U.S. Department of Transportation
National Highway Traffic Safety Administration
NHTSA
www.nhtsa.gov

TRAFIKVERKET
SWEDISH TRANSPORT ADMINISTRATION

SAFER

# Table of Contents

## Oral Papers

### Protection of Vulnerable Road Users


PaperNo.15-0051-O Integrated Bicyclist Protection Systems - Potential of Head Injury Reduction Combining Passive and Active Protection Systems
PaperNo.15-0059-O A New Strategy to Enhance Traffic Safety in Developing Countries
PaperNo.15-0084-O Car or Ground: Which Causes More Pedestrian Injuries?
PaperNo.15-0114-O Creating Pedestrian Crash Scenarios in a Driving Simulator Environment
PaperNo.15-0141-O Benefits Assessment of Autonomous Emergency Braking Pedestrian Systems Based on Real World Accidents Reconstruction
PaperNo.15-0169-O Fatal Urban Cyclist Collisions with Lorries: An In-Depth Study of Causation Factors and Countermeasures Using a System-Based Approach
PaperNo.15-0286-O Development of a Test Procedure for Driver Assist Systems Addressing Accidents Between Right Turning Trucks and Straight Driving Cyclists
PaperNo.15-0300-O Sensitivity of Q10 and Q6 Chest Measurements to Restraint and Test Parameters
PaperNo.15-0358-O Test Procedures and Results for Pedestrian AEB Systems
PaperNo.15-0319-O Guidelines for Pedestrian Friendly Windscreen Designs Considering Probabilistic Fracture Behaviour of Glass
PaperNo.15-0330-O Is Comfort Important for Optimal Use of Child Restraints?
PaperNo.15-0332-O Mechanisms of Head and Neck Injuries Sustained by Helmeted Motorcyclists in NSW, Australia
PaperNo.15-0375-O Countermeasures to Address Misuse in Child Restraint Installations: From Technical Solutions to Real World Evaluation
PaperNo.15-0391-O Pedestrian Response with Different Initial Positions During Simulated Impact with a Mid-Sized Sedan
PaperNo.15-0418-O Implication of Children in Road Accidents in France in 2011.


### Testing and Modeling of Structural Performance in Frontal Crashes


PaperNo.15-0343-O A Mobile Deformable Barrier Test for the Front Crash Assessment of Future Urban Microcars
PaperNo.15-0108-O Development of the Research Oblique Moving Deformable Barrier to Better Represent Real-World Frontal Oblique Crashes
PaperNo.15-0182-O The Incidence and Severity of Small Overlap Frontal Crashes in NASS-CDS
PaperNo.15-0183-O A Semi-Analytical Approach to Identify Solution Spaces for Crashworthiness in Vehicle Architectures
PaperNo.15-0244-O Small Overlap Frontal Impact – Experience and Proposal for a Future Approach
PaperNo.15-0254-O What Is the Benefit of a Frontal Mobile Barrier Test Procedure?
PaperNo.15-0081-O A Study of Gas Flow Behavior in Airbag Deployment Simulation
PaperNo.15-0100-O The Force Measurement of Primary Parts in Frontal Vehicle Crash Test and Those Test Methods
PaperNo.15-0217-O The Tracking Method of Vehicle Point or Dummy Point in the Vehicle Crash by Calculating Linear Accelerometer and Angular Velocity
PaperNo.15-0055-O Objective Evaluation Method of Vehicle Crash Pulse Severity in Frontal New Car

Assessment Program (NCAP) Tests

PaperNo.15-0038-O Feasibility Study of Airbag Concept Applicable to Motorcycles Without Sufficient Reaction Structure

PaperNo.15-0041-O Estimation of Front Underrun Protector Effectivity in Terms of Fatalities Reduction

## Crash Avoidance #1: Safety Performance and Effectiveness of Driver Assistance Technologies, Test & Evaluation Procedures, Benefits Assessment

PaperNo.15-0050-O The Real World Safety Potential of Connected Vehicle Technology

PaperNo.15-0370-O A Comprehensive and Harmonized Method for Assessing the Effectiveness of Advanced Driver Assistance Systems by Virtual Simulation: The P.E.A.R.S. Initiative

PaperNo.15-0063-O A Survey of Electrical and Electronic (E/E) Notifications for Motor Vehicles

PaperNo.15-0268-O Automated Generation of Virtual Driving Scenarios from Test Drive Data

PaperNo.15-0283-O Tools and Methods for Current and Future Controllability Assessment

PaperNo.15-0139-O Effectivity Analysis and Virtual Design of Integrated Safety Systems

PaperNo.15-0211-O Bicyclist Behavior Analysis for PCS (Pre-Collision System) Based on Naturalistic Driving

PaperNo.15-0097-O Real-Time Pedestrian & Driver Analysis by Neuromorphic Visual Information Processing

PaperNo.15-0040-O Fast Calculating Surrogate Models for Leg and Head Impact in Vehicle-Pedestrian Collision Simulations

PaperNo.15-0098-O Evaluation of the Effectiveness of Volvo‘s Pedestrian Detection System Based on Selected Real-Life Fatal Pedestrian Accidents

PaperNo.15-0354-O Aspects of Age Related Accident Causation Factors and Implication for Safety Measures

PaperNo.15-0212-O Road Departure Protection - A Means for Increasing Driving Safety Beyond Road Limits

PaperNo.15-0222-O Research on Driver Acceptance of LDA (Lane Departure Alert) System

PaperNo.15-0080-O Potential Safety Benefits of Lane Departure Warning and Prevention Systems in the U.S. Vehicle Fleet

PaperNo.15-0176-O Evaluation of a Pre-Production Head-On Crash Avoidance Assist System Using an Extended "Safety Impact Methodology" (SIM)

PaperNo.15-0437-O Development of a Standardized Method for Making Characteristic RADAR Measurements of Example Vehicles and Surrogate Targets

PaperNo.15-0015-O Unmanned Target Vehicle for Active Safety Evaluation in Cut-In Test Scenarios

PaperNo.15-0037-O Prospective Estimation of the Effectiveness of Driver Assistance Systems in Property Damage Accidents

PaperNo.15-0220-O Autonomous Emergency Braking for Cornering Motorcycle

PaperNo.15-0058-O AEB Real World Validation Using UK Motor Insurance Claims Data

PaperNo.15-0121-O Real-World Performance of City Safety Based on Swedish Insurance Data

PaperNo.15-0159-O The Development of a Test Procedure Suitable for Use in Consumer Information Programmes to Assess the Performance of AEB Systems in Collisions Involving Vulnerable Road Users

## Biomechanics #1: Development, Validation and Use of Human Body Models in Assessment of Crash Injury

PaperNo.15-0165-O Age and Sex-Specific Thorax Finite Element Model Development and Simulation

PaperNo.15-0166-O Age Dependent Factors Affecting Thoracic Response: A Finite Element Study Focused on Japanese Elderly Size Occupants

PaperNo.15-0313-O Rib Length Variation with Age and Sex - Measurements from High-Resolution Low-Radiation X-Ray Images of Volunteer Subjects
PaperNo.15-0387-O Unveiling the Structural Response of the Ribcage: Contribution of the Intercostal Muscles to the Thoracic Mechanical Response
PaperNo.15-0373-O Implementation of New Rib Material Models to a FE - Human Body Model for Evaluation of the PRE-SAFE Impulse Side Restraint System for Side Impact Protection
PaperNo.15-0148-O Effect of Age on Brain Injury Distribution in Rotational Head Trauma - A Parameter Study Using a Rat Finite Element Model.
PaperNo.15-0102-O Sensitivity of Head and Cervical-Spine Injuries to Impact Parameters Relevant to Rollover Crashes
PaperNo.15-0157-O Development and Validation of the Total HUman Model for Safety (THUMS) Toward Further Understanding of Occupant Injury Mechanisms in Pre- And Post- Crashes
PaperNo.15-0115-O Development of a Computationally Efficient Human Body Finite Element Mode
PaperNo.15-0247-O Aiming for an Average Female Virtual Human Body Model for Seat Performance Assessment in Rear-End Impacts
PaperNo.15-0345-O Muscle Activation Strategies in Human Body Models for the Development of Integrated Safety
PaperNo.15-0312-O Abdominal Characterization Test Under Lap Belt Loading

## Testing and Modeling of Structural Performance in Side Impact and Rollover Crashes

PaperNo.15-0068-O Simulation and Testing of Adaptive FRP-Substructures for Automotive Safety
PaperNo.15-0135-O Robust Design Method for Automotive and Aerospace Composite Structures Including Manufacturing Variations
PaperNo.15-0105-O The Force Measurement of Primary Parts in Vehicle Side/Smalloverlap Crash
PaperNo.15-0209-O Load Transfer of Passenger Car Compartment for Improvement of Structural Performance in Side Impact
PaperNo.15-0363-O Development of High Efficiency Load Path Structure to Enhance Side Impact Safety Performance
PaperNo.15-0034-O Potential of a Pre-Crash Lateral Occupant Movement in Side Collisions of (Electric) Mini Cars
PaperNo.15-0131-O Analysis of Vehicle Roof Weakness and Potential for Neck Injuries from Experimental and Simulated Dynamic Rollover Tests
PaperNo.15-0145-O Association Between Vehicle Panel Damage and Thoracic Injury in Rollover Crashes
PaperNo.15-0336-O Dynamic Validation of Rollover Buck Roof Structure
PaperNo.15-0350-O The Effect of Road Contact Angle and Pitchyaw Angle on the Injury of Drivers in Cris Test

## Crash Avoidance #2: Challenges for a Safe Human-Machine Interface Design

PaperNo.15-0359-O Fighting Driver Distraction – Recent Developments 2013 - 2015
PaperNo.15-0240-O Repeatability of the NHTSA Visual-Manual Guidelines Assessment Procedure
PaperNo.15-0057-O Using Sound to Reduce Visual Distraction from In-Vehicle Human-Machine Interfaces
PaperNo.15-0404-O Comparison Between Occlusion Methods for Measuring Distraction Caused by Smartphone Interaction
PaperNo.15-0398-O Reliability Improvement Needed in the Eye Glance Measurement Using Driving Simulator Test
PaperNo.15-0423-O Driver Behavior During Lane Change from the 100-Car Naturalistic Driving Study

PaperNo.15-0452-O Driver Vehicle Interface Design Assistance

PaperNo.15-0455-O Auditory Alerts in Vehicles: Effects of Alert Characteristics and Ambient Noise Conditions on Perceived Meaning and Detectability

PaperNo.15-0156-O Evaluation of Security Related Impacts on the Safety of Automotive Systems with Regard to Supporting Reaction Strategies for the Driver

PaperNo.15-0171-O Combining Coordination of Motion Actuators on a Truck Combination with Driver Characteristics

## Biomechanics #2: Advances in Crash Test Dummies, Instrumentation and Data Analysis

PaperNo.15-0048-O Injury Simulation of Rear Seat Child Occupant in Offset Deformable Barrier Frontal Impact

PaperNo.15-0432-O Injuries and Kinematics: Response of the Cervical Spine in Inverted Impacts

PaperNo.15-0170-O Lower Leg Injury Risk Curves Based on Survival Analysis - Meta Analysis of Normalized Post Mortem Human Subject Experiments for Applications to Dummy Tests in Crashworthiness

PaperNo.15-0272-O Comparison of HIC and BRIC Head Injury Risk in IIHS Frontal Crash Tests to Real-World Head Injuries

PaperNo.15-0288-O Instrumentation Technique for Measuring Six Degrees of Freedom Head Kinematics in Impact Conditions Using Six-Accelerometers and Three-Angular Rate Sensors (6a*f*ç Configuration) on a Lightweight Tetrahedron Fixture

PaperNo.15-0207-O A Study of Brain Injury Mechanisms in Vehicle Crashes

PaperNo.15-0397-O Occupant Behavior and Brain Injury in NHTSA Oblique Test

PaperNo.15-0216-O Proposal for a Modified THOR Lower Abdomen Including Abdominal Pressure Twin Sensors

PaperNo.15-0116-O Development of a High Energy Side Impact Dummy

PaperNo.15-0339-O Impact Responses of THOR Mod Kit Under Different Conditions in Sled Tests and Vehicle Crash Tests

## Restraint System Design and Performance Challenges: Addressing the Needs of Diverse Populations (Age, Gender, Stature)

PaperNo.15-0122-O A Simulation Study on the Efficacy of Advanced Belt Restraints to Mitigate the Effects of Obesity for Rear-Seat Occupant Protection in Frontal Crashes

PaperNo.15-0023-O Analysis of Abdominal Injuries Caused by the Submarining Phenomenon in the Rear Seat Occupants

PaperNo.15-0018-O Advanced Seat Belt Reminder System for Rear Seat Passengers

PaperNo.15-0263-O Influence of Impact Type and Restraint System Triggering Time on Injury Severity in Frontal Impact Crashes

PaperNo.15-0337-O Crash Protection Offered to Small Occupants in an Offset Frontal Crash

PaperNo.15-0371-O Innovative Seat Belt System for Reduced Chest Deflection

PaperNo.15-0381-O Innovative Restraints to Prevent Chest Injuries in Frontal Impacts

PaperNo.15-0443-O Investigation of Rear Seat Occupant Potential Injury Risk Based in Seat Belt Configurations

PaperNo.15-0130-O Preliminary Study of Roof Airbag Protecting Rear-Seat Occupants in Frontal Impact

PaperNo.15-0077-O Census Study of Real-Life Near-Side Crashes with Modern Side Airbag Equipped Vehicles

PaperNo.15-0384-O Gender Differences in Occupant Posture and Muscle Activity with Motorized Seat Belts

## Crash Avoidance #3: Connected and Automated Vehicles

PaperNo.15-0379-O Development of a Basic Safety Message for Tractor-Trailers for Vehicle-To-Vehicle Communications
PaperNo.15-0402-O Probabilistic Prediction Based Automated Driving Control in Urban Traffic Situation
PaperNo.15-0369-O Intelligent Infrastructure + Vehicles to Address Transportation Problems
PaperNo.15-0390-O A Multiple Target Tracking Strategy Using Moving Horizon Estimation Approach Aided by Road Constraint
PaperNo.15-0447-O Safety 2.0 – Potentials of Cooperative Safety by Vehicle-To-X Communication
PaperNo.15-0451-O Key Considerations in the Development of Driving Automation Systems
PaperNo.15-0457-O Analysis of Vehicle-Based Security Operations
PaperNo.15-0428-O Human Factors Evaluation of Level 2 and Level 3 Automated Concepts
PaperNo.15-0454-O An Overview of NHTSA's Electronic Reliability and Cybersecurity Research Programs
PaperNo.15-0109-O Automated Driving Functions Giving Control Back to the Driver: A Simulator Study on Driver State Dependent Strategies
PaperNo.15-0106-O Automatic Control of Vehicle Steering System During Lane Change
PaperNo.15-0431-O Improve Road Safety Using Combined V2V and Pre-Collision Systems
PaperNo.15-0206-O Safety Layer for Intelligent Transport Systems

## Advanced Fuels Crash Safety

PaperNo.15-0210-O An Analysis of Hybrid and Electric Vehicle Crashes in the U.S.
PaperNo.15-0164-O Fire Tests on E-Vehicle Battery Cells and Packs
PaperNo.15-0073-O Thermal Modelling of Fire Propagation in Lithium-Ion Batteries
PaperNo.15-0234-O Protection of Lithium-Ion Traction Batteries in the Electric Car
PaperNo.15-0163-O E-Vehicle Safety – Pyro Switch as High Voltage Circuit Breaker & Bypass
PaperNo.15-0252-O A Partnership Between Renault and French First Responders to Ensure Safe Intervention on Crash or Fire-Damaged Electrical Vehicles.
PaperNo.15-0361-O Recommendations for the Safe Handling of Damaged Electric Vehicles After Severe Road Traffic Accidents
PaperNo.15-0047-O Evaluation of Measurement Procedure for Post-Crash Hydrogen Concentration
PaperNo.15-0326-O Failure Analysis of Compressed Natural Gas Containers for Automotive Use
PaperNo.15-0405-O General Virtual Testing Methodology for Type IV CNG Tanks

## Consumer Information Approaches To Improve Global Safety

PaperNo.15-0314-O The Enhanced U.S. NCAP Five Years Later
PaperNo.15-0292-O Evaluation of Motorcycle Helmet Usability and Stability in the Consumer Safety Rating Program CRASH
PaperNo.15-0277-O Euro NCAP's First Step to Assess Autonomous Emergency Braking (AEB) for Vunerable Road Users
PaperNo.15-0258-O Beyond Safety Legislation: Contribution of Consumer Information Programmes to Enhanced Injury Mitigation of Pedestrians During Accidents with Motor Vehicles
PaperNo.15-0049-O Occurrence of Serious Injury in Real-World Side Impacts of Vehicles with Good Side-Impact Protection Ratings
PaperNo.15-0267-O Evaluation of the Euro NCAP Whiplash Protocol Using Real-World Crash Data

PaperNo.15-0315-O A Methodology to Derive Precision Requirements for Automatic Emergency Braking (AEB) Test Procedures

PaperNo.15-0093-O Development of a Methodology for Assessment of Integrated Pedestrian Protection Systems with Pre-Crash Braking and Passive Safety Components

PaperNo.15-0239-O Predicting the Impact of Vehicle Safety Developments in Emerging Markets Following the Industrialised Countries' Experience

PaperNo.15-0228-O Consumer Safety-Information Programs at IIHS

PaperNo.15-0376-O The Australian Child Restraint Evaluation Program: An Update on Dynamic Assessment Protocols and Observed Dynamic Performance of Child Restraint Systems

## Technologies and Policies of Driver Monitoring

PaperNo.15-0276-O Driver Alcohol Detection System for Safety (DADSS) – a Non-Regulatory Approach in the Development and Deployment of Vehicle Safety Technology to Reduce Alcohol-Impaired Driving – a Status Update.

PaperNo.15-0380-O Introduction of a Solid State, Non-Invasive, Human Touch Based Blood Alcohol Sensor

PaperNo.15-0410-O The Relationship Between BAC and BrAC of Healthy Korean Males

PaperNo.15-0458-O Unobstrusive Breath Alcohol Sensing System

PaperNo.15-0453-O Mitigating Drowsiness: Linking Detection to Mitigation

PaperNo.15-0226-O Analysis of the Robustness of Steering Pattern Based Drowsiness Detection

PaperNo.15-0377-O The Potential for Adaptive Safety Through In-Vehicle Biomedical and Biometric Monitoring

PaperNo.15-0150-O Application of Biologically Inspired Visual Information Processing in Affective Driver Status Monitoring

## Integrated Safety from Pre-Crash to Crash to Post-Crash

PaperNo.15-0060-O New Integrated Assistance Functions for Real World Accident Scenarios

PaperNo.15-0335-O The AEB System with Active and Passive Safety Integration for Reducing Occupans' Injuries in High-Velocity Region

PaperNo.15-0374-O Evaluation of Occupant Protection Systems: From a PREVENTIVE a PRE-IMPACTING RESTRAINT SYSTEM TO

PaperNo.15-0424-O Run Off Road Safety

PaperNo.15-0409-O Enhancement of Occupant Safety in Offset Frontal Vehicle Collision: Using Novel Mathematical Modelling Alongside Vehicle Dynamics Control Systems.

PaperNo.15-0215-O The Integrated Safety Concept of the Ultra-Compact Electric Vehicle Visio.M

PaperNo.15-0246-O Occupant Protection in Rear-End Collisions Preceded by Autonomous Emergency Braking Deployment

PaperNo.15-0137-O eCall – Defining Accident Conditions for Mandatory Triggering of Automatic Emergency Calls

PaperNo.15-0147-O Estimated Injury Risk for Specific Injuries and Body Regions in Frontal Motor Vehicle Crashes

PaperNo.15-0167-O Utilization of Crash Scene Photography Documenting Vehicle Damage and Intrusion to Improve Trauma Care Preparedness

PaperNo.15-0190-O Occupant Transportation Decision Algorithm: An Advanced Automatic Crash Notification Algorithm Developed and Evaluated for Motor Vehicle Crash Occupant Triage

PaperNo.15-0388-O Results from First Field Test of Telemetry Based Injury Severity Prediction

PaperNo.15-0415-O Pilot Study on AACN and HEMS System in Japan

PaperNo.15-0427-O Assessing Mechanisms of Injury as Predictors of Severe Injury for Adult Car and Truck Occupants

### Assessment of New and Improved Field Data Collection, Analysis and Benefits Assessment Methods

PaperNo.15-0124-O Features of Car–Cyclist Contact Situations in Near-Miss Incidents Compared with Real-World Accidents in Japan
PaperNo.15-0110-O Differences in Long-Term Medical Consequences Depending on Impact Direction Involving Passenger Cars
PaperNo.15-0394-O Analysis and Simulation of Occupant Injury Risk at NASS/CDS
PaperNo.15-0168-O Mathematical Modelling and Numerical Optimization of Three Vehicle Crashes Using a Single-Mass Lumped Parameter Model
PaperNo.15-0291-O Lives Saved by Vehicle Safety Technologies and Associated FMVSS
PaperNo.15-0266-O Validating Vehicle Safety Using Meta-Analysis: A New Approach to Evaluating Vehicle Safety Technologies
PaperNo.15-0372-O Extrapolation of GIDAS Accident Data to Europe
PaperNo.15-0368-O Analysis of Different Types of Winter Tires in Rear-End Injury Crashes and Fatal Loss-Of-Control Crashes with ESC
PaperNo.15-0253-O A Continuous Video Recording System on a Lap-Belt Equipped School Bus: Real-World Occupant Kinematics and Injuries During a Severe Side Impact Crash
PaperNo.15-0149-O Comparison of Event Data Recorder and Naturalistic Driving Data for the Study of Lane Departure Events
PaperNo.15-0133-O Analysis of Quad-Bike Loss-Of-Control Caused by Bump Perturbations Using Experimental and Simulated Dynamic Bump Tests
PaperNo.15-0284-O Opportunities for Injury Reduction in Rollover Crashes

## Written Papers

### Protection of Vulnerable Road Users

PaperNo.15-0111-W Active Hood Pedestrian Protection
PaperNo.15-0243-W Bicycle-To-Car Accidents - Their Consequences for the Bicyclists and Typical Accident Scenarios
PaperNo.15-0175-W Analysis of Children Strollers and Prams Safety in Urban Buses
PaperNo.15-0177-W Performance Comparison and Repeatability Evaluation of the Flex PLI and TRL Pedestrian Legform Impactors
PaperNo.15-0366-W Improvement of the Protection of Lower Extremities of Vulnerable Road Users in the Event of a Collision with Motor Vehicles
PaperNo.15-0416-W Finite Element Study of Effectiveness of  Modified Front-End Structure with Aluminium Foam in Reducing Pedestrian Injury
PaperNo.15-0433-W Improvements to the Flexible Pedestrian Legform Impactor: The Development of New Bone Cores
PaperNo.15-0421-W An Inverse Monte-Carlo Based Method to Estimate Pre-Crash Distribution for VRU Safety

### Testing and Modeling of Structural Performance in Frontal Crashes

PaperNo.15-0257-W Evaluation of Frontal Crash Stiffness Measures from the U.S. New Car Assessment Program

PaperNo.15-0282-W Preliminary Study of the Responses of Hybrid III 5th Female, 50th Male, Q6 and Hybrid III 5th Pregnant Female Dummy Seated in the 2nd Row Seats of Passenger Vehicles in Sled Tests

PaperNo.15-0261-W Consideration of Representativeness of Real-World Accidents and Repeatability of New NHTSA Oblique Offset Frontal Impact Test

PaperNo.15-0161-W A Model of Vehicle-Fixed Barrier Frontal Crash and Its Application in the Estimation of Crash Kinematics

PaperNo.15-0367-W Effect of FMVSS 226 Compliant Curtain Airbags on the BrIC Result of a Hybrid III 50th% Dummy During an Oblique Impact.

PaperNo.15-0033-W Study on the Safety Performance of the Rear Safety Guard with Air Bag for Truck

PaperNo.15-0389-W MOPDB- Mobile Offset Progressive Deformable Barrier: A New Approach to Cover Compatibility and Offset Testing

PaperNo.15-0096-W Critical Review of the Current Assessment Approaches for Frontal Crash Compatibility Regarding the Evaluation of Structural Interaction

PaperNo.15-0320-W The Trolley Test Way of IIHS Small Overlap and Side Test

## Crash Avoidance #1: Safety Performance and Effectiveness of Driver Assistance Technologies, Test & Evaluation Procedures, Benefits Assessment

PaperNo.15-0341-W Limitations of Use of an Inertial Positioning System in a Truck During a Maneuver of Avoiding a Suddenly Appearing Obstacle

PaperNo.15-0071-W How Is AstaZero Designed and Equipped for Active Safety Testing?

PaperNo.15-0125-W Virtual Experimental Environment Design of Camera-Sensor-Based Lane Detection System

PaperNo.15-0348-W Parking Crashes: The Rationale for Action and the Development of Test Procedures

PaperNo.15-0351-W Technologies for the Prevention of Run-Off Road and Head on Crashes

PaperNo.15-0227-W Determination of Pedestrian of Mannequin Clothing for the Evaluation of Image Recognition Performance of Pedestrian Pre-Collision Systems

PaperNo.15-0256-W Evaluation of Motorcycle Antilock Braking Systems

PaperNo.15-0245-W Analysis of Car Accidents Caused Due to Unintentional Run Off Road

PaperNo.15-0395-W Safety Assessment Procedure for Advanced Emergency Braking System

PaperNo.15-0355-W The Development of Assessment Technologies for Advanced Safety Vehicles

## Biomechanics #1: Development, Validation and Use of Human Body Models in Assessment of Crash Injury

PaperNo.15-0429-W Correlation Between THOR BrIC and TBI Risk from Full Body Human Model

## Testing and Modeling of Structural Performance in Side Impact and Rollover Crashes

PaperNo.15-0444-W Opportunities for Reducing Far-Side Casualties

PaperNo.15-0153-W Investigation of the Centre of Gravity Position on the Course of Vehicle Rollover

PaperNo.15-0016-W Characteristic Analysis of Passenger Cars' Side Impact Based on In-Depth Accident Research in China

PaperNo.15-0107-W Analysis of the Influence of Motor Cars’ Relative Positions During a Right-Angle Crash on the Dynamic Loads Acting on Car Occupants and the Resulting Injuries

## Biomechanics #2: Advances in Crash Test Dummies, Instrumentation and Data Analysis

PaperNo.15-0085-W Matching Structural Injury Risk Statistics and Dummy Injury Measures for Dynamic Compliance and Ratings Rollover Regulatory Test
PaperNo.15-0325-W First Generation Obese ATD (FGOA)

## Crash Avoidance #3: Connected and Automated Vehicles

PaperNo.15-0430-W Target Crash Population of Automated Vehicles

## Advanced Fuels Crash Safety

PaperNo.15-0074-W Detection of Fires in Heavy Duty (HD) Vehicles
PaperNo.15-0248-W High Risk E-Vehicle Battery Sled Testing

## Consumer Information Approaches To Improve Global Safety

PaperNo.15-0152-W A Study on Toughened Glass Used for Vehicles and Its Testing Methods
PaperNo.15-0144-W The Australian Terrain Vehicle Assessment Program (ATVAP)
PaperNo.15-0069-W Consumer Response to Vehicle Safety Ratings
PaperNo.15-0042-W Improving Vehicle Safety in Australia and New Zealand: The Role of ANCAP.
PaperNo.15-0328-W Vehicle Safety Trends and the Influence of NCAP Safety Ratings
PaperNo.15-0318-W Crashworthiness Testing of Electric and Hybrid Vehicles
PaperNo.15-0306-W Howsafeisyourfirstcar.com.au – a Website to Assist Young Drivers to Find a Safe Car, in Their Budget.
PaperNo.15-0275-W The Assessment Results of the Advanced Safety Technology in JNCAP and Its Future

## Integrated Safety from Pre-Crash to Crash to Post-Crash

PaperNo.15-0295-W Automatic Opening of Emergency Windows by Magnetic Release Mechanism
PaperNo.15-0310-W Occupant Protection Performance in Side Impact Collisions Preceded by Pre-Crash Deployment of On-Board Safety Systems
PaperNo.15-0329-W A Methodology and Tool Chain to Develop Integrated Safety Systems

## Assessment of New and Improved Field Data Collection, Analysis and Benefits Assessment Methods

PaperNo.15-0269-W Updated Estimates of Potential Traffic Fatality Reductions with Automatic Collision Notification
PaperNo.15-0259-W Airbag Related Injuries in NHTSA's Crash Databases
PaperNo.15-0435-W A Concept for Naturalistic Data Collection for Vulnerable Road Users Using a Smartphone-Based Platform
PaperNo.15-0287-W Identifying and Proving Automotive Algorithm Defects and Affecting Recalls
PaperNo.15-0260-W EDR Data Collection in NHTSA's Crash Databases

PaperNo.15-0270-W Real World Analysis of Fatal Rear-End Crashes

PaperNo.15-0323-W Improving the Swiss National Accident Statistics by Providing AIS Data to Classify Injury Severity

## Government Status Reports

PaperNo.15-0464-G Government Status Report for Japan

PaperNo.15-0465-G Government Status Report for United States

PaperNo.15-0466-G Government Status Report for Sweden

PaperNo.15-0467-G Government Status Report for Germany

PaperNo.15-0468-G Government Status Report for Australia

PaperNo.15-0469-G EEVSC

PaperNo.15-0470-G Government Status Report for Republic of Korea

PaperNo.15-0473-G Government Status Report for Poland

PaperNo.15-0478-G European Commission

PaperNo.15-0479-G Government Status Report for Italy

# INTRODUCTION

The Enhanced Safety of Vehicles (ESV) program originated in 1970 under the North Atlantic Treaty Organization (NATO) Committee on the Challenges of Modern Society, and was implemented through memorandums of understanding between the Governments of the United States, France, Germany, Italy, the United Kingdom, Japan, and Sweden. The participating nations agreed to develop experimental safety vehicles to advance the state-of-the-art technology in automotive safety engineering and to meet periodically to exchange information on their progress. Since its inception the number of international partners has grown to include the Governments of Canada, Australia, The Netherlands, Hungary, Poland, Republic of Korea, and two international organizations the European Enhanced Vehicle-safety Committee, and the European Commission. A representative from each country/organization serves as a Government Focal Point in support of the ESV program.

In the interest of information exchange, The U.S. Department of Transportation, National Highway Traffic Safety Administration (NHTSA), distributes the Proceedings of the 24th International Technical Conference on the Enhanced Safety of Vehicles. The technical papers in this publication detail safety research efforts underway worldwide, and share the common interest of reducing motor vehicle related fatalities and injuries.

The opinions, findings, and conclusions expressed in the publications are the original written work of the author(s) and not necessarily those of the U.S. Department of Transportation, National Highway Traffic Safety Administration. Traditional papers are accepted after the corresponding abstracts undergo technical review. To enhance the scientific content, twenty one papers were accepted for peer-review and published in a special edition of ***Traffic Injury Prevention*** 16(S1), by Taylor and Francis Group. These papers are available to the public via http://www-esv.nhtsa.dot.gov/.

On behalf of the Conference Organizing Committees we thank our international participants for their dedication and support of the 24th ESV Conference and look forward to your future participation.

Donna E. Gilmore
ESV Technical Coordinator & Scientific-Secretariat
USDOT/NHTSA

# 24th ESV INTERNATIONAL PROGRAM DELEGATES

## UNITED STATES – 24TH ESV CONFERENCE SPONSOR

**THE HONORABLE MARK R. ROSEKIND, PH.D.**
Administrator
National Highway Traffic Safety Administration

**NATHANIEL BEUSE**
Chairman, ESV Government Focal Points
Associate Administrator for Vehicle Safety Research
National Highway Traffic Safety Administration

**DONNA E. GILMORE**
ESV Technical Coordinator & Scientific-Secretariat
National Highway Traffic Safety Administration

**STEPHEN A. RIDELLA**
ESV Lead Technical Advisor
Director Office of Vehicle Crashworthiness Research
National Highway Traffic Safety Administration

**ARTHUR CARTER**
ESV Student Safety Technology Design Competition Coordinator
National Highway Traffic Safety Administration

## SWEDEN – 24TH ESV CONFERENCE HOST

**ANNA NILSSON-EHLE**
Director
SAFER Vehicle and Traffic Safety Centre

**ANDERS LIE**
ESV Government Focal Point
Specialist, Swedish Transport Administration

**LISA KNUTSSON**
Communications Manager
SAFER Vehicle and Traffic Safety Centre

**ULRIKA LANDELIUS**
Program Director FFI
Swedish Transport Administration

**ANDERS EUGENSSON**
Director Governmental Affairs
Volvo Car Corporation

**YNGVE HÅLAND**
Senior Advisor
SAFER Vehicle and Traffic Safety Centre

**PETER KRONBERG**
Safety Director
AB Volvo

**PER LÖVSUND**
Professor
Chalmers University of Technology

**HANS G PETTERSSON**
Ministry of Enterprise, Energy and Communications

**JAN OLSSON**
Senior Advisor
Autoliv

# 24th ESV CONFERENCE GOVERNMENT FOCAL POINT MEMBERS

**AUSTRALIA**

**Robert Hogan**
General Manager,
Vehicle Safety Standards Department of Transport and Regional Services

**CANADA**

**Peter Burns**
Chief, Ergonomics & Crash Avoidance, Transport Canada

**EUROPEAN COMMISSION**

**Philippe Jean**
Acting Director, European Commission

**EUROPEAN ENHANCED VEHICLE- SAFETY COMMITTEE**

**Bernd Lorenz**
Head of Section F2 – Passive Vehicle Safety, Biomechanics,
Federal Highway Research Institute (BASt)

**GERMANY**

**Stefan Strick**
President and Professor, Federal Highway Research Institute (BASt)

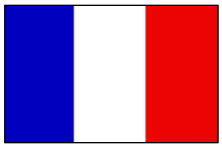

**FRANCE**

**Daniel Kopaczewksi**
Head – Department Vehicle Secuirty and Emissions,
Ministry of Ecology, Substainable Development and Energy

**HUNGARY**

**János Déak**
Head of the Technical Co-ordination Centre for EU and –UN-ECE Activities on Road Vehicles, KTI/Institute for Transport Sciences

**ITALY**

**Dott. Ing. Antonio Erario**
Head of Division I, International Regulation Affairs
Ministry of Infrastructure and Transport,Department for Transport

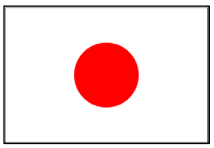

**JAPAN**

**Masayuki Shima**
Director of Engineering Policy Division,
Road Transport Bureau, Ministry of Land Infrastructure Transport and Tourism (MLIT)

**POLAND**

**Wojciech Przybylski**
Director for Technology and International Cooperation,
Motor Transport Institute (Instytut Transportu Samochodowego)

**REPUBLIC OF KOREA**

**Hyun Sung Shin**
Deputy Director, Motor Vehicles Management Divison, Ministry of Land,
Infrastructure and Transport (MOLIT)

**SWEDEN**

**Anders Lie**
Specialist, Traffic Safety Division Trafikverket,
Swedish Transport Administration

**THE NETHERLANDS**

**Peter E. Th. Striekwold**
Manager, Vehicle Standards Development, RDW

**UNITED KINGDOM**

**Bernie Frost**
Principal Engineer, Department for Transport

**UNITED STATES OF AMERICA**

**Nathaniel Beuse**
Associate Administrator for Vehicle Safety Research,
National Highway Traffic Safety Administration

# 24th ESV TECHNICAL SESSION CHAIRPERSONS/CO-CHAIRPERSONS

| Technical Session Topics | Chair | Country | Co-Chair | Country |
|---|---|---|---|---|
| Protection of Vulnerable Road Users | Suzanne Tylko | Canada | Jim Hand | UK |
| Testing and Modeling of Structural Performance in Frontal Crashes | Younghan Youn | Korea | Stephen Summers | U.S. |
| Crash Avoidance #1: Safety Performance and Effectiveness of Driver Assistance Technologies, Test & Evaluation Procedures, Benefits Assessment | Bernie Frost | U.K. | Anders Lie | Sweden |
| Biomechanics #1: Development, Validation and Use of Human Body Models in Assessment of Crash Injury | Matthew Craig | U.S. | Rainer Hoffmann | Germany |
| Testing and Modeling of Structural Performance in Side Impact and Rollover Crashes | Bengt Pipkorn | Sweden | Mark Terrell | Australia |
| Crash Avoidance #2: Challenges for a Safe Human-Machine Interface Design | Peter Burns | Canada | Jost Gail | Germany |
| Biomechanics #2: Advances in Crash Test Dummies, Instrumentation and Data Analysis | Philippe Vezin | France | Yasuhiro Matsui | Japan |
| Restraint System Design and Performance Challenges: Addressing the Needs of Diverse Populations (Age, Gender, Stature) | Lotta Jakobsson | Sweden | Lex van Rooij | The Netherlands |
| Crash Avoidance #3: Connected and Automated Vehicles | Tim Johnson | U.S. | Jonas Sjöberg | Sweden |
| Advanced Fuels Crash Safety | Jost Gail | Germany | Lars Hoffmann | Sweden |
| Consumer Information Approaches To Improve Global Safety | Andre Seeck | Germany | David Ward | U.K. |
| Technologies and Policies of Driver Monitoring | Trent Victor | Sweden | Dominique Cesari | France |
| Integrated Safety from Pre-Crash to Crash to Post-Crash | Stephen Ridella | U.S. | Jac Wismans | The Netherlands |
| Assessment of New and Improved Field Data Collection, Analysis and Benefits Assessment Methods | Rob Thomson | Sweden | Bernd Lorenz | EEVC |
| CONTINUATION Crash Avoidance #1: Safety Performance and Effectiveness of Driver Assistance Technologies, Test & Evaluation Procedures, Benefits Assessment | Clarie Rees | U.K. | Bernie Fronst | U.K. |

# U.S. GOVERNMENT AWARD RECIPIENTS
## Presented at the 24th ESV Conference
## Gothenburg, Sweden

**U.S. Government Special Awards of Appreciation**
In recognition of and appreciation for outstanding leadership and special contributions in the field of motor vehicle safety

| | |
|---|---|
| Robert Zobel | Germany |
| Dr. Sadayuki Ujihashi, | Japan |
| Jonas Ekmark | Sweden |
| Farid Ahmed-Zaid | United States |
| Matthew Reed, Ph.D. | United States |

**U.S. Government Awards for Safety Engineering Excellence**
In recognition of and appreciation for exceptional scientific contributions in the field of motor vehicle safety engineering and for distinguished service to the motoring public

| | |
|---|---|
| Gerhard Steiger | Germany |
| Naoto Muto | Japan |
| Jae Wan Lee, Ph.D. | Korea |
| Asso. Prof Astrid Linder | Sweden |
| Trent Victor | Sweden |
| Dr. David Hynd | United Kingdom |
| Dr. Hariharan Krishnan | United States |

# 24th ESV 2015 INTERNATIONAL STUDENT SAFETY TECHNOLOGY DESIGN COMPETITION FINALISTS

**ASIA PACIFIC – KOREA, REGION 1**
REGIONAL COORDINATOR: PROF. YOUNG HAN YOON, KOREA

KoreaTech University
*"Development of the Sensor and Motor Driven Automatic Height Adjustable Rear Seat Cushion to Best Fitting Adult Seat Belt for Older Child Protection"*

**ASIA PACIFIC – JAPAN, REGION 1**
REGIONAL COORDINATOR: MR. MASASHI YUKAWA, JSAE, JAPAN

Shibaura Institute of Technology
*"The Safety Avoidance System of Two-Wheel Vehicle Using Gyro Effect"*

**EUROPE, REGION 2**
REGIONAL COORDINATOR: BERND LORENZ, BASt, GERMANY

Chalmers University of Technology
*"Urban Personal Vehicle Safety Strategy"*

Technical University Berlin
*"Developing a Pedestrian Airbag for Secondary Impact"*

Hochschule für Technik und Wirtschaft des Saarlandes (University of Applied Sciences), Saarbrucken
*"High Dynamic Driving Simulator for ADAS HIL Testing"*

**NORTH AMERICA, REGION 3**
REGIONAL COORDINATOR: ARTHUR CARTER, NHTSA, UNITED STATES

University of North Texas
*"Motorcycle Helmet with Crash Detection and Airbag Deployment"*

Stanford University
*"The Obstacle is the Path"*

University of Alaska
*"Dynamic Lights"*

# UNMANNED TARGET VEHICLE FOR ACTIVE SAFETY EVALUATION IN CUT-IN TEST SCENARIOS

**Yeonggeol, Park**
**Jaejoon, Kwon**
**Kihong, Park**
**Jay, Jeong**
Kookmin University
South Korea

Paper Number 15-0015

## ABSTRACT

In recent years, active safety systems are introduced to the markets and many of them are adopted to improve the possibility to avoid the accidents. These active safety systems include AEBS (Automatic Emergency Braking System,) LKAS (Lane Keeping Assistant System,) BSD (Blind Spot Detection,) and so on. The evaluation methods for those systems also have been developed and determined as international standards. Additionally, target systems for evaluation have been developed too. However, they are usually designed for testing straight rear collision scenarios. To reproduce other scenarios such as cut-in situations, a new concept of the target system is needed. So, in this work, the unmanned target vehicle are designed and developed.
The target vehicle is developed as an unmanned vehicle for accurate path following performance. A DGPS with 2cm accuracy and heading angle IMU are installed for the path following function. A soft dummy which resembles a typical SUV is attached on the unmanned target vehicle. To reproduce accident scenarios safely, the target vehicle should be designed to protect the hunter vehicle and the target vehicle itself from the crash shock of the collision situation. The target vehicle in this work is developed with a shock absorber system in the rear part of the target vehicle.
The rear part of the target vehicle is designed to have similar characteristics with a real vehicles in visual shape for vision systems and radio frequency reflection for radar systems. The shape and the material of the part is selected for the hunter vehicle to recognize the target vehicle as a real SUV.
The structural and dynamic analysis are carried out for the target performance. Also, evaluation experiments of the cut-in scenarios are carried out to test the hunter vehicle with the AEBS.
The dynamic performance results of the target vehicle will be presented. The results include the limit of impact speed, maximum speed, maximum lateral speed and accuracy of path following logic. The AEBS performance results of the hunter vehicle will be presented in the test cut-in situation.
In this work, test scenarios to evaluate the hunter vehicles are carried out especially for the 'Rear collision and Cut-in' situations. Frontal collision and accidents in intersection situation are excluded. The hunter vehicles with AEBS are only tested for the evaluation experiments. The test speed is set less than 40km/h.

## INTRODUCTION

Currently, the vehicles that adopt the active safety system are launched in the market. There are AEBS, LKAS and BSD as such active safety system and the system of adding points is prepared to be adopted to such system in NCAP. And, the car manufacturing companies are accelerating the development of vehicles that adopt such functions along such trend. It is acknowledged that the test method for verification should be development for the active safety device as well like collision safety test that is carried out in NCAP necessarily. The evaluation methods of active safety performance are developed in Europe actively[1]. Euro NCAP is performing the evaluation of frontal collision prevention device[2].
And, the target vehicle that can represent the scenario is being developed together with the methodology. The target vehicle is the one that simulates accident-causing vehicles such as stop, decelerateing and cut-in vehicles to

represent the accident situation in the accident scenario. As the active safety vehicle test is the evaluation of the system for avoiding the collision in accident situation, it always contains the possibility of collision against target vehicle in case the system does not operate completely. So the target vehicle should perform the function that can protect each system against the collision that can occur in the test as well as representation of scenario. The vehicle should attach the shock-absorbing material to absorb the shock, however, the problem of difficulty to let the testing vehicle recognize the target vehicle as real one should be solved.
This study used the analysis of accident data in the advanced projects of Europe and selected the required specifications for the target vehicle using the accident scenario drawn from them. The target vehicles were developed to satisfy such specifications. And, they were developed as the unmanned vehicle was developed considering correct representation of scenario, repeatability of test and safety of test driver. The developed target vehicle verified the reproduction ability of scenario through the performance evaluation of trajectory tracking.

## Scenario selection

This study used the analysis results of accident statistical data in the other projects for scenario selection. The project called ASSESS[3] classified the kind of highest frequency and injury value by analyzing the accident data of Europe. It used the scenario classified in the project.
ASSESS analyzed it using several data base of Europe and selected the generalized analysis method for analysis of several data. The representative accident types were clasiffied for scenario classification
in advance and the representative ones were drawn considering the seriousness of accident. The importance was determined by giving the specific weight according to the seriousness of accident along its type for generalizing the frequency and seriousness. The whole generalization was done by giving the weight along the population of each country. The accident of single vehicle, longitudinal collision (including both same and opposiste direction), collision at intersection and pedestrian accident were drawn as the accident type and analyzed as the most important type. In here, the collision at intersection and longitudinal collision were finally selected from the accidents of vehicle-to-vehicle again.
It aimed to evaluate the active safety perforamce of state-of-the art vehicle and develop the device for that against all accident types ultimately but it aimed to develop the target vehicle that can represent the longitudinal collision (the same direction) in this study. In here, the selected specifications of target vehicle were the speed of 40 km/h to satisfy the low driving speed, trajectory tracking of unmanned driving for correct representation of scenario and deceleration performance of 6 m/s2.

## Development of target vehicle system

The efforts to develop the target vehicle were spent in the other researches[1],[4],[5]. The target vehicle developed in this thesis was produced by modifying the electric vehicle and installing the unmanned-controlling module. The dynamic performances were increased by lowering total weight of the vehicle through removing all exterior and interior materials of the vehicle. And the actuator and controller such as steering controling actuator, brake(deceleration) control, acceleration control actuator, speed change actuator, wheel encoder, remote controller, interface module box, control box, interface moduel box, power supply box were installed for unmanned driving and remote control.
To explain each actuator simply, steering controling actuator used MDPS module as the mechanical part that controls the steering of vehicle. The acceleration controlling actuator controls the accelerator pedal using the accelerator pedal of the vehicle with mechanical part and wire. Brake (deceleration) control actuator controls the brake pedal using the mechanical part to brake pedal. Remote controller can control power status of system, power of each actuator and operation mode of system at driver's seat. The rear side of vehicle had power supply box that supplies the power of operating system and control box that controls each actuator by processing the power and processing signal between actuator and controller (See Figure 1). The wheel and encoder were installed to measure the movement and moving speed of vehicle in this sytem. Wheel encoder (DMI) has the principle that forwards the value to the encoder as the bearing rotates when the wheel of vehicle rotates with the connection of encoder to bearing. Bearing was designed to increase the durability of abrasion against vehicle wheel by urethane-covering and measure the correct positional value with tighter adherence between the rotating part of wheel and encoder. 2 DMI's were installed at the rear wheel.

And remote control server (See Figure 2) was installed to control the target vehicle so that the tests of various collision evaluation scenarios could be conducted in the unmanned way.

## Development of soft crash

Soft crash was developed to protect the developed target vehicle from the collision. Soft crash should absob and disperse the collision energy generated from the collision enough and guarantee the safety of testing and target vehicles by minimizing the impulsive forece. Soft crash was developed to be installed at the height that the actual vehicle collides that is the position of bumper. As the position of vehicle frontal bumper ranges from 220mm to 720mm generally, soft crash was installed at the position that is suitable for that. Shock absorber and sponge were used to absorb the shock generated from the collosion. 4 shock absorbers were used and two of them were installed to disperse the shock by mounting at the height of 220mm and 700mm. They were developed to relieve the first shock and prevent the damage of bumper against the collision of metals as the sponge was attached to the rear side of shock absorber in case of vehicle collision.

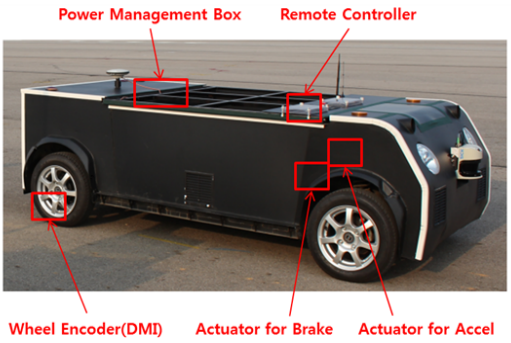


***Figure1. Layout of target vehicle.***

***Figure2.*** Control server and program of target system

## Performance evaluation of target vehicle

The specific track was composed for autonomic driving control algorithm performance evaluation for the developed target vehicle and one time of decelerating section and double lane change section were applied. And, in case of target speed, it was set as 45km/h for whole areas except the decelerating section. Its results were shown in Fig. 4 and Fig. 5.

Looking into autonomic driving control algorithm performance evaluation, it was known that the specific steering angle was input properly to track the designated route in real vehicle evaluation and the designated route was tracked as the result. But, it was recognized that the vehicle slightly got out of the coordinate of the designated way-point. It was judged that it came from GPS error generated from the influence of various surrounding environments including weather considering the characteristics of real vehicle that tracks the reference path based on the position of the vehicle that was input GPS actually.

## Real vehicle test of active vehicle

Real vehicle test was carried out using the developed target vehicle. The AEBS-adopted vehicle was selected as test vehicle for the test and the test was composed by mounting soft crash to the target vehicle (See Figure 4). The scenario used in the test was carried out at the difference of relative velocity of 10km/h in the condition of 0, 20, 30, 40km/h based on the speed of target vehicle in cut-in situation and it was programmed to implement cut-in and generate the steering at the time when TTC (Time To Collision) of both hunter vehicle and target vehicle became 4 seconds in case of cut-in scenario (See Figure 5). Looking into the test result of 40km/h, it was known that the speed of target vehicle kept 40km/h and the trigger was generated at the point when TTC of testing vehicle became 4 seconds in the test procedure. It could be checked out that TTC increased in a moment due to braking of testing vehicle at the testing time of 35 seconds. And, looking into the change of steering angle, it was checked out that steering began at the same time of generation of trigger and cut-in completed after 3.5 seconds (See Figure 6).

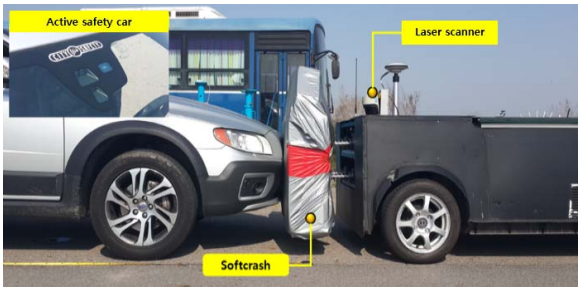


***Figure4. Active safety car test environment.***

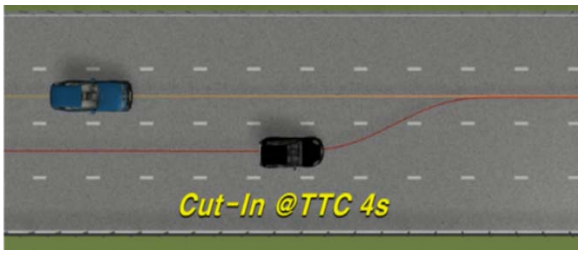


***Figure5. Cut-in scenario for the test***

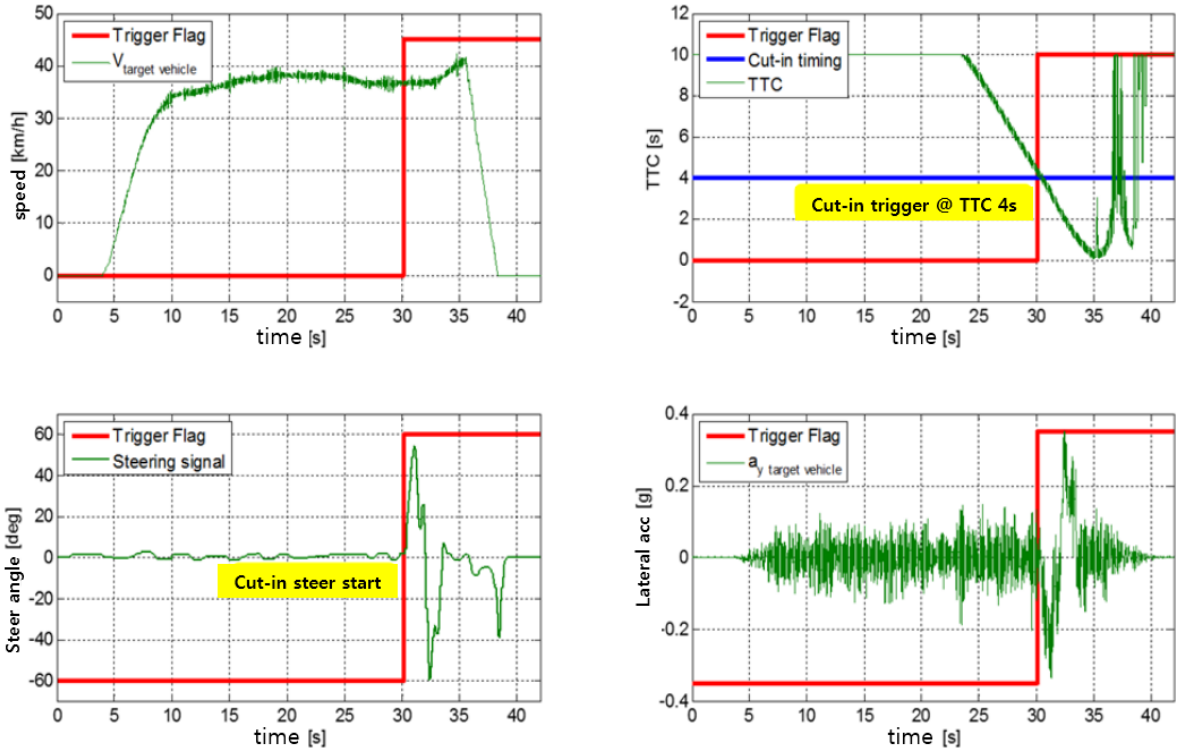


***Figure6. Test result at target speed 40km/h***

## DISCUSSION

Looking into the results of real vehicle test, it could be recognized that AEBS of testing vehicle operated approximately 5 seconds after target vehicle began to cut in, however, it was known that it performed the given scenario correctly. And, it was recognized that cruise driving of target vehicle could be performed well at the speed of 35~40km. The objective of target vehicle was to perform the testing situations correctly and repeatedly, however, it was regarded that such things could be satisfied well. And, it did cut in at TTC 4 seconds and finished cut-in in 3.5 seconds in respect of scenario, however, it was too much slow cut-in. TTC that began to cut in was needed to be performed in the reduced time to produce the more realistic accident situation and it was considered that the faster cut-in could be available by increasing the steering angle. It was considered that the additional performance improvement of vehicle and more precise speed control were required for that.

## CONCLUSIONS

The scenario to be applied to this study was selected to evaluate the active safety performance of active safety vehicle by investigating the projects of Europe that analyzed real accident data.

The target vehicle was developed to represent the accident situations of such scenario and the developed vehicle performed the test that conducted the designated scenario to verify the unmanned driving performance. As the results of test, it was checked out that it followed the route correctly in unmanned driving. It was checked out that it performed the scenario correctly by conducting the test that used the real vehicle. And, it was also checked out that the actual accident situation whose cut-in time had to be shortened could represented by increasing lateral acceleration through the additional performance improvement.

It is planned that system stabilization of system developed in this study and the research of the target vehicle that is capable of collision at high speed will be carried out continuously, the integration test of active safety vehicle will be possible hereafter if the system and methodology for the test are developed, and it is expected that it would suggest the more clear standards for consumers to choose the vehicles.

**ACKNOWLEDGEMENTS**

This research was supported by the Ministory of Land, Infrastructure and Transport. It was also supported by the Korea Agency for Infrastructure Technology Advancement(Project No.: 13PTSI-C054118-05)

**REFERENCES**

[1] Aparicio, Andres, et al. “Status of Test Methods for Active Safety Systems.” No. 2012-36-0214. SAE Technical Paper, 2012.
[2] Euro NCAP, “AEB Test Protocol”, 01/2014, V.1.0
[3] Assessment of Integrated Vehicle Safety Systems for improved vehicle safety, EU FP7 project ASSESS, SST.2008.4.1.1: 233942, Available at http://www.assessproject.eu
[4] Unselt, Thomas, et al. "Assessment of behavioral aspects in integrated safety systems (EU FP7 project ASSESS)." ESV Conference Paper. No. 11-0284. 2011.
[5] Sandner, Volker. "Development of a test target for AEB systems." ESV Conference Paper. No. 13-0406. 2013.

# CHARACTERISTIC ANALYSIS OF PASSENGER CARS' SIDE IMPACT BASED ON IN-DEPTH ACCIDENT RESEARCH IN CHINA

**Xiao, Xu**
**Junyi, Chen**
**Hongyan, Wang**
School of Automotive Studies, Tongji University
China

**Yutong, He**
Shanghai United Road Traffic Safety Scientific Research Center
China

Paper Number 15-0016

## ABSTRACT

Based on the in-depth accident study of 138 cases occurred in Shanghai, China, in which a passenger car got side impact, the characteristics of human - vehicle/equipment - environment factors were analyzed in order to reveal the causation and damage/casualty consequence of these side impact accidents. The results show that the average deformation of these side struck passenger cars was 22.4cm. Furthermore, the deformations caused by large striking vehicles (trucks and buses) were 52% larger and the ratio of critical casualty consequence (serious injury or death) hovered at 22%. On the other hand, the highest mortality occurred at both sides of rear seats, and was nearly 13%. The head and neck were the most prominent injured parts of the body, which occupied narrowly 64% of the casualties. These above objective characteristics of side impact accidents provide a reliable basis for the development and application of occupant protection system and collision avoidance technology in China.

## INTRODUCTION

Both of the accident rate and the injury rate of side impact accidents are highest among all the collision modes all over the world[1][2]. In the 2004 report of American Fatal Accidents, 22% of the road accidents were due to side impact and the cost of its damage exceeded 3 billion dollars every year[3]. Another statistical data collected by IHRA (International Holocaust Remembrance Alliance) also showed that about one third of the traffic accident casualties were caused by side impact[4]. Therefore, side impact accident has become a hot issue which needs to be further analyzed and dealt with. This paper analyzes the characteristics of side impact through concrete real-wold road traffic cases, to investigate the influencing factors of occupant protection and collision avoidance technology on the basis of the full research on motion response and injury severity in such accidents.

## SAMPLING CRITERIA

The research data were collected by Shanghai United Road Traffic Safety Scientific Research Center (SHUFO), which included 1097 serious traffic accidents[1] in Jiading district of Shanghai, China between June 2005 and March 2013. 23% of these accidents were side impact accidents, which is the leading collision mode.
The sampling criteria for this study is presented as followed: 1. Just two vehicles were involved; 2. A passenger car (included A00, A0, A, B, C and D segment) got side impact; 3. The first collision in the accident was side impact. According to the criteria, 138 accident cases involving 217 occupants in the struck cars (the positions of the 209 occupants were confirmed) were sampled.

---

[1] ***Sampling Criteria of SHUFO: 1. at least one accident vehicle was generally or seriously damaged, or any airbag of one accident vehicle was deployed; 2. at least one person involved in the accident was seriously injured or dead.***

## STATISTICAL ANALYSIS

Among the 217 occupants in the struck cars, 88 of them were not injured and 91 of them were slightly injured, while 10 of them were seriously injured and 13 were dead. The above injury severities accounted for 40.6%, 41.9%, 4.6% and 6% of the total respectively. The injuries of the other 15 occupants were unconfirmed.

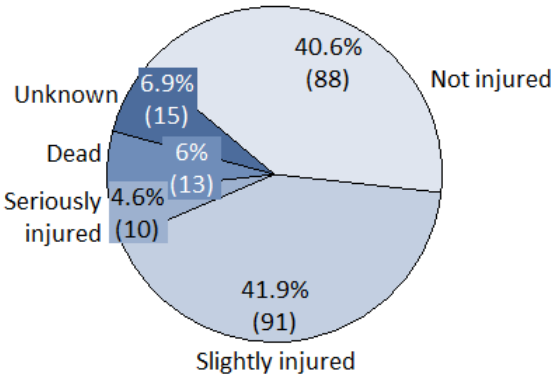


***Figure 1 distribution of occupants' injuries in struck car (N=217) ****

***Annotation: "Slightly injured" represents the not life-threatening injuries, such as bruises, fractures, etc. "Seriously injured" represents the life-threatening but not fatal injuries.***

## CHARACTERISTIC ANALYSIS OF SIDE IMPACT

### Accident Cause

About 81.9% of the side impact accidents were caused by violating traffic signal or right of way, which means that these accidents were mainly influenced by the subjective factors of driver.

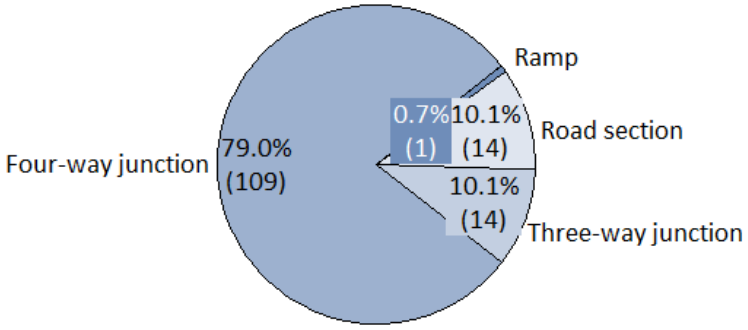


***Figure 2 distribution of accident sites (N=138)***

It is shown in the Figure 2 that 89.1% of the accidents happened at junction. Therefore, collision avoidance technology, such as Intersection Braking System[5], and IOV (Internet of Vehicles) [6] could improve the traffic safety in such conditions.

### Conflict Mode

73% of the accident cases concentrated on the three conflict modes: UTYP211, 301 and 321 (See Table 1). In the 24 accident cases of UTYP211, most of them were caused by A car's violating right of way. In this conflict mode all the A-cars were struck car. Generally speaking, in this conflict mode, the velocity of A-car (the left-turning vehicle) is remarkably lower than the velocity of B-car (the straight driving vehicle). If B-car get left side impact, such collisions are usually slight, which would not be collected in the database of SHUFO according to the sampling criteria of SHUFO. 22 accident cases of UTYP211 (accounting for 92%) took place at the intersections with at least four lanes in each direction, while 18 accident cases among them happened at the intersections without an

independent left-turn signal, where the A-cars drivers are more likely to violate right of way of B cars during left turning. Therefore, side impact accidents could be effectively reduced with the installation of independent left-turn signal.

**Table 1 distribution of conflict modes (N=101)**

| UTYP | 211 | 301 | 321 |
|---|---|---|---|
| Accident Amount | 24 | 77 | |
| Driving Direction | Straight driving + Left turning | Straight driving + Straight driving | |
| Sketch | 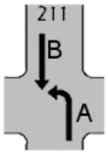  | 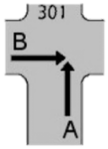  | 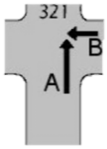  |

Most of the 77 accident cases with UTYP301 and 321 were caused by violating traffic signal. 34 cases (accounting for 44%) took place at the intersections with at most three lanes in each direction. At small intersection drivers are easier to lose vigilance, and the risk and severity of the side impact accidents could be increased by the unintentional or intentional violation of traffic lights. Otherwise, greenbelt on city road, which might influence driver's visibility to the side, was proved to be one of the influencing factors in the 35 accident cases (accounting for 45%). For the above two situations, IOV[6], which could provide effective conflict warning for driver, combined with Intersection Braking System[5] would contribute a lot to traffic safety at intersection. Meanwhile, regular safety education for driver and proper design and maintenance of greenbelt are necessary as well.

**Impacted Part**

Side impact accidents could be divided into three types according to the different impacted parts[2]. The collision, in which B-pillar is directly involved, is defined as middle-part-impact, while the collision in which B-pillar is not directly involved is defined as front-part-impact or rear-part-impact as shown in Figure 3.

***(a) Front-Part-Impact***

***(b) Middle-Part-Impact***

***(c) Rear-Part-Impact***

***Figure 3 classification of side impacted parts***

The statistics show that the right-side struck cars accounted for about 61.6% of the total, while the left-side struck cars accounted for 38.4%. The obvious difference between right and left side were mainly inluenced by the conflict mode UTYP211, in which all target cars were right-side impacted. When the striking vehicle was passenger car, SUV or van, the impacted part of the struck car concentrated mostly on front part (See Figure 4). When the striking vehicle was bus or truck, the impacted part of the struck car concentrated mostly on middle part, which could be due to the large width of bus and truck.

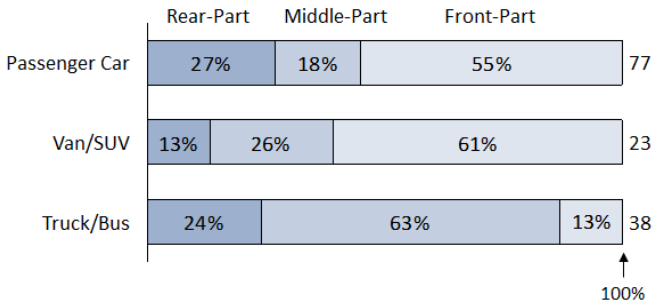


***Figure 4 distribution of impacted parts based on different striking vehicles (N=138)***

54.5% of the middle-part-impact accidents occurred when the striking vehicle was heavy vehicle (truck or bus), and in such accidents B-pillar was the main force-carrying component of the struck car. Improving the strength and stiffness of B-pillar is an essential issue of vehicle safety in side impact.

**Effective Impact Velocity**

The effective impact velocity is defined as the value of the striking vehicle's collision velocity in the y direction of the struck car. The distribution of effective impact velocities in the sample cases is shown in Figure 5. It could be found that side impact happened mostly with the effective impact velocity ranging from 45km/h to 60km/h, which accounting for 28.7%, followed by the velocity categories of 30km/h to 45km/h and of 15km/h to 30km/h.

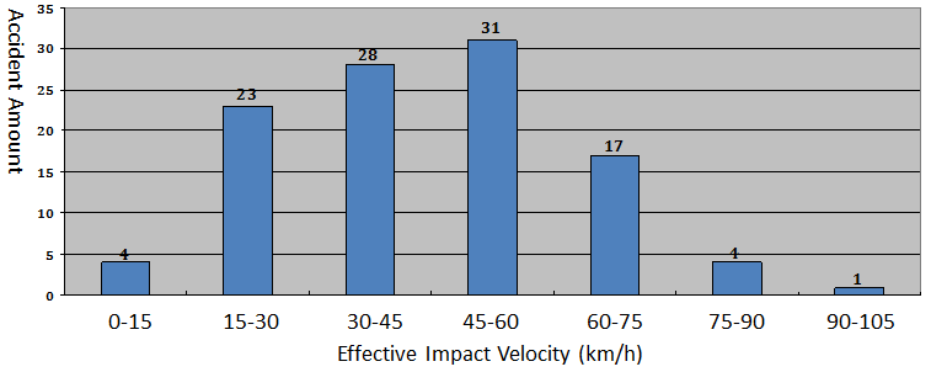


***Figure 5 distribution of effective impact velocities (N=108) ****

****Annotation: The effective impact velocities of 30 cases in the sample were unconfirmed.***

In the Side Impact Regulations of China, the testing velocity is determined as 50km/h[7]. The coverage of this velocity in the sample accident cases was 64%, while around 36% of the cases happened with the impact velocity higher than 50km/h. Higher impact velocity could lead to more serious accident consequences (will be analyzed in the following chapters). Therefore, side impact with high impact velocity deserves further attention.

**Maximum Deformation of Struck Car**

The maximum deformation of struck car mainly occurred at L2 and R2 in horizontal plane and LB and RB in vertical plane of struck car, as is shown in Figure 6. The maximum deformation position of struck car is mainly due to the impacted part and the structure and rigidity of the struck car in the accident. B2 region occupied 28.3% of the maximum deformations in the sample accidents, highest among all the positions. It is noteworthy that chest and abdomen of occupants are corresponded to B2 regions, which are the main impacted parts in Side Impact Test[7] as well.

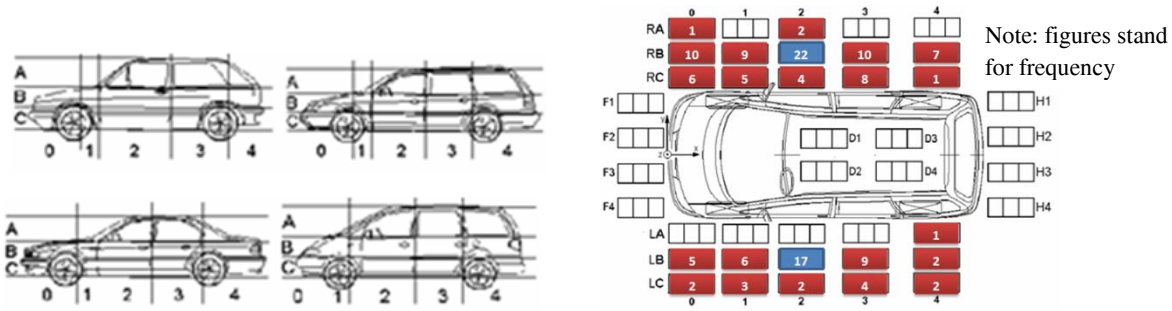


***Figure 6 distribution of struck cars' maximum deformations (N=138)***

According to the Side Impact Regulations of China[7], the test collision angle of side impact is 90°.In this study the collision angles in the sample accidents have been divided into 3 categories, 80°-100°, less than 80° and more than 100°. The category 80°-100°, which is corresponding to the test collision angle, accounted for aroud 49%. Meanwhile, the accidents cases with the impact angle of less than 80° or more than 100° still accounted for about 40% in the sample data, as shown in Figure 7, which would be mainly due to the steering maneuver of driver for collision avoidance before the impact and the influence of the conflict mode UTYP211. The oblique side impact collision is not covered in the Side Impact Regulations of China yet. In oblique side impact collision the motion response and the force direction of the struck car would be different, which could lead to sideslip, rotation and even rollover of the struck car after the impact. Then the motion response of the occupants in the struck car would be changed as well and different safety problems in side impact would be raised.

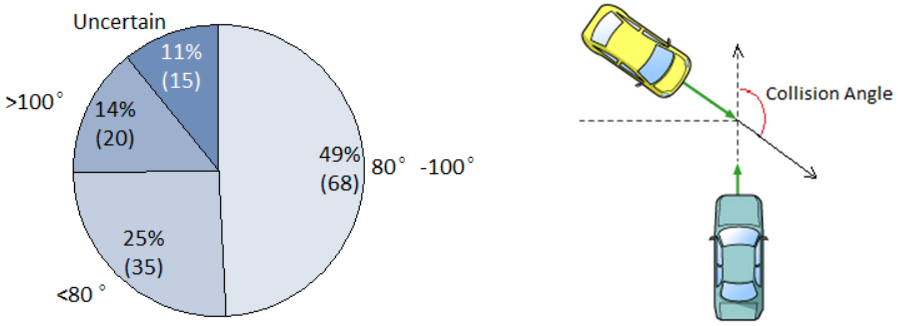


***Figure 7 distribution of collision angles at struck car's maximum deformation position (N=138)***

The results in Figure 8 and Figure 9 show that the maximum deformations of the struck cars were mainly less than 30cm (71%), with an average value of 22.4cm. Only 7% of the maximum deformations were more than 50cm. When the striking vehicle was passenger car, 62% of the maximum deformations were less than 20cm. When the striking vehicle was van or SUV, 52% of the maximum deformations were between 20cm and 40cm. When the striking vehicle was truck or bus, 39% of the maximum deformations were more than 40cm.

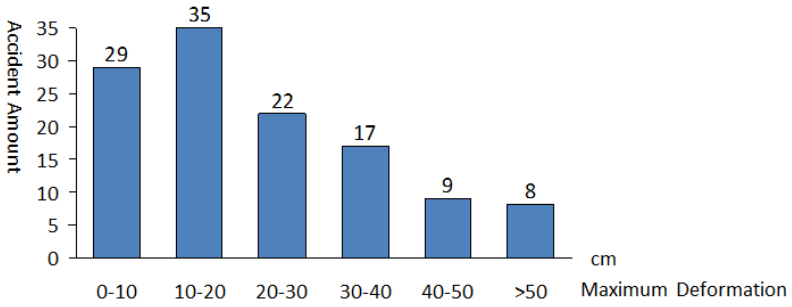


***Figure 8 frequency distribution of struck cars' maximum deformations (N=120) ****

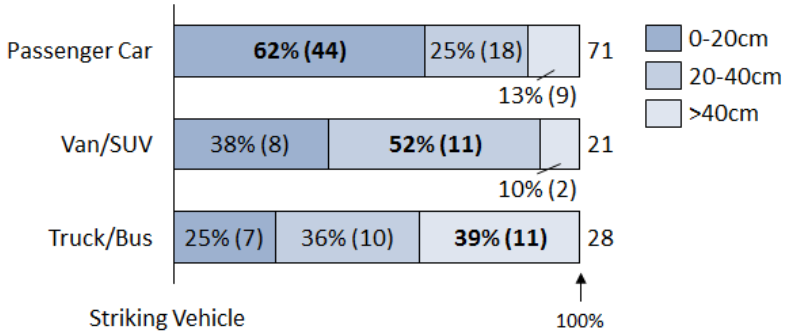


***Figure 9 distribution of struck cars' maximum deformations based on different striking vehicles (N=120) * *Annotation: The maximum deformations of 30 cases in the sample were unconfirmed.***

Therefore, with the increase of striking vehicle's height, width and weight, the maximum deformation of struck car rose rapidly, i.e. more serious the accident consequence would be.

**Table 2 distribution of struck cars' maximum deformations based on different striking vehicles with different effective impact velocities**

| | 0-30km/h | 30-50km/h | >50km/h | Avg. Maximum Deformations |
|---|---|---|---|---|
| **Passenger Car** | 15.5cm | 14.4 cm | 24.8 cm | **18.8 cm** |
| **Van/SUV** | 25.2 cm | 18.8 cm | 26.3 cm | **22.4 cm** |
| **Truck/Bus** | 19.8 cm | 33.6 cm | **42.7 cm** | **34.1 cm** |
| **Total** | **18.3 cm** | **19.2 cm** | **28.6 cm** | **22.4 cm** |

On the other hand, with the increase of effective impact velocity, the maximum deformation of struck car rose rapidly as well (See Table 2). When the striking vehicle was truck or bus and the effective impact velocity was more than 50km/h, the maximum deformation reached to about 42.7cm, which was almost double of the overall average.

**Injury**

In the struck cars of the accident cases, the use rate of seat belt for driver was highest (25%) among all the occupant positions, while that for front passenger took the second place (11%). No rear occupants were confirmed to be belted (See Figure 10).

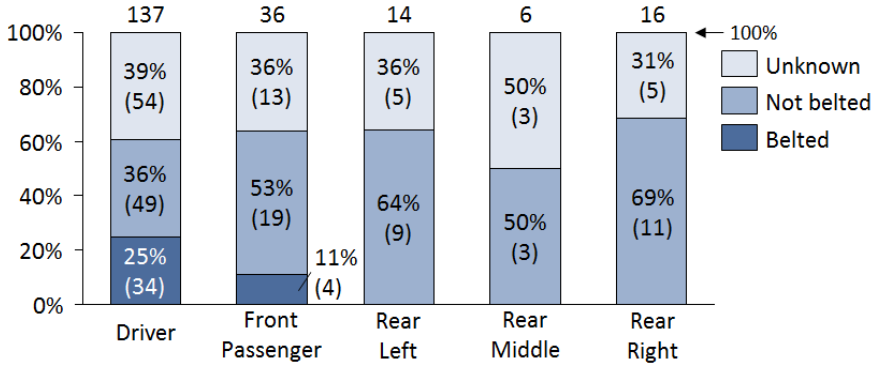


***Figure 10 use of seat belt in struck car (N=209)***

It is shown in Figure 11 that seat belt provided no definite protection for the occupants in struck car in side impact according to the injury distributions of the front occupants. The serious injury and death rates of the belted occupants and the unbelted occupants were similar.

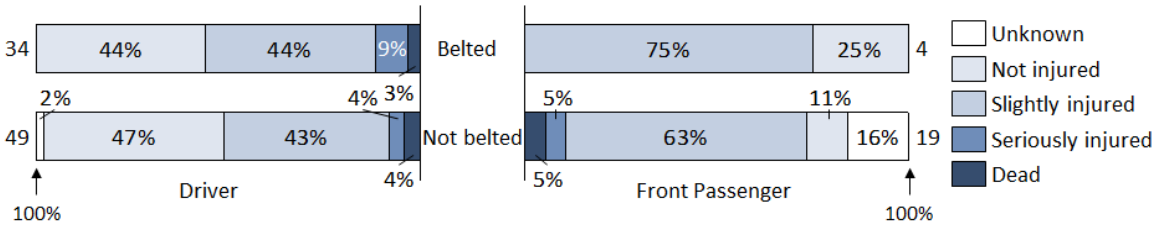


***Figure 11 effect of seat belt in struck car based on front occupants (N=106)***

Side airbag and inflatable curtain brought positive protection for the occupants in struck car, when the striking vehicle was passenger car. As Figure 12 shows, the occupants without the protection of side airbag/inflatable curtain in struck car were much more likely to get injured. Meanwhile there were no seriously or fatally injured occupants with the protection of side airbag/inflatable curtain.

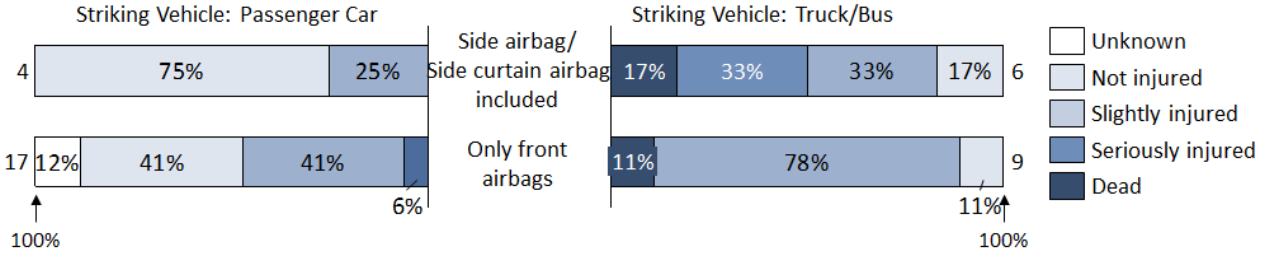


***Figure 12 effect of airbag in struck car based on different striking vehicles (N=36)***

However, when the striking vehicle was truck or bus, the protection of side airbag and inflatable curtain for the occupants in struck car was restricted. The serious injury and death rates of the occupants with the protection of side airbag/inflatable curtain were still very high. In the accidents stuck by heavy vehicle, occupants in struck car are easy to be involved in multiple collisions. Side airbag and inflatable curtain could provide at most once protection and could only protect the chest and abdomen of the occpuants. This protection seems to be not enough in such situation.

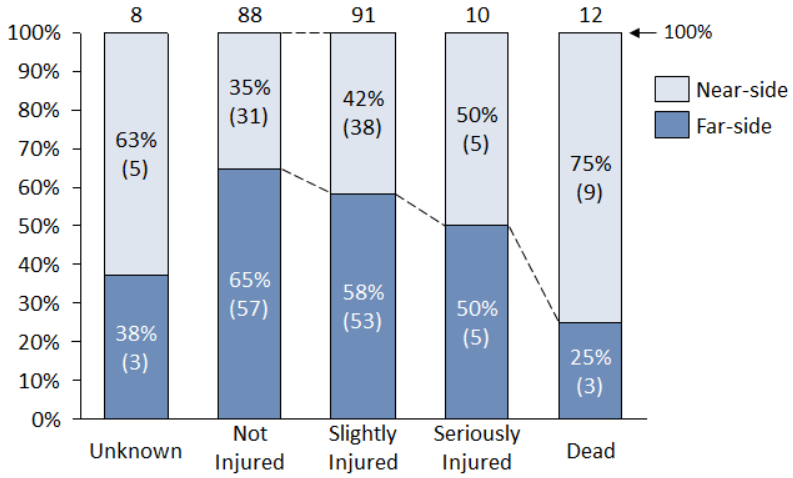


***Figure 13 relationship between injury severity and near-side/far-side occupants in struck car (N=209)***

It is defined that in left-side impact driver and left rear occupant in struck car are near-side occupants and in right-side impact front passenger and right rear occupant in struck car are near-side occupants. The other occupants in struck car are defined as far-side occupants. There were totally 88 near-side occupants and 121 far-side occupants, as Figure 13 shows.

75% of the fatally injured occupants in the side impact accidents were near-side occupants. Near-side occupants are seated close to the collision position and are much more likely to collide with door, window and interior of the struck car directly and suffer more serious injuries.

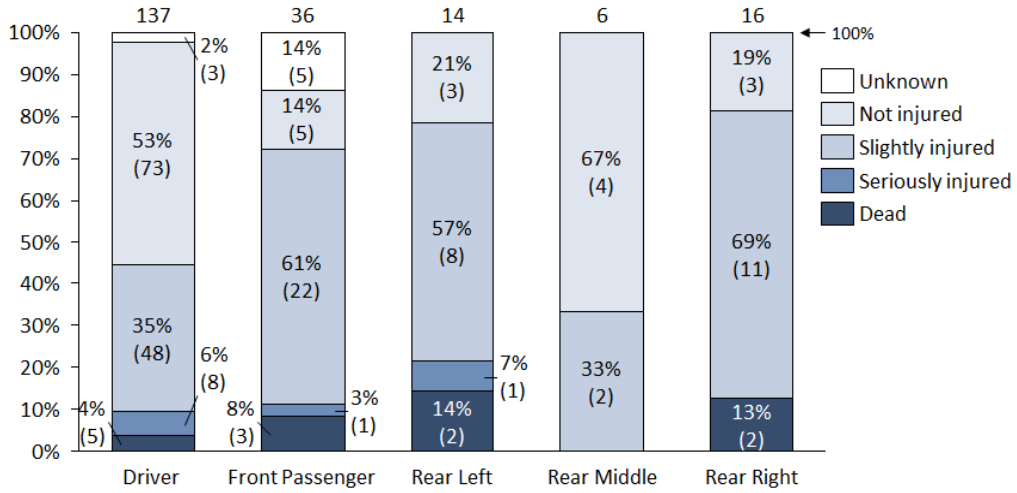


***Figure 14 relationship between injury severity and seat positions in struck car (N=209)***

The death rates of the rear left and rear right occupants in struck car were highest (14% and 13% respectively) among all the positions (See Figure 14). Compared to the front seats, most of the struck cars were not equipped with airbag at rear side seats. Meanwhile both of the rear side occupants are located at near-side positions and are very easy to get injured. Therefore, the protection for rear side occupants in struck car need to be improved.
On the other hand, the non-injury rates of the rear middle occupants and the drivers were highest, accounting for 67% and 53% respectively (See Figure 14). Rear middle occupants were always seated between the rear side occupants in the struck cars of the accident cases, which were the corresponding collision objects for the rear middle occupants in side impact as well. The corresponding rear side occupants are less stiffer compared to car componets and could work as a buffer during the collision, which would reduce the injury risk of the rear middle occupants. The driver position in struck car was relatively safer as well, for the driver in struck car were usually protected with restraint systems.

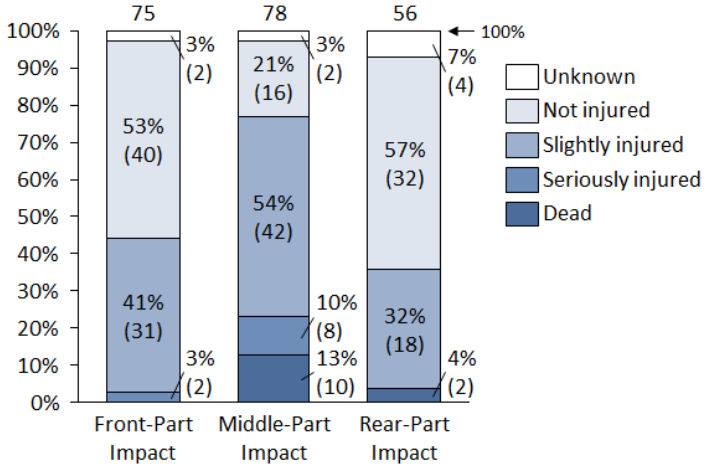


***Figure 15 relationship between impacted part and injury severity in struck car (N=209)***

Compared to front- and rear-part-impact, the injury risk and serverity of middle-part-impact were much higher. The injury risk of middle-part-impact reached to nearly 77% and the ratio of critical casualty consequences (serious injury or death) in middle-part-impact hovered at 23% (See Figure 15).72% of the seriously injured or dead

occupants were involved in middle-part-impact. According to the previous analysis, these middle-part-impact accidents, which led to serious accident consequences, were mostly struck by heavy vehile (bus or truck).

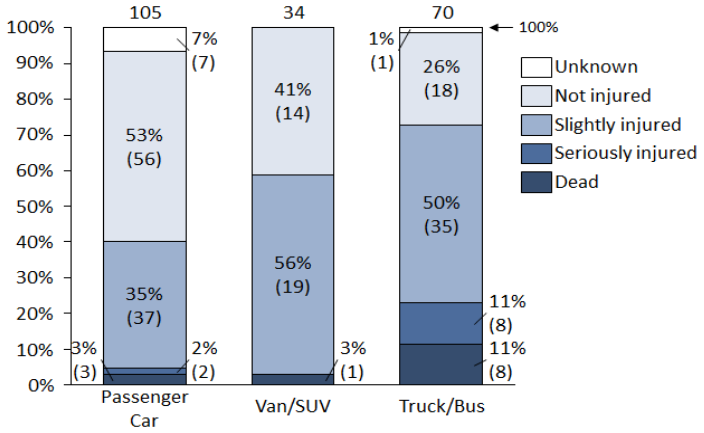


***Figure 16 relationship between striking vehicle and injury severity in struck car (N=209)***

As is shown in Figure 16, the injury risk and serious injury/death rate reached to respectively 72% and 22%, when the striking vehicle was heavy vehicle. 73% of the seriously injured or dead occupants were involved in this situation.

It is clear that under the influence of heavy weight, high stiffness and large size of heavy vehicle, it would be very difficult to prevent the occupants in struck car from injury, when struck by heavy vehicle. Therefore, it would be necessary to aim to avoid such accidents from the perspective of accident avoidance technology, which could fundamentally reduce the loss of such accidents.

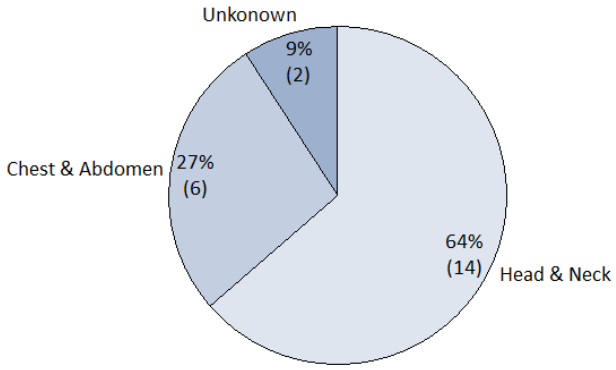


***Figure 17 distribution of seriously injured parts of the occupants in struck car (N=22)***

The distribution of occupants' seriously injured parts in struck car is shown in Figure 17. Head and neck, followed by chest and abdomen were the most prominent injured parts of the occupants in struck car in side impact, which occupied narrowly 64% and 27% of the casualties. The main causes for these injuries could be the collisions between occupant's head and door or window of the struck car, and the collisions between occupant's chest and abdomen and the deformed door of the struck car. Side airbag and inflatable curtain could provide good protection for head, neck, chest and abdomen of the occupants in side impact, which have been proved to be effective.

## SUMMARY AND CONCLUSIONS

Through the in-depth accident research of 138 side impact cases, the objective characteristics of these accidents could be obtained based on the impacted parts, the striking vehicles and the casualties of the occupants. The results could be concluded as follows:

1. 89.1% of the side impact accidents happened at junction and the drivers' violating traffic law was the most common cause (accounting for 81.9%).
2. With the increase of effective impact velocity, the severity of accident consequence rose rapidly. 36% of the side impact accident cases happened with more than 50km/h impact velocity. When the effective impact velocity was more than 50km/h, the maximum deformation of the struck car reached to about 28.6cm. These side impact accidents with high effective impact velocity should not be ignored during development process. Collision avoidance technology, such as Intersection Braking System, could function in these situation throug the reduction of the striking vehicle's velocity, to mitagate the severity of the accident or even avoid the impact.
3. 27.5% of the side impact accidents were struck by heavy vehicle and these accidents usually brought about serious accident consequences. In this situation the average deformation of the struck cars reached to 34.1cm. Meanwhile the injury risk and the ratio of critical casualty consequence (serious injury or death) reached to respectively 72% and 22%. It is clear that under the influence of heavy weight, large rigidity and large size of heavy vehicle, it would be very difficult to prevent the occupants in struck car (especially near-side occupants) from casualty, when struck by heavy vehicle. The application of IOV, which help remind the drivers when conflicting with heavy vehicle, could make a positive effect and fundamentally reduce the loss of such accidents.
4. Head and neck, followed by chest and abdomen were the most prominent injured parts of the occupants in struck car in the side impact accidents, which occupied narrowly 64% and 27% of the casualties. The main causes for these injuries could be the collisions between occupant's head and door or window of the struck car, and the collisions between occupant's chest and abdomen and the deformed door of the struck car. Side airbag and inflatable curtain could provide good protection for head, neck, chest and abdomen of the occupants during side impact, which have been proved to be effective.

## ACKNOWLEDGMENT

The accident data in this study are provided by Shanghai United Road Traffic Safety Scientific Research Center (SHUFO), which the authors particularly wish to acknowledge.

## REFERENCES

[1] Kamal, M.M. 1970. "Analysis and Simulation of vehicle to Barrier Impact." Society of Automotive Engineers, SAE Paper No. 700414

[2] Xu Guohong. "Analysis and Treatment of Traffic Accidents [M]." Beijing: People's Communications Press, 2003

[3] Fatal Accident Reporting System (FARS), 2004 http://www-Fars.Nhtsa.Dot.gov/queryReport.Cfm?stateid=0&year=2004, 2007(2/21)

[4] Samaha Radwan R., Elliott D.S. NHTSA side impact research: "motivation for upgraded test proceedings of the 18th International Technical Conference on the Enhanced Safety of Vehicles." Nagoya, Japan, May2003, Paper 492

[5] Dr.-Ing. Kai Frederik ZASTROW. "Regulatory Situation of Advanced Emergency Braking Systems." Workshop Active Test, Aachen, 28 September 2011

[6] NEKOUI M, NI D H, PISHRO-NIK H, et al. "Development of a VII-enabled prototype intersection collision warning system [J]." International Journal of Internet Protocol Technology, 2009, 4(3): 173-181

[7] GB 20071-2006. "Occupant Protection of Side Impact Collision." 2006

# ADVANCED SEAT BELT REMINDER SYSTEM FOR REAR SEAT PASSENGERS

**Thierry Mousel**
IEE S.A.
Luxembourg

**Keisuke Ueda**
Fuji Heavy Industries - Subaru
Japan

**Masaki Takahashi**
IEE Sensing Japan KK
Japan

Paper Number 13-0306

**ABSTRACT**

Advanced seat belt reminder systems with audiovisual warnings have proven to be highly effective in increasing the belt wearing rates of a vehicle's front seat occupants. While the availability of such advanced SBR systems for the front seats is almost common in some markets and fast-growing in others, also thanks to NCAP incentives, the systems available on the rear seats have so far only offered a basic functionality. In 2014, an upgraded SBR function entered the mass market, and the world's first car with an advanced rear seat SBR system including occupant detection was launched on the Japanese market. This vehicle, the Subaru LEVORG, offers an advanced audiovisual SBR warning for the rear outboard seating positions. This advanced function is enabled by occupant detection sensors designed to detect human rear seat occupants, while being robust against the detection of child restraint systems (CRS) or other objects frequently transported on a vehicle's rear seats. The robustness of the occupant detection and the object non-detection has been tested extensively. Occupants shifted their position forward and laterally away from the nominal seating position. A multitude of CRSs and objects were tested to ensure that they do not trigger unnecessary warnings. Advanced rear seat SBR systems have the potential to significantly increase the belt wearing rates, especially as those tend to be much lower on the rear than on the front seats in almost all countries. As belt load limiters and belt tensioners are more and more available for the rear seats, the advanced SBR systems ensure that more rear seat occupants will benefit from the restraint system enhancements.

## INTRODUCTION

Seat belts have proven to be highly effective in reducing the likelihood of severe or fatal occupant injuries in vehicle collisions. Additional technologies like seat belt tensioners and load limiters have helped to improve the seat belt effectiveness and to reduce belt induced injuries to the chest area. Many people, however, do not buckle up, for various reasons, often simply forgetting about it. Seat belt reminder (SBR) systems with audiovisual warnings have proven to be highly effective in increasing the seat belt use. The number of unbelted drivers is reduced by 80% in vehicles with advanced SBR systems meeting the Euro NCAP requirements [1]. For the front seat passengers the reminder effectiveness is comparable [2]. As seat belt reminders have such a significant impact on the belt wearing rates, the large majority of NCAP programs have decided to introduce incentives for front seat SBR systems into their rating. These incentives were very successful in motivating the vehicle manufacturers worldwide to fit SBRs in an increasing number of vehicle models [3]. In addition to the front seat SBR systems with audiovisual warnings, more simple systems had been developed for the rear seats, providing the driver with visual information on the buckle status on the rear seats. However, the effectiveness of those simple systems is limited as they are highly dependent on the driver response to the information. In 2014, a first car with an advanced seat belt reminder system also providing an audiovisual warning to the rear seat occupants entered the Japanese market. This paper describes the motivation behind this development, as well as the challenges that had to be solved with regards to occupant detection on the rear seats.

## MOTIVATION FOR ADVANCED REAR SEAT SBR

Subaru's roots go back to an aircraft manufacturer, so safety is one of the company's core values. In the domain of active safety, Subaru has proven this philosophy with its award-winning EyeSight technology, which was the first system ever to use only stereo camera technology to support functionalities like Adaptive Cruise Control, Lane Departure Warning and Autonomous Emergency Braking.
But also in the area of passive safety, Subaru identified additional road safety potential, aiming to reduce the number of vehicle occupant fatalities, namely by increasing the seat belt wearing rates on the rear seats. Although belt usage on rear seats has been mandatory since 2008, the rear belt wearing rates tend to be low in Japan, resulting in easily preventable occupant injuries and fatalities. Advanced seat belt reminder systems have

proven to be effective in raising the belt wearing rates on the front seats, but no such system had ever been implemented on a vehicle's rear seats. One key component for such a system, a rear seat occupant detection sensor simply did not yet exist.
In a joint development effort, Subaru and sensing system specialist IEE created the world's first advanced rear seat SBR system for a production vehicle, the Subaru LEVORG, launched in 2014. The expectation is that the system will increase the belt wearing rates, thus reducing the number of injuries or fatalities in Subaru vehicles.

**Rear Seat Belt Wearing Rates**

Seat belt wearing rates on the rear seats are lower than those for the front seats in all countries for which data is available. The reasons for this difference in belt usage behaviour are manifold, possible contributing factors are:

- rear seat occupants feel safer because of the backrest in front of them
- belt usage on the rear seats was mandated much later than for the front seats, so fewer people have acquired the habit to use the seat belt on the rear bench
- a lower enforcement level by police, also because belt usage is more difficult to verify
- unavailable or less effective seat belt reminders

**Seat belt wearing data from Japan** for front and rear seat vehicle occupants is shown in Figure 1 for the time frame 2005 to 2014. It shows the data for public highways (cities and rural roads). Additional data had been collected for express highways [4]. The belt wearing rates are highest for the driver (driver SBR fitment has been mandatory in Japan since 2005), closely followed by the front passenger. Belt wearing rates for the rear seat occupants are much lower, only about 1/3 (35.1 %) of the rear passengers buckle up on public highways. On express highways the belt usage increases to 70.3%, but is still far below the front seat usage rates. Seat belt usage on the rear seats was made mandatory in 2008, which explains the significant increase in the belt wearing rate for that year.

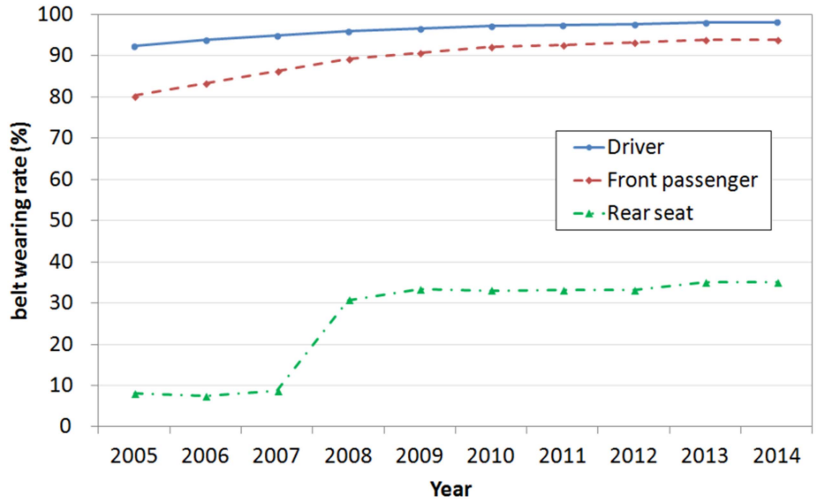


***Figure 1. Seat belt wearing rates in Japan on public highways.***

**Rear seat belt usage in the US** [5] is also lower than for the front seats, as shown in Figure 2. However, the difference is less important than in Japan. At 75%, the rear seat belt wearing rate in the US is only about 10% lower than the one for the front seats, while in Japan the rear seat usage rate is about 60% lower compared to the front seats. However, it should be noted that front seat belt usage in Japan (driver 98%, front passenger 94%) is about 10% higher than in the US (86%).
The US data also allows the analysis of rear seat belt usage by age group. The lowest belt wearing rate can be found for the age group teenagers and young adults (age 16 – 24), where only 67% buckle up, compared to the overall average of 75% belt users. The highest belt use can be found for children aged 8 to 15 (83%) and occupants aged 70 and higher (80%).

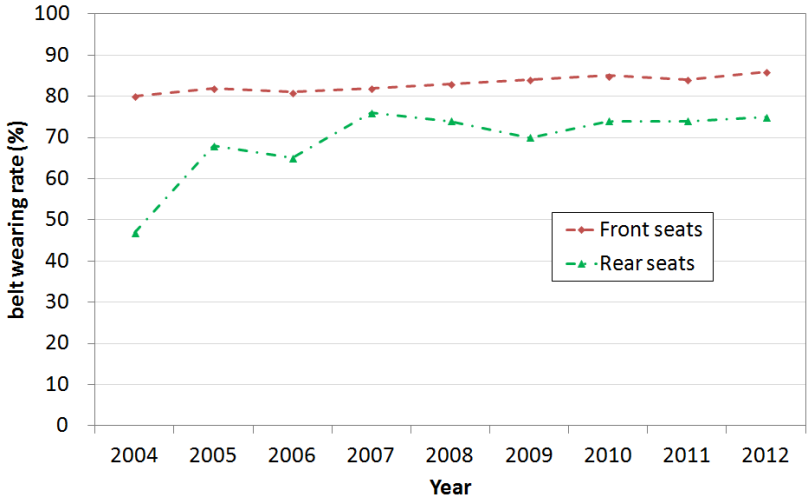


***Figure 2. US seat belt wearing rates for front and rear seat occupants.***

**In Europe, large differences in rear seat belt usage** can be found when comparing the different countries [6]. While the belt wearing rates of the rear seat passengers tend to be high with more than 80% for the Western and Northern European countries, much lower belt use is observed in most Eastern and Southern European countries.

***Table 1. Front and rear seat belt use rates for a selection of European countries.***

| Country | Belt use - front seat | Belt use - rear seat |
|---|---|---|
| Austria | 89% | 75% |
| Belgium | 86% | 80% |
| Czech Republic | 97% | 66% |
| France | 98% | 84% |
| Germany | 98% | 98% |
| Greece | 71% | 21% |
| Italy | 60% | 50% |
| Poland | 80% | 43% |
| Spain | 91% | 81% |
| UK | 95% | 89% |

**In Korea, belt usage on the rear seats** is significantly lower than on the front seats [7]. Only 19% of the rear seat occupants are belted, versus 84% of the front seat occupants.

**Rear Seat SBR Effectiveness**

The simple monitoring of the rear seat belt buckle status only allows for visual information to the driver and optionally the rear seat passengers at vehicle start. A brief audible warning can only be triggered if there is a "change of status", i.e. if a belted rear seat occupant unbuckles during the trip. The lack of a continuous audible alert limits the effectiveness of those simple systems.

Very little data is available on the effectiveness of such SBR systems. In a comment to NHTSA in 2010 [8], Volvo stated: *"…Volvo surveyed Volvo owners in Sweden and Italy in 2005. The survey clearly demonstrated that the belt usage rate in the rear seat, with the monitoring system as compared to without belt reminders, had increased from around 60% to around 82%"*. This would correspond to a reminder effectiveness of approximately 50%.

A laboratory study was conducted in Japan in 2012 [9], comparing the effect of various optical and audible SBR warnings on the belt use of rear seat passengers. Table 2 summarises the most important study results. The initial belt wearing rate without SBR warning was 38%. When an optical warning was only presented to the driver, who then reminded the rear seat passengers, the belt use increased to 56%. When both, driver and rear seat passengers were presented with an optical warning, the usage rose to 72%. And when an audiovisual

warning was used, 97% of the rear seat passengers buckled-up. So audiovisual SBR warnings motivated up to 95% of the initially non-belted rear seat occupants to buckle up. For visual-only warnings the effectiveness was limited to 50% (in line with the Volvo data above).

***Table 2. Belt wearing rates for various SBR warning systems.***

| | | Rear seat passenger information | | |
|---|---|---|---|---|
| | | No SBR information | Ceiling icon, blinking with frequency change, no audible signal | Ceiling icon, blinking with frequency change, audible signal with frequency change |
| Driver information | No SBR information | 38 % | - | - |
| | Meter cluster icon, blinking with frequency change, no audible signal | 56 % | 72 % | - |
| | Meter cluster icon, blinking with frequency change, audible signal with frequency change | - | - | 97 % |

As the first vehicle with an advanced rear seat SBR system only entered the market in Japan in June 2014, no field-data is available with regards to its effectiveness in increasing the belt wearing rates. But the laboratory study indicates a clear trend with regards to the effectiveness of various warning strategies.

## OCCUPANT DETECTION SENSOR DEVELOPMENT

Occupant detection on the rear seat can be achieved in principle in a similar way as on the front seat, a foil-based pressure sensitive sensor, integrated between seat foam and trim, is activated by the occupant's weight. However, some rear seat peculiarities have to be taken into consideration. The rear bench is often used to transport various objects, child restraint systems (CRS) are predominantly installed there, and the backrest can be folded down. For those scenarios sensor activation has to be prevented. In addition, the occupant himself often has a higher freedom of movement on the rear seat compared with the front seat, due to missing or less distinct side bolsters. Therefore sensor design and size have to be adapted to the specific rear bench needs.

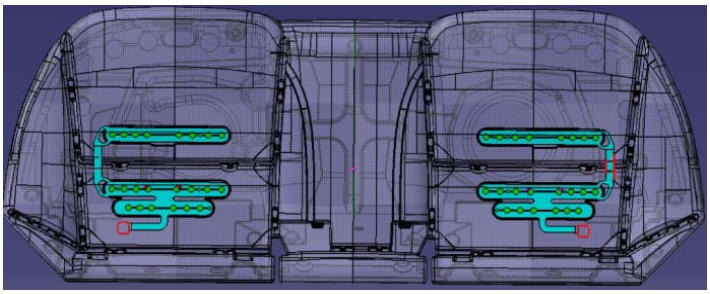

***Figure 3. Top view onto rear bench with occupant detection sensors on outboard positions.***

A dedicated test matrix has been developed to ensure robust sensor performance for occupant detection and object non-detection. Typically occupant detection has to be guaranteed for a 5% female, but also smaller occupants like young teenagers can be taken into consideration. Occupancy detection tests are performed with occupants of the specified size and weight. In addition to the nominal seating position, testing includes some forward and lateral position shifts. Non-detection is among others tested with beverage packs, rice and potato bags and a multitude of child restraint systems. In particular ISOFIX CRS with an integrated harness should not actuate the sensor, as those don't require the 3-point seat belt of the car to fix the CRS or to secure the child. Another non-detection test puts some weight onto the folded backrest to simulate a heavy trunk load.

A rear seat specific sensor layout and an IEE patented interconnection of the sensor's pressure sensitive cells allows the differentiation of the pressure profiles typically generated by humans from those generated by CRS or other test matrix objects. Figure 4 shows pressure profiles of a 5% female and various CRS, recorded with a high resolution pressure sensitive mat on a front passenger seat. The pressure distribution looks similar on the outboard rear seats. Although CRS or other objects can also exercise some load on the area usually covered by a human buttock, a smart senor design can almost entirely exclude unnecessary SBR warnings. For objects that are heavy enough to nevertheless activate the sensor, it is recommended to secure them with the belt or to load them into the trunk, as otherwise they are a potential danger for vehicle occupants if there is a crash.

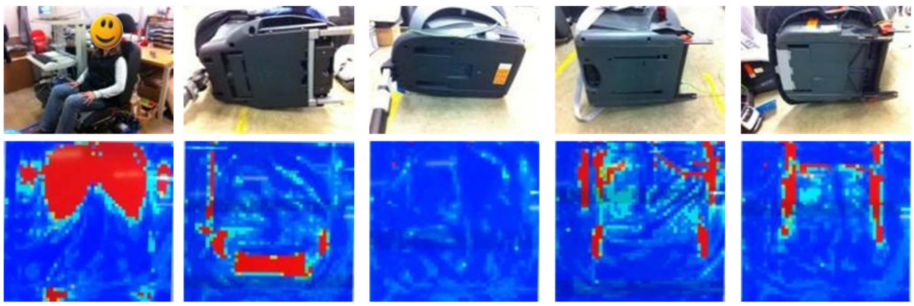

***Figure 4. High resolution pressure profiles of human and CRS on a vehicle seat.***

The system integrated into the Subaru model "LEVORG" has occupant detection only on the outboard seating positions. A system covering three positions on the rear bench is under development in order to cover all seating positions with an advanced seat belt reminder function.
The current system has the sensors and buckles connected to the car's wire harness via cables and connectors. For vehicles with highly flexible seat configurations or removable seats, a wired system layout could be considered a limiting factor. Therefore a wireless prototype concept has been developed by IEE to address those concerns. It is based on the same communication technology as currently used by tire pressure monitoring or keyless-go systems. A serial feasibility evaluation for the wireless system, as well as other occupant detection technologies that could be used for rear seat passenger detection, is currently under investigation.

## EXISTING AND FUTURE NCAP INCENTIVES

NCAP star ratings for a vehicle only have real-life relevance if occupants are belted during a collision. A five star car can only provide a "five star protection" if the occupants are buckled-up. That was the motivation for many NCAP programs to promote effective seat belt reminder systems, with a focus for the front seats. Several NCAP programs have now started to perform crash tests with adult dummies on the rear seats. One aim is to motivate the vehicle manufacturers to make restraint system technology that's widely available for the front seats, like belt tensioners and load limiters, also available on the rear seats in a larger number of vehicle models. However, as for the front seats, the rear seat occupants can only benefit from those improved belt systems if they are buckled up. Hence the NCAP programs have an increasing interest to promote more efficient SBR systems for the rear seat, especially taking into consideration the generally lower belt wearing rates on the rear compared to the front seats.

### Japan NCAP

When Japan NCAP introduced an overall rating scheme in 2011, SBR points became part of the evaluation. Since then, the overall rating score has been based on the sum of three elements: occupant protection (up to 100 points), pedestrian protection (up to 100 points) and seat belt reminder (up to four points for the front passenger seat and up to four points for the rear seats) [10].
J-NCAP was the first NCAP program to create an incentive for advanced seat belt reminders on the rear seats. Simple buckle monitoring only systems limited to telltale/display-type information are awarded with a maximum of two points, with the score depending on display location and its visibility to the occupants. Two additional points can be scored if the rear SBR alert includes an audible warning of at least 30 seconds. Such a warning, however, can only be triggered if passenger presence information is available.
The Subaru LEVORG is the first car where such an advanced SBR functionality will be assessed for the rear outboard seating positions, and it is expected to score between 3.0 and 3.33 points for the rear SBR system (official results not yet published at paper deadline).

**Euro NCAP**
Euro NCAP was the first NCAP to introduce SBR bonus points in 2002. Their SBR protocols evolved over time, and currently two combined points are available for advanced SBR systems covering both front seats, and one point for the buckle monitoring variant on the rear seats. The Euro NCAP protocol recommends occupant detection on the rear seats, but does so far not require it.
In its "2020 Roadmap" [11] Euro NCAP announced to introduce incentives for advanced rear seat SBR systems in 2018. Out of 2 points available for rear seat SBR, 1.5 points will be available for the buckle monitoring function (all rear seats), and 0.5 point will be allocated to additional occupant detection covering the 2nd row outboard seating positions, enabling an advanced reminder function.

**Australasia NCAP**
Australasia NCAP has announced it will fully harmonise with the Euro NCAP rating from 2018 on, so advanced rear seat SBR systems will become rating relevant in Australasia NCAP too.

**Other NCAPs**
Some NCAPs are now about to introduce incentives for the simple rear SBR systems into their rating (Korea NCAP in 2015, ASEAN NCAP in 2017, Latin NCAP – year to be confirmed). It can be assumed that incentives for more advanced systems will follow a couple of years later.

## CONCLUSIONS AND RECOMMENDATIONS

The relatively simple rear seat SBR systems so far used in cars, warning only via telltale or text message, have a limited effectiveness on increasing the belt wearing rate. Now the time has come to extend the concept of advanced SBRs to the rear seats and to address the issue of occupant detection in an environment with a higher variability than on the front seats.

Driven by Subaru's safety strategy and Japan NCAP incentives, a first vehicle model with an advanced rear seat SBR system has entered the Japanese market. Occupant detection sensors, dealing with the specific needs of the rear seat environment have been developed by IEE.

Although field data on the effectiveness of an advanced rear seat SBR system is not yet available, a laboratory study on various rear seat SBR variants and the proven effectiveness for front seat occupants raise the expectation that rear seat belt wearing rates, typically much lower than those for the front seats, can be increased significantly.

And with NCAPs worldwide increasingly addressing the safety of rear seat occupants, it makes sense that they also create incentives for systems that ensure high belt wearing rates for those occupants. Euro NCAP and Australia NCAP will follow Japan NCAP, and start rewarding advanced rear seat SBR systems from 2018 on. By achieving higher belt wearing rates in combination with improved rear seat restraint systems one can expect to achieve additional road safety benefits in the future.

## REFERENCES


[1] A. Lie, A. Kullgren, M. Krafft and C. Tingvall, “Intelligent Seatbelt Reminders: Do they change driver seat belt use in Europe,” in Paper 07-0388, ESV 2007.

[2] M. Freedman et al, “The Effectiveness of Enhanced Seat Belt Reminder Systems - Observational Field Data Collection Methodology and Findings,” NHTSA, DOT HS 810 844, 2007.

[3] T. Mousel, “Seat Belt Reminder Incentives in NCAP Programs: A Success Story,” in *Paper 13-0306*, ESV 2013.

[4] National Police Agency and Japan Automobile Federation, http://www.jaf.or.jp/eco-safety/safety/data/driver2014.htm

[5] T. Pickrell, “Occupant Restraint Use in 2012: Results From the National Occupant Protection Use Survey Controlled Intersection Study,” NHTSA, DOT HS 811 872, 2014.

[6] G. Jost, R. Allsop and A. Ceci, “ETSC PIN Flash Report 27: Ranking EU progress on car occupant safety,” European Transport Safety Council (ETSC), 2014.

[7] Republic of Korea, “Informal document GRSP-56-42,” http://www.unece.org/trans/main/wp29/wp29wgs/wp29grsp/grspinf56.html, 2014.

[8] A. Kopstein, “Docket reference: NHTSA-2010-0061-0018", www.regulations.gov, 2010.

[9] M. Akamatsu, H. Hashimoto and S. Shimaoka, “Assessment Method of Effectiveness of Passenger Seat Belt Reminder,” in SAE International 2012-01-0050, 2012.

[10] National Agency for Automotive Safety & Victim's Aid (NASVA), Car Safety Performance Guidebook, http://www.nasva.go.jp/mamoru/en/download/car_download.html, 2013.

[11] Euro NCAP, “2020 Roadmap,” http://www.euroncap.com/en/for-engineers/technical-papers/, March 2015.

# Analysis of Abdominal Injuries Caused by the Submarining Phenomenon in the Rear Seat Occupants

**Keita Nakane**
**Masayoshi Nojiri**
**Ryo Maekawa**
**Makoto Esaki**
Tokai Rika Co., Ltd.

**Shigeyuki Suzuki**
**Yasushi Masuda**
Toyoda Gosei Co, Ltd.
Japan

**Masahito Hitosugi**
Shiga University of Medical Science
Japan

Paper Number 15-0023

## ABSTRACT

Improvements to vehicle safety have targeted mainly the front seating positions, where the rate of seat belt usage was high and there were many casualties. Recently, rear seat occupant protection become an important challenge, with an increase in usage of seat belts by rear occupants due to new regulations and new performance criteria defined by Japanese and European vehicle assessment programs for rear seating occupants. Some prior analyses of accident data indicate that rear seat belted occupants tend to be injured in abdominal regions in comparison with front seat occupants. Due to this, the need to study the cause of abdominal injuries and how to countermeasure it is becoming indispensable for improving the protection performance of the rear seat occupants. The following two phenomenons are considered as factors which great impacts on abdominal injuries: the submarining phenomenon, lap belt intruding into abdominal region, and the incorrect routing of the belt, lap belt existing initially on abdominal region. However, the relationship between these probable causes and the abdominal injuries in the real world accident is not expressly described in prior studies. Therefore, first, the frequency of the abdominal injuries caused by the submarining phenomenon was estimated by micro analysis of the accident data. Second, the influence on abdominal internal organs, to which the lap belt load was applied, was analyzed using human body FE model THUMS. The results of this analysis indicated that the effect might be applied to abdominal internal organs. As the routing of the lap belt on the pelvis was shown as being very important in this study, a parametric study using Madymo was conducted to determine additional factors that might influence the proper routing of the belt on pelvis. This study narrowed down the factors with big contribution and explains how they were determined.

## INTRODUCTION

Crash data analysis clearly shows that seat belt use has an unquestionable advantage in occupant protection. A 2003 NHTSA research [1] estimated that 147,246 occupant lives were saved by seat belt use through 1975 to 2001 in US. The improvements of restraint systems such as seat belt and airbag has been pushed forward by changes in regulation and assessment programs mainly for the front seating positions, where the rate of seat belt usage was high and there were many casualties. In addition, requirements for improving the protection of rear seat occupants are increasing recently. In Japan New Car Assessment Program (JNCAP), off-set deformable barrier (ODB) test with Hybrid III 5%ile female dummy in rear seat started in 2009, while seat belt wearing for rear seat occupants was made mandatory by regulation in 2008 and usage rate is rising. [2][3] In addition, European New Car Assessment

Programme (ENCAP) is conducting frontal full width rigid barrier (FWRB) test with Hybrid III 5%ile female dummy in rear seat starting with January 2015. Due to the above, rear seat occupant protection is being regarded as more and more important.

R.Frampton et al. [4] reported that the abdominal injury risk for the rear seat occupants was higher than for front seat occupants based on UK accident data analysis. Additionally, the report on injuries to older passengers by the Institute for Traffic Accident Research and Data Analysis (ITARDA) [5] indicated that the rate of fatal and serious injuries for rear occupants involving elderly is higher due to abdominal injuries. The following two phenomenons are considered as factors which 1) submarining phenomenon, lap belt intruding into abdominal region, 2) belt malpositioning, lap belt existing initially on abdominal region. In particular, JNCAP and ENCAP put focus on the submarining phenomenon; the score is reduced when submarining occurs in the above-mentioned ODB (JNCAP) or FWRB (ENCAP) evaluations.[6][7]

However the above-mentioned accident data analysis [4][5] does not clearly refer to the relation between abdominal injuries and submarining phenomenon by lap belt. An in-depth analysis about the abdominal organs injuries of belted / non-belted front occupants by K. Ono et al.[8] also did not report any relationship. Due to this, the first objective of this study is to estimate the occurrence frequency of the submarining phenomenon based on accident data analysis and to simulate the severity to the abdominal organs when the submarining phenomenon occurs using the human finite element model. Second objective is to examine the effective control scenario to reduce the submarining phenomenon.

## METHODS

### Crash Data Analysis

The National Automotive Sampling System-Crashworthiness Data System (NASS-CDS) database was used to estimate the frequency of the submarining phenomenon occurrence. In the analysis, 555 injury cases of belted rear seat occupants were extracted from 2007 to 2011 (PDOF 11-1 o'clock).

### Analysis of the influence on abdominal organs

A series of simulations using 50%ile male human finite element model, THUMS Version3, was conducted to examine the influence to abdominal organs when the submarining phenomenon occurs. The severity of pressure to the abdominal organs due to the position of the lap belt, which assumed submarining phenomenon and belt malpositioning, was simulated and compared with the output of the lap belt worn appropriately. In this study, the geometry, seat belt parameters and deceleration of 56km/h full width rigid barrier test of actual vehicle were used. Abdominal organs deflection and deflection velocity were considered as characteristic indexes indicating the severity. However, the deflection mode and the injury mechanism of the abdominal organs were different because variation in structure (such as the solid and hollow). The characteristic value suitable for each internal organ was not expressly shown as various studies on those injury mechanism might be ongoing. Therefore, this study adopted both the deflection and the deflection velocity as the characteristic index.

### Parametric Study for Submarining Performance

A parametric study using Madymo was conducted to narrow down the parameters with large impact to anti-submarining performance and to clarify their proper design values. The angle between the belt-to-pelvis (abbreviated BTP from now on) from the submarining phenomenon index used in the study of J. Horsch and W. Hering [9] was used in this analysis. (Figure 1)

The mechanism of the submarining phenomenon was based on the following hypothesis:
"The pelvis receives the torso internal force $F_{Chest}$, the femur internal force $F_{Femur}$, the resistance force from the seat cushion $F_{Seat}$ as well as the lap belt force $F_{Belt}$ and moves forward with rotation. Due to this displacement of the pelvis, the lap belt direction for the iliac spine changes. As this displacement increases, the BTP increases counterclockwise and the force of the upper direction along the iliac spine increases. Due to the change in this load distribution, it becomes very likely that the submarining phenomenon will occur."

According to this hypothesis, "continuously maintaining a small BTP" is important to control the submarining phenomenon. Therefore, the extraction of the factors that influence the change of lap belt angle $\theta_B$ and iliac perpendicular angle $\theta_P$, and the contribution degree of each factor were derived.

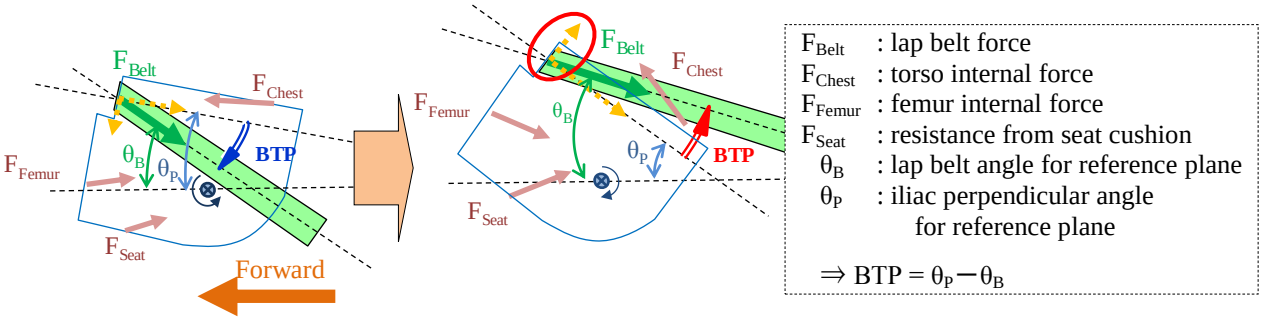


***Figure1. Force acting on pelvis and BTP***

## RESULTS

### Crash Data Analysis

According to the distribution ratio of the Abbreviated Injury Scale (AIS) from the extracted cases, 89% of the injuries in the rear seat were minor injuries with an AIS 1; the reduced severity of the injuries was attributed to the use of restraint system such as seat belt. This study researched the remaining 11% of AIS 2 and greater(AIS2+).

Injury source for the AIS2+ injuries in the rear seat (Figure 2a), injury description of the injuries by belt restraint system (Figure 2b), the rate of the injured abdominal organs (Figure 2c) are illustrated in below Figure 2. Results indicate that 28% of the injuries in the rear seat were caused by the belt restraint system, of which 34% were injuries to the abdominal region. In addition, 65% of the injured abdominal organs were distributed in the lower abdomen such as the intestine or the mesentery.

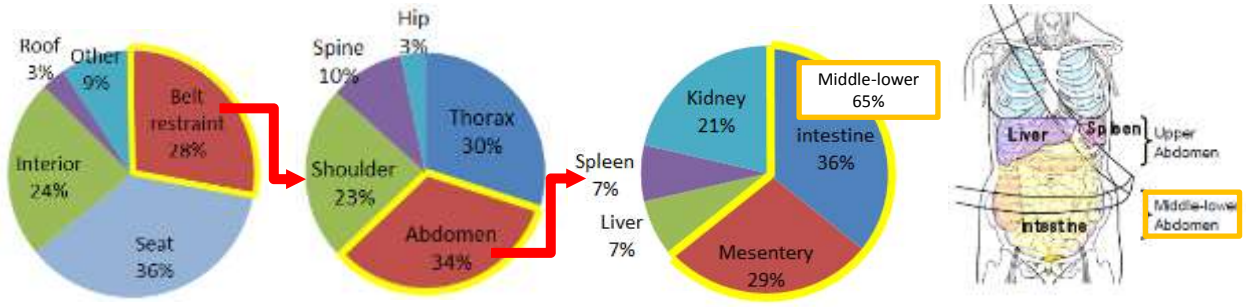


**Figure 2a** **Figure 2b** **Figure 2c** **Figure 2d [10]**

***Figure 2. Injury source for the AIS2+ injuries in the rear seat (Figure 2a), Injury description of the injuries by belt restraint system (Figure 2b), Rate of the injured abdominal organs (Figure 2c)***

Here, the micro-analysis of abdominal organs injury cases was researched to determine the relation between abdominal injuries and the submarining phenomenon. Results indicate that 30% of the abdominal organs injury cases were recieved abrasion and contusion to the hips by the belt restraint system. It was confirmed that the lap belt was fitted on the iliac spine at the start of the crash event and it became very likely for the submarining phenomenon to occur during the collision.

In four cases, rear seating occupants sustained the pelvic fractures with an AIS2 caused by the belt restraint system. After further analyzing these four cases, three were specified the fracture point and one of them was fracture of the anterior superior iliac spine on which the lap belt was fitted on; however, for this case, the cause of the fracture is believed to not be due to high load from the lap belt due to a low barrier equivalent speed of 45km/h. Two of the fractures were pelvic breaking away from iliac spine. From the collision velocity and involved region, it was assumed that the fractures were partly due to a contact with the buckle, the seat, another interior part or an unbalanced load by the vehicle behavior.

**Analysis of the influence on abdominal organs**

Vertical section views (in the initial stage of the restraint, in the maximum movement of the pelvis, and in the rebound of the pelvis) of the lap belt fitting on the iliac spine properly or the abdomen, maximum amount of abdomen deflection, and deflection velocity changes by time are illustrated in Figure 3. Here, the amount of abdomen deflection and deflection velocity were calculated using two places, top and bottom, that assume a division between spine and organs shown in vertical section views. This THUMS model used the abdominal organs model which is united; the upper part is equivalent to the upper abdomen including the liver and the spleen, and the lower part is equivalent to the lower abdomen including the intestine and the mesentery. Results indicate that the amount of abdomen deflection and deflection velocity in fitting of the lap belt on the abdomen were higher in the lower measurement part, equivalent to the lower abdomen, which has seen increased injury in the accident analysis compared to the upper part. This result matched the actual accident situation in the real-world. The maximum amount of abdomen deflection in fitting of the lap belt on the abdomen at the lower measurement part was increased by approximately 3.4 times compared with fitting of the lap belt on the iliac spine properly. Additionally, abdomen deflection velocity was increased by approximately 2.3 times. The above results showed that, when the lap belt was fitted on the abdomen, the characteristic value of abdominal injuries increased. This confirms the uttermost importance of properly routing the lap belt on the iliac spine in order to restrain the occupants properly.

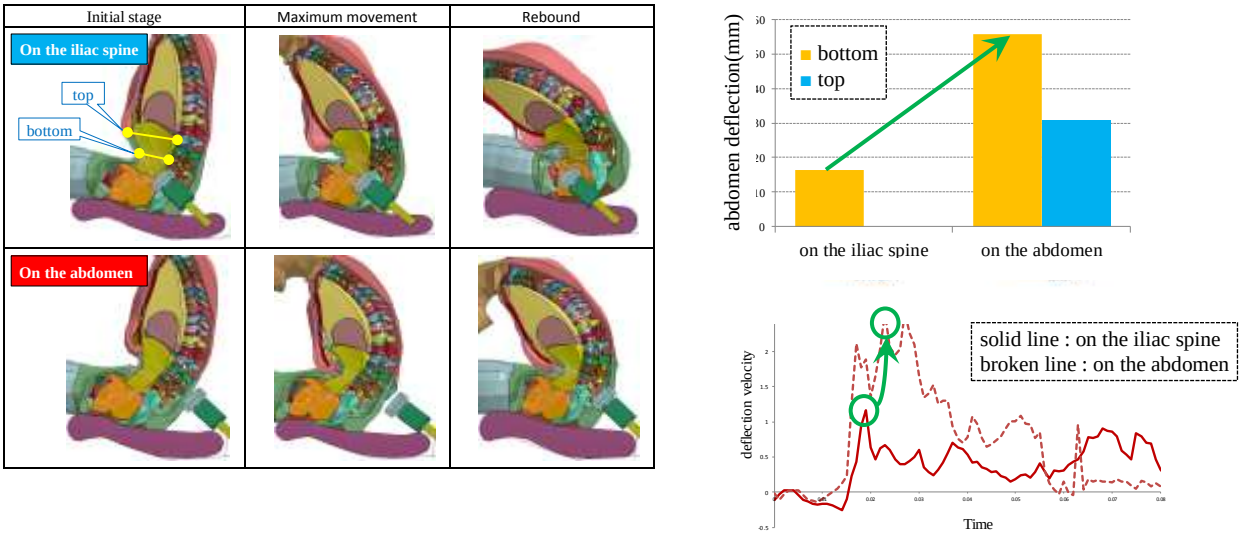


***Figure3. Vertical section views of fitting the lap belt on the iliac spine properly or the abdomen (Figure 3a), maximum amount of abdomen deflection (Figure 3b), time change of deflection velocity (Figure 3c).***

**Parameter Study of the Anti-Submarining phenomenon**

The above analysis of abdominal injuries showed that the submarining phenomenon may cause a significant load to the abdomen and it was also confirmed, by simulation, the importance of fitting the lap belt on the iliac spine. Therefore, it is essential to improve the anti-submarining performance as much as possible.

At the beginning of the study, the factors impacting the lap belt angle $\theta_B$ and the iliac perpendicular angle $\theta_P$ were selected as shown in Table 1 - seat belt specification, inner anchor point, seat cushion characteristic and front seat position. In addition, the levels were set in realistic range applied to actual vehicle and provided in regulation. Hybrid III 5%ile female dummy model was used as this was considered to be worst case for the submarining phenomenon because of its small pelvis. The initial sitting position and posture were neutral and the lap belt was fitted on the iliac spine.

Figure 4 shows the contribution degree to BTP of each factor listed in Table 1. All factors had some contribution degree to BTP, and it was confirmed to reduce the submarining phenomenon by proper parameter settings. In particular, it was determined that the contribution degree of the inner anchor point (longitudinal) and the seat cushion characteristic were particularly large.

**Table1.**
**Factor and Level**

| | | factor | level 1 | level 2 | level 3 |
|---|---|---|---|---|---|
| Seat Resistance force | A | Seat cushion caracteristic | Soft | Hard | |
| Torso internal force | B | Shoulder Force limiter | low | middle | high |
| Femur Internal force | C | Front seat position | front | middle | rear |
| Lap belt force | D | Inner anchor point (longitudinal) | forward | middle | rearward |
| | E | Inner anchor point (crosswise) | inner | middle | outer |
| | F | Inner length | short | middle | long |
| | G | Lap force limiter | | low | high |

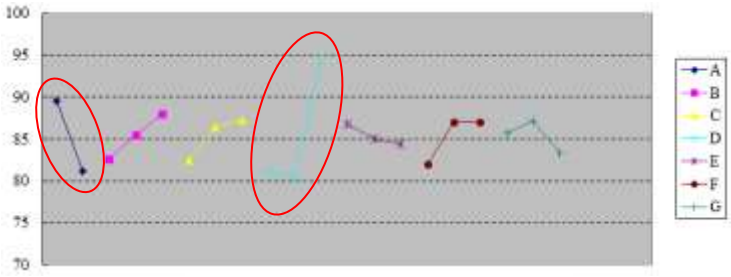


***Figur4. Cause and effect diagram***

Figure 5 shows the amount of BTP change (δBTP) during the crash event by changing the parameters of these two main factors. This shows that higher anti-submarining performance is achieved by following two items: ensure the initial relative angle by the front configuration of the inner anchor point, and reduce the relative angle change by the effect of the seat cushion caracteristic controlling the forward and downward pelvis displacement. In addition, the amount of BTP change (δBTP) was provided as the difference between the iliac perpendicular angle change ($\delta\theta_P$) and the lap belt angle change ($\delta\theta_B$); however, the change of $\delta\theta_P$ was small and the change in $\delta\theta_B$ was big. This confirmed that, in order to prevent the submarining phenomenon, the forward configuration of the inner anchor point, to make the initial BTP smaller, and moreso the pelvis restraint to reduce the forward and downward displacement during crash event were important.

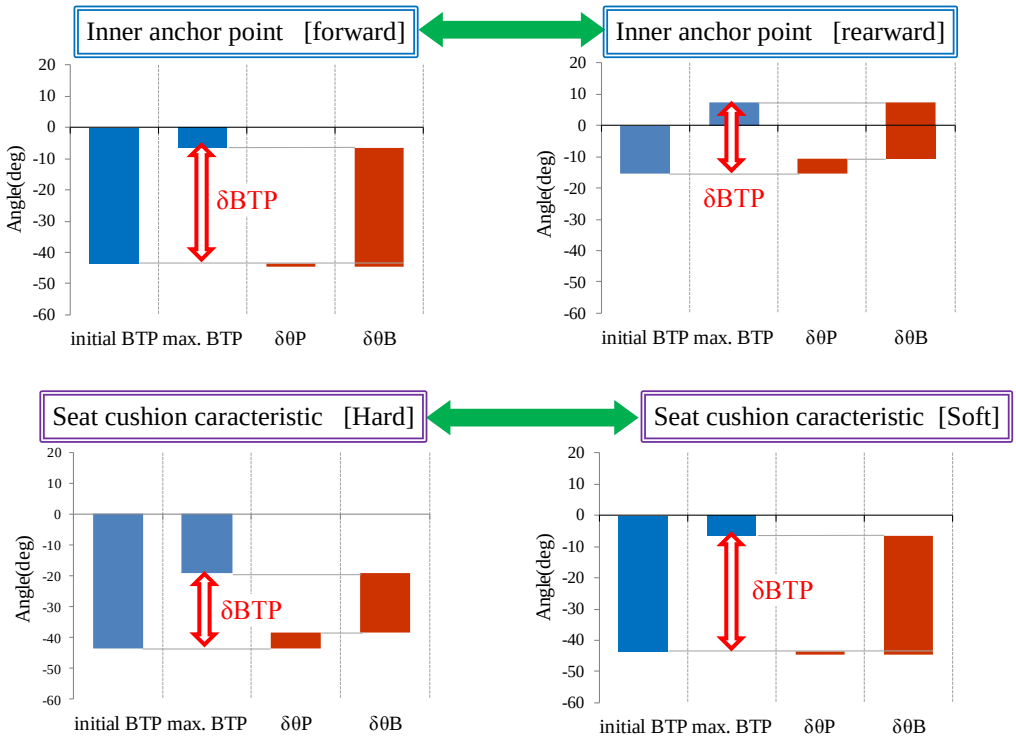


***Figur5. BTP change (δBTP) by changing the parameters of the inner anchor point (forward / rearward) and the seat cushion characteristic (Hard /Soft)***

## DISCUSSION

The accident analysis indicated that 65% of the injured abdominal organs were distributed in the lower abdomen such as the intestine or the mesentery. According to the simulation used FEM, it was confirmed that the lap belt positioned on the abdomen might be the cause for the large amount of deflection and deflection velocity, particularly in the lower abdomen. The conclusion, based on the above, is that it is important to hold the lap belt on the pelvis in order to reduce the load on the abdomen and prevent abdominal organs injuries. Although the combination of the anterior arrangement of inner anchor point and the measures for reducing the forward and downward movement of the pelvis described above are effective, the anterior arrangement is likely to increase the forward displacement of the pelvis by restraint performance degradation of the lap belt. Due to this, changes to the BTP should be considered but attention should be paid to the contradictory relationship with forward displacement suppression of the pelvis. However, in this analysis conditions, the effect of the initial BTP was larger than the BTP change during crash event and the most anterior arrangement, within the limit of regulation, was the optimum layout. Additionally, the decrease of pelvis restraint performance leads to the increase of the inner belt load and may have an influence to thoracic deflection. Therefore, it is necessary to design the proper location of the inner anchor in accordance with the geometry of vehicles or the crash characteristic.

## LIMITATION

The above study of submarining phenomenon was intended for the occupant sitting in proper position and with proper posture, but there may be various sitting conditions in the real-world. Research of sitting position and posture in the rear seat of sedan and minivan was conducted using 50 subjects (age; 24-51, gender; 76% male / 24% female). The results showed that the hip of 46% subjects were positioned in excess of 20mm forward compared to proper position and 15% were positioned in excess of 60mm. Because it is thought that when the pelvis is positioned forward, the lap belt will usually be fitted on the abdomen, it is important not only to sit down in a posture which easily fits the lap belt on the pelvis as much as possible, but also to promote education for understanding the importance of the correct use of seat belts.

As mentioned during the results of the accident analysis, the pelvic fractures are due to contact with the hard interior or unbalanced load by the vehicle behavior. However, the investigation of McCalden et al. [11] indicate that the breaking strain of the femur cortical bone decreases with age. Since the similar reduction can be considered against the pelvis, it is necessary to control of the seat belt force in consideration of elderly.

## CONCLUSIONS

The investigation into abdominal injuries due to the submarining phenomenon and the mesurements from this study were carried out with the aim to further improve the protection performance of the rear seat occupant. The findings of this study show that:

1. Accident analysis indicated that 65% of the injured abdominal organs were distributed in the lower abdomen such as the intestine or the mesentery.

2. Simulation using human finite element model found that fitting the lap belt on the abdomen might cause the abdominal injuries as the maximum amount of abdomen deflection was increased by approximately 3.4 times, and abdomen deflection velocity was increased approximately by 2.3 times relative to properly fitting the lap belt on the iliac spine. This confirmed that it is very important to route the lap belt on the pelvis in order to reduce the load on the abdomen and prevent abdominal organs injuries.

3. To prevent the submarining phenomenon, the forward configuration of the inner anchor point, to make the initial BTP smaller, and the countermeasure of increasing the restraint force of the pelvis to reduce the BTP change during crash event are valid.

4. The forward configuration of the inner anchor point can cause side-effects which impacts the lap belt angle during crash event or influence other injury values. Therefore, when designing the layout of the inner anchor point, the confirmation and the optimization based on the geometry and the crash characteristic of the target vehicle should be considered. And, in case of applying countermeasures to increase the restraint force of the pelvis, it is necessary to consider the pelvic tolerance of vulnerable population, such as elderly.

## REFERENCES

[1] D. Glassbrenner, NHTSA. 2003. “Estimating The Lives Saved by Safety Belts and Air Bags″ 18th ESV Conference Paper No. 500

[2] Ikari, T., Kawahara, H., 2009.“Rear Occupant Protection JNCAP Test” 21st ESV Conference, 09-0299

[3] Yamasaki, T., Uesaka, K., 2011.“Rear Occupant Protection JNCAP Test –Test Results and Findings” 22ndESV Conference, 11-0445

[4] Frampton, R., Lenard, J., Compigne, S., 2012. “An In-depth Study of Abdominal Injuries Sustained by Car Occupants in Frontal Crashes”, 56th AAAM Annual Conference
[5] ITARDA, 2014.“Injuries to Older Passengers in Traffic Accidents”, ITARDA Information, No.104
[6] JNCAP, 2014.“Car Safety Performance Guidebook”
[7] Euro NCAP, 2014.“Assessment Protocol - Adult Occupant Protection”, version 7.0.1
[8] Ono, K., et al., 2011.“In-Depth Analysis by using the New Advanced and Integrated Traffic Accident Datebase linked to Permanent Disability and Trauma Registry Data in Japan”, 2011 IRCOBI Conference, IRC-11-41
[9] Horsch, J., Hering, W., 1989. "A Kinematic Analysis of Lap-Belt Submarining for Test Dummies", SAE Technical Paper 892441
[10] Tachenatlas Der Anatomie, 4th edition, Bunkodo Co., Ltd. (2002)
[11] McCalden, R, McGeough, J., Barker, M., Court-Brown, C., 1993. “Age-related changes in the tensile properties of cortical bone. The relative importance of changes in porosity, mineralization, and microstructure”, J Bone Joint Surg Am, 1993 Aug; 75(8): 1193 -1205 .

# STUDY ON THE SAFETY PERFORMANCE OF THE REAR SAFETY GUARD WITH AIR BAG FOR TRUCK

**In-Song PARK,**
Smart Air Chamber Co., Ltd.
Republic of Korea

**Kyung-Won YUN, Kwang-Jong PARK, Hyo-Jun KIM**
Smart Air Chamber Co., Ltd.
Republic of Korea

Paper Number 15-0033

## ABSTRACT

Although the Korea government promotes the movement of safe traffic to reduce deaths in traffic accidents, the number increases every year.

Especially more and more accidents and casualties are reported from the cases of car collision to the back of the vehicles parked for managing car accident on road, cleaning of main roads, side roads and medial strip, and road repair.

Therefore, it has been along that the government should be responsible for taking a protective measure for road users.

71 cases have been reported to occur during highway repair and maintenance. As the result, 8 were dead and 76 were injured, showing the death rate of 11.3%, which is quite high.

So it seems urgent to take some action against it.

America and European countries legislate that vehicles of road repair and maintenance should be mandatorily equipped with shock absorber on car but our country lacks in a legislative measure, which is asked to be done.

Accordingly, this study compares the performance standards of shock absorber for road maintenance vehicle by applying country to establish the criteria.

In addition, it tries to interpret in theory the Rear Safety Guard using Air Bag and compare the safety performance test of a vehicle with the Rear Safety Guard manufactured in accordance with related laws and that using Air Bag.

Based on the result of the safety performance on the 60km/h Rear collision Test, this study proposes improvement in related regulations and laws in an attempt to reduce collision and death by proposing the Traffic Injury Prevention effect of the Rear Safety Guard using Air Bag.

## INTRODUCTION

Deaths & casualties by vehicles are getting grow though government provide more developed safety standard in order to reduce them.

Especially, rear-end collisions to the working trucks on the road, which are on cleaning road, treating accident or road maintenance, cause fatal injuries.

That's why social responsibilities for them has been issued since long time ago.

For the last 10 years, 71 cases of rear-end collisions to the working trucks in the highway have incurred, of which 8 persons were dead, 76 persons were injured, which shows remarkable 11.3% of death rate. Accordingly, we need to take urgent measurement against them.

Especially, Under-ride accident, which means rear-end collision car burrow down beneath under working truck, cause fatal influence to the passenger life.

Nowadays, it is compulsory to install Rear Safety Guard in order to prevent such under-ride accident.

It is possible to prevent under-ride accident if Rear Safety Guard is installed as per current installation intensity standard. However, it regulates only shock absorption which may cause fatal shock to the passenger.

This Study issues necessity of regulation amendment to reduce passenger casualties and guides characteristics of shock absorption Rear Safety Guard. In order to provide comparison data, we make use of both Airbag Rear Safety Guard and the Conventional Rear Safety Guard in the performance test of rear collision with 60km/h velocity.

**STRUCTURE OF REAR SAFETY GUARDAND THEORETICAL CONSIDERATION**

**Structure of Rear Safety Guard**

Comparing structure of both Rear Safety Guards, the Conventional Rear Safety Guard has cross section of quadrangle beam and Airbag Rear Safety Guard is consist of Control Case and Borer fixed bracket. Control Case prevents rebound of rear-end collision vehicle with air occupied space using TPU (Thermoplastic Polyurethane).

Therefore, difference between the both Rear Safety Guards is, the Conventional Rear Safety Guard has only quadrangle beam to endure loading specified installation intensity by standard, however, Air bag Rear Safety Guard consist of rear Bracket enduring loading specified by standard, at the same time, air in the TPU absorbing 1st shock by TPU Elongation & Control case under low velocity and Borer absorbing 2nd shock by emitting air, simultaneously, minimizing rebound of rear-end collision vehicle.

**Air bag Crush Movement Theory**

The follows theoretical formula becomes as follows

A body, which has mass m with initial velocity $V_0$, drops toward an elastic body.

Assume that the deformation of an elastic body is one-dimension and the material is compressible in order to make a formula for describing the moving of a colliding body.

σ is true stress and ε is true strain.

$$\sigma = f(\varepsilon),\ \varepsilon = \ln\frac{l}{l_0}$$

$l_0$ is the initial thickness of an elastic body, and $l$ is the thickness after deformation.

$$F = \sigma A = f(\varepsilon)A$$

Volume changes after deformation because an elastic body is compressible

$$\alpha A_0 l_0 = Al$$

$\alpha$ is the rate of volume, $A_0$ is the initial area of deformation, and $A$ is the area after deformation.

If $l_0 - l = x,$ then $A = \alpha\frac{l_0}{l_0 - x}A_0$

$$F = \alpha f(\varepsilon)\frac{l_0}{l_0 - x}A_0$$

Therefore, the momentum equation of the colliding body is

$$m\frac{d^2x}{dt^2} = -\alpha f(\varepsilon)\frac{l_0}{l_0 - x}A_0$$

Considering the effect of gravity, the equation is as follows

$$m\frac{d^2x}{dt^2} = -\alpha f(\varepsilon)\frac{l_0}{l_0 - x}A_0 + mg \quad \text{Formula of(1)}$$

Two initial conditions are necessary to solve the above equation. In case of small deformation, we can rewrite equation as

$$\frac{l_0}{l_0 - x} \cong 1$$

$$f(\varepsilon) = E\varepsilon = E\ln(\frac{l_0}{l_0 - x}) \cong E\frac{x}{l_0}$$

If we neglect the effect of gravity

$$m\frac{d^2x}{dt^2} = -\alpha E\frac{x}{l_0}A_0 \text{ Formula}$$

Formula of (2)

If we solve the equation (2) with two initial conditions, $x(0) = 0$ and $\frac{dx}{dt} = V_0$
The formula becomes as follows

$$x(t) = V_0\sqrt{\frac{ml_0}{\alpha EA_0}}\sin\sqrt{\frac{\alpha EA_0}{ml_0}}t$$

And equation (1) becomes

$$F = m\frac{d^2x}{dt^2} = -V_0\sqrt{\frac{\alpha EmA_0}{l_0}}\sin\sqrt{\frac{\alpha EA_0}{ml_0}}t$$

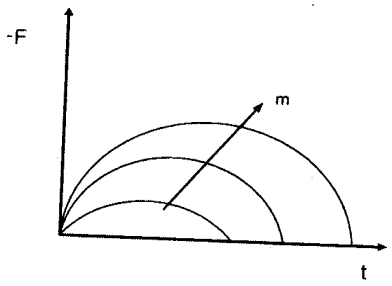


***Figure 1. F-t curve in the mass of the colliding body increase***

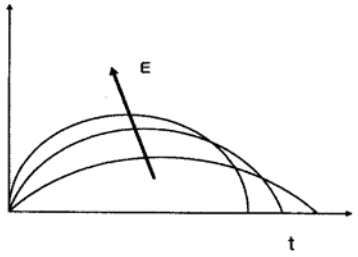


***Figu creases***

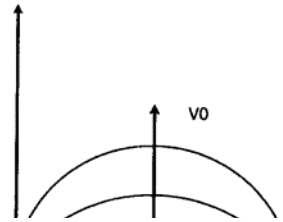


***Fig rease***

We can recognize that the relation between force and time is sine curve. Let us consider the effect of several variables.

The more the mass of the colliding body increases, the more the magnitude of the force and the period increase. When the elastic modulus increases, the force increases and the period become shorter.
When the initial velocity increases, the force increases, but the period stays same.

A body, which has mass m with initial velocity V0, drops toward an elastic body. Assume that the deformation of an elastic body is one dimension and the material is compressible in order to make a formula for describing the moving of a colliding body. σ is true stress and ε is true strain drops toward an elastic body. Assume that the deformation of an elastic body is one-dimension and the material is compressible in order to make a formula for describing the moving.

The tensile strength of the thermoplastic polyurethane is 440 kgf/cm² and the tensile stress(at 300% elongation) is 260 kgf/cm².

## TEST AND CONSIDERATION

### Test Facility

Collision test facility strictly follows clause No. 102 evaluation on passenger protection at the time of collision of Vehicle safety standard.

Towing collision test facility was made to test 60km/h velocity of collision.

Figure1, Figure2 shows collision test facility and test method respectively.
Test standard is Head-on center impact of Figure.2 (a).

**Figure 4-(a). Cable Draw Type collision Test Equipment**

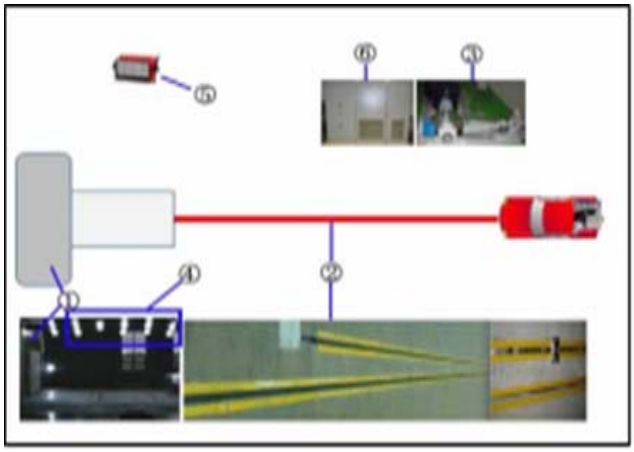

**Figure4-(b).System diagram**.

(Note)
①Collision test facility for this Study
consists of fixed collision wall
② Driving road
③ Driving motor
④ Lighting facility
⑤ Data accumulator
⑥ Control unit

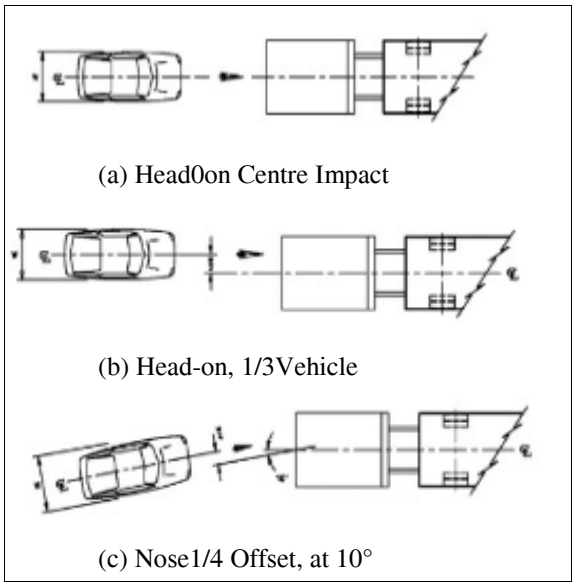


***Figure5. Test standard for crash absorption facilities***

**Testing**

**Collision testing** This is to find shock absorption performance of the Conventional Rear Safety Guard and mobility of rear-end collision vehicle at right after collision. We designed both types of Rear Safety Guard to meet the conditions of rear-end collision vehicle. Table.1 shows types of test specimens for trial impact tests.

**Table1**
**A kind of test specimens for trial impact test**

| Specimens | | Section(size) |
|---|---|---|
| Conventional Rear Safety Guard | NO.1 | 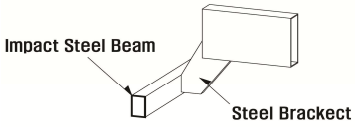  |

| | | |
|---|---|---|
| Air Bag Rear Safety Guard | NO.2 | 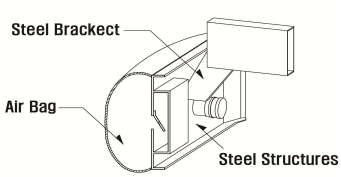 |

(Note) NO.1 : Steel impact beam + steel structure bracket
NO.2 : Air Bag impact cushion + Steelimpact structure + Steel structure bracket

The characteristics of respective tests are that fundamental structures of the both types of Rear Safety Guard are same.

However, Airbag Rear Safety Guard is assembled by air injected airbag. Those airbag's material, size, pressure, part price and weight are being studied through structure analysis and accurate testing.

Once it is accomplished, various types of products will be produced, which are able to meet each types of test.

**Collision test** Test performance of high speed rear-end collision tests follows American NCHRP Report 350 standard Shock Absorption Facility Test and U.K Design Manual for Roads and Bridges(TD49/07,Volume8 Section4, Part7), Requirements for Mounted collision Cushions standard. And 60km/h rear-end collision performance test was done in order to find collision performance of the both types of Rear Safety Guard.

Ten (10) tons of truck manufactured in 2003 for test installed both types of Rear Safety Guards with its total weight of 10,340kgs and midsized sedan of its weight of 10,340kgs was also used for rear-end collision vehicle.

The testing started that midsized sedan collided truck with Conventional Rear Safety Guard. After collision, its Conventional Rear Safety Guard was replaced with Airbag Rear Safety Guard for retesting. Same collision test method was applied to the Airbag Rear Safety Guard truck.

The test vehicle was installed with data accumulator inside test vehicle, acceleration meters at X,Y,Z axis and yaw sensor.

Tape switch for lighting was installed to sense impact at collision point.

500f/s high speed digital camera and video camera installed at left, right and upper right in order to record collision. Fig.3 shows collision test.

***Figure6. The scene of the car collision test ofRear Safety Guard for 10ton Truck.***

**ANALYSIS AND CONSIDERATION**

As follows Fig 7, Fig 8, Fig 9 Fig 10 showed that the 60km/h rear-end collision performance test results for both types of Conventional Rear Safety Guard and Air Bag Rear Safety Guard.

This study practical use evaluation standards is THIV 44km//h, PHD 20g, ASI 1.9G

The analysis for passenger protection performance index data by 60km/h collision performance test shows, at first, according to the test of Conventional Rear Safety Guard equipped truck, Yaw sensor detected data was maximum of +112.5˚ at 0.23 second and minimum of -51˚ at 0.24 second, and, acceleration index (ASI) was 50msec at composition of x,y,z axis direction, it was maximum 1.3(G'S) at 0.1890 ~ 0.239 second according to analysis result.

Theoretical Head Impact Velocity (THIV) shows 35.1km/h at 0.2149 second, which is synthesized value of x, y axis, and Post-Impact Head Deceleration (PHD) shows 17.1(G'S) at 0.2269~0.2369second, which is 10m second average synthesized value of x,y direction.

At second, in case Airbag Rear Safety Guard was installed, Yaw sensor detected data was maximum of -50° at 0.16 second and minimum of +19° at 0.45 second, and, Acceleration Severity Index (ASI) was 50msec at composition of x, y, z axis direction, it was maximum 0.9(G'S) at 0.0199~0.0609 second according to analysis result.

Theoretical Head Impact Velocity (THIV) shows 28.9km/h at 0.1269 second and Post-Impact Head Deceleration (PHD) shows 8.4(G'S) at 0.1269~0.1369second.

As follow in brief for above mentioned test data.

The results of data analysis, in case of Conventional Rear Safety Guard, shows Yaw effect based on z axis sharply rotate around 100~150° to the + direction at 0.15~ 0.25 second, however, in case of Airbag Rear Safety Guard, it shows 11~50° to the - direction at 0.15~ 0.25 second.

Especially, in case of Conventional Rear Safety Guard, it absorb collision force 0.10~ 0.20 second after collision, however, in case of Airbag Rear Safety Guard, it absorb whole collision force at the same time of collision.

From the under-ride's view, in case of Conventional Rear Safety Guard, passenger may have severe casualty because rear-end colliding car burrow down beneath under working truck, however, in case of Airbag Rear Safety Guard, passenger may have much less casualty because collision absorption occurs at the early time of collision.

The current regulation on Rear Safety Guard specifies to certify structure rigidity through only component test, which is revealed to be lack of prevention for the passenger casualties.

So, it is necessary to amend regulations on structure and test evaluation method of Rear Safety Guard because Rear Safety Guard bracket structure rigidity should be improved to prevent submarine effect by under-rider at collision.

Furthermore, there is no collision absorption performance standard.

So,we recognized that not only evaluation standards for injury THIV,PHD, ASI but also under ride situation level is should be provision of safety regulation.

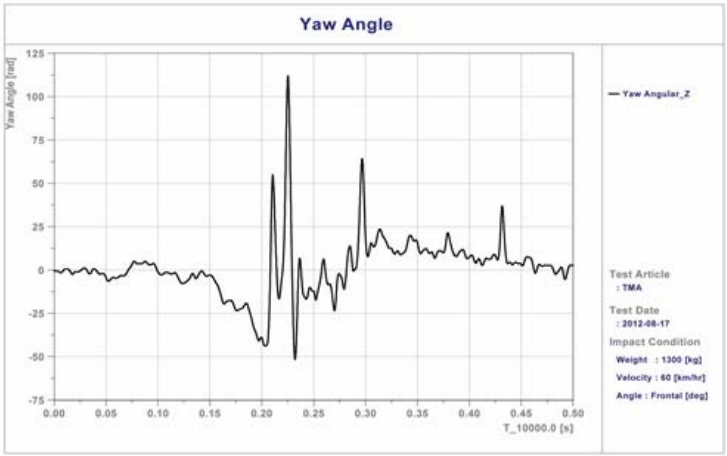


***Figure7-(a). YAW data-Conventional type installed***

*Figure7-(b). YAW data-Air bag type installed*

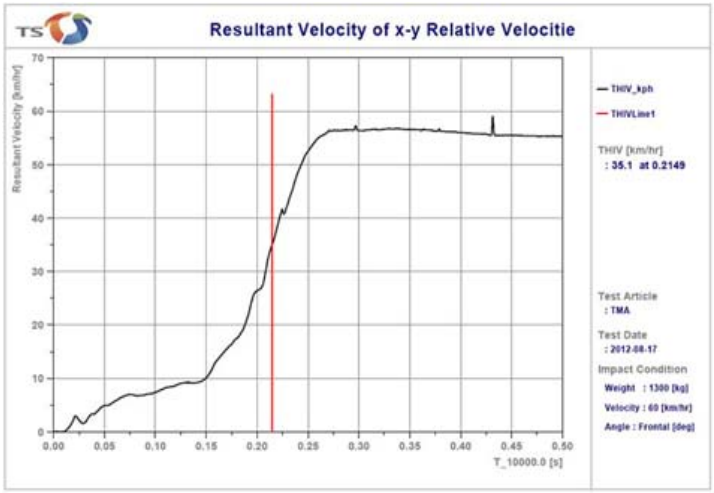


*Figure8-(a). THIV data- Conventional type installed*

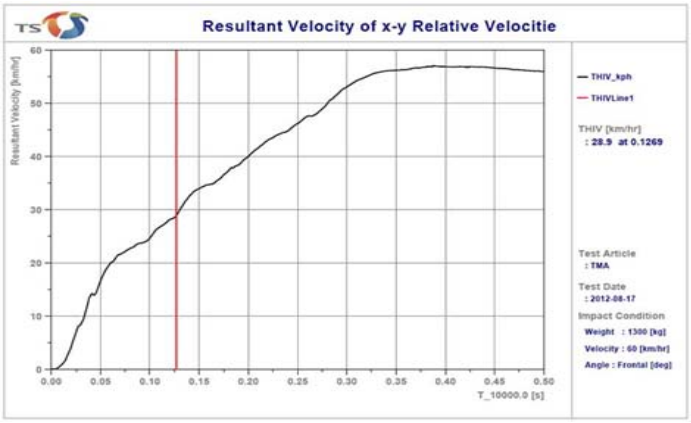


*Figure8-(b). THIV data-Air bag type installed*

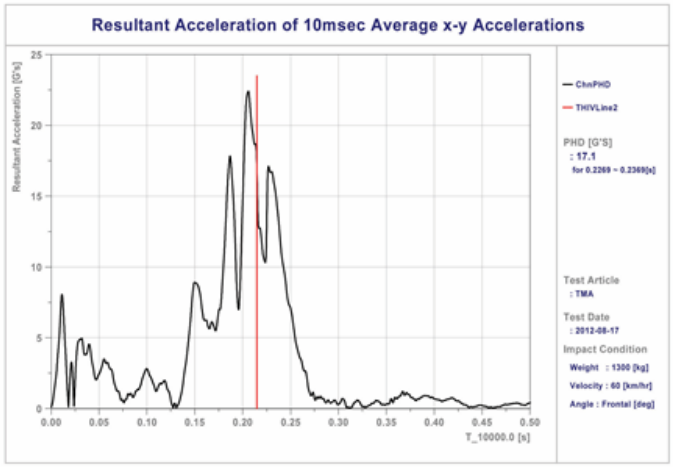


*Figure9-(a). PHD data- Conventional type installed*

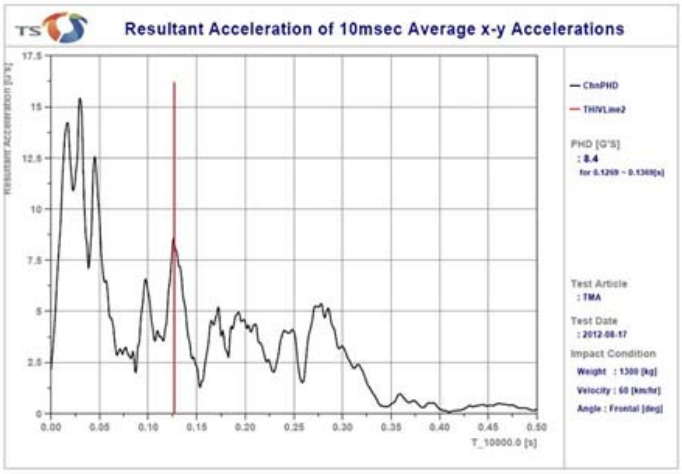


*Figure9-(b). PHD data-Air bag type installed*

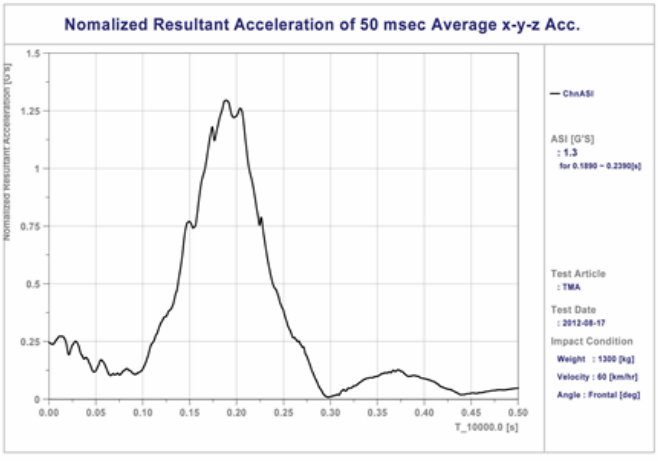


*Figure10-(a). ASI data- Conventional type installed*

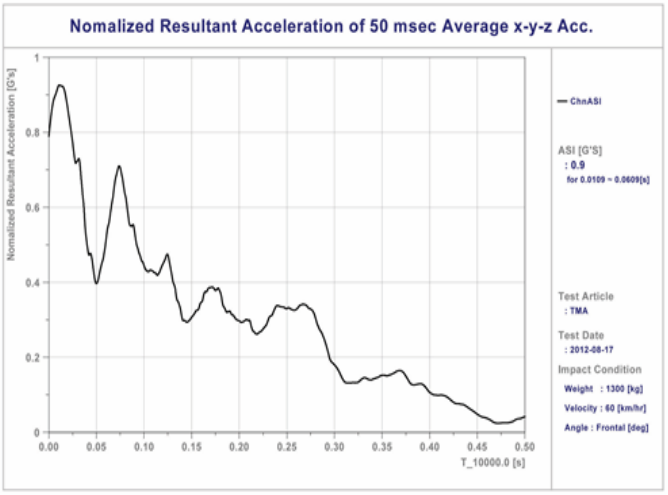


***Figure10-(b). ASI data-Air bag type installed***

## CONCLUSIONS

We have considered the related regulation to improve Rear Safety Guard. And, the analysis results of 60km/h rear-end collision performance test by installing both types of Rear Safety Guard are as follows.

1) Rear-end collision performance test of both types of Rear Safety Guard shows that Airbag Rear Safety Guard inferior 12% of THIV, 49% of PHD and 69% of ASI to them of Conventional Rear Safety Guard.

2) Mobility of rear-end collision vehicle at collision shows that Airbag type of Rear Safety Guard equipped vehicle less burrowed down beneath truck due to less Under-ride effect. Accordingly, airbag Rear Safety Guard with polyurethane revealed to much reduce passenger casualty.

3) Rear-end collision vehicle equipped with Conventional Rear Safety Guard burrowed down beneath the truck up to front window of rear-end collision vehicle because Conventional Rear Safety Guard couldn't absorb collision force.

It means that it is difficult for Conventional Rear Safety Guard to prevent passenger casualty. Therefore, structure rigidity and evaluation method for passenger casualty such as THIV, PHD and ASI should be improved by adopting Truck Mounted Attenuator (TMA) evaluation method.

4) Need to provision that the under ride situation levels on Rear-end collision vehicle because of cause to reduce deaths in traffic accidents,

5) We can recognize that Air Bag Truck Mounted Attenuator (TMA) is superiority absorbing performance on collision base on the showed similar trend for the Air Bag Theoretical Formula and 60km/h rear-end collision test result of complete vehicle attached Air Bag Truck Mounted Attenuator (TMA).

Hence, it is possible that reduce deaths traffic accidents on rear and the other dictions collision, in case of the much more study to commercialize and improvement of quality for Air Bag Truck Mounted Attenuator (TMA).

## REFFERENCE

[1] Ahn, K. H., “A study on the collision motion ofpolyurethane TPU airbag”, Seoul univ. Textilespolymer depart, pp. 20~32, 1992.
[2] Park, I. S., “A study on the vehicle safety at ahigh speed collision and the vehicle damageability and repairability at a low speed collision”, Kook min univ, pp. 40~60, 2000.
[3] Lee, H. B., Han, M. S., “Automobile design engineering”, Wonchang publish co., pp. 195~207,1998.
[4] S. P Timoshenko. J. N Goodier, "Theory of Elasticity", McGRAW-HILL, pp. 485~504, 1970.
[5] S. H. Crandall. et. al., "Introduction to the mechanics of Solid".McGraw-HILL, pp.323~325,1978.

[6] E.Kreyzig, "Advanced engineering mathematics", JOHN WILEY & SONS, pp. 73~75,1993.
[7] Ministry of Land, Transport and Maritime Affairsof Korea "Guidelines for installation andmaintenance of road safety facilities." 2012
[8] Ministry of Land, Transport and Maritime Affairsof Korea "Handbook for genuine vehicle collisiontest for protecting vehicle facilities" 2012
[9] Gyeong Woo, Kim "Study for mobility ofpassenger car collision and design of collisionabsorption facilities"
[10] DaeHyung, Jang "Study for collision mobilityof collision
absorption considering passenger safety"Korean Society
of Civil Engineers. 2006
[11] R.H. Macmillan, Dynamics of VehicleCollision," Proceeding of the InternationalAssociation for Vehicle Design, Special PublicationSP5 Channel Islands , UK, 1983
[12] H. E. Ross. Jr., D. L.Sicking, and R. A. Zimmer,ecommended Procedures for the SafetyPerformance Evaluation of Highway Features,"NCHRP Report 350, Transportation ResearchBoard, Washington, D.C., 1993
[13] CEN, "Road restraint systems Part 1:terminology and general criteria for test methods,EN 1317-1, European Committee for Standardization2010.
[14] Tae-Ho Yoon, Young-Me Cha, Jong-Il Yook,Jong-GyuBaek, Hee-Jae Kim "Study on Compositematerial's bullet-proof effect improvement by addingurethane resin." The Korean Society for CompositeMaterials 2011.

**DefinitionS/AbbreviationS**

**ATMA** Air Bag Truck Mounted Attenuator
**THIV** Theoretical Head Impact Velocity
**PHD** Post-Impact Head Deceleration
**ASI** Acceleration Severity Index

This paper has been peer-reviewed and published in a special edition of *Traffic Injury Prevention* 16(S1), by Taylor & Francis Group. The complete paper will be available on the *Traffic Injury Prevention and www.NHTSA.gov* websites on June 8, 2015.

To access all Peer-reviewed papers please copy and paste the link below into your browser to access the papers.

http://www.tandfonline.com/toc/gcpi20/16/sup1

# Prospective Estimation of the Effectiveness of Driver Assistance Systems in Property Damage Accidents

**Klaus Gschwendtner**
**Dr. Miklós Kiss**
AUDI AG
Germany

**Philip Feig**
**Prof. Dr.-Ing. Markus Lienkamp**
Institute of Automotive Technology, Technische Universität München
Germany

Paper Number 15-0037

## ABSTRACT

Projects for the analysis of traffic accidents are focused mostly on personal damage. But analyses show that property damage occurs 42 times more often than personal damage [4]. Officially registered accidents on German roads result in mere damage to property (2.1 mio accidents [1]). A significantly higher number of property damage accidents are not reported to the police. Some of which are reported to the insurers [2]. A significant number of minor damage does not appear in the statistics. According to [3] the number of minor damage cases amounts to 4.8 mio cases per annum. 35% of full comprehensive cover accidents occur at low speeds and pose a high potential for future advanced driver assistance systems (ADAS) [4]. Details of accidents involving minor damage cannot be found in official statistics. In "In-Depth" property damage analysis, the conflict leading to damage is of high relevance. Uncertainties need to be settled by means of an expansion of the existing accident conflict situations [4]. Currently, equipment rates of ADAS are low requiring a purchase incentive for customers. Based on [5] this paper describes how damages of vehicles can be classified and brought into relationship with ADAS functions and the vehicle itself. Various configurations and different materials of outer attaching parts (OAP), e.g. aluminum, CFRP or plastics induce variable costs of repair. For a prospective evaluation method of the monetary effect of ADAS it is necessary to know all influence parameters and to quantify them. The evaluation of vehicle concepts in combination with an ADAS is possible.
Keywords: In-Depth Property Damage Analysis, Field Effectiveness, Prospective Evaluation, Property Damage Risk Function, Accident Research.

## INTRODUCTION

Accident research units mainly analyze accidents involving personal injury. Derived findings run in the development of infrastructural arrangements or the vehicle safety. This has been mainly reflected in the decreasing number of traffic fatalities during the last decades. An investigation shows [4] that just every fourth of insurance cases of the property damage accident is reported officially. According to [3] the number of minor damage cases which do not appear in statistics amounts to 4.8 mio cases per year. Hence property damage occurs 42 times more often than personal damage. Official statistics only represent a fraction of real-world accidents involving property damage.
Up to now there is no detailed analysis of the accident characteristics and causes of accidents in large scale projects in the property damage field. Just pilot-studies like [4] deal with it. The objective is to make the „blank spot" on the accident scenario map disappear. Detailed information and knowledge about the emergence of accidents and the underlying conflict scenario are very helpful for developing and designing advanced driver assistance systems.
35% of full comprehensive cover accidents occur at low speeds and pose a very high potential for current and future advanced driver assistance systems (ADAS) [4]. Currently, equipment rates of ADAS are low requiring a purchase incentive for customers.
Safety systems are currently mainly intended for reduction of injury severity in accidents at high initial and collision speeds, as for instance Adaptive Cruise Control with emergency brake function [6]. However, fitting rates for such systems are small. Therefore, a purchasing incentive for the customer shall be established in order to trigger a higher effect on traffic safety. However, this requires knowledge of the effectiveness of the system prior to market introduction. Purchasing incentives for the customer can be saved repair costs or lower insurance premiums. Hence systems would partly or fully pay off in the course of their service life.

A retrospective effectiveness analysis of active systems is elaborate and time-consuming concerning the data collection and because of the low fitting rates only viable over a long period of time (approx. 3 years). Therefore a statement on the effectiveness of a system is only possible at a late stage after launch of sales. Prospective analysis methods of ADAS in the field of property damage accidents are rarely available.
This paper presents based on the methodology for the prospective determination of field effectiveness of ADAS focusing on the potential of reducing property damage accidents given in [5] a detailed evaluation of damages. Various equipment configurations and different materials of OAPs have a big impact on the repair costs. Furthermore the influence of the vehicle class has to be considered. An increasing number of automated systems is expected in the course of the next years and especially in the low speed range these systems could have a major influence on the number of occurring property damage accidents. Appropriate dimensions for the evaluation and comparability of the changing repair costs are needed.

## METHODS AND DATA SOURCES

For evaluating the benefit of ADAS in property damage accidents a systematic procedure like described in [5]. This method consist of the main parts of data collection, reconstruction and new simulation of accidents and a Damage Risk Function (SRF) for evaluating modified accident parameters.
The modified accident parameters are evaluated with the SRF. This function is build up modular for covering nearly every individual accident. Vehicles are divided into damage segments: Front, fender, doors, side panel and rear. Every area is related with components plugged in each.

### Damage points and Matching coefficients

The resulting damage of a collision is reflected as a standard value in relation to the volume model of the respective manufacturer. A standardized description of the damage allows a comparison over a long period of time. If the resulting damage is currency related there would be no possibility to do a comparison many years later because component costs and wages would have changed. A further reason for standardized representation is improved comparability of vehicle models. Besides validity over a long period of time the evaluation of damages should also be transferable to various models. In an identical damage scenario the resulting damage should be on the one hand be comparable and on the other hand individual influence factors regarding the extent of damage have to be considered.

These requirements can be achieved by means of the modular design of the SRF and using damage points (SP) as an independent damage value (Eq. (1)).The volume model of the respective manufacturer serves as a basis. Total cost of a repair consisting of component costs (ET), wages (LW) and paint-work costs (LACK) are under consideration. For every single part the total costs of replacing are considered and subsequently divided by the basic factor α.

Besides the complete replacement of components repair procedures like smart repair, paint work and removal of dents can be considered. The depth and surface area of the deformation are the main factors for the determination of the repair method.

$$SP_i = \frac{ET_i + AW_i + LACK_i}{\alpha} \qquad \textbf{(1)}$$

Mainly the OAPs are considered here since it can be assumed that in the low speed range without personal damage no significant structural elements are damaged. This was derived in other studies of [5].
The generated damage points are identical for each vehicle model in order to ensure comparability of components. Different materials of components, equipment speciation of vehicles and various vehicle classes have to be evaluated the same way. Therefore matching coefficients are necessary (Table 1). These coefficients are separated into different influence parameters as can be seen in the first column. The coefficients show the ratio of different prices of repair costs for different parts and vehicles. An estimator tool was used to determine repair costs.

**Table1.**
**Specifications of matching coefficients**

| Influence-parameter | Symbol | Example |
|---|---|---|
| Vehicle class | $\beta_{class}$ | small car, compact car, medium-sized vehicle, upper middle-sized vehicle, luxury class vehicle |
| Light | $\beta_{light}$ | Xenon-, LED- or laser-headlights |
| Material | $\beta_{material}$ | aluminum, CFRP or plastic |
| Dynamic Design packet | $\beta_{dynamic}$ | S-Line, M-packet, AMG- packets |
| Alloy rim size | $\beta_{rims}$ | 15“, 16“, 17“, 18“, 19“, 20“, 21“ |
| Type of varnish | $\beta_{varnish}$ | solid paint or special painting |
| Layout ADAS | $\beta_{ADAS}$ | ACC with one or two sensors |

For example if there is a damage on the right front edge all damage points of the components are taken into account. If the vehicle class is higher than the volume model, the material of the engine hood and the front fender have changed and also the technology of the headlights is a different one. The coefficients for class, light and material have to be multiplied to the individual damage points and are called damage units.
Figure 1 gives an overview over the range of the matching coefficients. This method can be applied for all manufacturers and would therefore provide a comparison option for damage scenarios.

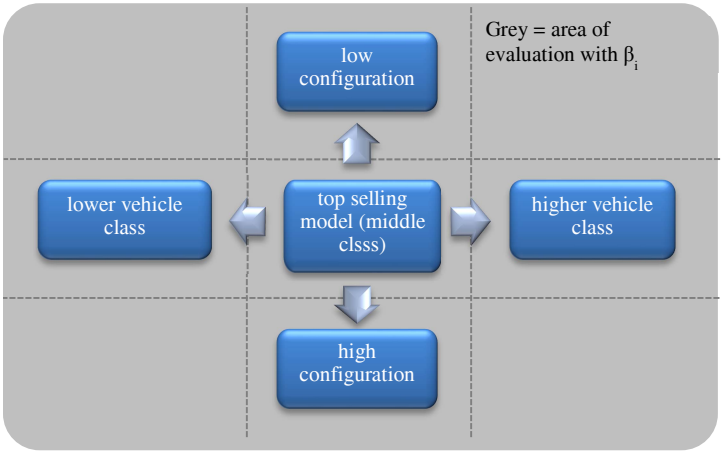


***Figure1. Matrix of matching coefficients***

**Damage units and real world repair costs**

The given example shows that a lot of different influence factors to the extent of damage have to be considered. Damage points derived for the volume model are calculated individually for each vehicle by means of the matching factors. Equation (2) shows the calculation of damage units (SE) of an individual component.

$$SE_i = SP_i \prod_n^m \beta_n \qquad (2)$$

$$m, n \in \{class, light, material, rims, dynamic, varnish, ADAS\}$$

In the most cases of an accident many components at once are damaged. Equation (3) contains all affected parts

$$SE_{sum\ of\ external\ components} = \sum_i^j (SP_i \prod_n^m \beta_n) \qquad \textbf{(3)}$$

In addition, there are basic costs which are identical for every repair job as for instance varnish preparation if paint work is required. The damage points and the damage units for the varnish-preparation are equal because there is no difference between various vehicle-models. They can be added to the total sum of damage units (Eq. (4)).

$$SE_{all} = SE_{sum\ of\ external\ components} + SE_{varnish\ prep} \qquad \textbf{(4)}$$

The back calculation to the damage extent in the used currency can be ensured all time. Therefore the sum of damage units including the varnish preparation is multiplied with the basic factor $\alpha$ (Eq. (5)). In the course of time only the basic factor has to be adjusted for considering changing prices.

$$SH = SE_{all}\,\alpha \qquad \textbf{(5)}$$

On the basis of this methodology it is possible to evaluate future vehicle concept without knowing the exact component costs. Only the vehicle class and the used materials have to be known for calculating the expected repair costs. The repair costs are in the first instance interesting for insurers.
The methodology of damage points and damage units facilitates a separate consideration: The ADAS can reduce damage points, the reduced damage points have vehicle individual impact on the resulting damage units. Both dimensions are referred to the basic factor.

**Property Damage Risk Score**

According to [7] risk is the combination of damage extent and the probability of occurrence. Using an overall statistical relevant damage frequency distribution like DEKRA, GIDAS or AZT can provide it, a basic risk can be calculated. If available even for different classes of vehicles. These information can be used in combination with vehicle specific information about materials of components and equipment. A property damage risk score (SSR score) can be calculated due to summing up all products of damage units and frequency in all damage segments around the vehicle (Eq. (6)).

$$SSR = \sum_i^j \left(SP_i \cdot \prod_n^m \beta_n \cdot p_{damage,i}\right) \qquad \textbf{(6)}$$

In application of the SSR Score a distinction between the upper and the lower SSR score. The difference between is the considered extent of damaged components. The lower SSR score considers bumpers, fenders, doors and side panel. The upper SSR score considers in addition lights on front and rear, ADAS sensors as well as front and boot lid. Therefore an interval between minor loss and bodily injury can be defined. A multiplication of these intervals with the annually expected damage frequencies a monetary potential of ADAS can be defined.
Based on this intervals a risk label is derived. It is divided in eight categories from A to H. In the categories from F to H a progressive rise is visible whereas the categories A to E show a linear rise. This is necessary because the rise

in repair costs for complex technologies like laser light or extreme lightweight constructions cannot be represented in a linear scale. Table 2 shows the intervals and the according risk labels.

**Table2.**
**Risk classification by means of property damage risk score (SSR)**

| risk label | lower boundary property damage risk score ($SSR_L$) | upper boundary property damage risk score ($SSR_U$) |
|---|---|---|
| **A** | > 0 | 40 |
| **B** | > 40 | 80 |
| **C** | > 80 | 120 |
| **D** | > 120 | 160 |
| **E** | > 160 | 200 |
| **F** | > 200 | 280 |
| **G** | > 280 | 400 |
| **H** | > 400 | |

A risk classification of vehicles has to be conducted because resulting repair costs in property damage accidents depend significantly of the equipment of the vehicles and the materials of the OAPs. Based on the findings in the risk classification an investment strategy could be derived how a vehicle should be protected by systems to achieve a good risk label. In order to achieve a positive effect on damage requirement there are two options: either reduction of frequency or reduction of damage extent. In both options ADAS functions can be a big advantage with a direct derive of a cost-benefit ratio.

## RESULTS

The most interesting thing of the evaluation method is the possibility to evaluate future vehicle concepts. A distribution of damage frequencies can be taken from a precursor or comparable model of a competitor.
The used material for OPSs is one of the main influence on the SSR score. Like Table 3 shows the influence of materials based on a middle class vehicle with OAPs of steel and a plastic bumper (ranking C). The adjustment to aluminum parts shows a little higher risk score but is in general a damage neutral possibility to use lightweight OAPs.
A complete change to CFRP parts results in a D label. This corresponds the risk score of a high class vehicle with aluminum structure and OAPs. An exact weighing up of the advantages of CFRP parts has to be done meticulous. There is a high potential for lightweight but also economical disadvantages.
Plastic OAPs lower down the SSR score and yield an B label. Additionally plastic parts can be brought to the workshop undercoat-varnished resulting in a shorter immobilization time of the vehicle and therefore lower cancelation expenses for customer and insurer.
Table 4 gives a overview of the influence regarding the light technology. This is the most considerabe factor. The reference model is equipped with a halogen headlight. Using xenon headlights increases the SSR score for 10%, LED for 38% and using laser-lights would be an increase of 129%. Damaging headlights causes high repair costs and additionally headlights have a very exposed position in case of a crash.

**Table3.**
**Influence of material of OAPs**

| middle class vehicle | steel | aluminum | CFRP | plastics |
|---|---|---|---|---|
| lower SSR score | 49 | 50 | 100 | 40 |
| upper SSR score | 83 | 86 | 156 | 67 |
| risk label | C | C | D | B |

**Table4.**
**Influence of headlight technology**

| middle class vehicle | halogen | xenon | LED | laser |
|---|---|---|---|---|
| upper SSR score | 83 | 91 | 115 | 191 |
| relative change | - | + 10 % | + 38 % | + 129 % |
| risk label | C | C | C | E |

The fitting position of ADAS sensors has also a high influence on the resulting risk score. For example the use of two radar sensors causes an increase of 34% compared to the reference vehicle without any sensors.
A minor influence can be found regarding alloy rims. Up to 19‘‘ there is just a little increase. Using 20‘‘ rims and higher there is an bigger influence because of the higher renewal costs.
Nearly every component brings a rise of the SSR score. Just plastic OAPs have a positive effect. ADAS functions therefore have to compensate this effect due to an active intervention for mitigating or avoiding a collision. This will be analyzed in further work.

## DISCUSSION AND LIMITATION

For validation of the systematic of damage points and matching coefficients real damage cases were taken into account and compered with the results out of the damage unit calculation. All considered cases of losses were taken out of the accident type extension analyzed in [4] and [5]. In every case damaged parts, manufacturer and model of vehicle, at hand ADAS and repair costs are known. Constitutive to this information the damage extent in damage units is calculated depending on vehicle class, materials and equipment options. The resulting damage is compared to the estimated damage of authorized experts.
Figure 2 shows the comparison of the resulting damage extents in motor-own-damage cases. The square shapes represent the findings of experts, the triangular shapes the ones of the described systematic. The dotted lines represent an equivalent SSR-score. In this figure the frequency and the specific scenarios are from no importance the interesting point is the deviation of the square and triangular shape.
The averaged deviation between the two different approaches is 2.9 percent. 64.1 percent of the analyzed cases were calculated directly under the assumption only to change OAPs. The amount of cases repaired by smart repair or repair varnish is 15.4 percent. In 20.5 percent of the cases slight structural damages occurred.

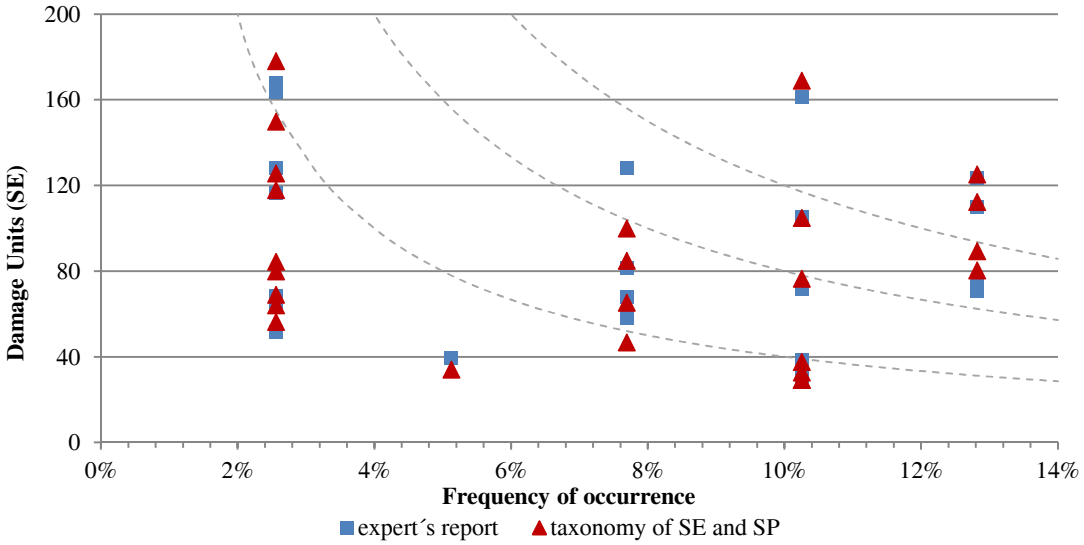


***Figure2. Validating the system of damage units (SE)***

The systematic of damage points and damage units is suitable for model and manufacturer independent calculation of repair damages in property damage accidents. The damage extent is given well in the retrospective consideration. The methodology is based on one manufacturer and on a limited number of vehicle models. However, the validation

shows the permissibility of assumptions und the transferability to other manufacturers and car models. The only larger deviation occurs in evaluating SUVs and high price models.
A use of the systematic for evaluating vehicles according to their class, materials and equipment in combination with an ADAS is possible and can be done while the development phase.
The methodology of evaluating the effectiveness of ADAS in property damage accidents should not serve as a new consultant-tool, but as a means to classify effects on vehicle damage in accident research. Up to now the methodology works for minor deformation depths which are very common in property damage accidents.

## CONCLUSIONS

In property damage different characteristics of accidents appear compared to personal damage [4]. Main influence parameters regarding the occurring repair costs are beside the deformation area and deformation dimensions the material of OAPs and the equipment of the vehicle.
ADAS with fully automated intervening functions have influence on property damage scenarios in the low speed range. The material and the configuration of vehicles have influence on the resulting damage in an accident. The procedure outlined here is a passible approach for evaluating damages of vehicles in the low speed range and compare them to other configurations in combination with an ADAS. This serves as a prospective method for deriving the customer value of systems and functions. Effectiveness of a system is stated in property points and individually calculated for vehicles in damage units. A validation of the systematics could have been shown by means of real world damage data.
More and more automated driving functions become of increasing importance in the driver assistance sector. If the frequency of various conflict scenarios in which an assistance system may intervene, it is possible to create a corresponding damage prevention or reduction potential of systems.
A bottom-up approach is pursued which allows an increase in system installation rates having a high impact on cost advantage as to damage reduction and prevention in the low speed range. Driver assistance systems which exhibit reliable function in the low speed range require high-end sensors. These sensors may also be utilized for further safety functions beyond parking and maneuvering actions and thus may significantly reduce accident numbers in a long term.
Accident research units, insurers and associations have to come to an arrangement of harmonized variables which are imposed similarly. This ensures that each other can benefit from the insights. If there is a proof of the benefit of an ADAS a purchase incentive for the customer can be created. A basic precondition for this is in-depth knowledge of property damage scenarios [4].

## REFERENCES

[1] Destatis;
https://www.destatis.de/DE/ZahlenFakten/Wirtschaftsbereiche/TransportVerkehr/Verkehrsunfaelle/Tabellen/PolizeilichErfassteUnfaelle.html; access: 07.03.2015.
[2] Gesamtverband der Deutschen Versicherungswirtschaft e.V. (GDV): Statistisches Taschenbuch der Versicherungswirtschaft 2013, Verlag Versicherungswirtschaft GmbH, Karlsruhe, S. 58-59.
[3] Gwehenberger, J.; Behl, T.; Lauterwasser, C.: Wie wirksam sind Fahrerassistenzsysteme – vom Bagatellschaden bis zum Schweren Unfall?, In: VKU - Verkehrsunfall und Fahrzeugtechnik, February 2012.
[4] Gschwendtner, Klaus; Kiss, Miklós; Gwehenberger, Johann; Lienkamp, Mar-kus: „In-Depth“-Sachschadenanalyse, Anforderungen und Potenziale. In: VKU - Verkehrsunfall und Fahrzeugtechnik, S. 272-284, Juli/August 2014.
[5] Gschwendtner, Klaus; Kiss, Miklós; Lienkamp, Markus: “Prospektive Analysis-Method for Estimating the Effect of Advanced Driver Assistance Systems on Property Damage”. Conference Paper. IEEE ITSC, Qingdao (China), Oktober 2014.
[6] Maier, F.: Wirkpotentiale moderner Assistenzsysteme und Aspekte ihrer Relevanz für die Fahrausbildung. Dissertation, Institute of Ergonomics, Technische Universität München, 2013.
[7] DIN 820-12, Normungsarbeit - Teil 12: Leitfaden für die Aufnahme von Sicherheitsaspekten in Normen (ISO/IEC Guide 51:2014), p.27. Principles of Standardization Standards Committee, DIN German Institute for Standardization, 2014.

This paper has been peer-reviewed and published in a special edition of *Traffic Injury Prevention* 16(S1), by Taylor & Francis Group. The complete paper will be available on the *Traffic Injury Prevention and www.NHTSA.gov* websites on June 8, 2015.

To access all Peer-reviewed papers please copy and paste the link below into your browser to access the papers.

http://www.tandfonline.com/toc/gcpi20/16/sup1

This paper has been peer-reviewed and published in a special edition of *Traffic Injury Prevention* 16(S1), by Taylor & Francis Group. The complete paper will be available on the *Traffic Injury Prevention and www.NHTSA.gov* websites on June 8, 2015.

To access all Peer-reviewed papers please copy and paste the link below into your browser to access the papers.

http://www.tandfonline.com/toc/gcpi20/16/sup1

# ESTIMATION OF FRONT UNDERRUN PROTECTOR EFFECTIVENESS IN TERMS OF FATALITIY REDUCTION

**Asao Koike**
**Yoshiaki Okami**
**Atsushi Miyamae**
**Ryota Yamamoto**
ISUZU Advanced Engineering Center
Japan

**Peter de Coo**
Coo-Consult
The Netherlands

**Sjef van Montfort**
TNO Integrated Vehicle Safety
The Netherlands

Paper Number 15-0041

## ABSTRACT

Frontal collisions between cars and trucks lead to high fatality rate of the car driver. Therefore the Japanese road administration established a directive, conformity to ECE-R.93 (2000/40/EC), compulsory since September 1st, 2011. As known, this directive describes a 'rigid' Front Underrun Protection (FUP) device installed on a truck. New developments are in the direction of energy absorbing devices in order to manage more severe impacts between both vehicles. The question is how to estimate the effectiveness of these devices.

Using a virtual car fleet, the effect of different FUP devices installed on or integrated with a truck front end can be estimated by simulation, in terms of injury severity and crash severity. The relationship between both makes it possible to estimate injury severity via crash severity. By transferring injury severity to AIS scale and fatality rate, a coupling can be made with real accidents and their effects on injuries. The other subject is to indicate the car severity by replacing a specific car fleet to a general device, in order to simplify the evaluation. The paper shows the steps from the simulations, to the analyses and simplifications, transfer to AIS scale and mapping on the real accident database, to predict the reduction of fatalities by using different types of energy absorbing FUPs (e.a.FUP).

In order to represent the car fleet, the Moving Progressive Deformable Barrier (MPDB) was selected. The MPDB was modelled to collide to a truck with an e.a.FUP. By this method, number of fatalities, or fatality reduction rate of the car for a certain e.a.FUP was estimated from the MPDB crash severity.

The processes in this study are based on simulations and accident investigation and analysis. The vehicle models used in the simulations are mainly validated on NCAP frontal impact tests. Some cars were validated at higher speeds, up to 90 km/h.

In this paper the prediction of injury levels is only based on the HIC to show the concept/principle of the method, but the method can be extended with other injury parameters.

The method described in this paper uses the Acceleration Severity Index (ASI) of a car-to-truck frontal collision in order to determine the probability of injury and fatalities. It uses AIS scaling and mapping on a matrix of relevant car to truck accidents. This simplified method can be applied to predict the e.a.FUP effectiveness in terms of injury reduction, and especially the fatality reduction.

## INTRODUCTION AND METHODOLOGY

New designs of safety structures need intensive testing and assessment before being realized and installed on vehicles on the road. However, the development of a realistic test setup is often a problem. Another problem is to find a way to value the usefulness and impact of the design on the society. In a previous paper [1] ways to test these structures, i.e. energy absorbing truck front underrun protection devices, were indicated. It was also suggested to use a generic test device instead of passenger cars with dummies for the final evaluation and assessment of newly designed truck front structures, and in particular an energy absorbing front underrun device. Using crash severity and accident severity information, the effect of a new design truck front structure can be estimated in terms of fatality reduction (See Figure 1).

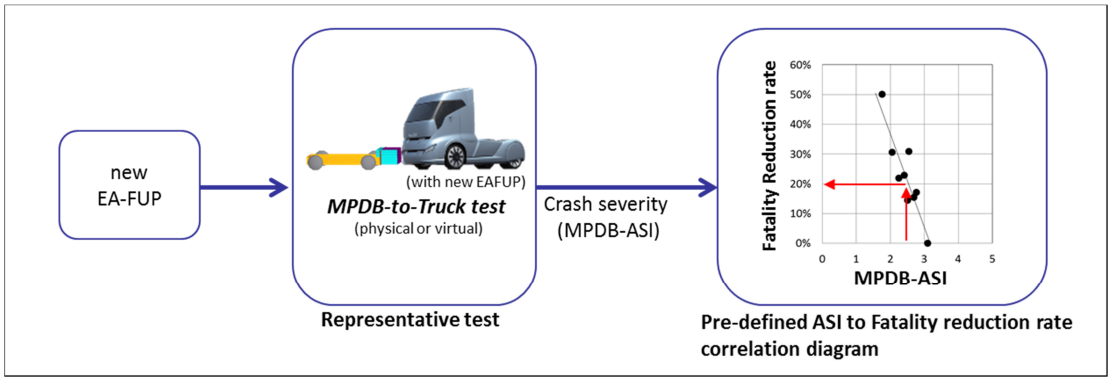


*Figure 1. General concept of estimating FUP effectiveness*

A similar idea but slightly different in implementation is given in [12]. The first steps to realize the above concept were made in [1]. In brief it boils down to the following. Based on accident investigation, vehicle registration and available test data a car fleet was selected and modelled. Also a 'standard set of FUP devices was defined, consisting of one 'rigid'FUP (fulfilling legal requirements) and 2 sets of 4 energy absorbing FUPs. Simulations of car-to-truck frontal collisions were carried out taking into account various accident parameters like relative speed and offset. This resulted in information about crash severity and injury severity. It appeared that a correlation can be indicated between the ASI and several injury parameters, like Head3msG, HIC, Thorax3msG, Chest deflection and Pelvis3msG. It also appeared that injury limit values for these injury parameters (e.g. HIC 1000) show an ASI limit value of 3 on an exponential curve. This process is visualized in the blue box, Figure 2-I.

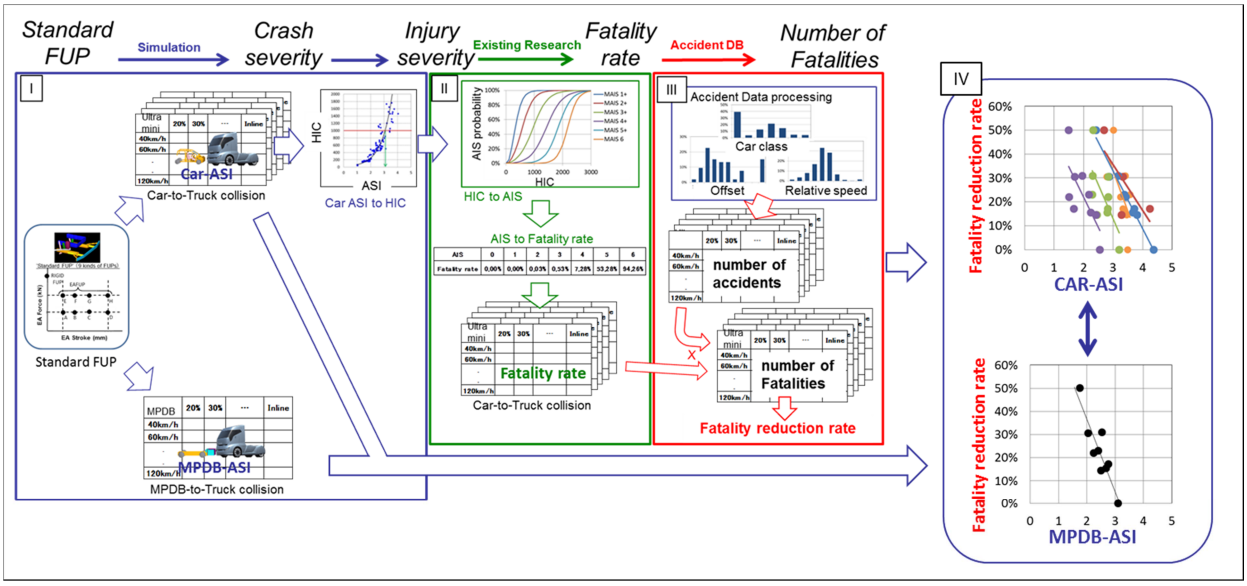


*Figure 2: Outline of the method*

The green box (Figure 2-II) shows how injury severity is transferred to Abbreviated Injury and subsequently to a Fatality Rate, which allows to transform the individual simulation data (Figure 2-I, blue box) to individual fatality data (Figure 2-II, green box). The next step is to associate this information with the information from accident data and fatality numbers (Figure 2-III, red box), resulting in a relationship between accident severity (CAR-ASI) and fatality numbers / fatality reduction rate (Figure 2-IV). In another line (bottom of Figure 2-I) the same batch of simulations is applied using a generic test device (MPDB) leading to a similar relationship between accident severity (MPDB-ASI) and the same fatality numbers / fatality reduction rate (Figure 2-IV). The relationship between CAR-ASI and MPDB-ASI will be shown in this paper, as well as the description of the consecutive steps mentioned above, starting with the green box.

## HIC TO FATALITY RATE

For the quantification of occupant head injury (HIC), the Abbreviated Injury Scale (AIS) is used. Formulas for the HIC versus injury probability for the 6 AIS+ levels are given in [5]. In a similar way as described in [3], the correlation between HIC and AIS can be developed (See Figure 3). Combining this figure with the AIS 6 (fatal) curve, the probability of fatality can be determined (See Figure 2-II and Table 1). The probability of fatality is used to transform all injury data from the simulations to a fatality rate for the individual simulated accident cases (See Figure 2-II, bottom picture in green box).

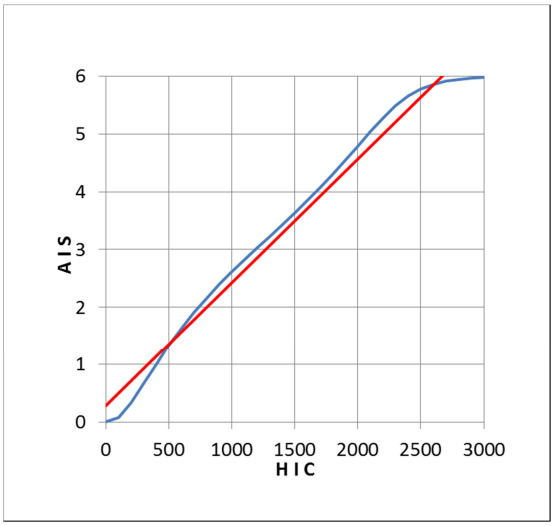


***Figure 3: HIC-AIS relationship (trendline red)***

***Table 1. Relationship between AIS, HIC and fatality rate***

| **AIS** | 0 | 1 | 2 | 3 | 4 | 5 | 6 |
|---|---|---|---|---|---|---|---|
| **HIC** | 0 | 329 | 798 | 1267 | 1736 | 2206 | 2675 |
| **HIC range** | ~ 93 | 94 ~ 562 | 563 ~ 1031 | 1032 ~ 1501 | 1502 ~ 1970 | 1971 ~ 2439 | 2440 ~ |
| **Fatality rate** | 0,00% | 0,00% | 0,03% | 0,53% | 7,28% | 53,28% | 94,26% |

## STATISTICS

The road vehicle registration database provides information about the amount of vehicles in different classes on the road. The traffic accident database provides information about the vehicle types involved in accidents and global information about collision type and injury. From in-depth accident analysis, more specific information on type of accident, speed and injury are known and can be rated in more detail.

Car distribution in car-to-truck head-on accidents
From the national accident database (2007 – 2011) [8] the representation of vehicles involved in car-to-truck head-on accidents can be obtained. As a standard for this database, the following classes have been defined: Ultra mini passenger car, ultra mini non passenger car, Sedan 1, Sedan 2, Mini vans, 1 box vehicles, SUV. In Figure 2-III the distribution of the cars in the different classes is shown. In the current study, however, another class definition was adopted: Ultra mini, Super mini, Small family, Saloon, SUV. This definition is more or less based on the one used by Euro NCAP. These vehicles represent 77% of the total registered cars. The numbers of vehicles in the 5 classes has been extrapolated to sum up to 100%.

Truck data
In the national accident database [8] most of the trucks were not supplied with a FUP (compulsory from September 2011 on new trucks). In the current paper it is assumed that trucks are fitted at least with a rigid FUP for determining the fatalities in these accidents. Therefore corrections were made on the number of fatalities, based on a study described in [4].

Relative speed
In the national accident database the traveling speeds of car and truck in the accidents is available. The relative or closing speed, however, is always lower than the sum of both speeds (braking). In this paper the relative speed is determined on the basis of an internal study by ISUZU. The distribution of the relative speed is shown in Figure 2-III. The relative speed concentration is around 80-100 km/h.

Offset distribution
From in-depth studies of special cases in the national accident database the offset distribution is estimated (See Figure 2-III). Especially in the high offset range this estimation is not always very precise. Offsets between 60% and inline can be everywhere in this range. Offsets collisions lower than 30% may result in a different event: the vehicle slides off instead of crashes into the truck front. Together with the offset limitation caused by the PDB width, the offsets in this paper range from 30% to 60%.

## NUMBER OF FATALITIES AND FATALITY RATE

From the national accident database a total number of 433 fatalities in car-to-truck head-on collisions in the period 2007 – 2011 could be subtracted. From this number of 433, 53 cases were selected for in-depth analysis. The analysis resulted in allocation of these fatalities in the above mentioned categories of vehicle class, relative speed and offset. With this classification, including all 433 fatalities, and using the fatality rate with AIS score, a number of fatalities could be associated with each type of collision. This resulted in the graph of Figure 4. Taking the number of fatalities using a rigid FUP as the standard, a fatality reduction rate can be determined along the vertical axis of this graph, ranging from 0% (FUP performance identical to rigid FUP) to ~60% (FUP performance better than rigid FUP).

It should be noted that the trendlines for the 5 selected vehicles almost have similar slopes. This means that it does not matter which trendline is used to determine the amount of reduction.

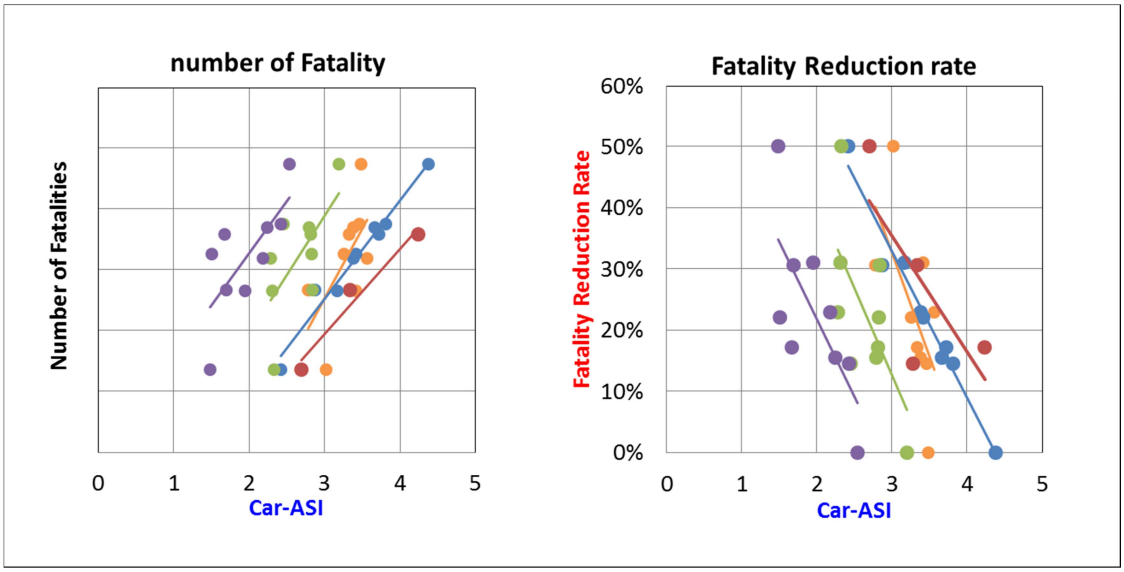


*Figure 4: Car-ASI versus Number of Fatalities and versus Fatality Reduction Rate for the vehicle fleet*

## MOVING PROGRESSIVE DEFORMABLE BARRIER

The assessment of an energy absorbing front underrun protection device in terms of fatality reduction can be done by using a passenger car with dummies in a car-to-truck frontal collision. Instead, a Moving Progressive Deformable Barrier (MPDB) will be used for simplicity reasons, cost reduction and generalization. The MPDB was investigated within the FIMCAR project [11] in frontal offset car-to-MPDB collisions with the purpose of assessing self-protection and partner protection of passenger cars. Focusing on partner protection, the MPDB may be used in frontal offset MPDB-to-truck tests. The MPDB is then used as a loading device, replacing the impacting passenger car. Based on the results, a statement can be given on crash severity, injuries to passengers and the compatibility of the e.a.FUP and the passenger car's front structure.

New PDB

The geometrical conformity between a MPDB (Progressive Deformable Barrier installed on a trolley) and a passenger car and between a MPDB and a truck is shown in Figures 5a and 5b.

*Figure 5a: Car front versus MPDB*

*Figure 5b: Truck front versus MPDB*

The size of the PDB [10] (especially the height) is hardly of influence on the outcome of the test with the passenger car. However, in a test with a truck the upper part of the PDB may contact the stiff longitudinal members, tilt mechanism or cabin floor. This will not happen in a car-to-truck collision, or at least at a much later stage. The current size of PDB may lead to incomplete contact between the PDB lower part and the e.a.FUP. Therefore the conditions of a resized PDB have been evaluated, in such a way that they do not affect the current stiffness properties of the PDB.

The misalignments of the PDB have also been recognized in other research [6]. In relation with a truck front end, a number of modifications are suggested. The current height of the (M)PDB (700mm + 150mm ground clearance) might not be realistic for interaction with trucks. In [6] suggestions for adjustments and tests are made, see Figure 6a.

From studies by GRSP ECE-TRANS-WP29-GRSP-2007-17e and VC-COMPAT [9], this barrier front face includes nearly all stiff structural components of a selection of passenger cars. The depth of the barrier, especially with the stiff 90mm honeycomb at the back, is adequate for impacts with passenger cars, due to the load spreading capability in the car front structure. When impacting a truck front structure with mainly a FUP beam, this may lead to bottoming out of the barrier. Therefore the bumper structure from the Offset Deformable Barrier (ODB) was used on the PDB (See Figure 6b) to spread the local load from a single FUP beam into the PDB.

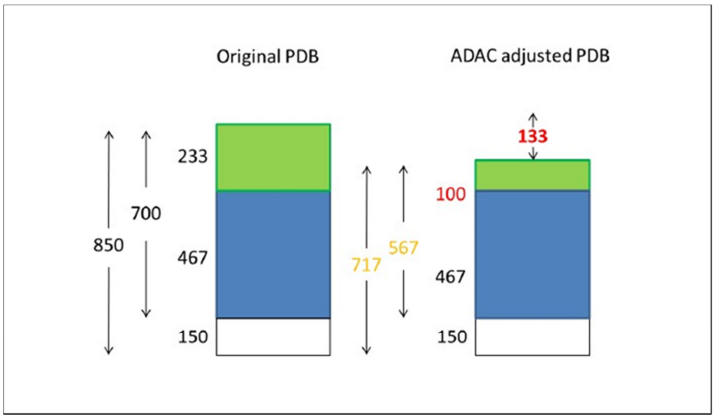


*Figure 6a: Original and alternative front of PDB*

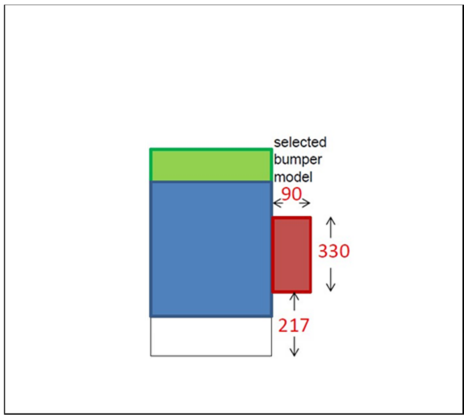


*Figure 6b: Alternative PDB front with bumper*

It is clear that the bumper structure does not allow aggressiveness assessment according to the standard PDB protocol. However, the modified PDB reflects better the load spreading by an average passenger car.

Regarding the width of the PDB, the MPDB-to-truck collision with the current barrier width of 1m limits the overlap of the car by approx. 60%. (see Figure 7). So higher overlaps and in-line collisions can not be tested in this way.

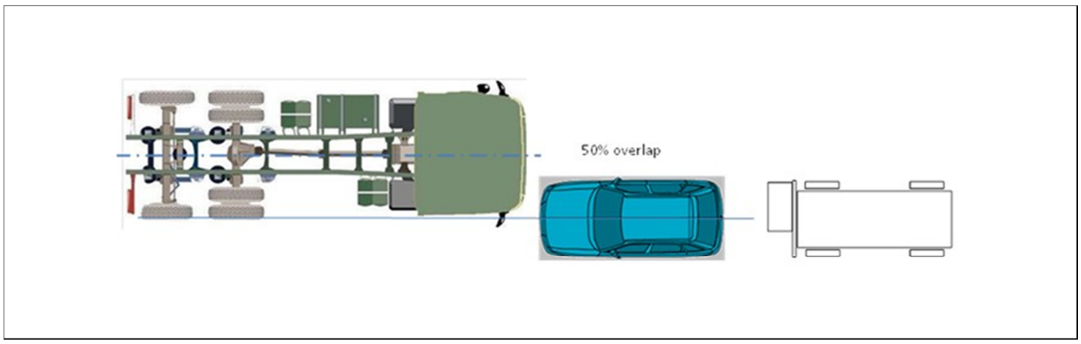


*Figure 7: Overlap of passenger car and MPDB*

MPDB simulations and ASI comparison
Using the modified PDB, a batch of simulations was carried out. The parameters relative speed, offset and FUP type were varied. The results of these simulations produced an accident severity value ASI for each case. Combining these MPDB-ASI values with the CAR-ASI values obtained from the batch of car simulations, the graphs of Figure 8 can be composed. It appears that a linear relationship can be indicated between car and MPDB ASI.

A linear relationship allows a transformation from the Fatality Reduction vs CAR-ASI graph to the same graph with the MPDB-ASI on the horizontal axis.

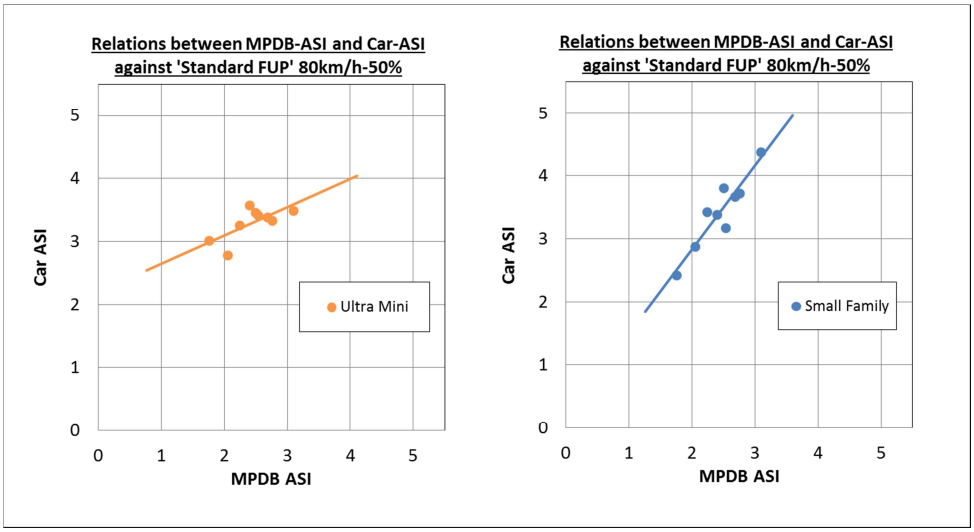


*Figure 8: Relationship between CAR-ASI and MPDB-ASI*

## SELECTION OF TYPICAL ACCIDENT

In order to estimate the effectiveness of a new FUP design, in terms of fatality reduction, relative to a legal rigid FUP, many simulations can be carried out and studied. These include ranges of relative speeds and offsets. From the accident investigations it appears that most accidents and fatalities occur in a speed range of 80-100 km/h. Collisions with relative speeds up to 90 km/h show that damage to the vehicles is large and that the energy absorbing capabilities of the vehicles are fairly to fully utilized. The offset concentration is around 40-50%. Close to 30% may lead to different impact behavior. Therefore a typical accident is chosen with relative speed of 80 km/h and 50% offset.

## EVALUATION NEW FUP DESIGN

The introduction of a rigid FUP on new trucks by enforcement through rule making is a very good step to reduce the seriousness of car-to-truck frontal collisions. Many studies, however, have shown that energy absorption by the truck front end is a good way of reducing the seriousness even further. By applying the method developed in this study the reduction can be quantified. A simulation of a collision (80 km/h, 50% offset) between the MPDB and the truck supplied with the new front structure results in an ASI value indication the severity of the crash. In Figure this value is put on the horizontal axis. When being left of the intersection of the trendline with the horizontal axis, the new front structure has a benefit on the fatality reduction. The reduction rate is determined by vertical intersection

with the trendline. An ASI value of 2.5 for instance results in a reduction rate of 20% with respect to a rigid front underrun protection device.

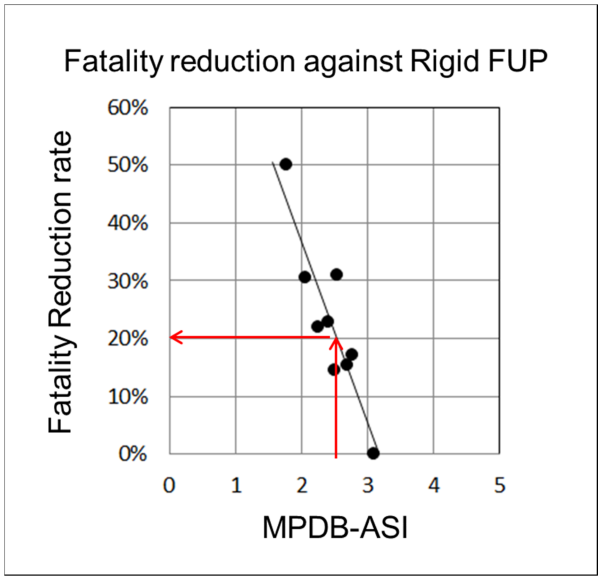


***Figure 9: Determination of FUP effectiveness in terms of fatality reduction rate.***

## DISCUSSION

There are a number of limitations to the study. The selection of car models which are defined as representative for the classes in the fleet is based on the availability of crash test results (from NCAP tests or private tests). Except for the in-house tests, which are carried out at high speeds, up to 90 km/h), the NCAP tests are normally carried out at speeds from 56 km/h to 64 km/h. In case overload situations (high speed impacts, up to 90 km/h) are simulated, the results may be different for models which have been validated against lower speed impacts. Therefore, the simulations outside the validation range are handled with care.

The width of the PDB is limited to 1000mm. As a consequence, only overlaps up to 60% be realized. Small overlaps are limited to approx. 30%. The PDB is uniform over the barrier width and smaller overlaps typically result in a different collision phenomenon. The MPDB is not representative for all type of cars.

Each simulation results in a set of injury values (head, chest, pelvis, etc.) for the occupant in the passenger car. In the study above only the HIC value is used to determine fatality via AIS. Other injury values can be involved in a similar way. However, AIS is a measure in accident investigation that describes the injury to a human per body region in real-world crashes. The different AIS values per body region can be combined to one overall injury criterion, known as the Injury Severity Score (ISS). The ISS predicts a percentage of mortality [7].

In this research, the interval in which the HIC reaches a maximum value was set to 36ms. This time interval affects the HIC calculation. In case of hard contact impacts this interval can better be 15ms, which is also applied in [5].

## CONCLUSIONS

The project described in this paper originally started with the aim of reducing injuries in car-to-truck frontal collisions by improving the compatibility of the truck front structure. Evaluation of a new truck front design is usually done by full scale testing using a passenger car with a dummy installed. This is a limited, costly and complicated way to obtain a feeling about possible reduction of injury to car occupants. Therefore a simplified and less costly method was developed by using a generic loading device replacing car and dummy, and by

doing computer simulations of these crash tests in order to evaluate more parameters which are involved in these collisions.

Although the national accident database includes 5 years of data, the amount of data related to car-to-truck frontal collisions is relatively low (433). Especially the number of in-depth cases from which detailed information about the accident is subtracted is low (53). This has consequences on the accuracy of the number of fatalities and on the fatality reduction rate. However, it is also recognized that by inclusion of new data (additional years) from the national accident database, the composition and distribution of the fatalities will also change, because of introduction of newer car and truck designs, new roads and road design, etc. In the current method the use of an MPDB replacing the car is therefore an advantage, but the influence of new statistic information should be faced.

The size of the standard PDB was adapted and a bumper element was added. The size was changed in order to have a better structural interaction with the energy absorbing front of the truck (the FUP). The influence of height reduction of the PDB may be small for the application in assessing car self-protection and partner protection. The bumper element was added to the PDB in order to have better load spreading from the (isolated and limited contact area) FUP to the MPDB. Especially in the lower offset cases the FUP, without any adjacent structures, may penetrate the honeycomb of the PDB till the end, resulting in bottoming out. A bumper element may reduce this, however, the possibility of aggressiveness evaluation is abolished.

The method described in this paper allows a quick evaluation of new truck front designs with respect to fatality reduction. Assuming that the accident statistics do not change abruptly from one year to another, the estimated reduction of fatalities might be valid for some time, especially when the fatality reduction rate is used.

## REFERENCES


[1] A. Koike, K. Toyofuku, N. Iguchi, K. Yamaguchi, R. Yamamoto, P. de Coo. “A new assessment method for car to truck compatibility”. DEKRA Symposium Safety of Commercial Vehicles, November 2012.
[2] A.Krusper. “Structural Interaction between Vehicles”. Thesis for the degree of doctor of Philosophy in Machine and Vehicle System. Dept. of Applied Mechanics, Chalmers University of Technology, Gothenburg, Sweden, 2014.
[3] M. Shojaati. “Correlation between injury risk and impact severity index ASI”. 3rd Swiss Transport Research Conference, Ascona, March 2003.
[4] Y. Sukegawa, H. Kubota, T. Hirase. “Japan’s Approach for Car to Truck Compatibilty in head-on Copllisions”. Japan Automobile Manufacturers Association, ESV Paper Number 7-0989.
[5] NHTSA. “Injury Risk Curves”. http://www.nhtsa.gov/cars/rules/rulings/AAirBagSNPRM/PEA/pea-III.n.html
[6] A. Radzek. “ADAC Compatibility-Crashtest”. Advanced Automotive Front-end 2012. Landsberg, November 2012, Munich.
[7] F. Leneman, on behalf of the VC-COMPAT truck leg consortium. “Assessment of Energy Absorbing Underrun Protection devices”. DEKRA Symposium Safety of Commercial Vehicles, October 2004.
[8] “Domestic accident statistics data (Macro data)”. Institute for Traffic Accident Research and Data Analysis (ITARDA).
[9] VC-Compat: http://vc-compat.rtdproject.net
[10] J. Saunders, P. Delannoy. “Results of NHTSA’s Comparison of the Offset Deformable Barrier and the Progressive Deformable Barrier Test Procedures”. Paper Number 09-0549
[11] FIMCAR: http://www.fimcar.eu
[12] J.Winnicki, R. Eppinger. “A Method For Estimating The Effect Of Vehicle Crashworthiness Design Changes On Injuries And Fatalities”. DOT HS 808 680, February 1998.

# IMPROVING VEHICLE SAFETY IN AUSTRALIA AND NEW ZEALAND: THE ROLE OF ANCAP

**Nicholas Clarke**
**Michael Paine**
**Rhianne Robson**
**Jason Smith**
ANCAP Australasia Limited
Australia

**Jack Haley**
NRMA Motoring & Services
Australia

Paper Number 15-0042

---

## ABSTRACT

The Australasian New Car Assessment Program (ANCAP) has had a significant impact on the Australian and New Zealand motor vehicle landscape over the past 20 years through its independent, non-regulatory, consumer-driven program. Five star cars are now available in all vehicle categories; the majority of manufacturers now approach ANCAP to obtain a rating prior to launch to leverage sales; and ANCAP assessments are now seen as the de facto standard, taking the place of regulation. Since 2011 ANCAP has been increasing the stringency of its requirements for each star rating level annually. In future years ANCAP will continue to raise the bar, updating and broadening its suite of physical crash tests and introducing performance testing of safety assist technologies (SAT). These advancements will see consumers provided with even safer vehicles, and in time, perhaps even cars that will not be able to crash at all.

NCAPs drive vehicle safety improvements through a non-regulatory approach. This paper examines the effectiveness of the Australasian NCAP, its achievements and its future direction.

## INTRODUCTION

The Australasian New Car Assessment Program (ANCAP) exists to provide consumers with independent, clear and concise vehicle safety information. The aim is to reduce death and injury on our roads and encourage manufacturers to supply - and consumers to demand and purchase - the safest vehicles. This is achieved through the communication and promotion of vehicle safety ratings. ANCAP uses a five star rating system (five stars being the highest rating) to communicate comparative levels of vehicle safety. While physical crash testing has dominated the program over time, advanced technology is becoming increasingly important. Historically it has been relatively simple for consumers to understand the apparent difference in safety between cars. As the photographs below illustrate, the differences were stark.

**Then**

**Now**

This is not the case today, where differences between cars may be substantial but not immediately discernible to consumers. Convincing consumers of the merits of safety technology is a huge challenge for ANCAP.

**DISCUSSION**

**Consumer Awareness**

Since the establishment of ANCAP in 1992, regular market research has been undertaken to track consumer awareness of the ANCAP brand, and also to monitor consumer uptake of the safer vehicles message and in turn, the purchase of safer cars.

Figure 1 shows the increase in consumer awareness of the ANCAP brand (both name and logo) across Australian and New Zealand new car buyers [1].

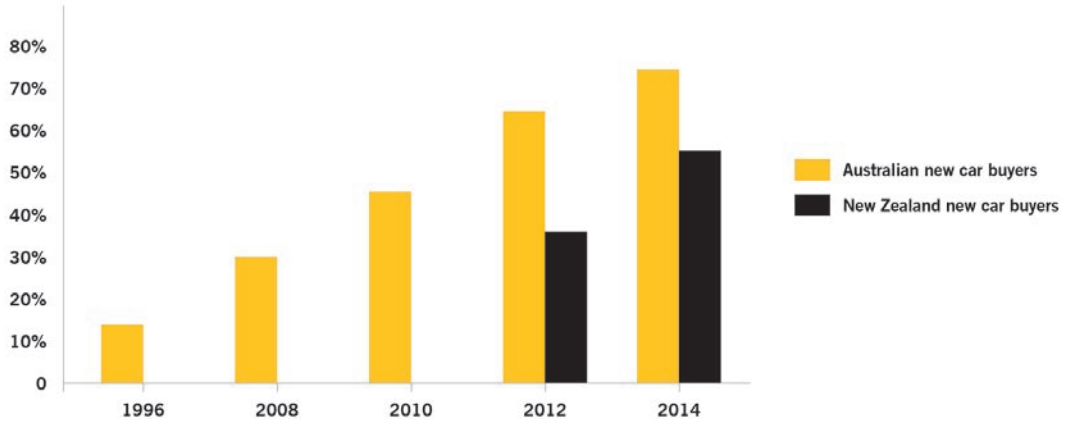


***Figure 1. Awareness of ANCAP amongst new car buyers in Australia & New Zealand.***

2014 results reveal that 74% of Australian new car buyers were aware of the ANCAP brand - an increase of 15% over 2012, and 60% more than 2010. Brand awareness amongst the New Zealand new car market was slightly lower at 54% in 2014, although showing significant growth since the first survey in 2012 (36%).

In order to reach these high levels of awareness ANCAP had to do two critical things. First, it had to establish itself as a professional organisation of integrity, with a strong focus on accuracy and reliability and demonstrated expertise in a complex technical field. Second, it had to convince manufacturers and consumers that this was indeed the case.

On reflection, it probably took the best part of a decade before ANCAP had made headway on the first critical point. There were many reasons for this including the fact that independent crash testing was a rather new and immature field (other than in the USA) and there was a belief in the community that if governments approved the sale of cars then *ipso facto* they must be safe. Early crash test results revealed the imprudence of this belief. Consumers were presented with the stark reality that by and large, cars were not particularly safe. Manufacturers were presented with a significant challenge in both a technical design and an ethical obligation sense. This challenge has been accepted.

As well as publishing test results, ANCAP undertook a range of marketing activities to explain and demonstrate its professional expertise and integrity of its processes. These included for example, test laboratory visits, consumer-focussed publications, greater interaction with the media, increased public advocacy for safety and closer ties with governments.

In relation to pursuing the second critical point, there were two significant events that occurred during the 2000s. The first was the awarding in 2001 of the first five star ANCAP safety rating – this made both consumers and manufacturers take notice of safety. The second was the awarding in 2008 of the first five star ANCAP safety rating for an Australian-built car. This resulted in a prominent advertising campaign during the 2008 Olympic Games where, for the very first time, a major local manufacturer extolled the benefits of an ANCAP rating to consumers.

Other manufacturers followed suit and what started as a trickle of five star ratings and associated marketing turned into an avalanche. It was clear that safety was becoming a major factor in selling cars and this was borne out in ANCAP's market research. In earlier research, safety had rated fourth or fifth in priority behind price, car type and performance.

Figure 2 shows that in 2014 Australian new car buyers ranked safety as a top priority when making purchasing decisions [1].

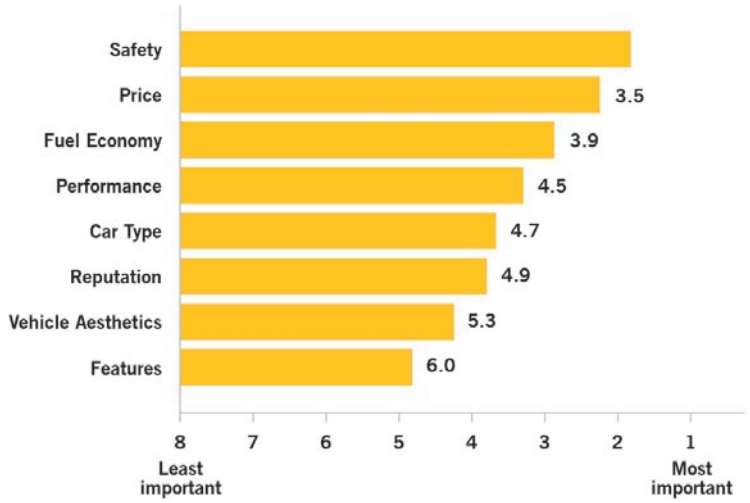


***Figure 2. Importance of Vehicle Attributes to New Car Buyers, 2014.***

**Market Penetration**

With awareness of ANCAP in Australia now high and growing quickly in New Zealand, ANCAP's influence on consumer purchasing was also apparent in the sale of five star rated cars.

Figure 3 reveals the portion of new cars sold in Australia in 2014 holding a five star ANCAP safety rating [2].

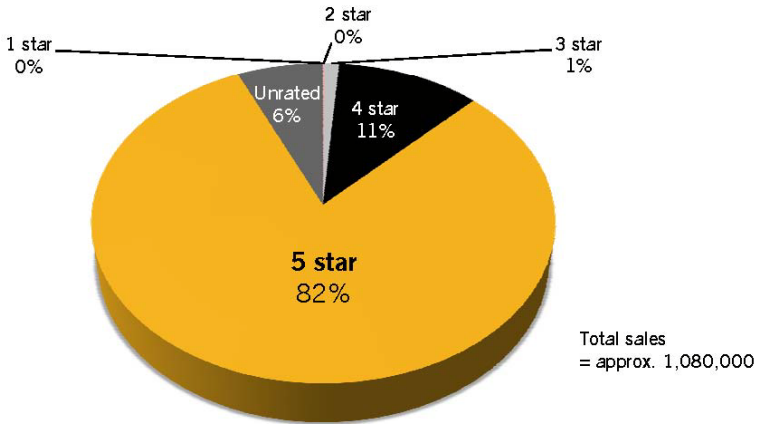


***Figure 3. 2014 Australian new motor vehicle (passenger, SUV & LCV) sales by ANCAP safety rating.***

In less than a decade, the penetration of five star cars in the Australian market has grown remarkably. In 2014, 82% of all new cars sold were models which held a five star ANCAP safety rating. In the relatively small Australian market this amounts to nearly 900,000 cars. A further 11% held a four star rating (~120,000 cars). Less than 2% (~20,000 cars) had a rating lower than four star, with just 6% (~65,000 cars) being models without a rating.

In New Zealand, 88% of all new *passenger* cars sold in 2014 held a five star ANCAP safety rating [3]. In both countries there are now numerous five star models available in all vehicle categories, providing a range of choices across all price points.

ANCAP's influence on five star vehicle sales can also be attributed to five star fleet purchasing policies implemented by governments and a range of private, domestic and multi-national organisations.

**Positive Outcomes**

With all the excitement about the prominence of ANCAP and the acceptance of safety ratings by consumers and manufacturers alike, it is easy to overlook an assessment of the outcomes of safer cars. Figure 4 sets out the reduction in fatalities on Australian roads over the last decade [4]. In that time there has been a 29% reduction in fatalities.

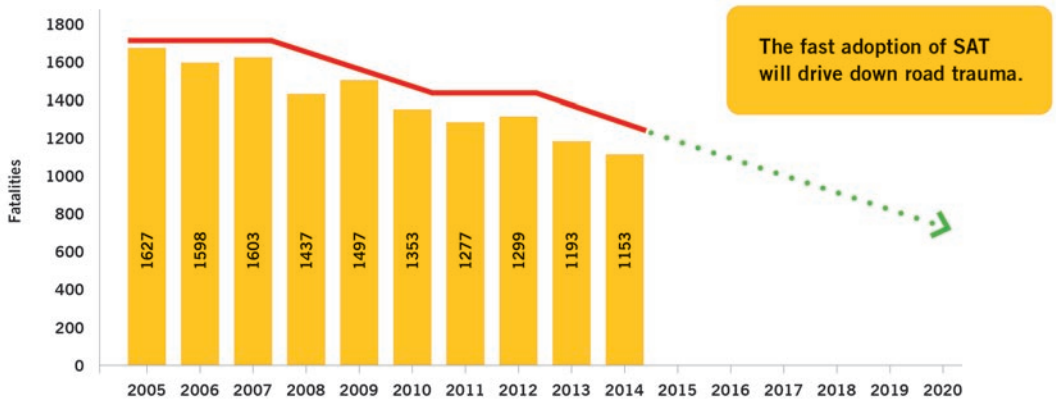


***Figure 4. Australian Road Fatalities 2005-2014.***

Clearly there are many factors that contribute to the reduction in fatalities, but what is also clear is that newer, safer cars play a very significant role. Figure 5 shows a snapshot of passenger vehicle fatalities and passenger vehicle registration by year of manufacture. It shows that older cars, while a smaller part of the fleet, account for a higher number of fatalities: the reverse is true for newer cars [5].

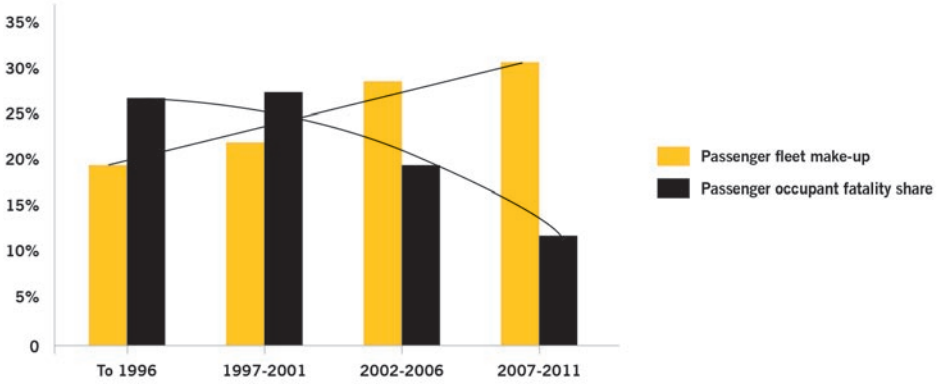


***Figure 5. Passenger Fleet: Share of Registration vs. Share of Occupant Fatalities 2011.***

**Autonomous Emergency Braking**

Since 2011, ANCAP has introduced stepped increases to the requirements vehicles must meet in order to achieve each of its five rating levels. These increases relate not only to physical crash test performance but also to the inclusion of safety assist technology (SAT) [6]. From 2015, ANCAP has taken another important step to further enhance vehicle safety, with a new focus on SAT and the substantial impact it will have on reducing road trauma. This will be achieved through ANCAP's alignment with Euro NCAP and the move to a more sophisticated test and assessment program encompassing performance assessments of active, life-saving SAT [7]. From 2018 ANCAP and Euro NCAP testing and assessment regimes will be effectively aligned.

In spite of the positive outcomes of recent road safety initiatives, over the last fifteen years Australia has slipped from eleventh to sixteenth place in the world in terms of road deaths per 100,000 population. More must be done to see this decline reversed and SAT has a huge role to play in achieving this.

Today, autonomous emergency braking (AEB) has already shown significant benefits in reducing the number of crashes. Early figures showed a 27% reduction in Europe [8] and 14% in US [9]. Recent Swedish research reveals AEB has reduced the risk of real world rear-end crashes in metropolitan areas by 54-57% and in all areas

by 35-41% [10]. These figures are largely supported by other, as yet unpublished, research (funded in part by ANCAP).

The central issue now is how we encourage consumers to demand, and manufacturers to supply, this technology. If left to the market alone it may be many years before the technology becomes available in all new cars and perhaps decades before it becomes ubiquitous in the fleet. Regulating the technology would likely lead to a similar outcome given the time it takes to develop and implement. The only practical way to ensure that this technology has an accelerated introduction into the market is for consumers, road safety practitioners and fleets to demand it. This puts a particular onus on ANCAP and other programs to pursue this with vigour.

**Autonomous Technology and the Consumer**

The idea of autonomous cars may well have its roots in the twentieth century development of the automatic transmission and other similar devices. Over time there have been many incremental advancements, but none is more exciting or arouses more fear than the prospect of the autonomous car. The move to autonomy has accelerated rapidly in the last decade and shows no signs of slowing. While it seems inevitable that at some time in the future all cars will operate this way, there are some challenges to face before we arrive at that future time.

The world is full of autonomous devices and machinery that once required specialised training and human control and intervention. Trains, ships, trucks, aeroplanes are all good examples and while most are happy to get on an aeroplane and fly thousands of kilometres at speeds approaching the sound barrier, there is something about owning and driving a car that on occasion provokes an irrational response to change, notwithstanding that the risk of death or serious injury is much higher in a car than in these other forms of transport.

The inevitable progression of advanced technology presents a new set of challenges for ANCAP in maintaining consumer trust. Having been exposed to the results of physical crash testing and graphic images of cars that perform well and those that perform poorly, the consumer has been an active participant in safety because the results are evident and the benefits apparent.

This may not be the case with some of the more technically complex SAT. There are no tangible images of good and bad performance to which the consumer can relate.

Surrendering control of the car will be difficult for those already driving. Driving skills are often worn like a badge of honour, particularly among younger people and if this is threatened, resistance will be strong. However, there is light at the end of the ‘generational’ tunnel and the existence of this light will ensure that subsequent generations of drivers will embrace technology and readily accept a new and different place for the car in society.

## CONCLUSIONS

ANCAP has had a significant impact on Australian and New Zealand motor vehicle safety over the past 20 years through its independent, non-regulatory, consumer-driven program. Five star rated cars are now common; manufacturers are embracing the ANCAP process by actively pursuing and promoting ratings; and consumer awareness and use of ANCAP ratings is at a record high. Accelerated introduction of life-saving technology is vital and new methods of communicating this to consumers and manufacturers will be required.

The era of autonomous technologies has commenced and consumers and NCAPs alike must acknowledge and embrace it if there is to be a further dramatic reduction in road trauma. ANCAP's future test, assessment and communications processes will therefore continue to evolve in order to ensure that consumers secure access to the safest cars, and in time, perhaps to cars that will not crash.

**REFERENCES**


[1] ANCAP brand tracking research, Intuitive Solutions (April 2014).
[2] ANCAP & VFACTS vehicle sales data analysis (January 2015).
SUV = sports utility vehicles, LCV = light commercial vehicles (excludes heavy vehicles).
[3] New Zealand Motor Industry Association new vehicle registration (sales) data (January 2015).
[4] BITRE Road Deaths Monthly Bulletins (January 2015).
[5] Compiled from 2012 Australian Bureau of Statistics Survey registration data & BITRE Australian Road Deaths Database (includes SUV).
[6] SAT is a generic acronym for active safety devices and systems (e.g. stability control, autonomous braking, fatigue warning, lane departure warning, adaptive headlights).
[7] ANCAP Transition to Alignment with Euro NCAP (October 2014).
[8] Euro NCAP Autonomous Emergency Braking Fitment Survey (June 2012).
[9] IIHS / HLDI News Statement: *Crash avoidance features reduce crashes, insurance claims study shows; autonomous braking and adaptive headlights yield biggest benefits* (3 July 2012).
[10] Rizzi, M., Kullgren, A., Tingvall, C. (2014). *Injury crash reduction of low-speed Autonomous Emergency Braking (AEB) on passenger cars*.

# EVALUATION ON MEASUREMENT PROCEDURE FOR POST-CRASH HYDROGEN CONCENTRATION

**Yohsuke Tamura**
**Hiroyuki Mitsuishi**
Japan Automobile Research Institute
Japan

Paper Number 15-0047

## ABSTRACT

To examine the measurement method for post-crash hydrogen or helium concentrations in the cabins and other enclosed spaces of vehicles which is provided in the UN Global Technical Regulation on hydrogen fuel cell vehicles (HFCV-gtr), the present study investigated 1) wind velocity conditions not affecting the hydrogen concentrations in the cabin, 2) the effect of the impact absorber of a moving deformable barrier, and 3) the feasibility of substituting the hydrogen concentration measurement with helium gas. The results indicated that the HFCV-gtr measurement method posed problems in its accuracy and reliability because hydrogen concentrations in the cabin varied under the influence of a 0.1 m/s wind and in the presence of an impact absorber in contact with the test vehicle. Furthermore it was found that although HFCV-gtr defines a permissible hydrogen concentration of 4vol% to be equivalent with a permissible helium concentration of 3vol%, this equivalence could not be verified. Consequently it is necessary to replace the HFCV-gtr measurement method for in-cabin hydrogen concentrations with a simpler method immune to external disturbances.

## INTRODUCTION

Currently the UN Global Technical Regulation on hydrogen fuel cell vehicles (HFCV-gtr)[1] regulates the hydrogen leakage of HFCVs and the hydrogen concentrations in enclosed spaces such as the cabin and the trunk room, after a crash test. HFCV-gtr permits a maximum hydrogen leakage of 118 NL/min and a maximum hydrogen concentration of 4vol%; in addition, HFCV-gtr allows the use of helium gas in place of hydrogen gas for ensuring the safety of crash tests. The maximum permissible helium leakage is set at 88.5 NL/min (= permissible hydrogen leakage flow rate x 0.75), and the maximum permissible helium concentration set at 3vol% (= permissible hydrogen concentration of 4vol% x 0.75) in view of the leakage-related properties of the two gases[2]. Nevertheless, in case hydrogen does not start leaking from the fuel system within 5 sec since the closure of the main stop valve after the crash, HFCV-gtr allows the omission of the hydrogen concentration measurement.

Unlike the gasoline vehicles and compressed natural gas vehicles that are required to measure only their fuel leakage flow rates after a crash test, HFCVs are required to measure both fuel leakage flow rate and hydrogen concentration, thus subjected to more complex measurement procedures.

Regarding the HFCV-gtr measurement methods for post-crash hydrogen and helium concentrations, there was a study on their possible replacement with the measurement of oxygen concentrations[2]. In another study, a crash test was performed with hydrogen sensors installed inside the test vehicle[3,4]. On the other hand, the present authors in their previous study investigated hydrogen concentrations in the vehicle underbody and the cabin with varied leakage locations, directions, flow rates and flow velocities (nozzle diameters) on the assumption that a side window pane is broken open in a side crash[5]. It was found that when hydrogen gas was leaked from the underbody, hydrogen rose along the side doors and infiltrated into the cabin from the lower side of the open window. This finding suggested that the presence of winds or a moving deformable barrier in the infiltration route of hydrogen

might affect the hydrogen concentrations in the cabin; also that for the cases where more complex hydrogen infiltration routes and more open windows are involved, it would be necessary to verify the validity of substituting hydrogen gas with helium gas, two types of gases with different diffusion coefficients.
Additionally the present study evaluated the hydrogen and helium concentration measurement methods by investigating , (1) wind velocities not affecting the hydrogen concentrations ,(2) the effects of moving deformable barriers (MDB), and (3) the reliability of the helium substitution test.

## DESCRIPTION OF EXAMINATIONS

**Test vehicles:** A 2,000cc gasoline vehicle (mini-van, sized L4,630 x W1,695 x H1,710mm, interior size of L2,775 x W1,505 x H1,350mm) was employed as the test vehicle, which was collided with a 950 kg carriage serving as MDB at a crash speed of 55 km/h according to the Japan New Car Assessment Program test method. Figure 1 shows the post-crash view of the test vehicle and the MDB both of which came to a stop with the MDB impact absorber (honey-comb structure made of aluminum) in contact with the crashed side door of the test vehicle. The lateral center window of the test vehicle had broken open as a result of the crash.

***Figure1. Test vehicle and side impact MDB after side crash test***

Because the post-crash measurement method of HFCV-gtr requires the measurement of hydrogen or helium concentrations and leakage, the crashed test vehicle was transported to the explosion resistance fire test cell of the Japan Automobile Research Institute in order to conduct an experiment in a safe, windless condition. The effect of the MDB was examined after placing a simulated impact absorber in contact with the test vehicle as shown in Figure 2.

***Figure2. Simulated side impact MDB***

**Leakage conditions:** Hydrogen (or helium) was leaked upward from the nozzles located at the center of the vehicle's underbody and at the center of the cabin floor, with the flow rate regulated by a mass flow controller. Only one (upward) nozzle direction was applied because previous studies[4,5] had found that hydrogen concentration distribution and the maximum concentration did not differ significantly between upward and downward nozzle directions when the hydrogen flow rate was about 2,000 LN/min.

In light of the fact that the fuel systems of HFCVs have pipes of a 1/4-inch (approx. 4 mm) inner diameter, nozzles of three different diameters (i.e., 1, 2, 4 mm) were applied. Considering the fact that HFCV-gtr permits a maximum hydrogen leakage of 118 NL/min, three different flow rates were applied--118 NL/min, 69 NL/min (a half), and 35 NL/min (a quarter). Two different leakage durations were applied--800 sec during which hydrogen concentrations were known to become constant inside the vehicle and 30 sec during which the hydrogen gas (estimated 59L) remaining in the piping after the closure of the main stop valve would be completely released at the maximum permissible hydrogen leakage of 118 NL/min for vehicle crash tests. To examine the effect of winds, an explosion-proof fan 600 mm in diameter was placed 5m away from the vehicle side.

Figure 3 shows the hydrogen concentration measurement positions in the cabin. Hydrogen and helium concentrations were measured using thermal conductivity hydrogen sensors (New Cosmos Electric Co., Ltd. XP-314).

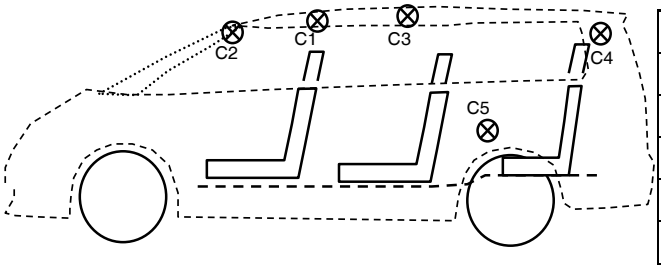


| Position | Hydrogen concentration measurement position |
|---|---|
| C1 | 50mm below the roof above the driver's seat |
| C2 | Near the mirror |
| C3 | The center of the vehicle roof |
| C4 | 50mm below the roof at cargo compartment center |
| C5 | 50 mm above the floor at rear seat |

***Figure3. Hydrogen concentration measurement positions in the cabin***

## RESULTS AND DISCUSSION

**Effect of winds on in-cabin hydrogen concentrations:** The effect of winds blown from a side of the test vehicle was investigated concerning hydrogen concentrations in the cabin. Hydrogen was leaked from the vehicle underbody center or the cabin floor center continuously at a flow rate of 118 NL/min when a wind of 0.1 m/s was applied from a side direction. Figure 4 shows the hydrogen concentrations measured under the above conditions. The wind blowing was started 600 sec after the crash in Figure 4(a), and 300 sec after in Figure 4(b).

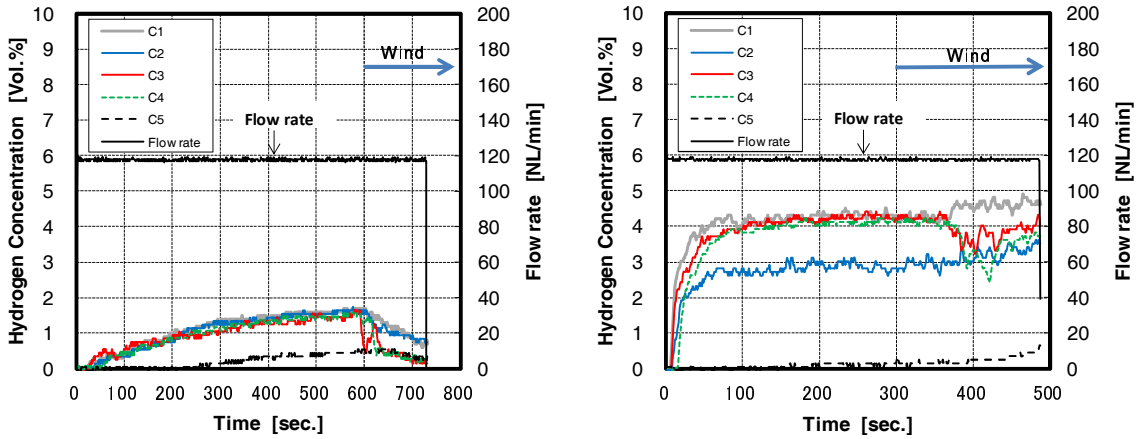


***(a) Leakage point: Center of vehicle underbody*** ***(b) Leakage point:Center of cabin floor***

***Figure4. Hydrogen concentrations in time sequence***
***(Wind velocity: 0.1 m/s and upward, Nozzle diameter: 4 mm, Flow rate: 118 NL/min)***

In both figures, in-cabin hydrogen concentrations were affected when winds were blown. Due to measurement accuracy limitations, the effect of winds below 0.1 m/s could not be examined in the present study. According to the Beaufort scale of wind force[5], a wind velocity of 0.1 m/s corresponds to a Beaufort number of 0 and is rated as "Calm". In other words, 0.1 m/s represents practically a windless state. Accordingly it can be considered problematic to conduct a measurement, verification or reproduction test on hydrogen concentrations in an outdoor testing facility where natural winds easily exceed 0.1 m/s. Similarly, it should be necessary to consider the effect of winds even in an indoor testing facility in warm seasons when the air conditioning is in operation. For example, the wind velocity around a test vehicle in the indoor crash test facility of the Japan Automobile Research Institute in summer (July) is an average of 0.5 m/s and a maximum of 3 m/s. Accordingly it is necessary to take account of wind factors even in an indoor testing sites.

**Effect of the MDB impact absorber:** The effect of the presence or the absence of an MDB impact absorber was examined in relation to in-cabin hydrogen concentrations. Figures 5, 6 and 7 show the hydrogen concentrations in time sequence measured under varied test conditions concerning the nozzle location (vehicle underbody center), nozzle diameters (1, 2, 4mm), flow rates (118 NL/min continuously), and the impact absorber's condition (present in contact with the vehicle side door, removal from the crash site).

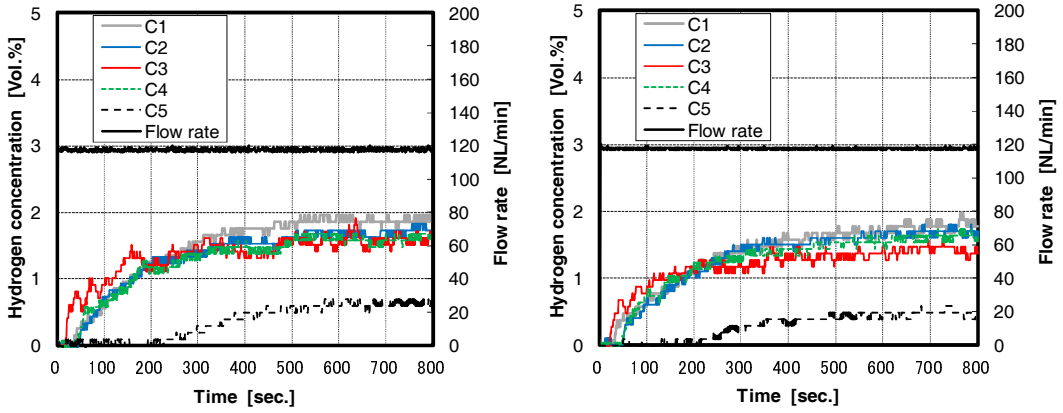


*(a) Impact absorber contact case* *(b) No impact absorber case*

***Figure5. Hydrogen concentrations in time sequence (Leak point: center of vehicle underbody, Leak direction: upward, Nozzle diameter: 4 mm, Flow rate: 118 NL/min)***

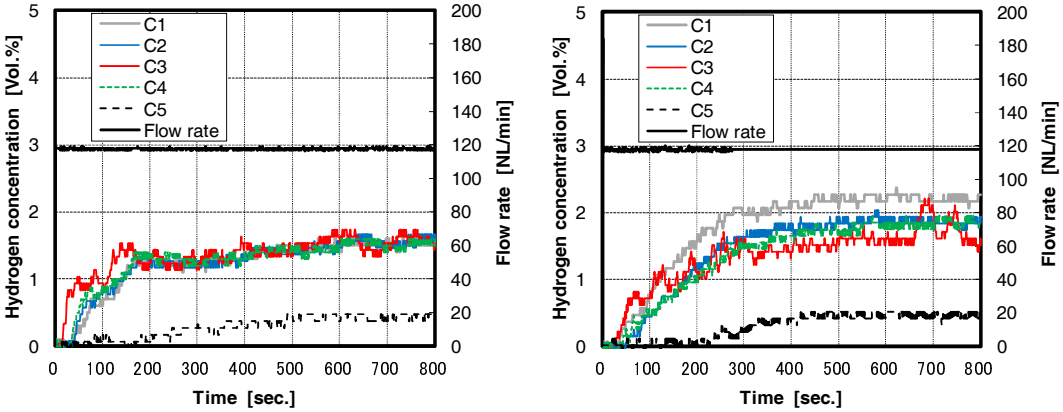


*(a) Impact absorber contact case* *(b) No impact absorber case*

***Figure6. Hydrogen concentrations in time sequence (Leak position: center of vehicle underbody, Direction: upward, Nozzle diameter: 2mm, Flow rate: 118 NL/min)***

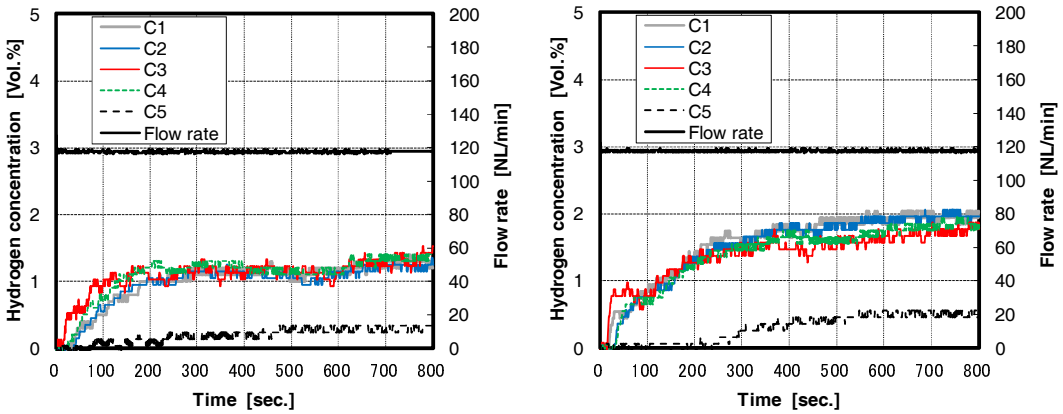


*(a) Impact absorbing contact case* *(b) No impact absorber case*

***Figure7. Hydrogen concentrations in time sequence (Leak position: center of vehicle underbody, Direction: upward, Nozzle diameter: 1mm, Flow rate: 118 NL/min)***

Comparison between an impact absorber in contact with the side door and the absence of an impact absorber at the crash site indicated differences in in-cabin hydrogen concentrations. Tables 2 and 3 show the comparison results in terms of maximum hydrogen concentrations under varied test conditions.

**Table2. Maximum hydrogen concentrations when in contact with impact absorber [vol%]**

| Leak position | Direction | Nozzle Dia. [mm] | Flow rate [NL/min.] | Door | Wind | Leak time [sec.] | C1 | C2 | C3 | C4 | C5 | Max (Position) |
|---|---|---|---|---|---|---|---|---|---|---|---|---|
| Underbody center | Upper | 4 | 118 | Close | No | 800 | 2.0 | 1.8 | 1.9 | 1.7 | 0.7 | 2.0(C1) |
| | | 2 | | | | | 1.6 | 1.7 | 1.7 | 1.6 | 0.5 | 1.7(C2,C3) |
| | | 1 | | | | | 1.4 | 1.3 | 1.5 | 1.4 | 0.3 | 1.5(C3) |
| | | 4 | 69 | | | | 1.4 | 1.3 | 1.5 | 1.2 | 0.5 | 1.5(C3) |
| | | | 35 | | | | 0.9 | 0.7 | 1.0 | 0.8 | 0.3 | 1.0(C3) |
| | | | 118 | | | 30 | 0.5 | 0.3 | 0.7 | 0.4 | 0.1 | 0.7(C3) |

**Table3.**
**Maximum hydrogen concentrations with only test vehicle (No impact absorber case) [vol%]**

| Leak position | Direction | Nozzle Dia. [mm] | Flow rate [NL/min.] | Door | Wind | Leak time [sec.] | C1 | C2 | C3 | C4 | C5 | Max (Position) |
|---|---|---|---|---|---|---|---|---|---|---|---|---|
| Underbody center | Upper | 4 | 118 | Close | No | 800 | 2.0 | 1.8 | 1.6 | 1.7 | 0.6 | 2.0 (C1) |
| | | 2 | | | | | 2.4 | 2.0 | 2.2 | 2.0 | 0.5 | 2.4(C1) |
| | | 1 | | | | | 2.0 | 2.1 | 1.9 | 1.9 | 0.6 | 2.1(C2) |
| | | 4 | 69 | | | | 1.3 | 1.3 | 1.3 | 1.2 | 0.5 | 1.3(C1,C2,C3) |
| | | | 35 | | | | 0.9 | 0.9 | 0.9 | 0.9 | 0.3 | 0.9(C1,C2,C3,C4) |
| | | | 118 | | | 30 | 0.5 | 0.4 | 0.7 | 0.5 | 0.1 | 0.7(C3) |

As indicated in Tables 2 and 3, the maximum hydrogen concentrations varied among the measurement positions, thus confirming the effect of impact absorbers on maximum hydrogen concentrations. The explanation of this effect is that as leaked hydrogen ascended along the doors and infiltrates into the cabin from an open window[4,5], the presence of the impact absorber in a hydrogen dispersion route affected the hydrogen infiltration into the cabin.

For the above reason, it should be difficult to accurately evaluate the diffusion behavior of hydrogen gas leaking from an HFCV in the presence of an MDB or a fixed barrier each equipped with an impact absorber.

Due to the HFCV-gtr requirement to measure in-cabin hydrogen concentrations immediately after a crash test, it should be necessary to remove the MDB near or in contact with the test vehicle to a sufficiently distant place so that the in-cabin hydrogen concentrations will not be affected.

**Helium substitution test procedure:** If the test condition of a 118 NL/min permissible hydrogen leakage is substituted with helium, the permissible helium leakage is 88.5 NL/min by applying a $He/H_2$ permissible leakage ratio of 0.75 (= 88.5/118). Based on the observation that gas concentrations in an enclosed space are in proportion to the gas leakage flow rate, HFCV-gtr[1] gives the following Equation **(1)** for the calculation of permissible helium concentration $X_{He}$ conducive to a permissible hydrogen concentration of 4vol%.

$$X_{He} = 4vol\%\ H_2 \times 0.75 = 3vol\% \qquad \textbf{(1)}$$

To verify if Eq.(1) is reliable under various test conditions, the present study investigated the $He/H_2$ ratios in the cabin under identical test conditions between hydrogen leakage at 118 NL/min and a helium leakage at 88.5 NL/min. Figures 8, 9 and 10 show the results of this test. Because the concentration values measured at the C5 position near the cabin floor proved exceptionally low, the concentrations only at C1 through C4 are shown in the following three figures.

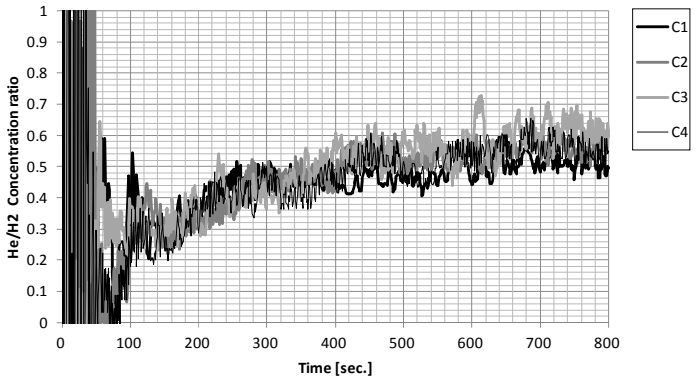


***Figure8. $He/H_2$ concentration ratios***
***(Leakage point: center of vehicle underbody, Nozzle direction: upward, Nozzle diameter: 4 mm, Hydrogen flow rate: 118 NL/min, Helium flow rate: 88.5 NL/min)***

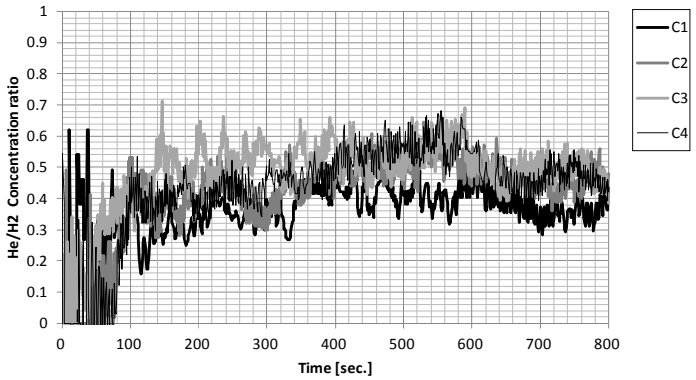


***Figure9. $He/H_2$ concentration ratios***
***(Leakage point: center of vehicle underbody, Nozzle direction: upward, Nozzle diameter: 1 mm, Hydrogen flow rate: 118 NL/min, Helium flow rate: 88.5 NL/min)***

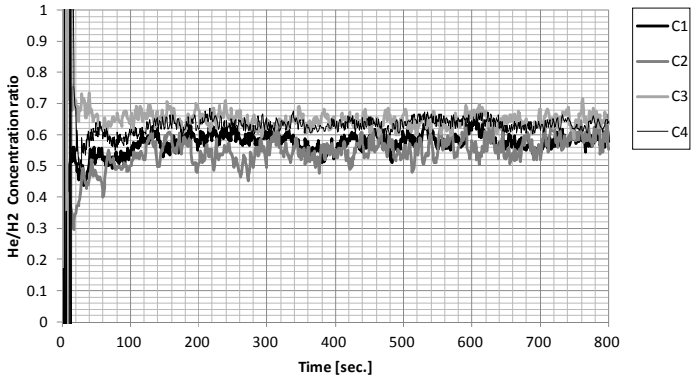


***Figure10. He/$H_2$ Concentration ratios***
***(Leakage point: center of cabin floor, Nozzle direction: upward, Nozzle diameter: 4mm, Hydrogen flow rate: 118 NL/min, Helium flow rate: 88.5 NL/min)***

The results indicated that the He/$H_2$ concentration ratio varied in the early phase of the test but gradually stabilized in the following phase onward. Nevertheless the ratio, instead of stabilizing at 0.75, varied according to leakage locations and nozzle diameters. The primary cause of this discrepancy was attributed to the fact that the aforementioned Equation (1) does not take account of differences in the diffusion behaviors of hydrogen and helium. Therefore, since no correspondence was found between a permissible hydrogen concentration of 4vol% and a permissible helium concentration of 3vol%, the validity of the helium substitution measurement method provided in HFCV-gtr was considered questionable.

## CONCLUSIONS

To examine the measurement method for post-crash hydrogen concentrations provided in HFCV-gtr, the present study investigated 1) wind velocity conditions not affecting the hydrogen concentrations in the cabin, 2) the effect of the impact absorber of a moving deformable barrier, and 3) the feasibility of substituting the hydrogen concentration measurement with helium concentration measurement. As the results indicated that hydrogen concentrations in the cabin were affected by the presence of a 0.1 m/s wind in the testing facility and an impact absorber in contact with the test vehicle, the HFCV-gtr measurement method is considered to pose some problems in its accuracy and reliability. In addition, since the correspondence between a permissible hydrogen concentration of 4vol% and a permissible helium concentration of 3vol% assumed in HFCV-gtr could not be confirmed, the existing helium substitution measurement method was also considered questionable. Consequently it is necessary to replace the HFCV-gtr measurement method for in-cabin hydrogen concentrations with a simpler method immune to external disturbances.

Finally, the present study was carried out as part of the “technology development project for hydrogen production, transport and storage systems” commissioned by New Energy and Industrial Technology Development Organization (NEDO), a national research and development agency of Japan.

## REFERENCES

[1] Global Technical Regulation (gtr) on hydrogen and fuel cell vehicles
[2] Isaac W. Ekotoa, Erik G. Merilob, Daniel E. Dedricka, Mark A. Groetheb, Performance-based testing for hydrogen leakage into passenger vehicle compartments, International Journal of Hydrogen Energy, Volume 36, Issue 16, 10169–10178, 2011

[3] Barbara Hennessey, James J Reuther, Jeffery S John, Paul E Shawcross, Gregory Kimmel, Post-crash fuel leakage and fire safety experiments for hydrogen vehicles, 22nd Enhanced Safety of Vehicle Conference, Paper Number 11-0439,2011

[4] Yohsuke Tamura, Noriaki Ohtsuka, Masayuki Takeuchi and Hiroyuki Mitsuishi, Determining hydrogen concentration in a vehicle after a collision test, Conference Proceedings on Fires in Vehicles (FIVE) 2012, SP Technical Research Institute of Sweden, September 27-28, 213-222, 2012

[5] Yohsuke Tamura, Masayuki Takeuchi and Kenji Sato, Effectiveness of a blower in reducing the hazard of hydrogen leaking from a hydrogen-fueled vehicle, International Journal of Hydrogen Energy, Volume 39, Issue 35, 20339–20349, 2014

# INJURY SIMULATION OF REAR SEAT CHILD OCCUPANT IN OFFSET DEFORMABLE BARRIER FRONTAL IMPACT

**Tomoshi Takahashi**
**Satoshi Fukushima**
**Yuichi Kitagawa**
**Tsuyoshi Yasuki**
Toyota Motor Corporation
Japan

Paper Number 15-0048

## ABSTRACT

From 2016, Euro NCAP plans to assess child occupant protection performance with Q6 and Q10 dummies in a 64 km/h offset deformable barrier (ODB) frontal impact test. This paper describes research simulating this frontal impact test using a ten-year old (10YO) version of the Total Human Model for Safety (THUMS) and an FE model of the Q10 dummy. The changes in impact kinematics and injury values of the 10YO THUMS model were compared with the Q10 dummy under various load limiter (L/L) values ranging from 2 to 5 kN, and the differences between the two were examined.

Differences in the kinematics between the two mostly appeared during the second half of the test. As a result, the displacement of the head and chest of the Q10 dummy was smaller than that of the 10YO THUMS model. This result was probably because the thoracic plate of the Q10 dummy hindered the flexion of the thoracic spine. In addition, the chest upper deflection of the Q10 dummy resulted in higher injury values. This result was assumed to be because the shoulder belt was positioned close to the chest upper deflection gauge. In addition, the change in the chest upper deflection of the Q10 dummy was greater than that of the 10YO THUMS model, with a sensitivity of approximately four times as large. This result was due to the high force transmission ratio from the clavicle to the sternum.

## INTRODUCTION

According to European accident statistics, the rate of child (0 to 14 year-old) occupant fatalities in the EU in 2009 amounted to 2.5 people in 100,000 (Kirk et al., 2012). As one measure to help improve the safety of child occupants, the EU enacted ECE R44 in 1981 to specify safety criteria for child seats. Euro NCAP then began assessing child occupant protection performance from 2003.

The development of the Q-series of child dummies began in 1993. Five completed dummies have already been completed, ranging in age from 0 to 6 years old, and the 10-year old Q10 dummy is due to be completed in the near future. Currently, Euro NCAP assesses child occupant protection performance using the 1.5-year old Q1.5 dummy and the 3-year old Q3 dummy. In addition, Euro NCAP has also announced plans to adopt the 6-year old Q6 dummy and the 10-year old Q10 dummy from 2016. Although various researches have examined the injury states, tolerances, and thresholds of child occupants, little information is available compared to research into adults. Physical tests on live subjects have been carried out at low force levels, assuming playground accidents. However, there is very little information related to tolerance and threshold at high forces such as in impact tests. For this reason, research using human finite element (FE) models is regarded as an effective means to better understand pediatric injuries.

The research described in this paper compared the occupant kinematics and injury values in a frontal impact using a ten-year old (10YO) version of the THUMS human FE model and an FE model of the Q10 dummy. Assuming the same conditions as the 64 km/h offset deformable barrier (ODB) frontal impact test used in Euro NCAP, the simulation placed the child occupant models in a junior seat (JRS) located in the rear. The impact kinematics and injury values of rear seat occupants are affected by the load limiter (L/L) device of the seatbelts. Therefore, this

research also examined changes in the displacement and injury value for each part of the occupant (i.e., the sensitivity) under various L/L values. After describing these simulations, this paper details the differences in impact kinematics and injury values of the 10YO THUMS and Q10 dummy models.

## METHOD

The first section of this paper describes an outline of the FE models used in the research.

### Vehicle FE Model

The simulated test vehicle was a B-segment compact car with a weight of 1,070 kg. The FE model of the test vehicle was created to represent its geometry and structure, including component parts. It was verified that the floor deceleration pulse, forward displacement, and yawing motion matched those measured in an ODB frontal impact test of this vehicle. The seatbelts in the rear seats for child occupants were equipped with a pretensioner to remove slack and an L/L function to control the occupant restraining force.

### JRS FE Model

A high-backed JRS in the 2-3 weight group was used. The FE model was created using external geometrical data obtained using optical measurement. The plastic and metal parts were modeled with shell elements, while solid elements were used for the foam parts. The average mesh size was 5 mm. It was verified that the deformation stiffness and strength of the head and lateral supports were consistent with those of actual JRS.

### 10YO THUMS Model

The 10YO THUMS model was created by changing the 6YO THUMS pedestrian model created by Nishimura et al. (2002) to a seated posture and scaling up the physique to that of a 10-year old child. The seated height of the 10YO THUMS model was changed to match that of the Q10 dummy. Both models had a weight of 35 kg. The impact response of the 10YO THUMS head was previously verified by Nishimura et al.(2002), while the chest response was verified in the research by comparison with the chest loading tests on post mortem human subjects (PMHS) of a 10-year old (Kent et al., 2012). The head displacement was measured at the center of gravity of the head and the chest displacement was measured at the fourth thoracic vertebra (T4). The displacement data was transferred to the vehicle (the rear floor) coordinate system. The upper and lower chest deflections were calculated in accordance with the measuring points on the Q10 dummy.

### Q10 Dummy FE Model

The Ver. 1.2.1 Q10 dummy FE model (Humanetics Innovative Solutions, Inc. ,2013) was used for the comparison with the 10YO THUMS model. The head and chest response were verified based on the details of Humanetics Technical Reports. The displacement and injury values of each part were outputted following the Humanetics User Manual from the sensors set inside the model. The displacement data was transferred to the vehicle coordinate system as processed in the 10YO THUMS model.

## Calculation Model and Conditions

The JRS model was placed on the right rear seat (i.e., the far side of the vehicle) assuming fixation through the ISOFIX anchors. Both the 10YO THUMS and Q10 dummy occupant models were seated so that their backs were in contact with the seatbacks. The seatbelts were wrapped around the torsos of the dummies passing through the belt guides. The pretensioner was activated at 20 msec after the impact, based on the specifications of the tested vehicle. Eight cases were simulated with the 10YO THUMS and Q10 dummy models, changing the L/L value from 2 to 5 kN. The kinematics of each part of the models and the injury values were compared for each case. Table 1 shows the calculation conditions for all eight cases.

***Table 1.*** **Simulation Matrix**

| CASE | | 1 | 2 | 3 | 4 | 5 | 6 | 7 | 8 |
|---|---|---|---|---|---|---|---|---|---|
| Test Condition | | 64kph ODB | | | | 64kph ODB | | | |
| Vehicle Type | | Compact Car | | | | Compact Car | | | |
| Occupant Position | | Rear Seat (Far Side) | | | | Rear Seat (Far Side) | | | |
| Child Occupant Model | | **10YO THUMS** | | | | **Q10 dummy** | | | |
| JRS | Seat Back | Available | | | | Available | | | |
| | Mount | ISO-FIX | | | | ISO-FIX | | | |
| Seatbelt | P/T | Available | | | | Available | | | |
| | L/L | 2kN | 3kN | 4kN | 5kN | 2kN | 3kN | 4kN | 5kN |

## RESULTS

This section compares the impact responses and injury values of the 10YO THUMS and Q10 dummy models between cases 3 and 7 (L/L value: 4 kN).

### Kinematics

Figure 1(a) superimposes the kinematics of the 10YO THUMS and Q10 dummy models at 0, 60 and 120 msec after the impact. In both models, the upper body flexed after the pelvis stopped. The head positions of two models were almost identical up to 60 msec but diverged after that. The upper body flexion and lateral bending of spine were greater in the 10YO THUMS model than those in the Q10 dummy. At 120 msec, the head forward displacement of the 10YO THUMS model was 547 mm and the chest (T4) forward displacement was 327 mm. These values were 179 mm (head) and 92 mm (chest) larger than those of the Q10 dummy, respectively. The lateral displacement of the 10YO THUMS model (chest) was 101 mm, larger than the 80 mm recorded by the Q10 dummy.

Figure 1(b) shows the changes in the maximum forward displacement of the head and chest under different L/L values. The maximum lateral displacement of the chest is also shown. Under the same L/L value, the 10YO THUMS model exhibited greater displacement than the Q10 dummy. The maximum forward displacement increased as the L/L value decreased. In contrast, there was little difference in the sensitivity of the maximum forward displacement against the L/L value. Under the impact conditions assumed in the research, the head of the 10YO THUMS model contacted the back of the front seat in case 1 (L/L value = 2 kN).

The maximum lateral displacement of the chest in the 10YO THUMS model was larger than that in the Q10 dummy. In this model, the lateral displacement increased as the L/L value decreased. However, in case 1 only, the lateral displacement of the 10YO THUMS model was smaller than that in case 2 even though the L/L value was smaller.

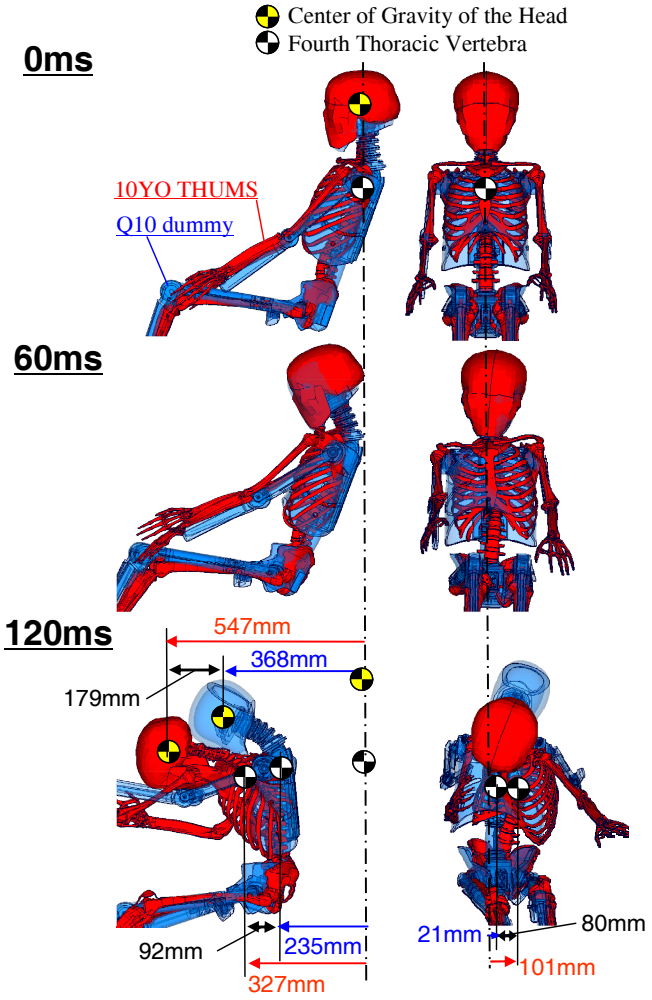


*(a)* Comparison of 10YO THUMS and Q10 dummy models (cases 3 and 7)

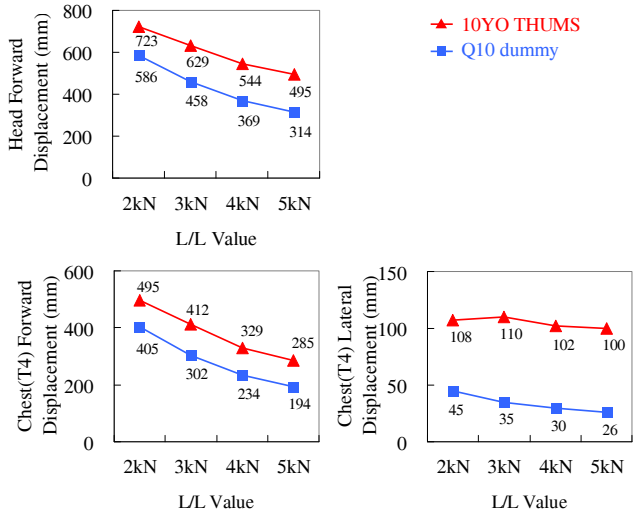


*(b)* Maximum displacement of head and chest at each L/L value

***Figure 1.*** Occupant displacement and sensitivity of displacement of each part to L/L value.

**Injury Values**

Figure 2(a) compares the time history curves of the head resultant acceleration, upper neck tension force, and chest deflections (upper and lower) of the 10YO THUMS and Q10 dummy models. The head resultant acceleration and upper neck tension force reached the maximum peaks at 116 msec, which was close to the timing of the maximum head forward displacement (120 msec). It should be noted that the maximum values in all cases were higher for the 10YO THUMS model. The chin and clavicle of the Q10 dummy came into contact at 85 msec, generating an initial peak for head resultant acceleration. Initial peaks for the chest upper and lower deflections appeared at 76 msec and the maximum values appeared after 116 msec. At 76 msec, the shoulder belt restrained the Q10 dummy from the chest to the abdomen. At 116 msec, the upper body flexed, causing the clavicle to be restrained by the shoulder belt. Although the maximum chest upper deflection of the 10YO THUMS model was smaller than that of the Q10 dummy, the chest lower deflection was greater.

Figure 2(b) shows the relationship between the L/L value and the head injury criteria (HIC), as well as the injury values for the neck (upper neck force) and chest (chest upper and lower deflections). Apart from the chest upper deflection, the injury values of the 10YO THUMS model were higher in all cases than the Q10 dummy. In the 10YO THUMS model, the HIC increased as the L/L value decreased. In contrast, the HIC of the Q10 dummy decreased as the L/L value decreased. The HIC was particularly high in case 1, in which the head contacted the back of the front seat. Although the upper neck force of the 10YO THUMS model increased as the L/L value decreased, the upper neck force of the Q10 dummy model decreased under the same conditions. The chest upper and lower chest deflection of both the 10YO THUMS and Q10 dummy models also decreased as the L/L value decreased. However, the change in the chest upper deflection of the Q10 dummy was greater than in the 10YO THUMS model, with a sensitivity of approximately four times as high.

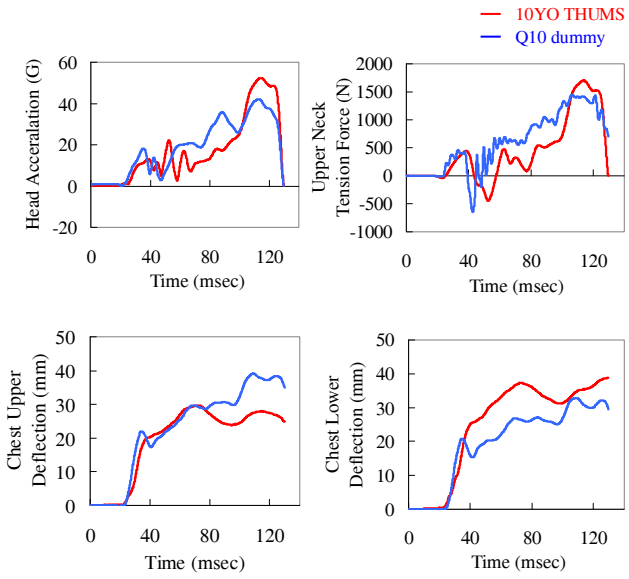


*(a)* Time history comparison of head resultant acceleration, upper neck tension force, and chest deflection (cases 3 and 7)

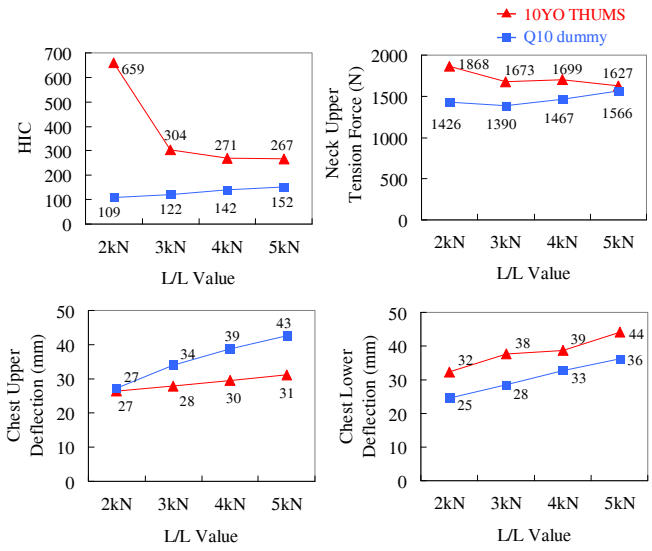


*(b)* Injury values of each part at each L/L value

***Figure 2.*** Injury value time history and sensitivity of displacement of each part to L/L value.

## DISCUSSIONS

### Cause of Smaller Head and Chest Displacement in Q10 Dummy Compared to 10YO THUMS Model

The mass distribution, dimensions and stiffness of body parts of the Q10 dummy closely match the average values of a 10-year old (Lemmen et al., 2012). However, the Q10 dummy has a rigid block, called a thoracic plate, for supporting the measurement instrumentation. The flexion range of the thoracic spine was relatively small due to the higher rigidity of this part compared to an actual human spine.

The smaller forward displacement of the Q10 dummy head compared to the 10YO THUMS head was analyzed comparing cases 3 and 7. The head forward displacement is mostly determined by the pelvis displacement and the flexion of the cervical, thoracic, and lumbar spines. Figure 3 compares the contributions of pelvis displacement and spine flexions between the 10YO THUMS and Q10 dummy. In the 10YO THUMS model, 328 mm (60%) of the head displacement amount of 544 mm was caused by the flexion of the thoracic spine. In contrast, the Q10 dummy had little flexion of the thoracic spine. This suggests that the thoracic plate of the Q10 dummy hindered the flexion of the thoracic spine. The rigidity of the thoracic plate was also a possible factor of the smaller chest forward displacement of the Q10 dummy.

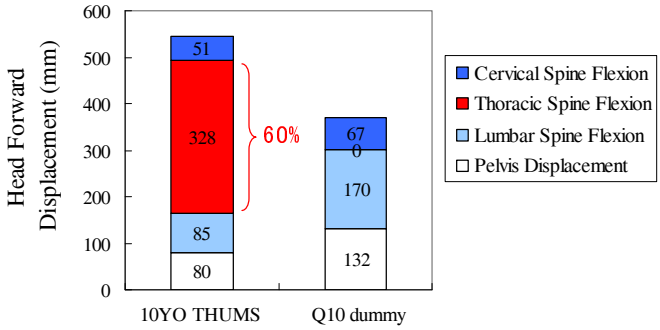


***Figure 3.*** Contributions of pelvis displacement and spine flexions to head forward displacement.

**Cause of Higher Chest Deflection in Q10 Dummy Compared to 10YO THUMS Model**

The contact force of the shoulder belt acting on the chest of the Q10 dummy (6,500 N, case 7) was lower than that of the 10YO THUMS model (8,300 N, case 3). Lemmen et al. (2012) reported that the chest deflection responses of the Q10 dummy are within the test corridor. These points indicate that the cause of the difference in chest deflection is neither the force of the shoulder belt nor the chest deflection responses of the Q10 dummy. This research focused on the relationship between the chest deflection measurement points and the position of the shoulder belt.
Figure 4 shows the positional relationship at the maximum chest deflection. The distance between the chest upper deflection measurement point and the center of the shoulder belt in the width direction was 89 mm in the 10YO THUMS model (case 3). This differed greatly from the distance in the Q10 dummy, which was only 7 mm (case 7). The shoulder belt contacted the area around the chest upper deflection measurement point in the Q10 dummy, while the belt was at the lower area in the 10YO THUMS model. This is thought to be the reason why the chest upper deflection of the Q10 dummy was greater than that of the 10YO THUMS model.

As shown in Figure 1(a), the Q10 dummy model exhibited much smaller chest lateral displacement (21 mm at 120 msec) compared to the 10YO THUMS model (101 mm), while there was little difference in the chest vertical displacement. The shoulder belt kept in contact with the area around chest upper deflection measurement point in the Q10 dummy while the chest upper deflection measurement point deviated from the shoulder belt contact in the 10YO THUMS model.

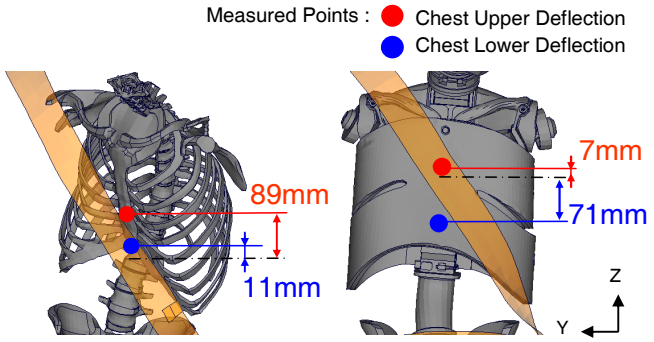


***Figure 4.*** Positional relationship between chest and shoulder belt.

**Cause of Higher Chest Upper Deflection Sensitivity to Changes in L/L value in Q10 Dummy**

In the 10YO THUMS model, the chest upper deflection decreased by 5.3 mm for each 1 kN of the L/L value. However, in the Q10 dummy, the chest upper deflection decreased by only 1.3 mm. The sensitivity of the chest upper deflection to the L/L value was roughly four times higher for the Q10 dummy than the 10YO THUMS model.

In cases 3 and 7, the shoulder belt contact area was divided into three regions (the clavicle, chest, and abdomen) for analyzing the force contribution to chest deflection. The clavicle region covers the right shoulder and the right rib 1, the chest region covered the area from the right rib 2 to the left rib 9, and the abdominal region covered the area below the left rib 9. At the maximum chest upper deflection, 48% of the force was generated at the clavicle region, 37% at the chest region, and 15% at the abdominal region. Of these, the forces at the clavicle and abdominal regions do not directly cause an increase in upper chest deflection. There were little differences in the change in clavicle force between both models with different L/L values.

The ratio of force transmission from the clavicle to the sternum (force transmission rate) was compared between the 10YO THUMS and Q10 dummy models. This ratio was 22% in the Q10 dummy but only 8% in the 10YO THUMS model, approximately 2.6 times higher (Figure 5(a)) than the rate for the Q10 dummy. In the human body, the left and right clavicles are completely separate and join to the sternum through ligaments. On the other hand, the clavicle

of the Q10 dummy is a single part extending laterally from the left to the right and bolted to the ribcage (Figure 5(b)). The high sensitivity of the chest upper deflection of the Q10 dummy is due to the smaller freedom of deformation of the joint between the clavicle and sternum, which facilitates transmission of the shoulder belt load acting on the clavicle to the sternum.

It is considered that the impact kinematics and responses of the Q10 dummy could be made closer to those of the 10YO THUMS model by improving the flexibility of the thoracic spine and the joint between the clavicle and sternum.

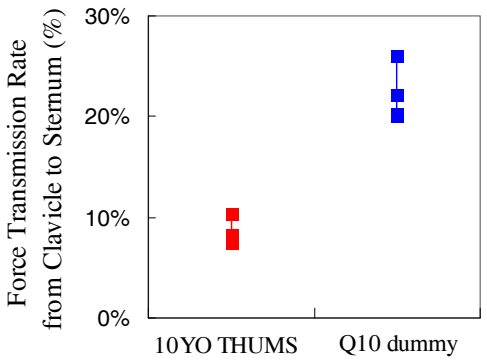


***(a)*** Force transmission rate from clavicle to sternum

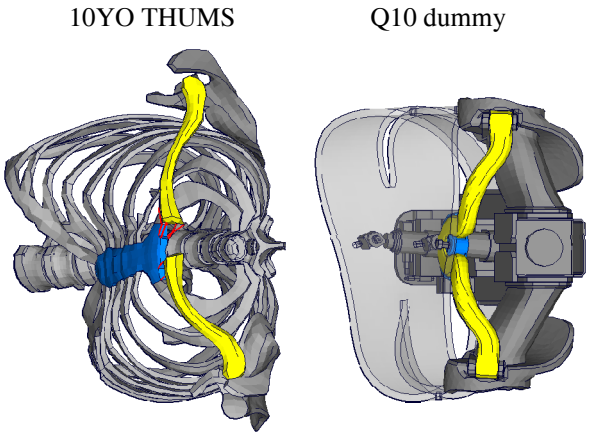


***(b)*** Deformation of clavicle and sternum with fixed spine (116 msec)

***Figure 5.*** Clavicle force transmission rate and structural differences.

Limitation

This research was conducted assuming particular impact conditions (vehicle, impact pattern, and speed). The investigation does not comprehensively cover all the types of accidents that occur in the real world and is not directly related to accident results.

## CONCLUSIONS

This paper described a simulated 64 km/h ODB frontal impact test using 10YO THUMS and Q10 dummy models. The changes in impact kinematics and injury values of the two models were compared under various L/L values ranging from 2 to 5 kN.

The kinematics of the 10YO THUMS and Q10 dummy models were almost identical up to 60 msec after the impact. However, the forward and lateral displacements of the 10YO THUMS model were larger than those of the Q10 dummy after 60 msec. The Q10 dummy exhibited lower head resultant acceleration, smaller upper neck tension force, greater chest upper deflection, and smaller chest lower deflection. The changes in the injury values under different L/L values were similar between the 10YO THUMS and Q10 dummy models. However, the change in the chest upper deflection of the Q10 dummy was greater than that of the 10YO THUMS model, with a sensitivity of approximately four times as high.

The smaller head and chest displacement in the Q10 dummy compared to the 10YO THUMS model was probably due to the thoracic plate of the Q10 dummy hindering the flexion of the thoracic spine. The greater chest upper deflection of the Q10 dummy was assumed to be because the shoulder belt was positioned close to the chest upper deflection gauge. The high sensitivity of the chest upper deflection of the Q10 dummy to the L/L changes was probably due to the high force transmission ratio from the clavicle to the sternum.

These results showed that the impact kinematics and responses of the Q10 dummy could be made closer to those of the 10YO THUMS model by improving the flexibility of the thoracic spine and the joint between the clavicle and sternum.

## REFERENCES


Humanetics Innovative Solutions, Inc. (2013). *Q10 Child Dummy Model LS-DYNA Model Version 1.2 User's Manual.* Humanetics Innovative Solutions, Inc. U.S.A.

Kent, R., Lopez-Valdes, F., Lamp, J., Lau, S., Parent, D., Kerrigan, J., et al. (2011). *Characterization of the Pediatric Chest and Abdomen Using Three Post-Mortem Human Subjects.* Proceedings of the 22nd ESV Conference. Paper No. 11-0394. Washington, D.C, U.S.A. : NHTSA

Kirk, A., Lesire, P., & Schick, S. (2012). *Project Deliverable 3.2.1 of the EC FP7 Project CASPER.* Retrieved from http://casper-project.eu/

Lemmen, P., Waagmeester, K., Burleigh, M., Lakshminarayana, A., & Korschdon, K. (2013). *Development of the Q10 10 Year-old Child Crash Test Dummy.* Proceedings of the 23rd ESV Conference. Paper No. 13-0348. Seoul, Republic of Korea. : NHTSA

Nishimura, R., & Hasegawa, J. (2002). *Development of the Human FEM Model for Child Pedestrian.* Proceedings of 2002 JSAE Autumn Congress. Paper No. 78-02. Kyoto, Japan. : JSAE

This paper has been peer-reviewed and published in a special edition of *Traffic Injury Prevention* 16(S1), by Taylor & Francis Group. The complete paper will be available on the *Traffic Injury Prevention and www.NHTSA.gov* websites on June 8, 2015.

To access all Peer-reviewed papers please copy and paste the link below into your browser to access the papers.

http://www.tandfonline.com/toc/gcpi20/16/sup1

This paper has been peer-reviewed and published in a special edition of *Traffic Injury Prevention* 16(S1), by Taylor & Francis Group. The complete paper will be available on the *Traffic Injury Prevention and www.NHTSA.gov* websites on June 8, 2015.

To access all Peer-reviewed papers please copy and paste the link below into your browser to access the papers.

http://www.tandfonline.com/toc/gcpi20/16/sup1

# INTEGRATED BICYCLIST PROTECTION SYSTEMS - POTENTIAL OF HEAD INJURY REDUCTION COMBINING PASSIVE AND ACTIVE PROTECTION SYSTEMS

**Rikard Fredriksson**
**Arian Ranjbar**
**Erik Rosén**

Autoliv Research
Sweden

Paper Number 15-0051

## ABSTRACT

In recent years both pedestrian passive and active safety systems, such as pedestrian bonnets/airbags and autonomous braking, have emerged on the market and are estimated to be effective to reduce injury of vulnerable road users in car crashes. A natural next step is to develop similar protection systems for bicyclists. The aim of this study was to investigate the potential bicyclist head injury reduction from passive and active protection systems compared to an integrated system.

The German In-Depth Accident Study (GIDAS) database was queried from 1999 to 2014 for severely (AIS3+) head injured bicyclists when struck by passenger car fronts. This resulted in 34 cases where information was sufficient for both the pre-crash and the in-crash part of the event. The default passive protection system was designed to mitigate head injuries caused by the bonnet area, A-pillars, and the lower windscreen (instrument panel) area (deployable hood and windshield airbag). To estimate the hood and airbag performance risk reduction functions were used based on experimental tests with and without the systems. The active protection system was an autonomous braking system, which was activated one second prior to impact if the bicyclist was visible to a forward-looking sensor. Maximum speed reduction was estimated using road condition information in each case. The integrated system was a direct combination of the passive and active protection systems. Case by case the effect from each of the active, passive and integrated systems was estimated. For the integrated system, the influence of the active system on the passive system performance was explicitly modelled in each case. A sensitivity analysis was performed varying the coverage area of the passive protection system and the activation criteria of the active system.

The integrated system resulted in 29%-62% higher effectiveness than the best single system of active respectively passive protection system in reducing the number of bicyclists sustaining severe (AIS3+) head injuries. These values were statistically tested and found to be significant. The study is based on representative data from Germany, but may not be representative to countries with a different car fleet or infrastructure. This study indicates that integrated systems of passive and active vulnerable road user countermeasures offer a significantly increased potential for head injury reduction compared to either of the two systems alone.

## INTRODUCTION

World-wide it is estimated that over 500 000 pedestrians and bicyclists are killed annually in road traffic (Naci, Chisholm et al. 2009). Virtually all road pedestrian fatalities and a majority of the cyclist road fatalities are caused by crashes with vehicles (SIKA 2009). In larger European cities, bicycle transportation is increasing (Thiemann-Linden 2010), likely due to congestion, fuel prices and an increasing awareness of its health benefits. Pedestrians and bicyclists already make up roughly half the traffic fatalities in urban areas in the EU (ERSO 2012), risking fatalities to increase with increased bicycle use.

In research studies pedestrians have been the dominant subject group. Legal regulations as well as consumer rating tests for pedestrians have influenced car design during the last decade in Europe and Japan. Cars on these markets are now often equipped with energy absorbing bumpers and hoods, as well as deployable hoods. Furthermore,

airbags for the windshield area, attempting to mitigate head injury have been introduced (Volvo 2012; Jaguar-LandRover 2014). Pedestrian passive countermeasures have proven effective in reducing pedestrian injury. Strandroth et al. (2014) showed, in a study on Swedish accidents, that cars with higher pedestrian ratings in EuroNCAP consumer tests resulted in less severe injuries. A natural next step is to design the airbag to protect also for bicyclists. The major difference between pedestrians and bicyclists is the higher head impact point of bicyclists on the car (Fredriksson, Bylund et al. 2012; Fredriksson and Rosén 2012). Fredriksson et al (2014) showed a potential protection system with a higher protection area designed to protect both pedestrians and bicyclists. Another way to reduce injury is to reduce impact speed, where even moderate speed reductions can significantly decrease risk for the vulnerable road user in an impact. For example, Rosén and Sander showed that reducing the impact speed from 50 km/h to 40 km/h reduced the pedestrian fatality risk by 50% while a reduction (from 50 km/h) to 30 km/h reduced the risk by as much as 80% (2009). Currently, active systems such as autonomous braking are being rapidly introduced on the market. These systems consist of a pre-crash sensor that detects a dangerous situation where a pedestrian is about to be hit. If unnoticed by the driver the system will automatically brake the car and prevent impact at low speeds and mitigate pedestrian injury at higher speeds by decreasing the impact speed. These systems are potentially very effective in reducing impact severity of pedestrian and bicyclist crashes (Rosén, Källhammer et al. 2010; Rosén 2013). In 2016 EuroNCAP begins assessing autonomous emergency braking (AEB) or warning for pedestrians (EuroNCAP 2014), and in 2018 it is planned to begin testing active systems also for bicyclists.

It has been argued by some that autonomous braking systems could even replace passive protection systems. It is then interesting to estimate how effective these systems are, and in particular, answer the question: if one of these systems, such as an active system, is implemented, would there be any additional benefit in adding a passive system, or vice versa? In an earlier study it was shown beneficial for pedestrians to combine active and passive systems regarding injury reduction potential.

The aim of this study was, therefore, to investigate the potential reduction of bicyclists sustaining severe head injury from either a passive (in-crash) or active (pre-crash) countermeasure compared to an integrated system that is a combination of both. Since these countermeasures do not yet exist in cars, or have just been introduced, no accident data, with these systems involved, is available to aid in estimating effectiveness. The alternative solution would then be to use crash tests and head injury criteria with accompanying risk curves along with incidence data to estimate effectiveness. Although legal and NCAP tests may be effective in leading the development towards safer car fronts for pedestrians, they have limitations in estimating real-life benefits, and the connection between selected injury criteria and pedestrian head injury risk has not been thoroughly investigated. Therefore, ideal passive and active countermeasures were considered in this study. The focus was not on estimating and comparing the exact effectiveness of the individual systems, but rather on the improved benefit of combining the two.

## METHOD

In this study three systems to reduce head injury of bicyclists in car crashes were considered, i.e. a passive deployable system, an active auto-brake system and finally a combined system of the active and passive system. The passive protection system consisted of a deployable hood and a windshield airbag and was designed to mitigate head injuries caused by the bonnet area, windshield frame and the lower windshield area where the instrument panel was in close proximity to the windshield glass. The active system was a so-called autonomous emergency braking (AEB) system that, if a bicyclist can be detected and is estimated to be impacted by the car, applies full braking to avoid or mitigate the crash. The combined system was a direct combination of the two systems with autonomous braking of the car first, followed by an activation of the passive system, in case the accident was not avoided and the remaining impact speed was sufficient to be estimated to cause severe head injury. This method was developed in an earlier study estimating effectiveness of pedestrian protection systems (Fredriksson and Rosén 2014).

We estimated the potential of these systems to reduce severe (AIS3+) head injury. Note that a bicyclist may sustain multiple severe head injuries from different impacts to the car, ground and other external objects in the same crash. In this study, bicyclists that sustained at least one of the severe head injuries from an impact to the ground, external objects or unprotected areas of the car were not considered helped by the passive

countermeasure. Only bicyclists that sustained all severe head injuries from impacts to the protected areas of the car were considered protected by the passive countermeasure.

To estimate the injury saving potential of the different systems we searched the GIDAS database for all cases where a bicyclist was severely (AIS3+) head injured when impacted by the car front. The database consisted of 4789 cases with bicyclists injured when struck by passenger cars between 1999-2014. When excluding the non-relevant cases (lower injury level, side/rear impacts to the car and cases when no severe head injury was sustained) it resulted in 34 cases where information was sufficient to estimate both passive and active protection potential. We then estimated the potential of the passive, active and the integrated system in reducing the risk of severe head injury case by case for the 34 cases.

**Passive protection system**

**Head impact speed** The head impact speed was, just like in the previous pedestrian study, assumed to be equal to the car impact speed. For pedestrians studies have shown head impact speeds both higher and lower than the car impact speed, ranging from 68%-146% in car-to-pedestrian post mortem human subject (PMHS) 40 km/h tests (Masson, Serre et al. 2007; Kerrigan, Crandall et al. 2008; Kerrigan, Arregui et al. 2009). For bicyclists no PMHS tests have been performed. Limited full-scale crash tests with the Polar II dummy showed head/car impact speed ratios of 87%-147% (van Schijndel, de Hair et al. 2012). Therefore the assumption that head impact speed was equal to car impact speed was made also in this study.

**Deployable hood system** The deployable hood performance was estimated in a previous study (Fredriksson and Rosén 2014) based on a study with headform tests at 40 km/h (Fredriksson, Håland et al. 2001) using a method by Searson et al (2012) to estimate performance at other impact speeds. Five different impact points were chosen distributed on the hood surface. The estimated HIC values for the reference hood and version 1 deployable hood was based on these tests. Since the active hood tested was designed to meet earlier Euro NCAP requirements on HIC1000 for full score with a 20% margin, it is likely that a system designed today would aim at keeping 20% below the current target of HIC650. Version 2 of the active hood was therefore estimated as a deployable hood designed to keep HIC 20% below the Euro NCAP level for full score in the hood area (HIC=0.8x650=520). The HIC values were used to calculate risk of AIS3+ head injury for the reference configuration and the active hood systems (Fredriksson and Rosén 2014).

**Windshield airbag** The airbag performance was also estimated in the previous study using the headform test method of Euro NCAP but varying the headform impact speed from 20-60 km/h for two different impact points (Fredriksson and Rosén 2014). One impact was chosen as the most severe, i.e. an impact directly to the A-pillar. The other impact was considered less severe, but still a frequent cause of severe head injuries, i.e. impact to the lower windshield glass with, in this case, 25 mm distance to the instrument panel. The tests were performed on a small family car in the standard condition as well as equipped with the windshield airbags as in Figure 1. Version 1 is a standard airbag design with a thickness of approximately 200 mm. Version 2 is a new design that increases the energy-absorbing distance achievable without increasing the airbag volume (Fredriksson and Rosén 2014).

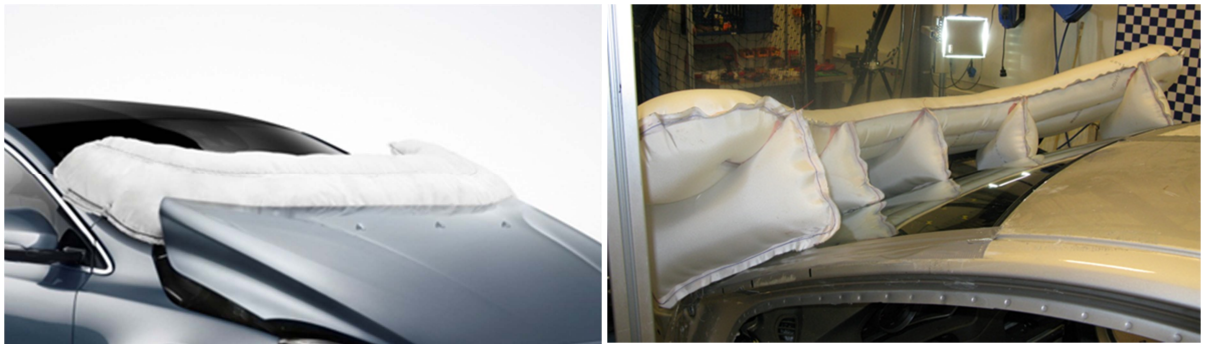

***Figure 1. Pedestrian airbags used in the headform tests in the previous study to estimate airbag performance, left: version 1 airbag, right: version 2 airbag (Fredriksson and Rosén 2014)***

For the effectiveness estimation it was assumed that the airbag was designed to cover the lower windshield, where the instrument panel is within the head line of motion, and the complete A-pillars for System 1 and 2. In System 3, version 2 airbag was extended to protect also in the area of the roof front edge. See Table 1. If the head injury or injuries resulted from what was judged as an A-pillar impact, fully or partially, or a direct hit to the lower windshield frame, we used the data from the A-pillar tests for estimation of the risk. If the impact was to lower windshield glass and instrument panel, we used the data from the lower windshield tests to estimate the risk.

**Table 1. Deployable system parameters for the three versions used in the study**

| ***Deployable system parameters*** | ***System 1*** | ***System 2*** | ***System 3*** |
|---|---|---|---|
| Hood lifter | Version 1 | **Version 2** | Version 2 |
| Airbag design | Version 1 | **Version 2** | Version 2 |
| Coverage area | Hood | Hood | Hood |
| | Low WS | Low WS | Low WS |
| | A-pillars | A-pillars | A-pillars |
| | | | **Roof front edge** |

When these data were collected, the severe head injury risk, for each impact speed and protection system, could be estimated for each case (i) using the risk function from NHTSA (1995). The risk reduction was then calculated (Fredriksson and Rosén 2014).

Note that if the impact location of any of the AIS3+ head injuries in a case is other than that protected by the protection system, i.e. other areas of the car or the surrounding/ground, then risk reduction potential in that case was set to 0. Also, for both systems, activation was limited to a minimum speed of 20 km/h.

**Risk reduction functions** In the earlier study (Fredriksson and Rosén 2014) risk reduction functions were developed for the two protection systems, deployable hood and windshield airbag (Figure 2). Linear interpolation between the data points was used for the airbag risk reduction functions. The risk reduction was 0 above 70 km/h for the active hood and above 60 km/h for the airbag in the A-pillar impact location. For the airbag lower windshield impact location the risk reduction was still 31% at 60 km/h. Since we did not have any test data above 60 km/h, we estimated the risk reduction function to continue linearly down to 0 at 70 km/h. Also the lower windshield reference test at 20 km/h was unsuccessful so the risk reductions from 20-29 km/h for lower windshield were estimated to be horizontal from the values at 29 km/h.

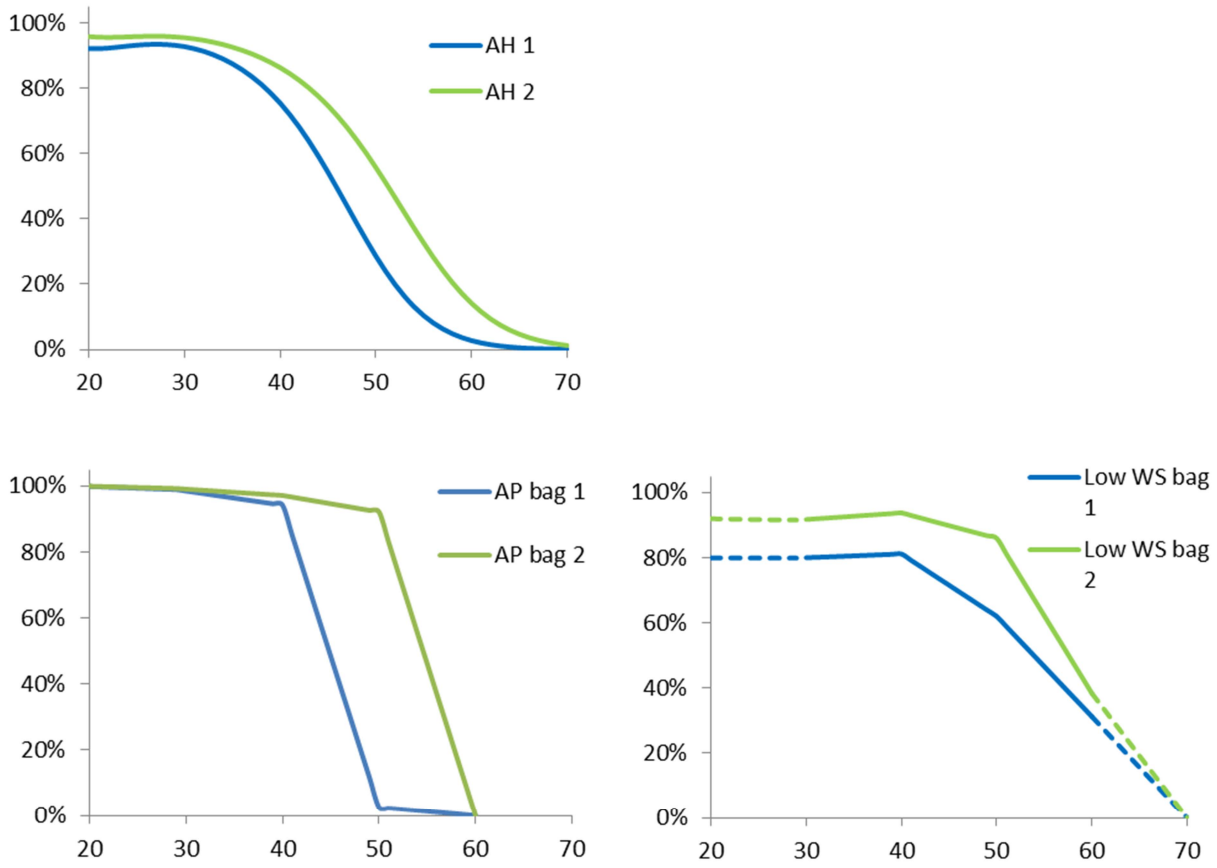


***Figure 2. Head AIS3+ injury risk reduction for active hood average (top) and windshield airbag (below) for two impact locations; A-pillar (left) and lower windshield (right)***

Using the risk reduction functions the possible effectiveness of the protection system could be estimated for each case. Note that if any of the AIS3+ head injuries was caused by a source outside the protected area, on the car or in the surrounding, the effectiveness of the protection system in that case was set to 0.

Finally, the total effectiveness of the passive protection system could be calculated as:

$$E_{passive}^{total} = \frac{1}{N}\sum_{i=1}^{N} \mathrm{e}_{passive}(v_i) \quad (1)$$

The rationale behind this effectiveness calculation method is described in more detail in a previous study (Fredriksson and Rosén 2012).

**Active protection system**

The active (AEB) system was estimated to detect all visible bicyclists within the field of view independent of weather and light conditions, and activate automatically the brakes up to 1.0 s before predicted impact. The braking system was estimated to have a ramp-up time of 300 ms and maximum braking level was set to 0.7 g, but reduced if road friction conditions were limited. Finally, three system parameters were varied: sensor field of view, trig width and cut-off speed for activation; the system was activated for bicyclists within the vehicle path or up to 1.0 or 3.0 m beside it (trig width), either up to 60 km/h or at all impact speeds, and during all light conditions (see Table 2). For further details on the AEB system, see earlier study by Rosén (2013).

**Table 2. AEB parameters for the three versions used in the study (in bold parameters that are varied)**

| *AEB parameters* | *System 1* | *System 2* | *System 3* |
|---|---|---|---|
| Field of view | 40° | 40° | **60°** |
| TTC max | 1.0 s | 1.0 s | 1.0 s |
| Trig width | 1 m | 1 m | **3 m** |
| Braking level max | 0.7 g | 0.7 g | 0.7 g |
| Ramp-up time | 300 ms | 300 ms | 300 ms |
| Cut-off speed | 60 km/h | **No limitation** | No limitation |
| Light conditions | All | All | All |

In order to derive injury risk functions for AIS3+ head injury, logistic regression analysis was conducted following Rosén and Sander (2009). The risk as a function of impact speed, p($v$), was assumed to have the following form (logistic regression) p($v$) = 1/(1 + exp(– a – b$v$)), where $v$ is the impact speed and a, b two parameters to be estimated by the method of maximum likelihood.

A bicyclist detected by the active system, so that autonomous braking could be activated, would be struck at an impact speed $v' \leq v$ (where v is the impact speed without activation). Hence, the relative risk becomes $p(v')/p(v)$ and so

$$E_{active}^{total} = \frac{1}{N}\sum_{i=1}^{N} 1 - \frac{1 + \exp(-a - bv_i)}{1 + \exp(-a - bv'_i)} \quad (2)$$

**Integrated protection system**

The integrated countermeasure combined both the passive and active countermeasures. To derive its effect, we first estimated new impact speeds from the active system and then estimated the risk reduction from the passive system with the same method previously used but using the new impact speeds.

Furthermore, the head WAD could change due to the autonomous braking. We know that the sliding effect of the bicyclist on the hood is speed dependent, leading to higher wrap around distance for higher impact speeds. On the other hand, pre-impact braking leads to pitching (lowering) of the car front which results in increased sliding. This was considered in a previous study for pedestrians and these two effects more or less cancelled

each other out and resulted in no total effect for pedestrians. We do not have this information for bicyclists so for simplicity we decided not to adjust the impact point for braking in this study.

A bicyclist that would have been helped only by the passive countermeasure has a relative risk of $1 - e(v)$. A bicyclist that would have been helped only by the active countermeasure has a relative risk of $(1 + \exp(-a - bv))/(1 + \exp(-a - bv'))$. Finally, a bicyclist that would have been helped by both countermeasures has a relative risk of $(1 - e(v'))(1 + \exp(-a - bv))/(1 + \exp(-a - bv'))$. Putting the pieces together, we get

$$E_{integrated}^{total} = \frac{1}{N}\sum_{i=1}^{N}(1 - (1 - e(v_i'))\frac{1+\exp(-a-bv_i)}{1+\exp(-a-bv'_i)}) \quad (3)$$

where $v_i' = v_i$ if the active countermeasure is not used and $e(v_i') = 0$ if the passive countermeasure is not helping. See also earlier study by Fredriksson & Rosén (2012) for more details and derivation of the effectiveness functions.

**Statistical methods**

To derive confidence intervals for the estimated effectiveness, we applied the bootstrap method (Efron and Tibshirani 1993). In this procedure, the original sample of 34 cases was used to generate another 1000 samples, each containing 34 cases, by random re-sampling with replacement from the 34 original cases. The effectiveness was then re-derived for each of the 1000 samples. Finally, the lower and upper 95% confidence bounds were chosen as the 2.5th percentile and 97.5th percentile of the 1000 estimates of effectiveness respectively (i.e. the value of the 975th largest and 25$^{th}$ largest estimates of effectiveness). The bootstrap samples were further used to compare the difference between the integrated system and the passive and active countermeasures respectively. For each bootstrap sample, the ratio of the integrated effectiveness and the passive and active effectiveness, respectively, were calculated. 95% confidence intervals for these ratios were formed as the 2.5$^{th}$ and 97.5th percentiles of the 1000 bootstrap estimates.

**RESULTS**

In total we had 34 cases with sufficient information to estimate both passive and active protection potential. The bicyclists, who had no limitation on age, were on average 48 years old with a body height of 169 cm, and the car mean model year was 1996. Note that information on stature and model year was not available for all cases. The impact speed for the 34 cases, which were all AIS3+ head injured when impacted by a passenger car front, ranged from 12-91 km/h, with a mean value of 43 km/h (Table 3). 8 of the 34 bicyclists were fatally injured. GIDAS does not conclude what injury was fatal.

**Table 3. Descriptive statistics for the bicyclists in the sample (N = 34)**

| | *mean* | *median* | *min* | *max* | *n* |
|---|---|---|---|---|---|
| age (years) | 48 | 55 | 13 | 81 | 34 |
| stature (cm) | 169 | 171 | 107 | 191 | 28 |
| car model year | 1996 | 1996 | 1986 | 2011 | 33 |
| car impact speed (km/h) | 43 | 38 | 12 | 91 | 34 |

In 1 of the 34 cases (3%) the bicyclist was severely head injured by the hood area alone, 6% from the lower windshield / I-panel area alone, 21% from the A-pillars alone, 24% from the roof edge alone, 9% from the remaining glass area alone, while 3% had at least one severe head injury from other parts of the car and 35% from the ground/surrounding. See Figure 3. This means that the passive system can potentially address all AIS3+ head injuries for 29% of the bicyclists for the system 1&2 protection systems and 53% for the more advanced system covering also the roof edge (system 3).

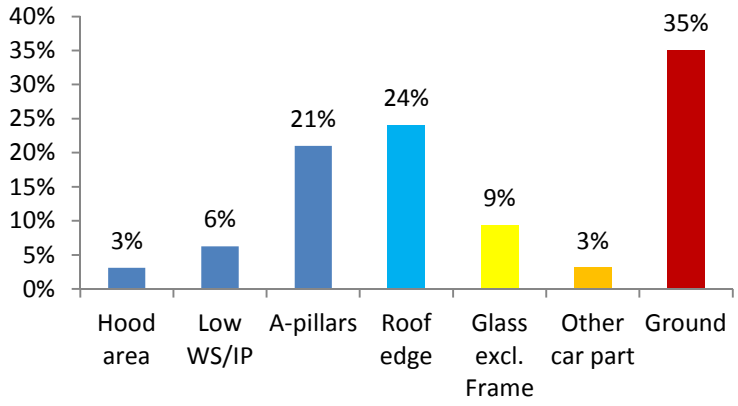


***Figure 3. Distribution of injury sources (all AIS3+ head injuries for an injured bicyclist caused by the given area, except for "other" where only one injury from this area is sufficient to classify as "other")***

The risk curve for AIS3+ bicyclist head injury was developed, see Figure 4. It shows the observed rates of AIS3+ head injured bicyclists at different intervals of impact speed and the best-fit logistic regression curves. The risk of severe (AIS3+) head injury is given in the function, $p(v) = 1/(1+\exp(6.1-0.080v))$.

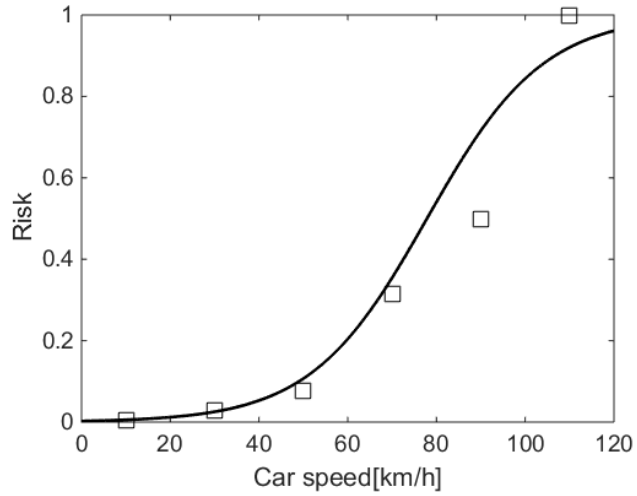


***Figure 4. AIS3+ head injury risk for bicyclists impacted by passenger cars, and the corresponding empirical injury rates***

Hence, the total effectiveness for active systems becomes:

$$E_{active}^{total} = \frac{1}{N}\sum_{i=1}^{N} 1 - \frac{1 + \exp(6.1 - 0.080 v_i)}{1 + \exp(6.1 - 0.080 v'_i)} \quad (4)$$

and for integrated systems:

$$E_{integrated}^{total} = \frac{1}{N}\sum_{i=1}^{N}(1 - (1 - e(v_i'))\frac{1+\exp(6.1-0.080 v_i)}{1+\exp(6.1-0.080 v'_i)}) \quad (5)$$

**Estimated effectiveness**

Using the risk reduction functions the possible effectiveness of the protection system could be estimated for each case. Note that if any of the AIS3+ head injuries was caused by a source outside the protected area, on the car or in the surrounding, the effectiveness of the protection system in that case was set to 0. Finally, the total effectiveness of the passive protection system for the 34 cases was summarized. The passive protection system, based on a deployable hood and a windshield airbag, was estimated in the baseline version to protect 21% of the severely head injured bicyclists from their AIS3+ head injury (system 1); that is, the AIS3+ head injury effectiveness was estimated to be 21% (CI: 10-34%). For system 2, with a different airbag design protecting better at higher speeds, but with the same coverage area, the effectiveness increased to 28% (CI: 14-45%). Finally if the passive system coverage area was increased to also protect the roof edge (system 3), the effectiveness increased to 38% (CI: 24-54%).

The effectiveness of the active AEB system was estimated in a similar manner, estimating in each case the reduction in risk achievable by applying the AEB system, by estimating the maximum time the brakes could be applied (depending on bicyclist visibility) and maximum braking level allowed depending on the road friction condition.

The AEB system was estimated to protect 26% (CI: 14-38%) with the baseline version (system 1), activated up to 60 km/h with the 40 degree field of view sensor and narrow trig width. When the active system was enhanced to activate for bicyclists in all impact speeds (system 2), the effectiveness increased to 30% (CI: 15-43%). Finally, if the system was enhanced further to activate also at a higher field of view and trig width (system 3), it could potentially save 48% (CI: 32-63%) of the bicyclists from their severe head injury.

By combining the passive and active protection systems a system is created that first brakes the car autonomously when a bicyclist is detected and if the impact cannot be avoided the passive system is activated to mitigate the head injury.

For the baseline system, with version 1 passive and active systems, the integrated system effectiveness was 38% (CI: 24-52%). The more advanced system, with version 2 passive and active systems, increased the effectiveness to 48% (CI: 32-64%), while the most advanced system, with version 3 passive and version systems, resulted in an integrated effectiveness of 62% (CI: 47-76%) (see Figure 5). The integrated systems had 29%-62% higher effectiveness than the best individual systems.

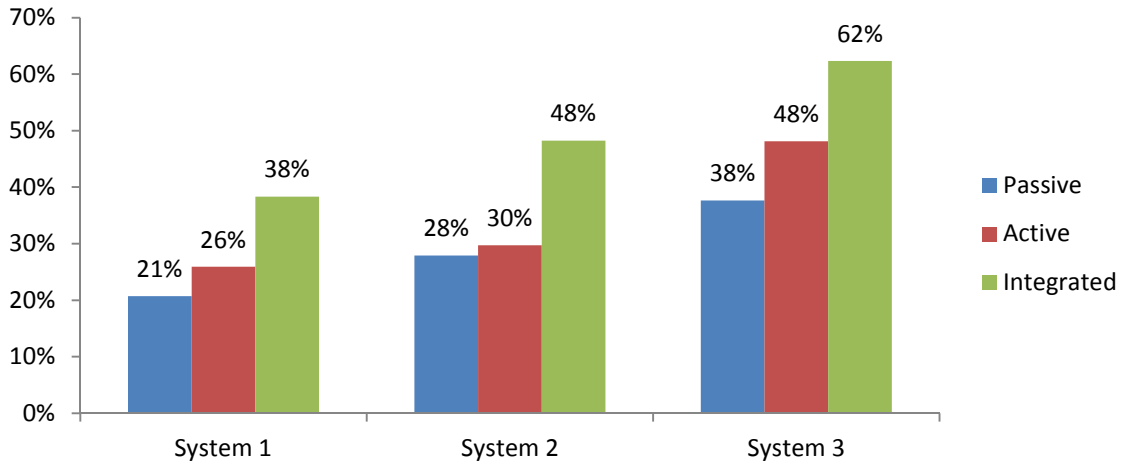


***Figure 5. Estimated effectiveness of the active, passive and integrated systems for three different combinations***

**Significance estimation** The ratios of the integrated and passive respectively active countermeasures were calculated, see Table 4. In all cases, the confidence intervals contained values constantly larger than 1. Thus, the effectiveness of the integrated countermeasures was significantly higher than either of the passive and active countermeasures alone.

**Table 4. Significance calculations of integrated effectiveness relative to active and passive effectiveness**

| | $E_{integrated}/E_{passive}$ *(95% CI)* | $E_{integrated}/E_{active}$ *(95% CI)* |
|---|---|---|
| Version 1 | 1.9 (1.2-3.2) | 1.6 (1.2-2.3) |
| Version 2 | 1.8 (1.2-2.9) | 1.7 (1.2-2.7) |
| Version 3 | 1.7 (1.2-2.5) | 1.3 (1.1-1.7) |

## DISCUSSION

Just like in the earlier study on pedestrians we made the assumption that head impact speed was equal to the car impact speed. Earlier studies on pedestrians and bicyclists have shown both higher and lower head impact speeds compared to the car impact speed. We also used the same passive risk curves for severe (AIS3+) head injury as in the previous study on pedestrians, since this is a risk curve based on HIC value, i.e. the loading that the head experiences, so it should not differ for different road users. However, the most important difference between pedestrians and bicyclists is the head impact point, the injury source on the car, and that was considered in this study.

For the active system we used a new risk curve since this is developed for the respective road user type and includes e.g. the difference in injury location. Here we assumed that the head impact point did not change however when an active protection system was introduced. This is a simplification, but as discussed in the method section, also this parameter could change in both directions. The decrease in impact speed by an auto-brake system is known to result in less sliding of the vulnerable road user on the car (less wrap around distance

to head impact) but in the same time the pitch of the car front leads to more sliding (larger wrap around distance). Therefore the assumption was made that the head impact point was unchanged. In a future study this could potentially be studied in full-body simulations with a human body model, but then very precise information about the accident, pedestrian direction, exact gait position, arm position, body angle etc is necessary which is often not known.

This study was performed using the same analysis method and data source as a previous study for pedestrians (Fredriksson and Rosén 2014). Bicyclist accidents are in one sense more challenging to the active sensor since bicyclists have a higher speed than pedestrians, but also to the passive system to some extent since bicyclists impact higher on the car. The current study on bicyclists accounted for this by increasing the field of view of the active sensor, and the coverage area of the passive systems for the most advanced system. But in the same time bicyclist accidents occur more frequently in day-light and dry conditions (Fredriksson, Bylund et al. 2012; Fredriksson and Rosén 2012) which increases the ability of especially the active sensor. These studies show that there is a benefit to combine active and passive protection for bicyclists as well as for pedestrians, which shows that that active and passive systems if designed right have the potential to protect both pedestrians and bicyclists in car crashes.

We performed this study using the probably most representative and extensive traffic injury database available. By doing so, and selecting the severely head injured bicyclists, we can estimate the effectiveness of reducing severe head injury of bicyclists with different countermeasures. (Note, that we make the assumption then that we do not raise the injury level for any person.) Although our estimations of the individual systems' effectiveness could be argued to be somewhat ideal (we estimate that the passive sensor activates for all crashes and that the active sensor has no other limitations than the parameters we chose), we made the same assumptions/simplifications for the integrated as for the individual systems so the conclusions of the benefit of the integrated system compared to the individual systems should therefore be sound.

**Limitations**

The data which this study is based on is from Germany, and the conclusions are therefore not valid for countries where the car fleet or infrastructure is different.

## CONCLUSIONS

This study analyzed the benefit of combining car-mounted passive and active protection systems for bicyclists. If more and more cars in Europe are equipped with auto-brake functions is there still a need for passive protection, or can the active systems replace the passive systems?
The analysis was performed using the most representative and extensive traffic injury database in Europe, GIDAS, where all severely head injured bicyclists in car crashes were selected to study how many of those could be protected with the different protection systems. The passive system consisted of deployable hood lifters and windshield airbag, while the active system used autonomous braking. To analyze the sensitivity of the analysis three different, but according to the authors reasonable, versions of passive respectively active protection systems were included in the study. The performance of the systems was estimated based on experimental tests at different impact speeds for the passive system, and by using computer reconstructions where the sensor system was modeled for the active system.
The study shows that there is a significant benefit in combining car-mounted active and passive protection systems for bicyclists. For the different versions of the systems, the integrated system was 29%-62% more effective in protecting from injury than the best individual system.

## REFERENCES

Efron, B. and R. J. Tibshirani, Eds. (1993). An introduction to the bootstrap, Chapman & Hall/CRC.

ERSO. (2012). "CARE database -Traffic safety basic facts 2012." Retrieved 2014-03-16, from http://ec.europa.eu/transport/road_safety/specialist/statistics/care_reports_graphics/index_en.htm.

EuroNCAP. (2014). "2020 ROADMAP." from http://www.euroncap.com/technical/technicalpapers.aspx.
Fredriksson, R., P.-O. Bylund, et al. (2012). "Fatal vehicle-to-bicyclist crashes in Sweden – an in-depth study of injuries and vehicle sources." Ann Adv Automot Med **56**: 25-30.
Fredriksson, R., M. Dahlgren, et al. (2014). "A Real-Life Based Evaluation Method of Deployable Vulnerable Road User Protection Systems." Traffic Inj Prev **15**: 183-189.
Fredriksson, R., Y. Håland, et al. (2001). Evaluation of a new pedestrian head injury protection system with a sensor in the bumper and lifting of the bonnet's rear part. 17th International Technical Conference on the Enhanced Safety of Vehicles (ESV). Amsterdam, Netherlands.
Fredriksson, R. and E. Rosén (2012). "Integrated pedestrian countermeasures – Potential of head injury reduction combining passive and active countermeasures." Safety Science **50**(3): 400-407.
Fredriksson, R. and E. Rosén (2012). Priorities for Bicyclist Protection in Car Impacts – a Real life Study of Severe Injuries and Car Sources. IRCOBI (International Research Council On the Biomechanics of Impact) Conference. Dublin, Ireland.
Fredriksson, R. and E. Rosén (2014). Head Injury Reduction Potential of Integrated Pedestrian Protection Systems Based on Accident and Experimental Data – Benefit of Combining Passive and Active Systems. IRCOBI (International Research Council On the Biomechanics of Impact) Conference. Berlin, Germany**:** 603-613.
Jaguar-LandRover. (2014). "New Discovery Sport: The most capable, versatile premium compact SUV." Retrieved 2015-03-16, from http://newsroom.jaguarlandrover.com/en-in/land-rover/press-kits/2014/09/lr_discovery_sport_launch_030914/lr_discovery_sport_launch_030914/.
Kerrigan, J. R., C. Arregui, et al. (2009). Pedestrian head impact dynamics: comparison of dummy and PMHS in small sedan and large SUV impacts. 21st International Conference on the Enhanced Safety of Vehicles. Stuttgart, Germany.
Kerrigan, J. R., J. R. Crandall, et al. (2008). "A comparative analysis of the pedestrian injury risk predicted by mechanical impactors and post mortem human surrogates." Stapp Car Crash J **52**: 527-567.
Masson, C., T. Serre, et al. (2007). Pedestrian-vehicle accident : analysis of 4 full scale tests with PMHS 20th International Technical Conference on the Enhanced Safety of Vehicles (ESV), Lyon, France.
Naci, H., D. Chisholm, et al. (2009). "Distribution of road traffic deaths by road user group: a global comparison." Inj Prev **15**(1): 55-59.
NHTSA (1995). Final Economic Assessment, FMVSS No. 201, Upper Interior Head Protection. Washington DC, USA, National Highway Traffic Safety Administration.
Rosén, E. (2013). Autonomous Emergency Braking for Vulnerable Road Users. IRCOBI (International Research Council On the Biomechanics of Impact) Conference, Göteborg, Sweden.
Rosén, E., J.-E. Källhammer, et al. (2010). "Pedestrian injury mitigation by autonomous braking." Accid Anal Prev **42**(6): 1949-1957.
Rosén, E. and U. Sander (2009). "Pedestrian fatality risk as a function of car impact speed." Accid Anal Prev **41**(3): 536-542.
Searson, D. J., R. W. G. Anderson, et al. (2012). "The effect of impact speed on the HIC obtained in pedestrian headform tests." Int J Crashworthiness **17**(5): 562-570.
SIKA (2009). Road traffic injuries 2008, Statens Institut för Kommunikationsanalys.
Strandroth, J., S. Sternlund, et al. (2014). "The Correlation Between Euro NCAP Pedestrian Test Results and Injury Severity in Real-Life Crashes with Pedestrians and Bicyclists." STAPP Car Crash Journal **58**.
Thiemann-Linden, J. (2010). Bicycle Use Trends in Germany. Berlin, German Institute of Urban Affairs (Deutsches Institut für Urbanistik).
van Schijndel, M., S. de Hair, et al. (2012). Cyclist kinematics in car impacts reconstructed in simulations and full scale testing with Polar dummy. IRCOBI (International Research Council On the Biomechanics of Impact) Conference. Dublin, Ireland.
Volvo. (2012). "Volvo Car Corporation's pedestrian airbag: here's how it works." Retrieved 2014-05-22, from https://www.media.volvocars.com/global/en-gb/media/pressreleases/43844.

# OBJECTIVE EVALUATION METHOD OF VEHICLE CRASH PULSE SEVERITY IN FRONTAL NEW CAR ASSESSMENT PROGRAM (NCAP) TESTS

**Chung-Kyu Park**
**Cing-Dao (Steve) Kan**
Center for Collision Safety and Analysis, George Mason University
USA

Paper Number 15-0055

## ABSTRACT

In this study, the available metrics for evaluating the crash pulse severity are reviewed and their accessibility is evaluated by using the frontal New Car Assessment Program (NCAP) test data. The linear regression analysis and sled test simulations are conducted. The new approach is proposed to evaluate the full vehicle crash performance by quantifying the crash pulse severity and restraint system performance separately and objectively.

## INTRODUCTION

The safety of occupants in a vehicle crash is highly dependent on the performance of vehicle structure and occupant restraint system. In vehicle crash safety, the role of a vehicle structure is absorbing crash energy efficiently as well as protecting the integrity of the occupant compartment. In general, the performance of vehicle structure is described by the occupant compartment intrusion and vehicle crash pulse. Basically, the occupant restraint system is designed based on the performance of the vehicle structure. So, it is desirable to evaluate the performance of vehicle structure objectively and quantitatively.

In frontal vehicle crash tests, occupant compartment intrusion and vehicle crash pulse are the most fundamental responses of a vehicle's structure. The occupant compartment intrusion is considered as an objective metric for quantifying the deformation severity of a vehicle structure. In general, a large compartment intrusion increases the injury probability of lower extremity of occupants. The vehicle crash pulse is the time history of vehicle acceleration and is used to calculate the changes of velocity and dynamic crush of a vehicle by integration. The vehicle crash pulse is closely related to the head and chest injuries of occupants. However, the severity of the vehicle crash pulse is difficult to be quantified objectively because the injury responses of dummy head and chest are also closely associated with restraint system performance. The crash pulse severity should be an objective measure of how severely the vehicle crash pulse has an effect on the occupant injury. Basically, it is regarded that less severe crash pulses possibly lead to less severe occupant injury.

Recently, there have been many vehicle safety research activities by re-designing current vehicles. For example, a current vehicle is light-weighted by using light-weight materials, and enforced structurally to meet the requirements of new regulatory tests (e.g. IIHS small-overlap frontal test and NHTSA oblique frontal test). When a current vehicle is re-designed, its crash pulse is changed accordingly and existing restraint system is not performing as it was designed any more. Then, it is difficult to conclude how its crash performance gets better or worse than the original one, especially in terms of crash pulse.

Many metrics were introduced and utilized to evaluate the severity of vehicle crash pulse [1-11]. Those metrics are derived from vehicle crash pulse in the frontal impact and can be categorized into 4 groups in the way of how occupant responses are considered. However, their assessability of the crash pulse severity is still uncertain. The objective of this study is to evaluate the assessability of available metrics for quantifying vehicle crash pulse severity in front crash. The vehicle crash pulses of the front New Car Assessment Program (NCAP) tests are utilized. Also, a new approach to evaluate the full vehicle crash performance is proposed.

## REVIEW OF EXISTING METRICS

In this study, some of existing metrics for evaluating vehicle crash pulses in frontal vehicle crash are reviewed. The existing metrics can be categorized into four groups: (1) metrics based on vehicle crash pulse only, (2) metrics based on vehicle crash pulse with assumed occupant response, (3) metrics based on vehicle crash pulse with actual

occupant response, and (4) combined metrics with the aforementioned metrics. The velocity $v(t)$ and displacement $d(t)$ are obtained by integration and double integration of the acceleration $a(t)$, respectively.

**Category1: Metrics Based on Vehicle Crash Pulse Only**

In the category1, the metrics are obtained from the vehicle crash pulse only. Dummy responses in the test are not considered. Therefore, these metrics are independent of occupant restraint system and represent an objective, quantified value of the vehicle crash pulse. However, they can hardly predict dummy responses.

- ***Maximum acceleration*** $(a)_{\max}$ is simply the maximum value of a vehicle acceleration curve over the duration of the crash event.

- ***Moving average acceleration*** $(\bar{a})^{\Delta t}$ is calculated as

$$(\bar{a})^{\Delta t} = \frac{1}{\Delta t}\int_{t}^{t+\Delta t} a(\tau)d\tau\,, \tag{1}$$

  where $t$ is time and $\Delta t$ is a moving time interval. If $\Delta t$ is the duration of the crash event, the moving average acceleration becomes the average acceleration. The upper bar indicates the average value. In general, ***maximum moving average acceleration*** $(\bar{a})^{\Delta t}_{\max}$ is used.

- ***Delta-V*** $\Delta V$ is the total vehicle velocity change over the duration of the crash event, as expressed by

$$\Delta V = (v)_{t=0} - (v)_{\min}\,. \tag{2}$$

- ***Time To Zero Velocity*** (TTZV) $(t)_{v=0}$ is the time when vehicle velocity becomes zero.

- ***Maximum dynamic displacement*** $(d)_{\max}$ is simply the maximum value of a vehicle displacement curve over the duration of the crash event.

**Category2: Metrics Based on Vehicle Crash Pulse with Assumed Occupant Response**

In the category2, an occupant restraint system is assumed and the metrics are derived from the dummy responses with the assumed restraint system under a given vehicle crash pulse. So, these metrics are independent of actual dummy responses in tests, but they are dependent on a virtual, uniform restraint system. Hence, they represent the objective quantified value of vehicle crash pulse and can predict dummy responses.

In general, the vehicle crash model and the restraint system are simplified in the category2. The common simplified model is a Spring-Mass (SM) system as shown in Figure1. In the SM model, the occupant is assumed as a point mass and the restraint system is a simple spring system. Subscripts $V$ and $O$ stand for vehicle and occupant, respectively. $M$ is the vehicle mass, $m$ is the occupant mass, $k$ is the spring stiffness, and $\delta$ is the initial slack between the occupant and restraint system. The upper wave indicates the prescribed motion which is a given vehicle crash pulse. In the actual crash test, the spring is highly nonlinear to represent the operation of seatbelt and airbag.

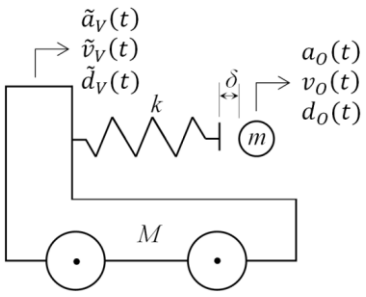


***Figure1. The model of a simple Spring-Mass (SM) system.***

- The Equation Of Motion (EOM) of the SM model is defined as

$$a_O(t) + \omega_n \cdot d_O(t) = \tilde{a}_V(t), \tag{3}$$

where $\omega_n = \sqrt{k/m}$. The ***analytical solution of the EOM*** $a_O^{SM}$ is in the form of the convolution integral expressed as

$$a_O^{SM}(t) = v_V(0) \cdot \omega_n \int_0^t \tilde{a}_V(\tau) \cdot \sin\{\omega_n(t-\tau)\} d\tau\,. \tag{4}$$

- In the flail-space model [1], the spring stiffness *k* is assumed to be zero, which indicates that no restraint system is present. So, the occupant moves freely. The allowable moving distance of the point mass is assumed to be 0.6 m. At the instant of occupant impact with the occupant compartment interior, the largest difference in velocity is termed the ***Occupant Impact Velocity*** (OIV). Once the impact with the interior occurs, the occupant is assumed to remain in contact with the interior and to be subjected to any subsequent vehicular acceleration.

Figure2 shows the velocity curves in a frontal NCAP test. The black curve is the test vehicle velocity and the red curve is the test occupant (chest) velocity. The occupant is restrained by a certain restraint system. In special cases, it can be assumed that the occupant velocity is prescribed, like the blue dot curve in Figure2, by a special restraint system. In this special case, the occupant translates freely with the initial velocity $v_O(0)$ until the point A. The point A represents the distance of the initial slack $\delta$. This phase is called free flight. After reaching the point A, the occupant is decelerating with a constant acceleration $a_O$ until it reaches the point B. At the point B, the relative velocity $v_{O/V}$ of the occupant to the vehicle becomes zero. This phase between the point A and the point B is called ideal restraint because the occupant has the constant minimum acceleration under a given crash pulse. So, this prescribed occupant velocity is the ideal velocity of the occupant in frontal crash and this special restraint system can be considered as the ideal restraint system. Compared to the SM model, the spring stiffness *k* will be nonlinear to maintain the constant deceleration of the occupant.

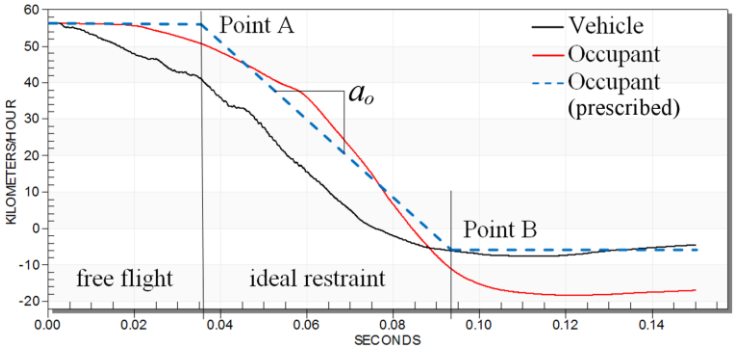


***Figure2. Prescribed occupant response in the NCAP test.***

- In the ***Occupant Load Criterion*** (OLC) metric [2], it is assumed that the initial slack $\delta$ is 65 mm and the distance between the vehicle and the occupant at the point B is an additional 235 mm. Then, given the point A and the point B, the constant acceleration $a_O$ becomes the critical occupant response which is called the OLC (G). Basically, the OLC means the minimum occupant acceleration induced by a given crash pulse under the protection of the ideal restraint system.

- In the ***Maximum Chest Travel*** (MCT) metric [3], it is assumed that the initial slack $\delta$ and the constant acceleration $a_O$ are predefined. Then, the distance between the point A and the point B is the critical occupant response. This distance is called the MCT (mm).

**Category3: Metrics Based on Vehicle Crash Pulse with Actual Occupant Response**

In the category3, metrics are obtained from both vehicle crash pulse and actual dummy responses in the test. The metrics are dependent on the dummy responses and restraint system performance in tests. Basically, those metrics identify the contribution of restraint system performance to the full vehicle crash performance. So, they quantify the vehicle structure performance in terms of crash pulse and the restraint system performance, but they are not the objective, quantified value. In general, they are in percentage terms.

- Occupant restraint performance during vehicle deceleration is measured as the relative velocity of the occupant in vehicle divided by the maximum velocity change of the vehicle which is $\Delta V$. This ratio is called the ***Restraint Quotient*** (RQ) [4] expressed as

$$RQ_C = \frac{v_{OC/V}}{\Delta V}, \tag{5}$$

where

$$v_{OC/V} = v_{OC} - v_V \tag{6}$$

and the subscript *C* stands for chest. It normally varies between 0 and 1. A RQ value of 0 represents an occupant rigidly coupled to the vehicle interior and a value of 1 indicates that the occupant attains the total velocity change of the vehicle before impacting the vehicle interior. The lower the RQ, the better the restraint performance in a crash. The relative kinetic energy per unit mass is calculated using the maximum relative occupant velocity normalized by a velocity of 5 m/s, which is called ***kinetic energy factor*** (*E*) [4] expressed as

$$E_C = \frac{(v_{OC/V})^2_{\max}}{5^2}. \tag{7}$$

- In the SM model in Figure1, the energy per unit mass (or energy density) of an occupant can be expressed as

$$e = \int_0^{d_V} a_O(x)dx_O = \int_0^{d_V} a_O(x)d(x_V + x_{O/V}) = e_{rd} + e_{rs}, \tag{8}$$

where

$$e_{rd} = \int_0^{d_V} a_O(x)dx_V, \tag{9}$$

$$e_{rs} = \int_0^{d_V} a_O(x)dx_{O/V} \text{ , and} \tag{10}$$

$$x_{O/V} = x_O - x_V . \tag{11}$$

$e_{rd}$ is called the ride-down energy density and $e_{rs}$ is the restraint energy density [5-10]. The ride-down energy is attributed to the crush of the front structures of the car and the restraint energy is dissipated by the crushing of the restraint system components. Then, the ***ride-down efficiency*** $\mu$ is obtained from

$$\mu = \frac{(e_{rd})_{\max}}{\{v(0)\}^2/2} . \tag{12}$$

This metrics reflect the percentage of total kinetic energy absorbed by the vehicle structure.

**Category4: Combined Metrics Using the Aforementioned Metrics**

In the category4, the metrics are defined as the linear combination of the aforementioned metrics. Mostly, certain metrics are combined to improve better prediction of occupant injury.

- In the ***Expanded ΔV*** [11], $\Delta V$ is expanded by combining with other metrics. Three expanded $\Delta V$ metrics were proposed as

$$\text{Expanded } \Delta V\text{-1} = a_1\Delta V + a_2\mu + a_3E_c , \tag{13}$$

$$\text{Expanded } \Delta V\text{-2} = a_1\Delta V + a_2(\bar{a})_{\max}^{\Delta t} + a_3RQ_c , \quad \text{and} \tag{14}$$

$$\text{Expanded } \Delta V\text{-3} = a_1\Delta V + a_2(\bar{a})_{\max}^{\Delta t} + a_3E_c , \tag{15}$$

where $a_1$,$a_2$, and $a_3$ are coefficients.

- In the **OLC++** [2], OLC was augmented as

$$\text{OLC++} = a_1\text{OLC} + \frac{a_2}{(t)_{v=0}} + a_3(\bar{a})_{\max}^{\Delta t} , \tag{16}$$

where $a_1$,$a_2$, and $a_3$ are coefficients.

**DATA ANALYSIS**

The aforementioned metrics' assessability of crash pulse severity is evaluated using frontal NCAP test data. A total of 60 frontal NCAP test data, collected from the MY 2012 vehicle test program, are analyzed. The linear regressions of each pair of all metrics and their $R^2$ values are examined. The larger value of $R^2$ indicates better fits. It is considered that the pair of two metrics has a linear correlation if the $R^2$ is greater than 0.5.

It seems that the metrics in Category2 are the fairly appropriate metrics for evaluating the crash pulse severity since they are the objective metrics associated with both vehicle crash pulse and uniform restraint system. So, the relationship between the metrics in Category2 and other metrics are investigated.

Table1 summarizes the linear regression results between Category1 and Category2. The $R^2$ values of each pair are shown in Table1. It is observed that the OLC and MCT have relatively high $R^2$ values with maximum acceleration,

maximum moving average acceleration, TTZV, and maximum dynamic crush. However, OIV has low $R^2$ values. Especially, Delta-V has very low $R^2$ values with OLC and MCT. Interestingly, although the metrics in Category1 are purely obtained from vehicle crash pulse only without dummy response information, the metrics in Category1 have a good linear correlation with the OLC and MCT in Category2.

**Table1. Linear regression results between Category1 and Category2 (highlighted cell indicates that $R^2$ is greater than 0.5).**

| $R^2$ | OIV | OLC | MCT |
|---|---|---|---|
| Max. Accel. | 0.214 | 0.527 | 0.445 |
| Max. Moving Average Accel. ($\Delta t$=25msec) | 0.477 | 0.735 | 0.607 |
| Delta-V | 0.395 | 0.002 | 0.029 |
| TTZV | 0.281 | 0.859 | 0.793 |
| Max. Dynamic Crush | 0.051 | 0.678 | 0.704 |

Table2 summarizes the linear regression results between Category2 and Category3. It is observed that the OLC and MCT have high $R^2$ values with the metrics in Category3, but OIV has very low $R^2$ values. Basically, the metrics in Category3 describe the actual effects of the vehicle crash pulse and restraint system on the dummy responses in the test. So, the high linear correlation between OLC and MCT in Category2 and the metrics in Category3 indicates that the OLC and MCT are able to predict the effect of the vehicle crash pulse on the dummy response and assess the crash pulse severity adequately.

**Table2. Linear regression results between Category2 and Category3 (highlighted cell indicates that $R^2$ is greater than 0.5).**

| $R^2$ | | OIV | OLC | MCT |
|---|---|---|---|---|
| Driver | $RQ_C$ | 0.051 | 0.669 | 0.679 |
| | $E_C$ | 0.098 | 0.705 | 0.680 |
| | Ride-Down Efficiency | 0.058 | 0.617 | 0.624 |
| Passenger | $RQ_C$ | 0.056 | 0.515 | 0.504 |
| | Ride-Down Efficiency | 0.120 | 0.474 | 0.447 |

Table3 summarizes the linear regression results between the aforementioned metrics and dummy injuries in the NCAP tests. It is observed that the $R^2$ values of all pairs between metrics and dummy injuries are very low. The Delta-V is commonly used to address the crash severity, but it can hardly predict the dummy injuries as well.

**Table3. Linear regression results between metrics and occupant injury responses.**

| $R^2$ | | Driver (H3 50% male) | | | Passenger (H3 5% female) | | |
|---|---|---|---|---|---|---|---|
| | | $HIC_{15}$ | Chest Peak Accel. | Chest Peak Deflection | $HIC_{15}$ | Chest Peak Accel. | Chest Peak Deflection |
| Max. Accel. | | 0.000 | 0.043 | 0.057 | 0.003 | 0.125 | 0.015 |
| Max. Moving Average Accel. ($\Delta t$=25msec) | | 0.002 | 0.139 | 0.064 | 0.013 | 0.284 | 0.005 |
| $\Delta V$ | | 0.003 | 0.007 | 0.019 | 0.005 | 0.001 | 0.055 |
| TTZV | | 0.005 | 0.101 | 0.060 | 0.018 | 0.339 | 0.016 |
| Max. Dynamic Crush | | 0.022 | 0.055 | 0.036 | 0.017 | 0.224 | 0.025 |
| OIV | | 0.023 | 0.070 | 0.039 | 0.001 | 0.186 | 0.002 |
| OLC | | 0.014 | 0.090 | 0.023 | 0.026 | 0.342 | 0.005 |
| MCT | | 0.021 | 0.075 | 0.016 | 0.026 | 0.305 | 0.012 |
| Driver | RQc | 0.009 | 0.086 | 0.056 | 0.028 | 0.178 | 0.069 |
| | Ec | 0.013 | 0.084 | 0.044 | 0.030 | 0.196 | 0.042 |
| | Ride-Down Efficiency | 0.010 | 0.113 | 0.052 | 0.052 | 0.201 | 0.081 |
| Passenger | RQc | 0.002 | 0.036 | 0.034 | 0.026 | 0.109 | 0.075 |
| | Ride-Down Efficiency | 0.001 | 0.106 | 0.067 | 0.020 | 0.137 | 0.120 |
| Expanded $\Delta V$-1 | | 0.012 | 0.082 | 0.037 | 0.024 | 0.192 | 0.030 |
| Expanded $\Delta V$-2 | | 0.005 | 0.110 | 0.053 | 0.022 | 0.220 | 0.042 |
| Expanded $\Delta V$-3 | | 0.010 | 0.096 | 0.043 | 0.025 | 0.217 | 0.030 |
| OLC++ | | 0.014 | 0.092 | 0.043 | 0.019 | 0.310 | 0.010 |

Based on the linear regression of the metrics shown in Table1 and Table2, it is found that some of metrics fairly can assess the crash pulse severity. Especially, it seems that the OLC has the high accessibility of crash pulse severity according to its high linear correlation to many metrics in Category1 and Category3. However, none of metrics can predict dummy injuries. Every vehicle has its own uniquely designed restraint system, and the dummy responds very

sensitively to various restraint system performances. Moreover, crash tests have very high dispersion errors in dummy injuries in general. In these circumstances, it is very difficult to predict dummy injuries in frontal crash using existing metrics.

## SLED TEST SIMULATIONS

In order to identify the effect of vehicle crash pulse and restraint system on dummy responses, sled test simulations with Hybrid III 50th male dummy FE model are conducted using all different 60 NCAP crash pulses. Two cases are considered for each sled test simulation; (1) fix dummy clearance dimensions and (2) adjust some of dummy clearance dimensions, such as CS (chest to steering hub), SCA (steering column angle), and KD (knee to dash). The uniform generic restraint system (seatbelt and airbag) is utilized for all sled test simulations. The dummy responses in sled test simulations are monitored.

Figure3 shows the linear regressions of chest peak accelerations in NCAP tests and sled test simulations. They show little correlation between two tests. Since the sled test simulations utilize the NCAP crash pulses, main difference between two tests is that all the different restraint systems are used in NCAP tests and one uniform restraint system is used in sled test simulations. It can be interpreted as the data dispersion is mainly caused by the various restraint system performances in the NCAP test vehicles.

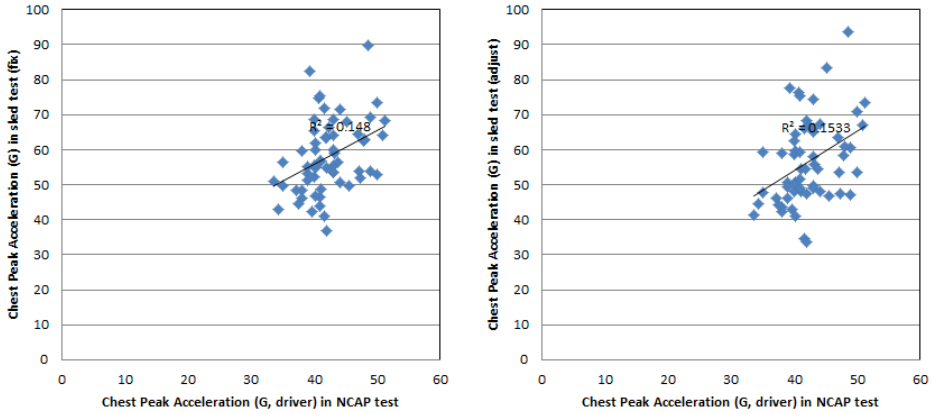


***Figure3. Data distribution of chest peak acceleration in NCAP tests vs. chest peak acceleration in sled test simulations***

Figure4 shows the linear regressions of chest peak accelerations in sled test simulations and the OLC metric. They show high correlation between two metrics. In other words, the OLC metric is able to predict dummy responses and injuries if the uniform restraint system is used in all test vehicles. Also, it can be observed that the different dummy clearance dimension makes the degree of data dispersion increase, but the linear correlation is still high.

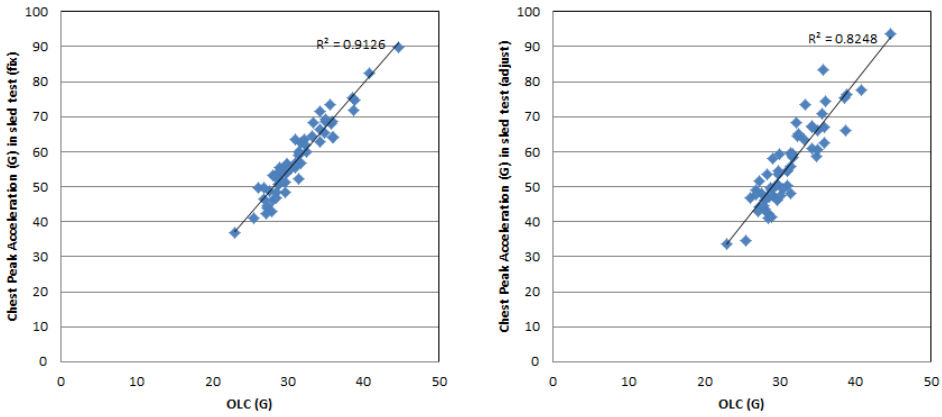


***Figure4. Data distribution of OLC vs. chest peak acceleration in sled test simulations***

## DISCUSSION

It seems that the Category3 provide an ideal approach to evaluate a full vehicle crash performance by quantifying both the vehicle structure performance and restraint system performance separately, where the vehicle structure performance includes only the crash pulse severity, but not the occupant compartment intrusion. However, the metrics in the Category3 are objective. The performance of the restraint system in vehicles are various in frontal crash tests. Moreover, the restraint system performance is dependent on the crash pulse severity, which means that the restraint system performance is coupled with crash pulse severity. So, it is difficult to quantify the restraint system performance objectively by de-coupling from the effect of a vehicle crash pulse. In this study, a new approach is proposed to evaluate the full vehicle crash performance by quantifying the crash pulse severity and restraint system performance separately and objectively. The new approach makes the restraint system performance de-coupled from the effect of the vehicle crash pulse.

Figure5 shows the three datasets of occupant chest peak accelerations with respect to maximum moving average acceleration of vehicles. The first dataset, red squares, is the OLC values. This dataset shows good linear correlation with high $R^2$ value. Basically, the OLC metric indicates the minimum occupant acceleration under a given crash pulse. Therefore, the OLC data forms the lower boundary in Figure5. The second dataset, green triangles, is the occupant peak accelerations obtained from the analytical solution (Eq. 4) of the SM model with the constant spring stiffness *k*. This dataset also shows good linear correlation with high $R^2$ value. Because the restraint system is regarded as a simple linear spring, the occupant response in the SM model under a given crash pulse is likely worse than the one with actual restraint system. Maybe the occupant response in the SM model with the linear spring will be the worst under the given crash pulse. Hence, it can be seen that the occupant peak acceleration in the SM model forms the upper boundary in Figure5. The linear regression slopes of two datasets (red squares and green triangles) are actually very close. So, the OLC metric with respect to maximum moving average acceleration of vehicles is considered as the crash pulse severity metric and the crash pulse severity index is defined by normalizing the crash pulse severity metric.

In Figure5, the third dataset, blue rhombuses, is the chest peak accelerations (driver) in the frontal NCAP tests. These data points are distributed between the lower and upper boundaries formed by two datasets (red squares and green triangles). Some data points are close to the lower or upper boundaries, that is, those data points are close to their minimum or maximum values in their crash pulse severity levels. The rational explanation of the data dispersion between two boundaries is because the different restraint system performance in every vehicle in the frontal NCAP tests. So, in order to de-couple the restraint system performance from the crash pulse effect, the third dataset is mapped to the OLC-axis plane and normalized to generate the restraint system performance index.

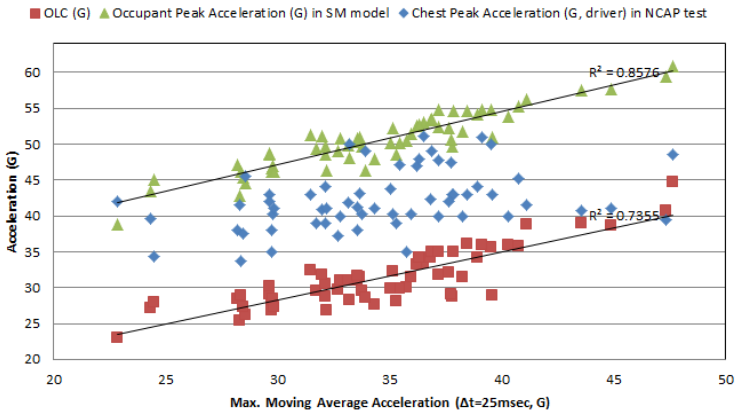


***Figure5. Data distribution of max. moving average acceleration vs. OLC, occupant peak acceleration in SM model, and chest peak acceleration (driver) in NCAP test.***

The crash pulse severity index and restraint system performance index are objective and independent each other. Two indices describe the full vehicle crash performance in the frontal NCAP test. Figure6 shows the data distribution of the full vehicle crash performance in two indices plane, which is very informative. For instance, the point A in Figure6 means low crash pulse severity but poor restraint system performance, and the point B indicates

high crash pulse severity but good restraint system performance. Practically, when the vehicle crash pulse is known, the plot in Figure5 shows the crash pulse severity and the range of the dummy chest peak acceleration, and the plot in Figure6 tells the performance of the current vehicle's restraint system in the frontal crash.

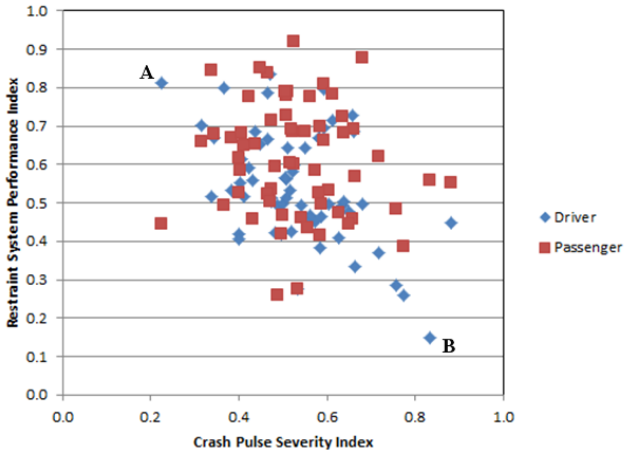


***Figure6. Data distribution of crash pulse severity index vs. restraint system performance index.***

## CONCLUSIONS

In this study, the existing metrics for evaluating the crash pulse severity are reviewed and categorized into four groups: (1) metrics based on vehicle crash pulse only, (2) metrics based on vehicle crash pulse with assumed occupant response, (3) metrics based on vehicle crash pulse with actual occupant response, and (4) combined metrics with the aforementioned metrics.

Their accessibility of crash pulse severity is evaluated by using the frontal NCAP test data. A total of 60 frontal NCAP test data, collected from the MY 2012 vehicle test program, are analyzed. The linear regression analysis shows that some of metrics fairly can assess the crash pulse severity. Especially, it seems that the OLC has the high accessibility of crash pulse severity according to its high linear correlation to many metrics in Category1 and Category3. However, none of metrics can predict dummy injuries.

The sled test simulations are conducted using the NCAP pulses. The uniform generic restraint system (seatbelt and airbag) is utilized for all sled test simulations. The results conclude that the various restraint system performances in the NCAP test's vehicles cause a big variation in dummy responses and make it difficult to predict dummy injuries in the frontal NCAP test.

The new approach is proposed to evaluate the full vehicle crash performance in the frontal NCAP test by quantifying the crash pulse severity and restraint system performance separately and objectively. The crash pulse severity index is defined by normalizing the OLC metric, and then the restraint system performance index is defined by de-coupling the restraint system performance from the crash pulse effect. Two indices describe the full vehicle crash performance in the frontal NCAP test. The new approach provides a quantitative and objective way to analyze the crash performance of a vehicle in the frontal NCAP test.

## ACKNOWLEDGEMENTS

The authors are grateful to Eun-Young Kim for data processing.

## REFERENCES

[1] J.D. Michie, "Collision risk assessment based on occupant flail-space model," *Transportation Research Record*, 1981, 796:1-9.

[2] L. Kübler, S. Gargallo, and K. Elsäßer, "Frontal crash pulse assessment with application to occupant safety," *ATZ worldwide*, 2009, 111(6):12-17.
[3] S.J. Song, S. Kim, and S. Bilkhu, "Front impact pulse severity assessment methodology," SAE Technical Paper #2005-01-1416.
[4] D.C. Viano and S. Arepally, "Assessing the safety performance of occupant restraint systems," SAE Technical Paper #902328.
[5] H. Katoh and R. Nakahama, "A study on the ride-down evaluation," Experimental Safety Vehicles, Proceeding of the 9th International Technical Conference on Experimental Safety Vehicles, pp. 190-195, 1982.
[6] N.C. Evans, L.M. Furton, and D.A. Cok, "Occupant energy management technique for restraint system analysis and design – theory and validation," SAE Technical Paper #922082.
[7] K.J. Bonello, "Occupant energy management technique for restraint system analysis and design - understanding the physics of the system," SAE Technical Paper #922083.
[8] M. Huang, J. Laya, and M. Loo, "A study on ride-down efficiency and occupant responses in high speed crash tests," SAE Technical Paper #950656.
[9] J. Wu, G.S. Nusholtz, and S. Bilkhu, "Optimization of vehicle crash pulses in relative displacement domain," *International Journal of Crashworthiness*, 2002, 7(4):397-414.
[10] J. Wu, S. Bilkhu, and G.S. Nusholtz, "An impact pulse-restraint energy relationship and its applications," SAE Technical Paper #2003-01-0505.
[11] D.J. Gabauer, "Predicting occupant injury with vehicle-based injury in roadside crashes," Dissertation, Virginia Polytechnic Institute and State University, 2008.

This paper has been peer-reviewed and published in a special edition of *Traffic Injury Prevention* 16(S1), by Taylor & Francis Group. The complete paper will be available on the *Traffic Injury Prevention and www.NHTSA.gov* websites on June 8, 2015.

To access all Peer-reviewed papers please copy and paste the link below into your browser to access the papers.

http://www.tandfonline.com/toc/gcpi20/16/sup1

# AEB REAL WORLD VALIDATION USING UK MOTOR INSURANCE CLAIMS DATA

**Murray Doyle**
**Alix Edwards**
**Matthew Avery**
Thatcham MIRRC Research
UK

Paper Number 15-0058

## ABSTRACT

City Safety is a low-speed autonomous emergency braking (AEB) technology, first made available as standard by Volvo on their XC60 model series, and released in the UK in 2008. This technology has since been made available on a growing number of models, including the high volume seller Volkswagen Golf 7. This paper presents an analysis of the impact of AEB in the UK on claim losses using real world Insurer claims data. Statistical regression was used to compare the claims losses for the XC60 to that of a SUV control cohort of vehicles without any such system, and quantify any AEB effects identified. The influences of calendar year and vehicle age on claim risk were accounted for in the analysis. Estimated claim frequencies for the XC60 were lower than those of the control cohort, in all liability types: 8% lower for Third Party Damage, 6% lower for Own Damage, and 21% lower for Third Party Injury. More recently this approach has been employed to compare claim frequencies for the Golf 7 with the Front Assist AEB system with that of a Small Family car control cohort of vehicles, with similar qualitative results observed from an analysis of the initial data available. Furthermore a study of claim damage severity based around claim costs and repair times estimated lower severity levels for the XC60 relative to control cohorts, for own damage liability, of the order of 10%-15%. This study is the first of its kind using UK claims and indicates the potential benefit of AEB technology. Further statistical analysis is intended with additional risk information for the XC60 and Golf 7, and other AEB study vehicles.

## INTRODUCTION

In recent years, collision avoidance or mitigation systems have become a feature on an increasing number of new vehicles, and show the potential to reduce injury and vehicle damage. Autonomous Emergency Braking or `AEB' is a safety technology which monitors the traffic conditions ahead and automatically brakes the car if the driver fails to respond to an emergency situation. AEB systems use various different names even where the functionality is similar. Systems also feature different sensors to monitor the traffic situation, such as cameras, lasers and radars. Some systems use a number of these together in sensor 'fusion'. These systems also have different speed ranges where they are active and they have different injury reduction potential. City Safety is a low-speed AEB technology, first made available as standard by Volvo on their XC60 model, and released in the UK in November 2008. The technology is designed to help prevent or mitigate front-to-rear impacts, at speeds up to 30 km/h, which is one of the common types of crashes. However City Safety may well have an effect in other crash configurations so long as the collision speeds are minimal and its sensor has time to allow a vehicle to react. City Safety works using a LIDAR (light detection and ranging) sensor mounted onto the upper windscreen to detect other vehicles travelling in the same direction around 6-8 metres in front of the vehicle. This technology has subsequently been fitted as standard to a number of other Volvo vehicles. This sensor is manufactured by Continental and is low cost, and as such has allowed proliferation.

The Volkswagen Golf 7 has the Front Assist AEB system fitted as standard to all of its trim levels with the exception of the base version, and has been available in the UK since November 2012. This system consists of a long-range RADAR (radio detection and ranging) manufactured by Bosch and fitted to the front grille, and can detect vehicles up to 80m ahead. Front Assist applies full braking up to 30km/h, and between 30-80km/h provides driver warning of a stationary object; between 30-200km/h the system applies its full capacity of driving warnings, partial braking and brake assistance.

A number of international studies have used real world data to establish the impact of AEB on claims' frequency and cost. In the USA the Highway Loss Data Institute (HLDI) have conducted statistical studies around the experience of the Volvo XC60 and S60 compared with appropriate vehicle control cohorts, while controlling for factors such as age, gender, population density, US State, and calendar year [1-2]. Since the City Safety system has been standard fit, identification of a cohort of appropriate vehicles was simple. Their research also addresses a possible `Volvo-effect' by comparing the loss experience of these Volvo City Safety vehicles against Volvos without it. Their most recent published results on this demonstrated frequency reductions arising from City Safety [3-4], for each of 1st and 3rd party damage and 3rd party injury liabilities. A similar analysis of damage severity using claim cost data generated mixed results.

A Swedish study carried out jointly by the Volvo Car Corporation and the leading Swedish Insurer Volvia focused solely on rear-end crashes [5]. In particular the real world data was used to measure the effectiveness of City Safety in avoiding crashes for the striking vehicle, by comparing the XC60 against other Volvo car models without this technology, while controlling for car ownership and size types. Their analysis demonstrated 23% effectiveness for City Safety in reducing front-into-rear crashes, when compared against a selection of other Volvo models, and 30% effectiveness when compared against XC70. Another recent Swedish study undertaken by Folksam [6] to analyse police reported front-into-rear crashes with at least one injured occupant, used the induced exposure method to compare a range of City Safety models to a selection of different control cohorts and for different impact speed ranges. Results demonstrated a range of levels of effectiveness of City Safety. A preliminary analysis was carried out by AZT Automotive/Allianz on the claims experience for the XC60 City Safety in Germany [7]. In their modelling of this they compared the XC60 to a number of its competitors, while controlling for a number of factors, for both comprehensive coverage and third party liability coverage. The conclusion of this study indicated no clear City Safety effect on claim frequency or average; however the selection of competitor vehicles was limited.

Because avoiding or mitigating the speed/severity of a crash is going to have a beneficial effect for society by reducing injuries and damage to vehicles, it is important to study the impact of such systems on UK roads. The research presented in this paper is concerned with an analysis of the effect of the Volvo City Safety and Volkswagen Front Assist on UK claim experience using available real world data, and the implications for injury reduction.

## METHODS

This study uses real world insurance claims data to analyse the effects of AEB on claim frequencies and costs, focusing primarily on the Volvo XC60 with City Safety fitted as standard since November 2008, but also the Volkswagen Golf 7 with its Front Assist system. All collision types are considered, not just front-into-rear impacts that AEB is designed to address. Potential AEB benefit is measured by comparing the XC60 against a control cohort of appropriate small SUV models without AEB fitted, and similarly for the Golf 7 (AEB) and a small family car control cohort.

The XC60 sits in the compact (small) SUV class, with a UK new purchase price varying between £25,000 and £40,000 at the time of writing. Some are fitted with 4-wheel drive whilst others with 2-wheel drive. A cohort of control vehicles were selected to include some 4x4s and some `cross-overs', all seen as being similar to the XC60 and also likely to feature in any such buyer's potential list. Of these vehicles only those with build dates of 2008 or later were used. The Golf 7 is a small family car and currently the third most popular selling vehicle in the UK, launched in late 2012. AEB is fitted as standard on all its trim levels with the exception of the base model. A control cohort of small family cars was selected to compare against, which includes the Golf 6 model and Golf 7 base model.

The analysis is carried out separately across the liability types Own Damage, Third Party Damage and Third Party Injury. An Own Damage claim relates to claims payable to the insured party for damage to their vehicle. In practice this primarily includes at-fault claims involving other vehicles or fixed objects, but also covers non-fault incidents

such as hit by unknown third party, weather damage, animal strike, and possibly vandalism. A Third Party Damage claim relates to the struck vehicle or object for the third/other parties. A Third Party Injury relates to third/other parties injured through the actions of the insured/policyholder.

**Data Sources**

Two datasets featured in this study, with key characteristics and differences listed in Table 1.

**Insurer Dataset:** A request for anonymous claims data was submitted to UK Insurers in 2013 to monitor the effects of AEB. This was completed by 12 Insurers and represents nearly 60% of the motor Insurance market in the UK by gross written premium. The resulting dataset includes claims count, cost and exposure information for the XC60 and Golf 7 and their respective control cohorts. For the XC60 study claims dating 2009 to Mid-2014 were collated, and for the Golf 7 this date range was 2013 to Mid-2014. Exposure is defined in Insured Vehicle Years (IVYs), whereby a vehicle insured for 6 months would have an exposure of 0.5.

**Research Claims Database:** This database of Insurer authorised vehicle repair claims is utilised by Thatcham for research purposes, and includes approximately 90% of the UK Insurance market by volume. The claims data held within the Research Claims Database lends itself to a study of damage severity, given that it contains information on repair costs and times, for a wide range of vehicles. Claims are for all liability types, but are mostly unidentifiable in this database; however the vast majority is related to vehicle collision damage. It has been assumed that claims involving damage to a front bumper are the striking vehicle, and therefore classifiable as Own Damage; however it is noted that front bumper damage could arise if a given vehicle is struck by a reversing vehicle, but this is a relatively minor subset. This analysis has been undertaken on the XC60 only to date.

**Table**1.
**Summary of available dataset characteristics and differences.**

| | Insurer Dataset | Research Claims Database Dataset |
|---|---|---|
| Liability Type | Identifiable by Own Damage, Third Party Damage, Third Party Injury | Not available; estimates with front bumper damage assumed to be Own Damage |
| Impact circumstance | Not available | Not available |
| Claim Status | Settled and outstanding | Authorised Insurer claims; some retail |
| Claim Count | Split by vehicle Make/Model/Variant | Split by vehicle Make/Model/Bodyshape |
| Claim Cost | Cost to Insurer; Include ancillary costs where appropriate | Repair costs and times; no ancillary cost information |
| Exposure | Included | Not available |
| Total Losses | Included; not identifiable | Included; identifiable |
| Claim Year | 2009 to Mid-2014 | 2009 to 2014 |
| Vehicle Age | 2008-on | 2008-on |

**Statistical Analysis**

Claim frequency is the number of claims in a period of unit exposure, typically recorded in insured vehicle years. Vehicle claim severity may be measured as an average claim cost or average repair time. A generalised linear model was employed to model this claim frequency (per 100 Insured Vehicle Years) or claim severity as response variables, with model series and claim calendar year as predictor variables. These statistical models were used to compare the AEB study vehicle (XC60 or Golf 7) loss experience with that of the weighted average of the appropriate control cohort, while controlling for effects of calendar year. A Poisson distribution was used for the

claim frequency analysis and a Gamma distribution for the claim severity analysis, in both cases using a logarithmic link function.

The AEB study vehicle was set as the baseline for the model series variable, and all its control cohort vehicles were calculated relative to it. Given that the response variable is related to model series categorical variables by a log link function, the relative ratio of a given model series to the AEB study vehicle baseline level is found by taking the exponential of its regression coefficient.

Frequency analysis was carried out using the Insurer dataset, given that this included data on exposure by model series. Severity analysis presented here utilised the Research Claims Database dataset, looking separately at estimate costs, parts costs and repair times. A number of key factors may potentially distort the findings of the analysis of claim severity, which are outlined here along with approaches adopted to counter their influence:

1) Claim costs are not only influenced by levels of damaged incurred, but also by the cost incurred in replacing the parts (the replacement parts cost). It is therefore sensible to control for the effect of varying parts costs in a severity analysis based around claim costs. This was achieved by limiting the control cohort vehicles to only those with comparable parts costs to that of the XC60.

2) Differences in vehicle design will result in variation in levels of damage sustained, and this must be taken into consideration when drawing conclusions from an analysis of impact severity based on repair times. For example, some of the SUV cohort will have different repair or styling strategies. This will also be affected by passive pedestrian protection strategies that can increase component damage in a given impact. This design issue has been investigated using an alternate measure of vehicle susceptibility to damage, discussed below (see Results: Severity Analysis).

3) Vehicle Age is an important factor in explaining claim frequency and cost, with newer vehicles likely to have higher claim incidence relative to older vehicles, but lower claim costs and times. Therefore vehicles registered pre-2008 have been excluded from the XC60 analysis, and vehicles registered pre-2013 have been excluded from the Golf 7 analysis. Also vehicle age where available has been used as a predictor.

4) Vehicle Mass in theory can influence damage severity, with a lighter vehicle more likely to sustain more damage than a heavier vehicle. However an analysis of vehicle kerb weight for the model series' under consideration here does not show any correlation with repair costs or times.

## RESULTS

### Frequency Analysis: Volvo XC60

A Poisson regression analysis was carried out separately for damage and injury liabilities. Table 2 summarises the results obtained for the predictors for Third Party Injury, while Table 3 provides details of the statistical model output for each control vehicle and calendar year. The intercept value corresponds to the claim frequency for the baseline, which is the claim frequency for the XC60 in 2014. All other coefficients are relative to these.

**Table2.**
**Predictors for Third Party Injury**

| | Degrees of Freedom | Wald Chi-Square | P-Value |
|---|---|---|---|
| Model Series | 27 | 106.5 | < 0.0001 |
| Calendar Year | 5 | 31.75 | < 0.0001 |

**Table3.**
**Frequency Analysis for Third Party Injury: Statistical Output**

| Category Variable | Coefficient | Standard Error | 95% Wald Confidence Interval Lower | Upper | Hypothesis Test Wald Chi-Square | Degrees of Freedom | P-Value |
|---|---|---|---|---|---|---|---|
| Intercept | -5.18 | .0840 | -5.345 | -5.016 | 3803.67 | 1 | <0.0001 |
| Chevrolet Captiva 2007 | .734 | .1615 | .417 | 1.050 | 20.64 | 1 | <0.0001 |
| Chevrolet Captiva 2011 | .534 | .2361 | .071 | .997 | 5.11 | 1 | .024 |
| Honda CRV 2010 | .088 | .1047 | -.118 | .293 | .69 | 1 | .403 |
| Range Rover Evoque 2011 | .400 | .1135 | .178 | .623 | 12.46 | 1 | <0.0001 |
| Land Rover Freelander 2007 | .212 | .0854 | .045 | .379 | 6.17 | 1 | .013 |
| Land Rover Freelander 2011 | .073 | .1833 | -.286 | .432 | .16 | 1 | .691 |
| Suzuki Grand Vitara 2007 | .106 | .1555 | -.199 | .411 | .47 | 1 | .494 |
| Suzuki Grand Vitara 2011 | .220 | .1874 | -.147 | .587 | 1.38 | 1 | .240 |
| Hyundai IX35 2010 | .194 | .1032 | -.008 | .396 | 3.54 | 1 | .060 |
| Renault Koleos 2008 | .433 | .1388 | .161 | .705 | 9.75 | 1 | .002 |
| Ford Kuga 2008 | .149 | .0862 | -.020 | .318 | 2.99 | 1 | .083 |
| Mercedes M Class 2009 | .428 | .1020 | .228 | .628 | 17.64 | 1 | <0.0001 |
| Mitsubishi Outlander 2007 | -.063 | .2414 | -.536 | .410 | .07 | 1 | .793 |
| Mitsubishi Outlander 2011 | .123 | .2176 | -.304 | .550 | .32 | 1 | .572 |
| Audi Q3 2011 | .218 | .1372 | -.051 | .487 | 2.52 | 1 | .112 |
| Audi Q5 2009 | .307 | .0966 | .117 | .496 | 10.08 | 1 | .001 |
| Nissan Qashqai 2009 | .287 | .0835 | .123 | .451 | 11.81 | 1 | .001 |
| Toyota Rav 4 2010 | -.042 | .1579 | -.351 | .268 | .07 | 1 | .792 |
| Lexus RX 2009 | .518 | .1232 | .276 | .759 | 17.65 | 1 | <0.0001 |
| Kia Sportage 2010 | .401 | .0950 | .215 | .588 | 17.87 | 1 | <0.0001 |
| Volkswagen Tiguan 2008 | .155 | .0873 | -.016 | .326 | 3.15 | 1 | .076 |
| Nissan X-Trail 2008 | .078 | .1336 | -.184 | .340 | .34 | 1 | .559 |
| BMW X1 2010 | .000 | .1143 | -.224 | .224 | .000 | 1 | .997 |
| BMW X3 2007 | .090 | .1602 | -.224 | .404 | .32 | 1 | .574 |
| BMW X3 2011 | .153 | .2555 | -.348 | .654 | .36 | 1 | .549 |
| Volvo XC90 2007 | .465 | .1013 | .266 | .663 | 21.04 | 1 | <0.0001 |
| Volvo XC90 2010 | .539 | .1291 | .286 | .792 | 17.45 | 1 | <0.0001 |
| Volvo XC60 2009 | 0 | 0 | 0 | 0 | 0 | 0 | |
| | | | | | | | |
| 2009 | .248 | .0879 | .076 | .421 | 7.99 | 1 | .005 |
| 2010 | .264 | .0624 | .141 | .386 | 17.85 | 1 | <0.0001 |
| 2011 | .263 | .0526 | .160 | .366 | 24.97 | 1 | <0.0001 |
| 2012 | .170 | .0486 | .074 | .265 | 12.17 | 1 | <0.0001 |
| 2013 | .125 | .0460 | .035 | .215 | 7.39 | 1 | .007 |
| 2014 | 0 | 0 | 0 | 0 | 0 | 0 | |

From the Insurer dataset there were 177 XC60 Third Party Injury claims from a corresponding 26,715 insured vehicle years. This actual claim frequency of 0.66 per 100 insured vehicle years is compared against those estimated for the control vehicles. The XC60 is found to have an injury claim frequency that is 21% lower than that of the weighted average of the control cohort, with a 95% confidence interval for this result estimated between 8% and 32%. Figure 1 depicts the actual claim frequency for the XC60, and the estimated claim frequency for control cohort vehicles with confidence intervals relative to the XC60. Three of the control vehicles are found to have lower claim

frequencies than the XC60, but these are not statistically significant. A number of the control vehicles with claims frequencies higher than the XC60 are also not significant.

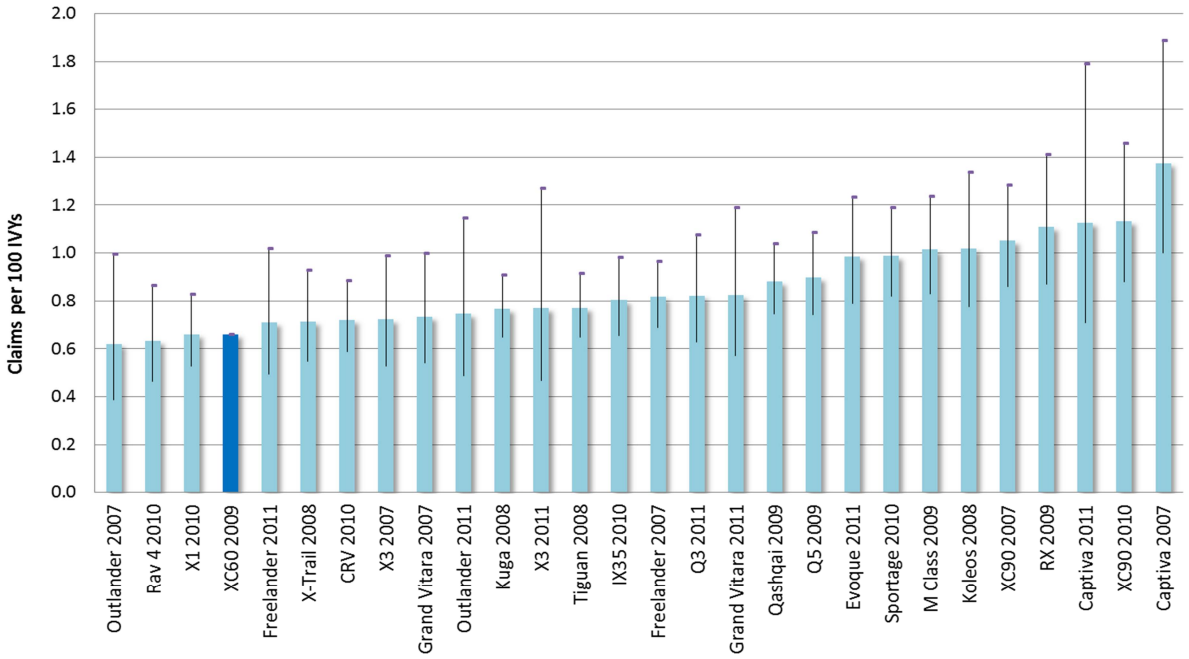


***Figure1. Claim frequency for Volvo XC60 compared to control SUVs: Third Party Injury.***

Table 4 summarises the results of the analysis across all three liability types, and a combined Own Damage and Third Party Damage category. In all liability types the model series and calendar year variables were statistically significant, and the XC60 is found to have a lower claims frequency compared to the weighted average of the control cohort.

**Table4.**
**Summary of Liability Results for XC60 compared to SUV Control Cohort**

| | XC60 | | | SUV Control | XC60 Claim Frequency Reduction | |
|---|---|---|---|---|---|---|
| | Exposure (IVYs) | Claim Count | Claims per 100 IVYs (Actual) | Claims per 100 IVYs (Estimated) | % Reduction | Confidence Interval |
| Own Damage | 26,715 | 1,757 | 6.58 | 7.00 | **-6%** | (-10%, -1%) |
| Third Party Damage | 26,715 | 844 | 3.16 | 3.45 | **-8%** | (-14%, -1%) |
| Own & Third Party Damage Combined | 26,715 | 2,601 | 9.74 | 10.49 | **-7%** | (-11%, -3%) |
| Third Party Injury | 26,715 | 177 | 0.66 | 0.84 | **-21%** | (-32%, -8%) |

Figure. 2 shows the loss experience for the XC60 and the individual control cohort vehicles, for Own Damage and Third Party Damage combined. Here again there are control vehicles with a claim frequency lower than that of XC60, which are in most cases not statistically significant; though one exception to this is the Ford Kuga. It is

suspected that the lack of further predictor variables available for claim frequency, such as driver age, annual mileage, urban versus rural etc., is impacting the claim frequency estimation for individual control vehicles here.

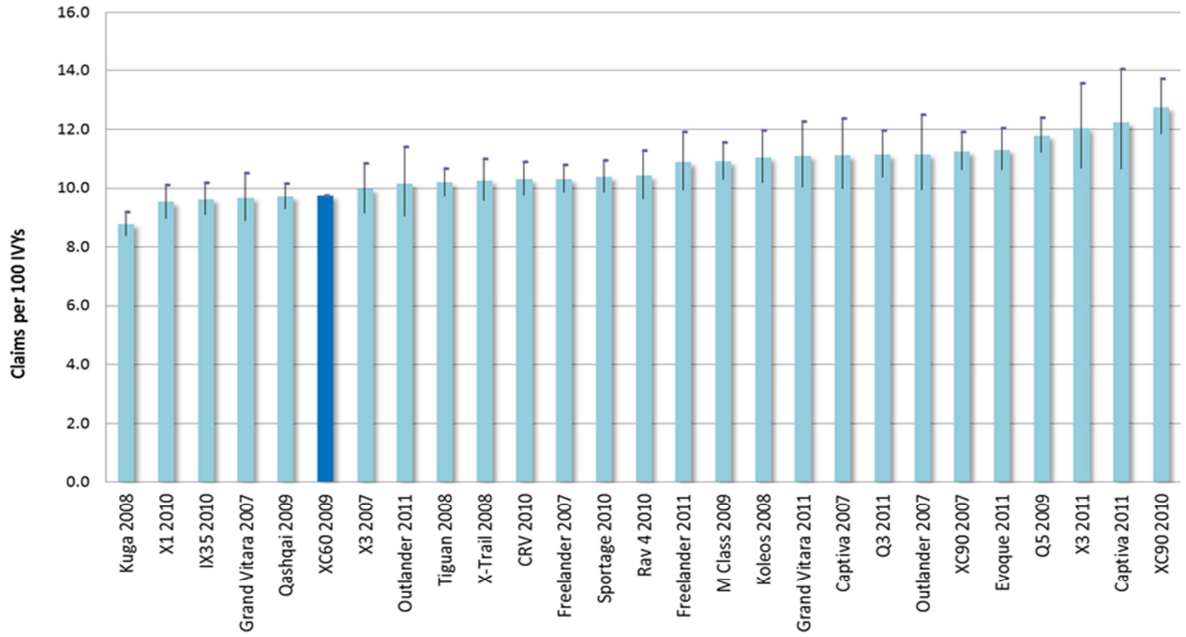


***Figure2. Claim frequency for Volvo XC60 compared to control: Own Damage & Third Party Damage combined.***

The `Volvo-driver' is an expression used to refer to the belief that individuals that buy a Volvo car are already safety-conscious, and are therefore pre-disposed to safe driving, with or without AEB. It is therefore sensible to consider this potential factor within this AEB benefit study: in this analysis the XC60 has a lower claims frequency than the Volvo XC90 for both damage and injury liabilities, which suggest the lower claim frequencies observed for the XC60 are not explained by this Volvo driver issue.

**Frequency Analysis: Volkswagen Golf 7 (AEB)**

Results for the analysis of Third Party Injury claims for the Golf 7 (AEB) when compared against the small family car control cohort are shown in Table 5. Calendar Year is not found to be statistically significant and is therefore excluded. Table 6 provides details of the statistical model output for each control vehicle. The intercept value corresponds to the claim frequency for the baseline, which in this case is the claim frequency for the Golf 7 (AEB); all other coefficients are relative to these. Figure 3 depicts the actual claim frequency for the Golf 7 (AEB), and the estimated claim frequency for control cohort vehicles with confidence intervals relative to the Golf 7 (AEB).

**Table5.**
**Predictor for Third Party Injury**

| | Degrees of Freedom | Wald Chi-Square | P-Value |
|---|---|---|---|
| Model Series | 13 | 32.1 | 0.002 |

**Table6.**
**Frequency Analysis for Third Party Injury: Statistical Output**

| Category Variable | Coefficient | Standard Error | 95% Wald Confidence Interval Lower | Upper | Hypothesis Test Wald Chi-Square | Degrees of Freedom | P-Value |
|---|---|---|---|---|---|---|---|
| Intercept | -5.273 | .1644 | -5.595 | -4.951 | 1028.84 | 1 | <0.0001 |
| BMW 1 Series 2011 | .682 | .1815 | .327 | 1.038 | 14.14 | 1 | <0.0001 |
| Peugeot 208 2012 | .527 | .1789 | .177 | .878 | 8.69 | 1 | .003 |
| Mercedes A Class 2012 | .632 | .2054 | .229 | 1.034 | 9.47 | 1 | .002 |
| Audi A3 2012 | .615 | .2160 | .192 | 1.039 | 8.12 | 1 | .004 |
| Vauxhall Astra 2010 | .823 | .1924 | .445 | 1.200 | 18.27 | 1 | <0.0001 |
| Toyota Auris 2010 | .396 | .3564 | -.302 | 1.095 | 1.24 | 1 | .266 |
| Toyota Auris 2012 | .677 | .2531 | .180 | 1.173 | 7.14 | 1 | .008 |
| Honda Civic 2012 | .237 | .2043 | -.163 | .638 | 1.35 | 1 | .245 |
| Ford Fiesta 2013 | .654 | .1743 | .312 | .995 | 14.06 | 1 | <0.0001 |
| Ford Focus 2011 | .536 | .1834 | .177 | .896 | 8.55 | 1 | .003 |
| VW Golf 2009 | .441 | .3434 | -.233 | 1.114 | 1.65 | 1 | .200 |
| VW Golf 2012 (no AEB) | .730 | .3138 | .115 | 1.345 | 5.42 | 1 | .020 |
| Renault Megane 2012 | .494 | .2621 | -.020 | 1.008 | 3.55 | 1 | .059 |
| VW Golf 2012 (AEB) | 0 | 0 | 0 | 0 | 0 | 0 | |

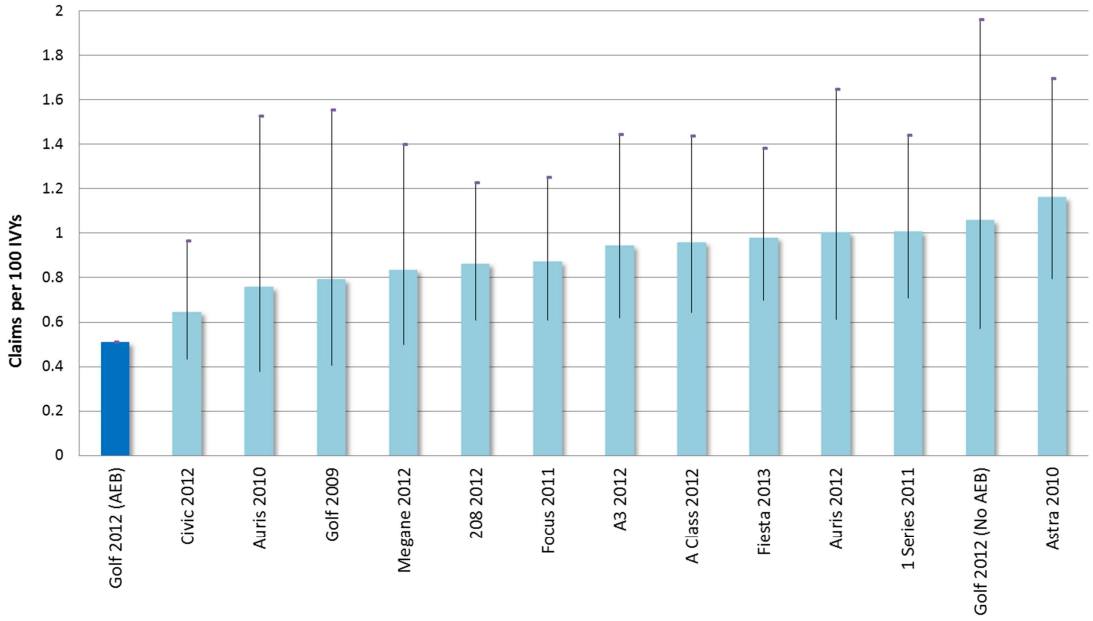


***Figure3. Claim frequency for Volkswagen Golf 7 (AEB) compared to control cohort: Third Party Injury.***

Table 7 summarises the results of the Golf 7 (AEB) analysis across all three liability types, and a combined Own Damage and Third Party Damage category. In all liability types the model series was statistically significant, while calendar year is also significant in the damage claims' analyses. For Third Party Injury and Third Party Damage liabilities the Golf 7 (AEB) is found to have a clearly lower claims frequency compared to the weighted average of the control cohort. For Own Damage liability this is not the case, with effectively no difference in claim frequency observed between the Golf 7 (AEB) and the weighted average of the control cohort. In general the Own Damage category includes a greater presence of claim types that are immune to AEB than is the case for Third Party

Damage, and it is therefore consistent that any Own Damage AEB effectiveness observed is lower than that of Third Party Damage. Additional exposure and claims volume for the Golf 7 (AEB) is required to further validate these results, and also whether differences between LIDAR and RADAR sensor technology are being manifested in these Golf 7 (AEB) and XC60 findings.

**Table7.**
**Summary of Liability Results for Golf 7 (AEB) compared to Small Family Car Control Cohort**

| | Golf 7 (AEB) | | | Small Family Car Control | Golf 7 (AEB) Claim Frequency Reduction | |
|---|---|---|---|---|---|---|
| | Exposure (IVYs) | Claim Count | Claims per 100 IVYs (Actual) | Claims per 100 IVYs (Estimated) | % Reduction | Confidence Interval |
| Own Damage | 7,216 | 610 | 8.45 | 8.51 | **-1%** | (-9%, 8%) |
| Third Party Damage | 7,216 | 844 | 2.55 | 3.18 | **-20%** | (-31%, -7%) |
| Own & Third Party Damage Combined | 7,216 | 2,601 | 11.00 | 11.81 | **-7%** | (-13%, 0%) |
| Third Party Injury | 7,216 | 177 | 0.51 | 0.94 | **-45%** | (-61%, -24%) |

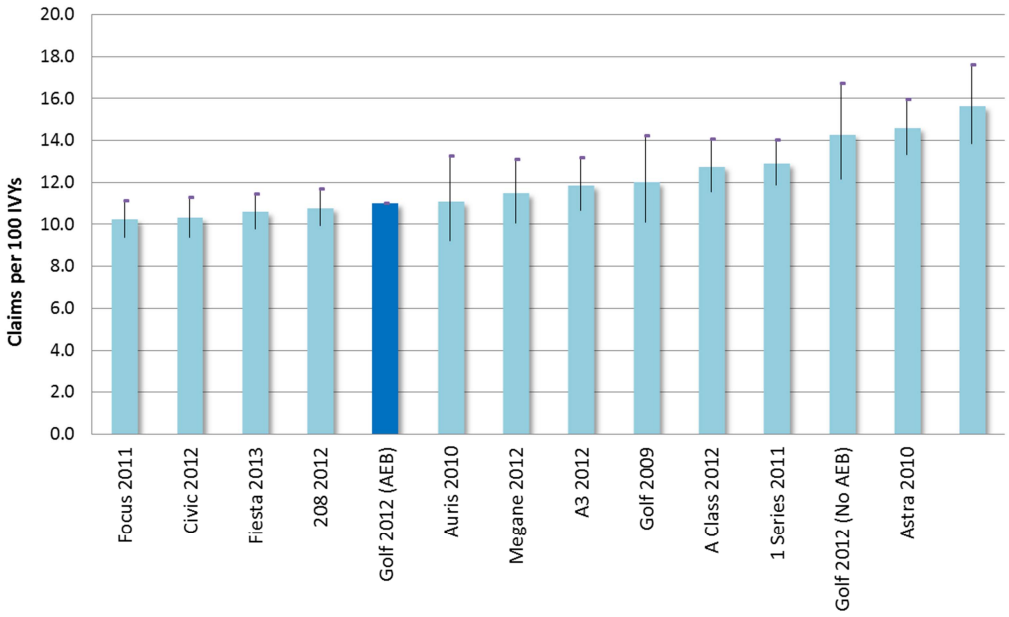


***Figure4. Claim frequency for Golf 7 (AEB) compared to control: Own & Third Party Damage combined.***

**Severity Analysis: Volvo XC60**

The Research Claims Database dataset is used to study the impact of AEB on claim severity, and is measured using claims costs and times. A subset of Own Damage claims, identified as those involving damage to the front bumper and registered 2008 or later, has been extracted for the XC60 and its control cohort. Gamma regression was used to model average cost and time quantities, with model series, calendar year and vehicle age as predictor variables.

For the regression analysis of average repair time the predictor variables model series, calendar year and vehicle age were all significant. The XC60 is found to have a repair time that is on average 10% lower than the weighted average of the SUV Control cohort, with a 95% confidence interval for this result estimated between 4% and 15%. Again a number of vehicles have an estimated average repair time that is lower than the XC60, but none of these reached statistical significance.

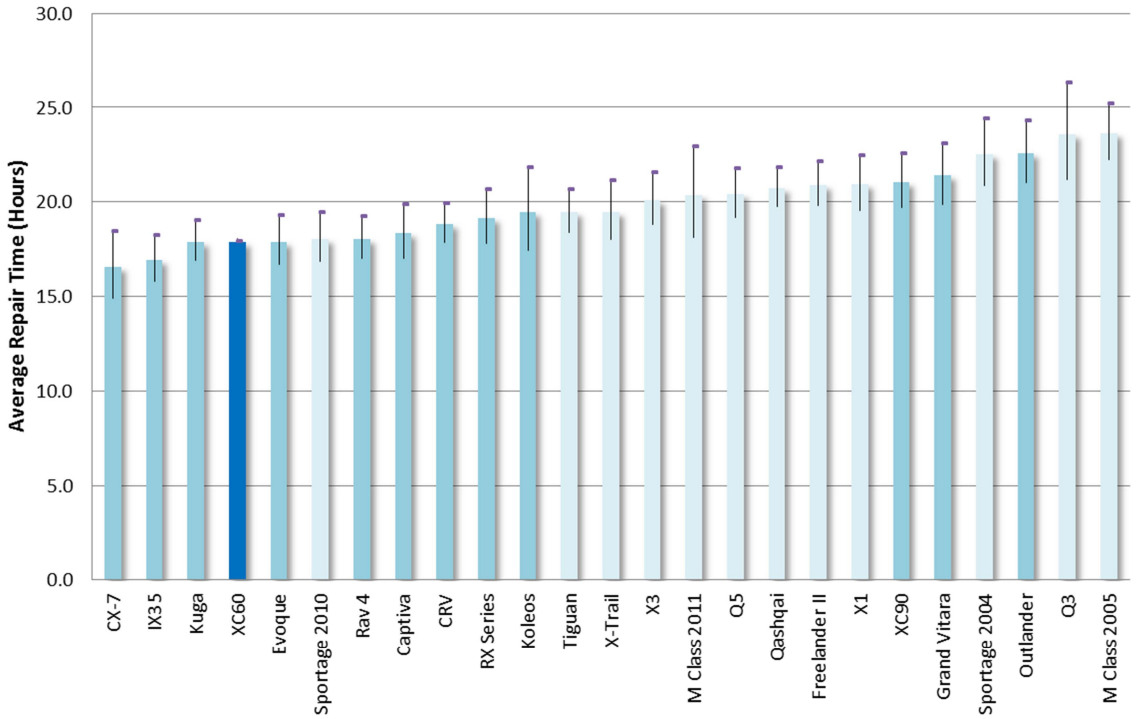


***Figure5. Average repair time for Volvo XC60 compared to control SUVs: Own Damage.***

Any discussion of severity as measured by repair time must also consider the issue of vehicle design susceptibility to damage. Thatcham Research carries out an assessment of every new vehicle to evaluate this issue, using a standardised 15 km/h offset barrier test. These damageability and repairability times, known more commonly as `D&R Times', form part of the UK Insurance group rating system, and have been used as a guide when considering this real world data. The D&R Times (unpublished) for the control cohort list range from 10 hours up to 31 hours; the XC60 lies in the mid-range. However it is noted that all of the control cohort vehicles with a D&R Time lower than that of the XC60 are estimated by the statistical model as having an average repair time greater than the XC60, indicated by the lighter-coloured bars in Figure 5. Or expressing this another way, the claim severity for the XC60 relative to the control cohort as estimated by the statistical model is lower than would have been expected by the D&R Times assessment data. This consideration of D&R Times does not remove the influence of vehicle design susceptibility to damage from this severity study, but does demonstrate that the XC60 severity reduction result is not explained by it.

Table 8 and Figures 6 and 7 summarise the findings from this repair time study, and also from analyses of claim repair costs and claim parts costs within the Research Claims Database dataset. For these costs studies only those

control cohort vehicles with parts costs comparable to that of the XC60 were included. Again the model series predictor variable was significant, but calendar year and vehicle age were not. For both the repair cost and parts cost studies the XC60 was found to have a lower average cost relative to the control cohort, by 14% and 13% respectively. Available D&R Times data suggests that vehicle design was not the explanation behind these severity results. For both of these repair cost studies the Renault Koleos had the lowest estimated cost, and in the parts cost study this was significantly lower compared to the XC60. Again vehicle design issues may play a role here.

Given that this analysis is of claims with front bumper damage, it is suggested that the observed cost and repair time reduction for the XC60 relative to the control cohorts is explained by the presence of impact mitigation as well as prevention. If all incidents are front-end Own Damage claims and therefore all equally preventable by AEB, then any reduction in frequency of these is unlikely to much alter the average claim cost or time for the XC60. It follows then that any reduction in the average cost or time could be brought about by mitigation of these impacts.

**Table8.**
**Summary of Damage Severity Results for XC60 compared to SUV Control Cohort**

| | XC60 | | SUV CONTROL | XC60 CLAIM SEVERITY EFFECT | |
|---|---|---|---|---|---|
| | Claim Count | Own Damage | Own Damage | % Reduction | Confidence Interval |
| Average Repair Time | 1,501 | 17.9 hours | 19.8 hours | -10% | (-15%, -4%) |
| Average Repair Cost | 1,501 | £2,683 | £3,111 | -14% | (-22%, -6%) |
| Average Parts Cost | 1,501 | £1,770 | £2,024 | -13% | (-23%, -4%) |

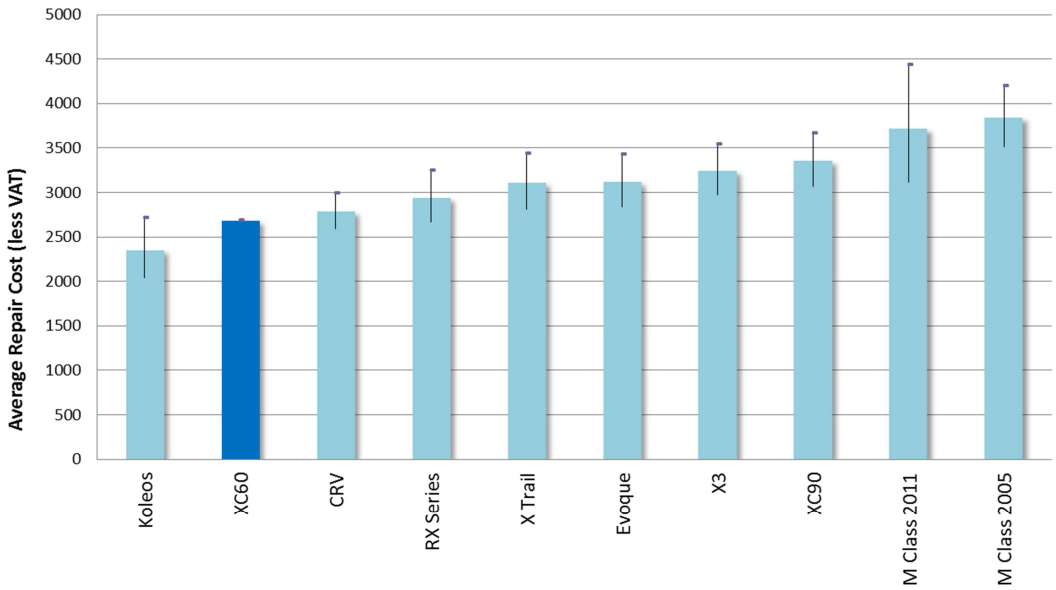


***Figure6. Own Damage Repair Cost Severity Analysis: Volvo XC60 v SUV Control Cohort***

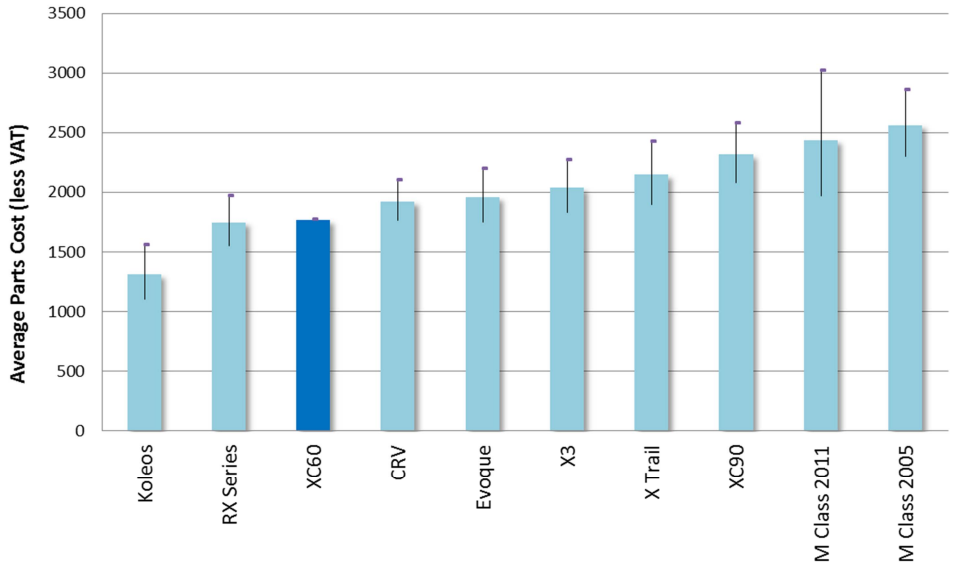


***Figure7.*** **Own Damage Parts Cost Severity Analysis: Volvo XC60 v SUV Control Cohort**

## DISCUSSION

A series of statistical analyses of claim frequency and severity for the Volvo XC60 and Volkswagen Golf 7 with their respective AEB standard-fit systems, compared against appropriate control cohorts, across damage and injury liability types, has generated a range of results that suggest an AEB benefit. Calendar year and vehicle age were controlled for throughout this study. Real world claims data was utilised from two different datasets, and the strengths and shortcomings of both of these have been outlined.

For frequency analysis an apparent AEB effect is detected across each liability type. Third Party Injury claim frequency for the XC60 was 21% lower than the control cohort. For Third Party Damage the XC60 has a claim frequency that is 8% lower than the control cohort, and for Own Damage the XC60 is 6% lower. Given that Own Damage includes more collision scenarios than Third Party Damage which are immune to AEB, the lesser frequency reduction observed for the Own Damage is in line with this. Analysis of the Golf 7 (AEB) also demonstrated substantial AEB benefits for Third Party Injury and Third Party Damage, of 45% and 20% respectively; however for Own Damage no AEB effect was observed. It may be the case that differences in sensor technology affecting target recognition and thus warning and auto-brake intervention strategies of the Volvo City Safety and Volkswagen Front Assist systems are being manifested in these results. The latter has functionality across the full range of driving speeds and therefore has the potential to be effective in some of the higher speed crashes and injuries that are beyond the speed range of Volvo City Safety system. Additional claims data for the Golf 7 will also help confirm these results. The injury reduction results reported here can be expected to have a substantial societal impact.

AEB also has the potential to reduce claim costs through prevention and mitigation of impacts, and results from severity analyses of the XC60 using claim costs and repair times suggest this is the case. An analysis of total repair cost and parts cost for claims with front bumper damage extracted from the Research Claims Database show respectively 14% and 13% cost reductions for the XC60 compared to an appropriate control cohort. A reduction in average claim cost may be interpreted in the context of the distribution of Own Damage claim costs, and whether those claims prevented by AEB have the effect of shifting the average of this distribution towards a lower value. This may indeed be the case if medium-high cost front-end impacts are being removed from this cost distribution. However this reduction may also be explained by impact mitigation having the effect of lowering the average repair cost, which is more applicable to the front bumper claims-only dataset, since distribution of costs are likely to be

less dispersed and its average claim cost less affected by the aforementioned impact prevention. Repair times were also employed as a measure of damage severity, and the average repair time for the XC60 was 10% lower than that of the control cohort. This repair time severity analysis lends itself to the same interpretations as the cost studies.

The available claims data analysed here does not feature factors such as driver age and gender, driver profession, annual mileage, previous driving offences, population density, and so on, which are generally known to be significant in the study of claim risk. Inclusion of factors such as these would improve the accuracy of the statistical modelling of claim frequency and severity, and assessment of AEB benefits. In the analysis reported here the XC60 has a lower claims frequency than the Volvo XC90 across all three liability types, and a lower average claim severity for Own Damage, which suggests the results observed for the XC60 are not explained by any `Volvo-driver' effect.

The UK frequency reduction results discussed here are broadly in agreement with those reported elsewhere, in particular those by HLDI. Compared to the 21% injury claim effectiveness for the XC60 and the 45% injury claim effectiveness for the Golf 7 (AEB) relative to their respective control cohort reported in this UK study, HLDI [3] observed a 33% lower claim frequency for the XC60 compared to an SUV control cohort and 34% lower than a Volvo control cohort; and the City Safety Volvo S60 has an 18% lower claim frequency than a midsize luxury car control cohort, and 22% lower relative to the Volvo control cohort. These USA results were generated from statistical models which included a number of significant claim risk predictors, which increased the accuracy of their AEB impact estimation. In the USA the closest equivalent to Own Damage is referred to as Collision coverage and is understood to include proportionally more crash types that are preventable by AEB. This may go some way to explaining the higher claim frequency reductions of 20% and 9% for XC60 and S60 respectively observed for this, compared to the 6% XC60 effectiveness result for UK Own Damage. For Third Party Damage the equivalent liability category results reported by HLDI were a 15% lower claim frequency for the XC60 and 16% for the S60, which are comparable with the 8% and 20% results for the XC60 and Golf 7 (AEB) studies respectively observed in UK data. Overall, given the agreement between this UK study and that from HLDI there is good evidence that AEB is having a significant effect to reduce both damage and injury claims.

Findings from the analysis of UK claim severity also shows some agreement with similar studies carried out by HLDI: for Collision coverage the XC60 had a 10% lower average claim cost relative to the control cohort, and 13% lower for the S60; UK results here were of the order of 10%-15%.

**CONCLUSIONS**

This paper summarises the findings from an analysis of UK Insurer claims data and appears to demonstrate that AEB is responsible for substantial claim prevention of Third Party Injury arising in vehicle claims. The study considered the Volvo XC60 with City Safety, and the Volkswagen Golf 7 with Front Assist, and these were compared to an appropriate control cohort and findings have been interpreted in terms of impact on claims. The absence of additional predictor variables is recognised as a shortcoming of this research, the inclusion of which would improve model accuracy and reliability of the findings. It is also the case that further clarity on crash circumstances within the liability data would be valuable in measuring AEB benefits, in particular front-to-rear claims data. This research is a first of its kind in the UK to look at the issue of AEB impact of claims experience, and further studies around Insurer claims data with enhanced detail and risk information are intended to build on the findings reported here. As more vehicles with this technology become available Thatcham Research will continue to monitor AEB performance trends.

This study shows the effectiveness and value of AEB systems, especially in the reduction of injuries and in particular whiplash cases. The results of these and other findings have supported the implementation of an insurance discount system for AEB systems, and also the testing of such systems with Euro NCAP and other consumer test organisations which will encourage the proliferation of AEB within the vehicle parc.

**ACKNOWLEDGEMENT**

The authors would like to acknowledge the contribution of the real world claims data from the Insurers, and to thank HLDI for their support with analytical methodology.

**REFERENCES**

[1] Highway Loss Data Institute (HLDI). 2011 Volvo City Safety Loss Experience – Initial Results. HLDI Bulletin, 2011, 28(6).
[2] Insurance Institute for Highway Safety (IIHS) 2010. Avoid crashes. Status Report, 2010, 46(6).
[3] Highway Loss Data Institute (HLDI) 2012. Volvo City Safety Loss Experience – an update. HLDI Bulletin, 2012, 29(3).
[4] Insurance Institute for Highway Safety (IIHS) 2013. Crash Avoidance. Status Report, 2013, 48(3).
[5] Isaksson-Hellman, I and Lindman, M. 2012. The Effect of a Low-Speed Automatic Brake System Estimated from Real Life Data. Annals of Advanced Automotive Medicine, 2012, 56, p. 231–240.
[6] Kullgren, A. AEB Analysis. 2014, RCAR P-Safe meeting, March.
[7] Lauterwasser, C and Redlich J. 2011. Preliminary Analysis of the Claims Experience with Standard City Safety based on GDV/Allianz data. 2011, RCAR AGM, presentation by AZT & German Insurance Research Association.

# A NEW STRATEGY to ENHANCE TRAFFIC SAFETY in DEVELOPING COUNTRIES

**Sarbaz Othman, Ph.D.**
**Joseph Carroll, Ph.D.**
**University of Kurdistan - Hewlêr**
**Kurdistan-Iraq**

**Paper Number: 15-0059**

## ABSTRACT

The rapid expansion of motor vehicle use in developing countries resulted in a sharp rise in road traffic–related deaths and injuries. The UN General Assembly recognized road deaths and injuries as a global epidemic since 2003. More than 90% of the 1.2 million people who die each year in traffic related crashes are from the developing countries in which more than 51% are vulnerable road users.

The Kurdistan region in Iraq has been chosen for this study where the number of registered vehicles has increased exponentially in the last decade, and the official number of fatalities in 2013 was 1,114. This number, however, is highly underreported; the actual figure of fatalities is estimated to be 100% more than the reported number according to World Health Organization. Pedestrians in the region are not separated from vehicles even on high speed roads, in front of schools, bus stops, parks and commercial areas. In addition, driving education and risk assessment is poor among drivers. A pre-study showed that only 5% of the current drivers in the largest city in Kurdistan, Erbil, know how to use a roundabout. Moreover, 0%, 1% and 12% could read and were knowledgeable about the signs of "One-way", "Give-Away" and" No-Entrance" respectively. The driving test and training systems are inadequate and inconsistent in the cities of Kurdistan. The test are performed in an isolated and controlled environment separate and far away from the everyday traffic. Moreover, the road network is non-standard and is lacking alignment and signs.

This study evaluates current traffic safety conditions in Kurdistan, and then proposes a new strategy to change the current driving license test system to a more realistic and educational test that is fair and promotes safe traffic flow. The new approach, in this study, is based on a new standard driving test and training system based on the 4 E's model which stands for: Engineering, Education, Enforcement, and Encouragement. The new proposed tests will be conducted on a limited, predefined, standardized and heavily monitored route within existing traffic environment.

This new testing system will focus on educating large groups of university students how to operate their vehicles more efficiently and safely. Moreover, the route within the existing road infrastructure that will be upgraded to standard and heavily monitored also allows licensed drivers, optionally or through an enforcement program, to retrain and experience driving on standard routes gradually leading to an improvement in drivers' awareness. The standard route can also be used as a model and starting point to successively standardize the current road network and when constructing new roads.

**Keyword:** Traffic Safety, Driving License, Developing Countries, Traffic System

# INTRODUCTION

The rapid expansion of motor vehicle use in developing countries resulted in a sharp rise in road traffic–related deaths and injuries [1]. The UN General Assembly recognized road deaths and injuries as a global epidemic since 2003 [2]. Nevertheless, resources devoted to assist effected countries to address the problem is still inadequate. Although more than 90% of the 1.2 million people who die each year in traffic related crashes are from the developing countries in which more than 51% are vulnerable road users [2]. Even efforts by the developing countries in the high income group, with a fully funded national road safety strategy, were unsuccessful at improving traffic safety and to implement advanced workable safety programs. In Saud Arabia, for instance, despite a fully funded program, traffic death almost doubled from 3500 in 2000 to 6500 fatalities in 2009, while the target was an annual reduction by 3%. Meanwhile, a similar national road safety strategy in France halved fatalities on the roads from 2001 to 2010 [3]. This attests that providing resources and replicating interventions of good practices that are implemented in countries with effective safety programs, will fail to yield sustainable results. Apart from political will to commit resources, a sustainable solution must consider institutional capacity weaknesses, social obstacles and best intervention practices based on scientific evidences [1]. Moreover, research is required to determine optimum standards before adopting elements of good practice observed in the developed countries.

In the Kurdistan region of Iraq, which is the scope of this study, registered vehicles increased exponentially over the past decade. The increase is still going on and is leading to more fatalities on the roads annually; in 2014, the number of registered vehicles was 1 250 000, an increase by 10%, compared to 2013. The official number of fatalities in 2013 were 1,114 [4]. This number, however, is highly underreported, the actual figure is estimated to be 100% more than the reported [3], especially when the country has no eligible death registration data.

An institutional framework together with a strong political will are the main factors that affect traffic safety conditions on the national level [5]. The framework is to, among others, organize national policy, set manageable goals and sub-goals, coordinate activities, and cooperation with international organizations.

The mechanism of road accidents is related to a number of explanatory factors which are deeply rooted and interrelated [6]. The most common being human errors, where deficient road design and planning will often have contributed to or compounded these errors [7]. Inadequate training and testing programs together with insufficient enforcement of traffic and transport regulations greatly affect road users' attitude and behavior [8]. In Kurdistan, the driving tests and trainings, which have direct influence on human errors, are applied differently in the cities of the region. The inconsistent driving tests are partially based on different modules used in developed countries. In addition, the tests, in practice, are not performed in the existing traffic environment, but rather in an isolated and controlled environment separate from other drivers. This limitation is due to several obstacles such as inadequate driving test systems, a nonstandard road network and the great danger of operating by the driving regulations on an uncontrolled road where the other drivers ignore many of the regulations. Thus, to improve traffic safety in Kurdistan, a comprehensive traffic safety system is essential. In particular, a new driving test model to gradually improve road users' behavior is required. Moreover, exploiting the model to successively upgrade the safety aspects of the road networks' standards in the region.

# AIM OF THE STUDY

The aim of this study is to evaluate current traffic safety conditions in the Kurdistan Region of Iraq, and then propose action plans to change the current system to a more fair and safe traffic flow. The action plan includes causal explanations of the persistence of poor traffic safety conditions in Kurdistan as well as long and short term strategies and approaches of improvement.

# CURRENT TRAFFIC SAFETY SITUATION

A comprehensive evaluation of the current traffic safety situations in Kurdistan is based on main factors that influence the safety level including data collection, political will, institutional framework and development goal, driving test system, human behavior, infrastructure, and vehicle factors.

**Data Collection:** Providing reliable data is important to review the mobility and traffic safety status which is to be used in development of any strategic plan. Kurdistan does not have an adequate system for data collection. The lack of reliable data is one of the most serious obstacles to conducting proper analysis. The limited available data is either incomplete or skewed, which creates great problems in the analyses. Hence, analyses of the factors, mentioned above, that affect traffic safety will be based on available data, visual evaluation and/or experiences. The available limited data will be used as a rough approximation of the real figures. Accident data as the most important indicator of traffic safety is unreliable, and only absolute numbers of fatalities exist. The official number of fatalities in 2013 was 1,114[4]. This number, however, is highly underreported, the actual figure is estimated to be 100% more than the reported [3], especially when the country has no eligible death registration data. An important measure to improve analyses is to adopt accident and/or fatality rate, instead of an absolute number independent of rate of change, which is the number of fatalities/ accidents per vehicle or person per kilometer. However, the data for distance travelled by people is unavailable. Hence, only absolute number of fatalities in relation to population and vehicles can be used. Thus, considering only registered deaths, Kurdistan has more than 22 fatalities per 100 000 population, while this figure is less than 3 fatalities in the safest countries. Fatality rate per 10 000 vehicles is 20 times more than in the safest developed countries, that's despite longer travelled distance and more vehicle trips in the developed countries.

**Political Will:** Decision makers in all countries agree and there seems to be a political will to decrease traffic road deaths [2]. Kurdistan is no exception as the highest authorities in Kurdistan, including the Regional President and the Prime Minster, announced and decided implementation of the necessary measures to reduce traffic accidents. However, no further nor concrete steps have been taken on the ground as a matter of fact. That is because accidents have not been considered by the society as public health problems similar to contemporary illnesses such as mad cow disease and bird flu. Hence, the society does not require special attention from the state to solve the problem.
Additionally, public policy makers point towards shortcomings in electricity and housing as major problems that need to be acknowledged by the state. Thus the state took great and expensive actions to solve the electricity and housing problems. Therefore, improving traffic safety is not among the region's developmental priorities. The main focus of traffic policy is to optimize mobility and flow of vehicles without proper plans to include traffic safety.

**Institutional Framework and Development Goal:** Kurdistan has not any institutional framework for coordinating activities and setting a practical goal to reduce fatalities and injuries on the roads. There is no fund from the national budget to improve road safety. Moreover, the region lacks a national research center to improve traffic and road safety. The roads and traffic are responsibilities of several departments without any department for traffic safety as in many other developing countries. The Interior Ministry has the main responsibility for the traffic safety in Kurdistan. Hence, traffic police stands for the poor traffic safety performance and its legal consequences. However, several other ministries are directly involved in the traffic safety performance without being responsible legally for the safety outcomes on the national level. The involved ministries are: The Ministry of Municipality that is responsible for planning and organizing urban roads and streets; Housing and Reconstruction Ministry deals with constructing, operation and maintenance of the main roads between the cities; Ministry of Transport and Communications is responsible for the administration and management of all areas of communications, including public transportation; other concerned Ministries are Education, Health and Planning.

**Driving Test System:** The driving test and training systems are inadequate and non-consistent in the cities of Kurdistan. The test are performed in an isolated and controlled environment separate and far away from the everyday traffic. The obstacles to perform the tests in the existing environment consist of a lack of experience by the traffic police and a non-standard road network in terms of alignment and signs. Moreover, the difficulty to perform driving tests according to the standards of uncontrolled roads where many regulations are ignored by licensed drivers and where the traffic environment is chaotic. The drivers learn the practiced driving by their own, friends or parents before or after acquiring driving license. In addition, the driving license is used for formalities and legal issues only. The common question to find out whether somebody drives is: "Do you drive?" and not "Do you have a driving license?" Which indicates the big gap between the driving test and the actual driving environment.There is a large number of unauthorized drivers using the roads before having a driving license. In addition to that, it is possible to obtain a driving license

through private connections without doing the test. Another serious deficiency is that there is only a slight difference, in practice, between tests for private vehicles and trucks. Truck accidents are more serious and cause greater damage which means that operating trucks demands different knowledge and experience.

**Human Behavior:** Individuals, in their nature, do not expect that they will be involved in accidents. They overestimate their ability and consider accidents as human errors made by road users without direct effect on them [9]. Human performance in terms of traffic safety is very weak in many aspects and includes a high number of road users. Driving education and risk assessment is poor among drivers. A pre-study showed that only 5% of the current drivers in the largest city in Kurdistan, Erbil, know how to use a roundabout. Moreover, 0%, 1% and 12% could read and were knowledgeable about the signs of "One-way", "Give-Away" and" No-Entrance" respectively. This indicates a serious lack in the driving test system and current road design and signposting. Even the traffic police do not seem to have enough knowledge in regard to organizing the traffic and investigating accidents. A traffic police officer with the lowest rank only goes through 40 days of training while an officer has completed 6 months of training. This short education, however, is mostly about disciplines and the use of weapons. Serious human errors are noticed in many cases, but there is no research or data collection to figure out the size of the problem. The main human errors are mentioned below and include:

- One of the main human errors in traffic is the fact that pedestrians are not separated from vehicles even on high speed roads, in front of schools, bus stops, parks and commercial areas. Moreover, the pedestrians very often choose to walk on and along the high speed streets in the direction of driving. Furthermore, roadwork is carried out without signposting on high speed roads. Opposite to what is stated in the traffic law, drivers do not stop at stop signs to allow pedestrians to cross the streets. The drivers and pedestrians have developed informal ways to divide space between them. The drivers have the priority of spatial appropriation where pedestrians by many drivers are considered as second class citizens. The reason behind this attitude is that most pedestrians are perceived as poor, while people from the middle and upper class are believed to be able to travel by car.
- Speeding is another major problems which also occurs in residential areas. The speed cameras are often not placed on the accident-prone roads to make driving safer on these roads. They are usually placed where the layout of the roads encourage speeding. Dangerous overtaking is very frequent on two lane rural roads even in the presence of oncoming traffic.
- A third common human error concerns the use of seatbelts. A few years ago, drivers and passengers were asked to show their identification card at the security checkpoints if they had fastened their seatbelt. Wearing the seatbelt was a clear indication that the traveler was not from the region. Enforcement of seatbelt use has changed the picture now, and a great improvement has been noticed in this area. However, wearing a seatbelt is still not common among passengers and child restraints are equally quite uncommon. To avoid using a seatbelt, there is even a cheap separated seatbelt buckle device in the market to turn off the acoustic signal of the seat belt reminder in case the driver or passenger do not wear the seatbelt. Other dangerous practices, which do not lead to action taken by traffic police, are riding passengers in moving truck beds, hanging out of sunroofs and vehicle windows.
- Unfortunately, drinking and driving is common, and an uncountable number of drivers drink and picnic along the roads outside the large cities.
- Helmet wearing is rare for both motorcyclists, moped drivers as well as cyclists.
- Parking and stopping on the roadway and in other dangerous places are frequent.
- Wrong side driving to shorten trips occur frequently.
- Driving despite red lights is not uncommon.
- Chaotic driving in roundabouts is also a common human error.

**Infrastructure:** The way residential areas and the connecting roads are built have a direct effect on the nature of traffic conflicts and traffic accidents. The environment is dangerous for all road users, in particular vulnerable road users like pedestrians and cyclists. The roads are built to allow maximum mobility and traffic flow. The streets lack proper sidewalks for pedestrians or they are occupied by the neighboring residential or commercial buildings which compels pedestrians to share the roads with vehicles. Moreover, uncontrolled urban growth and irregular land use have promoted dangerous sidewalks, or absence of sidewalks at all, adjacent to main and high speed roads. This increases the number of conflicts between vulnerable road users and vehicles. Moreover, street

widening is often made at the expense of sidewalks. The vulnerable road users have to face heavy vehicle traffic due to urban social networks being disturbed. A biographic survey showed that in the1960s and 1970s non-motorized transport modes such as walking and bicycle usage were competitive to motorized vehicles in the largest city Erbil in Kurdistan. The rate of bicycle commuters in the city, however, diminished dramatically starting from the early 1980s along with the increasing motorized travel modes. Though, the number of private vehicles increased by more than 1000% in the 1980s compared to the 1970s. While the increase, the last two decades, was 40000% compared to 1970s, from approximately 1000 private vehicles to more than 400,000 in 2014 [10]. The results of the survey showed that the rate of bicycle use has declined to 0.05% although the city has an excellent flat topography for cycling and a generous climate most days of the year. More specific deficiencies in regard to infrastructure are:

- Pedestrian cross/walks on high speed roads with heavy traffic roads. Moreover, the drivers hardly ever stop for pedestrians who want to cross the street using the crosswalks. Moreover, using the pedestrian crosswalks are dangerous due to broad roads, heavy traffic on the roads and the high speed of the vehicles. There are pedestrian crosses on 10 lane roads where the speed limit is 80 km/h with even higher actual operation speeds, so the pedestrians face a hard task to wait for all 10 lanes to be safe to cross. 10 experiments were conducted where a pedestrian waited 15 minutes at 3 pedestrian crosswalks during the rush hour without any success to cross the street. The few walkers who take the risk, usually cross the streets by crossing one lane at a time while vehicles at high speed pass the pedestrians on both sides.

- Building U-turns on roads where the speed limit is 80 but where the actual speed is greater than 100 km/h. The U-turns lead to blocking overtaking lanes in both driving directions followed by frequent incidents and serious accidents. That is because U-turns lead to a mix of high and low speed vehicles on heavily trafficked roads. On smaller roads, with 4 or 6 lanes, vehicles block half of the lanes, or the whole street while they are waiting to make a U-turn.
- Road lighting and alignment is another problematic aspect. Newly built roads are usually opened and used without completing lightning and alignments. Moreover, most of the two-lane rural roads are without edge and midline alignments to limit and separate opposite driving direction lanes. The roads lack roadside reflector posts which is very important when driving at night. Operation and maintenance of the existing lighting and alignments are additionally inadequate.
- Speed bumps, as a cost effective injury prevention measure, have widely been installed on the roads. However, poor signing prior to the high speed bumps becomes a serious hazard if it is not discovered well in advance by the driver. Moreover, the speed bumps are sometimes installed for one direction of the traffic which encourages drivers to drive on the wrong side of the road to avoid the speed bump.
- Most of the accident-prone existing roads lack roadside crash barriers. The newly built roads, however, include crash barriers but the appropriate operation and maintenance actions of the roads are not followed.
- Operation and maintenance of the roads are not followed by proper actions leading to quick physical failure and dangerous traffic states.
- Construction materials on the roads, coinciding with the new constructions of buildings and roads, are serious physical hazards on the roads. Moreover, poor temporary diversion of the roads and lack of information prior and during the diversion result in serious accidents and bad traffic flow.
- Many illegal markets, restaurants, houses and peddlers on the roads also lead to conflicts between high and low speed traffic including vulnerable road users.

**Vehicle Factor:** There are more than 1,250,000 registered vehicles in Kurdistan with an increase of 10% annually. The increase in developed countries, for instance Sweden, is 2% only. Vehicle conditions are good in general as they are equipped with relatively new passive and active safety devices. There are annual advanced vehicle controls. The problem, however, is the lack of qualified technicians to maintain the advanced systems. Another serious problem is, similar to deactivating the seatbelt warning system, that quite a few drivers deactivate the airbag system in order to keep their car from damage associated with the deployment of airbags.

# METHODOLOGY OF THE NEW STRATEGY

Many efforts by individuals and organizations have been conducted to create the political will to improve traffic safety on the national level. These efforts consisted of traditional approaches such as the political will to commit resources, establishing an institutional framework to coordinate activities concerning traffic safety, developing goals and sub-goals, gathering scientific evidence of the magnitude of the threat, identifying deficiencies in the current traffic safety system, and developing a social strategy for organizing effective interventions. However, the efforts were unsuccessful in affecting the decision-making process and the existing policy to prioritize traffic safety and to consider the problem as a public health issue. This lack of success is partly because public acknowledgment for the reasons of the problem range between seeing accidents as fatalistic, unavoidable outcomes of development, or simply placing the blame on the drivers. While it is clear that the current strategy for improving road safety in the Kurdistan Region is largely ineffective, certain aspects of the above mentioned interventions could still contribute in part to the long term goal and strategies to improve road safety in the region.

The new approach, in this study, is to develop a new driving test and training system based on the 4 E's model which are: Engineering, Education, Enforcement, and Encouragement. The current road network in the region lacks important features of safe driving and does not meet standards and regulations. Thus, a standardized route on a section of public roadway which includes the required road safety features, is required to conduct a safe driving test. This is the core of the methodology in this study. This study proposes that a limited route within the existing road network, no less than 10 kilometers and with moderate traffic density, be defined and upgraded according to the standards. The route should include important features of traffic flow and safety such as traffic signs, U-Turn, round about, lane-keeping, traffic light, give-away, primary-road, pedestrian crosswalks, alignments, residential area, etc. Further, the controlled route should be heavily monitored to limit traffic violations and enforce legal driving on this portion of the roadway.

The next step is to adapt the driver test and training, including a theory test, at a university as a part of the education program for a limited number of final year students. Further, it is important to publicize in the media the new strategy and goals of the controlled portion of the roadway prior to conducting the driving test. The aim of the test is to carefully evaluate the effectiveness of the new method and improve the model based on feedback from the test, which is important for untested assumptions. After an initial implementation, evaluation must be carried out on the effectiveness of conducting driving test on the controlled portion of roadway. From this evaluation, the new strategy can be adapted and generalized into a new method for driver education which can be applied in other cities as a part of the education program for final year student at all universities. The number of graduated students in Kurdistan in 2014 was 27,275 students. Therefore, the implementation of the university education portion of the project is a very large scale program. Many professional examiners and driving schools need to be prepared for both the training and driving tests to be conducted.

In this way, the new proposed system will teach a large group of the most educated class how to properly operate their vehicles more efficiently and safely. Moreover, the route allows licensed drivers, optionally or through an enforcement program, to retrain and experience driving on standard routes which may lead to a gradual improvement in drivers' awareness. The standard route can also be used as a model and starting point to successively standardize the current road network as new roads are constructed.

# CONCLUSIONS AND RECOMMENDATIONS

The political power is making motor vehicles the dominant mode of transport followed by extensive road building program. Moreover, the main focus in building the roads is to optimize mobility and flow of vehicles without proper plans to include traffic safety. Worsening traffic safety year after year is an indication that the practiced methods are not affective. Nonetheless, traditional views and approaches are still dominating. While the traditional strategy to improving road safety is ineffective, it is difficult to change from the top due to economic and political challenges. The rapid increase in the use of private car transport, upgrading old roads and constructing new roads that do not meet safety standards, and the lack of driver education led to increasing traffic accidents. Clearly, the traffic safety knowledge of drivers and the social environment were not prepared for the rapid changes leading to an increase in traffic accidents. Road safety in general, and the problems with vulnerable road users in particular, are not prioritized in updating the old road nor in constructing the new ones. Therefore, as new roads are built or old roads updated that

do not meet safety standards, they are building mistakes into their rapid growing road network which will require large amounts of money in the future to correct them. The blame of the poor safety performance, however, is mainly placed on the drivers. Based on the traffic safety research performed on developed countries, the main cause of accidents is human factors or automobile operator error. However, it is taken for granted that the developed countries already have a good road infrastructure, signing, and good vehicle condition.

Improving traffic safety in Kurdistan requires a strong political will, institutional framework to coordinate activities, feasible goals, funding from the national budget and interventions based on scientific evidences. The decision makers haven't prioritized traffic safety, despite more than 1,114 road deaths in 2013 and increasing fatalities annually. Thus, Kurdistan is 45 years behind developed countries when considering that road fatalities in the developed countries started to decline in the beginning of 1970's.

The suggested strategy in this study is based on the results of the survey which showed that licensed drivers do not know how to properly operate their vehicle according to driving regulations and were unable to correctly read road signs. The core of this method is to include an evaluated driving license tests in the universities final year program. This may gradually lead to an increased knowledge about the seriousness of the traffic safety problem among the public and politicians enabling them to rightly consider road deaths as a public health problem.

# REFERENCES


[1] Morris, Joseph R; Improving road safety in developing countries: opportunities for U.S. cooperation and engagement: workshop summary / Planning Committee for the Workshop on Traffic Safety in Developing Nations; p. cm. "National Research Council of the National Academies." ISBN 0-309-09423-2

[2] WHO; World Health Organization; GLOBAL STATUS REPORT ON ROAD SAFETY TIME FOR ACTION Dept. of Violence and Injury Prevention. ISBN 978 92 4 156384 0.

[3] WHO; World Health Organization; Global status report on road safety 2013: supporting a decade of action. ISBN 978 92 4 156456 4.

[4] Traffic Police, Ministry of the Interior, Kurdistan Regional Government, http://cabinet.gov.krd/, Erbil, November, 2014.

[5] Carlsson G. and Hedman K. O. (1990) A systematic approach to road safety in developing countries, Word Bank Report, Infrastructure and Urban Development Department.

[6] Othman S, Thomson R, Lannér G. Identifying Critical Road Geometry Parameters Affecting Crash Rate and Crash Type. 53rd AAAM Annual Scientific Conference; October 4–7, 2009; Baltimore, MD. Gothenburg, Sweden: Chalmers University of Technology; 2009. Oct, 2009. pp. 155–165

[7] NHTSA, U.S Department of Transportation. National Motor Vehicle Crash Causation Survey, DOT HS 811 059, Virginia, July 2008

[8] Salmon, P; Regan, M.; Johnston, I., Human Error and Road Transport: PHASE TWO – AFRAMEWORK FOR AN ERROR TOLERANT ROAD TRANSPORT SYSTEM, Monash University, Accident Research Center, Report No. 257, January 2006.

[9] VTI, Swedish Road and Transport Research Institute, Young drivers' overestimation of their own skill—an experiment on the relation between training strategy and skill. Linköping, Sweden, AAP, 1996 Mar;28 (2):243-50

[10] Othman, S. Why Cycling Vanished in the City of Erbil in Kurdistan, *University of Kurdistan Hewlêr, Poster Presentation, 3rd International Cycling Safety Conference November 2014, Gothenburg Sweden.,*

# NEW INTEGRATED ASSISTANCE FUNCTIONS FOR REAL WORLD ACCIDENT SCENARIOS

**Christoph Hartmann**
**Sakheen Harlapur**
**Thomas Brandmeier**
Technische Hochschule Ingolstadt
Germany

**Akshay Rajendra**
Continental, Chassis & Safety Division, Advanced Driver Assistance Systems Business Unit
Germany

**Holger Faisst**
Continental, Chassis & Safety Division, Passive Safety & Sensorics Business Unit
Germany

**Peter Lauer**
Continental, Chassis & Safety Division, Systems & Technology
Germany

Paper Number 15-0060

## ABSTRACT

Investigation of several accident databases consistently identified guardrail and embankment accidents as highly relevant in the context of real world accident scenarios that are not in the focus of today's vehicle safety functions. This work demonstrates the potential of future vehicle safety functions to reduce the severity of such accidents. To achieve this, two vehicle lateral controllers are in development that assist the driver in guardrail and embankment accident situations. A Linear Quadratic Regulator (LQR) approach, based on a single track model, is used to stabilize the vehicle in these situations with the goal to reduce the risk of secondary collisions and a rollover of the vehicle. Simulation results demonstrate the potential of the vehicle lateral controllers to stabilize the vehicle after a guardrail collision and to keep it in a safe area next to the guardrail. It is also demonstrated that the risk of a rollover in an embankment due to erroneous driver steering can be reduced. Further research is required to investigate the influence of driver inputs to the controllers in the mentioned accident situations. It needs to be discussed how the new controllers could be incorporated in the existing and future vehicle safety architecture.

## INTRODUCTION

According to the World Health Organization (WHO), road traffic accidents are the eighth leading cause of death worldwide and the leading cause of death among young people aged 19-25. While countries with a high income level have been able to reduce this number in the last years, the fatalities in low and middle income countries have increased (WHO 2013). The WHO has initiated the "Decade of Action for Road Safety" with the goal to safe five million lives in road traffic until 2020. The long term goal for countries with high safety standards is the "Vision Zero", meaning zero fatalities in road traffic. Car manufacturers, suppliers and legislative have worked hard on the improvement of vehicle safety in the last decades. The basis of today's passive safety systems is built on international standards and guidelines wherein the central components are highly reproducible crash tests. The PreCrash phase will have to be taken into account to achieve further improvement in the area of vehicle safety. Special attention should be put on real world accident scenarios that are not controllable by today's safety systems. Although the standardized laboratory crash tests are well representative for the majority of field crashes, it seems that a significant number of accident scenarios is not described completely (Allgemeiner Deutscher Automobil Club (ADAC) 2011). This requires the development of new Integrated Safety Algorithms based on the relevance of certain real world accident scenarios.

## ACCIDENT RESEARCH

Analyses of several accident databases identified significant accident scenarios that can no longer be neglected in the development of vehicle safety systems. Data obtained from the German In-Depth Accident Study (GIDAS), the United States Fatality Analysis Reporting System (FARS), the General Estimates System (GES) database as well as the ADAC accident research (ADAC 2013), illustrate consistently road departure accidents as the main cause for accidents involving severe injuries. GIDAS data shows that 20% of all accidents involving injured occupants have their root cause in unintentional leaving the road. Road departure as the consequence of a previous accident has been excluded in this analyses. The importance of road departure situations increases even more when the injury value is put into focus. Almost 49% of accidents involving fatally injured occupants have a road departure event as the initial starting point. In consequence, the need for new Integrated Safety Algorithms arises that concentrate on road departure accidents. A deeper analysis of road departue accidents identified situations involving an embankment or guardrail as primary accident event as highly significant in this accident category.

### Guardrail Accidents

Accidents that have a guardrail as the primary collision object are identified as the second most relevant scenario in the area of road departure accidents. They stand for 4.5%, or almost 7,000 injured people in the GIDAS analyses and they are also the fifth leading cause of accidents on German highways. Deeper analysis shows that 75% of the vehicles are involved in multiple collisions after they collided with a guardrail. This can either be another guardrail (52%), a vehicle (24%) or a different object (24%) like a tree. This is notable as the injury severity increases with multiple collisions. The delta-velocity, the velocity that is decomposed in the primary guardrail collision, is relatively low with a maximum of 20 km/h for more than half of the accidents. Therefore a high energy potential is left for secondary collisions, as the average collision velocity is more than 70 km/h for 51% of the vehicles during the primary guardrail contact. The analyses show also that the root cause of guardrail accidents are driving situations that relate to loss of control, inattention or fatigue of the driver. If proper reaction by the driver is initiated after the first guardrail contact, the risk of multiple collisions will be reduced. Support of the driver in such situations is therefore goal of the new vehicle safety functions.

### Embankment Accidents

Nearly 8% of all accidents involving injured occupants in a passenger car occur in the vicinity of an embankment, while the embankment can either go up or down. This corresponds to 12,000 people in Germany for the year 2010, according to the GIDAS analysis. Two thirds of the vehicles have a follow up collision after leaving the road. It is remarkable that 48% of the vehicles undergo a rollover that can be followed by a frontal or side impact. The initial angle between the vehicle's longitudinal axis and the roadside is for most of the accidents relatively small at the time the road is being departed; the maximum angle reached is 20° for in total 75% of the accidents. If attention is put on the root cause of such accidents, it is striking that over 90% of the accidents occur also due to loss of control, inattention or fatigue. This leads to the conclusion that a relatively harmless starting cause can lead to severe accidents, especially when a wrong reaction by the driver is initiated, like steering upwards in a downward embankment which increases the risk of a rollover. The new vehicle safety function currently under development aims on the support of the driver in such situations. The critical driving situation shall be detected by the function which leads to braking and steering actions by a vehicle lateral controller that brings the vehicle back to a state in which the driver can regain control over the vehicle.

## METHODS

The new integrated vehicle safety functions that are currently under development actively mitigate the severity of embankment and guardrail accidents during which the driver unintentionally worsens the situation with false lateral (Steering) and longitudinal (Brake and Gas pedal) control inputs to the vehicle. Existing safety functions like Electronic Stability Control (ESC) might even increase the severity of the situation in case of a panic reaction of the driver. The guardrail and embankment controllers presented in this paper use both longitudinal and lateral control inputs to stabilize and maneuver the vehicle to a safe state. Here, the safe state is defined by the reference trajectory which in case of the guardrail controller is defined as close to and parallel

to the guardrail. The embankment controller's main task is the reduction of the rollover risk by stabilizing the vehicle's dynamics.

**Vehicle Lateral Controller for Guardrail Accidents**

The guardrail controller stabilizes and keeps the vehicle at a certain lateral distance to the guardrail after a guardrail collision is detected. The states to be controlled are sideslip angle $\beta$, yaw rate $\dot{\psi}$ , deviation in yaw angle $\Delta\psi$ and deviation in lateral distance $\Delta y$. As cameras and other environmental sensors might not deliver trustable information after a collision, the curvature $\kappa_{ref}$ of the road for the next 80 – 100 m is continuously stored and referred to when a crash impulse is detected. The deviation in yaw angle $\Delta\psi$ and lateral distance $\Delta y$ is estimated using two fixed coordinate trajectory models, the vehicle trajectory model (VTM) and the virtual vehicle trajectory model (VVTM). The VTM calculates an estimated trajectory of the vehicle based on kinematic equations, while the VVTM acts as a reference trajectory and takes additionally the stored curvature $\kappa_{ref}$ into account. The controller itself is based on a linear single track model (Rajamani 2006) which can be given in state space representation, Eqs. (1-2).

$$\dot{X} = A(v)X + BU \tag{1}.$$

$$\begin{bmatrix}\dot{\beta}\\ \ddot{\psi}\end{bmatrix} = \begin{bmatrix} -\frac{C_f + C_r}{mv} & \frac{-C_f l_f + C_r l_r}{mv^2} - 1 \\ \frac{C_r l_r - C_f l_f}{J_z} & -\frac{C_f l_f^2 + C_r l_r^2}{J_z} \end{bmatrix} \cdot \begin{bmatrix}\beta\\ \dot{\psi}\end{bmatrix} + \begin{bmatrix}\frac{C_f}{mv}\\ \frac{C_f l_f}{J_z}\end{bmatrix} \cdot \delta \tag{2}.$$

$C_{f/r}$ are the tire cornering stiffness on the front and rear axle, $m$ denotes the overall vehicle mass, $v$ the vehicle velocity, $l_{f/r}$ are the distances of the front/rear axle to the vehicle's center of gravity, $J_z$ is the moment of inertia and $\delta$ is the steering wheel angle. The model is adapted to suit the needs of a lateral controller. The yaw moment $M_z$ is included as a second input to the model which results after some modifications and approximations in the adapted single track model, Eq. (3).

$$\begin{bmatrix}\dot{\beta}\\ \ddot{\psi}\\ \Delta\dot{\psi}\\ \Delta\dot{y}\end{bmatrix} = \begin{bmatrix} -\frac{C_f + C_r}{mv} & \frac{-C_f l_f + C_r l_r}{mv^2} - 1 & 0 & 0 \\ \frac{C_r l_r - C_f l_f}{J_z} & -\frac{C_f l_f^2 + C_r l_r^2}{J_z} & 0 & 0 \\ 0 & 1 & 0 & 0 \\ v & 0 & -v & 0 \end{bmatrix} \cdot \begin{bmatrix}\beta\\ \dot{\psi}\\ \Delta\psi\\ \Delta y\end{bmatrix} + \begin{bmatrix}\frac{C_f}{mv} & 0\\ \frac{C_f l_f}{J_z} & \frac{1}{J_z}\\ 0 & 0\\ 0 & 0\end{bmatrix} \cdot \begin{bmatrix}\delta\\ M_z\end{bmatrix} + \begin{bmatrix}0\\0\\v\\0\end{bmatrix} \kappa_{ref} \tag{3}.$$

The reference curvature $\kappa_{ref}$ is added as a disturbance to the model. The objective of the lateral controller is to bring the vehicle to stability, i.e. $\beta \to 0, \Delta\psi \to 0, \Delta y \to 0$, by applying active steering and active braking to the vehicle. The controller is designed as a Linear Quadratic Regulator (LQR) controller wherein the states are fed back to the input with a suitable gain feedback matrix $U = -K_c X$ (Lewis 1998). The feedback matrix $K_c$ is calculated by,

$$K_c = R^{-1} B^T P, \tag{4}.$$

wherein P is calculated by solving the algebraic Riccati equation,

$$A^T P + PA - BPR^{-1}B^T P + Q = 0. \tag{5}.$$

The matrices $Q$ and $R$ are weighting matrices between transient response and control effort. Larger $Q$ causes the states decay faster to zero while larger $R$ implies less control effort, e.g. less steering and/or braking. An approximate estimation method for $Q$ and $R$ is given in (Körtum et. al. 1993). The outputs of the LQR controller $\delta_{LQR}$ and $M_{z,LQR}$ are fed into a steer and brake controller respectively to convert steer angle to steer

torque and yaw moment to brake pressure. The steer torque is applied as an assisting torque to the steering wheel to support the driver while the brake pressure is used for wheel selective braking on the front axle to generate the required yaw moment. The complete controller concept is shown in Figure 1.

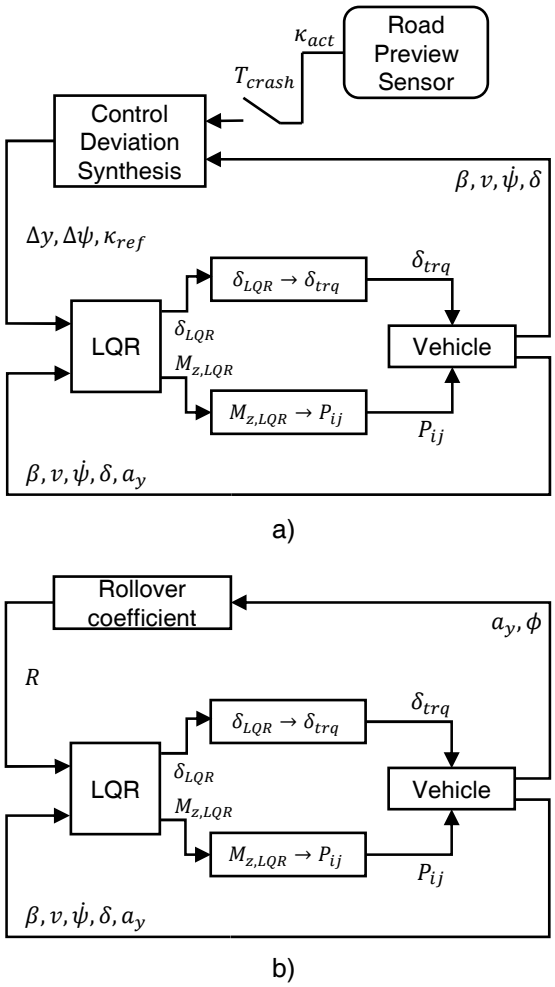


***Figure1. a) Flowchart of the lateral guardrail controller. b) Flowchart of the lateral embankment controller.***

**Vehicle Lateral Controller for Embankment Accidents**

The controller developed for embankment situations adopts the LQR approach for the design of the controller. Similar to the guardrail situation a triggering signal for the activation of the controller is needed, which indicates the vehicle is running into an embankment. This can be achieved by using inertial or environmental sensor based algorithms. The calculation of a rollover coefficient is used for the purpose of this work, Eq. (6). It is defined as,

$$R = \frac{F_R - F_L}{F_R + F_L} \tag{6}.$$

The value of $R$ is calculated accordingly to the changes in the normal loads on the wheels on the front axle. For example, if the right wheel lifts off, which is likely to happen in an embankment to the left side, the whole load is on the left wheel($F_R = 0, R = -1$). As the normal loads can usually not directly be obtained from sensors, the calculation of $R$ is approximated as given in Eq. (7), (Imine 2007).

$$R \cong \frac{2(h + h_R)a_y}{Tg} + 2\frac{h}{T}\phi \quad (7).$$

$h$ is the height of the center of gravity (CoG) of the sprung mass over the vehicle's roll centre, $h_R$ is the height of the roll axis, $T$ is the track width and $\phi$ is the roll angle. A more general approach of the kinematic single track model is used for the concept of the embankment controller as trajectory planning is not implemented in the current version, Eq. (8).

$$\begin{bmatrix} \dot{\beta} \\ \ddot{\psi} \end{bmatrix} = \begin{bmatrix} -\frac{C_f + C_r}{mv} & \frac{-C_f l_f + C_r l_r}{mv^2} - 1 \\ \frac{C_r l_r - C_f l_f}{J_z} & -\frac{C_r {l_r}^2 + C_f {l_f}^2}{J_z} \end{bmatrix} \cdot \begin{bmatrix} \beta \\ \dot{\psi} \end{bmatrix} + \begin{bmatrix} \frac{C_f}{mv} & 0 \\ \frac{C_f l_f}{J_z} & \frac{1}{J_z} \end{bmatrix} \cdot \begin{bmatrix} \delta \\ M_z \end{bmatrix} \quad (8).$$

The steering angle $\delta$ and the yaw moment $M_z$ calculated by the model act as inputs to the controller for the stabilization of the vehicle and the reduction of the rollover risk. The calculation of the feedback matrix $K_C$ and the matrix $P$ is done accordingly to the guardrail controller as the controller tries to reduce the states $\beta$ and $\dot{\psi}$ to a minimum.

**RESULTS**

Simulated test scenarios have been carried out in IPG CarMaker® to test the vehicle lateral controllers for guardrail and embankment accidents. The results of the tests concerning the guardrail controller are compared to results obtained by an ESC system and the simulated IPG Driver™ as guardrail accidents might also cause action by an ESC system due to high yaw rates induced by the crash impulse from the guardrail. Figure 2 shows a situation in which the vehicle left the road while it was driving through a curve and crashed into a guardrail on the right side of the road.

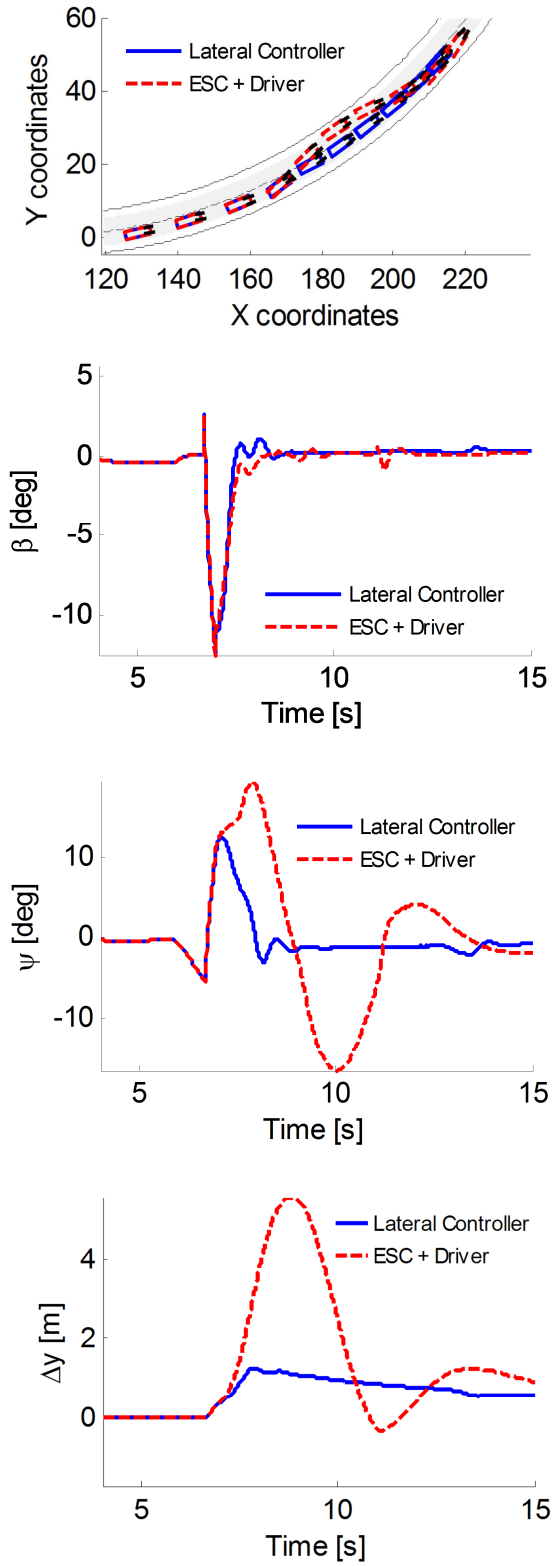


*Figure2. Lateral Guardrail Controller, Situation 1: Sideslip angle β, yaw angle ψ and lateral distance Δy.*

The initial velocity at the time of the crash was 70 km/h and the impact angle with the guardrail was 5.5°. It can be seen that the vehicle that is only equipped with an ESC system has a secondary impact on the other side of the road (146, 42) while the vehicle equipped with the lateral guardrail controller can be stabilized after the primary collision (139, 12). The sideslip angle and the yaw angle are also reduced faster to a minimum by the lateral guardrail controller as by ESC. Also the lateral distance to the guardrail is well under control as the vehicle stays in the safe area of 0.5 m next to the guardrail. The situation depicted in Figure 3 shows similar results.

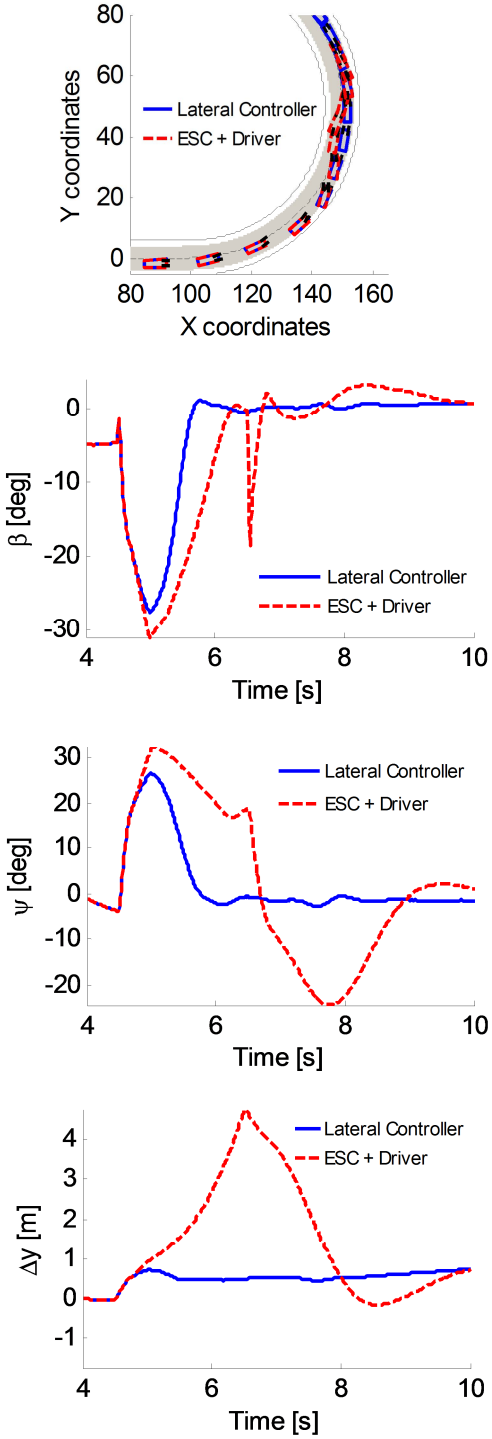


***Figure3. Lateral Guardrail Controller, Situation 2: Sideslip angle β, yaw angle ψ and lateral distance Δy.***

The driver of the vehicle only equipped with ESC is not able to keep the vehicle under control after the primary collision (166, 11) with 83 km/h and an impact angle of 4.2°, while the lateral controller keeps the vehicle within the driving lane. Also the yaw angle and side slip angle are reduced to a minimum within 1 s after the impact.
For the test of the embankment controller several downward embankments with an angle of 27° to 39° degree were created in CarMaker®, which represent the range of the standard embankments on German highways. The driving maneuver was constructed in a way that the driver wants to steer back onto the road after the vehicle went off the road and entered the embankment. This behavior is likely to cause a rollover as the lateral forces on the vehicle increase due to the embankment angle. Figure 4 shows a situation wherein the vehicle entered a 27° embankment while driving with 210 km/h.

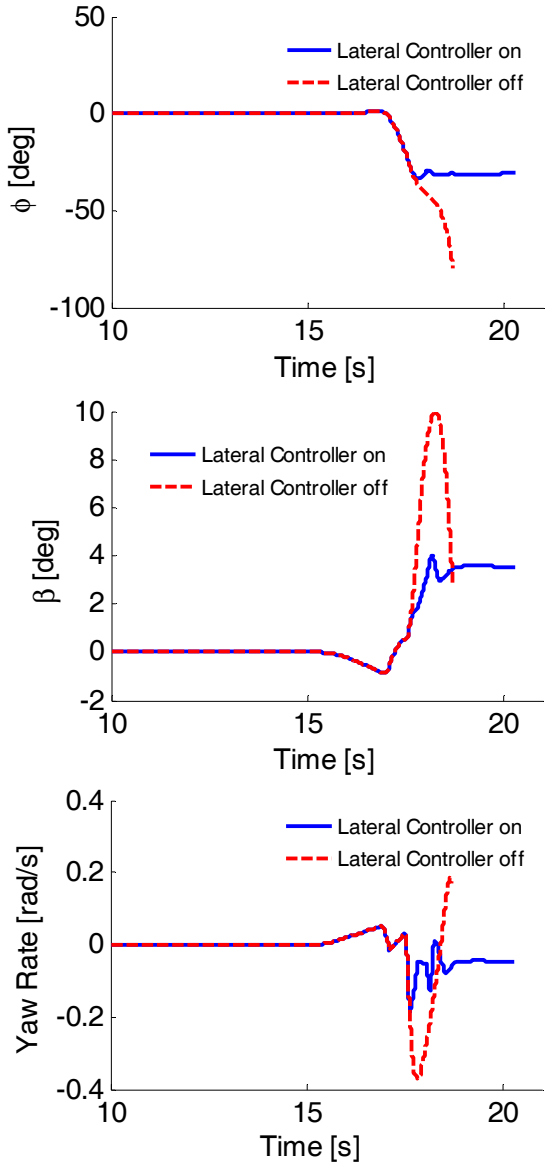


***Figure4. Embankment Controller, Situation 1: Roll angle $\phi$, sideslip angle $\beta$ and yaw rate $\dot{\psi}$.***

Here, the lateral controller is able to prevent the rollover while the roll angle of the uncontrolled vehicle increases until the simulation stops, around 80°. The same result is achieved for an embankment of 39° at 100 km/h as it can be seen in Figure 5.

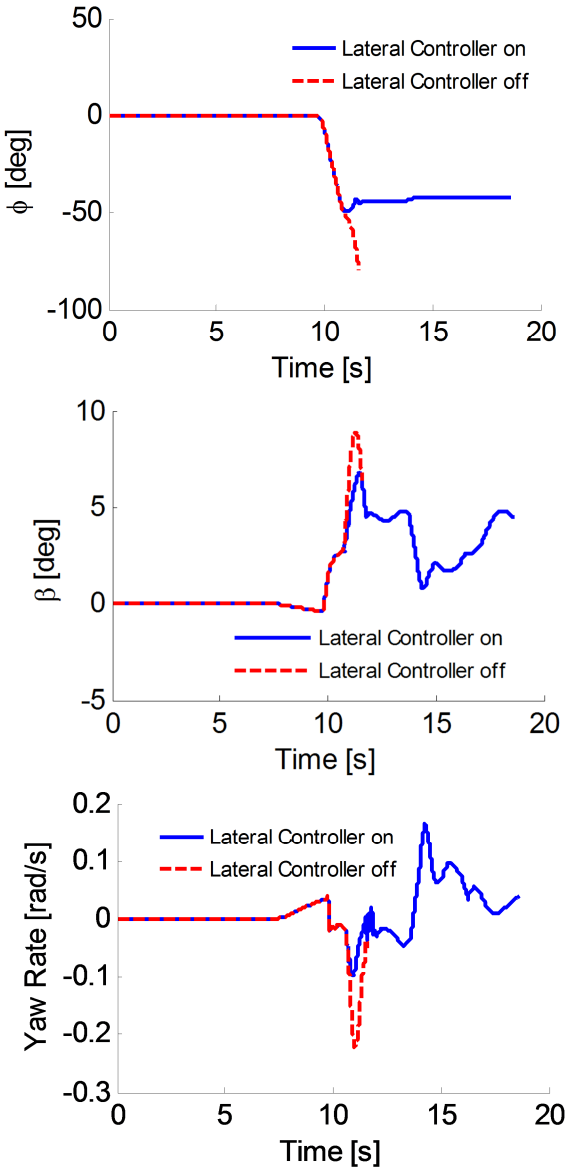


***Figure5. Embankment Controller, Situation 2: Roll angle ϕ, sideslip angle β and yaw rate ψ̇.***

From the further depicted results represented by the side slip angle and the yaw rate of the vehicle, it is shown that the driver's inputs to the vehicle worsen the stability of the vehicle and lead to a rollover. However, if the controller is active then the outputs of the controller act opposite to the driver and prevent the rollover by stabilizing the vehicle.

## DISCUSSION AND CONCLUSION

The analysis of several accident databases shows that accidents involving a guardrail or an embankment have a high relevance in the area of vehicle safety technologies. The developed vehicle lateral controllers for these two situations show that they have the potential to reduce the severity of such accidents by braking and steering interventions to the vehicle. Although the first simulation results are very promising, deeper analysis of the interaction between the vehicle and the driver in these situations has to be conducted. Governmental as well as functional safety requirements limit the maximum torque that can be superimposed onto the steering

wheel. This requires real world tests of the lateral controllers to understand the driver reaction to the applied torque. The introduction of an electronic steering and therefore the decoupling of steering wheel and steering axle might be a necessary step towards this topic. It is also necessary to investigate how a driving stability program like ESC interacts with the developed controllers. Usually, ESC tries to follow the desired driving direction of the driver, which in the discussed road departure situations might not always be the right choice. A discussion is needed to establish the new lateral controllers into the existing safety architecture. A highly automated driving level is needed in the mentioned guardrail and embankment situations as they are likely to be uncontrollable by the driver and today's safety functions alone.

## ACKNOWLEDGEMENTS

SPONSORED BY THE

Federal Ministry of Education and Research

This research work is being funded by the German Federal Ministry of Education and Research (Grant Number 16N11564K, Project HiPe-FiS, 2013 to 2016). The authors would like to thank their partners IPG Automotive GmbH in Karlsruhe, Ibeo Automotive Systems GmbH in Hamburg and Continental in Regensburg and Lindau.

## REFERENCES

[1] Allgemeiner Deutscher Automobil Club (ADAC). *Abkommensunfälle auf Landstraßen*; 2013.

[2] Allgemeiner Deutscher Automobil Club (ADAC). *Korrelation zwischen Crashtest Ergebnissen und realen Unfällen*; 2011.

[3] Imine H. *Heavy Vehicle Modeling: Evaluation and Prevention of Rollover Risk*; 2007.

[4] Körtum W., Lugner P. *Systemdynamik und Regelung von Fahrzeugen:* Springer; 1993.

[5] Lewis F. L. *Linear Quadratic Regulator (LQR): State Feedback Design*; 1998.

[6] Rajamani R. *Lateral Vehicle Dynamics: Vehicle Dynamics Control:* Springer; 2006.

[7] World Health Organization (WHO). *Global Status Report on Road Safety: Supporting a Decade of Action*; 2013.

# A SURVEY OF ELECTRICAL AND ELECTRONIC (E/E) NOTIFICATIONS FOR MOTOR VEHICLES

**Taylor T. Johnson**
Department of Computer Science and Engineering
University of Texas at Arlington
USA

**Raghunath Gannamaraju**
**Sebastian Fischmeister**
Department of Electrical and Computer Engineering
University of Waterloo
Canada

Paper Number 15-0063

**ABSTRACT**
Modern motor vehicles are becoming increasingly dominated by electrical and electronics (E/E) systems. While this trend is clear, its implications are uncertain. In this paper, we investigate data on safety-related notifications from the United States, Canada, and Europe to analyze questions and trends related to E/E systems. The data analysis indicates that E/E systems are a growing issue for motor vehicle safety, that the time delay for E/E notifications is longer than that for other notifications, and that specific subsystems are more prone to E/E problems than others.

## 1 INTRODUCTION

Modern motor vehicles are complex safety-critical systems that involve the coordination of dozens of computers, communication buses, actuators, and sensors [1, 2]. Their overall functionality and safety is dependent upon the correct and timely operation of electronics and software to sense and control physical states through sensors and actuators. Table 1 reports estimated numbers of ECUs (electronic control units; the usual term used for computers in cars) in recent model year vehicles and literature sources for these estimates. With approximately 50 to 75 ECUs, modern cars are truly distributed computer systems running on wheels.

Since motor vehicles are safety-critical systems, countries developed safety standards to protect consumers and the public. Regulatory standards such as the Federal Motor Vehicle Safety Standards and Regulations (FMVSS) [3] of the United States Department of Transportation (USDOT) codify required safety systems, their performance, and overall vehicle safety. For example, FMVSS Standard No. 126 governs electronic stability control (ESC) systems and includes the following requirement [3, Standard No. 126, § 5.1.1]: *"Is capable of applying brake torques individually to all four wheels and has a control algorithm that utilizes this capability."* Some countries have dedicated mandatory standards for tire safety. In addition to these regulatory standards on vehicle safety, the industry voluntarily has also created and uses domain-specific standards. For example the ISO 26262 [4] standard on *Road Vehicles: Functional Safety* is used for developing, maintaining, and decommissioning automotive components. The MISRA C [5] standard provides guidelines for source code in safety-critical applications using C and C++. Unlike FMVSS, complying with the ISO 26262 or MISRA C is optional.

Each country instated a regulatory agency in conjunction with these standards. These regulatory agencies police the mandatory safety standards and notify the public about non-compliance and safety-related concerns for products sold in their jurisdiction. In the United States, the National Highway Traffic Safety Administration (NHTSA) regulates vehicle safety through standards like the FMVSS. In Canada, Transport Canada is responsible for transportation policies and programs such as the *Motor Vehicle Safety Regulations* [6] and related acts. In the European Union (EU), the European Commission and member countries are jointly responsible for safety regulations such as the *General Safety Regulation* [7] and related laws. In addition, the European Commission administers the Rapid Alert System for non-food dangerous products (RAPEX) to facilitate the rapid exchange of information to the consumer on safety-related issues.

Each of these agencies maintains datasets (databases) on automotive safety notifications, potential hazards arising from the issues, and recommended corrective actions. Notifications in the datasets concern

| Year | List of: Vehicle (ECUs) [Source] |
|---|---|
| 2004 | VW Phaeton (61) [8], Current Upper Class (70) [9] |
| 2005 | Volvo cars (40) [10] |
| 2006 | Infiniti (11) [11], Toyota Prius (23) [11] |
| 2007 | Current Premium Car (70) [12] |
| 2009 | Current Premium Car (70-100) [13], Current Low-end Car (30-50) [13], Average Car (30-45) [14], Luxury Cars (70) [14] |
| 2010 | Jeep (7) [11], Range Rover (41) [11], Basic vehicles (30) [15], Some Luxury Cars (100) [15] |
| 2012 | Most new vehicles (100) [16] |
| 2014 | Infiniti (34) [11], Dodge Viper (19) [11], Range Rover (98) [11], Jeep (17) [11], Toyota Prius (40) [11], Average Vehicle (60) [17] |

Table 1: Reported and estimated numbers of ECUs in cars. *"Year"* is the year of reporting.

hazards and risks when operating motor vehicles, particularly as they pertain to non-compliance with standards like FMVSS. For instance, the purpose of the FMVSS ESC standard mentioned previously is *"...to reduce the number of deaths and injuries that result from crashes in which the driver loses directional control of the vehicle, including those resulting in vehicle rollover"* [3, Standard No. 126, § 2]. A malfunctioning component used in the ESC would then raise a hazard and thus a safety concern. A *hazard* is the possibility of suffering harm or injury of road participants (users). Road participants include, for instance, the driver, passengers, but also extends to pedestrians and cyclists. A hazard by itself is sufficient to cause an investigation; for example, the NHTSA may start an investigation upon receiving complaints from owners about defects. The level of risk of the hazard occurring during driving is a key element, with a *risk* being a situation that involves exposure to danger. There are many dangers present in the operation of motor vehicles, such as injuries due to collisions with other vehicles or objects, or burns due to engine fires or seat heater failures. Often a defect in the design or the implementation of a safety-related system in the motor vehicle will create an unanticipated risk that needs to be investigated. A safety-related *defect* in a motor vehicle or system thereof exists when there is increased risk beyond an acceptable level. In this situation, the defect causes the system to become unsafe and consequently corrective actions have to be taken, together with a notification of the public through the regulatory agency.

This paper presents an analysis of electrical and electronic (E/E) notification datasets from government regulatory agencies in the United States, Canada, and Europe. Since E/E encompasses software, notifications related to software are also part of our analysis. With this data, we explored several questions, such as the trend of E/E notifications over time in terms of the number of notifications and affected vehicles. We also analyzed E/E notifications in relation to Non-E/E notifications, and investigated the risk types associated with defects and the relationship between notifications and the model year for E/E vs. Non-E/E notifications. The paper concludes with additional observations made during the analysis and provides a call-to-action for researchers, the regulatory agencies, and also the automotive industry.

## 2 METHODS AND DATA SOURCES

This paper analyzes safety notification datasets from several data sources of regulatory agencies. The main aim of the study is to determine the prevalence and quantity of E/E notifications and compare them to Non-E/E notifications. To this end, we analyzed data from the NHTSA, Transport Canada, and RAPEX. These datasets are publicly available and provide a rich and diverse view into the nature of safety-related notifications and recalls in the three jurisdictions (the US, Canada, and Europe).

### 2.1 E/E Systems, Defects, and Notifications

We define our terminology following the vocabulary used in the ISO 26262 standard [4]. ISO 26262 is a comprehensive standard on functional safety of components (i.e., items) built into road vehicles.

We analyze datasets from three data sources: *"Complaints, Defect Investigations, Recalls, & Technical Service Bulletins"* (NHTSA) [18], *"Road Safety Recalls Database"* (Transport Canada) [19], and *"Rapid Alert System for non-food dangerous products"* (RAPEX) [20]. Each data source provides a dataset containing notifications. A *notification* is an entry that results from the process associated with the dataset. Each data source follows a different process for adding notifications to its datasets. Consequently a notification can be a compulsory recall, but it can also just be a benign complaint that led to an investigation, and ended in

| Data Source | Dataset | Contents | No. Entries | Model Years | Access Date | Source |
|---|---|---|---|---|---|---|
| NHTSA | *"Recalls"* | Vehicle safety recalls | 108 686 (18 768) | 1960–2015 | FEB-2015 | [21, 18] |
| Transport Canada | *"Road Safety Recalls Database"* | Vehicle safety recalls | 10 596 | 1970–2015 | JAN-2015 | [19] |
| European RAPEX | *"Rapid Alert System for non-food dangerous products"* | *Motor vehicles* category in non-food dangerous products | 1 246 | 2006–2015 | FEB-2015 | [20] |

Table 2: Summary of the datasets analyzed including the information contained. The access date is the date the dataset was downloaded for the analysis in this paper. While the datasets may already (as of February 2015) contain information for 2016 model year vehicles, only up to model year 2015 were included in the analysis in this paper. The NHTSA number in parenthesis is the number of unique campaign numbers.

the voluntary action of a press release. Section 2.2 discusses the data sources and datasets in more detail.

Since this paper is concerned with E/E artifacts, we must distinguish between E/E and Non-E/E artifacts. The ISO 26262 standard specifies *item* as the highest-level artifact. An item is then realized in systems, which are further broken down into elements. To keep the paper accessible to the general reader and because notifications in the datasets are usually related to specific artifacts, we will mostly use the term system for these instead of a specific breakdown of item, system, or element as defined in the ISO 26262 standard. We call a notification an *E/E notification*, if the reason for the notification originates from an E/E system and is not of mechanical or chemical nature. The ISO standard defines an E/E system as one that includes electrical or electronic elements, including (software) programmable electronic elements. Example E/E systems include power supplies, sensors, and other input devices, communication paths, and actuators and other output devices. For example, an E/E notification would be one related to stalls in hybrid vehicles due to the control software overheating power transistors. All notifications related to other technology (as defined for term 1.84 ISO 26262) are *Non-E/E notifications*. For example, a holding bracket loosening due to improper mounting is a Non-E/E notification.

### 2.2 Data Sources and Datasets

In our analysis, we use several datasets from the NHTSA, Transport Canada, and RAPEX from Europe to classify E/E and Non-E/E notifications. Table 2 provides a summary of the datasets and their contained information.

#### 2.2.1 Complaints, Defect Investigations, Recalls, & Technical Service Bulletins (NHTSA)

The NHTSA maintains extensive datasets of vehicle and system recalls and complaints online [18]. These are categorized into several major datasets including *"Complaints," "Defect Investigations," "Recalls," "Technical Service Bulletins"* [18, 21], as well as *"Foreign Campaigns"* [22]. The NHTSA is part of the US Department of Transportation, was established in 1970, and has a mission to reduce deaths, injuries, and economic losses arising out of motor vehicle crashes. As part of these responsibilities, the NHTSA sets and regulates safety performance standards for motor vehicles, such as through FMVSS [3], monitors and investigates consumer complaints regarding motor vehicles, and also conducts research on driver behavior and traffic safety, such as conducting crash tests [23].

The NHTSA maintains information about all safety-related defect and compliance campaigns that occur in all models of motor vehicles in the US starting from notifications made in the year 1967. Defects are defined in Section 1, and *compliance* means that a given motor vehicle and its systems comply with regulatory standards, such as FMVSS. A system is *non-compliant*, if it violates a regulatory standard, so non-compliance notifications correspond to violations of FMVSS and other regulations. As ISO 26262 is a voluntary standard, only federal regulations like FMVSS are considered in the definition of compliance. The dataset also contains information on model year vehicles before 1967, since defects reported in 1967 can affect older models. The NHTSA stores different categories of information in its *"Complaints"*, *"Defect Investigations"*, *"Recalls"*, and *"Service Bulletins"* datasets. Complaints are reports of problems from vehicle owners to the NHTSA, and are investigated by the NHTSA and tracked in an investigation dataset. Service bulletins are instructions from the manufacturer regarding how to correct defects. There is a process to be followed by a vehicle

owner to report problems with their vehicles. When there is a problem with their vehicle or equipment, the owner can file a complaint with the NHTSA, for example online at http://www.safercar.gov. As part of a complaint, the owner may provide the vehicle's VIN, the incident information including, if there was a crash, fire, injury, or fatality as a result of the incident, and other information. Complaints are entered into the NHTSA complaint dataset and will be used to determine, if a safety-related defect trend exists. These complaints are searchable on the NHTSA's website based on various criteria including the make, model, and year of the vehicle. Investigations are taken up by the NHTSA as a result of complaints by vehicle owners, and may result in a recall or other action if it is deemed necessary. The NHTSA also has the authority to fine automakers. Additionally, a manufacturer may notify the NHTSA of a potential defect, if they become aware of one, so the process of creating notifications may be driven either by the NHTSA or the manufacturer.

This paper uses the NHTSA *"Recalls"* dataset that contains all NHTSA safety-related defect and compliance campaigns since 1967 [21]. A *recall* is described [24] as: *"When a manufacturer or the National Highway Traffic Safety Administration determines that a car or item of motor vehicle equipment creates an unreasonable risk to safety or fails to meet minimum safety standards, the manufacturer is required to fix that car or equipment."* A manufacturer will have to rectify or replace parts, if the recall is a safety recall. The manufacturer will also have to inform the vehicle owner of the recall. More information about recalls and how they are notified and how to find if a particular vehicle is under recall or not are in the Vehicle Owners section [24]. The *"Recalls"* dataset consists of recall records. Information contained as part of a recall record includes the vehicle make, models, model years, component description, beginning and end dates of manufacturing, the potential number of affected vehicles, the date of notification to the owner, a defect summary, a consequence summary, a correction summary, and recall notes [18].

### 2.2.2 Road Safety Recalls Database (Transport Canada)

In Canada, transportation policies and programs are the responsibility of Transport Canada [25]. Transport Canada promotes safe, secure, efficient, and environmentally-responsible transportation. Transport Canada reports to Canadian Parliament and the Minister of Transport. Transport Canada administers various programs related to safety of vehicles such as importation of vehicles, advanced vehicle technologies, commercial vehicles, defect investigations, and vehicle recalls. The *"Road Safety Recalls Database"* in Canada is managed and maintained by Transport Canada. Transport Canada also documents recall campaigns, update the on-line recalls database, and monitor recall completion rates. Each record in the dataset contains the date of recall, make, model, system, model year(s) affected, recall details, category of the vehicle, etc. [19]. The records start from 1970 model year vehicles in Transport Canada database. Transport Canada defines safety-related defects as those that interfere with the safe functioning of the vehicle and are present in a group of similar vehicles [25]. Such defects are not due to normal wear and tear, operator negligence, nor inadequate maintenance, and may cause problems that occur with little or no warning that endanger the safety of road users. If motor vehicle owners in Canada suspect safety-related defects in their vehicles, they can report them to Transport Canada. Once a defect is reported, the defect complaint is entered into the *"Defect Complaints Database"* and reviewed by an analyst. If warranted, Transport Canada will initiate an investigation into the complaint that may result in recalls.

### 2.2.3 Rapid Alert System for non-food dangerous products (RAPEX)

RAPEX (*"Rapid Alert System for non-food dangerous products"*) was established in the EU as a rapid alert system that facilitates rapid exchange of information between member states of the EU and the European Commission on measures taken as a result of products posing risk to consumers. RAPEX relies on close cooperation between the Commission and individual national authorities of participating member countries.

RAPEX has notifications going back to the year 2006. In this dataset, each notification record has a risk level. The risk level can be "Serious" or "Other". The risk level is also classified based on the type of user distinguishing consumer or professional users. Each record has the week and year of notification, a reference number, the country that notified, and detailed description of the product including the name, category, type, batch number, and, in many cases, also a picture of the product. The notification also lists the risk type, which is the kind of injury that can result from the hazard, and includes risk types such as burns, electric shock, etc. [20]. Finally, a notification also includes information about the measures taken by the notifying country to mitigate risks from the product.

The notification process for RAPEX starts with the identification of a risk with respect to a product. The identification of risk can happen by a competent national authority, or the manufacturers and distrib-

utors of the product. Manufacturers and distributors must inform the national authority of any dangerous product, specifically consumer products that are on the market and present a risk to consumers (like electric shock, injury, etc.) such that the product may not remain on the market [26]. In this case, manufacturers and distributors should take appropriate preventative and corrective actions. When this identification happens, either the appropriate authority or the responsible business takes relevant measures to eliminate the risk. These measure can include withdrawing the product from the market, recalling the product from consumers, or issuing warnings. As a next step, each RAPEX national contact point informs European Commission about the product and all relevant information. The European Commission then disseminates this information to all participating countries [26].

#### 2.2.4 Differences between Datasets

Though the primary purpose of the data in these three datasets described above is to inform the consumer of issues that may be affecting a particular model of a vehicle, there are differences in the amount and format of data available in each dataset. The NHTSA and Transport Canada notifications do not contain columns to indicate the risk level of the problem. On the other hand, RAPEX notifications indicate risk level by classifying the notifications as serious or other. The NHTSA and Transport Canada datasets do not classify the risk into a fixed type of risk, and instead, their notifications describe the consequences of the defect. RAPEX classifies notifications based on a fixed number of risk types like asphyxiation, burns, chemical, fire, injuries etc. Another difference is that the NHTSA and Transport Canada datasets do not identify the country of origin of motor vehicle. However, RAPEX notifications have the country of origin of the vehicle. NHTSA does not regulate vehicles that are primarily intended for off-road use such as all-terrain vehicles (ATVs), snowmobiles, dirt bikes, etc.—which are regulated by the Consumer Product Safety Commission [CPSC])—while the Transport Canada and RAPEX datasets each have notifications about off-road vehicles.

### 2.3 Classifying E/E Notifications

We analyzed the datasets through two separate means. The first method used a manual classification involving two people and two reviewers and was performed for the Transport Canada, the RAPEX, and partially for the NHTSA dataset. The second method was an automated classification using text-based searches to classify notifications involving E/E systems and was performed for the NHTSA dataset.

A classified E/E notification is a *false positive*, if the actual cause of the corresponding defect was *not* due to problems in the E/E system. For example, if a notification was classified as an E/E notification in the tires that was in no way related to any E/E system (e.g., a tire pressure monitoring system) like improper tire pressure labeling, this would be a false positive. An E/E notification would be a *false negative*, if it was not identified. Any classification can include incorrect assignments, usually reported as *precision* and *recall*. In our case, precision is the fraction of notifications that were labeled as E/E notification and should be E/E notifications. Precision is degraded by false positives, which are notifications labeled as E/E, but that only mention other technologies. Recall, as a quantitative metric, is the fraction of E/E notifications relative to all E/E notifications. Recall targets characterizing false negatives, since recall is affected by classing notifications as Non-E/E although they are E/E notifications. In the ideal case, there are no false positives and no false negatives. There are several reasons this classification is performed for notifications and not for defects. First, the datasets only contain information on notifications that may or may not be correlated with known defects. This may occur in recent model year vehicles for which regulators and manufacturers have not yet initiated notifications, as defects may still be unknown. In the ideal case, this classification would find the set of all E/E defects and not the set of all E/E notifications, but this is impossible as these defects may be unknown. Additionally, the datasets themselves could contain false positives and false negatives, although the regulatory process should minimize these mis-classifications. Another reason for mis-classifications is due to grammatical and spelling errors, which may be detected and corrected easily in manual review, but is difficult to handle for automated classification, but may be handled with sophisticated natural language processing (NLP) techniques.

#### 2.3.1 Manual Classification and Review

We used full manual classification for the Transport Canada and RAPEX datasets, and partial manual classification for the NHTSA dataset. Full manual classification involved two persons categorizing the notifications into the categories of E/E or Non-E/E. For the RAPEX and the Transport Canada datasets, two undergraduate students investigated one notification at a time and assigned an appropriate label to them.

| | | | | | |
|---|---|---|---|---|---|
| computer | software | firmware | electronic control unit | ecu | engine control module |
| ecm | re-flash | re-program | control module | control unit | bug |
| version | update | program | overflow | electronic | electric |

Table 3: Keywords used for automatic classification of the NHTSA dataset.

To ensure high precision and high recall, and thereby high quality, we used an independent validation step after the manual classification. After the two undergraduate students completed the classification, one of the co-authors randomly selected a small subset to validate the classification. Any found mis-classification was subsequently corrected. On top of the validation, we also performed automated sanity checks to inspect specific notifications. For example, we carefully reinspected all notifications that carried the system type "Electrical" in the Transport Canada dataset, and double-checked all notifications that contained specific keywords, such as, for instance, motor, ECU, short circuit, and software. For the NHTSA dataset, one of the co-authors manually inspected the entries that we identified using a search-based classification. The purpose for this inspection was to identify and eliminate false positives to improve precision. In particular, it also highlighted certain bad keywords that resulted in high rates of false positives, such as "upgrade," that were excluded from subsequent keyword searches.

#### 2.3.2 Automated Classification

Automated classification was used for the NHTSA dataset, followed by the manual review discussed in Section 2.3.1. The NHTSA dataset contains several fields that have natural language data (i.e., English sentences and text), such as the "Defect Summary" (`DESC_DEFECT`) field. Specifically, each notification includes "Defect Description," "Defect Consequence," "Corrective Action," and "Notes" fields contain natural language descriptions of the defect, its correction, etc. that are used in classifying the notification as an E/E notification. Additionally, the "Component Name" field contains a semi-categorical name of the defective component (system) and was also used for classification. The "Component Name" field includes, for example, categories such as "ELECTRICAL SYSTEM: SOFTWARE". However, we did not classify by solely the "Component Name" field because many E/E notifications are not precisely categorized. For instance, some notifications for software defects, such as NHTSA notification 04V254000, are not correctly categorized as "ELECTRICAL SYSTEM: SOFTWARE," along with several others shown in Table 4. Each of these fields were searched using regular expressions for the set of keywords in Table 3.

Spacing was required between short keywords (e.g., for "ecu") and all standard permutations of keywords were used (e.g., "re-flash," "reflash," "re flash," etc.). If any substring in these fields matched any of these keywords (case insensitive and allowing permutations for spacing), they were classified as candidate E/E notifications that were then manually reviewed. Additionally, the NHTSA dataset contains many effectively duplicate entries that were accounted for (when necessary) by using the campaign number to uniquely identify the notifications to not duplicate counts of the number of affected vehicles or numbers of notifications.

## 3 RESULTS FROM ANALYSIS OF THE DATASETS

With access to these datasets, we could investigate a number of questions for E/E notifications. This section describes four questions we looked at in detail. Additional observations are part of Section 5.1.

### 3.1 E/E Systems are Increasingly Becoming a Problem

The dataset analysis indicates that E/E notifications have been increasing in recent model year vehicles and for notices issued in recent years. Specifically, E/E notifications are increasing over time in the Transport Canada and the NHTSA datasets in terms of all of the following: (a) the percentage of E/E notifications compared to Non-E/E notifications per model year (Figure 1), (b) the absolute numbers of vehicles and systems affected by E/E notifications compared to those affected by Non-E/E per notification year (Figure 2), and (c) the absolute number of notifications per vehicle model year (Figure 3). The RAPEX dataset also confirms this when looking at the total number of notifications over the years (Figure 6).

### 3.2 E/E Notifications have Greater Delay than Non-E/E Notifications

An interesting question is to determine whether certain types of notifications reach further back in time than others. We interpret this as being that the particular defect identified in the notification has taken longer to be detected than notifications that reach back fewer years.

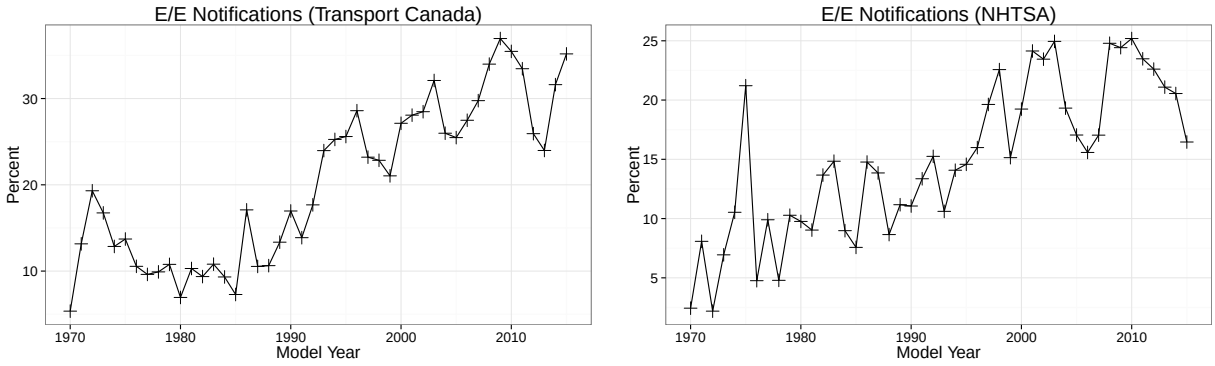


Figure 1: Transport Canada and NHTSA percentage of E/E notification out of all notifications across all makes and models versus model year.

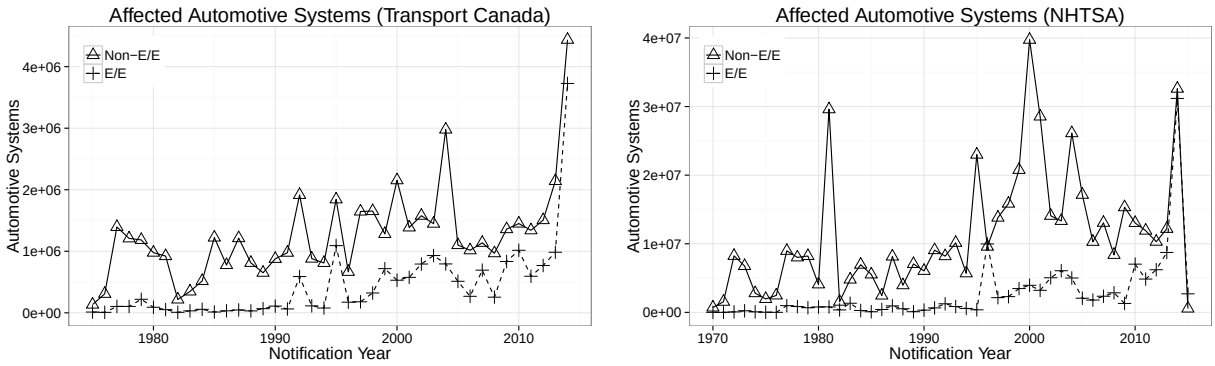


Figure 2: Transport Canada and NHTSA sum of the number of vehicles potentially affected by notifications versus notification year, categorized into E/E and Non-E/E notifications.

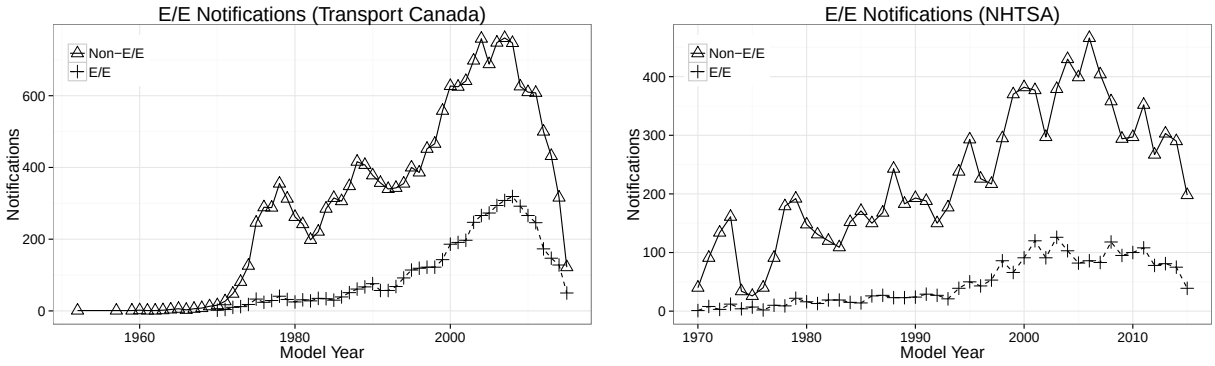


Figure 3: Transport Canada and NHTSA E/E and Non-E/E notification counts versus model year.

The delay of a notification is the date of the notification minus the starting manufacturing date. Figure 4 shows notification delays, categorized into E/E and Non-E/E notifications. In the Transport Canada dataset, the dates of manufacturing are not available, so the notification delay is approximated as the year of the notification minus the model year. If multiple models and model year vehicles are effected, the date or earliest model year across all the affected models will be used. For example, if a notification covered three models over different model years (2005 to 2010, 2007 to 2010, and 2005 to 2008), then the approximated delay will be $2011 - 2005 = 6$ years. While ideally the manufacturing date would be used instead of the

model year date, the manufacturing date is not always available in the datasets, while the notification date, affected models, and model year are more readily available.

Both datasets show that on average, E/E notifications reach back further than Non-E/E notifications. Thus, recent model year vehicles may also be correlated with having additional E/E defects that have not yet initiated notifications. In the Transport Canada dataset, the notification delay mean was 2.21 years for E/E defects and 1.83 years for Non-E/E. In the NHTSA dataset, the notification delay mean was 2.23 years for E/E defects and 2.14 years for Non-E/E. The differences between the notification delay was statistically significant (Wilcoxon rank sum test) for both datasets. These results are highlighted by E/E notifications such as NHTSA recalls 11V395000 and 14V047000 described in Table 4, that each had delays of around six years.

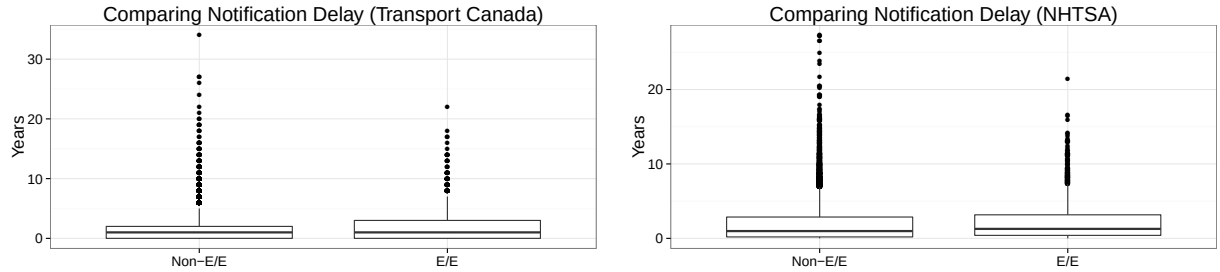


Figure 4: Transport Canada and NHTSA notification delay between E/E and Non-E/E notifications from 1970 to 2014 model years are illustrated as box plots.

### 3.3 E/E Notifications Appear for Electrical Components, Lights, and Airbags Most Frequently

The dataset from Transport Canada and the NHTSA categorized the notifications based on the vehicle subsystem that was affected. Transport Canada splits the data into 20 categories. The NHTSA uses 26 categories with additional sub-categories. The interesting question is which subsystems are prevalent in E/E notifications. Based on the datasets, we can identify the subsystems that are most likely affected by E/E problems within each jurisdiction. Figure 5 shows the frequency to which subsystem category the notification was assigned to in the different datasets.

A direct comparison is impossible, because the different datasets split up the notifications into different categories, and also the dataset from Transport Canada has generic category called *"Electrical"* that dominates the notifications related to E/E systems. Furthermore, due to regional influences, the datasets contain different data (see Section 2 for these differences). Nevertheless we can still provide a subjective, qualitative

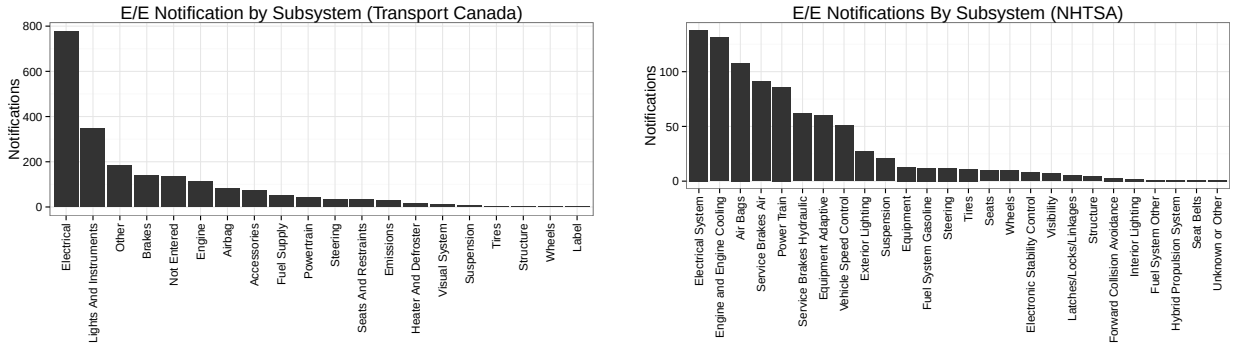


Figure 5: Subsystems specified for notifications related to E/E problems.

interpretation of the data in Figure 5. Subsystems that seem to rank highly when comparing notifications related to E/E problems are (in no particular order): air bags, lights and instruments, engines, brakes, and

the power train. For this categorization, we combined: brakes (i.e., "Service Brakes Hydraulic", "Service Brakes Air" in the NHTSA and "Brakes" in the Transport Canada dataset), power train (i.e., "Throttle Control", "Power train", "Transmission Control"), and instruments (i.e., "Lights and Instruments", "Lights", and "Instrument Cluster").

### 3.4 E/E Notifications Dominate Others with Respect to Fire Hazards

RAPEX provides detailed information on the risk types for the components involved in the notification. The dataset uses four distinct categories for the types of risk: burns, fire, injuries, and chemical. Some notifications list a combination of risk. For example, RAPEX notification 0615/11 lists a hazard involving a potential fuel leak and the ECU causing a fire by means of a short circuit. The notification therefore has the risk labels "Fire|Injuries". In our analysis, we will count this notification twice: once for the risk type being "Fire" and once for the risk type being "Injuries".

The RAPEX dataset distinguishes between the fire and burn hazards. The risk of a burn is one where a participant can get inured, but the failing component will not start a fire. As an example, two notifications that have the risk type "Burns," but not "Fire," are motorbike exhaust pipes that may lose their enclosure or seat heating elements that are overheating and charring the seat. Specific notifications in the RAPEX dataset are A12/1541/12, 0007/10, and 0767/11.

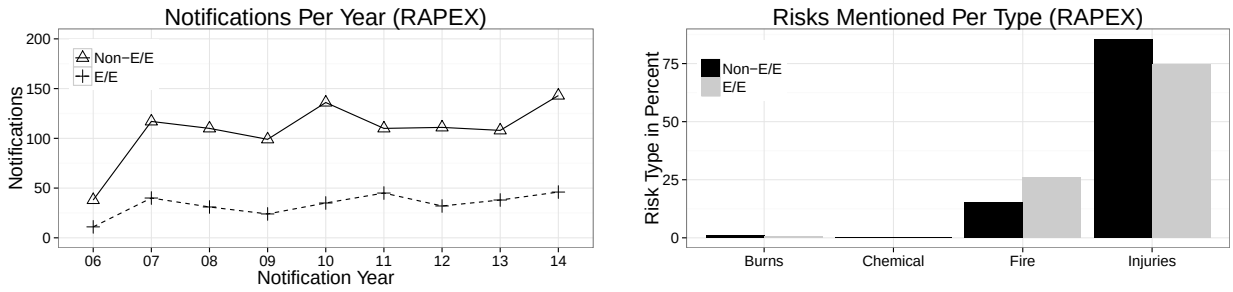


Figure 6: E/E and Non-E/E notifications in the RAPEX database (left). Comparison of the risk types for E/E vs. other components. Note: some notifications mention several risk types, so the total is not 1 (right).

Analyzing the RAPEX dataset, we discovered that E/E notifications dominate the risk type "Fire". Figure 6 shows a breakdown of the percentages for each risk type. About 25 percent of all notifications related to E/E systems specify a fire hazard, while only 15 percent of other notifications carry the risk type "Fire". Conversely, fewer E/E notifications are tagged with the risk type "Injury".

## 4 SPECIFIC E/E NOTIFICATIONS

This section describes specific E/E notifications identified in our analysis. Summaries of several specific E/E notifications appear in Table 4. As illustrated by Table 4, E/E notifications have involved nearly all types of motor vehicles, including buses, ambulances, motorcycles, passenger vehicles, passenger trucks, and cargo trucks. Additionally, E/E notifications have involved a diversity of energy sources, including gasoline, diesel, all electric, hybrid electric/gasoline, and natural gas. The affected systems involved in E/E notifications include airbags, seatbelt pretensioners, cruise control systems, electronic stability control systems, battery charging controllers, brakes, engine overheating, transmissions, engine and powertrain control, tire pressure monitoring systems, and many others. Additionally, there have been several instances of E/E notifications for unintended acceleration as summarized in Table 5. Of particular interest currently are notifications that involve computers and software. The root problems are also diverse, albeit somewhat difficult to ascertain from the data available, but certainly include wrong values specified in software (including calibration values), timing errors, wrong values computed by software, sign errors, among others. The earliest notification mentioning "computer" was in 1975 for 75V117000, the earliest notification mentioning "software" was in 1996 for 96V007000, and the earliest notification mentioning "over-the-air software update" was in 2014 for 14V006000. Additionally, while specific makes and models were explicitly not listed to avoid singling out particularly makers, models of all makes have been the subject of E/E notifications. Other authors have compiled interesting motor vehicle E/E issues previously [27].

| Camp. No. | Date | Pot. Aff. | Type | Model Years | Problem | Resolution |
|---|---|---|---|---|---|---|
| 75V117000 | JUN 23, 1975 | 8 500 | Cargo truck | 1971-1975 | Brake loss due to anti-lock computer malfunction | Replace computer |
| 85V134000 | OCT 22, 1985 | 3 988 | Passenger car | 1985 | ECU timing problem | Replace ECU |
| 96V007000 | JAN 16, 1996 | 10 600 | Passenger car | 1996 | Climate control module software failure | Replace module |
| 00V374000 | NOV 13, 2000 | 492 | Electric passenger truck | 1998 | Battery pack overheating | Battery pack module software update |
| 01V025000 | FEB 03, 2001 | 353 | Passenger car | 1999 | Brake warning light does not display due to software problem | Update software in instrument cluster |
| 99E023000 | JUL 29, 1999 | 1 362 | Engine | 1999 | Engine stall because of software | Update ECU software |
| 00V131003 | MAY 30, 2000 | 3 | Cargo truck | 2000 | Wrong gear selection in transmission due to software problem | Replace autoshift transmissions |
| 13V040000 | FEB 06, 2013 | 3 644 | Passenger car | 2003-2004 | Unintended airbag deployment | Replace controller |
| 04V254000 | MAY 27, 2004 | 8 189 | Motorcycle | 2004 | Wrong speedometer reading | Software update |
| 05V208000 | APR 27, 2005 | 153 | Natural gas bus | 2002-2005 | Unexpected throttle surge due to compressed natural gas ECU | Update ECU software |
| 05V153000 | APR 15, 2005 | 216 | Ambulance | 2002-2005 | Electric power sequencing problem causing overheating and fire risk | Install new transistor board |
| 11V395000 | AUG 04, 2011 | 1 512 107 | Passenger car | 2005-2010 | Stalls due to transmission damage | Update automatic transmission control module software |
| 14V047000 | FEB 10, 2014 | 2 190 934 | Passenger car | 2005-2011 | Engine and airbag disabling due to ignition switch disconnection | Replace ignition switch |
| 06V220000 | JUN 19, 2006 | 433 | Passenger car | 2006 | Certain operating conditions lead to engine compartment temperature increase that may damage alternator | Improve engine compartment cooling, modify ECU, and install new alternator |
| 06V493000 | DEC 29, 2006 | 50 665 | Passenger car | 2007-2008 | Brake lockup | Reprogram the ABS ECU |
| 13V500000 | NOV 01, 2013 | 344 187 | Passenger car | 2007-2008 | Unintended braking by Vehicle Safety Assist System (VSA) | Instal new yaw rate sensor |
| 08V595000 | NOV 14, 2008 | 2 500 | Passenger car | 2008 | Transmission software may perform a multistage downshift that could stall the car | Reprogram engine and transmission control unit software |
| 11V534000 | NOV 04, 2011 | 38 444 | Passenger car | 2008-2009 | Delay of 30ms between first and second dual-stage airbag deployment resulting in head injury criteria requirements non-compliance | Reprogram sensing and diagnostic module |
| 12V064000 | FEB 17, 2012 | 20 512 | Motorcycle | 2008-2011 | Insufficient battery charging leading to stalls | Replace voltage regulator |
| 13V233000 | JUN 04, 2013 | 254 396 | Passenger car | 2010-2012 | Seatbelt pretensioner and airbag non-deployment in crash | Software update |
| 14V053000 | FEB 12, 2014 | 698 457 | Hybrid passenger car | 2010-2014 | Stalls due to power electronics shorting | Software update for motor/-generator control ECU and hybrid control ECU |
| 14V522000 | SEP 02, 2014 | 1 810 | Electric car | 2010-2014 | Brake vacuum pump malfunction | Reprogram or replace brake vacuum pump controller |
| 13V283000 | JUL 02, 2013 | 224 264 | Passenger car | 2013 | Wrong side airbag deployment | Flash occupant restraint control module |
| 13V328000 | JUL 29, 2013 | 11 097 | Motorcycle | 2013 | Stall under deceleration | Replace ECU |
| 14V006000 | JAN 13, 2014 | 29 222 | Electric car | 2013 | Overheating power cables while charging | Over-the-air software update |
| 14V138000 | MAR 25, 2014 | 989 701 | Passenger car | 2013 | Occupant classification system (OCS) may classify seat as empty when occupied | Update OCS software |
| 13V506000 | OCT 17, 2013 | 207 | Passenger car | 2013-2014 | Remaining fuel overestimation leading to possible stalls | Update instrument cluster software |
| 14V173000 | APR 03, 2014 | 5 700 | Passenger car | 2014-2015 | Power Control Module (PCM) stops charging battery | Reprogram PCM |
| 14V551000 | SEP 10, 2014 | 19 | Diesel cargo truck | 2015 | Engine stalls due to incorrect parameter setting in software | Reprogram ECU |

Table 4: Specific E/E notifications from the NHTSA dataset, where *"Camp. No."* is the NHTSA campaign number, *"Date"* is the notification date, and *"Pot. Aff."* is the number of potentially affected units.

| Camp. No. | Date | Pot. Aff. | Type | Model Years | Resolution |
|---|---|---|---|---|---|
| 03V033000 | FEB 05, 2003 | 19 500 | Passenger truck | 2003 | Reprogram ECU |
| 10V231000 | JUN 01, 2010 | 372 | Low speed vehicle | 2010 | Accelerator pedal replacement |
| 13E068000 | DEC 12, 2013 | 496 | Transmission | 2010-2013 | Update hybrid control module software |
| 13V633000 | DEC 16, 2013 | 29 | Bus | 2013 | Update hybrid transmission software |
| 14V026000 | JAN 30, 2014 | 22 | Bus | 2014 | Update hybrid transmission software |
| 14V042000 | FEB 07, 2014 | 114 | Bus | 2014 | Update hybrid control module software |
| 14V303000 | MAY 28, 2014 | 2 | Bus | 2014 | Update hybrid control module software |
| 14V583000 | SEP 22, 2014 | 6 562 | Passenger car | 2015 | Reprogram engine control module (ECM) |

Table 5: E/E notifications for unintended acceleration, where *"Camp. No."* is the NHTSA campaign number, *"Date"* is the notification date, and *"Pot. Aff."* is the number of potentially affected units.

## 5 DISCUSSION AND LIMITATIONS

During the analysis of the different datasets, we made several observations that are relevant to put the work into context and should be interesting for work that repeats our analysis with future data.

### 5.1 Observations

The datasets show a clear upward trend in the number of E/E notifications. This trend has an obvious correlation with the number of ECUs reported for motor vehicles (Table 1). Our conjecture is that since recent motor vehicles have significantly more and more complex E/E systems (e.g., computerized control of all subsystems is standard and active driver assistance systems are becoming available), this inherently leads to more problems related to E/E systems. Consequently, the absolute number of E/E notifications increases over the years. Additionally, it is common to reuse E/E systems across vehicles, so the number of vehicles potentially affected by an E/E notification is also typically higher than for Non-E/E notifications.

Not all countries make their datasets accessible. We tried to obtain datasets from many different sources, however, the quality of the data available and the access methods vary. For example, the NHTSA and Transport Canada make the complete dataset available for download in one database file. The UK also provides a dataset that may be downloaded as one file, but that we did not analyze in this study [28]. RAPEX only provides an online interface that permits exports of at most 1000 entries at a time. The Kraftfahrt-Bundesamt (German) provides no download option and intentionally limits (as confirmed with the Kraftfahrt-Bundesamt) searching for notifications to only specific entries after entering brand, model, year, and type of notification (e.g., brakes). Australia provides static web pages with very limited ability to search [29]. Furthermore, the Australian site only lists rudimentary information about each notification. We contacted the Australian organization (the Australian Competition and Consumer Commission [ACCC]) to acquire the dataset, but at the time of this writing, we have not received a response. The inaccessibility of datasets limits the ability to perform an analysis of notifications on a global scale. We hope that in the future, more governments will embrace an open data mentality, and make the data easily accessible. Additionally, we hope that the regulatory authorities will make permanent URLs available for all notifications (e.g., using the campaign numbers), as the URLs we give in Table 4 and 5 may break over time.

Some datasets do not use a controlled vocabulary to ensure consistent labeling. Libraries use a controlled vocabulary, usually called thesaurus, to ensure that entries in the dataset are labeled consistently. The NHTSA and Transport Canada seem to use a controlled vocabulary, because we did not find many inconsistencies between entries. RAPEX does not seem to use a controlled vocabulary. Consequently, notifications concerning vehicle safety can be filed under, for instance, "passenger vehicle" or "passenger car". Furthermore, the lack of a controlled vocabulary permits spelling mistakes and makes certain notifications difficult to find. For example, we found one entry that misspelled the word "vehicle" and was consequently not found with the original search terms. Finally, the RAPEX database seems to contain a number of spelling mistakes across different columns in the notifications, as well as inconsistent style. For example, in the column on measures adopted by the notifying country, some entries have a colon symbol at the end (e.g., "Voluntary measures: Voluntary corrective action taken by the manufacturer:"); or just a typo as in "Voluntary measures: Voluntary corrective actions take by the importer". We have informed the maintainer of the dataset of these inconsistencies, but at the time of the submission have not heard whether they will address them.

The datasets provide different content and consequently a direct comparison to evaluate bias becomes impossible. Each dataset contains data that is not contained in the other datasets. For example, the RAPEX dataset contains a significant number of notifications for motorcycles, while the dataset from Transport Canada includes recreational vehicles, all-terrain vehicles (ATVs), and snowmobiles. Finally, the NHTSA dataset includes detailed supplemental information (e.g., how to fix the problem and the response from the manufacturer and access to significant supplementary documentation), while the other datasets only include short text fields. The significant differences between the type of data stored in the datasets unfortunately prevented us from more sophisticated comparisons. It would have been interesting to relate the data and identify potential bias of the different agencies involved in processing and publishing the notifications.

### 5.2 Threats to Validity

We actively tried to reduce classification errors in our manual classification. The classification completed by the two undergraduate students was reviewed by one of the co-authors of the paper. The review consisted of two phases. The first phase involved automated sanity checks on the data. For example, do all notifications with the same notification ID, but assigned to different vehicle models, have the same overall classification. In other words, we checked whether a notification has inconsistent labeling. Any elements found during the sanity checking were returned to the undergraduate students for re-classification. The second phase involved a review of a subset of the classified notifications to confirm that they are correctly labeled. Nonetheless, mis-classifications can still happen and judging whether a notification is an E/E notification based on a short textual description is subjective in several cases. Additionally, all analysis presented included all entries in the datasets, which may also cover systems like tires, child seats, etc., so many E/E results presented may be conservative estimates since tires and child seats are generally Non-E/E, although the total numbers of these notifications represent at most a few percent of the notifications.

An additional criticism of the analysis presented in this paper is that it could be subject to confirmation bias. As an attempt to avoid confirmation bias, we used multiple independent datasets, and the Transport Canada and RAPEX datasets were analyzed independently from the NHTSA dataset. The datasets were also compared for consistency to publicly available aggregate reports, such as the 2012 NHTSA Annual Report [30]. For the aggregate analyses presented in the figures in this paper, the Transport Canada and RAPEX datasets were analyzed using R and the NHTSA dataset was analyzed using MATLAB. All figures in this paper were created using R. Additionally, we do not make any claims that increasing numbers of E/E systems in motor vehicles is correlated with or decreases overall safety, such as measured using numbers of fatalities, injuries, or crashes.

Since the datasets can contain spelling mistakes, our data might be incomplete. For example, for the RAPEX dataset, we used specific search terms to extract notifications for motor vehicles. Spelling mistakes in the original dataset (e.g., "vehilce" instead of "vehicle") are not picked up by the search terms and consequently excluded from the list. Also in the automated classification performed on the NHTSA dataset, spelling mistakes will have significant consequences. We tried to counteract this by searching for slightly misspelled versions of the text, however, naturally, we might have missed something. A better solution would be to use natural language processing (NLP) tools, which we plan to do in the future. We still believe that our dataset is comprehensive and representative, because in the occasions where we found misspelled words, the search produced only a single or a few matching records.

### 5.3 Takeaway Messages: A Call to Action

Next, we discuss several takeaway messages from this survey of E/E notifications for motor vehicles.

**Fixing things late is expensive.** This discussion would be remiss without mentioning the recent Toyota unintended acceleration problems, which did not have E/E notifications in the datasets analyzed. Sudden unintended acceleration is the unintended, unexpected, uncontrolled acceleration of a motor vehicle [31]. As is well-known in software and systems engineering, correcting problems late in the development process, or after deployment, can be expensive (financially, in manpower, delays to market, reputation, etc.) [32, 33]. These unintended acceleration investigations highlight this observation, albeit in an extraordinary way beyond the typical finding a defect late in the development cycle and having to redesign and retest to fix it. This scenario did have two related Non-E/E notifications, together affecting over 4.5 million vehicles with model years from 2004 to 2010 of several models, for pedal sticking and floor mats (09V388000 and 07E082000). NASA and the NHTSA conducted a ten month study of the Electronic Throttle Control System (ETCS) and failed to find any definitive electronic or software causes for the unintended acceleration [34, 35, 36]. The

investigations concluded that the unintended accelerations were likely due to three possible reasons: operator misapplication, accelerator pedals sticking, or accelerator pedal entrapment in the floor mat. However, the 2013 Bookout v. Toyota case was premised partly on there being problems in the ECTS architecture and software [37]. During the testimony in this case, problems in the ETCS architecture and real-time software were explored, and a conclusion was drawn that some best practices were not followed that made the ETCS be another possible source of unintended acceleration [38, 39, 40].

In 2014, the US Department of Justice (DOJ) made a USD $1.2 billion criminal penalty charge as a part of the unintended acceleration problems [40, 41]. The NHTSA also levied the maximum fines, for a total cost of $48.8 million [42]. Additionally, in 2013, related class action lawsuits were settled for a total cost of USD $1.6 billion [40, 43]. Publicly available reports [34, 36] and additional details that arose in the Bookout v. Toyota case [38, 39, 40] suggest that the software codebase covered in the ETCS was on the order of 1 million source lines of code (LOC) [44, Table A.7-1]. Combining solely these three large legal costs to a total of approximately USD $2.85 billion suggests a per-LOC cost of between $285 to $2 850. This estimate of the per-LOC cost excludes other real costs such as those from development, testing, etc., but of course also excludes both (a) liability of the other possible sources of unintended acceleration (user error, pedal sticking, and floor mat entrapment), and (b) the cost of other (non-software related) aspects of the engineering, manufacturing, and other processes. Typical estimates of software development cost per-LOC range from around USD $10 in general embedded systems to USD $50 in aerospace and medical devices [45]. From this purely financial standpoint, perhaps additional investment in the earlier development, engineering, and verification and validation stages are warranted in motor vehicle engineering, particularly with regard to E/E systems and software, especially with the move toward autonomy and connected vehicles that will rely on more complex E/E systems.

**Need for better validation and verification methods.** With the surge of active driver assistance systems (ADAS), the number and complexity of E/E systems in cars will increase drastically. Consequently, the validation and verification methods used for E/E systems must scale with this surge. Furthermore, the integration of these new ADAS will require additional attention as the testing effort will grow exponentially with the increased number of E/E systems. Finally, the current methods will need to be adapted to cope with new challenges such as sensor fusion [46] and machine learning for ADAS.

**Improved collaboration between international data sources.** The datasets provided by the different regulatory agencies (the data sources) are not directly comparable. Additionally, while the NHTSA maintains information on foreign notifications (http://www-odi.nhtsa.dot.gov/frecalls/), this does not include the same information and is not in the same format as the US domestic notification information. The regulatory burden could perhaps be more easily spread across nations, or at least the information collected should be consistent.

**Security problems are ignored at the moment.** An interesting aspect is that the notification datasets lack information on security risks (other than some instances for vehicle entry and theft). Security is a serious threat to modern vehicles and can affect safety [47, 48, 11]. As vehicles become increasingly connected (such as through communications like vehicle-to-vehicle and vehicle-to-infrastructure [49]), security will play an increasing role in generating E/E notifications. It is not clear if including security notifications in the (primarily safety-related) datasets analyzed in this study is the right action plan. Creation of a motor vehicle security notification dataset and reporting service—similar to those operated by various companies and the US government through the US Computer Emergency Readiness Team, https://www.us-cert.gov/—may be the right path forward for tracking and reporting security defects in vehicles. Regardless, regulation of security in vehicles is likely to occur in the coming years (as indicated by recent legislative reports [50] and ongoing lawsuits [51]), and regulatory agencies should monitor security defects in motor vehicles and maintain notifications for them.

## 6 CONCLUSION

This paper used datasets on safety-related notifications for motor vehicles from three different jurisdictions (the United States, Canada, and Europe) to identify facts and trends related to E/E systems. We have identified the trend that E/E-related problems are increasing over time, shown evidence that E/E defects are latent for a longer time than Non-E/E defects, identified that E/E systems are more prone than Non-E/E systems to fire hazards when defective, and finally provided a ranking of the systems related to E/E notifications. Based on this analysis, a couple additional observations, and the compelling concrete examples, we formulated a call to action for researchers, regulators, and manufacturers. The analysis presented in this

paper is only the first step. In future work, we plan to further refine the labeling in the database, for example using NLP [52], and build prediction models based on the data.

## ACKNOWLEDGMENTS

We would like to thank and acknowledge Sunaal Mathew and Ben Mendis who helped with labeling the datasets. The research was in part sponsored by APCPJ (386797-09), ORF-RE (04-039), and the APMA-CVD related VIP grants from the Ontario Centres of Excellence. We were motivated in part to undertake this study by a similar study conducted for medical devices using datasets from the US Food and Drug Administration (FDA) [53].

## DISCLOSURE STATEMENT FOR CONFLICTS OF INTEREST

The authors of this paper have research support from motor vehicle manufacturers and suppliers (see the industry partners of the acknowledged grants). T. Johnson holds a small amount of stock in the Ford Motor Company. Any opinions and conclusions expressed herein are those of the authors and do not necessarily represent the views of any person or organization other than those of the authors'.

## REFERENCES

[1] M. Broy, "Challenges in Automotive Software Engineering," in *Proceedings of the 28th International Conference on Software Engineering*, ser. ICSE '06. New York, NY, USA: ACM, 2006, pp. 33–42.
[2] M. Broy, I. Kruger, A. Pretschner, and C. Salzmann, "Engineering Automotive Software," *Proceedings of the IEEE*, vol. 95, no. 2, pp. 356–373, Feb. 2007.
[3] *Federal Motor Vehicle Safety Standards and Regulations (US Code Title 49 - Transportation, Part 571)*, National Highway Traffic Safety Administration Std., Oct. 2010, http://www.nhtsa.gov/cars/rules/import/FMVSS/. [Online]. Available: http://www.ecfr.gov/cgi-bin/retrieveECFR?ty=HTML&n=pt49.6.571
[4] *ISO 26262-3: Road vehicles - Functional safety*, International Organization for Standardization (ISO) Std. ISO 26 262, 2011.
[5] *Guidelines for the Safety Analysis of Vehicle-based Programmable Systems (MISRA C:2012)*, Motor Industry Software Reliability Association (MISRA) Std., Mar. 2012. [Online]. Available: http://www.misra-c.com/
[6] "Motor Vehicle Safety Regulations (C.R.C., c. 1038)," http://www.tc.gc.ca/eng/acts-regulations/regulations-crc-c1038.htm.
[7] "General Safety Regulation (EC) No 661/2009," 2009, http://eur-lex.europa.eu/legal-content/EN/ALL/?uri=CELEX:32009R0661.
[8] J. Leohold, "Keynote – Automotive Communication: Communication Requirements for Automotive Systems," in *Proceedings of the IEEE International Workshop on Factory Communication Systems*, Sept. 2004, pp. 153–153.
[9] A. Bosch, "Comparison of Event-Triggered and Time-Triggered Concepts with Regard to Distributed Control Systems," in *Proceedings of Embedded World Exhibition&Congress*, Nürnberg, Germany, 2004, pp. 235–252.
[10] T. Nolte, H. Hansson, and L. Bello, "Automotive communications — Past, Current and Future," in *Proceedings of the IEEE Conference on Emerging Technologies and Factory Automation*, vol. 1, Sept. 2005.
[11] C. Miller and C. Valasek, "A Survey of Remote Automotive Attack Surfaces," in *black hat USA*, 2014.
[12] A. Pretschner, M. Broy, I. H. Kruger, and T. Stauner, "Software engineering for automotive systems: A roadmap," in *2007 Future of Software Engineering*, ser. FOSE '07. Washington, DC, USA: IEEE Computer Society, 2007, pp. 55–71.
[13] R. N. Charette, "This car runs on code," *IEEE Spectrum*, vol. 46, no. 3, Feb 2009.
[14] IHS Global Insight, "Resistance Is Futile – Electronics Are on the Rise: Electronic Control Units and Communication Protocols," *IHS Global Insight Perspectives*, Apr. 2009. [Online]. Available: http://www.ihsglobalinsight.com/Highlight/HighlightDetail16632.htm
[15] J. Motavalli, "The Dozens of Computers That Make Modern Cars Go (and Stop)," *New York Times*, p. B6, Feb. 2010. [Online]. Available: http://www.nytimes.com/2010/02/05/technology/05electronics.html
[16] C. Mann, "Look Out—He's Got a Phone!" *Vanity Fair*, Dec 2012. [Online]. Available: http://www.vanityfair.com/news/2012/12/microcomputers-weapons-smartphone
[17] K. Hill, D. Menk, B. Swiecki, and J. Cregger, "Just How High-Tech is the Automotive Industry?" *Center for Automotive Research*, Jan 2014. [Online]. Available: http://www.cargroup.org/?module=Publications&event=View&pubID=103
[18] (2015, Mar.) NHTSA/ODI Recall and Complaint Databases. National Highway Transportation Safety Agency. [Online]. Available: http://www-odi.nhtsa.dot.gov/downloads
[19] Transport Canada Road Safety Recalls Database. [Online]. Available: http://wwwapps.tc.gc.ca/Saf-Sec-Sur/7/VRDB-BDRV/search-recherche/menu.aspx?lang=eng
[20] RAPEX – Search Notifications. [Online]. Available: http://ec.europa.eu/consumers/safety/rapex/alerts/main/index.cfm?event=main.search
[21] (2015, Mar.) Flat File Copies of NHTSA/ODI Databases. National Highway Transportation Safety Agency. [Online]. Available: http://www-odi.nhtsa.dot.gov/downloads/flatfiles.cfm
[22] (2015, Mar.) NHTSA Foreign Campaigns Search Engine. National Highway Transportation Safety Agency. [Online]. Available: http://www-odi.nhtsa.dot.gov/frecalls/
[23] NHTSA – Who We Are and What We Do. [Online]. Available: http://www.nhtsa.gov/About+NHTSA/Who+We+Are+and+What+We+Do
[24] safercar.gov – Information for Owners. [Online]. Available: http://www.safercar.gov/Vehicle+Owners/
[25] Transport Canada. [Online]. Available: http://www.tc.gc.ca/eng/aboutus-menu.htm
[26] How does RAPEX work. [Online]. Available: http://ec.europa.eu/consumers/consumers_safety/safety_products/rapex/how_does_it_work/index_en.htm
[27] E. Nisley, "But I Never Did That Before!" *Dr. Dobb's Journal*, nov 2004. [Online]. Available: http://www.drdobbs.com/but-i-never-did-that-before/184405905

[28] (2015, Mar.) UK Automotive Recall System. Vehicle and Operator Services Agency. [Online]. Available: http://www.dft.gov.uk/vosa/apps/recalls/RecallsFile.csv
[29] (2015, Mar.) Product Safety Recalls Australia: Cars, Boats, Bikes. Australian Competition and Consumer Commission. [Online]. Available: http://www.recalls.gov.au/content/index.phtml/itemId/952839
[30] (2013, Jan.) National Highway Traffic Safety Administration 2012 Annual Report: All Recalls by Year. Washington, DC. [Online]. Available: http://www.nhtsa.gov/staticfiles/communications/pdf/2012_Recall_Annual_Report_Final.pdf
[31] S. Kirchhoff, *Unintended Acceleration in Passenger Vehicles*. DIANE Publishing Company, 2010.
[32] B. Beizer, *Software testing techniques*. New York, NY, USA: Van Nostrand Reinhold Co., 1990.
[33] D. Jackson, M. Thomas, and L. I. Millett, Eds., *Software for Dependable Systems: Sufficient Evidence?*, ser. Committee on Certifiably Dependable Software Systems, National Research Council. The National Academies Press, 2007.
[34] (2011, Apr.) NHTSA-NASA Study of Unintended Acceleration in Toyota Vehicles. U.S. Department of Transportation, National Highway Traffic Safety Administration. [Online]. Available: http://www.nhtsa.gov/UA
[35] "Technical Assessment of Toyota Electronic Throttle Control (ETC) Systems," U.S. Department of Transportation, National Highway Traffic Safety Administration, Tech. Rep., Feb. 2011. [Online]. Available: http://www.nhtsa.gov/UA
[36] "Technical Support to the National Highway Traffic Safety Administration (NHTSA) on the Reported Toyota Motor Corporation (TMC) Unintended Acceleration (UA) Investigation," NASA Engineering and Safety Center, Tech. Rep. TI-10-00618, Jan. 2011. [Online]. Available: http://www.nhtsa.gov/UA
[37] "Bookout et al vs. Toyota Motor Corporation et al (Case No. CJ-2008-7969)," 2008. [Online]. Available: http://www-odi.nhtsa.dot.gov/acms/cs/jaxrs/download/doc/ACM16847762/INRD-RQ10003-45440.pdf
[38] M. Barr. (2013) Bookout v. Toyota. [Online]. Available: http://www.safetyresearch.net/Library/BarrSlides_FINAL_SCRUBBED.pdf
[39] "Bookout et al vs. Toyota Motor Corporation et al (Case No. CJ-2008-7969): Transcript of Morning Trial Proceedings Had on the 14th Day of October 2013 before the Honorable Patricia G. Parrish, District Judge," 2013. [Online]. Available: http://www.safetyresearch.net/Library/Bookout_v_Toyota_Barr_REDACTED.pdf
[40] P. Koopman. (2014, Sept.) A case study of Toyota unintended acceleration and software safety. [Online]. Available: http://users.ece.cmu.edu/~koopman/pubs/koopman14_toyota_ua_slides.pdf
[41] (2014, Mar.) Justice Department Announces Criminal Charge Against Toyota Motor Corporation and Deferred Prosecution Agreement with $1.2 Billion Financial Penalty. [Online]. Available: http://www.justice.gov/opa/pr/justice-department-announces-criminal-charge-against-toyota-motor-corporation-and-deferred
[42] (2011, Feb.) U.S. Department of Transportation Releases Results from NHTSA-NASA Study of Unintended Acceleration in Toyota Vehicles. [Online]. Available: http://www.nhtsa.gov/PR/DOT-16-11
[43] "re Toyota Motor Corp. Unintended Acceleration Marketing, Sales, Practices, and Products Liability Litigation (Case No. 8:10ML 02151 JVS (FMOx)): Final Judgement (Document 3935)."
[44] "Technical Support to the National Highway Traffic Safety Administration (NHTSA) on the Reported Toyota Motor Corporation (TMC) Unintended Acceleration (UA) Investigation: Appendix A: Software," NASA Engineering and Safety Center, Tech. Rep. TI-10-00618, Jan. 2011. [Online]. Available: http://www.nhtsa.gov/UA
[45] W. Lobb and D. Warburton. (2011, June) How much does it cost to develop your software? (part 2). Foliage. [Online]. Available: http://www.foliage.com/images/How_Much_Does_It_Cost_To_Develop_Your_Software_Part2.pdf
[46] N.-E. E. Faouzi, H. Leung, and A. Kurian, "Data fusion in intelligent transportation systems: Progress and challenges – A survey," *Information Fusion*, vol. 12, no. 1, pp. 4–10, 2011, special Issue on Intelligent Transportation Systems.
[47] K. Koscher, A. Czeskis, F. Roesner, S. Patel, T. Kohno, S. Checkoway, D. McCoy, B. Kantor, D. Anderson, H. Shacham, and S. Savage, "Experimental Security Analysis of a Modern Automobile," in *Security and Privacy (SP), 2010 IEEE Symposium on*, May 2010, pp. 447–462.
[48] S. Checkoway, D. McCoy, B. Kantor, D. Anderson, H. Shacham, S. Savage, K. Koscher, A. Czeskis, F. Roesner, T. Kohno, *et al.*, "Comprehensive Experimental Analyses of Automotive Attack Surfaces," in *USENIX Security Symposium*, 2011.
[49] J. Harding, G. Powell, R. Yoon, J. Fikentscher, C. Doyle, D. Sade, M. Lukuc, J. Simons, and J. Wang, "Vehicle-to-Vehicle Communications: Readiness of V2V Technology for Application," National Highway Traffic Safety Administration, Washington, DC, Tech. Rep. DOT HS 812 014, Aug. 2014.
[50] E. J. Markey. (2015) Tracking & Hacking: Security & Privacy Gaps Put American Drivers at Risk. [Online]. Available: http://www.markey.senate.gov/imo/media/doc/2015-02-06_MarkeyReport-Tracking_Hacking_CarSecurity%202.pdf
[51] "Helene Cahen et al v. Toyota Motor Corporation et al (Case No. 4:2015cv01104)," 2015 Mar. [Online]. Available: http://dockets.justia.com/docket/california/candce/4:2015cv01104/285516
[52] M. Ghazizadeh, A. D. McDonald, and J. D. Lee, "Text mining to decipher free-response consumer complaints: Insights from the NHTSA vehicle owner's complaint database," *Human Factors: The Journal of the Human Factors and Ergonomics Society*, vol. 56, no. 6, pp. 1189–1203, 2014.
[53] H. Alemzadeh, R. Iyer, Z. Kalbarczyk, and J. Raman, "Analysis of Safety-Critical Computer Failures in Medical Devices," *Security Privacy, IEEE*, vol. 11, no. 4, pp. 14–26, 2013.

# Simulation and testing of adaptive FRP-substructures for automotive safety

**Gregor Gstrein**
Vehicle Safety Institute – Graz University of Technology
Austria

**Christian Kurzböck**
Virtual Vehicle Research Center
Austria

**Jan-Mark Opelka**
Daimler AG
Germany

**Jan Krollmann**
Institute of Carbon Composites – Technische Universität München
Germany

Paper Number 15-0068

## ABSTRACT

This paper describes the development of a basic finite element simulation model of a concept for an adaptive structure made with carbon fiber reinforced plastic materials. Thereby in particular the prediction of the mechanical properties of necessary deformation zones in the structure, that are realized with an elastomer matrix system, is challenging due to the different properties of this material compared to conventional composites. Available material models in the FE-Code LS-DYNA are analyzed for their usability in this task. For the parameterization of the material models a number of coupon tests are conducted and the deviations between the material with the elastomer matrix and the material with the conventional duromer matrix system is analyzed. The results of these tests is used to validate the material models for both, the material used in the expansion zone and the conventional composite material in the rest of the structure. It is shown, that the prediction of the shear properties of the elastomer based material creates difficulties with the used material model (MAT_54) but in total the correlation between test and simulation is good and comparable for both materials.
The first task that has to be approved for an adaptive structure made of FRP-materials is the expansion-process from the initial to the pressurized final geometry. For this purpose a quasistatic inflation test is performed. The results of the test and a corresponding simulation correlate well for the pressure at which the expansion of the structure begins. Regarding the maximum burst pressure and the location of the material failure deviations between test and simulation occur. Possible reasons for this deviations are analyzed and discussed.
Finally the additional necessary steps in the creation of a predictive simulation model for an adaptive FRP structure under crash-load and possible approaches for the latter are discussed.

## INTRODUCTION

Currently the automotive industry is highly demanding simulation models that are able to predict and optimise the crash behaviour of mass produced Fibre Reinforced Polymer (FRP) composite structures, which will be increasingly used in vehicles in the future. The ability to investigate crashworthiness of FRP vehicle structures by numerical simulation is very important for these lightweight materials to see widespread use in future cars.
In this paper, the current status of the development of simulation models for shape-adaptive FRP-Structures, as shown in (1), is described. It is analysed if state-of-the-art modelling-approaches and existing material models can be used, or if novel developments are necessary to predict the mechanical properties and behaviour of such components. The process of the parameterization of a material model, including the conduction of material tests as well as the validation of the models, is described.

## MOTIVATION

Shape-adaptive FRP-Structures address the demand for lightweight vehicles structures as well as the need for reduced injury-risk of car occupants. The potential benefits of those two topics are summarized in the following:

**Use of FRP-Materials in automotive application**

The increasing demand on reduced emissions, lower fuel consumption and higher safety in the automotive industry requires not only a development of alternatively powered vehicles, but also consistent lightweight design. The use of lightweight materials such as glass or carbon FRP is a possible approach to achieve these goals. In contrast to metal materials FRP have very high values for specific stiffness and strength. The usage of FRP structures within new vehicle concepts beneficially leads to a further enhancement of structural safety while lowering the vehicle's mass.
Compared to metal materials the use of FRP for the Body-in-White (BIW) shows a weight saving potential of up to 60% to 70% (2), (3). This potential has been exploited for many years in motorsport and comes more and more into focus for conventional cars. In particular for future alternatively powered vehicles, weight saving is directly linked to increased range which brings FRP-materials into such cars in greater extent (e.g. BMW i3 (4)).
In addition to the weight saving potential FRP also show a very high ratio of energy absorption per weight, compared to metal structures (CFK~ 100kJ/kg vs. Al ~50kJ/kg (5)). This makes it a very interesting material for the crash-structures in a car. Actual applications can be found predominantly in sports cars (e.g. Mercedes SLR (6)) but as soon as some shortcomings of those materials (e.g. cost, recycling, …) are solved, it is very likely that they are applied also in more vehicle types in the future.

**Adaptive structures in automotive application**

Recently expandable structures, which provide different mechanical properties due to a geometrical adaptivity, have come into focus of vehicle safety development. These structures are principally folded in their undeployed state to minimize the cross section. Thus these adaptive structures are very compact, which brings benefits regarding packaging in the vehicle. Due to the fact of cross sectional adaptivity, the structure shows very high potential concerning weight reduction. Wall thickness can be reduced due to increased stiffness, as a result of the increased moment of inertia by the expansion of the structure and additionally also due to the pressure within the structure (7).
Adaptive crash structures show potential for further increase of safety and lightweight performance. Different approaches with varying design goals and realisations have been discussed in recent publications. The main goals for the use of adaptive structures can be summarized as described in (8):

- Increase of deformation length
- Increase/decrease of crash load levels
- Increase of energy absorption
- Weight reduction
- Packaging benefits

One alternative approach describes the goal of improving the driver's vision by use of adaptive A-pillars (9).
Adaptive structures made of steel have already been developed by Daimler AG and used in prototype vehicles such as the Experimental Safety Vehicle (ESF 2009). For example, by expanding structural components to the ouside of the car, additional space for deceleration of impacting objects is created, which leads to a significant reduction of intrusion velocities of the door in case of a side impact (10).

When one tries to combine the above described benefits of FRP material and crash adaptive structures, an elementary question arises: Is it possible to realize a structure that allows for geometrical adaptivity with FRP-materials that are typically very stiff and allow only very low enlongations at failure?
One possible concept for a successful realisation of such a solution is described in (1). For a better understanding of the development of a corresponding numerical model, the chosen approach for this structure is summarized briefly.

For the realization of a shape adaptive CFRP (carbon fiber reinforced plastic) structure a novel hybrid-matrix approach is used to integrate multiple matrix materials into one CFRP structure. This hybrid-matrix approach allows the local integration of elastomer matrix material. Since the matrix material significantly influences the bending stiffness and strength in FRP, an elastomer matrix material leads to a strong flexibilization (11). Herewith, a large geometry change in FRP structures can be realized.
Based on the hybrid-matrix approach a suitable design concept for a reinforcing door structure is developed which is capable of a significant change in shape in case of an inner pressurization.
In the unpressurized state the hollow structure has a u-shape cross section at the expansion area (see Figure 1). In case of pressurization the cross section areas with the elastomer matrix material can change into a semicircle shape, which almost leads to a doubling of the structure's moment of inertia. The bottom area of the cross section geometry as well as the end area of the structure do not change their geometry due to the

rigidity of the thermoset matrix material. At the rigid end areas both, the fixation to the door frame and the integration of the pressurization device can be realized.

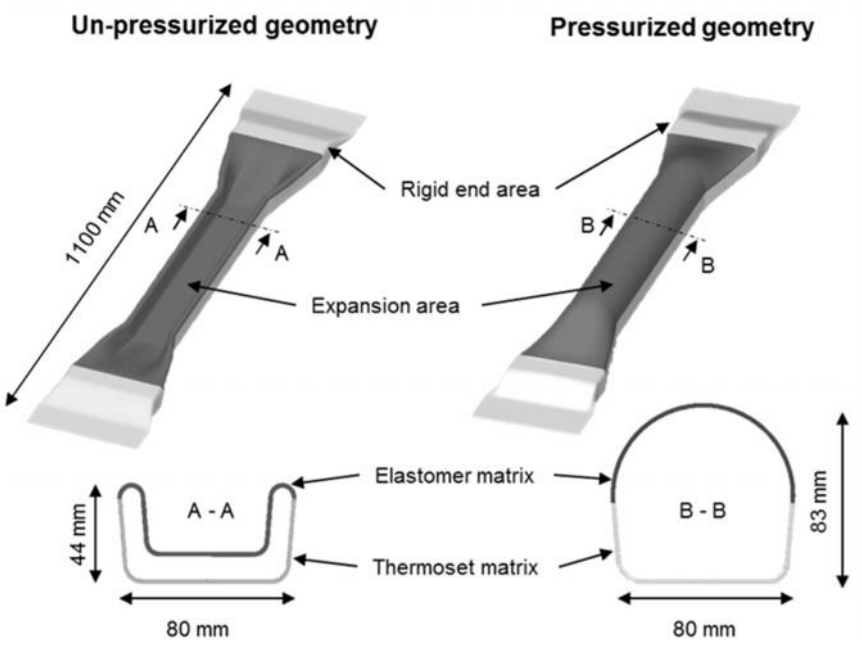


***Figure 1: Shape adaptive FRP-Structure***

This design concept represents the background for the manufacturing of prototypes which are tested regarding the inflation behaviour and their mechanical properties in pressurized and un-pressurized state.
The materials in the expansion area of this structure vary considerably to conventional FRP-materials with rigid thermoset resins as matrix materials. In particular the large strains that have to be sustained in the expansion-area require tailored material properties.
In addition to the proof of concept with prototypes as described above, numerical models of the used materials are developed and validated with coupon- and component-tests. In this paper the process of the development and validation of the material models, that are able to predict the mechanical behavior the adaptive FRP-Structure described in (1) is shown. Prior to that the state-of-the-art modelling techniques as well as the available standard material models are analyzed.

## METHODS

In general the FE-simulation models are set up based on a three level development process that is shown in Figure 2. This process consists of a basic material, a principle component and finally of a full vehicle implementation testing and validation level.

***Figure 2: Development process of FE-Model of adaptive FRP Structure***

At the material level, tests on coupon level are performed to derive the necessary data for the parameterization of the selected material models. In addition to the tests literature data is used (if available) for the verification of the test results.
At the principle component level the derived FRP simulation approaches are used to develop and evaluate the functionality and effectivity of design concepts of adaptive FRP structures. The FE models are used to investigate

and evaluate the adaptive behaviour of the FRP structure. Therefore all essential influencing parameters to the adaptive structure like, for instance, the use of different materials, wall thickness, FRP lay-up, position of the elastic areas, needed internal pressure for the unfolding process as well as the maximum burst pressure of such structures will be investigated in detail. Moreover, the FE simulation will be used to configure the setup for the component tests.
Once the second validation step is finished, the designed adaptive structure can be integrated into a full-vehicle simulation model and its potential regarding weight saving and increase of occupant safety can be assessed.

Beginning with a review of possible modelling techniques and available material models, a first simulation approach which is capable of predicting the behaviour of the laminate is defined. In order to derive the parameters necessary for the material models, a series of coupon tests are conducted and for each test a corresponding simulation model with the adjusted boundary conditions is created. Beginning with literature values and information of data-sheets, the material parameters are optimized iteratively to fit the test results as closely as possible. For this process also optimization tools (LS Opt) are applied.
In the following, the used data and the selected numerical tools are described in detail and the results of the first two validation steps are presented.

## MATERIAL TESTING AND VALIDATION

### Simulation approach for the laminate

In general, modelling techniques for FE simulation have to be classified into simulation of FRP UD (unidirectional) and woven laminates. First, UD laminates are simulated by the use of solid and layered shell element formulations in combination with special FRP material models. With the aid of these material models the elastic behavior as well as the failure and damage behavior can be simulated based on several available failure and damage criteria (e.g. (12)). Second, woven laminates are basically simulated by the use of two different modelling approaches (13), the cross ply and the smeared ply approach (see Figure 3).
These special approaches are motivated by the fact of interweaved, undulating fibers in warp (0°) and weft (90°) direction within one single layer. Within the cross ply approach interweaved fibers are split into two single unidirectional layers with half the thickness of the real woven single layer. One represents the warp and the other one the weft fibers. In contrast, within the smeared approach the warp and weft properties are smeared to one single layer.
In general the smeared approach is easier to apply concerning parameterization of the material models but gives less quality results regarding failure behavior. This is caused by the fact that existing failure criteria are designed for UD laminates but not for woven ones. In contrast, the cross ply approach is more elaborate regarding the parameterization of the material model caused by the split modelling of the woven fabric. Within this approach the failure and damage behavior can be simulated by using the existing failure criteria.
For this study the cross ply approach is used for simulation of woven laminates within the adaptive CFRP structure. The simulation of possible failure and damage mechanism during pressurization and external loading is of main interest to evaluate the structural effectivity of the adaptive structure.

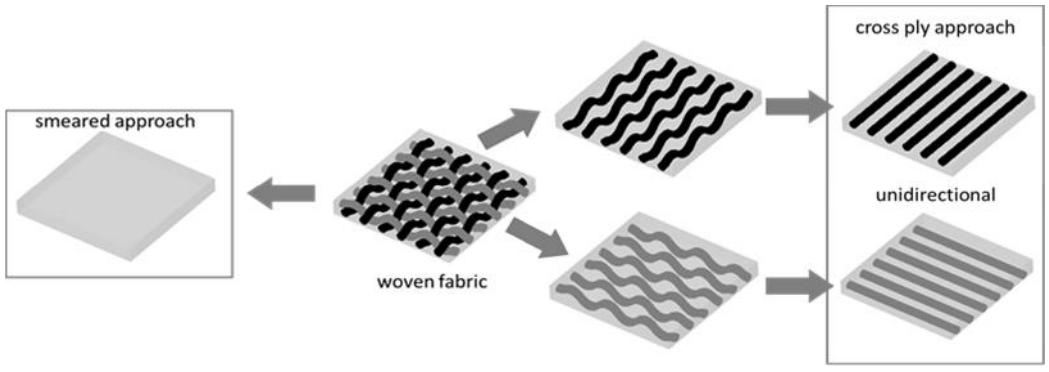


***Figure 3: Modelling approaches for woven fabrics***

### Selection of material model

Once the modelling approach is set, a suitable material model has to be selected. As the properties of the used materials (i.p. expansion zone) vary significantly from conventional thermoset FRPs, it has to be evaluated firstly which material model can describe the mechanical behavior in the best way. The used FE-Code LS-DYNA offers

a large variety of available material models dedicated for the simulation of FRP-materials (14) with different advantages and disadvantages (15).
With the chosen modelling approach of the laminate comes the need for the definition of material parameters that describe the integral mechanical properties of the FRP-material. A possible first step is to calculate the laminate properties (e.g. stiffness, strength in principal axis) based on the material properties of fiber, matrix system and the layup (16). This generally provides a good initial value for the subsequent validation with experimental data. With these determined first material parameters the different available material models of LS-DYNA were filled in, to provide an initial estimation of the usability of the different material models. With the comparably simple models: MAT_22, MAT_54 and MAT_58A, already a good correlation can be achieved. For those material models the previous calculation of the mechanical properties provide most of the required input parameters. For non-existing input parameters the material card must be completed with literature data and assumptions.
The application of more recent material models such as MAT_261 and MAT_262 is currently not considered, because they require very extensive material testing for the determination of the individual input parameters. For these material models many assumptions would have been necessary, which would have led to a worse predictability of the models.

**Performed coupon tests**

The data required for the parameterization of the models can be divided into “basic” data (e.g. Youngs modulus, poisson ration, etc. in longitudinal and transverse direction) and parameters that describe the material behavior after failure. In particular for the latter, the more complex material models (e.g. MAT_261, …) need more parameters for the definition and validation of the failure- and damage models and therefore require additional test configurations.
The values of the “basic” material parameters can be determined with tensile and compression tests in different layup configurations. For the shear properties a tensile test with a $[\pm 45°]_s$ laminate has to be carried out.
In order to be able to parameterize the material models used in the adaptive structure, the material used in the flexible areas as well as the stiffer material with the duromer resin system have to be examined.
An overview about the conducted tests is given in the following figure:

| Test | Norm | No. Of Tests | |
|---|---|---|---|
| Tensile Test $[0/90]_s$ | DIN EN ISO 527 | 5 | 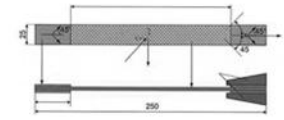 |
| Tensile Test $[+45/-45]_s$ | DIN EN ISO 527 | 5 | |
| Compression Test $[0/90]_s$ | Boeing Compression Test | 5 | 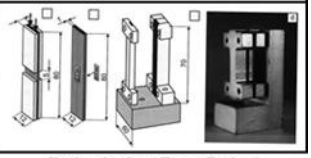 |
| Compression Test $[+45/-45]_s$ | Boeing Compression Test | 5 | |
| ENF $[0/90]_s$ | AECMA prEN 6034 | 5 | Sketches taken from: „Kunststoffprüfung“, Wolfgang Grellmann , Sabine Seidler, 2nd Edition, Hanser Verlag, 2005 |
| DCB $[0/90]_s$ | ASTM D5528-01 | 5 | |
| MMB $[0/90]_s$ | ASTM D6671 | 6 | |

***Figure 4: Overview of performed coupon tests in the MATISSE Project***

For the creation of the first simulation models, only the tension and compression tests are used. They are going to be analyzed further in the next chapters. The additional three tests (ENF, DCB and MMB) are used for the validation of a novel delamination model which is not part of this publication. This model has already been presented in (17) and (18).

**Results – Validation of material models**

In the following the results of test and simulation with the final material model are compared and discussed:

Elastomer matrix system – Expansion area of adaptive structure

For the expansion area of the shape-adaptive structure, which has to sustain large deformations during the unfolding process, the material model *MAT_54 was selected. The latter is a simple progressive failure model for FRP materials. It requires only a few input parameters, thus it reduces the difficulty and extensive material testing for input parameters. *MAT_54 describes a progressive failure within the limits of strength and strain (19).

For the determination of the input-parameters a number of material tests in longitudinal and transverse direction are performed. In 0° tension loading, the material shows an almost linear behavior up to failure (see Figure 5). This characteristic can be realized very well by the use of *MAT_54.
The shear component is adjusted by a 45° tension test. Typical duromer based FRPs show a non-linearity under shear loading (20). The elastomer based FRP does not show such a behavior, its force deflection curve is also nearly linear, as can be seen in Figure 5.

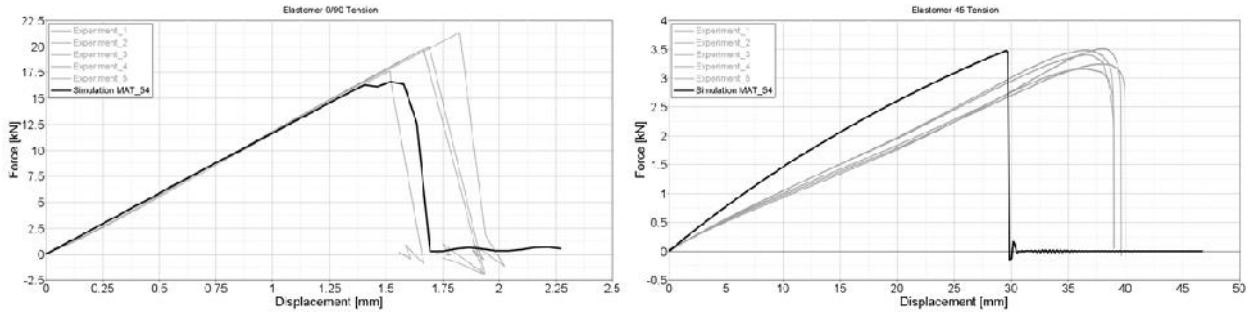


***Figure 5: Tension tests: Elastomer matrix system***

The simulation results of the $[0/90]_s$ laminate under tension loading show a high correlation to the test. In contrast the results of the tension test with a $[\pm 45°]_s$ laminate show a significant difference to the simulation. The increase of the reaction force under predominant shear loading of the material is overestimated, the elongation at break is too small whereas the maximum force correlates well with the test results. In the selected material model the ascent of the reaction force cannot be reduced without degrading the correlation in the $[0/90]_s$ configuration. Therefore for this first simulation approach the fair correlation in the shear properties is accepted.
Under compression load (see Figure 6) a higher variation in the test results can be seen. In the $[0/90]_s$ configuration the curves show a distinct peak value before first material failure occurs. In contrast at the $[\pm 45°]_s$ tests the force level is almost constant when the material begins to fail. After a certain value of deformation the reaction forces rise again in both test settings. This characteristic is mainly driven by the test setup.

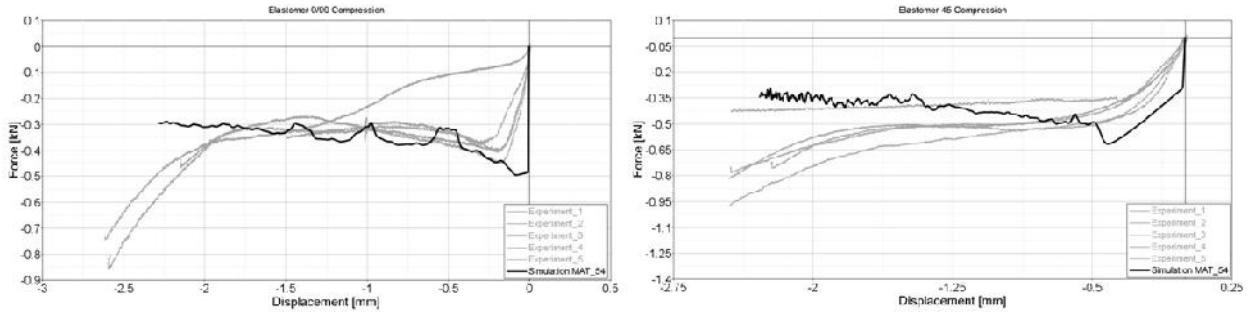


***Figure 6: Compression test: Elastomer matrix system***

When comparing the test results with the corresponding simulations it can be seen, that in particular at the $[0/90]_s$ configuration the ascent of the reaction force in the simulation is significantly higher. In this test-setup it has to be taken into account, that already smallest errors in the alignment of the upper and lower clamp of the specimen or deviations in the angle can artificially reduce the stiffness of the material. This effect is even higher, when testing soft materials such as the elastomer-matrix system used in this case. As the ascent of the reaction force in the area of elastic deformation correlates perfectly for the tension test with the $[0/90]_s$, layup it is assumed that the above mentioned effects influence the results to a certain extent.
For both cases the peak force before material failure is correlating well with the test results. After this initial peak the damage model in the simulation is obviously not capable of representing the real material characteristic. After failure the broken material is still supporting itself to some extent. In addition, the small test length leads to a buckling and an increase of thickness, which is not happening in the simulation model. An increase of the stiffness of the material after failure, which would be necessary to predict such a behavior, is not possible in any of the analyzed material models.

<u>Duromer matrix system – “Stiff” parts of adaptive structure</u>

To simulate the parts of the structure that are built with conventional carbon fiber/duromer material system, the material model *MAT_58 is used. *MAT_58 is a continuum damage model for representing unidirectional tape and woven fabric composite materials (21). The material behavior of a conventional carbon fiber/duromer material

system under a tension loading in $[\pm 45°]_s$ fiber direction shows a nonlinear load deflection curve, while a loading in fiber direction results in a linear response. Results for the different layups are shown in Figure 7.

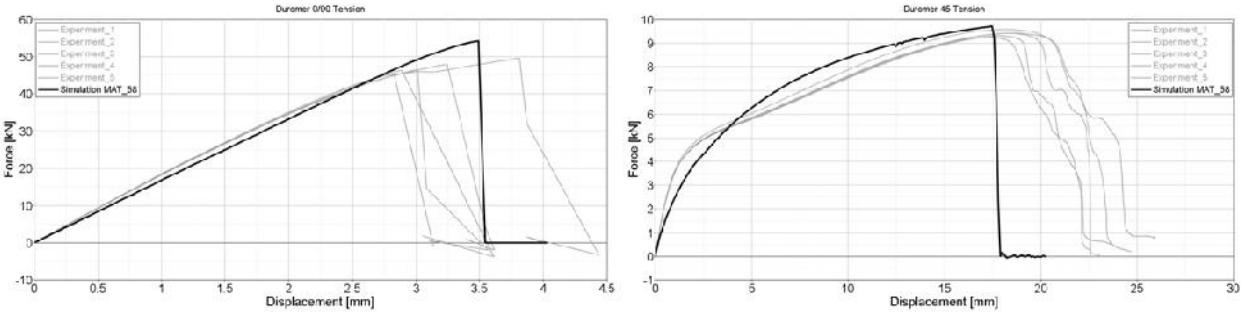


***Figure 7: Tension tests: Duromer matrix system***

It can be seen that in both configurations the results of simulation and test correlate regarding the peak force and also the elongation at break. For the $[\pm 45°]_s$ tests, the behavior after the peak force as well as the non-linear characteristic of the f-s-curve in particular in the initial ascent show a difference to the simulation results.
In case of the compression test with the duromer matrix system and a $[0/90]_s$ layup the material fails completely at very low strain levels. No residual force can be observed. In contrast the tests with $[\pm 45°]_s$ shows a certain residual force but the increase of the reaction forces at larger deformation, as seen with the elastomer matrix system under compression load, cannot be seen.

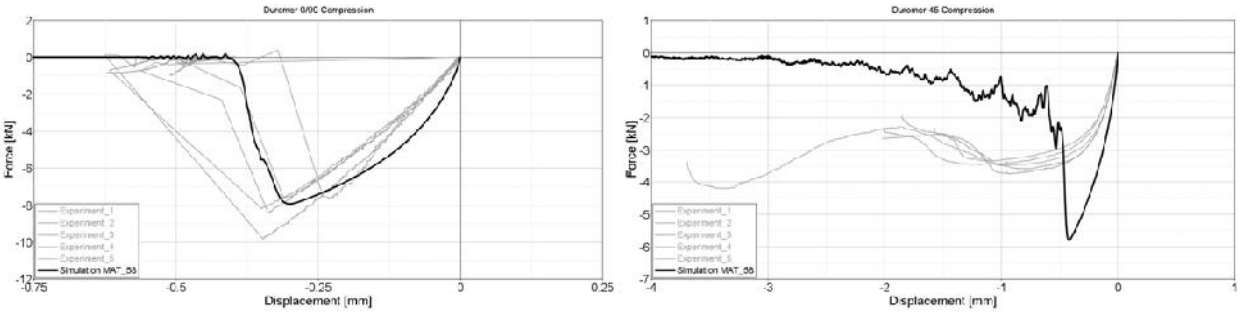


***Figure 8: Compression tests: Duromer matrix system***

Comparing the results of test and simulation the values for the initial ascent of the reaction forces correlate well. The peak force fits to the test results in case of the $[0/90]_s$ configuration, but is significantly too high for the $[\pm 45°]_s$ layup. The above mentioned issue with the damage model allowing no increase of stiffness after material failure leads to good results for the $[0/90]_s$ and comparable deviations as seen at the elastomer matrix system.

The shown correlation is the result of an iterative optimization of material parameters, whereby their respective physical boundaries are respected. A compromise setup is chosen in order to minimize deviations between test and simulation in all analyzed loading configurations.

It can be summarized that the available simple standard material models can be used in order to simulate the mechanical behavior of materials that allow for a shape adaptivity of a FRP structure. The correlation of the simulation with the conducted coupon tests is comparable for the conventional FRP based on a duromer matrix system and the material dedicated for the expansion-zones based on an elastomer matrix system.

## COMPONENT TESTING AND VALIDATION

Also for the testing, a stepwise approach for the proof of concept was chosen with the final goal to conduct a dynamic impactor test on an adaptive beam, which is expanded within few milliseconds by a pyrotechnical inflator. Before that a number of intermediate steps have to be carried out, beginning with the verification, that the actual expansion process of the beam can be realized without failure of the structure. For this purpose the structure is pressurized with water, slowly increasing the inner pressure.

**Inflation-Test of expandable beam with quasistatic pressure**

This test also gives some essential information for the validation of a corresponding numerical model:

- Pressure at which the structure begins to unfold
- Unfolded beam-geometry
- Burst pressure of entire beam

For that purpose the inflator is replaced by a water-pump that slowly increases the pressure within the structure. As the mountings for the inflator can be used for that purpose, there is no modification of the structure necessary. The following pictures show the attachment of the pressurization device and the beam in the process of unfolding.

***Figure 9: Mounting of pressure transducer***

***Figure 10: Unfolded shape of beam***

This test shows, that the static expansion process of the beam from the folded to the final shape begins at a very low pressure of around 100 to 200 kPa. After the expansion the elastic areas of the beam are creating a more or less semi-circular cross-section, whereas the areas with the duromer-resin maintain their initial shape.
The pressure is further increased to see at which level and at which location the first material failure occurs. At an inner pressure of around 4.400 kPa, a first small leakage can be observed in the transition area of the u-shape to the attachment points as displayed in Figure 11.

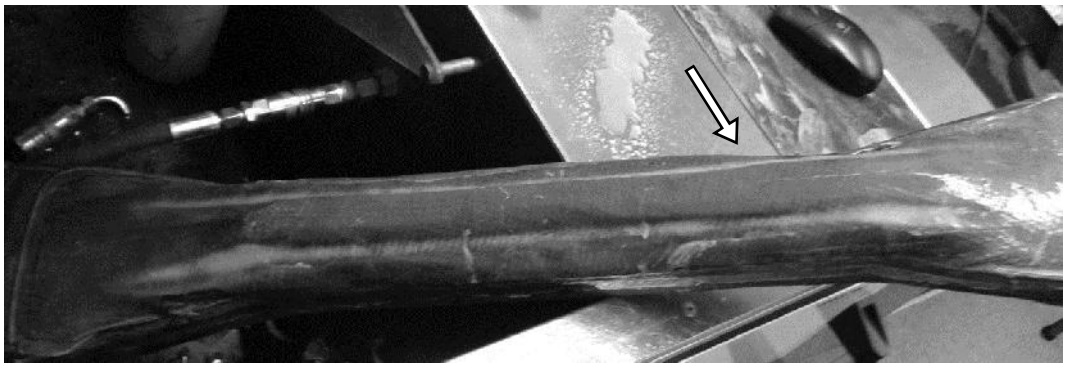

***Figure 11: Expanded structure with initial leakage at 4.400 kPa***

This leakage is not necessarily caused by a material failure as water could also have leaked through an area with higher porosity. Nevertheless, this pressure value gives a first idea of the possible pressure level that can be sustained.
In order to validate the simulation model of the component with this test, the same boundary conditions as in the test are applied to the model and the material data, which has already been validated with the coupon tests, is used.

**Simulation approach for the inner pressure**

Besides the availability of valid FRP material models a detailed approach to simulate the inflation process is mandatory for the cost and time efficient development of crash adaptive structures. Therefore, LS-DYNA offers three fundamentally different methods to mathematically model the inflation process of the expandable pressurized structures.

Depending on the optimization task and the level of detail, one of the following approaches can be used:

- Uniform Pressure Method (UP)
- Arbitrary-Lagrangian-Eulerian Method (ALE)
- Corpuscular Particle Method (CPM)

Typically, in the early development stage of crash adaptive structures no inflator specifications like heat capacity, mass flow rate and temperature profile of the inflowing gas mixture are known (22). Instead of calculating the inner pressure based on the inflator data the UP-approach offers the possibility to specify an idealized pressure versus time profile.
Due to the not existing discretization of the inflowing gas mixture the pressure distribution within the structural component is uniform. Accordingly, this yields to the following drawbacks:

- exact representation of the internal pressure requires technical measurement during inflation tests of the original component (hardware needed)
- no local interaction between gas and structure due to global pressure value
- evaluation of local temperature or pressure peaks (eg. close to the inflator) not possible

It is obvious that, as soon as the pressurization is realized with an inflator, the CPM or ALE-Method has to be applied in order to achieve a realistic loading of the structure in the simulation model. For the test with the quasistatic water-pressurization there is no benefit by applying this more complex approach, therefor the UP-Method is used.

**Results – Validation of component test**

In the selected simulation model of the structural member, both ends are constrained allowing only translational movement in the longitudinal direction of the beam. The structure can expand its shape without interacting with any other component. The pressure is steadily increased to reach 5.000 kPa after 500ms. These values are chosen to simulate the “slow” increase of pressure compared to an inflation with a pyrotechnical device. Even though the material properties are not modelled with strain rate dependency as described above, still the dynamic of the structure is influenced by the rate at which the inner pressure is rising in the simulation. The chosen configuration thereby is a compromise in order to limit the necessary calculation time. The inflation process as well as the curves for pressure and inner volume of the structure are displayed in Figure 12.

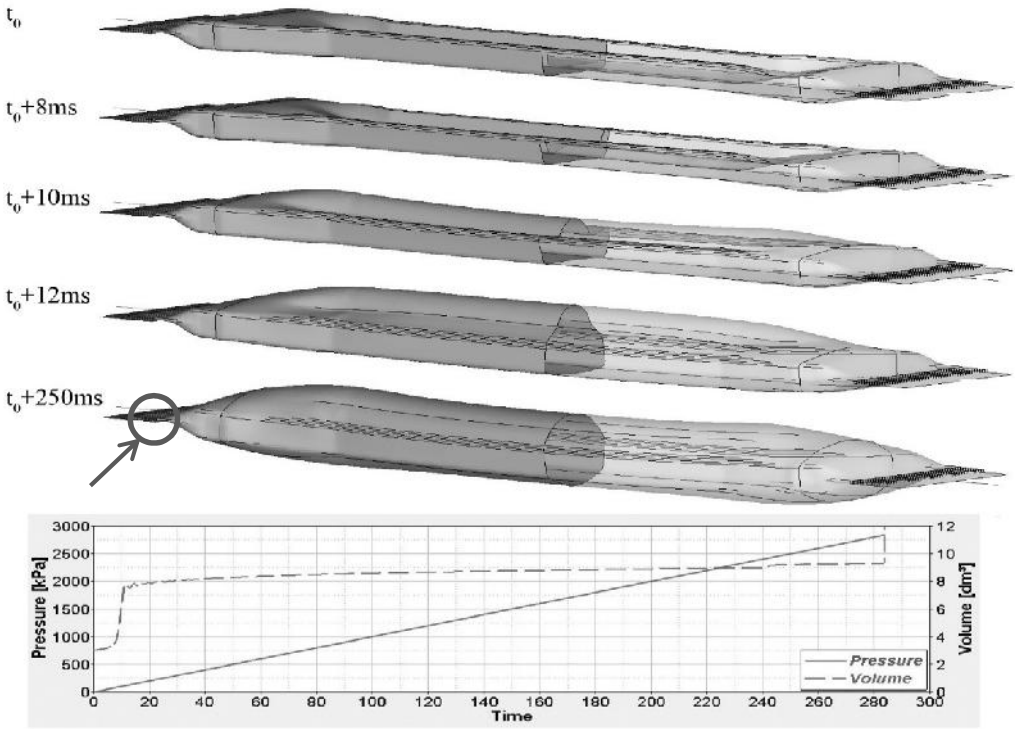


***Figure 12: Simulation of quasistatic pressurization***

It can be seen that the volume of the structure in the initial status is about 3 liters. The unfolding and thus the gain of volume begins at a pressure level of 100 kPa. At a pressure of around 150 kPa the expansion zone of the structure has completely unfolded and from that time on the increase of volume is caused by a transition to a more or less circular cross-section of the structure. Even though the pressure during the expansion process is low, the unfolding itself takes place with high dynamics. This effect correlates well with the conducted test in which the expansion process also begins already at very low pressure levels.
With increasing pressure also the volume slightly increases until the first material failure in the model at a pressure level of 2.800 kPa. This failure occurs in the transition area between the attachment and the expansion zone (see Figure 12, 250ms) which is not correlating with the location of the leakage in the test. By evaluating the stress-distribution within the layup areas with high loading can be identified. This analysis shows, that the area of the leakage in the test is the zone of the structure loaded with the highest shear-stresses. The part of the structure in which the failure occurs in the simulation is the zone with the highest principal normal stress.
This leads to the assumption, that the parameterization of the failure models for the two materials found in the coupon tests does not fit perfectly for the loading situation found in the structure.
Another issue is, that the geometry in the area of material failure shows some very small radii that lead to discretization errors caused by the mesh. That could be addressed with a refined mesh in that specific part of the model, which has the drawback of increased calculation time.

## SUMMARY/CONCLUSION

The goal of this study was to find suitable material models that are required to allow for an accurate simulation of the geometrical adaptivity of FRP structures. By comparing the results of conducted coupon tests with corresponding simulations it was demonstrated, that this goal can be achieved already with standard material models. The achieved correlation for the elastomer-based material in the expansion-zone is comparable to the standard-material used in the remaining parts of the structure. For the shear-stiffness of the elastomer-based CFRP only a fair correlation between test and simulation could be achieved with the used material model.

Whereas the results in the coupon tests match well, a significant deviation in the simulation of the component tests is noticed. With the performed coupon tests only in-plane compression and tension loading was analyzed. Based on these results the damage- and failure models in the chosen material models (MAT_54 and MAT_58) were parameterized. In the current structure obviously more complex loading conditions occur (inner pressure, bending load, …). That might be one reason, why the results for maximum pressure of the simulation is not matching the results of the component test. This issue suggests additional coupon tests (e.g.: 3 pt. bending, etc.) in order to have a wider basis for the parameterization of the damage models. With additional material data available also the application of more complex material models can be taken into account.

The first step in the development process for numerical models of shape adaptive beams is the capability of the simulation of the unfolding process. Based on this work it can be demonstrated that the used hybrid-matrix approach, which is one suitable concept for the realization of the necessary flexibility of the structure, can also be represented in a numerical model. Limitations of the chosen material models and the conducted coupon test lead to deviations in the correlation between simulation and tests. In order to improve the predictability of the simulations some possible approaches were discussed.

For the prediction of the mechanical properties of shape adaptive FRP-structures under crash-loads, the complexity of the modelling increases significantly:

Firstly it is assumed, that the unfolding process itself already causes local damage of the material which can lead to a weakening of the structure in the actual crash-load. First of all, this effect has to be analyzed by tests in order to understand the influencing parameters. Then basically two approaches are possible for the integration of this effect in the model of the structure: Either the used material model provides a “damage-history” that allows for the use of different parameters for the first loading (expansion – no damage) and the second loading (crash – pre-damage). Alternatively it is also feasible to run the expansion process in a pre-simulation and the actual crash-simulation with an exchanged material model.

Secondly it is known, that FRPs and hereby in particular the matrix materials show a high dependency of the mechanical properties to the loading velocity (23). This effect was not considered for the above presented numerical model but for the final purpose of this study it cannot be neglected. For the expansion process as well as the crash loading itself such effects can lead to a different stiffness and strength of the structure but

also to different failure modes. Strain rate dependencies can be considered also with the material models used in this study but the parameterization of these models requires an enormous amount of material testing.

Finally, it has to be considered that for the pressurization of the structure an inflator is used. Depending on the used inflator-technology the exhaust gas can reach several hundred degrees Celsius. The combination of hot gas and its high velocity in the area of the inflator, abrasive damage of the structure material can occur. This needs to be considered in the design of the structure. This effect cannot be simulated, so extensive testing is necessary.

The global heating of the structure during and after the inflation leads to varying material properties, which can be significant for plastic materials (24). Due to the very short time of interaction of the hot gas with the structure, this effect is possibly neglectable but it has to be confirmed for concept evaluation. A heat-dependency of material properties is not yet realized in available material models of LS-DYNA. So alternatively, after a pre-simulation for the expansion process the material model can be adjusted to simulate the material with the actual temperature during the crash-load.

It can be concluded that still a lot of research topics have to be solved in order to create a predictive numerical model of a shape-adaptive FRP structure but with this work a first step was achieved.

**ACKNOWLEDGEMENT**

The research leading to these results receives funding from the European Community's Seventh Framework Programme (FP7/2007-2013) under grant agreement no. 314182 (the MATISSE project). This publication solely reflects the author's views. The European Community is not liable for any use that may be made of the information contained herein.

## REFERENCES


1. Krollmann J. Design and Manufacturing of Shape Adaptive CFRP Structures in a Multi-Matrix Approach. SICOMP Conference on Manufacturing and Design of Composites; 2014 Jun 30; Lulea, Sweden.
2. Wacker M. Hochleistungsfaserverbunde in der Großserie [Internet]. 2012 Oct 17 [cited 2015 Feb 5]. Available from: www.fill.co.at
3. Giddons N, White, Mark. OEMs' Visions for Cost-Effective Adoption of Advanced Lightweight Materials to Deliver Improved Fuel Economy & CO2 reduction. Global Automotive Lightweight Materials 2012; 2012.
4. Scott P. The new BMW i3 [Internet]. 2013 Nov [cited 2015 Feb 6]. Available from: www.asymcar.com
5. Feindler N. Charakterisierungs- und Simulationsmethodik zum Versagensverhalten energieabsorbierender Faserverbundstrukturen. TU Munich; 2012.
6. Krüger J, Dölle N. FVK-Anwendungen bei Daimler - Lessons learned – [Internet]. [cited 2015 Feb 5]. Available from: http://www.carbon-composites.eu
7. Etzler M. Conceptual Study on adaptive crash structures. Bachelor Thesis, TU Graz;
8. Nohr M. Crash adaptive vehicle structures and components. 2009;
9. Pipkorn B, Lundström J, Ericsson M. Safety and vision improvements by expandable A-pillars. 2011.
10. Mellinghoff U. The Mercedes-Benz Experimental Safety Vehicle 2009. 2009.
11. Koschmieder M. Verarbeitung und Eigenschaften von Faserverbundkunststoffen mit Elastomermatrix. 2010.
12. Hartmann S. Neue Materialmodelle für Composites in LS-DYNA. 2013.
13. Hinterhölzl R. Auslegung und Bauweise von Composite Strukturen. Skriptum, TU München Institut für Carbon Composites; 2013.
14. LS-DYNA Keyword User's Manual, Version R7.0. LSTC;
15. Peinhaupt C. Numerische Untersuchung zur Eignung eines CFK-Crashelements als Energieabsorber. 2013.
16. Daniel IM, Ishai O. Engineering Mechanics of Composite Materials, 2nd Edition. Oxford University Press;
17. Brouzoulis J, Fagerström M. Modelling of multiple delaminations in shells using XFEM. 2013.
18. Brouzoulis J, Fagerström M, Svenning E. A shell element formulation for the simulation of propagating delamination and through-thickness cracks. 2014.
19. Wade B, Feraboli P, Osborne M. Simulating laminated composites using LS-DYNA material model MAT54 part I: [0] and [90] ply single-element investigation. 2012.
20. Schweizerhof K, Weimar K, Münz T, Rottner T. Crashworthiness analysis with enhanced composite material models in LS-DYNA–merits and limits. 1998.
21. LS-DYNA Keyword User's Manual. Livermore Software Technology Corporation (LSTC); 2014.
22. Opelka J-M, Nohr M, Blume K-H, Neutz J. PRE-SAFE® Structure als automobile Anwendung – Entwicklung intelligenter Tür-/Rohbaustrukturen. VDI Berichte 2204. 2013.
23. Eyerer P, Woidasky J, Dominighaus H, Elsner P. Einführung in Polymer Engineering. Springer Berlin Heidelberg; 2008.
24. Schürmann H. Konstruieren mit Faser-Kunststoff-Verbunden. Springer Berlin Heidelberg; 2006.

# CONSUMER RESPONSE TO VEHICLE SAFETY RATINGS

**Jessica B. Cicchino**
Insurance Institute for Highway Safety
United States

Paper Number 15-0069

## ABSTRACT

This study assessed how the release of the Insurance Institute for Highway Safety's (IIHS) new crashworthiness ratings based on a small overlap front crash configuration and ratings of front crash prevention systems affected consumer behavior. Telephone surveys were conducted with U.S. Volvo dealers after the August 2012 inaugural release of the IIHS small overlap frontal crash test ratings, in which the Volvo S60 was one of two models receiving the highest rating of good, and with U.S. Subaru and Jeep dealers after the May 2013 release of small overlap frontal test ratings of small SUVs, in which the Subaru Forester was the only model rated good and the Jeep Patriot was rated poor. Additional surveys were conducted following the September 2013 inaugural release of IIHS's front crash prevention ratings with U.S. Subaru, Volvo, and Cadillac dealers, automakers that offered automatic emergency braking systems receiving the top superior rating; U.S. Ford dealers, which offered a forward collision warning system rated basic; and U.S. Hyundai dealers, which had no rated system and offered little collision avoidance technology at the time.

Nearly half of Volvo dealers and 75% of Subaru dealers reported increased consumer interest in the S60 and Forester models, respectively, after their good ratings in the small overlap frontal test were broadcast. Volvo dealers reported a 41% increase in sales of the S60 and an 18% increase in sales of all Volvo models the week following this announcement compared with the week before. Subaru dealers reported a 14% increase in sales of the Forester and an 11% increase in all Subaru models compared with the week before the announcement, while Jeep Patriot sales declined slightly and sales of all Jeep models were essentially unchanged. About a third of Subaru, Volvo, and Cadillac dealers and 10% of Ford dealers reported increased consumer interest in front crash prevention systems after the inaugural ratings were released. Sales for all surveyed automakers declined from the week before the front crash prevention rating announcement to the following week. However, sales of Subaru, Volvo, Cadillac, and Ford models with rated systems declined 41% less than sales of Hyundai models, and sales of all models from these automakers declined 6% less than sales of Hyundai models. The findings suggest that well-publicized safety ratings can translate directly into changes in consumer vehicles purchases.

## INTRODUCTION

Surveys of the public [1-5] and of recent new vehicle buyers [6] in the United States, Canada, and Europe conducted during the past decade have found that consumers find safety to be an important consideration when purchasing a new vehicle. About half of drivers surveyed in the United States [4] and Europe [3] reported they have researched the protection vehicles would provide in a crash, or that such information has been useful to them in choosing a new vehicle to purchase. Drivers also consider technology that improves vehicle safety when choosing vehicles. In a survey of U.S. vehicle owners [2], 58% reported that a vehicle having proven and tested technology was highly influential in new vehicle purchases. Approximately half said they would be willing to pay extra for enhanced safety features in vehicles.

The Insurance Institute for Highway Safety (IIHS) has provided information to U.S. consumers about vehicle safety since the mid-1990s. IIHS introduced a new vehicle crashworthiness test, the small overlap frontal crash test, in 2012. The test is designed to replicate the vehicle damage and motion that occurs in a collision where a small

portion of the vehicle's front end contacts the struck object, such as when the front corner of a vehicle collides with another vehicle, or when a vehicle strikes a tree or utility pole. In the test, 25% of a vehicle's front end on the driver side is crashed into a rigid barrier at 64 km/h. Compared with the moderate overlap frontal crash test, involving 40% of the vehicle's front end, the small overlap test puts higher stress on the outer part of the vehicle's safety cage, which typically is less protected by the vehicle's crush zone structures. The top rating possible in this and IIHS's other crashworthiness tests is good, followed by acceptable, marginal, and poor ratings.

IIHS expanded its vehicle ratings program in 2013 to include front crash prevention systems. Vehicles that brake autonomously in the event of an imminent frontal collision can earn ratings of advanced or superior based on performance in tests conducted at 20 and 40 km/h. For the top rating of superior, vehicles with autobrake must avoid a crash or reduce speeds substantially in both tests. For a rating of advanced, vehicles with autobrake must avoid a crash or reduce speeds by at least 10 km/h in at least one of the two tests. Vehicles earn a rating of basic if they have a forward collision warning system that meets National Highway Traffic Safety Administration performance criteria.

New IIHS vehicle safety ratings are typically publicized to the U.S. public through hundreds and thousands of television broadcasts and extensive coverage by print and internet news media. Although there is evidence that many consumers factor safety ratings into their vehicle purchase decisions, it is unknown how safety ratings translate into sales of specific models that receive high and low ratings. To investigate this, IIHS conducted three surveys of dealers about consumer interest in and sales of recently-rated vehicle models.

Volvo dealers were interviewed following the inaugural release of small overlap crash test ratings with midsize luxury vehicles on August 14, 2012, in which the Volvo S60 was one of two of the 11 vehicles tested to earn the top rating of good. Suburu and Jeep dealers were interviewed following the May 16, 2013 release of small overlap crash test ratings of 13 small SUVs. The Suburu Forester was the only vehicle rated good in this round of small overlap crash testing and the first vehicle tested by IIHS in the small overlap configuration with top ratings in all aspects of the test. The Jeep Patriot was one of five vehicles rated poor. Press coverage of the test release tended to highlight the Subaru Forester and Jeep Patriot as examples of good and poor performers, respectively.

A final set of interviews with Volvo, Cadillac, Subaru, Ford, and Hyundai dealers was conducted following the September 27, 2013 inaugural release of front crash prevention ratings of midsize cars and SUVs. The Cadillac ATS and SRX equipped with Forward Collision Alert and Automatic Collision Preparation, the Subaru Legacy and Outback equipped with EyeSight, and the Volvo S60 and XC60 equipped with City Safety and Collision Warning with Full Auto Brake and Pedestrian Detection were six of the seven vehicles rated superior. The Volvo S60 and XC60 equipped only with City Safety, which brakes autonomously at low speeds and was standard equipment on these models, were two of the eight vehicles rated advanced. The Cadillac ATS and SRX equipped with Forward Collision Alert only, which warns of an imminent forward collision but does not include autobrake, and the Ford Edge, Explorer, Flex, and Fusion equipped with Collision Warning with Brake Support were six of the 28 vehicles that earned a basic rating. Hyundai had no models that were rated for front crash prevention in September 2013 and sold few vehicles with front crash prevention systems at the time.

**METHODS**

Telephone interviews were conducted by OpinionAmerica Group (Cedar Knolls, NJ), a professional survey organization. Phone numbers were obtained for dealerships from publicly available directories. Following the August 14, 2012 and May 16, 2013 small overlap ratings releases, interviews were attempted with all U.S. Volvo dealerships during August 28-September 6, 2012, and with all U.S. Subaru dealerships and a sample of the more than 2,200 U.S. Jeep dealerships during June 17-July 16, 2013. Of the 310 Volvo dealerships called with working phone numbers, interviews were completed with 206 (66%) and 2 (1%) refused. Subaru and Jeep dealerships were

called until 275 interviews were completed with each. Thus, among dealerships with working phone numbers, 47% of the 589 Subaru dealerships called completed interviews, 20 (3%) refused, and 4 (1%) began but did not complete the survey, and 28% of the 982 Jeep dealerships called completed interviews, 116 (12%) refused, and 6 (1%) began but did not complete the survey.

Following the September 27, 2013 announcement of front crash prevention ratings, interviews were attempted during October 28-December 3, 2013 with all U.S. Subaru, Volvo, Cadillac, and Hyundai dealerships, and a sample of the more than 3,100 U.S. Ford dealerships, with the goal of completing as many interviews as possible with Volvo dealers and 275 interviews with each of the remaining automakers. Among dealers with working phone numbers, 275 (48%) of the 572 Subaru dealers called completed interviews, and 59 (10%) refused; 176 (60%) of the 295 Volvo dealers called completed interviews, and 21 (7%) refused; 275 (26%) of the 1,080 Cadillac dealers called completed interviews, 268 (25%) refused, and 1 (<1%) began but did not complete the survey; 275 (35%) of the 792 Ford dealers called completed interviews, 74 (9%) refused, and 11 (1%) began but did not complete the survey; 275 (32%) of the 851 Hyundai dealers called completed interviews, and 125 (15%) refused. In all surveys, dealers that were called and did not refuse or begin the survey typically asked to be called back later or did not answer.

Interviewers asked to speak with the dealership's sales manager or with the general manager or owner if the sales manager was unavailable. Interviews were most often completed with sales managers (72% of interviews completed, ranging from 67%-80% among automakers). Surveys lasted about 5 minutes.

## RESULTS

### Surveys Following Small Overlap Crash Test Rating Releases

Dealers were asked if there was a change in the number of people who had contacted or visited their dealerships since the mid-August 2012 (Volvo) or mid-May 2013 (Subaru and Jeep) release of small overlap crash test ratings because they were interested in purchasing a Volvo S60, Subaru Forester, or Jeep Patriot, and if more, fewer, or the same proportion of customers who had contacted the dealership since the release had mentioned the safety performance of Volvo, Subaru, or Jeep as a reason for considering the brand. Larger percentages of Subaru (75%) and Volvo (49%) dealers than Jeep (12%) dealers reported an increase in calls and visits from customers interested in purchasing the tested vehicle (see Table 1). Subaru and Volvo dealers were likewise more likely to report that more customers had mentioned the safety performance of the automaker as a reason for considering it (55%-61% vs. 8%; see Table 1).

**Table 1.**
**Customer interest in Volvo, Subaru, and Jeep vehicles and mentions of automakers' safety and crash test performance since announcement of IIHS small overlap crash test results (percent).**

| | | Volvo (N=206) | Subaru (N=275) | Jeep (N=275) |
|---|---|---|---|---|
| Change in number of people who contacted or visited dealership because they are considering purchasing a Volvo S60, Subaru Forester, or Jeep Patriot | More | 49 | 75 | 12 |
| | Same | 50 | 24 | 86 |
| | Less | 1 | 1 | 2 |
| | Don't know/Refused | 0 | 1 | 0 |
| Change in number of customers who mentioned safety performance of automaker as reason for considering brand | More | 55 | 61 | 8 |
| | Same | 44 | 35 | 87 |
| | Less | <1 | 1 | 4 |
| | Don't know/Refused | <1 | 3 | 1 |
| Any customers mentioned automaker's performance in recent crash tests as reason for considering brand | Yes | 68 | 77 | 12 |
| | No | 30 | 22 | 88 |
| | Don't know/Refused | 2 | 1 | 1 |

More than two-thirds of Volvo and Subaru dealers reported that since the release at least some of their customers had mentioned performance in recent crash tests as a reason they were considering the automaker, compared with 12% of Jeep dealers (see Table 1). When Jeep dealers were asked if any potential customer since mid-May had mentioned Jeep's performance in recent crash tests as a reason why they were having second thoughts about buying a Jeep, 14 dealers (5%) said yes.

Volvo dealers were asked about the dealership's sales of the Volvo S60, and of all Volvo models, for four weeks in 2012: July 29-August 4 (two weeks before the release), August 5-11 (the week before the release), August 12-18 (the week during the release), and August 19-25 (the week after the release). Similarly, Subaru and Jeep dealers were asked about sales of the Subaru Forester or Jeep Patriot, and of all Subaru or Jeep models, for three weeks in 2013: May 5-11 (the week before the release), May 12-18 (the week during the release), and May 19-25 (the week after the release).

Sales numbers for all models and the rated model in each of the four weeks were provided by 156 Volvo dealers (78%), and in each of the three weeks by 261 Subaru dealers (95%) and 269 Jeep dealers (98%). Two Volvo dealers were unable to provide sales data for the period two weeks before the release but did provide data for the subsequent weeks. Response rates for these questions improved in the survey of Subaru and Jeep dealers because interviewers encouraged dealer representatives to look up sales numbers if they did not have them readily available, which was not done in the prior survey of Volvo dealers.

Changes in total sales were examined from the week before the release to the week after the release among dealers that reported data for all weeks (see Table 2). Volvo dealers reported a much larger increase in total sales of the S60 model (41%) than of all Volvo models (18%), and Subaru dealers reported a slightly larger increase in Forester sales (14%) compared with sales of all Subaru models (11%). Jeep dealers reported a small decrease in sales of the Patriot model (2%) and a small increase in total sales for all Jeep models (<1%).

**Table 2.**
**Sales of S60, Forester, Patriot, and all Volvo, Subaru, and Jeep models two weeks before and the week before, during, and after the release of IIHS small overlap test results, among dealers reporting for all weeks.**

| | | Two weeks before | Week before | Week of | Week after | Percent change, week before to week after |
|---|---|---|---|---|---|---|
| | | Jul 29-Aug 4, 2012 | Aug 5-11, 2012 | Aug 12-18, 2012 | Aug 19-15, 2012 | |
| Volvo | Volvo S60 | 317 | 261 | 329 | 369 | 41 |
| (N=156) | All Volvo models | 1,046 | 798 | 822 | 944 | 18 |
| | | | May 5-11, 2013 | May 12-18, 2013 | May 19-25, 2013 | |
| Subaru | Subaru Forester | — | 1,243 | 1,203 | 1,422 | 14 |
| (N=261) | All Subaru models | — | 3,970 | 3,795 | 4,397 | 11 |
| Jeep | Jeep Patriot | — | 426 | 398 | 419 | -2 |
| (N=269) | All Jeep models | — | 2,314 | 2,206 | 2,325 | <1 |

At the end of the survey, dealers were asked if they knew that the S60 or Forester model had earned a good rating or that the Patriot had earned a poor rating in a recent IIHS small overlap crash test. Nearly all Volvo (94%) and Subaru (93%) dealers were aware of the performance of the S60 and Forester, respectively, prior to the survey, but fewer Jeep (38%) dealers were aware of the Patriot's performance.

**Surveys Following Front Crash Prevention Rating Release**

Subaru, Volvo, Cadillac, and Ford dealers were asked a series of questions regarding customer interest in vehicles with front crash prevention systems since the late September 2013 inaugural release of IIHS front crash prevention

ratings. Subaru, Volvo, and Cadillac dealers were asked about interest in vehicles with systems rated superior (Subaru's EyeSight system, Volvo's City Safety and Collision Warning with Full Auto Brake and Pedestrian Detection systems, and Cadillac's Forward Collision Alert and Automatic Collision Preparation systems), and Ford dealers were asked about vehicles with a system that earned a basic rating (Collision Warning with Brake Support). The full names of the systems were used in questions to dealers.

When asked if there was a change in the number of people who had contacted or visited their dealerships since late September because they were interested in purchasing a vehicle with front crash prevention, between 25% and 47% of dealers of the automakers with systems rated superior and 10% of Ford dealers reported an increase in interest among consumers (see Table 3). Sixty percent of Subaru dealers, 49% of Volvo dealers, 31% of Cadillac dealers, and 20% of Ford dealers reported that at least some customers interested in purchasing the vehicles with rated systems since late September had mentioned that they had seen the system included in safety ratings (see Table 3).

**Table 3.**
**Customer interest in Subaru, Volvo, and Cadillac vehicles with front crash prevention systems rated superior and Ford models with front crash prevention systems rated basic, and mentions of safety ratings and autobrake since release of IIHS front crash prevention ratings (percent).**

| | | Subaru (N=275) | Volvo (N=176) | Cadillac (N=275) | Ford (N=275) |
|---|---|---|---|---|---|
| Change in number of people who contacted or visited dealership because they are considering purchasing a model with front crash prevention system rated superior (Subaru, Volvo, Cadillac) or basic (Ford) | More | 47 | 25 | 33 | 10 |
| | Same | 50 | 69 | 58 | 82 |
| | Less | 4 | 5 | 8 | 7 |
| | Don't know/Refused | 0 | 1 | 1 | 1 |
| Any customer interested in purchasing vehicle with system rated superior (Subaru, Volvo, Cadillac) or basic (Ford) mentioned seeing system included in safety ratings | Yes | 60 | 49 | 31 | 20 |
| | No | 39 | 50 | 69 | 79 |
| | Don't know/Refused | 1 | 1 | 0 | 1 |
| Any customer interested in vehicle with system rated superior mentioned system's autonomous braking as reason for considering system | Yes | 57 | 49 | 37 | — |
| | No | 41 | 49 | 63 | — |
| | Don't know/Refused | 1 | 2 | <1 | — |

Dealer representatives of Subaru, Volvo, and Cadillac, which offered front crash prevention systems with autobrake, were asked if customers interested in purchasing the rated vehicles with front crash prevention systems had mentioned the system's autonomous braking as a reason they were interested in purchasing them. Between 37% and 57% of dealers of each automaker reported that since late September at least some customers had mentioned autobrake as a reason for their interest (see Table 3). Among dealers reporting that customers mentioned autobrake, 58% of Subaru dealers, 51% of Volvo dealers, and 56% of Cadillac dealers said more customers than usual had mentioned autobrake since the release.

Dealer representatives of Ford, which did not offer a front crash prevention system with autonomous braking, were asked if customers interested in purchasing a Ford with front crash prevention had asked since late September if Ford's system brakes autonomously (not in table). About a quarter (23%) reported that at least some customers asked about autobrake, and among these dealers, 32% said that more customers than usual had asked about autobrake.

Dealer representatives from Hyundai, which sold front crash prevention on a limited proportion of their vehicles, were asked if any customers had questioned if Hyundai offered forward collision warning since late September. Fourteen percent reported that customers had asked about forward collision warning.

Sales figures were obtained for IIHS-rated vehicles with front crash prevention systems and for all vehicles sold by surveyed dealers during the week before (September 15-21, 2013), during (September 22-28, 2013), and after (September 29-October 5, 2013) the ratings release. The dealers were asked about sales of rated vehicles; Subaru offered a system rated superior, Volvo offered vehicles with systems rated superior and advanced, Cadillac offered vehicles with systems rated superior and basic, and Ford offered a system rated basic. The names of the packages that included the systems were used if package names differed from system names. A total of 269 (98%) Subaru, 168 (95%) Volvo, 257 (93%) Cadillac, 271 (99%) Ford, and 271 (99%) Hyundai dealers reported sales figures for all weeks for all vehicles and, if applicable, the rated vehicles. Sales reported by automakers with rated front crash prevention systems were compared with Hyundai sales.

Total sales and sales of rated vehicles declined for all automakers from the week before the ratings release to the week after (see Table 4). However, the combined sales of Subaru, Volvo, Cadillac, and Ford models with rated systems declined 41% less than sales of Hyundai models, and the combined sales of all models from these automakers declined 6% less than sales of Hyundai models. Sales of models with each rated system declined less

**Table 4.**
**Sales of all Hyundai, Subaru, Volvo, Cadillac, and Ford models, and sales of Subaru, Volvo, Cadillac, and Ford models with IIHS-rated front crash prevention systems the week before, during, and after the release of IIHS front crash prevention ratings, among dealers reporting for all weeks.**

| | | Week before Sept 15-21, 2013 | Week of Sept 22-28, 2013 | Week after Sept 29-Oct 5, 2013 | Percent change, week before to week after |
|---|---|---|---|---|---|
| Hyundai (N=271) | All Hyundai models | 5,604 | 4,633 | 3,900 | -30 |
| Subaru (N=269) | MY 2013-14 Legacy and Outback with EyeSight (superior) | 579 | 458 | 463 | -20 |
| | All Subaru models | 4,670 | 4,194 | 3,669 | -21 |
| Volvo (N=168) | MY 2013-14 S60 and XC60 with Technology Package and City Safety (superior) | 155 | 106 | 110 | -29 |
| | MY 2013-14 S60 and XC60 with City Safety and without Technology package (advanced) | 696 | 619 | 598 | -14 |
| | All Volvo models | 1,039 | 882 | 810 | -22 |
| Cadillac (N=257) | MY 2013-14 ATS and SRX with Driver Assist and Driver Awareness packages (superior) | 525 | 457 | 439 | -16 |
| | MY 2013-14 ATS and SRX with Driver Awareness package and without Driver Assist package (basic) | 412 | 380 | 339 | -18 |
| | All Cadillac models | 1,323 | 1,116 | 968 | -27 |
| Ford (N=271) | MY 2013- 14 Edge, Explorer, Flex, and Fusion models with Adaptive Cruise Control and Collision Warning package (basic) | 781 | 659 | 636 | -19 |
| | All Ford models | 6,228 | 4,576 | 4,005 | -36 |
| Total Subaru, Volvo, Cadillac, and Ford models with rated front crash prevention systems | | 3,148 | 2,679 | 2,585 | -18 |
| All Subaru, Volvo, Cadillac, and Ford models | | 13,260 | 10,768 | 9,452 | -29 |

than sales of Hyundai models, and total sales for each automaker offering vehicles with rated systems except Ford declined less than total Hyundai sales. There were no consistent differences among automakers in sales when comparing vehicles rated superior, advanced, and basic.

Because a lack of in-stock vehicles with systems could inhibit sales, dealers were asked if they had vehicles in stock with the rated systems at the time of the interview. More than 80% of dealers had vehicles with each optional system in stock, and nearly all (97%) Volvo dealers reported having S60 or XC60 models with the standard City Safety system in stock. It is unknown if dealers maintained the same stock levels in the weeks immediately surrounding the ratings release; historical stock was not assessed.

Dealers were told at the end of the survey that IIHS released front crash prevention ratings in late September and, if applicable, were informed how their systems were rated. Most Subaru (90%) and Volvo (85%) dealers, more than half of Cadillac (58%) dealers, and about a third of Ford (31%) and Hyundai (32%) dealers were aware of the ratings prior to the survey.

**DISCUSSION**

This study examined consumer interest in and sales reported by dealers of top- and poorly-rated vehicles in IIHS's small overlap crash test and of vehicles with and without front crash prevention systems rated by IIHS. A good rating in the small overlap crash test was associated with increased sales of the Volvo S60 and Subaru Forester models from the week before the ratings were released to the week after. These increases were larger than the rise in sales of all Volvo and Subaru models during this time, while sales of the poorly-rated Jeep Patriot remained flat. About half to three-quarters of Volvo and Subaru dealers also reported that customers mentioned seeing the vehicles included in crash tests, and that more customers were interested in purchasing the top-rated vehicles and mentioned the brand's safety performance as a reason they were considering them. These findings are consistent with prior research showing that consumers value safety when choosing vehicles [1-6] and demonstrate that this preference for safety extends to sales of specific vehicle models whose safety had received recent media attention.

Changes in consumer behavior following the inaugural release of IIHS front crash prevention ratings are less clear. Results indicated that some customers mentioned seeing systems included in safety ratings and some dealers reported increases in customer interest. However, reports varied by automaker and positive effects on sales were not as apparent as with the good ratings in the small overlap crash test. Sales declined for all vehicles examined from the week before the front crash prevention rating release to the week after. Sales trends likely reflected in part industry-wide factors, given that sales declined for all automakers surveyed, although it is unknown what such factors might have been. Thus, it is promising that declines were smaller among models with rated front crash prevention systems than among all vehicles and among Hyundai models, which sold few vehicles with front crash prevention at the time and did not offer vehicles with rated systems.

Consumer response to front crash prevention ratings may have been less positive than consumer response to small overlap crash test ratings because the public is less familiar with collision avoidance technologies than with crash tests. IIHS and the National Highway Traffic Safety Administration have been conducting crash tests in the United States since 1995 and the late 1970s, respectively. In comparison, front crash prevention is relatively new. A survey of Canadians during 2011-12 [7] found that only 24% were aware of forward collision warning.

Some limitations should be noted. Response rates were higher among automakers with top-rated vehicles, particularly among Volvo and Subaru dealers, than among other automakers. Volvo and Subaru dealers were also much more likely than other dealers to have known how their vehicles rated in IIHS tests. Dealers' enthusiasm to participate may have influenced their responses to questions on perceived consumer interest, and because of this limitation, it is encouraging that sales trends following small overlap crash test ratings corroborated subjective

judgments. Safety-conscious consumers may be attracted to particular automakers, which could also affect how potential customers of different automakers respond to safety ratings.

The Jeep Wrangler two-door model's marginal rating in the small overlap test was announced along with the ratings of the Subaru Forester and Jeep Patriot. Consumers' opinions of Jeep may have been affected by news reports regarding the performance of both the Patriot and Wrangler models. Finally, changes in vehicle sales were compared only between two weeks. Sales fluctuate week-to-week, and it is unknown if changes in sales persisted.

## CONCLUSIONS

The goals of IIHS's vehicle ratings programs are to inform the public about vehicle safety and to encourage automakers to improve vehicle designs to enhance safety. Since IIHS introduced its ratings programs [8], automakers continue to quickly modify vehicle designs to improve crashworthiness in response to safety ratings, and this has led to safer vehicles. For instance, virtually all new vehicles are now rated good in IIHS's moderate overlap frontal crash test, and drivers of vehicles with good ratings in this test have a lower risk of dying in a head-on collision than drivers of poorly rated vehicles [9].

Automakers also have improved the performance of their vehicles in the small overlap frontal crash test and added front crash prevention systems since the new ratings were introduced. Among 2012 vehicle models that underwent the small overlap test, 28% received the top two ratings of good or acceptable; among 2015 models, 64% had received good or acceptable ratings as of February 2015. Only 20 2013 model year vehicles had front crash prevention systems rated advanced or superior, compared with 63 2015 model year vehicles as of February 2015. Both of these ratings systems are now incorporated into IIHS's *TOP SAFETY PICK* and *TOP SAFETY PICK+* awards. The current evidence demonstrates that improving vehicle designs to boost safety ratings benefits not only consumers with safer vehicles but also automakers with increased sales.

## ACKNOWLEDGEMENTS

This work was supported by the Insurance Institute for Highway Safety.

## REFERENCES

[1] Johannson-Stenman O, Martinsson P. 2006. Honestly, why are you driving a BMW? *Journal of Economic Behavior & Organization* 60:129-46.

[2] Kaul V, Singh S, Rajagopalan K, Coury M. 2010. Consumer attitudes and perceptions about safety and their preferences and willingness to pay for safety. Report No. 2010-02-2336. Warrendale, PA: SAE International.

[3] Market & Opinion Research International. 2005. 10th anniversary consumer survey for Euro NCAP. London, England.

[4] McCartt AT, Wells JK. 2010. Consumer survey about vehicle choice. Arlington, VA: Insurance Institute for Highway Safety.

[5] Vrkljan BH, Anaby D. 2011. What vehicle features are considered important when buying an automobile? An examination of driver preferences by age and gender. *Journal of Safety Research* 42:61-5.

[6] Koppel S, Charlton J, Fildes B, Fitzharris M. 2008. How important is vehicle safety in the new vehicle purchase process? *Accident Analysis & Prevention* 40:994-1004.

[7] Robertson RD, Vanlaar WGM, Marcoux KD, McAteer HJ. 2012. Vehicle safety features: knowledge, perceptions, and driving habits. Ottawa, Ontario: Traffic Injury Research Foundation.

[8] Highway Loss Data Institute. 2013. IIHS crashworthiness evaluation programs and the U.S. vehicle fleet. *Loss Bulletin 30(7).* Arlington, VA.

[9] Farmer, C.M. 2005. Relationships of frontal offset crash test results to real-world driver fatality rates. *Traffic Injury Prevention* 6:31-37.

# HOW IS ASTAZERO DESIGNED AND EQUIPPED FOR ACTIVE SAFETY TESTING?

**Jan Jacobson**
**Henrik Eriksson**
SP Technical Research Institute of Sweden
Sweden

**Peter Janevik**
**Håkan Andersson**
AstaZero
Sweden

Paper Number 15-0071

## ABSTRACT

The Swedish test track AstaZero (Active Safety Test Area) is an open environment where vehicle OEMs, tier one suppliers, research institutes, and universities can come to perform development and research. AstaZero is located just outside the city of Borås in West Sweden and was inaugurated in August 2014. The initiative was taken to create an environment for innovation, testing, and research to develop new active safety functions for road vehicles. The four main environments of the facility are built especially for research and development of active safety functions. A city area for simulation of urban traffic, a multilane road, a 5.7 km long rural road, and an innovative high-speed area facilitate efficient testing. Equipment of different kinds is also at hand; test targets, position measurement and control systems, communication equipment, and driving simulators can be provided. However, the success of the AstaZero test bed is also depending on the existence of leading competence. The Swedish automotive cluster has the ability to perform research, industrial development, and rational production of road vehicles. It is essential for AstaZero to have access to strong competence in its vicinity. The organizations residing in the Gothenburg region can be reached in an hour by car. The Stockholm region is more distant but it is quite possible to travel by road in four hours. The success of AstaZero is built on the track, the competence, and all the partners supporting the facility.

## INTRODUCTION

Road safety has improved during the past years, but we are still far from the zero vision that no one should be killed or seriously injured in road traffic. The European Union has set ambitious goals for road safety. According to the 2011-2020 policy the objective is that member countries must together have reduced the number of road accidents by 50 per cent by the year 2020 [1]. Active safety, as well as test facilities where new techniques can be tested, will play an important part in the contribution of making this vision reality.

Active safety functions are regarded as key components to further increase safety on our roads. Due to safety and repeatability requirements, much of the development and research of these functions must be performed in a controlled environment such as a test track. For novel active safety functions many tests cannot be made in real traffic due to the risks of prototype malfunction. In terms of infrastructure, targets and their propulsion systems, as well as measurement systems, what resources are needed to evaluate the performance of active safety functions?

The AstaZero (active safety test area) [2] located just outside the city of Borås in West Sweden was inaugurated in August 2014. The initiative was taken to create an environment for innovation, testing and research to develop new active safety functions for road vehicles. The active safety functions are under rapid development and there are presently, and in contrast to passive safety, few generally accepted testing procedures in place. Performance testing methods for active safety are necessary to improve the safety performance of new safety functions in road vehicles. Suitable test procedures are key enablers. The tests must be repeatable and the results must be relevant to the safety benefits in real traffic. There is still much development and standardisation to be done for test procedures.

AstaZero is an open environment where industry (vehicle OEMs and tier one suppliers) and academia (institutes and universities) can come and perform development and research.

**TEST TRACK**

The AstaZero has been designed with four main environments. (Figure 1) There is a city area for simulation of urban traffic. Highway scenarios can be simulated at the multilane road. A 5.7 km long rural road is included for monotonous driving with sudden obstacles. Dynamics and fast scenarios can be tested using the high-speed area with acceleration stretches.

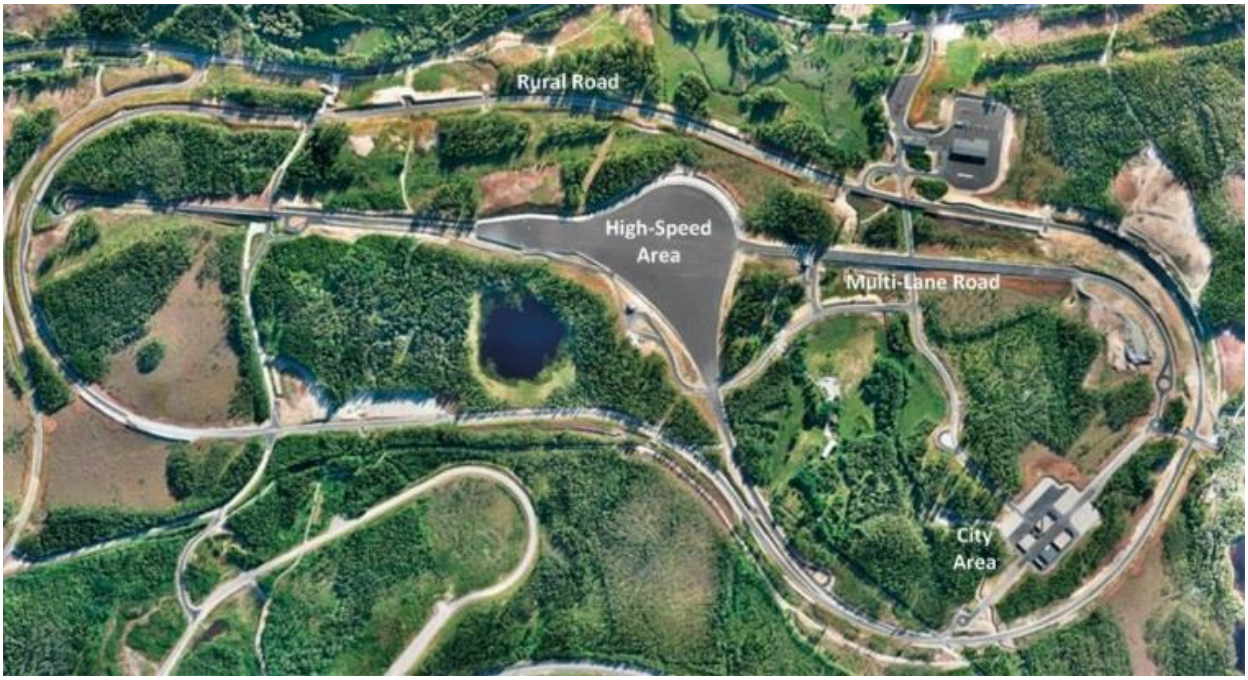


***Figure 1. Overview of the AstaZero facility.***

All paved surfaces are designed for 60 tons maximum vehicle weight and a 13 ton axel load. This will allow for researching scenarios where trucks with heavy load take part. A maximum vehicle length of 25.25 meters is planned. All internal roads have a width of 7 meters. They are designed for bi-directional traffic driving at the right-hand side of the road. There will be special areas for calibration made out of concrete. The calibration areas are 3 by 15 meters with flatness better than 0.1 degrees in all directions.

**The Rural Road**

The rural road encircles the facility. It is approximately 5.7 km long. Half of it is designed for travelling at maximum 70 km/h and to other half for maximum 90 km/h. The rural road is specially designed for different tests of driver behavior and is well-suited for the use of hidden or suddenly appearing obstacles. In several places there are scrubs or bushes growing near the road, which make it possible to conceal obstacles before they cross the road in front of the test vehicles. There are also two T-junctions and a crossroad that will be treated as real junctions changeable to suit customer requirements. The rural road will also have bus stops/lay-bys at two locations.

The road is not designed for advanced driving at high speed. It may be used for bi-directional traffic, but the normal setup is one-way traffic driving on the right-hand side of the road. There are some hills at the road, but the maximum incline is 4.5%. Initial feedback from users confirms that the rural road feels and looks like a conventional road and that “it is easy to forget that you are on a proving ground”. Communication links via optical fibers are prepared around the track, and it is ready to be populated with road-side units for ITS-applications.

*Figure 2. Emergency vehicle driver and platooning research on the rural road*

**The High-Speed Area**

The high-speed area is located at the center of the AstaZero facility. It consists of a circular area with drop-shaped entrances. The circle is 240 meters in diameter and has two acceleration roads. The main acceleration road is approximately 1 kilometer long. This will provide sufficient distance also for accelerating heavy trucks. In addition to the two acceleration roads, it is also possible to use the multilane road for acceleration. As a consequence, vehicles can enter the high-speed area from three different directions.

In this area, focus will primarily be on vehicle dynamics like avoidance maneuvers at very high speeds, but also "near misses" for active safety systems at high speeds. A large open asphalt area like the high-speed area is also useful for cases when virtual reality is combined with driving a real car.

The high-speed area slopes 1% in the lateral direction, but is completely flat in the longitudinal direction, (flatness 1.0 acc. to IRI). Asphalt is provided according to the specification SN75-80. There is a turning loop for long vehicles (25.25m) at the end of the acceleration road and halfway. It has a width of 7 meters. A calibration area is provided at the first turning loop (for gyros).

A separate control tower is overlooking the area. The tower is two stories high for good visibility, and it provides a platform on the roof for visitors. Remote control of targets, balloon cars and driving robots will be performed from the control tower.

*Figure 3. Virtual reality and trailer ESC tests on the high-speed area*

**The City Area**

The city area is located in the southern part of the facility and is connected to the rural road at two places. It consists of 4 building blocks (40 x 25 x 4 m), but there are plans to supplement it with additional five blocks. The city area will primarily be used to test the vehicle's capacity to interact with the surrounding environment. Test scenarios will include avoidance of collision with buses, cyclists, pedestrians or other road users. Streets have a 2.0% incline for good drainage into sewage drains. There are acceleration roads, longer than 150 m, before the intersection. The main street equipped with "portals" with traffic signs. The area therefore covers a number of different sub-areas, such as a town center with varying street widths and lanes, bus stops, pavements, bike lanes, street lighting and building backdrops. The city area also has a road system with different kinds of test environments such as roundabouts, T-junction, return loop and lab area (100x30 m). One block contains the control room and warehouse for dummies.

***Figure 4. Aerial and entrance view of the city area***

**The Multilane Road**

The Multilane Road is 700 meters long and consists of four lanes. These are connected to the high-speed area, and have an acceleration road that is approximately 300 meters long, 7 meters wide, and a turning loop for long vehicles. Several different scenarios can be tested on the multilane road, such as lane changes and departures, different collision scenarios, as well as crossing scenarios. For example, it will be possible to change the direction of travel in different lanes, as well as to build a temporary central barrier and different types of traffic barrier railings. The road has a 2 % lateral incline for good drainage, split between lane 1 and 2. There is a small intersection with the possibility to create intersection scenarios.

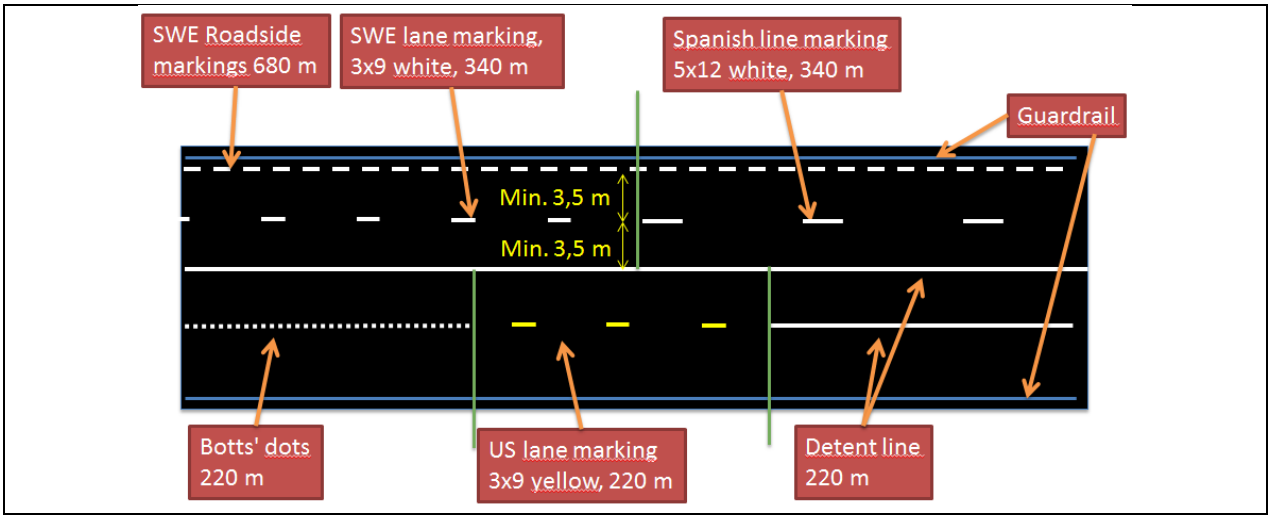


***Figure 5. Lane markings available on the multi-lane road***

## EQUIPMENT

Equipment of different kinds is needed to successfully perform development and research at a test track. Among these are: test targets to be used in different traffic scenarios, equipment for position measurement and control, communication test equipment, data acquisition, and simulation capabilities.

Researchers and engineers visiting the AstaZero facility expect the tests to be repeatable with a high degree of accuracy and efficiency. It is expected that the equipment will be reliable enough to provide a very high availability of the test environment. There are clear requirements for productivity and through-put also at a test track.

All equipment, including the test targets, has to be properly maintained and periodically calibrated. So far, no international practice for calibration of test targets has been established.

### Test Targets

The four main environments of the track are well suited to provide for many different traffic scenarios. But many traffic scenarios will also require other vehicles to be present. Safety precautions will in many scenarios require the use of test targets instead of real vehicles. Test targets are needed for cars, trucks, buses, pedestrians, bicycles and powered two-wheelers.

Test targets representing cars have been developed for rear-end collision scenarios [3,4,5]. Such a target must have a high fidelity of being perceived as a car both by the driver and by the sensor systems (radar, lidar, and/or camera) of the vehicle under test. At the same time, it must be possible to crash into without safety risks. The development of test targets for cars is towards correct representation of a car in all viewing angels, not only from the rear. Existing "balloon cars" have a three-dimensional structure, but do not provide a true 360 degree impression of the car. "360-targets" are under development and expected to be needed in future research and development.

Usually these car targets are towed or carried by a self-propelled flat platform such as the UFO [6] or LPRV [7]. However, being overrun by a heavy truck with full braking is a challenge for the platform-based solutions. It is also important to remember that the sensors on trucks could be placed in such a way that they "look down" at other road users which affect the design of targets.

### Position Measurement and Control

Testing of vehicles in traffic scenarios requires the possibility to measure and control the position with high accuracy. The accuracy possible to reach varies depending on the type of scenario, especially the speed of the vehicles involved, but ±20 mm is a state-of-the-art accuracy often mentioned. AstaZero is equipped with an RTK GPS base station which covers the entire test area. State-of-the-art GPS equipment is available as well as driving robots for driverless testing [8].

With the advent of automatically driven vehicles there will be a need for more complex traffic scenarios involving many road users. Here it will be necessary with interoperability between driving robots, target platforms, and overall scenario control. Standardized open communication interfaces will thus be needed. The trajectories of all targets and the test vehicle need to be synchronized, and the positioning of each actor needs to be sufficiently accurate. This calls for cost-efficient positioning based on local anchors and/or intelligent data fusion. In areas with poor GNSS reception, it might be necessary to augment the GNSS-based systems with a ground-based one [9].

Controlling test vehicles at high speed implies both safety risks for test engineers on the test track and the risk to severely damage expensive and unique prototype vehicles. All risks must be observed and the control system must be designed to provide adequate functional safety, i.e. to reduce all risks associated with malfunctioning of the control system to an acceptable level.

**Vehicle Communication Testing**

Communication between vehicles (”V2V”) and communication between vehicles and the infrastructure (“V2I”) will soon be offered in cars, trucks, and buses, The wireless communication facility will help to exchange data for safety applications, autonomous driving, traffic management and other applications. Communication facilities have to be offered by AstaZero.

The ETSI G5 standard defines a Basic Set of Application (BSA) for cooperative ITS. These applications are associated to a different number of use cases. Application classes have also been defined showing the potential of cooperative ITS for active safety as well as for efficiency and mobility. Among active road safety applications, three main blocks are also being defined by ETSI which group different applications: Road Hazard Signaling, Longitudinal Collision Risk Warning and Intersection Collision Risk Warning.

Communication nodes for application at AstaZero are under development. AstaZero has to be flexible and adopt the communication units since the test track will be used by several suppliers and vehicle OEMs.

**Test Data**

During product development testing a lot of test data is generated, especially raw data from sensors. Large amount of video data is not uncommon. In many cases the data collection is not centralized and integrated. Instead data is collected in different devices and tiresome post processing is needed to aggregate and align test data which in the worst case is out-of-sync. A secure and centralized data repository which collects test data in almost real-time could significantly improve the efficiency of proving ground testing.

The test track is used by several research groups and many companies. All partners need to know that the data collected from their test sessions is accessible only to them. Proper measures for IT security are deployed to ensure confidentiality of the data. Also the integrity of data and the availability of recorded data can be assured.

Analysis of the executed traffic scenarios will as good as always be performed off-line when the test is completed. Test data from several data loggers is synchronized and stored. One issue to handle is when data formats differ between the loggers used.

**Simulating the Test Track**

The use of the test track is considered as one of the tools to develop the automotive technology of the future. Research and development may start by simulation at a computer and then continue by simulation in a driving simulator. Vehicles will be driven at the test track and later in real traffic environments. Several tools will be needed to provide efficient research and development.

AstaZero has developed a model of the track to be used in driving simulators. The researchers and engineers have the possibility to try the test scenarios in a simulator before driving at the real test track. (Figure 6.) This will make it easier to plan the tests and run the most essential test cases on the track.

There is also a high-resolution three-dimensional model of the track which has been realized by on-site scanning of the four main environments. This precision model may be used for further enhancements of the driving simulations and planning of the test.

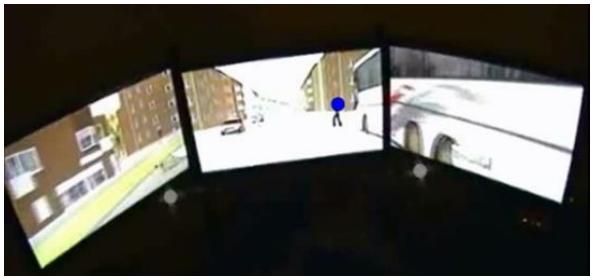

***Figure 6. Ambulance drivers have trained at AstaZero both by driving on the track and in a desktop simulator***

## COMPETENCE AND RESEARCH

### A Competence Cluster

A successful environment for automotive research and development certainly requires tools and equipment. In addition, the competence and the knowledge of the domain will be equally important. The Swedish automotive cluster has the ability to perform research, industrial development and rational production of road vehicles. The two major truck manufacturers Scania and Volvo Truck are together with the car manufacturer Volvo Cars the best known vehicle companies. There are also suppliers of world-leading reputation such as Autoliv. Research institutes offer possibilities for applied research together with all these industries, but also attract technology from small and medium sized enterprises (SMEs) in the automotive cluster. Several universities educate engineers for the automotive industry and provide automotive research together with European and international partners.

It is essential for AstaZero to have access to strong competence in its vicinity. The organizations residing in the Gothenburg region can be reached in an hour by car. The Stockholm region is more distant but it is quite possible to travel by road in four hours.

SAFER Vehicle and Traffic Safety Centre at Chalmers is a joint research unit where 30 partners from the Swedish automotive industry, academia, and authorities cooperate to make a center of excellence within the field of vehicle and traffic safety. The cooperation with authorities and local government is also essential for the development of AstaZero as a complete environment for automotive development and research.

The success of AstaZero is built on the track, the competence, and all the partners supporting the facility.

### Research to Develop Testing

Test and development of novel technology requires state-of-the-art test methods and equipment. AstaZero is cooperating with research institutes, universities, and industry to develop both equipment and ways of working.

Future road transport will be different from what we are used to today. The global urbanization and the aging population are two of the main factors driving the change. Perhaps the most important factor is to mitigate the consequences of the climate change. Reduction of the emission of greenhouse gases will require a change in the way we use the roads.

AstaZero must also be prepared to work with new types of road vehicles. Electric powertrains and hybridization has influenced the types of vehicles we find on our roads. Electrification and smart charging of electric vehicles will require facilities for test and demonstration.

Automatic and autonomous driving will require a lot of development effort. All autonomous functions will have to be carefully tested; at first in a controlled environment such as AstaZero and later in real traffic. Research to facilitate testing with optimized coverage of the shifting factors of the traffic environment is

important. It is also important to understand how much of the previously performed verification and validation that has to be repeated when a design is modified.

Sweden has a long tradition of supporting national research in vehicle technology and transport. The largest Swedish program for automotive research is called FFI - Strategic Vehicle Research and Innovation. This is a partnership between the Swedish government and automotive industry for joint funding of research, innovation and development concentrating on Climate & Environment and Safety. FFI has R&D activities worth approx. €100 million per year, of which half is governmental funding. The background to the investment is that development within road transportation and Swedish automotive industry has big impact for growth. FFI will contribute to three main goals: reducing the environmental impact of transport, reducing the number killed and injured in traffic, and strengthening international competitiveness.

**Standardization**

The automotive industry is depending on standardization. Standardization will reduce costs by making it possible to re-use solutions from one vehicle to another vehicle. Standardized features will enable drivers to easily drive vehicles of different type and manufacture. It will also make it possible for road vehicles to interact and use the same roads.

Passive safety testing has been developing up to a point where results are comparable between different test sites and different vehicles. Crash test dummies have been developed and test procedures to represent the important crash types have been agreed. Testing of active safety and road automation is far from this goal.

AstaZero is participating in the standardization work of ISO (the International Standardisation Organisation) as convener of the working group ISO/TC 22/WG 16 for Active Safety Test Equipment. Active safety and the related standardization subjects is of interest from both an ITS and a vehicle perspective. Both perspectives have to be considered when allocating the various aspects and work items. A first step in the standardization is expected two-dimensional vehicle targets and pedestrian targets. That may be followed by targets representing bicycles and other vehicles in a more three-dimensional way.

## CONCLUSIONS

The AstaZero facility has been designed and constructed according to plan. Operation started in the summer of 2014. New users of the proving ground are coming to join the competence cluster. There are already partners using AstaZero on a regular basis; vehicle manufacturers, suppliers and researchers come to AstaZero.

Equipment has been gathered and is still developing through several projects by industrial users and researchers. Also the competence network of AstaZero is under rapid development. Seminars have been held with researchers and two special “AstaZero Researchers Day” have been organized to make the research community in Sweden and internationally aware of the possibilities offered.

## REFERENCES

[1] The EC road safety web, European Commission, Transport, Road Safety. Official web page, http://ec.europa.eu/transport/road_safety

[2] The AstaZero Web, http://www.astazero.com/

[3] R. Schram, et al., “Implementation of Autonomous Emergency Braking (AEB), the Next Step in EURO NCAP’s Safety Assessment”, in Proceedings of 23rd ESV Conference, 2013.

[4] V. Sandner, “Development of a Test Target for AEB Systems”, in Proceedings of 23rd ESV Conference, 2013.

[5] D. J. LeBlanc, et al., “Advanced Surrogate Target Development for Evaluating Pre-Collision Systems”, in Proceedings of 23rd ESV Conference, 2013.

[6] DSD, http://www.dsd.at/

[7] Dynamic Research, http://www.dynres.com/

[8] H.-P. Schöner, et al., "Testing and Verification of Active Safety Systems with Coordinated Automatic Driving", in Proceedings of 21st ESV Conference, 2009.

[9] P. Perrone, et al., "Locata Positioning Used for World's First Fully-Autonomous Robotic Testing in Vehicle Collision Avoidance Systems ", in Proceedings of ION GNSS+, 2014.

# Thermal modeling of fire propagation in lithium-ion batteries

**Johan Anderson[1*], Fredrik Larsson[1,2], Petra Andersson[1] and Bengt-Erik Mellander[2]**
**[1] SP Technical Research Institute of Sweden, Borås, Sweden**
**[2] Applied Physics, Chalmers University of Technology, Göteborg, Sweden**
**[*] E-mail address: johan.anderson.br@sp.se**

Paper Number 15-0073

**ABSTRACT**

The objective of the present work is to assess the risk of spreading of fire between Lithium-ion battery cells initiated by a thermal runaway. In particular it aims at developing means to predict the temperature of cells in the vicinity of an overheated cell during the first 5-7 minutes after the thermal event in a Li-ion cell that has an organic based electrolyte which is flammable. Finite-Element (FE) modelling is used to compute the heat transfer between cells. The spreading model is assessed modeling a scenario where the cells are exposed to a 15 kW propane burner. Two different models where utilized, one that considers the conjugate heat transfer between the surrounding hot gases and the battery cells while the second is a thermal model where the boundary conditions are measured in a mock-up test. The results from the two models are contrasted to experimental data where the heat release rate (HRR) is utilized as an input to the simulation. It is found that the temperature increase in a neighboring cell can be quantitatively estimated in certain cases during the early stages of the fire taking into account the anisotropic thermal conductivity of the cells using the conjugate heat transfer model. Moreover, the thermal model captures the qualitative behavior of the test results, however, the temperature increase is slower in the computational model.

**KEYWORDS**: lithium-ion, battery, fire, propagation, thermal model, thermal runaway

**INTRODUCTION**

Lithium-ion (Li-ion) batteries offer great performance in form of e.g. energy and power densities, enabling their use for a wide range of applications including the use in electrified vehicles, an application that is steadily growing. If the temperature in a Li-ion cell is increased beyond a certain threshold, a thermal runaway can occur, resulting in a rapid temperature increase and possibly other adverse effects such as, release of gas, smoke, fire and rupture/explosion. There are numerous types of abuse situations that can result in elevated temperatures inducing a thermal runaway. For example, mechanical abuse, electrical abuse and thermal abuse [1-11]. In case of a thermal runaway in a single Li-ion cell it is important to stop or at least delay its spreading to adjacent cells, since the effects from a cascading thermal runaway scenario of a complete battery pack could be devastating. Battery packs in electrified vehicles can consist of thousands of battery cells. In general, the design of a battery pack plays an important role for fire propagation, e.g. the thermal management system, mechanical support structures cell-to-cell respective module-to-module, use of fire walls and division of the battery pack into different sub-packs are important aspects.

There are relatively many simulation studies regarding general heat generation and cooling of Li-ion batteries during normal cycling (battery charge/discharge) within the battery specifications. Furthermore, Li-ion cells and battery packs with multiple-cells have been simulated during abusive conditions; by external heating in oven, short circuiting, overchargeing and deformation/crash. For example, Spotnitz et. al. [12] performed a numerical study on the influence of various heat transfer modes for the propagation cell-to-cell for a battery pack with 8 cylindrical cells of type 18650.

However, only a limited number of simulations studies of lithium-ion battery fire abuse situations are available. For example, Anderson et. al. [7] used CFD simulations with subsequent thermal modeling to study the fire resistance of a battery pack in a gasoline pool fire test according to UNECE Regulation No. 100.

A heat propagation simulation of cell-to-cell fire propagation for 5 Li-ion cells has recently been performed by Anderson et. Al [8]. That utilized recent experiments performed at SP on five EiG Li-ion 7 Ah cells where a thermal runaway was initiated in a cell using a propane burner. The resulting temperatures were monitored by thermocouples and the experiments are well suited for modelling purposes. However the predicted temperatues were found to be lower than the measured counterparts partly due to the models inability to represent the boundary in the fire test.

The present work continues this work by utilizing additional measurements of the fire load on the batteries. The aim of this work is to develop a model suitable for predicting the propagation of thermal runaways in stacked Li-ion cells. The modelling was done using the COMSOL Multiphysics software package that can model conjugate heat transfer. The software is a Finite-Element (FE) tool and in order to successfully model the experimental set-up appropriate boundary conditions are needed for reliable results. The long term goal is to be able to study protective measures mitigating the propagation of a thermal runaway event. In this paper we will extend previous work done in Anderson et al. [8] where we make use of fire abuse tests of commercial Li-ion cells where detailed measurements of the temperatures between the cells as a result of the thermal runaway response of the cells were performed. These tests may be utilized to fine tune a numerical model of the phenomena.

## RESULTS FROM THE FIRE TESTS

Commercial Li-ion (EiG ePLB-F007A 7 Ah) pouch cells were exposed to a 15kW propane burner that initiated a thermal runaway event in the cell closest to the burner. During the tests heat release rates and temperatures, measured by thermocouples between the cells, were measured. The resulting HRRs have been published as well as one preliminary study on modeling one of the tests [6,8]. The tested EiG cell had a lithium-iron phosphate, $LiFePO_4$, cathode and a carbon based anode. Each of the tests consisted of five cells tightly packed together with steel wires, see Figure 1 (left). Also in Figure 1 (right), the mock-up used in to determine the impact from the burner can be seen and is described in detail below.

**Figure 1. Fire test on EiG 7 Ah LFP pouch cells (left) and measurement of the impact on a mock-up (right).**

The cell terminals (tabs) were cut-off prior to the tests for all but the middle cell. In the tests the thermal runaway was initiated by a LPG burner of approximately 15 kW placed underneath the packed cells, see Figure 1. Several tests with varying state of charge was done yielding cases with varying reactivity. The HRRs are presented in Figure 2, however in this paper we will focus on modeling the case with 75% state of charge (SOC) indicated by a dashed line, previously the case with 100% SOC was used.

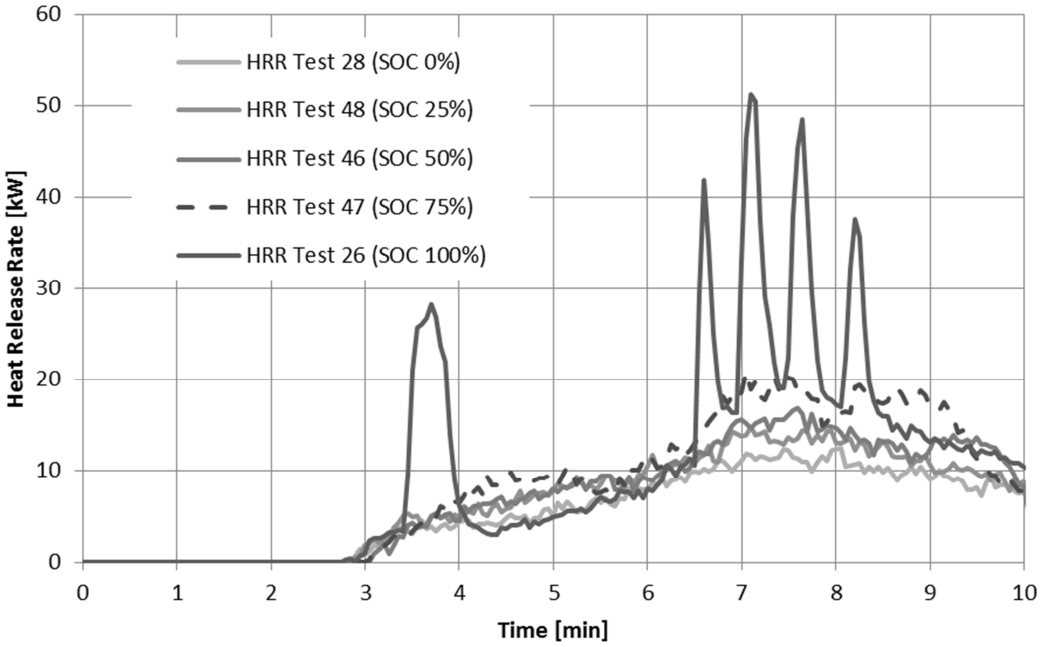


**Figure 2. The heat release rate of the EiG 7 Ah LFP pouch cells where the heat from the burner is subtracted.**

Additional quantities of interest was measured in each test such as cell voltage of the mid cell however this is out of the scope of the present work. We noted that the measured voltage breakdowns occurred earlier for increasing SOC values, in accordance with faster thermal response for increasing SOC shown by temperature and HRR measurements. During the test temperatures between some of the cells were carefully monitored in four positions, see Figure 3.

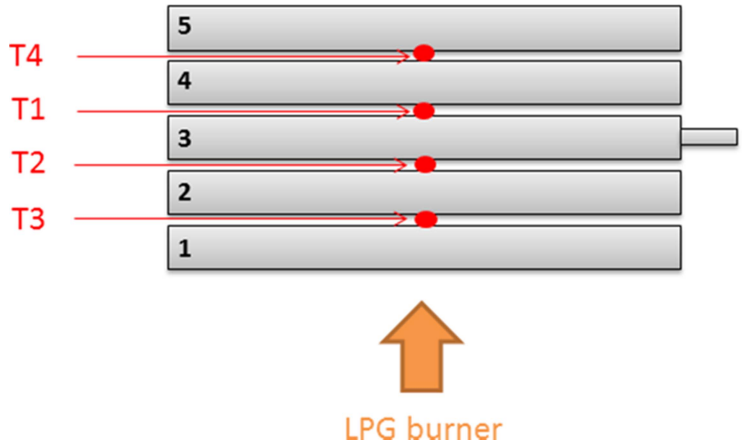


**Figure 3. The placement of thermocouples in the live fire test.**

In the previous paper by Anderson et al [8] it was identified that a well defined fire source is needed in order to more accurately describe the evolution of the temperatures between the cells. For modeling purposes one test with a

mock-up was performed where the impact of the burned was assessed. To achieve this the mock-up shown in Figure 1 was constructed of promatect clad with custom made plate thermometers. Although the moisture level in promatect is very low it was dried for around 48 h further reducing the moisture content. The plate thermometers were approximately 40 mm x 100 mm in size to fit on the side of the mock-up. The objective of the mock-up test is to estimate the fire source's impact on each side of the mock-up by measuring the adiabatic surface temperature (AST). The AST is an artificial effective temperature that replaces the gas and radiation temperature that describe the local conditions around the test object. It is defined as the temperature of a surface that cannot absorb any heat. However, due to the limitations of the physical extensions of the object the size of the plate thermometers were smaller than usual indicating that they may experience somewhat different convection radiation equlibrium since the estimation of the AST becomes more sensitive with smaller devices.

## THE SET-UP OF NUMERICAL SIMULATIONS

The modeling was performed in two stages; the first stage covered the fluid-structure interaction in a conjugate heat transfer model; the second stage was a thermal model where the boundary conditions were taken from measurements. Common in both models was to use the measured HRR produced in the thermal runaway event. The models were built in the multi-physics software COMSOL suitable for studying heat transfer problems. In the models the five battery cells have been implemented where bulk values of the density, specific heat and thermal conductivity are specified. Below we present the particulars of the models.

### The conjugate heat transfer model

The software solves the heat transport taking into account heat conduction and radiation as well as solving for the Navier-Stokes equations to assess the convection around the cells coming from the fluid movement of air around the cells. The software is a Finite-Element (FE) code and the Reynolds number is assumed to be small, such that turbulent fluctuations can be neglected. The model consists of around 10000 elements in order to have sufficient convergence and accuracy. The solution time of the model is about 10 minutes on an ordinary personal computer. A simplified 2D geometrical model was constructed for this work. In the model, the battery cells are in the same ambient conditions (T0) as the surroundings of that particular test and the cells are assumed to always be in perfect contact to each other. The ambient conditions give the boundary conditions for the thermal exchange between the cells and the surroundings by conduction, convection and radiation. The 15 kW heat of the propane burner was assumed as a boundary heat source placed directly beneath the first battery cell. The measured heat release rate was used as input in the model for the thermal energy which was deposited homogenously into the bottom cell. The heat generated by the propane burner was taken into account, however, the extra buoyancy of the exhaust gases from the burner was omitted since numerical instabilities occurred.

### The thermal model

Similarly to the conjugate heat transfer model the thermal model was built in COMSOL. The test specimen was modelled in 3D with half the amount of cells compared to the other model. The thermal model is considerably faster with runtimes of a few minutes. The boundary conditions were estimated by assuming a heat flow in to the specimen determined by the AST ($T_{AST}$) in the following manner,

$$\dot{q}'' = h(T_{AST} - T).$$

Here the heat flow is determined per unit of time and area where h is the heat transfer coefficient. The heat transfer coefficient is taken from Eurocode standard [13] to be h = 25 W/(m$^2$ K). No assumption was necessary for the propane burner since this is included in the AST. Otherwise the model had a similar set-up as the conjugate heat transfer model.

### Bulk material data

The physical structure of the pouch cells is complex with a repeatable layering of anode and cathode material. The total numbers of layers is of the order of 150 layers. The thermal properties of the materials vary significantly in terms of thermal conductivity, density and specific heat along and across the cell due to the layered structure. To be

able to accurately compute the temperatures in the 5-cell-pack realistic values of the thermal properties are needed in combination with a well-defined fire source in terms of the measured heat release rate. This complex structure of the cell makes detailed modeling impractical however for our purposes bulk values of the thermal properties are enough to capture the essential propagative features. In the present study these values are estimated from literature values by Spotnitz and Franklin, Fan et al., Wu et al and Chacko et al, [12], [14] –[16]. Ideally, careful measurements of these quantities at elevated temperatures are needed but generally difficult to obtain. The heat conductivity coefficient, k, was varied in the simulations since the multi-layered structure of the battery cell allows for this value to be highly anisotropic. Table 1 shows the thermal material properties of the cells used in the thermal simulations.

**Table 1. Values of the thermal properties of the cell used for the simulations.**

| Notation used in this paper | Density ρ [kg/m$^3$] | Specific heat $C_p$ [J/(kg K)] | Thermal conductivity k [W/(m K)] |
|---|---|---|---|
| Anisotropic k=13 | 1895 | 700 | $k_x$ = 13 and $k_z$ = 0.4 |
| Anisotropic k=27 | 1895 | 700 | $k_x$ = 27 and $k_z$ = 0.8 |

## RESULTS FROM THE NUMERICAL SIMULATIONS

In this section we will present the numerical results found using the developed models. We have chosen the test with 75% SOC as a representative case in the test series for corroborating the simulations. In this test four time series with temperature data, T1-T4, were recorded. In Figure 4, the results by comparing the experimental data with the simulations using isotropic (a) and anisotropic (b) thermal conductivity are presented using the conjugate heat transfer model. It is found that T1 and T2 of the middle cell can be modeled as described previously [8], but the temperatures are lower than the experimentally measured values. However, T3 at the top of the initiating (bottom) cell that undergoes thermal runaway deviates quite early.

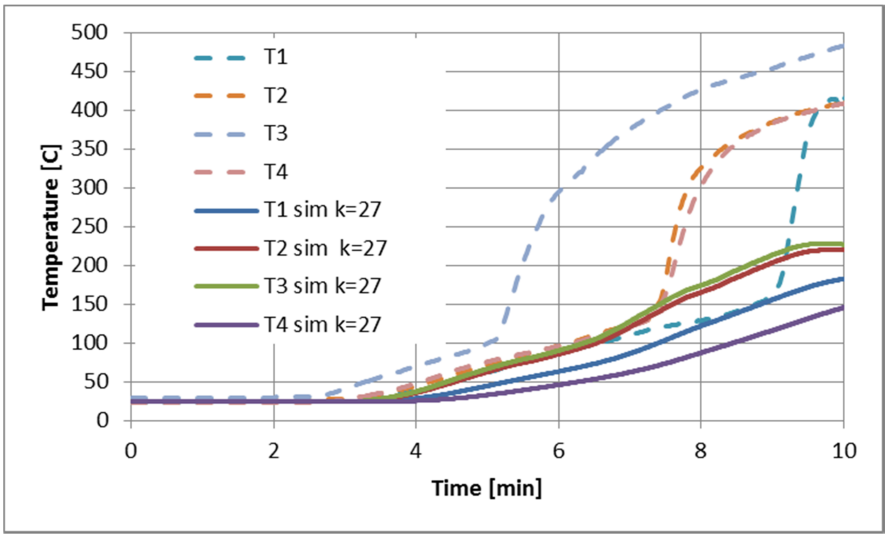


**Figure 4. Comparison between test results and simulated temperatures at 75% SOC using the conjugate heat transfer model. A comparison of temperatures T1, T2, T3 and T4 found in the experiment and the simulation assuming anisotropic heat conductivity k=27 (kx =27 W/(m K) and kz = 0.8 W/(m K)).**

In Figure 5, the same test is modelled using the thermal model with the AST used as boundary conditions however the same HRR is used. We find also in this case that the model yield lower temperatures compared to the experimental values. Interestingly, a higher value of the heat conductivity would yield lower temperatures through the whole test specimen.

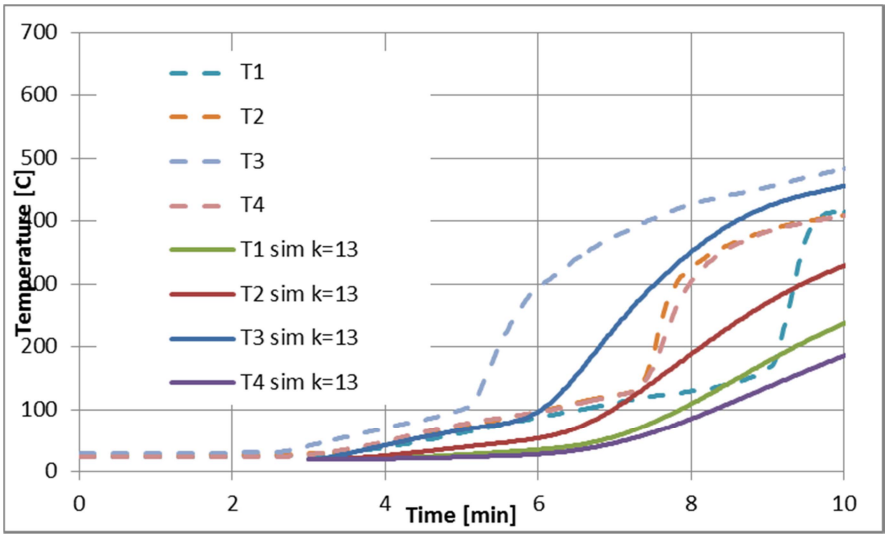


**Figure 5. Comparison between test results and simulated temperatures at 75% SOC using the thermal model. A comparison of temperatures T1, T2, T3 and T4 found in the experiment and the simulation assuming anisotropic heat conductivity k=13 (kx =13 W/(m K) and kz = 0.4 W/(m K)).**

However, the qualitative behavior is considerably better in the thermal model and it is very likely that using values corresponding to a lower thermal inertia would give a much better correspondence with the experimental results. In particular, the value for the specific heat and density may decrease considerably as the reactions progress. We note that in the experiment the measured temperature closest to the top is elevated, T4 is close to T2, indicating a significant amount of heat coming in from the top surface.

## DISCUSSION

This paper presents an attempt to predict the progress of a thermal runaway/fire in a cell to neighboring cell by simulating the temperature development on neighboring cells in the same lines as in our previous work, Anderson et al. [8]. Simulations and experiments have been conducted for varying SOC, this paper focuses on the case with 75% SOC as an example of results.

Modeling battery cells in such harsh conditions as that of a fire is a rather difficult task due to the lack of knowledge of the precise local conditions around the test object. This gives an uncertainty in the boundary conditions to be used. Another difficulty is the lack of knowledge of the material data. In order to have a reliable model the precise temperature dependency of the heat conductivity, specific heat and density are needed.

Using the conjugate heat transfer model we find that the model captures the first minutes of the test however as the runaway event progresses large deviations are found, this is partly due to that the thermal exposure in that case is only assumed to be underneath the cells and not around the entire object. In the thermal model a good qualitative match between the test and model is found however the thermal inertia in the model seems to be larger compared to the actual cell case. The thermal model uses the measured AST values as input however it is uncertain how representative this measurement is as in the real case the boundaries are not smooth/edges are sharp creating a complex convective heat transfer. Furthermore, radiative losses at the top surface are likely since the flames are rather thin resulting in a different boundary.

The simulations are in reasonable agreement with the experimental result up to the point where the thermal runaway is initiated but still the simulations under-predict the temperature in the neighboring cell somewhat in all cases.

However the model can be further developed by:

1. A two stage simulation using the methodology in Anderson et al [7] is likely to be a more proper representation of the turbulent driven convective heat transfer process.
2. Investigate in more detail different boundary conditions. Since the dimensions of the battery pack is rather small the influence of the boundary is important and can be a source for uncertainties. Both geometry at the edges and different forced convection boundaries should be investigated.
3. Simulating different contacts between the cells using a thin contact element with variable thermal resistance should be investigated.
4. More adequate values of the thermal properties data including temperature variation.

With these improvements there is great potential for the simulations to be able to better predict the temperature development in a neighboring cell. A conservative model of the propagation is desirable to be on the safe side in the predictions.

**ACKNOWLEDGMENTS**

The Swedish Energy Agency is greatly acknowledgment for its financial support. Several technical staff colleagues at the Fire technology have contributed to this work.

**REFERENCES**

[1] Roth EP, Doughty DH. Thermal abuse performance of high-power 18650 Li-ion cells. J Power Sources 2004; 128:308-318.

[2] Roth EP. Abuse response of 18650 Li-ion cells with different cathodes using EC:EMC/$LiPF_6$ and EC:PC:DMC/$LiPF_6$ electrolytes. ECS Transactions. 2008; 11(19):19-41.

[3] Jeevarajan J. Safety of commercial lithium-ion cells and batteries In: Gianfranco Pistoia (ed) Lithium-Ion Batteries Advances and Applications. Elsevier. Amsterdam. The Netherlands. 2014, p. 387-407.

[4] Zhang Z, Ramadass P, Fang W. Safety of lithium-ion batteries In: Gianfranco Pistoia (ed) Lithium-Ion Batteries Advances and Applications, Elsevier, Amsterdam, The Netherlands, 2014, p. 409-435.

[5] Doughty D, Roth EP. The Electrochem. Soc. Interface, summer 2012. 2012; 37-44.

[6] Andersson P, Blomqvist P, Lorén A, Larsson F. Investigation of fire emissions from Li-ion batteries. SP Report 2013:15, SP Technical Research Institute of Sweden, Borås; 2013.

[7] Anderson J, Sjöström J, Andersson P, Amon F, Albrektsson J. Experimental and numerical characterization of an electrically propelled vehicles battery casing including battery module. Journal of Thermal Science and Engineering Applications. 2014 Dec; 6: 041015-1 - 041015-7.

[8] Anderson J, Larsson F, Andersson P, Mellander BE. Fire spread due to thermal runaway in a lithium-ion battery cell. Conference proceedings of Fires in vehicles (FIVE) 2014, Andersson P, Sundström B, eds. SP Technical Research Institute of Sweden, Borås, Sweden; 2014: 268-271.

[9] Larsson F, Mellander BE. Abuse by external heating, overcharge and short circuiting of commercial lithium-ion battery cells. Journal of the Electrochem. Soc, 2014: 161 (10); A1611-A1617.

[10] Larsson F, Andersson P, Mellander BE. Battery Aspects on Fires in Electrified Vehicles. Conference proceedings of Fires in vehicles (FIVE) 2014, Andersson P, Sundström B, eds. SP Technical Research Institute of Sweden, Borås, Sweden; 2014: 209-220.

[11] Larsson F, Andersson P, Mellander BE. Are electric vehicles safer than combustion engine vehicles? In: Sandén B, Wallgren P, eds. Systems perspectives on Electromobility. Chalmers University of Technology. Göteborg. ISBN 978-91-980973-9-9; 2014:33-44.

[12] Spotnitz R, Franklin J. Abuse behavior of high-power, lithium-ion cells. Journal of Power Sources. 2003; 113:81-100.

[13] Eurocode EN 1991-1-2.

[14] Wu W, Xiao X, Huang X. The effect of battery design parameters on heat generation and utilization in a Li-ion cell. Electrochimica Acta 2012; 83:227-240.

[15] Chacko S, Chung YM. Thermal modelling of Li-ion polymer battery for electric vehicle drive cycles. 2012; 213:296-303.

[16] Fan L, Khodadadi JM, Pesaran AA. A parametric study on thermal management of an air-cooled lithium-ion battery module for plug-in hybrid electric vehicles. J Power Sources. 2013; 238:301-312.

**Detection of Fires in Heavy Duty (HD) Vehicles**

**Jonas Brandt**
**Ola Willstrand**
**Raúl Ochoterena**
**Alen Rakovic**
**Michael Försth**
SP Technical Research Institute of Sweden
Sweden

Paper Number 15-0074

## ABSTRACT

Detection of fires in the engine compartments, toilet compartments, baggage bays and sleeping cabins of Heavy Duty (HD) vehicles is arduous. The elevated air flows, concentration of pollutants and wide range of surface temperatures in the engine compartment together with the complicated geometries of the latter spaces complicate the operation of all types of detectors. These lead to difficulties defining the optimal type of detection technologies to be used as well as the adequate location of each detector.

This paper presents research for understanding the challenges and necessary characteristics of detection systems in compartments with high air flows, large temperature variations and complicated geometries. In particular, this work reports about literature surveys of existing standards, legislations and research in the field as well as experimental findings.

## INTRODUCTION

Fires in the engine compartments of surface and underground non-rail heavy duty (HD) vehicles are unfortunately still common around the world [1]. For instance, fires in the media drift and distribution level sections of Swedish non-coal mines and German potash and rock salt mining are predominantly caused by service vehicles, drilling rigs and loaders [2–4]. Furthermore, statistical data indicates that nearly one percent of the buses registered in northern Europe will suffer an incident related to fire during a one year period [5]. Although this quantity is alarmingly high, it does not necessarily denote that all these fires lead to fatalities or total property loss. However, statistical data do indicate that almost two thirds of the reported fires commenced in the engine compartment and that these fires were, in most cases, not promptly detected by the drivers. Late detection causes that nearly one in five of the aforementioned fires spread outside the firewall of the engine compartment putting in risk the security of its occupants [6, 7].

Engine compartments of heavy duty vehicles are, in general, spaces where detecting fires with inexpensive and simple detection systems is arduous. High air flows and large amounts of suspended pollutants in the compartment, together with the complicated geometry and the wide range of surface temperatures typically occurring during the normal operation of the vehicle, complicate the operation of all types of detectors. The deposition of pollutants on the components of optical detectors can impair their operation as well as obstruct the channels of aspirating systems, thus hindering their operation or shortening their service interval. In addition, thermal point detectors can have an extremely limited effectiveness under high air flow conditions unless these are located in the vicinity of an eventual fire where these can be effectively heated by the ensuing smoke and fire plumes [8].

UNECE Regulation No. 107 regulation stipulates that engine compartments of buses and coaches with rear mounted engines must be equipped with a fire detection system and that coaches should have fire detectors in the toilet compartments and sleeping cabins, but the regulation is unfortunately not specific about the performance and effectiveness of the employed detection system. This inaccurateness allows the employment of detection systems which would be incapable of detecting fires under high air flow conditions, providing a vague improvement regarding fire protection [9].

Although the engine compartment is the most common place of origin of fires in these types of vehicles, toilet compartments, baggage bays and sleeping cabins are not excepted of this problem. Although detecting fires in these compartments is not as difficult as detecting fires in engine compartments, the differences in geometries among vehicle fleets may lead to difficulties defining an optimal detection

technology and location of a detector to be installed in these compartments. Even though the mandatory implementation of detection systems is a fact, the effectiveness of the detectors will be highly suspected to their correct selection and placement.

Research for understanding the challenges and necessary characteristics of detection systems in compartments with high air flows, large temperature variations and complicated geometries is necessary. SP Fire Research conducts active research in the field of detection of fires in HD vehicles where different detection technologies and strategies are evaluated and compared. This paper reports experimental findings, a literature study about the existing standards and legislations in the field, and a study of bus fires in Sweden.

## BUS FIRE STATISTICS FROM SWEDEN

Data was collected from the Swedish Civil Contingencies Agency's (MSB) database on fires occurring in Sweden, which is based on incident reports from the emergency services. The study was confined to reports from 2005-2013, due to that before 2005 bus fires had no separate category in the incident reports. The study includes a total of 1255 records spread over this nine-year period. The data material was processed in a repetitive process in order to obtain relevant information. Loss of the records was 26 %, partly due to the study's limitation to commercial traffic as well as number of incidents being registered incorrectly in the bus category.

The average number of incidents per year related to fire between 2005 and 2013 was 104, which corresponds to 0.73 % of the buses in the commercial traffic. The highest number of incidents was recorded in 2006 with 130 cases; and fewest in 2012 with 88 cases and in 2013 with 81 cases. However, studying the whole period it is difficult to make a definitive conclusion on a decreasing trend regarding fire-related bus incidents.

In 61 % of the cases the incident originated in the engine compartment and in 20 % of the cases the incident originated in the wheel well. In 14 % of the cases the data was too flawed to obtain the information regarding origin area; in the remaining 5 % the incident originated inside the bus or in other area, see Fig. 1.

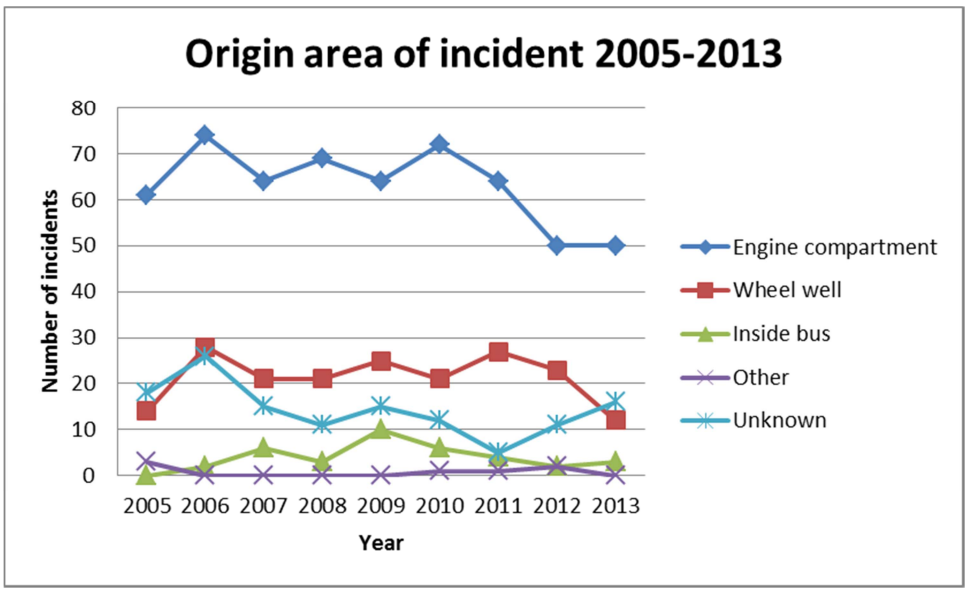


***Figure1. Origin area of incident 2005-2013.***

Flashover occurred in 7 % of all the registered incidents. The highest number of cases was registered in 2009 with 13 cases and in 2012 with 10 cases. There is no indication that the number of flashover fires is decreasing.

Fire and Rescue Service (FRS) carried out fire-fighting action in 55 % of the call outs between 2005 and 2013. In 73 % of these cases the FRS had to perform extinguishing action and in 27 % of the cases FRS conducted only cooling of the affected area.

The study shows that the bus drivers and staff have a very significant role in the initial stage of the fire-related incidents. Bus drivers extinguished the fire in 26 % of the cases prior to FRS arrival to the accident site.

## STANDARDS AND LEGISLATIONS

To our knowledge, there are no approval standards or test methods in use for fire detection in HD vehicles. There are some standards that point out minor requirements or risk assessment methods, but no approval test methods. E.g. the Australian Standard AS 5062 is a comprehensive standard regarding fire protection in vehicles, focused on risk analysis, and the Swedish Fire Protection Association publishes two guidelines, SBF 127 and SBF 128, which include minor requirements on fire detection in HD vehicles. Also a new standard from Israel for fire suppression systems in buses, I.S. 6278, includes a few tests for detection systems. Regarding environmental tests requirements, such as resistance to vibration, ambient temperature variations, and corrosion, EN 14604 and UL 217 set out requirements for recreational vehicles. Also the NATO standard STANAG 4317 have some relevant environmental requirements for main battle tanks.

For general use, the main standards for fire alarm systems in Europe and in the US are EN 54, ISO 7240, NFPA 72, FM (3210, 3230, 3232, 3260), and UL (268, 521). All of these, except NFPA 72, include approval test programs for different types of detectors. However, these should not be used for approval of detectors for use in e.g. the engine compartment of vehicles. There are several important parameters that are not adapted for vehicle application in these standards, such as ambient temperature, vibrations, high airflow, fire sources, and false stimuli/background level.

The European automotive legislation has very vague requirements on fire detection. For buses and coaches, UNECE Regulation No. 107 sets out some minor requirements, but the regulation is not specific of the performance or installation of the system.

The following two sections present fire detection tests conducted in the toilet compartment and in the engine compartment of buses. This and future work will be the basis for new improved standards of fire detection in HD vehicles.

## FIRE DETECTION IN BUS TOILET COMPARTMENTS

For the toilet compartment tests [10] a mockup was built, see Fig. 2, based on input from 26 different buses from a variety of suppliers. The most important influencing parameter was the ventilation condition, which may differ between buses. However, most buses have a fan positioned in a concealed space under the sink that extracts air from the compartment. The air enters the concealed space via air vents and in some cases also via the trash can opening (the largest hole to the left in Fig. 2). Gaps around the toilet door works as air inlet to the compartment and in the mockup these gaps are summed up in a larger gap at the upper right corner of the toilet door. Some real toilet compartments also have a feed from the air conditioning system.

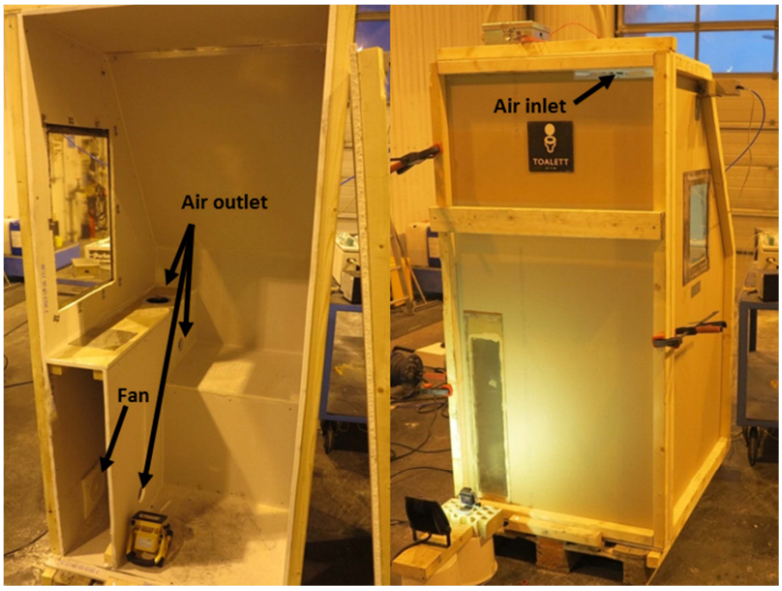


***Figure2. Mockup of bus toilet compartment.***

Five different fire detection systems were tested in different positions. The detectors included linear heat detection, point heat detection, point smoke detection, and aspirating smoke detection. Seven fire tests were conducted in accordance with Table1. The heptane pool is not a realistic fire source in the toilet compartment, but was used because of good repeatability compared to the other fire sources. The rubber and plastics were placed in the concealed space of the fan representing a pump, cables and other electronics normally contained there.

**Table1. Test scenarios.**

| Test | Fire source | Fire position | Ventilation condition |
|---|---|---|---|
| **1** | Cigarette | Seat level | Low fan speed |
| **2** | Paper | Trash can | Low fan speed |
| **3** | Paper | Trash can | High fan speed |
| **4** | Heptane pool | Floor level | Low fan speed |
| **5** | Heptane pool | Floor level | High fan speed |
| **6** | Plastics/rubber | Above fan | Low fan speed |
| **7** | Plastics/rubber | Above fan | High fan speed |

The main conclusions from the tests were:

Smoke detectors are generally much faster than heat detectors. Heat detectors should only be used in narrow spaces where the detector is close to a potential fire source, e.g. above the trash can.
The impact of the ventilation fan was very large. In several fire scenarios a detector in the ceiling of the toilet compartment would not give a fire alarm in the early stage of a fire. Fig. 3 shows the trash can paper fire, and no smoke entered the toilet compartment in this test.
Because of the impact of the fan, it is recommended to have fire detectors also in the concealed space of the fan, why aspirating systems may be considered due to their capability to sample air from several spaces.
Another advantage of aspirating systems is that the detector is hidden and protected.
Aspirating smoke detectors were not affected as much as point smoke detectors by high air flows.
It was only the most sensitive aspirating smoke detector that was activated by cigarette smoke.

*Figure3. Trash can paper fire.*

**FIRE DETECTION IN ENGINE COMPARTMENTS**

As part of an evaluation of fire detection systems for HD vehicles testing has been performed in the engine compartment of a city bus (See Fig. 4). Several systems were tested and compared regarding detection time, including heat, smoke and flame detectors.

Heat detection is the most used fire detection method in engine compartments of HD vehicles today. Flame detection is used to some extent, while smoke detection has until now not been much used in engine compartments of HD vehicles. Three widely used linear heat detectors were tested, two with fixed activation temperature of 170°C and 180°C respectively and one responding on the average temperature of the detector, with 139°C as activation temperature if the full length of the detector is heated. Also one IR/IR flame detection system and one aspirating optical smoke detection system were tested. The detection systems were installed in the engine compartment of the bus as it could have been installed in a real case with the aim of covering the entire engine compartment. Three fire scenarios were designed to simulate realistic fires and consisted of both slow developing electrically generated fires as well as a fast developing fuel leakage fire. Fig. 5 shows a fast propagating fuel spray fire. In all cases the air flow through the engine compartment was representing a stationary bus on idle speed. The rear hatch of the engine compartment was replaced with a glass window for increased visibility into the engine compartment as seen in the figures.

*Figure4. City bus prepared for performing fire detection tests*

*Figure5. Fast developing fuel spray fire*

The detection ability varied between the systems and between the fire scenarios. While the flame detector gave extremely fast response on the quickly developing fuel spray fire, it did not respond at all to the small and slow propagating electrically generated fires. The flame detector used in the test was designed to automatically adjust its detection alarm level to avoid false alarms, i.e. the detector does not respond if the radiation level increases too slowly. The results from the linear heat detectors shows that the tested systems has to be close to an open flame in order to activate, which may considerably delay the alarm time for small fires far away from the detection system. Moreover, the air flow from the engine compartment fan had a great impact on the heat transport by removing the heat from the fire area. It underlines the importance of covering the entire fire hazard area with the detectors and taking into account the heat transport direction. The tests did not show any significant differences in detection times between the different fixed temperature heat detectors. The results from the aspirating smoke detection system showed that the tested system was able to detect the fire at an early stage, i.e. already at small amounts of smoke. The test results show the importance of appropriate fire detection system design in order to avoid unwanted consequences in case of engine compartment fires.

## OUTLOOK

The work presented in this paper is part of the project “Fire detection & fire alarm systems in heavy duty vehicles – research and development of international standard and guidelines”. The aim of the project is to develop an international test method for fire detection systems in the engine compartment of buses and other heavy duty vehicles. Most work packages in the project are mainly focused on producing background material for the overall goal of defining an international test standard for engine compartments, but the project also includes work leading to recommendations on what type of fire detection system that is most suited in e.g. toilet compartments on buses and how the systems should be installed.

The remaining work consists of more testing, both full scale and small scale testing, more studies of background noise and fire causes in vehicles operating in different environments, e.g. in urban, in mines, or at construction sites, and in the end the development of an international test method.

## ACKNOWLEDGEMENTS

This work was financed by the FFI program of the Swedish Governmental Agency for Innovations Systems, VINNOVA.

## REFERENCES

[1] Meltzer N. R., Ayres G. and Truong M., Motorcoach Fire Safety Analysis: The Causes, Frequency, and Severity of Motorcoach Fires in the United States, FIVE - Fires in Vehicles 2012.
[2] Hansen R., Design fires in underground hard rock mines, Licentiate Thesis 127, School of Sustainable Development of Society and Technology, Mälardalen University, Sweden, 2011.
[3] Hansen, Site inventory of operational mines-fire and smoke spread in underground mines, Mälardalens Högskola, Västerås, 2009.
[4] Sønksen H., Oral presentation at the Symposium on Fire Protection for Vehicles and Work Equipment Underground, Freiberg, Germany, 2009.

[5] Hammarström R., Axelsson J. and Reinicke B., Fire Safety in Buses, WP1 report: Bus and coach fires in Sweden and Norway. SP Fire Technology, SP Report 2006:26, 2006.
[6] Brandt J. and Försth M., Testing active fire protection systems for engine compartments in buses and coaches - a pilot study, SP Report 2011:22, 2011.
[7] Kokki E., Bus Fires in 2010-2011 in Finland, FIVE - Fires in Vehicles 2012.
[8] Brandt J., Modin H., Rosen F., Försth M., and Ochoterena R., Test method for fire supression systems in bus and coach engine compartments, SAE 2013-01-0208, 2013.
[9] J. Eriksson and M. Mansoori, Branddetektion i motorrum (Fire detection in engine compartments), MSc. Thesis, Report 5206, Lund University of Technology, 2009.
[10]Willstrand O., Brandt J. and Svensson R, Fire detection & fire alarm systems in heavy duty vehicles, WP5 – Fire detection in bus and coach toilet compartments and driver sleeping compartments, SP Report 2014:28, 2014.

This paper has been peer-reviewed and published in a special edition of *Traffic Injury Prevention* 16(S1), by Taylor & Francis Group. The complete paper will be available on the *Traffic Injury Prevention and www.NHTSA.gov* websites on June 8, 2015.

To access all Peer-reviewed papers please copy and paste the link below into your browser to access the papers.

http://www.tandfonline.com/toc/gcpi20/16/sup1

# POTENTIAL SAFETY BENEFITS OF LANE DEPARTURE WARNING AND PREVENTION SYSTEMS IN THE U.S. VEHICLE FLEET

**John M. Scanlon**
Virginia Tech
United States

**Kristofer D. Kusano**
Virginia Tech
United States

**Rini Sherony**
Toyota Engineering & Manufacturing North America, Inc.
United States

**Hampton C. Gabler**
Virginia Tech
United States

Paper Number 15-0080

## ABSTRACT

Road departures account for nearly one-third of all fatal crashes. Lane departure warning (LDW) and lane departure prevention (LDP) have the potential to mitigate the number of crashes and fatalities that result from road departure crashes. The objective of this study was to predict the effectiveness of LDW and LDP in preventing road departure crashes if all vehicles in departure crashes in the U.S. fleet were equipped with either system. A set of 478 road departure crashes extracted from NASS/CDS 2012 were used to formulate a simulation case set. Each of these crashes were than simulated with and without LDW and LDP systems. The LDW system was assumed to alert the driver at the instance the leading wheel touched the lane marking. A steering-based LDP system was assumed to operate in conjunction with LDW (i.e. by alerting the driver of a lane departure) and directly modulate steering wheel angle at the instance the leading wheel touched the lane marking. Four hypothetical LDP designs were evaluated, using typical evasive maneuvering behavior from a lane departure, to be representative of "light", "moderate", "aggressive", and "autonomous" steering. The LDW system was estimated to reduce the number of crashes by 26.1% and the number of seriously injured drivers by 20.7%. In contrast, the light steering to aggressive steering LDP systems were estimated to reduce the number of crashes by 32.7% to 37.3% and the number of seriously injured drivers by 26.1% to 31.2%. The LDP system with autonomous driving characteristics were estimated to reduce the number of crashes by 51.0% and the number of serious injuries by 45.9%. This study shows that LDW and LDP could mitigate a large proportion of crashes and injuries in lane departure crashes. This paper is directly relevant to the design and evaluation of LDW and LDP systems.

## INTRODUCTION

Road departure crashes are one of the most harmful crash modes in the United States. A review of crashes in the National Automotive Sampling System (NASS) General Estimates System (GES) and Fatality Analysis Reporting System (FARS) databases from years 2010 to 2011 indicate that departure crashes accounted for only 10% of all crashes yet comprised 31% of all fatal crashes [1]. Lane departure warning (LDW) and lane departure prevention (LDP) are emerging active safety systems that have the potential to prevent departure crashes and injuries.

LDW works by alerting the driver, via an auditory, visual, or haptic warning [2], of a lane departure. However, the effectiveness of this system is limited by the driver's ability to respond to the departure event. In contrast, LDP can directly modulate vehicle trajectory using various modalities, including steering or selective braking of the vehicle's wheels.

There is a need to distinguish between the expected benefits of LDW and LDP, specifically for the implementation and design of these systems. In the U.S., the New Car Assessment Program (NCAP) tests for the presence of LDW only [3]. In the European NCAP (EuroNCAP), the presence of LDW or LDP is awarded equal points because of a lack of evidence that one system is more beneficial than the other [4].

The objective of this study was to compare the predicted safety benefits of LDW and LDP as if all vehicles in departure crashes in the U.S. fleet were equipped with either system. Two measures of safety benefits were evaluated: (1) the number of crashes that could have been avoided were investigated, and (2) the number of seriously injured drivers that could have been prevented.

## METHODOLOGY

Figure 1 summarizes the approach for estimating LDW and LDP benefits in the U.S. vehicle fleet. Each process in the model is discussed in detail in the following sections.

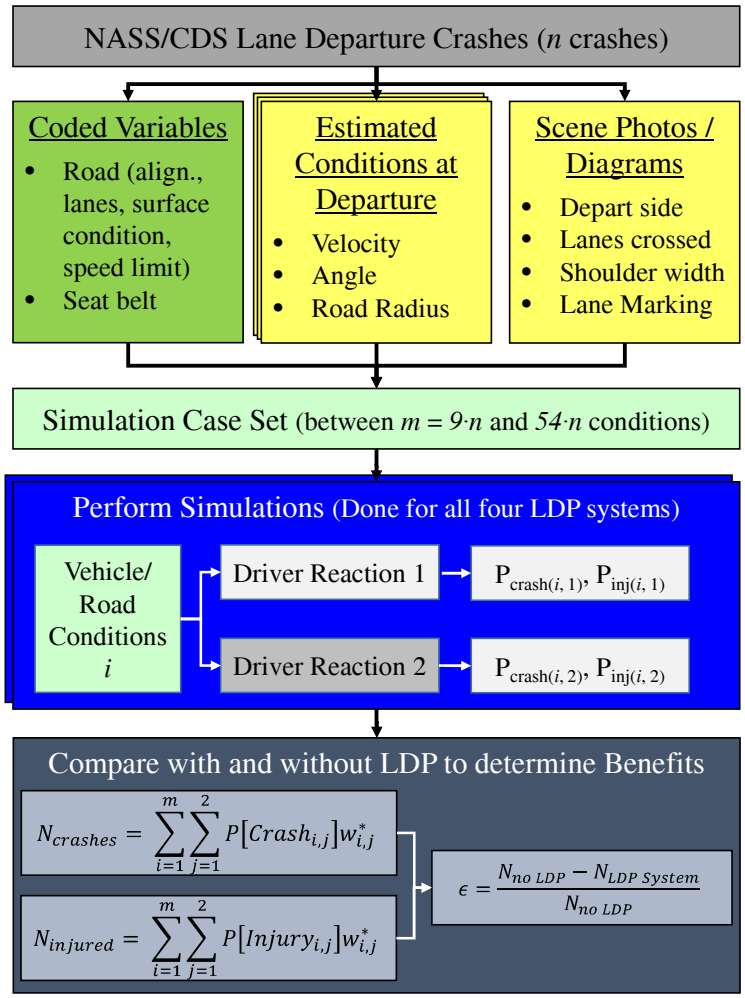


***Figure 1. Simulation of NASS/CDS Road Departure Crashes to Estimate Benefits of a Steering-Based LDP System.***

## Formulation of a Simulation Case Set

### Data Source

Crashes in the 2012 National Automotive Sampling System Crashworthiness Data System (NASS/CDS) were used to formulate the simulation case set. NASS/CDS is a nationally representative sample of crashes that occurred in the U.S. Approximately 5,000 crashes are investigated annually by the National Highway Traffic Safety Administration (NHTSA), and data collected by these investigators are compiled into the NASS/CDS database. To be included in the database, at least one vehicle had to have been towed from the scene due to damage. The database includes detailed medical records and information from the crash environment, such as road characteristics and vehicle information, which make it ideal for this study. Each case is assigned a national weight factor. The weight indicates the number of similar crashes that occurred annually in the United States. The results presented in this paper use these case weightings, in order to make them nationally representative. The simulation case set in this study included only single vehicle crashes where the driver drifted out of their lane, and excluded other single vehicle crashes, such as control loss or contact with animals in the roadway.

### Estimating Departure Conditions

Although a very detailed database, NASS/CDS lacks many of the lane departure conditions needed for this study, including departure speed, angle, and road radius of curvature. In order to estimate these missing parameters, the National Cooperative Highway Research Program (NCHRP) Project 17-22 was used to predict these missing parameters. The NCHRP 17-22 dataset consists of 890 NASS/CDS road departure crashes from 1997-2004 for which supplemental data collection was conducted on road departure conditions [5].

Statistical multivariate models for estimating departure conditions were formulated using the following process. First, one-way ANOVAs were used to determine which predictors significantly correlated with the departure conditions of interest. Second, models were developed to maximize the adjusted-$R^2$, or goodness of fit measure to the data. Three values were selected for each variable that represented the 17th, 50th, and 83rd percentiles of three equally portioned areas under a normal probability distribution. This model development strategy was previously implemented by Kusano et al. [6].

### Review of Event Records

The shoulder width of the road, the travel lane of the vehicle, and lane markings were required for the simulations. However, these parameters are not coded in the NASS/CDS database. Accordingly, these measures were determined through manual review of scene evidence. Shoulder width was estimated from scene photographs. Our approach was to categorize shoulder width as (a) zero-width, (b) between 0.3 and 1 m wide, (c) between 1 to 3.6 m wide, or (d) over 3.6 m wide. If the shoulder was less than 0.3 m, it was coded as zero-width. A width of 3.6 m was chosen because a typical highway lane in the U.S. is no wider than 3.6 m. Initial travel lane was determined through reading the written event narrative and review of the scene diagrams. Manual reviewers identified the presence of lane markings on scene photographs at the approximate point of the first lane departure that led to the crash.

### Driver Reaction Time

Drivers were simulated as having reaction times of either 0.38 s or 1.36 s. These values were chosen as upper and lower bounds on reaction times based on a past driving simulator study by Suzuki and Jansson [7]. They performed a study in a driving simulator with 24 drivers and 54 departure events. Depending on the warning

modality and if the driver was informed or not informed of the LDW system's function, the reaction times varied between 0.38 s to 1.36 s.

### Simulation Case Set Replications

Each case was represented in the simulation case set multiple times. Each replication was given an equal probability of occurring. The number of replications were determined using the possible crash conditions previously described. For example, a crash that occurred on a curved road and with a shoulder width between 0.3 and 3.6 m had the most number of simulations (2 reaction times x 3 departure velocities x 3 departure angles x 3 radius of curvatures x 2 shoulder widths = 108 simulations).

## Simulation of Lane Departure Crashes

Kinematics simulations were performed using CarSim® vehicle simulation software [8]. The CarSim vehicle model was of a model year 2000 Ford Taurus assumed to be a representative car in the fleet. This specific vehicle was selected to be consistent with the VFU driver model [9]. Trajectories were simulated using initial conditions from the simulation case set, the VFU ACAT driver model [9], the LDW model, and the LDP model. All numerical integration was performed using 4th order Runge-Kutta method, and the simulation time step was set to 0.01s. The travel lane in the simulations was 3.48 m wide for divided highways and 3.64 m wide for undivided highways, as found from cases in the NCHRP 17-22 database.

### Driver Model

To model driver control we used a driver recovery model developed by Volvo, Ford, and UMRTI (VFU) through the Advanced Crash Avoidance Technologies (ACAT) Program, with sponsorship from NHTSA [9]. This model was developed to study driver steering and speed response to lane departure warning systems. Steering is adjusted through a proportional control feedback loop based on the yaw rate of the vehicle. As the vehicle approaches the edge lines of the road, the driver model considers the yaw of the vehicle, identifies if that yaw will cause lane departure, and makes a proportional change to the yaw rate to maintain vehicle position in the lane [10]. The parameters for the driver model were based on driving simulator experiments performed in Ford's VIRTTEX driving simulator, which matches the 2000 Ford Taurus CarSim model that was developed for the VFU ACAT project and that was used in this study. Driver steering control was only implemented after vehicle departure occurred and the driver had become attentive.

### LDW and Steering-Based LDP modeling

In our simulations, the LDW system alerted the driver at the instance the leading wheel touched the lane markings. The modeled LDP system works by directly modulating steering wheel angle. Additionally, the LDP system was assumed to work in conjunction with an LDW system, i.e. the driver will still react after a lane departure occurs. When the driver became attentive, LDP was assumed to no longer contribute modulating steering.

Four potential LDP system designs were evaluated. Each LDP systems has unique steering wheel angular rates and maximum steering angles that were intended to replicate "light", "moderate", "aggressive", and "autonomous" LDP systems. As shown in Figure 2, when LDP became activated, steering wheel angle would change linearly at the prescribed angular rate, and would become saturated at the LDP maximum value. The "moderate" LDP system (rate = 20 degrees/second, maximum = 4 degrees) was designed using data from low severity departures. An analysis was performed on low angle departures that occurred during the IVBSS naturalistic driving [11]. The "light" (rate = 10 degrees/second, maximum = 2 degrees) and "aggressive" (rate = 40 degrees/second, maximum = 8 degrees) steering parameters were scaled to be one-half and two-times the "moderate" values, respectively. The "autonomous" LDP (rate = 100 degrees/second, maximum = 50 degrees)

steering parameters were determined using emergency driver steering data following severe lane departures. These values were taken from a previous study by Kusano and Gabler [12] that investigated severe lane departures during the Virginia Tech Transportation Institute (VTTI) 100-car study [13, 14].

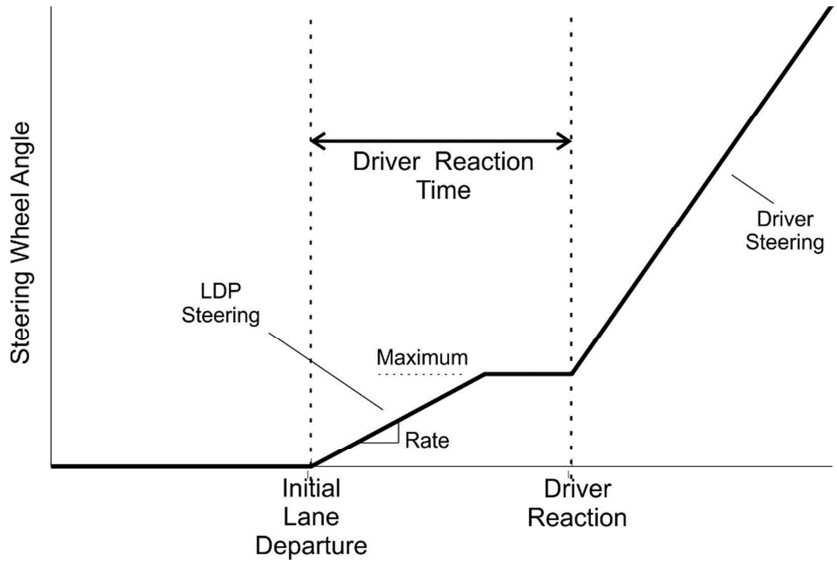


***Figure 2. Steering control with LDP system.***

**Benefits Estimation**

This study was interested in the number of crashes and seriously injured drivers that could have been prevented with LDW and LDP. The benefits estimation methodology used have been previously implemented and described by Kusano et al. [6].

**Probability of a Crash**

For a given simulation, indexed by i, the roadside terrain was discretized into zones, indexed by k, that were parallel to the road boundary. The road boundary was defined as the edge of the paved road, i.e. crashes were only assumed to occur off the paved road. We assume that the probability of a crash was dictated by two factors: 1) the distance travelled laterally from the road, and 2) the total distance travelled off-road.

The NCHRP 17-22 data was used to estimate collision risk in these zones. The 17-22 dataset was ideal for this, because the number of crashes in each of the roadside zones, $C_k$, and the distance traveled in each roadside zone, $\gamma_k$, could be determined. Given the total simulated trajectory length in each zone k, $L_{i,k}$, the probability of a crash $P[Crash_i]$, for a given trajectory could be calculated using Equation 1.

$$P[Crash_i] = 1 - \prod_{k=1}^{K} \exp\left(-\frac{C_k L_{i,k}}{\gamma_k}\right) \quad (1)$$

**Probability of Seriously Injury Driver**

The NCHRP 17-22 dataset was used to calculate probability of an injury given a simulated trajectory. For this study, a seriously injured driver was defined to be a driver with a Maximum Abbreviated Injury Score of 3 or greater using AIS98 [15]. In summary, the probability of a seriously injured driver was statistically modeled using logistic regression functions. Departure velocity and seat belt usage were used as independent variables, and injury outcome

was the dependent variable. After determining the probability of an injury given the departure conditions P[injury$_{IC}$], the probability of an injury given the simulated trajectory, P[injury$_i$], could be calculated using Equation 2.

$$P[Injury_i] = P[\boldsymbol{Injury_{IC}}]\, P[Crash_i] \quad (2)$$

**Effectiveness Calculation**

Benefits estimates were computed to determine the proportion of crashes and seriously injured drivers that could have been prevented if the vehicle had been equipped with LDW or LDP. As shown in Equation 3, this can be represented by an effectiveness measure, $\epsilon$, that is computed as the proportion of crashes reduced with LDW/LDP. Because the number of nationally representative crashes and seriously injured drivers without LDW are known, the simulated cases without LDW or LDP were additionally weighted to reflect these counts.

$$\epsilon = \frac{N_{without\ LDW/LDP} - N_{with\ LDW/LDP}}{N_{without\ LDW/LDP}} \quad (3)$$

## RESULTS

Table 1 summarizes the number of single vehicle drift out of lane road departure crashes in NASS/CDS 2012. Approximately 15% of all NASS/CDS 2012 crashes were drift out of lane departures. A manual review of cases was then performed to eliminate incorrectly coded cases within the database. Additional, cases were excluded for having disproportionally high case weight, for the departure being at a T-intersection, and for having multiple departure sides. Cases with weightings greater than 5,000, as others have done in the existing literature [16], were eliminated, because their simulated effectiveness greatly skew the data. The resulting 478 lane departure crashes formed the 20,118-simulation case set for making LDW/LDP benefits estimates, and are represented of 147,662 crashes nationally.

**Table 1. Case count summary. Cases were eliminated in the sequence described.**

| Group | | n | Freq. |
|---|---|---|---|
| All Crashes in CDS 2012 | | 3,581 | 1,996,016 |
| Drift out of Lane Departures | | 629 | 293,937 |
| Valid Departure after Manual Inspection | | 556 | 271,810 |
| Exclusions for Valid Departures | Weight > 5,000 | 5 | 91,577 |
| | End Departures | 8 | 1,767 |
| | Multi-side Departures | 65 | 30,804 |
| Final Dataset for LDW Modeling | | 478 | 147,662 |

Table 2 lists the number of crashes and injuries without LDW/LDP systems along with the predicted effectiveness of LDW and LDP systems. The LDW system was estimated to reduce the number of these drift out of lane road departure crashes by 26.1% and the number of seriously injured drivers by 20.7%. In contrast, the light steering to aggressive steering LDP systems were estimated to reduce the number of crashes by 32.7% to 37.3% and the number of seriously injured drivers by 26.1% to 31.2%. The LDP system with autonomous driving characteristics were estimated to reduce the number of crashes by 51.0% and the number of serious injuries by 45.9%.

**Table 2. Effectiveness of LDP in U.S. Vehicle Fleet.**

| Measure | | Values | Effectiveness (% Improvement) |
|---|---|---|---|
| | | | |
| **Crashes** | | | |
| No LDW or LDP | | 147,662 | --- |
| with LDW | | 109,404 | 26.1% |
| with LDP | Light | 99,412 | 32.7% |
| | Moderate | 96,939 | 34.4% |
| | Aggressiveness | 92,613 | 37.3% |
| | Autonomous | 72,403 | 51.0% |
| | | | |
| **Injuries (MAIS3+)** | | | |
| No LDW or LDP | | 30,098 | --- |
| with LDW | | 23,871 | 20.7% |
| with LDP | Light | 22,233 | 26.1% |
| | Moderate | 21,722 | 27.8% |
| | Aggressiveness | 20,694 | 31.2% |
| | Autonomous | 16,274 | 45.9% |

The effectiveness of LDW and LDP depended on the number of lanes crossed before departure. Figures 3 and 4 show the effectiveness of LDW and LDP by the number of lanes crossed before departure. Because this model assumes no objects or vehicles on the paved road, the effectiveness of LDW and LDP were expected to be dependent on the system's ability to prevent a departure from the paved road.

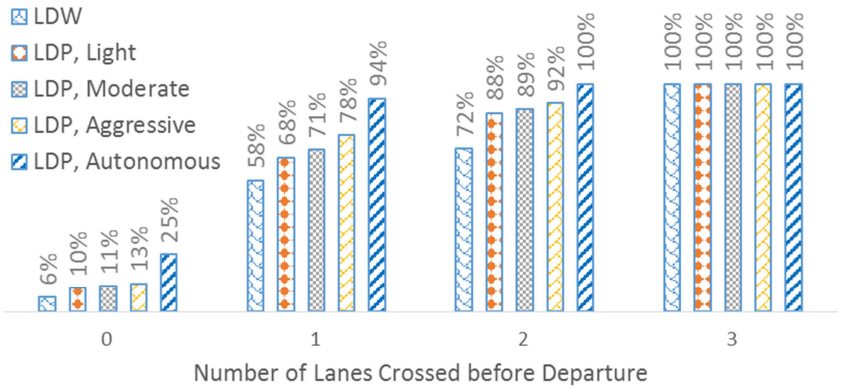


**Figure 2. Effectiveness of LDW and LDP in reducing the number of crashes given the number of lanes which needed to be crossed prior to leaving the road (n=20,118 simulations).**

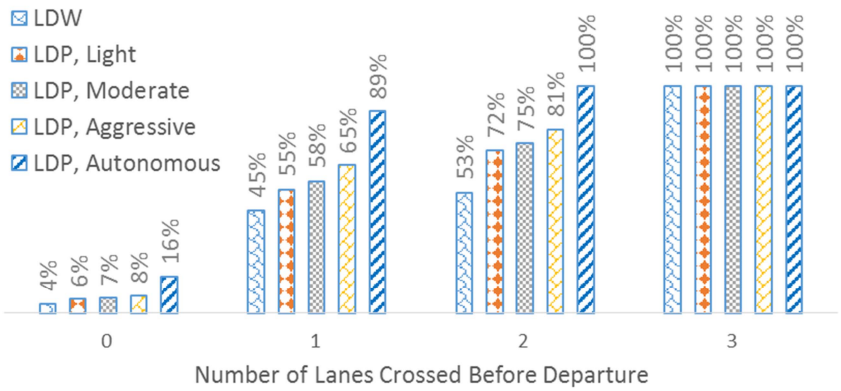


**Figure 3. Effectiveness of LDW and LDP in reducing the seriously injured drivers (MAIS 3+) as a function of shoulder width (n=16,920 simulations).**

Figures 3 and 4 show the effectiveness of LDW and LDP by shoulder width. Like number of lanes crossed before departures, wider shoulders provided additional time and space for returning the vehicle to the road. Only simulations that had no adjacent travel lanes crossed prior to departure, i.e. traveling in rightmost or leftmost lane, are tabulated to isolate the effect of shoulder width from number of lanes before departure.

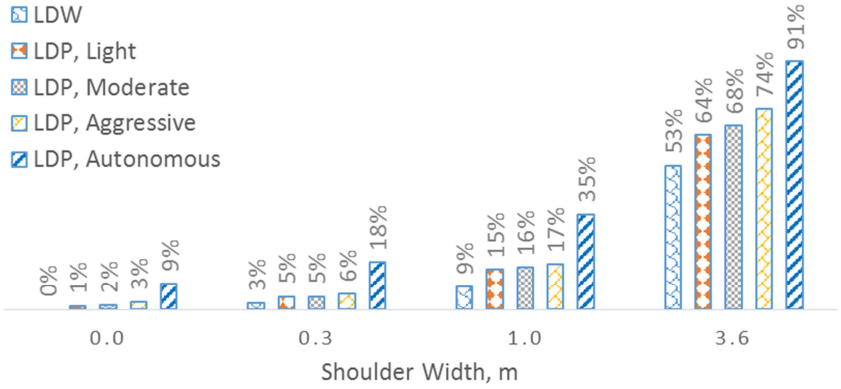


**Figure 3. Effectiveness of LDW and LDP in reducing the number of crashes as a function of shoulder width (n=16,920 simulations).**

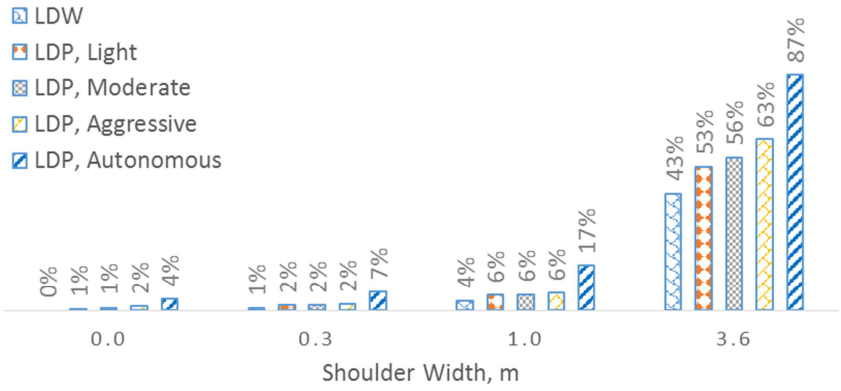


**Figure 4. Effectiveness of LDW and LDP in reducing the seriously injured drivers (MAIS 3+) as a function of shoulder width (n=16,920 simulations).**

## DISUSSION

These results indicate that LDP systems can prevent a larger number of crashes and seriously injured drivers than vehicles instrumented with only LDW. The potential benefits of LDP are dramatically influenced by the number of lanes crossed before departure and shoulder width. The influence of these factors on benefits is especially important when considering that 30% of crashes occurred on roads with no lane markings, and 29% of crashes occurred on roads with no shoulder.

Steering-based LDP systems are attractive for a number of reasons. First, by modulating vehicle trajectory, LDP not only warns the driver of a lane departure, but also gives the driver directional information about the required recovery maneuver. By its nature, this warning with directional information may serve to further improve driver reaction time and response. Second, steering-based LDP systems have the ability to begin returning the vehicle to the departed lanes prior to driver reaction. Even steering-based LDP system with relatively light steering input still yielded a substantially greater effectiveness than a simple LDW system.

There are several limitations to the current study. First, the mechanism which led to the lane departure was not considered. The reason for initial lane departure, such as distractive driving or drowsiness, may be important to consider when predicting driver response. Second, this model assumes that when the vehicle crosses adjacent lanes there is no contact with other objects or vehicles. This approach provides a best case scenario, and may lead to an overestimation of the systems effectiveness. Third, the LDP systems used in this study are simplistic representations of actual LDP systems. For instance, the current model applies an angular rate to the steering wheel that becomes saturated at some nominal value. Actual steering-based LDP systems may have more complex steering inputs that are dependent on a variety of factors, such as vehicle speed and trajectory. Also, LDP systems can provide other modes of lane departure prevention, such as through selective braking of wheels to direct the car back into the lane. Fourth, LDW and LDP were assumed to become activated when the leading wheel crosses the line. In reality, systems can become activated before or after lane departure occurs.

## CONCLUSIONS

This study shows that LDW and LDP could mitigate a large proportion of crashes and injuries in lane departure crashes. The results indicate that LDP systems are more effective than LDW systems at preventing the number or crashes and seriously injured drivers in the U.S. fleet. This data also demonstrates the sensitivity of these measures to LDP steering prior to driver reaction, and the dependency of effectiveness on number of lanes to road departure and road width. This paper is directly relevant to the design and evaluation of LDW and LDP systems. The results of this study could inform policy on regulatory and consumer rating tests.

## ACKNOWLEDGEMENTS

The authors would like to acknowledge the Toyota Collaborative Safety Research Center (CSRC) and Toyota Motor Corporation for funding this study. Our special thanks to Katsuhiko Iwazaki and Hiroyuki Takahashi of Toyota for sharing their technical insights and expertise throughout the project. We also gratefully acknowledge Kristin Dunford and Kaitlyn Wheeler for their assistance in examining NASS/CDS case documentation. The authors would like to thank Nicholas Johnson for his assistance reviewing the statistical models for predicting missing variables. The authors would also like to acknowledge Jackie Chen for his analysis of IVBSS lane departure crashes.

**REFERENCES**


1. Kusano, K.D. & Gabler, H.C., 2014. Comprehensive Target Populations for Current Active Safety Systems using National Crash Databases. *Traffic Injury Prevention*, 15(7), pp.753–761. doi:10.1080/15389588.2013.871003.
2. Beruscha, F., Augsburg, K. & Manstetten, D., 2011. Haptic warning signals at the steering wheel: a literature survey regarding lane departure warning systems. *Haptics-e*, 4, pp.1–6.
3. NHTSA, 2013. Lane Departure Warning System Confirmation Test, Washington, D.C.: U.S. Department of Transportation, National Highway Traffic Safety Administration.
4. Euro NCAP, *Euro NCAP Rating Review 2015*, in *Ratings Group Report*. 2015, European New Car Assessment Programme.
5. Mak, K.K. & Sicking, D.L., 2010. Identification of Vehicular Impact Conditions Associated with Serious Ran-off-Road Crashes, Transportation Research Board, National Cooperative Highway Research Program, NCHRP Report 665.
6. Kusano, K.D., Gorman, T.I., Sherony, R., Gabler, H.C.., 2014. Potential occupant injury reduction in the U.S. Vehicle fleet for lane departure warning-equipped vehicles in single-vehicle crashes. *Traffic injury prevention*, 15 Suppl 1(sup1), pp.S157–64. doi:10.1080/15389588.2014.922684
7. Suzuki, K. & Jansson, H., 2003. An analysis of driver's steering behaviour during auditory or haptic warnings for the designing of lane departure warning system. *JSAE Review*, 24(1), pp.65–70.
8. Mechanical Simulation, *CarSim*. 2012.
9. Gordon, T, Sardar, H., Blower, D., Ljung Aust, M., Bareket, Z., Barnes, M., Blankespoor, A., Isaksson-Hellman, I., Ivarsson, J., Juhas, B., Nobukawa, K., Theander, H., 2010. Advanced Crash Avoidance Technologies (ACAT) Program - Final Report of the Volvo-Ford-UMTRI Project: Safety Impact Methodology for Lane Departure Warning - Method Development and Estimation of Benefits, Department of Transportation.
10. Gordon, T., Blankespoor, A., Barnes, M., Blower, D., Green, P., Kostyniuk, L., 2009. Yaw rate error - a dynamic measure of lane keeping control performance for the retrospective analysis of naturalistic driving data. In Proceedings of the 20th International Enhanced Safety of Vehicles Conference. Stuttgart, Germany.
11. Sayer, J.R., Bogard, S.E., Buonarosa, M.L., LeBlanc, D.J., Funkhouser, D.S., Bao, S., Blankespoor, A.D., Winkler, C.B., 2011. Integrated Vehicle-Based Safety Systems Light-Vehicle Field Operational Test Key Findings Report, U.S. Department of Transportation, Research and Innovative Technology Administration.
12. Kusano, K.D. & Gabler, H.C., 2013. Driver Response to Road Departures in the 100-Car Naturalistic Study. In Proceedings of the 4th Road Safety and Simulation International Conference. Rome, Italy.
13. Dingus, T.A., Klauer, S.G., Neale, V.L., Petersen, A., Lee, S.E., Sudweeks, J., Perez, M.A., Hankey, J.M., Ramsey, D., Gupta, S., Bucher, C., Doerzaph, Z.R., Jermeland, J., Knipling, R.R., 2006. The 100-Car Naturalistic Driving Study - Phase II Results of the 100-Car Field Experiment, Washington, D.C.: National Highway Traffic Safety Administration.
14. McLaughlin, S.B., Hankey, J.M., Klauer, S.G., Dingus, T.A., 2009. Contributing Factors to Run-Off-Road Crashes and Near-Crashes, National Highway Traffic Safety Administration, Report DOT HS 811 079.
15. AAAM, *The Abbreviated Injury Scale-1990, Update 1998*. 1998: Des Plaines, IL.
16. Kononen, D.W., Flannagan, C.A. & Wang, S.C., 2011. Identification and validation of a logistic regression model for predicting serious injuries associated with motor vehicle crashes. Accid Anal Prev, 43(1), pp.112–122. doi: 10.1016/j.aap.2010.07.018

# A STUDY of GAS FLOW BEHAVIOR in AIRBAG DEPLOYMENT SIMULATION

**Hitoshi Ida**
**Masashi Aoki**
**Michihisa Asaoka**
Toyoda Gosei Co., Ltd.
Japan

**Kiyonobu Ohtani**
Institute of Fluid Science, Tohoku University
Japan

Paper Number 15-0081

## ABSTRACT

Airbag deployment simulation has been utilized as an important technique to predict the occupant protection performance in the development and design stages. One of the key elements of airbag deployment behavior is the gas flow behavior of jets from inflator. In this study, in order to understand the gas flow behavior of disk type inflator for driver side airbag, visualization experiments were conducted using the schlieren method. The gas flow from the inflator with a retainer has been found to have a strong directivity. Then, the gas flow simulation was conducted with a general purpose finite element program, LS-DYNA, it was possible to obtain a good reproducibility. For reproduction, it was found that jet direction and cone angle of gas diffusion were essential elements. Furthermore, comparison between simulation and experiments were conducted for deployment behavior of driver side airbag, the effect of gas flow on deployment behavior was analyzed. It was found from the results that the reproduction of gas flow from inflator was a major factor for reproduction on deployment behavior of driver side airbag.

## INTRODUCTION

To evaluate the occupant protection performance of the airbag, the airbag deployment simulation is an important and efficient one approach. The first developed approach was uniform pressure method, which obtained pressure from mixed jet gas property of inflator and equation of state was applied to entire inside of airbag. This method could evaluate energy absorption of airbag and used for occupants protection analysis combined with kinematic analysis.[1] However, Since the gas flow was not considered in this method, there were some issues that behavior and energy absorption of airbag in deploying process could not be obtained accurately. To resolve the issues, fluid and structure coupling method, ALE (Arbitrary Lagrangian-Eulerian) method has been introduced.[2]

When this method was applied to airbag deployment analysis, to represent the deployment of the folded airbag, enormous computational resources and cost were necessary.[3] To overcome the issue, a general purpose finite element program, LS-DYNA, implemented a new method CPM (Corpuscular Particle Method) which replace gas flow as particle movements. In this method, the gas was not treated as continuum and followed gas molecular dynamics. Instead of all models of the gas molecules, the overall translational kinetic energy are replaced with a number of particles to be equivalent.[4, 5]

It was not necessary to descrete entire space as same as ALE in this method, the deployment simulation has been executed in available computational resources and cost. When the gas flow in narrow tube such as curtain airbag, it was possible to predict the deployment behavior and an impact force property. The prediction is currently applied to products development.[6] However, the difference has occurred in actual phenomena and simulation results when the gas was evolved in large space such as driver side airbag. We focused the gas flow in the airbag, tried to visualize the gas flow from inflator using schlieren method. In the past study, there was a observation of the gas flow only inside the inflator.[7] Very few attemps have been made at such observation of the gas flow outside the inflator for airbag deployment behavior.

In this paper, the visualization experiments of the jet gas flow were conducted and reproduced the gas flow by CPM. Then we applied the study results to deployment simulation of driver side airbag, and present the deployment behavior was reproduced properly.

## METHODS

### Visualization Experiments of Gas Flow

To understand the jet gas flow from inflator, the visualization experiment using schlieren method was conducted in open atmosphere space. It was hard to perceive clearly the jet gas flow with high speed camera. There was a PIV method to observe velocity of marker particles which mixed in gas flow.[8] In this method, observation area was local and it was hard to visualize the range of gas flow. Therefore, we selected the schlieren method to visualize clearly and directly. The schlieren method is one method of observation for gas flow using difference of light refractive index. The method has been used to visualize a shock wave of explosion or aircraft.[9,10] The configuration of experiment apparatus are shown in Figure 1. A light from point light source was parallelized by parabolic mirror, object inflator gas was ejected in the parallelized light. The light was condensed by parbolic mirror again. The defocused light by difference of refractive index was removed by iris at focal point. Images of differece of light contrasting were recorded with a high speed camera. In generaly, Although a knife edge was used in schlieren method, to observe the diffusing gas from the center of inflator, iris was used to capture the gas clearly. To take a picture of gas flow in range of airbag deployment, the world's largest class parabolic mirror with a diameter of one meter and focal length of eight meter was used in this experiments. This apparatus could be visualized at least 3kPa pressure waves such as sound from trombone.[11]
For driver side airbag, the gas flow from inflator with or without a retainer was recorded with a high speed camera.

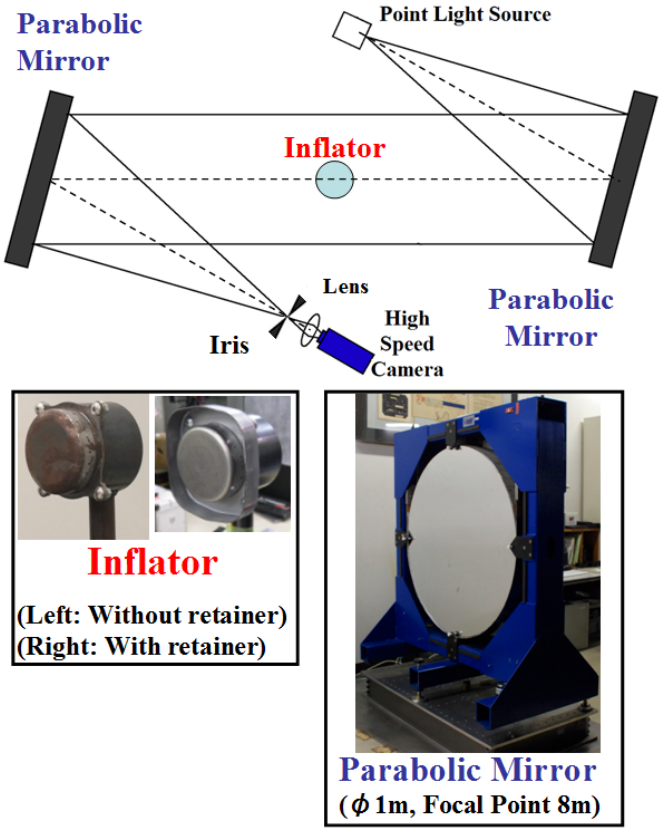


*Figure 1. Gas flow visualization apparatus of schlieren method at Tohoku University.*

## Gas Flow Simulation of Inflator

Gas flow simulation with or without a retainer using CPM of the LS-DYNA were conducted to reproduce the observed jet gas flow by visualization experiment. The research of seven CPM parameters is examined to reproduce the real gas flow. The examined parameters are shown in Table 1.

***Table 1.***
***Parameters of gas flow simulation***

| No. | Parameter | Without retainer | With retainer |
|---|---|---|---|
| 1 | Initial direction of gas inflow | Radial | Radial / Axial |
| 2 | Cone angle from orifices | Inactive / 16°/ 25° | Inactive / 0.1～25° |
| 3 | Friction factor | 0 (default) | 0 ～ -0.2 |
| 4 | Dynamic scaling of patricle | Inactive / Active | Inactive / Active |
| 5 | Initial gas inside airbag | CV method / Particle | CV method / Particle |
| 6 | Number of orifices | 16 (Inflator pinholes) | 16 / 4 (Retainer corner) |
| 7 | Number of gas components | Mixed / Multiple | Mixed / Multiple |

## Deployment Experiment of Driver Side Airbag

The static deployment behavior of driver side airbag was observed in an experiment. The experiment setting, the airbag configuration and deployment appearance are shown in Figure 2.

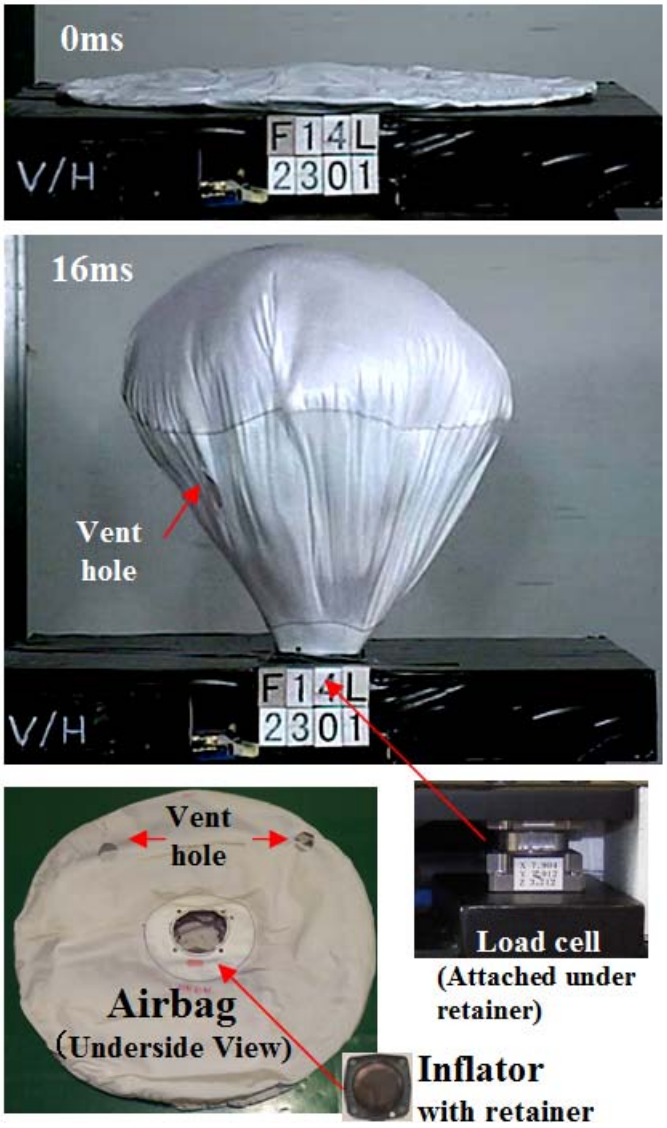


***Figure 2. Static deployment experiment of driver side airbag.***

The unfolded tether less airbag with retainer was installed for the experiment. A load cell was set under the retainer to measure a deployment force at installation point.

**Deployment Simulation of Driver Side Airbag**

A reproduce simulation shown in Figure 2 was conducted. A mechanical property of airbag fabric was from tensile, shear test and reflected to the property of input deck. A gas temperature and a mass flow rate were identified by tank test simulation. The parameter values of CPM were selected default condition on atmosphere space and the best conditions on Table 1 to reproduce the gas flow. The effect of gas flow reproduction in atmosphere space was examined to airbag deployment.

## RESULTS

### Visualization Experiments and Simulation of Gas Flow

The gas flow from inflator was clearly visualized as a dark image in schlieren method. The results of visualization are shown in Figure 3. The large distortion parts of parallel light were removed and observed as shadow. Since the inflator gas had a high temperature and a high pressure, the gas produced a distinct distortion that was different from the atmosphere. In these results, the difference of the flow with or without retainer was clearly observed. The gas trended to be released radially and vertically from orifices on the inflator for without a retainer. On the other hands, for with a retainer, the flow along the wall of retainer was observed. Additionally, the flow along the wall did not diffuse immediately after release.

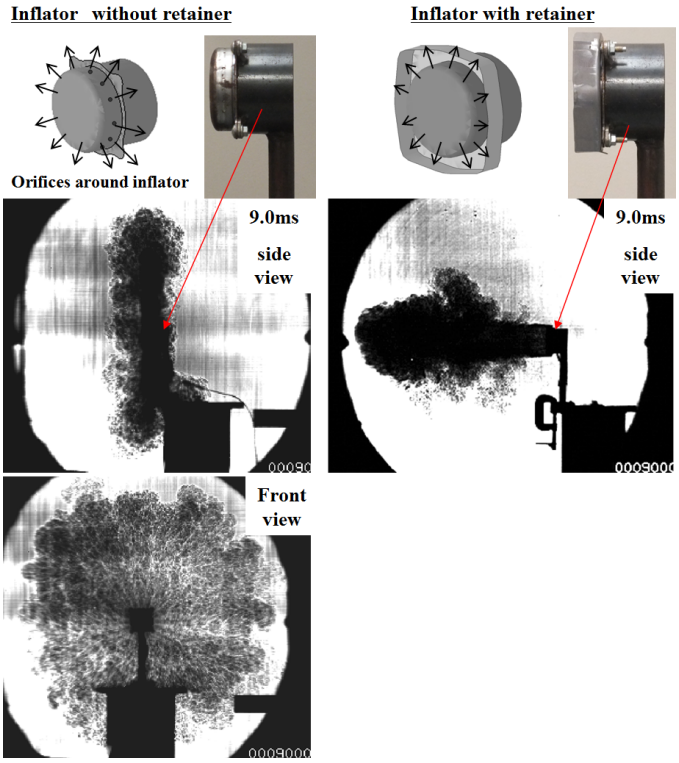


***Figure 3. Visualization of inflator gas by schlieren method (Left: without retainer, Right: with retainer).***

The gas flow of simulation by CPM for without the retainer in atmosphere space trended to be diffused randomly. The behavior of particles did not show radial flow. (See Figure 4A)
To reproduce this trend, when the cone angle parameter in Table 1 was set appropriately, radial flow was shown in Figure 4B.
On the other hands, for with retainer, the gas flow of simulation did not reproduce the experimental result. (See Figure 4C) The parameters from No. 3 to No. 7 in Table 1 did not affect to gas flow behavior. (See Figure 4D)
For with retainer, when jet direction was set as axial jet along the wall of retainer, the diffusion range of flow was slightly narrowed, however a directional flow was not reproduced. (See Figure 4E)
When additional parameter cone angle was set appropriately, the flow was reproduced as same as the experimental result. (See Figure 4F)

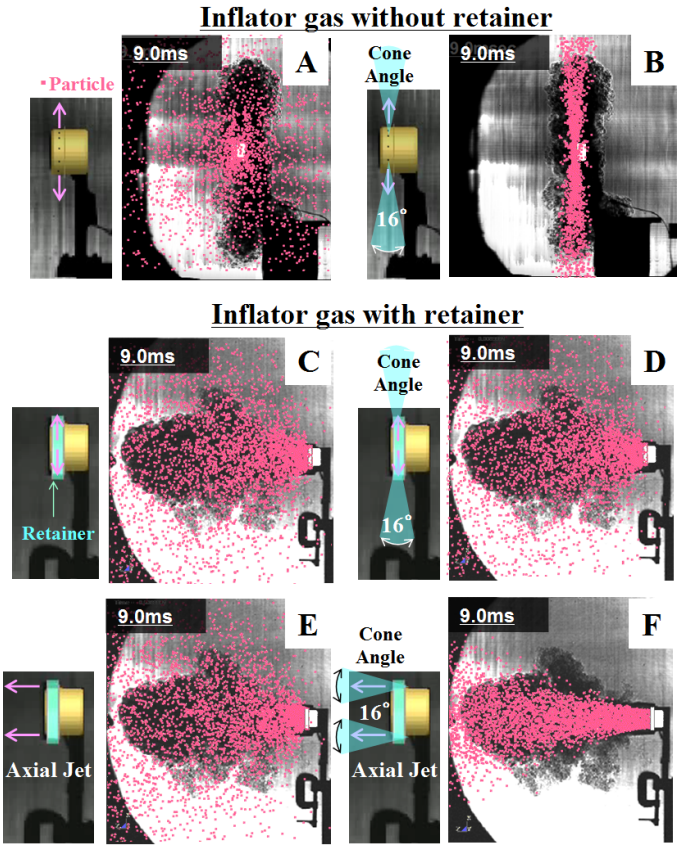


*Figure 4. Gas particle distribution of simulation result with retainer.*

**Deployment Experiments and Simulation of Driver Side Airbag**

Comparison between deployment experiment and simulation of driver side airbag was conducted. When the jet direction was set radially and vertically of the inflator in simulation, the result shows that the deployment behavior was delay against experiment. Approximately half force of the experimental result occurred in retainer fixed points. (See Figure 5A)

When the jet direction was set as axial and along the wall of retainer and cone angle was set appropriately, the deployment time and deployment force were almost reproduced the experimental results. (See Figure 5B)

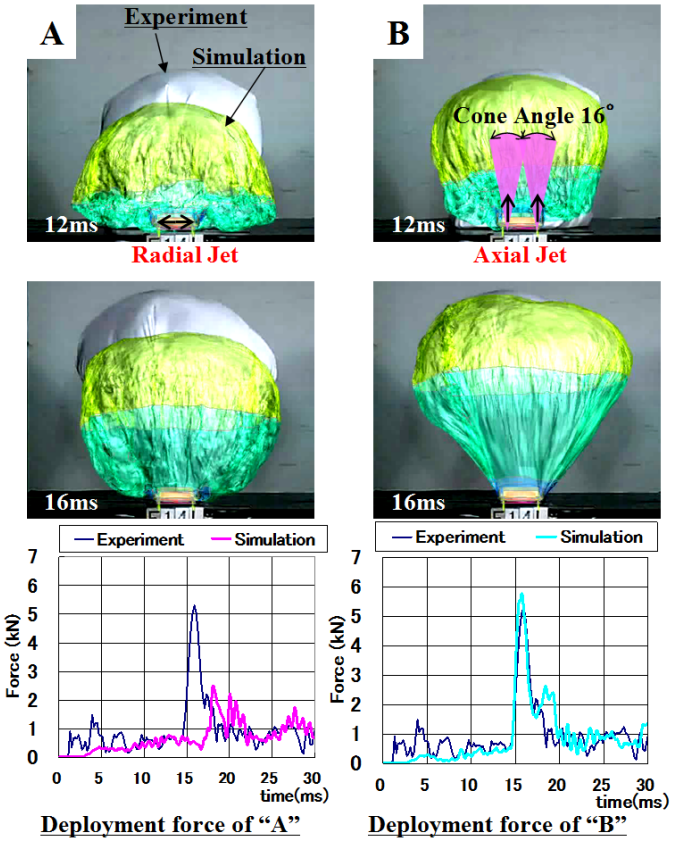


*Figure 5. Comparison of deployment behavior & deployment force between experiment and simulation (Left: Radial jet, Right: Axial jet with Cone angle).*

## DISCUSSION

According to the result comparison between experiment and simulation, when the particles were released to relatively wide space, random movement of each particle is dominant, the gas flow was found to be not sufficiently reproducible by CPM.
The actual gas flow from orifices on the inflator is released in vertical direction on orifices. When the gas flow from inflator with retainer is released, if it is assumed that the gas flow outlet faces open side of the retainer, the gas is released perpendicular to the open side of the retainer.
In CPM, because the particles diffuse randomly from orifices of the inflator, it should apply correction function such as cone angle.

## CONCLUSIONS

The visualization experiment and simulation of the gas flow from inflator provide the following findings.
Using schlieren method, the gas flow to atmosphere space is radially released perpendicular to orifices on the inflator. When the retainer is installed on inflator, the gas flow along wall of retainer is produced and the gas flow is perpendicular to open side of the inflator.
In simulation of CPM, particles from inflator behave randomly. To reproduce the actual radial flow, it should have a correction function, such as a cone angle. When the gas flow with retainer is reproduced, it should set the jet direction from open side of retainer and cone angle.
Applying the above conditions to deployment simulation of driver side airbag, the deployment behavior and the deployment force property are reproduced the experimental results.

**ACKNOWLEGEMENTS**

We wish to acknowledge valuable experiments and discussions with honorary Prof. Takayama at Institute of Fluid Science, Tohoku University.

**REFERENCES**

[1] Wang, J. T., & Nefske, D. J. (1988). A new CAL3D airbag inflation model. SAE Technical Paper 880654.

[2] Fokin, D., Lokhande, N., & Fredriksson, L. (2003). On airbag simulation in LS-DYNA with the use of the Arbitrary Lagrangian-Eulerian method. 4th European LS-DYNA Users Conference.

[3] Zhang, N., Shi, L., & Tzeng, B. (2006). Issues on Gas-Fabric interaction in airbag simulation using LS-DYNA ALE. 9th International LS-DYNA Conference.

[4] Olovsson, L. (2007). *Corpuscular method for airbag deployment simulations in LS-DYNA* (Report R32S-1). Huddinge, Sweden: Impetus Afea AB.

[5] Feng, B., & Coleman, D. (2008). Gas dynamics simulation of curtain airbag deployment through interior trims. 10th International LS-DYNA Conference.

[6] Sugaya, H., Imura, K., & Mae, H. (2014) . Development of Side Curtain Airbag Deployment Simulation Technology Using CPM. *Honda R&D Technical Review,* Vol. 26, No. 1.

[7] Kratz, H., Pührer, C., Takazono, K., & Yano, K. (2008). Shockwave characterisation, parameter studies and visualization for a cold gas curtain inflator. Airbag2008.

[8] Lee, J. S., Jang, G. Y., Kim, S., & Kim, S, C. (2006). Dynamic PIV measurement of a compressible flow issuing from an airbag inflator nozzle. *Journal of Thermal Science*, Vol. 15, No. 4, pp. 377-381.

[9] Mizukaki, T., Miura, A., & Takayama, K. (2004). Experimental simulation of large-scale explosion using a micro-charge explosion (1) - Behavior of shock waves in a complicated closed-space -. *Science and Technology of Energetic Materials,* Vol. 65, No. 5, pp. 180-188

[10] Ukai, T., Ohtani, K., & Obayashi, S. (2015). Validation of measurement accuracy for near-field pressure around supersonic projectiles in a ballistic range. *Measurement, Journal of the International Measurement Confederation*, Vol. 67, pp. 24-33.

[11] Takayama, K., Ohtani, T., Ogawa, T., Kikuchi, T., Takayama, R., & Takahashi, T. (2011). Visualization of weak shock waves emitted from trombone. *The Journal of the Acoustical Society of America 2011.* doi:10.1121/1.3588692

# CAR OR GROUND: WHICH CAUSES MORE PEDESTRIAN INJURIES?

**Anne Guillaume**
**Thierry Hermitte**
Laboratory of Accidentology Biomechanics and human behavior, PSA Peugeot-Citroën / RENAULT
France

**Véronique Hervé**
**Romain Fricheteau**
Centre Européen d'Etude de Sécurité et d'Analyse des Risques
France

Paper Number 15-0084

## ABSTRACT

The aim was to study the cause of the injuries of pedestrians when hit in frontal impacts by a vehicle. Depending on the impact speed, the type and severity of the injuries may be due partly to the vehicle and partly to the road/ infrastructure, when falling down. The study took into account the projection distance and the age of pedestrians.
The work has been supported by FSR (Fondation Sécurité Routière)
All the accident cases were reviewed by an expert committee composed by physicians and accident analysis experts. For each wounded pedestrian, the injuries were reviewed in order to determine their causing mechanism taking into account the accident occurrence circonstances, the vehicle deformations and the clues on the road or infrastructure.
The data base was a sample of 100 in-depth investigations and reconstructions of accidents from years 2009 to 2011 involving at least one injured pedestrian hit by a vehicle and continuously collected in a 20 km diameter area in the south of Paris (France). The accident analysis team was called with the emergency team on field where the data were collected.
In the sample, 89 pedestrians were injured in a frontal impact. For 83 of them, it was possible to evaluate the vehicle speed during the impact. In 12% of the cases the speed exceeded 50 km/h and all the pedestrians were severely injured (MAIS3+: pedestrian with at least one injury scored above AIS3) with a high projection distance. Therefore, we focused on frontal impact with vehicle speed below 50 km/h. In this configuration , considering injuries AIS2+, the head was the most often injured (53%) and then the lower limbs (21%). Among the wounding elements, the ground was incriminated in 27.5% of the cases, then the bonnet (22%), the windshield (17%) and the bumper (15.5%).When the vehicle speed was below 30 km/h, more than half of the injuries AIS2+ observed were caused by an impact with the ground. There was a compounding effect of age.

Though the sample is not representative of all French pedestrian accidents, it allows categorizing these accidents depending on the impact speed. For each speed range, the main causal factor of the injuries was determined.

The vehicle speed was the major factor in the determinism of the injury severity of pedestrians involved in frontal impact, firstly by direct impact secondly by increasing the projection distance and thus the severity of injuries due to ground impact. Primary safety systems should reduce the severity of pedestrian injuries by decreasing the impact speed.

## INTRODUCTION

The last WHO report relates that among the 1.24 milion deaths on the world's roads, 22% were pedestrians [1]. When focusing on European countries, they are representing 21% of the fatalities [2]. In France, the percent is lower but still high with 15% of the fatalities in 2014 [3]. In this context, a better understanding of the pedestrian injury mechanisms will help to orient the preventive actions. LAB and CEESAR carried out a specific study about this topic using in-depth accident analysis that was part of a larger project called CACIAUP supported by Fondation Sécurité Routière and the French car manufacturers. The aim of CACIAUP was to study three main topics: 1) to improve the in-depth accident analysis in order to specifically adapt them to pedestrian accidents. It means to optimize the alert, the way how data are collected and accident reconstruction techniques. 2) to follow the injured pedestrians until recovery or stabilization of injury sequelae in order to evaluate the efficiency of the Injury Impairment Scale (IIS) for this population of wounded people. 3) to identify main scenarios of accident involving a pedestrian in order to better specify the primary or secondary safety systems.
The paper focus on the evaluation of the type and severity of injuries depending on the impact speed in frontal impacts of pedestrians hit by a vehicle and of the determination of the cause of the injuries (part of the vehicle or road/ infrastructure).

## METHOD

Even a large part of the road fatalities are pedestrians, there is a lack of knowledge about the mechanisms of injuries. In fact in accidents involving pedestrians, numerous clues and parameters rapidly disapear from the scene and render difficult the analysis of the accident. That explains the necessity to adapt the current methodology of in-depth accident investigation.
The in-depth accident investigation is a method to collect detailed road accident data. The latter are useful to describe the circumstances leading up to the occurrence of road accidents. Experts collect transient clues concerning many aspects of road environment (infrastructure, trafic, weather, …), vehicles and road users that may have contributed to the accident. This detailed knowledge allows to understand the determinism of the accident and to reconstruct the accident with the pre and post crash periods by a PC crash simulation. Two ways to collect data are available:
- on-the-spot in real time
- in delayed time: several days after the accidents

In-depth accident investigation is limited to a study zone where the accident analysis team has obtained all the authorizations from different organizations: national commission for computing and liberties, the prosecutor of the district: judicial authority, the police, the emergency services, the medical services, etc.

### In-depth accident investigation in real time

A key point for the accident analysis experts is to be alerted at the same time as the emergency teams in order to arrive with them on the scene to note and figure out the meaning of the transient clues. Among the latter, were the locations of the involved vehicle and of the pedestrian in CACIAUP study. This point was specifically critical because in these accidents involving a pedestrian the damaged vehicle was often moved and the emergency and medical teams had to move the injured people in order to intervene as quickly as possible.
On the scene, experts collected transient data:

- Collection of the debriefings of the involved people and the potential witnesses,
- Collection of contextual information about infrastructrure, weather etc…
- Measures of the deformations of the involved vehicles and transcription of the clues

Though most of the information was collected on the scene, experts tried to keep in contact with the involved people in hospital or at home in order to complete the interview. They were also in contact with the police and hospital services.
This valuable method allows to collect very specific and useful data but has also drawbacks. It needs to be located in a limited geographical zone so that experts have time enough to join the accident location in a minimum time before transient clues disappear. Furthermore it is expensive and time consuming.

### In-depth accident investigation in delayed time

In-depth accident investigation was sometimes carried out in delayed time. Experts were kept informed of the accidents involving a pedestrian on the investigation area. They had to collect all the information from the police and the road safety district squadron in order to get the accident location and time, accident configuration, vehicle type, name and address of the involved people. Then the investigation went further by looking for additional data. Experts went to analyze car deformations, infrastructure on the accident location. They also met the pedestrian and the driver involved in the accident in order to determine the accident conditions and the performed maneuvers before and during the accident.
This method was less efficient that the previous one on-the-spot due to the fact that transient clues were sometimes lost. It was still informative and allows to incease the number of observations.

In both cases, a physician was in charge of collecting the medical data and to anonymize them.

### CACIAUP sample

The main interest of CACIAUP sample was to have numerous parameters and the reconstruction of the accidents in most of the cases. Though very useful, in-depth accident investigations addressed rather severe accidents and did not allow to gather a representative sample. Nevertheless, when possible, it will be compared to the French national road accident data base (BAAC: Bulletin d'Analyse des Accidents Corporels) collected in 2010.

The data base was a sample of 100 in-depth investigations and reconstructions of accidents from years 2009 to 2011 involving at least one injured pedestrian hit by a vehicle. They were collected in a 20 km diameter area in the south of Paris (France) in the timeframe ranging between 6 a.m. and 9 p.m.. A pedestrian was defined as one person who was on a roadway, a sidewalk, a path contiguous with a trafic way, or on a private property [4]. The road users in roller or in scooter were not considered as pedestrians in the study. Among 100 in-depth investigations, 67 were collected on-the-spot and in real time and 33 were collected a few days after the accidents.
Every accident was described in details using general variables in three areas (vehicle, occupant, and infrastructure). Up to 800 variables usable for future studies were coded for each accident. Medical data of every injured road users has been coded using AIS code revision 98 [5]. The score MAIS (Maximum AIS) was also used. It defined the overall level of severity of the injuries and was obtained by considering the highest level of AIS of a casualty having undergone multiple lesions. All the accident cases were reviewed by an expert committee composed by physicians and accident analysis experts. For each wounded pedestrian, the injuries were reviewed in order to determine their causing mechanism taking into account the accident occurrence circonstances, the vehicle deformations and the clues on the road or infrastructure. The categorization of the wounding elements was facilitated by the accident reconstructions.

## GENERAL RESULTS:

### General information on CACIAUP sample

#### Location

Among the 100 accidents, 95 of them were located in an urban area, 4 were on roads outside towns and 1 was on an highway. It is comparable to what was observed in the BAAC: 94% of the accidents involving a pedestrian against a car or a light truck were in urban areas.

#### Weather and light conditions

81% of the accidents occurred during the day, 4% at dawn or dusk and 15% during night. This differed from the accidents observed in the BAAC with 20% of the accidents during the night. It must be reminded that the timeframe of observation did not include a part of the night (from 9 p.m. to 6 a.m.).
81% of the accidents occurred under normal atmospheric conditions, 10% during rain, 6% under overcast and 3% in bright weather. This was approximatly the same in the BAAC.

### General information on the injured pedestrians

#### Description of the population of injured pedestrians

The 100 accidents involved 110 pedestrians including 50 males and 60 females. This corresponded to the percent observed in the BAAC.
The sample was different from the BAAC with regard to age (Figure 1). 17% were children under 11 years (12% in the BAAC) and 13% of the people older than 70 years (19% in the BAAC).

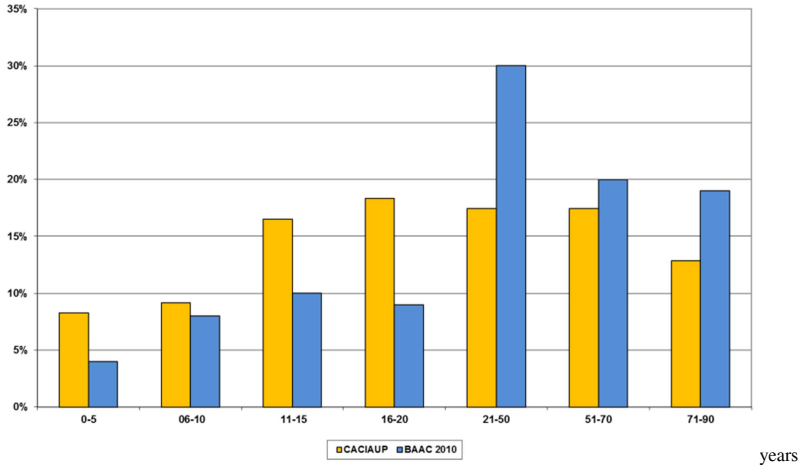


*Figure1. Distribution of age (in years) among injured pedestrians in CACIAUP compared to the BAAC*

**Injury severity**

The percent of pedestrians severely injured was similar in CACIAUP and in the BAAC (around 41%). Among them, the part of fatalities was higher in CACIAUP (14,5%) than in the BAAC (3,5%). Thus the CACIAUP sample included cases with a higher level of severity.

**Distribution by impact type**

The distribution was almost similar in CACIAUP sample and in the BAAC. In the sample, 82% of the vehicles hit the pedestrian by the frontal part, 10% by the rear part and 6% by the side part. Due to the limited size of the sample, further analysis was performed on the frontal impacts only.

## RESULTS FOR FRONTAL IMPACT:

Currently, the study focuses on the pedestrians injured in a frontal impact. In the sample, 89 pedestrians were hit by the frontal part of the vehicle. For 83 of them, it was possible to evaluate the vehicle speed during the impact.

**Distribution by accidental situations**

In-depth accident investigations have shown that the main maneuvers of the pedestrians while hit by the vehicle were the following:

- Road crossing: 56%
- Road crossing at an intersection: 27%
- Walk along the road: 7%
- Other maneuvers: 10%

To sum up, 83% of the accidents occurred while the pedestrian was crossing a road.

**Vehicle characteristics**

**Vehicle front shape**

The vehicle front shape is considered as an important factor in the determinism of the pedestrian injuries [6]. It was taken into account. Four vehicle front shapes were observed:

- the wedge shape (2%),
- the box shape (8%),
- the pontoon shape (10%)
- the trapezoidal shape (80%) that was largely the most frequent.

**Vehicle speed and projection of the pedestrian**

The speed at impact and the projection distance of the pedestrian were two main parameters that were obtained thanks to the in-depth investigations. The projection distance of the pedestrian was correlated to the speed as is shown on figure 2. The higher the speed the longer the projection distance. A few accidents occurred at a speed above 50km/h with a projection distance so high that the severe injuries could be the result of the direct impact of the vehicle and/or of the falling down. So it was decided to focus on the accidents with a speed below 50 km/h.
The mean speed at impact was 32 km/h ± 21.3.

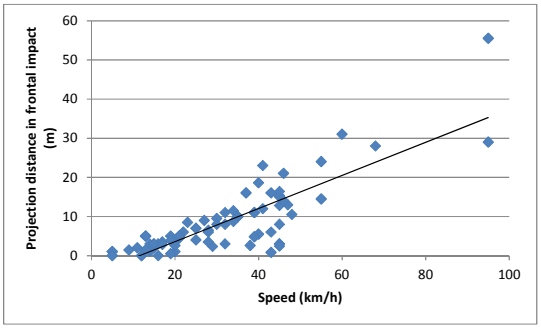


***Figure 2. Distribution of the pedestrians according to the speed and the projection distance in frontal impact.***

**Injuries of the wounded pedestrians**

87% of all the injuries , 97% of AIS2+ and 97% of AIS3+ were observed in frontal impacts.

**Injuries of the pedestrians for a speed lower than 50 km/h**

The sample of pedestrians hit by a vehicle at a speed lower than 50 km/h and for whom all the injuries were known included 71 persons. Thanks to the in-depth investigations, the wounding element was identified for 88% of the injuries. Table 1 describes the wounding elements incriminated to explain the injury AIS2+ of the different body areas.

| | Head | Upper limbs | Lower limbs | Thorax | Abdomen | Spine | Total |
|---|---|---|---|---|---|---|---|
| Ground | 19(15%) | 8 (6%) | 6 (4.5%) | 0 (0%) | 1 (1%) | 1 (1%) | **35(27.5%)** |
| Bonnet | 11 (9%) | 1 (1%) | 6(4.5%) | 7(6%) | 2 (1.5%) | 0 (0%) | **27(22%)** |
| Bumper | 2 (2%) | 0 (0%) | 12 (10%) | 1(1%) | 2 (1.5%) | 1 (1%) | **18 (15.5%)** |
| Windshield | 17(14%) | 0 (0%) | 0 (0%) | 1(1%) | 1 (1%) | 1 (1%) | **20(17%)** |
| Lower windscreen frame | 9(7%) | 0 (0%) | 0 (0%) | 0 (0%) | 0 (0%) | 0 (0%) | **9 (7%)** |
| Pilar | 5 (4%) | 0 (0%) | 0 (0%) | 0 (0%) | 0 (0%) | 0 (0%) | **5 (4%)** |
| Upper windscreen frame | 0 (0%) | 0 (0%) | 0 (0%) | 0 (0%) | 0 (0%) | 0 (0%) | **0 (0%)** |
| Front light | 0 (0%) | 1 (1%) | 1 (1%) | 3(2%) | 0 (0%) | 0 (0%) | **5 (4%)** |
| Rear view mirror | 3 (2%) | 0 (0%) | 0 (0%) | 0 (0%) | 0 (0%) | 0 (0%) | **3 (2%)** |
| Others | 0 (0%) | 0 (0%) | 1 (1%) | 0 (0%) | 0 (0%) | 0 (0%) | **1(1%)** |
| Total | **66(53%)** | **10 (8%)** | **26 (21%)** | **12(10%)** | **6 (5%)** | **3 (3%)** | **123(100%)** |

***Table 1- Distribution of the injuries AIS2+ per body area and vehicle impact part or ground – Speed ≤ 50 km/h***

The head was the most often injured (53%) and then the lower limbs (21%). Among the wounding element, the ground was incriminated in 27.5% of the cases, then the bonnet (22%), the windshield (17%) and the bumper (15.5%).

The severity of the injuries increased with the speed of impact (figure 3). 18% of the injuries were AIS3+.

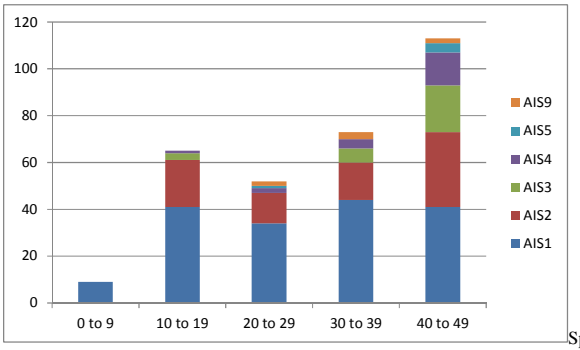


***Figure 3. Distribution of AIS according to the speed(km/h) in frontal impact (n=316 injuries).***

33% of the pedestrians were severely injured (MAIS3+). Among them, 59% had head injuries AIS3+. In about half the cases, the latter were the consequence of an impact with the windshield probably aggravated by the impact on the ground. 64% of the pedestrians were MAIS2+.
Considering the factor "age of the pedestrian", 63% of the wounded pedestrians with injuries AIS3+ were older than 51 years. Among them, 54% were older than 71 years.

**Injuries of the pedestrians for a speed lower than 30 km/h**

When the vehicle speed was below 30 km/h, still 11% of the pedestrians were severely injured (MAIS3+). In most of the cases, these severe injuries were related to the falling down. Considering now the injuries AIS2+ observed when the vehicle speed was below 30 km/h, thanks to the in-depth investigations, the wounding element was identified for 70% of the injuries. More than half of them were caused by an impact with the ground (table 2).

| | Head | Upper limbs | Lower limbs | Thorax | Abdomen | Spine | Total |
|---|---|---|---|---|---|---|---|
| Ground | 7(25%) | 3 (11%) | 4 (14%) | 0 (0%) | 1 (3.5%) | 1 (3.5%) | **16(57%)** |
| Bonnet | 1 (4%) | 0 (0%) | 1(3.5%) | 0(0%) | 0 (0%) | 0 (%) | **2(7.5%)** |
| Bumper | 0 (0%) | 0 (0%) | 3 (11%) | 0(0%) | 0 (0%) | 1 (3%) | **4 (14.5%)** |
| Windshield | 4(14%) | 0 (0%) | 0 (0%) | 0(0%) | 0 (0%) | 0 (0%) | **4 (14%)** |
| Lower windscreen frame | 0 (0%) | 0 (0%) | 0 (0%) | 0 (0%) | 0 (0%) | 0 (0%) | **0 (0%)** |
| Pilar | 0 (0%) | 0 (0%) | 0 (0%) | 0 (0%) | 0 (0%) | 0 (0%) | **0 (0%)** |
| Upper windscreen frame | 0 (0%) | 0 (0%) | 0 (0%) | 0 (0%) | 0 (0%) | 0 (0%) | **0 (0%)** |
| Front light | 0 (0%) | 1 (3.5%) | 0 (0%) | 0(0%) | 0 (0%) | 0 (0%) | **1 (3.5%)** |
| Rear view mirror | 0 (0%) | 0 (0%) | 0 (0%) | 0 (0%) | 0 (0%) | 0 (0%) | **0 (0%)** |
| Others | 0 (0%) | 0 (0%) | 1 (3.5%) | 0 (0%) | 0 (0%) | 0 (0%) | **1(3.5%)** |
| Total | **12(43%)** | **4 (14.5%)** | **9 (32%)** | **0(0%)** | **1 (3.5%)** | **2 (7%)** | **28(100%)** |

***Table 2- Distribution of the injuries AIS2+ per body area and vehicle impact part or ground – Speed ≤ 30 km/h***

The head was the most often injured (43%), then the lower limbs (32%) and the upper limbs (14.5%). Among the wounding element, the ground was incriminated in 57% of the cases, then the bumper (14.5%), the windshield (14%) and the bonnet(7.5%). 64% of the pedestrians were MAIS2+.
Considering the factor "age of the pedestrian", 30% of the wounded pedestrians with injuries AIS2+ were older than 51 years. Among them, 75% were older than 71 years.

## DISCUSSION

Though CACIAUP sample was not representative of the population of pedestrians injured on the French roads, the in-depth investigations were useful to study the determinism of the injuries. For each injury, the causing mechanisms were discussed among the accident experts and the physicians in order to take into account the entire course of the accident and not only the direct impact by the vehicle. The share of all the information about the accidents and their reconstructions enabled to perform this complex task. The final positions of both the vehicle and the pedestrian were so important for an accurate analysis, that the project had asked to the police to mark these positions when they arrived on the spot. Thus, it was possible to obtain the projection distance for the in-depth investigations either in real time or in delayed time. The results showed that the impact speed and the projection distance were correlated although there was a high variation among the different cases. Sometimes, pedestrians hit different obstacles in the infrastructure which reduced the projection distance but often led to severe injuries. The regression curve shows that the higher the speed the longer the projection distance. For speed close to 50 km/h, it could reach more that 20 m. Such distances imply a high risk of injuries during the falling down or at least a risk to worsen the initial injuries due to the direct car impacts.

Most of the CACIAUP results were in accordance with previous studies. The role of the vehicle speed has already been described. Rosen and Sander (2009) have shown a strong relation between the fatality risk and the car impact speed [7]. The circumstances of the accident have been described with a large majority of pedestrians crossing roadway [8] as was found in CACIAUP. However, previous studies found that pedestrians were coded to be not as frequently and severely injured by the ground during vehicle-to-pedestrian crashes [4].
Looking at the two tables describing the distribution of the injuries AIS2+ per body areas and per wounding impact elements, more than a quarter of the injuries were due to ground/infrastructure impacts for speeds below 50 km/h, and more than half of the injuries were due to ground/infrastruture impacts for speeds below 30 km/h. In many studies, these injuries were often underestimated or all injuries were often related by excess to the direct car impacts. The high percent of injuries aggravated or due to the falling down imply that they have to be taken into account. Secondary safety systems have no efficiency on these injuries. They have a limited efficiency on the occurrence of lesions: 1) concerning those related to the direct vehicle impact, secondary safety systems could not impede the abnormal movements of body segments with each other, 2) during the impact, the kinematic energy related to the velocity is transmitted to the pedestrian that is projected to a more or less longer distance. The projection distance increases rapidly with the speed and these systems have no protective effects on the lesions provoked by the falling out. Given the important role of the speed on both direct injuries and secondary injuries due to the falling down or the impact against infrastructure, the priority is to reduce the impact speed. Several solutions could be proposed. First of all, as it is a problem of interaction among the different road users, each of them have rules to respect in order to avoid dangerous conflicts. Especially in urban areas, speed limits help the drivers to adapt their speed to the context of the road and the presence of pedestrians. Primary safety systems could also help the drivers when there is a failure of perception or attention. The advanced emergency braking systems (AEBS) could be very relevant because they avoid contact with the pedestrian or reduce the impact speed if they can not prevent contact. In the latter cases, the resulting reduction of the impact speed decreases the severity of the injuries due to direct vehicle contact and also decreases those due to the falling down because the projection distance is reduced. At low speed, it could be vital for elderly people to avoid the contact as they can be seriously injured only by falling from their height without any injuries due to the vehicle. In CACIAUP, this point especially affects the population of pedestrians over 71.

## CONCLUSION

The vehicle speed was the major factor in the determinism of the injury severity of pedestrians involved in frontal impact, firstly by direct impact secondly by increasing the projection distance and thus the severity of injuries due to secondary impacts. CACIAUP results have showed a high number of the injuries due to the ground impact or aggravated by the falling down. Secondary safety has limited effects to protect the pedestrians due to the fact that it does not limit or impede the projection of the pedestrian when hit. Primary safety systems should more efficiently reduce the severity of pedestrian injuries by decreasing the impact speed. In that way, they decrease the energy of the direct impact and the projection distance and thus the severity of the injuries due to all the wounding elements in secondary impacts.

## ACKNOWLEDGEMENTS

The authors would like to acknowledge the “Fondation Sécurité Routière (FSR)” for its support during the project and the experts from CEESAR who collected the accident data.

## REFERENCES

[1] World health organization. 2013. “Global status report on road safety 2013”
[2] European Commission (2014). Fatalities at 30 days in EU countries. Source CARE.
[3] Observatoire National Interministériel de la Sécurité Routière (ONISR) (2015). L’accidentalité routière en 2014. Bilan sommaire (estimation janvier 2015)
[4] Zhang G.; Cao L.; Hu J. and Yang K.H. (2008). A field data analysis of risk factors affecting the injury risks in vehicle-to-pedestrian crashes. 52nd AAAM Annual Conference. Annals of Advances in Automotive Medicine.
[5] The Abbreviated Injury Scale – AIS, version 98

[6] Searle J.A. and Searle A. (1983). The trajectories of pedestrians, motorcycles, motocyclists, etc. Following a road accident. SAE Technical paper 831622.
[7] Rosen E. and Sander U. (2009). Pedestrian fatality risk as a function of car impact speed. Accid. Anal. and Prev. vol41. 536-42.
[8] Harruff R.C., Avery A. and Alter-Pandya A.S. (1998). Analysis of circumstances and injuries in 217 predestrian traffic fatalities. Accid. Anal. and Prev. vol30. 11-20.

# MATCHING STRUCTURAL INJURY RISK STATISTICS AND DUMMY INJURY MEASURES FOR A DYNAMIC ROLLOVER RATING AND REGULATORY COMPLIANCE TEST

**Donald Friedman**
Center for Injury Research
United States

**Josh Jimenez**
Consultant
United States

Paper Number 15-0085

**ABSTRACT**

A study was conducted on five different vehicles. Each vehicle was dynamically rollover tested using similar rollover test parameters. The study was performed to examine the major factors in a rollover that match structural injury risk to injury measures for occupants that were neither ejected nor partially ejected.

## RESEARCH OBJECTIVES

Identify major factors in a rollover that match structural injury risk to injury measures for occupants that were neither ejected nor partially ejected.

## INTRODUCTION

In recent years, efforts have been underway to develop a global full-scale dynamic rollover regulatory compliance test with instrumented anthropomorphic dummies. Compliance in this test is a function of both vehicle structural and dummy responses. In 2009, NHTSA amended the strength to weight ratio (SWR) requirement by increasing the criteria from 1.5 to 3.0 in the quasi-static FMVSS 216 Roof Crush compliance test. NHTSA also initiated research on a dynamic rollover compliance test. NHTSA pointed out that a regulatory compliance test be based on dummy injury measures and criteria that match the structural injury risk and criteria. Establishing the relationship between a vehicles structural performance and dummy injury measures became a primary objective of the (C*f*IR) Center for Injury Research recent research.

Until 2002 no direct measures of occupant responses and no data upon which to evaluate primary and supplemental restraint systems in a rollover environment have been available with the exception of virtual dummies. Virtual dummies are limited in that they cannot emulate the variable stiffness of human reactions over 0.9 seconds. A dynamic rollover test protocol can be used to determine the dummy kinematics in a rollover to better understand the relationship between the roof and occupant at the time of roof impact. Furthermore, the effectiveness of lap and shoulder belts in a rollover can be analyzed.

NHTSA has identified residual roof crush as the most important factor for determining structural injury risk in a rollover after an accident has occurred. Residual crush is the only data available to an investigator after a rollover accident. A specific injury is usually the result of a single impact not the result of a sequence of impacts. Dummy injury measures in a dynamic test can provide the time history of roof crush and crush speed. Structural injury risk, as used here, is a statistical term relating structural performance in terms of crush to the probability of human real-world injury. The probability of human real-world injury, or injury risk, could be defined with other factors as well.

Structural injury risk statistics were obtained from NHTSA's NASS (National Automotive Sampling System) and CIREN (Crash Injury Research) data. The data was then used to derive the "structural injury risk" criteria for the proposed compliance test. The probability of injury for a belted occupant is based on residual roof crush as well as the dynamic speed of roof crush. This means that for the same amount of roof intrusion the injury risk can be much higher for a scenario where the roof intrusion speed is high versus a lower intrusion speed. A NASS/CIREN statistical analysis of more than 20,000 model year 1993 to 2007 vehicles identified that the probability of injury is a function of maximum residual crush at the front seat occupant position as shown in Figure 1 by Mandell, et al. [1]. A rollover regulatory or NCAP injury measure system should match structural injury risk criteria with the predominant head, neck, and thorax injuries. The real-world rollover crash data files suggested that quadriplegia and paraplegia were consequences of lower neck bending injuries (bilateral locked

facets), while death was usually attributed to head injury, upper neck cord damage affecting pulmonary and circulatory functions at C1 to C3, and/or thorax injury.

Mortality (95% CI).

| Roof crush | Probability | Weighted probability | Unadjusted odds | Adjusted odds[a] | Conditional odds[b] (hazard ratio) |
|---|---|---|---|---|---|
| 0–3 cm | 3.41% | 0.38% | 1.0 | 1.0 | 1.0 |
| 3–8 cm | 2.03% | 0.35% | 0.588 (0.354, 0.977) | 0.606 (0.362, 1.013) | 0.577 (0.345, 0.963) |
| 8–15 cm | 2.64% | 0.28% | 0.769 (0.485, 1.218) | 0.794 (0.497, 1.268) | 0.759 (0.476, 1.210) |
| 15–30 cm | 6.86% | 1.63% | 2.089 (1.461, 2.987) | 2.452 (1.684, 3.569) | 2.253 (1.554, 3.267) |
| ≥30 cm | 18.18% | 3.08% | 6.301 (4.369, 9.087) | 7.241 (4.895, 10.710) | 6.548 (4.444, 9.647) |

[a] Adjustment was done on (conditioning variables for adjusted logistic regression) age + age-squared, front seat v. rear seat, left seat v. right seat, gender.
[b] Conditional models were matched on body type (Auto, SUV, Truck, Van/Minivan), # rolls (2–3, 4–5, 6+ or lateral), curb weight (<> mean 1490 kg), rollover as primary event.

Spine Injury AIS ≥ 3 (95% CI).

| Roof crush | Probability | Weighted probability | Unadjusted odds | Adjusted odds[a] | Conditional odds[b] (hazard ratio) |
|---|---|---|---|---|---|
| 0–3 cm | 1.96% | 0.46% | 1.0 | 1.0 | 1.0 |
| 3–8 cm | 1.92% | 0.37% | 0.978 (0.566, 1.690) | 0.958 (0.551, 1.665) | 0.935 (0.538, 1.624) |
| 8–15 cm | 3.79% | 0.94% | 1.968 (1.273, 3.043) | 1.883 (1.206, 2.940) | 1.838 (1.179, 2.865) |
| 15–30 cm | 4.82% | 1.38% | 2.530 (1.634, 3.917) | 2.341 (1.474, 3.718) | 2.343 (1.480, 3.708) |
| ≥30 cm | 5.09% | 1.01% | 2.682 (1.474, 4.877) | 2.690 (1.452, 4.983) | 2.588 (1.399, 4.789) |

[a] Adjustment was done on (conditioning variables for adjusted logistic regression) age + age-squared, front seat v. rear seat, left seat v. right seat, gender.
[b] Conditional models were matched on body type (Auto, SUV, Truck, Van/Minivan), # rolls (2–3, 4–5, 6+ or lateral), curb weight (<> mean 1490 kg), rollover as primary event.

Spinal cord injury (95% CI).

| Roof crush | Probability | Weighted probability | Unadjusted odds | Adjusted odds[a] | Conditional odds[b] (hazard ratio) |
|---|---|---|---|---|---|
| 0–3 cm | 0.62% | 0.06% | 1.0 | 1.0 | 1.0 |
| 3–8 cm | 0.56% | 0.09% | 0.911 (0.337, 2.460) | 0.868 (0.320, 2.355) | 0.854 (0.315, 2.315) |
| 8–15 cm | 0.69% | 0.19% | 1.113 (0.440, 2.812) | 1.083 (0.425, 2.760) | 1.071 (0.421, 2.724) |
| 15–30 cm | 1.90% | 0.56% | 3.104 (1.513, 6.366) | 3.062 (1.457, 6.439) | 3.195 (1.529, 6.673) |
| ≥30 cm | 2.18% | 0.26% | 3.579 (1.409, 9.092) | 3.483 (1.338, 9.067) | 3.434 (1.324, 8.906) |

[a] Adjustment was done on (conditioning variables for adjusted logistic regression) age + age-squared, front seat v. rear seat, left seat v. right seat, gender.
[b] Conditional models were matched on body type (Auto, SUV, Truck, Van/Minivan), # rolls (2–3, 4–5, 6+ or lateral), curb weight (<> mean 1490 kg), rollover as primary event.

Head injury AIS ≥ 3 (95% CI).

| Roof crush | Probability | Weighted probability | Unadjusted odds | Adjusted odds[a] | Conditional odds[b] (hazard ratio) |
|---|---|---|---|---|---|
| 0–3 cm | 3.82% | 0.76% | 1.0 | 1.0 | 1.0 |
| 3–8 cm | 2.26% | 0.84% | 0.582 (0.359, 0.942) | 0.603 (0.371, 0.981) | 0.580 (0.357, 0.942) |
| 8–15 cm | 4.25% | 0.77% | 1.117 (0.764, 1.634) | 1.188 (0.807, 1.749) | 1.136 (0.773, 1.669) |
| 15–30 cm | 5.69% | 1.05% | 1.520 (1.045, 2.211) | 1.678 (1.135, 2.480) | 1.545 (1.049, 2.277) |
| ≥30 cm | 12.73% | 2.11% | 3.672 (2.456, 5.490) | 4.088 (2.692, 6.209) | 3.694 (2.442, 5.588) |

[a] Adjustment was done on (conditioning variables for adjusted logistic regression) age + age-squared, front seat v. rear seat, left seat v. right seat, gender.
[b] Conditional models were matched on body type (Auto, SUV, Truck, Van/Minivan), # rolls (2–3, 4–5, 6+ or lateral), curb weight (<> mean 1490 kg), rollover as primary event.

***Figure 1.*** *NASS/CIREN statistical analysis.*

Precrash headroom, the effect dynamic intrusion has on headroom, and belt forces were identified as major factors that can be used for determining neck and head injuries in rollovers. Using a hybrid III, dummy lap and shoulder belt forces measured in a dynamic rollover test can be used to reasonably determine dummy motion and the amount of headroom loss for a specific vehicle.

Computer simulations of dummies with tensed and untensed necks, human volunteer drop testing from 12 to 36 inches [2], and comparative tests between dummies and humans determined that to better match human characteristcs in flexion the dummy neck should be 1/3 as stiff as the production Hybrid III neck and inclined at 30 degrees to the torso [3]. The ultimate value of a dynamic test is to not only assess structural injury risk such as intrusion, but also dummy injury criteria measured from transducers mounted in a reasonably-humanlike anthropometric test device. At present, most laboratories and finite element models utilize the Hybrid III dummy as the human surrogate. The Hybrid III dummy was modified with a low-durometer neck oriented in 30º pre-flexion and instrumented with a six-axis lower neck load cell. The IBM bending criteria was derived from the lower neck My and Mx momentum exchange, and the IHA was derived from the dummy head impact speed and displacement.

A match between roof intrusion measures and dummy injury measures was identified in the five dynamic rollover tests using five different vehicles. The study determined that when the lap and shoulder belt forces were high the belts were effective in minimizing the dummy's motion towards the roof. When occupant motion towards the roof in a rollover, or diving, and low structural injury risk existed (low intrusion and low intrusion speed) the dummy injury measures were small. However, when high structural injury risk existed the reduction in the dummy diving motion was not sufficient to minimize dummy injury risk.

## METHODS

Two generations of a mechanical rollover fixture called the Jordan Rollover System (JRS) were built and installed at C*f*IR, UVA (NHTSA), and UNSW. Over 50 vehicles have been evaluated for injury risk as defined by residual roof crush and crush speed using the JRS. The JRS rollover test protocol is used to examine the crash segment of a rollover that is further explained in ESV 11-0405 paper [4]. Moreover, it is used to assess what happens in a rollover crash after the vehicle begins to roll and two or more wheels of the vehicle have left the ground. Determining the factors such as vehicle handling and stability are assessed using other test methods.

Every rollover crash can be broken down into segments as defined by roll angle to evaluate the kinematics of a dummy/occupant. As a result the segment of the rollover crash with the greatest-injury potential was identified. The process of identifying the most serious injury potential required evaluating the injury potential sensitivity of each segment and its influence on the following segment. A real-world dynamic rollover test protocol should represent the injury consequences of FMVSS 216 and 226 compliant vehicles. This means that the injury criteria used in the protocol is not related to unbelted occupants or occupants that are partially ejected in a rollover. The test protocol is defined by road speed and roll rate to a 1-roll event at 33.6 kph (21 mph), 280°/sec roll rate, 10° of pitch, 145° contact angle and a drop height of 10 to 15 cm (4 to 6 inches) (See Table 1). The methodology for the development of the test protocol in Table 1 is explained in detail in ICrash paper ICR-14-33.

**Table 1.**
**The proposed real-world rollover protocol**

| |
|---|
| Impact Road speed 33.8 kph (21 mph) ± 1.6 kph (1 mph) |
| Roll rate @ near-side impact 270°/sec ± 10% |
| Pitch 10° ± 2° |
| Roll angle at impact 145° ± 5° |
| Drop height 10 cm ± 2 cm (3 to 4.5 inches ) |
| Yaw angle 10° ± 1° |
| Dummy initially tethered @ 1 g and 60° toward the nearside |

Consensus injury measures at 8 mph developed by McElhaney [5] and combined by Paver [6] are shown in Figure 2. The map of the injury measures was submitted to NHTSA in 2008. It describes the combination of an impact speed and head displacement and establishes areas of AIS values. The first integration over 60 ms of the resultant head acceleration represents the head velocity and the double integration represents the head displacement. The product of head velocity and displacement is the integrated head acceleration (IHA). For AIS 3+, the product of a 13 kph (8 mph) head impact velocity and a 15 cm (6 inches) head displacement yields an IHA criteria of 48. The only consensus injury measures were roof crush and roof crush speed based on criteria developed by McElhaney [6].

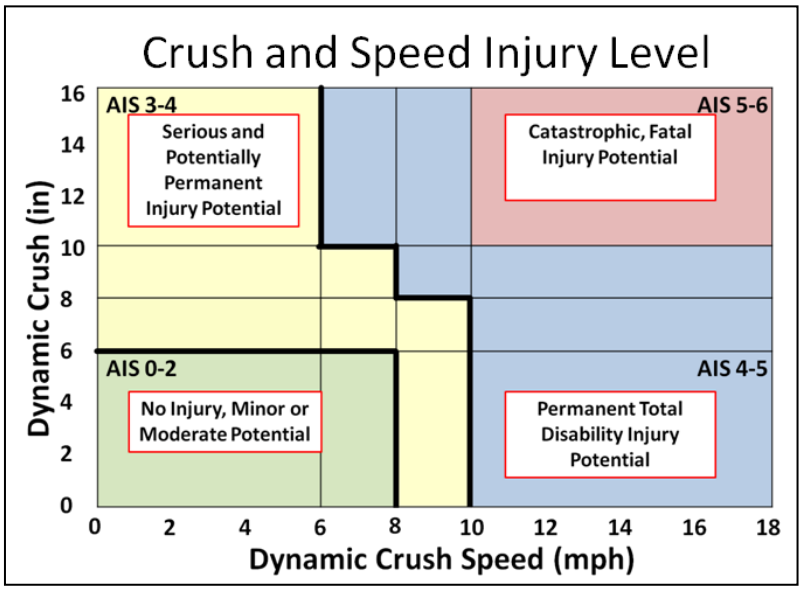


***Figure 2.*** *Dynamic crush and crush speed in relation to AIS injury levels.*

The dummy injury measure representing the momentum exchange between roof contact and neck flexion, called the IBM, was derived by integrating the resultant of Mx and My lower neck bending moments. Correlating results with residual crush values defined as injurious yielded the criteria as 13.5.

An example of an injury risk relationship was demonstrated by the IIHS analysis of the effect of SWR vs. injury rate. In 2008, C*f*IR compared the results of 21 JRS tests to IIHS statistical structural injury risk data which showed a substantial benefit from increased roof SWR [7]. NHTSA statistical analysis indicated that, when roof crush exceeded headroom, injury was five times more likely [8-9]. Moreover, the data indicated that the probability of death and serious-to-fatal head, spine, and spinal cord injury to belted occupants increases rapidly with cumulative vertical residual crush over the front occupant's seating position.

Since the real-world protocol described in Table 1 involves a 21 mph 10º pitch protocol, C*f*IR used a normalization procedure previously published [10] to represent most vehicles tested. The normalization procedure predicts the amount of residual crush based on SWR when a vehicle is tested using the real-world protocol. Validation of the normalization procedure is shown by the two bars corresponding to the 1999 Hyundai Sonata marked with an "x" as shown in Figure 3. One bar is the normalized value and the other bar is the JRS test result using the real-world protocol with less than a 10% error. The demonstration characterizes the probability of structural injury risk resulting from the proposed dynamic rollover test.

Vehicles with "acceptable" compliance have less than 6 inches of residual crush (and corresponding dummy injury measures). The colour bands identify the rating system. Although many vehicles tested would rate "poor" none were unacceptable. The chart is normalized to the 1st roll of a 2 Roll rollover representing 95% of all rollovers and AIS 3+ rollovers. Vehicles with residual crush less than 3.5 inches would be read "good", vehicles with residual crush up to 6 would be rated "acceptable", vehicles with residual crush between 6 and 12 inches would be rated "poor", and vehicles with residual crush more than 12 inches would be rated "unacceptable".

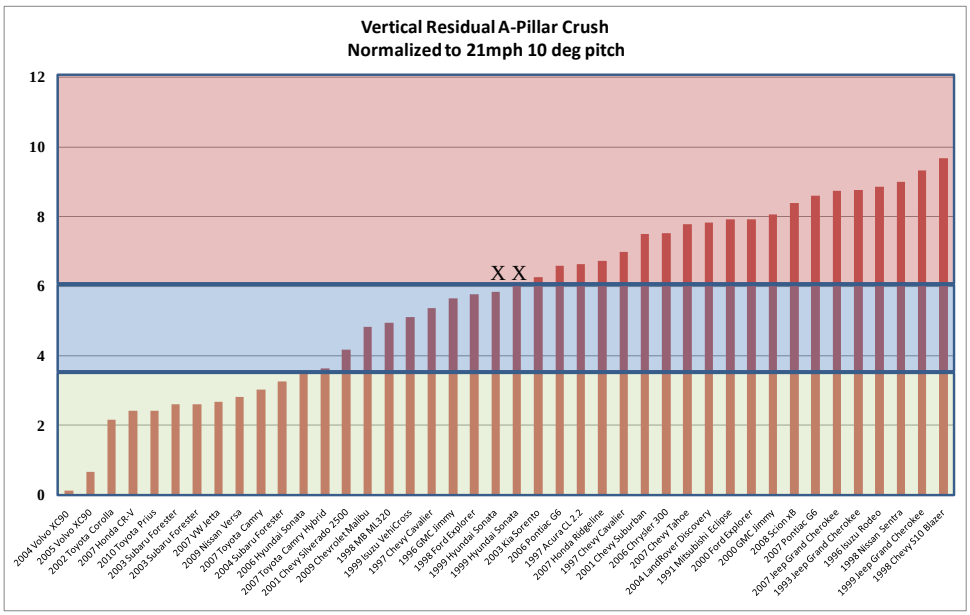


***Figure 3.*** *Normalized vertical residual A-pillar crush for various vehicles.*

**RESULTS**

There were five tests conducted using a "low-severity" protocol. The low-severity protocol differed from the proposed real-world protocol (Table 1) in that the translational speed was 15 mph versus 21 mph and the pitch angle was 5º pitch versus 10º. The structural injury risk relative to dummy injury criteria was matched in Figure 4. Based on a hybrid III dummy configured with a soft neck angled at 30 degrees, the dummy injury measures were found to be a function of headroom and belt loading. Dummy configuration was the same for each vehicle test.

The six bars in the figure from left to right represent corrected residual crush, dynamic injury risk, peak lower neck axial compression, peak lower neck flexion moment, the IBM, and the IHA.

- The royal blue (corrected from the string pot angle) and red (dynamic injury risk) bars represent residual roof crush and roof crush speed. Based on the structural injury criteria as defined by NASS/CIREN data the percentage probability of a AIS 3+ structural injury risk is 100 percent of Critical Value.

- The olive (peak axial lower neck compression) and purple (peak lower neck flexion moment) bars represent the percentage probability of AIS 3+ injury for traditional Injury Assessment Reference Values (IARV). Traditional IARV measures and criteria applicable to frontal and side impacts substantially underestimate rollover injury potential as result of the dummy stiffness being attuned to crash modes other than rollover.

- The turquoise (IBM) and orange (IHA) bars represent the percentage probability of AIS 3+ injury in a rollover crash.

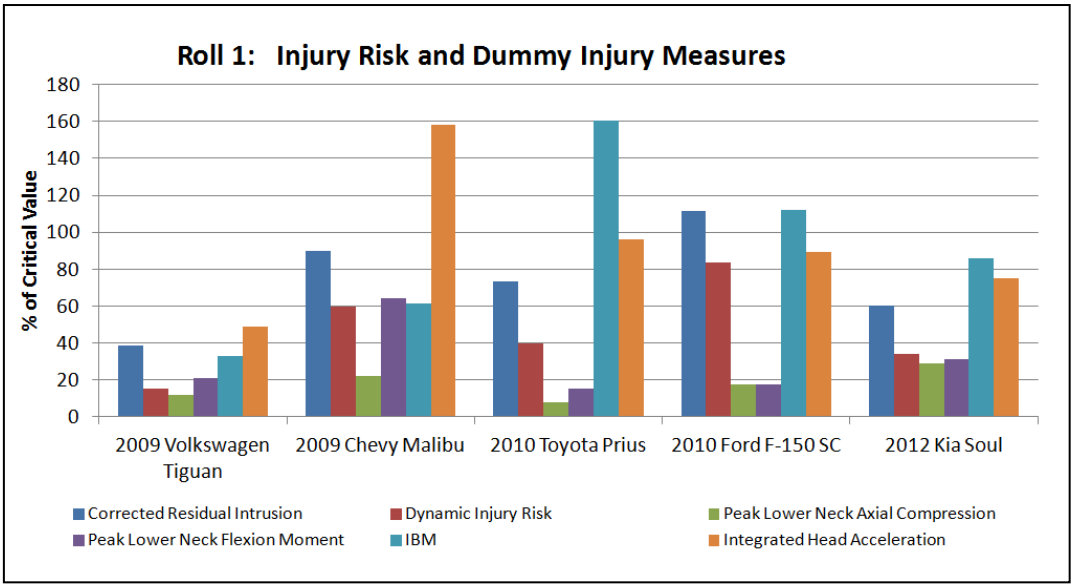


***Figure 4.*** *Structural injury risk and dummy injury measures of five production vehicles.*

The 2009 Volkswagen Tiguan precrash headroom measured from the header was approximately 5 inches using the dummy configuration described earlier. The dynamic speed of intrusion is only 18% of structural injury criteria and the headroom was reduced to approximately zero during the rollover crash test. The peak lap belt force was 247 pounds and the shoulder belt force was 250 pounds. The peak lap and shoulder belt forces occurred during the roll segment that spanned from 180 degrees (completely inverted) through the far side impact roof crush.

The 2009 Chevrolet Malibu precrash headroom measured from the header was approximately 6 inches. The Malibu residual intrusion is 90% of the structural injury risk criteria. The bending moment is consistent with the roof intrusion. However, the IHA is more than twice the dynamic intrusion speed and as a result of this was over 150% of the critical value. The peak lap belt force was 245 pounds and the shoulder belt force was 171 pounds. The lap and shoulder belt provided the dummy with adequate resistance to falling immediately before and at the time of the far side impact. The test video shows the collapse at the top of the A-Pillar to be timed with the dummy's rotation about the seat due to gravitational forces. No dummy motion in the direction of the vehicle's z-axis was observed.

The 2010 Toyota Prius precrash headroom measured from the header was approximately 4 inches. In terms of structural injury risk the 2010 Toyota Prius measured slightly less than the Malibu. However, for the Malibu the

IBM is more than twice its residual intrusion and dynamic speed. The peak lap belt force was 207 pounds and the shoulder belt force was 401 pounds. The shoulder belt force diminished quickly at the time of peak intrusion.

The 2010 Ford F150 precrash headroom measured from the header was approximately 10 inches. The F150 exhibits residual crush and dynamic intrusion speed at the critical limit of the structural injury measures. The peak lap belt force was 246 pounds and the shoulder belt force was 597 pounds. The shoulder belt force diminished at the onset of the far side impact. Although the headroom for this vehicle is much higher than the other four, the structural injury measures are high enough to affect the dummy injury measures.

The 2012 Kia Soul precrash headroom measured from the header was approximately 5 inches. Although the dummy did contact the roof intrusion and intrusion speed was so low that the dummy injury measures remained below the critical injury values. The peak lap belt force was 387 pounds and the shoulder belt force was 261 pounds.

## DISCUSSION AND LIMITATIONS

Precrash headroom for each vehicle is slightly higher than a typical seated $50^{th}$ percentile human because of the 30 degree soft neck angle used as an initial condition for the start of the rollover segment. The soft neck response to the dynamic forces involved in the rollover crash proved that the initial condition did not produce a negative effect on the test. Because the neck was able to respond quickly the dummy head position moved in the direction of the applied external forces. This meant that when the roof loading imparted an acceleration on the dummy and belts responded in the opposite direction the unrestrained head would move towards the roof as to be expected in a rollover.

The Tiguan showed correlation between relatively low residual crush and dynamic intrusion speed relative to dummy injury criteria. The values relative to criteria are so low that this vehicle is very safe in a rollover compared to the other four vehicles. Furthermore, the dynamic test validated the use of the lap and shoulder belts during the rollover. Because the belt provided the dummy with the necessary resistance to falling and the dynamic roof crush was minimal the magnitude of the impact with the header was minimized.

The Malibu vehicle as tested indicates a low force to the shoulder belt relative to other vehicles. In combination with a residual roof intrusion equal to 90% of the critical limit this allowed the upper torso of the dummy to rotate about the seat more rapidly and thus resulting in a high risk of serious head injury.

The Toyota Prius as a result of limited head room is very likely to result in a hyperflexion neck injury whenever the structural injury measures are close to the critical value. The small amount of headroom meant that the residual roof intrusion measure is more critical for the Toyota Prius to perform in terms of structural injury measures.

The Kia Soul has a little more than 5 inches of head room. With respect to the critical values, the residual intrusion and dynamic intrusion speed are not significally different from IBM and IHA measures. The peak lap belt force was 387 pounds and the shoulder belt force was 261 pounds. The belt forces diminished at the time of the far side impact indicating the roof was intruding on the occupant. The residual intrusion, IBM, and IHA support this finding. Because the intrusion measures were not exceeding the critical limit the IBM and IHA were also below the limit. The rollover test performed on the Kia Soul showed the vehicle to perform reasonably.

The F-150 has approximately 10 inches of headroom which is roughly 5 inches more than any of the other vehicles. The dummy injury measures match the structural injury risk measures. Furthermore, the structural injury criteria is near 100%. The peak lap belt force was 246 pounds and the shoulder belt force was 597 pounds. However, the belt forces diminished at the time of the far side impact indicating the roof was intruding on the occupant. The residual intrusion, IBM, and IHA support this finding. Figure 5 illustrates the percent of structural and dummy injury criteria for a 2010 Ford F150 pickup in a rollover [11].

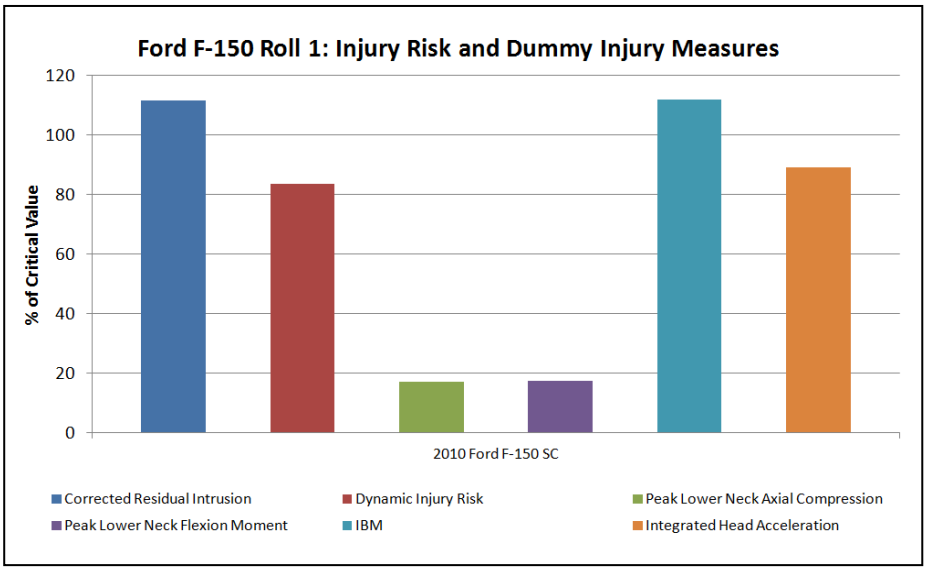


***Figure 5.*** *Structural injury risk and dummy injury measures for the 2010 Ford F-150.*

There is a good match between structural and dummy injury measures which suggests that the vehicle is not safe. In a more severe rollover where the translational speed is 20 mph as opposed to 15 mph, the residual intrusion and dummy injury measures would well exceed criteria.

## CONCLUSIONS

The five vehicle tests were conducted using a 24.1 kph (15 mph) translational speed, 190°/sec roll rate, and 5° of pitch. Studies of the vehicle trajectory preceding a near-side roll indicate that the far-side occupant experiences pre-trip yaw and trip accelerations of 0.7 to 1 G towards the near side. Experiments with human occupants and Madymo modelling (as part of the Far-Side Project) indicated that the subject leans to the nearside seat or center console so far that it is out of the shoulder belt [12]. Because of the occupant kinematics in a rollover lap belts need to be respond quickly to maintain the occupant seating position in a rollover. However, the loading associated with the lap belt can be excessive and therefore the best solution is one that maintains the occupant in its seating position by using both the shoulder and lap belt throughout the rollover segment. This can only be assessed using a dynamic test.

The JRS vehicle rollover dynamic testing apparatus has identified the 2010 Ford F150 as one of the vehicles which meets the most rigorous static roof strength criteria (SWR of 4 or greater) but fails to provide occupant protection from injury risk in a rollover consisting of more than one quarter turn. Results of JRS testing using a low-severity dynamic test protocol revealed it was possible for the side glazing to break causing a potential ejection portal in good SWR vehicles.

Because residual crush is measured post crash the factors that cause residual crush should be determined to better understand dynamic performance. Residual crush is found to be a function of vehicle strength to weight ratio, roof structure elasticity, and other geometric considerations [9]. When executing the IIHS roof strength protocol using a FMVSS 216 a roof crush test apparatus the elasticity of the roof structure can be measured as a second part of the roof crush test. The measurement would be added to the existing IIHS roof strength rating by measuring load and displacement (using the 13mm/sec speed) as the ram reverses direction until the load reading approached some number close to zero. This displacement value would then represent the elasticity of the roof structure.

An elasticity correction is necessary for better correlation of field data related to rollover injuries of late model vehicles with strong roofs. This is because the intrusion criteria was developed using earlier model vehicles with less elasticity. The NASS-CIREN files (Mandel probability of injury charts) are based on fleet average vehicles of the 90's with SWR's of about two and an elasticity of about 30%. Post 2005 vehicles have SWR's greater than four and an elasticity of 60%. Elasticity is a function of roof structure elements being less deformed as a result of a stronger roof structure.

A vehicle that can provide protection for its occupants in a rollover should be defined by a dynamic rollover test that is based on both structural and dummy injury measures. By using a dynamic test procedure roof strength, effectiveness of primary and supplemental restraints, and the effect interior components have on an occupant in a rollover can all be measured. Historically rollover regulations have been less rigorous than frontal and side crashworthiness regulations. However, rollovers have the highest percentage of fatalities and make up 30 percent of all deaths associated with vehicle crashes inside the U.S.

Similar to the existing US regulatory side impact test FMVSS 214 the rollover compliance test regulation would be a two part test. The first part would assess the static structural performance of the roof structure. The second part would require validation in the form of a dynamic test of the performance of the roof structure, restraints, and occupant compartment interior in order to reduce the probability of an injury in a rollover. The proposed real-world rollover protocol outlined in Table 1 is associated with the most common serious injury rollovers and is explained in further detail in ICrash paper ICR-14-33.

The dynamic tests performed on the five vehicles outlined above shows the importance of validating the roof structure and seatbelt performance in a dynamic test environment. Furthermore, using only the static roof strength test and strength to weight ratio can be limiting when considering the relationship between headroom and dynamic performance of the roof structure are not taken into account. Rollover crash safety measures outlined in this paper can be expanded on by using a dynamic test for development primary restraints and roll activated side curtain airbags with respect to near side occupants.

---

**REFERENCES**


[1] Mandell, S., R. Kaufman, C.D. Mack, E.M. Bulger. 2010. “Mortality and Injury Patterns Associated with Roof Crush in Rollover Crashes.” Accident Analysis and Prevention, 2010, 10.1016/j.aap.2010.02.013.
[2] Friedman, K., G. Gaston, J. Bish, D. Friedman, A. Sances, Jr., 2000. "An Investigation of Hybrid III and Living Human Drop Tests," Biomedical Engineering, 28(1&2):219-223.
[3] Echemendia, C., “Modeling Neck Compression in Rollovers,” George Washington University Report, http://www.ncac.gwu.edu, 2009.
[4] D. Friedman, G. Mattos, J. Paver, 2011., "The Development of a Dynamic Rollover Rating Test," 22nd Enhanced Safety of Vehicles Conference, Washington, DC.
[5] J McElhaney, R Snyder, J States, M A Gabrielsen, ‘Biomechanical Analysis of Swimming Pool Neck Injuries’, Society of Automotive Engineers, Inc., 1979.
[6] J G Paver, D Friedman, J A Jimenez, 2013. "Correlating Human and Flexible Dummy Head-Neck Injury Performance", Proceedings of the 23rd International Technical Conference on Enhanced Safety of Vehicles, Seoul, Korea, http://www.nhtsa.gov/ESV.
[7] Brumbelow, M. et. al., 2008. “Roof Strength and Injury Risk in Rollover Crashes.” Insurance Institute for Highway Safety. March 2008.
[8] A Strashny, 2007. "The Role of Vertical Roof Intrusion and Post-Crash Headroom in Predicting Roof Contact Injuries to the Head, Neck, or Face During FMVSS No. 216 Rollovers: An Updated Analysis", NHTSA Technical Report DOT HS 810 847.
[9] R Austin, M Hicks, S Summers, "The Role of Post-Crash Headroom in Predicting Roof Contact Injuries to the Head, Neck or Face During FMVSS No. 216 Rollovers", NHTSA.
[10] D Friedman, J A Jimenez, J G Paver, 2013. "Predicting a Vehicle's Dynamic Rollover Injury Potential from Static Measurements", Proceedings of the 23rd International Technical Conference on Enhanced Safety of Vehicles, Seoul, Korea, http://www.nhtsa.gov.my/ESV.
[11] Center for Injury Research JRS Dynamic Rollover Test for 2010 Ford F-150 Supercab, April 2010.
[12] C C Ward, H Der Avanessian, P Ward, J G Paver JG, 2001.“Investigation of Restraint Function on Male and Female Occupants in Rollover Events,” SAE Paper #01B-109, International Congress and Exposition.

This paper has been peer-reviewed and published in a special edition of *Traffic Injury Prevention* 16(S1), by Taylor & Francis Group. The complete paper will be available on the *Traffic Injury Prevention and www.NHTSA.gov* websites on June 8, 2015.

To access all Peer-reviewed papers please copy and paste the link below into your browser to access the papers.

http://www.tandfonline.com/toc/gcpi20/16/sup1

# CRITICAL REVIEW OF THE CURRENT ASSESSMENT APPROACHES FOR FRONTAL CRASH COMPATIBILITY REGARDING THE EVALUATION OF STRUCTURAL INTERACTION

**Emad Sadeghipour**
**Morris Fischer**
**Fabian Duddeck**
**Markus Lienkamp**
Technische Universität München
Germany

**Raffaele Ciardiello**
Politecnico di Torino
Italy

Paper Number 15-0096

## ABSTRACT

The assessment of structural interaction has been identified as the main challenge of the unresolved problem of frontal crash compatibility. With this background, two questions are raised: Does a better structural interaction correspond with higher safety and crash compatibility? Are current test approaches able to evaluate structural properties?
Considering the structural mechanics of collisions, it is hypothesized that a poor structural interaction does not necessarily result in lower safety and should be considered together with compartment strength and restraint systems. This hypothesis is confirmed by reviewing some crash results from other studies. A spring-mass vehicle model is also used to verify the hypothesis. Finally, a comprehensive simulation study is conducted to find the answers to the two questions. For this study three different variations of a vehicle model are created, which represent different structural properties of the passenger car fleet. The crash performance of these models is analyzed in different car-to-car and car-to-barrier tests.
Results of the car-to-car tests show that better structural interaction often makes the vehicle more aggressive. Generally, better structural interaction increases crash pulse and reduces intrusions. Depending on vehicle design and crash configuration, the intrusions or the crash pulse become more important as to why good or poor structural interaction cannot be overall related to more crash compatibility or occupant safety.
Our criticism of the current assessment approaches for frontal crash compatibility is the establishment of a direct link between good structural interaction and higher safety. These approaches do not consider the effect of higher crash pulses due to the better structural interaction. Our recommendation is to assess the partner protection through metrics about intrusions and crash pulse of the partner, without direct assessment of the structural interaction. Instead, the test configuration should be able to reflect structural properties in intrusions or crash pulse.
Results of the car-to-barrier tests show that the Progressive Deformable Barrier can reflect structural issues correctly. However, the developed metrics for this barrier result in incomprehensive interpretations. Results of the tests with other barriers are inconsistent with the structural properties of the vehicles.
Finally, an exemplary test concept with the Advanced European Mobile Deformable Barrier is presented as an alternative assessment approach. Simulation results of the proposed assessment approach show good consistency with the crash performance of the vehicles in the car-to-car tests. Combination of this test concept with the Full-Width Rigid Barrier test can be used to assess the safety and crash compatibility of passenger cars.

## 1. INTRODUCTION

Crash compatibility is known as a key component in improving vehicle safety and will become even more important in Europe's future road safety. This is due to the increasing market share of mini cars and sport utility vehicles in relation to other car segments [19], which increases the potential of incompatible collisions.
Although many studies [4, 15, 16] have been conducted in Europe to develop a proper assessment approach for crash compatibility, no assessment approach has been implemented yet. Important issues involving frontal crash compatibility for normal passenger cars have been identified as compartment strength, restraint systems, force levels and structural interaction (SI). Whereas restraint systems and compartment strength can be evaluated from dummy measurements and intrusion values, the assessment of SI is still an unresolved problem.
The issue of force levels consist of deformation forces of frontal structures and energy absorption management [4]. According to the matched pair analysis from the FIMCAR project, the deformation forces does not have a high

priority. Since the energy absorption management will also be considered in the assessment of SI, the focus of this study is on the issue of structural interaction.
Recently, two assessment approaches have been proposed from the FIMCAR project [1, 4]. The first approach is a combination of an offset test with the Offset Deformable Barrier (ODB) at 56 km/h and a full-width test with a Deformable Barrier and a load-cell wall (FWDB) at 50 km/h. A metric was developed in the FIMCAR project to establish a common interaction zone for the vertical SI; however, FIMCAR has not succeeded in developing a metric for horizontal SI in this approach.
The second approach is a test with a Progressive Deformable Barrier (PDB) or its mobile version. The developers see this barrier as the only configuration that can potentially assess horizontal load spreading. However, PDB still has validation and repeatability issues that must be resolved before its implementation. Furthermore, the association of the automotive industry worries about the misuse potentials of this barrier [17].

## 2. HYPOTHESIS: IMPACT OF STRUCTURAL INTERACTION ON OCCUPANT SAFETY

SI describes how the structures of a vehicle deform at the local level when interacting with a collision partner [14]. This definition includes two issues. First, with a poor load spreading, the energy absorption of the frontal structures is lower than its designed goal. The second issue is the structural stability, which prefers a homogeneous and robust reaction of the vehicle structures over different loading conditions. Neither of these aspects have a direct impact on occupants' injuries. The indirect impact has a dual meaning. On the one hand, poor SI can lead to intrusions by which occupants are exposed to contact injuries. On the other hand, poor SI can result in a higher deformation stroke that reduces the crash pulse in favor of restraint loadings on the occupants. Thus, poor SI does not necessarily correlate with lower safety and should be considered together with compartment strength and restraint systems.
Current assessment approaches define some requirements for good SI. In these approaches, the evaluation of separate metrics for SI, intrusions and dummy measurements determines the compatibility of the vehicle. This does not consider the influence of structural properties on crash pulse and intrusions.

### Review of Some Crash Test Results

It has been observed in some real crash tests from different studies that poor SI could result in better occupant safety. In the test series 1b from the FIMCAR project [11], some supermini cars were tested in aligned and misaligned configurations. It is obtained that if the vehicle has a strong passenger compartment and front-end design, then the misalignment does not necessarily result in higher intrusions. In this case, the misaligned configuration results in less intrusion for the firewall. Most dummy criteria were also better by the test series 1b with misalignment. Similar results have been observed in the test series 2 (small family car vs. sport utility vehicle) of the FIMCAR project and the test series 3 (supermini car vs. small family car) of the VC-COMPAT project [2]. This confirms that poor SI does not necessarily result in lower safety. The impact of SI on occupant safety depends on the compartment strength and restraint systems of the vehicle and also the crash configuration.

### Spring-Mass Vehicle Model

A spring-mass vehicle model from [7] has been further developed for this study. The model consists of two nonlinear springs as the main load paths and an elastic beam element as the bumper of the vehicle. The bumper represents load spreading on front structures; i.e. higher stiffness for the bumper corresponds with better SI for the vehicle. This model is calibrated to represent the Finite-Element-Model of the Toyota Yaris from [6]. The consistency between the kinematic of the spring-mass model and the Finite-Element-Model is verified in two tests against a rigid wall at 56 km/h with 50% overlap and full-width. The metrics of the Roadside Safety Verification and Validation Program from [8] are used for this verification.
Six variations of the spring model with different bumper stiffnesses are tested against a rigid wall at different speeds and with different overlap values. Figure 1 illustrates the results. The z-axis shows the maximum crash pulse in g. Colors indicate the value of the crash pulse, by which dashed red stands for high. The stiffness increases by a factor of two from SI-1 to SI-6. SI-2 represents the original Finite-Element-Model.
The results show that lower SI reduces the crash pulse by high overlaps. It is due to the extended deformation stroke. Higher SI is more desirable for low overlaps since the whole kinetic energy will be absorbed in crash structures, which prevents an impact of stiff compartment on the rigid wall. Hence, the ideal SI is a design parameter, which does not have an overall best case.

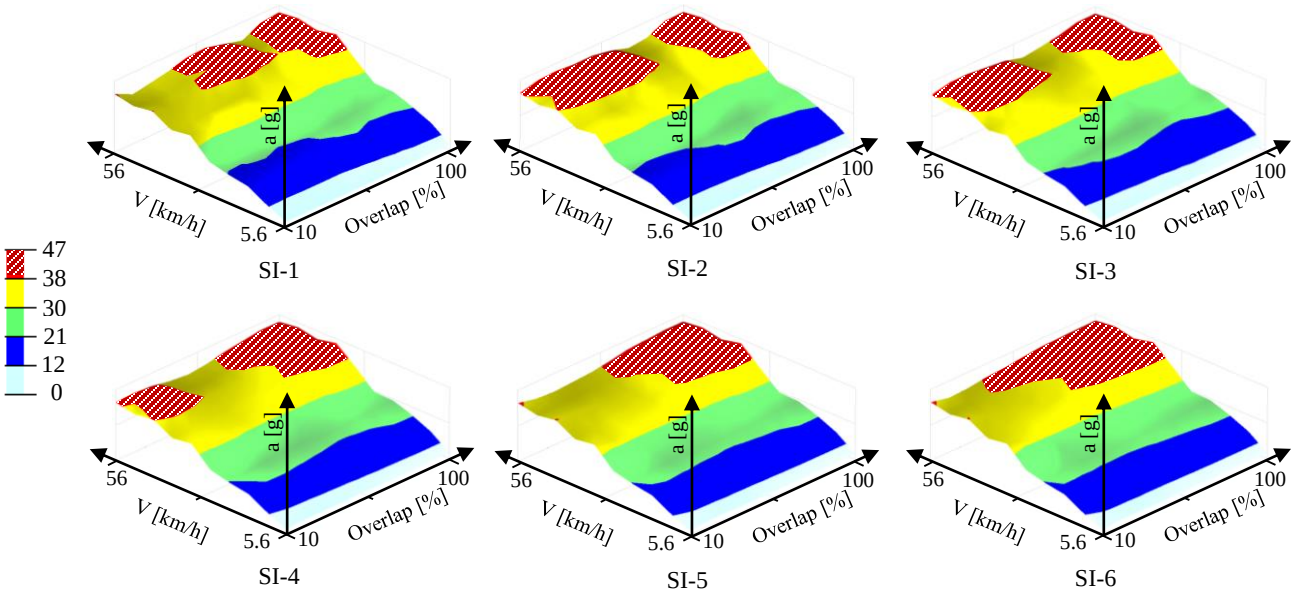


***Figure 1. Crash pulses for different structural interactions (prioritized from poor to good SI).***

## 3. SIMULATION STUDY

The previous section explained a hypothesis about the impact of SI on occupant safety. In this section, we are looking for answers to the following two questions:

1. Does a better SI correspond with higher safety and crash compatibility?
2. Are current test approaches able to evaluate structural properties?

To find the answers, a simulation study is conducted.

### Reliability of the Simulation Study

In this part, the question of reliability of the simulation results is addressed. The different aspects are categorized into simulation models, evaluation criteria and the test catalog.

**Simulation Models** The Toyota Yaris Finite-Element-Model from [6] is used as the basic simulation model[1]. This model is validated with crash tests against a Full-Width Rigid Barrier (FWRB) at 56 km/h and at 40 km/h and also against an ODB at 64 km/h with 40% overlap. The overall vehicle deformation and pulse were similar between tests and simulations [6]. This simulation model has also passed some additional tests with higher crash severity that confirmed the model robustness. Thus, this simulation model is considered a proper input for our qualitative simulation study.

The basic simulation model is changed to represent different structural properties of vehicles. Three variations are created from the basic model with considering the variations' feasibility. Each model represents a real car category with well-known SI characteristics. The models are ordered by their structural properties in Table 1.

To confirm the SI characteristics of the vehicle models, two simulation studies are conducted:

- The vehicles strike against the RCAR bumper from [18] at 56 km/h. This barrier can be used to evaluate the vertical homogeneity [9]. It is expected that vehicles with better structural properties have more homogeneity in the vertical deformations.
- The vehicles collide against the original Yaris model at 50 km/h with 50% overlap. This is the car-to-car baseline situation for the test ECE-R94, which is for the approval of vehicles in Europe with regard to the protection of the occupants in the event of a frontal collision. It is expected that vehicles with better structural properties have more homogeneity in the horizontal deformations.

[1] This model has been developed by The National Crash Analysis Center (NCAC) of The George Washington University under a contract with the FHWA and NHTSA of the US DOT.

**Table 1.**
**Simulation models and their variations, ordered by SI characteristics.**

| # | Model Name | SI characteristics | Changes of the model in relation to the original Yaris model |
|---|---|---|---|
| 1 | Mini Electric Car (Mini E-Car) | poor horizontal SI<br>poor vertical SI | 1- Represents an electric mini car without motor block and radiator, which eliminates a load path in the middle of the vehicle. This reduces the horizontal load spreading.<br>2- The height of the vehicle is reduced by 50 mm due to the configuration of the suspension systems. This increases the occurrence possibility of vertical SI problems (e.g. over-/underride).<br>3- A battery pack is added to the luggage compartment to balance the mass of this variation with the basic model. |
| 2 | Electric car (E-Car) | poor horizontal SI | 1- The same as No. 1 for the Mini E-Car<br>2- The height of the vehicle is the same as for the basic model<br>3- The same as No. 3 for the Mini E-Car |
| 3 | Basic-Model | Normal | Original Toyota Yaris model without any changes. |
| 4 | Strong-Car | good horizontal SI<br>good vertical SI | 1- The material of the front structure components (e.g. radiator frame) is changed to the highest-grade steel.<br>2- The thickness of the front structure components (e.g. radiator frame) is increased up to 100% (depending on the component).<br>3- The density of the changed components is scaled to maintain the same mass as the basic model. |

Figure 2 illustrates the results of these simulation studies. The results are comprehensive and confirm the ordering of the structural properties. For better visibility, the plastic bumper and the hood are hidden. The main load path and the front structure are colored in red and the wheels are colored in black. To highlight the structures' performance, a triangle is created for each vehicle that exhibits the homogeneity of the deformations. A triangle with a greater base shows more inhomogeneity.

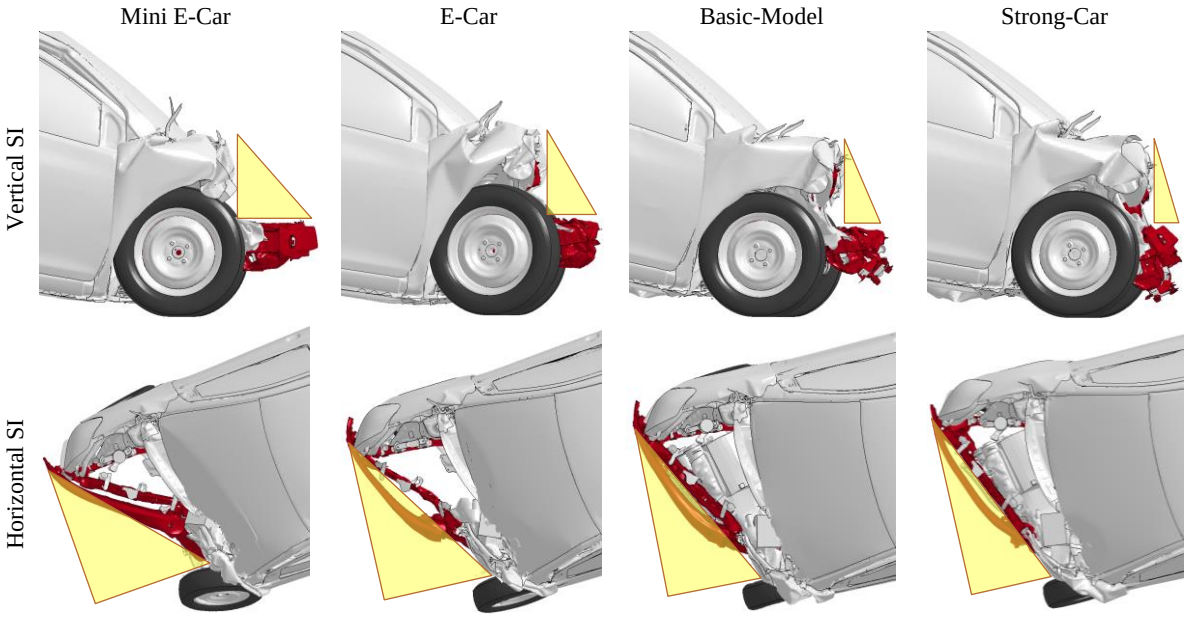


***Figure 2. Validation of SI characteristics for the vehicle models.***

**Evaluation Criteria** In this study, occupant safety is evaluated by intrusions and restraint loads. Points of vehicle crash metrics from [12] are used to measure the intrusions. This includes average intrusions in the toe-pan, maximum intrusion in the left and right knee-bolster for the driver, maximum displacement of the steering wheel and maximum displacement of the A-pillars.
The Occupant Load Criterion (OLC) is used to evaluate the restraint loads on the driver. OLC considers the principle physical behavior of restraint forces applied to the occupant's chest. At the beginning, the occupant has a free flight

phase of about 65 mm and then it will be ideally restrained with a constant deceleration over 235 mm. This constant deceleration defined the OLC value, which corresponds with head and chest injury criteria [5].
Use of intrusion values and OLC, instead of the implementation of a dummy in the vehicle model, removes the dependency of results on the specific configuration of the restraint systems of the test vehicle.

**Test Catalog** To answer the questions from the beginning of this section, two series of car-to-car and car-to-barrier tests are analyzed.
The most important types of frontal collisions are considered in the car-to-car test series, with the original Yaris model as the bullet vehicle. These configurations are:

- Baseline test of ECE-R94 with 50% overlap and 100 km/h collision speed (50 km/h for each vehicle). This test represents a collision with a high risk of intrusions in the passenger compartment.
- Car-to-car collision with 75% overlap and 100 km/h collision speed (50 km/h for each vehicle). This test represents a collision with a high crash pulse for the restraint systems. It been observed in [13] that there is a high proportion of fatal and severe injuries in accidents with high overlap.
- Baseline test of small overlap and oblique test from [12] with 15° and 17% overlap and 112 km/h for the bullet vehicle. This test represents a collision with highly misaligned loads and high crash severity.

The most important test configurations for safety and crash compatibility are included in the car-to-barrier test series. Aside from ODB (from Euro-NCAP) and FWRB (from US-NCAP), the studied cases are PDB and FWDB from the FIMCAR project [1, 4].

## 4. RESULTS

### Car-to-Car Tests

Simulation results are presented in Table 2. This section answers the first question: Does a better SI correspond with higher safety and crash compatibility?

**Self-Protection** Whereas vehicles with better structural properties have lower intrusions, better SI cause generally higher crash pulses and OLC values. Thus, there is no ideal structural property for all crash configurations.
There are two exceptions in the test results. By the high overlap test, the Mini E-Car with poor vertical SI has a higher OLC than the E-Car. This is due to a better coupling of wheels with the main load path because of the lower height of the vehicle, which causes a stiffer deformation zone. The other exception is that the Strong-Car with good SI has lower OLC values than the Basic-Model by the small overlap and oblique test. This is due to an impact on the stiff passenger compartment in the Basic-Model test, while the higher stiffness of the deformation zone by the Strong-Car avoids such an impact that reduces the crash pulse and the OLC value.

**Partner-Protection** Generally, the bullet vehicles have more intrusions and OLC values as they collide with vehicles with better structural properties. Hence, better SI makes the vehicles more aggressive.
There are two exceptions, by which the intrusion values of the bullet vehicle is less against the Strong-Car with good SI comparing to the test with the Basic-Model. By the small overlap and oblique test, better structural properties of the Strong-Car made it friendlier for the bullet vehicle regarding the intrusion values. The other exception is by the high overlap test, in which better structural properties resulted in less intrusion in the toe-pan and knee-bolster for the Strong-Car compared to the Basic-Model.

The results confirm the hypothesis that good or poor SI does not influence occupant safety directly. Structural issues, such as over-/underride, affect intrusion values and crash pulses. Depending on vehicle design and crash configuration, intrusion values or the crash pulse become more important as to why good or poor SI cannot be overall correlated to more or less occupant safety. It is also a design decision, if the passenger compartment should be stronger or the restraint systems should save occupants better. E.g., a supermini car could have a very short and stiff deformation zone, but a high-strength passenger compartment and good restraint systems. Therefore, an assessment of SI through some specific metrics that are independent from crash pulse and intrusions restricts the design's freedom.

**Table 2.**
**Results of the car-to-car test series.**

| Crash configuration | Car | OLC [g] | Intrusion / Displacement [mm] | | | |
|---|---|---|---|---|---|---|
| | | | Toe-pan | Knee-bolster | Steering wheel | A-Pillar |
| Baseline test of ECE-R94 vs. Yaris (bullet vehicle) 50% offset 50 km/h for each | Mini E-Car | 24.8 | 162 | 105 | 137 | 40 |
| | *Bullet* | *20.3* | *61* | *17* | *27* | *19* |
| | E-Car | 26.4 | 122 | 69 | 64 | 15 |
| | *Bullet* | *21.9* | *91* | *29* | *42* | *24* |
| | Basic-Model | 25.3 | 99 | 32 | 26 | 18 |
| | *Bullet* | *25.5* | *99* | *34* | *42* | *24* |
| | Strong-Car | 27.0 | 93 | 20 | 22 | 20 |
| | *Bullet* | *27.2* | *113* | *40* | *42* | *32* |
| High Overlap test vs. Yaris (bullet vehicle) 75% offset 50 km/h for each | Mini E-Car | 28.0 | 213 | 101 | 136 | 31 |
| | *Bullet* | *27.0* | *42* | *14* | *0* | *10* |
| | E-Car | 26.8 | 182 | 86 | 114 | 23 |
| | *Bullet* | *26.8* | *63* | *40* | *2* | *26* |
| | Basic-Model | 28.4 | 141 | 77 | 95 | 23 |
| | *Bullet* | *28.6* | *128* | *58* | *77* | *23* |
| | Strong-Car | 29.7 | 81 | 22 | 27 | 20 |
| | *Bullet* | *28.9* | *112* | *56* | *81* | *27* |
| Small overlap and oblique test vs. Yaris (bullet vehicle) 15°, 17% offset 112 km/h for the bullet vehicle | Mini E-Car | 22.6 | 317 | 267 | 420 | 287 |
| | *Bullet* | *27.5* | *76* | *7* | *11* | *17* |
| | E-Car | 27.5 | 251 | 207 | 251 | 75 |
| | *Bullet* | *28.0* | *132* | *26* | *38* | *24* |
| | Basic-Model | 30.2 | 174 | 92 | 111 | 54 |
| | *Bullet* | *34.5* | *171* | *73* | *84* | *31* |
| | Strong-Car | 29.2 | 158 | 82 | 128 | 46 |
| | *Bullet* | *37.4* | *159* | *54* | *57* | *67* |

**Car-to-Barrier Tests**

It is obtained in previous parts that good or poor SI cannot be overall correlated to more or less occupant safety. To consider the structural properties in the assessment of crash compatibility, either some metrics should predict the structural performance in real collisions, or the test configuration should reflect the structural issues in crash pulse and intrusions. This has been analyzed in this section for different barriers to answer the second question: Are current test approaches able to evaluate structural properties?
Simulation results are presented in Table 3.

**Full-Width Rigid Barrier** Vehicles with better SI had higher crash pulses and, consequently, higher OLC values. However, in this test configuration, better SI is penalized with more intrusions. It is due to the nature of the rigid wall that exerts forces to components, which are not designed as load paths. Displacement on these components results in intrusions in the compartment. Thus, this test configuration does not reflect structural properties correctly. There is also no metric for this barrier to predict the structural performance in real collisions.

**Offset Deformable Barrier** Generally, vehicles with lower SI had lower OLC values. However, the intrusions do not correspond with structural properties. The Strong-Car with good SI has more intrusions in the toe-pan and less in other zones. Intrusions of the Mini E-car with poor vertical SI do not reflect any over-/underride problem. On the contrary, the intrusion values in its toe-pan are higher than in other vehicle models. Although the E-Car has a poor horizontal SI, its intrusion values are slightly less than for the Basic-Model. There is also no metric for this barrier to predict the structural performance in real collisions.

**Full-Width Deformable Barrier** A metric has been developed in the FIMCAR project for the FWDB to assess the vertical structural alignment. The loads are measured in eight rows on a load cell wall behind the deformable block. The vehicle must achieve minimum load requirements in rows 3 and 4 and can use loads in row 2 to help fulfilling this requirement under certain conditions. The minimum load requirement promotes structural alignment and the credit of loads from row 2 encourages vertical load spreading [4]. FIMCAR did not succeed in developing a metric for horizontal SI, whereas the E-Car with poor horizontal SI has passed this test; it got even better results than the Basic-Model for both OLC and intrusions. The developed metric rejected the Mini E-Car due to its poor vertical SI. However, the Strong-Car with good SI is also failed. The most controversial part of these results is that the Mini E-Car failed due to only 6.4% lower loads than the limit of the metric, whereas the Strong-Car with good SI failed due to 28.1% lower loads. Therefore, it is doubtful that the developed metric could predict the structural performance in real collisions.
It is obtained that vehicles with better SI had higher OLC values. As it is mentioned in [10], the intrusion values in this test configuration are generally low and similar for different SI characteristics. A clear trend for different structural properties does not exist and this barrier cannot reflect structural properties correctly.

**Progressive Deformable Barrier** Deformations on the barrier can be used to evaluate SI of the vehicle. There is also a concept for a Fail/Pass metric, which is based on the measurements of the loads in different heights. The criterion 99%ile of Digital Derivative in Y (DDY) in common interaction zone from [1] has been estimated for each vehicle. Lower values correspond to more homogenous vehicle deformation, which is in contrast with the structural priorities of the vehicles. Criterion (d) is another developed metric from [1], which might detect the load path of the vehicles. This metric could generally detect SI problems. However, the (d) scores are similar and since limits are not yet adjusted, the evaluation of the simulation results with Fail/Pass is not possible.
Generally, vehicles with lower SI had lower OLC values and higher intrusions. The over-/underride issue is also observed in the results of the Mini E-Car with poor vertical SI relative to the E-Car. Hereby, the steering wheel's displacement is higher, while other intrusion values for the toe-pan and knee-bolster are lower.
This barrier can reflect structural properties in intrusions and crash pulse of the test vehicle. However, the metrics for the partner-protection are ineffective.

**Table 3.**
**Results of the car-to-barrier test series.**

| Crash configuration | Car | OLC [g] | Intrusion / Displacement [mm] | | | | Metrics for SI (if any) |
|---|---|---|---|---|---|---|---|
| | | | Toe-pan | Knee-bolster | Steering wheel | A-Pillar | |
| US-NCAP vs. FWRB 100% overlap 35 mph | Mini E-Car | 28.7 | 110 | 42 | 67 | 33 | - |
| | E-Car | 27.7 | 93 | 36 | 38 | 31 | - |
| | Basic-Model | 37.2 | 179 | 65 | 98 | 68 | - |
| | Strong-Car | 37 | 180 | 78 | 114 | 80 | - |
| EU-NCAP vs. ODB 40% overlap 64 km/h | Mini E-Car | 21 | 176 | 115 | 97 | 22 | - |
| | E-Car | 21.9 | 123 | 75 | 87 | 15 | - |
| | Basic-Model | 27.2 | 125 | 73 | 95 | 33 | - |
| | Strong-Car | 27.4 | 132 | 42 | 71 | 28 | - |
| vs. FWDB 100% overlap 50 km/h | Mini E-Car | 24.1 | 90 | 26 | 36 | 19 | Failed |
| | E-Car | 23.8 | 87 | 23 | 40 | 18 | Passed |
| | Basic-Model | 30.2 | 88 | 39 | 12 | 26 | Passed |
| | Strong-Car | 28.8 | 78 | 27 | 5 | 22 | Failed |
| vs. PDB 50% overlap 60 km/h | Mini E-Car | 23.0 | 168 | 83 | 120 | 23 | 99%ile DDY=1.4 (d) score = 3.4 |
| | E-Car | 21.8 | 193 | 86 | 80 | 24 | 99%ile DDY=1.7 (d) score = 3.2 |
| | Basic-Model | 28.0 | 106 | 37 | 38 | 25 | 99%ile DDY=2.8 (d) score = 3.6 |
| | Strong-Car | 27.4 | 89 | 27 | 23 | 22 | 99%ile DDY=2.8 (d) score = 3.5 |

## 5. ALTERNATIVE ASSESSMENT APPROACH

Our recommendation is to assess the partner protection through metrics about intrusions and crash pulse of the partner, without direct assessment of the structural interaction. Instead, the test configuration should be able to reflect structural properties in intrusions or crash pulse. An exemplary concept of such a test approach is presented in [10]. The vehicle strikes against the Advanced European Mobile Deformable Barrier (AE-MDB), the geometry and stiffness of which may represent the front-end of today's passenger car fleet [3]. Since the objective is the proof of this concept, the test configuration is not finalized in this study. The test vehicle collides at 50 km/h with 50% offset against the AE-MDB at 35 km/h. This results in an energy equivalent speed of about 56 km/h for both sides.
Besides the criteria for the crash pulse and intrusions of the test vehicle, acceleration pulse and forces behind the deformable blocks will be measured on the mobile barrier. Acceleration pulses will be converted to OLC and forces on the AE-MDB represent the risk of intrusions for the partner. Simulation results of the car-to-AE-MDB tests are presented in Table 4.

**Table 4.**
**Results of the test vs. AE-MDB.**

| Crash configuration | Car | OLC [g] | Intrusion / Displacement [mm] | | | | Other Criteria |
|---|---|---|---|---|---|---|---|
| | | | Toe-pan | Knee-bolster | Steering wheel | A-Pillar | |
| vs. AE-MDB 50% overlap AE-MDB 35 km/h Car 50 km/h | Mini E-Car | 19.3 | 139 | 80 | 68 | 21 | $OLC_{AE\text{-}MDB}$=16g max. F=73.2kN |
| | E-Car | 19.2 | 142 | 85 | 79 | 17 | $OLC_{AE\text{-}MDB}$=16.7g max. F=97.2kN |
| | Basic-Model | 26.5 | 91 | 38 | 31 | 22 | $OLC_{AE\text{-}MDB}$=25.1g max. F=222.8kN |
| | Strong-Car | 25.5 | 71 | 33 | 22 | 19 | $OLC_{AE\text{-}MDB}$=25.1g max. F=354.2kN |

The simulation results are consistent with the results of the car-to-car tests; i.e. vehicles with better SI result in higher crash pulses for both sides, while intrusions of the vehicles with better SI are smaller. Better SI makes the vehicle more aggressive and causes higher OLC values and forces on the barrier, which is in agreement with the car-to-car tests results.
The override issue is also reflected in the Mini E-Car case where the intrusion values in the toe-pan and knee-bolster are less comparing to those of the E-Car. It is noteworthy that the test severity is too low for the displacement of the A-pillar and all values are quite similar.

## 6. CONCLUSIONS AND RECOMMENDATIONS

Better SI increases crash pulse and reduces intrusions. Depending on the vehicle design and crash configuration, intrusion values or the crash pulse become more important as to why good SI cannot be overall related to more crash compatibility. It is obtained that better SI makes the vehicle more aggressive. Current assessment approaches for the frontal crash compatibility establish a direct link between good SI and higher safety. These approaches do not consider the effect of higher crash pulses due to better SI and limit the design's freedom.
Among the current assessment approaches, the PDB is found as the only barrier that can reflect SI issues correctly. However, the developed metrics for this barrier resulted in incomprehensive interpretations.
Our recommendation is to assess the partner protection through metrics involving intrusion and the crash pulse of the partner without direct assessment of the structural interaction. Instead, the test configuration should reflect the structural properties in intrusions or crash pulse values. An exemplary test concept is presented and proved by simulations. The combination of this test concept with FWRB test can assess the safety and crash compatibility of the vehicles.

**ACKNOWLEDGMENT**

The project was independently funded by the Institute of Automotive Technology at the Technische Universität München.

**REFERENCES**

[1] Del Pozo de Dios, E., Lázaro, I., Delannoy, P., Thomson, R., Versmissen, T. & van Nunen, E. (2013). *Development of a Structural Interaction Assessment Criterion Using Progressive Deformable Barrier Data*. 23rd ESV Conference Proceedings, Seoul

[2] Edwards, M.J., de Coo, P., van der Zweep, C., Thomson, R., Damm, R., Martin, T., Delannoy, P., Davies, H., Wrige, A., Malczyk, A., Jongerius, C., Stubenböck, H., Knight, I., Sjöberg, M., Ait-Salem Duque, O. & Hashemi., R. (2007). *Improvement of Vehicle Crash Compatibility through the Development of Crash Test Procedures*. Final Technical Report of VC-COMPAT

[3] Ellway, J.D., van Ratingen, M., Versmissen, T., van Montfort, S., Langner, T., Dobberstein, J., Goutas, P., Gay, P., Malak, A., Denker, C., Hallack, J., Odanaka, K. & Ogihara, T. (2013). *The Advanced European Mobile Deformable Barrier Specification for Use in Euro NCAP Side Impact Testing*. 23rd ESV Conference Proceedings, Seoul

[4] Johannsen, H., Adolph, T., Edwards, M., Lazaro, I., Versmissen, T., & Thomson, R. (2013). *Proposal for a Frontal Impact and Compatibility Assessment Approach Based on the European FIMCAR Project*. Traffic Injury Prevention, S105-S115, DOI: 10.1080/15389588.2013.790538.

[5] Kübler, L., Gargallo, S. & Elsäßer, K. (2009). *Frontal crash pulse assessment with application to occupant safety*. ATZ worldwide, Volume 111, Issue 6, pp 12-17.

[6] Marzoughi, D., Samaha, R.R., Cui, C. & Kan, C. (2012). *Extended Validation of the Finite Element Model for the 2010 Toyota Yaris Passenger Sedan*. Working paper of NCAC, 2012-W-005

[7] Huang, M. (2002). *Vehicle crash mechanics*. Boca Raton, Fla.: CRC Press.

[8] Mongiardini, M. & Ray, M.H. (2009). *Roadside Safety Verification and Validation Program (RSVVP)*. User's Manual of RVSSP 1.7

[9] O'Brien, S. (2011). *Priorities for the Assessment of Frontal Impact Compatibility*. 22nd ESV Conference Proceedings, Washington, D.C.

[10] Sadeghipour, E., Duddeck, F. & Lienkamp, M. (2014). *Crash Compatibility of Microcars: A Study on Current Test Approaches*. Crash.tech 2014, Munich (also published in Researchgate)

[11] Sandqyist, P., Thomson, R., Kling, A., Wågström, L., Delannoy, P., Vie, N., Lázaro, I., Candellero, S., Nicaise, J.L. & Duboc, F. (2012). *Report on Car-to-Car Test Results*. Deliverable 6.1 from FIMCAR project (FP7)

[12] Saunders, J., Craig, M.J. & Suway, J. (2011). *NHTSA's Test Procedure Evaluations for Small Overlap/Oblique Crashes.* 22nd ESV Conference Proceedings, Washington, D.C.

[13] Thompson, A., Edwards, M., Wisch, M., Adolph, T., Krusper, A. & Thomson, R. (2011). *Report detailing the analysis of national accident databases.* Deliverable 1.1 from FIMCAR project (FP7)

[14] Thomson, R., Johannsen, H., Edwards, M., Adolph, T., Lázaro, I. & Versmissen, T. (2012). *Documentation for a frontal impact and compatibility assessment approach: Part I*. Deliverable 6.3 from FIMCAR project (FP7)

[15] N.N. (2006). *Improvement of vehicle crash compatibility through the development of crash test procedures.* Final technical report of project VC-COMPAT

[16] N.N. (2007). *Car crash compatibility and frontal impact.* Final report of EEVC-WG 15 to steering committee

[17] N.N. (2008). *Detailed discussion of the VDA position on the proposal for draft amendments to UN-ECE R94*. Retrieved February 21, 2015, from http://www.unece.org/fileadmin/DAM/trans/doc/2008/wp29grsp/FI-03-09e.pdf

[18] N.N. (2010). *RCAR Bumper Test*. Issue 2.0 from Research Council for Automobile Repairs (RCAR)

[19] N.N. (2013). *European Vehicle Market Statistics*. Pocketbook 2013, the International Council on Clean Transportation (ICCT)

# REAL-TIME PEDESTRIAN & DRIVER ANALYSIS BY NEUROMORPHIC VISUAL INFORMATION PROCESSING

**IL SONG HAN**
**WOO-SUP HAN**
Korea Advanced Institute of Science and Technology
Korea, Republic of

Paper Number 15-0097

**ABSTRACT**

**Objective**
The safety enhancement of road users has begun to gain more attention, in particular the innovation and application of ADAS. The accurate and timely detection of the risk of accident has become an active area of research, with the focus on the drivers and other vulnerable road users.

The neuromorphic visual information processing method, inspired by Hubel and Wiesel's experiments on mammalian visual cortex, is proposed as a possible solution to these tasks. The proposed method replicates the performance of visual cortex in practical computing settings. By applying the orientation feature extraction and subsequently applying the neural network ensured robustness and accuracy.

**Method**
The proposed system has been evaluated on pedestrians/cyclists detection and driver monitoring, with a particular focus on emotion/stress detection. The tests have been carried out with video data sets of various conditions, with the experimentation and data set generation at public roads in every day settings.

The neuromorphic visual monitoring of drivers for the attentive or emotional status has been also evaluated, as approximately 15% of road accidents have been caused by the dangerous driving in 'anger and or/frustration'. The driver monitoring system by detecting the emotional state from the limited facial image of driver would make the measures of early warning against possible dangerous or inattentive driving. The neuromorphic system was evaluated to determine the warning signal based on the emotional state detection, based on the key feature extracted from the face images. The test was based on the facial database (JAFFE) of six basic emotional states.

**Results and Conclusion**
The performances of neuromorphic visual information system were measured to the success rate 99% of pedestrian/cyclist detection, and the successful recognition 91% of facial emotional states. The real-time

performance was evaluated with the neuromorphic ASIC, fabricated by the automotive CMOS technology. The processing speed of neuromorphic ASIC alone was tested for the speed of 30 frames per second, without the latency or external memory.

**KEYWORDS**

Pedestrian Detection, Cyclist Detection, Driver Status Monitoring, Advanced Driver Assistance Systems (ADAS), Image Processing, Neuromorphic Vision

## INTRODUCTION & BACKGROUND

In this paper, the elements of neuromorphic implementation of visual cortex are introduced with the orientation tuned function of synaptic connections and the spiking neuron, based on the electronically programmable MOSFET conductance (Hubel & Wiesel 1959, I Han 2006). The proposed neuromorphic visual signal processing is investgated for enhancing the vehicle safety by the pedestrian detection or the passenger detection as well as monitoring the driver status .

### Vulnerable Road Users (VRU)

Alongside pedestrians, cyclists and motorcyclists make up the category of road users regarded as vulnerable. These individuals are most exposed to the dangers of serious injury or fatality from a road accident. Furthermore, according to the CARE (Community database on Accidents on the Roads in Europe), as there is a 1-in-4 chance of having to be admitted to the hospital in case of a road accident, the risk doubles for pedestrian.
Statistics on cyclists also show similar trend. While the overall number of fatality is in a steady decline, the cyclists' ratio of road fatalities is now growing, with the percentage making up more than 21% in certain European countries.

These higher risks are also coupled with the fact that a pedestrian casualty of road accident would have the longest length of stay (10+ days) in hospital compared to any other groups, signifying the vulnerability of the pedestrians in road accident situations. In fact, 63% of non-fatal road casualties were from VRU, emphasising the need for improving safety for this group.

### Advanced Driver Assistance System (ADAS)

An increasing proportion of cars include ADAS to maximize the safety of road users (drivers, passengers, and pedestrians). European New Car Assessment Program (Euro-NCAP) initiatives support this trend by attributing a higher safety rating to cars that incorporate ADAS. Currently the NCAP ranking metrics focus on increased ADAS system performance. It is expected that after 2016, NCAP will introduce additional metrics that focus mainly on extending system functionality through the addition of pedestrian detection and automatic emergency braking, as well as lengthening operational up-time by requiring continued system functioning at night and during adverse weather conditions. This is logical as almost 60% of all road accidents happen in poor lighting conditions.

### Driver Monitoring/Emotion on Concentration and Driving

One of the issues of prime importance to traffic and transport psychologists is the possible effect that a particular emotional state would have on concentration in driving situations. Relationship between anger and the subsequent aggressive behaviour manifested in 'road rage' have been investigated in depth. And recently, more researches have been carried out on effect of other emotional states such as fear, anxiety, and surprise on driver's performance. Emotion affecting driving behaviour is widespread, with studies sometimes finding almost 90% of the questioned admitting to engage in behaviour motivated by their emotion. These behaviours ranged from sounding the horns to indicate annoyance, to chasing down other drivers as a display of hostility, and they were quite often regarded as a reckless or risky driving. This accentuates a need for monitoring the driver, and forewarning of any change in emotional status as a measure to improve road safety.

## NEUROMORPIC VISUAL INFORMATION PROCESSING

The proposed method of neuromorphic visual information processing has its basis on how we, humans process visual information. As the light enters the eye, it stimulates the sensors at the back of the retina, which in turn triggers a complex chemical reaction that results in electrical signals being sent to the brain through optical nerves. These signals travel through the optical nerve, and eventually reach the visual cortex at the back of the brain to be analysed. While visual cortex itself is still far from being fully understood, extensive studies of the mammalian brain including the 1960s research from Hubel and Wiesel have gave us basic understanding of how the visual cortex functions, as well as picture the physiology of the low-level human/mammalian visual systems (Fig. A1) (Hubel & Wiesel 1969).

**Primary Visual Cortex**
Hubel and Wiesel's research on cat's striate cortex have established the concept of the simple cell within the visual cortex. The simple cell responds to the orientated edges, and each types of cell responded specifically to the different inputs. Observations showed orientation based behavior evoked the reflection while the spike-based neuron signal is also an essential feature. Several theories and algorithms in image processing, object recognition and computer vision have been developed from this experiment and its findings (Risenhuber & Poggio 1999).

**Neuromorphic Neuron and Visual Information Processing**
The proposed neuromorphic visual information processing replicates the orientation selectivity of the simple cell. The neuromorphic neuron of visual cortex can be implemented by simulating the behavior of neuron in the Hubel and Wiesel's experimentation. The spike neural signal is explained by the widely adopted Hodgkin-Huxley formalism, based on the neurophysiological model of controlled conductance (Hauser 2000). The neuromorphic system of neuron and synaptic network was designed for evaluating the feasibility of mimicking the primitive behavior of brain neural system in electronic hardware using the CMOS neuromorphic circuit (I Han 2006, WS Han & I Han 2010, WS Han & I Han 2014). With the neuromorphic neuron formed the various stimuli of six 50 x 50 pixel sized rectangles at different angles are applied as the similar stimulus input to the cat in Hubel and Wiesel's experiment. The simulated result of neuromorphic neuron is demonstrated to be consistent to the outcomes from the Hubel and Wiesel's experiment, as shown in Fig. A1, where the tuned feature orientations are represented as the spike signal outputs (WS Han & I Han 2014].

The neuromorphic neuron of simple cell enables the neuromorphic vision system in Fig. A2, with the various orientation selective features. The system has three steps in its process which are: (1) orientation feature extraction using neuromorphic neuron, (2) neural network is then applied to the orientation extracted image and finally (3) the human head detection is made to detect the driver or the pedestrian depending on the system's application.

The proposed neuromorphic orientation feature extraction has the advantage of robust abstract image generation, under the limited situation like fuzzy human object image in the veil or in the dark/bad weather. The neuromorphic vision is based on the orientation feature processing using the scalar filter, where the filter shape is rotated with the designated orientation selectivity. Contrary to the complex computation of Gabor filter for the similar purposes, the neuromorphic visual signal processing has the feasibility of effective implementation for automotive applications because of its simpler integer computation.

**Detection of Vulnerable Road Users**
One of the major challenges in the pedestrian detection for the enhanced vehicle safety is that the reliability of the detection is strongly affected by illuminace conditions. For example, most pedestrian detection algorithms have significant drop in its detection rate at the night time or indoors compared to the day time or when operating in the bad weather such as rain or snow. The neuromorphic vision system is based on the orientation selectivity of simple cell, instead of the immediate pattern matching or complex figure pattern. The robustness in substantially weak illumination is observed by the successful detection at the indoor parking lot or the night time drive with the head light.

The test result has been summarized in Table. 1, and Fig. 3 demonstrates the process of detecting various types of VRUs. The data set is the captured video by on-board camera of passenger vehicle, on the turning road with slop at KAIST campus.

In addition to the pedestrian detection at various environments, the robustness of neuromorphic visual information processing is demonstrated by the successful cyclist detection in the crossing road as seen in Fig. A3. The data set for cyclist detection has been captured video by on-board DVR (a car blackbox with the lens of wide FOV) of moving passenger vehicle, on the cross road at KAIST campus.

The illumination for the pedestrian detection at night time is limited by the head light of passenger vehicle, with the low beam direction in the urban area. The earliest appearance of pedestrian is the lower part of body in this case, rather than the upper body of head and torso. The orientation feature at the scene of night time accident displays a clearly defined region of interest. The template of neural network detector is designed for detecting the lower body, as it is apparently required in this particular case. The saliency map is evaluated with the lower body template and, the result illustrates the condition required for lower body detector in the night time.

**Driver Monitoring System**

The proposed neuromorphic vision system is also applied inside the vehicle for the purpose of driver monitoring. For this purpose, only a minimal modification to the parameter is necessary to accommodate the difference of environment. The sensor used was identical, and the same template of head-torso and orientation features was reused. For the pedestrian detection, the environment at which the detection must be made is when the vehicle and/or pedestrian is in motion thus there is lot of change in the background such that frame difference cannot be used to reduce noise. The driver detection is in the quasi-stationary background condition, as the background of driver is mostly the vehicles stationary passenger cabin with minor variations in the window outlook. Hence, the frame difference of orientation features can be used to minimize noise detected during process.

To determine the head (equivalently face) of the driver, the template of head and torso is applied after evaluating the difference of orientation features extracted between the current frame and the previous frame. The processed orientation features in subsequent images yielded the clearer feature detection of head and particular object like driver's eye (W. J. Han & I. Han, 2013)

**Emotion Detection for Attentiveness Monitoring**

For the purpose of inattentiveness detection, we investigated on detecting emotive states from the abstract facial expression, based on neuromorphic processing as shown in in Fig. A4. This is due to the fact that the anger is the principal emotional state most linked to automobile accidents.

In order to detect emotional states, we have established three regions of interest (ROI) which would be obtained and processed. These regions are eye brows, cheeks and mouth. While the regions can be further divided into left and right eye brows and cheeks, since the expression would be similar within both sides of the face in most situations, we have processed each pair of them as one ROI.

The success rate for detecting happy emotion is 98%. This translates to one input being incorrectly classified from the 43 test images (from 5 individuals of JAFFE data set) used to evaluate the proposed framework. The one instance of detection failure occurred primarily due to the large displacement of face in the test image comparing to the reference point of neutral image.

The neural network of multi-layer perceptron (MLP) is applied for the autonomous or trainable detection of emotion state, instead of detection algorithm based on the statistical threshold value for evaluating orientation features.

The overall successful recognition of 91.4% is achieved, and has been presented in the confusion matrix of MLP classification of facial emotional states using JAFFE data set.

**Blind Spot Cyclist Detection**

The cyclist detection in the blind spot emerges as a serious issue as the population of cyclists grows rapidly due to its eco-friendly nature. It is particularly demanded for the commercial vehicles, as the tall and long

commercial vehicle is subject to the relatively limited sight of view. The neuromorphic processing is applied to the cyclist detection in the blind spot area of commercial vehicle. The captured video in Fig. A6 is for the test data, which was recorded from the upper deck of double decker bus (the public transportation in London). The orientation features extracted, which is illustrated in the second image of Fig. A6, has been evaluated by the same neuromorphic pedestrian detection system we have proposed in this paper. The nature of blind spot cyclist detection demands further enhancement as it is based on the view from the higher sensor location. The additional detector template is introduced to enhance the cyclist detection with the expected appearance in the blind spot analysis. The additional template of frontal part of cycle is designed and applied together in parallel with the existing human detector.

Bottom image of Fig. A5 show the successful cyclist detection in the shadow and blind spot area, simulated by the captured video from the double deck bus.

## REAL-TIME NEUROMORPHIC INFORMATION PROCESSING

The neuromorphic visual information processing is based on the multiple orientation filters mimicking the simple cell neuron of visual cortex, which are similar to the convolutional neural networks. The real-time operation requires the simple computational elements but parallel operation.

The processing speed of neuromorphic ASIC developed by the industry collaborator is the 30 frames per second for the orientation processing up to the HD video quality, without the latency or the external memory. The neuromorphic ASIC was fabricated in automotive CMOS 0.18um technology, and it performed the same orientation selective processing as simulated in the software.

## CONCLUSION

In this paper, the pedestrian/cyclist detection or driver monitoring by neuromorphic visual information processing is presented with the successful and robust performance in various application environments. The neuromorphic system demonstrated its versatile application to different objects and operation environments, with only the parameter tuning and the addition of necessary templates.

The overall performance of the pedestrian/cyclist detection in both under the nominal and the limited illumination shows that the robustness is sustained without the loss of accuracy as the 99% of successful detection rate. The neuromorphic vision processing demonstrated the 91% recognition rate of emotion detection for driver state monitoring.
In addition, the bio-inspired approach involved forming the neuron electronically using CMOS VLSI ASIC technology, which allows for financially advantageous implementation compared to using high-powered chips and computers that the computer vision algorithms requires frequently. The stand-alone neuromorphic ASIC demonstrated the speed performance of 30 frames per second and its practical advantage of working without any memory or complex programming,

The neuromorphic vision system is demonstrated by using a single camera, which suggests the further improvement in performance quality by employing the stereo camera or IR camera in harsh environment or more precise operation

## ACKNOWLEDGEMENT
The research was partly promoted as part of ‘Technology Development for Behavior Improvement and Violation Control of High Risk Drivers’ that was carried out by Ministry of Land, Infrastructure and Transport in Korea. We would like to thank Dr. S. H. Lee in i.A. for the sample of neuromorphic ASIC.

**REFERENCES**

Hubel DH, Wiesel TN. Receptive fields of single neurons in the cat's striate cortex, *J. Physiol.* 1959; 148: 574-591.

Han IS. Mixed-signal neuron-synapse implementation for large scale neural networks, Int. *Journal of Neurocomputing* 2006; pp. 1860-1867.

Risenhuber M, Poggio T. Hierachical models of object recognition in cortex, *Nature Neuroscience* 1999: pp.1019-1025.

Hausser M. The Hodgkin-Huxley theory of action potential, *Nature Neuroscience supplement* 2000; vol.3: pp.1165.

Han WJ, Han IS. Bio-Inspired Visual Signal Processing based on Neuromorphic Circuit, *Proc. WSEAS* 2010: pp.131-136

Han WS, Han IS. Robust Detection of Pedestrian/Cyclist by Neuromorphic Visual Processing, *Proc. FISITA* 2014: F2014-ASR-043

Han, W. J., & Han, I.S. Passenger/Pedestrian Analysis By Neuromorphic Visual Information Processing, *Proc. ESV 2013*:

## APPENDICES

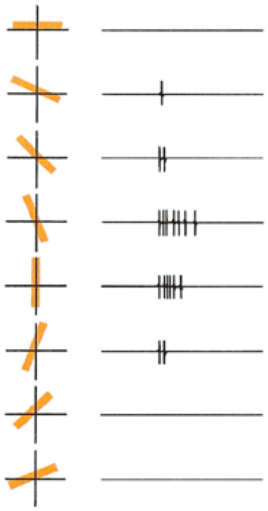

**FigureA1. Response of the cat's cortex when a rectangular slit of light of different orientations is shown**

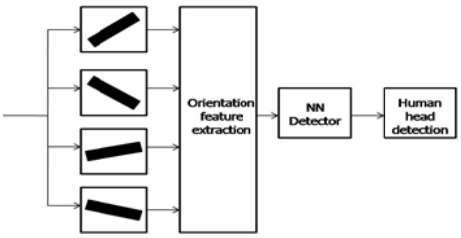


**Figure A2. Neuromorphic vision for human head figure detection, inspired by visual cortex.**

| Test Data Set | Total Frame s | Success Rate Frame s[%] | Undetected Failure Rate Frames[%] | Positive FailureRate Frames[%] |
|---|---|---|---|---|
| 1 | 60 | 58 [96.6%] | 0 | 2 [3.3%] |
| 2 | 36 | 36 [100%] | 0 | 0 |
| 3 | 150 | 150 [100%] | 0 | 0 |
| 4 | 162 | 160 [98.8%] | 2 [1.2%] | 0 |
| Total | 408 | 404 [99%] | 2 [0.5%] | 2 [0.5%] |

**Table 1. Test Result Summary for VRU detection.**

**Figure A3: Cyclist detection (bottom), (anti-clockwise from top left) input image with the box of detected cyclist, saliency map by neural network detector, and detected cyclist, crossing the road.**

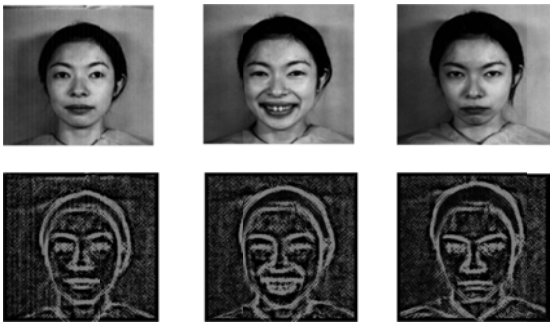

**Figure A4. Example of orientation processed images for subject "NA" (JAFFE) in various expressions: (top) original images - neutral, happy and angry, from left to right (bottom) orientation processed images –neutral, happy, and angry, from left to right. Notice the movements of mouth and cheeks in 'happy' image and lack of it in 'angry'.**

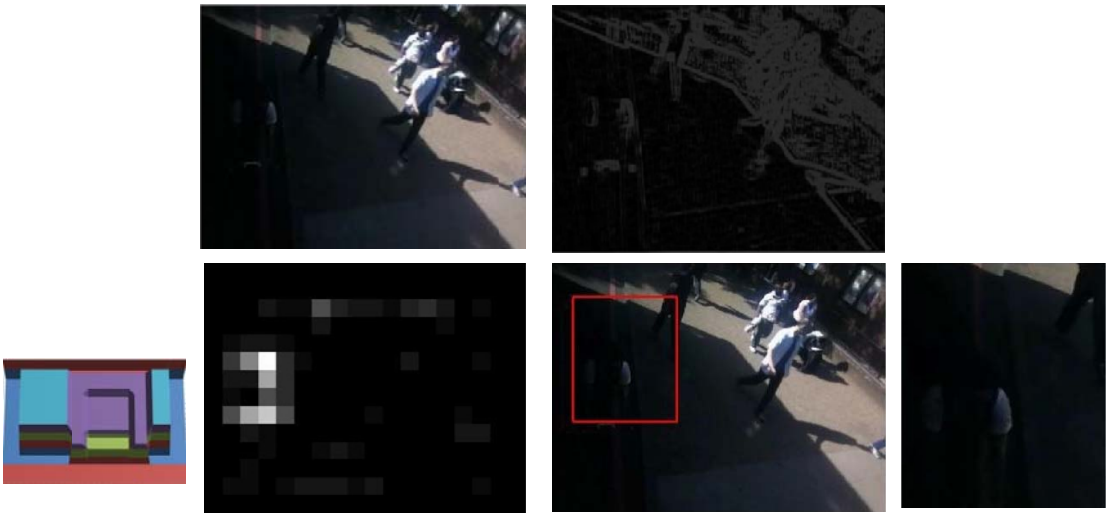

**Figure A5. (top-left)Video image captured by a smartphone, on the upper deck of London bus in the U.K.**
**(top-right) Neuromorphic orientation features of the image in Figure 18.**
**(bottom-left) Blind spot cyclist template enhancement (left) additional template configuration - the frontal part of cycle (right) saliency map processed by the parallel detectors applied.**
**(bottom-right). Resulting blind spot cyclist detection of Figure 18 (left) the detected cyclist in the red box, (right) the detail image inside the red box.**

# EVALUATION OF THE EFFECTIVENESS OF VOLVO'S PEDESTRIAN DETECTION SYSTEM BASED ON SELECTED REAL-LIFE FATAL PEDESTRIAN ACCIDENTS

**Peter, Vertal**
Institute of Forensic Engineering University of Zilina
Slovakia

**Assoc. Prof. Robert Kledus**
Institute of Forensic Engineering Brno University of Technology
Czech Republic
**Prof. Hermann, Steffan**
Vehicle Safety Institute Technische Universität Graz
Austria

Paper Number 15-0098

## ABSTRACT

The objective of this work is to test freely available system for active pedestrian protection. Tests are based on real fatal accidents that happened in the past with passenger cars that were not equipped with active safety systems. Tests have been conducted in order to evaluate what the real benefit of the active safety system is, and not to gain only a methodological prediction. The testing procedure was the first independent testing in the world which was based on real fatal pedestrian accidents. The aim of the tests is to evaluate the effectiveness of Volvo pedestrian detection system.

An in-depth accident database contains about 300 fatal pedestrian traffic accidents in urban areas. Eighteen cases of pedestrians hit by the front end of the passenger vehicle were extracted from this database. Cases covering an average traffic scenario have been reconstructed to obtain detailed model situations for testing. Simulations of accidents have been made in PC Crash 10.0 using a multibody object and a mesh model of vehicles. Active safety testing scenario was built on the basis of reconstructed accidents with Volvo V40 cc and a new dummy simulating a pedestrian. Before the tests the dummy was evaluated in anechoic room to gain required radar reflection properties which would be the same as those of a human body. The movement of the dummy was driven by the autonomous ultraflat overrunable robot (UFO) for experimental ADAS testing and synchronized with Volvo motion by D-GPS with high accuracy of motion.

## INTRODUCTION

The study is based on the measurements made under the leadership of Peter Vertaľ in 2014 in Linz, Austria, in cooperation Institute of Forensic Engineering Brno University of technology, Vehicle Safety Institute Technische Universität Graz, DSD Dr. Stefann Datentechnik and Institute of Forensic Engineering University of Zilina.

## SOFT DUMMY

The most important element in the experimental measurement of the conditions for the activation of the pedestrian detection system is a dummy representing a pedestrian. For the purposes of this paper, a pedestrian's movement was simulated using a dummy placed on an autonomous platform. The platform called "UFO" had a built-in D-GPS module for orientation in space and it was powered by two servomotors. The pedestrian dummy placed on the UFO platform had to undergo an evaluation process. The evaluation process guaranteed the achievement of the required reflective properties of the dummy identical to the human body. The reflective properties of the dummy for the short-range 24 GHz radar had to correspond to the reflective properties of the human body in order to avoid confusion of the dummy for an object that does not correspond to the properties of the human body.

For the purposes of reconstruction and expert activities related to the analysis of accident events, it was necessary to evaluate and re-create an ideal dummy whose reflective properties correspond to those of the human body. For the purposes of this paper, three basic positions of the dummy were determined that had to be evaluated by measurement for the subsequent use. The position of a standing person facing the radar source, the sideways

position and the position of a standing person with the back to the source. The dummy's positions were compared with the reflective properties of a test subject. For the purposes of this paper, the simulation involved only dry-weather conditions without the presence of significant moisture on the clothing of the pedestrian/dummy. During the measurements, it was necessary to compare the properties of the dummy with a human who is undressed, partially dressed and dressed in several layers in order to take into account all possible conditions of the pedestrian-car system.

Figure 1 shows a comparison of an empty anechoic chamber, with a test subject, a dummy before adjustments and after adjustments. The graph shows that the dummy without adjustments has approx. 15 dB lower values of reflection properties. The adjustments of the dummy resulted in identical properties to those of the human body. The value approx. 50 dB matches the test subject's value.

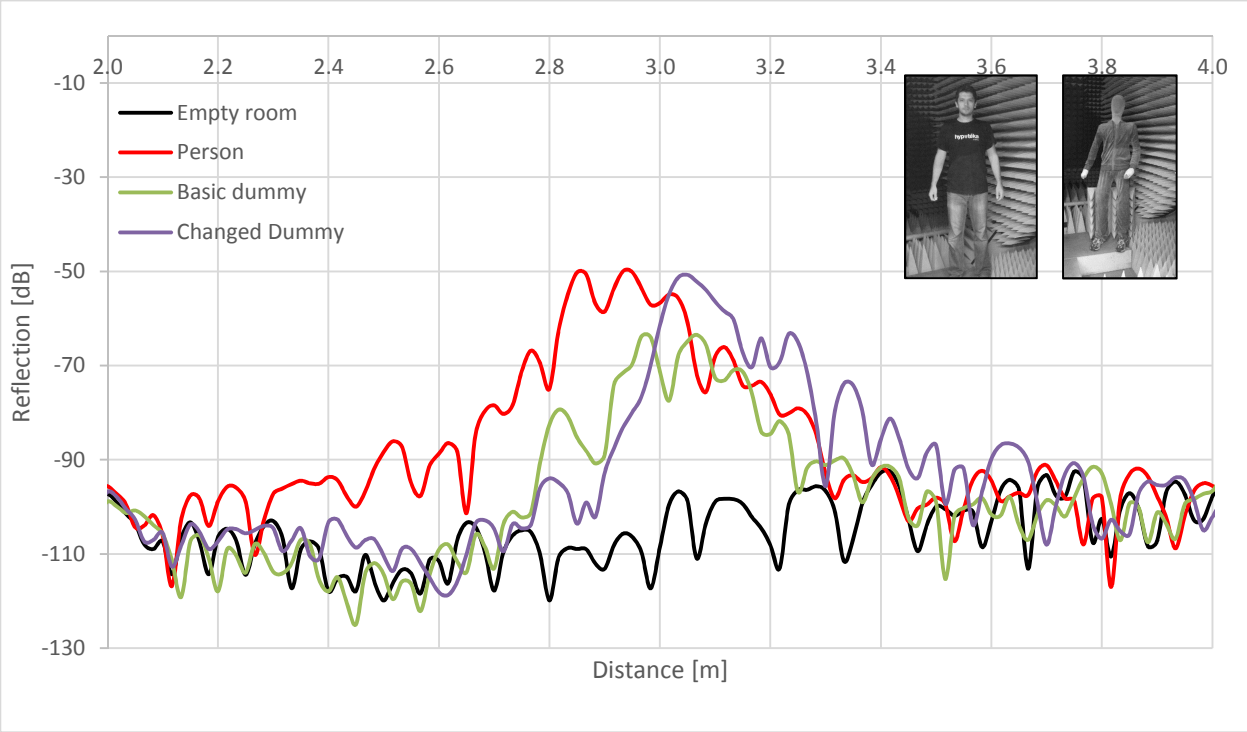


***Figure 1 Reflection of the person, basic dummy and changed dummy in anechoic chamber.***

After an in-depth analysis and measurements made in the anechoic chamber, it was possible to finalise the form of the dummy. During the experimental measurements, the dummy was adjusted using adhesive aluminium tape. The use of the aluminium tape increased and decreased the intensity of the reflected radar waves. After repeated measurements, tests and adjustments of the dummy, it was possible to a create dummy whose intensity of the reflected radar waves corresponded to the human body. This dummy was used for the experimental measurements with a Volvo vehicle.

## PROCESSING OF THE RESULTS

The measurements consisted of a series of tests based on selected real traffic accidents. For a complete test of the active safety system, it was necessary to choose accidents where the movement of the vehicle and the pedestrians cover the entire range of traffic accident situations. A full overview of the case studies and vehicle speeds at the time of collision resulting from the analysis of the accident studies is shown in Tab.1. Tests were performed under the conditions corresponding to the five characteristic types of traffic accidents with pedestrians. During the measurements, the following traffic situations were simulated: a pedestrian crossing the road in the perpendicular direction, in the oblique direction and in the direction towards the vehicle, a pedestrian standing on the roadside, a pedestrian coming from behind an object, a lying person, day and night conditions and situations combining the above.

**Table1. Overview of vehicles from traffic accidents and pedestrian motion**

| Case | Brand | Model | Registration year / Accident year | Impact velocity +/- 10% (km/h) | Direction of a pedestrian motion | Pedestrian age (years) |
|---|---|---|---|---|---|---|
| 1 | Opel | Astra | 1999 / 2003 | 23 - straight | → | W 69 |
| 2 | Citroen | AX | 1990 / 2003 | 47 - straight | → | W 71 |
| 3 | Opel | Corsa | 1990 / 2003 | 12 – cornering L | ← | W 78 |
| 4 | Peugeot | 306 | 1994 / 2003 | 50 - straight | → | M 96 |
| 5 | Volvo | S70 | 1997 / 2004 | 32 - straight | → | W 89 |
| 6 | VW | Multivan | 1989 / 2004 | 19 - straight | ← | W 84 |
| 7 | BMW | 3 | 1995 / 2004 | 41 – cornering L | ← | M 91 |
| 8 | Honda | Civic | 1990 / 2005 | 55 – overtaking R | → | M 43 |
| 9 | VW | Sharan | 2006 / 2006 | 18 – cornering R | ← | W69 |
| 10 | VW | 70D | 1993 / 2007 | 39 - straight | standing | M 12 |
| 11 | Mitshubishi | Pajero | 1992 / 2008 | 32 - straight | ← | M 61 |
| 12 | Ford | Transit | 1999 / 2004 | 36 – cornering L | → | W 45 |
| 13 | Toyota | Avensis | 2001 / 2003 | 45 - straight | lying | W 62 |
| 14 | Mazda | Demio | 1999 / 2004 | 42 - straight | ↘ 30 ° | M 81 |
| 15 | Renault | Twingo | 1993 / 2004 | 46 - straight | ↘ 60 ° | W 77 |
| 16 | Opel | Corsa | 2003 / 2004 | 39- straight | → | M 28 |
| 17 | VW | Passat | 1993 / 2005 | 30 - straight | → | W 92 |
| 18 | VW | Transporter | 2000 / 2005 | 47 - straight | ↙ 15 ° | M 84 |

The analysis of the data was used to identify the moment prior to a vehicle's contact with a pedestrian of the initial acoustic and visual warning of the driver against a potential barrier in the direction of the vehicle's movement. The measurements identified that the acoustic signal is always activated together with the visual warning. The visual warning of the driver is accompanied by a flashing light alarm which is located between the speedometer and the windscreen. It is a place with very good visibility for the driver. The light strip is approx. 15 cm long and its size is sufficient to alert the driver.

During the initial measurements, the vehicle was tested for the detection of pedestrians in the setting sun, i.e. when the sun is low over the horizon and dazzles the driver and also the camera. The measurements showed that when the sun is low over the horizon (15° and less), the functionality of the system will not deteriorate when driving in the direction of the sunlight ± 30 degrees (measured range) from the direction of the vehicle's movement.

Night measurements with no light source other than the vehicle's lighting showed that the system is unable to detect and react to a pedestrian. The system is able to detect a pedestrian at night up to the speed of approx. 20 km/h and brake subsequently. The system activates and identifies this manoeuvre based on a barrier (vehicle) and not based on the detection of a human figure. This fact was supported by a message "City Safety was activated", which appears upon the system's activation based on a critical situation ahead of the vehicle due to the presence of another vehicle. This conclusion follows from the functionality of the City Safety system, which is designed for driving the vehicle in traffic jams at low speeds, where the system reacts to objects or vehicles in the vehicle's traffic corridor and not to pedestrians.

During the tests with a lying dummy, the system was not activated in any event. The technical manual of the vehicle states that the system reacts to figures taller than 80 cm.

**An Example Case Study Analysis**

The study includes the acceleration curve derived from the measured data. It was subsequently converted to a video sequence which simplified video evaluation. It involved a vehicle moving at the speed of approx. 47 km/h at the time of the real collision. A pedestrian moving at approx. 4 km/h entered the vehicle's corridor from the left. The vehicle and the pedestrian were synchronised based on the result of an exact simulation of the PC Crash 10.0 programme. The visual representation of the course of case study No. 2.

1. The simulation started at the moment of a vehicle's passage through the light gate 5 s and 70 m before the collision with a pedestrian. The dummy is still standing at this moment. At the moment of the vehicle's passage through the light gate, UFO's control unit evaluates the right moment for the activation of UFO (pedestrian) based on the current speed of the Volvo vehicle.
2. The vehicle moves on at a constant speed of 47 km/h and at the time 4.3 s before the collision with the dummy, UFO is activated with an acceleration of 1 $m/s^2$. A fully automated and synchronised action reproduces a real accident.
3. At the time 2 s and 19 m ahead of the dummy movement corridor (Fig.2), the acoustic and visual warning of the driver is activated at the moment when the dummy is located at a distance approx. 0.7 m from the movement corridor of the Volvo vehicle driving at approx. 45 km/h. The Volvo does not brake autonomously at this moment.

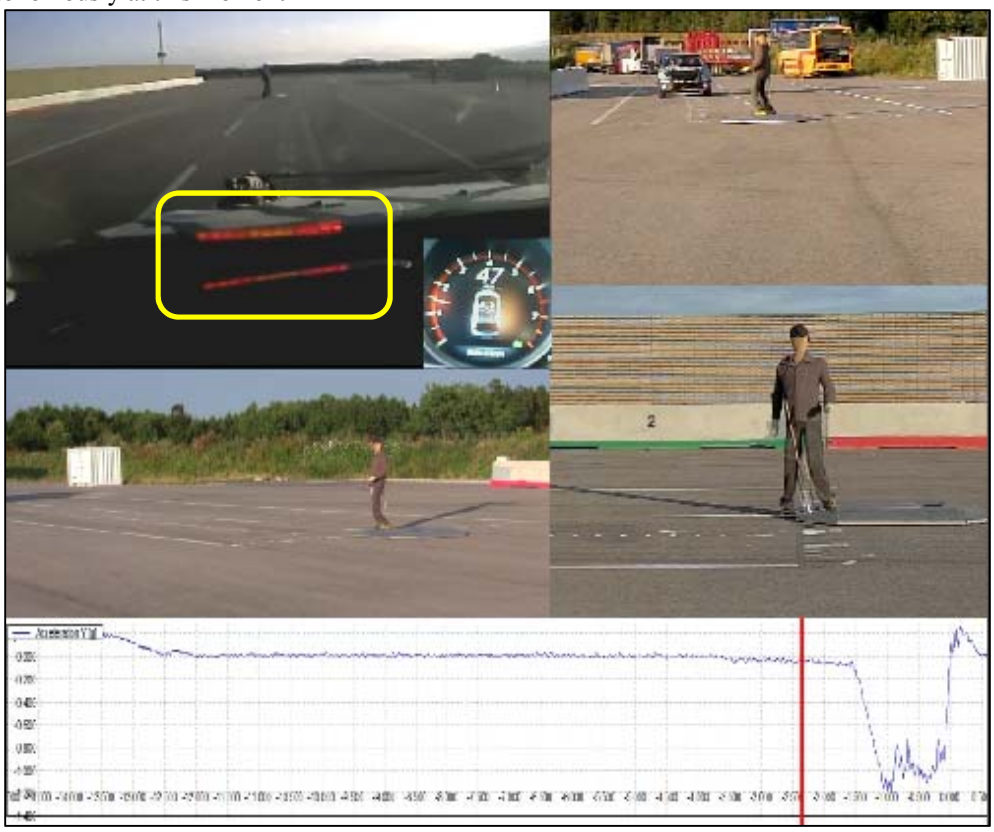


***Figure 2 Activation of the visual and acoustic alarm***

4. After less than 0.8 s from the activation of the alarm, the autonomous braking of the vehicle is activated at a distance of approx. 13 meters from the pedestrian movement corridor (Fig. 3). The vehicle brakes with an average deceleration of approx. $10ms^{-2}$. The driver did not interfere in the vehicle's driving when the autonomous braking was activated. During the autonomous braking, the brake pedal goes down to the floor as with normal braking.

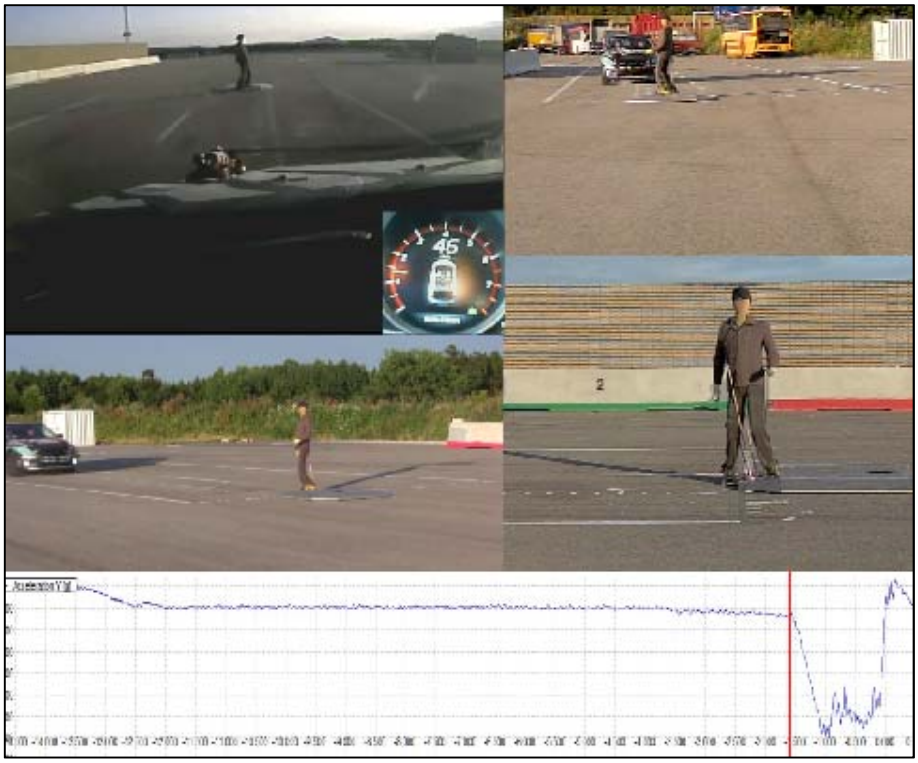

***Figure 3 Beginning of the autonomous braking***

5. After approx. 2 seconds from the initial acoustic signal, the vehicle collides with the dummy. The speed at the time of collision (Fig. 4) was approx. 12 km/h (base on acc and GPS) compared to 48 km/h in the real accident where the driver fails to react to a pedestrian.

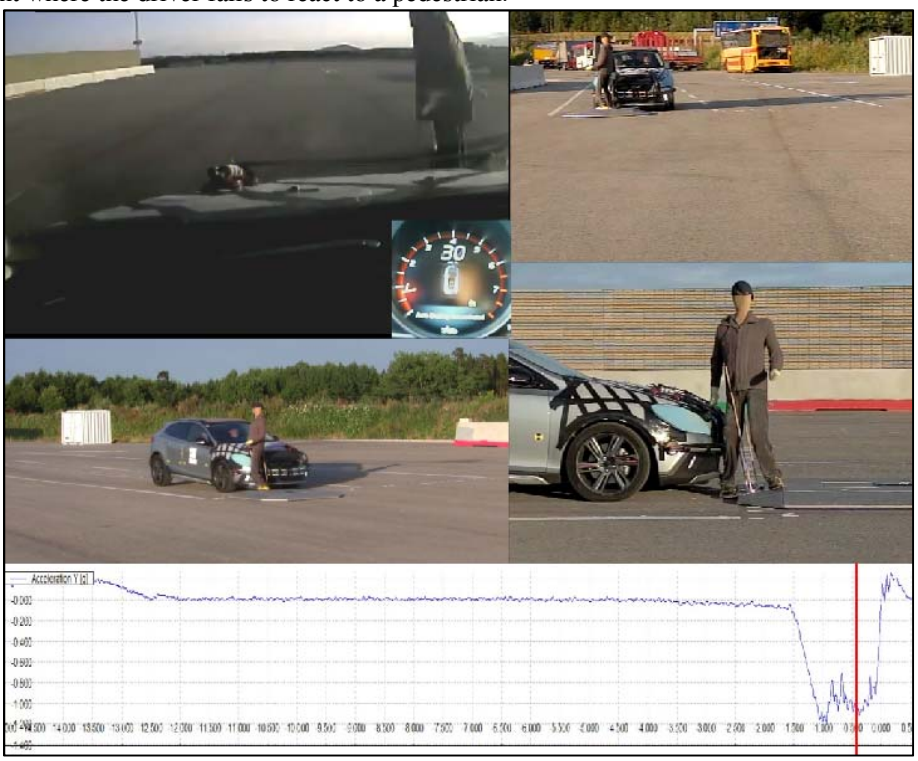

***Figure 4 Time of the first contact with dummy***

The course of the tested study allows us to clearly describe the entire accident depending on the time and distance of the vehicle from the dummy. If there was a collision with a pedestrian (a person weighing more than 15 kg), it is quite possible that the contact with the person would activate the active bonnet. This action would expand the clear space between the components in the engine compartment and the bonnet, which would contribute to a reduction in the pedestrian's injuries caused by solid parts. It is unlikely and questionable that the pedestrian airbag would be activated because the vehicle's speed at the moment of collision with the pedestrian was only approx. 12 km/h. These hypotheses are potential objectives for future research steps of the author of this paper.

**Acoustic and Visual Signalization of the System**

The analysis of the recorded data showed that in 69% of cases where the vehicle detected a pedestrian and evaluated it as an obstacle – "pedestrian", the driver was warned in time intervals before the collision with the pedestrian. The driver was warned more than **1 second (1-2,0s)** before the collision in nine case studies from the total number of measurements. It is a matter of further research to determine what is the time required for the driver's reaction to this alarm and the subsequent driver's action (dodging, braking etc.).

From the forensic point of view, it is important to identify the dependence of speed, distance and time of activation of the acoustic and visual alarm. In some case studies, the alarm was activated nevertheless a vehicle collided with a dummy. For a more accurate representation of the dependence, Figure 5 distinguishes the conditions for the activation of the alarm depending on the dummy's crash into a vehicle's outside corner, the middle or the inside corner. Except for one case, the points shown in the graph represent a vehicle driving straight. It is technically feasible that when driving in a curve the system's behaviour depends on the turn radius; hence, it may react to a dummy earlier.

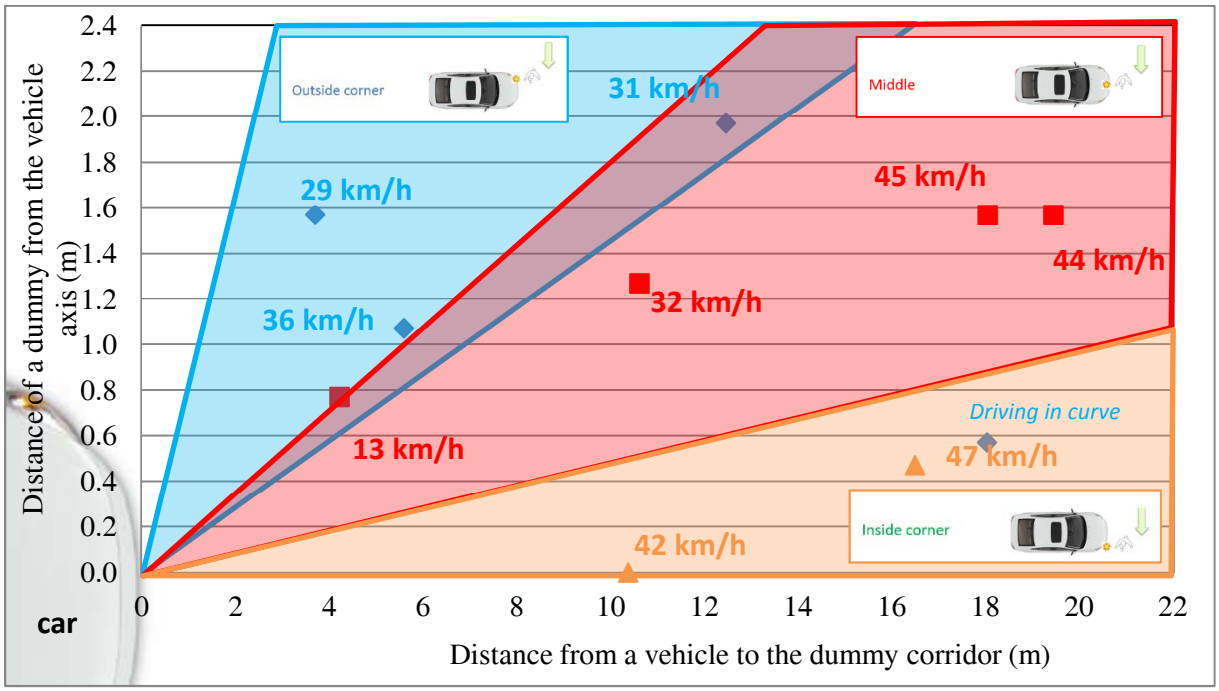


***Figure 5 Activation of the alarm depending on the speed and distance of a vehicle from the dummy's movement corridor, distance of the dummy from the vehicle axis and the subsequent contact of the vehicle with the dummy (the inside corner, the middle of the vehicle or the outside corner)***

**Autonomous Braking of the System**

Autonomous braking of the vehicle occurred in 63% case studies after the lapse of the acoustic warning of the driver. The time interval from the system's first acoustic and visual reaction until the initial moment of braking ranged from **0.1 to 0.8 seconds**. Braking was initiated without prior acoustic warning in one study case.

The measurements showed that the driver's sharp intervention with the vehicle's control at the time of warning or braking ends the process of warning and autonomous braking. It is the objective of further studies to determine what time interval after the initial warning is necessary for a distracted driver to react to objects in the driving corridor and, subsequently, to make the right manoeuvre to avoid collision with such object.

## BENEFITS OF AUTONOMOUS BRAKING FOR THE COURSE OF AN ACCIDENT EVENT

The analysis of the test studies identified that Volvo's pedestrian detection system in Volvo V40 of the model year 2014 can stop the vehicle autonomously in front of a pedestrian at low speeds up to 30 km/h if the pedestrian's movement is sufficiently predictable and the system is able to monitor the pedestrian with no object impeding the camera's view of the pedestrian. It is necessary to note in such cases where the system can stop the vehicle from low speed that there is no jump or a sudden change in the direction of the pedestrian's movement towards the road. At speeds above 30 km/h, there is always a significant reduction in the vehicle's speed before the actual collision with a pedestrian, but by a maximum of approx. 30 km/h compared to the vehicle's speed at the time of the initial reaction of the system. The overall summary of the reduction in speed as a result of the vehicle's autonomous intervention is shown in Table 2.

***Table 2 Decreasing of velocity the Volvo car during simulated scenarios***

| Case no. | 1 | 2 | 3 | 4 | 5 | 6 | 7 | 8 | 9 | 10 | 11 | 12 | 13 | 14 | 15 | 16 | 17 | 18 |
|---|---|---|---|---|---|---|---|---|---|---|---|---|---|---|---|---|---|---|
| Obstacle in driver view | yes | | | yes | | | | yes | | | | | | | | | yes | |
| Motion of the car | streight | streight | cornering L | streight | streight | streight | cornering L | overtaking R | cornering R | streight | streight | cornering L | streight | streight | streight | streight | streight | streight |
| Impact velocity in crash accident (km/h) | 23 | 47 | 12 | 50 | 32 | 19 | 41 | 55 | 18 | 39 | 32 | 36 | 45 | 42 | 40 | 39 | 30 | 30 |
| Alarm | | yes | yes | yes | yes | yes | yes | | | yes | yes | | | yes | | yes | | yes |
| Alarm before the crash (s) | | 2,0 | 1,0 | 1,7 | 1,5 | 0,5 | 1,6 | | | 1,9 | 1,5 | | | 1,1 | | 0,6 | | 1,5 |
| Decreasing of the velocity (%) | **0** | **74** | **100** | **48** | **0** | **0** | **59** | **0** | **0** | **64** | **34** | **0** | **0** | **57** | **0** | **0** | **0** | **30** |

All videos from measurements are available on youtube:
**www.youtube.com – than write "Peter Vertal" to the search line**
or
**https://www.youtube.com/channel/UCN6U-u4nQVjyCvSr8nm5eFg**

## CONCLUSIONS

In the near future, our expert deeds will increasingly often involve vehicles that are equipped with modern and sophisticated systems. These systems are intended to facilitate and secure the movement of vehicles on roads, but they also cause complications when dealing with such accidents from professional or expert perspective.

The measurements made with a highly sophisticated vehicle model Volvo V40 CC identified the vehicle's behaviour in different traffic situations, whose range covers normal movement of pedestrians and vehicles in urban traffic. These measurements can be summarised in a few points.

- The system does not react to a lying pedestrian.

- The system does not react to a standing pedestrian shorter than 80 cm.
- The system does not react to a pedestrian in the dark if the pedestrian is only illuminated with the vehicle's dipped or main beam.
- In good light conditions (until dusk), the system detects a person regardless of whether the pedestrian is wearing a reflective vest or not.
- When driving the vehicle into the sun that is low above the horizon, the system reacts to such situation and can detect a pedestrian (the camera is not dazzled).
- In daytime conditions, the system reacts to a pedestrian moving from 3.6 to 7.5 km/h (the speed from real tested accidents). Higher speeds of a pedestrian's movement were not tested.
- The system reacts to a pedestrian who is standing in the driving corridor of the vehicle.
- The system reacts to a pedestrian who is moving perpendicular to the direction of the vehicle's movement.
- The system reacts to a pedestrian who is moving at an angle in the direction or in the opposite direction of the vehicle's movement, but only up to an angle of the pedestrian's movement of +/- 45° from the plane perpendicular to the plane of the vehicle's movement.
- The driver was warned more than **1 second (1-2,0s)** before the collision in nine case studies from the total number of measurements. It is a matter of further research to determine what is the time required for the driver's reaction to this alarm and the subsequent driver's action (dodging, braking etc.).
- The time interval from the system's first acoustic and visual reaction until the initial moment of braking ranged from **0.1 to 0.8 seconds**. Braking was initiated without prior acoustic warning in one study case.
- The brakes lag time takes about **0.5 seconds**. Standart brakes lag time during a driver braking is 0.2s
- The system does not react to a traffic situation where the vehicle is moving in a laevorotatory corner and a pedestrian is moving into the road from the left.
- The system does not react to a traffic situation where the vehicle is moving in a dextrorotatory corner and a pedestrian is moving into the road from the right.
- The system that has detected a pedestrian can stop the vehicle completely only if the vehicle is moving at a speed up to 30 km/h and the pedestrian's movement is smooth and predictable.
- The system that has detected a pedestrian can reduce the vehicle's speed if the vehicle moves at a speed over 30 km/h and the pedestrian's movement is smooth and predictable.
- The vehicle's speed at the detection of a pedestrian can be reduced by a maximum of 30 km/h.
- If the driver intervenes with the vehicle's control during its autonomous intervention, the system deactivates autonomous braking.

The measurements show that the benefits of the system are noticeable and it is a good step to reducing the severity of pedestrian injuries caused by a collision with a car. Although a Volvo driving over 30 km/h will not stop in front of a pedestrian, the time interval when the driver is warned of an obstacle in front of the vehicle ranges up to 2.0 seconds, which may have a positive impact on the course of an accident event.

*This paper was created with the support of the OP Education for the project "Promoting quality education and research for the transport sector as the engine of the economy" (ITMS: 26110230076), which is co-funded by the European Social Fund.*

Európska únia
Európsky sociálny fond

Operačný program VZDELÁVANIE

Agentúra Ministerstva školstva, vedy, výskumu a športu SR pre štrukturálne fondy EÚ

*Moderné vzdelávanie pre vedomostnú spoločnosť/Projekt je spolufinancovaný zo zdrojov EÚ*

# The Force Measurement of Primary Parts in Frontal Vehicle Crash Test

## - by Strain Gauge Calibration -

**Park Un-chin** **Song Ha-jong*** **Kim Hyun-chul***
**Florian Ganz**** **Sudar Sankar**** **Mario Wohlfahrt****

ABSTRACT

In this research, the new calibration component test methodology and converted forces from strain gauge will be proposed about measuring real time force of frontal NCAP crash powertrain mounting and structure like front side member.

**Key Word** : Strain Gauge, Vehicle Crash, Force Calculation, Structure Force Distribution

## 1. Introduction

Strain gauges are commonly used in Aerospace and vehicle durability tests but not for the vehicle dynamic crash so often. Recently some vehicle crash institutes are applying the strain gauge to predict the vehicle deforming time in case of accelerometer measuring failure or dummy ribs displacement but not for the force measurement. [1)~4)]

To know the force distribution of structure in vehicle crash test is very important because all the strength design of each part can be changed by it. In the CAE, we can easily measure the value it but it's not easy in the real car crash test because the most of structure and inner steel parts like front side member and knee support bracket are in plastic deformation. If we insert the load cell device replacing measuring parts it is possible but this way cannot be used in so many developing tests because those device will influence the test result.

So in this research we will find how to attach strain gauges efficiently to know the component system level real-time force distribution in vehicle crash test with considering avoiding its plastic deformation area. To avoid the trial and error we also developed some component tests which can be tested easily and measured the force. It is very good to find force vs strain voltage synchronizations.

All the measurements are measured again in 14MY Kia YD real vehicle crash test. We could find the synchronization with dynamic component test. Also, we can compare the difference static and dynamic breakage force.

* Safety Performance Team 1 : Author or Co-Author
** Crash Simulation Team : Co-Author
*** ACTS (Advanced Car Technology System) : Co-Author

## 2. Main Subject

### 2.1 Powertrain Mounting Breakage Force

#### 2.1.1 Mounting breakage phenomena

Breakage itself cannot be judged as a bad thing because sometimes it helps vehicle crash pulse to stay in low level. But how to control is important if too easily broken there will too much deformation in the passenger compartment. This is the one purpose of this measurement research.

The used YD vehicle is the US model of 1.8 Nu engine auto transmission. Its mountings are 3 points-engine mounting, transmission mounting and roll rod. In case of roll rod the breaking direction and point are too various so we selected measuring position the engine mounting and transmission mounting. Also in the other mounting breakage measuring HKMC has measured its bolt z-direction force so this time we concentrated to these 2 mountings.

In case of YD vehicle crash the chain cover in the engine mounting side is broken. In case of transmission mounting side, there is no broken parts but during the crash the applied force angle is changed from 0 deg to 45 deg.

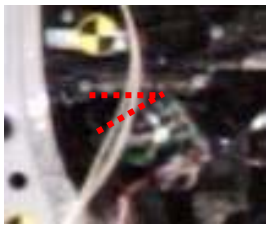

Fig.1 Post picture of YD engine mounting

### 2.1.2 Component test set-up

To make similar static tensile test of breakage condition with vehicle crash as static condition, we used side door strength test bench. The chain cover of engine is mounted on the jig and the engine mounting is connected to it with engine mounting bracket. We attached 3 strain gauges with x,y and z direction on the bracket considering its load path and flat surface to attach. The other test case is the usage of 3 axis loadcell, replacing the engine mounting bracket.

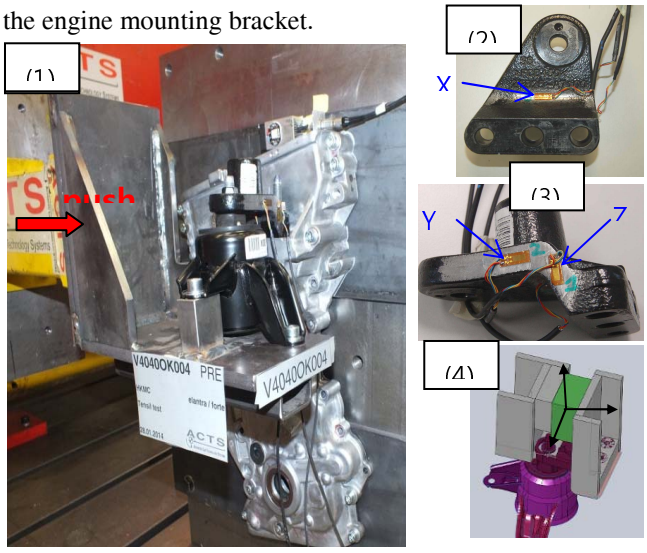


Fig.2 Chain cover breakage tensile test(1)/
Strain gauge position(2),(3)/3 Axis Load cell (4)

In case of transmission mounting breakage component test, we also used jig to mount transmission bracket and the transmission mounting,

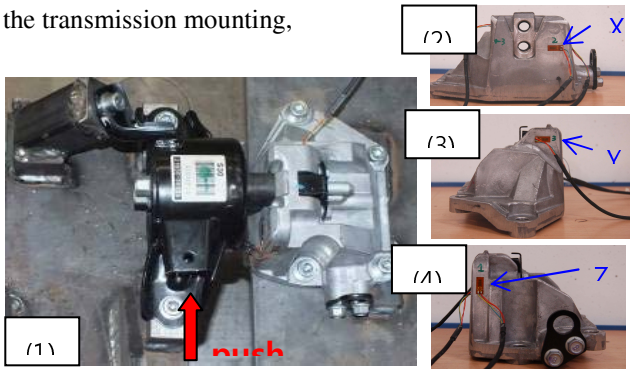


Fig.3 Transmission bracket breakage tensile test(1)/
Strain gauge position(2),(3),(4)

Also, in the crash CAE animation we already know the pushing angle is changed from 0 degree to 45 degree so we made another test chain pulling bench with seatbelt component test device.

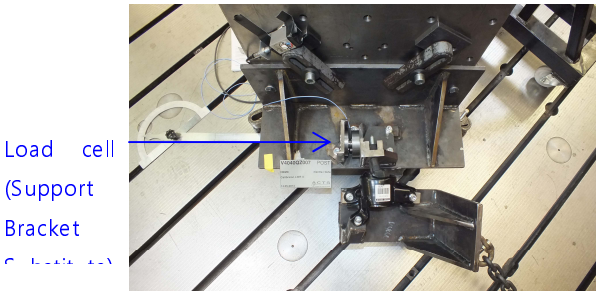


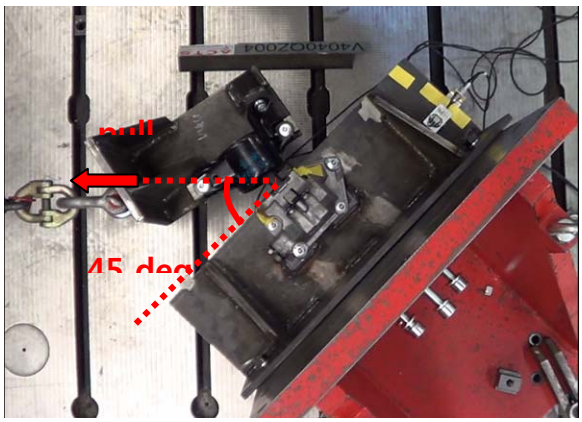


Fig.4 Transmission bracket breakage test with 45 degree
(with loadcell, without loadcell)

### 2.1.3 Component test result of engine mounting

We pushed the mounting jig in all case except first trial test with 200mm/min. The force limit was 10 ton at pushing test device. The result summary is below.

| Tests | | Pushing Force (t) | Loadcell (t) | Strain (0.01%) | | |
|---|---|---|---|---|---|---|
| | | | x | x | y | z |
| ENG | 1. Loadcell | **2.1** | **2.1** | - | - | - |
| | 2. Strain gauge | **2.7** | - | 2.2 | 4.5 | **2.3** |
| | 3. Loadcell jig | 3.0 | - | - | - | - |

Table 1. Summary of engine mounting breaking force

At the 1st engine mounting test, we used 3 axis load cell to confirm pushing force is equal to the force applied to the engine mounting bracket. Even if there was some breakage failure on the load cell mounting 4 bolts, we can check pushing force and load cell force was exactly same as 2.1 ton.

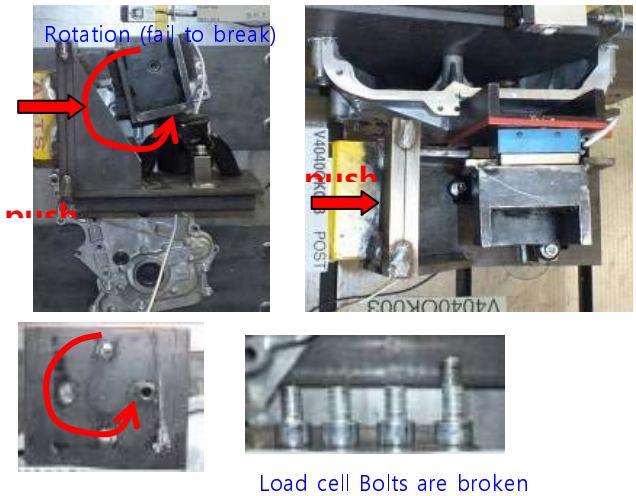


Fig.5 Engine mounting tensile test1 post picture

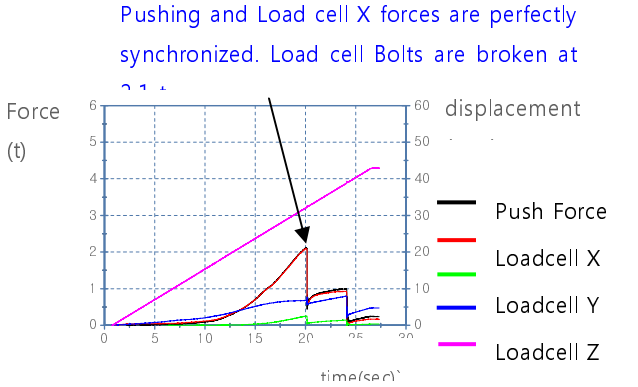


Fig.6 Engine mounting tensile test1 for

At the 2nd strain gauge test, we used the engine mounting bracket as the vehicle with 3 strain gauges attached. As a result, the chain cover rear hole is broken at 20mm displacement with 2.7 ton force. This breaking phenomena was very similar to the broken chain cover in high speed crash vehicle because the broken sequence is from the rear and the section surface is mostly vertical to y and z plane of vehicle.

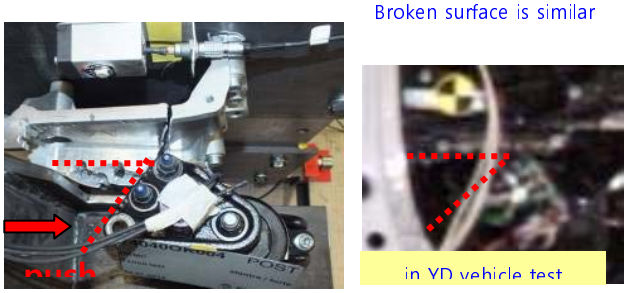


Fig.7 Engine mounting tensile test2 post picture

In this test the all the strain gauges are activated but x and y direction strain gauges activation was too small and the shape is not correspondent. The mode of z direction strain gauge is really synchronized very well to the pushing force. Now we can know this position is good elastic deforming place to measure its load and the load path is very unexpected because its direction is z.

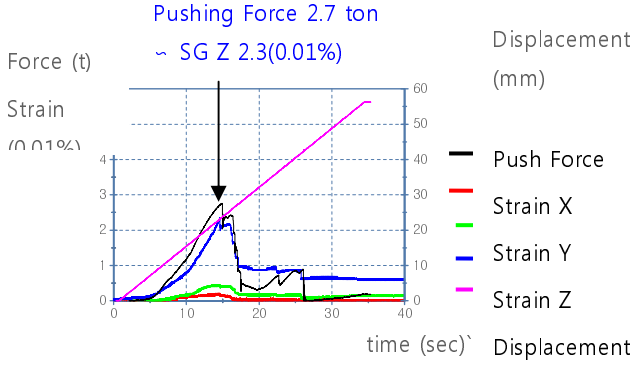


Fig.8 Engine mounting tensile test1 force graph

Also even if we have some rubber material like engine mounting bush on the calibration system we can use strain gauge to find the applied real time force. Now we can use this strain gauge position to fine the force in the vehicle crash test. This would be helpful to adjust the value of breaking force to improve the crash performance.

At the 3rd engine mounting test, we used 3 axis load cell jig again to check the variety of chain cover breaking force. Aluminum die casting breaking force tolerance is well known because it has a lot of air pouch inside when it is created. It has average 175~270Mpa tolerance at 1% strain-stress curve and to the amount of 310 MPa in case of 2% strain.

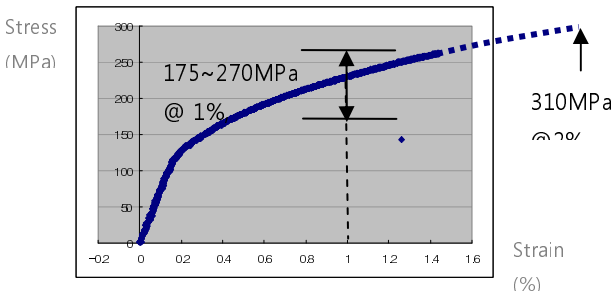


Fig.9 Aluminum die casting strain-stress curve

Because the load cell bolts were broken we attached 3 tucks to resist the breaking moments. As a result of 3rd engine mounting test, chain cover is broken at 3 ton pushing force with similar section surface to the test2. This is just 10% tolerance from 2.7 ton of 2nd test. So this kind of load cell can be used in the vehicle crash test to measure the breaking force instead of the engine mounting bracket only if it is not broken and deformed. The strong point of this load cell application is that it is possible to measure y and z direction force also. Most of engine rotates in y axis so there would be also z direction force.

Fig.10 Engine mounting tensile test3 post picture

### 2.1.4 Component test result of engine mounting

We pushed the mounting jig in all case except first trial test with 200mm/min. The force limit was 10 ton at pushing test device and 7 ton at pulling test device. The

result summary is below

| Tests | | Pushing Force (t) | Loadcell (t) | Strain (0.01%) | | |
|---|---|---|---|---|---|---|
| | | | x | x | y | z |
| TM | 1. 0 deg) Strain gauge | **5.0** | - | 4.3 | **5.5** | 3.4 |
| | 2. 45 deg) Strain gauge | **3.7** | **3.6** | | | |

Table2. Summary of transmission bracket breaking force

At the 1st transmission bracket test, we used the transmission supporting bracket as the vehicle with 3 strain gauges attached. As a result, the bracket is broken at 50mm displacement with 5.0 ton force. This breaking phenomenon did not happen in YD crash test but in case of next model of Elantra happened. So we can use this component test for both cases of transmission supporting broken or not broken to measure the real time force.

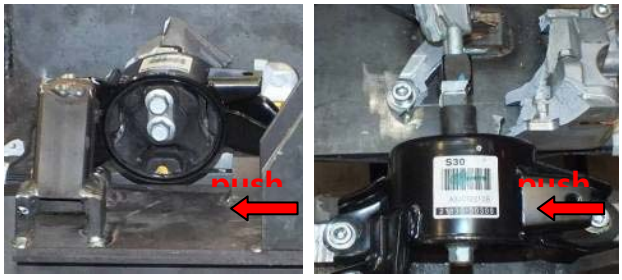


Fig.11 Transmission mounting tensile test1 post picture

In this test the all the strain gauges are activated but x and z direction strain gauges peak was delayed some. we can think this comes from the rubber bush absorbed the force till 23ms because x and z direction strain gauges are attached adjacent to the rubber bush. The mode of y direction strain gauge is really synchronized very well to the pushing force. The only differences are after being broken the smaller fall of strain y and the curve shape in detail. There seem to be come from the elastic system in including rubber but not difficult to see the peak force in transmission bracket.

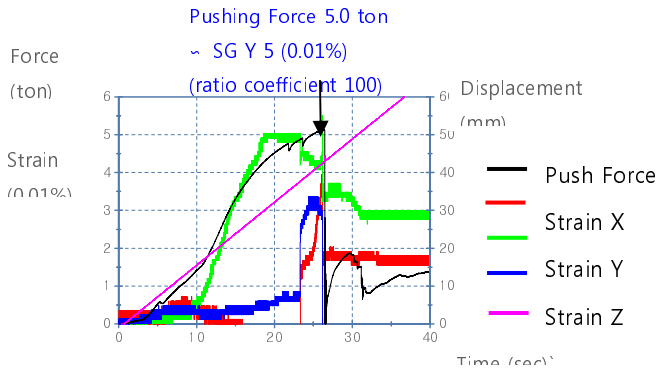


Fig.12 Transmission mounting tensile test1 force graph

Now we can know this position is good elastic deforming place to measure its load. In this case the load path is as expected because its direction is y. Also even if we have some rubber material like transmission mounting bush even there are hard steel bolts inside on the calibration system we can use strain gauge to find the applied real time force. Now we can use this strain gauge position to fine the force in the vehicle crash test. This would be helpful to adjust the value of breaking force to improve the crash performance.

Also we can see at test2 the pushing force is almost same as loadcell value like engine mounting breakage test.

## 2.2 Front Side Member Crushing Section Force

### 2.2.1 Calibration Condition

To calibrate the front side member its straightness is very important. In case of YD, the rear lower of front side member has some bending to be connected to the floor side member. So we cut the front side member at the end of its straightness.

To measure YD's front side member we selected 2 x-direction sections which were almost no deformation during the US NCAP crash because if there is some deformation strain gauge value doesn't show the actual applied force. We attached 4 x-direction strain gauges at section1 for each surface one and 10 x-direction strain gauges at section2 for each surface 2~3.

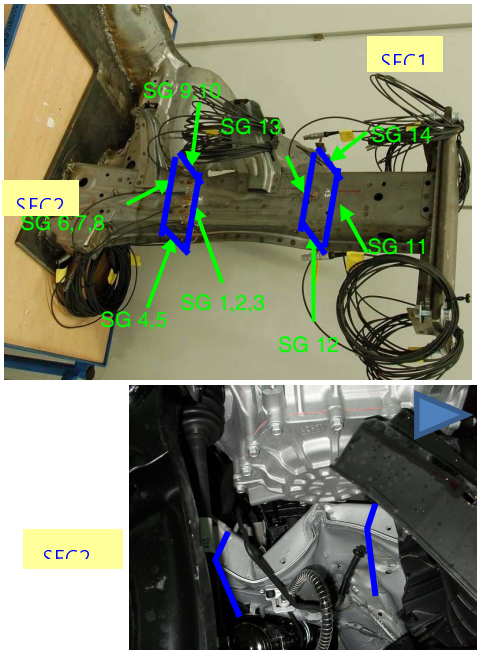


Fig.13 Front side member calibration sections

### 2.2.2 Calibration Result

We pushed front side member with 3 kinds of force- 2.5ton, 5ton and 10 ton because we already know the fact in RCAR frontal barrier test with load cell inserted to the member section the yielding force of the similar grade

compact car next model of Elantra front side member is 16 ton. As a reference in NCAP test its yielding force s 29 ton.

| Force | | Strain (mV) | | | |
|---|---|---|---|---|---|
| SG No | | 11 | 12 | 13 | 14 |
| 1st | 2.5t | 0.05 | 0.7 | 0.47 | 0.26 |
| 2nd | 5t | 0.08 | 1.36 | 1.08 | 0.63 |
| 3rd | 10t | 0.26 | 2.73 | 2.13 | 1.33 |
| Ratio coeffi. | | 0.98 | 1.00 | 1.00 | 1.00 |

Table3. SEC1 Summary of front side member calibration

| Force | | Strain (mV) | | | | | | | | | |
|---|---|---|---|---|---|---|---|---|---|---|---|
| SG No | | 1 | 2 | 3 | 4 | 5 | 6 | 7 | 8 | 9 | 10 |
| 1st | 2.5t | 0.12 | 0.07 | 0.08 | 0.03 | 0.95 | 1.08 | 0.55 | 0.56 | 0.5 | 0.03 |
| 2nd | 5t | 0.18 | 0.14 | 0.15 | 0.2 | 1.71 | 2.07 | 1.08 | 0.96 | 0.94 | 0.23 |
| 3rd | 10t | 0.51 | 0.25 | 0.25 | 0.1 | 3.29 | 4.01 | 2.12 | 2.09 | 2.02 | 0.43 |
| coeffi. | | 0.99 | 1.00 | 0.99 | 0.55 | 1.00 | 1.00 | 1.00 | 1.00 | 1.00 | 0.98 |

Table4. SEC2 Summary of front side member calibration

The correlation was so linear except strain gauge4.

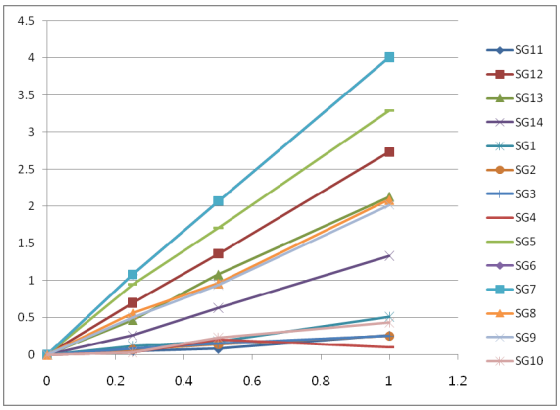


Fig.14 Front side member calibration result

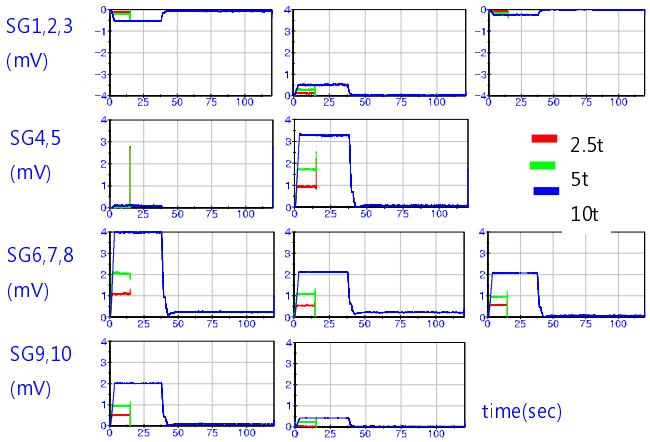


Fig.15. SEC2 calibration result of each strain gauges

The interesting thing is the ratio of each section strain peak average was similar for all 3 forces' test at section2 calibration. But in case of section1 calibration this ratio was not constant because we attached only 1 for each section. This can be useful to find initial yielding direction of the member and can be used to control the vehicle crash dipping value. In case of this YD member we can know the initial principle deformation surface is "inner" and "bottom". When we see Fig12, we can check the member was deformed mostly at inner and secondly at bottom.

| Force | outer | bottom | inner | upper |
|---|---|---|---|---|
| 2.5t | 1 | 4 | 8 | 2 |
| 5t | 1 | 4 | 9 | 2 |
| 10t | 1 | 3 | 8 | 2 |

Table5. The ratio of each surface strain at SEC2

### 2.2.3 Member Dynamic Component Test Condition

There are two frontal high speed modes in official crash tests. One is 56kph frontal to wooden flat barrier of US NCAP and KNCAP. The other one is 64kph 40% offset to aluminum honeycomb of EuroNCAP which are used in many country's NCAP. In case of 64kph offset there are some tolerance of honeycomb strength so 56kph frontal mode is better for the research of front side member characteristic.

To realize the YD 56kph frontal in component level, is we used 800kg rear half trolley. At the frontal center of barrier we attached YD's left frontal side member. We attached transmission with its linkage and subframe front mounting link because these have big influences to the member deformation in the real vehicle NCAP crash. as half rigid parts. We also attached 70mm distance the part of YD's crash box because too much hard contact can make some strain gauge noise peak value.

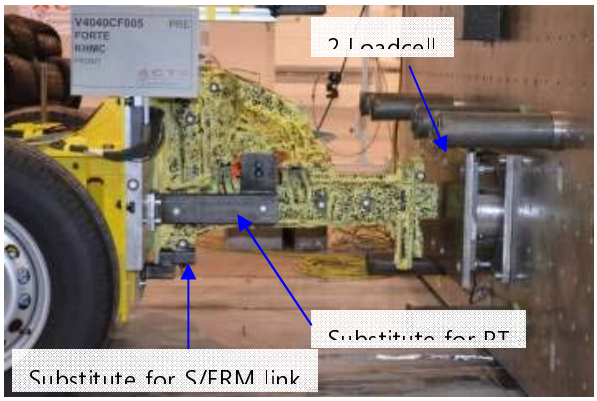


Fig.16. SEC2 calibration result of each strain gauges

It is well known fact when we should lessen the speed in the component level trolley test because the crushing energy is not absorbed by non-existing part. Experimentally we know in case of 56kph frontal, we use 35kph with same test weight for frontal member test. But in this test the trolley total weight was 940kg which is smaller than 1475kg of full car test and only left half hand side member was applied, we used 30.1kph after

calculating same energy. [5)~6)]

$$1/2m_1v_1^2=2*1/2m_2v_2^2 \quad m_1=1390\ v_1=35,$$

$$m_2=940 \quad \text{Then, } v_2=31\text{kph}$$

We also have the other experience, in case of frontal RCAR we use the same speed, 15kph at 70% mass. Even that is not full frontal mode, we know 30.1kph is appropriate number because 940kg is 64% of 1475kg.

At laser displacement measurement, we can know its dynamic peak collapsing was 352mm which is similar to acceleration calculation 372mm. When we compare the trolley x acceleration of the test with YD NHTSA official test x acceleration of rear side sill as a almost rigid part, those mode are similar at the 1st peak value.

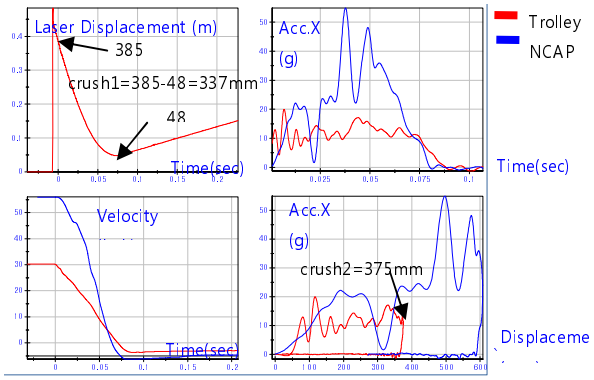


Fig.17. Member dynamic test characteristic

### 2.2.4 Measured and converted results in dynamic

By each trend line we did get the forces of the primary parts of frontal NCAP like the 2nd row of table.6. Comparing the breakage force of powertrain mountings in the dynamic situation it seems to be needed 2.5~5 times more force to be broken.

| Force | Eng MT'g | TM Mt'g | FR MBR SG5 | FR MBR SG6 |
|---|---|---|---|---|
| Vehicle | 6.9~7.3t | 25t | | 23.1t |
| MBR Dynamic | - | - | 19.7t<br>15.4t (Loadcell) | 21.5t |
| Static Component | 2.7t | 5t | - | |

Table.6 Max Force results

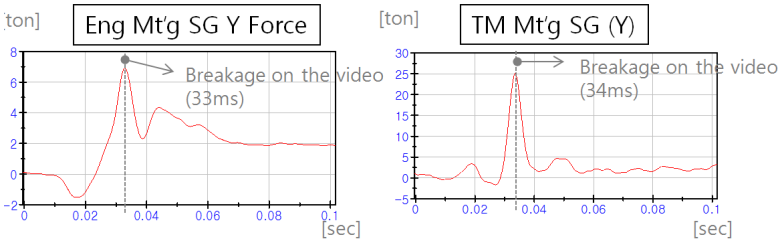


Fig.18. Powertrain breakage force converted from SG

For the member dynamic test, although we attached strain gauges in section1 and crash box there was no effective data but in section2 strain gauge 5 and 6 we got some valuable results when we converted the voltage to the force by previous calibration equations. Especially in strain gauge6, the synchronization is almost perfect. The time based curve shape matching and peak value similarity prove this strain conversion is right. So we can know the section 2 peak force is 21.5 ton. The raw data of barrier load cell has some oscillating we applied CFC60. Because the load was measured in the barrier and the strain conversion to force is for the member section2, the peak values don't have to be same. As we see fig.14 these were the most sensitive strain gauge positions among all the section2 strain gauges.

For the NCAP test measurement, the Force shape is similar to member dynamic test fom 25ms but before 20ms there is no value. We think the force is distributed to other components like hood and fender so there is no value on SG6, even section 2 has some compressing force. As a result we were successful to measure only the 1st highest force 23.1t in the real crash. Even if member dynamic test is not perfect.

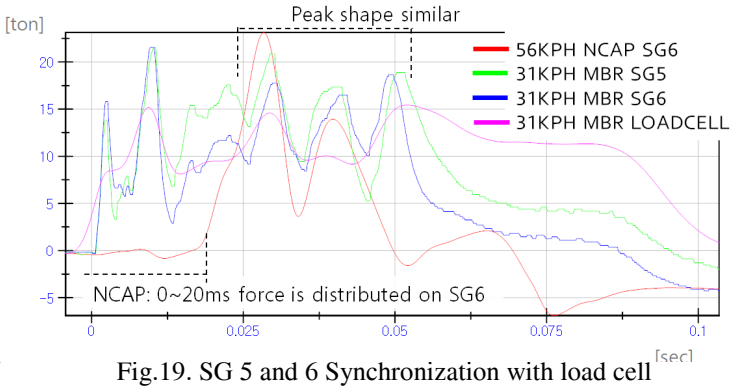


Fig.19. SG 5 and 6 Synchronization with load cell

## 3. Conclusion

As we discussed at the introduction, knowing the force of each part is very important. If we know, we can optimize the parts' weight and design for the good performance. To this time, those works were in the area of CAE but with this research we can also try more from test data. We expect test numbers frontal NCAP could be reduced half. For one vehicle development the developing cost saving would be over $120,000. We are planning this methodology adaptation from PD project.

We reviewed the component test method of powertrain mountings and front side member with those characteristics. Also wefound how to measure the real time force in powertrain mounting breakage tests and front side member dynamic crush test. The YD's chain cover breakage force in static test was about 3 ton and transmission 5 ton but 7ton and 25ton in dynamic. Front side member max force was 23.1t. These methods can be used in the full car crash tests.

If we stack these measurement and analyze we could

improve the prediction for the crash performance.

■ Patent: Be submitted "Powertrain load cell substitute"

## References


1. A. Muniappan, "Computational and Experimental Study on Lift Characteristics of Flapping Wing Micro Air Vehicle" MIT, 2006
2. P. K. C. Wood, " An Improved Test Procedure for Measurement of Dynamic Tensile Mechanical Properties of Automotive Sheet Steels" IARC, University of Warwick, 2007
3. P. K. C. Wood, " Characterising Dynamic Tensile Mechanical Properties of Automotive Materials at High Strain Rate" University of Warwick, 2007
4. Paul Lemmen, "Development of an Advanced Thorax / Shoulder Complex for the THOR Dummy" Paul Lemmen and Bernard Been, 2013
5. Karl Hoffmann, "Eine Einfüfrung in die Technik des Messens mit Dehnungsmeßstreifen", Herausgeber: Hottinger Baldwin Messtechnik GmbH, Sarmtadt
6. Herausgegeben von W.Beitz und K.-H., "DUBBEL TASCHENBUCH FÜR DEN MASCHINENBAU" 20. AUFLAGE


## ■ Author ■

Park Un-chin

Song Ha-jong

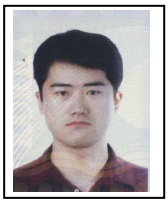
Kim Hyun-chul

Florian Ganz

Sudar Sankar

Mario Wohlfahrt

This paper has been peer-reviewed and published in a special edition of *Traffic Injury Prevention* 16(S1), by Taylor & Francis Group. The complete paper will be available on the *Traffic Injury Prevention and www.NHTSA.gov* websites on June 8, 2015.

To access all Peer-reviewed papers please copy and paste the link below into your browser to access the papers.

http://www.tandfonline.com/toc/gcpi20/16/sup1

# The Force Measurement of Primary Parts in Vehicle Side/Smalloverlap Crash

## - by Strain Gauge Calibration -

**Park Un-chin** **Song Ha-jong*** **Kim Hyun-chul****
**Florian Ganz***** **Sudar Sankar***** **Mario Wohlfahrt*****

ABSTRACT

In this research, the new calibration component test methodology and converted forces from strain gauge will be proposed about measuring real time force of side structure like B-pillar, roof rail, door beams and side sill of IIHS side crash and lower arm, A-pillar force of IIHS smalloverlap.

**Key Word** : Strain Gauge, Crash, side crash, smalloverlap, Force Calculation, Structure

## 1. Introduction

Strain gauges are commonly used in Aerospace and vehicle durability tests but not for the vehicle dynamic crash so often. Recently some vehicle crash institutes are applying the strain gauge to predict the vehicle deforming time in case of accelerometer measuring failure or dummy ribs displacement but not for the force measurement. [1)~3)]

To know the force distribution of structure in vehicle crash test is very important because all the strength design of each part can be changed by it. In the CAE, we can easily measure the value it but it's not easy in the real car crash test because the most of side structure and smalloverlap steel parts like lower arm and A-pillar are in plastic deformation. But even if they are in plastic deformation if the strain curve keep continuity and reasonable value we assume the converted force is closed to the real force. This would be profitable because we cannot insert the load cell device worrying about its breakage.

So in this research we will find how to attach strain gauges efficiently to know side structure force of IIHS side crash and lower arm/A-pillar of smalloverlap in real-time. IIHS side To calibrate the component we also developed some component tests which can be tested easily. The side structure deforming modes are simplified to make this calibration component tests.

* Safety Performance Team 1 : Author or Co-Author
** Crash Simulation Team : Co-Author
*** ACTS (Advanced Car Technology System) : Co-Author

## 2. Main Subject

### 2.1 Side Structure Force Measurement

#### 2.1.1 Simplifying deforming mode

The side crash deforming mode is not simple as front side member's initial simple compressing. But fortunately recent Hyundai-Kia vehicle are using hot stamping material in B-pillar so the most deformation of the structure is concentrated on the B-pillar, struck side doors, roof rail and side sill if there is no tearing and cut parts.

The used YD vehicle is the US model, it has Good grade in structural rating with over 160mm distance from B-pillar to seat centerline. There is almost no big deformation in Y direction on the floor and A&C –pillar. So we already made trolley test method for the only evaluation of side structure. [6)]

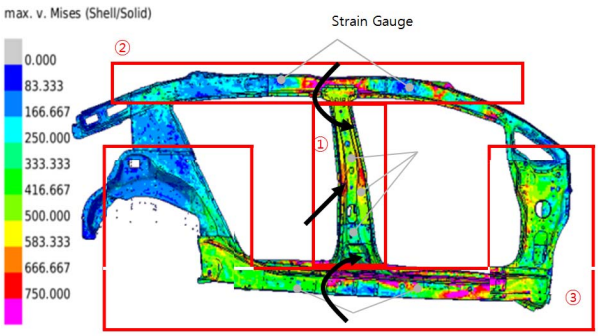


Fig.1 YD IIHS side trolley CAE model

When we review the strain distribution in YD IIHS side trolley CAE model in Fig.1 we can define the deforming modes as 3 types except doors. Firstly, the B-pillar is on the bending. Considering the modes we

attached rosette strain gauges at 3 positions of plane surface and no big deformation after crash. Secondly the roof rail is on the distorting mainly on the B-pillar connected position. Considering the modes we attached rosette strain gauges at 2 positions. Thirdly the side sill is also on the distorting mainly on the B-pillar connected position. Considering the modes we attached rosette strain gauges at 2 positions.

In case of doors, the major strength parts are door beams and they are in the simple bending mode with both ends restricted. So we can make component test for the calibration easily

### 2.1.2 Von Mises equation rosette calculation

The reason why we attached rosette strain gauge is we don't know the principle force, direction and equivalent stress. If we calculate the rosette by Von Mises equation we can get 2 principle stress value, 2 principle direction and 1 equivalent stress.

- Main stress formula:

$$\sigma_{1,2} = \frac{E}{1-\mu} \bullet \frac{\varepsilon_a + \varepsilon_c}{2} \pm \frac{E}{\sqrt{2}(1+\mu)} \sqrt{(\varepsilon_a - \varepsilon_b)^2 + (\varepsilon_c - \varepsilon_b)^2}$$

- Mohr circle:

$$\tan \Psi = \frac{2\varepsilon_b - \varepsilon_a - \varepsilon_c}{\varepsilon_a - \varepsilon_c} = \frac{N}{D}$$

- Direction:
  - If N>0 and D>0 then the direction is $\varphi = \frac{1}{2}(0° + \psi)$
  - If N>0 and D<0 then the direction is $\varphi = \frac{1}{2}(180° - \psi)$
  - If N<0 and D<0 then the direction is $\varphi = \frac{1}{2}(180° + \psi)$
  - If N<0 and D>0 then the direction is $\varphi = \frac{1}{2}(360° - \psi)$

Fig.2 Von Mises equation

The equivalent stress is a fictive, single directional stress amount that equals the deformation caused by the real, multi directional stress configuration. So it can be used for real force and torque calculation.

For a two dimensional strain configuration, the equivalent strain us given by:

$$\sigma_v = \sqrt{\sigma_x^2 + \sigma_y^2 - \sigma_x \cdot \sigma_y + 3 \cdot \tau^2}$$

Using the main stress configuration, the shear will be null and the equivalent stress. [4)~5)]

$$\sigma_v = \sqrt{\sigma_1^2 + \sigma_2^2 - \sigma_1 \cdot \sigma_2}$$

### 2.1.3 B-pillar calibration test and calculation

To calibrate the B-pillar with static we chose the side strength test machine. The pusher, if it is too narrow it can cause too partial bending, we selected 254mm round shape pole. The pushing position on the B-pillar we marked is the first plastic bending occurred place z=548mm in car coordinates from CAE model. By experience we selected maximum force 5.2ton and stroke 400mm with 1.66mm/s speed.

Fig.3 YD B-pillar component test

As a result, we got the F-D curve and strain gauges' value of 10Hz filtering by time. From 5 times test with 1,2,3,4 and 5 ton we can get the trend equation from Fig6. These values are equivalent stress from rosette macro calculation.

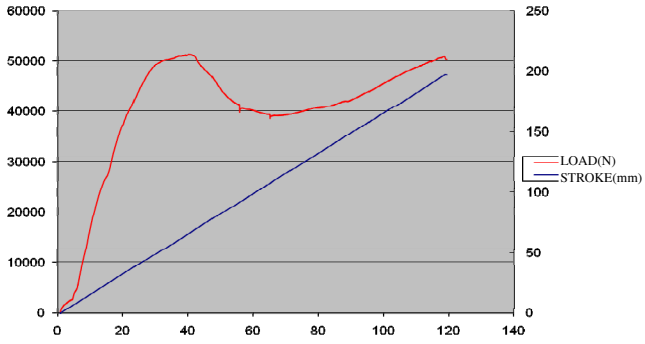


Fig.4 YD B-pillar component test F-D (5ton)

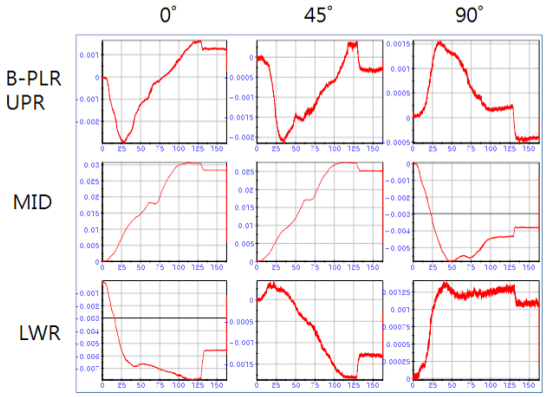


Fig.5 YD B-pillar component test SG graphs (5ton)

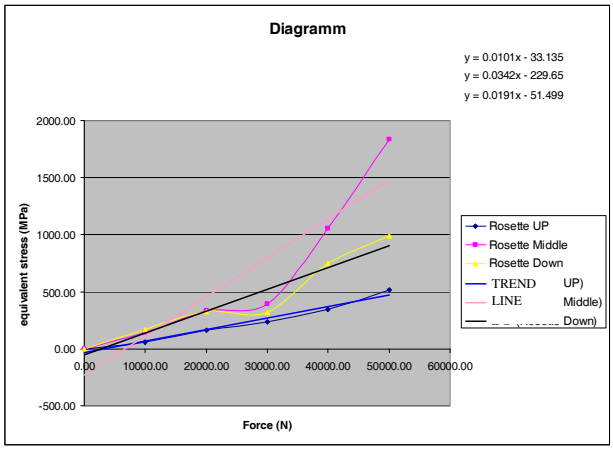


Fig.6 YD B-pillar component test trend line

### 2.1.4 Roof Rail calibration test and calculation

To calibrate the roof rail with static we chose the pulling test machine. We cut the B-pillar on the level of Z=548mm because it is the bending start point in the side crash and adequate to calculation the torque. The pusher, we used the steel chain, Also we welded B-pillar reinforcing stand because the B-pillar could be deformed without it before roof rail distorting. By experience we selected maximum torque 1kN with 1.66mm/s speed.

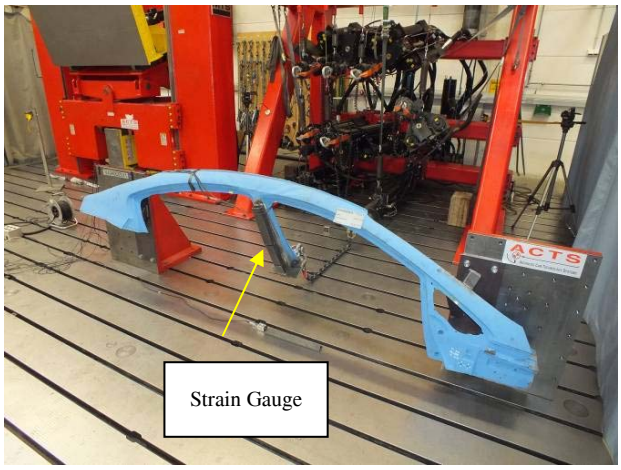


Fig.7 YD roof rail component test

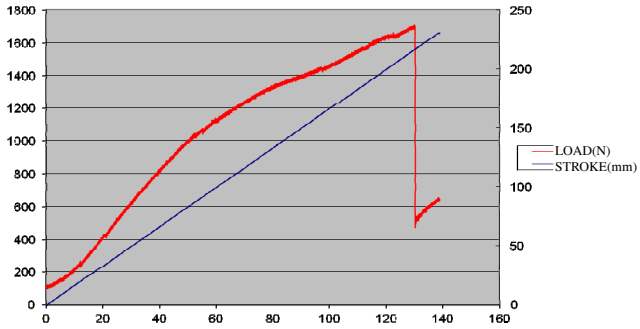


Fig.8 YD roof rail component test F-D

As a result, we got the F-D curve and strain gauges' value of 10Hz filtering by time. From 5 times test with 0.2, 0.4, 0.6, 0.8 and 1kNm torque we can get the trend equation from Fig10. These values are equivalent stress from rosette macro calculation.

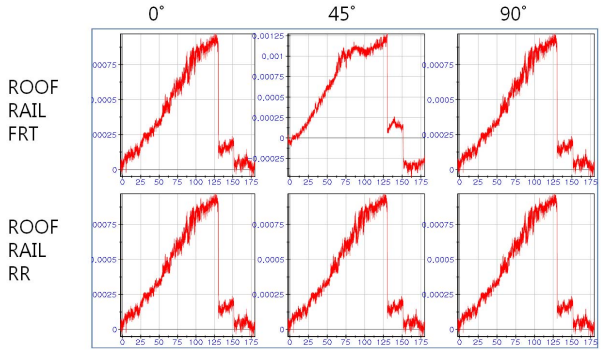


Fig.9 YD roof rail component test SG graphs

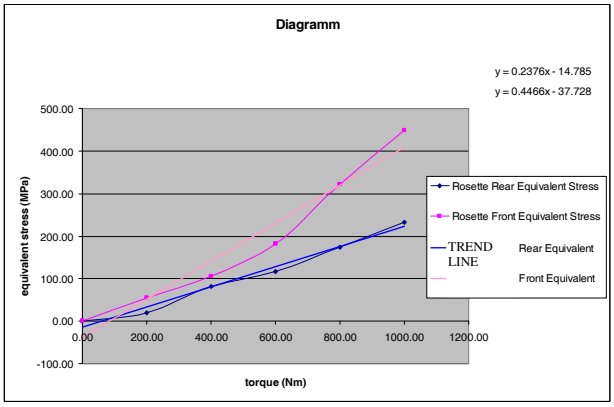


Fig.10 YD roof rail component test trend line

### 2.1.5 Side Sill calibration test and calculation

To calibrate the side sill with static we chose the pulling test machine again. We cut the B-pillar on the level of Z=548mm because it is the bending start point in the side crash and adequate to calculation the torque. The pusher, we used the steel chain, Also we welded B-pillar reinforcing stand because the B-pillar could be deformed without it before side sill distorting. By experience we selected maximum torque 10kN with 1.66mm/s speed.

Fig.11 YD side sill component test

As a result, we got the F-D curve and strain gauges' value by time. From 5 times test with 2, 4, 6, 8 and 10kNm torque we can get the trend equation from Fig14. These values are equivalent stress from rosette macro calculation.

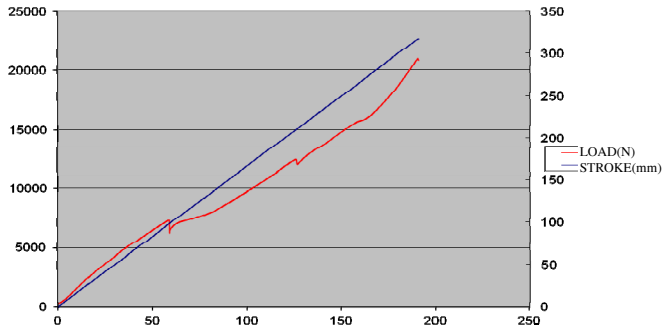


Fig.12 YD side sill component test F-D

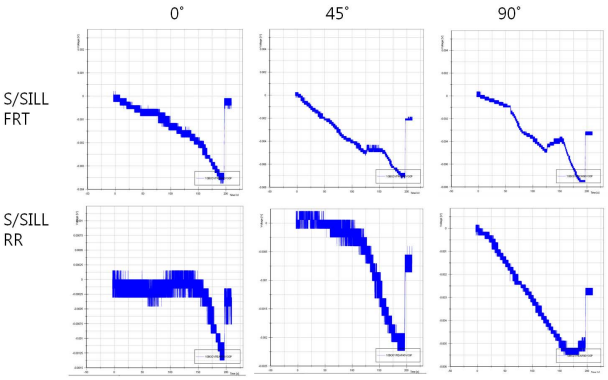


Fig.13 YD side sill component test SG graphs

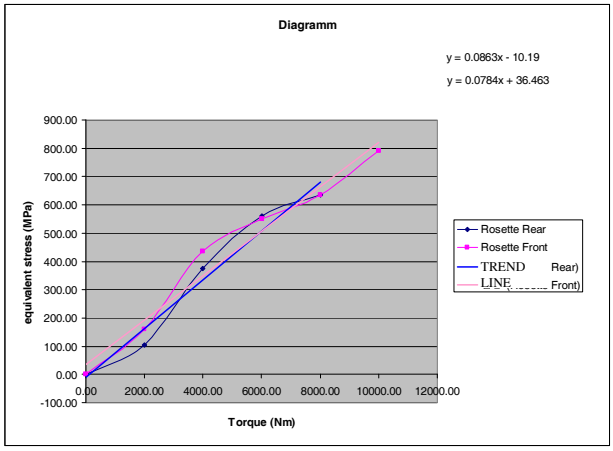


Fig.14 YD side sill component test trend line

### 2.1.6 Side door beams calibration test and calculation

To calibrate the door beams we chose the pulling test machine again. We mounted the 3 types of door beams (front, rear upper and lower) on the jig and pulled by 60mm width belt to prevent from point-concentrated load until plastic bending with 1.66mm/s speed.

Fig.14 YD door beam component test

The breakage force of door was 2.9 ton at front door beam and 3.3 ton at rear door upper beam. For the rear door lower beam the breakage force was not measured because we limited the maximum force as 4 ton.

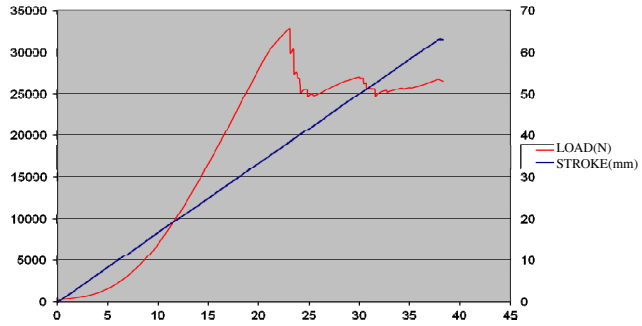


Fig.15 YD rear door upper beam component test F-D

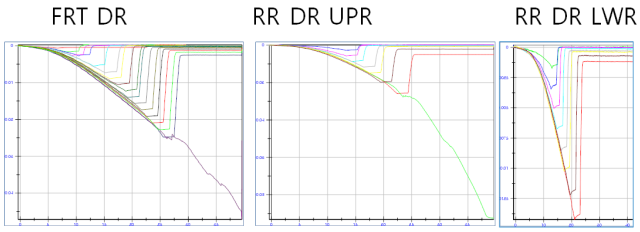


Fig.16 YD door beam component test SG graphs

As a result, we got the F-D curve and strain gauges' value by time. From 6~16 times test with different forces we can get the very linear trend equation from Fig16. These values are simple voltage because we think beam deformation is simple bending mode.

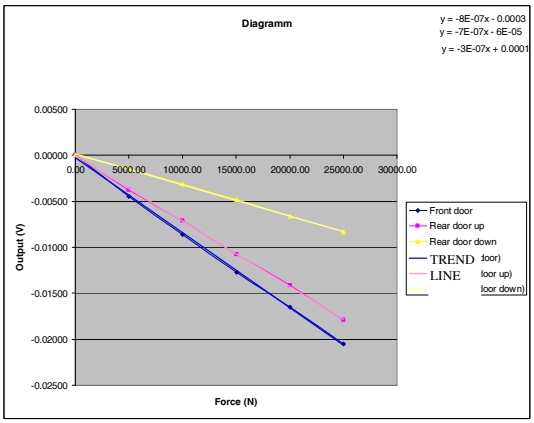


Fig.16 YD door beam component test trend line

### 2.1.7 Force calculation in YD IIHS side trolley test

By each trend line we did get the forces of the primary parts like table.1. We were successful for 8 points in 10 measuring place.

| DOOR BEAM | ROOF RAIL | B-PLR | S/SILL |
|---|---|---|---|
| 7.3t (FRT) | 1.2kNm (FRT) | 20t (UPR) | Error (FRT) |
| 3.4t (RR UPR) | Error (RR) | 26t (MID) | 7.1kNM (RR) |
| 21t (RR LWR) | - | 5t (LWR) | - |

Table.1 MaxForce and Torque results

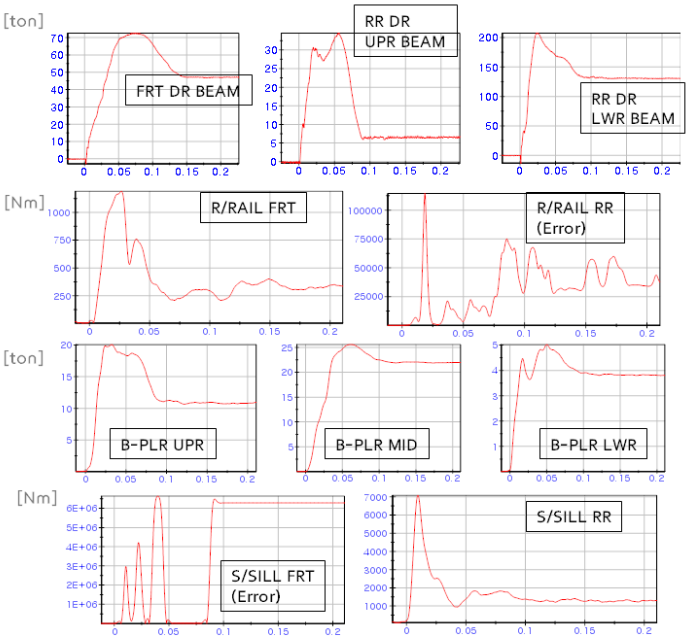


Fig.17 YD side trolley Converted to force graph

## 2.2 Smalloverlap Structure Force Measurement

### 2.2.1 A-pillar calibration test and calculation

We assumed the A-pillar deformation and attached 2 strain gauges on the edge place where there is no plastic deformation. We pushed at side door strength test bench with 0.33m/s speed until 400mm deformation. Because the vehicle test was MD, we carried out the component test also with MD A-pillar.

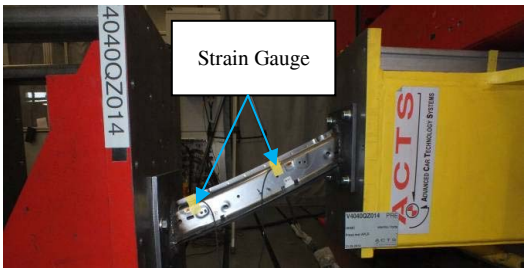


Fig.18 MD A-pillar component calibration test

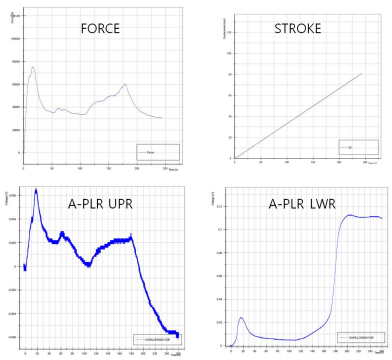


Fig.20 MD A-pillar component test SG graphs

As a result, we got the F-D curve and strain gauges' value by time. From 5 times test with 2, 4, 5, 6 and 7 ton force we can get the trend equation from Fig21. These values are equivalent stress from rosette macro calculation.

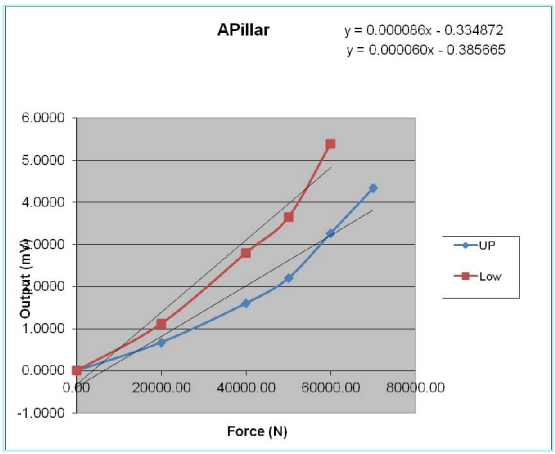


Fig.21 MD A-pillar component test trend line

### 2.2.2 Side sill calibration test and calculation

We assumed the side sill deformation and attached 2 strain gauges on the edge place where there is no plastic deformation. We pushed at side door strength test bench with 0.33m/s speed. But unfortunately, in the MD vehicle test, we didn't get meaningful voltage data. But this type of test method for side sill can be used in the next research.

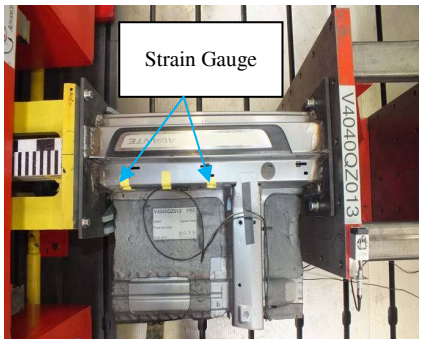


Fig.22 MD side sill component calibration test

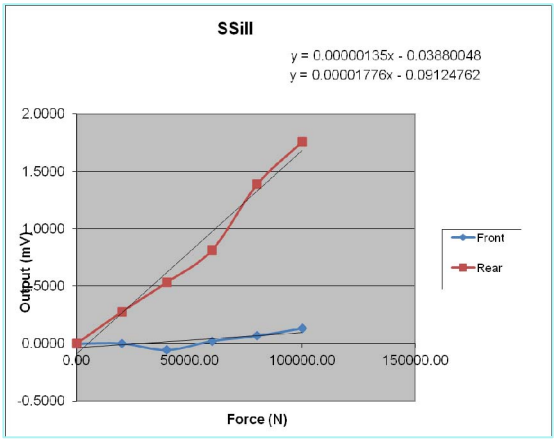


Fig.23 MD side sill component test trend line

### 2.2.3 Lower arm calibration test and calculation

We also tried to calculated YD smalloverlap lower arm A & B point removal force. We pulled G point at the chain pulling device with 3.33mm/s in 3 ways, firstly

only A point fixation and pulling in Y direction, secondly only B point fixation and pulling in Y direction and lastly A & B point fixation and pulling in X direction. We substitute YD smalloverlap trolley test which its structure deformation and movement was very close to the real crash.

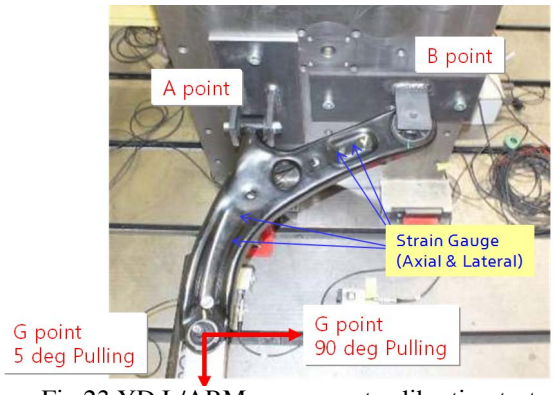


Fig.23 YD L/ARM component calibration test

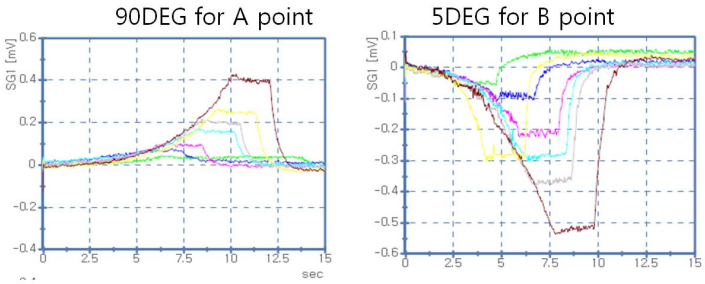


Fig.24 YD L/ARM component calibration test SG graphs

As a result, we got the F-D curve and strain gauges' value by time. From 8~9 times test with different forces we can get the linear trend equation from Fig25. These values are simple voltage because we think lower arm main load path is in axial direction.

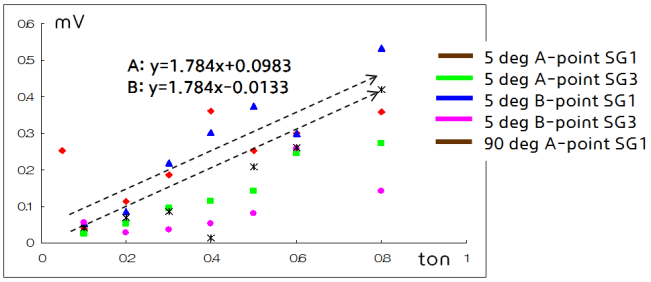


Fig.25 YD L/ARM component test trend line

### 2.2.4 Force calculation in YD smalloverlap trolley test

By each trend line we did get the forces of the primary parts of side and small overlap vehicle tests like table.2. We were successful for 6 points in 8 measuring place. In case of YD lower arm we selected the meaningful force measuring time with A point disconnection and the B point before being crushed from high speed video.

| MD A-PLR | YD L/ARM |
|---|---|
| 12t (UPR) | 13t@40ms (A point) |
| 11t (LWR) | 16.5t@44ms (B point) |

Table.2 Max Force results

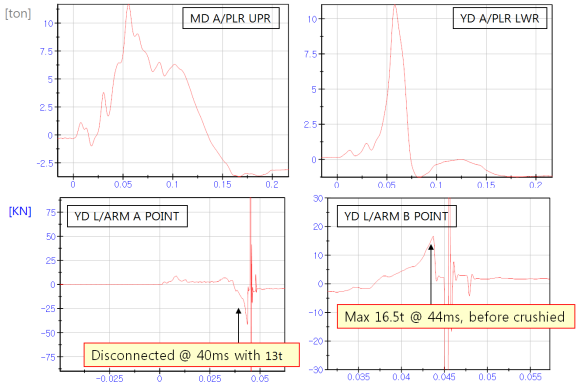


Fig.26 MD/YD smalloverlap converted to force graph

## 3. Conclusion

As we discussed at the introduction, knowing the force of each part is very important. If we know it, we can optimize the parts' weight and design for the good performance. To this time, those works were in the area of CAE but with this research we can also try more from test data. We expect test numbers side and smalloveralp could be reduced half. For one vehicle development the developing cost saving would be over $150,000. We are planning this methodology adaptation from PD project. We did know below facts in this research.

1) Even complicate deforming mode like side crash if we simplify the modes and use rosette strain gauge calibration, we can know its abbreviate real time force.

2) From the each part calibration test of the vehicle we can check its unique F-D curve. This could be used for the quality comparison.

3) For the YD IIHS side, the maximum force and torque of B-pillar 26t, door beam 21t, roof rail 1.2kNm and side sill 7.1kNm

4) For the MD smalloverlap, the maximum force of A-pillar 12t. For the YD smalloverlap, the maximum force of Lower arm A point was 13t and B point 16.5t.

If we stack these measurement and analyze we could improve the prediction for the crash performance.

■ Patent: Be submitted Diadem macro Rosette strain calculation

## References

1. A. Muniappan, "Computational and Experimental Study on Lift Characteristics of Flapping Wing Micro Air Vehicle" MIT, 2006

2. Janko Slavic, "Accelerated Fatigue and Modal Parameter Identification of Lightweight Structures" University of Ljubljana, 2014
3. Paul Lemmen, "Development of an Advanced Thorax / Shoulder Complex for the THOR Dummy" Paul Lemmen and Bernard Been, 2013
4. Karl Hoffmann, "Eine Einfüfrung in die Technik des Messens mit Dehnungsmeßstreifen", Herausgeber: Hottinger Baldwin Messtechnik GmbH, Sarmtadt
5. Herausgegeben von W.Beitz und K.-H., "DUBBEL TASCHENBUCH FÜR DEN MASCHINENBAU" 20. AUFLAGE
6. Park Un-chin "The trolley test way of IIHS small overlap and side test with minimized structure usage", HKMC, 2014

## ■ Author ■

Park Un-chin

Song Ha-jong

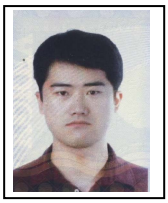
Kim Hyun-chul

Florian Ganz

Sudar Sankar

Mario Wohlfahrt

# AUTOMATIC CONTROL OF VEHICLE STEERING SYSTEM DURING LANE CHANGE

**Mirosław Gidlewski**
University of Technology and Humanities in Radom
Poland

**Dariusz Żardecki**
Military University of Technology
Automotive Industry Institute
Poland

Paper Number 15-0106

## ABSTRACT

Mechatronic systems assist drivers in safe driving of cars more and more often. A vision of a totally automated car realizing many manoeuvres without driver's participation becomes closer and closer. The lane change manoeuvre is one of the basic manoeuvres on the ground of which sequences of complex manoeuvres can be composed, e.g. vehicle passing or obstacle avoidance manoeuvre. For those reasons, automation of lane change manoeuvre appears to be essential for automation of vehicle driving and is a subject of numerous research studies. Within a research project, the authors have undertaken extensive analytical studies on application of active steering system EPS in automatic driving of a two-axis truck equipped with typical elements of ESC system and obstacle detectors, as well as road monitoring systems.
The present paper focuses on theoretical aspects of the synthesis of an automatic controller for the EPS active steering system. Simulation studies of an automatically controlled lane change manoeuvre illustrate the application of the methodology. The basis for theoretical considerations and numerical studies is the mathematic model of the controlled system (vehicle) and the controller. A complex, detailed description of the dynamics of a two-axis truck, taking into account nonlinearities and vehicle motion in 3D space, is included in the simulation model. The model of the controller is based on a reference model which is significantly simplified and hence is highly effective for carrying out necessary computations in real time. An algorithm of the controller operating as a Kalman regulator in a closed loop system is developed on the basis of this model. The time decomposition of the automatic control process into two phases –lateral displacement of the vehicle and stabilization of its position – is an essential, original distinguishing feature of the algorithm. Thanks to this decomposition, the structure of the control system is relatively simple. Feedback signals provided by the sensors available in a typical ESC system (lateral acceleration, yaw velocity) are used in the control process. The vehicle reference model and resulting control algorithms are presented in the paper. Simulation results refer to a two-axis truck travelling with a constant velocity on a straight, uniform road. At certain time instant the vehicle starts executing the lane change manoeuvre. Simulations were carried out for a number of cases with varying model parameters. That allowed estimating the sensitivity of the control algorithm to both perturbations of vehicle's physical and operational parameters and to perturbations of parameters related to the obstacle. The results of simulations show that the proposed concept of the vehicle automatic control performs well in computational tests. The method of automatic execution of the lane change manoeuvre presented in the paper can offer an attractive alternative for vehicle control engineers and researchers working in the fields of active steering systems of vehicles, including commercial trucks.

## INTRODUCTION

Development of modern automotive technology results in an increasing use of mechatronic systems assisting drivers in safe driving of road vehicles. The prospect of a totally autonomous vehicle performing a range of manoeuvres without driver's participation nears. The lane change manoeuvre is one of basic manoeuvres on the basis of which more complex manoeuvres such as vehicle overtaking or obstacle avoidance can be undertaken. Obstacle avoidance is necessary when an object suddenly appears on the vehicle path in a distance smaller than the estimated travel needed to stop. For these reasons, automation of the lane change manoeuvre is essential to achieve the goal of fully autonomous vehicle control. It is a subject of numerous research programs as well as prototype development and testing.
Publications on automation of lane change manoeuvre usually refer to the concept of automatic control including optimal path planning and then trajectory tracking [2, 4, 9, 10, 11, 12]. Trajectory planning is sometimes treated as a problem of parametric optimization of heuristically assumed forms of the desired path (segments of sinusoidal function, composition of arcs, line segments, parabola segments etc.). Optimization of the desired path should not only achieve short manoeuvre duration, desired smoothness of the trajectory, limitation of side jerks, but also ensure that the planned path will be feasible for efficient trajectory control. As known, trajectory tracking errors depend on

the quality of the desired path. Trajectory tracking controllers proposed in publications cited above are based on known algorithms from the control theory. Obviously, parameters of the vehicle, as well as parameters of its steering system, have significant influence on the optimal path and the choice of the tracking controller [13, 14].
Within the research project [7], comprehensive analytical studies have been carried out on the application of the active steering system EPS (Electric Power System) in automatic driving of a commercial truck of medium load capacity. Considered traffic situations included suddenly appearing obstacle potentially causing collision. The truck under consideration was equipped with typical elements of ESC (Electronic Stability Control) and obstacle detectors, as well as road monitoring systems.
This paper is based on a portion of the aforementioned studies [7]. It focuses on theoretical aspects of the synthesis of an automatic controller for the EPS active steering system. Simulation studies of an automatically controlled lane change manoeuvre illustrate the application of the methodology.
The basis for theoretical considerations and numerical studies is the mathematical model of the controlled system and the controller. A complex, detailed description of the dynamics of a two-axis truck, taking into account nonlinearities and vehicle motion in 3D space, is included in the simulation model representing the real system to be controlled. Complex nonlinear dynamics of the steering mechanism is included in the model, with free play and friction in the joints. The model of the controller is based on a simple reference model – known in the literature as a bicycle model of a car. Desired path as well as the structure and parameters of the controller are determined using this model.
An essential, distinguishing feature of the control algorithm is the decomposition of the lane changing manoeuvre into two phases: vehicle turning to move swiftly into the adjacent lane and then stabilization in the direction of the new lane. Owing to this decomposition, the structure of the control algorithm is relatively simple. Feedback signals provided by the sensors available in a typical ESC system (lateral acceleration, yaw velocity) are used in the control process. The vehicle reference model and resulting control algorithms are presented in the paper. Simulation results refer to a two-axis commercial vehicle of medium load capacity travelling with a constant velocity on a straight, uniform road. At certain time instant the vehicle starts executing the lane change manoeuvre. Simulations were carried out for a number of cases with varying model parameters. That allowed estimating the sensitivity of the control algorithm to both perturbations of vehicle's physical and operational parameters and to perturbations of parameters related to the obstacle. The results of simulations show that the proposed concept of the vehicle automatic control performs well in computational tests.

## LANE CHANGE MANOEUVRE IN THE FRAMEWORK OF THE CONTROL THEORY

### Assumptions

An obstacle suddenly appears on a straight stretch of the road in front of the travelling vehicle. The vehicle starts braking (manual or automatic process) until the time instant the control system discovers that further braking inevitably leads to a crash. After automatic monitoring of obstacle surroundings, if conditions allow for that, the rotation of the steering wheel is activated automatically in order to avoid the obstacle while travelling with a constant velocity that was reached at the final stage of braking. At the end of the manoeuvre vehicle should travel on the lane parallel to the primary lane. In that way, the control of the vehicle moves from the braking phase to the lane changing phase.
The purpose of the study presented in this paper is to show the concept of the steering wheel controller that would execute the lane change manoeuvre once it was automatically initiated. The method of setting controller parameters knowing the parameters of the vehicle reference model and allowable variable ranges will also be presented. The often challenging strategy of decision making to activate the automatic lane change operation will not be considered.

### Strategy for Steering Wheel Rotation Control

The control task involves two output variables – displacement of the centre of mass and angular position of the vehicle body in relation to the trajectory of the centre of mass – and is to be carried out with one control input (steering wheel rotation). It is convenient to divide the process of steering wheel control into two successive phases of "lateral displacement" and then "stabilization".
Realization of the task of vehicle lateral displacement allows for some level of vehicle yaw with respect to the roadway axis after required lateral displacement of the vehicle centre of mass has been achieved, ensuring obstacle avoidance with certain safety margin. The priority is on the fast execution of this phase of the manoeuvre.

The task of stabilization involves adjusting the angular orientation of the vehicle to become parallel to the roadway axis. Here, the priority is on accurately performing the procedure to ensure that the vehicle follows the new lane.
Such decomposition of the control tasks is consistent with practice of driving a car by experienced race drivers. Control in the first phase of the process can be carried out partly in an open loop ("blindly", "as quickly as possible") by generating an appropriate steering wheel rotation. Accuracy at this phase of the manoeuvre is ensured by the use of the earlier identified reference model. An additional corrective control will also be present during this phase. Namely, the correction of the steering wheel rotation angle is to be carried out in a closed loop, through the comparison of the lateral displacement of the vehicle (according to the reference model) with the measured position. Control in the second phase must be carried out completely in the closed loop, by regulating the angular orientation of the vehicle with respect to the roadway axis.
The concept of the control strategy based on the decomposition into two phases is shown in Fig.1.

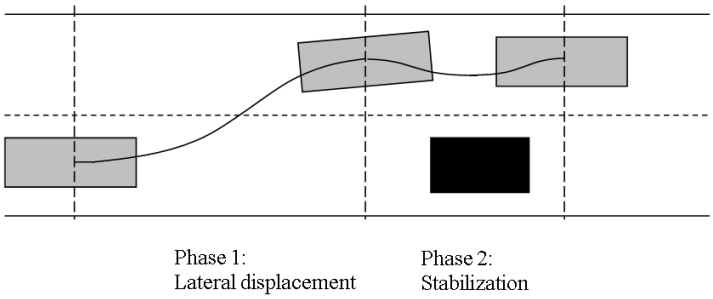


***Figure 1. Decomposition of the lane changing manoeuvre.***

Theoretical validation of this control strategy is presented in the subsequent part of the paper.

**The Reference Model**

Theoretical considerations will be conducted using the bicycle model of a car. The model describes the lateral dynamics of the vehicle travelling with constant velocity in the presence of small disturbances. This model is used in many studies related to the automatic control of vehicles. The bicycle model concept is illustrated in Fig. 2.

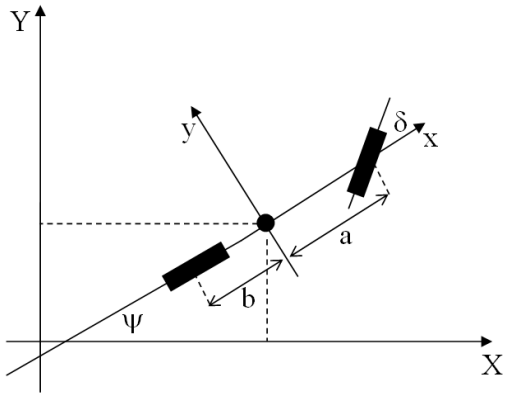


***Figure 2. Concept of the bicycle model of a car.***

Nomenclature of model variables and parameters:

| | | |
|---|---|---|
| t | – | time (t = 0 denotes the start of control), |
| δ(t) | – | steer angle of front wheels, |
| ψ(t) | – | vehicle yaw angle, |
| Ω(t) | – | yaw velocity of the vehicle ($\Omega(t) = \dot{\psi}(t)$), |
| U(t) | – | lateral velocity of the vehicle in the local coordinate frame, |
| V | – | longitudinal velocity of the vehicle (constant) in the local coordinate frame, |
| X(t), Y(t) | – | vehicle centre of mass coordinates in the global coordinate frame, |

m – mass of the vehicle,
J – moment of inertia of the vehicle with respect to the vertical axis passing through its centre of mass,
a, b – distances from the front and rear wheel axes, respectively, to the projection of the centre of mass,
$k_A$, $k_B$ – cornering stiffnesses at the front and rear wheel centres, respectively.

The mathematical model for the subsequent formulation is represented by linearized equations of motion derived from the balance of forces and moments acting on a two-wheeled vehicle. The equations expressed in the moving coordinate frame are:

$$m\dot{U}(t)+\frac{k_A+k_B}{V}U(t)+\frac{mV^2+k_Aa-k_Bb}{V}\Omega(t)=k_A\delta(t) \tag{1}$$

$$J\dot{\Omega}(t)+\frac{k_Aa^2+k_Bb^2}{V}\Omega(t)+\frac{k_Aa-k_Bb}{V}U(t)=k_Aa\delta(t) \tag{2}$$

Transformation from the moving coordinate frame to the frame connected to the road is described by the following relations:

$$\psi(t)=\int_0^t\Omega(\tau)d\tau \tag{3}$$

$$\dot{X}(t)=V\cos(\psi(t))-U(t)\sin(\psi(t)) \tag{4}$$

$$\dot{Y}(t)=V\sin(\psi(t))+U(t)\cos(\psi(t)) \tag{5}$$

Trajectory of the vehicle's centre of mass Y(X) can be determined from the following relationships:

$$X(t)=\int_0^t\dot{X}(\tau)d\tau=\int_0^t\left(V\cos(\psi(\tau))-U(\tau)\sin(\psi(\tau))\right)d\tau \tag{6}$$

$$Y(t)=\int_0^t\dot{Y}(\tau)d\tau=\int_0^t\left(V\sin(\psi(t))+U(\tau)\cos(\psi(\tau))\right)d\tau \tag{7}$$

The relationships (1-7) will be treated as an initial reference model of the vehicle.
With small and short time duration disturbances occurring during obstacle avoidance it is allowed to use linearized form of the transformation equations. Applying the Taylor series approximation gives:

$$\cos(\psi(t))\approx 1 \qquad \sin(\psi(t))\approx\psi(t) \tag{8, 9}$$

$$U(t)\sin(\psi(t))\approx 0 \qquad U(t)\cos(\psi(t))\approx U(t) \tag{10, 11}$$

Therefore, on the basis of (4-5):

$$\dot{X}(t)=V \tag{12}$$

$$\dot{Y}(t)=V\psi(t)+U(t) \qquad \ddot{Y}(t)=V\dot{\psi}(t)+\dot{U}(t) \tag{13, 14}$$

and also:

$$U(t)=\dot{Y}(t)-V\psi(t) \qquad \dot{U}(t)=\ddot{Y}(t)-V\dot{\psi}(t) \tag{15, 16}$$

After substitution into the equations of motion (1-2) and rearranging one gets:

$$m\ddot{Y}(t)+\frac{k_A+k_B}{V}\dot{Y}(t)+\frac{k_Aa-k_Bb}{V}\dot{\psi}(t)-\left(k_A+k_B\right)\psi(t)=k_A\delta(t) \tag{17}$$

$$J\ddot{\psi}(t)+\frac{k_Aa^2+k_Bb^2}{V}\dot{\psi}(t)-\left(k_Aa-k_Bb\right)\psi(t)+\frac{k_Aa-k_Bb}{V}\dot{Y}(t)=k_Aa\delta(t) \tag{18}$$

The trajectory of the vehicle's centre of mass Y(X) is determined by the relationships:

$$X(t)=\int_0^t\dot{X}(\tau)d\tau=\int_0^tVd\tau=Vt \tag{19}$$

$$Y(t)=\int_0^t\dot{Y}(\tau)d\tau \tag{20}$$

The above developed equations (17-20) will be treated as a simplified reference model of the vehicle.
In the initial reference model, the relationships (1, 2, 3) are linear and therefore can be subjected to the Laplace transformation. Then, at zero initial conditions of variables U(t) and Ω(t), an equivalent notation of the reference model can be defined in the transfer function form with the operator variable s.

$$\widetilde{U}(s)=G_{U\delta}(s)\widetilde{\delta}(s) \tag{21}$$

$$\widetilde{\Omega}(s)=G_{\Omega\delta}(s)\widetilde{\delta}(s) \tag{22}$$

$$\widetilde{\psi}(s)=\frac{1}{s}\widetilde{\Omega}(s) \tag{23}$$

where transfer functions have standard forms:

$$G_{U\delta}(s)=\frac{G_{U\delta 0}\left(T_{U\delta}s+1\right)}{T_0^2s^2+2\xi_0T_0s+1} \tag{24}$$

$$G_{\Omega\delta}(s)=\frac{G_{\Omega\delta 0}\left(T_{\Omega\delta}s+1\right)}{T_0^2s^2+2\xi_0T_0s+1} \tag{25}$$

The transfer function parameters can be described by the formulae:

$$T_0=V\sqrt{\frac{mJ}{k_Ak_B(a+b)^2-MV^2(k_Aa-k_Bb)}} \tag{26}$$

$$\xi_0=\frac{\left(m\left(k_Aa^2+k_Bb^2\right)+J\left(k_A+k_B\right)\right)}{2\sqrt{mJ\left(k_Ak_B(a+b)^2-mV^2\left(k_Aa-k_Bb\right)\right)}} \tag{27}$$

$$G_{U\delta 0}=\frac{\left(k_Ak_B(a+b)b-mV^2k_Aa\right)V}{k_Ak_B(a+b)^2-mV^2(k_Aa-k_Bb)} \tag{28}$$

$$T_{U\delta}=\frac{Jk_AV}{k_Ak_B(a+b)b-mV^2k_Aa} \tag{29}$$

$$G_{\Omega\delta 0}=\frac{k_Ak_B(a+b)V}{k_Ak_B(a+b)^2-mV^2(k_Aa-k_Bb)} \tag{30}$$

$$T_{\Omega\delta}=\frac{maV}{k_B(a+b)} \tag{31}$$

Operational calculus cannot be applied to Eqs. (4) and (5) due to the presence of nonlinear terms.
All relationships in the simplified reference model are linear and therefore the Laplace transformation can be applied and appropriate transfer functions can be determined. Then, at zero initial conditions of variables $\dot{Y}(t),\psi(t),\ \Omega(t)$, an equivalent notation of the simplified reference model in the transfer function form can be obtained as follows:

$$Y(s)=G_{Y\delta}(s)\delta(s) \tag{32}$$

$$\psi(s)=G_{\psi\delta}(s)\delta(s)=\frac{G_{\Omega\delta}(s)}{s}\delta(s) \tag{33}$$

where

$$G_{Y\delta}(s)=\frac{G_{\Omega\delta 0}V\left(T_1^2s^2+2\xi_1T_1s+1\right)}{s^2\left(T_0^2s^2+2\xi_0T_0s+1\right)} \tag{34}$$

$$T_1=\sqrt{\frac{J}{k_B(a+b)}}\qquad \xi_1=\frac{b}{2V}\sqrt{\frac{k_B(a+b)}{J}} \tag{35, 36}$$

**Responses to the Step Input of Wheels Rotation**

$$\text{If}\quad \delta(t)=\delta_0 1(t)\quad (1(t)-\text{Heaviside function}) \tag{37}$$

$$\text{then}\quad \delta(s)=\delta_0\frac{1}{s} \tag{38}$$

$$\lim_{t\to\infty}U(t)=\lim_{s\to 0}\left(sU(s)\right)=\lim_{s\to 0}\left(sG_{U\delta}(s)\delta(s)\right)=\lim_{s\to 0}\left(s\frac{G_{U\delta 0}\left(T_{U\delta}s+1\right)}{\left(T_0^2s^2+2\xi_0T_0s+1\right)}\delta_0\frac{1}{s}\right)=G_{U\delta 0}\delta_0$$

$$\lim_{t\to\infty}\Omega(t)=\lim_{s\to 0}\left(s\Omega(s)\right)=\lim_{s\to 0}\left(sG_{\Omega\delta}(s)\delta(s)\right)=\lim_{s\to 0}\left(s\frac{G_{\Omega\delta 0}\left(T_{\Omega\delta}s+1\right)}{\left(T_0^2s^2+2\xi_0T_0s+1\right)}\delta_0\frac{1}{s}\right)=G_{\Omega\delta 0}\delta_0 \tag{39}$$

When the time responses to the step input are available, these formulae can be used for identification of unknown parameters of the reference model.

**Steady State Responses Y(t) and ψ(t) to the Sharp Pull of the Wheels in One and Next in the Opposing Direction**

The two-sided sharp pull of the steering wheel with a hold time T can be described by a combination of step functions 1(t) of wheels rotation (see Fig. 3):

$$\delta(t)=\delta_0\left(1(t)-2*1(t-T)+1(t-2T)\right) \tag{40}$$

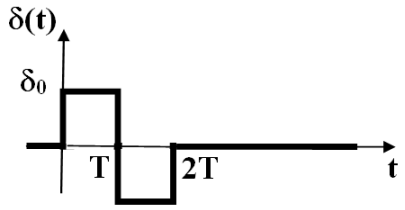


***Figure 3. Two-sided sharp pull of the wheels.***

An accurate analysis of the time histories of Y(t) and ψ(t) can be carried out on the basis of simulation results. The limits of ψ(t) and Y(t) at t → ∞ can be determined knowing the transform of the input function δ(t) and the appropriate transfer functions. For Y(t), due to the approximate character of the simplified reference model, this process will produce an estimated value.

The Laplace transform of δ(t) defined in formula (40) is given by:

$$\delta(s) = \delta_0\left(\frac{1}{s} - 2\frac{1}{s}e^{-sT} + \frac{1}{s}e^{-s2T}\right) = \delta_0\frac{1-2e^{-sT}+e^{-s2T}}{s} = \delta_0\frac{\left(1-e^{-sT}\right)^2}{s} \tag{41}$$

$$\lim_{t\to\infty} Y(t) = \lim_{s\to 0}\left(sY(s)\right) = \lim_{s\to 0}\left(sG_{Y\delta 0}(s)\delta(s)\right) = \lim_{s\to 0}\left(s\frac{G_{\Omega\delta 0}V\left(T_1^2s^2+2\xi_1T_1s+1\right)}{s^2\left(T_0^2s^2+2\xi_0T_0s+1\right)}\delta_0\frac{\left(1-e^{-sT}\right)^2}{s}\right) = T^2G_{\Omega\delta 0}V\delta_0 = Y_0 \tag{42}$$

$$\lim_{t\to\infty}\psi(t) = \lim_{s\to 0}\left(s\psi(s)\right) = \lim_{s\to 0}\left(sG_{\Omega\delta}(s)\delta(s)\right) = \lim_{s\to 0}\left(s\frac{G_{\Omega\delta 0}\left(T_{\Omega\delta}s+1\right)}{s\left(T_0^2s^2+2\xi_0T_0s+1\right)}\delta_0\frac{\left(1-e^{-sT}\right)^2}{s}\right) = 0 \tag{43}$$

The meaning of the above results is that vehicle steer through a sharp pull of the steering wheel in one direction, followed by another pull in the opposite direction, causes the vehicle to change the lane of travel. This conclusion is also supported by observations of real vehicle behaviour. For the development of the controller, it is crucial to note that according to the reference model on the new lane the vehicle will move with zero yaw angle. Of course, due to the presence of disturbances and imperfections of the reference model after reaching the steady state the vehicle may be moving along a straight path with nonzero yaw angle. Eliminating that error will be the subject of the corrective action of the controller.

To achieve the intended lane change represented by the lateral distance $Y_0$, it is necessary to appropriately choose the time duration T of the control impulse (square relationship) and its value $\delta_0$ (linear relationship). In this process it is necessary to take into account the value of the amplification parameter $G_{\Omega\delta 0}$ and vehicle velocity V.

The reference model proposed above can be used directly in the control of the trajectory of the vehicle centre of mass (the first phase of the manoeuvre) as well as in the vehicle yaw angle control (the second phase).

**Control of the Lateral Displacement of the Vehicle Mass Centre**

According to the proposed control approach, in the first phase of the process, the control of the steering wheel rotation angle will be executed in the open loop – on the basis of the reference model, taking into account signal limitations and minimization of the manoeuvre duration time. At the same time, the corrective action will be carried out based on the principles of automatic regulation. Accuracy of this operation should be ensured mostly by the quality of the identified reference model. The diagram of the control system for this phase is shown in Fig. 4.

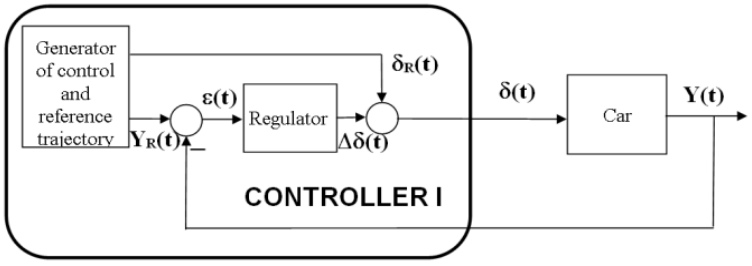


***Figure 4. Block diagram of the automatic control system in Phase I.***

**Generator of steering wheel angle and reference trajectory** Reference time profiles $\delta_R(t)$ and $Y_R(t)$ are generated.

The reference time profile of vehicle lateral displacement $Y_R(t)$ that ensures obstacle avoidance is determined by generation of the control input in the form presented in Eq. (40), with parameters $\delta_0$ and T chosen such that the conditions $|\ddot{y}(t)| \le \ddot{y}_{dop}$ and $|\dot{\psi}(t)| \le \dot{\psi}_{dop}$ are satisfied, and the steady state is achieved within the time not exceeding the allowed value resulting from current vehicle velocity and the distance from the obstacle. For the selection of $\delta_0$ and T, trajectory optimization can be used, for example with the objective to achieve the shortest time to reach the steady state. Such selection and representing the input function parameters in the tabular form are to be carried out off-line on the basis of simulations, for a broad range of design and operational parameters present in the initial reference model. The simplified reference model can facilitate that process.

**The regulator** The regulator can be developed on the basis of the classical control theory, or with the use of the optimal control theory applied to the linear-quadratic problem. As known, regulators determined from the solution of linear-quadratic problems are usually very effective and relatively simple for implementation. Such an approach is presented below.

The linear-quadratic problem is formulated as follows. For the model in the state-space matrix form

$$\dot{\mathbf{x}}(t) = \mathbf{A}\mathbf{x}(t) + \mathbf{B}\mathbf{u}(t) \tag{44}$$

with initial conditions $\mathbf{x}(0) = \mathbf{0}$ find the control vector $\mathbf{u}(t)$ that minimizes the functional:

$$Q = \int_0^\infty \left(\mathbf{x}(t)^T \mathbf{P}\mathbf{x}(t) + \mathbf{u}(t)\mathbf{R}\mathbf{u}(t)\right)dt \ . \tag{45}$$

with **P** and **R –** positively defined weight matrices.

According to Kalman theorem [1] the solution

of the linear-quadratic problem is:

$$\hat{\mathbf{u}}(t) = -\mathbf{R}^{-1}\mathbf{B}^T\mathbf{K}\mathbf{x}(t) \tag{46}$$

where **K** –symmetric matrix satisfying Ricatti equation: $-\mathbf{K}\mathbf{A} - \mathbf{A}^T\mathbf{K} + \mathbf{K}\mathbf{B}\mathbf{R}\mathbf{B}^T\mathbf{K} = \mathbf{P}$ (47)

The meaning of this solution is that the control vector is computed in the closed loop system, with feedback parameters depending on the model and the objective weight matrices, and determined as the solution of the nonlinear algebraic Ricatti equation.

In order to apply the theory of linear-quadratic systems it is necessary to formulate the linear mathematical model of the object in the state-space form. The control performance index should be presented in the form of integral functional with quadratic forms. Note that the earlier determined transfer function $G_{Y\delta}(s)$ describes also the dynamics for the perturbed states:

$\Delta\delta = \delta_R(t) - \delta(t)$ and $\Delta Y = Y_R(t) - Y(t) = \varepsilon(t)$ (tracking error), and therefore one also has:

$$\Delta Y(s) = G_{Y\delta}(s)\Delta\delta(s) = \frac{G_{\Omega\delta 0}V\left(T_1^2 s^2 + 2\xi_1 T_1 s + 1\right)}{s^2\left(T_0^2 s^2 + 2\xi_0 T_0 s + 1\right)}\Delta\delta(s) \tag{48}$$

For the purpose of illustrating the method by analytical means the simplified reference model will be used together with simplified form of the transfer function:

$$G_{Y\delta}(s) = \frac{\Delta Y(s)}{\Delta\delta(s)} = \frac{G_{\Omega\delta 0}V\left(T_1^2 s^2 + 2\xi_1 T_1 s + 1\right)}{s^2\left(T_0^2 s^2 + 2\xi_0 T_0 s + 1\right)} \approx \frac{G_{\Omega\delta 0}V}{s^2} \tag{49}$$

The model that corresponds to such transfer function has the following state-space form:

$$\begin{bmatrix}\dot{x}_1(t)\\ \dot{x}_2(t)\end{bmatrix} = \begin{bmatrix}0 & 1\\ 0 & 0\end{bmatrix}\begin{bmatrix}x_1(t)\\ x_2(t)\end{bmatrix} + \begin{bmatrix}0\\ 1\end{bmatrix}u(t) \tag{50}$$

where

$$x_1(t) = \Delta Y(t) \quad x_2(t) = \Delta\dot{Y}(t) \quad u(t) = G_{\Omega\delta 0}V\Delta\delta(t) \tag{51}$$

The control performance index can be defined as:

$$Q = \int_0^\infty \left(p_{11}x_1^2(t) + p_{22}x_2^2(t) + ru^2(t)\right)dt \text{ which means}$$

$$Q = \int_0^\infty \left(\begin{bmatrix}x_1\\ x_2\end{bmatrix}^T\begin{bmatrix}p_{11} & 0\\ 0 & p_{22}\end{bmatrix}\begin{bmatrix}x_1\\ x_2\end{bmatrix} + uru(t)\right)dt \tag{52}$$

In the typical notation of the linear-quadratic problem one gets:

$$\mathbf{A}=\begin{bmatrix}0 & 1\\ 0 & 0\end{bmatrix},\quad \mathbf{B}=\begin{bmatrix}0\\ 1\end{bmatrix}\quad \mathbf{P}=\begin{bmatrix}p_{11} & 0\\ 0 & p_{12}\end{bmatrix}\quad \mathbf{R}=r \tag{53}$$

The linear-quadratic problem has a solution according to Eqs. (46) and (47). For the considered case:

$$\mathbf{R}^{-1}=\frac{1}{r} \tag{54}$$

$$\mathbf{K}=\begin{bmatrix}K_{11} & K_{12}\\ K_{21} & K_{22}\end{bmatrix}=\begin{bmatrix}K_{11} & K_{12}\\ K_{12} & K_{22}\end{bmatrix}$$

The symmetric matrix **K** satisfies the equation:

$$-\begin{bmatrix}K_{11} & K_{12}\\ K_{12} & K_{22}\end{bmatrix}\begin{bmatrix}0 & 1\\ 0 & 0\end{bmatrix}-\begin{bmatrix}0 & 1\\ 0 & 0\end{bmatrix}^{T}\begin{bmatrix}K_{11} & K_{12}\\ K_{12} & K_{22}\end{bmatrix}+\begin{bmatrix}K_{11} & K_{12}\\ K_{12} & K_{22}\end{bmatrix}\begin{bmatrix}0\\ 1\end{bmatrix}r\begin{bmatrix}0\\ 1\end{bmatrix}^{T}\begin{bmatrix}K_{11} & K_{12}\\ K_{12} & K_{22}\end{bmatrix}=\begin{bmatrix}p_{11} & 0\\ 0 & p_{22}\end{bmatrix} \tag{55}$$

Carrying matrix operations in Eq. (55) leads to the equation:

$$\begin{bmatrix}rK_{12}^{2} & -K_{11}+rK_{12}K_{22}\\ -K_{11}+rK_{12}K_{22} & -2K_{12}+rK_{22}^{2}\end{bmatrix}=\begin{bmatrix}p_{11} & 0\\ 0 & p_{22}\end{bmatrix} \tag{56}$$

Considering stability requirements one finally gets:

$$K_{12}=\sqrt{\frac{p_{11}}{r}},\qquad K_{22}=\sqrt{\frac{p_{22}+2\sqrt{\frac{p_{11}}{r}}}{r}},\qquad K_{11}=\sqrt{p_{11}\left(p_{22}+2\sqrt{\frac{p_{11}}{r}}\right)} \tag{57}$$

Substituting calculated coefficients into Eq. (46) gives:

$$\hat{u}(t)=-\frac{1}{r}\begin{bmatrix}0\\ 1\end{bmatrix}^{T}\begin{bmatrix}K_{11} & K_{12}\\ K_{12} & K_{22}\end{bmatrix}\begin{bmatrix}x_1(t)\\ x_2(t)\end{bmatrix}=-\frac{1}{r}\begin{bmatrix}0 & 1\end{bmatrix}\begin{bmatrix}K_{11} & K_{12}\\ K_{12} & K_{22}\end{bmatrix}\begin{bmatrix}x_1(t)\\ x_2(t)\end{bmatrix}=-\frac{1}{r}\begin{bmatrix}K_{12} & K_{22}\end{bmatrix}\begin{bmatrix}x_1(t)\\ x_2(t)\end{bmatrix}=-\frac{1}{r}\left(K_{12}x_1(t)+K_{22}x_2(t)\right) \tag{58}$$

Hence

$$\hat{u}(t)=-\frac{1}{r}\left(\sqrt{\frac{p_{11}}{r}}x_1(t)+\sqrt{p_{11}\left(p_{22}+2\sqrt{\frac{p_{11}}{r}}\right)}x_2(t)\right) \tag{59}$$

$$\Delta\hat{\delta}(t)=-\frac{1}{G_{\Omega\delta 0}Vr}\left(\sqrt{\frac{p_{11}}{r}}\Delta Y(t)+\sqrt{p_{11}\left(p_{22}+2\sqrt{\frac{p_{11}}{r}}\right)}\Delta\dot{Y}(t)\right) \tag{60}$$

In the operator domain:

$$\Delta\hat{\delta}(s)=-\frac{1}{G_{\Omega\delta 0}Vr}\left(\sqrt{\frac{p_{11}}{r}}+s\sqrt{p_{11}\left(p_{22}+2\sqrt{\frac{p_{11}}{r}}\right)}\right)\Delta Y(s) \tag{61}$$

The transfer function of the proportional-plus-derivative regulator (PD):

$$G_{\Delta\delta\Delta Y}(s)=\frac{\Delta\delta(s)}{-\Delta Y(s)}=\frac{1}{G_{\Omega\delta 0}Vr}\left(\sqrt{\frac{p_{11}}{r}}+s\sqrt{p_{11}\left(p_{22}+2\sqrt{\frac{p_{11}}{r}}\right)}\right) \tag{62}$$

With the use of the vehicle lateral acceleration the controller becomes the regulator with integration.

**Stabilization of the Yaw Angle of the Vehicle**

Following the earlier described concept of vehicle control, in the second phase of the manoeuvre the control of the steering wheel rotation will be carried out as in the regulation system. Considering possible unification of the control system, it is useful to set the block structure of the controller in the form similar to the first phase controller. It is shown in Fig. 5.

In this case the generator of reference signals has a trivial form:

$$\psi_R(t)=0\qquad \delta_R(t)=0 \tag{63, 64}$$

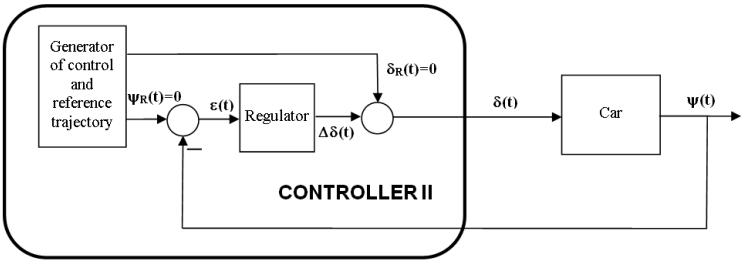


***Figure 5. Block diagram of the automatic control system in Phase II.***

The regulator adjusting the steering wheel rotation angle can be developed in the way similar to Phase I. Note that in this case the transfer function $G_{\Omega\delta}(s)$, determined from the initial reference model, can be also used for the description of the dynamics with angular perturbations:

$\Delta\delta(t) = \delta_R(t) - \delta(t)$ and $\Delta\psi = 0 - \psi(t) = \varepsilon(t)$ (regulation error), and thus one gets:

$$\Delta\psi(s) = \frac{1}{s} G_{\Omega\delta}(s)\Delta\delta(s) = \frac{G_{\Omega\delta 0}\left(T_{\Omega\delta}s + 1\right)}{s\left(T_0^2 s^2 + 2\xi_0 T_0 s + 1\right)}\Delta\delta(s) \tag{65}$$

Subsequent development follows an analogous path to the already presented and is omitted in this paper.

Note that due to identical structures of the controllers for the first and second phases of the manoeuvre, an universal controller device can be used, with a switchable algorithms and changing reference and feedback signals.

The developed algorithms of the controller, generating the reference signals and error feedback terms, constitute the basis of the active steering system controller. In the simplest approach, the steering wheel rotation angle $\delta_H(t)$ can be treated as a scaled version (through the steering gear ratio) of the steer angle of the wheels $\delta(t)$. In the more comprehensive solutions, additional corrective terms can be added in order to take into account the dynamics and nonlinearities of the real steering mechanism.

## SIMULATION RESULTS

Verification and validation of the proposed control approach was carried out through numerical simulations in which a comprehensive model of vehicle dynamics was used. That model was treated as a "real" vehicle. The model of a commercial truck [5,6] was adapted for that purpose and used in simulations. It represents a complex, 3D model of a two-axis commercial truck of medium load capacity, having twenty degrees of freedom, and built on the basis of studies and observations of the real vehicle (STAR 1142). The active steering system included in the model takes into account its geometry, kinematics, dynamics as well as elastic and damping properties. The tire model proposed by Dugoff, Fancher, Segel [3], completed with recommendations resulting from the research conducted under the guidance of Mitschke [7], was used for the description of interaction between vehicle tires and roadway surface. An important advantage of this tire model is that in spite of relatively simple mathematical formulation it allows for an easy introduction of vehicle parameters (traction coefficient, velocity, radial loads) and makes it possible to simulate vehicle motion in the full skid condition.

The model of the truck was subjected to a broad and thorough experimental verification [5]. The results obtained during tests of the real vehicle were used for the experimental verification of the model. Typical manoeuvres included driving along a circular path in steady conditions, quick turn of the steering wheel while driving straight ahead and braking while driving along a straight road and braking while turning. In order to determine the parameters of the tire model, thorough experimental tests of dynamic characteristics of vehicle tires were carried out on a drum dyno and with a dynamometer trailer.

Effectiveness of the control approach presented in this paper has been evaluated through simulations that involved avoiding suddenly appearing obstacle through single lane change on a shortest distance possible. During numerical experiments it was necessary to tune the values of parameters $p_{11}$, $p_{22}$ and r (Eq. 60). Adjusting those values was done by trial and error. A number of obstacle avoidance manoeuvres with different settings were carried out. The parameters that were changing in the consecutive tests included the initial velocity of the vehicle (in the range of V=40-80km/h), the friction coefficient between the tires and the road surface (in the range of $\mu$=0.1-0.5) and the weight of the load in the cargo section of the truck (not loaded, partly loaded and fully loaded). The objective was to find the settings that would allow successful completion of the obstacle avoidance manoeuvre in all trials that were conducted.

| Item | V=60km/h | V=70km/h | V=80km/h |
|---|---|---|---|
| μ=0.1 | 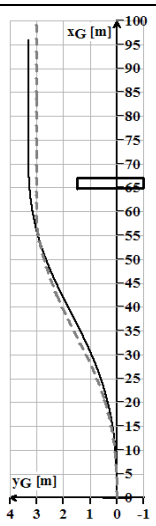 | 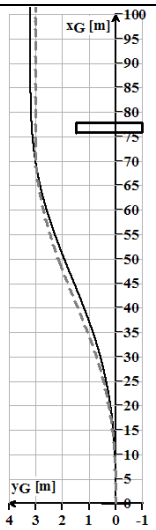 | 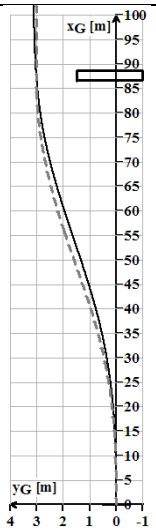 |
| μ=0.2 | 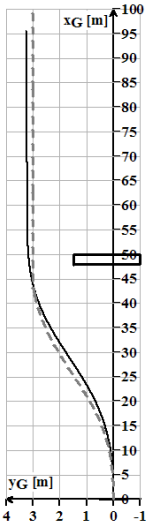 | 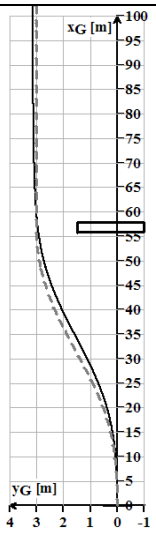 | 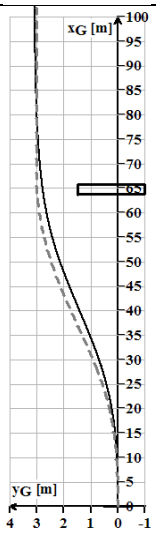 |
| μ=0.3 | 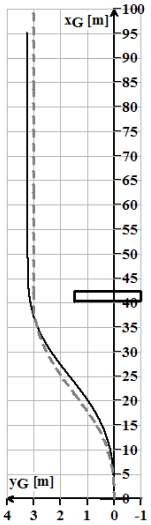 | 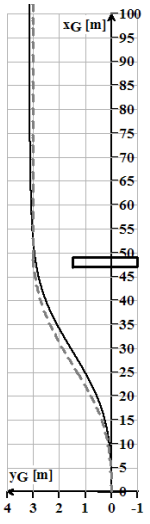 | 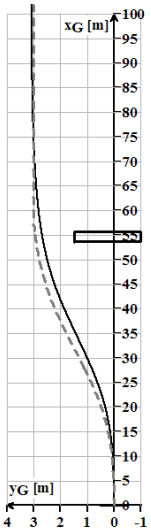 |

***Figure 6. The results of the simulation studies – the assigned (broken line) and realized (solid line) trajectory of the car's centre of mass.***

The obstacle avoidance manoeuvre, according to the earlier described approach, was implemented in two phases. The controller shown in Fig. 4 was used in the first phase. In that phase, the desired trajectories $Y_R(t)$ of the vehicle centre of mass had been generated using the bicycle model of the vehicle and Eq. (40). The time profiles of the steering wheel rotation angle $\delta_{HR}(t)$ had been determined using Eq. (40) and the mean value of the steering system ratio. For each test, the values of variables T and $\delta_0$ (Fig. 3) were determined taking into account the limit value of the radius of the circular path on which the vehicle could move without the loss of lateral traction. The lateral displacement $Y_0$=3 m of vehicle's centre of mass to the target lane was used. The controller shown in Fig. 5 was used in the second phase of the manoeuvre. In that phase, the vehicle yaw angle was set to zero ($\psi(t)=0$) and the steering wheel rotation angle was assigned as $\delta_{HR}=0$. In both phases, the instantaneous value of the steering wheel rotation angle $\delta_H(t)$ taken as the sum of the assigned value $\delta_{HR}(t)$ and the value $\Delta\delta_H(t)$ computed by the regulator was limited by the allowable values of vehicle velocity and the values of steering wheel angular acceleration. In all simulations that were carried out the controller II (Fig. 5) was taking over the control of the steering wheel rotation angle after the time period of $t_1$=1.5T (Fig. 3).
The results of simulations have shown that in all tests that were carried out the obstacle avoidance manoeuvre was accomplished successfully. A portion of simulation results is presented in Fig. 6. They were obtained for the fully loaded truck, with the low position of the centre of mass, on slippery pavements (friction coefficient of $\mu$ =0.1-0.3), and with vehicle velocities of 60-80km/h.
The automatically controlled vehicle was able to avoid the obstacle without losing directional stability, even though the conditions of vehicle operation were changing in a broad range. Therefore, it can be stated that the proposed concept of control and the developed regulators proved to be insensitive to varying road conditions, and with that, the control approach appeared to be effective in realization of the lane change manoeuvre on the shortest path possible.

## CONCLUSIONS AND CLOSING REMARKS

The adopted reference model of the lateral dynamics of the vehicle in its initial and simplified versions seems to provide an accepted basis for the development of controllers that automate the lane change manoeuvre. The proposed method of the decomposition of the control leads to two identical structures of the controller for both phases of the process. The results of simulations showing the use of such controller for the control of the commercial truck prove the correct direction of the research.
The method of automatic execution of the lane change manoeuvre presented in the paper can offer an attractive alternative for vehicle control engineers and researchers working in the fields of automatic steering systems and vehicle active safety systems. The results are especially important because they illustrate the application of the methodology for the case of a commercial truck.

## REFERENCES


[1] Athans, M., Falb, P. L.: Optimal control. An Introductionto the Theory and Its Applications. McGraf-Hill, 1966.
[2] Bevan, G. P., Gollee, H., Reilly, J.: Trajectory generation for road vehicle obstacle avoidance using convex optimization. Proceedings of the Institute of Mechanical Engineers PartD – Journal of Automobile Engineering, Vol 224 (4), 2010.
[3] Dugoff, H., Fancher, P. S., Guenther, D.A.: An analysis of tire traction properties and their influence on vehicle dynamic performance. SAE Transactions 700377, Vol. 79.
[4] Gao, Y., Lin, T., Borrelli, F., Tseng, E., Hrovat, D.: Predictive control of autonomous ground vehicles with obstacle avoidance on slippery roads. Dynamic Systems and Control Conference, 2010.
[5] Gidlewski, M.: Model of a dual axis heavy truck for handling studies in complex road situations. 11th European Automotive Congress. Budapeszt 2007.
[6] Gidlewski, M.: Opportunities to investigate the steering system for improvement of truck driving properties under critical road conditions. Archives of Transport No. 3/2011.
[7] Gidlewski, M.: Research project No. N N509 568439: Analysis of possibilities of using steer-by-wire system to improve driving properties of commercial truck in critical traffic situations. 2010
[8] Mitschke, M.: Dynamik der Kraftfahrzeuge. Band C. Springer –Verlag Berlin 1990.

[9] Moshchuk, N., Shih-Ken Chen, Zagorski, C., Chatterjee, A.: Path planning for collision avoidance maneuver. Proceedings of the ASME 2013 International Mechanical Engineering Congress and Exposition IMECE2013 November 15-21, 2013, San Diego, California, USA.
[10] Park, J.M., Kim, D.W, Yoon, Y.S., Kim, H.J., Yi, K.S.: Obstacle avoidance of autonomous vehicles based on model predictive control. Proceedings of the Institute of Mechanical Engineers PartD – Journal of Automobile Engineering, Vol 223, 2009.
[11] Shiller, Z., Sundar, S.: Optimal Emergency Maneuvers Of Automated Vehicles Research Reports California
[12] Partners for Advanced Transit and Highways (PATH) - UC Berkeley, 1996.
[13] Wieckowski, D.; Zardecki, D.: Sensitivity analysis of optimized overtaking manoeuvre in consideration of freeplay and dry friction parameters of steering system, Zeszyty Naukowe Instytutu Pojazdow. Politechnika Warszawska, Nr 1(77), 2010.
[14] Wieckowski, D.; Zardecki, D. Influence of freeplay and friction in steering system on double lane change manoeuvre, Logistyka, 4/2010.

# ANALYSIS OF THE INFLUENCE OF MOTOR CARS' RELATIVE POSITIONS DURING A RIGHT-ANGLE CRASH ON THE DYNAMIC LOADS ACTING ON CAR OCCUPANTS AND THE RESULTING INJURIES

**Mirosław Gidlewski**
Automotive Industry Institute
University of Technology and Humanities in Radom
Poland

**Leon Prochowski**
Military University of Technology
Automotive Industry Institute
Poland

**Karol Zielonka**
Automotive Industry Institute
Poland

Paper Number 15-0107

## ABSTRACT

Side collisions of vehicles participating in the traffic are very common road accidents in Poland. In 2013, such collisions amounted to 29% of all the traffic accidents and they were accountable for 31% of the injured and 18% of the killed among all the accident victims. In spite of a decline in the total numbers of road accidents and of the resulting casualties, recorded for more than the recent decade, the percentages of side collisions of vehicles in the traffic and of the resulting casualties in the total figures have been observed to grow. On the other hand, the severity rate of accidents of this type has been remaining for many years on a stable level while it has been decreasing for other vehicle crash types. This shows that the progress in the protection of motor car users from the effects of side impacts is too slow. Therefore, it seems reasonable to carry out research on the processes that take place during side collisions.
A research project, expected to facilitate the exploration of the course of some processes in result of which dynamic effects are produced by a right-angle collision of two motor cars on car occupants, has now been in progress at the Automotive Industry Institute (PIMOT) in Warsaw. Within the project, six crash tests were performed with the use of 12 passenger cars of the same make and model. At each test, the front of car A crashed into the left side of car B. The pre-impact speed of car A was about 50 km/h and it was twice as high as that of car B. At successive tests, different places on car B were struck by car A. In each car, a Hybrid III test dummy was placed on the front right seat and a Hybrid II dummy was placed on the front left seat.
The measuring systems used made it possible to determine the following:

- dynamic interactions between the cars;
- lateral displacements of the torsos and heads of the dummies placed on the front car seats;
- dynamic loads acting on dummies' heads and torsos;
- relations between the force applied to car B and the dynamic loads acting on the occupants of that car.

The paper includes test results, thanks to which the time histories of the force acting on the impacted car as well as the effect of this force on the displacements and accelerations of the test dummies could be presented.
An analysis of the test and computation results has shown that the location of the place of impact on car B has a considerable influence on the loads received by the car occupants. The knowledge of the dynamic loads acting on the occupants of front seats of car B makes it possible to predict the likelihood and scope of injuries to the occupants depending on the relative positions of the car during a collision.
The test and analysis results presented herein will be used for improving the construction of the system of individual protection of motor car occupants, including a system to restrain lateral displacements of car occupants during a side collision.

## INTRODUCTION

Side collisions of vehicles participating in the road traffic (referred to as broadside collisions, right-angle collisions, or T-bone collisions if the vehicles moved perpendicularly to each other before the crash) are very common road accidents in Poland. For more than ten recent years, the annual number of side collisions has been exceeding 25% of all the road accidents [3, 11]. The total number of vehicle collisions in the road traffic in Poland and the number of the resulting casualties show a downward trend (Fig. 1). However, the rates of decline in the number of side collisions of vehicles participating in the traffic (Fig. 1a) and in the number of the resulting deaths are far lower than

the rates of decline in the number of all the vehicle collisions in the traffic and in the number of deaths in such accidents [11].
At side collisions of motor vehicles, a vehicle may be struck either on the occupant's side of the impacted vehicle or on the side opposite to it (such collisions are often referred to as "near-side collisions" and "far-side collisions", respectively). Most of the research works dedicated to the side collisions of vehicles are focused on the analysis of the effects of near-side collisions because of the most severe injuries occurring in such a case due to the fact that the occupant (either the driver or the passenger) is exposed to direct contact with the deformed side structure of the vehicle body. However, side impacts are also dangerous to the car occupant seated on the non-struck side. Such collisions (i.e. far-side collisions) may result in severe injuries to occupant's neck, spine, and head because of the unrestrained lateral movements of these occupant's body parts in a typical passenger car.

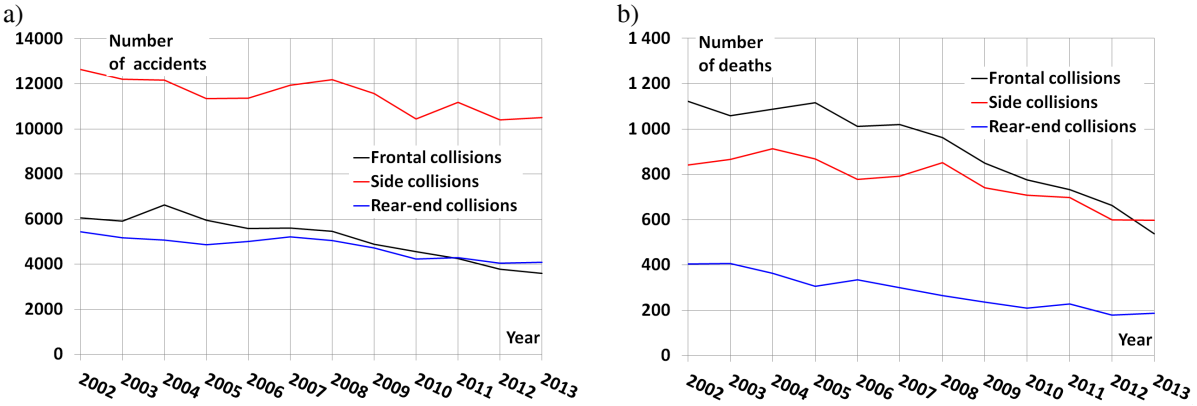


***Figure 1. Number of vehicle collisions in road traffic (a) and number of the resulting deaths (b) in Poland in the years 2002–2013 [11].***

Most of the biomechanical criteria commonly used to estimate the risk of vehicle occupants' bodily injury do not provide a possibility of evaluating the injuries that would result from a side collision of the impacted vehicle and no limiting values applicable to collisions of this type are known [1, 2].
All the above aspects justify the necessity of investigating the processes in result of which dynamic effects are produced by side collisions of motor cars on car occupants. This defines the objective of carrying out the experimental tests referred to herein. The test results and their analysis show, above all, the properties and characteristics of the process how the heads and torsos of occupants seated on front car seats (on both the struck side and the non-struck side) undergo the dynamic effects. The treatment of the results of many different tests as a whole will indicate new precautionary measures that would reduce the risk of injury to vehicle occupants and will help to improve the protection of motor car users from the effects of side collisions.

## METHODS OF THE EXPERIMENTAL TESTS

A research project, expected to facilitate the exploration of the course of some processes in result of which dynamic effects are produced by a right-angle collision of two motor cars on car occupants, has now been in progress at the Automotive Industry Institute (PIMOT) in Warsaw [7, 8, 9, 10]. Within the project, six crash tests were performed with the use of 12 passenger cars of the same make and model. At each test, the front of car A crashed into the left side of car B. The pre-impact speed of car A was about 50 km/h and it was twice as high as that of car B. The crash tests were carried out on a test yard with dry concrete surface, in good weather conditions. During the tests, the steering wheel was left free and the road wheels of the cars were not braked. In each car, a Hybrid III test dummy was placed on the front right seat and a Hybrid II dummy was placed on the front left seat.
At successive crash tests, the relative positions of cars A and B were changed as shown in Fig. 3. For each of the vehicle configurations, the tests were repeated twice in comparable conditions.

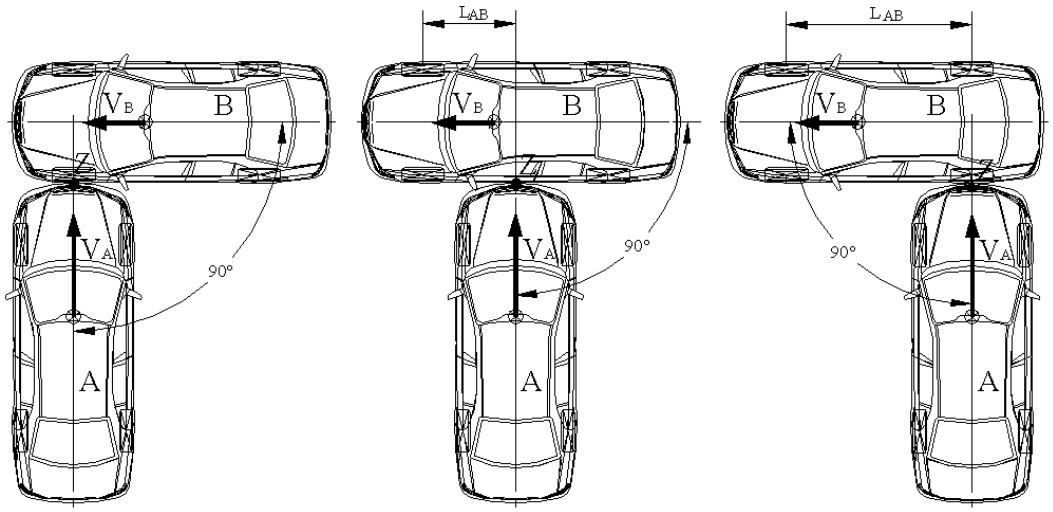


***Figure 2. Vehicle configuration options at the crash tests.***

The tests were carried out with the use of Honda Accord cars manufactured in 2000–2002, which were in good technical condition. The cars had undamaged and non-corroded bodies, which had not been previously repaired, as well as driver's and passenger's airbags and side airbags, with the latter having been mounted in the front seat backrests; all the airbags were in full working order.
Among the test parameters, the distance $L_{AB}$ between the longitudinal plane of symmetry of car A and the front wheel axis of car B was taken as a reference. This distance defined the vehicle configuration at the instant of the collision; at successive tests, it was $L_{AB}$ = 0.04 m, 0.17 m, 1.25 m, 1.34 m, 2.57 m, and 2.71 m.

**TEST RESULTS**

The results presented herein give grounds for evaluating the influence of the location of the place in which car B was struck on the generation of dynamic loads in vehicle occupants. Attention was also paid to the displacements of the dummies placed on the front car seats and on the influence of distance $L_{AB}$ on the values of some indicators characterizing the dynamic loads acting on dummies' heads and torsos.
The measuring systems used made it possible to determine the following:

- dynamic interactions between the cars;
- lateral displacements of the torsos and heads of the dummies placed on the front car seats;
- dynamic loads acting on dummies' heads and torsos;
- relations between the force applied to car B and the dynamic loads acting on the occupants of that car.

An analysis was carried out for the time histories of the above quantities measured during the period from the instant when car A just came into contact with car B, i.e. from t = 0 s, to t = 0.2 s. During this period, the following phases of the experiment were observed:

- collision of the cars and temporary contact between them;
- separation of the cars;
- separate post-impact movements of the cars.

**Displacements of the Heads and Torsos of the Dummies Placed on the Front Car Seats**

Figure 3 shows lateral displacements of the test dummies in car B, following the car impact at the crash test with $L_{AB}$ = 0.17 m (selected frames of the video record of the test). The values of the lateral displacements of the dummies in relation to the car seat remained insignificant until the instant of 0.04 s from the beginning of the process of car B being struck by the other car. The front airbags inflation process visibly began after a time of about 0.06 s had elapsed; the airbags were fully inflated at the instant of about 0.08 s. The video record of the test shows that the front airbags having been inflated did not limit the maximum displacements of the dummies because the airbags did not come into contact with the dummies. This can be seen from the trajectories of dummies' heads, which moved clear of the inflated airbags (Fig. 3). The shoulder strap of the seat belt of the right dummy did not

restrain the movement of the right dummy's torso. This means that the lateral movements of the torso and head of the dummy placed on the right side of the car was practically unrestrained by the individual vehicle occupant protection means, i.e. the protection system turned out to be ineffective in such a situation; the maximum lateral (linear) displacements of the centres of mass of dummy's torso and head to the left were in this case 0.26 m and 0.42 m, respectively.

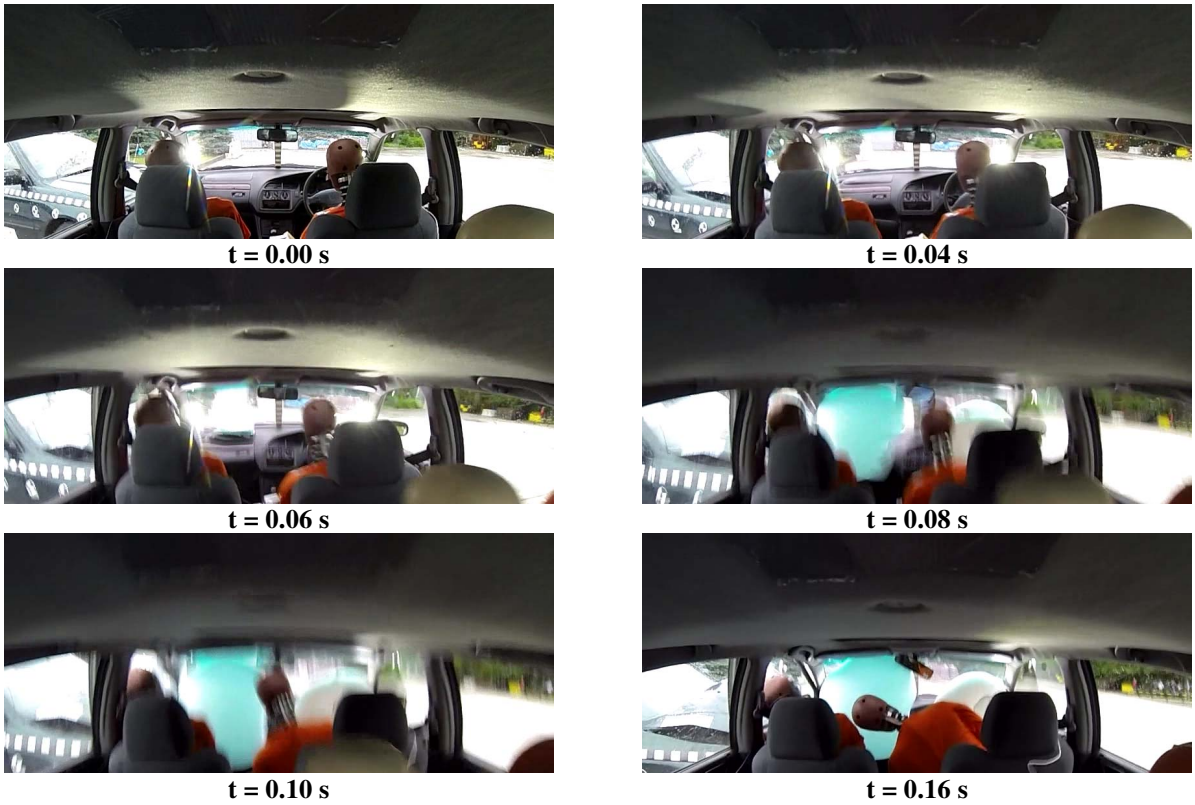


***Figure 3. Example of the lateral displacements of dummies' heads and torsos, $L_{AB}$ = 0.17 m.***

The lateral movement of the test dummy placed on the struck side of the car (left car side in this case) was restrained, at first, by the activated airbag mounted in the seat backrest and, afterwards, by the left part of the car body structure when it was deformed during the impact. The maximum lateral displacements of the centres of mass of dummy's torso and head to the left were now 0.16 m and 0.22 m, respectively.

To show the influence of the location of the place in which car B was struck by car A on the values of lateral displacements of the dummies, the trajectories of dummies' centres of mass were determined in the $O_Bx_By_Bz_B$ coordinate system rigidly connected with the centre of mass of car B. The computations were made with the use of time histories of the accelerations recorded by three-axial acceleration sensors located at the centres of mass of dummies' torsos and heads and at the vehicle centre of mass as well as the readings of sensors of angular velocities of the car body around individual axes of the $O_Bx_By_Bz_B$ coordinate system.

The curves in the graphs shown in Fig. 4 represent the lateral displacements (coordinate $y_B$ in the $O_Bx_By_Bz_B$ coordinate system) of the centres of mass of the torsos and heads of the dummies placed on front car seats (DL – dummy on the left seat, DR – dummy on the right seat) as functions of time, determined at four crash tests differing from each other in the distance between the place of impact on car B and the axis of the car's front wheels.

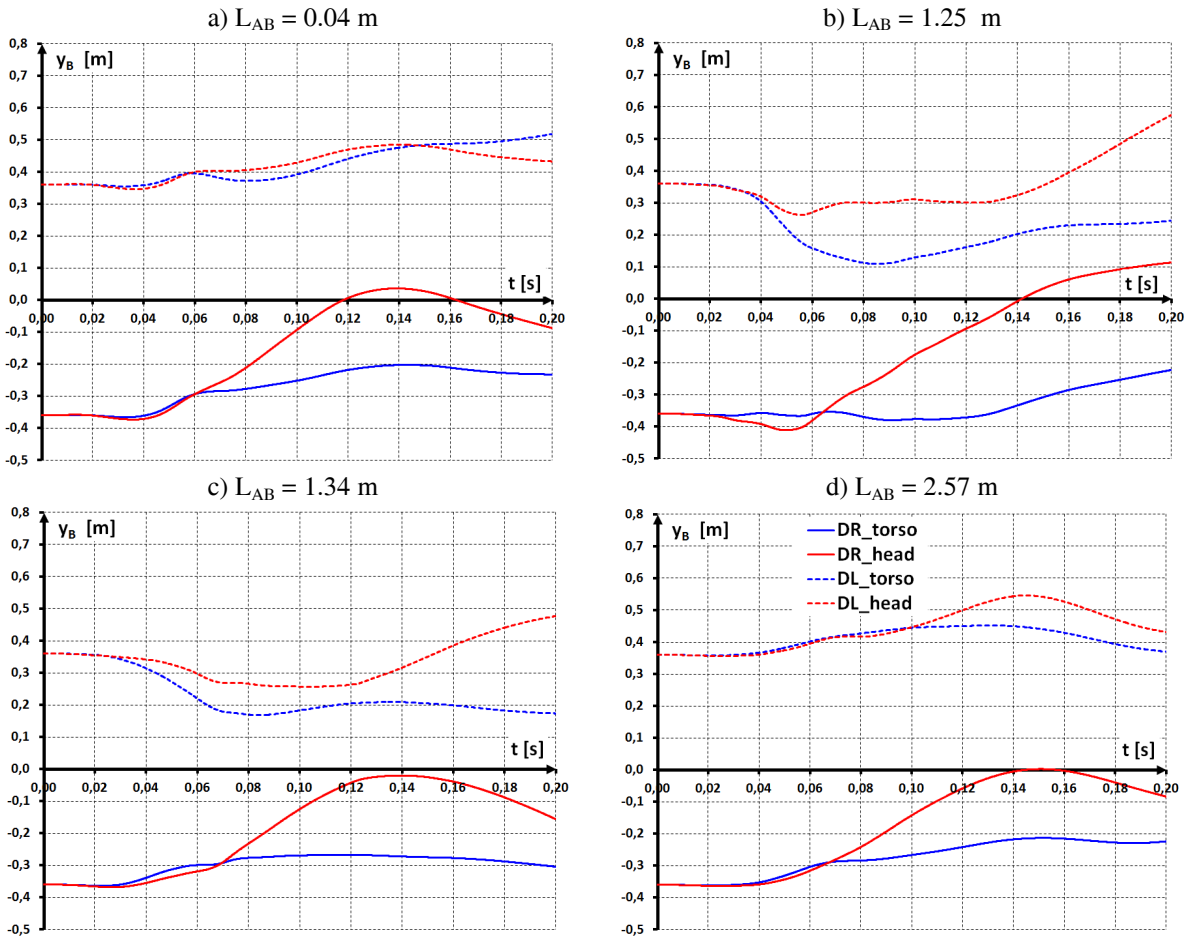


***Figure 4. Lateral (linear) displacements of the centres of mass of the torsos and heads of the right and left dummy in relation to the longitudinal plane of symmetry of car B.***

The graphs presented in Fig. 4 unequivocally show that for the right-angle impacts characterized by low and high $L_{AB}$ values, the time histories of lateral displacements of the torso and head of the right dummy (Figs. 4a and 4d) are practically identical to each other in qualitative terms and the quantitative differences between them are small.
Attention is attracted by high values of the lateral displacements of the centres of mass of the torso and head of the right dummy and high values of the difference between the lateral displacements of the head and torso, e.g. 0.24 mm for $L_{AB}$ = 0.04 m and 0.21 m for $L_{AB}$ = 2.57 m.
In the case of central impacts ($L_{AB}$ = 1.25 m and $L_{AB}$ = 1.34 m), the lateral dummies' displacements can be seen to have followed a different pattern. At these tests, the right and left dummies moved laterally towards the central plane of the vehicle, coming closer to each other in the culminating phase of the collision, i.e. at t = 0.04–0.12 s (Figs. 4b and 4c). The lateral displacement of the left dummy (together with the seat) was caused by inward deformation of the struck side of the car body. The centre of mass of the left dummy's torso moved laterally to the right (in relation to its initial position) by 0.26 m at $L_{AB}$ = 1.25 m and by 0.19 m at $L_{AB}$ = 1.34 m and this resulted in a collision between the two dummies on the level of their arms. In both cases, the collision between the dummies prevented the leftward movement of the right dummy. On the other hand, the right dummy's head did not meet any obstacle of this kind and kept moving laterally leftwards, which resulted in increased displacement of the head in relation to the torso having been stopped and in a dangerous reduction of its distance from the left dummy's head. During the test with $L_{AB}$ = 1.25 m, the clearance between the heads of both dummies was reduced to about 0.03 m. The difference in the values of the lateral displacements of the centres of mass of the head and torso of the right dummy reached as high a value as 0.34 m and was definitely bigger than that recorded at the other tests (Fig. 4b). During the test with $L_{AB}$ = 1.34 m, the lateral displacement of the head in relation to the torso of the right dummy was smaller but the heads of the two dummies hit on each other at an instant of 0.12 s from the beginning of the process of car B being

struck by the other car. In consequence of the collision between the dummies' heads, their resultant accelerations reached high values of 56 g and 73 g for the right and left dummy, respectively.
The tests carried out have shown that in the case of car B being struck in its central part, there is a risk of a collision between heads of the occupants of the front car seats. If such a collision does not occur, the head of the occupant of the right car seat will be significantly displaced in relation to the occupant's torso, which may result in neck injuries.

**Determining of the Impact Force Applied to the Vehicle Being Struck**

A matter of fundamental importance for the subsequent discussion is the determining of the time history of the force (i.e. the normal and tangential components and the resultant force vector) applied by car A to car B and the point of application of the force. The forces acting on car B during the impact were determined from the results of measurements of the vectors of acceleration of the centres of mass of car A ($ax_A$, $ay_A$, $az_A$) and car B ($ax_B$, $ay_B$, $az_B$) and the angular velocities of rotation of individual cars in relation to the axes of the local coordinate systems $O_Ax_Ay_Az_A$ ($P_A$, $Q_A$, $R_A$) and $O_Bx_By_Bz_B$ ($P_B$, $Q_B$, $R_B$) rigidly connected with cars A and B.
A model of the dynamics of a car collision was prepared and the model was used to calculate the force of impact applied to car B. The equations of motion of the model were derived with the use of the Boltzmann-Hamel equations for quasi-coordinates (1).

$$\begin{cases} m_A \cdot \dot{U}_A^* - m_A \cdot V_A^* \cdot \dot{\Psi}_A = R_{nA} + F_{xA1} + F_{xA2} \\ m_A \cdot \dot{V}_A^* + m_A \cdot U_A^* \cdot \dot{\Psi}_A = R_{sA} + F_{yA1} + F_{yA2} \\ I_A \cdot \ddot{\Psi}_A = R_{sA} \cdot x_A - R_{nA} \cdot y_A + F_{yA1} \cdot a_A + F_{yA2} \cdot b_A \\ m_B \cdot \dot{U}_B^* - m_B \cdot V_B^* \cdot \dot{\Psi}_B = R_{sB} + F_{xB1} + F_{xB2} \\ m_B \cdot \dot{V}_B^* + m_B \cdot U_B^* \cdot \dot{\Psi}_B = R_{nB} + F_{yB1} + F_{yB2} \\ I_B \cdot \ddot{\Psi}_B = R_{nB} \cdot x_B - R_{sB} \cdot y_B + F_{yB1} \cdot a_B + F_{yB2} \cdot b_B \\ R_{nB} = R_{nA} \cdot \cos(\gamma_{AB}) + R_{sA} \cdot \sin(\gamma_{AB}) \\ R_{sB} = R_{nA} \cdot \sin(\gamma_{AB}) + R_{sA} \cdot \cos(\gamma_{AB}) \end{cases} \quad (1)$$

where:

$m_A$, $m_B$ – masses of car A and car B;
$I_A$, $I_B$ – moments of inertia of car A and car B around the vertical axis;
$U_A^*$, $V_A^*$ – longitudinal and lateral components of the vector of velocity of the centre of mass of car A in the levelled coordinate system connected with car A;
$U_B^*$, $V_B^*$ – longitudinal and lateral components of the vector of velocity of the centre of mass of car B in the levelled coordinate system connected with car B;
$\dot{\Psi}_A$, $\dot{\Psi}_B$ – angular velocities of car A and car B around the vertical axis (yaw);
$\dot{U}_A^*$, $\dot{V}_A^*$, $\dot{U}_B^*$, $\dot{V}_B^*$ – components of the acceleration vectors;
$\ddot{\Psi}_A$, $\ddot{\Psi}_B$ – angular accelerations of car A and car B around their vertical axes;
$F_{A1}(F_{xA1}, F_{yA1})$, $F_{A2}(F_{xA2}, F_{yA2})$ – road reaction forces acting on the front and rear axle wheels of car A, with longitudinal and lateral components of the reaction vectors;
$F_{B1}(F_{xB1}, F_{yB1})$, $F_{B2}(F_{xB2}, F_{yB2})$ – road reaction forces acting on the front and rear axle wheels of car B, with longitudinal and lateral components of the reaction vectors;
$R_A(R_{nA}, R_{sA})$ – impact force applied to car A and its longitudinal and tangential components;
$R_B(R_{nB}, R_{sB})$ – impact force applied to car B and its longitudinal and tangential components;
$x_A$, $y_A$ – coordinates of the point of application of the impact force (point Z, Fig. 2) in the $O_Ax_Ay_Az_A$ coordinate system;
$x_B$, $y_B$ – coordinates of the point of application of the impact force (point Z, Fig. 2) in the $O_Bx_By_Bz_B$ coordinate system;
$\gamma_{AB}$ – included angle between the longitudinal symmetry planes of car A and car B.

The unknowns in these equations are the normal and tangential components of the impact forces $R_{nA}$, $R_{sA}$, $R_{nB}$, $R_{sB}$ and the lateral road reaction forces $F_{yA1}$, $F_{yA2}$, $F_{yB1}$, $F_{yB2}$.

After the system of equations (1), consisting of 6 equations of equilibrium and 2 equations describing the relations between the components of the impact forces applied to cars A and B, had been solved, the values and time histories of the normal and tangential components of the impact force applied to car B were determined.
Fig. 5 shows the results of computation of the normal component of force $R_B$. The time history of the normal component $R_{nB}$ depends to a significant extent on the location of the place of impact on car B. The average value of the normal component $R_{nB}$ calculated for a time period from 0 s to 0.1 s was:

- for $L_{AB}$ = 0.04 m, $R_{nB}$ = 132 kN;
- for $L_{AB}$ = 0.17 m, $R_{nB}$ = 121 kN;
- for $L_{AB}$ = 1.25 m, $R_{nB}$ = 128 kN;
- for $L_{AB}$ = 1.34 m, $R_{nB}$ = 96 kN;
- for $L_{AB}$ = 2.57 m, $R_{nB}$ = 74 kN;
- for $L_{AB}$ = 2.71 m, $R_{nB}$ = 75 kN.

The extreme values of the impact forces found to occur at successive tests depended on the force of inertia of car B, tangential reactions on the road wheels, and stiffness of the bodies of both cars in their crumple zones. Each of these factors has a complex influence on the time history and values of the impact force applied to car B.

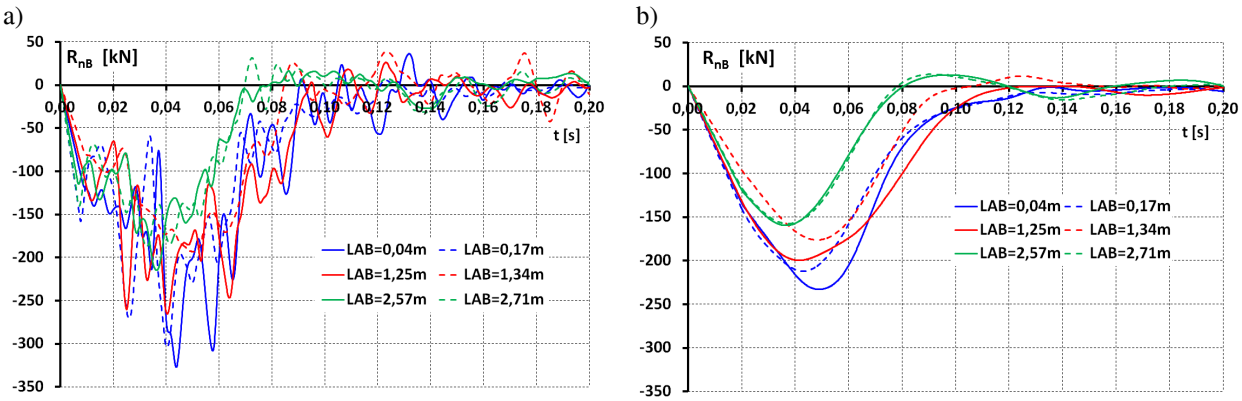


***Figure 5. Time histories of the normal component $R_{nB}$ of the impact force for various $L_{AB}$ values: a) CFC 60 filter; b) CFC 15 filter.***

**Dynamic Loads Acting on the Right Dummy in the Impacted Vehicle**

Fig. 6 shows some examples of the dynamic effects produced by a right-angle collision on car B and on the occupant of the front right seat. Results of three crash tests, with $L_{AB}$ = 0.04 m, $L_{AB}$ = 1.25 m, and $L_{AB}$ = 2.57 m, have been given.
The graphs in Fig. 6 represent the time histories of the following quantities:

- impact force applied to car B ("$R_B$");
- resultant acceleration of the floor of car B under the centre of the front right seat ("front right seat");
- resultant accelerations of the centres of mass of the torso and head of the right dummy ("torso" and "head", respectively).

The curves presented in Fig. 6 confirm the existence of a considerable relation between the effect produced by an external impact on car B and the time histories of the accelerations of right dummy's torso and head caused by the impact. For $L_{AB}$ = 0.04 m and $L_{AB}$ = 1.25 m, the process of growth in the acceleration of the floor under the front right seat became visible after as short a time as about 0.008 s from the instant when the value of the impact force began to rise. Conversely, this acceleration at $L_{AB}$ = 2.57 m could only be seen after a time of 0.02–0.025 s had elapsed. Interestingly, the beginning of growth in the accelerations of dummy's torso and head was practically independent of the location of the place of impact on car B; on the other hand, the rates of growth in these accelerations differed from each other. The characteristic values of the accelerations of right dummy's torso and head for different values of the distances $L_{AB}$ have been given in Table 1 in a subsequent part of this paper.

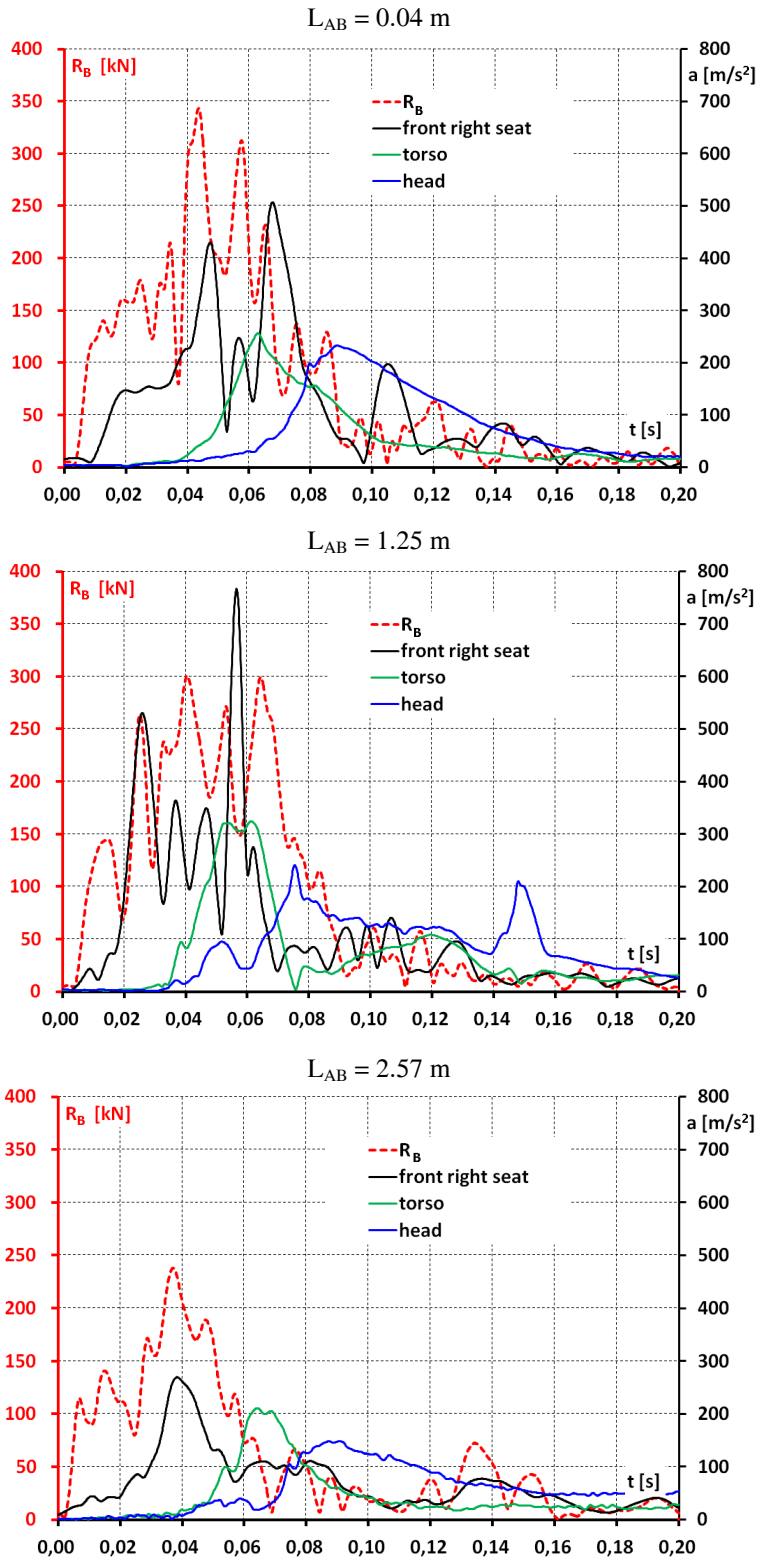


***Figure 6. Resultant impact force ("$R_B$"), resultant acceleration ("a") of the floor under the centre of the front right seat ("front right seat"), and resultant accelerations ("a") of the centres of mass of the torso and head of the dummy placed on the front right seat ("torso" and "head", respectively).***

## ANALYSIS OF THE TEST RESULTS

An analysis of the test and computation results has confirmed that the location of the place in which car B was struck by the other car significantly affected the loads received by that car and its occupants. The knowledge of the dynamic loads acting on the occupants of front seats of car B makes it possible to predict the likelihood and scope of injuries to the occupants depending on $L_{AB}$.

Two sets of indicators, i.e. W1, W2, and W3 as well as W4 and W5, have been proposed for the assessment and quantitative description of the dynamic loads received by motor car occupants during a side impact of the car. The indicators characterize the accelerations and, simultaneously, they are treated here as "per unit" values (related to the unit of mass) of the inertia forces acting on the car occupants. The values of these indicators were separately related to the torso and the head.

- W1 – average acceleration value for a time period from 0.04 s to 0.08 s;
- W2 – average acceleration value for a time period from 0.04 s to 0.10 s;
- W3 – average acceleration value for a time period from 0.04 s to 0.12 s;
- W4 – maximum acceleration value within a 0.005 s time range;
- W5 – maximum acceleration value within a 0.010 s time range.

The influence of the place of impact on car B on the Wi indicator values was analysed with taking into account the following factors that may characterize the impact:

- relative distance x between the point of impact on car B and the front wheel axis of this car ($x = L_{AB}/L$, where L is the wheelbase of car B);
- moment $M_S$ of an impulse of the force of impact against the car side; the arm of the impulse of the force has been assumed as the distance $L_{AB}$;
- moment $M_F$ of the average force of impact against the car side; the arm of the force of impact has been assumed as specified above.

The values of indicators W1–W5 were calculated for the torso and head of the dummy placed on the front right seat of the car and the calculation results have been presented in Table 1 and in Fig. 7.

**Table 1.**
**W1–W5 indicator values for the torso and head of the dummy placed on the front right seat of the car**

| $L_{AB}$ [m] | W1 [m/s$^2$] | W2 [m/s$^2$] | W3 [m/s$^2$] | W4 [m/s$^2$] | W5 [m/s$^2$] |
|---|---|---|---|---|---|
| Torso | | | | | |
| 0.04 | 150 | 136 | 113 | 245 | 231 |
| 0.17 | 85 | 90 | 83 | 175 | 162 |
| 1.25 | 195 | 147 | 133 | 317 | 315 |
| 1.34 | 134 | 110 | 93 | 198 | 183 |
| 2.57 | 117 | 99 | 81 | 205 | 202 |
| 2.71 | 119 | 94 | 79 | 190 | 180 |
| Head | | | | | |
| 0.04 | 51 | 106 | 121 | 230 | 226 |
| 0.17 | 28 | 57 | 79 | 156 | 152 |
| 1.25 | 100 | 115 | 117 | 211 | 193 |
| 1.34 | 37 | 69 | 87 | 384 | 284 |
| 2.57 | 43 | 74 | 83 | 147 | 145 |
| 2.71 | 43 | 76 | 89 | 148 | 147 |

The calculated values of the indicators characterizing the dynamic loads acting on the dummy's torso and head were presented as functions Wi(x), Wi($M_S$), and Wi($M_F$) and then trend functions in the form of second degree polynomials were determined for individual indicators. The approximating functions were selected that were characterized by the highest values of the coefficient of determination.

An analysis of the graphs presented in Fig. 7 made it possible to formulate an important conclusion: the values of the dynamic loads received by car occupants during a right-angle crash depend to a considerable degree on the distance of the point of impact from the front wheel axis (or, to be more precise, from the occupants' seats), on the moment of impulse of the impact force, and on the moment of the average impact force. Hence, these quantities may be considered as factors characterizing the effects of road accidents of this type. Noteworthy is the fact that each of the

curves presented (Fig. 7) has its maximum. This maximum occurred at the values of variables x, $M_S$, and $M_F$ approximately equal to x = 0.5, $M_S$ = (3…4) $10^3$ Nsm, and $M_F$ = $10^5$ Nm. When the point of impact was displaced from the centre towards the front or rear axle of the vehicle, the dynamic loads acting on the dummies were reduced. These conclusions are consistent with those formulated previously, which were drawn from an analysis of the influence of the location of the side impact place on the values of lateral displacements of dummy's torso and head. The highest values of the coefficient of determination, or simultaneously the trend functions that best describe the processes under analysis, lead to the following findings:

- The dependence of the dynamic loads acting on the torso on the location of the side impact place is best described by trend functions W1(x), W2(x), and W3(x).
- The above dependence for the head loads is best described by trend functions W4($M_F$) and W5($M_F$).

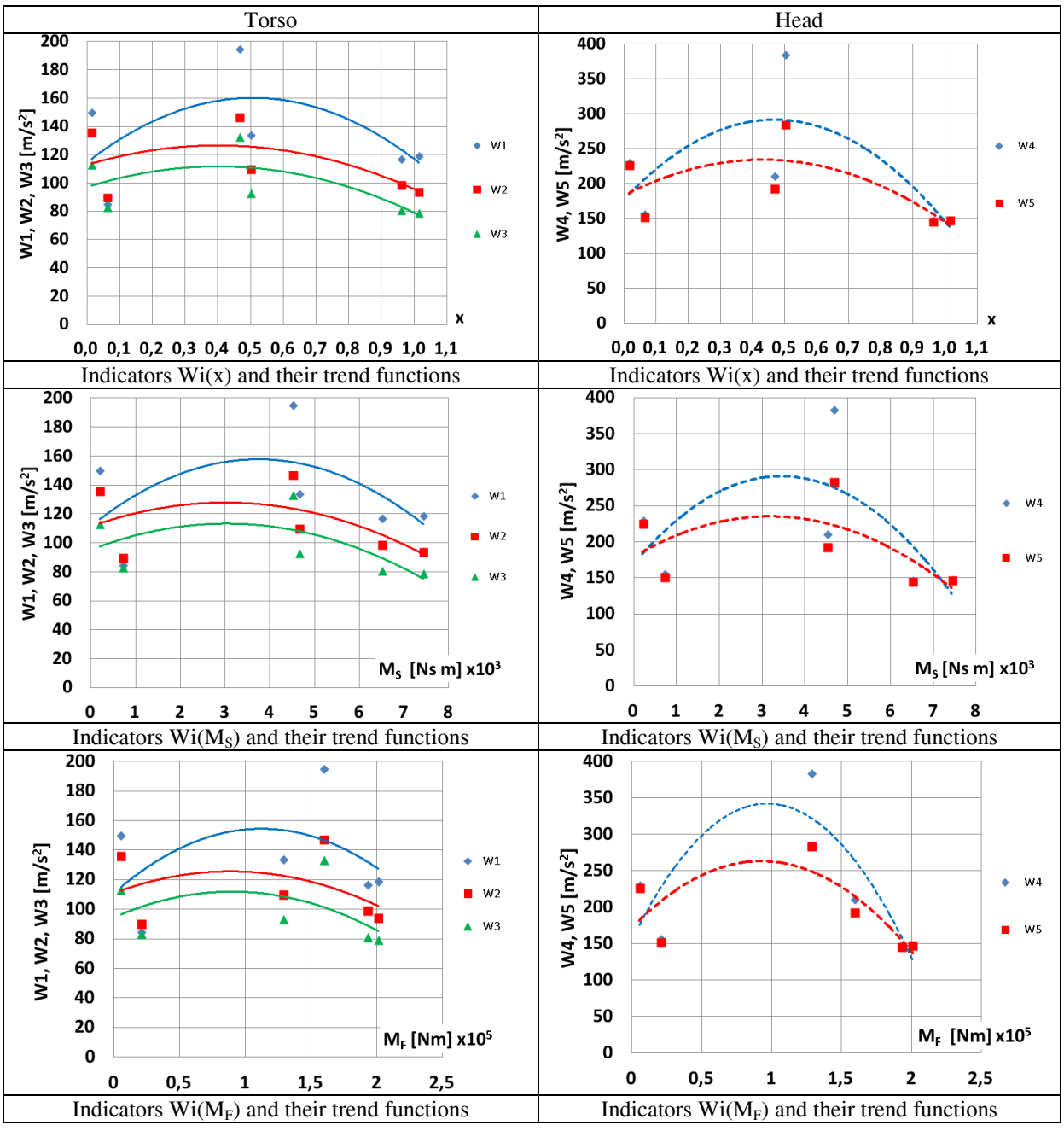


***Figure 7. Values and trend functions of indicators Wi(x), Wi($M_S$), and Wi($M_F$).***

## RECAPITULATION

Measurement results obtained from six right-angle (*T-bone*) crash tests of motor cars during a simulated crossing of a road intersection have been presented. The said results were used to analyse some properties and characteristics of the processes in result of which dynamic effects are produced on the torsos and heads of occupants of the front seats of the impacted car. Time histories and values of the force acting on the impacted car, referred to as "car B", were determined. As an effect of the impact force acting on car B, time histories of the displacements and accelerations of test dummies placed on the front car seats were recorded.
An analysis of the lateral displacements of occupants of the front seats of car B has provided grounds for the following conclusions to be drawn:

- The lateral displacements of the torso and head of the occupant of the seat on the non-struck side of the impacted car are much bigger than those on the struck side of the car (e.g. at $L_{AB} = 0.17$ m, the differences in the lateral displacements of the torso and head were 0.1 m and 0.2 m, respectively).
- The individual car occupant protection means practically do not participate in the restraining of lateral displacements of the occupants seated on the non-struck car side.
- Moreover, the absence of the said protective effect results in excessive lateral displacement of the head in relation to the torso (at $L_{AB} = 1.25$ m, the lateral displacement of the centre of mass of the head exceeded that of the torso by 0.34 m).
- At $L_{AB} = 1.25$ m, a collision took place between dummies' torsos in result of their lateral movements and the clearance between the heads of both dummies was reduced to about 0.03 m.
- At $L_{AB} = 1.34$ m, the lateral movements of the dummies caused dummies' heads to hit on each other and the acceleration of one of the heads reached a level of 73 g.

When the loads acting on motor car occupants were analysed, five indicators Wi were defined, which were then used to identify the factors that are decisive for the loads acting on the occupants during a side collision of the cars. In consideration of the fact that the dynamic loads acting on the occupant on the non-struck side of car B depend on the distance of the point of impact from the front wheel axis (or, to be more precise, from the occupants' seats), the following has been ascertained:

- The torso loads are best described by indicators W1, W2, and W3, defined as functions of the distance of the point of impact from the front wheel axis of car B.
- The head loads are best described by indicators W4 and W5, defined as functions of the moment of the average force of impact against the car side.

The test and analysis results presented herein will be used for improving the construction of the system of individual protection of motor car occupants, including a system to restrain lateral displacements of car occupants during a side collision.

The tests reported herein were carried out and their results were analysed within an authors' own research project No. N N509 559440.

## REFERENCES

[1] Prochowski, L.; Unarski, J.; Wach, W.; Wicher, J.: Podstawy rekonstrukcji wypadków drogowych (Fundamentals of the reconstruction of road accidents). WKiŁ, Warszawa, 2014.
[2] Wicher, J.: Bezpieczeństwo samochodów i ruchu drogowego (The safety of motor vehicles and road traffic). WKiŁ, Warszawa, 2012.
[3] Grzebieta, R.; Tingvall, C.; Rechnitzer, G.: Geometric compatibility in near side impact crashes. Paper number 243, The 17th International Technical Conference on the Enhanced Safety of Vehicles (ESV), Amsterdam, The Netherlands, 4–7 June, 2001.
[4] Digges, K.; Dalmotas, D.: Injuries to restrained occupants in far-side crashes. The 17th International Technical Conference on the Enhanced Safety of Vehicles (ESV), Amsterdam, The Netherlands, 4–7 June, 2001.
[5] Gabler, H.; Digges, K.; Fildes, B.; Sparke, L.: Side Impact Injury Risk for Belted Far Side Passenger Vehicle Occupants. SAE Technical Paper 2005-01-0287, 2005.
[6] Gidlewski, M.; Matuszewski, T.; Prochowski, L.; Wicher, J.: GAMBIT Mazowiecki. Program poprawy bezpieczeństwa ruchu drogowego na Mazowszu (GAMBIT Mazowiecki. Program to improve the road safety in the Mazovia region). WORD (Provincial Road Traffic Centre), Warszawa 2010.

[7] Gidlewski, M.; Jemioł, L.; Prochowski, L.; Zielonka, K.: Badanie procesów zachodzących podczas zderzenia samochodów (Investigation of processes occurring in car crashes). Paragraf na Drodze. Special issue 2013.
[8] Gidlewski, M.; Jemioł, L.: Badanie zderzeń bocznych samochodów. Prędkości samochodów po zderzeniu (Investigation of side crashes of motor vehicles. Post-crash vehicle velocities). Automotive Safety 2014. 9th International Science-Technical Conference. Slovakia 2014.
[9] Gidlewski, M.; Jemioł, L.: Zmiany parametrów ruchu samochodów w czasie zderzenia bocznego (Changes in the motor vehicle motion parameters during a side impact). In: Mitianiec, W. (ed): Badania pojazdów (Vehicle testing), Kraków 2014.
[10] Gidlewski, M.: Analiza przebiegu i skutków czołowo-bocznego zderzenia samochodów (Analysis of the course and effects of a frontal oblique offset collision of motor vehicles). A commissioned paper. Development of Automotive Engineering and Safety AES PROGRESS. Warszawa 2014.
[11] Database of the Central Statistical Office of Poland, www.stat.gov.pl

# NHTSA OBLIQUE CRASH TEST RESULTS: VEHICLE PERFORMANCE AND OCCUPANT INJURY RISK ASSESSMENT IN VEHICLES WITH SMALL OVERLAP COUNTERMEASURES

**James Saunders**
**Dan Parent**
**Eva Ames**
National Highway Traffic Safety Administration (NHTSA)
USA
Paper Number: 15-0108

## ABSTRACT

**Objective:** The National Highway Traffic Safety Administration (NHTSA) has been developing a research test protocol representative of real-world injury potential in frontal offset oblique impacts. This paper will address the vehicle and occupant responses from the latest research test series.
**Methods:** In this series, the Oblique Moving Deformable Barrier (OMDB) impacted stationery vehicles in both left and right side impacts. Vehicles were selected only if their performance in the Insurance Institute for Highway Safety (IIHS) Small Overlap (SOI) test condition earned a "Good" or "Acceptable" rating and had side curtain air bags meeting the requirements of Federal Motor Vehicle Safety Standard (FMVSS) No. 226, Ejection Mitigation. The vehicle responses studied included total velocity change (delta-V, DV), interior intrusion and steering wheel displacement, and the occupant responses studied included Brain Injury Criterion (BrIC), Multipoint Thoracic Injury Criterion, and Ankle Moment.
**Results:** Generally, delta-V (DV) in the X-direction decreased as the weight of the vehicle increased in both left and right side impacts, and the interior intrusion increased toward the center of the vehicle for both impact directions as well. A significant correlation between lap belt loads and vehicle mass was not found, but there was a general decreasing trend of peak lap belt loads with increase in vehicle mass. Occupant kinematics were generally mirror images for left and right side impacts, with the occupant's head moving forward and toward the direction of impact. The near-side occupants' heads moved toward the gap between the frontal and side curtain air bags, while the far-side occupants' heads rotated off of the frontal air bag and impacted the center instrument panel.
**Discussion:** The Honda Accord showed the greatest difference between left and right side impact vehicle response. The highest probability of injury for both near- and far-side occupants was predicted to occur in the head, chest, and ankle, agreeing with the findings from previous real-world oblique crash injury analysis. The test mode predicted a high risk of ankle injury, primarily due to ankle inversion and/or eversion. Left and right side impacts resulted in similar magnitudes of vehicle response, but occupant responses differed enough that it may be important to consider both left and right side oblique impacts in restraint system design.
**Conclusions:** The interior intrusions on the toe pan increased towards vehicle center, and toe pan point TP3 consistently showed the highest intrusion measurement. Vehicle deformation from left and right side impacts can differ due to the stack up of non-symmetrical vehicle component layouts. The latest NHTSA Oblique test series involving vehicles with a "Good" or "Acceptable" rating in the IIHS SOI test condition and with side curtain air bags meeting the requirements of FMVSS No. 226 suggest that additional countermeasures may reduce injury risk in this test mode.

## INTRODUCTION

A September 2009 report from the National Highway Traffic Safety Administration (NHTSA) investigated why occupant fatalities still occur in frontal crashes despite the presence of air bags and seat belts and the crashworthy structures of late-model vehicles [1]. It concluded that, aside from exceedingly severe crashes, the main cause of these deaths was poor structural engagement between the vehicle and its collision partner: corner impacts, oblique crashes, impacts with narrow objects, and heavy vehicle underrides. In response, the agency initiated a research program to develop a crash test procedure capable of replicating the injury potentials from real-world frontal offset oblique crashes.

The NHTSA Research Oblique Crash Test Protocol, illustrated below in Figure 1, involves a moving deformable barrier (MDB) weighing 2,486 kg (5,480 lb) which impacts a stationary vehicle at a speed of 90 km/h (56 mph), a 15 degree angle, and a 35 percent overlap. For an average mass 1,497 kg (3,300 lb) target vehicle, this barrier-to-vehicle crash has a delta-V of 56 km/h (35 mph), which is equivalent to a crash between two average mass vehicles with the bullet vehicle striking the target vehicle at a speed of 113 km/h (70 mph), a 15 degree angle, and a 50 percent overlap. For this test, a THOR 50th percentile male anthropomorphic test device (ATD) is seated in both the driver's and front passenger's positions.

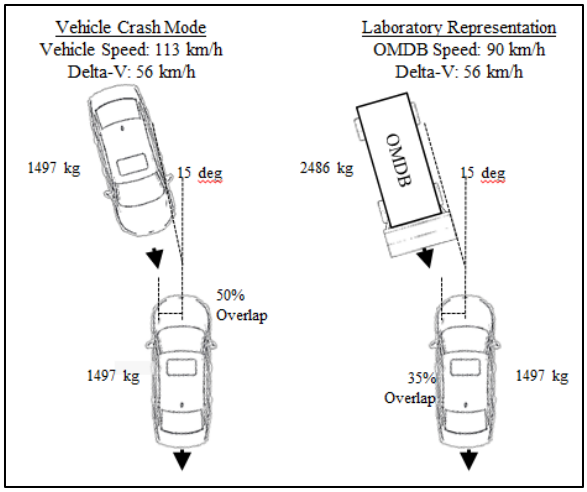


***Figure 1. Test Setup***

This test method is different from the existing New Car Assessment Program (NCAP) frontal tests in which the amount of test energy depends upon the mass of the vehicle. Because of the MDB impacting a stationary vehicle at the same speed regardless of the target vehicle's mass, the NHTSA Research Oblique Test Protocol is a constant-energy test, which encourages comparison of vehicle safety results between vehicle classes. As explained in Saunders 2012, the test speed was selected for consistency with the test severity of the NCAP frontal crash [2]. Saunders 2012 mistakenly noted that the NCAP test speed was 90 km/h (56 mph), but the proper speed, 56 km/h (35 mph), was actually used for the derivation of the speed for the NHTSA Oblique Test Protocol.

The research program started with a series of full-scale vehicle-to-vehicle crash tests to establish a baseline understanding of vehicle interaction and occupant kinematics. These full-scale vehicle-to-vehicle tests were then compared to results obtained in crash tests using an MDB, where it was determined that the MDB already in use in Federal Motor Vehicle Safety Standard (FMVSS) No. 214 would require modifications to produce equivalent test results. The face plate was enlarged to a width greater than the outer barrier track width to prevent wheel damage, a suspension was added to prevent the assembly from bouncing at high speeds, and the barrier honeycomb stiffness and thickness were optimized to prevent the barrier face from bottoming out too soon [3]. This modified version of the FMVSS No. 214 MDB is called the Oblique Moving Deformable Barrier (OMDB).

Previously, test procedure repeatability was demonstrated [4] and vehicle crash tests of high sales volume vehicles were performed to expand the database of OMDB-to-vehicle crash tests with THOR 50th ATDs [5]. Testing of vehicles redesigned or introduced in 2010 and 2011 with the highest ratings in US consumer rating programs has shown that there is potential for additional vehicle design improvements to mitigate real-world injuries and fatalities in frontal oblique crashes [5]. When comparing the average injury assessment values (IAVs) for each body region, trends appeared which mirrored the real-world data, including the risk of knee-thigh-hip, lower extremity, head, and chest injuries. Rudd, et al. 2011 also found similar injury incidence when they reviewed oblique crashes included in the Crash Injury Research and Engineering Network (CIREN) and National Automotive Sampling System Crashworthiness Data System (NASS-CDS) databases [6].

The current study presents both vehicle and occupant results from the latest series of OMDB-to-vehicle crash tests, in which vehicle selection was limited to those which received a "Good" or "Acceptable" rating in the Insurance Institute for Highway Safety (IIHS) Small Overlap Impact (SOI) crash test and also had side curtain air bags meeting the requirements of Federal Motor Vehicle Safety Standard (FMVSS) No. 226, "Ejection mitigation." These NHTSA Oblique tests were performed in both the left side impact (LSI) and right side impact (RSI) conditions, and kinematics for the occupants on both the struck and non-struck sides were evaluated.

## METHODOLOGY

### Oblique Crash Testing

Figure 21, in APPENDIX A, shows the left side impact (LSI) Oblique test procedure setup. In this setup, the OMDB impacts the target vehicle at 90 km/h (56 mph) and the stationary vehicle is positioned such that the angle between the OMDB and the vehicle is 15 degrees clockwise and the overlap is 35 percent on the driver side of the vehicle. For right side impacts (RSI) the OMDB impacts the target vehicle at 90 km/h (56 mph) and the stationary vehicle is positioned such that the angle between the OMDB and the stationary vehicle is 15 degrees counterclockwise and the overlap is 35 percent on the passenger side of the vehicle.

The vehicles were instrumented with a rear accelerometer on the left and right door sill to record the X and Y accelerations of the vehicle. APPENDIX B describes the intrusion points taken during the test. These points where placed according to IIHS "Moderate Overlap Frontal Crashworthiness Evaluation Crash Test Protocol (Version XV) dated May 2014. These points are listed in Table 3 and illustrated in Figure 23 and Figure 24, in APPENDIX B.

Table 1 shows the list of vehicles tested in the LSI condition, along with the naming convention for each vehicle, and Table 2 shows the list of vehicles tested in the RSI condition.

***Table 1: LSI matrix and vehicle naming convention***

| NHTSA TEST NUMBER | MAKE | MODEL | YEAR | TEST WEIGHT (KG) |
|---|---|---|---|---|
| 9043 | Honda | Fit | 2015 | 1426 |
| 8787 | Mazda | 3 | 2014 | 1588 |
| 8789 | Honda | Accord | 2014 | 1744 |
| 8788 | Mazda | CX-5 | 2014 | 1769 |
| 8478 | Subaru | Forester | 2014 | 1803 |
| 8488 | Volvo | S60 | 2012 | 1936 |

***Table 2: RSI matrix and vehicle naming convention***

| NHTSA TEST NUMBER | MAKE | MODEL | YEAR | TEST WEIGHT (KG) |
|---|---|---|---|---|
| 8999 | Mazda | 3 | 2014 | 1582 |
| 9042 | Honda | Accord | 2014 | 1749 |
| 8998 | Mazda | CX-5 | 2014 | 1777 |

### Occupant Response Assessment

Previous OMDB crash tests have included either a single THOR (Test Device for Human Occupant Restraint) anthropomorphic test device (ATD) seated in the driver (near-side) position, or THOR ATDs in both the driver and right front passenger positions. The tests presented in this paper (Table 1 and Table 2) included two THOR ATDs, one in the driver position and one in the right front passenger position. Both THOR ATDs met the specifications of the Mod Kit [7] with the addition of the SD-3 shoulder, a derivation of the Chalmers shoulder [8] which was further developed through the European Union's THORAX project [9]. For the LSI tests, the driver was on the near-side and the passenger on the far-side, while for the RSI tests, the passenger was on the near-side and the driver was on the far-side (further illustrated in Figure 22, APPENDIX A). In both the LSI and the RSI conditions, each ATD was positioned using the basic principles of the FMVSS No. 208 seating procedure, updated to account for the differences between THOR and Hybrid III.

### Injury Criteria

Occupant injury risk was assessed by determining the probability of given severity of injury based on the Abbreviated Injury Scale (AIS) [10] [11]. For the head, neck, chest, abdomen, femur, and acetabulum, the probability of an AIS score of three or higher (AIS $\geq$ 3) was calculated. For the lower extremity, the probability of an AIS score of two or higher (AIS $\geq$ 2) was calculated. As such, this injury assessment was limited to injury criteria for which injury risk functions were available in the literature. Table 8, in APPENDIX G, summarizes the calculation of each injury criterion, including the predictor variable, any intermediate variables and constant definitions, and the associated injury risk functions. Compared to previous NHTSA publications of Oblique test results and analysis, there are three notable changes to calculation of injury risk.

**BrIC.** Previous analysis of brain injury risk in the Oblique test condition was calculated using the kinematic brain injury criterion (BRIC) injury assessment metric calculated using the method and critical values described in Saunders et al., 2012 [2]. Since that publication, an updated methodology for brain injury assessment was published

by Takhounts et al., 2013 [12]. The revised rotational brain injury criterion (BrIC) does not consider angular acceleration, but does consider each individual local axis of angular velocity. The critical values are directionally dependent but not dummy-specific, so the critical values applicable to THOR are the average critical angular velocities for the BrIC formulation based on maximum principle strain (MPS), as summarized in Table 8 (APPENDIX G).

**Multipoint Thoracic Injury Criterion.** A relationship between chest deformation and injury risk was determined through a series of matched-pair sled tests conducted at the University of Virginia [13]. Sled tests were conducted in twelve conditions using the THOR ATD with SD-3 shoulder, for which thoracic biofidelity has been demonstrated [14]. The matched set of post-mortem human surrogate (PMHS) tests included 38 observations on 34 PMHS (four PMHS were subjected to a low-speed, non-injurious loading condition before injurious testing). A relationship was developed between the thoracic deflections measured in the THOR ATD tests to the incidence of injury in the PMHS in the same condition. Thoracic deflection was quantified by calculating the maximum resultant deflection at any of the four measurement locations on the THOR rib cage. Incidence of injury was quantified as AIS $\geq$ 3 thoracic injury to the PMHS, which represents three or more fractured ribs based on the 2005 (update 2008) version of AIS. The paired PMHS and THOR tests, along with associated test number in the NHTSA Biomechanics Database where available and the peak resultant deflection measured by the THOR ATD in each condition, are included in Table 7 (APPENDIX F).

**Ankle Moment.** Kuppa et al., 2001 proposed injury risk curves for the human lower extremity [15] and described their application to the lower extremity hardware of the THOR ATD [16]. Injury risk function were presented for the prediction of tibia plateau fractures (proximal or upper tibia axial force), tibia/fibula shaft fractures (Revised Tibia Index), calcaneus, talus, ankle, and midfoot fractures (distal or lower tibia axial force), and malleolar fractures and ankle ligament injuries (ankle rotation angle or moment). Previous analyses of ankle injury in the Oblique test condition were discarded due to measured ankle rotation data that were inconsistent with visual ankle kinematics from review of high-speed video. Since malleolar and ankle ligament injuries account for 60 percent of the lower extremity injuries in air bag equipped vehicles in frontal crashes, ankle injury risk was revisited by calculating ankle dorsiflection moment and inversion/eversion moment as described by Kuppa et al., 2001 [16].

## RESULTS

### Vehicle Response

In general, the total velocity change (delta-V (DV)) in the X-direction decreased as the weight of the vehicle increased for both LSI and RSI (Figure 2). The DV in the X-direction for the vehicles impacted on the RSI was higher than the DV for LSI impacts, but the same trend held for weight.

Figure 3 and Figure 4 show the interior intrusion of the vehicles tested in both LSI and RSI. Generally, intrusion increased toward the center of the vehicle for both RSI and LSI. Also, for the toe pan, point TP3 always displayed the highest intrusion. There was no apparent trend for the Left IP, Right IP, bottom A-pillar, and rocker panel intrusions.

Figure 5 shows the residual displacement of the steering wheel in the X-Y plane of the vehicle. From this figure it can be seen that the steering wheel moves toward the driver's door, and the Forester had about 100 mm of displacement toward the door.

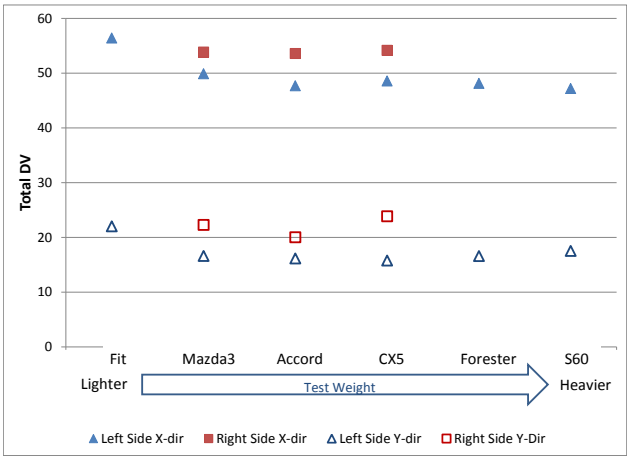


*Figure 2. X DV*

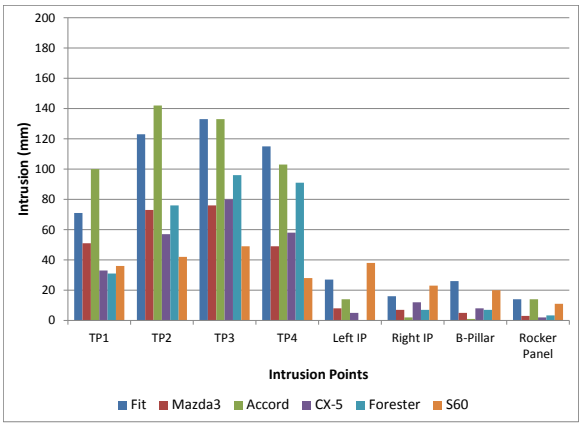


*Figure 3 – Interior intrusions for LSI*

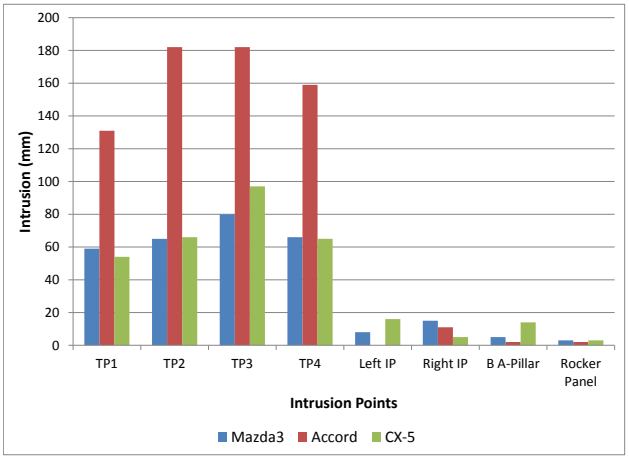


*Figure 4 – Interior intrusions for RSI*

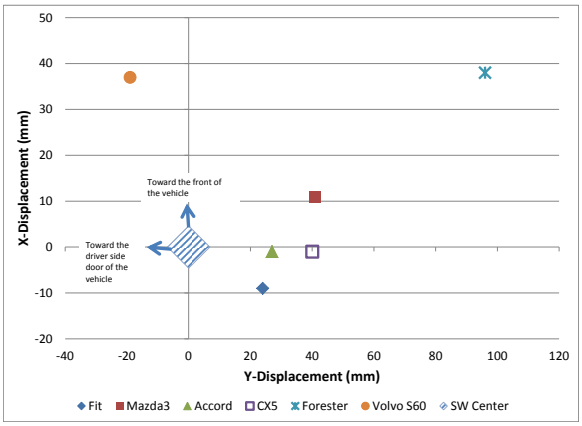


*Figure 5 – Steering wheel motion in the X-Y plane*

## Occupant Response

**Restraint Deployment.** In all nine tests presented in this paper (Table 1 and Table 2), the vehicles deployed retractor pretensioners, frontal air bags, and side curtain air bags to the near-side occupants. The vehicles deployed retractor pretensioners and frontal air bags to the far-side occupants. Since the far-side occupants primarily translated and rotated in the inboard direction, the far-side curtain air bags were disabled to allow for high-speed video coverage.

Frontal air bag deployment time varied across vehicles, but deployed no later than 22 milliseconds after barrier contact with the bumper of the target vehicle. Safety belt pretensioners triggered at roughly the same time as frontal air bag deployment, and triggered at the same time for both the driver and right front passenger. The side curtain air bags generally deployed later than the frontal air bags, the outliers being the Forester (25ms) and the S60 (18ms) which fired at similar times to the frontal air bags. Restraint deployment times and head contact locations are summarized in Table 4 (APPENDIX C). Note that in some cases, contact was not evidenced by paint transfer since either the air bag itself or the hand shielded the contact between the head and door panel or instrument panel, but there was evidence of contact in the high-speed video and head acceleration time-histories.

In this set of vehicles, there was a general decreasing trend of peak lap belt loads with increase in vehicle mass (Figure 7), likely resulting from the decrease in delta-V with increasing mass (Figure 2). Overall there is not a significant correlation between lap belt loads and vehicle mass. If the near-side occupants are isolated, there is a statistically-significant relationship between peak lap belt force and vehicle mass ($p = 0.036$), but not for the far-side

occupants (p = 0.154). The far-side occupant saw a higher peak lap belt load than the near-side occupant in all but one vehicle, which had the highest shoulder belt load of the group (Forester, as seen in Figure 6). Despite the shoulder of the far-side occupant slipping out of the shoulder belt in every instance, far-side shoulder belt peak forces were higher than equivalent near-side shoulder belt forces, where the shoulder belt was retained throughout the event, in almost half of the observations. There was no apparent relationship between shoulder belt forces and any vehicle parameters, which is not surprising since shoulder belt forces are controlled by load limiters in all of the present vehicles with the exception of the Forester.

To examine whether the high shoulder belt load seen in the Forster was anomalous or the result of a malfunction, the shoulder belt loads from a frontal rigid barrier test of the 2014 Forester were reviewed (NHTSA vehicle database test number 8313) and found to be similarly high at 6,640 N. Thus, the Forester may have a higher load limit for the driver-side seating position than the other vehicles in this group. The second-highest shoulder belt force occurred in the Honda Fit far-side occupant location, but a similar 50$^{th}$ percentile male test is not available for comparison.

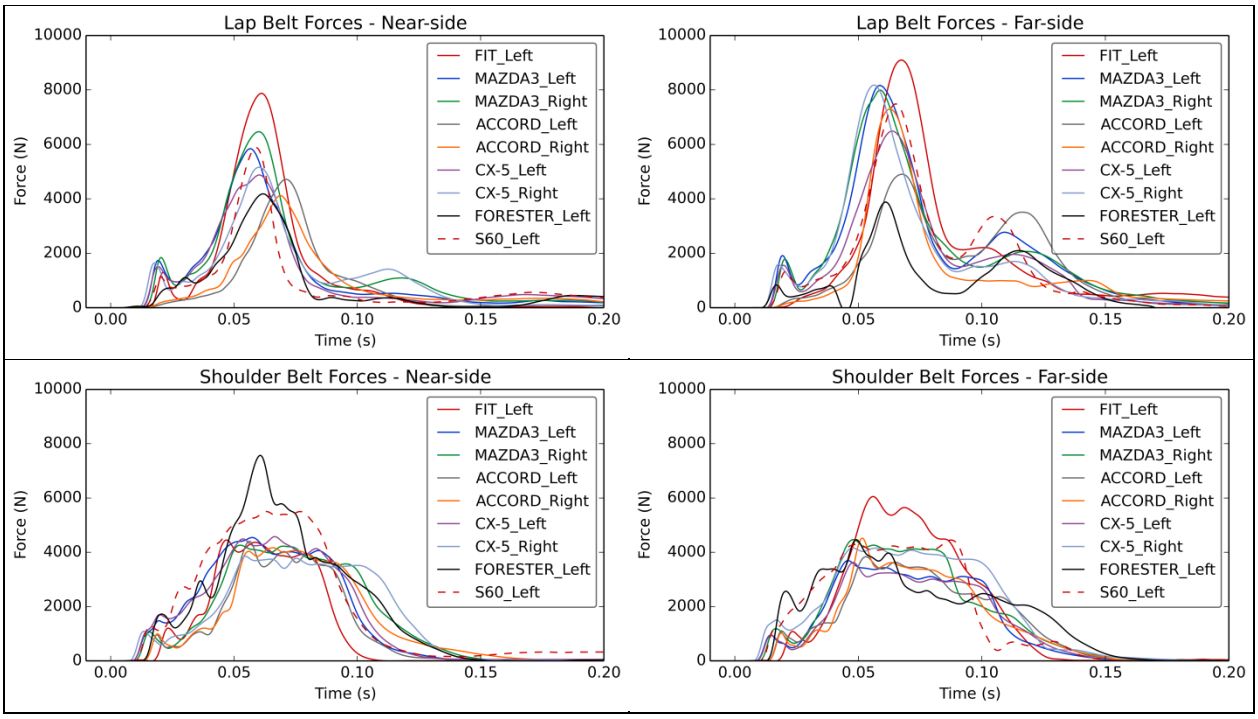


***Figure 6. Lap and shoulder belt forces for the near- and far-side occupants.***

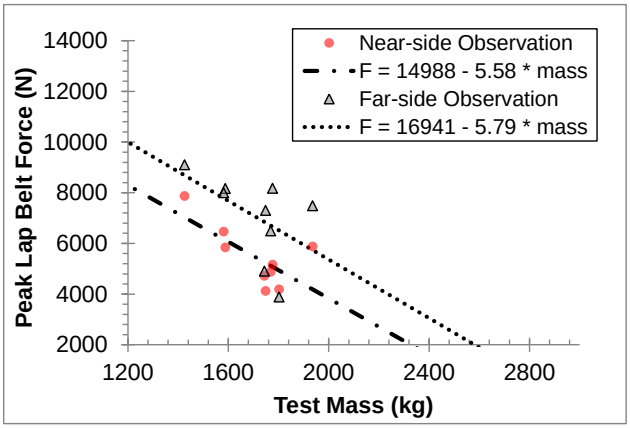


***Figure 7. Relationship between lap belt load and vehicle mass.***

**Near-side Occupant Kinematics.** In the LSI condition, the occupant in the driver's seat began moving directly forward with a gradually-increasing outboard translation. The frontal air bag was typically fully-deployed by the

time head contact was made, usually in the center or left-center of the bag. As the head contacted the frontal air bag, it continued to translate in an outboard direction, often having a rotational velocity about the local Z-axis induced as the face interacted with the frontal air bag. Contact with the side curtain varied greatly based on the vehicle and side curtain air bag design (Figure 25, APPENDIX H). In general, the head translated into the gap between the frontal air bag and the side curtain air bag and rotated about the local Y-axis. Depending on the extent of deployment and stiffness of the side curtain air bag, the head was either protected from contact (Accord, CX-5, and S60) or translated and rotated past the air bag and contacted the door panel (Fit, Mazda 3, and Forester).

In the RSI condition, the overall occupant kinematics were essentially a mirror-image of the kinematics in the LSI condition. As the occupant moved forward and to the right, the head interacted with the frontal air bag and translated to the right towards the gap between the frontal and side curtain air bags. However, in the case of the Accord, the side curtain air bag contacted the head before it interacted with the frontal air bag and imparted an outboard rotation about its the local Z-axis (Figure 8). The other RSI-P occupants showed similar kinematics to their LSI-D counterparts.

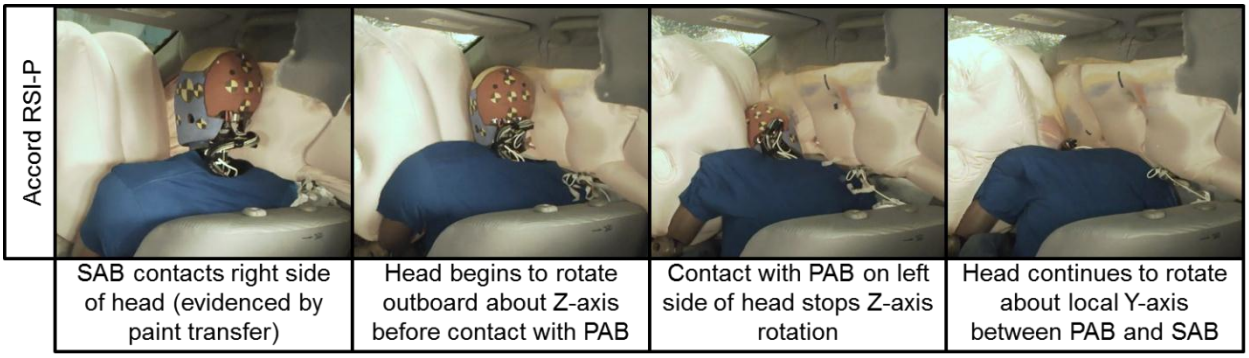


***Figure 8. Kinematics of near-side occupant (RSI-P) in right-side impact test.***

**Far-side Occupant Kinematics.** In the LSI condition, the far-side occupant was seated in the right front passenger seat. Like the near-side occupant location, the ATD began moving forward with an increasingly left lateral trajectory, inboard in this case. In all of the LSI vehicles, the frontal air bag appeared to be fully deployed by the time of head contact, and the head of the occupant contacted the left-hand side of the frontal passenger air bag. This contact initiated a positive Z-axis rotation of the head, and in all six of the LSI-P observations, the left side of the head contacted the center instrument panel (IP). In three of these six observations, contact was not evidenced by paint transfer but was apparent from high-speed video and head acceleration time-history (Figure 9). The peak head acceleration occurs in the Y-axis since it results from an impact to the side of the head, and occurs slightly after the peak head angular velocity since contact with the IP slows or stops the motion of the head. The earliest and most severe contact occurred in the Fit, where the head contacted the corner of a relatively narrow and visually stiff passenger air bag and rotated abruptly in the positive Z-axis direction to contact the center IP. On the other end of the spectrum was the CX-5, which had a wider and visually softer passenger air bag, which yielded under contact with the passenger's head until the point of maximum forward head excursion (Figure 10). Accordingly, out of all far-side occupants in this study, the Fit showed the highest head Z-axis angular velocity (4883 deg/s) while the CX-5 showed the lowest (1643 deg/s).

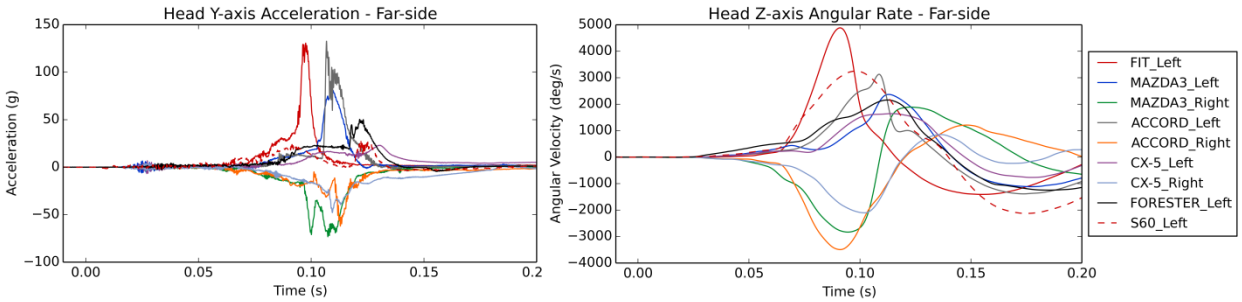


***Figure 9. Y-axis head accelerations (left) and Z-axis angular velocities (right) of the far-side occupants.***

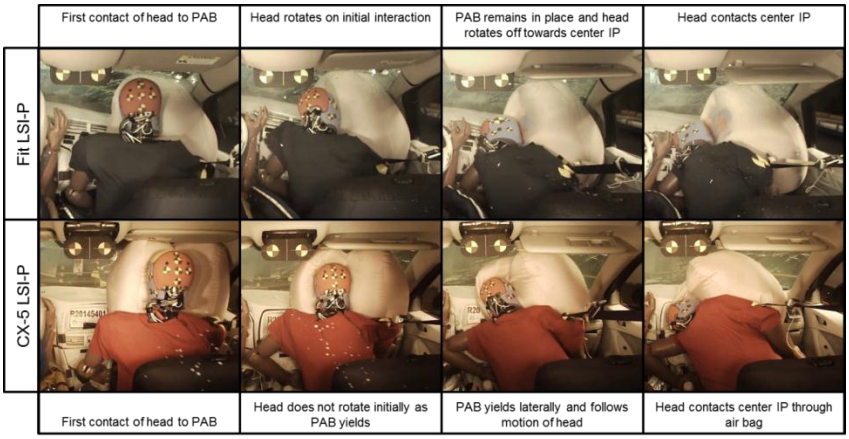


***Figure 10. Kinematics of far-side occupant in left side impact test (LSI-P), comparing head rotation and center IP contact with different passenger air bag (PAB) designs.***

In the RSI far-side condition, while the overall kinematics were a mirror-image of the LSI far-side condition, there were some localized changes due to differences in the driver-side and passenger-side restraints and interior features. The frontal air bag on the driver side was initially closer to the occupant but generally smaller and stiffer, so the initial interaction with the head may have differed from the passenger far-side condition. Also, since the hands of the driver were initially placed on the steering wheel, the right hand contacted the center IP and was subsequently impacted by the head in two of the three RSI-D observations. This did not occur for the passenger in the LSI far-side condition, as the hands of the passenger were initially placed on his lap. The differences in kinematics are shown in Figure 11 by presenting the LSI-P condition as-is and the RSI-D observation as a horizontal mirror-image at the same point in time during the crash. The head of the occupant in the RSI-D condition began rotating about the local Z-axis earlier and at a greater magnitude. This comparison is not too different from that shown in Figure 10, as the interaction of the RSI-D occupant with a stiffer, unyielding frontal air bag resulted in greater head rotational velocity and, visually at least, more forward and downward head excursion.

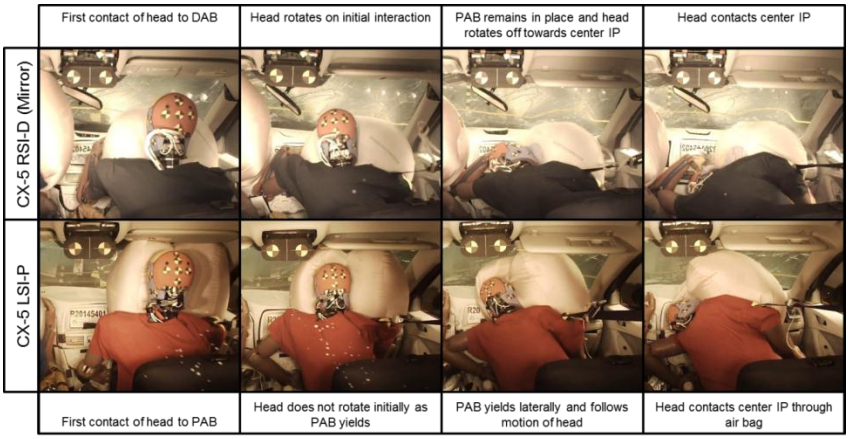


***Figure 11. Comparison of the far-side driver and far-side passenger observations, taken at identical time steps during the test. Note that the RSI-D images are mirrored horizontally.***

**Occupant Injury Assessment.**

For the purposes of this effort, occupant injury risk was assessed using the probability of an AIS $\geq$ 3 (or AIS $\geq$ 2 for the lower extremities) based on the injury criteria and underlying injury risk functions that can be applied to the THOR ATD. For the vehicles presented in Table 1 and Table 2, the body regions that showed the highest probability of injury include the brain (as predicted by BrIC), the chest (as predicted by the multipoint thoracic injury criterion), and the ankles (as predicted by ankle moment). These metrics show good agreement with the field injury exposure presented by Rudd et al. 2011 [6], where the body regions with the highest incidence of injury were the knee/thigh/hip, chest, lower extremity, and head. Summaries of the injury risk calculated by each criterion are

shown for the near-side (Table 5, APPENDIX D) and far-side (Table 6, APPENDIX E) occupants in the Appendix. This section will focus on the head, chest, knee/thigh/hip, and lower extremity. In the following bar charts, the shading of the bar represents the impact side (dark gray for left-side impact, light gray for right-side impact) while the fill pattern represents the occupant position (solid for near-side, cross-hatched far-side). RSI testing was not conducted for the Fit, Forester, and S60.

**Head.** Head injury predicted by the $HIC_{15}$ and BrIC injury criteria are shown in Figure 12. The highest injury risk predicted by $HIC_{15}$ occurs in the far-side condition, and three of the four observations above a 10 percent risk of AIS $\geq$ 3 injury occur in left-side impacts. Injury risk predicted by BrIC is notably higher, with a minimum of 23 percent risk AIS $\geq$ 3 injury in the Accord LSI-D observation. The average predicted BrIC injury risk for near-side occupants was 53 percent with five of the nine observations below a 50 percent risk of injury, while the far-side occupant average risk was 87 percent with all nine of the observations above a 50 percent risk of injury. The lowest-mass vehicles showed a higher injury risk as predicted by $HIC_{15}$, but there was no apparent relationship between BrIC and any vehicle structural response parameters. The measured BrIC value appears to be more sensitive to local interactions with the frontal air bags (as shown in **Figure 10**) and side curtain air bags than the differences in vehicle kinematics within the range of the current set of vehicles. Considering the three paired left-side to right-side comparisons, injury risk predicted by BrIC was higher in right-side impacts for all of the far-side occupants, while not consistently different for the near-side occupants.

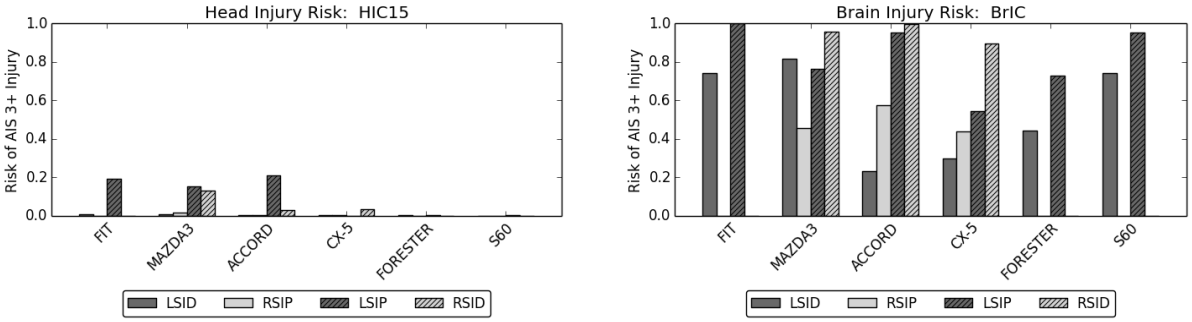


***Figure 12. Risk of AIS ≥ 3 injury as predicted by HIC15 (left) and BrIC (right).***

**Chest.** Chest injury risk presented in Figure 13 represent the injury risk predicted by the peak resultant chest deflection measured at any of the four rib deflection measurement locations on the THOR ATD at any point in time. This deflection is calculated as spatial resultant representing the length of the vector between the initial rib location and the current rib location, as measured in a coordinate system on the local spine segment. In all but one of the tests in this series (Fit LSI), chest deflection was higher for the near-side occupant than for the far-side occupant. Comparing left-side impacts to right-side impacts, all three near-side conditions showed a higher risk of chest injury in the right-side impact than the left-side impact, while the difference was not consistent for the far-side occupants.

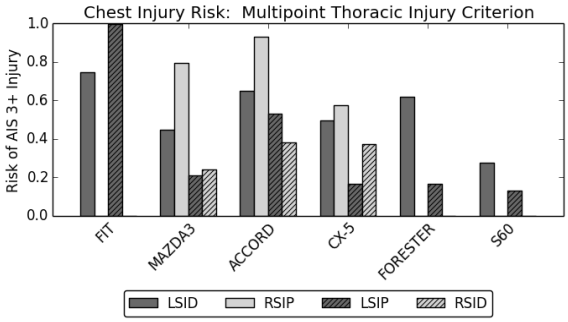


***Figure 13. Risk of AIS ≥ 3 injury as predicted by multipoint thoracic injury criterion.***

**Knee/Thigh/Hip.** While the axial load measured by the distal femur and the load measured at the acetabulum are intrinsically related due to the shared load path, the injury risk to the body regions in question is not necessary linearly related. This has been observed in field data, as only 50 percent of the occupants in oblique crashes who sustained pelvis and/or hip injury also sustained femur shaft fracture [6]. Femur fracture risk was generally low, with

only one observation predicting greater than a 10 percent risk of injury (S60 LSI-D) which resulted from compressive loading of the right femur. The risk of acetabulum fracture in the same observation was greater than 50 percent, also occurring in the occupant's right leg. Three out of the four highest acetabulum injury risks were predicted to the far-side occupant in a left-side impact (Figure 14).

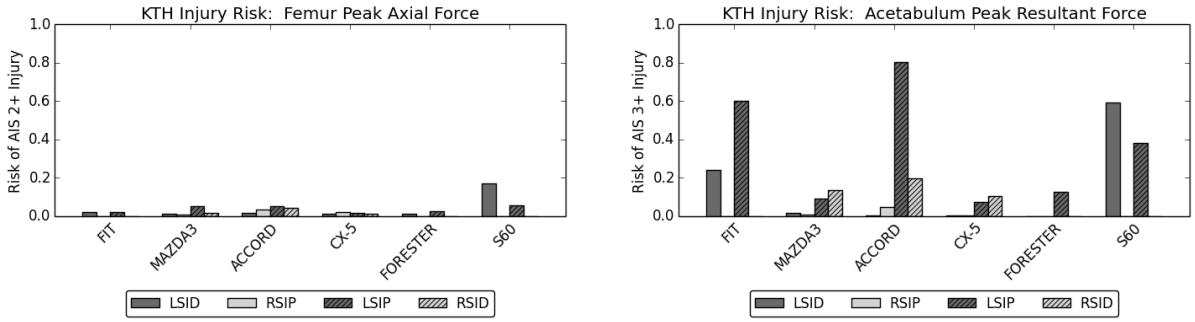


***Figure 14. Risk of AIS ≥ 2/3 injury as predicted by femur axial force (left) and acetabulum force (right).***

**Lower Extremity.** Risk of lower extremity injury was assessed using the Revised Tibia Index (RTI), which is summarized in Figure 15 as the maximum risk predicted using RTI for either the upper or lower tibia and either left or right leg. Injury risk predicted by RTI was generally low, with all but one observation predicting less than 25 percent risk of AIS ≥ 2 injury to the lower leg, specifically a tibia or fibula shaft fracture. The highest injury risk occurred again in the S60 LSI-D observation, again in the right leg which also saw a high risk of femur and acetabulum fracture. The S60 did have the highest right IP intrusion (see Figure 3), though this intrusion was only 22 millimeters. As shown in the past [5], the near-side occupant was expected to see a higher injury risk than the far-side due to intrusion into the occupant compartment. However, only five out of nine near-side occupants saw a higher injury risk than their far-side counterparts as predicted by RTI.

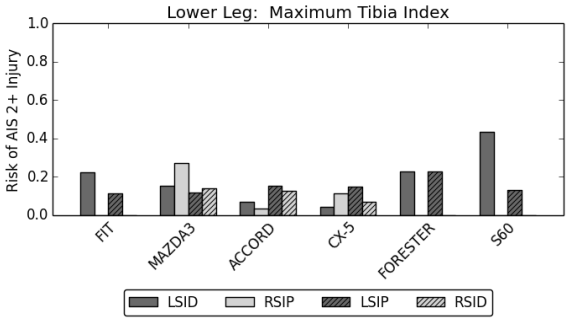


***Figure 15. Risk of AIS ≥ 2 injury as predicted by Revised Tibia Index.***

The prediction of ankle injury based on ankle moment was prevalent across all vehicles and occupant positions included in this study (Figure 16), especially due to ankle inversion/eversion. The average risk of ankle injury due to dorsiflexion moment was roughly 25 percent, while the average risk of ankle injury due to inversion/eversion moment was nearly 90 percent. Risk to near-side and far-side occupants were generally similar, as were risk of left and right ankle injury. Ankle inversion/eversion moment is generally induced by intrusion of the toe pan for the near-side occupant, as can be seen in high-speed video (Figure 26). However, high-speed video was not recorded in the far-side occupant seat position, so ankle kinematics can only be speculated based on occupant measurements. Another limitation in this assessment is that the tibia accelerations and lower tibia shear forces (FX, FY) were not measured in these tests due to channel count restrictions. However, based on the data presented by Kuppa et al. [16], the ankle moment measured at the lower tibia load cell may be an under-prediction of the peak ankle joint moment.

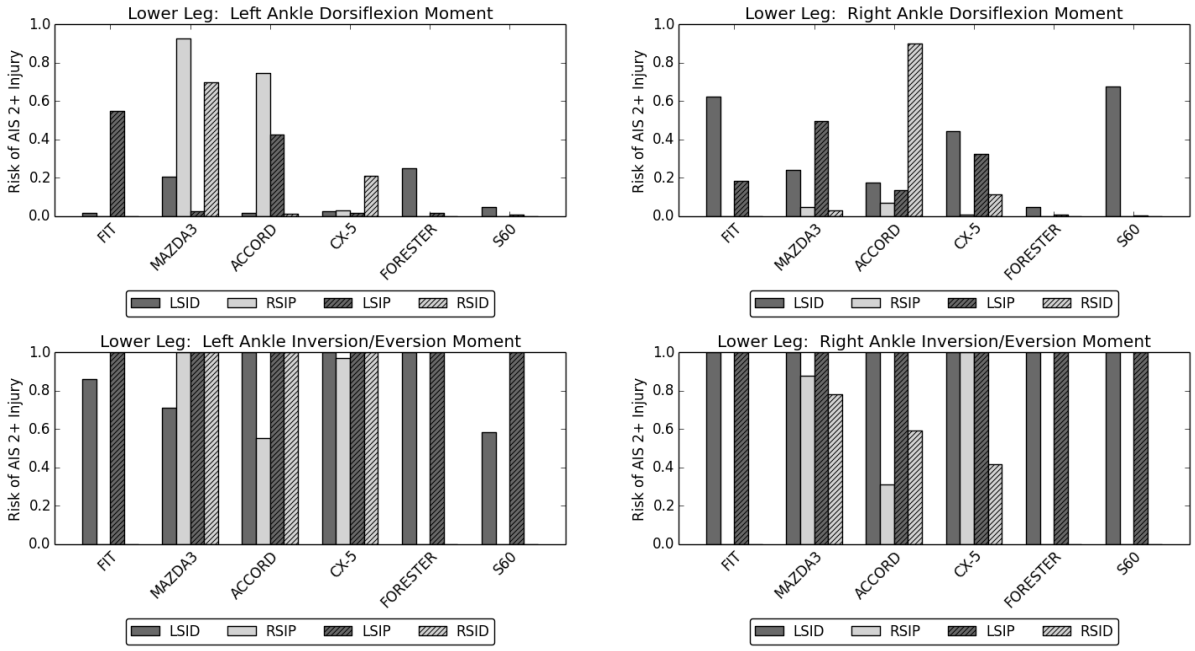


***Figure 16. Risk of AIS ≥ 2 left and right ankle injury as predicted by ankle dorsiflexion (top) and inversion/eversion moment (bottom).***

## DISCUSSION

### Vehicle Response

When comparing the intrusions of an LSI and RSI vehicle, the Accord had the greatest difference between left and right side (Figure 17). Figure 18 shows the post-test picture of the underbody for the Accord. The RSI picture was flipped in the figure to be able to make a better comparison. Figure 18 shows the Accord underbody had three different locations with different bending or pieces breaking off. The differences in this deformation may be due to the stack up of vehicle components on each side of the vehicle.

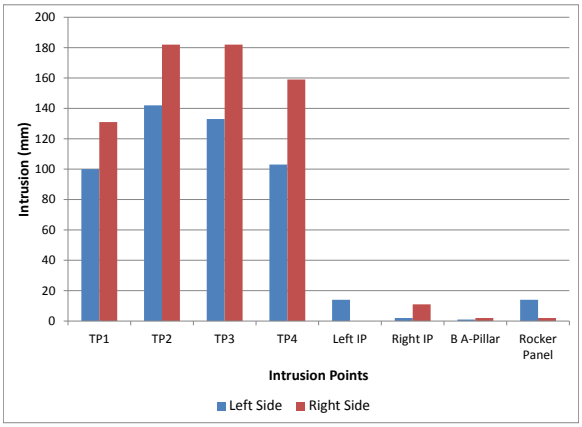


***Figure 17 - Honda Accord interior intrusions***

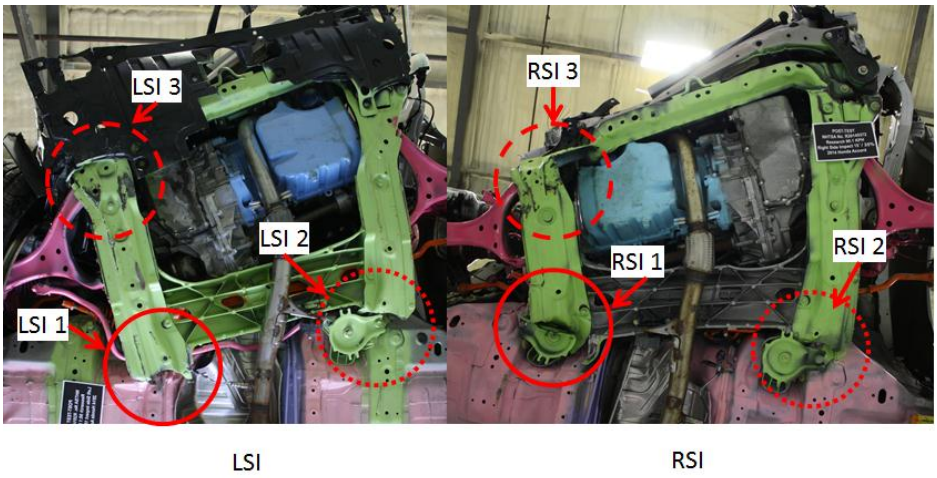


***Figure 18 - Underbody of Honda Accord LSI and RSI***

**Occupant Response**

**Injury Risk.** The current study implemented THOR ATDs to predict injury risk in a simulated frontal oblique impact for a group of nine vehicles. Overall, the highest probability of injury for both occupants in these nine vehicles was predicted to occur in the head, chest, and ankle. Correspondingly, the most frequently injured body regions in oblique crashes were the knee/thigh/hip, chest, leg/foot, and head, as presented by Rudd et al. [6]. While knee/thigh/hip injuries were not shown to have a proportionally high injury risk in the current set of tested vehicles, high acetabulum and femur forces consistent with a high risk of injury have been measured in previously-tested vehicles [5].

**Ankle Injury.** This test mode indicated a high risk of ankle injury, primarily due to ankle inversion and/or eversion as predicted by the ankle moment measured by the THOR ATD. These high ankle moments were induced by intrusion into the toe pan coupled with interaction with the pedals for the occupants in the driver's seat. However, there was no clear disadvantage to the driver seat location compared to the passenger seat location, nor to the inboard limb compared to the outboard limb. There was also no distinct correlation between peak intrusion and ankle injury risk, as highlighted by the fact that the Accord RSI-P seating location showed the largest toe pan intrusion (Figure 4), yet measured the lowest ankle inversion/eversion moment for both the left and right ankles (Figure 16).

**Near-side versus Far-side.** Visually, one of the key differences between the near-side and the far-side occupant kinematics is that the far-side occupant appears to slip out of the shoulder belt before the point of peak head excursion. One would expect to see a difference in the measured shoulder belt forces between the near-side and far-side occupants at the point that the shoulder appears to escape the shoulder belt, roughly 100 milliseconds after impact. However, the timing of shoulder belt unloading is similar between the near-side and far-side observations (Figure 6), which suggests that the shoulder escaping the shoulder belt does not mean that the shoulder belt is not still restraining the occupant. Instead, the shoulder belt loads the lower torso, evidenced by the lower left being the quadrant of peak chest deflection in 5 of the 6 LSI observations. Interestingly, the quadrant of peak chest deflection for the three RSI far-side observations is the upper right, perhaps a result of the arms being initially positioned with the hands on the steering wheel.

Another notable difference between the near-side and far-side occupant kinematics is the rotation of the head. This can be demonstrated by calculating the individual components of BrIC by dividing the peak angular velocity about each axis of the head by its respective critical value. In six of the nine near-side observations, the Y-axis angular rate is the peak axis of rotation (Figure 19, left), similar to what would be expected in a full-frontal impact. Peak angular rates for the far-side occupant are noticeably higher than those of the near-side occupant, and dominated by Z-axis angular rate for all far-side observations (Figure 19, right).

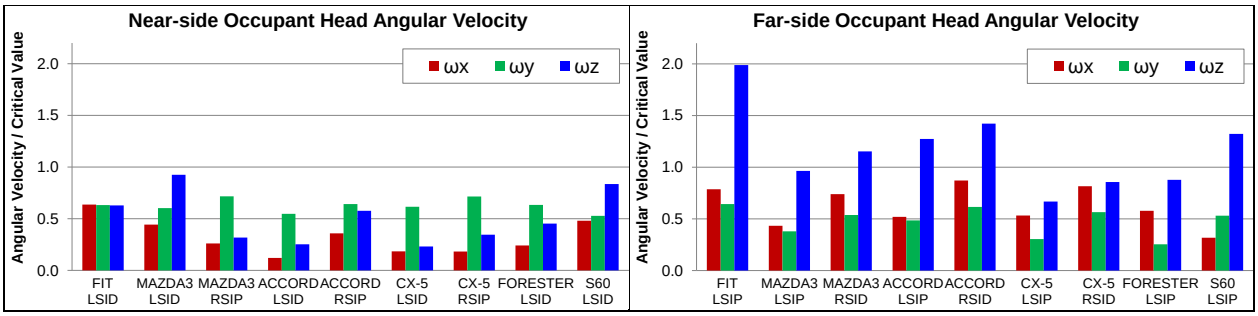


***Figure 19. Components of head angular velocity for the near-side (left) and far-side (right) occupants.***

**LSI versus RSI.** While the left-side and right-side impacts resulted in similar magnitudes of vehicle response, there were some differences in the occupant response that highlight important restraint system considerations. Comparing the three paired test conditions (Mazda 3, Accord, and CX-5 were all tested in both the LSI and RSI condition), the differences were more pronounced in the near-side occupant location than the far-side location. The far-side kinematics were generally a mirror image for the left- and right-side impacts, which can be seen in the head rotational velocity about the Z-axis (Figure 20, left). As the head interacted with the frontal air bag, it rotated outboard about its local Z-axis, resulting in positive angular velocity for the far-side passengers and negative angular velocity for the far-side drivers. However, the responses were not quite mirrored since the driver began to interact with the frontal air bag earlier than the passenger, with peak angular rates for the driver occurring earlier than their passenger counterparts in all three paired observations. The differences were less apparent for the near-side occupants (Figure 20, right), as the peak local Z-axis rotation was not consistently positive or negative for either group. Unlike the far-side occupant whose head interacted with only the frontal air bag, the head of the near-side occupant interacted with both the frontal air bag and the side curtain air bag. The driver-side frontal air bag and the passenger-side frontal air bag may have interacted with the side curtain air bag differently. Thus, it may be important to consider both left- and right-side oblique impacts in restraint system design.

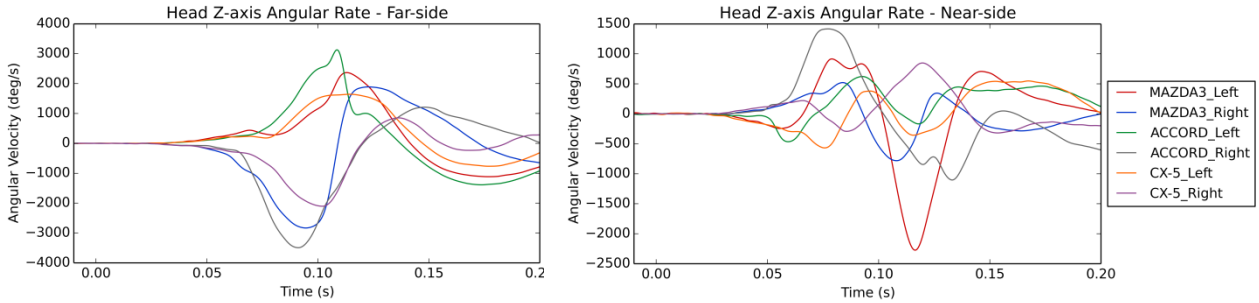


***Figure 20. Comparison of head angular velocity in paired left- and right-side impact tests.***

## CONCLUSIONS

The interior intrusions on the toe pan increased moving toward the center of the vehicle and the highest point of intrusion on the toe pan was TP3. The deformation on the LSI and RSI can be different due to the stack up of non-symmetrical vehicle component layouts.

The current set of vehicles tested in the NHTSA Oblique condition suggest that additional countermeasures to reduce injury risk may be needed, despite these vehicles being rated "Good" or "Acceptable" in the IIHS Small Overlap Impact test condition and including side curtain air bags meeting the requirements set forth by FMVSS No. 226. The body regions for which the highest risks of injury were predicted were the head, chest, and lower extremity, consistent with injury incidence found in previously-published reviews of NASS and CIREN data. This study reviewed the differences between left-side and right-side impacts and found that neither was of notably higher risk, though there were localized differences in the interaction of the occupants with the frontal air bag. These differences were more pronounced in the near-side occupant location, where the interaction with the frontal air bag and side curtain air bag differed noticeably between left- and right-side impacts of the same vehicle design.

**REFERENCES**


1. Bean, J.D., et al., "Fatalities in Frontal Crashes Despite Seat Belts and Air Bags – Review of All CDS Cases – Model and Calendar Years 2000-2007 – 122 Fatalities," NHTSA Technical Report, Report No. DOT HS 811 202, September 2009.
2. Saunders, J., Craig, M. and Parent, D., "Moving Deformable Barrier Test Procedure for Evaluating Small Overlap/Oblique Crashes," SAE World Congress, paper no. 2012-01-0577, 2012.
3. Saunders, J., Craig, M. and Suway, J., "NHTSA's Test Procedure Evaluations for Small Overlap/Oblique Crashes," 22nd ESV Conference, Paper No. 11-0343, 2011.
4. Saunders, J. and Parent, D., "Repeatability of a Small Overlap and an Oblique Moving Deformable Barrier Test Procedure," SAE World Congress, paper no. 2013-01-0762, 2013.
5. Saunders, J. and Parent, D., "Assessment of an Oblique Moving Deformable Barrier Test Procedure," 23rd ESV Conference, Paper No. 13-0402, 2013.
6. Rudd, R., Scarboro, M., Saunders, J., "Injury Analysis of Real-World Small Overlap and Oblique Frontal Crashes," 22nd ESV Conference, Paper No. 11-0384, 2011
7. Ridella, S., Parent, D., "Modifications to Improve the Durability, Usability, and Biofidelity of the THOR-NT Dummy," 22nd ESV Conference, Paper No. 11-0312, 2011.
8. Lemmen, P., Been, B., Carroll, J., Hynd, D., Davidsson, J., Song, E., Lecuyer, E., "Development of an advanced frontal dummy thorax demonstrator," Proceedings of the 2012 IRCOBI Conference, 2012.
9. Törnvall, Fredrik. A New Shoulder for the THOR Dummy Intended for Oblique Collisions. Chalmers University of Technology, 2008.
10. AAAM: The Abbreviated Injury Scale – 1990, Update 1998. Des Plaines, Il. 2008.
11. AAAM: The Abbreviated Injury Scale – 2005, Update 2008. Des Plaines, Il. 2008.
12. Takhounts, E.G., Hasija, V., Moorhouse, K., McFadden, J., Craig, M., "Development of Brain Injury Criteria (BrIC)", Proceedings of the 57th Stapp Car Crash Conference, Orlando, FL, November 2013.
13. Crandall, J., "Injury Criteria Development: THOR Metric SD-3 Shoulder Advanced Frontal Crash Test Dummy," NHTSA Biomechanics Database, Report b11117-1, September 2013.
14. Parent, D., Craig, M., Ridella, S., McFadden, J., "Thoracic Biofidelity Assessment of the THOR Mod Kit ATD," 23rd Enhanced Safety of Vehicles Conference, Paper No. 13-0327, 2013.
15. Kuppa, S., Wang, J., Haffner, M., Eppinger, R., "Lower Extremity Injuries and Associated Injury Criteria," 17th ESV Conference, Paper No. 457, 2001.
16. Kuppa, S., Haffner, M., Eppinger, R., Saunders, J., "Lower Extremity Response And Trauma Assessment Using The THOR-Lx/HIIIr And The Denton Leg In Frontal Offset Vehicle Crashes," 17th ESV Conference, Paper No. 456, 2001.

**APPENDIX A.**

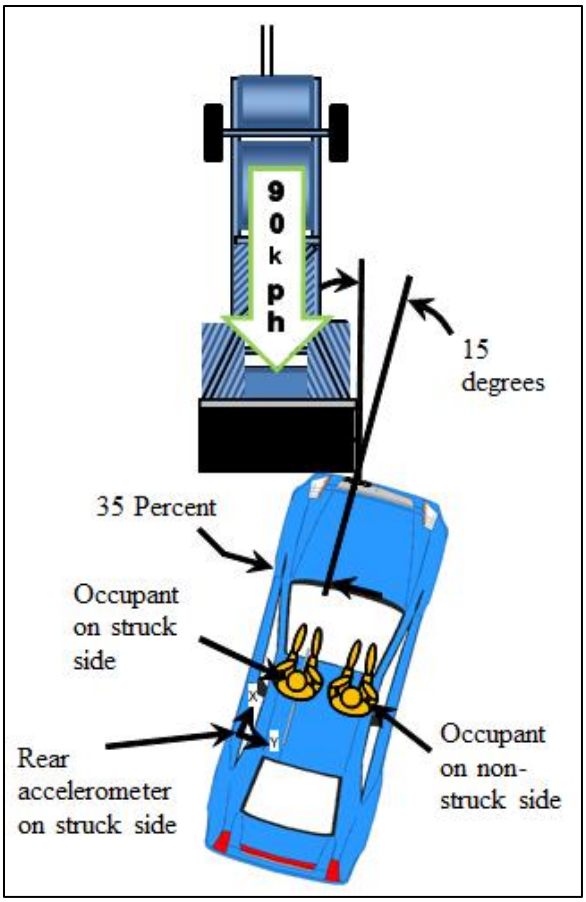


*Figure 21. Test setup for Left Side Impact (LSI)*

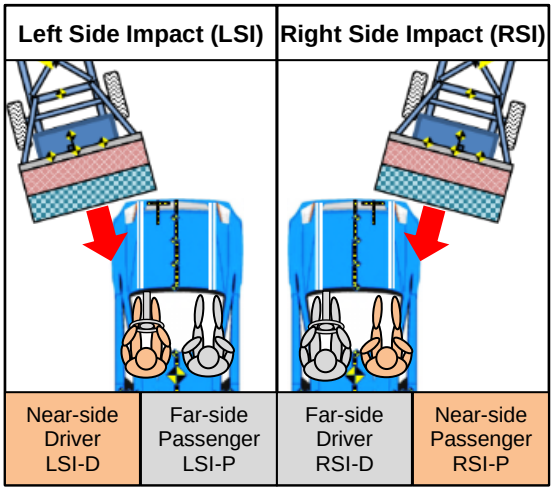


*Figure 22. Occupant location terminology.*

**APPENDIX B.**

**Table 3. Intrusion Points**

| Description | Abbreviation | Figure |
|---|---|---|
| Left Footrest | TP1 | Figure 23 |
| Left Toe Pan | TP2 | Figure 23 |
| Center Toe Pan | TP3 | Figure 23 |
| Right Toe Pan | TP4 | Figure 23 |
| Left Instrument Panel | Left IP | |
| Right Instrument Panel | Right IP | |
| Center Steering Wheel | SW | |
| Bottom A-pillar | B A-pillar | Figure 24 |
| Rocker Panel | | Figure 24 |

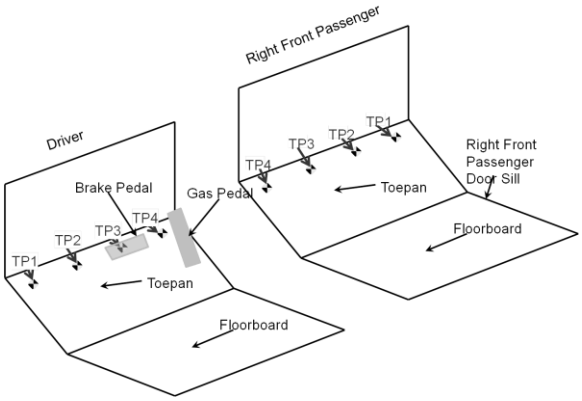


***Figure 23: Interior intrusion measurements***

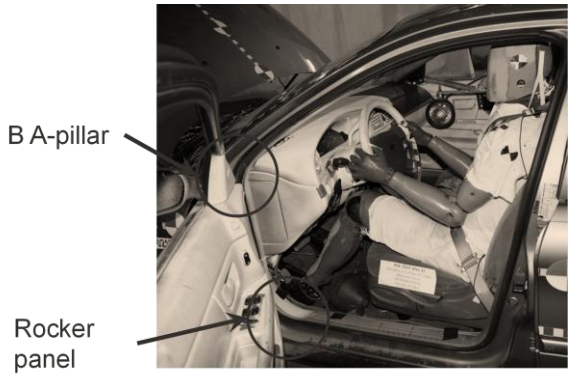


***Figure 24: Location of B A-pillar and rocker panel intrusion points***

**APPENDIX C.**

***Table 4. Head contact locations and restraint deployment timing.***

| Mode | Vehicle | Contact Location (Evidence) | Frontal Air Bag Deployment | Side Curtain Air Bag Deployment | HIC15 | Safety Belt Pretensioner |
|---|---|---|---|---|---|---|
| **Left Front Driver** | | | | | | |
| LSI Oblique | Fit | AB (V, PT), SAB (V, PT), DP (V, PT) | AD (21) | AD (35) | 264 | AD (21) |
| | 3 | AB (V, PT), SAB (V, PT), DP (V, TAB) | AD (14) | AD (42) | 268 | AD (14) |
| | Accord | AB (V, PT), SAB (V, PT) | AD (16) | AD (46) | 191 | AD (18) |
| | CX-5 | AB (V, PT), SAB (V, PT) | AD (13) | AD (43) | 219 | AD (13) |
| | Forester | AB (V, PT), SAB (V, PT), DP (V, PT) | AD (17) | AD (25) | 193 | AD (17) |
| | S60 | AB (V, PT), SAB (V, PT) | AD (12) | AD (18) | 152 | AD (14) |
| RSI Oblique | 3 | AB (V, PT), IP (V, PT, TH) | AD (14) | | 750 | AD (14) |
| | Accord | AB (V, PT), IP (V, PT) | AD (18) | | 419 | AD (18) |
| | CX-5 | AB (V, PT), IP (V, TH) | AD (12) | | 453 | AD (12) |
| **Right Front Passenger** | | | | | | |
| LSI Oblique | Fit | AB (V, PT), IP (V, PT) | AD (22) | | 910 | AD (22) |
| | 3 | AB (V, PT), IP (V, TAB) | AD (16) | | 806 | AD (13) |
| | Accord | AB (V, PT), IP (V, PT) | AD (18) | | 947 | AD (18) |
| | CX-5 | AB (V, PT), IP (V, TAB) | AD (15) | | 113 | AD (15) |
| | Forester | AB (V, PT), IP (V, TAB) | AD (22) | | 200 | AD (17) |
| | S60 | AB (V, PT), IP (V, PT) | AD (14) | | 227 | AD (15) |
| RSI Oblique | 3 | AB (V, PT), SAB (V, PT) | AD (14) | AD (42) | 356 | AD (14) |
| | Accord | AB (V, PT), SAB (V, PT), DP (V, PT) | AD (19) | AD (42) | 190 | AD (18) |
| | CX-5 | AB (V, PT), SAB (V, PT) | AD (16) | AD (44) | 247 | AD (12) |

| | | | |
|---|---|---|---|
| **AB** | Air Bag | **AD ( )** | Available and Deployed (time deployed in ms) |
| **SAB** | Side Curtain Air Bag | | |
| **RR** | Roof Rail | **AN** | Available and Not Deployed |
| **IP** | Instrument Panel | **N** | Not Available |
| **DP** | Door Panel | | |
| **V** | Video | | |
| **PT** | Paint Transfer | | |
| **TAB** | Contact Through Air Bag | | |
| **TH** | Contact Through Hand | | |

## APPENDIX D.

***Table 5. Summary of injury risk for near-side occupants in LSI and RSI Oblique crash tests***

| | | | | | | | | | | | |
|---|---|---|---|---|---|---|---|---|---|---|---|
| | | **Test Number** | 9043 | 8787 | 8999 | 8789 | 9042 | 8788 | 8998 | 8478 | 8488 |
| | | **Vehicle Model** | Fit | Mazda3 | Mazda3 | Accord | Accord | CX-5 | CX-5 | Forester | S60 |
| | | **Impact Side** | Left | Left | Right | Left | Right | Left | Right | Left | Left |
| | | **Occupant Location** | D | D | P | D | P | D | P | D | D |
| **Body Region** | **Metric** | **AIS ≥ n** | | | | | | | | | |
| **Head** | HIC15 | 3 | 0.006 | 0.006 | 0.016 | 0.001 | 0.001 | 0.003 | 0.004 | 0.002 | 0.001 |
| | BrIC | 3 | 0.740 | 0.818 | 0.454 | 0.230 | 0.576 | 0.297 | 0.440 | 0.442 | 0.743 |
| **Neck** | Nij | 3 | 0.463 | 0.374 | 0.463 | 0.251 | 0.545 | 0.342 | 0.499 | 0.351 | 0.492 |
| **Chest** | Multipoint Deflection | 3 | 0.747 | 0.448 | 0.793 | 0.650 | 0.929 | 0.497 | 0.572 | 0.617 | 0.277 |
| **Abdomen** | Peak Deflection | 3 | 0.198 | 0.049 | 0.127 | 0.143 | 0.259 | 0.076 | 0.189 | 0.000 | 0.000 |
| **Left Leg** | Acetabulum Force | 2/3 | 0.241 | 0.000 | 0.005 | 0.000 | 0.049 | 0.000 | 0.001 | 0.000 | 0.003 |
| | Femur Force | 2 | 0.019 | 0.010 | 0.009 | 0.017 | 0.023 | 0.014 | 0.019 | 0.012 | 0.019 |
| | Tibia Index, Proximal | 2 | 0.026 | 0.008 | 0.223 | 0.029 | 0.030 | 0.030 | 0.113 | 0.046 | 0.006 |
| | Tibia Index, Distal | 2 | 0.028 | 0.021 | 0.273 | 0.035 | 0.032 | 0.035 | 0.035 | 0.115 | 0.017 |
| | Tibia Proximal Force | 2 | 0.005 | 0.004 | 0.001 | 0.005 | 0.003 | 0.004 | 0.001 | 0.002 | 0.006 |
| | Tibia Distal Force | 2 | 0.000 | 0.000 | 0.000 | 0.000 | 0.002 | 0.000 | 0.001 | 0.000 | 0.001 |
| | Ankle Dorsiflexion Moment | 2 | 0.858 | 0.711 | 1.000 | 0.999 | 0.555 | 1.000 | 0.970 | 1.000 | 0.584 |
| | Ankle [in/e]version Moment | 2 | 0.016 | 0.204 | 0.924 | 0.018 | 0.745 | 0.025 | 0.028 | 0.251 | 0.048 |
| **Right Leg** | Acetabulum Force | 2 | 0.001 | 0.016 | 0.006 | 0.001 | 0.033 | 0.003 | 0.003 | 0.000 | 0.590 |
| | Femur Force | 2 | 0.020 | 0.009 | 0.008 | 0.009 | 0.036 | 0.007 | 0.010 | 0.012 | 0.168 |
| | Tibia Index, Proximal | 2 | 0.144 | 0.075 | 0.069 | 0.015 | 0.010 | 0.032 | 0.016 | 0.041 | 0.143 |
| | Tibia Index, Distal | 2 | 0.221 | 0.153 | 0.020 | 0.069 | 0.006 | 0.044 | 0.022 | 0.226 | 0.433 |
| | Tibia Proximal Force | 2 | 0.010 | 0.002 | 0.001 | 0.004 | 0.003 | 0.003 | 0.002 | 0.003 | 0.003 |
| | Tibia Distal Force | 2 | 0.000 | 0.000 | 0.001 | 0.000 | 0.002 | 0.000 | 0.001 | 0.000 | 0.000 |
| | Ankle Dorsiflexion Moment | 2 | 1.000 | 1.000 | 0.876 | 1.000 | 0.309 | 1.000 | 1.000 | 1.000 | 1.000 |
| | Ankle [in/e]version Moment | 2 | 0.622 | 0.240 | 0.048 | 0.176 | 0.067 | 0.441 | 0.008 | 0.048 | 0.676 |

## APPENDIX E.

*Table 6. Summary of injury risk for far-side occupants in LSI and RSI Oblique crash tests*

| | | | | | | | | | | | |
|---|---|---|---|---|---|---|---|---|---|---|---|
| | | **Test Number** | 9043 | 8787 | 8999 | 8789 | 9042 | 8788 | 8998 | 8478 | 8488 |
| | | **Vehicle Model** | Fit | Mazda3 | Mazda3 | Accord | Accord | CX-5 | CX-5 | Forester | S60 |
| | | **Impact Side** | Left | Left | Right | Left | Right | Left | Right | Left | Left |
| | | **Occupant Location** | P | P | D | P | D | P | D | P | P |
| **Body Region** | **Metric** | **AIS ≥ n** | | | | | | | | | |
| **Head** | HIC15 | 3 | 0.194 | 0.152 | 0.130 | 0.209 | 0.028 | 0.000 | 0.035 | 0.002 | 0.003 |
| | BrIC | 3 | 1.000 | 0.764 | 0.955 | 0.952 | 0.995 | 0.545 | 0.894 | 0.727 | 0.952 |
| **Neck** | Nij | 3 | 0.585 | 0.296 | 0.468 | 0.308 | 0.441 | 0.223 | 0.544 | 0.125 | 0.230 |
| **Chest** | Multipoint Deflection | 3 | 0.998 | 0.211 | 0.240 | 0.529 | 0.380 | 0.164 | 0.374 | 0.166 | 0.131 |
| **Abdomen** | Peak Deflection | 3 | 0.100 | 0.127 | 0.268 | 0.205 | 0.201 | 0.110 | 0.086 | 0.000 | 0.000 |
| **Left Leg** | Acetabulum Force | 2/3 | 0.271 | 0.014 | 0.136 | 0.804 | 0.000 | 0.001 | 0.106 | 0.125 | 0.382 |
| | Femur Force | 2 | 0.013 | 0.050 | 0.009 | 0.043 | 0.042 | 0.017 | 0.005 | 0.024 | 0.054 |
| | Tibia Index, Proximal | 2 | 0.114 | 0.117 | 0.140 | 0.010 | 0.128 | 0.146 | 0.035 | 0.228 | 0.092 |
| | Tibia Index, Distal | 2 | 0.103 | 0.036 | 0.105 | 0.153 | 0.050 | 0.114 | 0.000 | 0.084 | 0.128 |
| | Tibia Proximal Force | 2 | 0.001 | 0.001 | 0.002 | 0.003 | 0.006 | 0.001 | 0.004 | 0.003 | 0.002 |
| | Tibia Distal Force | 2 | 0.001 | 0.001 | 0.000 | 0.001 | 0.001 | 0.001 | 0.001 | 0.000 | 0.000 |
| | Ankle Dorsiflexion Moment | 2 | 1.000 | 1.000 | 1.000 | 1.000 | 1.000 | 1.000 | 0.000 | 1.000 | 1.000 |
| | Ankle [in/e]version Moment | 2 | 0.547 | 0.024 | 0.699 | 0.426 | 0.011 | 0.017 | 0.005 | 0.017 | 0.006 |
| **Right Leg** | Acetabulum Force | 2 | 0.600 | 0.090 | 0.005 | 0.024 | 0.198 | 0.072 | 0.006 | 0.009 | 0.364 |
| | Femur Force | 2 | 0.022 | 0.008 | 0.014 | 0.051 | 0.044 | 0.007 | 0.012 | 0.017 | 0.006 |
| | Tibia Index, Proximal | 2 | 0.028 | 0.062 | 0.038 | 0.002 | 0.045 | 0.090 | 0.014 | 0.048 | 0.098 |
| | Tibia Index, Distal | 2 | 0.027 | 0.045 | 0.014 | 0.010 | 0.023 | 0.114 | 0.000 | 0.138 | 0.115 |
| | Tibia Proximal Force | 2 | 0.002 | 0.001 | 0.003 | 0.004 | 0.003 | 0.001 | 0.004 | 0.002 | 0.004 |
| | Tibia Distal Force | 2 | 0.001 | 0.001 | 0.000 | 0.002 | 0.001 | 0.001 | 0.003 | 0.000 | 0.001 |
| | Ankle Dorsiflexion Moment | 2 | 1.000 | 1.000 | 0.782 | 1.000 | 0.593 | 1.000 | 0.414 | 1.000 | 1.000 |
| | Ankle [in/e]version Moment | 2 | 0.181 | 0.496 | 0.028 | 0.136 | 0.898 | 0.324 | 0.115 | 0.009 | 0.002 |

## APPENDIX F.

***Table 7. THOR-PMHS paired tests used in development of multipoint thoracic injury criterion.***

| Occupant Position | Environment | Restraint | Delta-V (km/h) | Age | Sex | Mass (kg) | Height (cm) | AIS 3+ | PMHS BioDB | THOR BioDB | THOR Peak Res Defl (mm) |
|---|---|---|---|---|---|---|---|---|---|---|---|
| Front Driver | Gold Standard | 3-point standard belt | 10 | 59 | F | 80 | 167 | No | | 11125 | 12.62 |
| | | | | 69 | M | 84 | 178 | No | | 11126 | |
| | | | | 60 | M | 81 | 191 | No | | | |
| Front Driver | Gold Standard | 3-point standard belt | 40 | 59 | F | 80 | 167 | Yes | | 11123 | 49.4 |
| | | | | 69 | M | 84 | 178 | Yes | | 11124 | |
| | | | | 60 | M | 81 | 191 | Yes | | | |
| Front Passenger | 1997 Ford Taurus | 3-point force-limited belt plus air bag | 48 | 57 | M | 70 | 174 | No | 8371 | 11129 | 51.3 |
| | | | | 69 | F | 53 | 155 | Yes | 8372 | 11130 | |
| | | | | 72 | F | 59 | 156 | Yes | 8373 | | |
| | | | | 57 | M | 57 | 177 | No | 8374 | | |
| Front Passenger | 1997 Ford Taurus | Lap belt with air bag | 48 | 40 | M | 47 | 150 | Yes* | 8377 | 11131 | 30.08 |
| | | | | 70 | M | 70 | 176 | No | 8378 | 11132 | |
| | | | | 46 | M | 74 | 175 | No | 8379 | | |
| Front Passenger | 1997 Ford Taurus | 3-point standard belt with air bag | 48 | 55 | M | 85 | 176 | Yes | 8382 | 11127 | 54.83 |
| | | | | 69 | M | 84 | 176 | Yes | 8383 | 11128 | |
| | | | | 59 | F | 79 | 161 | Yes | 8384 | | |
| Front Passenger | 1997 Ford Taurus | 3-point standard belt | 29 | 49 | M | 58 | 178 | No | | 11133 | 42.75 |
| | | | | 44 | M | 77 | 172 | No | | 11134 | |
| | | | | 39 | M | 79 | 184 | No | | | |
| Front Passenger | 1997 Ford Taurus | 3-point standard belt | 38 | 44 | M | 77 | 172 | No | | 11135 | 51.17 |
| | | | | | | | | | | 11136 | |
| Front Passenger | Gold Standard 1 | 3-point standard belt | 40 | 76 | M | 70 | 178 | Yes | 9546 | 11117 | 47.73 |
| | | | | 47 | M | 68 | 177 | Yes | 9547 | 11118 | |
| | | | | 54 | M | 79 | 177 | Yes | | 11119 | |
| | | | | 49 | M | 76 | 184 | Yes | | | |
| | | | | 57 | M | 64 | 175 | Yes | | | |
| | | | | 72 | M | 81 | 184 | Yes | 11014 | | |
| | | | | 40 | M | 88 | 179 | Yes | 11015 | | |
| | | | | 37 | M | 78 | 180 | No | 11016 | | |
| Front Passenger | Gold Standard 2 | 3-point force-limited belt | 30 | 59 | M | 68 | 178 | No | | 11120 | 26.78 |
| | | | | 66 | M | 70 | 179 | No | | 11121 | |
| | | | | | | | | | | 11122 | |
| Rear Passenger | 2004 Ford Taurus | 3-point standard belt | 48 | 51 | M | 55 | 175 | Yes | 9337 | 11143 | 57.96 |
| | | | | 57 | F | 109 | 165 | Yes | 9338 | 11144 | |
| | | | | 57 | M | 59 | 179 | Yes | 9339 | 11145 | |
| Rear Passenger | 2004 Ford Taurus | 3-point force-limited belt with pretensioner | 48 | 67 | M | 71 | 175 | Yes | | 11140 | 46.66 |
| | | | | 69 | M | 60 | 171 | No | | 11141 | |
| | | | | 72 | M | 73 | 175 | Yes | | 11142 | |
| Rear Passenger | 2004 Ford Taurus | 3-point inflatable force-limited belt with pretensioner | 48 | 72 | M | 88 | 173 | Yes | | 11137 | 29.66 |
| | | | | 69 | M | 69 | 175 | No | | 11138 | |
| | | | | 40 | M | 83 | 186 | No | | 11139 | |

## APPENDIX G.

***Table 8. Summary of injury criteria and associated injury risk functions used to assess injury risk using THOR test results.***

| Criterion [ref] | Calculation | Vars | Variable Definition | Risk Function |
|---|---|---|---|---|
| $HIC_{15}$ | $HIC_{15} = \left\lvert (t_2 - t_1)\left[\frac{1}{(t_2 - t_1)}\int_{t_1}^{t_2} a(t)dt\right]^{2.5}\right\rvert_{max}$ | $t_1$ | Beginning of time window in $s$ | $p(AIS \geq 3) = \Phi\left[\frac{\ln(HIC_{15}) - 7.45231}{0.73998}\right]$ |
| | | $t_2$ | End of time window in $s$ | |
| | | $a(t)$ | Head CG resultant acceleration in Beginning of time window in $g$ | |
| $BrIC$ | $BrIC = \sqrt{\left(\frac{\max(\lvert\omega_x\rvert)}{\omega_{xC}}\right)^2 + \left(\frac{\max(\lvert\omega_y\rvert)}{\omega_{yC}}\right)^2 + \left(\frac{\max(\lvert\omega_z\rvert)}{\omega_{zC}}\right)^2}$ | $\omega_{[x,y,z]}$ | Angular velocity of the head about the local [x, y, or z] axis, in $rad/s$, filtered at CFC60 | $p(AIS \geq 3) = 1 - e^{-\left(\frac{BrIC}{0.987}\right)^{2.84}}$ |
| | | $\omega_{[x,y,z]C}$ | Critical angular velocities in $rad/s$ | |
| | | $\omega_{xC}$ | 66.25 $rad/s$ | |
| | | $\omega_{yC}$ | 56.45 $rad/s$ | |
| | | $\omega_{zC}$ | 42.87 $rad/s$ | |
| $N_{ij}$ | $N_{ij} = \frac{F_z}{F_{zc}} + \frac{M_y}{M_{yc}}$ | $F_z$ | Z-axis force measured at upper neck load cell in $N$ | $p(AIS \geq 3) = \frac{1}{1 + e^{3.227 - 1.969 N_{ij}}}$ |
| | | $F_{zc}$ | Critical force (tension or compression) in $N$ [2520/-3640] | |
| | | $M_y$ | Y-axis moment measured at upper neck load cell $Nm$ | |
| | | $M_{yc}$ | Critical moment (flexion or extension) in $Nm$ [48/-72] | |
| Multi-point Thoracic Injury Criterion | $R_{max} = max(UL_{max}, UR_{max}, LL_{max}, LR_{max})$ where $[U/L\lvert R/L]_{max} = max\left(\sqrt{[L/R]X^2_{[U/L]S} + [L/R]Y^2_{[U/L]S} + [L/R]Z^2_{[U/L]S}}\right)$ | $R_{max}$ | Overall peak resultant deflection in $mm$ | $P(AIS \geq 3 \mid age, R_{max}) = 1 - exp\left(-\left[\frac{R_{max}}{exp(4.4853 - 0.0113age)}\right]^{5.03896}\right)$ |
| | | $[U/L\lvert R/L]_{max}$ | Peak resultant deflection of the [upper/lower \| left/right] quadrant in $mm$ | |
| | | $[L/R][X/Y/Z]^2_{[U/L]S}$ | Time-history of the [left/right] chest deflection along the [X/Y/Z] axis relative to the [upper/lower] spine segment in $mm$ | |
| Compression | $A_{max} = \frac{\max(\delta L, \delta R)}{d_{abd}}$ | $\delta[L, R]$ | Peak X-axis deflection of the left or right abdomen in $mm$ | $p(AIS \geq 3) = 1 - e^{-\left(\frac{A_{max}}{0.4247}\right)^{3.6719}}$ |
| | | $d_{abd}$ | Undeformed depth of the abdomen [238.4 $mm$] | |
| Acetabulum Load | $F_R = \sqrt{{F_x}^2 + {F_y}^2 + {F_z}^2}$ | $F_{[x,y,z]}$ | X-, Y-, and Z- axis force measured at the acetabulum load cell in $kN$ | $p(AIS \geq 3) = \Phi\left[\frac{\ln(F_R/0.72) - 1.6526}{0.1991}\right]$ |
| Femur Axial Load | | $F_z$ | Z-axis femur load in $kN$, filtered at CFC600 | $p(AIS \geq 2) = \frac{1}{1 + e^{5.7949 - 0.5196 F_z}}$ |
| Revised Tibia Index | $RTI = \frac{F}{F_c} + \frac{M}{M_c}$ | $F$ | Measured compressive axial force in $kN$ | $p(AIS \geq 2) = 1 - exp\left(-exp\left[\frac{ln(RTI) - 0.2468}{0.2728}\right]\right)$ |
| | | $F_c$ | Critical compressive axial force [12 $kN$] | |
| | | $M$ | Measured bending moment in $Nm$ (resultant of medial-lateral and anterior-posterior directions) | |
| | | $M_c$ | Critical bending moment [240 $Nm$] | |
| Proximal Tibia Axial Force | | $F_z$ | Z-axis upper tibia load in $kN$, filtered at CFC600 | $p(AIS \geq 2) = \frac{1}{1 + e^{5.6654 - 0.8189 F_z}}$ |
| Distal Tibia Axial Force | | $F_z$ | Z-axis lower tibia load in $kN$, filtered at CFC600 | $p(AIS \geq 2) = \frac{1}{1 + e^{4.572 - 0.670 F_z}}$ |
| Dorsiflexion Moment | $M_{y_{ankle}} = M_Y - F_x D - \frac{m a_x D}{2}$ | $M_Y$ | Y-axis moment measured at lower tibia load cell in $Nm$ | $p(AIS \geq 2) = \frac{1}{1 + e^{6.535 - 0.1085 M_y}}$ |
| | | $F_x$ | X-axis force measured at lower tibia load cell in $N$ | |
| | | $D$ | Distance between ankle joint and lower tibia load cell [0.0907m] | |
| | | $m$ | Mass between ankle joint and lower tibia load cell [0.72kg] | |
| | | $a_x$ | X-axis acceleration of the tibia in $m/s^2$ | |
| Inversion/ Eversion Moment | $M_{x_{ankle}} = M_x - F_y D - \frac{m a_y D}{2}$ | $M_x$ | X-axis moment measured at lower tibia load cell in $Nm$ | $p(AIS \geq 2) = \Phi\left[\frac{M_x - 40Nm}{10Nm}\right]$ |
| | | $F_y$ | Y-axis force measured at lower tibia load cell in $N$ | |
| | | $D$ | Distance between ankle joint and lower tibia load cell [0.0907m] | |
| | | $m$ | Mass between ankle joint and lower tibia load cell [0.72kg] | |
| | | $a_y$ | Y-axis acceleration of the tibia in $m/s^2$ | |

**APPENDIX H.**

***Figure 25. Interaction of LSI-D occupants with driver air bag (DAB) and side curtain air bag (SAB).***

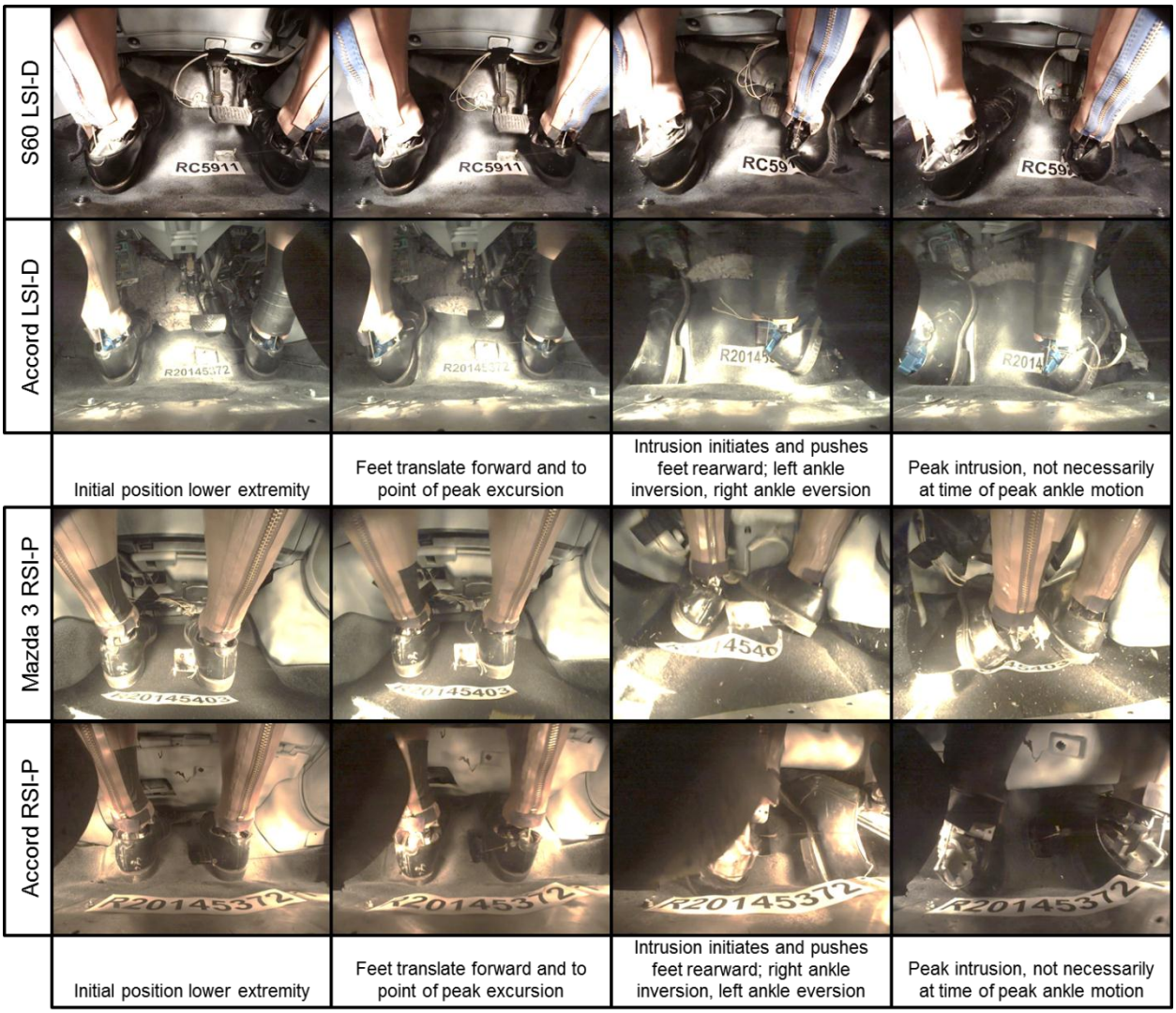


***Figure 26. Lower extremity interaction with toe pan for vehicles with least (top of each pair) and most (bottom of each pair) toe pan intrusion.***

# AUTOMATED DRIVING FUNCTIONS GIVING CONTROL BACK TO THE DRIVER: A SIMULATOR STUDY ON DRIVER STATE DEPENDENT STRATEGIES

**Dehlia Willemsen**
**Arjan Stuiver**
**Jeroen Hogema**
TNO
The Netherlands

Paper Number 15-0109

## ABSTRACT

Many car companies and other organisations are working hard to get automated driving on the road. Where some prefer driverless cars, most foresee a future where control of the vehicle will be shared between the driver and automated functions in the coming years. Sharing tasks and responsibilities creates the interesting challenge of transition of control of the vehicle between driver and automation. This paper presents research into this transition. By taking into account the attentiveness of the driver, different strategies were evaluated in a simulator study to create an optimal transition given the situation at hand. The study concentrates on an automated platoon system 'Virtual Tow Bar'. The results show that the differences among the tested conditions are small and no large trends are visible in either the subjective or the objective results. Hence it is concluded that the experiment should be repeated with a larger group naïve participants and probably more extreme parameter settings.

## INTRODUCTION

Many car companies and other organisations are working hard to get automated driving on the road (see e.g. Hoeger et al. 2008; Jootel 2013; Kameda 2013). Where some prefer driverless cars, most foresee a future where control of the vehicle will be shared between the driver and automated driving functions in the coming years.

Sharing control of the vehicle means that the driver must be able to hand over the control to the automated driving function and either actively regain control from the automation function or get handed over control by the system. These transitions must be designed well as they take place while driving. TNO has taken up research to gain insight in the process of transition of control and the related research questions ('how should the system take over', 'how can the driver take back control', 'can the driver be regarded as a backup if the system fails', etc.). By designing and evaluating the different transitions of control, it is the long-term goal of the research to come to architectures and model-based designs for the transition of control and techniques and guidelines on how to evaluated these transitions.

As a case study, TNO's automated system Virtual Tow Bar (VTB) is taken. The VTB is an automated system that allows a vehicle to follow its predecessor at a relatively short following distance, controlling both the longitudinal and lateral motion. The VTB system is designed to operate on public motorways (i.e. without using dedicated lanes), initially limited to platoons of two vehicles. The first vehicle is driven by a human operator and (once engaged) the second vehicle is controlled by the VTB. The VTB is designed with the goals to reduce fuel consumption (especially for trucks) and improve traffic throughput. To achieve these goals, the system must maintain relatively short headways, in the order of magnitude of 0.2-0.3 s (see e.g. Jootel, 2013), i.e., much smaller than headways normally adopted by drivers.

This paper reports on an explorative driving simulator study conducted to evaluate different strategies to come to an optimal transition from automated driving to manual driving, where the state of the driver is taken into account. The transition was initiated by the automated system when approaching the highway exit to be taken by the driver to contiue his journey on the desired route. The upcoming automatic disconnect was preseded by a warning. The warning process asked for a confirmation from the driver that he/she was ready to regain the driving task. The timing of the warning and the confirmation process was made dependent on the driver state. (Note that the situation where the driver is not capable to regain control must ultimately be dealt with, but is beyond the scope of out current work).

For the driver state we concentrated on the topic of attentiveness of the driver. It was the goal of the project to investigate different strategies to re-involve the driver and not to measure his/her level of attentiveness. In the simulator study the level of attentiveness was maninupated by instructing the participants either to be attentive, or to engage in a secondaty task that was designed to be highly distracting. For next steps in the research eye tracking may be used as a basis to measure driver attentiveness (Ahlstrom, 2013).

Previously research was conducted on finding the most important parameters that influence the transition of control when the driver switches the VTB system on and off, and on driver behaviour after he/she switched the VTB system off (Willemsen et al. 2014a; Willemsen et al. 2014b). Results of this research were taken into account in the reported study in the settings of several parameters of the VTB system and in the driver interface.

## VIRTUAL TOW BAR SYSTEM

As explained in the Introduction the VTB system uses short following distances, which means the driver cannot be regarded as a backup to take over in case of system failure or any other emergency. To create a safe transition towards the small following distance, a scheme was designed to let the driver switch the system on from a safe following distance. Once activated, the automated system decreased the following distance to the desired (small) following distance. When switching off, either by the driver or by the automated system itself, the system first increases the following distance to a safe length before giving back control to the driver.

### System Model

The VTB was modelled as a combination of a Cooperative Adaptive Cruise Control (CACC) controller (Ploeg et al., 2014) and a Lane Keep Assist (LKA) system. The Cooperate part of the system consisted of short-range communication between the two vehicles in the platoon. Via this channel, the longitudinal following controller had access to the current acceleration command of the lead vehicle, which provides additional damping with respect to an autonomous ACC that only has distance and relative speed as control inputs. The LKA algorithm was used to provide lateral control of the vehicle with respect to the middle of the lane. The controllers were combined and logic was added to create different system modes to switch the system on and off (Willemsen et al. 2014a; Willemsen et al. 2014b).

### System Interface

A dedicated user interface was developed for the earlier experiments and improved based on the feedback from these experiments (Figure 1). A touchscreen visual display was mounted in the mid console (see Figure 2) of the mock-up of the driving simulator, as high as possible without blocking the view on the road. On this display the current system status was shown together with a graphical indication of the current time headway and guidance to help te user engage the system. Moreover, this display was used to also notify the driver of an upcoming automated switch off (Figure 2) and request confirmation of this notification of the driver. Lower in the mid-console, within easy reach for the participants, a pushbutton was placed which they could press to engage or disengage the system. Pressing the brake pedal would also initiate a disengagement of the system.

***Figure 1. Driver display showing the confirmation request of the driver.***

The goal of the study was to develop strategies for the automation to notify the driver of a switch off by the automation, not to develop a specific HMI. We therefore wanted the user experience with the system to be as good as possible, i.e. without flaws in the interface that might disturb the experience. We therefore needed an interface of which we could assume it would be understood and accepted by the user. Experiences in previous studies were taken into account in the design of the basic interface. Using an iterative process we designed, developed and tested the additional warning towards the driver for an automated switch off in a low-fidelity simulator. Besides the visual display, acoustic warnings were provided to the driver at the moment information or warnings were presented to alert the driver to the new visual information.

## METHOD

Because of the safety implications of automated driving and the wish to have a natural driving environment (i.e. no test track environment) the experiment was conducted in a moving base driving simulator.

### Driving Simulator and Scenario

The experiment was carried out in a high fidelity moving base driving simulator (Van den Horst and Hogema, 2011). It consisted of a BMW mock-up mounted on a 6DOF moving base. The road and traffic environment was projected on cylindrical screens around the vehicle. The projection system for the front view had a horizontal viewing angle of 180 degrees, realized by three projectors. The vertical viewing angle was 41 degrees (22 degrees above and 19 degrees below the neutral viewing direction). The driver could use the existing BMW external rear view mirrors to look at two screens placed behind the vehicle displaying the environment behind. Similar, the internal rearview mirror could be used to look at a 32 inch LCD screen placed in the back of the car. Feedback of steering forces was given to the driver by means of a high-fidelity electrical torque engine.

***Figure 2. Setup of displays in the driving simulator.***

Participants drove on the right-hand lane (the slower lane) of a two-lane motorway behind a lead vehicle that was driving with an average speed of 120 km/h. The participants were instructed to follow this lead vehicle and switch the automated function on when possible. There were no entries or exits on the route until the very end of the run. The participants were instructed to take this exit after the automated function had switched itself off. Slight curves, surrounding traffic, and two signs indicating the upcoming of the exit made the experience more realistic.

**Parameters and Experimental Setup**

Goal of the study was to investigate different strategies for the automated function to switch itself off in case of an attentive or an inattentive driver. Hence the participants drove one run where they were asked to stay attentive and two runs where they were asked to perform a demanding secondary task. This secondary task consisted of the HASTE task (Engström, Johansson, & Östlund, 2005): participants were presented with matrices of arrows on an additional LCD touch screen. An example can be seen in Figure 2, in which also the position of the touch screen in the simulator mock-up shown can be seen. The task was to determine whether an arrow pointing upwards was present. Participants gave their answers by pressing ‘‘yes’’ or ‘‘no’’ on the touch screen. A new matrix was presented every 10 seconds. Each matrix remained on the display for 2 s before a new matrix was presented. Participants were instructed perform as good as possible on the HASTE task by getting as much answers right as they could during their whole trip.

The time gap of the VTB system was 0.3 s. Hooking on and off phases took 15 s and the transition just before hooking on and after hooking off were instant (no additional countdown from 5 s as presented in Willemsen et al. (2014b).

At a certain distance upstream from the exit, the participant was warned and requested to provide a confirmation by pushing a button on the touch screen of the interface (Figure 2). If the driver did not confirm within a certain time the warning and confirmation request was repeated. Closer to the exit, irrespective of the driver reacting to the confirmation request, a warning was displayed that provided the amount of meters till the exit (Figure 1 without the confirmation request and button). The timings of the warnings and feedback requests were different between the attentive and inattentive driver states (see Table 1). The unadapted transition strategy was to warn the participant and ask for confirmation the first time at 1000 m before the exit. From 500 m before the exit the participant was continously informed on the distance (‘count down’) till the VTB system would switch off. In the adapted strategy,

the participant was warned and asked for confirmation earlier, at 2000 m before the exit and the 'count down' was shown from 1000 m before the exit. In both strategies, if the participant did not react to the first confirmation request, a second one was issued at 750 m before the exit.

***Table1. Parameter combinations in the simulator experiment.***

| Condition | Driver distraction | Transition strategy |
|---|---|---|
| 0 | - | Familiarization run |
| 1 | attentive | Unadapted |
| 2 | inattentive | Unadapted |
| 3 | inattentive | Adapted |

The order of presentation of the second and third condition were balanced over the participants.

### Participants

A total of 16 participants attended the experiment. It shoud be noted that all participants were research colleagues with a background outside the automotive domain to prevent they had too much information about automated driving and the transition of control before the experiment. First the subjective results, aqcuired through questionnairs is discussed followed by analyses of the logged signals.

## RESULTS AND DISCUSSION

### Subjective Results

Drivers judged the amount of information or understanding they had about the environment when they had to take over control to be in the middle between *more than enough* and *not enough*. They rated the unadapted strategy slightly lower than the adapted strategy when they were distracted by the secondary task (see Figure 3, on the left). This suggests that the adapted strategy helped the participants to take over control with more information about the traffic situation.

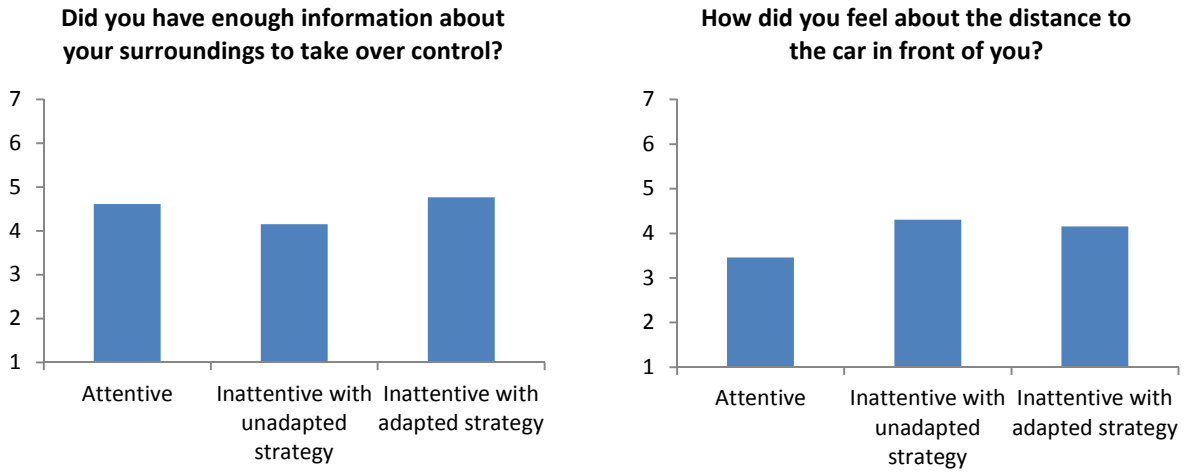


***Figure 3. Left: Situational awareness (1 = not enough, 7 = more than enough), right: Experienced time headway (1 = too close, 7 = too far).***

Figure 3 on the right shows that the participants experienced the car in front of them too close when they were paying attention. Note that the car was driving at 0.3 s behind the lead vehicle, which is much closer than these drivers would normally drive. Since they always received the attentive condition before both inattentive conditions, this might be an order effect, meaning that drives got used to driving (being driven) so close to a preceding vehicle. It could also mean that when engaged in a secondary task reliance on the system is higher and a closer gap becomes acceptable. This should be investigated in follow-up research.

When asked about their feelings of safety when taking over control, particpants on average answered only slightly above the mid value (4) and with very small differences among conditions, as can be seen in Figure 4 (left). Some participants felt much safer than others, values ranging from 2 to 6. The average not being higher than 4 does suggest there is concern with the drivers about their safety when taking over. Apparantly these concerns were there both with and without the adapted strategy.

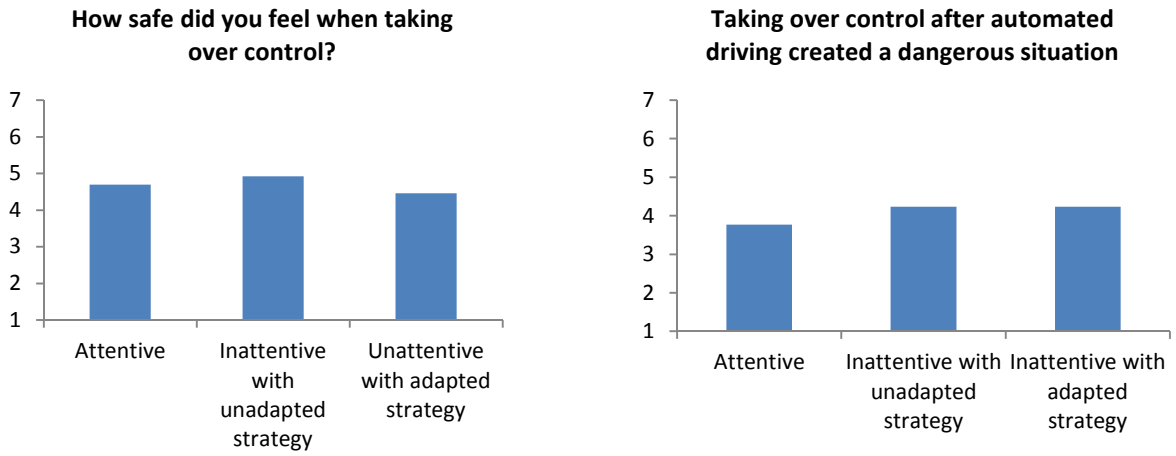


***Figure 4. Left: Experienced safety (1 = not safe at all, 7 = very safe), right: Automated driving creates a dangerous situation, (1 = strongly disagree, 7 = strongly agree).***

The results for the question about whether taking over control after being driven autonomously created a dangerous situation again suggests the drivers had concerns about safety and dangerous situations. In Figure 4 (right) it can be

seen that they felt a dangerous situation was more likely to arise when they had been inattentive. In contrast to the result from Figure 3 (left), there is no evident difference between the condtion with and without the adapted strategy.

It seems that participants found the amount of warnings neither too few nor too many for any of the conditions (Figure 5). This could mean that the the extreme values of number of warnings was not reached and that drivers accepted both the maximum as well as the minimum amount of warnings. This would mean that the difference between conditions as presented in this experiment was not large and minimal warnings were enough to alert the driver again. This could be different when either the automation switches off more often, making the warning more annoying, or when the time of distraction becomes longer or more intense, which means that the minimum amount of warnings is not sufficient anymore.

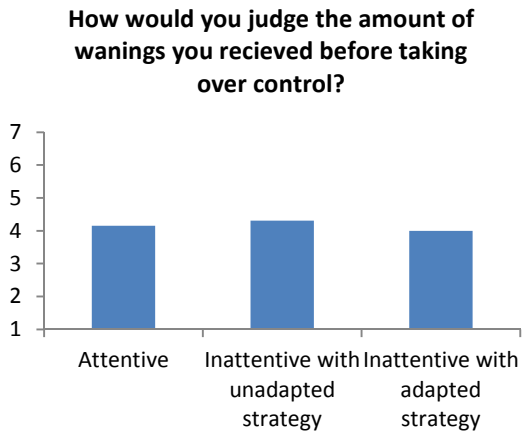


*Figure 5. Amount of warnings (1 = too few, 7 = too many).*

## Objective Results

The effect of the additional task is evaluated through the reaction time of the drivers on the confirmation request, and the steering behaviour after regaining control and taking the exit. This is shown in Figure 6.

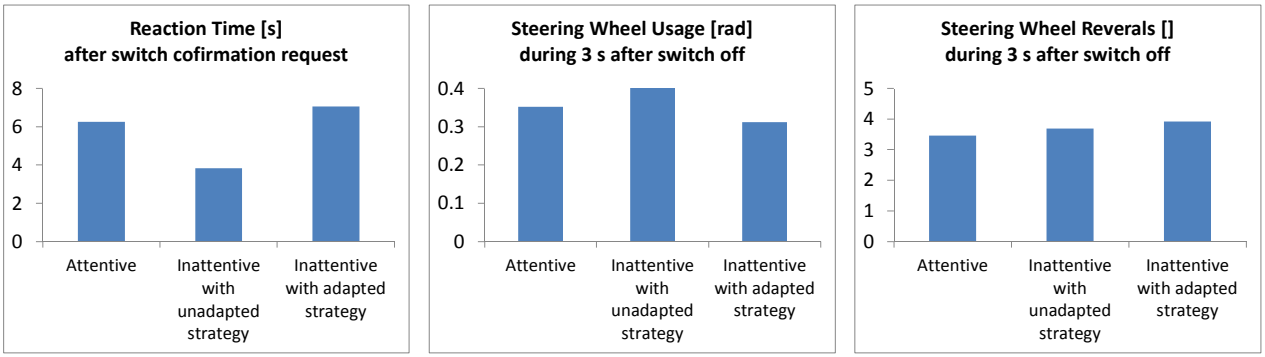


*Figure 6. Left: Reaction times, Middle: Steering Wheel usage, right: Steering Wheel Reversals (cond1: attentive, cond2: inattentive with unadapted strategy, cond 3: inattentive with adapted strategy).*

The reaction time was calculated as the time between the first confirmation request and the driver pushing the confirmation button. In some cases the driver did not react to the confirmation request: one in each tested condition. These data were not taken into account.

In the inattentive case the reaction time is lower than in the attentive case for the unadapted warning strategy, for the adapted warning strategy (earlier warning) the reaction times are larger. This could mean that the drivers were anticipating the warning, however, in the adapted warning strategy the warning may have come earlier than expected by the drivers, as they drove at least the attentive run before the other inattentive runs. Furthermore a large reaction time is not critical as the situation is not urgent. Moreover in the adapted strategy the warning was even 1000 m earlier than in the other two cases, so even with an increase of the reaction time of about 3 s, the reaction is in fact still further upstream from the merging point.

For the calculations of the steering wheel usage, data of three participants were excluded as they switched off the VTB bar system too early. In that case they were not at the highway exit they should steer onto and the required steering was less than for the other cases.

The amount for steering used after switch off (middle chart in Figure 6) shows differences: the inattentive participant with the unadapted warning strategy uses largest steering angle range and the inattentive paricipant with the adapted strategy the smallest. This may suggest that earlier warnings prepare the driver better to take over the steering of the vehicle. This needs further detailted research.

Regarding the steering wheel reversals the results are quite the same for the different conditions. Although it was expected that the first run would show more reversals as the participants would learn to take over control after more practice and this seems not to be the case.

## CONCLUSIONS

Results of a small driving simulator (16 participants, runs of nearly 5 minutes) experiment are shown, in which an automated driving system hands back the control to the driver on initiative of the automated driving system. Immediately after getting back the control the drivers had to take an exit. Different timings of take over warnings were tested with attentive and inattentive participants.

Overall it can be concluded that the differences between the tested conditions are small and no large trends are visible in either the subjective or the objective results. Probably the participants were able to rebuild their situation awareness in a short time. Further, only distraction was differed over the tests (fatigue, drowsiness, absence were not investigated). In general the participants were moderately positive about the system, though there were concerns about the safety with the short following distances. Hence it is concluded that the experiment should be repeated with a larger group naïve participants and probably more extreme parameters (longer distraction times, larger difference between conditions).

## REFERENCES

Ahlstrom, C., Kircher, K., & Kircher, A. (2013). A gaze based driver distraction warning system and its effect on visual behavior. IEEE Transactions on Intelligent Transportation Systems, 14 (2), 965 973.

Engström, J., Johansson, E., & Östlund, J. (2005). Effects of visual and cognitive load in real and simulated motorway driving. Transportation Research Part F: Psychology and Behaviour, 8, 97–120

Hoeger, R, Amditis, A, Kunert, M, Hoess, A, Flemisch, F, Krueger, H.P , Bartels, A, Beutner, A. (2008, November). Highly Automated Vehicles For Intelligent Transport: HAVEit Approach. ITS World Congress, New York, USA.

Van der Horst, A.R.A., Hogema, J.H. (2011), Driving simulator research on safe highway design and operation. Transportation Research Record: Journal of the Transportation Research Board (2248), pp. 87-95.

Jootel, P.S. (2013) SARTRE Safe Road Trains for the Environment. Final Report. Retrieved 20 February 2015 from: http://www.sartre-project.eu/en/publications/Documents/SARTRE_Final-Report.pdf.

Kameda, M. (2013, November 25) Nissan road-tests self-driving vehicle. The Japan Times, Retrieved 20 February 2015 from: http://www.japantimes.co.jp/news/2013/11/25/business/nissan-road-tests-self-driving-vehicle.

Ploeg, J, Van de Wouw, N, Nijmeijer, N. (2014, March) Lp string stability of cascaded systems: Application to vehicle platooning. IEEE Transactions on Control Systems Technology, Vol. 22, No. 2. Retrieved 20 February 2015 from: http://ieeexplore.ieee.org/stamp/stamp.jsp?arnumber=06515636.

Willemsen, D, Stuiver, A, Hogema, J, Kroon, L, Sukumar, P. (2014, June) Towards Guidelines for Transition of Control. Paper F2014-ACD-009 presented at the 2014 FISITA World Automotive Congress, Maastricht, Netherlands.

Willemsen, D, Stuiver, A, Hogema, J. (2014, July) Transition of Control: automation giving back control to the driver. Proceedings of the 5th International Conference on Applied Human Factors and Ergonomics (AHFE), Kraków, Poland.

This paper has been peer-reviewed and published in a special edition of *Traffic Injury Prevention* 16(S1), by Taylor & Francis Group. The complete paper will be available on the *Traffic Injury Prevention and www.NHTSA.gov* websites on June 8, 2015.

To access all Peer-reviewed papers please copy and paste the link below into your browser to access the papers.

http://www.tandfonline.com/toc/gcpi20/16/sup1

# POP-UP HOOD PEDESTRIAN PROTECTION

**Eva Ames**
**Peter Martin**
National Highway Traffic Safety Administration
United States of America
Paper Number 15-0111

## ABSTRACT

**Objective:** One means of protecting pedestrians is through vehicle safety systems that are built into a vehicle's front-end to protect pedestrians should a vehicle impact occur. These pedestrian protection systems include hood structures aimed at reducing pedestrian head injuries. Pop-up hoods function by increasing the head penetration space beneath the hood by quickly lifting upon vehicle contact with a pedestrian. This paper explores the prevalence of vehicles with pop-up hoods to show that their market penetration and performance benefits merit consideration in standardized pedestrian protection test protocols.
**Methods:** Euro NCAP test scores and the Parkers United Kingdom (UK) vehicle database were used to better understand the fleet performance and market penetration of vehicles with pop-up hoods. An analysis of Euro NCAP pedestrian test results and overall vehicle test scores was performed to compare the performance of vehicles equipped with pop-up hoods to those without, and the Parkers UK vehicle database was used to estimate historical vehicle prices and demonstrate that pop-up hoods are available on both high- and low-cost vehicles.
**Results:** There are many different types of systems that operate pop-up hoods, and their architectures vary widely from one vehicle to the next; however, they typically create an increase in the distance from the hood to rigid components in the engine bay, thus reducing the probability and/or severity of a head injury of a struck pedestrian. Compared to vehicles with non-deploying hoods, vehicles with pop-up hoods rated by Euro NCAP had better pedestrian protection scores on average. In the European Union (EU), pop-up hood systems, which have become more prevalent over time, were found on vehicles outside the oft-assumed market of only low-volume luxury models.
**Discussion and Limitations:** Pedestrian Protection is mandatory on all vehicles sold in the EU Conformity of pop-up hoods is based largely on headform impact tests conducted on a fully popped-up hood. During the Type Approval process, the determination of system reliability and consistency also must be demonstrated by the vehicle manufacturer, but the means and requirements to do so are not defined within the regulation itself. Because the operation of pop-up systems varies widely and they are generally unique to specific vehicle models, the demonstration of system functionality is agreed upon between the manufacturer and the Type Approval Authority. Euro NCAP operates in a similar manner.
**Conclusions:** Pop-up hoods generally perform better than non-deploying hoods in headform impact tests. As their development matures and vehicle styling progresses towards low, sleek, aerodynamic hood profiles, demand as well as variation in these systems may grow. To date there is not a published, fully prescriptive test protocol that tests the full functionality of such systems, including reliability and deployment thresholds, to objectively ensure that they function properly during an actual collision with a pedestrian.

## INTRODUCTION

Fatal injuries to pedestrians from motor vehicles often result from the pedestrian's head striking either the vehicle or the ground. There are two primary means of protecting pedestrians through vehicle safety systems: one involves the use of crash avoidance safety systems, such as those for braking and lighting, to help the driver see the pedestrian and avoid a collision, and the other involves structural designs and mechanisms built into the vehicle front-end that reduce the injury potential to pedestrians should a crash occur. This paper will discuss pop-up hood systems, which increase the distance to rigid components in the engine bay, potentially reducing the head injury risk of a struck pedestrian [14], by quickly lifting the rear edge of the hood a few inches when triggered.

A sleek vehicle profile, and therefore a low hood profile, is often desirable by vehicle manufacturers for both styling purposes and aerodynamic performance. These low hood profiles are contrary to what is desired for good pedestrian head protection because they leave less space between the hood and underlying hard surface components, a clearance necessary for energy absorption during impact through free deformation of the hood. Though many manufacturers are able to provide the desired clearance through other means such as structural changes and component layout adjustments, some use pop-up hoods as an alternate strategy [5].

Pop-up hoods are particularly beneficial because they provide head penetration clearance near the hinges and at the rear edge of the hood along the cowl, where the windshield, hood, and firewall all intersect. It is in this area where pedestrian heads often strike. But it is also the area where non-deploying hoods are typically stiffest – even those

designed to conform to pedestrian safety standards. The beneficial qualities of pop-up hoods have been demonstrated in numerous studies [8][12][14].

Also, the addition of a pop-up hood to an existing vehicle designed for a market without pedestrian protection requirements may allow a vehicle manufacturer to sell vehicles in additional marketplaces while avoiding major structural and styling changes.

The basic premise behind pop-up hood deployment is that the vehicle is outfitted with a control unit which triggers hood deployment when the vehicle senses a pedestrian collision and is traveling within a predetermined threshold for which the control unit knows hood deployment will be effective. The control unit receives input from a contact sensor and/or pre-crash sensing technologies. Contact sensors in the bumper, in the form of accelerometers, pressure tubes, or resistive/capacitive sensors, detect that the vehicle has struck a pedestrian's leg (rather than a tree, pole, or other inanimate roadside object) through classification of the impact pulse. Some new vehicles are outfitted with pre-crash sensing technologies such as radar and LIDAR, which are able to influence the control unit's hood deployment algorithm through identification of a pedestrian prior to vehicle-pedestrian impact.

Deployment (lifting) technologies vary from springs and motors to pyrotechnic actuators using rapidly expanding gas to provide the necessary lift, similar to the devices used in air bag deployment. The lifting actuators are located at the rear corners of the hood at the hinge locations, and they lift the hood up as it pivots at the latch in the front [12]. The spring and motor method is considered to be desirable because the hood could be fully reset post-impact or after a false trigger, whereas the pyrotechnic method would require the replacement of certain components. Conversely the pyrotechnic method is desirable because of its ability to deploy the hood faster than the other option, and most research has focused in this area. Also, pyrotechnic components are generally smaller and weigh less. Minimizing the repair costs of a vehicle equipped with pop-up hood deployment also requires a hood that could be reused, which would depend upon a hood rigid enough to resist deformation from the impact of a head or torso. This may conflict with the ability of a hood to absorb energy when not deployed [11]. A newer pop-up hood system, first seen in mass production on the Volvo V40, is the pedestrian air bag [8]. Triggered with the same sensing methods as used for traditional pop-up hood actuation systems, an inflator fills the pedestrian air bag which then lifts the hood. This air bag is located at the base of the windshield, and it not only lifts the hood for additional clearance but also provides air bag coverage to the vehicle's A-pillars and lower windscreen, which are relatively very hard surfaces.

**METHODS**

The United States does not currently have pedestrian protection requirements applicable to vehicles, so vehicles in markets with pedestrian protection requirements were studied to examine trends regarding pop-up hood systems. Pedestrian safety systems such as pop-up hoods are not new to Europe. Euro NCAP, a non-regulatory consumer ratings group in Europe, supported by various European governments and motoring organizations, has been testing pedestrian protection for more than a decade. Additionally, many European countries are subject to pedestrian protection regulations.

In this paper, 498 Euro NCAP test reports from 2000-2014 were entered into a database. Next, the Parkers database of United Kingdom (UK) vehicle prices was consulted to assign new vehicle prices to each vehicle in the database. The Parkers information was consulted because it includes a wealth of historical vehicle pricing information, and the UK market was deemed large and varied enough to be an appropriate sample.

From these 498 database entries, 63 were excluded from the following calculations regarding test scores and price, leaving 435 unique vehicle entries with full Euro NCAP test scores and Parkers vehicle pricing information. Of the excluded entries, 33 were repeated entries, 1 was a Euro NCAP test report (the 2008 Mercedes Viano) that did not include pedestrian protection scores, and 29 were vehicles that lacked historical price information through Parkers.co.uk or were not offered for sale in the UK. The 33 Euro NCAP vehicle retests came from both the 2009 Euro NCAP test protocol change regarding rescoring and retesting and also from design changes stemming from poor initial Euro NCAP scores. In all of these cases, the most recent test report was kept. These repeat test vehicles had identical pedestrian scores except for the Mazda 6 retest in 2005, VW Passat retest in 2010, and Jaguar XF in 2011. The Passat and XF tests were redone specifically for pedestrian protection. The complete list of these

vehicles, as well as 12 additional European vehicles with pop-up hoods but not tested by Euro NCAP which were identified through various media outlets, is included in Appendix A.

Euro NCAP assigns an overall vehicle score on a five star scale, similar to the star assignment system used by NHTSA's own NCAP program. The number of overall stars is determined by the scores a vehicle receives in four main areas: Adult Occupant, Child Occupant, Pedestrian, and Safety Assist. For the year 2015, a vehicle must achieve 65 percent of the total possible points in the pedestrian test to qualify for a five star rating, and the pedestrian score comprises 20 percent of the overall score [1]. The pedestrian scores are compiled from three tests: headform, upper legform, and legform. The headform test is potentially 24 of the 36 total possible pedestrian points, and it tests for both child and adult impacts [3].

A vehicle equipped with a pop-up hood is tested with the pop-up hood only if the sales volume of vehicles with this feature is high enough according to the Euro NCAP sales volume specifications for that model year and if the vehicle manufacturer can work with the Euro NCAP Secretariat prior to testing to prove system functionality and reliability. Otherwise, it is tested without having its hood activated. In the Euro NCAP headform test, point values are assigned based on the HIC value from free motion headforms fired at the hood, targeting a grid of impact locations for both children and adults. This physical testing validates a simulation model provided by the vehicle manufacturer prior to the test [4].

**RESULTS**

Listed in Appendix B, there are 24 vehicles sold with pop-up hoods that Euro NCAP has tested, and they span the whole gamut of vehicle sizes and prices, going from the Fiat Freemont and Hyundai Santa Fe to the Mercedes M-Class, BMW 5-series and Jaguar XF. This is not to say that vehicles must have an pop-up hood to achieve a good head impact test score or that a pop-up hood guarantees a good head impact score – the 2012 Subaru Forester (without an pop-up hood) scored 20.3 of 24 potential points for head impact, and the 2011 Dodge Caravan (with an pop-up hood) scored only 11 points for head impact. Additionally, not all luxury vehicles have pop-up hoods – the Maserati Ghibli uses passive pedestrian protection without a pop-up hood. Inclusion of pop-up hoods in new vehicles has become more common over time.

As seen **Error! Reference source not found.** in Figure 1, the percentage of vehicles with pop-up hoods in the Euro NCAP test inventory has increased over time. Euro NCAP cannot test every vehicle so their inventory is not a census, but each year's vehicle selection is made in order to provide the broadest range of consumer information possible by collecting information about the most popular and interesting vehicle models [5]. Assuming the sample selection to be consistent over time, it can be posited that though pop-up hoods remain a small part of the vehicle fleet, they already have a high enough market penetration to have a tangible effect on overall pedestrian safety in the EU. However, we have no data on hood activations and pedestrian injury outcomes in real-world pedestrian crashes in the EU.

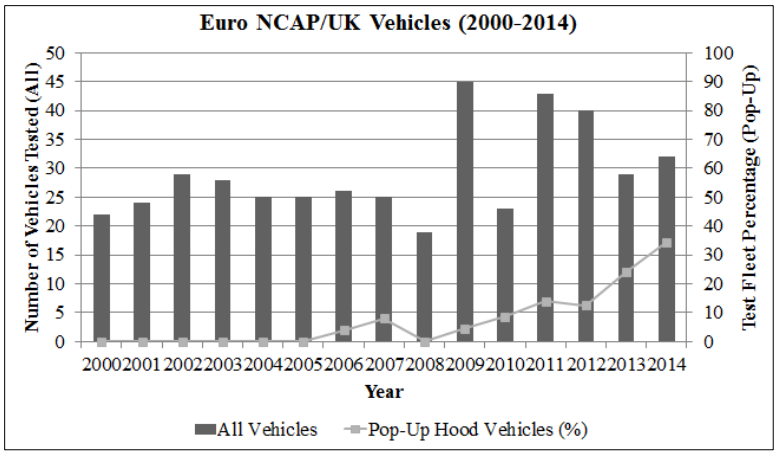


***Figure 1. Pop-up Hood Market Penetration for 2000-2014 Euro NCAP/UK Vehicles Tested***

Figure 2, below, shows the pedestrian protection scores for all vehicles. Those vehicles without pop-up hoods have increased their scores over time. Figure 3, below, shows that this trend is consistent with that for looking only at the scores from the headform test. Though the sample size is relatively small for vehicles with pop-up hoods, score gaps in both figures indicate that they yield higher scores than those without pop-up hoods.

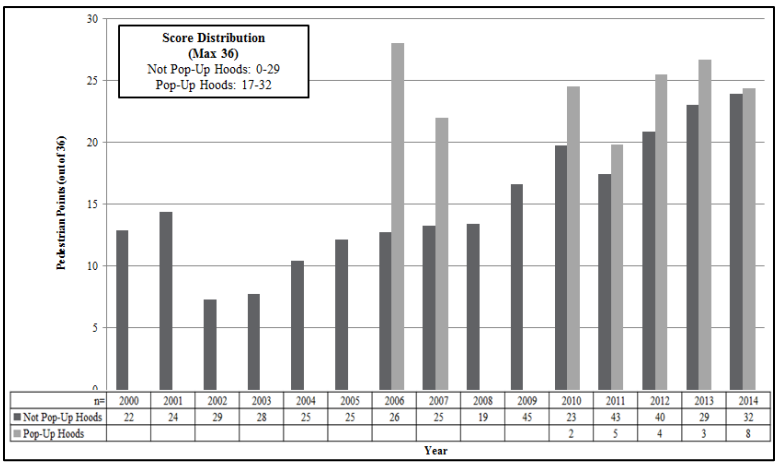


***Figure 2. 2000-2014 Euro NCAP/UK Vehicle Overall Pedestrian Scores over Time***

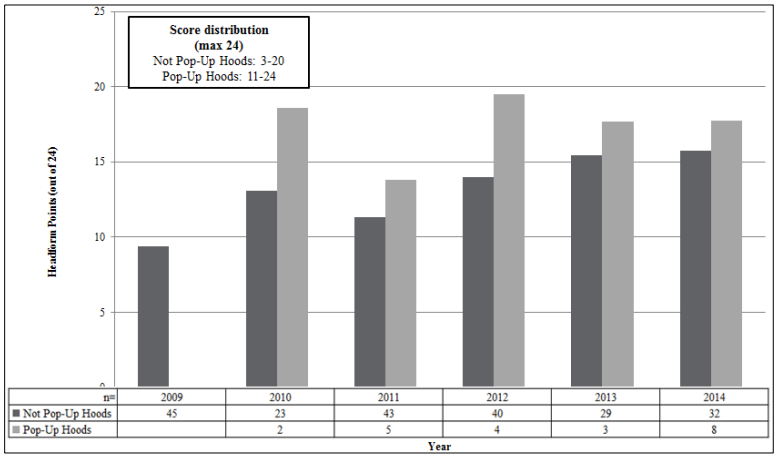


***Figure 3. 2000-2014 Euro NCAP/UK Vehicle Average Pedestrian Headform Scores***

To date, the 2012 Volvo V40 is the only vehicle in the Euro NCAP database to achieve a perfect 24 point score for the head impact testing. (The V40 is not sold in the U.S.) Note that prior to 2009, publically reported Euro NCAP pedestrian protection scores were given as overall scores and not broken into separate head, upper leg, and leg scores as they are currently. This result was achieved with a pedestrian air bag that deploys when the vehicle is moving at speeds between 20 and 50 km/h to not only lift the hood, but to also cushion the windshield wiper, windscreen, and A-pillar areas in case of a strike from a pedestrian head [6]. The 2010 BMW 5-series, equipped with a pop-up hood, also scored highly in both child and adult head impact tests, receiving 22 of 24 possible points. The 2006 Citroen C6 is also noteworthy because it is one of the earliest vehicles featuring a pop-up hood. Until 2009, Euro NCAP translated the overall pedestrian point score into a separate rating out of 4 stars. The 2006 Citroen C6 was the first vehicle to achieve that top 4 star pedestrian rating with a score of 28 of 36 points. This pre-2009 Euro NCAP pedestrian score was a single score with all of the three factors combined into a single score.

The effectiveness of the pop-up hood technology alone is seen with the 2013 Skoda Octavia and the 2010-2012 Jaguar XF. The 2013 Skoda Octavia's test results were updated in June 2013 because Skoda made the decision to remove the pop-up hood, which had previously been standard equipment on vehicles sold throughout the EU. The Euro NCAP test report states that the full pedestrian protection score, not specific to only head impact, was 30 points

with the pop-up hood technology or 24 without, out of a potential 36 points. Without the pop-up hood, the head impact score was only 16.5 out of a potential 24 points. Conversely the Jaguar XF was tested in 2010 without pop-up hood technology, where it scored 16 points out of a potential 24 for head impact testing. The 2010 XF was outfitted with pop-up hood technology, but was tested without it because the sensors in the bumper did not meet Euro NCAP standards. The XF was tested again in 2012 with the pop-up hood technology activated, which improved that score to 22 out of 24 points.

The historical pricing information from the Parkers database was used to characterize original, new vehicle sales prices for the vehicles in the database. The Parkers database provided a range of prices for the various option levels, and the median of this range was calculated for each vehicle and used to create Figure 4, below. Median new vehicle sales prices for vehicles with pop-up hoods are higher than those for vehicles without a pop-up hood, but as seen in Figure 4, not all vehicles with pop-up hoods are at the absolute top end of the price spectrum.

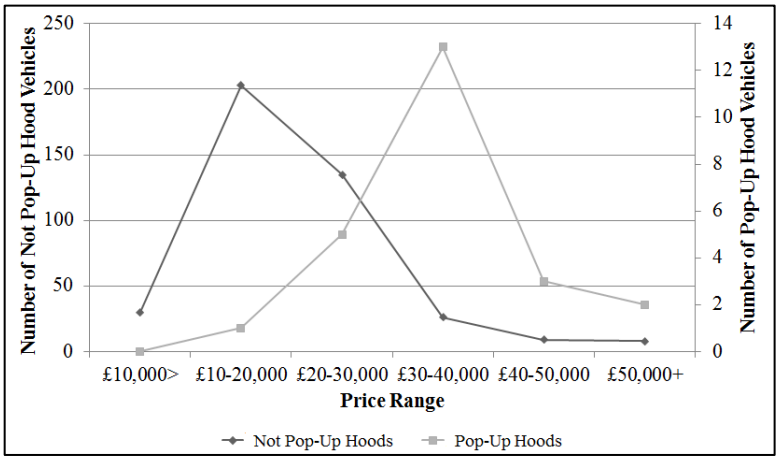


***Figure 4. 2000-2014 Euro NCAP/UK Vehicle Median Price Distribution***

The analysis of the vehicles in the database showed that while pop-up hoods can help to get a high pedestrian headform score in the Euro NCAP test, it was not essential to doing so. below, in Figure 5, it can be seen that the 2012 Subaru Forester, without a pop-up hood, scored 20.3 out of 24 headform points, while the comparably priced 2011 Dodge Caravan, with an pop-up hood, only scored 11 out of 24 headform points.

***Figure 5. Pedestrian Protection Vehicle Comparison With and Without Pop-Up Hood***

**Market Penetration**

We identified 40 vehicle models with pop-up hoods that have been marketed in Europe, as shown in Table 1 below. Only two of them are no longer produced: the Citroen C6 (ceased production in 2012) and the Acura RL (also ceased in 2012 but reintroduced in 2015). Of the current European models with pop-up hoods, most are versions of similar models sold in the U.S. without a deployment actuator.

One such vehicle is the Dodge Caravan, sold in the Europe as the Lancia Voyager. The Caravan is an example of a vehicle not originally designed for a market with pedestrian protection requirements (only 4,140 sales units in the EU vs. 272,191 in the U.S. for 2014). In light of these sales figures and its marginal headform score of 11.0 (lowest of all vehicles with pop-up hoods and below average for all), it would appear that the pop-up hood provided the manufacturer with a more economic option to allow an existing vehicle design entry into the European market. Otherwise, a costly redesign of the whole front end including hood under-components may have been required to achieve comparable pedestrian headform scores.

As seen in Table 1, about 8% of new cars sold in Europe have pop-up hoods and the U.S. market share of the North American versions is about the same. The market share of vehicles with pop-up hoods could increase further as the systems mature. Aside from the benefits to pedestrians discussed in the Introduction, a pop-up hood offers other advantages. From a vehicle styling viewpoint, a pop-up hood provides a means to achieve a desired appearance of a sleek vehicle with a low hood profile, which may provide better aerodynamic performance.

**Table 1. European Passenger Cars with Pop-Up Hoods**

| Make | Model | United States version | | European version | | Euro NCAP head score /36 | European name |
|---|---|---|---|---|---|---|---|
| | | Sales 2014 | Median Price | Sales 2014 | Median Price | | |
| Acura | RL | Discont. | $49,490 | Discont. | £37,713 | n/a | Honda Legend |
| Aston Martin | DB9 | 1,224 | $191,200 | 285 | £140,527 | not tested | |
| Aston Martin | Vanquish | | $279,995 | 325 | £198,640 | not tested | |
| Audi | A3 | 22,250 | $29,060 | 199,537 | £29,158 | 18 | |
| BMW | 2-Series | 7,345 | $33,000 | 26,215 | £26,993 | 14.9 | |
| BMW | 6-Series | 8,647 | $53,253 | 7,902 | £67,050 | not tested | |
| BMW | 5-Series | 52,704 | $50,950 | 98,519 | £44,080 | 22 | |
| Cadillac | ATS | 29,890 | $40,445 | 365 | n/a[1] | not tested | |
| Cadillac | CTS | 31,115 | $63,215 | | n/a[1] | not tested | |
| Citroen | C6 | not sold in U.S. | | Discont. | £33,578 | n/a[2] | |
| Chrysler | 300 | 53,382 | $33,745 | 487 | £38,000 | 15.3 | Lancia Thema |
| Dodge | Journey | 93,572 | $27,945 | 17,417 | £20,970 | 12 | Fiat Freemont |
| Dodge | Caravan | 272,192 | $34,710 | 4,140 | £32,265 | 11 | Lancia Voyager |
| Hyundai | Genesis | 29,992 | $42,125 | 247 | n/a[3] | 16.7[3] | |
| Hyundai | Santa Fe | 107,906 | $27,075 | 13,332 | £30,363 | 18.6 | |
| Infiniti | Q50 | 36,899 | $41,200 | 2,426 | £69,253 | 19.1 | |
| Jaguar | F-type | 4,112 | $80,500 | 4,654 | £69,253 | not tested | |
| Jaguar | XF | 5,880 | $65,150 | 20,328 | £40,670 | 16.2 | |
| Jaguar | XK | 1,452 | $77,835 | 1,882 | £81,965 | not tested | |
| Kia | Sorento | 102,520 | $28,275 | 9,325 | £31,900 | 18.3 | |
| Land Rover | Discovery Sport | n/a | $41,320 | n/a | £39,195 | 19.2 | |
| Lexus | IS | 51.358 | $50,979 | 9,552 | £33,643 | 16.9 | |
| Mazda | MX-5/Miata | 4,745 | $26,485 | 5,787 | £21,095 | not tested | |
| Mercedes | A-Class | not sold in U.S. | | 121,321 | £26,058 | 18 | |
| Mercedes | CLA-Class | 27.365 | $38,675 | 38,423 | £30,155 | 17 | |
| Mercedes | GLA-class | 6,884 | $39,800 | 44,930 | £30,218 | 18.4 | |

| Make | Model | United States version | | European version | | Euro NCAP head score /36 | European name |
|---|---|---|---|---|---|---|---|
| | | Sales 2014 | Median Price | Sales 2014 | Median Price | | |
| Mercedes | C-Class | 75,065 | $49,275 | 136,431 | £32,580 | 21 | |
| Mercedes | C-Class Coupe | | $46,095 | | £33,725 | 14.6 | |
| Mercedes | E-Class | 66,400 | $66,900 | 99,441 | £37,563 | 15.2 | |
| Mercedes | S-Class | 25,276 | $114,070 | 17,694 | £74,900 | not tested | |
| Mercedes | SL | 5,030 | $101,565 | 2,638 | £78,190 | not tested | |
| Mercedes | SLK | 4,737 | $51,150 | 11,107 | £38,705 | not tested | |
| Mercedes | M-Class | 46,726 | $71,990 | 23,710 | £48,035 | 17.4 | |
| Mini | Cooper | 33,467 | $22,900 | 94,909 | £19,053 | 18.1 | |
| Nissan | GT-R | 1,436 | $77,965 | 275 | £81,610 | not tested | |
| Peugeot | RCZ | not sold in U.S. | | 5,772 | £27,050 | not tested | |
| Porsche | Panamera | 5,740 | $111,200 | 5,647 | £97,603 | not tested | |
| Tesla | Model S | 36,400 | $81,650 | 8,841 | £75,535 | 13.9 | |
| Audi | TT | 1,158 | $40,795 | 9,786 | £32,320 | 17.7 | |
| Volvo | V40 | not sold in U.S. | | 80,948 | £25,388 | 24 | |
| Total vehicles w/ pop-up hoods | | 1,174,225 | | 1,043,650 | | | |
| Total all light vehicles | | 16,531,070 | | 12,939,046 | | | |

[1] Cadillac ATS and CTS not sold in U.K. Estimated price for the CTS in EU: 56,200 € (£40,800). No estimate for the ATS.
[2] Citroen C6: Separate headform score not reported.
[3] Hyundai Genesis not sold in U.K. Estimated price in EU: 65,000 € (£47,200). Headform score of 16.7 reported by Australia NCAP.

**Standardized Test Protocols**

Test protocols for pop-up hoods and associated requirements are discussed below. In addition to Euro NCAP's five star consumer ratings, which are consumer information ratings and not regulations, some countries also subscribe to various United Nations agreements and are therefore subject to United Nations regulations. United Nations Global Technical Regulation No. 9 (GTR No. 9), *Pedestrian Safety*, which applies to WP29 1998 Agreement signatory countries, includes a test protocol for evaluating the pedestrian friendliness of light duty vehicles. GTR No. 9 provides general guidance as to how testing of vehicles with pop-up hoods could be done.

**GTR No. 9.** GTR No. 9 [15] addresses pedestrian safety, targeting the energy absorption abilities of the bumper and hood areas in 40 km/h vehicle-to-pedestrian crashes. GTR No. 9 is broken into two main parts: Section A, the Statement of Technical Rationale and Justification, and Section B, the Text of the Regulation. The regulatory requirements are prescribed in Section B, where it is stated: "[a]ll devices designed to protect vulnerable road users when impacted by the vehicle shall be correctly activated before and/or be pop-up during the relevant test. It shall be the responsibility of the manufacturer to show that any devices will act as intended in a pedestrian impact." However, there are no specifics on how this demonstration is carried out. Pop-up hoods were still conceptual during the 1990s when the work of the ISO, IHRA, the EEVC, and NHTSA formed the building blocks of the GTR.

Section A, however, does provide informal guidance on pop-up hoods. It states that pop-up hoods "must not create a higher risk of injuries for the pedestrians." In conjunction with this point, working paper INF GR/PS/141, Certification Standard for Type Approval Testing of Active Deployable Systems of the Bonnet/Windscreen Area, is offered as a guideline for the certification of deployable devices by Contracting Parties looking to implement test procedures in their home countries, with previous working papers giving additional insight [1][16].

Another working paper provides a decision tree analysis for a Type Approval system of compliance in which the vehicle manufacturer and a type approval authority agree on the timing between a headform launch and a hood activation [17]. The guidelines serve mostly to specify terminology for defining the timing of a launch as provided by the manufacturer. They do not specify the timing itself, nor do they provide requirements for the triggering threshold or any requirements for hood activation.

**Euro NCAP.** Though not a regulatory body, Euro NCAP has had a pedestrian testing protocol in place for more than a decade, which covers headform, legform, and upper legform impact tests. The first vehicle tested with a pop-up hood in the Euro NCAP database of test results was the 2006 Citroen C6, followed by the 2007 Honda Legend and several others.

Since Version 5.2 (implemented in 2009), Section 2 in the Euro NCAP pedestrian testing protocol has been dedicated to the "assessment of vehicles with active bonnets," laying out detailed information for how Euro NCAP will assess not only the deployment but also the triggering and sensing capabilities of these pop-up systems. As the pop-up systems have matured, the Euro NCAP testing protocol has undergone periodic refinement to provide more objective assessment procedures.

Notwithstanding higher Euro NCAP scores, uncertainty remains over the true effectiveness of pop-up hoods. Absent a real-world analysis of pedestrian collisions, it is unknown whether higher headform scores for pop-up hoods have translated into reduced injury risk for pedestrians. Much of the uncertainty surrounds questions on how well pop-up hoods function in the real-world. The discussion below highlights these uncertainties and explains how they are treated under the current Euro NCAP protocol (Version 8.0, implemented in 2014).

## DISCUSSION

### Questions Regarding Real-World Effectiveness

The effectiveness of pop-up hoods has been questioned since the early stages of pedestrian safety standards development. The original uncertainties are perhaps best summarized in a 2006 feasibility report by Lawrence and Hardy [11]. The authors expressed low confidence for pop-up systems due to their complexity and the amount of tuning needed for them to work properly. The device must trigger and then physically push the bonnet upwards, before the pedestrian's head strikes, and the lifting mechanism must be strong enough for not only the initial lift but also to support the weight of the pedestrian's head and torso. The lift timing must be precise, and the sensors must be calibrated as to prevent false triggering. They must be able to differentiate between pedestrians about to be or having just been struck versus non-pedestrians, and a triggering threshold for a minimum vehicle collision speed must be established. The introduction of vehicles with active suspensions only serves to complicate the matter further.

In Euro NCAP, the functionality of the pop-up hood system is demonstrated through computer simulations carried out by the vehicle manufacturer. This exercise must adhere to a set of guidelines laid out in Section 2 of the Euro NCAP protocol and the integrity of the analysis must be approved by the Euro NCAP Secretariat. The protocol is not prescriptive of the system. Instead, Euro NCAP allows manufacturers to set their own sensing and triggering criteria and then performs a limited number of verification tests based on these provided criteria. System reliability and consistency is largely left to the discretion of the vehicle manufacturer. Some of the more prominent functionality concerns are discussed below.

**Pedestrian sensing.** All vehicles with pop-up hoods have some sort of pedestrian sensing mechanism to trigger the deployment of the hood. In Euro NCAP, this functionality is demonstrated by the manufacturer through computer simulations of knee-to-bumper interactions using full body models of pedestrians of various sizes. The simulations are run using models of various pedestrian sizes, but only for stances in which the pedestrian is walking perpendicular to the line of vehicle travel.

Hence, there is no physical test method for assuring that the sensors detect pedestrians in various gaits and stances and in a range of collision speeds, vehicle maneuvers (turning or braking) and environmental conditions (temperature, icy vs. dry). To verify sensing and deployment through a physical test, a special pedestrian manikin may be needed. Such a manikin would likely differ in form and function from the legform impactor used by Euro NCAP (and known as the Flex-PLI) to assess pedestrian leg injury risk.

There are also concerns that pedestrians will be left unprotected in a collision that is not initiated by leg-to-bumper contact so that the hood does not deploy. And since the sensors are located on the bumper, a criterion may be needed to assure that they do not become easily damaged. Also, it is also entirely possible that future systems would

use visual detection and not require actual contact, which would require even another manikin with considerations for environmental operating conditions (dirt, rain and snow, lighting).

**Timing.** In Euro NCAP, computer simulations are carried out by the manufacturer to demonstrate that the hood is fully deployed before landed upon by a pedestrian. However, it may be necessary to account for various pedestrian gaits and stances since they can influence the time lapse between the initial bumper-to-pedestrian contact and the subsequent head-to-hood impact. In Euro NCAP, there are no physical tests associated with this demonstration due in part to the absence of a standardized pedestrian test dummy.

**Deployment threshold.** In Euro NCAP, the manufacturer specifies the hood deployment thresholds (both at a speed below 40 km/h and at a speed of 50 km/h or higher), which are then verified through physical testing. Triggering thresholds generally differ from one vehicle to the next. The vehicle speed at which activation occurs may depend upon the protectiveness of the hood in its undeployed state, which is dependent on under-hood clearances and the size of the hood. Thus, a blanket requirement for a single threshold for all vehicles might not achieve all the potential benefits it could otherwise achieve if, for example, it did not deploy at a low enough speed. . However, a protocol may be needed to verify the thresholds are met under a variety of collision scenarios.

**Head impacts below the deployment threshold**. If a low-speed collision occurs below the hood activation threshold, a pedestrian may be placed in undue risk if the undeployed hood is overly stiff. In Euro NCAP, manufacturers are required to show that HIC values in actual headform impact tests on an undeployed hood are not exceedingly high (HIC values must be less than 1350) when the tests are run at the deployment threshold speed.

**Width of bumper sensitivity.** Relative to the width of the hood, the front-end vehicle width over which trigger sensors apply should be sufficiently wide. However, the legform test area specified by Euro NCAP (used in conjunction with the Flex-PLI to assess lower leg injuries) only extends to the edges of the bumper support structure. In the case of a vehicle with beveled front corners, the test area can be quite narrow (less than half the full width of some vehicles). Therefore, added assurance may be needed to verify that the hood deploys for any bumper-to-leg impact that could precede a head-to-hood impact.

**Lifting device.** The actuators used to raise the hood pose one of the greater risks to failure of the entire pop-up hood system. Test procedures may be needed to assure that the lifting linkages are strong enough for not only the initial lift but also to support the weight of the pedestrian's torso so that the hood does not collapse prior to or upon head-to-hood impact. In Euro NCAP, such assurances are provided by the manufacturer through computer simulations of vehicle-to-pedestrian collisions. For pyrotechnic devices, further requirements may be needed to assure that their performance does not degrade over time due to the harsh environmental conditions under a hood.

**False deployments.** Bumper sensors are tuned in some manner to differentiate between a human leg and an object of a similar shape. A test method for a pedestrian detection sensor may be needed to show that the trigger sensor is able to differentiate between a pedestrian and a common roadside object, such as a garbage can. False deployments are not explicitly covered by the Euro NCAP protocol. However, there could be visibility risks for occupants of a vehicle in motion whose pop-up hood deploys from a false-positive trigger event. Furthermore, deployed hoods have cost implications which require additional consideration. Not only is a pop-up hood system added cost to the vehicle at purchase, but it is also potentially an area for costly repairs. Will the driver be able to drive the vehicle with deployed hood to a repair shop, or will a tow truck be required? These are factors which need to be balanced when assessing false deployments. [11]

**Overall objectivity.** Standardized test methods with objective assessment criteria may be needed in order to fully assess the overall effectiveness of pop-up hood systems on real-world pedestrian safety. They may also be needed to assure conformity to given level of pedestrian safety by a third party. A performance requirement for a device that is reliant on a manufacturer to prescribe how it should be tested and assessed may lessen the ability of an independent evaluator to provide such assurances.

## CONCLUSIONS

The range of vehicles in the Euro NCAP database shows that the early concerns about prohibitive cost and reliability of pop-up hoods did not appear to come to fruition. Our observations revealed the following:

• Since 2010, vehicles with pop-up hoods generally produced better Euro NCAP headform scores on average: 17.2 (out of a possible 24) for cars with pop-up hoods vs. 13.8 for cars with non-deploying hoods.

• From year-to-year, the Euro NCAP headform scores of cars with traditional, non-deploying hoods have been trending upwards. Nonetheless, in the latest year of our assessment (2014), the scores of cars with pop-up hoods were still higher.

• In 2014, there were 38 European new car models with pop-up hoods. The models tended to be in a higher price range (such as several Jaguar and Mercedes Benz models), but there are exceptions (examples: Hyundai Santa Fe, Mini Cooper).

• Cars with pop-up hoods comprise about 8% of all new light vehicles in Europe. These same vehicles comprise about 7% of new light vehicles sold in the U.S.

• Only one vehicle so far, the 2013 Skoda Octavia, has introduced pop-up hood technology as standard and later removed it.

• Pop-up hood technology is generally more costly than other passive strategies for protection pedestrians, but this examination of pop-up hood trends showed that sometimes a pop-up hood can lead to lower HIC values while enabling the vehicle to attain a better Euro NCAP score and still achieving a desired vehicle style.

• The Dodge Caravan exemplifies a situation where a pop-up hood provided an expedient means to achieve an acceptable pedestrian rating in a vehicle not originally designed for a market with pedestrian protection requirements. By fitting the sensing and lifting components to an existing design (rather than engaging in a lengthy and costly redesign of the vehicle front-end using a non-deploying hood), the vehicle was brought to the European market promptly.

• Notwithstanding the guidelines laid out in Section 2 of the Euro NCAP protocol, there is no standardized means to independently test and assess entire pop-up hood systems because of their unique and vehicle-specific operations. The basic technologies vary widely, and pop-up hoods activate within different speed ranges depending on the vehicle. These conditions make it difficult to develop a standardized test and criteria that is objective, uniform, and repeatable during testing across a fleet of vehicles with differing pop-up deployment designs.

Given the number of these systems in production today, it is clear that engineering has been able to overcome the initial technical challenges in a safe and reliable manner regardless of the remaining testing standardization challenges. Pop-up hoods are now yet another technical advance in the field of automotive engineering. The trends in the preceding analysis show that pop-up hoods are worthy of consideration for the development of new standardized test methods and assessment criteria.

**ACKNOWLEDGMENTS**
The authors would like to thank Euro NCAP for their support in the collection of vehicle test reports.

**REFERENCES**


[1] CLEPA European Association of Automotive Suppliers (2004). *INF GR/PA/67 Pedestrian Protection Test method – Active hood/bonnet systems.* [Working Paper]

[2] Euro NCAP (July 2012). *European New Car Assessment Programme (Euro NCAP) Assessment Protocol – Overall Rating, Version 6.0.* [Test Protocol].

[3] Euro NCAP (June 2014). *European New Car Assessment Programme (Euro NCAP) Assessment Protocol – Pedestrian Protection, Version 8.0.* [Test Protocol].

[4] Euro NCAP (June 2014). *European New Car Assessment Programme (Euro NCAP) Pedestrian Testing Protocol, Version 8.0.* [Test Protocol].

[5] Euro NCAP (2015). *The Car Selection Explained | Euro NCAP – For Safer Cars Crash Test Safety Rating.* [Web]. Retrieved January 8, 2015 from http://euroncap.com/ourtests/selectionexplained.aspx.

[6] European Motor News. (2013, May 30). *THE ALL-NEW VOLVO V40 – PEDESTRIAN AIRBAG TECHNOLOGY* [Video File]. Retrieved from http://www.youtube.com/watch?v=NCjVS_-6hYs

[7] Evrard, Borg (2011). *Innovative Bonnet Active Actuator (B2A) For Pedestrian Protection*, Proceedings of the 22nd International Technical Conference on the Enhanced Safety of Vehicles, paper 11-0113, Washington, D.C.

[8] Fredriksson, R., Boström, O., Chang, L.Y., Yang, K., (2006). *Influence of pop-up hood systems on brain injuries for vulnerable road users*. In: 2006 International IRCOBI Conference on the Biomechanics of Impact, Madrid, Spain.

[9] Key, Edwin (2012). "Volvo S40 Comes with Pedestrian Airbag." *Ubergizmo*.

[10] Honeywill, Tristan. (2013, June 27). Skoda withdraws pedestrian-friendly pop-up hood on Octavia [Online Article]. *Car Safety Rules*. Retrieved August 28, 2013 from http://www.carsafetyrules.com/skoda-withdraws-pedestrian-protecting-hood-on-octavia/0627/.

[11] Lawrence, G J L, Hardy, B J, et al. (2006). *A study on the feasibility of measures relating to the protection of pedestrians and other vulnerable road users* [Project Report]. Berkshire, England, United Kingdom: Transportation Research Laboratory Limited (TRL), EC Contract No. UPR/VE/045/06 ENTR/05/17.01.

[12] Nagatomi K, Hanayama K, Ishizaki T, Sasaki A, Matsuda K (2005), *Development and full-scale dummy tests of a pop-up hood system for pedestrian protection,* Proceedings of the 19th International Technical Conference on the Enhanced Safety of Vehicles (ESV) - Washington D.C. June 6-9, 2005.

[13] *Road Safety Information: Pop Up Bonnet* [Pamphlet]. September 2005, Birmingham, England, United Kingdom: The Royal Society for the Prevention of Accidents (RoSPA).

[14] Takahashi, H, Miyazaki, H, et al. (2013). *Development of Pop-Up Hood System for Pedestrian Protection*, Proceedings of the 23rd International Technical Conference on the Enhanced Safety of Vehicles, paper 13-0126, Seoul, Korea.

[15] United Nations (18 November 2004). *Global technical regulation No. 9: Pedestrian Safety* [Addendum to GTR]. Geneva, Switzerland.

[16] United Nations (6 December 2003). *INF GR/PS/104 Minimum Standard for Type Approval Testing of Active Deployable Systems of the Bonnet/Windscreen Area.* [Working Paper]

[17] United Nations (6 December 2003). *INF GR/PS/141 Certification Standard for Type Approval Testing of Active Deployable Systems of the Bonnet Area.* [Working Paper]

**APPENDIX A**

Table 2, below, includes the processed list of vehicles described above in the Methods section. At the end of the list of vehicles used in the above calculations, 12 additional vehicles which were sold in Europe with pop-up hoods but not tested by Euro NCAP are listed. These 12 additional vehicles were identified through other media outlets.

**Table 2. Vehicle Database**

| Vehicle Information | | | | | Euro NCAP Scores | | | | | |
|---|---|---|---|---|---|---|---|---|---|---|
| | | | | | Overall | Pedestrian Scores | | | | |
| Yr | Make | Model | Ctgry | Pop Up ? | Stars (/5) | Stars (/4) | Pts (/36) | Head (/24) | Pelvis (/6) | Leg (/6) |
| 2000 | Citroen | Saxo | 3 door hatch | no | n/a | 2 | 10 | n/a | n/a | n/a |
| 2000 | Daewoo | Matiz | 5 door hatch | no | n/a | 2 | 15 | n/a | n/a | n/a |
| 2000 | Daihatsu | Sirion | 3 door hatch | no | n/a | 3 | 19 | n/a | n/a | n/a |
| 2000 | Fiat | Seicento | 3 door hatch | no | n/a | 2 | 13 | n/a | n/a | n/a |
| 2000 | Ford | Fiesta | 3 door hatch | no | n/a | 1 | 8 | n/a | n/a | n/a |
| 2000 | Ford | Ka | 3 door hatch | no | n/a | 1 | 9 | n/a | n/a | n/a |
| 2000 | Honda | Accord | 4 door saloon | no | n/a | 2 | 16 | n/a | n/a | n/a |
| 2000 | Honda | Logo | 3 door hatch | no | n/a | 2 | 14 | n/a | n/a | n/a |
| 2000 | Lancia | Ypsilon | 3 door hatch | no | n/a | 2 | 12 | n/a | n/a | n/a |
| 2000 | Nissan | Micra | 3 door hatch | no | n/a | 2 | 16 | n/a | n/a | n/a |
| 2000 | Opel/Vauxhall | Corsa | 3 door hatch | no | n/a | 2 | 14 | n/a | n/a | n/a |
| 2000 | Peugeot | 206 | 3 door hatch | no | n/a | 2 | 11 | n/a | n/a | n/a |
| 2000 | Renault | Clio | 3 door hatch | no | n/a | 2 | 13 | n/a | n/a | n/a |
| 2000 | Saab | 9-3 | 5 door hatch | no | n/a | 1 | 4 | n/a | n/a | n/a |
| 2000 | Seat | Ibiza | 3 door hatch | no | n/a | 2 | 17 | n/a | n/a | n/a |
| 2000 | Skoda | Fabia | 5 door hatch | no | n/a | 2 | 12 | n/a | n/a | n/a |
| 2000 | Smart | City Coupe | 2 door saloon | no | n/a | 2 | 14 | n/a | n/a | n/a |
| 2000 | Toyota | Yaris | 3 door hatch | no | n/a | 2 | 13 | n/a | n/a | n/a |
| 2000 | Volvo | S80 | 4 door saloon | no | n/a | 2 | 14 | n/a | n/a | n/a |
| 2000 | VW | Beetle | 2 door saloon | no | n/a | 2 | 14 | n/a | n/a | n/a |
| 2000 | VW | Lupo | 3 door hatch | no | n/a | 2 | 13 | n/a | n/a | n/a |
| 2000 | VW | Polo | 3 door hatch | no | n/a | 2 | 13 | n/a | n/a | n/a |
| 2001 | Alfa Romeo | 147 | 3 door hatch | no | n/a | 2 | 17 | n/a | n/a | n/a |
| 2001 | Audi | A4 | 4 door saloon | no | n/a | 1 | 7 | n/a | n/a | n/a |
| 2001 | BMW | 3 Series | 4 door saloon | no | n/a | 1 | 8 | n/a | n/a | n/a |
| 2001 | Citroen | C5 | 5 door hatch | no | n/a | 2 | 16 | n/a | n/a | n/a |
| 2001 | Citroen | Picasso | 5 door MPV | no | n/a | 2 | 12 | n/a | n/a | n/a |
| 2001 | Fiat | Multipla | 5 door MPV | no | n/a | 2 | 13 | n/a | n/a | n/a |
| 2001 | Honda | Civic | 5 door hatch | no | n/a | 3 | 26 | n/a | n/a | n/a |
| 2001 | Hyundai | Elantra | 4 door saloon | no | n/a | 2 | 16 | n/a | n/a | n/a |
| 2001 | Mazda | Premacy | 5 door MPV | no | n/a | 3 | 19 | n/a | n/a | n/a |
| 2001 | Mercedes | C-Class | 4 door saloon | no | n/a | 2 | 12 | n/a | n/a | n/a |
| 2001 | Mitsubishi | Carisma | 5 door hatch | no | n/a | 2 | 16 | n/a | n/a | n/a |
| 2001 | Mitsubishi | Space Star | 5 door MPV | no | n/a | 2 | 14 | n/a | n/a | n/a |
| 2001 | Nissan | Almera | 5 door hatch | no | n/a | 2 | 16 | n/a | n/a | n/a |
| 2001 | Nissan | Almera Tino | 5 door MPV | no | n/a | 2 | 16 | n/a | n/a | n/a |
| 2001 | Opel/Vauxhall | Vectra | 5 door hatch | no | n/a | 2 | 14 | n/a | n/a | n/a |
| 2001 | Opel/Vauxhall | Zafira | 5 door MPV | no | n/a | 2 | 13 | n/a | n/a | n/a |

| Vehicle Information | | | | | Euro NCAP Scores | | | | | |
|---|---|---|---|---|---|---|---|---|---|---|
| | | | | | Overall | Pedestrian Scores | | | | |
| Yr | Make | Model | Ctgry | Pop Up ? | Stars (/5) | Stars (/4) | Pts (/36) | Head (/24) | Pelvis (/6) | Leg (/6) |
| 2001 | Peugeot | 307 | 5 door hatch | no | n/a | 2 | 14 | n/a | n/a | n/a |
| 2001 | Peugeot | 406 | 4 door saloon | no | n/a | 2 | 14 | n/a | n/a | n/a |
| 2001 | Renault | Scenic | 5 door MPV | no | n/a | 2 | 10 | n/a | n/a | n/a |
| 2001 | Rover | 25 | 3 door hatch | no | n/a | 2 | 18 | n/a | n/a | n/a |
| 2001 | Rover | 75 | 4 door saloon | no | n/a | 2 | 13 | n/a | n/a | n/a |
| 2001 | Skoda | Octavia | 5 door hatch | no | n/a | 2 | 14 | n/a | n/a | n/a |
| 2001 | Volvo | S60 | 4 door saloon | no | n/a | 2 | 14 | n/a | n/a | n/a |
| 2001 | VW | Passat | 4 door saloon | no | n/a | 2 | 13 | n/a | n/a | n/a |
| 2002 | Audi | A2 | 5 door hatch | no | n/a | 1 | 5 | n/a | n/a | n/a |
| 2002 | Chrysler | PT Cruiser | 5 door MPV | no | n/a | 1 | 3 | n/a | n/a | n/a |
| 2002 | Citroen | C3 | 5 door hatch | no | n/a | 2 | 11 | n/a | n/a | n/a |
| 2002 | Ford | Fiesta | 3 door hatch | no | n/a | 2 | 14 | n/a | n/a | n/a |
| 2002 | Ford | Mondeo | 5 door hatch | no | n/a | 2 | 13 | n/a | n/a | n/a |
| 2002 | Honda | CR-V | 5 door | no | n/a | 3 | 19 | n/a | n/a | n/a |
| 2002 | Hyundai | Santa Fe | off-roader | no | n/a | 1 | 4 | n/a | n/a | n/a |
| 2002 | Jaguar | X-Type | 4 door saloon | no | n/a | 1 | 2 | n/a | n/a | n/a |
| 2002 | Land Rover | Freelander | off-roader | no | n/a | 1 | 7 | n/a | n/a | n/a |
| 2002 | Land Rover | Range Rover | Large Off-Road 4x4 | no | n/a | 1 | 2 | n/a | n/a | n/a |
| 2002 | Mazda | MX-5 | 2-seater roadster | no | n/a | 1 | 7 | n/a | n/a | n/a |
| 2002 | Mercedes | E-Class | 4 door saloon | no | n/a | 1 | 4 | n/a | n/a | n/a |
| 2002 | Mercedes | M-Class | off-roader | no | n/a | 1 | 4 | n/a | n/a | n/a |
| 2002 | Mercedes | SLK | 2-seater roadster | no | n/a | 1 | 8 | n/a | n/a | n/a |

| Vehicle Information | | | | | Euro NCAP Scores | | | | | |
|---|---|---|---|---|---|---|---|---|---|---|
| | | | | | Overall | Pedestrian Scores | | | | |
| Yr | Make | Model | Ctgry | Pop Up ? | Stars (/5) | Stars (/4) | Pts (/36) | Head (/24) | Pelvis (/6) | Leg (/6) |
| 2002 | Mercedes | Vaneo | 5 door MPV | no | n/a | 2 | 10 | n/a | n/a | n/a |
| 2002 | MINI | One | 3 door hatch | no | n/a | 1 | 8 | n/a | n/a | n/a |
| 2002 | Nissan | Primera | 5 door hatch | no | n/a | 1 | 9 | n/a | n/a | n/a |
| 2002 | Nissan | X Trail | 5 door | no | n/a | 2 | 10 | n/a | n/a | n/a |
| 2002 | Opel/Vauxhall | Corsa | 3 door hatch | no | n/a | 1 | 9 | n/a | n/a | n/a |
| 2002 | Opel/Vauxhall | Frontera | 5 door | no | n/a | 1 | 2 | n/a | n/a | n/a |
| 2002 | Opel/Vauxhall | Vectra | 4 door saloon | no | n/a | 1 | 5 | n/a | n/a | n/a |
| 2002 | Peugeot | 607 | 4 door saloon | no | n/a | 1 | 3 | n/a | n/a | n/a |
| 2002 | Proton | Impian | 4 door saloon | no | n/a | 1 | 4 | n/a | n/a | n/a |
| 2002 | Renault | Megane | 5 door hatch | no | n/a | 2 | 11 | n/a | n/a | n/a |
| 2002 | Saab | 9-3 | 4 door saloon | no | n/a | 1 | 7 | n/a | n/a | n/a |
| 2002 | Seat | Ibiza | 5 door hatch | no | n/a | 2 | 14 | n/a | n/a | n/a |
| 2002 | Suzuki | Grand Vitara | off-roader | no | n/a | 0 | 0 | n/a | n/a | n/a |
| 2002 | Toyota | Corolla | 5 door hatch | no | n/a | 2 | 11 | n/a | n/a | n/a |
| 2002 | VW | Polo | 5 door hatch | no | n/a | 1 | 6 | n/a | n/a | n/a |
| 2003 | Audi | A3 | Small Family | no | n/a | 1 | 8 | n/a | n/a | n/a |
| 2003 | Audi | TT | 2-seater roadster | no | n/a | 0 | 0 | n/a | n/a | n/a |
| 2003 | BMW | X5 | 5 door | no | n/a | 1 | 2 | n/a | n/a | n/a |
| 2003 | Citroen | C2 | Super mini | no | n/a | 2 | 12 | n/a | n/a | n/a |
| 2003 | Citroen | C3 Pluriel | Super mini | no | n/a | 2 | 13 | n/a | n/a | n/a |
| 2003 | Ford | Focus C-MAX | Small MPV | no | n/a | 2 | 14 | n/a | n/a | n/a |
| 2003 | Ford | Fusion | Small MPV | no | n/a | 2 | 11 | n/a | n/a | n/a |
| 2003 | Honda | Accord | 4 door saloon | no | n/a | 2 | 16 | n/a | n/a | n/a |
| 2003 | Hyundai | Trajet | MPV | no | n/a | 1 | 9 | n/a | n/a | n/a |
| | | | | | | | | | | |

| Vehicle Information | | | | | Euro NCAP Scores | | | | | |
|---|---|---|---|---|---|---|---|---|---|---|
| | | | | | Overall | Pedestrian Scores | | | | |
| Yr | Make | Model | Ctgry | Pop Up ? | Stars (/5) | Stars (/4) | Pts (/36) | Head (/24) | Pelvis (/6) | Leg (/6) |
| 2003 | Jeep | Cherokee | Small Off-Road 4x4 | no | n/a | 1 | 3 | n/a | n/a | n/a |
| 2003 | Kia | Carnival/Sedona | MPV | no | n/a | 1 | 4 | n/a | n/a | n/a |
| 2003 | Kia | Sorento | Large Off-Road 4x4 | no | n/a | 1 | 3 | n/a | n/a | n/a |
| 2003 | Mitsubishi | Pajero Pinin | off-roader | no | n/a | 1 | 1 | n/a | n/a | n/a |
| 2003 | Nissan | Micra | Super mini | no | n/a | 2 | 12 | n/a | n/a | n/a |
| 2003 | Opel/Vauxhall | Meriva | Small MPV | no | n/a | 1 | 3 | n/a | n/a | n/a |
| 2003 | Opel/Vauxhall | Signum | 5 door hatch | no | n/a | 1 | 1 | n/a | n/a | n/a |
| 2003 | Peugeot | 807 | MPV | no | n/a | 1 | 6 | n/a | n/a | n/a |
| 2003 | Peugeot | 307CC | Cabriolet | no | n/a | 2 | 10 | n/a | n/a | n/a |
| 2003 | Renault | Espace | MPV | no | n/a | 2 | 10 | n/a | n/a | n/a |
| 2003 | Renault | Kangoo | Small MPV | no | n/a | 1 | 2 | n/a | n/a | n/a |
| 2003 | Renault | Laguna | 5 door hatch | no | n/a | 2 | 12 | n/a | n/a | n/a |
| 2003 | Renault | Scenic | Small MPV | no | n/a | 2 | 11 | n/a | n/a | n/a |
| 2003 | Saab | 9-5 | 4 door saloon | no | n/a | 2 | 12 | n/a | n/a | n/a |
| 2003 | Skoda | Superb | 4 door saloon | no | n/a | 0 | 0 | n/a | n/a | n/a |
| 2003 | Toyota | Avensis | 4 door saloon | no | n/a | 1 | 8 | n/a | n/a | n/a |
| 2003 | Toyota | Previa | MPV | no | n/a | 1 | 5 | n/a | n/a | n/a |
| 2003 | Volvo | XC90 | Large Off-Road 4x4 | no | n/a | 2 | 10 | n/a | n/a | n/a |
| 2003 | VW | Touran | Small MPV | no | n/a | 3 | 19 | n/a | n/a | n/a |
| 2004 | Audi | A6 | 4 door saloon | no | n/a | 1 | 3 | n/a | n/a | n/a |
| 2004 | BMW | 1 Series | 5 door hatch | no | n/a | 1 | 2 | n/a | n/a | n/a |
| 2004 | BMW | 5 Series | Executive | no | n/a | 1 | 2 | n/a | n/a | n/a |
| | | | | | | | | | | |

| Vehicle Information | | | | | Euro NCAP Scores | | | | | |
|---|---|---|---|---|---|---|---|---|---|---|
| | | | | | Overall | Pedestrian Scores | | | | |
| Yr | Make | Model | Ctgry | Pop Up ? | Stars (/5) | Stars (/4) | Pts (/36) | Head (/24) | Pelvis (/6) | Leg (/6) |
| 2004 | BMW | Z4 | 2-seater roadster | no | n/a | 2 | 13 | n/a | n/a | n/a |
| 2004 | Citroen | C4 | Small Family | no | n/a | 3 | 22 | n/a | n/a | n/a |
| 2004 | Citroen | C5 | Large Family | no | n/a | 1 | 8 | n/a | n/a | n/a |
| 2004 | Fiat | Doblo | Small MPV | no | n/a | 1 | 1 | n/a | n/a | n/a |
| 2004 | Fiat | Panda | Super mini | no | n/a | 1 | 6 | n/a | n/a | n/a |
| 2004 | Ford | Focus | 5 door hatch | no | n/a | 2 | 15 | n/a | n/a | n/a |
| 2004 | Honda | Jazz | Super mini | no | n/a | 3 | 19 | n/a | n/a | n/a |
| 2004 | Hyundai | Getz | Super mini | no | n/a | 1 | 5 | n/a | n/a | n/a |
| 2004 | Kia | Picanto | Super mini | no | n/a | 1 | 6 | n/a | n/a | n/a |
| 2004 | Mazda | 2 | Super mini | no | n/a | 2 | 10 | n/a | n/a | n/a |
| 2004 | Opel/Vauxhall | Astra | 5 door hatch | no | n/a | 1 | 3 | n/a | n/a | n/a |
| 2004 | Opel/Vauxhall | Tigra | 2-seater roadster | no | n/a | 2 | 10 | n/a | n/a | n/a |
| 2004 | Peugeot | 407 | 4 door saloon | no | n/a | 2 | 15 | n/a | n/a | n/a |
| 2004 | Renault | Megane CC | Cabriolet | no | n/a | 2 | 11 | n/a | n/a | n/a |
| 2004 | Renault | Modus | Super mini | no | n/a | 1 | 6 | n/a | n/a | n/a |
| 2004 | Saab | 9-3 Convertible | Convertible | no | n/a | 1 | 7 | n/a | n/a | n/a |
| 2004 | Seat | Altea | Small MPV | no | n/a | 3 | 22 | n/a | n/a | n/a |
| 2004 | Skoda | Octavia | Family Saloon | no | n/a | 2 | 17 | n/a | n/a | n/a |
| 2004 | Toyota | Prius | 4 door | no | n/a | 2 | 13 | n/a | n/a | n/a |
| 2004 | Volvo | S40 | Family Saloon | no | n/a | 2 | 18 | n/a | n/a | n/a |
| 2004 | VW | Golf | 5 door hatch | no | n/a | 3 | 19 | n/a | n/a | n/a |
| 2004 | VW | Touareg | Large Off-Road 4x4 | no | n/a | 1 | 7 | n/a | n/a | n/a |

| Vehicle Information | | | | | Euro NCAP Scores | | | | | |
|---|---|---|---|---|---|---|---|---|---|---|
| | | | | | Overall | Pedestrian Scores | | | | |
| Yr | Make | Model | Ctgry | Pop Up ? | Stars (/5) | Stars (/4) | Pts (/36) | Head (/24) | Pelvis (/6) | Leg (/6) |
| 2005 | BMW | 3 Series | Large Family | no | n/a | 1 | 4 | n/a | n/a | n/a |
| 2005 | Chevrolet | Matiz | 5 door hatch | no | n/a | 2 | 13 | n/a | n/a | n/a |
| 2005 | Citroen | C1 | Super mini | no | n/a | 2 | 14 | n/a | n/a | n/a |
| 2005 | Daihatsu | Sirion | 5 door hatch | no | n/a | 2 | 15 | n/a | n/a | n/a |
| 2005 | Fiat | Croma | Large Family | no | n/a | 1 | 6 | n/a | n/a | n/a |
| 2005 | Fiat | Grande Punto | 3 door hatch | no | n/a | 3 | 19 | n/a | n/a | n/a |
| 2005 | Fiat | Stilo | Small Family | no | n/a | 1 | 8 | n/a | n/a | n/a |
| 2005 | Honda | FR-V | Small MPV | no | n/a | 3 | 20 | n/a | n/a | n/a |
| 2005 | Jeep | Grand Cherokee | Large Off-Road 4x4 | no | n/a | 0 | 0 | n/a | n/a | n/a |
| 2005 | Kia | Rio | 5 door hatch | no | n/a | 2 | 13 | n/a | n/a | n/a |
| 2005 | Lexus | GS | Executive | no | n/a | 2 | 18 | n/a | n/a | n/a |
| 2005 | Mazda | 5 | Small MPV | no | n/a | 2 | 12 | n/a | n/a | n/a |
| 2005 | Mazda | 6 | 5 door hatch | no | n/a | 1 | 5 | n/a | n/a | n/a |
| 2005 | Mercedes | A-Class | Small Family | no | n/a | 2 | 17 | n/a | n/a | n/a |
| 2005 | Mitsubishi | Colt | 5 door hatch | no | n/a | 1 | 7 | n/a | n/a | n/a |
| 2005 | Opel/Vauxhall | Zafira | Small MPV | no | n/a | 2 | 16 | n/a | n/a | n/a |
| 2005 | Peugeot | 1007 | 3 door hatch | no | n/a | 2 | 10 | n/a | n/a | n/a |
| 2005 | Peugeot | 407 Coupe | | no | n/a | 2 | 15 | n/a | n/a | n/a |
| 2005 | Renault | Clio | Super mini | no | n/a | 1 | 9 | n/a | n/a | n/a |
| 2005 | Renault | Vel Satis | 4 door saloon | no | n/a | 1 | 2 | n/a | n/a | n/a |
| 2005 | Seat | Leon | 5 door hatch | no | n/a | 3 | 24 | n/a | n/a | n/a |
| 2005 | Smart | forfour | Super mini | no | n/a | 1 | 7 | n/a | n/a | n/a |
| 2005 | Suzuki | Swift | Super mini | no | n/a | 3 | 20 | n/a | n/a | n/a |
| 2005 | Toyota | Yaris | 5 door hatch | no | n/a | 2 | 18 | n/a | n/a | n/a |

| Vehicle Information | | | | | Euro NCAP Scores | | | | | |
|---|---|---|---|---|---|---|---|---|---|---|
| | | | | | Overall | Pedestrian Scores | | | | |
| Yr | Make | Model | Ctgry | Pop Up ? | Stars (/5) | Stars (/4) | Pts (/36) | Head (/24) | Pelvis (/6) | Leg (/6) |
| 2005 | VW | Fox | 3 door hatch | no | n/a | 2 | 12 | n/a | n/a | n/a |
| 2006 | Alfa Romeo | 159 | 4 door saloon | no | n/a | 1 | 9 | n/a | n/a | n/a |
| 2006 | Audi | Q7 | 5 door SUV | no | n/a | 2 | 15 | n/a | n/a | n/a |
| 2006 | Chevrolet | Aveo | 4 door saloon | no | n/a | 3 | 19 | n/a | n/a | n/a |
| 2006 | Chevrolet | Kalos | 5 door hatch | no | n/a | 2 | 11 | n/a | n/a | n/a |
| 2006 | Citroen | C6 | 4 door saloon | yes | n/a | 4 | 28 | n/a | n/a | n/a |
| 2006 | Fiat | Idea | 5 door MPV | no | n/a | 1 | 8 | n/a | n/a | n/a |
| 2006 | Ford | Galaxy | 5 door MPV | no | n/a | 2 | 15 | n/a | n/a | n/a |
| 2006 | Ford | S-MAX | 5 door MPV | no | n/a | 2 | 13 | n/a | n/a | n/a |
| 2006 | Hyundai | Santa Fe | off-roader | no | n/a | 0 | 0 | n/a | n/a | n/a |
| 2006 | Hyundai | Sonata | 5 door sedan | no | n/a | 2 | 12 | n/a | n/a | n/a |
| 2006 | Hyundai | Tucson | 5 door | no | n/a | 1 | 4 | n/a | n/a | n/a |
| 2006 | Kia | Carnival /Sedona | 5 door MPV | no | n/a | 1 | 3 | n/a | n/a | n/a |
| 2006 | Kia | Cerato | 5 door hatch | no | n/a | 1 | 8 | n/a | n/a | n/a |
| 2006 | Kia | Magentis | 4 door saloon | no | n/a | 1 | 3 | n/a | n/a | n/a |
| 2006 | Land Rover | Discovery | Large Off-Road 4x4 | no | n/a | 1 | 8 | n/a | n/a | n/a |
| 2006 | Lexus | IS | 5 door saloon | no | n/a | 2 | 15 | n/a | n/a | n/a |
| 2006 | Mazda | 3 | 5 door hatch | no | n/a | 2 | 15 | n/a | n/a | n/a |
| 2006 | Mercedes | B-Class | 5 door MPV | no | n/a | 2 | 12 | n/a | n/a | n/a |
| 2006 | Nissan | Note | 5 door hatch | no | n/a | 2 | 15 | n/a | n/a | n/a |
| 2006 | Nissan | Pathfinder | 5 door | no | n/a | 2 | 18 | n/a | n/a | n/a |
| 2006 | Opel/Vauxhall | Corsa | 3 door hatch | no | n/a | 3 | 19 | n/a | n/a | n/a |
| 2006 | Peugeot | 207 | 5 door hatch | no | n/a | 3 | 19 | n/a | n/a | n/a |
| 2006 | Skoda | Roomster | 5 door MPV | no | n/a | 2 | 14 | n/a | n/a | n/a |

| Vehicle Information | | | | | Euro NCAP Scores | | | | | |
|---|---|---|---|---|---|---|---|---|---|---|
| | | | | | Overall | Pedestrian Scores | | | | |
| Yr | Make | Model | Ctgry | Pop Up ? | Stars (/5) | Stars (/4) | Pts (/36) | Head (/24) | Pelvis (/6) | Leg (/6) |
| 2006 | Suzuki | SX4 | 5 door hatch | no | n/a | 3 | 22 | n/a | n/a | n/a |
| 2006 | Toyota | Auris | 5 door hatch | no | n/a | 3 | 21 | n/a | n/a | n/a |
| 2006 | Toyota | RAV4 | 5 door SUV | no | n/a | 3 | 21 | n/a | n/a | n/a |
| 2007 | Chrysler | Voyager | 5 door MPV | no | n/a | 0 | 0 | n/a | n/a | n/a |
| 2007 | Daihatsu | Materia | 5 door hatch | no | n/a | 2 | 16 | n/a | n/a | n/a |
| 2007 | Dodge | Caliber | 5 door hatch | no | n/a | 1 | 5 | n/a | n/a | n/a |
| 2007 | Fiat | 500 | 3 door hatch | no | n/a | 2 | 14 | n/a | n/a | n/a |
| 2007 | Fiat | Bravo | 5 door hatch | no | n/a | 2 | 16 | n/a | n/a | n/a |
| 2007 | Ford | Mondeo | 5 door hatch | no | n/a | 2 | 18 | n/a | n/a | n/a |
| 2007 | Honda | Civic Hybrid | 4 door sedan | no | n/a | 3 | 21 | n/a | n/a | n/a |
| 2007 | Honda | CR-V | 5 door SUV | no | n/a | 2 | 13 | n/a | n/a | n/a |
| 2007 | Honda | Legend | 4 door saloon | yes | n/a | 3 | n/a | n/a | n/a | n/a |
| 2007 | Kia | Carens | 5 door MPV | no | n/a | 1 | 9 | n/a | n/a | n/a |
| 2007 | Kia | Cee'd | 5 door hatch | no | n/a | 2 | 11 | n/a | n/a | n/a |
| 2007 | Land Rover | Freelander | 5 door SUV | no | n/a | 1 | 7 | n/a | n/a | n/a |
| 2007 | Mazda | 2 | 5 door hatch | no | n/a | 2 | 18 | n/a | n/a | n/a |
| 2007 | MINI | Cooper | 3 door hatch | no | n/a | 2 | 14 | n/a | n/a | n/a |
| 2007 | Mitsubishi | Outlander | 5 door SUV | no | n/a | 2 | 17 | n/a | n/a | n/a |
| 2007 | Nissan | Qashqai | 5 door | no | n/a | 2 | 18 | n/a | n/a | n/a |
| 2007 | Nissan | X Trail | 5 door SUV | no | n/a | 2 | 12 | n/a | n/a | n/a |
| 2007 | Peugeot | 207CC | 2-seater roadster | no | n/a | 2 | 16 | n/a | n/a | n/a |
| 2007 | Renault | Laguna | 5 door hatch | no | n/a | 2 | 10 | n/a | n/a | n/a |
| 2007 | Renault | Twingo | 3 door hatch | no | n/a | 2 | 11 | n/a | n/a | n/a |
| 2007 | Skoda | Fabia | 5 door hatch | no | n/a | 2 | 17 | n/a | n/a | n/a |

| Vehicle Information | | | | | Euro NCAP Scores | | | | | |
|---|---|---|---|---|---|---|---|---|---|---|
| | | | | | Overall | Pedestrian Scores | | | | |
| Yr | Make | Model | Ctgry | Pop Up ? | Stars (/5) | Stars (/4) | Pts (/36) | Head (/24) | Pelvis (/6) | Leg (/6) |
| 2007 | Smart | fortwo | 2 door | no | n/a | 2 | 10 | n/a | n/a | n/a |
| 2007 | Suzuki | Grand Vitara | 5 door SUV | no | n/a | 3 | 19 | n/a | n/a | n/a |
| 2007 | VW | Caddy | 5 door MPV | no | n/a | 2 | 13 | n/a | n/a | n/a |
| 2007 | VW | Eos | 2 door cabriolet | no | n/a | 2 | 13 | n/a | n/a | n/a |
| 2008 | Alfa Romeo | MiTo | 3 door hatch | no | n/a | 2 | 18 | n/a | n/a | n/a |
| 2008 | BMW | X3 | 5 door SUV | no | n/a | 1 | 5 | n/a | n/a | n/a |
| 2008 | Citroen | Berlingo | 5 door MPV | no | n/a | 2 | 10 | n/a | n/a | n/a |
| 2008 | Daihatsu | Terios | 5 door SUV | no | n/a | 3 | 19 | n/a | n/a | n/a |
| 2008 | Ford | Fiesta | 5 door hatch | no | n/a | 3 | 20 | n/a | n/a | n/a |
| 2008 | Ford | Ka | 3 door hatch | no | n/a | 2 | 11 | n/a | n/a | n/a |
| 2008 | Ford | Kuga | 5 door SUV | no | n/a | 3 | 20 | n/a | n/a | n/a |
| 2008 | Hyundai | i10 | 5 door hatch | no | n/a | 3 | 21 | n/a | n/a | n/a |
| 2008 | Hyundai | i30 | 5 door hatch | no | n/a | 2 | 14 | n/a | n/a | n/a |
| 2008 | Lancia | Delta | 4 door saloon | no | n/a | 2 | 15 | n/a | n/a | n/a |
| 2008 | Mercedes | M-Class | Large Off-Road 4x4 | no | n/a | 1 | 6 | n/a | n/a | n/a |
| 2008 | Mitsubishi | L200 | 4 door pickup | no | n/a | 1 | 2 | n/a | n/a | n/a |
| 2008 | Nissan | Navara | 4 door pickup | no | n/a | 2 | 14 | n/a | n/a | n/a |
| 2008 | Renault | Kangoo | 5 door MPV | no | n/a | 2 | 14 | n/a | n/a | n/a |
| 2008 | Renault | Koleos | Small Off-Road 4x4 | no | n/a | 2 | 14 | n/a | n/a | n/a |
| 2008 | Renault | Megane | 5 door hatch | no | n/a | 2 | 11 | n/a | n/a | n/a |
| 2008 | Seat | Ibiza | 5 door hatch | no | n/a | 3 | 19 | n/a | n/a | n/a |
| 2008 | Suzuki | Splash | 5 door hatch | no | n/a | 3 | 19 | n/a | n/a | n/a |
| 2008 | VW | T5 | MPV | no | n/a | 1 | 3 | n/a | n/a | n/a |

| Vehicle Information | | | | | Euro NCAP Scores | | | | | |
|---|---|---|---|---|---|---|---|---|---|---|
| | | | | | Overall | Pedestrian Scores | | | | |
| Yr | Make | Model | Ctgry | Pop Up ? | Stars (/5) | Stars (/4) | Pts (/36) | Head (/24) | Pelvis (/6) | Leg (/6) |
| 2009 | Audi | A4 | Large Family | no | 5 | n/a | 14 | 7.9 | 0.0 | 6.0 |
| 2009 | Audi | Q5 | Small Off-Road 4x4 | no | 5 | n/a | 12 | 5.5 | 0.0 | 6.0 |
| 2009 | Chevrolet | Cruze | Small Family | no | 5 | n/a | 12 | 6.2 | 0.0 | 6.0 |
| 2009 | Chevrolet | Spark | Super mini | no | 4 | n/a | 16 | 9.6 | 0.0 | 6.0 |
| 2009 | Citroen | C3 | Super mini | no | 4 | n/a | 12 | 5.8 | 0.0 | 6.0 |
| 2009 | Citroen | C3 Picasso | Small MPV | no | 4 | n/a | 16 | 5.6 | 4.0 | 6.0 |
| 2009 | Citroen | C4 Picasso | Small MPV | no | 5 | n/a | 16 | 8.0 | 2.4 | 6.0 |
| 2009 | Citroen | C5 | Large Family | no | 5 | n/a | 11 | 5.4 | 0.0 | 6.0 |
| 2009 | Citroen | DS3 | Super mini | no | 5 | n/a | 13 | 6.3 | 0.3 | 5.9 |
| 2009 | Honda | Accord | Large Family | no | 5 | n/a | 19 | 13.3 | 0.0 | 6.0 |
| 2009 | Honda | Civic | Small Family | no | 5 | n/a | 24 | 12.2 | 6.0 | 6.0 |
| 2009 | Honda | Insight Hybrid | Small Family | no | 5 | n/a | 27 | 15.4 | 6.0 | 6.0 |
| 2009 | Honda | Jazz | Super mini | no | 5 | n/a | 22 | 10.4 | 5.2 | 6.0 |
| 2009 | Hyundai | i20 | Super mini | no | 5 | n/a | 23 | 12.0 | 5.2 | 5.8 |
| 2009 | Infiniti | FX | Large Off-Road 4x4 | no | 5 | n/a | 16 | 10.2 | 1.6 | 4.2 |
| 2009 | Kia | Sorento | Large Off-Road 4x4 | no | 5 | n/a | 16 | 10.2 | 0.0 | 5.7 |
| 2009 | Kia | Soul | Small MPV | no | 5 | n/a | 14 | 8.0 | 0.0 | 5.9 |
| 2009 | Mazda | 3 | Small Family | no | 5 | n/a | 18 | 10.2 | 2.0 | 6.0 |
| 2009 | Mazda | 6 | Large Family | no | 5 | n/a | 18 | 10.1 | 1.5 | 6.0 |
| 2009 | Mercedes | C-Class | Large Family | no | 5 | n/a | 11 | 3.7 | 1.5 | 5.6 |
| 2009 | Mitsubishi | Lancer | Small Family | no | 5 | n/a | 12 | 7.5 | 0.0 | 4.7 |
| 2009 | Opel/Vauxhall | Astra | Small Family | no | 5 | n/a | 16 | 10.4 | 0.0 | 6.0 |

| Vehicle Information | | | | | Euro NCAP Scores | | | | | |
|---|---|---|---|---|---|---|---|---|---|---|
| | | | | | Overall | Pedestrian Scores | | | | |
| Yr | Make | Model | Ctgry | Pop Up ? | Stars (/5) | Stars (/4) | Pts (/36) | Head (/24) | Pelvis (/6) | Leg (/6) |
| 2009 | Opel/Vauxhall | Insignia | Large Family | no | 5 | n/a | 14 | 8.3 | 0.0 | 6.0 |
| 2009 | Peugeot | 308 | Small Family | no | 5 | n/a | 19 | 7.7 | 5.3 | 6.0 |
| 2009 | Peugeot | 3008 | Small Family | no | 5 | n/a | 11 | 3.0 | 2.1 | 6.0 |
| 2009 | Peugeot | 5008 | Small MPV | no | 5 | n/a | 13 | 7.4 | 0.0 | 6.0 |
| 2009 | Peugeot | 308CC | Small Family | no | 5 | n/a | 12 | 4.9 | 0.8 | 6.0 |
| 2009 | Renault | Grand Scenic | Small MPV | no | 5 | n/a | 15 | 6.8 | 2.3 | 6.0 |
| 2009 | Saab | 9-5 | 4 door saloon | no | 5 | n/a | 16 | 9.9 | 0.0 | 6.0 |
| 2009 | Skoda | Superb | 5 door saloon | no | 5 | n/a | 18 | 12.0 | 0.0 | 6.0 |
| 2009 | Skoda | Yeti | 5 door SUV | no | 5 | n/a | 17 | 10.7 | 0.0 | 6.0 |
| 2009 | Subaru | Impreza | 5 door hatch | no | 4 | n/a | 26 | 16.2 | 3.6 | 6.0 |
| 2009 | Subaru | Legacy | 5 door | no | 5 | n/a | 21 | 15.1 | 0.0 | 5.8 |
| 2009 | Suzuki | Alto | Super mini | no | 3 | n/a | 13 | 9.5 | 0.0 | 3.3 |
| 2009 | Toyota | Avensis | Large Family | no | 5 | n/a | 19 | 12.6 | 0.5 | 6.0 |
| 2009 | Toyota | iQ | Super mini | no | 5 | n/a | 19 | 11.8 | 1.7 | 6.0 |
| 2009 | Toyota | Prius | Large Family | no | 5 | n/a | 24 | 14.9 | 4.3 | 5.2 |
| 2009 | Toyota | Urban Cruiser | Small MPV | no | 3 | n/a | 19 | 13.1 | 0.0 | 5.9 |
| 2009 | Volvo | C30 | Small Family | no | 5 | n/a | 9 | 5.2 | 0.0 | 4.0 |
| 2009 | Volvo | V70 | Large Family | no | 5 | n/a | 16 | 9.6 | 0.0 | 6.0 |
| 2009 | Volvo | XC60 | Small Off-Road 4x4 | no | 5 | n/a | 17 | 11.3 | 0.0 | 6.0 |
| 2009 | VW | Golf | Small Family | no | 5 | n/a | 22 | 12.0 | 3.9 | 6.0 |
| 2009 | VW | Polo | Super mini | no | 5 | n/a | 15 | 8.5 | 2.4 | 4.0 |
| 2009 | VW | Scirocco | Small Family | no | 5 | n/a | 19 | 7.1 | 6.0 | 6.0 |
| 2009 | VW | Tiguan | Small Off-Road 4x4 | no | 5 | n/a | 17 | 11.2 | 0.0 | 6.0 |

| Vehicle Information | | | | | Euro NCAP Scores | | | | | |
|---|---|---|---|---|---|---|---|---|---|---|
| | | | | | Overall | Pedestrian Scores | | | | |
| Yr | Make | Model | Ctgry | Pop Up ? | Stars (/5) | Stars (/4) | Pts (/36) | Head (/24) | Pelvis (/6) | Leg (/6) |
| 2010 | Alfa Romeo | Giulietta | Small Family | no | 5 | n/a | 23 | 13.5 | 3.1 | 6.0 |
| 2010 | Audi | A1 | Super mini | no | 5 | n/a | 18 | 11.6 | 0.2 | 6.0 |
| 2010 | BMW | 5 Series | Executive | yes | 5 | n/a | 28 | 22.0 | 0.0 | 6.0 |
| 2010 | Citroen | C4 | Small Family | no | 5 | n/a | 15 | 7.9 | 4.5 | 6.0 |
| 2010 | Citroen | Nemo | Small MPV | no | 3 | n/a | 20 | 9.0 | 4.8 | 6.0 |
| 2010 | Ford | C-MAX | Small MPV | no | 5 | n/a | 18 | 13.0 | 0.9 | 4.0 |
| 2010 | Ford | Grand C-MAX | Small MPV | no | 5 | n/a | 18 | 13.0 | 0.9 | 4.0 |
| 2010 | Honda | CR-Z | Super mini | no | 5 | n/a | 25 | 15.5 | 6.0 | 4.0 |
| 2010 | Hyundai | ix35 | Small Off-Road 4x4 | no | 5 | n/a | 20 | 14.0 | 0.0 | 5.6 |
| 2010 | Kia | Sportage | Small Off-Road 4x4 | no | 5 | n/a | 18 | 11.6 | 1.2 | 4.9 |
| 2010 | Kia | Venga | Small Off-Road 4x4 | no | 5 | n/a | 23 | 12.8 | 4.2 | 6.0 |
| 2010 | Mazda | CX-7 | Small Off-Road 4x4 | no | 4 | n/a | 16 | 6.5 | 3.1 | 6.0 |
| 2010 | Mercedes | E-Class | Executive | yes | 5 | n/a | 21 | 15.2 | 0.0 | 6.0 |
| 2010 | MINI | Countryman | Small MPV | no | 5 | n/a | 23 | 15.3 | 1.5 | 6.0 |
| 2010 | Nissan | Cube | Small MPV | no | 4 | n/a | 20 | 14.0 | 0.3 | 6.0 |
| 2010 | Nissan | Micra | Super mini | no | 4 | n/a | 21 | 13.4 | 1.6 | 6.0 |
| 2010 | Opel/Vauxhall | Meriva | Small MPV | no | 5 | n/a | 20 | 15.0 | 0.9 | 4.0 |
| 2010 | Seat | Alhambra | Large MPV | no | 5 | n/a | 16 | 12.4 | 0.0 | 4.0 |
| 2010 | Seat | Exeo | 4 door saloon | no | 4 | n/a | 18 | 12.2 | 0.0 | 5.9 |
| 2010 | Suzuki | Swift | 5 door hatch | no | 5 | n/a | 22 | 18.4 | 0.0 | 4.0 |
| 2010 | Toyota | Verso | Small MPV | no | 5 | n/a | 25 | 18.8 | 0.0 | 6.0 |

| Vehicle Information | | | | | Euro NCAP Scores | | | | | |
|---|---|---|---|---|---|---|---|---|---|---|
| | | | | | Overall | Pedestrian Scores | | | | |
| Yr | Make | Model | Ctgry | Pop Up ? | Stars (/5) | Stars (/4) | Pts (/36) | Head (/24) | Pelvis (/6) | Leg (/6) |
| 2010 | VW | Passat | Large Family | no | 5 | n/a | 19 | 14.0 | 0.0 | 5.3 |
| 2010 | VW | Sharan | Large MPV | no | 5 | n/a | 16 | 12.4 | 0.0 | 4.0 |
| 2011 | Audi | A6 | Executive | no | 5 | n/a | 15 | 8.7 | 0.0 | 6.0 |
| 2011 | Audi | Q3 | Small Off-Road 4x4 | no | 5 | n/a | 19 | 12.8 | 0.0 | 6.0 |
| 2011 | BMW | X3 | Small Off-Road 4x4 | no | 5 | n/a | 19 | 13.1 | 0.0 | 6.0 |
| 2011 | Chevrolet | Aveo | Super mini | no | 5 | n/a | 19 | 13.7 | 0.2 | 5.3 |
| 2011 | Chevrolet | Captiva | Small Off-Road 4x4 | no | 5 | n/a | 17 | 14.0 | 0.0 | 3.3 |
| 2011 | Chevrolet | Orlando | Small MPV | no | 5 | n/a | 18 | 13.1 | 0.0 | 4.5 |
| 2011 | Chevrolet | Volt | Small Family | no | 5 | n/a | 15 | 8.9 | 0.0 | 6.0 |
| 2011 | Citroen | C-Zero | Super mini | no | 4 | n/a | 17 | 11.2 | 0.0 | 6.0 |
| 2011 | Citroen | DS4 | Small Family | no | 5 | n/a | 15 | 7.5 | 2.0 | 6.0 |
| 2011 | Citroen | DS5 | Large Family | no | 5 | n/a | 15 | 6.3 | 2.2 | 6.0 |
| 2011 | Dacia | Duster | Small Off-Road 4x4 | no | 3 | n/a | 10 | 10.0 | 0.0 | 0.0 |
| 2011 | Fiat | Freemont | Large MPV | yes | 5 | n/a | 18 | 12.0 | 0.0 | 6.0 |
| 2011 | Fiat | Panda | Super mini | no | 4 | n/a | 18 | 10.7 | 0.8 | 6.0 |
| 2011 | Hyundai | i40 | Large Family | no | 5 | n/a | 16 | 8.1 | 1.5 | 6.0 |
| 2011 | Hyundai | ix20 | Small MPV | no | 5 | n/a | 23 | 12.8 | 4.2 | 6.0 |
| 2011 | Hyundai | Veloster | Small Family | no | 5 | n/a | 18 | 7.3 | 4.4 | 6.0 |
| 2011 | Jaguar | XF | Executive | yes | 4 | n/a | 22 | 16.2 | 0.0 | 6.0 |
| 2011 | Jeep | Grand Cherokee | Large Off-Road 4x4 | no | 4 | n/a | 16 | 10.1 | 0.0 | 6.0 |

| Vehicle Information | | | | | Euro NCAP Scores | | | | | |
|---|---|---|---|---|---|---|---|---|---|---|
| | | | | | Overall | Pedestrian Scores | | | | |
| Yr | Make | Model | Ctgry | Pop Up ? | Stars (/5) | Stars (/4) | Pts (/36) | Head (/24) | Pelvis (/6) | Leg (/6) |
| 2011 | Kia | Picanto | Super mini | no | 4 | n/a | 17 | 9.2 | 1.5 | 6.0 |
| 2011 | Kia | Rio | Super mini | no | 5 | n/a | 17 | 11.3 | 0.0 | 5.4 |
| 2011 | Lancia | Thema | Executive | yes | 5 | n/a | 21 | 15.3 | 0.0 | 6.0 |
| 2011 | Lancia | Voyager | Large MPV | yes | 4 | n/a | 17 | 11.0 | 0.0 | 6.0 |
| 2011 | Land Rover | Range Rover Evoque | Small Off-Road 4x4 | no | 5 | n/a | 15 | 8.8 | 0.0 | 6.0 |
| 2011 | Lexus | CT200h | Small Family | no | 5 | n/a | 20 | 13.5 | 0.2 | 6.0 |
| 2011 | Mercedes | B-Class | Small MPV | no | 5 | n/a | 20 | 14.1 | 0.0 | 6.0 |
| 2011 | Mercedes | C-Class Coupe | Small Family | yes | 5 | n/a | 21 | 14.6 | 0.0 | 6.0 |
| 2011 | Mitsubishi | ASX | Small Family | no | 5 | n/a | 22 | 17.6 | 0.0 | 4.0 |
| 2011 | Mitsubishi | i-MiEV | Super mini | no | 4 | n/a | 17 | 11.2 | 0.0 | 6.0 |
| 2011 | Nissan | Juke | Super mini | no | 5 | n/a | 15 | 9.5 | 0.8 | 4.4 |
| 2011 | Opel/Vauxhall | Ampera | Small Family | no | 5 | n/a | 15 | 8.9 | 0.0 | 6.0 |
| 2011 | Opel/Vauxhall | Astra GTC | Small Family | no | 5 | n/a | 18 | 12.0 | 0.0 | 6.0 |
| 2011 | Opel/Vauxhall | Zafira Tourer | Small MPV | no | 5 | n/a | 19 | 14.0 | 0.0 | 4.9 |
| 2011 | Peugeot | 508 | Large Family | no | 5 | n/a | 15 | 9.1 | 1.5 | 4.0 |
| 2011 | Peugeot | iOn | Super mini | no | 4 | n/a | 17 | 11.2 | 0.0 | 6.0 |
| 2011 | Renault | Fluence ZE | Small Family | no | 4 | n/a | 13 | 7.2 | 0.1 | 6.0 |
| 2011 | Seat | Ibiza | Super mini | no | 5 | n/a | 21 | 15.3 | 0.0 | 6.0 |
| 2011 | Seat | Mii | Super mini | no | 5 | n/a | 17 | 11.7 | 0.0 | 4.9 |
| 2011 | Skoda | Citigo | 3 door hatch | no | 5 | n/a | 17 | 11.7 | 0.0 | 4.9 |
| 2011 | Toyota | Yaris | Super mini | no | 5 | n/a | 21 | 15.3 | 0.1 | 6.0 |
| 2011 | VW | Beetle | Small Family | no | 5 | n/a | 19 | 15.0 | 0.0 | 4.0 |
| 2011 | VW | Golf Cabriolet | Small Family | no | 5 | n/a | 19 | 11.3 | 3.9 | 3.8 |
| | | | | | | | | | | |

| Vehicle Information | | | | | Euro NCAP Scores | | | | | |
|---|---|---|---|---|---|---|---|---|---|---|
| | | | | | Overall | Pedestrian Scores | | | | |
| Yr | Make | Model | Ctgry | Pop Up ? | Stars (/5) | Stars (/4) | Pts (/36) | Head (/24) | Pelvis (/6) | Leg (/6) |
| 2011 | VW | Jetta | Small Family | no | 5 | n/a | 20 | 11.7 | 2.5 | 6.0 |
| 2011 | VW | up! | Super mini | no | 5 | n/a | 17 | 11.7 | 0.0 | 4.9 |
| 2012 | Audi | A3 | Small Family | no | 5 | n/a | 27 | 19.6 | 1.0 | 6.0 |
| 2012 | BMW | 1 Series | Small Family | no | 5 | n/a | 23 | 16.6 | 0.0 | 6.0 |
| 2012 | BMW | 3 Series | Large Family | no | 5 | n/a | 28 | 15.9 | 6.0 | 6.0 |
| 2012 | BMW | X1 | Small Off-Road 4x4 | no | 5 | n/a | 23 | 16.9 | 0.0 | 6.0 |
| 2012 | Citroen | C1 | Super mini | no | 3 | n/a | 19 | 13.2 | 0.0 | 6.0 |
| 2012 | Citroen | Jumpy | Van-based people carrier | no | 3 | n/a | 8 | 7.8 | n/a | 0.0 |
| 2012 | Fiat | 500L | Small MPV | no | 5 | n/a | 23 | 15.0 | 2.5 | 6.0 |
| 2012 | Fiat | Scudo | Van-based people carrier | no | 3 | n/a | 8 | 7.8 | 0.0 | 0.0 |
| 2012 | Ford | B-MAX | Small MPV | no | 5 | n/a | 24 | 15.0 | 3.0 | 6.0 |
| 2012 | Ford | Fiesta | Super mini | no | 5 | n/a | 23 | 12.2 | 5.1 | 6.0 |
| 2012 | Ford | Focus | Small Family | no | 5 | n/a | 26 | 16.0 | 6.0 | 4.0 |
| 2012 | Ford | Kuga | Small Off-Road 4x4 | no | 5 | n/a | 25 | 15.4 | 3.7 | 6.0 |
| 2012 | Honda | Civic | Small Family | no | 5 | n/a | 25 | 12.9 | 6.0 | 6.0 |
| 2012 | Hyundai | H-1 | Van-based people carrier | no | 3 | n/a | 10 | 4.2 | n/a | 6.0 |
| 2012 | Hyundai | i30 | Small Family | no | 5 | n/a | 24 | 14.3 | 4.0 | 6.0 |
| 2012 | Hyundai | Santa Fe | Large Off-Road 4x4 | yes | 5 | n/a | 25 | 18.6 | 0.9 | 6.0 |
| 2012 | Isuzu | D-Max | 4 door pickup | no | 4 | n/a | 18 | 12.4 | 0.0 | 6.0 |

| Vehicle Information | | | | | Euro NCAP Scores | | | | | |
|---|---|---|---|---|---|---|---|---|---|---|
| | | | | | Overall | Pedestrian Scores | | | | |
| Yr | Make | Model | Ctgry | Pop Up ? | Stars (/5) | Stars (/4) | Pts (/36) | Head (/24) | Pelvis (/6) | Leg (/6) |
| 2012 | Jeep | Compass | Small Off-Road 4x4 | no | 2 | n/a | 8 | 8.4 | 0.0 | 0.0 |
| 2012 | Kia | Cee'd | Small Family | no | 5 | n/a | 22 | 12.6 | 3.6 | 5.8 |
| 2012 | Land Rover | Range Rover | Large Off-Road 4x4 | no | 5 | n/a | 23 | 16.6 | 0.0 | 6.0 |
| 2012 | Mazda | CX-5 | Small Off-Road 4x4 | no | 5 | n/a | 23 | 17.0 | 0.2 | 6.0 |
| 2012 | Mercedes | A-Class | Small Family | yes | 5 | n/a | 24 | 18.0 | 0.0 | 6.0 |
| 2012 | Mercedes | M-Class | Large Off-Road 4x4 | yes | 5 | n/a | 21 | 17.4 | 0.0 | 4.0 |
| 2012 | Mitsubishi | Outlander | Small Off-Road 4x4 | no | 5 | n/a | 23 | 16.9 | 0.0 | 6.0 |
| 2012 | Nissan | Leaf | Small Family | no | 5 | n/a | 23 | 15.2 | 3.0 | 5.1 |
| 2012 | Opel/Vauxhall | Mokka | Small Family | no | 5 | n/a | 24 | 18.0 | 0.0 | 6.0 |
| 2012 | Peugeot | 107 | Super mini | no | 3 | n/a | 19 | 13.2 | 0.0 | 6.0 |
| 2012 | Peugeot | 208 | Super mini | no | 5 | n/a | 22 | 12.5 | 3.5 | 6.0 |
| 2012 | Peugeot | Expert | Van-based people carrier | no | 3 | n/a | 8 | 7.8 | n/a | 0.0 |
| 2012 | Renault | Clio | Super mini | no | 5 | n/a | 24 | 11.8 | 5.9 | 6.0 |
| 2012 | Renault | Trafic | Passenger Van | no | 2 | n/a | 8 | 8.5 | n/a | 0.0 |
| 2012 | Seat | Leon | 5 door hatch | no | 5 | n/a | 25 | 16.9 | 2.2 | 6.0 |
| 2012 | Seat | Toledo | 5 door hatch | no | 5 | n/a | 25 | 16.6 | 2.1 | 6.0 |
| 2012 | Skoda | Rapid | 5 door hatch | no | 5 | n/a | 25 | 16.6 | 2.1 | 6.0 |
| 2012 | Subaru | Forester | 5 door SUV | no | 5 | n/a | 26 | 20.3 | 0.0 | 6.0 |
| | | | | | | | | | | |

| Vehicle Information | | | | | Euro NCAP Scores | | | | | |
|---|---|---|---|---|---|---|---|---|---|---|
| | | | | | Overall | Pedestrian Scores | | | | |
| Yr | Make | Model | Ctgry | Pop Up ? | Stars (/5) | Stars (/4) | Pts (/36) | Head (/24) | Pelvis (/6) | Leg (/6) |
| 2012 | Subaru | XV | 5 door hatch | no | 5 | n/a | 23 | 16.9 | 0.0 | 6.0 |
| 2012 | Toyota | Aygo | Super mini | no | 3 | n/a | 19 | 13.2 | 0.0 | 6.0 |
| 2012 | Volvo | V40 | Small Family | yes | 5 | n/a | 32 | 24.0 | 2.0 | 5.8 |
| 2012 | Volvo | V60 | Large Family | no | 5 | n/a | 23 | 14.7 | 2.8 | 5.7 |
| 2012 | VW | Golf | Small Family | no | 5 | n/a | 24 | 14.8 | 2.8 | 6.0 |
| 2013 | BMW | i3 | Small Family | no | 4 | n/a | 21 | 14.8 | 0.0 | 6.0 |
| 2013 | Chevrolet | Trax | Small Family | no | 5 | n/a | 23 | 17.1 | 0.0 | 6.0 |
| 2013 | Citroen | C4 Picasso | Small MPV | no | 5 | n/a | 25 | 15.3 | 3.3 | 6.0 |
| 2013 | Dacia | Sandero | Super mini | no | 4 | n/a | 21 | 14.8 | 0.0 | 6.0 |
| 2013 | Ford | EcoSport | Small Family | no | 4 | n/a | 21 | 14.7 | 0.4 | 6.0 |
| 2013 | Ford | Tourneo Connect | Small MPV | no | 5 | n/a | 22 | 16.2 | 0.3 | 6.0 |
| 2013 | Honda | CR-V | Small Off-Road 4x4 | no | 5 | n/a | 25 | 15.8 | 2.9 | 6.0 |
| 2013 | Infiniti | Q50 | Executive | yes | 5 | n/a | 24 | 19.1 | 0.0 | 5.1 |
| 2013 | Jeep | Cherokee | Small Off-Road 4x4 | no | 5 | n/a | 24 | 16.9 | 1.6 | 6.0 |
| 2013 | Kia | Carens | Small MPV | no | 5 | n/a | 23 | 15.4 | 1.7 | 6.0 |
| 2013 | Lexus | IS 300h | Large Family | yes | 5 | n/a | 29 | 16.9 | 6.0 | 6.0 |
| 2013 | Maserati | Ghibli | Executive | no | 5 | n/a | 27 | 14.8 | 6.0 | 6.0 |
| 2013 | Mazda | 3 | Small Family | no | 5 | n/a | 24 | 17.1 | 0.5 | 6.0 |
| 2013 | Mazda | 6 | Large Family | no | 5 | n/a | 24 | 17.8 | 0.0 | 6.0 |
| 2013 | Mercedes | CITAN Kombi | Small MPV | no | 4 | n/a | 20 | 14.0 | 0.5 | 5.9 |
| 2013 | Mercedes | CLA-Class | Small Family | yes | 5 | n/a | 27 | 17.0 | 4.0 | 6.0 |
| 2013 | Mitsubishi | Space Star/Mirage | Super mini | no | 4 | n/a | 26 | 16.5 | 3.8 | 6.0 |
| | | | | | | | | | | |

| Vehicle Information | | | | | Euro NCAP Scores | | | | | |
|---|---|---|---|---|---|---|---|---|---|---|
| | | | | | Overall | Pedestrian Scores | | | | |
| Yr | Make | Model | Ctgry | Pop Up ? | Stars (/5) | Stars (/4) | Pts (/36) | Head (/24) | Pelvis (/6) | Leg (/6) |
| 2013 | Nissan | Evalia | Small MPV | no | 3 | n/a | 24 | 14.4 | 5.0 | 4.8 |
| 2013 | Nissan | Note | Super mini | no | 4 | n/a | 21 | 15.0 | 0.0 | 6.0 |
| 2013 | Opel/Vauxhall | Adam | Super mini | no | 4 | n/a | 24 | 13.6 | 4.0 | 6.0 |
| 2013 | Peugeot | 308 | Small Family | no | 5 | n/a | 23 | 12.2 | 5.2 | 6.0 |
| 2013 | Peugeot | 2008 | Super mini | no | 5 | n/a | 26 | 16.0 | 4.2 | 6.0 |
| 2013 | Renault | CAPTUR | Super mini | no | 5 | n/a | 22 | 13.4 | 2.7 | 6.0 |
| 2013 | Renault | ZOE | Super mini | no | 5 | n/a | 24 | 14.2 | 3.9 | 6.0 |
| 2013 | Skoda | Octavia | 5 door hatch | no* | 5 | n/a | 24 | 16.5 | 1.6 | 6.0 |
| 2013 | Suzuki | SX4 | Small Family | no | 5 | n/a | 26 | 20.2 | 0.0 | 6.0 |
| 2013 | Toyota | Auris | Small Family | no | 5 | n/a | 25 | 16.8 | 2.0 | 6.0 |
| 2013 | Toyota | RAV4 | Small Off-Road 4x4 | no | 5 | n/a | 24 | 18.0 | 0.0 | 6.0 |
| 2013 | VW | T5 | Business and family van | no | 4 | n/a | 10 | 9.8 | 0.0 | 0.0 |
| 2014 | Audi | A3 Saloon | Small Family | yes | 5 | n/a | 24 | 18.0 | 0.1 | 6.0 |
| 2014 | BMW | 2 Series Active Tourer | Small Family | yes | 5 | n/a | 22 | 14.9 | 2.0 | 4.9 |
| 2014 | Citroen | Berlingo | Small MPV | no | 3 | n/a | 23 | 13.3 | 3.5 | 6.0 |
| 2014 | Citroen | C4 Cactus | Small Family | no | 4 | n/a | 29 | 17.1 | 6.0 | 6.0 |
| 2014 | Dacia | Logan MCV | Small MPV | no | 3 | n/a | 20 | 14.8 | 0.0 | 5.2 |
| 2014 | Ford | Mondeo | Large Family | no | 5 | n/a | 24 | 17.9 | 0.0 | 6.0 |
| 2014 | Ford | Tourneo Courier | Super mini | no | 4 | n/a | 27 | 16.3 | 4.6 | 6.0 |
| 2014 | Hyundai | i10 | Super mini | no | 4 | n/a | 26 | 16.0 | 3.7 | 6.0 |
| 2014 | Kia | Sorento | Large Off-Road 4x4 | yes | 5 | n/a | 24 | 18.3 | 0.0 | 5.9 |
| | | | | | | | | | | |

| Vehicle Information | | | | | Euro NCAP Scores | | | | | |
|---|---|---|---|---|---|---|---|---|---|---|
| | | | | | Overall | Pedestrian Scores | | | | |
| Yr | Make | Model | Ctgry | Pop Up ? | Stars (/5) | Stars (/4) | Pts (/36) | Head (/24) | Pelvis (/6) | Leg (/6) |
| 2014 | Kia | Soul | Small MPV | no | 4 | n/a | 21 | 15.3 | 0.0 | 6.0 |
| 2014 | Kia | Soul EV | Small MPV | no | 4 | n/a | 21 | 15.3 | 0.0 | 6.0 |
| 2014 | Land Rover | Discovery Sport | Small Off-Road 4x4 | yes | 5 | n/a | 25 | 19.2 | 0.0 | 5.9 |
| 2014 | Lexus | NX | Small Off-Road 4x4 | no | 5 | n/a | 25 | 18.8 | 0.1 | 6.0 |
| 2014 | Mercedes | C-Class | Large Family | yes | 5 | n/a | 28 | 21.0 | 0.8 | 5.9 |
| 2014 | Mercedes | GLA-class | Small Off-Road 4x4 | yes | 5 | n/a | 24 | 18.4 | 0.0 | 6.0 |
| 2014 | MG Motor | MG 3 | Super mini | no | 3 | n/a | 21 | 16.4 | 0.0 | 5.1 |
| 2014 | Mini | Cooper (F56) | Super mini | yes | 4 | n/a | 24 | 18.1 | 0.0 | 6.0 |
| 2014 | Nissan | Pulsar | Small Family | no | 5 | n/a | 27 | 15.8 | 5.5 | 6.0 |
| 2014 | Nissan | Qashqai | Small Family | no | 5 | n/a | 25 | 15.8 | 3.1 | 6.0 |
| 2014 | Nissan | X Trail | Small Off-Road 4x4 | no | 5 | n/a | 27 | 15.4 | 5.8 | 6.0 |
| 2014 | Opel/Vauxhall | Corsa | Super mini | no | 4 | n/a | 26 | 14.3 | 5.3 | 6.0 |
| 2014 | Porsche | Macan | Small Off-Road 4x4 | no | 5 | n/a | 22 | 15.6 | 0.0 | 6.0 |
| 2014 | Renault | Megane Hatch | Small Family | no | 4 | n/a | 22 | 14.2 | 1.6 | 6.0 |
| 2014 | Renault | Twingo | Super mini | no | 4 | n/a | 25 | 15.3 | 3.2 | 6.0 |
| 2014 | Skoda | Fabia | Super mini | no | 5 | n/a | 25 | 14.6 | 4.4 | 6.0 |
| 2014 | Smart | forfour | Super mini | no | 4 | n/a | 24 | 15.2 | 2.4 | 6.0 |
| 2014 | Smart | fortwo | Super mini | no | 4 | n/a | 20 | 13.3 | 1.2 | 6.0 |
| 2014 | Subaru | Outback | Large Family | no | 5 | n/a | 25 | 18.9 | 0.4 | 6.0 |
| 2014 | Tesla | Model S | Executive | yes | 5 | n/a | 24 | 13.9 | 4.1 | 5.8 |

| Vehicle Information | | | | | Euro NCAP Scores | | | | | |
|---|---|---|---|---|---|---|---|---|---|---|
| | | | | | Overall | Pedestrian Scores | | | | |
| Yr | Make | Model | Ctgry | Pop Up ? | Stars (/5) | Stars (/4) | Pts (/36) | Head (/24) | Pelvis (/6) | Leg (/6) |
| 2014 | Toyota | Aygo | Super mini | no | 4 | n/a | 23 | 16.3 | 0.2 | 6.0 |
| 2014 | VW | Golf Sportsvan | Small MPV | no | 5 | n/a | 22 | 16.4 | 0.0 | 6.0 |
| 2014 | VW | Passat | Large Family | no | 5 | n/a | 24 | 15.3 | 2.6 | 6.0 |
| 2007 | Jaguar | XK | | yes | | | | | | |
| 2009 | Nissan | GT-R | | yes | | | | | | |
| 2009 | Porsche | Panamera | | yes | | | | | | |
| 2011 | Peugeot | RCZ | | yes | | | | | | |
| 2012 | BMW | 6-Series Coupe | | yes | | | | | | |

| Vehicle Information | | | | | Euro NCAP Scores | | | | | |
|---|---|---|---|---|---|---|---|---|---|---|
| | | | | | Overall | Pedestrian Scores | | | | |
| Yr | Make | Model | Ctgry | Pop Up ? | Stars (/5) | Stars (/4) | Pts (/36) | Head (/24) | Pelvis (/6) | Leg (/6) |
| 2013 | Cadillac | ATS | | yes | | | | | | |
| 2013 | Cadillac | CTS | | yes | | | | | | |
| 2013 | Fiat | Punto | | yes | | | | | | |
| 2013 | Mazda | MX-5 Roadster (Miata) | | yes | | | | | | |
| 2014 | Aston Martin | DB9 | | yes | | | | | | |
| 2014 | Aston Martin | Vanquish | | yes | | | | | | |
| 2014 | Jaguar | F-type | | yes | | | | | | |

*The Skoda Octavia was originally to be sold with a pop-up hood as standard equipment and was tested by Euro NCAP as such. Later, Skoda announced the pop-up hood would no longer be included as standard, so Euro NCAP retested the vehicle without the pop-up hood. The scores on the report for this vehicle are for the test without the pop-up hood deployment [10].

**APPENDIX B**

**Table 3. Vehicles With Pop-up Hoods and Euro NCAP Scores**

| Year | Make | Model |
|---|---|---|
| 2006 | Citroen | C6 |
| 2007 | Honda | Legend |
| 2010 | BMW | 5-series |
| 2010 | Mercedes | E-class |
| 2011 | Fiat | Freemont |
| 2011 | Lancia | Thema |
| 2011 | Lancia | Voyager |
| 2011 | Mercedes | C-Class Coupe |
| 2012 | Hyundai | Santa Fe |
| 2012 | Jaguar | XF |
| 2012 | Mercedes | M-Class |
| 2012 | Volvo | V40 |
| 2013 | Infiniti | Q50 |
| 2013 | Lexus | IS 300h |
| 2013 | Mercedes | A-Class |
| 2013 | Mercedes | CLA-Class |
| 2014 | Audi | A3 Saloon |
| 2014 | BMW | 2 Series Active Tourer |
| 2014 | Kia | Sorento |
| 2014 | Land Rover | Discovery Sport |
| 2014 | Mercedes | C-Class |
| 2014 | Mercedes | GLA-Class |
| 2014 | Mini | Cooper (F56) |
| 2014 | Tesla | Model S |

This paper has been peer-reviewed and published in a special edition of *Traffic Injury Prevention* 16(S1), by Taylor & Francis Group. The complete paper will be available on the *Traffic Injury Prevention and www.NHTSA.gov* websites on June 8, 2015.

To access all Peer-reviewed papers please copy and paste the link below into your browser to access the papers.

http://www.tandfonline.com/toc/gcpi20/16/sup1

This paper has been peer-reviewed and published in a special edition of *Traffic Injury Prevention* 16(S1), by Taylor & Francis Group. The complete paper will be available on the *Traffic Injury Prevention and www.NHTSA.gov* websites on June 8, 2015.

To access all Peer-reviewed papers please copy and paste the link below into your browser to access the papers.

http://www.tandfonline.com/toc/gcpi20/16/sup1

# DEVELOPMENT OF A HIGH ENERGY SIDE IMPACT DUMMY

**Zhenwen Wang**
Humanetics Innovative Solutions, Inc.
USA

**Donald Sherman**
Wayne State University
USA

**Nickolas Kloppenborg**
S-E-A Ltd.
USA

**Cynthia Bir**
University of Southern California
USA

Paper Number 15-0116

## ABSTRACT

A high energy side impact dummy (HE-SID) was developed for special vehicle development used for law enforcement and VIP protections subjected to improvised explosive device (IED). MIL-SID, i.e. ES-2 ATD with Hybrid III head/neck and MIL-LX design, was used to develop the test rig and define inputs to mimic the IED test conditions. It was found that the MIL-SID shoulder and rib modules were not durable enough to survive the impact during the testing. In addition, the shoulder biofidelity was lacking and requires improvement. A new shoulder structure was designed to improve the shoulder biofidelity. Finite element analysis was conducted to optimize the shoulder design according to the target biofidelity as defined by a series of 12 PMHS shoulder impacts. The MIL-SID shoulder cam design was replaced with a single shoulder rib integrated with damping materials. A 3D deflection measurement system was developed to measure the shoulder deflections. The 3D deflection measurement system consists of a linear potentiometer and two rotary potentiometers. An algorithm was developed to calculate the deflections at its shoulder joint attachment location. Hardware was fabricated and retrofitted in a MIL-SID for verification and validation. The preliminary test shows that the thorax durability issue was addressed. The ATD was able to withstand numerous tests without any damage. The new shoulder design demonstrated good biofidelity under high energy test conditions.

## INTRODUCTION

Mines have been a major threat for military vehicles and their occupants since World War I [Radonic, 2004]. Improvised Explosive Devices (IEDs) were one of the major threats in Mideast conflict in the last two decades. In peacekeeping and peace-enforcing, occupant safety has the highest priority. Military and law enforcement personnel are becoming more aware that, apart from vehicle integrity, personnel safety is crucial in operations where IEDs pose a threat. In the past 15 years, national and international projects for the improvement of the mine protection of several military vehicles have been performed to study the injury mechanisms under the IED. To systematically approach the issue, HFM-090/TG25, a team of experts developed an injury assessment methodology for light armored and logistic vehicles landmine protection systems [RTO TR-HFM-090]. Hybrid III anthropomorphic test devices (ATD) and ES-2RE were specified for the injury assessment surrogates [RTO TR-HFM-148]. ES-2RE is used for lateral loading test conditions. MIL-SID is an ES-2RE design with the Hybrid III 50$^{th}$ percentile ATD head, neck and MIL-LX lower extremities. The MIL-LX leg provides superior biofidelity and instrumentation capability for under-body blast test.

Shoulder injury is the one of the major injuries for occupant injuries from side impact. The most common injury in low-speed automotive impacts is distal clavicle fracture [Bolte et al 2003]. The Post Mortem Human Subjects (PMHS) tests conducted in the Bolte study are conducted at 4.4 m/s for majority of the tests. Two of the tests were conducted at 7.6 m/s velocity. The duration of the impact was slightly over 60 milliseconds. In loading conditions generated from IED detonation in the lateral direction, the impact velocity can be as high as 27 m/s [Lebarbe et al 2013], and the duration of the impact is near 10 milliseconds. Clavicle fracture was rare in high speed tests. Instead, it was found that humerus, coracoid process and scapula fractures were present frequently. Lebarbe observed that that there was a good correlation between the force, impact speed and injury. It was observed that the force alone was not sufficient to predict the injuries. He also noticed the shoulder deflection was associated with the humerus and scapular fractures. In the current MIL-SID design, the ATD shoulder structure does not have the capability of measuring the shoulder deflection. There is a need to develop an ATD that has the ability to measure shoulder deflection for injury prediction. In this paper, a new shoulder design was developed and can be retrofitted into the MIL-SID dummy. The revised ATD is named High Energy Side Impact Dummy (HE-SID). HE-SID has a shoulder design that provides motion with a degree of freedom in vertical direction. It also has a 3D linear potentiometer in the shoulder structure to provide deflection measurement in x, y and z directions.

## METHOD

### HE-SID Design

The design of HE-SID was developed from MIL-SID. Three major changes were conducted in the design: 1) the thoracic rib durability improvement, 2) the shoulder complex, 3) arm flesh thickness.

The existing MIL-SID was tested using a high rate loading condition (20 m/s, 50 mm deflection) to determine a baseline response. For the thoracic rib module, several durability issues were found from the high rate testing. The potentiometer shaft for the rib module was pulled out of its housing during the rib rebound. The rib module rubber stops were sheared off during the initial loading phase. The housing bracket for the rail bent during testing. Under such loading conditions, the thoracic rib model spring was bottoming out. The strong rebound requires a large travel distance to damp out the energy. This additional travel distance exceeded the travel range of the potentiometer and caused damage. The strong rebound also generated higher force and sheared off the rubber stops.

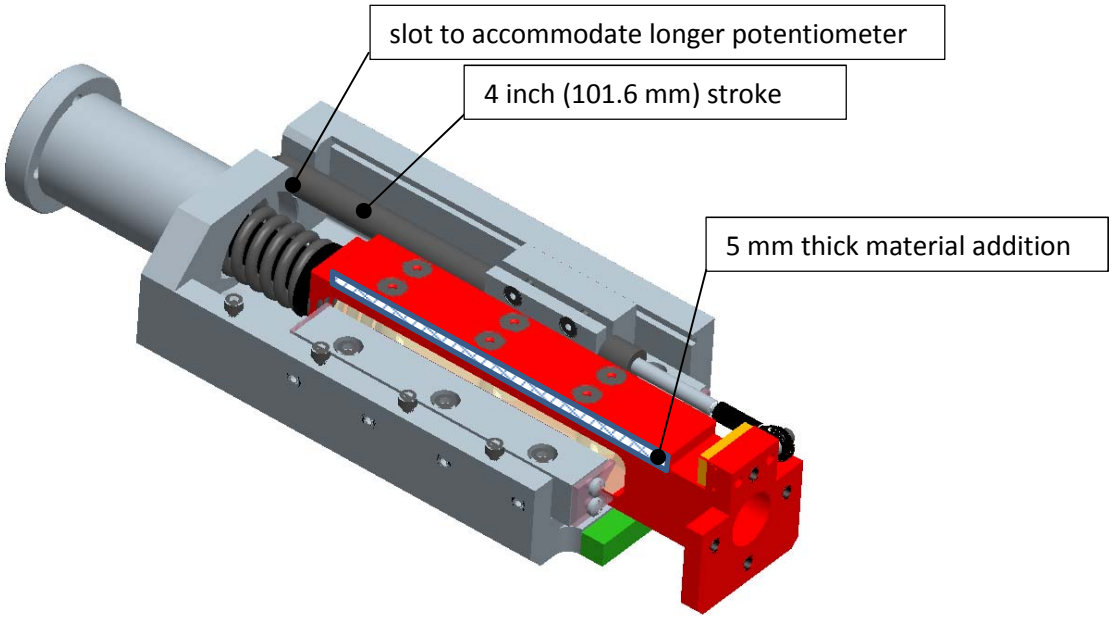


Figure 1, Thoracic rib module design changes - 4 inch potentiometer and stronger rail mounting bracket

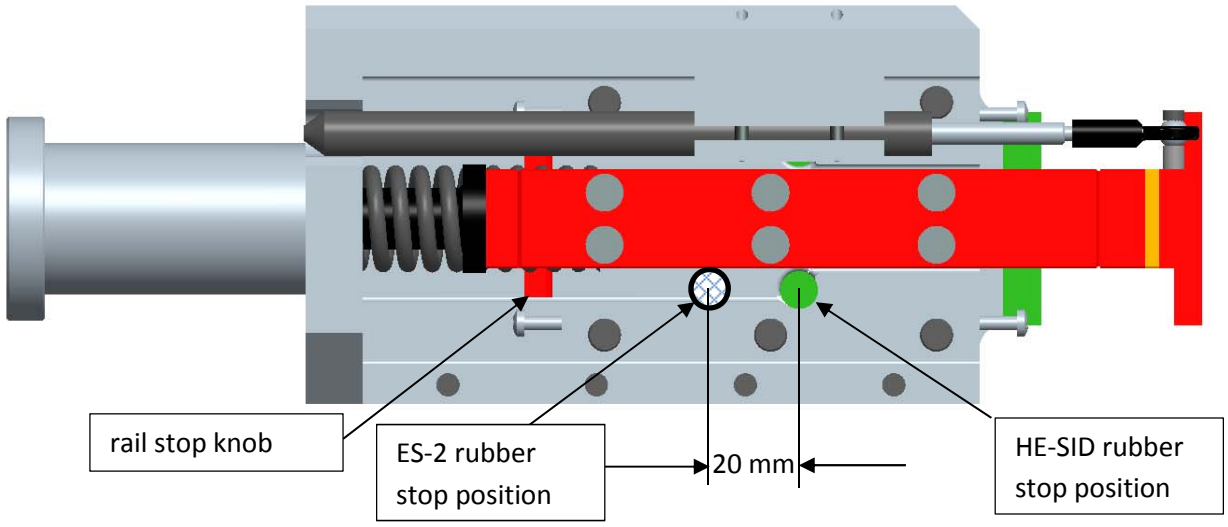


Figure 2, Thoracic rib model rubber stop shifted by 20 mm

To address the above durability issues, design changes were made accordingly. A 4-inch (101.6 mm) stroke potentiometer was chosen to replace the 3-inch (76.2 mm) stroke potentiometer, shown in Figure 1. The 4-inch potentiometer had a longer barrel, which required a slot cutout on the guidance bracket to accommodate the additional length and allow enough space for cable exit. When installed, the 4-inch potentiometer shaft was compressed back by 25 mm more to allow additional motion for the rebound. The rubber stops were shifted laterally toward the struck side by 20 mm to allow more energy dissipation before the rail stop knob engages with the rubber stop. The design was proven to effectively address the durability issue in testing.

Test results show the MIL-SID shoulder stiffness is much higher than that of PMHS shoulder. It was desired to improve the ATD shoulder biofidelity. The MIL-SID shoulder structure limits the range of motion in its horizontal plane. The shoulder has a leaf spring and a shoulder cam. When the shoulder is impacted, it rolls inboard. No vertical or posterior range of motion is allowed in the design, shown in Figure 3. In addition, the MIL-SID shoulder design does not provide the ability to measure the shoulder deflection and acceleration in the shoulder joint.

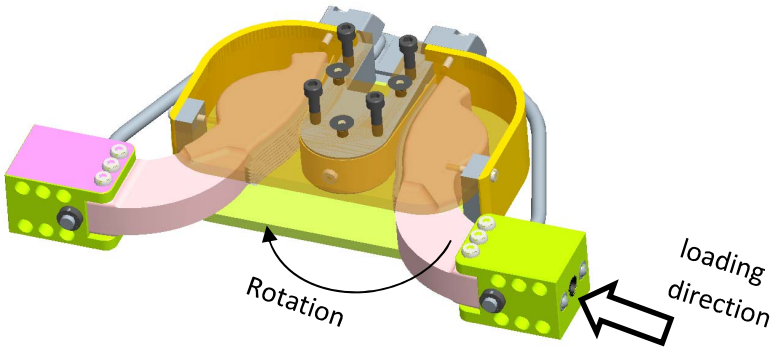


Figure 3, ES-2 shoulder design

It was desired to have a new shoulder design that was able to provide a long range of motion not only in the lateral direction, but also in the vertical and posterior directions. Due to the budget and time limitation, the project would not permit the exploration of a more complex design, such as the THOR-SD3. It was proposed to develop a simple

solution similar to the SID-IIs design – a steel shoulder rib with damping material. 3D shoulder deflection measurement was also desired to develop deflection based injury criteria. Considering the constraints above, a shoulder girdle was designed as shown in Figure 4. The design consists of a spring steel rib with the blue damping material developed in the WorldSID program, an interface bracket for the MIL-SID arm, a linear potentiometer and two rotary potentiometers system to provide 3D calculation of the shoulder joint motion, and a triaxial block for 3 linear accelerometers to measure the acceleration in X, Y and Z directions.

The linear potentiometer range of motion was designed to allow ±32° rotation in the transverse plane (rotation along z axis), and ±90° rotation in coronal plane (along the x axis). The design is shown in Figure 4.

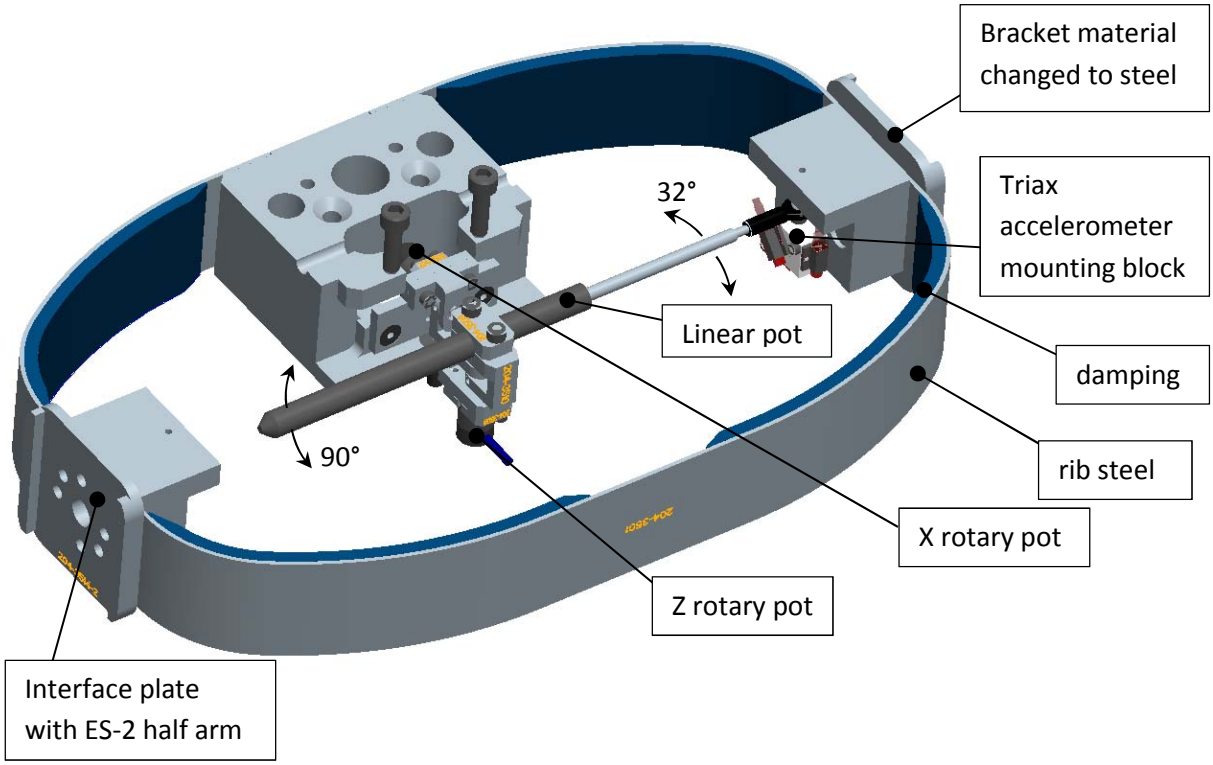


Figure 4, HE-SID shoulder design

Arm flesh provides damping to the skeletal structure of the shoulder. The flesh plays an import rule to mitigate the load. It is important to have a representative flesh in the ATD design. To gain knowledge of the flesh thickness, 8 PMHS MRI images were evaluated; the average flesh thickness at the glenohumeral joint was measured to be 14.3 mm with a standard deviation of 4.8 mm. The MIL-SID arm flesh thickness, shown in Figure 5, is between 27-35 mm, which is much thicker than that in human beings.

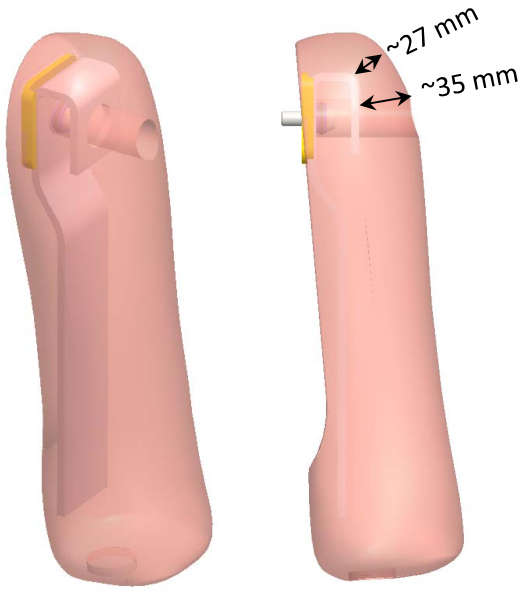


Figure 5, ES-2 arm flesh thickness near acromion

In order to bring the flesh thickness closer to human thickness values, a nylon insert was designed and attached to the existing MIL-SID arm bone in proximal humerus, which brought the thickness to approximately 15 millimeters, shown in Figure 6. In addition, the edges of the block were rounded to provide a smooth profile in order to minimize the potential damages to the ATD flesh during the impact.

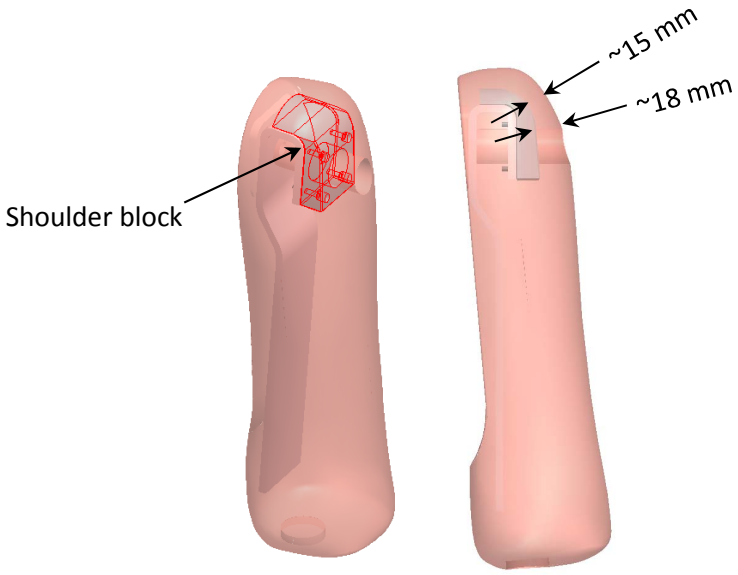


Figure 6, HE-SID arm design

**Shoulder Joint Location**

The MIL-SID shoulder joint is defined by where the shoulder is located in driving posture, which is in a forward (anterior) position relative to that of a (passively seated?) human. HE-SID was designed to represent the impact scenario of a passenger occupant. The shoulder joint center was aligned with the thorax to reflect the real shoulder joint position of the occupants. The HE-SID arm position is shown in Figure 7. The distance between the two

positions is 46.5 mm. The HE-SID shoulder position allows the arm to have more realistic arm/thorax engagement during the impact.

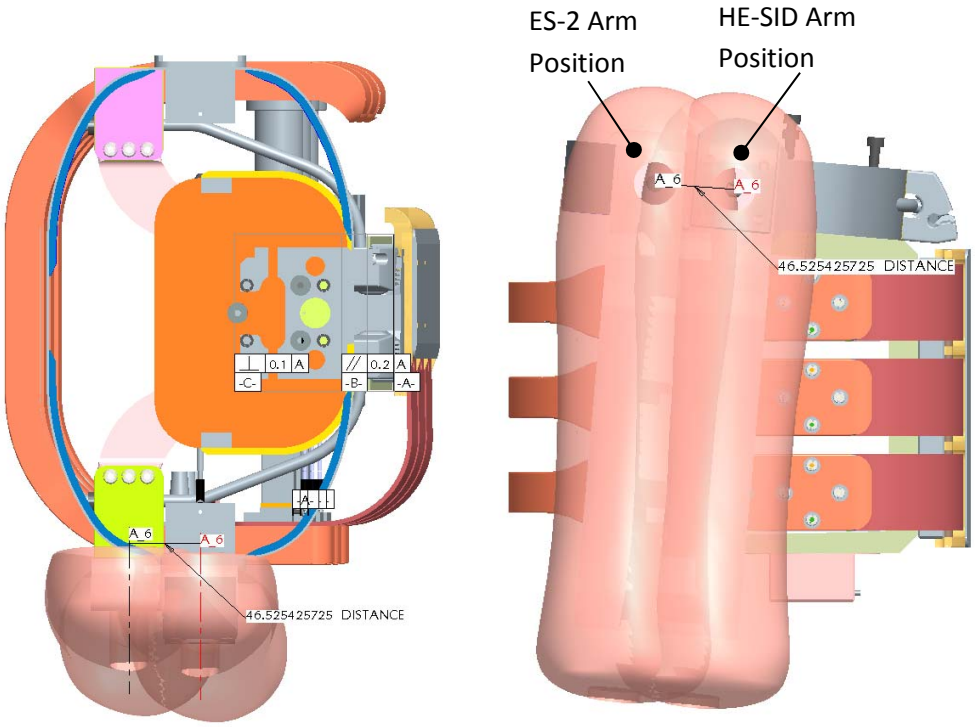


Top View Side View

Figure 7, ES-2 and HE-SID arms overlayed for position comparison

**Shoulder Deflection Calculation**

In the HE-SID shoulder design, a linear potentiometer and two rotary potentiometers were designed in the shoulder to provide the capability for the shoulder joint motion calculations in all three directions. The initial position is aligned with the ATD shoulder local coordinate system, shown in Figure 8.

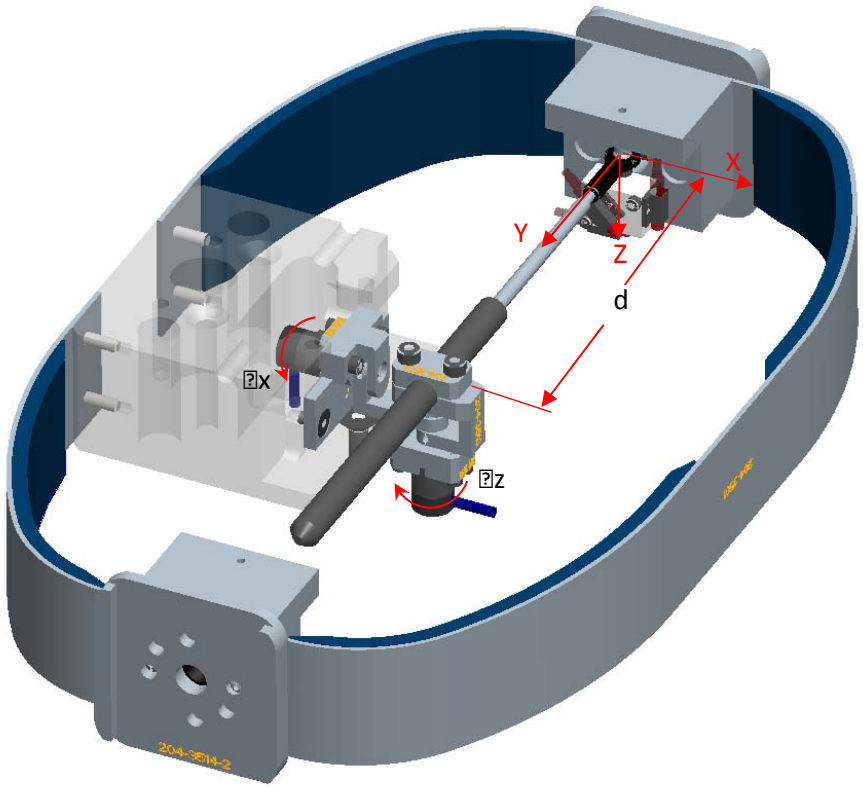


Figure 8, Shoulder deflection measurement system

The calculation can be carried out with the following formula

$$d_x = (d_0 + d_{pot}) * \sin(\theta_z)$$

$$d_y = (d_0 + d_{pot}) * \cos(\theta_z)$$

$$d_z = (d_0 + d_{pot}) * \sin(\theta_x)$$

Where:

$d_0$ is the initial distance (pre-impact condition) between the rotary pot pivot center to the linear pot rod end pivot center.

$d_{pot}$ is deflection at the rod end pivot center of the linear potentiometer attached to the rib.

$\theta_x$and $\theta_z$ are the rotation angles of the two rotary potentiometers from their initial ( pre-impact) positions.

For a brand new rib assembly, the rib was very close to the designed orthogonal planes. $d_0$ is very close to the designed dimension of 129.66 mm. If the rib is off the orthogonal planes due to small permanent deformation, the rotary potentiometer offset from its orthogonal position and $d_0$ at the deformed condition can be measured and taken into consideration in the calculation for better calculation accuracy.

After the above calculation, the data can be filtered according to SAE J211 filter class recommendation if appropriate. The absolute deflection time history in X, Y and Z directions can be calculated by subtracting its pre-impact values from $d_x$, $d_y$ and $d_z$.

**Finite Element Analysis**

Preliminary PMHS test results were used to evaluate the biofidelity of the HE-SID design. Finite Element models were built to analyze the design for durability, biofidelity and sensitivity to the shoulder impactor alignment.

Quasi-static analysis was conducted for the rib rail mounting bracket with AutoDesk Inventor 2012 Professional (stress results from LS-DYNA). The MIL-SID design with aluminum 6061-T6 was loaded until it yielded. The stress distribution is shown in Figure 9. The same load was applied to the HE-SID design, which has 5 mm additional thickness with aluminum 7075-T6 material, shown in Figure 10.

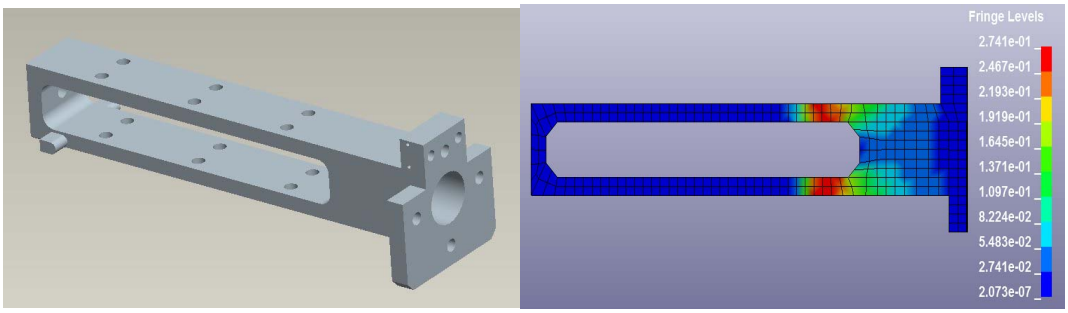


Figure 9, Load to yield for the ES-2 rail mounting bracket

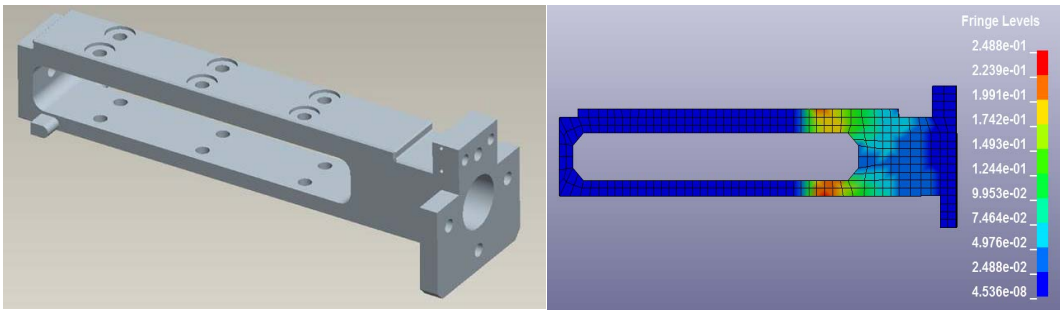


Figure 10, HE-SID rail mounting bracket stress distribution with the same load to yield ES-2

The analysis is summarized in Table 1. HE-SID rib module rail mounting bracket strength was increased by approximately 90%.

Table 1 Stress analysis results of the thoracic rib module rail mounting bracket

| ATD | Materials | Load | Max Von Mises Stress | Yield Stress |
|---|---|---|---|---|
| ES-2 | Aluminum 6061-T6 | 5.2 KN | 274 MPa | 276 MPa |
| HE-SID | Aluminum 7075-T6 | 5.2 KN | 264 MPa | 503 MPa |

Stress analyses were conducted for the shoulder rib to analyze the durability of the rib. For spring steel 1095, the Von Mises stress is well below the yield stress level for 60 mm compression, which is well above the estimated shoulder injury threshold.

In PMHS tests, the center of the impactor is aligned with the glenohumoral joint. Due to the irregular geometry in the shoulder girdle, the alignment is critical for achieving consistent test results. An FEA study was conducted to investigate the sensitivity of the impactor alignment with the ATD shoulder. Two positions were analyzed for comparison – 1) the impactor center is aligned with the ATD shoulder joint pivot center, 2) the impactor center is aligned with the ATD shoulder corresponding to the human glenohumoral joint.

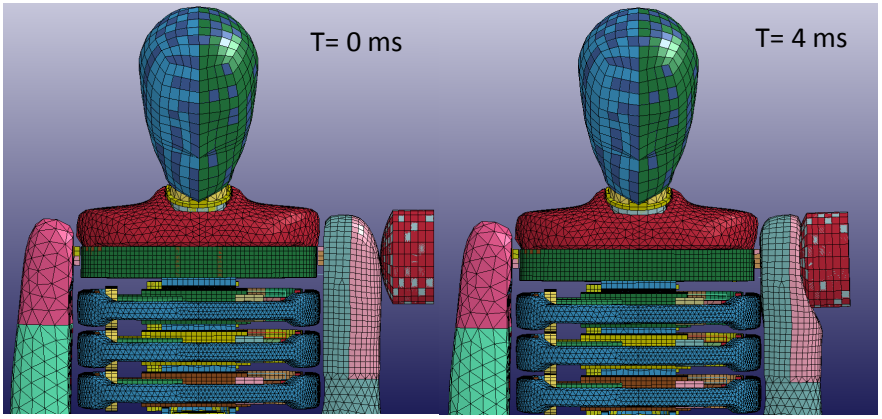


Figure 11, Shoulder impactor aligned with shoulder joint pivot center

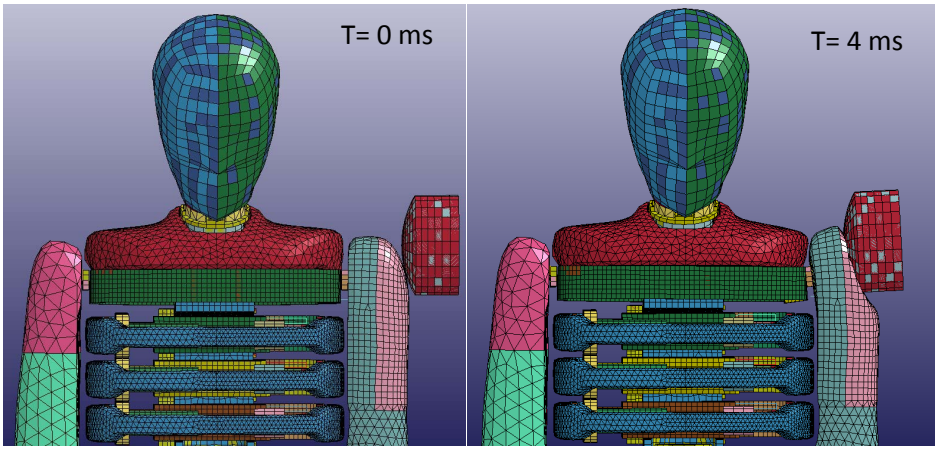


Figure 12, Shoulder impactor aligned with glenohumoral joint

From the kinematics analysis, it was observed that the HE-SID upper torso does not move much at all when the shoulder was maximally compressed (~50 mm). This is consistent with the observation in PMHS impact tests. Due to its impact speed and high energy impact, the PMHS and ATD upper torso remains its position due to its inertia. The deformation happened mainly in the local girdle of the shoulder, shown in Figure 11 and Figure 12. The low reaction of the torso kinematics is also evidenced by the relatively low T1 displacement, less than 3.5 mm in both cases.

Between the two alignment positions, a large deflection difference, up to 14 mm from both skeleton or arm flesh, was observed. It is important to align the impactor with glenohumeral joint for ATD biofidelity validation and verification test so that the results are comparable.

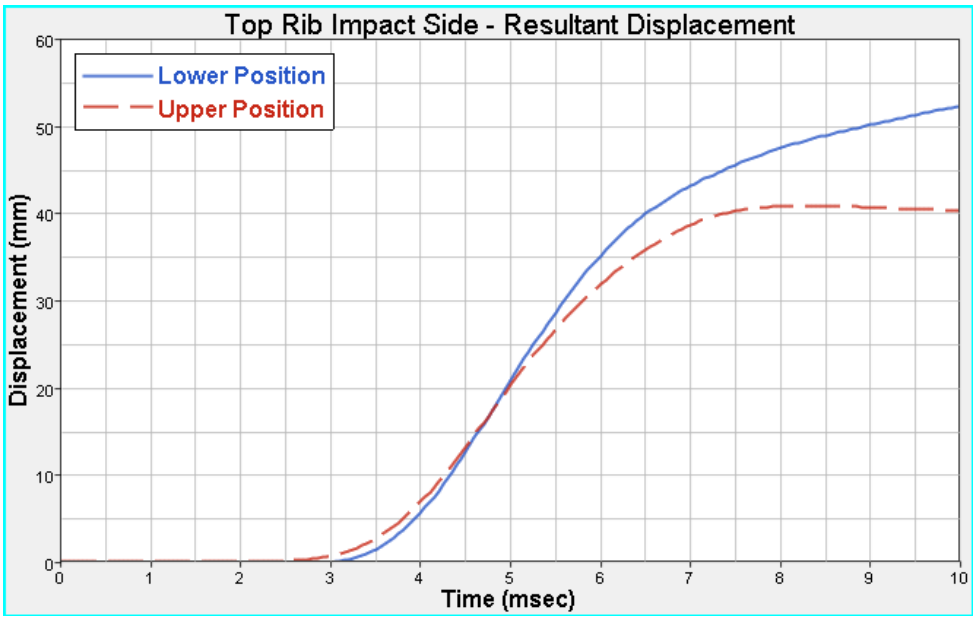


Figure 13, Deflection from ATD linear potentiometer measurement

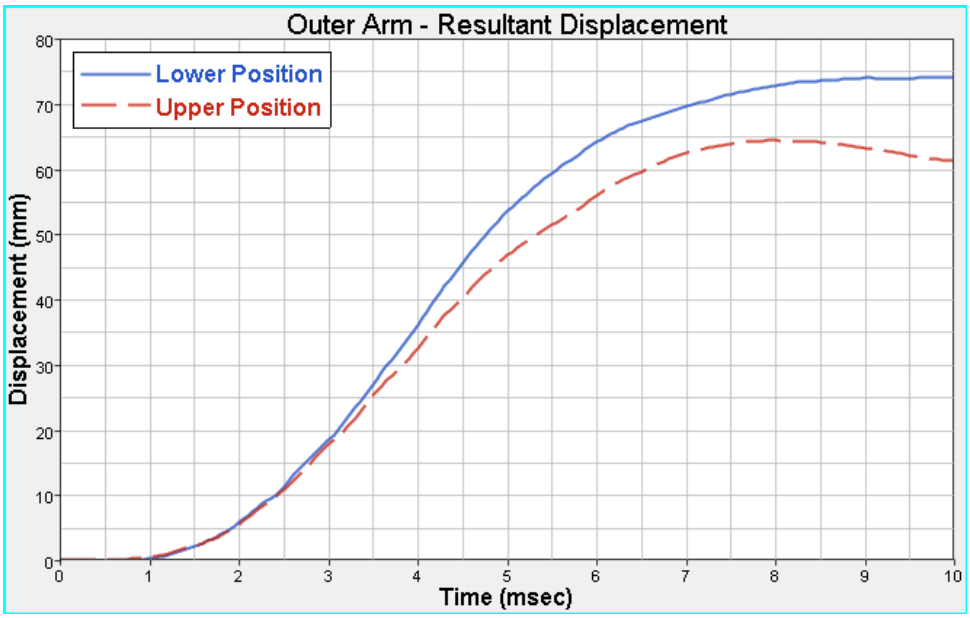


Figure 14, Deflections from the exterior arm flesh measurement

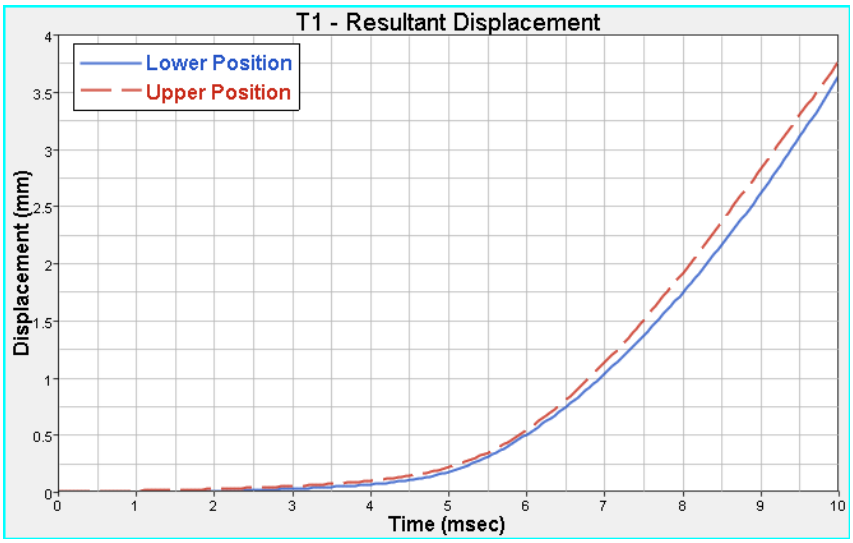


Figure 15, T1 Accelerations

## RESULTS

### Durability

Upon the completion of the HE-SID design, prototype ATD hardware was fabricated for validation and verification testing. After the first test, it was found that the shoulder rib was bent. The rib was brought to Humanetics for analysis and it was discovered that the spring steel was not properly heat treated. A second rib was treated with the proper heat treat process and the rib survived numerous impact tests without damage. No durability issue was observed for the thoracic rib module. The thoracic rib potentiometer was functioning well without any issue. The analysis and the design successfully addressed the MIL-SID durability issue.

### ATD Responses

The prototype HE-SID was tested in the same rig that was developed for PMHS tests to verify the ATD biomechanical response. A series of 12 PMHS were tested to develop a biofidelity guideline and also the injury criteria. The force-deflection relationship of the PMHS tests is summarized in Figure 16, Figure 17 and Figure 18. The ATD demonstrates that the biomechanical parameters are similar to those of the PMHS. Specifically, the third test in the series aligns well with the PMHS corridors. Additional testing will need to be completed to fully characterize the variance shown in the initial test series.

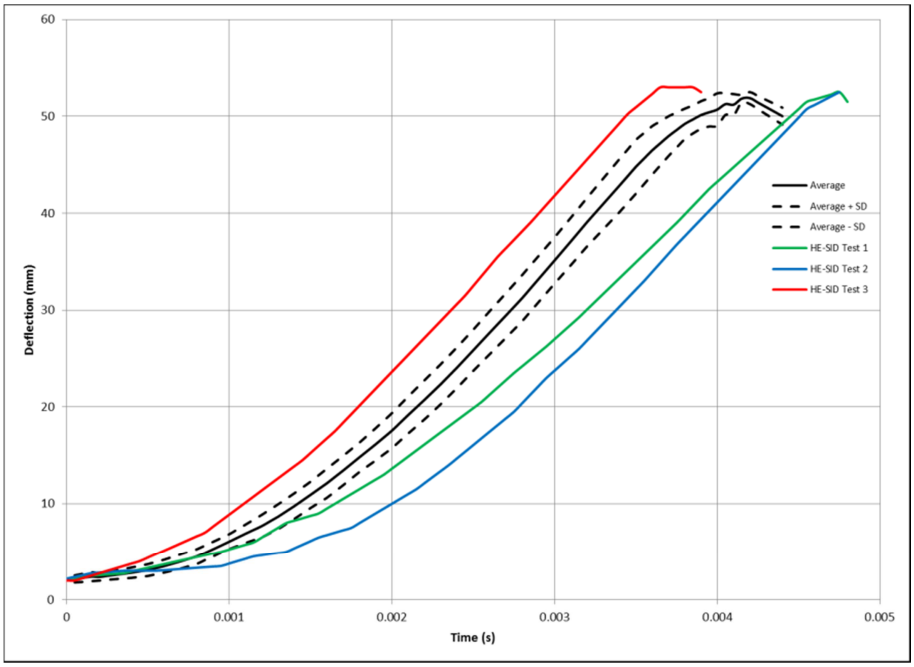


Figure 16, ATD and PMHS shoulder deflection comparison

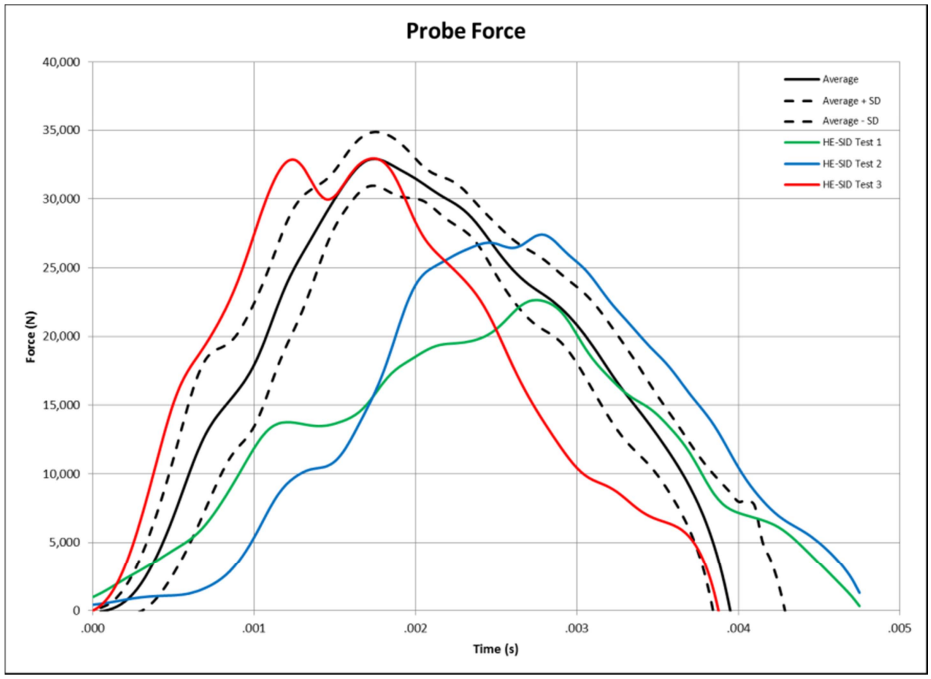


Figure 17, HE-SID and PMHS shoulder probe force comparison

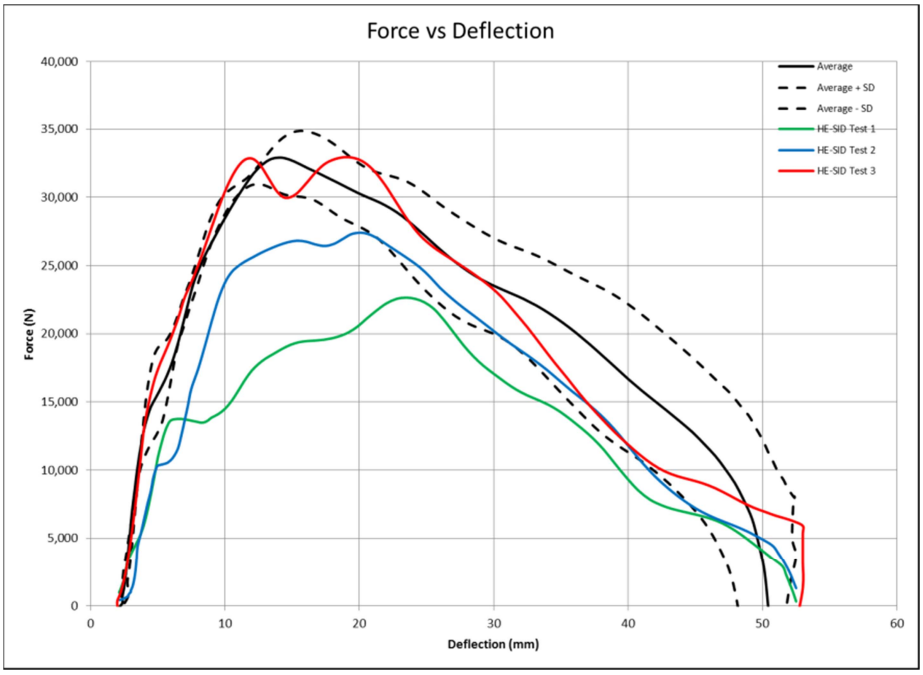


Figure 18, HE-SID and PMHS force vs deflection comparison

## CONCLUSIONS

HE-SID was developed to address the need for a durable and biofidelic ATD in high speed testing for injury predictions. The design is based on the ES-2RE design with improved durability of the rib modules and a new shoulder design. The HE-SID shoulder design allows motion in more degrees of freedom and also offers a 3D deflection measurement ability with a linear potentiometer and two rotary potentiometers. The shoulder joint of the HE-SID is located closer to the anatomical location and the arm skin thickness now resembles that of the human. The testing of the prototype design shows good durability at the high impact speed. Compared to PMHS shoulder response, the ATD shows similar results to human response. Further testing will be conducted to evaluate the HE-SID biomechanical response and injury criteria will be developed accordingly in the future.

## REFERENCES

Bolte IV, J., Hines, M.H., McFadden, J.D., and Saul, R.A., 2000. Shoulder response characteristics and injury due to lateral glenohumeral joint impacts, 44th Stapp Car Crash Journal.

Bolte IV, J., Hines, M. H., Herriott, R.G., McFadden, J.D., Donnelly, B.R., 2003. Shoulder impact response and injury due to lateral and oblique loading, 47th Stapp Car Crash Journal.

Lebarbe, M., Lafont, D., Uriot, J., Potier, P., Baudrit, P., Vallencien, G., 2013. Study of the shoulder response to a high speed – short displacement lateral impact using PHMS and ES-2re, IRCOBI Conference, Gothenburg, Sweden, September 11-13.

TR-HFM-090, Final Report of HFM-090 Task Group 25, 2007. Test methodology for protection of vehicle occupants against anti-vehicular landmine effects.

Radonić, V., Giunio, L., Biočić, M., Tripković, A., Lukšić, B. and Primorac, D., 2004. Injuries from Antitank Mines in Southern Croatia, in Military Medicine, Vol. 169, April, pp. 320-324.

# REAL-WORLD PERFORMANCE OF CITY SAFETY BASED ON SWEDISH INSURANCE DATA

**Irene Isaksson-Hellman**
If P&C Insurance
Sweden

**Magdalena Lindman**
Volvo Car Corporation
Sweden

Paper Number 15-0121

## ABSTRACT

The number of passenger cars equipped with Auto Brake functionalities in traffic is increasing rapidly. Following this, the opportunity to study real world performance of these systems is growing. The low-speed Auto Brake system City Safety, launched in 2008 and a standard feature on all recent Volvo Cars' models, is a technology designed to help the driver mitigate and in certain situations avoid rear-end collisions at low speed by automatically braking the vehicle. Previous analysis of the City Safety technology showed promising results in terms of reducing real world crashes.
In this study, further evaluation of City Safety was performed based on insurance claims data. Using a unique dataset containing all new Volvo cars in traffic in Sweden from 2010 to 2014, including the possibility to control for other advanced driver assistance systems such as ACC, FCW and Auto Brake functionalities, the rate of rear-end frontal collisions per insured vehicle years was studied. First, car models with and without City Safety were compared. Second, the same car model with and without City Safety was compared, thereby controlling for specific characteristics in different models. Finally, the second generation of City Safety, that operates at speeds up to 50 km/h, was compared to the first generation (<30 km/h). Results showed that the overall claim frequency of rear-end frontal collisions was 28% lower for City Safety equipped models than for other Volvo models without the system. The result of the comparison between the same models was similar while no significant collision avoidance effect of the upgraded system to speeds up to 50 km/h was found. The expected crash mitigating effect of City Safety can be added to these results, providing a further potential to be explored in future real world follow-up studies.
This study confirms previous encouraging results of the crash reducing effect of the City Safety functionality. The findings of Auto Brake safety performance in real world traffic, shows the relevance of this type of vehicle systems for increased traffic safety and emphasizes the importance of the introduction of such systems on the market.

## INTRODUCTION

In 2008, the world first standard mounted passenger car collision avoidance system was introduced in Volvo cars, targeting low-speed rear-end frontal collision situations. City Safety uses a lidar sensor monitoring the area in front of the vehicle and initiate braking if a crash is imminent (Distner et al., 2009). A limited number of real world follow-up studies are available. HLDI (2011, 2013) presented the first indications of the real-world effect of City Safety, as insurance claims data for cars with and without City Safety were compared. Claim frequency rates for the XC60, equipped with City Safety, were lower than for all other midsize luxury SUVs combined. A similar effect was found for other Volvo cars. When studying Swedish insurance claims, it was found that the rate of rear-end frontal collisions was significantly reduced by 23% in the Volvo XC60 equipped with City Safety compared to other Volvo car models without City Safety registered during the same period of time (Isaksson-Hellman and Lindman, 2012). In Swedish police-reported injury crashes 2010-2014, a reduction of striking rear-end crashes was found that ranged between 35% and 41% for cars with City Safety (Rizzi et al., 2014). The limited number of real world follow-up studies on collision avoidance systems indicates that finding datasets of appropriate content is challenging. Fields et al. (2013) suggest improving the follow-up study process by combining data from several databases using meta-analyses and thus obtain results more quickly, but so far, research into this approach has been limited.
The aim of this study was to calculate the effect of City Safety by comparing cars with and without the standard mounted low speed Auto Brake system. The overall effectiveness was studied as well as the specific performance of selected car models. Also, the first and second generations of the system were compared. A dataset comprising all new Volvo cars in crashes in Sweden noted in insurance claims was analyzed to evaluate

the real world performance of City Safety. The influence of non-standard mounted advanced driver assistance systems (ADAS) was considered in the effect estimations.

## METHODS

Crashes in Sweden form the basis for this evaluation of City Safety. By using data from claims at the insurance company Volvia/If, rear-end frontal collisions were identified and the rate per insured vehicle years was calculated. Three different analyses were performed. First, an aggregated group of Volvo models with City Safety was compared with a group of models without the system. Then, the effectiveness of City Safety was evaluated for two selected Volvo car models, V70 and XC70. Finally, the updated version of City Safety launched in MY 2013, which operates at speeds up to 50 km/h, was compared with the first generation of the City Safety, with functionality at speeds up to 30 km/h. Separate analyses were performed in order to control for the effect of other (non-standard mounted) ADAS, e.g. Adaptive Cruise Control (ACC), Forward Collision Warning (FCW) and Auto Brake functionalities, that partly address the same crash situations.

### Data

Insurance data is an important source of information regarding real world crashes. A comprehensive motor insurance for cars covers both injuries to people involved in a crash as well as damage to vehicles and property. The collision damage insurance pays for vehicle damage to the policy holder's own car, while the third party liability insurance covers personal injuries and damage to other vehicles and property. CDW (Car Damage Warranty) is a unique Swedish concept, valid the first three years and covers damage to the policy holder's own car. This warranty has been a Swedish competitive standard a long time and is funded by each car manufacturer. On behalf of Volvo Cars, Volvia Insurance handles this unique warranty which provides an excellent opportunity to study the number of collisions for all new Volvo cars in traffic.
Crashes reported to the insurance company cover all levels of crash severity, from slight crashes with only minor damages to the car to severe crashes with fatal injuries and heavily damaged cars. These data are advantageous compared to other crash databases where the quantity and the representativeness of data often is a problem in car safety evaluations. For example, considering low speed collision avoidance system effectiveness evaluations, the collection criteria in crash databases often exclude low-severity crashes. The insurance claim data include information on crash type, damaged parts, car model, ownership, insured vehicle years, and estimated mileage per year. The variable crash type makes it possible to identify rear-end frontal collisions, giving the opportunity to evaluate the conflict situation for which City Safety was designed.
Data from SMHI, (Swedish Meteorological and Hydrological Institute) was used to evaluate temperature variations for the winter season.

### Data Selection

The data selected for this study cover insurance claims from 1 July, 2012, to 30 June, 2014. The number of rear-end frontal collisions, see Figure 1, were counted for each model, and the exposure was calculated by summing up the number of insured vehicles from vehicle years starting on July 1, 2012 and ended on June 30, 2014. Only cars with model year 2010 and later were included. Situations taken into account were collisions with vehicles in traffic, collisions with parked vehicles were excluded.

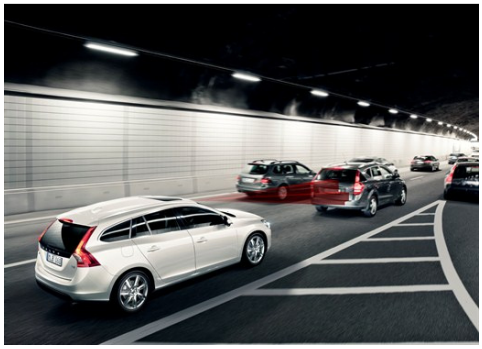

***Figure1. Illustration of a rear-end frontal collision situation (white car).***

Three subsets were selected for the different analyses. First, for an overall estimation of the effectiveness, a group of Volvo vehicle models with City Safety was selected to be compared with a group of vehicle models without the system, Table 1. Next, the rate of rear-end collisions and the effectiveness of City Safety was evaluated for the same Volvo car models: V70 and XC70 in order to control for possible unique

characteristics in different car models. The Volvo car models XC60, V60, and S60, were introduced with City Safety as standard mounted equipment, while the Volvo car models S80, V70 and XC70 were first introduced without the system, see Table 1. From MY 2012 and onwards, the City Safety functionality was available also in these models.

**Table1.**
**Exposure (number of insured vehicle years) and model years for car models with and without City Safety included in the study.**

| | With City Safety | | Without City Safety | |
|---|---|---|---|---|
| | All | | All | |
| | MY | Insured vehicle years | MY | Insured vehicle years |
| **S80** | 2012-2014 | 1632 | 2010-2011 | 2902 |
| **V70** | 2012-2014 | 30724 | 2010-2011 | 36271 |
| **XC70** | 2012-2014 | 12549 | 2010-2011 | 6275 |
| **S60** | 2011-2014 | 10172 | | |
| **V60** | 2011-2014 | 35912 | | |
| **XC60** | 2010-2014 | 27733 | | |
| **Total** | | **118722** | | **45448** |

Finally, the second generation of City Safety, operating at speeds up to 50 km/h, was compared with the first generation with functionality at speeds up to 30 km/h. In Table 2, the vehicle models, model years included and exposure are presented. Cars of MY 2012 were compared with cars of MY 2013-2014 during a one year period, between 1 July, 2013 and 30 June, 2014.

**Table2.**
**Vehicle models, model years and exposure for the first and second generation of City Safety.**

| Models: | City Safety 30km/h | | City Safety 50km/h | |
|---|---|---|---|---|
| | MY | Insured vehicle years | MY | Insured vehicle years |
| S80, V70,XC70 S60 V60,XC60 | 2012 | 22163 | 2013-2014 | 37642 |

Along with City Safety, other ADAS addressing the same crash situations were introduced as optional features in the same car models. The number of cars with these optional systems is increasing as shown in Figure 2. Samples with car individuals not equipped with optional ADAS were identified, to control for the effect in rear-end frontal collisions not related to City Safety, see Table 3.

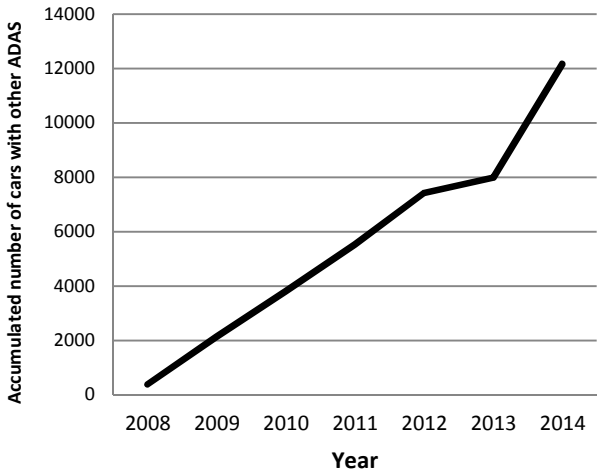


***Figure2. Accumulated number of cars equipped with optional advanced driver assistance systems (ADAS), 2008-2014.***

**Table3.**
**Exposure and model years for models with and without City Safety and optional ADAS functionalities**.

| | MY | With City Safety | | | MY | Without City Safety | |
|---|---|---|---|---|---|---|---|
| | | With ADAS | Without ADAS | | | With ADAS | Without ADAS |
| | | Insured vehicle years | Insured vehicle years | | | Insured vehicle years | Insured vehicle years |
| **S80, V70, XC70** | 2012-2014 | **15848** | **102874** | **S80, V70, XC70** | 2010-2011 | **2681** | **42767** |
| **S60, V60** | 2011-2014 | | | | | | |
| **XC60** | 2010-2014 | | | | | | |

Additionally, the rate of rear-end frontal collisions per insured vehicle years for the Volvo XC60 was studied by stratifying for seasonal effects. Road conditions, an important factor influencing the rate of rear-end collisions, varies a lot in Sweden due to variations in climate between summer and winter, (Isaksson-Hellman et al., 2012). Road conditions during the winter also vary a lot between years, and between different geographical locations in Sweden. The rate of rear-end frontal collisions for the winters in the study presented in Isaksson-Hellman et al., (2012), December 2009-February 2010 and December 2010-February 2011 and for the winters in the present study, December 2012-February 2013 and December 2013-February 2014 was compared together with the average temperature (°C) retrieved from SMHI, at three different locations in Sweden.

**Statistical methods**
To evaluate the effect of City Safety, the rates of rear-end frontal collisions per insured vehicle years were calculated and vehicle models with and without the system were compared.

The rate of rear-end frontal collisions was estimated by the number of claim frequency per insured vehicle years

$$Rate_{w\,CS} = ( n_{w\,CS} / VY_{w\,CS})$$

Where

$n_{w\,CS}$ = Number of rear-end frontal collisions for cars with City Safety

$VY_{w\,CS}$ = Number of insured vehicle years for cars with City Safety

The rate of rear-end frontals for cars without City Safety was defined in the same way. The number of claims occurring over insured vehicle years can be considered using a Poisson distribution, and the 95% confidence interval for the rate was calculated by using a normal approximation to this distribution.

$$\text{Rate}_{\text{w CS}} \pm 1.96 * \sqrt{\text{Rate}_{\text{w CS}}/\text{VY}_{\text{w CS}}}$$

To evaluate if City Safety equipped vehicles have a different rate of rear-end frontal collisions, the difference between the rates for vehicles with and without the system was calculated together with a 95% confidence interval.

$$\text{RD} = \text{Rate}_{\text{wo CS}} - \text{Rate}_{\text{w CS}}$$

Poisson distribution and test-based methods were used to construct the confidence interval. (Sahai and Kurshid, 1995).

$$\chi^2 = \left(\text{n}_{\text{w CS}} - \frac{\text{m} * \text{VY}_{\text{w CS}}}{\text{VY}}\right)^2 / \left(\frac{\text{m} * \text{VY}_{\text{w CS}} * \text{VY}_{\text{wo CS}}}{\text{VY}^2}\right)$$

Where

m= the total number of events observed

VY= the total number of insured vehicle years

The confidence limits were then calculated by

$$\text{RD}_{\text{L}} = \text{RD} \pm 1.96 * \sqrt{\text{RD}^2/\chi^2}$$

The effectiveness of City Safety can also be presented as a difference between rates for models without and with City Safety divided by the rate for models without City Safety:

$$\text{e} = \frac{\text{Rate}_{\text{wo CS}} - \text{Rate}_{\text{w CS}}}{\text{Rate}_{\text{wo CS}}}$$

**RESULTS**

First, Volvo car models equipped with City Safety, and Volvo car models without City Safety were compared to estimate the overall effect of the system. The rate of rear-end frontal collisions estimated by insurance claims per 1,000 insured vehicle years, was 4.0, 95% CI [3.6, 4.3] for vehicle models with City Safety and, 5.5, 95% CI [4.9, 6.2] for vehicle models without the system. The results showed a significant difference between the rates of rear-end frontal collisions in models with and without City Safety on the 95% significance level;

$$5.5 - 4.0 = 1.5,\ 95\%\ \text{CI}\ [0.8, 2.3]$$

The effectiveness was estimated to

$$\text{e} = \frac{5.5 - 4.0}{5.5} = 28.3\ \%.$$

The result was estimated for vehicle models where an optional ADAS were available. Considering City Safety only, the rate of rear-end frontal collisions estimated by insurance claims per 1,000 insured vehicle years was 4.2, 95% CI [3.8, 4.6] for the cars with City Safety and without ADAS, and 5.6, 95% CI [4.9, 6.3] for cars without City Safety and without ADAS. The results showed a significant difference between the rates of rear-end frontal collisions, comparing groups of Volvo models with and without City Safety with any optional ADAS;

$$5.6 - 4.2 = 1.4,\ 95\%\ \text{CI}\ [0.6, 2.2]$$

The effectiveness for City Safety when controlling for non-standard ADAS was estimated to

$$\text{e} = \frac{5.6 - 4.2}{5.6} = 25\ \%.$$

Specifically, the effectiveness of City Safety was evaluated for the same Volvo car models: V70 and XC70. These models were first introduced without the system but from a certain MY, the City Safety

functionality was available also in these models. In the comparison of the same Volvo car models with and without City Safety, the rate of rear-end frontal collisions was 4.1, 95% CI [3.5, 4.7] for the car models with City Safety, while the rate for the same models without City Safety was 5.8, 95% CI [5.1, 6.5]. Considering the comparison for the same models without ADAS the rate per 1000 insured vehicle years was 4.3, 95% CI [3.6, 4.9] and 5.8, 95% CI [5.1, 6.6] respectively for cars with and without City Safety. Both results showed a significant difference between the rates of rear-end frontal collisions on a 95% level;

With non-standard ADAS 5.8 - 4.1 = 1.7, 95% CI [0.7, 2.6]

Without non-standard ADAS 5.8 - 4.3 = 1.5, 95% CI [0.5, 2.5]

The effectiveness was estimated to; 29% and 26% respectively.

Finally, the evaluation of the City Safety systems' update to its second generation showed that for cars with the City Safety version operating at speeds up to 30 km/h, the rate of rear-end frontal collisions was 3.7, 95% CI [2.9, 4.5], while for the system operating at speeds up to 50 km/h, it was 3.6, 95% CI [3.0, 4.2]. The rate of rear-end frontal collisions was lower, but no significant difference was found:

3.7 – 3.6 = 0.1, 95% CI [-0.9, 1.1]

The effectiveness was estimated to 3% for the second generation of City Safety compared to the first generation of the system.

In Figure 3a, average temperatures (°C) for winter seasons in Isaksson-Hellman et al. (2012), (December 2009-February 2010 and December 2010-February 2011) and winter seasons included in the present study (December 2012-February 2013 and December 2013-February 2014) were compared for three different locations in Sweden. The average temperature during the previous winter seasons was lower than in the present study. The rate of rear-end frontal collisions was shown to be larger during the previous winters than during the winters in the present study.

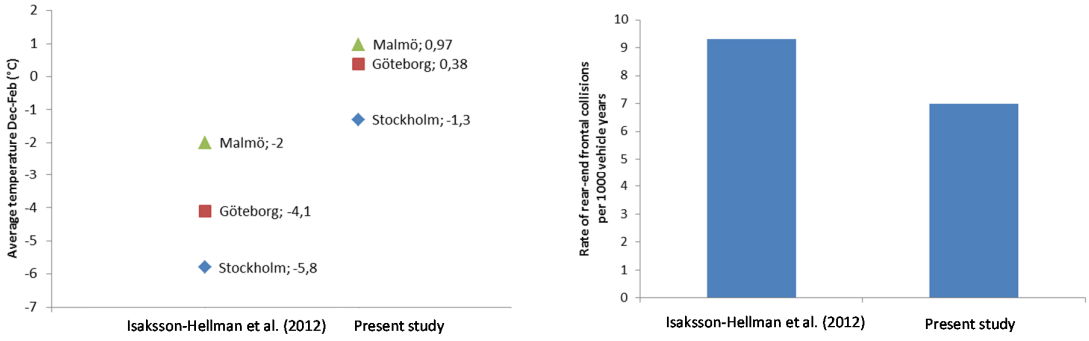


***Figure3a. Average temperature (°C) during the winters for three geographical locations in Sweden. Figure3b. Rate of rear-end frontal collisions in corresponding time periods.***

## DISCUSSION

This evaluation of the City Safety performance, based on insurance claims from real world traffic crashes in Sweden, strengthen the previously presented findings that City Safety is effectively preventing rear-end frontal collisions. The benefit of City Safety is reflected in lower rates of crashes per insured vehicle years. This study shows that cars with City Safety were exposed to 28% less rear-end frontal collisions than cars without the system.

The overall crash reduction effect was slightly larger than the one reported in Isaksson-Hellman et al. (2012). In the present study, additional car models with the City Safety functionality were available and a different period of time was studied. Also, two influencing factors were further explored, providing insight into the performance of City Safety. First, and most significant, the importance of considering non-standard mounted ADAS in a City Safety evaluation was confirmed in this study. This has been presented as one of the main limitations in previous real world follow up studies presented (HLDI, 2011, 2013; Isaksson-Hellman et al., 2012; Rizzi et al., 2014). A notable increase of ADAS take-rate over the last years was found in the Volvo car population, Figure

2. When controlling for optional ADAS, the benefit of City Safety was estimated to 25%. The other aspect considers the refined City Safety technology. In MY 2013 the second generation of City Safety was launched, which operates at speeds up to 50 km/h in comparison to 30 km/h in the first generation. A non-significant effect of 3% less rear-end frontal collisions from the increase in operating speed was noted. In a prospective study (Lindman et al., 2012) no additional crashes avoided were predicted for the 50 km/h City Safety compared to the 30 km/h version based on a sample of crashes with at least one injured occupant. Considering that the data in the present study also comprised crashes of lower severity as it was collected from a larger sampling frame, the result was sound in relation to the prediction study. Adding up to the collision avoidance effect there is a crash mitigating effect expected that was not estimated in this study. Since the relative risk for injuries in frontal impacts increases with impact speed up to high crash severity levels (Kullgren et al., 2000), decreasing the impact severity by means of autonomous braking will contribute to occupant injury reduction.

When comparing the same vehicle model with and without City Safety, the bias resulting from different car model characteristics was decreased. For example, it is possible that drivers that chose to purchase car models with City Safety differ in ways that could affect crash likelihood. The effectiveness of City Safety for the V70 and XC70 models was estimated to 29% for all cars and 26% when controlling for other ADAS. This is only slightly different from the overall effectiveness, indicating robust overall results.

There is also a possibility that traffic environmental aspects influence the results. Road conditions due to seasonal changes was shown to influence the rate of rear-end collisions (Isaksson-Hellman et al., 2012). In the present study, it was shown that in the cold winters included in the 2012 analysis, a higher rate of rear-end frontal collisions was found compared to in the relatively mild winters in the present study. Reports from SMHI (Swedish Meteorological and Hydrological Institute) confirmed presence of more snow and ice resulting in more adverse road conditions all over Sweden during the period studied in Isaksson-Hellman et al., (2012). Despite the differences in rear-end frontal collision rates, the effect presented in 2012 and in this study were similar suggesting that the findings on the City Safety performance were robust.

A challenge when evaluating the safety performance in real world traffic is to secure the amount and quality of data needed to be able to perform reliable analyses. Data from insurance claims is one excellent source of information for that purpose. This was demonstrated as the three first real world data analyses of City Safety were performed by using insurance data (HLDI, 2011, 2013; Isaksson-Hellman et al., 2012). Still, some limitations are obvious. While the insurance data used for the present analysis were detailed enough for classifying the collision type of interest, rear-end frontal collisions, there was still fine points missing in the information needed to isolate the exact operating situations of City Safety. It was not possible to control for driving speed in order to evaluate the driving situation for which City Safety was designed.

Additionally, it was not known whether the driver had turned off the system prior to the crash. However, since turning off the functionality requires substantial navigation in the car settings menu and since the system always is default on at every start, it is not likely that many trips were driven with the system disabled.

In future research, the additional effect of crashes mitigated due to City Safety lowering the speed in the crash should be studied. Concerning occupant injuries, a significant reduction of soft tissue neck injuries in rear-end impacts is expected since these are frequent in occupants of both the impacting and the impacted car, (Avery and Weekes, 2008; Jakobsson, 2004; Jakobsson et al., 2004; Kullgren et al., 2000). In this study, only reductions of host vehicle rear-end frontal collisions were evaluated. Occupant injury reduction in the host and lead vehicle is yet to be quantified in future studies.

## CONCLUSIONS

The overall benefit of City Safety is estimated to 28% fewer rear-end frontal impacts for cars with the system than for cars without it. When controlling for non-standard mounted collision avoidance systems such as ACC, FCW and Auto Brake functionalities, the effect was 25%. The pronounced collision avoidance performance was confirmed in a comparison of the same car models with and without the system. When evaluating the second generation of City Safety that operates in higher speeds than the first generation, a non-significant collision avoidance effect of 3% was found. Adding up to the collision avoidance effect, there is a crash mitigating effect expected that was not estimated in this study. The possibility to control for the presence of ADAS represents a significant improvement of the Auto Brake safety evaluation method.

## REFERENCES

Avery, M., Weekes, A. (2008). Volvo City Safety – Collision Avoidance Technology and its Potential to reduce Whiplash Injuries. *Conf. Neck Injuries in Road Traffic and Prevention Strategies*, Munich, Germany.

Distner, M., Bengtsson, M., Broberg, T. and Jakobsson, L. (2009). City Safety – A System Addressing Rear-end Collisions at Low Speeds. *Proceedings of the 21st ESV Conference*. Paper No. 09-0371-O. Stuttgart.

Fildes, B., Keall, M. D., Thomas, P., Parkkari, K., Pennisi, L. and Tingvall, C. (2013). MUNDS: A New Approach to Evaluating Safety Technologies. *International Technical Conference on the Enhanced Safety of Vehicles (ESV)*, Paper No. 13-0073.

Insurance Institute of Highway Safety. (2011). *Status Report Vol. 46*. No.6.

Insurance Institute of Highway Safety. (2013). *Status Report Vol. 48*. No.3.

Isaksson-Hellman, I. and Lindman, M. (2012). The Effect of a Low-Speed Automatic Brake System Estimated from Real Life data. *Proceedings of the Ann Adv Automot Med. 56*, 3-12.

Jakobsson, L. (2004). Evaluation of Impact Severity Measures for AIS1 Neck Injuries in Frontal Impacts using Crash Recorder Data. *Int. J of Crashworthiness*, *9(1)*: 105-111.

Jakobsson, L., Norin, H., Svensson, M. Y. (2004). Parameters Influencing AIS 1 Neck Injury Outcome in Frontal Impacts. *Traffic Injury Prevention*, *5(2):* 156-163.

Kullgren, A., Krafft, M., Malm, S., Ydenius, A., Tingvall, C. (2000). Influence of Airbags and Seatbelt Pretentioners on AIS1 Neck Injuries for Belted Occupants in Frontal Impacts. *Stapp Car Crash Journal 44,* 117-125.

Lindman, M., Nyström, J., Jakobsson, L. and Ödblom, A. (2012). Monitoring the past and the future of a passenger car auto brake system. *Proc. of IRCOBI Conference on Biomechanics of Impacts*, Paper number: IRC-12-46.

Rizzi, M., Kullgren, A., Tingvall, C. (2014). The injury crash reduction of low-speed Autonomous Emergency Braking (AEB) on passenger cars. *Proc. of IRCOBI Conference on Biomechanics of Impacts*, Paper number IRC-14-73.

Sahai, H., Kurshid, A. (1995). *Statistics in Epidemiology: Methods, Techniques and Applications*. CRC Press.

SMHI, Swedish Meteorological and Hydrological Institute, Available on line at: http://www.smhi.se/klimatdata/meteorologi/temperatur.

This paper has been peer-reviewed and published in a special edition of *Traffic Injury Prevention* 16(S1), by Taylor & Francis Group. The complete paper will be available on the *Traffic Injury Prevention and www.NHTSA.gov* websites on June 8, 2015.

To access all Peer-reviewed papers please copy and paste the link below into your browser to access the papers.

http://www.tandfonline.com/toc/gcpi20/16/sup1

# FEATURES OF CAR–CYCLIST CONTACT SITUATIONS IN NEAR-MISS INCIDENTS COMPARED WITH REAL-WORLD ACCIDENTS IN JAPAN

**Yasuhiro Matsui, Shoko Oikawa**
National Traffic Safety and Environment Laboratory
Japan

**Kunio Takahashi**
Saisei Engineering
Japan

**Masahito Hitosugi**
Shiga University of Medical Science
Japan

Paper Number 15-0124

## ABSTRACT

The use of active safety devices that can detect cyclists is considered an effective countermeasure for the reduction of the severity of injuries and number of deaths of cyclists. The detailed features of car–cyclist contact scenarios need to be clarified to develop such safety devices. Because there is limited information on real-world accidents, the present study investigates near-miss scenarios captured by drive recorders installed in passenger cars.

The first purpose of the present study is to ascertain the utility of using near-miss scenarios in clarifying the features of situations of contact between cars and cyclists. The similarities of data of near-miss incidents including video captured by drive recorders and national data of real-world fatal cyclist accidents in Japan are investigated. We used 229 videos of near-miss car–cyclist incidents collected by the Society of Automotive Engineers of Japan (J-SAE) from 2005 to 2009. In scenarios where the car travels straight ahead, 70–84% of cyclists on straight roads or at intersections crossed the road in front of the forward-moving cars both in accidents and near-miss incidents. There are thus similarities between accidents and near-miss incidents and it is possible to estimate the situations of cyclists' accidents from near-miss incident data including video that captures cyclist behavior.

The second purpose of the study is to calculate the time to collision (TTC) from the near-miss incident data. The study analyzed data for 166 near-miss car–cyclist incidents in which cyclists crossed the road in front of forward-moving cars on straight roads or at intersections. We calculated the TTC from the velocity of the car with an installed drive recorder and the distance between the car and the cyclist at the moment the cyclist appeared in the video captured by the drive recorder. The average TTC was 2.1 s (Standard Deviation (SD) of 1.6 s). In terms of the manner in which cyclists emerged in front of cars, the average TTC was the shortest (1.9 s) when cyclists emerged from behind a building or moving vehicle in the opposite lane. We propose that the specifications of a safety device developed for cyclist detection and automatic braking should reflect detailed information that includes the TTC obtained for near-miss situations.

## INTRODUCTION

The number of traffic deaths in Japan decreased in the past 20 years to 4373 in 2013[1)]. The Japanese government has an aim to reduce the annual fatality count to less than 2500 by 2018[2)]. Among types of road fatalities between 2012 and 2013, only cyclist fatalities increased in number, from 563 to 600 (by 7%). As an example of a countermeasure implemented by the Japanese government to reduce pedestrian deaths, the safety performances of car bonnet tops have been assessed since 2005. However, there has been no effective regulation for cyclist protection.

To reduce the severity of injuries and the number of deaths, active safety devices such as crash severity mitigation systems using sensors for cyclist detection are regarded as effective countermeasures. Currently, cars installed with crash severity mitigation systems that include a stereo camera as a sensor and automatic braking have been

developed in Japan [3, 4]. Such cars are expected to be further designed with consideration of aspects of car–cyclist contact situations including the time to collision (TTC). However, the contact situations of accidents have not been clarified, because there is limited detailed information on real-world accidents. Rosen et al.[5] investigated the positions of pedestrians and cars at a time 1 s prior to impacts that resulted in fatal accidents, but there have been few other representative examples of research on cyclists and car positions. The present study therefore focused on near-miss incidents captured by drive recorders installed in passenger cars.

A near-miss incident is a situation that a car accident involving a cyclist is avoided by the attention and braking of a driver. Near-miss incidents occur more frequently than accidents. Recently, drive recorders were installed in taxis in metropolitan, Tokyo for the purpose of investigating causes of car accidents and educating car drivers. The data of the drive recorder consist of video captured by a forward-facing camera and a car's velocity, acceleration, and braking signals. If near-miss incidents are similar in nature to accidents, then car–cyclist contact situations or the TTC can be calculated from near-miss incidents. The authors thus analyzed the near-miss incident data captured by drive recorders installed in taxis.

The first purpose of the present study is to ascertain the usefulness of using near-miss situations in clarifying the features of situations of contact between cars and cyclists. The study investigated similarities between the data of near-miss incidents including video captured by drive recorders and the data of real-world fatal cyclist accidents in Japan.

The second purpose of the present study is to calculated the TTC from the near-miss incident data so as to help develop a crash severity mitigation system for the active safety of cars in the future. The study analyzed near-miss car–cyclist incident data where cyclists crossed the road in front of forward-moving cars on straight roads or at intersections. The TTC was calculated from the velocity of the car with an installed drive recorder and the distance between the car and the cyclist at the moment the bicycle appeared in the video captured by the drive recorder. The worst situation was assumed to be that when a car moved toward a cyclist without the driver noticing the cyclist or braking.

## NEAR-MISS IN-DEPTH DATA

J-SAE has collected near-miss incident data[6] consisting of forward-oriented video and the car velocity, acceleration and braking signal obtained from drive recorders for more than 100 taxis in Tokyo from 2005. Each drive recorder was installed on the inside of the front window and consisted of a camera and a three-dimensional accelerometer. The near-miss incident data include events of car–car, car–cyclist, car–bicycle, and car–motorcycle impacts.

The drive recorder's collection of data is triggered by a driver's sudden braking with deceleration exceeding 0.5 G, and the recorder collects data for 10 seconds before and 15 seconds after the triggering. In the present study, the authors used data for 229 near-miss car–cyclist incidents from 2005 to 2009 consisting of 150 incidents during the day and 79 incidents at night.

## CONTACT SCENARIOS IN REAL-WORLD ACCIDENTS AND NEAR-MISS INCIDENTS

The Institute for Traffic Accident Research and Data Analysis of Japan investigated car–bicycle contact scenarios in real-world fatal cyclist accidents from 1999 to 2003 in Japan[7]. In accidents on straight roads or at intersections, the fatality rates for working-age and elderly cyclists crossing the road in front of forward-moving cars were 83% and 90%, respectively. We thus compared scenarios of contact between near-miss car–cyclist incidents and real-world fatal car–cyclist accidents when cyclists crossed the road in front of forward-moving cars to clarify the utility of using near-miss car–cyclist incident data. We investigated video captured by drive recorders for 229 near-miss incidents from 2005 to 2009 and national records for 2818 real-world fatal cyclist accidents from 1999 to 2003 in Japan[7], in which cyclists crossed the road in front of forward-moving cars on straight roads or at intersections. The relationships of the moving directions of vehicles and cyclists on straight roads and at intersections are defined in Figure 1. On straight roads, the cyclist crosses the road in front of a forward-moving car in case A while the cyclist travels in the parallel direction as the moving car in case C. At an intersection, the cyclist crosses the road in front of the forward-moving car in what is referred to as case B.

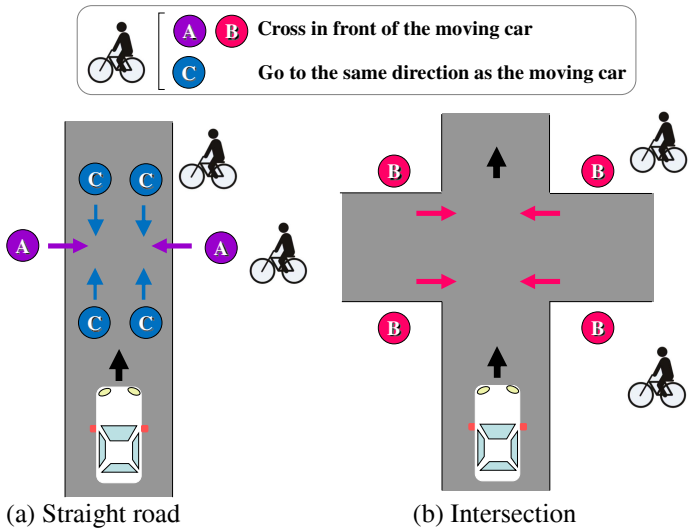


*Fig.1. Relationships of moving directions of a vehicle and cyclist.*

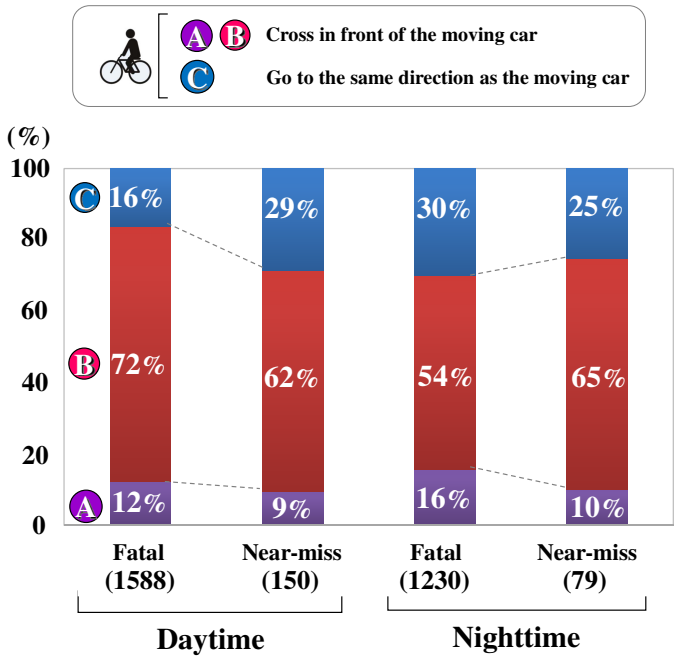


*Fig.2. Relative directions of travel of a vehicle and cyclist in accidents and near-miss incidents.*

Figure 2 presents the distribution of relative directions of travel of a vehicle and cyclist in accidents and near-miss incidents. Cases A and B together accounted for 84% (fatal) and 71% (near-miss) of incidents during the day and 70% (fatal) and 75% (near-miss) of incidents at night; i.e., 70–84% of incidents involved cyclists on straight roads or at intersections crossing the road in front of forward-moving cars. These results show similarities in cyclists' behavior between accidents and near-miss incidents. Cyclist accident situations can thus be predicted by analyzing near-miss incident data including video that captures the cyclist behavior. The next section investigates situations of cars and cyclists approaching each other in detail using near-miss incident data.

## IN-DEPTH ANALYSIS OF NEAR-MISS EVENTS

### In-depth analysis of data of near-miss events

In this section, the TTC is calculated from near-miss car–cyclist incident data where cyclists crossed the road in front of forward-moving cars on straight roads or at intersections. A near-miss incident is a situation that an accident is avoided through the attention and braking of the driver of the car. In the present study, the TTC was calculated from the near-miss incident data considering the worst case that the driver did not brake (through, for example, a lack of attention or insufficient reaction time).

The near-miss incident data for situations in which cars and cyclists approached each other were selected for analysis. As a result, 166 near-miss car–cyclist incident data were used, where cyclists crossed the road in front of forward-moving cars on straight roads or at intersections.

### Calculation of the TTC

The TTC (s) was calculated as

$$\mathbf{TTC = L/V, (1)}$$

where V (m/s) is the velocity of a car with an installed drive recorder and L (m) is the forward distance between the car and the cyclist at the moment when a cyclist appears in the video captured by the drive recorder as shown in Figure 3. Here, V is the running velocity of the car just before the driver applies the brake after realizing the existence of the cyclist. It was determined whether a driver applied the brakes by checking the braking signal and deceleration signal recorded by the drive recorder.

The study also investigated the lateral distance Ld (m) between one side of the car and the cyclist obtained as

$$\mathbf{Ld = LL - 0.85, (2)}$$

where LL (m) is the distance between the center of the drive recorder camera (the center of the car) and the cyclist (approximately 1.7 m), and the value 0.85 m is half the full width of the car.

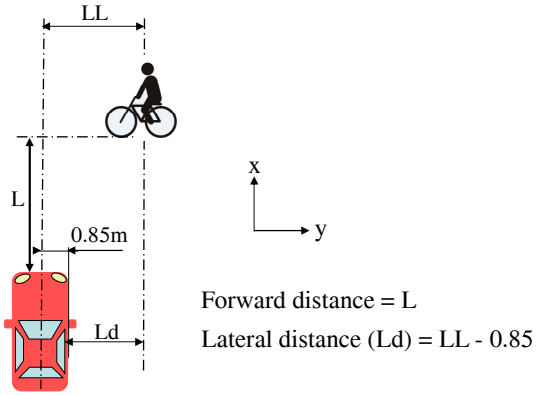


***Fig.3. Definitions of forward and lateral distances.***

Figure 4 shows the distribution of the calculated TTC the lateral distance (Ld) from the side of the car to the cyclist at the moment the cyclist appears in the video captured by the drive recorder. The TTCs ranged from 0.5 to 10.0 s. In determining the location of a cyclist relative to the center of a car, it was observed that the cyclist was to the right of the car in 86 cases and to the left in 80 cases. The average TTC was 2.2 s (standard deviation (SD) of 1.7 s) for the cases on the right-hand side and 2.1 s (SD of 1.7 s) for the cases on the left-hand side. Because the average TTC was similar for the two sides, the following analyses were performed regardless of whether the cyclist to the left or right of the vehicle. The average TTC was 2.1 s (SD of 1.7 s) for the total 166 cases.

The distribution of the calculated TTC and forward distance (L) between a car and a cyclist is shown in Figure 5. Theoretically, the TTC should increase as the forward distance increases. The figure reveals direct proportionality between the forward distance and TTC.

The distribution of the calculated TTC and the car velocity (V) is shown in Figure 6. Theoretically, the TTC should decrease as the car velocity increases. However, no linear correlation between the car velocity and TTC is observed. There are several possible reasons for the widely scattered data in Figure 6. Therefore, the next section investigates the features of cyclist behavior in detail.

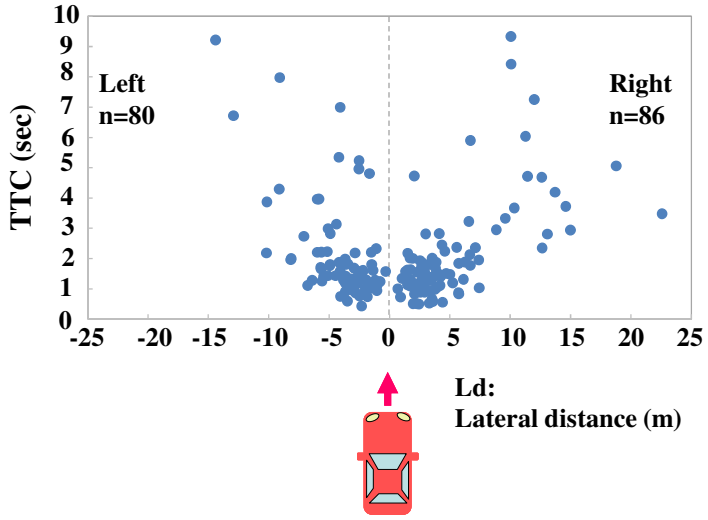


*Fig.4. Distribution of the calculated TTC and lateral distance (Ld).*

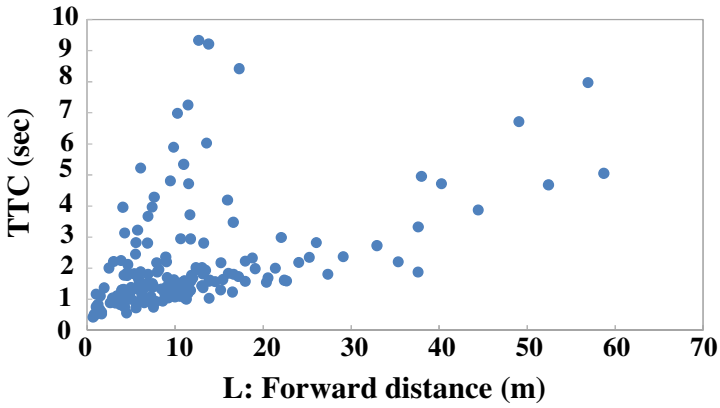


*Fig.5. Distribution of the calculated TTC and forward distance (L).*

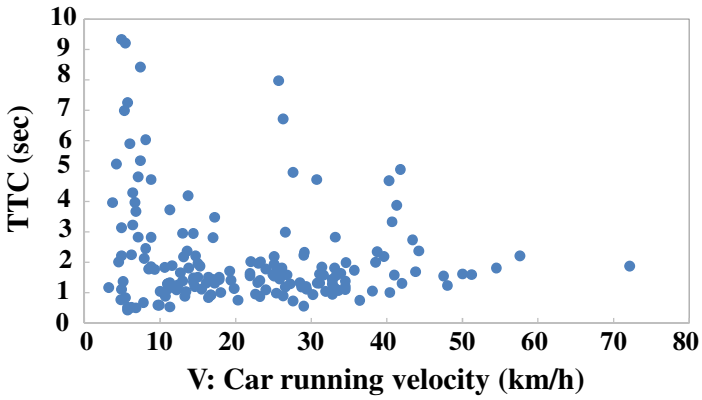


*Fig.6. Distribution of the calculated TTC and car velocity (V).*

**Detailed Features of Cyclist Behaviors**

The manner in which cyclists appeared in front of the car was classified into four categories as shown in Table 1. The classifications are (1) the driver having an unobstructed view, (2) the cyclist emerging from behind a building, (3) the cyclist emerging from behind a parked vehicle, and (4) the cyclist emerging from behind a moving vehicle. The average values of the TTC, the forward distance between the car and the cyclist, and the car velocity for the four classifications are presented in Figure 7. The average TTC was longest (3.3 s) for the unobstructed view (1), presumably because of the longer forward distance (averaging 19.5 m) regardless of the higher velocity of the car (averaging 24.7 km/h). The average TTC was shortest (1.9 s) when a cyclist emerged from behind a building (2) or moving vehicle (4), presumably owing to the shorter forward distance between the car and the cyclist (averaging 9.9 m for (2) and 8.7 m for (4)).

**Table1.**
**Four classifications of situations in which the cyclist appears in front of a car.**

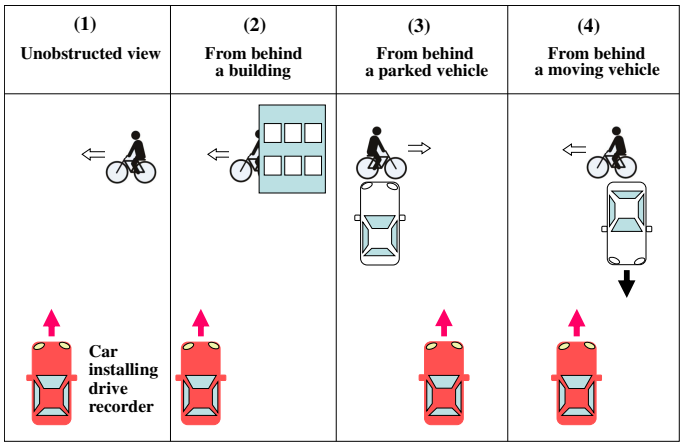


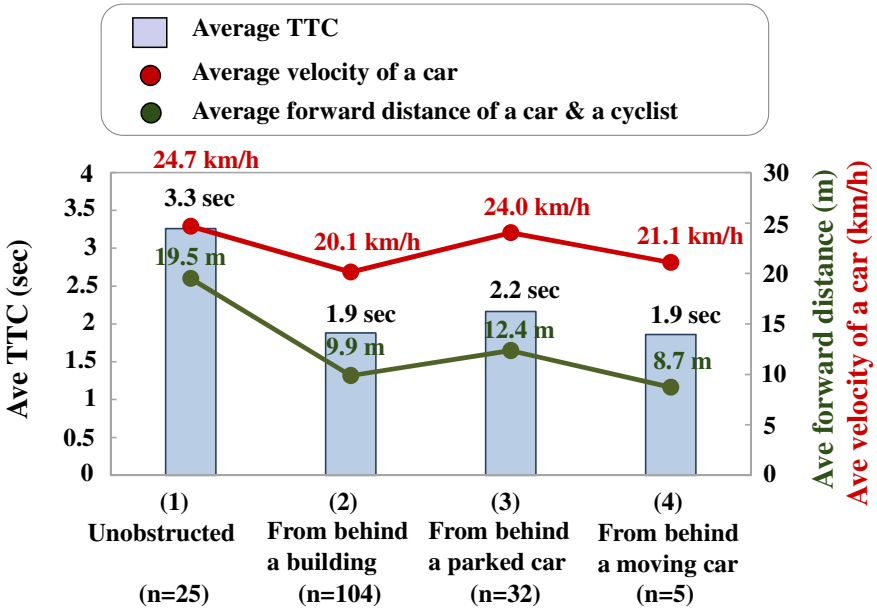


*Fig.7. Average values of the TTC, forward distance between the car and the cyclist, and car velocity in the four categories of cyclist emergence.*

## DISCUSSION AND CONCLUSIONS

The present study investigated the usefulness of near-miss situations in clarifying the features of situations of contact between cars and cyclists, and calculated the TTC using near-miss incident data. A near-miss incident was considered a situation that an accident was avoided through the attention and braking of the driver of the car.

The similarities between the data of near-miss incidents including video captured by drive recorders and national data of real-world fatal cyclist accidents in Japan were investigated. It was found that 70–84% of cyclists involved in accidents on straight roads or at intersections crossed the road in front of forward-moving cars both in cases of accidents and in cases of near-miss incidents. There were thus similarities between accidents and near-miss incidents. It was determined that the situations of car–cyclist accidents could be calculated from near-miss incident data including video capturing cyclist behavior.

The study analyzed data for 166 near-miss car–cyclist incidents in which cyclists crossed the road in front of forward-moving cars on straight roads or at intersections. It is noted that, in the present study, the TTC was calculated from near-miss incident data considering the worst case that the car hits the cyclist without braking. The TTC was calculated from the velocity of the car installed with a drive recorder and the distance between the car and the cyclist at the moment the cyclist appeared in the video captured by the drive recorder. The average TTC was obtained as 2.1 s (SD of 1.7 s). In terms of the manner in which cyclists emerged in front of cars, the average TTC was shortest (1.9 s) when cyclists emerged from behind a building or from behind a moving vehicle in the opposite lane. The authors propose that the specifications of a safety device developed for cyclist detection and automatic braking should reflect detailed information including the TTC obtained for near-miss situations.

As described, the present study obtained TTCs for 166 near-miss car–cyclist incidents. Currently, definition of the near-miss incident has not been determined quantitatively. Because the features of the 166 near-miss car–cyclist incidents were similar to features of accident records, it was possible to define a near-miss incident level for estimating accident situations according to the present analysis results, such as an average TTC of 2.1 s (SD of 1.7 s).

## ACKNOWLEDGMENTS

The authors appreciate the assistance of Mr. Katsumi Moro, formerly at the Society of Automotive Engineers of Japan (J-SAE) and currently with the Tokyo University of Agriculture and Technology, in the analysis of near-miss incident data.

## REFERENCES

[1] Institute for Traffic Accident Research and Data Analysis of Japan (ITARDA), ‘Annual Traffic Accident Report in 2013’, Tokyo, 2014 (in Japanese).
[2] Cabinet Office, White Paper on Traffic Safety, 2009 (in Japanese).
[3] E. Shibata, Development of Driving Assist System “EyeSight” by New Stereo Camera, Journal of Society of Automotive Engineers of Japan Vol.63, No.2, pp.93-98, 2009, paper number 20094102 (in Japanese).
[4] S. Kuzumaki, Our Approach to a Safe Sustainable Society, Journal of Society of Automotive Engineers of Japan Vol.63, No.12, pp.11-19, 2009, paper number 20094737 (in Japanese).
[5] E. Rosen, J. Kalhammer, D. Eriksson, M. Nentwich, R. Fredriksson and K. Smith, Pedestrin Injury Mitigation by Autonomous Braking, 21st International Technical Conference on the Enhanced Safety of Vehicles (ESV) 2009, paper number 09-0132.
[6] M. Nagai, Current Situation in Registration and Application of Drive Recorder Data Base, Forum in JSAE Spring Convention in 2009 “What the Drive Recorder can contribute for Traffic Safety”, pp.31-40 2009 (in Japanese).
[7] Institute for Traffic Accident Research and Data Analysis of Japan, ITARDA Information No.53 (in Japanese), Tokyo, 2004 (in Japanese).

# VIRTUAL EXPERIMENTAL ENVIRONMENT DESIGN of CAMERA-SENSOR-BASED LANE DETECTION SYSTEM

**Ziyi, Peng**
Chinesisch-Deutsches Hochschulkolleg, Tongji University
China

**Junyi, Chen**
**Hongyan, Wang**
**Lulong, Cai**
School of Automotive Studies, Tongji University
China

**Yutong, He**
Shanghai United Road Traffic Safety Scientific Research Center
China

Paper Number 15-0125

## ABSTRACT

Based on the application of software model building, virtual experiment can be conducted with vehicle model, road environment model and sensor model building to develop camera-sensor-based lane detection system in PreScan. These three types of models are connected and the virtual experimental environment is built. Sensor-extracted data are processed by Matlab/Simulink to acquire the accurate ground truth. Meanwhile, images from camera sensor are processed with standard size for further application. The virtual experimental environment design is the foundation for the analysis and comparison of ground true and camera-detected data, as well as for accuracy evaluation in system pre-development. In conclusion, the virtual experimental environment design can be used in camera-sensor-based lane detection system development and is a supplement to traditional system development.

## INTRODUCTION

In recent years, with rapid development and comprehensive application of computer vision and image processing technology, more and more products about pilotless automobiles and Advanced Driver Assistance Systems (ADAS) are coming to the market.
Camera-sensor-based vision and image processing technology are suitable for application of trajectory recognition and tracking. A lot of scientific achievements have been already applied in the real world. For example, a six-wheeled autonomous off-road vehicle (called an Argo vehicle) was equipped with various sensors at the University of Waterloo. 3D objects on the road can be dectected by the sensor on the Argo vehicle [1]. In Highway Lane Change Assistant (HLCA) system which was designed by M.Ruder from BMBF in Germany, vision and radar sensors were combined to detect dangerous objects in the neighboring lanes [2]. The system which was applied to Lane Departure Warning was connected to computers with Controller Area Network (CAN) and controlled by CAN. AutoVue System from Iteris Inc was also applied to Lane Departure Warning. The system was controlled by an integrated unit which consisted of camera and computer [3]. Currently most research focuses on application and optimization of lane detection algorithm in ADAS and pilotless automobiles [4]. There are basically two major research focuses in algorithm development. One is trajectory recognition and tracking with Hough Transform and other related algorithm. The other is based on the existing lane marker models. Parameters of the lane markers are detected by camera and matched with models [5]. The suitable lane marker model will be selected, if the information of lane markers and the model is similar or identical.
With deeper and more intensive research in development and evaluation of camera-sensor-based driver assistance system, a new method is expected to ensure the effectiveness and efficiency of system development process [6]. Meanwhile, due to high cost and long term of field experiment, virtual experiment is suggested as a good support and supplement of traditional field experiment by R&D engineers. Thus, design and development of virtual experiment is a new research focus of camera-sensor-based driver assistance system development.

## 1 BACKGROUND

This paper focuses on virtual experimental environment of camera-sensor-based driver assistance system, especially lane detection systems, for instance, Lane Departure Warning (LDW), Lane Keeping Assist (LKA), Lane Centering Assist (LCA) etc. Camera-sensor-based driver assistance system aims to identify various types of lanes on different roads and help cars drive in the right lane [7].

Traditional evaluation method of camera-sensor-based driver assistance system development is to apply advanced data process technology such as VBOX or TRC to extract ground truth [8]. Taking VBOX for instance, it is a GPS based data acquisition system, which can extract the real-time location and dynamic parameters of the vehicle. Extracted data will be transmitted to computers without delay [9]. Meanwhile, VBOX can process image data of lanes from the camera and output the distance between the lane markers and the vehicle. By comparing this information with data from lane detection algorithm, the accuracy of the algorithm can be evaluated.

In the course of research and development in real life, a major problem of field experiment is that the system cannot be tested and evaluated exhaustively under every operating condition. Besides, the cost of traditional field experiment is relatively high. Thus, it is quite difficult to achieve the effectiveness of experiment. Under this circumstance, virtual experiment by software is regarded as a good supplement of traditional experiment. A vehicle dynamic model is needed to calculate dynamic parameters in camera-sensor-based driver assistance system virtual experiment. A standard road environment model along with weather and traffic condition is designed in the experiment. A camera sensor and a lane marker sensor should be also included to extract real-time image data and ground truth. In total, the vehicle model, road environment model and sensor models are mutually dependent and interacting.

The PreScan Software developed by TNO provides the possibility of design of the above three kinds of models under request of different parameters and conditions. PreScan is a physics-based simulation platform that is used for development of ADAS that are based on sensor technologies such as camera and GPS [10]. Meanwhile, PreScan can be connected with Matlab/Simulink for further data processing and calculation.

## 2 VIRTUAL EXPERIMENT MODELS

In order to design the virtual experimental environment of camera-sensor-based lane detection system, a vehicle model, a road environment model and sensor models should be set up in the related simulation software separately. The three types of models should work together so that the model can calculate vehicle dynamic data and the sensor can receive the signal of the road environment model at the same time. The vehicle dynamic model is primarily used to simulate the vehicle motion in reality, meanwhile the sensor is equipped on the vehicle, so the motion state of the vehicles can directly influence the signal received by the sensor. The road environment model, as one of the most important parts in this virtual experiment, is the source of the information collected by the sensor. This model should contain not only the information of national standards of roads, but also the driving route and the velocity of the vehicle.

### 2.1 Vehicle Model

In the test experiment of lane detection system vehicle model is basically focused on vehicle dimensions and dynamic model. Vehicle dimensions can affect the location of camera, while dynamic model is to calculate dynamic parameters. Audi A8, the software built-in dimension model, is chosen for the experiment as a dimension model in this paper. A suitable vehicle dynamic model can calculate real-time dynamic parameters for development and test of lane detection system. The Two-wheeled vehicle dynamic model is selected as a dynamic model, because there is no specific requirement for more sophisticated dynamic in the lane detection

system experiment. The Two-wheeled vehicle dynamic model will calculate longitudinal and lateral velocity and acceleration, as well as yaw angle and pitch angle etc. For instance, pitch angle of the vehicle is different at different accelerations. As figure 1 shows below, the right image is in the course of acceleration, while the left one shows vehicle without acceleration. It is obvious that the horizon in the right image is higher because of the different pitch angle under conditions of different accelerations.

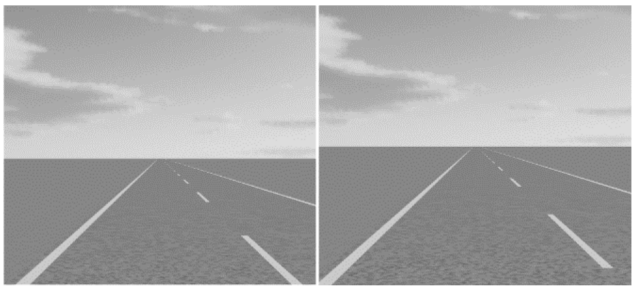


***Figure1. Comparison of output images at different accelerations***

It should be noted that, a customized, more sophisticated vehicle dynamic model can be called into PreScan if there is higher requirement for the virtual experimental environment.

**2.2 Road Environment Model**

**2.2.1 Road model** Lane detection systems are usually designed for expressways or other well-structured roads. Thus, the chosen road model in this paper is based on expressway model.

There are rigorous rules and regulations in Standard of Chinese Highway Route Design [11]. Direction of roads, as well as numbers and width of lanes are considered in the virtual experiment. Length, width and interval of lane markers and other related information is also important to the reality of the virtual road model.

According to the Standard of Chinese Highway Route Design, the radius of curves ranges from 250m to 1500m, and a total of 6 groups of bend road are designed. In order to test the fault tolerance of misstatement and omission of lane detection systems, missing lane markers are designed in the virtual experiment. In this paper the length of missing lane markers is 5m, 10m, 20m and 50m respectively. In addition, the color of lane markers, the luminance of lane markers, dashed/solid lane markers and bumpy/flat roads etc. can be defined as well.

**2.2.2 Trajectory** In the virtual experiment, the trajectory of the vehicle can be identified under specific request. However, due to the Two-wheeled vehicle dynamic model, the actual trajectories of the vehicle might be slightly different with the identified ones when vehicles change lanes or make a turn in the virtual experiment.

**2.2.3 Vehicle velocity** Vehicle velocity is essential to the result of virtual experiment. Since lane detection systems are mainly applied on expressways, the velocity is set at the range over 80km/h in the experiment. The performance of lane detection system is tested under different driving scenarios, including acceleration, deceleration, uniform motion and constant acceleration motion, etc.

**2.3 Sensor Models**

**2.3.1 Camera sensor** **A** camera sensor is one of the most important sensors in lane detection systems. All the extracted data are from the video images that captured by the camera sensor.

Parameters of the camera sensor can be set according to the specific sensor applied in traditional experiments, including location coordinates, range of sight, focal length, resolution of the output images, the video frames and the bit rate and so on. In this paper the frequency of the camera sensor is set as 25 Hz, that is, the video frame of the output images is 25.

**2.3.2 Lane marker sensor** Besides camera sensor, a lane marker sensor is quite necessary to extract accurate and real-time ground truth in the virtual experiment. The lane marker sensor is a built-in virtual sensor. It can provide the accurate information of the lane markers. The specific form of the lane marker information is the absolute coordinates of intersection between the center line of the lane marker and the sensor scanning line, as well as the distance from the intersection to the sensor. The accuracy of the data is 0.01m. According to the sensor settings, it can detect and record 3 points of the intersections at most each time. The frequency of the lane marker sensor is identical to the camera sensor, which is 25 Hz. In order to facilitate data processing and calculation afterwards, the lane marker sensor is located at the center position of the rear axle.

### 2.4 Build of Virtual Experiment Models

After setting the parameters of the above three types of models, different models can be connected and built in the Matlab/Simulink and the parameters of connections which are shown in Figure 2 can be further set according to specific requirements.

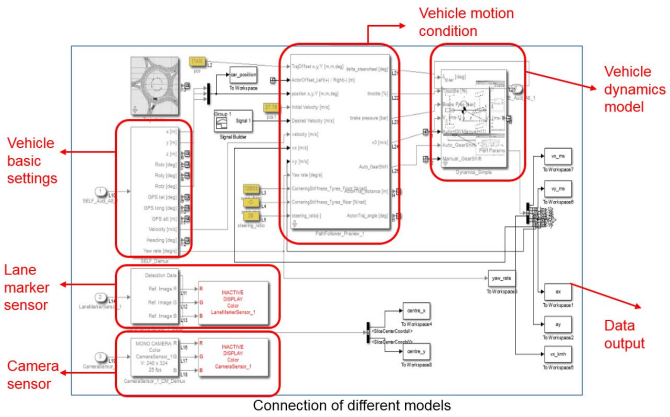


***Figure2. Connections and control strategy diagram of lane detection system***

## 3 DATA PROCESSING

In order to facilitate simulation data processing for the subsequent Software or Hardware in the Loop (SiL or HiL), the output data should be real-time data of ground truth and vehicle dynamic based on every video frame. These data can be regarded as the accurate vehicle dynamic and ground truth in the experimental environment. The results come from camera video image processing can be validated by comparing with the accurate data mentioned above.

### 3.1 Lane Marker Model

This paper only introduces two-dimensional lane marker models. Two-dimensional lane marker models can be divided into straight lane marker model, curve lane marker model and combined model, etc. A combined model of lane marker is chosen in this paper. At certain time, the lane marker model function below can describe the lane marker ahead [12].

$$y(x) = y_0 + \tan(\varepsilon)\, x + \frac{C_0}{2} x^2 + \frac{C_1}{6} x^3 \qquad \textbf{(1)}$$

Where,

$y_0$ : the distance from the center line of lane marker to the center of the rear axle

$\varepsilon$ : the angle between travel direction of vehicle and the lane marker

$C_0$, $C_1$ : coefficients

The origin of the coordinate system is the center of the rear axle as shown in Figure 3.

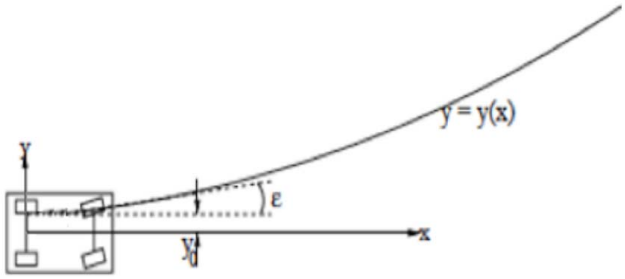


***Figure3. Sketch of the lane marker model and vehicle-rear-axle-based coordinate system***

### 3.2 Ground Truth Data Processing

In order to determine the coefficients of the lane marker model, points on the lane marker should be recorded for data fitting as many as possible at every moment. However, the lane marker sensor can detect and record only 3 points of the intersections at most each time and data are based on absolute coordinate system.

Under this circumstance, two tasks should be completed to determine the coefficients of function (1). The first task is to extract as many points as possible. The lane marker sensor is required to cover 100m lane marker ahead and extract about 1000 points in total each time, which means the points are extracted about every 0.1m on average. As a result, the vehicle should run two times in the virtual experiment.

For the first time the vehicle runs at the velocity of 2.5m/s (about 9 km/h) from the beginning of the lane to the end, by which the points on the lane marker can be extracted. The extracted data are in the absolute coordinate system. Because the frequency of the lane marker sensor is 25Hz and the velocity of the vehicle is 2.5m/s, the points can be extracted every 0.1m on the road. It can meet the requirements of data density which mentioned above.

For the second time the vehicle runs at the previous set velocity and follows the set trajectory on the road. The real-time vehicle-rear-axle-GPS data, as well as the vehicle dynamic data such as velocity, yaw rate, pitch, etc. can be extracted by PreScan. As the frequency of camera video is 25Hz, the absolute coordinate of the vehicle rear axle on each image can be known by reading the GPS data.

The second task is to transform the absolute coordinates to vehicle-rear-axle-based coordinates and determine the coefficients of function (1). The following data processing procedure is used to complete the second task:

Step 1. Coordinate transformation. The data of points on the lane marker should be transformed into the real-time vehicle-rear-axle-based coordinate system by applying the two-dimensional coordinate transformation formula.

Step 2. Data selection. All the points on the lane marker are extracted at the first time of the vehicle motion. In order to extract the points within about 100m ahead, the distance from the vehicle rear axle to the farthest points should be a little more than 100m.

Step 3. Determination of the coefficients. All the selected data should be stored by cell function. With the help of Polyfit function in data fitting tool box in Matlab, the coefficients of function (1) can be fitted. In this way, the accurate real-time ground truth can be acquired based on every frame of the camera video images.

Taking one of the lane markers on the curve road as an instance, the fitting results of these 1021 points are in the following.

$$\begin{cases} y_0 = 5.6356 \\ \varepsilon = 0.0015 \\ C_0 = -0.0044 \\ C_1 = -2.128E-05 \end{cases}$$

The fitted curve whose standard deviation is 0.0117 is shown in Figure 4.

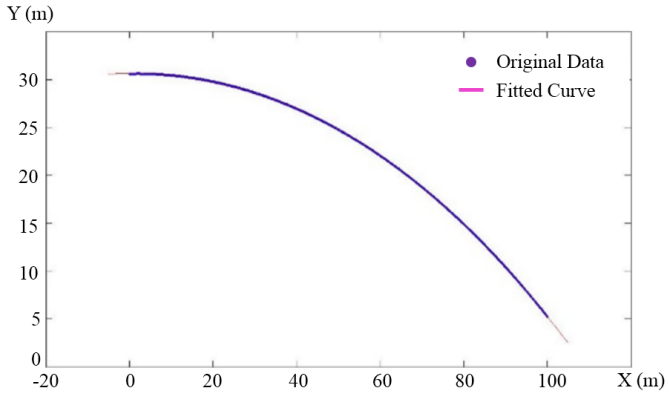


***Figure4. Scatter and fitted curve of the curved lane (t=48.25s)***

### 3.3 Video Images Output

Besides the data extracting and data processing, the video images from camera sensor should also be output and processed. In order to prepare for application of algorithm verification, the output images should be scale and processed to fitting size by batch processing in Matlab. The suitable image recognition algorithm, such as Hough Transform, is applied to extract the information of the lane markers on the image. By comparing the coefficients of function (1) determined by the image recognition algorithm with the above mentioned coefficients, the accuracy of the lane marker fitting algorithm in the virtual experimental environment can be identified.

## CONCLUSIONS AND DISCUSSIONS

The design of virtual experiment for lane detection system can simulate the vehicle model, road environment and camera and lane marker sensors in PreScan. With the help of virtual experiment, vehicles, roads and

sensors in different conditions can be designed and tested in short time. The cost can be much less than field experiment and the efficiency can be much higher. The accurate ground truth of the road and vehicle dynamic data can be acquired by running of the virtual experiment and the data processing.
In conclusion, the virtual experimental environment design and development can be used in camera-sensor-based lane detection system development and is a supplement to traditional system development.
However, this paper only introduces the design of basic road models of straight and curve road with a two-dimension combined lane marker model. More types of road models should be considered in further study, such as spiral road model and bumpy road model. Thus, a three-dimension lane marker model is required to acquire the accurate ground truth. In addition, complex traffic conditions, as well as different lighting conditions and weather conditions can also be added in the further study of virtual experiment design.

## REFERENCES


[1] Javed, M.A., Spike, J., Waslander, S., Melek, W., Owen, W. 2001. "Argo Vehicle Simulation of Motion Driven 3D LIDAR Detection and Environment Awareness." Autonomous and Intelligent Systems, Volume 6752: 284-293
[2] Ruder, M., Enkelmann, W., Gamitz, R. 2002. "Highway Lane Change Assistant". In Proceedings of Intelligent Vehicle Symposium (Versaille, France, June 17-21). IEEE, 240-244
[3] Wang Rongben, Guo Lie, Jin Lisheng, et al. 2007. "Recent Research of Safety Driving Assistance Technology in Intelligent Car". Journal of Highway and Transportation Research and Development, 24(7): 107-111
[4] Qu Yang, Feng Huanqing, Ding Feng. 2013. "A Lane Detection Algorithm Based on Real-Time Video Process." Application Research of Computers, 30(3): 930-932
[5] Sun Yanbiao, Liu Wei, Wang Shaoping, et al. 2014. "Design and Implementation of Lane Detection System Based on DSP." Electronic Measurement Technology Press, April: 83-86
[6] Tideman, M., Versteegh, T., Bouts, R. 2012 "Developing Methodology for Design and Assessment of Active and Integrated Safety Systems for Automobiles." Journal of Automotive Safety and Energy, 3(2)
[7] Borkar A. 2011. "Multi-viewpoint lane detection with applications in driver safety systems." PhD thesis
[8] Preda, I., Covaciu, D., Ciolan, Gh., et al. 2008. "Vehicle Dynamic Behaviour Analysis Based on GPS Data." In Proceedings of "SMAT2008" International Conference (Craiova, Romania)
[9] Wang Liang. 2010. "Performance Test and Result Analysis of Abs Based On VBOX Equipment." Light Vehicles
[10] Tideman, M., Van Noort, M. 2013. "A Simulation Tool Suite for Developing Connected Vehicle Systems." In Proceedings of Intelligent Vehicles Symposium (IV), IEEE
[11] JTG D20—2006, "Standard of Chinese Highway Route Design."
[12] Southall, B., Taylor, C.J. 2001. "Stochastic road shape estimation." In Proceedings of Eighth International Conference on Computer Vision, IEEE

**Preliminary Study of Roof Airbag Protecting Rear-Seat Occupants in Frontal Impact**

**Chun-Tao, Wu**
**Kai, Zhang**
Great Wall Motors Co., Ltd.
People's Republic of China

Paper Number 15-0130

## ABSTRACT

A kind of innovative Airbag, Roof Airbag (RAB), with external straps is studied via virtual engineering, which provide protection to rear-seat occupants in frontal impact. Frontal sled model with AF05 female dummy is generated in LS-DYNA, which is well correlated with full vehicle frontal crash tests in terms of the kinetics and injuries of the dummy. In addition, it is adapted for AF50 and AF95. Based on above models, different configurations of restraint system are studied, different levels of load limiter, belt with or w/o pretensioner, with or w/o RAB for instance. It can be summarized that roof airbag with low level of belt load limiter and pretensioner could provide protection to most size of rear-seat adult occupants as good as that of front-seat occupants in frontal impact.

## 0 INTRODUCTIONS

Frontal Airbag, Driver Airbag (DAB) and Passenger Airbag (PAB), has been fitted in most of the vehicles as standard safety restraints, which provide inevitable protection to drivers and passengers in frontal accidents. This is benefitted from the requirements of regulations and consumer metric protocols, such as NCAP. It is reported that 40% fatal and serious injuries is caused by frontal accidents for rear-seat occupants [4]. However, for rear seat occupants, such helpful restraint equipments are not fitted in any commercial vehicle, yet. Anyway, the protection to rear seat occupants in frontal impact has been paid more attentions since last decay. NHTSA funded Rear Seat Occupant Protection Research Program. In 2005, Kuppa[1] and etc. reported that protection performance of rear-seat occupants is related with the age of the occupants in frontal impact. For the children and young adult people, age below 50, it is safer seated in rear seats than in the frontal-row seats, which is opposite for older people. It may be caused by misuse of frontal airbag. In 2007, Richard Kent[2] and etc. revealed that newer vehicle models, after 1999, with better restraints has improve the benefit to occupants younger than 50 seated in frontal seats compared with vehicle models before 1999, which is similar to those seated in rear seats. Meanwhile, Koji Mizuno[3] and etc. carried out couples of full vehicle frontal impact tests at 50km/h, which emphasis the necessaries of using seatbelt to avoiding fatal injuries during frontal impact for adults and children. Lotta Jakobsson and her partners have introduced integrated booster cushion with progressive torsion bar of seatbelt to provide protection for growing Children in frontal accidents[5]. Katarina Bohman and etc. has studied the rear seat child protection due to different type of seatbelt retractors, which shown that seatbelt with load limiter and pretensioner can not only constrained the occupants well to avoiding secondary impact but also reduce the injuries by 10% to 40%[6]. Above development and research work has consolidated current vehicle fitments for protection to rear seat occupants in frontal impact.

## 1.0 ROOF AIRBAG WITH EXTERNAL STRAPS

Seiji Aduma[7] and etc. has studied airbag integrated with seat belt via virtual simulation and sled test, which would provide improved protection performance in terms of head and neck, fatal injuries reduced by 30% appropriately. For chest injuries, the protection of the airbag is not mentioned in the paper, which takes 35% of the fatal locations of human body. Seatbelt Airbag has advantages in no requirements of mounting or supporting system in front of occupants, which is different from traditional airbag system, shown as Figure 1. Unfortunately, it has not been implemented to automotive industry to improve frontal protection to rear seat occupants, yet.

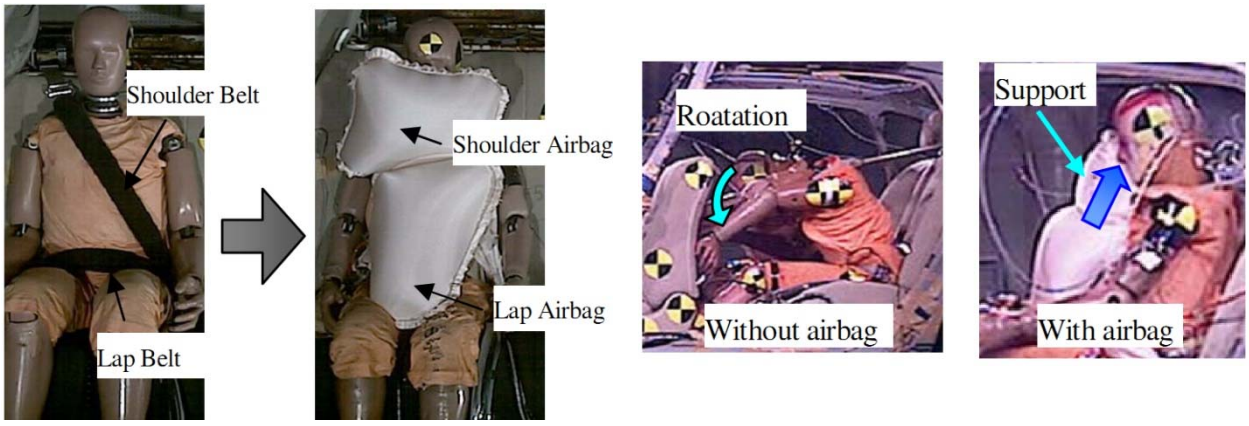


a) Seatbelt Airbag deployments b) Seatbelt Airbag Working Senario

***Figure 1 Seatbelt Airbag provides protection to rear-seat occupants in frontal impact.*** [7]

### 1.1 DESIGN IDEA

According to the Rating results released by EuroNCAP, some vehicles could achieve merely maximum score, 98.8%, in frontal impact, which could be considered as perfect protection. Frontal airbag, belt load limiter, belt pretensioner and even knee airbag could be used to presuming better protection for front-seat occupants. Due to lacking head restrained, for the rear-seat occupants low level of belt load limiter is not recommended in risk of secondary contact to frontal seats. To absorb energy of the head of occupants, the airbag for rear-seat occupants should be constrained in the front of the occupants. Generally, there are frontal seats for outboard occupants. It has been designed as container of rear-row airbag. The position of frontal seats are not fixed, which cause challenges to restraint system as smart as possible. The system needs to recognize the position of the frontal seats and accordingly the airbag can be scaled to interact with the occupants well. Here, a roof airbag with external straps is studied, shown in figure 2. The housing of airbag is fixed in frontal roof cross member and the cushion attaches to external straps. The rear end of straps is fixed at rear roof cross member. So, the external straps can constrain the airbag when it interacts with rear-seat occupants in frontal impact. The airbag does not need any external support, supported by frontal seat back for instance. It covers the shortage of the head restrained in frontal impact.

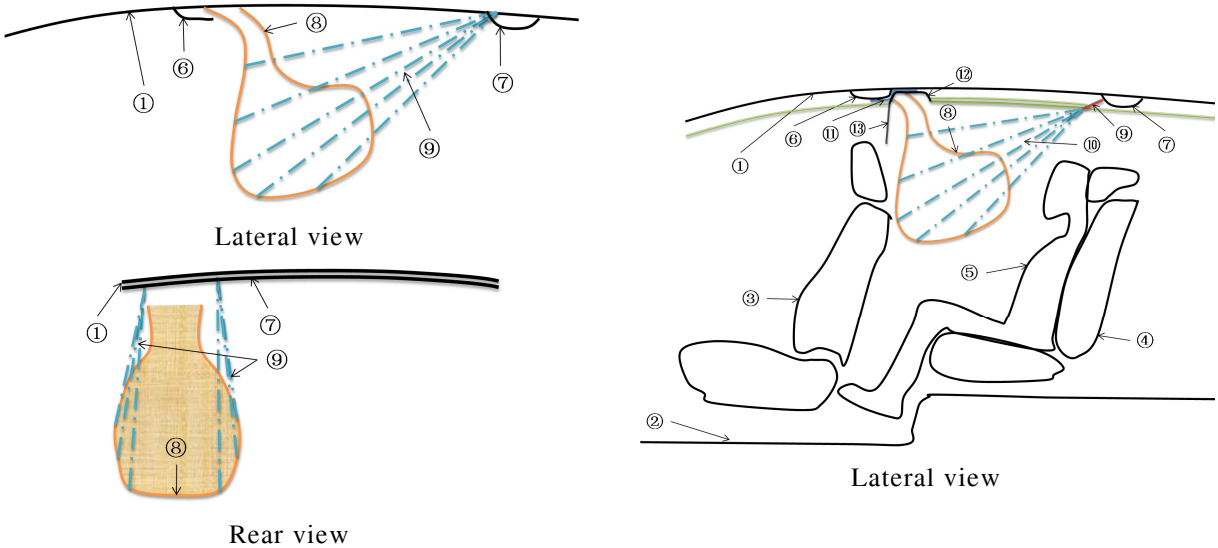


a) Roof Airbag deployment b) Roof Airbag Layout

***Figure 2 Deployment and layout of Roof Airbag***

The influence by add-in the roof airbag to occupant protection is discussed in the following paragraphs via virtual engineering.

## 2.0 SLED MODEL GENERATION

To carry out virtual engineering of restraint system development, the models should be correlated overally, from materials to parts, subsystem and full models[8]. Regarding rear occupants protection, the sub system including compartment, seats, seat belts, occupants and the roof airbag, shown as figure 3, which is generated within LS-DYNA.

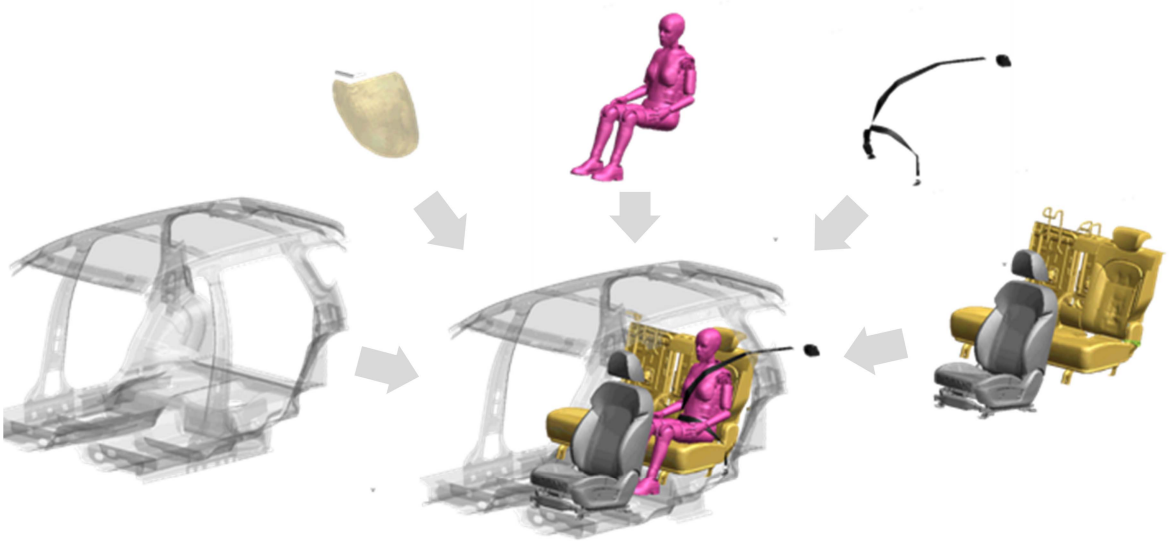

*Figure 3 Rear seat occupant protection model for frontal impact*

### 2.1 Full Vehicle Frontal Impact Tests with HIII 5% Female Dummy

According to the protocol of C-NCAP[9], full-wrap frontal barrier impact at 50km/h, called FFB, and 40% overlap frontal deformable barrier impact at 64km/h, called ODB, are carried out with one under development vehicle model. HIII 5% Female dummy is seated at rear seats in both tests, shown as Figure 4. The Seatbelt is normal emergency locking retractor with extra high level of belt load limiter, about 5kN.

a) Dummy at the seat

b) Dummy in the vehicle

*Figure 4 Full vehicle test with AF05 female dummy*

The injury possibility of dummy in both tests is shown as figure 5. Here, the injury possibility of individual location is assessed by the method as the same as that of US-NCAP [10]. The joint injury possibility is about 41.5% in FFB at 50km/h and 31.2% in ODB at 64km/h respectively. It is reasonably that the injury possibility of lower limbs is neglect-able, 0.0%, resulted from merely no hazardous deformation to rear occupants in frontal impact.

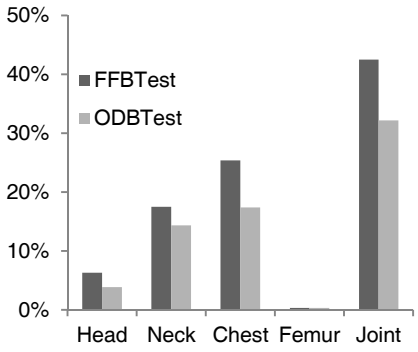


*Figure 5 ASI 3+ possibility of HIII 5% Female dummy in frontal impact tests*

## 2.2 Correlation of Sled model with HIII 5% Female Dummy

Based on the data of accelerometers from the tests, the motion of the vehicle is assigned to the virtual model, shown as figure 3. Correspondingly, the seatbelt and position of dummy is adjusted as that of tests. The results of simulation are compared with tests are shown as Figure 6, which shown good correlation level between simulation and tests in FFB.

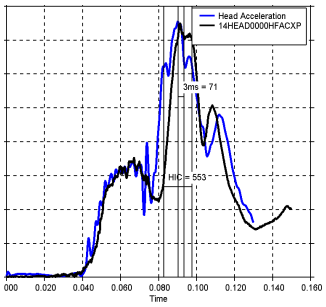


a) Head Acceleration

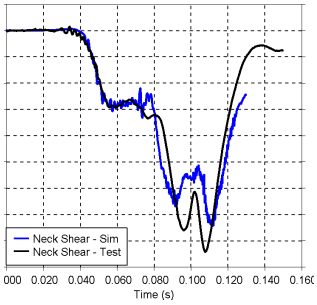


b) Neck Shear

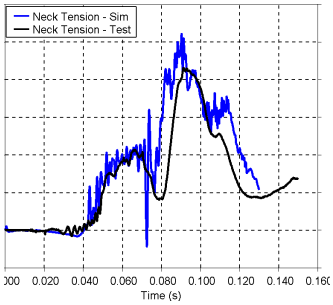


c) Neck Tesion

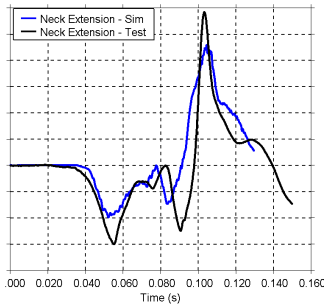


d) Neck Moment

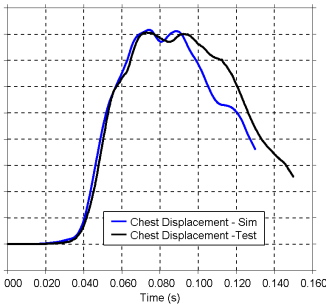


e) Chest Displacement

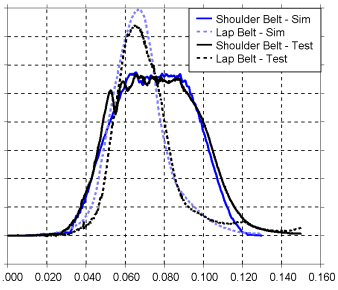


f) Belt Force

*Figure 6 Injury and kinemics of AF05 predicted by sled model compared with that of test in FFB*

The comparison of injury possibility between sled model and test are shown in figure 7. In FFB, the error of body locations predicted by sled model is less than 4%, which resulted in good joint injury possibility, 46.1%, error about 3.6%. In ODB, the injury possibility predicted by sled model is about 26.1%, 6.1% less than that of test. The injury possibility of chest predicted by sled model is 8% lower than that of test. Except for the chest, the injury possibility of other locations has good accuracy, error less than 2.4%. The error of injury possibility predicted by sled models is shown in table 1. The accuracy of sled models is acceptable to study parameters of restraint system.

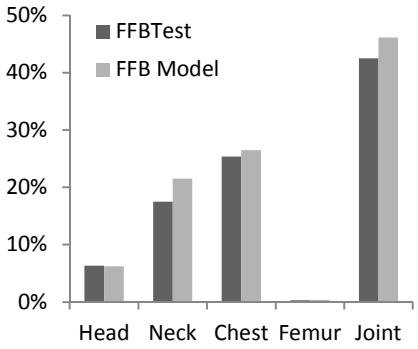


a) ASI 3+ possibility of AF05 in FFB

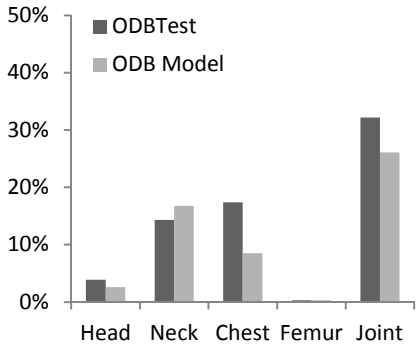


b) ASI 3+ possibility of AF05 in ODB

***Figure 7 Comparison injury possibility of rear-seat AF05 in frontal impact between sled models and tests***

**Table1. Error of ASI 3+ possibility predicted by sled models compared with tests**

| Cases | Head | Neck | Chest | Femur | Joint |
|---|---|---|---|---|---|
| **FFB** | -0.1% | 4.0% | 1.1% | 0.1% | 3.6% |
| **ODB** | -1.3% | 2.4% | -8.9% | 0.0% | -6.1% |

### 2.3 Adapted Sled models with HIII 50% and 95% Dummies

For the rear occupants, not only female dummy seated, normal gentle man and bigger size of occupants seat there in real life. Respectively, AF50 and AF95 dummy are adapted to the correlated sled model. The injury possibility of AF50 predicted by sled models is about 24.5% in FFB and 20.9% in ODB respectively. That of AF95 is about 18.8% in FFB and 14.0 in ODB respectively. Here, the injury limits of AF50 are used for assessment of AF95. The injury possibility of AF50 and AF95 is shown as Figure 8.

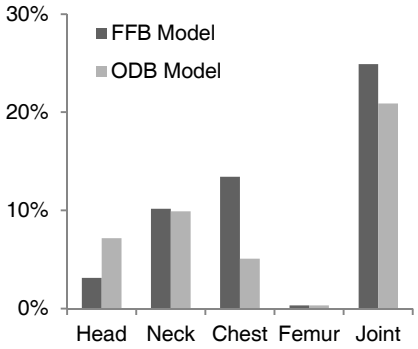


a) ASI 3+ possibility of AF 50

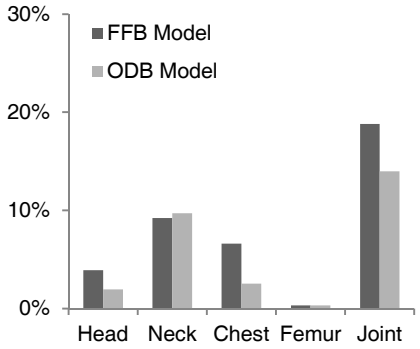


b) ASI 3+ possibility of AF 95

***Figure 8 Injury possibility of AF 50 and AF95 in frontal impact at rear seat predicted by adapted sled models.***

As the dummy size increased, the trend of injury possibility shows reduction, which is appropriate to common sense, shown as figure 9. How to provide good protection to smaller female occupants will be challenge for current restraint system. FFB load cased and AF05 will be focused in following paragraphs to improve performance of protection to rear-seat occupants.

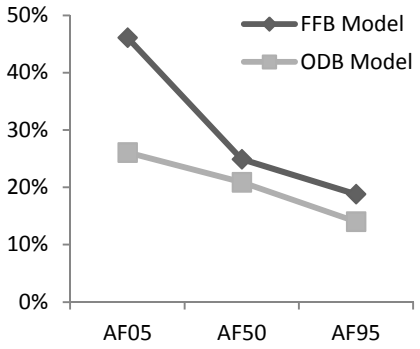


***Figure 9 The trend of ASI 3+ possibility respects to dummy size in frontal impact.***

## 3.0 RESTRAINT SYSTEM STUDY

In 2013, Jeongkeun Khim[11] and etc. studied protection performanceof different kind of seatbelt to rear occupant, AF 05 Female, via correlated sled model within LS-DYNA,which prepared for EuroNCAP FFB implemented in 2015[12]. It is reported that the pretensioner with constant load limiter will improve the dummy injuries in reduction of HIC15, Neck tension and Chest compression. As the load limiter level reduce, the chest displacement will be reduced as well, which are coincident between simulation and tests.

### 3.1 Affect of Load Limiter Levels

Based on correlated sled model with AF05, different levels of load limiter are studied. The injury possibility is shown as figure 8. The trend of injury possibility shows reduction overly, including head, neck and chest, as the level of load limiter decreased. The joint injury possibility ranges from 32.5% to 50.2%.

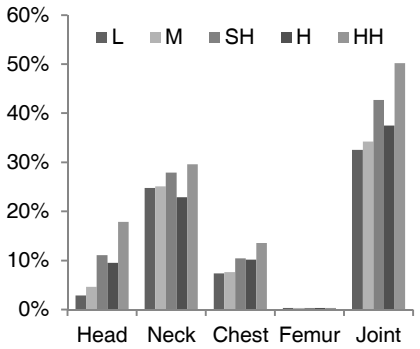


***Figure 10 ASI 3+ possibility of rear-seat AF05 in FFB predicted by sled models regarding different level of load limiter:***

***L: Low M: Mid SH: Sub-High H: High HH: Hyper-High***

However, the joint injury possibility is still very high, more than 30%, even for vehicles fitted with low level of belt load limiter of emergency retractor.

### 3.2 Affects of Retractor with or w/o Pretensioner

Pretenioner is common for front seats, which can constrained the occupants earlier during impact compared with emergency seat belt. Different levels of load limiter with pretensioner are studied in the sled models. As load limiter level reduced, the trend of injury possibility shows reduction overly, which is similar to the trend of emergency seatbelt, shown as Figure 11. The injury possibility can be reduced to about 20% for rear seat AF05 using low level of load limiter seatbelt with pretentioner. In addition, adding pretensioner can reduced the injury possibility of AF05 by 10% to 20% at least comparing with corresponding load-limiter level of emergency seatbelt, shown as Figure 12.

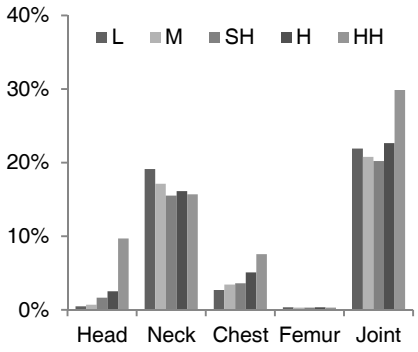


***Figure 11 ASI 3+ possibility of rear-seat AF05 due to belt pretensioner respects to different levels of belt load limiter:***

***L: Low M: Mid SH: Sub-High H: High HH: Hyper-High***

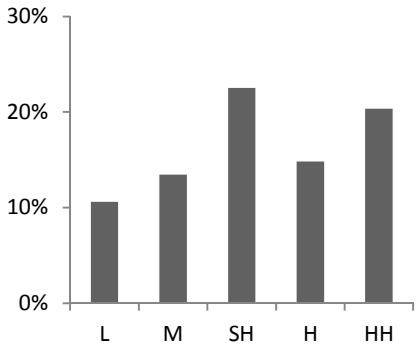


***Figure 12 Improvement of ASI 3+ possibility due to belt pretensioner respects to different level of load limiter:***

***L: Low M: Mid SH: Sub-High H: High HH: Hyper-High***

However, the lower level of load-limiter, the dummies will move more displacement. The bigger size of occupant, the dummies will moves more displacement as well. For AF05, the low level of load limiter seatbelt can be fine, there is no secondary contact. According to the results of simulation, the secondary contact can be observed for AF 50 and AF95 with low level of load limiter seatbelt, shown as Figure 13. The joint injury possibility is increased by 4.6% from 14.3% to 18.9% for AF50 and by 11.2% from 12.9% to 24.0% for AF95 respectively due to secondary impact, shown as figure 14. The fatal injury comes from head and neck. For AF50, the injury possibility is increased by 3.7% for head and by 2.6% for neck respectively. For AF95, bigger size body, the injury possibility of head is increased much more than that of AF50, mediate body, 11.1% increased. For bigger size of occupants, the injury may severer using seatbelt of low-level load limiter and pretentioner in risks of secondary contact.

a) Secondary Contact of AF50 @100ms b) Secondary Contact of AF 95 @100ms

***Figure 13 Observed secondary contact between head and front seats for AF50 and AF95 using low level of belt load limiter***

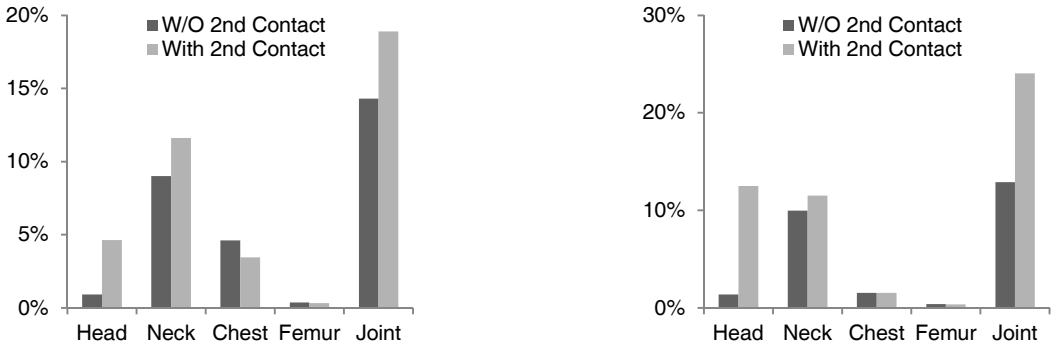


a) ASI 3+ Possibility of AF50 b) ASI 3+ Possibility of AF95

***Figure 14 Comparison of injury possibility of AF50 and AF95 between with and w/o secondary contact predicted by sled models***

### 3.3 Affects of Roof Airbag

As discussed above, the belt with low level of load limiter and pretensioner could provide better protection to rear seat occupants if there was no secondary contact, which is not suitable for most of current commercial vehicle due to constraint of the space. The roof airbag can protect the head from secondary contact even working with low level of belt load limiter. Interaction between roof airbag and different size of dummy is illustrated in Figure 15. There is no secondary contact observed. The ASI 3+ possibility of rear-seat occupants is reduced to 14.5% for AF05, 12.5% for AF50 and 10.1% for AF95 respectively, shown as Figure 16.

a) AF05@125ms b) AF 50@125ms c) AF95@125ms

***Figure 15 Interaction between roof airbag and different size of rear-seat occupants in frontal impacts***

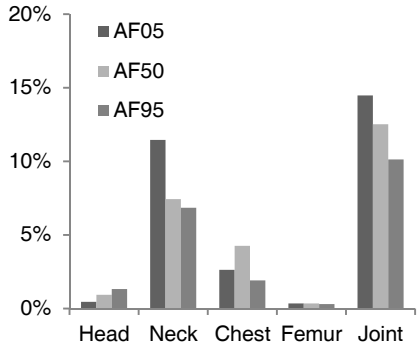


***Figure 16 ASI 3+ possibility of rear-seat AF05, AF50 and AF95 with Roof Airbag in frontal impact predicted by sled models***

Regarding risks of secondary contact, compared with that of w/o roof airbag, the joint injury possibility of occupants protected with Roof Airbag is reduced by 6.3% for AF05, 6.4% for AF50 and up to 13.9% for AF95

respectively, shown as figure 17. Restraint system having low-level belt load limiter, belt pretensioner and roof airbag can provide better protection to rear-seat occupants in frontal impact.

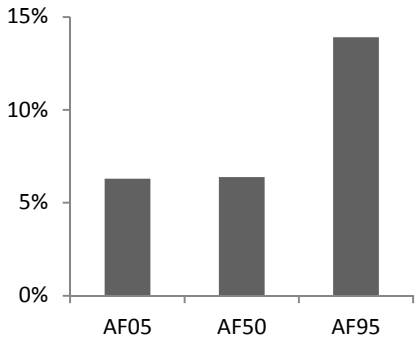


***Figure 17 Benefit to ASI 3+ possibility of rear-seat AF05, AF50 and AF95 due to Roof Airbag in frontal impact predicted by sled models.***

### 3.4 Engineering Approach of Roof Airbag

**3.4.1 Interaction Stability** In ODB impact, the benefit of protection to rear-seat occupants maybe not as good as that in FFB impact. Due to the rotation of vehicle, the head may rotate and pass by the side of the Roof airbag, shown as figure 18. The rotation of head may result in severer neck injury. It could be solved by modifying the shape of the airbag.

a) Head of AF05 passes by roof airbag b) Head of AF05 is restrained by roof airbag

***Figure 18 Head of AF05 interacts with roof airbag in ODB impact.***

**3.4.2 Customer Survey** The idea has been shown on The 3rd Technology Day of Great Wall Motors at first time, which was held in October of 2014, shown as figure 19.

***Figure 19 Sample of Roof Airbag shown on the 3rd Tech. Day of Great Wall Motors***

Meanwhile, customer survey has been conducted on the show. The questionnaire includes seven closed questions, covering users' safety consciousness, recognization of design purpose, protection effects, demanding, numbers, impact by sunroof and price acceptance, and one open question for suggestions. 300 pieces of sheet were finished during the events. According to the investigation data, the typical number of Roof Airbag is about 2.5, which depends on the vehicle seats. As concerned, the demand of sunroof and roof airbag is about 40% and 60% respectively, shown in figure 20. More surprising, a reasonable price is appropriately accepted by customers to fit Roof Airbag, which reduces the pressure of cost due to low volume at early stage.

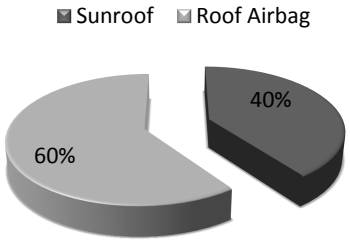


***Figure 20 Demand of Roof Airbag vs. Sunroof***

**3.4.3 Package, Transportation and Hazardous deployment** The airbag should cover most sizes of occupants. The shown sample can covers typical short female adult, nominal 50% and 95% male adults, shown as Figure 21.

The external straps need to be hidden inside of roof interior to minus impact on styling. Additional effort is needed to package the module during transportation.

In real life, people may sit forward, which is out of position. In this case the airbag deployment will be hazardous to occupants. Seatbelt reminder will remind people to be belted, when vehicle drive forward. Intellectual system is needed to suppress the roof airbag in case the deployment being hazardous to occupants.

a) Anologous 5% female adult b) Anologous 50% male adult c) Anologous 95% male adult

***Figure 21 Deployment of roof airbag covers most of general rest-seat occupants***

## 4.0 DISCUSSION

Through out the world, the regulations and mandatory standards require vehicle providing protection to front-seat occupants in high speed frontal impacts. Lots of attentions has been paid to frontal-row occupants protection in frontal impact. However, the requirements of protection to rear-seat occupants are required mostly by cosumer protocols. In 2004, EuroNCAP started to assess vehicle performance of child protection in frontal ODB impact. In 2012, C-NCAP started to have AF05 in rear seat in frontal impact and the head, neck and chest injury is assessed. In 2015, FFB is integrated to EuroNCAP protocol, which focus on protection to AF05. The head, neck, chest and femur will be assessed and the limits is more serious than that of AF50. According to the data released by Euro-

NCAP from 2009 to mid of March 2015, about 7%, 17 out of 242, vehicle models are fitted with belt load limiter and pretensioner for rear seats. The trend of fitment ratio of belt load limiter and pretensioner for rear seats is shown as Figure 22. So far, 3 vehicle ratings is released and 1 of them is fitted with rear-seat belt load limiter and pretentioner. The fitment ratio soaring to about 33%. The new FFB of EuroNCAP has pushed the evolution of fitments for rear-seat occupants protection forward.

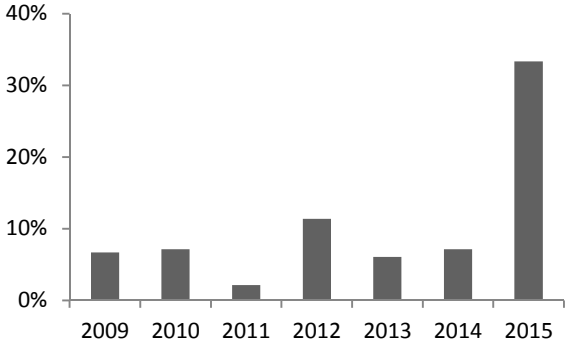


***Figure 22 Fitment ratio of rear-seat belt load limiter and pretensioner by years, up to March 2015.***

It can be estimated that if new protocol assessing more size of occupants will encourage the implement of roof airbag, which provide better protection to rear-seat occupants with belt load limiter and pretensioner.

## 5.0 CONCLUSIONS

Well correlated sled model is developed to study rear-seat occupants protection due to belt load limiter, pretensioner and roof airbag. The followings could be summarized:

1. The smaller size of occupants, the severer of injury possibility for specific restraint system.
2. For emergency belt, the lower level of load limiter, the better of protection to rear-seat AF05. The joint injury possibility of AF05 ranges from 32.5% to 50.2%.
3. Adding belt pretensioner, the joint ASI 3+ possibility of AF05 will be reduced by 10% to 20% compared with corresponding level of load limiter of emergency seatbelt. However, the ASI 3+ possibility of bigger rear-seat occupants may be increased by 6.4% for AF50 and by 13.9 for AF95 respectively in risk of secondary contact.
4. Roof airbag with low level of load limiter and pretensioner can protect all size of rear-seat occupants from secondary contact and provide better protection in frontal impact. The ASI 3+ possibility of rear-seat occupants can be reduced to 14.5% for AF05, 12.5% for AF50 and 10.1% for AF95, respectively.
5. Consumer protocols persuming better occupant protection has benefitted to rear-seat protection in frontal impact.

Protection to rear-seat occupants in frontal impact has come to vision of safety engineers. More efforts will be made to improve the performance. It will and must be stimulated by new protocol or standards requiring assessing more sizes of rear-seat occupants in frontal impact. The roof airbag or similar equipement will come true.

## ACKNOWLEDGEMENTS

The study is based on teamwork. The authors would like to acknowledge all of those supporting the work, especially: Xiao-Chao An, Bing-Bing Peng and Kelvin Tong at Autoliv (Shanghai) Vehicle Safety System Technical Center, who had made efforts to provide sample used in the Tech. Show, and all of the volunteer colleagues in Vehicle Safety Engineering Dept. of Great Wall Motors, who had supported to customer survey.

## REFERENCES

[1] Shashi Kuppa, James Saunders, Osvaldo Fessahaie. Rear Seat Occupant Protection in Frontal Crashes. 19th Enhanced Vehicle Safety, 05-0212.
[2] Richard Kent, Jason Forman, Daniel P. Parent, Shashi Kuppa. 20th Rear Seat Occupant Protection in Frontal Crashes and its Feasibility. Enhanced Vehicle Safety, 07-0386.

[3] Koji Mizuno, Takahiro Ikari, Kenich Tomita and Yasuhiro Matsui. Effectiveness of Seatbelt for Rear Seat Occupants in Frontal Crashes. 20th Enhanced Vehicle Safety, 07-0224.
[4] Report of Traffic Accident Case Study in 2007. ITARDA.
[5] Lotta Jakobsson, Henrik Wiberg, Irene Isaksson-Hellman, Jörgen Gustafsson. Rear Seat Safety for The Growing Child - a New 2-Stage Integrated Booster Cushion. 20th Enhanced Vehicle Safety, 07-0322.
[6] Katarina Bohman, Ola Boström, Anna-Lisa Osvalder, Maria Eriksson. Rear Seat Frontal Impact Protection for Children Seated on Booster Cushions – an Attitude, Handling and Safety Approach. 20th Enhanced Vehicle Safety, 07-0268.
[7] Seiji Aduma, Kouichi Oota, Hiroshige Nagumo, Tomosaburo Okabe. Development of New Airbag System For Rear-Seat Occupants. 21th Enhanced Vehicle Safety, 09-0288.
[8] Chun-Tao Wu, Ling-Jun Yang, Xian-Ling Chen, Kai Zhang. Methodology of Restraint System Engineering Directed by Virtual Simulation. The Proceedings of China 17th Conference of Automotive Safety Technology. P. 699-714, in Chinese.
[9] C-NCAP Protocol, http://www.c-ncap.org/index.html.
[10] CARHS.Safety Companion 2015, P40.
[11] Jeongkeun Khim, Changkyu Son, Jeongmin Kim, Huijeong Jeon, Jungbum Ha, Kwanho Seo and Dongseok Kim. A Study of the Relationship between Seatbelt System and Occupant Injury in Rear Seat Based on EuroNCAP Frontal Impact. 23th Enhanced Vehicle Safety, 13-0153.
[12] EuroNCAP Full Width FrontalImpact Test Protocol v1.0. http://www.euroncap.com.

# ANALYSIS OF VEHICLE ROOF WEAKNESS AND POTENTIAL FOR NECK INJURIES FROM EXPERIMENTAL AND SIMULATED DYNAMIC ROLLOVER TESTS

**Mario Mongiardini**
**Raphael H. Grzebieta**
**Garrett A. Mattos**
**Mike Bambach**
**George Rechnitzer**
Transport and Road Safety (TARS) - University of New South Wales,
Australia

**Andrew S. McIntosh**
McIntosh Consultancy & Research Pty Ltd,
Australia

**Ross Dal Nevo**
Roads and Maritime Services (RMS), Crashlab, New South Wales
Australia

Paper Number 15-0131

## ABSTRACT

Despite the considerable rollover crashworthiness research carried out to date, there is still a need to establish exactly how spine and neck injuries occur to a seat-belted occupant during a rollover. This paper details an experimental and Finite Element (FE) analysis aimed at demonstrating how a stronger vehicle roof can reduce the potential for neck injuries to a seat belted occupant seated in the front on the rollover far-side.

An analysis was carried out of the head-torso kinematics of a seat-belted Anthropomorphic Test Device (ATD) measured during two rollover crash tests conducted on a weak- and strong-roof sport utility vehicle (SUV), respectively. Both experimental laboratory rollover tests were performed under the same nominal conditions using the original Center for Injury Research (CFIR) Jordan Rollover System (JRS) located in Goleta, California. Further, a comparison of the ATD kinematics was then carried out using data obtained from detailed FE simulations of vehicle rollovers carried out using the FE model of the University of New South Wales (UNSW) JRS located in Sydney Australia, and an FE model of a SUV, first with the original production roof and then with a reinforced roof.

The analysis of the experimental tests indicated that an excessive roof crush would likely cause the head to be captured within the crush zone long enough for the torso to apply a large inertial axial-compression load to the neck. In contrast, a stronger roof continuously guides the occupant's head moving it along an arc in a smoother manner, thus reducing any significant change in velocity between the head and torso, and any consequent inertial axial-compression loading. However, preliminary computer simulations confirm this mechanism only in part, and further simulations of the refined computer model of the UNSW JRS and SUV models are being conducted and will be reported on when completed.

## INTRODUCTION

Although vehicle rollovers are relatively rare events, they are particularly dangerous crash modes with one of the highest fatality rates per crash. Generally, rollovers are responsible for 20 to 35 percent of the total fatalities in vehicle crashes, with specific percentages varying from country to country. Specifically, in the USA, vehicle rollover crashes account for around 35 percent of the total motor-vehicle road crash fatalities [1]. Similarly, in Australia, coronial investigations indicated that 27 percent of the occupants killed in a vehicle crash are involved in vehicle rollovers. Studies of rollover-related deaths in Australia found that around half of the victims were not wearing a seat belt [2,3], with the majority being ejected from the vehicle. Nonetheless, the remaining half of rollover-related fatalities involved properly restrained occupants, clearly indicating the magnitude of the risk for serious injuries and fatalities during vehicle rollover crashes, even for restrained occupants.

Understanding the mechanisms that cause severe injuries during vehicle rollovers is essential to develop future effective countermeasures, such as restraints and curtain airbags. In rollover crashes, spine and neck injuries account for around one-third of the total serious or fatal injuries [4,5]. There are a range of mechanisms proposed among researchers in regards to how an occupant's neck and spine are being injured in rollover crashes. Initially, Moffat [6] and others [7-9] proposed that such injuries result from a diving-type mechanism and that, consequently, roof strength is not causal to the degree of injury. He claimed that it did not matter that the roof crushed around the head, neck and torso of the occupant once that part of roof where the head was located inside the vehicle came into contact with the ground [10]. According to the diving theory, occupant injuries occurring in rollover crashes are simply associated with the severity of the rollover. In contrast, work by Brumbelow [11,12] and others [13-17] using real-world statistical crash data reveal some form of a relationship existing between serious and fatal injuries and roof crush and/or roof strength. Moreover, some of the authors have previously shown mathematically that when roof

crush occurs, neck loading is exacerbated [10,18,19]. More interesting is that Rechnitzer and Lane [18] indicated more than 20 years ago that entrapment of the occupant's head by the side header rail could lead to spinal cord injuries even under low levels of roof intrusion. However, when there is considerable roof crush the neck loading is exacerbated and significantly higher in these circumstances than in the case of low intrusion as discussed below.

However, the arguments presented by researchers advocating a causal relationship between roof crush and neck injuries are still being debated. In particular, the diving and the roof crush mechanisms have been found difficult to separate because neck loading resulting from either mechanism cannot be distinguished mathematically from each other [10]. Either mechanism appears to occur when observing the vehicle and occupant relative to the roadway inertial frame. Camera views taken inside the vehicle (i.e., relative to the vehicle reference system) highlight neck compression resulting from roof crush but, when viewed outside the vehicle (i.e., the roadway inertial reference system), the Anthropomorphic Test Device (ATD) appears to be diving into the roadway when the vehicle's far-side roof crushes against it. However, the difference is subtle albeit noticeable as pointed out in [20] and in Figure 1. Nonetheless, injuries occur in conjunction with considerable roof crush.

Despite extensive rollover crashworthiness research having been carried out so far, there is still a need to establish exactly how spine and neck injuries occur to a seat-belted occupant during a rollover. This paper aims at demonstrating how a stronger vehicle roof can reduce the potential for neck injuries to a properly restrained occupant seated in the front seat on the rollover far-side (i.e., the side opposite to the leading side of the rollover). The authors propose as a potential injury mechanism that, when considerable roof crush occurs, the head movement relative to the vehicle's center of mass (CoG) is associated with an amplification of the neck loading (Figure 2). This is due to an increase in inertial compressive load being applied by the torso to the neck as it keeps moving towards the head [20]. In contrast, when a strong roof limits the extent of the roof crush, the ATD's head position relative to the vehicle's CoG does not change to the same extent as in the case of the weak roof vehicle. The head is effectively guided away by the strong roof and allowed to continue smoothly in its motion path relative to roadway. Whilst some torso augmentation occurs to the neck, the neck load induced is smaller than that when the roof is weak (Figure 3).

An analysis was carried out of the head-torso kinematics of a seat-belted ATD measured during two rollover crash tests conducted on a weak- and strong-roof vehicle, respectively. Both rollover tests were performed under the same nominal conditions using the CFIR JRS [21]. Further, a comparison of the ATD kinematics was then carried out using data obtained from detailed FE simulations of vehicle rollovers carried out using the FE model of the UNSW JRS (located in Sydney Australia) and an FE model of a SUV, first with the original production roof and then with a reinforced roof.

The analysis of the experimental tests indicated that excessive roof crush in the right circumstances can cause the head to be captured within the crush zone long enough for the torso to apply a large inertial axial load onto the neck. However, the author's preliminary computer simulations have yet to fully demonstrate this mechanism using FE modelling. Nevertheless, some interesting results were generated and are discussed. Further analysis with both experimental tests and refined computer models of the UNSW JRS and SUV models are being conducted and will be reported on when completed.

## EXPERIMENTAL ANALYSIS

An analysis was carried out of the ATD kinematics and dynamics during two rollover crash tests conducted using the CFIR JRS [22,23]. Each test was performed on a different SUV: a Jeep Grand Cheeroke with a roof Strength to Weight Ratio (SWR) of 2.2; and a Volvo XC90 with an SWR of 4.6. The SWR is the peak load measured within 127 mm (5 in) of platen displacement divided by the kerb weight of the vehicle during a one-sided quasi-static roof crush test. The crush test is carried out using a rigid flat platen 762 mm (30 in) wide and 1829 mm (72 in) long applied to the vehicle front A-pillar at a pitch angle of 5º and roll angle of 25º.

### Measurement of the ATD's Head Motion

For both the cases of a strong- and weak-roof vehicle, frames from the high-speed videos were used to measure the movement of the ATD's head and the vehicle's Center of Gravity (CoG) relative to the roadway inertial reference system. The angle swept-arc relative to the vehicle's CoG and the front header rail were considered, as shown in the lines drawn in Figure 1. For both tests, the angular displacements, i.e., the change of the angular position between two consecutive lines drawn on the considered frames, were computed and presented as shown in Figure 2. Similarly, the distance between the ATD's head and CoG of the vehicle were also measured and compared and shown in Figure 2.

### Kinematics of ATD's Head with Strong and Weak Roof

Interestingly, in the test with the strong-roof vehicle, the ATD's head continued to move through an arc, albeit the velocity of the ATD's head slows down more rapidly for the stronger roof vehicle compared to the weak roof vehicle. In the weak roof vehicle, the distance between vehicle's CoG relative to the ATD's head increases to a lesser extent than in the case of a strong roof vehicle (Figure 2). Moreover, in the case of the weak-roof vehicle, the

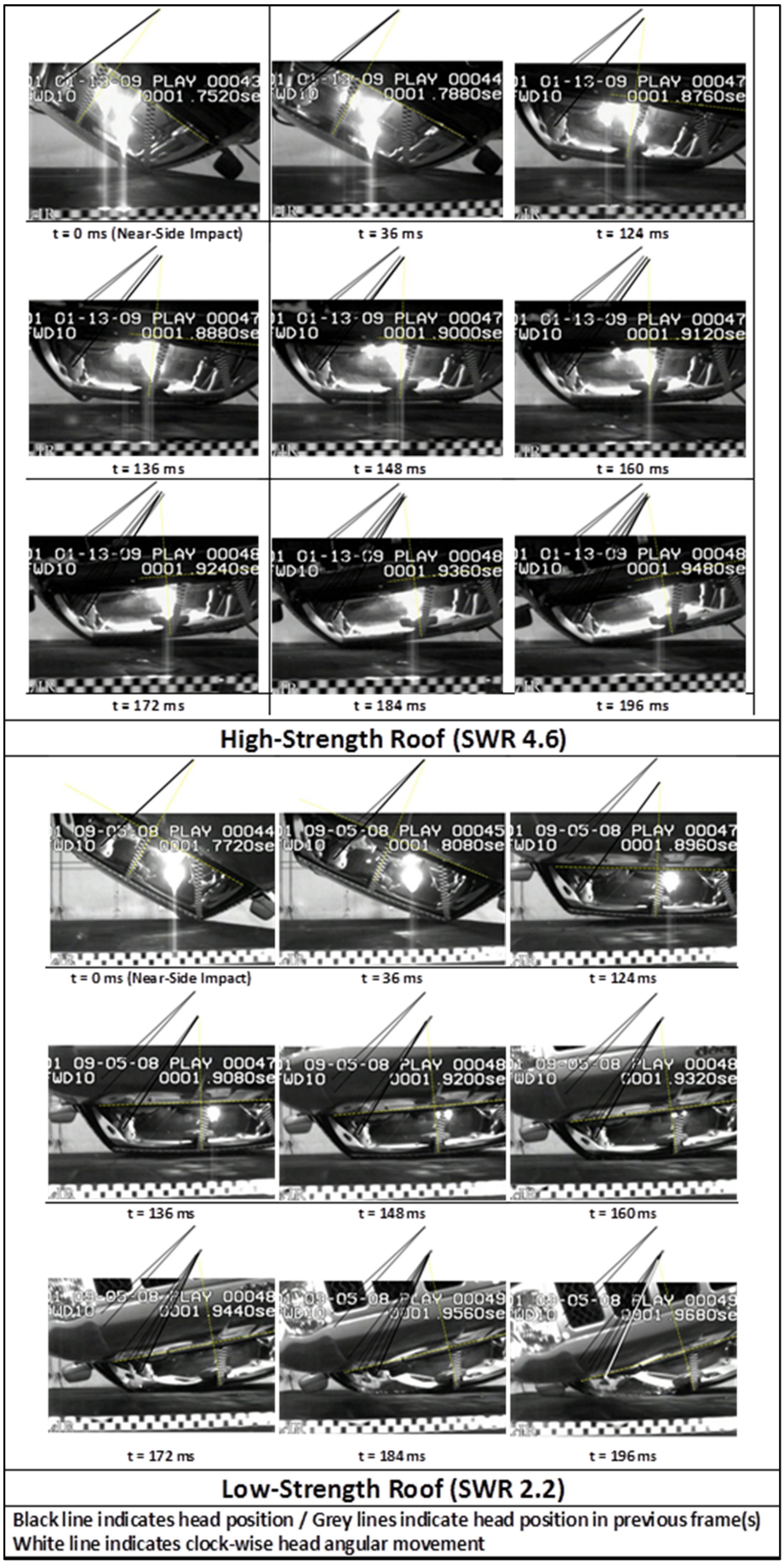


*Figure 1. Movement of ATD's head relative to the vehicle's CG and the roadway – high- and low-strength roof.*

ATD's head was entrapped in the roof, which subsequently buckled, pushing the head back up relative to the vehicle's CoG and the roadway, as indicated in Figure 2. The ATD torso continued to move towards the relatively entrapped (reverse thrusting) head, thus resulting in a greater axial compressive load being applied on the ATD's neck in the case of the weak roof compared to the strong roof vehicle.

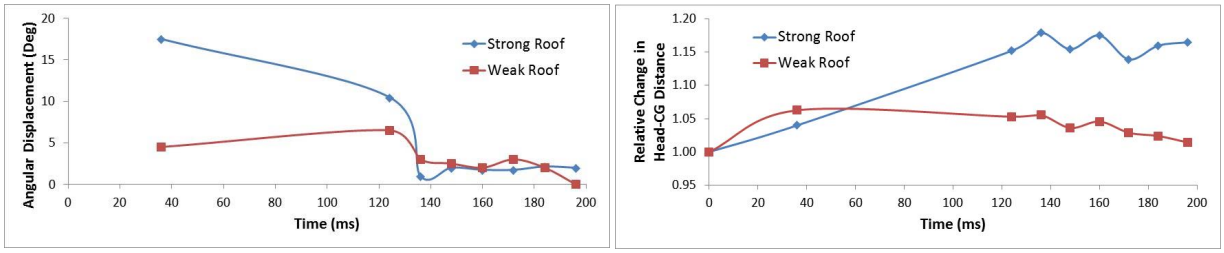


*Figure 2. Left: Angular displacement of the ATD from CFIR JRS rollover crash tests of a strong roof SUV and weak roof SUV, Right: Relative change of distance from ATD head position to vehicle CoG.*

### ATD's Neck Load with Strong and Weak Roof

The plot of the compressive load measured by the ATD's upper-neck load cell during the two tests, an SUV with a strong-roof and an SUV with a weak-roof vehicle, are shown in Figure 3. A much higher peak compressive load of around 10 kN was measured in the test in the case of the weak-roof vehicle, compared to a peak load of about 3 kN in the case of a strong-roof vehicle.

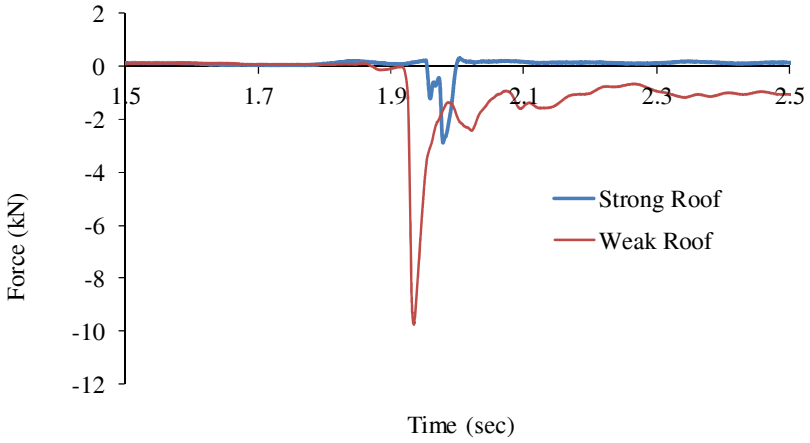


*Figure 3. ATD's upper neck load from CFIR JRS rollover crash tests of a strong roof SUV and weak roof SUV [22,23].*

## COMPUTER SIMULATIONS

Computer simulations of a vehicle rollover crash were also conducted in order to confirm the observations presented above regarding the two experimental rollover crash tests of the strong roof SUV and weak roof SUV. Simulations were performed using the non-linear FE solver LS-DYNA [24].

### FE Model

A detailed FE model was constructed of the UNSW JRS, which was previously developed by some of the authors [25,26]. The UNSW JRS operates under the same functional principles of the original CFIR JRS [27]. Results obtained from simulations with the UNSW JRS model were expected to be consistent with the experimental results of the two tests conducted with the CFIR JRS that were used to identify the injury mechanism. A FE model was not available for either of the two different vehicles that were used in the experimental tests (i.e., a Volvo XC90 and a Jeep Cherokee). Nevertheless, assuming that the injury mechanism is independent of any specific vehicle model and it depends on the magnitude of roof crush, it was assumed the FE model of a 2003 Ford Explorer should be capable of simulating such a neck axial loading mechanism. The Ford Explorer is a SUV, which is in the same vehicle category as the two vehicles used in the experimental tests conducted using the CFIR JRS. The FE model of the Ford Explorer was obtained from the National Analysis Crash Center (NCAC) [28] on-line calibrated models freely available and further modified to more closely simulate the actual vehicle deformation. The modifications consisted of changes to both the material and element properties of the windshield and some of the roof components. The FE model of the UNSW JRS coupled with the modified FE model of the Ford Explorer was previously validated against an experimental rollover crash test conducted using the UNSW JRS [26]. A FE model of the Hybrid III ATD, which was obtained from Livermore Software Technology Corporation (LSTC) [29], was seated in the driver position (right-hand drive configuration) and restrained using a generic three-point seatbelt model. The seatbelt model used a

combination of both shell elements and discrete elements and included slipring and retractor modelling features available in LS-DYNA.

To limit the time necessary to simulate the rollover test, as well as to minimise the potential for numerical instabilities associated with excessively long simulation periods, the FE analysis was carried out in two phases, i.e. Phase I – ATD, seatbelt and vehicle positioning simulation, and Phase II – reduced model impact simulation. In Phase I the whole vehicle in the UNSW JRS is gradually accelerated to the desired roll rate, then it is released at the appropriate roll angle and allowed to free drop under gravity similar to how it occurs in the actual experimental crash test. This ensures that the ATD position, seatbelt configuration and vehicle response during a rollover just prior to the roof impacting the roadbed is simulated accurately. Thus the ATD position, seatbelt configuration and vehicle conditions just prior to the roof impacting roadbed are noted and stored. For Phase II the model was reduced as shown in Figure 4 and Figure 5, and the initial conditions retrieved from Phase I were assigned to the reduced Phase II FE model, i.e. set to the same conditions as those that were measured at the time the vehicle's roof started impacting the roadbed.

**Modelling Issues and Validation**

Determining the proper ATD initial conditions during Phase I as well as implementing these conditions at the beginning of Phase II proved to be more challenging than what was initially thought. In the Phase I simulation, the sash part of the three-point FE seatbelt had not slipped off the FE ATD's right shoulder in contrast to what occurred in the actual experimental CFIR JRS test where the sash had slipped off the ATD's shoulder. Also, the Phase I simulation did not completely replicate the change in direction of the ATD's movement that was observed in the experimental test just before the vehicle impacted the roadbed. An analysis of the test high-speed videos showed that the initial ATD movement towards the vehicle's center console gradually slowed down and the ATD eventually started to swing back towards the far-side door. In contrast, in the Phase I simulation, the FE ATD kept moving in the direction of the center console until the FE vehicle's roof impacted the roadbed. Both these differences in the FE seatbelt and FE ATD's movement appear to have affected establishing the initial position of the FE ATD and FE seat belt model for the Phase II simulation. This resulted in some differences in the simulated FE ATD response during the impact compared with the experimental test results. Further, a limitation in LS-DYNA prevented imposing independently an initial velocity field to the ATD and the vehicle model at the start of the Phase II impact simulation, making the simulation task challenging.

A partial validation of the FE model of the UNSW JRS and the FE vehicle coupled with the FE ATD was accomplished. However further work is required. The FE model (UNSW JRS, vehicle, ATD and seat belt) validation was based on the ATD kinematics that was measured during an experimental test of the UNSW JRS combined with the Explorer [25,26,27]. A comparison of the simulated FE ATD kinematics and the kinematics observed during the experimental test is shown in the sequential frames in Figure 4. The simulated ATD kinematics were different from what was observed during the actual rollover crash test, which was likely due to the above mentioned issues related to the ATD and seatbelt initial configurations at impact.

There was a further complicating modelling issue. In the experimental test, at the start of the vehicle's roof impact with the roadbed, the ATD was offset from the seat cushion due to the vehicle roll position. During the first 150 ms after the initial vehicle impact, the ATD's posterior offset from the seat cushion remained constant. Unfortunately, in the simulation, the FE ATD kept moving away from the FE seat cushion, towards the FE vehicle roof. This incompatibility between the test and FE simulation resulted in two subsequent major differences when comparing the results of the FE simulation to the experimental test in terms of (i) location where the head impacted the roof and (ii) magnitude of bending of the ATD's neck. Further, in the experimental test, the ATD's head impacted the side of the roof in proximity to the far-side rail. In contrast, in the simulation the initial impact of the FE ATD's head against the roof occurred at a location directly above the center of the driver's seat, i.e. further inboard of the side header rail. Also, more extensive bending of the FE ATD's neck occurred in the simulation, likely due to the FE ATD's posterior continually moving away from the seat cushion towards the roof.

**Analysis of Simulations with Weak and Strong Roof**

The FE model was then used to simulate a rollover under the same initial conditions as in the baseline experimental test, but using a modified version of the Explorer model with a stronger roof. To increase the roof strength, the yield stress and the wall thickness of the A- and B-pillars and the roof header were increased by 50 percent and one millimeter, respectively. A comparison of the roof crush and ATD kinematics between the simulations with the original and a strengthened roof is shown in Figure 5. Apart from the extent of the roof crush, the main difference was that the FE ATD's head stayed in contact with the far-side roof rail in the case of a stronger roof, while it was pushed towards the near side by the crushing roof in the case of with the lower roof strength. This contrasted to the experimental test with the weak-roof vehicle, where the ATD's head was mainly held (entrapped [18]) in close proximity of the far-side header rail during the roof crush. Moreover, the ATD neck load for the weak roof SUV [22] was around 10 kN whereas the simulated FE ATD load for the strong roof vehicle shown in Figure 6 was around 7.5 kN. This compares to the ATD's neck load of around 3 kN for the strong roof vehicle [23] tested using the CFIR JRS.

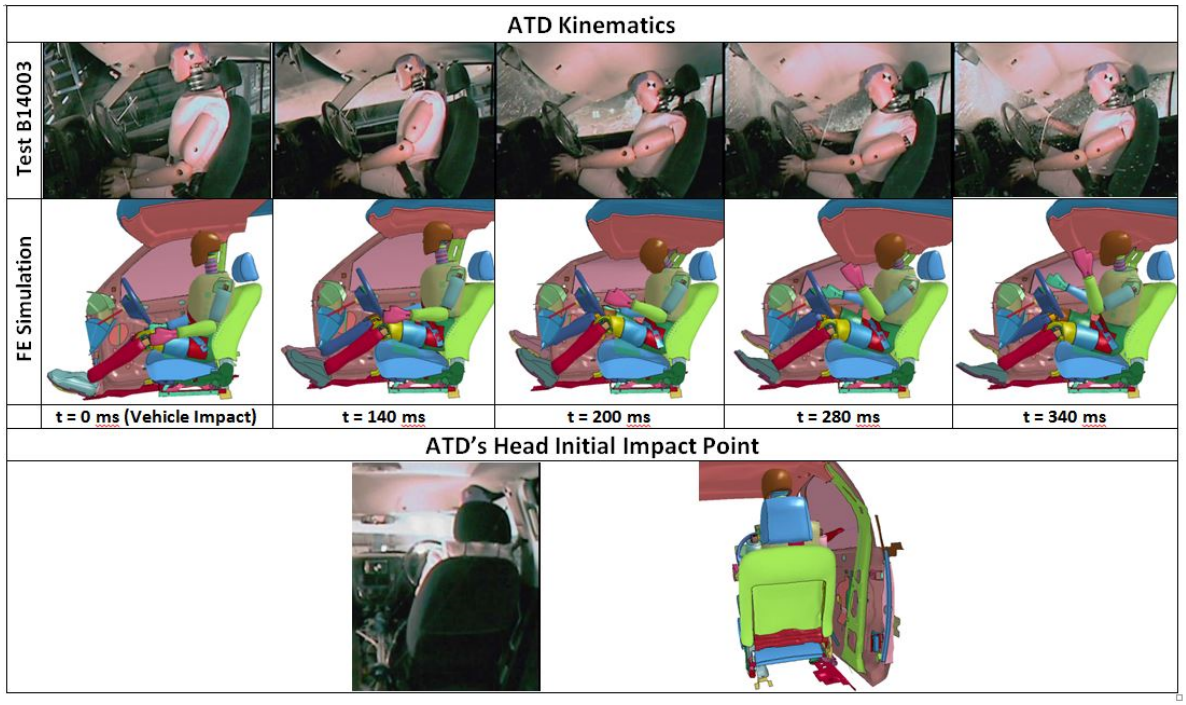


*Figure 4. Experimental and simulated ATD kinematics and comparison of initial ATD head impact on vehicle roof [25,26,27].*

The simulated angular speed of the FE ATD's head for both cases (original and strengthened vehicle roof) is shown in Figure 6. Although crush of the weak roof contributed to slowing the FE vehicle's roll motion as a result of dissipating more roll energy than in the case with a stronger roof, it caused the FE ATD's head to be pushed inboard (left bottom frame in Figure 5). This in turn resulted in a smaller upper-neck compressive peak load being imparted in the case with a weak roof compared to the case with a strengthened roof. In fact, in the case with a weak roof the FE ATD head was forced to tilt laterally with a consequent bending of the neck, which mitigated the compressive load applied onto the neck.

A possible explanation for the apparently opposite trends in terms of neck loading when comparing the CFIR JRS experimental test results and the FE simulations is related to the different magnitudes of roof crush that occurred in the weak-roof vehicle used in the experimental test compared with the FE vehicle model in the simulations. Also the interior shapes and sizes of the Jeep Grand Cherokee and Ford Explorer interior is different to the Volvo XC90 causing the head to interact and move differently within the vehicle when in contact with the roof, i.e. the head tilts rather than becoming entrapped.

In the experimental test, the weak-roof vehicle (i.e., Jeep Grand Cherokee) underwent larger roof crush than what was observed in the FE simulation using the original Ford Explorer FE model. A bimodal non-linear relationship between neck axial loading and the amount of roof crush seems to be consistent with a recent analysis of real-world NASS CDS rollover crashes conducted by Bambach et *al.* [5] as shown in Figure 7. In that study, a higher frequency of AIS 3+ occupant neck and spine injuries was found for either relatively small or very large magnitudes of vertical roof crush. However, the number of AIS 3+ injuries was reduced for magnitudes of roof crush between these two extremes.

A similar relationship would be expected between the neck axial compressive load and increasing amount of roof crush (or weaker roof), assuming that neck axial compression was causal to the cervical and upper thoracic spine injuries. Indeed, this trend was observed when comparing the simulated FE ATD neck load obtained using the Ford Explorer FE model when the roof was further weakened as shown in Figure 7. The FE ATD's Neck load for the 'weaker roof' (green curve) increased in magnitude compared to the 'weak roof' (red dashed cure). In other words, a very weak roof will likely result in increased neck loading. As a further observation, bending of the neck during roof crush may also be affected by other factors, such as localised buckling of the roof structure and/or roof interior padding. These factors, may contribute to either entrapping the head in position [18] or force it to move laterally. Whilst more detailed simulation work needs to be carried out, it appears that the orientation of the head relative to the torso and head entrapment are critical factors in terms of axial compressive loads imparted to the occupant's head during a rollover crash.

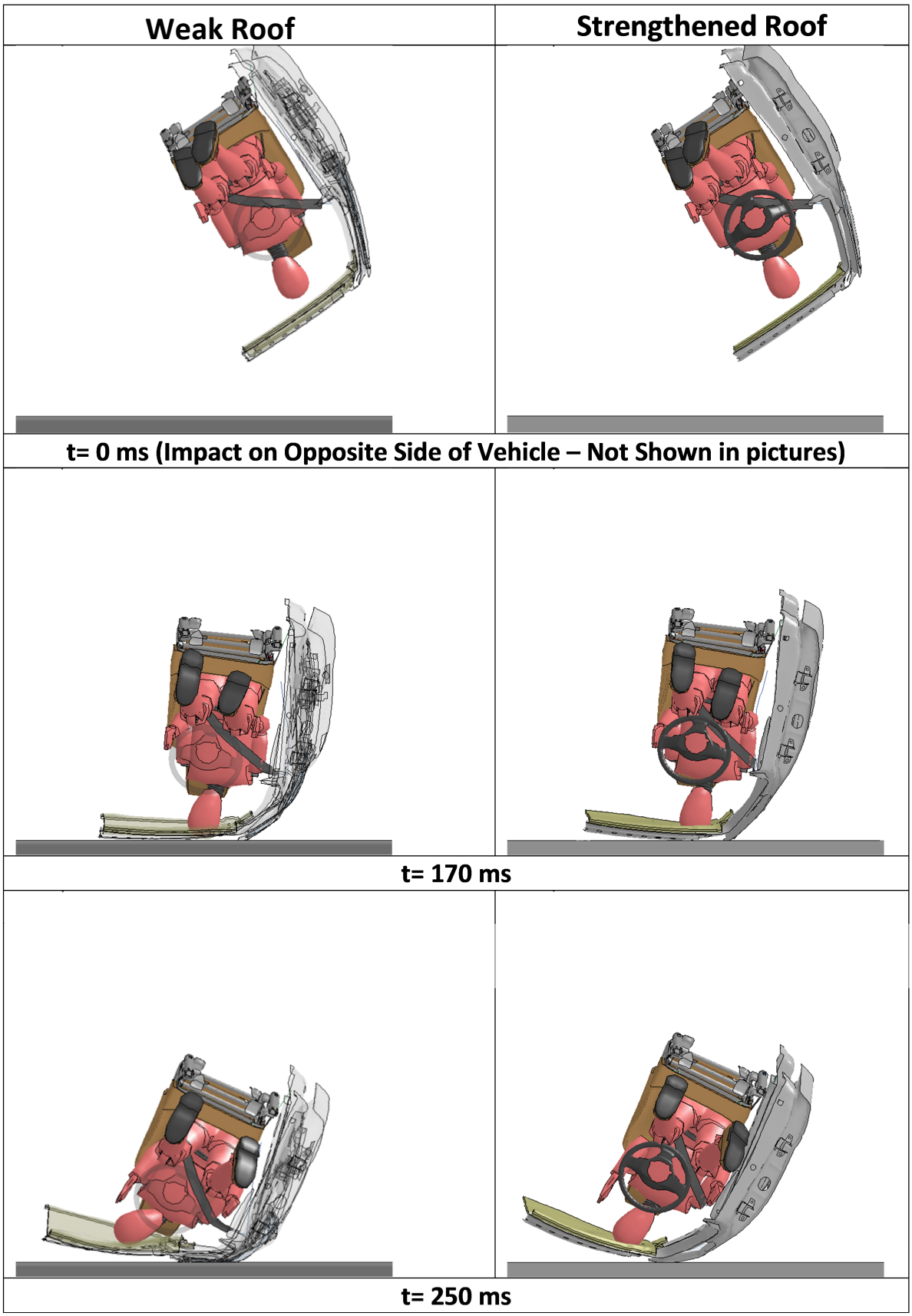


*Figure 5. Simulated roof crush and FE ATD kinematics using Explorer model: strong (right) and weak (left) roof configurations.*

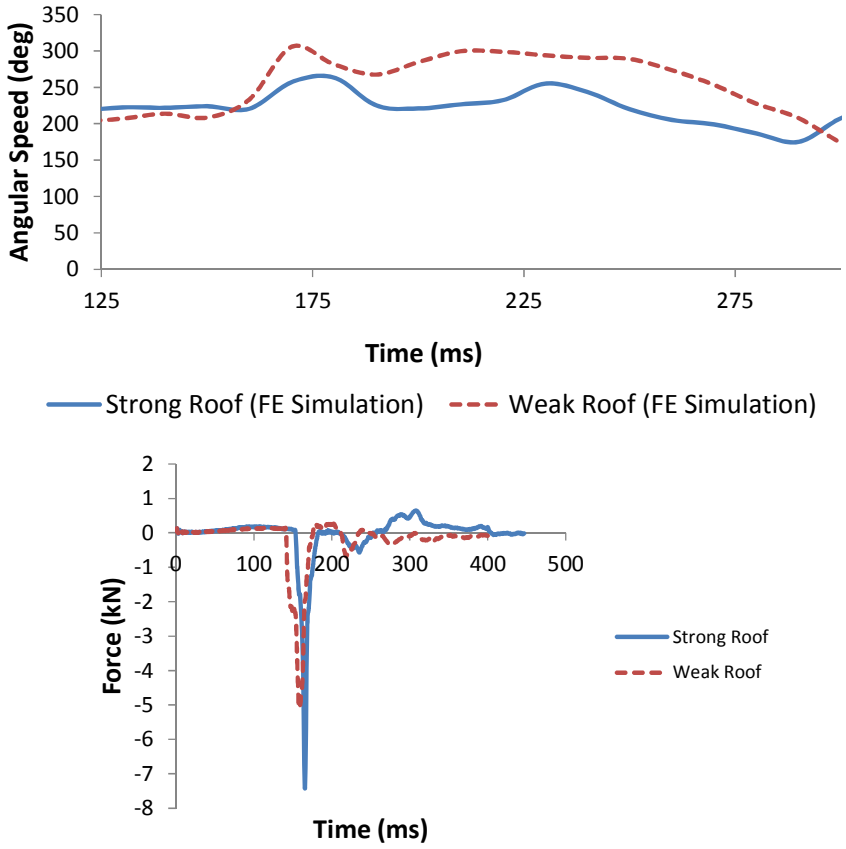


*Figure 6. Simulated angular speed of the FE ATD head and upper-neck load: strong- and weak-roof configurations.*

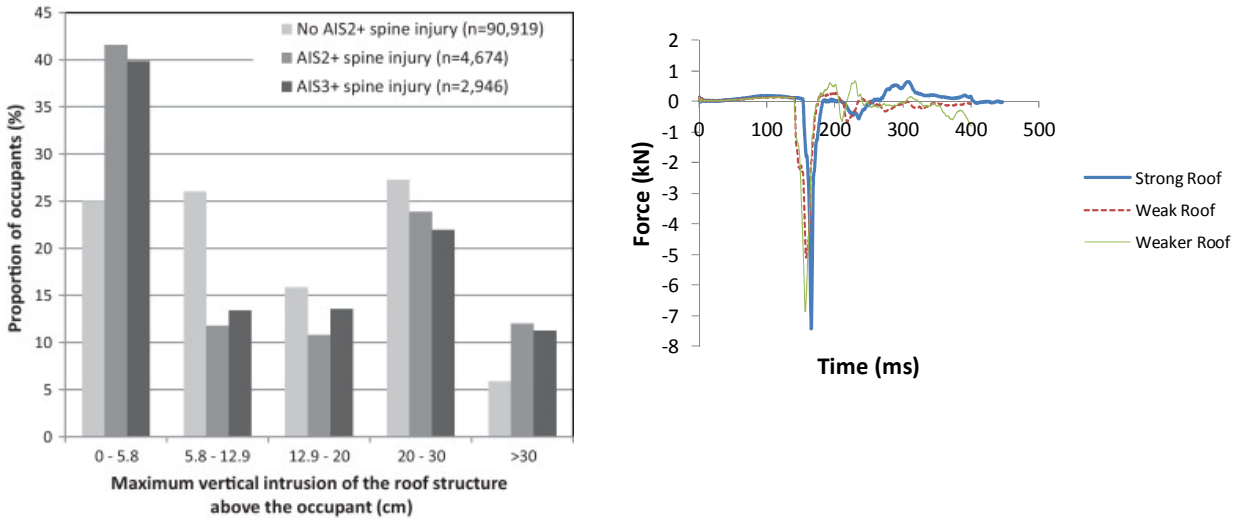


*Figure 7. Distribution of occupant neck and spine injuries in rollover crashes based on vertical roof intrusion [5] (left) and simulated FE ATD neck load with a decreased levels of roof strength (right).*

## CONCLUSIONS

This paper describes how neck injuries can occur to a seat-belted occupant, seated in the front of the vehicle on the far-side opposite to the leading side of rollover, and are exacerbated in the case of a weak roof vehicle compared to a strong-roof vehicle. An analysis of experimental rollover crash test results, on two SUVs carried out using a JRS, indicate that in the case of a weak roof, the head can be entrapped within the crush zone. As a result, the distance between vehicle's CoG relative to the ATD's head increases to a lesser extent than in the case of a strong roof vehicle.

However, the analysis conducted using FE simulations resulted in different compressive neck loading with the FE ATDs. In the case of a weak roof, the simulated FE ATD's head was pushed towards the FE vehicle's near side exerted by the crushing far-side of the weaker roof. This had the effect of reducing the compressive peak load in the

FE ATD's neck. In contrast, in the strong roof FE Vehicle the FE ATD's head remained aligned with the torso and hence was subjected to a higher torso augmentation load (7.5 kN), albeit the load was less than that observed in the CFIR JRS tested weak roof vehicle (10 kN). This in turn indicates that inducing an offset to the head, e.g. side header rail air bag, that tilts the head inboard may alleviate the neck load in rollover crashes. This needs further investigation.

Whilst this analysis focused on the magnitude of the axial compressive force on the neck, which is indeed an important contributor to neck injury, future analysis should also consider neck flexion moments and shear forces. Although the Hybrid III is widely used for many crash applications, including rollover crash tests, the neck of the ATD has been observed to have limited biofidelity [30]. In particular, the neck response of the Hybrid III has been shown to be stiffer than the actual human neck [31]. Further investigations should be conducted using simulations with a detailed and validated human body FE model, such as the Total Human Model for Safety (THUMS) or Global Human Body Model Consortium (GHBMC). Ultimately, experimental tests with post-mortem human specimens should be considered as well.

## ACKNOWLEDGEMENTS

The work described in this paper was part of the TARS UNSW Dynamic Rollover Protection (DROP) Project [27,32]. The authors would like to thank the Australian federal government's Australian Research Council for providing funds to carry out this research through the Linkage Projects grants scheme (No. LP110100069). The authors would also thank the industry partners for providing industry funding as Partner Organisation to the ARC Linkage project, namely, the New South Wales state government's Centre for Road Safety at Transport for New South Wales, the Victorian state government's third-party insurer Transport Accident Commission (TAC), the West Australian (WA) state government's Office of Road Safety at Main Roads WA, the mining company BHP Billiton Ltd., and the U.S. Center for Injury Research (CFIR).

The rollover crash test results [22,23] using the CFIR JRS was provided by the Center for Injury Research (CfIR). The authors would also like to acknowledge the staff at the Road and Maritime Services (RMS) Crashlab for the setup and carrying out of the rollover crash tests using the UNSW JRS and the Explorer vehicle for FE model calibration purposes [25,27].

## REFERENCES

1 National Highway Traffic Safety Administration (NHTSA), Traffic Safety Facts 2012, A Compilation of Motor Vehicle Crash Data from the Fatality Analysis Reporting System and the General Estimates System, National Center for Statistics and Analysis, U.S. Department of Transportation, DOT HS 812 032, 2012.

2 Fréchède, B., McIntosh A.S., Grzebieta R.H., and Bambach M.R., (2010). "Characteristics of Single-Vehicle Rollover Fatalities in Three Australian States (2000-2007)." Accident Analysis and Prevention, Vol. 43, Issue 3, pp. 804-12.

3 Young, D., Grzebieta R.H., Rechnitzer G., Bambach M., and Richardson S., (2006). "Rollover Crash safety: Characteristics and Issues." 5th International Crashworthiness Conference (ICRASH 2006), Athens, Greece.

4 Grzebieta, R.H., Bambach M., McIntosh A.S., Digges K., Mattos G., Simons K., and Rechnitzer G., (2013). "Replicating Real-World Rollover Crash Injuries." 23rd International Technical Conference on the Enhanced Safety of Vehicles (ESV), Seoul, Korea.

5 Bambach, M., Grzebieta R.H., McIntosh A.S., and Mattos G., (2013). "Cervical and Thoracic Spine Injury from Interactions with Vehicle Roofs in Pure Rollover Crashes." Accident Analysis and Prevention, Vol. 50, pp. 34-43.

6 Moffatt E.A., (1975). "Occupant Motion in Rollover Collisions." 19th Conference of the American Association of Automotive Medicine. San Diego, California, USA.

7 Bahling, G. S., Bundorf R.T., Kaspzyk G.S., Moffatt E.A., Orlowski K.F., and Stocke J.E., (1990). Rollover and Drop Tests: The influence of Roof Strength on Injury Mechanics using Belted Dummies. SAE Paper 902314, Society of Automotive Engineers, Warrendale, PA, USA.

8 Piziali, R., Hopper R., Girvan D., and Merala R., (1998). Injury Causation in Rollover Accidents and the Biofidelity of Hybrid III Data in Rollover Tests. SAE Paper 980362, Society of Automotive Engineers, Warrendale, PA, USA.

9 James, M. B., Nordhagen R.P., Schneider D.C., and Koh S.W., (2007). "Occupant Injury in Rollover Crashes: A Reexamination of Malibu II." SAE Paper 2007-01-0369, Society of Automotive Engineers, Warrendale, PA, USA.

10 Grzebieta R.H., Young D., Bambach M., McIntosh A., (2007). Rollover Crashes: Diving Versus Roof Crush, Proc. 20th International Technical Conference on the Enhanced Safety of Vehicles, Lyon, France.

11 Brumbelow, M.L., Teoh E.R., Zuby D.S., and McCartt A.T., (2008). Roof Strength and Injury Risk in Rollover Crashes. Proceedings of the 2008 IRCOBI Conference, Bern, Switzerland.

12 Brumbelow, M. L. and Teoh E.R., (2009). Roof strength and injury risk in rollover crashes of passenger cars and SUVs. 21st International Technical Conference on the Enhanced of Safety of Vehicles (ESV), Stuttgart, Germany.

13 Friedman D. and Grzebieta.R.H., (2009). "A Proposed Rollover and Comprehensive Rating System." 21st International Technical Conference on the Enhanced Safety of Vehicles (ESV), Stuttgart, Germany.

14 Mandell S.P., Kaufman R., Mack C.D., and Bulger W.M., (2010). Mortality and Injury Patterns Associated with Roof Crush in Rollover Crashes. Accident Analysis and Prevention, Vol. 42, pp. 1326–1331.

15 Conroy, C., Hoyt D.B., Eastman A.B., Erwin S., Pacyna S., Holbrook T.L., Vaughan T., Sise M., Kennedy F., and Velky T., (2006). Rollover Crashes: Predicting Serious Injury Based on Occupant, Vehicle, and Crash Characteristics. Accident Analysis and Prevention, Vol. 38, pp.835-842.

16 Kahane, K.J. (1989). An Evaluation of Door Locks and Roof Crush Resistance of Passenger Cars – Federal Motor Vehicle Safety Standards 206 and 216, DOT HS 807 489, NHTSA Technical Report.

17 Strashny A. (2007). The Role of Vertical Roof Intrusion and Post-Crash Headroom in Predicting Roof Contact Injuries to the Head, Neck or Face During FMVSS No.216 Rollovers; An Updated Analysis. DOT HS 810 847.

18 Rechnitzer G. & Lane J., (1994) Rollover Crash Study - Vehicle design and occupant injuries. Monash University Accident Research Centre (MUARC) Report No. 65, Monash University, Melbourne, Australia.

19 Young, D.P., Grzebieta R.H., McIntosh A.S., Bambach M., and Fréchède B., (2007). Diving Versus Roof Intrusion: A Review of Rollover Injury Causation. International Journal of Crashworthiness, Vol. 12, Issue 6, pp. 609-628.

20 Grzebieta, R.H., McIntosh A.S., and Bambach M., (2010). How Stronger Roofs Prevent Diving Injuries In Rollover Crashes. In Proceeding of the 7th International Crashworthiness Conference (ICRASH), Washington D.C, USA.

21 Jordan, A. and Bish J., (2005). Repeatability Testing of a Dynamic Rollover Test Fixture. In Proceedings of the International Technical Conference on the Enhanced Safety of Vehicles (ESV), Paper Number 05-0362, Washington D.C., USA.

22 Center for Injury Research (CfIR), (2008). JRS Dynamic Rollover Test of a 2007 Jeep Grand Cherokee." Test Report submitted to Santos Family Foundation.

23 Center for Injury Research (CfIR), (2009). JRS Dynamic Rollover Test of a 2005 Volvo XC90. Test Report submitted to Santos Family Foundation.

24 Hallquist, J.O. (2014). LS-DYNA - Keyword User's Manual LS-DYNA R 7.1 (revision: 5471). Livermore Software Technology Corporation (LSTC), Livermore, CA.

25 Mongiardini, M., Mattos G., and Grzebieta R., (2014). Computer Modelling of a Test Device for Investigating Injury Causes in Vehicle Rollovers. Journal of the Australasian College of Road Safety, Vol. 25, No. 2, pp. 16-23.

26 Mongiardini, M., Grzebieta R., and Mattos G., (2015). Computer Modelling of Vehicle Rollover Crash Testing with the UNSW JRS. (In Preparation).

27 Grzebieta, R., McIntosh A., Mattos G., Simmons K., Rechnitzer G., Mongiardini M., Dal Nevo R., and Jackson C., (2013). Implementation of the UNSW Jordan Rollover System at Sydney's Crashlab Test Facility. In Proceeding of the International Technical Conference on the Enhanced Safety of Vehicles (ESV), Paper Number 13-0120, Seoul, Republic of Korea.

28 National Crash Analysis Center (NCAC), (2014). Finite Element Model Archive. http://www.ncac.gwu.edu/vml/models.html (Last accessed: Sep. 19, 2014).

29 Livermore Software Technology Corporation (LSTC), (2015). Dummy and Barrier Models for LS-DYNA:. http://lstc.com/download/dummy_and_barrier_models (Last accessed: Jan. 19, 2015).

30 Fréchède BO, McIntosh AS, Grzebieta RH & Bambach M, (2009) Hybrid III ATD in inverted impacts: influence of impact angle on neck injury risk assessment, Annals of Biomedical Engineering; 37: 1403-1414.

31 McIntosh A.S., Frechede B., Grzebieta R.H. and Bambach M.R., (2010). Biomechanical considerations for a dynamic rollover crash test, Proc. 7th Int. Crashworthiness Conf. ICRASH 2010, ed. Chirwa E.C. and S. Kan, Washington DC.

32 Grzebieta R.H., Bambach M., McIntosh A.S., Digges K., Mattos G., Simons K., Rechnitzer G., (2013). Replicating Real World Rollover Crash Injuries, Proc. 23rd International Technical Conference on the Enhanced Safety of Vehicles, Seoul, Korea, Paper Number 13-0098-O.

# ANALYSIS OF QUAD-BIKE LOSS-OF-CONTROL USING EXPERIMENTAL AND SIMULATED DYNAMIC BUMP TESTS

**David, Hicks**
**Mario, Mongiardini**
**Raphael, Grzebieta**
**George, Rechnitzer**
Transport And Road Safety (TARS) Research, University of New South Wales, Sydney, NSW 2052
Australia

**Keith, Simmons**
KND Consulting Pty Ltd, 20 Castle Rock Court, Wattle Grove, NSW, 2173
Australia

Paper Number 15-0133

## ABSTRACT
Quad-bikes, also known as all-terrain vehicles in the United States of America, continue to be a major contributor to fatal and serious injuries in Australia as well as in many other countries all over the world, both for recreational use and in the workplace. There have been over 150 fatalities caused by quad-bike incidents in Australia since 2000 with around 70 percent of these attributed to rollovers. In 2011, quad-bikes overtook tractors as the leading cause of injury and death on Australian farms.

There is a significant portion of quad-bike fatalities that are identified as being caused by riding over a raised obstacle (i.e. bump, log, tree stump, etc.), which causes the vehicle to lose control and rollover. However, the authors are not aware of any research that has been published to date in regards to identifying the mechanism that causes this loss-of-control situation in the case of quad-bikes. This paper details a novel method used to identify this mechanism.

Preliminary testing conducted with a human test rider, identified that a rider can be significantly displaced across the seat when riding a quad-bike over a semi-circular raised obstacle placed on one side of the vehicle wheel track. A formal test procedure was then developed to measure the pelvis kinematics of an Anthropomorphic Test Device mounted on a quad-bike moving over a 150mm high bump obstacle placed on one side of the vehicle wheel track. This procedure was then simulated using a Finite Element (FE) model of a quad-bike that was validated against experimental tests. The analysis of both experimental and FE simulation results presented here clearly demonstrate how a quad-bike loss-of-control event, leading to rollover, can be triggered by a bump-like raised obstacle.

## INTRODUCTION

### Background
Small vehicles including two-wheeled motorcycles, four-wheeled quad-bikes and Side-by-Side Vehicles (SSVs) are now being used for a variety of applications on Australian farms. Over the last decade, there has been a steady increase in the number of quad-bikes in use in the agricultural and recreational sectors both in Australia and in many other developed countries [1]. The increasing popularity of quad-bikes can be attributed to their ability to undertake, in a more efficient manner, activities previously performed using horses, tractors or two-wheeled motorcycles.

It is well known that an improperly negotiated raised obstacle can be dangerous to a rider and potentially cause a loss-of-control event [2].Quad-bike stability and manoeuvrability can be improved through active riding techniques, i.e., requiring the rider to actively change their body position on the quad-bike according to any specific situation where there is a risk of loss-of-control [3]. Due to the need for vigilant active riding, quad-bikes may become particularly unstable if the operator begins riding in a passive mode or performs active body movements counter to the stability of the vehicle. To maintain full control of the vehicle, it is suggested by manufacturers that when traversing a raised obstacle with a quad-bike, active riding from a standing position should be used [1]. However, *Grzebieta et al.* [4] highlighted that often in a loss-of-control situations where riders are injured they may not necessarily be aware of the obstacle. Moreover, riding continuously in an ‘active mode’ is unrealistic particularly in farming environments, and especially with older riders.

There has been a growing concern over the number of fatalities and serious injuries caused by quad-bikes, both in Australia and overseas [5,8]. A recent study of the Australian National Coroner's Information System (NCIS) data of 109 fatalities that occurred in the twelve-year period between 2000 and 2012 identified that in an estimated twenty six percent (n=29) of fatalities, the rider lost control of the vehicle as a result of riding over an obstacle. In most of these loss-of-control cases the quad-bike also rolled over [6].

In regards to the United States of America (USA), an analysis of 2,718 quad-bike fatalities that occurred between the years 2000 and 2010 [6], thirty-four percent (n=916) of the fatalities noted the initiator as 'hit stationary object'. In around half, forty-six percent (n=409) of these fatalities, the quad-bike rolled over as a result of hitting the stationary object. Unfortunately, a more detailed description of the types of object (e.g., tree, rock, etc.) that was hit and whether a collision occurred or the object was riden over was not available. However, these statistics suggests that riding over a raised obstacle is one of the significant causes of quad-bike fatalities in the USA.

**Research Objectives**

The objective of this research was to investigate how riding over a relatively small raised obstacle could cause a quad-bike rider to lose control. Both experimental testing and computer simulations, using both a human rider and an Anthropomorphic Test Device (ATD), were used to observe the vehicle and rider kinematics when a quad-bike moved over a relatively small raised obstacle on level terrain at low speed. Both testing and simulations were purposely designed to observe the reaction of a rider seated in a neutral and relaxed seating position, i.e., without undertaking any active riding or bracing themselves against the impact in any way. This, in effect, allowed a situation where a rider who was not anticipating riding over an obstacle, to be observed.

## METHOD

**Human Rider Bump Test**

A preliminary qualitative investigation was conducted to identify how riding over a raised obstacle could potentially cause a quad-bike to rollover with a human rider [7]. A volunteer test rider rode a Honda TRX250 quad-bike over several obstacles varying in height from 100 mm to 200 mm and at speeds of 10, 15, 20 and 25 km/h. The raised obstacles were asymmetrically placed and in line with either the left or right front wheel of the quad-bike. A moment just before impacting the obstacle, the rider released the throttle in order to 'free-wheel' over it. As the quad-bike moved over the obstacle, the rider maintained a neutral (i.e., relaxed) seating position to replicate a rider who was not anticipating riding over the raised obstacle.

**ATD Bump Test**

A controlled reproducible test, was then developed using an ATD instead of a human test rider [7]. The 'ATD bump test' consisted of towing the quad-bike, a Honda TRX500, along a straight line, over a 150-mm high semi-circular obstacle, which was in line with either the left or right wheel track. The tow vehicle stopped towing before the quad-bike hit the obstacle so that the quad-bike could 'free-wheel' over it. A Hybrid III 95$^{th}$ percentile ATD was positioned on the quad-bike in an upright seating position. The hands were ratchet strapped to the handle bars to prevent the ATD from becoming detached from the vehicle. A visual representation of the initial test setup including the initial seating position of the ATD is shown in Figure 1.

The quad-bike was towed from a standstill to approximately 25 km/h before being released in front of the obstacle. This ATD bump test was repeated three times for the case with the obstacle placed on either side of the vehicle wheel track in order to assess repeatability. The lateral and vertical accelerations of the ATD pelvis were used to determine the consistency of any particular test. The vehicle yaw rate and roll angle were also measured at the centre of the quad-bike's rear tray. The pelvis lateral displacement was also measured using a string potentiometer. The velocity of the vehicle was measured using a Global Positioning System (GPS) device positioned on the front tray.

The ATD bump test was then simulated using previously developed quad-bike and ATD Finite Element (FE) models [9], as shown in Figure 1. The FE quad-bike model reproduces in detail a Honda TRX500 quad-bike. The model consists of a series of shell, solid and beam elements linked together to represent the main components of the quad-bike that affect its stability and handling. These include: steering and suspension control arms, frame, fairings tyres, seat and handle bars. The suspension and steering system components of the vehicle were calibrated against the physical components. A series of dynamic and static test procedures were also performed to verify and validate the static stability and dynamic handling of the FE quad-bike model.

A validated FE model of a 95th percentile Hybrid III ATD provided as a standard software component by Livermore Software Technology Corporation (LSTC) was used for the simulations [10]. A 95th percentile ATD was used instead of a 50th percentile since the former represents the worst-case scenario in terms of both ATD mass and location of the centre of gravity above the vehicle seat. The ATD model used for these simulations is shown in Figure 1.

Simulation of the ATD bump test was performed in order to validate the response of the FE quad-bike and ATD models to moving over a raised obstacle. This allowed the use of simulations to further highlight the rollover mechanism observed in the human rider bump testing. The validation procedure involved comparing the experimental and simulation results. This included comparing the lateral and vertical pelvis accelerations of the ATD as well as the vehicle roll angle and speed while the quad-bike and rider moved over the obstacle. A qualitative visual comparison of the tyre deformation and the final resting position of the ATD on the quad-bike post ATD bump test was also conducted. A comparison of the setup and initial conditions between the actual experimental tests and the simulation is shown in Figure 1.

***Figure 1: Initial simulations setup: testing and FE simulation using a Honda TRX500.***

## FE Tyre Model Calibration

The tyres of the original quad-bike model were further improved to ensure their calibration for the intended use in this research. A simplified tyre model consisting of solid elements with isotropic and nearly incompressible rubber properties were sufficient to reproduce with good approximation both the tyre deformation and damping in the radial direction. The LS-DYNA airbag modelling feature was used to simulate the tyre internal pressure, which was set to an initial value of 30 kPa (4.4psi).

### *Radial Compression*

Radial tyre compression tests were performed to determine the vertical stiffness of the physical tyres. The calibration process, which was performed separately for both the front and rear tyres, was based on the force-versus-displacement curves obtained from the corresponding experimental tests. A constant displacement rate of 10 mm/min was applied. Adjustments to the shear modulus of the tyre material in the FE tyre model matched the experimental radial stiffness.

### *Radial Damping*

Vertical tyre drop tests were also performed to determine the vertical damping properties of both the physical front and rear tyres. In the calibration test, the wheel was raised 750 mm from the ground and released to bounce over a smooth surface under its own weight, until it naturally came to rest. The vertical displacement of the rim was measured over time (displacement per fractions of a second) as the wheel bounced. The damping properties of the FE tyre model were calibrated such that they accurately reproduced the vertical displacement time domain response obtained from the testing.

### ATD Bump Test with Increased Obstacle Height

The ATD bump test was also simulated for increased obstacle heights of 200 and 250 mm. This was in order to replicate the large displacement of the rider vertically and laterally across the seat as seen during the human rider bump test. Since the FE quad-bike model represents a larger, heavier quad-bike with greater suspension travel than the TRX250 that was used for the human rider bump test, a taller bump obstacle was required to reproduce the same rider displacement. Another difference between the preliminary testing and this simulation is the weight of the rider. The volunteer test rider used during the human rider bump test had an approximate mass equivalent to a 50$^{th}$ percentile adult male (approximately 78 kg) whereas the ATD bump test and simulations used a 95$^{th}$ percentile adult male weighing approximately 101 kg.

## RESULTS

### Human Rider Bump Test

The human rider bump test demonstrated that riding over an asymmetric raised obstacle could cause the rider to become displaced laterally across the seat. It was observed that the larger the obstacle the further the rider was displaced. The sequence of events as the rider moves over the 200 mm high bump obstacle at 25 km/h is presented in Figure 2. It was observed that when the front-right wheel moved over the raised obstacle, the front suspension system allowed the quad-bike to maintain stability, which in turn allowed the rider to maintain a balanced seating position, as shown in frames 2 and 3 of Figure 2. In other words, the suspension of the front wheel and the riders arms adequately dampened the impact with the obstacle. However, when the rear-right wheel hit the raised obstacle, the rider became elevated and was thrown sideways across the vehicle seat, as shown in frames 4 through 6 of Figure 2. It is clear that suspension cannot adequately dampen the rear tyre impact with the obstacle. Using the rear tyre to absorb most of the impact energy subjects the rider to a high risk of losing control of the vehicle. This impact also caused the quad-bike to yaw at an angle towards the side of the obstacle i.e. clockwise towards the obstacle if it was on the right side. The rider's spontaneous reaction to this lateral movement was to increase the grip on the handle bars and pull on the right side of the handle bars in order to relocate their posterior squarely back on the seat. This in turn caused the rider to suddenly turn the vehicle towards the right hand side, i.e., the side where the obstacle was located. Such sudden steering combined with the vehicle yaw increased the roll rate of the vehicle and had not the rider taken a quick and active counter-response manoeuvre, rollover would have likely occurred.

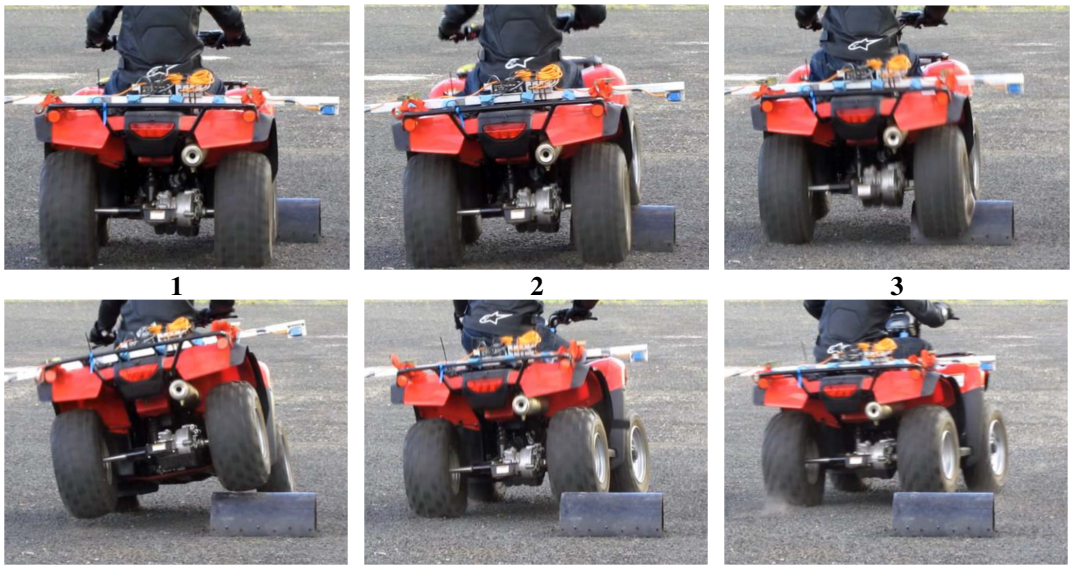


***Figure 2: Rider on a Honda TRX250 moving over a 200mm high asymmetric raised obstacle at 25 km/h. <u>Note:</u> in frame 5 the rider's pelvis has lifted off the seat in response to the accelerations imparted by the bump. In frame 6, the rider's pelvis can clearly be seen relocated to the left side of the quad-bike and the rider is beginning to slide off the saddle.***

**<u>Tyre Calibration</u>**

Before the bump test could be simulated using the FE model of the quad-bike and ATD the tyres in the FE model had to be calibrated against test results first. The results of the front and rear tyre vertical stiffness tests are shown in Figure 3. The results show that good calibration of the vertical stiffness was achieved. Good calibration of the vertical damping properties of the front and rear tyres was also achieved.

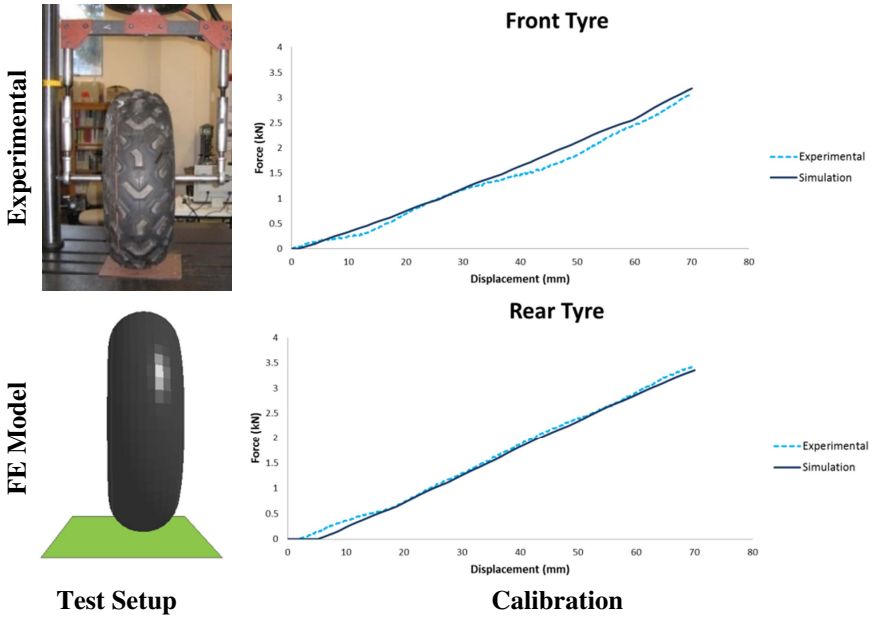


***Figure 3: Vertical compression calibration of a Honda TRX500 tyre– test and model setup (left) and comparison of experimental and simulated force-displacement curves (right).***

**ATD Bump Test**

There was sound repeatability evident between any three 'ATD bump tests' conducted on either side of the vehicle wheel track [7]. Good correlation between the experimental and simulated results was also evident. The speed at which the FE quad-bike model impacted and moved over the obstacle as well as the vehicle roll angle closely matched those observed during testing. The displacements and accelerations imparted to the ATD were similar between the tests and the simulation. The FE ATD also simulated the kinematics of the actual ATD during the tests well. In the simulation, the pelvis was displaced laterally across the seat by a similar distance as observed in the test.

During the ATD bump test, a large compression of both the front and rear tyres occurred as they rolled over the obstacle. This large deformation confirms that the tyres are absorbing a large part of the energy that would have otherwise increased the suspension travel when the vehicle moved over the obstacle. A comparison of the experimental and simulated tyre deformation is shown in Figure 4.

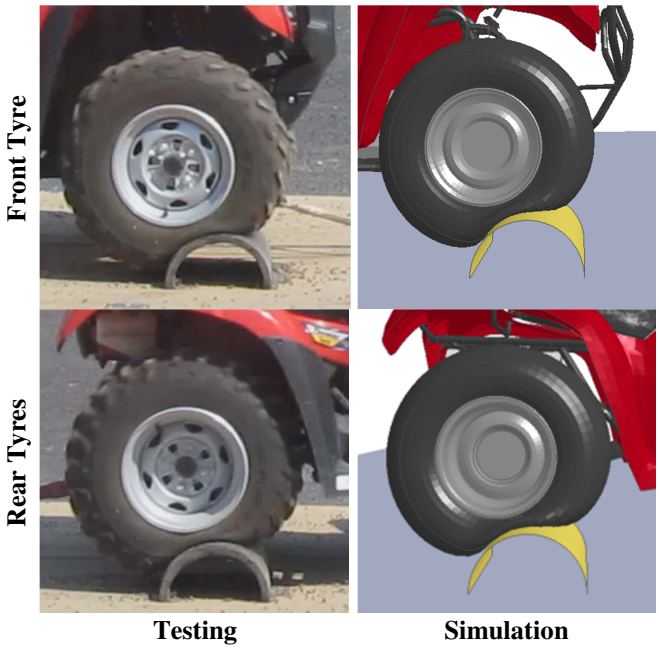


***Figure 4: Comparison of a Honda TRX500 tyre deformation – testing and FE simulation.***

Both the experimental and simulated kinematics of the quad-bike and the ATD as they moved over the raised obstacle are shown in Figure 5. It can be seen that, as a result of the right-front wheel hitting the obstacle, the ATD was able to maintain a stable seating position (frames 1 and 2 in Figure 5) as the ATD's arms acted as shock absorbers to manage the movement of the handlebars. The ATD's upper body adjusted by leaning back slightly against this and pulling forward again as the handlebars fell back down, but there was no significant change of location on the saddle and no resultant imbalance. However, when the right-rear wheel impacted the obstacle, the ATD's pelvis was displaced outward across the seat with respect to the obstacle (frame 5 in Figure 5). This resulted in the ATD leaning both sidewards and forwards due to the rear suspension system being unable to smoothly absorb the impact energy. The simulated kinematics was very similar to that observed in the experimental test. However, overall both the simulated ATD forward and lateral movements were slightly smaller than in the corresponding experimental test.

*Figure 5: Asymmetric-obstacle test using a Honda TRX500 - sequence of events of test and simulation: rear and side views.*

**ATD Bump Test with Increase Obstacle Height**

The 'bump test' simulation at a raised obstacle height of 250 mm demonstrated the large lateral displacement and steering effect observed during the human rider bump testing. It can be observed from the simulation that when the front wheel moved over the obstacle, the ATD maintained a balanced seating position, as shown in frames 1through 3 of Figure 6. However, when the rear wheel impacted the obstacle, the rider became elevated and thrown sidewards across the seat, as shown in frames 4 through 6 of Figure 6. This impact has also caused the quad-bike to yaw clockwise towards the obstacle. Also similar to the human rider bump testing, it can be observed in frames 6 of Figure 6 that the ATD has induced a steering input as a result of being shifted across the seat.

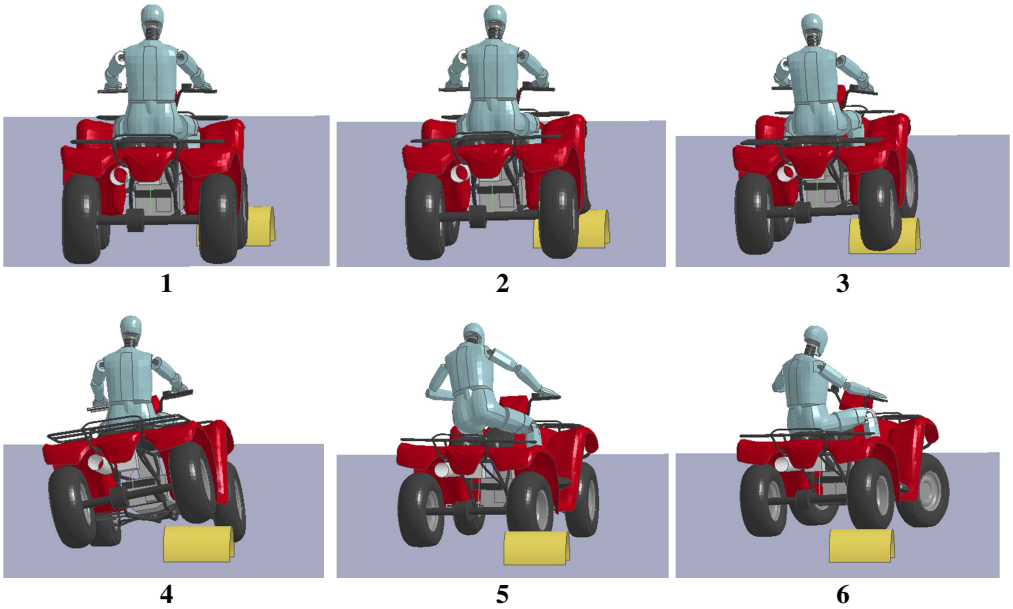


***Figure 6: Modelling of quad-bike (Honda TRX500) and ATD moving over a 250mm high raised obstacle.***

**SUMMARY AND CONCLUSIONS**

Both the experimental and simulated bump tests outlined the potential risks associated with riding over an asymmetric raised obstacle, even at a relatively low speed of 25 km/h. The experimental test (both human rider and ATD) demonstrated that an obstacle may cause the rider to become displaced laterally across the seat of the quad-bike when the rear wheel hits an obstacle placed asymmetrically on one side of the wheel track. Simulations further demonstrated that, in case of a bigger obstacle, hitting an asymmetric obstacle could cause the rider to steer the quad-bike into a loss of control situation. These results show the potential risk of riding over an asymmetric obstacle in a neutral seating position if the quad-bike's suspension has not been designed to dampen such rear tyre impacts that can lead to the loss-of-control situation identified in this research.

Further investigation should be done to assess what combination of speed, obstacle height and slope combined with this mechanism can cause a quad bike to rollover. Modifications to the existing quad-bike suspension setup could then be simulated to optimise the vehicle stability when moving over an obstacle with a passive seated rider. Also, a detailed model of a high-grip soil, such as sand or soft ploughed soil, would better assist in investigating the traction provided by the tyres and its causal relationship with a quad-bike rollover.

**ACKNOWLEDGEMENTS**
The Authors would like to gratefully acknowledge: the Workcover Authority of NSW for funding the majority of the experimental research and in particular Mr. Tony Williams and Ms. Diane Vaughan. The Australian Consumer and Competition Commission (ACCC) also contributed funds for the test program. The authors are also grateful to Ross Dal Nevo, Drew sherry and staff from Crashlab, Roads and Maritime Services, for their assistance with testing and to Bruce Oliver and Seetha Mahadevan from the School of Mechanical and Manufacturing engineering at the University of New South Wales, for assistance with the tyre calibration testing.

**REFERENCES**

[1] FCAI (Accessed: 12/05/2013). *Australian Motorcycle Market in 2012*. Available: http://www.fcai.com.au/motorcycles/australia%27s-motorcycle-market-in-2012

[2] Elder J, Leland E. (2006). CPSC Staff Response Regarding Follow-Up Questions from Commissioner Moore after the June 15, 2006, ATV Safety Review Briefing, Consumer Product Safety Commission.

[3] SVIA. (2010). American National Standard for Four Wheel All-Terrain Vehicles, ed, 2010.

[4] Grzebieta R, Rechnitzer G, Simmons K, McIntosh A. (2015). Final Project Summary Report: Quad Bike Performance Project Test Results, Conclusions and Recommendations, TARS Research Report, Submitted to The Workcover Authority of New South Wales, UNSW, Australia.

[5] Knight S, Franklin R, Lower T. (2012). Mouint Isa Statement on Quad Bike safety, Mount Isa Centre for Rural and Remote Health (Media Release 03/08/2012).

[6] Grzebieta R, Rechnitzer G, McIntosh A, Mitchell R, Patton D, Simmons K. (2015). Supplemental Report: Investigation and Analysis of Quad Bike and Side by Side (SSV) Fatalities and Injuries, Quad Bike Performance Project, TARS Supplemental Research Report submitted to the Workcover Authority of New South Wales, UNSW, Australia.

[7] Grzebieta R, Rechnitzer G, Simmons K. (2015). Dynamic Handling Test Results, Quad Bike Performance Project, TARS Research Report No. 2 submitted to The Workcover Authority of New South Wales, UNSW, Australia.

[8] Rechnitzer G, Grzebieta R, McIntosh A, Simmons K. (2013). Reducing All Terrain Vehicle Injuries (ATVs) and Deaths - A Way Ahead, presented at the 23rd International Technical Conference on the Enhanced Safety of Vehicles, Seoul, South Korea, 2013.

[9] Mongiardini M, Hicks D, Grzebieta R, Rechnitzer G. (2014). Modeling a Quad Bike (All-Terrain Vehicle) for Simulating Rollover Events, *Journal of the Transportation Research Board,* vol. 1, pp. 50-60, 2014.

[10] LSTC. (Accessed: 15/04/2013). *Dummy Model Archive*. Available: http://www.lstc.com/products/models/dummies/H3_Adult_FAST

# A DESIGN METHOD FOR ROBUST AUTOMOTIVE AND AEROSPACE COMPOSITE STRUCTURES INCLUDING MANUFACTURING VARIATIONS

**AUTHOR:** Dr Dirk Lukaszewicz, BMW AG, Research and Innovation Centre, Knorrstraße 147, 80788 München, Germany, Email: Dirk.Lukaszewicz@bmw.de

Paper Number: 15-0135

## ABSTRACT

**Objective**
Composites may enable further weight reductions for plastic composite intensive vehicles. Among the challenges associated with greater adoption of composites in the automotive industry are the need for novel design procedures, the use of composites in impact applications and the greater variability during composite manufacture. Here, are method is presented to account for composite manufacturing variability in the design phase.

**Methods**
The method is based on measuring the variability in a part and the translation into a simulation. As an example a side-pole impact into a doorsill subassembly was chosen. The test data are used to validate numerical simulations models for the impact situation. The simulation is then used to study the sensitivity of the system with respect to manufacturing variability. A novel optimization was also used that decouples multiple manufacturing variations and allows identifying limits on acceptable variability levels.

**Results**
The experimental tests exhibit changes in mechanical performance due to the existence of manufacturing variations. The numerical simulation including these manufacturing variations shows reasonable agreement with the experimental data. The FE model was then used to vary the manufacturing variations and to identify allowable intervals within defined performance criteria.

**Conclusion**
The design methodology has significant benefits for automotive composite design and manufacturing since it may enhance the robustness of composite crash-structures, reduce part cost and eliminate excessive safety factors to account for unknown manufacturing variations.

**KEY WORDS: Crash, Crashworthiness, Finite Elements, Vehicle Design**

## INTRODUCTION

To enable further weight reductions and fuel savings for future vehicles, Plastic Composite Intensive Vehicles (PCIVs) (Barnes, Coles, Roberts, Adams, & Garner 2011) may become more widespread. Advanced Fibre Reinforced Plastics (FRPs) exhibit excellent mechanical and crash performance when compared with conventional metallic structures. Both the specific stiffness and energy absorption capability of FRPs exceed common automotive materials, such as aluminium and steel, making them highly suitable for crash application for frontal, side and rear impact.
However, composites exhibit different deformation behaviour than steel or aluminium, thus requiring an adaptation of design philosophies for vehicle safety (Ferenczi, Kerscher, & Möller 2014). In addition, FRP mechanical performance may vary significantly due to manufacturing variations (MV) such as fibre misalignment, fibre waviness, gaps or folding. Safe structural design of composite vehicles containing MVs may thus require enhanced design methods and processes. An example for this is introduced here.

### Impact Of Imperfections On Mechanical Performance

Some of the most common MVs are fibre misalignment, fibre waviness, laps and gaps, and porosity. The focus of this work will be on preforming MVs, which include in- and out-of-plane waviness and longitudinal and transverse folding. An early study into the impact of fibre waviness by Mrse and Pigott (Mrse & Piggott 1993) studied the compressive properties of thermoplastic carbon fibre prepreg, which had some initial waviness and were crimped to introduce additional waviness. The authors observed some reduction in compression modulus but a significant reduction of compressive strength with increasing wave character.
Daniel and co-workers (Chun, Shin, & Daniel 2001; Hsiao & Daniel 1996a, 1996b) focused on the impact of fibre waviness on the elastic properties of carbon-fibre reinforced epoxy prepreg. An analytical model was used to evaluate the impact of waviness on tensile and shear modulus as well as Poisson's ratio. In-plane tensile modulus was found to degrade significantly as a function of waviness, up to 35% for a graded wave with characteristic value of 0.1, while transverse in-plane tensile modulus were found to increase.
Compressive stiffness and strength were more significantly affected and the reduction in compressive strength could be up to 80% for a graded wave with a characteristic value of 0.1. Similar observations were made for Poisson's ratios and shear moduli. Trends were consistent for uniform and graded waviness but significantly less pronounced for localized waviness, which had only a small impact on overall property changes. Garnich and Karamani (Garnich 2005; Garnich & Karami 2004a, 2004b) used Finite Element (FE) simulations to demonstrate that fibre waviness had increasing impact on mechanical performance with increasing fibre misalignment and obtained stiffness reductions of up to 70%. Chan and Chou (Chan & Chou 1995) studied the impact of misalignment on the flexural properties of laminates and observed that waviness yielded more severe stiffness and strength reductions in highly stressed plies.
Most of this early numerical work assumed either some form of symmetry, such as a sinusoidal waviness, or that the waviness would be confined. However, as mentioned previously out-of-plane waviness may affect neighbouring plies making it very difficult to separate the effects of waviness in individual plies. For example, Joffe et. al. (Joffe, Mattsson, Modniks, & Varna 2005) studied the mechanical properties and deformation behaviour of NCF using both FE-models and extensive testing proposing a linear approximation between misalignment angle and obtaining a reduction of 40% in mechanical performance for a misalignment angle of 15°. A linear relationship between MV and mechanical property had previously not been predicted. In addition the reduction was lower than what might have been expected. Pansart, Sinapius and Gabbert (Pansart, Sinapius, & Gabbert 2009) presented a coupled FEM/analytical approach to study the impact of both fibre misalignment and fibre waviness on the compressive strength of NCF and reported increasing reductions in compressive strength with increasing fibre waviness angle and wave half wavelength of up to 40% for 10deg waviness and a half wavelength of 5. El-Hajjar and Petersen (El-Hajjar & Petersen 2011) proposed a new approach to model waviness using a Gaussian function as opposed to the sinusoidal approach used previously and tested the tensile stiffness and strength of wavy laminates with reported strength reductions of up to 60%. Potter and co-workers (Bloom, Wang, & Potter 2013; Lightfoot, Wisnom, & Potter 2013a, 2013b) have studied waviness including wrinkles experimentally and observed a reduction of up to 50% for the tensile strength. While most of the experimental work thus tends to confirm the initial analytical predictions we can conclude that experimentally measured reductions in mechanical properties are lower than the predictions from early models. In addition most experimental results tend to show a linear relationship between MV characteristics and mechanical property.
Since the focus of this work is the crashworthiness of composite vehicle structure an important aspect is the impact of such MVs during dynamic deformation as opposed to the quasi-static tests commonly employed. This has been studied by Hsiao and Daniel (Hsiao & Daniel 1999) for fibre waviness. It was demonstrated that the effect of waviness was less severe for increasingly dynamic loading due to the strain rate dependent increase in

stiffness. It can thus be concluded that the used of quasi-static test data to model the impact of MVs on the crashworthiness will represent a conservative estimate.

## METHODS

Two sets of carbon fibre reinforced plastic (CFRP) subassemblies of a doorsill were manufactured with different MV distributions. The sets where then mechanically tested to measure the maximum deformation into the doorsill assembly, representing a loading situation comparable to an FMVSS214 side pole impact (Anon 1998). Additionally, MVs were recorded through destructive testing and the information was incorporated into a numerical simulation to replicate the test results. The simulation was then validated against the test data. Based on this validated FE simulation a method is introduced that enables direct simulation of MVs and their impact on structural performance for a side pole impact. Latin hypercube (LHC) sampling is then used to vary the characteristics of the MV. The sampling results are then used to generate an analytical regression model. A novel optimization method is then used that aims at finding the largest hyperbox containing good designs within the solution space, thus generating limits on the characteristics of the MV.

### Component Manufacture

The subassembly studied here is the side frame of a composite vehicle body structure made from carbon fibre reinforced epoxy. Within the vehicle architecture one of the functions of the side frame is protection of the passengers in an impact event, such as a side pole test. During a side pole test the intrusion into the passenger cell have to be mitigated, while the supplementary restrained systems, i.e. airbags and curtains, are being deployed and the vehicle is stopped at the pole.

This occurs while the side frame undergoes significant deformation, which can exceed 100mm locally. To prevent large deformations of the side frame the incoming loads are normally redistributed in the floor structure and then to the vehicle non-struck side. Consequently, the side frame is supported by cross members and ancillary structural elements, which enable load transfer to the non-struck side of the impact, Figure 1. The side frame is an assembly of individual parts through co-curing for the inside and outside parts and adhesive bonding for the inside and outside. The key components under investigation here are the inner and outer doorsill parts, the inner reinforcement and the inner top cap and frontal cap, five parts in total, Figure A 1. This assembly is referred to as side frame-set of which a total of six was manufactured for two different MV combinations, referred to as “A” and “B”. To manufacture parts with different MV severities and types the temperature of the mould as well as the mounting of the plies in the frame was modified. Of the six side frame-sets each, three were visually inspected and three were cured with resin and tested mechanically. This way it was ensured that the side frame-sets for inspection and mechanical inspection were from the same batch. This was important as the MVs were assumed to be identical between visually inspected and mechanically tested subassemblies. For visual inspection the parts were segmented into plies again and for each segment the MV’s in the plies were recorded. To record the MV’s a grid with a side length of 50x50mm was projected onto the vehicle in all projection planes. Here we are concerned with a side frame subassembly only and consequently only the y-z-vehicle plane is used to record MV’s. For each ply the part was then inspected visually progressing from one quadrant of the grid to the next.

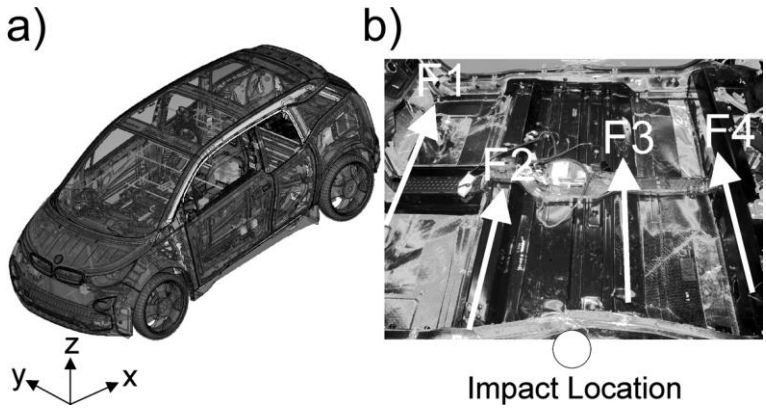


Figure 1a) Overview of the vehicle layout and coordinate system with the side frame highlighted and b) Illustration of principal loading of a doorsill in a side pole impact. The loading conditions are comparable to a five point bending configuration.

For each quadrant the in- and out-of-plane waviness, longitudinal and transverse folding amongst other MV's such as tearing of the stitching yarn was recorded. Then each MV was categorized according to its characteristics, with six different characteristics categories for each MV. The categories are dependent on the MV type but can generally be related to physical variables for a given MV, for example for waviness the MV category is related to the waviness height and length. This process for both MV locations as well as MV characteristics was then carried out by three different quality inspection staff to ensure that all MVs were recorded and that the characteristics was recorded correctly. In case of disagreement between individual recordings the defect with the highest severity was retained. This process was then repeated for each ply in the part and for all three produced parts. The result was a feature map for all three parts combined for every ply were both the location of the MV's as well as their characteristics could be easily accessed. Table 1 provides an overview of the recorded MVs that were used in this study to develop the simulation model.

Table 1: Varied MVs and Characteristic Range. The Characteristic Range is a normalized classification relating to the physical dimensions or shape of a given MV.

| MV | Out-of-plane waviness | In-plane waviness | Longitudinal Folding | Transverse Folding |
|---|---|---|---|---|
| Size Range | 1-6 | 1-6 | 1-6 | 1-6 |

**Testing**

The principal loading of a side frame in a vehicle may be approximated using a five-point bending configuration, Figure 1. Consequently, the test set-up was designed to replicate this vehicle situation as shown in Figure 2. A loading frame consisting of two supports on the lower and two supports on the upper side was manufactured. The mounting positions were equipped with machined interfaces that would fit the complex geometry of the doorsill and would prevent torsion and bending while allowing some transverse movement. The entire setup with the side frame section mounted into the loading frame was placed into a drop tower where an impactor with a diameter of 254mm would impact the side frame in the same position as the side pole in a full vehicle test. An accelerometer on the impactor was used after testing to calculate the force on the impact side. A laser beam system was used to measure the displacement of the impactor. This was levelled to zero on top of the side frame for each test. The loading frame was then aligned with the impactor and fixed to the ground to prevent further movement during testing.

An initial FE simulation was setup to generate a test configuration, were the load level and energy absorption of the side frame were comparable to the full vehicle loading. From the FE-simulation a total drop weight of 352kg and a test speed of 5.65m/s were found to be comparable to the full vehicle-loading situation. For each feature map "A" and "B" three side frames were tested and the acceleration and displacement at the impactor were recorded. After recording, the data were filtered using a Butterworth filter with a channel frequency class of 60 (Anon 1995). The experimental results are summarized in Table 2.

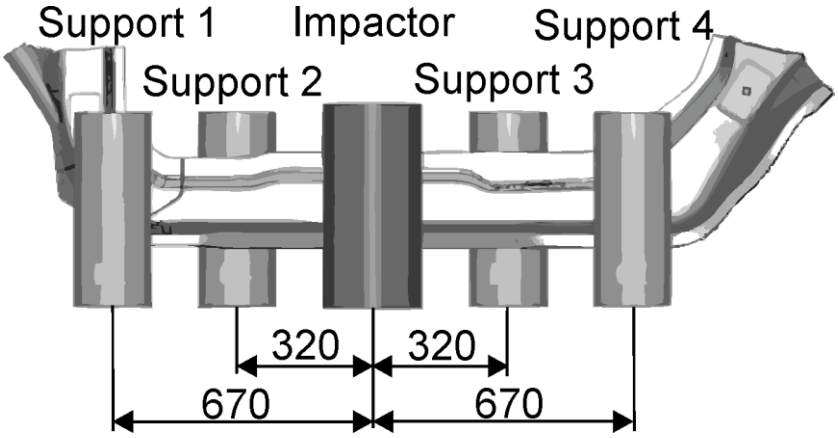


Figure 2: Test setup for dynamic five-point-bending of a doorsill in a drop tower.

Table 2: Experimental Results. The labels “A” and “B” designate two subassembly configurations with known, but different MVs in the parts.

| Test [-] | Maximum Intrusion [mm] | Mean [mm] | |
|---|---|---|---|
| A1 | 99.7 | | |
| A2 | 101.9 | 101.1 | ± 1.2 |
| A3 | 101.7 | | |
| B1 | 111.4 | | |
| B2 | 105.7 | 108.9 | ± 3.0 |
| B3 | 109.7 | | |

**FE Model with Manufacturing Variations**

To replicate the experimental results a baseline model was set up in the commercial FE-Code Abaqus 6.11-2A *(Dassault Simulia 2013)*. The composite parts were modelled using the ABQPly-Fabric composite material model within Abaqus using a single shell element over the thickness incorporating the physical layers into a shell section. Typical mesh size was 10mm for the composite parts. In total the model consists of 240613 elements, while the composite parts were modelled using 67107 shell elements of the type S4R. The composite parts stacking sequence, ply thickness and ply orientation were modelled as composite sections with an offset from the respective shell element plane. The inner and outer side frame were glued together, this was modelled by cohesive elements along the bond line, which had energy based material degradation behaviour.

The Impactor and the four supports were modelled as rigid bodies. The impactor had a reference node on the perimeter in line with the impact point to enable simple comparison with experimental results. All six degrees of freedom of the supports were fixed. The impactor was attached to a reference point, with and impact mass of 352kg and the impact velocity of 5.65m/s as initial condition with displacement in the z-direction (vehicle y-direction) only. Total simulation time was 0.7s. Forces and displacements from the simulation were measured at the reference node, which was identical to the accelerometer location in the physical test. To translate the MVs from visual inspection onto the FE-model material definitions were necessary. These were generated through extensive mechanical testing of coupons, for example in tension and compression. The generation of these FE material definitions are not the focus of this paper. As a result specific material data for different MV types and their characteristics were available.

The MV’s from specimen manufacture that were translated into the FE model were in- and out-of-plane waviness, longitudinal and transverse folding, Table 1. The mapping of the MV’s was scripted in ANSA *(Beta CAE 2014)*. First the visual inspection data was used to segment the side frame into areas with different material behaviour, depending on whether defects were present or not and taking into account individual plies as well. This information was recorded in the shell section definition of each element by modifying the material definition of all the affected plies. As an example in one element the third ply and sixth ply might be associated with in-plane waviness material definition while all remaining plies would retain their nominal material definition. A neighbouring element might be associated with through-thickness waviness in the $4^{th}$ to $6^{th}$ ply of the shell section.

Then, for each area the plies were associated with the corresponding MV severity ranging from 1 to 6 from the visual inspection data. The result is a model with a significant number of unique shell sections.

This is illustrated in Figure A 2 where the different shell section definitions are shown through colour coding. The grey area contains nominal material properties, while the coloured areas are associated with MVs in the shell sections. Since data from multiple preforms and inspectors were mapped simultaneously an approach was needed to identify which MVs would be mapped onto the final simulation part. As mentioned previously the aim was to map the most severe MV onto the geometry. Here a stiffness based mapping approach was used, where the MV’s were ranked according to their combined impact on tensile and compressive stiffness in the fibre direction, $E_{11+}$ and $E_{11-}$. The plies were then associated with appropriate material definitions, which were generated through testing. Since material definitions for out-of-plane waviness were not available the material definition for in plane waviness was used here as well.

**Optimization**

The goal of the optimisation proposed here is to simultaneously define allowables for multiple optimisation goals, such as multiple MVs. In other words the process is aimed at defining a maximum solution space. To achieve this, the approach proposed by Zimmermann and Edler von Hoessle (Zimmermann & von Hoessle 2013) is adapted here for the optimisation of composite structural MVs. The optimization algorithm by

Zimmermann and Edler von Hoessle combines stochastic sampling and Bayesian interference to generate a feasible maximum solution space.

Initially, a good design is created using classical optimization techniques such as gradient based optimization or genetic algorithms (GA). Starting from this good design a randomly defined search box is populated with sampling points. The iteration can be divided into two phases, Phase 1 and Phase 2.

In the first phase the search box is generated and the results are evaluated with respect to a performance criterion, for example the maximum intrusion. By removing poor designs from the initial search box the largest possible box is computed that contains no poor designs and a maximum of good designs. This may not necessarily be the largest bounding box for all good designs. In additional steps this box is extended or reshaped and new Latin Hypercube samples in the bounding box are calculated. This process is repeated until the bounding box is stationary and at maximum size.

In the second phase new samples are generated inside the box and the box is shrunk or reshaped until the bounding box contains only good designs. The new box is then populated again using Latin Hypercube sampling. This process is repeated until a number of consecutive Latin Hypercube seeds within a bounding box produce only good designs, after which the process is stopped.

**Performance criterion:** Since the optimization approach described above uncouples all MVs, which are simulated simultaneously, it is possible to generate allowable intervals for each MV independent of the others. All repeated tests including full vehicle crash tests exhibit a standard deviation that is their tests results vary to a certain extent between nominally identical tests. This may be due to the fact that no vehicle undergoing testing is free of MVs, variability in the test facility or the accuracy of the measurement equipment to name a few here, this fact is being used as definition for the performance criterion for the MV optimization. If the scatter between two nominally identical tests is equal to or greater than the change in performance that can be attributed to different MVs in the vehicle, then MVs are having an insignificant impact on vehicle performance since a distinction between scatter due to MVs and the test configuration cannot be made. This may be defined as

$$\Delta d_{MV} \leq \Delta d_{Test} \tag{1}$$

where $\Delta d_{MV}$ is the relative change in Intrusion due to MV's and $\Delta d_{Test}$ is the relative change between tests. While this repeatability of the BMW test facility is established it is not being used in this paper for confidentiality reasons. Instead, the scatter of the impact tests for side frame configuration "A" of 1.2% is being used here. This value has no connection to the repeatability of the full vehicle test facility and is simply used here to illustrate the process. Since the base simulation without any MVs had a maximum intrusion of 97.6mm, the maximum allowable intrusion in a model containing any MVs is 98.8mm.

**Workflow:** The following section introduces a workflow, which controls the creation, execution and result handling for the FE simulation and optimization. The goal of the optimization procedure is to identify allowable intervals for MVs, which will ensure that the variability of the response, or intrusion, stays within certain limits.

The optimization workflow is shown in Figure A 3. The optimization starts with the setup of the initial model. Here all MVs are mapped onto the respective locations on the part and plies as described previously for the validation simulation. Lastly, all characteristics are set to zero, i.e. the material card without knockdown is used to calculate the baseline result for the simulation. From this model variants are then generated using a scripted Latin Hypercube simulation approach. By varying the characteristics of the MVs 400 variants were generated. They location on the part and the ply was fixed. The models were then solved in parallel on an HPC Cluster with 16 CPUS for variant. Abaqus Explicit 6.11-2A was used as solver. Typical runtime was 75 minutes.

From the simulation the intrusion of the Impactor was evaluated as Latin Hypercube Output. The nodal displacement of the impactor was extracted using a python script and the maximum value was recorded. ClearVuAnalytics (Divis 2014) was then used to generate a Response Surface Model (RSM). From the available methods within the software the random forest tree algorithm consistently generated the highest degree of correlation $R^2$ between the FE-data and the regression model for the optimization. It was thus used to compute the RSM. Allowable intervals for the MV characteristics were then calculated based on the RSM using the bounding box optimization described previously. This process was then repeated by setting the maximum severity of the MV characteristics to the allowable intervals from the previous optimization. Here, the process was stopped after two iterations. Lastly, the allowable intervals form the optimization were validated using 10 FE simulations with discreet MV characteristics.

## RESULTS

The FE-simulation was computed using Abaqus 6.11-2A on 16 cores with double precision. Results are shown in Figure 3.

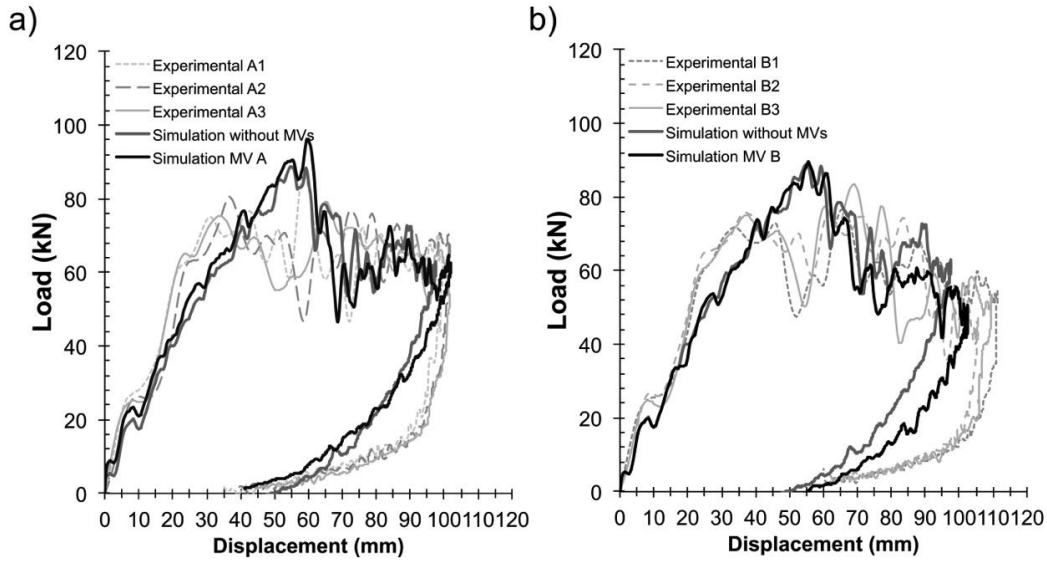


Figure 3a): Experimental and numerical load-displacement curves for MV's for subassembly A with comparison to the baseline simulation and MV simulation and b) for subassembly B.

The base simulation without any MV's yielded a maximum intrusion of 97.6mm, 101.9mm for MV map A and 102.5mm for MV map B. When comparing the simulation results with the experimental results in Table 2 it can be seen that the simulation replicates the experimental results well for MV map A, while it significantly under predicts the experimental results for MV map B. This may be explained through the fact that now all MVs are mapped and that the mapping of through-thickness waviness is based on the material data for in-plane waviness. For the subsequent optimization of the limiting samples for each part model A was used.

Two consecutive iterations of the Latin Hypercube Simulation Process were conducted to develop the analytical model for the MV optimization. From the first 400 variants that were generated for the Latin Hypercube simulation 391 design points were simulated successfully. Based on this data set an analytical model was generated using a random forest algorithm. The $R^2$ of the RSM was 0.91. For the second 400 variants the $R^2$ of the RSM was 0.9. The results of the Latin Hypercube simulation are summarized in Table A 1. The results of the corridor calculation are shown in Table 3. The numbers indicate the allowable intervals for the MVs characteristic for each MV.

## DISCUSSION

The optimization generates limits on the maximum characteristics of the MV that do not detrimentally affect mechanical performance. The optimization demonstrates that MVs have different bearing on the change in functional performance, which is governed by both the characteristics of the MV, such as the angle of fibre waviness, as well as the location. The method thus enables safe structural design of advanced composites by linking manufacturing and structural design.

Variability of the MV location was typically very low since the MV locations remained relatively constant for all visually inspected side frames. MV characteristics fluctuated, which could be explained amongst other things by the variability of the areal weight of the incoming NCF. This validates the assumption that the MV location in the mechanically tested side frames is comparable to the visually inspected side frames.

Table 3: Allowable Intervals for the MV Characteristics investigated in the FE simulation and optimization.

| MV | Out-of-plane waviness | In-plane waviness | Longitudinal Folding | Transverse Folding |
|---|---|---|---|---|
| First Iteration | 3 | 5 | 6 | 6 |
| Second Iteration | 3 | 5 | 6 | 6 |
| Final | 2 | 3 | 5 | 4 |

This is a significant shortcoming of the results presented herein, and further work is aimed at addressing this in the future *(Deobald et al. 2014)*. Further, it should be noted that not all manufacturing variations present in the as manufactured side frames were translated into the model.

One Interesting result is the fact that certain combinations of manufacturing variations result in a reduction of the maximum intrusion. There are several possible explanations for this that need to be explored further. The first would be numerical noise, for example due to different domain decompositions for various models. The second is the fact that certain MV's, such as longitudinal and transverse folding as well as in-plane waviness can actually improve the stiffness of a ply either in the fibre direction or transverse which may improve stiffness locally and this effect was also captured by the FE model. The third explanation would be a change of failure sequence due to MV's which would result in a redistribution of the load on a part and could change the severity of a MV, this effect is explored in more detail for out-of-plane waviness in another paper (Deobald et al. 2014).

Here, a novel concept for designing composite structures has been shown which is based around optimization of the entire product development including manufacturing. Historically, most MVs in composite parts are not accepted because they may be detrimental to safety and are difficult to reproduce in a serial prototype-manufacturing environment often encountered in the aerospace industry. In addition, they are detrimental to achieving ultimate lightweight designs. However, ultimate lightweight design is not desirable if cost and production volume constraints are taken into account. Consequently, designing with MVs becomes a potential target for improving the composite development process with respect to automotive requirements. Potential improvements include a direct link between manufacturing and design to simultaneously optimize both. Further, design with MVs may enable a trade-off between lightweight design, cost and production volume.

A workflow that enables safe structural design with MVs is demonstrated here for a generic composite crash structure. An approach for translating MVs from testing into an FE simulation is first shown. The FE model that was developed here demonstrated reasonable correlation between the simulated and experimentally observed structural response for two representative MVs maps. One model was then subsequently used to optimize the manufacturing variations with respect to their impact on structural performance. The method and simulation approach shown herein may enable significant improvements to production cost, rate and part quality for composites components for the aerospace and automotive industry.

## ACKNOWLEDGEMENTS

The author would like to thanks BMW Group for the opportunity to carry out and publish this research. The author acknowledges the support from David Becherer, Viorel-Constantin Ionescu and Dr Stefan Kerscher from the BMW Group. The author would also like to thank Lyle Deobald, Chul Y. Park, Nihar Desai and Mary Matthews from the Boeing Company for the invaluable feedback and discussions.

## REFERENCES

Anon. (1995). Instrumentation for impact test - Part 1 - Electronic Instrumentation (Vol. J211-1): SAE International.

Anon. (1998). U.S. Department of Transportation: Federal Motor Vehicle Safety Standards and Regulations. Retrieved 23rd February 2013, from http://www.nhtsa.gov/cars/rules/import/fmvss/index.html

Barnes, G., Coles, I., Roberts, R., Adams, D. O., & Garner, D. M. J. (2011). Crash Safety Assurance Strategies for Future Plastic and Composite Intensive Vehicles (PCIVs). Cambridge, Massachusetts, USA: Volpe National Transportation Systems Centre.

Beta CAE. (2014). ANSA.

Bloom, L., Wang, J., & Potter, K. (2013). Damage progression and defect sensitivity: An experimental study of representative wrinkles in tension. *Composites Part B, 45*(1), 449-458.

Chan, W., & Chou, C. (1995). Effects of delamination and ply fibre waviness on effective axial and bending stiffness's in composite laminates. *Composite structures, 30*, 299-306.

Chun, H. J., Shin, J. Y., & Daniel, I. M. (2001). Effects of material and geometric nonlinearities on the tensile and compressive behaviour of composite materials with fibre waviness. *Composites Science And Technology, 61*(1), 125-134.

Dassault Simulia. (2013). Abaqus 6.11-2A.

Deobald, L., Park, C., Desai, N., Ramnath, M., Jin, O., Lukaszewicz, D., & Kerscher, S. (2014). *Simulation of Composite Manufacturing Variations to Determine Stiffness and Strength Reductions in Automotive and Aerospace Structure*. Paper presented at the ACS 29th Technical Conferences, San Diego

Divis. (2014). ClearVu Analytics.

El-Hajjar, R. F., & Petersen, D. R. (2011). Gaussian function characterization of unnotched tension behaviour in a carbon/epoxy composite containing localized fibre waviness. *Composite structures, 93*(9), 2400-2408.

Ferenczi, I., Kerscher, S., & Möller, F. (2014). *Energy Dissipation and structural integrity in frontal impact*. Paper presented at the 23rd ESV 2013 International Technical Conference on the Enhanced Safety of the Vehicles, Seoul, Korea.

Garnich, M. (2005). Localized Fibre Waviness and Implications for Failure in Unidirectional Composites. *Journal Of Composite Materials, 39*(14), 1225-1245.

Garnich, M., & Karami, G. (2004a). Finite element micromechanics for stiffness and strength of wavy fibre composites. *Journal Of Composite Materials, 38*, 273.

Garnich, M., & Karami, G. (2004b). Finite Element Micromechanics for Stiffness and Strength of Wavy Fibre Composites. *Journal Of Composite Materials, 38*(4), 273-292.

Hsiao, H. M., & Daniel, I. M. (1996a). Effect of fibre waviness on stiffness and strength reduction of unidirectional composites under compressive loading. *Composites Science And Technology, 56*, 581-593.

Hsiao, H. M., & Daniel, I. M. (1996b). Elastic properties of composites with fibre waviness. *Composites Part A-Applied Science And Manufacturing, 27*, 931-941.

Hsiao, H. M., & Daniel, I. M. (1999). *Effects of strain rate and fibre waviness on the compressive behaviour of composite laminates*. Paper presented at the ICCM-12, Paris France.

Joffe, R., Mattsson, D., Modniks, J., & Varna, J. (2005). Compressive failure analysis of non-crimp fabric composites with large out-of-plane misalignment of fibre bundles. *Composites Part A: applied science and manufacturing, 36*, 1030-1046.

Lightfoot, J. S., Wisnom, M. R., & Potter, K. (2013a). Defects in woven preforms: formation mechanisms and the effects of laminate design and layup protocol. *Composites Part A*, 1-35.

Lightfoot, J. S., Wisnom, M. R., & Potter, K. (2013b). A new mechanism for the formation of ply wrinkles due to shear between plies. *Composites Part A, 49*(C), 139-147.

Mrse, A., & Piggott, M. (1993). Compressive properties of unidirectional carbon fibre laminates: II. The effects of unintentional and intentional fibre misalignments. *Composites Science And Technology, 46*, 219-227.

Pansart, S., Sinapius, M., & Gabbert, U. (2009). A comprehensive explanation of compression strength differences between various CFRP materials: Micro-meso model, predictions, parameter studies. *Composites Part A, 40*(4), 376-387.

Zimmermann, M., & von Hoessle, J. (2013). Computing solution spaces for robust design. *International Journal for Numerical Methods in Engineering, 94*(3), 290-307.

**APPENDIX**

Table A 1: Latin Hypercube Simulation Results And No. Of Designs above Critical Limit

| Iteration | $R^2$ | Misclassifications [-] | Misclassifications [%] |
|---|---|---|---|
| 1st | 0.91 | 125 | 31.9 |
| 2nd | 0.90 | 72 | 18.3 |
| Final | - | 43 | 10.8 |

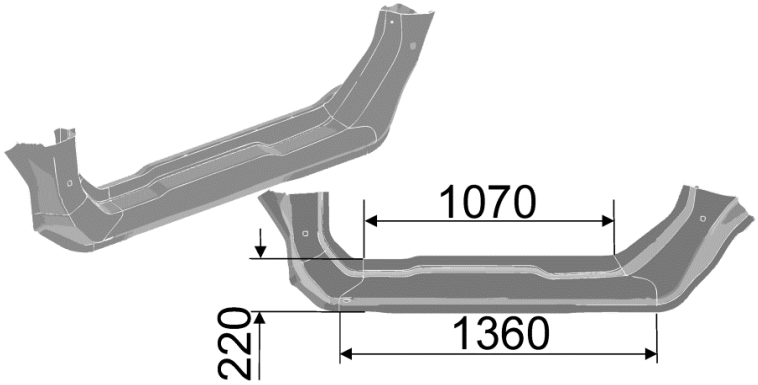


Figure A 1: Segment of a side frame and overall dimensions of the doorsill section.

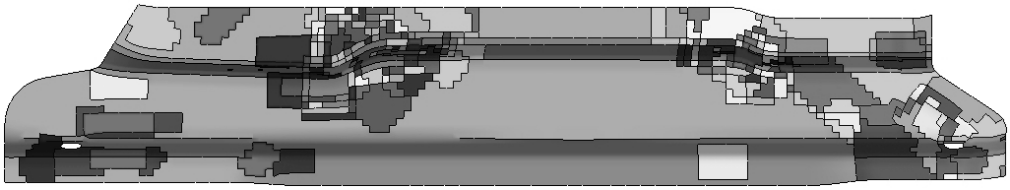

Figure A 2: Example of a simulation model for the doorsill outside with mapped MV's. The patches on the parts represent discreet material definitions for the respective elements.

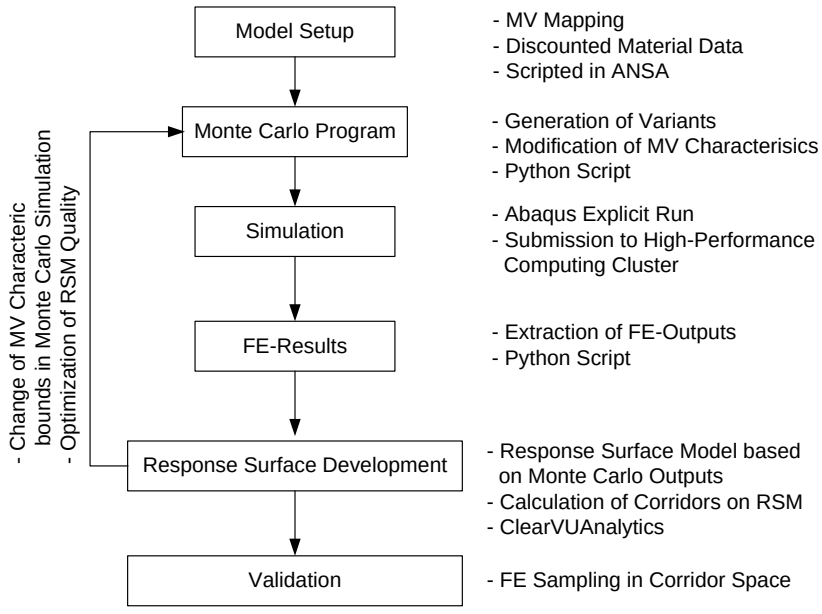


Figure A 3: Simulation Workflow for the MV corridors and the maximum allowable characteristic. The right-hand side description provides details of the operations for each step of the simulation workflow.

# ECALL – DEFINING ACCIDENT CONDITIONS FOR MANDATORY TRIGGERING OF AUTOMATIC EMERGENCY CALLS

**Matthias Seidl**
**Jolyon Carroll**
**Richard Cuerden**
Transport Research Laboratory
United Kingdom

Paper Number 15-0137

## ABSTRACT

eCall, the pan-European automatic crash notification system, will facilitate road vehicles to contact emergency services autonomously when a potentially injurious crash has been detected by vehicle sensors. Type-approval requirements will set out conditions for assessing systems under which automatic triggering of eCalls will be mandatory. Research is needed to specify the accident typologies and severities represented by these conditions.

This paper analyses what definition of accident conditions would ensure that a high number of casualties benefit from automatic eCalls. The conditions should also allow cost-effective type-approval testing, avoid excessive numbers of superfluous eCalls, and not restrict manufacturer's design freedom.

Two conditions were considered as being particularly suitable for the European type-approval system:

- Condition A: Trigger in accident conditions similar to, and at least as severe as, a mandatory frontal or lateral full-scale crash test.
- Condition B: Trigger in conjunction with deployment of any airbag.

In-depth accident data from the Road Accident In-Depth Studies (RAIDS) database, collected between 2000 and 2010 for the Co-operative Crash Injury Study (CCIS), was analysed to produce an estimate of the proportion of car occupant casualties captured by each of these conditions and subsequently scaled to a national level for Great Britain.

The analysis found that Condition A captured only 34.7% of fatally and seriously injured casualties whereas Condition B would apply to 81.0%. For Great Britain, with about 9,335 fatally or seriously injured car occupants annually, this is a difference of 4,330 fatal or serious casualties which could benefit from automatic eCall triggering each year. However, if Condition B was applied, automatic eCalls would be triggered for 74,390 slight casualties per annum in GB (and for an additional unknown number of damage-only accidents).

The sensitivity of Condition B, i.e. the proportion of casualties successfully selected, is considerably higher compared to Condition A. Nevertheless, accident types where airbags are deliberately not deployed would not be captured. Condition B exhibited an almost unvaryingly high sensitivity in selecting fatal casualties and serious casualties respectively.

The higher sensitivity of Condition B is achieved at the expense of specificity in selecting fatal or severe casualties, i.e. more of the collisions for which an eCall is triggered would be slight casualties. There are indications, however, that the negative consequences of superfluous eCalls could be mitigated.

The results are based on British data and cannot be transferred in detail to other countries. The general trends identified would be expected to also appear in reproductions of this analysis using data from other European countries.

The most preferable mandatory automatic eCall triggering condition for type-approval legislation appears to be triggering in conjunction with deployment of any airbag. Nevertheless, up to 19.0% of fatal and serious car occupant casualties might not be captured by this condition. To allow this problem to be overcome using advanced triggering algorithms, a non-restrictive approach could be taken with regard to the triggering requirement, i.e. require triggering in the presence of the condition yet not prohibit triggering in its absence.

## INTRODUCTION

### eCall and the Associated Regulatory Process in the European Union

eCall, the pan-European accident emergency call system (AECS), will facilitate road vehicles to contact emergency services autonomously when a potentially injurious crash has been detected by vehicle sensors. The in-vehicle system (IVS) will contact a public safety answering point (PSAP) via the pan-European emergency number 112. Once the connection is established, it will transmit a minimum set of data (MSD), containing information such as the exact location of the accident and the vehicle involved, and open a duplex voice channel to allow communication between vehicle occupants and PSAP operators. Shortly after the accident, emergency services therefore know that there has been an accident, and where exactly it occurred and can request additional detail, if needed, from the occupants. The safety benefit of eCall arises through the potential reduction in response times for emergency services attending to the accident, thus helping to treat injuries more rapidly which can contribute to a reduced probability of death in road accidents (Sánchez-Mangas et al. 2010).

The European Commission (EC) has adopted a proposal in June 2013 to make eCall mandatory for passenger cars in the near future (European Commission 2013). This was followed in February 2014 by the European Parliament's Legislative Resolution (European Parliament 2014). The subsequent Council's General Approach from May 2014 sets out the high level expectation with regard to the automatic triggering of eCall systems in Article 5.2 (Council of the European Union 2014): An eCall shall be triggered automatically "*in the event of a severe accident, detected by activation of one or more sensors or processors within the vehicle*". This expectation awaits translation into specific requirements for minimum triggering conditions that ensure effective system performance in passenger cars.

The objective of this study is, therefore, to assess the suitability of different accident condition definitions as minimum triggering conditions for type-approval requirements to ensure a high number of casualties benefit from automatic eCalls, while avoiding excessive numbers of superfluous eCalls and fulfilling constraints for implementation in type-approval legislation.

**Review of Accident Conditions in Discussion for Automatic Triggering**

As reported in (Carroll et al. 2014), a review of international legislation, technical standards, cost-benefit studies and international voluntary system implementations provided a selection of different accident conditions for automatic triggering.

The set of European technical standards with regard to eCall does not set out specific mandatory triggering conditions. prEN 16454 Sections 9.4.9 and 9.4.10 refer to full-scale crash tests according to UN Regulation No. 94 (UN R94; frontal impact protection) and UN Regulation No. 95 (UN R95; lateral impact protection) to define shock resistance requirements. Section 9.4.11 defines a test to demonstrate that the automatic trigger is activated by different crash types. However, these sections do not provide any stipulation as to whether triggering should activate the automatic eCall during UN R94 or UN R95 crash tests or any other crash types, but simply that it performs in accordance with the manufacturer's intention.

Studies have been performed by McClure & Graham (2006), Stevens & Hopkin (2010), the European Commission (2011) and Hayden (2014) to determine the costs and benefits of a mandatory implementation of pan-European eCall. These studies did not report the specific triggering conditions used for the underlying benefit calculations and do therefore not constitute a source of accident conditions to assess for the present study.

The European Union (EU) is also involved in the legislative process at the UN level through the Informal Working Group on Automatic Emergency Call Systems (IWG AECS) under the Working Party on General Safety Provisions (GRSG) within WP.29 (1958 Agreement). The draft UN Regulation on AECD/AECS sets out the expectations with regard to automatic triggering in Part III, Section 24.2.2: An automatic call shall be triggered at least by the "*occurrence of a frontal collision according to Regulation No. 94 (frontal collision); or occurrence of a lateral collision according to Regulation No. 95 (lateral collision)*". In order to simplify type-approval, the EU is aiming to keep the European legislation closely aligned with Regulations under the 1958 Agreement (CARS21, 2012). Therefore, the triggering conditions proposed at the UN level are considered in this study as a possible option for EU legislation.

The upcoming mandatory AECS implementation of the Russian Federation, ERA-GLONASS, will reference the technical standard GOST R 54620, which sets out that automatic triggering must occur "*in the event of an accident in which there is a substantial likelihood of threat to life and health of people in the vehicle*". This is further detailed to include front-, side- and rear-impacts. The exact triggering conditions are left to the manufacturer's discretion; however, it is recommended to trigger an automatic call if the acceleration severity index (ASI) of a collision event exceeds a certain score. The ASI algorithm is commonly used as a vehicle-based way to predict the likelihood of injuries in full-scale roadside barrier tests because these are performed without crash test dummies. It is not deemed a suitable mandatory triggering condition for the present study: Given the development effort and complexities surrounding modern crash sensors in vehicles, the prescription of a specific algorithm in not considered suitable for European type-approval legislation with regard to the design freedom of vehicle manufacturers.

Voluntary implementations of AECSs exist in many world regions, including Japan, the United States of America (USA) and the EU. The Japanese implementation, HELPNET, links the automatic triggering of emergency calls to accidents where an airbag was deployed (IWG AECS-Representation of Japan 2014). The American voluntary AECSs are expected to also rely mainly on deployment of an airbag (Kononen et al. 2011). As to the voluntary systems in the EU, it was inferred from communications with vehicle manufacturers that, again, airbag deployment was an important condition for automatic triggering. Therefore, the condition of airbag deployment for automatic triggering forms the second option investigated as legislative triggering condition.

## METHODS

### Data Sources

Two sources of road casualty data were used, the UK's detailed Road Accident In-Depth Studies (RAIDS) database and the British road casualty database, referred to as STATS19. The in-depth accident data were used to identify the proportion of casualties where automatic eCalls were likely to have been initiated under certain definitions of accident conditions for automatic triggering. The RAIDS data were scaled to British national casualties with respect to injury severity using STATS19 data.

**RAIDS** RAIDS is one of the most comprehensive in-depth accident studies in the world; it is funded by the UK Department for Transport (DfT) to provide an evidence source to help prevent future road collisions and mitigate the injuries suffered. RAIDS pulls together four separate historical studies that ran from 1982 to 2010 into one database, including the Co-operative Crash Injury Study (CCIS). RAIDS currently collects information on approximately 500 accidents per year.

The CCIS project collected in-depth real world car occupant injury data from 1983 to 2010. Vehicle examinations were undertaken at recovery garages several days after the collision. Car occupant injury information was collected from hospitals and HM Coroners and questionnaires were sent to survivors. All injuries were coded using the Abbreviated Injury Scale (AIS) 1990 Revision (AAAM 1990). Accidents were investigated according to a stratified sampling procedure, which favoured cars containing fatal or seriously injured occupants as defined by the British Government definitions of fatal, serious and slight. Fatal injury includes only casualties who died less than 30 days after the accident, not including suicides or death from natural causes. Serious injury includes casualties who were admitted to hospital as an in-patient. Slight injury includes minor cuts, bruises, and whiplash. The CCIS project also favoured newer vehicles.

**STATS19** STATS19 is the database of all police reported injury accidents on public roads in Great Britain (GB). About 50 fields are recorded for each accident, including details of the accident circumstances, any vehicles involved and the resulting casualties. Driver and passenger casualties are linked to the vehicle that they were in or on at the time of the accident and pedestrian casualties are linked to the vehicle which hit them.

The injury severity of the casualties involved in the accident is assessed by the investigating police officer. Each casualty is recorded as being either slightly, seriously, or fatally injured. Further details of what is recorded are given in STATS20 (Department for Transport 2011).

### Analysis

CCIS data from phases 6, 7 and 8, which encompasses accidents collected from 2000 to 2010, were used for this analysis. The primary selection criteria for the CCIS in-depth accident cases were:

- Cars registered between 2000 and 2009 and involved in an accident occurring between 2000 and 2010
- Cars towed from the scene
- Cars fitted with front and side airbags (to represent modern vehicle fleet)
- Car occupants with known injuries

This formed the base sample of car users (drivers and passengers). Two principle automated eCall triggering options were considered:

- Condition A: Trigger in accident conditions similar to, and at least as severe as, a mandatory frontal or lateral full-scale crash test according to UN R94 or UN R95 respectively.

  CCIS car occupants were differentiated, with those who experienced collisions similar to UN R94:
  - The car did not roll over
  - Experienced a frontal impact according to Collision Deformation Classification (CDC) SAE J224b (CDC side = 'F')
  - With a Principal Direction of Force (PDF) of $\pm$ 30° (CDC PDF of 11, 12 or 01)
  - With significant residual frontal crush (CDC extent $\geq$ 3)

  And those who experienced collisions similar to UN R95:
  - The car did not roll over
  - Experienced a side impact according to CDC SAE J224b
  - For CDC side = 'R', PDF between 60° to 120° (CDC PDF of 02, 03 or 04)
  - For CDC side = 'L', PDF between 240° to 300° (CDC PDF of 08, 09 or 10)
  - With significant residual frontal crush (CDC extent $\geq$ 3)

- Condition B: Trigger in conjunction with deployment of any airbag.

This sets a lower deployment threshold than the first option and may include more accident modes.

The CCIS car users were classified by those who experienced an airbag deployment and those who did not.

The resulting numbers from the CCIS analysis were scaled to match those of GB national casualty numbers. STATS19 data for accidents of the years 2010, 2011 and 2012, involving car users only, were used (Department for Transport 2013).

## RESULTS

### Results of the Analysis

There are an estimated 125,945 vehicle occupant casualties in road collisions per annum in GB, with 9,335 of these being fatally or seriously injured (KSI). Considering all injury severity levels, automatic triggering Condition A was found to capture 24,913 casualties, whereas Condition B captured 81,955 casualties. Limiting the analysis to KSI casualties, Condition A captured 3,235 casualties compared to Condition B capturing 7,565 casualties (see *Table 1*).

***Table 1*. Annual GB casualty numbers and number of casualties selected by automatic triggering Conditions A and B respectively; reported for different injury severity levels and different positions**

| | | All severities | KSI | Fatal | Serious | Slight |
|---|---|---|---|---|---|---|
| Annual GB casualties | All occupants | 125,945 | 9,335 | 839 | 8,496 | 116,610 |
| | Drivers | 84,989 | 6,247 | 576 | 5,671 | 78,742 |
| | Passengers | 40,956 | 3,088 | 263 | 2,825 | 37,868 |
| Selected by Condition A | All occupants | 24,913 | 3,235 | 394 | 2,841 | 21,678 |
| | Drivers | 16,641 | 2,243 | 283 | 1,960 | 14,398 |
| | Passengers | 8,271 | 992 | 111 | 881 | 7,279 |
| Selected by Condition B | All occupants | 81,955 | 7,565 | 703 | 6,862 | 74,390 |
| | Drivers | 55,246 | 5,017 | 475 | 4,542 | 50,229 |
| | Passengers | 26,709 | 2,548 | 228 | 2,320 | 24,161 |

This means the sensitivity of the assessed automatic triggering conditions, i.e. the proportion of casualties successfully selected from all casualties of the corresponding severity level, compares as follows: The sensitivity in capturing casualties of any injury severity level was found to be 19.8% for Condition A and 65.1% for Condition B. When focussing on KSI casualties only, the sensitivities were 34.7% for Condition A compared to 81.0% for Condition B.

Conversely, this means if Condition A was applied, up to 6,100 KSI casualties per annum in GB (65.3%) might not be covered by automatic eCalls. For Condition B this number would reduce to 1,770 (19.0%).

The sensitivity of Condition B is elevated by the factor 3.3 for all injury severity levels and by the factor 2.3 for KSI compared to Condition A. Sensitivities split by injury severity and between drivers and passengers are given in *Table 2*; a comparison is visualised in *Figure 1*.

***Table 2.*** **Sensitivity of automatic triggering Conditions A and B, i.e. proportion of casualties successfully selected from all casualties of the corresponding severity level; reported for different injury severity levels and different positions**

| | | All severities | KSI | Fatal | Serious | Slight |
|---|---|---|---|---|---|---|
| Condition A | All occupants | 19.8% | 34.7% | 47.0% | 33.4% | 18.6% |
| | Drivers | 19.6% | 35.9% | 49.1% | 34.6% | 18.3% |
| | Passengers | 20.2% | 32.1% | 42.2% | 31.2% | 19.2% |
| Condition B | All occupants | 65.1% | 81.0% | 83.8% | 80.8% | 63.8% |
| | Drivers | 65.0% | 80.3% | 82.5% | 80.1% | 63.8% |
| | Passengers | 65.2% | 82.5% | 86.7% | 82.1% | 63.8% |

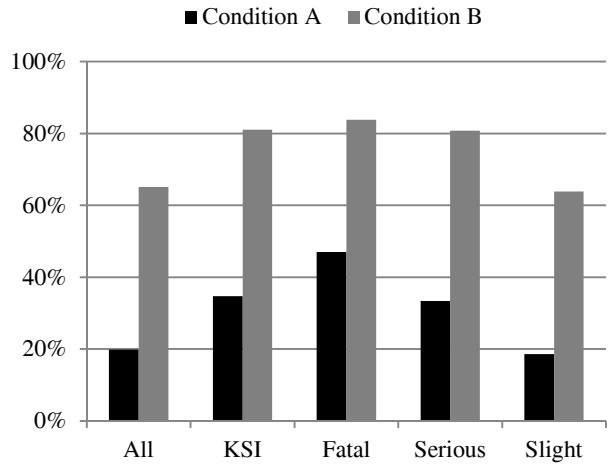


***Figure 1.*** **Comparison of the sensitivity of automatic triggering Conditions A and B for different injury severity levels (all vehicle occupants)**

It can be seen for both conditions that the sensitivity is decreasing with decreasing injury severity level. This trend is more obvious for Condition A with a particularly marked drop in the sensitivity in selecting serious casualties compared to fatal casualties. The sensitivity of Condition B in selecting fatal and serious casualties is at a comparable level.

The sensitivity of both conditions does not vary markedly between drivers and passengers. For KSI casualties the variation is 3.8 percentage points for Condition A and 2.2 percentage points for Condition B.

The specificity of the assessed conditions, i.e. the proportion of non-KSI casualties (that is, slightly injured casualties) that were successfully not selected, compares as follows: Condition A provides a specificity 81.4% for all vehicle occupants compared to 36.2% for Condition B (see *Table 3* and *Figure 2*). Note that the reported specificity is based on recorded injury collisions only, because no data is available for damage-only collisions.

***Table 3*. Specificity of automatic triggering Conditions A and B, i.e. proportion of non-KSI casualties (that is, slightly injured casualties) not selected; reported for different positions**

| | | KSI |
|---|---|---|
| Condition A | All occupants | 81.4% |
| | Drivers | 81.7% |
| | Passengers | 80.8% |
| Condition B | All occupants | 36.2% |
| | Drivers | 36.2% |
| | Passengers | 36.2% |

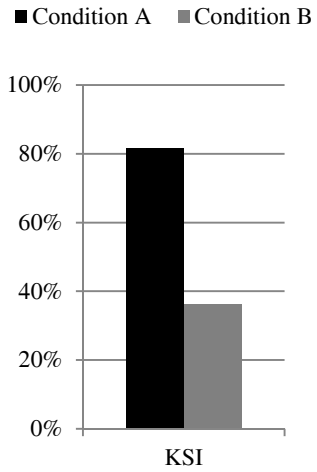


***Figure 2*. Comparison of the specificity of automatic triggering Conditions A and B in selecting KSI casualties (all vehicle occupants)**

The specificity of Condition B is markedly lower than that of Condition A. This means if Condition A was applied, automatic eCalls would be triggered for 21,678 slight casualties per annum in GB (18.6% of all slightly injured casualties). For Condition B this number would increase to 74,390 (63.8%).

The specificity of both conditions varies only slightly between drivers and passengers.

### Limitations of the Analysis

The present analysis was performed based on in-depth accident data from GB. The analysis cannot be transferred in detail to the whole EU because impact typology varies across the member states. The authors have, however, no reason to believe that the general trends observed will differ or that the magnitude of the results would be of a different order. *Table 4* details the collision type distribution of the underlying GB in-depth accident data, i.e. the 3,351 CCIS cases identified by applying the primary selection criteria.

***Table 4.*** **Collision typology of cases selected for analysis from the in-depth CCIS accident database; absolute numbers and proportion of collision types; reported for different injury severity levels**

| | All severities | KSI | Fatal | Serious | Slight |
|---|---|---|---|---|---|
| Front | 1,406 (42.0%) | 500 (41.9%) | 64 (28.1%) | 436 (45.1%) | 906 (42.0%) |
| Side | 783 (23.4%) | 252 (21.1%) | 68 (29.8%) | 184 (19.0%) | 531 (24.6%) |
| Rear | 201 (6.0%) | 28 (2.3%) | 5 (2.2%) | 23 (2.4%) | 173 (8.0%) |
| Multi | 343 (10.2%) | 133 (11.1%) | 28 (12.3%) | 105 (10.9%) | 210 (9.7%) |
| Rollover | 597 (17.8%) | 267 (22.4%) | 57 (25.0%) | 210 (21.7%) | 330 (15.3%) |
| Other | 21 (0.6%) | 14 (1.2%) | 6 (2.6%) | 8 (0.8%) | 7 (0.3%) |
| Total | 3,351 (100%) | 1,194 (100%) | 228 (100%) | 966 (100%) | 2,157 (100%) |

In-depth CCIS accident data was scaled up because the STATS19 database itself does not provide enough detail to estimate whether the assessed triggering conditions would have been met. It is assumed that, accounting for deliberate case selection strategies, the CCIS data is broadly representative of national crashes. However, the CCIS data collection followed a tow-away model, which means that less damaged cars are underrepresented because these are less likely to be towed away from the scene. Compared to STATS19 the cases within each severity level will be biased towards the more severe collisions of the respective level. This might lead to an overestimate of the sensitivity of both conditions.

The analysis was limited to vehicles fitted with front and side airbags which is expected to be the case for the vast majority of passenger cars sold in Europe after mandatory introduction of eCall. However, a smaller proportion of the vehicles in the database than is to be expected in future vehicles are fitted with side-curtain airbags that are prepared to be deployed in rollover accidents. This means that some rollovers will not see airbag triggering in the database, which is why the sensitivity of Condition B might be somewhat underestimated.

Further, for the analysis of Condition A only those casualties whose car principally experienced a front- or side-impact were included. This might lead to a certain underestimate of the real-world sensitivity of Condition A, because an unknown proportion of the oblique, multi-impacts and rollover events may have involved dynamic loading conditions similar to those experienced in the UN R94 and UN R95 tests and therefore triggered an automatic eCall during the course of the real event.

Lastly, the results of this study are not intended to be absolute measures of likely automatic eCall numbers; rather they provide a comparison between the two options. Absolute numbers of expected superfluous eCalls could not be estimated because the accident data does not include damage-only collisions, for which no data was available that would allow an analysis of the specific accident conditions.

## DISCUSSION

### Sensitivity of the Assessed Triggering Conditions

A suitable triggering condition has to provide a high level of sensitivity to ensure that a high proportion of the relevant casualties benefits from the automatic eCalls. The assessment focussed on KSI casualties because the prevalence of incapacitating injuries (preventing a manual emergency call) as well as the prevalence of conditions resulting in long term disabilities (or death) without rapid medical treatment in this group is higher than among the slightly injured casualties.

The results of the accident analysis confirmed that Condition B is more sensitive than Condition A, i.e. successfully captures a higher proportion of all KSI casualties. This result confirmed expectations based on the fact that the accidents selected by A can be considered a sub-set of those selected by B: A captures crashes whose impact angle resembles UN R94 or UN R95 tests and which are of comparable or higher severity. Because vehicles always deploy the respective airbags in these tests, all of these cases are, among others, included in B.

However, the difference in sensitivity was found to be large: Condition A captures only 34.7% of KSI casualties, whereas B captures 81.0%. This would result in a difference of up to 4,330 KSI casualties per annum in GB. Even in light of the fact that the formal interpretation of Condition A applied for this analysis represents a worst case that might be somewhat unrealistic from a practical real-world implementation perspective, this difference appears high.

Condition B also exhibited an almost unvarying sensitivity in selecting fatal casualties and serious casualties respectively, whereas the sensitivity of Condition A already dropped considerably at the serious casualty level. Further, Condition B is slightly superior in equally selecting drivers as well as passengers, however the difference to Condition A is small. Considering the marked difference in sensitivity and the low level of Condition A in absolute terms, clear preference should be given to Condition B based on sensitivity.

Nevertheless, 19.0% of KSI casualties would not be captured by this condition, which is 1,770 KSI casualties per annum in GB. Although the sensitivity is expected to be higher among more recent vehicles due to the higher fitment rate of side-curtain airbags prepared for rollover protection, there will remain a proportion of collisions not captured: Airbag systems are deliberately not deployed in certain accident types (such as rear shunt accidents where the vehicle is accelerated forwards) or are not deployed because of insufficient detection capabilities (such as certain cases of under-run accidents with low deceleration levels yet high injury risk due to large intrusion).

This shortcoming of Condition B could be addressed by pursuing a non-restrictive approach when implementing the triggering condition in type-approval legislation, i.e. require triggering in the presence of the condition yet not prohibit triggering in its absence. This would ensure, via regulation, that a reasonable minimum proportion of casualties are captured, while allowing vehicle manufacturers to apply more advanced algorithms tuned to the specific vehicle characteristics and making use of the full available sensor infrastructure to cover additional KSI casualties.

**Specificity of the Assessed Triggering Conditions**

Besides sensitivity, the triggering condition also needs to provide a high level of specificity to avoid a high number of superfluous eCalls. These two targets are of somewhat conflicting nature because the severity of injuries sustained in accidents varies not only with external accident conditions or characteristics of the vehicles involved, but also with factors which are unknown to the vehicle's triggering logic, such as the occupants' individual physiology (size and mass), injury resistance or pre-impact posture.

The specificity in selecting KSI casualties of Condition B (36.2%) was found to be markedly reduced compared to Condition A (81.4%). This means for Condition B, which is preferable based on sensitivity, approximately 74,390 of the 81,955 annually reported casualties via automatic eCalls in GB will only be slightly injured. This is also an indicator of the protection afforded by airbags where a high deceleration crash can result only in slight injuries. The overall number of automatic eCalls will be even higher and include an unknown number of additional calls from damage-only accidents (which are not quantified in this analysis). While superfluous automatic eCalls do not create dis-benefits for the road users concerned, the work of PSAPs and the correct targeting of those persons most in need of emergency medical treatment might be hampered if the number of eCalls is excessive.

It can be expected that a certain proportion of the slightly injured casualties would also call emergency services manually and there might be certain benefits from automatic eCalls, although the major part of this group will not be reliant upon the automatic triggering. The number of additional eCalls from damage-only accidents is unknown. However, there are indications that PSAPs and emergency services would be able to mitigate the negative consequences of superfluous eCalls from Condition B:

- Even among conventional emergency calls approximately 60% are reported to be non-emergencies (European Commission 2011);
- PSAPs receive ample information for triage via the MSD and the voice communication channel with the occupants. Advanced injury prediction algorithms can be applied as suggested by Bahouth *et al.* (2014) and Kusano & Gabler (2014);
- Emergency services already attend most injury collisions, even with only slightly injured occupants. Experience from the RAIDS programme also shows, that many ambulances attend collisions and treat casualties who do not appear in the STATS19 statistics (either because their injuries are relatively minor or because not every case is reported by the police); and
- The already existent implementation of Condition B in certain voluntary AECSs in the EU, Japan and USA is not known to have led to major disruptions of third party service providers (TPSPs). Furthermore, TPSPs having a system in coexistence with the mandatory eCall could help by filtering minor calls and only transferring the more severe cases.

**Suitability for Implementation in Type-Approval Legislation**

Airbags are not mandatory equipment for any vehicle sold in the EU. Nevertheless, to pass the performance criteria of the regulatory full-scale crash tests UN R94 and UN R95 and to score sufficiently in Euro NCAP, including the pole-impact test where a head-protecting airbag is a prerequisite, virtually all passenger cars are

equipped with frontal airbags and a high and increasing proportion is also equipped with side-torso and side-curtain airbags. Hence, Condition B can be applied to virtually all passenger cars. The specific implementation of the triggering requirement could cater for the theoretically remaining vehicles that are not equipped with any airbag; for example, via implementation as an 'if fitted' requirement.

A feasible and low-cost means of demonstrating adherence to the triggering requirement for type-approval would be a paper-based process. The vehicle manufacturer or IVS supplier could, for example, hand in a dossier of documents that assures the type-approval authority of the non-restrictive link between airbag deployment and automatic eCall triggering.

To prevent undue restriction of design freedom, the triggering algorithm should be left to the vehicle manufacturer's discretion within certain boundaries. This is also due to the fact that only vehicle manufacturers have advanced knowledge of the vehicle models and should therefore be enabled to tune the eCall triggering to the properties and sensors of the specific model. Implementing Condition B for mandatory triggering in a non-restrictive way does comply with these aims: Firstly, the algorithm under which conditions to trigger an airbag (and hence also trigger a mandatory eCall) is fully at the vehicle manufacturer's discretion. The automatic eCall requirement would just ensure that emergency services are notified after collisions which the vehicle manufacturer considered severe enough to deploy non-reusable restraint systems that need to be replaced. Secondly, an implementation of the requirement that allows triggering also under different accident conditions ensures that vehicle manufacturers can apply their expertise to also cover the remaining proportion of casualties in non-airbag deployment collisions.

### Conclusions

This study found that mandatory triggering of automatic eCalls under accident conditions similar to, and at least as severe as, the frontal and lateral full-scale crash tests defined in UN R94 and UN R95 respectively cannot successfully ensure via regulation that a high proportion of casualties will benefit from automatic eCalls. In contrast, a non-restrictive requirement to trigger automatic eCalls after collisions where an airbag deployed was found to cover up to 4,330 fatally or seriously injured casualties more per annum in GB (57,042 casualties when considering all injury severity levels) and is, therefore, considered a more suitable candidate for implementation in type-approval legislation.

## ACKNOWLEDGMENTS

The authors wish to acknowledge the European Commission (EC) for funding this project.

The paper used accident data from the United Kingdom Co-operative Crash Injury Study (CCIS) collected during the period 2000–2010. CCIS was managed by the Transport Research Laboratory, on behalf of the DfT (Transport Technology and Standards Division) who funded the project along with Autoliv, Ford Motor Company, Nissan Motor Company and Toyota Motor Europe. Previous sponsors of CCIS have included Daimler Chrysler, LAB, Rover Group Ltd, Visteon, Volvo Car Corporation, Daewoo Motor Company Ltd and Honda R&D Europe (UK) Ltd. Data were collected by teams from the Birmingham Automotive Safety Centre of the University of Birmingham; the Vehicle Safety Research Centre at Loughborough University; the Transport Research Laboratory and the Vehicle & Operator Services Agency of the DfT.

## REFERENCES

Association for the Advancement of Automotive Medicine (AAAM). *The Abbreviated Injury Scale 1990 Revision*. Des Plaines, Illinois, U.S.A.: Association for the Advancement of Automotive Medicine (AAAM). 1990.

Bahouth G, Graygo J, Digges K, Schulman C, Baur P. The Benefits and Tradeoffs for Varied High-Severity Injury Risk Thresholds for Advanced Automatic Crash Notification Systems. *Traffic Injury Prevention*. 2014; 15:sup1: S134-S140.

Carroll J, Seidl M, Cuerden R, Stevens A. *Technical considerations regarding type-approval testing of eCall in-vehicle systems. Client Project Report CPR1868.* Crowthorne, UK: Transport Research Laboratory. 2014.

CARS 21 High Level Group on the Competitiveness and Sustainable Growth of the Automotive Industry in the European Union. *Final Report 2012*. Brussels, Belgium: European Commission. 2012.

Council of the European Union. *Proposal for a Regulation of the European Parliament and of the Council concerning type-approval requirements for the deployment of the eCall in-vehicle system and amending Directive 2007/46/EC - General approach, dated 19 May 2014*. Available at: http://register.consilium.europa.eu/doc/srv?l=EN&f=ST%209879%202014%20INIT. 2014.

Department for Transport. *STATS20 Instructions for the Completion of Road Accident Reports from non-CRASH Sources*. London, UK: Department for Transport. 2011.

Department for Transport. *Reported road casualties in Great Britain: main results 2012*. London, UK: Department for Transport. 2013.

European Commission. *Commission staff working paper - Impact assessment - Accompanying the document commission recommendation on support for an EU-wide eCall service in electronic communication networks for the transmission of in-vehicle emergency calls based on 112 ('eCalls'), dated 8 September 2011*. 2011.

European Commission. *Proposal for a Regulation of the European Parliament and of the Council concerning type-approval requirements for the deployment of the eCall in-vehicle system and amending Directive 2007/46/EC, dated 13 June 2013.* Available at: http://eur-lex.europa.eu/legal-content/EN/TXT/PDF/?uri=CELEX:52013PC0316&from=EN. 2013.

European Parliament. *European Parliament legislative resolution of 26 February 2014 on the proposal for a regulation of the European Parliament and of the Council concerning type-approval requirements for the deployment of the eCall in-vehicle system and amending Directive 2007/46/EC, dated 26 February 2014*. Available at: http://www.europarl.europa.eu/document/activities/cont/201403/20140312ATT81008/20140312ATT81008EN.pdf. 2014.

GOST R 54620-2011 *Global Navigation Satellite System. Emergency Response System in case of Accidents. Car System Call Emergency Services. General Technical Requirements*. 2011.

Hayden J. *eCall UK 2013 Review and Appraisal. Final Report. Department for Transport*. Manchester, UK: Atkins Limited. 2014.

IWG AECS-Representation of Japan. *HELPNET System Specifications*. Document number: AECS 03-05. Available at: https://www2.unece.org/wiki/download/attachments/16449877/AECS-03-05%20%28J%29%20HELPNET.pdf?api=v2. 2014.

Kononen DW, Flannagan CA, Wang SC. Identification and validation of a logistic regression model for predicting serious injuries associated with motor vehicle crashes. *Accid Anal Prev*. 2011; 43:112–122.

Kusano K, Gabler HC. Comparison and Validation of Injury Risk Classifiers for Advanced Automated Crash Notification Systems. *Traffic Injury Prevention*. 2014; 15:sup1: S126-S133.

McClure D, Graham A. *eCall – The Case for Deployment in the UK. Final report*. Milton Keynes, UK: SBD Limited. 2006.

prEN 16454. *Intelligent transport systems. ESafety. ECall end to end conformance testing*. Brussels, Belgium: European Committee for Standardization (CEN). 2014.

Sánchez-Mangas R, García-Ferrrer A, de Juan A, Arroyo AM. The probability of death in road traffic accidents. How important is a quick medical response?. *Accid Anal Prev*. 2010; 42(4): 1048-56.

Stevens A, Hopkin, J. *UK eCall impact assessment. Published Project Report PPR470*. Crowthorne, UK: Transport Research Laboratory. 2010.

UN Regulation No. 94. *Uniform provisions concerning the approval of vehicles with regard to the protection of the occupants in the event of a frontal collision.* Revision 2. Available at: http://www.unece.org/fileadmin/DAM/trans/main/wp29/wp29regs/updates/R094r2e.pdf. 2013.

UN Regulation No. 95. *Uniform provisions concerning the approval of vehicles with regard to the protection of the occupants in the event of a lateral collision.* Revision 2. Available at: http://www.unece.org/fileadmin/DAM/trans/main/wp29/wp29regs/updates/R095r2e.pdf. 2013.

UN Regulation on AECD/AECS (draft). *Uniform provisions concerning the approval of: I Emergency call devices (AECD), II Vehicles with regard to the installation of an AECD of an approved type, III Vehicles with regard to their AECS*. Document number: AECS 03-04e. Available at: https://www2.unece.org/wiki/download/attachments/16449877/AECS%2003-04e.pdf?api=v2. 2014.

# RECENT ADVANCES IN EFFECTIVENESS ANALYSIS AND VIRTUAL DESIGN OF INTEGRATED SAFETY SYSTEMS

**Izabella Ferenczi**
**Dr. Thomas Helmer**
BMW Group
Germany

**Peter Wimmer**
VIRTUAL VEHICLE Research Center
Austria

**Dr. Ronald Kates**
REK Consulting
Germany

Paper Number 15-0139

## ABSTRACT

Design, optimization, and assessment of integrated safety systems (combining active and passive elements) pose considerable challenges. For example, the spectrum of potential situations in the field in which active elements might be triggered is considerably larger than one can achieve under controlled testing conditions.

In this context, it is crucial to evaluate quantitative metrics relating as closely as possible to human risks and benefits, such as avoidance of injuries or reduction of injury severity. The consequences of unnecessary interventions and other side effects on passengers or traffic also need to be quantified. This paper describes a generic approach to assessment of field effectiveness and evaluation of active and integrated safety systems. The approach, based on virtual experiments, is holistic, in that both active and passive safety elements are evaluated using a common metric while seeking the most effective solutions regarding overall improvement of vehicle safety. The complexity of process models and their interactions utilizes an advanced knowledge base. In order to achieve this goal, the whole sequence of events in a hazardous situation is virtually implemented in a tool chain. The tool chain includes stochastic (or "Monte-Carlo") traffic simulation, generating large samples of accident sequences but also near-misses, as well as detailed, high-resolution crash simulations of resulting accidents. The methods are useful not only for assessment of existing integrated safety designs, but also for comparing different system concepts or optimizing performance within a complex design concept. The potential of this approach is illustrated for several key accident scenarios.

## INTRODUCTION

Although prevention of all accidents is still out of reach, integrated approaches, combining elements of active and passive safety, appear quite promising in terms of human benefits. Active safety components are designed to reduce crash severity or avoid a crash entirely in situations with high collision risk, while minimizing unnecessary interventions. In accidents that cannot be prevented entirely by active strategies, it may still be possible to reduce severity of injuries by passive safety elements. However, design, optimization, and assessment of integrated safety systems pose considerable challenges. For example, the spectrum of potential hazardous situations in the field in which active elements might be triggered is considerably larger than one can achieve under controlled testing conditions.

In this context, it is crucial to define and evaluate appropriate quantitative metrics relating (as closely as possible) to human risks and benefits, such as avoidance of injuries or reduction of injury severity. These metrics are generally quite difficult to measure directly in field operating tests (FOT) or naturalistic driving studies (NDS), even retrospectively, because the number of injury accidents required for statistically significant injury probability differences to emerge is typically in the hundreds or thousands; the total accident

rate is, for example, a few hundred per billion kilometers on German autobahns. FOT and NDS are appropriate for evaluating the impacts of safety systems on normal driving situations and driving errors that occur with much higher frequency, such as lapses of attention or unintended lane crossings. These observations can play an important role in accident risk modeling, but they do not directly provide the required metrics.

This paper describes the application of a generic safety evaluation algorithm to integrated safety systems. The basic idea is to estimate field effectiveness by virtual experiments carried out on a large sample of representative situations. The experimental design generally compares a safety system to a reference or basis situation without the system; a typical metric for comparison is the relative reduction in frequency and/or severity of accident injuries. The frequency and consequences of unnecessary interventions and other side effects on passengers or traffic can also be quantified in this approach. The virtual experiments are performed in the framework of a tool chain, which is illustrated below for several scenarios and safety systems of interest.

**Knowledge base for virtual experiments on integrated safety systems**

In order to perform virtual experiments, an advanced knowledge base is required. The knowledge base contains detailed models of all safety relevant processes in the traffic scenarios under consideration. In this context, "processes" include vehicle and traffic dynamics, as well as human sensory and physiological performance.

In addition, the possible influences of a proposed safety system on all these processes need to be modeled. To this end, specifications of sensors, algorithms, and actuators are required, as well as models of the human machine interface. The level of detail needs to be adequate to predict if and when a system would trigger during a simulated critical situation and how the system could influence the driver. Active safety modes of influence include acoustic or visual warnings, haptic feedback, pre-filling brakes or changing brake assist thresholds, direct intervention in longitudinal or lateral vehicle control, etc.

For evaluation of integrated safety systems including systems both of active and passive safety (such as pre-tensioning restraint systems or airbag deployment), the approach described below is to implement the knowledge base models within a virtual tool chain for virtual experiments.

## TOOL CHAIN ELEMENTS FOR INTEGRATED SAFETY SYSTEMS

Figure 1 illustrates the process steps within a virtual tool chain for pedestrian safety systems:

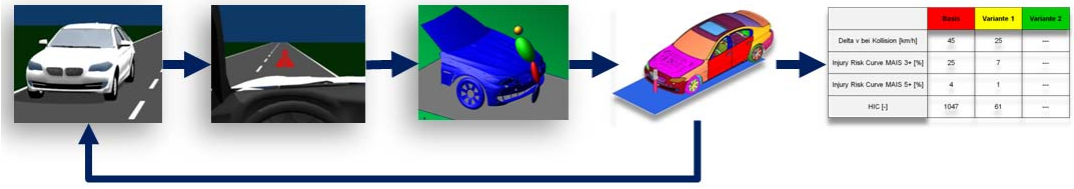


***Figure 1: Virtual Tool Chain (for the case of a pedestrian crossing scenario)***

The virtual tool chain for a typical integrated safety system includes several steps:

1. Stochastic traffic simulation including preventive safety systems
2. Multibody simulations determining precise collision constellations
3. Finite-element simulation of representative collision constellations

4. Surrogate models for injury criteria in collisions (for example support vector machines)

5. Determination of injury risk based on injury criteria, such as Head Injury Criterion (HIC) etc.

The processes represented by the simulation models include behavioral and physical characteristics of all traffic participants, the environment, the vehicle, the safety function, and all possible interactions. A key characteristic of most models in traffic safety is the inherently stochastic nature of the processes, particularly those that depend on human factors. Collisions are generally rare events, even in potentially risky situations. Hence, in order to simulate a sufficiently large sample of "true" virtual accident situations, a correspondingly large number of potential conflicts or hazardous situations need to be simulated, requiring high computational efficiency during the stochastic simulation step.

When evaluating overall safety performance in case of unavoidable accidents, a detailed representation of the vehicle, occupants (dummies, human models) or pedestrians/cyclists (impactors, human models) is necessary. For example, detailed determination of injury characteristics and their improvement due to passive safety systems (e.g., active bonnet for pedestrian safety, reversible belt pre-tensioning during pre-crash phase) usually demand finite-element simulations. The highly dynamic processes during the relatively short crash phase require higher resolution and thus several orders of magnitude more computational time per virtual accident than the pre-crash phase although being significantly longer (usually several seconds of pre-crash phase are followed by only some hundred milliseconds during the crash phase). For virtual statistical evaluation of a particular system configuration, several hundred accidents need to be generated and simulated. Considering the many possible variants within a system, surrogate models, which allow rapid calculations, offer a useful approach to achieving manageable overall computing times.

Regarding kinematic occupant behavior in the pre-crash phase (such as during braking), standard finite element models have only limited validity: first of all, crash test dummies (both, numerical and hardware dummies) are validated for massive crash impacts and are quite rigid under low-g impacts. The second limitation is that under low impacts, the occupants have the ability to actively control their behavior. Therefore, active human models seem to have a more realistic behavior in these scenarios, [KH14].

**CONFLICT SCENARIOS ADDRESSED BY INTEGRATED SAFETY SYSTEMS**

In the following, we focus on methods for evaluating integrated systems including automatic emergency braking (AEB) features in three conflict scenarios:

1. Pedestrian/vehicle conflicts (→ AEB pedestrian)
2. Cyclist/vehicle conflicts (→ AEB cyclist)
3. Vehicle/vehicle rear-end conflicts (→ AEB city/AEB interurban)

For these AEB systems, the traffic contexts are different (highway traffic vs. city scenarios, rear-end braking scenarios, lane changing, crossing/turning, occlusion), the driver models are in general similar but may differ regarding their parameterization (e.g., regarding awareness, response times), and also the behavior of pedestrians is completely different from that of cyclists (regarding for example acceleration/deceleration, inertia, evasion). Therefore each traffic scenario needs careful and detailed modeling. The AEB systems under investigation have typical key characteristics which are the similar for all systems mentioned above: sensor opening angles (horizontal, vertical), sensor range, latency, sensor quality, brake ramp, maximal deceleration. Beside these similarities, the algorithms (e.g. the underlying intelligence) are completely different and independent and therefore result in differing behavior.

Regarding cases where the accident cannot be avoided completely or the accidents which happen without an AEB system, the collisions cyclist/vehicle, pedestrian/vehicle, and vehicle/vehicle each have different kinematics and

require validated multibody or suitable finite-element models to determine the exact collision constellation and injury outcomes.

In case of an active or integrated cyclist safety system the tool chain itself is identical to the one which is described below for the pedestrian. Evidently, every single module requires different models. The stochastic traffic simulation must be able to reproduce all critical cyclist conflict scenarios (crossing, turning, overtaking…). The multibody models have to be validated for the cyclists (different bicycle geometries, cyclists' body forms (children, adults…)). In addition, the determination of the injury criteria is not trivial, since the model choice is not predetermined (impactors vs. hybrid dummy models vs. active/passive human models). The tool chain for active and integrated cyclist safety systems is under current development.

Similarly, the tool chain for vehicle/vehicle active safety systems is currently under further development. The first module, the stochastic traffic simulation of highway scenarios with and without automatic emergency braking systems is available (highway scenarios including lane change, traffic jams; city scenarios) and presented in this paper. In case of an accident, the injury risks can be estimated based on the resulting crash-constellations (impact speed, masses, impact direction); however, detailed models for vehicle/vehicle crashes at different angles, speeds etc. are still subject of research (available finite-element-models are too time-intensive in computation for this field of application). In the future we will also provide appropriate models for the pre-crash phase (including active safety systems) and surrogate models for the crash phase so that the comparison of passive safety systems is also possible within the tool chain.

## TOOL CHAIN FOR INTEGRATED PEDESTRIAN SAFETY SYSTEMS

### Stochastic traffic simulation of pedestrian crossing scenarios

Effectiveness analysis for preventive safety systems starts with the generation of representative initial conditions for potentially critical situations using appropriate exposure models. An exposure model describes the distribution of key characteristics that are likely to affect the probability of a conflict (and consequently that of an accident or a system response).

Consider for example an inherently hazardous crossing scenario known as the "midblock dash": a pedestrian decides to cross an urban street (from the passenger side) at an unregulated spot between intersections, i.e., without traffic lights, crosswalks, or any other form of infrastructure support, see figure 2. For the example presented in this paper, we consider one-way traffic on a single, straight, one-lane road and assume that there are no obstructions, such as parked delivery trucks, to obstruct the drivers' view of the roadway and the traffic stream. For other applications different street layouts, obstructions etc. are also available.

In the paradigm of virtual testing by stochastic simulation, the aim is to obtain and simulate large, representative samples of virtual sequences of traffic situations. As an example, the pedestrian model consists of various key characteristics; specific parameters are drawn from multivariate distributions, such as:

- Context variables: distribution of pedestrian crossing volume during the course of the day (by age and gender)
- Pedestrian attributes, such as age- and gender-adjusted distributions of height and weight, as well as fatigue and alcohol levels (both related to time of day)
- Distributions of cognitive characteristics, such as alertness, visual and reactional performance (related to age, gender, alcohol, fatigue)

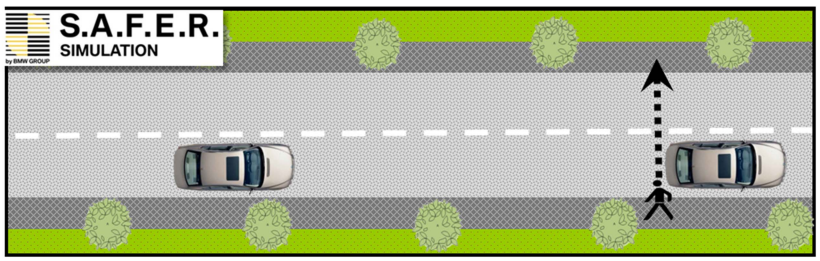


***Figure 2: Stochastic Simulation of a pedestrian crossing: the midblock***

Exposure also deals with generation of realistic traffic contexts and representative drivers, who might be confronted with an unexpected crossing pedestrian. The model distributions involve:

- traffic volume and average traffic flow speed during the course of a day
- speeds and gaps within a traffic stream

Once a representative virtual pedestrian has been "created", processes governing the dynamics of the pedestrian are simulated. These include, for example:

- Gap acceptance to begin crossing of the road
- Decision to walk or run
- Initial walking or running speed
- Initial heading
- Angular gaze distribution
- Possible speed and course correction

The willingness of the pedestrian to wait for an acceptable gap decreases with increased waiting time. As a consequence, the pedestrian "becomes impatient" and will accept smaller gaps. More generally, there are several mechanisms of cognitive error for estimating gaps and crossing times, all of which can contribute to a particularly hazardous crossing. An additional characteristic that needs to be respected is the response of the pedestrian, once he perceived a critical situation: possible reactions include freezing on the spot, jumping forwards, or moving backwards; all responses are associated with cognitive processing demands.

Similarly, driver performance including alertness, visual acuity, perception of hazards, cognitive processing (reactions), and response (such as braking) are also modeled in detail using appropriate probability distributions. These depend in turn on relevant driver attributes, e.g., age or fatigue, but may also depend on context (e.g. lighting conditions). A detailed model description is given in [HSSEK11] and [HNRGKK12].

In the scenarios considered here, available driver responses to a critical situation are limited to braking, but in general, emergency evasive steering would be another option for the driver.

Preventive safety systems – such as AEB systems – have different options for influencing the situation, such as driver information and warning, automatic braking, or rather indirect strategies, such as adaptation of brake assist thresholds. Thus, system safety performance is clearly mediated in many cases by the driver's actions, and these in turn depend on individual characteristics. As a consequence, performance evaluation requires stochastic models that include the relevant individual driver characteristics.

In addition, safety performance is affected by the range of cognitive and dynamic responses of pedestrians: for example, there are two mechanisms for avoiding collisions by braking of the vehicle: The first is obvious, i.e., the vehicle stops before crossing the pedestrian's path. The second is less obvious: even if a vehicle cannot stop before

crossing the *pedestrian's* path, some pedestrians might move fast enough to get out of the *vehicle's* path (an extra 300 ms at 3 m/s means 90 cm, or about half the width of a vehicle).

In case of ideal weather and illumination conditions camera systems used for automotive applications show a good performance concerning object detection and classification. Nevertheless in order to ensure a realistic model of the AEB system, probability of failure and limited functionality are also considered.

The possibilities of the virtual simulation are currently extended by considering more crossing scenarios (far side, obstructed), other vulnerable road users (cyclists), other traffic scenarios (turning, oncoming traffic, etc.) and more elaborate preventive safety systems (such as the fusion of camera and radar sensors).

Most active safety algorithms have to deal with uncertainties related to human performance. Effective prevention or mitigation of an accident may require system response before the accident is 100% certain to occur. For example, an acutely endangered pedestrian could jump back at the last minute. The result is that an active safety device can trigger even if no collision would have occurred without it. Because the exposure models generate situations that do not necessarily lead to accidents (even without a safety system), virtual stochastic simulation enables quantification of how often such "unnecessary" responses occur in relation to the "necessary" ones. Moreover, possible side effects of AEB systems, such as secondary rear-end collisions, can be quantified for all responses, not just the necessary ones. In this way, the advantages and disadvantages of a triggering decision under uncertainty can be quantified and incorporated into system optimization.

Since the virtual simulations provide data such as gender, age, height, and weight in addition to collision speed and position, it is possible to model the effectiveness of the AEB systems not only in terms of speed reduction, but also with respect to changes in injury severity. One approach is to interface the stochastic simulation with empirically generated injury probability models. This approach does not require detailed vehicle models and provides a good assessment of the effectiveness of the active system. However, whenever conclusions for specific vehicles and their passive safety systems are required, one has to follow the subsequent steps of the described tool chain.

**Collision constellation via multibody simulation for pedestrian impact**

In cases where the accident cannot be avoided completely, or for the basis simulation without any active safety systems, the collision constellations need to be determined. Stochastic traffic simulation, as described above, calculates the trajectories of involved traffic participants, but is not designed for delivering exact collision details, such as exact points of impact (especially of specific body parts), exact impact speed etc. These parameters can be simulated using fast, multibody simulation models. The pedestrian is modeled by 4 body elements (head, torso, femur, and tibia) joined by 3 joints (neck, hip, knee); the models are scalable for different body heights (children, adults). The pedestrian models have been validated based on available PMHS tests (Post Mortem Human Subjects), [KMDKBC05].

The vehicle is modeled as a rigid surface. Since these models are fast calculating (i.e. few seconds per run), it is possible to determine the exact collision constellation for a considerable number of accidents.

Current developments include enhancement of multibody models for cyclists. In this case, the validation is more difficult, since cyclist data is scarce. It is planned to use the results of finite element simulations for the validation of the multibody kinematics.

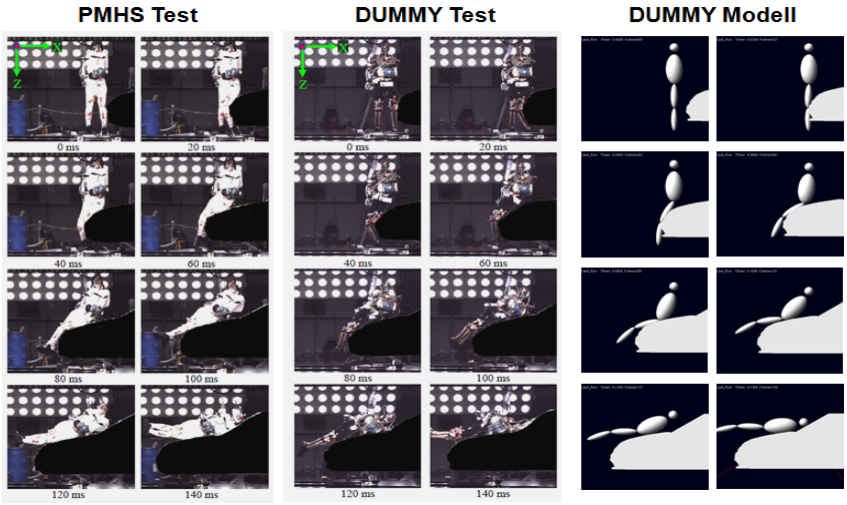


*Figure 3: Kinematics Comparison PMHS vs. Multibody Simulation*

**Injury criteria via finite element simulation for pedestrian impacts**

The next step is the determination of the injury criteria of the pedestrians based on the exact collision constellations. These depend not only on parameters like speed, acceleration or the exact point of impact, but also on the stiffness and geometry of the vehicle and its passive safety features, like active hoods etc.

The finite element models of the vehicle and the pedestrian (THUMS, finite element dummy, head impactor, TRL leg impactor, flex pli …) have the main disadvantage of requiring long calculation times in order to deliver accurate responses. Of course, there are some ways to optimize these calculation times, like reducing the models to the absolutely required model parts and omitting everything which is not needed directly. Nevertheless, depending on the IT-infrastructure, each simulation still requires at least some hours.

For example, considering one million stochastic simulations without preventive safety systems, probably thousands of collision scenarios would have to be simulated using these models (either THUMS Simulation for the whole body or head & leg impact); this would require about 1-2 months calculation times, which is not feasible in this developmental context. To overcome these long waiting times, surrogate models for each vehicle/impactor combination have been developed.

**Surrogate models for injury criteria**

Surrogate models are mathematical, non-physical models describing input/output relations of given data pairs. There are several, well known approaches, such as fuzzy models, linear models, support vector machines, local linear model trees… Since these models are non-physical, one has to calibrate them for each problem and check carefully, if they are truly valid by considering appropriate error measurements, [WBHF15]. When the underlying physical problem changes (e.g., new vehicle geometry), the model has to be rebuilt or at least re-parameterized.

When building surrogate models, the first step is the selection of training data. Beside the appropriate distribution of chosen points, the number of training points is crucial. Too few result in imprecise surrogate models; too many require long calculation times. Regarding the distribution, we found that accounting the problem structure sometimes improves the result quality, for example the use of more training data in areas of higher in-homogeneity. In case of pedestrian protection, all available information has been considered, when

choosing training data. For example, in areas with known changes in stiffness, more data have been chosen than in areas with little changes. Our goal was to achieve acceptable results using data of about 100 head-impacts and 100 leg-impacts. The head- and leg-impacts didn't necessarily belong to the same collision. Calibration of the surrogate models can be done using different methods for example by using differential evolution algorithms to find optimal model parameters. We tested different regression methods namely LOLIMOT (Local Linear Model Tree), support vector machines and Kriging. These standard methods are available in different (commercial) optimization and machine learning software. We found that different injury criteria demand different surrogate models.

**Injury risk**

Based on the calculated and predicted injury criteria (in our case HIC-values of the head impactor and leg acceleration, shear- and bending forces of the TRL impactor), injury risk curves are used to determine the risk of injury with and without the integrated safety system or in order to compare different systems.

These impactor values give a first impression of the passive safety performance of a certain vehicle and have the advantage of being established measurement criteria. Further enhancements of the tool chain for cyclists and occupants will also imply the use of biofidelic human models and the deduction of suitable injury criteria.

**Example: Stochastic Simulation of the pedestrian crossing scenario with an integrated safety system**

The next example uses the complete tool chain for effectiveness analysis of an exemplary active pedestrian safety system compared with an active bonnet.

The active pedestrian safety system is camera-based with very limited functionality during night and a maximal automatic deceleration of 4 m/s².

For this example about 1 million stochastic runs of the crossing scenario were performed (pedestrian crosses a single lane street from the right side without traffic signs or obstructions) with and without the preventive pedestrian safety system. The remaining collisions (head to bonnet impacts) were simulated with and without

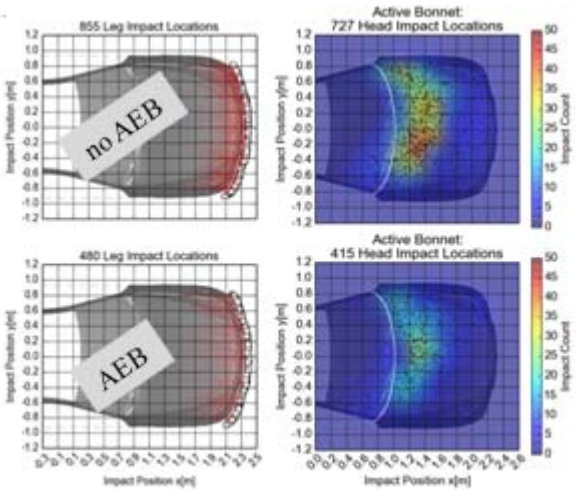


***Figure 4: Impacts on vehicle in pedestrian/vehicle collisions***

an active bonnet.

In order to avoid long calculation times, a surrogate model was used for the prognosis of the injury criteria.

In this example, the preventive safety system succeeds in avoiding 46% of the accidents. In the remaining accidents, the integrated safety system achieves the following injury risk reductions based on HIC15 and lower leg acceleration, bending and shear forces:

- 16% reduced injury risk through the active bonnet
- 29% reduced injury risk through the preventive pedestrian safety system
- 39% reduced injury risk through the combination of both systems

For the interpretation of these figures, one should note that:

- The driver reactions vary due to the underlying probability distributions, so that some drivers show very fast reaction and some show no reaction at all.
- The active bonnet has some effect on the head to bonnet impacts but of course none on the other impact locations (windshield, A-pillar, leg impacts).
- The preventive pedestrian system considered in the stochastic simulation is camera-based and has very limited functionality during nighttime. Additionally, accidents occurring at night are usually with faster vehicle speeds than during daytime.

## EFFECTIVENESS ANALYSIS FOR AEB SYSTEMS DESIGNED FOR VEHICLE/VEHICLE SCENARIOS

### Stochastic Simulation of rear-end conflict scenarios

Another important application of AEB systems is the prevention or mitigation of rear-end vehicle/vehicle conflicts. On highways for example, rear-end conflicts are particularly common when drivers encounter a strong negative gradient in traffic flow speed (a sharp slowdown) that they fail to anticipate. An acutely hazardous scenario can occur for example if traffic flows at a speed requiring a sight distance that exceeds the true visibility distance, for example due to a curve or hilltop, and if a vehicle does not observe the actual braking of traffic ahead. In addition, even if the first driver approaching a slowdown does manage to brake sharply, a second driver who has not been able to observe the primary conflict is also at high risk for a rear-end collision. If there is one collision, then secondary or tertiary collisions become even more likely, for example due to extreme decelerations and loss of control. In either case, avoidance of a collision in an unequipped vehicle (without AEB) depends critically on driver response. The driver must perceive the conflict or the brake lights of a preceding vehicle, properly orient and understand the potential severity, and apply the brakes quickly and decisively. Obviously, if we consider a typical distribution of drivers on a highway, some will not be looking directly forward at the crucial moment. Even without “distractions”, there are many visual cues competing for the driver’s attention.

Under these circumstances, it is intuitively clear that sensor-supported AEB systems could help prevent or mitigate rear-end collisions. The clear advantage is that an AEB sensor (e.g., radar) will not be subject to the same distractions as the driver.

We have developed a knowledge base including stochastic models appropriate for describing traffic flow in rear-end conflict scenarios such as those described above. As in the case of pedestrian protection, the knowledge base begins with appropriate exposition models. For example, an important parameter is the frequency of negative speed gradients as a function of severity – large negative gradients are the most dangerous, but occur less often. Exposition models also describe representative initial conditions for a sequence of vehicles with realistic initial TTC (time to collision) and spatial headways, based on analysis of highway vehicle data. It is also possible to model the effects of traffic context (e.g., traffic volume). The knowledge base further includes observation-based models of the

distributions of the key human factors that determine driver braking performance in an acute rear-end conflict. Possible driver swerving will also be taken into account.

A particularly important feature is the percentage of drivers not looking directly ahead. The human factor models take into account the fact that these drivers will tend to have longer reaction times and that they tend to brake more abruptly when they do finally perceive a conflict.

In a typical AEB system, the sensor information can be combined with additional signals from the vehicle. For example, it is an advantage if the algorithm can classify whether the driver is in fact "in the loop" or not. If the driver is in the loop, a delayed system response can avoid unnecessary interventions, [KFS04]. If the driver appears not to be attentive, then an early system response may be advantageous. The stochastic simulation methodology provides a virtual experimental framework for tuning these algorithms and determining an appropriate operating point.

Another key aspect concerns possible secondary or following accidents. It might be assumed that AEB systems will induce more following accidents due to the sharp braking of the system, than would occur without AEB. However, note that in an acute rear-end conflict without AEB, if a rear-end collision does occur, then the effective deceleration is also quite large, and, moreover loss of control can induce a spectrum of additional conflicts. Hence, for a comprehensive analysis, it is important to take following vehicles and their human drivers into account to model the complete situation.

### PERSPECTIVE: EXPANSION OF THE VIRTUAL TOOL CHAIN FOR CYCLIST SAFETY AND OCCUPANT SAFETY

The virtual tool chain including stochastic simulation for the effectiveness analysis of integrated pedestrian safety systems has been designed to provide a valid representation of real-world accident occurrence and system behavior.

The outlined tool chain will be extended for other vulnerable road users, mainly cyclists. The extensions will include a broader spectrum of traffic scenarios for stochastic simulation (turning scenarios…) including several street layouts and a more complex preventive safety system. The cyclist's behavior must be carefully modeled (maximum deceleration rates, swerving). Challenges include validation of the cyclist dynamics and modeling of bicycle-vehicle collisions, including injury characteristics. In addition, surrogate models must be calibrated for each case separately.

Regarding rear-end collision and AEB systems, occupant behavior in these scenarios must also be carefully validated, since it could have a major impact on crash results. Since crash test dummies are too stiff under low g impacts, other models have to be used, such as active human models.

## CONCLUSIONS

This paper has illustrated some recent advances in virtual design and effectiveness evaluation of integrated safety systems, using the example of AEB systems for pedestrians. The approach described above is holistic, in that both active and passive safety elements can be assessed on a common basis. The methods are useful not only for assessment of existing integrated safety designs, but also for comparing different system concepts or optimizing performance within a complex design concept. In order to achieve this goal, the whole sequence of events in a hazardous situation is virtually implemented in a tool chain. The tool chain includes stochastic (or "Monte-Carlo") traffic simulation, generating large samples of accident sequences but also near-misses, as well as detailed, high-resolution crash simulations of resulting accidents. The approach was illustrated in detail for key accident scenarios in pedestrian protection. The virtual-experiment approach using a tool chain generates assessment metrics relating to human risks and benefits, such as avoidance of severe injuries. Comparative evaluation of human-oriented metrics provides important information for stakeholders in safety system development.

**REFERENCES**


[EHSS11] Ebener, A.; Helmer, T.; Samaha, R.; Scullion, P.:"Identifying and Analyzing Reference Scenarios for the Development and Evaluation of Active Safety: Application to Preventive Pedestrian Safety." International Journal of Intelligent Transportation Systems Research, 9(3), p. 128–138, 2011.

[GWMS12] Gruber, C.; Wimmer, P.; Marbler-Gores, H.; Sinz, W.:"Integrale Sicherheit. Durchgängige Methode zur numerischen Simulation." Grazer Symposium Virtuelles Fahrzeug., 2012.

[HEH09] Helmer, T.; Ebner, A.; Huber, W.:"Präventiver Fußgängerschutz - Anforderungen und Bewertung." 18. Aachener Kolloquium Fahrzeug- und Motorentechnik, 2009.

[HSSEK11] Helmer, T.; Scullion, P.; Samaha, R.; Ebner, A.; Kates, R.: "Predicting the Injury Severity of Pedestrians in Frontal Vehicle Crashes based on Empirical, In-depth Accident Data." International Journal of Intelligent Transportation Systems Research, 9(3), p. 139–151, 2011.

[HNRGKK12] Helmer, T.; Neubauer, M.; Rauscher, S.; Gruber, C.; Kompass, K.; Kates, R.: "Requirements and methods to ensure a representative analysis of active safety systems, 11th International Symposium and Exhibition on Sophisticated Car Occupant Safety Systems" Fraunhofer-Institut für Chemische Technologie ICT, 2012, 6.1-6.18

[HKGK12] Helmer, T.; Kühbeck, T.; Gruber, C., Kates, R.: "Development of an integrated test bed and virtual laboratory for safety performance prediction in active safety systems" FISITA 2012 World Automotive Congress - Proceedings and Abstracts, 2012

[KH14] Kirchbichler, S., Huber, P.: "Human Modeling and Integrated Safety" Safety Update Graz, 2014

[KMDKBC05] Kerrigan, J., Murphy D., Drinkwater D., Kam C., Bose D., Crandall J.: "Kinematic corridors for PMHS tested in full-scale pedestrian impact tests" Proceedings 19th International Technical Conference on the Enhanced Safety of Vehicles, 2005

[KFS04] Kopf, M.; Farid, M.N.; Steinle, J.: "Bausteine zur Entwicklung eines Systems der aktiven Sicherheit." 1. Tagung Aktive Sicherheit durch Fahrerassistenzsysteme, 2004

[Wim13] Wimmer P.:"A New Simulation Method for Virtual Design and Evaluation of Integrated Vehicle Safety Systems" NAFEMS World Congress 2013

[WBHF15] Wimmer P., Benedikt M., Huber P., Ferenczi I.:"Fast Calculating Surrogate Models for

Leg and Head Impact in Vehicle-Pedestrian Collision Simulations" Proceedings 24th International Technical Conference on the Enhanced Safety of Vehicles, 2015

# BENEFITS ASSESSMENT OF AUTONOMOUS EMERGENCY BRAKING PEDESTRIAN SYSTEMS BASED ON REAL WORLD ACCIDENTS RECONSTRUCTION

**Francisco Javier, Páez**
**Arturo, Furones**
University Institute of Automobile Research (INSIA) – Technical University of Madrid (UPM)
Spain
**Alexandro, Badea**
Vehicle Safety, Jaguar Land Rover Ltd.
United Kingdom

Paper Number 15-0141

## ABSTRACT

Despite the success in reducing Spanish traffic fatalities by 65 percent in the past decade (2004 - 2013), pedestrian fatalities only have diminished by 45% (decreased by 35% in urban areas).

This paper describes the main findings of a coordinated study performed by INSIA-UPM aimed to assess the potential influence of two active safety systems, a brake assist system (BAS) and an autonomous emergency braking system (AEB), in vehicle-pedestrian collisions through reconstruction of real-world accidents occurred in the city of Madrid (Spain).

A total number of 50 vehicle-pedestrian collisions have been in-depth investigated following a common methodology, including on the spot data collection, analysis and reconstruction to estimate the collision speed and the pedestrian kinematics. Every single case has been virtual simulated twice using PC-Crash® software: the first is a reconstruction of the real accident and the second is a simulation in which the operation of active safety systems is emulated.

The performance of the BAS system acts together with the antilock braking system (ABS). The AEB system emulated in this paper through computer simulations is based on the DaimlerChrysler's PROTECTOR system.

The benefit is assessed in terms of both collision speed and Injury Severity Probability (ISP) by comparing the reduction of their values from the real conditions to the virtual simulations. The pedestrian ISP was estimated, depending on the collision speed and the pedestrian head impact point, using a specific application to calculate its value based on the results of head form impact laboratory tests.

The findings show that in several cases the collision could be avoided by implementing the active safety systems (12% if the vehicle was fitted with BAS+ABS system; 42% with PROTECTOR system); and it would reduce their consequences in terms of the estimated ISP. It was also found that in few cases a low reduction of the collision speed would increase the head injury severity (10%).

Further research should include injury information and/or estimation (HIC). Other limitations are the sample size (only one city and frontal collisions) and no unhurt accidents have been included.

The injury severity assessment within this study only considers head impacts to the front surface of the vehicle, injuries provoked by subsequent impacts were not taken into account. Hence it can be an interesting subject for further research.

This is new because: it is a prospective assessment of active safety systems and autonomous emergency braking systems; it is based on accurate reconstructions, highly detailed parameters; the behavior of the system is simulated according to design parameters.

Multi-disciplinary approaches such as this study make the identification of critical parameters easier and simplify the development of practical solutions by quantifying their potential impact on future actions to improve pedestrian safety. The active safety braking pedestrian systems have a potential benefit in real conditions. It also has limitations so we cannot rely just on it. It has to act together with other passive features and the driver has to keep aware. This methodology can serve to test the benefit of forthcoming active safety technologies.

## INTRODUCTION

Pedestrians are the most vulnerable road users and when involved in traffic accidents often suffer severe and fatal injuries. In year 2013 a total of 378 pedestrians were killed in the Spanish roads (22.5% of the overall traffic fatalities), 224 fatalities ocurred in urban areas (49.8% of the urban traffic fatalities). Compared with the year 2004 figures, the pedestrian fatalities percentage of total fatalities has increased (in 2004, 14.4% of national traffic fatalities, 38.1% of urban traffic fatalities).

This high vulnerability has its response in the manufacturers and the Public Administrations, which adopt different measures to protect these road users, e.g. driver and pedestrian education, urban planning, vehicles design and equipment...

The technological advances for vehicles adopted to enhance road users' protection have been primarily focused on secondary safety; however there are a number of recent developments aimed to avoid the collisions. Many accidents are caused by late braking and/or braking with insufficient force. In this way, the European Parliament and the Council have enacted Regulation (EC) 78/2009 (The European Parliament and the Council of the European Union, 2009 [11]) "on the type-approval of motor vehicles with regard to the protection of pedestrians and other vulnerable road users..." binding the manufacturers to equip the new vehicles placed on the European market with a type-approved brake assist system (BAS). According to the text of the Regulation, a brake assist system is a function of the braking system that deduces an emergency braking event from a characteristic of the driver's brake demand and, under such conditions assists the driver to deliver the maximum achievable braking rate; or is sufficient to cause full cycling of the Anti-lock Braking System (ABS).

The brake assist system was originally introduced to compensate the insufficient brake rates due to unexpected driver reactions discovered in rear-end collisions. It was found that despite the antilock braking system, the braking distance in critical situations was not significantly reduced. The reason was that drivers were not pushing the brake pedal strong and quick enough to its full stroke. The advantages of BAS as an active safety system were soon evidenced to avoid collisions and reduce the impact speed when the collision was inevitable. Thus the European Commission decided to make mandatory the fitting of BAS in new vehicles, representing one of the first active safety requirements for type-approval of motor vehicles with regard of the pedestrian protection (Badea-Romero et al, 2013 [1]).

Additionally primary safety systems have been developed for vehicles in order to autonomously detect a pedestrian and to avoid or mitigate the impact. The global functioning of these systems is based on analyzing the forward path of the vehicle in real time in order to try to identify a pedestrian on the road. If it is determined that the pedestrian trajectory is across the forward path of the vehicle, as a countermeasure to avoid an imminent crash, these systems employ emergency braking and some may potentially employ emergency steering (Hamdane et al, 2014 [4]). The systems they have developed can be grouped under the title AEB: Autonomous (the system acts independently of the driver to avoid or mitigate the accident); Emergency (the system will intervene only in a critical situation); and Braking (the system tries to avoid the accident by applying the brakes). AEB systems improve safety in two ways: firstly, they help to avoid accidents by identifying critical situations early and warning the driver; and secondly they reduce the severity of crashes which cannot be avoided by lowering the speed of collision ([14]).

The evaluation of the benefit of two active safety systems, a brake assist system (BAS) and an autonomous emergency braking system (the DaimlerChrysler's PROTECTOR system), for pedestrians involved in accidents is tackled in this paper which describes an in-depth accident investigation performed by INSIA-UPM. Data of 50 frontal vehicle-pedestrian collisions occurred in the city of Madrid between 2002 and 2006 were collected. Every single case has been virtual simulated twice using PC-Crash® software: the first is a reconstruction of the real accident and the second is a simulation in which the operation of the two active safety systems, BAS and PROTECTOR systems, is emulated modifying the collision parameters and its potential consequences.

To harmonise the process, a simulation procedure with simplified hypotheses about the driver's reactions, the brake assist system and the autonomous emergency braking pedestrian system operation was previously adopted. Collision speeds and pedestrian kinematics have been obtained from the reconstructions, which

allowed estimating the Injury Severity Probability (ISP) as the parameter considered for assessing the benefit of the active safety systems in terms of injury mitigation.

## METHODOLOGY

The methods presented in this section were developed within the framework of a research project (INSIA et al., 2008 [5]). The methodology was established to encompass into one optimal procedure to investigate on the spot every single accident, perform reconstructions and simulations, and analyse the obtained data and the results.

### Accident investigation and reconstruction

To investigate and reconstruct accidents occurred in Madrid, a multidisciplinary team was created with the support of local police forces, emergency services and hospitals.

The sampling was based in three main criteria: first, according to the road characteristics, the selected accidents should occur in urban areas; the second criterion is about the vehicle type, considering only accidents in which the striking vehicle was a passenger car (86%), a SUV (2%) or a people carrier (12%); the third is related to the accident configuration, only where the pedestrian was struck by the front of a passenger car. No restrictions about pedestrian characteristics such us gender, age, height or weight were imposed.

On the spot accident investigation and data collection was the first step of the process. The investigation teams in collaboration with the police forces attended the scene to collect all the available information about the scenario, geometry of the roads, visibility, visual evidence such as skid marks and traces, and also vehicle damages, dents and marks. Information about the injuries was obtained from paramedics and hospital data and used in the analysis phase for determining the injury mechanisms.

Once the investigation and data compilation phases were finished, the available information was analyzed, revised and prepared to be used in the reconstruction. Fully detailed scene plans were drown to be used in the reconstruction process.

Next the corresponding vehicle was selected in each case and loaded from the vehicle database available in the computer program; its characteristics were set up according to the real vehicle. The frontal shapes of real vehicles were accurately measured for this purpose.

Based on anthropometric studies (Spanish Ministry of Health, 2008 [10] and Benjumea, 2001 [2]), multi-body pedestrian models have been defined, representative of the up-to-date Spanish population for both male and female, and for a wide range of ages.

Finally, the virtual simulations of the accidents were performed using a reconstruction software. As it has been recently shown (Untaroiu et al., 2010 [12]) the initial conditions have a strong influence on the reconstruction kinematics. Many parameters such as approaching speed, path, position, pedestrian motion, driver maneuvers and sequences are slightly modified and tested in different combinations in an iterative process that leads to a reliable reconstruction, matching both the impact points with the visual evidence such as dents or marks and with the injury locations and mechanisms, and the vehicle and pedestrian rest positions.

Some simplifying hypotheses were established so all the simulations were performed from a common approach. These basic simplifications were: 1) the reaction time of the driver was considered to be one second for all cases; 2) the lag for a conventional brake system was 0.25 s; 3) the Possible Perception Point (PPP) of the driver was the instant in which the pedestrian stepped onto the pavement and no obstacle covered the driver's field of vision; 4) three intensity levels were established for the pre-collision brake force: no brakes when the evidence show that the driver had no time to react or was completely unaware of the pedestrian presence on the vehicle path, a default medium intensity brake for most accidents and a full brake when evidence such as skid marks leaded to it.

**Simulation of BAS+ABS operation**

The BAS operation can be described in three steps: a) detection of the pedal signal; b) interpretation and decision; and c) actuation.

At the first step a sensor detects a signal from the brake pedal. At the second phase the input signal is processed by the electronic central unit which decides if it corresponds to an emergency braking situation, triggering the system or keeping it in standby when normal braking. Next, if the control unit estimates that the signal corresponds to an emergency braking, an electric valve is opened and the pressure of the system increases to its maximum operating level activating the antilock system that prevents the vehicle from skidding.

The BAS operation features specified for its approval were taken into account when performing the virtual simulations. The parameters used to emulate the BAS in the virtual simulations are presented in table 1.

**Table1. BAS and PROTECTOR systems variables used in the virtual simulations.**

| Variable Name | Notation | Unit | Source |
|---|---|---|---|
| Pre-collision braking distance | $S_k$ | m | Reconstruction |
| Approaching speed | $V_0$ | km/h | Reconstruction |
| Braking deceleration with BAS+ABS | $a_{BAS}$ | $m/s^2$ | BAS-simulation |
| Braking deceleration with PROTECTOR | $a_{PROT}$ | $m/s^2$ | PROT-simulation |
| Braking deceleration | $a_k$ | $m/s^2$ | Reconstruction |
| Reaction time | $t_0$ | s | Average values |
| Pre-collision braking time | $t_k$ | s | Reconstruction |
| Lag of the brake system with BAS+ABS | $t_{BAS}$ | s | SAVE-U ([6]) |
| Collision speed | $V_k$ | km/h | Reconstruction |
| Collision speed with BAS+ABS | $V_{kBAS}$ | km/h | Reconstruction |
| Collision speed with PROTECTOR | $V_{kPROT}$ | km/h | Reconstruction |
| Brake distance with BAS | $S_{BAS}$ | m | BAS-simulation |
| Collision speed with BAS | $V_{BAS}$ | m | BAS-simulation |
| Brake distance with PROTECTOR | $S_{PROT}$ | m | PROT-simulation |
| Collision speed with PROTECTOR | $V_{PROT}$ | m | PROT-simulation |

Starting from the initial driving speed ($V_0$) obtained from the real accident reconstruction; a second virtual simulation was performed considering the BAS. The hypotheses adopted for the pre-impact phase were: when the BAS starts to operate, the ABS has to be activated and its operation frequency set up at the correct value to prevent from skidding, regardless if the original vehicle was fitted or not with such system. The PPP remains the same as also does the reaction time of the driver ($t_0$) but the lag of the brake system is reduced from 0.25s in normal conditions to 0.1s when the BAS is activated according to the results presented by Meinecke et al. (2003 [6]) within the SAVE-U project.

After the reaction and the lag sequences, the braking phase was established at the maximum deceleration ($a_{BAS}$) allowed by the computer program according to the friction conditions, which was considered equal to the deceleration that can be achieved with full cycling of the ABS ($a_{ABS}$). Then new values of the braking distance and the impact velocity were obtained and the difference was evaluated. If the braking distance to the collision point with the BAS ($S_{BAS}$) was less than the pre-collision braking distance ($S_k$) obtained from the reconstruction, then the collision could have been avoided due to the BAS; otherwise new simulations of the collision and post-collision phases had to be performed modifying the values of both the impact velocity and brake deceleration ($V_{BAS}$ and $a_{BAS}$ respectively). The modifications of the relative position between the vehicle and the pedestrian and the pitch angle of the vehicle at the collision point were also considered.

**Simulation of the DaimlerChrysler's PROTECTOR system**

The DaimlerChrysler's PROTECTOR system (SAVE-U consortium, 2005 [9]) has been tested in the EC-Project "SAVE-U. Sensors and system Architecture for VulnerablE road Users protection (Project IST - 2001 - 34040)".

Two strategies for the protection of vulnerable road users (VRU) have been implemented in the DaimlerChrysler vehicle: acoustical driver warning and automatic braking. In case of a high risk of a collision, automatic braking tries to either avert the crash at all or to mitigate the impact if the collision is unavoidable.

The deployment strategy of these protection measures consists of three phases:

- Phase 1: Early Detection. The sensor platform detects and tracks all VRUs in front of the vehicle (within the sensor coverage area), but none of protection measures are activated yet.
- Phase 2: Acoustical Driver Warning. A VRU is detected to enter the vehicle's path, but there is no risk of an immediate collision yet. The driver is alerted by an acoustical signal about this potentially dangerous situation.
- Phase 3: Automatic Braking. A high risk of a collision has been identified. The vehicle is decelerated in order to avert the collision or, in case a collision is unavoidable, mitigate the impact.

The decision about the activation of a protection measure is made from the position and heading direction of the pedestrian, and the current vehicle path. For that purpose, the detection area is divided into three zones, see figure 1:

- The red zone, 1.5m to each side, approximately represents the vehicle path. VRUs within this area are considered of being in risk of collision.
- VRUs in the yellow zone, from 1.5m to 3m to each side, are considered only if they are heading towards the vehicle path.
- VRUs in the green zone are not considered for the activation of one of the protection measures.

The automatic brake system operation features specified for the DaimlerChrysler's PROTECTOR system were taken into account when performing the virtual simulations. The parameters used to emulate this system in the virtual simulations are presented in table 1.

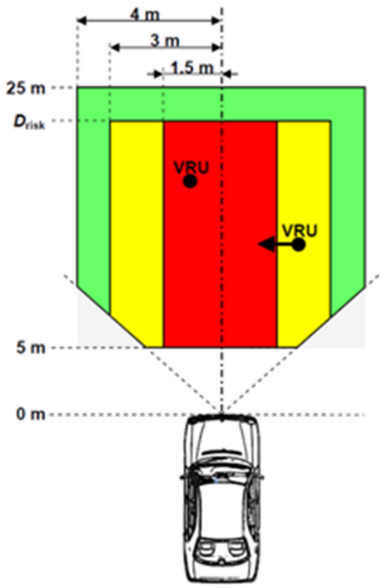


***Figure1. DaimlerChrysler's PROTECTOR system. Subdivision of the detection area into 3 risk zones.***

Starting from the approaching speed ($V_0$) obtained from the real accident reconstruction; a second virtual simulation was performed considering the PROTECTOR system. The hypotheses adopted for the pre-impact phase were: when the pedestrian goes into the red zone an automatic brake system starts to operate, the ABS has to be activated and its operation frequency set up at the correct value to prevent from skidding, regardless if the original vehicle was fitted or not with such system. The PPP (Possible Perception Point) remains the same as also does the reaction time of the driver ($t_0$).

After the reaction and lag sequences, the braking phase was established at the maximum deceleration ($a_{PROT}$) allowed by the computer program according to the friction conditions, which was considered equal to the deceleration that can be achieved with full cycling of the ABS. Then new values of the braking distance and the impact velocity were obtained and the difference was evaluated. If the braking distance to the collision point with the PROTECTOR system was less than the pre-collision braking distance ($S_k$) obtained from the reconstruction, then the collision could have been avoided due to the PROTECTOR system; otherwise new simulations of the collision and post-collision phases had to be performed modifying the values of both the impact velocity and brake deceleration ($V_{PROT}$ and $a_{PROT}$ respectively). The modifications of the relative position between the vehicle and the pedestrian and the pitch angle of the vehicle at the collision point were also considered.

**Estimation of the Injury Severity Probability (ISP)**

Head injuries are the most severe and with threat to life that pedestrians suffer when struck by a vehicle (Yao et al., 2008 [13]). The severity of the injuries depend on many parameters such as the collision speed, head impact point, collision configuration, vehicle shape, anthropometric measures of the pedestrian and rigidity of the component hit by the head.

The intensity of head impact is often assessed by the head injury criterion (HIC) (Mizuno and Ishikawa, 2001 [7]). The HIC can be correlated to the risk of severe injury, which gives a much clear idea of the how serious the head impact might be.

The methodology used in this research to estimate the head injury severity is described in figure 2 (Badea-Romero et al., 2013 [1]). First, the location of the head impact point is obtained from the computer simulation and represented by a row and a column corresponding to the wrap around distance (WAD) and the distance across the frontal respectively.

Then data from several laboratory tests performed at Applus+ IDIADA are used to estimate the correspondent HIC.

To estimate the injury severity, the value of the HIC obtained from the test is then derived into the probability of suffering a severe (AIS3+) head injury (ISPHIC,H,3). Thus the intensity of the head impact given by the HIC is translated into the injury severity that it can potentially cause. This is not a novel procedure, it has been previously presented by Fröming et al. (2006) [3].

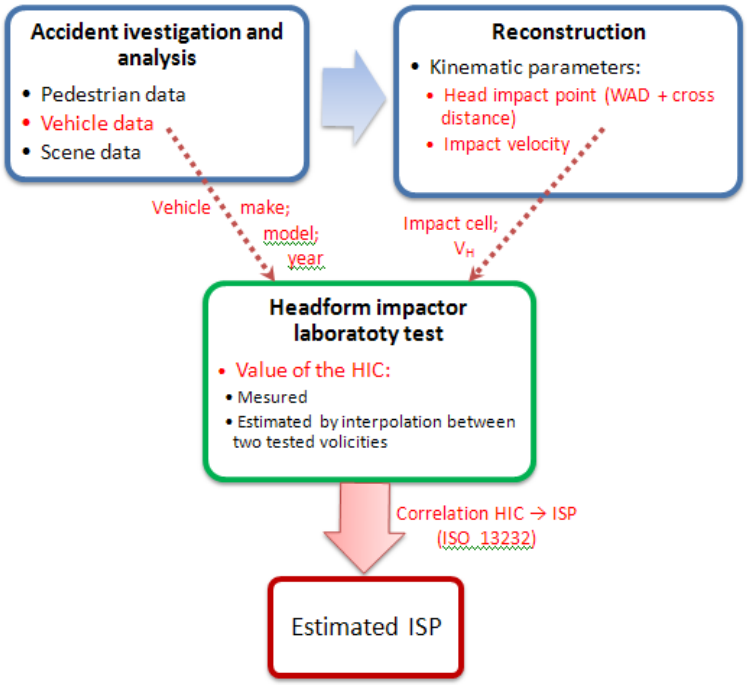


***Figure2. Methodology to estimate the Injury Severity Probability (ISP)*** [1].

**RESULTS AND DISCUSSION**

All the 50 reconstructions of the real accidents have been obtained with reliable results matching the impact points and rest positions for both vehicle and pedestrian with the visual evidence collected on the spot.

By modifying the parameters that affect the braking sequences according to the active safety systems characteristics, a second set of virtual simulations for all the cases has been obtained. Both BAS+ABS and PROTECTOR system simulation outputs were compared by pairs.

It was found that in the 88% of the accidents, the vehicle started to brake during the pre-collision phase. No evidence of braking maneuvers was found for the other 12% of the cases, this hypothesis was confirmed by the reconstructions. I was proved that the driver was probably unaware of the pedestrian on his path, or the pedestrian was detected too late leaving no time to react.

Related to the ISP estimation, the pedestrian head impact point was located out of the car frontal in the 20% of the accidents so the ISP value could not be calculated. The Injury Severity Probability (ISP) estimated versus collision speed (Vk) is shown in figure 3.

Figure 4 shows the distribution of the cases according to the reduction in percentage between real and the BAS+ABS/PROTECTOR systems simulated collision speeds ($V_{kBAS}/V_{kPROT}$ reduction in %); and figure 5 the distribution of the cases according to the reduction in percentage between real and the BAS+ABS/PROTECTOR systems simulated ISP ($ISP_{kBAS}/ISP_{kPROT}$ reduction in %).

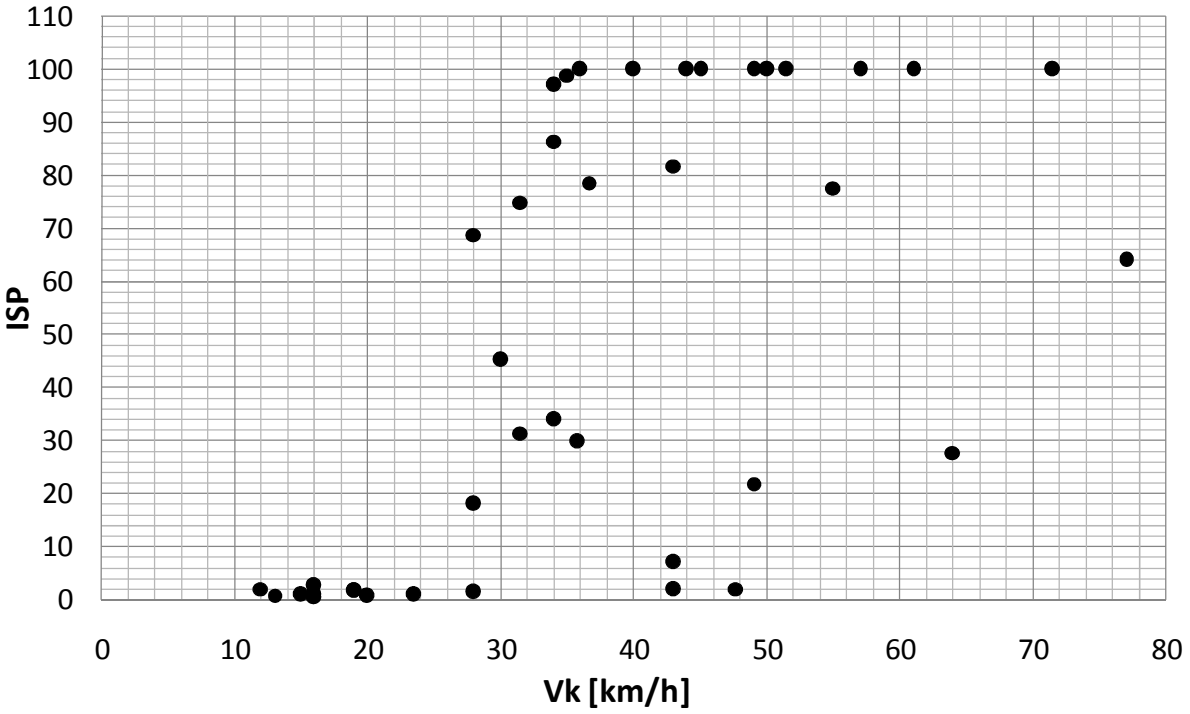


*Figure3. Injury Severity Probability (ISP) versus collision speed ($V_k$).*

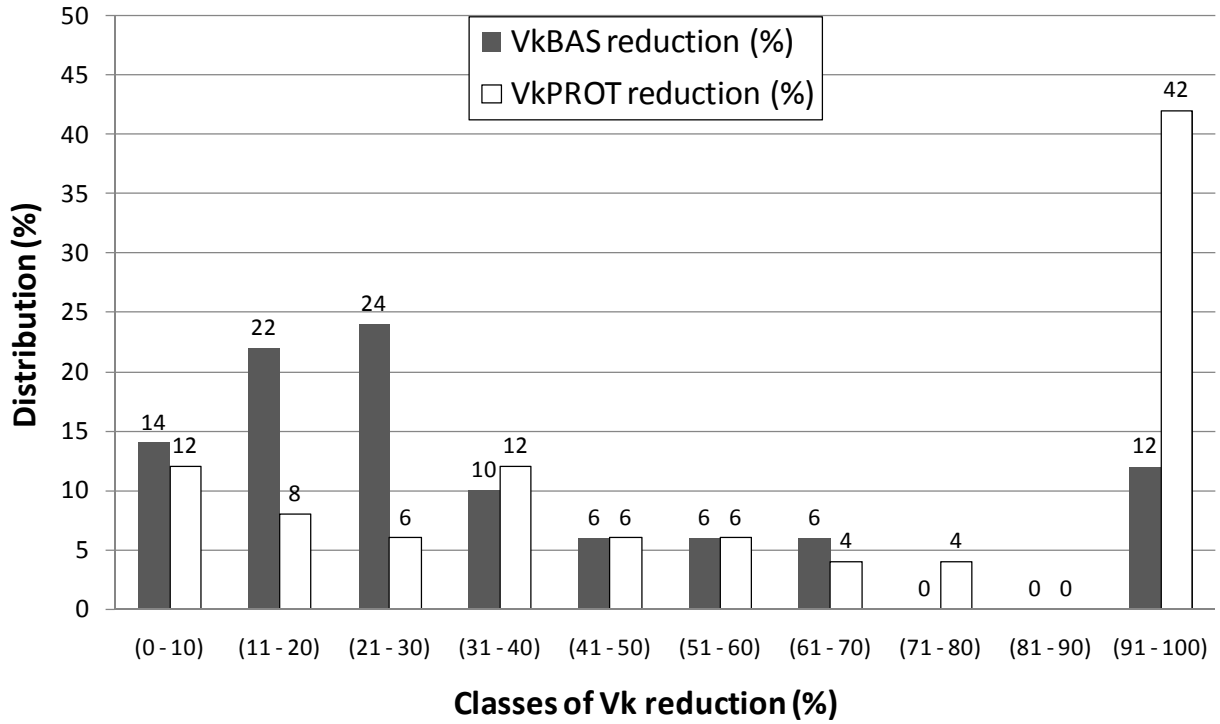


*Figure4. Distribution of the cases by the percentage of collision speed ($V_k$) reduction.*

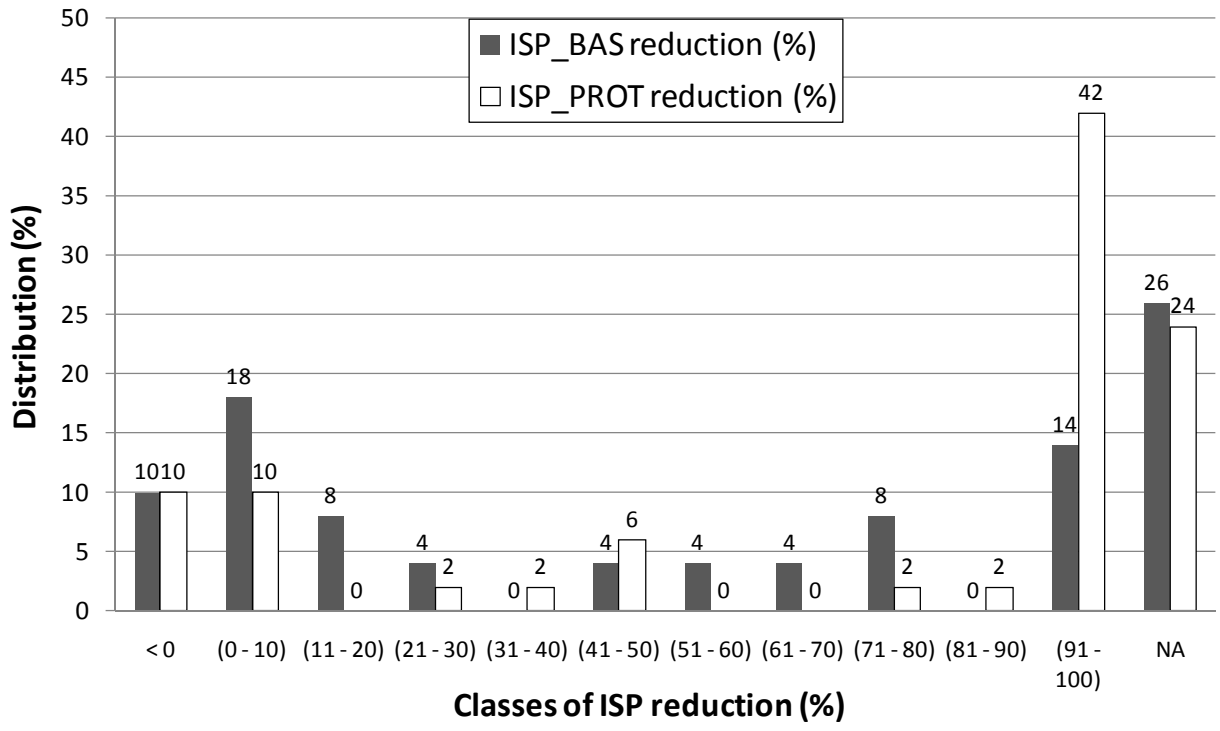


***Figure5. Distribution of the cases by the percentage of Injury Severity Probability (ISP) reduction.***

The collision could have been potentially avoided in 12% of the cases if the vehicle was fitted with BAS+ABS system ($V_{kBAS} = 0$) and in these accidents the $ISP_{BAS}$ reduction is 100%. In 55% of the cases of the studied sample, the speed reduction achieved is less than 5 km/h. In 26% of the cases the $ISP_{BAS}$ reduction value could not be calculated (NA) due to the pedestrian head impact point was located out of the car frontal (in the real accident and/or in the BAS+ABS system simulated). The data show that 18% of the cases in the sample present a percentage $ISP_{BAS}$ reduction less than 10%, and in a 10% that reduction is negative (there is an increase in the value of ISP; these cases commented below).

In 42% of the cases with the PROTECTOR system simulated the percentage of the speed reduction achieved is more than 90% ($V_{kPROT} = 0$, the collision has been avoided due to the PROTECTOR system) and in these accidents the $ISP_{PROT}$ reduction is 100%. In 70% of the cases of the studied sample, the speed reduction achieved with the PROTECTOR system is greater than 10 km/h, and in 44% of the cases the percentage of the $ISP_{PROT}$ reduction achieved is greater than 80%. In 24% of the cases the $ISP_{PROT}$ reduction value could not be calculated (NA) due to the pedestrian head impact point was located out of the car frontal (in the real accident and/or in the PROTECTOR system simulated). The data show that only 10% of the cases in the sample present a percentage $ISP_{PROT}$ reduction less than 10%, and in a 10% that reduction is negative (there is an increase in the value of ISP; these cases commented below).

Reductions of ISP up to 50% correspond to low levels of collision speed reduction. This fact evidences that improvements of pedestrian protection in frontal collisions depend not only on speed but on other parameters (in our study, these parameters are those from which the ISP is calculated: characteristics of the vehicle and head impact point).

In 10% of the cases (both BAS+ABS system and PROTECTOR system simulated) the percentage of the ISP reduction is negative; it was found that the head impact location changed to a stiffer area of the vehicle causing a more severe head impact

Since vehicle-pedestrian collisions are complex phenomena in which many parameters are involved, some simplification hypotheses were made in order to make the reconstruction process easier and quicker. These simplifications are related to parameters that can hardly be estimated such as the driver behavior.

The injury severity assessment within this study only considers head impacts to the front surface of the vehicle, injuries provoked by subsequent impacts were not taken into account. Hence it can be an interesting subject for further research.

The accident sampling is specific for this study and their characteristics are limited by the criteria that the Local Police Forces use for attending within their coverage area. So the 50 cases cannot be considered a representative sample for the whole pedestrian accidents that occur in the Spanish cities and the findings of this investigation might be different for other samples.

## CONCLUSIONS

Multi-disciplinary approaches such as this study make the identification of critical parameters easier and simplify the development of practical solutions by quantifying their potential impact on future actions to improve pedestrian safety.

Using this methodology, a database containing 50 pedestrian accidents was created, including in detail information of the vehicle, person (anthropomorphic variables, injury codification); scene and pedestrian kinematics. Reconstructions of these accidents were performed using advanced techniques to accurately estimate multiple parameters from the collision, the pre- and post-impact phases.

The gathered information has been used for the evaluation of the effectiveness of two active safety systems, a brake assist system (BAS+ABS) and an autonomous emergency braking system (AEB). The performance of these systems has been simulated in the reconstructions, so it was possible to analyze their capacity for severity reduction in pedestrian accidents or even its avoidance.

Both analyzed systems (BAS + ABS and PROTECTOR) proved to be efficient for reducing severity of pedestrian accidents in most of the studied cases. In the case of the BAS+ABS system the findings show that even though most of the collisions could not have been avoided by implementing these systems, their consequences would have been reduced in terms of the estimated ISP. The PROTECTOR system proved to be efficient for reducing collision speed of pedestrian accidents in most of the studied cases so the effect in terms of the estimated ISP reduction is greater than the case of the BAS+ABS system simulated.

In some cases a low reduction of the collision speed due to the simulated systems would increase the estimated ISP. The interaction between collision speed, vehicle frontal design and pedestrian parameters –height, weight, speed – is more relevant for the severity of the pedestrian head impact than the speed by itself, because it determines the head trajectory, acceleration and impact point. Thus, these primary safety systems should be combined with other secondary safety devices, such as the pop-up bonnet or the windscreen airbag.

## ACKNOWLEDGEMENTS

This study was partially funded by the Spanish Ministry of Industry, Tourism and Commerce within the framework of the “FIT project (370100 – 2007 – 51)” on pedestrian protection research, and the Community of Madrid (SEGVAUTO TRIES: “SEGuridad de los Vehículos AUTOmóviles, por un TRansporte Inteligente,

Eficiente y Seguro", P2013/MIT2713). The authors would like to thank the Local Authority of Madrid for their support in the investigations. The research work was also supported by the Madrid Regional Ministry of Education and the European Social Fund (ESF) through the Research Personnel Support Program of Madrid Autonomous Community

**REFERENCES**

[1] Badea-Romero, A., Paez, F.J., Furones, A., Barrios, J.M., de-Miguel, J.L. "Assessing the benefit of the brake assist system for pedestrian injury mitigation through real-world accident investigations" [J]. Safety Science, 2013, 53, p. 193-201 Communications of the ACM 24, No. 4, April: 19-197.
[2] Benjumea, A. "Datos antropométricos de la población laboral española" [M]. Instituto Nacional de Seguridad e Higiene en el Trabajo, 2001.
[3] Fröming, R., Schindler,V. and Kühn, M. "Requirement Engineering for Active Safety Pedestrian Protection Systems based on Accident Research" [J]. Advanced Microsystems for Automotive Applications, 2006, p. 79-106.
[4] Hamdane, H., Serre, T., Anderson, R. , Masson, C., Yerpe, J. "Description of pedestrian crashes in accordance with characteristics of Active Safety Systems". In proceedings of the IRCOBI 2014 Congress, 2014. (Berlin, Germany, 10 - 12 September 2014).
[5] INSIA, Applus IDIADA, CENTRO ZARAGOZA and SERNAUTO. "Investigación industrial en la protección de peatones a partir del estudio en profundidad de accidentes de tráfico en Madrid, Zaragoza y Barcelona. FIT 370100-2007-51 project report" [M]. Madrid, 2008.
[6] Meinecke, M-M., Obojski, M., Gavrila, D., Marc, E., Morris, R., Töns, M. and Letellier, L. (2003). "Strategies in Terms of Vulnerable Road User Protection. (Project IST – 2001 – 34040)".Germany.
[7] Mizuno, Y. and Ishikawa, H. "Summary of IHRA pedestrian safety WG activities – Proposed test methods to evaluate pedestrian protection afforded by passenger cars" [J]. Proceedings 17th International Technical Conference on the Enhanced Safety of Vehicle, 2001.
[8] Páez, F.J., Furones, A. and Badea, A. "Simulating the impact of automatic brake on real pedestrian collisions". In proceedings of the FISITA 2014 World Automotive Congress, 2014. (Maastricht, the Netherlands, June 2-6).
[9] SAVE-U consortium. "Deliverable 22: Driver Warning and Vehicle Actuator Concepts" [M]. Commission of the European Communities - Directorate-General Information Society, 2005.
[10]Spanish Ministry of Health. "Estudio antropométrico de la población femenina española" [M]. Ministerio de Sanidad y Consumo, 2008.
[11]The European Parliament and the Council of the European Union. (2009). "Regulation (EC) No 78/2009 on the type-approval of motor vehicles with regard to the protection of pedestrians and other vulnerable road users, amending Directive 2007/46/EC and repealing Directives 2003/102/EC and 2005/66/EC.(Official Journal of the EU L 35/1)". Brussels.
[12]Untaroiu, C. D., Crandall, J. R., Takahashi, Y., Okamoto, M., Ito, O. and Fredriksson, R. "Analysis of running child pedestrians impacted by a vehicle using rigid-body models and optimization techniques" [J]. Safety Science, 2010, 48, p. 259-267.
[13]Yao, J., Yang, J.and Otte, D. "Investigation of head injuries by reconstructions of real-world vehicle-versus-adult-pedestrian accidents" [J]. Safety Science, 2008, 46, p. 1103-1114.
[14]http://www.euroncap.com/en/vehicle-safety/the-rewards-explained/autonomous-emergency-braking/ (web consulted on January 18th, 2015).

# THE AUSTRALIAN TERRAIN VEHICLE ASSESSMENT PROGRAM (ATVAP)

**Raphael Grzebieta**
**George Rechnitzer**
**Keith Simmons**
**David Hicks**
**Declan Patton**
**Mario Mongiardini**
Transport And Road Safety (TARS) Research, University of New South Wales, Sydney, Australia

**Andrew McIntosh**
McIntosh Consultancy & Research Pty Ltd, Australia

**Drew Sherry**
**Ross Dal Nevo**
Roads and Maritime Services, Crashlab, NSW, Australia

Paper Number 15-0144

## ABSTRACT

Around 12 to 14 people are killed and 1400 injured annually in Australia resulting from Quad bike (All- Terrain Vehicle - ATV) and Side by Side Vehicle (SSV) incidents. The Australian Terrain Vehicle Assessment Program (ATVAP) consumer safety star rating system has been developed on the basis of a series of tests assessing a vehicle's static stability, dynamic handling and rollover crashworthiness and is being proposed as a method to reduce these serious and fatal injuries mainly resulting from Quad bike rollovers.

The ATVAP objective is to introduce a robust, test based rating system, in order to provide consumer based incentives for informed, safer and appropriate vehicle purchase, highlighting 'Fit For Purpose' criteria, with corresponding incentives and competition amongst the Quad-bike and SSV industry for improved designs and models. This paper presents an overview of the testing basis on which the proposed rating system was developed.

## INTRODUCTION

### Background

In Australia, the term for vehicles commonly used on farms over rougher terrains is Quad Bikes or Side-by-Side Vehicles (SSVs) depending on their size and farming task. Quad bikes (Figure 1: top left frame) are distinguished from SSVs (Figure 1: top right frame) in Australia by their design, namely the Quad bike's straddle seating, steering via handlebars with a small thumb operated throttle on the right side and low pressure tyres. This compares to the SSV's operator configuration which is more akin to a traditional car where seating is upright, a steering wheel is used to direct the vehicle, brakes and accelerator are operated by the drivers right foot and wheel tyre pressures are higher.

The Quad bike is called an All-Terrain Vehicle or ATV in the United States of America (USA). However, both an Australian Coroner and the USA Federal Government's Consumer Product Safety Commission (CPSC) have indicated that the term 'All-Terrain Vehicles' is misleading and may result in false assumptions as to the terrain that such vehicles can safely traverse [1, 2]. Hence, there is considerable resistance by Australian safety stakeholders in regards to the use of the term All-Terrain Vehicles or ATV. In this paper the term Quad bike will be used throughout to describe this vehicle type as shown in top left frame of Figure 1.

The SSV shown in the top right frame of Figure 1 is also referred to as a Recreational Off-Highway Vehicle (ROHV) in the USA. In this paper the term SSV will be used throughout to describe this vehicle type. Another term sometimes used in the USA for SSVs is Utility Task Vehicle (UTV). SSVs are distinguished from various larger four wheel drive or sports utility vehicles (SUV) off-road vehicles by their limited width, limited gross vehicle weight rating and limited engine capacity. However, the term All-Terrain Vehicle or ATV is sometimes used in Australia inadvertently to describe a SSV. One potential confusing factor in Australia is the continuing use of the terms 'Quad', 'Quad bike', 'ATV' and 'All-Terrain Vehicle' by the media, by accident investigators, by Coroners, and by others, which has often been used to refer to both Quad bikes and Side-by-Side Vehicles.

It is estimated that there were approximately 270,000 Quad bikes (ATVs) and SSVs in use in Australia in 2010 [3]. This compares to an estimated 80,000 Quad bikes and SSVs in use in New Zealand agriculture in 2010 [4]

and an estimated 10 million Quad bikes and SSVs in use by 16 million individuals in 2008 in the United States (US) [5]. However, SSVs are increasingly being used on farms and workplaces in place of Quad bikes, and are part of the 'Fit For Purpose' vehicle selection for farming and workplace environments being promoted by the Quad bike safety stakeholder groups. Some advantages of SSVs when compared to Quad bikes are: greater carrying capacity; standard driving configuration (e.g. steering wheel and pedals); no specific physical capacity for performing "active riding" as required with quad bikes; roll cages or rollover occupant protection systems; and, occupant restraint systems.

A detailed study of Australian fatalities from the Australian National Coronial Information System (NCIS) involving Quad-bikes and SSVs from 2001 to 2012 was carried out to establish injury mechanisms associated with their usage [6]. Around 141 fatalities were identified of which 109 were relevant to the study described here, and were studied in detail by the authors. Approximately 75% occurred on farms. A rollover occurred in 71% of all cases and of these 85% of the work related fatal cases involved a rollover compared to 56% of recreational cases. Around 28% involved mechanical asphyxia where 50% were 'pinned' by the Quad bike and for the 53 farm cases identified 68% were 'pinned'. Regarding Quad bike & SSV injuries, based on hospital and other injury databases [7], it is estimated that there are approximately 1,400 presentations per annum at hospitals in Australia, from minor to severe injuries.

In response to the incidence of fatal and serious injury rollovers involving Quad bikes it has been proposed by some authorities and other safety stakeholders that, as a minimum, Operator Protection Devices (OPDs) such as those devices highlighted by the Authors in a previous paper [8], be installed on all workplace Quad bikes. That proposal is based mainly on the observation that a two post Rollover Protection System (ROPS) fitted to old and new tractors has resulted in a marked reduction of tractor fatalities [9, 10, 11] and hence, by analogy, might be effective in reducing Quad bike rollover harm.

While in principle it appears that such systems may have a protective benefit in some rollovers, it is also clear that fitment of OPDs will not prevent rollovers from occurring in the first instance and OPDs may not be effective in all rollover situations [12], as active separation or ejection still occurs and impact or crush by stiff areas on the Quad bike or the OPD itself may result. Other than the reports by the Authors, Australian research on the 'in service' effectiveness of OPDs based on fatality and hospital data has yet to be done. Some USA research has been done and published based predominantly on computer simulations and some limited field rollover tests on full ROPS designs [13-19], but similarly no US cohort studies have been carried out to assess the effectiveness of OPDs in the field or laboratory tests of Quad bikes fitted with an OPD.

Thus, there has been little agreement on the way forward in improving Quad bike safety in regard to rollover [20]. The Australian Industry manufacturers represented by the Federal Chamber of Automotive Industries (FCAI) policy position for Quad bikes is that while some design and safety performance measures have been standardised and introduced (mandatory under US law), they remain focused on rider training, active riding and administrative controls such as personal protection equipment (PPE), e.g. such as helmets [8].

The Authors note that in the hierarchy of control measures for managing risks, engineering controls which design out the hazard are considered a more effective control measure than training courses which seek to change human behaviour. The authors note from Australian regulations covering mobile plant and structures in Australia, that persons with management or control of plant at a workplace are required to prevent mobile plant from overturning or the operator from being ejected from the plant. This person(s) must ensure, so far as is reasonably practicable, that a suitable combination of operator protective devices (OPD) for the plant is provided, maintained and used. A person who neglects their 'duty of care' to prevent mobile plant from overturning or the operator from being ejected from the plant, can be criminally charged in the event of serious injury or death of an employee.

Increasing rollover resistance and enhancing rollover crashworthiness design, should be one of the first components in the hierarchy of controls for managing risks within a Safe System Approach [21] in the workplace. Control should include engineering approaches, e.g. increasing rollover resistance and enhancing rollover crashworthiness design, while still maintaining the operational capabilities of the vehicles. Nevertheless, the authors also support administrative controls, but as a complimentary component of a larger holistic Safe System Approach based on the Swedish 'Vision Zero' criteria (i.e., no deaths in the workplace). Even higher-level controls in work situations would be to (a) ban quad bikes and/or (b) substitute SSVs for Quad bikes.

Administrative controls are generally accepted as the lesser effective form of control in a Vision Zero (no deaths) Safe System Approach, in the hierarchy of safety controls. Nevertheless, the Industry (FCAI) have advised the Authors that:

*"In the USA, where since 1991 the only increases in control have been in administrative controls (i.e., increasing passage of state laws regarding Quad bike usage, increasing to 47 out of 50 states as of 2013), during 1999 – 2006 Quad bike fatality rates (per 10,000 vehicles in use) decreased by 29%, and during 2001-2010, Quad bike emergency department rates (per 10,000 vehicles in use) decreased by 56% (Garland (2011, Tables 4 and 7)* [22]*, demonstrating the effectiveness of administrative controls."*

However, this statement fails to recognise the significant limitations that the CPSC note in all their reports regarding collection of fatality and injury data and the number of vehicles in use. Whilst the authors agree with the Quad bike Industry (FCAI) regarding their call for further in-depth research of injury and vehicle data relating the characteristics of Quad bike and SSV rollover crashes in general and also in relation to vehicle stability, handling and crashworthiness design would be of benefit, the authors disagree that vehicle design safety advances cannot proceed until such data is fully obtained and analysed. This argument should not be used to hinder safety design advancement for Quad bikes and SSVs. The authors consider that until such data can be obtained, the principles established over the past 50 years in mobility safety for all vehicle types can be usefully and appropriately applied to Quad bike and SSV safety design.

For this reason, Australian users of Quad bikes, farm safety stakeholder groups, government occupational health and safety regulators, and safety researchers, see from the history of safety advances in road vehicle transport that design countermeasures are possible, practical and effective, and that fitment of OPDs to Quad bikes is seen as a means of harm minimisation. In contrast, the Quad bike Industry (FCAI) continues to negate promotion of any design solutions concerning fitment of OPDs. The Quad bike Industry's resistance to fitment of OPDs (in their view) is that there is no scientifically valid 'in service' research data indicating that fitment of OPDs would be effective, not harmful and not compromising the capabilities of the vehicle. Hence, there exists a decades-long impasse on advancing Quad bike rollover crashworthiness safety and the need for a new approach, as a way ahead to reduce Quad bike trauma until such data is collected [8].

What is clear is that rollover is a major contributor to fatal and serious injury outcomes involving Quad bikes and SSVs, and therefore measures aimed at reducing both the incidence and severity of rollover are obvious injury prevention countermeasures that should be strongly advanced. The authors do not agree with Industry (FCAI) that Quad bikes and SSVs are exempt from such fundamental safety principles which apply to all mobile vehicles that transport people (e.g., cars, trucks, trains, trams, buses, motorcycles, bicycles, etc.). A pro-active approach should be taken rather than waiting another decade until such in-depth data may become available, with many additional casualties occurring as a consequence of such delays. We are reminded here of the wise aphorism "Do not let the *best* be the enemy of the *good*", with regard to progressing Quad bike and SSV safety.

On this basis, in order to assist consumers and workplace plant managers to address their current technical and political challenges to improving the design of Quad bikes and SSVs in regards to rollover safety, particularly in the farm environment, the Australian Terrain Vehicle Assessment Program (ATVAP) Star Rating System for Quad bikes and SSVs was developed. While clearly the authors make no claim that a 'newly-born' ATVAP can draw on a long and well validated history, as can the NCAP (worldwide New Car Assessment Programs), with its now 36 years history of development, innovation and robust validation (NCAP, started in the USA in 1978), it is apparent that such testing based star rating system for consumer information has been a major catalyst for and helped promote large technological safety advances in automobile safety [23].

The objective is to introduce a robust, test based rating system, in order to provide workplace and consumer based incentives for informed, safer and appropriate vehicle purchase (highlighting 'Fit For Purpose' criteria), and at the same time generate corresponding incentives and competition amongst the Quad bike Industry for improved designs and models for the workplace environment. The premise is that Quad bikes and SSVs with a higher resistance to rollover and improved rollover crashworthiness will result in reduced rollover related fatalities and serious injuries. It is proposed that those vehicles receiving high stability and crashworthiness overall rating index values, will in fact be found to have lower fatality and serious injury rates as has occurred with other vehicle types [24, 25]. This opinion takes its basis from the NCIS Coronial data [6], which indicates overwhelmingly that rollover, pinned entrapment and asphyxiation are the major casual factors involved in farm place deaths related to Quad bikes. It is hoped that ATVAP will be implemented in Australia (and internationally) to provide design safety gains for Quad bikes, SSVs and similar type vehicles for farm, workplace and indeed eventually in recreation use, over the years as it matures and accumulates further real world data to provide appropriate development, validation and refinement.

The following sections provide an overview of the components of the ATVAP rating system.

## ATVAP METHOD

The Australian national Heads of Workplace Safety Authorities (HWSA) committee identified in 2011 Quad bike safety to be a major issue on farms in Australia and New Zealand. As a result the ATVAP Star Rating method was developed within a major program of tests, namely the Quad bike Performance Project (QBPP), managed and carried out at the TARS unit at the University of New South Wales (NSW), Australia [26]. The QBPP was funded by the New South Wales Workcover Authority with a contribution from the Australian Competition and Consumer Commission (ACCC). The series of tests were carried out on a selection of 16 production vehicles consisting of 8 Quad bikes, 3 recreational Quad bikes and 5 SSVs. Testing was carried out at the NSW state government's Roads and Maritime Services Crashlab crash testing facility. The test program essentially consisted of three Parts, namely, Part 1: Static tests, Part 2: Dynamic handling tests and Part 3: Rollover crashworthiness tests.

While initially, the project was limited to testing Quad bikes only, it became apparent early in the test program that it would have been far too limiting in scope to simply restrict testing to only Quad-bikes, and that Side by Side vehicles (SSVs) should also be included as they were increasingly being used on farms and as possible safer alternatives to Quad bikes. This was a fundamental (yet still controversial to some) decision made early in the program to expand the mix of 'workplace' and 'recreational' Quad bikes and SSVs. This was also the first time that such a comparison of vehicle stability, handling and crashworthiness has been made across such a diverse range of terrain vehicle types. This decision has proven to be valid and invaluable. It has enabled the focus of the testing to broaden from just considering what improvements to Quad bikes could be made by manufacturers. What has resulted is a much more fundamental approach to risk reduction/management options involving, in principle, appropriate vehicle selection and 'fitness for purpose' criteria, and provision of previously unavailable comparison of Star Rating information for Quad bikes and SSVs for consumers. Hence, the ATVAP rating should be of both Quad bikes and SSVs compared together.

### Part 1 - Static Stability Tests.

Static Stability tests provide the first arm of the assessment and rating of Quad bikes and SSVs for rollover propensity (Figure 1). This test series should be comprised of tilt table tests for rollover resistance in lateral roll,

***Figure 1: Photographs from the tilt table tests, showing Quad bike with ATD for a lateral roll tests, and SSV for lateral roll, rear and forward pitch tests.***

forward and rearward pitch. The tests use a 95th percentile Hybrid III Anthropomorphic Crash Test Dummy (ATD) as a surrogate rider with a test mass of 103kg. The test matrix should include the vehicle on its own and then with a rider, and with combinations of maximum cargo loads on the front and rear. The Tilt Table Ratio (TTR), which is approximately the Tan of the angle of the tilt table shown in Figure 1, from the project tests for the Quad bikes, ranged from as low as 0.41 to at most 0.6 in the lateral roll direction with the ATD seated on the vehicle. The TTR for the SSVs were notably higher than for the Quad bikes, on the other hand, and ranged from 0.64 to 0.96 in the same (lateral) roll direction also with the same ATD. It was also found that OPDs had little effect on static stability measures.

It is important to highlight that a relative index which compares one vehicle with another should be developed. As such no one vehicle is then being disadvantaged against another as the same criteria and weighting is applied to all vehicles. Preliminary parametric analyses of the effect of any weighting variations from the test program [27] indicate that the relative static stability index of one vehicle compared with another is relatively insensitive to such variations. The stability indices are firstly based on the TTR values for each of three tilt test directions, by summing and then averaging the TTR values for each loading combination within those test directions:

1. Lateral Roll
2. Forward Pitch
3. Rear Pitch

The final Static Stability Overall Rating Index for each vehicle is then derived from weighted average TTR values for each of the three test directions.

In order to show a perspective regarding the stability of Quad bikes and SSVs in the lateral roll direction, Figure 2 provides a comparison of the author's postulated rollover crash rate versus Static Stability Factor (SSF) for Quad Bikes and SSVs compared to NHTSA's Mengert (1989) rollover crash rates for cars and SUVs [24], and New Zealand's (DIER, 2006) rollover crash rates for heavy articulated and rigid trucks [25]. Figure 2 is essentially a composite with the addition of the author's postulated curve, showing the relationship between the TTRs measured for Quad bikes and SSVs [26, 27] versus relative rollover crash rate. Furthermore, Figure 2 shows that the stability of Quad bike's TTR (SSF and TTR are similar measures) is in the lower range and not dissimilar to trucks; whereas the TTR (SSF) for higher stability SSVs overlaps with a four wheel drive/ Sports Utility Vehicles (SUVs). The authors postulate that the likely rollover risk for lower stability Quad bikes could be as much as four times (or higher) as the highest stability SSVs. Better data collection is required for Quad bike and SSV crashes to determine the actual rollover risk curve for these vehicles, as has been done for the other motor vehicle types.

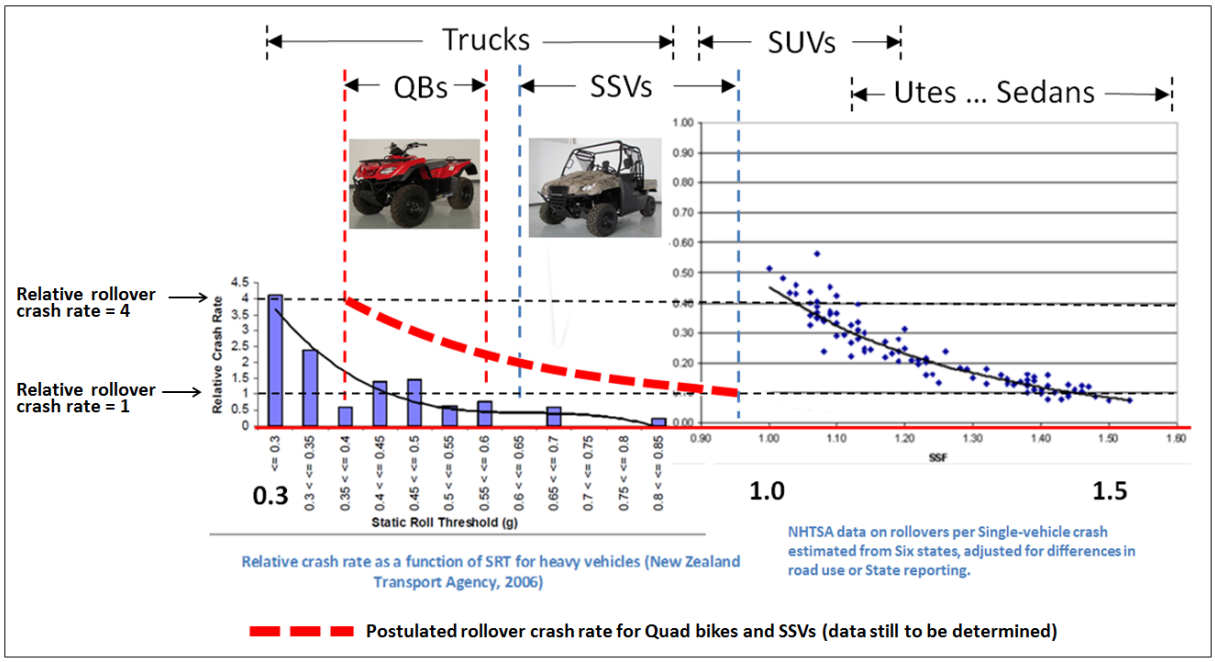


***Figure 2: The Author's postulated crash rate versus Static Roll Threshold (SSF ≈ TTR) for Quad Bikes and SSVs with rider/driver (with 95th% ATD) compared to NHTSA's Mengert chart for relative rollover crash risk for cars and SUVs [24] and to New Zealand Transport Agency's Relative Rollover crash rate for trucks [25].***

Hence, the authors are of the opinion that history has clearly demonstrated that advances in safety for all types of land mobile vehicles are correlated with improvements in stability, handling and crashworthiness. There is no reason why Quad bikes and SSVs should be any different and not obey the same laws of physics and vehicle dynamics.

**Part 2 - Dynamic Handling Tests.**

This Part was comprised of dynamic handling tests [Figure 3] which included the ISO 4138: 2012 Passenger Cars - Steady State Circular Driving test method and the ISO 7401: 2011 Road Vehicles - Lateral Transient Response – open loop test method [28]. Both these test methods were modified for a Quad bike and a SSV. An obstacle perturbation bump test (simulating riding one side over a rock like object) was also included and is presented in a companion ESV paper [29]. Components of these dynamic handling tests complemented the static stability evaluation.

The proposed Dynamic Handling Overall Rating Index is based on the summation of the Index values from the following four dynamic test results with rider/ driver for each vehicle:

1. **Steady-state circular driving behaviour dynamic tests** - the limit of lateral acceleration, Ay (g)
2. **Steady-state circular driving behaviour dynamic tests** - scores either the understeer or oversteer characteristic. The point of transition between understeer and oversteer is also rated.
3. **Lateral transient response dynamic tests** - the steering response time.
4. **Bump obstacle perturbation tests** - the measured acceleration of the ATD pelvis.

Figure 3 shows the test setup for both the Quad-bikes and the SSVs. The circular tests provide information on the vehicle's limit of lateral acceleration and whether it has an understeer, oversteer or neutral steering characteristic, and the point of transition between them, if it transitioned from one characteristic to another. The step steer response tests provide information on the vehicle's lateral transient response time. The perturbation bump test provided information on pitch and yaw response and how much the perturbation disturbs and displaces the rider from their riding position. Details of the tests and results and how the vehicles were rated are presented in [28].

The focus of the dynamic handling rating index is to encourage those dynamic characteristics that provide predictable and forgiving handling characteristics while remaining responsive and highly mobile in a farming and workplace environment. Moreover, in order to provide predictable and forgiving handling characteristics while remaining responsive and highly mobile, in the author's opinion a vehicle should be designed to provide a light understeer response of between 1 to 2 degrees per g lateral acceleration. In light off-road vehicles, this understeer characteristic should continue to at least 0.5g lateral acceleration. Those vehicles that demonstrated this characteristic are provided with a higher rating Index value.

Most Quad bikes had a fixed rear differential, which meant that the rear wheels rotated in unison, even when on a curve. Most SSVs that had an open differential (or the option to switch from an open to fixed differential and vice versa), all exhibited light understeer handling characteristics. When the rear differential was locked, the vehicle demonstrated oversteer characteristics. For those that had an open differential did not tip but either simply broke traction on the rear inside wheel and reduced speed or slid out, under the test conditions.

**Part 3 - Rollover Crashworthiness Tests.**

This Part of the proposed ATVAP was comprised of tests that focused mainly on rollover crashworthiness. Some exploratory testing and procedures were carried out for the purposes of developing a rollover crashworthiness rating (see: Figures 4 and 5). A Motorcycle 50$^{th}$ % ATD (MATD) was used as the rider/driver in the exploratory rollover crashworthiness tests that were undertaken for the purposes of developing the rollover crashworthiness rating Index. The MATD is based on the HIII ATD but with enhanced features.

The tests carried out were:

1. Measurements of static ground contact force for a Quad bike with and without an OPD on its left and right side and when inverted (Figure 4: top left frame). The mass difference between different model Quad bikes was not sufficient to provide significant discrimination in terms of asphyxia potential [6, 26], as in most cases the 50 kg asphyxia load criterion would be exceeded.
2. Inspection and measurements of Side by Side Vehicle (SSV) occupant retention (Figure 4: top right frame) in accordance with the United States (US) American National Standard for Recreational Off-

***Figure 3: Steady state circle testing on asphalt and on grass. Top left: Rider on Quad bike following circle. Top right: Rider on Quad bike following grass circle at point of tilt. 2nd row: Grass circle test site 3rd row: Typical Quad bike circular driving behaviour test where both wheels lifted. Bottom: An SSV that was tested with outrigger wheels fitted.***

***Figure 4: Examples of: 1. (top left) Quad bike contact force tests using load scales; 2. (top right) Side-by-Side Vehicle occupant retention; 3. (bottom left) SSV Roll-Over Protective Structure (ROPS) lateral pull test; and 4. (bottom right) Rollover test with occupant and Lifeguard OPD.***

Highway Vehicles ANSI/ROHVA 1-2011 with additional constraint requirements applied [30], i.e. points are deducted if there is extension of any part of the ATD outside the plane of the vehicle width when the vehicle is tilted over on the tilt table; and the seat belts in all seats are not a 3 point seat belt or harness (4 or 5 point). Bonus points are awarded if there is a seat belt warning light which switches off when the seat belt is locked in, for a seat belt audible alarm that is maintained for at least 5 minutes when a person is seated in the vehicle and turns off when the seat belt is locked in, and for a seat belt interlock system that is ignition or speed interlock based.

3. SSV ROPS structure load tests consisting of applying a lateral load (Figure 4: bottom left frame) followed by a vertical load then a longitudinal load to the vehicle ROPS whilst recording the deflection and noting the structural integrity, in accordance with the ISO (2008) test option [31] for the US ANSI/ROHVA 1-2011 requirements [30].
4. Vehicle and rider/driver dynamic rollover tests consisting of positioning a MATD in the operator's position of a Quad bike or Side by Side Vehicle, tilting the vehicle to an angle at which rollover would occur, and releasing the vehicle from an initial static position to rollover to observe 'survival space' and functionality of the OPD (Figure 5), and in the case of the SSVs the ROPS and restraints (Figure 4: top right frame). Lateral roll (Figure 5), forward pitch (Figure 4: bottom right frame) and rearward pitch was carried out for the Quad bike. Two SSVs were also tested in lateral roll.

It became apparent that it was unrealistic currently to be able to discriminate the rollover crashworthiness between different Quad bike models [32]. However, discrimination between vehicle types, e.g. Quad bikes and SSVs, was realistic. Further, it was also evident from preliminary rollover, forward pitch and rearward pitch testing, that due to the stochastic ('hit and miss') nature of severe injury risk to a rider and the large range of possible relevant rollover test permutations, it was unrealistic to continue with such tests for rating Quad bikes. Indeed it was deemed by the authors that the term "Crashworthy Quad bike" was essentially a contradiction in terms. For this reason for the Quad bike type, all were assumed to be rated equally for rollover crashworthiness, and all were assigned the same arbitrarily low minimum value points rating when assessing rollover

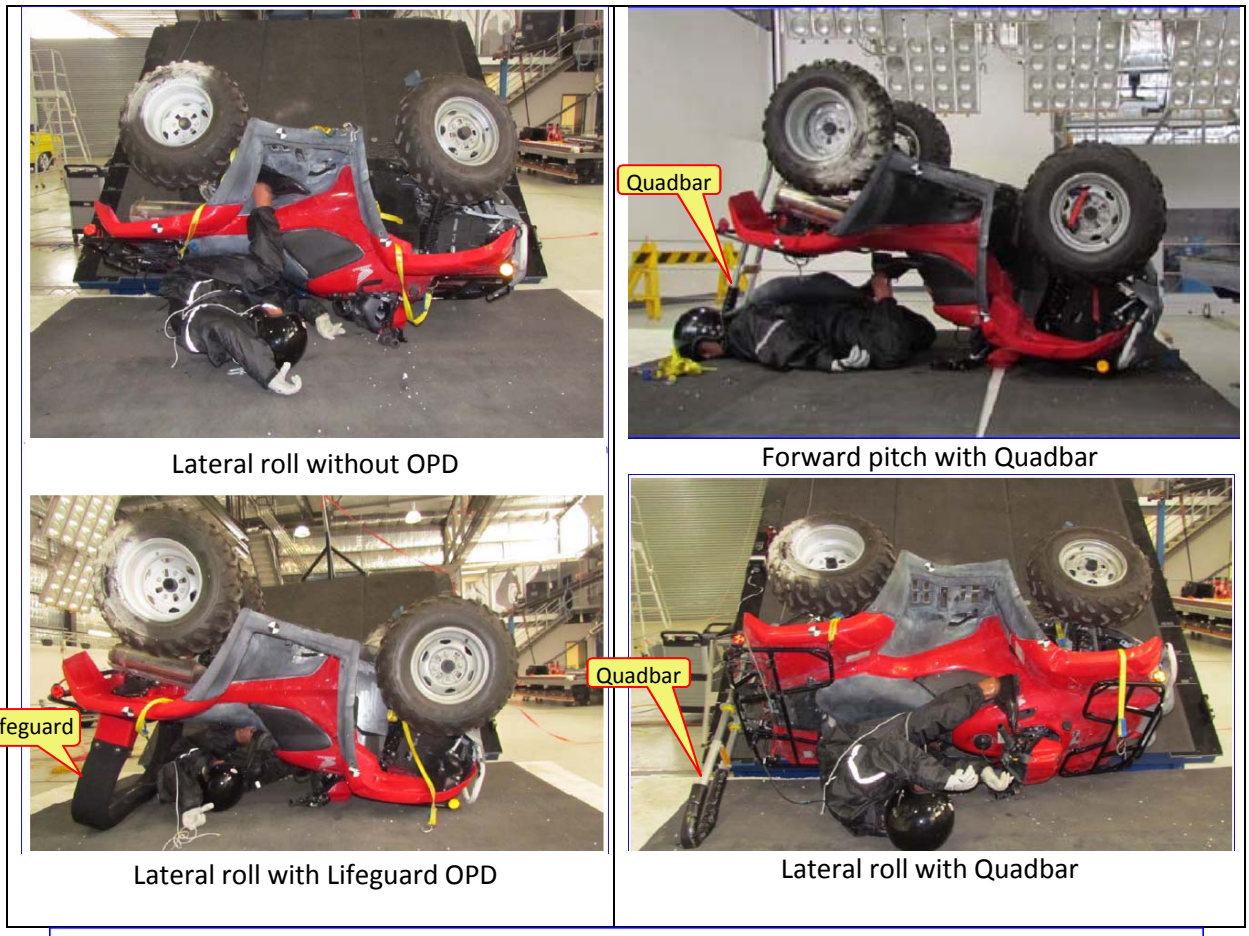


Lateral roll without OPD

Forward pitch with Quadbar

Lateral roll with Lifeguard OPD

Lateral roll with Quadbar

Forward pitch roll - No OPD

**Figure 5: Examples of Quad bike lateral rollover and forward pitch tests with and without OPDs [32]. For more details see 'Part 3: Rollover Crashworthiness Test Results' report.**

crashworthiness protection. Fundamentally Quad bikes do not and cannot satisfy fully the well-known principles of occupant protection in rollover crashes even with an OPD attached, i.e. good containment and crush prevention. If the straddle position is maintained with respect to the vehicle's design and 'separation' is the crashworthiness criterion adopted by the Industry (FCAI) then it is unlikely the Quad bikes would not achieve any points higher than the lowest range (approximately 1/5$^{th}$ of maximum score). The main reason the Quad bikes can be allocated some points even though they were at the lowest range of values, is that riders have survived when a Quad bike has rolled and indeed when the vehicle has rolled over the rider.

In contrast to Quad bikes, the SSVs do adhere in general to rollover crashworthiness principles, in that they are typically fitted with ROPS, seatbelts and various degrees of containment measures which combine to keep the occupants within a protected space. As the effectiveness of such designs in terms of severe injury prevention can vary widely, it is possible to discriminate and rate SSVs. Hence, the rollover crashworthiness of SSVs tested were evaluated against the ANSI/ROHVA standard [30] and fundamental crashworthiness principles of rider/occupant protection in rollovers. In contrast to the Quad bikes, well designed SSVs offer superior rollover crash protection in a typical farming environment. This is provided that three point (or harness) seatbelts and helmets are worn and other occupant lateral restraints are fitted and are in place, e.g. doors, side meshing, etc. The results from the rollover crashworthiness tests provide sufficient discrimination in the range of vehicles tested (Quad bikes and SSVs) to use as a basis for the rollover safety rating system.

**The ATVAP Star Rating System**

The Star Rating is the sum of the points for the three tests (Parts 1 to 3), with equal points allocated to each test performance requirement, i.e. Static stability, Dynamic Handling and Rollover Crashworthiness. Additional bonus points (approximately 10% to 15%) can be provided for vehicles that have an open rear differential, both a seat belt warning light and audible sound which turns off when the seat belt is locked in, and a seat belt interlock which either prevents vehicle startup or restricts the maximum speed of the vehicle to around 5 to10 km/h.

Figure 6 shows the final graph of the 16 production vehicles tested in the Quad Bike Performance Project albeit the particular models have been masked at this point in time. The graph shows that the SSVs outperformed the Quad bikes significantly. The star rating shows that the SSVs demonstrated superior static stability (see Figure 2), superior dynamic handling reflecting a slight understeer characteristic, minimal disturbance of steering in the bump test [29], and superior rollover crashworthiness, when compared to the Quad bikes. The Recreational Quad bikes have no physical provision (e.g. load rack, etc.) to carry loads. Two of these vehicles (3 star) demonstrated superior static stability and dynamic handling characteristics indicating these design features can be improved for Quad bikes. For SSVs, it is however vital to recognize, that as with passenger vehicles, the significant variation in the Star rating between different SSVs.

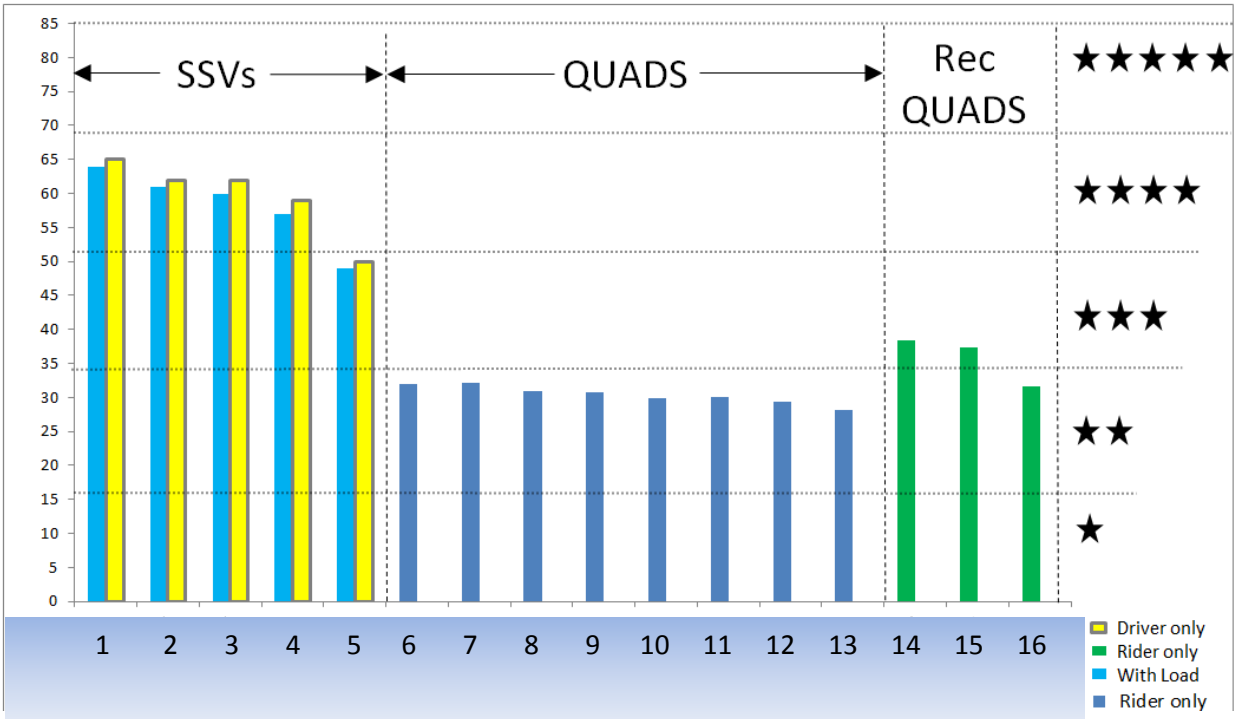


**Figure 6: Final Points and Star Rating of the 16 production Quad bikes and SSVs tested.**

## CONCLUSIONS

The aims of the project were to also introduce a robust, test based Star Rating system, similar to other product rating systems, in order to provide consumer based incentives (and assist workplace plant managers) for informed, safer and appropriate vehicle purchase (highlighting 'Fit For Purpose' criteria) that reduced the risk of being injured in a rollover in a workplace setting, and at the same time generate corresponding incentives and competition amongst the Quad bike and SSV Industry for improved designs and models. Those aims were met. It was possible to develop a Star Rating system, that was capable of providing sufficient discrimination in the range of vehicles tested and commonly used, (Quad bikes and SSVs) as a basis for consumers to be able to choose a vehicle that provides a lower risk of rollover, and lower risk of injury if the vehicle does roll.

There are no standards or compliance requirements in Australia for Quad bikes or SSVs. The proposed Australian Terrain Vehicle Assessment Program (ATVAP) consumer Star Rating system presented provides a rapid means of applying a performance benchmark testing protocol that can lead to significantly reduce rollover injury risk. Using the Star Rating system, manufacturers would be encouraged to compete with each other in order to make their products attractive to potential consumers and workplace plant managers wanting to purchase a safer workplace/farming vehicle and comply with workplace regulations.

## ACKNOWLEDGEMENTS

The Authors would like to gratefully acknowledge the Workcover Authority of NSW for funding the majority of the experimental research and in particular Mr. Tony Williams and Ms. Diane Vaughan. The Australian Consumer and Competition Commission (ACCC) also contributed funds for the test program. The authors are also grateful to staff at the Roads and Maritime Services Crashlab crash test facility for their assistance with testing.

The authors would like to also acknowledge and thank the members of the international QBPP Project Reference Group, and the Australian Federated Chamber of Automotive Industries (FCAI) representatives, for their valuable input to the project; and the Victorian Institute of Forensic Medicine (VIFM) as the source organisation of the National Coroners Information System (NCIS) from which rollover crash data was extracted for the Australian fatality data presented in this paper. In particular the authors would like to thank Ms. Joanna Cotsonis, for her assistance as the NCIS Access Liaison Officer for the Quad Bike Performance Project, and all the State Coroners for allowing access to the full brief of evidence for the Australian Quad bike fatality cases. The opinions expressed in this paper are those of the authors.

## REFERENCES

[1] Olle J, (2009). Investigation into deaths of Vince Tobin, Joseph Jarvis Shepherd, Jye Kaden Jones, Peter Vaughn Crole, Thomas James Scutchings, John Neville Nash, Patricia Murray Simpson, Elijah Simpson with inquest, Melbourne: State Coroner Victoria, Australia.

[2] Elder J, Leland E, (2006). CPSC Staff Response Regarding Follow-Up Questions from Commissioner Moore after the June 15, 2006, ATV Safety Review Briefing, in editor: http://www.cpsc.gov/LIBRARY/FOIA/FOIA06/brief/atvmoore.pdf

[3] Australian ATV Distributors, Australian ATV Distributors position paper, January, 2010. http://www.fcai.com.au/library/publication/1302069213_document_5_january_2010_industry_position_paper.pdf

[4] Carman A., Gillespie S., Jones K., Mackay J., Wallis G., and Milosavljevic S., All terrain vehicle loss of control events in agriculture: Contribution of pitch, roll and velocity. Ergonomics, 2010. 53(1): p. 18-29.

[5] Helmkamp, J., Marsh, S., and Aikten, M., Occupational all-terrain vehicle deaths among workers 18 years and older in the United States, 1992-2007. Journal of Agricultural Safety and Health, 2011. 17(2): p. 147-155.

[6] Grzebieta R.H., Rechnitzer G., McIntosh A., Mitchell R., Patton D., and Simmons K., (2014). Investigation and Analysis of Quad Bike and Side By Side (SSV) Fatalities and Injuries, Quad Bike Performance Project (QBPP) Report 3-2014: Supplemental Report, Transport and Road Safety (TARS) Research Report, submitted to The WorkCover Authority of New South Wales, University of New South Wales, Sydney, Australia.

[7] Mitchell R. Grzebieta R. Rechnitzer G., Capture and surveillance of quad bike-related injuries in administrative data collections. International Journal of Injury Control and Safety Promotion, published on-line January 7, 2015. DOI:10.1080/17457300.2014.992353.

[8] Rechnitzer G, Grzebieta R, McIntosh A, Simmons K. (2013). Reducing All Terrain Vehicle Injuries (ATVs) and Deaths - A Way Ahead, presented at the 23rd International Technical Conference on the Enhanced Safety of Vehicles, Seoul, South Korea, 2013.

[9] Day L & Rechnitzer G, Evaluation of the Tractor Rollover protective Structure Rebate Scheme, May 1999, Monash University Accident Research Centre. Report 155.

[10] Scott M., Willaims R., Day L., Rechnitzer G., Walsh P., and Boyle S., 2002. Safe Tractor Assessment Rating System, Technical Reference Documant, Monash University Accident Research Centre and Kondinin Group.

[11] Franklin R.C., Stark K.L. and Fragar L.J., (2005). Evaluation of the New South Wales Rollover Protective Structure Rebate Scheme 2000 - 2004. Australian Centre for Agricultural Health and Safety (ACAHS), University of Sydney, Moree.

[12] Grzebieta R.H. and Achilles T., (2007). Report on Quad-bar in Relation to ATV Rollover Crashworthiness, submitted to Victorian Coroner Inquest into ATV deaths, Dept. Civil Engineering, Monash University, Victoria, Australia.

[13] Van Auken R.M. and Zellner J.W., Preliminary Analysis of the Effects of ATV ROPS on Rider Injury Potential, Volume 1: Technical Report, DRI-TR-96-4B, October 1996, Second Revision Issued February 1997, Dynamic Research, Inc., California, USA.

[14] Van Auken, R.M., and Zellner, J.W., ATV ROPS/CPD Tests and Simulations, Dynamic Research, Inc. Technical Report DRI-TR-98-2, October 1998.

[15] Zellner JW, Kebschull SA, Van Auken RM, Lenkeit JF, Broen PC, (2004). Review And Analysis Of MUARC Report "ATV Injuries And Deaths," And Additional Simulation And Initial Testing of MUARC ATV Rollover Protection System (ROPS), Volumes I to III, Report submitted to Victorian Coroner Inquest into ATV deaths, Dynamic Research Inc.

[16] Zellner JW, Kebschull SA & Van Auken RM, (2006). Updated Injury Risk/Benefit Analysis Of Quadbar Crush Protection Device (CPD) For All-Terrain Vehicles (ATVs); DRI-TR-12-06.

[17] Zellner, J., Kebschull, S., and Van Auken, R., (2013), Evaluation of Injury Risks and Benefits of a Crush Protection Device (CPD) for All-Terrain Vehicles (ATVs)," SAE Int. J. Passeng. Cars – Electron. Electr. Syst. 7(1):2014, pp 41-72, doi: 10.4271/2013-32-9173.

[18] Grzebieta RH, Rechnitzer G, Richardson S, (2005). Comments on video evidence of rollover tests presented by Breen; Calculations regarding additional weight to ROPS to account for increased weight of ROPS; and Brief statement regarding human impact and acceleration [G-force] tolerance, Supplementary Report submitted to Victorian Coroner Inquest into ATV deaths, DVExperts International Pty Ltd.

[19] Van Ee C., Toomey D. and Moroski-Browne B., (2012). ATV Rollover, Operator Response, and Determinants of Injury: Implications for CPDs, Design Research Engineering. Presentation made at US Consumer Product Safety Commission ATV Safety Summit, Bethesda, USA, October.

[20] FCAI, (2012). ATV Industry opposes rollover devices on safety grounds. http://www.fcai.com.au/news/news/all/all/311/atv-industry-opposes-rollover-devices-on-safety-grounds.

[21] Grzebieta R.H., Mooren L., and Job S., Introduction (or Reintroduction) to the Safe System Approach, Roadside Safety Design and Devices, International Workshop July 17, 2012, Milan, Italy, Ed. R. Troutbeck, Transportation Research Board, Washington DC, Transportation Research Circular Number E-C172, February 2013, http://onlinepubs.trb.org/onlinepubs/circulars/ec172.pdf.

[22] Garland S. 2010 Annual report of ATV-related Deaths and Injuries. Bethesda, MD: Consumer Product Safety Commission, 2011.

[23] Paine M, and Haley J, (2008). Crash testing for safety - possible enhancements to ANCAP test and rating methods, Proc. 2008 Australasian Road Safety Research, Policing and Education Conference, Adelaide, South Australia.

[24] Mengert, P., Salvatore, S., DiSario, R., Walter, R., Statistical estimation of rollover risk, DOT-HS-807-466, U.S. Department of Transportation, August, 1989.

[25] Department of Infrastructure, Energy and Resources (DIER), Land Transport Safety Authority, SRT Calculator User Guide, TERNZ Ltd, Manukau, New Zealand, 25 May 2006.
http://fuelsaver.govt.nz/srt-calculator/user-guide.pdf

[26] Grzebieta R, Rechnitzer G, Simmons K and McIntosh AS (2015) Final Summary Project Report: Test Results, Conclusions, and Recommendations, Quad Bike Performance Project TARS Research Report No 4, submitted to the WorkCover Authority of New South Wales, University of New South Wales, Sydney, Australia.

[27] Grzebieta R, Rechnitzer G, Simmons K. (2015) Static Stability Test Results, Quad Bike Performance Project TARS Research Report No 1, submitted to the WorkCover Authority of New South Wales, University of New South Wales, Sydney, Australia.

[28] Grzebieta R, Rechnitzer G, Simmons K. (2015) Dynamic Handling Test Results, Quad Bike Performance Project TARS Research Report No 2, submitted to the WorkCover Authority of New South Wales, University of New South Wales, Sydney, Australia.

[29] Hicks D., Mongiardini M., Grzebieta R, Rechnitzer G, and Simmons K, (2015). Analysis Of Quad-Bike Loss-Of-Control Using Experimental And Simulated Dynamic Bump Tests, Proc. 24th Enhanced Safety of Vehicles (ESV) Conference, Gothenburg, Sweden, Paper No. 15-0133.

[30] Recreational Off-Highway Vehicle Association, (2011). American National Standard for Recreational Off-Highway Vehicles, ANSI/ROHVA 1 - 2011, Recreational Off-Highway Vehicle Association, California, USA.

[31] International Standard (ISO), ISO 3471:2008(E), Fourth edition 2008-08-15, Earth-moving machinery - Roll Over protective structures - Laboratory tests and performance requirements.

[32] Grzebieta R, Rechnitzer G, McIntosh A. (2015) Rollover Crashworthiness Test Results, Quad Bike Performance Project TARS Research Report No 3, submitted to the WorkCover Authority of New South Wales, University of New South Wales, Sydney, Australia.

# ASSOCIATION BETWEEN VEHICLE PANEL DAMAGE AND THORACIC INJURY IN ROLLOVER CRASHES

**Tana Tan**
**Raphael Grzebieta**
**Mike Bambach**
Transport and Road Safety, The University of New South Wales
Australia

**Jake Olivier**
School of Mathematics and Statistics, The University of New South Wales
Australia

**Andrew McIntosh**
Monash Injury Research Institute, Monash University
Australia

Paper Number 15-0145

## ABSTRACT

Rollover crashes are infrequent and account for approximately 2% to 3% of all vehicle crashes in the US annually. However, when they do occur they are more likely to result in a serious injury or fatality than some other types of crashes. In rollovers, the thorax has been identified as one of the three most frequently seriously injured body regions. As such, research has been carried out over the last few decades to understand better environmental, vehicle and occupant variables in a rollover crash which contribute to an occupant sustaining a serious, i.e. of severity greater than or equal to three on the Abbreviated Injury Scale (AIS 3+), thoracic injury. The findings from the research described in this paper will provide information for the development of a dynamic rollover crash test protocol which includes assessment of thoracic injuries. The aim of this study is to determine if there is an association between vehicle panel damage and AIS3+ thoracic injuries. NASS CDS data from 2001 to 2012 was examined for single vehicle rollover crashes with occupants receiving serious thoracic injuries (cases) and those without thoracic injuries (controls). Vehicle panel damage for both cases and controls were coded and logistic regression performed to determine if there is an association between serious thoracic injury and vehicle panel damage.

The result of this study indicates that there is an association between thoracic injury and damage to the top-half of the left front door, top-half of the right front door and left side of the vehicle rearwards of the B-pillar.

## INTRODUCTION

In 2012, rollovers constituted 2.4% of all vehicle crashes in the United States of America (USA) but they contributed to 34.6% of all motor vehicle crash fatalities equating to approximately 7,500 deaths (NHTSA, 2012b) . To date a widely accepted dynamic rollover crashworthiness crash test protocol has not been developed. In order to establish a valid protocol, the environmental, vehicle and occupant variables that are associated with serious injuries in a rollover need to be identified and a method of replicating these variables in a simulated rollover crash needs to be developed.

In a rollover crash, the head, spine and thorax are the three most commonly injured body regions for contained and restrained occupants (Mattos, Grzebieta, Bambach, & McIntosh, 2014; Parenteau, Gopal, & Viano, 2001) with the thorax being the second most commonly injured region (Bedewi, Godrick, Digges, & Bahouth, 2003; Moore, Vijayakumar, Steffey, Ramachandran, & Corrigan, 2005). Vital organs such as the heart and lungs are located within the thorax. Thus, protecting this region in a rollover crash is important and often under-researched in comparison to the head and spine. One of the more recent studies conducted to understand thoracic injuries in vehicle rollover crashes sustained by restrained and contained occupants was carried out by Bambach *et al.* (2013). Their study found that lung contusions are the most frequently reported thoracic injury followed by rib fractures. The main sources of these injuries were the door interior, seatbelt and seatback. The mechanisms of these injuries in rollover crashes is still being investigated through crash data, crash reconstruction, physical modelling and numerical modelling.

It was initially hypothesized that occupant injuries in rollovers are the result of intrusion into the occupant space (Conroy et al., 2006; Sharma & Singh, 2009). However, recent examination of NASS CDS rollover crash data by Bambach *et al.* (2013) found that only 7.4% of thoracic injuries are directly associated with any intrusion. As such, they proposed that thoracic injuries are likely to occur due to the occupant traversing laterally towards and impacting internal components of a vehicle. This finding shifts the focus to developing an understanding as to how vehicle roll kinematics results in an occupant traversing laterally into the vehicle's interior thus causing thoracic injury. Bambach *et al.* (2013) also noted that there was not an obvious correlation between vehicle damage and thoracic injury citing, "…typically the side of the vehicle displayed some damage, indicating ground contact. However, a wide variety of vehicle damage occurred, varying from no damage (indicating no ground contact) to significant damage (indicating significant ground contact)." Digges *et al.* (2013) examined this in more and sought to find an association between vehicle crash damage patterns and thoracic injury but their study was only based on eight rollover crashes. That is, there was insufficient data to establish a comprehensive relationship between vehicle crash damage patterns and thoracic injury.

This study extends the work carried out by Digges *et al.* (2013) and Bambach *et al.* (2013) by determining if there is an association between vehicle crash damage patterns and thoracic injuries quantitatively.

## METHOD

### Data

The US National Automotive Sampling System (NASS) Crashworthiness Data System (CDS) collects data from approximately 5,000 police reported passenger car, light truck, van and utility vehicle crashes each year. In order to be selected in the sample, a crash must involve personal or property damage; be reported to the police; and the vehicle towed away. The CDS is a probability sample and each case is provided with a weighting factor to represent police reported crashes occurring in the US during that year thus allowing population estimates to be calculated (NHTSA, 2012a).

NASS CDS from 2001 to 2012, inclusive, was queried in SAS Enterprise Guide 5.1 (SAS Institute) with the following filters: single-vehicle tripped rollover crash with at least one quarter rollover where the front seat occupants were 16 years or older; were restrained and contained in the vehicle; the vehicle did not contact another object prior to, during or after rolling over; and no airbags were deployed. The vehicles included in this study were sedans, utilities, vans and light trucks with the steering wheel located on the left side. Multiple vehicle crashes with a vehicle undergoing a rollover prior to or subsequent to the impact with another vehicle produces different injury patterns thus were excluded (Digges, Eigen, & Dahdah, 2005). Additionally, it has been noted that 80% of all rollovers in the US are single vehicle rollovers (Eigen, 2003). From the filtered cases, two groups were created. Cases consisted of occupants with thoracic injuries of severity equal to or greater than three on the Abbreviated Injury Scale (AIS3+) (Champion, 2012) while controls consisted of occupants without thoracic injuries.

The query returned 43 cases and 761 controls. The weighting factor, $n_{weighted}$, was 4,573 and 325,067 for cases and controls respectively. From the 761 controls, 200 were randomly selected for vehicle panel damage coding. This was reduced to 181 ($n_{weighted}$ = 55,905) controls, thus achieving a ratio of cases to controls of 1:4 to 1:5, after filtering out vehicles deemed unsuitable for inclusion in this study. These included vehicles where vehicle panel damage was obscured by plastic sheets used to prevent ingress of water into the vehicle; vehicles which were cut open and it was unclear if the panels were bent by rescue workers or damaged during the crash; or when vehicles were undergoing repairs when the photos were taken.

### Coding of Vehicle Panel Damage

The panels forming the exterior of each vehicle was divided into eleven segments for each vehicle class (sedans, utilities, vans and light trucks). The segments consisted of the front fender, front door upper half, front door lower half, vehicle side rearwards of the B-pillar for either side and the front hood, glasshouse roof and boot lid for the top. These segments were titled as Left/Right 1, Left/Right 2, Left/Right 3, Left/Right 4, Top 1, Top 2 and Top 3 respectively for entry into SAS (See Figure 1).

| Vehicle Class | Vehicle Segments |
|---|---|
| Sedans | 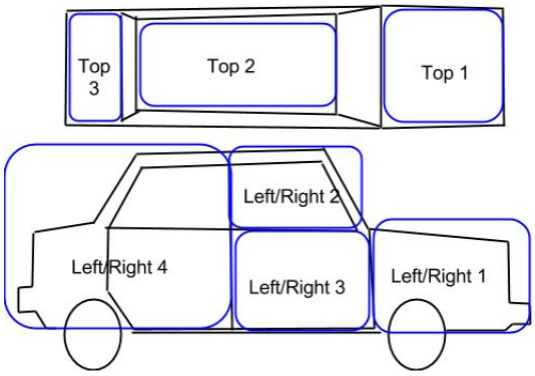 |
| Utilities and Vans | 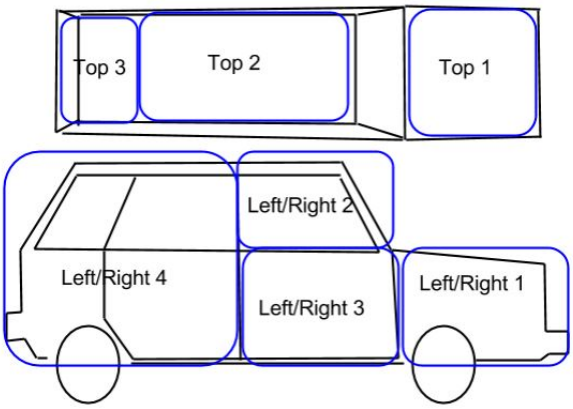 |
| Light Trucks | 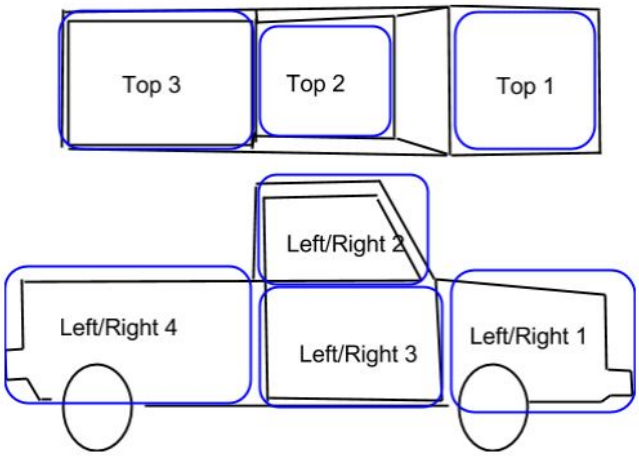 |

***Figure1. Each class of vehicle (sedans, utilities, vans and light trucks) was divided into 11 segments.***

Coding of vehicle segment damage was then performed. Segment damage was dichotomously coded with segments receiving either no to minor damage, coded as zero, or segments receiving major damage, coded as one, from vehicle-to-ground contact. No or minor damage is defined as segments which have sustained scratches or small dents from the vehicle-to-ground impact and is unlikely to have substantially affected the vehicle's rollover kinematics. Major damage is defined as segments which have sustained substantial damage to the vehicle's panel and/or structure upon vehicle-to-ground impact sufficient to alter the vehicle's rollover kinematics. An example of minor and major damage is provided in Figure 2. Where it is unclear as to whether a segment has moderate or major damage, a conservative approach was taken and the segment damage was coded as zero.

***Figure2. Examples of vehicle panels with minor damage (left) versus major damage (right).***

In the event that two adjacent segments received major damaged directly from the vehicle-to-ground impact, both segments would be coded as receiving major damage. However, if one segment received major damaged from the vehicle-to-ground impact and subsequently affected an adjacent segment thus causing major damage, then only the segment damaged from the vehicle-to-ground contact was coded as receiving major damage and the adjacent segment was coded as receiving minor damage.

The weighting of each NASS CDS case was not applied to vehicle segment damage as it is applicable to the type of vehicle crash and not to segment damage.

**Statistical Method**

A multiple variable logistic regression model was developed in SAS Enterprise Guide 5.1 (SAS Institute) to assess the association between predictor variables and the response variable. The predictor variables for the model consisted of variables from the vehicle, occupant and the crash environment. They were evaluated for inclusion in the model based on the possibility that they may be associated with serious

thoracic injury and guided by previous reports (Bambach et al., 2013; NHTSA, 2002). The variables considered for inclusion in the model were: vehicle quarter rollover, occupant age, occupant gender, roll direction relative to the occupant, vehicle class (sedan, utility, van and light truck), roadway alignment (straight road, left curve or right curve), rollover initiation location (roadway, paved shoulder, unpaved shoulder or roadside/median), surface condition (dry, wet, snow, slush, ice or sand/dirt/oil/gravel) and roadway profile (level, uphill, hill crest, downhill or sag). Other variables such as occupant height, weight and BMI were considered. However, due to missing observations for several cases, these variables were not included as this would have reduced the number of already limited cases in this study.

The aforementioned variables were classified as either continuous (vehicle quarter rollover, speed limit and occupant age), dichotomous (occupant gender and roll direction relative to the occupant) or polytomous (vehicle body type, rollover location, roadway alignment, surface condition and roadway profile). Due to the small sample size in this study, polytomous variables were classified as dichotomous in the following manner: vehicle body type was either a utility/van/light truck or sedan; rollover location was either on the roadway or otherwise; roadway alignment was either straight or curved; surface condition was either dry or otherwise; and roadway profile was either level or otherwise.

The response variable was the presence, coded as one, or its absence, coded as zero, of a serious (AIS 3+) thoracic injury.

Purposeful selection was used to determine significant variables, evaluated to a significance level of 0.20 for the initial stage and 0.05 for subsequent stages of the model, associated with serious thoracic injuries that were to be included in the base model (Hosmer, Lemeshow, & Sturdivant, 2013). The dichotomously coded segment damage variables were then added to the base model and were evaluated to a significance level of 0.05. Non-significant segment damage variables were then removed to create the final model. Additionally, checks for linearity between each continuous variable and the logit was also performed (Friendly, 2012; Hosmer, Lemeshow, & May, 2008).

## RESULTS

The base model from the logistic regression analysis includes the following variables: vehicle quarter rollover, dichotomously coded rollover location (off roadway versus on road way), dichotomously coded vehicle class (utility/van/light truck versus sedans), and dichotomously coded surface condition (dry or otherwise) (See Table 1). The dichotomously coded segment damage variables were then added to this model and all non-significant segment damage variables removed thus resulting in the final model (See Table 2). It is noted that the dichotomously coded surface condition was removed from the final model as it became insignificant (p=0.41, OR= and 1.67). Additionally, the Left 2 segment damage was kept in the final model even though its p-value of 0.058 is higher than the statistical significance level of 0.05. However, its odd ratio point estimate of 2.46 is high and thus an important factor (Olivier & Bell, 2013). The final model consists of the following variables: vehicle quarter rollover; dichotomously coded rollover location (off roadway versus on road way); dichotomously coded vehicle class (utility/van/light truck versus sedans); Left 4; Right 2; and Left 2 segment damage.

**Table1.**

**Multiple variable logistic regression results for thoracic injury (AIS 3+) and base model covariates.**

| Variable | MLE Ratio Estimate | Standard Error | Odds Ratio Point Estimate | 95% Confidence Interval | p-Value |
|---|---|---|---|---|---|
| Increase in One Quarter Roll | 0.82 | 1.40 | 2.26 | 1.73, 2.95 | <0.001 |
| Rollover off Roadway | 1.22 | 0.61 | 3.40 | 1.04, 11.13 | 0.043 |
| Utility/Van/Light Truck | 1.59 | 0.59 | 4.90 | 1.55, 15.52 | 0.007 |
| Dry Surface | 1.13 | 0.56 | 3.10 | 1.04, 9.24 | 0.042 |

**Table2.**

**Final logistic regression model.**

| Variable | MLE Ratio Estimate | Standard Error | Odds Ratio Point Estimate | 95% Confidence Interval | p-value |
|---|---|---|---|---|---|
| Increase in One Quarter Roll | 0.74 | 0.15 | 2.09 | 1.57, 2.79 | <0.001 |
| Rollover off Roadway | 1.36 | 0.64 | 3.90 | 1.11, 13.72 | 0.034 |
| Utility/Van/Light Truck | 1.31 | 0.64 | 3.71 | 1.06, 12.93 | 0.039 |
| Left 4 Segment | 1.21 | 0.48 | 3.35 | 1.30, 8.62 | 0.012 |
| Right 2 Segment | 1.30 | 0.50 | 3.68 | 1.37, 9.85 | 0.009 |
| Left 2 Segment | 0.90 | 0.47 | 2.46 | 0.97, 6.22 | 0.058 |

## DISCUSSION

The results from the multiple variable logistic regression model indicate that the number of vehicle quarter rollovers; the vehicle is a utility, van or light truck; the rollover occurred off the roadway and there is major damage to the Left 4, Right 2 and Left 2 segments are associated with a front seat occupant sustaining a serious thoracic injury. An increase in one quarter rollover is associated with a 2.1 times increase in the odds of receiving a serious thoracic injury, a finding similar to that from previous studies (Bambach et al., 2013; Moore et al., 2005; Viano & Parenteau, 2007). This increase in odds is likely due the higher velocity or crash energy and greater opportunity for occupants to impact the vehicle's interior. This study also shows that being an occupant in a utility, van or light truck, as opposed to those in a sedan, is associated with a four fold increased in the odds of sustaining serious thoracic injury and confirms the findings of a previous study by Bambach *et al.* (2013). It is possible that this is due to the higher aspect ratios of utilities, vans and light trucks compared to sedans resulting in a higher deceleration rate as the vehicle rolls. Rollovers that are initiated on the shoulder or the median are 3.7 times more likely to result in a front seat occupant sustaining a serious thoracic injury than if the initiation occurred on the roadway. This is possibly due to the higher friction forces that occur when a vehicle furrows into the soft surface (Allen, Rosenthal, & Chrstos, 1997; Warner, Smith, James, & Germane, 1983) resulting in a higher deceleration than if the vehicle tripped on a paved surface.

Intuitively, an increase in occupant age would be associated with an increased probability of sustaining an injury in a rollover crash. However, this was found not to be a significant variable in this study and is likely to be due to the small sample size and that age was treated as a continuous variable. It is noted that age was also entered into the model as an interval variable. However, this did not affect the outcome of the model.

Previous studies (Bambach et al., 2013; Cuerden, Cookson, & Richards, 2009; Parenteau et al., 2001) have found that rollover direction was associated with an increased probability of sustaining an injury. However, this study has not come to that same conclusion with findings similar to the studies by Bedewi *et al.* (2003), Conroy *et al.* (2006) and Viano & Parenteau (2007).

Damage to the Right 2 and Left 2 segment is associated with a 3.1 and 2.5 increase in the odds of sustaining a thoracic injury respectively. An explanation of the vehicle kinematics resulting in damage to these segments is provided below followed by a discussion on the possible relationship between damage to these segments and thoracic injury.

A vehicle in a clockwise rollover (right side leading), as viewed from the rear, may receive damage to the Right 2 segment as it impacts the ground on entering the $2^{nd}$, $6^{th}$ and $10^{th}$ quarter rollover, noting that most rollovers do not exceed 12 quarter rollovers (Bambach et al., 2013). The vehicle may also receive damage to the Left 2 segment as it impacts the ground on entering the $3^{rd}$, $7^{th}$ and $11^{th}$ quarter rollover. Similarly, a vehicle in a counter clockwise rollover (left side leading), as viewed from the rear, may receive damage to

the Left 2 segment as it impacts the ground when it enters the 2nd, 6th and 10th quarter rollover and damage to the Right 2 segment as it impacts the ground when it enters the 3rd, 7th and 11th quarter rollover.

In a clockwise rollover, thoracic injury may be occurring at the 2nd quarter rollover as the driver and passenger's thorax might be oriented approximately horizontally (Heller et al., 2010), relative to the ground, with gravitational force acting on both occupants so that the driver and passenger is accelerated into the centre console and the right door interior respectively resulting in a thoracic injury (See Figure 3). In a counter-clockwise rollovers the driver and passenger are accelerated into the left door interior and centre console respectively. The occupant's thorax position is less clear once the vehicle rotates past the 2nd quarter rollover thus making it difficult to form a plausible cause of thoracic injury.

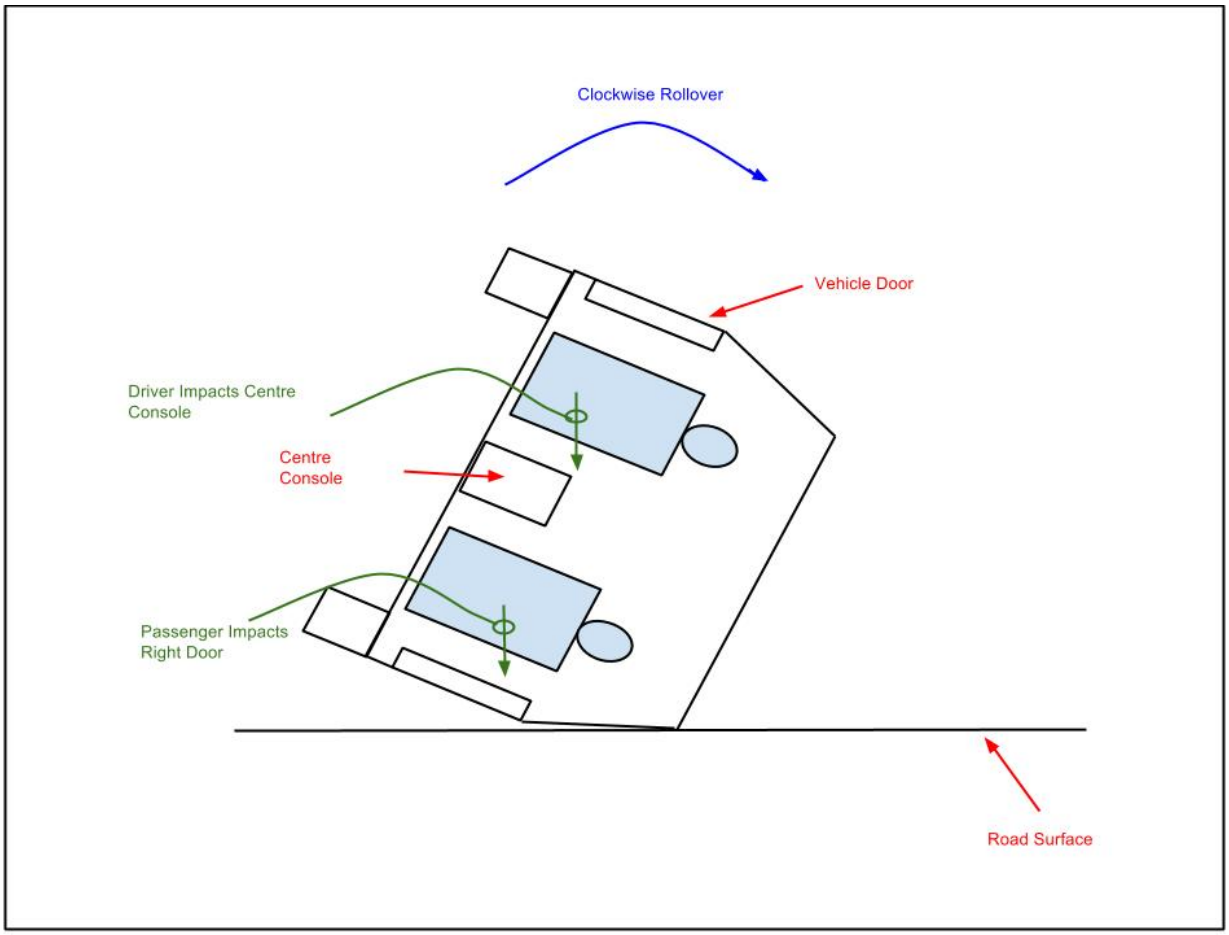


***Figure3. Vehicle right rollover, as viewed from the rear of the vehicle, impacting the ground at the Right 2 segment with the driver impacting the center console and passenger impacting the right door interior.***

Damage to the Left 4 segment was found to be associated with serious thoracic (OR=3.9). The vehicle kinematics and damage mechanism is similar to that which results in Left 2 damage. However, it is likely a negative vehicle pitch, as defined by the SAE sign convention for vehicles, would be present thus allowing the rear of the vehicle to contact the ground as it enters the 2nd, 6th and 10th quarter rollover, for counter clockwise rotations, and as the vehicle enters the 3rd, 7th and 11th quarter rollover for clockwise rotations.

It is interesting to note that damage to the rear right of the vehicle rearwards of the B-pillar, Right 4 segment, is not associated with thoracic injury and is likely to be due to the small number of cases and, to a lesser extent, controls.

**Limitations**

The limitations of this study should be noted. The NASS CDS data is a probability sample rather than a census and the data is dependent on the investigation and data entry accuracy of the NASS investigator. Logistic regression models can be biased towards a particular sample. Occupant height and weight were not included as variables in the analysis. The coding of vehicle panel damage is subjective and is based on residual deformation only. Sheet metal strength varies from vehicle model to model thus two different vehicle models subjected to the same impact force will deform to different extents. Certain parts of a vehicle, such as the A-pillar, are significantly stronger than the panels forming the exterior of the vehicle thus if the vehicle in a rollover impacted the ground with a structural component first, this may result in the panels receiving minor damage. The regression model establishes associations between the predictor variables and response variable but it does not imply causality.

## CONCLUSION

In this study, coding of vehicle panel damage was carried out for a total of 224 vehicles involved in pure rollover crashes. The association between vehicle panel damage; vehicle class; occupant variables; and the crash environment variables and serious, AIS 3+, thoracic injury was assessed. Vehicle quarter rollover, rollovers involving Utilities/Van/Light trucks, rollovers occurring off the roadway, damage to the vehicle rearwards of the left B-pillar (Left 4 segment), damage to the top-half of the right front door (Right 2 segment) and damage to the top-half of the left front door (Left 2 segment) were associated with serious thoracic injury in rollover crashes.

Although this study has identified damage to the left rear of the vehicle rearwards of the B-pillar and top-half of the right and left front door are associated with serous thoracic injury and may need to be taken into account in rollover reconstructions, future studies are still needed to verify this finding and to develop a better understanding as to how damage to these areas of the vehicle is associated with thoracic injuries. Future studies could also include vehicle roof strength to weight ratio and roof shape as variables in the logistic regression model as well as increasing the number of cases and controls.

**REFERENCES**


Allen, R. W., Rosenthal, T. J., & Chrstos, J. P. (1997). A Vehicle Dynamics Tire Model for Both Pavement and Off-Road Conditions (Paper No. 970559): SAE Technical Paper.

Bambach, M. R., Grzebieta, R. H., & McIntosh, A. S. (2013). Thoracic Injuries to Contained and Restrained Occupants in Single-Vehicle Pure Rollover Crashes. *Accident Analysis and Prevention*(50), 115-121.

Bedewi, P. G., Godrick, D. A., Digges, K., & Bahouth, G. T. (2003). *An Investigation of Occupant Injury in Rollovers: NASS-CDS Analysis of Injury Severity and Source by Rollover Attributes.* Paper presented at the Proceedings of the 18th International Technical Conference on the Enhanced Safety of Vehicles, USA.

Champion, H. R. (2012). Abbreviated Injury Scale. In J.-L. Vincent & J. Hall (Eds.), *Encyclopedia of Intensive Care Medicine* (pp. 1-5): Springer Berlin Heidelberg.

Conroy, C., Hoyt, D. B., Eastman, B. A., Erwin, S., Pacyna, S., Holbrook, T. L., . . . Velky, T. (2006). Rollover Crashes: Predicting Serious Injury Based on Occupant, Vehicle and Crash Characteristics. *Accident Analysis and Prevention*(38), 835-842.

Cuerden, R., Cookson, R., & Richards, D. (2009). *Car Rollover Mechanisms and Injury Outcome.* Paper presented at the Proceedings of the 21st Conference on the Enhanced Safety of Vehicles, Stuttgart, Germany.

Digges, K., Eigen, A. M., & Dahdah, S. (2005). *Injury Patterns in Rollovers by Crash Severity.* Paper presented at the Proceedings of the 19th International Technical Conference on the Enhanced Safety of Vehicles, USA.

Digges, K., Tahan, F., Grzebieta, R. H., Bambach, M. R., Mattos, G. A., & McIntosh, A. S. (2013). Crash Damage Patterns Associated with Chest Injuries in Far-Side Rollovers.

Eigen, A. M. (2003). *Examination of Rollover Crash Mechanisms and Occupant Outcomes.* (DOT HS 809 692). Washington DC.

Friendly, M. (2012). Visualizing Categorical Data with SAS and R. York University.

Heller, M. F., Newberry, W. N., Smedley, J. E., Eswaran, S. K., Croteau, J. J., & Carhart, M. R. (2010). Occupant Kinematics and Injury Mechanisms During Rollover in a High Strength-to-Weight Ratio Vehicle. *SAE International Journal of Passenger Cars-Mechanical Systems, 3*(1), 450-466.

Hosmer, D. W., Lemeshow, S., & May, S. (2008). Model Development *Applied Survival Analysis* (pp. 132-168): John Wiley & Sons, Inc.

Hosmer, D. W., Lemeshow, S., & Sturdivant, R. (2013). *Applied Logistic Regression* Wiley Series in Probability and Statistics, (pp. 528).

Mattos, G., Grzebieta, R., Bambach, M., & McIntosh, A. S. (2014). *Roof Damage Patterns and Serious Head Injuries in Pure Rollover Crashes.* Paper presented at the Transport Research Board Annual Meeting, Washington D.C.

Moore, T., Vijayakumar, V., Steffey, D. L., Ramachandran, K., & Corrigan, C. F. (2005). Biomechanical Factors and Injury Risk in High-Severity Rollovers. *Association for the Advancement of Automotive Medicine, 49*.

NHTSA. (2002). *Characteristics of Fatal Rollover Crashes.* (DOT HS 809 438).

NHTSA. (2012a). *NASS Analytical Users Manual.*

NHTSA. (2012b). *Traffic Safety Facts 2012*.

Olivier, J., & Bell, M. (2013). Effect Sizes of a 2x2 Contingency Table. *PLoS One, 8*(3).

Parenteau, C., Gopal, M., & Viano, D. (2001). *Near- and Far-Side Adult Front Passenger Kinematics in a Vehicle Rollover.* Paper presented at the Proceedings of the 45th Stapp Car Crash Conference.

SAS Institute. SAS Enterprise Guide (Version 5.1).

Sharma, D., & Singh, S. (2009). *A Classification Model for Prediction of Rollover Crash Severity.* Paper presented at the Proceedings of the 21st Internatioal Technical Conference on the Enhanced Safety of Vehicles, Stuttgart, Germany.

Viano, D. C., & Parenteau, C. S. (2007). Rollover Injury: Effects of Near- and Far-Seating Position, Belt Use, and Number of Quarter Rolls. *Traffic Injury Prevention*(8), 382-392.

Warner, C. Y., Smith, G. C., James, M. B., & Germane, G. J. (1983). Friction Applications in Accident Reconstruction: SAE Technical Paper.

This paper has been peer-reviewed and published in a special edition of *Traffic Injury Prevention* 16(S1), by Taylor & Francis Group. The complete paper will be available on the *Traffic Injury Prevention and www.NHTSA.gov* websites on June 8, 2015.

To access all Peer-reviewed papers please copy and paste the link below into your browser to access the papers.

http://www.tandfonline.com/toc/gcpi20/16/sup1

This paper has been peer-reviewed and published in a special edition of *Traffic Injury Prevention* 16(S1), by Taylor & Francis Group. The complete paper will be available on the *Traffic Injury Prevention and www.NHTSA.gov* websites on June 8, 2015.

To access all Peer-reviewed papers please copy and paste the link below into your browser to access the papers.

http://www.tandfonline.com/toc/gcpi20/16/sup1

# COMPARISON OF EVENT DATA RECORDER AND NATURALISTIC DRIVING DATA FOR THE STUDY OF LANE DEPARTURE EVENTS

**Kristofer D. Kusano**
**Rong Chen**
**Ada Tsoi**
**Hampton C. Gabler**
Virginia Tech
U.S.A.

Paper Number 15-0149

## ABSTRACT

Naturalistic Driving Study (NDS) data are an important source for driver behavior data to design and evaluate autonomous vehicles and driver assistance systems. The number of serious crash events in NDS, however, is often small. As a result, surrogates such as "near crashes" or events identified using vehicle instrumentation are used with the assumption that they are relevant to real crash events. The objective of this study is to determine if NDS crash and near-crash data are indeed representative of crash events. To examine this issue, we focused on one subset of crash events, lane departure events where the vehicle drifts out of its lane. These are the events most likely to be mitigated by lane departure warning systems.

Four naturalistic datasets that covered the full range of events from lane departures during normal driving, to near-crashes, to crashes were compared to data from a crash database. Our hypothesis is that the crash and near-crash NDS events will have the most similar vehicle kinematics compared to the crash database. Normal driving departure events were extracted from the Integrated Vehicle-Based Safety Systems (IVBSS) field operation test. Two departure event datasets from IVBSS were identified using the lane tracking cameras. The first dataset consisted of 12,760 cases of the vehicle departing and returning to its lane and the second consisted of 7,750 events where the equipped LDW systems were triggered. Thirty-two (32) near-crash lane departure events were analyzed from the 100-Car NDS. Finally, 49 curb strike events were analyzed from the SHRP-2 NDS. Data from lane departure crashes was extracted from the National Automotive Sampling System, Crashworthiness Data System (NASS/CDS). Event Data Recorders (EDRs) downloaded from 482 NASS/CDS crash investigations were analyzed.

There were important sampling differences between datasets. Younger drivers were overrepresented in the 100-Car near-crash and SHRP-2 curb strike events and crash data while the IVBSS participants were uniformly distributed over age and gender groups. The vehicle speeds from IVBSS were restricted to over 42 kph (25 mph), whereas the crash data had vehicles speed that contained both low and high speed events. The 100-Car near-crash and SHRP-2 curb strike departures had larger departure angles (2.6° and 14.1° median, respectively) and lateral excursion (0.63 m and 0.50 m median, respectively) compared to the IVBSS data (0.6° and 0.7° departure angle and 0.19 m and 0.10 m excursion for LDW and lane departure datasets, respectively). The differences in departure conditions may have also affected driver maneuvers after the departure. In 52% of crashes with EDRs there was a brake application in the last second before the crash compared with 38% of 100-Car near-crash and 33% of SHRP-2 curb strike events. The selection criteria for the IVBSS departures excluded almost all brake application, with only 4% of the IVBSS LDW events having brake application. Steering wheel input was also substantially larger in the 100-Car near-crashes (48°) compared to the IVBSS (4°-5°).

These results show that crash and near-crash events from NDS produce datasets that are most consistent with crash data compared to datasets generated using lane tracking information. If the research question involves replicating conditions relevant to departure crashes, such as in the design of test track experiments, crash and near-crash events should be used over less severe NDS departure events.

## INTRODUCTION

Naturalistic Driving Studies (NDS) have become an important data source for studying driver behavior to design and evaluate active safety systems, such as lane departure warning (LDW) systems. NDS involve instrumenting drivers' personal vehicles and recording all normal driving for a period of months or years. Participants are given no

special instructions and researchers are not present during driving. The result is often thousands to millions of vehicle miles of instrumented driving. The instrumentation, including cameras and vehicle sensors, provide a high level of detail to study driver behavior in a variety of driving scenarios. LDW systems will mostly likely mitigate crashes caused by the driver inadvertently drifting out of the vehicle's lane, i.e. not changing lanes or turning. This study focuses on examining lane departure events where the driver drifted out of their lane. These drift out of lane events are important for developers of LDW systems because they represent the scenarios where LDW will most likely activate.

Because crashes are extremely rare in NDS, analysis is often based on near-crashes or other crash surrogates that are correlated with crash risk (Guo et al. 2010). The assumption of researchers is that these NDS critical events, whether identified through manual review or aggregated from vehicle sensor data, are representative of crashes and crash risk. The validity of this assumption is on open research question (Ljung Aust 2013), but is difficult to evaluate because the type of driver behavior data obtained from NDS are not available in most crash datasets. Using critical event data may be appropriate for some research questions, such as exposure to lane departures, but not for other research questions, such as how drivers steer to avoid serious departure events. Although a researcher's choice of dataset may affect the results of studies, little previous work has been done to directly compare different NDS data sources.

Most crash databases are investigated retrospectively and do not contain detailed pre-crash information that is available in most NDS. One promising data source for obtaining driver behavior from crashes are Event Data Recorders (EDRs). EDRs are able to record data both after a crash occurs as well as pre-crash vehicle data in some modules. This study uses a set of EDR modules downloaded from investigated crashes from a nationally representative crash database. In addition to the vehicle speed and brake pedal data recorded on the EDR, supplemental analysis of the scene diagrams prepared by investigators was performed to measure the approximate departure angle and impact location.

Even between different NDS, the selection criteria to generate lane departure event datasets may affect the composition of the lane departure datasets. Some selection criteria may result in a dataset of more severe driver corrective action than other selection criteria, for example. Where along the continuum of departure severity a departure dataset falls, from moderate departures requiring little driver intervention to near-crashes involving emergency maneuvers, may have implications for the study of active safety systems. For example, selecting a dataset that has only small driver steering input may result in evaluations that do not include departure conditions relevant to crashes.

The objective of this study was to determine how representative lane departure event datasets extracted from NDS are of real crashes investigated in crash databases. This study is unique in that it directly compares the completely different NDS to real-world crash data.

## METHODS

### Comparison of Datasets

The data sources for this study were the 100-Car NDS, the Integrated Vehicle-Based Safety Systems (IVBSS) NDS, the SHRP-2 NDS, and EDRs downloaded from crashes in the National Automotive Sampling Systems, Crashworthiness Data System (NASS/CDS). A description of each data source and selection criteria of departure events are described in the following sections. This first section describes how data sources were compared.

Figure 1 shows the relationship of the data sources examined for this study. The NDS and crash data sources are arranged in increasing severity. The hypothesis that will be examined in this paper is that the more severe NDS lane departure events are most similar to crash events. The crash data from the NASS/CDS was used as the "gold standard" that represents serious crashes that result in tow-away damage to vehicles.

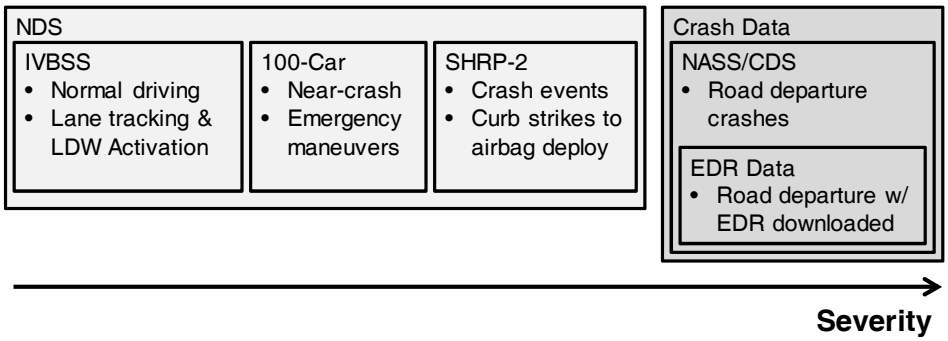


***Figure 1. Comparison of Lane Departure Events from NDS and Crash Databases.***

The data sources will be compared in two ways: 1) the drivers and vehicles that make up each data source and 2) the characteristics of the vehicle during the departure events. The first comparison of participant and vehicle makeup will determine how selection criteria may bias the observed behavior. Age and gender can affect driver behavior (Montgomery et al. 2014). The age of the vehicle may also affect handling and the availability of safety equipment such as electronic stability control. The second comparison of the departure events will determine how the departure characteristics differ between critical events and crashes. These characteristics include departure angle and vehicle speed, brake application, steering wheel angle, and maximum lateral excursion.

**100-Car NDS**

The 100-Car NDS was a landmark study of approximately 100 vehicles instrumented between 2002 and 2004 in the Washington D.C. metropolitan area (Dingus et al. 2006). There were 108 primary drivers that enrolled in the study. A primary driver was the owner(s) or lessee(s) of the vehicles who most often drove the vehicle. These primary drivers drove approximately 1.1 million miles during the study and drove an average of 224 unique days while their vehicles were instrumented (McClafferty and Hankey 2010). The instrumentation on the vehicles included cameras, inertial sensors, and monitoring of the vehicle network (CAN) data. Some vehicles were fitted with a prototype lane detection system, but not in sufficient numbers to identify a representative sample of departure events. Participants that were new drivers and that had high self-reported driving mileage were oversampled in the study design.

Lane departure crash and near-crash events from the 100-Car study were first identified by McLaughlin et al. (2009). They identified 121 lane departure events, 28 of which were crashes and the remaining 93 were near-crashes. Crashes included any physical contact with objects, including vehicles striking curbs. A near-crash was defined as the vehicle leaving the road or a vehicle leaving the lane and having to take emergency maneuvers to avoid impacting another vehicle or object. Near-crashes were found by first identifying potentially dangerous events using lateral acceleration and yaw rate sensors and then by a manual review of events. Of these 121 lane departure events, many were scenarios that LDW systems will likely not mitigate, such as leaving the road after avoiding a stopped lead vehicle, changes in road geometry in or around intersections, or as the result of turning maneuvers. Our study examined the video and instrumentation data for the 121 departure events. Our analysis identified 32 events were the driver unintentionally drifting out of their lane, which is the scenario most applicable to LDW systems. Of these events, 5 were classified as crashes and 27 as near-crashes. All 5 crash events were curb strikes that did not result in vehicle damage. These 32 events are the basis for the 100-Car events analyzed for this study. These events will be referred to as the "100-Car near-crash events" in this study. Even though 5 events were classified as crashes, these curb strikes do not rise to the same severity as tow-away crashes extracted from NASS/CDS.

**Integrated Vehicle-Based Safety Systems Field Operational Test**

The IVBSS NDS was conducted by the University of Michigan Transportation Research Institute (UMTRI) (Sayer et al. 2008, Sayer et al. 2011a, Sayer et al. 2011b, Nodine et al. 2011). IVBSS was designed to assess the effectiveness of prototype crash warning systems designed to mitigate the risk of rear-end, roadway departure, and lane change-merge crashes. In the light vehicle portion of IVBSS, vehicles were installed with forward collision warning (FCW), lane departure warning (LDW), lane-change/merge warning (LCM), and curve speed warning (CSW).

Participants of the program included 108 drivers randomly selected and stratified by age and gender. State driving records were used to identify an equal proportion of males and females in the age groups of 20 to 30 years, 40 to 50 years, and 60 to 70 years. Participants were equally distributed over the three age groups, but the exact number of participants by age and gender was not disclosed by the study designers. The drivers were given a 2006 or 2007 model year Honda Accord equipped with retrofitted prototype crash warning systems. The instrumented test vehicles recorded driving during a 40 day period. During the first 12 days, or the "baseline period", the system gave no warnings from the crash avoidance systems. The activation of the systems, however, was recorded during the baseline period. During the "treatment period", or the last 28 days of data collection, the system provided audible, visual warnings, and tactile warnings. Instrumentation in the study included video, inertial sensors, lane tracking information (lane width, vehicle position in lane, lane marking type), and LDW system activation.

Two datasets from the IVBSS were examined for this study: 1) lane departure events as identified by the lane tracking cameras and 2) lane departure events that triggered the LDW system (Sayer et al. 2011a). The selection criteria, number of events, and human review status is summarized in Table 1. Vehicle instrumentation and forward video data were provided to the authors by UMTRI.

**Table 1.**
**Summary of IVBSS Departure Data Sets.**

| Attribute | Lane Departure Event | Valid LDW Triggered |
|---|---|---|
| Condition for Inclusion | Vehicle leaves and returns to lane; no lane change, braking, or large steering input activity 5 seconds before, after, or during departure; no braking during event; speed above 25 mph | LDW delivered, reviewer confirmed system operated correctly, and driver had steering reaction to return to lane |
| Number of Events | 12,760 | 7,750 |
| Generated by Human Review | No | Yes |

The IVBSS lane departure event dataset was collected by selecting driving where the lane tracking system had high confidence of lane tracking and the vehicle was traveling above 42 kph (25 mph). A departure event was defined as one of the vehicle's wheels crossing the lane boundary followed by the vehicle returning to the lane within 20 s of the departure. Any events that had intentional maneuvers (e.g., lane changing or turning) within 5 s of the start or end of the departure event were excluded. Any departure events with braking during the departure were also excluded. The result was a dataset of 12,760 lane departure events generated automatically without manual review of events.

The LDW triggered event dataset was constructed from LDW warnings that were triggered during the study. These events included LDW activation during both the baseline period, where no warnings were delivered to the drivers, and the treatment period, where warnings were delivered. There were two levels of LDW alerts: 1) a "cautionary" alert (LDW-C) and 2) an "imminent" alert (LDW-I). The LDW-C was delivered when the driver was drifting out of their lane into an unoccupied space, such as a clear lane or the shoulder. The LDW-I alert was delivered when the side-looking sensors detected a hazard, such as another vehicle or roadside object. The LDW-C alert presented only a seat vibration in the direction of the lane departure and the LDW-I alert delivered seat vibrations as well as audio and visual warnings. All warnings were suppressed at vehicle speeds less than 40.2 kph (25 mph). In total there were 20,005 LDW-C and LDW-I warnings triggered. Of these, a video review performed by UMTRI found that 94% of warnings were valid (Sayer et al. 2011a). A valid LDW was defined as a warning that was delivered as intended by the design of the system. Many warnings, however, were delivered when a driver changed lanes without using a turn signal or intentionally left the lane, for example to avoid construction equipment. A video review performed by UMTRI researchers found that 7,385 LDW events had a driver reaction to steer back toward the lane.

The lane departure event and LDW triggered event datasets had little overlap. Out of the 12,760 departure events, only 2,165 (17% or departure events) had an LDW during or within 1 second of the departure. Of the 7,750 LDW events with driver correction that were validated by manual review, 1,343 were on the departure data set (17.3% of valid LDW events). The design of LDW used in IVBSS was proprietary. The result that many drift out of lane

events did not trigger an LDW may suggest that the design of the LDW was dependent on other vehicle dynamics, such as lateral speed, other than lateral distance to the lane line.

**SHRP-2 NDS**

The Strategic Highway Research Program 2 (SHRP-2) NDS was a follow-on to the 100-Car study and was funded by the Transportation Research Board of the National Academies. A total of 3,362 vehicles were instrumented in 6 study locations throughout the U.S. Collection of the field data was completed in 2013. The analysis of the data is ongoing. In total 6.7 million trips were recorded resulting in 49.7 million miles traveled, which is approximately 45 times more distance traveled than was recorded during the 100-Car study.

Part of the initial analysis of the SHRP-2 NDS was identifying all crash and near-crash events that occurred. Identification of crash and near-crash events followed a protocol similar to the 100-Car study. First, risky driving events were identified by using the instrumentation signals. Second, risky events were manually reviewed by data reductionists to classify the events as crashes, near-crashes, or non-critical events. For this study, all crash events with a precipitating event of the vehicle departing its lane were analyzed. Crashes were defined as any physical contact between the vehicle and its surroundings. The lowest severity crashes, as defined by the SHPR-2 analysis, involved the tires of the vehicle striking a curb. The most severe event was a vehicle departing the road into a ditch resulting in a rollover.

A total of 49 lane departure crash events were extracted from the data reduction performed for the SHRP-2 study. Events were selected by extracting all events that had an event severity of "crash" (i.e., not near-crash) and an incident type of "lane departure – left or right." At the time of writing, there were 264 such events in the SHRP-2 database. The data reduction is ongoing and it is expected that more events will be added to the database as analysis is completed. Some lane departure crash events were associated with turning or other another vehicle maneuver (163), occurred in a parking lot (107), and/or were caused by control loss (33). These departure crash events which included maneuvers, parking lots, and control loss were excluded from this analysis because these scenarios would not likely be mitigated by LDW systems. The final dataset of SHRP-2 lane departure crashes consisted of 49 events. From the event narratives, all crash events from SHRP-2 involved minor impacts with a curb and none were police reported.

**Event Data Recorders from NASS/CDS**

In a growing number of NASS/CDS crashes, investigators are able to download the EDR data from the involved vehicles. Since calendar year 2000 NASS/CDS investigators have downloaded over 8,000 EDRs from General Motors (GM), Ford, Chrysler, and Toyota vehicles. Some EDR are able to store vehicle data up to 5 seconds before the crash occurred.

An example of the pre-crash data that is available from some EDRs is NASS/CDS crash 2013-11-049. This crash involved a 2003 GMC G-Series van departing a two-lane undivided road and striking a large tree resulting in the driver being fatally injured. There was no police reported alcohol involvement and the crash occurred during daylight, clear weather, and dry pavement conditions. Figure 2 shows the pre-crash data downloaded from the EDR. The throttle application was constant at 31% prior to the crash, resulting in the vehicle accelerating from 68 to 76 kph (42 to 47 mph). There was no brake application recorded by the EDR prior to the crash. This EDR sampled pre-crash data once every second. Newer modules sample pre-crash data more frequently at 2 or 10 samples per second.

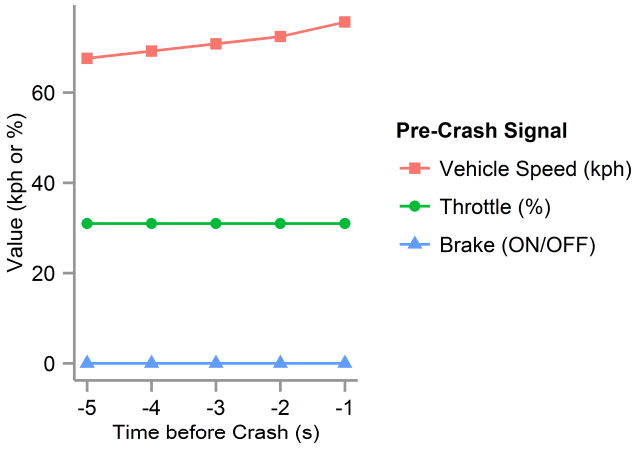


***Figure 2. Example of EDR Pre-Crash Data from NASS/CDS Case 2013-11-049.***

Table 2 summarizes the number of crashes and vehicles from NASS/CDS involved in single vehicle, drift out of lane crashes with an EDR download. From 2000 to 2013, the years EDRs were downloaded in NASS/CDS, there were 3.8 million weighted single vehicle lane departure crashes, which accounted for 12% of all NASS/CDS crashes. Drift out of lane crashes were identified using pre-crash scenarios developed in a previous study and excluded single vehicle crashes where the vehicle lost control before departing the lane (Kusano and Gabler 2014). Of these lane departure crashes, 249,572 weighted crashes, or 6%, had an EDR downloaded. Some EDRs are able to store events that did not result in a deployment of an air bag, also called non-deployment events. Non-deployment events are not locked in the memory of the EDR and can be overwritten by subsequent events. As a result of the volatile storage of non-deployment events, only EDRs with locked deployment events were analyzed. This final sample of EDRs from drift out of lane departure crashes consisted of 482 modules corresponding to 126,532 crashes or 3% of all drift out of lane crashes in NASS/CDS.

**Table 2.**
**Selected Lane Departure Crashes with EDRs from NASS/CDS Years 2000-2010.**

| Group | Cases | Weighted Frequency |
|---|---|---|
| All NASS/CDS Crashes (2000-2013) | 64,189 | 31,487,174 |
| All Vehicles with EDRs (2000-2013) | 8,426 | 3,895,698 |
| Single Vehicle, Lane Drift Crashes | 10,808 | 3,898,012 |
| Lane Drift Crash with EDR | 808 | 249,572 |
| Lane Drift with locked EDR Record | 482 | 126,532 |

## RESULTS

### Comparison of Drivers and Vehicles

Table 3 shows the distribution of age groups in each of the datasets. Proportions are shown for all departure crashes in NASS/CDS (3.9 million crashes) and for NASS/CDS crashes with EDR downloads (126,532 crashes). The 32 departure near-crash events from the 100-Car study involved 19 drivers, 5 of which were non-primary drivers who did not have age information collected as part of the study. Non-primary drivers were those who did not enroll formally in the study but were recorded driving the instrumented vehicles. The final distribution of demographics from the IVBSS study was not published, but the study design stated that subjects were selected to balance participants in three age groups (20-30, 40-50, and 60-70 years). In the crash data, there were more young drivers under age 21(23.7%) and fewer drivers with age over 60 (8.2%) compared to departures with EDR downloads (17% young driver and 17.5% 60+ drivers). The difference in driver age between NASS/CDS crashes with EDR downloads and all NASS/CDS departure crashes was statistically significant according to a Wald chi-squared test ($p = 0.0181$). The IVBSS drivers were equally distributed and thus contained more older drivers compared to the crash

data. The 100-Car drivers followed the same trend as the crash data with 64% of drivers under the age of 31, however fewer were under the age of 21. The SHRP-2 curb strike events had more drivers over the age of 60 (22.9%) compared to the crash data, but also had a large proportion of young drivers.

**Table 3.**
**Distribution of Driver Age Group for Crash, EDR, 100-Car, and IVBSS Lane Departure Datasets.**

| Age Group | NASS/CDS Departure Crashes | NASS/CDS Departure Crash EDRs | IVBSS* Normal Driving | 100-Car Near-Crashes | SHRP-2 Curb Strike |
|---|---|---|---|---|---|
| < 21 | 23.7% | 17.0% | 0% | 14.3% | 27.1% |
| 21-30 | 30.9% | 30.0% | 33% | 50.0% | 27.1% |
| 31-40 | 16.3% | 13.0% | 0 | 7.1% | 6.3% |
| 41-50 | 13.6% | 10.8% | 33% | 0% | 10.4% |
| 51-60 | 7.4% | 11.6% | 0% | 28.6% | 6.3% |
| 60+ | 8.2% | 17.5% | 33% | 0% | 22.9% |
| Total | 100% | 100% | 100% | 100% | 100% |

* Demographic information for IVBSS drivers was not disclosed, but the study design attempted to equally distributed among age groups.

Table 4 summarizes the distribution of gender in the crash, EDR, 100-Car, and IVBSS lane departure datasets. Real-world crashes involved more male than female drivers with approximately 59%-65% of drivers being male. The 100-Car near-crashes follow this trend with 58% male. The gender of IVBSS participants was assumed to be equally distributed. The SHRP-2 curb strike events were reversed, with almost two-thirds (65%) of drivers being female.

**Table 4.**
**Distribution of Driver Gender for NASS/CDS, EDR, 100-Car, and IVBSS Lane Departure Datasets.**

| Dataset | Male | Female |
|---|---|---|
| NASS/CDS Departure Crashes | 65% | 35% |
| NASS/CDS Departure EDRs | 59% | 41% |
| IVBSS* | 50% | 50% |
| 100-Car Near-Crashes | 58% | 42% |
| SHRP-2 Curb Strike | 35% | 65% |

** Demographic information for IVBSS drivers was not disclosed, but the study design attempted to equally distributed among gender.*

Figure 3 shows the cumulative distribution of vehicle model year for departure events. The CDS departure events were shown for the entire dataset (2000 – 2013), a subset of CDS departures with vehicle model year 1995 and greater (the first year EDRs were downloaded using a public tool, MY1995+), and CDS departures with EDR downloads. All vehicles from the IVBSS were either 2006 or 2007 model year vehicles and were not included in Figure 3. The vehicles with EDR downloads had a higher model year than all CDS crashes and near-crash events from the 100-Car database. When the CDS departure crashes are restricted to those involving model year 1995 and great vehicles (MY1995+), the distributions of model year was more similar to the EDR sample. However, all three CDS samples were statistically different from one another according to a simultaneous test using Tukey contrasts ($p < 0.0001$). This result suggests that vehicles with EDR data downloaded are newer than the general departure crash population. The newest vehicle population was from the SHRP-2 study.

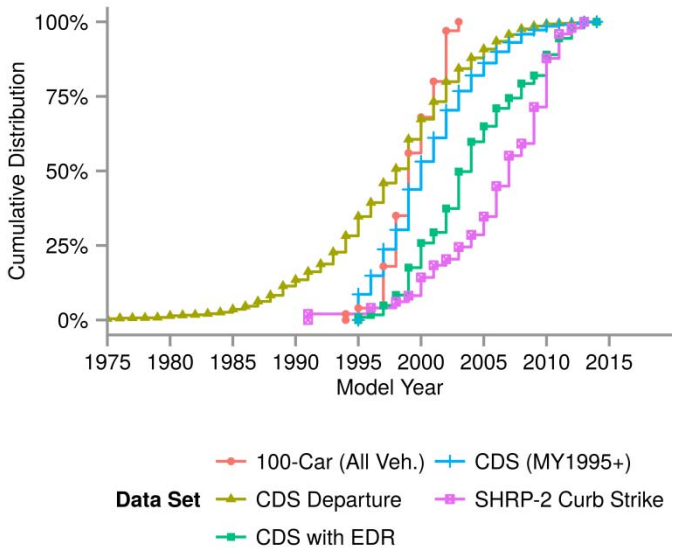


***Figure 3. Cumulative Distribution of Vehicle Model Year for Departure Event Datasets.***

**Comparison of Departure Characteristics**

Figure 4 shows the cumulative distribution of vehicle speed in departure events. Not all EDR modules were equipped to record pre-crash vehicle speed. In the sample of lane departures with EDRs, 109 had valid pre-crash speed data. The time that the vehicle departed the road is not known in the EDR data and here we used maximum pre-crash speed as a surrogate for departure speed. The maximum pre-crash speed recorded by the EDR was plotted in Figure 4 using the national weighting factors included in NASS/CDS. In IVBSS, the LDW system was suppressed at travel speeds under 42 kph (25 mph). The SHRP-2 curb strike events occurred at the lowest speeds with a median speed of 44.8 kph (27.8 mph), followed by the 100-Car near-crashes with a media speed of 69.7 kph (43.3 mph). The IVBSS LDW dataset had a median of 86.5 kph (53.7 mph), which was close to the EDR dataset median speed of 85.3 kph (53.0 mph). The IVBSS lane departure events had the highest median speed at departure with 113.4 kph (70.5 mph). The mean departure speeds for the IVBSS lane departure, and IVBSS LDW, 100-Car near-crash, and SHRP-2 curb strike sets were significantly different according to an Analysis of Variance (ANOVA, $p < 0.0001$). The EDR data was not included in the ANOVA because the sample design variables (clustering, stratification, and weighting) cannot be combined with the other data. This limitation of the data is discussed further in the Discussion section.

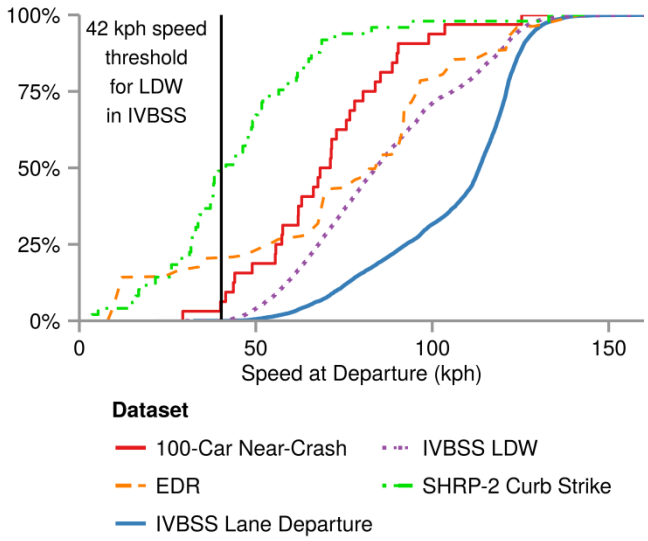


***Figure 4. Cumulative Distribution of Vehicle Speed in Lane Departure Events.***

Table 5 lists events with and without brake application. The pre-crash EDR records display brake switch status, i.e. ON or OFF, but not brake magnitude. In 60% of crashes with EDRs, there was braking during the pre-crash record. This estimate may include some non-event related braking, because most EDR pre-crash records span up to 5 seconds prior to the crash. If restricted to the last second of the pre-crash record, 52% of crashes with EDRs had brake application. This result shows that much of the braking recorded by the EDR in departure crashes is in the last second before the crash. In the IVBSS event datasets, brake application was rare. A condition of selection for the lane departure events was that there was no brake application. In IVBSS LDW events, only 4% of events had brake application. In the 100-Car near-crash events, approximately 38% of events had brake application between 0.5 s before and 2 s after the start of the departure events. Similarly, the SHRP-2 curb strike events had approximately one-third of drivers apply the brakes (32.7%) between 0.5 s before and 2 s after the curb strike.

***Table 5. Brake Application in EDR, 100-Car, and IVBSS Departure Events***

| Group | Brake Application | No Brake Application |
|---|---|---|
| EDR (Any Braking) | 60% | 40% |
| EDR (Any Braking 1 second before crash) | 52% | 48% |
| IVBSS Lane Departure* | 0% | 100% |
| IVBSS LDW | 4.2% | 95.8% |
| 100-Car Near-Crashes | 37.5% | 62.5% |
| SHRP-2 Curb Strike | 32.7% | 67.4% |

* Lack of brake application was a condition of selection for LDW lane departure events

**Comparison of NDS Departure Characteristics**

The instrumentation available on NDS allow for examination of additional departure conditions, such as departure angle, maximum lateral excursion, and steering wheel input, which are not available on most EDR modules. This section compares these additional departure conditions in the IVBSS LDW, and IVBSS lane departure, 100-Car near-crash, and SHRP-2 curb strike datasets. Only IVBSS LDW departures that did not occur within 5 seconds of a lane change event were included in this analysis because characteristics due to correcting the lane drift were difficult to discern from the lane change. This lane change exclusion eliminated 1,569 (20.2%) of the IVBSS LDW events. The 49 SHRP-2 curb strike events occurred mostly on roads without road markings and as a result the lane tracking

cameras used to calculate departure angle and excursion were not available. This section includes 9 departure events that had high lane tracking confidence during the departure.

Figure 5 shows the cumulative distribution of maximum lateral distance vehicles traveled out of the lane for the IVBSS LDW dataset, and the IVBSS lane departure dataset, 100-Car near-crashes, and SHRP-2 curb strike events. Lateral excursion from the IVBSS and SHRP-2 vehicles was estimated using the lane width and vehicle positioning provided by the lane tracking camera. The 100-Car vehicles were not all instrumented with lane tracking cameras. Trajectories for the 100-Car departures were computed using the vehicle forward speed and yaw rate to estimate the vehicle's position. The methodology used to reconstruct trajectories in the 100-Car near-crashes is detailed in the appendix. The median lateral distance was 0.10 m for the IVBSS departure dataset, 0.19 m IVBSS LDW dataset, 0.63 m for the 100-Car dataset, and 0.50 m for the SHRP-2 curb strikes. The vehicle did not leave the lane (negative maximum excursion) in approximately 10% of the IVBSS LDW events. Excluding these negative events, the median maximum excursion was 0.20 m. Most of the curb strikes from the SHRP-2 data redirected the vehicles, limiting the maximum excursion. The higher excursions, i.e., those above 0.5 m were mostly the result of vehicles overriding the curb before the driver steered back into the lane. The mean excursions were significantly different from each other using a post-hoc Tukey's test (all $p < 0.0001$).

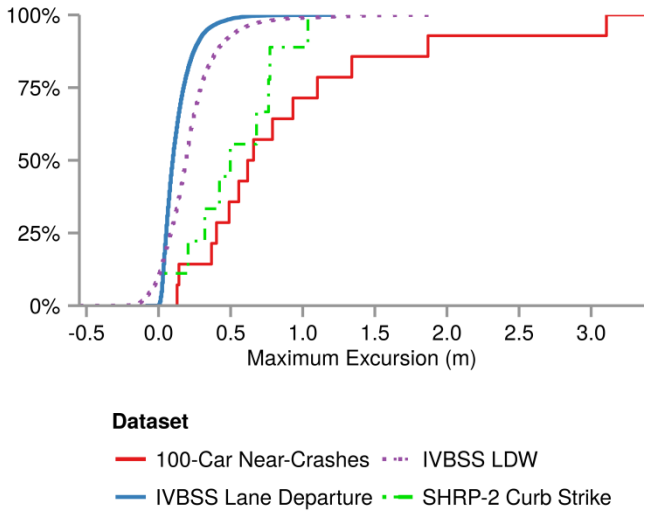


***Figure 5. Cumulative Distribution of Maximum Lateral Excursion in NDS Events. SHRP-2 curb strike data includes 9 events with lane tracking during departure.***

Figure 6 shows the distribution of departure angle in the NDS events. The departure angle from the 100-Car near-crash events was found in the reconstruction of the vehicle trajectory used to determine the lateral excursion. The IVBSS and SHRP-2 departure angle was estimated using the distance to the lane line 0.1 s prior to the lane departure and the vehicle forward speed at departure. Like lateral distance traveled outside of the lane, the 100-Car near-crash events had higher departure angle (median 2.6°) compared to the IVBSS departure (median 0.6°) and IVBSS LDW (median 0.7°). The SHRP-2 curb strike events (median 14.1°) had several high angle departures. One possible explanation for the high departure angles could be the tires entering the gutter portion near the curb causing the vehicle to rotate before striking the curb. Steering wheel angle was only available for 4 of the 9 SHRP-2 events. Two of these events had high angles and showed evidence of driver steering prior to the departure event. The mean departure angles were significantly different from each other using a post-hoc Tukey's test (all $p < 0.0001$).

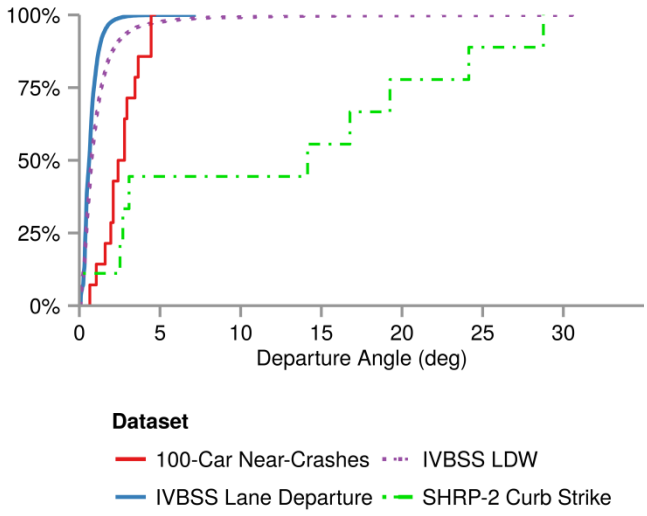


***Figure 6. Cumulative Distribution of Departure Angle in NDS Departure Events. SHRP-2 curb strike data includes 9 events with lane tracking during departure.***

Figure 7 shows the cumulative distribution of steering magnitude for the IVBSS LDW, IVBSS lane departure, and 100-Car near-crash datasets. Steering magnitude was defined as the largest absolute change in steering wheel angle from the steering wheel angle at departure. Data from the SHRP-2 curb strikes was excluded from the figure because few vehicles were equipped with steering wheel sensors. The instrumentation from the 100-Car study did not include a steering wheel sensor. Steering wheel angle was estimated for the 100-Car departure events by video tracking analysis using the over shoulder video view. Of the 32 departures, 18 had the steering wheel visible for video tracking analysis. Reasons for a non-visible steering wheel were dark conditions in the vehicle or the steering wheel being blocked by objects, e.g. papers or a book. The IVBSS vehicle instrumentation reported steering wheel angle to the nearest degree. The median steering magnitude was 5° for the IVBSS LDW events, 4° for the IVBSS lane departure events, and 48° for the 100-Car near-crashes. Because near-crashes often included emergency maneuvers to return to the lane to avoid a crash, the steering magnitudes were substantially higher than in the IVBSS datasets, where non-emergency maneuvers were taken to return to the lane. The mean steering wheel angle from the lane departure and LDW departures from IVBSS were statistically different according to an ANOVA.

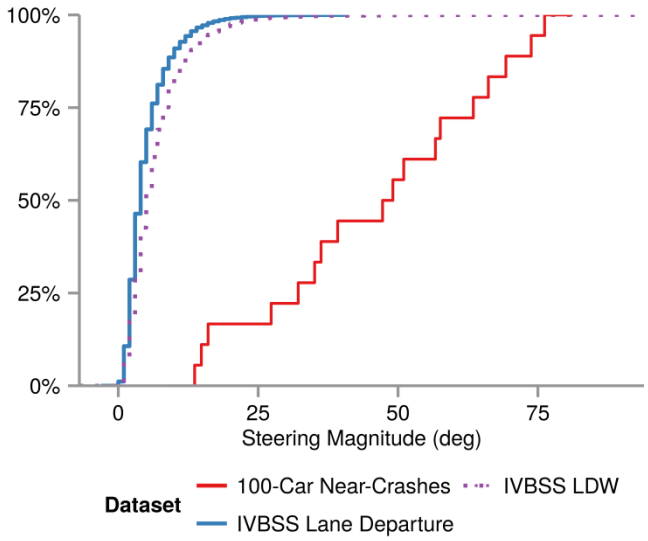


***Figure 7. Cumulative Distribution of Steering Input Magnitude after Departure in NDS Events.***

## DISCUSSION

This study compared several NDS lane departure event datasets to crash data with EDR downloads with the goal of determining how representative NDS events are of serious, tow-away severity crashes. This comparison was accomplished in two ways: 1) by comparing the sample of drivers and vehicles in each dataset and 2) by comparing the departure conditions and driver reactions after departure. The results showed that the populations included in each NDS dataset were different and therefore it is not surprising that the characteristics of these departures were also different.

The near-crash events from the 100-Car study and the SHRP-2 curb strike events more closely matched the conditions of the crash data than did the normal driving datasets from IVBSS. Younger drivers were overrepresented in the crash data, which was true for both the 100-Car and SHRP-2 samples, while IVBSS had a uniform distribution of ages by design. Males were also overrepresented in the crash data, which was true for the 100-Car near-crash events. The SHRP-2 curb strikes had a majority of female drivers. The IVBSS sampled was evenly distributed between males and females. Driver demographics may play an important role in driver behavior, as risk evaluation differs by both age and gender (Harris et al. 2006, Charlton et al. 2006). The datasets also differed in how lane departures were selected. The IVBSS events were selected using the lane tracking cameras, and as a result were restricted to highway driving at high speeds. The 100-Car near-crash and SHRP-2 curb strikes occurred at a larger range of speeds, similar to the crash data.

The differences in departure conditions between the crash/near-crash NDS and IVBSS were also reflected in the severity of departures and driver reactions to the departures. The near-crash and crash datasets had much higher departure angles and maximum lateral distance out of the lane. There was brake application before over half (52%) of departure crashes. By design, the IVBSS data excluded events with brake application, while the near-crash and curb strike data had 38% and 33% of events with brake application, respectively. Steering wheel input was also much larger in the 100-Car near-crashes compared to the IVBSS data (SHRP-2 near-crashes did not have sufficient steering wheel data to evaluate).

The differences in departure conditions in the NDS data may be important if the goal of the research is to replicate departure conditions and driver input in lane departure crashes. For example, designing a test track evaluation using the IVBSS data may produce departure conditions that are not representative of crash events. The moderate departure events, however, may still be correlated with crash risk (Guo et al. 2010) and thus are appropriate to use to evaluate the overall impact of LDW on drivers' lane keeping safety. The results of two previous analyses of the IVBSS LDW data found a statistically significant improvement in lane keeping safety metrics. One study found that the presence of LDW improved driver's lane keeping ability and decreased the number of departures per mile driven

(Sayer et al. 2011a). An independent analysis of the IVBSS also found a decreased rate of departure events with LDW active (Nodine et al. 2011). These trends are likely correlated with a driver's risk for involvement in serious departure crashes.

The NDS had different purposes and subject recruitment strategies. The 100-Car and IVBSS recruited drivers from a single geographical area (Washington D.C. and Ann Arbor, MI, respectively), while SHRP-2 was conducted in 6 study areas. IVBSS, however, had the purpose of evaluating prototype safety equipment while 100-Car and SHRP-2 had the sole purpose of monitoring normal driving in unmodified vehicles. It is possible the subjects recruited for IVBSS were early adopters of safety technology and as a result safer drivers than the subjects in the 100-Car and SHRP-2 studies. A limitation of the current study is that it is difficult to address subject recruitment differences in the post-hoc fashion used for this study.

From a statistical perspective, comparing the NASS/CDS data to the NDS datasets is a challenge. A standard technique to compare variables across multiple datasets is to perform an ANOVA on all data. The response in the model is the variable of interest and the main effect is the data source. This ANOVA will determine if there are significant differences in the mean of the variable across data sources. The NASS/CDS data are collected using a probability weighted complex survey design, not a random sample. In order to estimate variance, the survey design variables (clustering and strata) must be taken into account. The result is that traditional statistical analyses techniques, such ANOVA, cannot be performed on the NASS/CDS data.

Another statistical challenge is analyzing the large volume of events in the modern NDS datasets like IVBSS. Because traditional statistical methods like ANOVA are highly dependent on sample size, the massive number of samples makes almost all tests significant to the 95% confidence level. Another statistical challenge is modeling within- and between-driver variability. Research on appropriate statistical techniques for NDS data is ongoing (Kim et al. 2013; Zhang et al. 2012). There is a need for consensus on the methods that researchers should use when analyzing NDS data.

## CONCLUSIONS

The objective of this study was to compare departure events where LDW could have intervened that were extracted from crash and NDS data in order to determine if NDS data are representative of the crash data. The departure events examined were extracted from the NASS/CDS crash database, the IVBSS (two separate instrumentation triggered events), the 100-Car NDS (near-crash events), and the SHRP-2 NDS (curb strike events). The 100-Car and SHRP-2 NDS had a distribution of driver age and gender more similar to the crash data than the IVBSS subjects, who were equally distributed by design. Age and gender may affect risk of a departure occurring as well as driver response once a departure occurs. These differences in demographics may help explain why there were large differences in the departure characteristics between NDS and crash data. The IVBSS departure datasets had almost no brake application while the crash, 100-Car, and SHRP-2 data had 52%, 38%, and 33% of drivers applying the brakes, respectively. The IVBSS data were also selected using the lane tracking cameras, which restricted vehicle travel speeds above 42 kph (25 mph). The 100-Car and SHRP-2 events were selected by manual review of risky driving events identified from the instrumentation data. The near-crash and curb strike occurred at a wide range of travel speeds, although the median speeds were lower than the crash data. The differences in conditions may have also affected the severity of departure. The 100-Car near-crash and SHRP-2 curb strike departures had larger departure angles (2.6° and 14.1° median, respectively) and lateral excursion (0.63 m and 0.50 m median, respectively) compared to the IVBSS data (0.6° and 0.7° departure angle and 0.19 m and 0.10 m excursion for LDW and lane departure datasets, respectively). The results of this study suggest that both driver composition and event selection criteria in NDS datasets affect the evaluation of departure characteristics. Near-crash and crash severity NDS events are more representative of crash events compared to the normal driving used to create the IVBSS departure datasets. These differences are important when answering research questions where replicating conditions similar to crashes are important.

## ACKNOWLEDGEMENTS

The research team would like to acknowledge the Toyota Collaborative Safety Research Center (CSRC) and Toyota Motor Corporation for funding this study. The authors would like to thank Rini Sherony, Hiroyuki Takahashi, and Katsuhiko Iwazaki from Toyota for their helpful feedback to improve this research. The team would also like to

acknowledge the University of Michigan Transportation Research Institute (UMTRI) for providing access to the IVBSS data. We would also like to thank Jonathan Rupp, Scott Bogard, David LeBlanc, and Jim Sayer from UMTRI for their assistance in accessing and analyzing the IVBSS data. The research team would like to acknowledge the Virginia Tech Transportation Institute (VTTI) for providing access to the 100-Car and SHRP-2 data. The authors would like to thank Miguel Perez, Shane McLaughlin, Julie McClafferty, and Joel Kady from VTTI for their assistance.

**REFERENCES**

Charlton JL, Oxley J, Fildes B, et al. Characteristics of older drivers who adopt self-regulatory driving behaviours. *Transp. Res. Part F Traffic Psychol. Behav.* 2006;9(5):363-373. doi:10.1016/j.trf.2006.06.006.

Dingus TA, Klauer SG, Neale VL, et al. *The 100-Car Naturalistic Driving Study - Phase II Results of the 100-Car Field Experiment*. Washington, D.C.: National Highway Traffic Safety Administration; 2006.

Guo F, Klauer SG, Hankey JM, Dingus TA. Near Crashes as Crash Surrogate for Naturalistic Driving Studies. *Transp. Res. Rec. J. Transp. Res. Board* 2010; 2147: 66-74.

Harris CR, Jenkins M, Glaser D. Gender Differences in Risk Assessment: Why do Women Take Fewer Risks than Men? *Judgm. Decis. Mak.* 2006;1(1):48-63.

Kim S, Chen Z, Zhang Z, Simons-Morton B, Albert P. Bayesian hierarchical poisson regression models: an application to a driving study with kinematic events. *J American Statistical Association*. 2013;108(502):494-503.

Kusano KD, Gabler HC. Characterization of Lane Departure Crashes Using Event Data Recorders Extracted from Real-World Collisions. *SAE Int J Passeng Cars - Mech Syst* 2013;6(2):705-713. doi:10.4271/2013-01-0730.

Kusano KD, Gabler HC. Comprehensive Target Populations for Current Active Safety Systems using National Crash Databases. *Traffic Inj. Prev.* 2014;15(7):753-761. doi:10.1080/15389588.2013.871003.

Ljung Aust M. Defining Critical Events in Theory and in Practice, using the EuroFOT Database. In: *Second International Symposium on Future Active Safety Technology Toward Zero Traffic Accidents (FAST-zero'13).*; 2013.

McClafferty J, Hankey JM. *100-Car Reanalysis: Summary of Primary and Secondary Driver Characteristics*. Blacksburg, VA: The National Surface Transportation Safety Center for Excellence; 2010.

McLaughlin SB, Hankey JM, Klauer SG, Dingus TA. *Contributing Factors to Run-Off-Road Crashes and Near-Crashes*. Washington, D.C.: National Highway Traffic Safety Administration; 2009: Report Number DOT HS 811 079.

Montgomery J, Kusano KD, Gabler HC. Age and gender differences in time to collision at braking from the 100-car naturalistic driving study. Traffic Inj. Prev. 2014: 15 Suppl 1:S15-20.

Nodine E, Lam A, Stevens S, Razo M, Najm W. *Integrated Vehicle-Based Safety Systems (IVBSS) Light Vehicle Field Operational Test Independent Evaluation*. Washington D.C.: Research and Innovative Technology Administration; 2011: Report Number DOT HS 811 516.

Sayer J, LeBlanc D, Bogard S, et al. *Integrated Vehicle-Based Safety Systems Field Operational Test Plan*. University of Michigan Transportation Research Institute; 2008. Report Number UMTRI-2005-51. Available at http://deepblue.lib.umich.edu/bitstream/2027.42/62108/1/102281.pdf

Sayer JR, Bogard SE, Buonarosa ML, LeBlanc DJ, Funkhouser DS, Bao S, Blankespoor AD, Winkler CB. *Integrated Vehicle-Based Safety Systems Light-Vehicle Field Operational Test Key Findings Report*. Washington, D.C.: U.S. Department of Transportation, Research and Innovative Technology Administration; 2011a: Report Number DOT HS 811 416.

Sayer JR, LeBlanc DJ, Bogard SE, Funkhouser DS, Bao S, Buonarosa ML, Blankespoor AD. *Integrated Vehicle-Based Safety Systems Field Operational Test Final Program Report*. Washington, D.C.: U.S. Department of Transportation, Research and Innovative Technology Administration; 2011b: Report Number DOT HS 811 482.

Zhang Z, Albert PS, Simons-Morton B. Marginal analysis of longitudinal count data in long sequences: methods and applications to a driving study. *Annals of Applied Statistics*. 2012; 6(1):27-54

**APPENDIX: METHODOLOGY FOR RECONSTRUCTING DEPARTURE TRAJECTORIES FROM VEHICLE INSTRUMENTATION**

The method for reconstructing the departure events is summarized in Figure 8. First, the yaw rate and forward vehicle speed were integrated to determine the change in heading angle and curvature of the vehicle's path. These two signals were used to reconstruct the vehicle's X-Y position. If the road was curved, satellite imagery of the event site was used to determine the radius of curvature of the road. The vehicle GPS location data was used to locate the sites and the radius of curvature of the road was estimated using publically available satellite imagery and tools, Google Earth. The forward video view was used to approximate when the vehicle departed its lane and when it returned to its lane. The departure point was defined as when the vehicle's leading wheel first touched the lane line or road edge if there was no lane line. The end of the departure event was when the same wheel crossed the same lane line or road edge. Using the X,Y trajectory from the vehicle data, the road data, and the time off the road the departure angle of the trajectory was iteratively varied until it matched the recorded time off road. The departure angle was iterated by 0.05°. The departure angle that had the lowest error to the observed time out of lane was chosen as the departure angle.

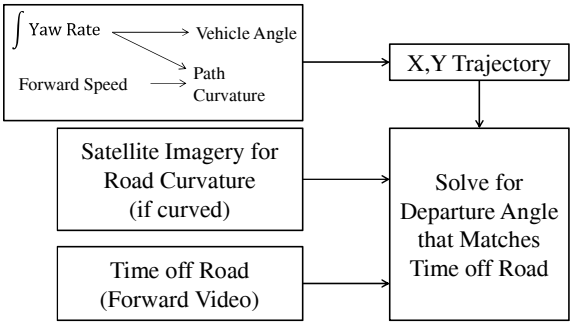


***Figure 8. Procedure for Determining Vehicle Trajectory from Naturalistic Driving Data.***

Consider a vehicle trajectory that has discrete points corresponding to each successive instrumentation measurement, shown in Figure 9. At time $j$ the vehicle has a heading angle $\theta_j$ and speed $v_j$. At the next time point, $j+1$, the vehicle has a heading $\theta_{j+1}$ and speed $v_{j+1}$.

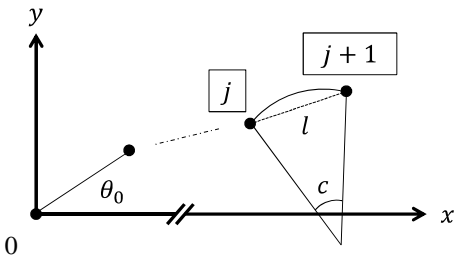


***Figure 9. Schematic of Determining Vehicle X-Y Trajectory from Vehicle Data.***

Between the time points, we assume the vehicle moves in a circular path that has a radius of curvature defined by the vehicle's yaw rate, $\omega_j$, and forward speed, $v_j$

$$r_j = \frac{v_j}{\omega_j} \quad (1).$$

The change in angle between point $j$ and $j+1$ is the difference between heading angles

$$c_j = \theta_{j+1} - \theta_j \quad (2).$$

Next, the chord length can be found using the geometric relationship

$$l_j = 2r_j \sin\frac{c_j}{2} \quad (3).$$

Finally, the coordinates of the next point can be found as

$$x_{j+1} = x_j + l_j \cos\theta_j \quad (4)$$

and

$$y_{j+1} = y_j + l_j \sin\theta_j \quad (5).$$

# Application of Biologically Inspired Visual Information Processing in Affective Driver Status Monitoring

**IL SONG HAN**
**WOO-SUP HAN**
Korea Advanced Institute of Science and Technology
Korea, Republic of

Paper Number 15-0150

**ABSTRACT**

Recent times have seen an increased interest in technologies of driver assistance. Understanding the driver's current status is crucial for the implementation of Advanced Driver Assistance System (ADAS) and Driver Status Monitoring (DSM). Emotional factors such as anger have been long attributed to aggressive driving behaviours and increased likelihood of road accidents. Therefore, being able to accurately detect the affective states of the vehicle occupant will be critical for enhanced safety and comfort.

In this paper, we present a methodology for the evaluation of the emotional states of vehicle drivers. The proposed approach performs an assessment of the emotional states by using combination of biologically inspired visual information processing and neural networks coupled with feedback mechanisms. The system consists of the following stages: (1) biologically inspired image pre-processing; (2) facial feature extraction; (3) multilayer perceptron for classification; and (4) feedback mechanism. The system has been preliminary validated by using data available from Japanese Female Facial Expression (JAFFE) database. Four affective states were identified and tested, which includes anger, sadness, and happiness. Subsequent tests have shown the successful detection rate of 91.3% with test images, and over 70% correct classification in images with Gaussian noises, respectively.

## INTRODUCTION

Recently there has been increasing attention towards automobile safety. According to the recent report by the UK government, road deaths have increased by 4% in the first quarter of 2014 compared to the previous year [**1**]. While the overall figure of fatalities has been under decline for the past decade, thanks to the improvement in medical treatment as well as the greater attention shown to the vulnerable road users such as the pedestrians and motor cyclists, the issue of road safety remains a key area for almost all nations in the world regardless of their wealth, with the fatality figure reaching over 1.2 million in the year 2010. Yet, only 28 nations in the entire world, which account for less than 450 million peoples of 7 billion world populations, are deemed to have sufficient legal measures to protect road users [**2**].

On the other hand, recent trends have shown that the developed nations are devoting a substantial amount of resources to improve road safety. In Britain, the government has spent £15.1 billion on the prevention of road accidents alone [**3**]. On a continental level, European Commission has launched a new EU Road Safety programme in 2010 as part of drive to cut the number of road fatalities by half between 2011-2020. All these findings show that the issue of road safety goes beyond the scope of industry.

Improving road safety comes in many different forms. The EU Road Safety programme has been divided into seven sub-sections: improving the education and training of road user; better enforcement of road rules; providing safer transport infrastructures; developing safer vehicles; promoting the use of modern technology to increase road safety; improving emergency and post-injuries services; and increased effort to protect vulnerable road users.

Within this paper, we have identified human emotions as one of the key influencers of driving performance. While most of existing Driver Monitoring System (DMS) focuses on drivers' concentration or drowsiness, another aspect of driver's status that deserves our attention is in emotion. Certain states of emotion, such as anger, and frustration can lead to aggressive and risky driving, which could result in accidents and fatalities. We believe that the accurate detection of emotional states from facial expressions is an important method to analyse and provide feedback to the vehicle driver's concentration level. Through successful recognition of emotional status, such as distraction, anger or frustration, it will be possible to improve the driving conditions and thereby safety of the vulnerable road users such as the pedestrians and cyclists.

We have applied image processing techniques and neural networks in the measurement of affective states based on still facial images in this study. The result of the finding can be used as a basis for future research in the application of affective computing in DMS.

There have been a number of studies which looked to present the feasibility of affective computing for improving road safety, and testing various methods of image processing in affective computing. It is notable that, despite numerous papers in the literature, there have been a minimal number of studies carried out on the use of image processing techniques coupled to neural networks in order to create an intelligent vision system which could evaluate human emotions.

## METHODS

### Biologically Inspired Orientation Filters

We claim that biologically inspired visual information processing offers a robust method for mimicking the robustness and flexibility of the primary visual cortex. One major strand of knowledge behind our current understanding of the behaviour of the primary visual cortex, an important brain area for vision, comes from the set of experiments by Torsten Hubel and David H. Wiesel [**4**]. Their experiment consisted of inserting microscopic electrodes into the visual cortex of experimental animals. This was used to read the activity of single cells in the visual cortex while presenting various stimuli to the animal's eyes.

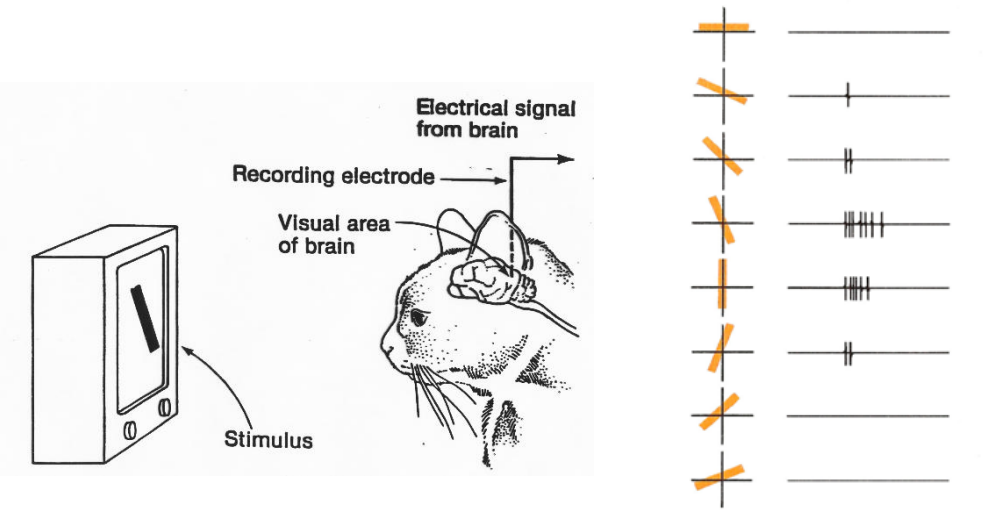


***Figure 1. Hubel & Wiesel's Experiment Setup (left), and the responses of the cat's cortex when a rectangular slit of light of different orientations is shown (right)***

They discovered that a topographical mapping in the cortex, i.e. that nearby cells in the cortex represented nearby regions in the visual field, i.e. that the visual cortex represents a spatial map of the visual field. Individual cells in the cortex, they found responded to the presence of edges in their region of the visual field. Furthermore, cells were found which would fire only in the presence of a vertical edge at a particular location in the visual field, while other nearby cells responded to edges of other orientations in that same region of the visual field. These orientation-sensitive cells were called "simple cells", and were found all over the primary visual cortex [**5**][**6**]

Based on Hubel and Wiesel's experimentation, the biologically inspired visual information processing incorporates the orientation selectivity of simple cell neurons to extract the features of facial images. The bahviour of the simple cells suggest that these cells possessed a patterned receptive field, with excitatory and inhibitory regions so that the cell would activate only if it received input (due to light) in the excitatory portion of its receptive field in the absence of input from the inhibitory portion. This operation is comparable to the operation of edge detection in image processing, which would process an image by spatial convolution with an edge filter [**7**].

We have simulated these biological operations through the application of multiple orientation filters for the feature processing of the facial expression. Our aim was to develop a filter which could accurately recreate the characteristics of the simple cells in mammalian visual cortex. These filters consist of six filters, each with specific orientation selectivity, yielding outputs of six orientation images for each input image (test image and reference image). Each set of six orientation filters provided orientation-selectivity for 0, 30, 45, 60, 90, and 135, degrees, and represents the receptive field properties of simple (linear) cells in V1.

Thus, the facial images were processed through this simulated simple cell function of the orientation selectivity and the six orientation images would then be combined to provide a resultant orientated image.

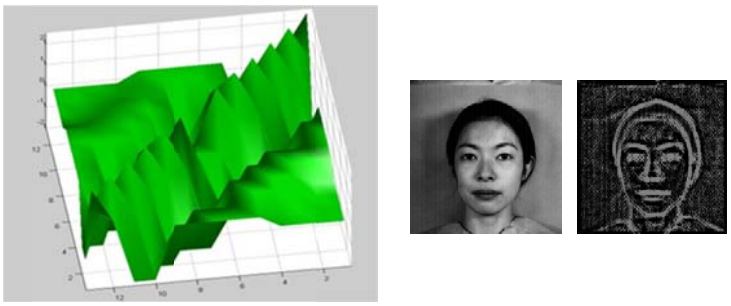

***Figure 2. Image filter for 45 degrees orientation selectivity (left), and how the input image (middle) compares to the image processed by the image filter (right)***

**Affective Computing and Facial Action Coding System (FACS)**

The resulting images have been then further processed to focus on the key 'regions of interest' (ROI). For determining the ROI, we have referenced results from contemporary researches in facial affect detection in the fields of affective computing. The detection and processing of facial expression has already been done through various methods such as, optical flow analysis, neural network, and active appearance model [**8**][**9**]. Facial affect detection can be done as a stand-alone affective computing system, and it can also be combined or fused alongside other modality (multimodal recognition, such as facial expression + speech pattern analysis or facial expression + hand gestures) to deliver a more robust analysis of the subject's emotional status. In this case, we have made use of Facial Action Coding System (FACS) for the purpose of determining ROI. FACS is one of the products of efforts to taxonomies human facial movements, and can be understood as an index list of facial expressions. Its foundation lies in Paul Ekman's cross-cultural research from the 1960s. His work suggested that affective expressions in face are not culturally determinant, but rather universal [**10**]. To support his points, Ekman carried out tests on Fore tribesmen in Papua New Guinea. The members of this tribe were not exposed to any contemporary emotional expressions, yet certain emotions – in particular six basic emotions: *anger*, *disgust*, *fear*, *happiness*, *sadness*, and *surprise*, were classified in the similar manner [**11**][**12**]. Thus, Ekman's study implied that certain facial expressions are biological in origin, and can be categorised with the same criteria.

While types of expressions which could be classified as the basic emotion have been under debate, the idea behind the various theories of emotion is the same. It suggests that the excluding core emotions, which could range between six to ten, all the other emotional states are simply synonyms of these core sets [**13**]. For our study, we have limited the emotive categories to be tested to four affective states of *happiness*, *sadness*, *anger* and *neutral*.

Thus, it is possible to demonstrate almost all facial expressions in terms of the fundamental actions of muscles, otherwise known as Action Units (AU) [**14**]. Every AU is independent of each other, and as such, a collection of AUs can be used to describe facial muscle movements including description of basic emotions. Ekman have incorporated FACS (Facial Action Coding System) into his research and provided corresponding AUs for each of the basic emotions, in addition to his own interpretation of their meaning. The six basic emotions of Ekman

would be described as shown in Table 1. In the context of affective computing, identification of emotional states using FACS code is known as EMFACS (Emotional facial Action Coding System), and they would concentrate on AU combinations related to emotional states. [**15**]

**Table 1.**
**Basic Emotions and Corresponding Action Units**

| **Emotion** | **Action Units (AU)** |
|---|---|
| Happiness | 6 ( 'cheek raiser') + 12 ('lip corner puller') |
| Sadness | 1 ('inner brow raiser') + 4 ('brow lowerer') + 15 ('Lip Corner Depressor') |
| Surprise | 1 ('inner brow raiser') + 2 ('outer brow raiser') + 5B ('Upper Lid Raiser*') + 26 ('Jaw Drop') |
| Fear | 1 ('inner brow raiser') + 2 ('outer brow raiser') + 4 ('brow lowerer') + 5 ('Upper Lid Raiser') + 7 ('Lid Tightener')+ 20 ('Lip Stretcher') + 26 ('Jaw Drop') |
| Anger | 4 ('brow lowerer') + 5 ('Upper Lid Raiser') + 7 ('Lid Tightener') + 23 ('Lip Tightener') |
| Disgust | 9 ('Nose Wrinkler') + 15 ('Lip Corner Depressor') + 16 ('Lower Lip Depressor') |

**Determining Regions of Interest (ROI)**

The actual process of calculating ROI has been done through detection of eyes and subsequent establishment of centre points between the eyes as the reference point through template based object recognition of eyes. From here, relevant AUs can be analysed for both the input image and neutral 'reference' image to which it would be compared against, as shown below. (**figure!**)

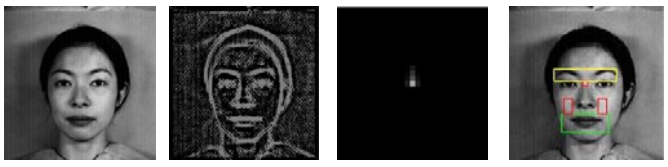

***Figure 3. (from left) Input image, orientation image, detection of central point between two eyes as the reference location of calculating the ROIs, and how the calculated ROIs appear in the original input image.***

Tests show that eye locations were detected successfully in both frontal and side facial image, demonstrating the effectiveness of combination of orientation selective feature extraction and feature based object recognition. This would, in turn, allow for measuring the level of driver attentiveness in road driving

situations. Subsequently, the detection of emotion (happiness, anger, or etc.) was based on the evaluation of processed facial features of selected areas.

**Neutral Network**

One of the requirements in developing a reliable warning system would be to provide feedback to the driver, whenever the driver would go into an extreme emotional state. To achieve this aim, it was important to detect which emotional state was the subject under, as certain emotive states are more counterproductive to safe driving than the other. However, more crucial aspect was in ensuring that neutral states of the subject was not being misinterpreted as an emotional state of any category. In this regards, an output of 1 (safe / neutral state) or 0 (unsafe / emotional state) would provide a sufficient result. The proposed system is designed to improve the successful detection of safe or unsafe emotional status of a driver, by tuning the ROI salience data encoding with the weight to the neural network input for improving the ordinary neural networks of Multi-Layer Perceptron (MLP).

Our input data would consist of analysed ROIs from the test and the reference images. This would be yielded by the data set of 90 images processed by the multiple orientation filters. The six data extracvted from six ROI were applied to the MLP to be classified into four emotional status, i.e. 'Neutral', 'Angry', 'Happy' and 'Sad'. The MLP of two hidden layers is designed to produce 4 outputs, which was implemented using the MATLAB neural network tool box.

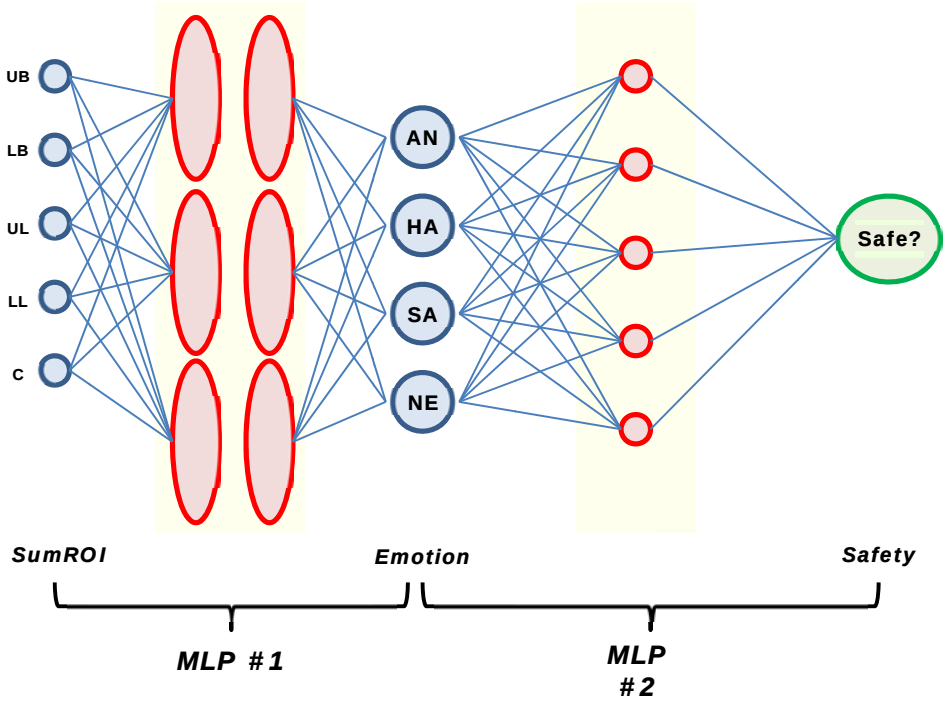


*Figure 4: Design of proposed neural network system*

During the design phase, the optimum network structure of 5x10x10x4 was determined by iterative trials of various network architectures with the observation of weight value distribution. The image processed by multiple orientation filters is assumed to be consistent in facial direction, size or scale.

The purpose of monitoring the driver's emotional status is attained by detecting the neutral emotional status as *safe* and the other status as *unsafe*, using the MLP of 4x10x5x1. The upper part of networks (4x10x5x1) is trained by an ideal situation, while lower part of networks (5x10x10x4) is trained by the back propagation learning using processed image data set.

**Feedback Mechanism**

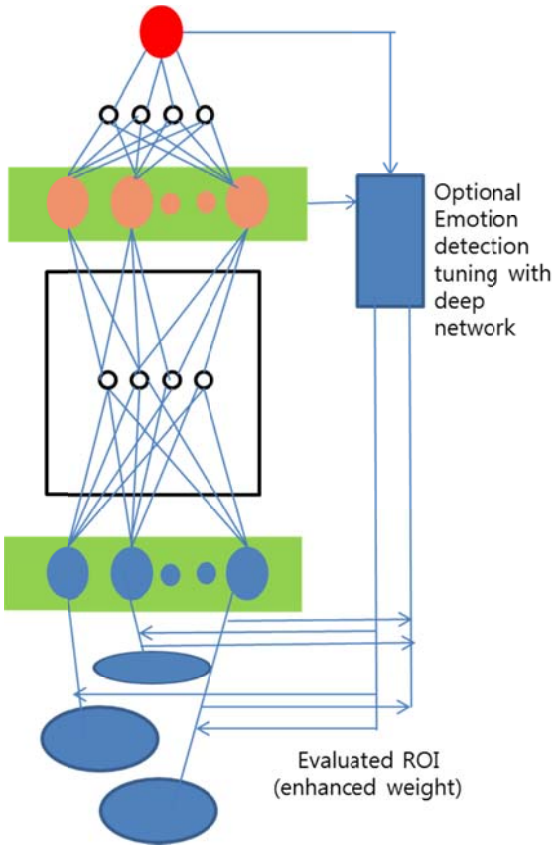


***Figure 5. Proposed emotion classification system with weight tuning or learning at an early stage.***

We stated in the introduction that our initial purpose was to develop a warning system which could provide an alert to the driver, whenever the driver would go into an extreme emotional state. To achieve this aim, it was important to detect which emotional state was the subject under, as certain emotive states are more counterproductive to safe driving than the other. However, more crucial aspect was in ensuring that neutral states of the subject was not being misinterpreted as an emotional state of any category. In this regards, an output of 1 (safe / neutral state) or 0 (unsafe / emotional state) would provide a sufficient result. The proposed system is designed to improve the successful detection of safe or unsafe emotional status of a driver, by tuning the ROI salience data encoding with the weight to the neural network input for improving the ordinary neural networks of MLP.

In addition to cascaded neural networks of MLP explained previously, the feedback to ROI is applied by the trained upper and lower networks of MLP. In case of failed detection of safety monitoring output, the encoding of ROI values to neural input is subject to the feedback with the lower weight, for the pre-analysed ROI for the largest value of emotional status – which is the main contributor to the detection failure. The feedback rate to ROI applied to neural network is a fixed value and the selection of ROI is controlled by the ROI value and the input status of upper network when feedback is required, for this framework. The method of deep network is scope of investigation by evaluating the effectiveness and relevance to the performance of the target function.

## DATA SOURCES

The accuracy of the emotion detection was measured by tests carried out on the JAFFE database, through processing with two feedforward neural networks (multi-layer perceptrons) and the feedback mechanism based on a deep learning concept. The biologically inspired visual information processing showed a significantly high accuracy to emotion recognition without the need for precise matching or complex computation. This was superseded by mimicking the primary function of the simple cell of visual cortex, which provided a degree of robustness by maintaining accuracy even in test images with Gaussian noises.

## RESULTS

Based on the data set of 360 images, the overall rate of detection returned over 91.3% accuracy, as shown in the Table 2 below. The proposed method of combining biologically inspired visual information processing with multilayer perceptron also gave a satisfactory performance, maintaining a 70+% accuracy level up to 5% Gaussian noise level. Investigation of deep-learning inspired feedback mechanism also yielded an improved performance, resulting in 27.2% reduction in the occurrence of false-positives.

**Table 2.**
**Result of Biologically Inspired Visual Information Processing & Multilayer Perceptron**

| Input Class | Output Classification Result | | | | Accurate Classification Rate |
|---|---|---|---|---|---|
| | Happy | Angry | Sadness | Neutral | |
| Happy | 81 | 1 | 7 | 1 | 90.0 % (81 / 90) |
| Angry | 0 | 90 | 0 | 0 | 100.0 % (90 / 90) |
| Sad | 2 | 2 | 78 | 8 | 86.7 % (78 / 90) |
| Neutral | 2 | 0 | 8 | 80 | 88.9 % (80 / 90) |

Compared to the comparative studies carried out in affective computing, combination of biologically inspired visual information processing and MLP have outperformed methods based on artificial neural networks (ANNs; 84% accuracy) and combination of Sequential Floating Forward Search (SFFS), Fisher Projection (FP), and K-nearest neighbour algorithm (KNN; 81% accuracy) [**16**].

In depth review of biologically inspired visual information processing approach revealed certain patterns of interest. It was demonstrated that four emotional states (happiness, anger, sadness, and neutral) can be successfully classified with a small number of variables. Yet there were some level of differences as to how accurately each emotion was classified by biologically inspired visual information processing approach.

Angry emotional state was most likely to be detected with accuracy, with 100.0% successful detection rate, followed by happy emotional state with 90.0% classification accuracy. Sad emotional state had the most inaccurate incidents of classifications, which has also been documented in previous researches [**17**]. Reason for this difficulty could be attributed in parts to the comparative lack of facial expression in sad emotional state.

Compared to anger, which involves composite movements of eyebrows, competitive movements of eyelids, and major movement in lip areas, sadness would be expressed by movement of eyebrows and small movement to the corner of the lips. Even in real-life situations, detecting expression of subtle sadness is a challenge, and it is possible to infer such factors have been represented in the test results as well.

Further tests were carried out to determine the robustness of biologically inspired visual information processing approach, through introducing Gaussian noise to the images. This was done in order to examine its applicability in real life situations, where the image data is often corrupted. The results of classification with noisy test images showed a reduction of 16.01% in detection rate at 1% noise level, and maintained over 70% level of accuracy even at 10% noise level.

**Table 3.**
**Detection rate (%) of biologically inspired visual information processing method with different level of Gaussian noise**

| Noise Level | SumROI(G) | SumROI(M) |
|---|---|---|
| 0.0% | 78.7 | 91.7 |
| 1.0% | 76.4 | 79.1 |
| 2.5% | 73.1 | 75.7 |
| 5.0% | 68.8 | 73.5 |
| 10.0% | 64.1 | 65.9 |

## DISCUSSIONS AND LIMITATIONS

In this study, our proposed model for identifying affective states required the presence of a neutral emotive state, which would be used as a reference. While it is theoretically possible to process an individual's emotional status from a single image without any reference, in reality, there is a wide variability to the strength of human expression even within same emotive state. This variability is deemed dependent on the cultural, national, regional and gender difference of the subject [**18**]. This had also been reinforced during the analysis of datasets: that absolute values of expression within an individual cannot be used as a reliable measure. Further tests and statistical analysis could be carried out in the future as a means to develop an accurate and reliable indicator of emotive states based on input image alone.

Another challenge we have recognised during the experiments was that there are at least two kinds to the expression of emotions – genuine and fake. A fake expression often differs from a genuine expression. For example, in case of happiness, only the zygomatic major muscle, which runs from the cheekbone to the corner of lips, moves in case of fake emotional status. On the other hand, a genuine expression of happiness would involve movement of orbicularis oculi and pars lateralis (eyebrows) as well as zygomatic major. In addition to limited facial muscle movements, fake emotive states are also known to contain a certain degree of asymmetry [**19**],[**20**].

On the other hand, for certain emotional states in JAFFE dataset, there were very little expressions present. In comparison to the neutral image, even human vision had difficulty in determining the emotional state without the label.

Further investigation of other facial affection database has shown that this issue isn't unique to JAFFE database, as demonstrated in the figures below.

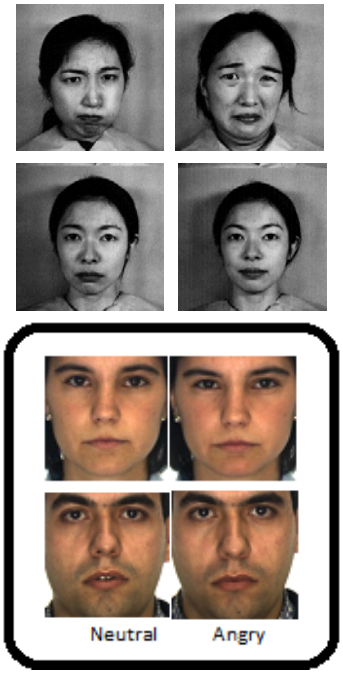


***Figure 6.Limitations of dataset***
***Top Row: Examples of 'fake' emotion – asymmetry is clearly visible in the fake facial expression***
***Middle Row: Images displaying supposed expression of sadness (left) and neutral (right).***
***Notice the lack of difference between this image and that of the neutral state (right).***
***Black Box: Example of angry and neutral emotion from an alternative database.***
***Without the labels, it would be challenging to determine that left image is demonstrating anger and the right one is of the neutral emotional state.***

## CONCLUSIONS AND RELEVANCE TO THE SESSION SUBMITTED

We believe this research has produced a foundation from which further studies could be carried out. For example, would be in refining the biologically visual information processing approach. We have recognised that there are at least two kinds to the expression of emotions – genuine and fake. Within the context of driver monitoring system, fake emotions are unnecessary and should be ignored. Further studies carried out with images of emotions in real-life situations could provide a better training for the monitoring system capable of demarcating two categories.

Secondly, we have worked with the assumption of only neutral emotional states allowing for ideal driving situations. This hypothesis is under discussion within affective computing research, and will be given further updates in the coming time.

## ACKNOWLEDGEMENT

The research was partly promoted as part of 'Technology Development for Behavior Improvement and Violation Control of High Risk Drivers' that was carried out by Ministry of Land, Infrastructure and Transport in Korea.

## REFERENCES


[1] Reported Road Casualties in Great Britain: Quarterly Provisional Estimates Q1 2014. (2014). London: Department for Transport.

[2] World Health Organization. (2013). *WHO global status report on road safety 2013: supporting a decade of action*. World Health Organization.

[3] Reported Road Casualties in Great Britain: 2012 Annual Report. (2014). *Statistical Releases.* London: Department for Transport.

[4] Hubel, D. H., & Wiesel, T. N. (1962). Receptive fields, binocular interaction and functional architecture in the cat's visual cortex, *The Journal of Physiology*, 160(1), 106.

[5] Han, W. S., & Han, I. S. (2014). All Weather Human Detection Using Neuromorphic Visual Processing. In *Intelligent Systems for Science and Information* (pp. 25-44). Springer International Publishing.

[6] Han, I. S. and Han, W. S. (2014). Robust Detection of Pedestrian/Cyclist by Neuromorphic Visual Processing, In *FISITA 2014 World Automotive Congress, 2-6 June 2014.*

[7] Jhuang, H., Serre, T., Wolf, L., & Poggio, T. (2007, October). A biologically inspired system for action recognition, *IEEE 11th International Conference on Computer Vision, 2007. ICCV 2007.* (pp. 1-8). IEEE.

[8] Picard, R. W. (2010). Affective computing: from laughter to IEEE, *IEEE Transactions on Affective Computing*, 1(1), 11-17.

[9] Hudlicka, E. (2003). To feel or not to feel: The role of affect in human–computer interaction. *International Journal of Human-Computer Studies*, 59(1), 1-32.

[10] Ekman, P. (1992). An argument for basic emotions, *Cognition and Emotion*, 6(3-4), 169-200.

[11] Ekman, P. E., & Davidson, R. J. (1994). *The Nature of Emotion: Fundamental Questions*, Oxford University Press.

[12] Izard, C. E. (1992). Basic emotions, relations among emotions, and emotion-cognition relations, *Psychological Review*. 99(3):561-5

[13] Beck, J. S. (1995). *Cognitive Therapy*. John Wiley & Sons, Inc.

[14] Ekman, P., & Rosenberg, E. L. (eds.). (1997). *What the Face Reveals: Basic and Applied Studies of Spontaneous Expression Using the Facial Action Coding System (FACS).* Oxford University Press.

[15] Kanade, T., Cohn, J. F., & Tian, Y. (2000). Comprehensive database for facial expression analysis, *Proceedings of Fourth IEEE International Conference on Automatic Face and Gesture Recognition, 2000.* (pp. 46-53). IEEE.

[16] Kolodyazhniy, V., Kreibig, S. D., Gross, J. J., Roth, W. T., & Wilhelm, F. H. (2011). An affective computing approach to physiological emotion specificity: Toward subject-independent and stimulus-independent classification of film-induced emotions, *Psychophysiology*, 48(7), 908-922.

[17] Picard, R. W., Vyzas, E., & Healey, J. (2001). Toward machine emotional intelligence: Analysis of affective physiological state, *IEEE Transactions on Pattern Analysis and Machine Intelligence*, 23(10), 1175-1191.

[18] Ekman, P., & Rosenberg, E. L. (eds.). (1997). *What the Face Reveals: Basic and Applied Studies of Spontaneous Expression Using the Facial Action Coding System (FACS).* Oxford University Press.

[19] Ekman, P., Davidson, R. J., & Friesen, W. V. (1990). The Duchenne smile: Emotional expression and brain physiology: II. *Journal of Personality and Social Psychology*, 58(2), 342.

[20] Shackelford, T. K., & Larsen, R. J. (1997). Facial asymmetry as an indicator of psychological, emotional, and physiological distress. *Journal of personality and social psychology*, *72*(2), 456.

[21] W. Han (2014). Multiple Direction Filter as the Feature Map for Image Analysis of Affective Computing. MSc thesis. Imperial College London

# A STUDY ON TOUGHENED GLASS USED FOR VEHICLES AND ITS TESTING METHODS

**Kwang-bum, Lee**
**Hae-boung, Kwon**
**Ho-soon, Ahn**
**Sang-woo, Jeon**
TS KATRI(Korea Automobile Testing & Research Institute )
Republic of Korea
**Young-sam, Son**
MOLIT(Ministry of Land, Infrastructure and Transport)
Republic of Korea

Paper Number 15-0152

Key words: toughened glass, ball drop test, ceramic-printed toughened glass.

## ABSTRACT

Toughened glass for vehicles is used for most window glass, except for windshield glass, and in particular is also generally used for sunroofs installed on the roofs of vehicles. Toughened glass is known to have external impact resistance that is about four times stronger than original glass.
We would like to verify that ceramic-printed toughened glass does not meet of GTR(Global Technical Regulations) No. 6 and its strength is lower than original glass through tests.
The tests were conducted with the test piece of original glass, toughened glass, and ceramic-printed toughened glass from five glass manufacturers. In Test 1, a 227g steel ball was dropped from a height of 2 meters, and damage was checked according to the test method of GTR No. 6, and in Test 2, a steel ball was freely dropped from different heights and limited damage height was determined.
In the result of Test 1 according to the test method of GTR No. 6, while all five test pieces of toughened glass were not damaged, all the ceramic-printed toughened glass from the five manufacturers were damaged.
In the result of Test 2, none of the five test pieces of toughened glass were damaged by a 10m ball drop, the original glasses were damaged by an average of 3m ball drop, and the ceramic-printed toughened glasses were damaged by an average of 1.4m ball drop.
As the results of the tests show, ceramic-printed toughened glass does not have the features of toughened glass due to its very low strength.
Therefore, we would like to contribute to the safety of consumers by considering the GTR No.6, and by revising the toughened glass test method.

## 1. INTRODUCTION

Vehicle manufacturers have broadened the ceramic-printed area of toughened glass to improve the external design of vehicles and the attachment of glass to the vehicle body.
The panoramic sunroofs of vehicles are mainly made of toughened glass, and the ceramic-printed area accounts for 30~70%.
According to the details of reports from a vehicle defect reporting center of the Republic of Korea, the defect reports related to panoramic sunroof damage have been increasing in recent years. Therefore, we believe that as the ceramic-printed area has been broadened, the damage of toughened glass that is vulnerable to external impacts have also been increasing, and so have the complaints of consumers.
Hence, we would like to verify the vulnerability of ceramic-printed toughened glass through the test and consider the test method of GTR No. 6.

## 2. TYPE AND DEFINITION FOR VEHICLE GLASS

**a.** **Laminated Glass:** Means glazing consisting of two of more layers of glass held together by one or more inter-layers of plastic material.

**b.** **Toughened glass:** Means glazing consisting of a single layer of glass which has been subjected to special treatment to increase its mechanical strength and to condition its fragmentation after shattering.

**c. Double Glazing:** Double-glazed unit means an assembly of two panes permanently assembled in manufacture and separated by a gap.

**d. Glass-plastic Combination Glass:** Glass-plastic means glazing consisting of any glazing material which comprises one layer of glass and one or more layers of plastic in which a plastic surface of the product faces the inner side.

**e. Original Glass:** This is the glass pane before the process to make safe glass for vehicle.

**f. Ceramic-printed Toughened Glass:** This is the toughened glass which has been toughened after ceramic printing.

## 3. BALL DROP IMPACT STRENGTH TEST FOR GLASSES

### a. Test Purpose

The purpose is to investigate what result comes out when ceramic-printed toughened glass is tested for GTR No. 6 and to compare the impact strength of ceramic-printed toughened glass and original glass.

### b. 227 g Ball Drop Test

- **<u>Test equipment</u>**

  - Steel ball: Hardened-steel ball with a mass of 227 g ± 2 g and a diameter of approximately 38 ㎜.
  - Support for ball tests: Supporting fixture, such as that shown in Figure 1, composed of steel frames, with machined borders 15 mm wide, fitting one over the other and faced with rubber gaskets 3 mm thick and 15 mm wide and of hardness 50 ±10 International Rubber Hardness Degree (IRHD).
    The lower frame rests on a steel box 150 mm high. The test piece is held in place by the upper frame, the mass of which is 3 kg. The supporting frame is welded onto a sheet of steel 12 mm thick resting on the floor with an interposed sheet of rubber 3 mm thick and of hardness 50 ± 10 IRHD.
    Figure 1 shows the supporting fixture used for the test and Figure 2 shows the whole device for the ball drop test.

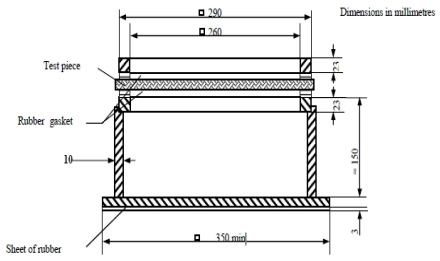


*Figure 1. Drawing of Supporter*

*Figure 2. The test equipment for the ball drop test*

- **<u>Test piece</u>**

  - The test piece is manufactured flat, with a size of 300 X 300 ㎜.
  - The thickness of the test piece, which is used for panoramic sunroofs, is 4 ㎜ ± 0.2 ㎜.
  - Type of test piece: Three type of toughened glass, ceramic-printed toughened glass, and original glass from five manufactures. The test piece are marked A, B, C, D, and E.

- **Test 1**

  - Test method: Test according to GTR No. 6
  - Procedure
    ① When a 227 g ball drop test is conducted at a height of 2.0 m $\pm {}^{5}_{0}$ ㎜, the test piece shall not break.
    ② Six test pieces shall be tested and at least five shall meet the requirements.
  - Result of Test 1

**Table 1. Result of Test 1(Number of Pass/Number of Tests)**

| Type of Glass | A | B | C | D | E |
|---|---|---|---|---|---|
| Original Glass | Pass(6/6) | Fail(4/6) | Pass(6/6) | Pass(6/6) | Pass(6/6) |
| Toughened Glass | Pass(6/6) | Pass(6/6) | Pass(6/6) | Pass(6/6) | Pass(6/6) |
| Ceramic-printed Toughened Glass | Fail(0/6) | Fail(0/6) | Fail(0/6) | Fail(0/6) | Fail(1/6) |

As shown in Table 1, the original glass met of GTR No. 6 except for test piece B, and all test pieces of toughened glass met the regulation. However, none of the test pieces of ceramic-printed toughened glass met GTR No. 6.

- **Test 2**

  - Test method: A 227 g ball is dropped every 20 ㎝ from a higher position starting at 1 m till the test piece is broken. When the test piece is broken, the same test piece is tested at the same height.
  - Procedure: When two sheets are damaged at the same height in a row, the height at which test pieces broken shall be taken.
  - Result of Test 2.

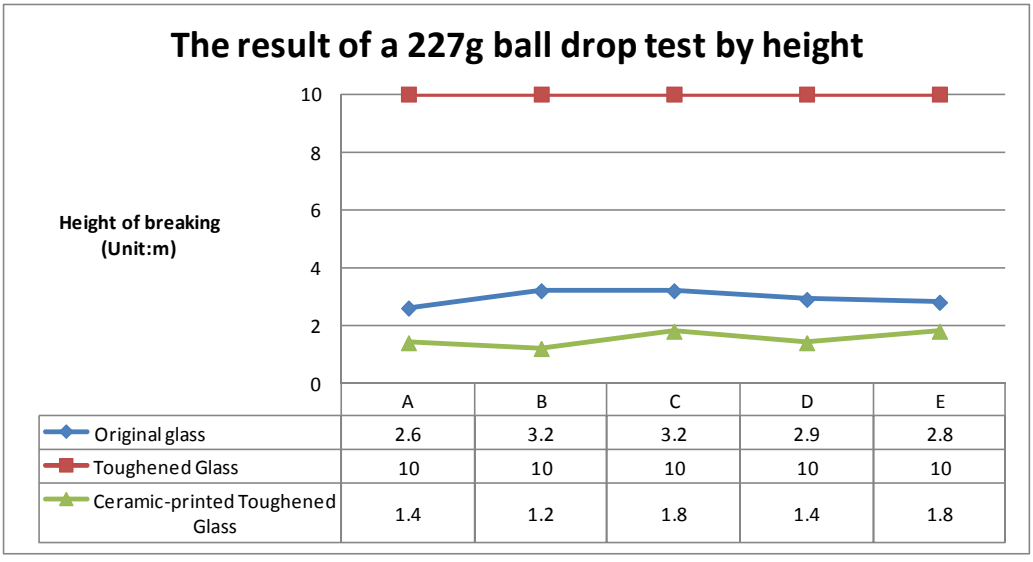


***Figure 3. Result of Test 2***

As shown in Figure 3, original glass was damaged at an average ball drop height of 3 m. while toughened glass was not damaged at a ball drop height of 10 m. However, ceramic-printed toughened glass was damaged at average height of 1.4 m. Also, the damage height of ceramic-printed toughened glass is lower than the damage height of original glass, showing vulnerability to external impact strength.
Ceramic-printed toughened glass does not meet the feature of toughened glass defined in GTR No. 6 in terms of strength.

## 4. VULNERABILITY OF CERAMIC-PRINTED TOUGHENED GLASS

### a. Toughened Glass Manufacturing Process

The manufacturing process of toughened glass is divided into a pre-treatment process and a toughening process. During the pretreatment process, original glass is cut and ceramic is printed and dried. And during the toughening process, pretreated glass is put into a heating furnace and heated at 600~700℃. And then curvature is given to the glass and it is toughened through a cooling technique (rapid cooling, etc.). Figure 4 shows the manufacturing process of toughened glass by phase.

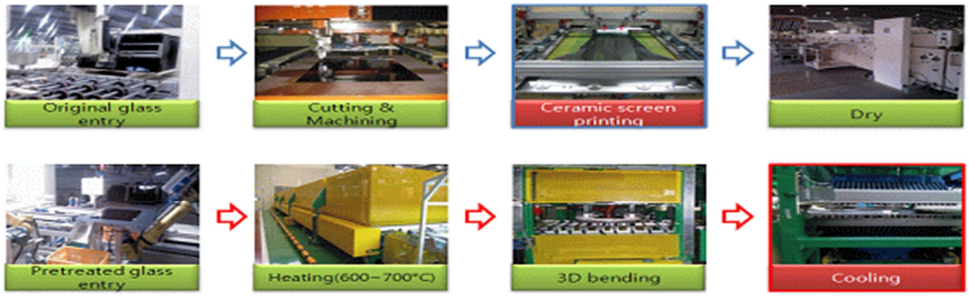


*Figure 4. Manufacturing process of toughened glass*

### b. Stress Distribution of Toughened Glass

In toughened glass finished with a toughening treatment, both outside surfaces are very stable due to compression stress, while the inside is very unstable due to tension stress. Figure 5 shows the stress distribution of general toughened glass.

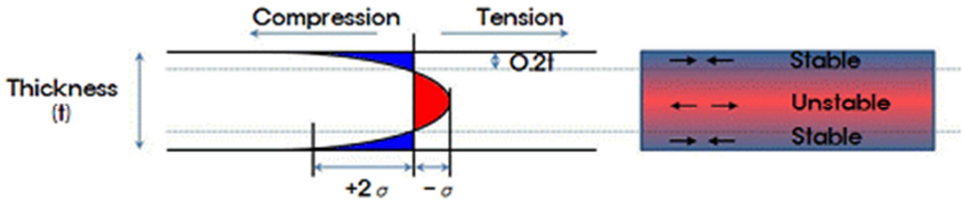


*Figure 5. Stress distribution map of cross section of toughened glass*

### c. Ceramic Printing of Toughened Glass

During the pretreatment process, enamel paint, which is composed of frit, pigment, and medium, is printed on original glass and dried. The glass is then fused with high heat in a furnace at a high temperature. Figure 6 shows the ceramic printing and fusing process of toughened glass.
The reason for ceramic printing is the necessity of having a rough ceramic surface to maintain strong adhesive strength when glass is attached to a vehicle body. The other reasons are the concealment of interior materials and blocking of UV rays.

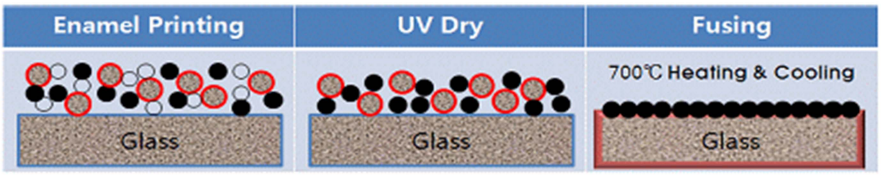


*Figure 6. Ceramic melting process of toughened glass*

※ **Enamal materials:** **Frit,** **Pigment(Ceramic),** **Medium**

### d. Reason why Ceramic-printed Toughened Glass is Vulnerable

Ceramic fusion of toughened glass makes the glass surface very unstable because it hampers the formation of compression stress on the surface. Figure 7 shows the stress distribution of ceramic-printed toughened glass. The ceramic-printed layer hampers the toughening of glass on the outside surface and marks unstable tension stress work.
Therefore, it can be damaged by a small impact more easily than original glass.

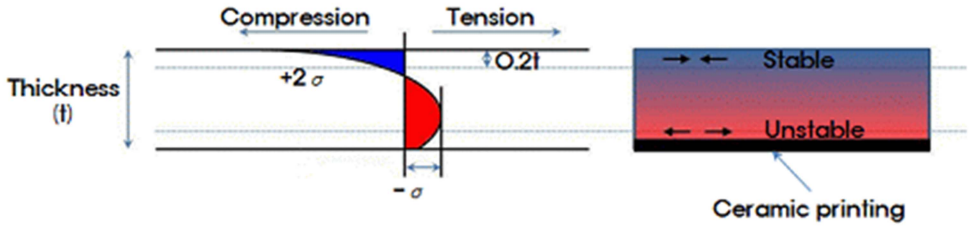


*Figure 7. Stress distribution of ceramic-printed toughened glass*

### e. Case of Ceramic-printed Toughened Glass

Ceramic-printed toughened glass is used for most vehicles. As shown in Figure 8, it is used for sunroofs, side window glass, and rear window glass.

| | | |
|---|---|---|
| | | |
| Panoramic sunroof | Side window glass of van | Rear window glass of sedan |

*Figure 8. Use case of ceramic-printed toughened glass*

### f. Damage Cases of Ceramic-printed Toughened Glass

Figure 9 shows cases of damage to ceramic-printed toughened glass by external impacts. In all cases, the ceramic-printed area is damaged.

*Figure 9. Damage case of ceramic-printed toughened glass*

## 5. CONSIDERATION OF SAFETY REGULATION FOR TOUGHENED GLASS FOR VEHICLES

### a. The Global Technical Regulation of Toughened Glass for Vehicles(GTR No. 6)

**Global technical regulation No. 6**

<A. STATEMENT OF TECHNICAL RATIONALE AND JUSTIFICATION>

30. The purpose of the 227 g steel ball test is to assess the resistance of the glazing to impacts from stones or other flying objects that might be encountered in everyday use.

<B. TEXT OF REGULATION>

3.3.7. **Uniformly toughened -glass** : means glazing consisting of a single layer of glass which has been subjected to special treatment **to increase its mechanical strength** and to condition its fragmentation after shattering.

6.3.4.1. The test pieces shall be flat samples measuring 300 x 300 mm, **specially made or cut** from the flattest part of a windscreen or pane.

6.3.4.2. Test pieces **can alternatively be finished products** that may be supported over the apparatus described in paragraph 6.3.1.

6.3.4.3. If the test pieces are curved, care should be taken to ensure adequate contact with the support.

6.3.2.3. The point of impact shall be within 25 mm of **the centre of the supported area** for a drop height less than or equal to 6 m, and within 50 mm of the centre of the supported area for a drop height greater than 6 m.

### b. Analysis of GTR No. 6

The features of toughened glass for vehicles can be divided into two things. First, the external impact strength is three to four stronger than original glass. Second, when it is damaged it breaks into small pieces without sharp points.
GTR No. 6 provides a 227 g ball drop test to evaluate external impact strength, the feature of toughened glass, and fracture test to evaluate if it is broken into small pieces without sharp points.
The height of the ball drop test provided in GTR No. 6 is 2 m. This is lower than the height of damage of original glass in our test. Therefore, to evaluate the mechanical strength of toughened glass, setting the 227 g ball drop height as more than or equal to 3 m should be considered.
Also, if toughened glass has a ceramic-printed area, it cannot be regarded as equal to toughened glass. Therefore, the test method for ceramic-printed toughened glass needs to be provided separately.
For your reference, there is the item that heated wire installed in window glass is excluded from tests in UN Regulation No. 43, “Uniform provisions concerning the approval of safety glazing materials and their

installation on vehicles." It is considered that the device needed to secure a view rather than the strength of glass is allowable regardless of strength.

**Regulations No. 43**

**<ANNEX 5>**

3.1. 227g ball test
3.1.1. Indices of difficulty of the secondary characteristics.

| Material | Index of difficulty | Colouring | Index of difficulty |
|---|---|---|---|
| Polished glass<br>Float glass<br>Sheet glass | 2<br>1<br>1 | Colourless<br>tinted | 1<br>2 |

The other secondary characteristic (**namely, incorporation or otherwise of conductors**)is not involved.

## 6. CONCLUSION

Ceramic printing technology, the surface process technology of toughened glass, was evaluated as an innovative technology when it was developed. It is said the development of this technology has reduced the production process for the attachment of window glass to vehicle bodies and improved durability. Also, the design of a vehicle body has freely gone luxe, and UV rays can be blocked. In this way, ceramic printing has a lot of benefits.
Because of these many benefits, the ceramic-printed area in the toughened glass has been broadened. In particular, as panoramic sunroof-equipped vehicles became popular, the ceramic area went bigger in design, and vehicles with ceramic-printed toughened glass account for as much as over 70% of vehicles.
However, it was confirmed that the ceramic-printed area of toughened glass has the drawback that its strength was lower than original glass, as shown in table 1 and Figure 3.
Therefore, as it is vulnerable to small external impacts or vibration, it leads to the damage of the whole toughened glass. In particular, in the case of a sunroof, which is installed above the head of a driver, if the glass is damaged, the glass fragments fall onto the head of the driver and threaten safe driving.
Hence, it is considered that if ceramic printing is necessary for toughened glass for a vehicle, it should be applied in the minimum area needed for the attachment of glass to the vehicle body.
The low strength of the ceramic printed area of toughened glass, which was determined in this study, is expected to be overcome through technology development for ceramic painting or various kinds of surface treatment technology. If it cannot be overcome with current technology, the safety regulation for window glass should be revised to minimize the risk. Therefore, it is believed that regulation of the ceramic-printed area of glass through the revision of the current regulation can contribute to safe driving.

RERERENCE

[1] Motor Vehicle Safety Standard of Korea, Article 34 "Window Glass", Article 105 "Stability of Window Glass"

[2] UN ECE Regulation No. 43 "UNIFORM PROVISIONS CONCERNING THE APPROVAL OF SAFETY CLAZING MATERIALS" Revision 1, Revision2 and Revision 3.

[3] FMVSS 571.205 Standard No. 205 "Glazing materials".

[4] SAE Standard ANSI / SAE Z26.1-1996.

[5] UN Global Technical Regulation No. 6 "SAFETY GLAZING MATERIALS FOR MOTOR VEHICLE AND MOTOR VEHICLE EQUIPMENT" 12 March 2008.

[6] KAC Homepage 'http://kac.kccworld.co.kr'

[7] HANGLAS Homepage ‘http://www.hanglas.co.kr/auto/’

[8] NSG Group Homepage ‘http://www.nsg.com/en/our-businesses/automotive’

**Investigation of the Influence of the Centre of Gravity Position on the Course of Vehicle Rollover**

**Andrzej Reński**
Warsaw University of Technology,
Poland

Paper Number 15-0153

## ABSTRACT

Rollover crashes belong to the most danger type of road accidents. Particularly vehicles with a high situated center of gravity are exposed to this type of accidents. The basic measure of vehicle resistance to rollover is Static Stability Factor SST, i.e. the ratio of half the track width to the height of the center of gravity. In the quasi-static rollover limit it is assumed that the SST should not be less than the tire-to-road friction coefficient. This follows from the assumption that the side skid is less dangerous than the rollover. Most of the passenger cars are designed in order to prevent the rollover on flat surface with normal friction. However from several reports it is known that the quasi-static rollover limit can be not met in the case of vehicles with the high center of gravity position (in relation to the tread): heavy trucks, delivery vans or busses, especially high-floor coaches and double-deckers. Also other cars especially, very trendy at present, SUVs and trucks could also undergo the rolling over when the tire-to-road friction coefficient would be extremely high, namely its value would exceed 1 or more. The rollover can happen on a flat surface also when the height of the centre of gravity is higher then the height assumed by the designers.
In the paper the method of calculation of the course of rollover in time domain is described and it is investigated the influence of the height the centre of gravity on the increase of the rollover angle velocity. The conducted calculations show that during rollover the rotation angle of the vehicle increases progressively. It can be noted that the higher the vehicle centre of gravity is located, the faster the rotation angle increases. On the basis of calculation results it is discussed whether the drive has a chance to counteract the rollover of the vehicle. It is shown, that in a few first tenth parts of the second the angle of the rotation is small enough that it gives the driver a chance to correct the movement of the car using the steering wheel or by reducing speed, even when the rollover process has already begun.

## INTRODUCTION

Rollover crashes belong to the most danger type of road accidents. Admittedly accidents of this type constitute only 3% of all accidents; fatalities of these accidents constitute is as many as 33% of all fatalities [3] . It is the reason why the problem of rollover accidents is discussed in many papers, e.g.: [10], [5], [11], [6]. Particularly vehicles with high situated centre of gravity are exposed to this type of accidents. Most dangerous are accidents with buses, especially with double-decker and high-floor buses [4].
In the vehicle dynamics the rolling over is treated as the case of loss of stability, which is one of the most important problems of lateral vehicle dynamics. The loss of stability consists on a rapid, uncontrolled by the driver, increase of vehicle deviance from its assumed trajectory. The loss of stability is a great danger, because it can cause departure of the car from the road, rollover or collision with other vehicle. The loss of lateral stability can happen mostly by cornering with great velocity or by avoiding an obstacle. Two cases of the stability loss are discussed:

- Side skid, caused by so great increase of outside forces acting on the car (e.g. centrifugal force, side wind force) that these forces can not be counterbalanced by tyre to road friction forces.
- Rollover which consists on rotation of the vehicle about its longitudinal axis. It happens when roll moment in cornering can not be counterbalanced by the moment of the vehicle weight.

## SIDE SKID LIMIT

The side skid on a level road does not occur when the lateral forces $Y$ acting in the ground plane counterbalance external lateral force $F_y$ acting on the car. Thus the safety requirement is

$$\sum Y \geq F_y \tag{1}$$

In the cornering manoeuvre the centrifugal force is the predominating lateral force

$$F_y = \frac{m\,v^2}{R} \tag{2}$$

where:
$m$ – vehicle mass,
$v$ – longitudinal velocity,
$R$ – radius of the curve.
With friction forces

$$Y = Z\,\mu \tag{3}$$

where:
$\mu$ - tyre-to-road friction coefficient
$Z$ – vertical road-to-tyre reaction force
and with the sum of vertical road reactions equal to vehicle weight: $\Sigma Z = mg$

$$\sum Y = m\,g\,\mu \tag{4}$$

Finally the safety requirement

$$m\,g\,\mu \geq \frac{m\,v^2}{R} \tag{5}$$

And the maximum velocity on the curve with given radius $R$ is

$$v \leq \sqrt{R\,g\,\mu} \tag{6}$$

**QUASI-STATIC ROLLOVER LIMIT**

The vehicle loaded with the lateral force $F_y$ acting in its centre of gravity is shown in Figures 1 and 2. The vehicle here is treated as a rigid body, which means that the elasticity of the suspensions and tyres is not being taken into consideration. The rollover of the vehicle does not occur when the roll moment $F_y\,h$ can be counterbalanced by the moment of the vehicle weight

$$F_y\ h \leq m\,g\,\frac{b}{2} \tag{7}$$

where:
$h$ – centre of gravity (CG) height over ground,
$b$ – wheel track.
In the cornering manoeuvre the centrifugal force is the lateral force, also with $F_y$ according to Equation (2)

$$\frac{m v^2}{r}\,h \leq m\,g\,\frac{b}{2} \tag{8}$$

Thus the safety requirement preventing the rollover is so that the vertical forces acting on the inside wheels should not decrease below zero (Figure 1). It means that in unstable equilibrium state the resultant force (i.e. the sum of centrifugal force and the vehicle gravity force $mg$) should not cross the ground outside the wheel track, also outside the line which joins outside wheels/road contact points (Figure 1). In the case of rollover the car rotates about this line. Thus this line can be called rollover axis.

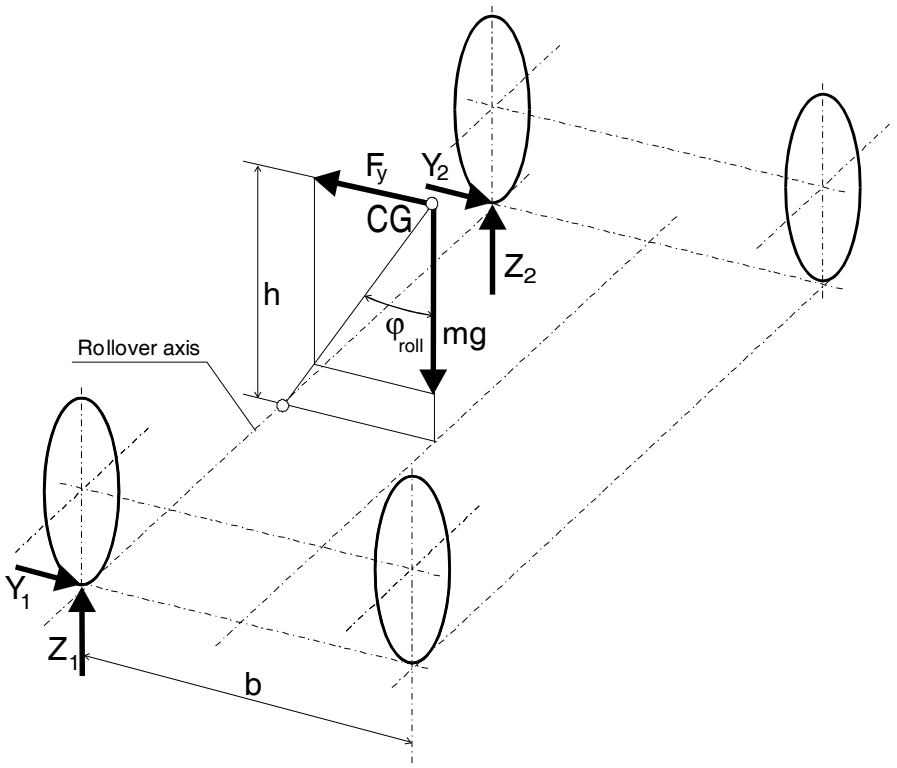


*Figure 1. Forces acting on the car by cornering in the rollover limit condition, $F_y$ – centrifugal force, mg – vehicle weight, Y, Z – lateral and vertical road reaction forces, CG – centre of gravity, h – CG height over ground, b - track*

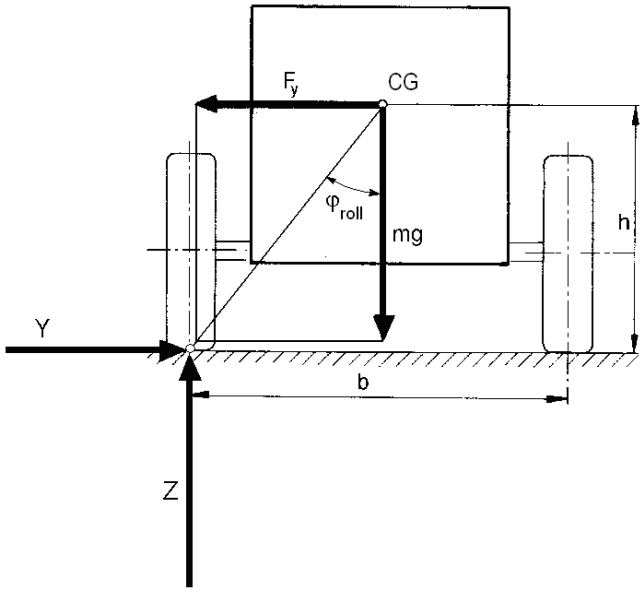


*Figure 2. Forces acting on the vehicle (treated as a rigid body) in its cross section in unstable equilibrium*

And finally the maximum velocity which does not cause rollover of the vehicle is

$$v \le \sqrt{R\,g\,\frac{b}{2h}} \tag{9}$$

It is commonly assumed that the side skid is less dangerous than the rollover. Also the maximum velocity calculated from the side skid limit should be smaller than the velocity calculated from the rollover limit

$$\sqrt{R\,g\,\mu} \le \sqrt{R\,g\,\frac{b}{2h}} \tag{10}$$

also

$$\mu \le \frac{b}{2h} \tag{11}$$

From the formula (11) it is evident that the rollover risk depends on one hand from the centre of gravity height in relation to the wheel track, on the other from the tyre-to-road friction condition. The value $b/(2h)$, called Static Stability Factor (SSF),

$$SSF = \frac{b}{2h} \tag{12}$$

is the first order measure of the vehicle resistance to rollover. However the influence of the tyre-to-road friction condition is so: The higher friction coefficient the higher possibility that the vehicle will roll instead slide.
In the Table 1 data of different types of motor vehicles are collected. They can be compared with the values of tyre-to-road friction coefficient which are being met on roads (Table 2). In most cases values of the friction coefficient do not exceed 0,9, also the vehicles mentioned in the Table 1 characterized with SSF value higher than 0,9 are not threatened with rollover. However in particular situations the friction coefficient can achieve value of 1,0 or more (very rough dry surface and good tyres) and the cars with relatively high CG position (vans, suvs or trucks) can be threatened with rollover.

**Table 1.**
**Approximate values of the Static Stability Factor of different types of motor vehicles,**

| **Vehicle type** | **Static Stability Factor (SSF)** |
|---|---|
| Cars[1] | 1,35 – 1,45 |
| Vans[1] | 1,10 – 1,25 |
| Sport Utility Vehicles – SUV[1] | 1,05 – 1,20 |
| Trucks, pick-ups[1] | 1,10 – 1,25 |
| Double-decker buses[2] | 0,60 – 0,75 |

[1]) based on [1]
[2]) calculated (see Appendix)

Buses with very high CG position (particularly double-deckers and high-flour buses) are much less safe. They can rollover even on the surface with the friction coefficient smaller than 0,8, that is with the value normally met on roads.

**Table 2.**
**Exemplary values of tyre to road friction coefficient measured on dry road surfaces for summer and winter tyres of two manufacturers according to [7]**

| v [km/h] | manufacturer 1 | | manufacturer 2 | |
|---|---|---|---|---|
| | summer tyre | winter tyre | summer tyre | winter tyre |
| 30 | 0,74 | 0,88 | 0,79 | 0,86 |
| 60 | 0,64 | 0,81 | 0,64 | 0,78 |

Thus the first safety requirement is to prevent the roll-over, also the vertical forces acting on the inside wheels should not decrease below zero (Figure 1). It means that in unstable equilibrium state the resultant force, i.e. the sum of centrifugal force and the vehicle gravity force *mg* should not cross the ground outside the wheel track, also outside the line connecting outside wheels/road contact points. In the case of rollover the car rotates about this line. Thus this line can be called rollover axis.
It can be also introduced the rollover angle $\varphi_{roll}$ as an angle between vertical line and the line drawn from centre of gravity perpendicularly to the roll axis (Figure 2).

$$\varphi_{roll} = \arctan\left(b/(2h)\right) \tag{13}$$

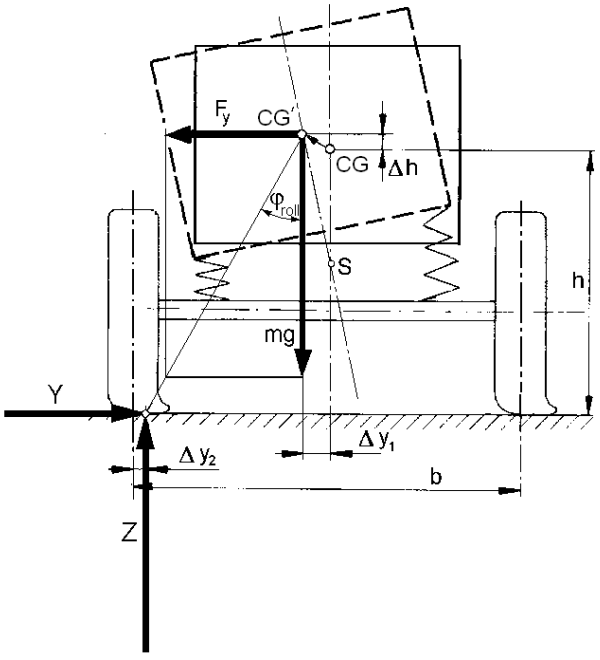


*Figure 3. Forces acting on the vehicle in its cross section in unstable equilibrium, when elasticity of suspensions and elasticity of tires are taken into consideration*

**ROLLOVER ANGLE**

Scheme shown in Figure 2 doesn't demonstrate all factors influencing the lateral stability of the vehicle. Therefore in Figure 3 it is shown the influence of body roll caused by compression and rebound of suspension and elasticity of tyres. Moreover one should notice that due to nonlinearities of suspensions characteristics their compression on outer side is smaller than rebound on inside site. As a result of these influences the centre of gravity is moving up and outside and the rollover angle is decreasing:

$$\varphi_{roll} = \arctan\left(\frac{0{,}5b - \Delta y_1 - \Delta y_2}{h + \Delta h}\right) \tag{14}$$

In consequence the stability of vehicle is decreasing and the roll-over limit can be modified as follows:

$$\mu \leq tg\,\varphi_{roll} \tag{15}$$

Based on comparing data from tables 1 and 2 it is possible to state, that in most cases requirement not to roll over is accomplished. However some accidents with rollover occur not rare.

**TRIPPED ROLLOVER**

It appears from statistics that about 63% of all rollover accidents is happening as a result of the blow of the car wheels in the curb or in the other similar obstacle ([3], [11]). The tripped rollover can be treated as the special case of rollover when the tyres coming across the surface with infinitely high value of friction coefficient, e.g. a quicksand on the shoulder of roadway or the curb.
The mechanics of rollover after contact with the curb will be discussed for an idealized situation when after loss of the adhesion the car slides with the velocity $v_y$ at right angle to the curb and finally it hits the curb simultaneously with both wheels of one side. The movement of the car will be treated as the flat movement in the plane perpendicular to its longitudinal axis (Figure 4). In the Figure 4 the axis of rotation is represented by the point O. Force impulse, which appears as result of the hitting, causes that the side movement of the car is converted into a rotational movement about the impact point O (more precise - about rotation axis). It can be assumed that the car will roll over when the kinetic energy of its rotational movement will be enough to raise the car CG in this way that the CG will be placed direct over the rotation axis (Figure 4).
In this case the vehicle movement can be divided into 2 phases [2]:

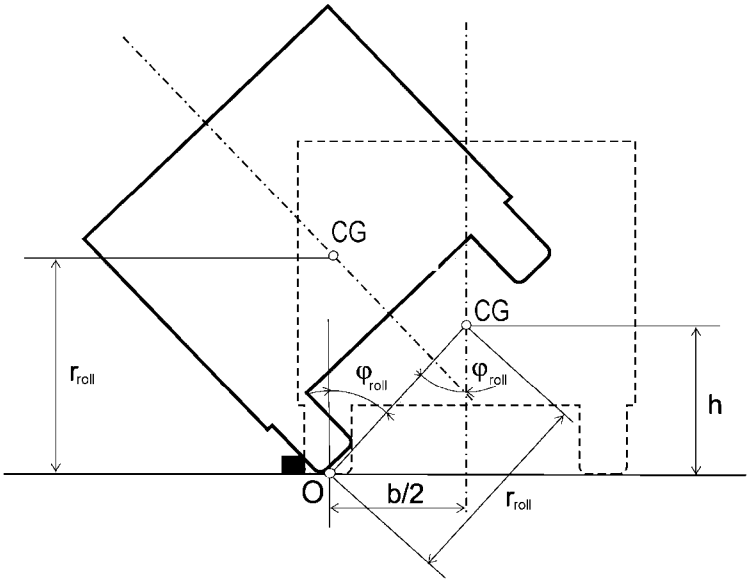


*Figure 4. Vehicle rolling over after hitting in the kerb*

Phase I – the hitting in the curb and the conversion of the translational movement into the rotational movement. From the law of conservation of angular momentum arises that the rotational momentum of the car after hitting $J_{\text{roll}}\,\dot{\varphi}$ should be equal to its moment of momentum around its rotation axis before hitting $mv_y h$

$$m v_y\, h = J_{roll}\,\dot{\varphi} \tag{16}$$

where:
- $J_{roll}$ is the moment of inertia of the vehicle about its roll axis

$$J_{roll} = J_x + m\, r_{roll}^{\,2} \tag{17}$$

- $J_x$ is the moment of inertia of the vehicle about its central longitudinal axis x and
- $r_{roll}$ is the distance of CG from the roll axis

$$r_{roll} = \sqrt{(b/2)^2 + h^2} \tag{18}$$

Also after the conversion of Equation (16) the rotational speed after hitting is equal to

$$\dot{\varphi} = \frac{m v_y\, h}{J_{roll}} \tag{19}$$

Phase II – rotational movement. The kinetic energy of the rotational movement should be enough big in order to raise the car CG to its possibly highest position, also to the position in which the CG will be direct over the rotation axis. The kinetic energy of the rotational movement will be converted into an increase of the potential energy

$$\frac{1}{2} J_{roll}\,\dot{\varphi}^2 = m\, g\, (r_{roll} - h) \tag{20}$$

Also the rotational speed after hitting should be equal to

$$\dot{\varphi} = \sqrt{\frac{2 m\, g\, (r_{roll} - h)}{J_{roll}}} \tag{21}$$

After conversion of Equation (19)

$$v_y = \dot{\varphi}\, \frac{J_{roll}}{m h} \tag{22}$$

and with the use of Equation (21) it can be calculate the value of the lateral velocity $v_y$ which is necessary to cause the rollover of the vehicle. This velocity is called Critical Sliding Velocity - CSV

$$\text{CSV} = v_y = \sqrt{\frac{2\, g\, J_{roll}}{m h^2}\left(r_{roll} - h\right)} \tag{23}$$

In praxis the value of CSV is higher then the value calculated from Equation (23) because in the calculation the car was treated as the rigid body and the losses of energy in shock absorbers and caused by tyres deflection are not taken into consideration.
The value of Critical Sliding Velocity is recognized as the evaluation criterion of the resistance of the vehicle to rolling over as the result of hitting the curb. In the Table 3 approximate values of CSV are presented for the same group of vehicles as in the Table 1. It can be observed from the table, that particularly buses on account of the very small value of CSV can roll over after hitting the obstacle on the roadway even at the slight skid.

**Table 3.**
**Approximate values of Critical Sliding Velocity**

| **Vehicle type** | **Critical Sliding Velocity (CSV)** |
|---|---|
| Cars[1] | 19 – 21 km/h |
| Vans[1] | 17 – 19 km/h |
| Sport Utility Vehicles – SUV[1] | 15 – 17,5 km/h |
| Trucks, pick-ups[1] | 15,5 – 19 km/h |
| Double-decker bus without passengers[2] | 14,4 km/h |
| Double-decker bus with passengers[2] | 12,2 km/h |

[1]) based on [1]
[2]) calculated (Appendix 1)

**COURSE OF ROLLOVER ON THE FLAT SURFACE**

The vehicle travelling in the steady state condition (with constant lateral velocity and constant angular velocity) on the flat surface can roll over in the case when the condition described with formula (5) or (6) is not met. This condition can not be met in the case of car with the big CG height (in relation to the tread): heavy trucks, delivery vans or busses, especially high-floor coaches and double-deckers. However other cars mentioned in table 1, especially very trendy at present SUVs and truck, can also undergo rolling over when the tyre-to-road friction coefficient would be extremely high, namely its value would exceed 1 or more.
The process of rollover begins, when $F_y/(mg) > \text{tg}\,\varphi_{roll}$. Because of a big value of the vehicle rolling moment of inertia about roll axis the angle of vehicle rotation $\varphi$ is increasing gradually. The determining of the course of changes of this angle will allow assessing whether the driver can counteract the rollover when the process already began.

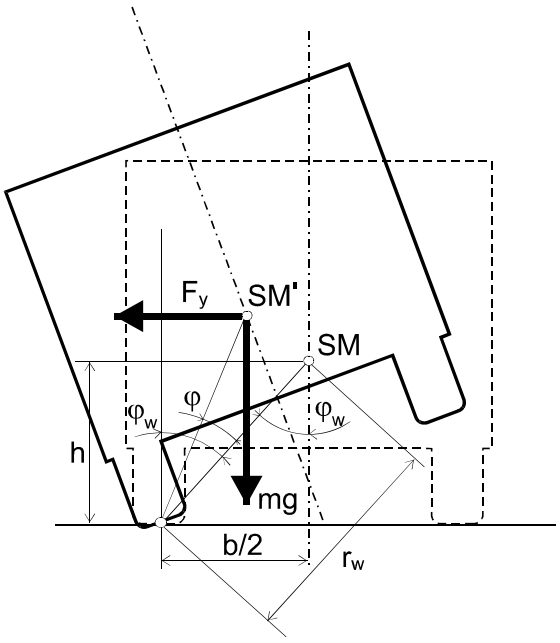


*Figure 5. The car while rolling over for the angle φ*

The moment $M_\varphi$ which causes rollover is equal the difference between the moment of lateral force $F_y$ and the moment of vehicle weight $mg$ (Figure 5)

$$M_\varphi = F_y\, r_{roll} \cos(\varphi_{roll} - \varphi) - m\, g\, r_{roll} \sin(\varphi_{roll} - \varphi) \tag{24}$$

Since the angular acceleration $\ddot{\varphi}$ is proportional to the rolling moment $M_\varphi$ and inversely proportional to the moment of inertia $J_{roll}$

$$\ddot{\varphi} = \frac{M_{roll}}{J_{roll}} \tag{25}$$

is also a function of the rotation angle $\varphi$.
During the rotation of the vehicle for the angle $\varphi$ the rolling moment $M_\varphi$ does the work

$$L_\varphi = \int_0^\varphi M_{roll}\, d\varphi = \int_0^\varphi \left[F_y\, r_{roll} \cos(\varphi_{roll} - \varphi) - m\, g\, r_{roll} \sin(\varphi_{roll} - \varphi)\right] d\varphi \tag{26}$$

After integration

$$L_\varphi = F_y\, r_{roll}\, [-\sin(\varphi_{roll} - \varphi) + \sin\varphi_{roll}] + m\, g\, r_{roll}\, [-\cos(\varphi_{roll} - \varphi) + \cos\varphi_{roll}] \tag{27}$$

On the flat surface, if the deflections of suspensions are neglected, it can be assumed that $\sin\varphi_{froll} = 0{,}5\, b/r_{roll}$ and $\cos\varphi_{roll} = h/r_{roll}$. Thus

$$L_\varphi = [0{,}5\, b - r_{roll} \sin(\varphi_{roll} - \varphi)] + m\, g\, [h - r_{roll} \cos(\varphi_{roll} - \varphi)] \tag{28}$$

An effect of the done work is an increase in the kinetic energy

$$E_\varphi = \frac{J_{roll}\, \dot{\varphi}^2}{2} \tag{29}$$

After comparing of the kinetic energy and the done work the angular velocity $\dot{\varphi}$ can be calculated

$$\dot{\varphi} = \sqrt{\frac{2 L_\varphi}{J_{roll}}} \tag{30}$$

Since the work $L_\varphi$ is a function of the angle $\varphi$, for the small increase of the rotation angle $\Delta\varphi = \varphi_i - \varphi_{i-1}$, it is possible to calculate angular velocities $\dot{\varphi}_{i-1}$ and $\dot{\varphi}_i$ for two successive values of rotation angles, and next its increase $\Delta\dot{\varphi} = \dot{\varphi}_i - \dot{\varphi}_{i-1}$, beginning from its null value. With the use of earlier calculated from Equation (25) values of angular accelerations $\ddot{\varphi}_i$ and $\ddot{\varphi}_{i-1}$ and their mean value $\ddot{\varphi}_{sr} = 0{,}5(\ddot{\varphi}_i + \ddot{\varphi}_{i-1})$ it can be calculated the time interval $\Delta t$ in which this increase took place

$$\Delta t = \frac{\Delta\dot{\varphi}}{\ddot{\varphi}_{sr}} \tag{31}$$

After adding values of time intervals $\Delta t$ calculated for successive values of rotation angles $\varphi$ the times of achieving these angles can be calculated. Finally it is possible to obtain the course of the rotation angle $\varphi$ as the function of time $t$.
Exemplary calculations of the course of vehicle rollover were carried out for the double-decker bus in two loading states: without passengers and with passengers. In calculation data taken from [8] and [9] was used. Data and preliminary calculations are placed in the Appendix. The bus with passengers is characterized by

greater mass, the higher put centre of gravity and the greater moment of inertia. In calculations a radius of the curve was assumed equal 60 m, and the vehicle velocity equal 80 km/h, that is higher than rollover limit for the bus without passengers (see the Appendix).
The results of calculations are shown on the Figure 6 and they are compared with the values of roll angles (Equation (13)) for both states of loading. From the diagram it is evident, that the higher the centre of gravity is located the faster the rotation angle increases. The vehicle with the higher position of the centre of gravity reaches the roll angle in the shorter time then the vehicle with lower centre of gravity; here appropriately in circa 1,05 s and 1,3 s.
Furthermore the increase in the rotation angle is progressive. In a few first tenth parts of the second the angle of the rotation is still small. For example, in the case 1 (bus without passengers) it does not exceed the value of 10° during 0,85 s from the beginning of rolling over and for the case 2 (the bus with passengers) respectively 0,65 s. It gives to the driver the chance to correct the movement of the vehicle using steering wheel or decreasing the velocity. However the driver has this time less, if the centre of gravity is put higher (case 2, bus with passengers).

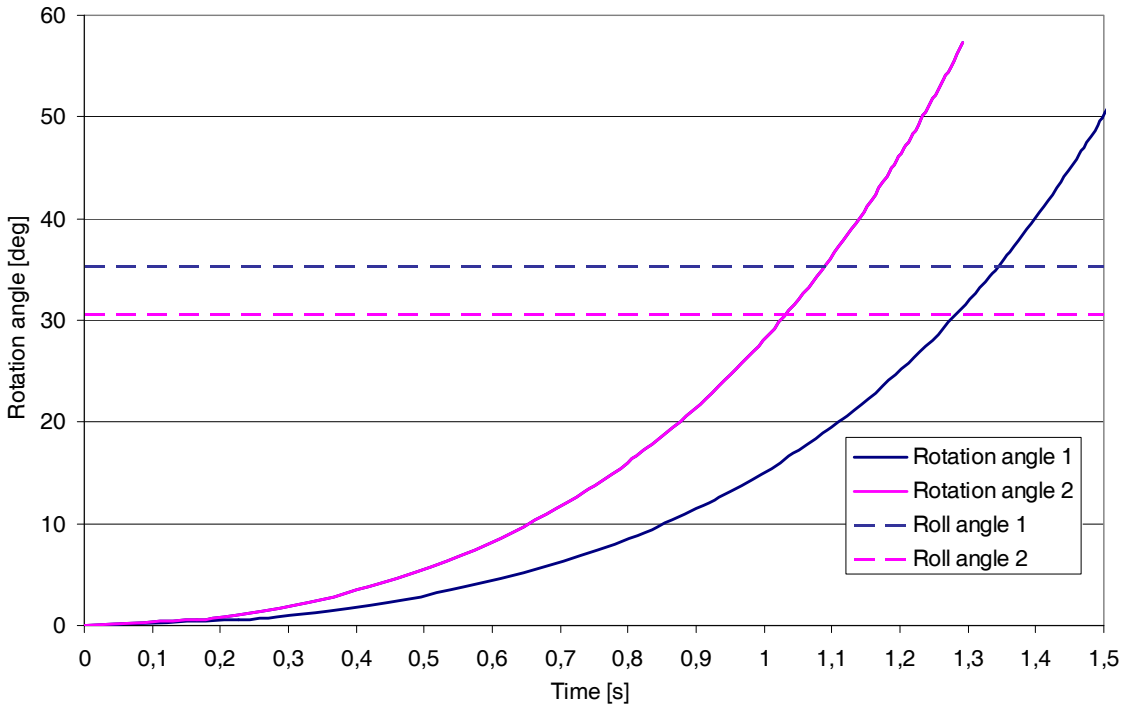


*Figure 6. The rotation angle of the bus as the function of time for two loading states: without passengers (1) and with passengers (2). Curve radius - 60 m, vehicle velocity - 80 km/h*

## CONCLUSIONS

The majority of passenger cars is designed in order to prevent the rollover on flat surface with normal friction coefficient. Their Static Stability Factor is higher than the tyre-to-road friction coefficient. However in the case of these vehicles the rollover can also happen when the friction coefficient will be extremely high or the height of the centre of gravity will be bigger then the height assumed by the designers, e.g. as the result of improper loading.
In case of the tripped rollover, which can be treated as the special case of rollover, when the tyres coming across the surface with infinitely high value of friction coefficient, the Critical Sliding Velocity is assumed as the safety criterion. Its value is about 20 km/h for passenger cars or respectively smaller for vehicles with

higher positioned centre of gravity (vans, trucks, SUVs) and especially small (less than 15 km/h) for double-deckers and high-floor buses.
The conducted calculations show that during the rollover the rotation angle of the vehicle increases progressively. It can be noticed that the higher is positioned the vehicle centre of gravity the increase the rotation velocity is the greater. Furthermore it can be stated, that in the initial phase of the rollover the increase in the angle of the rotation is enough small, that is giving to the driver the chance to correct the vehicle motion.

## REFERENCES


[1] Heydinger G.J., Bixel R.A., Garrott W.R., Pyne M., Hove J.G., Guenther D. A. 1999. "Measured Vehicle Inertial Parameters – NHTSA's Data Through November 1998". SAE Paper 1999-01-1336
[2] Huang M. 2002. "Vehicle crash Mechanics". CRC Press 2002
[3] Linstromberg M., Scholpp G., Scherf O. 2005. "Test and Simulation Tools in a Rollover Protection Development Process". 19th International Technical Conference on the Enhanced Safety of Vehicles (ESV). Paper No. 05-0122
[4] Matolcsy M. 2007. "The Severity of Bus Rollover Accidents". 20th Conference. ESV. Lyon 2007. Paper No. 07-0989.
[5] McLean J., Kloeden C., Ponte G. 2007. "Characteristics of Rollover Creshes". 20th International Technical Conference on the Enhanced Safety of Vehicles (ESV). Paper No. 07-0479
[6] NHTSA Report. 2002. "Characteristics of Fatal Rollover Crashes". NHTSA Technical Report DOT HS 809 438, April 2002
[7] Pokorski J., Reński A., Sar H. 2012. "Investigation of adhesion characteristics of different tyre types in different weather conditions". Journal of KONES Powertrain and Transport, Vol. 19, No. 3, 2012
[8] Prochowski L., Zielonka K, Muszyński A. 2012. "Analysis of the Process of Double-deck Bus Rollover at the Avoidance of an Obstacle Having Suddenly Sprung up". Journal of KONES Powertrain and Transport, Vol. 19, No. 3, 2012
[9] Prochowski L., Zielonka K. 2014. **"**Analysis of the risk of double-deck bus rollover at the avoidance of an obstacle (analytical approach and computer simulation)". Eksploatacja i Niezawodnosc – Maintenance and Reliability 2014; 16 (4)
[10] Viano D.C., Parenteau, Ch.S. 2004. "Rollover Crash Sensing and Safety Overview". SAE Technical Paper No. 2004-01-0342
[11] Young D., Grzebieta R.H., Rechnitzer G., Bambach M., Richardson S. 2008. "Rollover Crash safety. Characteristics and issues". Accident Reconstruction Newsletter. Issue 95, June 2008


## APPENDIX. CALCULATION

Data for the exemplary calculation related to the rollover of the double-decker bus in two states of loading was taken from [8] and [9].

The bus without passengers:
- vehicle mass $m$ = 17 300 kg,
- mass moment of inertia about the vehicle centre longitudinal axis $J_x$ = 34 600 kg m$^2$
- wheel track $b$ = 2,05 m,
- CG height $h$ = 1,45 m.

The Static Stability Factor (SSF) for the bus without passengers according to Equation (12) is equal to

$$SSF = b/(2h) = 2{,}05/(2\cdot 1{,}45) = 0{,}71$$

and roll angle (Equation (13))

$$\varphi_{roll} = \arctan\left(b/(2h)\right) = \arctan\left(2{,}05/(2\cdot 1{,}45)\right) = 35{,}3\ [^\circ]$$

The radius of rotation of the centre of gravity about the rotation axis (Equation (18)) is equal to

$$r_{roll} = \sqrt{(b/2)^2 + h^2} = \sqrt{(2{,}05/2)^2 + 1{,}45^2} = 1{,}78 \text{ [m]}$$

Also according to Equation (17) the mass moment of inertia $J_{roll}$ about the rotation axis can be calculated as follows:

$$J_{roll} = J_x + m\, r_{roll}^2 = 34\,600 + 17\,300 \cdot 1{,}78^2 = 89\,400 \text{ [kg m}^2\text{]}$$

and finally according to Equation (23) the Critical Sliding Velocity is equal to

$$\text{CSV} = \sqrt{\frac{2\,g\,J_{roll}}{m\,h^2}\left(r_{roll} - h\right)} = \sqrt{\frac{2 \cdot 9{,}81 \cdot 89400}{17300 \cdot 1{,}45^2} \cdot \left(1{,}78 - 1{,}45\right)} = 4{,}0 \text{ [m/s]} = 14{,}4 \text{ [km/h]}$$

In the similar way for the bus with passengers:
- vehicle mass $m$ = 25 000 kg,
- mass moment of inertia about the vehicle centre longitudinal axis $J_x$ = 48 700 kg m$^2$
- wheel track $b$ = 2,05 m
- CG height $h$ = 1,73 m

$$\text{SSF} = b/(2h) = 2{,}05/(2 \cdot 1{,}73) = 0{,}59$$

$$\varphi_{roll} = \arctan\left(b/(2h)\right) = \arctan\left(2{,}05/(2 \cdot 1{,}73)\right) = 30{,}6 \text{ [°]}$$

$$r_{roll} = \sqrt{(b/2)^2 + h^2} = \sqrt{(2{,}05/2)^2 + 1{,}73^2} = 2{,}01 \text{ [m]}$$

$$J_{roll} = J_x + m\, r_{roll}^2 = 48\,700 + 25\,000 \cdot 2{,}01^2 = 153\,000 \text{ [kg m}^2\text{]}$$

$$\text{CSV} = \sqrt{\frac{2\,g\,J_{roll}}{m\,h^2}\left(r_{roll} - h\right)} = \sqrt{\frac{2 \cdot 9{,}81 \cdot 153000}{25000 \cdot 1{,}73^2} \cdot \left(2{,}01 - 1{,}73\right)} = 3{,}4 \text{ [m/s]} = 12{,}2 \text{ [km/h]}$$

Since in both cases SSF is smaller than the friction coefficient the bus is exposed to rolling over on the ordinary, flat road surface ($\mu \approx 0{,}8$).
If the bus without passengers is moving on the curve with radius equal of 60 m, the rollover limit can be calculated from the Equation (9)

$$v = \sqrt{R\,g\,\frac{b}{2h}} = \sqrt{60 \cdot 9{,}81 \cdot \frac{2{,}05}{2 \cdot 1{,}45}} = 20{,}4 \text{ [m/s]} = 73{,}4 \text{ [km/h]}$$

and for the bus with passengers

$$v = \sqrt{R\,g\,\frac{b}{2h}} = \sqrt{60 \cdot 9{,}81 \cdot \frac{2{,}05}{2 \cdot 1{,}73}} = 18{,}7 \text{ [m/s]} = 67{,}2 \text{ [km/h]}$$

# EVALUATION OF IMPACTS OF IT-INCIDENTS ON AUTOMOTIVE SAFETY WITH REGARD TO SUPPORTING REACTION STRATEGIES FOR THE DRIVER

**Sven Kuhlmann**
**Robert Altschaffel**
University of Magdeburg
Germany

**Tobias Hoppe**
**Jana Dittmann**
**Christoph Neubüser**
University of Magdeburg
Germany

Paper Number 15-0156

## ABSTRACT

### Objectives

The integration of modern IT technologies into vehicles brings up several new challenges in automotive systems engineering. While current technology aspires an exclusive use of electrical and electronic control systems for relevant functions, such as engine control or X-by-wire systems, growing dependency on electronic systems increases the vulnerability of modern cars to both accidental and intentionally forged IT incidents. Especially the constantly increasing complexity of and interdependencies between different automotive IT systems makes it difficult for the developers to foresee all potential fault conditions or to prevent unauthorized actions from taking effect. As if these problems were not enough of a challenge, especially in automotive IT environments IT- incidents can possibly also affect the safety of the car, its passengers and other road users.
Building on a study on IT security warnings [1] and comparing with corresponding ASIL levels, we carried out a driving simulator study to evaluate driver reactions to various error and security relevant scenarios.

### Methods

Assuming that malfunctions of electronically supported control systems will endanger the safety of the car, a driving simulator study was designed and executed. These tests cover both security-related and safety-related lsources of failures (i.e.: accidental or provoked malfunctions) and scenarios with different criticality (based on ASIL A, B, C, D – [2]). The reactions of 40 uninformed drivers were observed and analyzed. In particular failures of engine, steering and brakes were executed in different road and traffic scenarios (e.g.: slow vs. high speed, low vs. high traffic density). The reactions of the drivers were recorded and, additionally, the controllability of the situation was observed as perceived by the drivers (using a think-aloud test). Furthermore, the study evaluated the potential of appropriate warning and reaction strategies that could support the reaction of the driver in critical situations as developed in [1].

### Results

The results show differences in driver behavior within a specific failure situation and an even greater degree between various failure situations. We found different types of accidents following the loss of steering and braking function – but no accidents caused by the loss of engine function. Interestingly, the results show the highest rate of recognition for the engine turn off scenario, where as in the autonomous acceleration and loss of brake function 15-17% of drivers did not recognize the malfunction. Besides this, we introduce different strategies to warn and support drivers in such situations. Especially when losing the ability to steer and brake, the warnings showed positive impact if the driver is warned ahead and stops the car before the complete loss of those functions. When the warning appears together with the function loss, a significant improvement of crash count and severity could not be observed.

## Conclusions

This work shows the impact security-related incidents can have on the safety of concurrent and future vehicles. It shows the potential of decreasing the severity of these incidents by using tailored warnings and shows a first evaluation of the feasibility of such an approach. It was shown that a loss of engine function leads to a safe stop of the car while a loss of steering or braking ability or an autonomous acceleration lead to an accident in 45% up to 71% of all cases. The severity of those accidents is not significantly correlated to the type of malfunction.

## INTRODUCTION

Concurrent automotive systems are more than mere mechanical systems. With a broad array of embedded systems, a modern car is akin to a driving computer network. This network consists of various electronic control units (ECU) which communicate using different bus-systems (see [3] for further details). These ECUs implement various functions. Simple ECUs control simple components like the window openers while more complex ECUs handle more complex tasks like engine control. Other embedded systems support the driver by giving him information about the environment or suggesting a route. All these factors establish cars as complex multimedia systems (as discussed in [4] On one hand this opens a broad range of possibilities to interact with and support the driver. On the other hand all these interconnected electronic components enlarge the error-proneness and attack surface of the automotive system. Looking at the security aspect, in automotive scenarios there is always the risk that unauthorized tampering with car IT can escalate into a safety incident – with the risk of the driver losing control of his car. Based on prior work from us where we demonstrated real IT attacks on several automotive subsystems ([5], [6]), such common automotive vulnerabilities have also been illustrated later on full cars by [7] and [8]. The spectrum of observed results leads up influencing the brakes, the steering wheel or disabling the engine by specially crafted CAN bus commands. As these practical analyses have substantiated, unforeseen IT incidents (like intentional, IT-based attacks) also bear severe safety implications. This contribution therefore focuses on the impact of (e.g. security-related) IT incidents on the safety of automotive systems. However, also unintended malfunctions (e.g. caused by system/component defects, software coding errors, or unforeseen and unhandled system interdependencies) could cause similar results. With reference to different examples of such potential incident causes, the aim of this paper is to analyze reactions of drivers in different incident scenarios with different grades of safety criticality.

### A Model to Describe Safety and Security Relevant Consequences

As a first step we revert to the Automotive Safety Integrity Level (ASIL), a model to describe consequences of safety and security-related incidents. This model allows us to specify various safety-related incidents and to evaluate their severity with regard to automotive scenarios. ASIL is defined in ISO 26262 ([2]) and consists of three components:

- Severity (S) is the severity of potential harm caused by an incident (similar to the SIL). It ranges from S0 (no injuries) via S1 (light and moderate injuries) and S2 (severe and life-threatening injuries with probable survival) to S3 (life-threatening with uncertain survival or fatal injuries)
- Probability (E) shows how probable it is that such an incident occurs. The levels range from E0 (incredible) via E1 (very low probability), E2 (low probability), E3 (medium probability) to E4 (high probability)
- Controllability (C) evaluates if the driver would be able to control the situation if such an incident occurs. It ranges from C0 (controllable in general) via C1 (simply controllable) and C2 (normally controllable) to C3 (difficult to control or uncontrollable)

These three categories allow a categorization of various incidents in respect of their severity. As a further concept ASIL contains an overall integrity level based on these three components. Similar to SIL, four different levels of differing severity (ASIL A, B, C and D) exist with an additional level for no or very low severity (QM – Quality managementt). Table 1 gives an overview on the impact of the three categories on the overall safety integrity level.

**Table1.**

***Overview on the impact on the overall safety integrity level with highlighted cells representing the tested scenarios***

| | | C1 | C2 | C3 |
|---|---|---|---|---|
| **S1** | **E1** | QM | QM | QM |
| | **E2** | QM | QM | QM |
| | **E3** | QM | QM | A |
| | **E4** | QM | A | B |
| **S2** | **E1** | QM | QM | QM |
| | **E2** | QM | QM | A |
| | **E3** | QM | A | B |
| | **E4** | A | B | C |
| **S3** | **E1** | QM | QM | A |
| | **E2** | QM | A | B |
| | **E3** | A | B | C |
| | **E4** | B | C | D |

Using ASIL we are able to evaluate different scenarios in respect of their severity. This allows us to create different test scenarios with varying severity either in respect to their overall ASIL or its components.

**Factors in an Automotive Environment**

In an automotive environment various factors contribute to othe ASIL. We identify three basic groups of factors which can influence the severity of an incident. These groups deal with the vehicle, the traffic condition and the driver himself. It is important to evaluate all these factors to determine a reliable ASIL for the current situation. As an exhaustive list of factors would exceed the scope of this paper we give a few examples for the various groups of factors.

- Vehicle-dependent factors: This group consists of factors which are inherent to the vehicle and generally don't change rapidly. They consist, for example of:
    - Vehicle type (e.g sports car, bus, transporter, truck)
    - Implemented driver assistance systems (e.g. adaptive cruise control with inherent autonomous acceleration and brake functionality or lane keeping assistant with inherent autonomous steering functionality)
- Traffic-dependent factors: These factors describe the current situation of the traffic or the road. They can change rapidly. Examples consist of:
    - Speed of the vehicle
    - Current lane conditions (e.g. clean or dirty street, potholes)
    - Traffic density (e.g. rural road with no other traffic participants or inner city during work traffic)
    - Weather conditions (e.g. sunny and warm or cold and rainy)
    - Noise (e.g. no outside noises or a lane directly next to a noisy construction site)
- Driver-dependent factors:
    - Response time of the driver for the perception of a certain situation
    - Response time of the driver for the execution of a reaction on a certain situation
    - Quality of the reaction of the driver
    - Interpretation of occurred errors or situations by the driver
    - Physical condition of the driver (e.g. fit or drowsy)
    - Distractions that could influence the attentiveness of the driver (e.g. a nearby airport with a starting plane nearby)

## METHODS

We decided to simulate various scenarios of differing severity to record and evaluate the reactions of various drivers. Since the failure of electronic computing control functions endangers the safety of the car, its driver and other traffic participants, we decided to perform these tests using a driving simulator. We created the scenarios according to the formerly discussed ASIL.

### The Driving Simulator

We used a driving simulator situated in our lab as the hardware for the tests. It consists of electronic control units (ECUs) and the dashboard of a VW Passat B6 with the ability to trigger instruments such as the tachometer. Furthermore, a forceable and force-feedback steering wheel from Logitech with additional accelerator and brake pedal is integrated into the driving simulator. During the simulation, the driving lane is displayed in front of the vehicle on a semi-transparent screen via rear video projection. We used commercial driving simulation software ([9]) for the simulation of the various test tracks. It provides the adjustment of several factors such as traffic density or the type of vehicle, which will be regarded during the evaluation. Furthermore it offers the possibility to create tracks and specify scenarios.
In order to achieve proper evaluation results 46 test persons were invited to take part in the tests. Thereby each test person has performed four test runs including different scenarios. In the different scenarios the failure of various vehicle components was simulated. As result of the evaluation the reactions of all test persons on these situations were observed, as well as the influence of acoustic and visual warnings on the reaction of the test persons. It should be noted that each test person was only warned in one of the four test runs to prevent the drivers of special expectations during the test runs. Furthermore the appearance of the warning was varied for different test persons, as well as the order of the four chosen scenarios. This was done for the prevention of coherent results and succession effects, which could occur if some combinations of scenario orders with the same appearance of warnings are used to often and could therefore distort the overall evaluation. In total one test run took 1 ½ hour including questionnaires.

### Scenarios and derived Hypothesis (ASIL Classification)

We based our scenarios on the different ASIL defined in ISO 26262 ([2]). We created a theoretical scenario for each of the four levels.
**ASIL A:** In this scenario the engine control unit is manipulated in order to allow law enforcement to safely stop the vehicle using remote access. This scenario implies that the law enforcement agents choose a situation in which the forced stop doesn't endanger other traffic participants. Such a situation implies sparse traffic and low speeds. Hence the severity is rated as S1. The manipulation performed by experts implies a high probability of E4 (e.g. by the means of electromagnetic pulses as researched in [10]. In general the driver will still be able to control the vehicle after the engine is shut down and should be able to stop safely. Therefore, as the derived hypothesis we rate the controllability of this scenario as C2 yielding an ASIL A classification.
**ASIL B:** In this scenario the car owner tries to manipulate the engine of his car himself, aiming to gain better performance. A failure caused by such manipulation could lead the car to accelerate autonomously while driving, endangering the safety of the driver and other vehicles in the surrounding area. In this scenario we choose an urban area and dense traffic. Hence the rapid acceleration of the car would cause a higher severity of S2. It is not certain that a manipulation of the engine would lead to a malfunction as described. The probability would be rated as E3 though, since most home tuners lack the expertise of professional automotive mechanics. Looking at the high traffic density in this scenario, an affected vehicle would be hard to control. Controllability is rated as C3 in this scenario which leads to an overall ASIL B classification.
**ASIL C:** This scenario covers another manipulation done by the driver. In this case the driver manipulates his infotainment system to show video (e.g.: TV) while driving. In general this functionality is disabled if the current speed exceeds walking pace. In this scenario, a 3rd party tool to inject forged bus messages with a lower speed signal has been installed by the driver, which would allow him to watch video while driving. As a side effect, this could also set steering support to maximum which could lead to fatal effects especially in high speed scenarios taking place on a speedway (Severity S3) – because these usually require little or no steering support. This causes a relative low controllability for the driver (Controllability C3). As in the previous scenario it is not certain that such a signal manipulation would necessarily propagate to all ECUs. Therefore we rate the probability as E3 again and get an overall ASIL C classification.

**ASIL D:** In this scenario a potential attacker manipulates the compressor of a heavy transporter. The compressor is also responsible to provide air pressure for the braking process. Such a manipulation would make it impossible for the driver to brake. In this scenario we assume that the transporter reaches the end of a tailback with an option of steering on the hard shoulder and slow down the transporter by engine break function. The momentum of the transporter would ensure fatal consequences which we rated as severity S3 – due to the lack of a higher possible rating. As there would be no control over the brakes any more, the controllability is rated as C3 – again, due to the lack of a higher possible rating. As this manipulation would be performed by an expert, the probability is rated as E4 leading to an overall ASIL D classification.

**General Hypothesis**

Following the results in the automotive warning research our test drivers should benefit from a warning in general [1]. We expect positive effects especially in ASIL A, B and C scenarios, due to the possibility to brake the car in these scenarios. We used a general warning without any information about the affected system (engine, steering, acceleration pedal or brakes) or reaction strategies (e.g. "Stop car immediately!"). This allows us to investigate the reaction of the drivers as a direct response to the vehicles system failure. Given the timeframe necessary to process incident, deriving, planning and executing an action, we expect a higher amount of false reactions (or no reactions at all) to critical incidents, like the loss of brake or control functionality, due to time constraints. For ASIL A scenario we expect the highest number of correct reactions.

**Test Drivers**

46 test persons took part in our tests. These persons had an average age of 26.9 years and an average driving experience of 7.3 years. Each test person performed one test for each of the four scenarios. From these 46 test persons 42 where able to finish all our tests. The remaining four persons needed to drop out due to simulator sickness at various stages of the test. For three of them a partial evaluation of their results was done. Before the start of our tests the participants weren't familiar with the test scenarios and the failures.

**Measurement**

We observed the reactions of all test persons on the given scenarios as well as the influence of acoustic and visual warnings. To prevent the test persons from having expectations during the test runs, each subject was only warned during one of the four scenarios. To prevent coherent results and succession effects, we changed the order of the various tests between different test persons. Furthermore the appearance of the warning was varied for different test persons.
The tests themselves started with a questionnaire and an initial trial run to get familiar with the simulator. Afterwards the respective scenarios started. During these scenarios the test persons committed thoughts and feelings using the think-aloud-method [11]. We combined these protocols with the observation how the test persons reacted inside the simulation and what result (accident or no accident) concluded. For doing so we used a simple coding scheme (Did the driver notice anything is wrong? Did the driver brake? Did the driver try to move the car to the sideline? Did an accident occur?). This allowed us to determine if the test persons correctly recognized the situation and if accidents could be avoided. We also looked closely on the health condition of the test persons in order to prevent negative influence due to simulator sickness [12]. In case of simulator sickness, a short break was scheduled and the test was either repeated aborted.

**Warnings**

Three different types of warnings are mainly used in current automotive and related research: visual, acoustic and haptic warnings. In general visual warnings are displayed on the head-up display (HUD) of the vehicle to inform the driver about possible critical situations. The size and position of the warning sign on the HUD is of great importance because of its influence on the reaction of the driver. An Evaluation of size and position of visual warning signs and their effect on the driver has been performed in [13]. Acoustic signals are also frequently used in current vehicles to direct the attention of the driver to critical situations. In this case duration and frequency of the acoustic warning signal are the decisive factors for the success of the warning. In [13] an analysis of different acoustic signals with different length and frequencies has also been performed to observe how different test persons react on such signals in critical situations. The third type of warning signals, which is used in vehicles, are so called haptic warnings. In

this case the driver is for instance warned through tactile vibration of the steering wheel during his drive. In current vehicles this is for instance used for lane tracking support in case the driver is about to leave his current lane [14]. Following the previous research we selected visual and acoustic warnings for this experiment. The acoustic warning was a sine tone with the duration of one second and a frequency of 1320 Hz which was repeated 4 times. The visual warning was provided as a red triangle with a black exclamation mark inside. It was presented virtually inside the projection of the simulation scene as a head-up display warning. Additional instructions were not given to avoid influences to the subject's reaction.

## RESULTS

Due to our observations the majority of test persons were able to determine the particular situation or failure in each of the four scenarios. We observed the highest rate of correct detection in the ASIL A scenario. This is mostly due this being the least severe scenario which also does not require a sudden reaction by the driver. 94.1% perceived this situation correctly. Regarding the other three (more critical) scenarios, we observed a higher rate of misinterpretations. We see the reason for this higher rate in the fact that these situations require a much faster reaction of the driver which leads to greater attention on the task itself. One example can be seen in the circumstances that several test persons failed to notice the fact that the vehicle accelerated by itself in the ASIL B scenario. They blamed a failure of breaking for the fact that the vehicle didn't slow down and didn't notice that the vehicle even accelerated. In the ASIL C scenario most wrong determinations resulted from problems of some test persons to track the lane while driving with high speed.
At first glance it appears that the provided warning has not improved the correct determination of the provided situation. This is due to the fact that most test persons already stopped the vehicle in safe place immediately after the warning was provided. Hence the test persons were not able to correctly determine the situation since they reacted on the warning before the situation itself manifested. By sorting out these occurrences, we observed the results shown in figure 1.

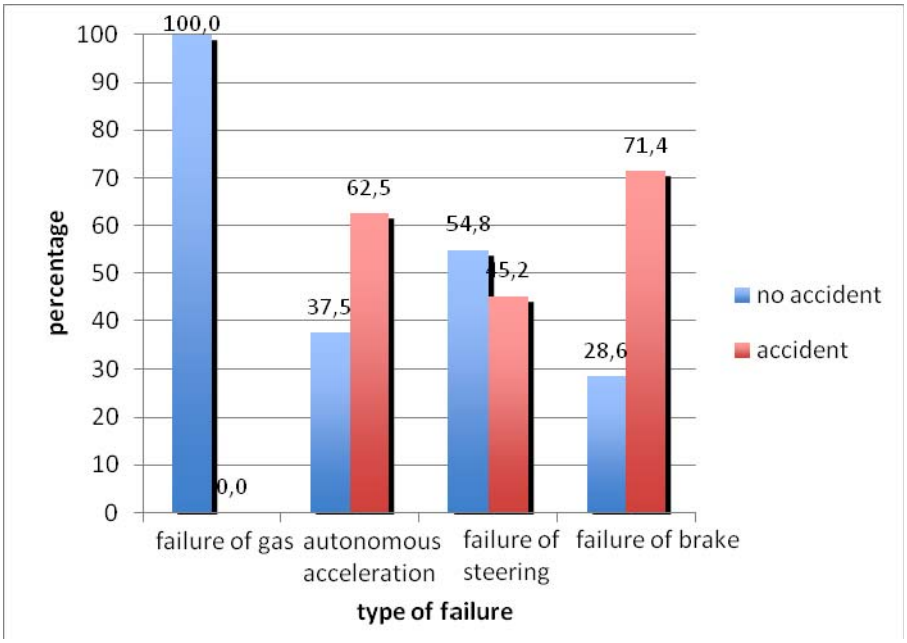


***Figure1. Observed reactions of the test persons without a warning***

We observed a correct determination rate of 100% in ASIL A (10 out of 10) and ASIL C (7 out of 7). In ASIL B and ASIL D these rates were lower with 82% (9 out of 11) and 87% (7 out of 8) respectively. Therefore it can be assumed that the provided warning had a positive influence on the number of correct determinations although the number of results led to this not being provable by our tests.

The second focal point for our research was how the persons reacted in these situations with regard to prevent harm for themselves and other traffic participants. At first we observed the occurrence of accidents in test runs without a warning before the respective situation. We predicted that the rate of accidents would increase according to the rising severity of the various scenarios. This prediction proved correct in general with 0% accidents in scenario ASIL A while ASIL B, ASIL C and ASIL D led to 62.5%, 42.2% and 71.4% accidents, respectively.

By the inclusion of an error warning before the occurrence of the situation we could reduce the number of accidents in general as shown in figure 2. ASIL B went down from 62.5% to 50% and ASIL D from 71.4% to 55.6%. ASIL C however suffered an increase in the number of accidents to 45.5%.

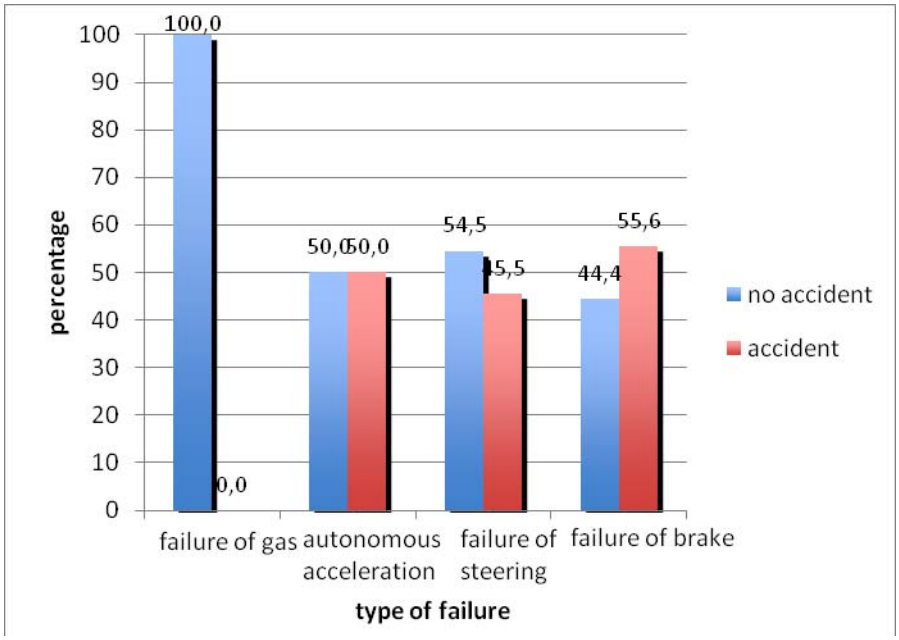


***Figure2. Observed reactions of the test persons supported by a warning***

This better overall performance is supported by the fact that some test persons almost instantly reacted on the warning by turning on the hazard lights and trying to stop their vehicle in a safe place. The overall attentiveness was also increased since the test persons were more concentrated on determining the reason for the failure. This became most obvious due to the think-aloud-tests. However avoiding an accident was still dependant on the skill of the driver in these sudden occurrences of critical situations as observed in ASIL B scenario. Although traffic density and average speed was rather low for the ASIL B scenario, because of strictly urban traffic, this rather high percentage of accidents had not been expected first. The main reason therefore was that many of the test persons were quite startled of this situation which often led to uncontrolled steering to avoid collisions, because of the decreased braking effect (according to the acceleration of the vehicle). Those who were able to control the car properly, for instance by activating the emergency brake and shifting down the engine, could avoid accidents because they remained concentrated. As this is a situation that rather does not seem likely, the reaction of most of the test persons is not surprising in the end because of its rather sudden appearance in compare to the ASIL A scenario. The results from the think aloud test revealed a general inhibition of the positive warning effect if the expected failure from a warning does not match the failure situation. In the think aloud test and the interview after the simulator study, those drivers reported that it leads to surprise and confusion and therefore to the inadequate reaction. This also applies if the driver is not able to derive a reaction strategy from the given warning, e.g. if the warning is missed, unspecific, appears too early or late or leads interpretation to a wrong system (brake vs. steering). Beside the slight decrease in the statistical numbers it could be observed that the severity of the accidents which still happened decreased. The increase in overall driver attentiveness led to better reaction even if an accident could not been avoided.

Overall the evaluation shows that a preceding warning decreased the amount of accidents or at least their severity. Further research questions were related to the design of the warnings. In summary, the chosen warning design was reflected as appropriate and helpful. Nevertheless, the test drivers suggested additional clear advice for an appropriate reaction strategy (e.g. stop the car immediately).

**Inferential Statistics**

First of all it was tested if the assumed hypothesis, that a preceding warning affects the number of correct determinations of each situation, could be verified. Therefore a chi square test was performed and the contingency table was created for each of the four observed scenarios regarding the warning condition and the determination condition. As some of the test persons were not able to determine the actual situation according to their immediate reaction on the warning, these test persons were excluded for the chi squared test to gather the correct values. This has been performed for each scenario to verify if the features warning condition and determination condition are stochastically independent.

As each value is lower than the critical value of the chi squared test of 3.841 [15], it could not be verified that the samples differ significantly. Therefore it could not initially be stated that the provision of a preceding warning influences the correct determination of a certain scenario. To prove if the calculated value was just received randomly according to the samples, the p-values for each scenario were calculated as seen in table 2: Failure of gas (p=0.5), autonomous acceleration (p=0.48), failure of steering (p=0.37) and failure of brake (p=0.47).

**Table2.**

***Chi squared values by scenario***

| Scenario | Chi Squared Value |
|---|---|
| failure of gas | 0.0 |
| autonomous acceleration | 0.057 |
| failure of steering | 0.48 |
| failure of brake | 0.103 |

Afterwards it was proven if the assumed hypothesis, that a preceding warning has a positive effect on the reaction of the driver, could be verified. As for the verification of the previous hypothesis, the contingency table was created for each of the four scenarios, regarding the warning condition and the accident condition. According to this the chi squared values were calculated for each scenario to verify if the two observed features are stochastically independent. As each value is lower than the critical value of the chi squared test of 3.841 it could not be verified that the samples differ significantly. Because of that it could not initially be stated that the provision of a preceding warning has a positive effect on the reaction of the driver. To prove if the calculated value was just received randomly according to the samples, the p-values for each scenario were calculated: Failure of gas (p=0.5), autonomous acceleration (p=0.375), failure of steering (p=0.49) and failure of brake (p=0.304).

## CONCLUSIONS

The evaluation of the performed tests has provided interesting results for security related considerations for present and upcoming x-by wire systems. However, a critical discussion of these results is needed.
First of all the test setup does not precisely reflect the feeling of real driving. This is due to the use of a driving simulator and its properties such as the missing movement of the body and limited field of view provided for the test persons. Therefore they may lack the ability to judge the overall traffic situation. Beside this general limitations the wrong interpretation of the failure in our study may have an important effect on the results. It might happen that a test person attributes the failure (e.g. engine stop) rather to the simulation itself than to the vehicle in the simulation. We implemented engine sound and the real dashboard (incl. warning lights) to avoid a misattribution. Additionally we asked the test subjects during (think-aloud test) and after the tests about their thoughts about the failures. All of them reported that they were confident that the failure was a part of the test and in time critical scenarios they did not reason the cause of failure. We also observed some oddities in the behavior of the computer-controlled traffic.

The test track we used in our driving simulator proved to be appropriate for our evaluation as it included all necessary properties of our test scenarios.
The think-aloud-test we used to gather information about feelings and thoughts of the test persons has been discussed in recent literature. One source [16] points out the unnatural process which could change the demands of the task. This could imply for instance that the test persons believe that they have to fulfill certain expectations which could lead to a distortion of the results. Nevertheless it provided appropriate results for the purpose of the evaluation while different variations could be used to reduce such negative impact.
While the amount of tests persons is appropriate for a first test, the results presented here are not statistically provable but reveal tendencies and qualitative results for further studies.

## ACKNOWLEDGMENTS

This work was partly supported by German Research Foundation, project ORCHideas (DFG GZ: 863/4-1).

This work was also partly supported by European Research Foundation, project SAVELEC (Safe control of non cooperative vehicles through electromagnetic means, FP7- SEC-2011, Grant Agreement Number 285202).

## REFERENCES

[1] Tuchscheerer, S., Dittmann, J., Hoppe, T., and Krems, J. F. Theoretical Analysis of Security Warnings in Vehicles and Design Challenges for the Evaluation of Security Warnings in Virtual Environments. In G. Saake and V. Koeppen (Ed.). IWDE '10 - Proceedings of the First International Workshop on Digital Engineering (pp. 33-37). New York: ACM Digital Libary, 2010

[2] ISO/FDIS 26262:2010(E). Road vehicles - functional safety, 2010. Available at http://www.iso.org/iso/catalogue_detail?csnumber=43464 Accessed November 14, 2014.

[3] Paar, C. Embedded Security in Automobilanwendungen. Elektronik Automotive, 1:1–6, 2004.

[4] Dittmann, J., Hoppe, T., Vielhauer, C. Multimedia Systems as Immune System to Improve Automotive Security? Safecomp 2013 FastAbstract, Toulouse:
France (2013), Hyper Articles Len ligne (HAL), HALid: hal-00926391, URL: http://hal.archivesouvertes.fr/hal-00926391; SAFECOMP 2013, 24.-27. Sept. 2013, Toulouse, France, 2014.

[5] Tobias Hoppe, Stefan Kiltz, Jana Dittmann: Security threats to automotive CAN networks – practical examples and selected short-term countermeasures. In: Computer Safety, Reliability, and Security, Proceedings of the 27th International Conference SAFECOMP 2008, Newcastle, UK, September 2008; Springer LNCS 5219; S. 235-248; Editors: Michael D. Harrison, Mark-Alexander Sujan; ISBN 978-3-540-87697-7, 2008.

[6] Tobias Hoppe, Stefan Kiltz, Jana Dittmann: Automotive IT-Security as a Challenge: Basic Attacks from the Black Box Perspective on the Example of Privacy Threats. In: Computer Safety, Reliability, and Security, Proceedings of the 28th International Conference SAFECOMP 2009, Hamburg, Germany, September 2009; Springer LNCS 5775; S. 145-158; Editors: Bettina Buth, Gerd Rabe, Till Seyfarth; ISBN 978-3-642-04467-0, 2009.

[7] K. Koscher, A. Czeskis, F. Roesner, S. Patel, T. Kohno, S. Checkoway, D. McCoy, B. Kantor, D. Anderson, H. Shacham, S. Savage: Experimental Security Analysis of a Modern Automobile. In: The IEEE Symposium on Security and Privacy, Oakland, CA, May 16-19, 2010.

[8] Charlie Miller, Chris Valasek: Adventures in Automotive Networks and Control Units. In: DEF CON 21 Hacking Conference, 1.-4. August 2013, Las Vegas, USA, White Paper at http://illmatics.com/car_hacking.pdf (last access: 2015-01-20), 2013.

[9] Astragon Fahr-Simulator 2009. 2009. Available at http://www.astragon.de/produktdetails/article/fahr-simulator-2009.html Accessed November 14, 2014.

[10] Savelec-Project. 2012. Available at: http://savelec-project.eu/ Accessed November 14, 2014.

[11] Janni Nielsen, Torkil Clemmensen, and Carsten Yssing. Getting access to what goes on in peoples heads? - Reflections on the think-aloud technique. In Proceedings of the second Nordic conference on Human-computer interaction, pages 101–110, 2002.

[12] Sonja Hoffmann, Hans-Peter Krüger, and Susanne Buld. Avoidance of simulator sickness by training the adaptation to the driving simulation. VDI- Berichte Nr. 1745. Simulation und Simulatoren - Mobilität virtuell gestalten, 1745:p. 385–404, 2003.

[13] Diana Rösler, Anja Naumann, Sven Tuchscheerer, and Josef F. Krems. Warnen im Kraftfahrzeug: Experimentelle Untersuchung zur Detektion und Bewertung optischer und akustischer Signale. In M. Röttig, G. Woszny, A. Klostermann, and J. Huss, editors, Prospektive Gestaltung von Mensch- Technik-Interaktion, pages 209-214. VDI Verlag, 2007.

[14] Jens E. Gayko. Lane departure and lane keeping. Handbook of Intelligent Vehicles, Volume 1:689-708, 2012.

[15] P.E. Greenwood and M.S. Nikulin. A guide to chi-squared testing. Wiley, 1996.

[16] Sharon McDonald, Helen M. Edwards, and Tingting Zhao. Exploring think-alouds in usability testing: An international survey.IEEE Transactions on Professional Communication, Volume 55:2 19, 2012.

This paper has been peer-reviewed and published in a special edition of *Traffic Injury Prevention* 16(S1), by Taylor & Francis Group. The complete paper will be available on the *Traffic Injury Prevention and www.NHTSA.gov* websites on June 8, 2015.

To access all Peer-reviewed papers please copy and paste the link below into your browser to access the papers.

http://www.tandfonline.com/toc/gcpi20/16/sup1

# THE DEVELOPMENT OF A CONSUMER TEST PROCEDURE FOR PEDESTRIAN SENSITIVE AEB

**Colin, Grover**
**Matthew, Avery**
Thatcham Research
UK

**Iain, Knight**
Apollo Vehicle Safety Limited
UK

Paper Number 15-0159

## ABSTRACT

In Europe, nearly 20% of all road deaths are pedestrians (Pace et al, 2012). Pedestrians have been protected only by the requirements for passive protection at the front of passenger cars and there has been little evidence to show that this measure has been effective. Autonomous Emergency Braking (AEB) systems have been clearly demonstrated to substantially reduce the incidence of car-to-car rear crashes and manufacturers have now extended the functionality to pedestrian, and in some cases pedal cyclist, collisions. If a comparable level of effectiveness is proven, then these systems will offer substantial reductions in the number of those killed and seriously injured on our roads. The research challenge described by this paper was the development of a test procedure that could be used to encourage the fitment of these systems and the development of high levels of performance in a way that could be linked to real world safety.

Thatcham Research led the AEB Group (a partnership of insurance research centres, OEMs and Tier ones) in the development of test procedures. This contributed substantially to the Harmonisation Platforms in a major collaboration with the vFSS group and the EU funded ASPECCS project. Work began with studies of real-world accident data. A cluster analysis identified the most prevalent collision scenarios and smaller samples of more detailed data were used to characterise each scenario in terms of speeds, impact points, relative positions and sight lines. Physical testing identified the characteristics required of the pedestrian test target and the performance of production and advanced prototype vehicles as well as establishing the conditions required for repeatability and reproducibility.

In Europe almost 75% of serious pedestrian crashes can be characterised by three scenarios: walking from the nearside of the road with open sight lines; running from the far side of the road; and walking out from behind a parked vehicle. In the vast majority of crashes the vehicle involved was travelling at 60 km/h or less. To ensure the systems worked well in the real world it was found that the test should involve adults and children, different impact points and different pedestrian speeds. The pedestrian target found to be most effective was the 4A design, and this was further tuned to optimise the radar and visual signatures to ensure consistent function across different sensor types and proving ground locations.

AEB has considerable potential to reduce the frequency and severity of vulnerable road user collisions. Robust test procedures, representative of real world collisions, have been developed and adopted by Euro NCAP for implementation in the 2016 ratings. However, VRU collisions are a problem in many areas of the world and the harmonisation of these tests and assessments in other NCAP regimes remains a priority, alongside the continuous technical development to expand the tests to include night-time performance and functionality in pedal cycle collisions.

## INTRODUCTION

While collisions between cars and pedestrians are relatively rare (for example, representing approxiamtely 1% of insurance claims in the UK) they tend to be very severe in terms of injury outcome, representing 20% of all road deaths in Europe (Pace et al, 2012). While Regulations and consumer test procedures have been implemented in order to reduce severity of injury when a collision does occur, the number of deaths and serious injuries remains

substantial and does not appear to be reducing as fast as for other collision types. Autonomous Emergency Braking (AEB) systems have been clearly demonstrated to substantially reduce the incidence of car-to-car rear crashes and manufacturers have now extended the functionality to pedestrian, and in some cases pedal cyclist, collisions. If a comparable level of effectiveness is proven, then these systems will offer substantial reductions in the number of those killed and seriously injured on our roads. The research challenge described by this paper was the development of a test procedure that could be used to encourage the fitment of these systems and the development of high levels of performance in a way that could be linked to real world safety.

The work involved collating evidence on the circumstances of pedestrian collisions from around the world in order to develop a small number of generalised collision scenarios that could be considered representative of a large proportion of all pedestrian crashes. These scenarios were then converted to test scenarios and procedures that assessed the performance of vehicles equipped with pedestrian sensitive AEB.

## USING REAL WORLD COLLISION DATA TO DEFINE TEST SCENARIOS

An extensive analysis of GB accident data was undertaken in order to provide the primary evidence under-pinning the development of the test procedures, and this was reported in full by Lenard & Danton (2010). Studies were made of police reported crash data covering the whole of Great Britain (STATS19) and of a detailed sample of crashes that were attended by research personnel On-The-Spot (OTS) of the accident. Both data sets were subjected to a multi-variate cluster analysis, which defined several groups of accidents with common features. In both sets of data, it was found that the single largest cluster involved pedestrians crossing from the nearside during daylight in fine conditions with moderate speeds (average 43 km/h). Less than half of the vehicles involved braked and the average speed reduction was 7 km/h. Children were over-represented in the data but remained a minority.

The next largest cluster (14%) was characterised by children crossing from the nearside (running) during fine daylight conditions but masked by vehicles or other obstruction of view.

Clusters 3 and 4 were similar and in combination represented 21% of the population with common characteristics including crossing from both farside and nearside in darkness and sometimes wet weather without obstructions to the field of view. On average the speeds were slightly higher at 50 km/h. It is worthy of note that the analyses above are for all casualties. When considering only fatalities, clusters 3 and 4 combined represent 42% of the populations, showing that darkness is associated with lower frequency but higher severity crashes.

When all frontal collisions with pedestrians were considered in terms of the lateral position at which the collision occurred, it was found that 42% occurred in the nearside quarter of the front and a further 22% the most offside quarter. Thirty-six percent collided with the two quarters either side of the vehicle centerline.

Children under the age of 16 were frequently involved in the crashes (43% of those with known age) but less frequently killed (11% of those with known age). Conversely, those over the age of 65 were less frequently involved (11%) but more frequently killed (33%). However, it was young adults between the age of 19 and 45 that were most likely to be killed (50%).

Information from these analysis was collated into a subset of collision types and international comparisons were sought from other partners in the AEB Group (a partnership of insurance research centres, OEMs and Tier one suppliers). The results are shown in summary form in **Table *1***, below.

**Table 1.**

**International comparison of the frequency of different pedestrian crash types.**

| Combining accident data from international sources | UK<br>STATS 19<br>n=10,574<br>cluster analysis<br>frontal collisions | UK<br>OTS<br>n=175<br>cluster analysis<br>frontal collisions | Germany<br>UDV<br>n=234<br>(N=18,571)<br>3rd party vehicle claims 2002-2006<br>frontal collisions | USA<br>IIHS<br>1997-2006 FARS & GES<br>all car-pedestrians |
|---|---|---|---|---|
| Pedestrian walks from nearside | 51% | 59% | 32% | 27% |
| Pedestrian walks out from behind obstruction | 14% | | 7% | |
| Pedestrian runs out from the far side | 9% | 37% | 28% | |
| Pedestrian walks along in the dark | 3% | 5% | 8% | 9% |
| Pedestrian walks out into the path of turning car | 6% | Overall: going ahead 87%, Turning 13% | 18% | - |

It can be seen that, within Europe at least, there is broad agreement that in the region of three quarters of all frontal collisions with pedestrians fall within the first 3 groups listed of walking from the nearside, walking out from behind an obstruction and running from the far side. Within this, there was variation between UK and Germany with UK finding collisions with obscured pedestrians more of a problem and Germany finding pedestrians crossing from the far side more of a problem.

The data also suggested that the vast majority of collisions occurred when cars were travelling at less than 60 km/h before the collision.

## DEVELOPING REPRESENTATIVE TEST TARGETS

The development of the test targets has been the subject of a previous ESV paper (Lemmen et al, 2013) so within this paper the results will simply be summarized briefly and updated for the latest status. The previous work identified a range of dummy attributes that were important enablers of recognition by different sensors and proposed specifications for them. These included:

- Size and posture
- Infra-red reflectivity
- Radar Cross Section (RCS)
- Contrast with background

In terms of the propulsion system required to deliver the dummy to the point of impact, it was decided to use a low profile platform approach rather than an overhead gantry. The rationale for this was the reduced visual and radar signature of the platform and the more realistic appearance of the test, from a consumer point of view. At that stage, a range of dummy and delivery system solutions remained under consideration. However, since that

time extensive further development was undertaken such that the static dummy produced by 4A emerged as a leading contender. Preliminary testing in partnership with Thatcham and Continental in Austria and the UK showed that the dummy was remarkably robust, surviving regular impacts at 60 km/h with only very minor cosmetic damage to either dummy or vehicle. The preliminary tests also suggested that the recognition by visual sensors was good but that variations in performance were found between the two test sites, suspected of being a contrast problem as a result of different backgrounds. The radar signature was found to be adequate for some vehicles. However, for the Mercedes E class, it was found to be inadequate, discussion with the manufacturer suggesting that this was because the radar signature was "brighter", i.e. a stronger radar return, than that of a real pedestrian and this reduced detection confidence for their algorithm, whereas for the algorithms of other manufacturers this was not considered a problem.

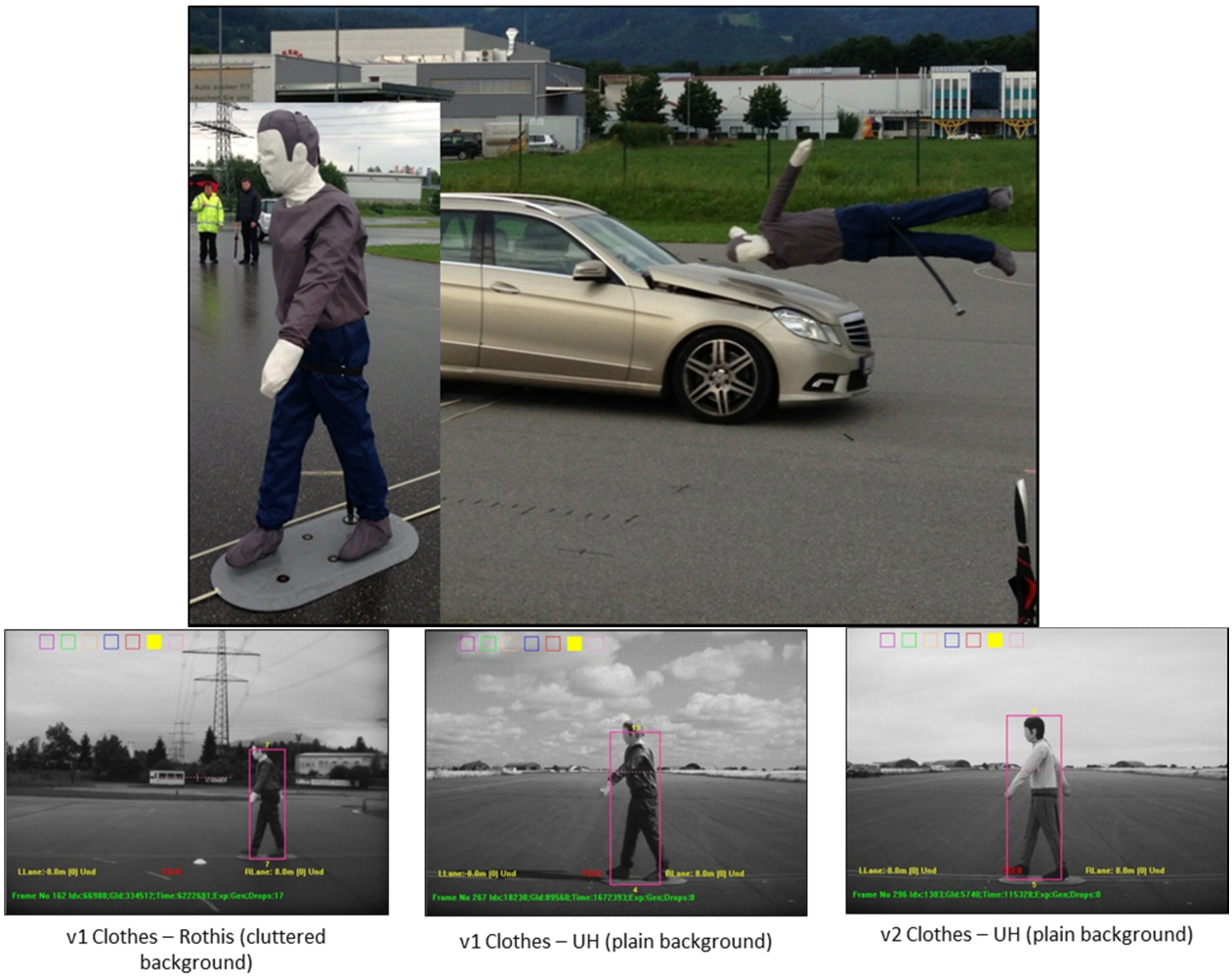


***Figure 1: Illustrations of the 4A dummy, it's durability and contrast.***

In late 2014, two further dummy workshops were organized by the Harmonisation Platforms, one hosted by BASt in Germany to fine tune the radar signature of the dummy and the other hosted by Thatcham in the UK to consider the effects of different colour clothes and the contrast with the background. At each event a wide variety of manufacturers brought their instrumented vehicles to test for recognition of the dummy and 4A had prepared different versions of key components such as clothes to allow for tuning.

The results of these workshops were such that modifications were made to interior components of the dummy and the dummies foot in order to amend the radar cross section and the colouring selected as the most suitable against a variety of backgrounds was blue trousers with a black top and black hair, as illustrated below.

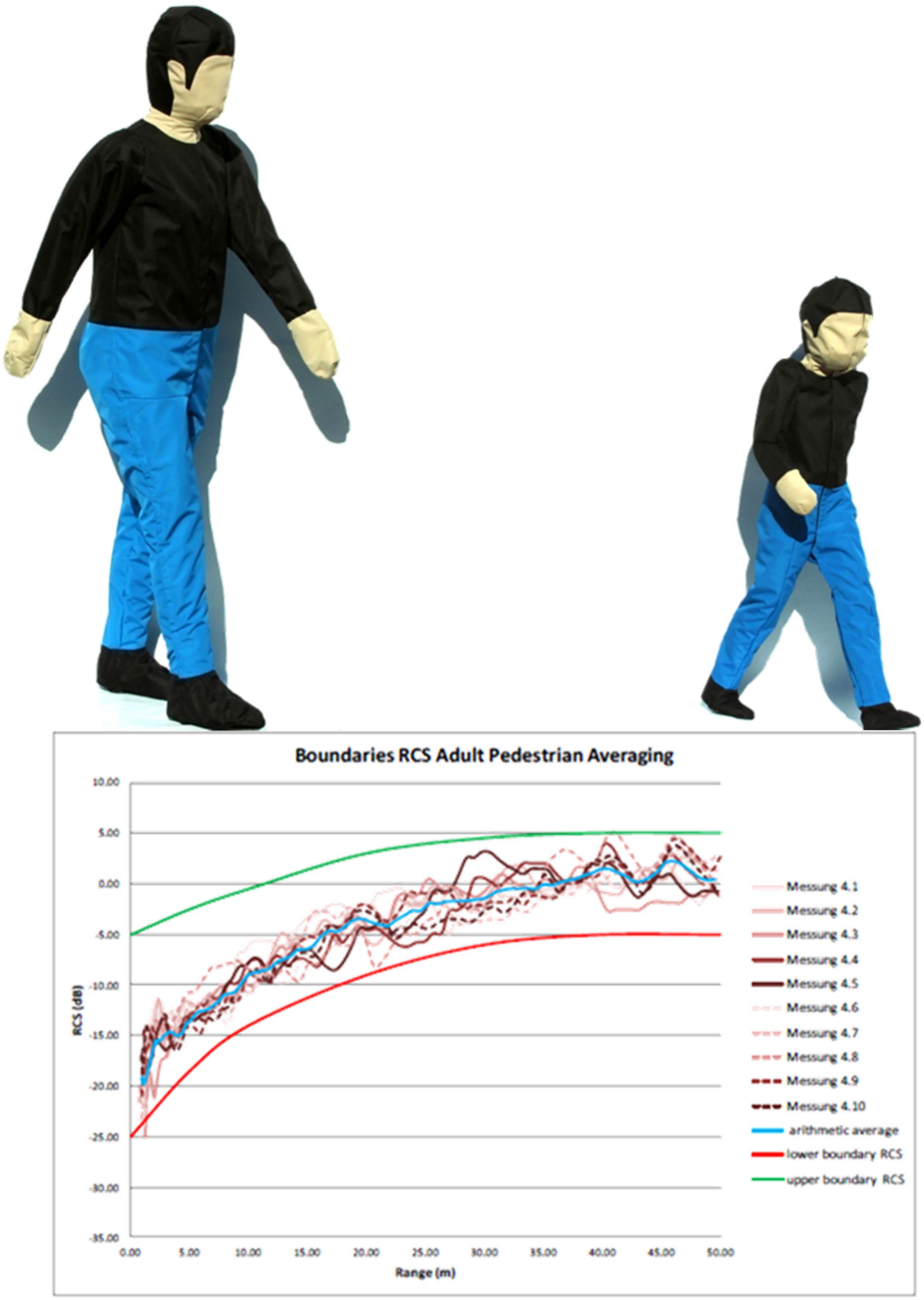


***Figure 2: Final version of the static dummy arising from the 2014 Harmonisation Platform Events (Source: 4A)***

The OEMs involved in the event considered that this dummy was acceptable for current sensors. However, reservations remained in terms of its future performance for more sophisticated radar systems that were being developed to recognize the radar signature of arm and leg movement in order to provide a more confident classification of the target as a pedestrian, potentially without fusion with a camera sensor. It was, therefore, agreed that if industry successfully developed a dummy with articulated arm and/or leg movement that could operate on the low profile platform delivery systems with levels of robustness and acceptability to visual systems at least equal to that of the standard dummy then this would be accepted.

Such a dummy is under development by industry in partnership with 4A. There has been limited independent testing of this new solution at the time of writing but first experiences suggest that the result is very impressive. The dummy survived high speed collisions well and was easy to re-assemble and the adult version

tended to produce similar results (with current sensor systems) to the static dummy. In the version presented, the dummies feet were considered to be too far from the floor, and the articulated child dummy was less well recognized than its static counterpart. This was considered likely to be a postural problem and suitable amendments are underway. If these final modifications are successful then the articulated dummy will be adopted for the final procedure.

***Figure 3: Image of the proposed adult articulated dummy (source: 4A).***

## EVALUATING CANDIDATE TEST SCENARIOS

During the development of the test procedure, a wide range of test scenarios proposed by the various stakeholders. Each of these could have been justified on the basis of the available accident data and each had advantages and disadvantages. However, it was considered that to minimize the test burden the number of test scenarios had to be kept low. The results of preliminary rounds of testing and analysis involving these scenarios is described below.

### Testing in Darkness

The accident data showed that for killed and seriously injured pedestrians, performance in darkness would be very important. Some AEB Pedestrian systems will not work in darkness whereas others will. There is, therefore, a strong rationale for implementing a test in darkness. However, such a test would add considerable technical and operational complexity to an already difficult test. For example, to ensure reproducibility the actual level of light would need to be closely controlled to defined levels. Given that most pedestrian collisions occur in urban areas with street lighting then the test should be representative of that condition, however, street lighting can vary considerably by region. Additionally, tuning the characteristics of the dummy to be sufficiently representative of a real human has proved complex. It remains unknown whether those same properties are adequate to be representative of a real human at night.

It was considered that overcoming these difficulties would be likely to take considerable time and delay the introduction of a test procedure. For that reason, it was agreed at an early stage that tests in darkness would not be considered for the protocol due to be implemented in 2016. Instead, it is proposed that manufacturers be awarded additional points on confirmation that the system continues to work at low levels of illumination. Additional night-time performance tests will be considered for inclusion as an update to the protocol for 2018.

**Adult walks from nearside, no obstruction**

The accident evidence reviewed in this paper agreed closely with that from all other stakeholders that this scenario represented the most common accident mechanism by a substantial margin. Walking speed was generally agreed to be 5 km/h. The main variable considered for discussion was the impact point on the front of the car, whether this should be at a point 25% of the vehicle's width from the nearside, 50% or 75%.

Most of the early testing was done at an impact point of 50%. In this test scenario it was found that all vehicles tested generally showed considerable performance but variation between models existed. For example, a production radar camera fusion system would typically avoid collisions at vehicle speeds of up to 30 km/h and would mitigate a small amount (10 km/h) even at a test speed of 60 km/h. However, an advanced prototype stereo camera (tuned for highest possible avoidance) was capable of avoiding collision from a vehicle speed of 50 km/h. None of the vehicles tested offered performance at a vehicle speed of 10 km/h. This is a function of the lateral field of view of the sensor. When the vehicle is travelling very slowly it is not much faster than the pedestrian dummy, which means the pedestrian dummy does not begin to move until the vehicle is very close. At this point it is not within the field of view of the sensors tested, and then reappears back in the field of view at short Time To Collision (TTC), limiting the opportunity available for the AEB system to activate.

Engineering analysis of this scenario suggests that the time that the sensor detects the pedestrian with sufficient confidence to act should not be affected by different impact points on the front of the car. Thus, the closer the impact point is to the nearside, the less time is available for the car to brake. Thus, it would be expected that performance would be reduced compared to the results above at 25% impact point and increased at a 75% impact point, though in the 75% scenario the system may not fully exploit that opportunity if it does not have early confidence that the pedestrian will not fully pass the vehicle before impact or that the collision cannot be avoided by steering.

**Adult walks from farside, no obstruction**

It was also clear from the accident data that an adult crossing the road from the farside of the vehicle was one of the more common situations. However, the evidence was more conflicting about the speed of the movements. In this scenario the adult was assumed to walk at 5 km/h.

The lateral separation between the starting position of the pedestrian and the impact point on the car is greater in the scenario than in the one where the pedestrian walks from the nearside. So, the time available for the system to detect and react to the pedestrian is theoretically greater, offering the opportunity for superior AEB performance. However, this is limited by two factors:

- Sensor field of view: the sensor field of view will continue to limit performance at low vehicle speeds
- Confidence in impact prediction: Moving human beings are highly dynamic and can stop or change direction quickly so most AEB systems will not be sufficiently confident of an imminent collision to autonomously brake until the pedestrian is either in the direct path of the vehicle or close to entering the path. This threshold is likely to be symmetrical around the vehicle so in fact the time available to brake in this farside scenario will actually be the same as that for the nearside walking scenario.

**Adult runs from farside, no obstruction**

In the UK data from the OTS study, it was identified that adults crossing from the farside were often running. It was not possible to identify the actual speed of these pedestrians but it was assumed that this translated to a pedestrian speed of 8 km/h.

In terms of layout and sequence of events this scenario is identical to the adult walking from the farside one. However, the increased pedestrian speed has the effect of exacerbating the sensor field of view difficulty at low speeds because the car will be closer (longitudinally) to the pedestrian at the point the pedestrian first begins to cross the road. Thus, the pedestrian will enter the sensor field of view with a smaller time to collision than at lower pedestrian speed. The additional speed also reduces the time available to brake for systems that will only apply braking when the pedestrian crosses into the vehicle path. Systems that use path prediction might suffer less with the latter problem because a pedestrian moving more quickly will also take longer to stop or change direction so the point at which the algorithm decides a collision is imminent may also become earlier.

As such this is a more challenging scenario for the technology than either of those previously discussed. However, technological opportunities do exist to overcome those challenges and improve performance. This is reflected in preliminary test results at a 50% impact point that suggest a simple mono camera installation was inoperative at speeds below about 25 km/h and above about 50 km/h. At test speeds in-between it reduced collision speeds by a few km/h. However, an advanced sensor fusion system was able to mitigate a 20km/h test speed to a 5 km/h impact speed and was able to fully avoid higher speed impacts from travel speeds of up to 55 km/h. At a test speed of 60 km/h the impact speed was reduced to less than 30 km/h.

**Elderly adult walks slowly from farside**

Accident data presented by the ASPECCS project suggested that a substantial proportion of those crossing from the farside were elderly and thus moving slowly, estimated to be represented by a test speed for the pedestrian of 3 km/h.

In terms of detection, a slow pedestrian speed could potentially be more challenging, because very low speed movement can be harder to quantify accurately than higher speeds. However, if detected, the slower pedestrian speed would reduce the problems with sensor field of view and allow more time for braking for those systems that will only brake once the pedestrian has entered the path.

**Child runs out from behind parked vehicles at the nearside.**

The accident data was generally agreed that collision mechanisms involving obstructed line of sight and children were common and that such accidents often involved running. Initially, this was assumed to be represented by a dummy speed of 8 km/h, the same as assumed for the running adult in the farside scenario. In physical terms, the obstruction was achieved by parking a small car immediately in front of the pedestrian and a larger car in front of that. The obstructed view meant that the time for which the pedestrian was visible between emerging from behind the car and entering the path of the test vehicle was very small. This severely limits the amount of time the sensing system has to detect and track the pedestrian. Although it is possible that future sensing systems may find ways of detecting the movement of the pedestrian behind the obstruction, none of those tested to date have demonstrated such performance.

Initial tests of this scenario were undertaken at impact points positioned 25% of the vehicles width in-board of the nearside of the vehicle. This impact point limits the time available for braking, if braking is initiated at a fixed geometric boundary (i.e. when the pedestrian crosses into the vehicle's path). The 8 km/h pedestrian speed also reduces the time available for braking, compared with the benchmark walking scenarios.

The test results for this scenario supported the theory that this was a very challenging one for AEB systems to prevent. Of those systems tested in this scenario, the best performance was modest speed reductions of around 5 km/h from tests speeds of around 20 to 25 km/h. Simulations of the performance that might be expected from future systems suggested that this could be improved upon somewhat but not substantially.

**ANALYSIS AND SCENARIO SELECTION**

The preliminary tests and analyses of the candidate test scenarios identified a range of variables that were important in relation to the accident data and/or to the ability of current systems to perform. These were:

- Impact point (25%, 50% or 75%): The 25% point is more representative of the most frequent collisions and is more technically challenging for systems
- Pedestrian speed (3, 5 or 8 km/h): Evidence was mixed from the accident data, higher pedestrian speeds are more technically challenging in respect to time available to brake and sensor field of view but the low speed was potentially more challenging for detection and classification.
- View (obstructed or clear): Collisions where the view of the pedestrian is clear 2 seconds before impact are more common than those that are masked from view. However, the latter represents a substantial and sensitive minority, often involving children, and is more technically demanding.
- Pedestrian age/size (adult or child): Adults are more frequently involved but children represent a substantial, over-represented and sensitive minority and could be more technically challenging, particularly in the presence of an obstructed view.

The two most closely agreed scenarios in the preliminary list of candidate scenarios were the adult walking from the nearside unobstructed and the child running from behind cars parked at the nearside. The first of these was a test that closely represented common accident types and the available AEB systems were able to demonstrate a strong positive effect, though the magnitude of effect varied for different systems. However, with respect to each of the variables above it involved the less challenging options for all of them. The second scenario was also representative of the accident data but combined the most challenging option for all of the above variables in one test. Thus, it was found that current and likely future systems would be able to offer only very small benefits.

It was, therefore, considered that the challenging options should be distributed around the test scenarios more evenly. This resulted in the final selection of test scenarios shown in ***Table 2***, below.

**Table 2: Final selection of test scenarios for implementation in Euro NCAP in 2016**

| | | | |
|---|---|---|---|
| PEDESTRIAN | Far side | Near side | |
| | Adult | Adult | Child |
| | 8km/h | 5km/h | 5km/h |
| | 50% (central) | 25% & 75% | 50% (central) |
| VUT | 20-60km/h | 20-60km/h | 20-60km/h |

In this way, the child emerging from behind a parked car is still represented but with a slightly lower dummy speed than originally considered (though still within the range of a running child) and involving a collision with the centre point of the front of the car. The main baseline scenario remains the adult walking from the nearside but this test should be undertaken at impact points towards the edges of the car, which is representative of collision data and fairly reflects the challenge of avoiding such collisions. The farside test is

undertaken with the higher speed dummy, which is representative of the UK association with adults running from that side and which also acts to ensure symmetry of performance, while challenging the sensor field of view and the braking performance.

Of the list of key variables identified above, a 3 km/h elderly pedestrian is the only one not represented in this matrix. The rationale behind this was that for this type of pedestrian the key element was almost binary; could the pedestrian be detected reliably or not. Once detected reliably, such pedestrians would be easier to avoid than those represented by the other scenarios. The ability to detect 3 km/h pedestrians has therefore been included as a pre-requisite of the test and is demonstrated by a single test at one vehicle test speed.

## VERIFICATION OF PROPOSED PROCEDURES

Tests have now been undertaken with a range of vehicles against all of the defined procedures to assess how well they work and to test the repeatability & reproducibility of the test procedures and to assess the scoring system (reported separately). In order to demonstrate the effectiveness of the procedures the results from two vehicles, representing the outliers of current production cost and performance, have been shown below. The Mini One is equipped with a single mono-camera AEB and the Lexus LS460 is equipped with a very sophisticated sensor fusion system comprising radar, stereo camera and infra-red sensors.

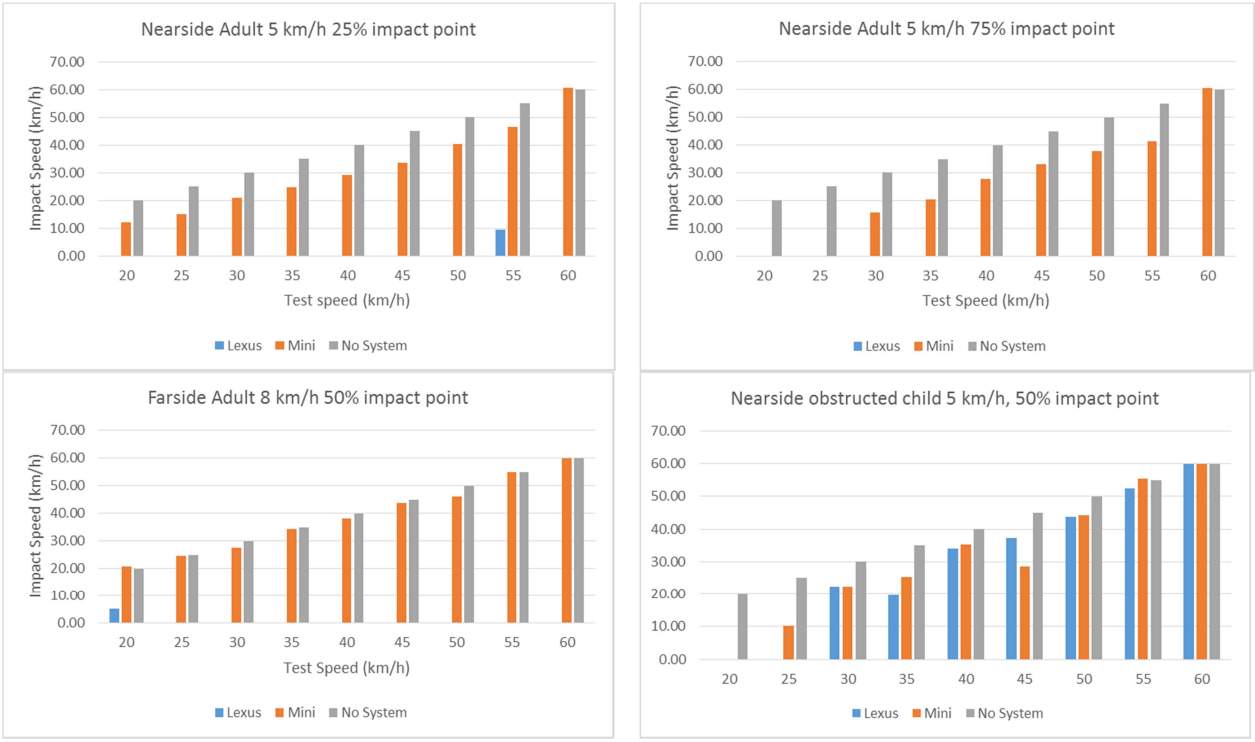


***Figure 4: Results of final test procedures applied to single mono-camera and sophisticated sensor fusion systems.***

It can be seen that the mono-camera system fitted to the Mini is mainly a mitigation system. There are only a very few scenarios where it is capable of avoidance but it offers useful speed reductions in the baseline nearside adult scenarios and nearside child scenario. By contrast, the sophisticated sensor fusion system fitted to the Lexus avoids in almost every test except the nearside obstructed child test. It is understood that the extremely good performance of the Lexus is enabled by the use of a path prediction algorithm that enables the brakes to be applied a short time before the pedestrian enters the vehicle path. However, the advantage of this system is denied in the obscured scenario where the pedestrian is hidden for large parts of the time required to produce the path prediction.

## CONCLUSIONS

Pedestrians remain a serious road safety concern in Europe, representing almost 20% of all fatalities from road traffic accidents. Analyses of the circumstances of those crashes involving the front of the car show that the vast majority involve pedestrians crossing the road approximately perpendicularly to the direction of travel of the car. The largest group of such collisions involve adults walking from the nearside without being masked by parked vehicles or other obstructions. This is followed by adults crossing from the farside of the road. Children crossing from behind parked vehicles represents a significant and over-represented minority of crashes.

Developing test targets that appear sufficiently 'human-like' in the eyes of a range of different sensor systems, whilst being sufficiently cheap and robust to be used in full contact testing has proved challenging. However, a static dummy that is effective for all current production sensors tested to-date is now commercially available. An articulated dummy that will future proof the test against the future development of radar sensors that rely on the movement of limbs is in the final stages of development and will be adopted for the test.

Test procedures have been developed based on a combination of the evidence from real world accident data and the ability of current and likely future AEB systems to influence the outcome in such scenarios. A set of three test scenarios have been proposed, offering comprehensive coverage of the variable identified as most important, including varying impact point, pedestrian speed, and vehicle speed, nearside and far side approach, adult and child pedestrians, obstructed and clear views.

These test procedures have been applied to a range of vehicles and do successfully reward fitment of even simple systems while also clearly discriminating between the different levels of performance found in the market today. It is expected that these developments, once fully implemented in consumer testing will be expected to drive significant reductions in pedestrian casualties.

Euro NCAP has agreed to implement these procedures within it's protocols in 2016 but pedestrian crashes are a problem across the developed world and the globalization of the vehicle industry means that there will be considerable benefits to implementing a harmonized test in as many international programs as possible.

## REFERENCES

Lemmen, Stoll, Bergelt, Seiniger, Wisch, Bartels, Schubert, Kunert, Knight, Brookes, Ranovona, Okawa, Domsch, Schaller (20130. *"Evaluation of pedestrian targets for use in autonomous emergency brake system testing – A report from the harmonization platform 2 dealing with test equipment*." Proceedings of the 23rd ESV conference, Seoul, Korea, 2013 paper number 13-0124

Lenard, J. and Danton, R. (2010). *"Accident data study in support of development of autonomous emergency braking test procedures"*. Loughborough University LUEL 5989/6175.

Pace J. F., et al. (2012) *Basic Fact Sheet "Pedestrians*", Deliverable D3.9 of the EC FP7 project DaCoTA.

# A MODEL OF VEHICLE-FIXED BARRIER FRONTAL CRASH AND ITS APPLICATION IN THE ESTIMATION OF CRASH KINEMATICS

**Zuolong, Wei**
**Hamid Reza, Krimi**
**Kjell Gunnar, Robbersmyr**
University of Agder
Norway

Paper Number 15-0161

## ABSTRACT

The study of vehicle crash process is of great importance in transportation safety. The crash pulses of vehicles during the fixed barrier impacts can reflect the crashworthiness of the vehicle structure. In this paper, a mathematical model of vehicle kinematics during the frontal crash is investigated. This work is based on the analysis of crash response signals and vehicle structure. The proposed model uses piecewise linear functions to describe the trend of crash impulse and ignores the residual oscillations. To study the model variance, the crashes in various speeds and a full car crash in complex condition are compared. At the end of paper, the crash performance of a vehicle crash is predicted according to the proposed model and therefore demonstrates its effectiveness and usability.

## INTRODUCTION

Crashworthiness is one of the core topics in the passive safety of vehicles and plays an important role in the condition that the impact cannot be avoided. Generally, the analysis of crashworthiness is based on the related crash responses, i.e. the displacement, velocity and acceleration, of critical parts of a vehicle in full car crash tests. However, these tests are required appropriate facilities, one or more cars with measuring devices, experienced staff and a long time to prepare. It means they are complicated, expensive, long-lasting and therefore not easy to realize [1]. This is especially true in the early stage of vehicle design. Therefore, vehicle designers and researchers made a lot of effort to build numerical models to describe the crash processes.
Up to now, various technologies are used to model the vehicle crash. Typical crash models may be classified into three broad categories [2]: 1) Detailed nonlinear finite element models. These models have excellent performance in the estimation of structural crashworthiness. However, before these crash models could be used, they usually require the details of the vehicle structure and materials. This limits the use of FE models in the design process. 2) Multibody models and multibody based lumped parameter models. As FE models, the multibody models also suffer the complexity. Consequently, the multibody based lumped parameter models make a compromise between the accuracy and complexity. Most of these models consist of energy absorbing (EA) elements with masses connected to both ends [3]. Reference [4 and 5] are typical studies on the lumped parameter models. 3) Functional approximation or response surface models. The functional approximation method is widely used in academia and industry. And reference [6] provides an overview of its use in the research of crashworthiness. To achieve better approximation, some advanced technologies are also introduced in this area, such as wavelet [7] and neural network [8]. Most of these models focus on the crash response signals themselves and can hardly be related to the vehicle structure. So the physical meaning of these modes is not clear.
In the proceeding of the study, a piecewise linear model is proposed to represent the vehicle-rigid wall frontal crash. Compared to existing models, this model is developed based on the analysis of crash responses and therefore can reflect the performance of vehicle structures in crashes.
The rest part of this paper is organized as follows: In the next section, the crashworthiness structure is introduced firstly. Afterwards, the proposed model is proposed. In this section, the modelling procedures will be presented in detail and the influences of crash condition are also discussed. After that, an estimation of vehicle kinematics is given as an application of the proposed model. The conclusion goes finally.

## VEHICLE STRUCTURE

Most of modern commercial cars have unibody construction, i.e. a single entity forms a car's body and frame. The vehicle body is usually made of steel or aluminum that is stamped with the appropriate cross members and everything is mounted directly to it. In this paper, only the frontal crash of unibody construction is studied.

To improve the crashworthiness, the vehicles are meticulously designed. As an integration, the vehicle structure would transmit the impact load in a proper way, i.e. load-carrying path. In addition, there are some weak components arranged as crumple zone. During the crash, the crumple zone will deform and absorb energy and ensure the rest parts of the vehicle are safe. In the local design, the material and shape of beams, shells and connectors are also considered to achieve better energy-absorbing performance.

**Load-carrying Path and Crash Process**

Generally, vehicles have a high relative velocity in the crashes. For this reason, the frontal structures always have enough space for the crashworthiness design. In many vehicles, there are three paths to transmit the impact load:

1) Path1: Accessories - Front bumper and Crash box - Front longitudinal beam-Engine - Firewall
2) Path2: Upper wing beam - A pillar - Guard beams of door;
3) Path3: Sub-frame - Sill beam

For most cases, the first path affords more than half of the total energy in crashes. Accordingly, the ideal crash process contains several stages:

1) Accessory crush. This is designed to protect the pedestrian. This stage is very short and nearly has no influence on the energy and velocity of vehicles.
2) Bumper crash and Crash box. The bumper is helpful in the low-speed crashes. Its ability for the energy absorbing is limited.
3) Longitudinal beam collapse. This part is responsible for crash compatibility, i.e. to protect the opposing vehicle in some extent and make the total lost lower in crashes.
4) Engine compression. Engine should be seen as a mass with limited deformation in crashes. In some high speed crashes, it will crush into the firewall and be compressed a little.
5) Firewall deformation. Firewall is much stronger than other components to protect the passenger cabin.

**Crashworthy Structures**

In most vehicles, longitudinal beams are designed as the crashworthy structures and employed for the energy absorbing. Although, the longitudinal beams can be various in terms of the material, section shape and processing technology, they follow the same requirement in design to optimise its performance:

1) No deformation in low speed crashes; Collapse progressively and absorbing the energy effectively in high speed crashes.
2) Having repeatable and reliable failure mode to ensure its performance in different crashes.

For this reason, the crashworthy structures of vehicles always experience a stables process of collapse during different crashes. In this process, the deformation follows a linear trend and have a series of oscillations.
To sum up, the crash processes of vehicles yield to an internal pattern, which is controlled by the load-carrying path and beam collapse mode. For this reason, a functional model is proposed to present the vehicle crash process.

**CRASH MODEL**

During a crash, the response signals contain several parts, which are corresponding to the crash stages. A piecewise model can be therefore identified by the accelerations and external force.

**Piecewise Linear Model**

There are some mathematical models of crash response in the literature, such as sine, triangular, and haversine [9]. However, none of them consider the vehicle structure and consequently are neither precise enough nor adjustable for different crash scenarios. To illustrate the proposed modelling process, NHTSA Test 5677, in which Yaris is crashing to a rigid wall in 56km/h, is employed for example.

**Model structure** The response of vehicle crashes can be recorded by the acceleration signals (crash impulses). Figure 1 shows the acceleration signal of the left rear seat during the crash and the proposed model structure.

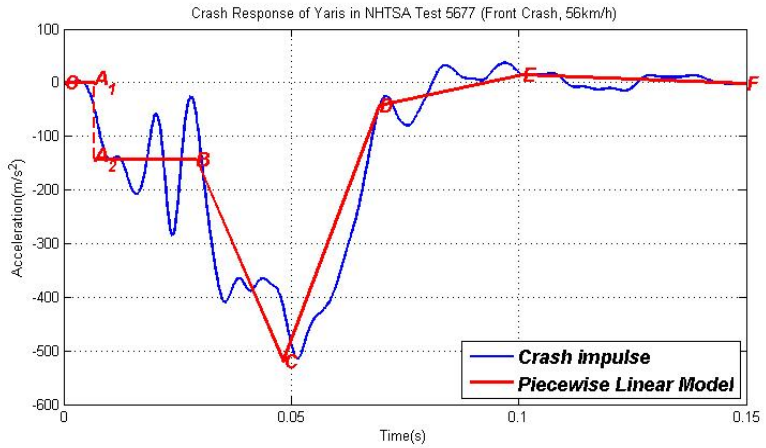


***Figure1. Piecewise linear model structure for front crash of sedans.***

Comparing with load-carrying path and crash stages presented above, the physical meaning of the model structure is as follows:

1) Original-A1 segment: The accessory are crushed and bumper deform. In this stage, there is no significant acceleration.
2) A2-B segment: The crash box and longitudinal beam are working. During this time, the acceleration is stable around a level.
3) B-C-D segment: The longitudinal beam keeps working and the engine is crashing to the firewall. The force worked on the firewall makes the sharp slowdown of the cabin.
4) D-E-End segment: Restitution process. The crumple area is fully compressed and most energy are absorbed. Some internal energy is released and leads the oscillation of velocity.

Although some local oscillations (the high frequency component of acceleration signals) are lost in this model structure, it reflects the trend (base mode) of acceleration in a full crash. Because the integration of the oscillations approaches zero [10], this model can keep a good performance in the estimation of velocity and displacement.

**Time of model nodes** In the presented model structure, the time and value of each node (i.e. A1, A2, and B~F) are to be decided. For O-$A_1$ stage, the acceleration is small and the variation of velocity is tiny. The end of this stage can be set as:

$$T_A = t_0, \text{when } \Delta v(t_0) = \int_0^{t_0} a(t)\,dt = 1\% \times v_{init} \quad (1)$$

and

$$Acc_{A_1} = 0 \quad (2)$$

For node F, $T_F$ is the end time of signals and the acceleration $Acc_F$ is the value of end time. The times of other nodes are discussed in this part and the accelerations will be studied in the next part.

Comparing to $A_2$-B, the main feature of B-C-D process is that the engine is compressed by the firewall. The contact force slowdowns the cabin drastically. Correspondingly, the reacting force makes the deceleration of engine turn smaller (See Figure 2). So the time of B, $T_B$, is the time of minimum engine deceleration.

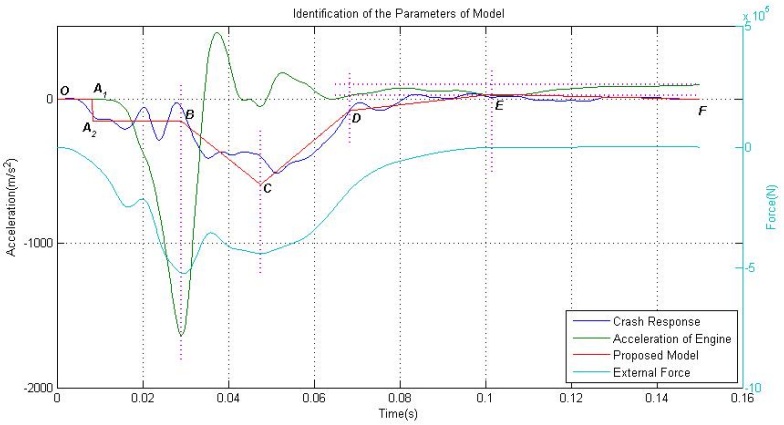


***Figure2. Time Identification of Proposed Model Structure.***

After $T_B$, the engine experiences a "step response" like process with the input of the reacting force from firewall and finally arrives the stable value when the time finished. So $T_B$ can be set as the time when engine acceleration arrives the steady area. A recommended steady area can be seen from the maximum to the minimum value of engine acceleration after the $T_E$ (will be given later).

Node C refers to the maximum deceleration in the crash process. Of course, it can be decided directly by the minimum point of crash response. However, in some cases, $Acc_C$ is not significantly lower than the neighborhood and therefore $T_C$ suffers a great uncertainty. This is because of the combined effect of the oscillations from engine and rest part of the vehicle. And neither of them plays a leading role. For these cases, an alternated method is given as below.

It should be noted that the crash response signal is measured from one point of the vehicle body. That means it cannot reflect the general response exactly perfect. To solve this problem, the external force, which works on the vehicle is to be studied (See Figure 2).

As shown, the first maximum force is corresponding to the node B and contributes to the maximum deceleration of the engine. The second maximum force is related to the Node C, as the engine acceleration is not significant at that period. So, $T_C$ equals to the time of the second maximum force.

For the restitution stage, $T_E$ is the time when external force falls to 1% of the maximum value.

**Accelerations of model nodes** The proposed model is hoped to make the error of acceleration and velocity small. For convenience in computation, the accelerations of B~E should ensure 1) $Acc_B$~$Acc_E$ locate near the real crash response; 2) the interaction of the proposed model, i.e. the velocity of model, is same with the real crash response at times $T_B$, $T_D$ and $T_F$. So we can set $Acc_D = a(T_D)$ arbitrarily and decide the rest accelerations as follows:

1) To ensure

$$\int_0^{T_B} Acc(t)\,dt = Acc_B * (T_B - T_A) = \Delta v(T_B) \quad (3)$$

$Acc_B$ is set as

$$Acc_B = \frac{\Delta v(T_B)}{T_B - T_A} \quad (4)$$

2) To ensure

$$\int_{T_B}^{T_D} Acc(t)\,dt = \frac{1}{2}Acc_B * (T_C - T_B) + Acc_C * (T_D - T_B) + \frac{1}{2}Acc_D * (T_D - T_C) = \Delta v(T_{D-B}) \quad (5)$$

$$\int_{T_D}^{T_F} Acc(t)\,dt = \frac{1}{2}Acc_D * (T_E - T_D) + Acc_E * (T_F - T_D) + \frac{1}{2}Acc_F * (T_F - T_E) = \Delta v(T_{F-D}) \quad (6)$$

$Acc_C$ and $Acc_E$ are set as

$$Acc_C = \frac{1}{T_D - T_B}\left[\Delta v(T_{D-B}) - \frac{1}{2}Acc_B * (T_C - T_B) - \frac{1}{2}Acc_D * (T_D - T_C)\right] \quad (7)$$

$$Acc_E = \frac{1}{T_F - T_D}\left[\Delta v(T_{F-D}) - \frac{1}{2}Acc_D * (T_E - T_D) - \frac{1}{2}Acc_F * (T_F - T_E)\right] \quad (8)$$

**Models for Various Speed**

To show the variance of the proposed model, a series of crashes are simulated by the FE method. In these crashes, the 2010 Toyota Yaris is crashing to a rigid wall at the speed of 20km/h, 25km/h, 32km/h, 40km/h,

48km/h, 56km/h and 65km/h. The FE model of Yaris comes from the National Crash Analysis Center (NCAC) of George Washington University.
The parameters of the modelling results are shown in the table (See Table 1).

**Table1.**
**Parameters of modelling results for crash simulations in various initial velocities.**

| No. | Initial Velocity | At(s)/ A1(m/s$^2$) | Bt(s)/ B(m/s$^2$) | Ct(s)/ C(m/s$^2$) | Dt(s)/ D(m/s$^2$) | Et(s)/ E(m/s$^2$) | Ft(s)/ F(m/s$^2$) | Note |
|---|---|---|---|---|---|---|---|---|
| 1 | 20km/h | 0.0203<br>0 | *0.0473*<br>*-114.4992* | *0.1159*<br>*-127.7229* | 0.0736<br>-93.6547 | 0.1026<br>22.6533 | 0.1499<br>2.0482 | Bad |
| 2 | 25km/h | 0.0172<br>0 | 0.0368<br>-125.1086 | 0.0569<br>-199.2543 | 0.0749<br>-87.6170 | 0.0985<br>20.3931 | 0. 1499<br>-0.5908 | Good |
| 3 | 32km/h | 0.0145<br>0 | *0.0541*<br>*-178.0036* | *0.1058*<br>*35.2196* | 0.0933<br>-3.2184 | 0.0989<br>-1.1863 | 0. 1499<br>14.3759 | Bad |
| 4 | 40km/h | 0.0125<br>0 | 0.0403<br>-187.4030 | 0.0516<br>-285.4251 | 0.0774<br>-84.9810 | 0.1030<br>37.3893 | 0.1499<br>-17.9486 | Good |
| 5 | 48km/h | 0.0111<br>0 | 0.0337<br>-195.5635 | 0.0578<br>-379.2445 | 0.0745<br>-110.9681 | 0.0927<br>25.4419 | 0.1499<br>17.3587 | Good |
| 6 | 56km/h | 0.0102<br>0 | 0.0330<br>-195.0890 | 0.0474<br>-484.4808 | 0.0873<br>40.1901 | 0.0963<br>40.0699 | 0.1499<br>-12.1832 | Good |
| 7 | 65km/h | 0.0096<br>0 | 0.0278<br>-202.8010 | 0.0456<br>*-399.5320* | *0.1042*<br>*44.3387* | 0.1049<br>*21.1624* | 0.1499<br>-22.8631 | Bad |
| 8 | 20km/h | 0.0203<br>0 | 0.0323<br>-97.2563 | 0.0481<br>-172.514 | 0.0736<br>-93.6547 | 0.1026<br>22.6533 | 0.1499<br>2.0482 | Good after adjustment |
| 9 | 32km/h | 0.0145<br>0 | 0.0362<br>-150.5192 | 0.0503<br>-229.4992 | 0.0933<br>-3.2184 | 0.0989<br>-1.1863 | 0.1499<br>14.3759 | Good after adjustment |
| 10 | 65km/h | 0.0096<br>0 | 0.0278<br>-202.8010 | 0.0456<br>-500.0374 | 0.0905<br>38.564 | 0.1049<br>35.1197 | 0.1499<br>-22.8631 | Good after adjustment |

This table shows that:

1) Generally speaking, the model has good applicability for the crashes with the initial velocity from 25~56km/h.
2) For the No. 3, the model has a wrong identification of $T_B$ and $T_C$ and therefore fails to fit the crash response. By studying the crash responses of 32km/h crash (See Figure 3b), it can be found that the engine acceleration at 0.0362s is the first local minimum value with the abrupt turn of trend. According to the physical meaning, this abrupt turn refers to the contact between the engine and firewall and $T_B$ should be 0.0362s. Consequently, $T_C$ is 0.0503s. After this adjustment (as No. 9), the model fits the crash response well. This is because of the less compression of the engine in the lower speed crashes. So for the crashes with initial speed lower than 32km/h, it is highly recommended to check the model again according to the physical meaning.
3) No. 1 suffers similar problems with Test 3 and can be adjusted (as No. 8) to achieve good performance. However, the minimum value is not much lower than other values in this crash response (See Figure 3a). Specifically, the process B~D (i.e. the engine influence) is not as significant as other crashes. This means the crash process, as well as model structure, is different from high speed crashes. For this reason, the proposed model may cannot represent the responses well for the crashes with initial velocity lower than 20km/h.
4) No. 7 is for the 65km/h crash and have a problem in the identification of $T_D$. In the crash responses (See Figure 3c), there are oscillations with big amplitude in the process D~E and lead the wrong identification. Obviously, in this crash, the vibration of the engine is much stronger than 56km/h crash. An adjustment can be made manually to improve the model (as No. 10). But it should be mentioned that for a higher speed crash, the model can hardly present the crash process very well.

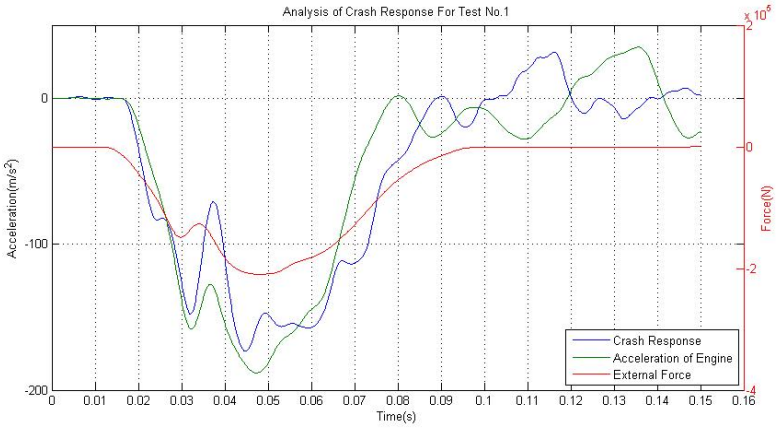


a) Crash Responses and References of No.1 Simulation

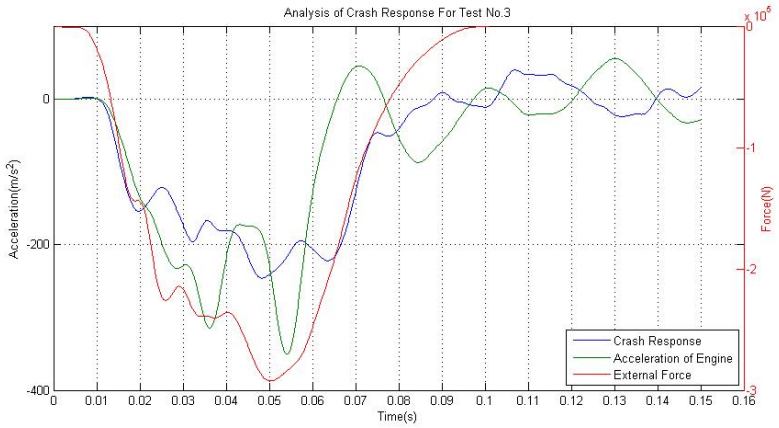


b) Crash Responses and References of No.3 Simulation

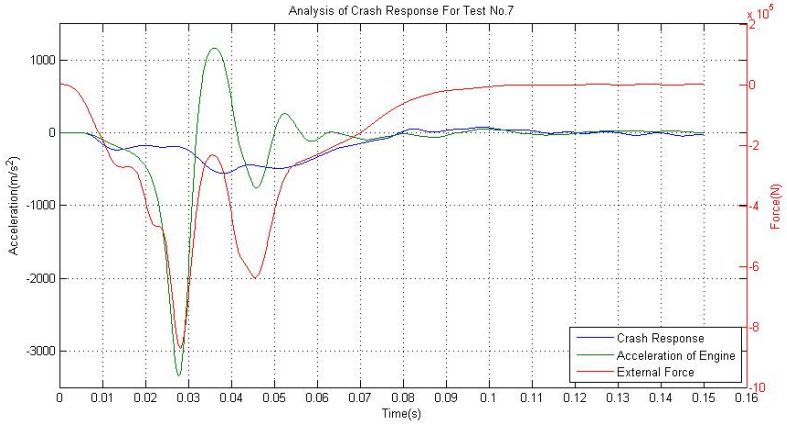


c) Crash Responses and References of No.7 Simulation

***Figure3. Crash Responses and References (a. No.1; b. No.3; c. No.7).***

**Complex Condition**

In this subsection, a full car crash test will be studied. In this crash, the Yaris is crashed by a moving deformable barrier (RMDB) with a target speed of 86.7 km/h. The crash mode is 7° angle and 20.6% offset (See Figure 4a). The test data come from NHTSA Test 7434.

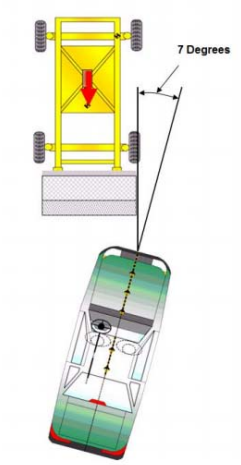


a) Configuration of NHTSA Test 7434

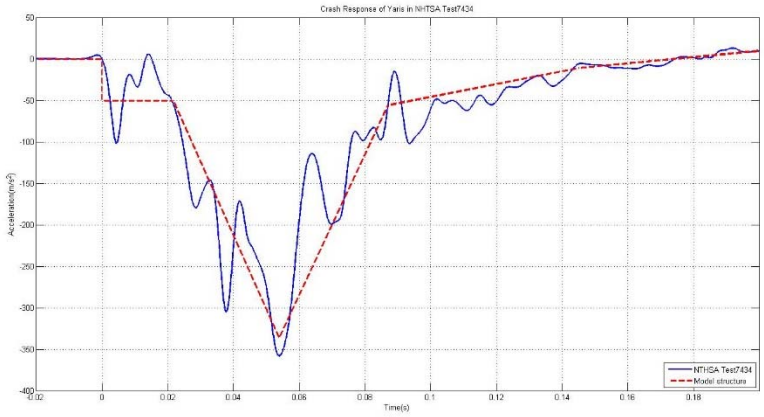


b) Crash Responses and Modelling of NHTSA Test 7434

***Figure4. NHTSA Crash Test 7434 (a. Crash Configuration; b. Crash Response)***

From this response, we can find that:

1) Because of the deformable barrier, the maximum acceleration in this test is 358.3208m/s$^2$ in negative direction, which is near the value in 40km/h rigid wall crash. So it is possible to have an experience that the maximum acceleration of a deformable barrier crash can be estimated by the rigid wall crash with half speed. Of course, this is a rough estimation and the barrier should have similar mechanical characteristics as the vehicle body.
2) In 0~0.02s, the bumper, crash box and longitudinal beam are deforming. But due to the offset, only left half part of the crush zone is crushed and therefor this crash response during this time is different from 100% overlap crash. The most important difference is the average value in this period is about 50m/s$^2$, which is about only 1/ the $Acc_B$ in No. 4 of Table 1. In other words, the absorbed energy is much lower than the full overlap crash
3) There is also a process like B-D in the model, which indicates that the engine is also crushed into the firewall and compressed. This shows all the crashworthiness structures will work in the crashes with an offset.

In conclusion, this crash test can also be described roughly by the proposed model structure, shown as the red dash line in Figure 6b. However, some local performances are different, such as the mode of B-C stage. And consequently the related parameters should also be revalued.

## ESTIMATION OF VEHICLE KINEMATICS

The proposed model can be used for the estimation of vehicle kinematics. The NTHSA Test 6069 can be used as an example. The crash condition is: 39.6km/h full overlap crash to a rigid wall barrier. To make an

estimation, the parameters of the proposed model can be set as the average value of No. 5 and No. 9 in Table 1. That is $A_t = 0.0128$, $Acc_A = 0$, $B_t = 0.0350$, $Acc_B = -173.0414$, $C_t = 0.0541$, $Acc_C = -304.3719$, $D_t = 0.0825$, $Acc_D = -40.4034$, $E_t = 0.958$, $Acc_E = 12.3273$, $F_t = 0.1499$ and $Acc_F = 15.8673$.
Note: the $T_D$ of No. 9 is obviously higher than other $T_D$. This may be because of the uncertainty of simulations. To get better estimation, the estimation of $T_D$ and $Acc_D$ should be adjusted as the average of No. 2~6, as the 39.6km/h is the average of the corresponding velocities.
The estimated model will be compared with the Test 6069 and simulation result (See Figure 5).

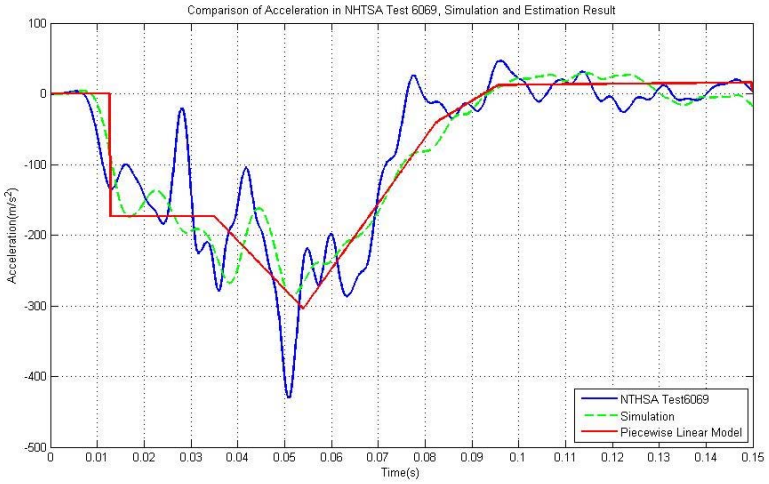


a) Acceleration Signals

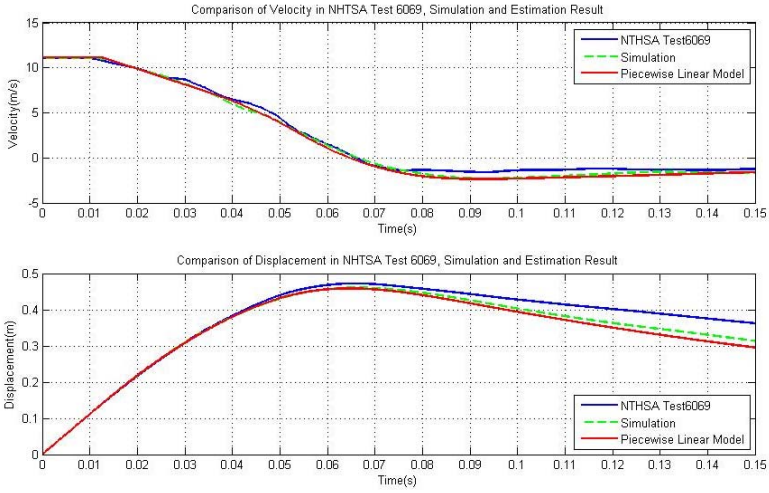


b) Velocity and Displacement Signals

***Figure5. Validation of the estimation (a. Acceleration; b. Velocity & Displacement)***

As shown in Figure 5, the estimated results fit the test and simulation very well. The displacement error (about 0.0668m) at the end of time, which is similar with the simulation (about 0.0460m).

## CONCLUSIONS

Comparing to finite element models and multibody modes, the mathematical models have advantages on conciseness and usability. For this reason, the mathematical models can be used in the early design of vehicles, as well as accident reconstruction. This paper presents a novel modelling scheme of crashes, which is based on the acceleration signals and vehicle structure. The proposed model can reflect the crash process clearly and therefore describe the crash response exactly. In addition, this model suits for the crash in various conditions

by adjusting the parameters. At the end of paper, an estimation of vehicle kinematics shows the good performance of the proposed model for a frontal crash at 40km/h.

**REFERENCES**

[1] Pawlus, W., Robbersmyr, K. G. and Karimi, H. R. 2014. "Investigation of vehicle crash modeling techniques: theory and application." International Journal of Advanced Manufacturing Technology, 70(5-8), 965-993.
[2] Hamza, K. T. 2008. "Design for vehicle structural crashworthiness via crash mode matching". ProQuest.
[3] Huang, Matthew. 2010. "Vehicle crash mechanics". CRC press.
[4] Kamal, M. M. 1970. "Analysis and simulation of vehicle to barrier impact." No. 700414, SAE Technical Paper.
[5] Pawlus, W., Robbersmyr, K. G. and Karimi, H. R. 2011. "Mathematical modelling and parameters estimation of a car crash using data-based regressive model approach." Applied Mathematical Modelling, 35(10), 5091-5107.
[6] Simpson, T. W., Booker, A. J., Ghosh, D., Giunta, A. A., Koch, P. N. and Yang, R. J. 2004. "Approximation methods in multidisciplinary analysis and optimization: a panel discussion." Structural and multidisciplinary optimization, 27(5), 302-313.
[7] Karimi, H. R. and K.G. Robbersmyr. 2011. "Signal analysis and performance evaluation of a vehicle crash test with a fixed safety barrier based on Haar wavelets." International Journal of Wavelets, Multiresoloution and Image Processing, 9(1), 131-149.
[8] Zhao, L., Pawlus, W., Karimi, H. R. and Robbersmyr, K. G. 2014. "Data-based modeling of vehicle crash using adaptive neural-fuzzy inference system." Mechatronics, IEEE/ASME Transactions on, 19(2), 684-696.
[9] Varat, M. S. and Husher, S. E. 2003. "Crash pulse modelling for vehicle safety research. In Proceedings of International Technical Conference on the Enhanced Safety of Vehicles. " National Highway Traffic Safety Administration.
[10] Chou, C. C., Le, J., Chen, P. and Bauch, D. J. 2001. "Development of CAE simulated crash pulses for airbag sensor algorithm/calibration in frontal impacts." In 17th International Technical Conference on the Enhanced safety of Vehicles, Amsterdam.

**E-Vehicle Safety – Pyro Switch as High Voltage Circuit Breaker & Bypass**

**David, Sturk**
**Per, Gustafsson**
Autoliv Development AB
**Alf, Holgers**
**Håkan, Sundmark**
Autoliv Sweden AB
Sweden
**Christian, Cavell**
Autoliv Germany
Germany
**Francois Gaudinat**
**Etienne Dugast**
Autoliv NCS
France

Paper Number 15-0163

## ABSTRACT

An E-Vehicle (i.e. electrified vehicle such as EV and HEV) is often equipped with a traction battery with voltage of as high as 200 to 600 Volt dc. It is critical that such voltage shall not be put in circuiting contact with any person at any point – workshop, crash or post-crash rescue. NHTSA have defined testing procedures in FMVSS 305 so as to assure that a basic level of safe guard systems shall be utilized by conventional E-Vehicles. The paragraph S5.3 (b) demands that the traction battery shall present an external voltage <60 Volt dc after crash. This is commonly solved with relays and melting fuses which have their Pros and Cons. Relays/contactors have the benefit of being a reversible active component but are limited to operative currents and are prone to switching bounces and they are relatively heavy, large and expensive. A melting fuse is a passive component that can operate at extreme currents but is irreversible and their cutting speed is dependent on the magnitude of the fault-current.

In this paper Autoliv will present a methodology on how to disconnect a faulty battery unit rapidly (in milliseconds) regardless of the magnitude of the fault-current. This methodology can also be used to divide a traction battery down to minor units of <60 Volt dc or even bypass and disconnect a faulty battery module with maintained power electronics in order to retain mobility as well as adding the option of discharge the disconnected module so as to prevent stranded energy.

Autoliv has investigated how to use pyrotechnic switches for disruption of over-currents in a traction system with battery packs of about 300-400 Volt dc. Those tests, aiming at safe disconnection without lasting arcs, included static faulty-current tests and tests simulating an E-Vehicle traveling 50-70 km/h on a horizontal surface. Autoliv's Pyro Safety Switch (PSS) arrangement proved capable to safely disconnect both a complete battery pack (ranging from 300 to 400 Volt dc) and the intended battery module (30-60 Volt dc) in less than 0.5 milliseconds.

## INTRODUCTION

While the number of E-Vehicles on our roads is steadily increasing, new safe guard systems are continuously being developed in order to extend their electric range in terms of higher energy density without compromising safety. Safe disconnection of high voltage battery in the event of an error is mandatory and conventionally relays and fuses are used to manage such safety issues. Continuous efforts to reduce component size and weight are challenged by

issues such as arcing and switching bounces as well as unintended division of the electric energy over relays and fuses in case of harmful over-currents. The latter may occur during exposure to high over-currents if relays experience electromagnetic repulsion or bad contacts.
In his article "Hochvolt-Relais von morgen: Sichere Minimalisten" product manager Thomas Merkel of Panasonic Electric Works Europe AG educate the reader on the potential consequences if the interaction between relays and fuses does not work properly. Mr. Merkel offers an illustration to clarify this interaction between relays and fuses in general; hence the lack of definite figures for Current respectively Time in Figure 1. In tests done by Autoliv on fuses the corresponding results to the yellow curve indicate that its delta time to completion of disconnection can vary from tens of milliseconds (at over-currents of several thousands of Amps) to seconds (at lower fault currents).

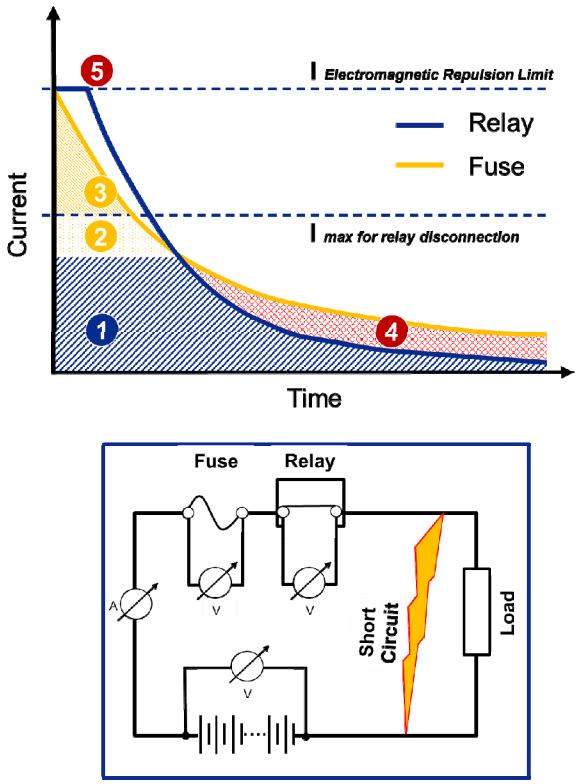


***Figure 1.*** **a) A comparison of characteristics of conventional relays and fuses when circuit disconnect is demanded. b) Simplified representation of the High Voltage circuit. (Merkel, 2014).**

In Figure 1a the blue line represent the maximum current that a relay may carry whereas the yellow line represent the characteristics of a fuse and the condition at which it will disconnect the circuit. The curve of the fuse present the dependence between the magnitude of the over-current and the rate at which the current is reduced when the fuse performs its disconnection. Figure 1b illustrates a simplified representation of a High Voltage circuit related to Figure 1a. The five areas represent the following conditions (Merkel, 2014):

1. This is the area in which a relay can comply with electrical conditions and successfully act upon activation signal.
2. Although relays can operate in this area they are often designed not to disconnect the circuit because the fuse act faster than the relay and thereby protect the relay from potenially harmful exposure to over-currents.
3. Under these conditions the relay must stay closed. Instead, the fuse shall disconnect the circuit as it is faster than a relay at these over-currents. If the relay fail to stay firmly closed and do open, a difference in

potential will be established across the contacts of the relay and the electric energy required for disconnection by the fuse will not be sufficient. A risk of severe damage to electrical components in the circuit will be imminent.

4. In this region, the system is exposed to an unacceptably long-lasting faulty-current. The fault current is not high enough for the fuse to disconnect the circuit before the relay is damaged. The system must rapidly regulate down the power in order to avoid harming the relay.
5. Fault/over-currents above the Electromagnetic Repulsion limit cannot be safely handled by neither fuse nor relay. Electrical components in the circuit will be severely damaged.

Permanent damage to the electrical system and/or its safeguard components is commonly related to overheating that is induced by over-currents and/or arcing. The time to successfully complete a disconnection of a circuit that is experiencing an over-current must be minimized in order to assure that irreversible damage to electrical components in a high voltage system also is minimized.

In contrast to a fuse, the time to achieve a complete disconnection of a circuit by means of a pyrotechnic circuit breaker will not be dependent on the magnitude of the over-current. In general, Autoliv's series of pyrotechnic switches utilizes a miniature guillotine that is propelled by a pyrotechnic charge to achieve the force required to cut through a metallic conductor. The first generation of these PSS devices have been designed for disconnection of 12 Volt batteries in the event of a traffic accident (Autoliv, n.d.) and is widely used by automanufacturers. Later PSS versions address the issue of high voltage disconnection and a methodology for such an action is presented in this article.

In the tests presented in this article, the bypass and disconnection sequence was executed by one PSS that closes a circuit so as to establish the bypass path (i.e. *a PSS which is Normally Open* – ***PSS/NO***), and a second PSS that opens a circuit in order to disconnect the faulty unit (i.e. *a PSS which is Normally Closed* – ***PSS/NC***). In later versions those two types of PSS:s are combined into one unit. By the use of Autoliv's pyrotechnic switches this bypass and disconnection sequence offers an safe high voltage disconnection with minimized risk of arcing and an extraordinary short delta time to complete the disconnection of less than 0.5 ms. The pyrotechnic switch design assure that the delta time of bypass and disconnection is kept to a minimum. This is of most importance since it will provide that the heat generated by a fault current and its harmful effects on electrical components are also put at a minimum.

## METHOD

The fundamental idea is to "redirect" the main current so as to bypass the "faulty battery unit(s)" before it is to be disconnected. At that point an extreme over-current will develop through the faulty battery unit and therefore rapid disconnection is of vital importance. Moreover, the load applied need to take into account the range of inductance that is experienced by an E-Vehicle traction system. Preparatory tests (conducted at inductance levels within a range from 0 to 154 µH) proved that when performing a direct cut off to a traction system or sub-units thereof, the higher the inductance is, the greater the propensity is of developing lasting arcs across the gap between the formerly connected conductors. Hence, the key tests (i.e. to measure the performance of the bypass and disconnection methodology) were those with the inductance above 100 µH.

The bypass of the faulty unit is the key of solving the issue with the risk of harmful arcing when cutting off an inductive circuit. A simplified explanation for this is that the circuit with inductive current is reluctant to change. This reluctance causes a harmful arc to develop between two formerly connected conductors at the moment of disconnection. In contrast to the type of "soft" arc that appear anytime when a circuit with no inductance (i.e. a capacitive circuit) is disconnected, an arc under influence of inductance will not be easily extinguished. By first establishing the bypass path, the influence on the faulty unit by the inductance from the

electric traction system will be greatly reduced. Thereafter, a rapid disconnection of the faulty unit can be achieved with minimum risk for harmful arcing.

This PSS arrangement was tested in two major setups – Complete High Voltage Disconnection and Partial High Voltage Disconnection. In the former test series, the tests were performed on a complete battery pack with test voltage ranging from 300 Volt dc up to 400 Volt dc where the arrangement replaced a Main Fuse. The latter test series were conducted on the same battery pack but the arrangement acted as a pack-internal bypass and disconnection device that allow a "faulty battery module" to be selectively disconnected while retaining operative conditions for the remaining traction system.

**Complete High Voltage Disconnection**

The diagram and photographs in Figure 2 present the test setup and the key equipment. In order to substitute a Main Fuse the PSS arrangement, i.e. a bypass switch (PSS/NO) and disconnection switch (PSS/NC), was located outside the battery pack. The intention with this test was to expose this "main fuse substitute" to an extreme condition of 5000 Amp of short circuit current carrying an inductance of 154 µH. A coil was used as static load and all power was supplied by the battery pack after a contactor (i.e. an ASEA EG315 that normally operate for steady three-phase current up to 690 Volt ac and present a very low resistance) had established the short circuit across the coil. In order to assure that the circuit carried 154 µH of inductance the short circuit was allowed to prolong for about 20 ms before the PSS/NO and PSS/NC arrangement was activated (i.e. time 0 ms). The bypass and disconnection sequence was performed in less than 0.5 ms. An additional 20 ms of data was acquired in order to visualize the relaxation of the system after the short circuit had been eliminated.

Three shunts (60 mV @ 400 Amp) measured currents as experienced by the battery pack ($I_{Batt}$ Battery Current), by the bypass circuit ($I_{BP}$ Bypass Current), and through the load ($I_L$ Load Current). All data was acquired by use of a data acquisition unit with a sampling rate of 100 kHz.

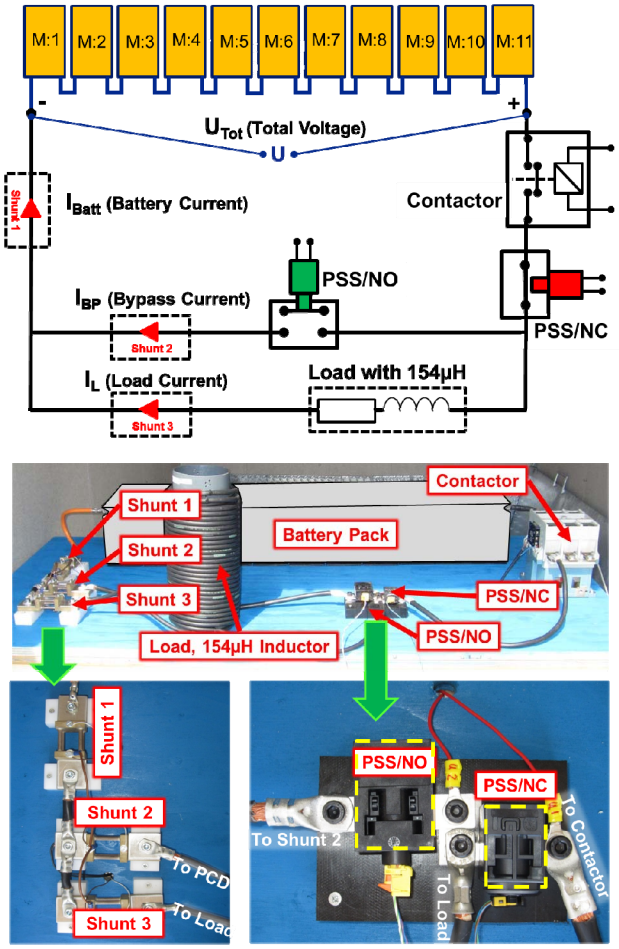


*Figure 2.* **Complete HV disconnection. Diagram on test setup, and picture of the physical test setup.**

**Partial High Voltage Disconnection**

In Figure 3 a diagram is presented where the PSS arrangement has been mounted inside the battery pack in order to allow the removal of a "faulty battery module" while retaining the main current flow through the neighboring battery modules. A Resistor-Inductor-Capacitor (i.e. RLC) load that provided a load representative for an electric car driving at steady state of 50-70 km/h on a horizontal surface regulated the main current to 25 Amp. The inductance of the system was 108 µH, which is a result of a capacitive impedance of 0.19 Ohm @300 Hz, inductive impedance of 3.4 Ohm, and a resistance of 4.5 Ohm of the RLC load.

The RLC load included a current converter with six silicon-controlled rectifiers (SCR) in bridge feeding the power from the complete battery power pack back to the national power grid. This power electronics had also a capacitor bank on the DC side to simulate the commutation capacitance in the inverter. Between the power grid and the current converter a three phase coil was located to simulate the induction in an automotive traction machine. This three phase coil also ensured that a smooth current was fed to the grid (dI/dt).

The instruments used to observe the wave forms were two Fluke® oscilloscopes of model 199C respectively 99B. Both of these were triggered by a step response, i.e. when a large change in voltage and current were evident in the circuit.

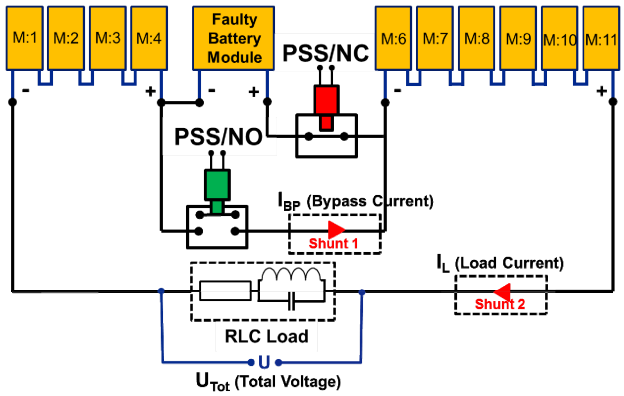


***Figure 3.*** **Partial HV disconnection. Diagram on test setup, and picture of the physical test setup.**

## RESULTS

In both test series – i.e. Complete HV Disconnection and Partial HV Disconnection – a battery pack (ranging from 300-400 Volt dc) was used together with a load that was designed to simulate an E-Vehicle electric traction system. Test results showed that breaking the high voltage circuit or isolating a faulty battery subunit, by the use of the PSS arrangement, was successfully achieved without harmful arcing or electrical fluctuations of a magnitude that may damage the surrounding electronics. As can be seen in Figure 4 and Figure 5, this action was performed in less than 0.5 ms and only minor current spikes (i.e. the integral of such a spike represent little electrical energy) and momentarily voltage variations were seen in the traction system. After a test the total battery voltage showed a reduction corresponding to the unit disconnected.

### Complete High Voltage Disconnection

At the start of the Complete High Voltage Disconnection test the contactor was closed to create a hard short circuit across the poles of the battery pack. The inductance of the system (i.e. 154 µH) delayed the balancing current conditions, which are presented in Figure 3a (between approximately -10 ms to 0 ms), i.e. the plateau for *Battery Current*, *Load Current* and Total Voltage. Meanwhile the *Bypass Current* is zero since the bypass circuit is not yet connected. See Figure 4a.

Starting at the time of the connection of the bypass circuit (i.e. at 0 ms) and prolonging for 0.5 ms (i.e. throughout the bypass/disconnect delta time) the *Battery Current* experience an even higher extreme current than before, while the *Load Current* only experience very short current spikes at the point in time of disconnection (i.e. at 0.5 ms). See Figure 4b.

After the disconnection of the battery pack the inductive circuit relaxed. This is seen in Figure 4a as the *Bypass Current* (negative direction) and *Load Current* (positive direction) decreased.

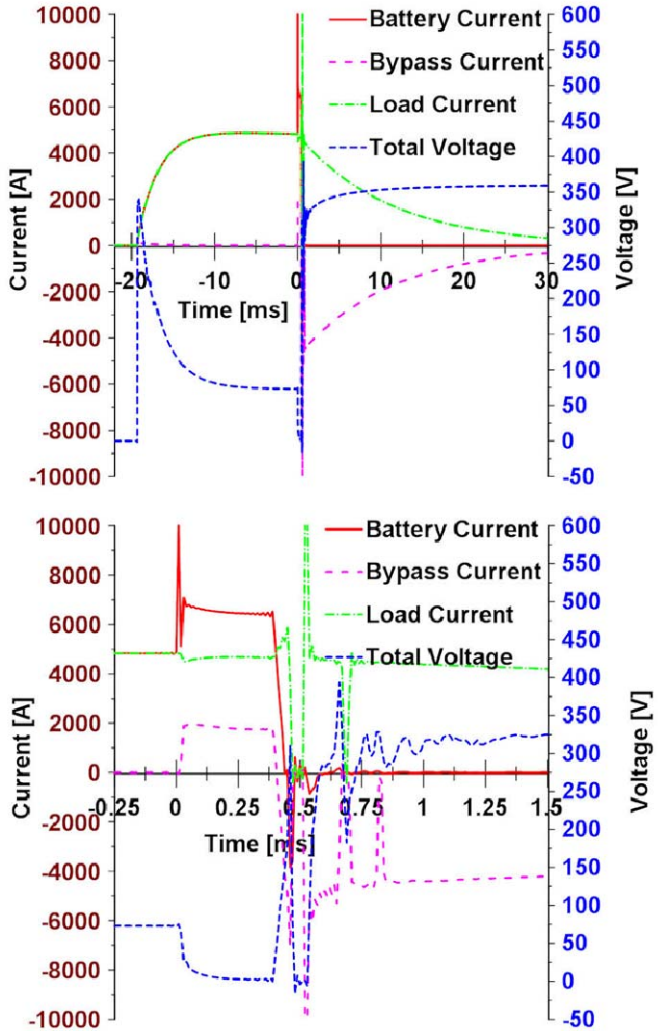


***Figure 4.*** **Complete HV disconnection. a) Current flow and voltage change during test (range -20 to 30 ms). b) Current flow at time of disconnection (range -0.25 to 1.5 ms).**

**Partial High Voltage Disconnection**

The delta time for the process of active bypass and disconnection in the Partial HV Disconnection test series was about 0.35 ms. At the time of the activation of the bypass circuit (time 0 ms) a very rapid negative current spike was seen in the main circuit (see Figure 5a), while the battery module to be disconnected experienced an extreme short circuit that rushed to a peak of at above 3000 Amp just before the action of disconnection (see Figure 5b). At the time of disconnection the Load Current experienced one rapid positive spike followed by one rapid negative spike, while the short circuit current across the Bypass path was sharply terminated.
After the completed process of active bypass and disconnection in the Partial HV Disconnection test series the battery pack offered a total voltage equivalent to the original voltage minus the disconnected battery module (see Figure 5a)

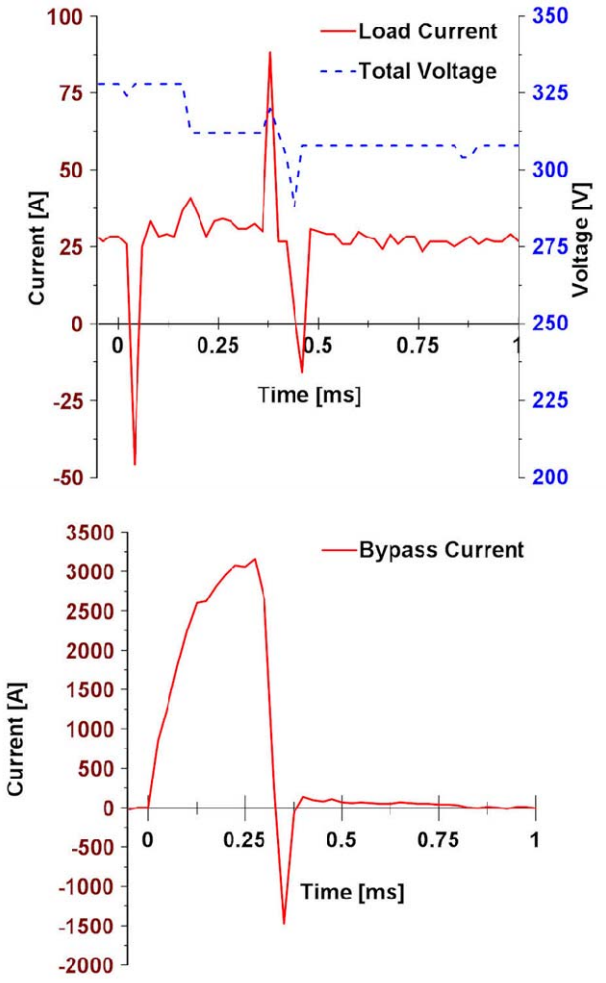


***Figure 5.*** **Partial HV disconnection. a) Main current flow and total voltage change across the bypass and disconnect sequence. b) Short circuit current flow through the bypass path and the faulty module.**

## DISCUSSION

The tests series presented in this report were performed on battery packs of ranging from 300 to 400 Volt dc and the disconnected unit was either the complete battery pack or a constituent battery module of the pack. The risk of generating a severe arc when cutting off a complete battery pack of 300-400 Volt dc or disconnecting subunits of such a battery pack, is greatly reduced by the presented methodology. However, this methodology demands a very short delta time between the connection of the bypass circuit and the disconnection of the battery unit. This short delta time is vital in order that the extreme short circuit, which instantaneously develops across the battery unit to be disconnected through the bypass circuit, shall not generate heat or other phenomena that are harmful to the battery system.

Autoliv achieved the required short delta time by using pyrotechnic switches (i.e. the PSS/NO and PSS/NC) which are available in Autoliv's product portfolio. A later version of PSS offers a single unit with those two functionalities combined. Furthermore, in order to deal with the risk of stranded energy of a disconnected battery unit an additional PSS/NO functionality can be incorporated in order to engage a Drain Unit after the sequence of bypass and disconnection has been completed (see Figure 6).

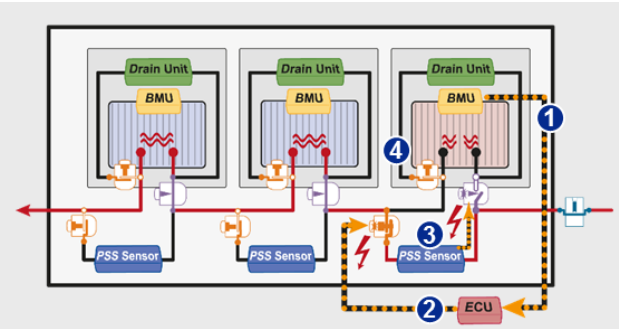


**1.** The Battery management unit (BMU) signals a confirmed failure to the ECU.

**2.** The ECU triggers a pyrotechnic connector to close the bypass circuit. The main current will then choose the bypass since it offers the lowest Ohm.

**3.** After the PSS sensor has detected a current in the bypass, the pyrotechnic disconnection device removes the failing battery unit.

**4.** A second pyrotechnic connector activates a drainage circuit to prevent stranded energy to remain in the disconnected battery unit.

***Figure 6.*** **Concept sketch with separated PSS/NO and PSS/NC units for clarity. In later PSS version, a single unit of combined functionalities of PSS/NO and PSS/NC offers a multiple connection/disconnection opportunity.**

The Complete HV Disconnection that is achieved with the methodology of Active Bypass & Disconnection can alternatively be achieved with a single 'one-stage' pyrotechnic switch that perform a disconnection of the HV battery but no bypass (i.e. a 'one stage' PSS/NC). Such a device must be very robustly designed to anticipate the extreme conditions of arcing that evolves within the device when carrying out a disconnection without first diverting the inductive current. This type of device is defined in Autoliv's product portfolio as PSS/NC High Power. However, it has not been subject to the test series presented in this paper as it is using a different methodology.

## CONCLUSIONS

The key feature of the successful disconnection and bypass, seen in the tests presented, is the diversion of the electrical traction system's inductive influence away from a faulty battery pack or battery subunit, right before that unit is disconnected. This diversion of the influence of the inductance on the pyrotechnic circuit breaker prevent the formation of harmful arcs across the divided conductor.

When the bypass has been established it is crucial that the subsequent disconnection of the faulty battery unit (i.e. complete battery pack or a battery subunit) is performed extraordinary quick in order to minimize the effects of the short circuit current that is rushing between the "faulty unit" and the bypass circuit. Autoliv is capable of achieving this by using a pyrotechnic switch sequence with a delta time of less than 0.5 ms between bypass and disconnection. This extraordinary short delta time provides that the otherwise harmful effects of an extreme short circuit remain at a minimum, and therefore damage to the battery system as well as potential repair costs can be kept at a minimum.

### Complete High Voltage Disconnection

Autoliv's PSS arrangement can offer an alternative to main fuses and, in contrast to a conventional fuse; it will perform a clean cut-off of the conductor at a speed that is independent of the magnitude of the fault current.

### Partial High Voltage Disconnection

Autoliv's PSS arrangement can offer an alternative to relays/contactors when reversibility is less important than speed, physical weight and size as well as cost and the ability to act properly beyond current levels during the E-Vehicle's operational driving conditions. The risk of switching bounces is eliminated when using Autoliv's pyrotechnic switches.

Furthermore, when a faulty battery sub-unit is bypassed and disconnected properly, a "limp-home" ability can be offered since the battery power electronics are remained unharmed due to the extraordinary short delta time and the minimized effects of inherent current spikes during process of the bypass and disconnection.

### General

The setup of Pyro Switches for High Voltage Circuit Breaking & Bypass not only prove to assist in solving the acceptance criteria of the FMVSS 305 for E-Vehicle crashes, but also offers a tool to achieve retained mobility after a faulty battery unit(s) have been disconnected. Additionally, by using the Autoliv's PSS arrangement the faulty battery unit(s) will be isolated from the rest of the traction system and thus will not experience further electric exposures that otherwise may cause more damage to such unit(s). Instead, a discharge unit may be connected in order to release stranded energy in a safe manner.

## REFERENCES


Autoliv. (n.d.). Life saving in only a few milliseconds. Retrieved March 2015, from Autoliv Pyroswitch: http://www.pyroswitch.com

Merkel, T. (2014). Hochvolt-Relais von morgen: Sichere Minimalisten. Hanser Automotive - OEM Supplier - Elektro und zukunftsmobilität, 106-108. Retrieved March 2015, from https://www.panasonic-electric-works.com/cps/rde/xbcr/SID-13796B8A-54077247/pewnew/fb_x61_de_oemsupplier_201409.pdf?type=target

This paper has been peer-reviewed and published in a special edition of *Traffic Injury Prevention* 16(S1), by Taylor & Francis Group. The complete paper will be available on the *Traffic Injury Prevention and www.NHTSA.gov* websites on June 8, 2015.

To access all Peer-reviewed papers please copy and paste the link below into your browser to access the papers.

http://www.tandfonline.com/toc/gcpi20/16/sup1

This paper has been peer-reviewed and published in a special edition of *Traffic Injury Prevention* 16(S1), by Taylor & Francis Group. The complete paper will be available on the *Traffic Injury Prevention and www.NHTSA.gov* websites on June 8, 2015.

To access all Peer-reviewed papers please copy and paste the link below into your browser to access the papers.

http://www.tandfonline.com/toc/gcpi20/16/sup1

This paper has been peer-reviewed and published in a special edition of *Traffic Injury Prevention* 16(S1), by Taylor & Francis Group. The complete paper will be available on the *Traffic Injury Prevention and www.NHTSA.gov* websites on June 8, 2015.

To access all Peer-reviewed papers please copy and paste the link below into your browser to access the papers.

http://www.tandfonline.com/toc/gcpi20/16/sup1

**Utilization of crash scene photos of vehicle damage and intrusion to improve trauma care preparedness**

Daniel V. McGehee [1,3]
Robert P. Kaufman [2]
Christopher T. Buresh [1,3]
Karisa K. Harland [3]
Michele A. Lilienthal [4]

[1] Transportation and Vehicle Safety Research Division, Public Policy Center, 205 South Quadrangle, University of Iowa, Iowa City, Iowa 52242
[2] University of Washington, Harborview Injury Prevention and Research Center, Seattle, Washington
[3] Department of Emergency Medicine, University of Iowa, Iowa City Iowa
[4] Department of Surgery, Division of Acute Care Surgery, University of Iowa, Iowa City, Iowa

E-mails: daniel-mcgehee@uiowa.edu; rkaufman@uw.edu; christopher-buresh@uiowa.edu; kari-harland@uiowa.edu; michele-lilienthal@uiowa.edu

Journal: Traffic Injury Prevention
Word Count: ~ 3,400
**Paper # 15-0167**

**ABSTRACT**

**Objective**

To design, develop, and field test a smartphone app (called TraumaHawk) that would transmit photographic vehicle crush information to a trauma center in advance of patient arrival, then determine whether such information increases the amount of lead time the trauma center has to activate and prepare for treating crash injured patients.

**Methods**

TraumaHawk, a smartphone app for law enforcement and first responders, was designed by the University of Iowa to send photographs showing extent of intrusion and vehicle damage in a vehicle's occupant compartment to the receiving trauma center. With some basic training, first-responders and law enforcement personnel were taught how to photograph vehicles at a crash scene; trauma staff similarly received training regarding crash injury biomechanics and traumatology. For TraumaHawk cases received October 2013–August 2014, electronic medical records and trauma team notification pages were examined. Time of notification and actual time of patient arrival were noted. Time of TraumaHawk alert for these cases was also recorded. Traditional paging and TraumaHawk lead-times (minutes) were calculated. A paired *t*-test was used to determine if the mean lead-times for the Paging and TraumaHawk alerts differed significantly.

**Results**

During the study period, 35 TraumaHawk cases were identified, and 32 met trauma team activation criteria. For these 32, actual mean time between the trauma team page and patient arrival was 12 min; for TraumaHawk, advance notice was received at the trauma center 26 minutes before patient arrival, more than doubling notification time ($p<0.001$).

**Conclusions**

Utiltizing TraumaHawk to identify serious crashes remotely allowed the trauma team significantly more time to prepare for incoming trauma patients than the conventional ambulance crew notification. This allotted time allowed trauma staff to assemble a more complete and appropriate level of care by specialists, as well as to arrange other vital aspects of care—such as scheduling operating rooms.

Keywords: Motor vehicle crashes, traumatic injury, injury mechanism, prehospital

## INTRODUCTION

Photographic documentation of crashed vehicles at the scene can be used to improve triage of crash victims. A U.S. expert panel developed field triage rules to determine the likelihood of occupants sustaining serious injuries based on vehicle damage that would require transport to a trauma center (Sasser et al., 2011). The use of photographs for assessing vehicle damage and occupant compartment intrusion as it correlates to increased injury severity has been validated (Davidson et al., 2014). Providing trauma staff with crash scene photos remotely could assist them in predicting injuries, or in the least, determine when a crashed vehicle damage indicates severe forces to the occupants. This would allow trauma care providers to easily assess when a more traumatic crash occurred, determine the appropriate transport mode, as well as develop mental models of treatment options prior to patient arrival at the emergency department (ED).

Crash-scene medical response has improved tremendously in the past 20-30 years. This is in part due to the increasing number of paramedics who now have advanced life support (ALS) training that allows independence in the field. By adopting more advanced procedures involving a more streamlined and efficient field treatment, the paramedics are more focused on treating crash victims and may have less time, or the need, to communicate with trauma centers regarding the crash severity and potential injury mechanisms. As a result, trauma centers may not learn about severe trauma patients until just a few minutes before they arrive. If the damaged vehicle photos could be electronically transmitted from the scene to the trauma center, this would allow an advanced remote interpretation of the crash severity prior to ED arrival and provide clues about the type and severity of injury.

With strategic crash scene photo documentation, trauma professionals have been trained to assess the severity and patterns of injury based on exterior crush and occupant intrusion. In past years, training was conducted during surgery grand rounds and to ED staff at the pilot trauma center as well as at paramedic training in the region. This training focused on the principles to assess occupant compartment intrusion that increases the force that translates into injury severity and also assess the amount of exterior crush that determines the severity of force all the occupants experienced. (Tencer et al., 2005; Assal et al., 2002; Mandell et al., 2010). Again, first responders have the unique opportunity to assess and visualize the severity of damaged vehicles at the crash scene, but often the information regarding the mechanism of injury and crash severity is limited due to time constrains in the field and may not be relayed to ED trauma staff.

To integrate photographic and scene information, an app called “TraumaHawk” was created to capture images of crash vehicles and send them electronically to the trauma center. If efficiently implemented, the crash scene photos would provide the potential advantage of increasing the lead-time for ED arrival of known severely injured crash patients. Ideally, this advanced interpretation could result in better treatment and outcomes for crash victims by determining a need for airlift versus ground transport, allow more lead times for trauma preparedness for arrival, and possibly prioritize treatment plans that focus on potential injury mechanisms. In addition advanced notice can make the overall operation more efficient. Trauma staff is frequently utilized during non-emergent periods to do other

inpatient operative and bedside procedures that once started cannot be interrupted. Having some advanced lead-time for patient arrival could allow time to finish the procedure, or postpone and reschedule.

The objective of this paper is to describe the design, development, and field testing of a smartphone app (called TraumaHawk) that transmits photographic vehicle crush information to a trauma center in advance of patient arrival. We then determine whether such information increases the amount of lead time the trauma center has to activate and prepare for treating crash injured patients.

## METHODS

### Background and TraumaHawk Development

Development of the TraumaHawk app was a team collaboration that included law enforcement from the Iowa State Patrol, first responders, ALS paramedics, trauma doctors, nurses and app developers. Involving all parties was crucial in ensuring that both the app and reporting process would be intuitive and practical for all users. Figure A1 displays several screen shots from the TraumaHawk app. The design allows on-scene personnel to create a report in about one minute and transmit it electronically to the ED. The app alerts trauma staff to the exact location of the crash, and its distance from the trauma center. The report displays a series of relevant photos of the vehicles involved in the crash, and allows for added contextual information. Icons help first responders easily select specific photos to document the exterior and interior of the crashed vehicles. The few images captured allow assessment of steering wheel deformation, A-pillar compromise, roof crush and other intrusions into the occupant compartment of the vehicle that are correlated with increased injury severity (Tencer et al., 2005; Assal et al., 2002; Mandell et al., 2010).

### TraumaHawk User Procedures

TraumaHawk is currently implemented on Apple iPhone® 5s smart phones supplied by the state. To create a report, law enforcement or a first responder clicks on the App (Figure A1A) and then clicks “New Report” on the first screen (Figure A1B). Within the new report, the user is asked to state the type of crash (frontal, side, rollover, or rear-end); meanwhile, GPS location is also automatically logged, and calculates the distance the crash is from the Level 1 Trauma Center (Figure A1C). As can be seen in Figure A1D, the user is then guided as to what areas of the automobile should be photographed. The six areas chosen by the research team were selected based on the work by Davidson et al. (2014) that demonstrated these particular regions are most predictive of injury severity. Figure A1E shows the screen that pops up when the “Driver’s Side” option is selected in Figure A1D. The user is asked to provide three pictures of the driver’s side that together create a full side view of the vehicle, as well as 45º angled views at both corners of the damaged plane. If the user is unclear as to where the pictures should be taken, he/she can click on “Help” and view example photos of how to capture or frame the damaged side of the vehicle. Figure A1e is an example of photos taken at a TraumaHawk alert crash that illustrate the result of a high-speed near-side impact that met the intrusion rule for transport of the front right passenger to the trauma center. The field users are also allowed to include additional textual information on the crash. Nighttime photos have been successfully taken

utilizing the iPhone 5s internal flash. Additional lighting can also be provided from the high intensity flashlights that are used by law enforcement.

Finally, users have the ability to 'sanitize' each image by using their fingers to 'smudge' out crash victim faces (if present) and vehicle license plates to ensure confidentiality and protect the privacy of crash victims.

**TraumaHawk in the Emergency Department**

Once a report has been submitted, it is electronically transmitted to the ED trauma center where the patient will be transported and displayed as an iPad® text alert; a signature auditory alarm alerts staff at the charge nurse's station that a report has been delivered. A copy of the report is also sent to the research team via secure e-mail. The iPad report is then viewed by the ED charge nurse, who alerts the ED staff physician of the TraumaHawk notification. The ED physician reviews the TraumaHawk report and shares the photos with the Trauma team to assess crash severity, the potential for traumatic injuries, and how best to activate the trauma team most efficiently. A flow diagram of the overall process is presented in Figure 1. After the images have been received, a member of the research/trauma team communicates with the field users, mainly State troopers, who sent the photos to give them feedback on the image quality and contents. This promoted better personal communication from the field users and also provided an opportunity to discuss any factors influencing the ability or inability to capture the required photos.

TraumaHawk cases are received at the University of Iowa Hospital, which is an American College of Surgeons Committee on Trauma accredited Level 1 Trauma Center with over 600 adult and pediatric trauma beds. At this Trauma Center, in order for a trauma notification to be sent, a patient must meet certain CDC Field Triage criteria. Paramedics utilize these triage rules, examining the physiological and anatomic criteria to assess whether a patient qualifies for notification (Sasser, et al., 2011). A patient may also be considered a trauma notification for certain levels of crush and intrusion for a high-risk automobile crash. Some of the indicators of a high-risk automobile crash are defined as:

1. Component intrusion greater than 12 inches at the occupant's site that includes the roof; or greater than 18 inches of crush at any location.
2. Patient is ejected (partial or complete) from the automobile, or
3. A death occurred in same passenger compartment, or
4. Vehicle telemetry data are consistent with a high risk of injury

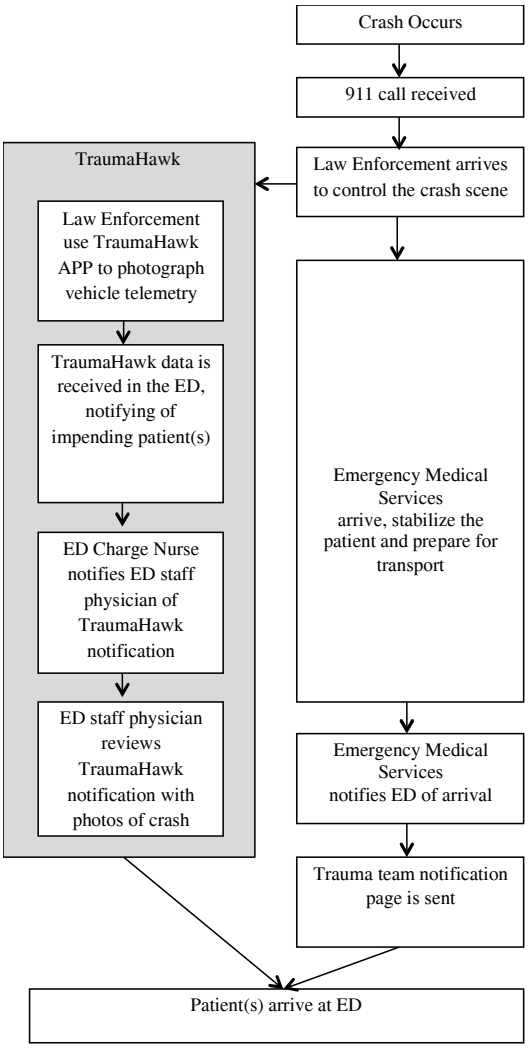

Figure 1. TraumaHawk flow diagram from crash to ED arrival

In October 2013, 15 phones with the TraumaHawk App were distributed to a convenience sample of prehospital providers, mainly to law enforcement (Iowa State Patrol), along with local county and city-based ALS ambulance services. In the first few months of deployment, we observed that the State Patrol and/or law enforcement were generally in the best position to complete and transmit the TraumaHawk reports at the crash scene. After providing first aid and traffic control, the on-scene law enforcement officer has a short window in which to capture a report once the paramedics arrive to help manage the scene. Having the on-scene photo documentation done by law enforcement does not impede on any emergency activities or delay extrication, or any patient care. The paramedics were frequently too busy with patient care priorities to pause and document the scene. However, on ambulances that carried a three-member crew, the designated driver was able to take pictures and submit a report. It should be noted, however, that each crash can have a different order of first responders to a crash scene. Depending on the crash location, particular in rural areas, law enforcement may be one of the last parties to arrive. However, they were still able to document the scene prior to patient transport, or ED arrival.

After the photos are received in to the secure email inbox and utilized in the trauma bay, they are then entered in to the patient's permanent medical record as photo attachments by hospital staff. Privacy concerns and compliance with the Health Insurance Portability and Privacy Act (HIPPA) were discussed with hospital legal counsel and the hospital compliance office. It was determined that photos that were taken by law enforcement did not constitute protected health information until they were viewed by the trauma team. However, it was felt that photos taken by EMS crews would constitute protected health information because they are using the photos as part of a medical evaluation. In these cases, any photos that contained identifiable information would need to be 'sanitized' as described above. The photos can only be sent to a password protected email inbox so that they are secure and only accessible by attending medical staff and the research team. Additional security is built into the app itself. Crash scene photos can only be accessed through the TraumaHawk app, not through the phone's camera or other photographic software. Finally, photos taken by the TraumaHawk app are perishable and are automatically deleted from the iPhone two hours after they are taken and the reports were submitted.

**Trauma Alert Times and Trauma Registry Data Collection**

For TraumaHawk cases received from October 2013–August 2014, electronic medical records and trauma notification pages were examined to document the time and content of trauma notification pages, and the actual time of patient arrival. Time of the TraumaHawk alert cases were identified and recorded. The difference between traditional paging and TraumaHawk lead-times was calculated in minutes. A paired *t*-test was used to determine if the mean lead-times for the Paging and TraumaHawk alerts differed significantly.

To examine how TraumaHawk motor vehicle crashes (MVC) differed from all MVCs seen at the Trauma Center over the study period, hospital-based trauma registry data were abstracted for all MVCs (ICD-9 CM E-codes =E810.0-E825.7) from October 2013 through June 2014, and then analyzed. Trauma notifications were excluded if the crash involved a motorcycle or moped, all-terrain vehicle, or snowmobile that did not include a collision with a passenger vehicle; if patients were not brought directly to the Trauma Center (transferred from an outside hospital to trauma center); or if they were not brought via ground or air ambulance. Differences in proportions of TraumaHawk versus other MVCs were compared using Pearson chi-square test and differences in means were examined using a Student's *t*-test

**RESULTS**

From October 2013 through August 2014, 35 TraumaHawk reports were received, of which 32 met the criteria for a trauma team notification. During this time, 319 eligible MVC were seen at the Trauma Center, of which 10.0% (n=32) had TraumaHawk reports.

TraumaHawk-reported patients had an average injury severity score (ISS) of 6.4 (standard deviation=11.4), 50% (n=16) were male, their mean length of hospital stay was 5.6 days (standard deviation=7.9), and the majority

(93.8%, n=30) arrived by ground ambulance. These characteristics did not differ between TraumaHawk and Non-TraumaHawk patients (see Table 1). TraumaHawk patients were less likely to be admitted (25.0% vs. 44.8%, p=0.0325) and were, on average, younger than non-TraumaHawk patients (30.8 vs. 38.6 years, p=0.0365).

**Table 1. Patient, Emergency Dept. and Hospital Stay Characteristics by Presence of TraumaHawk Photos**

| | TraumaHawk | | |
|---|---|---|---|
| | Yes (%) | No (%) | p-value |
| Age, years (mean, std) | 30.8 (19.4) | 38.6 (20.0) | 0.0365 |
| Male | 16 (50.0) | 153 (53.5) | 0.7070 |
| Arrival Mode | | | |
| Air ambulance | 2 (6.3) | 55 (19.2) | 0.1797[1] |
| Ground ambulance | 30 (93.8) | 230 (80.4) | |
| Police | 0 | 1 (0.4) | |
| Injury Characteristics | | | |
| ISS | 6.4 (11.4) | 8.0 (10.5) | 0.5020 |
| Max AIS | 1.7 (1.3) | 2.0 (1.2) | 0.1721 |
| ED GCS | 14.6 (1.3) | 14.3 (2.7) | 0.2256 |
| TRISS | 0.97 (0.07) | 0.95 (0.16) | 0.2383 |
| Admitted to Hospital | 8 (25.0) | 128 (44.8) | 0.0325 |
| Length of stay, days (mean, std) | 5.6 (7.9) | 5.2 (8.3) | 0.8811 |
| Died | 0 | 7 (2.5) | 0.9999[1] |

[1] Fisher's exact test

Of the 32 TraumaHawk cases who were also trauma notifications, the actual mean time between the trauma team page and patient arrival was 12 minutes; with TraumaHawk, the advanced notice was received at the trauma center 26 minutes before patient arrival, more than doubling notification time ($p<0.001$). On average, the ED doctor saw patients 69 minutes after they sustained their injury. These times were significantly lower for TraumaHawk patients (56.7 minutes, standard deviation=23.3) than for non-TraumaHawk patients (70.2 minutes, standard deviation=43.8) ($p=0.03$). In addition, the trauma surgeon responded, on average, 66 minutes after the injury. TraumaHawk patients saw the trauma surgeon, on average, 58.1 minutes (standard deviation=22.1) after their injury vs. 67.3 minutes (standard deviation= 36.0) for non-TraumaHawk patients ($p=0.07$).

The TraumaHawk reports averaged six (range 1-14) photos per report. In the 35 TraumaHawk reports, 88.6% included interior images of the driver area with a view of the steering column, and 80% showed a view of the driver floorboard. In all cases, the damage planes were documented.

**DISCUSSION**

Advanced warning and trauma page activation regarding an incoming crash allows ED personnel to allocate resources more efficiently. They are able to order the disposition of patients and allocate adequate staff to receive incoming crash victims. The increased time afforded by a trauma alert also allows trauma surgeons and specialty services to adjust schedules accordingly (i.e., they might delay the start of a non-urgent scheduled procedure to provide time to assess the incoming trauma victim).

While all trauma staff receive a standardized page with a report from the field, this often includes only the most basic information about the manner of collision such as frontal crash, rollover; some vital sign information and potential body region injury may also be described. It is said that, "a picture is worth a thousand words". Some of the feedback from trauma staff indicated that the viewing of the TraumaHawk report images prior to a patient's arrival allowed a much better assessment of potential injury than a brief radio report would. This assessment did enable the trauma team to prepare and plan for specific key treatment and specialties services (orthopedics, neurosurgeon, etc.) such was the case in identifying the potential for a pelvic fracture for the patient in Figure A1E.

TraumaHawk is a useful tool to teach the basics of automotive traumatology. This is a complex science that involves an understanding of restraint systems, physics, occupant factors, and crash dynamics. Having a basic understanding of traumatology, one can correlated the damage crush and intrusion into the vehicle to potential severe injury patterns, as well as measure the extent of force in which the passengers may have sustained. This then can help shape the mental model of treatment by EMS and trauma care providers. A crash injury mechanism curriculum had been created by the team and delivered to all users by an in-person presentation during this pilot phase. The course has been certified to provide continuing medical education (CME) credits. The course illustrates the basic methods on how to interpret the Step 3 CDC rule examining damage planar crush and the potential injury patterns from intrusion. Currently several short topic modules are being created from this curriculum that can be reviewed electronically by law enforcement, prehospital personnel, nursing, and trauma staff. This curriculum will be a required component of the using the information generated from the app and the modules would also be available to the users on the iPhone. We see that such a series of courses would become standard training for all personnel involved in the treatment of crash victims.

Improving the mental model of crash dynamics and potential injury has several potential advantages on patient care. In the prehospital setting, when used in conjunction with the CDC trauma guidelines it can help to determine whether to take the patient to a level II or III trauma center for treatment or whether to bypass one of these closer

hospitals in favor of going directly to a level I trauma center. TraumaHawk reports can help to make determinations about which patients should be transported by air ambulance versus the standard ground transport. The research did not evaluate if TraumaHawk impacted these decisions or transport modes. Further research is planned to evaluate after the pilot with TruamaHawk procedures are in place.

Once in the hospital, all patients undergo a standardized and very thorough exam. The photos generated by the TraumaHawk app can help the team focus on particular parts of the exam where the data would indicate there is a high risk for injury. Conversely, if a patient appears to be uninjured or has very mild injuries after a full and thorough exam, having an understanding of the crush patterns of the vehicle (or lack thereof) can provide the treating team with reassurance that the patient is safe for discharge and could reduce the need for invasive procedures and radiological images. Current prehospital treatment protocols are always in place to examine patients, and even in low speed crashes occupants can still be severely injured and not have significant crush. As this was an implementation pilot, trauma staff feedback and communication regarding it use was conducted. This generated some positive responses from ED staff, especially the additional time to prepare trauma bays and schedule the potential need for operating rooms and some pre diagnosis of potential mechanism of injury.

There are limitations to this study. First, TraumaHawk crashes tended to occur in closer proximity to the ED than did non-TraumaHawk crashes; therefore we cannot say if the shorter time between patient injury and the ED/Trauma physician was perhaps due to the shorter distance traveled. Second, because there are only a small proportion of MVCs seen at the ED with TraumaHawk reports, the generalizability of the current results are limited, although, the characteristics of TraumaHawk patients and their injuries did not differ greatly from non-TraumaHawk patients.

From these pilot data, TraumaHawk was shown to increase the advance time for trauma notification and preparedness at a trauma center for identified trauma patients. Because of the added context, patients were seen more quickly than non-TraumaHawk cases. Since the initial 15-phone deployment, we have increased the number of phones to 35 in state trooper vehicles, and more data will be available soon. With the success in the implementation of TraumaHawk, further research and evaluations are planned to examine the benefits in the triage, transport and treatment of crash victims.

**CONCLUSIONS**

Utilizing TraumaHawk to identify serious crashes and potential injury mechanisms allowed the trauma team significantly more time to prepare for incoming trauma patients than the conventional ambulance crew notification. This allotted time allowed trauma staff to assemble a more complete and appropriate level of care by specialists, as well as to arrange other vital aspects of care—such as scheduling operating rooms.

## REFERENCES


Assal M, Huber P, Tencer AF, Rohr E, Mock C, Kaufman R (2002). Are drivers more likely to injure their right or left foot in a frontal car crash: a crash and biomechanical investigation. *Annual proceedings / Association for the Advancement of Automotive Medicine. Association for the Advancement of Automotive Medicine.* 2002;46:273-288.

Davidson GH, Rivara FP, Mack CD, Kaufman R, Jurkovich GJ, Bulger EM (2014). Validation of prehospital trauma triage criteria for motor vehicle collisions. *J Trauma Acute Care Surg.* Mar 2014;76(3):755-761.

Mandell SP, Kaufman R, Mack CD, Bulger EM (2010). Mortality and injury patterns associated with roof crush in rollover crashes. *Accid Anal Prev.* Jul 2010;42(4):1326-1331.

Sasser SM, Hunt RC, Faul M, et al. (2011). Guidelines for field triage of injured patients: recommendations of the National Expert Panel on Field Triage, 2011. *MMWR. Recommendations and reports : Morbidity and mortality weekly report. Recommendations & reports/Centers for Disease Control.* Jan 13 2012;61(Rr-1):1-20.

Tencer AF, Kaufman R, Mack C, Mock C (2005). Factors affecting pelvic and thoracic forces in near-side impact crashes: a study of US-NCAP, NASS, and CIREN data. *Accid Anal Prev.* Mar 2005;37(2):287-293.


## ACKNOWLEDGEMENTS


This study was funded by the Iowa Department of Transportation. Special thanks goes to Sandra Larson and Steve Gent for the Iowa DOT's support of this project. We also thank Dr. Denise Szecsei who coded the app and to Dieter Friton, EMT-P, who coordinated communication with law enforcement, paramedics and the University of Iowa Emergency Department. We have also received overwhelming support from many Iowa State Troopers, namely Trooper Eric Payne, and many other dedicated first responders and paramedics.

FIGURE A1

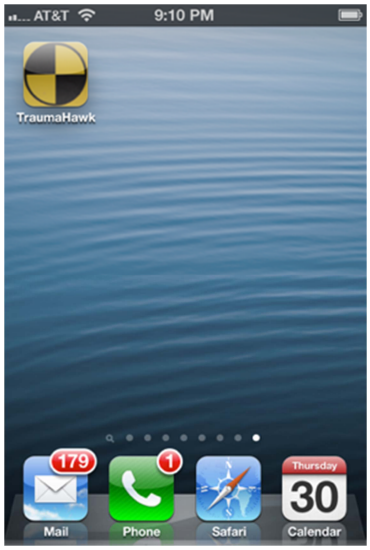


Figure A1a

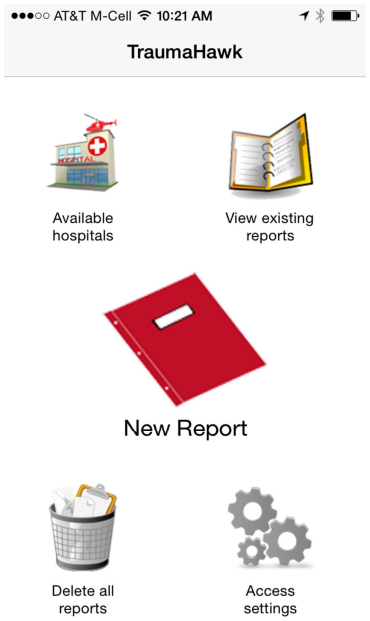


Figure A1b

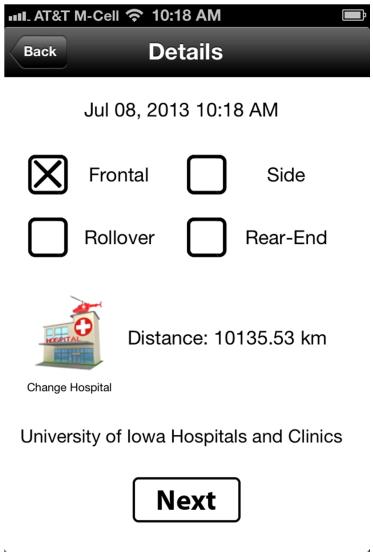
AT&T M-Cell 10:18 AM
Back
Details
Jul 08, 2013 10:18 AM
Frontal
Side
Rollover
Rear-End
Distance: 10135.53 km
Change Hospital
University of Iowa Hospitals and Clinics
Next

A1c

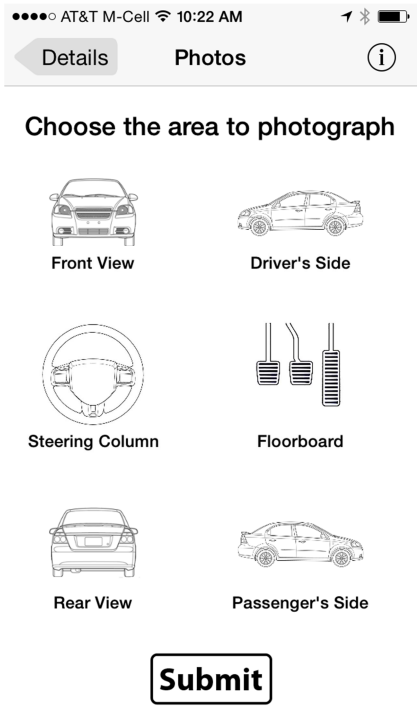
AT&T M-Cell 10:22 AM
Details
Photos
Choose the area to photograph
Front View
Driver's Side
Steering Column
Floorboard
Rear View
Passenger's Side
Submit

A1d

A1e

Figure A1. TraumaHawk iPhone 5S interface and screen shots

FIGURE A2

Figure A2. Example images from a TraumaHawk crash file

# MATHEMATICAL MODELING and NUMERICAL OPTIMIZATION of THREE VEHICLE CRASHES using a SINGLE-MASS LUMPED PARAMETER MODEL

**Andreas Klausen,**
**Sondre Sanden Tørdal,**
**Hamid Reza Karimi,**
**Kjell G. Robbersmyr,**
University of Agder
Norway

**Mladen Ječmenica,**
**Ole Melteig**
Telemark University College
Norway

Paper Number 15-0168

## ABSTRACT

In this paper mathematical modelling of a vehicle crash based on a lumped parameter model is studied. The vehicle is modelled as a single mass connected to a non-linear spring and damper system. The characteristics of the non-linear behaviour of the model is identified with a hybrid Firefly/Harmony Search optimization algorithm that minimizes the deviation between experimental test data and a simulated response. The experimental data is taken from three crashes of an identical vehicle that crashes into a wall at different initial velocities. The aim of this paper is to find a piecewise-linear function for the spring and damper coefficients which is scaleable to reconstruct the three different experimental crashes at different impact velocities. Numerical results are provided to illustrate the applicability of the proposed algorithm. Three data sets will be used for parameter identification and a fourth data set will be used for verification.
Keywords: Vehicle crash, crashworthiness, LPM, parameter identification, simulation, Firefly/HS

## INTRODUCTION

Numerous studies have been devoted to the area of vehicle crashworthiness to improve the safety for occupants and pedestrians in the last decade. In order to test a vehicle prototype on how it reacts to a crash, and how it affects occupants or pedestrians, a physical crash test of the vehicle is often constructed. This however requires trained personnel, a facility, measurement devices, sensors, a great deal of planning and a vehicle. This is a costly and time consuming process, but is the most reliable method for testing the crashworthiness of a vehicle. The amount of crash tests needed for a given prototype could however be reduced. If an accelerometer is placed at the center of mass of the vehicle and its acceleration is measured during the crash, that data could be used to create a mathematical model of the vehicle and tune its parameters based on the experimental crash response. If the mathematical model is verified, it could be used to simulate crashes on modified designs hence identifying the most promising version before staging a real crash.
In the literature, there are two general ways to make a model of a vehicle; Lumped Parameter Models (LPMs) and Finite Element Method (FEM) Models. An LPM utilizes up to several masses connected with each other and surroundings with springs and dampers. The masses are often determined by dividing the total mass of the vehicle into strategic parts of the model. The spring and damper coefficients are estimated by using experimental crash data. Several studies of crashworthiness used analytic methods and numerical optimization to tune the parameters for an LPM of the crash. In [1] Elmarakbi et al. presented a new mathematical model to optimize the crashworthiness using vehicle dynamics control systems. In [2], Pawlus et al. proposed a method for modelling a vehicle crash based on viscous and elastic properties of the materials. In [3] Jonsén et al. presented a method for identifying a lumped parameter model of the frontal bumper on a Volvo S40. In [4] Lu et al. established the LPV-ARMAX model for a vehicle crash in order to calculate a single LPM that can handle any initial impact velocity. In [5] Pawlus et al. developed an LPM of a crash consisting of two sets of mass-spring-damper systems, and verified the model from a vehicle crash in a pole. LPM is often easier to model and their parameters are simpler identified than FEM models, but the results may not be as accurate. FEM models are more accurate but time consuming to model and simulate because they usually contain more accurate material specifications, stresses and deformation in the vehicle during a crash. In [6] the energy absorbed in

a crash was used to optimize energy absorption by remodelling the motor room. In [7] an analytical method was presented to identify the critical velocity of a transverse rigid body impact on a steel column. In [8], Tang et al. presented a new Black Box optimization algorithm that is used to optimize the frontal member of a vehicle in terms of energy absorption. A different, but effective method of modelling a vehicle crash is shown by Zhao et al. in [9] where they developed a novel adaptive neurofuzzy inference system (ANFIS-based) approach to reconstruct the kinematics of a vehicle crash.
In this paper, a non-linear mathematical model for a vehicle crash scenario is obtained using three experimental crash data sets. The main contribution of this paper is to find a scaling function between the response of three experimental data sets in order to make a mathematical model of the vehicle crash with only the initial velocity as input. The connection between the crashes is to be found as a function of the initial velocity. After parameters of the model are identified, a fourth experimental data set is used to verify the model and its performance.

## METHOD

### Experimental data sets

The experimental data used in this article is of a 1986 model Ford Taurus with a mass of $m = 1591kg$. This car was crashed into a wall at different impact velocities. For parameter identification, three crashes occurring at an impact velocity $v_0 = \{15.5, 32.4 \text{ and } 48.3\}km/h$ are used. To verify the model, a similar crash at impact velocity of $v_0 = 29.9km/h$ is used. An accelerometer was placed at the centre of mass in each of the crashed cars, which logged the acceleration in all three directions. The experimental data is the acceleration of these three vehicles in the forward direction (facing the wall). It is important that the accelerometer was placed in the centre of mass to conform to Newton's laws of motion. This article uses this principle law to develop a mathematical model for the crash, and this law breaks if the acceleration is measured somewhere else than the centre of gravity. Possible sources of an error in these data sets are:

1. The logging device may be experiencing noise from several sources, which could potentially create errors.
2. The centre of gravity of the car may move because of the deformations, which could lead to inaccurate measurements if the accelerometer moves outside the centre of mass.

Since the experimental data sets downloaded from NHTSAs web page [10] contain raw acceleration data, they are filtered before they are analysed. The raw acceleration data is filtered using a CFC180 filter. This filter is a low-pass filter with a -3$dB$ limit frequency at 300$Hz$. The requirement for this filter is a sampling frequency of at least 1800$Hz$. The measuring frequency of the raw data set is 8000$Hz$ which means that the time step between each measurement is $dt = 1.25ms$. For convenience, all time simulations are carried out with this time step, which is small enough for accurate forward Euler time integration.
The time scope of the experimental data sets are adjusted to only include the time from impact until the vehicle is positioned at the origin. Afterwards the adjusted acceleration data is time integrated using a forward Euler time integration formula to obtain the velocity and position of the car. This time integration is given in Equations (1) and (2):

$$v(t) = \int a(t) \cdot dt \tag{1}$$

$$s(t) = \int v(t) \cdot dt \tag{2}$$

where $a(t)$ is the acceleration of the vehicle, $v(t)$ is the velocity of the vehicle and $s(t)$ is the position of the vehicle. Before the acceleration is integrated, the start and end time is adjusted to only include the start of the crash pulse up until the rebound position is $0m$. This is done to remove any position change before the car hits the wall. Figure 1 shows the filtered and adjusted acceleration for the first crash and its velocity and position. The red curve shows acceleration in per gravity constants ($-9.81m/s^2$), the green line shows velocity in $km/h$ and the blue line shows the position of the car in $cm$. These units are used instead of SI units in order to fit all three graphs on a single y-axis.

### Mathematical model

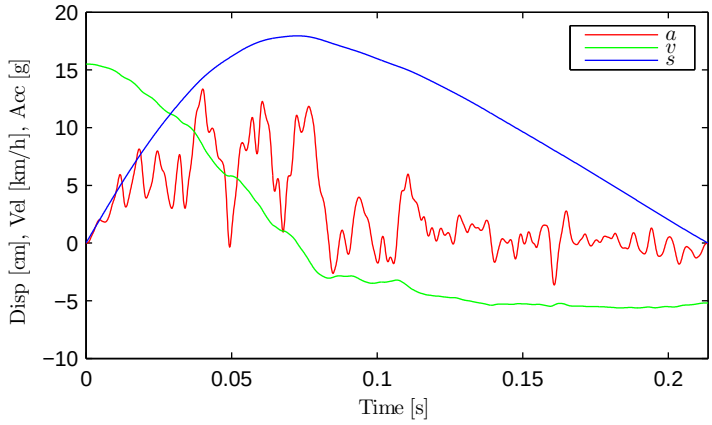


***Figure 1:*** **Experimental crash data for the first test, $v_0 = 15.5$km/h.**

The mathematical model under consideration is a mass connected to a non-linear spring and damper system. The model is shown in Figure 2a and the differential equation for the system is represented as:

$$m\ddot{x} + c(|x|, v_0)\dot{x} + k(|x|, v_0)x = 0 \tag{3}$$

where $m$ is the mass of the vehicle, $x$ is the position of the simulated vehicle relative to its impact position, $\dot{x}$ and $\ddot{x}$ is the speed and acceleration of the simulated vehicle respectively, $c(x, v_0)$ is the damping coefficient of the vehicle as a function of the current displacement and initial velocity ($v_0$) of the vehicle, $k(x, v_0)$ is the spring coefficient of the crash as a function of the current displacement and initial velocity of the vehicle. Remember $s$, $v$ and $a$ represents the position, velocity and acceleration of the real experimental crash, while $x$, $\dot{x}$ and $\ddot{x}$ represents the position, velocity and acceleration of a simulated crash.

This non-linear model is used in favour of connecting several linear mass-spring-damper systems in order to keep a simple differential equation. It is also simpler to increase the complexity of the model by modifying the non-linear spring and damper characteristics instead of dividing the car mass into additional mass-spring-damper systems. The characteristics of the non-linear spring and damper are shown in Figure 2b. This figure shows two arbitrary piecewise linear functions; one for the non-linear spring characteristics $k_s(|x|)$ and one for the non-linear damper $c_s(|x|)$. These spring and damper characteristics are functions of the absolute value of the position of the vehicle. $C$ is the maximum displacement of the car (maximum crush) during the crash. $p_{1,s}, p_{2,s}, p_{3,s}$ and $p_{4,s}$ are percentages of the maximum crush. $k_{1,s}, k_{2,s}, k_{3,s}$ and $k_{4,s}$ are the heights of the piecewise linear functions in the spring setpoint function and $c_{1,s}c_{2,s}, c_{3,s}$ and $c_{4,s}$ are the heights of the damper setpoint function.

As these spring and damper characteristics are setpoint functions, they have to be scaled to fit a certain crash scenario. Equations (4), (5) and (6) show the relationship between the setpoint functions and the actual spring and damper functions used in a simulation:

$$k(|x|, v_0) = S_k(v_0) \cdot k_s(|x|) \tag{4}$$

$$c(|x|, v_0) = S_c(v_0) \cdot c_s(|x|) \tag{5}$$

$$p_i = C_{est}(v_0) \cdot p_{i,s} \qquad i \in [1, 4] \tag{6}$$

where $k(x, v_0)$ is the spring function, $c(\dot{x}, v_0)$ is the damper function and $p_i, i \in [1, 4]$ are breakpoints for the spring and damper functions. $S_k(v_0)$ and $S_c(v_0)$ are scaling functions which will scale the spring and damper to fit a crash with a given initial velocity. A representation of this scaling function is shown in Figure 2c. A separate scaling function is created for the spring and damper functions.

$C_{est}(v_0)$ is an estimate of the maximum displacement of the car in a given crash. Since the maximum crush is never known before a simulation, it is estimated in order to limit the spring and damper characteristics. This estimate is a function of the initial velocity, and it is created by curve fitting the maximum crush of all three experimental data sets to a function. This curve fitting is shown in Figure 2d where the blue curve shows the curve fitted function, and the red dots shows the maximum crush of the three experimental crash test data sets. This curve fitting returned the following

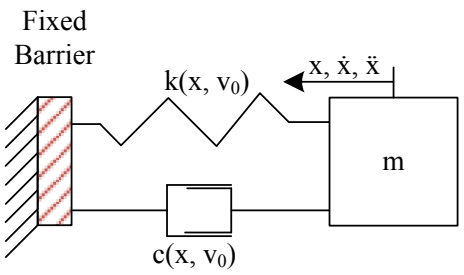


*(a)* **The non-linear mathematical model.**

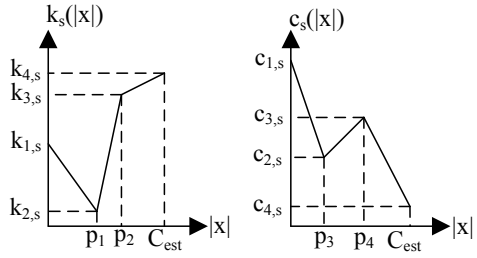


*(b)* **A piecewise linear characteristic for the spring and the damper.**

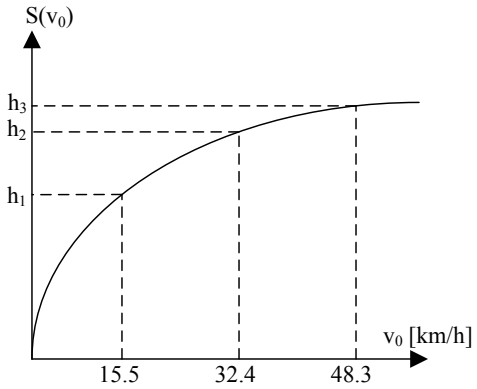


*(c)* **A representation of the scaling function.**

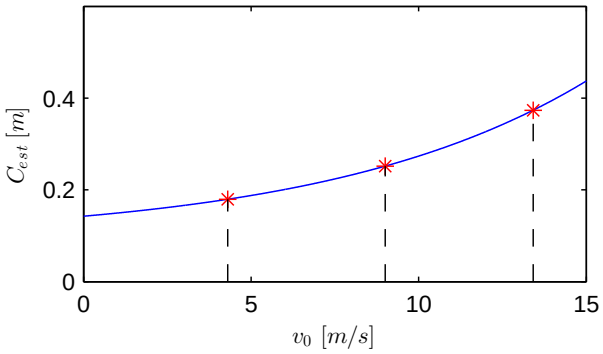


*(d)* **Curve fitting results to make a $C_{est}$ function.**

***Figure 2:*** **Mathematical model of the vehicle crash.**

function:

$$C_{est}(v_0) = 0.04992 \cdot e^{0.1288 \cdot v_0} + 0.09263 \tag{7}$$

where $e$ is Euler's number. The goodness of the fit is given by an R-square which was returned as 1. This estimate is used before every simulation to set the last breakpoint on the spring and damper characteristics. One issue with this curve fitted equation is that it doesn't start with zero maximum crush at zero initial velocity. However, the purpose of this function is to use it in between the given initial velocities.

**Hybrid Firefly/Harmony Search algorithm**

The lumped parameter model is optimized by using a hybrid Firefly/Harmony Search algorithm [11]. The Firefly algorithm is a nature inspired meta heuristic search algorithm that is used to find near-optimal solutions of a global optimization problem. The algorithm was written by Yang and He in 2008, and a recent result in [12] explained the algorithm and its advantages compared to other swarm intelligence algorithms. The algorithm itself is based on the attraction between fireflies, and the core of the algorithm is based on the movement of fireflies that are attracted by each other. In this context, a firefly is a vector containing parameter values, and the upper and lower bounds of each parameter determines the field in which these fireflies can move within. Fireflies are unisex and will be attracted to any firefly that shines brighter than itself. The light intensity of a given firefly is determined by the value of the cost/objective function of its parameter values. In general, this means that a firefly with a high light intensity (a good objective value) will attract more fireflies to search the same area for possible local minimas. This allows the fireflies

***Table 1:*** **Optimizeable parameters and upper and lower bounds.**

| Parameter | Lower bound (Lb) | Upper bound (Ub) | Unit |
|---|---|---|---|
| $k_{1,s}$ | 0 | 100000 | N/m |
| $k_{2,s}$ | 0 | 100000 | N/m |
| $k_{3,s}$ | 0 | 100000 | N/m |
| $k_{4,s}$ | 0 | 100000 | N/m |
| $c_{1,s}$ | 0 | 100000 | Ns/m |
| $c_{2,s}$ | 0 | 100000 | Ns/m |
| $c_{3,s}$ | 0 | 100000 | Ns/m |
| $c_{4,s}$ | 0 | 100000 | Ns/m |
| $p_{1,s}$ | 0 | 1 | - |
| $p_{2,s}$ | 0 | 1 | - |
| $p_{3,s}$ | 0 | 1 | - |
| $p_{4,s}$ | 0 | 1 | - |
| $h_{1,d}$ | 0 | 4.3 | - |
| $h_{2,d}$ | 0 | 9 | - |
| $h_{3,d}$ | 0 | 13.41 | - |
| $h_{1,k}$ | 0 | 4.3 | - |
| $h_{2,k}$ | 0 | 9 | - |
| $h_{3,k}$ | 0 | 13.41 | - |

to divide in groups in the parameter field to exploit several local minimas. This allows the algorithm to quickly search a wide range of parameter values, as well as finding a near optimal solution to the problem. For for information of the Firefly algorithm, see Ref. [12].
There is only a movement if firefly $i$ is attracted to firefly $j$, but nothing happens in the original Firefly algorithm if it is not attracted. The inclusion of a Harmony Search (HS) under those circumstances changes that by performing a Harmony Search mutation on the superior firefly, $i$, while the parameter values belonging to the other fireflies are used as harmony memory. If the objective value of the new parameter set is better than the worst firefly, its parameters are swapped with the new parameters coming from the harmony search mutation. This allows for fireflies in bad positions to be reset. More information about the Harmony Search algorithm is found in Ref. [13].

**Objective Function**

The experimental data sets are used to optimize the design parameters for the mathematical model in. A list of parameters for the optimization algorithm to determine and their corresponding upper and lower bounds are shown in Table 1. The objective function value, or the cost, is the sum of the squared error between the three simulated responses and their corresponding experimental crash data set. For crash $n$ the squared error is calculated with Eq. (8):

$$E_n = \frac{|x_n(t) - s_n(t)|^T |x_n(t) - s_n(t)|}{L(t)} \cdot 1000, \qquad n \in [1, 3] \tag{8}$$

where $L(t)$ is the amount of data points in the time vector $t$, $x_n(t)$ is a vector containing the simulated displacement for crash $n$ and $s_n(t)$ is a vector containing displacement of the experimental crash test $n$. The reason for dividing by $L(t)$ and multiplying by a thousand is to make each crash test data set count equal on the total error, as neither of the experimental crash tests have the same number of datapoints. The total error (the objective value) is calculated as:

$$E_{tot} = \sum_{n=1}^{3} E_n \tag{9}$$

***Table 2:*** **Optimized values for each parameter.**

| Parameter | Value | Unit | Parameter | Value | Unit |
|---|---|---|---|---|---|
| $k_{1,s}$ | 28,668 | N/m | $p_{1,s}$ | 0.247 | - |
| $k_{2,s}$ | 55,478 | N/m | $p_{2,s}$ | 0.459 | - |
| $k_{3,s}$ | 86,759 | N/m | $p_{3,s}$ | 0.482 | - |
| $k_{4,s}$ | 99,668 | N/m | $p_{4,s}$ | 0.931 | - |
| $c_{1,s}$ | 60 | Ns/m | $h_{1,d}$ | 1.871 | - |
| $c_{2,s}$ | 13,016 | Ns/m | $h_{2,d}$ | 4.017 | - |
| $c_{3,s}$ | 13,043 | Ns/m | $h_{3,d}$ | 3.587 | - |
| $c_{4,s}$ | 22,731 | Ns/m | $h_{1,k}$ | 4.285 | - |
| $h_{2,k}$ | 6.084 | - | $h_{3,k}$ | 5.932 | - |

The objective is to minimize the error between a simulated response and experimental test data, $E_{tot}$.

**Constraints**

The firefly/HS algorithm allows for both linear and non-linear equality and inequality constraints. The non-linear constraints are handled by using a Penalty Method, which punishes the objective value of a firefly if the constrains are violated. The penalty method is very effective for swarm optimization algorithms. If a non-linear constraint is violated by a firefly, its objective value is added with the degree of violation squared multiplied by a large number like $10^{15}$. The light intensity of that firefly is therefore low and it will easily move out of the constraint by being attracted to almost every other firefly. The linear constraints are shown as bounds in Table 1. The non-linear inequality constraints used are given by Equations (10) and (11):

$$p_{2,s} \geq p_{1,s} \tag{10}$$

$$p_{4,s} \geq p_{3,s} \tag{11}$$

**RESULTS**

The firefly/HS optimization algorithm is run with the following parameter values: $n = 25$; $\beta_0 = 1$; $alpha_0 = 0.01$; $delta = 0.99931$; $HMCR = 0.85$; $PAR = 0.3$; $bw = 0.02$. The resulting parameter values are shown in Table 2 and the resulting objective value became $E_{tot} = 0.0984$ after 268 epochs. The percentage of the total objective value each crash test amount to is 10.32%, 63% and 26.62% for crash numbers 1, 2 and 3 respectively. A comparison between a simulated response and their corresponding experimental data sets are shown for the three crashes on Figures 3a, 3b and 3c. The verification of the model with the impact velocity $v_0 = 29.9km/h$ is shown in Figure 3d. Here, the stapled lines show the experimental crash test data acquired from NHTSA, and the continuous lines shows the simulated response from the mathematical model. For both cases, the red lines show acceleration in per gravity constant (-9.81 $m/s^2$), the green lines show velocity in $km/h$, and the blue lines show displacement in $cm$.

**DISCUSSION**

In this paper a mathematical model of a vehicle crash test was identified. The model consisted of a mass connected to a non-linear spring and damper system and the parameters were found by optimizing the squared error between the displacement of the model and the experimental data. This model is used to reproduce the three experimental crashes with little deviation. A fourth experimental data set is used to verify the models integrity, and results from using the model on this data set is shown in Figure 3d. This figure shows that the model does a good job of reproducing the crash, but it is not perfect. There are large deviations around the maximum displacement and during the rebound phase. However the parameter identification algorithm also struggled to fit the crash at $v_0 = 32.4km/h$ shown in Figure 3a which is a

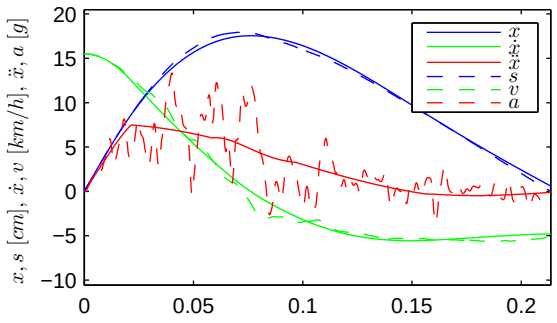


***(a)* Parameter identification test no. 1 at $v_0 = 15.5$km/h.**

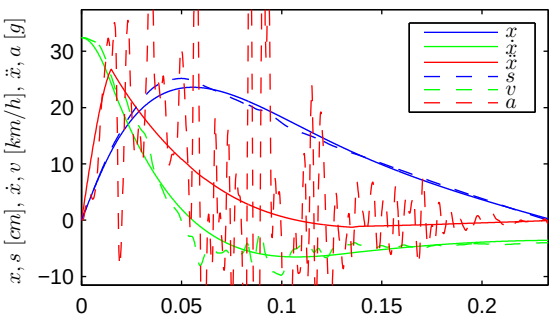


***(b)* Parameter identification test no. 2 at $v_0 = 32.4$km/h.**

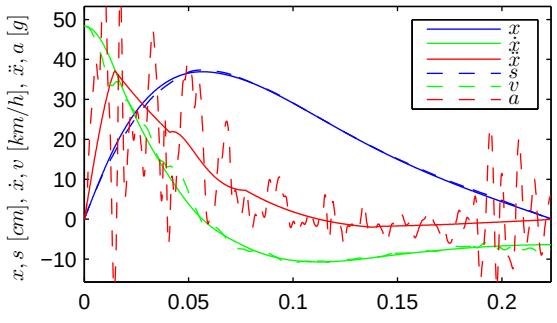


***(c)* Parameter identification test no. 3 at $v_0 = 48.3$km/h.**

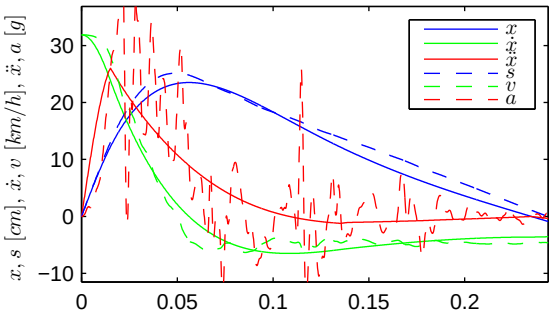


***(d)* Model verification test at $v_0 = 29.9$km/h.**

***Figure 3:* Results and comparisons between simulated response and experimental crash data sets.**

similar impact velocity as the verification data set. This indicates that a single non-linear mass-spring-damper system is not complex enough to model a vehicle crash at different initial velocities.
It was shown that the hybrid Firefly/Harmony Search optimization algorithm is able to find a good solution to the optimization problem despite having many parameters to tune. This is mainly because the Harmony Search mutation adds possibilities to try completely new parameter values which increases the diversity drastically. Therefore this algorithm is suitable for large optimization problems with many local minimas. For future work, the model should be improved to remove the remaining deviations from the experimental data.

**ACKNOWLEDGEMENT**

This work is supported by the grant of the collaborative research project between the University of Agder and Telemark University College.

# References

[1] A. Elmarakbi, M. Elkady, and H. El-Hage. Development of a new crash dynamics control integrated mathematical model for crashworthiness enhancement of vehicle structures. *International Journal of Crashworthiness*, 18:5:444--458, 2013.

[2] W. Pawlus, H. R. Karimi, and K. G. Robbersmyr. Development of lumped-parameter mathematical models for a vehicle localized impact. *Journal of Mechanical Science and Technology*, 25(7):1737--1747, 2011.

[3] P. Jonsén, E. Isaksson, K. G. Sundin, and M. Oldenburg. Identification of lumped parameter automotive crash models for bumper system development. *International Journal of Crashworthiness*, 14:6:533--541, 2009.

[4] Q Lu, H. R. Karimi, and K. G. Robbersmyr. A Data-Based Approach for Modeling and Analysis of Vehicle Collision by LPV-ARMAX Models. *Journal of Applied Mathematics*, 2013:9, 2013.

[5] Witold Pawlus, Hamid Reza, and Kjell Gunnar Robbersmyr. Application of viscoelastic hybrid models to vehicle crash simulation. *International Journal of Crashworthiness*, 16(2):195--205, 2011.

[6] B. Y. Kim, C. M. Jeong, S. W. Kim, and M. W. Suh. A study to maximize the crash energy absorption efficiency within the limits of crash space. *Journal of Mechanical Science and Technology*, 26(4):1073--1078, 2012.

[7] H. Al-Thairy and Y. C. Wang. A simplified analytical method for predicting the critical velocity of transverse rigid body impact on steel columns. *International Journal of Impact Engineering*, 58:39--54, 2013.

[8] L. Tang, H. Wang, G. Li, and F. Xu. Adaptive heuristic search algorithm for discrete variables based multi-objective optimization. *Stuructural and multidisciplinary optimization*, 48(4):821--836, 2013.

[9] L. Zhao, W. Pawlus, H. R. Karimi, and K. G Robbersmyr. Data-Based Modeling of Vehicle Crash using Adaptive Neural-Fuzzy Inference System. *IEEE/ASME Transactions on Mechatronics*, 19(2):684--696, April 2014.

[10] NHTSA. National Highway Traffic Safety Administration webpage http://www.nhtsa.gov/.

[11] L Gou, G. G. Wang, H. Wang, and D. Wang. An Effective Hybrid Firefly Algorithm with Harmony Search for Global Numerical Optimization. *The Scientific World Journal*, 2013:9, 2013.

[12] X. Yang and X. He. Firefly Algorithm: Recent Advances and Applications. *International Journal of Swarm Intelligence*, 1:36--50, 2013.

[13] Z. W. Geem, J. H. Kim, and G. V. Loganathan. A new heuristic optimization algorithm: harmony search. *Society for Modeling and Simulation International*, 76:2:60--68, 2001.

# FATAL URBAN CYCLIST COLLISIONS WITH LORRIES: AN IN-DEPTH STUDY OF CAUSATION FACTORS AND COUNTERMEASURES USING A SYSTEM-BASED APPROACH

**Pete Thomas**
**Rachel Talbot**
**Steve Reed**
**Jo Barnes**
Loughborough University, United Kingdom

**Nicola Christie**
University College London, United Kingdom

Paper Number 15-0169

## ABSTRACT

In the UK and other countries cyclists are the only group of road users with increasing fatalities and cyclist protection has become a high priority both to reduce the risks of cycling and the perception of risks amongst cyclists. The objective of this study is to apply a systems approach to a causation analysis of fatal crashes in order to identify key risk factors and countermeasures associated with all vehicles involved, the infrastructure, road users and road safety management.

The paper presents an analysis of fatal cyclist collisions that took place in London in the years 2007 to 2011. Case materials included police reports, witness statements, vehicle inspections, scene plans and photographs, collision reconstructions, post-mortem and other medical reports. The sample comprised a total of 53 fatal cyclist collisions that occurred during the five year period.

The most common collision type resulting in a fatal cyclist was an impact with a large vehicle >3.5T including 27 lorries and 3 buses. The most common manoeuvre involved the large vehicle turning left resulting in a low speed interaction with the cyclist. Generally impacts occurred to the front left side or left front side of the truck (24 cases, 89%). Insufficient direct vision of the cyclist was a factor in all of these cases with additional risks associated with driver attention and mirror limitations. The availability of Class V side and Class VI front mirrors did not prevent all fatalities.

12 (45%) of the lorries were equipped with side guards while 11 were exempt, however all of the fatally injured cyclists were on the ground before any side-guard interaction could have occurred and side guards were not seen to be effective in this sample.

## INTRODUCTION

Although there has been a longer term reduction in fatalities of all road users in Great Britain, between 2009 and 2013, the number of pedal cycle fatalities fluctuated between 100 and 120 with some evidence of a slight upwards trend (DfT 2013). This has led to an increased focus on cycle safety in the UK – especially in areas such as London where there has also been an increase in the number of pedal cyclists on the road as a result of healthy mobility initiatives.

Cyclists, along with pedestrians and motor-cyclists are considered to comprise the group of “Vulnerable Road Users”. Compared with the occupants of motorised vehicles they have very few opportunities for protection and injury mitigation and casualty reduction measures focus predominantly on collision avoidance measures. Unlike

other vulnerable road users however cyclists frequently do not have the segregation from traffic experienced by pedestrians but they do have increased conflicts with motorised vehicles due to the frequent speed differentials.

This paper describes the results of a study conducted on behalf of Transport for London that examined fatal along with a small number of very serious injury pedal cyclist crashes that occurred in London between 2007 and 2011 (Talbot et. al. 2014).

## SYSTEMS APPROACH

The first step in developing countermeasures to road traffic crashes is to identify what factors contributed to their occurrence in the first place. Accident causation models have been developed to improve the safety of industrial processes for many years. An early model of accident causation was developed in the context of industrial accidents by Heinrich (1931). The model explained an accident as a step in a sequential chain of events or circumstances, each of which was dependent on the previous event. By removing one of the events the consequent circumstance would be avoided and the accident prevented. More recent models of accident causation developed for industrial processes have come to consider the development of risks within a closely coupled, integrated system of which humans are a part. All components of all systems have a variation in performance whether they are human, mechanical or algorithmic. Systems that are increasingly tightly coupled are less resilient to the effects of adverse circumstances. Humans in the control loop have the opportunity to adapt behaviour to enable the system to accommodate adverse conditions but in a tightly coupled system a minor human error can result in a major outcome.

In considering the behaviour of systems Reason (2000) identified two types of error that may occur. Active failures are unsafe acts that are committed by people who are components in the system. He states that they may take a variety of forms including slips, lapses, fumbles, mistakes, and procedural violations. Secondly he identifies latent conditions, which represent attributes of the system – design, functionality, operation. Normally these deficiencies have no consequence and there are no adverse outcomes. However when the trigger of an active failure aligns with the latent conditions of the system it may result in an adverse outcome.

The principles of the accident causation models discussed above have guided the approach used in the collection of data, the analysis of that data, as well as the identification of potential countermeasures. To this end, it can be said the crashes are failures in a road traffic system made up of four components:

- Environment: This includes aspects such as infrastructure and weather conditions.
- Vehicle: All vehicles (including bicycles), their design and safety systems.
- Road user: The human behaviour element in the system - drivers, pedestrians, pedal cyclists, motorcycle riders etc.
- Management: These are the indirect influences of the system including legislation, policy and procedures e.g. licensing, congestion charging, fleet management, which in turn influences factors such as who is on the road and when.

These components are not considered in isolation as they are all interlinked and each component can affect another in the system. For example a driver may drive differently (road user) in different weather conditions (environment) or misinterpret unfamiliar infrastructure.

## METHODOLOGY

In the UK, specialist police officers, who are trained in road traffic crash investigation methodologies, attend crashes that are fatal or considered to be life threatening. They conduct detailed investigations and where possible reconstructions to gain as thorough as possible understanding about the crash and how it occurred. Data was collected from the resulting police files that were accessed in paper form at a London police station under conditions of a confidentiality agreement. A set of key documents from which the most data could be extracted were identified:

- the police collision investigation report;
- scene and vehicle photographs;
- scene plan and reconstruction;
- CCTV images;
- driver interview transcripts;
- witness statements;
- Post-mortem reports.

A simple database was created to allow quantitative data to be recorded such as time and date of crash, vehicle type, age, gender, impairment, as well as more detailed qualitative descriptions such as crash description, vehicle defects, information about road narrowing and route information. Other supplementary information such as mirror positions and vehicle damage was recorded on paper and copies of scene plans and photos were also obtained. Injury data collected from post-mortems and hospital consultant witness statements were recorded separately including Abbreviated Injury Scale (AIS, 2005) codes, injury descriptions, toxicology and date of death. Transport for London also provided context data such as the number and type of crashes that had occurred at each crash location during the previous three years.

A case review approach was adopted to analyse the crashes whereby the complete dataset (including the database variables, scene plan, photos, injury and context data) for each crash was reviewed by two or more researchers to identify factors that contributed to the crash. Contributory factors were not assigned according to a pre-defined list but the system approach as previously discussed was used to ensure factors relating to the environment, road user, vehicle and management were identified as appropriate.

## RESULTS

Seventy-nine fatal and very serious crashes occurring in London were investigated by specialist police offices between 2007 and 2011. Of these, 53 were available for data collection. Forty-six were fatal pedal cyclist crashes, using the internationally accepted definition of death within 30 days. A further 7 involved a seriously injured pedal cyclist whose injuries were considered to be life threatening at the time of the crash. In the following results and analysis, the fatal and serious crashes have been grouped together the characteristics of the serious crashes, in terms of crash causation, were very similar to those of the fatal crashes.

Some differences were observed between the sample of 53 crashes occurring in London and the fatal pedal cyclist crashes occurring in Great Britain as a whole (See Figure 1). In London there were

- Fewer cyclist crashes in the summer months, more in winter (73% London, 42% GB)
- Fewer weekend crashes (7% London, 31% GB)
- A larger early morning peak (8:00 – 10:00) in collisions (25% London,12% GB)
- More cyclist crashes on A-roads (76% London, 53% GB)
- More cyclist crashes in 30 mph speed limits (89% London, 48% GB)
- More cyclist crashes on or on the approach to junctions (74% London,48% GB)

### Collision partner

Table 1 shows the primary collision partner for the 53 fatal and serious crashes examined and the manoeuvres conducted by the two vehicles. The primary collision partner is defined as the vehicle that was involved in the initial interaction with the pedal cyclist. The most common collision partner was a goods vehicle corresponding to 29 (55%) of the total collisions while 15 (28%) of the collisions were with a car. In 17 crashes a motorised vehicle turned left across the path of the cyclist and 15 of these were goods vehicles. A further four collisions occurred when the cyclist and motorised vehicle were both turning left and three of these again involved a goods vehicle. In nine collisions the bicycle was struck in the rear by another vehicle and three of these involved goods vehicles.

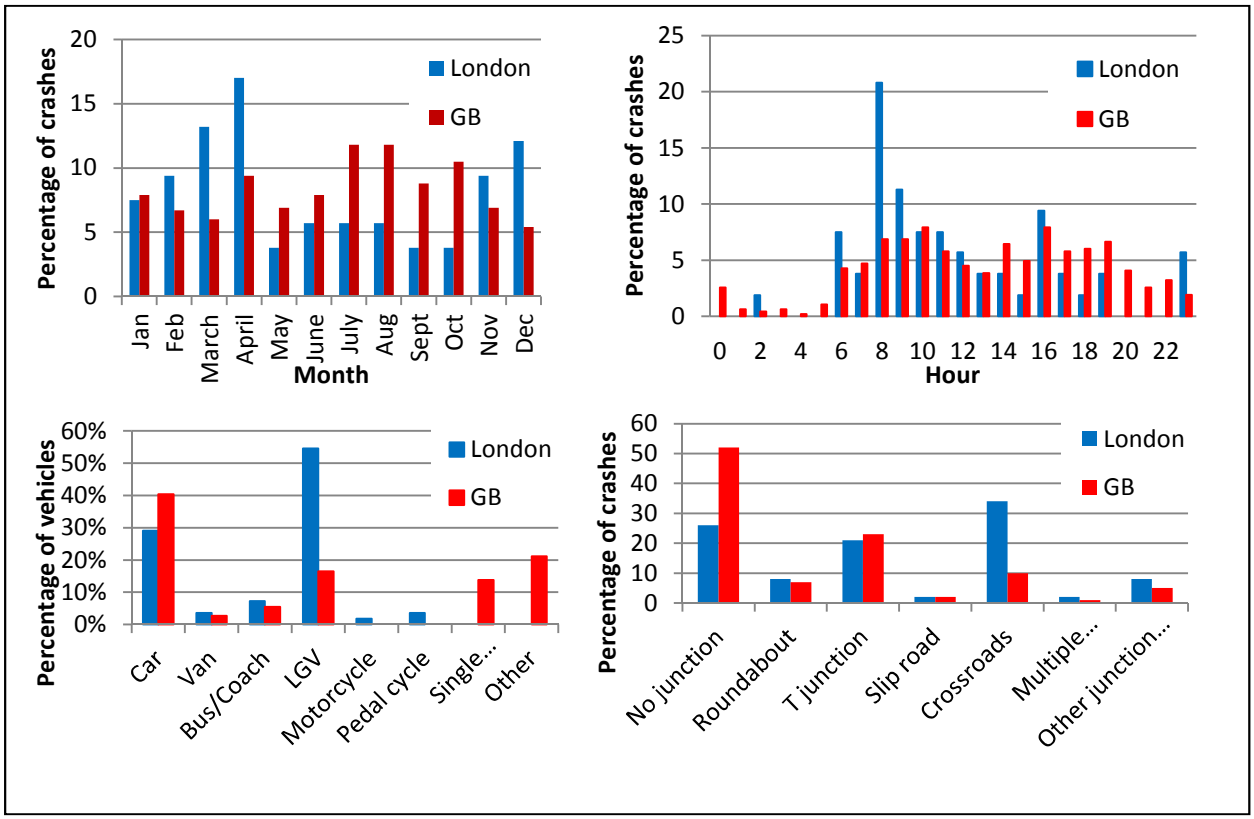


*Figure 1. Comparison of London and GB accident circumstances*

Table 2 shows the distribution of the relative movement between the cyclist and the large vehicles within the sample. There were 32 large vehicles, lorries and buses, of which the motion was identified in 30 cases. Most commonly the cyclist was undertaking – moving forward relative to the large vehicle – on the vehicles left-side, closest to the kerb. Out of the 32 cases there were 20 in which the cyclist undertook the large vehicle and a further three cases where the large vehicle overtook the cyclist. There were only two cases where the cyclist passed the large vehicle on its right side.

**Direct and indirect vision of the cyclist**

Each case file was examined in order to identify evidence relating to the location of the first contact between the large vehicle and the cyclist. Figure 2 shows the location of the first contact between the large vehicle and the bicycle for the 29 cases where there was information available within the case material. In the UK vehicles drive on the left side of the road and the most locations of the contact with the fatally injured cyclists were clustered around the front left corner either on the front or the side face of the large vehicle.

At the time of the analysis it was compulsory for large vehicles to be fitted with Class IV wide angle side mirrors and Class V close proximity side mirrors with very few exemptions and Table 3 shows that only one large vehicle was identified without one fitted. Fitting in a further three cases was unknown. Large vehicles manufactured after January 2007 were also required to be equipped with a front mounted Class VI mirror to identify close situated road users. Table 3 shows the numbers of contacts between cyclist and vehicle distributed to the relevant zone for each combination of mirrors. There were 26 large vehicles were the type of mirrors fitted was known and only one was not equipped with a class V mirror while only 14 were equipped with Class VI mirrors.

Eight of the 14 cyclists with first contacts on the side of the vehicle were in zones S1, S2 which were judged to lie within the vision zone of Class V mirrors according to the specification (European Commission regulation 2003/97/EC) and all of these vehicles were equipped with Class V mirrors. 13 of the 15 cyclists struck by the front of the vehicle were in zones F2 and F3, the area covered by Class VI mirrors and in eight of the 13 cases Class VI mirrors were available.

**Table 1**

**Crash manoeuvre by collision partner**

| Manoeuvre | Diagram | Car | Van | Bus/ Coach | Goods vehicle >=3.5 T | Other | Total |
|---|---|---|---|---|---|---|---|
| Other vehicle turns left across the path of P/C | | 1 | | | 15 | 1 | 17 (32%) |
| Other vehicle runs into rear of P/C | | 2 | 1 | 1 | 5 | | 9 (17%) |
| P/C and other vehicle travelling alongside each other | | 1 | | | 3 | 1 | 5 (9%) |
| P/C fails to give way or disobeys junction control & collides with other vehicle | | 4 | | | | | 4 (8%) |
| P/C and other vehicle collide when both turning left | | | | 1 | 3 | | 4 (8%) |
| Head on collision between P/C and other vehicle | | 2 | | | | | 2 (2%) |
| Other vehicle fails to give way or disobeys junction control & collides with P/C | | 1 | | | 1 | | 2 (2%) |
| No other vehicle hit by P/C. Various manoeuvres or loss of control only | | | | | | 2 | 2 (2%) |
| Other | | 4 | 1 | 1 | 2 | | 8 (15%) |
| Total | | 15 (28%) | 2 (4%) | 3 (6%) | 29 (55%) | 4 (8%) | 53 (100%) |

**Table 2**
**Relative movement of cyclists and large vehicles at point of collision**

| Relative motion | Number of crashes |
|---|---|
| Cyclist overtaking stationary large vehicle | 2 |
| Cyclist overtaking moving large vehicle | 0 |
| Cyclist undertaking stationary large vehicle | 11 |
| Cyclist undertaking moving large vehicle (not turning) | 1 |
| Cyclist undertaking moving large vehicle which was turning right | 0 |
| Cyclist undertaking moving large vehicle which was turning left | 8 |
| Both moving together (similar speed) | 2 |
| Large vehicle overtaking stationary cyclist | 0 |
| Large vehicle overtaking moving cyclist | 3 |
| Other crash configuration | 3 |
| Unknown | 2 |
| Total | 32 |

**Table 3**
**Mirror fitting and contact zone**

| Zone | Mirrors Fitted | | | | Total |
|---|---|---|---|---|---|
| | No Class V or VI | Class IV or V only | Class IV, V & VI fitted | Not known | |
| F1 | 0 | 0 | 0 | 1 | 1 |
| F2 | 1 | 0 | 3 | 1 | 5 |
| F3 | 0 | 4 | 3 | 1 | 8 |
| F4 | 0 | 1 | 0 | 0 | 1 |
| S1 | 0 | 1 | 1 | 0 | 2 |
| S2 | 0 | 2 | 4 | 0 | 6 |
| S3 | 0 | 1 | 1 | 0 | 2 |
| S4 | 0 | 2 | 2 | 0 | 4 |
| Total | 1 | 11 | 14 | 3 | 29 |

**Table 4**

**HGV and 3.5-7.5 tonne truck types included in sample**

| HGV/3.5-7.5 tonne type | Image | Number of HGV/3.5-7.5 tonne | Side guard | | |
|---|---|---|---|---|---|
| | | | Fitted | Not fitted | Unknown |
| Tipper | | 11 (37%) | 0 | 9 | 2 |
| Flat or drop side | | 5 (17%) | 4 | | 1 |
| Box | | 4 (13%) | 3 | | 1 |
| Skip carrier | | 3 (10%) | | 3 | |
| Curtain sided articulated vehicle | | 3 (10%) | 3 | | |
| Refuse Lorry | | 2 (7%) | | 2 | |
| Tractor Unit only | | 1 (3%) | | 1 | |
| Cement mixer | | 1 (3%) | | 1 | |
| Total | | 30 | 10 | 16 | 4 |

**SIDE UNDERRUN GUARDS**

Table 4 shows the body style of the 30 goods vehicles involved in the collisions. 11 (37%) of the vehicles were tipper lorries and overall 19 of the vehicles – tipper, flat/drop side and skip carriers – were related to the construction industry and 12 were not fitted with side guards.

The trajectory of the interaction of the cyclist in the interaction with the lorry was established by reviewing the locations of contact marks and the final rest position of the cyclist. In 29 of the 30 cases the cyclist was run over by the wheels of the lorry sustaining the fatal injuries. Only four cyclists collided with the lorry in a zone that was a candidate and all of these were run over by a rear wheel.

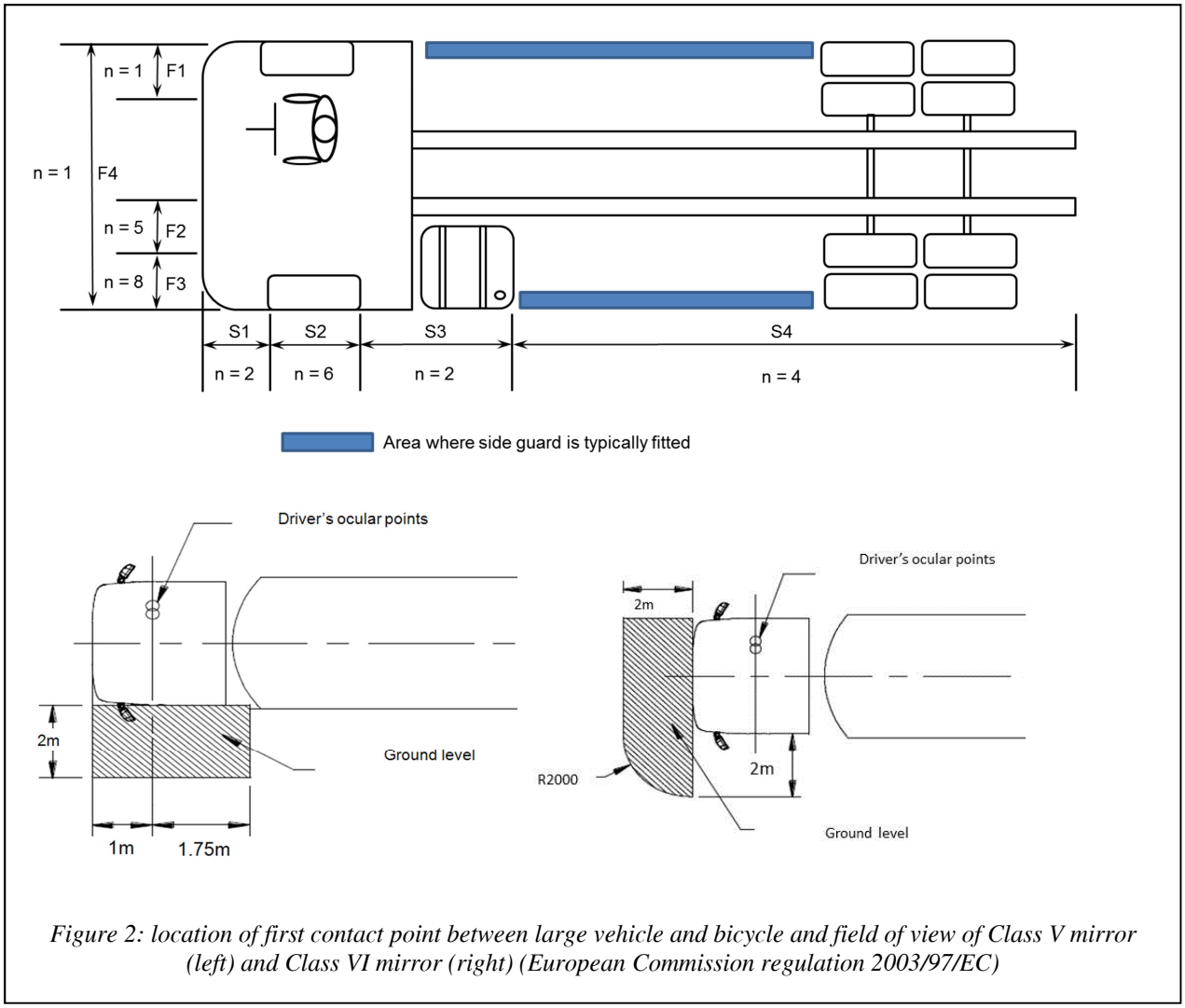


*Figure 2: location of first contact point between large vehicle and bicycle and field of view of Class V mirror (left) and Class VI mirror (right) (European Commission regulation 2003/97/EC)*

## DISCUSSION

This analysis has been part of a wider research programme intended to form the evidence base for a range of actions that will improve the safety of cyclists in London and is reported by Talbot et al. 2014. The main objective was to identify beneficial interventions that could be applied within the context of the Metropolitan region. The approach, based on a systems analysis of all related factors, has enabled the principal road, vehicle and user factors to be fully established and their interactions to be identified. Using the systems analysis Talbot et al identify several risk factors related to the causation of lorry collisions with cyclists including

- conflicts between cyclists and lorries due to an overlap in peak lorry and cyclist traffic at specific times of the day and week
- installation of cycle lanes on roads with high lorry traffic
- road infrastructure design that increases the conflicts between cyclists and left-turning lorries
- lorry driver workload at busy junctions
- the entry points and design dimensions of Advanced Stop Lines
- late or no left turn signalling by lorry

This analysis has focussed on the interactions between cyclists and lorries to provide a more detailed description of the precise nature of the safety problem and support the development of new countermeasures.

The analysis is based on the data contained within the police accident records. In the UK fatal crashes are investigated by specialist police officers and the nature of the examination and reconstructions results in a detailed, reliable source of information. The 53 fatally injured cyclists in the sample form one of the largest groups of in-depth studies of cyclists available and the detailed nature of the data has been used to examine specific accident and injury risk factors.

The comparison between fatal cyclist collisions in London and elsewhere in Great Britain has identified that there are differences, mostly related to the characteristics of London. In particular a greater proportion of collisions occurred during weekdays, during the winter months, near junctions and on A-class roads. Therefore the overall distributions of the key accident risk factors may not be generalizable to the UK, however the present analysis focusses on the nature of the interaction between cyclists and large vehicles and therefore is highly relevant when considering the revision of the EU lorry dimensions (see EU Directive 96/53/EC). The data analysed only concerns fatally injured cyclists and therefore all crashes in the sample can be considered system failures, this means that the results cannot be taken to provide estimates of the effectiveness of safety systems.

The in-depth analysis of the fatal collisions indicates the typical sequence of events prior to the collision (see Figure 3). In Figure 3a the cyclist moves towards a lorry that is moving slowly or stopped at a junction and decides to pass on the left side, dedicated cycle paths or the availability of an advanced stop line may encourage the cyclist. The lorry driver intends to turn left but is either not indicating or the indicators are not visible to the cyclist. The cyclist moves to a zone around the front left corner of the lorry, either to the left side front or the front left, as illustrated in Figure 3b. The cyclist intends to continue ahead or to turn left but is not observed by the lorry driver who steers the lorry around the corner, being a long vehicle the front end takes a wider curve than the rear which moves close to the curb. The bicycle is struck at slow speed as the lorry moves away, the cyclist falls to the ground and passes underneath any side underrun guards to be run over by the following wheel either on a second front or a rear axle as in Figure 3c.

The conflict that leads to the collision typically occurs when the lorry driver is unable to perceive the presence of the cyclist and the cyclist does not recognise that the lorry is about to turn left. Schoon et al (2007) examined the Dutch national accident data to identify the frequency with which right-turning (in the case of the Netherlands) lorries collided with cyclists. They surmised that poor direct vision of the cyclist and insufficient field of view of side mirror systems was a relevant risk factor. Cook et al (2011) used human modelling methods and identified the presence of significant blind spots to the side of the lorry, even when equipped with both Class IV and Class V

mirrors. Niewohner and Berg (2005) similarly identified blind spots associated with side mirrors and proposed a range of countermeasures. Nevertheless there has been little research on the real-world performance of class VI mirrors.

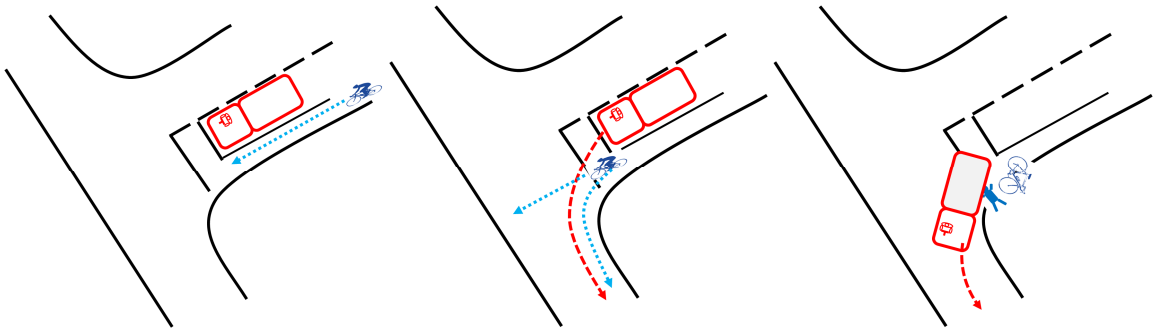

*Figure 3a* *Figure 3b* *Figure 3c*

*Cyclist – lorry collision sequence*

This analysis has shown that fatal collisions with cyclists occur despite the presence of Class V and Class VI mirrors and where contact zones are expected to be in view. 14 cyclists had their initial contact with the side of the lorry and eight of these were in zones expected to be covered by Class V mirrors. There was no definitive evidence available in the case reports of the reasons why the cyclists were not detected by the lorry drivers however some drivers reported the demands on attention of a busy traffic environment, others reported they did look at the mirrors but did not see the cyclist. It was observed that the frequent relative movement between the cyclist and the lorry meant that the cyclist would only be visible in a Class V mirror for a short period of time if moving at a normal speed due to the convex profile. The lorry driver would then have to be looking at the mirror during this time in order to detect the cyclist. Further anecdotal problems of the lorry driver identified in the case reports included incorrect mirror adjustment and incorrect understanding of the purpose of the mirrors.

The current EU requirements (2007/38/EC) for Class V mirrors were introduced in 2007 and the Directive included the requirement to retrofit older vehicles. Class VI mirrors were introduced in 2003 but there was no requirement for retrofit. This analysis has shown that Class VI mirrors were only fitted to 14 of the 29 lorries in the sample and 15 cyclists died after being struck by the front of the lorry. 13 of these were located in the zone covered by Class VI mirrors which were fitted to eight of these vehicles. This indicates that Class VI mirrors do not completely prevent fatal cyclist collisions with the front left of the lorry, cyclists can be located in this position yet still not be observed by the driver. There were six cases where no mirror was available however it cannot be concluded these would have been prevented the fatality.

**Side underrun**

Side underrun guards have been primarily developed to reduce the risks of injury to car occupants when in collision with the side of a lorry or its trailer. Pedestrians and cyclists are assumed to have protection by being diverted away from the rear wheels when colliding with the vertical face of the guard. This protection is determined on the basis that the cyclist or pedestrian will be vertical at the time of impact. The performance is specified in Council Directive 89/297/EEC which defines the dimensions of the underrun guard and requires the height above ground to be no more than 550mm. The present analysis has shown that 14 of the 29 fatally injured cyclists were in collision with the side of the lorry however only 4 of these contacts were in a zone covered by a side underrun guard and only one of these case files showed clear evidence of cyclist contact on the underrun guard. Overall the case reviews indicated that the cyclists struck by the side of the lorry, together with many of those struck by the front, were already on the ground before the approach of the following axle. Only 10 of the lorries were known to be equipped with side underrun guards, the remainder being considered exempt as a result of their purpose. It cannot be concluded that

side underrun guards do not offer any protection for cyclists since this data sample does not include collisions involving non-fatal cyclists. However the protection is considered to be limited and further investigation is recommended of the protection offered by a side guard to a cyclist lying on the ground.

## CONCLUSIONS

This paper has examined the case reports of 53 fatally injured cyclists died in London between 2007 and 2011. The main conclusions are

1. Lorries are the most frequnt collision partner and further actions are necessary to reduce crsh risks
2. There is no single countermeasure that is available that will prevent all fatal cyclist collisions with lorries, a systems approach is required including veicle design measures
3. The most common crash scenario involves a slow-moving lorry turning across the path of an unidentified cyclist, the cyclist having a contact around the are of the front left corner of the lorry, falling off the bicycle and then being run over by the lorry wheels.
4. Even when Class V and Class VI mirrors are available on trucks the cyclist may not be observed by the driver
5. Many lorries are not equipped with side underrun guards
6. Side underrun guards do not prevent cyclists being run over by the rear wheels of lorries

## REFERENCES


COOK, S., SUMMERSKILL, S., MARSHALL. R. et al., 2011. The development of improvements to drivers' direct and indirect vision from vehicles - phase 2. Report for Department for Transport DfT TTS Project Ref: S0906 / V8. Loughborough: Loughborough University

Council Directive 89/297/EEC of 13 April 1989 on the approximation of the laws of the Member States relating to the lateral protection (side guards) of certain motor vehicles and their trailers

Department for Transport. Reported Road Casualties Great Britain: 2013 Annual Report Focus on pedal cyclists.

Directive 2007/38/EC of the European Parliament and of the Council of 11 July 2007 on the retrofitting of mirrors to heavy goods vehicles registered in the Community

Heinrich, H. W. (1931) Industrial accident prevention: a scientific approach McGraw-Hill

Niewoehner, W., Berg, A. Endangerment of Pedestrians and Bicyclists at Intersections by Right Turning Trucks. ESV 2005 paper 05-344. DEKRA Automobil GmbH

Reason, J. (2000) Human error: models and management. British medical Journal, 320:768–70

Schoon, C. C. dr... Doumen, M.J.A, de Brui, D. The circumstances of blind spot crashes and short- and long-term measures : a crash analysis over the years 1997-2007, traffic observations, and surveys among cyclists and lorry drivers. SWOV report 2008

Talbot, R., Reed, S., Barnes, J., Thomas, P., Christie, N. Pedal Cyclist Fatalities in London: Analysis of Police Collision Files (2007-2011). 2014 accessed at http://www.tfl.gov.uk/cdn/static/cms/documents/pedal-cyclist-fatalities-in-london.pdf March 2015.


## ACKNOWLEDGEMENT


This research project was funded by Transport for London. The authors acknowledge the financial support of TfL to conduct the project and the organisational support of the Metropolitan Police Service of London in providing access to the fatal accident reports. The views expressed in the paper are those of the authors.

This paper has been peer-reviewed and published in a special edition of *Traffic Injury Prevention* 16(S1), by Taylor & Francis Group. The complete paper will be available on the *Traffic Injury Prevention and www.NHTSA.gov* websites on June 8, 2015.

To access all Peer-reviewed papers please copy and paste the link below into your browser to access the papers.

http://www.tandfonline.com/toc/gcpi20/16/sup1

This paper has been peer-reviewed and published in a special edition of *Traffic Injury Prevention* 16(S1), by Taylor & Francis Group. The complete paper will be available on the *Traffic Injury Prevention and www.NHTSA.gov* websites on June 8, 2015.

To access all Peer-reviewed papers please copy and paste the link below into your browser to access the papers.

http://www.tandfonline.com/toc/gcpi20/16/sup1

# ANALYSIS OF CHILDREN STROLLERS AND PRAMS SAFETY IN URBAN BUSES

**Luis Martínez, Antonio García, Manuel Espantaleón, Enrique Alcalá.**
UPM. Universidad Politécnica de Madrid.
INSIA. Instituto Universitario de Investigación del Automóvil.
SPAIN.

**Juan Dols.**
UPV. Universidad Politécnica de Valencia.
IDF. Instituto de Diseño y Fabricación.
SPAIN.

Paper Number 15-0175.

## ABSTRACT

The wide incorporation of low floor buses in our cities encourages that child younger than three years, seated on their stroller could use the buses. Currently, the UNECE Regulation No 107 at its revision 5 has included general provisions for the accessibility and basic safety for this type of users. An applied research has been performed to analyze the level of protection offered for the stroller restraint systems included in R107, by performing dynamic tests with instrumented dummies.
More than 20 dynamic sled tests were performed to assess the child safety in urban buses. Two types of configurations have been tested: a vehicle specific CRS for urban buses and the own stroller with different restraint systems.
The specific vehicle built-in CRS tested is a rearward facing group 0/I that is currently in use in the city of Madrid (Spain) by the public urban buses. This CRS was tested in frontal and rear impact with the acceleration pulse defined in the UNECE regulation No 80.
On the other hand, to make suggestions for using the stroller in urban buses, a very low severity crash pulse (up to 2 g peak acceleration and $\Delta V = 20$ km/h) was defined and used in this study. Four stroller models with three types of restraint devices (safety belt, PRM wheelchair backrest and a folding backrest device) were tested with this pulse. The strollers were selected in order to reduce biasing of the results.
Several dummies (P3, Q3 and Q1) were used to evaluate the injuries and the kinematics. Furthermore, different sources of IRAV have been applied for the Q dummies (R94 and FMVSS 208 scaled by applying Mertz 2003 techniques), an extended range of injury criteria is obtained and an in depth analysis of the protection offered by the different restraints systems used is performed.

## INTRODUCTION

The use of public transport is a need and a right for all citizens. However, there are still some groups who experience difficulty travelling on buses – such as users who travel with pushchairs or strollers. These users also face safety problems as it is often necessary for children to be taken out of their strollers and held in the arms of their accompanying person. From the standpoint of operating companies, the use of buses by this group represents a design problem that has not yet been satisfactorily and effectively resolved at the moment of perform this research study.

One of the studies published regarding the use of buses by passenger travelling with pushchair [1], analyze the response of a survey applied to 44 Spanish transport companies (69% of the total). The results show that 32% of bus companies use local legislation to regulate the access to buses by pushchair users, 27% applies internal regulations, 11% respond to regional legislation, and up to 30% of companies do not apply any regulations. Of all the companies surveyed, 45% allow pushchairs to be open inside the bus, while 32% prohibit pushchairs from being open. Most companies (41%) have not defined the number of pushchairs allowed on a bus, while 34% allow access for up to two pushchairs, and 25% allow only a single pushchair. Note that priority is given to wheelchair users over pushchairs by 23% of these companies, while the remainder (77%) does not specify priority. Access for pushchairs is usually (preferably) through the front door, although central door entry is allowed (even without using the ramp), while exiting is normally made through the central or rear doors.

Pushchairs are usually positioned parallel to the longitudinal axis of the vehicle and facing backwards. Some 25% of bus companies require that the pushchair brake is applied to the wheels during transport (as the pushchair is open), while no indication is provided by the remaining 75%. Finally, only 18% of the companies surveyed explicitly deny access to tandem (twin) pushchairs.

Recently, at June 2014, the UNECE regulations (United Nations Economic Commission for Europe) in its regulation 107R05 (current version of the regulation 107 is R06 from March 2015), has modified the accessibility requirements of Class I vehicles (urban buses), extending the previous requirement of at least one wheelchair user to also at least one pram or unfolded pushchair at same time.

The work reported in this paper is focus on the child safety (children under 3 years old) in urban buses. Children under 3 usually used Child Restraint System – CRS (approved under regulation 44 or in future the i-Size category according regulation 129). Nevertheless in urban buses this type of CRS could not be used (technically because there is no safety belt or ISOFIX installed in urban buses seats; and it is not practical for the user that must wear their own CRS for buses). There are clearly two tendencies: on one hand to use a specific built-in child restraint system (with national or regional approval) and on the other hand to establish prescriptions for use the strollers or prams inside the urban buses in order to obtain a certain level of safety (the same direction than regulation 107), however R107 does not require any dynamic evaluation of the restraint system included into vehicles.

To bring some information to the previous mentioned options, dynamic sled tests have been performed in order to assess the safety behaviour in urban buses with different safety devices, and oriented to achieve the following objectives:

- Know the accelerations of a specific built-in child restraint system for urban buses tested with the acceleration profile as defined in the regulation 80 (for coaches). The safety assessment is evaluated objectively in order to obtain the accelerations levels as a maximum in order that this level could be useful to establish a reference for the child safety evaluation in urban buses.
- Evaluation of the child safety behaviour in urban buses using strollers or prams. In this case, it has been developed a low severity pulse in order to assess this behaviour.
- Analyze the safety of different systems (safety belt, PRM backrest or a prototype [2] of folding backrest), using different types of strollers. It is not the objective of the study to evaluate if one stroller is better or worse than others.

## METHODS

Two severity pulses are used in this study. For the strollers, several frontal low severity impact sled tests were performed in order to assess the safety performance of different strollers restrained with different systems to the urban bus (a PRM backrest, a folding backrest and a 2P stroller safety belt). Furthermore, for the specific built-in CRS, three sled tests (2 frontals and 1 rear) were performed with the acceleration profile defined in regulation 80R03, more severe than previous ones. The next figure shows the differences of the two severity pulses carried out (these pulses are obtained from real sled test deceleration). The low severity pulses represents conditions more severe than the emergency manoeuvres (limited by the friction coefficient between the tire and the road), but there is not intended to replicate a bus crash, therefore the acceleration should be greater than 1 g. An increase of 50% was imposed (i.e. an acceleration of at least 1.5 g). The duration of the dynamic impact was limited by the capabilities of the sled facility used, with a maximum stroke of 1200 mm. Finally it was established a $\Delta V = 20$ km/h (compatible with the total braking distance available).

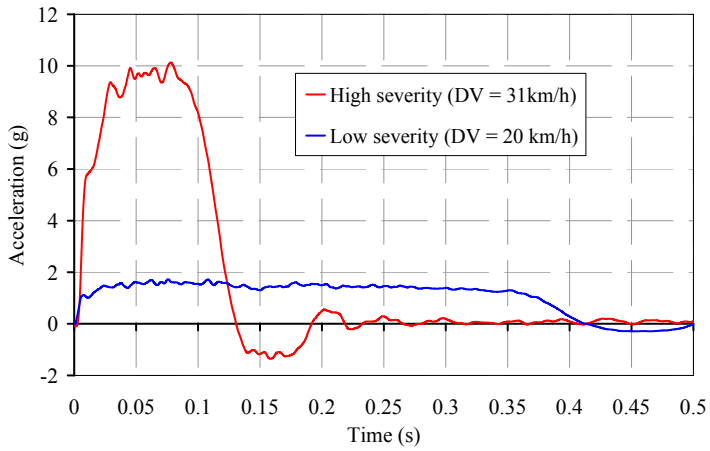


***Figure 1. Sled acceleration for the two severities.***

Four types of occupants were used to perform the dynamic sled tests:

- Ballasted mannequin of 9MO: with a total mass of 9 kg. Used to assess the kinematics response.
- Q1 dummy. The measurement capabilities used in tests are: head acceleration (X, Y, Z), upper neck forces (X, Y, Z), upper neck moments (X, Y, Z), chest acceleration (X, Y, Z), chest deflection and pelvis acceleration (X, Y, Z).
- P3 dummy with head acceleration (X, Y, Z) and chest acceleration (X, Y, Z).
- Q3 dummy with chest acceleration (X, Y, Z).

Furthermore to the dummy measuring capabilities, two or three high speed cameras (1000 fps) were used to evaluate the impact kinematics of the dummies and the strollers. The next figure shows a sketch of the sled test with the views of the two high speed cameras (the third camera is a zenithal view). As it can be seen, a representative urban bus floor was installed on the sled. This floor includes the PRM backrest, the folding backrest and the 2P stroller safety belt.

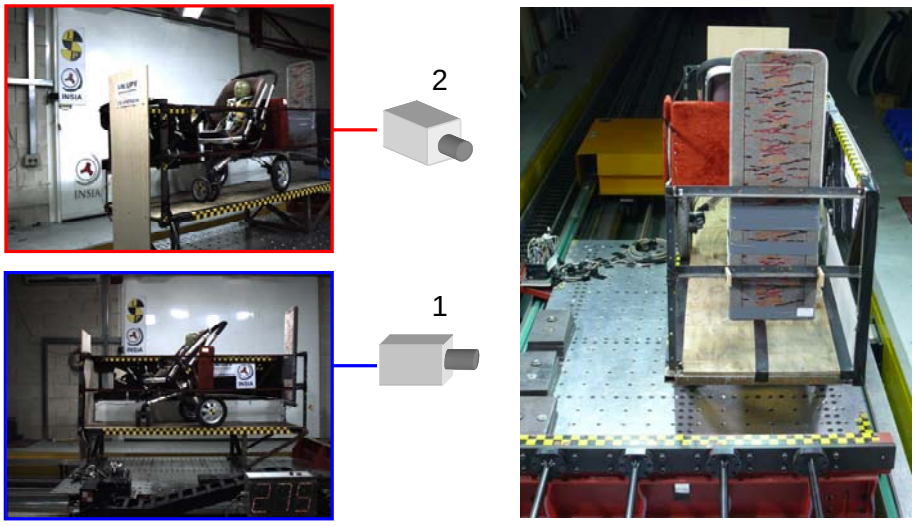


***Figure 2. High speed cameras and test ring set up.***

The dynamic sled tests were performed in two phases:

- **Phase1**: High severity dynamic tests (according regulation 80R03) with a specific built-in rearward facing child restraint system. The objective of this phase is to obtain the safety performance of a specific child restraint system built in an urban bus.

- **Phase2**: Low severity dynamic tests (ΔV = 20 km/h; 1.5 g) with strollers and baby carriage with different safety devices:
    - **Phase2A**. Larger number of dynamic tests with: folding backrest, PRM backrest and 2P safety belt as safety devices used to restraint the strollers. Four types of strollers have been tested in this phase. The objective of this phase is to analyze the general behaviour of the strollers and the safety devices.
    - **Phase2B**. Finally, in this latter phase a Q1 dummy (with larger measurement capabilities) was used in order to study in detail the behaviour of the strollers with the safety devices. Two types of strollers and two types of safety devices were studied.

**Samples**

Different samples have been tested during the dynamic tests (see Figure 3). For the dynamic tests, the strollers have been used in the configuration of the bigger child (i.e. the worst situation for the restraint and stability of the stroller is produced with the heavier child). The strollers have been selected with different configurations or features but all of them are current market representatives. The main characteristics of them are summarized:

- For the high severity pulse, a **specific built-in** (in an urban bus – **M3 vehicle category, Class I**) child restraint system was used. This CRS is rearward facing oriented and incorporates an integral 5p safety harness. This system is based on the design of the traditional CRS according regulation 44R04 for group I rearward facing oriented. The buckle and the straps fulfil the requirements of the regulation 44R04.
- **Stokke Xplory**. Incorporates a telescopic rod for height adjustment. The main characteristic of this stroller is the height of the centre of gravity that is greater than the other models. The child is restrained to the stroller using a 5p harness.
- **Quinny Buzz**. This stroller has been selected because it has 3 wheels (the frontal is twin wheel). This produced a potential instability of the stroller. The child is restrained to the stroller using a 5p harness.
- **Bebeconfort Streety**. This stroller has a large wheelbase compare with the rest of the dimensions. It was tested in a lateral configuration in order to produce more instability. The child is restrained to the stroller using a 5p harness.
- **Maclaren Quest**. It is the "traditional stroller", with four wheels (same track width front and rear). The child is restrained to the stroller using a 5p harness.

***Figure 3. Built-in (M3 vehicle) CRS and strollers used (figures are not to same scale).***

**Injury Assessment Reference Values (IARV) – extended range**

The anthropomorphic tests devices (ATD) or dummies are very useful and a good measurement tool as a substitute for the human body under crashes. Thanks to their measurements capabilities is possible to establish a baseline or boundaries to determine whether there is a likelihood of injury.
The injury criteria are primarily developed for adult size dummies (specifically for the Hybrid III 50$^{th}$ male). The reference values for child dummies should be scaled form the data of average size adult occupant. The

injury criteria used in this paper (for the Q1 dummy) are obtained from information contained in the regulation 94R02 and FMVSS 208, scaled with the information provided by Mertz et al [3] (where it is described the scaling process for developing the IARV for different sizes and ages). Current IARV used for Q1 at R129 were not used because the pulse severity used at present study is much lower than in R129 (20 kph versus 50 or 30 kph), also and a extended set of IARV with respect to R129 is used and to avoid any collateral effects for use different sources of the IARV, a common procedure were used to obtain the set of injury criteria.

| Dummy part | Parameter | Unit | Limit |
|---|---|---|---|
| Head | $HIC_{15}$ | | 389.00 |
| | HPC ($HIC_{36}$) | | 555.71 |
| | Acceleration | g | 154.00 |
| | 3ms acceleartion | g | 68.44 |
| Upper neck | Shear force Fx | N | 740.00 |
| | Tension force +Fz | N | 783.45 |
| | Compression force -Fz | N | 960.00 |
| | Lateral moment Mx | Nm | 21.00 |
| | Flexion moment +My | Nm | 27.00 |
| | Extension moment -My | Nm | 8.31 |
| | Twist moment Mz | Nm | 14.00 |
| | Nij | | 1.00 |
| | · FT | N | 1610.00 |
| | · FC | N | 1470.00 |
| | · MF | Nm | 42.50 |
| | · ME | Nm | 18.60 |
| | NIC | | Corridor |
| Chest | Sternum deflection Dx | mm | 24.00 |
| | T4 acceleration | g | 87.00 |

NOTE: All the values in the table are peak values, except the 3ms head acceleration.
Grey data are obtained based on the regulation 94R02 and scaled to Q1 dummy.

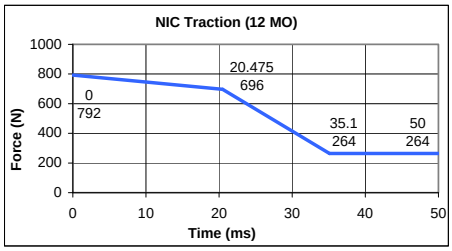


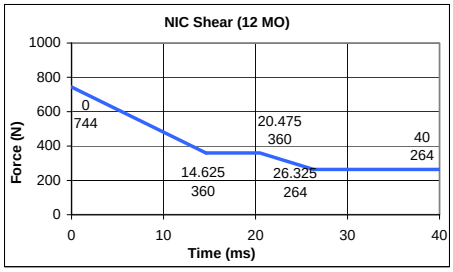


***Figure 4. IARV obtained for a Q1 dummy.***

## RESULTS

This section summarized the results of the dynamic sled tests performed with different severities, strollers, dummies and restraint systems (as mentioned before):

- **Phase1**: High severity dynamic tests (according regulation 80R03) with a specific rearward facing child restraint system.
- **Phase2A**: Low severity dynamic tests ($\Delta V$ = 20 km/h; 1.5 g) with strollers and baby carriage with different safety devices (folding backrest, PRM backrest, safety belt).
- **Phase2B**: Low severity dynamic tests ($\Delta V$ = 20 km/h; 1.5 g) with the most unstable strollers with folding table and PRM backrest and misuse evaluation. These tests have been performed with a Q1 dummy.

### Phase1 (P1)

In this phase, a Q3 instrumented dummy has been used for assess the performance of a rearward facing child restraint system built-in in a urban bus (M3 category, class I). This system was manufactured using components with the individual approval of regulation 44R04 for the group I, therefore this system may offer safety performance equivalent to the CRS used in M1 vehicles. Three tests have been performed in this phase:

- 2 rearward facing impact tests (P1-1 and P1-2).
- 1 forward facing impact test (P1-3).

The next table summarized the chest acceleration of the Q3 dummy in the tests and a picture obtained from the High Speed camera register.

**Table 1. Summary results of the phase 1, (urban bus with specific vehicle CRS).**

| Test ref | Sled Vel (km/h) | Chest AccR 3ms (g) | Chest Vert AccZ (g) | RF (t = 100 ms) | FF (t = 100 ms) |
|---|---|---|---|---|---|
| P1-1 | 30.78 | 14.82 | 4.08 | 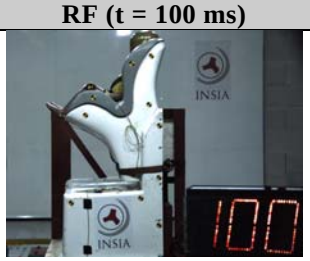 | 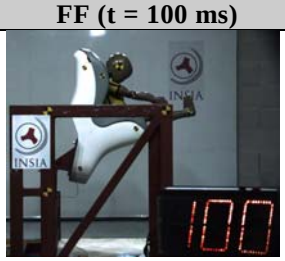 |
| P1-2 | 31.16 | 15.64 | 10.97 | | |
| P1-3 | 31.19 | 20.83 | 8.94 | | |

**Phase2A (P2A)**

The second phase is focused on the assessment of the safety performance of restraint devices with the strollers in the urban bus. Initially (in phase2A) a large number of samples were tested (see Figure 3) with three types of safety devices:

- 2P safety belt (Br3 according regulation 16R08, i.e. two point belt with retractor and automatically locking retractor).
- PRM backrest installed in the urban bus
- Folding backrest (developed in ASUCAR project under P-201131557 patent [2]). It is objective of these test to evaluate this device and provide (if necessary) solution for improved it.

The next figure shows a picture of the sled with a representative section of the urban bus. This section is used for the three types of safety devices.

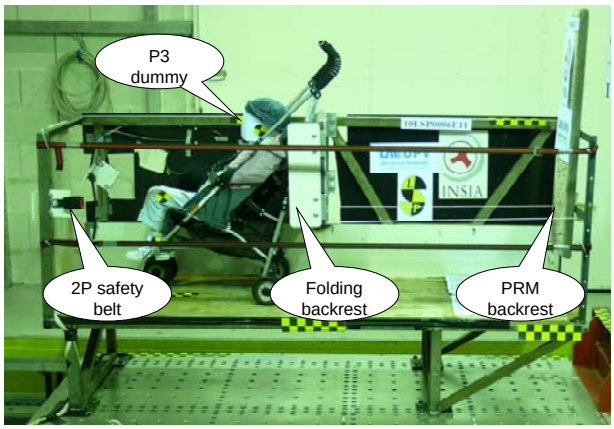


***Figure 5. Urban bus module with three safety device types installed.***

14 sled tests were performed with:

- P3 dummy and Ballast 9MO dummy. One tri-axial accelerometer was installed in each stroller for measure its acceleration during the dynamic tests.
- 4 types of strollers (see Figure 3).
- 3 types of safety devices (described above).
- Different configurations: rearward facing, forward facing, misuse in the belt path, break and without break the strollers' wheels, etc)

In this phase, kinematics analysis was made in order to verify the restraint of each type of the safety device. The results of these test have allow to design the test matrix for the phase2B, with has been performed with a Q1 dummy (more biofidelic dummy and instrumentation capabilities).

**Phase2B (P2B)**

The next table shows the test matrix of the phase2B.

**Table 2. Test matrix of the phase2B.**

| Test ID | Stroller | Safety device | Comments |
|---|---|---|---|
| **P2B-1** | Stokke Xplory | Prototype #1 | Stroller placed 89 mm from the first contact of the folding backrest. The stroller breaks are deactivated |
| **P2B-2** | Stokke Xplory | PRM backrest | 150 mm gap between the stroller and the PRM backrest. The stroller breaks are deactivated |
| **P2B-3** | Stokke Xplory | Prototype #2 | 150 mm gap between the stroller and the folding backrest. The stroller breaks are deactivated |
| **P2B-4** | Quinny Buzz | Prototype #3 | The stroller in contact with the backrest with the breaks activated (this is the recommended usage). |
| **P2B-5** | Quinny Buzz | Prototype #3 | 150 mm gap between the stroller and the folding backrest. The stroller breaks are deactivated |
| **P2B-6** | Quinny Buzz | PRM backrest | The stroller in contact with the PRM backrest with the breaks activated (this is the recommended usage). |

As it can be seen, there are three types of prototype folding backrests. The three prototypes are manufactured with metal frame and covered with wooden plates. The first prototype has a total height of 500 mm, whilst the second has 400 mm. The third prototype has as well 400 mm of total height but is covered by a padded surface (similar to a carpet).
All the tests were performed with a Q1 dummy instrumented as mentioned in "**METHODS**" section, except the test P2B-1 with a P3 dummy.

The objective of test **PB2-1** was to verify the structural strength of the pushchair panel prototype#1 using the heaviest dummy (TNO type P3 weighing 15 kg). This configuration was considered as a "misuse" as it aimed to verify the behaviour of the least stable pushchair, with the tallest panel prototype, and without brakes applied to the wheels. The pushchair was placed facing backwards and in its lowest position. The free flight distance between the rear wheels and the restraint system (prototype #1) was 89 mm.
The aim of test **PB2-2** was to verify the structural strength and behaviour of a restraint for wheelchair users (PRM backrest) using the instrumented Q1 dummy (representing a one-year-old child). This configuration is considered as "misuse" as it was intended to verify the behaviour of the least stable pushchair when interacting with the panel used by wheelchair users. In this case, the stroller was configured in its highest position, with a distance from the pushchair grab-bar to the panel (in a horizontal position) of 150 mm – and without brakes applied to the wheels.
The aim of test **PB2-3** was to verify the structural strength of the prototype #2 using the Q1 instrumented dummy. These conditions represented a "misuse" because the stroller was the least stable pushchair and was positioned facing backwards in its highest position with a distance of the centre bar to the panel of 150 mm – and without brakes applied to the wheels.
Test **PB2-4** aimed to verify the structural strength of the prototype #3 using the Q1 dummy. This configuration was considered as "correct use". The stroller was located with the side bars of the pushchair touching the panel – and with brakes applied to the wheels.
Test **PB2-5** was intended to verify the structural strength of the prototype #3 using the Q1 dummy. This configuration is considered a "misuse" as it examined the behaviour of the backward facing stroller when interacting with the prototype #3 when the sidebars of pushchair were 150 mm from the panel – and without brakes applied to the wheels.
Finally, test **PB2-6** aimed to verify the structural strength and behaviour of the panel for wheelchair users (PRM backrest) using the Q1 dummy. This configuration is considered "correct use" as it verified the behaviour of the widest pushchair when interacting with the PRM backrest. In this case, the stroller was located with the handle (horizontal) touching the PRM backrest, and brakes applied to the wheels.

It should be noted that the goal of tests **PB2-2** and **PB2-6** was not only to verify the structural strength of the new pushchair restraint but to compare dynamic behaviour in settings of correct use and misuse in relation to the technical requirements defined in UNECE regulation 107.

The next table shows the results of the Q1 dummy with respect to the IARV obtained in Figure 4.

**Table 3. Q1 dummy results relative to the IARV obtained.**

| Dummy part | Parámetro | Value (% wrt the IARV) | | | | |
|---|---|---|---|---|---|---|
| | | P2B-2 | P2B-3 | P2B-4 | P2B-5 | P2B-6 |
| Head | $HIC_{15}$ | 3.5 | 1.2 | 0.3 | 6.1 | 0.2 |
| | HPC ($HIC_{36}$) | 2.5 | 0.8 | 0.3 | 4.3 | 0.3 |
| | Acceleration | 12.6 | 11.8 | 4.2 | 21.6 | 3.5 |
| | 3ms acceleartion | 27.6 | 21.2 | 9.3 | 40.8 | 7.9 |
| Upper neck | Shear force Fx | 16.4 | 10.0 | 9.7 | 22.8 | 3.2 |
| | Tension force +Fz | 11.5 | 10.1 | 2.4 | 17.2 | 3.9 |
| | Compression force -Fz | 6.2 | 4.5 | 1.0 | 8.0 | 1.4 |
| | Lateral moment Mx | 8.0 | 3.2 | 4.4 | 4.0 | 1.4 |
| | Flexion moment +My | 7.0 | 2.3 | 3.2 | 11.0 | 1.1 |
| | Extension moment -My | 112.7 | 94.8 | 58.5 | 126.4 | 44.2 |
| | Twist moment Mz | 13.7 | 4.9 | 9.4 | 10.6 | 3.6 |
| | Nij TF (Tensile-Flexion) | 5.4 | 2.9 | 2.4 | 8.6 | 0.8 |
| | Nij TE (Tensile-Extension) | 41.1 | 44.6 | 20.8 | 59.9 | 21.5 |
| | Nij CF (Compression-Flexion) | 5.3 | 2.1 | 0.7 | 5.4 | 1.4 |
| | Nij CE (Compression-Extension) | 54.3 | 39.3 | 26.4 | 56.3 | 10.7 |
| | NIC Tensile | 11.4 | 10.8 | 5.2 | 17.0 | 8.2 |
| | NIC Shear | 18.4 | 10.3 | 14.4 | 23.8 | 7.1 |
| Chest | Sternum deflection Dx | 3.4 | 4.4 | 0.5 | 3.1 | 0.1 |
| | T4 acceleration | 13.7 | 16.5 | 5.3 | 21.5 | 4.0 |

As it can be seen in the previous table, the extension moment has values that exceed the IARV. All the tests with "misuse" configuration have obtained values greater than 90% (and in two tests over exceed the limit). The tests performed according with the recommendations (PB2-4 & PB2-6) has been obtained values around the 50% of the limit. The rest of the parameters have not got value potentially injurious. Two comparisons in detail are made: P2B-2 vs P2B-3 and P2B-4 vs P2B-5.

**P2B-2 vs P2B-3**

In this case, two test configurations, classified as misuse, were compared. The least stable stroller due to its high centre of gravity was used, and in one of the tests it was supported by the PRM backrest and in the other test (P2B-3) was supported by the folding backrest (prototype #2). Figure 6 shows a superimposed image of the two configurations with the relative position of the pushchair during free flight of 150 mm towards each of the restraint systems.

Table 3 shows the results of the tests. Although the distance of free flight in both cases were the same (150 mm), the difference in height between the two panels and the contact point of the pushchair with them, produces differing behaviour in each case. Thus, while the contact of the pushchair with the PRM backrest system occurs with the back of the (horizontal) pushchair handgrip, the contact with the folding backrest (prototype #2) occurred lower down with the central telescopic rod on which the chair is mounted. Although the distance of free flight is the same, the horizontal displacement of the pushchair in the case of the PRM backrest is greater, because the handgrip bends when it comes into contact with the panel and the pushchair continues travelling until the telescopic mast strikes the panel (see Figure 7). As a consequence, all the values obtained in the test with the PRM backrest system (P2B-2) are higher than those obtained with the folding backrest (P2B-3).

The most critical parameter in both cases corresponds to neck extension moment of the dummy. The limit was exceeded by 12% in the case of the PMR backrest, while in the case of the folding backrest the values did not reach the limit of tolerance (5% below the limit).

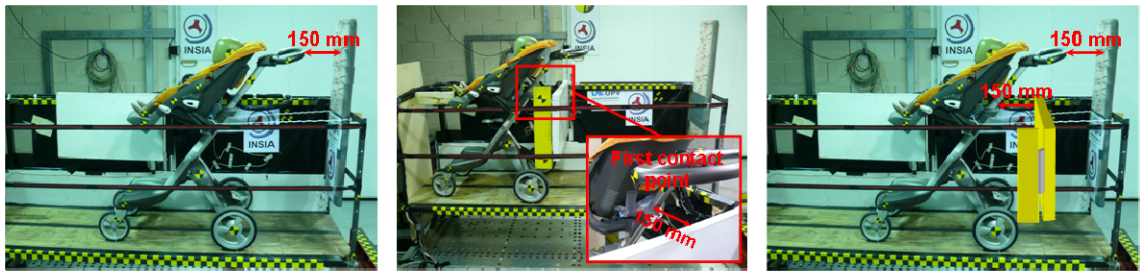


*Figure 6. P2B-2 & P2B-3 configurations and a superimposed figure.*

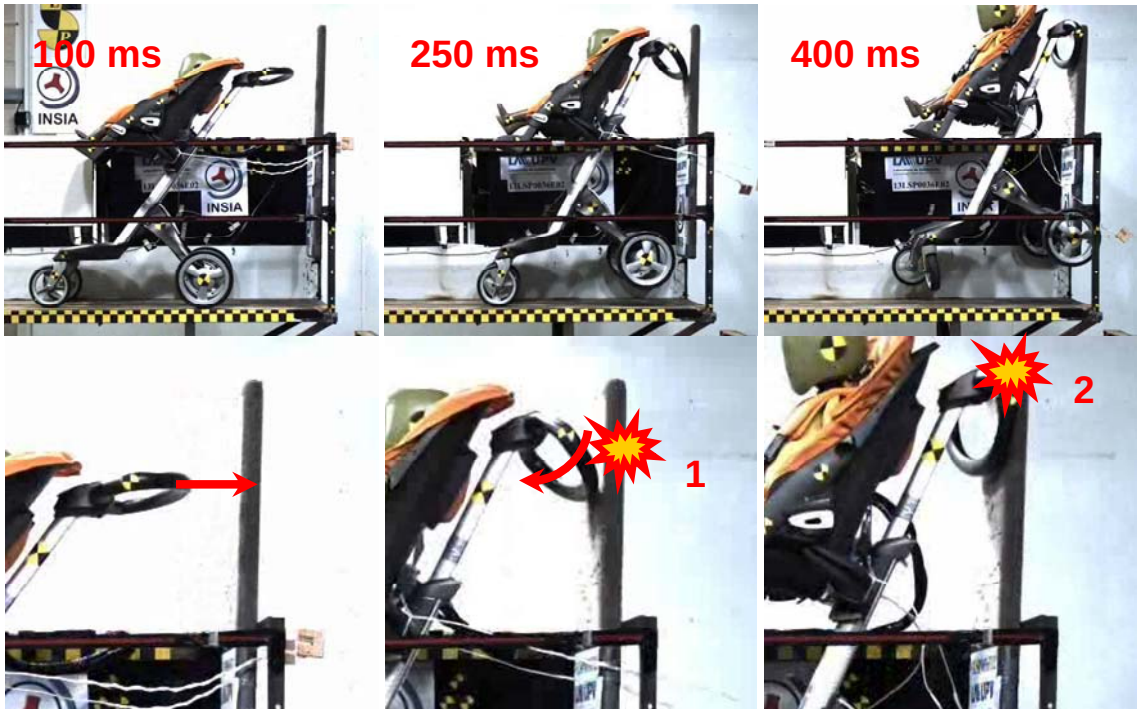


*Figure 7. Kinematics analysis of the P2B-2.*

**P2B-4 vs P2B-5**

In this case, two configurations were tested using the same stroller, one of the widest models and a model with three wheels (twin wheels for the frontal). The analysis compared a "correct" configuration (P2B-4 test) in which the stroller was in contact with the folding backrest (prototype #3) and the brakes were applied to the wheels, with a "misuse" configuration (PB2-5 test) with the PRM backrest, with a free flight distance of 150 mm and finally, the brakes were not applied to the wheels.

Table 3 shows the results of the tests, and it can be seen that all the parameters obtained for the PB2-5 test ("misuse") were worse than those obtained for the PB2-4 test ("correct use"). Only a small gap of 150 mm between the pushchair and the panel caused all the registered levels to double or more. The highest critical values exceeding the tolerance level were reached for the vertical extension of the neck, which exceeded the level of tolerated damage by 26%. Values increased by up to four times for head and chest accelerations, although critical values were not exceeded.

## CONCLUSIONS

The main conclusions of the analysis of children strollers' safety in urban buses are:

- The safety belt has probed that is able to restraint the strollers and baby carriages in low severity frontal impact. Although there are potential risk configuration (the path of the belt in the strollers), it has not been able to reproduce any unstable configuration in the tests. This system is the only device that guarantees the retention of the child whatever be the impact direction.
- The folding backrest (tested in phase2B) is able to withstand the loads of the stroller occupied by one dummy (total mass 25 kg). As mentioned before, the folding backrest has being developed under patent [2].
- The misuse configuration tested in phase 2B has probed that the measurement on the dummy parts (injury readings) has grown up from 2 up to 5 times with respect to the recommended or standard situation. Therefore, it is highly recommended to follow the directions noted by usage recommendations.
- With respect to the folding backrest or the PRM backrest, neither of them have got positively restrained the stroller. In crash configuration or acceleration fields that are not longitudinal, there may be an uncontrolled movement of the stroller inside the urban bus.
- Despite the low severity tested, potentially injury situations have been reproduced.
- Currently the regulation 107R06 only provides as safety device the PRM backrest for restraint the strollers. The folding backrest (from the ASUCAR project) provides a similar solution that complements the requirements of the regulation. Furthermore, the regulation framework does not provide a solution for cases in which a wheelchair user and stroller coincide on the same journey on the urban bus. Therefore the folding backrest could be an alternative solution for transportation compatibility of different users.
- The specific built-in child restraint system has obtained four times chest acceleration with respect to the "correct use" in low severities, but the same levels with respect to the "misuse" configuration. The specific built-in CRS has been tested with a crash severity more than 6 times greater than the low severity. That means that this system is safer than the other systems (as it has been estimated).

## ACKNOWLEDGEMENTS

This research has been held with the support of the Spanish Ministry of Science and Innovation who funded the project 'Accessibility Requirements and the Safe Use of Baby Carriages in Public Buses' (ASUCAR) (PET2008_0328) in the 2008–2011 National Research Program, and the University Polytechnic of Valencia who funded the project "Experimental validation of a restraint system for the transport of children prams in public transportation vehicles" (Ref. SP20120893) in the UPV innovative program (INNOVA-01-12). The development of the injury criteria used in this study has been supported by the Spanish Ministry of Science and Innovation who funded the project 'Children and Elderly Safety in Bus Accidents' (CESBA/SANCA), (TRA2011-26313) in the 2008–2011 National Research Program (Basic Research). Our acknowledgement is also to the Public Transportation Operators of Madrid and Valencia (Spain) for their contribution and collaboration in the development of the practical trials scheduled in the project.

## REFERENCES

[1] Dols, J.; Aparicio, F.; Alcalá, E.; Pons, V.; Martínez, L.; Martín, A.L.; Valles, B. (2012). Código de Buenas Prácticas para la utilización de carritos de niños en vehículos de transporte público. Ed. UNIVERSITAT POLITÈCNICA DE VALÈNCIA. ISBN: 978-84-8363-810-1.

[2] Dols, J.; Pons, V.; Alcala, E.; Martínez, L.; Martín, A.; Valles, B. (2011). Sistema de Seguridad Pasivo para carritos de niños en vehículos de transporte público. University Polytechnic of Valencia and University Polytechnic of Madrid. Patent No. P-201131557. Priority country: Spain. 27 SEPT. 2011.

[3] Mertz , H.J., Irwin, A.L. and Prasad P. 2003. "Biomechanical and Scaling Bases for Frontal and Side Impact Injury Assessment Reference Values". Stapp Car Crash Journal, Vol. 47, pp. 155-188 (2003-22-0009).

**Evaluation of a Pre-Production Head-on Crash Avoidance Assist System using an Extended "Safety Impact Methodology" (SIM)**

**John W. Zellner**
**R. Michael Van Auken**
**Jordan Y. Silberling**
**Joseph Kelly**
**Brad K. Hagoski**
Dynamic Research, Inc.
United States of America

**Yoichi Sugimoto**
Automobile Technology Research Division, Honda R&D Americas, Inc.
United States of America

**Yoshihiro Urai**
Honda R&D Co., Ltd.
Japan

Paper Number 15-0176

## ABSTRACT

Objective: This paper describes the results of the Honda-DRI ACAT-II program initiated by the National Highway Traffic Safety Administration (NHTSA) to develop test and evaluation procedures and methods to assess the safety benefits and effectiveness of advanced driver assistance technologies. The objectives of the ACAT-II program were further development of a formalized Safety Impact Methodology (SIM) for estimating the capability of advanced technology applications installed in vehicles to address specific types of motor vehicle crashes, and to evaluate driver acceptance of the technologies.

Methods: This particular ACAT study extended earlier work by Honda and DRI in the NHTSA ACAT-I program by extending the SIM so as to be able to analyze head-on crashes more completely, and by using the extended SIM to evaluate of a pre-production version of a Honda Head-on Crash Avoidance Assist System (H-CAAS). More than 25 substantial SIM extensions and refinements were implemented, including: updated and extended FARS and NASS database extractions; improving the accident reconstruction process for NASS/CDS cases and developing a new special purpose reconstruction algorithm applicable to head-on cases with low lateral acceleration "drifts;" extending the driver-vehicle-ACAT-environment simulation to include a post-conflict recovery phase; and further automating the overall safety benefits evaluation steps. The extended SIM and results from objective tests were used to evaluate the safety impact of Honda's pre-production H-CAAS based on a large number of simulations of a sample of reconstructed real-world head-on crashes.

Results: The effectiveness of the H-CAAS in reducing the number of two-vehicle "Same Trafficway, Opposite Direction" crashes (including non-H-CAAS technology relevant crashes) and fatalities if the H-CAAS were installed on one of the crash involved vehicles were estimated to be a 2.6% reduction in these types of crashes and a corresponding 11.3% reduction in fatalities based on simulation results. The overall benefits of the H-CAAS, in terms of reduction in number of crashes and fatalities, when projected to the annual US level were estimated to be a 2,966 reduction in the number of US crashes and a corresponding reduction of 450 US fatalities per year. The results are based on various assumptions, approximations, and limitations that are summarized herein and further documented in the supporting references, such as the representativeness and accuracy of the supporting data and reconstructed accident pre-crash scenarios.

Conclusions: Overall, this ACAT-II program was successful in extending and demonstrating a methodology that can be used to estimate the effectiveness and safety benefits and driver acceptance of frontal crash avoidance and mitigation countermeasures. The methods used are directly relevant to the test and evaluation procedures to assess the safety benefits and effectiveness of advanced driver assistance technologies.

Keywords: active safety, crash avoidance, countermeasures, driver assistance systems, evaluations

## INTRODUCTION

The National Highway Traffic Safety Administration (NHTSA) initiated the Advanced Crash Avoidance Technologies (ACAT) program in 2006 to determine the safety impact of new and emerging crash avoidance technologies. This involved developing a Safety Impact Methodology (SIM) and framework, including objective tests, as summarized in Carter et al. (2009) and Funke et al. (2011). In 2008 NHTSA initiated a second phase of this program (ACAT-II), the primary objective being to further develop a formalized SIM methodology in order to evaluate specific types of vehicle crashes.

## BACKGROUND

Honda, Dynamic Research Inc. (DRI) and many others have been developing and applying safety impact analysis methods for many years. These methods are multi-disciplinary, involving accident data analysis, accident reconstruction, driver and vehicle modeling and simulation, and injury and fatality risk modeling, based on models ranging from theoretical to empirical depending on the sought for accuracy and available information. For example, Suzuki et al. (2006) described a prototype safety analysis system to forecast vehicle safety benefits using a fleet systems model based on real-world crash scenarios, accident and exposure data for existing vehicles, and estimated sales and technology effectiveness for future vehicles. The systems model incorporates the estimated effectiveness of various existing and proposed safety technologies in order to estimate the incremental and combined effects of these technologies, which may be complimentary or redundant. This tool was inspired by previous work by Henson (1978), Najm (1999, 2000), Kuchar (2001), and others. Sugimoto et al (2005) described a method to estimate the effectiveness of advanced driver assistance systems in avoiding or mitigating crashes using simulations of the driver, vehicle, technology, and environment during the pre-crash phase of reconstructed real-world crash scenarios. The driver model for these simulations was structured based on the NASA MIDAS model (Hart et al. 2001).

More recently Honda and DRI and other researchers have had Cooperative Agreements with NHTSA for either the ACAT-I program or subsequent ACAT-II program, or both programs. The ACAT-I program (Carter et al. 2009; Funke et al. 2011) comprised four research teams from Honda and DRI; Volvo, Ford, and the University of Michigan Transportation Research Institute (UMTRI)); Toyota; and General Motors and Virginia Tech Transportation Institute (VTTI). In the ACAT-I program Honda and DRI extended the ACAT SIM tool based on their earlier work and used the SIM to evaluate a prototype Honda Advanced Collision Mitigation Braking System (A-CMBS), as described in Zellner et al. (2009), Sugimoto et al. (2010), and Van Auken et al. (2011a, 2011b). The Volvo-Ford-UMTRI team developed a SIM to estimate the benefits of a Lane Departure Warning (LDW) system (Gordon et al. 2010), Toyota developed a SIM to estimate the benefits of a Pre-Collision Safety System (PCS) (Aoki et al. 2009), and the GM-VTTI team developed a SIM to estimate the benefits of a Backing Crash Countermeasure (Perez et al. 2011).

The ACAT-II program comprised two research teams from Honda and DRI; and Nissan and UMTRI (NHTSA 2009). This paper summarizes the cooperative research by Honda and DRI under the ACAT-II program, which involved further extensions to the previously developed SIM tool and applying it to evaluate the effectiveness and safety benefits of a pre-production Honda Head-On Crash Avoidance Assist System (H-CAAS). Progress reports for this study were presented in Van Auken et al. (2011c), Sugimoto et al. (2011), and Zeller et al. (2012). More detailed methods and results from this study are presented in Zellner et al. (forthcoming).

In addition to the two NHTSA ACAT programs, the ACAT teams and other researchers are continuing to develop and refine ACAT SIMs. For example, Kusano et al. (2013) has developed a methodology for using advanced event data recorders (EDRs) to reconstruct vehicle trajectories for use in the SIMs. Kusano et al. (2012) has investigated the identification of target populations for active safety systems. Both of these examples correspond to activities in the NHTSA ACAT SIM framework described in Carter et al. (2009).

### Project Aims

The primary objective of the NHTSA ACAT-II program was to further develop a formalized SIM to estimate the capability of advanced technology applications installed in vehicles to address specific types of motor vehicle crashes. A secondary objective was to evaluate driver acceptance of the technologies and, if applicable, how that acceptance could be improved.

### Scope of the Study

The scope of this study involved:

- Theoretical and software extensions to the existing Honda-DRI ACAT-I SIM tool, which provides an estimate of advanced technology safety benefits at the US level;
- Refinement of the objective test procedures and apparatus (i.e., car Guided Soft Target (GST)) and the slowly increasing steer (SIS) test procedure in order to facilitate the use of the steering wheel torque model in the Crash Sequence Simulation Module (CSSM) simulations;
- Using the data from previous objective tests to parameterize, calibrate and validate the SIM tool;
- Delivering an extended SIM tool which includes improved modules for automated reconstruction of conflict and crash scenarios from available databases; automated definition and sampling of Technology Relevant Crash Types (TRCTs); dynamic simulations involving a human-vehicle-device-environmental model; and an overall safety effects estimator;
- An example application of the extended SIM tool using objective test data which involved safety effectiveness and benefits estimation for Honda's pre-production Head-on Crash Avoidance Assist System (H-CAAS).

## SAFETY IMPACT METHODOLOGY

NHTSA's Safety Impact Methodology framework (Carter et al. 2009) is illustrated in Figure 1. This framework comprises 22 different Functions (e.g., "Archival Data"). These functions are grouped into seven different activities illustrated by the large open boxes (e.g., "Data Usage"), which are also grouped into three main areas indicated by the box color coding (i.e., orange, blue, and purple). Of the 22 different Functions, 11 Functions were implemented by the Honda-DRI SIM tool and the other 11 Functions were accomplished "off-line".

An overview of the Honda-DRI ACAT SIM and the extensions made during the ACAT-II program are summarized in Zellner et al. (2012). The SIM is described in further detail in Van Auken et al. (2011b) and Zellner et al. (forthcoming). The extensions made to the SIM for the ACAT-II program are further described in Zellner et al. (forthcoming).

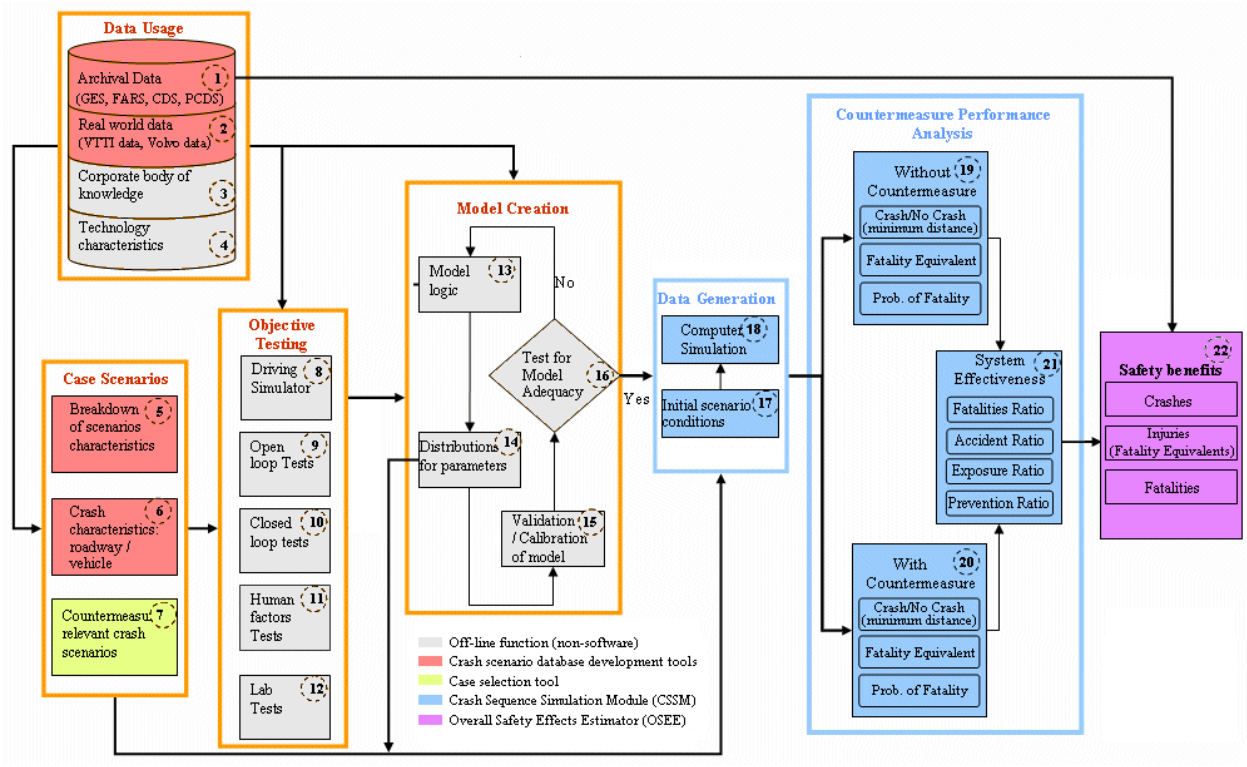


***Figure 1. NHTSA ACAT SIM Framework (Carter et al. 2009).***

## ADVANCED TECHNOLOGY AND SAFETY AREA ADDRESSED

A pre-production Honda Head-On Crash Avoidance Assist System (H-CAAS) was selected as an example of an advanced technology to be evaluated using the ACAT-II SIM. The pre-production H-CAAS was designed to be installed on light passenger vehicles (i.e., passenger cars and light trucks) to prevent or mitigate certain types of head-on crashes. These crash types primarily include head-on crashes where driver inattention (e.g., distraction, drowsiness, and/or impairment) is a contributing factor. It is assumed that the subject vehicle in these cases drifts with up to 0.05 g lateral acceleration, which is assumed to be not noticeable kinesthetically (i.e., sub-threshold) by the driver in the absence of visual cues (e.g., visual distraction, drowsiness, etc.) based on published literature (e.g., Young (1973)).

### The Size of the Crash Problem

The potential numbers of crashes, involved vehicles, and fatalities that represent the size of the problem for the entire US motor vehicle fleet are listed in Table 1 in terms non-technology specific crash types that have been broadly defined in terms of NASS Crash Configurations (e.g., “Same Trafficway, Opposite Direction” or simply “Opposite Direction”) (NASS 2000). Some of these crashes were not expected to be addressable by the H-CAAS due to either vehicle application (e.g., passenger car vs. motorcycle), vehicle role (e.g., struck vehicle), or other technology relevant factors. For example, the results in Table 1 include 239,000 crashes involving non-light passenger vehicles (e.g., motorcycle only crashes), on which the pre-production H-CAAS was not designed to be installed, involving 253,000 vehicles and 3,953 fatalities.

**Table 1.**
**Estimated Crash Problem Size for the Entire US Motor Vehicle Fleet in the 2009 Calendar Year**

| Crash Category | Crash Type | Estimated Number of | | |
|---|---|---|---|---|
| | | Crashes (1000s) | Vehicles (1000s) | Fatalities |
| 1-vehicle | All | 1,749 | 1,749 | 19,869 |
| 2-vehicle | Opposite Direction | 116 | 232 | 4,024 |
| | Other 2-Vehicle | 3,303 | 6,605 | 7,747 |
| 3 or more Vehicles | 3 or More Vehicles | 328 | 1,048 | 2,168 |
| Total | | 5,496 | 9,635 | 33,808 |

**H-CAAS Description**

The pre-production Head-on Crash Avoidance Assist System (H-CAAS) is illustrated in Figure 2. The H-CASS automatically predicts certain types of impending head-on collisions, warns the driver, and applies braking in order to reduce the effects of an impact on occupants and vehicle damage as illustrated in Figure 3. The H-CAAS sensors, operation scenario, and mapping between the crash sequences and the H-CAAS internal and warning states are described in Zellner et al. (2012). Note that this pre-production H-CASS was still under development at the time of this evaluation. Many issues (e.g., reliability verification through field operational tests using product level sensors) were yet to be resolved before any mass production could occur. Therefore the performance and effectiveness of the pre-production H-CAAS for this program is not related to any current or possible future production H-CAAS or other ACAT.

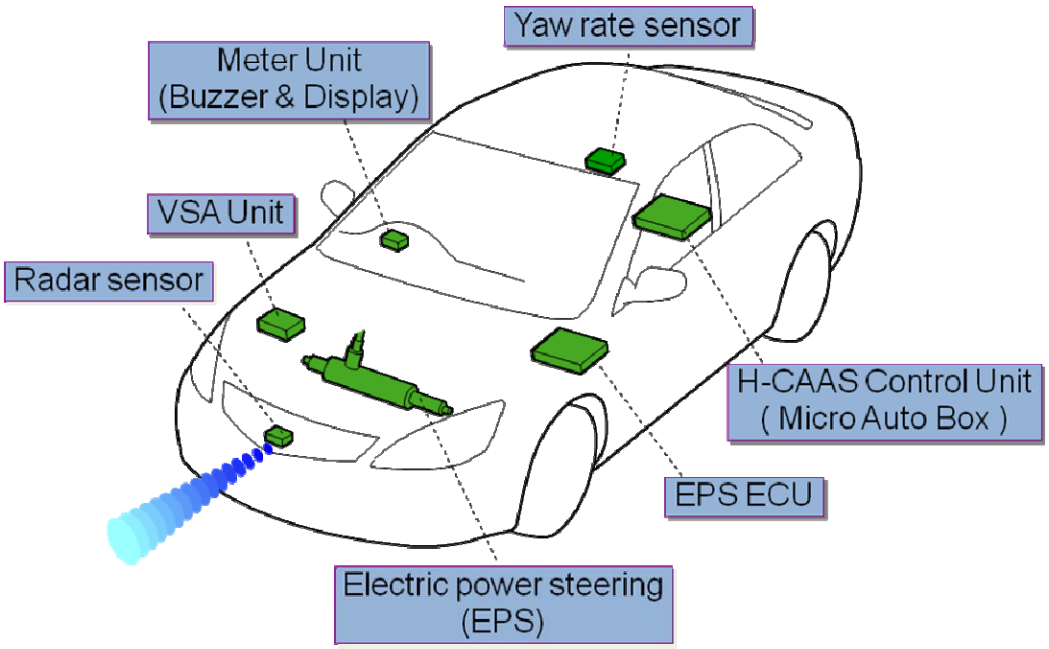


***Figure 2. H-CAAS System Configuration.***

1. Subject Vehicle travels forward along its intended path.

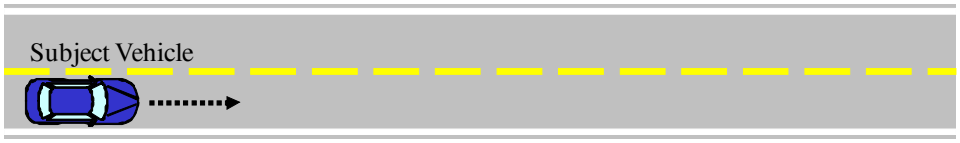


2. When the driver is inattentive (e.g., distracted, drowsy and/or impaired), the Subject Vehicle begins departing from its intended path. Then an oncoming vehicle approaches.

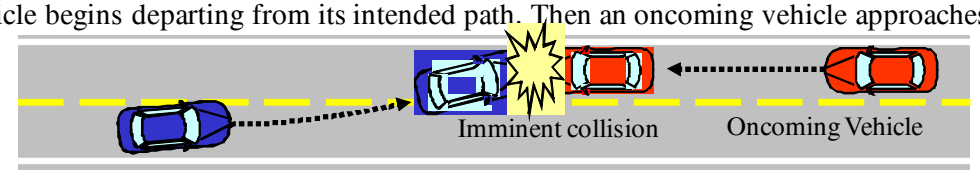


3. H-CAAS activates steering control and gives a warning (buzzer) to the driver.

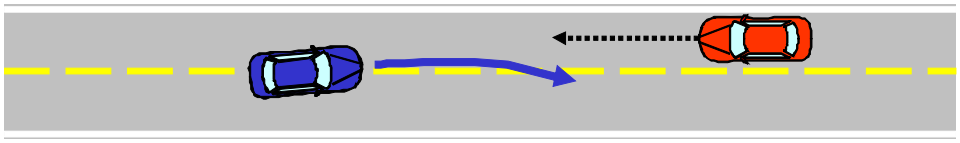

4. The driver reacts to the warning and steers to avoid crash and resumes its intended path.

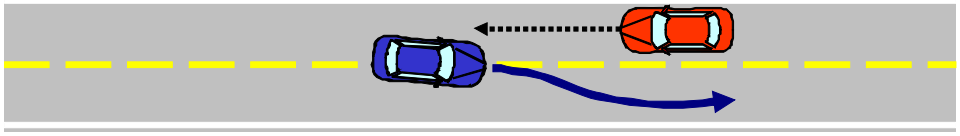

***Figure 3. Proposed Head-On Crash Avoidance Assist System Operation Scenario.***

**Technology Relevant Crash Types**

It is generally assumed that the ACAT effectiveness in reducing the probability of conflicts, crashes, injuries, and fatalities depends on the numerous variables related to the crash circumstances. In order to estimate the safety benefits it is necessary to first quantify the ACAT collision and fatality effectiveness in Technology Relevant Crash Types (TRCTs) for which the ACAT is intended to be effective, based on a detailed technical understanding of the ACAT functionality. The H-CAAS has seven TRCTs that were defined by the ACAT designer based on coded crash scenario database variables as described in Zellner et al. (2012).

**The Size of the Problem Addressed**

The numbers of addressable crashes, fatalities, and vehicles involved in each H-CAAS TRCT listed in Table 5 of Zellner et al. (2012) were then estimated using the OSEE Fleet Systems model as described in Van Auken (2011b). The Fleet Systems model was used with the H-CAAS TRCT classification criteria in Tables 3 and 4 of Zellner et al. (2012) in combination with the corresponding in-depth crash scenario database, in order to effectively interpolate the FARS (Tessmer 2006) and GES (NASS 2009) results in Table 1 to the H-CAAS TRCT level of detail (see, for example Najm et al. (2007)).

**OBJECIVE TESTS**

Objective testing in the ACAT-II program involved upgrades to the Guided Soft Target (GST) developed during ACAT-I; and detailed analysis of driver responses collected in previous Driving Simulator tests using an earlier prototype Crash Avoidance Assist System (CAAS). The second generation GST system is described in further detail in Kelly et al. (2011).

**Driving Simulator Tests**

Data from a previous series of driving simulator tests using a prototype Crash Avoidance Assist System (CAAS) were used to quantify driver responses to (and corresponding driver response parameter values for) head-on conflicts with and without the ACAT, and also driver acceptance of the ACAT. The prototype CAAS system was an earlier version of the pre-production H-CAAS system, and was assumed to be sufficiently similar to the H-CAAS system for the purposes of this program. The driving simulator tests were conducted using the DRI Driving Simulator, as using established internal protocols for treatment of participants, as described in Zellner et al. (2012). These tests, which included 8 "distracted" driver subjects and 5 "drowsy" driver subjects, are further described in Zellner et al. (2012).

**Driver Model Parameters**

During emergency driving it was assumed that the driver uses a pre-cognitive emergency driving procedure to attempt to avoid the crash. This emergency driving procedure was modeled by switched, open-loop driver braking and steering wheel angle or torque time histories. The emergency driving response time histories were modeled by a parsimonious set of parameters described in Zellner et al. (2012) in order to characterize different "driver behaviors." The parametric steering time history was also refined for the H-CAAS evaluation in order to allow for asymmetric steering responses as illustrated in Figure 4, which was the typical steering response observed in the Driving Simulator tests for head-on drift scenarios. The asymmetric steering response represents a half sinusoid emergency steering maneuver followed by a second half sinusoid recovery maneuver with smaller amplitude and longer duration intended to bring the driver back into the original travel lane.

The driver specific emergency steering and braking response parameter values were determined by fitting the driving simulator test data for each driver subject, as described in Zellner et al. (2012). The resulting modeled emergency responses for the driver subjects are then assumed to be a representative distribution of "driver behaviors".

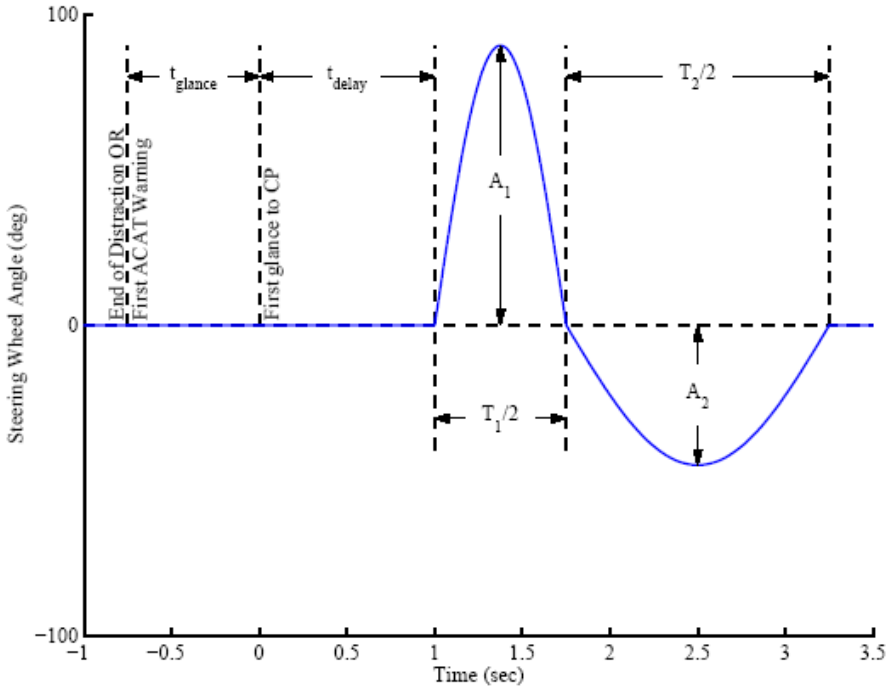


***Figure 4. Parametric Form of the Assumed Driver Pre-Cognitive Emergency Steering Procedure.***

## SIMULATION RESULTS

The effectiveness and benefits of the H-CAAS were estimated based on the results from the Crash Sequence Simulation Module and Overall Safety Effects Estimator.

### CSSM Simulation Results

The CSSM was used to simulate the conflict scenario with each of the unique driver-behavior combinations and with and without the ACAT, in order to estimate the relative reductions in numbers of crashes, injuries, and fatalities due to the ACAT. There were 106 unique simulation cases that were sampled using the Technology Relevant Case Sub-Sampling Tool (SIM Module 2) covering 5 of the 7 TRCTs (The other two TRCTs were the "S2" TRCT, which involved loss-of-control and were therefore not reconstructable by the current AART, and the "S6" TRCT, for which there were also no reconstructable cases in the 2000 through 2007 calendar year crash scenario dataset used; therefore these TRCTs have been omitted from the remainder of this analysis and are treated as H-CAAS having no safety effect.). There were a total of 26 different driver-behavior combinations observed in the simulator test results, which were simulated both with and without the ACAT. Therefore the total number of CSSM simulations was 103 x 26 x 2 = 5,512 simulations. With an approximate time per simulation of 1.5 minutes, the total simulation run time was about 138 CPU-hours or 5.75 CPU-days. The CSSM simulation results are further described in Appendix A.

### OSEE Results

The Overall Safety Effects Estimator was used to estimate at the US level the number of crashes, vehicles, and fatalities for the 2009 model year modeled fleet with and without the ACAT in the 2009 calendar year based on the CSSM results which are summarized in Table A3. These estimates were based on actual accident and exposure data for individual make-model vehicles in the 2008 model year fleet in the 2008 calendar year, using the Fleet Systems model described in Suzuki et al. (2006) and Van Auken et al. (2011b). The modeled fleet comprised Honda and Acura vehicles.

For example, one exemplar make-model vehicle in the modeled fleet (a 2008 model year 4-door Honda Civic) was involved in 1,830 accidents involving 2 vehicles in the 2008 calendar year resulting in 14 fatalities, based on VIN decoded NASS/GES and FARS data. Based on this information and other information about the 2008 and 2009 make-model vehicle (i.e., vehicle size, weight, safety equipment, sampled distribution of driver ages and sexes, and assumed vehicle registration year exposure), it was estimated by the Fleet Systems model that the 2009 model year make-model vehicle would have been involved in 1,276.5 accidents and 7.9 fatalities in the 2009 calendar year without the H-CAAS, and 1,274.4 accidents and 7.5 fatalities with the H-CAAS. These results are based on the assumption that the 2-vehicle crash cases in the Fleet Systems model, which were derived from NASS/CDS, PCDS, GES data (NASS 2000, 2002, 2009), are a representative sample of 2-vehicle crashes in the US. Therefore the number of crashes, vehicles, and fatalities can in effect be interpolated to the non-technology specific crash type and by TRCT level of detail by the Fleet Systems Model.

Repeating these assumptions and analysis for 1-vehicle, 2-vehicle, and 3-vehicle crashes and summing the results, it was estimated that the 2009 model year exemplar make-model vehicle would have been involved in 2,437.7 accidents and 15.5 fatalities in the 2009 calendar year without the H-CAAS, and 2,435.7 accidents and 15.1 fatalities with the H-CAAS.

The total number of accidents, vehicles, and fatalities in the modeled fleet with and without the H-CAAS were then estimated, at the same level of crash type detail, by repeating this process using the Fleet Systems Model for all make-model vehicles in the modeled fleet. The results were that the 2009 model year modeled fleet would have been involved in 10,221 accidents and 55.4 fatalities in the 2009 calendar year without the H-CAAS, and 10,208 accidents and 54.0 fatalities with the H-CAAS. Of these totals it was estimated that there were 495 accidents and 12.8 fatalities in non-technology specific "Opposite Direction" crashes without the H-CAAS, and 482 accidents and 11.3 fatalities with the H-CAAS.

**US Level Safety Benefits**

The benefits of the Honda H-CAAS projected to the entire US Light Passenger Vehicle Fleet in the 2009 calendar year were estimated according to the methods described in (Burgett et al. 2008). The results are based on the size of the crash problem listed in Table 1 and the estimates of effectiveness for each TRCT from the Overall Safety Effects Estimator that are listed in Table A3. The overall benefits for each crash type listed in Table 2 can be calculated by multiplying the TRCT effectiveness values in Table A3 by the corresponding ratio of the number of TRCT crashes in Table 5 of Zellner et al. (2012) to the total number of crashes in Table 1. The benefits for each TRCT in Table 3 are then equal to the baseline problem size in Table 1 times the overall effectiveness in Table 2 according to Eq. (2) in Zellner et al. (2012).

**Table 2.**
**Overall Estimates of Effectiveness of the H-CAAS by Non-Technology Specific Crash Type Projected to the Entire US Light Passenger Vehicle Fleet in the 2009 Calendar Year**

| Non-Technology Specific Crash Type | Estimated Effectiveness | | |
|---|---|---|---|
| | Crashes | Vehicles | Fatalities |
| 2-Vehicle Opposite Direction | 2.6% | 2.6% | 11.3% |
| Other crash types | 0.0% | 0.0% | 0.0% |
| Overall | 0.1% | 0.1% | 1.3% |

**DRIVER ACCEPTANCE**

Preliminary subjective ratings and objective data related to "driver acceptance" were also collected in the previous Driving Simulator tests with a prototype CAAS described herein. These data indicated that, in regard to CAAS "effectiveness," the driver subjective ratings were favorable, indicating that the participants found the system to be helpful, with most ratings among distracted and drowsy drivers being similar. Eighty-two percent found the system to be “Effective,” “Very Effective” or “Extremely Effective.” Eighteen percent rated the system “Somewhat Effective,” while none of the participants rated the system “Not at All” effective. Drowsy drivers found the system to be more effective than distracted drivers, with 79% rating the system as “Very Effective” or “Extremely Effective.” When asked if the participant would like to have the system installed in their vehicle, only two of the 20 participants said “No.” Interestingly, the two participants who indicated “No” were from the drowsy group, which rated the system more favorably, on average.

Participants placed a monetary value on the prototype CAAS system somewhere between $250 and $1000. Seventy-seven percent of all participants placed the value of the system above $250, while 55% valued the system at a level above $500. Again, the drowsy drivers tended to assign a higher value than did the distracted drivers.

In regard to the "acceptance" (i.e., annoyance) evaluation tests, which were intended to quantify the effect of the False Positive steering wheel torque pulses, the subjective ratings were very favorable (i.e., not annoying) in terms of Ease of Performing the Driving Task and Sense of Discomfort/Risk, for all chosen steering torque pulse levels. In addition, objective measurements showed no appreciable degradation of driver performance over baseline driving during the False Positive events.

**ASSUMTIONS AND LIMITATIONS**

The accuracy of the ACAT-II SIM and results presented herein are based on various assumptions, approximations, and limitations in data, which are described in detail in Van Auken et al. (2011b) and Zellner et al (forthcoming). For example, it is assumed that the reconstructed crash cases in the simulation and test case samples are representative of all H-CAAS technology relevant crashes. However since the outcome of each crash (in general) is assumed to depend on numerous factors, including the time-space trajectories of the vehicles, the driver behaviors, environmental factors, and other crash circumstances, all of which are subject to some form of random variation, the accuracy of the results depends on the number of cases in the

representative case samples that were used at each stage of the SIM analysis (e.g., testing, simulations, overall safety effects estimation. The OSEE Fleet Systems model currently assumes that the ACAT is only installed on one vehicle in each crash. The projection to the US level does not account for the potential benefits of the ACAT if it were to also be installed on the crash partners as well.

## SUMMARY AND CONCLUSIONS

The Advanced Crash Avoidance Technology (ACAT) Phase II program was a proof-of-concept effort that sought to determine the feasibility of developing estimates of effectiveness for specific safety technologies in the absence of data from real world crashes or field operational tests. This project was successful at developing and demonstrating a methodology that could be used to estimate the safety benefits of the particular crash countermeasure evaluated in this research project.

The Safety Impact Methodology (SIM) tool developed was used to provide an estimate of safety benefits of a pre-production Honda Head-on Crash Avoidance Assist System (H-CAAS) in terms of reduction in crashes and fatalities. When projected to the US level (including all non-Technology Relevant Crashes) in the calendar year 2009, this corresponded to estimated total collision and fatality effectiveness values for all police-reported crashes of 0.1% and 1.3% respectively, and this corresponds to estimated safety benefits of 2,966 fewer head-on collisions and 450 fewer fatalities, as summarized in Table 3. These overall safety benefits are estimated based on more detailed safety benefits and effectiveness results described in Zellner et al. (forthcoming).

**Table 3.**
**Overall Estimates of Benefits of the H-CAAS Projected to the Entire US Light Passenger Vehicle Fleet in the 2009 Calendar Year**

| Crash Type | | Estimated Benefits | | |
|---|---|---|---|---|
| | | Crashes | Vehicles | Fatalities |
| H-CAAS Technology Relevant Crash Type (See Zellner et al. (2012) | Primary (P1) | 1,790 | 3,581 | 120 |
| | Secondary 1 (S1) | 506 | 1,013 | 44 |
| | Secondary 3 (S3) | 0 | 0 | 0 |
| | Secondary 4 (S4) | 670 | 1,339 | 277 |
| | Secondary 5 (S5) | 0 | 0 | 9 |
| Other crash types (Non-H-CAAS Technology Relevant) | | 0 | 0 | 0 |
| Total Estimate | | 2,966 | 5,933 | 450 |

## REFERENCES


Aoki, H, Aga, M, Miichi, Y, Matsuo, Y. Development of a Safety Impact Estimation Tool for Advanced Safety Technologies. Paper presented at: 21st International Technical Conference on the Enhanced Safety of Vehicles (ESV); June 15-18, 2009; Stuttgart, Germany. Paper Number 09-0025.

Burgett, A, Srinivasan, G, and Ranganathan, R. A Methodology for Estimating Potential Safety Benefits for Pre-Production Driver Assistance Systems. Washington, DC: National Highway Traffic Safety Administration; 2008. DOT HS 810 945.

Carter, AA, Burgett, A, Srinivasan, G, Ranganathan, R. Safety Impact Methodology (SIM): Evaluation of Pre-Production Systems. Paper presented at: 21st International Technical Conference on the Enhanced Safety of Vehicles (ESV); June 15-18, 2009; Stuttgart, Germany. Paper Number 09-0259.

Fleck, JT, and Butler, FE, *Validation of the Crash Victim Simulator, Vol. 1: Engineering Manual – Part 1: Analytical Formulation*. Washington, DC: Calspan for the National Highway Traffic Safety Administration; 1981. DOT HS 806 279.

Funke, J, Srinivasan, G, Ranganathan, R, and Burgett A. Safety Impact Methodology (SIM): Application and Results of the Advanced Crash Avoidance Technologies (ACAT) Program. Paper presented at: 21st International Technical Conference on the Enhanced Safety of Vehicles (ESV); June 13-16, 2011; Washington, DC. Paper Number 11-0367.

Gordon, T, Sardar, H, Blower, D, Ljung Aust, M, Bareket, Z, Barnes, M, Blankespoor, A, Isaksson-Hellman, I, Ivarsson, J, Juhas, B, Nobukawa, K, and Theander, H. *Advanced Crash Avoidance Technologies (ACAT) Program – Final Report of the Volvo-Ford-UMTRI Project: Safety Impact Methodology for Lane Departure Warning – Method Development and Estimation of Benefits*. Washington, DC: Ford, Volvo, UMTRI for the National Highway Traffic Safety Administration; 2010. DOT HS 811 405.

Hart, SG, Dahn, D, Atencio, A, and Dalal, KM. Evaluation and application of MIDAS v2.0. Warrendale, PA: SAE; 2001. Paper 2001-01-2648, DOI: 10.4271/2001-01-2648.

Henson, SE, *Safety Systems Optimization Model (SSOM) Final Report - Volume I: Introduction and Executive Summary*. Washington, DC: Ford Motor Company for the National Highway Traffic Safety Administration; November 1978. DOT HS 804 771.

Kelly, J, Broen, P, Silberling, J, Bozin, N, Zellner, J. Development of a Guided Soft Target for Crash Avoidance Technology Evaluation. *SAE Int. J. Passenger. Cars – Mech. Syst.* 2011; 4(1):479-487. DOI: 10.4271/2011-01-0580.

Kuchar, AC. A Systems Modeling Methodology for Estimation of Harm in the Automotive Crash Environment. Paper presented at: 17th International Technical Conference on the Enhanced Safety of Vehicles (ESV); June 4-7, 2001; Amsterdam, The Netherlands. Paper No. 354.

Kusano, KD, and Gabler, HC. Identification of Target Populations for Current Active Safety Systems using Driver Behavior, 2012 Intelligent Vehicles Symposium; June 3-7, 2012; Alcalá de Henares, Spain.

Kusano, KD, Sherony, R, and Gabler, HC. Methodology for Using Advanced Event Data Recorders to Reconstruct Vehicle Trajectories for Use in Safety Impact Methodologies. *Traffic Injury Prevention* 2013;14(S):77-86.

Najm, WG, daSilva, MP, and Wiacek, CJ, Safety Benefits Estimation of an Intelligent Cruise Control System Using Field Operational Test Data. Warrendale, PA: SAE International; 1999. Paper No. 1999-01-2950, DOI: 10.4271/1999-01-2950.

Najm, WG, daSilva, MP, and Wiacek, CJ. Estimation of Crash Injury Severity Reduction for Intelligent Vehicle Safety Systems. Warrendale, PA: SAE International; 2000. Paper No. 2000-01-1354, DOI: 10.4271/2000-01-1354.

Najm, WG, and Smith, DL. Definition of a Pre-Crash Scenario Typology for Vehicle Safety Research. Paper presented at: 20th International Technical Conference on the Enhanced Safety of Vehicles (ESV); June 18-21, 2007; Lyon, France. Paper No. 07-0412.

NASS, *National Automotive Sampling System Crashworthiness Data System, 2000 Coding and Editing Manual*. Washington, DC: National Highway Traffic Safety Administration; 2000.

NASS, *National Automotive Sampling System Pedestrian Crash Data Study, 1996 Data Collection, Coding, and Editing Manual*. Washington, DC: National Highway Traffic Safety Administration; 2002.

NASS, *National Automotive Sampling System (NASS) General Estimates System (GES), Analytical User's Manual 1988-2008*. Washington, DC: National Highway Traffic Safety Administration; 2009.

NHTSA, Research In Progress - Advanced Crash Avoidance Technologies Program (ACAT) II – Nissan/University of Michigan Transportation Research Institute (UMTRI). 2009, Available at: http://www.nhtsa.gov/DOT/NHTSA/Traffic%20Injury%20Control/Research%20In%20Progress/files/AdvancedCrashAvoidanceTechnologiesProgram(ACAT)IINissanUMTRI.pdf. Accessed February 9, 2015.

Perez, M, Angell, LS, Hankey, J, Deering, RK, Llaneras, RE, Green, CA, Neurauter, ML, and Antin, JF. *Advanced Crash Avoidance Technologies (ACAT) Program - Final Report of the GM-VTTI Backing Crash Countermeasures Project*. Washington, DC: General Motors for the National Highway Traffic Safety Administration; 2011. DOT HS 811 452.

Sugimoto, Y, and Sauer, CW. Effectiveness Estimation Method for Advanced Driver Assistance System and its Application to Collision Mitigation Brake System. Paper presented at: 19th International Technical Conference on the Enhanced Safety of Vehicles (ESV); June 6-9, 2005; Washington, DC. Paper No. 05-0148-O.

Sugimoto, Y, and Zellner, JW, Effectiveness Estimation Simulation using US Accident Data and its Application to Collision Mitigation Brake System. Tokyo, Japan; JSAE; 2010. Paper No. 20104049. (Japanese)

Sugimoto, Y, Kawakami, K, Hashimoto, T. Zellner, JW, Van Auken, RM. Safety Impact Methodology for Advanced Crash Avoidance Technology (ACAT) Program and Application to Advanced Collision Mitigation Braking System and Head-on Crash Avoidance Assist System. First International Symposium on Future Active Safety Technology Toward Zero-Traffic-Accident, JSAE; September 5-9, 2011; Tokyo, Japan.

Suzuki, H, Sugimoto, Y, Van Auken, RM, and Zellner, JW. Development of a Prototype Safety Analysis System to Assess and Forecast Vehicle Safety. Warrendale, PA,: SAE International; 2006. Paper No. 2006-01-0718, DOI: 10.4271/2006-01-0718.

Tessmer, JM, *FARS Analytic Reference Guide 1975 to 2006*. Washington, DC: National Highway Traffic Safety Administration; 2006.

Van Auken, RM, Zellner, JW, Silberling, JY, Kelly, J, Chiang, DP, Broen, P, Kirsch, A, Sugimoto, Y. Extension of the Honda-DRI Safety Impact Methodology for the NHTSA Advanced Crash Avoidance Technology (ACAT) Program and Application to the Evaluation of an Advanced Collision Mitigation Braking System – Final Results of the ACAT-I Program, *SAE Int. J. Passenger Cars – Mech. Syst.* 2011a; 4(1):488-508. DOI: 10.4271/2011-01-0581.

Van Auken, RM, Zellner, JW, Chiang, DP, Kelly, J, Silberling, JY, Dai, R, Broen, PC, Kirsch, AM, Sugimoto, Y. *Advanced Crash Avoidance Technologies (ACAT) Program – Final Report of the Honda-DRI Team, Volume I: Executive Summary and Technical Report*. Washington, DC: Honda and DRI for the National Highway Traffic Safety Administration; 2011b. DOT HS 811 454.

Van Auken, RM, Zellner, JW, Silberling, JY, Sugimoto, Y, Urai, Y. Progress Report on Evaluation of a Pre-Production Head-On Crash Avoidance Assist System Using an Extended "Safety Impact Methodology" (SIM). Paper presented at: 21st International Technical Conference on the Enhanced Safety of Vehicles, Washington, DC, June 13-16, 2011c. Paper Number 11-0270.

Young, LR. On Adaptive Manual Control, *Ergonomics*, 1969; 12(4): 635-675 (Also in Parker, JF Jr., and West, VR. *Bioastronautics Data Book, Second Edition*. Washington, DC: National Aeronautics Space Administration; 1973. NASA SP-3006, pp. 593-595)

Zellner, JW, Van Auken, RM, Chiang, DP, Broen, PC, Kelly, JK, Sugimoto, Y. Extension of the Honda-DRI "Safety Impact Methodology" (SIM) for the NHTSA Advanced Crash Avoidance Technology (ACAT) Program and Application to a Prototype Advanced Collision Mitigation Braking System. *SAE Int. J. Passenger. Cars – Mech. Syst.* 2009; 2(1):875-894. DOI: 10.4271/2009-01-0781.

Zellner, J, Van Auken, M, Silberling, J, Kelly, J, Hagoski, B, Sugimoto, YS, and Urai, Y. Extension of the Honda-DRI "Safety Impact Methodology" (SIM) for the NHTSA Advanced Crash Avoidance Technology (ACAT) II Program and Application to the Evaluation of a Pre-Production Head-On Crash Avoidance Assist System - Progress Report. SAE Int. J. Passeng. Cars - Electron. Electr. Syst. 2012; 5(2):385-402. doi:10.4271/2012-01-0291.

Zellner, JW, Van Auken, RM, Kelly, J, Silberling, JY, Hagoski, BK, Sugimoto, Y, "*Advanced Crash Avoidance Technologies (ACAT) II Program – Final Report of the Honda-DRI Team, Volume I: Key Findings Report*. Washington, DC: Honda and DRI for the National Highway Traffic Safety Administration; forthcoming.

## APPENDIX A - SIMULATION RESULTS

This appendix further describes the CSSM crash avoidance and mitigation and post-conflict conflict recovery simulation results.

**Crash avoidance and mitigation results:**

If the pre-crash simulation results in a collision, then the CSSM uses a US Air Force Articulated Total Body (ATB) crash simulation (Fleck 1981) to estimate the crash Delta-V, and an Injury Outcome Estimator to estimate the Fatality Equivalent injuries and the probability of fatality for the both the subject vehicle and collision partner drivers. The weighted number of collisions and fatalities are used to calculate the effectiveness of the ACAT within each TRCT.

The estimated annual numbers of collisions for each TRCT, without and with the ACAT, based on the CSSM simulations, are listed in Table A1. The product of the Exposure Ratio (ER) and Prevention Ratio (PR) can be calculated from the information in this table. For example, the annual numbers of vehicles involved in the Primary TRCT crashes without and with the H-CAAS technology were estimated to be 1,654 and 1,497 respectively. These results are based on simulation results from 41 different Primary TRCT crash scenarios, each with up to 26 different driver-behavior combinations for a total of 1,066 different crash scenarios x driver-behavior combinations. Assuming that the Exposure Ratio is 1, the ERxPR product for the Primary TRCT crashes is 0.905, which is equal to 1,497 divided by 1,654.

**Table A1.**
**Estimated Effect of H-CAAS on the Number of Collisions by TRCT**

| H-CAAS Technology Relevant Crash Type (See Zellner et al. (2012)) | Estimated Number of Collisions Based on Simulations | | Estimated ERxPR |
|---|---|---|---|
| | Without H-CAAS | With H-CAAS | |
| Primary (P1) | 1,654 | 1,497 | 0.905 |
| Secondary 1 (S1) | 2,187 | 2,098 | 0.959 |
| Secondary 3 (S3) | 24 | 24 | 1.000 |
| Secondary 4 (S4) | 985 | 860 | 0.873 |
| Secondary 5 (S5) | 5,307 | 5,307 | 1.000 |

The annual number subject vehicle drivers and collision partner fatalities and Fatality Equivalent injuries were also estimated without and with the exemplar ACAT using the simulations. Example results for the subject vehicle driver are listed in Table A2. The data in this table was used to calculate ERxPRxFRsv, which is the number of subject vehicle driver fatalities with the H-CAAS divided by the number of fatalities without the H-CAAS (i.e., the same basic approach that was used to calculate ERxPR), and where FR is the Fatality Ratio. For example, the annual number of subject vehicle driver fatalities (in this weighted simulation sample) in Primary TRCT crashes without and with the H-CAAS technology was estimated to be 204.6 and 138.6 respectively, and the resulting ERxPRxFRsv product is 0.667. The Fatality Ratio can then be determined by dividing the ERxPRxFRsv product by the ERxPR product, resulting in FRsv=0.748.

**Table A2.**
**Estimated Effect of H-CAAS on the Number of Subject Vehicle Driver Fatalities by TRCT**

| H-CAAS Technology Relevant Crash Type (See Zellner et al. (2012)) | Estimated Number of Subject Vehicle Driver Fatalities Based on Simulations | | Estimated ERxPRxFRsv |
|---|---|---|---|
| | Without H-CAAS | With H-CAAS | |
| Primary (P1) | 204.6 | 138.6 | 0.677 |
| Secondary 1 (S1) | 169.6 | 158.8 | 0.936 |
| Secondary 3 (S3) | 1.2 | 1.2 | 1.000 |
| Secondary 4 (S4) | 214.5 | 104.8 | 0.489 |
| Secondary 5 (S5) | 368.9 | 368.3 | 0.998 |

The resulting estimates of H-CAAS collision and fatality effectiveness based on these CSSM simulation results are listed in Table A3. The collision effectiveness is equal to the (1-ERxPR)x100%; the fatality effectiveness is (1-ERxPRxFR)x100%. These results were used to estimate the overall effectiveness and benefits of the H-CAAS.

**Table A3.**
**Estimated H-CAAS Effectiveness by TRCT**

| H-CAAS Technology Relevant Crash Type (See Zellner et al. (2012)) | Collision Effectiveness (1-ERxPR) | Fatality Effectiveness (1-ERxPRxFR) | |
|---|---|---|---|
| | | SV | CP |
| Primary (P1) | 9.5% | 32.3% | 39.3% |
| Secondary 1 (S1) | 4.1% | 6.4% | 6.9% |
| Secondary 3 (S3) | 0.0% | 0.0% | 0.0% |
| Secondary 4 (S4) | 12.7% | 51.1% | 58.9% |
| Secondary 5 (S5) | 0.0% | 0.2% | 0.7% |

**Post-conflict recovery results:**

The CSSM was also extended to simulate the post-conflict recovery phase of the scenario in order to consider this phase in the ACAT evaluation as well. The simulation results for the recovery phase are used to assess the ability of the simulated driver to maneuver the vehicle back into the intended travel lane, after the driver's response to the warning.

The recovery phase was implemented in the CSSM simulations by transitioning back to normal driving (i.e., closed-loop path following) either after the completion of the open-loop emergency steering (half-sine) crash avoidance maneuver, or as soon as the collision partner is no longer visible in the forward view (i.e., is next to or behind the subject vehicle), whichever is sooner. The simulated driver attempts to regain the "intended path" by means of combined feed-forward/feedback control during the recovery phase, as opposed to following the reconstructed trajectory that resulted in a collision.

Application of the model in the CSSM simulations indicated that modeled drivers that successfully avoided the crash were also able to recover from the crash avoidance maneuver without overshoot. This result is consistent with the recorded trajectories of distracted and drowsy drivers in the original Driving Simulator experiments used to develop the driver models.

# PERFORMANCE COMPARISON AND REPEATABILITY EVALUATION OF THE FLEX PLI AND THE TRL PEDESTRIAN LEGFORM IMPACTORS

**Lan Xu**
**Sukhbir Bilkhu**[1]
**Iskander Farooq**
**Jeff Hickman**
**Jack Jensen**
**Ken McCabe**
**Guy Nusholtz**

*The USCAR/OSRP Pedestrian Task Group*

*United States*

**Paper Number** 15-0177

## ABSTRACT

The objectives of this study were to compare the response differences of the Flex PLI and TRL legforms under various test conditions and to assess their repeatability. A test fixture with four control factors was designed and fabricated to simulate a generalized front structure of a light truck. Using this fixture, thirty-six impact tests with the Flex PLI and the TRL legforms were performed at an impact speed of 32 km/h.

The responses from the two legform impactors, specifically, moments in the Flex PLI and acceleration in the TRL, MCL elongation in the Flex PLI and bending angle in the TRL, and ACL elongation in the Flex PLI and shear displacement in the TRL were compared. The Taguchi method was applied to compare the responses from these three pairs of measurements. The shape and magnitude of the response time histories were used to evaluate the repeatability of the Flex PLI and TRL legforms.

Some results from this limited study indicate that the two legforms did not consistently respond to the same test conditions in the same way and could potentially drive countermeasures in opposite directions. For example, increasing the protrusion of the lower bumper stiffener relative to the bumper generally resulted in lower moments in the upper tibia with the Flex PLI, but higher accelerations with the TRL legform. However, the MCL from the Flex PLI and bending angle of the TRL legform trended consistently with changes of all four fixture factors, although with differing sensitivity.

A repeatability analysis indicated that most measurement parameters of each legform were repeatable or marginally repeatable across the spectrum of the test conditions. However, the MCL elongation of the Flex PLI and the bending angle of the TRL were non-repeatable in some test conditions.

## INTRODUCTION

Currently, two legforms are available for pedestrian impact tests: the TRL Pedestrian Legform Impactor, originally developed by the EEVC (European Enhanced Vehicle Safety Committee) consortium [1] and the Flexible Pedestrian Legform Impactor (Flex PLI) [2]. The TRL Legform was incorporated into the ECE (Economic Commission for Europe) regulations in 2003 [3, 4]. The European New Car Assessment Program (EuroNCAP) has been using the TRL legform since 1997. The Flex PLI was developed by the Japanese Automobile Research Institute (JARI) in the early 2000's and over time, various versions have been evaluated [5]. EuroNCAP included the latest version of the Flex PLI GTR (Global Technical Regulation) in their 2014 vehicle tests [6]. Considering that these two legforms are used for the same type of test, it is important to understand their performance differences.

Various versions of the TRL legform and Flex PLI have been evaluated and compared by a number of organizations under different test conditions. A series of pedestrian impact tests involving five vehicles was performed using both

[1] Retired from Chrysler in 2014

legforms [7]. The major findings from these tests were that the two legforms had marked differences in how they interacted with vehicle front structures. Another series of tests on eight vehicles was performed with both legforms [8]. This work concluded that the TRL legform predicted a higher risk of tibia fracture but a lower risk of knee ligament injury than the Flex PLI. In addition, several bumper designs were tested with both legforms [9]. These results indicated that the bumper system that performed well with the TRL legform did not necessarily perform well with the Flex PLI.

The repeatability of the two legforms has also been studied by different organizations. Most repeatability analyses used the Coefficient of Variance, CV, which was based on the International Organization for Standardization document, ISO/TC22/SC12/WG5 N 751, regarding methods to assess the repeatability and reproducibility [10]. A repeatability and reproducibility study using six TRL legforms in 76 tests was conducted by Siems et al. in 2007 [11]. Repeat tests were performed on each legform with a linearly guided impactor. The CV values calculated from the parameter peaks of the repeat tests were all below 5% which indicated "acceptable" repeatability. Another study by Zander et al. [12] concluded that CV values from certification tests with the Flex PLI demonstrated that all tibia moments had acceptable repeatability while some knee ligament elongations had unacceptable repeatability, with CVs >10%. In the same study, two different locations at the front end of two vehicles were each impacted three times with a Flex PLI. Most of the tibia bending moments were repeatable, with CVs <5%; however, some of the knee elongations (ACL, PCL, and MCL) were non-repeatable with CVs >10%. The repeatability of the Flex PLI was then further assessed by the inverse calibration impact tests. The repeatability for the inverse calibration impact was acceptable since all the CV values were less than 4%. Another repeatability study with a later version of the Flex PLI was conducted [13] using two sedans and one (SUV) Sport Utility Vehicle. For each vehicle, two selected locations were each impacted three times. The CV results indicated that all the tibia moments were either repeatable or marginally repeatable. However, elongations of the knee ligaments did not have acceptable repeatability; their repeatability depended on vehicle front end geometry.

The OSRP (Occupant Safety Research Partnership) of USCAR (United States Council for Automotive Research) evaluated these pedestrian legforms. A unique test fixture was designed and used which allowed understanding of the response differences between the two legforms in this evaluation. The objectives were to compare the performance of the TRL legform and Flex PLI, and to assess the repeatability of some of the responses of the two legforms.

## METHODOLOGY

### Legform Impactors

The TRL legform consists of two rigid segments covered with foam and neoprene skin (Figure A1 in Appendix A) [1, 14]. The segments represent the lower leg (tibia and foot) and upper leg (femur) of an adult, connected by a simulated knee joint that can rotate and translate. The motion of the knee joint is resisted by two deformable elements (ligaments as shown in Figure A1) which are replaced after each test.

The Flex PLI consists of an upper leg (femur) and lower leg (tibia) composed of fiberglass bone cores and several plastic segments attached to its impact side (Figure A2) [2, 14]. The knee element consists of two complex blocks containing over twenty four springs. The entire assembly is wrapped in a thin rubber and neoprene skin.

The TRL legform and Flex PLI instrumentation locations are shown in Figures A3 and A4, respectively [15, 16]. The standard TRL legform instrumentation includes two transducers to measure the relative rotation (bending angle) and relative translation (shear displacement) between the femur and tibia. There is also an accelerometer fitted to the non-impact side of the tibia, close to the knee joint (66mm below its knee as shown in Figure A3).

The Flex PLI has four strain gauges glued to its fiberglass core to estimate the tibia moments at four different locations. These are labeled Leg-1 through Leg-4 in Figure A4, but identified as Tb1 through Tb4 throughout the text. The standard Flex PLI also includes four string potentiometers in its knee to measure the elongations of the Anterior Cruciate Ligament (ACL), Medial Collateral Ligament (MCL), Posterior Cruciate Ligament (PCL) and Lateral Collateral Ligament (LCL). Although the thigh has instrumentation, the moments in the thigh and the LCL elongation were not measured in this evaluation program.

To minimize the potential damage to the Flex PLI (GT version), the owner of the legform (JARI) advised that the maximum tibia bending moment should not exceed 380Nm during any test. A series of tests was performed using the Flex PLI, starting from a low impact speed which was increased gradually, to determine the impact speed for this test program. An impact speed of 32km/h kept the bending moments less than 380 Nm. Both the TRL and the Flex PLI legforms were tested at this speed.

**Test Fixture Design**

The test fixture was designed to represent a front end of a generic Light Truck and Van (LTV) and is shown in Figure 1. The fixture had three horizontal components which represented the hood edge, bumper, and lower bumper stiffener (LBS). The LBS was adjustable in both horizontal and vertical directions. The fixture was bolted to a heavy bed plate and secured to the test area floor. The foam placed in front of bumper face was expanded polypropylene (EPP) with a density of 32g/l and a thickness of 75mm. It was replaced for each test.

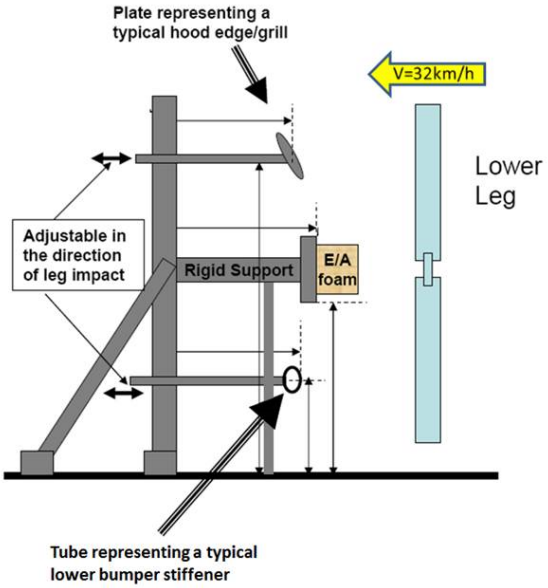


***Figure 1. Fixture Design***.

**Test Matrix Design**

**Taguchi method** A procedure used to analyze the data from this test series was the Taguchi method [17, 18]. The Taguchi method utilizes orthogonal arrays in the design of experiments to significantly reduce the number of experimental configurations compared to a full factorial array. Control factors such as the bumper foam height and LBS position were varied and evaluated.

**Test matrix** An L9 orthogonal array was used in this study. It had four control factors with 3 different levels. This resulted in 9 tests for each legform. The required number of tests, if a full factorial array were used, would be 162. The factors are given in Table 1. Factor A, the bumper foam section height, was the vertical length of the cross section. Factor B, height of the bumper, was the vertical distance from the ground plane to the bumper lower edge. Factor C, LBS fore/aft position, was its alignment with respect to the bumper contact surface in the horizontal direction. Factor D, the height of LBS, was the vertical distance from the ground plane to the LBS. Photographs of the nine test configurations are shown in Figure B1 (Appendix B). To assess the repeatability of the legforms, two tests were conducted for both legforms in each of the nine configurations.

All four control factors were tested using three levels except for the bumper foam height (Factor A). Only two levels of the bumper foam height were used in the test. The Taguchi method allows for substitution for variables that were not represented in testing. Thus, Level 2 of factor A is the same as Level 1 (A2=A1). A 100 mm bumper section was used in test configurations 1 through 6 in this test series. The factor levels are shown in Table 2.

**Table 1.**
**Test Matrix.**

| **L9 Taguchi Experimental Layout Inner Array - Control Factors and Levels** | | | | |
|---|---|---|---|---|
| *Confg.** | *Bumper Foam Height (z)* | *Bumper Lower Edge From Ground* | *Lower Bumper Stiffener offset to bumper face* | *Lower Bumper Stiffener from ground* |
| | **A** | **B** | **C** | **D** |
| **1** | **1** | **1** | **1** | **1** |
| **2** | **1** | **2** | **2** | **2** |
| **3** | **1** | **3** | **3** | **3** |
| **4** | **2** | **1** | **2** | **3** |
| **5** | **2** | **2** | **3** | **1** |
| **6** | **2** | **3** | **1** | **2** |
| **7** | **3** | **1** | **3** | **2** |
| **8** | **3** | **2** | **1** | **3** |
| **9** | **3** | **3** | **2** | **1** |

*Confg. = configurations

**Table 2.**
**Factor Levels.**

| **Control Factors and Levels for Taguchi L9** | | | |
|---|---|---|---|
| | ***Level 1*** | ***Level 2*** | ***Level 3*** |
| **A** *Bumper Foam Height (mm)* | 100 | 100 | 200 |
| **B-***Bumper lower edge from Ground (mm)* | 350 | 400 | 450 |
| **C-***Lower Bumper Stiffener Offset to bumper face (mm)* | -50 | 0 | +50* |
| **D-***Lower Bumper Stiffener from ground (mm)* | 180 | 230 | 280 |

*Positive is in the legform initial travel direction

**Data Processing**

For the Flex PLI legform, the directions of the tibia moments (Tb1, Tb2, Tb3 and Tb4) were about the legform X axis. The MCL, PCL, and ACL extension measurements were in the local (dummy) coordinate systems (as opposed to the vehicle coordinate system). For the TRL legform, the directions of tibia acceleration and shear displacement were in the Y-direction (legform travel direction), and the knee bending angle was about the leg's X-axis. Data was recorded at a sample rate of 10,000 samples per second and filtered with a SAE CFC180 filter. Sign conventions, filtering and data processing followed standard industry practices (as described in SAE J211.)

**Analysis Method**

The measurements from the Flex PLI and TRL legforms that were hypothesized and proposed to assess the same injury type were compared. Moments from the Flex PLI and acceleration from the TRL were hypothesized to assess the risk of bone fracture. MCL elongation in the Flex PLI and bending angle in the TRL were hypothesized to assess the risk of injuries to the collateral ligaments. ACL elongation in Flex PLI and shear displacement in the TRL were hypothesized to assess the risk of injuries to the cruciate ligaments. Since some pairs measured different physical metrics, the trends of both their peak responses and their signal to noise ratios for each control factor were compared.

Factor A in the test fixture, size of the bumper foam, controlled the amount of energy that was absorbed. Factor B, the height of the bumper, controlled the relative height between the bumper and the knee and accelerometer location for the TRL legform, and between the bumper and the Tb1 and Tb2 for the Flex PLI. Factor C, LBS fore/aft position,

is the horizontal distance between the contact surfaces of the bumper and LBS. C2 is aligned with the bumper beam, C3 is towards the rear of the fixture (recessed rearward of the bumper surface), and C1 is towards the front of the fixture (protruded forward of the bumper surface). Factor D is the LBS height relative to the ground.

The relationship between moment distribution and loading conditions in a beam is illustrated in Figure C1 of Appendix C. Considering that the shape and construction of the tibia in the Flex PLI is essentially a beam, it is possible to use beam theory for pictorial estimation of the moment distribution in its tibia, as shown by Figure C1. The pictorial estimation indicates that the maximum moments occur near the locations of the reaction forces, which would be the bumper force and LBS force.

The signal to noise (S/N) function used in this analysis is of the smaller-the-better type exhibited in Eq. (1),

$$S/N = -10\,log(\frac{1}{n}\sum_{i=1}^{n} y_i^2) \qquad (1)$$

where $y_i$ are responses and n is the number of repeats from a test configuration. In this study, n=2, $y_1$ and $y_2$ are the peaks from the two repeat tests.

Repeatability was assessed by shape and magnitude correlation method. The repeatability between the two signals was measured through the use of cross correlations of the time-histories [19]. The two signals are considered repeatable if both the shape correlation is at least 0.98 and the magnitude correlation is at least 0.95. On the other hand, the two signals are considered not repeatable if either the shape is below 0.92 or the magnitude is below 0.9. In between, the repeatability is marginal. The definition of the shape and magnitude correlations and the repeatability criterions are included in Appendix E. All of the correlations were calculated from 0 to 80 milliseconds.

## RESULTS AND DISCUSSION

### Peak Response Analysis

The data from the PCL transducer could not be recorded because of faulty instrumentation. Therefore, it was not included in this analysis.

Peak tibia accelerations from the TRL legform and peak moments in the Flex PLI from all the tests are presented in Figures 2 and 3 (t1= test 1, t2=test 2) below and Figure D1 in Appendix D. Among the measured moments at four locations in the Flex PLI, the majority of the maximum moments occurred at Tb1 (at the top location), possibly due to the inertial loading from the knee and its contact with the bumper. Moments in Tb2 were close to Tb1 in configurations 7 and 9. Moments in Tb2 were larger than Tb1 in configurations 4 and 8. Beam theory seems to explain this result: the closer the bumper and LBS reaction points are to the transducer location, the higher the moment. For example, in configuration 4, the bumper was below the Tb1 location and both the bumper and the LBS are nearer to Tb2 than to Tb1; in configuration 8, both the bumper and the LBS are nearer Tb2 again. Therefore, only the Tb1 moments from the Flex PLI are compared to the tibia accelerations from the TRL legform in peak response analysis.

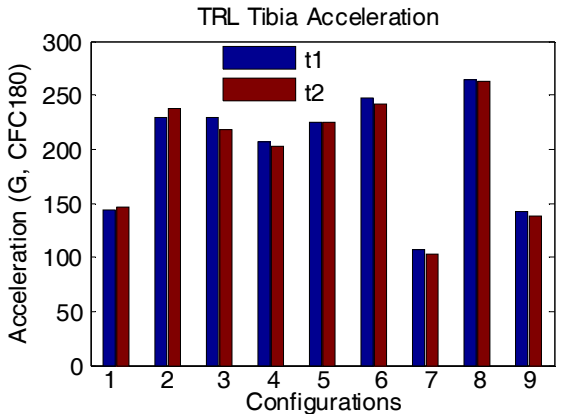


*Figure 2. Peak Tibia Accelerations (TRL).*

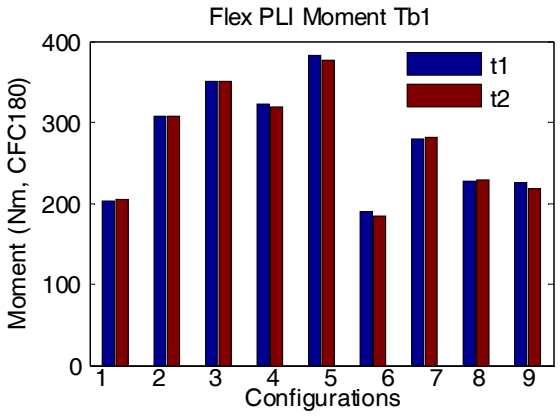


*Figure 3. Peak Tb1 Moments (Flex PLI).*

The configurations that produced maximum or minimum peaks for the tibia acceleration and Tb1 moment are presented in Table 3. The configurations that resulted in the maximum acceleration from the TRL legform included C1 (protruded LBS), while the configurations that resulted in the maximum Tb1 moment from the Flex PLI included C3 (recessed LBS). C3 created more rotation around the knee (observed from the video) which increased the moments in the tibia. The highest acceleration in the TRL legform occurred when it was impacted at the top quarter of the tibia, but the highest Tb1 in the Flex PLI occurred when both the top quarter and bottom quarter of the tibia were impacted. Similarly, the TRL legform obtained the minimum accelerations in the configuration that included C3, and the Flex PLI Tb1 tended to obtain the minimum in the configurations that included C1.

**Table 3.**
**Maximum or Minimum Peaks in Terms of Configurations.**

| Variables | Configurations | Comments |
|---|---|---|
| **Tibia Acc. Max (TRL)** | 8: A3B2C1D3 | contains C1; |
| | 6: A2B3C1D2 | contains C1 |
| **Tb1 moment Max (Flex PLI)** | 5: A2B2C3D3 | contains C3; |
| | 3: A1B3C3D2 | contains C3; |
| **Tibia Acc. Min (TRL)** | 7: A3B1C3D2 | contains C3; |
| **Tb1 moment Min (Flex PLI)** | 6: A2B3C1D2 | contains C1; |

Peaks of the bending angle in the TRL legform and the MCL displacement in the Flex PLI are presented in Figures 4 and 5. Both legforms demonstrated considerable similarity in the ranking of the three maximum peaks. This might be due to the similar parameters measured in the two legforms. Bending angle in the TRL legform measures the relative rotation between the femur and the tibia. As the femur rotates with respect to the tibia, the MCL is approximately proportional to the multiplication of the relative rotating angle (similar to bending angle in the TRL legform) and the distance (almost constant) from the pivot point to the location of the measurement device of the elongation. It was observed that C3 is included in the two maximum peak response configurations (3 and 5).

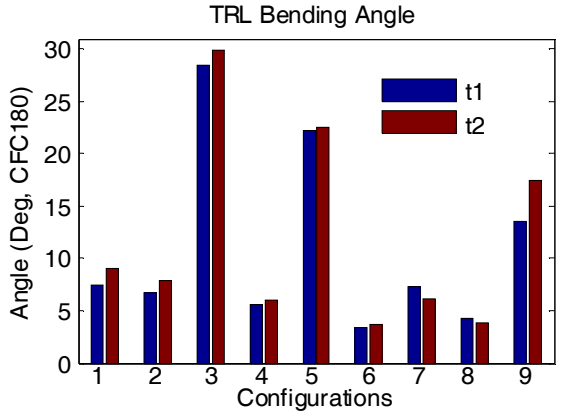


*Figure 4. Peak Bending Angles (TRL).*

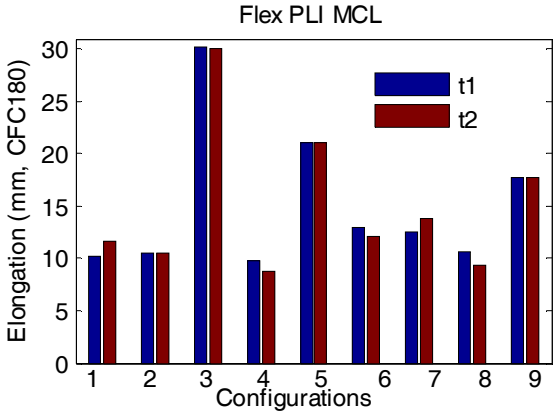


*Figure 5. Peak MCL Elongations (Flex PLI).*

The peaks of the shear displacement in the TRL legform and the ACL elongation in the Flex PLI are presented in Figures 6 and 7. These two parameters measure the relative translational motion between the femur and tibia. The two legforms responded to most test configurations inconsistently. The trends from one legform could not be predicted from the trends of the other legform. For example, configurations 3 and 9 produced peak shear

displacement responses in the low range for the TRL legform, but they produced peak ACL elongation responses in the high range for the Flex PLI. Configuration 4 produced peak responses in the high range for the TRL legform, but it produced the peak responses in the low range for the Flex PLI.

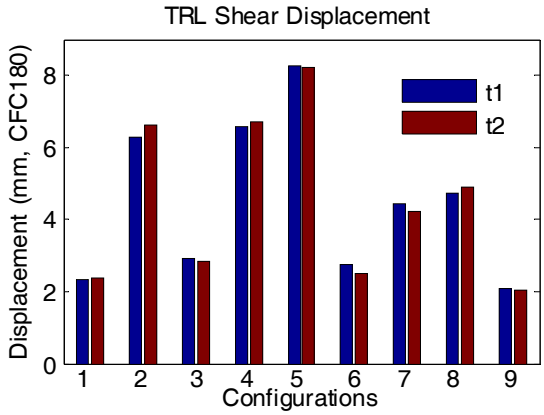


*Figure 6. Peak Shear Displacements (TRL).*

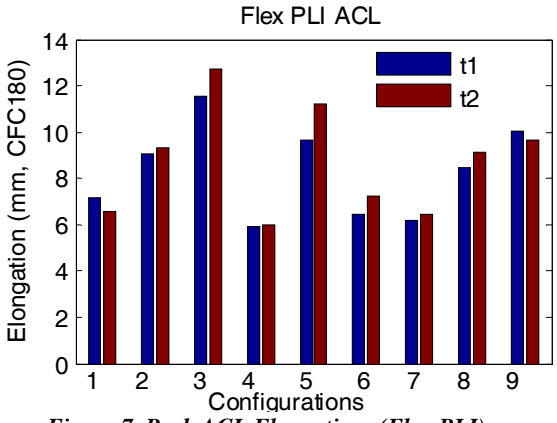


*Figure 7. Peak ACL Elongations (Flex PLI).*

**Control Factor Analysis**

The trends and sensitivities of S/Ns (signal to noise ratios) of the two legform responses due to the changes in the levels of the four factors are compared below. S/Ns for tibia acceleration from the TRL legform and Tb1 from the Flex PLI are overlaid in Figure 8. In general, the larger the change in the S/N with respect to an increment in a factor indicates the more sensitive the response is to that factor.

Tibia acceleration and Tb1 moment were affected by Factor A in a similar way, presumably due to the similar transducer locations. Both legform peak responses were influenced by Factor B consistently: there was a bumper position between B1 and B3 that would produce a minimum S/N. However, tibia moment Tb1 peak response in the Flex PLI and the acceleration in the TRL legform were influenced by Factor C in opposite directions. Tibia moment Tb1 peak response in the Flex PLI and the acceleration in the TRL legform were influenced by changing from factor D2 to D3 similarly but with different sensitivities.

The S/Ns for the bending angle from the TRL legform and the MCL elongation from the Flex PLI are presented in Figure 9. All four factors tended to affect the two parameters consistently, but with different sensitivities. The TRL legform was more sensitive to Factors A, C and D than the Flex PLI. The larger bumper section (A3), the lower bumper height (B1), and more forward alignment (protrusion) of LBS (C1) produced less rotation between the femur and tibia. Additionally, it indicates that there was a position between D1 and D3 for the LBS that would produce a maximum S/N.

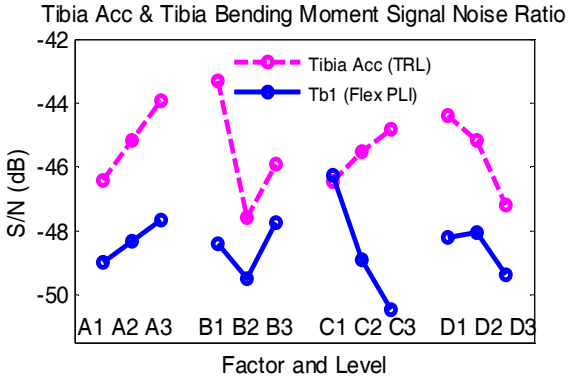


***Figure 8. Factor Effects to Tibia Accelerations (TRL) and Tb1 Moments (Flex PLI).***

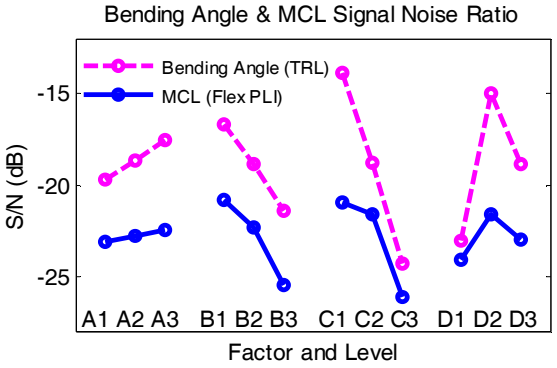


***Figure 9. Factor Effects to Bending Angles and MCL Displacements.***

The S/Ns for the shear displacement from the TRL legform and ACL elongation from the Flex PLI are presented in Figure 10. The two legforms were inconsistent in their responses to the factors changed in most configurations. With respect to the height of the bumper foam face (Factor A), the Flex PLI ACL was insensitive to the bumper face size. Recall that for control factor A only two values were tested (A1 and A2 were both 100 mm and used for configurations 1 through 6). The differences in S/N ratios between A1 and A2 are attributed to variability in the testing. Because the Taguchi method predicts trends from test outputs and test outputs are affected by test variability and noise factors it is not unusual for an S/N ratio to change for two control factors that are the same. The changes in S/N between A1 and A2 could be considered the limitations of the analysis (at least for control factor A, but not necessarily for the other control factors.) The differences between S/N ratios between A1 and A2 are, however, relatively low, as expected.

Control factor A3 (large bumper face) spans the tibia / femur interface in configuration 9 (see Figure B1). Thus tibia measurement trends would be expected to have discontinuities as the leg is moved up and down with the larger bumper face. This challenges the Taguchi method and trends with respect to control factor A should be interpreted accordingly. However, this geometric configuration is realistic and vehicles could indeed have bumper faces that span this area. As such trends identified in this study (such as the different trends between the two legs) are meaningful.

With respect to the location of the bumper (Factor B), the Flex PLI ACL was insensitive to the bumper height change from B2 (400mm) to B3 (450 mm) above the ground, while the TRL legform shear displacement was significantly sensitive to this change. The trends for both shear displacement and ACL varied differently to the heights of the LBS (Factor D). Only the protrusion of the LBS relative to the bumper (Factor C) affected both legform shear displacement and ACL displacement similarly, however with different sensitivities.

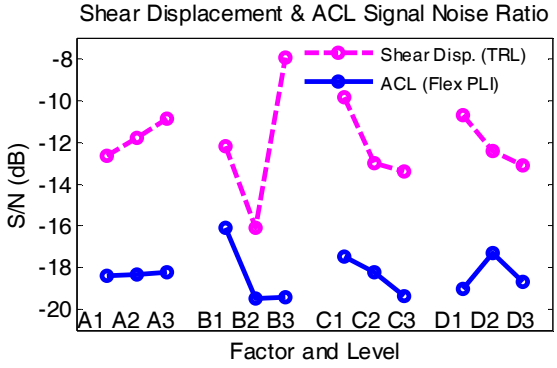


***Figure 10. Factor Effects to Shear Displacement and ACL Displacement.***

**Repeatability Analysis**

**TRL legform** The shape and magnitude correlations for the three parameters from the TRL legform tests are shown in Figures D2 and D3 (Appendix D). The shape and magnitude correlations of the TRL legform measurements are categorized in Table 4. Tibia acceleration of the TRL legform was repeatable in both shape and magnitude for all test configurations. Bending angle was repeatable in both shape and magnitude in only two of the nine test configurations. Shear displacement was repeatable in both shape and magnitude in six of the nine test configurations. Examples of repeatable time-histories for tibia acceleration, bending angle, and shear displacement from test configuration 4 are shown in the subplots of Figure D6, while non-repeatable time-histories for bending angle from test configuration 2 are shown in Figure D7.

**Table 4.**
**Repeatability of TRL Legform Measurements.**

| Config. | Acc | | Bending Angle | | Shear Disp. | |
|---|---|---|---|---|---|---|
| | Shp | Mag | Shp | Mag | Shp | Mag |
| 1 | Y | Y | Y | N | Y | Y |
| 2 | Y | Y | M | N | Y | M |
| 3 | Y | Y | Y | M | M | N |
| 4 | Y | Y | Y | Y | Y | Y |
| 5 | Y | Y | Y | Y | Y | Y |
| 6 | Y | Y | Y | N | M | N |
| 7 | Y | Y | Y | N | Y | Y |
| 8 | Y | Y | Y | M | Y | Y |
| 9 | Y | Y | Y | N | Y | Y |

Config. = Configuration
Shp=shape; Mag=magnitude;
Y: Repeatable; M: Marginal; N: Non-repeatable;

**Flex PLI legform** The shape and magnitude correlations from the Flex PLI tests for the six parameters are shown in Figures D4 and D5 (Appendix D). The results of the repeatability level for each parameter from the Flex PLI are categorized in Table5. Tb1, Tb2, Tb3, and ACL were repeatable or marginally repeatable in both shape and magnitude for all test configurations. Tb4 had non-repeatable shape for test configuration 3. It also had non-repeatable magnitudes for test configurations 1 and 7, but they were below the non-repeatable criteria (0.9) with small margin (0.90 and 0.89, respectively). MCL had a non-repeatable magnitude for test configuration 8. It was below the non-repeatable criteria (0.9) with a considerable margin (0.61). As an example, repeatable time-histories for moments Tb1 through Tb4 and MCL and ACL elongations from test configuration 4 are shown in the subplots of Figure D6, while non-repeatable time-histories for MCL from test configuration 8 are shown in Figure D8.

**Table 5.**
**Repeatability of Flex PLI measurements by test Configuration.**

| Config. | Tb1 | | Tb2 | | Tb3 | | Tb4 | | MCL | | ACL | |
|---|---|---|---|---|---|---|---|---|---|---|---|---|
| | Shp | Mag | Shp | Mag | Shp | Mag | Shp | Mag | Shp | Mag | Shp | Mag |
| 1 | M | Y | Y | Y | M | Y | Y | N | Y | M | M | Y |
| 2 | Y | Y | Y | Y | Y | Y | Y | M | Y | Y | M | M |
| 3 | Y | Y | Y | Y | M | Y | N | M | Y | Y | Y | Y |
| 4 | Y | Y | Y | Y | Y | Y | Y | Y | Y | Y | M | Y |
| 5 | Y | Y | Y | Y | Y | Y | Y | Y | Y | M | Y | M |
| 6 | Y | Y | Y | Y | Y | Y | Y | Y | Y | Y | Y | Y |
| 7 | Y | Y | Y | M | Y | M | Y | N | Y | M | Y | M |
| 8 | M | M | Y | M | Y | Y | Y | Y | M | N | M | M |
| 9 | M | Y | M | Y | M | M | Y | M | Y | Y | Y | Y |

Config. = Configurations;
Shp=shape; Mag=magnitude;
Y: Repeatable; M: Marginal; N: Non-repeatable;

**Repeatability comparison** The mean and standard deviation (Std) for the shape and magnitude repeatability were obtained by combining the 9 shape and magnitude correlations[2]. The mean plus and minus one Std of the correlations for all the parameters in the TRL legform and the Flex PLI are presented in Figures 11 and 12. In terms

[2] This does not imply that every configuration results in similar measured responses. The correlation coefficient across the two repeat tests for one configuration was then combined with the correlation coefficients from the other 8 configurations.

of the means of shape correlations and magnitude correlations, the tibia acceleration from the TRL legform and Tb1, Tb2, Tb3, and ACL from the Flex PLI were repeatable. The magnitude of bending angle in the TRL legform was non-repeatable. The magnitude of shear displacement in the TRL legform and Tb4 and MCL in the Flex PLI were marginally repeatable. However, the magnitude of the MCL in the Flex PLI had large standard deviation (Figure 12) which indicated that its repeatability was dependent on the test configurations: non-repeatable responses might be produced under some test conditions.

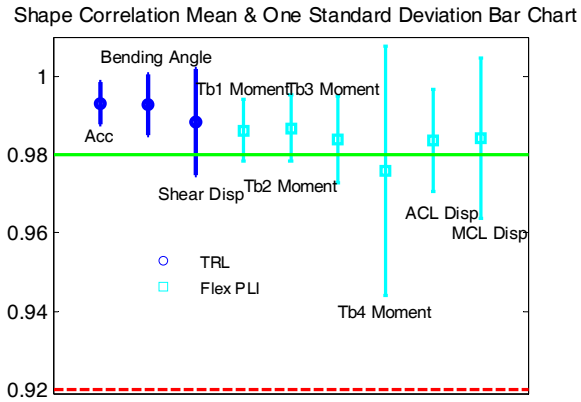


*Figure 11. Means and one Std of Shape Correlations.*

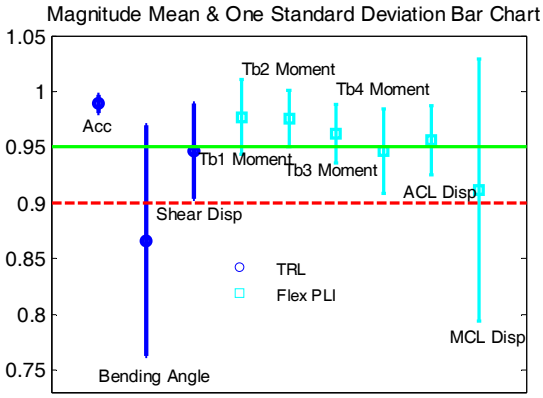


*Figure 12. Means and one Std of Magnitude Correlations.*

**Limitations**

The result on the level of the repeatability for these two legforms is limited in this study as there were only two repeat tests in this analysis. More repeat tests should be conducted to confirm the observations of this study.

The control factor analysis provided insights into the trends for the measured parameters with respect to the factor level changes. These trends could be further verified through additional confirmation tests. As an example, the limitation of only 2 repeat tests may have failed to fully quantify the trends associated with bumper foam height. The analysis suggested trends between A1/A2 (which were the same physical dimension) and A3 (which was larger) were insignificant, however more testing repeats may have better quantified the effects of the larger bumper foam height.

All tests were conducted at 32 km/h and neither legform was damaged. Additional tests at 40 km/h or higher should be conducted to confirm the durability of the legforms and if the repeatability changes.

**Summary**

Tibia acceleration in the TRL legform and tibia Tb1 bending moment in the Flex PLI reached their maximum peaks from different test configurations. The trends from the two legforms were inconsistent (in opposite directions) with respect to the change of LBS alignment with the bumper. This is possibly due to the difference in the mechanisms for producing the force/acceleration and the mechanism for producing the moment. As an example, for producing force/acceleration, the impact to the legform only occurs at one point. However, to produce a significant moment, either two (or more) impact points or one impact point and one (or more) fixed point reactions is required.

Shear displacement in the TRL legform and ACL elongation in the Flex PLI achieved the maximum peaks from different test configurations as well. In addition, to the increments of the four adjustable factors in the fixture, their sensitivities were different and some trends were inconsistent. The inconsistency might be due to the differences in transducer locations and knee designs.

Bending angle in the TRL legform and MCL elongation in the Flex PLI reached the maximum peaks from various configurations consistently, but with different levels of sensitivity.

Observations from the data indicate that the lowest responses (optimal responses) from the instrumentations between two legforms do not occur at the same vehicle front geometries. This could guide the design of the vehicle front structure differently.

Repeatability analysis indicated that across the spectrum of the test conditions in this study, some measured parameters had acceptable repeatability, but others were only marginal. Bending angle in the TRL legform had unacceptable repeatability. The MCL elongation in the Flex PLI is borderline non-repeatable under some test conditions, considering that its mean of overall magnitudes was close to the non-repeatable criteria (magnitude =0.9, Figure 12) and it exhibited a large standard deviation.

## CONCLUSIONS

In general, inconsistencies in the responses between the TRL and Flex PLI legforms for the same changes to a generic LTV front geometry are identified in this study. These inconsistencies likely would drive differing vehicle designs depending on what legform was used.

The change to the horizontal alignment between the bumper and the lower bumper stiffener (Control Factor C) affected the "risk of leg bone fracture" assessment values (tibia acceleration in the TRL legform and tibia moments in the Flex PLI) in opposite directions. Contradictory design directions are likely depending on which legform is used.

The "risk of leg ligament tear by bending" assessment values (tibia bending angle in the TRL legform and MCL elongation in the Flex PLI) produced consistent trends but with different sensitivities in most impact configurations.

The "risk of leg ligament tear by shear" assessment values (shear displacement in the TRL legform and ACL elongation in the Flex PLI) produced inconsistent trends in most impact configurations.

Overall, the MCL displacement responses in the Flex PLI were marginally repeatable.

With the TRL legform, the tibia acceleration response was repeatable, but bending angle was not repeatable in some test conditions.

## ACKNOWLEDGEMENT

JARI/JAMA loaned their Flex PLI Pedestrian Legform Impactor which made this evaluation program possible.

## REFERENCES

[1] TRL, Transport Research Laboratory, *TRL Pedestrian Legform User Manual, version 2.0*, 2000

[2] Humanetics Innovative Solutions, *Flex PLI GTR User Manual, GRR9-3-04,* 2011

[3] UNECE, European Directive 2003/102/EC, 2003

[4] UNECE, European Directive 78/2009/EC, 2009

[5] GTR 9, Flex PLI SubGroup - Informal Group on Pedestrian Safety - Flex-PLI Technical Evaluation Subgroup at http://www.unece.org/trans/main/wp29/wp29wgs/wp29grsp/pedestrian_flexpli.html, 2005-2010

[6] EuroNACP Group, EUROPEAN NEW CAR ASSESSMENT PROGRAMME (Euro NCAP); PEDESTRIAN TESTING PROTOCOL, Version 7.1.1, December 2013

[7] Mallory, A., Stammen, J., and Legault, F., "*Component Leg Testing of Vehicle Front Structures*", ESV 2005, 05-0194. 2005

[8] Matsui, Y., Takagi, S., Tanaka, Y., Hosokawa, N., Itoh, F., Nakasata, H., Watanabe, N., and Yonezawa, H., "*Characteristics of the TRL Pedestrian Legform and the Flexible Pedestrian Legform Impactors in Car-front Impact Tests*", ESV, 09-0206, 2009

[9] Kinsky, T., Friesen, F., and Buenger, B., "*The Flexible Pedestrian Legform Impactor and Its Impact on Vehicle Design*", ESV, 11-0328, 2011

[10] Mertz, B., "*Calculation Method & Acceptance Levels for Repeatability and Reproducibility*", ISO/TC22/SC12/WG5 N 751, Dec. 6, 2004

[11] Siems, S., Zander, O., Leβmann, P., Gegring D., Bortenschlager, K., Barnsteiner, K., Ferdinand, L., Hartlieb, M., Kramberger, D., and Zeugner, M., "*Evaluation of the Effects of Test Parameters on The Results of the Lower Legform Impactor*", ESV 07-0009, 2007

[12] Zander, O., Lorenz, B., Gehring, D., and Lebmann, P., "*Prediction of Lower Extremity Injury Risks During an Impact on Modern Car Fronts with a Flexible Pedestrian Legform Impactor and the Pedestrian Legform Impactor According to WWVC WG17*", ESV 07-0206, 2007

[13] Zander, O.B., Gehring, D., Lebmann, P., and Bovenkerk J., "*Evaluation of a Flexible Pedestrian Legform Impactor (Flex-PLI) for the Implementation within Legislation on Pedestrian Protection*", ESV 09-0277, 2009

[14] GRSP, "*Difference Of TRL Legform Impactor/Injury Criteria And Flex Pedestrian Legform Impactor/Injury Criteria*", Informal Document GRSP-49-24 (49th GRSP, 16-20 May 2011

[15] 7 EEVC Working Group 17 Report, *IMPROVED TEST METHODS TO EVALUATE PEDESTRIAN PROTECTION AFFORDED BY PASSENGER CARS* (December 1998 with September 2002 updates).

[16] Dr. Konosu / JARI, UNECE,http://www.unece.org/fileadmin/DAM/trans/doc/2006/wp29grsp/teg-002e.pdf, 2006

[17] Wu, Y., Wu, A., "*Taguchi Methods for Robust Design*", 2000

[18] Taguchi, G., Chowdhury, S., Wu, Y., *"Taguchi's Quality Engineering Handbook"*, 2004

[19] Xu, L., Agaram, V., Rouhana, S., Hultman, R., Kostyniuk, G., McCleary, J., Mertz, H., Nusholtz, G. and Scherer, R., *"Repeatability Evaluation of the Pre-Prototype NHTSA Advanced Dummy Compared to the Hybrid III"*, SAE2000-01-0165, 2000

## APPENDIX A: TWO LEGFORMS

The TRL legform and Flex PLI are illustrated in Figures A1 and A2. The locations of their instrumentations are presented in Figures A3 and A4.

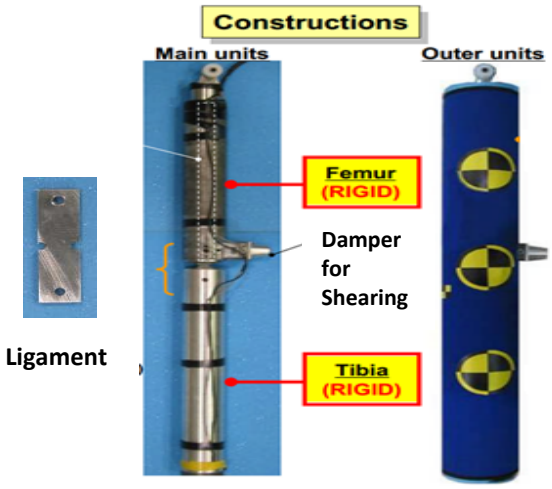


*Figure A1. TRL Legform Construction.*

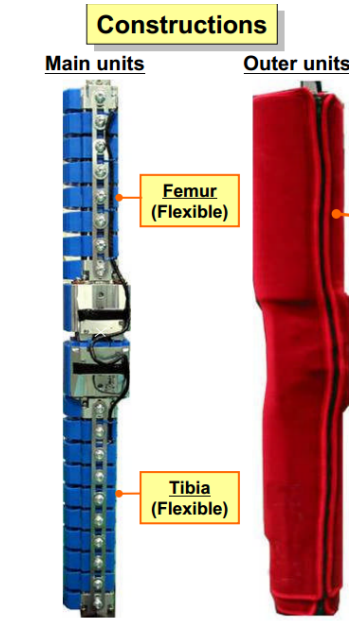


*Figure A2. Flex PLI GT Legform Construction.*

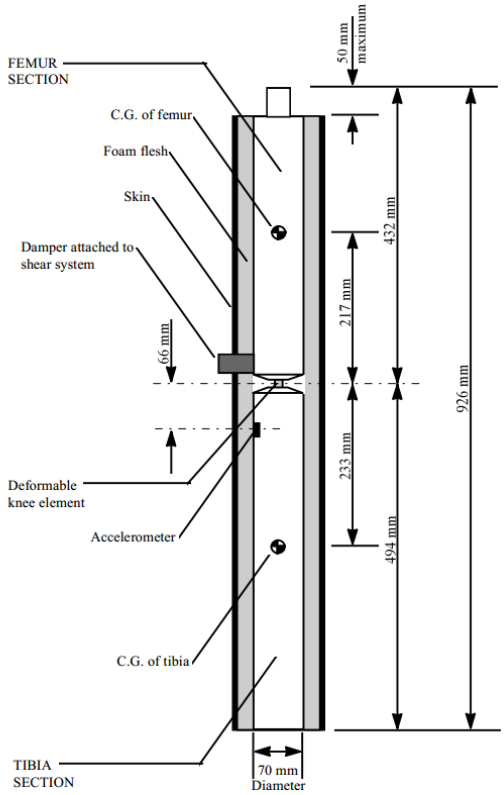


*Figure A3. TRL Legform Instrumentation.*

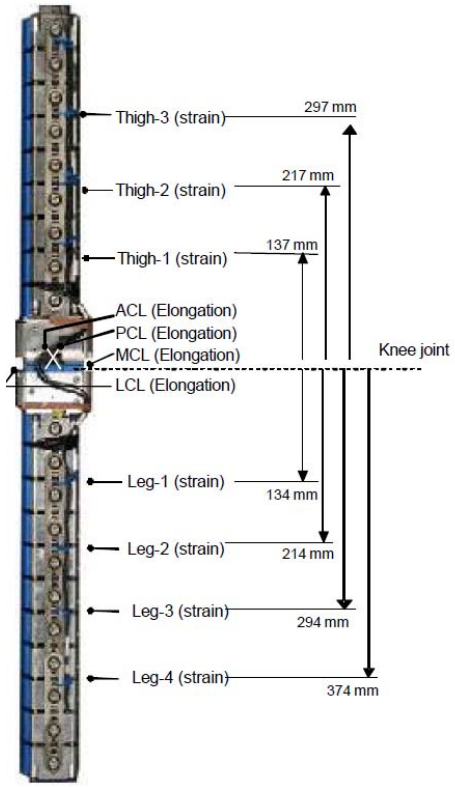


*Figure A4. Flex PLI Instrumentation.*

## APPENDIX B: TEST CONFIGURATIONS

Nine test configurations with the TRL legform and its alignment with the fixture are presented in Figure B1. The configurations with the Flex PLI are similar. The distances from the bottom of the legform to the ground are different for the two legforms: 25mm for the TRL legform and 75mm for the Flex PLI according to the test protocols for the standard tests. With the additional information provided in Tables 1 and 2, as well as in Figures A3 and A4, the positions of the transducers in the legforms with respect to the test fixture can be obtained.

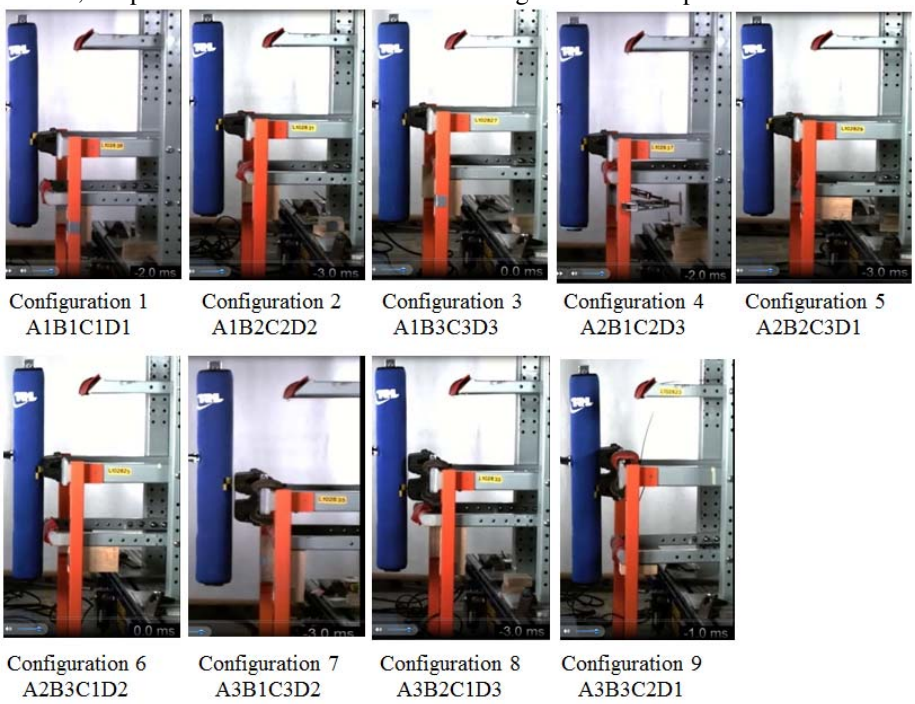


***Figure B1. Nine Test Configurations.***

## APPENDIX C: ILLUSTRATION OF LOAD AND MOMENT TO THE LEGFORM

The moment distribution estimated from elementary linear beam theory for a beam subjected to concentrated and distributed loads is shown in the Figure C1. $F_{kn}$ represents the force from the knee and $w_1$ and $w_2$ represent the inertial loading distributions.

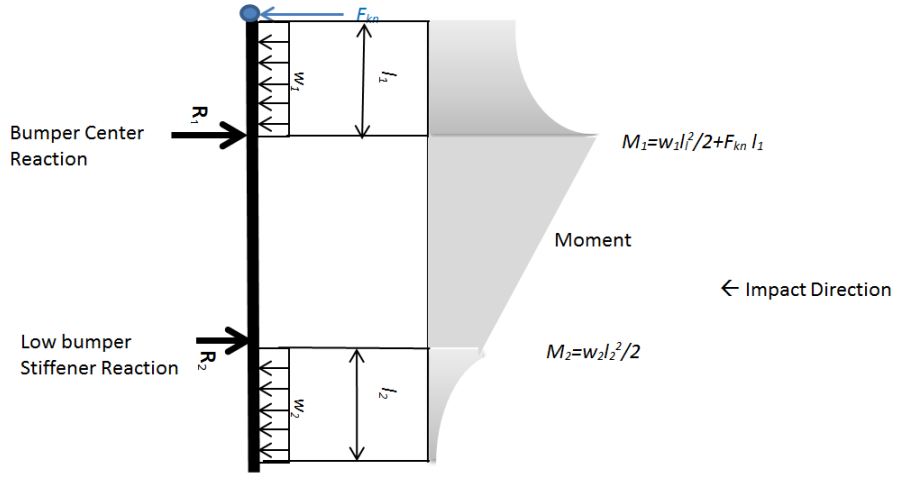


***Figure C1. Illustration of Moments in a Beam.***

## APPENDIX D: TEST RESULTS

### Peak Moment Response and Signal to Noise Ratio

Peak responses (absolute peak values) for four tibia moments from the Flex PLI are presented in Figure D1.

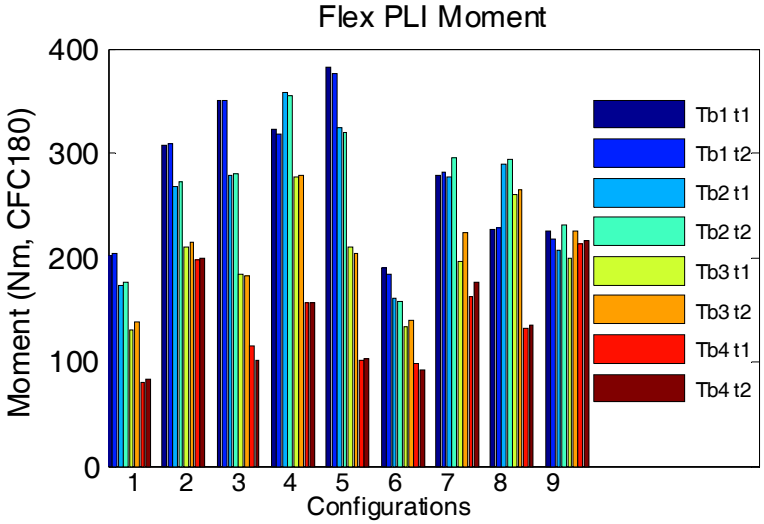


***Figure D1. Peak Moments from the Flex PLI.***

Signal to noise ratios, S/Ns, are contained in Table D1. The S/Ns for each factor level are in Table D2. The procedure to compute the S/Ns from B1, B2, B3, C1, C2, C3, D1, D2, and D3 are similar: take the S/Ns from the three configurations that include a factor at the same level, and then average them. As an example, when calculating the effect from factor B1 for parameter Tb1 (column 5), the S/N values in Table D1 from configurations 1, 4, and 7 (rows 3, 6, and 9) are used.

There is a slight difference in calculating the effects from factor A, considering A2=A1 in this series of tests. When calculating the effects from A1, the average of six S/N values from six configurations including A1 is the S/N value from A1. The calculation of S/N from A3 is the same as those from the Bs, Cs, and Ds. Once the S/Ns from A1 and A3 were obtained, the S/N from A2 is just the average of the S/Ns from A1 and A3.

**Table D1.**
**Signal Noise Ratios from the TRL and the Flex PLI Legforms.**

| | Acc | Angle | Shear | Tb1 | Tb2 | Tb3 | Tb4 | MCL | ACL |
|---|---|---|---|---|---|---|---|---|---|
| **Configuration** | | | | | | | | | |
| **1 A1B1C1D1** | -43.2 | -18.3 | -7.4 | -46.2 | -44.8 | -42.6 | -38.2 | -20.8 | -16.8 |
| **2 A1B2C2D2** | -47.4 | -17.4 | -16.2 | -49.8 | -48.6 | -46.5 | -45.9 | -20.5 | -19.3 |
| **3 A1B3C3D3** | -47.0 | -29.3 | -9.2 | -50.9 | -48.9 | -45.3 | -40.7 | -29.6 | -21.7 |
| **4 A2B1C2D3** | -46.2 | -15.2 | -16.4 | -50.1 | -51.0 | -48.9 | -43.9 | -19.4 | -15.5 |
| **5 A2B2C3D1** | -47.0 | -27.0 | -18.3 | -51.6 | -50.1 | -46.3 | -40.2 | -26.5 | -20.4 |
| **6 A2B3C1D2** | -47.8 | -11.0 | -8.4 | -45.4 | -44.1 | -42.7 | -39.6 | -22.0 | -16.7 |
| **7 A3B1C3D2** | -40.4 | -16.6 | -12.7 | -49.0 | -49.1 | -46.4 | -44.6 | -22.4 | -16.0 |
| **8 A3B2C1D3** | -48.4 | -12.2 | -13.7 | -47.1 | -49.3 | -48.4 | -42.5 | -20.1 | -18.9 |
| **9 A3B3C2D1** | -43.0 | -23.9 | -6.3 | -46.9 | -46.8 | -46.6 | -46.6 | -25.0 | -19.9 |

**Table D2.**
**Signal Noise Ratios Affected by Different Control Factors and Levels.**

| Factor | Acc | Tb1 | Tb2 | Tb3 | Tb4 | Angle | MCL | Shear | ACL |
|---|---|---|---|---|---|---|---|---|---|
| **A1** | -46.4 | -49.0 | -47.9 | -45.4 | -41.4 | -19.7 | -23.1 | -12.7 | -18.4 |
| **A2** | -45.2 | -48.3 | -48.2 | -46.2 | -43.0 | -18.6 | -22.8 | -11.8 | -18.3 |
| **A3** | -43.9 | -47.7 | -48.4 | -47.1 | -44.6 | -17.6 | -22.5 | -10.9 | -18.2 |
| **B1** | -43.3 | -48.4 | -48.3 | -46.0 | -42.2 | -16.7 | -20.8 | -12.2 | -16.1 |
| **B2** | -47.6 | -49.5 | -49.4 | -47.1 | -42.9 | -18.8 | -22.3 | -16.1 | -19.5 |
| **B3** | -45.9 | -47.7 | -46.6 | -44.8 | -42.3 | -21.4 | -25.5 | -8.0 | -19.4 |
| **C1** | -46.5 | -46.3 | -46.1 | -44.5 | -40.1 | -13.8 | -20.9 | -9.8 | -17.5 |
| **C2** | -45.5 | -48.9 | -48.8 | -47.3 | -45.5 | -18.8 | -21.6 | -13.0 | -18.2 |
| **C3** | -44.8 | -50.5 | -49.4 | -46.0 | -41.8 | -24.3 | -26.1 | -13.4 | -19.4 |
| **D1** | -44.4 | -48.2 | -47.3 | -45.2 | -41.7 | -23.1 | -24.1 | -10.7 | -19.0 |
| **D2** | -45.2 | -48.1 | -47.3 | -45.2 | -43.4 | -15.0 | -21.6 | -12.4 | -17.3 |
| **D3** | -47.2 | -49.4 | -49.8 | -47.5 | -42.4 | -18.9 | -23.0 | -13.1 | -18.7 |

## Shape and Magnitude Correlations

The results for shape and magnitude correlations are presented in Figures D2 to D5. The green lines are the repeatable criterions and the red lines are the non-repeatable criterions in those figures (conf.=configurations).

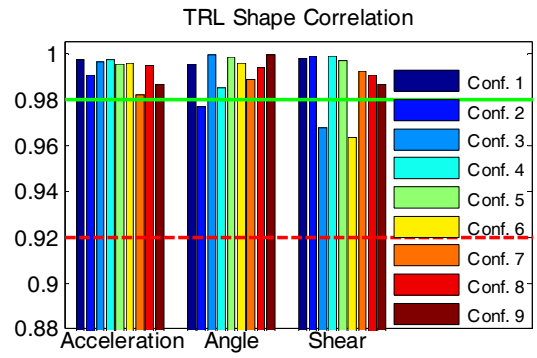


*Figure D2. Shape Correlations (TRL).*

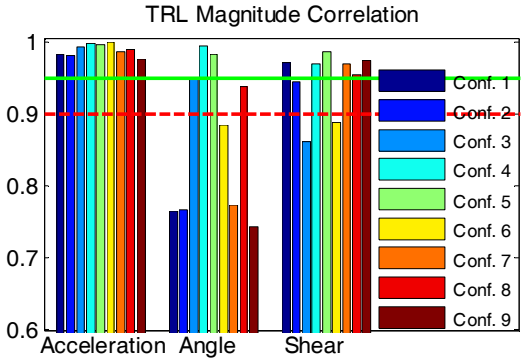


*Figure D3. Magnitude Correlations (TRL).*

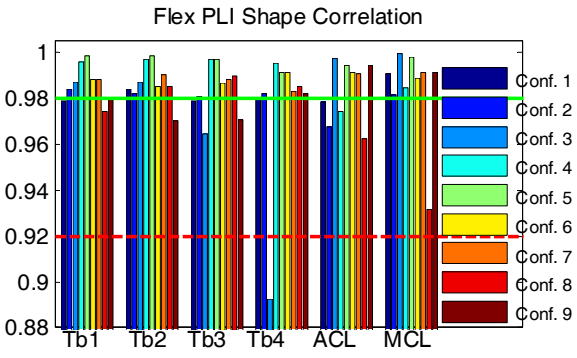


*Figure D4. Shape Correlations (Flex PLI).*

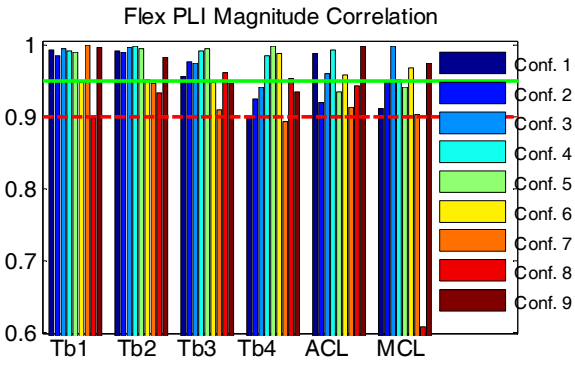


*Figure D5. Magnitude Correlations ( Flex PLI).*

**Selected Time Histories**

The time histories from test configuration 4 for nine measurements of both legforms are presented in Figure D6 to illustrate the repeatable time-histories. The time histories for the bending angles from test configuration 2 and MCL from test configuration 8 are presented in Figures D7 and D8 to illustrate the non-repeatable time-histories.

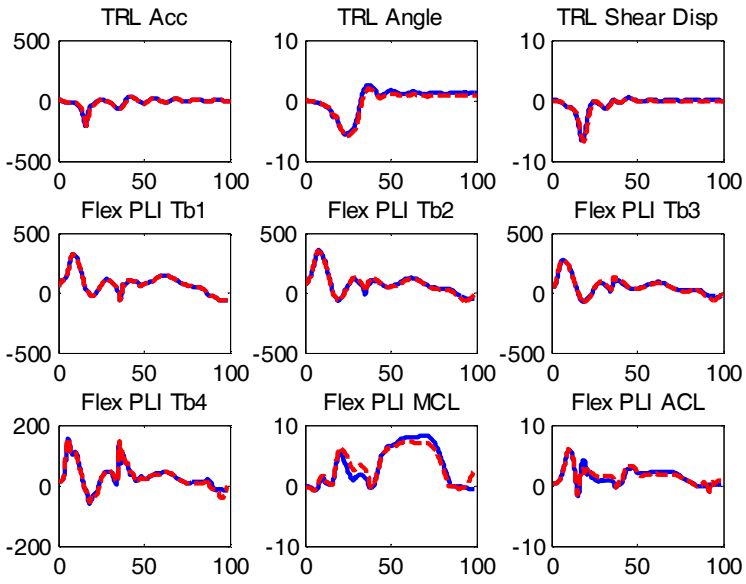


***Figure D6. Nine Measurement Response Time-histories from Test Configuration 4.***

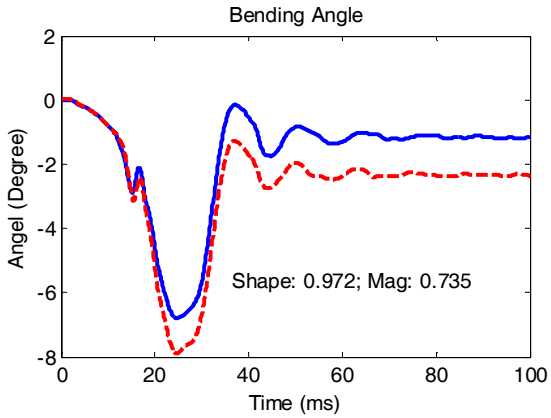


***Figure D7. Bending Angles from Test Configuration 2.***

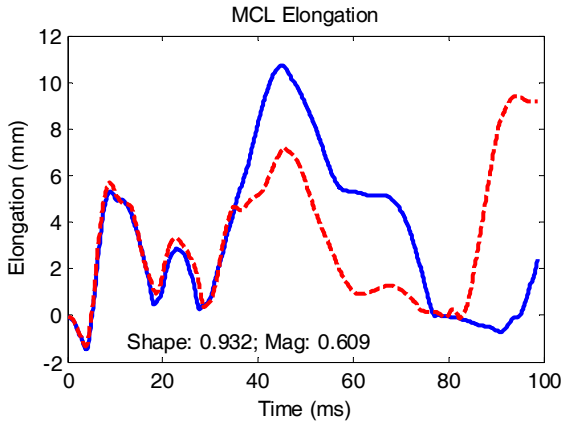


***Figure D8. MCLs from Test Configuration 8.***

**APPENDIX E: SHAPE AND MAGNITUDE CORRELATION METHOD**

**Definitions**

Given two signals denoted as, X: $x_i$; and Y: $y_i$. The definitions for the shape correlation and magnitude correlation between X and Y are given in the following.

1. Norm $||X|| = \sqrt{\sum x_i^2}$; $||Y|| = \sqrt{\sum y_i^2}$;
   The average of the two is
   $Mxy = (||X|| + ||Y||)/2;$ (E1)

2. *Shape* correlation:

In general, the shape correlation is defined as

$\max(\sum_j x_i * y_{i+j}/(||X|| * ||Y||))$ (E2)

3. Magnitude correlation: $Mx = ||X|| / Mxy;$ $My = ||Y|| / Mxy;$ $Mx+My=2$ (E3)

It should be noted that one of the magnitudes is greater than or equal to one and the other less than or equal to one. Magnitude that is less than or equal to one is used throughout this study.

**Repeatability Standards**

Two signals with both the shape correlation greater than 0.98 and the magnitude correlation greater than 0.95 are deemed to have acceptable repeatability. Two signals with the shape correlation less than 0.92 or the magnitude correlation less than 0.9 are deemed to have unacceptable repeatability. Two signals with the shape correlation between 0.92 and 0.98 and the magnitude correlation of 0.9 or above, or with the magnitude correlation between 0.9 and 0.95 and the shape correlation of 0.92 or above are deemed to have marginal repeatability.

Figures E1 illustrated the signals that have both repeatable shape and magnitude correlations (shape > 0.98 and magnitude >95) for any set of two curves. Figures E2 illustrated the signals that have both non-repeatable shape and magnitude correlations (shape < 0.92 and magnitude <0.9) for any set of two curves.

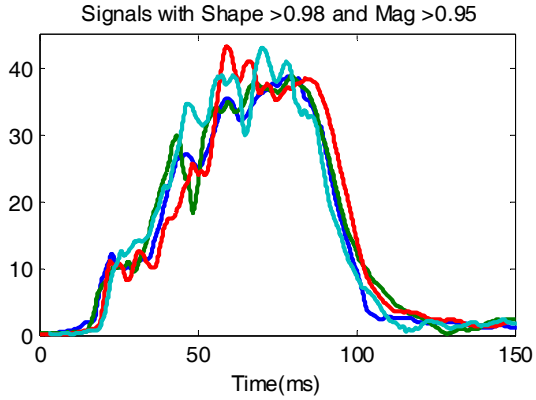


***Figure E1. Repeatable Signals.***

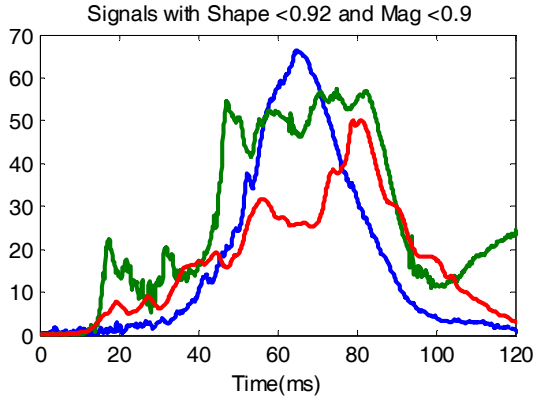


***Figure E2. Non-repeatable Signals.***

# THE INCIDENCE AND SEVERITY OF SMALL OVERLAP FRONTAL CRASHES IN NASS-CDS

**Priya Prasad**
Prasad Engg, LLC
USA

**Dainius Dalmotas**
**Alan German**
D.J. Dalmotas Consulting, Inc.
Canada

Paper Number 15-0182

## ABSTRACT

The Insurance Institute for Highway Safety has recently introduced a small overlap frontal crash test in its frontal rating scheme. Another small overlap frontal crash test is under development by the National Highway Traffic Safety Administration (NHTSA). Whereas the IIHS test is conducted against a fixed rigid barrier, the NHTSA test is conducted with a moving deformable barrier that overlaps 35% of the vehicle being tested and the angle between the longitudinal axis of the barrier and the longitudinal axis of the test vehicle is 15 degrees. The field relevance of the IIHS test and the NHTSA test has been the subject of papers by Prasad et al. (2014a,b). The current study is aimed at examining the combined relevance of the two tests as representing frontal corner impacts involving small overlap. The field relevance is indicated by the frequency of occurrence of real world crashes that are simulated by the test conditions, the proportion of serious-to-fatal real world injuries explained by the test conditions, and rates of serious injury to the head, chest and other body regions in the real world crashes resembling the test condition. The database examined for real world crashes is NASS-CDS. The frontal corner impacts as represented by the 25% Small overlap frontal and the NHTSA tests together address slightly less than 9% of all frontal crashes and 6% to 12% of all MAIS3+F injuries to the drivers in these crashes. The IIHS test has a somewhat higher contribution in both the incidence and severity. The two crash modes together address 4.6% to 8.2% of all MAIS3+F head injuries. Similarly, the proportion of all frontal MAIS3+F chest injuries addressed by the two crash modes or corner tests is estimated to be 6% to 10.6%.

The available data for the passenger involved in driver-side frontal corner crashes indicate that elderly female occupants predominantly experience serious head and chest injuries. All, except one, injured passengers were females. The average age of injured females who had chest injuries was slightly over 65 years. Injury rates of the head and the chest are substantially lowered in far-side than in near-side frontal impacts. Crash test ATD rotational responses of the head in the tests substantially over predict the real world risk of serious-to-fatal brain injuries.

## INTRODUCTION

Light vehicles are currently designed to meet or exceed the requirements of the FMVSS 208 in frontal impacts. This regulation includes perpendicular and angular tests against a rigid barrier and a 40% offset test against a deformable barrier. The rigid barrier tests are conducted at 25 mph with unbelted dummies, and at 35 mph with belted dummies. Whereas the offset, deformable barrier test is conducted at 25 mph for the FMVSS 208, vehicles are also designed to perform well in the IIHS 40% offset, deformable barrier tests. Over the years, most vehicles had achieved the highest ratings in the IIHS frontal tests, and also good ratings in NHTSA's frontal NCAP. This prompted the IIHS and NHTSA to investigate additional test configurations for frontal impacts. The IIHS has adopted a 64 kph frontal crash test in which 25% of the front-end of a vehicle is engaged by a rigid barrier, generally referred to as a Small Overlap Impact (SOI) test, and is shown in Figure 1. The structural and dummy responses are used to rate the vehicle as Good, Acceptable, Marginal or Poor. To get the highest rating, Top Safety Pick+ (TSP+), the vehicle has to achieve at least an acceptable rating in the new test. Mueller et al. of the IIHS have reported on various structural design strategies adopted in vehicles redesigned to perform well in the SOI mode.

Simultaneously, NHTSA conducted a meeting of NHTSA experts to examine the reasons why vehicle occupants are killed despite being belted and protected by airbags in frontal Impacts (Bean et al. and Rudd et al. (2009)). A detailed study of 122 fatal frontal crashes in NASS was performed in which primary and secondary causes were subject to group consensus. 49 of the 122 crashes (40%) were considered to be exceedingly severe or had anomalies. 29 of the 122 (24%) were **corner and/or oblique impacts** in which it was judged that the primary factor affecting fatalities was limited structural engagement of the front longitudinal rails of vehicles that are designed for energy absorption. The frequency of occurrence of the corner and/or oblique crashes in the NASS database was not estimated. This study led to a research program of crash testing by NHTSA and some of the test results have been reported by Saunders et al. (2011, 2012, 2013 and 2014).

After conducting a large number of developmental frontal crash tests, NHTSA has selected a movable deformable barrier crash test, shown in Figure 1, in which a Research Moving Deformable Barrier (RMDB) impacts the test vehicle on its left or on its right front corner a vehicle. The test vehicle is stationary and positioned at a target angle of 15˚ and at a target overlap of 35% to the forward line of motion of the RMDB. The RMDB is towed down the test track in a full forward direction, without any crabbing, and at the targeted impact velocity of 90.12 kph (56.0 mph) into the test vehicle. Regardless of the test vehicle's mass, RMDB's mass is 2490.7 kg (5491 lbs.). At the time of writing of this paper, results of eighteen (18) crash tests conducted by NHTSA have been placed in the public domain. Test reports of 6 RMDB tests of vehicles rated "Good" in the IIHS SOI test have also been added to the website. NHTSA's rationale for selecting the Oblique RMDB test has been outlined in several papers by Saunders et al referenced earlier.

It is worth noting that both tests shown in figure 1 could be classified as corner impacts. In the IIHS SOI test the stationary barrier overlaps the front end of the tested vehicle by 25% leading to missing the front rail entirely in virtually all vehicles in the US fleet. This test comes close to the definition of a corner crash not involving the front rails as in Bean et al. In the RMDB test, the barrier overlaps the front-end of the impacted vehicle by 35%. This initial impact geometry ensures that the barrier impacts the front-rail in the vast majority of light vehicles, but at an angle. Both test conditions are also referred to as "small overlap" frontal tests.

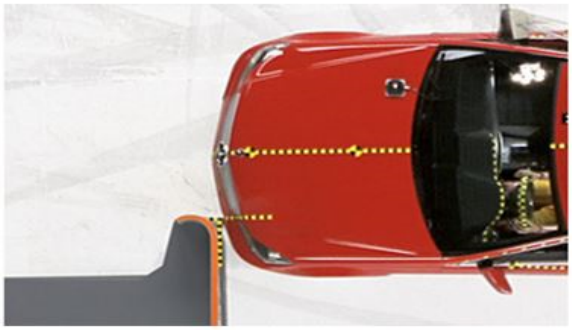

IIHS Small Overlap Impact (above)

NHTSA Oblique-frontal Impact (right)

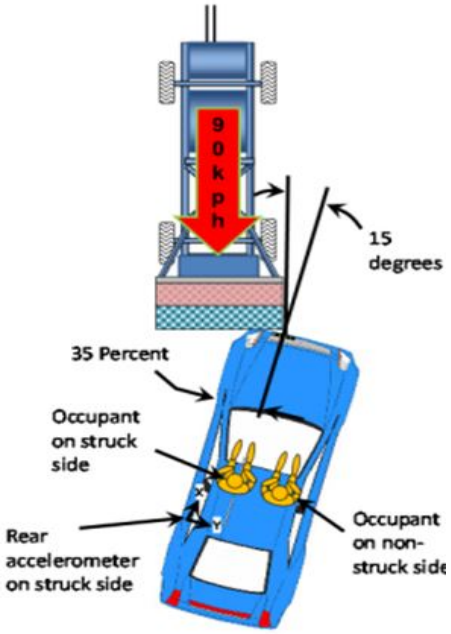


*Figure 1. Small Overlap Crash Tests*

Saunders and Parent (2014) summarized the status of NHTSA's research in January 2014 and have placed their analysis on NHTSA's website. Their analysis of existing data indicates that the Oblique RMDB test is representative of vehicle-to-vehicle crashes and the test procedure is repeatable. Testing of newer, high sales volume vehicles show injury risk trends similar to previous older vehicles. Far-side dummy occupant responses in these tests show head rotational velocities associated with high risk of brain injury.

Saunders and Parent (2014) also tested six vehicles that had achieved the IIHS Top Safety Pick+ (TSP+) rating utilizing the Oblique RMDB test procedure and compared their results with those of non-TSP+ vehicles. In general, the five TSP+ vehicles in the NHTSA Oblique RMDB tests yielded lower passenger compartment intrusions than the fourteen non-TSP+ vehicles, however injury risks as determined from the THOR dummy responses were similar in the two groups of vehicles. A particularly important finding was that the provisional Injury Assessment Reference Value (IARV) for rotational velocity of the head, BrIC, was exceeded in both the TSP+ and the non-TSP+ group of vehicles. Additionally, the average BrIC was higher for the far-side occupants than near side occupants, i.e. front seat passenger involved in a left corner impact as in figure 1.

**FIELD RELEVANCE OF THE CORNER TESTS**

The relative importance of the two tests in Figure 1 has been covered by several studies aimed at identifying the real world distribution of frontal crashes, in terms of frontal engagement and the proportion of all serious-to-fatal occupant injuries addressed in frontal crashes. A brief review of these studies follows.

The earliest study somewhat addressing small overlap frontal crashes in Sweden was reported by Planath et al. In 1993, Planath et al. reported the results of a study of frontal crashes in Sweden. A class of frontal crashes labeled as Severe Partial Overlap Crash (SPOC) occurred 3% of the time, but accounted for 14% of AIS2+ injuries to occupants of vehicles involved in frontal crashes. In a subsequent paper, Planath and Nilsson compared several frontal crash tests in regulations and mentioned that Volvo had developed an additional test procedure for SPOC that consisted of a 35% overlap, frontal test against a rigid barrier at 64 km/h. It was also stated "Exclusive use of SPOC in the development process would however be detrimental." This test did not gain too much attention, perhaps due to the introduction of the European 40% overlap against a fixed deformable barrier in the European regulation and by the IIHS in the USA and by NCAPs around the world. The results of further crash studies in Sweden performed by Lindquist et al. in 2003 and 2004 once again focused the attention of researchers to Small Overlap Impacts (SOI). Lindquist claimed that nearly half of all frontal crash fatalities in Sweden were in these SOI's. In these crashes the front longitudinal members were not engaged resulting in substantially greater passenger compartment intrusions than in frontal crashes in which the rails were were engaged. The 2003 and 2004 studies kicked off similar studies in US and Europe. The IIHS conducted a study of frontal crashes of vehicles that were rated "Good" in their frontal crash program and at least one front-outboard occupant had an AIS>=3 injury unless the only such injury was to the extremities. Brumbelow and Zuby reported results of the study in 2009. They defined small overlap as being when the major load path was outboard of all major longitudinal members. The small overlap accounted for nearly 25% of all the cases included in the study. The IIHS followed up by conducting several frontal crash tests to help them develop the test shown in Figure 1.

Kuehn et al. (2013) from the German Insurers Accident Research Group conducted a retrospective analysis of 3242 accidents involving passenger cars- 1930 of these were frontal collisions and 485 of which involved collisions in which the frontal engagement was considered to be small overlap. Unlike the results from Sweden, their conclusion was that "In terms of fatalities, the relevance of small-overlap car accidents is low. In terms of serious injuries (AIS2+) to the lower extremities, the relevance of small-overlap car accidents is high."

A Frontal Impact Taxonomy study was conducted by Sullivan et al. (2008), in which all NASS frontal crashes were distributed in eight different bins. The proportional contribution of each bin was determined in terms of frequency of occurrence and injury severity. Sullivan et al. reported that nearly two-thirds of all frontal crashes were full-engagement and offset with a nearly even split. A bin classified as SS/Corner

accounted for slightly less than 14% of all frontal crashes, slightly less than 12% of all vehicles in which at least one occupant had an MAIS3+ injury and slightly over 10.5% of all vehicles in which at least one occupant was fatally injured. This bin would contain the IIHS 25% offset and NHTSA's Oblique RMDB test conditions and vehicle deformations, and would give an upper limit of the incidence of the two crash types combined and injuries associated with them.

Scullion et al. (2010) modified the Frontal Impact Taxonomy study of Sullivan et al. into seven bins and concentrated on identifying the frequency of occurrence of and injury rate in small overlap frontal crashes in NASS. They defined small offset as a case in which the frame rail was not engaged and the center of damage was located entirely outside the frame rails. This case would fit the conditions produced in the IIHS SOI tests. In this study, slightly over 69% of all frontal crashes could be described by offset plus full engagement and 7.5% could be classified as small offset. The MAIS3+ injury risk was slightly lower than that in full-engagement crashes. Although the relative contribution of the small offset crashes as a proportion of all MAIS3+ frontal crashes was not reported, it had to be much less than that of offset plus full engagement crashes. In subsequent papers by Scullion et al. and Morgan et al. the small offset crashes continued to show up as relatively much smaller proportion of frontal crash modes than the full engagement and offset crashes.

Samaha et al. have reported the results of a more detailed FIT study of the NASS CDS cases for MY 1985-2011 vehicles involving belted drivers in vehicles equipped with airbags. In this study, the light vehicle fleet was partitioned into four weight classes and the FIT of individual weight classes was determined. In their crash classification the corner impact bin was separated into two classes- "small offset front" and "small offset side." The combined corner bin accounted for 7% of all crashes and 10% of all MAIS3+ driver injuries. The vehicle fleet was also divided in two groups of MY's- 1985 to 1999 and 2000+. Two driver age groups were also studied- 16 – 50 years and 50+ years. For both age groups, the involvement and injury rates were estimated as a function of FIT classification. The distribution of various body regions with moderate- and serious-to-fatal injuries by FIT classification was also determined for the two MY groups and age groups. For example, in the 16-to-50 yr. age group, full engagement and offset crashes accounted for approximately 79% of all serious-to-fatal head injuries and the corner crashes accounted for approximately 10% of all serious-to-fatal head injuries. Similar results were observed for lower extremity injuries- the corner crashes accounted for approximately 8% of all serious-to-fatal lower extremity injuries.

During the course of the Samaha et al. study, random check of photographs of case vehicles binned in the "small offset side" category, showed that some of them would not fit the damage patterns produced in either the IIHS SOI tests or in the Oblique RMDB tests conducted by NHTSA. Subsequently, a NASS case review process was used by Prasad et al. (2014a,b) that relied on hard copy reviews of frontal crashes in NASS-CDS. This involved binning potential corner crashes in either the IIHS like crashes or in NHTSA's Oblique RMDB like crashes.

**Objective**

The objective of this paper is to consolidate the main results of the two studies as they relate to frontal corner impacts and add further observations not covered in the earlier studies.

To establish the field relevance, the frequency of occurrence of the crash types and the resulting rates of serious-to-fatal injuries in real world frontal crashes were estimated from the publicly available database, NASS.

**Collision Deformation Classification (CDC):** Since these studies utilize the Collision Deformation Classification (CDC) as the first filter of the frontal crash data in NASS for comparison with test data, a brief introduction of the CDC is deemed appropriate in this section. A simplified description of the CDC is shown in Figure 2. It is important to note that a CDC code for any given vehicle is based solely on contact damage; any damage that is induced to the vehicle structure as a result of an impact is specifically excluded from consideration. Essentially, the front end of a vehicle is divided into three sections- L, C and R. L covers the left one-third of the vehicle, R covers the right one-third of the vehicle and C covers the center one-third of the vehicle. By the definition of the IIHS test with only 25% overlap of the barrier all IIHS

test like deformations should be in the L section (or R for right-front impacts). Since the overlap of the front-end of a test vehicle with NHTSA's barrier is 35%, the deformation of the front-end should be in the Y (or Z) section by definition. Therefore, all crashes that have CDC classification FY or FZ would contain the CDC observed in NHTSA's tests, and similarly all FL or FR crashes would contain the CDC observed in the SOI crashes conducted by the IIHS. Based on the definitions of FY and FL, given any error in the direct damage estimate, it is quite possible that some of the FY's could be FL's and some of the FL's could be FY's.

**METHODOLOGY**

Two crash test databases maintained by the IIHS and the NHTSA were interrogated. In the IIHS database there were results of 65 vehicle crashed in the SOI crash mode. In the NHTSA database results of 18 vehicles crashed in the Oblique RMDB mode were available. The damage patterns of the vehicles were assigned CDC classifications. The IIHS CDC classifications were 12FLXXXX and the NHTSA test vehicles 11FYXXXX. As shown in Figure 3, NASS frontal crash database was interrogated with the following restrictions: 3-point belted front-outboard occupants involved in planar impacts (i.e. no rollovers), airbags fitted on driver and passenger sides, direction of force 11, 12, 01, and all CDC extents. NASS calendar years were restricted to 1988 to 2010. The age of the front-outboard occupants was restricted to 15 years or older. This Subset of frontal crashes was referred to as Subset 03 in the two Prasad et al. papers. It contained 21,433 cases representing 9,793,461 cases when weighted. Hard copy reviews of all FL and FR crashes (not restricted by the PDOF) identified by the search in which a front outboard occupant had an MAIS3+F injury were conducted. Damage patterns of the involved vehicles were compared to those observed in the IIHS SOI tests and binned as "Good", "Moderate" or "poor" match with those observed in the SOI tests. The "Poor" matched cases were further examined to see if they could be classified in the Oblique RMDB crash bin. A similar process was followed for the FY and FZ classification of crashes as shown in Figure 3. Once again, the cases rated as "Poor" match with damage patterns observed in the Oblique RMDB were reviewed to verify if they could be classified in the IIHS bin. Details of the process can be found in the Prasad et al. papers. In this paper only the main results will be presented.

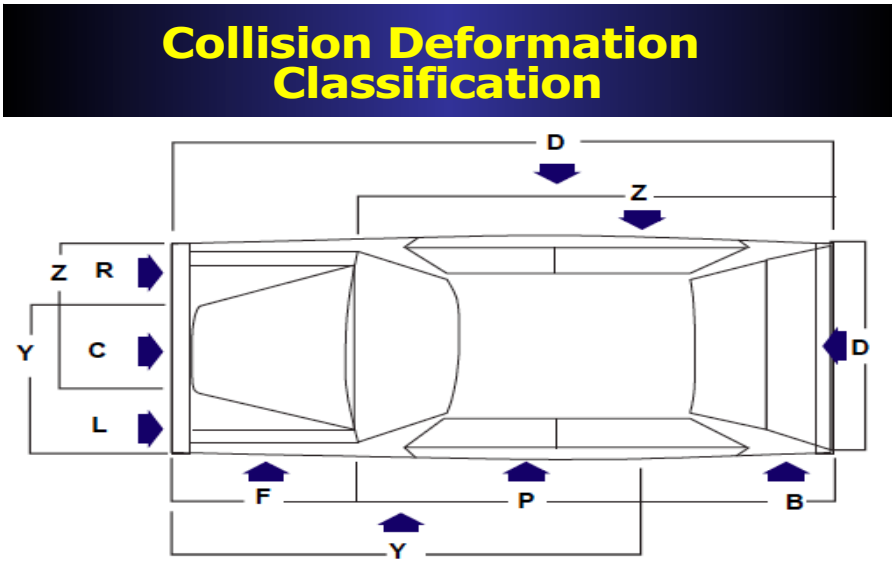


***Figure 2***. *Schematic Of the Collision Deformation Classification*

Prasad et al.(2014a) have reported the results of the CDC-FL branch shown in Figure 3 for all MY vehicles, MY2000+ vehicles and the 2000+ MY vehicles that were rated "Good" in the IIHS Moderate Offset tests to be consistent with the Brumbelow and Zuby study. Both the FIT analysis and hard copy reviews of the NASS cases were performed. The FIT analysis indicated that 7.5% of all frontal crashes

could be represented by the IIHS SOI tests. The frequency of occurrence of the NHTSA test like deformations was estimated by Prasad et al (2014b) as 1.24%. Therefore, the two small overlap corner crashes account for approximately 9% of all frontal crashes. The IIHS test condition also accounted for 6.1% of all MAIS3+F injuries to the front outboard occupants. These proportions were similar for the 2000+ MY vehicles as shown in Table 1. Note that Table 1 contains data for paired driver and passenger, i.e. driver side and passenger side crashes with occupants on the side impacted. Considering that the Samaha et al. study included "small offset side" also, the results of the FIT analysis in the two studies are similar. Samaha et al. also found little difference in injury distribution between all MY vehicles and 2000+ MY vehicles. Based on the above, hard copy reviews of the NASS cases in FY or FZ branch in Figure 3 was limited to the 2000+ MY vehicles. The results of the hard copy analysis are shown in Figure 4.

**Table 1. Summary of Estimated Contribution of IIHS SOI- like Crashes**

| | All MY | MY2000+ | MY2000+ & Good |
|---|---|---|---|
| SOI % MAIS3+F | 2.9% to 6.8% | 3.9% to 7.1% | 3.0% to 7.5% |
| SOI %MAIS3+F | 6.1% FIT Analysis<br>5.2% to 9.3% | 4.5% to 8.8% | 4.7% to 9.2% |

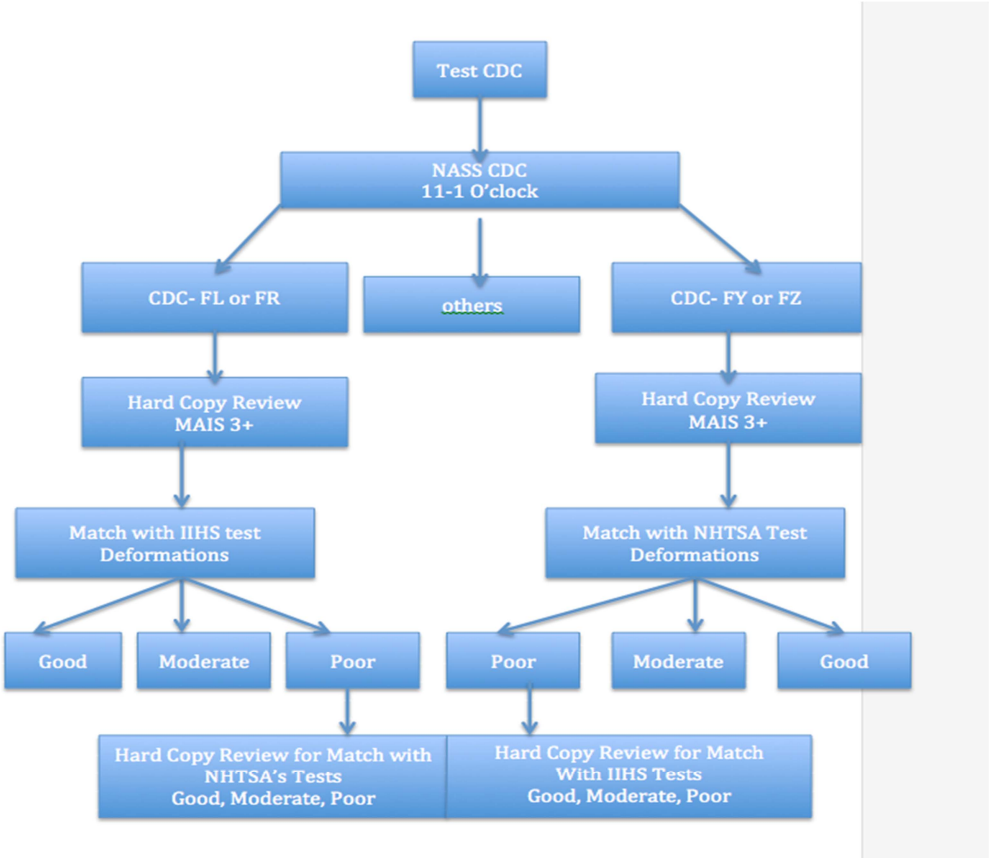


***Figure 3:*** *Schematic of the process used to identify NASS Frontal crashes that could be represented by NHTSA's Oblique RMDB Tests or by the IIHS SOI*

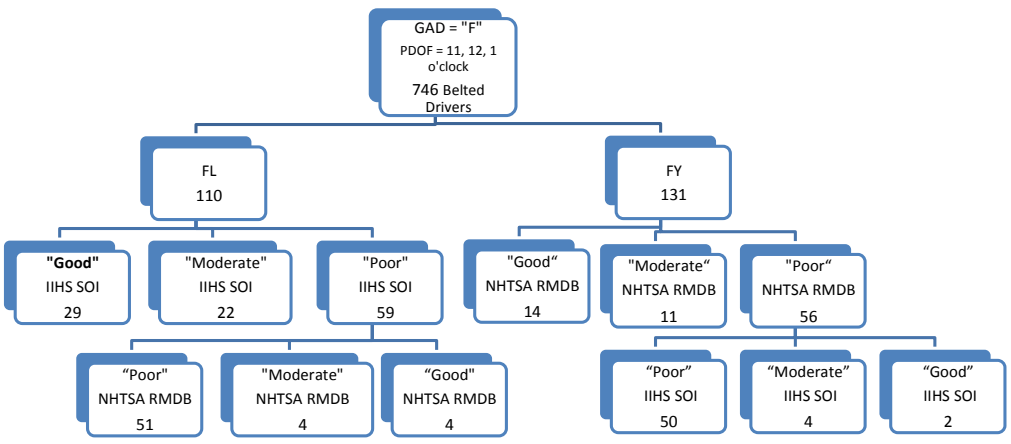


*Figure 4: Distribution of Driver MAIS3+F Injuries by FL and FY Damage Locations*

Figure 4 shows that there were 746 drivers with MAIS3+F injuries in 2000+ MY vehicles that were involved in frontal crashes. Of these, 110 were in crashes with frontal damage classified as FL. Hard copy analysis of these 110 cases showed that 29 had a "good" match with the IIHS tests and 22 had "moderate" match with the IIHS tests. Out of the 59 cases with poor match with the IIHS tests, 4 were considered to be a "Good" match with NHTSA's Oblique RMDB tests. There were 131 cases with FY classification. Out of these, 14 were considered to be "Good" match with the RMDB tests and 11 had a "moderate " match. Out of the 56 with "Poor" match with the RMDB test, 2 were considered to have "Good" match with the IIHS test and 4 had "Moderate" match with the IIHS tests. Adding up, there are 31 "Good" matches with the IIHS tests and 18 "Good" matches with the Oblique RMDB tests. The total number of "Good" matches is assumed to indicate the lower bound of the estimated proportion of all frontal crash MAIS3+F injuries. There are 31 "Good" matches with the IIHS SOI test yielding 31/746 or 3.9% of all frontal MAIS3+F injuries. Similarly there are 18 "Good" matches with the NHTSA RMDB test yielding 2.4% of all frontal injuries considered. The two tests together address 6.3% of all MAIS3+F frontal injuries to belted drivers. If the sum of the "Good" and "Moderate" matches is assumed to be the upper bound of injuries addressed by either test, the IIHS test represents approximately 7.6% and the RMDB test represents approximately 4.4% all MAIS3+F driver injuries in frontal crashes. Therefore, an upper-bound of approximately 12% is estimated as being addressed by the two small overlap corner tests discussed in this paper. Therefore the two small overlap corner tests address 6.3% to 12% of all driver frontal MAIS3+F injuries. The authors believe that a point estimate closer to the lower bound is more likely outcome of the current analysis described in the paper, since the upper estimates contain cases with "Moderate" match with the test data several of which have extent 9 with massive damage not seen in the IIHS tests. The estimates made by Sullivan et al. and Samaha et al. are within the range of estimates in this analysis.

**Distribution of injuries by damage location**

With insights gained from the hard copy reviews, further interrogation of the Subset 03 reported in Prasad

et al. was conducted to estimate MAIS3+ injury rates by damage locations for belted Front Outboard Occupants (FOO). Particularly, AIS3+ head/face and chest injuries were investigated as a function of seating position, Direction of Force and Damage Extent.

**RESULTS of NASS Data Analysis:**

The overall composition of frontal crashes being considered in this paper is shown in Tables 2. In Tables 2, numbers in parentheses give the percentage of the total of the individual cell, e.g. 12.8% of the drivers are involved in crashes whose damage location is coded as FL. Table 3 contains the injury rates for the drivers and passengers based on weighted data. The raw counts are also shown. Note that in order to have increased raw sample size, all MY's counts were used. In spite of that, the raw numbers for the passenger side are relatively small.

Table 2: Involved Driver and Passenger By Damage Location (All MY) Subset 03 Prasad et al.

| Subset 03 Drivers GAD/SHL1 | Driver Raw count | Driver weighted | Passenger Raw count | Passenger weighted |
|---|---|---|---|---|
| FL | 2154 | 1,066,113 (12.8%) | 448 | 200,952 (13.7%) |
| FY | 2586 | 1,137,490 (13.7%) | 499 | 173,508 (11.8%) |
| FD | 8873 | 3,929,359 (47.2%) | 1798 | 708,527 (48.2%) |
| FC | 273 | 91,581 (1.1%) | 60 | 18701 (1.3%) |
| FZ | 2187 | 1,122,328 (13.5%) | 455 | 173,517 (11.8%) |
| FR | 1739 | 976,964 (11.7%) | 361 | 194,421 (13.2%) |
| All | 17,812 | 8,323,834 (100%) | 3621 | 1,469,626 (100%) |

Table 3: MAIS3+F Injury rates by Damage Location (All MY)

| Subset 03 Drivers GAD/SHL1 | Driver Raw count | Driver weighted (%) | Passenger Raw count | Passenger weighted (%) |
|---|---|---|---|---|
| FL | 224 | 2.0 | 28 | 0.9 |
| FY | 285 | 2.0 | 34 | 4.1 |
| FD | 832 | 1.6 | 160 | 1.6 |
| FC | 48 | 2.3 | 8 | 11.4 |
| FZ | 148 | 1.0 | 42 | 1.2 |
| FR | 83 | 1.0 | 38 | 0.8 |
| All | 1620 | 1.6 | 310 | 1.7 |

Examination of table 3 indicates that the driver injury rates in the near-side frontal impacts, i.e. in the FL and FY damage locations, are nearly two times those in far-side damage locations, i.e. in FR and FZ locations. This trend does not appear to be true for the passenger, especially when the far-side is the FY location. The FY location is slightly over three times more injurious than the FZ location for the passenger. The passenger injuries in the FY damage location were examined further in terms of the demographics of those injured.

**Passenger Head and Chest injuries in FY damage location crashes**

There were only six passengers with MAIS3+ head injuries and all were females. Three of the six were in multiple impact crashes. One had a head contact coded as Center IP and below, one contacted the right B-pillar, one the right Grab Handle, one had contact with the passenger airbag and one showed only belt contact, one had an unknown contact. Based on the small numbers other more detailed analysis was not conducted.

There were 18 cases of MAIS3+F chest injuries. All except one were female occupants whose average age was slightly over 65 years. The source of injury for all except one was coded as the belt restraint and hardware. One injury source was coded as Floor or console. Based on the chest injuries and source, there is no evidence of passenger occupant slipping out of the shoulder belt in the far-side crashes.

**Driver Head and Chest Injuries by Damage Location:**

The distribution of driver head and chest injuries by frontal damage location was studied next and is shown in Table 4. Nearly half of all MAIS3+F head injuries occur in crashes with damage location coded FD, i.e. both rails were engaged. The corner impacts would include a subset of the FL and FY damage locations that account for nearly 27% of all head injuries. However, not all FL crashes are represented by the IIHS test and not all FY crashes are represented by the Oblique RMDB test. Based on Figure 4, approximately 26.4% to 46% of MAIS3+F injury producing FL crashes are like the IIHS SOI, and 10.7% to 19% of all FY crashes are like the Oblique RMDB crash. Applying these to the numbers in Table 4, one would estimate that the two crash modes together address 4.6% to 8.2% of all MAIS3+F head injuries. Similarly, the proportion of all frontal MAIS3+F chest injuries addressed by the two small overlap or corner tests is estimated to be 6% to 10.6%.

Table 4. Composition of Frontal Sample by Damage Location (Drivers Only)

(From Prasad et al. 2014b)

| Subset #03 Drivers | Sample Counts | | % Composition by GAD1/SHL1 | | | | | |
|---|---|---|---|---|---|---|---|---|
| | | | Head/Face AIS>=3 | | Chest AIS>=3 | | Fatality or MAIS>=3 | |
| GAD/SHL1 | Unweighted | Weighted | Unweighted | Weighted | Unweighted | Weighted | Unweighted | Weighted |
| FC | 273 | 91,581 | 2.4% | 3.4% | 3.3% | 1.7% | 3.0% | 1.6% |
| FD | 8,873 | 3,929,359 | 48.1% | 49.9% | 53.7% | 49.7% | 51.2% | 48.3% |
| FL | 2154 | 1,066,113 | 17.4% | 11.0% | 12.7% | 15.1% | 13.8% | 16.4% |
| FR | 1739 | 976,964 | 6.1% | 12.9% | 5.0% | 6.9% | 5.4% | 7.5% |
| FY | 2586 | 1,137,490 | 20.5% | 15.9% | 16.3% | 19.4% | 17.5% | 17.6% |
| FZ | 2187 | 1,122,328 | 5.5% | 7.0% | 9.0% | 7.3% | 9.1% | 8.6% |
| **All** | **17,812** | **8,323,834** | **100.0%** | **100.0%** | **100.0%** | **100.0%** | **100.0%** | **100.0%** |

The MAIS3+F head, chest and overall are shown in Table 5 for the driver. These rates are for frontal crashes in which the damage extent is between 3 to 6 which is the range of extent of frontal damage produced in the regulatory and public domain tests (IIHS 40% and 25% Overlap, the NCAP and RMDB Small Overlap tests). Examination of Table 5 shows that the head injury rate in highest in FD crashes and lowest in the FR and FL crashes. Similarly, the chest injury rate is highest in the FD crashes and lowest in the FR and FL crashes.

Table 5. Frontal Injury Rates by Damage Location Drivers only/ CDC Damage Extents: 3 to 6
(From Prasad et al, 2014b)

| Subset #03 Drivers CDC Exts: 3-6 | Sample Counts | | Injury Rates ( % ) | | | | | |
|---|---|---|---|---|---|---|---|---|
| | | | Head/Face AIS>=3 | | Chest AIS>=3 | | Fatality or MAIS>=3 | |
| GAD/SHL1 | Unweighted | Weighted | Unweighted | Weighted | Unweighted | Weighted | Unweighted | Weighted |
| FC | 82 | 11,538 | 4.88% | 1.08% | 15.85% | 4.14% | 32.93% | 8.22% |
| FD | 1,528 | 262,248 | 5.82% | 2.09% | 13.74% | 5.32% | 32.79% | 14.36% |
| FL | 872 | 350,921 | 1.83% | 0.19% | 3.44% | 1.15% | 12.50% | 2.97% |
| FR | 732 | 397,919 | 0.96% | 0.12% | 1.91% | 0.41% | 6.56% | 1.13% |
| FY | 595 | 139,669 | 7.90% | 1.86% | 11.76% | 2.53% | 33.61% | 10.53% |
| FZ | 367 | 110,873 | 1.91% | 0.44% | 8.17% | 1.33% | 22.62% | 5.56% |
| **All** | **4,176** | **1,273,167** | **4.07%** | **0.77%** | **8.79%** | **1.97%** | **23.18%** | **5.84%** |

## DISCUSSION

A historical review of various studies aimed at examining the real world relevance of frontal corner crashes as represented by the IIHS 25% overlap and the NHTSA RMDB test conditions has been presented. The estimated proportion of serious-to-fatal injuries addressed by the corner impacts varies substantially depending on the sampling scheme of the different datasets studied and reported. Some studies in Europe show high proportions of fatal frontal crashes that could be explained by the small overlap tests and some show very little if any. In the US, NASS-CDS is a nationally representative accident sampling scheme from which the field relevance of these crashes can be estimated for the US. Towards this end, the authors of this paper have estimated the frequency of occurrence and the proportion of frontal crash injuries addressed by the tests simulating frontal corner impacts. The estimates are similar to those by other authors who have attempted to estimate the frequency of occurrence of these crashes and the population affected by them using the NASS-CDS database.

### Comparison of the Results With Current Test Data

The results shown in Table 5 indicate good correlation with the results of the IIHS 25% overlap tests. Prasad et al. (2014a) have reported their analysis of the 25% overlap IIHS crash test data that indicate head and chest injury risks predicted by dummy responses to be low but lower extremity injury responses to be higher than those observed in the 40% overlap tests. The NHTSA tests also indicate lower extremity injuries in the RMDB tests to be important. However, very little data with the THOR dummy exist in other frontal crash modes to evaluate the relative importance of the RMDB tests conducted so far. Based on the analysis of Samaha et al. the corner tests (IIHS and the RMDB tests together) potentially address slightly less than 10% of all AIS3+ lower extremity injuries. When the limited existing test data from the RMDB tests are examined, the projections from the tests do not agree with the field data as analyzed in this report or others by Prasad et al. (2014b), Samaha et al., Sullivan et al. and Scullion et al.. The serious head injury risks predicted by the dummy responses are substantially higher than those observed in the field. This prediction is traced to be due to the utilization of the new rotational injury criteria, BrIC (Takhounts et al.), to predict head injury risk in the tests. The brain injury risk

predicted by the dummy head responses for the passenger in driver-side RMDB tests are substantially over-predicting head injury risks. As discussed earlier in this paper, only six serious head injuries were identified in all serious injury producing FY crashes and all were to females and some were in multiple event crashes. Similarly, chest injury of passengers in FY type of corner crash appears to be an issue with elderly females (average age 65+ years) with injury source identified as the belt system. In the RMDB tests, the dummy kinematics is such that it slips out of the belt. This slipping out of the shoulder belt is not supported by the field data. It is not clear if the passenger dummy kinematics is due to artifacts of the dummy design, the RMDB or the initial test conditions.

## CONCLUSIONS

1. The frontal corner impacts as represented by the 25% Small overlap frontal and the Oblique RMDB tests together address slightly less than 9% of all frontal crashes and 6% to 12% of all MAIS3+F injuries to the drivers in these crashes.

2. The two crash modes together address 4.6% to 8.2% of all MAIS3+F head injuries. Similarly, the proportion of all frontal MAIS3+F chest injuries addressed by the two crash modes or corner tests is estimated to be 6% to 10.6%.

3. The available data for the passenger involved in driver-side frontal corner crashes indicate that female occupants predominantly incur serious head and chest injuries. All, except one, injured passengers were females. The average age of injured females who had chest injuries was slightly over 65 years.

4. Injury risks in far-side frontal corner crashes are lower than those in near-side frontal corner crashes.

5. The field data do not support the RMDB test data in terms of predicted head injury risks and observed kinematics of the passenger dummy in far-side frontal crashes.

## REFERENCES


Bean, J., Kahane, C. K., Mynatt, M., Rudd, R. W., Rush, C. J. and Wiacek, C. (2009), Fatalities in Frontal Crashes Despite Seat Belts and Air Bags- Review of All CDS Cases- Model and Calendar Years 2000-2007 – 122 Fatalities. Report No. DOT HS 811 102. US DOT, Sept. 2009.

Kuehn, M., Hummel, T. and Bende, J., Small-Overlap Frontal Impacts Involving Passenger Cars, Paper No. 13-0370, ESV Conference, 2013.

Lindquist ,M., Hall ,A., and Björnstig ,U. (2003), Real world car crash investigations — A new approach. IJCrash. (4) 375-384. 2003.

Lindquist, M., Hall, A. and Bjornstig (2004), Car Structural Characteristics of fatal frontal crashes in Sweden, IJCrash, 2004 Vol 9.

Morgan, R. M., Cui, C., Marzougi, D., Digges, K. H., Cao, L. and Kan, C-D (2012), Frontal Pole Impacts, Proc. IRCOBI Confc., 2012.

Morgan, R. M., Cui, C., Digges, K. H., Cao, L. and Kan, C-D. (2012), Impact and Injury Patterns in Between-Rails Frontal Crashes of Vehicles with Good Ratings for Frontal Crash Protection, Proc. 56th AAAM Conference, 2012.

Becky C. Mueller, Andrew S. Brethwaite, David S. Zuby, Joseph M. Nolan (2014), Structural Design Strategies for Improved Small Overlap Crashworthiness Performance, Stapp Car Crash Journal, Vol. 58, 2014.

Planath, I., Norin, H., and Nilsson, S., Severe Frontal Collisions with Partial Overlap - Significance, Test Methods and Car Design, SAE Technical Paper 930636, 1993.

Planath-Skogsmo, I. and Nilsson, R., Frontal Crash Tests – A Comparison of Methods," SAE Technical Paper 942228, 1994,

Prasad, P., Dalmotas, D., and German, A. (2014b), The Field Relevance of NHTSA's Obliqoue Research Moving Deformable Barrier Tests, Stapp Car Crash Journal, Vol. 58, 2014.

Prasad, P., Dalmotas, D., and German, A. (2014a), An Examination of Crash and NASS Data to evaluate the Field Relevance of IIHS Small Offset Tests, SAE 2014-01-1989, SAE International Journal of Transportation Safety, July 2014.
Rudd, R. W., Bean, J., Cuentas, C., Kahane, C. J., Mynatt, M. and Wiacek, C. (2009), A Study of the Factors Affecting Fatalities of Airbag and Belt Restrained Occupants in Frontal Crashes, Proc. ESV Conference, 2009.
Rudd, R. W., Scarboro, M., Saunders, J. (2011), Injury Analysis of Real-World Small Overlap and Oblique Frontal Crashes, Proc. ESV Conference, 2011.
Samaha, R, R., Prasad, P., and Nix, L. (2013), Opportunities for Injury Reduction in US Frontal Crashes: An Overview by Structural Engagement, Vehicle Class, and Occupant Age, Stapp Car Crash Journal, Vol. 57, 2013.
Saunders, J. and Parent, D. (2014), Update on NHTSA's Oblique Research Program, SAE 2014 Government Industry Meeting, NHTSA Website, Public Meeting, http://www.nhtsa.gov/Research/Public+Meetings/SAE+2014+Government+Industry+Meeting.
Saunders, J., Craig, M. J. and Suway, J. (2011), NHTSA's Test Procedure Evaluations for Small Overlap/Oblique Crashes, Proc. ESV Conference, 2011.
Saunders, J., Craig, M. and Parent. D. (2012), Moving Deformable Barrier Test Procedure for Evaluating Small Overlap/Oblique Crashes, SAE World Congress, Paper No. 2012-01-0577, 2012.
Saunders, J. and Parent, D. (2013), Repeatability of a Small Overlap and an Oblique Moving Barrier Test Procedure, SAE World Congress, Paper No. 2013-01-0762, 2013.
Saunders, J. and Parent, D. (2013), Assessment of an Oblique Moving Deformable Barrier Test Procedure, Paper No.: 13-0402, 23rd ESV Conference, Seoul, Korea, 2013.
Scullion, P., Morgan, R. M., Mohan, P., Kan, C-D, Shanks, K., Jin, W. and Tangirala, R. (2010), A Reexamination of the Small Overlap Frontal Crash, Proc. 54th AAAM, 2010.
Scullion, P., Morgan, R. M., Digges, K. H. and Kan, C-D (2011), Frontal Crashes Between the Logitudinal Rails, Proc. ESV Conference, 2011.
Sullivan, K., Henry, S. and Laituri, T. R. (2008), A Frontal Impact Taxonomy for USA Field Data, SAE 2008-01-0526.

**ACKNOWLEDGEMENTS**

The authors would also like to acknowledge the support of the Alliance of Automobile Manufacturers who funded this study.

# A SEMI-ANALYTICAL APPROACH TO IDENTIFY SOLUTION SPACES FOR CRASHWORTHINESS IN VEHICLE ARCHITECTURES

**Lailong Song**
**Johannes Fender**
BMW Group, Research and Innovation Center
Germany

**Fabian Duddeck**
Technische Universität München
Germany

Paper Number 15-0183

## ABSTRACT

In an early design phase for vehicle crashworthiness, the use of classical optimization is limited. One reason for this is that development of structural components is distributed over different departments. Additionally, crash performance depends on several components and their interaction. Common components in vehicle architectures are subject to various load cases in multiple vehicles. Thus, the entire vehicle architecture has to be considered during optimization. In order to enable distributed development the system needs to be decoupled, which means that a variation in one component does not require modifications of other components in order to reach the global structural performance goal.
The objective of this paper is to introduce a method to define the component-wise force-deformation requirements of vehicle architectures for front crash structure design. The force-deformation properties of the components are subject to constraints, from which an analytical description of the design space of the vehicle architecture is derived. The optimal orthogonal solution space within this design space is identified via optimization process. This results in maximal intervals for variations of the component forces over their deformations under the given boundary conditions. The validity of the solution space is proven through explicit FE simulation.

## INTRODUCTION

### 1.1 Load Case (USNCAP)

In 1978, the U.S. National Highway Traffic Safety Administration (NHTSA) introduced the crash test to evaluate the crashworthiness of the vehicles on market. This result is published in the U.S. New Car Assessment Program (USNCAP). One of the test scenarios is a vehicle impact against a fixed rigid barrier with 56km/h. Two dummies, which are protected by the restrain system, are seated in the front seats. The injury criteria are assessed based on the data collected during the crash by the dummies.
In vehicle crashworthiness design, the system is decomposed into two main sub-systems: vehicle structure system and restraint system. The analyse on the vehicle structure response, which is fundamental to the occupant protection, is the primary focus in this paper.

### 1.2 Structure Design

The crash relevant components are designed to absorb the kinetic energy of the vehicle by plastic deformation. These components usually form several parallel load paths going through the front structure of the vehicle in driving direction. During the deformation of the load paths, the **acceleration at the B-pillar** must not exceed the critical value. The B-pillar acceleration is correlated with the dummy acceleration, which is restricted by the injury criteria (Huang, 2002). Furthermore, the compartment deformation is constrained to prevent the occupants from crushing and penetration injury. The **firewall intrusion** is considered as a measurement of the severity of the compartment deformation in front crash. In addition to the dummy protection, the **number of the affected components** depending on the crash velocity is considered due to the structural reparability and reusability.

### 1.3 The Vehicle Cluster within Architecture

For economical reasons, the vehicle are desired to share as many components as possible. The vehicles are grouped into one cluster if they are coupled in the following ways:

**Direct coupling:** When several vehicles share common components, they are directly coupled. (shown in Figure 1)

**Indirect coupling:** The indirect coupling denotes the situation, in which several vehicles don't have common components. Nevertheless they have common components with the same vehicle(s) as shown in Figure 1.

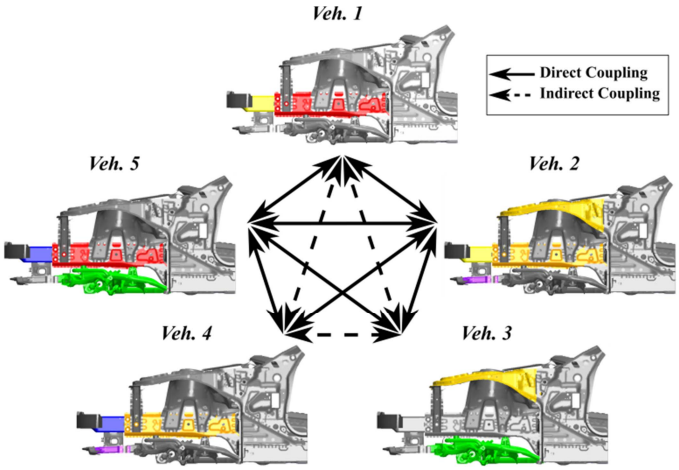


***Figure 1. The coupling relation of a cluster with five vehicles.***

The common components, which are assembled in different vehicles, must fulfill the functional requirements of each vehicle respectively. The design of common components is difficult if the mass distribution and feasible deformable lengths of the vehicles vary. Therefore, an approach to coordinate the local requirements from all the individual vehicle structures into one requirement for the component design should be established. These requirements defined in early phase can guide the later component design.

### 1.4 Simplified Modeling

The simplified model can be used to derive the functional requirement of the original structure effectively in the whole vehicle design process.
One prominent approach to simplify the structure is the lumped mass-spring (LMS) model. It was introduced by Kamal in the early 1970s. The frontal structure of the vehicle is represented one-dimensionally by masses and springs. This model delivers acceptable results seeing that the main features of the structure behavior in the crash are captured (Kamal, 1970). However, the characteristics of the springs must be collected from experiment, which limits the applicable field of the approach. Based on this, Ni and Song built a new model, in which the springs are substituted by shell and beam. This frame structure is analyzed by the finite element simulation to identify its behavior in the crash, based on which a study is conducted to define appropriate force-deformation curves for all the components (Ni & Song, 1986). Lust established a two-phase approach to study the connection between component property and the response of the overall vehicle structure in crash. In the first phase, the force-deformation curve of the component is individually analyzed. The identified force-deformation curve is considered to be scalable regarding the wall thickness of the component. In the second phase, the mass-spring model is built to obtain the overall structural response (Lust, 1992). Due to the increasing demand on the accuracy of the simplified model in prediction, the deviation between static crush test and real dynamic crash load case was put into consideration. Kim developed a mass-spring model for a quasi-static load case (Kim, Mijar, & Arora, 2001).
For the simplified model stated above, if the force-deformation curves of the component are calibrated to achieve the overall structural performance goal in crash, in the further component design process, optimizing the component to match the predefined force-deformation curve is not plausible. On this account, the concept of solution space was

developed by Zimmermann (Zimmermann & von Hoessle, 2013). The simplified model provides intervals for the force-deformation curves. The intervals calculated for all the components form the solution space of component design. This solution space is applied during component design: if the force-deformation curve of the component lies inside the solution space, the entire structure fulfills the expected functional goal. The solution space is identified with two approaches: the stochastic approach requires an FE model for the calibration of a load path model, which has its limitations in the early phase (Zimmermann & von Hoessle, 2013); the analytical approach includes a two-level solution procedure which sometimes over constrains the solution space. When calculating the solution space for vehicle architecture with common components in different vehicles, the analytical approach confronts an over determined system and thus delivers no solution space (Fender J. , 2013).

### 1.5 Vehicle Architectures

In order to minimize the development cost of the vehicle, the concept of the vehicle platform is introduced. A platform denotes a technical basis, on which various vehicle models can be constructed. The platform is also called vehicle architecture. In practice, besides the economical reason, the producers can take more advantage of the concept, e.g. less variant in components, efficient innovation, stronger global standardization and diversity in product (Gonçalves & Ferreira, 2005).
The common parts that make up an automotive platform are: chassis, suspension, steering mechanism and drive train components (WhyHighEnd.com, 2010). Analogously the platform concept is also applied for the corresponding components in Crash. The vehicles, which share the common components in the passive safety design, are grouped in one cluster. The solution spaces for the different vehicles with common components are identified by the stochastic approach based on a simplified load path model. The common components obtain a single functional requirement which fulfills the structural goal in different vehicles respectively.

## ANALYTICAL SOLUTION SPACE

### 2.1 Analytical Solution Space for Single Vehicle

**2.1.1 Basic Concepts** The process of the vehicle structure design is divided into several phases. The V-model shown in Figure 1 illustrates the detailed division of the phases. In the early phase, the package and platform of the new vehicle are decided. Thereby the rough mass distribution and topology are available. The structural parameters are thus extracted.

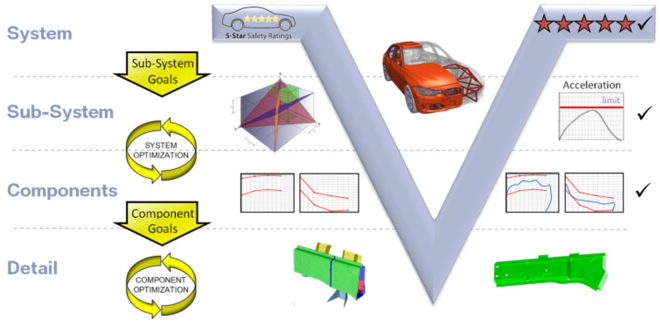


*Figure 2. The process of structure crashworthiness design.* **(Fender J. , 2013)**

**Available deformation length:** The available deformation of the front structure is the primary factor for the energy absorption. The total deformation length can be derived from the length of the frontal structure, the drive type, predefined topology and the firewall intrusion. This information is available and used for crashworthiness design in the early phase.

**Mass:** In the USNCAP front crash test, the impact velocity is predefined. Hence the mass of the vehicle determines the kinetic energy of the system to be dissipated. For the design of frontal structures, the total mass is divided into

two parts. The mass of the rear part of vehicle is concentrated at one point behind the firewall. The mass of the front end is distributed over the structure. Each component is attached with a concentrated mass, this simplification is proved to maintain the sufficient accuracy (Fender, Duddeck, & Zimmermann, 2014).

**The geometry space and deformation space:** The vehicle structure can be modeled using surrogate elements and concentrated mass points. In the symmetric front-crash, since the dominant momentum change happens in the driving direction (x direct), only the resistance forces in this direction are taken into consideration. The deformation conjugated to the force regarding energy is thus the deformation in x-direction. The maximal deformable length of the component is estimated in the early design phase. When integrated into the structure, the components are blocked often by rigid devices in between. In order to predict the actual available deformation of each component, a geometry space is first built up. The deformation space, which is significant for kinetics and energy absorption, is constructed by trimming the geometry space. Sections are inserted where a mass point or an ending of the component are met. The shortest load path is the bottle neck of the feasible deformation of the structure as shown in Figure 3.

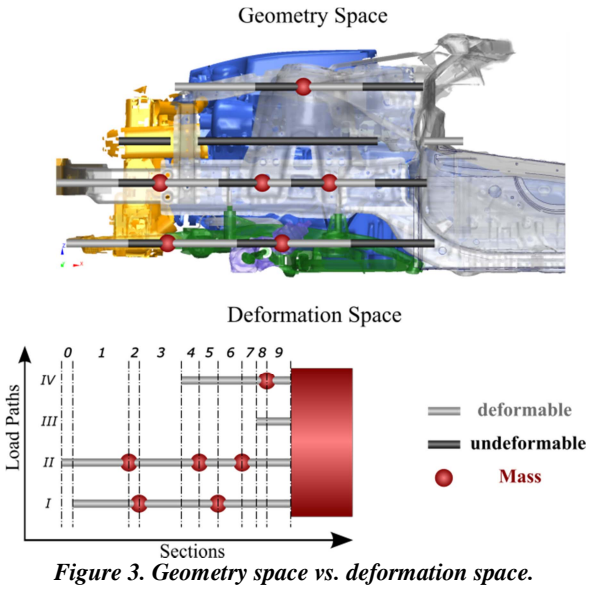


***Figure 3. Geometry space vs. deformation space.***

**2.1.2 Constraints** As discussed in section 1.2, three criteria are defined, in order to describe the performance of the structure in crash. In this section, the functional constraints are discussed based on information included in the deformation space.

**Critical acceleration:** The acceleration of the vehicle compartment is evaluated section wise in the deformation space. Therefore, the critical acceleration gives out the critera on the force levels in components:

$$a_i = \frac{F_i}{M_{act,i}} \leq a_{crt.i} \qquad (1).$$

In which $F_i$ is the sum of the axial resistant forces of all parallel load paths in section $i$. $M_{act,i}$ is the sum of the masses whose velocities are bigger than zero. This results in a system with $N$ inequalities. $N$ is the number of the sections of the system. If the acceleration in each section is smaller than the critical value, the structure fulfills the acceleration criterion.

**Firewall intrusion:** The criterion on the maximal firewall intrusion is satisfied if the velocities of all the mass point are null, before the feasible deformation is totally used up. In the deformation space, this condition can be described thusly:

In section $i$:

$$\int F_i(u)du \geq \frac{1}{2}M_{act,i}v_i^2 - \frac{1}{2}M_{act,i}v_{i+1}^2 \quad (2).$$

In which,
$F_i(u)$ : is the sum of the axial force from all the components in section $i$ over $u$
$u$ : is the deformed length of section $i$
$M_{act,i}$: is the active mass of section $i$
$v_i$: is the velocity of the structure when the section $i$ starts to deform
The final velocity of the previous section and the initial velocity of the subsequent section are the same. And the velocity of the compartment should be zero after the last section in front structure deforms. In consequence, when the inequalities are summed up section wise, the terms with the intermediate velocities are eliminated, which yields the inequality:

$$\sum_{i=0}^{N} \frac{\int F_i(u)du}{M_{act,i}} \geq \frac{v_0^2}{2} \quad (3).$$

If Eq. (3) is fulfilled, the firewall intrusion is restricted.

**The order of deformation:** If the impact velocity is relatively low, it is not necessary to absorb energy by collapsing all the components. Moreover, the successive deformation behavior mitigates the dependencies of the components. On this account, the order of deformation criterion requires that:

$$F_1(u_1) - M_1 a(u_1) \leq F_2(u_2 = 0) \quad (4).$$

The indices represent the component 2 locates after component 1 in the same load path.
Up to here, the three constraints for the force-deformation curve of each component are introduced based on the information in deformation space.

**2.1.3 The Concept of Solution Space** One of the basic goals for the passive safety design in the early phase is to set up the expected force-deformation characteristic for the components. However this goal is ambitious because of the limited available information.
Zimmermann established an approach to find out a robust, compatible and flexible guideline for the component design. The fundamental concept can be explained in an example with a primitive deformation space, shown in Figure 4. The three boundary conditions are applied onto the axial resistance force of the components. The feasible field of designs is the triangle, in which the optimal design $A$ is located. The optimum offers not only the lowest acceleration but fulfills the firewall intrusion and order of deformation constraints as well. However, this design is neither robust nor independent, i.e. If $F_1$ is changed, the design may violate the constraints. $F_2$ must be adjusted correspondingly to bring the design back to the feasible field.
The solution space approach creates in this situation a suitable rectangle (a hypercube in high dimensional space) inside the design space. All the designs inside this solution space fulfill the three constraints. In each dimension, the level of the resistance forces is restricted by an interval. For a component with several sections, the intervals form a corridor for the force-deformation curve of the component.
Inside the solution space, the change of the resistance force level in one dimension doesn't lead to constraint violations in other dimensions, which means that the change of force level in one component doesn't require the adaption of the others to fulfill the overall structural requirments.
With the solution space concept, the passive safety design in early phase can be transformed into the problem: calculate the solution space of the structure; i.e. identify the corridors for the force-deformation curves of the components. In the component design phase, if the force-deformation curve of individual component locates inside the corridor, the total structure fulfills the three constraints.

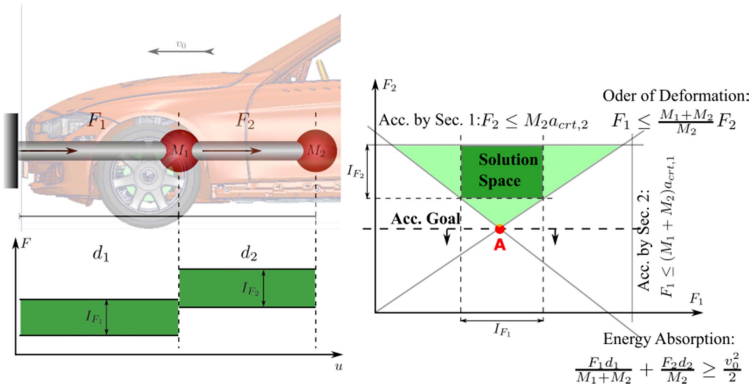


*Figure 4. Solution space of a structure with two components.* (**Zimmermann & von Hoessle, 2013**)

## 2.2 Solution Space for One Cluster within Vehicle Architecture

If the components have identical length and concentrated mass in the geometry space, these components can in principle be defined as common components. However, the commonality is in reality based on more criteria from other disciplines. Therefore, the common components are manually pre-defined.

**2.2.1 Construction of the Coupled Deformation Spaces** The common components are marked with the same name in the deformation space. The relationships are managed using a mapping. The structure of the mapping is shown in Figure 5.

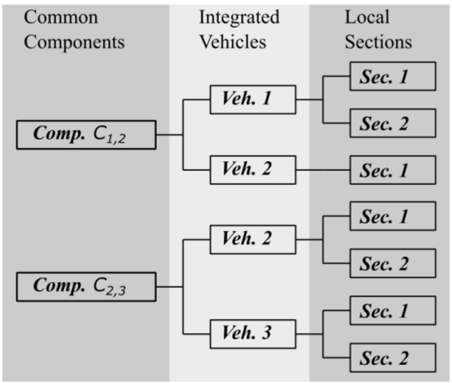


*Figure 5. Mapping list of the vehicle relationship in cluster.*

The force-deformation curve of the component is discretized by sections. As a consequence, the common components, which share the same corridor, must have the same section discretization. In another words, the section division of common components should have identical distances and count. For this reason, the artificial sections are inserted into the deformation spaces to synchronize the section division of the common components. For instance, three deformation spaces with common components are synchronized in the following way:

**a. Independent construction of the deformation space**

As shown in Figure 6 in step I, the three deformation spaces are built independently for each structure. The building process is the same as for single structure – sections are inserted where a mass point or an ending of the component are met.

**b. Consecutive synchronization of sections for each component**

The new artificial sections are inserted, so that the common components have the identical section division as shown in Figure 6 in step II and III. Since the sections are transversely through all parallel load paths, the parallel components are affected as well. This synchronization leads to a finer discretization for the deformation space. When the common components have comparable relative spatial positions among structures, the section count for the common components converges. Important positions (mass point and ending of component) within the spatial range of the common components are eventually marked with section bounds. In the case of a cluster with *N*

vehicles, each has $p_i$ components and $q_i$ mass points, the synchronization converges before maximal $\sum_{i=0}^{N}(p_i + q_i)$ iterations.

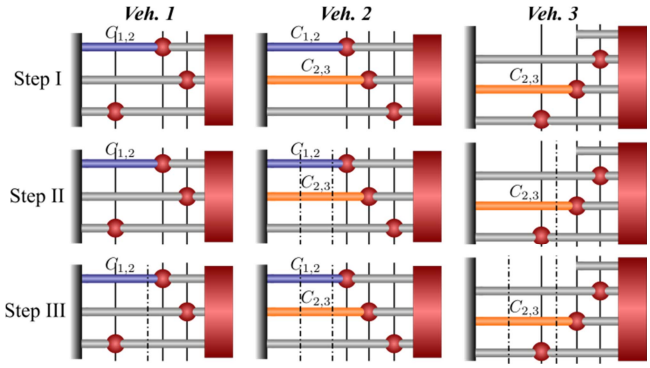


***Figure 6. Artificial sections are inserted to synchronize the deformation spaces.***

### 2.3 Solution Space Identification

The goal of this solution process is to find the largest possible solution space in the design space, which is described by the three constraints. The notations used in the solution process are the following:
$F_{u(pper),ij}/F_{l(ower),ij}$ : the upper and lower boundaries of the force interval in section $i$, load path $j$.
$M_{ij}$ : the value of the mass point at section $i$, on load path $j$.
$M_{act,i}$ : the active mass when the system deforms till section $i$.
$d_i$ : the length of the section $i$.
$a_{crt,i}$ : the critical acceleration of the section $i$.
$v_0$ : the initial velocity of the vehicle

**2.3.1 Constraints** The upper and lower boundaries of the intervals are the unknowns to be identified in the solution process. Suppose that the system has N sections and M load paths. The constraints for an optimization problem can be formulated as follows:
The upper boundaries of force-deformation curves in each component should satisfy the inequalities for critical acceleration:

$$\sum_{j=1}^{M} F_{u,ij} \le M_{act,i} \cdot a_{act,i} \qquad (5).$$

The lower boundaries of force-deformation curves in each component should satisfy the equalities Eq. (6) w.r.t. the energy absorption criterion:

$$\sum_{i=1}^{N}\left(\sum_{j=1}^{M} F_{l,ij}\right)\frac{d_i}{M_{act,i}} = \frac{v_0^2}{2} \qquad (6).$$

The order of deformation between components in the same load path applies constraints between the upper and lower boundaries of the intervals. If a component ends at section $i$, the constraint is:

$$F_{u,ij} - \frac{M_{ij}}{M_{act,i}}\sum_{j=1}^{M} F_{u,ij} \le F_{l,(i+1)j} \qquad (7).$$

These constraints are applied to the intervals of the force-deformation curves for each vehicle structure in the cluster. Among the vehicles, extra equalities are needed to ensure the identical corridors for common components. For instance, components $C_A$ and $C_B$ are common in deformation spaces $D_A$ and $D_B$, which are built from the structure of vehicle $A$ and $B$ respectively. $F^A_{u,ij}$, $F^A_{l,ij}$ are the upper and lower boundaries of the force intervals for $C_A$ in $D_A$ with the section set $I_A$ while $F^B_{u,mn}$, $F^B_{l,mn}$ are the boundries of the force interval for $C_B$ in $D_B$ with the section set $M_B$. The section set $I_A$ and $M_B$ have an offset $\delta$, i.e. $I_A = M_B + \delta$. The commonality requires that:

$$F^A_{u,ij} \equiv F^B_{u,(i+\delta)n}\ , F^A_{l,ij} \equiv F^B_{l,(i+\delta)n}\quad \forall i \in I_A \cap \{M_B + \delta\} \qquad (8).$$

**2.3.2 Objective Functions** Under these constraints, the optimal values of the upper and lower boundaries are calculated by quadratic programming. The objective function is defined as follows:

**Width of the corridor**: In the application, it is more flexible to design the component with wider corridor for the force-deformation curve. Thus, the largest solution space is desired within the design space. The closer the corridor boundaries approach to the constraints, the wider the corridors are. In order to maintain the convexity of the optimization problem, the objective function is formulated with sum of squares (SoS).
The widths of the corridor for different components are controlled by a weighting factor. This is practical, when the force-deformation behavior of one component is easier to control (e.g. crushing component) than that of another component (e.g. buckling component). Thus, the widest corridor is achieved by finding the minimum of Eq. (9).

$$\text{min.} \quad \Psi = \sum_{i=0}^{N} \left[ \left( \sum_{j=0}^{M} \omega_{ij} \right) \left( \sum_{j=0}^{M} F_{u,ij} - M_{act,i} \cdot a_{crt,i} \right)^2 \right] \tag{9}$$

In which $\omega_{ij}$ denotes the weighting factor of the corridor segment at section i and load path j .

**Smoothness of the corridor:** If dramatic overshootings exist in the corridor, it is difficult to design the force-deformation curve of the component to fulfill the corridor. Therefore, the smoothness of the corridor should be tuned to reduce the complexity of the engineering work. For component $C_k$ with $S$ corridor segments, the objective function for corridor smoothness is written as:

$$\text{min.} \quad \phi_k = \frac{1}{S-1} \sum_{i=1}^{S} \left( F_{m,ij} - \bar{F}_M \right)^2 \tag{10}$$

In which $\bar{F}_M = \frac{1}{S} \sum_{i=1}^{S} \left( F_{u,ij} + F_{l,ij} \right)/2$. $\Phi$ is the sum over the objective functions of each corridor.

**Uniform distribution of the corridor widths:** The force-deformation curve to be designed may not fulfill an extreme narrow corridor. Therefore, the widths of the corridors should be be as uniform as possible. If the influence of the pre-defined weighting factors is eliminated, the objective function is formulated to minimize the variation of the corridor widths:

$$\text{min.} \quad \Theta = \frac{1}{D-1} \sum_{i=1}^{N} \sum_{j=1}^{M} \left( \frac{F_{u,ij} - F_{l,ij}}{\omega_{ij}} - \overline{\Delta \mathrm{F}} \right)^2 \tag{11}$$

In which $\overline{\Delta F} = \frac{1}{D} \sum_{i=1}^{N} \sum_{j=1}^{M} \left( F_{u,ij} - F_{l,ij} \right)/\omega_{ij}$ , and $D$ is the number of corridor segments.
As a concequence, the solution process is transferred into a multi-objective optimization problem. The overall objective function is built by weighted sum of the sub-objective functions Eq. (9-11):

$$\text{min.} \quad \Sigma = \Omega_{\mathrm{w(idth)}} \cdot \Psi + \Omega_{s(moothness)} \cdot \Phi + \Omega_{d(istribution)} \cdot \Theta \tag{12}$$

The objective function is formed by SoS and therefore semi-positive definit.The equality and inequality constraints are linear. As a result, a unique optimum of this convex problem can be found by interior point method (IPM) (Nocedal & Wright, 2006) (Vandenberghe, 2010).

## RESULTS

### 3.1 Solution Space Calculation

The upper and lower boundaries of the force interval in each section and load path are packed into the solution vector $\vec{x} = [F_{l,ij}, F_{u,ij}]^T, i \in [0, N], j \in [0, M]$ . This solution vector is obtained by solving the quadratic optimization problem:

$$\min. \quad \vec{x}^T H \vec{x} + b^T \vec{x} \qquad (13).$$

under the equality and inequality constraints. In which $H$ is the Hessian matrix of Σ and $b$ is the first derivative of Σ. Tuning the weighting factor of the sub-objective functions leads to different optimal solution spaces as shown in Figure 7.

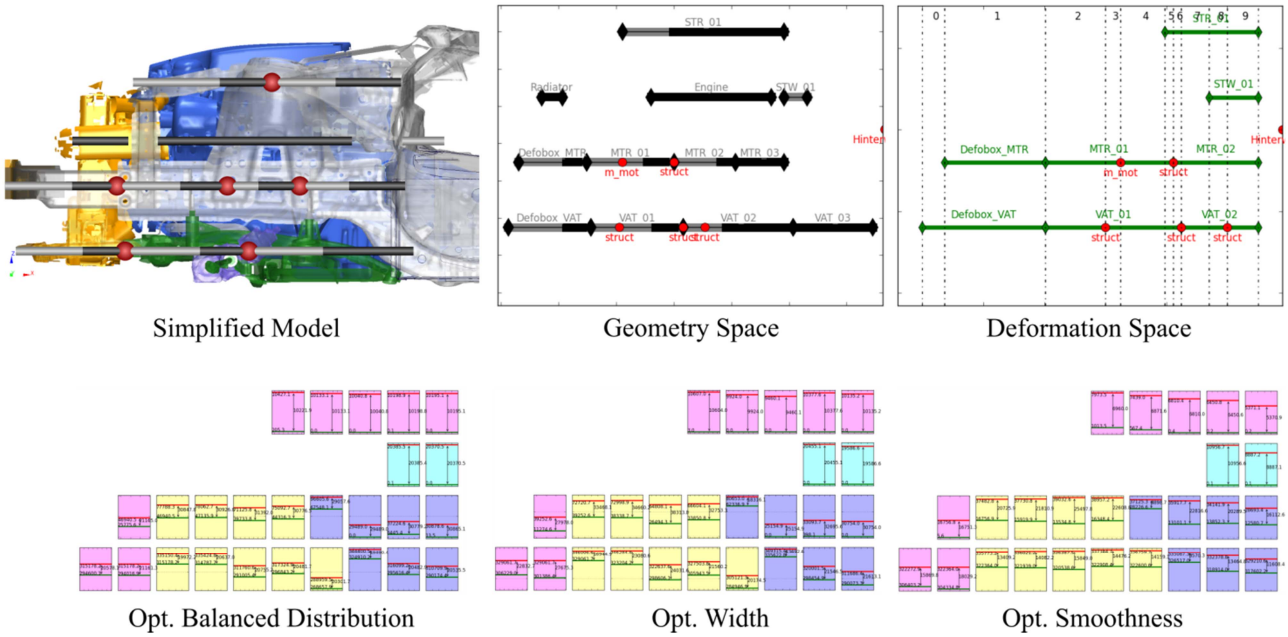


***Figure 7. Calculation of the solution space concerning different applications.***

A solution of the cluster is shown in Figure 8, which shows that the common components (marked with red and green respectively) integrated in different vehicles are constrained with the identical corridors. For each vehicle, the deformation spaces before and after synchronization are shown on the left in Figure 8.

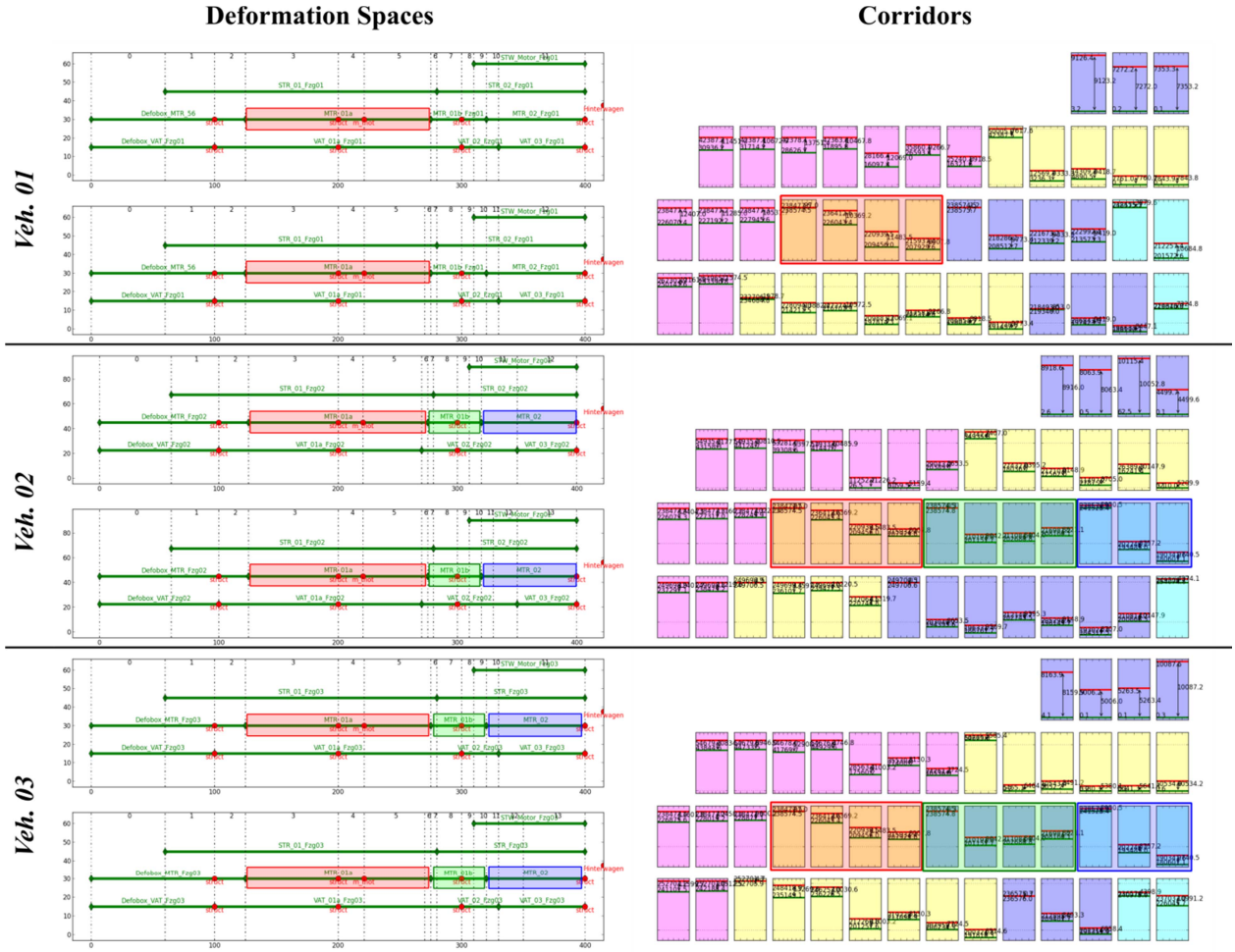


*Figure 8. Corridor calculation for vehicle cluster.*

### 3.2 Validations of the Component Functional Goals

In order to validate the method, a simplified FE model is constructed. The structure with four thin-wall components is crashed against a rigid barrier. The acceleration of the mass at the back of the structure is constrained. The solution space of the structure is calculated with the method stated above. In the initial design, the force-deformation curve of the last component violates its corridor; the acceleration of the mass exceeds the critical value as shown in Figure 9. In order to fulfill the goal of structural design, the component is modified (e.g. variation in wall thickness, introduction of beads and holes) to yield a force-deformation response which lies inside its corridor. The acceleration goal is subsequently achieved as shown in Figure 9.

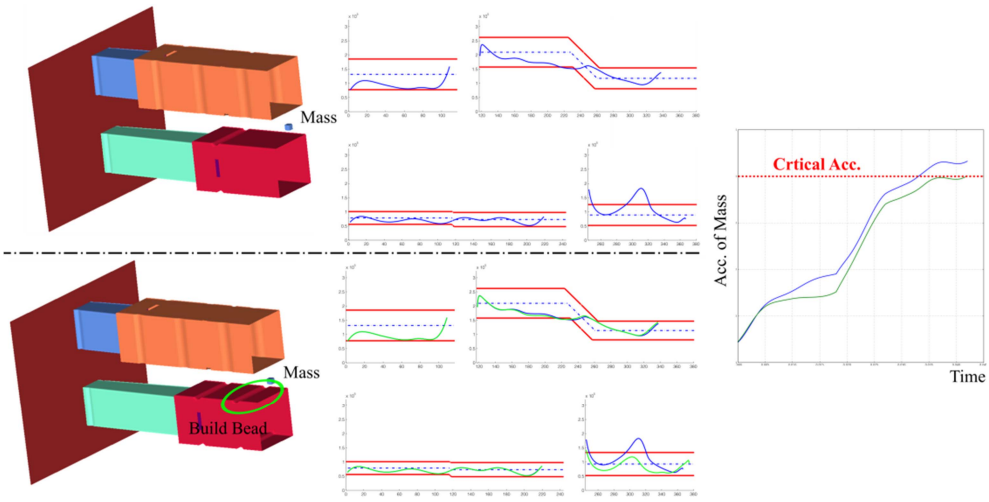


***Figure 9. Component design based on corridors.***

## CONCLUSIONS

The solution space of the vehicle cluster is described analytically and identified through the numerical optimization. The approach can be used to decouple the design of the components while maintaining the commonality of the vehicle architecture. This solution space provides each component an interval for force-deformation responses. These intervals as the functional goals, compared with a single curve, ensure more flexibility for the component design.

With the solution process established in this work, the features of the solution space can be adjusted by tuning the weighting factors in Eq. (12) in order to minimize the effort of the structural optimization in component design.

As a conclusion, this approach can serve the V-model design process by establishing the functional goals for individual components within vehicle architecture.

## REFERENCES

Fender, J., Duddeck, F., & Zimmermann, M. (2014, Vol. 49 No. 3). On the Calibration of Simplified Vehicle Crash Models. *Structural and Multidisciplinary Optimization*, pp. 455-469.

Gonçalves, A., & Ferreira, N. (2005). *Automobile Front-end Structure: Modularity and Product Platform.* Instituto Superio Técnico: tech. rep.

Graff, L. (2013). *A Stochastic Algorithm for the Identification of Solution Spaces in High-dimensional Design Spaces.* Philosophisch-Naturwissenschaftlichen Fakultät der Universität Basel: Doctoral Dissertation.

Huang, M. (2002). *Vehicle Crash Mechanics.* CRC Press LLC.

Kamal, M. M. (1970, Feb.). Analysis and Simulation of Vehicle to Barrrier Impact. *SAE Paper No. 700414.*

Kim, C., Mijar, A., & Arora, J. (2001, vol. 22 no. 4). Development of Simplified Models for Design and Optimization of Automotive Structures for Crashworthiness. *Structural and Multidisciplinary Optimization*, pp. 307-321.

Lust, R. (1992, vol. 4 no. 2). Structural Optimization with Crashworthiness Constraints. *Structure Optimization*, pp. 85-89.

Ni, C. M., & Song, J. (1986, vol. 79). Computer-aided Design Analysis Methods for Vehicle Structural Crashworthiness. *Proc. of Symposium on Vehicle Crashworthiness Including Impact Biomechanics*, pp. 125-139.

Nocedal, J., & Wright, J. (2006). *Numerical Optimization.* Springer.

Vandenberghe, L. (2010). *The cvxopt Linear and Quadratic Cone Program Solvers.* UCLA Engineering Henry Samueli School of Engineering and Applied Science: tech. rep.

WhyHighEnd.com. (2010). Retrieved from Automobile Platform and Platform Sharing: http://www.whyhighend.com/automobile-platform.html

Zimmermann, M., & von Hoessle, J. E. (2013, vol. 94 no. 3). Computing Solution Spaces for Robust Design. *Numerical Methods in Engineering*, pp. 290-307.

# OCCUPANT TRANSPORTATION DECISION ALGORITHM: AN ADVANCED AUTOMATIC CRASH NOTIFICATION ALGORITHM DEVELOPED AND EVALUATED FOR MOTOR VEHICLE CRASH OCCUPANT TRIAGE

**Joel Stitzel, Ashley Weaver, Samantha Schoell**
Virginia Tech-Wake Forest Center for Injury Biomechanics
United States

**Ryan Barnard, Jennifer Talton, R. Shayn Martin, J. Wayne Meredith**
Wake Forest School of Medicine
United States

Paper Number 15-0190

## ABSTRACT

The objective was to develop an Advanced Automatic Crash Notification (AACN) algorithm and evaluate its performance in making optimal occupant triage decisions. The developed AACN algorithm known as the Occupant Transportation Decision Algorithm (OTDA) uses measurements obtainable from vehicle telemetry to predict risk of overall occupant injury and recommend a transportation decision for the occupant following a motor vehicle crash (MVC), particularly whether transport to a Level I/II trauma center is recommended. A list of injuries necessitating treatment at a Level I/II trauma center (TC) was determined using an injury-based approach based on three facets (severity, time sensitivity, and predictability). These three facets were quantified for each injury from expert physician and emergency medical services (EMS) professional opinion and database analyses of the National Trauma Data Bank and National Inpatient Sample. Severity, Time Sensitivity, and Predictability Scores were summed for each injury to compute an Injury Score. Injuries with an Injury Score exceeding a particular threshold were included on the Master Target Injury List, which is a list of injuries more likely to require Level I/II TC treatment. OTDA inputs for development include the Master Target Injury List and 38,970 National Automotive Sampling System-Crashworthiness Data System (NASS-CDS) 2000-2011 occupants. The OTDA uses multivariate logistic regression to predict an occupant's risk of sustaining an injury on the Master Target Injury List from the following model variables: longitudinal/lateral delta-v, number of quarter turns (in rollover only), belt status, multiple impacts, and airbag deployment.

A parametric OTDA was developed with five tunable parameters allowing for extensive optimization. The OTDA was optimized with a genetic algorithm that compared the OTDA transportation decision for each NASS-CDS occupant to a dichotomous representation of their Injury Severity Score (ISS). Occupants with ISS 16+ should be transported to a Level I/II TC. OTDA optimization minimized under triage (UT) and over triage (OT) rates with the goal of producing UT rates < 5% and OT rates < 50% as recommended by the American College of Surgeons (ACS). For the optimized OTDA, UT rates by crash mode were 5.9% (frontal), 4.6% (near side), 2.9% (far side), 7.0% (rear), and 16.0% (rollover). OT rates by crash mode for the optimized OTDA were 49.7% (frontal), 47.9% (near side), 49.7% (far side), 44.0% (rear), and 49.7% (rollover).

The OTDA was developed with an injury-based approach that examined three injury facets to identify injuries necessitating treatment at a Level I/II TC. Large hospital and survey datasets containing information on injuries, mortality risk, treatment urgency, and hospital transfers were used in conjunction with large crash datasets with crash, vehicle, occupant, and injury data. The OTDA has been rigorously optimized and has demonstrated improved UT rates compared to other AACN algorithms in the literature and OT rates meeting ACS recommendations. Since the OTDA uses only vehicle telemetry measurements specified in Part 563 regulation, this AACN algorithm could be readily incorporated into new vehicles to inform emergency personnel of recommended triage decisions for MVC occupants. The overall societal purpose of this AACN algorithm is to reduce response times, increase triage efficiency, and improve overall patient outcome.

## INTRODUCTION

There are approximately 6.4 million motor vehicle crashes (MVCs) annually in the United States (US) [1]. These crashes killed 33,000 people and injured 3.9 million people in 2010 [2]. Many crashes leave a heavy burden of

morbidity that can affect victims throughout the rest of their lives. While the advent of passive safety standards (seat belts, airbags, etc.) has lowered the morbidity and mortality of motor vehicle crash victims, there are significant barriers to further improvements. Most experts believe that an important future avenue for progress is to improve the trauma triage process, that is, the process whereby patients are given the "right care" at the "right place" at the "right time." Optimizing this process is difficult due to timing, decision making, resources, and access to care.

Advanced Automatic Crash Notification (AACN) has shown promise in improving the trauma triage process by predicting occupant injury severity using vehicle telemetry data to recommend a transportation decision. Event data recorders (EDRs) use electronic sensors in the car to collect crash data and AACN systems can transmit this data to the proper authorities. The 49 CFR Part 563 regulation for EDRs released by NHTSA specifies the data elements required for all vehicles equipped with an EDR [3]. Required data elements include longitudinal delta-v, seat belt status, frontal airbag deployment, and multiple events. The regulation also includes data elements required for vehicles under specified conditions. Data elements for these include lateral delta-v, vehicle roll angle, and side airbag deployment. Using the information collected from a vehicle, the risk of an occupant sustaining an injury can be calculated, and a decision process for determining the level of care for the occupant can be presented to emergency medical personnel. The National Study on the Costs and Outcomes of Trauma (NSCOT) identified a 25% reduction in mortality for severely injured patients who received care at a Level I trauma center rather than at a non-trauma center [4]. AACN technology can provide data on the vehicle location, delta-v, principal direction of force (PDOF), airbag deployment, and the occurrence of rollover or multiple event collisions which may be valuable in estimating the occupant's injury risk following a MVC.

Current AACN algorithms include OnStar and URGENCY which incorporate model variables such as crash direction, delta-v, multiple impacts, belt use, vehicle type, age, and sex [5-11]. Both of these algorithms use Abbreviated Injury Scale (AIS) metrics to define severely injured patients. Although AIS-based metrics are most commonly used, other methods of injury scoring have been developed to better discriminate severely injured patients.

The objective of this study was to develop an AACN algorithm and evaluate its performance in making optimal occupant triage decisions using an injury-based approach. The developed AACN algorithm, known as the Occupant Transportation Decision Algorithm (OTDA), uses measurements obtainable from vehicle telemetry to predict risk of overall occupant injury and recommend a transportation decision for the occupant following a MVC.

## METHODS

An injury-based approach quantifying three facets of individual injuries was developed to improve upon the severity scoring systems and better evaluate the risk of occupant injury. This approach focused on 240 injuries comprising the top 95% most frequently occurring AIS 2+ injuries in the National Automotive Sampling System-Crashworthiness Data System (NASS-CDS) 2000-2011. The injury-based approach identifies injuries requiring Level I/II trauma center (TC) level treatment by quantifying three facets of injury: severity, time-sensitivity, and predictability. Severity is associated with injuries which have a high mortality and high threat-to-life. Severity was scored based on mortality risk ratios (MRRs) obtained from the National Trauma Data Bank (NTDB) [12]. Time Sensitivity is associated with the urgency with which a particular injury requires treatment. Time Sensitivity was scored using expert physician survey data which incorporated the recommended treatment location and a rank of urgency [13]. Predictability is associated with injuries with a propensity to be missed on evaluation at the scene. Predictability was scored using two components: an Occult Score and a Transfer Score. The Occult Score is a measure of the likelihood that an injury is missed using expert survey data from physicians and emergency medical services (EMS) professionals. The Transfer Score is a measure of the likelihood that an injury is present in patients that require transfer from a non-trauma center to a Level I/II TC using the National Inpatient Sample (NIS) database [14]. The scores of each of these facets (Severity, Time Sensitivity, and Predictability) were computed for each of the 240 injuries on the top 95% most frequently occurring AIS 2+ MVC injuries list. Each score was normalized on a zero to one scale in which scores closer to one were more severe, more time sensitive, and less predictable.

The inputs to the OTDA include a Master Target Injury List and NASS-CDS 2000-2011 cases. The Master Target Injury List is determined by multiplying the Severity, Time Sensitivity, and Predictability Scores by a weighting coefficient and then summing these values to produce a Target Injury Score. Injuries exceeding a defined Injury Score Cutoff are then included on the Master Target Injury List. The Master Target Injury List is not a static list and

is capable of being varied in order to optimize the algorithm. An example computation of the Target Injury Score is provided in Figure 1 for an AIS 3 vault fracture. The injury had Severity, Time Sensitivity, and Predictability Scores of 0.73, 0.93, and 0.48, respectively. These scores indicated a severe and time sensitive injury that has moderately high predictability and the Target Injury Score was 2.14. For this example, the weighting coefficients were set to one. However, optimization of the algorithm allows the weighting coefficients to vary as will be explained later.

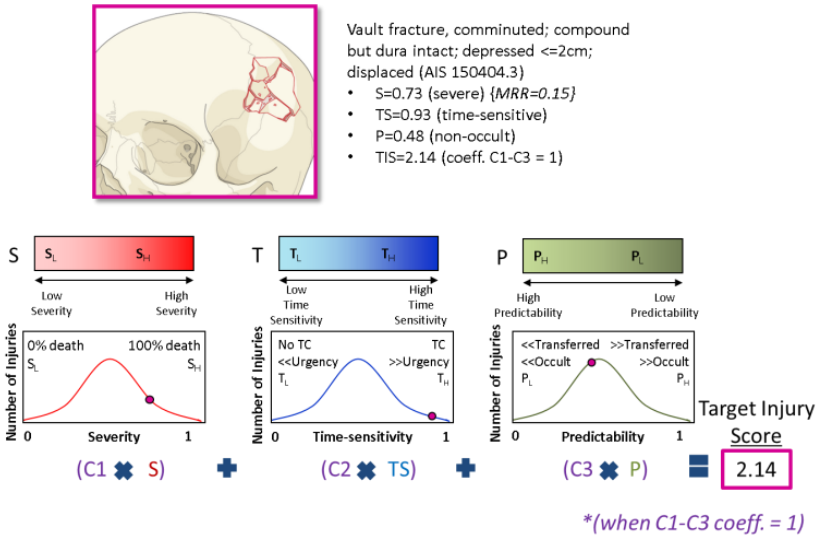


***Figure 1. Example computation of a Target Injury Score for an AIS 3 vault fracture.***

NASS-CDS 2000-2011 cases were used to train and evaluate the OTDA. Cases from NASS-CDS 2009-2011 with a model year greater than 10 years were excluded due to missing injury and occupant information (11,814 distinct occupant IDs excluded). After applying the exclusion criteria, the resulting NASS-CDS 2000–2011 dataset contained 54,703 cases, 94,283 vehicles, 115,159 occupants, and 303,230 injuries.

The OTDA uses multivariate logistic regression to predict the risk of an occupant sustaining an injury on the Master Target Injury List for specified crash conditions. Weighted NASS-CDS 2000-2011 data was used to select frontal, near side, far side, rear, and rollover crashes for driver and front right passengers 16 years and older. Five separate multivariate logistic regression models were created according to crash type: frontal, near side, far side, rear, and rollover crash. For determining the outcome measure, each occupant's injuries were assessed to determine if any one of the injuries was on the Master Target Injury List. If at least one injury appeared on the Master Target Injury List that occupant was coded as sustaining a Target Injury; if none of the occupant's injuries were on the Master Target Injury List, that occupant was coded as not sustaining a Target Injury.

Longitudinal delta-v was used for the frontal and rear models. Lateral delta-v was used in the near side and far side models. EDR correction factors for delta-v were implemented to adjust for differences in the delta-v estimated by WinSMASH in NASS and the delta-v obtained directly from the EDR [15-18]. For the rollover crash type, the number of quarter turns was binned into six categories: 1, 2, 3-4, 5-6, 7-8, 9-17. Any MVC with a quarter turn greater than 1 was categorized as rollover even if it met other crash mode criteria. Models for frontal, rear, and far side were adjusted for belt status, multiple impacts, and frontal airbag deployment. Models for near side and rollover were adjusted for belt status, multiple impacts, frontal and side airbag deployment. The majority of the variables included in the OTDA (longitudinal delta-v, belt status, multiple impacts, and frontal airbag deployment) were selected because they are EDR variables required for all vehicles in the EDR regulation, 49 CFR Part 563 [3]. Lateral delta-v and side airbag deployment were included because of their importance in defining crash severity for side impacts and they are EDR variables required for vehicles under specified conditions in 49 CFR Part 563. Occupants with any missing data for variables of interest were not included in the analysis. The Risk of any Target Injury is calculated with the cumulative distribution function for frontal, rear, and far side in Equation 1 and for near side and rollover in Equation 2. Logistic regression analyses were performed using SAS 9.4 (SAS Institute, Cary, NC) and R 3.0.2 (R Foundation for Statistical Computing, Vienna, Austria).

$$\frac{e^{(\alpha + \beta_1 DV + \beta_2 Belt + \beta_3 AB + \beta_4 MI)}}{1 + e^{(\alpha + \beta_1 DV + \beta_2 Belt + \beta_3 AB + \beta_4 MI)}} \quad \textbf{(1).}$$

where α= intercept, $\beta_1$, $\beta_2$, $\beta_3$, $\beta_4$=parameter coefficients for DV= longitudinal delta-v/lateral delta-v; Belt= belt status (0=no, 1= yes); AB= frontal airbag deployment (0= no, 1=yes); MI= multiple impacts (0= no, 1= yes).

$$\frac{e^{(\alpha + \beta_1 DV + \beta_2 Belt + \beta_3 AB + \beta_4 MI + \beta_5 SAB)}}{1 + e^{(\alpha + \beta_1 DV + \beta_2 Belt + \beta_3 AB + \beta_4 MI + \beta_5 SAB)}} \quad \textbf{(2).}$$

where α= intercept, $\beta_1$, $\beta_2$, $\beta_3$, $\beta_4$=parameter coefficients for DV= lateral delta-v/number of quarter turns; Belt= belt status (0=no, 1= yes); AB= frontal airbag deployment (0= no, 1=yes); MI= multiple impacts (0= no, 1= yes); SAB= side airbag deployment (0=no, 1=yes).

The OTDA features five tunable parameters (termed "Variable Parameters") allowing for extensive optimization. The five Variable Parameters include the Severity Multiplier, Time Sensitivity Multiplier, Predictability Multiplier, Injury Score Cutoff, and a Risk Cutoff. The Severity Multiplier, Time Sensitivity Multiplier, and Predictability Multiplier are the weighted coefficients used to produce the Target Injury Score. The Injury Score Cutoff is the threshold at which an injury is deemed to be included on the Master Target Injury List. The Risk Cutoff is the threshold above which a case is deemed recommended to be sent to a Level I/II TC.

The OTDA was optimized with a Covariance Matrix Adaptation- Evolution Strategy (CMA-ES) genetic algorithm that compared the OTDA transportation decision for each NASS-CDS occupant to a dichotomous representation of their Injury Severity Score (ISS). Occupants with ISS 16+ should be transported to a Level I/II TC. OTDA optimization minimized under triage (UT) and over triage (OT) rates with the goal of producing UT rates < 5% and OT rates < 50% as recommended by the American College of Surgeons (ACS) [19]. OT was assessed using the False Positive Rate (FPR) metric, also known as 1-Specificity [20-22]. This represents the proportion of mildly injured patients that went to a Level I/II TC. UT was assessed using the False Negative Rate (FNR) metric, also known as 1-Sensitivity [20-23]. This represents the proportion of seriously injured patients that did not go to a Level I/II TC. A graphical representation of the OTDA is provided in Figure 2.

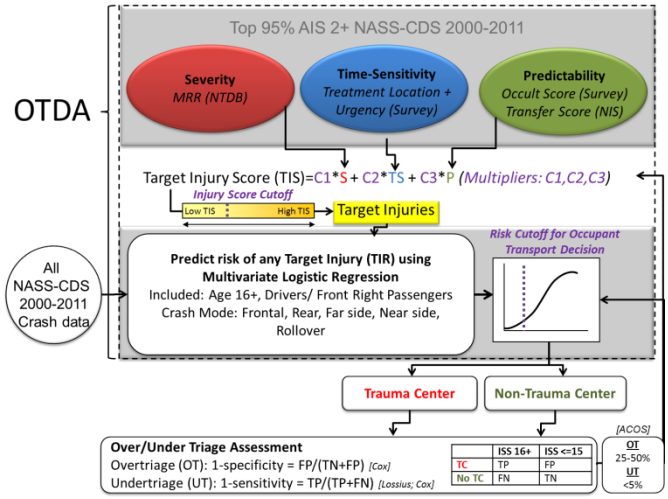


***Figure 2. Overview of OTDA.***

## RESULTS

A total of 38,970 NASS-CDS 2000-2011 cases met the inclusion criteria and the number of cases by crash mode is summarized in Table 1.

**Table 1.**
**Cases meeting inclusion criteria by crash mode.**

| Crash Mode | # of Cases |
|---|---|
| Frontal | 21,273 |
| Rear | 2,667 |
| Far side | 3,608 |
| Near side | 3,890 |
| Rollover | 7,082 |
| Total | 38,970 |

The resulting OT and UT metrics for the optimal Variable Parameters are listed in Table 2.

For the optimized OTDA, UT rates by crash mode were 5.9% (frontal), 7.0% (rear), 2.9% (far side), 4.6% (near side), and 16.0% (rollover). OT rates by crash mode for the optimized OTDA were 49.7% (frontal), 44.0% (rear), 49.7% (far side), 47.9% (near side), and 49.7% (rollover). The UT rates for far side and near side met the 5% ACS recommendation. The OT rates for frontal, rear, far side, near side, and rollover all met the 50% ACS recommendation.

**Table 2.**
**OT/UT metrics by crash mode for the optimal Variable Parameters.**

| Crash Mode | OT Metric (FPR) | UT Metric (FNR) | TP | FP | TN | FN |
|---|---|---|---|---|---|---|
| Frontal | 49.7% | 5.9% | 903 | 10451 | 10312 | 57 |
| Rear | 44.0% | 7.0% | 40 | 1470 | 1154 | 3 |
| Far side | 48.7% | 2.9% | 232 | 1727 | 1642 | 7 |
| Near side | 47.9% | 4.6% | 559 | 1723 | 1581 | 27 |
| Rollover | 49.7% | 16.0% | 871 | 3040 | 3005 | 166 |

## DISCUSSION

The OTDA was developed with an injury-based approach that examined three injury facets to identify injuries necessitating treatment at a Level I/II TC. Large hospital and survey datasets containing information on injuries, mortality risk, treatment urgency, and hospital transfers were used in conjunction with large crash datasets with crash, vehicle, occupant, and injury data. The OTDA has been rigorously optimized and has demonstrated improved UT rates compared to other AACN algorithms in the literature and OT rates meeting ACS recommendations. For studies using URGENCY where separate models were created by crash mode, the UT rates ranged from 29-49% for frontal crashes, 6-33% for near side crashes, and 19-46% for far side crashes [8-11, 24]. For the OT rates, the values ranged from 3-18% for frontal crashes, 5-46 % for near side crashes, and 10-15% for far side crashes.

Traditionally, priority has been given to the reduction of UT to prevent mortality & morbidity with the understanding that some elevation in OT is necessary to prevent seriously injured patients from being under triaged. The OTDA significantly reduced UT for all crash modes without elevating OT beyond the ACS guidelines. These results are very encouraging as the OTDA uses only crash characteristics that are obtainable from vehicle sensors, whereas the majority of AACN algorithms in the literature use variables such as occupant age or gender that are not obtainable directly from the vehicle. In short, the OTDA appears to be doing “more with less” than several algorithms to which it has been compared and shows great promise as an improved approach for triaging patients.

Additional reduction in UT and OT would be expected if additional variables such as occupant age and gender were included in the OTDA. There is some room for improvement in UT for rollover crashes. Rollover crashes are complex events and determining the severity of the event is difficult due to many factors. These factors include vehicle geometry, vehicle deformation, and subsequent impacts which can alter the number of quarter turns a vehicle experiences. Several studies have taken different approaches to determine rollover severity by using the number of quarter turns [25], the number of ground to roof impacts [25], the extent of roof crush [26], pre-roll speed [6], and primary area of damage [26]. The NASS rollover variable which designates the number of quarter turns has

been previously used in URGENCY and other studies involving rollover research [8, 11, 27-31]. Additional data elements could be incorporated in the future to better quantify the severity as well as a better differentiation of the types of rollovers.

Overall, side airbag deployment resulted in little difference in the OT/UT rates for near side and rollover crashes. However, for the cases that involved vehicles that deployed a side airbag, the UT rates were improved, but this is less evident when looking at the entire NASS-CDS sample since only 5-10% of the vehicles were equipped with side airbags. Therefore, with the inclusion of the side airbag variable there would be a benefit for the occupant in vehicles where a side airbag is equipped.

Since the OTDA uses only vehicle telemetry measurements specified in Part 563 regulation, this AACN algorithm could be readily incorporated into new vehicles to inform emergency personnel of recommended triage decisions for MVC occupants. The overall societal purpose of this AACN algorithm is to reduce response times, increase triage efficiency, and improve overall patient outcome.

## CONCLUSION

An AACN algorithm, known as the OTDA, was developed that utilizes MVC characteristics obtainable from vehicle telemetry data and estimates the risk of serious injury for occupants. This risk for injury is used to recommend a transportation decision for the occupant (Level I/II TC versus non-trauma center). A parametric algorithm was developed with tunable parameters to allow for extensive optimization. Adjusting the Severity, Time Sensitivity, and Predictability Multipliers changes the taxonomy of injuries on the Master Target Injury List. The Injury Score Cutoff changes the number of Target Injuries that are included on the Master Target Injury List. The Risk Cutoff adjusts the level of risk that defines whether an occupant should be treated at a Level I/II TC versus a non-trauma center. The rigorous optimization of the OTDA produced improved UT rates compared to other AACN algorithms in the literature and OT/UT rates that met the ACS recommendations.

## ACKNOWLEDGEMENTS

Funding has been provided by Toyota Motor Corporation and Toyota's Collaborative Safety Research Center. Views expressed are those of the authors and do not represent the views of any of the sponsors.

## REFERENCES

[1] NHTSA. Traffic Safety Facts: Research Note. In: US DOT, editor.2010.
[2] Blincoe LJ, Miller, T. R., Zaloshnja, E., & Lawrence, B. A. The economic and societal impact of motor vehicle crashes, 2010. Washington, DC: National Highway Traffic Safety Administration; 2014.
[3] NHTSA. Event Data Recorders; Final Rule. In: NHTSA, editor.: Department of Transportation; 2006. p. 150.
[4] MacKenzie EJ, Rivara FP, Jurkovich GJ, Nathens AB, Frey KP, Egleston BL, et al. A national evaluation of the effect of trauma-center care on mortality. N Engl J Med. 2006;354:366-78.
[5] Kononen DW, Flannagan CA, Wang SC. Identification and validation of a logistic regression model for predicting serious injuries associated with motor vehicle crashes. Accid Anal Prev. 2011;43:112-22.
[6] Malliaris AC, Digges KH, DeBlois JH. Relationships between crash casualties and crash attributes. SAE International Congress & Exposition. Detroit, MI: Society of Automotive Engineers; 1997.
[7] Augenstein J, Digges K, Ogata S, Perdeck E, Stratton J. Development and validation of the URGENCY algorithm to predict compelling injuries. Enhanced Safety of Vehicles2001.
[8] Bahouth G, Digges K, Schulman C. Influence of injury risk thresholds on the performance of an algorithm to predict crashes with serious injuries. Ann Adv Automot Med. 2012;56:223-30.
[9] Bahouth GT, Digges KH, Bedewi NE, Kuznetsov A, Augenstein JS, Perdeck E. Devleopment of URGENCY 2.1 for the prediction of crash injury severity. Top Emerg Med. 2004;26:157-65.
[10] Rauscher S, Messner G, Baur P, Augenstein J, Digges K, Perdeck E, et al. Enhanced automatic collision notification system - improved rescue care due to injury prediction - first field experience. Enhanced Safety of Vehicle Conference. Stuttgart, Germany2009.
[11] Augenstein J, Perdeck E, Bahouth GT, Digges KH, Borchers N, Baur P. Injury identification: priorities for data transmitted. Enhanced Safety of Vehicles2005.

[12] Weaver AA, Barnard RT, Kilgo PD, Martin RS, Stitzel JD. Mortality-based quantification of injury severity for frequently occuring motor vehicle crash injuries. Ann Adv Automot Med. 2013;57:235-45.
[13] Schoell SL, Doud AN, Weaver AA, Talton JW, Barnard RT, Martin RS, et al. Development of a time sensitivity score for frequently occurring motor vehicle crash injuries. Journal of the American College of Surgeons. 2014.
[14] Schoell SL, Doud AN, Weaver AA, Barnard RT, Meredith JW, Stitzel JD, et al. Predicting patients that require care at a trauma center: analysis of injuries and other factors. Injury. 2014.
[15] Hampton CE, Gabler, H.C., Gabler HC. Evaluation of the Accuracy of NASS/CDS Delta-V Estimates from the Enhanced WinSMASH Algorithm. Annals Advancement Automotive Medicine: Association for the Advancement of Automotive Medicine; 2010. p. 241-52.
[16] Johnson NS, Gabler HC. Evaluation of NASS-CDS Side Crash Delta-V Estimates using Event Data Recorders. Traffic Inj Prev. 2014.
[17] Sharma D, Stern, S., Brophy, J., Choi, E. An Overview of NHTSA's Crash Reconstruction Software WinSMASH. The Proceedings of the 20th International Conference on the Enhanced Safety of Vehicles2007.
[18] Johnson NS, Gabler HC. Accuracy of a damage-based reconstruction method in NHTSA side crash tests. Traffic Inj Prev. 2012;13:72-80.
[19] American College of Surgeons Committee on Trauma. Resources for Optimal Care of the Injured Patient. Chicago, IL2006.
[20] Simmons E, Hedges JR, Irwin L, Maassberg W, Kirkwood HA, Jr. Paramedic injury severity perception can aid trauma triage. Ann Emerg Med. 1995;26:461-8.
[21] Wuerz R, Taylor J, Smith JS. Accuracy of trauma triage in patients transported by helicopter. Air Med J. 1996;15:168-70.
[22] Cox S, Currell A, Harriss L, Barger B, Cameron P, Smith K. Evaluation of the Victorian state adult pre-hospital trauma triage criteria. Injury. 2012;43:573-81.
[23] Lossius HM, Rehn M, Tjosevik KE, Eken T. Calculating trauma triage precision: effects of different definitions of major trauma. J Trauma Manag Outcomes. 2012;6:9.
[24] Augenstein J, Perdeck E, Stratton J, Digges K, Bahouth G. Characteristics of crashes that increase the risk of serious injuries. Annu Proc Assoc Adv Automot Med. 2003;47:561-76.
[25] Digges KH, Eigen AM. Crash attributes that influence the severity of rollover crashes. PROGRESS IN TECHNOLOGY. 2004;101:299-308.
[26] Cohen D, Digges K, Nichols RH. Rollover crashworthiness classification and severity indices: NHTSA; 1989.
[27] Conroy C, Hoyt DB, Eastman AB, Erwin S, Pacyna S, Holbrook TL, et al. Rollover crashes: predicting serious injury based on occupant, vehicle, and crash characteristics. Accident Analysis & Prevention. 2006;38:835-42.
[28] Viano DC, Parenteau CS, Edwards ML. Rollover injury: effects of near-and far-seating position, belt use, and number of quarter rolls. Traffic injury prevention. 2007;8:382-92.
[29] Gabauer DJ, Gabler HC. Differential rollover risk in vehicle-to-traffic barrier collisions. Annals of advances in automotive medicine/Annual Scientific Conference Association for the Advancement of Automotive Medicine Association for the Advancement of Automotive Medicine Scientific Conference: Association for the Advancement of Automotive Medicine; 2009. p. 131-40.
[30] Viano DC, Parenteau CS. Ejection and severe injury risks by crash type and belt use with a focus on rear impacts. Traffic injury prevention. 2010;11:79-86.
[31] Ridella SA, Rupp JD, Poland K. Age-related differences in AIS 3+ crash injury risk, types, causation and mechanisms. Proceedings of the International Research Council on the Biomechanics of Injury conference: International Research Council on Biomechanics of Injury; 2012. p. 43-60.

# SAFETY LAYER for INTELLIGENT TRANSPORT SYSTEMS

**Benedikt Schonlau**
**Dr. Klaus Krumbiegel**
**David Seidel**
IAV GmbH
Germany

Paper Number 15-0206

## ABSTRACT

Intelligent Transport Systems are currently being developed in many different industry sectors.
These developments range from highly automated land vehicles, robots for mail delivery, agricultural drones up to ships automating vehicle ferry operations or automating the transportation of oil from the corresponding platforms.
Virtual drivers are a big challenge for implementation of these systems, and there is currently much activity in this area. But this is not the major challenge; which is making those systems safe and reliable. The following article shows an approach to realize safety and reliability of Intelligent Transport Systems by separating the functional components into a driver model with limited safety and reliability, and an additional safety layer.
In this approach, the driver model takes care of putting the required application case into practice and tries, similarly to a human driver, to continuously optimize the driving task. It is also possible to use training programs in productive operations for such driver models.
The driver model is supported by a static safety layer. This safety layer implements all safety targets that have been defined in the development phase and ensures that all safety targets are continuously being adhered to during the operation. This article shows an overview of the relevant safety targets for Intelligent Transport Systems and demonstrates strategies for implementing the security layer.

## INTRODUCTION

Intelligent Transport Systems in combination with Highly Automated Driving are a frequent topic for research and development. IAV GmbH showed different use-cases with different speed levels of highly automated driving at the ITS World Congress in Detroit [1]. In Las Vegas the BMW Group presented technologies up to fully automated driving with the Remote Valet Parking Assistant [2]. Daimler AG introduced “The Truck of the Future”, an autonomously driving truck with the “Highway Pilot” system [3]. In Europe the first autonomous delivery flights of parcelcopters have been authorized for Deutsche Post DHL AG [4]. So compared to highly automated driving in Intelligent Transport Systems, there are also many similar technologies for automation and autonomous enabling of mechatronic systems in this area.
The objective of this technology is to provide a comfortable and safe future in all situations and numerous companies and institutions are putting a big effort into this [5]. But instead the big issue is to make these systems reliable and safe. The public acceptance of such high technology in their environment can only be achieved by a policy such as that aimed for in the “Vision Zero” initiative [6].
The goal of “Vision Zero”, introduced by the European Commission in 2011, aims for no fatalities or serious injuries by the year 2050. To accomplish a full acceptance it is necessary to put these goals into practice and familiarize the public with these technologies by continuous exhibiting [7].
Currently available assistance systems have a high level of safety, while their main features can be identified by availability and performance. These systems are primarily the basis of future highly automated or autonomous systems in Intelligent Transport Systems. The following article shows an approach to realize safety and reliability of Intelligent Transport Systems by separating the functional components into the comfort function with the main focus on availability and performance (i.e. assistance functions) and an additional safety layer as the safety function. (See Figure 1)

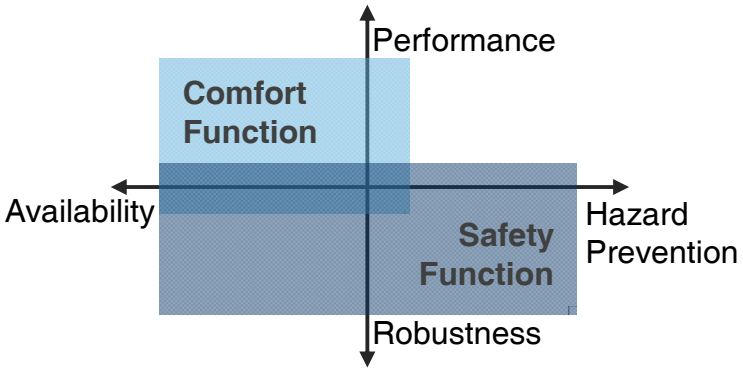


*Figure 1: Characteristics of Comfort and Safety functions*

## CURRENT STATE OF ART

For a better comprehension of Intelligent Transport Systems (Abbr. ITS) and their safety issues, it is necessary to determine all essential system elements within the scope of this article. Starting in the lowest layer with assistance systems, followed by the Highly Automated Driving Systems (Abbr. HAD) and finally showing their part in ITS.
The "autonomous" character of driver assisting functions can be defined as decisions made by the car without the intervention of the driver [7].

### Assistance Systems

Current driver assistance systems help drivers by way of a comfort function in standard situations as well as a safety function in critical situations [8]. Normally their function is limited to one problem and independent of other assistance systems [9]. There are two main types of systems: passive and active, not to be confused with categories of safety engineering. While the passive system works in background and the driver won't notice their assistance except for signaling, i.e. the Electronic Stability Control (ESC). The active system has to be turned on and/or adjusted by the driver. Situations the assistance function can't handle, the driver has to take over in around one to two seconds [11][15].
Input data can come from function-exclusive sensors. Shared input sources are a common way to distribute sensor data to the relevant functions. Objects already compiled from different input sources, e.g sensor data fusion, is also an increasingly popular method.
The function can be implemented as part of several functions on a control unit or alone on a control unit [10].

### Highly Automated Driving

In contrast to assistance systems, here the car mostly operates by itself. The car controls the longitudinal and lateral directions. In first developments the driver sits in the loop with the automated system to intervene in situations the system can't handle. This take over action should have 8-10s to guarantee a smooth handover to the driver. With further research and development fully automated systems should be able to handle most situations. Then drivers won't be required and the handover request should give them several minutes time. The goal is an autonomous system which can handle every situation and where no drivers are necessary (See Figure 2) [5][11][15].

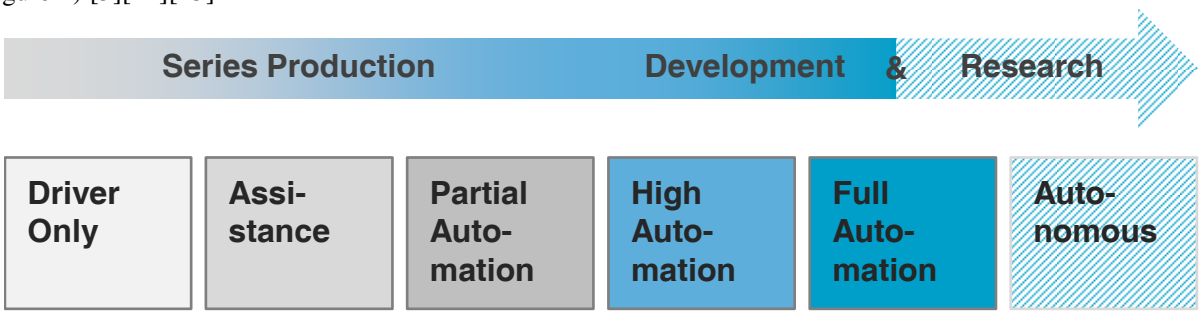


*Figure 2: Levels of Automated Driving*

Highly automated or autonomous systems require detailed environmental information, which can be achieved by data fusion of different sensor's data and information by communication between all participants. A verification of the presence of objects is possible with different sources of data.

**Safety Functions & System Restrictions**
Actual HAD Systems include state-of-the-art safety functions like redundancy, watchdogs etc. In addition the driver is sitting every time in the loop of the system [9]. When the automatic system fails, the driver has to take over. In emergency situations safety systems can support the driver or try by them self to bring the car into a safe state [8].
Moreover the German regulatory body doesn't support highly or fully automated driving systems, because the driver has to pay permanent attention to the traffic situation [12].

**Fully Automated & Autonomous Systems**
Furthermore highly automated or autonomous systems are more and more being introduced into ITS. They range from autonomous multicopters for parcel delivery [4] to fully automated public services [13] and unmanned cargo ships [14].

## ANALYSIS OF APPLICATION

In the following illustration a scheme of different ITS participants and their interactions are characterized. It shows a possible example of a future application. Afterwards the limitations of highly automated and autonomous systems are demonstrated for the example with special focus on safety matters. The example also serves as the basis for practical application of the proposed safety concept.

**Scheme of an ITS Interaction**
The example is shown in Figure 3. It describes situations in an urban area with several participants such as pedestrians, cyclists, cars, public services and delivery services. The description is situation based. All cars are equipped with Highly Automated Driving. The public service and delivery service are also capable of autonomous or highly automated acting. Communication between most participants is possible.

**Situation 1** Two cars are reaching an intersection at the same time. There is no direct visual contact between them. Because of car-to-car communications, the vehicles know each other's position, direction and velocity. The HAD System can handle this situation by cooperative actions, e.g. based on the most energy-efficient decision or the traffic rules.

**Situation 2** A careless cyclist isn't paying attention to the traffic and just wants to reach the cycle path on the other side of the road. A car, equipped with HAD, is approaching the virtual crash point between these two participants. Even with the knowledge of the cyclist the car can't avoid a crash just by using emergency braking.

**Situation 3** A car is approaching a crash site. The crash happened seconds before, so the car is entering a critical phase. Left of the car is a lane of oncoming traffic. On the other side is the sidewalk. The HAD System decides to brake and change to another lane.

**Situation 4** A full autonomous delivery service distributes parcels by car and for the last meters to the house by multicopter. The multicopter drops off the parcel in a parcel box next to the house. On the way all sensors for obstacle detection fail.

**Situation 5** A fully automated public bus is reaching a bus stop. Sensing an approaching passenger, the bus wants to pull over and stop, but a subsystem fails and is in danger of suffering damage.

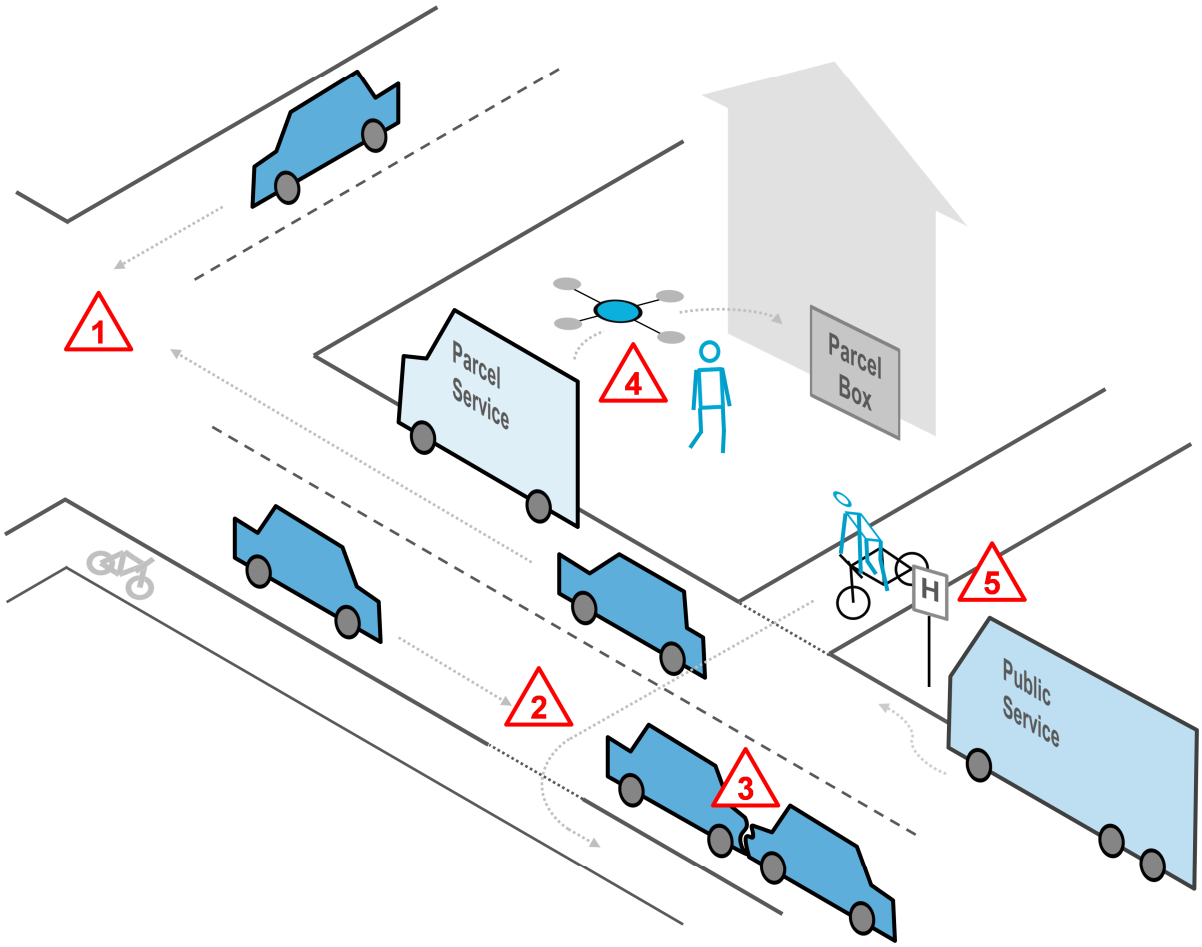


*Figure 3: Scheme of danger situations in Intelligent Transport Systems*

**Limitations to Highly Automated Systems**

To point out the limitations of highly automated systems, problems are explained for each proposed situations.

**Situation 1** It might use a special implementation to detect other cars, their trajectory and a possible collision point. So for every unique situation like intersection crossing, turning or driving on the highway, there's a corresponding unique detection function for such problems.

**Situation 2** The HAD System has to make a tough decision. The first objective is to avoid the crash or in the case it is unavoidable, to minimize the consequences of the accident. The HAD System chooses a process of avoidance, but can't guarantee a successful outcome with regard to the time-critical situation.

**Situation 3** The car decides to change to another lane to avoid the crash. The system requests a steering angle, which exceeds the actual possible steering angle of the car. The HAD System thinks it's avoiding the crash, but actually it is not.

**Situation 4** The multicopter's autonomous system still wants to deliver the package. It's actually possible, because of the knowledge of the position of the drop-off zone. But it is not safe to go there, because of the failure of the detection sensors.

**Situation 5** The fully autonomous bus' system tries to reach the bus stop, but it doesn't recognize the failing system. If it keeps going, it may result in damaged subsystems.

## CONCEPT PROPOSAL

This section introduces the Safety Layer Concept. This includes a theoretical explanation of the concept and a detailed description of all components. The concept is then applied to the proposed situations from the above section and the advantages are pointed out.

**Safety Layer Concept**

If assistance, automated and autonomous systems have a system failure, there is a probability for human or object damage. The concept aim is making these systems safer by separating the functions or subsystems in a comfort part and a safety part as fallback layers (See Figure 1). These fallback layers serve as basis to transfer the system with the failure condition into a safe state. The fallback layer initiates a plan of actions to achieve the safe state.

The procedure can be applied to different assistance functions and automated or autonomous systems, especially in situations where the function or system leads to undefined states, guides into accidents or where components and functions aren't executable. Furthermore the multiple variants of applied applications will be summed up as *functions*.

So the main purpose of monitoring the *functions* is to evaluate their output for regularity, check for possible hazard outcomes and verify for operability of relevant components. The input data can contain condition parameters of the vehicle and environment parameters, which may include information of mobile and stationary objects. The output contains the original output of the *function* or the corrected output in the case that one or more safety functions take control.

**Plausibility Layer** The first layer of the concept evaluates the output data of the *function* for their plausibility. If the output data exceed a defined interval, the plausibility of the data is not fulfilled.

If the plausibility of the data is not performed, plausible or none data will be forwarded. The check for plausibility can be performed on the basis of defined faults, tables, characteristic diagrams, functional relations, look-up tables or similar methods. The usage of more than one method is also possible.

A feedback to the *function* allows a recalculation for the next period or the deactivation of the *function*. If the *function* is deactivated, a notification to the driver can be given to take over, or another assistance function tries to bring the system into a safe state.

**Accident Layer** The second layer checks for possible hazard outcomes of the performed action of the *function*. This layer calculates on the basis of the new trajectory of the car and all objects in the environment, a value of accident risk. If the value exceeds a threshold, measures will be initiated to prevent or to reduce the consequences of the accident. This layer can be used for the whole system, even when there is no *function* in use.

Objects can be all other transport systems and users as well as infrastructure elements. So hazard outcomes are defined as damages to people and inanimate objects. Along with the calculated value of accident risk, it is also possible to include the expected hazard or the criticality of the accident in the calculation.

**Function Layer** The third layer verifies the operability of all relevant components, which are used in context with the *function*. If components are not functional, the layer tries to replace them or deactivates the relevant one.

Relevant components are sensors, actuators, control units, computing resources and algorithms which are used by the *function*. The replacement can be an adequate component or a substituted function by emulation or simulation, where the output data of the component is determined by other components data. If the component is deactivated, the driver should be informed to take over.

**Complete Concept** All layers are displayed in Figure 4. They are working constantly and monitor the *function* the whole time. It is possible to prioritize all layers differently, but to release output data all layers have to consent. The advantage of this concept is the provision of three independent layers to localize all cause-specific failure sources and eliminate them. All layers can adjust the output data of the function or execute a special action plan to reach a safe state.

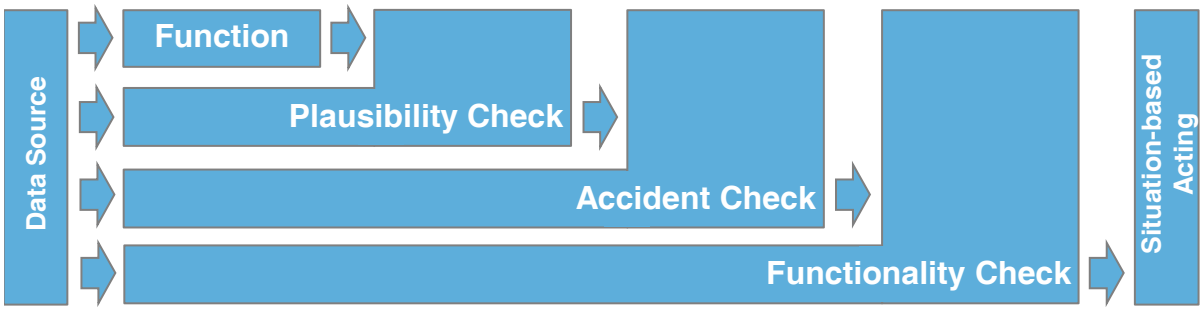


***Figure 4: Scheme of Safety Layer Concept***

To apply the concept to multiple systems, it is advisable to develop a configurable variant to adapt the layers to a specific system. So the development effort covers several systems and the costs can be divided between them. Also the development effort on the *functions* is a far less, because failures originating from systems, algorithms, undefined conditions or correlation of *functions* don't have any hazard-relevant effects. Further tests on the *functions* and defined threshold values are not necessary. So *functions* can be developed as platform-independent. With an already developed Safety Layer Concept it is easier to test *functions* and re-fit them in running systems.
It is possible to deactivate all relevant components which are associated with a failed component, to suppress false system activity and the usage of unnecessary system resources. After substituting a component, the system should assign a lower confidence value to it, maybe because of inaccuracy, to accomplish a higher safety in the system by adding additional safety tests based on this value.

**Implementation in Scheme**
In the following, the capabilities of the Safety Layer Concept are shown by applying it to the proposed situations. Application possibilities and advantages are presented.

**Situation 1** The *Accident Layer* can operate as the detection function for external objects like other cars. So there is no need for multiple functions to detect outside objects. The HAD System can handle the longitudinal and lateral direction. If the *Accident Layer* detects a possible accident, it handles the specific situation on the basis of regulations and cooperative acting, and reports the takeover to the HAD System.

**Situation 2** The HAD System has to handle a time-critical situation. The *Plausibility* and *Accident Layer* work in parallel with it. The layers can support the HAD System, which can only work as a comfort function, by monitoring steering angle and braking force plus adding more braking force. It is also possible to let the layers control the mechanical system, while the HAD System has more system resources to calculate the best avoidance procedure.

**Situation 3** The *Plausibility Layer* detects a limit exceedance of the steering angle by the subsystem "Lane Change". By overwriting it to the maximum value, the *Accident Layer* detects a possible crash and decides to steer into the other lane, which is reachable with the maximum steering angle and also free of objects. The layers initiate an action plan to bring the car to a safe state by avoiding a crash with the cyclist.

**Situation 4** The *Function Layer* detects the failing sensors. The layer decides to bring the multicopter into a safe state, because it is not safe for the environment to continue the flight. It initiates an action plan and overrules the autonomous system.

**Situation 5** The system may end up with damaged parts. Instead the *Function Layer* also detects the failing subsystem and the consequences of its breakdown. The layer executes an action plan to reach a safe state with no further usage of the failing subsystem. The system can call another bus for exchange and a service to make repairs.

## CONCLUSIONS

Assistance functions as well as highly automated and autonomous systems may contain possible failure effects like exceeding limit values, going into unknown states, guiding into accident situations or experiencing function losses and suchlike. By introducing the Safety Layer Concept it is possible to counteract these failures based on several layers to evaluate the output of functions for regularity, check for possible hazard outcomes and verify for operability of relevant components. These three layers are designated as *Plausibility Layer*, *Accident Layer* and *Function Layer*.
The concept can be applied to every level of a system, to monitor and control functions, subsystems or the whole system. With the possibility of feedback to the monitored element, overruling and deactivating, the layer concept includes several opportunities to act. By paralleling the layers themselves and to the *function*, it has high potential in time-critical situation to solve complex tasks by distributing the work between different methods. Also the concept can and should be used in every ITS participant, regardless to a possible superior functional unit, to improve the safety of all systems.
The introduction of highly automated and autonomous systems in daily life can only be achieved when these systems are totally reliable and do not present any hazards to people or objects. These goals are equal to the ones of the "Vision Zero" policy. Also the regulations in European States will only be adapted to this technology if sufficient activity on these features will be made. To fulfil such high standards in Intelligent Transport Systems, the use of the Safety Layer Concept is absolutely recommended.

**REFERENCES**


[1] IAV GmbH. (2014, September 3). *IAV bietet Testfahrten in eigenem hochautomatisierten Demofahrzeug an.* Press release.
[2] BMW Group. (2014, December 19). *BMW TO SHOWCASE INNOVATIONS INCLUDING HIGHLY & FULLY AUTOMATED DRIVING, DRIVER INTERFACE ADVANCEMENTS AND NEW LIGHTING TECHNOLOGIES AT THE LAS VEGAS CONVENTION CENTER SOUTH PLAZA DURING THE 2015 CONSUMER ELECTRONICS IN LAS VEGAS.* Press release.
[3] Daimler AG. (2014, July 3). *Weltpremiere für das Verkehrssystem von morgen – effizienter, sicherer, vernetzter – und autonomy.* Press release.
[4] Deutsche Post DHL. (2014, September 24). *DHL parcelcopter launches initial operations for research purposes.* Press release.
[5] Meyer, Gereon; Deix, Stefan. (2014). *Road Vehicle Automation. Research and Innovation for Automated Driving in Germany and Europe*. Springer International Publishing.
[6] European Commission. (2011, March 28). *White Paper: Roadmap to a Single European Transport Area - Towards a competitive and resource efficient transport system.*
[7] Özgüner, Ümit; Stiller, Christoph; Redmill, Keith. (2007). *Systems for safety and autonomous behavior in cars: The DARPA Grand Challenge experience.* IEEE (Vol. 95, No. 2), S. 397–412.
[8] Kämpchen, Dr.-Ing. Nico; Aeberhard, Kämpchen; Ardelt, Michael; Rauch, Sebastian. (2012). *Technologies for highly automated driving on highways.* ATZ worldwide (06/2012), S. 34–38.
[9] Cieler, Stephan; Konigorski, Ulrich; Lüke, Dr.-Ing. Stefan; Winner, Prof. Dr.rer.nat. Hermann. (2014). *PRORETA 3 Project-Aautomation. Safety with Assistance Systems.* autotechreview (Vol 3, Issue 11), S. 30–34.
[10] Winner, Hermann; Hakuli, Stephan; Wolf, Gabriele. (2012). *Handbuch Fahrerassistenzsysteme.* Wiesbaden: Vieweg+Teubner Verlag.
[11] Ebner, Hans-Thomas. (2013, December 11). *DVR-Kolloquium Automatisiertes Fahren. Motivation und Handlungsbedarf für Automatisiertes Fahren.* Deutscher Verkehrssicherheitsrat e. V. Bonn.
[12] Gasser, T. (2012). *Rechtsfolgen zunehmender Fahrzeugautomatisierung. Gemeinsamer Schlussbericht der Projektgruppe.* Bremerhaven: Wirtschaftsverlag NW (Berichte der Bundesanstalt für Straßenwesen, F 83). MA: C. ARZT, M. Ayoubi, A. Bartels, L. Bürkle, J. Eier, F. Flemisch et al.
[13] Siemens EOOD Bulgaria. (2007, July 3). *Another fully automatic metro system from Siemens goes into commercial.* Press release.
[14] Levander, Oskar. (2014). *Voyaging into the future.* Rolls-Royce. England.
[15] Petermann-Stock, I.; Hackenberg, L.; Muhr, T.; Mergl, CH. (2013). *Wie lange braucht der Fahrer? Eine Analyse zu Übernahmezeiten aus verschiedenen Nebentätigkeiten während einer hochautonmatischen Staufahrt.* TU München und TÜV Süd Akademie GmbH (Hg.): 6. Tagung Fahrerassistenz.

# A STUDY OF BRAIN INJURY MECHANISMS IN VEHICLE CRASHES

**Takahiro Kikuchi**
**Atsushi Togawa**
**Daisuke Murakami**
**Kaoru Tatsu**
**Chinmoy Pal**
**Tomosaburo Okabe**
Nissan Motor Co., Ltd.
Japan

Paper Number 15-0207

## ABSTRACT

Brain injury has been researched since the 1940s and various methodologies have been discussed for evaluating brain injury risk in vehicle crash tests. In recent years, an angular velocity based brain injury criterion (BrIC) has been proposed by the National Highway Traffic Safety Administration (NHTSA) for use in regulatory or consumer vehicle safety assessment tests. One of the brain injury mechanisms can be explained by relative displacement between the brain and skull, resulting in brain deformation and strain. This paper states a hypothesis of this brain injury mechanism using a simple mass-spring-damper model. Then the hypothesis was verified by the Simulated Injury Monitor (SIMon) version 4.0, a finite element model of the human head developed by NHTSA, using a cumulative strain damage measure (CSDM) as the brain injury metric. In consequence, CSDM varies according to the input loadings, which have the same peak angular velocity but different levels of peak angular acceleration and loading durations. These results suggest that in order to evaluate brain injury risk accurately, an angular velocity based criterion may not always be sufficient and it may be necessary to consider the peak value of angular acceleration and the corresponding loading duration. This hypothesis was applied to NHSTA's research test data to prove its validity. It was found that brain injury risk predicted by CSDM can be comparatively lower than that predicted by BrIC and vice versa.

## INTRODUCTION

Brain injury is caused by either a direct contact force to the head or inertial loading from an indirect impact. In either case, the head undergoes both translational and rotational motion. Rotational motion of the head is purported to be the major factor of causing strain-induced brain injury [1-4]. CSDM is widely employed in this field as an injury metric for strain-related brain injury which is calculated by the fraction volume of brain which exceeds a prescribed strain level threshold. The accumulated volume fraction of damaged brain are thought to be related to diffuse axonal injury [2-4].
SIMon was used to examine the effect of head rotational motion on CSDM using NHTSA's research test data. Three variations of input to the skull were parametrically used: (i) both translational and rotational acceleration, (ii) only translational acceleration and (iii) only rotational acceleration. In both frontal and side impact tests, case (iii) showed that CSDM was approximately at the same level as that seen for the combined acceleration loading in case (i). By contrast, CSDM was almost zero in case (ii). These results indicated that rotational motion of head was the major contributor to CSDM [5].
In recent years, BrIC has been proposed as a brain injury predictor by NHTSA. It is calculated with Eq. (1).

$$\mathbf{BrIC} = \sqrt{\left(\frac{\omega_x}{\omega_{xc}}\right)^2 + \left(\frac{\omega_y}{\omega_{yc}}\right)^2 + \left(\frac{\omega_z}{\omega_{zc}}\right)^2} \quad (1)$$

where $\omega_x$, $\omega_y$ and $\omega_z$ are maximum angular velocities about the coronal, sagittal and transverse planes. $\omega_{xc}$, $\omega_{yc}$ and $\omega_{zc}$ are the critical angular velocities around each axis based on CSDM shown in Table 1.

**Table 1.**
**Critical angular velocity $\omega$ (rad/s) around each axis**

| | |
|---|---|
| $\omega_{xc}$ | 66.20 |
| $\omega_{yc}$ | 59.10 |
| $\omega_{zc}$ | 44.25 |

The heads of anthropomorphic test devices (ATDs) were impacted using a pendulum with and without a pad, and the resultant translational and rotational accelerations were measured. SIMon was used with translational and rotational data measured with the sensors on ATDs' heads to calculate CSDM and the maximum principal strain (MPS) on the brain. Risk curves for diffuse axonal injury were proposed with regard to BrIC [6].
The purpose of this study was to examine the effect of the peak value and loading duration of the angular acceleration on CSDM. The present hypothesis of brain injury is that the brain displacement depends on the peak angular acceleration and the loading duration, resulting in brain strain as a consequence. Firstly, brain displacement is explained with a simple mass-spring-damper model (simple model) in which physical paramaters are roughly estimated in reference to cadaveric experiments [7]. Loading pulses to the skull were parametrically input as sinusoidal functions which cover more than 95% of the loadings in 74 NHTSA research tests (Tabel A1) used in the literature [8]. The results were validated with SIMon. Secondly, NHSTA's reserch test data are applied to SIMon to calculate CSDM. The angular velocity based predictor, BrIC, is examined as to whether it is a rational predictor of CSDM, one of the brain injury metrics. Close examination of the plots of CSDM vs. BrIC can show that brain injury risk predicted by CSDM can be comparatively lower than that calculated by BrIC and vice versa. The reasons for this inversion are examined in terms of the peak and the duration of the resultant angular acceleration.

## METHODS

To examine the relationship between the relative displacement of brain and the loading pulse, a hypothesis for the mechanism of brain displacement is explained using a simple model as shown in Fig.1. Direct contact to the head or indirect inertial loading induces skull rotation indicated by the blue arrow in the left diagram, while the brain has a tendency to keep its position with respect to the inertial frame at $t = t_0$. After some delay ($\Delta t$) following the impact, the brain then starts to rotate (indicated by the green arrow in the right diagram), consequently producing relative displacement between the brain and skull ($\Delta Y$,$\Delta Z$), which induces brain deformation and strain.

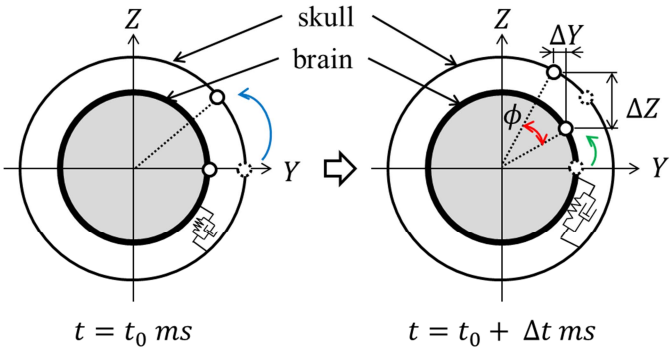


***Figure 1. A Simple Brain Displacement Model***

Assuming the input loading pulse to the head as a sinusoidal function [8-10], the equation of motion of the brain with respect to the skull, $\phi$ shown by red arrow in the right diagram, takes the form of Eq. (2).

$$I\ddot{\phi} + c\dot{\phi} + k\phi = A\Omega \sin \Omega t \tag{2}$$

The steady-state solution of Eq.(2) can be expressed by Eq. (3).

$$\boldsymbol{\phi} = \frac{\mathbf{A\Omega}}{\sqrt{\left(\Omega_0^2 - \Omega^2\right)^2 + 4\alpha^2\Omega}} \mathbf{sin}(\boldsymbol{\Omega t + \delta}) \tag{3}$$

where, A: peak of the loading pulse, Ω: driving frequency, $\Omega_0$: undamped angular frequency of the oscillator and δ : induced phase change. It is seen that the peak relative angle of the brain with respect to the skull is a function of the amplitude of the driving force A and the driving frequency Ω which is the inverse of loading pulse duration. Coefficients of damper, c, and spring, k, were roughly estimated from the results of a cadaver head impact test C386-T6 in the literature [7] in which one of the test was conducted in the coronal plane and the specimen was impacted in the left-side temporal region.

To determine the loading pulse to the simple model, the peak values of both angular velocity and angular acceleration were investigated using 80 NHTSA research tests (Tabel A1) used in the literature [8]. The test data were for frontal impacts, side impacts with a moving deformable barrier (MDB), side impacts to a rigid pole and vehicle-to-vehicle side impacts. The ATDs used were the Hybrid-III 50th Male and the ES-2. Six out of 80 tests were excluded because the peak angular acceleration or the peak angular velocity in these tests were more than three standard deviations away from the mean value of those 80 tests. Fig.2 shows the peak angular velocity vs. peak angular acceleration of the 74 tests (blue dots). The red dots mean loading pulses which cover more than 95% of the tests as shown by shaded area in red. These three input pulses shown with the red dots were applied as the sinusoidal functions shown in Fig.3. For validation of the brain displacement results calculated with the simple model, CSDM was calculated by the SIMon version 4.0, using a strain threshold of 0.25 [6]. The loading pulses were the same as the ones used with the simple model and were applied around the coronal axis.

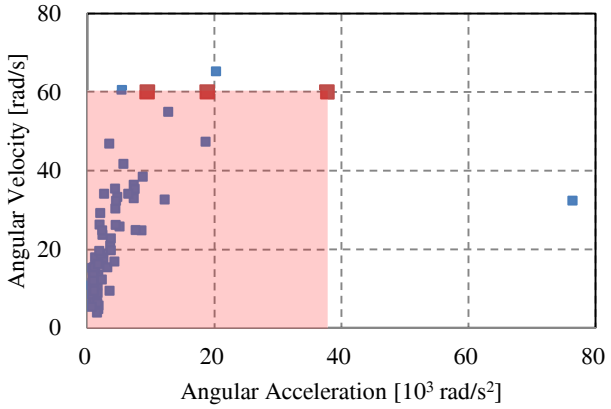


***Figure 2. Peak Angular Velocities and Angular Accelerations from 74 NHTSA Tests and Loading Pulses***

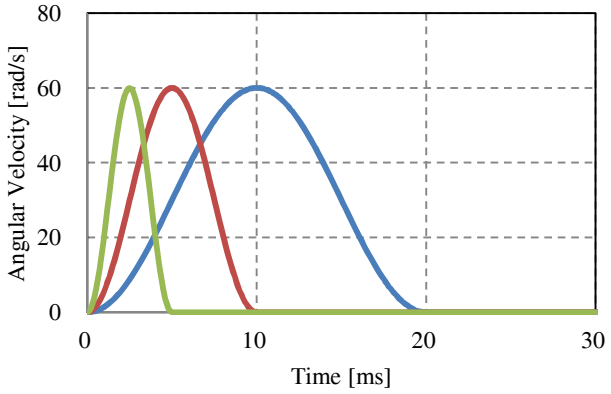


***Figure 3. Angular Velocities as Input Pulses***

In addition to the calculation above, the nine accelerometer data measured on ATDs' heads in 74 NHTSA research tests were applied to SIMon to calculate CSDM values under the loadings in vehicle crashes. BrIC was also calculated to examine whether it is a rational brain injury metric for predicting CSDM. In addition, the correlation between the angular acceleration and the gradient of CSDM, which is calculated from the difference of CSDM at time t and t+Δt (Δt=1ms), was examined by plotting their distributions with respect to time in order to estimate when and how much volume fraction of the brain exceeds the threshold strain level of 0.25.

## RESULTS

The relative displacements between the brain and skull calculated with the simple model are shown in Fig.4. The colors of curves correspond to the ones of the input loadings shown in Fig.3. The graph legend means the peak values of the angular acceleration of the input loading pulses. The results show that the relative displacements varied even though the peak angular velocities did not change as shown in Fig.3. The loading pulse having the longest loading duration due to the lowest peak acceleration shown with blue curve produces the largest relative displacement of the brain. This suggests that the longer is the loading duration due to the lower peak acceleration, the larger is displacement.

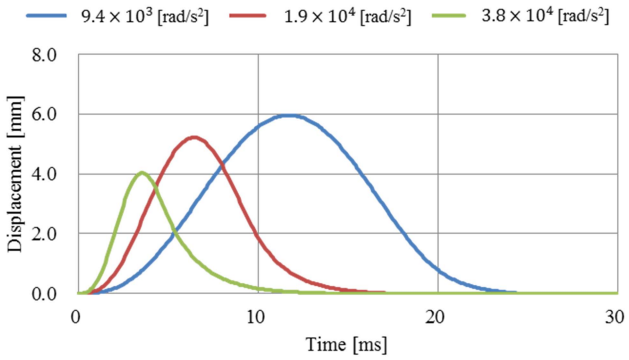


***Figure 4. Relative Displacement between the Brain and Skull calculated by Simple Model***

Fig.5 shows the time histories of CSDM calculated by SIMon using the same input pulses of the simple model shown in Fig.3. The legends of the graph correspond to the peak values of the angular acceleration of the input loading pulse. Referring to the blue curve, the CSDM value for the loading pulse having the longest loading duration and the lowest peak angular acceleration, reaches a level of 50% at around 25 ms. On the other hand, referring to the green curve, the CSDM value for the input loading having the shortest loading duration and the highest peak angular acceleration, reaches a level of 22% at around 10 ms.

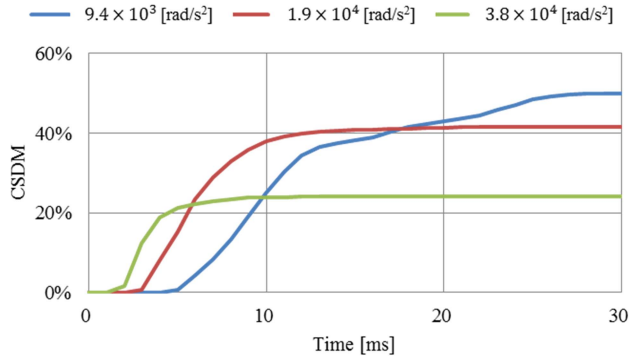


***Figure 5. CSDM Data calculated with SIMon***

Next, the above hypothesis obtained from the calculation by the simple model and SIMon was applied to NHSTA's research test data to prove its validity. In consequence, comparison of a pair of research tests (v03800 and v04292) shows that the brain injury risk predicted by CSDM can be comparatively lower than that calculated by BrIC and vice versa as shown Fig.6. The CSDM (Fig. 6a) and BrIC (Fig. 6b) values of these two tests, corresponding to their individual AIS 4+ brain injury risk curves, are plotted in blue and red squares on the dotted curves [6]. The CSDM value in the v03800 test is about two times higher than that of the v04292 test; while the BrIC value in v03800 is 0.05 lower than that in v04292.

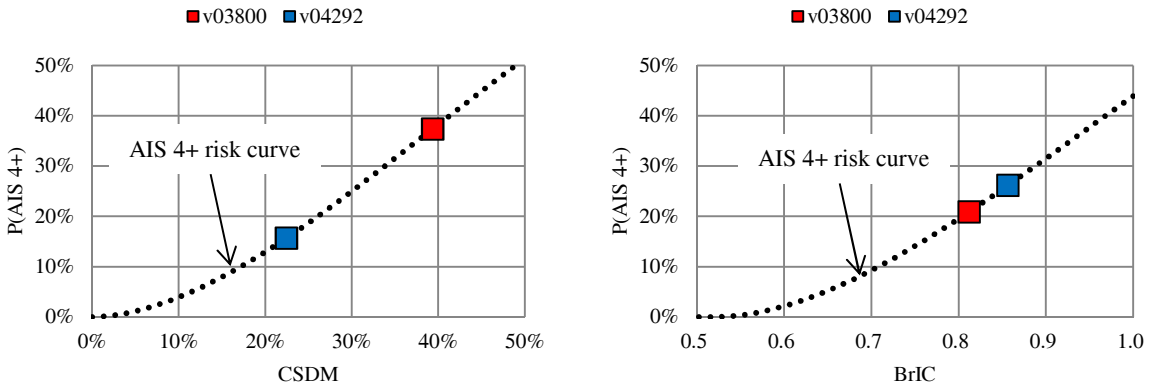


***(a)*** ***(b)***

***Figure 6. AIS 4+ Risk Curves for (a) CSDM and (b) BrIC based on CSDM of Brain Injuries***

Fig.7 shows time histories of the angular velocities and CSDM in (a) v03800 and (b) v04292. In both tests, the maximum angular velocities in the three axes are marked by dotted ellipses, which are used to calculate BrIC. Thorough observation of Fig.7 (a) shows the results for the v03800 test in which an increase of CSDM is seen after 50 ms. At nearly the same time, the angular velocity around the x-axis and y-axis changes from positive (A-A) to negative peak (B-B). Hence, the change in angular velocity, i.e. the angular acceleration in this period seems to cause the increase in CSDM from 0 to 39%. On the other hand, Fig. 7(b) shows the results for the v04292 test in which an increase of CSDM is seen around 50 ms (C-C). In this test, the value of the change in angular velocity may be about one half of that for v03800. The CSDM value is also about one half of that for v03800. These results suggest that the magnitude of the change in angular velocity seems to be related to the value of the CSDM.

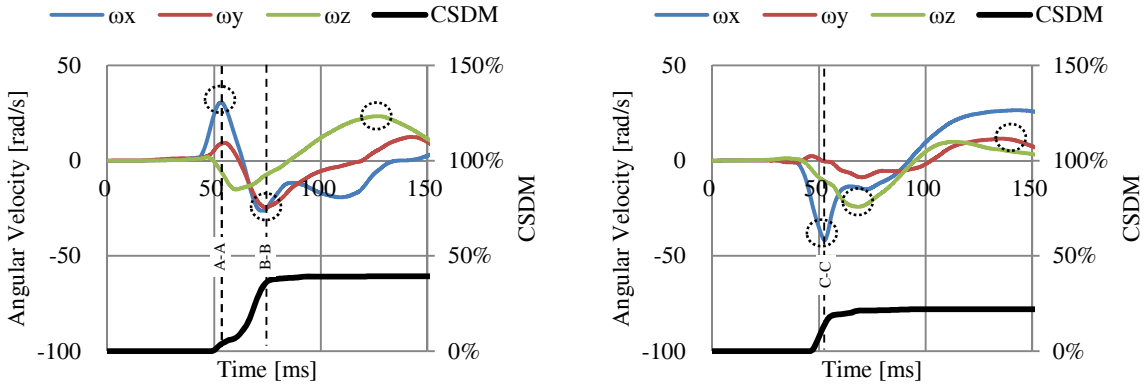


***(a)*** ***(b)***

***Figure 7. Angular Velocities and CSDM in (a) v03800 and (b) v04292***

Fig.8 shows CSDM versus BrIC plot of 74 tests. Among the tests results as marked in dotted ellipse as shown in Fig.8, the pair of tests, such as shown above in Fig.6 and Fig.7, can be seen frequently. For example, within one dotted ellipse, the lower right plots have relatively higher BrIC values than the upper left plots, while CSDM values of the lower right plots are lower than the ones of the upper left plots. The pair of tests shown above in Fig.6 and Fig.7 are marked in black.

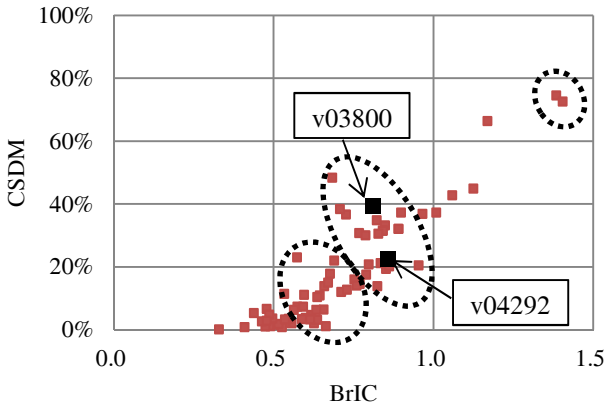


***Figure 8. CSDM versus BrIC of 74 tests calculated by SIMon***

Fig.9 shows time histories of the resultant angular acceleration and the volume fraction of the brain in 4 tests. The test numbers are shown below the corresponding graphs. These graphs show that the volume fraction of the brain that exceeds the strain level of 0.25 increases just after the resultant angular acceleration increases. These results suggest that the rate of change in CSDM might be influenced by the resultant angular acceleration.

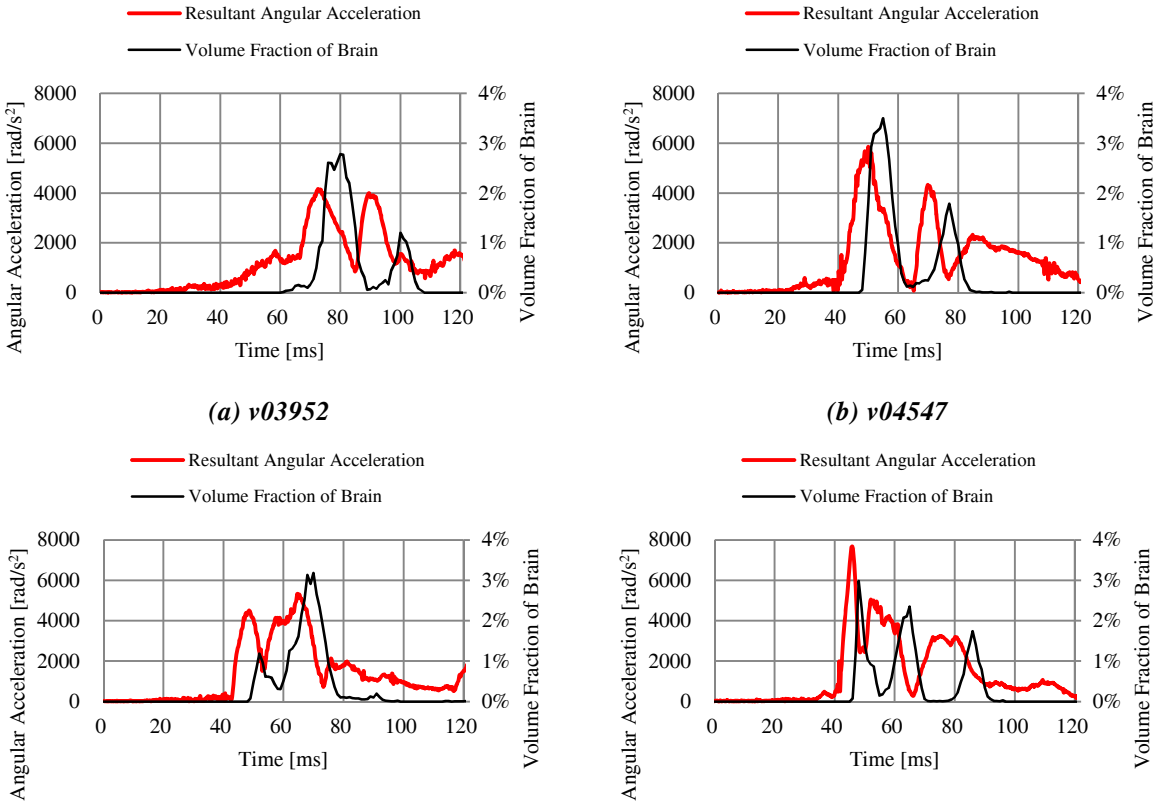


***(a) v03952***

***(b) v04547***

***(c) v03800***

***(d) v04380***

***Figure 9. Resultant Angular Acceleration and Volume Fraction of Bran in 4 tests***

## DISCUSSION

An injury criterion based only on angular velocity might not be an accurate brain injury metric for predicting CSDM values. The peak values of relative displacement between brain and skull calculated by simple model varied under the different loading pulses with the same peak angular velocity. The results of simple model were verified by FEM

based SIMon model. The CSDM values calculated by SIMon showed the same tendency as that of the simple model. In the vehicle crash test, BrIC, one of the angular velocity based injury criterion, not always accord with the predicted result based on CSDM value calculated by SIMon as shown in Fig.6 and Fig.7. The CSDM value in the v03800 test is approximately twice as large as the value in the v04292 test. However, the BrIC value in the former test hovers at a level of just 0.05 lower than that in the latter test. Such pairs of tests are found frequently as shown in Fig.8. Within one dashed ellipse in Fig.8, the lower right plots have relatively higher BrIC values than the upper left plots, but CSDM values of the lower right plots are lower than the upper left ones. This inversion of the relationship between CSDM and BrIC might lead to mislead consumers about the crash safety performance of vehicles, if the present BrIC estimation is used in regulatory or consumer vehicle safety assessment tests.
Presumably, one of the reasons why BrIC does not necessarily predict CSDM value is that BrIC considers only the absoulte peak angular velocity and does not take into account the peak value of angular acceleration and corresponding loading duration. The peak value and loading duration of angular acceleration might affect the relative displacement of the brain as shown Eq.(3) and Fig.4. This hypothesis was verified by SIMon as shown in Fig.5. The loading pulse having the longest loading duration due to the lowest peak acceleration produces the largest relative displacement of the brain and CSDM value. The gradient of CSDM with respect to time showed when and how much volume fraction of the damaged brain swelled. Fig.9 indicated that the volume fraction of the damaged brain increased with increasing resultant angular acceleration with some delay. These results suggest that the rate of change in CSDM might be influenced by the resultant angular acceleration.

## CONCLUSIONS

This study highlighted the importance of considering the peak value of angular acceleration and the corresponding loading duration when evaluating brain injury risk based on CSDM. In addition, an injury criterion based only on an angular velocity might cause misunderstanding of consumers about the crash safety of vehicles with respect to brain injury risk. More research is needed before adopting such criteria for evaluating brain injury risk in regulatory or consumer vehicle safety tests.

## REFERENCES


[1] Holbourn, A. H. S., 1943. "Mechanics of head injuries." Lancet 2:438-441.
[2] Bandak, F.A. and Eppinger, R.H. 1995. “A three-dimensional finite element analysis of the human brain under combined rotational and translational acceleration.” Proc. 38th Stapp Car Crash Conference, pp. 145-163.
[3] Bandak, F.A., 1995. “On the Mechanics of Impact Neurotrauma”, Journal of Neurotrauma 12, 4, pp.635-649
[4] DiMasi, F.P., Eppinger, R.H., Bandak, F.A., 1995. “Computational analysis of head impact response under car crash loadings.” Proc. 39th Stapp Car Crash Conference, pp. 425-438.
[5] Zhang, J., Yoganandan, N., Pintar, F. A., Gennarelli, T. A., 2006. “Brain Strains in Vehicle Impact Tests.” 50th Annual Proceedings Association for the Advancement of Automotive Medicine, Vol.50, pp. 1-12.
[6] Takhounts, E.G., Craig, T. J., Moorhouse, C. K., McFadden, J., Hasija, V., 2013. “Development of Brain Injury Criterion (BrIC).” Stapp Car Crash Journal, Vol. 57, pp. 243 - 266.
[7] Hardy, W.N., Mason, M.J., Foster, C.D., Shah, C.S., Kopacz, J.M. Yang, K.H., King, A.L., Bishop, J., Bey, M., Andrest, W., Tashman, S. 2007. "A Study of the Response of the Human Cadaver Head to Impact." Stapp Car Crash Journal, Vol. 51, pp. 17 - 80.
[8] Takhounts, E.G., Eppinger, R.H., Campbell, J.Q., Tannous, R.E., Power, E.D., Shook, L.S., 2003. “On the Development of the SIMon Finite Element Head Model.” Stapp Car Crash Journal, Vol. 47, pp. 107-133.
[9] Takhounts, E.G., Hasija, V., Ridella, S.A., Tannous, R.E., Campbell, J.Q., Malone, D., Danelson, K., Stitzel, J., Rowson, S., Duma, S., 2008. “Investigation of Traumatic Brain Injuries Using the Next Generation of Simulated Injury Monitor (SIMon) Finite Element Head Model.” 52nd Stapp Car Crash Conference.
[10] Zhang, L., Yang, K.H., Dwarampudi, R., Omori, K., Li, T., Chang, K., Hardy, W.N., Khalil, T.B., King, A.I, 2001. “ Recent advances in brain injury research: a new human head model development and validation.” Stapp Car Crash Journal, Vol. 45, pp. 369-394.
[11] Hardy, W.N., Foster, C., Mason, M., Yang, K., King, A., Tashman, S., 2001. “Investigation of head injury mechanisms using neutral density technology and high-speed biplanar X-ray.” Stapp Car Crash Journal, Vol. 45, pp. 337 – 368.

## Appendix

Table A1. NHTSA's research tests data.

| Frontal impact tests | | | Side impact tests | | |
|---|---|---|---|---|---|
| **Test Number** | **Occupant** | **Test Condition** | **Test Number** | **Occupant** | **Test Condition** |
| v04303 | Driver | Vehicle into barrier | v03800 | Driver | MDB into vehicle |
| v04242 | Driver | Vehicle into barrier | v04551 | Driver | MDB into vehicle |
| v04205 | Passenger | Vehicle into barrier | v03875 | Driver | MDB into vehicle |
| v04273 | Driver | Vehicle into barrier | v03899 | Driver | MDB into vehicle |
| v04198 | Driver | Vehicle into barrier | v03818 | Driver | Vehicle into pole |
| v03897 | Driver | Vehicle into barrier | v04547 | Driver | MDB into vehicle |
| v04266 | Passenger | Vehicle into barrier | v04380 | Driver | MDB into vehicle |
| v04247 | Driver | Vehicle into barrier | v03845 | Driver | Vehicle into pole |
| v03916 | Driver | Vehicle into barrier | v04497 | Driver | Vehicle into pole |
| v04081 | Passenger | Vehicle into barrier | v04547 | Passenger | MDB into vehicle |
| v04264 | Passenger | Vehicle into barrier | v03898 | Driver | Vehicle into pole |
| v03901 | Passenger | Vehicle into barrier | v04551 | Passenger | MDB into vehicle |
| v04250 | Driver | Vehicle into barrier | v03799 | Passenger | MDB into vehicle |
| v04251 | Driver | Vehicle into barrier | v04380 | Passenger | Vehicle into pole |
| v04215 | Passenger | Vehicle into barrier | v03820 | Driver | Vehicle into pole |
| v04237 | Passenger | Vehicle into barrier | v04456 | Passenger | MDB into vehicle |
| v04080 | Driver | Vehicle into barrier | v03819 | Passenger | MDB into vehicle |
| v04205 | Driver | Vehicle into barrier | v04378 | Driver | Vehicle into pole |
| v04090 | Driver | Vehicle into barrier | v04292 | Driver | Vehicle into vehicle |
| v04264 | Driver | Vehicle into barrier | v04498 | Driver | Vehicle into pole |
| v04090 | Passenger | Vehicle into barrier | v03803 | Passenger | MDB into vehicle |
| v04223 | Passenger | Vehicle into barrier | v03802 | Driver | Vehicle into pole |
| v04267 | Passenger | Vehicle into barrier | v04292 | Passenger | Vehicle into vehicle |
| v04215 | Driver | Vehicle into barrier | v03803 | Driver | MDB into vehicle |
| v04242 | Passenger | Vehicle into barrier | v04482 | Driver | Vehicle into vehicle |
| v04259 | Driver | Vehicle into barrier | v03800 | Passenger | MDB into vehicle |
| v03987 | Driver | Vehicle into barrier | v04471 | Driver | Vehicle into pole |
| v03915 | Driver | Vehicle into barrier | v04313 | Driver | Vehicle into pole |
| v04255 | Passenger | Vehicle into barrier | v03819 | Driver | MDB into vehicle |
| v04235 | Driver | Vehicle into barrier | v04086 | Driver | MDB into vehicle |
| v04235 | Passenger | Vehicle into barrier | v04284 | Driver | Vehicle into pole |
| v04265 | Passenger | Vehicle into barrier | | | |
| v04292 | Passenger | Vehicle into barrier | | | |
| v04240 | Driver | Vehicle into barrier | | | |
| v04237 | Driver | Vehicle into barrier | | | |
| v04259 | Passenger | Vehicle into barrier | | | |
| v04198 | Passenger | Vehicle into barrier | | | |
| v03915 | Passenger | Vehicle into barrier | | | |
| v03952 | Driver | Vehicle into barrier | | | |
| v03901 | Driver | Vehicle into barrier | | | |
| v04241 | Driver | Vehicle into barrier | | | |
| v04252 | Driver | Vehicle into barrier | | | |
| v03952 | Passenger | Vehicle into barrier | | | |

**GLOSSARY**

ATD: anthropomorphic test device
BrIC: brain injury criteria
CSDM: cumulative strain damage measure
MPS: maximum principal strain
NHTSA: National Highway Traffic Safety Administration
SIMon: Simulated Injury Monitor

# LOAD TRANSFER OF PASSANGER CAR COMPARTMENT FOR IMPROVEMENT OF STRUCTURAL PERFORMANCE IN SIDE IMPACT

**Satoshi Akima**
Keio University, Graduate School of Science and Technology
Japan

**Masaki Omiya**
**Kunihiro Takahashi**
Keio University
Japan

Paper Number 15-0209

## ABSTRACT

We demonstrate the effectiveness of a new method for expressing the load transfer in passenger car bodies to improve structural performance in order to protect occupants in side impact. For vehicle structures, one of the most important goals is the reduction of compartment deformation. For this purpose, indicating the load transfer paths in a vehicle compartment is fundamentally significant. The present authors previously developed an index Ustar (U*) to express the load paths in structures. Our purpose in the present study is to express the load transfer using U* in a vehicle compartment in side impact.

The index U* is defined as $U^* = 1 - U/U'$, where U is the work done at the loading point and U′ is the work done when an arbitrary point is constrained. We can say that U* shows the connectivity between the loading point and an arbitrary point. It is natural to think that the force is transferred along the highest part of the U* distribution. The index U* can realize a way to obtain the overall view of load transfer in the vehicle compartment during collisions.

We introduce the extended U* in which the effect of inertial force is included for the calculation of vehicle collision. The calculated distribution of U* for a sample passenger car shows that the impact force is transferred mainly to the lower structure of the compartment. However, the load is not transferred to the opposite body side, because of the separation caused by the center tunnel structure. The U* distribution shows that among the several transverse cross-members, the cross-member under the B-pillar plays a key role in load transfer. In contrast, the cross-member under the front seat has a small effect for load transfer. These results of load transfer are demonstrated by the colored U* contour lines in the entire compartment for any specified instant during impact. The calculated results are expected to improve the side impact crashworthiness to reduce the risk of injury to occupants.

As an example, to increase the load transfer of the cross-member under the front seat, we locate the stiffener member between the side sill and the tunnel structure. The designation of the stiffener location is pinpointed by the distribution of U*. A crash simulation of a sample vehicle equipped with the stiffened cross-member reveals that the side sill intrusion deformation decreases by more than 30%. The value of the decrease rate itself is not a key point of the result. The point of importance is the effectiveness of the deduction process by U* for the strict determination of structural improvement.

## INTRODUCTION

Occurrence of traffic accidents is a social problem, and reduction of injuries to vehicle occupants is the inevitable research subject. Side impact accounts for a relatively large fraction of the total numbers of accidents

and fatal injuries.

In order to decrease injuries caused by side impacts, improvement of both the occupant protection system and the vehicle body structures is important. In the present study, we focus on the investigation of the vehicle body structure. Reduction of the intrusion velocity of the vehicle body-side structure into the compartment is the aim of the structural improvement [1] [2]. Understanding the load transfer from a moving deformable barrier (MDB) into the body structure is highly effective in increasing the stiffness of the compartment.

Load transfer in structures has been generally studied by examining the stress distribution [3]. However, observing the load transfer using stress distribution is rather difficult because of the effect of stress concentration around holes or notches. It is unreasonable to conclude that a hole or notch is effective for the load transfer. A novel index Ustar (U*) previously developed by the authors has been used to express the load transfer and load paths, thereby overcoming the abovementioned problem of stress concentration [4].

The concept of U* has been used in vehicle body structures [5] [6]. For the calculation of U* under dynamic loading, a method has been proposed that includes the effect of inertial forces [7]. Previously, using this approach, we calculated the load transfer in a passenger car compartment during frontal collision [8].

Extending the study of frontal impact, in the present study, we introduce similar methods for side impact. We apply the index U* to numerically depict the load transfer and load paths in a compartment structure during a side impact.

In the U* calculation under side impact, the compartment structure except for the front-end structure of a finite element model is assumed to be elastic. As will be mentioned later, we also use the assumptions of a "dynamic-static method" and "equivalent inertial force method". Through application of these methods for the side impact of a sample passenger car, the obtained U* distribution shows that the cross-member under the front seat should especially be stiffened. A dynamic crash simulation demonstrates the significant effectiveness of the newly stiffened cross-member.

## METHODS

### Index U* and Load Transfer

The concept of the index Ustar (U*) that was previously developed by the authors [4] is summarized as follows. Figure 1 shows a linear elastic body in which an external force $\boldsymbol{p}_A$ is applied at Point A. Point B is a support end, and Point C is an arbitrary point. The relationship between forces and displacements for these three points is

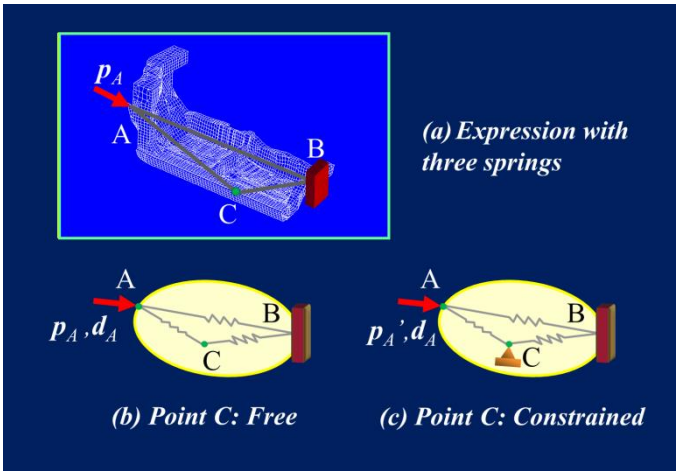


***Figure1. Ustar calculation.***

$$\begin{Bmatrix} \boldsymbol{p}_A \\ \boldsymbol{p}_B \\ \boldsymbol{p}_C \end{Bmatrix} = \begin{bmatrix} \boldsymbol{K}_{AA} & \boldsymbol{K}_{AB} & \boldsymbol{K}_{AC} \\ \boldsymbol{K}_{BA} & \boldsymbol{K}_{BB} & \boldsymbol{K}_{BC} \\ \boldsymbol{K}_{CA} & \boldsymbol{K}_{CB} & \boldsymbol{K}_{CC} \end{bmatrix} \begin{Bmatrix} \boldsymbol{d}_A \\ \boldsymbol{d}_B \\ \boldsymbol{d}_C \end{Bmatrix} \tag{1}$$

where $\boldsymbol{K}$, $\boldsymbol{p}$, and $\boldsymbol{d}$ with suffixes are the internal stiffness tensor, force vector, and displacement vector, respectively. The expression of Eq. (1) is not the elementary formulation of the finite element method (FEM) but rather the representation of the overall behavior of an entire structure.

The work done by the force $\boldsymbol{p}_A$ and the displacement $\boldsymbol{d}_A$ at Point A in Fig. 1(b) is denoted as $U$. When Point C is constrained as shown in Fig. 1(c), the work done under the same displacement $\boldsymbol{d}_A$ at Point A is denoted as $U'$. A non-dimensional value

$$U^* = 1 - \frac{U}{U'} \tag{2}$$

indicates the definition of the index U* at an arbitrary point in the structure. The index U* means the stiffness between the loading point A and an arbitrary point.

From Eqs. (1) and (2), we have

$$U^* = \left( 1 - \frac{2U}{(\boldsymbol{K}_{AC}\boldsymbol{d}_C) \cdot \boldsymbol{d}_A} \right)^{-1} \tag{3}$$

where tensor and vector notations are employed instead of matrix notation for the products. The value of $U^*$ is unity at the loading point A and zero at the support B. It can be seen that the index $U^*$ is expressed by $\boldsymbol{K}_{AC}$ which is a tensor value stiffness between the loading points and an arbitrary point. Although we can calculate Eq. (2) by FEM, the inspection load methods [9] based on Eq. (3) can reduce the calculation time remarkably.

**Load Path and Optimization**

Figure 2(a) shows schematic U* distributions and contour lines. The ridgeline of a three-dimensional curved surface is defined as the line that connects the highest points of stiffness in series from the loading point. We define this ridgeline as a load path because it can be regarded that the line that connects the highest stiffness points transfers the largest loading.

The actual U* contour lines and the load paths are calculated for a simple plate model shown in Fig. 2(b). The stress concentration does not affect the load paths.

To confirm the concept of U* being applicable to structures, an optimization process using a genetic algorithm (GA) for U* was previously tested [10]. In the optimization process, the objective function was determined based on the following three conditions for desirable structures.

(a) Uniformity: Uniform decrease in U* along a path (Fig. 3(a))

(b) Continuity: Smoothness of the curvature of U* along a path (Fig. 3(b))

(c) Consistency: Coincidence between a path from Point A and a path from Point B ($S_1$ and $S_2$ in Fig. 3(c))

For the flat plate model shown in Fig. 4(a), the design parameter of optimization was the thickness of each element. The optimized structure obtained using U* in the 50th generation of the GA is shown in Fig. 4(b). For comparison, the result of sensitivity analysis, which is one of the conventional optimization methods for strain energy density, is shown in Fig. 4(c). There is no significant difference in the thickness distribution, and this indicates the validity and effectiveness of the U* theory.

During both the optimization processes, the thickness distribution developed once into the Michell truss pattern but then eventually attained a simple pattern using the operation of intensification.

It is important to see that this objective function using U* has no relationship to the concepts of stress. Generally, the concept of stress is suitable as the parameter of strength, and U* is adequate for the index of load transfer.

Since the above reference is for the confirmation of the concept of U*, hereafter we do not intend to

discuss the optimization in the present paper.

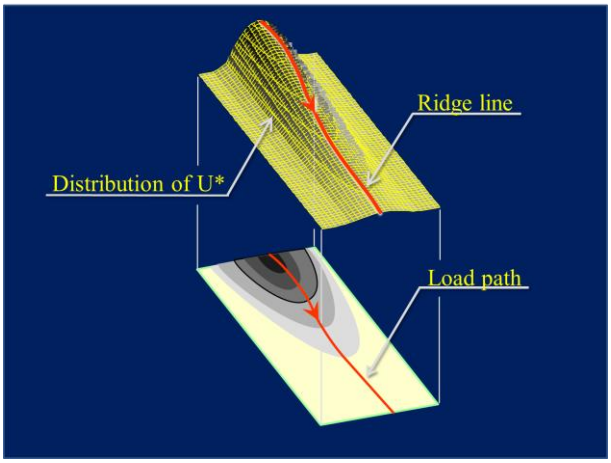


*(a) Load path*

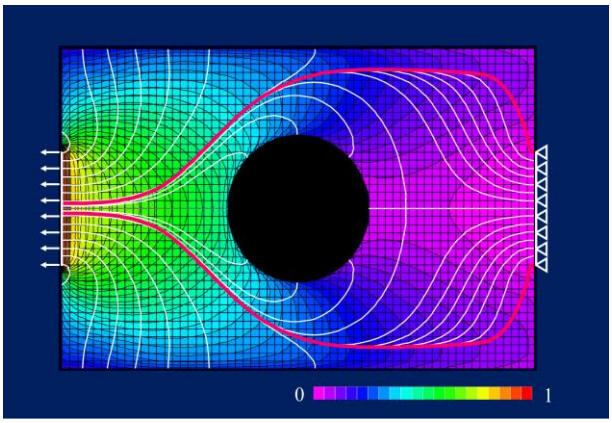


*(b) Distribution of U**

***Figure2. Definition of load path and distribution of U*.***

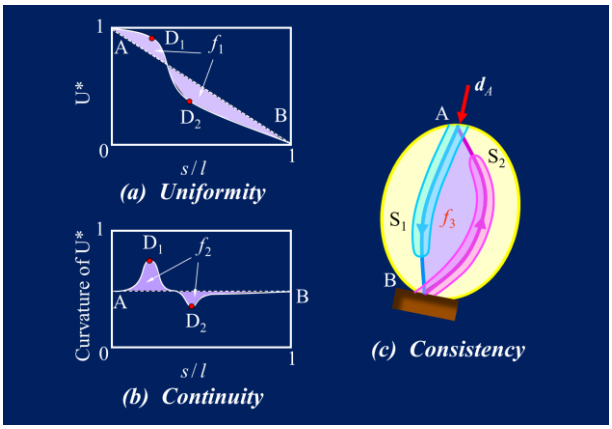


***Figure3. Conditions of desirable structure.***

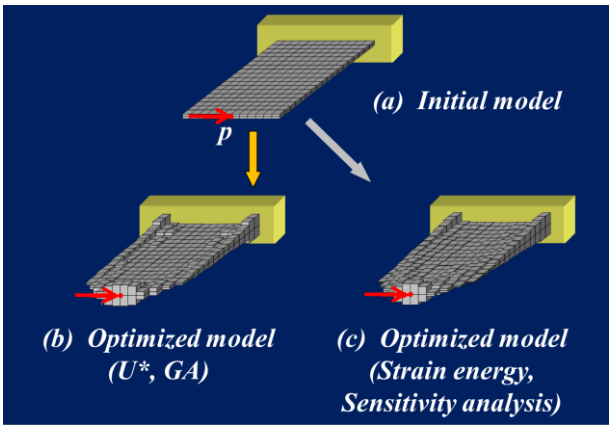


***Figure4. Structural optimization.***

**Effect of Inertial Force**

For the calculation of side impact, the definition of U* under dynamic loading including the effect of inertial force is required. Since we already developed the calculation method of U* under the effect of inertial force [7], here, we present only the abbreviated summary.

Figure 1 shows the loading point A, support point B, and arbitrary point C. Here, for the inertial force, we introduce other points $D_i$ (i = 1, 2, 3, …, n, n: number of nodes) shown in Fig. 5.

For simplicity, we consider the case of n = 1, which means that the inertial force is applied to only one node of a finite element. In Fig. 1, an elastic body with Points A, B, and C is expressed by three springs. Introducing the new Point D, we should use the six-spring model as shown in Fig. 6. For the new model, the definition of U* is given as

$$U^* = \left\{ 1 - \frac{2U}{[(\boldsymbol{k}_{AC} - \boldsymbol{k}_{AD}\boldsymbol{k}_{DD}^{-1}\boldsymbol{k}_{DC})\boldsymbol{d}_C]\cdot\boldsymbol{d}_A} \right\}^{-1} \tag{4}$$

instead of Eq. (3), where $\boldsymbol{k}$ with suffixes expresses the internal stiffness tensor between two points. The suffixes represent the two related points. The stiffness in the six-spring model is different from the stiffness in the three-spring model: $\boldsymbol{k}_{AC} \neq \boldsymbol{K}_{AC}$.

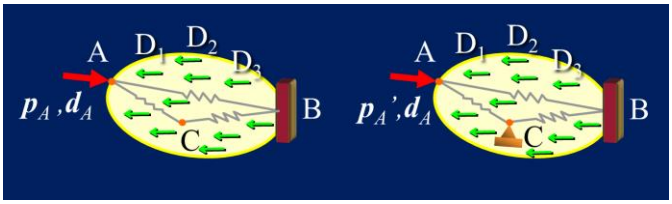


***(a) PointC: Free*** ***(b) PointC: Constrained***

***Figure5. Elastic structure with three springs.***
***($D_1$, $D_2$, $D_3$, … : inertial forces)***

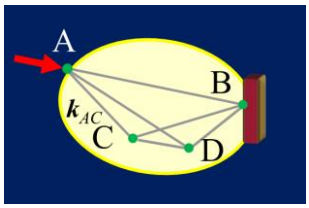


***Figure6. Elastic structure with six springs.***

For the case of zero inertial force, the U* value of Eq. (3) should coincide with that of Eq. (4). Remembering that the displacement $\boldsymbol{d}_A$ or $\boldsymbol{d}_C$ can be given independently of the stiffness and that the stiffness is constant for a given structure, the following equation

$$\boldsymbol{K}_{AC} = \boldsymbol{k}_{AC} - \boldsymbol{k}_{AD}\boldsymbol{k}_{DD}^{-1}\boldsymbol{k}_{DC} \qquad (5)$$

is obtained. Equation (5) shows that it is unnecessary to calculate its right side; rather, it is sufficient to know the left side, which can be determined by the static U* calculation using Eq. (4) with the inspection load method. However, in Eq. (4), we should adopt the value of $\boldsymbol{d}_C$ under dynamic loading.

## FULL-WIDTH FRONTAL COLLISION [8]

### Application of U* to Frontal Collision

In our previous report [8], we applied the index U* to the full-width frontal collision (56 km/h) for a sample vehicle structure. Since the index U* is applied only for elastic structures, we used the following assumption of structural separation. Namely, we assumed the passenger compartment as an elastic body for the calculation of the load transfer by using U*. The original material properties of the vehicle front-end crash region were not changed, and the rear end was assumed to be rigid (Fig. 7).

The dynamic crash behavior for the vehicle model was calculated by LS-DYNA. A deformed body at an arbitrary instant in the crash was extracted. The extracted compartment model was used for the static U* calculation by MSC Nastran. The combined operation above using the dynamic simulation and static calculation is called the "dynamic-static method."

The loading area for the static U*calculation was located at the boundary between the front-end structure and the passenger compartment. The support area was located at the boundary between the compartment and the rear end (Fig. 8).

### Equivalent Inertial Force

We used the abovementioned definition of U* (Eq. (4)) under the dynamic condition. In this calculation, inertial

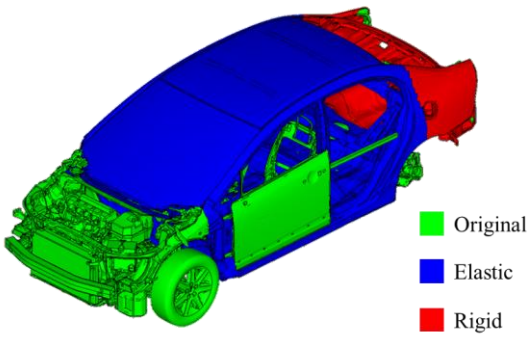


***Figure7. Structure separation.***

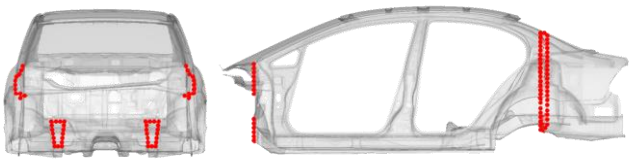

***Figure8. Loading and support.***

force should be applied to every FE node. Using the abovementioned dynamic-static method, we obtained displacement vectors of every node for the extracted compartment at any instant during collision. The necessary static force on each node for reproducing the obtained displacement was inversely calculated by NASTRAN. The necessary forces for such displacements from the initial configuration can be regarded as inertial forces. We call the present process the "equivalent inertial force method."

Although the calculation of the above-described entire process requires complicated operation, automated software that had been developed beforehand was used.

**Load Transfer in Frontal Collision** [8]

The load transfers from the front-end structure and the rear end are shown in Fig. 9 using U* at 30 ms after frontal barrier collision. Although the maximum U* value from the front-end structure is 1, we set the maximum value from the rear end to 0.034, which is decided by the ratio of the frontal force to the rear supporting force.

By inspecting the U* value from the front-end structure shown in Fig. 9(a), we can see that the frontal loading is transferred mainly to the under-floor member. In contrast, as shown in Fig. 9(b), the supporting force from the rear end is transferred to the side sill. We call such a discrepancy the inconsistency of load paths (Fig. 3(c)). This discrepancy indicates that an increase in the stiffness of the connecting member between the under-floor member and the side sill is required.

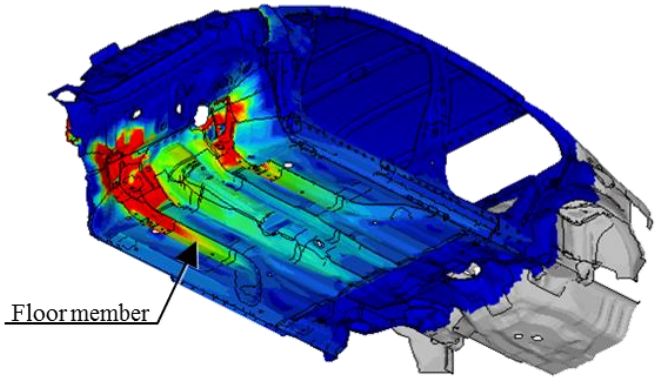


***(a) Distribution of U* from loading area***

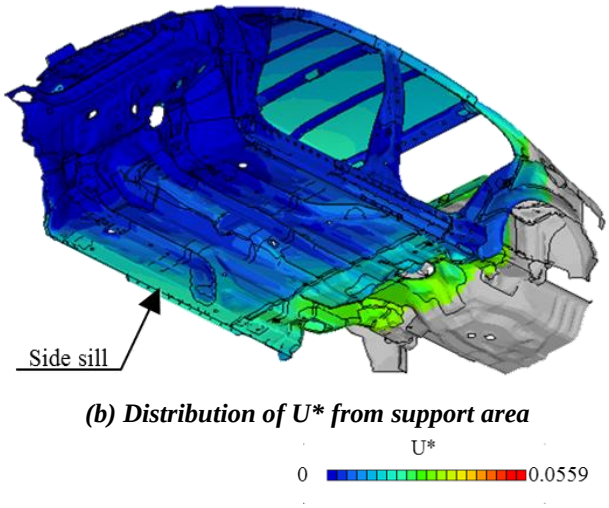


***(b) Distribution of U* from support area***

***Figure9. Distribution of U* (30ms).***

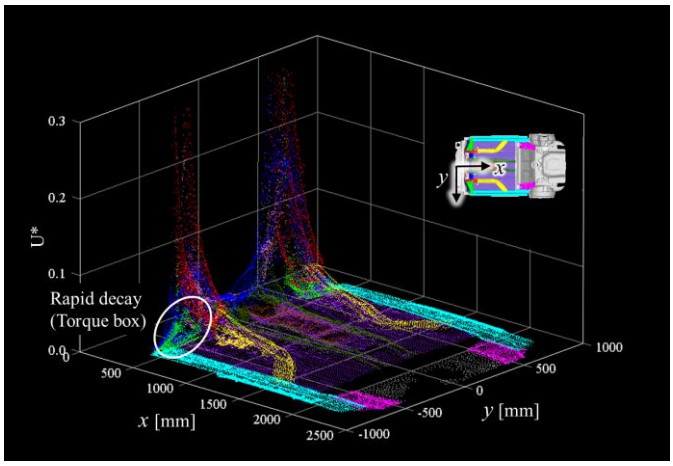


***Figure10. Disutribution of U* scatter diagrams (30ms).***

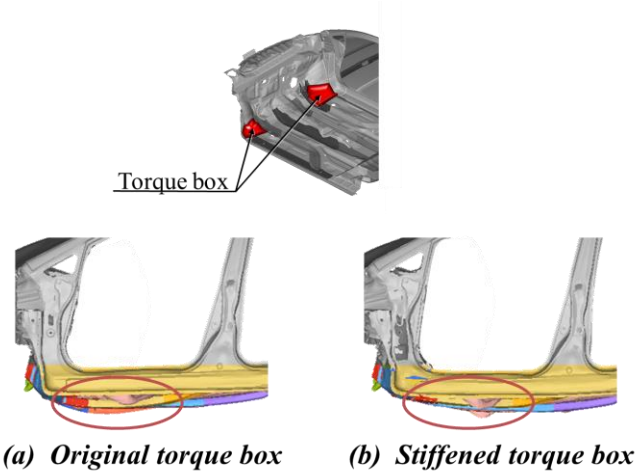


***Figure11. Comparison of deformation (x40 deformation, 40ms).***

For a clearer observation, the scatter diagram of U* is shown in Fig. 10, where the U* value of each FE node is plotted on the *x*-*y* plane (*x*, *y*: longitudinal and lateral coordinates, respectively, of a compartment structure). The FE nodes of the connecting member (torque box) between the under-floor member and the side sill are indicated in the figure, which shows the rapid decrease in U* along the connecting member.

Based on these results, the torque box was stiffened for a remodeled vehicle. The vehicle with such a stiffened body was calculated for the frontal impact by LS-DYNA. Comparison of deformation between the original body and the stiffened body is shown in Fig. 11. As expected, an undesirable large deformation of the under-floor member in the original body was improved by the use of the stiffened torque box.

## SIDE IMPACT

### Calculation Model

Application of the U* calculation to side impact is the final goal of the present study. The FE model of a passenger car with 272,485 elements for side impact is shown in Fig. 12(a). The model type of the MDB is ECE-R95 (Fig. 12(b)). The impact speed is 55 km/h. For the dynamic and static calculations, LS-DYNA and MSC Nastran, respectively, are used. The loading area and the supporting area are shown in Fig. 13.

***(a) Passenger car*** [(#)]

***(b) Moving deformable barrier***

(#) National Crash Analysis Center, Dodge Neon, Detailed model, Date posted: 2006 Jul. 3, available from (http://www.ncac.gwu.edu/vml/models.html)

***Figure12. Calculation model.***

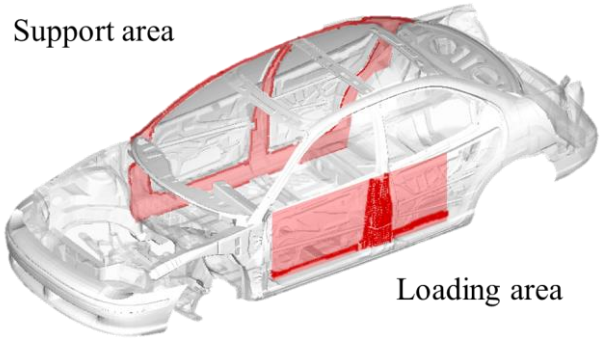


***Figure13. Loading and support (Static U* calculation).***

**Calculation Process**

Since the U* calculation is applied to only elastic bodies, as mentioned above, it is necessary to assume that the material property of the passenger compartment is elastic. However, based on the assumption of structural separation as shown in Fig. 14, the original material property is used for the outer panels of both the body sides of the compartment including doors as the crash area and the supporting area.

The dynamic vehicle behavior under side impact is calculated by LS-DYNA, and the deformation of the compartment structure at an arbitrary instant is extracted. In the same manner as described above for frontal collision, using the dynamic-static method, we statically calculate the extracted frozen compartment model to obtain the U* distribution by MSC Nastran (Fig. 15).

For the definition of U* under dynamic condition (Eq. (4)), the equivalent inertial force is applied to every FE node as the distributed external force in the static U* calculation (Fig. 16). For retaining the deformation of the extracted compartment at any instant, the necessary static force on each node for reproducing the deformed shape of the body is conversely calculated by NASTRAN. The calculated forces can be regarded as the equivalent inertial forces.

**Selection of U* Theory**

From the definition of U* (Ustar), the forced deformation at the loading points is constant during the calculation of load transfer. Namely, deformation is the parameter of the applied work. From the definition of

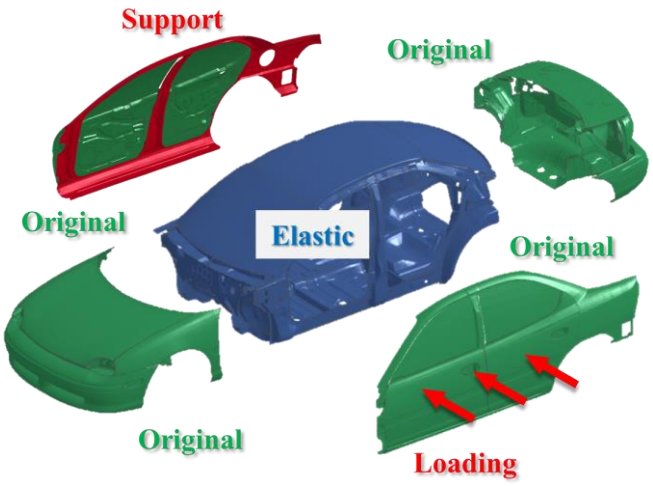


*Figure14. Structure separation.*

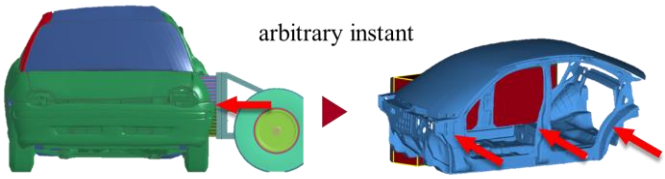


*(a) Dynamic calculation* *(b) Static calculation (Extracted compartment)*

*Figure15. Dynamic-static method.*

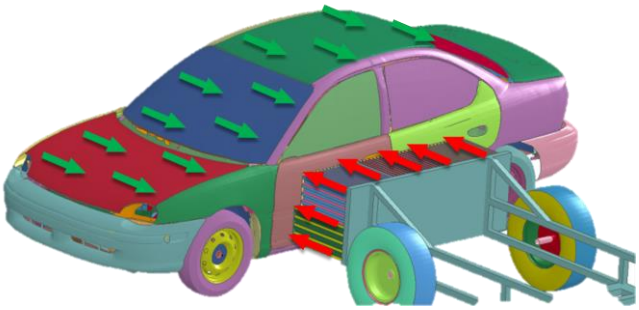

*Figure16. Equivalent inertial force.*

another index U** (Ubistar), on the contrary, force at the loading points is constant during the calculation, wherein force is the parameter of applied complementary work [11].

Since the MDB is equipped with an aluminum honeycomb, the applied force is almost constant during impact. Thus, for side impacts, application of U** is more desirable than application of U*. However, the MSC Nastran U*Toolkit [12] saves calculation time, and FRONE U*PRE [13] performs systematic dynamic calculation for U*. For these reasons, here, we use the conventional U*.

**Load Transfer in Side Impact**

For the above passenger vehicle, U* values from the loading area under side impact are shown in Fig. 17 for 10, 20, 30, and 40 ms after impact. From the definition of U*, which is non-dimensionalized, the maximum value of U* is 1 at any instant during a collision. However, to express the process during impact, the maximum

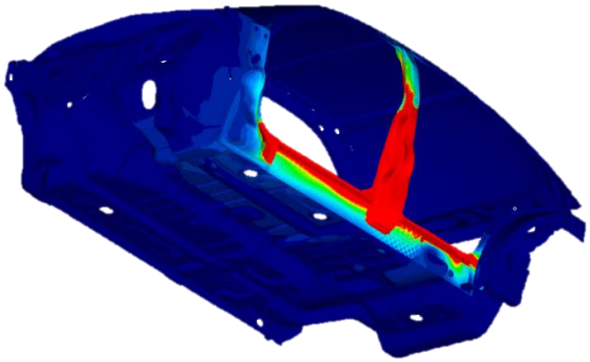

*(a) 10ms (max: 1)*

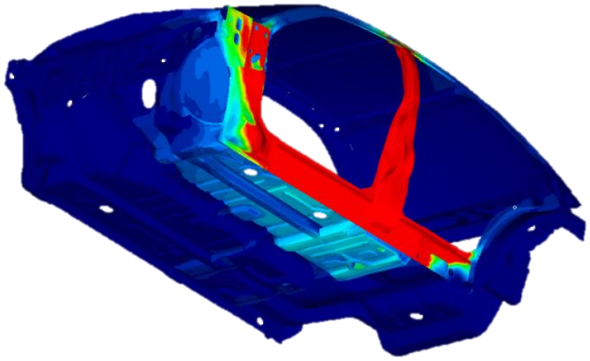

*(b) 20ms (max: 17.4)*

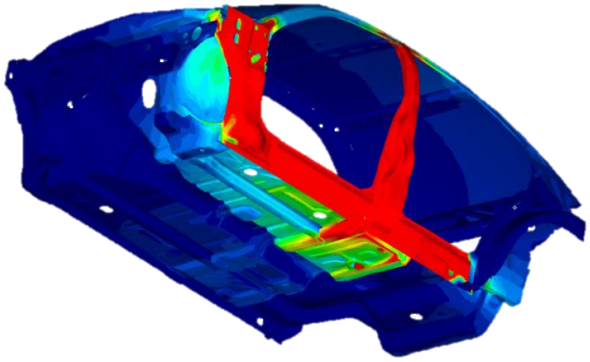

*(c) 30ms (max: 87.1)*

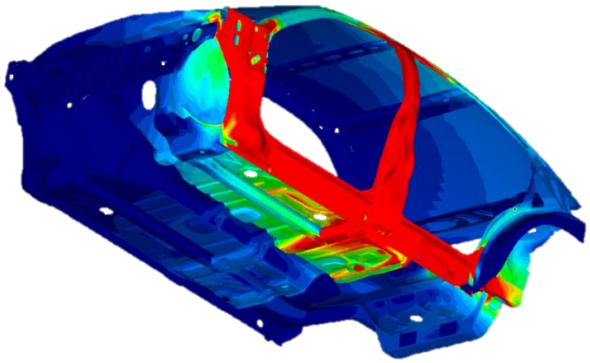

*(d) 40ms (max: 121)*

***Figure17. Distribution of U* from loading area during side impact.***

value of 1 is multiplied by the resultant crash force of each instant. The ratio of the resultant crash force is shown in the figure.

From Fig. 17, we can see that the input loading is transferred mainly to the lower structure. Despite the important role of the lower structure, the load transfer is interrupted by the tunnel structure. The floor structure is explicitly separated from the viewpoint of stiffness continuity, and the degree of separation is clearly represented by the U* distribution.

Figure 17 shows that among the several cross-members located across the floor panel, the cross-member located under the B-pillar is intensively effective. The impact force from the MDB presses the B-pillar strongly, and the force is transferred directly to the cross-member that is beneath the B-pillar.

On the other hand, the second cross-member that is located under the front seat has a small effect for the load transfer. Actually, by observing the scatter diagram in Fig. 18, which shows the U* distribution of the lower structure, we can clearly see the rapid decay of U* at the second cross-member.

The U* distribution from the support end is shown in Fig. 19, which indicates the support capability of the opposite body side. Because of the existence of inertial force, the upper structure including the roof panel has relatively large U* value. Figure 19 indicates that the upper structure has effective support capability, though the

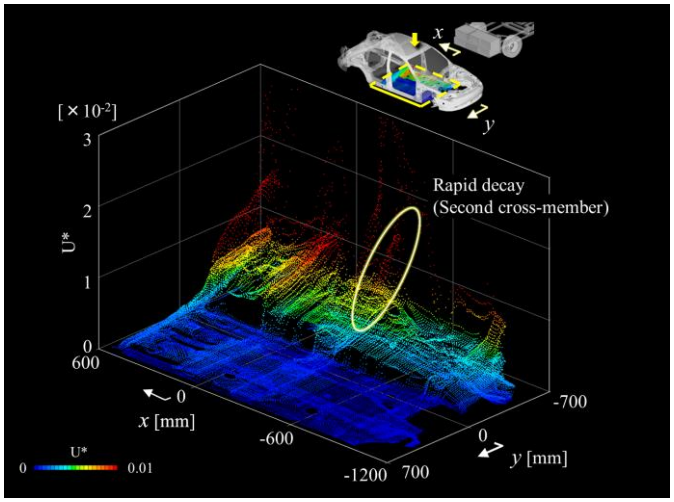


*(a) 30ms*

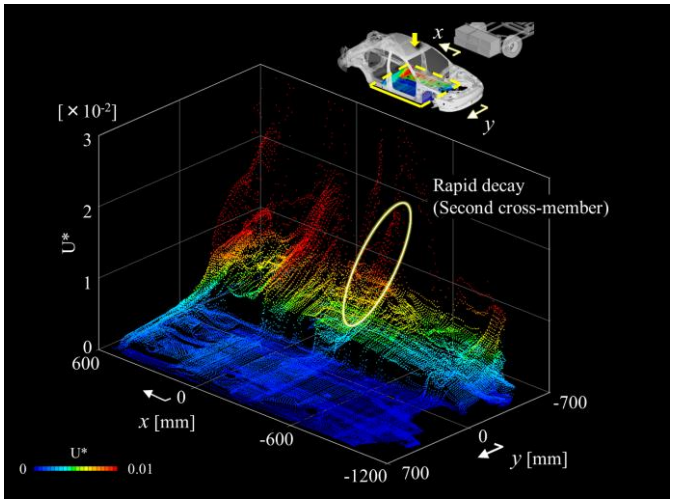


*(b) 40ms*

***Figure18. Disutribution of U* scatter diagrams.***

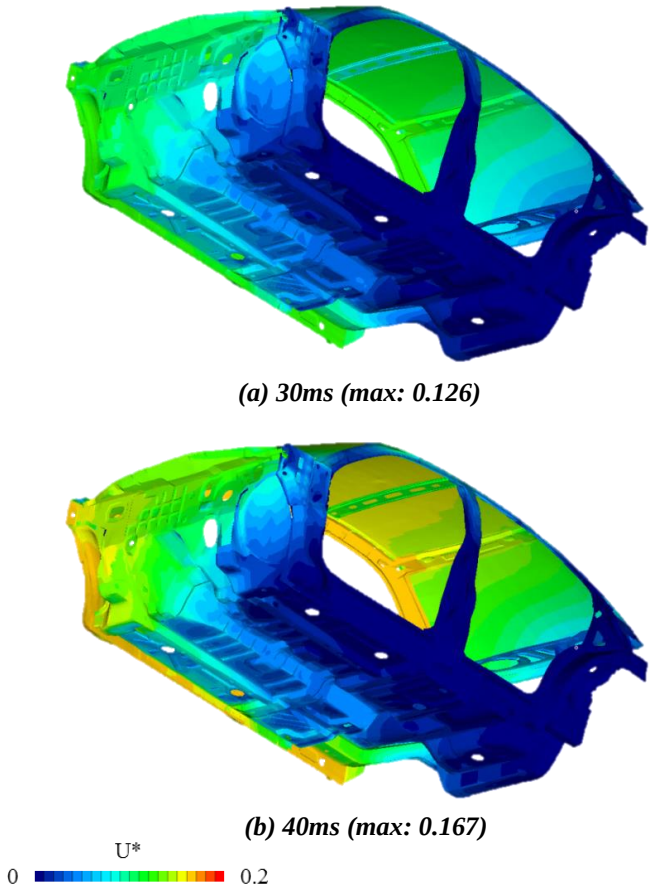


*(a) 30ms (max: 0.126)*

*(b) 40ms (max: 0.167)*

***Figure19. Distribution of U* from support area during side impact.***

transferred impact force from the B-pillar to the roof panel is small.

**STIFFENED CROSS-MEMBER**

As shown above, the load transfer along the second cross-member located under the front seat is relatively small. To improve the stiffness of the second cross-member, we locate the stiffener member between the side sill and the tunnel structure. The beam model of a steel pipe (length: 606 mm, diameter: 48.6 mm, thickness: 3.2 mm) is used for the stiffener. The location of the pipe is shown in Fig. 20. The pipe end at the side sill is located at a point where the stiffness decreases rapidly.

The rapid decrease point of the stiffness is determined using U* from the loading area (Fig. 20(a)). Another pipe end at the tunnel structure is decided by the rapid change point of U* from the support (Fig. 20(b)).

In general, for determining the location of a stiffener, it is necessary to connect the following two points:

(1) the point with the maximum U* from the loading area

(2) the point with the maximum U* from the support area

In the present study, we used the determination process of the stiffener location by inspecting the U* distribution from both sides as a typical example of the above general application method of U*.

Using the above stiffened body, we recalculated the side impact by LS-DYNA under the same crash condition as that for the original vehicle. The calculated result is shown in Fig. 21, where the side-sill intrusion deformation along the side sill upper edge at an instant 60 ms after the crash is plotted.

Although the maximum side sill intrusion deformation decreased by more than 30%, the value of the decrease rate itself is not a key point of the result. The point of importance is the effectiveness of the deduction

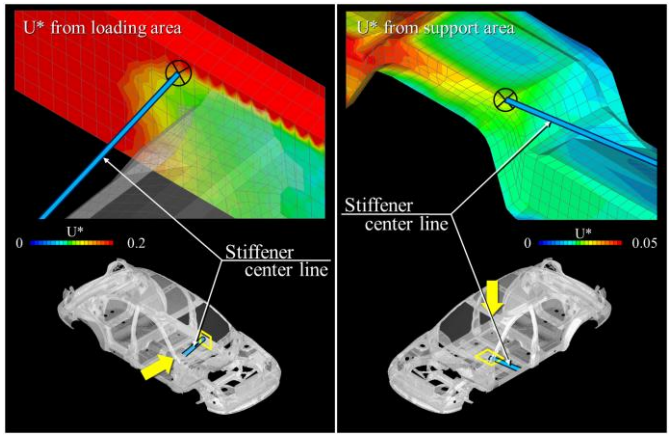


*(a) Side sill* *(b) Cross-member*

***Figure20. Stiffener location.***

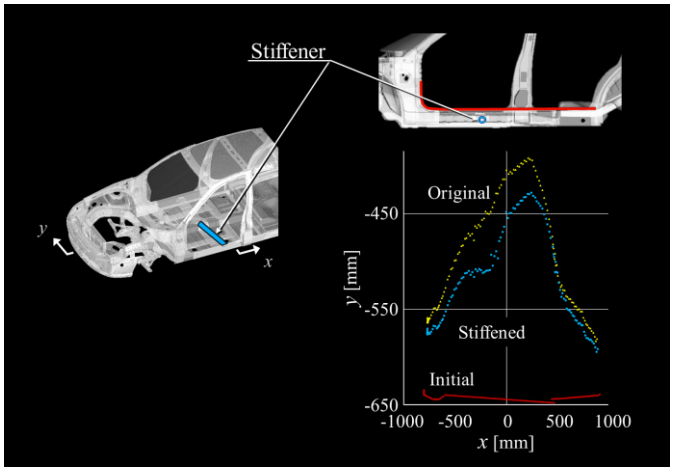


***Figure21. Side sill intrusion (upper edge, 60ms).***

process by using U* for the strict determination of structural improvement.

## CONCLUSIONS

With the aim of increasing the stiffness of a vehicle body structure in side impact, we investigated the load transfer and load paths into the passenger compartment from a moving deformable barrier (MDB) by using the new theory of Ustar (U*).

(1) The dynamic crash behavior for a sample vehicle model was calculated by a dynamic simulation. A deformed body at an arbitrary instant during the crash process was extracted, and the extracted compartment model was used for the U* calculation by a static simulation.

(2) The input loading to the sample vehicle structure is transferred mainly to the lower structure. Despite the important role of the lower structure, the load transfer is interrupted by the tunnel structure. The U*distribution shows that in contrast to the effective cross-member located under the B-pillar, the cross-member under the front seat has only a small effect for the load transfer.

(3) To improve the stiffness of the cross-member under the front seat, we located the stiffener member between the side sill and the tunnel structure. The designation of the stiffener location was pinpointed by inspecting the distribution of U*. With the use of the stiffened body, the side sill intrusion

deformation improved by more than 30%.

**ACKNOWLEDGEMENT**

The authors would like to express their deepest gratitude to Prof. T. Maki, Prof. T. Sakurai, Mr. T. Iso, and Mr. Y. Zaiki for their helpful collaboration.

**REFFERENCES**

[1] Mangala, M. J., "2-Door Vehicle Body Local Force Evaluation with the IIHS, EuroNCAP and LINCAP Side Impact Barriers", SAE Technical Papers, 2004-01-0333 (2004)
[2] Abe, A., Sunakawa, T., Fujii, S., Fukushima, M. and Ogawa, S., "Aggressivity-Reducing Structure of Large Vehicle in Side Vehicle-to-Vehicle Crash", SAE Technical Papers, 2005-01-1355 (2005)
[3] Marhadi, K. and Venkataraman, S., "Comparison of Quantitative and Qualitative Information Provided by Different Structural Load Path Definitions", Int. J. Simul. Multidisci. Des. Optim., Vol.3, p.384-400 (2009)
[4] Takahashi, K. and Sakurai, T., "Expression of Load Transfer Paths in Structures", Trans. JSME Ser. A, Vol.71, No.708, p.1097-1102 (2005) (in Japanese)
[5] Hoshino, H., Sakurai, T. and Takahashi, K., "Vibration reduction in the Cabins of Heavy-Duty Trucks Using the Theory of Load Transfer Paths", JSAE Review, Vol.24, p.165-171 (2003)
[6] Naito, T., Kobayashi, H., Urushiyama, Y. and Takahashi, K., "Introduction of New Concept of U*sum for Evaluation of Weight-Efficient Structure", SAE Int. J. Passeng. Cars – Electron. Electr. Syst., Vol.4, Issue 1 (2011)
[7] Takahashi, K., Omiya, M., Iso, T., Zaiki, Y., Sakurai, T., Maki, T., Naito, T. and Urushiyama, Y., "Load Transfer Ustar (U*) Calculation in Structures under Dynamic Loading", Trans. JSME Ser. A, Vol.79, No.807, p.1657-1668 (2013) (in Japanese)
[8] Sakurai, T., Nonaka, D., Takahashi, K., Omiya, M., Naito, T., Urushiyama, Y. and Maki, T., "Application of Load Transfer Ustar Calculation to Cabin Structures under Frontal Collision", Proceedings of 2014 JSAE Annual Congress, No.78-14, p.3-6 (2014) (in Japanese)
[9] Sakurai, T., Takahashi, K., Kawakami, H. and Abe, M., "Reduction of Calculation Time for Load Path U* Analysis of Structures", Journal of Solid Mechanics and Materials Engineering, Vol.1, No.11, p.1322-1330 (2007)
[10] Kamimura, M., Hatta, Y., Ito, S., Koga, Y., Sakurai, T. and Takahashi, K., "Structural Optimization and Load Paths", Trans. JSME Ser. A, Vol.74, No.737, p.6-12 (2008) (in Japanese)
[11] Wang, E., Yoshikuni, Y., Guo, Q., Nohara, T., Ishii, H., Hoshino, H. and Takahashi, K., "Load Path U** Analysis of Truck Cab Structure under Frontal Collision", Proceedings of 2009 JSAE Annual Congress, No.21-09, p.5-8 (2009)
[12] MSC Nastran U*Toolkit, available from
(http://pages.mscsoftware.com/rs/mscsoftware/images/NastranUserMeeting-MSC-Ustar.pdf),
(accessed 2015-3-16)
[13] FRONE U*PRE, available from
(https://drive.google.com/folderview?id=0B23OQ8Pgk40VX3hubUpJaXNFaTA&usp=sharing),
(accessed 2015-3-16)

# AN ANALYSIS OF HYBRID AND ELECTRIC VEHICLE CRASHES IN THE U.S.

**Rong Chen**
Virginia Tech
United States

**Kyu-Sang Choi**
Hyundai Motor Group
Republic of Korea

**Allison Daniello**
Virginia Tech
United States

**Hampton Gabler**
Virginia Tech
United States

Paper Number 15-0210

## ABSTRACT

The growing popularity of hybrids and electric vehicles in the U.S. has raised questions about whether they might pose a different crash risk than conventional vehicles. In particular, there have been anecdotal reports of fires associated with the battery system in these advanced fuel vehicles. The objective of the study was to characterize the factors that influence the risk of serious to fatal injury in U.S. hybrid and electric passenger vehicle crashes.

Our approach in this study was to compare the crash performance of the conventional passenger vehicle fleet with hybrid/electric passenger vehicles in the U.S. The study was based upon the analysis of three U.S. crash databases: the Fatal Analysis Reporting System (FARS), the National Automotive Sampling System / Crashworthiness Data System (NASS/CDS), and the National Automotive Sampling System / General Estimates System (NASS/GES). Cases recorded by the databases between the years 1999 and 2013, and involving passenger vehicles model year 2000 and newer were extracted from all three databases.

Hybrid vehicles constituted less than 1% of the total vehicle population in all three databases. FARS contained no fatalities in electric vehicles, and less than 0.01 % of cases in NASS/CDS and NASS/GES involved electric vehicles.

The incidence of fire was lower for hybrid vehicles than the conventional fleet in all three databases. Fatal crashes involving fire constituted 2.6% of hybrid vehicle cases and 4.4% of conventional vehicle cases. No cases of fire or electric shock injury associated with hybrid vehicles were found in NASS/CDS. Only 1 case of a hybrid fire was found in NASS/GES and 5 cases of hybrid fire were found in FARS. No fires involving electric vehicles were found in any of the three databases.

Similar crash characteristics were found for both hybrid and conventional vehicle populations. Median longitudinal delta-V was 18 km/hr for hybrid vehicles and 14 km/hr for conventional vehicles. Hybrid vehicle occupants were found to have higher risk of AIS2+ upper extremity injury but lower risk of AIS2+ lower extremity injury than conventional vehicle occupants. Similar risk of AIS2+ head and chest injury was observed between the two groups.

The most notable difference between hybrid vehicles and conventional passenger-vehicles was that occupants of hybrid vehicle were more likely to be older than occupants of conventional vehicles. In FARS, the median age of fatally injured hybrid vehicle occupants was 59 years versus 36 years for conventional vehicle occupants. In NASS/CDS, the median age of hybrid vehicle occupants was 42 years and the median age of conventional vehicle occupants was 29 yrs. In NASS/GES, the median age of hybrid/electric vehicle occupants was 44 years, as compared to the median age of 32 years for conventional vehicle occupants.

The present study characterized the crash and occupants of hybrid and electric vehicles. The comparison between hybrid and conventional vehicle crashes showed little difference in the crash performance and injury outcome between the two groups. The incidence of fire was actually lower in hybrid vehicles than in the rest of the fleet.

## INTRODUCTION

Hybrid and electric vehicles have been gaining popularity in the U.S. market since their introduction. Nearly 500,000 hybrid vehicles and 100,000 electric vehicles were sold in the U.S. market in the year 2013 [1]. Although the improved fuel economy offered by hybrid and eletric vehicles have made them very attractive to consumers, the advanced battery systems utilized by these vehicles have raised questions whether they pose a different crash risk than conventional fuel vehicles. It is still unknown whether hybrid and electric vehicles' reliance on heavy battery packs lead to different crash outcomes as compared to similar size conventional vehicles.

Several instances of battery fire associated with hybrid and electric vehicles have been reported. In 2011, The National Highway Traffic Safety Administration (NHTSA) reported that a Chevrolet Volt, which had undergone the side impact pole test as part of the New Car Assessment Program (NCAP), had sustained damage to the lithium-ion battery during the crash test and subsequently experienced a fire [2]. In March 2013, Mitsubishi Motors reported two instances of battery fire associated with the Mitsubishi i-MiEV and Mitsubishi Outlander P-HEV. Both fires occurred at Mitubishi's battery pack assembly plant during testing [3]. Although these fires occurred in unusual conditions, the concern remains that a real world crash of sufficient severity could trigger a fire event.

The objective of this study is to characterize the factors which influence the risk of serious to fatal injury in U.S. hybrid and electric passenger vehicle crashes. Specifically, we would like to answer the following three questions:

1. What is the frequency of fire in these crashes?
2. What are the characteristics of the occupants in these crashes?
3. What types of crashes and injury outcomes are associated with each vehicle fleet?

## METHOD

Our approach in this study was to compare the crash performance of the conventional passenger vehicle fleet with the crash performance of hybrid and electric passenger vehicles in the U.S. The study was based upon the analysis of three U.S. crash databases: (1) the Fatal Analysis Reporting System (FARS), (2) the National Automotive Sampling System / Crashworthiness Data System (NASS/CDS), and (3) the National Automotive Sampling System / General Estimates System (NASS/GES).

FARS is a census of all traffic fatalities in the U.S. and was used in this study to determine the characteristics of fatal crashes. NASS/CDS is a sample of 4000-5000 in-depth crash investigations collected each year at 24 sites nationally. NASS/CDS provides exhaustive detail on injuries suffered in these crashes and, in this study, was used to explore the factors associated with injury. To be included in NASS/CDS, cases must involve at least one passenger car or truck and be of sufficient severity that one vehicle was towed from the scene. NASS/GES is a database of approximately 60,000 crashes/year sampled from U.S. police reported crashes, and was used for computation of exposure in this study. Both NASS/CDS and NASS/GES are weighted to be representative of crashes nationally.

Cases were extracted from all three databases using the criteria listed below.

- Case Year 1999-2013
- Model Year (MY) 2000+
- Cars, light trucks, and vans only
- Hybrids identified by Make/Model codes and Fuel Code Variable (hybrid)

These criteria were chosen to include only vehicles with the latest safety technologies. All MY 2000+ passenger vehicles would have been equipped with both driver and right front passenger airbags.

NASS/CDS describes the severity of these injuries based on the Abbreviated Injury Scale (AIS). AIS ranks injuries on a scale of 1-6 based on the threat to the life of the occupant, AIS 1 is a minor injury and AIS 6 is an unsurvivable injury. Here we focused on AIS2+ injured occupants – those occupants with moderate (AIS2) to unsurvivable (AIS6) injuries. Our analysis classified injury severity by the maximum AIS (MAIS) level injury sustained by an occupant. In the analysis which follows, weighted values based on NASS sample weight were used in order to better represent the larger population.

Hybrid and electric vehicles were identified in two ways. For most cases in FARS and NASS/CDS, hybrid and electric cars were identified by using the NASS and FARS FUELCODE variable, which denotes the type of fuel

used in the vehicle. In the event of a missing FUELCODE, the make-model codes of known hybrid and electric vehicles models, e.g. the Toyota Prius and the Chevrolet Volt, were used to identify hybrid and electric vehicles. NASS/GES does not contain a similar FUELCODE variable which describe the type of fuel used in the vehicle. For cases in NASS/GES, make-model codes of known hybrid and electric vehicle models were used to identify hybrid and electric vehicles.

## RESULTS

### Dataset Composition

Table 1 shows the composition of vehicles in all three databases used in the study. Hybrid vehicles made up approximately 0.3% of the fatal crashes in FARS, 0.7% of the weighted cases in NASS/CDS, and 0.3% of the weighted cases in NASS/GES. No fatalities associated with electric vehicles were found in the FARS databases. Only 2 electric vehicles were found in the NASS/CDS database, representing approximately 0.002% of the weighted vehicle sample, and 18 electric vehicles were found in the NASS/GES database, representing approximately 0.003% of the weighted vehicle sample in NASS/GES. Given the small proportions of electric vehicles in the databases, the following analysis only focuses on the comparison between hybrid and conventional vehicles.

**Table 1.**
**Dataset Composition of Vehicles in All Databases (Case Year 1999-2013)**

| Database | Hybrid Vehicles (%) | Electric Vehicles (%) | Conventional Vehicles (%) | Total Vehicles (%) |
|---|---|---|---|---|
| **FARS** | 421 (0.3%) | - | 128,119 (99.7%) | 128,540 (100%) |
| **NASS/CDS (Unweighted)** | 377 (0.7%) | 2 (0.004%) | 55,696 (99.3%) | 56,075 (100%) |
| **NASS/CDS (Weighted)** | 165,932 (0.7%) | 553 (0.002%) | 25,308,829 (99.3%) | 25,475,314 (100%) |
| **NASS/GES (Unweighted)** | 1,863 (0.3%) | 18 (0.003%) | 561,812 (99.7%) | 563,693 (100%) |
| **NASS/GES (Weighted)** | 233,796 (0.3%) | 2,310 (0.003%) | 68,280,880 (99.7%) | 68,516,986 (100%) |

### Dataset Composition

Table 2 shows the distribution of body types for vehicles in the databases. Weighted percentages are shown for NASS/CDS and NASS/GES databases. As shown by the table, conventional vehicles contains approximately equal percentage of cars and LTV, while hybrid vehicles are predominantly passenger cars.

**Table 2.**
**Distribution of Vehicle Body Type in All Databases (Case Year 1999-2013)**

| Database | Hybrid Vehicles | | Conventional Vehicles | |
|---|---|---|---|---|
| | Cars (%) | LTV (%) | Cars (%) | LTV (%) |
| **FARS** | 94% | 6% | 55% | 45% |
| **NASS/CDS (Weighted)** | 87% | 13% | 57% | 43% |
| **NASS/GES (Weighted)** | 100% | 0% | 57% | 43% |

### Incidence of Fire in Vehicles

Table 3 shows the number of vehicles involved in crashes with fire in all three databases. In fatal vehicle crashes extracted from FARS, incidence of fire was found in 11 of the 421 hybrid vehicles (2.6%). In comparison, 5,619 of 128,119 conventional vehicles (4.4%) involved in fatal crashes had fire occurrence.

Similar to the FARS analysis, Table 3 shows that vehicle fire was also rare for cases included in NASS/CDS. No hybrid vehicles in the sample experienced a vehicle fire and only 330 of 56,075 conventional vehicles had a fire. Using weighted numbers, this comprised approximately 0.1% of all conventional vehicles in crashes.

The incidence of fire was similarly rare in NASS/GES. Only 1 hybrid vehicle was reported to be involved in a fire, while 974 conventional vehicles were involved in crashes with fire incidences in NASS/GES. Using the NASS/GES weighting factor, fire occurred in 0.03% of all hybrid vehicles and 0.07% of all conventional vehicles.

**Table 3.**
**Vehicles in Crashes Involving Fire in All Databases (Case Year 1999-2013)**

| Database | Hybrid Vehicles (% of All Hybrid) | Electric Vehicles (% of All Electric) | Conventional Vehicles (% of All Conventional) |
|---|---|---|---|
| **FARS** | 11 (2.6%) | - | 5,619 (4.4%) |
| **NASS/CDS (Unweighted)** | - | - | 330 (0.6%) |
| **NASS/CDS (Weighted)** | - | - | 37216 (0.1%) |
| **NASS/GES (Unweighted)** | 1 (0.05%) | - | 974 (0.2%) |
| **NASS/GES (Weighted)** | 61 (0.03%) | - | 48,685 (0.07%) |

**Incidence of Electric Shock**

In addition to the incidence of fire, we also searched for any reports of electric shock. Using the sample of crashes from NASS/CDS, AIS codes for all occupants were searched for cases of electric shock. However, no such cases were found in our dataset for either hybrid, electric, or conventional vehicles. Note however, that NASS/CDS only contains vehicles involved in towaway crashes. These results should not be generalized to non-towaway crashes on other non-crash situations.

**Occupant Characteristics**

**Occupant Composition and Gender** Table 4 shows the occupant distribution by gender in all three databases. Only weighted gender percentages are shown from both NASS/CDS and NASS/GES datasets. A total of 465 fatally injured hybrid vehicle occupants and 142,821 fatally injured conventional vehicle occupants were found in the FARS data set. Of all fatally injured hybrid vehicle occupants, 58% were male and 42% were female. On the other hand, 62% of all fatally injured conventional vehicle occupants were male and 38% were female.

In NASS/CDS, the distribution of gender between all exposed occupants was almost equal. 43% of hybrid vehicle occupants and 51% of conventional vehicle occupants in NASS/CDS were male. However, only 11% of all MAIS2+ injured hybrid occupants were male, while 47% of all MAIS2+ injured conventional vehicle occupants were male and 53% were female.

Similar to occupants in NASS/CDS, the distribution of gender in NASS/GES was found to be fairly equal. 50% of conventional vehicle occupants were male, while 47% of hybrid occupants were male.

**Table 4.**
**Occupant Count and Gender Distribution in All Databases (Case Year 1999-2013)**

| Database | Hybrid Vehicle Occupants | | | Conventional Vehicle Occupants | | |
|---|---|---|---|---|---|---|
| | Occ. Count | % Male | % Female | Occ. Count | % Male | % Female |
| **FARS** | 465 | 58% | 42% | 142,821 | 62% | 38% |
| **NASS/CDS (All Occ. Unweighted)** | 407 | - | - | 66,037 | - | - |
| **NASS/CDS (MAIS2+ Unweighted)** | 62 | - | - | 11,430 | - | - |
| **NASS/CDS (All Occ. Weighted)** | 165,070 | 43% | 57% | 25,029,076 | 51% | 49% |
| **NASS/CDS (MAIS2+ Weighted)** | 24,821 | 11% | 89% | 1,306,918 | 47% | 53% |
| **NASS/GES (All Occupants Unweighted)** | 2,523 | - | - | 802,523 | - | - |
| **NASS/GES (All Occupants Weighted)** | 301,992 | 47% | 53% | 94,734,122 | 50% | 50% |

**Occupant Age** The following subsection presents the distribution of occupant age in the three databases. Only occupants with known age are shown in the distributions. Occupants less than one year old are listed as having an age of 0.

Figure 1 shows a summary of median occupant age in all three databases. As shown by the figure, the median age of occupants in hybrid vehicles are generally older than occupants of conventional vehicles. In fatal crashes extracted from FARS, the median age of fatally-injured hybrid occupant was 59 years while the median age of fatally-injured conventional vehicle occupants was 36 years. For all occupants with MAIS2+ injuries in NASS/CDS, the median age for MAIS2+ injured hybrid vehicle occupants was 53 years, and 35 years for conventional vehicle occupants. For all exposed occupants in NASS/CDS, the median age for hybrid occupants was 42 years while the median age for conventional fleet occupants was 29 years. For all occupants in NASS/GES, the median age for conventional vehicle occupants was 32 years while the median age for hybrid occupants was 44 years old.

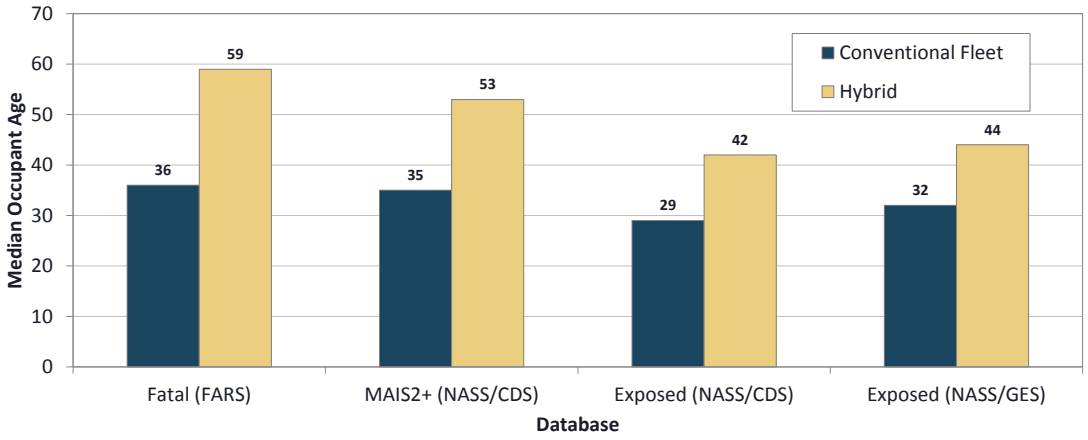


***Figure 1. Summary of Median Occupant Age in Crashes (1999-2013)***

**Occupant Restraint Use** The following subsection presents the occupant restraint use in each of the three databases. Only occupants with known restraint use are included in the distributions shown. The "Other" restraint category includes occupant wearing restraint other than lap and shoulder belt or a child restraint, such as lap belt only, shoulder belt only, or wearing the restraint improperly.

Figure 2 shows the distribution of occupant restraint use in fatal crashes extracted from FARS. The comparison between fatalities in hybrid occupants and fatalities in conventional vehicle occupants shows that belt usage was much higher in hybrid fatality crashes. Approximately 75% of occupants in hybrid vehicles were belted, while only 47% of occupants in the conventional fleet were belted.

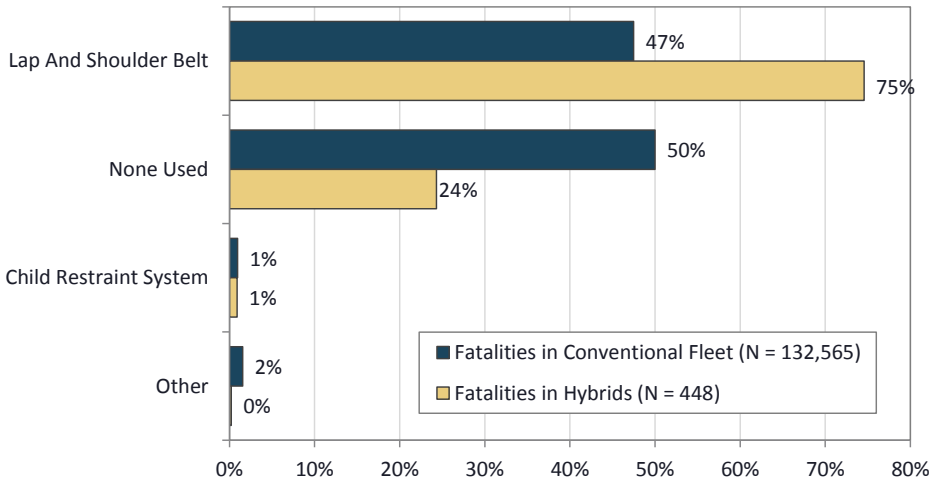


***Figure 2. Distribution of Occupant Restraint Use in Fatal Crashes (FARS 1999-2013)***

Figure 3 shows the restraint use distribution for all occupants exposed to crashes in NASS/CDS. Approximately 90% of both hybrid and conventional fleet occupants were belted.

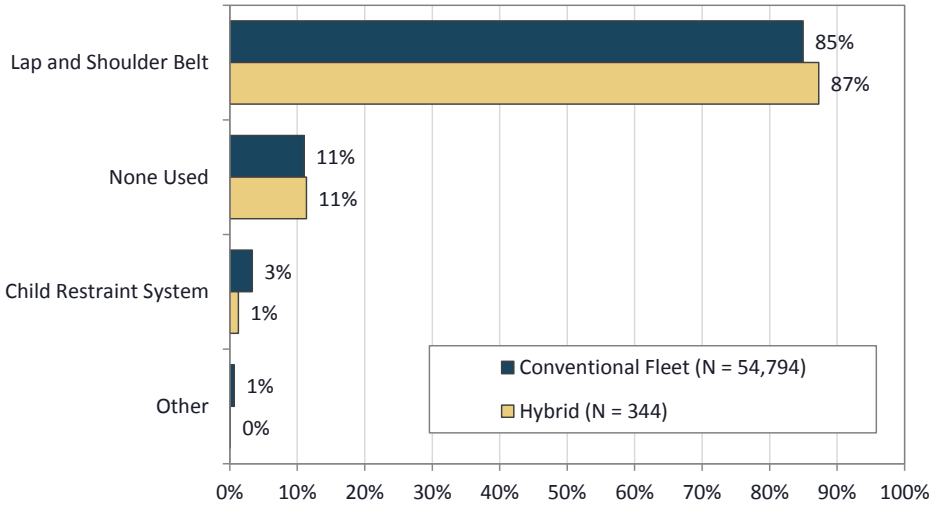


***Figure 3. Distribution of Restraint Use in All Exposed Occupants (NASS/CDS 1999-2013)***

Figure 4 shows the distribution of distribution of restraint use in MAIS2+ injured occupants in NASS/CDS. Compared to the distribution of all exposed occupants, the restraint use in MAIS2+ injured conventional vehicle occupants decreased from 85% to approximately 67%. On the other hand, the restraint use for hybrid vehicle occupants increased from 87% to 98%.

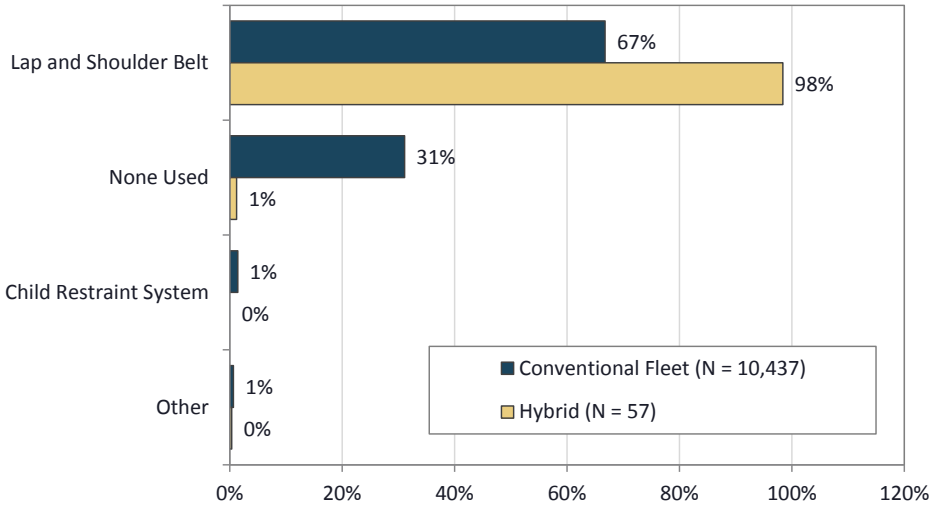


***Figure 4. Distribution of Restraint Use in MAIS2+ Injured Occupants (NASS/CDS 1999-2013)***

Lastly, Figure 5 shows the distribution of restraint use in all occupants involved in crashes in NASS/GES. As shown from the figure, conventional fleet occupants and hybrid occupants have similar restraint use. Approximately 88% of occupants in the conventional fleet were belted, and about 92% of hybrid occupants were belted.

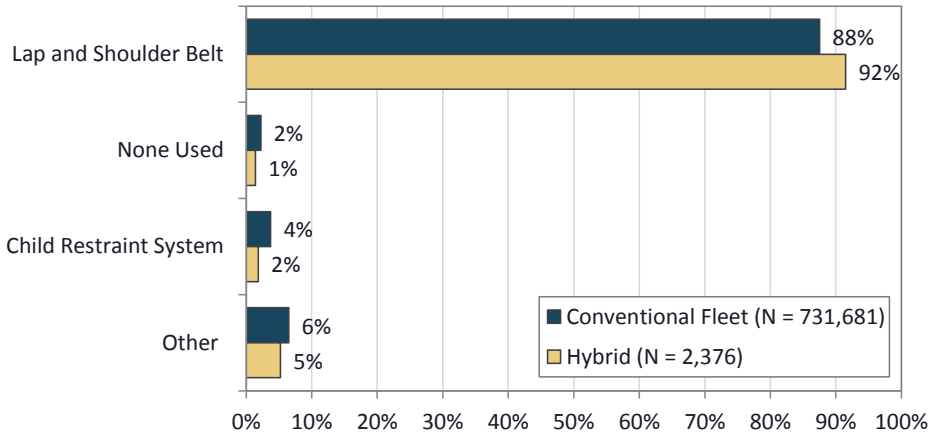


***Figure 5. Distribution of Occupant Restraint Use in All Occupants (NASS/GES 1999-2013)***

Figure 6 shows the summary of occupant restraint use in all three databases. In the distribution shown, restrained occupant refers to any occupant wearing a lap and shoulder belt, lap belt, shoulder belt, or child restraint. As shown in Figure 6, occupants in hybrid vehicles were generally more likely to be restrained.

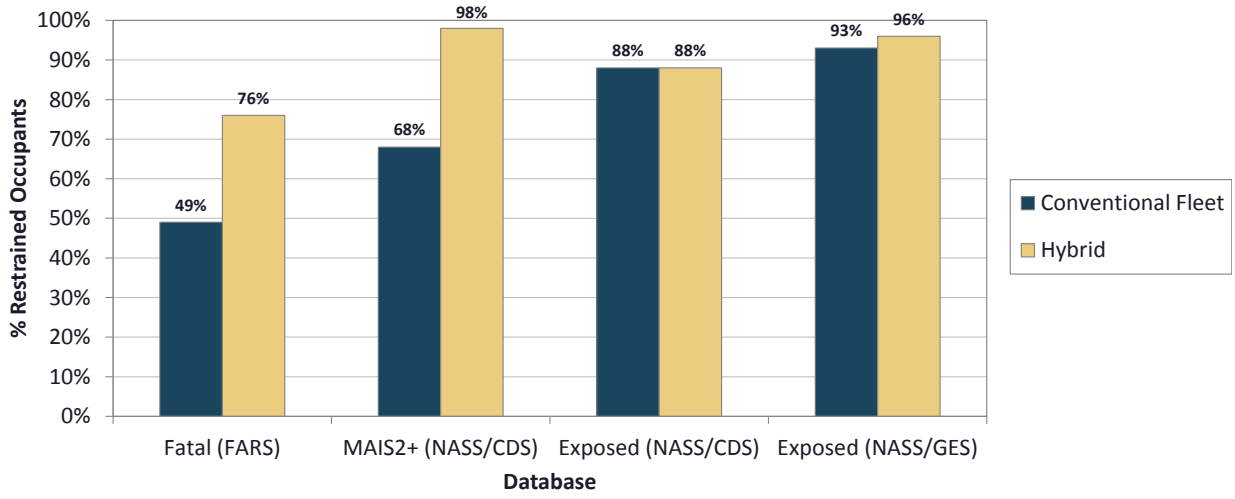


***Figure 6. Summary of Occupant Restraint Use (1999-2013)***

**Occupant Risk of Injury** The comparison of occupant injury was conducted using injury information reported from NASS/CDS. In this study, the risk of injury for a particular body region is calculated as fraction of cases at a given severity, as shown in Equation 1.

$$Risk\ of\ Injury = \frac{Number\ of\ Injuries\ to\ Body\ Region}{Total\ Number\ of\ Known\ Injuries} \quad (1)$$

Figure 7 compares the risk of AIS2+ injury by body regions for each occupant of hybrid and conventional vehicles. For both vehicle types, the risk of head injury was very similar (2.5% vs. 2.0%). Similarly, there was little difference in risk of chest injury (1.6% for conventional vehicle occupants and 1.2% for hybrid occupants). However, our sample predicted a higher risk of upper extremity injury for hybrid occupants (2.9% vs. 1.6%), and a lower risk of lower extremity injury for hybrid occupants (0.5% vs. 1.9%). When interpreting this plot, we caution again that the hybrid AIS2+ injuries are based upon a very small number of cases for occupants in hybrid vehicles.

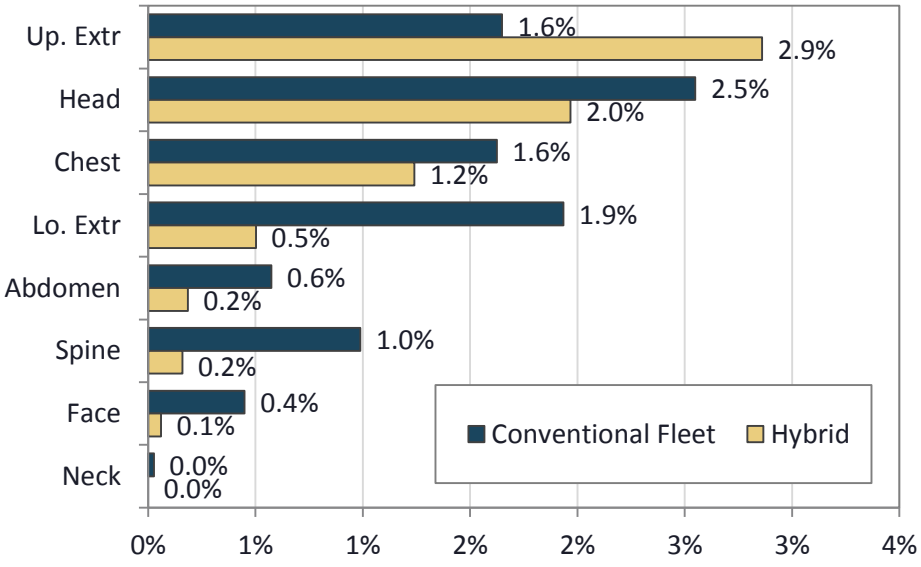


***Figure 7. Risk of AIS2+ Injury by Body Region (NASS/CDS 1999-2013)***

## Crash Characteristics

**Crash Mode** Figure 8 presents the distribution of fatal crash modes for hybrid and conventional fleet vehicles. The distribution of crash mode is based on the most harmful event during the crash. However, after

year 2011, the definition of crash mode was changed in FARS. Therefore, the distribution shown in Figure 8 is limited to case year 1999-2011.

As shown by the figure, frontal crashes comprise the majority (50%) of fatal crashes, and side impact accounts for the second most common fatal crash mode (28%). For conventional vehicles however, rollover crashes and frontal crashes account for nearly equal percent of fatal crashes (37% and 35%, respectively). The increased incidence of rollover in conventional vehicles may be due to the large number of SUVs and pickup trucks in the fleet, which have a much higher risk of rollover.

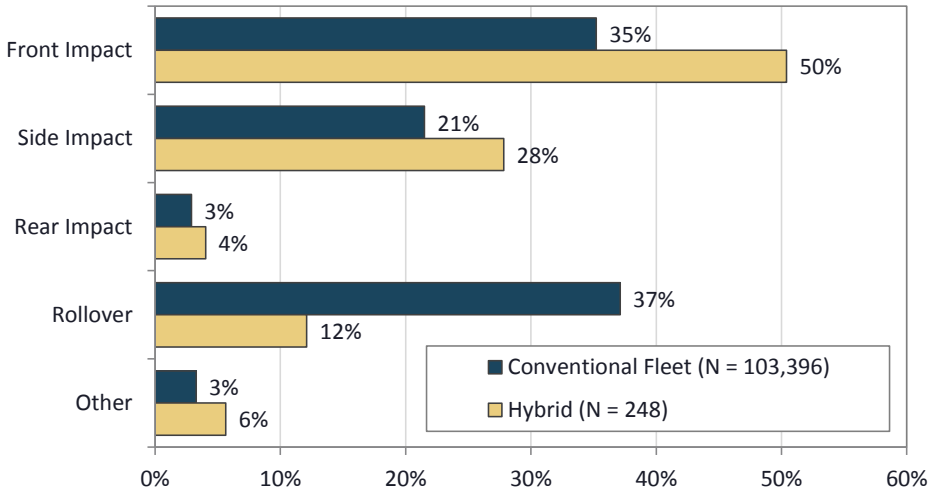


***Figure 8. Distribution of Crash Mode in Fatal Crashes (FARS 1999-2011)***

In the NASS/CDS dataset, the most common crash mode for MAIS2+ injured occupants in conventional vehicles was frontal impact, as shown by Figure 9. Over half of all MAIS2+ injured occupants in conventional vehicle were involved in a frontal impact. Side impact, including impacts to both the left and right side of the vehicle, was the most frequent crash mode for hybrid vehicles. Over 80% of all MAIS2+ injured hybrid occupants involved in a side impact. Rollover was more frequent in conventional vehicles as compared to hybrid vehicles, with 18% of all MAIS2+ injured conventional vehicle occupants exposed to rollover and less than 1% of all MAIS2+ injured hybrid vehicle occupants were exposed to rollovers.

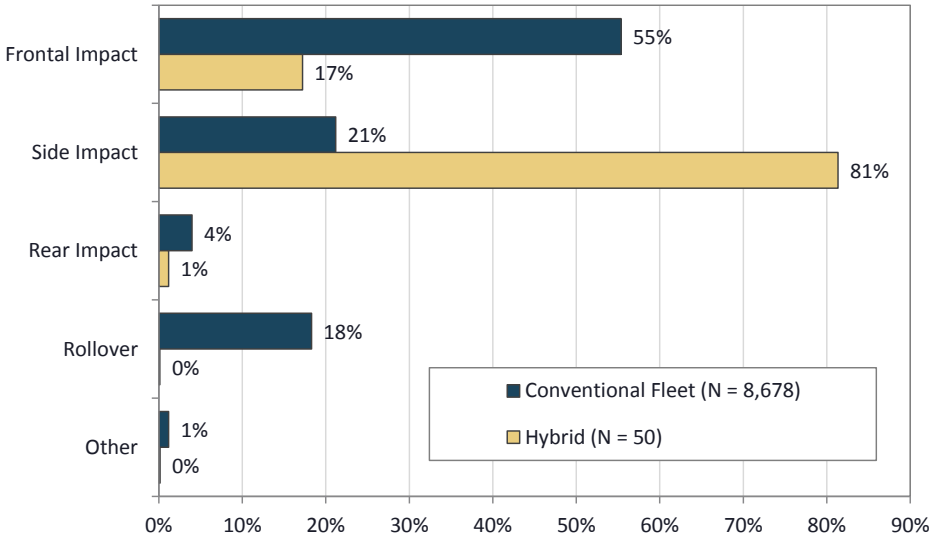


***Figure 9. Distribution of Crash Mode in MAIS2+ Injured Crashes (NASS/CDS 1999-2013)***

Figure 10 presents the distribution of crash modes in the NASS/GES database. As observed in the FARS and NASS/CDS analyses, frontal impact was the most common crash mode for both vehicle types, and accounted for

approximately 40% of all crashes for both vehicle types. However unlike FARS and NASS/CDS, rear impact was a close second in frequency with 26% of crashed conventional vehicles and 33% of crashes hybrid-vehicles. Rear impact is a common crash mode, but does not carry the injury risk of other crash modes. We hypothesized that rear impact was more common for hybrid vehicles as these are more likely to be drive in urban environments where frequent stop-and-go traffic leads to increase chance of rear end crashes.

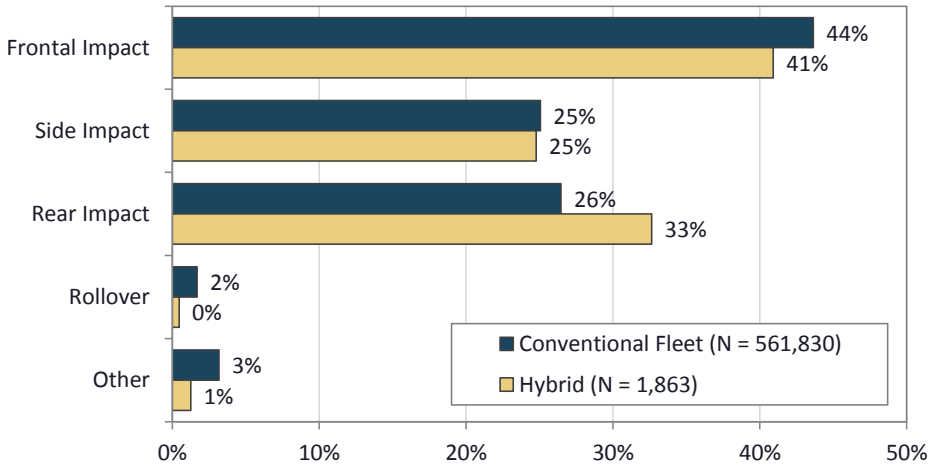


***Figure 10. Distribution of Crash Mode in All Crashes (NASS/GES 1999-2013)***

**Crash Severity** The struck vehicle change in velocity, or delta-V, is a widely used measure of crash severity. Longitudinal delta-V for all exposed occupants is presented in Figure 11. The median longitudinal delta-V for hybrid vehicles was 18 km/hr while the median delta-V for conventional vehicles was 14 km/hr. The delta-V for hybrid vehicles was higher as hybrids are in general lighter than conventional vehicles, which include a large number of SUVs and pickup trucks.

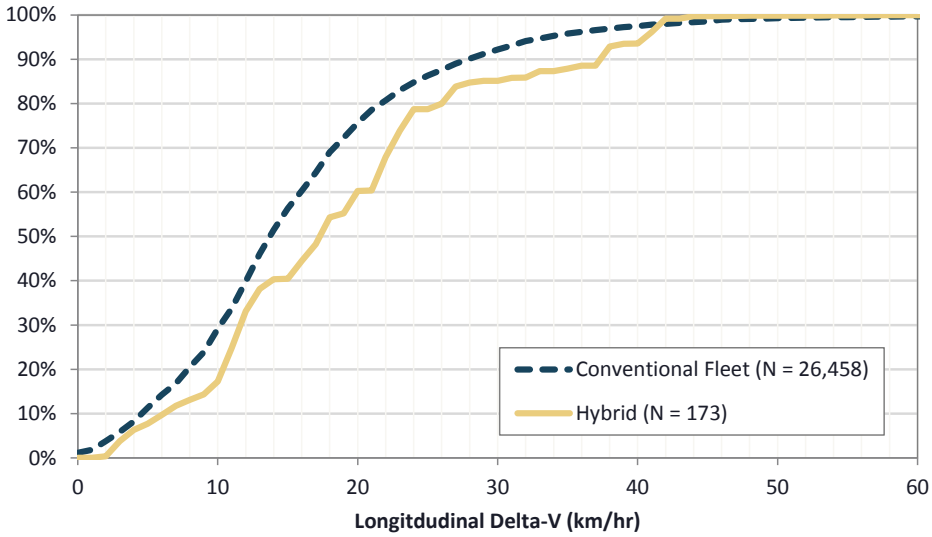


***Figure 11. Distribution of Longitudinal Delta-V for All Occupants (NASS/CDS 1999-2013)***

The lateral delta-V distribution was very similar for occupants of both hybrid and conventional vehicles. As shown by Figure 12, the median lateral delta-V was approximately 5 km/hr for hybrid vehicles and 3 km/hr for conventional fleet vehicles.

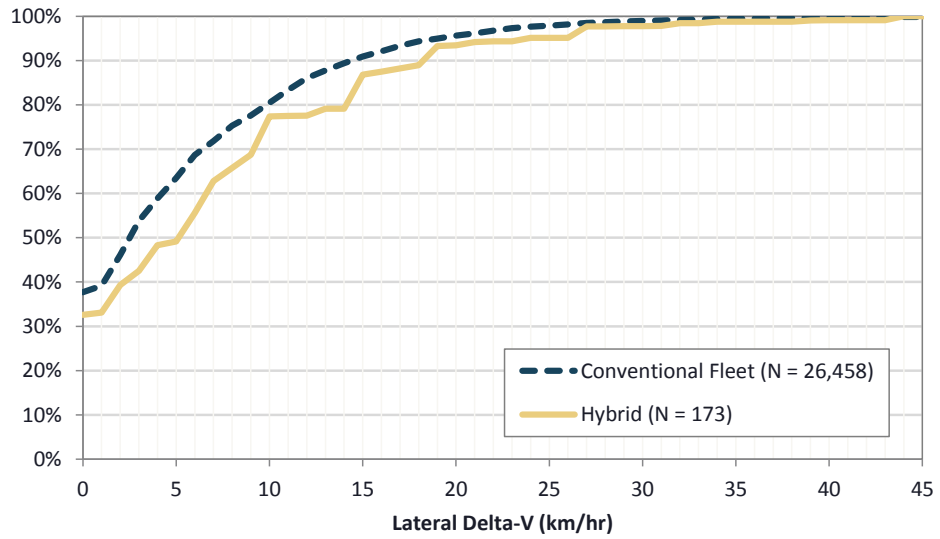


***Figure 12. Distribution of Lateral Delta-V for All Occupants (NASS/CDS 1999-2013)***

## CONCLUSIONS

The goal of this study was to characterize the factors which influence the risk of serious to fatal injury in U.S. hybrid and electric passenger vehicle crashes. The study was based upon the analysis of three U.S. crash databases: (1) the Fatal Analysis Reporting System (FARS), (2) the National Automotive Sampling System / Crashworthiness Data System (NASS/CDS), and (3) the National Automotive Sampling System / General Estimates System (NASS/GES).

The analysis datasets included 421 hybrid vehicles from FARS, 377 hybrid vehicles from NASS/CDS, and 1,863 vehicles from NASS/CDS. Only 2 electric vehicles were found in NASS/CDS, and 18 electric vehicles were found in NASS/GES and, therefore, we could not further investigate electric vehicles in this study.

Fires were rare in both hybrid and conventional vehicles. Fatal crashes involving fire constituted 2.6% of hybrid cases and 4.4% of conventional vehicle cases. No cases of fire or electric shock injury for hybrids in NASS/CDS 1999-2013. Only 1 case of a hybrid fire was found in NASS/GES. The incidence of fire was lower for hybrids than conventional vehicles in all three databases.

The gender of fatally injured hybrid and conventional vehicle occupants was very similar. Males were more likely than females to be fatally-injured. For the population as a whole as described in GES, hybrid occupants were more likely to be female (53%) than conventional vehicle occupants (50%).

Hybrid occupants were more likely to be older than conventional vehicle occupants in all three databases. In FARS, the median age of fatally injured hybrid occupants was 59 yrs vs. 36 years for conventional vehicle occupants. In NASS/CDS, hybrid occupants were more likely to be older (42 yrs) than conventional vehicle occupants (29 yrs). In GES, hybrid occupants were more likely to be older (44 yrs) than conventional vehicle occupants (32 yrs).

The risk of MAIS2+ head and chest injury was very similar for both hybrid and conventional vehicles. Upper extremity injury risk was higher while lower extremity risk was lower for occupants of hybrids than those in conventional vehicles.

Frontal impact was more frequently the fatal crash mode for hybrid (50%) than conventional vehicles (35%). In NASS/CDS, frontal impact was more frequently the injury crash mode for conventional vehicles (53%) than hybrid vehicles (40%). In GES, frontal impact was most frequently the crash mode for both hybrids (41%) and conventional vehicles (44%).

Hybrids and conventional vehicles had similar crash severity based on cases included in NASS/CDS. Longitudinal delta-V for hybrids was 18 km/hr and 14 km/hr for conventional vehicles. Lateral delta-V were similar for both vehicle types.

Our study found little difference between hybrid/electric and conventional vehicle crashes, in either crash performance or injury outcome between the two groups. No unique factors that could influence the crash outcome of these advanced fuel vehicles were found in this study. However, the hybrid/electric vehicle population is currently only a small percentage of the market share. Future studies will benefit from examination of larger population of hybrid/electric vehicles.

## ACKNOWLEDGEMENTS

Hyundai Motor Corporation is gratefully acknowledged for providing the funding for this study.

## REFERENCES

[1] S. C. Davis, S. W. Diegel, R. G. Boundy, and S. Moore, "2013 Vehicle Technologies Market Report." Oak Ridge National Laboratory, Oak Ridge, TN, 2014.

[2] B. Smith, "Chevrolet Volt Battery Incident Overview Report," DOT HS 811 573, January 2012.

[3] Mitsubishi Motors, "Press Release: Fire of Electric Vehicle Battery Pack in Mizushima Plant," 2013. [Online]. Available: http://www.mitsubishi-motors.com/publish/pressrelease_jp/corporate/2013/news/detaild327.html. [Accessed: 27-Jan-2015].

# BICYCLIST BEHAVIOR ANALYSIS FOR PCS (PRE-COLLISION SYSTEM) BASED ON NATURALISTIC DRIVING

**Ryo Fujishiro**
Toyota Motor Corporation
Japan

**Chao Liu**
**Lauren Christopher**
**Jiang Yu Zheng**
Transportation Active Safety Institute, Indiana University-Purdue University Indianapolis
United States

Paper Number 15-0211

## ABSTRACT

In recent years, automakers have introduced the PCS (Pre-Collision System) which is designed to warn a driver or to brake automatically to help avoid or mitigate accidents. One of the significant aspects of this system is to help protect vulnerable road users such as pedestrians and bicyclists. In this paper, the research is introduced which analyzes normal bicyclist behavior in order to design and evaluate PCS systems. The attributes of normal bicyclist behavior investigated are: TTC (Time-To-Collision), lateral position, vehicle speed and bicycle speed. This behavior was analyzed using TASI's (IUPUI's Transportation Active Safety Institute) naturalistic driving data from 110 cars.

## INTRODUCTION

The PCS (Pre-Collision System) is designed to warn a driver or brake automatically to help avoid or mitigate potential accidents. This system is needed to detect and robustly classify surrounding objects. Therefore, a broad range of sensors are utilized for PCS systems such as: millimeter-wave radar [1], LIDAR [2], camera [3] and the combination of some sensors [4][5]. Each sensor choice has pros and cons. For instance, radar is good at detecting distances and relative speeds of an object, but not good at classifying the type of an object. On the other hand, a camera is good at classifying the type of an object, but not good at detecting distances and relative speeds of an object. Therefore, those sensors are selected by manufacturers to classify target objects such as vehicles, pedestrians and bicyclists. The number of targets is expanding with improved sensor technology. Consequently, one of the significant aspects of PCS systems is considered to help protect vulnerable road users such as pedestrians and bicyclists. In fact, a non-negligible number of fatalities in regard to pedestrians and bicyclists are reported by NHTSA (National Highway Traffic Safety Administration) [6][7]. According to [6] and [7], of all traffic fatalities in 2012, 14% were pedestrian deaths and 2% were pedalcyclist deaths.

This research is targeting normal bicyclist behavior in order to help design and evaluate PCS systems. By knowing what is considered normal, the PCS can concentrate on the abnormal behavior and react in the dangerous situations. Of course, bicyclist accident data analysis is also important for PCS design and testing. However, the accident data lacks some detailed parameters in general. Some bicyclist parameters which are needed to design or evaluate PCS systems should be analyzed in both accident analysis and normal bicyclist behavior analysis. For normal behavior analysis, an enormous data set, called TASI 110-Car Naturalistic Driving Data [8], is utilized for understanding bicyclist behavior relative to the driving vehicles. This data set includes 120 degree viewing angle videos observing traffic in front of the vehicles, together with Global Positioning System (GPS) location data and G-sensor information of the vehicles. From this data set, bicyclists were extracted using machine learning and pattern recognition techniques [9]. Pattern recognition enables the computer to find specified objects automatically. From these bicycle video clips, the bicyclist movement was tracked using visual tracking techniques [10]. Once an initial position is given, the tracking follows a bicyclist. From these tracking results and the GPS information, the TTC (Time-To-Collision), lateral position, vehicle speed and bicycle speed were calculated. Several important and intriguing findings were observed.

## METHOD

### Data Set and Tracking of Bicyclists

The TASI 110-Car Naturalistic Driving Data [8] was utilized and more than 10,000 videos containing bicyclists were extracted. The data has 120 degree viewing angle videos of observed traffic in front of the vehicles, GPS location, speed data and G sensor information. The data collection was conducted mainly in Indiana, United States from 2012 to 2013. The data consist of a total of 1.1 million miles (2T bites) in length. This data set was first used to analyze pedestrian behavior in a naturalistic driving condition. This paper presents the bicyclist research from this huge data set. Subject vehicles drove in the downtown area where many bicyclists were found.

Bicyclists were extracted from all the recorded videos using pattern recognition techniques in [9]. The results contained false positives (unsolicited detection), which were eliminated manually. Bicyclist position in an image was specified as a rectangle, but the detected position was not necessarily accurate. Therefore, the bicyclist position was corrected manually. This correction was conducted at one video-frame for one bicyclist video clip of 5 seconds. Once an accurate bicyclist position at one video-frame was obtained, that bicyclist was tracked using the referenced visual tracking techniques [10]. Bicyclist movement was represented as a sequence of a size-varying rectangle. The rectangle size information was used for calculation of TTC, lateral position, vehicle speed and bicycle speed.

### TTC Calculation

TTC is one of the most significant variables for PCS systems since this signifies the level of danger in a convincing and direct manner. This section details TTC calculation method as the ratio of the depth over the first derivative of the depth. TTC is defined as Equation (1) provided that the distance from the camera is defined as Z.

$$TTC = -\frac{Z}{\dot{Z}} \qquad \text{Eq. (1).}$$

However, one problem of using this method is inaccuracy of Z. Generally, camera recognition is good at detecting object angle, but not good at detecting object distances. Since the TTC calculation is central to PCS systems, a different method was utilized to calculate TTC as described in [11]. In Figure 1, X, Y and Z denote world coordinates, S denotes the size of the bicyclist, s denotes the size of the bicyclist in the image, and F denotes the focal length.

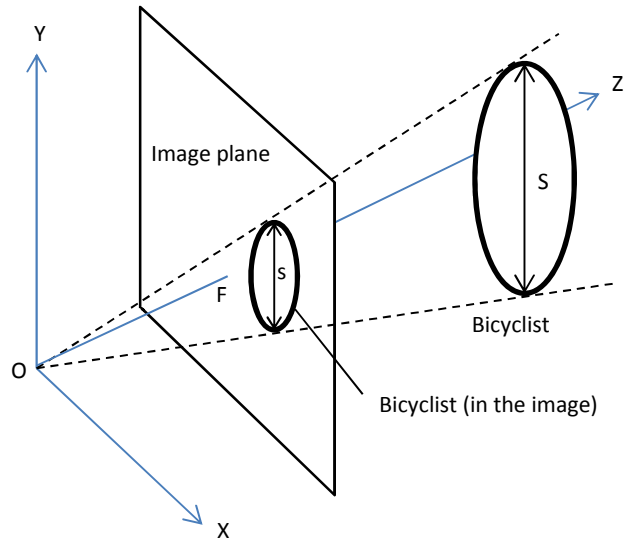


***Figure 1. Geometrical relationship between a bicyclist and the projection to the image plane.***

Equation (2) is derived from the geometrical relationship.

$$\frac{1}{s} = \frac{Z}{S \cdot F} \quad \text{Eq. (2).}$$

Substituting Equation (1) for Equation (2), TTC is calculated as Equation (3).

$$TTC = \frac{s}{\dot{s}} \quad \text{Eq. (3).}$$

In Equation (3), the only value necessary to calculate TTC is the size of the bicycle in the image. This size was detected using tracking techniques as stated above.

**Lateral position calculation**

Although TTC is central to PCS systems, TTC is not enough information to analyze bicyclist behavior since TTC signifies only longitudinal relative movement. This research also analyzed the lateral position of the bicyclist to the vehicle. In order to calculate the lateral position, the distance to the bicyclist was calculated first as described in [12], and then lateral position was calculated next.

In Figure 2, H denotes the height of the camera, $Z_c$ denotes the distance between the camera and the bicyclist on the road, $\theta_h$ denotes the vertical angle of the horizon in the camera axis, and $\theta_{bv}$ denotes the vertical angle of the bicyclist's bottom in the camera axis. Provided that the horizon and bicyclist bottom are specified in the image, the angles of $\theta_h$ and $\theta_{bv}$ can be obtained. Horizon position was specified with human operators examining the videos, and bicyclist bottom was obtained from a rectangle which is the result of the tracking discussed above. Equation (4) details how to calculate the distance, $Z_c$.

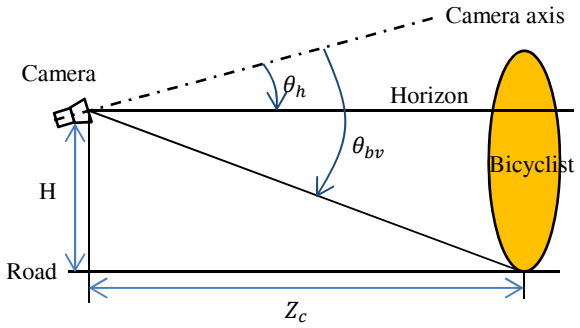


***Figure 2. Geometry of a bicyclist (side view).***

$$Z_c = \frac{H}{\tan(\theta_{bv} - \theta_h)} \quad \text{Eq. (4).}$$

The camera height H should be a fixed value of each vehicle. However, there were some cases in which cameras dropped and were attached again in the naturalistic driving. That is why the camera height H was not able to be maintained strictly. One fixed value per vehicle was chosen that was considered to be the most likely.

In Figure 3, $X_c$ and $Z_c$ denote the bicyclist position in the camera coordinate system, $X_v$ and $Z_v$ denote the bicyclist position in the vehicle coordinate system, $\theta_c$ denotes the angle between the camera axis and the vehicle moving direction, and $\theta_{bh}$ denotes the horizontal angle of the bicyclist in the camera coordinate. The vehicle moving direction was specified with human operators examining the videos, and the angle $\theta_{bh}$ was obtained from a

rectangle which is the result of the tracking stated above. Equation (5) and (6) detail a rotation of the coordinate system, which was used to calculate the lateral position $X_v$.

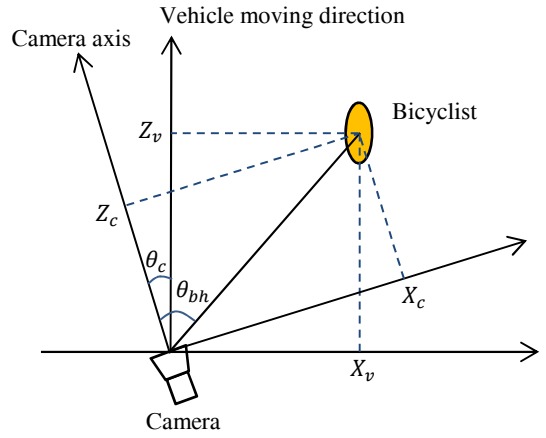


***Figure 3. Geometry of a bicyclist (top view).***

$$X_c = Z_c \tan \theta_{bh} \quad \text{Eq. (5).}$$

$$\begin{bmatrix} X_v \\ Z_v \end{bmatrix} = \begin{bmatrix} \cos\theta_c & -\sin\theta_c \\ \sin\theta_c & \cos\theta_c \end{bmatrix} \begin{bmatrix} X_c \\ Z_c \end{bmatrix} \quad \text{Eq. (6).}$$

**Vehicle and bicycle speed calculation**

Vehicle speed was obtained by the GPS devices. The speed information was extracted from the videos in which the subject vehicles encountered bicyclists.

Bicycle speed is also an important variable to design and evaluate PCS systems. Since bicyclist distance $Z_v$ is calculated as in Equation (6), longitudinal bicyclist speed $V_{br}$ relative to a vehicle is calculated by differentiating this value. Using the vehicle longitudinal speed $V_v$ which is obtained by GPS, the longitudinal bicyclist speed $V_b$ is calculated as in Equation (7).

$$V_b = V_{br} + V_v \quad \text{Eq. (7).}$$

In light of the fact that vehicle turning motion is not recorded in this data set, lateral bicyclist speed is difficult to calculate because the lateral position X and its speed are strongly affected by the vehicle turning. Therefore, we chose not to calculate the horizontal bicyclist speed.

**RESULT**

The pattern recognition techniques stated above extracted bicyclists from all the videos corresponding 1.1 million miles, and the false positives were eliminated manually. The total of 4,259 cases has been processed so far. Then, the tracking was applied to them, and the results were narrowed down to 1,969 cases since some of them were excluded because of the stopped subject vehicles or false tracking. Cases in which subject vehicles were stopped are out of the scope of the PCS actions.

Figure 4 is a heatmap which shows TTC on a vertical axis and lateral position of the bicyclists on a horizontal axis. Each blue point shows the existence of a bicyclist in that position, and each red point shows it as well and means a bicyclist heading toward the vehicle. If the bicyclist direction was heading within +/- 1.5 m at TTC of 0 second, it was deemed heading toward the vehicle. Therefore, red points can be considered more dangerous than blue points. The darkness of the color signifies the frequency of appearances in that position. Therefore, the darker the color is, the higher the probability of existence of a bicyclist in that position. Moreover, the pink dashed line is depicted in Figure 4. This line shows the approximate boundaries between red point areas and the vehicle side.

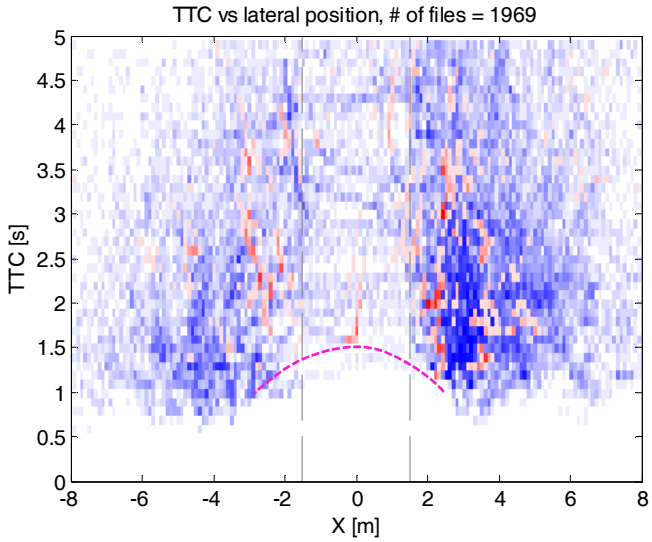


***Figure 4. Heatmap of TTC and lateral position.***

Several findings are observed from Figure 4. First, bicyclists were found more on the right side of the vehicles. This is due to US traffic rules which adopt right-hand traffic. This is why the bicyclists were captured by the cameras more on the right side. Second, the minimum TTC at each lateral position looks larger when lateral position is relatively small, e.g. within +/- 1.5 m. This might be understood as follows. Even if the TTC is small, a far lateral position from the vehicle does not cause dangerous situation. That is why a small TTC is quite normal outside the region where the lateral position is small. However, if a bicyclist is near the center of the vehicle, small TTC might lead to dangerous situation. Incidentally, there is no bicyclist whose TTC is less than 0.6 second in Figure 4. This comes from the limitation of the camera viewing angle. Third, red points imply that collision between a vehicle and a bicyclist might happen if either of them does not take an evasive action. In addition, there was no bicyclist heading toward a vehicle in the bell-shaped region specified by the pink line in this huge naturalistic driving data. This makes sense, as there were no traffic accidents in the entire data set. One conclusion we can find is that if a bicyclist is in this region and heading toward a vehicle, it can be considered abnormal and dangerous. The summit of this region is 1.6 seconds in TTC.

Those findings could be used to design PCS systems. For instance, if a bicyclist heading toward the vehicle is detected inside the region specified by the pink lines, the system may start warning since it can be considered dangerous. On the other hand, if a bicyclist is situated outside the region, PCS warning may be suppressed. Frequent warning should be avoided since it causes drivers to consider PCS systems annoying and switch them off.

Figure 5 shows a histogram of bicyclist lateral position. Only bicyclists moving in the direction parallel to the vehicle path were extracted. The cases were narrowed down to 478. The median of the right side was 3.9 m, and that of the left side was 4.4 m. Those data might be useful to establish PCS testing scenarios.

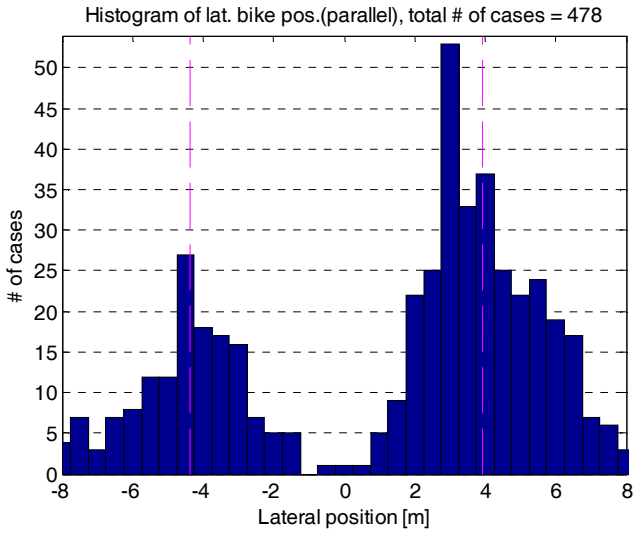


***Figure 5. Histogram of bicyclist lateral position (parallel cases).***

Figure 6 (a) shows a histogram of vehicle speed. Speed was detected by GPS device. The total of 17.4 hours in which the vehicles encountered bicyclists was used for this calculation. The median of the vehicle speed was 32 km/h. As described at the beginning of this section, cases in which vehicles were stopped were excluded since these are out of the scope of the PCS actions.

Figure 6 (b) shows a histogram of vehicle speed. Only bicyclists which satisfy following two conditions were extracted. First condition is that the bicycle is moving in the direction parallel to the vehicle path. Second condition is that the vehicle is moving at constant speed. The data set includes vehicle speed information using the GPS devices, but it contains time-varying delay. In order to evade the erroneous speed estimation, only the referenced-above cases were used. The cases were narrowed down to 198. The median of the bicycle speed was 7.5 m/s. This information might be useful to establish PCS testing scenarios. It has to be brought to attention that the direction of the bicyclists is parallel to the vehicle. In other words, the speed of bicyclists in cross traffic might be different.

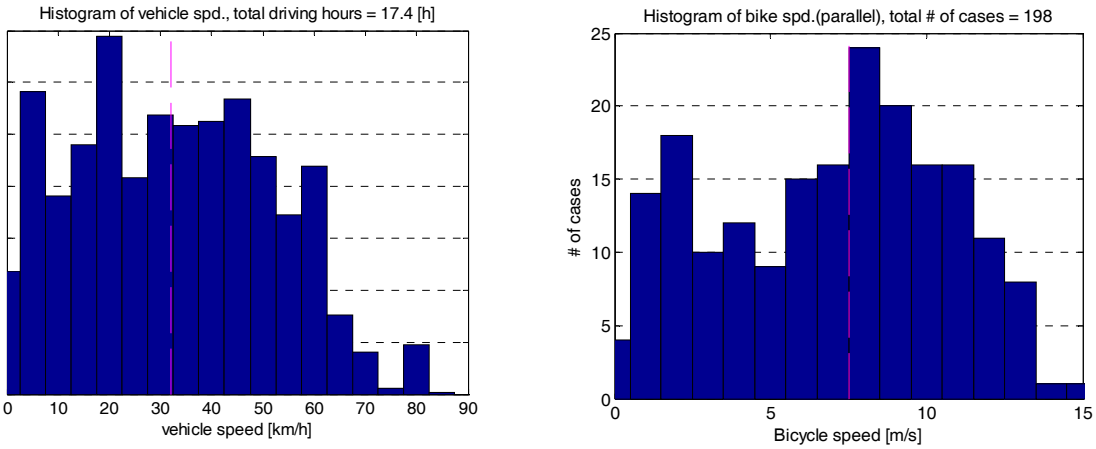


(a) Histogram of vehicle speed

(b) Histogram of bicycle speed

***Figure 6. Histogram of vehicle & bicycle speed (parallel cases).***

## CONCLUSIONS

This research analyzed normal bicyclist behavior to help design and evaluate PCS systems. TTC (Time-To-Collision), lateral position, vehicle speed and bicycle speed were calculated using TASI 110-Car Naturalistic Driving Data. Several important and intriguing findings were observed. First, there is bell-shaped region in front of the vehicle which can be considered abnormal and dangerous. This region might be used when PCS systems are designed. Second, lateral position of the bicyclists when they move in the direction parallel to the vehicle path was estimated. The median of the right side was 3.9 m, and that of the left side was 4.4 m. Those data could be useful to establish PCS testing scenarios. Third, vehicle and bicycle speed were estimated in limited conditions. The median of the vehicle speed was 32 km/h and that of bicycle speed was 7.5 m/s. This information might be useful to establish PCS testing scenarios. The results uncovered in this paper are based exclusively on US data. Those results might differ depending on the country or region.

## REFERENCES


[1] Tokoro, S., Kuroda, K., Kawakubo, A., Fujita, K., & Fujinami H. (2003). Electronically Scanned Millimeter-wave Radar for Pre-Crash Safety and Adaptive Cruise Control System. *Intelligent Vehicles Symposium, 2003. Proceedings. IEEE*, 304-309

[2] Distner, M., Bengtsson, M., Broberg, T., Jakobsson, L. (2009). City Safety - A System Addressing Rear-end Collisions at Low Speeds. *Proceedings of the 21rd International Technical Conference on the Enhanced Safety of Vehicles (ESV), 09-0371*.

[3] Saneyoshi, K. (1996). Drive Assist System Using Stereo Image Recognition. *Intelligent Vehicles Symposium, 1996., Proceedings of the 1996 IEEE*, 230-235.

[4] Hayashi, H., Inomata, R., Fujishiro, R., Ouchi, Y., Suzuki, K., & Nanami, T., (2013). Development of Pre-crash Safety System with Pedestrian Collision Avoidance Assist. *Proceedings of the 23rd International Technical Conference on the Enhanced Safety of Vehicles (ESV), 13-0271*.

[5] Coelingh, E., Eidehall, A., & Bengtsson, M. (2010). Collision Warning with Full Auto Brake and Pedestrian Detection - a practical example of Automatic Emergency Braking. *Intelligent Transportation Systems (ITSC), 2010 13th International IEEE Conference on*, 155-160.

[6] National Highway Traffic Safety Administration. (2014). Pedestrians. *Traffic Safety Facts: 2012 Data, DOT HS 811 888*.

[7] National Highway Traffic Safety Administration. (2014). Bicyclists and Other Cyclists. *Traffic Safety Facts: 2012 Data, DOT HS 812 018*.

[8] Du, E.Y., Yang, K., Jiang, F., Jiang, P., Tian, R., Luzetski, M., Chen, Y., Sherony, R., & Takahashi, H. (2013). Pedestrian Behavior Analysis Using 110-Car Naturalistic Driving Data in USA. *Proceedings of the 23rd International Technical Conference on the Enhanced Safety of Vehicles (ESV), 13-0291*.

[9] Yang, K., Liu, C., Zheng, J.Y., Christopher, L., & Chen, Y. (2014). Bicyclist detection in large scale naturalistic driving video. *Intelligent Transportation Systems (ITSC), 2014 IEEE 17th International Conference on*, 1638-1643.

[10] Jia, X., Lu, H., & Yang, M.H. (2012). Visual tracking via adaptive structural local sparse appearance model. *Computer Vision and Pattern Recognition (CVPR), 2012 IEEE Conference on*, 1822-1829.

[11] Nègre, A., Braillon, C., Crowley, J.L., & Laugier, C. (2008). Real-Time Time-to-Collision from Variation of Intrinsic Scale. In O. Khatib, V. Kumar, & D. Rus (Eds). *Experimental Robotics: The 10th International Symposium on Experimental Robotics* (pp. 75-84). Springer Berlin Heidelberg.

[12] Stein, G.P., Mano, O. & Shashua, A. (2003). Vision-based ACC with a single camera: bounds on range and range rate accuracy. *Intelligent Vehicles Symposium, 2003. Proceedings. IEEE*, 120-125.

# ROAD DEPARTURE PROTECTION - A MEANS FOR INCREASING DRIVING SAFETY BEYOND ROAD LIMITS

**Dr. Benedikt Lattke**
**Alfred Eckert**
**Harald Feifel**
Continental AG – Chassis & Safety Division
Germany

**Dr. Dominik Fröhlich**
**Jeremy McClain**
**Ganesh Adireddy**
Continental AG – Chassis & Safety Division
United States of America

**Florian Janda**
**Dr. Erich Fuchs**
FORWISS - Universität Passau
Germany

Paper Number 15-0212

## ABSTRACT

Despite great technical progress in vehicle safety, according to the WHO approximately 1.2 million fatalities occur on the world's roads every year. Thus great efforts are undertaken to reduce the number of road fatalities and serious accidents, or at least to mitigate their impact on road users. The introduction of environment perception based Advanced Driver Assistance Systems (ADAS) in road vehicles is expected to improve traffic safety significantly. In today's vehicles, the prevalent ADAS focus primarily on the longitudinal driving direction, e.g. Autonomous Emergency Braking (AEB) systems and Adaptive Cruise Control. Whilst the functional range of these systems continues to expand, there exists a very large portion of critical vehicle crashes which are not addressed, mainly caused by vehicles leaving the roadway laterally.

Today, Electronic Stability Control (ESC) is one of the only established Active Safety Systems covering emergency situations in the lateral direction, and always dealing within the physical limits of vehicle dynamics. Despite the very high effectiveness of ESC systems, there remain many cases in which it is not possible to prevent unintended lateral roadway departures, especially in cases of driver drowsiness or inattention, e.g. on American highways or European rural roads. Preventing roadway departure crashes, which cannot be covered by today's lateral guidance/lane keeping ADAS, is motivation behind developing a system for road departure protection. Road Departure Protection systems expand today's lateral ADAS by active road keeping in emergency situations before reaching the physical limits of vehicle dynamics. Based on environment perception means like road edge detection or road course preview, the system should actively intervene when unintentionally leaving the roadway. By automated vehicle control, the system keeps the vehicle on the roadway, thereby protecting against roll-over accidents or collisions with roadside obstacles or oncoming traffic.

This paper presents the roadway departure problem we face today via accident data and different use cases and gives insight into the state of the art Active Safety functions and research activities. The functionalities to address the selected use cases will be described, including functional architectures, a road edge detection algorithm, approaches to preview the course of the road, sensor fusion concepts, a function cascade, and activation strategies. First test data will illustrate the function and working area of a Road Departure Protection system.
A reliable and real-time capable perception algorithm will be demonstrated. For this algorithm, different image processing techniques are applied to mono camera images to estimate the parameters of a geometric model of the road edge. It works without any supplementary knowledge about the road infrastructure.

Two system architectures will be presented, which differ in the used surrounding sensors, actuators, functional capabilities, and system cost. One variant uses a radar sensor, stereo camera and an Electric Power Steering (EPS) system, whereas another solution uses a mono camera and an ESC system. The vehicle steering capabilities and limitations of the ESC based steering are discussed in the paper. Finally, an outlook to future work and possible extensions will be given.

## INTRODUCTION

Despite a tangible increase in the volume of traffic in the United States (US), European Union and Japan for more than a decade, the numbers of fatalities in the same time have been significantly reduced. Along with traffic policy and road-safety education measures, the main contributory factors here have been safety technology measures such as the continuous improvement of active and passive vehicle safety.
Continental has demonstrated with the integral safety system ContiGuard that further development in traffic safety must include – in addition to the individual active/passive safety domains – in particular the complete network and the integration of vehicle surrounding information, including as well the Human Machine Interface (HMI). ContiGuard therefore covers all safety functions by integration of crash prevention and injury mitigation measures, vehicle surrounding sensors, HMI and Safety Telematics, including driver assistance functions. Instead of "Comfort ADAS", which addresses mainly enhanced driving comfort, this paper considers "Safety ADAS" to address challenging driving situations where the safety of vehicle occupants and other road users is endangered. To identify relevant use cases for new "Safety ADAS", US and German accident data is examined in the paragraphs below.

For the United States, the NHTSA "Traffic Safety Facts" 2011 and 2012 [NHTSA11, NHTSA12] report that approximately 1.6 million and 1.75 million single vehicle accidents happened in 2011 and 2012 respectively, of which nearly 55% were related to road departure crashes, out of which 36% caused fatalities or injuries. This amounts to approximately 6% of all accidents in the U.S. in 2011 and 2012. In 2011, of all road departure crashes, 311,000 crashes with fatalities or injuries were due to a collision with fixed objects, such as parked vehicles, poles, or trees. The same data shows, once a vehicle has left the road the risk of fatalities and injuries raises significantly.
On looking further, [NHTSA02] presents more data on crashes related to off-roadway and classifies them into different crash scenarios and their frequencies. As shown in Figure 1, departing road edge without losing the control of the vehicle (straight: 36%, curve: 17%, maneuver: 7%), a scenario which can easily be avoided, totaled to 55% (525,000) of all off-roadway related crashes.

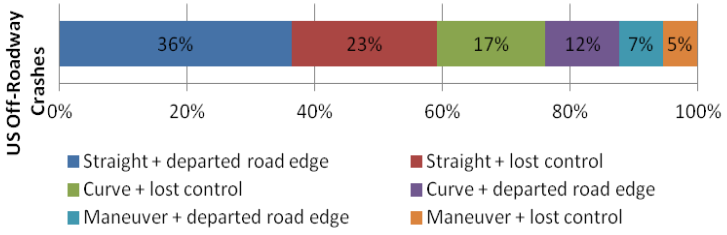


***Figure 1: Off-Roadway crashes on US roads***

In Germany, 60% of road accidents with fatalities and 25% of road accidents with non-fatal injuries occur on rural roads. In 2012, this accounted for 2,151 killed and 25,766 seriously injured persons. Out of all accident victims on rural roads, more than 60% are car occupants [DESTATIS13]. This makes the rural road a focus for developing new safety systems, particularly in passenger cars.
As demonstrated in Figure 2, a first more detailed analysis of rural road accidents shows that 47% of accidents are driving accidents that are caused by car drivers losing control of their vehicle. 86% of these driving accidents lead to the vehicles run-off the carriageway to either side (46% right, 40% left) [GIDAS13]. Car safety systems could address these accidents by stabilizing the vehicles or by protecting them from road departure.

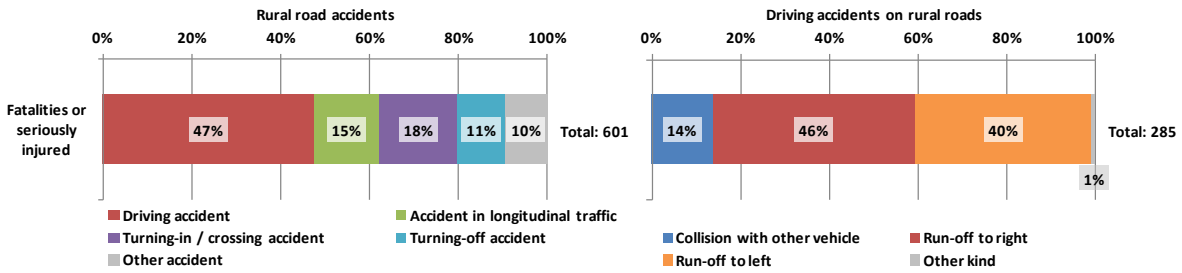


***Figure 2: Accident types on German rural roads (left figure) and accident kinds of driving accidents on German rural roads (right figure) [GIDAS13]***

In a second step, all car accidents on rural roads are analyzed, where the vehicle runs-off the road resulting from a driving accident, i.e. the driver losing control of the vehicle [GIDAS13]. Hereby, accidents with ESC-fitted vehicles are considered only, as those are regarded state of the art. The causes of accidents with fatalities or seriously injured are examined as this information delivers necessary input for the system development.
As shown in Figure 3, 38% of all driving accidents on rural roads with the vehicle running of the road are caused by "other mistake made by the driver" (e.g. inattention, drowsiness), 27% are caused by inappropriate speed (within speed limits) and 14% are caused by excessive speed (speeding).

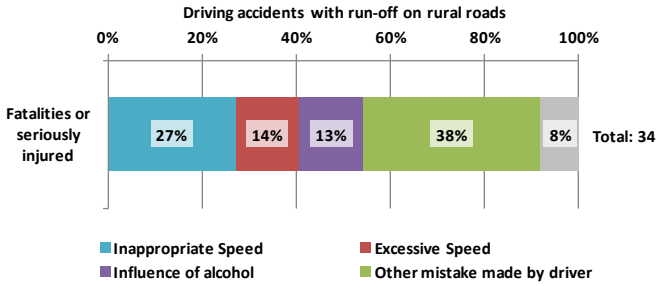


***Figure 3: Accidents caused by cars on rural roads (accident type = driving accident, accident kind = run-off road, ESC fitted) [GIDAS13]***

Similar to the provided US statistics, the German accident data demonstrates that there is a lack in vehicle safety regarding the protection from unintended road departure. Regarding vehicle dynamics, the relevant accidents can be divided into two main groups:

1.) Reaching the physical limits ("lost control", "speed") which counts for 45% (US) resp. 41% (GER) of relevant accidents (Figure 1, Figure 3).
2.) Not reaching the physical limits ("departed road edge", "other mistake") which counts for 55% (US) resp. 38% (GER) of relevant accidents (Figure 1, Figure 3).

To address the second group of these dangerous off-roadway related accidents, in this paper a comprehensive Road Departure Protection system is presented. The goal of such a function is to protect against unintended departure of a vehicle from the used roadway. If the risk of roadway departure is high, the driver will be warned. Should the driver not react to the warning, the Road Departure Protection system will intervene by automatically adjusting the vehicle course towards a safer, road departure avoidance path.

## STATE OF THE ART

The first Lane Departure Warning (LDW) systems were introduced into the market in 2000. Lane Keeping Support (LKS) systems followed two years later [Winner09]. Since that time, the market increased and these systems are available for a magnitude of vehicles. Both types of systems monitor the lane boundaries to protect from lane departure. A study by the Highway Loss Data Institute finds LDW ineffective at preventing collisions in the field [HLDI12]. The authors of that study assume that drivers are getting too many false alarms, which could make them tune out the warnings or turn them off completely. Whatever the actual reason,

it seems that warning only systems are not effective and therefore active systems, which are not reacting solely on lanes, must be considered.
Among other topics, the European research project interactIVe (accident avoidance by active intervention for Intelligent Vehicles) investigated such systems. Towards the goal of accident-free traffic, the so-called run-off road prevention took a key role inside the project activities [interactIVe14].
A serial system addressing road departure accidents was announced by Volvo. In case of a detected run-off road accident, this system tightens the front safety belts to keep the occupants in position [Volvo14].

## SYSTEM OVERVIEW

### System Functionality

Road Departure Protection expands today's lateral ADAS by active road keeping in emergency situations before reaching the physical limits of vehicle dynamics. The system continuously monitors the road ahead looking for road edges along with the vehicle position with respect to the road. A road edge is defined as the border of the drivable area. For instance, the transition from road surface to grass, gravel or a solid barrier like guard rails. In contrast to LKS systems, the Road Departure Protection system does not react solely on line markings.
Once an unintended road departure is detected, the driver is warned with visual and audible warnings. If the driver fails to correct the vehicle path, and also does not indicate that the departure is intended, the function actively intervenes with the intent to steer the vehicle back onto the roadway while at the same time aligning the vehicle with the boundary. In case the vehicle cannot be brought back onto the road within the system's operational constraints the Road Departure Protection function attempts to stop the departure and aligns the vehicle with the roadway. The operational limits and effectiveness are determined by the capabilities of the sensors, actuators, and functional safety analysis.

### System Architecture

Figure 4 illustrates the Road Departure Protection system architecture of a Base System and an Enhanced System. At the upstream, the Base System gathers camera image and road surface roughness information as inputs, to extract attributes of lane marker, road edge and road surface roughness. In addition to mono camera image and road surface information, the Enhanced System utilizes data of a radar sensor and a stereo camera. As the curbstone detection module extracts an additional attribute, the occupancy map of the Enhanced System delivers further information for the detection of solid boundaries. All attributes are combined together to form a hypothesis of the existence and position of the road edge
At downstream, the Road Departure Protection function calculates the vehicle motion required to avoid the road departure and the request is sent to the actuator(s). To steer the vehicle back to the road, differential braking via Electronic Stability Control (ESC), controlling the brake pressures independently at each wheel, or optionally electrical steering via Electric Power Steering (EPS) is utilized.

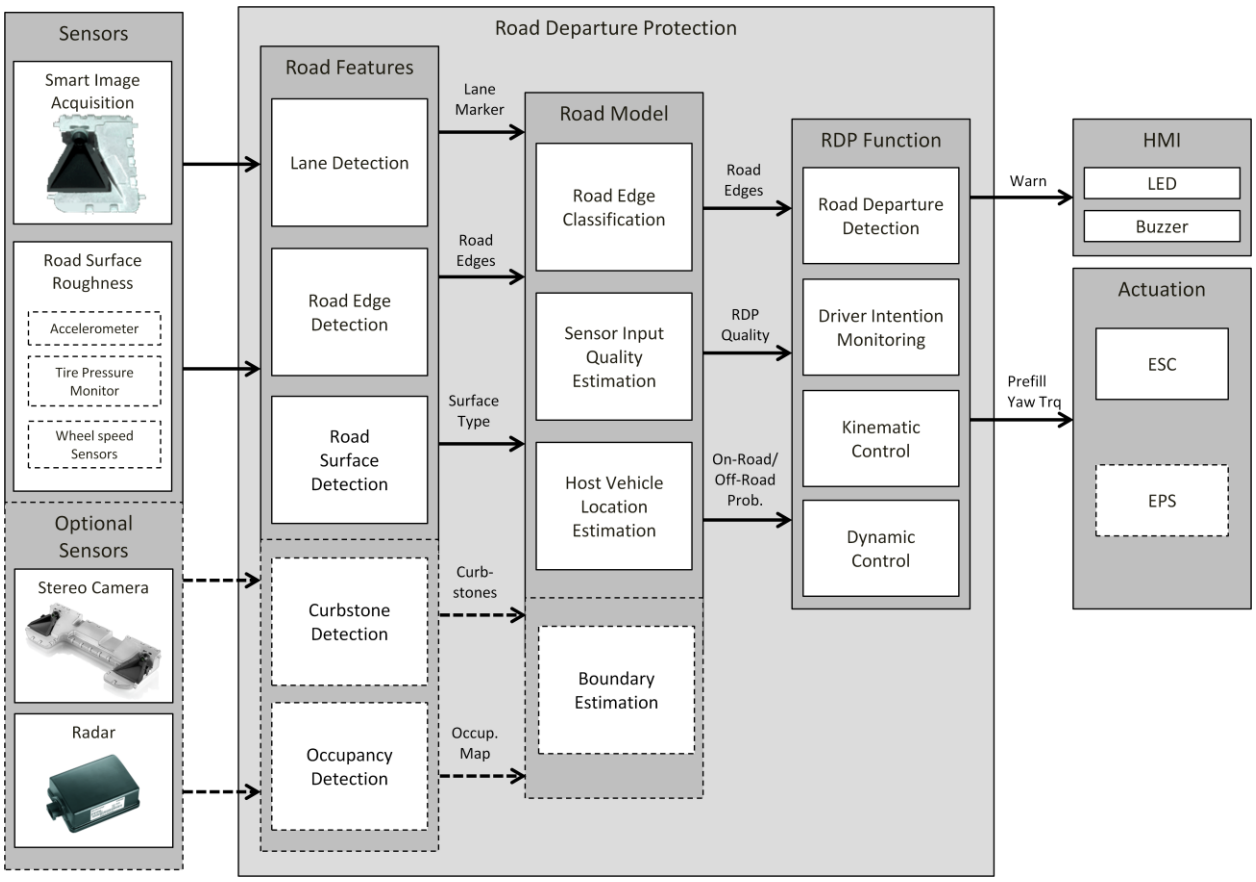


***Figure 4: Road Departure Protection architecture (solid lines: modules of Base System, dashed lines: additional modules of Enhanced System)***

Figure 4 shows major components of the developed Road Departure Protection system, broadly classifying them in major functions interfaced with sensors and actuation system. With images as input from camera, the road edge detection function extracts road edge attributes such as lateral offset, relative heading angle and curvature. Similar attributes for lane markers and curbstones are collected by lane marker and curbstone detection functions respectively. Road edge, lane marker and curbstone detections provide primary confirmation of road departure and this can be strengthened by a secondary confirmation from a measured change in road surface roughness. Different sensors like accelerometers, tire pressure monitors or wheel speed sensor can be used to detect the change in roughness of the road. This choice of sensors allows the use of different sensor configurations with same Road Departure Protection system function.

Radar sensor and stereo camera of the Enhanced System allow the generation of an occupancy map which contains information about the occupancy state of a tessellated area in the vehicle's field of view. Based on this map, the boundary estimator module extracts the solid borders of the vehicle surrounding. This provides a further confirmation of road departure and potential collisions with solid borders (e.g. guard rails, construction site equipment).

The Road Departure Protection function shares some use-case scenarios with LDW and LKS. Though, it is not a sub-set of LDW and LKS however. The main environmental information used by LDW and LKS are lane markers. Lane departures are critical only if there is a risk of collision with other objects and/or a risk of leaving the road. Such scenarios and their criticality cannot generally be assessed by using lane markers only. Road Departure Protection limits and extends the operating scenarios of LDW/LKS to provide protection in a roadway departure event. The Road Departure Protection function can either be implemented as a standalone active safety function or as extension to functions like LDW, LKS, Lane Center Assist (LCA), and Active

Blind Spot Detection (BSD). In any case the integration of Road Departure Protection functionality into either of these functions is beneficial because of the similarity of concepts, designs, and implementations. LDW, LKS, and Road Departure Protection may be implemented as modes of a lateral departure protection function. An even higher level of integration can be achieved by combining Road Departure Protection, LDW, LKS, LCA, and Active BSD into a comprehensive Lateral Support Systems component. This way these functions jointly provide all lateral safety support to the driver.

Road Departure Protection integrates driver intention monitoring, road departure detection, kinematic control and dynamic control, calculating required yaw moment using inputs from road edge detection, vehicle states and driver's inputs such as steering torque, accelerator and braking. In the following sections, the two main components of the proposed system, road edge detection and Road Departure Protection function are discussed in detail.

## ROAD EDGE DETECTION

In general, the road edge estimation is a challenging task in case of arbitrary combinations of lane markings and unmarked road sides. It has to deal with different types of roads as highway, country, rural, tunnel, etc., where lane markings are visible, scarce or missing at all. This problem is faced by combining the techniques of a multi-lane detection and road segmentation in order to determine the road boundary on asphaltic roads. Additionally, illumination changes like shadows or irregularities on the road surface make a separation from road to non-road area very difficult. There are a lot of approaches given in literature that deal with the multi-lane recognition on well-structured roads [Zhao12]. A particle filter is used to identify hypotheses for the road edges by analyzing image features. The integration of a multi-lane detection system makes the algorithm unaffected by the road type and the number of lanes.
A popular technique to separate the homogeneous road surface from the non-road area is texture analysis [Rasmussen04]. The approach is designed for country roads and might not return the road boundary if markings are present. In [Enzweiler13] a stereo camera system in combination with a high precision digital map is used, which has to contain some information about the road edge already. Although, color information [Alvarez11] seems to be a promising feature after a transformation to a color space that is more robust for illumination changes, a monochrome camera image is used here. In contrast to a feature based approach with a neural network like [Strygulec13] which requires a lot of training data for road segmentation, it is relied on the estimation of a geometric road model by online calculated image features without the need of any additional training data. A camera-only approach was developed that does not need any other sensor information. The basic concept has been shown in [Janda13a, Janda13b].
Nearly every road follows a clothoid, which is a curve with linearly changing curvature with respect to its run length. The calculation of a first-order Taylor approximation of this clothoidal model leads to a third order polynomial. Both road edges are defined in the same vehicle coordinate system. In our local vehicle coordinate system the x-axis points in the longitudinal direction of the vehicle, the y-axis points to the left and the z-axis points upwards. In ascending order, the coefficients of the polynomial identify, the distance to the center of the origin of the road coordinate system (o), the ascending slope between the longitudinal vehicle axis and the tangent at the start point ($\lambda$), as well as the curvature ($c_0$) and the curvature change rate ($c_1$). Furthermore an adequate dynamic model is used to represent the vehicle movement between two points in time, such that the change of orientation is compensated. Those parameters form the state space of the considered estimation problem. The state probability density of the state space is approximated discretely by a finite set of particles. Hence, a particle filter is applied. Each particle consists of a state hypothesis $x = (o, \lambda, c_0, c_1)$, which is a realization of the state space and an importance weight. The importance weight is proportional to the likelihood of state x for observing some measurements. Finally, a point estimation of the particles is utilized to get the most likely road edge hypothesis. The most challenging task is the identification of image features which are appropriate to deduce suitable weighting functions for the task of estimating road edges.
At first, each road edge hypothesis is transformed to the image domain. This is done by sampling the polynomial up to a certain distance. Then, each of the sampled points is projected into the image domain with the help of the known camera calibration. Finally, the sampled and projected points are approximated, to get a continuous representation of a road edge hypothesis in the image. A weighting function for a hypothesis takes into account either the image area covered by a hypothesis of a road edge or the neighborhood of a hypothesis in the image. Given a road edge hypothesis x, the pixels that belong to the projected hypothesis are indicated

by $B_R(x)$. Pixels in a neighborhood on the left of the road edge hypothesis for right borders are denoted by $B_A(x)$ and pixels in a neighborhood on the right of the hypothesis are contained in $B_G(x)$. Remember, that for a left road edge hypothesis the meaning of these two sets changes. An important requirement is to know the image areas which are covered by road markings. However, it is sufficient to identify longitudinal road markings in the direction of motion. Image processing algorithms are applied exclusively to pixels which do not belong to any road marking. Removing road markings in the preprocessing makes the road edge estimation algorithm more robust and more accurate.
Importance functions for edge gradient images and texture images were introduced in [Janda13b]. Longitudinal contours in images might be the result of a road edge. For each pixel in $B_R(x)$ the distance to the pixel with the biggest gradient norm within a local neighborhood of ten pixels is calculated. A weighting function for contours takes into account the biggest gradient norm in the neighborhood of a road edge hypothesis. The weight $w_K(x)$ is the geometric mean of the biggest gradient norms in the neighborhoods of the pixels of $B_R(x)$. By contrast, the texture feature evaluates $B_A(x)$ and $B_G(x)$. Furthermore, a two dimensional discrete cosine transform is applied to those image areas taking into account another 8x8 sized pixel neighborhood. As described in [Janda13a], the result of the transform is 64-dimensional vector. The first value is the mean gray value over the 8x8-window. The remaining entries contain the frequency spectrum of this part of the image. The variance of these 63 coefficients is computed and it shows that for asphalt the variance is slightly lower than for most of the other image parts. Consequently, the ratio of the geometric mean of the variances belonging to $B_G(x)$ and the geometric mean of the variances that belong to $B_A(x)$ are interpreted as an importance weight $w_T(x)$. If one of the three sets $B_R(x), B_G(x)$ or $B_A(x)$ is empty, the weight is set to one. Finally, the overall weight for a hypothesis is the product of the results of the single image weighting functions: $w(x) = w_K(x)\, w_T(x)$.

## ROAD DEPARTURE PROTECTION

### Road Model

As mentioned, the Road Departure Protection function receives camera images as input from which attributes and confidence of lane markings along with road edge is extracted. This is fused with the change in road surface roughness information to estimate the confidence of detected road edges. The advantage of using this approach of fusing the inputs from different sensors to reinforce the confidence of road edge is to keep the sensor interface open and extensible. The sensor fusion can easily be extended to include the objects or infrastructure details like road side curbs, guardrails, barrels and dividers, improving the ability of road model function to identify the road edges and their relative confidence.
The fusion is based on Bayesian Belief Network [Barber12] where the inputs include, but are not limited to, probability of adjacent lane, marker position, color, quality, type, road edge, probability of road merge, road exit and road surface roughness. The Road model function provides the estimates of left and right road edge along with the attributes such as lateral offset from vehicle center of gravity, relative heading angle, curvature and curvature derivative, to represent them as clothoids [Dickmann92] which is used for estimation of road departure.

### Road Departure Detection

The Road departure detection component is responsible for correctly identifying the road departure scenarios based on inputs from road model and the vehicle motion with respect to the road. It estimates Distance-to-Edge (DTE), lateral offset from the vehicle to closest road edge, Time-to-Edge (TTE), a time estimate of when the vehicle might cross the road edge, and the corresponding lateral Velocity-to-Edge (VTE).
Before Road Departure Protection interventions are activated, the impending road departure is notified to the driver in two stages, pre-warning and acute warning. The pre-warning is an early warning, suggesting a mild corrective action by the driver, whereas, a more aggressive intervention is needed to correct the vehicle course after the acute warning. Road departure detection component calculates Time-to-Steer (TTS), which corresponds to the available time to steer the vehicle to avoid road departure while limiting the lateral acceleration ($a_y$) to a pre-specified safe value. TTS can be customized by selecting the maximum allowable $a_y$ values for pre-warning and acute warning, to suit the reaction time and potential of the driver to avoid road departures.

**Driver Intention Monitoring**

A crucial aspect of active safety systems like Road Departure Protection is to avoid intrusive intervention to the driver and therefore the system should always honor the driver's request to take over the control of the vehicle. If not done, drivers may lose confidence in the safety system and might even turn the function off thereby negating any benefit which otherwise may have been provided. The driver intention monitoring component is responsible for identifying different aspects of driver behavior like driver feedback, activity, lane change intention and intention to overtake, by monitoring the vehicle and actuators states like steering, brake and throttle pedals as well as the turn indicators and other driver inputs. These measures help to limit the Road Departure Protection system intervention to minimize the intrusion to driver, avoiding interventions when driver wants otherwise, and assisting when driver needs the intervention.

**Kinematic Control**

Kinematic control component takes the inputs from road model, driver intention monitoring component and vehicle states to calculate the intervention and classify it into cascaded phases, as shown in Figure 5. When an unintended departure is detected, a warning is issued and if no corrective action is taken by the driver, Road Departure Protection enters into a pre-fill phase, where the brake system is prepared for the further intervention. The prefill phase is later followed by a first lateral control phase (L1).

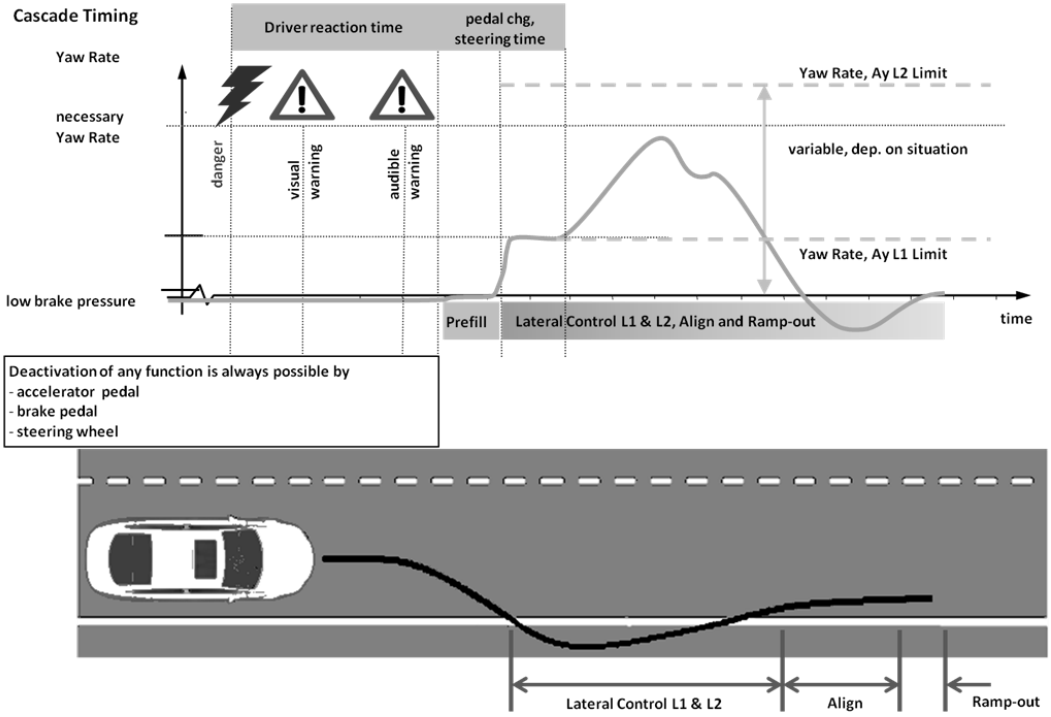


***Figure 5: Road Departure Protection control phases***

The L1 lateral control phase is further cascaded into a second lateral control phase (L2), followed by alignment and ramp-out sub phases. When in lateral control phase, the kinematic control calculates a correction path to correct the position and heading error of the vehicle with respect to the detected road edge. The correction of the heading error should always have a higher priority than the position correction as preventing or mitigating the road departure is of upmost importance. The calculated correction path is represented as a clothoid, from which the desired curvature is derived (Eq. 1).

$$C_{0_latctrl} = 2 * \left( \left( \frac{\Delta Y_Y}{\Delta x^2} \right) W_y - \left( \frac{\Delta Y_\varphi}{\Delta x^2} \right) W_\varphi \right) \quad (1)$$

Based on the vehicle states and position of the vehicle relative to the road, available longitudinal distance for correction ($\Delta x$), available lateral distance for position correction ($\Delta Y_Y$), available lateral distance for heading angle correction ($\Delta Y_\varphi$), and a set of dynamic weights for position correction ($W_y$) and heading correction ($W_\varphi$) are computed. When the vehicle is getting closer to the road edge in an impending departure (departure scenario), these weights are computed to cooperate and request higher curvature whereas soon after the intervention when the vehicle is moving away from the road edge onto the roadway (return scenario), these weights compete to reverse the curvature request. This dynamic weighing helps in faster position and heading correction in departure scenarios and limits the overcorrection during return scenarios.
The lateral control intervention is further cascaded, to escalate the interventions from moderate to strong in order to give the driver additional reaction time while still offering support through the automatic path correction and the reduction in kinematic energy. The gradual increase of the steering authority may also be used to allow for higher $a_y$ and yaw rate ($\omega_z$) but still ensure driver controllability.
Following the lateral control phase, during the alignment phase, the objective is to ensure that the vehicle is aligned with the road edge before giving the control back to the driver. As the objective is to correct the heading, the position correction term is not included in curvature request calculation (Eq. 2).

$$C_{0_align} = 2 * \left( \left( \frac{\Delta Y_\phi}{\Delta x^2} \right) \tan(\phi) \right) \tag{2}$$

In the final ramp-out sub phase, kinematic control prepares to give the control back to the driver by ramping down the curvature request to zero.

**Dynamic Control**

The dynamic control component takes the desired curvature request as input from the kinematic control and responds to it by calculating a steering angle request for EPS or a yaw moment request for ESC. In the second case, ESC accordingly applies differential braking by requesting brake pressures at each wheel. With ESC, the performance of steering correction is influenced by the vehicle's steering geometry, as higher positive scrub radius is favorable for steering with differential braking. The dynamic control limits the requested yaw moment and its gradient to a value which can be overridden, in case the driver wishes to do so, ensuring an additional layer of safety to avoid an excessive steering intervention.

## EXPERIMENTAL RESULTS

### Road Edge Detection

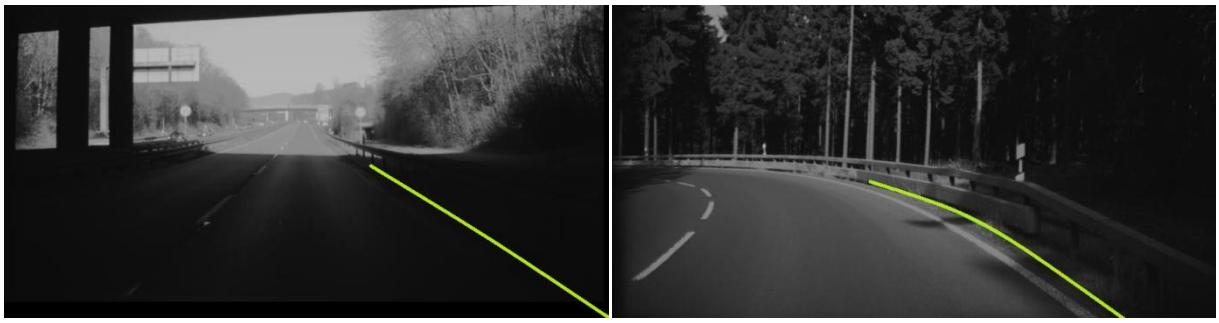

***Figure 6: Road edge with line markings and guard rails under various lighting conditions***

*Figure 7: Roads with grass edge and partly shadowy surface*

*Figure 8: Road edge with gravel and with curbstone*

In order to evaluate the capability of the road edge detection algorithm, test drives on various German roads were conducted. Figure 6 to Figure 8 show the estimated right road edge for sample driving scenarios. Various road edges like curbstones, guard rails, gravel, and grass were detected. Tests under various lighting conditions demonstrated the capability to detect the road edge also under harsh environment conditions, like partly shadowy road surface or bridge/tunnel passages.

**Road Departure Protection**

**Prototype Vehicle Setup** To develop and validate the whole Road Departure Protection function concept, two prototype vehicles were built. One, a pick-up truck, was equipped with the Base System and the other, a sedan, was equipped with the Enhanced System. For this paper, the test results for the Base System will be described. The developed prototype under test includes a mono camera, mounted near the rear-view mirror behind the windshield, and a pair of accelerometers, mounted on the upper control arm of each front wheel to measure the vertical acceleration of the wheel. For the purpose of this study, the road surface roughness detection was configured to detect rumble strips, which are very common in the U.S. to mark the road boundaries. In this prototype the Electronic Stability Control (ESC) system was used as the primary lateral control actuator.

**Vehicle Steering Capability** Before testing the Road Departure Protection function, the steering capability of the prototype vehicle was evaluated. Open loop curvature requests were sent to the lateral dynamic controller to investigate the maximum curvature capability and accuracy of the system control. This testing is especially important in the case of steering by differential braking as the steering capability depends highly on the vehicle's steering and suspension geometry. Figure 9 shows the curvatures defining the potential capability and limitations of the system relative to the possible road curvatures. 'Max. ESC Steer' represents the steering capability of the prototype, which, above the lower operational speed limit of 55km/h, exceeds the most extreme road curvatures, represented by 'Max. Road (e=10%)' (Maximum curvatures for a banking angle of

10%). The maximum curvature supported by the camera used in the prototype vehicle is shown in the plot as 'Max. Camera'. At approximately 80km/h and above the lane marker detection capability exceeds the steering capability and the maximum road curvatures. With the components currently used in the developed prototype, the region 'Avoidance' indicates the potential road departure avoidance region and region 'Mitigation' indicates the curvatures on which road departures can be mitigated. This however may change with components used and functional limits.

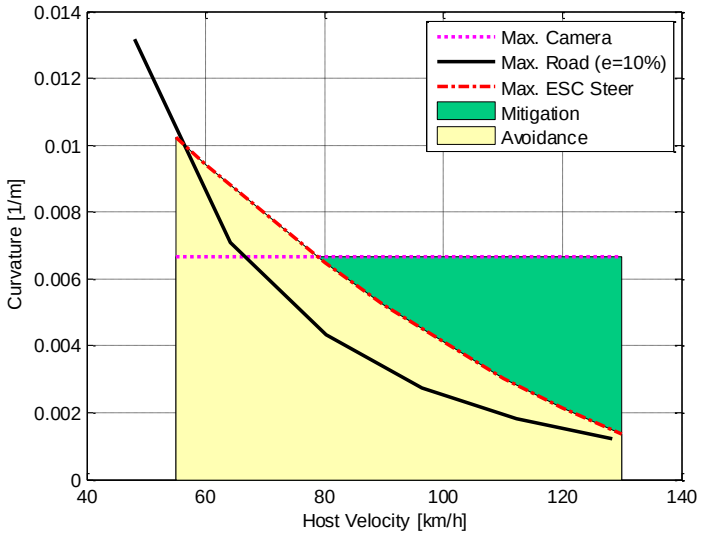


***Figure 9: Potential benefits and limitations***

**Use Case Validation Results** The use-case behavior and performance of the Road Departure Protection function has been tested on a closed course test track. To study the performance at different speeds, road departure use cases were tested at velocities between 64 km/h and 129 km/h (40 mi/h and 80 mi/h) in increments of 16 km/h (10 mi/h). Under curved road use case conditions, lower speeds were tested 64 km/h (40mi/h). In 23 out of 25 tested use cases, the road departure was completely corrected ending with the vehicle back on the road and aligned with the road boundary.

Figure 10 shows the effectiveness of intervention with DTE, intervention phases and requests on a straight road at 95 km/h speed. As the vehicle gets closer to the road edge and DTE drops to 0.4 m, a warning is issued. With the vehicle being 0.3 m over the edge, steering intervention starts with lateral control phase L1, honoring curvature request from kinematic control and requesting yaw moment at front and rear independently. The lateral control phase extends to L2 bringing the vehicle back onto the road. At approximately 8.3 s, Road Departure protection system enters into align phase and ending the intervention with ramp-out phase.

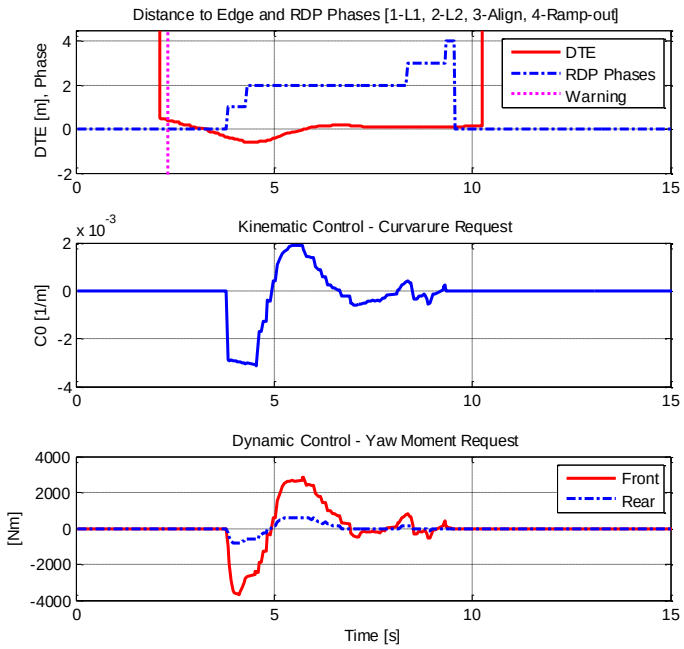


***Figure 10: Road departure protection phases and requests***

## CONCLUSION AND OUTLOOK

The developed and presented Road Departure Protection system integrates an effective road edge detection function with cascaded kinematic and dynamic control functions to protect against unintended road departures. The proposed function can be integrated with different possible sensor configurations to enhance the ability to detect road departures. The steering capability of the prototype system proves that the differential braking based Road Departure Protection system is capable of avoiding road departures even on roads with very high curvature values in some vehicle configurations.

The presented system provides all required functionalities for Road Departure Protection. It has the potential to further increase vehicle safety and to contribute to traffic with zero accidents. Thus, product development is ongoing at Continental.

The tested Road Departure Detection system takes advantage of differential braking via ESC. Utilizing electrical steering via Electric Power Steering (EPS) offers further possibilities to keep the vehicle on the road and to protect from road departure.

The presented system reacts after an impending road edge crossing has been detected. In case of inappropriate or excessive speed, the influence on the vehicle dynamics is limited because the physical limits have been reached. These accident cases could be covered by PreView ESC which detects the course of the road before entering a curve [Schaefer12]. Based on the predicted upcoming road curvature the driver is supported when the vehicle is approaching the curve too fast. The new active safety system identifies the critical situation with road map data and on-board GPS. The target vehicle speed is a function of road curvature and friction. The function is initiated when the driver releases the accelerator pedal and starts steering in the curve direction. The function commands a smooth but resolute brake intervention as long as the vehicle is too fast. In the critical curve driving phase the vehicle is guided by ESC wheel individual brake intervention. Experiments have shown that in a situation where the vehicle is close to instability, the system is very effective to assist the driver safely through the maneuver. Research is ongoing in this direction.

## REFERENCES


[Barber12] David Barber, 2012. “Bayesian Reasoning and Machine Learning”, ISBN-13: 978-0521518147.

[DESTATIS13] German Federal Statistical Office DESTATIS, 2013. “Verkehr - Verkehrsunfälle 2012. Fachserie 8, Reihe 7“, Statistisches Bundesamt, Wiesbaden, Germany

[Dickmanns92] Dickmanns, Ernst D. and Mysliwetz, Birger D, 1992. “Recursive 3-d road and relative ego-state recognition”, Transactions on pattern analysis and machine intelligence, IEEE, vol. 14, no. 2, February, 199-213

[Enzweiler13] Enzweiler, M.; Greiner, P.; Knoppel, C.; Franke, U., 2013. "Towards multi-cue urban curb recognition," Intelligent Vehicles Symposium (IV, 23-26 June), IEEE , 902-907

[GIDAS13] German In-Depth Accident Study GIDAS. 2005-2012

[HLDI12] Highway Loss Data Institute, 2012. “Crash avoidance features reduce crashes, insurance claims study shows; autonomous braking and adaptive headlights yield biggest benefits”, HLDI News July 3)

[interactIVe14] interactIVe, 2014. ”interactIVe - accident avoidance by active intervention for Intelligent Vehicles” http://www.interactive-ip.eu

[Janda13a] F. Janda, S. Pangerl, E. Lang und E. Fuchs, 2013. “Road boundary detection for run-off road prevention based on the fusion of video and radar“, IEEE Proceedings on the Intelligent Vehicles Symposium (IV, 23-26 June), 1173–1178

[Janda13b] F. Janda, S. Pangerl und A. Schindler, 2013. “A road edge detection approach for marked and unmarked lanes based on video and radar“, International Conference on Information Fusion (FUSION ’13), 871–876.

[NHTSA02]. NHTSA, 2002. “Development of test scenarios for off-roadway crash countermeasures based on crash statistics”, (DOT HS 809 505).

[NHTSA11] Traffic Safety Facts 2011. A Compilation of Motor Vehicle Crash Data from the Fatality Analysis Reporting System and the General Estimates System (http://www-nrd.nhtsa.dot.gov/Pubs/811754AR.pdf).

[NHTSA12] Traffic Safety Facts 2012. A Compilation of Motor Vehicle Crash Data from the Fatality Analysis Reporting System and the General Estimates System (http://www-nrd.nhtsa.dot.gov/Pubs/812032.pdf ).

[Rasmussen04] C. Rasmussen, 2004. “Texture-based vanishing point voting for road shape estimation“, British Machine Vision Conference, 470–477

[Schaefer12] J. Schäfer, C. Kuhrt, M. Feser, H. Faisst, T. Raste, P. Lauer, 2012. „Contiguard® - Driving You Safely: Integrated Occupant Protection Beyond Today’s Passive Safety”, 11th International Symposium & Exhibition on Sophisticated Car Occupant Safety Systems (airbag 2012, 3-5 December)

[Strygulec13] S. Strygulec, D. Müller, M. Meuter, C. Nunn, S. Ghosh und C. Wohler, 2013. “Road Boundary Detection and Tracking using monochrome camera images“, International Conference on Information Fusion (FUSION ’13), 864–870

[Volvo14] Volvo Car Group, 2014. “All-new Volvo XC90: two world-firsts, one of the safest cars in the world” Press release ID: 148123 (Jul. 22). Volvo Car Group, Gothenburg, Sweden

[Winner09] Winner, H.; Hakuli, S.; Wolf, G.; Gayko, J., 2009. „Lane Departure Warning“, Handbuch Fahrerassistenzsysteme. Vieweg + Teubner, Wiesbaden, 543-553

[Zhao12] K. Zhao, M. Meuter, C. Nunn, D. Muller, S. Muller-Schneiders, and J. Pauli, 2012. “A novel multi-lane detection and tracking system,” Intelligent Vehicles Symposium (IV), IEEE, 1084-1089.

# THE INTEGRATED SAFETY CONCEPT OF THE ULTRA-COMPACT ELECTRIC VEHICLE Visio.M

**Thomas, Unselt**
Daimler AG
Germany

**Johann, Unger**
Autoliv B.V. & Co. KG
Germany

**Mathias, Krause**
IAV GmbH
Germany

**Thomas, Hierlinger**
Technische Universität München
Germany

Paper Number 15-0215

## ABSTRACT

A great opportunity for increasing range and decreasing the production costs of battery-powered vehicles is to lower vehicle weight as far as possible. To this end, designers not only can incorporate lightweight materials, but also reduce the size of the vehicle and limit the equipment installed as excellent weight-saving strategies. Since this strategy could lead to crash incompatibility, ultra-compact electric cars are subjected to enormous loads in the event of a collision with a heavier vehicle. The high structural rigidity and limited deformation paths produce a high crash pulse, with higher forces acting on occupants than are experienced in conventional vehicles. The objective of the safety task force within the Visio.M project funded by the German government was to draft, implement, and test a concept that resolves these conflicting interests and provides sufficient protection for ultra-compact vehicles. Using an analysis of the potential accident scenario involving ultra-compact electric vehicles as a starting point, specific safety requirements were derived for these vehicles. To meet these requirements, a strategy for an integrated safety design was developed to reduce the occupant loads. The integrated safety concept incorporates pre-crash systems, occupant protection systems, and a CFRP monocoque, among other features, and was developed using numeric simulations. Verifiable proof of the operative function and benefit of the safety concept was provided by leveraging numerical simulation techniques, carrying out comprehensive component tests, and conducting a series of full-scale crash tests using a Visio.M prototype. In the end, the integrated safety strategy is the key to realizing a sufficient level of protection for sub-compact vehicles.

## INTRODUCTION

According to targets set by the German federal government, one million vehicles powered by alternative technologies should be running on German roads by 2020. By 2030, this figure is expected to grow to 6 million. Efficient, electrically powered small motorized vehicles have the potential of driving the expansion of electromobility forward. Yet most previous concepts have either been too heavy or too expensive, or do not reach the safety level expected by the market. Traffic experts have expressed concern that the current safety level for vehicles of the L7E homologation category (quadricycle category) is insufficient for mass traffic. Tests by Euro NCAP partially revealed serious deficiencies in vehicles of the L7E homologation category. Currently, safety requirements in the quadricycle category are low, but safety experts are demanding effective occupant protection if the number of ultra-compact vehicles circulating on roads should increase. The Visio.M Consortium has taken on

this challenge and is developing concepts for electric vehicles that are not only efficient and cost-effective to manufacture but are also considered to be safe. In particular, the Safety workgroup led by Daimler AG was working with its partners Autoliv, IAV and the Technical University of Munich on developing and implementing an integrated safety concept (See Figure 1) and verifying its worthiness.

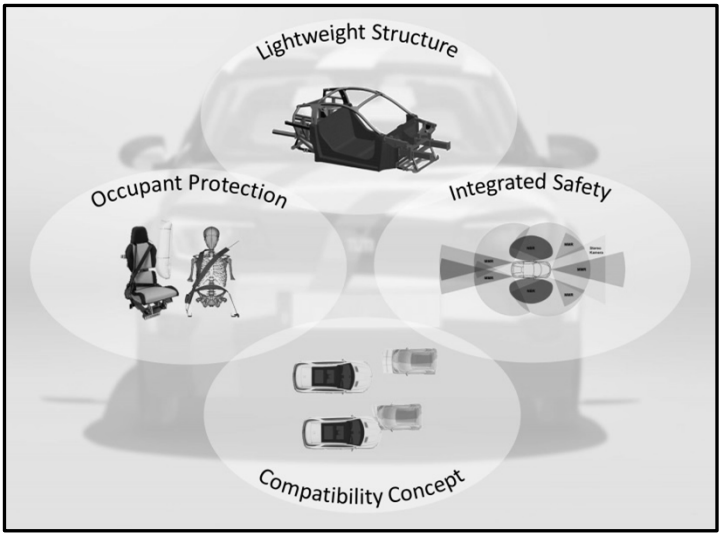


***Figure1. The integrated safety concept of the ultra-compact vehicle Visio.M.***

## BOUNDARY CONDITIONS

### Ultra-compact vehicles and safety

Discussions concerning the appeal and acceptance of battery-powered vehicles center on their limited range. A major opportunity for increasing their range while decreasing production costs is to lower vehicle weight as far as possible. Weight-saving strategies with considerable potential that are being employed by designers are the incorporation of lightweight materials, the reduction in vehicle size and limiting the equipment installed in the vehicle. This opens up new possibilities in terms of vehicle homologation. Vehicles with a curb weight of up to 400 kg (450 kg beginning in 2016) without an energy storage unit and a maximum continuous output of 15 kW are not considered to be conventional passenger cars of the M1 vehicle class, but can be homologated as category L7E vehicles. The limited requirements that apply to vehicles of this category, which are similar to today's passenger cars both in terms of their characteristics and usage, result in the risk that important yet non-regulated safety standards will be disregarded. Ultra-compact vehicles that circulate on public roads are particularly vulnerable to the high forces which occur during a collision with heavier vehicles since their reduced weight and the resulting large differences in mass to conventional vehicles on the market today lead to crash incompatibility. The necessarily high structural stiffness as well as the smaller deformation zones inherent to ultra-compact vehicles lead to a high crash pulse and, compared to conventional vehicles, to considerably higher forces that act on the occupants. In conjunction with reduced safety features, this crash incompatibility results in a greater risk to the occupants. However, to avoid negatively impacting the broad acceptance of electric vehicles and to ensure occupant safety, there should be no discrepancies to conventional vehicles regarding the level of occupant protection in actual accident situations. Against this background, the approach used in the Visio.M project, which is to align the vehicle target weight with the weight limit of the L7E approval category, presents a major challenge to the design of the occupant protection systems. Despite the limited requirements for this category, the vehicle should reach an adequate safety level that is in accordance with the specific requirements dictated by how the vehicle is used and the expectations of

customers and society. An analysis of the actual accident situation is the basis for defining the requirements placed on the safety concept of the Visio.M. The goal is to evaluate the potential risks of this vehicle type under the boundary conditions related to its specific usage in general traffic situations.

**Analysis of potential accident situations of ultra-compact vehicles**

In cooperation with the traffic accident research department at the Technical University of Dresden, one aspect of the Visio.M project was to analyze the potential accident situations of ultra-compact vehicles in comparison with current general accident situations. The analysis is based on the GIDAS (German In-Depth Accident Study) database, in which around 2000 accidents from the greater Dresden and Hannover areas have been documented and reconstructed since 1999. Based on accident data from all accident passenger cars of model year 1995 or later, which were used as the control group, general statements were first made on the overall accident situation in Germany. In contrast, however, there are almost no accident data on ultra-compact vehicles because of their limited presence on the market at this time. The potential accident situation of these vehicles was therefore analyzed using the GIDAS data for passenger cars most closely related to ultra-compact vehicles because of their small size, usage characteristics and use conditions. The analysis concentrates on making a prognosis of the accident situation that can be expected to develop in the next several years for electric ultra-compact vehicles. The evaluation of the accident data shows a significant shift of the accident type toward urban scenarios for ultra-compact vehicles compared to other groups (See Figure 2). Thus, compared to accidents in general, ultra-compact vehicles can be expected to be considerably less involved in front/rear collisions yet will be more subject to lateral collisions due to the growth of intersection accidents. The analysis of the impact distribution shows that the great majority of front/rear collisions are frontal impacts in which a considerable overlap occurred. Side pole collisions, which frequently lead to serious injury in accidents in general, played a subordinate role in accidents involving ultra-compact vehicles in urban use. While the share of collisions with bicyclists increased for ultra-compact vehicles in urban use, no difference could be determined between the two groups regarding the frequency of pedestrian collisions, rollovers and tipping. The shift of accident situations toward urban accident scenarios means that only approx. two in three urban accidents result in an endangerment of occupants.

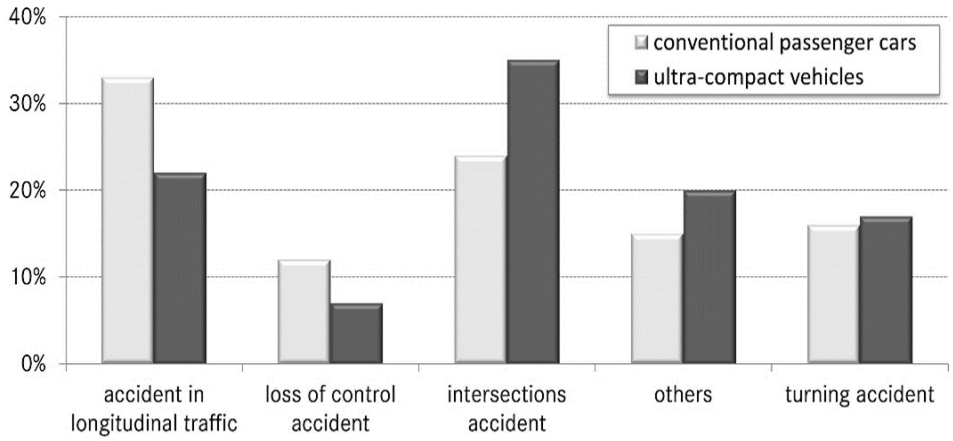


***Figure2. Distribution of accident types for conventional passenger cars and ultra-compact vehicles.***

The analysis also showed that because accident situations involving ultra-compact vehicles are concentrated in urban traffic regions, collision speeds are considerably lower. In conjunction with the low mass of ultra-compact vehicles, this results in a general reduction in the overall collision energy. However, in a collision with a heavy accident counterpart, these smaller and lighter vehicles can only partially benefit from this advantage since they must absorb a large share of the collision energy. The accident severities resulting for an ultra-compact vehicle with a curb weight of approx. 450 kg in frontal and side collisions were predicted by the accident analysis based on energy-equivalent computations. To evaluate the accident severity of frontal collisions, the respective energy equivalent speed (EES) was computed. The distribution functions of the respective EES values show that ultra-compact vehicles are subjected to an EES of more than 30 km/h in 40% of all frontal collisions, while this is the case in only 20% of all frontal collisions of accidents in general. The majority of frontal accidents expected for ultra-compact vehicles have an EES of up to 55 km/h. To estimate the accident severity of side collisions, the energy-equivalent value was calculated for the collision speeds observed for the group of ultra-compact vehicles relative to the mass of the side impact barrier used by Euro NCAP. A comparison with the distribution of the equivalent collision speeds of the impact vehicles in the current accident situation in general shows that similar accident severities can be expected on average for both groups.

**Requirements placed on the safety of the Visio.M vehicle**

The evaluation and assessment of accident data show that special safety requirements exist for electric ultra-compact vehicles compared to conventional passenger cars due to the urban nature of the accident situations, crash compatibility and the associated changes in the collision speeds. The test scenarios used to verify the crash safety of electric ultra-compact vehicles in frontal and side impacts under the current traffic and infrastructure conditions are orientated on the predicted energy-equivalent values, taking into account the expected impact constellations. The performance of the vehicle structure should be in accordance with today's established safety standards: It must ensure a stable passenger compartment and prevent battery intrusions while providing deformation areas specifically designed for energy absorption. These considerations along with assessments of the potential risk for the group of ultra-compact vehicles give rise to the demand for equipping these vehicles with comprehensive integrated safety systems that prevent accidents or reduce their severity. In addition, the vehicle structure and occupant protection systems should be designed for the following load cases:

- Frontal impact: 40% offset, ODB, 64 km/h; Euro-NCAP
- Side impact: MDB, 50 km/h, ECE R95
- Criteria:
  - Stable passenger cell, no battery intrusion
  - Occupant load values fulfill legal requirements, ideally Euro NCAP 5 stars

For both load cases, the design is confirmed in full scale crash tests with a prototype. In addition, further load cases such as rear crashes as per ECE R32, pole side impacts as per Euro NCAP configuration and a roof depression test were examined and verified by simulation with respect to the vehicle structure. Based on these requirements, an overall safety concept was drafted initially and the individual elements were then designed and worked out in detail.

**Safety concept**

The requirement for a stable passenger compartment results in a very stiff design of the vehicle structure in small and very light vehicles. In conjunction with the great speed changes that ultra-compact vehicles experience due to the differences in mass of the collision partners, this high stiffness leads to a hard crash pulse and thus to high occupant loads. This must be taken into account by the occupant protection concept. In addition to these requirements, steps should be taken to reduce the accident severity or ideally to prevent

accidents altogether. This results in an integrated safety concept consisting of a vehicle assistance system, pre-crash and in-crash measures and a hybrid vehicle structure. A comprehensive system consisting of radar and camera sensors provides 360° detection of the vehicle environment and thus forms the basis of accident prevention and collision mitigation systems such as autonomous emergency braking and lane departure warning systems. To counteract the increase in turning/intersection accidents, an intersection assistance system is considered to have great potential. In addition, to prevent impending rear collisions, various strategies are being examined that enable vehicle evasion toward the front. In this connection, the electrical drive and the low weight of ultra-compact vehicles are proving to be highly advantageous. During an accident, the vehicle structure plays a key role. In the defined load cases, it must provide for a stiff passenger compartment to secure the occupant survival space on the one hand, while also providing a sufficient deformation range for absorbing collision energy on the other. The lightweight structure concept of the Visio.M vehicle is therefore based on an aluminum and carbon fiber reinforced plastic (CFRP) hybrid design. The closed passenger cell is built using an innovative, multi-part monocoque of CFRP and is characterized by a particularly high degree of stiffness. The structure of the front and rear sections of the vehicle consists of aluminum profiles to achieve the highest possible defined energy absorption with sufficient strength and stiffness. However, because of the small dimensions of ultra-compact vehicles, the deformation path made available by the crash structures in the front and rear sections of the vehicle are limited. The innovative safety concept being developed therefore focuses on a needs-oriented extension of the effective deformation zones in the front and side areas of the vehicle in the form of pyrotechnically deployed structure-airbags. To ensure that the deformation zones required to absorb the impact energy are available at the time of the collision, these crash-active systems must be triggered in the pre-crash phase, in the last few milliseconds before an accident that has been assessed as being unavoidable occurs. The crash pulse resulting from frontal impacts in ultra-compact vehicles, which exerts a larger influence on occupants than in conventional vehicle designs, is counteracted by means of an innovative seat belt system consisting of a three-point seat belt and an additional two-point seat belt. Because there is a high risk of serious injury to occupants on the impact side of the vehicle due to the close distance between the door and the occupant in ultra-compact vehicles e.g. caused by vehicle elements intruding into the passenger compartment, an active lateral displacement of the occupant on the impact side of the vehicle toward the middle of the vehicle is provided in the final milliseconds prior to a side collision. As a result of this pre-acceleration, the crash pulse acting on the occupant can be further reduced. The integral protection strategy can be summarized as follows, subdivided into the particular load cases:

- Frontal impact: Pre-crash sensing / initiation of automatic emergency braking / active extension of the crash length through deployment of a structure-airbag / positioning and optimal restraint of the occupants with high performance belt tensioners and a 3+2-point seat belt system / energy absorption through the crash structure / prevention of intrusions through sturdy CFRP monocoque / controllable force limitation/deployment of airbags to prevent collision with hard interior structures
- Side collisions: Pre-crash sensing / intersection assistant activation / optimal restraint of occupants with high performance belt tensioners and a 3+2-point seat belt system and activation of a lateral occupant displacement / active increase of the side stiffness of the vehicle through deployment of a structure-airbag / prevention of intrusions through sturdy CFRP monocoque / deployment of airbags for early restraint and prevention of contact with hard interior structures, penetrating structures / deployment of airbags to prevent crash-related interactions between vehicle occupants
- Rear impact: Pre-crash sensing / activation of automatic evasion toward the front / positioning and optimal restraint of passengers with high performance belt tensioners and a 3+2-point seat belt system / energy absorption through crash structure / prevention of intrusions into the passenger compartment through sturdy CFRP monocoque

An additional requirement in electric ultra-compact vehicles is that the high-voltage system must be electrically disconnected from the battery as soon as a heavy impact is detected to prevent electric shock and the risk of fire. A detailed description of the components and functions and their design is provided in the following chapters.

## SAFETY COMPONENTS AND SYSTEMS

### Assistance systems/environment sensing electronics

A complex sensor and control system was designed for the Visio.M vehicle with respect to the needs-oriented control of restraint components. A combination of radar and camera sensors creates a "virtual 360° safety cocoon" around the vehicle. The principle of sensor redundancy was applied for the planned pre-crash deployments. The sensors are designed for a comprehensive vehicle assistance package (e.g. Euro NCAP 2020). They help to prevent critical driving situations as well as accidents and were used to trigger pre-crash systems. The evaluation of the integral functions of the individual components was conducted in a simulation using selected urban intersection scenarios.

### Restraint systems

The core element of the restraint system is a highly adaptive belt system consisting of a three-point seat belt with an additional two-point seat belt. This 3+2 seat belt design (See Figure 3, left) provides for optimal occupant restraint and largely prevents uncontrolled occupant movement during frontal and side impacts and rollovers. The forces on the occupants during a crash are controlled by optimally coordinated actions of electrically controlled, adaptive belt tensioner and force limiter systems. The electrically controlled high performance belt tensioner achieves a restraint force of up to 900 N. In connection with the pre-crash sensing of frontal and rear collisions, this makes is possible to keep occupants in their optimal seating position, or even to pull them back from an unfavorable position, even in the case of an autonomous full brake application. Airbag systems in passenger compartments are consistently only used where an impact with a hard vehicle structure or an interaction between the passengers must be prevented. A conventional driver airbag module is used in the steering wheel. Adaptive components such as multistage deployment or active venting can be added if required. Lateral protection is afforded by the combination of a head airbag mounted on the roof frame and a thorax-pelvis airbag attached to the body shell. Because of the specific seating design of the Visio.M vehicle in which there is no seat adjustment along the vehicle longitudinal axis (fixed-eye-point design), it is impossible for a belted front passenger to make contact with the dashboard. For this reason, standard installations of a front passenger airbag and knee airbag are not required. The fixed-eye-point design additionally makes it possible to precisely define the area in which protection must be provided and helps in designing compact modules. A special feature is the protection system against interaction between the driver and front passenger. In the event of a crash, an airbag is deployed between the shoulders and heads of the vehicle occupants to prevent them from being thrown against each other. The airbag is mounted at shoulder height on the driver's seat in the vehicle interior.

### Active lateral occupant displacement

Another innovation is the active lateral displacement of the vehicle occupant (See Figure 3, left) on the impact side in the event of side collisions. Investigations have shown that it is possible to displace the seat and the occupant by approx. 100 mm toward the center of the vehicle through a pre-crash triggering that occurs approx. 150 ms before a collision. Simulations demonstrate that the load reduction averages 22.3 %. In addition, the boundary conditions for designing the side airbags are improved. The occupant displacement mechanism is implemented using a pyrotechnical actuator in the seat. The seat also houses the unlocking mechanism, the shock absorption at the end of the movement and the seat fixation after displacement. Use of

this function requires the space in the center of the vehicle, which exists in the Visio.M (missing center console/tunnel), and an interaction protection mechanism between the occupants.

***Figure3. Active lateral occupant displacement, 3+2 seat belt design and sidebag (early design phase) and Frontal structure-airbag.***

**Structure-airbags**

Another innovative feature is the structure-airbag concept (See Figure 3, right) for actively influencing the crash pulse during frontal and side collisions. Triggered before a collision, a hose fabric is filled with gas (approx. 16 bar) and supports the composite structure of the vehicle as a load-absorbing element. For frontal protection, this structure airbag is mounted on the cross member behind the bumper covering. When activated, the covering is pushed forward by approx. 12 cm directly prior to the crash (approx. 50 ms) and the structure-airbag behind it contributes to an effective extension of the useable crumble zone. To fill the structure airbag, a gas generator technology is used which largely operates without pyrotechnics and whose performance is therefore minimally dependent on temperature and which is especially aging resistant. Operating pressures up to 30 bar achieve support forces of up to 300 N/cm². Burst membranes are used to specifically release pressure in the structure airbag by means of controlled venting of the stored energy. The same technology is used to provide protection during side collisions. Integrated in the door module, this structure-airbag pushes the lower area of the door outward immediately prior to a collision, establishes a stiffening connection between the A and B-pillars and counteracts overriding of the door sill. The design of the structure airbag and the occupant protection components is closely coordinated with the performance of the vehicle structure.

**VEHICLE STRUCTURE**

**Structure concept**

The structure concept of the Visio.M vehicle is based on the requirement for lightweight design on the one hand, and on the safety requirements for ultra-compact vehicles on the other. The hybrid structure (See Figure 4) enables a stiff vehicle passenger compartment for securing the survival space in the presence of a sufficient deformation path for specific energy dissipation through the use of different materials in different areas of the vehicle. To secure the survival space, the passenger compartment is built with an extremely stiff, multi-part monocoque in a shell design. The low seating position in the vehicle permits an almost complete protection of the occupants while material use through the monocoque is kept to a minimum. The monocoque consists of CFRP materials. With the "tub-like" shape of the monocoque, the lightweight construction material – which is still expensive at this time – is used to preserve the passenger compartment in the event of a crash. All other crash-related areas in the structure are made of the less-expensive standard aluminum profiles to achieve the greatest possible energy absorption levels with sufficient strength and stiffness.

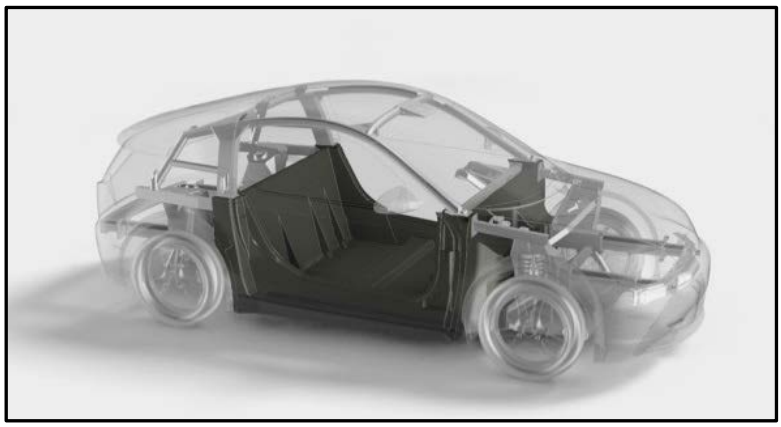

***Figure4. Hybrid structure of the Visio.M vehicle.***

**Monocoque**

The structural design of the monocoque consists of 11 single parts which were manufactured from CFRP using prepreg as semi-finished material with CFRP tools. The low number of components made it necessary to develop single parts in such a manner that their package, design and structure are multi-functional and optimally designed in terms of production and joining. In light of the possibility of a small series production, CFRP tools were selected because they achieve a considerably higher number of pieces while reaching smaller production tolerances than epoxy tools. The prepreg semi-finished products used were both woven and unidirectional mats, which were used in various areas of the monocoque depending on the load and design. By means of the local use of lightweight cores, such as Rohacell and aluminum honeycombs, the single parts were joined in a device with structure adhesive and then hardened using the autoclave process to form the component. By designing the adhesive flanges according to the applied load, it was possible to eliminate the need for other joining methods. After completion of the monocoque, all joints were analyzed for uniform thickness distribution and voids using ultrasound technology to rule out the possibility of errors in the joining process. To ensure the integrity of the structure, multiple quasi-static pressure tests were conducted. The monocoque was clamped into a device and forces derived from the crash simulation were applied to the points of load application in the front, rear and side wall areas. To perform an acoustic analysis, measurement heads were attached to the surface of the monocoque. The evaluation and analysis of the acoustic signals are used to detect and localize situations critical to the fiber composite. By steadily increasing the load, the load limit of the component is slowly approached without destroying the component, and in this way the computational design of the component can be validated. In addition, the ultrasound test and noise emission test are used for component analysis after the conduction of the crash tests to identify inside or outside damage to the fiber matrix composite and joints that may not be visible.

**Doors**

The multi-part door design consisting of an inner and outer part with an integrated shaft reinforcement and side collision brackets is also made of CFRP and closes off the passenger compartment on the side. The small installation space between the driver and the outer part make a very stiff door structure necessary. Because of the broad overlap with the door, the monocoque also contributes to the safety of the occupants with its especially high sill in the transition area to the B-pillar. With a total of only 4 structure-related components, the doors contribute to a reduction in the production costs thanks to the integration of functions as well. In addition to the usual components such as the door lock, window lift, loudspeaker, sensors and electrics, the door also incorporates the structure-airbag (see above).

### Crash structure

The crash structure in the front section of the vehicle, roof frame and rear section of the vehicle consists of a wide variety of conventional standard aluminum profiles and sheets. Aluminum alloys of the 6000 series were used, which were produced specifically for prototypes using WIG manual welding on a welding device and which then obtained their final strength through T6 heat treatment.

## LAYOUT AND VALIDATION

The following paragraphs will give some examples of the different methods which were used during the development phase of the integrated safety concept of the Visio.M vehicle.

### Simulations of the integrated safety concept

Many of the components of the integrated safety concept are activated before an accident occurs. The data required for deployment are provided by the environment sensors. Because deployment of irreversible safety components such as the structure-airbag or the active lateral occupant displacement must be absolutely reliable, their validation is closely linked to that of the sensor system. In addition, the safety components only develop their full potential if they are activated in a defined time period prior to the accident. Typical sensor characteristics such as the latency periods, as well as the run times of the associated algorithms, can have a considerable impact on the performance of the safety components (See Figure5). Consequently, the expense of validating these system is high, but can be moderated through the use of simulations. Another advantage is the fact that it is possible to begin with the simulation-based validation very early in the development process since it does not rely on the availability of the components. The simulation of traffic scenarios has the big advantage that they are reproducible, unlike tests on the vehicle testing site. Thus it is possible to focus on a range of different aspects of the safety concept, since the input data are always the same. Based on the use characteristics of the Visio.M vehicle, an entire catalog of urban scenarios was developed and the interplay of the integrated safety concept was designed accordingly. In this way, it was possible to specify the safety concept at a very early stage of development without a prototype. The definition of an accident situation and non-accident situation for these scenarios makes it possible to easily and fully classify the simulation space. Moreover, the following tests and validations of the synthetic sensor system can be performed based on this material. Thus, a procedure was used that can specify, test and validate the sensor and safety features being used for a large number of specific traffic scenarios.

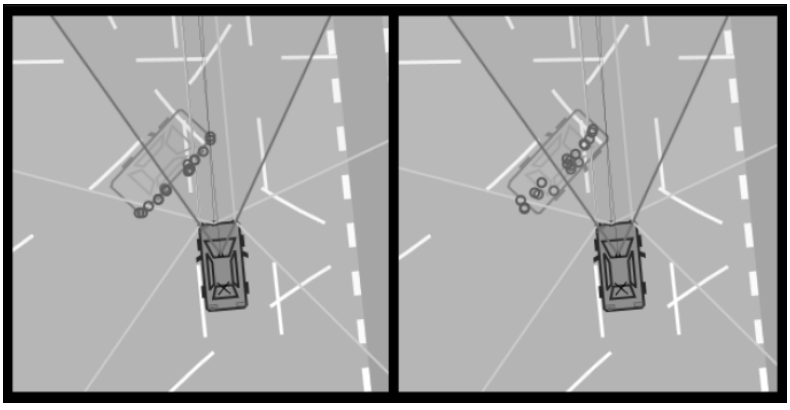

***Figure5. Comparison of an ideal sensor and a sensor considering latency period and noise.***

Based on this, the installation position, angle of view and range of the environment sensors were defined so that especially critical intersection scenarios can be detected almost as early as necessary. A variety of sensor technologies were used for the integrated safety concept to ensure redundant coverage of critical areas around the vehicle and to make use of the advantages of the different technologies in an optimal fashion. Based on a synthetic sensor concept, the environment sensor system is simulated independently of the technology. For the individual sensors, specific properties such as the cycle rates, ranges, detection probabilities, occlusion probabilities and overlap signals are modeled. Using this principle, the safety concept can be initially validated for a 100% sensor to identify limitations early on and to counter these effectively. In the next step, the influences of the sensors on the performance of the safety concept were examined to determine if the individual components can be triggered reliably. In particular, the simulation of the cycle rates, the latency periods during sensing and the estimates of the run times of the underlying algorithms are coordinated so that the components can develop their full potential in protecting passengers.

**Simulations and tests regarding the vehicle structure**

The monocoque, doors and aluminum structure packages were subjected to multiple optimization loops overall. To develop a lightweight structure that is appropriate for the load path, one of the techniques applied was the topology optimization method. This optimization method is used to identify load paths within the available installation space. Based on structural mechanical requirements, a static load spectrum was derived for the finite element model, which contained chassis loads, stiffnesses and impact loads. The identified optimal load paths were used in the course of the project as a basis for developing the body shell. To be able to perform design calculations for the specific materials, precise material models are required. The aluminum alloys EN AW-6060 T6 and EN AW-6082 T6 are used in the front and rear sections of the vehicle and in the roof frame. Because the characteristic material parameters vary with heat treatment, for example, the samples of the materials used were characterized. The characteristic material parameters are critical for simulating the impact behavior because they have a highly sensitive response to the material modeling. Based on various tests, these materials were characterized and the corresponding material models were derived from the findings. Although the material EN AW-6082 T6 has a higher yield point than EN AW-6060 T6 (230 MPa compared to 200 MPa), the elongation after fracture is considerably lower (approx. 12% compared to approx. 17%). The material EN AW-6082 T6 is more suitable for structural areas with static loads. However, if high energy absorptions are required that are associated with high plastic deformations, material EN AW-6060 T6 is used. Furthermore, the calculation was validated using component tests (quasistatic pressure tests) with the longitudinal members from the aluminum front section structure. The goal was to determine the deformation behavior and the force level of the longitudinal members using the previously established characteristic material parameters and to compare these results with the calculation results. The findings from the component test and simulations were used to adapt the aluminum crash structure to the design load cases. The design began with a “0° rigid wall“ test with full-width impacts. The overlap of the structural deformation values obtained from the calculation and from the test showed very good agreement and confirmed the calculated design of the aluminum structure. For the design of the CFRP monocoque as the central component of the structural concept, a "zero intrusion cell" for frontal and rear impacts was defined as a requirement on account of the small size of the passenger compartment. It was based on static and dynamic calculations. The dynamic calculations involved implementation of the characteristic material parameters of the various CFRP materials into the calculation model. For this purpose, component tests were performed to establish the corresponding damage parameters for the constitutive laws in use. The material models determined in this way were used to identify areas in the monocoque that are subject to high loads.

## RESULTS OF FULL SCALE CRASH TESTS

According to the load cases which were defined as requirements on the integrated safety concept of the Visio.M vehicle at the beginning of the development phase three full scale crash tests using a Visio.M prototype were conducted to prove the efficiency of the concept:

1. Frontal impact: 40% offset, ODB, 64 km/h; Euro-NCAP, without deployment of structure-airbag

2. Frontal impact: 40% offset, ODB, 64 km/h; Euro-NCAP, with deployment of structure-airbag

3. Side impact: MDB, 50 km/h, ECE R95

The two frontal impact tests differed in the deployment of the structure-airbag with the objective of figuring out its benefit.

### Frontal and side impact

The tests were conducted with a total mass of the Visio.M prototype (See Figure 6, left) including measurement instrumentation, Dummies etc. of 700 kg. The vehicle structure and the occupant restraint systems were acting in accordance with their design. The monocoque kept stable and avoided the intrusion of components into the passenger compartment. The analysis of the occupant load values according to the Euro-NCAP [1] test protocol for the adult occupant protection box and the offset frontal impact show a result with 15,74 (driver) and 16 (passenger) of 16 possible points. The side impact (See Figure 6, right) was conducted with just one dummy located on the driver's seat. Its load has also a respectable value of 13,704 of 16 possible points.

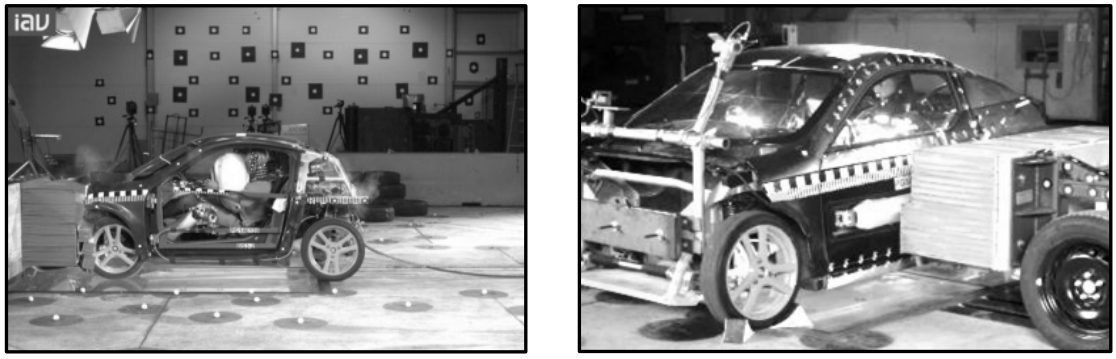


***Figure6. Frontal impact: 40% offset, ODB, 64 km/h, Euro-NCAP and Side impact: MDB, 50 km/h, ECE R95.***

## CONCLUSION

The work and the results of the Safety workgroup of the Visio.M project indicate that, by the use of innovative safety systems and methods, it seems to be possible to reach an acceptable level of occupant safety for ultra-compact vehicles which is comparable to those of compact cars. Even if most of the specified systems and components have just reached a prototype status, the integrated safety concept of the Visio.M vehicle could be beneficial to push the acceptance and thus the market penetration of electrically powered small motorized vehicles in recent years. On the other hand it is questioned if the safety requirements of the L7E vehicle class are sufficient for ultra-compact

[1] Just one test scenario of the Euro-NCAP test protocol was part of the Visio.M load cases – Thus, prediction of a star rating and is not feasible and even was not goal of the working group

vehicles with the character of the Visio.M or a separate homologation class for such vehicles is reasonable. However, this paper shows that higher levels of safety are achievable.

## ACKNOWLEDGEMENT

Participants in the Visio.M consortium are, in addition to the automotive companies BMW AG (lead manager) and Daimler AG, the Technische Universitaet Muenchen as a scientific partner, and Autoliv BV & Co. KG, the Federal Highway Research Institute (BAST), Continental Automotive GmbH, E.ON AG, Finepower GmbH, Hyve AG, IAV GmbH, InnoZ GmbH, Intermap Technologies GmbH, LION Smart GmbH, Amtek Tekfor Holding GmbH, Siemens AG, Texas Instruments Germany GmbH and TÜV SÜD AG as industrial partners. The project is funded under the priority program "Key Technologies for Electric Mobility – STROM" of the Federal Ministry for Education and Research (BMBF).

## REFERENCES

[1] „Elektromobilität und Sicherheit“ In Positionspapier, Verein Deutscher Ingenieure e.V., 2013
[2] Hierlinger, T.; Unger, J.; Khazami, M.; Netzker, C.; Lienkamp, M. 2014 “Presentation of innovative protection systems of a side impact protection concept for micro cars with potential analysis based on FE simulations”
crash.tech 2014, München, April 09th 2014
[3] Hierlinger, T.; Netzker; C.; Unger, J.; Lienkamp, M. 2013 „Aktive seitliche Insassenverschiebung in Seitenaufprall“
9. VDI-Tagung Fahrzeugsicherheit 2.0, Berlin, November 19th–21th 2013
[4] Justen, R.; Schöneburg, R.; Unselt, T. 2014 „Ein neues Sicherheitskonzept für Elekrokleinstfahrzeuge“
In Elektronik automotive, Weka Fachmedien GmbH, Haar, July 2014
[5] Marschner, M.; Liers, H. 2013 „Untersuchung des potentiellen Unfallgeschehen eines zukünftigen urbanen Elektrofahrzeuges auf Basis Realunfalldaten“
9. VDI-Tagung Fahrzeugsicherheit 2.0, Berlin, November 19th–21th 2013
[6] Netzker, C.; Justen, R.; Schöneburg, R. 2013 „Aspekte und Herausforderungen an die Sicherheit von Kleinstfahrzeugen.“
9. VDI-Tagung Fahrzeugsicherheit 2.0, Berlin, November 19th–21th 2013
[7] Netzker, C.; Lang, R.; Quedenbaum, L.; Schonlau, B.; Hierlinger T. 2013 „Elektrokleinstfahrzeuge – Herausforderung an die Fahrzeugsicherheit“
In Automobiltechnische Zeitschrift - ATZ 115 (2013) extra: Automotive Engineering Partners
[8]..Schonlau, B.; Krumbiegl, K.; Quedenbaum, L.; Serka, A. 2013 „Auslegung eines integralen Sicherheitskonzepts für das Kleinstfahrzeug Visio.M“
9. VDI-Tagung Fahrzeugsicherheit 2.0, Berlin, November 19th–21th 2013

# PROPOSAL FOR A MODIFIED THOR LOWER ABDOMEN INCLUDING ABDOMINAL PRESSURE TWIN SENSORS

**Sabine Compigne**
Toyota Motor Europe NV/SA
Belgium

**Mitsutoshi Masuda**
Toyota Motor Corporation
Japan

**Gaëtan Hanen**
**Philippe Vezin**
**François Bermond**
Université de Lyon, Université Claude Bernard Lyon 1, IFSTTAR, LBMC UMR_T 9406
France

Paper Number 15-0216

## ABSTRACT

This paper presents the evaluation of a modified THOR-NT lower abdomen which includes two abdominal pressure twin sensors (APTS®) as replacement for the displacement measurements. Further small changes such as the addition of small masses in front of the abdomen have also been made to better mimic the response of the PMHSs under seat belt loading. As a result, the biofidelity of the prototype abdomen was improved compared to THOR-NT standard abdomen. The addition of the small masses succeeded in increasing the initial peak force of the force-penetration response under seat belt tests. In rigid bar impacts, the prototype force-deflection response stayed longer in the corridor. The pressure measurement was repeatable and discriminated the various impact speeds as well as the impact direction. The pressure peaks were proportional to force and penetration peaks. This study demonstrates the feasibility of introducing the APTSs into THOR lower abdomen and makes proposals for further biofidelity enhancements.

## INTRODUCTION

The Test Device for Human Occupant Restraint (THOR) is an advanced anthropomorphic test device designed to represent the automotive occupants in the sophisticated restraint systems, such as force-limited three-point belts and air bags. The first THOR version, THOR alpha, was released in 2000. Since then the dummy version has evolved into THOR-NT (NHTSA, 2005), THOR Mod Kit (Ridella et al., 2011) and THOR Metric (Parent, 2014). The current study focuses on the THOR lower abdomen which design has not changed along THOR versions except for the instrumentation. THOR abdomen biofidelity specifications are defined for a 6.1 m/s rigid-bar test simulating an impact to the lower rim of the steering wheel as previously tested by Cavanaugh et al. (1986) on Post Mortem Human Subjects (PMHSs). However, the seatbelt is reported nowadays as the most common abdominal injury source of belted occupants involved in a frontal collision (Huelke et al., 1993; Klinich et al., 2008). Rear seat occupants are especially concerned since they are reported to have a significantly higher rate of sustaining a moderate or severe abdominal injury compared to front seat occupants (Lamielle et al., 2006; Martin et al., 2010; Frampton et al., 2012). Several biomechanical studies investigated swine (Miller et al., 1989; Kent et al., 2008) or human abdomen responses (Hardy et al., 2001; Trosseille et al., 2002; Foster at al., 2006; Lamielle et al., 2008) under seatbelt loading which allow the evaluation of the dummy response. Some of the mentioned biomechanical studies investigated various abdominal injury predictors such as abdominal compression, belt tension, penetration speed, viscous criterion, force “viscous criterion”, work of belt tension. Arterial and venous pressure peaks have also been proposed to serve as injury predictor of abdominal organs (Miller et al., 1989; Ruan et al., 2005; Kremer et al. 2011). Beillas et al. (2012) demonstrated the ability to measure pressure inside child Q-dummy abdomen using the Abdominal Pressure Twin Sensors (APTS®). The APTSs could detect injurious abdominal loading for child Q3 and Q6 dummies with an estimated risk of sustaining an AIS3+ abdominal injury of 50% at 1.09 bars. Hanen et al. (2011, 2012), Masuda et al. (2012) investigated the introduction of the APTSs inside the THOR lower abdomen. This paper presents the results of the prototype delivered in 2012 and developed from THOR-NT dummy version.

## MATERIAL AND METHOD

### THOR lower abdomen prototype

THOR-NT lower abdomen is made of two foam blocks and of an internal mounting weld assembly enclosed in a Cordura nylon bag. Two DGSPs (Double Gimbaled String Potentiometer) go through two holes in the foam blocks. They are attached to the rear on each side of the spine to mounting brackets and to the front of the abdominal bag. The DGSPs measure the three dimensional displacements of the two points on the bag surface. The whole lower abdomen assembly can be accessed by opening a zipper placed on the abdomen bag (NHTSA, 2005) (Figure 1).

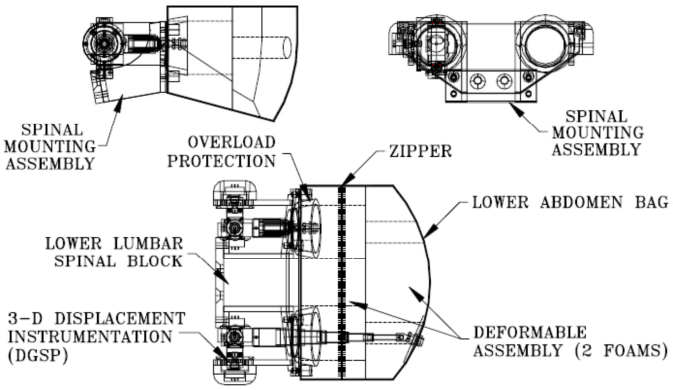


***Figure 1. THOR-NT lower abdomen assembly (NHTSA, 2005).***

The THOR lower abdomen prototype is made from THOR-NT abdomen components. An exploded view of the prototype assembly is shown in Figure 2. New front and rear foam blocks were ordered without holes as DGSPs are not used anymore. Instead two new vertical holes of 51 mm diameter with center axes spaced by 90 mm were made in the front foam block to receive the APTSs (Figure 3). The APTSs (version 2) were inserted with their caps downwards. The version 2 is composed of a 50 mm diameter soft polyurethane bladder filled with paraffin oil. The APTS has one cap through which oil is entered using a pressure column to provide consistent filling conditions. Pressure measures are made by XPR30 subminiature pressure sensors (Measurement Specialties, Les Clayes, France) placed in the balled cap at the interface with the oil (Beillas et al., 2012). Mounting brackets to the spine and abdomen internal plate geometries were simplified. The brackets allow a simpler mounting and dismounting of the entire abdomen assembly from the spine (Figure 4, Figure 5). The wires of the APTSs exit from the bottom of the front foam, go through two cuts made in the rear foam and finally pass through the holes of the modified internal plate and the abdomen bag.

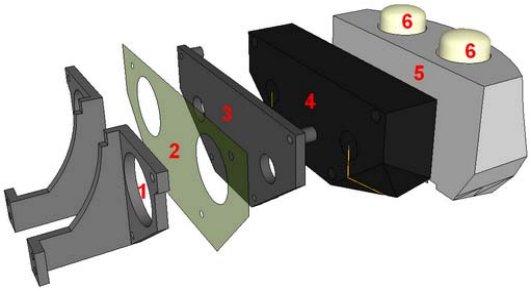


***Figure 2. Abdomen prototype exploded view: (1) Right and left modified mounting brackets (2) Cordura bag (3) Modified internal plate (4) Rear foam block (5) Front foam block (6) Right and left APTSs.***

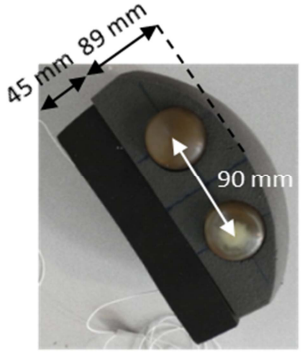


***Figure 3. Top view of abdomen prototype equipped with the APTSs (dimensions measured from dummy parts) .***

*Figure 4. Standard (top) and modified (bottom) abdomen internal plate.*

*Figure 5. Standard (top) and modified (bottom) mounting bracket to the spine.*

Fifteen steel cylinders of 30 mm diameter and 10 mm thickness are attached to the front of the abdomen bag using a Velcro® layer (Figure 6). They represent an additional mass of 825 g. The total mass of the prototype with the attachment brackets is 3.12 kg (THOR-NT abdomen assembly is 2.60 kg). The prototype abdominal depth is 292 mm and 282 mm without the small masses. This has to be compared with the THOR-NT abdominal depth of 265 mm. The abdomen prototype can similarly be mounted on THOR Mod Kit and THOR-Metric thanks to similar lower abdomen/spine assemblies between the dummies.

*Figure 6. Abdomen prototype assembly with the small masses attached to the Cordura bag.*

**Test set-ups**

The abdomen prototype response was evaluated under rigid bar impact and seatbelt loading as performed previously by Hanen at al. (2011) on THOR-NT standard abdomen. Its response was compared to available Post Mortem Human Subject (PMHS) corridors and standard THOR-NT abdomen response re-analysed from Hanen et al. (2011). Additional tests at various speeds (1 to 6.1 m/s) and different impact angles (0° and 20°) were performed to evaluate the sensitivity of the APTS measurement.

**Rigid bar impact** The THOR-NT dummy equipped with the abdomen prototype was submitted to 32 kg impactor tests according to Cavanaugh et al. (1986) test set-up. The impactor was equipped with a 25 mm diameter rigid bar of length 300 mm. Initial impact speed was varied from 1 to 6.1 m/s. The dummy was placed on a table covered by a Teflon® sheet with outstretched legs. The lumbar spine joint was in slouch position (9° between lumbar bracket and pelvis bracket) and the back was unsupported. The hands were attached at the head level. The table height was adjusted to align the rigid bar with the line joining the centers of the attachment nuts of the DGSPs (Figure 7).

The impactor was instrumented with a 20 kN SEDEME SAM-load cell and a 100 g ENTRAN EGCS-S067 uniaxial accelerometer. A light gate measured the impact speed just prior to the contact between the impactor bar and the dummy. The THOR dummy pelvis was instrumented with a 250 g ENTRAN EGAS-S077B three-axis accelerometer. A laser ODS 1150 (900 mm range, 0.1 mm resolution) was positioned in the back of the dummy and measured its pelvis displacement. Data acquisition was made at 20 kHz using Kistler acquisition system and channels were filtered according to SAE J211 using a low pass band Butterworth filter (CFC180 for the accelerations, pressures and laser displacement, CFC600 for the force).
Two high-speed cameras (Photron SA3 black and white) recorded the impact at a rate of 2000 frames/s with a resolution of 1024×1024 pixels. One camera filmed the overall scene and the other one was placed perpendicular to the dummy sagittal plane to measure the impactor and dummy pelvis displacements using Motion Track® software. The time "zero" was identified on the video by a flash which was lit up when the rigid bar came in contact with the dummy suit.
Impact force could be obtained by multiplying the impactor longitudinal acceleration by its mass (32 kg) or by the impactor load cell once corrected for the mass placed in front of the sensor (2.62 kg). Consistency of the force response obtained by these two means was checked. Abdomen penetration was measured as the difference between the impactor displacement and the one of the dummy pelvis obtained by the video analysis. Consistency with other measurements (difference of the double integration of impactor and dummy pelvis longitudinal accelerations) was also checked.
Abdominal penetration measured from the video was re-sampled using linear interpolation at 20 kHz to draw the force-penetration response.

**Seatbelt loading** The THOR-NT dummy equipped with the abdomen prototype was submitted to seatbelt loading according to Foster at al. (2006) test set-up. The dummy was seated on the floor covered by a Teflon® sheet with the legs outstretched and the back against a vertical rigid plate. The dummy lumbar spine joint was in slouch position and its arms were attached to the vertical structure at the head level. The seatbelt was wrapped around the abdomen at mid height and guided from the lateral aspects of the dummy abdomen. The same pretensioner systems as in Foster et al. (2006) study were used and denoted similarly Type A, B and C. Type B and C consisted of a single pretensioner (at different levels of pretension, respectively) whereas Type A consisted of two Type B pretensioners. In addition to Foster's configurations, two Type C pretensioners were also tested. In the case of a single pretensioner system, the webbing was attached on itself using a clamp whereas in the case of a dual pretensioner system, a webbing piece was wrapped around the dummy and its extremities were sewn to each pretensioner webbing. The longitudinal position of the pretensioner support was adjusted to set an initial small tension inside the webbing (10 to 20 N) (Figure 8).
Two 500 g ENTRAN EGAS-S077D uniaxial accelerometers were mounted on each side of the webbing together with two 16 kN MEAS EL20-S458 seatbelt load cells. The same laser as in the rigid bar impact was positioned in front of the dummy and targeted the dummy umbilicus. The dummy pelvis was instrumented with a 250 g ENTRAN EGAS-S077B three-axis accelerometer. Data acquisition was made at 20 kHz using Kistler acquisition system and channels were filtered according to SAE J211 using a low pass band Butterworth filter (CFC180 for the accelerations, pressures and laser displacement, CFC600 for the force).
Two Photron high-speed cameras recorded the impact at a rate of 2000 frames/s. One camera was placed in front of the dummy and the other one was placed to the right of the dummy, perpendicular to the dummy sagittal plane to record the seatbelt and the dummy pelvis displacements. Motion Track® software was used to perform the video analysis. The time "zero" was identified on the video by a flash which was lit up when firing the pretensioner.
Applied force to the abdomen was obtained by adding the forces recorded by both seatbelt load cells. Abdomen penetration was measured as the difference between the seatbelt displacement at dummy umbilicus level and the displacement of the dummy pelvis obtained by the video analysis. Consistency with other measurements (abdominal displacement measured by the laser and pelvis displacement obtained by the double integration of the pelvis longitudinal acceleration) was also checked.
Abdominal penetration measured from the video was re-sampled using linear interpolation at 20 kHz to draw the force-penetration response.

The prototype abdomen responses were overlaid in each test configuration with THOR-NT standard abdomen and, when available, with PMHS corridors. Dummy responses under rigid-bar impacts were compared with Cavanaugh et al. (1986) and Hardy et al. (2001) PMHS corridors defined using average force-penetration responses firstly filtered at 100 Hz and CFC60 respectively and scaled to a 76 kg subject using Eppinger

(1976) equal-stress/equal-velocity technique. Dummy responses under seatbelt loadings were compared with Foster et al. (2006) PMHS corridors defined using average force-penetration responses firstly filtered at CFC600 and scaled to a 78 kg subject using Eppinger (1976) equal-stress/equal-velocity technique.
In all studies, the corridors were calculated from the average response plus and minus one standard deviation. The linear approximations of corridors established in Hardy's and Foster's papers are used here. Cavanaugh's corridor was digitised from the paper.

*Figure 7. Rigid bar impact test set-up.*

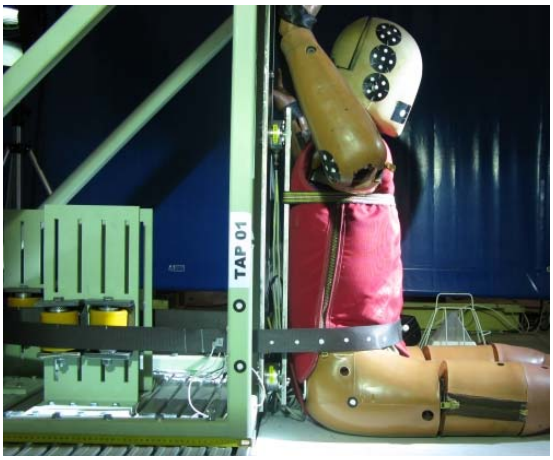


*Figure 8. Seatbelt loading test set-up.*

**Test matrices** Rigid bar impacts were performed with impact speeds ranging from 1 to 6.1 m/s. Each test condition was at least repeated twice. Oblique impacts at 20° towards the right side of the dummy were also conducted at 3 m/s impact speeds to assess directional sensitivity. One test at 3 m/s was performed without the prototype front masses to quantify their effect. The prototype abdomen response was compared to the standard abdomen one at 3 and 6.1 m/s impact speeds (Table 1).

*Table 1. Rigid bar impact test matrix.*

| Test Id (Prototype abdomen) | Velocity (m/s) | Impact angle (°) | Test Id (Standard abdomen, Hanen et al., 2011) |
|---|---|---|---|
| TME82, 83 | 1 | 0 | NA |
| TME84, 85 | 2 | 0 | NA |
| TME79, 80, 81[(1)] | 3 | 0 | TME02, 03 |
| TME77, 78, 88, 89 | 3 | 20 | NA |
| TME90, 91 | 4 | 0 | NA |
| TME92, 93 | 5 | 0 | NA |
| TME94, 95 | 6.1 | 0 | TME04, 05 |

[(1)]The masses in front of the abdomen were removed.

Seatbelt tests were conducted according to Table 2. Four loading conditions were applied to the abdomen. Each test condition was at least repeated twice. The prototype abdomen response was compared to the standard abdomen one under Type B and C test conditions.

*Table 2. Seatbelt test matrix.*

| Test Id (Prototype abdomen) | Loading type | Test Id (Standard abdomen) |
|---|---|---|
| TAP39, TAP40 | C | TAP04, TAP05 |
| TAP41, TAP42, TAP47[(2)] | B | TAP02, TAP03 |
| TAP43, TAP44 | 2×C | NA |
| TAP45, TAP46 | A (2×B) | NA |

[(2)]The masses in front of the abdomen were removed.

## RESULTS

### Prototype biofidelity

**Rigid bar impact** Figure 9 shows the force-time and the penetration-time responses of the standard and the prototype abdomen under 6.1 m/s rigid bar impact. The changes in force-time slopes and small peaks were correlated with the events observed on the video. Overall, the force peaks recorded for the standard abdomen are higher than those of the prototype abdomen and the penetration peaks are slightly higher for the prototype.
The first slope of the force curve of the standard abdomen is related to the abdomen jacket and front foam compression whereas in the prototype, the addition of the small masses gives first a steeper rise of the force during approximately the first 10 mm of penetration. At around 13 ms, the impactor hits the pelvis flesh of the dummy equipped with the standard abdomen. The effect of this contact is visible on the force slope of the standard abdomen due to the stiffness difference between the front abdomen foam and the pelvis flesh. At the moment the impactor slides over the flesh pelvis, the force drops suddenly for the standard abdomen and the penetration continues to increase. The impactor starts to move the dummy at around 27-30 ms, almost 10 ms after the force peak.
The contact with the pelvis flesh happened later with the prototype abdomen (at around 21 ms, 8 ms later than the standard abdomen). The compression of the APTS which happened in addition to the flesh compression increased more gradually the force before the impactor contacts the pelvis flesh. The force peak and the start of the dummy motion happened almost at the same time. The penetration peak occurred around 6 ms after the force peak due to the fact that the impactor continued to move inside the dummy after going above the pelvis flesh. By looking at the movie, this phenomenon was related to the impactor rigid bar mounting which was not sufficiently reinforced to avoid the impactor upwards bending due to the abdomen /pelvis reaction force (Figure 10). The movie showed that the impactor bar slid along the pelvis flesh whereas for the standard abdomen, a significant compression of the pelvis flesh was seen before the impactor could ride above it. For the prototype abdomen, it is expected that such ride off the pelvis flesh may not happen for a more rigidly mounted impacting face and therefore, the maximum penetration would correspond to the maximum force and would likely be lower.

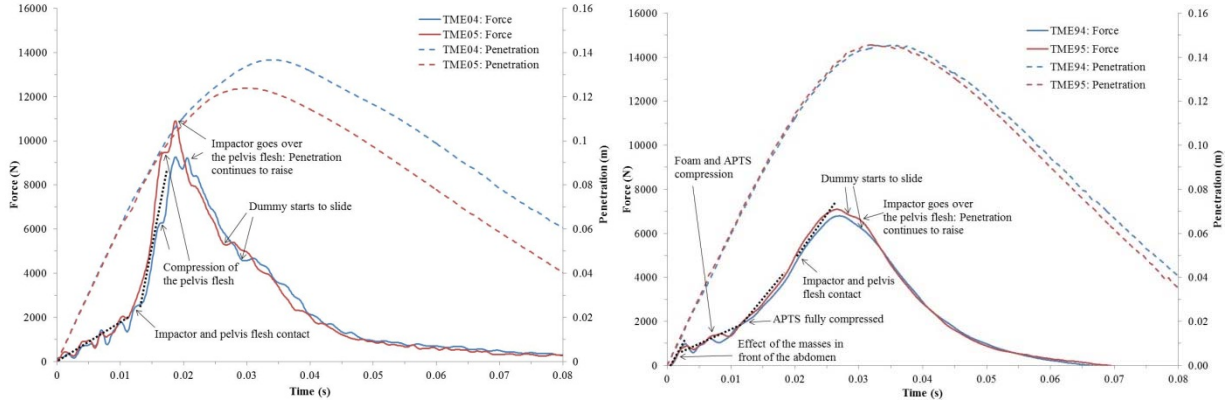


***Figure 9. Force-time and Penetration-time responses of the standard (left) and the prototype (right) abdomen for 6.1 m/s rigid bar impact.***

The difference in time for the impactor contact with the pelvis flesh between the standard and the prototype abdomens was mainly due to their abdomen width difference. Figure 11 shows both abdomens in front of the impactor. By looking at the jacket profile, it is visible that the prototype abdomen protrudes more outside of the pelvis flesh. The small masses and the APTS increase the prototype depth whereas in the standard abdomen, the DGSPs attached at the front of the abdomen bag compress the front foam. Approximately an additional 45 mm penetration was measured at the time of impactor-pelvis contact in the case of the prototype compared to the standard abdomen.

*Figure 10. Impactor rigid-bar upwards bending.*

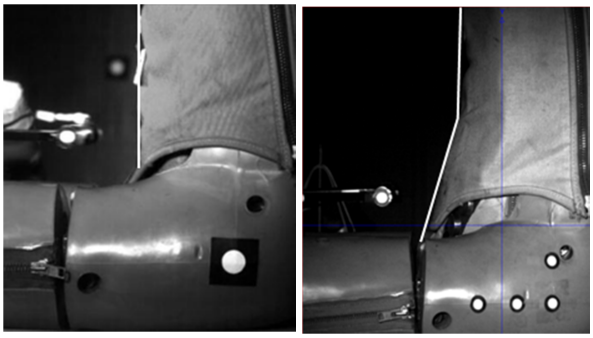

*Figure 11. Depth of standard abdomen (left) and prototype abdomen (right).*

Figure 12 and Figure 13 show the force-penetration responses of the two abdomens. Peak values are reported in Table 3. At 3 m/s, no contact was recorded between the impactor and the pelvis flesh for the dummy equipped with the prototype abdomen. On the opposite, this contact occurred at around 33 ms (88 mm penetration) with the standard abdomen. This increased the force peak (Figure 12). At 6.1 m/s, the prototype abdomen response stayed a bit longer in the PMHS corridors. This was due to a later contact with the pelvis flesh (at 119 mm penetration compared to 80 mm for the standard abdomen). Before that point, between 90 and 120 mm penetration (front foam block and APTS were fully compressed), the response of the prototype exceeds the upper bound of the PMHS corridor which seems to highlight a too stiff response of the abdomen rear foam block (Figure 13).

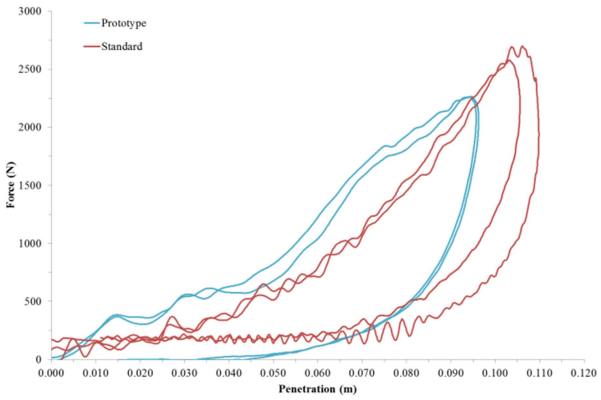


*Figure 12. Force-penetration of the standard (in red) and prototype (in blue) abdomens at 3 m/s rigid bar impact.*

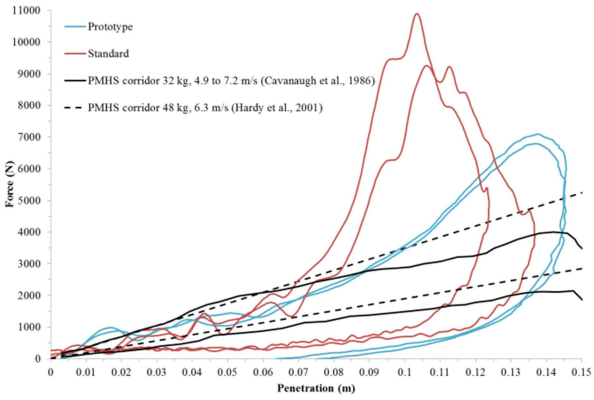


*Figure 13. Force-penetration of the standard (in red) and prototype (in blue) abdomens overlaid with the scaled PMHS corridor at 6.1 m/s rigid bar impact.*

*Table 3. THOR-NT and Prototype peak values under rigid-bar impacts.*

| | Force Peak (N) | | Penetration Peak (mm) | |
|---|---|---|---|---|
| **Velocity (m/s)** | **NT** | **Prototype** | **NT** | **Prototype** |
| 3 | 2578 / 2699 | 2263 / 2265 | 106 / 110 | 96 / 96 |
| 6.1 | 9255 / 10902 | 6791 / 7088 | 137 / 124 | 146 / 146 |

**Seatbelt loading** Figure 14 and Figure 15 overlay the force-penetration responses of the standard THOR-NT abdomen, the prototype abdomen, the responses of a single PMHS (for Type C) and the PMHS corridors as defined by Foster et al. (2006) (for Type B and A). On Figure 14, the large force variations seen from 8 to 12 mm penetration were attributed to the left seatbelt sensor. The reason for these sudden variations is unknown and could not be checked from the video as the camera was on the right side of the dummy. Generally, the force measured at the webbing is increased for the prototype compared to the standard abdomen. However, this increase is still not sufficient to match PMHS responses. The penetration is also much lower than that of the PMHSs (Table 4). Foster et al. (2006) obtained 25%, 35% and 55% PMHS abdominal compression for

pretensioner Type C, B and A respectively, whereas 8%, 20% and 28% abdominal compression was reached with the abdomen prototype (292 mm abdominal depth is considered for the abdomen prototype). The standard abdomen gave similar compression to the prototype: 6% and 18-19% under pretensioner Type C and B (265 mm abdominal depth is considered for THOR-NT).

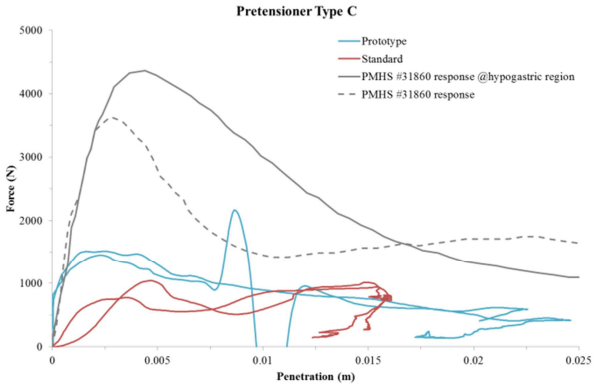


***Figure 14. Force-penetration response of the standard and prototype abdomen compared to Foster et al. (2006) PMHS scaled responses (seatbelt load CFC180 versus penetration CFC60) for pretensioner Type C.***

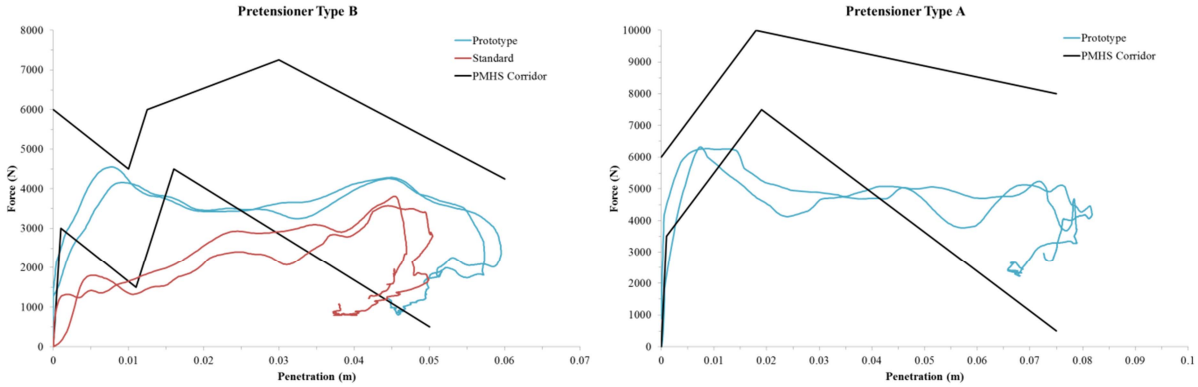


***Figure 15. Force-penetration response of the standard and prototype abdomen compared to Foster et al. (2006) PMHS scaled corridors for pretensioners Type B (left) and A (right, only prototype).***

***Table 4. THOR-NT, Prototype and PMHS peak values under pretensioners Type C, B, A.***

| | Force Peak (N) | | | Penetration Peak (mm) | | |
|---|---|---|---|---|---|---|
| **Loading Type** | **NT** | **Prototype** | **PMHS (Scaled)** | **NT** | **Prototype** | **PMHS (Scaled)** |
| C | 939 / 1039 | 1451 / 1513 | 4363 / 3636 | 16.1 / 15.9 | 24.6 / 22.6 | 63.6 / 66.1 |
| B | 3573 / 3811 | 4257 / 4551 | 5593/5128/6726 | 50.4 / 47 | 57.3 / 59.5 | 97.6/93.6/107.4 |
| A | NA | 6318 / 6265 | 8289 / 7938<br>9737 / 9370 | NA | 78.9 / 81.8 | 123.6 / 112.1<br>153.2 / 128.5 |

**Effect of the APTS and small masses** Force-compression responses of the standard abdomen, of the prototype abdomen without the small masses, and of the prototype with the small masses are compared in Figure 16 and Figure 17 under rigid bar impact and pretensioner loading respectively. Compression is considered here to take into account the differences in abdomen depth between the THOR-NT (265 mm), the prototype without the small masses (282 mm) and the prototype abdomen (292 mm). Starting from the THOR-NT response, the addition of the APTS and of the small masses allowed the gradual increase of the force. The compression of the three abdomens is similar under the Type B seatbelt loading and smaller for the prototype under the 3 m/s rigid bar impact.

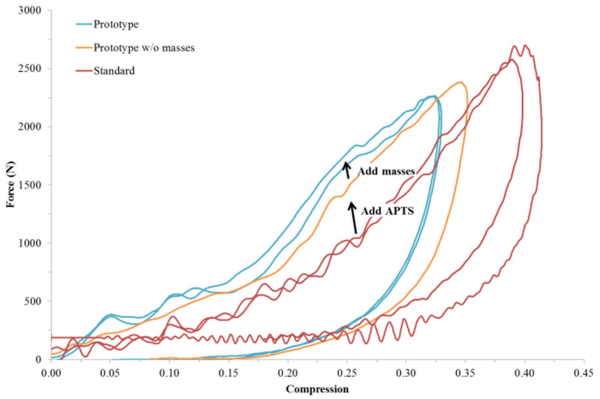


*Figure 16. Force-compression responses of THOR-NT abdomen, prototype without small masses and prototype under 3 m/s rigid bar impact.*

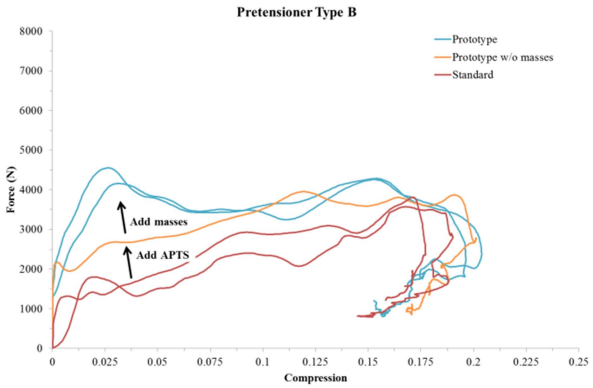


*Figure 17. Force-compression responses of THOR-NT abdomen, prototype without small masses and prototype under pretensioner Type B loading.*

**Sensitivity to speed**

Figure 18 shows the force-penetration responses of the prototype abdomen under 32 kg rigid-bar impacts and for speed variations between 1 and 6.1 m/s. The force and the penetration peaks raise with increasing speed. The force peaks vary between 400 and 7100 N and the penetration peaks vary between 46 mm and 145 mm. The loading slope also increases with the increased penetration at higher speed due to the compression of abdomen components. The contact between the rigid-bar and the pelvis flesh only occurred at 6.1 m/s. For 4 and 5 m/s impacts, the rigid bar rode over the pelvis flesh without touching it. This explains why the penetration peak occurred after the force peak. This kind of behaviour would not be expected with a reinforced rigid bar and in that case, the loading force would increase with a steeper slope up to the peak. Figure 19 overlays the force-penetration responses of the prototype for the various pretensioner types. The average retraction speeds of the seatbelt measured by video analysis using the targets placed on the side of the webbing are mentioned in the figure key. The retraction speed varied from 6.5 to 16 m/s. A first force peak is observed on all the curves at the very beginning of the penetration (at 2 and 10 mm for the slower and the higher retraction speed respectively). For Type B and A, this initial peak is followed by a decrease in force and a plateau almost up to the maximum penetration. For Type C and 2C, the force decreases after the initial peak until the maximum penetration. The force and the penetration peaks are increased with the retraction speed. A large jump in absorbed energy (area under force-penetration curves) is seen between Type 2C and B from 50 to 200 J.

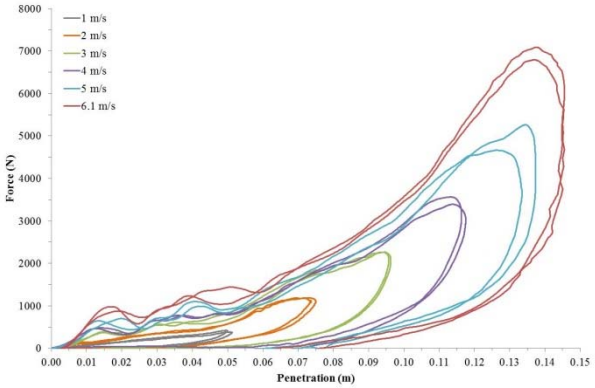


*Figure 18. Prototype abdomen force-penetration responses under 32 kg rigid-bar impacts for impact speed ranging from 1 to 6.1 m/s.*

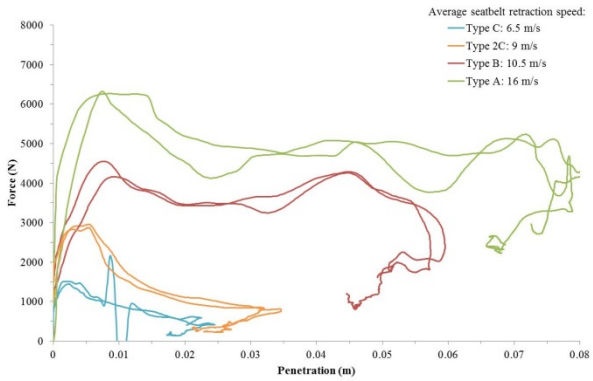


*Figure 19. Prototype abdomen force-penetration responses under pretensioners Type C, 2C, B and A.*

**APTS measurements**

Figure 20 to Figure 23 show APTS pressure versus abdomen penetration for rigid bar impacts and seatbelt loading. Under seatbelt loading, the pressure peaks are observed at the beginning of the penetration. The APTS pressure peaks occur between 10 mm (pretensioner Type C) and 35 mm (pretensioner Type A) penetration. Figure 24 and Figure 25 reveal that pressure peaks are synchronized with force peaks in the case of the prototype without the small masses and delayed by around 4 ms in the case of the prototype. Indeed, with the little masses, the first force peak is linked to the masses inertia whereas there is little abdomen penetration.

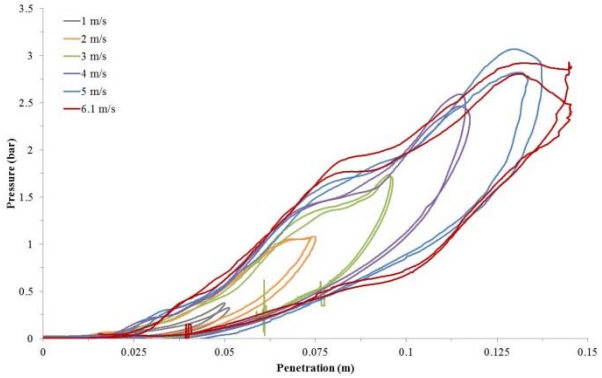


***Figure 20. Left APTS pressure versus abdomen penetration for rigid-bar impacts from 1 to 6.1 m/s.***

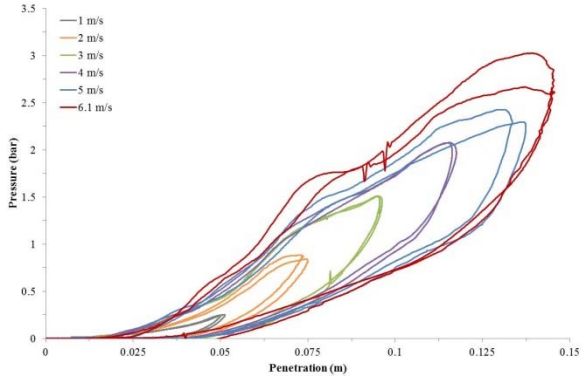


***Figure 21. Right APTS pressure versus abdomen penetration for rigid-bar impacts from 1 to 6.1 m/s.***

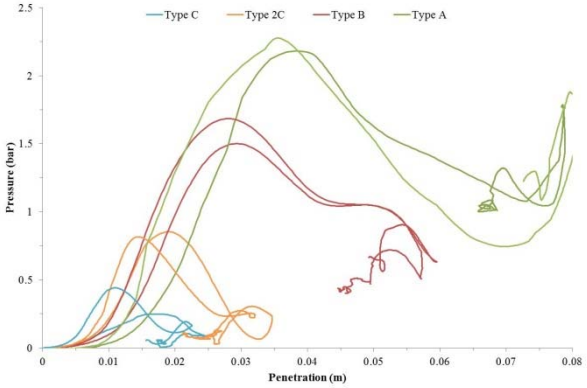


***Figure 22. Left APTS pressure versus abdomen penetration for seatbelt loading using pretensioner Type C, 2C, B and A.***

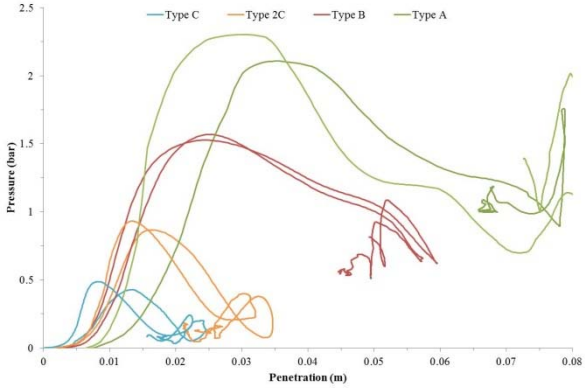


***Figure 23. Right APTS pressure versus abdomen penetration for seatbelt loading using pretensioner Type C, 2C, B and A.***

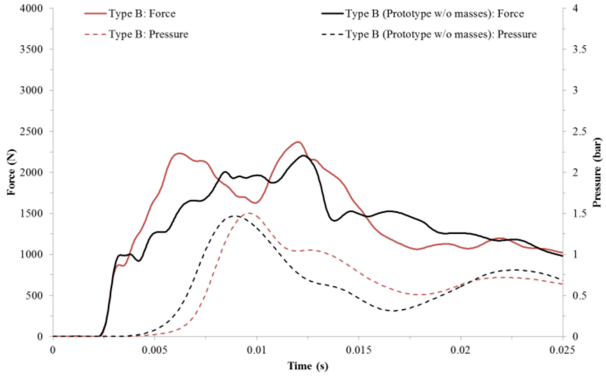


***Figure 24. Left seat belt force (y-axis1) and left APTS pressure (y-axis2) versus abdomen penetration for pretensioner Type B.***

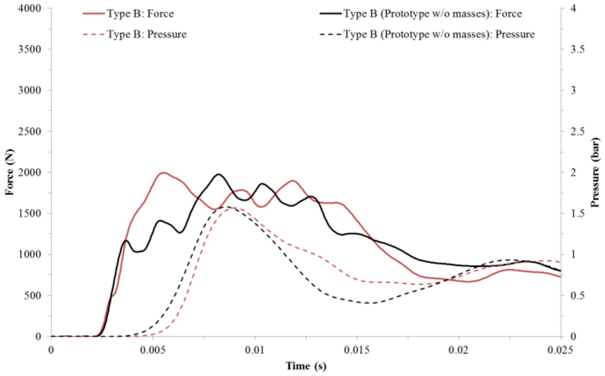


***Figure 25. Right seat belt force (y-axis1) and right APTS pressure (y-axis2) versus abdomen penetration for pretensioner Type B.***

Rigid-bar impacts performed with the dummy rotated by 20° to its left side, exposing more the right APTS, showed the ability of the APTS to discriminate the loading direction. Almost twice higher pressure peaks were recorded by the right APTS (Figure 26).

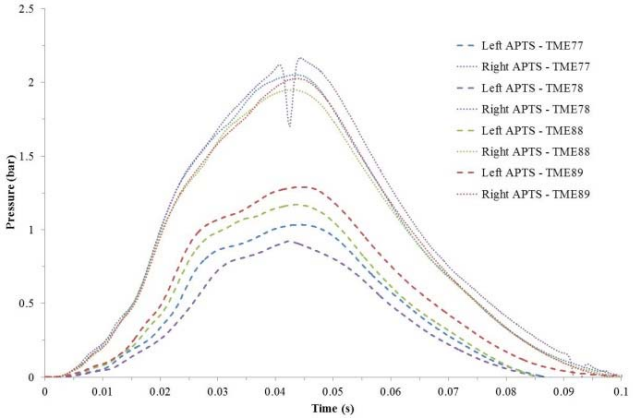


***Figure 26. Left and right APTS pressure for 20° rigid-bar impacts at 3 m/s (4 tests).***

## DISCUSSION

**Biofidelity** The prototype biofidelity was improved under rigid-bar impacts thanks to the addition of the small masses and the higher stiffness of the APTS compared to the front foam. The increased abdominal depth in the prototype made the contact between the rigid-bar and the pelvis flesh occurring later than with the THOR-NT abdomen. In the THOR-Mod Kit and THOR-Metric (most recent version of THOR released by NHTSA), the pelvis flesh at the antero-superior iliac spine (ASIS) are shortened by 20 mm. It is therefore expected that such contact with the rigid-bar impact will not occur anymore. It will remain that the stiffness observed between 90 and 120 mm penetration is still higher than PMHS corridors. This might be solved by changing the abdominal rear foam block properties.

The human response under the seatbelt/pretensioner loading is much more challenging to mimic. The force can be increased, but not to a sufficient level compared to PMHS. The penetration remains lower than that of the PMHSs. A comparison between the prototype and the average scaled PMHS response under pretensioner Type B gives further insight into these differences compared to the corridor (Figure 27-Left). A similar curve shape is in fact observed but it appears that the force plateau after the initial force peak is longer for the prototype (around during 15 mm penetration compared to 5 mm for the PMHSs). A second higher force plateau exists for the PMHS response whereas the penetration of the prototype is stopped. It is therefore necessary to reduce the first plateau in the prototype and increase the force between 20 and 50 mm penetration. This might be done by changing the front foam characteristics to a stiffer material.

Finally, the first force peak should be at the really beginning of the impact (Figure 27). This should be achieved by placing the small masses inside the dummy suit instead of the surface of the abdomen Cordura bag.

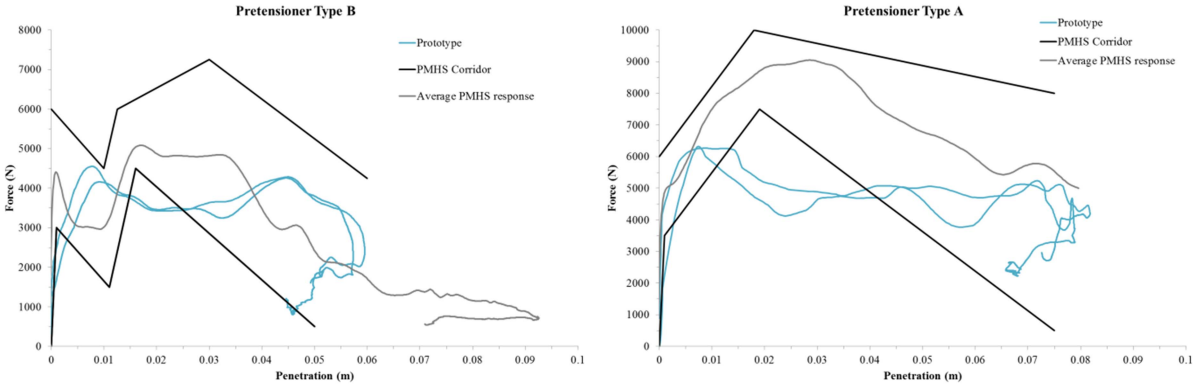


***Figure 27. Force-penetration response of the prototype compared to Foster et al. (2006) PMHS corridors and average PMHS response scaled with Eppinger technique (Lebarbé, 2011)(Left: Type B, Right: Type C).***

**Instrumentation** The abdomen prototype is equipped with two APTSs. In THOR-Mod Kit and THOR-Metric, the pelvis ASISs are equipped with load cells (Ridella et al., 2011). This will provide information on the lap belt and the pelvis interaction in addition to the lap belt and abdomen interaction given by the APTS. The pressure peaks measured by the APTSs corresponded to the force and the penetration peaks measured under the rigid-bar impacts (Table A 1). Under the seatbelt loading, the pressure peak corresponded to the force peak in the prototype without the small masses (Figure 24 and Figure 25). In the prototype (including the small masses), this is not the case as explained earlier. Regarding the penetration peak, there is always a significant time delay (around 10 ms) between the pressure and the penetration peaks as between the force and the penetration peaks (Table A 2). The pressure curves follow force history curve shapes.

**Injury prediction** Cavanaugh et al. (1986) PMHS tests led to abdominal AIS4 injuries for speeds higher than 6 m/s. In Foster et al (2006) study, only tests with pretensioner Type A created AIS2 to AIS3 abdominal injuries. In these two test configurations, the APTS pressure peaks were above 2.7 bars and 2 bars respectively. Beillas et al. (2012) estimated a threshold of 1 bar for the child Q-dummies. This is of course not possible to compare since the tolerance of adult and child is certainly different and since the dummy abdomen designs are also different.

## CONCLUSIONS

The APTSs already used in 3 and 6 years old Q-dummies were introduced into THOR lower abdomen front foam block. Small masses were added on the abdomen Cordura bag and the assembly was mounted on THOR-NT dummy. The response of the abdomen prototype was then compared to the THOR-NT abdomen and to PMHS corridors under 6.1 m/s rigid-bar impact and Foster's seatbelt/pretensioner loadings. Generally, the force-penetration response of the prototype was closer to PMHS response and the APTS pressures accounted well for the impact severity as measured by external force measurements or dummy abdominal penetration. Along the analysis, below proposals were made to further improve the abdomen response:

1. Moving the small masses inside the dummy suit to create earlier the initial peak force seen on PMHS responses,
2. Changing rear foam block properties to a softer material to allow a larger penetration and a lower force after 90 mm penetration,
3. Increasing front foam stiffness to raise further force up to 50 mm penetration,
4. Proceeding with 2/ and 3/ above might lead to using a single lower abdominal foam block since the front foam is too soft and the rear foam is too stiff.

In the component tests performed in this study, the interaction between the pelvis flesh and the rigid-bar or the seatbelt webbing influenced largely the results. This could be easily identified in the rigid-bar tests but less easily in the seatbelt tests. The THOR-Metric is equipped with ASIS load cell and its pelvis flesh has been shortened by around 20 mm. Together with the prototype abdomen, THOR-Metric will allow measurement of the load applied to the pelvis and to the abdomen, discretely.

Interaction between the lower abdomen and the upper torso will need to be considered. Evaluation in sled tests highlighted that further work is also needed to understand the influence of the dummy kinematics on the pressure measurements.

## REFERENCES

Beillas P., Alonzo F., Chevalier M-C., Lesire P., Leopold F., Trosseille X., Johannsen H. (2012) Abdominal twin pressure sensors for the assessment of abdominal injuries in Q dummies : In-dummy evaluation and performance in accident reconstruction. Stapp Car Crash Journal 56: 387-410.

Cavanaugh J. M., Nyquist G. W., Goldberg S. J., King A. I. (1986) Lower abdominal tolerance and response. Proceedings of 30th Stapp Car Crash Conference, pp. 41-63, SAE technical paper No 861878. Society of Automotive Engineers, Warrendale, PA.

Eppinger R. H. (1976) Prediction of thoracic injury using measurable experimental parameters. Proceedings of 6th international ESV Conference, p. 770. Washington, DC, USA. 1976.

Foster C. D., Hardy W. N., Yang K. H., King A. I. (2006) High-speed seatbelt pretensioner loading of the abdomen. Stapp Car Crash Journal 50: 27-51.

Frampton R., Lenard J., Compigne S. (2012) An in-depth study of abdominal injuries sustained by car occupants in frontal crashes. Proceedings of 56th Association for the Advancement of Automotive Medicine, Chicago, Illinois. October, 2012.

Hanen G., Bermond F., Compigne S., Masuda M. (2011) Contribution to the improvement of crash test dummies in order to decrease abdominal injuries in road accidents. Proceedings of 22nd international ESV Conference, Paper No 11-0218. Washington, DC, USA. June 13-16, 2011.

Hanen G, Vezin P., Bermond F., Masuda M., Compigne S. (2012) A pressure-based abdominal insert for THOR-NT. JSAE Annual Congress, Pacifico Yokohama, Japan. May 2012.

Hardy W. N., Schneider L. W., Rouhana S. W. (2001) Abdominal impact response to rigid-bar, seatbelt, and airbag loading. Stapp Car Crash Journal 45: 1-31.

Huelke D. F., Mackay G. M., Morris A. (1993) Intraabdominal injuries associated with lap-shoulder belt usage. SAE paper n°930639.

Kent R., Stacey S., Kindig M., Woods W., Evans J., Rouhana S. W., et al. (2008) Biomechanical response of the pediatric abdomen, Part 2: Injuries and their correlation with engineering parameters, Stapp Car Carsh Journal 52: 135-166.

Klinich K. D., Flannagan C. A., Nicholson K. et al. (2008) Abdominal injury in motor vehicle crashes. UMTRI technical report UMTRI-2008-40.

Kremer M. A., Gustafson HM, Bolte J. H., Stammen J., Donnelly B. (2011) Pressure-based abdominal injury criteria using isolated liver and full-body post-mortem human subject impact test. Stapp Car Crash Journal 55: 317-350.

Lamielle S., Cuny S., Foret-Bruno JL., Petit P., Vezin P., Verriest JP., Guillemot H. (2006) Abdominal injury patterns in real frontal crashes: Influence of crash conditions, occupants seat and restraint systems. Association for the Advancement of Automotive Medicine, Chicago, Illinois. October 16-18, 2006.

Lamielle S., Vezin P., Verriest JP., Petit P., Trosseille X., Vallancien G. (2008) 3D deformation and dynamics of the human cadaver abdomen under seatbelt loading. Stapp Car Crash Journal 52: 267-294.

Lebarbé M. (2011) Contribution to the definition of biofidelity corridors in frontal impact for an adult male 50th percentile – Abdomen. ACEA report Revision 9. September 2011.

Martin JL., Lardy A., Compigne S. (2010) Specificities of rear occupant protection: Analysis of French accident data. Proceedings of IRCOBI Conference, Hanover. September 2010.

Masuda M., Compigne S. (2012) Dynamic response of the THOR-NT: Thorax and Abdomen. SAE 2012. Government/industry meeting. Washington, DC, USA. January 25-27, 2012.

Miller M.A. (1989) The biomechanical response of the lower abdomen to belt restraint loading. Journal of trauma 29 (11): 1571-1584.

National Highway Traffic Safety Administration, THOR-NT user manual 50% male frontal dummy, Revision 2005.1, Report No: GESAC-05-02, U.S. Department of Transportation, Washington, DC, March 2005.

Parent D. P. (2014) Applications of the THOR ATD in NHTSA research. . SAE 2014. Government/industry meeting. Washington, DC, USA. January 22-24, 2014.

Ridella S. A., Parent D. P. (2011) Modifications to improve the durability, usability and biofidelity of the THOR-NT dummy. Proceedings of 22nd international ESV Conference, Paper No 11-0312. Washington, DC, USA. June 13-16, 2011.

Ruan J. S., El-Jawahri R., Barbat S., Prasad P. (2005) Biomechanical analysis of human abdominal impact responses and injuries through finite element simulations of a full human body model. Stapp Car Crash Journal 49: 343-366.

Trosseille X., Le-Coz JY., Potier P., Lassau JP. (2002) Abdominal response to high-speed seatbelt loading. Stapp Car Crash Journal 46: 71-79.

**APPENDIX I**

*Table A 1. Peak values and timing in rigid-bar impacts.*

| | | Rigid-bar impact | | | |
|---|---|---|---|---|---|
| **Impact speed (m/ss)** | **Test Id** | **Force (N) @ Time (ms)** | **Penetration (mm) @ Time (ms)** | **Left Pressure (bar) @ Time (ms)** | **Right Pressure (bar) @ Time (ms)** |
| 1 | TME82 | 384@75 | 51@84 | 0.33@79.2 | 0.25@76.9 |
| | TME83 | 419@73.3 | 50@79.5 | 0.38@75.2 | 0.25@75.2 |
| 2 | TME84 | 1183@44.2 | 74@55 | 1.1@51.3 | 0.9@50.4 |
| | TME85 | 1185@47.1 | 75@56.5 | 1.1@51.8 | 0.8@51.1 |
| 3 | TME79 | 2263@41.8 | 96@47 | 1.7@43.6 | 1.5@43 |
| | TME80 | 2265@41.8 | 96@47 | 1.7@44 | 1.5@42.4 |
| 4 | TME90 | 3563@35.3 | 116@40.5 | 2.6@36.9 | 2.1@37.3 |
| | TME91 | 3389@36 | 118@42.5 | 2.5@36.7 | 2.1@37.4 |
| 5 | TME92 | 4661@30.9 | 134 @38 | 2.8@34.5 | 2.4@33.3 |
| | TME93 | 5261@33.7 | 137@39 | 3.1@30.8 | 2.3@35.4 |
| 6.1 | TME94 | 6791@27 | 146@35 | 2.8@25 | 3.0@28 |
| | TME95 | 7088@26.6 | 146@32 | 2.9@33.7 | 2.7@26.3 |

*Table A 2. Peak values and timing in seatbelt loading.*

| | | Seatbelt loading | | | | |
|---|---|---|---|---|---|---|
| **PT** | **Test Id** | **Left Force (N) @ Time (ms)** | **Left Pressure (bar) @ Time (ms)** | **Right Force (N) @ Time (ms)** | **Right Pressure (bar) @ Time (ms)** | **Penetration (mm) @ Time (ms)** |
| Type C | TAP39 | 563@4.6 | 0.25@11.6 | 888@4.5 | 0.43@9.9 | 17@20.5 |
| | TAP40 | 730@6.1 | 0.44@10.6 | 917@4.6 | 0.49@9.3 | 23@19 |
| Type B | TAP41 | 2370@12 (*) | 1.5@9.6 | 1996@5.5 | 1.6@9 | 57@16.5 |
| | TAP42 | 2479@12.2 (*) | 1.7@9.7 | 2278@5.7 | 1.5@9.3 | 60@17 |
| Type 2C | TAP43 | 1616@5.1 | 0.85@8.6 | 1346@5.2 | 0.87@8.2 | 35@17 |
| | TAP44 | 1592@4.5 | 0.82@9.2 | 1315@5.3 | 0.9@8.8 | 32@16.5 |
| Type A | TAP45 | 3492@3.8 | 2.2@7.9 | 2832@3.7 | 2.1@7.6 | 79@23 |
| | TAP46 | 3480@3.8 | 2.3@7.4 | 3166@4.8 | 2.3@6.8 | 82@16.5 |

(*) This time corresponds to the second peak force. The first one is slightly lower but occurs at 6 ms.

# The tracking method of vehicle point or dummy point in the vehicle crash by calculating linear accelerometer and angular velocity

**Park Un-chin** **Song Ha-jong*** **Kim Hyun-chul****
**Florian Ganz***** **Sudar Sankar***** **Christian Santos*****

ABSTRACT

From the mathematical equations we can get the point coordinates with 3 axis linear accelerometer and 3 axis angular velocity by integration. In this research, we will introduce two unique algorithms-acceleration method and velocity method of Hyundai-Kia motors and ACTs and prove the accuracy from many kinds of dummy inboard or outboard tracking case and vehicle body point.

**Key Word** : Gyro, Tracking, Vehicle Crash, Dummy, accelerometer, angular velocity

## 1. Introduction

Target tracking is useful in the vehicle crash test analysis because we can check the contact of 2 objects and compare what is different on the moving among the several tests.

If we use video target tracking, it takes some more time than point tracking by calculating 3 axis linear accelerometer and 3 axis angular velocity because we should convert the high speed film file and analyze by video tracking program like TEMA. Also, the resolution of tracking data become lower because the resolution of high speed film is 1,000Hz and that of sensor data is 10,000 Hz. The most important thing is video target tracking time is restricted in case of the head tracking because the head is commonly covered by curtain airbag and passenger airbag by test modes or rotates so the target is untraceable.

But we cannot conclude the point tracking by calculating 3 axis linear accelerometer and 3 axis angular velocity is always more useful, because we cannot use it on the deforming area of crash vehicle. The vibration during the deformation makes a kind of noise so the calculation becomes inaccurate. Also there must be some tolerance in the calculation method. (IMU company says the maximum tolerance is about 12mm in case of frontal sled head tracking). [1)~3)]

So we should mix these two types of method for proper purpose. In this research we will introduce two unique algoritms-acceleration method and velocity method of Hyundai-Kia motors and ACTs. We need only common 3 axis linear accelerometer and 3 axis angular velocity data and diadem software, not expensive sensor or software, so we believe this can be widely and easily used in crash analysis.

## 2. Main Subject

### 2.1 Theories and related formula in physics.

#### 2.1.1 The velocity relative to fixed system "S"

Considering two axis systems, "S" fixed to ground and "S'" moving relative to "S".

Considering a point in space, coordinates relative to the two systems are:

To "S": $\vec{r} = x\vec{i} + y\vec{j} + z\vec{k}$ (1)

To "S'": $\vec{r}' = x'\vec{i} + y'\vec{j} + z'\vec{k}$ (2)

in velocity from position, the position must be differentiated through time.

$$\vec{v} = \frac{d\vec{r}}{dt} \quad (3)$$

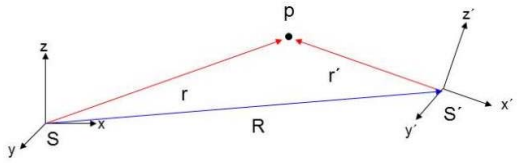


To obtain the velocity relative to the fix systems "S",

* Safety Performance Team 1 : Author or Co-Author
** Crash Simulation Team : Co-Author
*** ACTS (Advanced Car Technology System) : Co-Author

the position has to be differentiated relative to the fix system "S".

$$(\vec{v})_S = \left(\frac{d\vec{r}'}{dt}\right)_S = \frac{dx'}{dt}\vec{i}' + \frac{dy'}{dt}\vec{j}' + \frac{dz'}{dt}\vec{k}' + x'\left(\frac{d\vec{i}'}{dt}\right)_S + y'\left(\frac{d\vec{j}'}{dt}\right)_S + z'\left(\frac{d\vec{k}'}{dt}\right)$$

(4)

The variation through time of the axis vectors represent the angular velocity of the axis. Therefore, the velocity of the point calculated relative to the fix system "S" is:

$$(\vec{v})_S = \left(\frac{d\vec{r}'}{dt}\right)_S + (\vec{w} \times \vec{r}') \qquad (5)$$

To obtain the velocity variation through time of the axis vectors represent the angular velocity of the axis. Therefore, the velocity of the point calculated relative to the fix system "S" is:

$$(\vec{v})_S = \left(\frac{d\vec{R}}{dt}\right)_S + \left(\frac{d\vec{r}'}{dt}\right)_S + (\vec{w} \times \vec{r}') \qquad (6)$$

But if S' is rotating in pitching sled, oblique or offset crash we should consider its velocity factor also.

$$(\vec{v})_S = \left(\frac{d\vec{R}}{dt}\right)_S + (\vec{w}' \times \vec{R}') + \left(\frac{d\vec{r}'}{dt}\right)_S + (\vec{w} \times \vec{r}') \qquad (6)'$$

**2.1.2 The acceleration relative to fixed system "S"**

To get acceleration, relative to the fix systems "S" the velocity has to be differentiated.

$$\vec{a} = \left(\frac{d\vec{v}}{dt}\right)_S = \left(\frac{d\vec{v}'}{dt}\right)_S + \left(\frac{d\vec{V}}{dt}\right)_S + \left(\frac{d(\vec{w} \times \vec{r}')}{dt}\right) \qquad (7)$$

The third term differentiates as follows:

$$\left(\frac{d(\vec{w} \times \vec{r}')}{dt}\right) = \left(\frac{d\vec{w}}{dt}\right)_S \times \vec{r}' + \vec{w} \times \left(\frac{d\vec{r}'}{dt}\right)_S = \left(\frac{d\vec{w}}{dt}\right)_S \times \vec{r}' + \vec{w} \times \left[\left(\frac{d\vec{r}'}{dt}\right)_S + \vec{w} \times \vec{r}'\right] =$$

$$= \left(\frac{d\vec{w}}{dt}\right)_S \times \vec{r}' + \vec{w} \times \left(\frac{d\vec{r}'}{dt}\right)_S + \vec{w} \times (\vec{w} \times \vec{r}') \qquad (8)$$

Remembering that from equation (5):

$$\left(\frac{d\vec{r}'}{dt}\right)_S = \left(\frac{d\vec{r}'}{dt}\right)_S + (\vec{w} \times \vec{r}')$$

Final acceleration relative to fixed system "S" is:

$$\vec{a} = \left(\frac{d\vec{V}}{dt}\right)_S + \left(\frac{d\vec{v}'}{dt}\right)_S + \left(\frac{d\vec{w}}{dt}\right)_S \times r' + \vec{w} \times (\vec{w} \times \vec{r}') + 2\vec{w} \times v' \qquad (9)$$

Which is same as

$$\ddot{\vec{x}}_{31} = \ddot{\vec{x}}_{32} + \ddot{\vec{x}}_{21} + \dot{\vec{w}}_2 \times \vec{x}_{32} + \vec{w}_2 \times (\vec{w}_2 \times \vec{x}_{32}) + 2 \cdot \vec{w}_2 \times \dot{\vec{x}}_{32} \qquad (10)$$

4)~5)

**2.1.3 Two methods - from velocity or acceleration**

To obtain position from the velocity calculation, one integration must be done from equation (6). In case of a sled test, the calculated point acceleration has to be integrated two times (ax,ay,az) to obtain point position (x,y,z). Also sled acceleration has to be integrated one time to obtain sled velocity which is considered the moving system's velocity and angular velocity is given.

To obtain position from acceleration calculation, two integration must be done. in case of a crash test, the calculated point has to be integrated two times (ax,ay,az) to obtain point position (x,y,z). Sled acceleration does not need to be integrated. Angular velocity is given. Then, acceleration can be calculated from equation (8).

For velocity method calculation in a crash test, only one point acceleration needs to be integrated. In order to obtain position, one integration of the complete velocity needs to be done. Consequently 3 integrations are needed.

For acceleration method calculation in a crash test, only one point acceleration needs to be integrated. In order to obtain position, two integration of the complete velocity needs to be done. Consequently 4 integrations are needed.

Comparing these two method in a crash test, we can expect velocity method would be more accurate because its integration number are smaller one time.

For velocity method calculation in a sled test, point acceleration and sled acceleration needs to be integrated. In order to obtain position, one integration of the complete velocity needs to be done. Consequently 4 integrations are needed.

For acceleration method calculation in a sled test, only one point acceleration needs to be integrated. In order to obtain position, two integration of the complete velocity needs to be done. Consequently 4 integrations are needed.

Comparing these two method in a sled test, we can expect acceleration method would be more accurate because there is no integration of sled axis which has bigger value than the others.

## 2.2 How to insert channels in diadem macro

We should be careful about the polarity and each axis definition when we use this macro. The inserting

sequence can be list like Fig1.

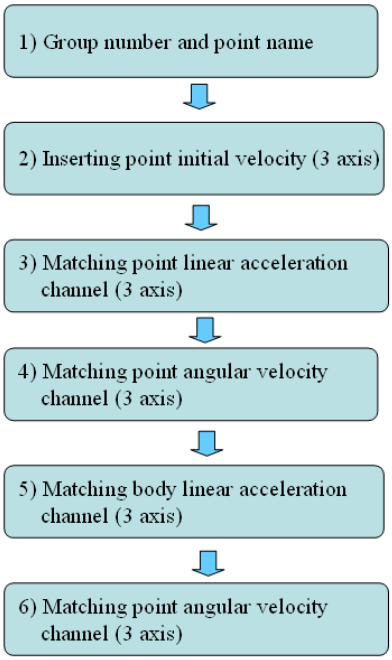


Fig.1 inserting sequence of the macro

Firstly, we should differentiate the group number and point name because when we do multi-calculation in one diadem file the previous calculation can be deleted unless we don't differentiate.

Secondly, we should insert point's 3 axis initial velocities because these are used to calculate the position. We should be careful for the macro unit, here we are using m/s, so NCAP x speed 56kph is 15.57 and Offset x speed 64kph is 17.78. The others be inserted as 0.

Thirdly, we should match the point's linear acceleration channels of 3 axis. We are using m/s2 and the polarity is same as SAE1733's which deceleration is plus in case of dummy contact to front airbag.

Fourthly, we should match the angular velocity channels of 3 axis. We are using rad/s and the polarity is same as SAE1733's.

Fifthly, we should match the body linear acceleration channels of 3 axis. We are using m/s2 and the polarity can be different by the case. In case of frontal sled test dummy head tracking the sled x axis pulse polarity is plus because when we compare and analyze it with video tracking the camera is onboard and it pushed the sled buck rear. In case of frontal crash test dummy head tracking the body x axis pulse polarity is minus because when we compare and analyze it with video tracking the camera is outboard and it pushed the car rear. If there is not y and z acceleration, we should match it with null channel which is automatically made by macro.

Sixthly, we should match the angular velocity channels of 3 axis. We are using rad/s and the polarity is same as SAE1733's. This terms are from equation (6)' and used only for body rotating case like pitching sled, oblique or offset crash.

## 2.3 Usage and confirming accuracy

### 2.2.1 Head tracking in YD NCAP sled and crash case

To confirm the accuracy, we chose YD US NCAP sled and crash case.

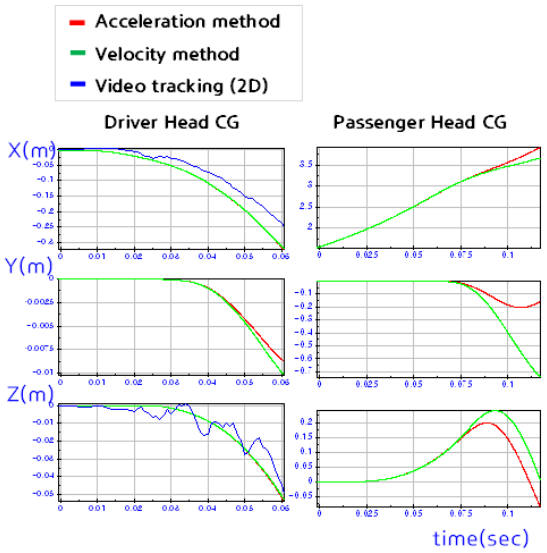


Fig.2 Head target tracking result in YD NCAP sled

When we review the sled target tracking, the acceleration method is very close to the velocity method till 100ms. But in case of passenger dummy the difference between them goes bigger (over 25cm), we can guess it comes from angular velocity tolerance which is 0.5˚/sec in H3 50% percentile dummy but of 5˚/sec in H3 5% percentile(10 times bigger tolerance).

The comparison with 2D video target tracking was not successful because there was big oscillation on the sled onboard camera. We compare it only for the driver.

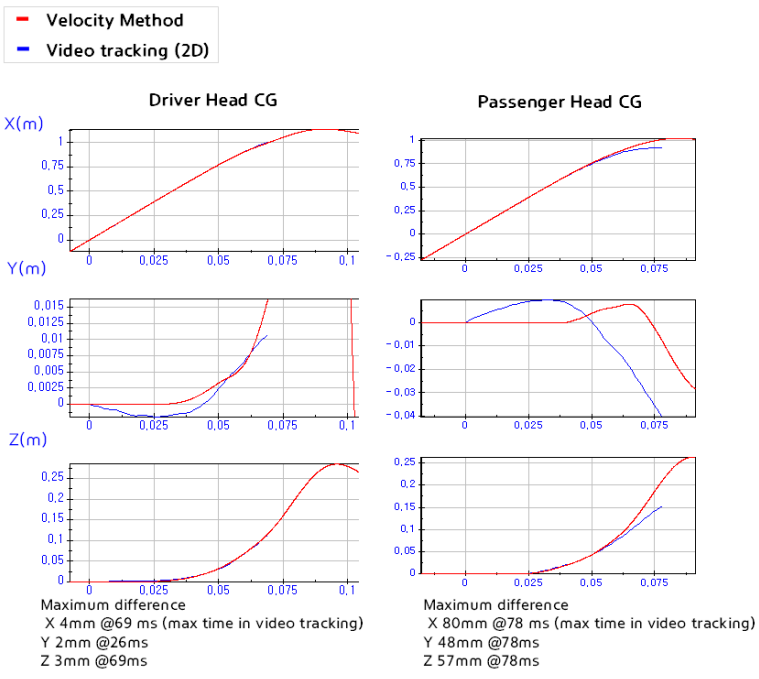

Fig.3 Head target tracking result in YD NCAP crash

In NCAP crash the comparison with 2D video target tracking was successful. The maximum tracking difference was 4mm below in driver. But in case of passenger it was much higher than driver, we guess this comes from also angular velocity tolerance which is 0.5˚/sec in H3 50% percentile dummy but of 5˚/sec in H3 5% percentile(10 times bigger tolerance).

Now the thinking in 2.1.3 that " we can expect acceleration method would be more accurate because there is no integration of sled axis which has bigger value than the others." in not so meaningful because the tolerance is too low in comparison with video tracking.

Comparison between sled and crash is not meaningful because sled test was done just as a base to confirm measuring method so we skip it here.

### 2.2.2 YD smalloverlap trolley ACU tracking case

In HKMC research with ACTs, we make YD smalloverlap trolley test for chassis and structure evaluation and its realization was quite close to the real crash. [6)]

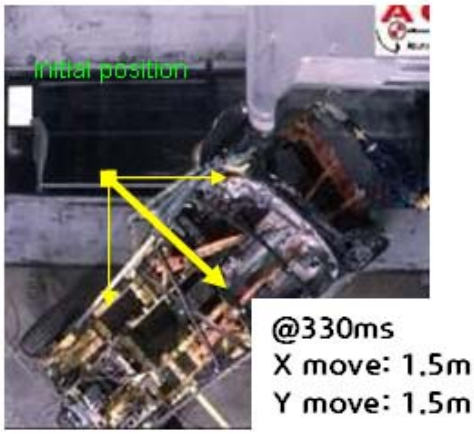


Fig.4 YD smalloverlap trolley video@330ms

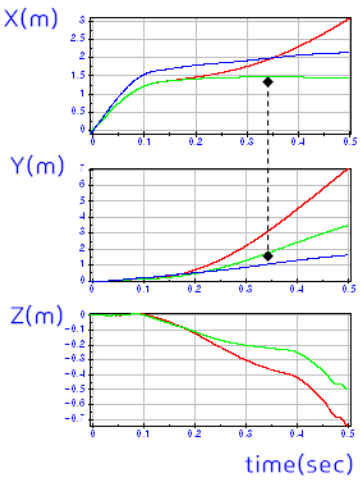


Fig.5 YD smalloverlap ACU positon tracking

In this test, we attached 3 axis linear accelerometer and 3 axis angular velocity sensorr to ACU (airbag control unit) position. Like NCAP sled head tracking result, acceleration method and velocity method tracking is close each other in 100ms but it becomes far. When we checked the video ACU position roughly which is possible to check to the time 330ms they matches to the tracking value x:1.5m and y:1.5m. We added similar place video tracking (cowl top tracking) in the graph, it is similar to the velocity tracking. So we can confirm the thinking in 2.1.3 that "we can expect velocity method would be more accurate because its integration number are smaller one time."

### 2.2.3 YD IIHS side trolley CG tracking case

In HKMC research with ACTs, we make YD IIHS side trolley test for the side structure evaluation and its realization was quite close to the real crash.

Fig.6 YD IIHS side trolley video@240m

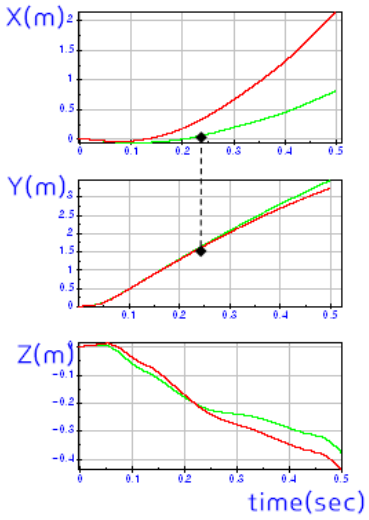


Fig.7 YD IIHS side trolley CG positon tracking

In this test, we attached 3 axis linear accelerometer and 3 axis angular velocity sensor to trolley CG. Like NCAP

sled head tracking result, acceleration method and velocity method tracking is close each other in 100ms but it becomes far. When we checked the video CG position roughly which is possible to check to the time 240ms they matches to the tracking value x:0.1m and y:1.7m. There was no good video tracking position close to the trolley so we skipped to compare with video tracking. But we can confirm the thinking in 2.1.3 that "we can expect velocity method would be more accurate because its integration number are smaller one time."

#### 2.2.4 YD US NCAP crash ACU tracking case

For more usage, in HKMC research with ACTs, we run the YD NCAP crash test with 3 axis linear accelerometer and 3 axis angular velocity sensor to ACU position

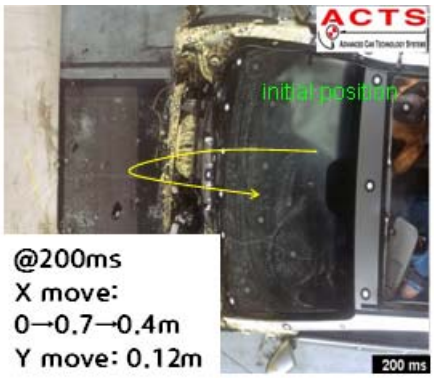


Fig.8 YD NCAP ACU video@200m

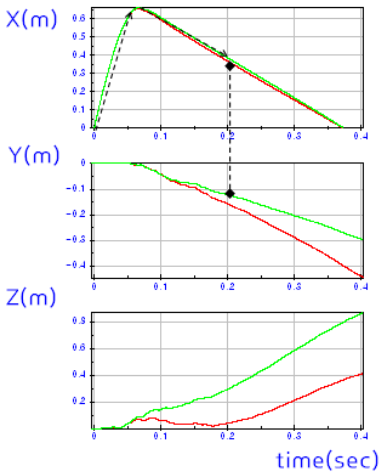


Fig.9 YD NCAP ACU positon tracking

In this test, like NCAP sled head tracking result, acceleration method and velocity method tracking is close each other in 100ms but it becomes far. When we checked the video ACU position roughly which is possible to check to the time 200ms they matches to the tracking value x: once maximum 0.7m and rebound to 0.4m and y:0.12m. There was no good video tracking position close to the trolley so we skipped to compare with video tracking. But we can confirm the thinking in 2.1.3 that "we can expect velocity method would be more accurate because its integration number are smaller one time."

## 3. Conclusion

As we discussed target tracking by calculating sensors is very useful in the vehicle crash test analysis because we can check the invisible area also. Now we developed HKMC and ACTS' unique calculating algorithm by the physical points moving vector equation. We did know below facts in this research.

1) The acceleration method is very close to the velocity method till 100ms.

2) The accuracy of velocity method was in 4mm in NCAP crash test H3 50% driver head tracking.

3) In case of passenger dummy the difference between them goes bigger (over 25cm), we can guess it comes from angular velocity tolerance which is 0.5˚/sec in H3 50% percentile dummy but of 5˚/sec in H3 5% percentile(10 times bigger tolerance).

4) For the body point tracking, only velocity method was accurate because its integration number are smaller one time than acceleration method.

■ Patent No. : Be submitted Diadme macro target tracking by 3 axis accelermeter and 3 axis angular velocity sensor

## References

1. Peter Björkholm, "Inertial Navigation of Crash Dummies Phase II", Imego 2011
2. Sangram Redkar, "USING INERTIAL MEASUREMENT TO SENSE CRASH-TEST DUMMY KINEMATICS" Arizona State University, 2010
3. Wolfgang Sinz. Simulation Based Analysis of Test Results Graz University of Technology, 2010
4. Karl Hoffmann, "Eine Einfüfrung in die Technik des Messens mit Dehnungsmeßstreifen", Herausgeber: Hottinger Baldwin Messtechnik GmbH, Sarmtadt
5. Herausgegeben von W.Beitz und K.-H., "DUBBEL TASCHENBUCH FÜR DEN MASCHINENBAU" 20. AUFLAGE
6. Park Un-chin "The trolley test way of IIHS small overlap and side test with minimized structure usage", HKMC, 2014

## ■ Author ■


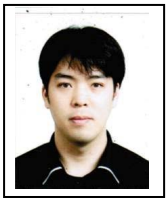
Park Un-chin

Song Ha-jong

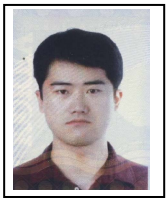
Kim Hyun-chul

Florian Ganz

Sudar Sankar

Christian Santos

# AUTONOMOUS EMERGENCY BRAKING FOR CORNERING MOTORCYCLE

**Giovanni Savino**
Dept. of Industrial Engineering, University of Florence
Italy
Accident Research Centre, Monash Injury Research Institute, Monash University
Victoria, Australia

**Federico Giovannini**
**Simone Piantini**
**Niccolò Baldanzini**
**Marco Pierini**
Dept. of Industrial Engineering, University of Florence
Italy

Paper Number 15-0220

## ABSTRACT

**Research question**
Autonomous emergency braking (AEB) has been indicated as a potential safety application not just for passenger cars and heavy goods vehicles, but also for motorcycles and powered two-wheelers (PTWs) at large. Motorcycle AEB (MAEB) was designed to produce autonomous deceleration of a host PTW in case of inevitable collision. Previous studies limited MAEB to the case of a PTW travelling along a straight, as the activation of AEB was considered hazardous for a leaning vehicle. This study aims to extend the applicability of MAEB to cornering scenarios.
**Methods**
A virtual PTW in a simulated environment was equipped with MAEB and Active Braking Control (ABC). MAEB consisted of a virtual obstacle detection device, triggering algorithms that identify inevitable collision states, and an automatic braking device. When an inevitable collision is detected for the host PTW and at the same time the rider is applying some braking force, MAEB deploys enhanced braking, which assists the rider reaching the maximum feasible deceleration. ABC consisted of control algorithms for the automatic braking device that stabilise the vehicle along the curved path. The complete system named MAEB+ was tested using detailed computer simulation reproducing real world crashes.
**Data sources**
The crash cases used for the simulations were selected from the in-depth crash dataset "InSAFE", which collects severe road crashes in the metropolitan area of Florence. The selection criteria were the following: a) the PTW crashed into another vehicle; b) the PTW was travelling along a curved path with roll angle above 15 deg; c) the rider applied some braking force prior to impact; d) PTW loss of control was not the main contributing factor.
**Results**
In the simulation, MAEB+ was able to assist the rider in reducing the motorcycle speed prior to impact with higher deceleration compared to baseline MAEB and in maintaining the stability of the motorcycle.
**Limitations**
The potential benefits of the proposed system, expressed in terms of impact speed reduction or avoidance of fall events, cannot be directly correlated with actual benefits for the rider in terms of injury mitigation. In fact, risk curves expressing the level of injury for the rider as a function of kinematic quantities (such as impact speed) are not currently available for riders.
**Significance of results**
Previous studies showed that MAEB would typically apply to situations where the motorcycle is travelling along a straight path. However, this paper shows that MAEB associated to ABC can apply also to those cases where the PTW is leaning, thus contributing to prove and extend the robustness of MAEB.

## INTRODUCTION

An advanced emergency braking system, often referred to as Autonomous Emergency Braking (AEB), indicates a system that detects imminent collisions and activates emergency braking to decelerate the vehicle with the purpose of avoiding or mitigating the crash [1].
The first patent disclosing this specific concept was published in 1992 [2]. In 2006 the first high-end passenger cars able to brake without input from the driver were released on the market by Volvo and Mercedes Benz. Only few years later the first city car model was fitted with AEB (Fiat Panda, 3rd generation). AEB is nowadays available for a range of passenger cars [3], whereas since the 1st November 2014 AEB has become mandatory in the European Union for buses, coaches and trucks.
The scientific literature of the last decade is rich in studies discussing triggering algorithms, system architectures, evaluations, human related aspects of AEB for passenger cars [1, 4-10]. More recently, in 2012, the authors presented a simple prototype of AEB for powered two-wheelers (PTWs) [11], after the concept being introduced independently in 2009 by two research projects funded by the European Commission, namely

PISa [12] and SiM [13]. The prototype of MAEB described in [11] applied to straight path scenarios with roll angles up to 10 deg. This limit was due to avoid the risks for the rider associated with an unexpected, automatic braking action produced by MAEB while the vehicle was leaning in a curve.
In previous studies the authors investigated the applicability of MAEB via case-by-case retrospective analysis based on in-depth crash datasets from different countries [14-16]. In most of the cases where automatic braking may have applied, the motorcycle was travelling along a straight path. However, the extension of MAEB applicability to larger roll angles would represent an important step of development. Firstly, this improvement would enhance the applicability of MAEB. For example, in the multinational datasets presented in [16] the percentage of cases where MAEB was considered 'not applicable' due to PTW roll angles greater than 10 deg ranged between 5% and 28% for the Italian and Swedish datasets, respectively. Secondly, the acceptability of MAEB among riders is expected to be higher if the system can safely deploy even when the PTW is cornering, due to increased usability (additional details on the indicators of acceptability can be found in [17]).
This paper introduces a system named MAEB+ combining the functionalities of MAEB with an Active Braking Control (ABC) that maintains vehicle stability during hard braking while cornering. An analysis of the effects of MAEB+ was performed via computer simulations reproducing three real world crashes selected from the in-depth motorcycle crash dataset InSAFE (In-depth Study of Accidents in FlorencE).

## METHODS

From the InSAFE database, three suitable PTW-to-car crash cases were identified and reconstructed via numerical simulations. For each case, a baseline simulation was tuned in order to reflect the kinematics and the collision configuration identified by the original InSAFE crash reconstruction. Then, for each crash case two additional simulations were performed, assuming that MAEB and MAEB+ respectively were active on the PTW at the time of the crash. Finally, the baseline results and the results obtained with MAEB and MAEB+ were compared to analyse the possible effects of these crash mitigation systems.

## SYSTEM DEFINITION

The MAEB+ system combined two subsystems: MAEB and ABC, presented by the authors respectively in [11, 18] and [19, 20]. MAEB was designed to monitor the vehicles around the host powered two-wheeler and to deploy automatic braking in case of inevitable collision with an opponent vehicle. ABC was designed to optimise the braking action of the rider while guaranteeing the capsize stability. ABC can potentially assist MAEB in safely achieving the desired emergency deceleration both in straight and, more importantly, in curved path. In this study MAEB and ABC were combined to assist the rider in case of imminent collision in a curve. In this situation both MAEB and ABC are engaged, thus enhancing rider's braking action (MAEB) and keeping the vehicle stable along the curved trajectory (ABC). In the following paragraphs, each subsystem and their interaction will be described.

### MAEB subsystem

MAEB monitored the vehicles in the frontal surroundings of the host PTW and when an inevitable collision was detected the automatic brake was deployed. A full prototype of MAEB was developed within PISa and implemented on a large-size scooter. The obstacle detection device was a compact, multi-layered laser scanner mounted in front of the vehicle. The triggering algorithm was designed for the simple scenario in which the host PTW approached a fixed obstacle moving along a straight path. The algorithm deployed autonomous braking as soon as the collision became inevitable – either by braking or swerving at the physical limits [11].
Recently, new triggering algorithms were developed by the authors to apply to a wider range of pre-crash scenarios, including intersection scenarios. These algorithms were based on the concept of Inevitable Collision State (ICS) defined by Fraichard and Asama [21]. Given the current state $s = \{v_{PTW}, v_{car}, P_{car}, \theta_{car}\}$, where $v_{PTW}$ and $v_{car}$ represent the speed of the host PTW and opponent car, respectively, and $P_{car}$ and $\theta_{car}$ are respectively the relative position and relative heading of the opponent car with respect of the host PTW, $s$ is an inevitable collision state if, no matter what the future manoeuvres of host and opponent vehicles are, a collision will eventually take place. Inevitable collision states can be pre-computed and implemented via triggering look up tables, as described in detail in [18]. The analysis of these look up tables indicated that in typical pre-crash situations the ICS can be identified up to 0.5 s before collision. This study adopted the triggering algorithms computed for a case in which the PTW is initially travelling along a straight path [16].
Concerning the deployment of automatic braking once the collision becomes inevitable, two different modes were identified. The first one was a proper autonomous braking (AB) with moderate deceleration deployed by

the system when the collision was inevitable and the rider was not braking. The second method was the enhanced braking (EB), deployed when the collision was inevitable and the rider applied some braking action. In this case, the system amplified the braking force up to the limit imposed by the road-tyre friction coefficient.
Previous studies recommended limitations for the deceleration level in AB mode. In fact, the unexpected autonomous deceleration may destabilise the rider with dangerous consequences. Symeonidis, Kavadarli, Shuller, Graw and Peldschus [22] performed experiments with volunteers in controlled conditions using a sled to produce different levels of decelerations simulating AB. Their results indicated that a deceleration of 0.35 g was acceptable for AB. The initial prototype vehicle equipped with MAEB was tested on the road by professional riders, confirming the feasibility of AB deceleration at 0.3 g [23]. However, in these tests the riders were aware of the imminent automatic deceleration produced while approaching foam obstacles. Other tests were conducted by the authors involving common riders in order to validate the feasibility of genuinely unexpected AB events along a straight path [24].

**ABC subsystem**

The aim of ABC was to provide the maximum deceleration and, in case of critical events, improve vehicle stability via longitudinal forces modulation. Similar concepts were described in the literature [25] and at present this technology is available on the market [26]. The basis of the ABC was a system integrating combined braking (CB) and antilock braking (ABS), indicated here as C-ABS. CB converted a braking input into reference braking pressures on front and rear wheels for a steady state optimal braking [27]. Force modulation downstream of the CB adjusted the braking pressures to avoid wheel lock and improve stability during unsteady braking and cornering.
Figure 1 depicts the layout of the ABC system, which included Combined Braking (CB, yellow), Antilock braking (AL, light blue), risk evaluation module (green) and Active Braking (or braking modulation) module (AB, white). The hierarchy of the functions is described hereafter: 1) combined braking applied to every manoeuvre, aiming to maximise vehicle deceleration in every braking scenario; 2) in case of wheel slip over a threshold, antilock braking unit was activated; 3) the vehicle state was constantly under control during every manoeuvre: as soon as a critical event was detected, the RISK unit sent a warning signal to the AB unit; 4) active braking unit was activated as soon as the RISK unit sent an alert; AB acted directly on the CB function.
The braking forces modulation was based on the application of the correction $\rho_c$ to the actual braking force distribution. The correction was computed so that the desired stability target was addressed maximizing the deceleration. The correction was a function of the total longitudinal force and therefore it was a function of the maximum acceleration/deceleration that the rider tried to achieve.
The factor $\rho_c$ was computed according to the following equation:

$$(1) \quad \rho c = \frac{-Izz \cdot \ddot{\psi}}{FxT \cdot a \cdot \delta \cdot cos(\phi)}$$

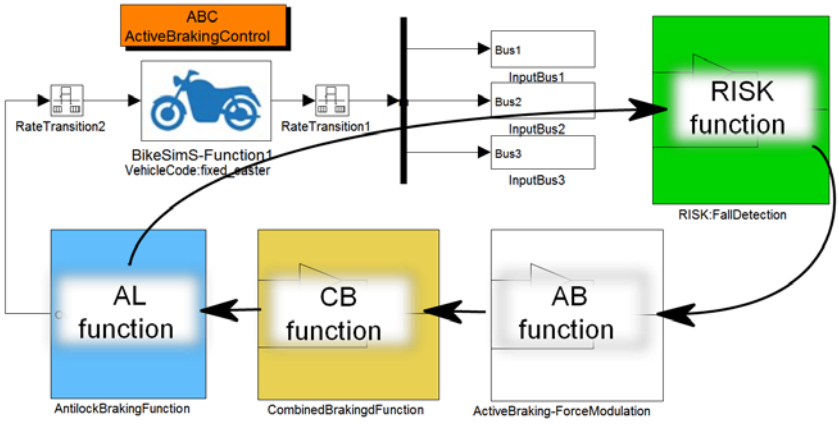


***Figure 1. General layout of the Active Braking Control: Combined Braking function (CB, yellow); Anti-Lock function (AL, light blue); RISK function (green); the Active Braking, or braking modulation, function (AB, white)***

where *Izz* represents the yaw inertia of the PTW in the body-fixed system of reference, $\ddot{\psi}$ the yaw acceleration, *FxT* is the total longitudinal tyre force, *a* is the longitudinal distance between the CG and the centre of the front wheel, $\delta$ is the steering angle and $\phi$ is the vehicle roll angle.
The intervention of the braking modulation control unit applied to the original braking force distribution, $\rho_x$. The correction $\rho_c$ was subtracted from the original force distribution. When the AB unit deployed, the correction was computed, and the braking force distribution was modulated in order to produce the new braking balance.
The *RISK* unit detected a potential fall and activated the AB unit. The *RISK* function integrated in the risk unit was the implementation of the equations described in [20]. This unit was composed of a number of algorithms, named *RISKi*, able to detect potential fall events that are critical for PTW stability and safety. The parameters were designed to identify incipient fall events produced by braking intensity or heavy oscillations of vehicle body and steering bar.
The minimum working frequency adopted for the AL module was 10 Hz. It should be noted that current ABS working frequencies are typically lower (3-4 Hz).

**MAEB+ system**

MAEB+ was designed to extend the applicability of MAEB beyond the straight path scenario and cover situations in which the PTW is cornering by incorporating AB and EB functions with the braking control algorithms of ABC.
As previously described, the ABC received braking inputs and modulated them to produce optimally distributed braking and vehicle stability during the braking manoeuvre. In the MAEB+, the braking inputs of the ABC module were either the rider's control actions or – in case of inevitable collision scenario – MAEB control actions.
As the aim of the present study was an overall evaluation of the influence of MAEB+ in real world crash circumstances, and not the development of the physical system, the system modelling was highly simplified as follows.
The rider action was modelled in BikeSim as an open loop force applied on the brake levers in order to produce the deceleration profile described in the crash reconstruction report. MAEB module received three inputs: a triggering signal from the ICS module and front/rear braking signals from the rider. MAEB module provided the adjusted front/rear brake delivery pressures, which followed the states described in Table 1.
MAEB outputs were passed to the ABC module, together with vehicle state data. The outputs of ABC module were the modulated front/rear brake pressures provided to the BikeSim module as braking pressure inputs at the callipers. A scheme of MAEB+ is provided in Figure 2.

***Table 1.***
***In&Out MAEB State Chart***

| MAEB inputs | | | MAEB outputs | |
|---|---|---|---|---|
| Front brake pressure @ master cylinder (from rider) | Rear brake pressure @ master cylinder (from rider) | ICS signal (True or False) | Front brake pressure @ delivery | Rear brake pressure @ delivery |
| 0 | 0 | T | AB pressure | 0 |
| 0 | 0 | F | 0 | 0 |
| α | 0 | T | EB pressure | 0 |
| α | 0 | F | α | 0 |
| 0 | β | T | EB pressure | β |
| 0 | β | F | 0 | β |
| α | β | T | EB pressure | β |
| α | β | F | α | β |

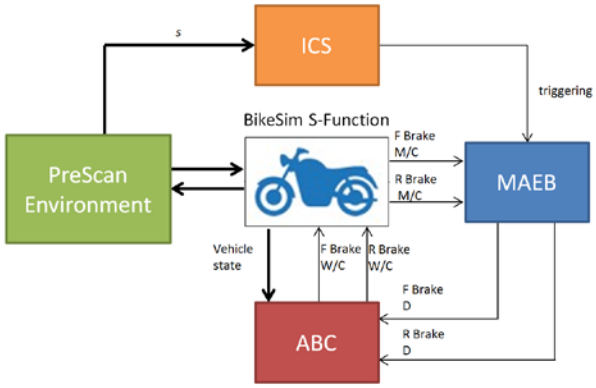


***Figure 2. Scheme of MAEB+: bold lines indicate multiple signals; s is the current state of host motorcycle and opponent vehicle used to determine inevitable collision states; M/C is the master cylinder braking pressure; D is the braking pressure at delivery; W/C is the braking pressure at callipers; F and R indicate front and rear brakes, respectively.***

## CASE STUDIES

### InSAFE crash database

The InSAFE study is conducted by the University of Florence with the Intensive Care Unit (ICU) of the Emergency Department of the Careggi Hospital. InSAFE has been collecting road accident data since 2009 in the cities of Florence and Prato and their surroundings [28, 29]. The data collection protocol of InSAFE complies with the guidelines defined by the European funded Project DaCoTA [30]. The selection criteria consist in urban and non-urban road crashes (not only with PTWs) involving at least one seriously injured person (Injury Severity Score, ISS $\geq$ 15) admitted to ICU. Investigators inspect vehicles involved in the crash to collect data on vehicular deformation, seat-belt usage, and protective garment including helmets and motorcycle clothing. Furthermore, for each case, retrospective site inspection and witness interviews are carried out in order to identify relevant pre-crash events. The ICU involved in the study alerts the InSAFE team providing information on injuries typologies and severities codified using the Abbreviated Injury Scale (AIS). A biomechanical correlation between injury and cause is conducted for each case by a panel of physicians and engineers. Through vehicular deformation, skid marks and witness accounts, collision speeds are computed and then validated using the accident simulation software Virtual Crash [31].
In the period 2009-2014, the InSAFE team has collected 206 serious road accidents of which 94 cases (45%) were fully reconstructed and studied (Table 1 reports the road accident typologies in the latter subset of records). Forty in-depth cases involved PTWs (Table 3 for details). The most frequent PTW crash configurations were head-on-side collisions (66%) followed by the head-on collisions (27%) (Table 4). Concerning the injury outcomes, the most severe configurations were head-on collisions, leading to a mean ISS of 22.0 and mean MAIS of 3.3.
For the present study, the selection criteria for the identification of the cases to be considered in the simulations were the following: a) the PTW collided with another vehicle; b) the PTW was travelling along a curved path with roll angle equal or above 15 deg; c) the rider applied some braking force prior to impact; d) PTW loss of control was not the main contributing factor. These criteria led to the identification of three crash cases, described in the following paragraphs. (Right hand side driving is in place in Italy, where these cases took place.)

***Table 2.***
***Accident types of fully reconstructed accidents in the InSAFE database***

| Type | N. | % |
|---|---|---|
| Single Vehicle | 9 | 9.5 |
| Vehicle-to-Pedestrian | 38 | 40.5 |
| Vehicle-to-Bicycle | 14 | 15.0 |
| Vehicle-to-Vehicle | 33 | 35.0 |
| Total cases | 94 | 100 |

***Table 3.***
***Accident types of events involving PTWs in the InSAFE database***

| Type | N. | % |
|---|---|---|
| Single Vehicle | 5 | 12.0 |
| PTW-to-Pedestrian | 7 | 17.0 |
| PTW-to-Bicycle | 3 | 7.5 |
| PTW-to-Car | 23 | 56.0 |
| PTW-to-Van | 2 | 7.5 |
| Total cases | 40 | 100 |

***Table 4.***
***PTWs accident configurations (opponent vehicle: car or van)***

| Type | N. | % | Mean impact speed (km/h)* | Mean MAIS* | Mean ISS* |
|---|---|---|---|---|---|
| Head-on crash | 7 | 28.0 | 50.7 | 4.0 | 28.7 |
| Head-on-side crash** | 17 | 68.0 | 46.2 | 3.1 | 19.6 |
| Sideswipe crash | 1 | 4.0 | 53.0 | 3.0 | 14.0 |
| Total cases | 25 | 100 | 47.7 | 3.3 | 22.0 |

* Referred to PTW user

** PTW impacting on side of opponent vehicle

**Case study 1 – ID-16**

This case involved a 37-year-old male rider fatally injured in a head-on collision with a medium-sized car (Figure 3). The accident happened in a rainy winter night in low traffic conditions at signalised intersection with fully controlled cross-traffic light. A Mercedes E280 approached the crossroad with green light travelling straight at 65.8 km/h (±5 km/h). A Yamaha Cygnus scooter was approaching the same junction from opposite direction at 56.5 km/h (±5 km/h). The rider, eventually found to be positive to the alcohol test, did not stop at the red light and turned left. The roll angle of steady-state cornering was approximately 23 deg. Due to the weather conditions, the adherence was supposed to be in the range 0.55-0.60 (typical values from literature [32, 33]), leading to a maximum deceleration of 5.4-5.9 $m/s^2$. Skid marks were not reported. In the crash reconstruction both vehicles were assumed to start decelerating at 0.3 g (corresponding to 50% of the maximum braking force) one second before the crash (assuming typical reaction times). The impact speed was 55 km/h (±5 km/h) for the car and 50 km/h (±5 km/h) for the PTW. The rider suffered injuries with ISS of 36. The three most serious injuries were reported at the head and chest (MAIS 4), and face (MAIS 2). The accident took place on urban roads in residential area, where a 50 km/h speed limit was in place.

***Figure 3. Case study 1, head-on collision at urban crossroad (ID-16)***

**Case study 2 – ID-10**

In this accident, a 25-year-old male rider was seriously injured as result of head-on collision with a small-size car (Figure 4). The crash scenario was an S-curve in a dual lane, two ways, non-urban road with a speed limit of 60 km/h during a sunny day (no dazzling involved). A Suzuki GSX R750 was travelling at 94 km/h (±5 km/h). Before entering the first of the two curves, the motorcycle was in the opposite lane to negotiate the right hand side bend with a roll angle of approximately 40 deg. A FIAT Punto car was oncoming in the opposite direction at 57 km/h (±5 km/h). The rider started braking 0.5 s before the impact, with a peak deceleration of 0.7 g reached at impact. In addition, also the driver applied a braking action of 0.3 g at 0.5 s from the crash. The impact speed was 88 km/h (±5 km/h) for the PTW and 50 km/h (±5 km/h) for the car. The rider was subjected to multiple injuries (ISS of 29). The most severe ones were located in the chest (MAIS 4) and in the pelvic region (MAIS 3).

***Figure 4. Case study 2, head-on collision at non-urban road (ID-10)***

**Case study 3 – ID-30**

The third accident involved a 20-year-old male rider seriously injured in a sideswipe collision with a small-sized car. The accident happened in a sunny spring day with moderate traffic conditions. The accident scenario was a non-signalised crossroads (Figure 5). A Renault Clio car approached the intersection from right to left hand side of the rider path. The driver reached the crossing (signalised with STOP signal) slowing down the vehicle up to 17 km/h (±5 km/h) and then accelerating until the crash. A Honda SH300 scooter was traveling on the main road at 77 km/h (±5 km/h). The rider realised the driver's intentions too late. One second before impact the rider applied a braking action resulting in a deceleration of 0.3 g and made an evasive manoeuvre towards the left hand side with a maximum roll angle of approximately 15 deg. The impact speeds were 65 km/h (±3 km/h) and 37 km/h (±3 km/h) for the PTW and for the car respectively. The rider was assigned an ISS of 19 with MAIS 3 injuries to head and thorax and MAIS 2 injuries to the spine. All the injuries were caused by the impact of the rider with the road environment (a post and the concrete shoulder).

***Figure 5. Case study 3, sideswipe collision in urban scenario (ID-30)***

## SIMULATIONS

The three in-depth crash cases were reconstructed using the software tool PreScan (TASS International, Helmond, The Netherlands) [34]. Motorcycle dynamics was simulated using BikeSim software (Mechanical Simulations, Ann Arbor, MI, US). The algorithms of MAEB+ were modelled in Matlab Simulink software environment. The three software packages were interfaced with each other to run simulations that included road geometries, reconstructed trajectories of the opponent vehicles, detailed vehicle dynamics, and control algorithms for the safety system.
Baseline cases and variant cases were simulated. The baseline simulations aimed to obtain realistic reconstructions of the actual cases in last 2-3 seconds prior to crash. The simulation results were compared with the original reference cases as described in the crash reports, to check the agreement in terms of: initial position, path, and speed profile of the vehicles involved, driver and rider's control actions (type, timing, and intensity), impact point, and relative heading at collision.
Variant simulations used the same conditions defined for the baseline cases, and included virtual MAEB and MAEB+ to evaluate the effects that these systems may have produced compared to the baseline cases.
For each case (baseline and variants), a simplified reference trajectory was defined using the original crash reconstruction developed with Virtual Crash software. Reference trajectories were obtained assembling only straight and constant radius stretches for both car and motorcycle. The reference trajectory of the motorcycle was passed to BikeSim as a target path for the virtual rider. Details of the virtual rider are available elsewhere [35, 36].
Driver and rider inputs were defined based on the information available from the crash investigations and the Virtual Crash reconstructions. Open-loop throttle and brake controls were defined via step functions for host and opponent vehicles. Trial-error procedure was adopted to identify timing and intensity of the longitudinal controls.
The PTWs were modelled in BikeSim using the model of a scooter reproducing a Piaggio Beverly 300.

## RESULTS

According to the simulations, in one case analysed (ID-10) MAEB and MAEB+ would have deployed in autonomous braking mode (AB) followed by enhanced braking mode (EB), as the rider started braking after reaching the ICS condition (inevitable collision state). In the remaining cases the simulations indicated that MAEB and MAEB+ would have deployed in EB mode only, as the riders applied the brakes before reaching the ICS condition.
Impact speed reductions were estimated in the range from 0.8 km/h to 3.0 km/h for MAEB, and from 1.3 km/h to 6.1 km/h for MAEB+. In all three cases the activation of MAEB and MAEB+ would have increased the mean deceleration in the time frame between the ICS detection and the collision.
Results showed higher decelerations for MAEB+ compared to simple MAEB. In two of the cases, the impact speed reduction was more than double with MAEB+ compared to MAEB. This outcome is mainly due to MAEB operating on the front disk only, with limitations compared to the combined braking operated by MAEB+, especially on damp and wet road conditions. Speed profiles, longitudinal accelerations, and brake pressure values for the three simulations are provided in Figure 7.
In addition, the simulations showed that the hard braking with braking modulation operated by MAEB+ obtained lower destabilisation of the vehicle with respect to MAEB deployment, as visible in the diagrams in Figure 8. With MAEB+, the absolute value of the roll angle tended to reduce while braking, as the vehicle tended to maintain the original path at decreasing speed.
In the following paragraphs, the main results for each case will be briefly presented. The results are also synthesised in Table 5.

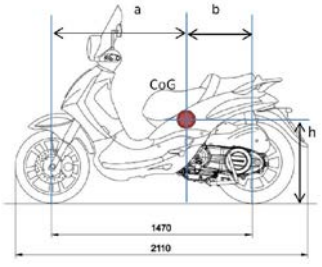


***Figure 6. Wheelbase and centre of gravity of the Piaggio Beverly 300. Experimental measurements with rider: a=925 mm; b=545 mm; h= 500 mm.***

a) ID-16

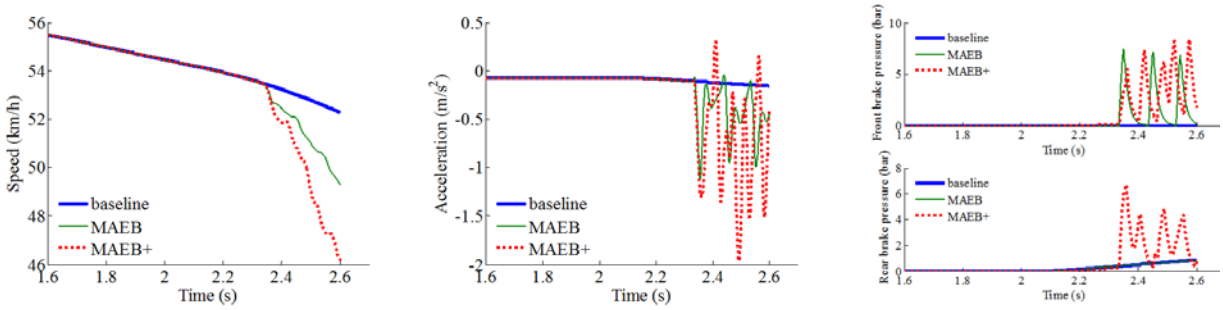


b) ID-10

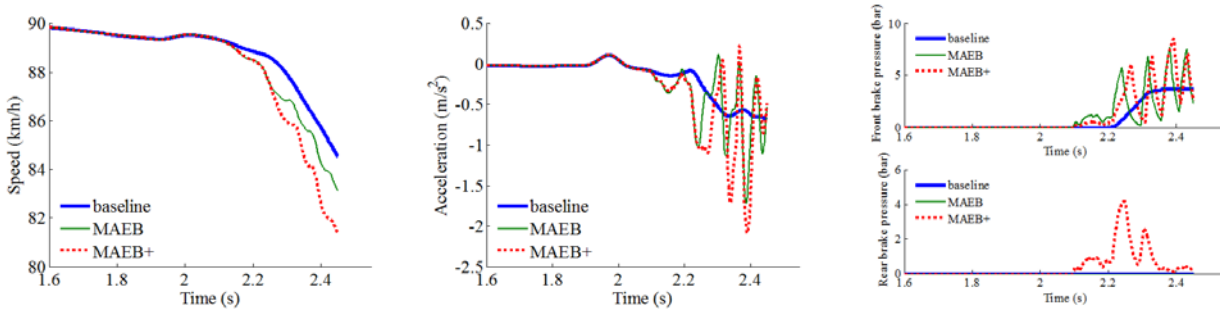


c) ID-30

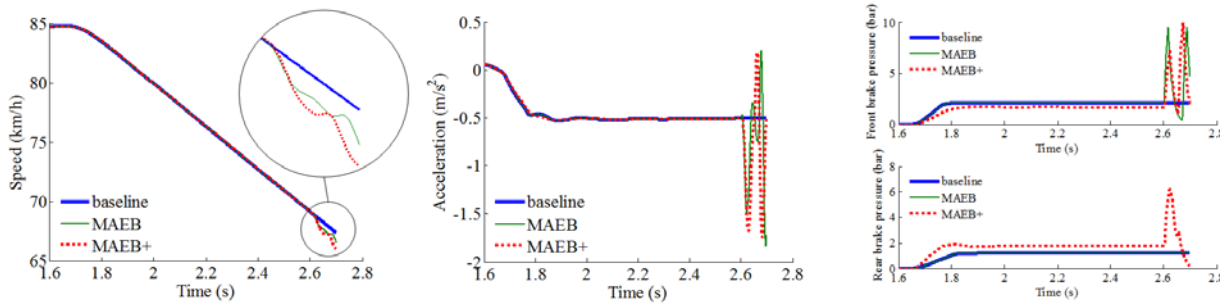


***Figure 7. Diagrams showing speed profile, acceleration, and front and rear braking pressures of the PTW in the simulations: a) case ID-16; b) case ID-10; c) case ID-30.***

**ID-16**

The benefits of autonomous emergency braking in terms of increased average deceleration and consequent impact speed reduction were noticeable in case ID-16 (PTW turning in front of opponent vehicle), in which the rider was reported to brake with low deceleration only. However, the deployment of MAEB produced a quick increase in the absolute roll angle, which was a sign of an incipient loss of control and subsequent fall. With MAEB+ the vehicle achieved similar decelerations without noticeable destabilisation.

**ID-10**

The benefits of MAEB and MAEB+ were less tangible in case ID-10 (head on crash scenario). The impact speed reduction produced by autonomous emergency braking was moderate. The deployment of EB produced additional vibrations of the vehicle (less evident when using MAEB+), as a consequence of the large roll angle at triggering.

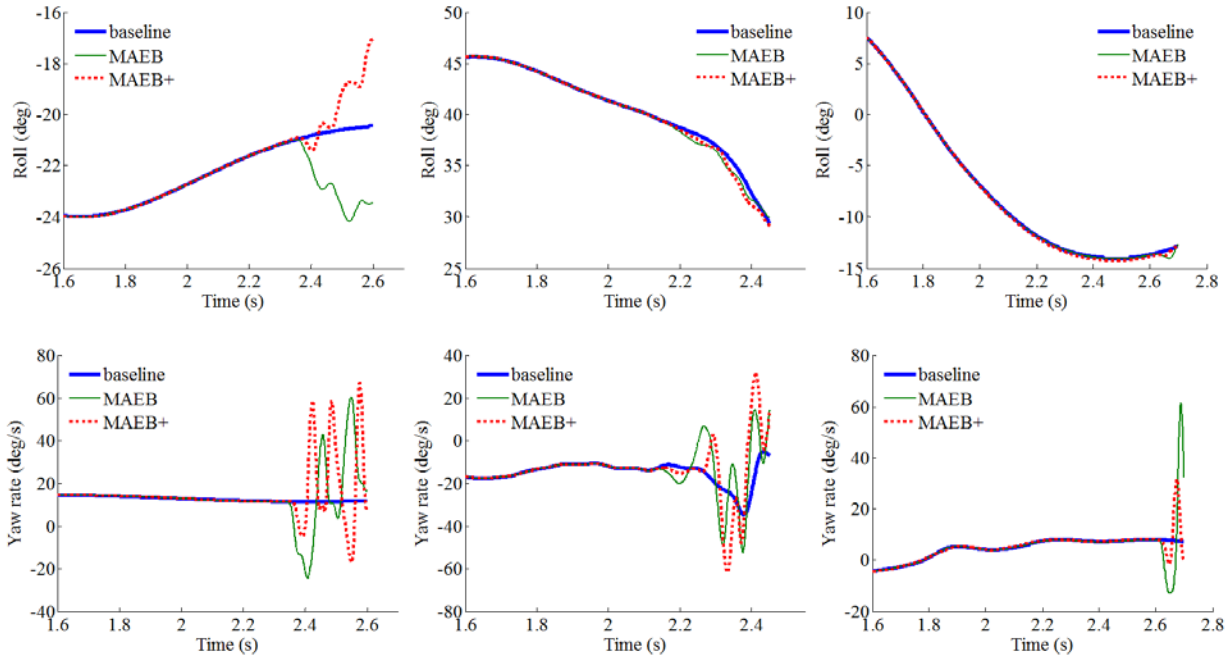


a) ID-16 b) ID-10 c) ID-30

***Figure 8. Diagrams showing roll angle and yaw rate of the PTW in the simulations: a) case ID-16; b) case ID-10; c) case ID-30.***

**ID-30**

Also in this case (sideswipe scenario) the benefits of autonomous emergency braking in terms of impact speed reduction were moderate. However, the benefits of MAEB+ in terms of vehicle stabilisation were noticeable. In fact, in the initial phase of the curve the brake modulation reduced the braking force on the front wheel and built up braking pressure to the rear. In conclusion, the vehicle appeared to be stable while negotiating the curve even under hard braking conditions.

## DISCUSSION, LIMITATIONS AND FUTURE PERSPECTIVES

The values of impact speed reduction obtained with MAEB in the simulations were in line with the values estimated in previous studies, although derived from different configurations (with roll angle smaller than 10 deg). The introduction of MAEB+ has allowed generalizing speed reduction benefits of MAEB to a larger set of accident configurations. In addition, the improved management of braking forces allowed higher decelerations in all the case studies, while the PTW stabilization, achieved with the ABC subsystem, prevented the vehicle capsizing prior to the impact in ID-16. In the latter case the deployment of the system in EB mode while the

***Table 5.***
***Synthesis of the results for the three simulated cases in baseline, MAEB, and MAEB+ configurations***

| Case | Initial speed (km/h) | Time to collision at ICS (s) | Configuration | Impact speed (km/h) | Impact speed reduction compared to baseline (km/h) | Average deceleration from ICS to collision ($m/s^2$) |
|---|---|---|---|---|---|---|
| ID-16 | 56.5 | 0.26 | Baseline | 52.3 | - | 1.3 |
| | | | MAEB | 49.3 | 3.0 | 4.5 |
| | | | MAEB+ | 46.2 | 6.1 | 7.8 |
| ID-10 | 91.0 | 0.37 | Baseline | 84.5 | - | 3.7 |
| | | | MAEB | 83.1 | 1.4 | 4.8 |
| | | | MAEB+ | 81.4 | 3.1 | 6.0 |
| ID-30 | 85.0 | 0.38 | Baseline | 67.4 | - | 4.4 |
| | | | MAEB | 66.5 | 0.8 | 5.0 |
| | | | MAEB+ | 66.0 | 1.3 | 5.4 |

rider was applying mild braking allowed to capitalize an impact speed reduction close to the theoretical values presented in previous studies, which turned in more than 20% of PTW kinetic energy reduction at impact. The analysis of case ID-16 showed the peculiar relevance of MAEB+ in situations where human factor failures are key elements and roll angles are not close to the limit. These results also suggest that autonomous emergency braking is likely to produce higher benefits when the rider is only able to achieve low deceleration prior to the collision, possibly due to lack of confidence in applying strong braking while turning, or as a result of panic, uncontrolled reaction in the imminence of a crash.

Despite the lower impact speed reduction obtained by the autonomous emergency braking, also in the other case studies MAEB+ outperformed MAEB. The limited speed reduction derived from higher braking forces applied by the riders in the simulations. (Maximum decelerations are similar in ID-10 and ID-16, but in the latter case a larger speed reduction was obtained.) It is worth noticing that the dynamical model of a scooter was used in case ID-10, despite the actual PTW involved was a sports motorcycle. Similar results would be expected when adopting a dynamical model of a sports motorcycle, in agreement with the similar results obtained with a scooter and a sports motorcycle in the computer simulations used for the assessment of the ABC system [19, 20].

In the proposed simulations, the position, the speed, and the heading of the opponent vehicle were assumed to be available for the MAEB and MAEB+ systems (as long as the obstacle was in the field of view of the PTW). Possible obstructions in the field of view, although not reported for the cases considered, could represent a strong limitation to a system that adopts an optical sensing device, especially in urban scenarios. In addition, the use of an optical sensing device to identify and track obstacles is particularly challenging when the roll angle is greater than 10 deg [11]. The adoption of V2X communication in order identify the triggering event will represent a fundamental step in the development of MAEB+.

In the simulations, the ABC subsystem provided enhanced stability to the PTW while hard braking along a curve, in the assumption that when EB deploys – thus abruptly increasing the deceleration of the vehicle – a real rider would be able to hold themselves firmly on the vehicle. Initial tests with professional riders experiencing EB deployment were conducted in the past [23], showing the feasibility of such system along a straight path with alerted rider. As far as the authors are aware, there are no other similar studies available in the literature. This important question regarding the feasibility of EB, and especially in emergency situations while negotiating a turn, should receive adequate attention in the future.

The braking stabilisation potential of ABC, when confirmed with larger set of simulations and with practical tests, would then enable MAEB deploying while negotiating a curve. But first and foremost, it would make MAEB deployment more reliable in a pre-crash scenario along a straight path, by compensating for possible last-second swerve avoidance manoeuvres operated by the rider in proximity of MAEB activation. In this context, such safer deployment of MAEB in the future may allow anticipating AB and EB intervention in time (higher TTC at triggering leading to higher effectiveness in impact speed reduction or even crash avoidance). In other words, MAEB+ has a potential to enable the application of MAEB to “avoidable impact conditions” and not just after the collision has become inevitable. However, the development of a MAEB+ for collision avoidance shoud be accompanied by the elaboration of appropriate overriding strategies. Best practice indicates human factor to be integrated since the initial design phase through extensive rider characterization and testing on volunteers.

As final limitation, the potential benefits of the proposed system expressed in terms of impact speed reduction or avoidance of fall events cannot be directly correlated with actual benefits for the rider in terms of injury mitigation. In fact, risk curves expressing the level of injury for the rider as a function of kinematic quantities (such as impact speed) are not currently available for riders.

## CONCLUSIONS

MAEB+ was presented as an evolution of MAEB that incorporates optimal braking distribution and cornering stability. MAEB+ and baseline MAEB were tested in computer simulations reproducing three real world crash cases selected from the InSAFE database of crashes in the metropolitan area of Florence, Italy. The results showed that both MAEB and MAEB+ systems reduced the impact speed of the PTW compared to the cases in the actual configuration without braking assistance systems. In addition, MAEB+ was able to obtain higher decelerations and improved stability with respect to baseline MAEB, thanks to special algorithms of braking modulation. MAEB+ extends the applicability of autonomous emergency braking to a set of crash scenarios that so far were excluded from the evaluations of the potential benefits of MAEB. The results of this study also suggested that the effectiveness of MAEB+ is likely to be higher when the rider applies early, poor braking, and when roll angles are far from the limit, compared to cases in which the rider is able to apply late, nearly optimal braking, and in tight corners requiring high roll angles. When further validated, MAEB+ or similar systems could also enable the deployment of emergency braking when the collision between PTW and opponent vehicle

is still preventable. This concept is inspiring, especially considering that in the current literature such futuristic scenario of motorcycle autonomous emergency braking has not even been mentioned.

## ACKNOWLEDGMENTS

GS is supported by the European Commission's Seventh Framework Programme FP7/2007-2013 under the Grant Agreement n.328067 (ABRAM project).

## REFERENCES

[1] Labayrade, R., Royere, C., Aubert, D., "Experimental Assessment of the RESCUE Collision-Mitigation System," IEEE Transactions on Vehicular Technology, vol. 56, no. 1, pp. 89-102, Jan, 2007.
[2] Chen, G.J., "Automatic Braking Apparatus with Ultrasonic Detector." U.S. Patent No. 5,170,858. 15 Dec. 1992.
[3] Hulshof, W., Knight, I., Edwards, A., Avery, M., Grover, C., "Autonomous Emergency Braking Test Results," Proceedings of the 23rd International Technical Conference on the Enhanced Safety of Vehicles (ESV). 2013.
[4] Dietmayer, K., Kaempchen, N., Fuerstenberg, K., Kibbel, J., Justus, W., Schulz, R., "Roadway Detection and Lane Detection using Multilayer Laserscanner," Advanced Microsystems for Automotive Applications 2005, pp. 197-213: Springer, 2005.
[5] Coelingh, E., Jacobsson, L., Lind, H., Lindman, M., "Collision Warning with Auto Brake: A Real-Life Safety Perspective," Proceedings of the 20th International Technical Conference on the Enhanced Safety of Vehicles (ESV). 2007.
[6] Kaempchen, N., Schiele, B., Dietmayer, K., "Situation Assessment of an Autonomous Emergency Brake for Arbitrary Vehicle-to-Vehicle Collision Scenarios," IEEE Transactions on Intelligent Transportation Systems, vol. 10, no. 4, pp. 678-687, Dec, 2009.
[7] Coelingh, E., Eidenhall, A., Bengtsson, M., "Collision Warning with Full Auto Brake and Pedestrian Detection - a practical example of Automatic Emergency Braking," in 13th International IEEE Conference on Intelligent Transportation Systems, 2010.
[8] Brannstrom, M., Coelingh, E., Sjoberg, J., "Model-Based Threat Assessment for Avoiding Arbitrary Vehicle Collisions," IEEE Transactions on Intelligent Transportation Systems, vol. 11, no. 3, pp. 658-669, Sep, 2010.
[9] Kobiela, F., Engeln, A., "Autonomous Emergency Braking Studies on Driver Behaviour," ATZ worldwide, vol. 112, no. 10, pp. 4-8, 2010.
[10] Rizzi, M., Kullgren, A., Tingvall, C., "Injury Crash Reduction of Low-Speed Autonomous Emergency Braking (AEB) on Passenger Cars," in IRCOBI Conference, 2014.
[11] Savino, G., Pierini, M., Baldanzini, N., "Decision Logic of an Active Braking System for Powered Two Wheelers," Proceedings of the Institution of Mechanical Engineers, Part D: Journal of Automobile Engineering, vol. 226, no. 8, pp. 1026-1036, 2012.
[12] Savino, G., Penumaka, A.P., Pierini, M., Baldanzini, N., Roessler, B., "Design of the Decision Logic for a PTW Integrated Safety System," in Proceedings of the 21st International Technical Conference on the Enhanced Safety of Vehicles (ESV), 2009.
[13] Roll, G., Hoffmann, O., Konig, J., "Effectiveness Evaluation of Antilock Brake Systems (ABS) for Motorcycles in Real-World Accident Scenarios," in Proceedings of the 21th International Technical Conference on the Enhanced Safety of Vehicles (ESV). 2009.
[14] Savino, G., Pierini, M., Rizzi, M., Frampton, R., "Evaluation of an Autonomous Braking System in Real-World PTW Crashes," Traffic Injury Prevention, vol. 14, no. 5, pp. 532-543, 2012.
[15] Savino, G., Giovannini, F., Baldanzini, N., Pierini, M., Rizzi, M., "Assessing the Potential Benefits of the Motorcycle Autonomous Emergency Braking Using Detailed Crash Reconstructions," Traffic Injury Prevention, vol. 14, no. S1, pp. S40-S49, 2013.
[16] Savino, G., Rizzi, M., Brown, J., Piantini, S., Meredith, L., Albanese, B., Pierini, M., Fitzharris, M., "Further Development of Motorcycle Autonomous Emergency Braking (MAEB), What Can In-Depth Studies Tell Us? A Multinational Study," Traffic Injury Prevention, vol. 15, no. S1, pp.S165-S172, 2014.
[17] Beanland, V., Lenné, M.G., Fuessl, E., Oberlader, M., Joshi, S., Bellet, T., Banet, A., Rößger, L., Leden, L., Spyropoulou, I., Yannis, G., Roebroeck, H., Carvalhais, J., Underwood, G., "Acceptability of Rider Assistive Systems for Powered Two-Wheelers," Transportation Research Part F: Traffic Psychology and Behaviour, vol. 19, pp. 63-76, 2013.
[18] Savino, G., Giovannini, F., Fitzharris, M., Pierini, M., "Inevitable Collision States for Motorcycle-to-Car Collision Scenarios," Forthcoming.

[19] Giovannini, F., Savino, G., Pierini, M., Baldanzini, N., "Analysis of Stability of Motorcycles During Braking Manoeuvres," Doctoral Thesis, Department of Industrial Engineering, University of Florence, 2013.
[20] Giovannini, F., Baldanzini, N., Pierini, M., Development of a Fall Detection Algorithm for Powered Two Wheelers Application, No. 2014-32-0022, SAE Technical Paper, 2014.
[21] Fraichard, T., Asama, H., "Inevitable Collision States — A Step Towards Safer Robots?," Advanced Robotics, vol. 18, no. 10, pp. 1001-1024, 2004.
[22] Symeonidis, I., Kavadarli, G., Shuller, E., Graw, M., Peldschus, S., "Analysis of the Stability of PTW Riders in Autonomous Braking Scenarios," Accident Analysis & Prevention, vol. 49, pp. 212-22, Nov, 2012.
[23] Savino, G., Pierini, M., Grant, R., Frampton, R., Talbot, R., Peldschus, S., Schuller, E., Oudenhuijzen, A., Pauwelussen, J., Scheepers, B., Teerhuis, A., "PISa – Powered Two-Wheeler Integrated Safety. Development, Implementation and Testing of PTW Integrated Safety Systems," in Proceedings of the IFZ International Motorcycle Conference, 2010.
[24] Savino, G., Pierini, M., Thompson, J., Fitzharris, M., Lenne, M., "Towards Motorcycle Autonomous Emergency Braking: Testing Human Reaction to Unexpected Automatic Deceleration," Forthcoming.
[25] De Filippi, P., Tanelli, M., Corno, M., Savaresi, S.M., Santucci, M.D., "Electronic Stability Control for Powered Two-Wheelers," IEEE Transactions on Control System Technology, vol.22, no.1, pp.265-272, 2014.
[26] Matschl, G., "Motorcycle Sability Control - MSC. The Next Step into Safety Solutions for Motorcycles," in Proceedings of the IFZ International Motorcycle Conference, 2014.
[27] Cossalter, V., Lot, R., Maggio, F., "On the Braking Behavior of Motorcycles," Washington, USA: SAE International (20044305), 2004.
[28] Piantini, S., Grassi, D., Mangini, M., Pierini, M., Zagli, G., Spina, R., Peris, A., "Advanced Accident Research System based on a Medical and Engineering Data in the Metropolitan Area of Florence," BMC Emergency Medicine, vol. 13, no. 1, pp. 3, 2013.
[29] Piantini, S., "In-Depth Metropolitan Road Accident Database Development and Accident Analysis," Doctoral Thesis, Department of Industrial Engineering, University of Florence, 2013.
[30] Del Pozo De Dios, E., Ferrer, A., Hill, J., Fagerlind, H., Giustiniani, G., Persia, L., "Towards a Global and Harmonized Database for In-Depth Accident Investigation in Europe: The Dacota Project," in Proceedings of the 23rd International Technical Conference on the Enhanced Safety of Vehicles (ESV), 2013.
[31] Belobrad, Meleg, Sucha, Vida, "Virtual Crash Technical Manual," Virtual Crash Software.
[32] C. Y. Warner et al., "Friction Applications in Accident Reconstruction," SAE Technical Paper no. 830612, 1983.
[33] Nakao, Y., Kawasaki, H., Major, D.J., "Estimation of Friction Levels between Tire and Road," SAE Technical Paper no. 2002-01-1198, 2002.
[34] Gietelink, O.J., Verburg, D.J., Labibes, K., Oostendorp, A.F., "Pre-crash System Validation with PRESCAN and VEHIL," 2004 IEEE Intelligent Vehicles Symposium, pp. 913-918, 2004.
[35] BikeSim, "BikeSim Rider Controls (Motorcycle) - User guide," 2013.
[36] Sharp, R.S., "Motorcycle Steering Control by Road Preview," Journal of Dynamic Systems, Measurement, and Control, vol. 129, no. 4, pp. 373, Jul, 2007.

# RESEARCH ON DRIVER ACCEPTANCE OF LDA (LANE DEPARTURE ALERT) SYSTEM

**Ryo Fujishiro**
**Hiroyuki Takahashi**
Toyota Motor Corporation
Japan

Paper Number 15-0222

## ABSTRACT

The purpose of this research is to identify whether the road departure accident reduction performance of the Lane Departure Alert (LDA) system is consistent with driver acceptance. If a vehicle deviates from the lane, the LDA system warns the driver and/or automatically steers the vehicle back into the lane to help avoid an accident. However, the system cannot perform as expected if the driver feels that the system is annoying and turns it off. Therefore, the consistency between the accident reduction performance and driver acceptance of LDA was studied by investigating driving behavior based on a new form of two-dimensional analysis using the distance to the lane boundary (DTLB) and the lateral velocity of the vehicle.

## INTRODUCTION

In Japan, in 2013, single-vehicle accidents (such as rollovers and collisions with stationary objects or vehicles) and frontal collision accidents accounted for approximately 21% and 10% of fatal accidents, respectively. A high proportion of these accidents occurred when the vehicle departed from the road [1]. Reducing such road departure accidents is a major challenge in the development of technology to help achieve the ultimate target of zero fatalities and injuries from traffic accidents.
The importance of reducing road departure accidents has also been recognized at a governmental level. For example, in 2011, the National Highway Traffic Safety Administration (NHTSA) in the U.S. began assessments of lane departure warning (LDW) systems developed to help reduce these accidents [2]. Similar assessments have also been introduced in Europe and Japan.
In Japan, human factors such as drowsiness, distraction, and intoxication are involved in approximately 80% of road departure accidents (Figure 1) [3]. Furthermore, it was found that roughly 70% of drivers performed no steering or braking operations after departing the road in these accidents [3]. This suggests that many road departure accidents occur without the driver realizing that the vehicle is departing from the lane.

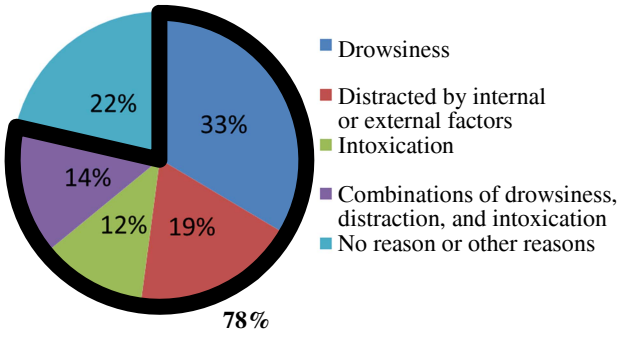


***Figure1. Human factors of road departure accidents.***

The Lane Departure Alert (LDA) system was developed as a driver support system to help prevent road departure accidents. It uses a forward monitoring camera to recognize the markings that identify lane boundaries. If there is a high probability of lane departure, LDA warns the driver and/or performs control to steer the vehicle back inside the lane. When in operation, this system is reported to be an effective way of helping to prevent road departure accidents [4].

However, if LDA activates frequently in non-dangerous situations, the driver will feel annoyance and switch the system off. Since LDA can have no accident reduction effect if it is not switched on, it is important to design a system that is both effective at reducing accidents and that will not be turned off by the driver.
This paper describes research into the feasibility of reducing both accidents with the LDA steering control and driver annoyance by investigating and analyzing driving behavior.

## RELATIONSHIP ANALYSIS OF LDA ACTIVATION FACTORS

To study how to help reduce accidents while minimizing driver annoyance with the system, this section analyzes the relationship between the key LDA control factors. As shown in Figure 2, there are three control factors: the maximum lateral distance traveled out of the lane (A), the steering control magnitude (B), and the intervention timing (C). Since the maximum lateral distance traveled out of the lane must be restricted to help reduce road departure accidents, the research first examined a control target for this factor.
Figure 3 shows the distribution for the lateral distance traveled beyond the lane boundary in road departure accidents, as described in the 2007 Traffic Accident Investigation and Analysis Report by the Japanese Institute for Traffic Accident Research and Data Analysis (ITARDA) [3]. The bars in the graph show the number of road departure accidents and the line shows the cumulative distribution. This figure indicates that at least 80% of road departure accidents occur with lateral distance traveled out of the lane of 0.5 m or more. In other words, activating the LDA system so that the lateral distance traveled out of the lane is 0.5 m or less may be an effective measure for at least 80% of road departure accidents. Therefore, the development aimed to restrict the maximum lateral distance traveled out of the lane to less than 0.5 m using the functions of the LDA system.

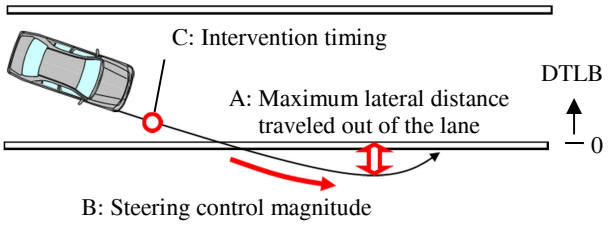


***Figure2. LDA control factors.***

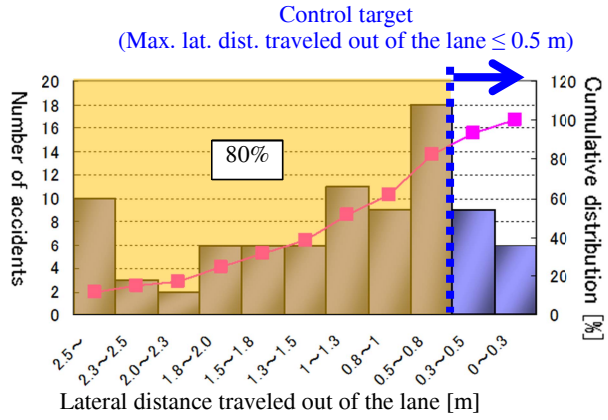


***Figure3. Distribution of lateral distance traveled out of lane in road departure accidents.***

Next, the research examined the relationship of the lateral distance traveled out of the lane with the steering control magnitude and intervention timing. To restrict the lateral distance traveled out of the lane, it is possible to either increase the steering control magnitude (proposal 1) or adopt the earlier intervention timing (proposal 2). In contrast, however, smaller steering control magnitude and later intervention timing are preferable conditions for minimizing driver annoyance with the system. As shown in Figure 2, this paper expresses the intervention timing using the

distance to the lane boundary (DTLB) variable. DTLB defines the direction toward the inside of the lane as a positive value, taking the lane boundary as the origin point.
Figure 4 shows the results for proposal 1 (greater steering control magnitude) and the results for proposal 2 (earlier intervention timing). Each graph indicates how the maximum lateral distance traveled out of the lane (i.e., the minimum DTLB) varies with different steering control magnitudes and intervention timings, respectively. The simulations assumed the following conditions for calculation: a vehicle speed of 100 km/h, an initial lateral velocity (i.e., the speed at which the vehicle approaches the lane boundary) of 1.0 m/s, and a vehicle response delay for the steering control after lane boundary recognition of 0.5 s. The maximum lateral acceleration was set to 1.0 m/s$^2$ in accordance with the technical guidelines established by the Japanese Ministry of Land, Infrastructure, Transport and Tourism (MLIT) [5]. The intervention timing in proposal 1 was fixed at the DTLB of 0.2 m and the yaw acceleration in proposal 2 was fixed at 3.5 deg/s$^2$ in Figure 4.

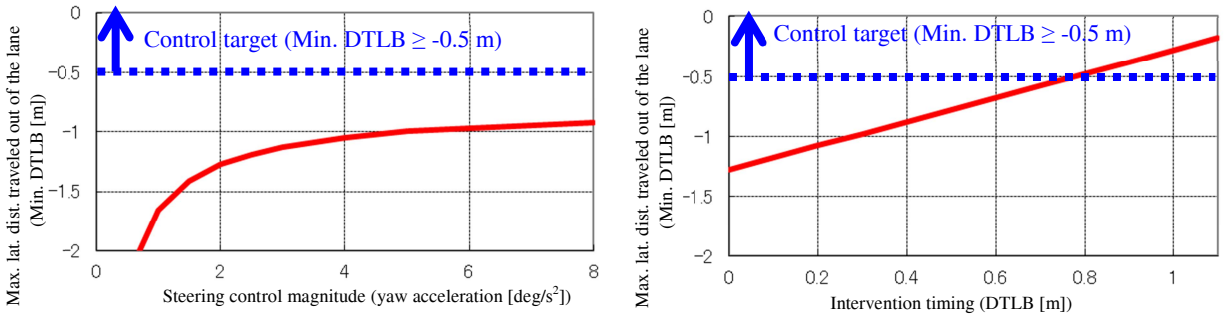


proposal 1 (greater steering control magnitude)

proposal 2 (earlier intervention timing)

***Figure4. Results for proposal 1 (greater steering control magnitude) and proposal 2 (earlier intervention timing).***

When the steering control magnitude was increased with proposal 1, the reduction in maximum lateral distance traveled out of the lane (i.e., the increase in minimum DTLB) became markedly less pronounced after the steering control magnitude exceeded 4 deg/s$^2$. This is because the maximum lateral acceleration of the steering control has an upper limit, regardless of the speed by which the control starts up. For another reason, the ECU processing time, communication delay, and vehicle response time must be considered before the vehicle responds to the steering control after lane boundary recognition. As a result, the vehicle has already started to depart from the lane when the vehicle response occurs.
In this case, adopting earlier intervention timing in proposal 2 should help to reduce the maximum lateral distance traveled out of the lane (i.e., increase the minimum DTLB). The maximum lateral distance traveled out of the lane decreases by the amount that the intervention timing is speeded up. The gradient in proposal 2 is linear.
Therefore, based on the results for proposal 2, it was concluded that earlier intervention timing would be more effective than greater steering control magnitude in helping to reduce the maximum lateral distance traveled out of the lane.

## INVESTIGATION AND ANALYSIS OF DRIVING BEHAVIOR

The previous section identified earlier intervention timing for the steering control as a potentially effective way of reducing the maximum lateral distance traveled out of the lane. However, adopting earlier intervention timing for the steering control may trigger LDA activation in non-dangerous situations, potentially annoying the driver.
For example, the LDW assessment performed by NHTSA defines a warning that starts at DTLB of 0.75 m or more as too early and not in compliance with the assessment criteria [2]. The standard issued by the International Organization for Standardization (ISO) also contains the same requirement [6]. These requirements were probably established because a system that activates too early is unlikely to be accepted by drivers.
Proposal 2 in Figure 4 indicates that to achieve maximum lateral distance traveled out of the lane of less than 0.5 m, the system must activate at DTLB of approximately 0.8 m when the lateral velocity is 1.0 m/s. However, this means that the system will activate from a position close to the center of the lane, which is highly unlikely to be accepted by drivers.

Therefore, this research examined this issue from another standpoint by investigating driving behavior using a new two-dimensional (2D) form of analysis that incorporates lateral velocity as well as DTLB. It was hypothesized that drivers would drive closer to the lane boundary when the lateral velocity is low but would tend to drive further away from the lane boundary when the lateral velocity is high. This hypothesis was then verified as described below.

**Test conditions**

Data was acquired by a forward monitoring camera. The DTLB and lateral velocity detected by the camera were then recorded. Table 1 shows the detailed test conditions.

**Table1.**
**Test conditions.**

| Item | Content |
|---|---|
| Vehicle | Lexus GS |
| Market | Japan |
| Model year | 2012 |
| Camera | Originally equipped on the vehicle for the Lane Keeping Assist (LKA) system |
| Position of camera | Top center of windshield |

**Test method**

Informed consent was obtained from at least ten test subjects, who were asked to drive the vehicle described in Table 1 in a normal driving style. The driving behavior of these drivers was then recorded. Table 2 shows an outline of the test scenario and Table 3 describes how the data was acquired.

**Table2.**
**Test scenario.**

| Item | Content |
|---|---|
| Period | Apr. 5, 2013 – Dec. 13, 2013 |
| Route | Mainly Aichi, Shizuoka, and Yamanashi in Japan Incl. both highways & general roads |
| Drivers | More than 10 people |
| Driving style | Normal |

**Table3.**
**Data acquisition methods.**

| Variable | Method |
|---|---|
| Vehicle speed | Vehicle CAN |
| DTLB | Recognized by camera |
| Lane width | Recognized by camera |
| Lateral speed | Differential of DTLB |
| Road curve radius | Recognized by camera |

The measured data includes different lane widths and curve radii. However, it is thought that the lane width and the size of the curve radius change the positional relationship between the vehicle and the lane marking. Therefore, the lane width and the size of the curve radius were categorized from (a) to (i) as shown in Table 4 and then analyzed. Since the inside of a curve is more likely to intersect with the driving region, the DTLB and lateral velocity at the inside of the curve were used. The “Curve G” value in Table 4 is the square of the vehicle speed divided by the curve radius.

**Table4**
**Classification of recorded data.**

| | | Curve G [m/s$^2$] | | |
|---|---|---|---|---|
| | | Up to 0.5 | 0.5 to 1.5 | 1.5 to 2.5 |
| Lane width [m] | From 3.25 | a | b | c |
| | 2.75 to 3.25 | d | e | f |
| | Up to 2.75 | g | h | i |

**Test results**

In the test, normal driving behavior was recorded over total distance of 16,285 km. Most data was recorded at a speed of 50 to 60 km/h on general roads and at around 100 km/h on highways. In all regions where a lane marking was detected by the camera, 2D distribution of the DTLB and lateral velocity was plotted and the distribution indicated by color. The red areas indicate high frequencies and represent normal driving behavior. The blue areas indicate low frequencies. Figure 5 shows the plotted results for category (a) in Table 4.

According to Figure 5, the highest frequency is obtained at a lateral velocity of 0 and DTLB of 0.8. This has ellipsoidal distribution. When driving straight in the center of the lane, the driving behavior is likely to be close to the center of this ellipsoidal region.
An approximation was carried out using 2D normal distribution to analyze the distribution in Figure 5 statistically. First, the correlation coefficient between the DTLB and lateral velocity was calculated to be -0.0076. Since this indicates virtually no correlation, the probability density distribution $f(v_y, D)$ of the 2D normal distribution was calculated following Equation 1, where, $v_y$ is the lateral velocity, $D$ is the DTLB, $\sigma_{v_y}$ is the standard deviation of $v_y$, $\sigma_D$ is the standard deviation of $D$, $\overline{v_y}$ is the average of $v_y$, and $\overline{D}$ is the average of $D$.

$$f(v_y, D) = \frac{1}{2\pi\sigma_{v_y}\sigma_D} \exp\left[-\frac{1}{2}\left(\frac{(v_y-\overline{v_y})^2}{\sigma_{v_y}{}^2} + \frac{(D-\overline{D})^2}{\sigma_D{}^2}\right)\right] \qquad (1)$$

To calculate the regions with the highest probability in which normal driving occurs, an ellipsoidal isopleth drawn between positions of equal values in the 2D normal distribution was used. The probability of data falling inside this ellipsoid was calculated following Equation 2 by integrating Equation 1 using the region inside the ellipsoid (S) defined when the exponential part of Equation 1 is set to $-C^2/2$.

$$P = \iint_S f(v_y, D)dS = \iint_S \frac{1}{2\pi\sigma_{v_y}\sigma_D} e^{-\frac{c^2}{2}} dv_y dD = 1 - e^{-\frac{c^2}{2}} \qquad (2)$$

This calculation was applied to the data in Figure 5. Figure 5 also shows the ellipsoid drawn when the result of Equation 2 is 99%. The actual proportion of data inside the ellipsoid is 98.2%, indicating that the margin of error for the 2D normal distribution model is 0.8%, which is regarded as a comparatively close approximation.
The 99% ellipsoidal isopleth indicates that virtually all driving behavior is within this ellipsoid. Therefore, Figure 5 shows that, as the lateral velocity increases, the ellipsoid (lower limit) moves further away from the lane boundary (DTLB=0). This result quantitatively verifies the hypothesis for category (a).

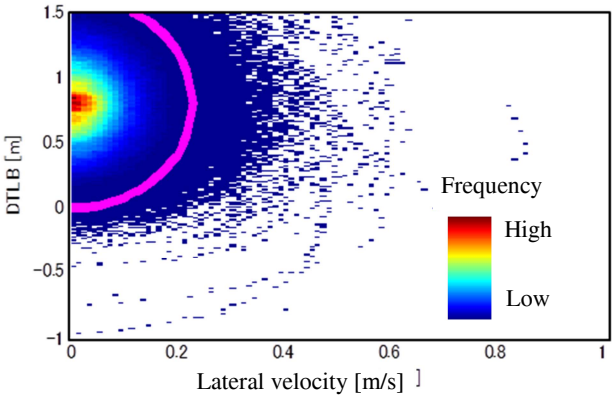


***Figure5. Driver behavior analysis using 2D normal distribution.***

Categories (a) to (i) in Table 4 were analyzed in the same way. Figures 6 shows the 99% ellipsoidal isopleth results for each lane width. All results follow the hypothesis.
In addition, Figures 6 also indicates an increasing trend for vehicles to depart from the lane as the curve radius becomes sharper and the lane becomes narrower, and at lower lateral velocities.

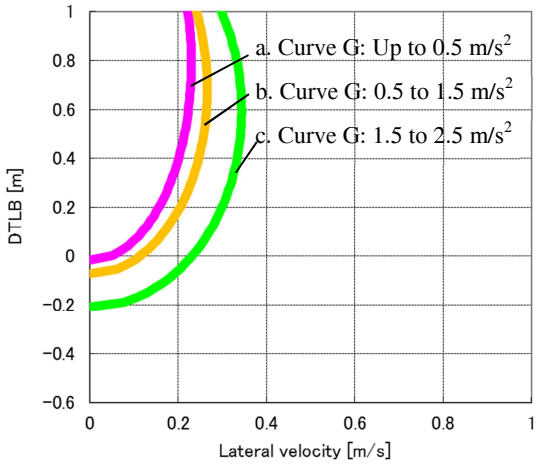


Driving regions (width: from 3.25 m)

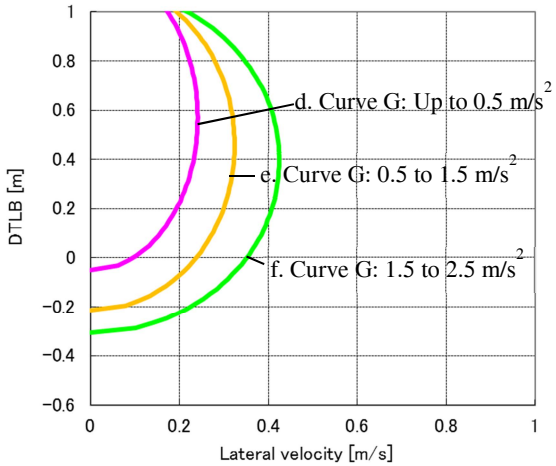


Driving regions (width: 2.75 m to 3.25 m)

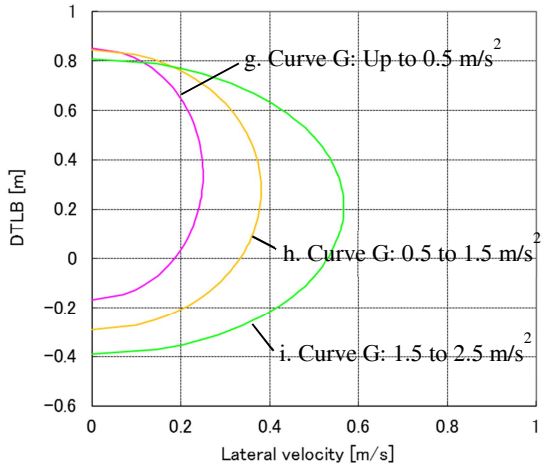


Driving regions (width: up to 2.75 m)

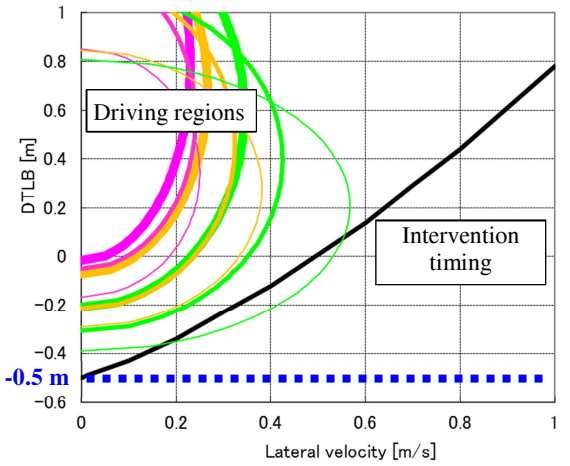


Relationship between intervention timing and driving regions

***Figure6. Driving regions in each lane width and relationship with intervention timing.***

## DISCUSSION

Driving behavior was identified in the previous section. The following section discusses the driving regions analyzed above and the consistency of the target maximum lateral distance traveled out of the lane (0.5 m).
The required intervention timing to achieve maximum lateral distance traveled out of the lane of 0.5 m was calculated and the driving regions were plotted on the same graph (Figure 6). This graph assumes a vehicle speed of 100 km/h, a yaw rate gradient of 3.5 deg/s$^2$, and a vehicle response delay for the steering control after lane boundary recognition of 0.5 sec.

Figure 6 indicates that, as the lateral velocity increases, the target of 0.5 m is not achieved without earlier intervention timing. In addition, the driving regions analyzed above (i.e., the 99% ellipsoidal isopleth results) were plotted on the same graph. The DTLB lower limit values for the driving regions also increase in accordance with the lateral velocity. As a result, the figure shows that the required intervention timing almost entirely does not intersect with the driving regions. This means that it should be possible to achieve the target maximum lateral distance traveled out of the lane of 0.5 m when LDA control is started outside the driving regions.
From these results, the newly proposed 2D analysis of driving behavior using DTLB and lateral velocity shows that it may be possible to help reduce both accidents and driver annoyance with the system by adopting later intervention timing when the lateral speed is low, and earlier intervention timing when the lateral speed is high.

## CONCLUSIONS

This paper studied how to help reduce both accidents and driver annoyance with the LDA system by investigating and analyzing driving behavior. The following results were obtained.

- Normal driving behavior was identified using a 2D analysis method incorporating DTLB and lateral velocity. It was found that drivers approached or crossed the lane boundary when the lateral velocity was low, but drove further away from the lane boundary as the lateral velocity increased.
- The normal driving position is affected by the size of the curve radius and the lane width. It was found that drivers tended to depart from the lane as the curve radius becomes sharper and the lane becomes narrower, and at lower lateral velocities.
- The possibility of intersection between the driving region and LDA activation falls when later intervention timing is adopted at low lateral speeds and earlier intervention timing is adopted at high lateral speeds. Based on this concept, it may be possible to help reduce both accidents and driver annoyance with the system.

This research assumed that activation of the system would not be invasive outside the 99% driving region. However, if strong steering control is applied in this case, the system is unlikely to be accepted by drivers. Therefore, further research is needed into the relationship between the steering control magnitude and driver acceptance.

## REFERENCES

[1] Traffic Planning Division, Traffic Bureau, National Police Agency of Japan. 2014. “Characteristics of Fatal Traffic Accidents and Road Traffic Law Violations in 2013” (in Japanese).
[2] National Highway Traffic Safety Administration. 2010. “Lane Departure Warning System Confirmation Test.”
[3] Japanese Institute for Traffic Accident Research and Data Analysis (ITARDA). 2008. “2007 Traffic Accident Investigation and Analysis Report” (in Japanese).
[4] Tanaka S. et al. 2012. “Benefit Estimation of a Lane Departure Warning System using ASSTREET.” SAE Paper No. 12AC-0016.
[5] Japanese Ministry of Land, Infrastructure, Transport and Tourism (MLIT). 2013. “Technical Guidelines for Lane Keeping Assist Systems” (in Japanese).
[6] ISO 17361. 2007. “Intelligent transport systems – Lane departure warning systems – Performance requirements and test procedures.”

# ANALYSIS OF THE ROBUSTNESS OF STEERING PATTERN BASED DROWSINESS DETECTION

**Christiane Spindler**
**Frauke Driewer**
**Lorenz Schäfers**
Daimler AG
Germany

Paper Number 15-0226

## ABSTRACT

Several studies show that up to one in four severe traffic accidents can be attributed to drowsiness. Drivers often over-estimate their fitness level or are not aware of the danger that always accompanies drowsy driving.
Since associations like the NHTSA pointed to the relevance of this topic, more and more research has been conducted and in the meantime there is also a variety of commercial systems on the market to address this risk.
In this paper, we do not aim to find new methods of detecting drowsiness of a driver. Our approach is rather to choose an established method and enhance it in a way that it not only performs well in a driving simulator but also in real world drives.
The chosen drowsiness detection method is the observation of the steering wheel angle signal. It has been shown that the frequency of occurrence of a typical steering pattern, which can roughly be described as a deadband followed by a rather fast correction, is an indicator for the state of drowsiness of a driver. The advantage over other techniques like camera-based detection is that it can run in standard equipped cars. Thus it is available for the largest number of drivers and can thereby achieve the greatest effect on accident avoidance.
We investigate the chosen detection method in real world drives and discuss which other effects not related to drowsiness can evoke the described steering pattern. We focus on environmental effects like crosswind and can show that those events may lead to an increase of the amount of steering patterns. Finally, we quantify the influence on drowsiness measures. The underlying database comprises more than two million kilometers of more than one thousand drivers, all real-world drives.
Our evaluation shows that particularly on routes or in situations where those environmental influences accumulate, the drowsiness measure can be affected to an extent that leads to false triggering of the system. Therefore, we suggest measures that can be taken to reduce the influence of steering patterns that are not related to the driver's drowsiness state.
The aim of most drowsiness detection systems is to inform a driver when his state has reached a critical level and to motivate him to take appropriate measures. This presupposes confidence in the system. False warnings will negatively affect the credibility of the system.
Our purpose is to show the importance of enabling this kind of system to recognize external influences, thus making detection more robust. We consider it very important to make such systems as reliable and credible as possible, as otherwise the driver will not take the advice the system will give him. Limiting the influence of external factors is a key to achieving this goal.

## INTRODUCTION

Numerous reports name drowsiness and distraction as the cause of alarming numbers of accidents. The National Highway Traffic Safety Administration (2010) reports that in 2009 16% of all fatal crashes in the United States involved distracted driving. As regards drowsiness, Horne and Reyner (1995) found that 20% of all accidents on motorways in Southwest England to which the police was present were sleep-related. According to Langwieder et al. (1994), 24% of all fatal crashes in Bavaria, Germany, in 1991 happened because the driver fell asleep. NHTSA (Royal, 2002) reports 56,000 crashes annually to be related to drowsiness as mentioned by the police, resulting in 1,550 fatalities. In the same report, NHTSA lists reasons why these numbers are presumed to be conservative. Furthermore, crashes due to drowsiness tend to have a severe outcome (Wang et al., 1996).
The focus on the topic is still increasing. NHTSA names distracted and drowsy driving as one of the traffic safety problem areas (Goodwin et al., 2013) and the Euro NCAP 2020 Roadmap aims to reward manufacturers in the area of driver state monitoring in order to bring down the numbers of vehicles departing the road (European Car Assessment Programme, 2014).

A lot of research has been conducted in the field of drowsiness recognition and in the last years several commercial systems have become available on the market, using different methods. Dong et al. (2011) and Platho et al. (2013) give an overview of driver monitoring systems and also mention the commercial products of Ford, Mercedes-Benz, Volvo and VW. All those systems aim to suggest the driver to take a rest when he has reached a critical level. Many different algorithms were developed that analyze the driving performance, e.g. based on steering behaviour or lane keeping ability. These algorithms normally detect drowsiness if the driver shows an unusal driving behaviour (e.g. leaving the lane too often) or if the driving behaviour changes significantly from the beginning (e.g. lane keeping ability decreases).

A problem of methods that use driving performance as criteria for drowsiness detection is that only the reaction of the driver can be analyzed, not the reason for certain driving manoeuvers. Attwood (2014) mentions that systems, though they work in driving simulators, may fail on real roads, as they are not able to detect what the driver is responding to, considering environmental characteristics related to road, traffic and weather.

In the present paper we discuss which environmental characteristics may have an impact on driver monitoring systems. In detail, the influence of crosswind and road disturbances is analyzed and it is estimated to what extent those events have an impact on drowsiness recognition. Finally it is shown how these external factors are taken into account in the system under consideration.

The following evaluation is based on the steering wheel angle signal as the main information source. The main advantage of this method is that no special sensor, e.g. lane detection or driver monitoring camera, is needed. The steering wheel angle signal is part of the standard equipment of present-day cars. By this means, it is possible to integrate the drowsiness detection as a standard feature and thus reach a high number of drivers.

## APPROACH

### Steering wheel angle based drowsiness detection

Several studies investigating the use of the steering wheel angle signal for drowsiness detection have been carried out. Dingus et al. (1987) found that the number of steering wheel velocities over 150deg/s is an indicator for drowsiness. Bouchner et al. (2006) show a positive correlation of the ratio of fast and slow steering corrections with drowsiness.

A combination of slow and fast steering velocities is also used in this study. It is based on the Mercedes-Benz Attention Assist, which is a system that detects drowsiness and long-term distraction. Both kinds of driving impairment affect the steering behavior in a similar way. The steering pattern we evaluate consists of a deadband (phase without or with very slow steering) and a subsequent fast steering correction. Friedrichs and Yang (2010) show that this pattern correlates with drowsiness.
In our experience, steering velocities differ widely between drivers. Therefore, several thresholds in the algorithm are adapted continuously during the drive and according to the behavior in the first minutes of a drive, when the driver is presumed to be rather awake.
The accumulated steering pattern is the basis for the drowsiness measure. Figure 1 shows other factors that are taken into account to make the system more robust and useable in real road environment.

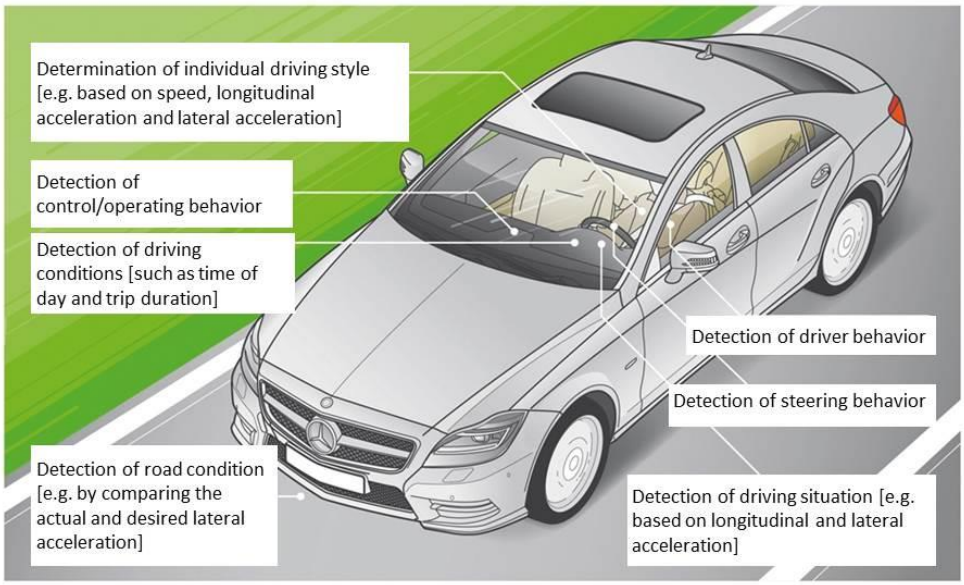


***Figure1. Features of the Mercedes-Benz Attention Assist.***

**Situations potentially provoking steering patterns**

Friedrichs et al. (2011) identified external influences on the driving behavior. We refer to the factors listed in that study and cluster them as shown below.

**Gaze direction, distraction, vehicle operation.** Factors describing different kinds of driver action. These include for example eating or drinking, which can lead to abnormal steering behavior as the driver does not operate the vehicle with both hands. It may also be the driver not keeping his eyes on the road because he is attending to his children on the back seat or reading messages on his smartphone. The steering patterns arising from these actions can be classified as indicators of distraction and are thus treated by the system in the same way as steering patterns evoked by drowsiness. Vehicle operations on the other hand are part of the driving task. They can be detected by the system and the related steering patterns can be filtered out.

**Vehicle type/motorization, posture.** Influences that can be summarized as characteristics of the vehicle and the driver. A key issue of these factors is that they normally do not change during a drive. Hence, adaptive systems are able to minimize the influence.

**Rain/fog/snow, traffic density, lane width/-number, speed, curvature.** Description of the driving situation. An impact on the driving behavior is probable. Those situations are usually of longer duration. Some of these situations can easily be detected with standard sensors, e.g. speed or curvature. Others are more complicated to be analyzed online, e.g. traffic density. Nevertheless, as the factors are usually of longer duration, adaptive algorithms can react on the change in an adequate time.

**Road condition, road bumps, crosswind, warping.** Single, strong events with sudden occurrence that may have immediate impact on the driving behavior. Crosswind often occurs unexpectedly, laterally displaces the vehicle and thus requires a fast counter-steering. Road bumps, warping or potholes can also lead to unintentional steering corrections. Steering corrections that potentially arise from these environmental influences are neither related to drowsiness nor to distraction and should therefore not be considered for driver state monitoring.

In this study, we concentrate on the environmental events and investigate the influence of crosswind and road irregularities (road bumps, potholes) in detail. Friedrichs et al. (2011) conducted special drives for their evaluation in order to keep the dimension of the influences as small as possible. In the following evaluation real road data from naturalistic driving is used. Some restrictions were made on speed range and rated

drowsiness. Therefore, a much larger number of drives are part of the evaluation and the study of Friedrichs et al. (2011) is extended towards real driving situations.

**Recognition of environmental influences**

A prerequisite for all further evaluation is the ability to detect the presence of environmental influences. The detection of potholes and road bumps is based on an algorithm that looks for characteristics in the rotational speed of the wheels. The occurrence of crosswind is detected by comparing the steering angle, which provides information regarding the driver's intention, to the lateral acceleration, which supplies the actual lateral vehicle movement. This approach of crosswind detection also includes the recognition of road warping. Often a mixture of road bumps and warping occurs, which means that the detection of crosswind, warping and road bumps is not always separable. Hence, some events are recognized by both algorithms. All signals mentioned are available in standard equipped cars.

The algorithms described have been extensively proven in real world drives. For the following evaluations, the results of those algorithms have been used as labels for the presence of environmental influences.

## EVALUATION

**Underlying Database**

All data used comes from naturalistic drives. Driving simulator data is not included. The database comprises more than two million kilometers conducted by more than one thousand drivers. Self-rating of driver drowsiness is available for each drive. This rating has been conducted according to the Karolinska Sleepiness Scale (KSS) (Âkerstedt & Gillberg, 1990). Every single drive has undergone a validation process to make sure quality standards like consistent values of the KSS-rating are fulfilled. All drives come from Mercedes-Benz cars, but have been conducted in different models from the A-Class (compact car) to the S-Class (luxury large car).

**Evaluation of steering behavior**

Prior to the investigation of the occurrence of steering patterns, a more general look at the steering behavior was taken. Steering velocities were explored regarding the influence of crosswind or road bumps.

As there are significant differences in steering behavior between individuals the analysis was conducted separately for single drivers. From the entire database, the ten drivers with the largest amount of recorded data were selected. Since Friedrichs et al. (2011) have shown that speed has a strong impact on the steering velocities, distributions of this signal in different speed ranges were compared for single drivers. Afterwards, the speed range under consideration was limited to velocities between 100km/h and 200km/h, as the signal values vary more at lower speeds. In addition, only parts of the drives were considered in which the driver was awake and alert.

For each drive of the ten selected drivers the ratio of the presence of crosswind to the duration of the whole drive in the considered speed range was calculated. The lower quartile $Q_1$ and the upper quartile $Q_3$ of this ratio were then used for each driver to group his measurements into rather smooth drives (*group 1*) and drives under windy conditions (*group 2*). The same was done for proportions of the presence of road bumps and warping. Accordingly, *group 1* comprises smooth drives and *group 2* drives on roads with frequent disturbances.

Subsequently, mean (*mean*) and variance (*var*) of the steering wheel velocity (*swv*) of each group of drives was calculated.

Table 1 shows the results for the crosswind comparison. The calculated ratios are defined according to Eqs. (1-2).

$$ratio\ mean = \frac{mean(swv)_{group2}}{mean(swv)_{group1}} \quad (1)$$

$$ratio\ var = \frac{var(swv)_{group2}}{var(swv)_{group1}} \quad (2)$$

From the values in $Q_1$ and $Q_3$ it can be seen how much crosswind was present in *group 1* and *group 2*. The interquartile range *IQR* shows how strong the two groups differ in their amount of crosswind.

It can be seen from the table that driver A sticks out, having the highest *ratio mean* and *ratio var*, which means that the mean value of his steering velocity is higher for drives under windy conditions while also the distribution is spread more widely. In comparison, for driver E both ratios are still greater than one but with much smaller values. Hence, this driver also has higher steering velocities with a higher variance for his drives of *group 2*, but the effect is less marked than for driver A. A look at the quartiles gives an explanation for this difference. The value of $Q_3$, which is the threshold for drives under windy conditions, is much higher for driver A than for driver E, while $Q_1$ is the same for both drivers. Thus, data from more windy conditions is existent for driver A than it is for driver E, which results in a higher effect on the steering velocities.

In summary, for all drivers the mean value and the variance of *swv* is higher for drives of *group 2* than *group 1*. A look at the individual thresholds $Q_1$ and $Q_3$ and the *IQR* shows that this effect is stronger for individuals for which a greater difference in the ratio of crosswind occurrence is present. Taken together, these results reinforce the expectation that higher steering velocities occur with environmental disturbances.

**Table1.**
**Comparison of steering velocity mean and variance for drives with different ratios of crosswind occurrence.**

| Driver | data selection | number of drives | evaluated time [min] | *mean(swv)* [°/s] | *var(swv)* [°/s] | *ratio mean* | *ratio var* | $Q_1$ | $Q_3$ | *IQR* |
|---|---|---|---|---|---|---|---|---|---|---|
| A | Group 1 | 79 | 6369 | 1.00 | 2.17 | 2.84 | 10.06 | 0.03 | 0.13 | 0.10 |
| | Group 2 | 79 | 4420 | 2.84 | 21.79 | | | | | |
| B | Group 1 | 44 | 3608 | 1.44 | 4.04 | 1.41 | 1.92 | 0.03 | 0.10 | 0.07 |
| | Group 2 | 44 | 2751 | 2.04 | 7.75 | | | | | |
| C | Group 1 | 43 | 3879 | 1.38 | 3.18 | 2.01 | 3.18 | 0.03 | 0.18 | 0.15 |
| | Group 2 | 43 | 2234 | 2.78 | 10.12 | | | | | |
| D | Group 1 | 87 | 7276 | 1.72 | 4.12 | 1.93 | 4.51 | 0.03 | 0.11 | 0.08 |
| | Group 2 | 87 | 4668 | 3.33 | 18.56 | | | | | |
| E | Group 1 | 37 | 2942 | 1.27 | 2.86 | 1.18 | 1.22 | 0.03 | 0.07 | 0.04 |
| | Group 2 | 37 | 2923 | 1.51 | 3.48 | | | | | |
| F | Group 1 | 39 | 2766 | 1.68 | 4.37 | 1.19 | 1.46 | 0.02 | 0.04 | 0.02 |
| | Group 2 | 39 | 2832 | 2.01 | 6.38 | | | | | |
| G | Group 1 | 44 | 4110 | 1.09 | 1.94 | 1.19 | 1.48 | 0.02 | 0.06 | 0.04 |
| | Group 2 | 44 | 2636 | 1.29 | 2.88 | | | | | |
| H | Group 1 | 47 | 3203 | 1.22 | 2.72 | 1.27 | 1.53 | 0.03 | 0.09 | 0.06 |
| | Group 2 | 47 | 3017 | 1.54 | 4.14 | | | | | |
| I | Group 1 | 29 | 1768 | 1.28 | 2.64 | 1.22 | 1.42 | 0.02 | 0.06 | 0.04 |
| | Group 2 | 29 | 2335 | 1.57 | 3.75 | | | | | |
| J | Group 1 | 36 | 3872 | 1.04 | 1.81 | 1.27 | 1.63 | 0.02 | 0.07 | 0.05 |
| | Group 2 | 36 | 2346 | 1.32 | 2.95 | | | | | |

The same procedure was applied for the presence of road disturbances. The result is presented in Table 2. Though not as definitive as for crosswind, the findings are the same. For all drivers, both mean and variance of the steering velocity are higher for data of *group 2*, which are the drives with a high amount of road disturbances. The tendency of a higher portion of road irregularities leading to higher mean values and higher variance of the steering wheel velocity can also be observed: driver I has the smallest *IQR*, which means the

difference of the ratio of road disturbance occurrence between his drives in *group 1* and *group 2* is smaller than for the other drivers. This explains why the mean steering velocity differs less between *group 1* and *group 2* than it does for example for driver D, whose drives in *group 2* feature a larger ratio of road irregularities.

**Table2.**
**Comparison of steering velocity mean and variance for drives with different ratios of road bumps occurrence.**

| **Driver** | **data selection** | **number of drives** | **evaluated time [min]** | ***mean(swv)* [°/s]** | ***var(swv)* [°/s]** | ***ratio mean*** | ***ratio var*** | $Q_1$ | $Q_3$ | ***IQR*** |
|---|---|---|---|---|---|---|---|---|---|---|
| A | Group 1 | 79 | 6701 | 1.01 | 2.15 | 2.47 | 8.46 | 0.03 | 0.18 | 0.15 |
| | Group 2 | 79 | 5487 | 2.51 | 18.22 | | | | | |
| B | Group 1 | 44 | 3040 | 1.53 | 4.20 | 1.43 | 2.06 | 0.03 | 0.13 | 0.10 |
| | Group 2 | 44 | 2464 | 2.19 | 8.66 | | | | | |
| C | Group 1 | 43 | 3849 | 1.62 | 3.98 | 1.50 | 2.14 | 0.04 | 0.23 | 0.19 |
| | Group 2 | 43 | 2504 | 2.42 | 8.54 | | | | | |
| D | Group 1 | 87 | 6853 | 1.82 | 4.47 | 1.65 | 3.59 | 0.03 | 0.14 | 0.11 |
| | Group 2 | 87 | 5824 | 3.00 | 16.04 | | | | | |
| E | Group 1 | 37 | 2991 | 1.27 | 2.89 | 1.18 | 1.24 | 0.07 | 0.18 | 0.11 |
| | Group 2 | 37 | 2875 | 1.50 | 3.60 | | | | | |
| F | Group 1 | 39 | 3068 | 1.76 | 5.01 | 1.01 | 1.07 | 0.04 | 0.10 | 0.06 |
| | Group 2 | 39 | 2315 | 1.78 | 5.35 | | | | | |
| G | Group 1 | 44 | 3762 | 1.05 | 1.94 | 1.22 | 1.40 | 0.02 | 0.10 | 0.08 |
| | Group 2 | 44 | 2160 | 1.28 | 2.71 | | | | | |
| H | Group 1 | 47 | 3542 | 1.33 | 3.28 | 1.10 | 1.05 | 0.02 | 0.10 | 0.08 |
| | Group 2 | 47 | 3155 | 1.47 | 3.45 | | | | | |
| I | Group 1 | 29 | 2163 | 1.37 | 3.04 | 1.06 | 1.14 | 0.02 | 0.08 | 0.06 |
| | Group 2 | 29 | 1859 | 1.46 | 3.45 | | | | | |
| J | Group 1 | 36 | 3647 | 1.05 | 1.92 | 1.11 | 1.19 | 0.03 | 0.09 | 0.06 |
| | Group 2 | 36 | 3382 | 1.17 | 2.28 | | | | | |

**Evaluation of the occurrence of steering patterns**

To find out whether there are peculiarities in the number of steering patterns with the presence of crosswind, all time instances of onsets of crosswind in the speed range 60-200km/h were identified for 11,604 drives. Afterwards a time range of ten seconds before and ten seconds after those time instances was investigated for steering patterns.

Figure 2 provides the cumulated result for all time instances in which crosswind was detected. Zero on the time axis marks the beginning of crosswind. As the duration differs, the red vertical line marks the median of the end of the detected crosswind. The number of steering patterns have been counted and plotted at their instant of occurrence, relative to the beginning of crosswind and normalized with the number of crosswind events. As can be seen, in general the number of steering patterns moves around a certain level. After the onset of crosswind, a very strong rise can be observed. The subsequent lower amount is attributable to the violation of the deadband criteria caused by the counter-steering. It is apparent from this data that more steering corrections are produced under the influence of crosswind.

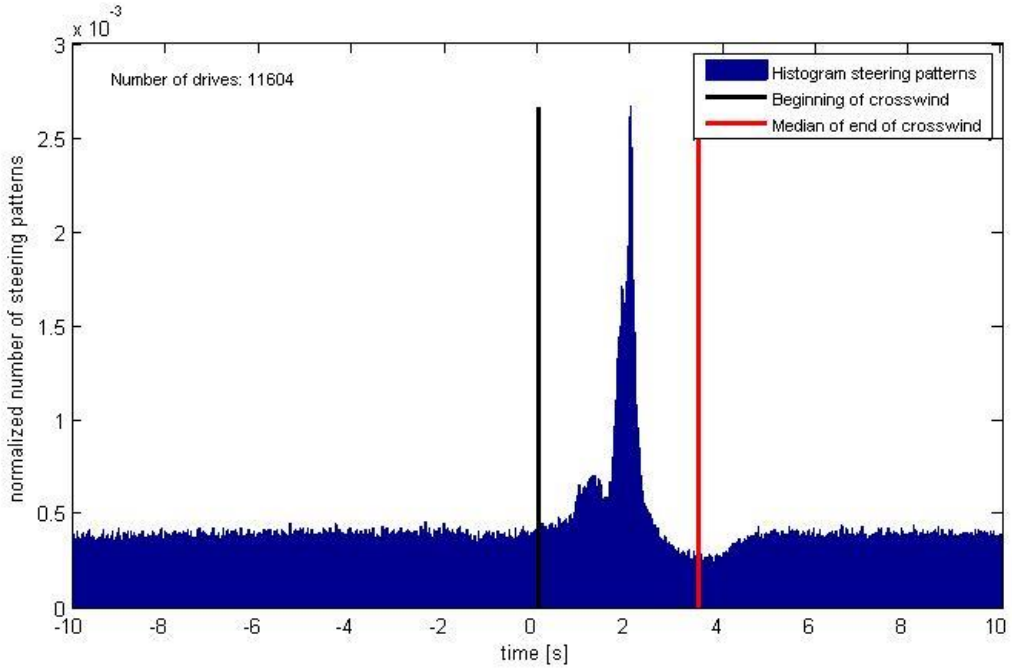


***Figure2. Histogram of steering patterns around crosswind events.***

The same procedure was applied for road surface irregularities. The results obtained from 11,638 drives are shown in Figure 3. The observation is the same as for crosswind. The number of steering patterns varies little around a certain level and increases strongly when road bumps occur. It is thus confirmed that road disturbances can lead to steering corrections.

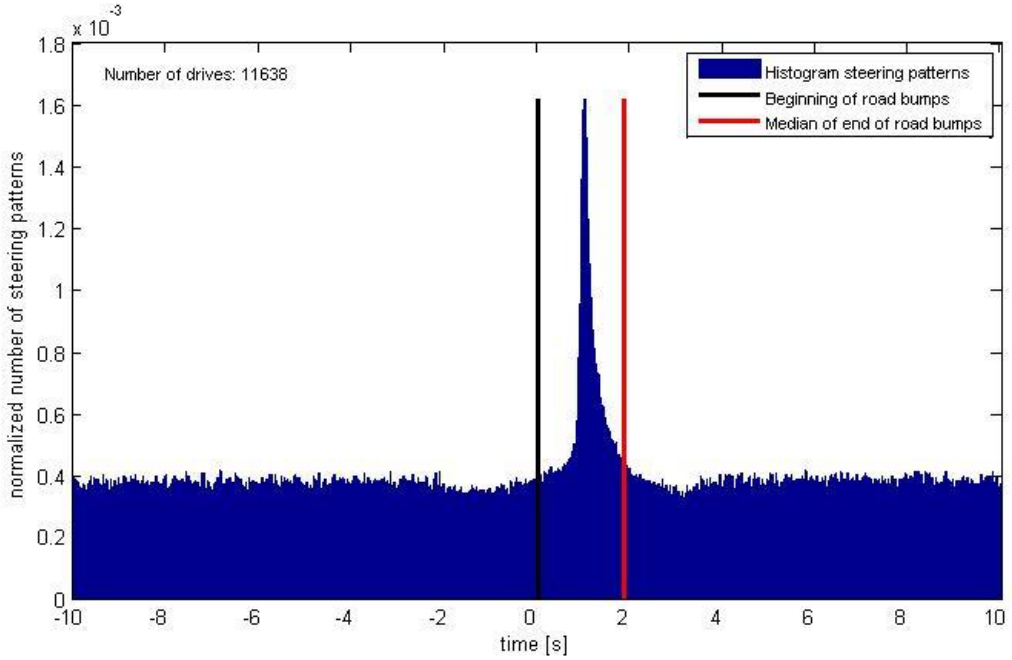


***Figure3. Histogram of steering patterns around road disturbances.***

**Quantification of influence on drowsiness detection**

The previous evaluation proofed that environmental characteristics can evoke steering patterns. In the next step the dimension of the influence on a possible drowsiness measure was estimated. Based on this final evaluation it could be determined whether environmental influences present a severe problem or if effects are minor and can be neglected.

This estimation was performed by calculating the factor by which the number of steering corrections increases if environmentally influenced ones are taken into account. Only data was used, in which the driven speed lay for at least 30min in the range of 60 to 200km/h. This led to 6075 evaluable drives. For each drive, the ratio of the amount of steering corrections that were detected during the presence of crosswind to the amount of steering patterns that occurred when no environmental disturbances were present was calculated. The result shows by which factor the number of steering patterns would increase if those evoked by crosswind were ignored. It also represents an estimation of how much a drowsiness measure, based only on a summation of steering patterns, would be affected.

The same principle was applied for the computation of the increase of steering patterns as a result of road disturbances. Figure 4 presents the distributions of the results for both kinds of environmental influences in a boxplot. A factor of increase of one means that the number of steering patterns would double by taking into account the environmental disturbance-evoked ones. For a better readability, only values up to 1.5 are shown. This was done due to some striking outliers, which may occur for special driving conditions, e.g. extraordinary windy conditions.

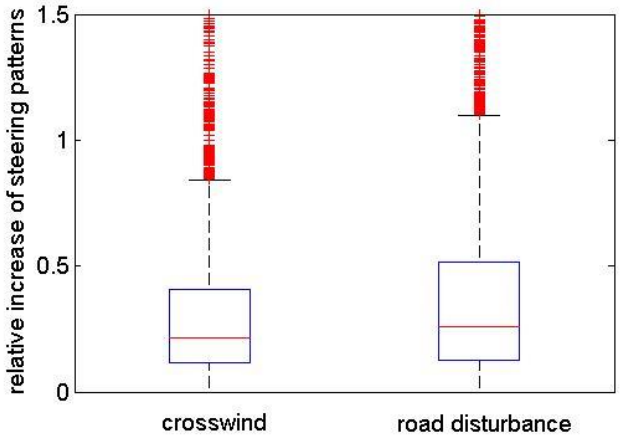


***Figure4. Increase of number of steering patterns with environmental disturbances.***

The median for the factor of increase on account of crosswind lies at a value of 0.215, due to road irregularities at 0.258. As explained before, the crosswind recognition and the detection of road bumps may sometimes be effective for the same events, thus it has not to be assumed that both factors of increase would add up. But, for half of the drives in the existing database, a possible drowsiness measure increases by more than 20% even regarding only one of the influences, which may indeed lead to false warnings. The problem is less severe for drives under smooth conditions and more severe if more disturbances occur. Figure 5 shows that the rise of steering patterns and the relative amount of crosswind is highly correlated, as can be expected. The same observation can be made for road irregularities, as shown in Figure 6. Especially for drives under more extreme conditions, measures have to be taken to increase the robustness of the drowsiness recognition system to prevent false alarms.

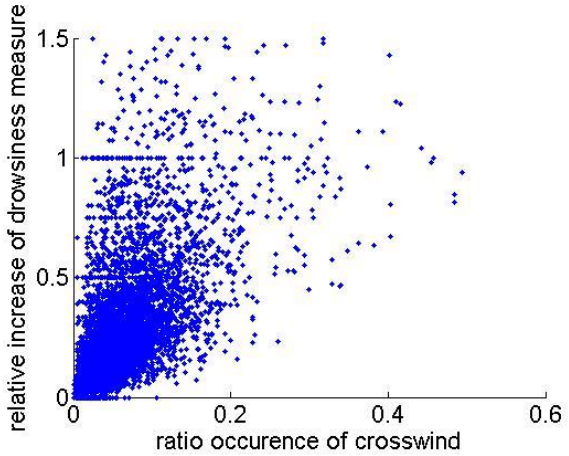


*Figure5. Relation between amount of crosswind and increase of steering patterns.*

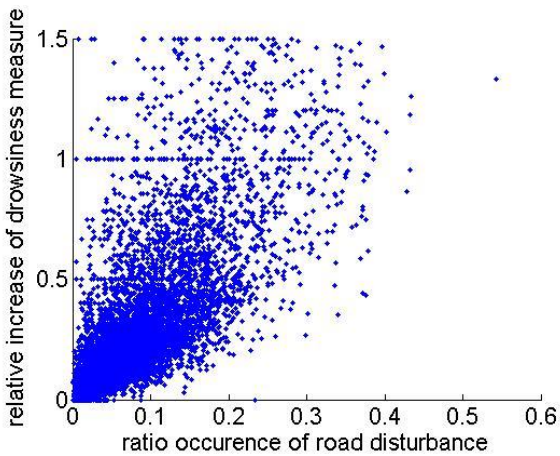


*Figure6. Relation between amount of road disturbances and increase of steering patterns.*

## PROPOSAL OF MEASURES

The evaluations show that the impact of environmental influences on steering pattern based drowsiness detection systems is too strong to be neglected. In the following we propose measures that increase the robustness as they are implemented in the Mercedes-Benz Attention Assist system.

### Masking

In the first step, steering corrections evoked from events like crosswind or road bumps are left out of the estimation of drowsiness. A prerequisite for this is the possibility of recognizing such disturbing influences. Not to consider those steering patterns means that the system cannot evaluate the driver's steering behavior during the presence of the environmental disturbance. This leads to some kind of system inactivity. Inactivity due to environmental influences is of short duration. Figure 2 and Figure 3 depict the median of the duration of disturbing environmental events, about 3.5s and 2s respectively. In our database, crosswind led to 4.3% of overall system inactivity, while masking due to road disturbances concerned 6.2% of all data. Both values were obtained from data in the speed range 60-200km/h. Hence, the inactive periods have only minor influence on the overall system performance.

If the system is inactive for a long time, we recommend letting the driver know that he cannot expect it to work without restrictions. This is for example the case if the system works only in a certain speed range. Transparency, such as displaying inactivity, can lead to better understanding and thus more trust in the system.

### Adaption

While masking is effective for determined events, another measure is needed for all non-specific influences that cannot be detected as single environmental events can be. Increased robustness can also be achieved by making algorithms adaptive, not only to the driver but also to changes in the driving situation that cannot be attributed to special events. For example thresholds for the recognition of steering patterns should adapt during the whole drive.

## CONCLUSIONS

The purpose of the current study was to determine the necessity of making driving-performance based driver state monitoring systems, especially those that rely on steering patterns, robust against environmental influences. The results of the investigations have shown that environmental influences have a significant

impact on the steering behavior and can lead to steering patterns that are not related to drowsiness or distraction.

It has also been found that the number of unwanted steering patterns cannot be disregarded. The influence on the drowsiness measure is significant, especially with higher presence of disturbances. The implementation of possibilities to detect environmental events and ignore the consequent steering corrections helps to achieve better performance of such systems in real road scenarios. The performance can be further improved by designing adaptive algorithms, e.g. by fitting certain parameters to the special driving situation.

The effectiveness of drowsiness detection systems that are limited to give advice depends on the driver's confidence. An increase in the drowsiness measure because of environmental influences can lead to false triggering of the system and thus to the driver not taking it seriously.

The presented method of evaluating influence of certain events on drowsiness detection algorithms can also be used to study the effect of other events, e.g. certain vehicle operations. It allows estimating the scale of the effect and helps deriving measures to decrease the negative consequences on the system performance. The method shows especially an efficient way to extract this information in a huge amount of existing real road data.

## REFERENCES


Åkerstedt, T., & Gillberg, M. (1990). *Subjective and objective sleepiness in the active individual.* International Journal of Neuroscience, 52, 29-37.

Attwood, D. (2014). *Vehicle-based driver interlocks: After 50 years of research, can we now design an on-board, real-time system to detect abnormal driving behavior?* SAE Technical Papers, 1.

Bouchner, P., Piekník, R., Novotný, S., Pěkný, J., Hajný, M., & Borzová, C. (2006). *Fatigue of car drivers - detection and classification based on the experiments on car simulators.* WSEAS Transactions on Systems, 5(12), 2789-2794

Dingus, T., Hardee, H., & Wierwille, W. (1987). *Development of models for on-board detection of driver impairment.* Accident Analysis & Prevention, 19(4), 271-283.

Dong, Y., Hu, Z., Uchimura, K., & Murayama, N. (2011). *Driver Inattention Monitoring System for Intelligent Vehicles: A Review.* IEEE Transactions in Intelligent Transportation Systems, 12(2), 596-614.

European Car Assessment Programme (2014). *2020 Roadmap.* Retrieved from www.euroncap.com.

Friedrichs, F., & Yang, B. (2010). *Drowsiness monitoring by steering and lane data based features under real driving conditions.* European Signal Processing Conference, 209-213.

Friedrichs, F., Hermannstädter, P., & Yang, B. (2011). *Consideration of Influences on Driver State Classification.* 2nd Conference on Driver Distraction and Inattention (DDI), Gothenburg.

Goodwin, A., Kirley, B., Sandt, L., Hall, W., Thomas, L., O'Brien, N., & Summerlin, D. (2013). *Countermeasures that work: A highway safety countermeasures guide for State Highway Safety Offices.* Washington, DC: National Highway Traffic Safety Administration.

Horne, J., & Reyner, L. (1999). *Vehicle accidents related to sleep: A review.* Occupational and Environmental Medicine, 56(5), 289-294.

Horne, J., & Reyner, L. (1995). *Sleep related vehicle accidents*. British Medical Journal, 310(6979), 565-567.

Langwieder, K., Sporner, A., & Hell, W. (1994). *Struktur der Unfälle mit Getöteten auf Autobahnen im Freistaat Bayern im Jahr 1991.* München: HUK-Verband, Büro für Kfz-Technik.

National Highway Traffic Safety Administration (2010). *Traffic Safety Facts: Distracted Driving 2009.* Washington, DC: NHTSA's National Center for Statistics and Analysis.

Platho, C., Pietrek, A., & Kolrep, H. (2013). *Erfassung der Fahrermüdigkeit.* Berlin: Bundesanstalt für Straßenwesen.

Royal, D. (2002). *National Survey of Distracted and Drowsy Driving Attitudes and Behavior.* Washington, DC: National Highway Traffic Safety Administration, 1.

Wang, J.-S., Knipling, R. R., & Goodman, M. J. (1996). *The Role of Driver Inattention in Crashes; New Statistics from the 1995 Crashworthiness Data System.* 40th Annual Proceedings of the Association for the Advancement of Automotive Medicine, Vancouver.

**Determination of Pedestrian Mannequin Clothing Color for the Evaluation of Image Recognition Performance of Pedestrian Pre-Collision Systems**

**Libo Dong, Stanley Chien, Kai Yang, Yaobin Chen**
Transportation Active Safety Institute, Indiana University-Purdue University Indianapolis, USA

**David Good**
Transportation Research Center, Indiana University, USA

**Rini Sherony**
Toyota Motor Engineering & Manufacturing North America, Inc. USA

**Hiroyuki Takahashi**
Toyota Motor Corporation, Japan

**Keyword**: Pre-collision systems, PCS mannequin, cloth color

Paper Number 15-0227

## ABSTRACT

Pedestrian Pre-Collision Systems (PPCS) for helping avoid or mitigate pedestrian crashes have been equipped on many vehicles [1]. At present, there is no common standard for the performance evaluation of PPCSs. The Transportation Active Safety Institute (TASI) at Indiana University-Purdue University-Indianapolis with support from Toyota's Collaborative Safety Research Center (CSRC) has been studying the various issues to support the effort of developing such a standard. An important component in the PPCS evaluation is the development of a standard mannequin. This paper describes the approaches used to determine the color of the clothing on the mannequins based on the data obtained from the TASI 110 car one year naturalistic driving data collected in the greater Indianapolis area in USA.

## 1. Introduction

Pedestrian Pre-Collison System (PPCS) is an active safety system component to help avoid or mitigate the collision with pedestrians [1]. Many automotive companies have been developing PPCSs and have started to equip them in their vehicles [2]. The performance of different PPCS systems varies significantly. Many research groups and government agencies are actively studying various methods for the evaluation of PPCSs [3]. At present, there is no common evaluation standard for PPCS. The Transportation Active Safety Institute (TASI) at Indiana University-Purdue University-Indianapolis has been conducting research related to the establishment of such a standard with the support from Toyota Collaborative Safety Research Center (CSRC). Many PPCS use mono or stereo cameras for pedestrian detection which is an important part of the PPCS. One factor that may significantly affect the performance of the pedestrian detection is the color of the clothing worn by the mannequins. In order to define testing scenarios for evaluating and comparing PPCS systems, representative clothing colors for both adult and children needs to be selected to dress the dummies used in PPCS testing. This paper describes a method for determining the clothing colors for adult and child mannequins in the United States for PPCS evaluation based on pedestrian cloth color data obtained from the TASI 110 car one year naturalistic driving study.

The paper is organized as follows. Section 2 describes the process of getting the pedestrian upper and lower cloth colors. Section 3 explains the process of dividing the color space into color regions and selecting the representative color. Sections 4 and 5 are discussion and conclusion, respectively.

## 2. Pedestrian cloth color data collection and preprocessing

Many PPCS use mono or stereo cameras for pedestrian detection. One factor that may significantly affect the effectiveness of a PPCS is the color of the clothing worn by the pedestrians. In order to define testing scenarios for evaluating and comparing the PPCSs, representative clothing colors for both adult and children need to be selected for the performance evaluation. The color of the mannequin's clothing is one of the many variables that can affect

the performance of PPCSs. To limit the number of tests needed for PPCS performance evaluation, it is imperative to select a standard color of clothing that represents US adult pedestrians and a standard color of clothing that represents US children pedestrians. This problem involves two issues, the first is to get the data and d3escribe the pedestrians clothing color distributions, and the second is to choose specific representative colors.

From 2012 to 2013, TASI equipped 110 cars with systems capable of recording naturalistic driving data, and collected naturalistic driving data in the greater Indianapolis Indiana USA area. The purpose was to study the pedestrian behaviors in various conditions. An HD CMOS camera with GPS and G-sensor was installed on each vehicle to gather video of what the driver would see out of the front windshield. Each car collected video data for one year amounting to 100 TB of video data. 60,000 Pedestrians were identified in the video, then the clothing colors of the pedestrians were recorded by choosing one point on the pedestrian's upper body and one point at pedestrian's lower body. The RGB values at these points were recorded.

By examining the clothing colors on the pedestrian images, it was noticed that the color of the clothing is not only affected by the fabric itself, but also affected by brightness of the environment. The same clothing appears darker in a darker environment. The brightness of the environment is affected by weather, the time of the day, and the shade under a tree or building. Since these factors are controllable in the PPCS testing, only the true colors of the clothes is useful for this study. Therefore, around 8,439 pedestrian videos were manually selected from the 60,000 pedestrians such that the pedestrians in the frame were well lit by sun light during clear weather and not under any shade. Then, RGB values of the upper clothes and lower clothes were extracted.

The upper clothing colors of adult pedestrians are shown in a 3d RGB gamut space (Figure 1). The RGB gamut space is modeled as a cube with three axes Red, Blue and Green. The value range of each axis is normalized between 0 and 1. Black is at the corner of the cube that all R, G, B values are zero and white is at the opposite corner with all RGB values equal to 1. Each black dot on the diagram represents the cloth color of a pedestrian.

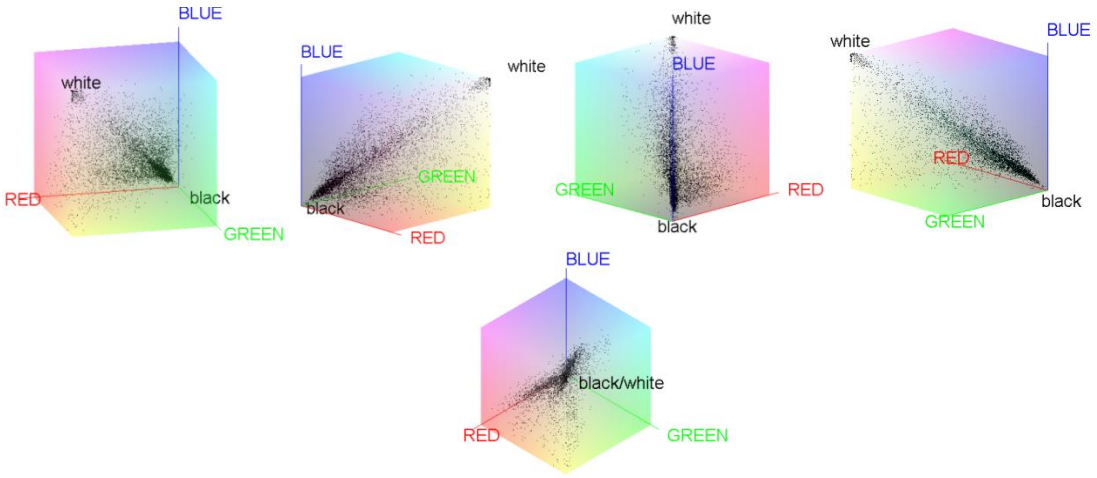


*Figure 1. The colors of the top cloth of adult pedestrians plotted in five viewing angles in the RGB space.*

These 3d gamut diagrams show that (1) the adult upper clothing colors are concentrated around the diagonal from the black to white axis, and (2) the colors tend to have a larger variance (span) on the axis when moving from black to white (This is reasonable due to Webber's law [4]).

### 3. Selection of the representative colors

The first approach for selecting the representative color is to find a color that has minimum sum of the mean square error to all the color points in the pedestrian cloth color poll. However, due to the shape of the distribution of the

pedestrian's cloth value, the resulting color is between gray and black for upper and lower cloths of both adults and children. It is concluded that this approach is not optimal.

The second approach is to divide the 3D space into seven color regions and the find which regions cover the most number of pedestrians. The seven regions are black-white, red, red-green, green, green-blue, blue, and blue-red. The boundaries of the seven color regions are determined according to the ratio of the two adjacent color values, as described as follows,

Black/White region: $(R/B \leq 1+\Delta)$ && $(B/R \leq 1+\Delta)$ && $(B/G \leq 1+\Delta)$ &&
$(G/B \leq 1+\Delta)$ && $(R/G \leq 1+\Delta)$ && $(G/R \leq 1+\Delta)$

Red region: $((R+G)/2 \geq B)$ && $((R+B)/2 \geq G)$ && $((R/G > 1+\Delta) \,||\, (R/B > 1+\Delta))$
Blue region: $((B+R)/2 \geq G)$ && $((B+G)/2 \geq R)$ && $((B/R > 1+\Delta) \,||\, (B/G > 1+\Delta))$
Green region: $((G+B)/2 \geq R)$ && $((G+R)/2 \geq B)$ && $((G/B > 1+\Delta) \,||\, (G/R > 1+\Delta))$

Magenta region: $((R+G)/2 < B)$ && $((G+B)/2<R)$ && $((R/G > 1+\Delta) \,||\, (B/G > 1+\Delta))$
Cyan region: $((B+R)/2 < G)$ && $((R+G)/2<B)$ && $((B/R > 1+\Delta) \,||\, (G/R > 1+\Delta))$
Yellow region: $((G+B)/2 < R)$ && $((B+R)/2<G)$ && $((G/B > 1+\Delta) \,||\, (R/B > 1+\Delta))$

Where $\Delta$ defines the boundaries of the black-white region around the black-white diagonal line. The value of $\Delta$ is chosen as between 0.1 and 0.2. These seven regions are shown in Figure 2.

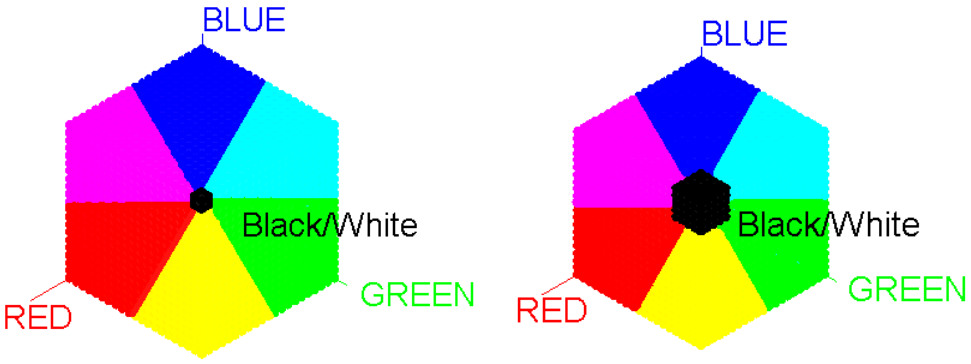


*Figure 2. Seven color regions. (Left: $\Delta$ = 0.1; Right: $\Delta$ = 0.3)*

To be able to distinguish the shade of the color, each of these seven regions is divided into 3 sub regions according to the color intensity. The intensity division is based on the following method,

Dark shade: $(R \leq 1/3)$ && $(G \leq 1/3)$ && $(B \leq 1/3)$
Medium shade: $(1/3 < R \leq 2/3)$ && $(1/3 < G \leq 2/3)$ && $(1/3 < G \leq 2/3)$
Light shade: $(R > 2/3)$ && $(G > 2/3)$ && $(G > 2/3)$

An example of 3 shades within the white-black region is shown in Figure 3. Therefore, a total of 21 non-overlapping regions completely cover the 3D color space is generated (Figure 4).

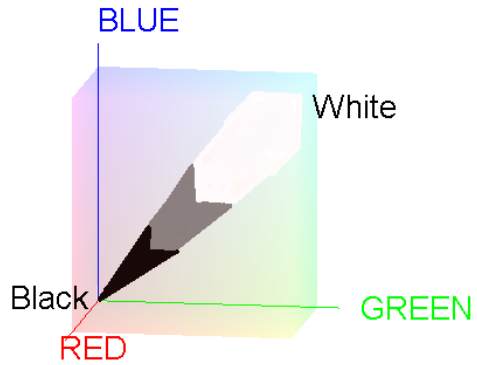


*Figure 3. An example of 3 color shades in a region.*

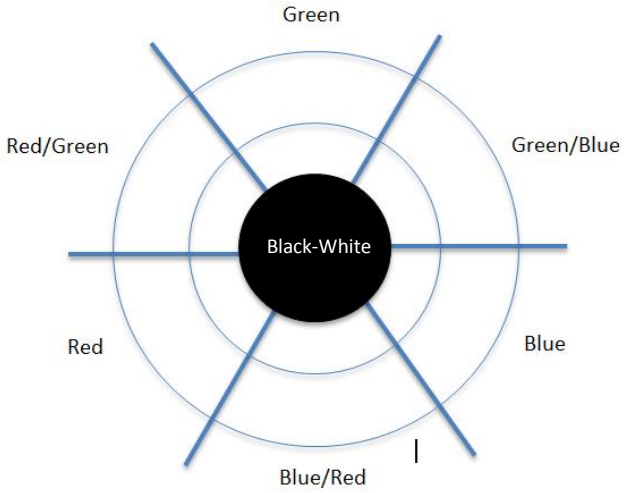


*Figure 4. 21 color regions in the color space. The Black-White regions are divided in the axis perpendicular to the figure.*

In order to illustrate the distribution for clothing colors in a visual friendly way, a chromaticity diagram is introduced. A chromaticity diagram can define the hue and colorfulness [5] [6] regardless of its luminance by compressing its luminance information to 2-dimentions. In this method, the luminance is less important than hue since the frame selected guarantees that colors can be interpreted correctly. The 2D chromaticity diagram source code is inspired from ECE 637 from Professor Bouman, Purdue University [7].The outer red line of the chromaticity diagram represent all the color that human can perceive [8], the CIE 1931 standard and Rec.709 standard are part of all perceivable color.

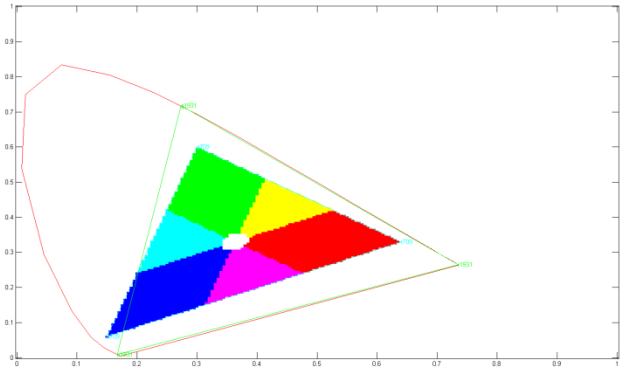

*Figure 5. 2D chromaticity diagram of the color of children upper cloths.*

## A. Adult upper cloth color

The number of the adult upper cloth and lower cloth in each color region is shown in Figure 6 and 7, respectively. The three numbers in the parentheses are the average RGB values of clothing colors in that region, respectively.

When Δ=0.1, dark/medium red, dark red/blue, and dark/medium blue are the most popular colors for adult upper cloth (see Figure 6a). Since there are more than one basic color region included, the color population in Δ=0.2 cases are checked. When Δ is increased to 0.2, a significant number of upper cloth from dark red, dark red/blue, and dark blue regions is moved to dark black-white region so that black becomes the dominate population(see Figure 6(b)). Therefore, the black color (RGB = 43, 41, 44) is selected as the adult upper cloth color. The corresponding point is shown as a black dot in Figure 6(c).

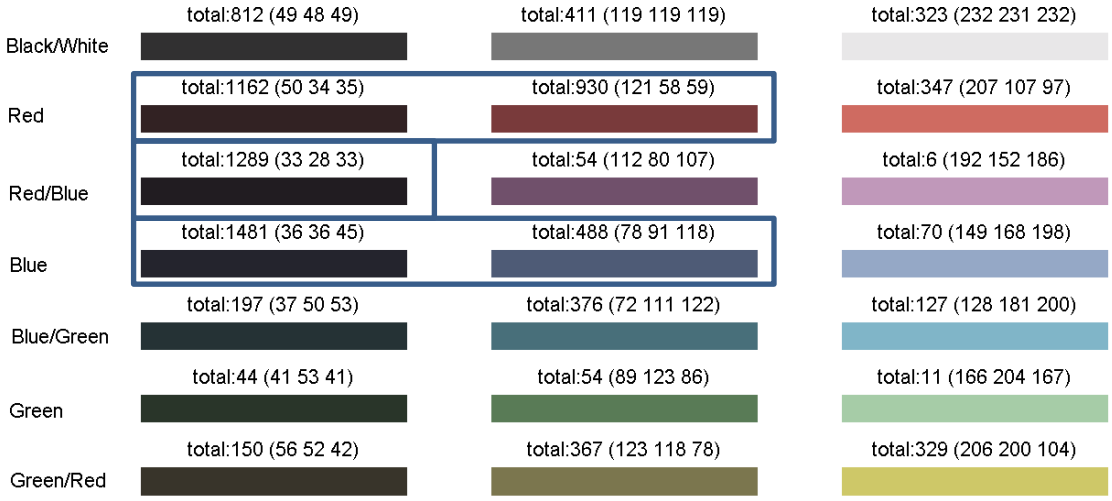


*(a) Adult upper cloth. Δ = 0.1*

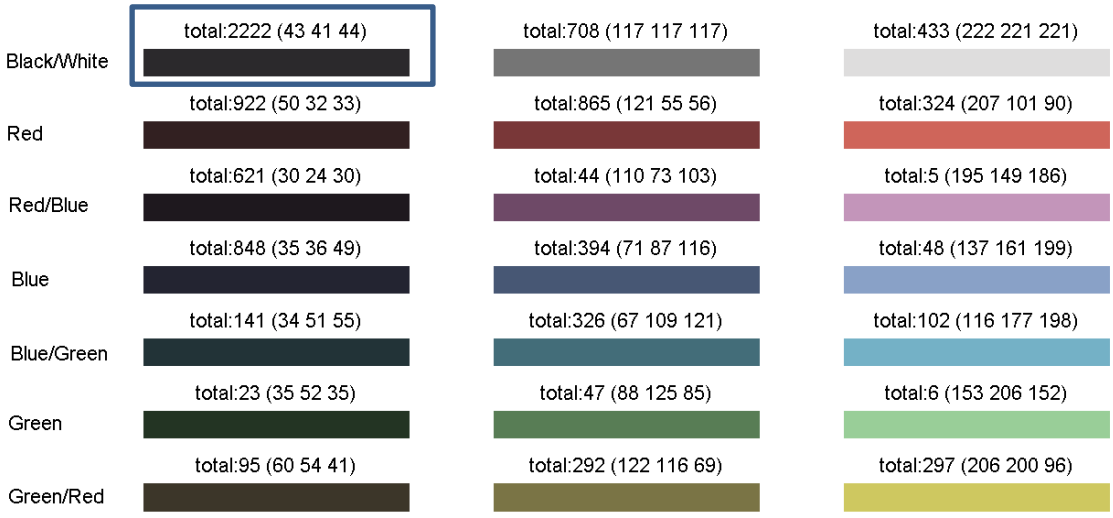


*(b) Adult upper cloth. Δ= 0.2*

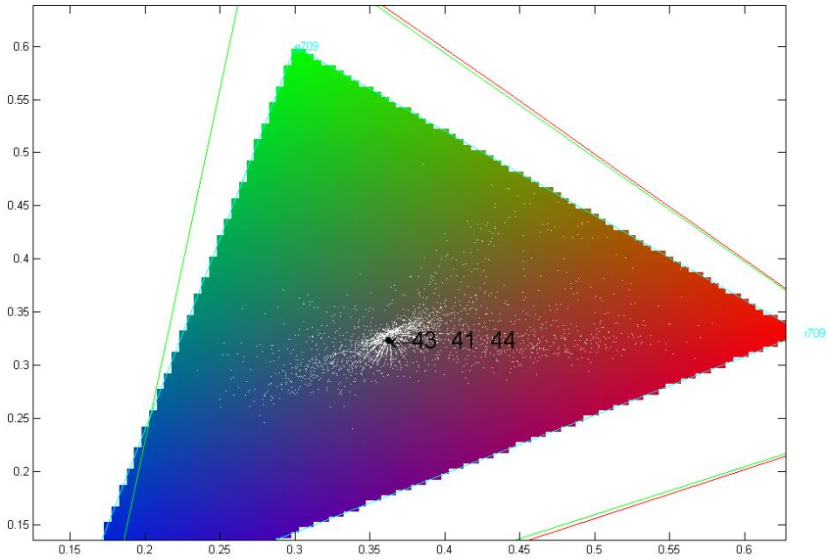


*(c) 2D chromaticity diagram of the color of adult upper cloths. Black dot shows the selected color.*

*Figure 6. The selection of the mostly wore adult upper cloth color based on TASI 110 car naturalistic driving data.*

## B. Adult lower cloth color

The number of adult lower clothing colors in each color region is shown in Figure 7. When Δ=0.1, dark blue (43, 44, 53) is significantly more favorable than other colors. Therefore, dark blue color (RGB= 43, 44, 53) is selected for adult lower cloth color. The corresponding point is shown as a black dot in Figure 7(c).

| | | | |
|---|---|---|---|
| Black/White | total:47 (52 52 53) | total:66 (119 120 119) | total:30 (212 210 207) |
| Red | total:32 (47 38 37) | total:38 (119 84 81) | total:13 (218 177 163) |
| Red/Blue | total:50 (37 32 38) | total:3 (116 70 95) | total:0 (200 69 200) |
| Blue | total:89 (43 44 53) | total:36 (83 96 115) | total:8 (142 155 180) |
| Blue/Green | total:23 (48 56 62) | total:68 (90 110 121) | total:9 (156 183 198) |
| Green | total:1 (50 54 49) | total:0 (54 136 54) | total:0 (88 219 88) |
| Green/Red | total:8 (60 56 47) | total:39 (133 122 99) | total:26 (204 188 159) |

*(a) Adult lower part Δ= 0.1*

*(b) Adult lower part Δ= 0.2*

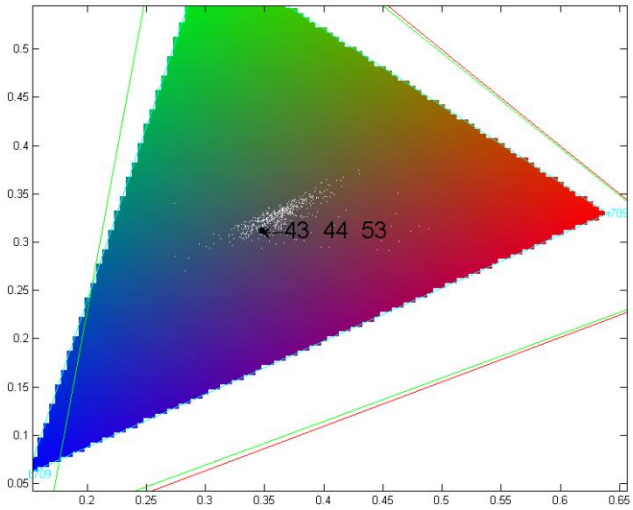


*(c) 2D chromaticity diagram of the color of adult lower cloths. Black dot shows the selected color.*

*Figure 7. The selection of the mostly wore adult lower cloth color based on TASI 110 car naturalistic driving data.*

## C. Child upper cloth color

The number of the child upper cloth colors in each color region is shown in Figures 8. When Δ=0.1, dark/medium red, dark red/blue, and dark/medium blue were the most popular colors for adult upper clothing. Since there is more than one pure color region having high population, the color population in Δ=0.2 cases is checked. When Δ is increased to 0.2, a significant number of the population from dark red, dark red/blue, and dark blue regions are moved to dark black-white region so that black becomes the dominate population. Therefore, the black color (RGB = 48, 46, 48) is selected as the child upper clothing color. The corresponding point is shown as a black dot in Figure 8(c).

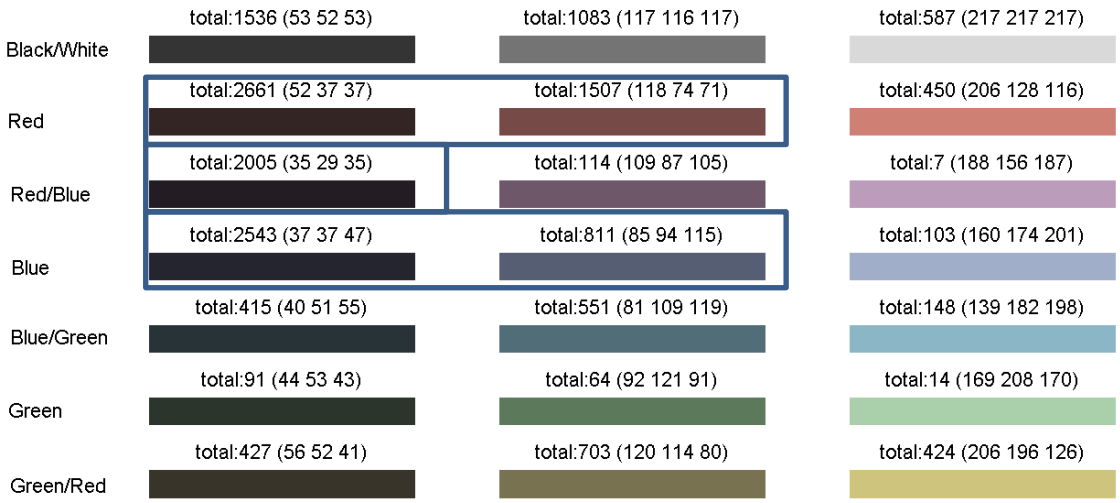


*(a) Children upper cloth. part* $\Delta = 0.1$

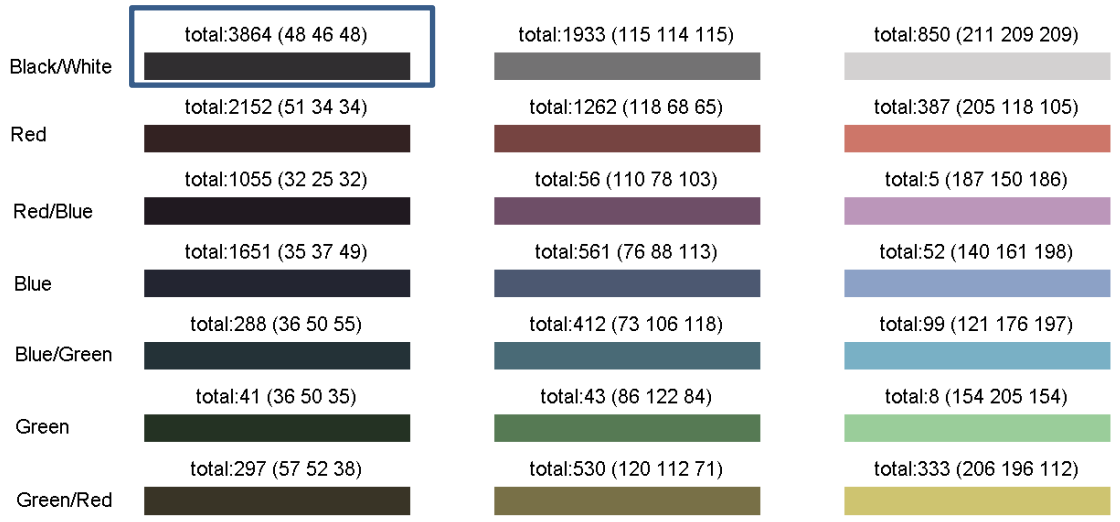


*(b) Children upper cloth.* $\Delta = 0.2$

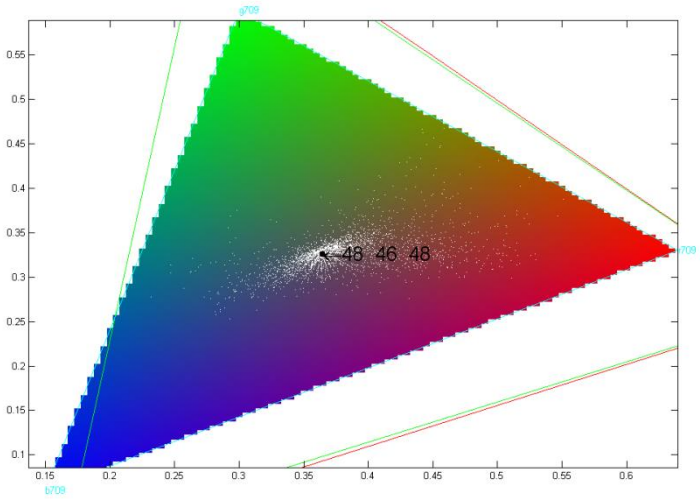


*(c) 2D chromaticity diagram of the color of child upper cloths. Black dot shows the selected color.*

*Figure 8. The selection of the mostly wore children upper cloth color based on TASI 110 car naturalistic driving data.*

### D. Chile lower cloth color

The number of the child lower clothing colors in each color region is shown in Figure 9. Since there are close counts in the dark blue and medium blue regions, the average color (65, 71, 88) of these two blue shades is selected to represent the child lower cloth color. The corresponding point is shown as a black dot in Figure 9(c).

| | | | |
|---|---|---|---|
| Black/White | total:13 (56 56 57) | total:14 (115 116 117) | total:14 (229 227 229) |
| Red | total:10 (56 43 42) | total:18 (117 79 82) | total:14 (210 149 142) |
| Red/Blue | total:16 (41 36 41) | total:1 (134 116 131) | total:0 (200 69 200) |
| Blue | total:33 (41 43 54) | total:34 (89 99 121) | total:1 (224 229 248) |
| Blue/Green | total:3 (55 64 69) | total:9 (95 110 120) | total:2 (109 191 203) |
| Green | total:0 (25 63 25) | total:0 (54 136 54) | total:0 (88 219 88) |
| Green/Red | total:3 (75 72 60) | total:12 (127 115 92) | total:7 (197 177 150) |

*(a) Children lower part Δ= 0.1*

*(b) Children lower part Δ= 0.2*

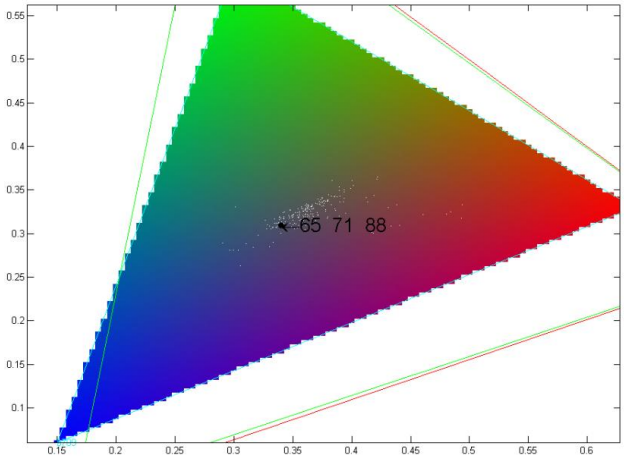


*(c) 2D chromaticity diagram of the color of child lower cloths. Black dot shows the selected color.*

*Figure 10. The selection of the mostly representative child lower cloth color based on TASI 110 car naturalistic driving data*

**Summary of cloth colors**

The representative the upper cloth color for adult is black (RGB=43, 41, 44)
The representative the lower cloth color for adult is deep dark blue (RGB=43, 44, 53)
The representative the upper cloth color for children is black (RGB=48, 46, 48)
The representative of the lower cloth color for children is medium blue. (RGB=65, 71, 88)

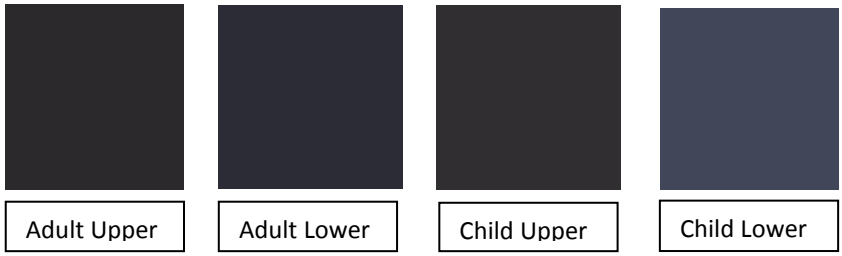


*Figure 11. The representation of upper/lower adult and upper/lower children cloth color from left to right.*

## 4. Discussion

The goal in this paper is to select one set of colors for dressing the mannequins for PPCS evaluation. The proposed method is to determine the color based on the popularity of the colors seen from video cameras. It is well known that lighting affects the perceived color. Even through the data preparation tried to remove the lighting influences, the color seen in the image are still darker than the original color. There are other possible ways to consider the clothing color, such as contrast to the background. Contrast base study is currently ongoing and will be reported in the future.

## 5. Conclusion

A method for finding the representing upper and lower clothing colors for both child and adult mannequins is described in this paper. The paper is based on the pedestrian data collected from TASI 110 car one year naturalistic driving in Greater Indianapolis area in USA. This data can be considered as an accurate representation for the whole Midwest region in USA. The method can be applied to additional pedestrian clothing color data from other naturalistic driving studies.

## Acknowledgments

This project is sponsored by Toyota's Collaborative Safety Research Center

## References

[1] Toyota, "Pre crash," Toyota, 16 Feb 2015. [Online]. Available: http://www.toyota-global.com/innovation/safety_technology/safety_technology/technology_file/pre_crash/.

[2] Dailmer, "PRE-SAFE® Brake: The Anticipatory Brake," Dailmer, 16 Feb 2015 . [Online]. Available: http://www.daimler.com/dccom/0-5-1210220-1-1210348-1-0-0-1210338-0-0-135-0-0-0-0-0-0-0-0.html.

[3] NHTSA, "Objective Tests for Automatic Crash Imminent Braking (CIB) Systems," NHTSA, Washington,DC, 2011.

[4] E.H.Weber, E.H.Weber on the tactile senses, Erlbaum (UK): Taylor & Francis, 1996.

[5] E. Wolf, Progress in Optics, Volume 1, North-Holland Publishing Company, 1966.

[6] CIE, "Commission internationale de l'Eclairage proceedings," Cambridge: Cambridge University Press, 1931.

[7] C. A. Bouman, "Image Processing Laboratories," 11 May 2011. [Online]. Available: https://engineering.purdue.edu/~bouman/grad-labs/Colorimetry/pdf/lab.pdf.

[8] G. W. a. W. S. Stiles, Color Science: Concepts and Methods, Quantitative Data and Formulas, London: John Wiley & Sons, Inc., 1967.

# CONSUMER SAFETY INFORMATION PROGRAMS AT IIHS

**David Zuby**
Insurance Institute for Highway Safety
United States

Paper Number 15-0228

## ABSTRACT

Since 1969, when the Insurance Institute for Highway Safety (IIHS) began publishing results of low-speed crash tests to highlight differences in vehicle bumpers, it has been a significant source of information about how the safety of different vehicle designs varies. Currently, IIHS maintains crashworthiness ratings covering five crash modes along with ratings of front crash prevention (FCP) systems and children's booster seats, as well as annual updates of insurance loss reports from its affiliate, the Highway Loss Data Institute (HLDI).

This report describes the experience with IIHS's latest consumer information efforts and identifies the next areas of consumer information to come online. It presents information about the number of vehicle models and booster seats evaluated; their ratings assigned as well as media, consumer, and manufacturer response; and small overlap crashworthiness and FCP ratings. Research underpinning future rating programs addressing Lower Anchors and Tethers for Children (LATCH) and advanced head lighting systems also is summarized.

Since launching its booster seat ratings, IIHS has evaluated 200 designs for their ability to adjust rear seat belt fit to booster-age children across a wide variety of rear seat belt configurations. The number of models rated Best Bet, indicating they will provide good belt fit in common passenger vehicles, has increased from a low of 10 in 2008 to 69 in 2014. Media coverage of these annual ratings announcements is estimated to average an audience of 88 million people in the United States. IIHS internet pages with booster ratings are among the most viewed, with an average of 102,800 page views monthly.

IIHS began rating vehicle front crashworthiness on the basis of a 64 km/h small overlap crash against a rigid barrier in 2012. Of the 118 currently rated 2015 models, 49 are good, 25 acceptable, 23 marginal, and 21 poor. Several models have been tested in two design iterations with improved performance in the second test, indicating automakers are able to design vehicles to better protect occupants in similar crashes. It is estimated that the media coverage across all small overlap ratings announcements has achieved 1.1 billion views. Surveys of automobile dealers indicate that good ratings in this test have led to increased sales, at least in the short term.

IIHS ratings of vehicle FCP systems include both warning and autobraking functions. The proportion of new models available with FCP of any kind has increased from 30 to 60 percent. The combined media coverage of three announcements featuring FCP ratings were viewed 212 million times. While not as strong as for crash test ratings, there was indication that these announcements positively affected sales of vehicles with these systems.

Large audiences for IIHS consumer information programs have prompted manufacturers of rated products to make changes in ways indicated by IIHS tests. Based on this experience with current programs, there is good reason to believe that IIHS ratings of LATCH and advanced head lighting systems can also improve vehicle safety.

## INTRODUCTION

The Insurance Institute for Highway Safety (IIHS) was founded in 1959 as a nonprofit research and communications organization. Its mission is to conduct and publish research that will lead to the reduction of deaths, injuries, and property damage associated with crashes on roads in the United States of America. One of the ways in which IIHS uses its research to motivate improvements in vehicle designs has been through consumer information programs that

highlight differences in safety among different vehicles. The most recognizable form of such programs are crashworthiness ratings based on crash tests, the first of which were published by the New Car Assessment Program of the U.S. Department of Transportation [1]. However, such consumer information can take other forms such as the publication of insurance losses by make and model, which have been produced by IIHS affiliate the Highway Loss Data Institute (HLDI) since 1973 [2]. More recently, IIHS has applied the consumer information model to motivate improvements to child restraint systems and commercial truck underride guards.

IIHS's first foray into providing information about crash differences among contemporary vehicle models was bumper tests in 1969, which ultimately led to regulatory bumper performance requirements. In 1972, HLDI was formed to examine highway safety issues through analysis of insurance loss data provided by a subset of IIHS sponsors. The compilation of data from the largest insurers in the United States allows HLDI analyses to ascertain the model-specific contribution to losses under different types of insurance coverage. HLDI has published annual comparisons of losses by make and model since 1973. While not fully explaining the differences in insurance costs paid by different insurance customers, these analyses partly explain the differences an individual will pay depending on the model insured. Results are published on a scale that relates the insurance experience of a specific model to the average for all contemporary passenger vehicles. This type of information was considered so important to consumers that the Motor Vehicle Information and Cost Savings Act of 1972 required the U.S. Department of Transportation to devise a means of distributing it wherever new vehicles were sold [3]. From 1993 until 2013, when the availability of information via the internet obviated the need for auto dealers to keep printed brochures on hand, HLDI's data have helped the National Highway Traffic Safety Administration fulfill this requirement [4].

Since 1995, IIHS has created a rigorous program of crash test ratings that have led to measureable improvements in the crash protection offered by modern vehicles. Its first crash rating program involved front crashes at 64 km/h with a 40 percent overlap against a deformable barrier. Test results are graded on a scale of good, acceptable, marginal, and poor to reflect the relative protection for occupants exposed to similar crashes. The ratings are based not only on measurements made by sensors in the test dummy but also on analysis of the dummy's observable motion and measurements of safety cage deformation. Figure 1 illustrates the increasing availability of good-rated vehicles across model years, and these improvements have been associated with a lower risk of death in front crashes [5].

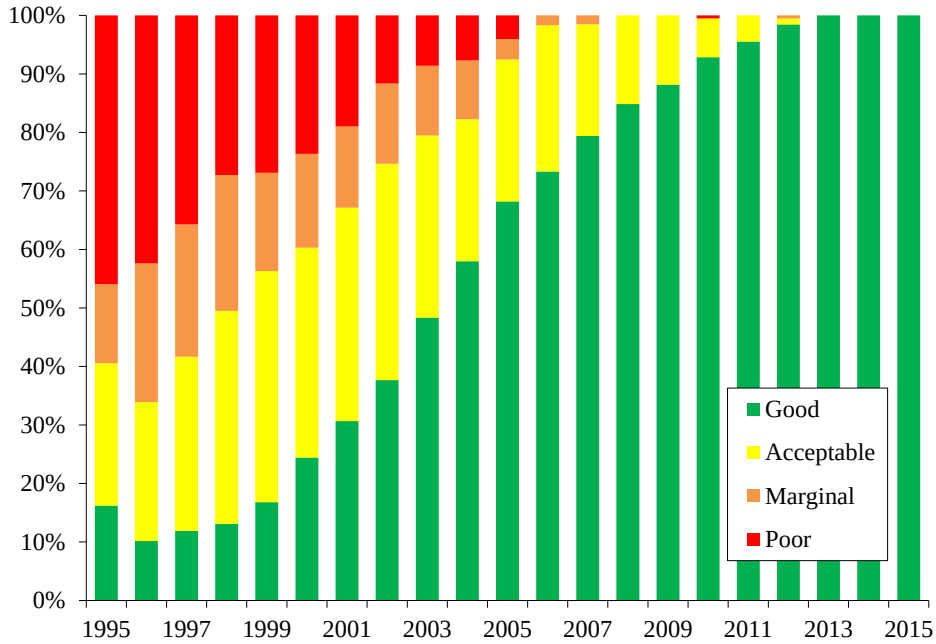


***Figure 1. IIHS moderate front overlap crash test ratings by model year.***

The IIHS crashworthiness program currently consists of five tests, all using the poor-to-good scale of ratings: two front (moderate and small overlap impacts at 64 km/h), a side impact at 50 km/h, a quasi-static test of roof strength, and a simulated rear crash used to evaluate the ability of vehicle seats and head restraints to mitigate neck injury. Like IIHS's original front crash test, the side and rear crashworthiness evaluations have resulted in measurable changes in the likelihood that vehicle occupants will be injured or killed in crashes represented by the corresponding evaluation [6][7]. The roof strength test was initiated based on research establishing the protective effect of strong roofs in rollover crashes [8][9]. All of these programs have led to meaningful improvements in the safety of the U.S. passenger vehicle fleet.

IIHS *Top Safety Pick* awards were launched in 2005 to recognize those 2006 model year designs that offered the highest levels of crash protection, as indicated in IIHS tests. In addition to rewarding automakers whose products offer the highest level of safety, the rewards also generate a single list of recommendations to consumers. The annual announcement of these ratings is widely covered by the U.S. news media. Table 1 shows the number of times an IIHS-produced video was broadcast for each of the *Top Safety Pick* announcements since 2006, along with the estimated size of the audience that saw those broadcasts. Also, automakers increasingly use *Top Safety Pick* claims in their advertising, as Table 2 attests. Public attention to this award amplifies the incentive for automakers to improve the safety of their products.

**Table 1.**
**Number of television broadcasts and estimated audience for IIHS *Top Safety Pick* announcements.**

| Award year | Number of broadcasts | Estimated audience (millions) |
|---|---|---|
| 2006 | 1,123 | 95.0 |
| 2007 | 1,365 | 102.3 |
| 2008 | 1,051 | 100.0 |
| 2009 | 1,880 | 115.1 |
| 2010 | 2,580 | 149.4 |
| 2011 | 2,052 | 114.2 |
| 2012 | 637 | 41.3 |
| 2013 | 1,262 | 155.5 |
| 2014 | 856 | 74.8 |
| 2015 | 1,083 | 76.7 |

**Table 2.**
**Number of requests to approve *Top Safety Pick* advertising claims.**

| Award year | Advertising approval requests |
|---|---|
| 2006 | 218 |
| 2007 | 288 |
| 2008 | 361 |
| 2009 | 328 |
| 2010 | 341 |
| 2011 | 646 |
| 2012 | 635 |
| 2013 | 573 |
| 2014 | 614 |

The criteria for earning *Top Safety Pick* was made more stringent twice between its introduction and 2012. The *Top Safety Pick+* was introduced in 2014 as a type of "soft landing" for the introduction of new front crashworthiness requirements. Designs that met the previous year's criteria kept their *Top Safety Pick* accolades, but an acceptable or good rating in the new test was required to earn the new award. Table 3 shows the criteria for *Top Safety Pick* and *Top Safety Pick+* awards during their history. For the foreseeable future, *Top Safety Pick+* will continue to be the way to identify IIHS's latest safety recommendations.

Ratings of small overlap front crashworthiness and front crash prevention systems are the latest additions to IIHS consumer information programs encompassed by *Top Safety Pick.* Also, IIHS has rated belt-positioning booster seats for children since 2009 and has published a one-time comparison of commercial truck underride guards. Evaluations for vehicle LATCH (Lower Anchors and Tethers for Children) and advanced headlights are also being developed. The remainder of this paper describes these programs and the safety improvements they have compelled or intend to once launched.

**Table 3.**
**IIHS *Top Safety Pick* criteria, 2006-15.**

| Award year | Moderate overlap front crash | Side impact | Rear crash | Electronic stability control | Roof strength | Small overlap front crash | Front crash prevention |
|---|---|---|---|---|---|---|---|
| 2006 | Good | Good | Good or acceptable | | | | |
| 2007 | Good | Good | Good | Available | | | |
| 2008 | Good | Good | Good | Available | | | |
| 2009 | Good | Good | Good | Available | | | |
| 2010 | Good | Good | Good | Available | Good | | |
| 2011 | Good | Good | Good | Available | Good | | |
| 2012 | Good | Good | Good | * | Good | | |
| 2013 | Good | Good | Good | | Good | Acceptable | |
| *TSP+* | Good | Good | Good | | Good | Good | |
| 2014 | Good | Good | Good | | Good | Good or acceptable | |
| *TSP+* | Good | Good | Good | | Good | Good or acceptable | Basic or better |
| 2015 | Good | Good | Good | | Good | Good or acceptable | |
| *TSP+* | Good | Good | Good | | Good | Good or acceptable | Advanced or better |

*TSP+ = Top Safety Pick+*
*Electronic stability control became required by regulation beginning September 1, 2011

## LATEST CONSUMER INFORMATION PROGRAMS

### Booster Seat Belt Fit Ratings

Booster seats are intended to improve the fit of vehicle seat belts for children who have outgrown child restraint systems with internal harnesses and that are anchored to the vehicle with the seat belts or dedicated attachments. The simplest boosters are cushions that raise the child above the vehicle seating surface such that the lap belt crosses the bony pelvis and the shoulder belt does not interfere with the neck or face. This improves the comfort for young vehicle occupants and, more important, helps the seat belts restrain them more effectively in a crash. Children riding in boosters are much less likely to be injured in a crash than children secured by vehicle seat belts alone [10].

Due to the variation in rear seating areas of modern vehicles and the variety of booster seat configurations, some combinations do not result in good belt fit for some children. This complication leads to a high rate of booster misuse in the field [11]. To address this problem, IIHS researchers worked with the University of Michigan Transportation Research Institute (UMTRI) to develop a method for evaluating which booster seat designs provide the best belt fit across a range of vehicles [12]. The evaluation uses a 6-year-old Hybrid III dummy to represent the relevant child population. The dummy is seated on each booster, which is installed on a test fixture representing a rear seat with variable seat belt anchor positions. Both lap and shoulder belt positions on the dummy are recorded for four seat belt anchor configurations representing the variation in the modern vehicle fleet. Boosters that provide ideal fit — lap belt lying flat on the thighs and close to the hip with the shoulder belt crossing the middle of the sternum — in all four configurations are rated Best Bet, reflecting the notion that the design provides sufficient control of the belt routing that it would be expected to provide correct fit for all booster-age children in almost any vehicle. Boosters rated Good Bet also would be expected to provide no more than slight deviations from ideal fit in almost any vehicle. The Check Fit rating means that acceptable fit is possible for some, but not all, seat belt anchor configurations. Consumers are advised to check whether such boosters provide good belt routing for their children in the vehicles in which the boosters will be used. Seats rated Not Recommended fail to provide acceptable belt fit in any of the four tested belt anchor configurations.

The booster seat belt fit evaluations were first published in 2008 and have been repeated every year since. Among the 41 booster designs evaluated in the first year, 10 were rated Best Bet, 5 were Good Bet, and 13 were Not

Recommended. The rest were rated Check Fit. The availability of Best Bet boosters has increased in every update of the IIHS ratings, indicating that child restraint manufacturers are taking the rating guidance into account when developing new products. Figure 2 compares the current distribution of seat ratings with those from 2008. These improvements also have led to customer satisfaction for those boosters earning Best Bet ratings, as this email correspondence from Michael Noah, president of Harmony Juvenile Group, attests:

> I'm happy to report that over the past year many customers with some of our Best Bet boosters experienced only good outcomes from some pretty severe crashes. It is nice to know that the combination of technology in the seat design along with the good work that you do — truly leads to the outcomes we are all working towards.

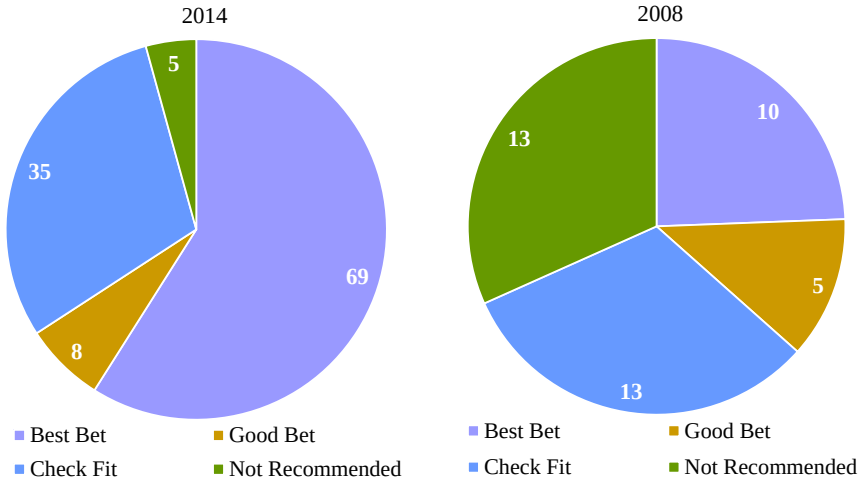


***Figure 2. IIHS Booster seat ratings published in 2014 compared with those published in 2008.***

The public is very much interested in information about child safety. The booster ratings pages of the IIHS internet website are among the most frequently visited, receiving an average of 102,800 page views monthly. Likewise, the television audiences for announcements of new booster ratings are regularly large. Table 4 shows the number of television broadcasts and estimated audience for each update of IIHS booster ratings.

**Table 4.**
**Number of television broadcasts and estimated audience for IIHS booster seat ratings announcements.**

| Award year | Number of broadcasts | Estimated audience (millions) |
|---|---|---|
| 2008 | 1,384 | 87.1 |
| 2009 | 3,669 | 182.9 |
| 2010 | 2,575 | 153.3 |
| 2011 | 739 | 44.5 |
| 2012 | 864 | 42.6 |
| 2013 | 1,452 | 53.7 |
| 2014 | 1,299 | 53 |

**Truck Underride Guards**

During the past 5 years, the number of passenger vehicle occupants killed each year in crashes with large trucks has averaged more the 2,400 in the United States. According to a 1997 study, about half of these deaths involve the passenger vehicle underriding some portion of the truck [13]. Approximately one-fifth of the underride deaths occur in crashes to the rear of the truck, despite requirements that many heavy trucks be equipped with underride prevention guards.

Research by IIHS identified the nature of underride guard failures, and testing showed there was a range of effectiveness among designs meeting U.S. regulatory requirements [14]. Specifically, two of the three tested guards prevented underride of a midsize car in full-overlap crash tests at 56 km/h, and only one prevented underride when overlap with the guard was reduced to 50 percent [15]. This research received moderate amount of media attention and was featured in 1,296 broadcasts with a total estimated audience of 64 million viewers.

Follow-up testing during 2012-13 involving truck trailers from the eight largest manufacturers in the U.S. market already showed improvements for the guards that performed least well in earlier testing [16]. All eight guards prevented underride in the full-overlap test, all but one prevented underride in the 50 percent overlap condition, and only one prevented underride when the overlap was reduced to 30 percent. This test program also received media attention and was featured in 811 broadcasts with a total estimated audience of 37 million viewers. This attention has resulted in six of the seven trailer manufacturers whose guards could not prevent underride in all three test conditions to report they are developing more effective guards. In 2014, one company, Vanguard, whose guard failed to prevent underride in the 50 percent overlap condition in both rounds of tests, tested an improved design at IIHS that successfully prevented underride in this condition. These observations suggest that comparative safety evaluations can be an effective means of stimulating improvements in the commercial fleets as it has for private passenger vehicles.

**Small Overlap Front Crashworthiness Ratings**

By the 2008 model year, 85 percent of passenger vehicles rated by IIHS earned good ratings in the moderate overlap front crash test and the remainder were rated acceptable, indicating the evaluation was no longer providing significant discriminating information to consumers nor spurring further improvements in front crashworthiness design. So IIHS researchers examined crashes of good-rated vehicles to ascertain whether further improvements in front crashworthiness were possible. This research focused on crashes resulting in serious injury or fatality and found that many had damage patterns indicating overlaps smaller than the 40 percent overlap of the crash tests [17]. In such crashes, the energy absorbing structures in the crush zones often were minimally damaged while the safety cages were severely collapsed. Crash testing showed that some vehicles provided better protection with less collapse of the safety cage than others in the same small overlap test configuration. This led to the development of IIHS's newest crash test evaluation, which involves crashing a vehicle at 64 km/h with 25 percent of its width overlapping a rigid barrier with a rounded edge (Figure 3).

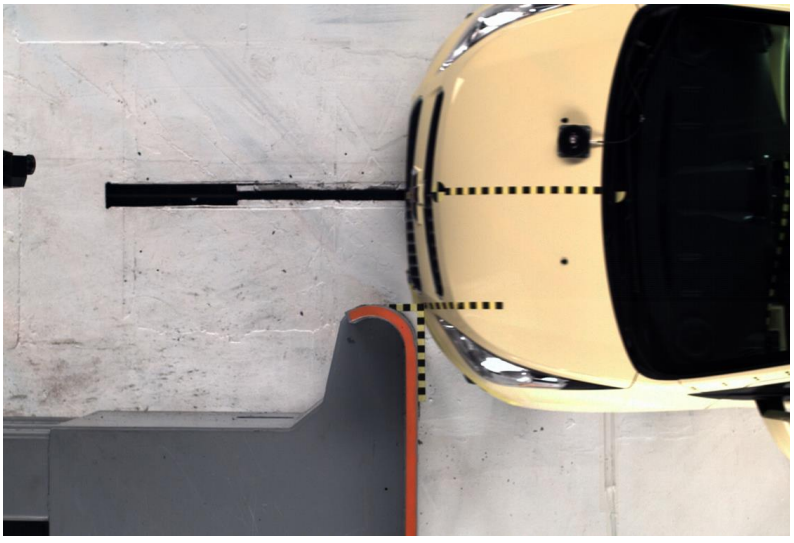

***Figure 3. Small overlap crash test configuration (overhead view at t = 0).***

Small overlap front crash test ratings of new vehicles were first published in August 2012. Eleven midsize luxury cars were tested, with two rated good, one acceptable, four marginal, and four poor. Since that time, 133 model designs have been evaluated in this test. Figure 4 shows an example the survival space difference for a vehicle rated good compared with one rated poor. In addition to structural differences, these tests also show differences in the ability of restraint systems to prevent impacts between the driver dummy's head and instrument panel (Figure 5). Figure 6 shows ratings in the small overlap front test by vehicle type for the 2015 model year. Eight models have been tested both before and after modifications or redesigns intended to improve front crashworthiness. All eight modifications/redesigns showed increased survival space compared with their predecessors, and six of the eight had improved overall ratings [18]. It is too early to know the extent to which such changes are affecting real crash outcomes.

These new crash test ratings received considerable news media and public attention (Table 5). In addition to traditional television news, IIHS's YouTube channel also attracted large numbers of viewers. Table 6 shows the number of views for the YouTube videos associated with each of the public releases of small overlap crash test ratings. The combined number of views for all small overlap crash test videos, including individual crash tests, exceeded 37 million as of mid-December 2014.

***Figure 4. Comparison of survival space in Mazda CX-9 (poor) and Chevrolet Equinox (good) following a 64 km/h 25 percent overlap crash against a rigid barrier.***

***Figure 5. Comparison of driver dummy motion during a 64 km/h 25 percent overlap crash against a rigid barrier.***

All of this attention to the new crash test ratings has also elevated consumer interest in vehicles earning good ratings, at least in the short term. Surveys of vehicle dealerships indicated that announcements of crash test ratings increased consumer interest in and sales of good-rated models in the week following ratings announcements compared with the week before [19]. Thus, it seems worth automakers' efforts to design their products to earn good crash test ratings.

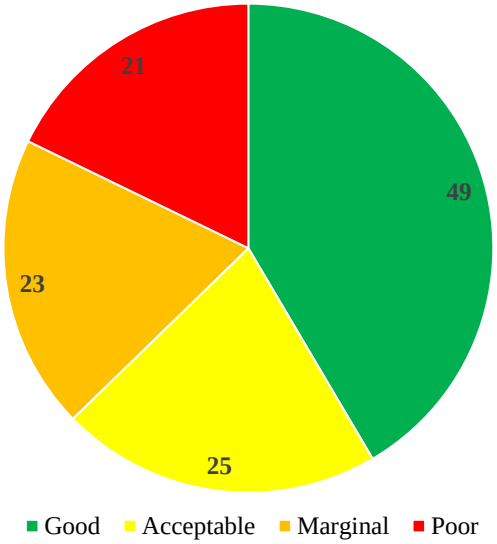


***Figure 6. Small overlap front crash test ratings for 2015 model year vehicles.***

**Table 5.**
**Number of television broadcasts and estimated audience for IIHS front small overlap crash test ratings announcements.**

| Date | Vehicle group | Number of broadcasts | Estimated audience (millions) |
|---|---|---|---|
| November 20, 2014 | Minivans | 1,905 | 129.2 |
| July 30, 2014 | Small cars 2 | 3,245 | 165.5 |
| April 8, 2014 | Midsize SUVs | 2,441 | 146.2 |
| January 22, 2014 | Minicars | 2,048 | 121.9 |
| August 8, 2013 | Small cars 1 | 1,129 | 110 |
| May 16, 2013 | Small SUVs | 790 | 63.4 |
| December 20, 2012 | Midsize non-luxury cars | 1,262 | 155.5 |
| August 14, 2012 | Midsize luxury cars | 2,751 | 212.3 |

**Table 6.**
**Number of views for IIHS small overlap crash test ratings news videos on YouTube, as of January 23, 2015.**

| Date | Vehicle group | Number of YouTube views |
|---|---|---|
| November 20, 2014 | Minivans | 209,845 |
| July 30, 2014 | Small cars 2 | 174,944 |
| April 8, 2014 | Midsize SUVs | 229,127 |
| January 22, 2014 | Minicars | 426,338 |
| August 8, 2013 | Small cars 1 | 179,066 |
| May 16, 2013 | Small SUVs | 235,290 |
| December 20, 2012 | Midsize non-luxury cars | 951,370 |
| August 14, 2012 | Midsize luxury cars | 816,218 |

**Front Crash Prevention Systems Ratings**

HLDI published a series of analyses using insurance data that evaluated the benefit of new crash avoidance technologies [20][21][22]. These analyses showed that all of the systems intended to help drivers avoid being in front-to-rear collisions were preventing some crashes reported to insurers. Vehicles with forward collision warning (FCW) from three automakers had 7-10 percent fewer liability claims for damage done to other vehicles and 4-7 percent fewer collision claims for own damage compared with the same year/make/models without FCW. The frequency of injury claims also was reduced. The results for automatic braking systems were even better. Volvo vehicles with City Safety (a standard feature) have 15 percent fewer liability claims and 18 percent fewer collision claims than their market competitors without automatic braking systems, and injury claims are reduced by more than 25 percent. Similarly, optional automatic braking systems from four different automakers also reduce liability claims compared with their counterparts without it. There is an indication that own damage and injury claims also are reduced with these systems, but the confidence intervals for the estimated reductions are large.

Based on these crash and injury reductions and consistency across different automakers' implementations of FCP systems, IIHS began rating them in 2013. The ratings — basic, advanced, and superior — are intended to reflect the level of benefit consumers could expect from systems with different characteristics. The basic level is intended to identify models available with FCW, although it is possible to earn the basic rating with automatic braking that produces small speed reductions in one of two simulated front-to-rear crashes. The FCW performance requirements are the same as those that the National Highway Traffic Safety Administration uses to identify FCW in its New Car Assessment Program. The advanced rating is intended to represent models with the availability of automatic braking systems similar to Volvo's City Safety or the optional systems studied by HLDI. Typically this requires collision prevention or near prevention through automatic braking in one of two simulated front-to-rear collisions at 20 and 40 km/h. However, it is possible to earn the advanced rating with moderate speed reductions in both tests. Models that combine FCW with automatic braking earn more points toward their ratings than those with automatic braking alone. The superior rating is intended to identify models with more capable automatic braking and requires that both simulated collisions be avoided or nearly so through the automatic application of brakes. Figure 7 shows that the availability of these systems at every rating level has increased in the 2015 model year compared with 2013.

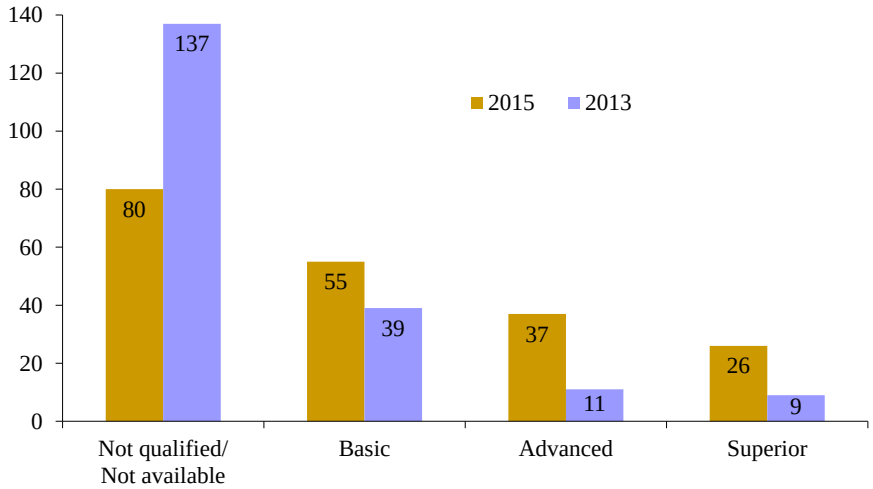


***Figure 7. Comparison of the availability of FCP systems with different IIHS ratings, 2015 vs. 2013 model year***

IIHS FCP ratings were first published in September 2013, and an update was published in May 2014. Both received a moderate amount of news and public attention, with estimated audiences of 58 and 79 million, respectively, in addition to being highlighted in *Top Safety Pick* announcements since 2013. Consumer response, as measured by reported level of interest and sales at automobile dealerships, was muted in comparison with what was observed for

crashworthiness ratings [19]. Nevertheless, compared with dealerships whose marquis brands did not offer FCP technology on any product, those that were mentioned in the FCP ratings announcements had better new vehicle sales experience.

## FUTURE CONSUMER INFORMATION PROGRAMS

### Vehicle LATCH Evaluations

All passenger vehicles sold in the United States have been required to be equipped with Lower Anchors and Tethers for Children (LATCH) since September 1, 2002 [23]. The purpose of LATCH, which is similar to ISOFIX, is to facilitate the proper installation of child restraint systems (CRS) and to provide top tether anchors for CRS installed with vehicle seat belts. Since its earliest implementation, however, many LATCH systems have failed to achieve this basic function, and observations of child restraint installations indicate that only slightly more than half of CRS in vehicles equipped with LATCH were installed using it [24][25]. Use of the top tether on forward-facing CRS is similarly low [26][27].

The Society of Automotive Engineers (SAE) Child Restraint Systems Subcommittee and ISO TC22/SC12/WG1/TF2 have drafted procedures and tools for assessing LATCH usability and the compatibility between vehicles and child restraints when using LATCH [28][29]. IIHS researchers working with UMTRI have established that the measures recommended by SAE and ISO do predict correct use of LATCH to install CRS [30][31][32][33]. Clear space around the anchor measured as an angle in a vertical plane, a low force to attach a simulated CRS LATCH connector, and a shallow depth of the anchor within the seat bight all were associated with higher rates of correct CRS installation using LATCH. This research will be the basis of a LATCH evaluation that IIHS intends to begin publishing in 2015. The evaluation will emphasize the ease-of-use characteristics in seating positions that are required by regulation to be equipped with LATCH and offer additional credit toward the highest rating for additional seating positions also equipped with easy-to-use LATCH.

In January 2015, NHTSA published a notice of proposed rulemaking that announced its intention to require easier-to-use LATCH [34]. The proposed requirements are consistent with IIHS and UMTRI's research, so the new LATCH evaluation will serve as a guide to parents purchasing new vehicles until all passenger vehicles are required to be equipped with better LATCH.

### Advanced Head-lighting Evaluations

HLDI's studies of optional crash avoidance systems also found a significant benefit of adaptive headlights that was consistent across four automakers' implementations [20]. The frequency of property damage liability claims was reduced by 5-10 percent and collision claims were reduced by 1-6 percent for vehicles equipped with headlights that point in the direction the car is being steered, compared with their counterparts with traditional fixed-aim headlights. Large reductions of injury claim frequencies were also associated with steerable headlight systems.

The demonstrated benefits of these new headlight systems has inspired IIHS researchers to begin developing an evaluation of headlight systems to promote, through consumer recommendations, those that provide a better view of the road ahead. The main focus of this effort is identifying systems that enhance forward view on curved roads because this is the situation in which the steerable headlights studied by HLDI offer the greatest benefit over fixed-aim systems [35].

Ideally, the evaluation will not specify the technology by which enhanced lighting is achieved, so work has concentrated on making measurements of illumination as the tested vehicles are driven toward sensors placed on the test track (Figure 8). Curved paths are deemed necessary to assess how well each system illuminates curved roads. The curve radii will be based on locations of nighttime fatal crashes. Likely, tests will also include measurements

from straight approaches to the sensors because more injurious and fatal crashes at night occur on straight roads than on curves (Figure 9). Furthermore, initial measurements indicate a large range in straight-line distance that different headlight systems illuminate the road (Figure 10). The initial evaluations of new car headlight systems are expected to be published in 2015 with possible integration into the *Top Safety Pick* program in 2017.

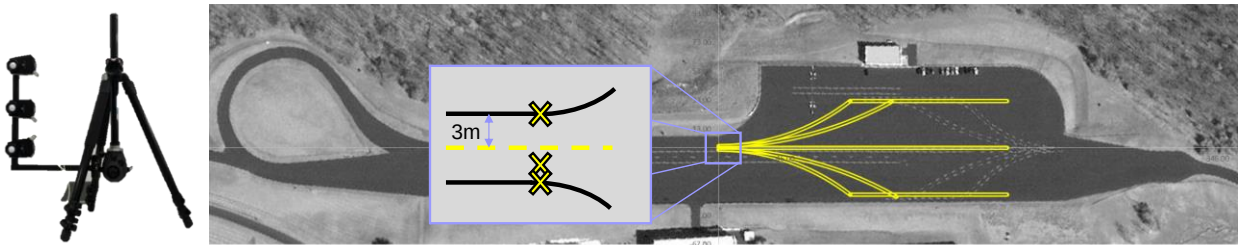


***Figure 8. Conceptual set-up for IIHS headlight evaluations.***

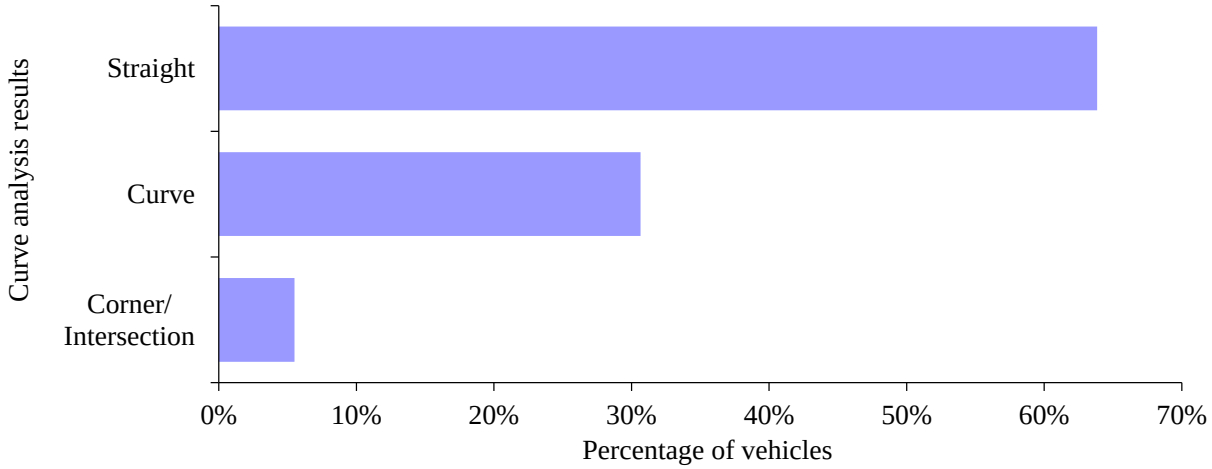


***Figure 9. Distribution of road types for nighttime fatal crashes based on 2012 Fatal Analysis Reporting System.***

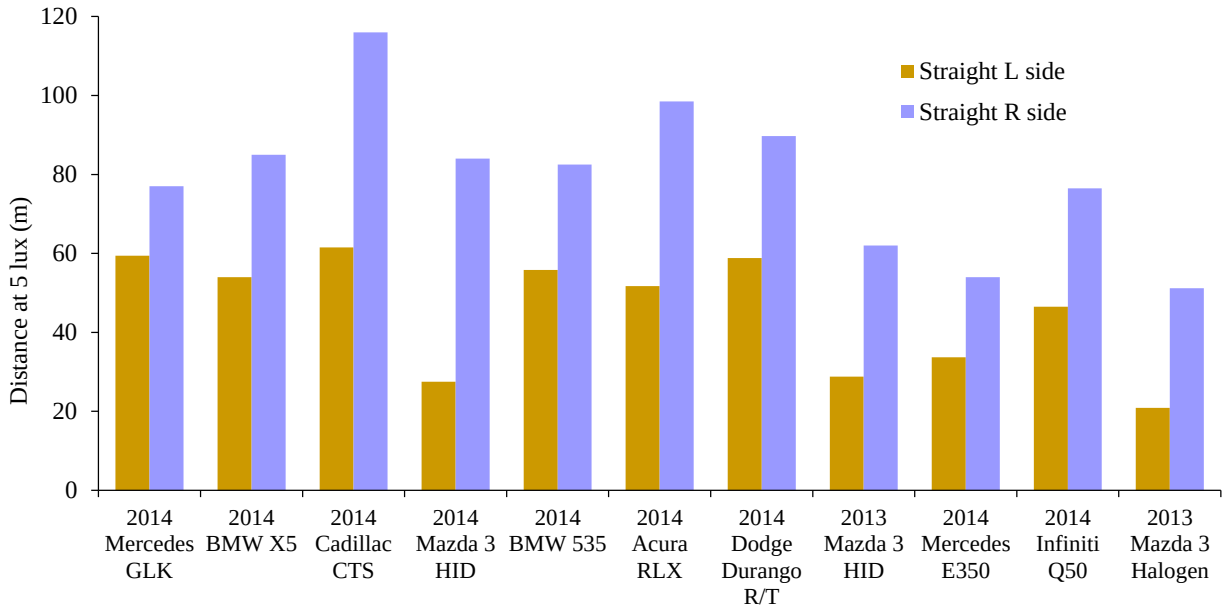


***Figure 10. Maximum straight-line distance for 5 lux illumination at 25 cm above road level by year/make/model.***

## CONCLUSIONS

IIHS and HLDI have a long history of publishing comparisons of the crash safety of different vehicles. In some cases, this effort has led to legislative requirements for the distribution of information or regulatory requirements for the design of vehicles. More recently, large audiences for IIHS consumer information programs have prompted manufacturers of rated products to make changes in ways indicated by IIHS tests, and models achieving better ratings have been rewarded by increased sales. IIHS experience with truck underride guard testing also suggests that the consumer information model can promote improved safety in the commercial vehicle fleet. Based on its experience with current programs, there is good reason to believe that IIHS ratings of LATCH and advanced head lighting systems can also improve vehicle safety.

## REFERENCES


[1] Hershman LL. 2001. The U.S. New Car Assessment Program (NCAP): past, present and future. Paper presented at the 17th International Technical Conference on the Enhanced Safety of Vehicles. Washington, DC: National Highway Traffic Safety Administration.

[2] Highway Loss Data Institute. 1973. Automobile insurance losses, collision coverages: variations by make and series, 1972 models. Washington, DC.

[3] Motor Vehicle Information and Savings Act, 92 P.L. 513, 86 Stat. 947 (1972)

[4] Repeal of Requiring Motor Vehicle Insurance Cost Reporting, 112 P.L. 252, 126 Stat. 2406 (2013)

[5] Farmer CM. 2005. Relationships of frontal offset crash test results to real-world driver fatality rates. *Traffic Injury Prevention* 6:31-37.

[6] Teoh ER.; Lund AK. 2011. IIHS side crash test ratings and occupant death risk in real-world crashes. *Traffic Injury Prevention* 12:500-07.

[7] Farmer CM, Zuby DS, Wells JK, Hellinga LA. 2008. Relationship of dynamic seat ratings to real-world neck injury rates. *Traffic Injury Prevention* 9:561-67.

[8] Brumbelow ML, Teoh ER, Zuby DS, McCartt AT. 2009. Roof strength and injury risk in rollover crashes. *Traffic Injury Prevention* 10:252-65.

[9] Brumbelow ML, Teoh ER. 2009. Roof strength and injury risk in rollover crashes of passenger cars. *Traffic Injury Prevention* 10:584-92.

[10] Arbogast KB, Jermakian JS, Kallan MJ, Durbin DR. 2009. Effectiveness of belt positioning booster seats: an updated assessment. *Pediatrics* 124:1281-86.

[11] O'Neil J, Daniels DM, Talty JL, Bull MJ. 2009. Seat belt misuse among children transported in belt-positioning booster seats. *Accident Analysis and Prevention* 41:425-29.

[12] Reed MP, Ebert SM, Sherwood CP, Klinich KD, Manary MA. 2009. Evaluation of the static belt fit provided by belt-positioning booster seats. *Accident Analysis and Prevention* 41(3):598-607.

[13] Braver ER, Cammisa MX, Lund AK, Early N, Mitter EL, Powell MR. 1997. Incidence of large truck-passenger vehicle underride crashes in the Fatal Accident Reporting System and the National Accident Sampling System. *Transportation Research Record* 1595:27-33.

[14] Brumbelow ML, Blanar L. 2010. Evaluation of U.S. rear underride guard regulation for large trucks using real-world crashes. *Stapp Car Crash Journal* 54:119-131.

[15] Insurance Institute for Highway Safety. 2011. Crash tests demonstrate the need for new underride guard standards. *Status Report* 46(2). Arlington, VA.

[16] Insurance Institute for Highway Safety. 2013. Not good enough: Underride guards on big rigs can be lifesavers, but most leave passenger vehicle occupants at risk in certain crashes. *Status Report* 48(2). Arlington, VA.

[17] Brumbelow ML, Zuby DS. 2009. Impact and injury patterns in frontal crashes of vehicles with good ratings for frontal crash protection. *Proceedings of the 21st International Technical Conference on the Enhanced Safety of Vehicles* (CD-ROM). Washington, DC: National Highway Traffic Safety Administration.

[18] Mueller BC, Brethwaite AS, Zuby DS, Nolan JM. 2014. Structural design strategies for improved small overlap crashworthiness performance. *Stapp Car Crash Journal* 58:145-74.

[19] Cicchino J. 2015. Consumer response to vehicle safety ratings. *Proceedings of the 24th International Technical Conference on the Enhanced Safety of Vehicles* (CD-ROM). Washington, DC: National Highway Traffic Safety Administration.

[20] Moore M, Zuby D. 2013. Collision avoidance features: initial results. *Proceedings of the 23rd International Technical Conference on the Enhanced Safety of Vehicles* (CD-ROM). Washington, DC: National Highway Traffic Safety Administration.

[21] Insurance Institute for Highway Safety. 2014. Honda warning system trims insurance claims. *Status Report* 49(4). Arlington, VA.

[22] Insurance Institute for Highway Safety. 2013. First crash avoidance ratings under new test program: 7 midsize vehicles earn top marks. *Status Report* 48(7). Arlington, VA.

[23] Office of the Federal Register. 2011. *Code of Federal Regulations*; Title 49 Transportation, Part 571 Federal Motor Vehicle Safety Standards, Standard No. 225 Child Restraint Anchorage Systems. Washington, DC: National Archives and Records Administration.

[24] Insurance Institute for Highway Safety. 2003. LATCH kids in cars. *Status Report* 38(5). Arlington, VA.

[25] Decina LE, Lococo KH. 2007. Observed LATCH use and misuse characteristics of child restraint systems in seven states. *Journal of Safety Research* 38:273-81.

[26] Eichelberger AH, Decina LE, Jermakian JS, McCartt AT. 2014. Use of top tethers with forward-facing child restraints: observations and driver interviews. *Journal of Safety Research* 48:71-76.

[27] Jermakian JS, Wells JK. 2011. Observed use of tethers in forward-facing child restraint systems. *Injury Prevention* 17:371-74.

[28] Society of Automotive Engineers. 2009. Guidelines for implementation of the child restraint anchorage system or LATCH system in motor vehicles and child restraint systems. Document no. J2893. Child Restraints Systems Committee, Troy, MI. Warrendale, PA.

[29] International Organization for Standardization. 2010. Road vehicles: Methods and criteria for usability evaluation of child restraint systems and their interface with vehicle anchorage systems; Part 1 Vehicles and child restraints equipped with ISOFIX anchorages and attachments. Report no. CD 29061-1. Geneva, Switzerland.

[30] Klinich KD, Manary MA, Flannagan CAC, Moore JL, Jermakian JS. 2013. Evaluation of proposed protocols for assessing vehicle LATCH system usability. *SAE International Journal of Transportation Safety* 1:32-45.

[31] Klinich KD, Flannagan CAC, Jermakian JS, McCartt AT, Manary MA, Moore JL, Wells JK. 2013. Vehicle LATCH system features associated with correct child restraint installations. *Traffic Injury Prevention* 14:520-31.

[32] Jermakian JS, Klinich KD, Orton NR, Flannagan CAC, Manary MA, Malik LA, Narayanaswamy P. 2014. Factors affecting tether use and correct use in child restraint installations. *Journal of Safety Research* 51:99-108.

[33] Cicchino JB, Jermakian JS. 2014. Vehicle characteristics associated with LATCH use and correct use in real-world child restraint installations. Arlington, VA: Insurance Institute for Highway Safety.

[34] Office of the Federal Register. 2015. *Federal Register*, vol. 80, no. 15, pp. 3744-3785. National Highway Traffic Safety Administration, Notice of Proposed Rulemaking, Docket no. NHTSA-2014-0123; 49 CFR Part 571, Federal Motor Vehicle Safety Standards, Child Restraint Systems, Child Restraint Anchorage Systems. Washington, DC: National Archives and Records Administration.

[35] Reagan IJ, Brumbelow ML, Frischmann T. 2015. On-road experiment to assess drivers' detection of roadside targets as a function of headlight system, target placement, and target reflectance. *Accident Analysis and Prevention* 76:74-82.

# Protection of Lithium-Ion Traction Batteries in the Electric Car

**Michael Funcke**
Forschungsgesellschaft Kraftfahrwesen Aachen mbH
Germany
**Sebastian Lovski**
**Sebastian Schäfer**
Institute for Automotive Engineering RWTH Aachen University
Germany
**David Sturk**
**Dominique Dufaut**
**Hakan Sundmark**
**Kyriakos Vavalidis**
**Per Gustafsson**
Autoliv
Sweden

Paper Number 15-0234

## ABSTRACT

The storage elements in an electric vehicle (EV) remain a key challenge to wide-scale, successful deployment of EVs that are appealing to customers and are adequately functional (e.g. in terms of range and drivability). State-of-the-art electric storage systems are lithium-ion batteries, offering approximately 0.5 km driving range per 1 kg of battery pack mass (see Funcke et al [1]). However, these battery packs require high level safety measures to avoid e.g. mechanical damage of the cells, which increases the pack mass again. In order to make a reliable statement about the battery safety at an early stage of development, detailed knowledge of the mechanical behavior of the cells as well as its reproduction in the virtual development process is necessary.
Based on a sample design of a main battery structure, the development process of the cell model is explained. The first steps are the integration of the design in a full vehicle and the determination of the dominant cell deformations, which are transferred to cell load cases. These mechanical abuse tests of cells deliver the input data for generating an adequate finite-element (FE) model, which offers the opportunity to dimension the battery pack and to add safety measures. With this simulation model inflatable structures as well as passive reinforcements for the traction battery are investigated.
To validate the simulation results, component tests on system level, i.e. complete battery packs, are conducted. The test is based on the full vehicle reference design load case, in this case the EuroNCAP pole side impact with a modified pole position and an impact velocity of 50 km/h. An analysis of the impact position is needed since the vulnerabilty to intrusion of the battery pack and the stiffness of the vehicle structure varies along the vehicle longitudinal axis.
These component tests confirm the simulation results and show the potential of inflatable structures and passive protection systems. Furthermore, it is possible to generate a FE model for lithium-ion batteries, which is applicable to full vehicle simulations.
Although it is possible to map the mechanical characteristics to the generated cell model, this model is limited to the investigated load cases, which have been the result of the battery position within the vehicle and the corresponding critical design load case. Since the battery may be placed in another position within the vehicle and the arrangement of the cells may change, the cell model is not universal. However, it is extensible to other load cases.
Overall, the results from the study with the inflatable elements show clearly the benefit of those structures. With low additional mass a high positive effect (e.g. lower intrusion) is achieved, which means the ratio of the incorporated mass to the reached protective effect is lower than with passive protection systems.

## INTRODUCTION

In the field of electric vehicles, lithium-ion batteries are widely utilized. In general three major types of battery cells are used: prismatic, cylindrical and pouch cells. A representative prismatic cell is protected by a case made of metal or hard plastic. Cylindrical cell cases often consist of aluminium. Pouch cells use lightweight cases made of layered foil consisting of sheets of polymer and aluminium jointed at the edges of the flat cell. Usually multiple cells are grouped into modules and several modules are grouped into a battery pack. Using different circuit conditions (in parallel, in series) different voltages or different capacities at the same voltage are achievable. The assembled main battery pack (MBP) is installed within the electric vehicle, mostly in the safest position e.g. in the tunnel area.

Sahraei et al [2] as well as Choi et al [3] reported their effort on modelling lithium-ion pouch cells using FE. Sahrei et al [2] model covered the force-displacement behaviour for 3-point bending as well as for axial and through thickness compressions. The FE model of Choi et al [3] focussed on a more detailed behaviour of the cell layers e.g. local stress and strain. Therefore three-layered shell elements were used, which represented the pure metal substrate (Al or Cu) and the coating (e.g. Cobalt or Carbon coating). The electrolyte layers, which nodally connects the shell layers, were modeled using link elements. However, both simulation models are limited to the tests used for the validation which do not necessarily represent the loads acting when the MBP is placed in an electric vehicle. In addition, the high number of nodes and elements restricts the use of the model to cell tests. With the aim to design a MBP and to apply a passive as well as an active protection system, in means of inflatable elements, for the OSTLER project a battery model was needed which was applicable to full vehicle simulations.
The following study was part of the european founded project OSTLER which focused on the development of smart concepts for physical integration of battery packs in electric vehicles. For this purpose, the MBP was placed outside the common safe zone in an area that presents higher frequency of intrusions – i.e. MBP under the front seats, transverse to the driving direction and stretching out into areas close to the vehicle sill. Using a simplified battery cell model, for the given battery location relevant full vehicle load cases as well as associated cell load cases were derived using a simplified FE cell model. For these load cases mechanical tests were carried out and gradually built up a full vehicle-enabled cell model, which enabled the investigation of inflatable elements and passive systems to provide protection to the battery. Using systems tests, the final design of the systems was validated against the simulation results. The following investigation was carried out using the explicit solver LS-DYNA.

## DEVELOPMENT OF A FE MODEL FOR LITHIUM-ION POUCH CELL

First, the selection of cell type for this study was carried out. For this purpose, it was necessary to determine the full vehicle load cases, which had to be considered for the crash simulations. By analysing the German In-Depth Database (GIDAS) (see Funcke et al [1]) the impact velocity, direction and the impacting object of the 2 % of accidents with the highest intrusion was evaluated.

### Relevant Full Vehicle Load Cases And Derivation of Cell Load Cases

The 2 %-tile area consisted of 82 collisions. If the incident direction is numbered according clockwise, with 12 clock corresponds to a frontal impact, it was found that in 45 cases the impact object was another vehicle with the predominant impact direction between 12 and clockwise to 7. In the other cases the impact object was an object which were predominant in the area between 8 and 2 with major peaks at 9 and 12.
Beside the impact direction the impact velocities were analysed with the result that to cover at least 50 % of all crashes the following load cases had to be considered within the project:

- EuroNCAP ODB
- FMVSS 208 (56 km/h, 0° impact, 50 % male dummies)
- FMVSS 301
- EuroNCAP pole side impact with 50 km/h and varied pole position

First draft designs for MBP, containing the three different cell types each, were installed as part of the electrification process in the FE model of a Toyota Yaris model which was publicly available. Placing the MBP transverse underneath the frontal seats meant the battery reaches in an area where frequently deformations occur in case of an accident. Performing the four load cases and analysing the deformations of the MBP housing as well as the deformation of the cells inside, the pouch cell was identified as cell with the highest deformation and most critical cell type for this MBP location and design. Due to the location relevant intrusions only occurred within the high speed EuroNCAP pole side impact. Out of the occurring cell deformations as well as the plastic strains within the cells (*see Figure 1*), three load cases were identified, which the simulation model of the cells had to fulfil and which were used for the built-up process. Specifically, these were the load cases through thickness compression, three-point bending and the clamped cell. Within the last-mentioned load case the pouch cell is clamped according to the installation condition in the MBP between two frames.
For the following study, lithium-ion pouch cells with a capacity of 40 Ah and 3.7 V were used, which were fully charged for the tests. This enabled to detect whether a short circuit or internal damage occurs during the

test. To avoid personal injury and to increase security the cell tests were carried out using a freestanding and foreclosed housed test bench, which enables the application of a maximum force of 30 kN. Any escaping gas could get vacuumed by the built-in ventilation.

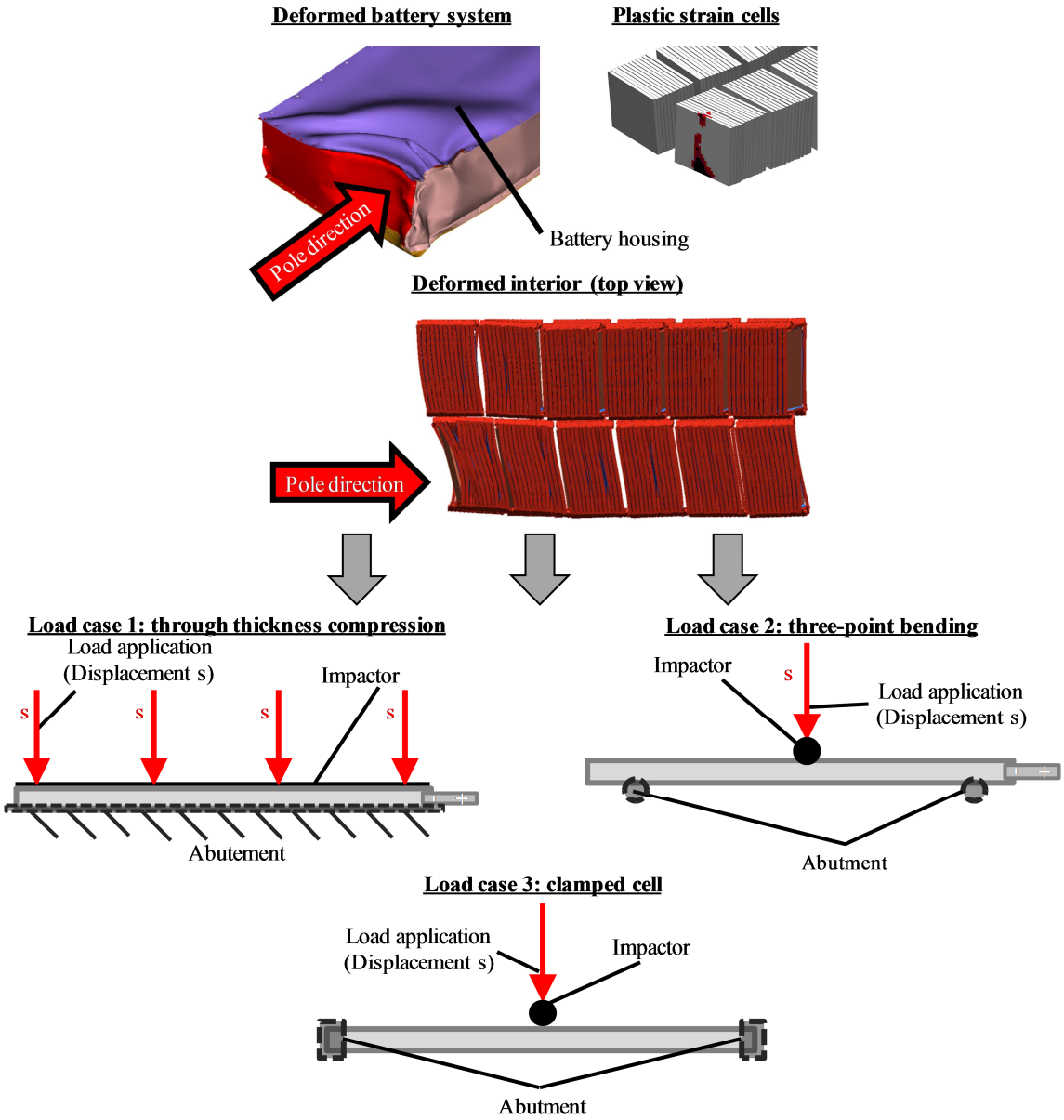


***Figure1. Determination of cell load cases.***

Based on the experiences made by Sahraei et al [2] the test series began with the through thickness compression in order to determine the material parameters for the solid layers representing the electrolyte. Therefore, the assumption was made that the other layers do not contribute to the overall performance within this load case. Starting from this load case, the simulation model was gradually expanded.

**Through Thickness Compression Test**

Although a pouch cell consists of a high number of layers (e.g. ~205, Choi et al [3]), the number of layers was reduced in order to reduce simulation time and to generate a simulation model applicable to full vehicle simulation. The simulation time step, which depends on the smallest element length within the simulation model and is called courant criterion [4], should not be lower than the value $1.112e^{-6}$ s, which was the time

step defined in the full vehicle simulation. The cell model (*see Figure 2*) consisted of five solid layers representing the electrolyte layers, six layers of aluminum representing the pure metal layers, a layer representing the border area of the cell which was used for clamping the cell as an element row closing the cell at the sides. The different layers were not coincident connected using shared nodes, like done by Sahraei et al [2]. Instead, the layers could slide to each other using a common LS-DYNA single surface contact [5]. As input for the material model MAT_83 served a stress-strain curve which was calculated out of the testing force-displacement-curves.

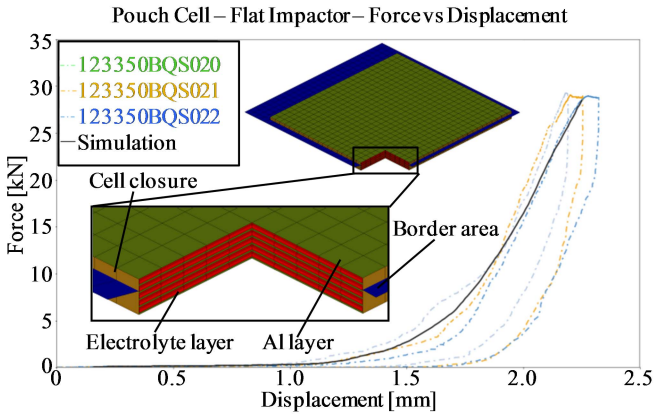


***Figure2. Cell modeling and through thickness compression test results vs. simulation.***

Using this approach provided very good results which can be seen comparing the force-displacement curves of the simulation compared to the three tests (*see Figure 2*).

**Three-Point Bending Test**

The determination of the Al layer thickness, the contact parameters between the electrolyte and the Al layers as well as the cell closure thickness formed the next step. For this purpose, the three-point bending test was the best choice since the cell surrounding does not contribute, or only to a very small part, to the bending stiffness within this load case. As abutment as well as impactor served round profiles with 40 mm diameter (*see Figure3*), which covered the entire width of the battery cell. The bending load case was carried out as in the entire vehicle occurring about the vertical axis in parallel to the electrical contact areas of the cell. Using a layer thickness of 0.4 mm for the pure metal layers, a thickness of 0.04 mm for the closure and a friction of 0.15 between the layers it was noted that a good correlation between simulation results and the tests was achieved. Both the force-displacement curves as well as the qualitative behavior were in good agreement.

**Clamped Battery Test**

In the last validation step, the cell was fitted under mounting conditions between two frames similar to the MBP (*see Figure4*). As required by the cell manufacturer, the through the frames transmitted clamping force was applied only to the border area of the battery. Since the behavior of the battery should be examined and the mechanical effect of the framework should be kept as low as possible, an impactor with a length of 100 mm and a diameter of 40 mm was used, which was placed centered in height and width of the battery. During the load application, on the one hand the battery slid out of the frames; on the other hand the battery was locally deformed in the impact area as well as in the border area. As a result, the material and the thickness of the border area could be determined as well as the friction parameters between border and frame. The highest agreement with the experimental results could be achieved by using a Part_Composite [5], which enables to apply multiple materials and associated thicknesses to one single layer of shell elements. Most suitable was a layout consisting of a layer of aluminum (thickness 0.4 mm) surrounded by a layer of a plastic material (thickness 0.25 mm).

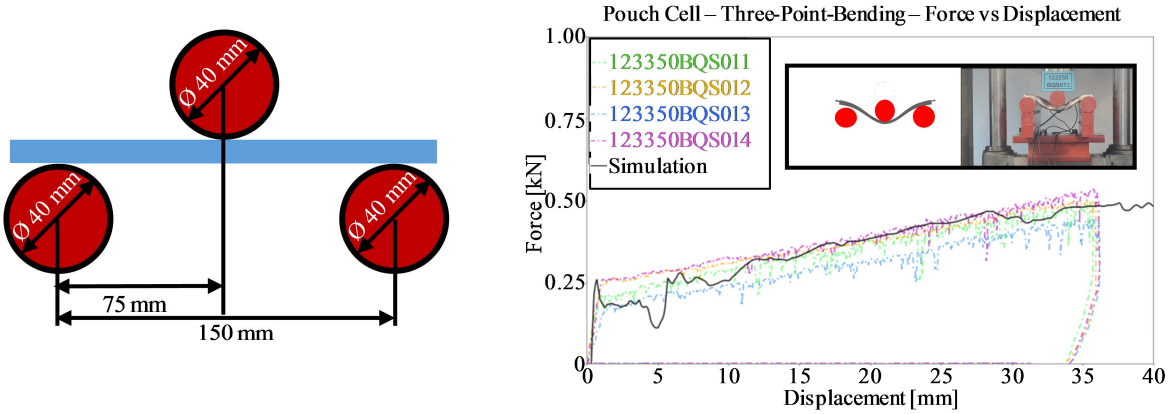


***Figure3. Results testing vs. simulation three-point bending.***

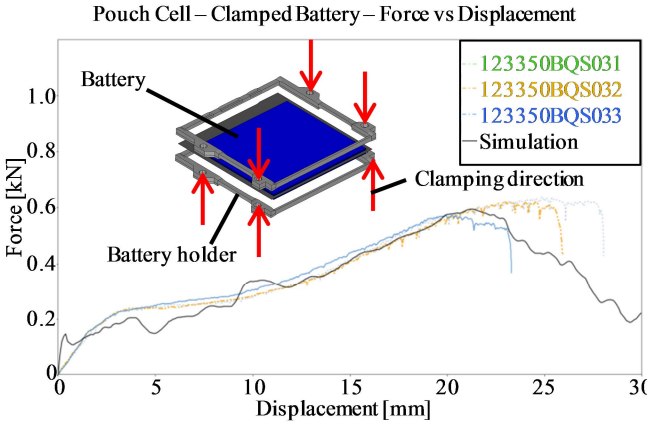


***Figure4. Results testing vs. simulation clamped battery.***

Both initial force and the force-displacement curves of simulation and experiments were in a good agreement (*see Figure4*). It must nevertheless be noted, that the simulation model considered no strain rate as well as temperature effects. After generating a simulation model for the pouch cells the design process of the inflatable element and the passive reinforcement as battery pack protection started.

## PROTECTION OF BATTERY SYSTEMS USING INFLATABLE ELEMENTS

Including the gained CAE model of the pouch cells into the full vehicle simulation model, the loads as well as the geometrical interaction between battery system and the surrounding vehicle structure were analysed using different impact points of the pole. In this analysis, it was found the highest intrusion into the battery system occurred when the pole hits the center of the modules. Another finding was that the vehicle structure in means of the inner sill hit the battery with a velocity of 9 ms/s and thereby increased the pole diameter due to the wrapping to 325 mm (see Funcke et al [1]). These parameters were transferred into a battery system test, where the vehicle structure was skipped and the battery was hit directly by the pole with the higher diameter. This test was used to further speedup the virtual design process as well as to run the final physical evaluation of the protection concepts.
Since the development of a passive protection is state of the art in protecting battery systems, the following passages focus on the development process of the active protection system. Nevertheless, there is some information included since the passive protection was used as benchmark for the active system.

### Concept of Passive Protection

The passive reinforcement consisted of three stages compared to the unreinforced battery pack; an increased wall thickniss, an additional load path by adding longitunal beams within the battery housing and an energy

absorbing foam block between the battery and the vehicle structure. After the virtual optimisation of the named measures, the passive reinforcement caused a weight increase of 37 kg but reduced the intrusion into the main battery pack (MBP) from 157 mm to 66 mm (58 %) compared to the unreinforced reference structure. The reduction within the simulation loop was predicted with 69 % (from 157 mm to 48 mm). Since the intrusion of the unreinforced battery pack was predicted with a high accuracy, the reason for the inconsistency is not located in the cell model. Rather, the reason is suspected in other model parameters.

**Concept of Active Protection using Inflatable Elements**

The installation of inflatable elements made it possible to create new energy absorption paths and to reduce the load onto the MBP.
As a consequence it was possible to reduce the deformation and the stress of the cells in case of a crash. As shown in *Figure5*, in the case of a pole side impact with a current lateral in-crash sensing, the active solution of battery pack protection consisted of a "structural" airbag, which provided both a certain structural rigidity against intrusions as well as good energy absorption potential.

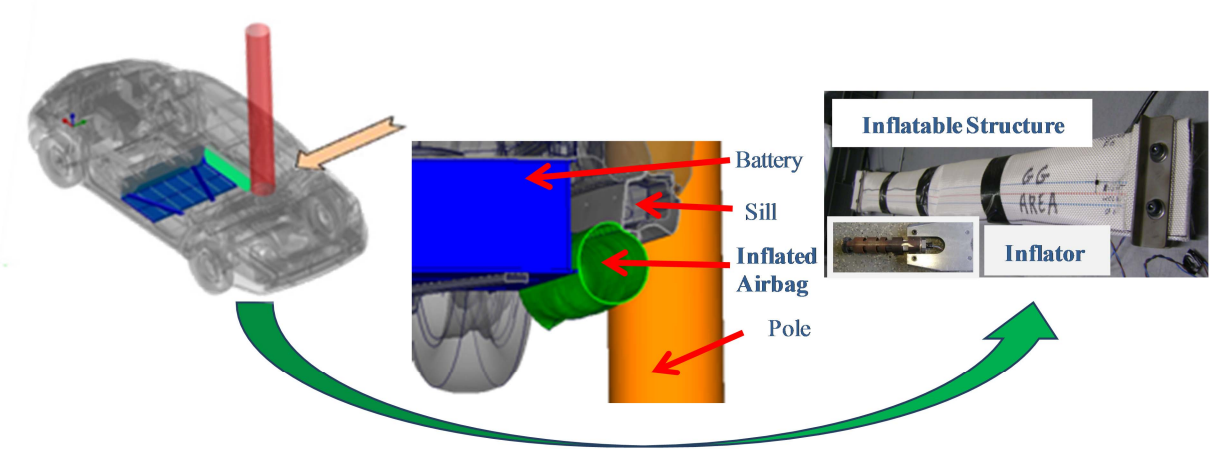


***Figure 5. Active Protection concept***

Such a structural airbag resembles a normal airbag from the point of view of its constituent components, i.e. mainly a fabric cushion, a pyrotechnic inflator and a wire harness to the standard airbag ECU, but differs greatly in the performance characteristics. The cushion consists of a highly reinforced fabric capable to withstand gas pressures more than 20-30 times that of a passenger airbag and also capable to resist mechanical aggressions from its surroundings.
This high pressure made the cushion becoming almost rigid and, compared to metal reinforcement, had the potential of a lower weight and a reduced packaging (both critical to EVs). It was placed in the free space between the battery pack and the sill, right in front of the lower part of the battery pack in order to take advantage of its rigid bottom plate.
The FE model of the battery pack including the FE model of the pouch cells made it possible to define the mechanical requirements for such a structural airbag.

**Active Protection efficiency**

With an added weight of 4 kg (2 kg for both sides of BP) compared to the unreinforced reference structure, the intrusion into the battery pack was reduced from 157 mm to 121 mm in the physical tests. This was a reduction of 23 % taking the unreinforced battery pack as reference. The reduction within the simulation loop was predicted with 28 % (157 mm to 116 mm). Compared to the passive reinforcement of the battery structure, the weight-specific intrusion reduction (intrusion reduction [%]/ added weight [kg]) of the active system was over four times higher (1.57 %/kg passive system to 7 %/kg active system).

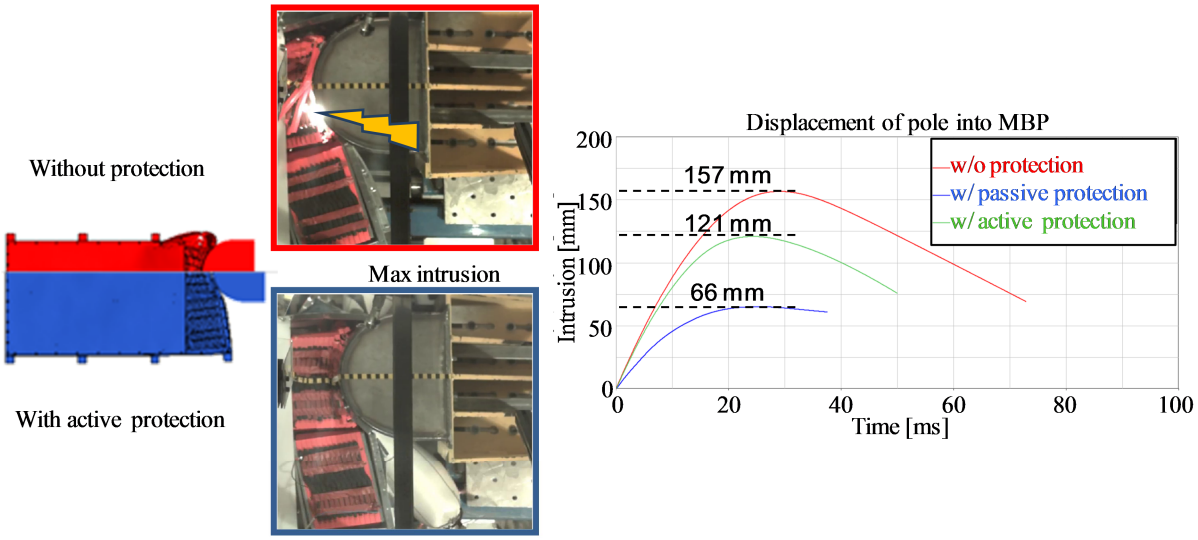


***Figure 6. Effects of active structure (targeted load case: pole side impact at 50km/h)***

## CONCLUSIONS

The relevant modeling of cells, which could be elaborated through the approach presented, offered the opportunity to dimension and design the battery pack casing and the associated safety measures. It enabled to investigate the protection of the battery pack using an alternative system in means of an inflatable element. The investigation showed that the protection of the main battery pack by an active structure is possible (as presented for the worst load case, with the MBP as defined above). It successfully reduced the intrusion into the battery system. The additional mass of the active system was small compared with the mass of the passive reinforcement.

Smartly combining benefits of the active protection with a passive protection according to the protection requirements of the MBP, along with an optimization of MBP construction allows for a wider MBP and therefore an increase in EV's driving range with favorable weight balance (added weight by active structure, reduced weight of casing of MBP).

The used approach of identifying the cell loads, generating a cell simulation model and the afterwards design process can also be seen as guideline for future investigation concerning the crash safety of battery packs. Once generated, the cell model can be applied to various investigations (battery pack position, pack dimensions,..) as long as the cells experience the same type of mechanical loads the model was validated for. In the case the loads are different; the simulation model can be adapted to this by means of additional cell tests.

## REFERENCES

[1] Michael Funcke, Sebastian Schäfer, Roland Wohlecker, Dominique Dufaut, David Sturk, Kyriakos Vavalidis „Evaluation report in active and passive protection solutions", www.ostlerproject.com/Downloads

[2] Elham Sahraei, Rich Hill, Tomasz Wierzbicki "Calibration and finite element simulation of pouch lithium-ion batteries for mechanical integrity", 201, 307– 321, Journal of Power Sources, 2011

[3] Hyung Yun Choi, Inhyeok Lee, June Soo Lee, Young Man Kim, Hyunjin Kim "A Study on Mechanical Characteristics of Lithium-Polymer Pouch Cell Battery for Electric Vehicle", Paper Number 13-0115, 23rd International Technical Conference on the Enhanced Safety of Vehicles (ESV), Seoul, Republic of Korea, May 27-30, 2013

[4] Lutz Eckstein, "Strukturentwurf von Kraftfahrzeugen", p. 183, Schriftenreihe Automobiltechnik, Germany, 2010

[5] LS-DYNA Manual, DYNA MORE, 2014

# Predicting the Impact of Vehicle Safety Developments in Emerging Markets following the Industrialised Countries' Experience

**Louise Lloyd, Richard Cuerden, Caroline Wallbank, Matthias Seidl**
Transport Research Laboratory, UK

ID#: 15-0239

## ABSTRACT

Vehicles in emerging markets are not typically regulated to the same extent as seen in industrialised regions. Casualty rates are considerably higher in these emerging markets, and the lack of vehicle safety regulation is responsible for at least some of the difference. With rapid growth in passenger cars expected, the number of road deaths and casualties in emerging markets is likely to rise, unless targeted and efficient interventions are planned and initiated urgently.

The objective of this work was to quantify the casualty benefit that could be realised in an emerging market, if the experiences and lessons learned in the Europe Union (EU), including minimum car safety standards and consumer testing, were efficiently applied. Malaysia was selected as the emerging market for study in this paper, because it is a Contracting Party to the UN 1958 Agreement and has recently applied the major UN vehicle safety regulations.

Clear differences in vehicle safety developments in Britain compared with Malaysia were identified through analysis of NCAP results and accident data. Frontal impact performance varied, with some cars tested in ASEAN NCAP performing to levels similar to those seen in Euro NCAP today, whilst others were significantly worse. Based on this evidence, in broad terms, this study assumes that new car models sold in Malaysia are approximately 10 years behind today's (2014/15) equivalent European cars, in terms of vehicle safety developments. However, the fleet in Malaysia is older than that seen in Britain, so it is possible that the entire fleet (with many older cars) could reflect a level of safety more like Britain before 2004. Therefore, the Malaysian casualty benefits predicted by this study represent a conservative estimate.

By taking the vehicle safety development experience witnessed in the EU and applying it to the situation in an emerging market, this work quantifies the casualty reduction potential could be a saving of between 1,200 and 4,300 Malaysian fatalities by 2030.

## INTRODUCTION

Road vehicles in some of the world's emerging markets are not currently regulated to the same extent as industrialised regions. The combination of growing fleet sizes, made-up of vehicles that do not have to meet basic safety standards, contributes to today's casualty rates, which are considerably higher in emerging markets compared to Europe and other industrialised regions. The lack of vehicle safety regulation is responsible for at least some of the difference. With rapid growth in passenger cars expected to continue, the number of road deaths and casualties in emerging markets is likely to rise, unless targeted and efficient interventions are planned and initiated urgently.

In the automotive sector, minimum safety regulations and standards have evolved in Europe, the US, Japan and other world regions over the last 50 years. There are differences with regard to the nature of tests and criteria which must be met, but the current regulations that apply in the industrialised regions share the objective to provide the highest level of cost-effective safety performance. It is recognised that there are specific differences between the EU and US Regulations, if compared line by line, but it is the outcome mandated by these regulations in real-world car accidents that is important.

Therefore, for practical reasons and to align with the UN Decade for Action for Road Safety, UN Regulations and Global Technical Regulations (GTRs) are referenced as our assumed baseline for minimum mandatory Standards. The UN Decade of Action for Road Safety encourages all countries to apply and promulgate motor vehicle safety regulations as developed by the UN's World Forum for the Harmonization of Vehicle Regulations (WP29). This paper identifies five car regulations, which are defined as a minimum for today's world markets:

- Approved seat belts and anchorages for all seating positions (UN Reg. 14 and 16).
- Occupant protection in frontal collision (UN Regulation 94)
- Occupant protection in side or lateral collisions (UN Regulation 95)
- Pedestrian protection (GTR 9)
- Electronic Stability Control (ESC) (GTR 8)

The UN Decade of Action also has a stated activity to: '*Encourage implementation of new car assessment programmes in all regions of the world in order to increase the availability of consumer information about the*

*safety performance of motor vehicles*'. The European New Car Assessment Programme (Euro NCAP) was launched at TRL in 1997 to provide an independent assessment of the safety performance of popular cars sold in Europe; the aim was to encourage, on the one hand, consumer awareness of the safety performance of the cars they buy and on the other, to motivate manufacturers to exceed the minimum requirements set out by legislation. Over time Euro NCAP has become more sophisticated, and as well as maintaining its original methodology, which provides a star rating (between one and five stars) based on the car's performance in a number of secondary safety crash tests, including adult and child occupant and pedestrian protection assessments, it also assesses the primary safety or crash avoidance and mitigation credentials of the vehicle.

This paper aims to highlight the combined safety benefits that are realised through the establishment of minimum mandatory car standards enforced through regulation, in conjunction with consumer (NCAP) programmes, which seek to set more challenging vehicle safety design safety targets. Global NCAP has established testing programmes in a number of emerging markets.

Malaysia was selected as the emerging market for this study because it is a Contracting Party to the UN 1958 Agreement and has a vehicle safety improvement strategy, which recently included applying most of the major UN Regulations. Malaysia hosts ASEAN NCAP tests and so it was possible to evaluate the safety performance of some of the vehicles currently sold and to bench-mark performance against similar European vehicles.

Specifically, this paper aims to quantify how many car user fatalities are likely to be prevented in Malaysia between 2014 and 2030, as a combined result of adopting the basic secondary safety measures, namely seat belt standards and UN Regulations 94 and 95 and the impact that ASEAN NCAP will provide on further real world vehicle improvements.

## METHOD

Information from Great Britain and Malaysia forms the basis of the study, including accident data, exposure data, and historic and expected developments in fleets. From these data and NCAP test results, the relative safety status of cars in the emerging market compared to the history of European vehicle safety developments is identified. A series of statistical models on British data measure the effect of developments in secondary vehicle safety and apply these effects to the potential impact on casualties in Malaysia if similar developments were seen.

### Secondary safety modelling

Car safety has improved in Britain over the past two decades, but how much of this improvement is due to secondary safety features and how much is due to changes in the conditions in which vehicles are driven, for example due to improvements to the road system or changes in the weather, or the way in which they are driven is difficult to define. Statistical modelling is required to disaggregate these effects. The models (Broughton, 2003) use data from the British STATS19 database to model the proportion of casualties killed in road accidents (the severity proportion). The details of the model are shown in the Technical Annex. From these results it is possible to predict the number of casualties which would have occurred if secondary safety had not improved over time.

### Prediction modelling

In order to predict the possible future effect of secondary safety improvements in cars in Malaysia we use a scenario based modelling method derived initially in Broughton et al (2000).

The models derived start with a set of possible baseline models, which predict the number of casualties over the next few years if the number of registered vehicles (a proxy for traffic) follows a series of possible scenarios and basic vehicle safety developments continue in the way that has been observed up until the current time. The impacts of further vehicle safety interventions can then be added to the baseline model to predict the impact of these additional measures.

The baseline model is defined as:

$$C'(2030) = C(2012) [ T(2030) / T(2012) ] (1-\alpha)^{19}$$

where:

- C'(2030) is the predicted adjusted number of car occupant fatalities in 2030 given current progress in vehicle safety
- C(2012) is the number of car occupant fatalities in 2012 (the latest known year)
- T(2030) is the expected number of registered cars in 2030 based on a series of scenarios

- T(2012) is the number of registered cars in 2012
- α is the average annual fatality rate of reduction (adjusted rate) predicted over the 19 year period 2012-2030

For the baseline model, the expected number of registered cars is predicted based on the following broad scenarios:

a) Similar growth or decline to that observed in recent trends.
b) No change in current level.
c) Increased or decreased growth or decline relative to current trend.

Some possible scenarios for changes to vehicle safety progress are added to the baseline model. These new measures have been defined as:

1) Introduction of similar regulations and adaptations to the NCAP testing regime, similar to those seen in Europe over the same time period.
2) Introduction of regulations and NCAP adaptations as above, but over a shorter period.

Application of the scenarios is based on a number of assumptions:

i. Accident types for cars are similar in Britain and Malaysia.
ii. The uptake rate of these regulations and the relative timing is the same in Malaysia as in Britain.
iii. The impact of NCAP in Malaysia is insignificant, but grows as we have seen in Britain in terms of individuals' buying habits. Since the introduction of ASEAN NCAP in Malaysia, we have seen very little evidence of a change in the buying habits in the new sales data as the poorer safety performing cars remain popular.

The results of the secondary safety modelling are used to provide the predicted casualty saving due to secondary saving improvements. In order to apply these to the Malaysian data it is necessary to understand the current state of the Malaysian fleet in terms of fleet renewal and safety standards, relative to a specific point in time in the British fleet. The fleet renewal has been determined from data on the sales of new cars from 2005 to 2010 from Motor Trader (2014). NCAP tests were the most accessible and robust method for comparing safety levels of different cars, however it was not possible to compare star ratings or scores across different NCAPs as the methods vary. Therefore, simple subjective safety levels have been identified by experienced vehicle engineers comparing the visible structural stability of the most popular cars in the most recent NCAP tests in the Malaysian region compared to those in Britain over the last 20 years. These structural scores take into account the visible deformation of the A-pillar and the sill, along with any movement in the steering column and the airbag positioning/ interaction with the dummy's head.

There were some limitations in the method partly due to the video formats. Firstly, these results are based on expert, but subjective opinions. In many cases it was difficult to code exactly into one category and the most appropriate category has been chosen according to the judgment of the experts. Secondly, many of the videos from the different tests in different years and different countries had different views – some just included a side view, others included a frontal view and a view from an internal camera. From some of the camera views it was easier to see steering column and wheel movement compared to others, which may mean that movement was more easily picked up in some types of videos. The NCAP tests are based on the newest car model derivative at the time of the test.

## DATA

This section compares vehicle fleet and road fatality figures for Malaysia in the latest available year and for Britain in 1999, 2004, 2009 and 2013. The years covered by the British data reflect the investigation to determine where the current car safety standard in Malaysia is in relation to the British developments.

### Casualty data

MIROS provided the total number of road fatalities in Malaysia from 1995 to 2013. This can be combined with information from WHO (2009, 2013) which provide the distributions of these fatalities by road user type for 2007 and 2010. Interpolating from these figures enables us to derive estimates of the number of car occupant fatalities from 2007 to 2012 as shown in Table 1.

**Table 1. Estimated number of car occupants from 2007 to 2012 in Malaysia (red numbers are extrapolated)**

| Year | Deaths | Proportion of car occupants in deaths | Car occupant deaths (estimated) |
|---|---|---|---|
| **2007** | 6,282 | 23% | 1,445 |
| **2008** | 6,527 | 24% | 1,566 |
| **2009** | 6,745 | 25% | 1,686 |
| **2010** | 6,872 | 26% | 1,787 |
| **2011** | 6,877 | 27% | 1,857 |
| **2012** | 6,917 | 28% | 1,937 |

In 2012, relative to the population the car death rate in Malaysia was 66.1 per million population. In comparison, the highest equivalent rate in Britain was in 1972 (60 per million population) with rates between 31 and 13 from 1999 to 2012.

## NCAP comparisons

As of December 2011 new cars in the Asean region could be tested by the New Car Assessment Programme (ASEAN NCAP). A total of nine cars in the top 20 most popular cars in Malaysia were tested by ASEAN NCAP. For the purposes of comparing vehicle safety across Malaysia and Britain, these nine cars and a further 31 cars in the top 10 new sales in 1999, 2004, 2009 and 2013 across Euro NCAP from 1997 to 2014 were observed and scored based on structural deformation in the frontal test which is broadly comparable across the two NCAPs. Structural deformation was classified into one of nine categories:

1. No intrusion
2. Mild A-pillar damage
3. Severe A-pillar damage
4. Mild vehicle sill (base of door) or footwell movement/damage
5. Severe vehicle sill movement/damage
6. Mild A-pillar and sill damage
7. Severe A-pillar damage and mild sill damage
8. Mild A-pillar damage and severe sill damage
9. Severe A-pillar and sill damage

The distribution of the structural deformation score is shown in Table 2. This shows a mixture of scores across the different NCAP regions and years.

**Table 2. Count of cars tested by NCAP by structural deformation score**

| Structural deformation | 1 | 2 | 3 | 4 | 6 | 7 | 9 | Proportion of new sales |
|---|---|---|---|---|---|---|---|---|
| **Asean** | 4 | 3 | 1 | | | | 1 | 45% |
| **Euro 1999** | | 1 | 2 | | | 3 | 4 | 35% |
| **Euro 2004** | 4 | 1 | 1 | | 1 | 1 | | 26% |
| **Euro 2009** | 3 | | | 2 | | | | 16% |
| **Euro 2013** | 5 | 1 | | 2 | | | | 24% |

Broadly, the Asean cars appear to be performing somewhere around the Euro 2004 level.

## Fleet data

Table 3 compares car fleet facts in Malaysia in 2012 and Britain in 2004. In Malaysia, 10.5m cars were registered which included 0.6m new cars (OICA (2013) for registrations and Malaysian Automotive Association (MAA, 2014) for sales data). The number of registered cars is growing substantially each year.

**Table 3. Comparison of registered car facts in Malaysia and Britain**

| | Britain: 2004 | Malaysia: 2012 |
|---|---|---|
| **No. reg cars (DfT, 2013a)** | 25.8m | 10.5m |
| **Growth in reg cars from previous year** | 3.1% | 6.5% |
| **Proportion of reg cars new (DfT, 2013b)** | 9.7% | 5.3% |
| **Proportion of cars aged 6 years or less (DfT, 2014)** | 53% | 28% (2010) |
| **Motorisation rate (DfT, 2013b)** | 0.44 | 0.36 |

Detailed registered car data were not available to the research team for Malaysia during the research. However, based on sales data from 2005-2010 (Best Selling Cars Blog, 2014) we estimated that 28% of the Malaysian car fleet is at most six years old. In comparison, the number of cars and the proportion of these cars that are 6 years or younger is twice as high in Britain in 2004. Given the information in Table 3, there is some suggestion that the current fleet in Malaysia contains older cars relative to Britain in 2004, therefore any expected casualty savings are likely to be underestimates.

## RESULTS

### Secondary safety in Britain

The secondary safety modelling is shown in detail in the Technical Annex. This shows that there have been considerable reductions in fatalities in Britain since 1990 due to developments in secondary safety. It is estimated based on these models that 302 lives have been saved between 2004 and 2013 in Britain due to secondary safety which is a reduction in car driver fatalities of 4.2%.

### Predictive modelling in Malaysia

Based on the number of registered cars and the car occupant fatality estimates shown in Table 1, the fatality rate for car occupants can be estimated. These are shown in Figure 1 with two possible trends. Both trends are based on a linear function. A longer term analysis (1995 – 2013) was carried out on all fatalities and all registered vehicles and this suggested that a linear trend was more appropriate than a log linear trend. There is a longer trend which takes into account data from 2007 to 2012 and a shorter trend (based on 2009-2012), which encompasses what appears to be a possible change in trend in 2009, when the car occupant fatality rate started to decrease. It was decided that, given these trends are based on relatively few data points, the longer trend should be used as this is less likely to contain as much random fluctuation as the shorter trend.

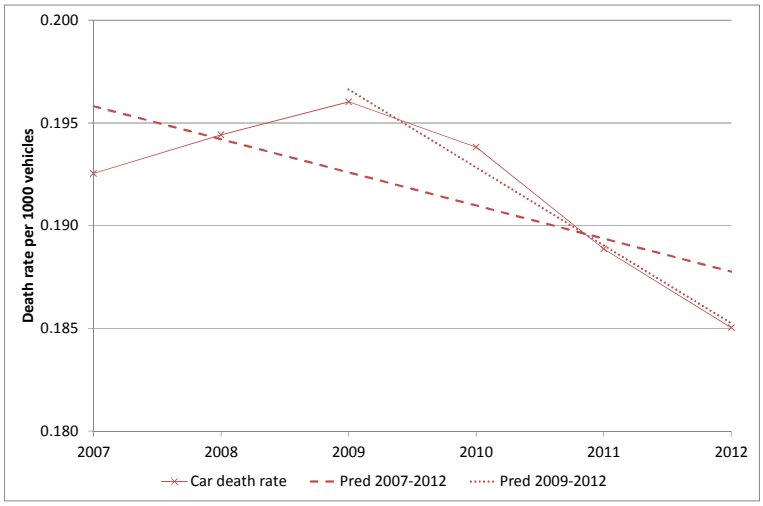


**Figure 1. Car occupant fatality rate per 1000 registered cars in Malaysia (2007-2012)**

The possible baseline scenarios for car registration growth in Malaysia from 2012 to 2030 have been devised as:

A. The trend in car registrations continues to grow linearly at the current rate: an average annual rate of 5.4% relative to 2012
B. The trend in car registrations continues to grow linearly at an average annual rate of 0.7% relative to 2012. This is equivalent to the growth rate in Britain between 2004 and 2013.
C. The trend in car registrations continues to grow linearly at an average annual rate of 14.8% relative to 2012. This is equivalent to the highest annual average increase in car registrations in Britain, in the 1950s.
D. The trend in car registrations continues to grow linearly at an average annual rate of 5.4% as in scenario a) but also encompasses a gradual move from motorcycles to cars resulting in half of the number of motorcycles in the fleet in 2030. This is equivalent to an annual average increase of 7.0% per year.

Relative to the population (and assuming a constant linear growth), the associated motorisation rates by 2030 are 0.52 (A), 0.29 (B), 0.96 (C) and 0.59 (D). The current motorisation rate in Malaysia is 0.36 and in Britain is 0.45

as shown in Table 3. This shows that scenario C is highly unlikely, and further calculations do not consider this scenario.

Assuming that the relationship between car occupant fatalities and registered cars remains the same as in the current trend, the derived number of car occupant fatalities that could be expected under the three feasible scenarios A, B and D are shown in Figure 2. The associated increase in car occupant fatalities in 2030 compared to 2012 for the three remaining baseline scenarios 68% (A), -5% (B) and 92% (D).

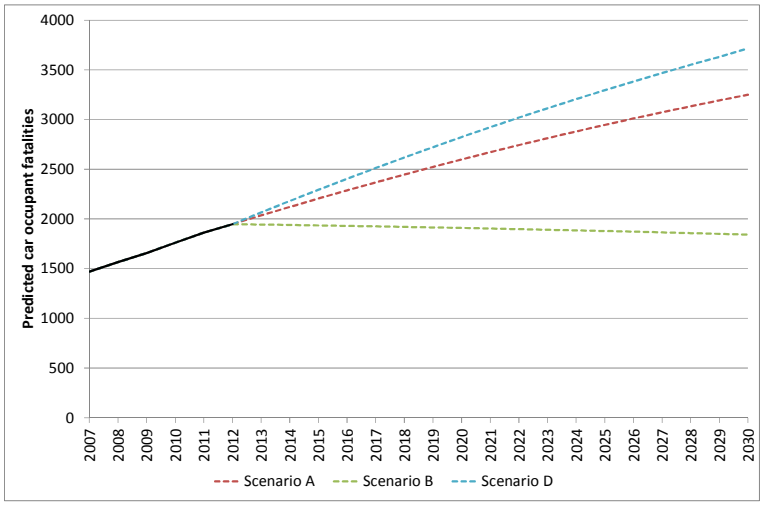


**Figure 2. Predicted number of car occupant fatalities in Malaysia 2007-2030 based on three scenarios**

These baseline scenarios assume that vehicle safety developments continue at the current rate. However, if the impact of regulations on vehicle manufacturers and NCAP on buying habits that were seen in Europe could be replicated in Malaysia, then we would expect a reduced number of fatalities over the same period. Based on the comparisons shown in vehicle safety between Malaysia and Britain on new cars tested in NCAP programmes, the suggestion is that the current vehicle safety standard in Malaysia could be equivalent to the 2004 standards in Europe. We know that Malaysia is not exactly as Europe was in 2004. In particular, as shown in Table 3, the proportion of the cars in the fleet that were reasonably new (6 years or under) is approximately half that in Britain in 2004. This suggests that the fleet renewal rate in Malaysia is currently slower than observed in Britain in 2004, and therefore any regulations or new safety technologies or features would likely infiltrate the fleet at a much slower pace than observed in Britain. As discussed above, in Britain, 4.2% fewer car drivers died between 2005 and 2013 due to the progression in secondary safety.

We have predicted the impact on fatalities of two future scenarios:

1. A proportional reduction in the baseline scenarios fatalities equivalent to half the proportional reduction observed in Britain to take into account the difference in fleet turnover rate observed in Britain.
2. The same proportional reduction in the baseline scenarios as observed in the Britain which might reflect a quicker fleet turnover or a quicker uptake of regulations than observed in Britain.

Table 4 shows the estimated potential car occupant fatality savings over 17 years between 2014 and 2030 based on the potential baseline trends in car occupant fatalities in Malaysia shown in Figure 2, and the two named future scenarios 1 and 2 above.

**Table 4. Estimated potential car occupant fatality savings between 2014 and 2030 given future scenarios 1 and 2**

| | Future scenario 1 | | Future scenario 2 | |
|---|---|---|---|---|
| **Baseline scenario** | **Potential total fatality saving** | **Potential fatality saving proportion** | **Potential total fatality saving** | **Potential fatality saving proportion** |
| **A** | 1,914 | 4.1% | 3,827 | 8.3% |
| **B** | 1,225 | 3.8% | 2,449 | 7.6% |
| **D** | 2,139 | 4.2% | 4,278 | 8.4% |

## CONCLUSIONS

In 2012, the car user death rate was 66.1 per million Malaysian population compared to 13 per million British population. This represents a significantly higher casualty rate, and this is only partially associated with differences in vehicle safety standards.

Comparing the performance of cars in Asean and Euro NCAP frontal impact tests, we concluded that broadly, today's Asean cars could be performing somewhere around the Euro 2004 level. This was based on an engineering visual assessment of the cars' structural behaviours during the impact tests. However, it is not known how well the Asean cars would perform in equivalent Euro NCAP side impact conditions, or the level of secondary safety offered by cars in the current fleet, which have not undergone NCAP testing.

The casualty modelling assumes that recent car safety regulations that have come into force in Malaysia, have improved the secondary safety protection afforded to new car model users, to a level similar to that seen in Europe in 2004. Based on information on the age of the car fleet in Malaysia, it is possible that the entire fleet (with many older cars) could reflect a level of safety more like Britain before 2004. Therefore, the casualty benefits predicted for Malaysia by this study represent a conservative estimate.

In Britain from 2005-2013, the estimated effectiveness of improvements in car secondary safety, since 2004-05 registered vehicles, was 4.2% for car driver fatalities. That is, 4.2% fewer car drivers died between 2005 and 2013 due to improvements in secondary safety in cars.

The current motorisation rate in Malaysia is 0.36 and in Britain is 0.45. Depending upon the change in motorisation rates and the uptake of new cars, we estimate that between 1,200 (scenario B, 0.29 motorisation rate) and 4,300 (scenario D, 0.59 motorisation rate) car user fatalities could be prevented on Malaysia's roads between 2014 and 2030. This assumes that the car secondary safety improvements seen in Britain since 2004 are transferred to the Malaysian vehicle fleet.

This paper has provided estimates for fatality reductions associated with secondary safety measures for car users that are likely to be seen in Malaysia because of the adoption of UN Regulations. Establishing minimum mandatory regulations within the marketplace has been a significant step and provides a real world example of what can be achieved.

Further work will summarise the potential benefits for pedestrian protection and ESC advances in Malaysia and other emerging markets.

**Acknowledgements**
This research was funded by Global NCAP.

**References**

Broughton, J. (2003). *The benefits of improved car secondary safety.* Accident Analysis & Prevention, Volume 35, Issue 4, 527-535.

Broughton J, Allsop RE, Lynam DA and McMahon CM (2000). *The numerical context for setting national casualty reduction targets.* TRL Report 382, Transport Research Laboratory, Crowthorne.

Broughton J and Keigan M (2010). *Linking STATS19 and Scottish Hospital In-Patient data for the SafetyNet project.* TRL Report PPR207, Transport Research Laboratory, Wokingham.

Department for Transport (DfT) (2013a). *Vehicles (TSGB09) - Statistical data sets - GOV.UK. [ONLINE]* Available at: https://www.gov.uk/government/statistical-data-sets/tsgb09-vehicles#ASEAN NCAP-TSGB0901-VEH0103 [Accessed 4 Mar. 2015].

DfT (2013b). *Vehicles (TSGB09) - Statistical data sets - GOV.UK. [ONLINE]* Available at: https://www.gov.uk/government/statistical-data-sets/tsgb09-vehicles#ASEAN NCAP-TSGB0901-VEH0103 [Accessed 4 Mar. 2015].

DfT (2014). *Number of registered cars by make, model and year of first registration.* Data direct from DfT.

Gasnier, M (2014). *Best Selling Cars – Matt's blog » 2014*. *[ONLINE]* Available at: http://bestsellingcarsblog.com/2014 [Accessed 4 Mar. 2015].

Lloyd, L.K., Reeves, C., Broughton, J. and Scoons, J. (2012). *Investigating the reduction in fatal accidents in Great Britain from 2007-2010.* TRL Published Project Report PPR663.

Motor Trader (2014). *New Vehicle Sales by brand. [ONLINE]* Available at: http://www.motortrader.com.my/ . [Accessed 02 March 15].

OICA (2013). *PC World Vehicles In Use. [ONLINE]* Available at: http://www.oica.net/wp-content/uploads/2013/09/pc-wviu.pdf . [Accessed 03 March 15].

MAA (2014). *Malaysia Automotive Info – Summary of sales and production data. [ONLINE]* Available at: http://www.maa.org.my/info_summary.htm . [Accessed 03 March 15].

WHO (2009). *Global status report on road safety 2009*. *[ONLINE]* Available at: http://www.who.int/violence_injury_prevention/road_safety_status/2009/en/ [Accessed 4 Mar. 2015].

WHO (2013). *Global status report on road safety 2013*. [online] Available at: http://www.who.int/violence_injury_prevention/road_safety_status/2013/en/ [Accessed 4 Mar. 2015].

## TECHNICAL ANNEX – Secondary safety modelling

### Method

The following variables are included in logistic regression models:

- **Registration year of the vehicle**: used to estimate the reduction in the severity of drivers' injuries linked to changes in succeeding 'cohorts' in the car fleet
- **Accident year**: accounts for the fact that other road safety measures and conditions will have affected the road system
- **Age and sex of the casualty**: to allow for the differences in injury severity and car choice for different demographics of drivers
- **Vehicle type of striking car**: controls for the differences in protection offered to occupants of different sizes of cars.
- **Road type**: is a proxy for speed of accident and controls for the influence of speed on injury severity.

The modelling is used to predict the number of casualties which would have occurred if secondary safety had not improved. This calculation assumes that improving car secondary safety cannot prevent occupants from being injured in an accident, but can reduce the severity of the injuries suffered. As a result, this model is likely to underestimate the actual benefit as some car occupants who would previously have been slightly injured may now not be injured.

### Results

In total, 2,802,648 car driver casualties were injured in accidents recorded in STATS19 between 1989 and 2013. Of these 83% (2,329,292) had a valid age, vehicle registration year, vehicle type and speed limit and these data have been used for this analysis. It has been assumed that excluding those vehicles where the data is unknown does not bias the results of the model, and the casualty estimates presented are weighted to take into account those that are unknown.

***Modelling results*** Figure 3 shows the proportion of male 25-59 year old small family car driver casualties killed by registration year in 2013 on built up and non-built up roads. The blue dots show the result of the model when year of registration is included as a factor, and the red line shows the model results when a linear trend is assumed for the improvements to secondary safety. A break-point in the linear trend occurred in 1990-91 registered vehicles on both built-up and non-built-up roads.

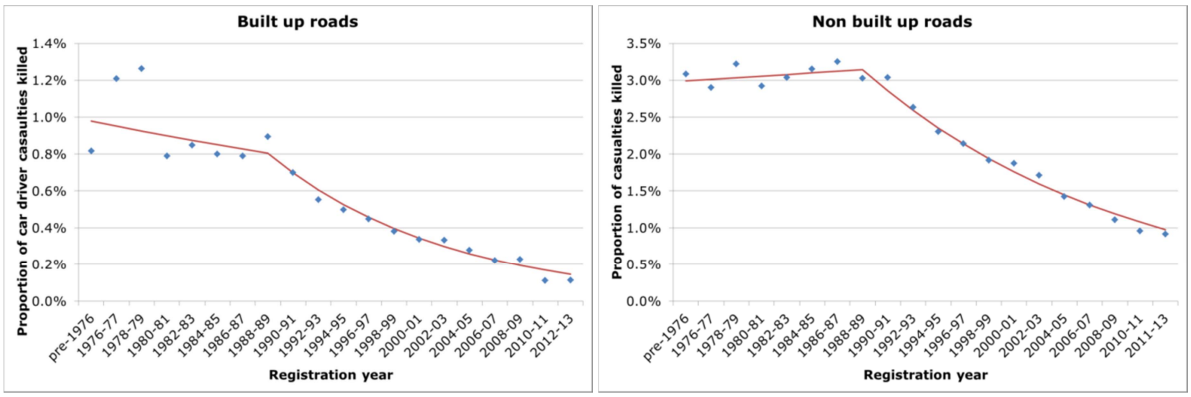


**Figure 3: Modelled fatality proportion by registration year for car drivers (males 25-59, small family cars, 2013)**

Figure 3 indicates that, for accidents on built-up and non-built-up roads, since 1990-91, improvements to secondary safety for car occupants have improved more rapidly than pre-1990. It is suggested that this is due to the impact of manufacturers starting to consider the impact of possible regulations on the car industry.

One other possible explanation for this trend is a change to the level of underreporting in STATS19. If slight and/or serious casualties were being reported less over time, but the level of fatality reporting remained the same then the proportion of casualties killed would appear to increase. In June 2006, the Department for Transport commissioned some work to match STAT19 data to hospital data in an attempt to determine levels of underreporting (Broughton and Keigan, 2010); however the conclusions are hard to draw out and the trend over time was not investigated. Even if this trend is true, the changes in reporting rate do not bias the crucial results relating to registration year as we are interested in the trend from 2004 onwards when applying the data to Malaysia.

***Estimated casualty benefits*** Following the methodology outlined in Broughton (2003), the models described above can be used to estimate the number of lives that have been saved by improvements to the secondary safety of cars. For example, it is possible to determine if the safety of cars had remained at the level of the 2004-05 registered cars how many additional fatalities would have occurred up to 2013.

These calculations assume that the total number of collisions remains unchanged, but that more drivers would have been killed because of the lower secondary safety. The model is used to adjust the severity proportions of the modern cars to match with those registered in 2004-05. Casualties in cars registered before 2004-05 are assumed to remain unaffected.

Improvements to secondary safety are likely to have reduced the total number of casualties as some casualties who would have previously been slightly injured in the collision are not injured in more modern cars. As a result, the casualty estimates presented in Table 5 are an underestimate for the actual casualty benefit. The total figure shown in Table 5 is based on modelled data to smooth out variability in the trend due to random variation.

**Table 5: Actual and estimated car driver fatality numbers in 2007, 2010, 2013 if secondary safety had remained at level of 2004-05 registered vehicles**

| Accident year | Actual fatality numbers | Estimated fatality numbers if secondary safety had not improved | Reduction in fatalities due to secondary safety improvements | Proportional reduction due to secondary safety |
|---|---|---|---|---|
| **2007** | 934 | 990 | 56 | 5.7% |
| **2010** | 568 | 583 | 15 | 2.5% |
| **2013** | 543 | 602 | 59 | 9.8% |
| **Total (modelled) 2005-2013** | 6,874 | 7,176 | 302 | 4.2% |

Hence, between 2005 and 2013 the estimated effectiveness of improvements in secondary safety since 2004-05 registered vehicles was 4.2% for car driver fatalities. That is, 4.2% fewer car drivers died between 2005 and 2013 due to improvements in secondary safety in cars.

# REPEATABILITY OF THE NHTSA VISUAL-MANUAL GUIDELINES ASSESSMENT PROCEDURE

**Annie Rydström**
**Mikael Ljung Aust**
**Robert Broström**
**Trent Victor**
Volvo Car Corporation
Sweden

Paper Number 15-0240

## ABSTRACT

The Visual-Manual NHTSA Driver Distraction Guidelines for In-Vehicle Electronic Devices includes the Eye Glance Measurement Using Driving Simulator Testing (EGDS) task acceptance test. This paper describes the outcome of two EGDS tests, where both tests assessed the same set of 10 in-vehicle tasks, though each test employed a different group of 24 test participants, randomly sampled according to the proscribed EGDS procedure. Thus, in total 48 test participants drove on a simulated motorway in a lead vehicle following scenario while performing tasks such as changing temperature, setting destination in the navigation system and selecting and playing music using a prototype in-vehicle infotainment system located on the center panel. When comparing the test outcomes between the two groups, it was found that for 6 of the 10 tested tasks, pass/fail outcomes differed between the two groups on one or more of the proposed criteria. This high level of inconsistency in outcome between two identical tests using ten identical tasks raises questions regarding the repeatability of the proposed NHTSA EGDS procedure.

## INTRODUCTION

Human-Machine Interface (HMI) guidelines and standards to promote safe design are important tools during the design of in-car interfaces. Several design guidelines and standards have been published, including the European Statement of Principles [1] the JAMA guidelines [2] and the Alliance guidelines [3] (see [4] for an extensive overview of guidelines and standards to use to enhance safety and ease of use, and reduce distraction). Lately authorities have expressed increased concern about a potential intensification in hazardous driver behavior following the functionality growth in infotainment systems in cars and smartphones. As a part of the Driver Distraction Program the National Highway Traffic Safety Administration (NHTSA) in 2012 issued additional guidelines, the Visual-Manual NHTSA Driver Distraction Guidelines for In-Vehicle Electronic Devices. The guidelines provide interface recommendations and performance-based acceptance criteria. After some criticism from both the car industry and the academia on first and foremost the task acceptance testing described in the guidelines, the final version of the guidelines was published April 26 2013 [5] (and some additional clarifications has been published after that [6]). The guidelines are valid for all new cars sold in the USA 3 years after the date of publication.

The guidelines include the task acceptance testing procedure Eye Glance Measurement Using Driving Simulator Testing (EGDS). Volvo Car Corporation (VCC) has for many years used test methods similar to EGDS to evaluate in-car HMIs during their development phase, and has in previous years performed numerous EGDS tests. However, when analyzing the test data according to the EGDS acceptance criteria, it has been found that a task which passes the test at one test occasion does not necessarily pass at another occasion.

A key property of any performance assessment procedure is reliability, i.e. for outcomes to be consistently similar when a test is repeated. If results are not repeatable, the whole idea behind the test fails. The lack of test repeatability when applying the NHTSA EGDS criteria at VCC has therefore raised concerns. However, since the testing performed at VCC has not strictly followed the prescribed EGDS procedure, it is possible that the lack of repeatability may be due to differences in test setups rather than an inherent property of the criteria formulation.

The objective of this study was to assess whether the lack of repeatable outcomes previously found at VCC is methodological or structural in character. To this end, two identical EGDS task acceptance tests were performed at a professional test facility external to VCC. The same 10 in-vehicle tasks were used for both tests, and the NHTSA

proposed EGDS test protocol was strictly followed in terms of recruiting and test setup, in order to have exactly the same trial conditions for the two test groups.

## METHOD

The test was performed in the test facilities of Ergoneers GmbH in Manching, Germany.

### Participants

A total of 48 participants, i.e. two test samples, were recruited in the area around Manching in Germany. Each test sample conformed to the test participant recommendations in the NHTSA guidelines in terms of general criteria, test participant impartiality, mix of ages (six participants in each of the age groups 18-24, 25-39, 40-54, and 55+) and an equal balance of men and women [5].

### Equipment

The test was conducted in an Ergoneers Sim-Lab left-hand drive, fixed base and open cab driving simulator (Figure 1). The simulator is designed as a replica of an actual production vehicle and is adapted to the driving simulator recommendations in the NHTSA guidelines [5].

***Figure 1: The Ergoneers Sim-Lab driving simulator***

The driving simulation used in the study was a car following scenario on an undivided, four lane wide highway with a speed limit of 50 mph, designed in accordance with the driving simulator scenario recommendations [4]. The Ergoneers Dikablis head mounted eye tracking system was used to record the eye movements of the participants. A touch-screen tablet with a prototype infotainment HMI implemented on it was mounted at the center panel of the simulator. Tasks 1-9 were performed on this tablet. An additional, conventional Panasonic car stereo was installed in the simulator to be able to test the AAM radio manual tuning reference task [3].

### Tasks

The prototype infotainment system was designed to replicate a typical in-car center stack interface. Nine tasks were included for the in-vehicle interface, and an additional radio manual tuning reference task was added for the conventional car stereo (Table 1). I line with the guideline recommendations, all tasks started from a home screen view and ended when the task had been executed correctly [5].

*Table1: Tasks*

| Task no. | Task | Task description |
|---|---|---|
| 1 | Activate vehicle function | Access menu and activate a specific vehicle function (on/off option) |
| 2 | Activate USB | Access menu and activate USB |
| 3 | Set a new destination | Access navigation menu and activate a search field and tap in a destination of 10 characters and start guidance |
| 4 | Seta a favorite destination | Access navigation menu and a favorite menu, choose a specific destination and start guidance |
| 5 | Select and play music from USB | Access menu and activate USB and find a specified song in a list |
| 6 | Call contact from recent calls list | Access phone menu and recent calls list and choose a specified contact in the list to call |
| 7 | Dial a phone number manually | Access phone menu and keypad and tap in a 10 digit phone number and call |
| 8 | Change temperature | Access climate and increase temperature with 2 degrees |
| 9 | Set seat heat | Access seat heat and set it to a mid-level |
| 10 – AAM reference task | Manual radio tuning | Access FM1 and adjust to 106.7 (starting position FM3, presetting 97.4) |

**Procedure**

The test procedure, including test participant training, was arranged in alignment with the recommendations in the guidelines [5]. Upon arriving to the test facilities, the participants were given a brief description on the test procedure and they were asked to fill in a consent form and a demographic questionnaire. Then they were asked to sit down in the simulator and adjust the seat. They got to put on the eye tracking glasses and the eye tracking system was calibrated. The user interface and the tasks were demonstrated to the participants and they were able to practice each task as many times as they wanted to. The participants were then given instructions on the driving scenario and got to practice driving the simulator. When they felt comfortable driving the simulator they got to practice to perform the tasks as many times as needed while driving. After the training session the data trial was performed, i.e. the participants performed the tasks and data was collected.

**Acceptance criteria**

Eye movements were analyzed in accordance with the EGDS acceptance criteria [5, 6], which proscribes that no more than 3 out of 24 of the participants shall fail to meet each of the following criteria:

- **Acceptance criteria 1 (AC1):** For at least 21 of the 24 test participants, no more than 15 percent (rounded up to the next whole number) of each participant's total number of eye glances away from the forward road scene have durations of greater than 2.0 seconds while performing the testable task one time.
- **Acceptance criteria 2 (AC2):** For at least 21 of the 24 test participants, the mean duration of each participant's eye glances away from the forward road scene is less than or equal to 2.0 seconds while performing the testable task one time.
- **Acceptance criteria 3 (AC3**): For at least 21 of the 24 test participants, the sum of the durations of each individual participant's eye glances away from the forward road scene is less than or equal to 12.0 seconds while performing the testable task one time.

## RESULTS

When comparing the acceptance test outcomes between the two groups of test participants, results show that for the 10 tested tasks, outcomes were the same in four instances and different in six instances.

Tasks 1, 2, 3 and 9 had the same outcome in both test groups. Tasks 1, 2 and 9 passed on all criteria, while task 3 failed on all criteria (Table 2). The other tasks had different outcomes. Task 8 failed on AC1 and AC2 with group 1, but passed on AC1 and AC2 with group 2. Tasks 4 and 6 passed on AC1 but failed on AC2 with group 1, while the inverse was true for group 2, i.e. failed on AC1 but passed on AC2. Tasks 5 and 7 failed on AC1 and AC2 with

group 1 but passed on AC2 with group 2. Task 10 failed on AC1 with group 1 but passed on AC1 with group 2 and failed on AC3 with both groups.

***Table 2: The number of participants that failed to meet criteria, green = pass and red = fail***

| Task no. | Task | Group 1 | | | | Group 2 | | |
|---|---|---|---|---|---|---|---|---|
| | | AC1 | AC2 | AC3 | | AC1 | AC2 | AC3 |
| 1 | Activate vehicle function | 2 | 2 | 0 | | 3 | 3 | 0 |
| 2 | Activate USB | 3 | 3 | 0 | | 1 | 1 | 0 |
| 3 | Set a new destination | 8 | 6 | 9 | | 10 | 4 | 13 |
| 4 | Seta a favorite destination | 2 | 6 | 0 | | 4 | 2 | 0 |
| 5 | Select and play music from USB | 8 | 6 | 3 | | 6 | 3 | 1 |
| 6 | Call contact from recents list | 3 | 4 | 0 | | 4 | 3 | 0 |
| 7 | Dial a phone number manually | 11 | 9 | 3 | | 10 | 3 | 3 |
| 8 | Change temperature | 6 | 6 | 0 | | 2 | 2 | 0 |
| 9 | Set seat heat | 1 | 1 | 0 | | 0 | 0 | 0 |
| 10 | AAM ref. task: Manual radio tuning | 5 | 2 | 12 | | 3 | 1 | 16 |

## DISCUSSION AND CONCLUSIONS

The objective of this study was to assess whether the lack of repeatable outcomes previously found at VCC when applying the NHTSA acceptance criteria to EGDS test type methods was primarily methodological or structural in character. The results of the two identical EGDS acceptance tests reported above indicate that the lack of repeatability stems from how the criteria are designed, rather than how the test is performed. In this case, the two tests were set up following the proscribed protocol as strictly as possible, and the tested tasks were the same between the groups. Yet 6 out of 10 tasks came out different in terms of pass or fail on at least one of the proposed criteria.

From the above table, it mainly seems like acceptance criteria 1 and 2 have the most inconsistent outcomes, while acceptance criteria 3 (total eyes-off-road time) seems quite stable. Notable is the inconsistent outcome on task 10, which is a radio task that is supposed to work as a reference task, i.e. a task that has been prevalent throughout traffic through the ages and which drivers are thought to accept the risk of performing.

It is of course possible that some of the inconsistencies may still be due to methodological issues. In a perfect world, if two samples are recruited from the same population, and the same task is tested using the same test leaders, test method, equipment and logging apparatus, the outcome of a test should be consistent. In the real world on the other hand, differences may still occur due to different test leaders sometimes giving instructions in slightly different manners, and the environmental conditions and other factors may vary slightly. However, in this study, since the outmost care was taken to achieve an identical test setup for the two groups, it is unlikely that any unintended difference in the methodology would by itself lead to such a differentiated outcome. Moreover, since it would be a very large effort to reach a higher level of between test consistencies than the one in the current study, going for higher methodological precision does not seem to be an option. For an acceptance test to work in practice, it has to be robust enough to be applied at any certified test facility, without leading to inconsistent test outcomes.

Given that this study did have a high level of between test consistency, it thus seems like the problem with inconsistent outcomes have to do with how the acceptance criteria are formulated rather than with inconsistencies in

the EGDS testing. It is thus recommendable to investigate what it is in the criteria formulation that leads to these inconsistent outcomes, before applying the NHTSA EGDS method for assessment of production vehicles.

The results have some additional interesting properties. For one, the only tasks that passed all three criteria were the really simple ones that require only one or two button presses, such as activate a vehicle function, activate USB and set the seat heat. While that these simple tasks would pass was expected, it was not expected that a fourth task that presumably should belong to the same category of simple tasks, i.e. change the temperature in the vehicle, would fail (though it only failed in group 1, it passed in group 2). Looking at the detailed glace data from the two groups above, it can be seen that many drivers have long mean glance durations for these simple tasks. This suggests that drivers strive to complete these tasks in one go, rather than use multiple off-road glances.

This further highlights the need to understand what it is in the acceptance criteria formulation that leads to inconsistent outcomes. If future studies verify that mean glance durations indeed are longer for short and simple tasks, then this illustrates a deliberate driver strategy that has to be accommodated both in task development and testing. NHTSA has partially taken this into account by allowing a limited number of glances over 2.0 seconds for a task [6].

However, the results from this study shows that this topic still needs further investigation. For example, as the criteria are currently formulated, a person who uses a single glance of 3 seconds to complete a task will fail on both AC1 and AC2, but if that person uses a single glance of 3 seconds and then adds a check glance of 0.5 seconds (e.g. to verify that a setting has been updated), that person will pass both on AC1 and AC2. In the raw data from the two studies above, there are many examples of drivers who consistently fall into either of these two categories (i.e. they either use one long glance, or one long glance combined with a check glance). The behavior thus clearly is there empirically speaking, and therefore has to be considered in the acceptance criteria formulation.

In summary then, the difference in outcome between two identical tests using ten identical tasks raises questions regarding the repeatability of assessment outcome of the proposed NHTSA EGDS procedure and criteria. Since the need for an assessment method of this type is clear, and projected to lead to increased safety on the roads, further research into what exactly would need reformulation in criteria and method for the assessment procedure to fulfill its intended purpose is urgently needed.

## REFERENCES


[1] European Commission. 2008. “Commission Recommendation of 26 May 2008 on Safe and Efficient In-Vehicle Information and Communication Systems; Update of the European Statement of Principles on Human-Machine Interfaces.”

[2] JAMA. 2004. “Guideline for In-Vehicle Display Systems, Version 3.0”. Japan Automobile Manufacturers Association, Tokyo, Japan, August 2004.

[3] Alliance of Automobile Manufacturers. 2006. “Statement of Principles, Criteria and Verification Procedures on Driver-Interactions with Advanced In-Vehicle Information and Communication Systems”, Driver Focus-Telematics Working Group, Washington, DC., June 26, 2006 update.

[4] Green, P. 2009. “Driver Interface Safety and Usability Standards: An Overview”. In K. Young, J. D. Lee and M. A. Regan (Eds.) Driver Distraction: Theory, Effects, and Mitigation. Boca Raton, FL: CRC Press.

[5] Visual-manual NHTSA Driver Distraction Guidelines for in-Vehicle Electronic Devices (2013). Docket no. NHTSA-2010-0053, National Highway Traffic Safety Administration, April 2013.

[6] Visual-manual NHTSA Driver Distraction Guidelines for in-Vehicle Electronic Devices (2014). Docket no. NHTSA-2014-0088, National Highway Traffic Safety Administration, September 2014.

# CYCLIST-CAR ACCIDENTS – THEIR CONSEQUENCES FOR CYCLISTS AND TYPICAL ACCIDENT SCENARIOS

**Matthias Kuehn**
**Thomas Hummel**
**Antje Lang**
German Insurers Accident Research
Germany

Paper Number 15-0243

## ABSTRACT

The structure of the official German statistics does not permit in-depth analyses to be carried out, so the UDV built up a set of representative case material in order to examine accidents between cars and cyclists in more detail and derive effective measures to improve the safety of cyclists. This material was formed from accidents with personal injury from the years 2002 to 2010 that were covered by motor third-party insurance and involved injury and damage costs of 15,000 euros or more. The cyclist accident material consists of a total of 407 accidents between cars and cyclists. This paper describes how and under what circumstances cyclist-car accidents occur, the maximum levels of injury severity sustained by the cyclists and the impact constellations that occur particularly frequently. In 84% of the cases, the impact between the bicycle and the car occurred at the front part of the vehicle (the front of the car plus the left- and right-hand front wings). In 42% of these cases, the bicycle was coming from the right (as seen by the driver), and in 34% of the cases from the left. Moreover, the analysis of the cyclist-car accidents revealed that the average speed of the cars was a relatively low 24 km/h. The speed of the cyclists often could not be ascertained from the available documents. However, it is known from the UDV's measurements of the speeds of 20,000 cyclists that they travel at an average speed of 18.6 km/h. Three typical scenarios were obtained from the accident material that together account for 42% of all cyclist-car accidents. These three scenarios are "car traveling straight ahead, cyclist coming from the right" (15%), "car turning right, cyclist coming from the right" (15%) and "car traveling straight ahead, cyclist coming from the left" (12%). Another key finding is that the collisions in these three scenarios often (in 47% to 85% of the cases) took place at the entries to or exits from properties or parking lots and at junctions. The findings described make it possible both to work out the requirements that have to be met by future systems for preventing cyclist-car accidents and to design effective test procedures.

## INTRODUCTION

In the last 10 years, the number of people killed on the roads has fallen significantly. That is true not just in Germany but also in the European Union as a whole [1]. However, the picture for cyclists is not quite as positive. In Germany in 2013, for example, 43% fewer road users were killed than in 2004. Fatalities among car occupants fell by as much as 51%, whereas those among cyclists fell by only 25%. The improvement in cyclists' safety thus has not kept pace with the general trend. However, future technical systems in cars (such as emergency brake assist systems with cyclist detection) will have a positive effect on the accident statistics of cyclists. Before such systems can be designed, however, it is essential to have detailed information on how cyclist-car accidents happen and the course they take. The purpose of this paper is to add to this information.

## DATABASE OF THE UDV

The UDV (German Insurers Accident Research) is a department of the GDV (the Gesamtverband der Deutschen Versicherungswirtschaft e.V. or German Insurance Association). It has access to all of the third-party vehicle insurance claims reported to the GDV. In 2013, for example, there were 3.9 million of these claims [2]. For the purposes of accident research, the UDV has created a database (the UDB) that contains a representative cross-section of the data (from the years 2002 to 2010) in this large pool. The data collected is conditioned for interdisciplinary purposes to facilitate research in the fields of vehicle safety, transportation infrastructure and behavior on the roads. The UDB is based on the contents of insurers' claim files. Around 700 to 1,000 new cases are added to the UDB each year. Only accidents with personal injury and a total claim value of 15,000 euros or more are added to the UDB.

## DESCRIPTION OF THE CYCLIST ACCIDENT MATERIAL

### Areas of impact on the car

In 356 of the total of 407 cyclist-car accidents it was possible to ascertain what part of the car was involved in the impact with the bicycle. The distribution of the areas of impact was as follows:

- Front of the car: 218 cases (61%)
- Left-hand side of the car: 55 cases (15%)
- Right-hand side of the car: 69 cases (20%)
- Rear of the car: 14 cases (4%)

### Areas of impact on the car and the cyclist's maximum level of injury severity

If we group together all of the impacts between the bicycle and the front part of the car (the front of the car plus the left- and right-hand front wings), we get the following picture:

- Front part of the car: 299 cases (84%)
- Passenger compartment plus left-hand rear wing: 23 cases (6%)
- Passenger compartment plus right-hand rear wing: 20 cases (6%)
- Rear: 14 cases (4%)

**Figure 1** indicates how seriously the cyclists were injured in collisions involving each of these areas of impact. Figure 1 clearly shows that measures to improve the safety of cyclists need to be focused primarily on the front of the car. This is true in relation to both the frequency of the impacts and cyclists' maximum level of injury severity [3].

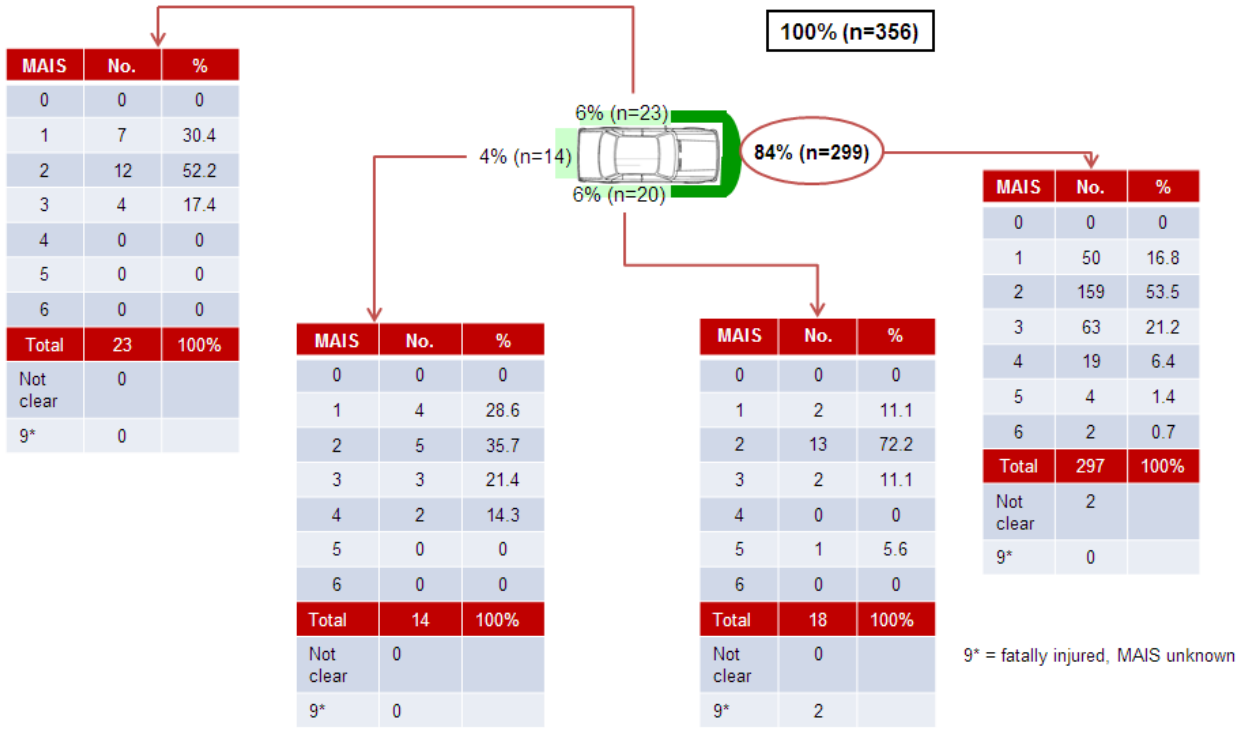


| MAIS | No. | % |
|---|---|---|
| 0 | 0 | 0 |
| 1 | 7 | 30.4 |
| 2 | 12 | 52.2 |
| 3 | 4 | 17.4 |
| 4 | 0 | 0 |
| 5 | 0 | 0 |
| 6 | 0 | 0 |
| Total | 23 | 100% |
| Not clear | 0 | |
| 9* | 0 | |

| MAIS | No. | % |
|---|---|---|
| 0 | 0 | 0 |
| 1 | 4 | 28.6 |
| 2 | 5 | 35.7 |
| 3 | 3 | 21.4 |
| 4 | 2 | 14.3 |
| 5 | 0 | 0 |
| 6 | 0 | 0 |
| Total | 14 | 100% |
| Not clear | 0 | |
| 9* | 0 | |

| MAIS | No. | % |
|---|---|---|
| 0 | 0 | 0 |
| 1 | 2 | 11.1 |
| 2 | 13 | 72.2 |
| 3 | 2 | 11.1 |
| 4 | 0 | 0 |
| 5 | 1 | 5.6 |
| 6 | 0 | 0 |
| Total | 18 | 100% |
| Not clear | 0 | |
| 9* | 2 | |

| MAIS | No. | % |
|---|---|---|
| 0 | 0 | 0 |
| 1 | 50 | 16.8 |
| 2 | 159 | 53.5 |
| 3 | 63 | 21.2 |
| 4 | 19 | 6.4 |
| 5 | 4 | 1.4 |
| 6 | 2 | 0.7 |
| Total | 297 | 100% |
| Not clear | 2 | |
| 9* | 0 | |

***Figure 1. Maximum levels of injury severity (MAIS) in the cyclists by area of impact on the car***

## TYPICAL ACCIDENT SCENARIOS IN CYCLIST-CAR ACCIDENTS

Figure 1 illustrates that most collisions between bicycles and cars involve impact with the front part of the car (n = 299 cases). In 23 of these cases the car was parked. Consequently, only 276 cases are included in our consideration of typical accident constellations. Thus, both parties involved were in motion at the time of the accident in these remaining cases.
**Figure 2** shows four different impact constellations, to which all the observations that follow apply:

- **A**: The car is traveling straight ahead or turning left or right, and the bicycle is coming from the right.
- **B**: The car is traveling straight ahead or turning left or right, and the bicycle is coming from the left.
- **C**: The car is traveling straight ahead or turning left or right, and the bicycle is approaching head-on.
- **D**: The car is traveling straight ahead or turning left or right, and the bicycle is moving in the same direction.

Constellation A is the most common one (with 116 cases), followed by constellation B (94 cases) and then constellations C (35 cases) and D (31 cases).
The box in the upper-left corner of Figure 2 shows the subset of the cyclist-car accident material to which the information in the main part of Figure 2 applies. The same principle applies to the boxes in Figures 3 to 5.

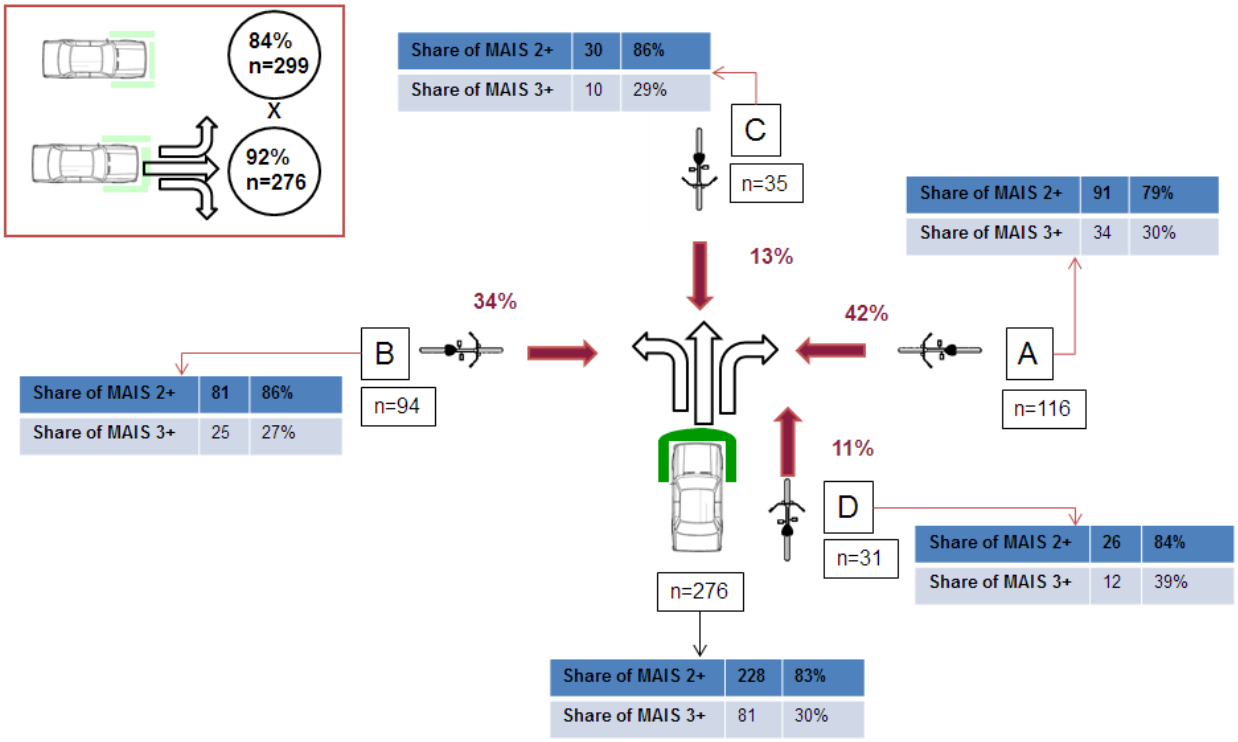


***Figure 2. Frequency of different impact constellations at the front part of the car with the corresponding distributions of MAIS 2+ and MAIS 3+ in the cyclists***

### Speeds of the cars and bicycles and severity of the cyclists' injuries

**Figure 3** shows the average speeds of the cars for these four constellations. The average speeds of the cars in constellations A, B and C were very similar (19 km/h to 23 km/h), while for constellation D the average speed was significantly higher (51 km/h).
The different speeds of the cars are also reflected in the maximum level of severity of the injuries of the cyclists involved in the accidents: The percentage of serious to fatal injuries (MAIS 3+) in constellation D was

thus significantly higher (at 39%) than in constellation A (30%), constellation B (27%) or constellation C (29%). As shown in Figure 2, however, constellation D is the least common of the accident constellations investigated here (at 11%).
The insurers' claim files often contain no information, or only very vague information, on the speeds of the cyclists immediately before the collision with the car, which is why these cannot be specified here. However, in an observational study on the speeds of almost 20,000 cyclists [4], the UDV found that their average speed on a clear run was 18.6 km/h. Moreover, the speed measurements indicated that cyclists on mountain bikes (at 20.5 km/h) and road or racing bikes (25.5 km/h) were significantly faster than average, and cyclists on "Dutch" bicycles (17.0 km/h) were significantly slower. The average speed of cyclists on city bikes (18.3 km/h) was about the same as the average speed for all cyclists, and the same can be said for riders of pedelecs 25 (electric-assist bicycles), whose average speed was 18.5 km/h.

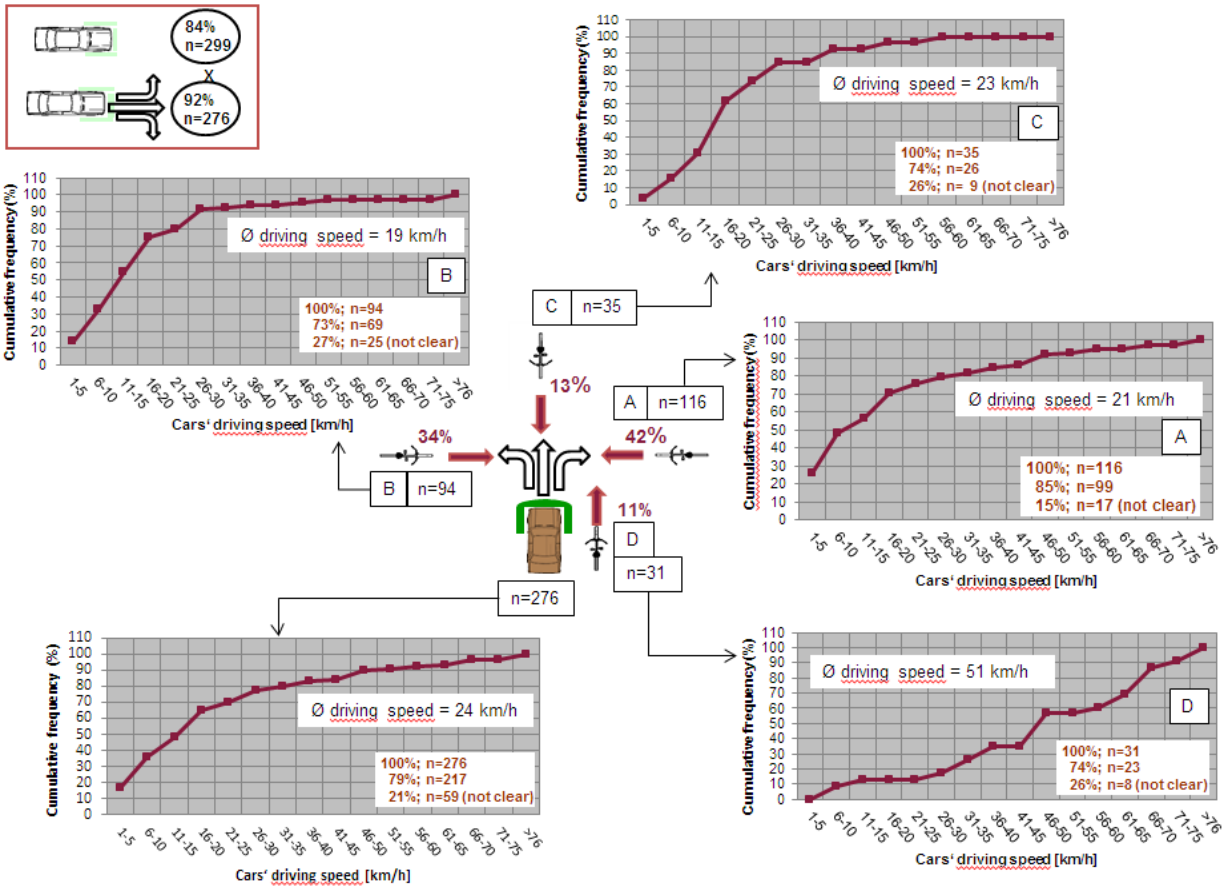


***Figure 3. Average speeds of the cars by impact constellation***

**In-depth analysis of the two most common accident constellations**

It can be seen from Figures 2 and 3 that accident constellations A (116 cases) and B (94 cases) are clearly more common than the other constellations in this accident material. These two accident constellations will be described in depth below.

**<u>Accident constellation A, bicycle coming from the right:</u>** Accident constellation A can be subdivided into three separate scenarios (see **Figure 4**):

- A1: The car is turning left, and the bicycle is coming from the right.
- A2: The car is traveling straight ahead, and the bicycle is coming from the right.
- A3: The car is turning right, and the bicycle is coming from the right.

Accident scenarios A2 and A3 occur with almost exactly the same frequency, accounting for 46% and 45% of the cases. Scenario A1, on the other hand, occurs much more rarely (9%). The lower part of Figure 4 sets out concrete situations for each of the three accident scenarios (A1, A2 and A3) that show the circumstances of the cyclist-car collision in more detail.

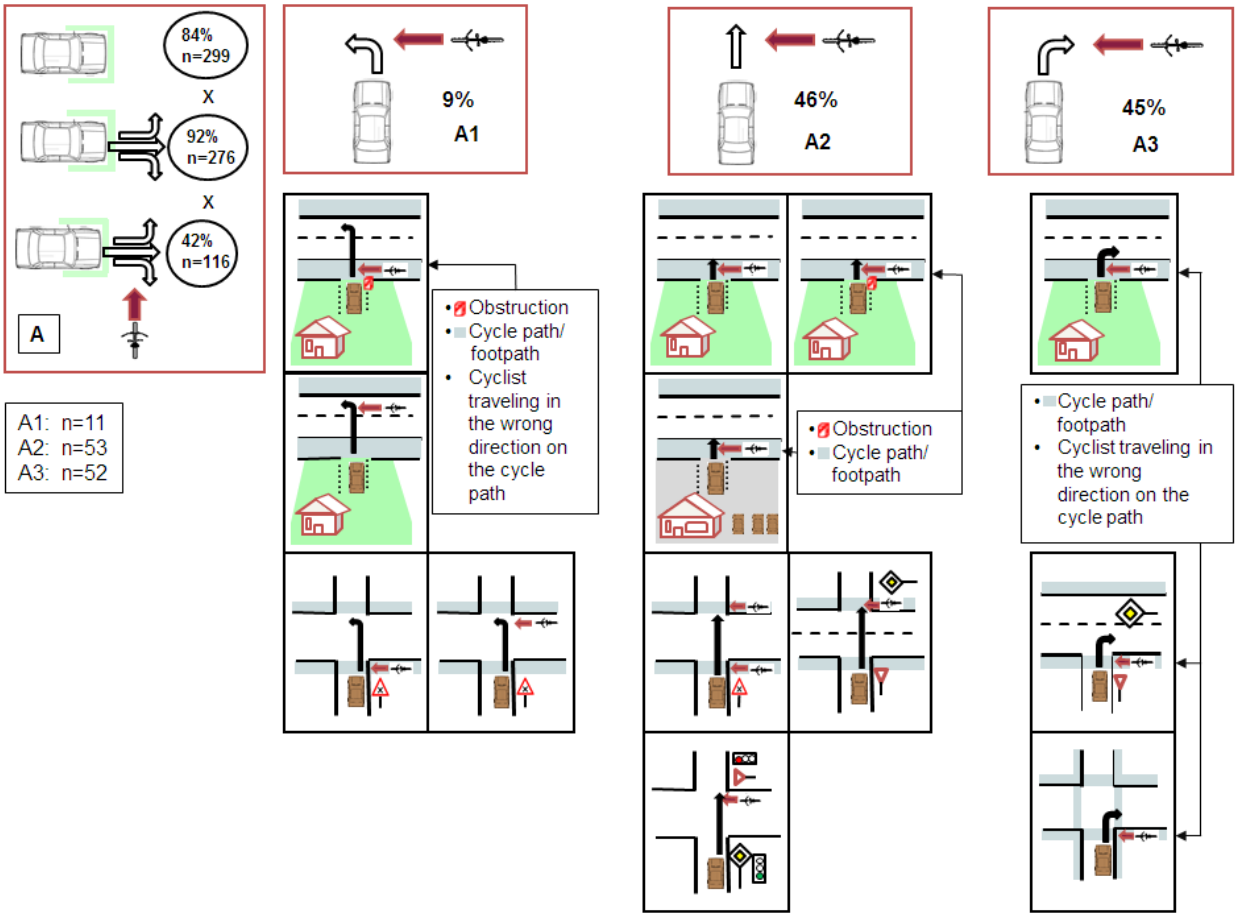


***Figure 4. Distribution of accident scenarios A1, A2 and A3 and illustration of typical cases***

The following are typical accident scenarios for A1:

- The car is coming out of an exit and wants to turn left into the road. A cyclist is approaching from the right on the footpath or cycle path and is partially or totally concealed by an obstruction (such as a hedge or wall).
- The car is coming out of an exit and wants to turn left into the road. A cyclist is approaching from the right on the road.
- The car is turning left at an intersection and collides with a cyclist coming from the right.

The following are typical accident scenarios for A2:

- The car is coming out of an exit straight onto the road. A cyclist is approaching from the right on the footpath or cycle path and in some cases may be concealed by an obstruction (such as a hedge or wall).
- The car is coming out of a parking lot (of a supermarket, for example) straight onto the road. A cyclist is approaching from the right on the footpath or cycle path.
- The car is traveling straight ahead across an intersection and collides with a cyclist coming from the right on the footpath, cycle path or road.

The following are typical accident scenarios for A3:

- The car is coming out of an exit and wants to turn right into the road. A cyclist is approaching from the right on the footpath or cycle path.
- The car is turning right into a road where the traffic has priority and collides with a cyclist coming from the right on the footpath or cycle path.
- The car is turning right at an intersection and collides with a cyclist coming from the right on the footpath or cycle path.

**Accident constellation B, bicycle coming from the left:** Like accident constellation A, accident constellation B can also be subdivided into three separate scenarios (see **Figure 5**):

- B1: The car is turning left, and the bicycle is coming from the left.
- B2: The car is traveling straight ahead, and the bicycle is coming from the left.
- B3: The car is turning right, and the bicycle is coming from the left.

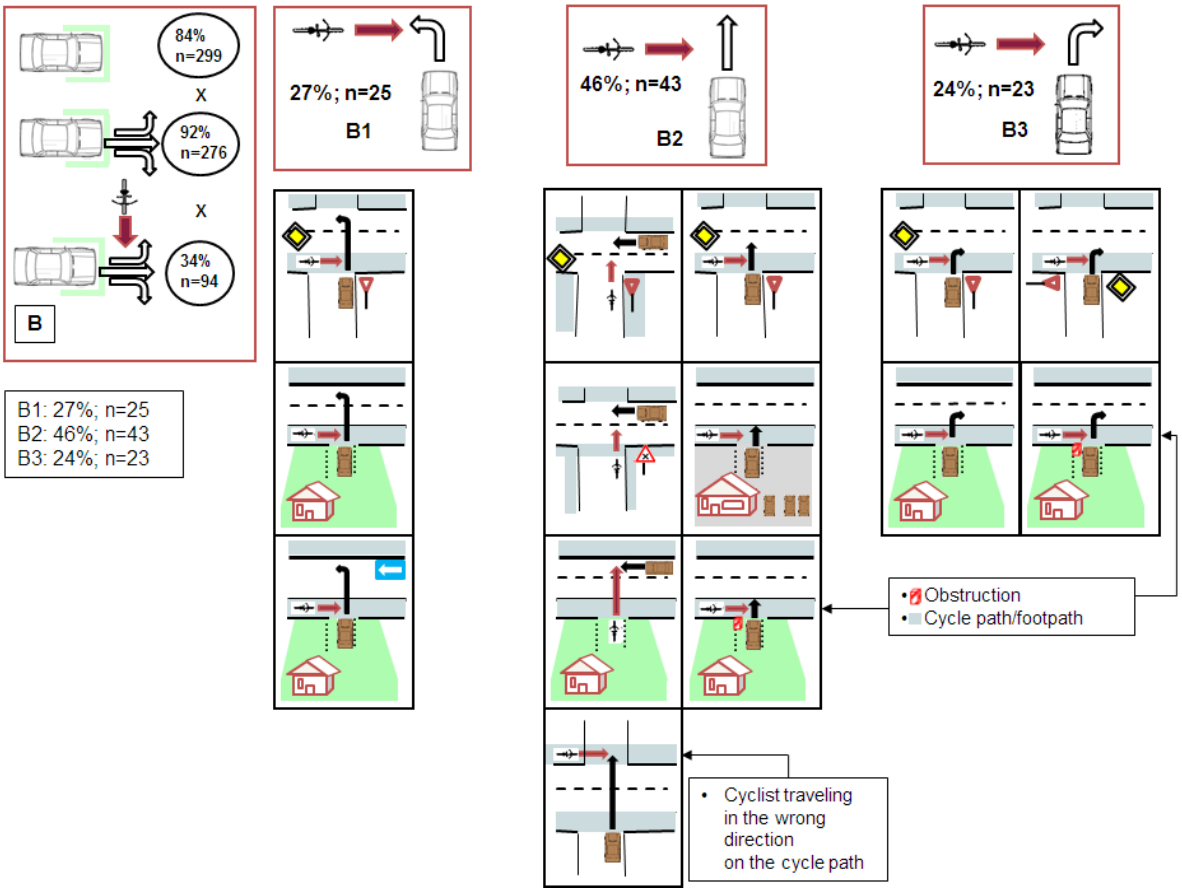


***Figure 5. Distribution of accident scenarios B1, B2 and B3 and illustration of typical cases***

B2 is the most common accident scenario (accounting for 46% of the cases), while scenarios B1 and B3 occur with a similar frequency (27% and 24%). The lower part of Figure 5 sets out concrete situations that show the circumstances of the cyclist-car collision in more detail.

The following are typical accident scenarios for B1:

- The car, which does not have priority, is turning left at an intersection and collides with a cyclist coming from the left on the footpath or cycle path.
- The car is coming out of an exit and wants to turn left into the road or one-way street. A cyclist is approaching from the left on the footpath or cycle path.

The following are typical accident scenarios for B2:

- The car is traveling straight ahead across an intersection and collides with a cyclist coming from the left on the footpath, cycle path or road.
- The car is coming out of an exit or a parking lot onto the road. A cyclist is approaching from the left on the footpath or cycle path and in some cases may be concealed by an obstruction (such as a hedge or wall).
- The car is traveling straight ahead on a road and collides with a cyclist who comes out of an exit on the left.
- The car is traveling straight ahead across an intersection and collides with a cyclist coming from the left on the other side of the road.

The following are typical accident scenarios for B3:

- The car is turning right at an intersection and collides with a cyclist coming from the left on the footpath or cycle path.
- The car is coming out of an exit and wants to turn right into the road. A cyclist is approaching from the left on the footpath or cycle path and in some cases is concealed by an obstruction (such as a hedge or wall).

**Summary assessment of the three most common accident scenarios** In addition to the findings described in this paper, a range of further analyses were also carried out and assigned to the various accident scenarios. Moreover, extrapolation factors were used to extrapolate the cyclist-car accident material described here to all claims reported to the GDV. When all these findings are combined, the picture shown in **Figure 6** is obtained: Scenarios A2 and A3 are the most common, followed by B2. These three scenarios alone account for 42% (15% + 15% + 12%) of all cyclist-car accidents.
Two out of three A2 accidents take place at entrances or exits, the average speed of the car is 30 km/h, and the driver does not brake in 55% of all cases. In scenario A3, 85% of the collisions between cyclists and cars take place at entrances or exits, and the driver does not brake in three of every four cases. This suggests that the driver either does not see the cyclist or does not have enough time to brake. The average speed of the car in scenario A3 is 11 km/h. The percentage of entrances and exits involved in scenario B2 is also very high (47%). The average speed of the cars in scenario B2 is 27 km/h, and the driver does not brake in 42% of the collisions. Further characteristics of scenarios A2, A3 and B2, such as light conditions, the condition of the road and the injury severity and age distribution of the cyclists, are also shown in Figure 6.

## CONCLUSIONS

In the past, researchers focused primarily on pedestrians rather than other unprotected road users. However, cyclists are now becoming an increasingly important focus of research. In 84% of the cases in the UDV's cyclist-car accident material, the impact between the bicycle and the car occurred at the front part of the vehicle. The most common accident scenarios are "cyclist coming from the right" and "cyclist coming from the left". There are only a few cases in which the car is behind the bicycle and hits the back of it. In this impact constellation, however, serious to fatal injuries (MAIS 3+) occur more often than in other impact constellations. Accidents in which the cyclist is coming from the right or left

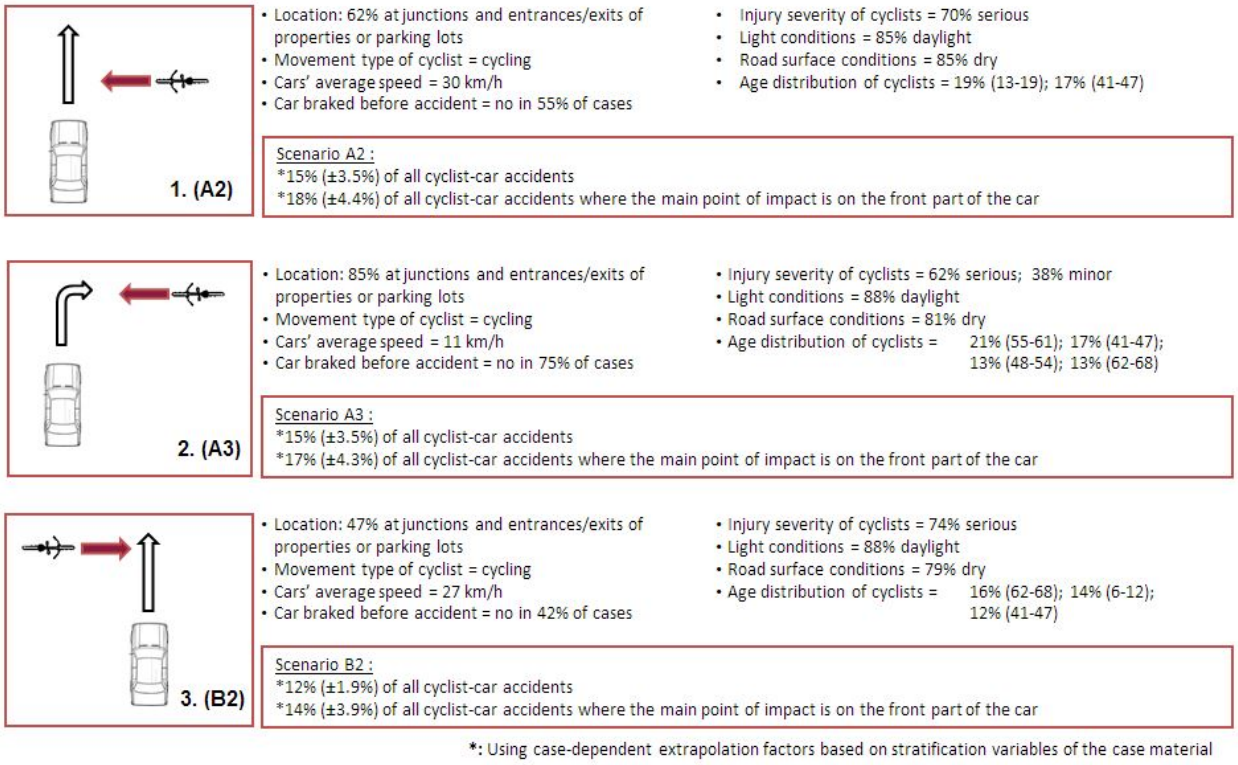


***Figure 6. The three most common accident scenarios, their significance in relation to all cyclist accidents and characteristic features of these accident scenarios***

very often occur at the entrances or exits of properties or parking lots and at junctions. It is essential to take this into account when developing advanced driver assistance systems designed to prevent collisions between cars and cyclists – but also when developing test procedures. Poor light or road conditions, on the other hand, are of only minor significance.

## REFERENCES


[1] German Federal Statistical Office. 2014. Verkehrsunfälle 2013 [Traffic accidents 2013]. Fachserie 8, Reihe 7. Wiesbaden, July 2014. Article no. 2080700137004

[2] German Insurance Association (GDV). 2014. Statistical Yearbook of German Insurance – 2014. Distributed by Verlag Versicherungswirtschaft GmbH, Karlsruhe, Germany. ISSN 0936-1960

[3] Association for the Advancement of Automotive Medicine. 1990. Abbreviated Injury Scale – 1990 Revision.
Des Plaines, IL

[4] Alrutz, D., Bohle, W., Maier, R., Enke, M., Pohle, M., Zimmermann, F., Ortlepp, J. and M. Schreiber. 2015. Einfluss von Radverkehrsaufkommen und Radverkehrsinfrastruktur auf das Unfallgeschehen [Influence of cycling traffic volume and cycling infrastructure on accident occurrence].
German Insurers Accident Research (UDV), Berlin

# SMALL OVERLAP FRONTAL IMPACT – EXPERIENCE AND PROPOSAL FOR A FUTURE APPROACH

**Bengt Larsson**
**Joerg Bakker**
Daimler AG
Germany

Paper Number 15-0244

## ABSTRACT

This paper examines the field relevance regarding frequency and severity of small overlap accidents by comparing accident data from GIDAS, NASS and Mercedes-Benz accident research and from this perspective shows a proposal of a more realistic small overlap test configuration. The result shows a field relevance of approx. 7% in relation to all frontal impact accidents. With respect to an occupant injury severity of MAIS3+ the field relevance is reduced to approx. 3%. Detailed investigations regarding vehicle deformations and occupant loadings on a Mercedes Benz C-Class (MJ 2013 and earlier) show significantly higher severity in the IIHS load case compared to a typically small overlap field accident. Furthermore, a better severity correlation between field accidents and a car-to-car small overlap or the NHTSA small overlap research load case has been observed. In case of the IIHS small overlap test mode some preferential vehicle concepts related to the results has been observed. Investigations show that front wheel drive vehicles with a "east-west" (lateral) engine mount design seem to have some advantage compared to rear wheel drive vehicles with a "north-south" (longitudinal) engine mount design. Accident data analysis confirms that small overlap accidents have field relevance, although the severity of the accidents is lower compared to the IIHS small overlap test mode. In order to obtain a more realistic test configuration the proposal is to use a deformable barrier in order to simulate this kind of accidents.

## INTRODUCTION

The IIHS Small Overlap test program is one of the latest challenges for the automotive development. This load case was implemented in order to simulate the severity of small overlap field accidents, and since the introduction there is a discussion if this load case accurately enough reflects real world accidents. In the first step a review of accident data from GIDAS(Germany), NASS (US) and Mercedes-Benz accident research and published studies was conducted in order to give an overview of the relevance of frontal impact collisions where a small overlap without engagement of the front longitudinal members and an injury severity of MAIS3+ occured. In the second step a case-by-case study of the relevant small overlap accidents with involvment of Merdedes-Benz vehicles was done to compare with the results obtained in IIHS small overlap crashtests. The objects for the comparison were vehicle deformation paths and vehicle collision kinematics. In the third step a closer investigation of the specific IIHS load case was done in order to better understand and classify the test and to answer regarding questions robustness, what kind of field collisions are adressed and if certain vehihle concepts like front wheel drive or rear wheel drive are preferential. In the fourth step a closer look on the repeatability of the IIHS load case was taken: result comparison of two identical vehicle crash tests and simulations test setup variations. Finally in the fifth step different test configurations were investigated that first better reflect real world accidents and second show more robustness and repeatabillity regarding vehicle kinematics and deformations, because it is important that a test configuration is driven by the most typical types of crashes occurring in the field so that potential design changes will lead to benefits in real-world crashes.

## 1. Field relevance regarding frequency, severity and opponents of small overlap accidents

### 1.1 Frequency

There have been many publications about the relevance of the IIHS small overlap test in real world accident scenarios, for example [1],[2],[3], and [4]. Especially, when the test was introduced in 2012, many numbers were quickly published in the press that assessed the relevance in the range 20 – 25% of all frontal collisions. However, there is a simple relation between overlap degree and the frequency of its occurrence in crashes. This relation is valid for the whole range of overlap degrees in frontal offset collisions and basically reflects the frequency

distribution of overlap degree in a random impact into the car front. Accident data shows this relation, which can be seen in figure 1-1 (left) where the cumulative frequency of frontal collisions up to a certain overlap degree with different injury severity levels (from uninjured MAIS 0+ to MAIS 2+) is shown. We can see a linear increase with the level of overlap, independent of the injury severity. According to this distribution, the relevance of a small offset crash with 25% overlap degree could be determined as 25%. The question is, can we derive a relevance of an offset crash from this relation? It seems like no particular overlap degree has a special relevance and one could argue that the bigger the overlap, the bigger the relevance. However, technical considerations come into play when considering the range of accidents one specific offset crash test should represent. In case of the small overlap crash, the crash structure, i.e. the longitudinal members should not be impacted so that they would have the ability to absorb energy. This is the specific characteristic of this crash, separating it from other possible offset configurations, and should be reflected in a corresponding accident analysis. Obviously, having 25% overlap as the only selection criterion for accident data is not enough, as many of these cases also overlap with the structure of the car, due to a bigger variance of impact situations and vehicles in real world accident data than in the crash test. Also, within the group of small overlaps that do not impact the longitudinal members, there are types of accidents with very different characteristics, such as super small overlaps (sideswipes) or impacts with a small oblique component resulting in deformations mostly more on the side than at the front of the vehicle.

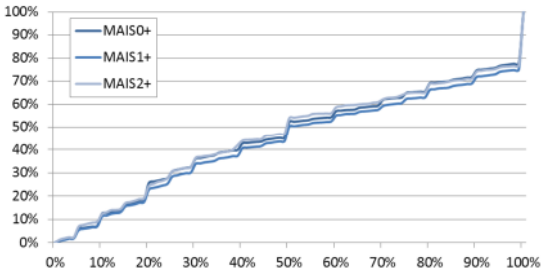


| Source | Country | Data | Year | All Frontal Collisions | Severe Injuries | Fatalities |
|---|---|---|---|---|---|---|
| Prasad et. al, [1] | USA | NASS | 2014 | 7.5 % | 4.6 % to 9 % (MAIS 3+) | 3 % to 8 % |
| George Washington University, [4] | USA | NASS | 2014 | 6 % | 3 % (MAIS 2+) | |
| Mercedes Accident Research | Germany | GIDAS | 2014 | 7 % | 3 % (MAIS 3+) | |

***Figure 1-1. Cumulative frequency of overlap degree in car frontal collisions at different injury levels (left) and different studies with in-depth analysis of small overlap crashes and their relevance (right)).***

In order to filter out the cases with a small overlap and no impact on the longitudinal members, a detailled and manually conducted study of single accident cases is a reliable but costly method. Automatic selection is usually not very accurate with current accident databases in this situation as they lack the exact detail of deformation of the longitudinal members. Figure 1-1 (right) shows the results of several different and recent efforts to conduct such a manual analysis and it turns out that they are comparable, even when based on different datasets. With respect to all frontal collisions and independent of the injury severity, the small overlap represents about 7 %. These numbers also show that the overall relevance of small overlap impacts is comparable in the US and Germany.

In an analysis of GIDAS data (German In-Depth Accident Study as of 07.2013) from Germany, 2524 frontal car crashes were classified into different overlap characteristics shown in figure 1-2. Full overlap takes up to 41% of all impacts. Partial overlaps can roughly be devided into three big groups: large (50 – 75% overlap), moderate (30 – 50% overlap), and different types of small overlap (up to 30%). The rest is made up of central impacts and others. The variaty of small overlap crashes ranges from super small overlaps, which are basically sideswipes, to impacts more into the side structure of the vehicle. Due to the nature of impacting the corner of the vehicle, there is a greater variaty of different types of crashes in the group of small overlaps, than in the other partial overlaps. Some of these differences are shown in the following sections, when injuries and collision opponents are examined for each group.

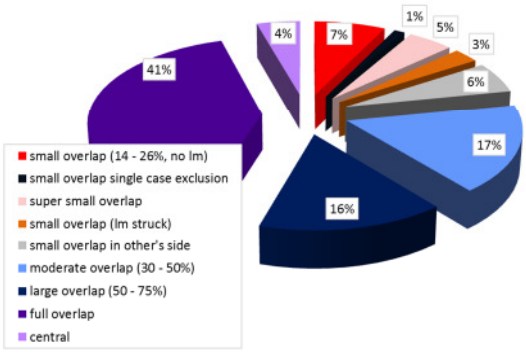


***Figure 1-2. Distribution of severe frontal collisions with different overlap characteristics.***

## 1.2 Injury severity

In the previous section, the relevance of small overlap has been discussed on the accident level. When it comes to injuries, the type of injuries sustained in small overlap crashes is different than in other frontal crashes which has an influence on the injury severity. Serious injuries (AIS 2+) in small overlap crashes are mostly located in lower and upper extremities (figure 1-3) opposed to head/neck and chest in other frontal crashes with the latter injury types are generally more serious than the former ones. Thus, the overal relevance is different and decreases at different injury levels to about 3% for MAIS 3+ injuries (and fatalities) in small overlap crashes (figure 1-3). This pattern is not only observed in accident data, but also in the crash test dummy loads of small overlap crashes vs. other frontal crashes, that have been conducted so far. Also, other studies on US accident data show similar results [4].

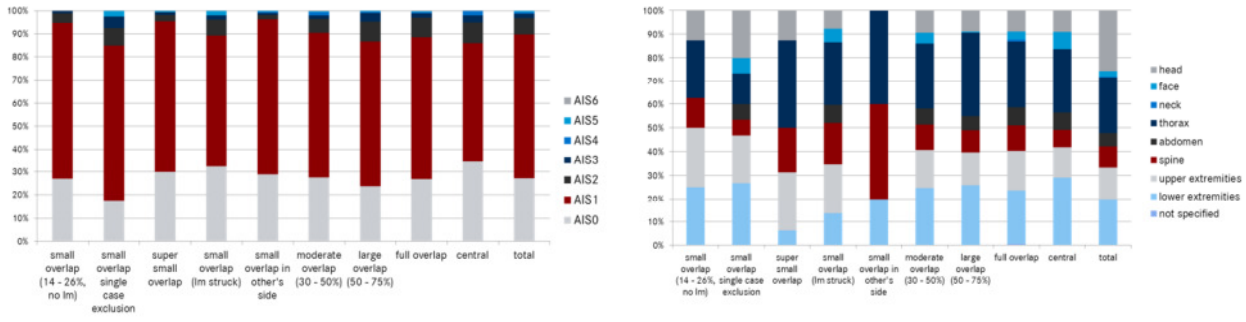


***Figure 1-3. Injury severity and body regions of AIS2+ injuries in crashes with different overlap characteristics.***

## 1.3 Collision opponent

The most striking difference between real world accidents and the small overlap crash test configuration gets obvious when looking closer to the impact opponent. In general, when looking at all types of frontal collisions, object collisions are not as frequent as vehicle collsions. This holds also true for small overlap crashes and is in the same order of magnitude as in all severe frontal impacts. Vehicle opponents occure four times as often as object collisions (figure 1-4). Looking at the small overlap object collisions only, it is not surprising that nearly all of them are collisions against a tree or pole. Out of the 49 object collisions, 28 hit a tree and another 9 a pole. In sum these are 76% tree/pole collisions of all small overlap object collions, which is 20% of all small overlap impacts. To

summarize, the collision opponent in a small overlap accident is in most cases (94%) either a vehicle or a tree/pole where vehicles are clearly dominant with 74%. Similar results were found by [1], [2] where in 22 small overlap crashes, 19 were impacts with the front or side of another vehicle (86%) and 3 were impacts with a pole, post, or tree (14%).

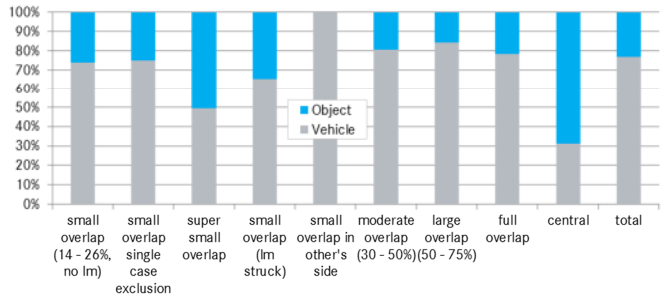


***Figure 1-4. Collision opponent in crashes with different overlap characteristics.***

## 2. Small overlap field accidents versus IIHS small overlap crashtest results

To get a picture how IIHS small overlap test results match to known field accidents a comparison of the deformation patterns and kinematics between tested vehicles and real world collisions was investigated. In this case field accidents analyzed from the Mercedes–Benz accident research were compared to the same Mercedes-Benz carline tested in the IIHS crash test setup. As a representative example for this research a Mercedes-Benz C-Class (MJ 2013 and earlier) involved in a vehicle-to-vehicle accident to a mid-size car with an overlap of 23% for the C-Class is shown below (fig. 2-1 above). The C-Class had a calculated Energy Equivalent Speed (EES) of approx. 60 km/h at collision, which is comparable to the EES severeness of the IIHS small overlap test (58- 60 km/h). The occupant in the C-Class suffered no injuries.

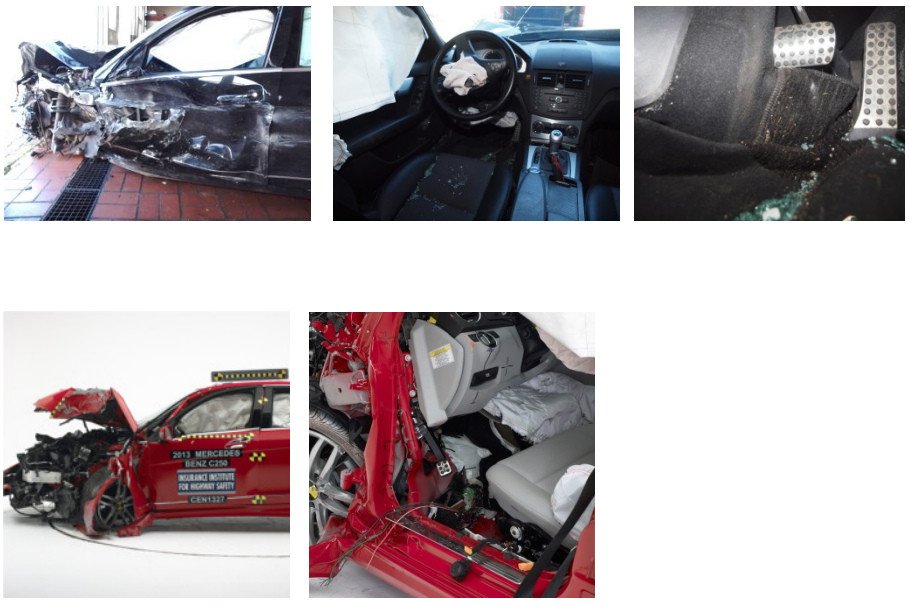

***Figure 2-1. Small overlap field accident, C-Class (MJ 2013 and earlier) vs. IIHS small overlap test result C-Class (MJ 2013 and earlier) [IIHS data]***

The occupants head, neck and chest was well protected by the seatbelt, driver airbag and side- and curtain airbag. Further the intrusion in the foot area was on a low and therefore acceptable level: no structural rupture and no trapping of the lower extremities. The C- Class (MJ 2013) was official tested in the IIHS small overlap and some test results, especially regarding the intrusion at the lower occupant compartment, were unfavorable (fig. 2-1 below).

Although the collision severeness between the field accident and the IIHS test is comparable, significant differences particularly at the lower compartment intrusions are observed. The explanation for these discrepancies is assumed to be the different collision partners: the rigid barrier in the IIHS test setup induces higher and compared to field accidents not representative intrusions.

## 3. IIHS small overlap crashtest - working range and limits

To better understand the IIHS small overlap crash configuration the published data from IIHS crash test during the development of the load case was investigated. Additional car-to-car tests with same and different vehicle test partners were conducted in order to examine the vehicle kinematics and how these fits to the IIHS test configuration. Furthermore vehicle tests in the IIHS setup with different vehicle design concepts, longitudinal ("north-south") and lateral ("east-west") engine mount were reflected, to find out possible differences in output and behavior.
For development of the IIHS small overlap crash configuration a Volvo S60 was often used as a test vehicle. The data from these tests is available on the home page of IIHS and tests were conducted both against barriers (rigid and deformable) and vehicle-to-vehicle configuration. At first car-to-car tests were studied in order to investigate the vehicle kinematics. As an example two car-to-car configurations are shown below (figure 3-1 above):

- Volvo S60 vs. Volvo S60 with 28% overlap, v= 64 km/h [data from IIHS home-page]
- Volvo S60 vs. Volvo S60 with 22% overlap, v= 64 km/h [data from IIHS home-page]

In both cases both vehicles more (28% overlap) or less (22% overlap) stuck to each other and rotated around the vertical axis. A fully glancing off behavior, which has been observed in the IIHS small overlap crash setup of the Volvo S60 (figure 3-1 below), did not occur

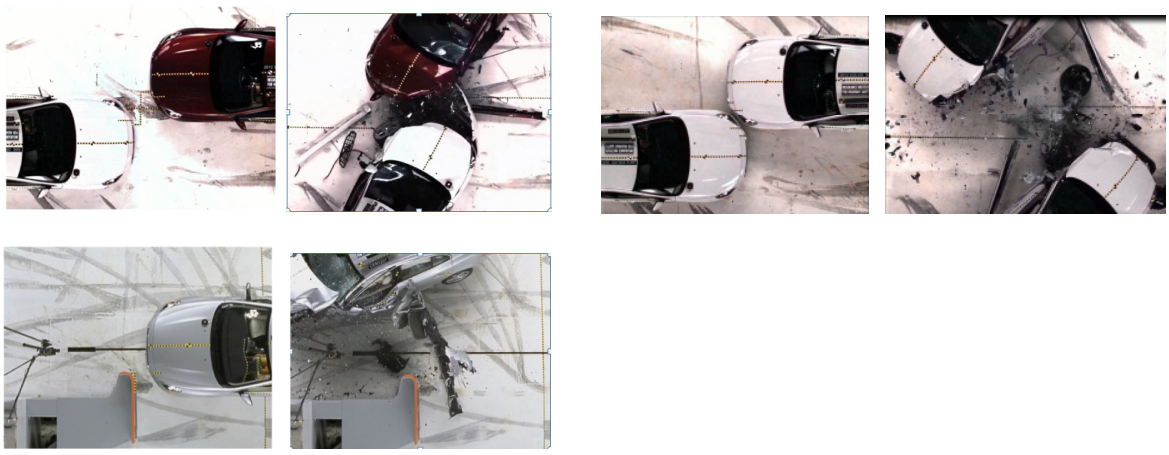

***Figure 3-1. Volvo S60 vs. Volvo S60, 28% overlap (above left), Volvo S60 vs. Volvo S60, 28% overlap (above right) and Volvo S60 tested in the IIHS small overlap test configuration (below) [IIHS data]***

The first conclusion is that the IIHS test setup more simulates a collision against a rigid object like a pole, post or tree prior to a deformable vehicle-to-vehicle collision. The second conclusion concerns the question of the repeatability (see also step 4 below): a minor variation of the overlap 25% +/-3%, seen in the vehicle-to-vehicle tests, causes a major change of the vehicle kinematics regarding the degree of glancing off.

During the development of the load case the IIHS tested different barrier types. The examples in figure 3-1 and figure 3-2 are showing the rigid barrier with two different radius of the barrier edge: 50 mm vs 150 mm. The test with the Volvo S60 shows a different kinematics between these two barriers: a glancing off with the 150 mm radius and a stuck behavior against the 50 mm radius barrier. Thus, a smaller change of the barrier geometry leads to major change of the vehicle kinematics. In fact, the kinematic result at the barrier with the smaller radius is fitting better to the vehicle-to-vehicle tests.

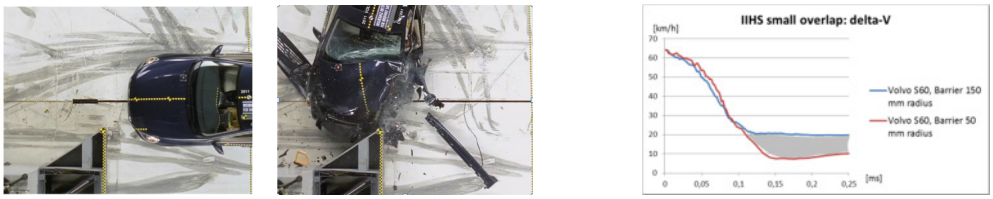


***Figure 3-2. Volvo S60 tested in the IIHS small overlap test configuration overlap 20% with a 50 mm radius edge (left) and delta-V characteristic of the Volvo S60 tested in the IIHS small overlap test configuration 25% overlap with a 150 mm barrier radius edge vs. 20% overlap with a 50 mm barrier radius edge (right) [IIHS data]***

A glancing off kinematic also leads to less reduction of the kinetic energy at the barrier, what firstly means that the vehicle moves uncontrolled forward with a residual amount of velocity, and secondly to less vehicle structural stress (figure 3-2 right: e.g. Volvo S60 approx. 20 km/h residual velocity after impact). Certainly a glancing off behavior obtains a higher amount of lateral velocity than a sticking behavior that could lead to higher injury risk for the occupants at head and chest, but on the other hand the intrusions and structural stress at the upper compartment area normally are lower compared to a sticking behavior.

The cars that up to now have been rated in IIHS small overlap impact have a vehicle architecture either with a longitudinal engine mount (normally rear wheel drive) or a lateral engine mount (normally front wheel drive).

Two characteristics are observed

- None of the vehichle concepts with a longitudinal engine mount ("north-south") have a glancing off tendence at impact.
- For vehichle concepts with a lateral engine mount ("east-west") every degree of glancing off seems to be possible, but a major part (81%) of the invesigated vehichles have a clear glancing off tendence at impact

To get one explanation for the reason of these differences the two concepts below are compared with regard to the barrier impact.

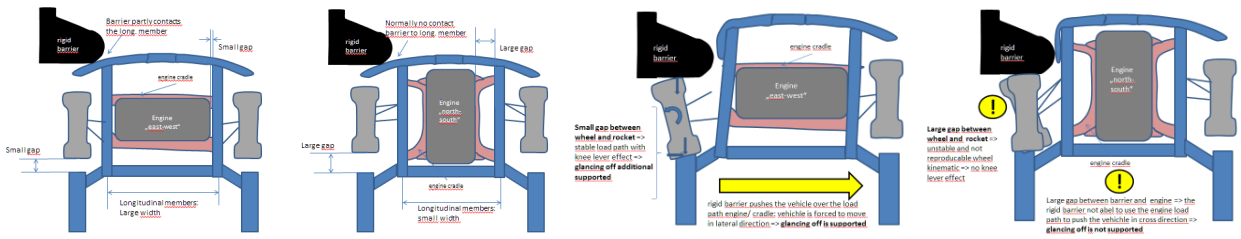


***Figure 3-3. Vehicle concept engine mount "east-west" (left) and "north-south" (right)***
***Schematic results: vehicle concept engine mount "east-west" (left) and "north-south" (right)***

Viewed in figure 3-3 are two structures with the same vehicle width. The main differences between the two concepts that have an important impact on the degree of glancing off at the rigid barrier are:

- The width of the longitudinal members: a large width can allow a partly barrier impact to the longitudinal member
- The gap between the longitudinal member and engine: a small gap allows a lateral engine load path, that pushes the vehicle in lateral direction away from the rigid barrier during the impact
- The gap between wheel and rocket (side member): at the barrier wheel impact a small gap allows a stable and reproducable contact to the rocket and during the impact phase the wheel works like a knee lever to support a vehicle glancing off kinematic. A large gap results in an instable an non-reproducable wheel contact to the rocket.

Conclusion:
For this reasons vehicles with a lateral engine mount concept have benefits in the IIHS small overlap crash mode: the geometry of the rigid barrier allows a pushing effect away from the barrier and increase the degree of glancing off possibility.

In the same way vehicles with a longitudinal engine mount do not benefit from the glancing off effect: almost the whole input kinetic energy has to be managed by the vehicle structure.

## 4. IIHS small overlap – repeatability

During the development of countermeasures and vehicle improvements it was observed that the results of identical vehicle tests didn't give a reasonable repeatability: abnormal large result deviation compared to deviations occurring in for example moderate frontal offset crash configurations. To investigate this, simulations of a large luxury vehicle with a) slightly different overlaps (30%, 20%) and b) different positions of the wheel rim at impact to the barrier were done. Another factor that in a major way influences the test result deviations is the wheel rim styling. In two IIHS small overlap configuration tests of a Mercedes-Benz vehicle with identical body structures and configurations except for the 5 spoke wheel rim styling (fig 4-1) indicate this. In these two cases the rim impact to the barrier for the both vehicles was similar: impact between two rim spokes. However, during the ongoing crash phase the deformation and kinematic of the wheels differs successively, which at the end leads to a complete different structural result especially with respect to the toepan intrusion. These results were also confirmed in numerical simulations with different rim designs and stylings.

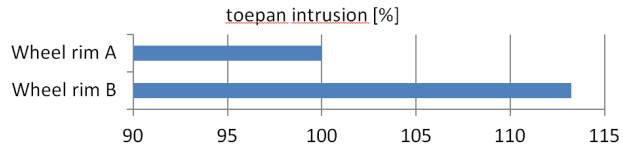


***Figure 4-1. Vehicle with wheel rim A (left) and rim B (right, [IIHS data]): rim impact at the rigid barrier, wheel kinematic during crash and structure response at the rocket (vehicle side member, front view)***

Numerical simulations of an identical wheel rim but with different rim positions at the rigid barrier impact shows large differences of the rim deformations and wheel kinematic, which causes a variation of body structure intrusions (fig 4-2 above). Depending on the rim deformation and rim impact to the body structure the vehicle intrusions differs up to 30 - 40%. In this case especially a wheel rim styling with fewer spokes seems to be more critical (rim strength distribution more inhomogeneous). Further, other parts like the size and thickness of the brake disc and its rupture behavior and the position of the brake caliper have an additional impact on variation of the wheel kinematic and crash results.

Next, a simulation reflects the influence of a smaller variation of the degree of overlap in the IIHS small overlap setup. The overlap was varied between 20% and 30% and compared to the basis setup 25% in all cases the longitudinal member was not struck (fig. 4-2 below). A slightly smaller overlap (20%) shows results with intrusion deviations up to >20% and a slightly higher overlap (30%) induce intrusion deviations even up to >30%. Thus, a smaller change of the vehicle overlap against the IIHS rigid barrier would significant change the vehicle intrusion values.

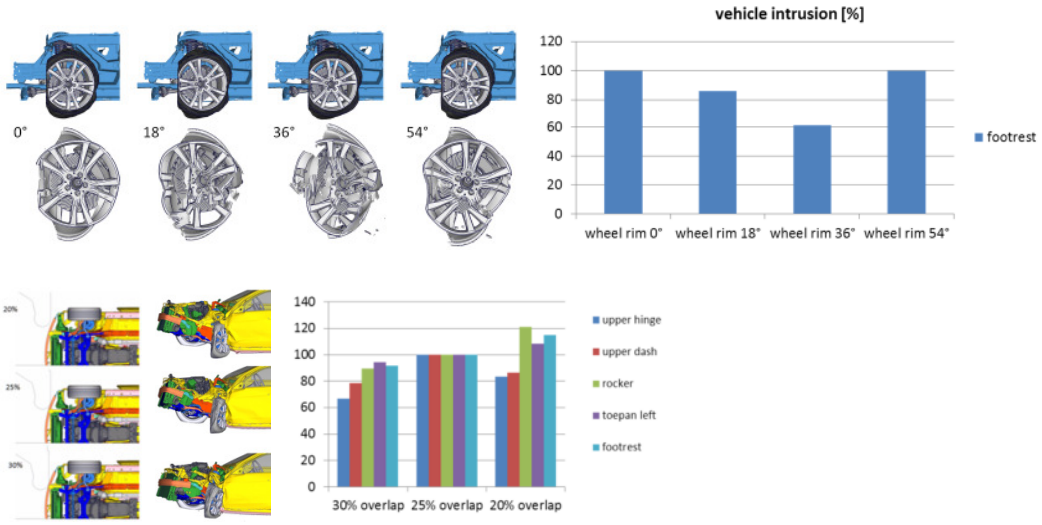


***Figure 4-2. above: Wheel rim deformations at different wheel positions at impact to the rigid barrier (0° = 54°)***
***below: overlap variation at impact and influence on the vehicle intrusions (large luxury vehicle)***

Conclusions:

In the shown examples minor variations to the vehicle setup or test setup causes significant deviations to the test result output. Claiming the same high safety requirement for all vehicle configurations and options, for example wheel rim styling, this lack of repeatability and high deviations makes it hardly feasible to reach that claiming goal. On the other hand this means that the IIHS small overlap configuration with the chosen rigid barrier geometry and shape could lead to a point optimization of a certain vehicle setup.

## 5. Investigations of further small overlap crash test configurations

At the introduction of the IIHS small overlap one main intention was to address severe injuries (MAIS3+) at head and chest areas [Zuby paper 09-0257]. However, almost every tested vehicle since the introduction in 2012 has shown only minor occupants loadings of the 50% HIII in these areas. The major occupant loadings are located to the dummy extremities (femur, tibia and foot) often due to high vehicle body intrusion values in the foot / floor area. For this reason Mercedes-Benz has made further considerations and investigations towards a small overlap load case that could better cover both field accidents severity and also be a robust test

configuration with an acceptable repeatability for the vehicle development. The starting point for finding such a load case the objects were:

- no involvement of primary crash structure like longitudal frame members
- test velocity that covers 90% of the relevant field accidents
- barriere configuration that covers the most common field accidents impact objects
- get a stable and reproducable behavior of the suspension and wheel kinematics with a insignisficant impact of for example wheel rim stylings and wheel rim position at barrier contact
- better balancing of the occupant loadings: vehicle kinamatic that for both glancing off and/or sticking behavieur stronger adresses the head/ neck / chest loadings prior to leg and lower extremities loadings

Relevant conclusions and evaluations that have been shown in the previous steps and could be considered for an optimization of a small overlap test configurations are:

- in the examined field accidents a 40 km/h Delta-V covers more than 90% of the real cases, or in other words
- an Energy Equivalent Speed (EES) of 46 km/h covers 90 % of the reviewed relevant accidents
  - ⇒ This gives a representative velocity of 56- 58 km/h against a rigid barrier or 64km/h against a deformable (ODB) barrier.
    (In comparison: EES for IIHS Small Overlap is approximately 55-60 km/h. In GIDAS, this value represents a cumulative frequency of approx. 98%)
- As shown in the first step obove the most small overlap accidents two vehicles are involved. In GIDAS this represent approx. 75% of the cases. Only 25% are vehicle-to-object accidents. This means, that the most common real collision objects are prevalent deformable and not rigid.
- a rigid barrier causes issues regarding repeatabillity especially with respect to wheel kinematics for longitudinal engine mount vehicle concepts.
- the geometry of the rigid IIHS barrier seems to benefit lateral engine mount vehicle concepts where a glacing off effect reduces the needed energy absorbing capacity for the vehicle.

In order to match the requirements to the above conclusions Mercedes-Benz started a simulation and test evaluation program to find an adequate small overlap test configuration. The main result of that work was the recommendation to use a deformable element in front of a rigid barrier. In the investigation the common ODB deformable barrier (Euro-NCAP / IIHS) and the discussed NHTSA oblique/ small overlap deformable barrier were used. The tested configuration with the deformable ODB barrier is as follow

- ODB barrier in front of a rigid block
- Rigid block w/o edge rounding
- 25% overlap, 0° obliqueness
- Vehicle velocity v= 64 km/h
- Vehichle weight and equipment in accordance to the IIHS test protocol

The first observation of the test result is that the use of the deformable barrier makes the reproducibility of the wheel kinematics much higher: due to the deformation of the barrier the wheel displacement is more defined guided towards the side member (rocket). Also the influence of different wheel rim designs and/or wheel rim positions at impact to the barrier is much lower and makes the evaluation of developed vehicle changes much more accurately and predictably (fig 5-1 above).

With this test vehicle (longitudinal engine mount) a sticking kinematic behavior at the barrier impact occurs. The wheel kinematic with a stable contact to the side member leads to a robustly load path on the axis barrier-wheel- side member. This load path increases the rotating velocity of the vehicle and induces a stronger occupant lateral movement towards the vehicle side structure (fig 5-1 mid, below).

The higher lateral excursion of the occupant in the test mode with the deformable barrier increases the injury risks for head and neck. On the other hand the floor intrusions and injury risks for the lower extremities are reduced. In the overall evaluation and comparison of the two test setups the use of the deformable barrier results in a more balanced injury risk distribution: higher injury risks for head/neck/chest and lower injury risks for feet and legs, which also shows a good alignment to the results from the real life accident analysis.

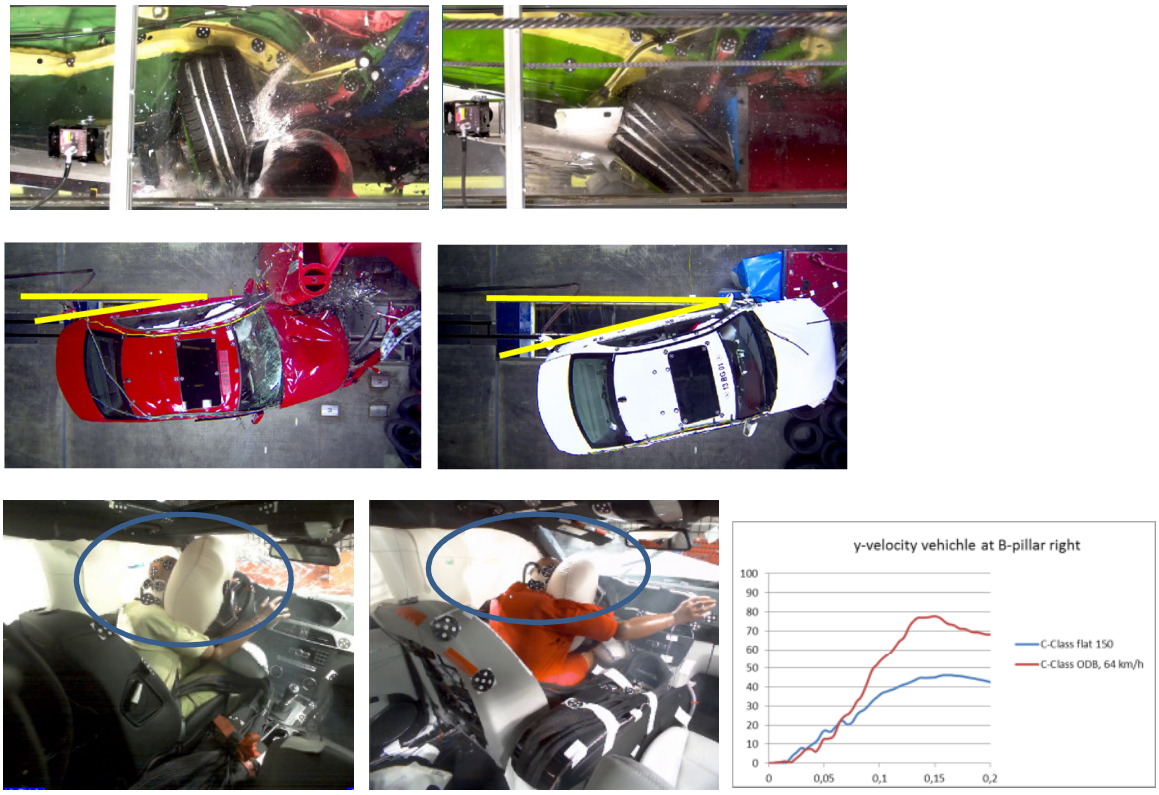


***Figure 5-1. above and mid: IIHS small overlap test mode (left), small overlap w. deformable barrier (right) below: Occupant at maximum excursion; IIHS small overlap test mode (left), small overlap w. deformable barrier (mid), vehicle lateral velocity (right), C-Class (MJ 2013 and earlier)***

To review the results above an additional study was done with the discussed crash mode NHTSA small overlap:

- Movable deformable barrier, mass 2500 kg, barrier velocity 90 km/h, vehicle velocity 0 km/h
- 20% overlap, 7° obliqueness

The result is similar to the outcome of the deformable ODB test: the deformable barrier guides the wheel to stable contact with the side member and a high lateral vehicle movement. The intrusions at upper and lower area are good balanced: compared to the IIHS small overlap configuration the upper area is more and the lower area less loaded. Thus, this configuration reflects the original target requirements in a good way (fig 5-2 above and mid).

The occupant kinematic in NHTSA small overlap setup also differs compared to the IIHS small overlap: the upper torso rotates more around the vertical axis, which could increase the injury risk to head/ neck and chest if the coverage of the driver- and curtain airbag is insufficient (fig 5-2 below)

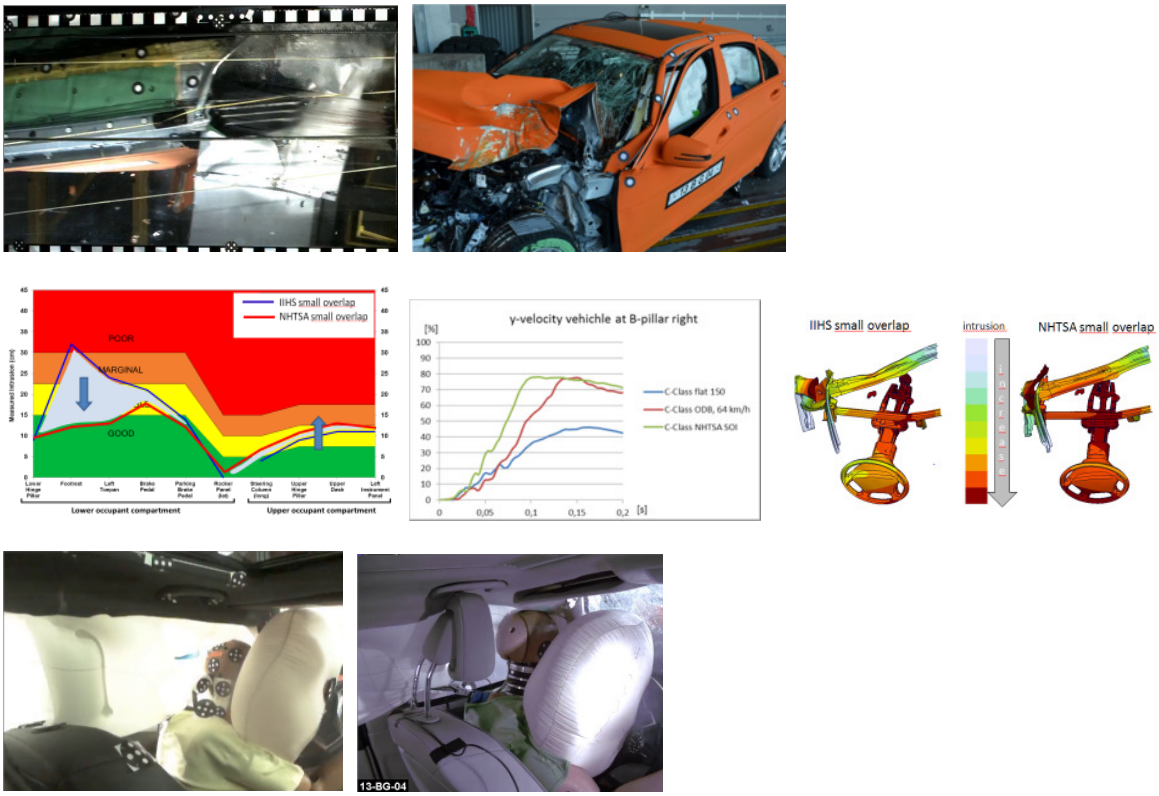


***Figure 5-2. above: NHTSA small overlap - wheel kinematic (left) and A-pillar deformation (right)***
***mid: NHTSA small overlap vs. IIHS small overlap - intrusions and lateral vehicle velocity***
***below: Dummy kinematic / torso rotation: IIHS small overlap (left) and NHTSA small overlap (right), C-Class (MJ 2013 and earlier), HIII- dummy.***

The two examples small overlap with the ODB barrier and the NHTSA small overlap configuration shows that it is reasonable to use a deformable barrier in front of a rigid or movable block. This configuration is able to address the most of previously formulated objects and would make the development more precise and robust. In the investigated setups with the deformable barrier reflects a sticking vehicle kinematic at the barrier impact. In order to also address lateral engine mount vehicle concepts, which have a higher tendency to glancing off, it could be discussed to combine a deformable barrier in front of a rigid block with rounded edge (similar to the IIHS rigid barrier). Such a combination could have the potential to fulfill the previously formulated objects even better.

## CONCLUSIONS

Field accident data shows that severe small overlap frontal impacts occurs but have comparatively a low relevance. Most of the cases are vehicle-to-vehicle impacts, so this should be the focus for a realistic near-to-real-world crash test setup. The experience and investigations of the IIHS small overlap test configuration shows that the load case only partly covers the real world accidents, emphasizing injury risks occurring at the lower extremities of the occupants. The chosen rigid barrier with a large rounded edge also gives a benefit for lateral engine mount vehicle concepts, where the barrier can be used to push the vehicle laterally away from the barrier. Further the rigid barrier has an influence on occurring test result deviation, inter alia, depending on wheel rim positions. To get a more general small overlap crash test configuration, which can cover a larger part of the field accidents and shows more robustness in vehicle development process, the use of a deformable barrier layer in front of the rigid block should be considered.

**REFERENCES**

[1] P. Prasad, D. Dalmotas and A. German, “An Examination of Crash and NASS Data to Evaluate the Field Relevance of IIHS Small Offset Tests.”, 2014 SAE International
[2] M. L. Brumbelow and D. S. Zuby, “Impact and Injury Patterns in Frontal Crashes of Vehicles with Good Ratings for Frontal Crash Protection.”, 21st International Technical Conference on the Enhanced Safety of Vehicles, Stuttgart, Germany – June 2009
[3] B. C. Mueller, A. S. Brethwaite, D. S. Zuby and J. M. Nolan “Structural Design Strategies for Improved Small Overlap Crashworthiness Performance.”, Stapp Car Crash Journal, Vol. 58 (November 2014)
[4] P. Scullion, R. M. Morgan, P. Mohan, C.-D. Kan, K. Shanks, W. Jin, and R. Tangirala “A Reexamination of the Small Overlap Frontal Crash.”, 2010

# ANALYSIS OF CAR ACCIDENTS CAUSED BY UNINTENTIONAL RUN OFF ROAD

**Matthias Kuehn**
**Thomas Hummel**
**Jenö Bende**
German Insurers Accident Research
Germany

Paper Number 15-0245

## ABSTRACT

Car accidents caused by unintentional run off road (in this paper the term "inadvertent lane departure" is used) have become an important topic within world wide accident research activities. These accidents can be addressed by lateral support systems (e.g. Lane Departure Warning) which are considered by experts to be the second most important active safety countermeasures after forward collision intervention systems.

There is no common understanding for "run off road" yet. This term is being used both for the event of a departure from the own driving lane and for the event of a departure from the road. But it is known that when a driver leaves its driving lane unintentionally, it mostly results in a severe crash involving an oncoming vehicle or an obstacle (e.g. tree).

The importance of this topic is also visible as efforts have already been made in order to adopt this issue in current and future testing procedures (eg. NHTSA, IIHS, Euro NCAP).

In Germany, the relevance of unintentional run off road accidents can hardly be estimated when using only official numbers. Official statistics categorize accidents by the parameter "leaving the carriageway" without any differentiation between intentional or unintentional lane departure. However, in the year 2013, these accidents made up 14% of all accidents with personal injury involving all kinds of road users but 30% of all fatalities and 23% seriously injured persons. A more accurate view on the accidents that match the definition "unintentional run off road" was given by UDV in an earlier study (paper-09-0317).

This paper presents now the results of a second more detailed analysis which was carried out with up-to-date accident data. For the analysis, the In-depth database of the German Insurers (UDB) was used. It contains a representative cross section of all third party insurance claims reported between 2002 and 2011. The group of car accidents analyzed was defined as "unintentional run off road accidents" and implies only cases where a car had left his driving lane unintentionally. The aim of the analysis was to get a better understanding of the circumstances at which these incidents occur and to derive key accident scenarios.

From a total of 118 relevant cases in the database, which account for 5% of all accidents caused by a car, five accident scenarios were deduced. These make up 68% of the accidents and 66% of the fatalities in the datapool. Some of the main results were: A lane departure to the left occurred more frequently than a lane departure to the right. Generally, the lane departure was followed by a collision with an oncoming vehicle (in 70% passenger car) rather than by a run off from the road. Regarding behavioral issues, health problems of the driver were found to be twice as frequent as distractions of any kind.

## INTRODUCTION

Car accidents caused by inadvertent lane departure now feature significantly in accident research around the world. Systems for lateral support (or lane departure warning systems) can have a positive effect on these accidents and are seen by experts as being the second most important active safety measure that can be taken, right after advanced emergency braking systems. Accidents caused by inadvertent lane departure are generally very serious because they often result in collisions with oncoming traffic or roadside obstacles such as trees at relatively high speeds. The significance of these accidents is also evident from the level of attention now being given to them by international

test institutes (e.g. NHTSA, IIHS, Euro NCAP). At the European level, Euro NCAP has already made progress toward including systems for lateral support in its test program in future. Euro NCAP's current roadmap [1] includes the objective of providing a test procedure for lane departure warning systems from 2016. From 2018, a procedure will also be available for active lane keeping systems, which constitute a further development of lane departure warning systems.

The relevance of accidents caused by inadvertent lane departure has not yet been extensively investigated in Germany. The official accident statistics do not allow concrete statements to be made about these kinds of accidents. The reason for this is that the road accident reports on which the official statistics [2] are based do not contain any information on inadvertent lane departure because this is not recorded in police accident records.

A previous UDV study [3] provided an initial overview of car accidents caused by inadvertent lane departure. The aim of the present study is to describe these accidents in more detail and identify the main accident scenarios in order to assist with the development of realistic future test procedures. The study also describes the complex methodology that is required for the identification of the relevant accidents and underlines the priority and challenge of this important part of the analyses.

## CASE MATERIAL

The accident material on which the study is based covers the years 2002 to 2011 and comprises 4,245 car accidents, in which 339 people were killed, 2,756 sustained serious injuries, and 4,592 sustained minor injuries. A total of 6,822 cars (not including vans) were involved in these accidents, and 41% of them were the main causer of the accident. All types of road users were taken into account as the other parties in the collisions (cars, vans, trucks, buses, two-wheel motor vehicles, bicycles and pedestrians). Single-vehicle accidents were also included. However, single-vehicle accidents are underrepresented in this case material because, for methodological reasons, cases not involving injury or damage to a third party are not included in the UDV's accident database (UDB).

## TERMINOLOGY AND FORMULATIONS

It is best to begin by explaining some of the terminology and formulations used in this study:

- **Accident type**: Designated by a code of up to three digits. Describes the initial conflict between two road users that led to the accident [4].
- **Kind of accident**: Designated by a single-digit code. Indicates the position of the parties to the collision in relation to each other immediately before the impact [2].
- **Person-related misbehavior** (cause 01-69): This term is taken from the translation of the official accident statistics and essentially refers to a personal error. It is assessed and assigned to the relevant road user by the police officer recording the accident on the basis of a list of accident causes [2].
- **Lane and carriageway**: The carriageway (roadway) consists of at least two lanes, which separate it into two directions of travel; the borders of a lane are generally indicated by markings (Figure 1).
- **Case car**: This is the car that leaves its lane, without the driver intending to do so, and thus causes the accident. In this study, the case car is always the main causer of the accident. In the course of the accident, other road users may leave their lanes either intentionally (to get out of the way) or inadvertently (following a collision), but they are not considered to be the case car.
- **Lane departure**: This is when at least one wheel of the case car leaves its lane. This can be either to the left, which means it crosses the center line, or to the right, in which case it crosses over the border of the carriageway.
- **Leaving the carriageway**: This happens when the case car leaves not just its lane but the entire carriageway (roadway). Leaving the carriageway thus always involves lane departure.

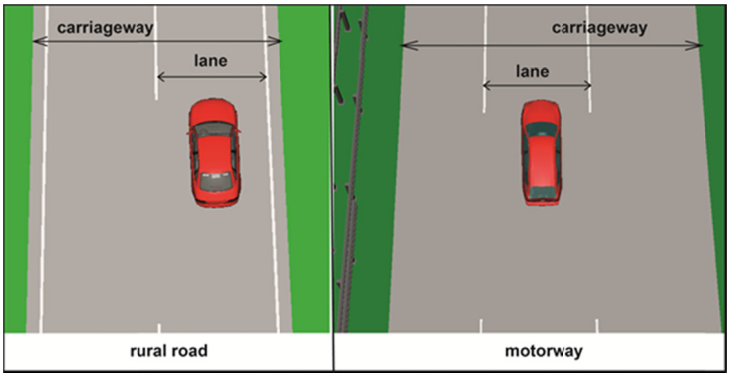


***Figure 1. Illustration of the terms "lane" and "carriageway"***

## METHODOLOGICAL APPROACH

The methodology used in the study involves the following steps:

a. Pre-analysis of a random sample of cases in order to ascertain the defining factors for identifying accidents caused by inadvertent lane departure
b. Selection of factors that indicate inadvertent lane departure and identification of the relevant case material by means of a database query
c. Case-by-case analysis of the relevant case material with descriptions of the accidents and identification of the main accident scenarios.

### a: Pre-analysis

Information on inadvertent lane departure is not recorded in police accident records and thus does not exist in this form in the accident database. It was possible to obtain this information subsequently by utilizing expert knowledge and by taking into account relevant factors that made it possible to conclude from the course of an accident that inadvertent lane departure had occurred. To begin with, the defining factors were ascertained by means of a brief analysis of a random sample of cases. The ten kinds of accident were selected here as the filter criterion, and ten cases were then randomly selected for each kind of accident. The kind of accident [2] has the advantage that it describes the collision position of the vehicles at the time of the accident and thus reveals a key aspect of the accident. In addition, by taking into account all kinds of accident, we ensured that the random sample covered all the accident constellations contained in the database. In the pre-analysis of individual cases, we investigated whether any cases of each kind of accident were caused by inadvertent lane departure, and we examined which factors indicated this.

The pre- analysis resulted in two important findings: Firstly, a combination of different factors and their refinements was required in order to properly identify the cases we were looking for. Secondly, it became clear that a vehicle that causes an accident as a result of inadvertent lane departure is almost always the main causer of an accident. It was thus possible to clearly identify the case car in the subsequent analyses.

### b: Selection of factors that indicate inadvertent lane departure

The relevant cases were selected by using expert knowledge on the basis of the following factors:

- Kind of accident
- Accident type (three-digit code)
- General accident cause
- Person-related misbehavior (cause per road user involved)
- Location

- Soft shoulder
- Single-vehicle accident (yes/no)
- Party with which the car collides.

Taking into account the above factors, the methodology involved combining the ten kinds of accident with the following three-digit accident types [4]:

- "Other accident" (761-763; 771-775; 799)
- All "driving accidents" (in which the driver loses control over the vehicle), filtered by the criteria "rural road" and "soft shoulder".

After preselecting the accidents with the car as the main causer of the accident (n=2,475), a new set of case material was formed by means of a database query using the factors specified above (n=118 cases). This contained only cases that could be attributed to the inadvertent departure of the car from the lane. In other words, it was the case material we were looking for.

**Description of the methodology by means of an example**

In the following example the methodology is explained with respect to the identification of the relevant cases:

The case material involving accidents in which the car was the main causer of the accident was filtered on the basis of the fourth kind of accident, "collision with another oncoming vehicle". This kind of accident provides important information on the accident, such as that it was not a single-vehicle accident and that it was a collision with oncoming traffic in which none of the road users involved intended to turn off across the lane of the oncoming traffic. In order to establish the relevance of the case material conclusively, the following questions also had to be answered:

- Which of the road users left their lane?
- Was this road user a car (case car)?
- Did the driver of the car leave the lane intentionally (e.g. in order to overtake) or inadvertently?

In addition to the kind of accident, accident type 7 ("other accident") was included as a further factor. For this accident type, the refinement "sudden physical incapacity" (two-digit code 76) was set as the filter criterion, for example, together with the additional refinement "asleep at the wheel" (three-digit code 761). This three-digit accident type indicates that the accident was caused by a driver who lost control of his or her vehicle as a result of falling asleep. Together with the information "collision with another oncoming vehicle" and the pre-selected criteria "car driver was the main causer of the accident", it was possible to conclude that the accident occurred because the driver left his or her lane inadvertently as a result of falling asleep. Further factors such as "person-related accident cause" (with the refinement "overfatigue") and "location" (with the refinement "rural road without motorway") confirmed this picture.

## RESULTS OF THE ANALYSES

The following chapters give a first general description of accidents caused by inadvertent lane departure and they then present the results of the analyses with respect to the main accident scenarios.

**Relevance of accidents caused by inadvertent lane departure**

From the case material of n=2,475 accidents in which the car was the main causer, a total of n=118 relevant cases were identified by means of the methodology described. In these cases, 33 people were killed, 153 people sustained serious injuries, and 148 sustained minor injuries. Accidents caused by inadvertent lane departure thus made up only 3% of all car accidents and 5% of all accidents caused by cars. However, they accounted for almost 10% of the total of 339 fatalities involved in all car accidents, and are thus highly relevant in terms of accident severity.

**Causes of the lane departure**

In order to obtain a better understanding of the course of these accidents, the causes of the departure from the lane were examined in relation to the case car.

It was possible to clearly identify the causes in half of the cases (n=50). In descending order of importance, these were:

a. Physical problems and health problems such as overfatigue and faintness or loss of consciousness (66%)
b. Distraction/inattentiveness, e.g. caused by adjusting the navigation system or radio or engaging in some other activity in the car (26%)
c. Alcohol/drugs (6%)
d. Weather conditions, such as heavy rain or fog (2%).

The causes were almost exclusively driver related. The comparatively low number of usable cases was due to the fact that a rather conservative approach was taken to analyzing them. In other words, only cases in which at least one clear cause was ascertained were included. These accident causes were ascertained on the basis of police inquiries, witness statements and medical reports (of low blood sugar or pre-existing medical conditions, for example).

The analyses revealed that physical and health problems were the cause of the inadvertent lane departure in two-thirds of the cases. This cause was twice as common as inattentiveness/distraction (26%). Drugs and/or alcohol (three cases) and severe weather conditions (one case) were found to be the cause far less often.

The distractions involved in the inattentiveness/distraction category originated almost exclusively in the vehicle itself. Examples included adjusting the navigation system, conversations with passengers and searching for things. In a few cases, nothing more was known than that the driver of the case car left the lane due to inattention. These cases were also included in the subsequent analyses.

**a: Collision events caused by "physical and health problems":** For the above mentioned "physical and health related causes", the collisions that occurred after the lane departure were investigated. The results were as follows:

a. Collision with oncoming traffic on a rural road (n=19)
b. Subsequent collisions on the motorway (n=6)
c. Single-vehicle accident including a collision with an obstacle such as a tree (n=3)
d. "Other", such as a collision with a pedestrian at the side of the road (n=2)

In over half of the cases caused by physical problems, the case car collided with oncoming traffic on a rural road (n=19 cases). It is worth noting here that the underlying case material originated from third-party claims, which means that collisions with oncoming traffic (i.e. with third parties) may be overrepresented, just as single-vehicle accidents are underrepresented, as already mentioned.

The second most common collisions were motorway accidents in which the case car and/or further road users collided with each other (n=6 cases). The accidents often took the following course: The case car left its lane, hit the crash barrier and came to a standstill on the carriageway. Subsequent collisions then occurred between the case car and other road users or between other vehicles without any direct involvement of the case car.

**b: Collision events caused by "distraction/inattentiveness":** Collisions with oncoming traffic on rural roads were also clearly the most common accidents caused by "distraction/inattentiveness" (nine out of twelve cases).

It was noticeable in five of the nine cases that the case car first went onto the soft shoulder at the side of the road before ending up in the lane for oncoming traffic as a result of the driver overcorrecting. Despite the low number of cases, this result is worthy of note in that the soft shoulder did not play a role in any of the accidents caused by the driver experiencing physical or health problems. One possible explanation for the high proportion of cases in which the car departed from its lane on the right-hand side is that the distracting activities described above generally took

place on the driver's right-hand side. In consequence, the driver unintentionally moved the steering wheel to the right while moving to the right.

**Main accident scenarios**

In the subsequent analyses, the 118 accidents were subdivided into predefined categories in order to identify the main accident scenarios. For these analyses, vehicle-specific and infrastructure-related aspects were taken into account in order to form these categories. The following factors and their refinements were taken into account and applied in terms of an "analysis path":

- State of the road surface (dry, wet/damp)
- Course of the road (straight road, bend)
- Radius of the bend (greater or less than 200 m)
- Light conditions (daylight, dawn/darkness)
- Severe weather conditions (heavy rain, fog)

Due to a lack of information, 18 cases could not be allocated to any category. This reduced the case material to be analyzed to n=100 cases with n=32 fatalities.

**Relevance of the main accident scenarios:** A total of five scenarios were identified. These are shown in figure 2 together with the factors described. The five main accident scenarios together account for 68% of the accidents and 66% of the fatalities in the case material of 100 cases.

It has to be mentioned that other combinations of these "analysis paths", resulting in other scenarios, are also possible. Against the background of the planned test procedures for lateral support systems and the use of accident data to support them, this approach was considered to be reasonable. This ensures that the scenarios also address those aspects that describe the characteristics of the sensors of lateral support systems and can also be tested in future.

| | | Scenario 1 | Scenario 2 | Scenario 3 | Scenario 4 | Scenario 5 |
|---|---|---|---|---|---|---|
| Relevance and brief description | | | | 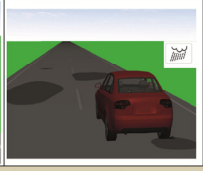 | | 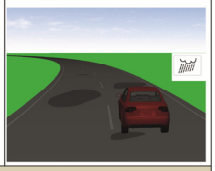 |
| Filter criteria for assignment to a scenario | | | | | | |
| Road surface | | Dry | Dry | Damp/wet | Damp/wet | Damp/wet |
| Course of the road | | Bend | Straight | Straight | Straight | Bend |
| Radius of the bend | | ≥ 200 m | - | | - | ≥ 200 m |
| Light conditions | | Daylight | Daylight | Daylight | Dawn/darkness | Daylight |
| Severe weather conditions | | None | None | None | Heavy rain | None |
| Additional information | | | | | | |
| Relevance in relation to all accidents (n=100) | n | 27 | 23 | 7 | 6 | 5 |
| | % | **27** | **23** | **7** | **6** | **5** |
| Relevance in relation to all fatalities (n=32) | n | 12 | 2 | 3 | 3 | 1 |
| | % | **38** | **6** | **9** | **9** | **3** |
| Average speed of the case car | | 85 km/h | 90 km/h | 75 km/h | Unknown | 70 km/h |

***Figure 2. Main accident scenarios for accidents caused by inadvertent lane departure***

For example, according to figure 2 all accidents that met the following criteria were allocated to Scenario 1:

- Dry road surface
- Daylight
- Accident in the vicinity of a bend with a radius of at least 200 m
- No severe weather conditions such as heavy rain or fog.

**In-depth analysis of the main accident scenarios**

In the course of a more in-depth analysis, the following aspects were examined more closely, allowing the scenarios to be described in greater detail in relation to the test procedures mentioned:

- Location
- Lane width
- Type and location of the road markings
- Speed of the case car
- Typical collision opponent of the case car
- Direction of the lane change before the collision
- Driver-related causes
- Age of the driver.

The results are shown in Table 1.

| Scenario | Percentage (n=100) | Location | Typical lane width | Typical speeds | Lowest speed | Highest speed | Type and location of the road markings | | Typical collision opponent and direction of the lane change before the collision | | Average age of the drivers (only cases with a known cause) | Typical driver-related causes for inadvertent lane departure | Average age of drivers with health problems |
|---|---|---|---|---|---|---|---|---|---|---|---|---|---|
| S1 | 27 | Rural roads | 2-3 m | 86 km/h | 45 km/h | 160 km/h | Left | Broken | Car | To the left | 59 | Health problems (45%), distraction/inattention (36%), overfatigue (9%), drugs (9%) | 72 |
| | | | | | | | Right | Continuous | | | | | |
| S2 | 23 | Rural roads | 2-3 m | 91 km/h | 50 km/h | 140 km/h | Left | Broken | | | 51 | Health problems (38%), overfatigue (23%), distraction/inattention (38%) | 61 |
| | | | | | | | Right | Continuous | | | | | |
| S3 | 7 | Rural roads | 3-4 m | 68 km/h | 40 km/h | 90 km/h | Left | Both | | | 55 | Health problems (50%), overfatigue (25%), alcohol/drugs (25%) | 52 |
| | | | | | | | Right | Both | | | | | |
| S4 | 6 | Both urban and rural roads | 2-3 m | 100 km/h (one case) | | | Left | Broken | | | 22 | Overfatigue (75%), alcohol/drugs (25%) | - |
| | | | | | | | Right | Continuous | | | | | |
| S5 | 5 | Rural roads | 2-3 m | 67 km/h | 50 km/h | 90 km/h | Left | Broken | | | 48 | Health problems (25%), overfatigue (25%), distraction/inattention (25%), severe weather conditions (25%) | 25 |
| | | | | | | | Right | Continuous | | | | | |

***Table 1. Descriptive details of the five main accident scenarios***

The in-depth analysis revealed following results:

- With only a few exceptions, all accidents took place on rural roads with typical lane widths of 2 to 3 meters.
- There was at least one road marking present in all cases.
- The most frequent collision opponent of the case car was another car (in 70% of the cases). The case car always departed from its lane on the left-hand side before colliding with the other car.
- The average age of the drivers who had inadvertently left their lane due to health problems was 67 in the two most common scenarios (S1 and S2, which accounted for 50% of the case material).
- The most common health-related cause was faintness (as a result of low blood sugar, for example).
- Falling asleep at the wheel was specified most often in connection with the cause “overfatigue”.

- The following ranking was obtained for driver-related causes:
    - Health problems: e.g. faitness (36%)
    - Distraction/inattention (27%)
    - Physical problems: e.g. overfatigue (25%)
    - Alcohol/drugs (8%).

**Main accident scenarios under the consideration of test procedures**

As a result of the finding that over a third of the cases were attributable to health problems of the driver, and that these were thus cases in which the driver's reaction and acting were significantly impaired, the scenarios had to be adjusted. In the cases described, it is highly unlikely that the accidents could have been prevented by lateral support systems, and the scenarios would thus not be suitable for the planned test procedures.

Figure 3 therefore shows what the structure of the scenarios would look like if only cases with known causes were used, and cases caused by health problems were excluded. For this new structure the analysis revealed that the five scenarios would remain the same but their ranking would change. Within the individual scenarios marginal changes in the average driven speeds of the case car could be observed.

| Relevance and brief description (only cases with a known cause, excluding the cause "health problems") n=23 accidents; n=4 fatalities | | Scenario 1 | Scenario 2 | Scenario 3 | Scenario 4 | Scenario 5 |
|---|---|---|---|---|---|---|
| | | 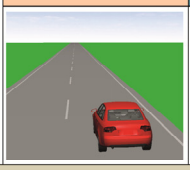 | 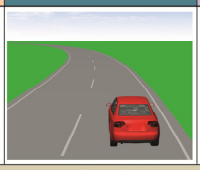 | 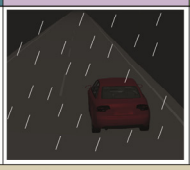 | 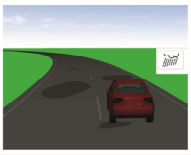 | 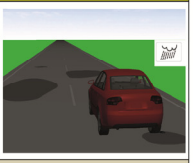 |
| Filter criteria for assignment to a scenario | | | | | | |
| Road surface | | Dry | Dry | Damp/wet | Damp/wet | Damp/wet |
| Course of the road | | Straight | Bend | Straight | Bend | Straight |
| Radius of the bend | | - | ≥ 200 m | - | ≥ 200 m | - |
| Light conditions | | Daylight | Daylight | Dawn/darkness | Daylight | Daylight |
| Severe weather conditions | | None | None | Heavy rain | None | None |
| Additional information | | | | | | |
| Number of accidents | n | 8 | 6 | 4 | 3 | 2 |
| Number of fatalities | n | 1 | 2 | 0 | 0 | 1 |
| Average speed of the case car | | 71 km/h | 77 km/h | Unknown | 70 km/h | 80 km/h |

***Figure 3. Rearrangement of the main accident scenarios with the following constraint: only cases with a known cause of the inadvertent lane departure and excluding cases caused by health problems***

## CONCLUSIONS

The analysis of car accidents caused by inadvertent lane departure showed that, although these accidents only occur rarely (accounting for 3% of all car accidents), they have serious consequences (accounting for 10% of all fatalities in car accidents). The most common reasons for inadvertent lane departure were physical and health problems and distraction/inattention. The main accident scenarios that were deduced from the analyses account together for 68% of the accidents and 66% of the fatalities in the case material (n=100 cases).

It was found that, in the main accident scenarios, most drivers inadvertently left their lane on a straight road, in daylight and on a dry road surface (i.e. in nearly ideal driving conditions). However, it was also found that over a third of these cases could be attributed to health problems of the driver and that over half of the drivers affected were over 60 years old. In view of the high percentage of accidents caused by health problems (36%), it is clear that there are limits on how effective current lateral support systems can be. The systems are not capable of preventing these

accidents. For the future there is a need to consider systems that are effective regardless of the location (on rural roads or on motorways) and that bring the vehicle to a standstill safely when the driver is no longer in a fit state to drive. Consequently, for the scenarios identified for the purpose of testing the features of lateral support systems, only those cases that are not attributable to health problems should be taken into account.

The following findings were also obtained in relation to these scenarios:

- 75% of the accidents occurred on a dry road surface, with 25% thus taking place on a wet road surface.
- Most case cars initially left their lane on the left-hand side.
- They then collided with an oncoming vehicle.
- At the point at which they left their lane, the case cars were generally traveling at over 70 km/h.
- At least one road marking was present in all cases. In cases where the case car left the lane on the left-hand side, there were both broken and continuous markings (to indicate that overtaking was prohibited, for example).
- Dawn/darkness and severe weather conditions (heavy rain, fog) were not significant factors in lane departure.

## REFERENCES


[1] Euro NCAP: Euro NCAP`s Road map 2020, June 2014.
[2] German Federal Statistical Office (2013): Road traffic accident statistics, Wiesbaden.
[3] Kuehn, M., Hummel, Th. and Bende, J. (2009): Benefit Estimation of Advanced Driver Assistance Systems for Cars Derived from Real-Life Accidents. 21st ESV Conference, Paper No 09-0317, Stuttgart, June 15-18, 2009.
[4] GDV (1998): Accident type catalogue - A guide to determine the accident type, Köln.

# OCCUPANT PROTECTION IN REAR-END COLLISIONS PRECEDED BY AUTONOMOUS EMERGENCY BRAKING DEPLOYMENT

**Salvatore Battaglia**
**Kajetan Kietlinski**
**Michiel Unger**
Tass International
Germany

**Martin Tijssens**
Tass International
The Netherlands

Paper Number 15-0246

## ABSTRACT

The safety of vehicle occupants has evolved recently due to the market implementations of new sensing technologies that enable predicting and identifying hazardous road traffic situations and thus actively prevent or mitigate collisions. The obvious benefits of the active safety systems has also been recognized and acknowledged by the regulatory and consumer bodies responsible for transportation, and as a result, the new standards, regulations and public rewards are being introduced.
The active safety systems can prevent or mitigate collisions by controlling the motion of the vehicles through autonomous actuation of either: braking, steering or both simultaneously. The autonomous control of the vehicle inevitably affects the motion of the travelling occupants with respect to the vehicle interior. Depending on the severity of the maneuver, the occupant motion may lead to non-optimal postures for the in-crash phase if the collision is unavoidable. This consideration creates the direct need for developing the active systems together with passive systems with the ultimate objective to best protect the occupants. This paper presents a simulation methodology for developing new automotive safety systems in an integrated manner that ensures optimal exploitation of benefits of predictive sensing and occupant restraints. It also demonstrates the application of the above methods, to investigate and optimize the occupant whiplash protection in rear-end collisions occurring during the autonomous emergency braking of the collided vehicle.

The investigation was performed using simulation techniques (MADYMO software). The driver occupant is initially exposed to the low-g longitudinal acceleration resulting from emergency braking, during which the rear-end acceleration pulse is applied, representing the collision conditions (following the High Severity Sled Pulse of Euro NCAP Whiplash testing protocol). Two different models of anthropometric test devices are used and compared: BioRID-II facet Q model and Active Human Model (AHM) to predict occupant motion while braking and assess injury risk as a result of the rear-end collision.

The results obtained showed the severity of the out-of-position occupant posture created by the autonomous braking maneuver, and its effect on injury risk in the consecutive collision. It was observed that the occupant motion resulting from braking is more pronounced in case of AHM than BioRID-II. Increased occupant travel during pre-braking impairs significantly the effectiveness of occupant rear-end protection restraint systems, thus increasing the whiplash injury risk. Further study demonstrates conceptual, pre-crash deployed safety solutions that alleviate the negative effects of the out-of-position postures created by pre-braking.

The study shows the need for developing the new safety systems in an integrated manner. It was performed based on the numerical simulations and some of the model components were not fully validated. The simulation methods and techniques will play a significant role in the integrated safety systems development processes, allowing testing the conditions of high complexity in order to represent the real life scenarios and thus ensuring better occupant protection.

## INTRODUCTION

The introduction of Advanced Driver Assistance Systems (ADA systems or ADAS) generates new opportunities to mitigate the damage caused by traffic accidents or, in many cases, prevents them from happening. ADA systems such as Autonomous Emergency Braking System (AEBS) or lane change assist (LCA) support the driver in hazardous traffic situations by controlling longitudinal (by braking) and lateral (by steer torque) motion of the vehicle in case of collision risk. These systems, though relatively new to the market, have proved their significance for vehicle safety and are recognized already by legislative authorities and consumer bodies. The European Commission has introduced legislation for AEB and Lane Departure Warning (LDW) systems in commercial vehicles [1], and consumer testing protocols are currently available for AEB systems in the standard Euro NCAP protocol dedicated for city and interurban traffic.

Previous studies have shown that autonomous systems, such as AEB or autonomous steering, can lead to a non-optimal occupant posture and position resulting in reduced performance of the occupant restraint systems in case of a collision [2]. At the same time, the increasing presence of surround sensors allows for an improved performance of the passive safety systems by using information from before the crash. This information can be used to trigger restraint systems during the pre-crash phase e.g. pre-pretentioning of safety belts to reduce the occupant misalignments during pre-crash lateral or longitudinal loadings.

Previous studies [2], [3] have shown that the on-board restraint systems can be optimized in an integrated manner for a specific load case, i.e. frontal or side. The wide range of ADA systems available in the new vehicles can provide information about the vehicle's surrounding and can therefore be used to estimate the interaction with other vehicles resulting from the activation of a single ADA system. This plays an important role not only on the level of controllers implementation, but also on the occupants' protection: given a certain flow of actions initiated by the ADA controllers, the injuries suffered in an imminent collision might depend on the occupant Out Of Position (OOP) resulting from the avoidance of a preceding potential collision. With the more and more extensive implementation of AEB systems the urban areas have become a potential scenario for the combination of AEB actuations followed by a rear-end collision.

A first attempt of correlating the performance of an AEB system with the performance of the vehicle's restraint system in protecting the occupants in a rear collision has been done and described within this paper. The performance of the AEB system and the vehicle's restraint potential in limiting the whiplash injuries are awarded separately in the Euro NCAP protocol, with the only requirement of a minimum whiplash score for the vehicle to be eligible for the AEB City award.

This study presents a new application of the integrated safety method described in [2] with the analysis of the out of position resulting from the actuation of an AEB system before a rear collision. In line with the methodology, the advantage of predictive sensing for the optimization of the on-board restraint systems is confirmed, along with the difference in the injuries estimation between the BioRID-II dummy model and the active human model. The analysis is performed on a simulation level and extended with the activation of a selection of on-board restraint systems prior to the rear collision with the main objective of showing the different risk of high whiplash injuries with and without the preceding actuation of the AEB system.

## METHODOLOGY

Currently, no experimental methods or simulation tools exist for evaluating the effects of pre-crash dynamics on the occupant injury risk during the crash phase. In this paper, the use of two software packages that together provide the potential to cover all critical aspects of the design of an integrated safety system is shown. One of the software packages (PreScan) focuses on the sensing and active control systems of a vehicle, and the other package (MADYMO) predicts an occupant response and injury risk throughout the whole pre- and potential in-crash event.

The methodology used in this study has been previously presented [2] when applied for the investigation into the frontal collision load case with pre-crash autonomous braking and the side collision load case with pre-crash triggered restrained systems [3]. In the current study, the methodology was appropriately adjusted to best represent

the phenomena characteristic for the problem of out-of-position while emergency braking, followed by a rear-end impact load case (See Figure 1).
The real world traffic situation is represented in PreScan in which the vehicle model under investigation, equipped with predictive sensors, is exposed to the collision risk situation. A control system based on the predictive sensors provides detection and initial classification of collidable objects (here referred to as targets), with respect to which the Time To Collision (TTC) information is estimated. Once the crash detection system model classifies the collision risk, the occupant's injury analysis is initiated in MADYMO with the initial conditions imported from PreScan. Based on the estimated TTC information sent to MADYMO, on-board restraint systems (e.g. belt pre-pretensioners) are triggered in case of an unavoidable collision with the target. MADYMO uses the above listed information to calculate the deployment of restraints and compute the resultant occupant's posture. The outputs from MADYMO analysis is used to quantify the significance of active restraint systems in the rear-end collision.

The presented approach assumes that the pre-crash control system for rear-end collision placed on the struck vehicle does not affect the vehicle motion itself. Therefore, the collision conditions remain unchanged with and without the system. The pre-crash control system affects only the motion of the occupants by deploying the on-board restraint system before the crash in order to mitigate the injuries.

In the current study the methodology has been further extended to investigate the effects of AEBS actuations (vehicle pitching and braking) prior to the predicted rear collision. The origin of the pre-crash vehicle motion is not investigated in this study, but simply adopted as input to the MADYMO simulation to quantify the significance of occupant's misalignments and thus the out of position posture in the rear-end collision. The AEBS-induced vehicle motion is prescribed in MADYMO and synchronized with the rear-end crash pulse. The AEBS controller principle, its application and effects on the vehicle motion have been studied and described in [2].

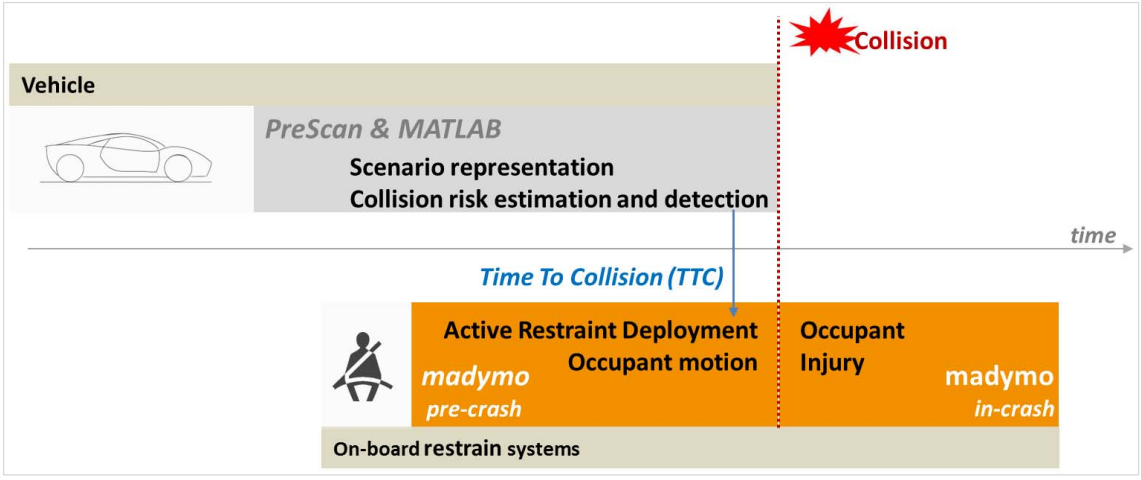


***Figure1. Method.***

**Traffic scenario identification**

Recent studies [4] confirm that in Germany rear-end collisions represent the third most common impact scenario after frontal and side impacts, and amount to 15% of all car accidents. Most of the car-to-car single rear-end collisions occur on urban roads [5] and 80% of rear-end collisions include accidents in longitudinal traffic conditions in which vehicles are stuck in a traffic jam or queuing at the traffic light [4].
Two traffic scenarios have been selected for this study and developed in the PreScan software, each representing a rear-end collision caused by a car (striking vehicle) failing to brake in the vicinity of a red traffic light and impacting the preceding car (struck vehicle) at the speed of 48 km/h. Two scenarios conditions for the struck vehicle are investigated:

1. The struck vehicle is stationary queuing at the traffic light
2. The struck vehicle drives at 56 km/h and comes to a full stop after the intervention of an AEB system to avoid a collision with the preceding stationary vehicle queueing at the traffic light.

The simulations of both traffic scenarios are shown in the Figure 2.

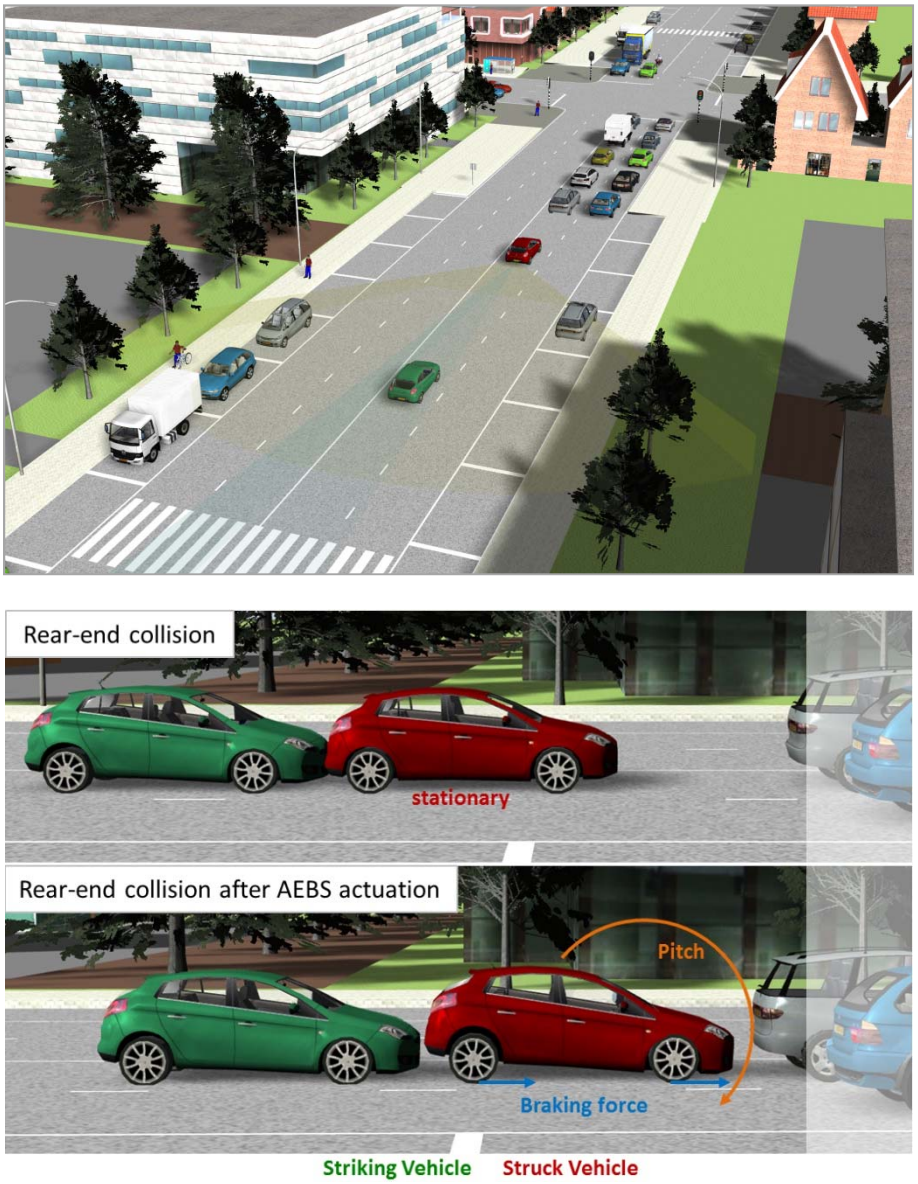


***Figure2. Traffic Scenarios - Overview (top), details (bottom).***

**Maneuver dynamics of the struck vehicle model due to AEBS intervention**

The deceleration and pitching profiles resulting from the activation of the AEB system have been computed by means of the PreScan embedded vehicle dynamics model [6]. A mid-class vehicle has been used for this study and it has been assumed that the maximum longitudinal braking force can be generated (dry asphalt, high friction). Supposing that the collision between the two vehicles is fully inelastic and both vehicles are of the same mass, the velocity change of 24.45 ±1.2 km/h required by the Euro NCAP protocol (See section "Collision condition and investigated injuries") implies a striking vehicle driving at the speed of 48 km/h.
In line with the controller principles described in [2] due to the AEB intervention the struck vehicle undergoes a maximum longitudinal deceleration of 0.79 [g] and a maximum pitch angle of 1.4 [deg].

**Collision condition and investigated injuries**

In order to assess the occupant whiplash injury risk, the High Severity crash pulse of the Euro NCAP Whiplash protocol has been used [7]. The adopted crash pulse has been registered in a laboratory and complies with the Euro NCAP protocol requirements (not shown in this paper).
The same crash pulse has been used also in the traffic scenario involving the actuation of the AEB system. Although the initial conditions of the struck vehicle (pitching) do not fully comply with the sled test requirements (horizontally placed sled), it can be assumed that the small pitch angle does not compromise the validity of the crash pulse.

In line with the Euro NCAP dynamic test protocol, the injuries on the neck and thoracic spine are registered by means of a Bio-RID-II dummy, and quantified in terms of:

1. NIC peak
2. Maximum Nkm
3. Peak of Head rebound velocity
4. Maximum vertical and shear force on the Upper Neck
5. Peak of T1 acceleration
6. Time to first contact between the Head and the headrest

According to the protocol, all parameters except the rebound velocity are calculated up to the end of head to headrest contact.
The Euro NCAP parameters are calculated for both occupant models and it is therefore assumed that the limits (See Table 1) defined by the protocol are applicable also to outputs of the human model.

***Table1.***
***Euro NCAP High Severity Pulse limits.***

| | **Higher Performance Limit** | **Lower Performance Limit** | **Capping Limit** |
|---|---|---|---|
| **NIC [-]** | 13.00 | 23.00 | 25.50 |
| **Nkm [-]** | 0.22 | 0.47 | 0.78 |
| **Head Rebound Velocity [m/s]** | 4.10 | 5.50 | 6.00 |
| **Upper Neck Shear Force [kN]** | 30.00 | 210.00 | 364.00 |
| **Upper Neck Tension Force [kN]** | 470.00 | 770.00 | 1024.00 |
| **T1 acceleration [g]** | 12.50 | 15.90 | 17.80 |
| **Time to head- headrest contact [ms]** | 53.00 | 80.00 | 92.00 |

**Rear collision detection principles**

A controller algorithm and two radar sensors have been modelled to estimate the risk for the vehicle (host/struck vehicle) of being rear-struck by the vehicle coming from the back (striking vehicle). By means of a Long Range Radar (LRR, with one beam 150 [m] long and 8 [deg] wide) and a Short Range Radar (SRR, with one beam 30 [m] long and 80 [deg] wide) the area behind the host vehicle is scanned for targets. The sensors' readings are processed by the controller algorithm that computes the Time To Collision (TTC) based on which the on-board restraint systems can be triggered before the collision. The system (controller and sensors) acts in four steps to produce the TTC information with respect to the identified target vehicle (striking vehicle):

1. The LRR scans the surrounding of the host vehicle and identifies approaching objects. The TTC is calculated for each of them
2. Based on TTC $\leq$ 1.6 [s] the target type identification process (object vs vehicle) is initiated
3. The SRR scans the surrounding of the host vehicle and identifies targets
4. If the same target is detected by both sensors and has been classified as a vehicle, the related TTC information is made available for the on board restraint systems to be triggered

The controller and the sensors have been implemented in PreScan, using Matlab/Simulink for the sensors' readings processing and for the computation of the TTC information.

**Test sled and restraint systems models**

The Euro NCAP Whiplash sled test has been reproduced in MADYMO with a seat including headrest, cushions and structure, a safety belt and a foot rest. The seat geometry is represented using facet surface technique and its compliance is expressed in terms of stress-strain characteristics representative of a generic middle-class vehicle seat. The model represents a generalized mid-size class passenger car and is validated for the three Euro NCAP whiplash sled pulses. The characteristics and properties of the seat are not shown in this paper. The belt is modelled with FE technique and represents the functionality of a belt system without locking mechanism and retraction functionality. To investigate the effectiveness of pre-crash deployed injury countermeasures the model is additionally equipped with the retractor pre-pretensioner (here referred to as pretensioner) and the active headrest prior to collision. The actuation of the active headrest aims at reducing the gap between the occupant's head and the seat and is implemented by prescribing the angular motion to a maximum angular displacement of 10 [deg]. The active headrest is actuated before the crash and can be triggered at the desired TTC based on the pre-crash vehicle sensors (i.e. radar sensor models). The actuation of the active retractor pretensioner to reduce the gap between the occupant and the backrest can be triggered with a pre-defined load at the desired TTC based on the pre-crash vehicle sensors (i.e. radar sensor models).
The design and optimization of the restraint systems actuation has been performed by means of simulations and has not been validated. The optimization enabled to define the triggering time (TTC) and the type of actuation (amount of angular headrest displacement and pretensioner loading force), and is not described in this study. The active restraint systems under investigation have been optimized for both load-cases and are listed in Table 2 together with the reference model (seat and seat-belt with no pre-crash activation).

***Table2.***
***Restraint systems under investigation.***

| | **Headrest forward rotation [deg]** | **Pretensioning load [kN]** | ***Reference in the paper*** |
|---|---|---|---|
| **Reference model** | *n.a.* | *n.a.* | *Ref* |
| **Active Headrest rotated forward** | 10 | *n.a.* | *AH_10deg* |
| **Retractor Pretensioner (1)** | *n.a.* | 0.15 | *RPT_0.15kN* |
| **Retractor Pretensioner (2)** | *n.a.* | 0.50 | *RPT_0.50kN* |
| **Combination of Active Headrest and Retractor Pretensioner (1)** | 10 | 0.15 | *AH+RPT_0.15kN* |
| **Combination of Active Headrest and Retractor Pretensioner (2)** | 10 | 0.50 | *AH+RPT_0.50kN* |

**INVESTIGATION APPROACH**

The paper describes the investigation into the effect of OOP induced by the (autonomous) actuation of an AEB system prior to a rear-end collision. The intervention of an AEB system alters the occupant's position with respect to the seat, thus affecting the restraining capabilities of the safety system. In the specific case, the AEB system actuation increases the relative distance between the occupant's head and the headrest, thus compromising the Euro NCAP Geometry assessment. As a consequence, the advantage of the restraint systems optimized according to (static) in-position requirements might be compromised.
In addition, the potential of triggering the on-board whiplash protection system prior to the rear-end collision is investigated. Based on the analysis of the whiplash injuries as required by Euro NCAP, the actuation and combination of active restraint systems is eventually analyzed.

Two occupant models are selected for the investigation, the MADYMO Active Human Model 50th percentile (here referred to as AHM) and the MADYMO BioRID-II Q facet dummy. The BioRID-II facet dummy is a well-

established ATD (Anthropometric Test Device), typically used in rear crash test protocols. It is extensively validated in numerous component, full scale and full system tests for in-plane rear loading [8].
The active human model has an improved biofidelity and includes muscle activity and posture maintenance activation: the neck, spine, elbows and hips can be controlled in order to try to maintain the initial position under the influence of external loading. The active human model is validated against volunteer and PMHS (Post Mortem Human Subject) test data for occupant pre-crash simulation of low-g frontal, as well as high- and low-g rear load-cases [9], [10], [11].
In the study, the neck, spine, elbows and hips of the human model are activated. The muscle activation settings used in the investigation represent an occupant that is aware about the upcoming collision and his muscles are initially braced (isometrically pre-tensed due to the psychological stress resulting from being in a dangerous situation). Occupant awareness/unawareness and bracing/relaxation are represented on the modeling level with two parameters: Muscle reaction time – time from 0 to 30ms represent an aware occupant Co-contraction – values above 0.5 represent braced occupant.

For both occupant models the same seat model is adopted, with the same initial orientation of both backrest and headrest. The BioRID-II has been placed into the seat making sure that the vertical and horizontal distances of the head with respect to the headrest are within the Euro NCAP corridors. The human model has been positioned assuring that the head-to-headrest position is as close as possible to the one of the BioRID-II (a maximum difference of 16 mm in the longitudinal direction). The seating procedure for both occupant models has been implemented by means of pre-simulations and is not described in this paper. The Figure 3 compares the position of both occupant models at the end of the AEBS intervention (before the rear-end collision) when placed on the same seat model. Due to the vehicle's deceleration and pitching, the occupant is displaced out of his initial position and the distances to the headrest and backrest increase. The Bio-RID-II shows a more significant out of position, with a longitudinal distance to the headrest five times higher than the initial value (41 [cm] versus 7.5 [cm]).

***Figure3. Reference Model - Occupant models posture before the crash with and without previous AEB activation.***

The sequence of events in case of a regular rear-end collision and a rear-end collision following the activation of an AEB system is shown in the Figure 4. In the regular rear-end collision all the active restraint systems are actuated based on the estimated risk of rear-end collision. With the AEBS intervention the retractor pretensioner is controlled by the AEB controller and triggered when the braking phase is initiated, while the headrest deployment is triggered based on the estimated rear-end collision.

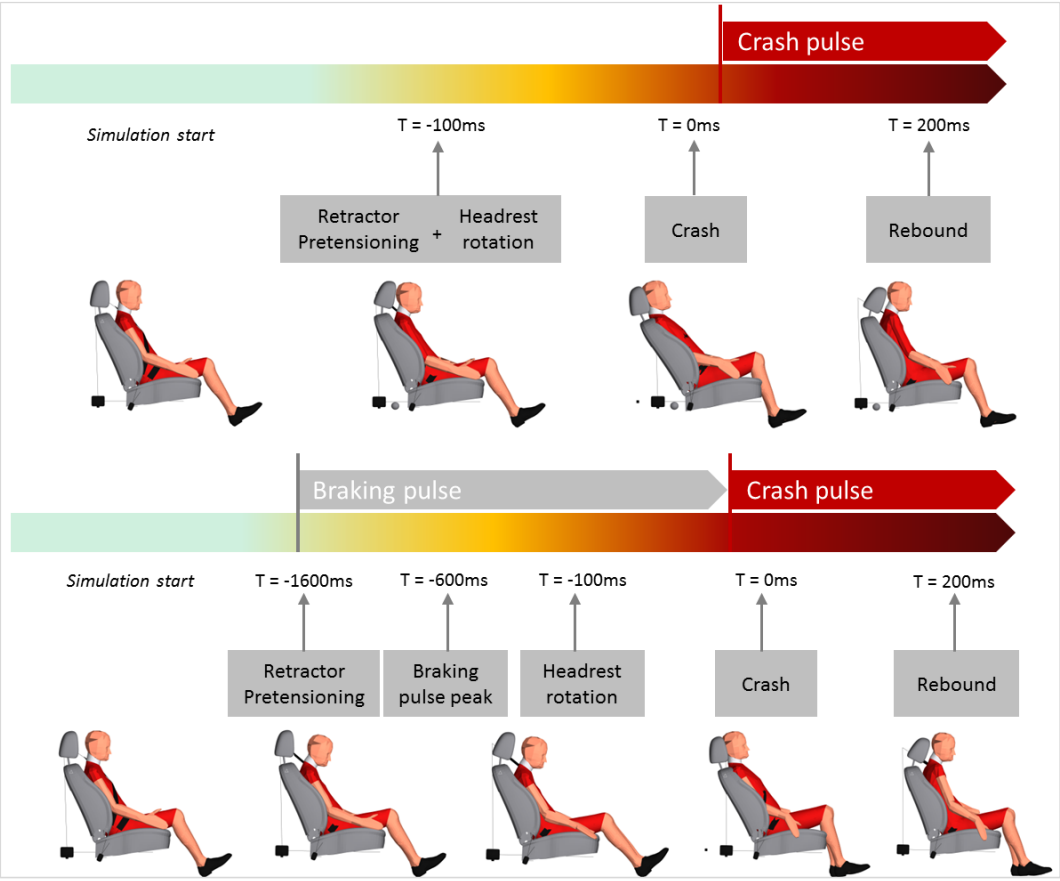


***Figure4. Sequence of events - Regular rear-end collision (top), rear-end collision after AEBS intervention (bottom).***

In order to quantify the overall risk of high whiplash injuries, the Euro NCAP Lower Performance limits are assumed to be the maximum value (100%) with respect to the ideal situation of no injuries (0%): according to the Euro NCAP Whiplash test protocol, a criterion is awarded a "null score" if its value exceeds the Lower Performance Limit. The ratios (here referred to as Injury Ratios) between the in-simulation-observed injury values and the corresponding Lower Performance limits have been calculated and expressed in terms of percentages (100% corresponds to injury values equal to the Lower Performance limits). The injury ratios have been calculated for each of the seven injury criteria required by the Euro NCAP Whiplash test protocol and eventually averaged for each simulation (one simulation corresponds to one occupant model, one restraints configuration and one load case).
It should be noted that the results evaluation has been carried out only with the Euro NCAP injury parameters and no analysis of the neck in jury mechanisms has been performed.

## WHIPLASH INJURY ANALYSIS RESULTS

The sensitivity of the reference restraint system to the load-case and to the occupant model is shown in the Figure5. The activation of an AEBS always increases the risk of high whiplash injuries in a consequent rear-end collision, but the effect is differently quantified by the two occupant models: for the BioRID-II model the average injury ratio of 111% increases to 194%; a similar trend, though less pronounced, can be observed for the Active Human Model registering an average injury ratio increasing from 74% to 107%. The intervention of the AEBS amplifies also the difference between the occupant models: in a regular rear-end collision the BioRID-II produces whiplash injuries around 37% higher than the AHM, with the intervention of the AEBS the whiplash injuries are almost 90% higher for the BioRID-II.

The results with the reference models show a significant decrease in occupant protection resulting from the AEB-induced OOP, and thus create the need for the pre-crash intervention to correct the position of the occupant before entering the rear-end in-crash phase.

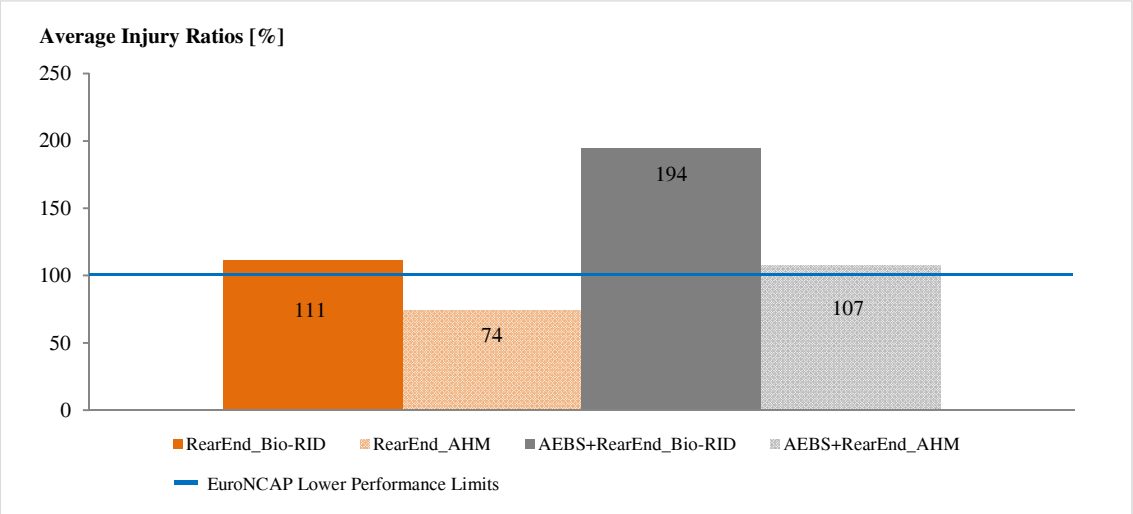


***Figure5. Whiplash injuries in the reference models.***

The effectiveness of different active restraint systems in reducing occupant injury values in rear-end load case with respect to the reference system is presented in the Figure 6. The two bar plots show the results for different ATD models: BioRID-II and AHM.

In case of the BioRID-II the 83% increase in the risk of high whiplash injuries caused by the AEBS (grey vs. orange bar) could be limited to a minimum of 74% by combining the active headrest and belt pretensioning. However, unlike the rear-end-only load case, triggering active systems in the pre-crash phase after an emergency braking always showed injury values still higher than the Euro NCAP Lower Performance limits.
The potential of actuating the restraint systems before the rear-end collision proved always beneficial and similar trends in the injuries reduction after the AEBS actuation are observed. Depending on the applied system configuration the injuries are reduced by 18% - 55%.

In case of the AHM the 33% increase in the risk of high whiplash injuries caused by the AEBS (grey vs. orange bar) could be limited to a minimum of 5% by combining the active headrest and the belt pretensioning. Besides, triggering active systems in the pre-crash phase after an emergency braking always resulted in whiplash injuries equal to or lower than the Euro NCAP Lower Performance limits.
The potential of actuating the restraint systems before the rear-end collision proved beneficial only after the AEBS deployment, with 8% - 25% lower injuries. In the rear-end-only load case the active restraint systems did not significantly affect the performance of the reference system: although no benefits have been found, a 5% increment has been observed.

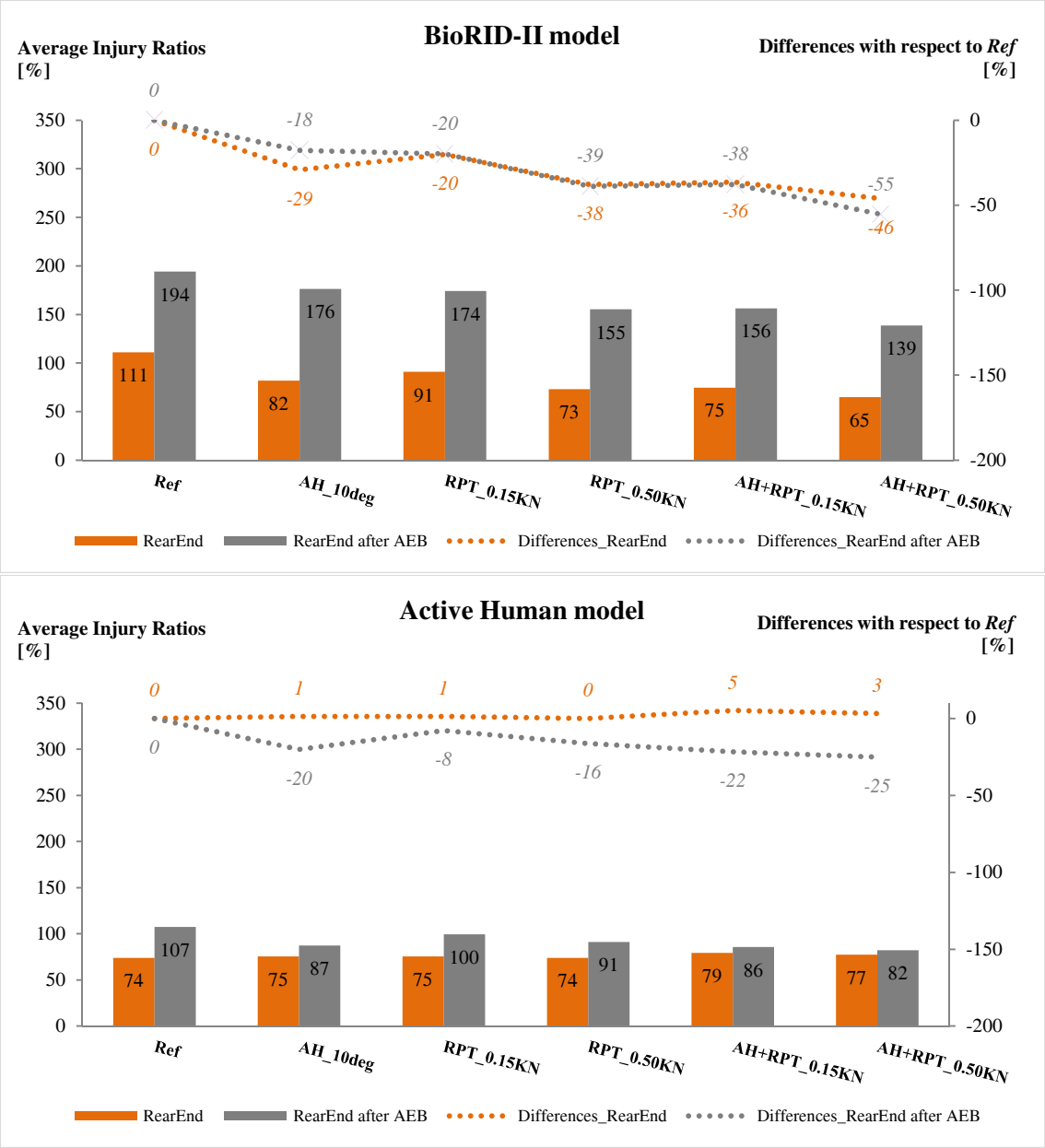


***Figure6. Average Injury Ratios with and without the intervention of the AEBS - BioRID-II (top) and Active Human Model (bottom).***

The direct comparison between the injury results obtained with two ATD models (BioRID-II and AHM) throughout the active restraint systems under investigation is presented in the Figure 7.
The AEBS-induced OOP has differently affected the injury prediction of the occupant models. The difference in the injury values varies between 57% and 87% depending on the applied system configuration. In contrast with the simulations with the BioRID-II, triggering active systems in the pre-crash phase always showed average whiplash injuries lower than or equal to the Euro NCAP Lower Performance limits when simulating with the AHM: with the BioRID-II the risk of high whiplash injuries is in the range of 139% - 194%, while a much lower range of 82% - 107% has been observed with the human model.
The potential of actuating the restraint systems before the rear-end collision proved always beneficial and showed similar trends in the injuries reduction. However, with the AHM, the observed reduction of whiplash injuries is less than with the BioRID-II.

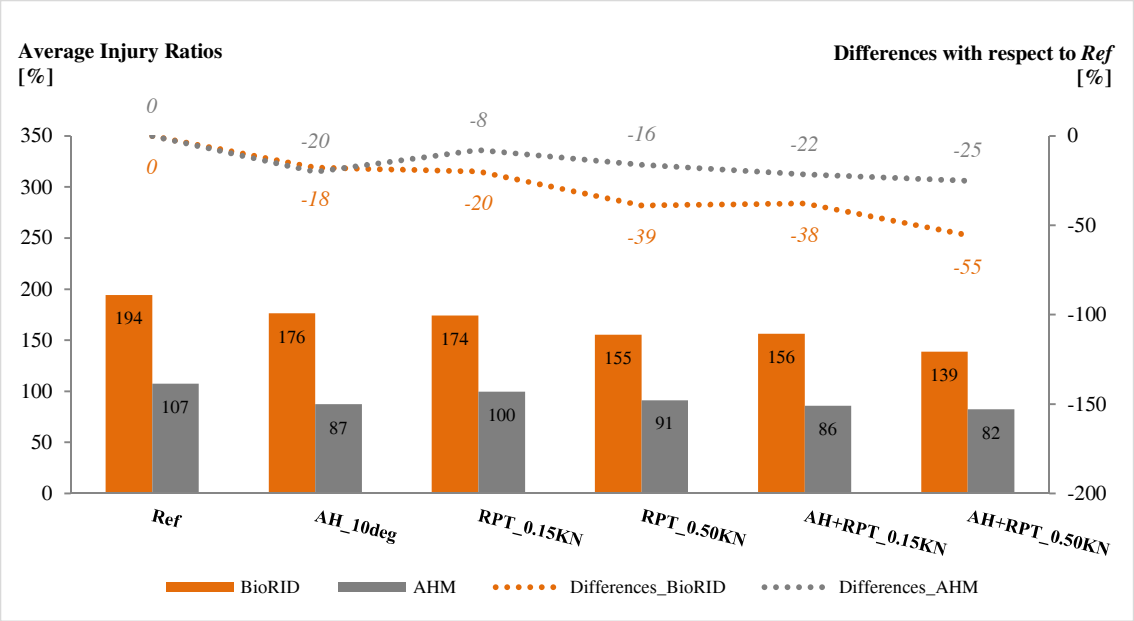


***Figure7. Average Injury Ratios in the Rear-end collision after the AEBS intervention - Comparison between the occupant models.***

Previous studies [11] prove that the initial seating posture and the head restraint position strongly influence the model response. In the study, the ratio between the head distance to the headrest and resulting injury values was found to be non-linear. In a regular rear-end collision reducing the initial gap between the head and the headrest reduces the risk of high whiplash injuries as long as the BioRID-II is used; with the human model no significant effect in the whiplash injuries has been observed when reducing the head to headrest gap (maximum increment of 5% in the injuries). In the Figure 8 the injury ratios observed with both occupant models are plotted with respect to the head-headrest distances (for clarity reasons, the results of the BioRID-II in the AEB scenarios are not entirely plotted). The reduction of the gap reduces the difference between the whiplash injuries of the BioRID-II and the AHM from 37% to 14%. In case of AEB-induced OOP, reducing the initial gap reduces the risk of high whiplash injuries. However, the gap reduction does not bring the risk of high whiplash injuries of the BioRID-II close to the ones of AHM, with differences in the range of 32% to 87%.

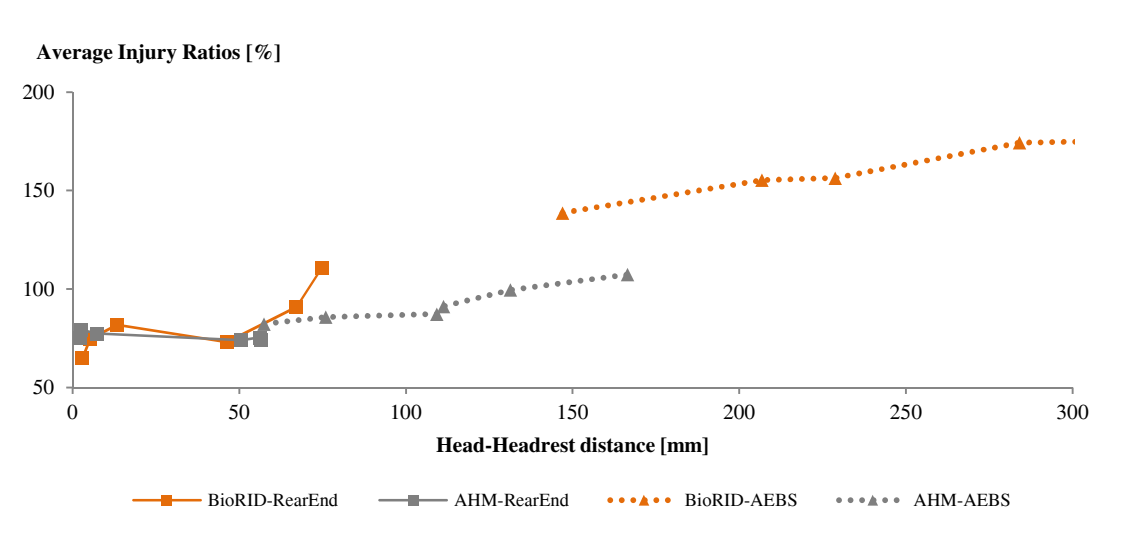


***Figure8. Average Injury Ratios vs Head-Headrest distance***

**Results summary**

With the intervention of an AEB system prior to a rear-end collision the risk of high whiplash injuries as a result of an altered seating position for the occupant (OOP) increases. The risks predicted by the BioRID-II increase by 83%, while in case of the AHM, the risks increase by 37%. For both occupant models the adoption of the active restraint systems cannot fully compensate the higher risk of high whiplash injuries caused by AEB-induced OOP, thus offering an overall protection level lower than in the regular rear-end collision (with no OOP).

The difference in the whiplash injury prediction between the occupant models changes radically between a regular rear-end collision and a rear-end collision after the actuation of an AEBS. Even though used with the same restraint systems and under the same loading conditions, in a rear-end collision the difference is in the range of 1% - 37%, while after the activation of the AEBS the difference can be as high as 57% - 89%.

The study shows that the intervention of active systems prior to a rear-end-only collision reduces the injuries to values lower than the Euro NCAP Lower Performance limits for both occupant models. The adoption of active restraint systems during the actuation of an emergency braking may result in an improvement with respect to the passive-only systems for both occupant models, but the whiplash injuries estimated by the BioRID-II remain above the Euro NCAP higher limits.

The BioRID-II model showed a consistent behavior in the prediction of the whiplash injury values with or without the intervention of the AEB system: in terms of risk reduction with respect to the reference model, the actuation of each active system has proved equally beneficial in both cases. On the other hand, with the AHM, only the AEBS-induced pre-collision loading shows the need for additional active restraint systems (which proved to be able to reduce the injury risk with a trend similar to the BioRID-II), while in a regular rear-end collision the level of protection of the reference system is neither improved, nor significantly worsened with the addition of active systems.

Reducing the head to headrest gap reduces the difference in the whiplash injuries estimation between the two occupant models for the regular rear-end collision. In case of AEB-induced OOP, the distances observed with the BioRID-II are significantly higher than the ones of the human model (150 – 400 [mm] range for the first, 55 – 180 [mm] range for the latter).

## CONCLUSIONS

A methodology for the development of passive and active safety systems in an integrated manner has been drafted and motivated in this paper. Due to the increased implementation of autonomous functions in the new vehicles (e.g AEBS), there is also an increased need for investigating and testing the consequences of operation of such systems on occupant safety. The protocols assessing the whiplash injury risk in a rear-struck vehicle adopt a BioRID-II dummy in the dynamic tests for which a crash pulse is applied to an initially stationary sled, thus assuming no prior AEBS actions. With the analysis of an altered initial state of the vehicle (due to AEBS) the established protocols and the occupant model (dummy) may become obsolete or less applicable

The study shows that the AEB-induced OOP results in an increased risk of whiplash injuries in the follow-up rear-end collision. The increase of injury risk depends on the type of occupant model used in the simulation and has been done for only one collision severity case, one braking pulse and one vehicle. However, the initial results of this study indicate already that the whiplash assessment protocols for cars equipped with AEB systems should include the effect of AEB-induced OOP. Addressing the above problem would require, though, a robust method to identify the position of the occupant (including dynamic effects) at which he or she enters the in-crash phase.

The negative effect of AEB-induced OOP in the rear-end collision can be alleviated effectively by applying different occupant motion control measures deployed in the pre-crash phase. The main mechanical principle of the investigated system configurations is the reduction of the distance between the occupant and the backrest and headrest. The highest effectiveness in reducing the negative effect of AEB-induced OOP was obtained for the system with active headrest and motorized belt pretensioner.

Both investigated occupant models showed significant differences in predicting the pre-crash occupant motion resulting from AEB deployment, and thus also in the injury results in the follow-up rear-end collision. The severe OOP recorded with the BioRID-II model can be explained with the fact that the dummy is not validated for frontal loading, neither is it mechanically designed for use outside the in-plane rear loading and rebound phase. No mechanism in the BioRID-II can provide thoracic stiffness in flexion, thus resulting in an excessive (when compared to testing with volunteers in similar testing configuration [12]) forward motion of the upper torso under a braking loading.

It can be concluded that the BioRID-II and its model cannot represent the forward motion of the occupant during the pre-crash phase and cannot be used for these purposes. Further studies should include feasibility and effectiveness of using AHM to predict the forward OOP induced by AEBS and then swap the BioRID-II model at the moment of rear-end crash start (T=0.0 [s]). This approach ensures that in both pre- and in-crash phases the adopted ATDs are adequate and validated for the loading conditions of pre- and in-crash phases.

Further studies into this problem should increase the confidence in the conclusive statements of this paper by:

- broadening the scope of the investigation (different rear-end crash severity, braking pulse)
- sensitivity study into testing condition parameters: seat geometry, seat characteristic compliance, seating position of the occupant

In conclusion, given the significant injury risk typically accompanying rear impact collisions also at very low relative speeds [4] and the yet limited understanding of the potential for integrated safety to address this issue, this paper intends to initiate the interest in further research that can exploit new predictive technologies to reduce the harm caused by rear-end impact.

**REFERENCES**


[1] EC/No 661/2009. Type-approval requirements for the general safety of motor vehicles, their trailers and systems, components and separate technical units intended therefor.

[2] Bours, R.; Verhoeve, R.; Kietlinski, K. and Tideman, M. (2012, May 23–25). *Enhancing Real-Life Safety by Integration of Active and Passive Safety System Simulation*. In Proceedings of the 2012 Annual Congress of the Society of Automotive Engineers of Japan. JSAE Technical Paper 20125200.

[3] Velardocchia, M; Unger, M; Vigliani, A; Leone, N; Kietlinski, K; Galvagno, E. (2013, August 4). *Integrated Active and Passive Systems for a Side Impact Scenario*. SAE Technical Paper 2013-01-1162.

[4] Bogenrieder, R; Fehring, M; Bachmann, R. (2009). *Pre-Safe in Rear-End Collisions Situations*. Paper 09-01229 presented at the ESV Conference, Stuttgart, Germany.

[5] Eis, V; Sferco, R; Fay, P. (2005). *A Detailed Analysis of the Characteristics of European Rear Impacts*. Paper 05-0385 presented at the ESV Conference, Washington DC.

[6] PreScan R7.0 Theory Manual.

[7] Euro NCAP. *The Dynamic Assessment of Car Seats for Neck Injury Protection Testing Protocol* (version 3.2, November 2014).

[8] MADYMO Quality Report Release Update (2011). *BioRID-II facet Q model version 3.3 (R7.4)*. Report number QBioRIDII-111101.

[9] MADYMO Quality Report Release Update. (2013). *Active Human 50$^{th}$ Facet Q Model, version 1 (R7.4)*. Report number QAHM50FC-130603.

[10] Meijer, R., van Hassel E., Broos J., Hala W., van Rooij L. and van Hooijdonk P. (2012, September 12-14). *Development of a Multi-Body Human Model that Predicts Active and Passive Human Behaviour.* In Proceedings of the IRCOBI Conference , Dublin, Ireland.

[11] Horst van der, M.J.; Bovendeerd, P.H.M; Happee, R; Wismand, J.S.H.M; Kingma, H. (2001). *Simulation of Rear End Impact with a Full Body Human Model with a Detailed Neck: Role of Passive Muscle Properties and Initial Seating Posture*. Paper 119 presented at the ESV Conference, Amsterdam, The Netherlands.

[12] Mages, M.; Seyffert, M. and Class, U. (2011, June 13-16). *Analysis of the Pre-Crash Benefit of Reversible Belt Pre-Pretensioning in Different Accident Scenarios.* Paper 11-0442 presented at the ESV Conference, Washington, D.C.

# AIMING FOR AN AVERAGE FEMALE VIRTUAL HUMAN BODY MODEL FOR SEAT PERFORMANCE ASSESSMENT IN REAR-END IMPACTS

**Karin Brolin**
**Jonas Östh**
**Mats Svensson**
Chalmers University of Technology
Sweden

**Fusako Sato**
**Koshiro Ono**
Japan Automotive Research Institute
Japan

**Astrid Linder**
Swedish National Road and Transport Research Institute, VTI
Sweden

**Anders Kullgren**
Folksam
Sweden

Paper Number 15- 0247

**ABSTRACT**

The female part of the population suffers more Whiplash Associated Disorders (WAD) in car crashes than males. Several studies have illustrated the need to consider the female population when developing and assessing the WAD prevention performance of advanced restraint systems in rear-end collisions. Presently only one crash test dummy is available, the average sized male BioRID. Recently a virtual dummy model of an average female, EvaRID, was developed and used in rear impact simulations. The results stressed the need for models representing the female part of the population, as well. Virtual crash simulations have become essential in traffic safety and with models of both an average male and female, further steps in addressing improved assessment of WAD prevention can be taken. The present paper presents a starting point of research aiming to develop an open-source average female Finite Element (FE) model with an anatomically detailed cervical spine. This paper provides a review of the literature to identify gender specific neck biomechanics and anatomical differences, followed by a review of published FE models of the cervical spine.

Data on vertebral body dimensions (height, width, depth, spinal canal diameter, facet joint angles) have been compiled from biomechanical literature. Significant gender differences exist for the vertebral body depth and width, the spinal curvature in the seated posture, and the spinal stiffness and range of motion. All have the potential to influence the outcome of an impact and should be accounted for in the development of WAD prevention.

The review of FE models of the cervical spine presented 17 models based on male geometry but only one model scaled to represent a female. An overview of the models are given with respect to the solver, geometry source, number of elements, and implementation of the facet joints, ligaments, and muscles. It is recommended that an average female model is developed with focus on; 1) the shape of the female vertebral body, especially the depth and width that provides less support area than for males, 2) defining the spinal curvature representative of seated female volunteers who generally display less lordosis than males, 3) the dimensions of the spinal ligaments, rather than the material properties, to capture the larger range of motion and less spinal stiffness of female subjects compared to males, and 4) validation to female volunteers and PMHS tests for range of motion, while failure prediction seem less gender sensitive.

KEYWORDS**:** Whiplash Associated Disorders, gender, biomechanics, finite element human body model

## INTRODUCTION

Whiplash Associated Disorders (WAD) is the common denomination for a range of neck related symptoms that typically occur in vehicle collisions. During a rear-end collison, the torso of a properly restrained occupant will be accelerated while the head tends to lag behind causing inertial loading to the neck. This loading causes a so called whiplash motion of the neck in which the neck is forced into an unphysiological s-curved shape that later evolves into a c-shape (Ono et al, 1997). For example, in Sweden WADs account for ~70% of all injuries leading to disability due to vehicle crashes (Kullgren et al. 2007). The majority of victims experiencing initial WAD symptoms recover within a few weeks or months of the crash (The Whiplash Commission 2005), however, 5–10% of individuals experience different levels of medically classified permanent disabilities (Nygren 1983, Krafft 1998, The Whiplash Commission 2005). WADs occur at relatively low velocity changes, typically <25 km/h (Eichberger et al. 1996, Kullgren et al. 2003), and in impacts from all directions, although rear impacts are most frequently featured in accident statistics (Watanabe et al. 2000). Since the mid-1960s, injury statistical data have shown that females have a higher risk of sustaining WAD than males, even in similar crash conditions (Narragon 1965, Kihlberg 1969, O'Neill et al. 1972, Thomas et al. 1982, Otremski et al. 1989, Maag et al. 1990, Morris & Thomas 1996, Dolinis 1997, Temming & Zobel 1998, Richter et al. 2000, Chapline et al. 2000, Krafft et al. 2003, Jakobsson et al. 2004, Storvik et al. 2009, Carstensen et al. 2012). According to these studies, WAD risk is 1.4 to 3 times higher for females compared to males.

Currently rear impact tests are performed using the only available dummy developed for low severity testing, the Biofidelic Rear Impact Dummy, BioRID II (Davidsson et al. 1999), which represents a 50$^{th}$ percentile male. The BioRID II is used in test protocols, i.e. Euro NCAP, for assessing the risk of whiplash injuries when seated in the front seat. The BioRID was developed in the late 1990s to evaluate the protective performances of car seats in low severity rear impacts. However, real world accident analysis has shown that seats designed to prevent WAD are more effective for males (Kullgren et al., 2013). Therefore, there is an urgent need to better represent the whole adult population in the development and assessment of WAD prevention systems and develop models representing females, as well as males for assessing the prevention performance.

The initial step in the work towards addressing WADs in females was recently taken in the ADSEAT project (Linder et al. 2013) that adopted a broad approach when developing the world first average female virtual dummy model, EvaRID (Carlsson et al. 2014). Virtual impact simulations with seats showed, using the virtual male and female dummy models, that differences were found in the response of the BioRID II and EvaRID models for some of the seat concepts tested (Linder et al 2013). Furthermore, a prototype dummy of an average female was developed and run in the same test set-up as the Euro NCAP tests performed with the BioRID II (Schmitt et al. 2012). Four different seat types were tested and the results confirmed that the size of males and females interact differently with the seat and the head restraint. Based on the dummy responses, male and female occupants would thus obtain different levels of protection when seated in the same seat. Hence, having access to models of both an average male and female, further steps in addressing improved assessment of WAD prevention can be taken. Virtual models offer a greater variety of seated postures and the potential to evaluate a wider range of parameters, compared to what is practically possible in physical testing.

Virtual crash simulations using the Finite Element (FE) method has become an essential tool in traffic safety and with increasing computer capacity the size and complexity of the models has increased. Traditionally, FE occupant models were virtual copies of crash test dummies but more recently there has been a strong progression in the development of Human Body Models (HBMs). The latter have been designed to represent the human body rather than a dummy and have the potential to allow for much more detailed studies of injury mechanisms than physical or virtual dummies. A number of occupant HBMs have been released, primarily of the average male anthropometry, but are not widely used due to a number of reasons such as model quality, restricted availability or high licencing fees. Therefore, the need for open source models where knowledge and experience can be shared and continued improvements of the models can be provided by any user is apparent. Our overall aim is to develop an open-source FE model of an average female, with an anatomically detailed cervical spine suitable for assessment of seat performance.

This paper provides a review of the literature to identify gender specific neck biomechanics and anatomical differences followed by a review of published FE models of the cervical spine. Lastly, a short complementary discussion presents the conlusion on requirements for the development of an average female HBM. The resulting

recommendations have the potential to improve the biofidelity of female HBMs and thereby enhance the development and assessment of safety systems that can reduce the incidence of WAD in traffic accidents.

## INJURY MECHANISMS

Despite much research, WAD is still one of the most poorly understood traffic injuries. Literature supports an organic basis for WADs (Siegmund et al. 2009; Curatolo et al. 2011). Several anatomical sites have been proposed, including, facet joints, spinal ligaments, intervertebral discs, vertebral arteries, dorsal root ganglia, and neck muscles. Each of these tissues is strained during a whiplash motion exposure. Two mechanisms of facet joint lesions have been proposed: pinching of the synovial fold and excessive capsule strain. The cervical vertebrae have been shown to rotate about an elevated instantaneous centre during whiplash motion in a rear-end collision. This may compress the posterior facet surfaces, pinching the synovial fold (Ono et al. 1997; Kaneoka et al. 1999). Excessive facet capsule strain has been demonstrated during rear-end collision whiplash motion experiments where, in a functional cervical spinal unit, the upper vertebrae was exposed to excessive rearward shear (Pearson et al. 2004; Yang and King 2003). Lesions to the other neck ligaments and intervertebral discs have been reported by Krakenes and Kaale (2006), for instance. Ligament lesions may cause acute neck pain and lead to chronic spinal instability. Lesion to mechanoreceptors may corrupt the normal sensory signals and can lead to abnormal muscle response patterns, decreased neck mobility and proprioception (Panjabi et al. 2006).

Chronic symptoms such as headache, blurred vision, tinnitus, dizziness, and vertigo have been proposed to be associated with altered blood flow rates due to spasm and/or narrowing of vertebral arteries in WAD patients (Reddy et al. 2002; Seric et al. 2000). Intimal tears of the vertebral artery are most common at the atlanto-axial joint. This has been hypothesized to be caused by coupled extension and axial rotation of the upper cervical spine. Also, many WAD symptoms could be explained by lesion to the dorsal root ganglia that contain the cell bodies of most peripheral sensory nerves, at each spinal level. Increased electrical activity in the spinal cord and widespread reductions in electrical and pressure thresholds after whiplash motion exposure suggest altered central pain processing (Banic et al. 2004, Curatolo et al. 2001, Kasch et al. 2001a, Scott et al. 2005). During whiplash motion, pressure transients have been registered in the spinal canal (Örtengren et al. 1996, Svensson et al. 2000). These are hypothesized to be the cause of spinal ganglion nerve cell membrane dysfunction. Direct deformation of the nerve roots is another possible cause as the diameter of the neural foramina decrease during extreme neck motions.

Muscle pain is a common WAD symptom, although evidence of direct lesions in muscles remains inconclusive. Direct muscle lesions may not be responsible for chronic pain, but may play an indirect role in modulating pain caused by injuries to other structures. The direct mechanism of muscle lesions occur due to imposed lengthening during active contraction. Both anterior and posterior muscles experience active lengthening (Brault et al. 2000; Vasavada et al. 2007). Neck muscles interact with other anatomical sites: 1) they attach to the facet capsule; 2) they indirectly load other neck structures; and 3) altered neuromuscular control may contribute to chronic pain.

For each of the above mentioned tissues, continued research is needed to help improve diagnosis and treatment. Simulations with HBMs can help shed light on the strain in different neck tissues during the multitude of different loading scenarios that occur in traffic accidents and are known to produce WADs. Also, in order to assess the protective properties of vehicle seats and other safety systems it is necessary for the HBMs to be detailed enough to provide metrics for all or at least most of the above mentioned injury mechanisms. To predict tears of the vertebral arteries and excessive strain of upper cervical ligaments, it is essential to model the complex structure of the upper cervical joints with sliding contacts between the joints and soft tissues limiting the motion. Facet joint motion and strain in the spinal ligaments are highly dependent on the vertebral kinematics and therefore it is essential the HBMs have biofidelic relative motion in the vertebral segments.

## ANTHROPOMETRY AND MATERIAL PROPERTIES

There are significant differences in neck anthropometry based on gender. The female neck is more slender than the male neck, for example Harty et al. (2004) found the female neck circumference to be 84% of the male neck circumference and female neck length was 91% of the male. There is little gender differences in the head circumference while the neck circumference is smaller for females (Vasavada et al. 2001, Harty et al. 2004,

Mordaka 2004, Valkeinen et al. 2002, Vasavada et al. 2008, DeRosia 2008). Hence, females support more head mass per neck cross-sectional area. These gender differences may to some extent depend on stature and not directly on gender. To distinguish the effects of gender from stature, size matched male and female subjects were studied by Vasavada et al. (2008) and DeRosia (2008) (Table 1). It can be seen that head circumference varied by only 3%, irrespective of size matching based on neck length, seated height, or stature. On the other hand, the female neck circumference was 84 – 86 % of the male measurements for all groups. Hence, gender have significant effect on neck circumference, which is not an effect of differences in overall body dimensions. Gender differences for neck length were less than the difference for neck circumference, supporting previous findings that female necks are more slender (Vasavada et al. 2008, DeRosia 2008).

**Table 1. Body Dimensions for Size Matched Volunteers**

F = Females, M = Males, No. = Number of subjects, Circumf. = Circumference.

*Neck length measure: C7 spinous process - tragus of the ear (Vasavada 2008), C2-C6 length (DeRosia 2008).

| | | average ± SD | | | | |
|---|---|---|---|---|---|---|
| **References** | | Schneider et al. 1983 | Vasavada et al. 2008 | DeRosia 2008 | DeRosia 2008 | DeRosia 2008 |
| **Size Matched** | | 50th percentiles | neck length | seated height | head circumf. | stature |
| **No. F** | | | 14 | 11 | 19 | 11 |
| **No. M** | | | 14 | 17 | 15 | 10 |
| **Head Circumf.** | F | | 562 ± 15 | 561 ± 14 | 559 ± 7 | 548 ± 15 |
| [mm] | M | | 577 ± 13 | 580 ± 15 | 561 ± 8 | 564 ± 21 |
| | F/M | | 97% | 97% | 100% | 97% |
| **Neck Circumf.** | F | | 331 ± 20 | 324 ± 12 | 322 ± 14 | 318 ± 22 |
| **[mm]** | M | | 394 ± 22 | 376 ± 16 | 379 ± 20 | 379 ± 23 |
| | F/M | | 84% | 86% | 85% | 84% |
| **Neck length*** | F | | 107 ± 5 | 88 ± 6 | 86 ± 6 | 86 ± 7 |
| [mm] | M | | 108 ± 5 | 95 ± 6 | 97 ± 6 | 97 ± 6 |
| | F/M | | 99% | 94% | 88% | 89% |
| **Stature** | F | 1618 | 1690 ± 30 | 1677 ± 60 | 1645 ± 69 | 1687 ± 18 |
| [mm] | M | 1753 | 1690 ± 30 | 1745 ± 44 | 1785 ± 92 | 1693 ± 18 |
| | F/M | 92% | 100% | 96% | 92% | 100% |
| **Seated height** | F | 844 | | 879 ± 10 | 859 ± 24 | 851 ± 19 |
| [mm] | M | 901 | | 886 ± 9 | 900 ± 41 | 875 ± 18 |
| | F/M | 94% | | 99% | 95% | 97% |
| **Mass** | F | 62 | 66 ± 9 | 64 ± 6 | 61 ± 6 | 60 ± 12 |
| [kg] | M | 77 | 74 ± 9 | 76 ± 8 | 79 ± 14 | 75 ± 7 |
| | F/M | 81% | 89% | 84% | 77% | 80% |

Vertebral body dimensions are smaller for females than males (Table 2), irrespecitve if measured on skeletal bone specimen or from medical images of patients and volunteers. This is expected as the female population is overall smaller than the male population. Frobin et al. (2002) found that the vertebral body height divided by depth ratio was smaller for females than males, indicating that the female cervical spine has less support area. When this ratio was calculated for other studies where both depth and height were reported, similar trends were seen (Table 2, last three columns). Vasavada et al. (2008) matched volunteers with regards to seated height and neck length, and found the female dimensions to be 86-98% of the male dimensions. Gender differences were most prominent for the C3-C5 vertebral bodies. DeRosia (2008) and Stemper et al. (2008, 2009) pusblished results with size matched volunteers in three groups based on either seated height, head circumference, or stature. They found that the female dimensions were 86-95% of the male dimensions and significantly smaller with regards to width and depth for females among the head circumference matched volunteers. The results from the head circumference matched group compare well with a large survey without size matching by Parenteau et al. (2014), which is likely because the head circumference matching provides a large spread in stature and other dimensions. Hence, even when size-matched, females have smaller vertebral bodies than males, which is most prominent for the vertebral depth.

A narrow spinal canal could possibly increase the risk of nervous tissue lesions. Significant gender differences in spinal canal dimensions have been found in studies of skeletal specimens and patients (Table 3). The spinal canal was widest in the upper cervical spine and narrowest at the C4-C6 levels. The largest gender differences were found at the C4-C5 level, where the spinal diameter was 4-6% narrower for females (Tatarek 2005 and Evangelopoulos et al. 2012, Parenteau et al. 2014). On the other hand, differences of less than 2% were reported for all levels (Hukuda and Kojima 2002) and for C4 and above (Parenteau et al. 2014). None of these studies comprised size-matched subjects and the gender differences may stem from a difference in overall size rather than gender.

**Table 2. Vertebral Body Dimensions**

F = females, M = males, No. = number of, skel. = skeletal specimen, vol = volunteers.

| | | **Height*** | | | | **Depth**** | | | | | | **Width***** | | | | | | **Height by Depth** | | |
|---|---|---|---|---|---|---|---|---|---|---|---|---|---|---|---|---|---|---|---|---|
| | | average ± SD [mm] | | | | average ± SD [mm] | | | | | | average ± SD [mm] | | | | | | [mm/mm] | | |
| | **References** | Boyle et al. 1996 | Hukuda and Kojima 2002 | Vasavada et al. 2008 | Milne 1991 | Kasai et al. 1996 | Ebraheim et al. 1998 | Hukuda and Kojima 2002 | Vasavada et al. 2008 | DeRosia 2008 | Stemper et al. 2009 | Stemper et al. 2009 | Parenteau et al. 2014 | Milne 1991 | Vasavada et al. 2008 | DeRosia 2008 | Stemper et al. 2009 | Stemper et al. 2009 | Frobin et al. 2002 | Hukuda and Kojima 2002 | Vasavada et al. 2008 |
| **Size Matched** | | no | no | neck length | no | no | no | no | neck length | stature | sitting height | head circumf. | no | no | neck length | stature | sitting height | head circumf. | no | no | neck length |
| **Subjects** | | skel. | skel. | vol. | skel. | skel. | skel. | skel. | vol. | vol. | vol. | vol. | patients | skel. | vol. | vol. | vol. | vol. | skel. | skel. | vol. |
| **No. F** | | 25 | 114 | 14 | 21 | 10 | 11 | 114 | 14 | 11 | 11 | 18 | 176 | 21 | 14 | 11 | 11 | 18 | 100 | 114 | 14 |
| **No. M** | | 26 | 105 | 14 | 40 | | 16 | 105 | 14 | 10 | 17 | 9 | 251 | 40 | 14 | 10 | 17 | 9 | 35 | 105 | 14 |
| **C1** | F | | | | | | | | 45,1 ± 1,9 | | | | | | | | | | | | |
| | M | | | | | | | | 47,6 ± 4,5 | | | | | | | | | | | | |
| | F/M | | | | | | | | 95% | | | | | | | | | | | | |
| **C2** | F | | | | | | 13,7 ± 1,3 | | 13,1 ± 1,0 | 15,7 ± 1,1 | 15,9 ± 1,2 | 15,4 ± 0,9 | 14,4 ± 1,4 | | | 19,6 ± 2,3 | 20,4 ± 2,4 | 20,2 ± 1,7 | | | |
| | M | | | | | | 14,6 ± 1,2 | | 14,2 ± 1,0 | 16,8 ± 0,9 | 17,5 ± 0,9 | 17,0 ± 0,8 | 16,7 ± 1,6 | | | 21,8 ± 1,0 | 22,3 ± 1,3 | 21,9 ± 1,0 | | | |
| | F/M | | | | | | 94% | | 92% | 93% | 91% | 91% | 86% | | | 90% | 91% | 92% | | | |
| **C3** | F | 13,0 ± 1,2 | | 12,0 ± 0,9 | 13,8 ± 0,2 | | 13,6 ± 1,4 | 16,0 ± 1,2 | 12,8 ± 0,8 | 15,4 ± 1,0 | 15,7 ± 0,8 | 15,1 ± 0,9 | 15,0 ± 1,6 | 18,2 ± 0,3 | 14,6 ± 2,6 | 20,4 ± 1,8 | 20,9 ± 1,9 | 20,7 ± 1,7 | 0,94 | 0,81 | 0,94 |
| | M | 14,6 ± 1,5 | | 13,5 ± 0,9 | 15,3 ± 0,2 | | 14,6 ± 1,2 | 18,1 ± 1,3 | 14,2 ± 1,6 | 16,6 ± 1,0 | 16,8 ± 1,1 | 16,9 ± 1,2 | 17,2 ± 1,9 | 19,1 ± 0,3 | 16,9 ± 1,6 | 22,0 ± 1,3 | 22,9 ± 1,4 | 22,2 ± 1,9 | 0,91 | 0,81 | 0,95 |
| | F/M | 89% | | 89% | 90% | | 93% | 88% | 90% | 93% | 93% | 89% | 87% | 95% | 86% | 93% | 91% | 93% | 103% | 101% | 99% |
| **C4** | F | 12,7 ± 1,2 | | 11,6 ± 0,9 | 14,4 ± 0,3 | | 13,5 ± 1,4 | 15,7 ± 1,3 | 13,0 ± 1,0 | 15,3 ± 0,9 | 15,7 ± 0,8 | 15,2 ± 1,0 | 15,3 ± 2,0 | 20,9 ± 0,3 | 16,9 ± 1,2 | 20,6 ± 2,0 | 21,9 ± 1,7 | 21,3 ± 1,5 | 0,88 | 0,81 | 0,89 |
| | M | 14,2 ± 1,4 | | 12,6 ± 0,8 | 16,0 ± 0,3 | | 14,8 ± 1,6 | 17,6 ± 1,4 | 14,8 ± 1,2 | 16,9 ± 1,0 | 16,8 ± 1,1 | 17,1 ± 1,6 | 17,5 ± 2,1 | 19,3 ± 0,3 | 17,8 ± 2,1 | 22,2 ± 1,6 | 23,2 ± 1,3 | 22,7 ± 1,3 | 0,84 | 0,81 | 0,85 |
| | F/M | 89% | | 92% | 90% | | 91% | 89% | 88% | 91% | 93% | 89% | 87% | 108% | 95% | 93% | 94% | 94% | 105% | 100% | 105% |
| **C5** | F | 12,7 ± 1,2 | | 11,3 ± 0,7 | 14,0 ± 0,2 | 17,1 ± 0,6 | 13,4 ± 1,3 | 15,3 ± 1,3 | 13,0 ± 0,9 | 15,5 ± 0,9 | 15,8 ± 0,8 | 15,6 ± 1,2 | 16,6 ± 2,5 | 20,4 ± 0,3 | 18,3 ± 1,5 | 21,1 ± 1,5 | 22,1 ± 1,3 | 21,6 ± 1,8 | 0,85 | 0,83 | 0,87 |
| | M | 13,9 ± 1,4 | | 12,2 ± 0,6 | 16,2 ± 0,3 | 18,2 ± 0,5 | 14,6 ± 1,4 | 17,4 ± 1,4 | 15,2 ± 1,1 | 17,7 ± 1,2 | 16,9 ± 0,8 | 17,6 ± 1,2 | 18,7 ± 2,6 | 21,6 ± 0,2 | 19,0 ± 2,0 | 23,5 ± 1,7 | 23,8 ± 2,2 | 23,2 ± 1,5 | 0,81 | 0,80 | 0,80 |
| | F/M | 91% | | 93% | 86% | 94% | 92% | 88% | 86% | 88% | 93% | 89% | 89% | 94% | 96% | 90% | 93% | 93% | 104% | 104% | 108% |
| **C6** | F | 11,1 ± 1,1 | 12,8 ± 1,3 | 11,6 ± 0,8 | 14,9 ± 0,5 | | 13,3 ± 1,0 | 15,9 ± 1,3 | 14,0 ± 1,0 | 15,9 ± 0,9 | 16,3 ± 1,0 | 16,2 ± 1,0 | 16,9 ± 2,2 | 22,1 ± 0,4 | 19,8 ± 1,6 | 24,5 ± 1,8 | 24,7 ± 1,3 | 24,1 ± 1,8 | 0,83 | 0,81 | 0,83 |
| | M | 11,8 ± 0,9 | 13,7 ± 1,2 | 12,0 ± 0,7 | 16,6 ± 0,3 | | 14,8 ± 1,3 | 18,1 ± 1,4 | 15,6 ± 1,0 | 18,4 ± 2,0 | 18,0 ± 1,3 | 18,8 ± 2,0 | 19,0 ± 2,4 | 23,7 ± 0,3 | 20,9 ± 2,3 | 27,0 ± 1,6 | 26,0 ± 2,0 | 27,0 ± 1,2 | 0,85 | 0,76 | 0,77 |
| | F/M | 94% | 93% | 97% | 90% | | 92% | 88% | 90% | 86% | 91% | 86% | 89% | 93% | 95% | 91% | 95% | 89% | 99% | 106% | 108% |
| **C7** | F | 12,9 ± 1,2 | 14,1 ± 1,2 | 12,8 ± 0,6 | 14,7 ± 0,3 | | 12,9 ± 0,7 | 16,6 ± 1,3 | 13,7 ± 1,2 | | | | 15,6 ± 1,7 | 23,4 ± 0,3 | 22,6 ± 2,4 | | | | 0,91 | 0,85 | 0,93 |
| | M | 13,3 ± 1,3 | 15,6 ± 1,5 | 13,0 ± 1,0 | 16,5 ± 0,3 | | 14,3 ± 1,0 | 18,7 ± 1,2 | 15,5 ± 1,3 | | | | 17,7 ± 1,9 | 25,2 ± 0,2 | 24,6 ± 2,7 | | | | 0,92 | 0,83 | 0,84 |
| | F/M | 97% | 90% | 98% | 89% | | 90% | 89% | 88% | | | | 88% | 93% | 92% | | | | 98% | 102% | 111% |
| **T1** | F | 14,3 ± 1,3 | | | 14,4 ± 0,3 | | | | | | | | | 23,4 ± 0,3 | | | | | | | |
| | M | 15,3 ± 1,1 | | | 16,2 ± 0,2 | | | | | | | | | 25,2 ± 0,3 | | | | | | | |
| | F/M | 94% | | | 88% | | | | | | | | | 93% | | | | | | | |

* Height was measured at the middle of the vertebral body or the average of anterior and posterior height. ** Depth was measured at the middle of the vertbral body or the average of the superior and inferior surfaces, except for Milne 1991 (superior surface), Parenteau et al. 2014 (inferior surface), Stemper et al. 2009 and DeRosia 2008 (maximum measurement). *** Width was measured at the superior surface by Milne 1991, average of superior and inferior surface in Vasavada et al. 2008, and the maximum measurement in Stemper et al. 2009 and DeRosia 2008.

The facet joints are important for the biomechanical response. Gender differences in facet joint angles have been hypothesized as one explanation to the increased WAD risk for females. Measured relative to the vertebral body, very small and contradictory gender differences have been reported by Milne (1991), Boyle et al. (1996), Kasai et al. (1996), and Parenteau et al. (2013) (Table 3). Any difference in facet joint angle must thus stem from a difference in posture and/or spinal curvature. The variations in cervical spine alignment have been investigated extensively. For a majority of the population lordosis of the cervical spine is normal. The proportions of non-lordosis (straight or kyphosis) were 36% (Matsumoto et al. 1998) and 38% (Takeshima 2002) for an asymptomatic population measured in a seated position. Matsumoto et al. (1998) showed that females more frequently presented non-lordosis than males and that gender was an independent factor significantly associated with non-lordosis. Likewise, Helliwel et al .(1994) reported that the cervical spine was more likely to be straight in females than in males. Haedacker et al. (1997) observed that statistically cervical lordosis in males was more pronounced than in females. Additionally, Lee et al. (2014) focused on the cervicothoracic junction. Females had a thinner thoracic cage than males and males had a more forward-inclined thoracic inlet (angle between lines drawn from the top of the manubrium to the centroid of the cranial T1 end plate and the horizontal plane) than females. They concluded that a small anteroposterior diameter in the upper most thoracic cage was associated with cervical hypolordosis, whereas an inclined thoracic inlet was associated with pronounced cervical lordosis. Klinich et al. (2004) investigated the relationship between stature and type of cervical spine alignment. Tall females were more likely to have a straight cervical spine than short females. On the other hand, there was no significant relationship between stature and curvature for males. Hence, accounting for the spinal curvature, less lordosis will give a more horizontal orientation of the facet joint surfaces. An average female occupant HBM should include a seated posture with less lordosis than the average male models, based on these data. Also, the height of the female HBM should be considered when the seated lordosis is defined.

Dynamic response of occupants in rear impacts have been analysed with volunteer and post mortem human subject (PMHS) tests in order to understand the biomechanics of whiplash motion. In volunteer tests (Siegmund et al. 1997), females had greater head and neck kinematics compared to males in the overall motion analysis. In addition, cervical vertebral kinematics were also greater for females compared to males, when analysing sequential cineradiography images of cervical spines (Ono et al. 2006, Sato et al. 2014). Likewise, in rear impact sled tests with PMHS head-neck complexes, cervical vertebral kinematics were significantly greater for the female specimens than for the male specimens (Stemper et al. 2003, 2004). Initial alignment of cervical vertebrae has been considered as one of possible causes of the experimental gender difference seen. The alignment influences load transmission between the head and trunk of the body through the cervical spine, and can affect vertebral kinematics. Previous experimental studies (Maiman et al. 1983, Maiman et al. 2002, Yoganandan et al. 1986, Yoganandan et al. 1999, Liu and Dai 1989, Pintar et al. 1995) showed that changes in the initial alignment of the cervical spine had an influence on the severity of injury. Ono et al. (1997) conducted rear impact sled tests with a volunteer and quantified the effect of the initial alignment of the cervical spine on vertebral kinematics. They reported that rotational angles of cervical vertebrae were significantly greater in kyphotic alignment than in lordosis. Hence, as females are more likely to present with non-lordosis this implies that females inherently will suffer greater vertbral rotations. Likewise, Stemper et al. (2005) and Frechede et al. (2006) investigated elongation of the facet joint capsular ligaments (CL) in lordotic, straight and kyphotic cervical alignment with a FE head/neck model and reported that facet joint ligament elongations increased with kyphotic cervical alignment and concluded that kyphosispresented a higher risk for WAD than lordosis or straight spinal aligment.

Alongside anthropometry and spinal alignment, gender differences in material properties can influence the risk of lesions. Nightingale et al. (2002, 2007) tested upper and lower cervial spine specimen (4 female, 7 male) in flexion and extension bending load to failure. They found the mean upper cervical flexion and extension strength to be greater for males than females, however only significantly for flexion. The mean angle at failure were not significantly different for the genders. The female upper cervical spine was significantly less stiff than the male. Hence, the male range of motion was significantly greater than the female. Similar differences were seen also for the lower cervical spine. This, could be because of gender differences in cross sectional area of the ligaments or in the material properties. In sports, female athletes sustain more anterior cruciate ligament lesions (Elliot 2010), and some studies indicate that the influence of sex hormones on the material properties of the ligament may provide part of the explanation to increased risk (Wild 2012). Osakabe et al. (2001) studied the elastin and collagen content of lumbar ligaments with aging and found gender difference. The elastin content decreased with age for males but not for females. They suggested that sex steroid hormones may regulate the metabolism and thus effect how the elastin and collagen contents change with age. Stemper et al. (2010) tested thoracic specimen and found gender to influence the

elastic modulus in tension and compression, with female specimen having significantly greater moduli. Contrary, Bass et al. (2007) did not find any gender dependence for the failure true stress and failure true strain in cervical specimen (6 male, 5 female) tested for anterior longitudinal ligament (ALL), posterior longitudinal ligament (PLL), and ligamentum flavum (LF). Mattucci et al. 2012 tested the ALL, PLL, LF, CL, and interspinous ligament (ISL) from 8 male and 8 female cadavers in quasi-static (0.5 s-1) and dynamic (up to 250 s-1) load rates. Stiffness and strength were consistently lower for female specimen, although significant gender differences were only found for the Young's modulus of the ALL and the failure force of the CL (Mattucci 2012). Hence, it seems likely that the gender difference due to anthropometry have a larger influence than gender difference in the material properties of the ligaments.

**Table 3. Spinal Canal Diameter and Facet Joint Angles**

None of these studies included size matched subjects. F = Females, M = Males, No. = Number of, skel. = skeletal specimen. * Spinal canal anterior-posterior diameter in the sagittal plane. For Parenteau et al. 2014 the diameter was recalculated by doubling the reported radius. Tatarek 2005 values are the average of the two reported groups. ** The angle of the superior facet to the plane of the end plate, except for Parenteau et al. 2013 (inferior facet). Data from Kasai et al. 1996 was recalculated from the angle to the posterior vertebral line by adding 90 degrees.

| | **Spinal Canal Diameter *** | | | | **Facet Joint Angles **** | | | |
|---|---|---|---|---|---|---|---|---|
| | average ± SD [mm] | | | | average ± SD [degrees] | | | |
| **References** | Hukuda and Kojima 2002 | Tatarek 2005 | Evangelopoulos et al. 2012 | Parenteau et al. 2014 | Milne 1991 | Boyle et al. 1996 | Kasai et al. 1996 | Parenteau et al. 2013 |
| **Subjects** | skel. | skel. | patients | patients | skel. | skel. | patients | patients |
| **No. F** | 114 | 321 | 100 | 176 | 21 | 25 | 10 | 173 |
| **No. M** | 105 | | | 251 | 40 | 26 | | 250 |
| **C1** F | | | 16,3 ± 1,6 | | | | | |
| M | | | 16,6 ± 1,9 | | | | | |
| F/M | | | 98% | | | | | |
| **C2** F | | 15,9 ± 1,4 | 13,3 ± 1,3 | 13,7 ± 1,6 | | | | 126,5 ± 14,0 |
| M | | 16,6 ± 1,4 | 13,6 ± 1,6 | 13,7 ± 1,9 | | | | 122,1 ± 12,3 |
| F/M | | 95% | 97% | 100% | | | | 104% |
| **C3** F | 16,8 ± 1,7 | 13,9 ± 1,4 | 12,9 ± 1,3 | 12,9 ± 1,5 | 126,2 ± 1,2 | | 128,4 ± 3,8 | 127,0 ± 11,4 |
| M | 16,6 ± 1,5 | 14,7 ± 1,3 | 13,3 ± 1,7 | 13,0 ± 1,7 | 122,8 ± 1,2 | | 129,5 ± 4,2 | 124,1 ± 9,1 |
| F/M | 101% | 94% | 97% | 99% | 103% | | 97% | 102% |
| **C4** F | 15,8 ± 1,7 | 13,4 ± 1,4 | 12,5 ± 1,5 | 12,7 ± 1,5 | 124,8 ± 1,23 | | 129,7 ± 2,8 | 128,4 ± 11,5 |
| M | 15,8 ± 1,4 | 14,3 ± 1,3 | 13,1 ± 1,0 | 13,0 ± 1,9 | 124,5 ± 0,81 | | 131,2 ± 4,1 | 129,0 ± 8,8 |
| F/M | 100% | 94% | 96% | 98% | 100% | | 96% | 100% |
| **C5** F | 15,7 ± 1,6 | 13,4 ± 1,3 | 12,7 ± 1,7 | 12,3 ± 1,7 | 125,7 ± 1,5 | | 131,7 ± 3,0 | 128,0 ± 11,3 |
| M | 15,9 ± 1,3 | 14,3 ± 1,3 | 13,4 ± 1,2 | 13,0 ± 1,6 | 127,6 ± 0,8 | | 132,3 ± 2,5 | 129,3 ± 10,2 |
| F/M | 99% | 94% | 94% | 95% | 99% | | 99% | 99% |
| **C6** F | 15,6 ± 1,6 | 13,5 ± 1,1 | 12,5 ± 1,8 | 12,7 ± 1,5 | 124,8 ± 1,42 | 124,4 ± 5,7 | 125,3 ± 2,7 | 120,9 ± 11,9 |
| M | 15,9 ± 1,3 | 14,3 ± 1,3 | 13,3 ± 1,9 | 13,3 ± 1,7 | 126 ± 0,89 | 125,7 ± 5,5 | 126,1 ± 4,5 | 124,5 ± 9,3 |
| F/M | 98% | 95% | 94% | 96% | 99% | 99% | 98% | 97% |
| **C7** F | 15,5 ± 1,6 | 13,5 ± 1,1 | | 13,6 ± 1,5 | 116,0 ± 1,1 | 115,8 ± 5,7 | 115,2 ± 2,8 | 124,2 ± 14,4 |
| M | 15,8 ± 1,4 | 14,4 ± 1,2 | | 14,2 ± 1,4 | 115,6 ± 0,9 | 118,7 ± 5,1 | 117,4 ± 4,0 | 125,4 ± 11,4 |
| F/M | 98% | 94% | | 96% | 100% | 98% | 92% | 99% |
| **T1** F | | | | | 111,1 ± 1,13 | 108,5 ± 6,1 | | |
| M | | | | | 112,2 ± 1,05 | 112,2 ± 6,6 | | |
| F/M | | | | | 99% | 97% | | |

## FINITE ELEMENT HUMAN BODY MODELS

A number of whole body FE occupant models have been released, primarily of the 50$^{th}$ percentile male anthropometry as defined by Schneider et al. 1983. A first generation of models developed in the late 1990s and early 2000s are the THUMS v3 (Iwamoto et al. 2002), HUMOS (Robin 2001), and the JAMA model (Sugimoto and Yamazaki 2005). In the THUMS v3, 7 400 elements of the total 143 000 are located in the cervical region. However, quite substantial simplifications such as the the facet joints being represented by single hexahedral elements in shear, rather than a sliding contact, makes soft tissue injury prediction difficult. A second generation of whole body HBMs have more recently been released, with an increased number of elements by an order of

magnitude; the THUMS v4 (Watanabe et al. 2011) includes 1.7 million elements and the GHBMC model (Vavalle et al. 2013) 2.2 million elements to represent a 50$^{th}$ percentile male occupant. To date, the most advanced cervical model in a whole body HBM appears to be the GHBMC model, that includes sliding contact facet joints with articular cartilage, failure criteria for the interverterbral discs to represent disc avulsion, failure criteria for 1D cervical ligaments and bone, and 3D musculature with superimposed active 1D elements. For the GHBMC, 12% of the elements are located in the cervical region, while in the THUMS v4 only 1.6 % is used. For some of the models mentioned above, 95$^{th}$ percentile male and 5$^{th}$ percentile female versions have been developed and released. However, to the best of our knowledge, no 50$^{th}$ percentile female whole body HBM has been released to date.

Many models of the isolated cervical spine have been developed and used to study impact biomechanics problems. The first models employed multibody dynamics modelling techniques (de Jager 1996, Deng and Goldsmith 1987, van der Horst 2002), and were used to show the importance of musculature in capturing volunteer responses in multi-directional impacts (de Jager 1996, van der Horst 2002). The multibody approach is numerically more efficient than FE simulations, an important property for early models. When applied to whiplash motion, one major drawback of the multi body models is that the spinal joints were modelled with kinematic joints instead of facet surfaces restrained by soft tissues. One of the first FE models to inlude the complex joints of the upper cervical spine with sliding surfaces between the occiput and second cervical vertebra was Brolin and Halldin (2004), illustrating the benefit of this modelling approach when studying how material properites of ligaments influence kinematics. More recent studies have successfully been used to study the effect of cervical muscle activity, using optimisation (Chancey et al. 2003, Brolin et al. 2005, Dibb et al. 2013) or neuromuscular control schemes (de Bruijn 2014) for the cervical musculature. In order to capture the response of live human subjects through numerical simulation, detailed representation of the cervical musculature and at least a basic muscle activation scheme are necessary (Brolin et al. 2008, Hedenstierna and Halldin 2008). For rear-end impacts the importance of cervical muscle activation has also been confirmed through numerous experimental studies, e.g. by Siegmund et al. 2003.

The overwhelming majority of the developed impact biomechanics FE cervical spine models, summarised in Table 4, are based on the average male anthropometry. In general no stringent definition of the average male subject used for model development appear to have been used, such as defined for the GHBMC model (Gayzik et al. 2011), but rather a male volunteer or PMHS of arbitrary average size has provided the template geometry for the models. Interesting exceptions are the Duke University models, which have been scaled to represent the cervical spine of 6 and 10 year old children (Dibb et al. 2013), and the Nottingham Trent University model which was scaled to an average female size (Mordaka 2004). Although a limited number of publications were made with the average female model, it was concluded that scaling alone is not sufficient to capture gender differences in head-neck kinematics during rear-end impact simulations (Mordaka 2004). Furthermore, an expected trend of increasing number of elements with later years can be found, with the exception of the parametric model of Laville et al.(2009). By parameterizing and simulating 16 different individual cervical spine geometries, almost all variation present in experimental moment-rotation corridors for the C5–C6 spinal unit was captured, although material properties were kept constant (Laville et al. 2009). As shown by the review of female anthropometry in this paper, significant differences between female and male cervical vertebral geometry exist; hence, the findings of Laville et al. 2009 support the need for HBMs based on female anthropometry.

The strength of the FE method for impact biomechanics modelling is that it allows for localised injury prediction, rather than using global kinematic and force criteria, as used for assessment with anthropomorphic test devices. In about half of the publications included in Table 4, no assessment of soft tissue injury has been considered. For the rest, the most commonly assessed parameter is ligament strain, which can either be relative between simulations (Brolin et al. 2008, Kitagawa et al. 2008), or compared with experimentally recorded failure levels (Cronin et al. 2012, DeWit and Cronin 2012, Fice and Cronin 2012, Fice et al. 2011, Panzer et al. 2011). Peak intervertebral annulus fibrosus strain has been considered (Panzer et al. 2011), as well as shear deformation of the disc (Fice et al. 2011), the change in intervertebral disc pressure and cross-sectional force between simulations (Brolin et al. 2008), and disc avulsion by tied contact failure (Cronin et al. 2012). For the hard tissues, bone fracture simulation by element elimination is quite common (Cronin et al. 2012, DeWit and Cronin 2012, Halldin et al. 2000, Panzer et al. 2011, Zhang et al. 2005), although some questions about post failure response accuracy have been raised (DeWit and Cronin 2012). Furthermore, global injury criteria that have been suggested, or used as complements to local criteria, were the neck injury criterion (Kitagawa et al. 2008) and cervical spine tensile or compressive forces (Camacho et al. 1997, Dibb et al. 2013).

**Table 4. Summary of FE Cervical Spine Models for Impact Biomechanics**

Anthrop. = Anthropometry, No. Elem. = Number of elements, M50 = average male, F50 = average female, PMHS = Post Mortem Human Subject. CT = Computed Tomography. MRI = Magnetic Resonance Imaging. 1,2,3D = One, two, or three dimensional elements. *Only elements in the cervical spine are reported here. The number of elements may vary with different versions of the models.

| References | Anthrop. | Skeletal geometry | No. Elem.* | Solver | Facet Joints | Ligaments | Muscles |
|---|---|---|---|---|---|---|---|
| Camacho et al. 1997<br>Chancey et al. 2003<br>Dibb et al. 2013 | M50<br>6-year-old<br>10-year-old | Visible Human Database. Child models scaled based on anatomical literature. | 1137 | LS-DYNA | Non-linear kinematic joints govern intervertebral joint motion, soft tissues not modelled individually. | | Active 1D |
| Yang et al. 1998 | M50 | Volunteer MRI data. | 14700 | PAM-CRASH | Sliding contact | Non-linear 1D and 2D | Not included |
| Halldin et al. 2000<br>Brolin and Halldin 2004<br>Brolin et al. 2005<br>Brolin et al. 2008<br>Hedenstierna et al. 2008 | M50 | Volunteer CT data. | 8400 | LS-DYNA | Sliding contact | Non-linear 1D | Active 1D and 3D |
| Jost and Nurick 2000 | M50 | Anatomical literature. | 3000 | ABAQUS | Not included | 2D | Passive 2D |
| Gentle et al. 2001<br>Mordaka 2004 | M50<br>F50 | Visible Human Database. F50 scaled from M50 based on anatomical literature. | Not reported | LS-DYNA | Not reported | Non-linear 1D and 3D | Passive 1D |
| Meyer et al. 2004 | M50 | Volunteer CT data. | 73185 | RADIOSS | Sliding contact | 1D | Passive 3D |
| Zhang et al. 2005<br>Zhang et al. 2006 | M50 | Volunteer external measurements. | 22094 | LS-DYNA | Sliding contact | Non-linear 1D | Not included |
| Eijima et al. 2005 | M50 | JAMA model [x] and volunteer MRI scan | 14300 | LS-DYNA | Solid elements | 2D | Passive 3D |
| Panzer 2006<br>Panzer and Cronin 2009<br>Fice et al. 2011<br>Panzer et al. 2011<br>Cronin et al. 2012<br>DeWit and Cronin 2012<br>Fice and Cronin 2012 | M50 | Commercial geometry package. | 108300 | LS-DYNA | Sliding contact with synovial fluid | Non-linear 1D with failure | Active 1D |
| Wheeldon et al. 2008 | M50 | PMHS CT data and cryomicrotome data. | Not reported | ABAQUS | Sliding contact with synovial fluid | Non-linear 1D | Not included |
| Kitagawa et al. 2008 | M50 | From THUMS v.4 (Watanabe et al. 2011) | 80000 | LS-DYNA | Sliding contact with synovial fluid | 2D | Passive 1D |
| Laville et al. 2009 | Subject specific | Volunteer CT | 5350 | RADIOSS | Sliding contact | Non-linear 1D | Not included |
| **Cervical spine models in whole human body models** | | | | | | | |
| Iwamoto et al. 2002<br>THUMS v3 | M50 | Commercial geometry package. | | LS-DYNA,PAM-CRASH | Solid element in shear | Linear 2D | Passive 1D |
| Watanabe et al. 2011<br>THUMS v4 | M50 | CT Scan data set. | | LS-DYNA, PAM-CRASH | Solid element in shear | Linear 2D | Passive 1D |
| Robin et al. 2001<br>HUMOS/HUMOS2 | M50 | Photos of PMHS slices. | | MADYMO, RADIOSS, PAM-CRASH | Sliding contact | Non-linear 1D | Passive 1D |
| Vavalle et al. 2013<br>GHBMC | M50 | Volunteer CT and MRI data sets. | | LS-DYNA | Sliding contact | Non-linear 1D with failure | Active 1D |
| Sugimoto and Yamazaki 2005, JAMA | M50 | Based on other FE models. | | LS-DYNA, PAM-CRASH | Unknown | Unknown | Unknown |

In relation to proposed injury mechanisms for WAD, summarised in the Injury Mechanisms section, synovial fold pinching, tension of dorsal root ganglia or vertebral arteries, and musculoskeletal injury appear not to have been covered in detail in studies with FE impact biomechanics models of the cervical spine. It is likely that further model development is nescessary to assess these mechanisms. Another mechanism not investigated by the models summarised in Table 4 is cervical canal pressure transients that may load and deform nerve tissue such as the spinal ganlia, which require coupled fluid dynamic and solid mechanics simulations in the HBM or in a submodel that use the output from the HBM as input in order to model local phenomena.

## SUMMARY AND CONCLUSIONS

Real-world data has identified the female occupant to be at more risk for WAD in traffic accidents and many studies illustrate important differences in the kinematic response of male and female subjects, volunteers and PMHSs. The review of FE models of the cervical spine presented 17 models based on male geometry but only one model that was scaled to represent a female. It is obvious that current tools are not adequate for assessing seat performance or develop protection against WAD with the female population in focus. An average female HBM has the potential to improve WAD prevention and assessment of seat performance to reduce traffic injuries in the population most at risk of these injuries. When the EvaRID model was developed, the average female was defined on the anthropometric measures of the 50$^{th}$ percentile female from the UMTRI study (stature 161.8 cm, mass 62.3 kg, Schneider et al. 1983) as it was considered a reasonable representation of the worldwide population at risk (Carlsson 2014). Another advantage of using the data by Schneider et al. (1983) for the average female HBM is that it would be consistent with several of the average male models developed based on the 50$^{th}$ percentile male (stature 175.3 cm, 77.3 kg, , Schneider et al. 1983). This approach would provide stronger comparisons between average male and female responses for seat assessment and other safety applications.

The literature review leaves no doubt that female HBMs should be developed directly based on female anthropometry and not scaled from male data because females have more slender necks and less muscle mass than males. Gender significantly influences the shape of the vertebral body, with the female vertebral body being less deep and not as wide. There was no or very little influence of gender on the height of the vertebral bodies and the diameter of the spinal canal. The facet joint angles compared to a reference in the vertebral body did not seem to depend on gender. Instead, gender significantly influenced the spinal alignment in the seated posture, where females on average present a straighter spine and males show more lordosis. There may be an effect of gender on the material properties of the ligaments in the cervical spine; however it is probably less important than gender differences in the cross sectional area of ligaments. In future studies on gender dependence, using size matched male and female subjects based on neck length or seated height rather than head circumference is recommended to distinguish the effect of gender from size.

To conclude, we recommend that average female HBMs are developed with focus on;

- The shape of the female vertebral body, especially the depth and width that provides less support area than for males,
- Defining a spinal curvature representative of seated female volunteers that on average present with less lordosis than males,
- The dimensions of the spinal ligaments, rather than the material properties, to capture the larger range of motion and less spinal stiffness of female subjects compared to male, and
- Validation of female volunteers and PMHS tests for range of motion, while failure prediction seem to be less gender sensitive.

## ACKNOWLEDGEMENT

The work presented in this paper was partly funded by VINNOVA, the Swedish Governmental Agency for Innovation Systems and the Strategic Area of Advance (Transport), Chalmers. The work was conducted within the SAFER Vehicle and Traffic Safety Centre at Chalmers, Gothenburg, Sweden and it was also partly performed by the Advanced Research Project, the Safety Research Division at JARI, Japan Automobile Research Institute, Tsukuba, Japan.

## REFERENCES


Banic B, Petersen-Felix S, Andersen O, Radanov B, Villiger P, Arendt-Nielsen L, Curatolo M. (2004) Evidence for Spinal Cord Hypersensitivityin Chronic Pain after Whiplash Injury and in Fibromyalgia. Pain 107: 7–15.

Bass CR, Lucas SR, Salzar RS, Oyen ML, Planchak C, Shender BS, Paskoff G (2007) Failure Properties of Cervical Spinal Ligaments under Fast Strain Rate Deformations. Spine 32(1): E7–13.

Boyle J, Singer K, Milne N. (1996) Morphological survey of the cervicothoracic junctional region. Spine 21(5): 544-548

Brault JR, Siegmund GP, Wheeler JB. (2000) Cervical Muscle Response during Whiplash: Evidence of a Lengthening Muscle Contraction. Clin. Biomech. 15: 426–435.

Brolin K, Halldin P. (2004). Development of a Finite Element Model of the Upper Cervical Spine and a Parameter Study of Ligament Characteristics, Spine 29(4): 376-385.

Brolin K, Halldin P, Leijonhufvud I. (2005) The Effect of Muscle Activation on Neck Response, Traffic Inj Prev. 6(1): 67–76.

Brolin K, Hedenstierna S, Halldin P, Bass C, Alem N. (2008). The Importance of Muscle Tension on the Outcome of Impacts with a Major Vertical Component. International Journal of Crashworthiness 13(5): 487–498.

Camacho D, Nightingale R, Robinette J, Vanguri S, Coates D, Myers B. (1997). Experimental Flexibility Measurements for the Development of a Computational Head-Neck Model Validated for Near-Vertex Head Impact, In Proceedings of the 41st Stapp Car Crash Conference (Orlando, FL, USA). Paper no. 973345.

Carlsson A, Chang F, Lemmen P, Kullgren A, Schmitt KU, Linder A, Svensson M. (2014) Anthropometric Specifications, Development, and Evaluation of EvaRID - A 50th Percentile Female Rear Impact Finite Element Dummy Model. Traffic Inj Prev. 15(8): 855-865.

Carstensen T, Frostholm L, Oernboel E, Kongsted A, Kasch H, Jensen T, Fink P (2012) Are There Gender Differences in Coping with Neck Pain Following Acute Whiplash Trauma? A 12-Month Follow-Up Study, Eur J Pain. 16(1): 49–60.

Chancey V, Nightingale R, Van Ee C, Knaub K, Myers B. (2003) Improved Estimation of Human Neck Tensile Tolerance: Reducing the Range of Reported Tolerance Using Anthropmetrically Correct Muscles and Optimized Physilogic Initial Conditions, Stapp Car Crash J. 47: 135–153.

Chapline J, Ferguson S, Lillis R, Lund A, Williams A (2000) Neck Pain and Head Restraint Position Relative to the Driver's Head in Rear-End Collisions, Accid Anal Prev. 32(2): 287–297.

Cronin D, Fice J, DeWit J, Moulton J. (2012) Upper Cervical Spine Kinematic Response and Injury Prediction, In Proceedings of the IRCOBI Conference (Dublin, Ireland, Sept. 12–14), 225–234.

Curatolo M, Bogduk N, Ivancic P, McLean S, Siegmund G, Winkelstein B (2011) The role of tissue damage in whiplash associated disorders: Discussion paper 1. Spine. 36(25 Suppl): S309–315.

Curatolo M, Petersen-Felix S, Arendt-Nielsen L, Giana C, Zbinden AM, Radanov BP. (2001) Central Hypersensitivity in Chronic Pain after Whiplash Injury. Clin J Pain. 17(4): 306–315.

Davidsson, J., Lövsund, P., Ono, K., Svensson, M. Y., & Inami, S. (1999). A comparison between volunteer, BioRID P3 and Hybrid III performance in rear impacts. In Proceedings of the International Research Council on the Biomechanics of Injury conference (Vol. 27, pp. 165-178). International Research Council on Biomechanics of Injury.

de Bruijn E. (2014) Isometric and Dynamic Control of Neck Muscles – Reflexive Contributions and Muscle Synergies, Doctoral Thesis, Delft University of Technology, Delft, the Netherlands.

de Jager M. (1996) Mathematical Head-Neck Models for Acceleration Impacts, Doctoral Thesis, Eindhoven University of Technology, Eindhoven, the Netherlands.

Deng Y-C, Goldsmith W. (1987) Response of a Human Head/Neck/Upper-Torso Replica to Dynamic Loading – II. Analytical/Numerical Model, J Biomech. 20(5): 487–497.

DeRosia J (2008) Role of Gender and Size in Biomechanics of Rear Impact. Doctoral Dissertation, Marquette University, USA, UMI Number: 3357947.

DeWit J, Cronin D (2012) Cervical Spine Segment Finite Element Model for Traumatic Injury Prediction, J Mech Behav Biomed Mater. 10: 138–150.

Dibb A, Cox C, Nightingale R, Luck J, Cutcliffe H, Myers B, Arbogast K, Seacrist T, Bass C. (2013) Importance of Muscle Activation for Biofidelic Pediatric Neck Response in Computational Models", Traffic Inj Prev. 14 Suppl: S116–127.

Dolinis J (1997) Risk Factors for "Whiplash" in Drivers: a Cohort Study of Rear-End Traffic Crashes, Injury 28(3): 173–179.

Ebraheim N, Fow J, Xu R, Yeasting R. (1998) The Vertebral Body Depths of the Cervical Spine and Its Relation to Anterior Plate-Screw Fixation. Spine 23(21): 2299-2302.

Eichberger A, Geigl BC, Moser A, Fachbach B, Steffan H. (1996) Comparison of Different Car Seats Regarding Head-Neck Kinematics of Volunteers During Rear End Impact. Proceedings of the International Research Conference on the Biomechanics of Impact, IRCOBI, Dublin (Ireland).

Ejima S, Ono K, Kaneoka K, Fukushima M. (2005) Development and Validation of the Human Neck Muscle Model Under Impact Loading, In Proceedings of the IRCOBI Conference (Prague, Czech Republic, Sept. 21–23), 245–255.

Elliot D, Goldberg L, Kuehl K. (2010) Young Women's Anterior Cruciate Ligament Injuries An Expanded Model and Prevention Paradigm. Sports med 40(5): 367-376.

Evangelopoulos D, Kontovazenitis P, Kouris S, Zlatidou X, Benneker L, Vlamis J, Korres D, Efstathopoulos N. (2012) Computerized Tomographic Morphometric Analysis of the Cervical Spine. Open Orthop J. 6: 250-254.
Fice J, Cronin D. (2012) Investigation of Whiplash Injuries in the Upper Cervical Spine using a Detailed Neck Model, J Biomech. 45(6): 1098–1102.
Fice J, Cronin D, Panzer M. (2011) Cervical Spine Model to Predict Capsular Ligament Response in Rear Impact, Ann Biomed Eng. 39(8): 2152–2162.
Frechede B, Bertholon N, Saillant G, Lavaste F, Skalli W (2006) Finite Element Model of the Human Neck during Omni-directional Impacts. Part II: Relation between Cervical Curvature and Risk of Injury. Comput Methods Biomech Biomed Engin. 9(6): 379-386.
Frobin W, Leivseth G, Biggemann M, Brinckmann P. (2002) Vertebral height, disc height, posteroanterior displacement and dens–atlas gap in the cervical spine: precision measurement protocol and normal data. Clin Biomech. 17: 423-431.
Gayzik F, Moreno D, Geer C, Wuertzer S, Martin R, Stitzel J. (2011). Development of a Full Body CAD Dataset for Computational Modeling: A Multi-Modality Approach, Ann Biomed Eng. 39(10): 2568–2583.
Gentle, C.R., Golinski, W.Z., and Heitplatz, F. (2001) Computational Studies of 'Whiplash' Injuries, Proc Inst Mech Eng H. 215(2): 181–189.
Haedacker JW, Shuford RF, Capicoto PN, Pryor PW (1997) Radiographic Standing Cervical Segmental Alignment in Adult Volunteers without Neck Symptoms. Spine. 22(13): 1472-1480.
Halldin P, Brolin K, Kleiven S, von Holst H, Jakobsson L, Palmertz C. (2000) Investigation of Conditions that Affect Neck Compression-Flexion Injuries Using Numerical Techniques, In Proceedings of the 44th Stapp Car Crash Conference (Atlanta, GA, USA, Nov. 6–8). Paper no. 2001-01-SC10.
Harty J, Quinlan J, Kennedy J, Walsh M, O'Byrne J. (2004) Anthropometrical analysis of cervical spine injuries. Injury 35(3): 249-252.
Hedenstierna S, Halldin P. (2008) How Does a Three-Dimensional Continuum Muscle Model Affect the Kinematics and Muscle Strains of a Finite Element Neck Model Compared to a Discrete Muscle Model in Rear-End, Frontal, and Lateral Impacts, Spine. 33(8): E236–245.
Helliwel PS, Evans PF, Wright V (1994) The Straight Cervical Spine: Does it Indicate Muscle Spasm? J Bone Joint Surg Br. 76(1): 103-106.
Hukuda S, Kojima Y. (2002) Sex Discrepancy in the Canal/Body Ratio of the Cervical Spine Implicating the Prevalence of Cervical Myelopathy in Men. Spine 27(3): 250-253.
Iwamoto M, Kisanuki Y, Watanabe I, Furusu K, Miki K. (2002) Development of a Finite Element Model of the Total Human Model for Safety (THUMS) and Application to Injury Reconstruction, In Proceedings of the IRCOBI Conference (Munich, Germany, Sep. 18–20)
Jakobsson L, Norin H, Svensson M. (2004) Parameters Influencing AIS 1 Neck Injury Outcome in Frontal Impacts. Traffic Inj Prev. 5(2): 156–163.
Jost R, Nurick G. (2000) Development of a Finite Element Model of the Human Neck Subjected to High G-Level Lateral Deceleration, International Journal of Crashworthiness, 5(3): 259–269.
Kaneoka K, Ono K, Inami S, Hayashi K (1999) Motion analysis of cervical vertebrae during whiplash loading. Spine. 24(8): 763-769.
Kasai T, Ikata T, Katoh S, Miyake R, Tsubo M. (1996) Growth of the Cervical Spine With Special Reference to Its Lordosis and Mobility. Spine 21(18): 2067-2073.
Kasch H, Stengaard-Pedersen K, Arendt-Nielsen L, Staehelin Jensen T. (2001) Pain Thresholds and Tenderness in Neck and Head Following Acute Whiplash Injury: A Prospective Study. Cephalalgia 21(3): 189–197.
Kihlberg JK (1969) Flexion-Torsion Neck Injury in Rear Impacts. Proceedings of the 13th Association for the Advancement of Automotive Medicine (AAAM) Conference, pp. 1–16.
Kitagawa Y, Yasuki T, Hasegawa J. (2008) Research Study on Neck Injury Lessening with Active Head Restraint Using Human Body FE Model", Traffic Inj Prev. 9(6): 574–582.
Klinich KD, Ebert SM, Van Ee CA, Flannagan CAC, Prasad M, Reed MP, Schneider LW (2004) Cervical Spine Geometry in the Automotive Seated Posture: Variations with Age, Stature , and Gender. Stapp Car Crash J. 48: 301-330.
Krafft M. (1998). Non-fatal injuries to car occupants, Injury assessment and analysis of impacts causing short- and long-term consequences with special reference to neck injuries. Doctoral thesis, Karolinska Institutet, Stockholm, Sweden.
Krafft M, Kullgren A, Lie A, Tingvall C. (2003) The Risk of Whiplash Injury in the Rear Seat Compared to the Front Seat in Rear Impacts, Traffic Inj Prev. 4(2): 136–140.
Krakenes J, Kaale BR. (2006) Magnetic Resonance Imaging Assessment of Craniovertebral Ligaments and Membranes after Whiplash Trauma. Spine. 31(24): 2820–2826.
Kullgren A, Krafft M, Tingvall C, Lie A. (2003) Combining crash recorder and paired comparison technique: Injury risk functions in frontal and rear impacts with special reference to neck injuries. Proc. 18th ESV Conf, Paper No. 404, Nagoya (Japan).
Kullgren A, Krafft M, Lie A, Tingvall C (2007) The Effect of Whiplash Protection Systems in Real-Life Crashes and Their Correlation to Consumer Crash Test Programmes, Proc. 20th ESV Conf. (07-0468), Lyon (France).

Kullgren A, Stigson H, Krafft M (2013) Development of Whiplash Associated Disorders for Male and Female Car Occupants in Cars Launched Since the 80s in Different Impact Directions. Proceedings of the International Research Conference on the Biomechanics of Impact, IRCOBI, pp 51-62.
Laville A, Laporte S, Skalli W. (2009) Parametric and Subject-Specific Finite Element Modelling of the Lower Cervical Spine. Influence of Geometrical Parameters on the Motion Patterns. J Biomech. 42(10): 1409–1415.
Lee JH, Park YK, Kim JH (2014) Chronic Neck Pain in Young Adults: Perspectives on Anatomic Differences. Spine J. 14(11): 2628-2638.
Linder A, Schick S, Hell W, Svensson M, Carlsson A, Lemmen P, Schmitt K-U, Gutsche, A, Tomasch E. (2013) ADSEAT – Adaptive Seat to Reduce Neck Injuries for Female and Male Occupants, Accid Anal Prev. 60: 334-343.
Liu YK, Dai QG (1989) The Second Stiffest Axis of a Beam-Colum: Implications for Cervical Spine Trauma. J Biomech Eng. 111(2): 122-127.
Maag U, Desjardins D, Bourbeau R, Laberge-Nadeau C (1990) Seat Belts and Neck Injuries, Proceedings of the IRCOBI Conference, Bron (France), pp. 1–14.
Maiman D, Sances A Jr, Myklebust J, Larson S, Houterman C, Chilbert M, El-Ghatit A (1983) Compression Injury of the Cervical Spine. Neurosurgery. 13(3): 254-260.
Maiman D, Yoganandan N, Pintar F (2002) Preinjury Cervical Alignment Affecting Spinal Trauma. J Neurosurg. 97(1 Suppl): 57-62.
Matsumoto M, Fujimura Y, Suzuki N, Toyama Y, Shiga H (1998) Cervical Curvature in Acute Whiplash Injures: Prospective Comparative Study with Asymptomatic Subjects. Injury. 29(10): 775-778.
Mattucci S, Moulton J, Chandrashekar N, Cronin D. (2012) Strain rate dependent properties of younger human cervical spine ligaments. J Mech Behav Biomed Mater. 10: 216-226.
Meyer F, Bourdet N, Deck C, Willinger R, Raul J. (2004) Human Neck Finite Element Model Development and Validation against Original Experimental Data, Stapp Car Crash J. 48, Paper no. 2004–22–0008.
Milne N. (1991) The role of zygapophysial joint orientation and uncinated processes in controlling motion in the cervical spine. J. Anat. 178: 189-201.
Mordaka J. (2004) Finite Element Analysis of Whiplash Injury for Women, Doctoral Thesis, Nottingham Trent University, Nottingham, UK.
Morris AP, Thomas PD (1996) Neck Injuries in the UK Co-operative Crash Injury Study, Proc. 40th Stapp Car Crash Conf., SAE 962433), pp. 317–329.
Narragon EA (1965) Sex Comparisons in Automobile Crash Injury, Cornell Aeronautical Laboratory (CAL) Report No. VJ 1823-R15.
Nightingale R, Chancey C, Ottaviano D, Luck J, Tran L, Prange M, Myers B. (2007) Flexion and extension structural properties and strengths for male cervical spine segments. J Biomech 40(3): 535-542.
Nightingale R, Winkelstein B, Knaub K, Richardson W, Luck J, Myers B. (2002) Comparative strengths and structural properties of the upper and lower cervical spine in flexion and extension. J Biomech 35(6): 725-732.
Nygren, Å. (1983). Injuries to Car Occupants - Some Aspects of the Interior Safety of Cars. Acta Oto-Laryngologica. 95(s395): 1-135, doi: 10.3109/00016488309139642.
O'Neill B, Haddon W Jr, Kelley AB, Sorenson WW (1972) Automobile Head Restraints: Frequency of Neck Injury Claims in Relation to the Presence of Head Restraints. Am J Public Health. 62(3): 309–406.
Ono K, Ejima S, Suzuki S, Kaneoka K, Fukushima M, Ujihashi S. (2006) Prediction of Neck Injury Risk based on the Analysis of Localized Cervical Vertebral Motion of Human Volunteers during Low-speed Rear Impacts. Proceedings of IRCOBI Conference, Madrid, Spain.
Ono K, Kaneoka K, Wittek A, Kajzer J. (1997) Cervical Injury Mechanism Based on the Analysis of Human Cervical Vertebral Motion and Head-Neck-Torso Kinematics during Low-speed Rear Impacts. Proc.41st Stapp Car Crash Conference, pp. 339–356.
Örtengren T, Hansson HA, Lövsund P, Svensson MY, Suneson A, Säljö A. (1996) Membrane Leakage in Spinal Ganglion Nerve Cells Induced by Experimental Whiplash Extension Motion: A Study in Pigs. J Neurotrauma. 13(3): 171–180.
Osakabe T, Hayashi M, Hasegawa K, Okuaki T, Ritty T, Mecham R, Wachi H, Seyama Y. (2001) Age- and Gender-Related changes in ligament components. Ann Clin Biochem. 38(Pt 5): 527- 532.
Otremski I, Marsh JL, Wilde BR, McLardy Smith PD, Newman RJ (1989) Soft tissue cervical injuries in motor vehicle accidents. Injury. 20(6): 349–351.
Panjabi MM. (2006) A Hypothesis of Chronic Back Pain: Ligament Subfailure Injuries Lead to Muscle Control Dysfunction. Eur Spine J. 15(5): 668–676.
Panzer M. (2006) Numerical Modeling of the Human Cervical Spine in Frontal Impact. Master Thesis, University of Waterloo, Waterloo, ON, Canada.
Panzer M, Cronin D. (2009) C4–C5 Segment Finite Element Model Development, Validation, and Load-Sharing Investigation, J Biomech. 42(4): 480–490.
Panzer M, Fice J, Cronin D. (2011) Cervical Spine Response in Frontal Crash, Med Eng Phys. 33(9): 1147–1159.
Parenteau C, Wang N, Zhang P, Caird M, Wang S. (2014) Quantification of Pediatric and Adult Cervical Vertebra—Anatomical Characteristics by Age and Gender for Automotive Application. Traffic Inj Prev. 15(6): 572-582.

Parenteau C, Zuby D, Brolin K, Svensson M, Palmertz C, Wang S. (2013) Restrained Male and Female Occupants in Frontal Crashes: Are We Different? International IRCOBI Conference on the Biomechanics of Impact, September 11-13, Gothenburg, Sweden.
Pearson AM, Ivancic PC, Ito S, Panjabi MM. (2004) Facet Joint Kinematics and Injury Mechanisms during Simulated Whiplash. Spine. 29(4): 390–397.
Pintar F, Yoganandan N, Voo L, Cusick JF, Maiman DJ, Sances A Jr (1995) Dynamic Characteristics of the Human Cervical Spine. 39th Stapp Car Crash Conference Proceedings, pp. 195-202.
Reddy M, Reddy B, Schoggl A, Saringer W, Matula C. (2002) The Complexity of Trauma to the Cranio-Cervical Junction: Correlation of Clinical Presentation with Doppler Flow Velocities in the V3- Segment of the Vertebral Arteries. Acta Neurochir (Wien). 144(6): 575–580.
Richter M, Otte D, Pohlemann T, Krettek C, Blauth M (2000) Whiplash-Type Neck Distortion in Restrained Car Drivers: Frequency, Causes and Long-Term Results, Eur Spine J. 9(2): 109–117.
Robin S. (2001) HUMOS: Human Model for Safety – A Joint Effort Towards the Development of Refined Human-like Car Occupant Models. 17th ESV Conference (Amsterdam, the Netherlands, June 4–7). Paper no. 297.
Sato F, Nakajima T, Ono K, Svensson M, Brolin K, Kaneoka K (2014) Dynamic Cervical Vertebral Motion of Female and Male Volunteers and Analysis of its Interaction with Head/Neck/Torso Behavior during Low-speed Rear Impact. Proceedings of IRCOBI Conference, Berlin, Germany.
Schmitt K-U, Weber T, Svensson M, Davidsson J, Carlsson A, Björklund M, Jakobsson L, Tomasch E, Linder A (2012) Seat testing to investigate the female neck injury risk - preliminary results using a new female dummy prototype, Proceedings of the International Research Conference on the Biomechanics of Impact, IRCOBI, Dublin (Ireland).
Schneider LW, Robbins DH, Pflüg MA, Snyder RG. (1983) Development of Anthropometrically Based Design Specifications for an Advanced Adult Anthropomorphic Dummy Family, Final Report, UMTRI-83-53-1, University of Michigan Transportation Research Institute, Ann Arbor, Michigan, USA.
Scott D, Jull G, Sterling M. (2005) Widespread Sensory Hypersensitivity Is a Feature of Chronic Whiplash-Associated Disorder but Not Chronic Idiopathic Neck Pain. Clin J Pain. 21(2): 175–181.
Seric V, Blazic-Cop N, Demarin V. (2000) Haemodynamic Changes in Patients with Whiplash Injury Measured by Transcranial Doppler Sonography (TCD). Coll Antropol. 24(1): 197–204.
Siegmund GP, King DJ, Lawrence JM, Wheeler JB, Brault JR, Smith TA (1997) Head/neck kinematic response of human subjects in low-speed rear-end collisions, Proceedings of 41th Stapp Car Crash Conference, Lake Buena Vista, FL, USA, SAE paper 973341.
Siegmund G, Winkelstein B, Ivancic P, Svensson M, Vasavada A (2009) The anatomy and biomechanics of acute and chronic whiplash injury. Traffic Inj Prev. 10(2): 101-112.
Siegmund G, Sanderson D, Myers B, Inglis J. (2003) Rapid Neck Muscle Adaptation Alters the Head Kinematics of Aware and Unaware Subjects Undergoing Multiple Whiplash-Like Perturbations. J Biomech. 36(4): 473–482.
Stemper B, Board D, Yoganandan N, Wolfla C. (2010) Biomechanical properties of human thoracic spine disc segments. J Craniovertebr Junction Spine 1(1): 18-22.
Stemper B, DeRosia J, Yogananan N, Pintar F, Shender B, Paskoff G (2009) Gender Dependent Cervical Spine Anatomical Differences in Size-Matched Volunteers. 46th International ISA Biomedical Science Instrumentation Symposium, Milwaukee WI, 17-19 April, 149-154.
Stemper B, Yoganandan N, Pintar F. (2005) Effects of Abnormal Posture on Capsular Ligament Elongations in a Computational Model Subjected to Whiplash Loading. J Biomech. 38(6): 1313–1323.
Stemper B, Yoganandan N, Pintar FA. (2004) Gender- and Region- Dependent Local Facet Joint Kinematics in Rear Impact. Spine 29(16): 1764–1771.
Stemper B, Hallman J, Pintar F, Maiman D. (2012) Gender and Aging: Considerations for Orthopaedics. In Orthopaedic Biomechanics, Editor: Beth A. Winkelstein, Published: December 18, 2012 by CRC Press
Stemper B, Yoganandan N, Pintar FA, Maiman DJ, Meyer MA, DeRosia J, Shender BS, Paskoff G (2008) Anatomical Gender Differences in Cervical Vertebrae of Size-Matched Volunteers. Spine. 33(2): E44–E49.
Stemper B, Yoganandan N, Pintar F. (2003) Gender Dependent Cervical Spine Segmental Kinematics during Whiplash. J Biomech. 36(9): 1281–1289.
Storvik S, Stemper B, Yoganandan N, Pintar F. (2009) Population-Based Estimates of Whiplash Injury Using NASS CDS Data, Biomed Sci Instrum. 45: 244–249.
Sugimoto T, Yamazaki K. (2005). First Results from the JAMA Human Body Model Project. 19th ESV Conf. (Washington D.C., US), Paper no. 05–0291.
Svensson MY, Boström O, Davidsson J, Hansson H-A, Håland Y, Lövsund P, Suneson A, Säljö A. (2000) Neck Injuries in Car Collisions—A Review Covering a Possible Injury Mechanism and the Development of a New Rear-Impact Dummy. Accid Anal Prev. 32(2): 167–175.
Takeshima T, Omokawa S, Takaoka T, Araki M, Ueda Y, Takakura Y (2002) Sagittal Alignment of Cervical Flexion and Extension. Spine. 27(15): E348–355.
Tatarek N. (2005) Variation in the human cervical neural canal. Spine J. 5(6): 623-631.
Temming J, Zobel R (1998) Frequency and Risk of Cervical Spine Distortion Injuries in Passenger Car Accidents: Significance of Human Factors Data, Proceedings of the IRCOBI Conference, Göteborg, Sweden, pp. 219–233.
The Whiplash Commission (2005) *Final Report* http://www.whiplashkommissionen.se/pdf/WK_finalreport.pdf.

Thomas C, Faverjon G, Hartemann F, Tarriere C, Patel A, Got C (1982) Protection Against Rear-End Accidents, Proceedings of the IRCOBI Conference, Cologne, Germany, pp. 17–29.
Valkeinen H, Ylinen J, Malkia E, Alen M, Hakkinen K. (2002) Maximal force, force/time and activation /coactivation characteristics of the neck muscles in extension and flexion in healthy men and women at different ages. Eur J Appl Physiol. 88(3): 247–254.
van der Horst M. (2002) Human Head Neck Response in Frontal, Lateral, and Rear End Impact Loading – Modelling and Validation, Doctoral Thesis, Eindhoven University of Technology, Eindhoven, the Netherlands.
Vasavada A, Brault J, Siegmund G. (2007) Musculotendon and Fascicle Strains in Anterior and Posterior Muscles during Whiplash Injury. Spine 32(7): 756–765.
Vasavada A, Danaraj J, Siegmund G. (2008) Head and neck anthropometry, vertebral geometry and neck strength in height-matched men and women. J Biomech. 41(1): 114-121.
Vasavada A, Li S, Delp S. (2001) Three-Dimensional Isometric Strength of Neck Muscles in Humans. Spine. 26(17): 1904-1909.
Vavalle N, Moreno D, Rhyne A, Stitzel J, Gayzik F. (2013) Lateral Impact Validation of a Geometrically Accurate Full Body Finite Element Model for Injury Prediction, Ann Biomed Eng. 41(3): 497–512.
Watanabe Y, Ichikawa H, Kayama O, Ono, K, Kaneoka K, Inami S (2000) Influence of Seat Characteristics on Occupant Motion in Low-Velocity Rear-End Impacts, Accid Anal Prev 32(2): 243–250.
Watanabe R, Miyazaki H, Kitagawa Y, Yasuki T. (2011) Research of Collision Speed Dependency of Pedestrian Head and Chest Injuries Using Human FE Model (THUMS Version 4). 22nd ESV Conf. (Wasington D.C., June 13–16). Paper no. 11–0043.
Wheeldon J, Stemper B, Yoganandan N, Pintar F. (2008) Validation of a Finite Element Model of the Young Normal Lower Cervical Spine, Ann Biomed Eng. 36(9): 1458–1469.
Wild CY, Steele JR, Bridget J, Munro BJ (2012) Why Do Girls Sustain More Anterior Cruciate Ligament Injuries Than Boys? A Review of the Changes in Estrogen and Musculoskeletal Structure and Function During Puberty. Sports Med. 42(9): 733–749.
Yang K, King A. (2003) Neck Kinematics in Rear-end Impacts. Pain Res Manag. 8(2): 79–85.
Yang K, Zhu F, Luan F, Zhao L, Begeman, P. (1998) Development of a Finite Element Model of the Human Neck. In Proceedings of the 42nd Stapp Car Crash Conference (Tempe, AZ, USA). Paper no. 983157.
Yoganandan N, Pintar F, Gennarelli T, Eppinger R, Voo L.(1999) Geometrical Effects on the Mechanism of Cervical Spine Injury due to Head Impact. Proceedings of IRCOBI Conference, Sitges, Spain.
Yoganandan N, Sances A Jr, Maiman DJ, Myklebust JB, Pech P, Larson SJ (1986) Experimental Spinal Injuries with Vertical Impact. Spine. 11(9): 855–860.
Zhang Q, Teo E, Ng H. (2005) Development and Validation of a C0–C7 FE Complex for Biomechanical Study, J Biomech Eng. 127(5): 729–735.
Zhang Q, Teo E, Ng H, Lee V. (2006) Finite Element Analysis of a Moment-Rotation Relationship for Human Cervical Spine, J Biomech., 39(1): 189–193.

# High-Risk E-Vehicle Battery Sled Testing

**David, Sturk**
**Per, Gustafsson**
Autoliv Development AB
**Håkan, Sundmark**
**Robert, Persson**
Autoliv Sweden AB
Sweden
**Kyriakos, Vavalidis**
**Dominique, Dufaut**
**Nicolas, Evrat**
Autoliv France
France

Paper Number 15-0248

## ABSTRACT

Crash testing of E-Vehicles (electrified vehicles, e.g. electric and hybrid electric vehicles) is required to assure compliance with global safety regulations and standards as well as the even higher requirements set by the car manufacturers themselves. The introduction of E-Vehicle battery systems of as much as 200 to 600 Volt dc presents new safety considerations when performing crash tests. At a crash test, safety by regulations, standards and ratings as well as the limits of durability are investigated. If investigating the limits of durability, scenarios such as release of harmful gases and thermal events must not be disregarded. In order to ensure safe testing conditions, regardless of the severity of impact to be evaluated, new risk analysis, routines and laboratory designs need to be assessed when a new technology, such as high voltage (HV) battery systems, are introduced to the vehicle market.

Autoliv has a long experience in crashworthiness testing and offers car manufacturers assessments of crash safety in laboratories and crash tracks available on all continents. E-Vehicles are being crash tested as well, and for that reason Autoliv have established research and testing capabilities for HV batteries as well as updated routines and laboratory designs. Besides Autoliv's full size crash tracks around the world a new laboratory facility for battery sled testing is now available in Sweden for high-risk durability-limit testing.

## INTRODUCTION

Range anxiety is often defined as one of the key limitations of E-Vehicles. It is often considered that the limited range can be extended by means of research on more energy dense battery chemistries. Currently, the Li-ion chemistry is the predominant battery on the market because it currently presents the highest energy density. A great deal of successful research on the constituent materials and molecules have contributed to the introduction of the current Li-ion battery technology. Although this family of battery chemistries have proven to be the key to the present global launch of E-Vehicles, the importance of system and structural design achievements cannot be underestimated.

Another key for the global launch of E-Vehicles is the battery safety. Traditionally the crashworthiness of a battery system installed in an E-Vehicle is solved by locating it in the "safe zone" where mechanical damage from a crash is limited according to crash statistics. Additionally, battery systems are equipped with rigid

housings and other means of structural protection in order to prevent intrusions upon the battery. Crashworthiness testing is a vital part of the safety research that in the years to come will assure that the range anxiety issue will become less of a hurdle. New designs of HV battery systems will permit them to be located closer to frequent deformation zones rather than restricted to the safe zone. The risk that any vehicle crash could reach a worst scenario consequent continuous to diminish as capabilities and routines for safe crash testing and mechanical abuse testing on cars and components are constantly being developed. However, in the world today, there exist only few laboratories for dynamic mechanical abuse testing on HV battery systems, which offers a complete methodology and testing experience in order to replicate the crash environment suffered by such a battery system in a full vehicle crash. The key issue is the concern for the safety of the testing personnel, the facility and the testing equipment since the structural and chemical response of a battery under dynamic sled tests and crash test is not common knowledge. Such a safe testing environment is now offered by Autoliv in Sweden.

**Issues to be anticipated when performing high-risk battery testing**

**The influence of battery material and chemistry**

As mentioned Li-ion batteries offer an out-standing energy and power density in comparison to other battery chemistries (e.g. NiMH and lead acid). The key is the high nominal voltage per cell that is a consequence of the large difference in standard reduction potential between the material of the anode and the cathode. Because of this high nominal voltage water cannot be used as electrolyte solvent in Li-ion batteries. Instead, organic solvents are used together with a salt to form the required electrolyte. Commercial Li-ion batteries use a mixture of alkyd carbonates as solvent and the $LiPF_6$ as the salt to form their electrolyte. This salt is completely predominant because of its extraordinary performance in comparison to other salts. If the battery cell is exposed to elevated temperatures (commonly starting within the range from 80 to 170 ºC), the material of the two electrodes have a tendency to start reacting with the components of the electrolyte (Huang, Yan, & Jiang, 2008). Under such conditions, the pressure will build up inside a battery cell because of those reactions as well as the gradual vaporization of the organic solvents.

In order to prevent rupture at higher pressures Li-ion cells are designed with soft-spots or venting mechanisms that will release the gases from the cell at a prefered lower internal pressure. This is a safeguard feature which in many scenarios mitigate further escalation of a cell failure. Another safeguard feature is the characteristics of the separators that ensure that only Li-ions can move from one electrode to the other. Commonly, the separator constitutes of a multilayer structure of polyethylene (PE) and polypropylene (PP) with a thickness between 10 to 40 µm. The two polymer melts at 135ºC (PE) and 165ºC (PP) and the 30ºC buffer allow the PP to retain the separator structure while the PE melts and make the separator impenetrable to Li-ions which consequently prevents Li-ion transport at the location of the damage and thus impedes the current in the circuit (Zhang, 2007). Therefore, they are named shutdown separators. Many battery cells are equipped with additional safeguard systems that intend to prevent an escalation of a cell failure, such as Current Interrupt Devices (CID) or poly-thermal switch (PTC).

Nevertheless, all these safeguard systems have an upper limit of operation at which they are overridden. A common cause for a safeguard system to be overridden is when the thermal exposure onto, as well as inside, a battery cell lead to a temperature increase at a rate that is higher than those safeguard systems are capable of handling. Under such circumstances, a battery cell risk to reach a second stage of critical failure that is defined as thermal runaway. Among conventional Li-ion batteries, this may occur at temperature ranging between 170 to 250ºC depending on the constituents of the cathode material (Yang, Amiruddin, Bang, Sun, & Prakash, 2006). As of 2014, the two predominant Li-ion chemistries are denoted NMC (based on the use of a cathode material composed of Nickel Manganese and Cobolt) and LFP (based on the use of a cathode material composed of iron phosphate). At best, a thermal runaway remain isolated to the original cell but it is not

unlikely that the heat-up of the first cell increases several hundreds of degrees rapidly that then provokes the neighboring cells into thermal runaway. If propagation of thermal runaway starts between cells it becomes nearly impossible to extinguish until the fuel, (i.e. the cell material) is consumed. This scenario will generate large quantities of gases, as presented by the picture of a faulty battery module in Figure 1a. In the presence of a sufficient source for ignition, the electrolyte vapor might ignite (Figure 1b).

***Figure 1.*** **Under tough crashworthiness testing conditions, an E-Vehicle battery may experience thermal runaway. Such a critical cell failure cause the faulty cell to heat up rapidly, which may lead to propagation of the failure to neighboring cells. The first indication of a damage battery cell is gas ventilation (a) and the worst scenario of a fire might occur if the organic electrolyte vapors get access to a sufficient ignition source (b).**

**A simplified fault tree analysis for a Li-ion battery cell**

Three major abusive conditions can be illustrated with a simplified fault tree diagram (Figure 2). Those three conditions are:

- Mechanical Abuse
- Electrical Abuse
- Thermal Abuse

A worst-case scenario, in the event of a traffic accident or as a consequence of tough durability testing the mechanical abuse generated onto the battery, would be that the whole failure sequence described above is not impeded. In such a scenario, the mechanical abuse could result in a fault current(s) that heat up the internal components of the battery cells. If the rate of heat-up exceeds the shut-down capacity of the safeguard systems,

thermal runaway might start and the quantity/pressure of electrolyte vapor and gaseous species, which are generated by the decomposition of the cell's material, cause the cell to rupture. At that point, large quantities of gases are emitted to the surrounding and in the presence of a sufficient ignition source; a battery fire might start (Figure 1b).

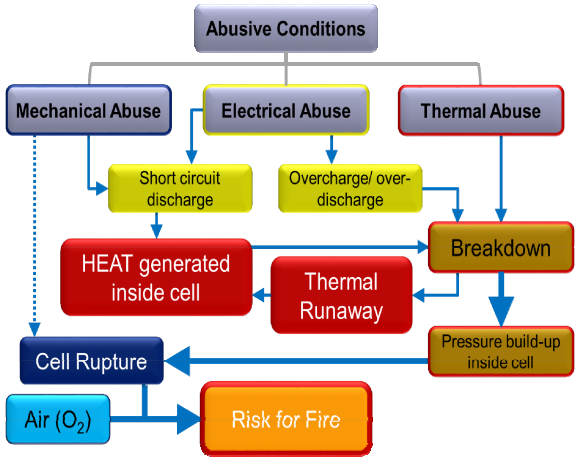


***Figure 2.*** **Fault tree analysis for a battery cell. There are three major abusive conditions – Mechanical, Electrical and Thermal Abuse. When thermal runaway have started the cell-internal pressure quickly increases and the cell soon rupture and gases are emitted to the surrounding. (Sturk, 2011) Autoliv ©.**

There is of course no fire without a fuel. For the internal breakdown of Li-ion cells, the fuel is the mix of organic electrolyte and the active materials of the electrolytes, while a battery cell external fire is fueled by the electrolyte vapors emitted by a critically damaged battery.
The internal breakdown can progress without visual flames but it will generate much gases. Predominant species is carbon dioxide and carbon monoxide. However, it has been documented that lesser quantities of more toxic species such as hydrogen fluoride or other fluoro-organics are generated. (Hammami, Raymond, & Armand, 2003) (Sturk & Hoffmann, 2013) (NIOSH, 1996) (AFS, 2011)The toxic fluoro-species derive from the breakdown of the salt $LiPF_6$. (Yang, Zhuang, & Ross Jr., 2006) (Wilken, Treskow, Scheers, Johansson, & Jacobsson, 2013) Hence, extensive ventilation of gases from a critically damaged Li-ion battery must be anticipated when preparing for a crash test of an E-Vehicle or a battery component test.
In the event of a battery fire, the composition of gases emitted may alter somewhat, but the risk for harmful fluoro-organics and hydrogen fluoride remains. (Sturk, Hoffmann, & Tidblad, 2015)

## METHOD

Autoliv's battery abuse testing facility is designed for dynamic mechanical abuse testing, i.e. separate acceleration or deformation tests, or a combination of the two. The specifications defining how to perform such a battery test are developed by means of full vehicle crash test with dummy/inert batteries and/or CAE crash simulations on E-Vehicle and battery pack or subsystem in order to assure the best possible replication of the target crash conditions.

### The characteristics and safety feature of the battery sled track

As for all types of crash related testing, sensors and cameras are used to provide qualitative data acquisition during and after test so as to fulfill customer specifications and maintain high level of post-crash safety. In order to offer customers a high-end sled track for battery systems, the 15 meter of track utilize up to 9 meters

for acceleration of the sled that can be propelled, by up to 10 bungee ropes, to a maximum velocity of close to 100 km/h. An empty sled weight 196 kg and the maximum added weight of battery unit is 200 kg. In comparison to regular crash tests some extra sensors and monitoring equipment is added to this test setup because of the need for monitoring the temperature and electrical properties of the battery unit to be tested. (Figure 3)

Additional requirements when performing high-risk battery abuse tests involves a stringent FMEA and routines that ensures that:

1) No test operators or other people are exposed to potentially harmful situations or substances caused by the test.
2) No collateral or unforeseen damage should be caused to the facility or neighboring facilities or property.
3) Any damage to test equipment shall be kept to a minimum.

Based on these priorities Autoliv has equipped the new facility with a test chamber by the barrier-end of the track. This test chamber is surrounded with transparent removable walls that will ensure that no physical parts of the test setup or object will be expelled from the chamber. The chamber offers an enforced environment for fire suppression and forced cooling measures as it limits the air volume, and restrict the area where any critical battery failure may occur. For flame suppression a stationary $CO_2$ system is dedicated, and for fire suppression and forced cooling water spray is used. Water (with or without additives) is the preferred cooling and fire suppression medium according to research published by (Egelhaaf, Wolpert, & Lange, 2014) and (Sturk, et al., 2014). Besides sensors for electrical characteristics and temperature monitoring a gas-detection warning system ensures an early alert for emissions of species such as carbon monoxide, organic vapors, hydrogen and hydrogen fluoride. All liquids released or leaked during or after a test will be collected and safely handled. For the safety of test operators, multiple cameras allow visual monitoring of the track and test chamber to be viewed from a separate control room with no direct air-contact with the testing room.

***Figure 3.*** **Autoliv's laboratory for high-risk sled testing of E-Vehicle batteries offers a testing environment with multiple layers of safety. A key safety feature is the enforced test chamber, at the barrier-end of the sled track, which is equipped with gas detection warning, fire suppressions, forced ventilation and collection of liquids. (Autoliv ©)**

**Defining specifications for physical testing**

Regardless of the choice of preferred physical testing setup – i.e. separate acceleration or deformation tests, or a combination of the two – the customer specification, upon which the final battery sled test is designed, can be derived from one out of two alternatives:

A. Battery crash environment characteristics acquired by complete E-Vehicle crash testing with low state of charge (SOC) battery, dummy battery or inert battery system. Tests performed by either Autoliv or the customer.
B. Battery crash environment characteristics acquired by CAE simulations on complete E-Vehicle crash model. Simulations performed by either Autoliv or the customer.

Alternative A is preferred when a comprehensive simulations model of all relevant parts of the E-Vehicle, the battery system and electronics are not yet fully validated. It shall offer the characteristics of the mechanical abuse that a battery system and its subcomponents experience under the complete vehicle crash. The necessity of replacing the active battery with dummy or inert battery, or using a low SOC is analog to the procedures of conventional crash testing where all liquids, which possess a fire risk (e.g. petrol and diesel), are replaced by inert liquids in prior to crash testing.

Alternative B is preferred when a validated simulation model with sufficient details of the E-Vehicle as well as the battery system is available. This offers a cost effective and fully risk free investigation of the mechanical abuse that may compromise the battery integrity.

Either way, Autoliv will utilize the data acquired to establish a best possible replication of the battery system and/or the subcomponents and run the corresponding simulations with the object to be tested in a detailed model of the battery sled track in order to ensure a high-end of equivalence between the crash scenario and final physical battery sled test (Figure 4). Autoliv's methodology behind this has been publicly presented through the OSTLER project that was cofunded by the European Commision through the 7$^{th}$ Framework Programme. (Funcke, et al., 2014)

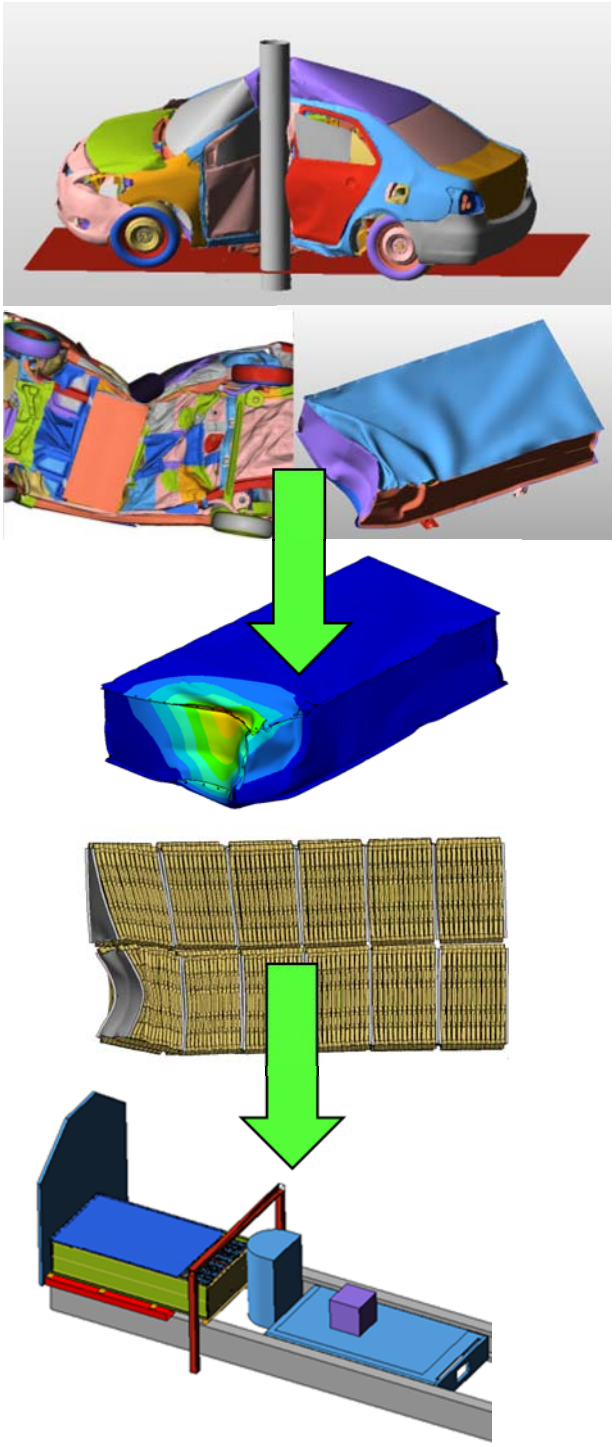

***Figure 4.*** **CAE simulations on the crash scenario to be investigate offers a more cost effective alternative than complete E-Vehicle testing when the crashworthiness of the battery system and its subcomponents are to be physically tested. (Funcke, et al., 2014)**

## RESULTS

As mentioned, when performing a replication of the crash environment experienced by the battery pack in an E-Vehicle crash scenario or when plainly investigating the crashworthiness limits of a battery system, the physical test setup can be optimized for either battery deformation tests or acceleration tests. A combination of them both is also possible. However, it will involve a larger physical setup in order to provide the correct synergy effects of testing the acceleration and deformation characteristics simultaneously. Hence it may put restrictions as to the size of the battery object to be tested.

### Battery Deformation Test

In the OSTLER project a scenario of an E-Vehicle crashing into a pole (sideways) at 50 km/h plus the corresponding damage to the "floor-battery" was investigated (Figure 4). For this physical test setup of the battery sled track, the battery pack was mounted to a rigid barrier and a pole-impactor was mounted on the moving sled. The conversion from the complete E-Vehicle crash characteristics to the physical test setup proved successful and a satisfying match of the compared crash environments was achieved. Figure 5 show the setup prior to testing as well as the arcing-event that occurred during the intrusion of the pole. It is also possible to mount the battery pack or its sub-components on the sled and the impactor or deformation element onto the barrier.

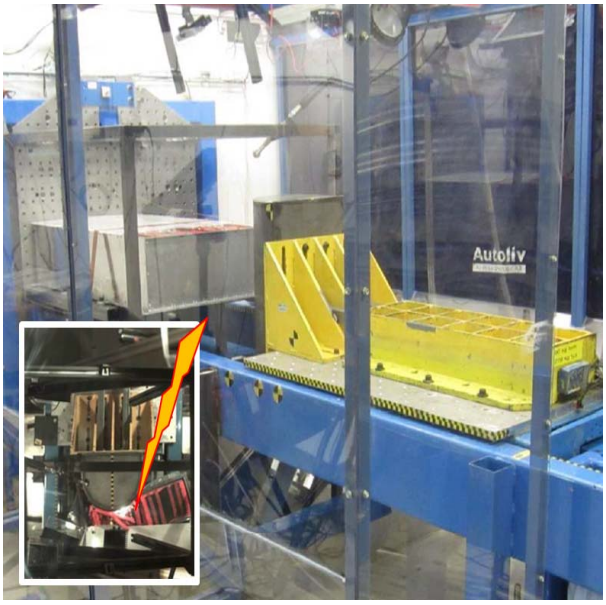


***Figure 5.*** **A battery deformation test with a pole impact. After the characteristics that a battery experience in a specified vehicle crash have been simulated in a CAE model of the track, the physical setup is constructed to offer a crash-matching environment for the battery system and its subcomponents to be tested. (Autoliv ©)**

### Battery Acceleration Tests

Conventional E-Vehicles are traditionally designed to assure the battery system integrity by means passive protective structures. Figure 6a presents a successful FMVSS 305 rear end collision (FMVSS 305, 2015) where the integrity of the battery system proved tough enough to prevent any intrusions. Consequently, in this example a deformation test on battery subcomponent proved not to be needed. In the research project E-Vehicle Safe Rescue, Autoliv performed the corresponding acceleration exposure onto battery modules in order to visualize the high level of robustness of a conventional battery system to the project's target group of first responders. (Sturk, et al., 2014)

At an acceleration test the battery or sub-component to be tested is mounted on the sled and the dedicated acceleration pulse is achieved by means of different types of breaking elements, such as tubes, bending bar or honey-comb structures.

Regulation UN ECE 100 requires that battery systems are tested for “Mechanical Shock” and show complience with a set of specifications. In its Annex 8C, figure 1 presents an accelration pulse corridor with nodes defined by the tables 1-3. (Economic Commission for Europe, 2014) Such a regulatory pulse requirement is physically possible to perform at Autoliv’s battery sled track facility.

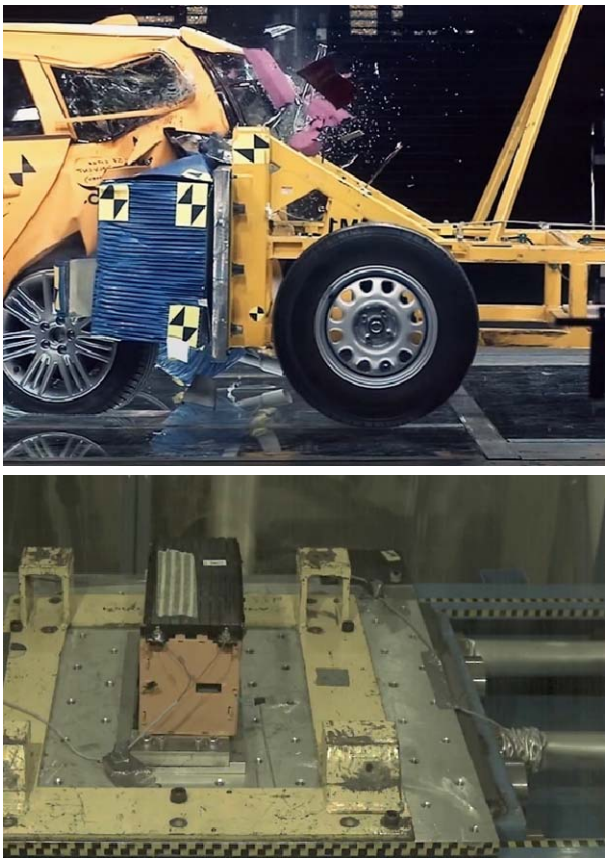

***Figure 6.*** **A battery acceleration test. FMVSS 305 rear impact is a tough test that US market E-Vehicle must comply to; in order to avoid over-engineering of protective structures, the battery and its subcomponents can be tested separately to offer more precise testing feedback on the design. Picture from a video available at (Swedish Civil Contingencies Agency, n.d.).**

## SUMMARY

Conventional E-Vehicles of today present a high level of safety but at a cost of range and battery weight since the structural integrity of their battery systems are commonly ensured by passive protection and its location is often restricted to the “safe zone”. Continuous efforts to develop lighter batteries and protective structures demand for dynamic abuse testing that is capable of replicating any foreseeable crash scenarios of future E-Vehicles in order to modify the battery system design without compromising battery crashworthiness.
Moreover, regulations, standards and ratings are adressing battery safety more precisely by every subsequent amendment process. The need for test facilities that are prepared for the increase demand of battery crash testing and all the safety concerns related thereto, are not always fully anticipated by current laboratories on the testing market.

For this reason, Autoliv have developed its new battery laboratory for dynamic mechanical abuse tests on E-Vehicle battery systems and their subunits.

**General risk factors when testing battery systems**

When performing durability and crashworthiness tests on battery systems and their sub-components it is of outmost importance to have updated routines and fully understand the potential risks associated with provoked batteries in order that any critical battery failure may not compromise the safety of test personnel, the facility and test equipment.

The constituent material of a battery cell influence its failure response in the event of a critical battery failure. As of 2014, the two most common Li-ion chemistries are denoted NMC and LFP based on their respective cathode material. However, all commercial Li-ion battery cells use the salt $LiPF_6$ together with alkyd carbonates solvents in their electrolytes. As the electrode materials have advanced to higher levels of stability the electrolyte is often considered as the weak link as it starts to decompose when being exposed to temperatures above 80ºC and risk to start reacting exothermally with the electrode materials if the temperature becomes even higher.

Depending on the choice of active materials in a Li-ion battery, the onset temperature of thermal runaway can be experience in the range from 170 to 250ºC for most of the commercial battery cells. At elevated temperatures (i.e. starting at 80ºC) the cell-internal pressure of these batteries rapidly increases and if the heat-up rate is too fast for the safeguard systems to comply, extensive ventilation of electrolyte vapor and other gases risk to be emitted to the surrounding of the battery. If there exists a sufficient ignition source, a fire could be the worst-case scenario. The gases released during ventilation and the gases during battery fire have proven to be unhealthy to people since they may constitute of species such $CO_2$, CO, various organics, fluoro-organics, and possibly hydrogen fluoride.

**Efficient and Safe Methodology**

In order to reduce the number of unknown parameters related to a battery system of an E-Vehicle that is exposed to a crash test, it is beneficial to study a smaller system (i.e. the battery system or sub-components) than the complete E-Vehicle. The mechanical interaction between the battery and its surrounding can be extracted from either, complete E-Vehicle crash tests with dummy/inert batteries or low SOC batteries, or stringent CAE simulation models of the vehicle and the battery. By avoiding complete E-Vehicle tests with active high-SOC battery systems, safety during testing is enhanced. This is analog to the requirements of conventional vehicle crash testing when all flammable liquids such as fuels are replaced with inert liquids prior to crash tests. The mechanical characteristics that is extracted from complete (electrically inactive) E-Vehicle crash tests are subsequently transferred into CAE models of the battery sled track together with the model of the battery and/or its sub-components. After optimizations have been done with these models, a physical test setup can be constructed. The final test can be either deformation tests or acceleration tests, or a combination of the two.

Autoliv's methodology, in combination with the new battery-sled-track laboratory, ensures that the unit to be tested experience a good representation of the dedicated crash environment while the risk factors associated with critical battery failure are safely anticipated.

## FINAL REMARKS

Autoliv's battery-crash test facility in Sweden can provide dynamic crashworthiness investigative testing on E-Vehicle battery systems and its sub-components in a dedicated laboratory environment. Severe mechanical abuse testing can be pushed beyond the limit of critical battery failure without compromising the safety of test operators as

well as neighboring facilities. Testing beyond this limit is key to develop lighter battery designs for further extension of the range of future E-Vehicles without compromising battery integrity and crashworthiness.

## REFERENCES


AFS. (2011). *Hygieniska gränsvärden.* Arbetsmiljöverkets författningssamling. doi:AFS 2011:18

Economic Commission for Europe. (2014). Vehicles with regard to specific requirements for the electric power train. *ECE 100-02*. UN: InterRegs Ltd.

Egelhaaf, M., Wolpert, D., & Lange, T. (2014). Fire Fighting of Battery Electric Vehicle Fires. *Proceedings from 3rd International Conference on Fires in Vehicles - FIVE 2014* (pp. 221-230). Berlin: SP Technical Research Institute of Sweden.

FMVSS 305. (2015). ELECTRIC-POWERED VEHICLES: Electrolyte spillage and electrical shock protection. *FMVSS 305 (49 DFR Part 571)*. USA: InterRegs Ltd.

Funcke, M., Schäfer, S., Wohlecker, R., Dufaut, D., Sturk, D., & Vavalidis, K. (2014). *Physical testing to validate simulations and demonstrate feasibility of solutions.* ika, fka & Autoliv. Brussels: FP7 The OSTLER Project. Retrieved from http://www.ostlerproject.com/Documents/OSTLER%20%20R140210-08%20D3.21%20Evaluation%20report%20on%20active%20and%20passive%20protection%20solutions.pdf

Hammami, A., Raymond, N., & Armand, M. (2003, August 7). Runaway risk of forming toxic compounds. *Nature, 424*, 635-636. doi:10.1038/424635b

Huang, Q., Yan, M., & Jiang, Z. (2008). Thermal study of organic electrolytes with fully charged cathodic materials of lithium-ion batteries. *12*, 671-678.

NIOSH. (1996, Aug 16). *Hydrogen Fluoride*. (NIOSH) Retrieved February 20, 2011, from IDLH Documentation: www.cdc.gov/niosh/idlh/7664393.html

Sturk, D. (2011). *Risk Analysis from an EV/HEV collision point of view.* Research. Vårgårda: Autoliv Development AB.

Sturk, D., & Hoffmann, L. (2013). *Fundamental Analysis for Risk assessment of E-Vehicles Involved in Traffic Accidents.* Borås: SP Technical Research Institute of Sweden. Retrieved from http://www-v2.sp.se/publ/user/default.aspx?RapportId=15651#15651

Sturk, D., Hoffmann, L., & Tidblad, A. A. (2015). Fire tests on E-Vehicle Battery Cells and Packs. *Traffic Injury Prevention, 16*. doi:10.1080/15389588.2015.1015117

Sturk, D., Näsman, Y., Hoffmann, L., Gusfafson, H., Östrand, L., & Björnstig, U. (2014). E-Vehicle Safe Rescue - Investigation of risk factors and rescue tactics in a traffic incident event involvin an E-Vehicle. *Proceedings from 3rd International Conference on Fires in Vehicles - FIVE 2014* (pp. 255-265). Berlin: SP Technical Research Institute of Sweden.

Swedish Civil Contingencies Agency. (n.d.). *Fronter Login*. Retrieved March 2015, from Produkter & tjänster: https://www.msb.se/sv/Produkter--tjanster/Fronter/

Wilken, S., Treskow, M., Scheers, J., Johansson, P., & Jacobsson, P. (2013, June 27). Initial stages of thermal decomposition of LiPF6-based lithium ion battery electrolytes by detailed Raman and NMR spectroscopy. *RSC Advances*, 1-6. doi:10.1039/c3ra42611d

Yang, H., Amiruddin, S., Bang, H. J., Sun, Y.-K., & Prakash, J. (2006). A Review of Li-Ion Cell Chemistries and their Potential use in Hybrid Electric Vehicles. *12*(1), 12-38.

Yang, H., Zhuang, G. V., & Ross Jr., P. N. (2006). Thermal stability of LiPF6 salt and Li-ion battery electrolytes containing LPF6. *161*, 573-579.

Zhang, S. S. (2007). A review on the separators of liquid electrolyte Li-ion batteries. *Journal of Power Sources, 164*, 351-364. doi:10.1016/j.jpow.sour.2006.10.065

# A PARTNERSHIP BETWEEN RENAULT AND FRENCH FIRST RESPONDERS TO ENSURE SAFE INTERVENTION ON CRASH OR FIRE-DAMAGED ELECTRICAL VEHICLES.

**Claire, Petit Boulanger ; Jacques, Thomazo ; Bruno, Azmi**
Renault SAS
France

**Olivier, Labadie**
Yvelines Firefighters Brigade
France

**Bruno, Poutrain,**
Paris Firefighters Brigade
France

**Michel, Gentilleau**
Vienne Firefighters Brigade
France

**Hervé, Bazin**
Laboratoire Central de la Préfecture de Police
France

Paper Number 15-0252

## ABSTRACT

In order to ensure first Responder safety, Renault set up a collaborative approach to involve rescuers in our electrical vehicle conception. The breakthrough came from the integration of crash and fire deterioration from the earliest stages of vehicle development.
Collaboration with fire brigades revealed 5 key areas which were then dealt with: electrical vehicle identification; prevention of electrical risk during emergency intervention; the impact of Li Ion batteries on occupant extrication and fire; co-creation of decision-making tools (Emergency Response Guide or ERG, rescue cards); training sessions on electrical vehicles.
EV prototypes were provided to study how the 400V system affected fire brigade intervention. Extrication tests were led on the full range of Renault electrical vehicles to take into account the different locations of the 400V battery. Fire tests were carried out until total combustion of the 400V batteries was reached. Then, extinction tests in open and closed environments were conducted, led by French scientific laboratories. Temperatures, thermal radiation, and concentrations of flue gases effluents were measured in most of these tests.
A large number of electrical vehicles were donated to French and European fire brigades for extrication training and fire demonstration. Bespoke electrical vehicles were produced as training supports and offered to fire brigades.
Trainings are given for free to French rescuers all around the year by an engineer from Renault, expert in electrical vehicle interventions.Finally, Renault regularly participates in national working groups with fire brigades and contributes to the ISO initiative on ERG writing and templates.
This combination of actions and results removed doubts as to the safety of electrical vehicle 400V batteries in a deteriorated state; enabled the proposal of a modus operandi for fire brigade intervention; led to the modification of the architecture of the 400V battery casing and the vehicle itself to improve rescuer intervention; highlighted the need to standardize service plug location across the range of Renault electrical vehicles.

Thanks to this fruitful collaboration between Renault and French fire brigades, rescuers acquired knowledge and skills for intervention on Li Ion battery electrical vehicles.

## INTRODUCTION

When launching the Renault Electric Vehicles (EV) programs, the overall safety of these vehicles along their life cycle was a major concern for the company, as it already was for Internal Combustion Engine vehicle (ICE). The safety was integrated in the technical specifications by a careful selection of Lithium ion batteries safety concepts: electric architecture, service disconnect switch (SD/SW) integration, mechanical structure, " Battery Management System " ( BMS) protection strategy of the battery for a maximal safety level in all use cases. Many validation tests were led to guarantee the battery safety, including in abusive conditions such as: electrical abuse, thermal abuse, mechanical abuse and cell internal defect.
Renault's innovative way was to get involved, from the design of vehicles, first responders to study incindental situations of EV life cycle, such as road accidents and vehicles fires. Those sharing seemed particularly useful as it could raise relevant questions coming from fire brigades interventions habits and not yet identified by development teams.

## GOALS

The five actions areas identified with firefighters to guarantee their safety and the victims one in emergency interventions were the need of :

- Efficiently identifying the vehicle as electric.
- Getting the vehicle safe easily
- Keeping low the Li-Ion battery effect on extrication and extinguishing situations
- Creating common standards to help first responders decision (Emergency Response Guides, and Rescue Cards)
- Training them free of charge by our EV experts

## METHODS

The first step was to understand the difficulties of fire brigades during their interventions on crashed, burning, or immersed vehicles … During their intense exchanges, Renault and first responders drafted together the technical specifications of EV Emergency Response Guide to be sure to answer the real needs of the firefighters. To fill some chapters of this ERG and validate its EV safety level during rescuers future interventions, Renault conducted field testing together with fire brigades.

### EV Identification and safety

Fire brigades expressed their need to be able to distinguish the EV from an ICE in case of emergency intervention.
Renault took into account this necessity with standard distinctive visual elements in its EV; special Headlights, lack of exhaust pipe, logos Z.E. lack of petrol filling flap, underhood orange wires and connectors, specific elements on the dashboard
The BMS is in charge of managing the battery functional and dysfonctional safety , this is achieved by controlling both temperature and voltage and ensuring they remain in between the defined functional tresholds. Furthermore, aiming to guarantee the best safety level for people, Renault recommends beforehand in any intervention of extrication, to isolate the electric 400V circuit of the battery from the vehicle by disconnecting the SD/SW.
A 2 steps cut-off mechanism ensures the lack of electric arc during the operation of service plug disconnexion.

**First extrication tests on Electric Vehicles**

Renault was willing to verify before the selling of its two first EV models (Kangoo Z.E. and Fluence Z.E.) if the 400V battery and wires could affect usual extrications technics. A prototype of each EV model was thus given to French fire brigades so that they could check the possibility of keeping their usual cutting techniques .

They concluded that Renault EV wedging could be done the same way as ICE, including by applying rams directly on the battery casing. Weight distributions are different between EV and ICE, because of the lack of internal combustion engine and the presence of 300kgs batteries under the vehicle for Kangoo Z.E. and in the trunk for Fluence Z.E. As a matter of fact, if it lies on the roof after a crash, the EV is in balance (figure 1). It requires more wedging elements than for ICE which tilts forwards, because of its engine weight. Rescuers confirmed that Kangoo Z.E. floor had no risk of downward movement when positioned on the roof, in spite of the weight of the underfloor battery. They also showed that it was possible to extricate a victim through the Fluence Z.E. rear window when on the roof, using rams for example, in spite of the weight of the battery in the trunk (figure 1).

All the techniques of intervention used usually for extrication have been tested and rescuers concluded that none of their manoeuvre was forbidden by the presence of the battery or electric wires in Renault EV, because none is located in cutting areas. These results were used to fill in Renault EV ERGs and Rescue Cards .

*Figure 1 : a-Fluence Z.E. in balance on the roof ; b-poosible wedging on Kangoo Z.E. battery ; c- no downward movement of Kangoo Z.E. on the roof ; d-possible exit of victims from Fluence Z.E. on the roof despite battery located in the trunk.*

**Electric Vehicles first tests of fire in closed environment**

The aim of these tests was to answer the questions of fire brigades about EV (with Li-Ion batteries) behavior when involved in a fire. These first fire tests were organized by Renault and performed in the Centre National de Prevention et Protection (CNPP), in partnership with fire brigades.

They included bruning a Fluence Z.E. and a Kangoo Z.E. (with batteries at 100% charge level) in closed environment (16m x 19m x 2.9m) by placing them on an aluminum pan of 150 x 100 x16 cms filled with 150 l of alcohol, to ensure at least 15 mn to fire exposure.

After ignition started, each EV was left until total combustion (body and battery), without any external intervention. These tests led to the following conclusions: the kinetics of the fire of Fluence Z.E. and Kangoo Z.E. is similar to ICE fire. Without any extinguishing, the Li-Ion battery has a total combustion duration of 1 hour without any explosion. The EV close neighbooring temperature tops 900°C during the burning of the car and decreases to 350°C during the combustion of the battery. 5m away, the maximal temperature does not overtake 350°C (figure 2).

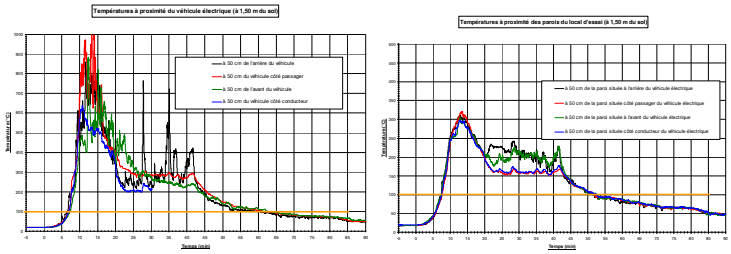


*Figure 2: EV close neighbooring temperature and at 5 meters distance*

Firefighters were able to conclude that this Renault EV fire behavior was similar to ICE fires they have experience with. Nevertheless, it was deemed necessary to perform comparative fire tests on EV and ICE to confirm these observations with quantified data.

**Comparative tests of EV and ICE fires in closed environment**

The purpose of this second test was to have comparative data between EV and ICE fire behaviour. These tests were performed by the "Institut National de l'Environnement Industriel et des Risques" (INERIS) on a conventional Fluence and a Fluence Z.E. . The only difference between these two cars is the presence of a Li-Ion battery instead of a diesel fuel tank. The Li-Ion battery of Fluence Z.E. was charged up to 100 % capacity and the diesel tank of the Fluence full (50L of fuel). The ignition was started into the passenger compartment from the driver seat with a gas burner.

As described in the first tests, there was no evidence of projections nor explosion resulting from the battery fire. The fire maximal thermal power and the total energy released are lower for the EV than for ICE: respectively 4.7MW against 6.1 MW, and 8 500 MJ against 10 000 MJ. The toxic effects during the combustion of the EV and the ICE were also compared.

Total quantities of CO2, CO, HCl, hydrocarbons, NO, NO2, HCN emitted during the combustion of EV are close or lower than those of the ICE (table 1).

**Table 1: Pollutants measurements [1]**

| Emitted gas (g) | ICE | EV |
|---|---|---|
| $CO_2$ | 722 637 | 618 487 |
| CO | 15 732 | 11 700 |
| HCl | 2 139 | 1 933 |
| NO | 740 | 770 |
| $NO_2$ | 410 | 349 |
| HCN | 178 | 148 |
| HF | 813 | 1472 |

Significant quantity of HF was emitted during combustion of both the EV and the ICE: a first peak of HF emission 14 min after the beginning of the test was observed in both cases. It results from the combustion of air conditioning fluid (figure 3).

A second wave of HF emission is observed in the case of the EV, linked to the presence of fluorinated salts in the Li-Ion battery. The associated kinetic is relatively slow and the instantaneous flow rates remain much lower than those from the the air conditioning liquid combustion. Moreover, it is interesting to notice that the overall amount of emitted HF from the battery is relativeley low compared to the potential content. Indeed, except the part linked to the A/C liquid combustion, assuming all the HF emitted from the vehicle comes from the battery, this is approximately 1050g of HF. Compared to about 5050g potentially contained into the battery, it is roughly only 20% of effective emission. This can be explained by the high affinity of HF for common metals present all over the vehicle frame (iron, steel, aluminum,...) thus it will react with apparent metallic surfaces and therefore will be less

present in gaseous emissions. The total quantity of HF remains superior to the ICE, without preventing fire brigades from applying their usual intervention procedures [1]. During later intervention testing of Fluence Z.E. fire, a HF detector positionned on the first fireman shoulder never measured concentration exceeding the tolerated threshold in intervention.

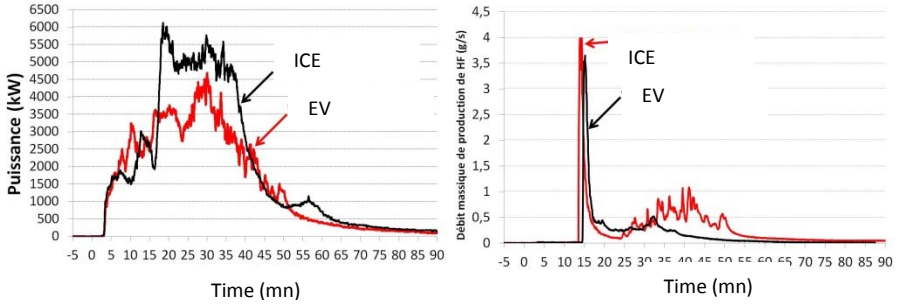


*Figure 3: comparison of released energy and HF emission during the EV and the ICE combustion.*

**First EV extinguishing tests by fire brigades.**

Prior to the selling of its two first EV models, Renault gave the fire brigades 2 Fluence Z.E. to perform outdoor fire and extinguishing tests. Firefighters wanted to reproduce the fire context of the most common vehicle fire situation : vandalism ignition, throwing a flammable object on the rear seats. As the objective was ensure the Li-Ion battery would catch fire, firefighters waited for 30 mn from the fire beginning and until launching the extinguishing intervention. At this moment, they could visually confirm the Li-Ion battery combustion, thanks to flames behind the vehicle. The firefighters extinguishing strategy was similar to ICE one: start from the front of the car, get rid of engine compartment fire, then move to the body and the peripherals (tires). Fire brigades *finally* focused on the Li-Ion battery extinguishing by spraying water on its casing for cooling . It was an ineffective attempt because the fire started again after every stop of water spraying, this until battery total combustion (~ 1h ). Following this extinguishing failing attempt, a reflection was led to define the best strategy to stop the Li-Ion battery fire.The second test of Fluence Z.E. fire and extinguishing was set up by flooding the battery from firefighters hose, directly into the battery cooling system. This second attempt appeared to be particularly effective because the complete and definitive extinguishing of the Li-Ion battery was achieved within 5min.

The following recommendation was thus proposed: the extinguishing of a Li-Ion battery is possible and effective only by filling it with common water in the aim to flood it.

As Kangoo Z.E. didn't provide direct access to the Li-Ion battery (whereas Fluence Z.E. did) , the question of how to flood the battery remained. Several tests of fire and extinguishing of Kangoo Z.E. were thus performed in partnership with fire brigades and the "Laboratoire Central de la Prefecture de Police" ( LCPP) to make sure that it was also possible to fill in the Li-Ion battery of this EV with water.

As the *main* objective was to be sure that the Kangoo ZE Li-Ion battery would *catch* fire during the test, firefighters filled the passenger compartment of wood pieces , and added some also on the ground underneath the battery. This set up was chosen to ensure a sufficient heat capacity to trigger the battery combustion. In every fire test, the Kangoo Z.E.battery, located under the vehicle, caught fire approximately half an hour after the beginning of vehicle fire. With the intense heat of the fire, it appeared that the Li-Ion battery aluminum casing melted in different points, allowing direct injection of water inside the battery, consequently the complete and definitive extinguishing was achieved in approximately 15 mn after the beginning of its combustion. [2]

The third Renault EV, ZOE, took experience from these fire tests results and integrated an innovative technical solution for allowing a fast and effective extinguishing of its Li-Ion battery: the "fireman access". It is a thermal fuse part based on plastic, located on the body of the vehicle, under the the rear passenger seat cushioning, which will melt because of the fire heat and therefore provide to firefighters a direct access to the vents of the Li-Ion battery (figure 4).

*Figure 4: Fireman Access on ZOE before, during and after the fire test.*

This worldwide innovation, allows efficient Li-Ion battery fire extinguishing within one minute, by flooding it with the fire nozzle. This shows a typical example of OEM taking in account the fire brigades needs. Since these tests took place, Renault integrated an additional requirement for this specific access dedicated to firefighters in the specifications of development of all its embedded Li-ion batteries. This "fireman access" presents a double interest: a direct and easy access for fire nozzle, and a direct view on the battery flames which makes easier the hole localisation , even for a first responder unaware of its existence. This improvement of rescuers intervention efficiency and safety was confirmed during others fire tests realized on ZOE in partnership with fire brigades and LCPP according to the same protocol as for Kangoo Z.E. (wood pieces inside the passenger compartment and under the vehicle). [2]. After usual extinguishing of the EV body, its Li-Ion battery was quickly and definitely extinguished by flooding it within one minute.

**Simulation test of fire coming from inside the Li-Ion battery.**

When it has been decided to add a "fireman access" in the passenger compartment of ZOE, the engineering team worried about a possible side effect in the highly improbable case of Li-Ion battery thermal runaway. Indeed, if a fire departure occurred inside the battery, would there be a life threatening risk (toxic gazs and smokes or flames) for the car passengers? To answer this difficult question and make sure that the "fireman access" would not decrease the safety level of the vehicle, a simulation test of fire coming from inside the Li-Ion battery was conducted, by overcharging a cell in the battery, considering this was the worst case possible of battery malfunction. This test was led once again in partnership with fire brigades and LCPP [ 3 ]. The heat increase of the overcharged cell was observed only after 1:30 hour of charging, and was associated with emission of smokes observed only outside of the vehicle (figure 6a). This phenomenon was observed during the heat propagation from cell to cell during 90 mn. During the same period, the heavily instrumented vehicle cabin (thermosensors, gas sensors & cameras) could not see any evidence of smoke nor flame presence inside the car. The LCPP and the fire brigades suggested to stop the test at this moment, concluding that if such a situation would occurred in the reality on EV with passengers blocked inside the car, rescuers would have enough time to extricate them .

After this test, the good behaviour of the "fireman access" *part* has been proved in spite of a skin temperature measured at 200°C (Figure 5 b and c).

*Figure 5 : a – external smokes during heat increase distribution in nearby cells of Li-Ion battery ; b &c - Fireman Access after heat increase distribution in nearby cells of Li-Ion battery.*

The conclusion of this test is that there is no increase of toxic risk or fire in the passenger compartment due to the presence of the fireman access.

**CONCLUSIONS**

All these tests contributed to improve knowledge on Renault EV safety when submitted to abuse situations such as road accidents and fire. Thanks to the intrinsic safety *level* of Li-Ion batteries on EV Renault and their BMS, as well

as to all the tests described in this paper, there is no particular risk found associated to EV for people (rescuers and car occupants). All the EV fire and extinguishing tests conducted in partenrship with fire brigades, that is 16 since 2011, guaranteeing a good reproducibility of the behavior of the Renault EV and their batteries (kinetics, intensity). Water was found an effective extinguishing agent for Renault EV battery Li-Ion. It is nevertheless necessary that the first responders are informed about the recommendations given by Renault. These knowledge, shared during the tests with some fire brigades experts, were thus *widely* distributed *to* fire brigades, by publishing on-line documents such as Emergency Response Guides (ERG) [ 4] [ 5 ] [ 6 ] ) and Rescue Cards [ 7 [ 8 ] [ 9 ].

At the same time, trainings on Renault EV intervention are given free of charge in French fire brigades *by* a Renault expert, also volunteer fireman. A partnership French Renault / fire brigade was also set up to propose these trainings in the fire brigades of other countries wishing to benefit from it.

These actions and the results obtained allowed to provide answers to the fire brigades questions on EV safety when involved in abuse situations. Operating procedures have been adjusted by fire brigade. Renault found how to modify the battery casing architecture and the vehicle itself to improve first reponders interventions, and integrated the necessity of homogenizing the location of its SD/SW in spite of the associated stresses *on* mechanical and electrical architecture.

These works have been made possible thanks to a close partnership between French fire brigades and Renault EV engineering teams. Each part has been able to deepen its knowledge, to make sure Renault EV safety level is at least equivalent to ICE one. Fire brigades were able to adapt their methods of intervention and Renault learned how to integrate into its specifications the particular needs of first responders.

**REFERENCES**

[1] Rapport d'Etude INERIS, « Essais d'incendie de véhicules et de batteries » 17/11/2011 DRA-11-123008-09671A

[2] Rapport d'étude LCPP « Étude de l'impact de feux de véhicules électriques (RENAULT) sur les intervenants des services de secours » 20 janvier 2012

[3] Rapport d'étude LCPP n°13/11747, « Évaluation du comportement de la trappe thermo-fusible sur la propagation d'effluents gazeux dans l'habitacle d'un véhicule de type ZOE (RENAULT) en cas d'emballement thermique de sa batterie de traction

[4] Emergency Response Guide Fluence Z.E. Renault - http://www.infotech.renault.com/fo/accueil.action

[5] Emergency Response Guide Kangoo Z.E. Renault - http://www.infotech.renault.com/fo/accueil.action

[6] Emergency Response Guide ZOE Renault - http://www.infotech.renault.com/fo/accueil.action

[7] Rescue Sheet Fluence Z.E. Renault - http://www.infotech.renault.com/fo/accueil.action

[8] Rescue Sheet Kangoo Z.E. Renault - http://www.infotech.renault.com/fo/accueil.action

[9] Rescue Sheet ZOE Renault - http://www.infotech.renault.com/fo/accueil.action

# A CONTINUOUS VIDEO RECORDING SYSTEM ON A LAP-BELT EQUIPPED SCHOOL BUS: REAL-WORLD OCCUPANT KINEMATICS AND INJURIES DURING A SEVERE SIDE IMPACT CRASH

**Kristin Poland**
**Thomas H. Barth**
National Transportation Safety Board
USA

**Kristy B. Arbogast**
**Mark R. Zonfrillo**
Children's Hospital of Philadelphia
USA

**Richard Kent**
University of Virginia
USA

Paper Number 15-0253

## ABSTRACT

A loaded truck-tractor semitrailer severely impacted the side of a lap-belt-equipped large school bus in which 30 students, age 5 to 11 years, were riding. The crash investigation obtained on-board video and audio from the school bus recording system, which had four active cameras that recorded at 15 frames per second. A total of 55 minutes 39 seconds of video and audio was obtained, including over 15 minutes after the bus came to final rest. Qualitative descriptions of occupant motion during the crash sequence were documented based on the time sequence of vehicle motion, including kinematics of lap-belted pediatric occupants, occupant-to-occupant interactions, and occupant-to-vehicle interactions. Further, quantitative measurements of occupant motion were performed by tracking visible body regions such as the head or center of the pelvis using commercially available motion analysis software. Occupant injuries were coded using hospital medical records and according to the Abbreviated Injury Scale 2008 manual.

Injury severity was higher in the rear of the bus near the region of impact, maximum intrusion, and maximum lateral accelerations. The injury severity scores (ISS) ranged from 1 to 6 in the front of the bus and from 1 to 57 at the rear, including the one student seated at the rear of the bus who was fatally injured. Head injuries included several mild to moderate traumatic brain injuries. Lateral head translations and velocities were evaluated. The lateral head displacements toward the impacted side in the front of the bus were similar to those in the rear during the initial impact, but the head displacements for occupants in the rear of the bus were greater during the secondary and tertiary rebound motions toward alternating sides of the bus. Lateral head velocities relative to the bus interior were generally almost twice as high in the rear of the bus as in the front. In addition, the magnitude of whole body pediatric occupant motion in the absence of injury was notable. Further, loss of consciousness negatively affected occupants' ability to self-evacuate, even when subjects regained consciousness.

The qualitative and quantitative descriptions represent the first time that lap-belted school bus pediatric occupant motion during a crash has been documented from continuous onboard video recordings. This unique data source allows the rare correlation of occupant kinematics with crash severity and injury outcomes in living humans.

## INTRODUCTION

Pediatric biomechanics is a critical area of research to ensure the protection of these vulnerable occupants. Key data has been gathered from research through academic and industry partnerships. [1] Government programs, such as the National Highway Traffic Safety Administration (NHTSA) National Automotive Sampling System (NASS) and Crash Injury Research (CIREN), generate critical databases, crash reconstructions, and associated research. Although a significant amount of real-world information for a large number of crash types and scenarios has been

obtained in the past, there is still limited information available about real-world pediatric occupant kinematics and interactions with seats, restraints, and interior systems during the impact sequence.

Seat and restraint designs are developed using anthropomophic test devices (ATD), which have biofidelity limitations, including seat positioning differences between the ATD and a human. [2] Further, pediatric ATDs are often scaled from adult ATDs and suffer from a lack of information establishing range of motion and injury thresholds. [3] Human volunteer research partially addresses the differences between ATDs and humans, but this research is conducted in sub-injurious settings. [4, 5] Naturalistic driving studies have the potential to provide information on a range of event severities as long as the appropriate data can be collected. [6] Accident reconstructions in conjunction with post mortem human subject (PMHS) testing address injurious crash levels, but pediatric PMHS testing is extremely rare [7] and does not include muscle response.

The objectives of this analysis were to document pediatric occupant injuries, qualitative observations from the continuous onboard video system, and quantitative measurements from the onboard video of occupant kinematics during the crash phase. The results present a unique data source to study the real-world movement and associated injuries of pediatric occupants.

## METHODS

In this crash, a loaded truck-tractor semitrailer severely impacted the side of a lap-belt-equipped large school bus occupied by the driver and 30 students, age 5 to 11 years. (See ***Figure 1***.) The school bus was equipped with a continuous audio and video recording system manufactured by Seon Design, Inc. The system had four active cameras, which recorded at 15 frames per second. The videos began prior to student loading of the bus and continued through the bus trip to the point of the collision and after. A total of 55 minutes 39 seconds of video and audio was obtained, including over 15 minutes after the bus came to final rest. The continuous video system captured useful data prior to, during, and after the crash.

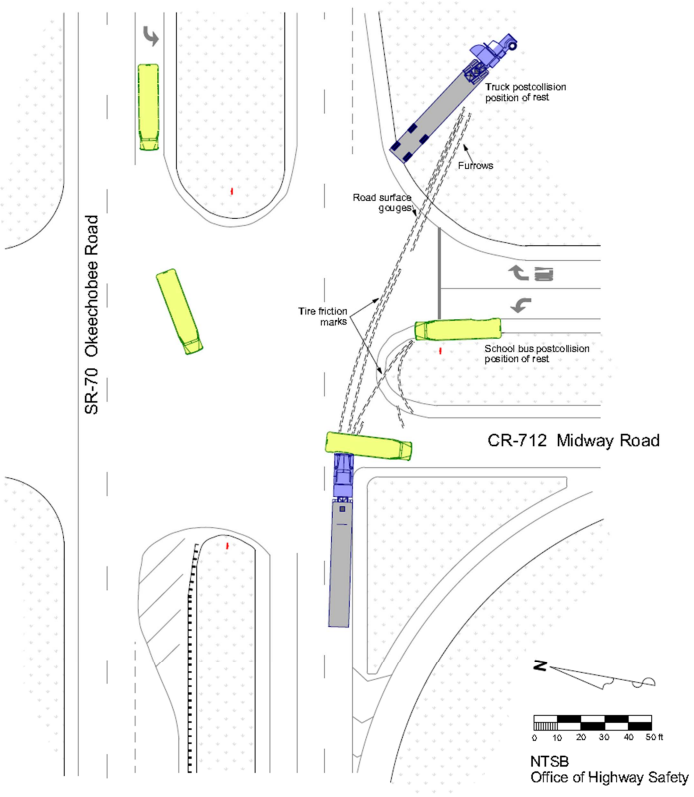


***Figure 1. The crash scene diagram.***

**Vehicle and Occupant Descriptions**

Each of the four camera positions was individually labeled, by the Seon Design, Inc. video system, as "Step", "Front", "Mid", and "Rear" according to their location and orientation. ***Figure 2*** shows a still image with four frames from each of the four onboard video cameras prior to the loading of the school bus. (By statute, the NTSB is prohibited from releasing onboard video and audio recordings that show occupants.) All four camera views were evaluated for the entire recorded duration to describe the motion of the school bus and the occupants using both qualitative and quantitative methods. During the precrash phase, qualitative descriptions of the driver's actions, communications, the vehicle motion, and any relevant video overlay information, such as "RT" indicating the right turn signal was illuminated or "BRK" indicating that the brake was applied, were documented based on the crash timeline. In addition, qualitative descriptions of each visible occupant's belt use, seating position prior to impact, position at final rest, whether the occupant was ejected from the seat compartment, occupant-to-occupant interactions, occupant-to-vehicle interactions, and state of consciousness postcrash were documented based on the timeline developed for the vehicle motion.

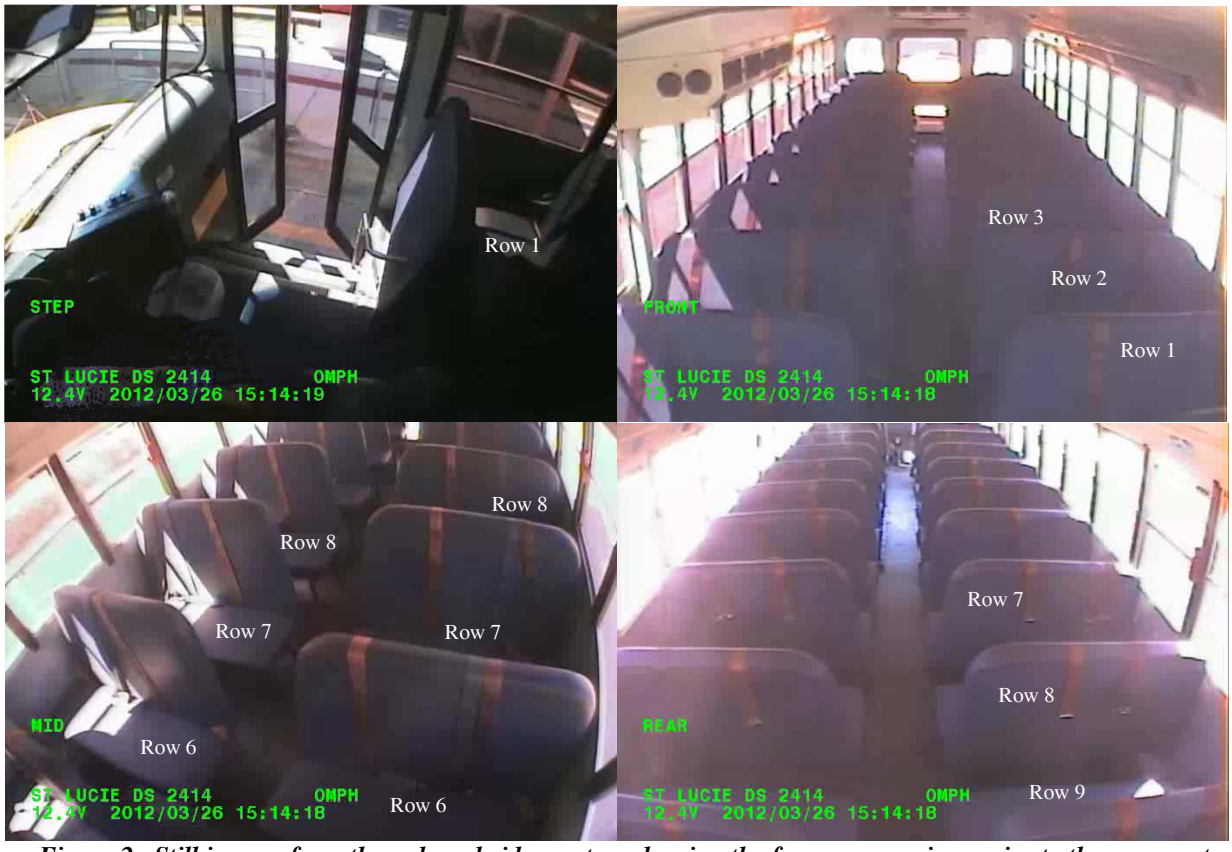


***Figure 2. Still images from the onboard video system showing the four camera views prior to the occupants loading onto the school bus. The four camera views, starting in the upper left corner and moving clockwise, are "Step", "Front", "Rear", and "Mid". Text detailing the row numbers is overlayed on the images for clarity.***

Further, quantitative positions and velocities of the school bus and the visible occupants were calculated. The process to estimate the dynamic school bus motion history has been described previously. [8] Briefly, a model of the camera was developed and calibrated. In an iterative process, each video frame from the camera was matched to a synthesized video frame, including known landmarks outside the bus, generated by the camera model. When the frames matched, the bus position and orientation was established. For the quantitative occupant motion, the "Front" and "Mid" cameras provided the clearest view of the occupant motion and were the source of this documentation. The basic method to calculate the occupant motion required the calibration of the visible occupant space within the two-dimensional recorded video frame. ProAnalyst Professional Edition (Version 1.5.6.5) was used to calibrate the local occupant seating coordinate system, based on interior bus dimensions measured from the three-dimensional laser scans of the school bus, and to track the occupants' (or interior surfaces') motion.

The "Front" camera was centered in the middle of the school bus interior. As a result, the perspective calibration was used in ProAnalyst, using four points representing the base and top of the windows on each side of the bus in a position closely matching the occupant's initial seated position. Row 2 and row 3 were calibrated. Seat spacing and seat width were used to verify the calibrations. The "Mid" camera was offset toward the driver's side of the bus looking toward the passenger side of the bus. The perspective calibration was implemented again for row 7, using four points representing the base and top of the windows on both sides of the bus in a position closely matching the tracked occupant's initial seated position. For row 6, because the top of the windows were not visible in the camera view, the perspective calibration was used but the four points represented the base of the windows and the base of the seat pan on both the driver and passenger side of the bus. The perspective calibration was adjusted to most closely match the tracked occupant's motion within a seat row. As a result, there were multiple calibrations defined for both row 6 and row 7. Seat spacing and seat width were used to verify the calibrations. The motion in the local occupant seating coordinate system was then transformed into the bus body coordinate system. Positions and velocities were calculated relative to the bus body coordinate system.

The videos documented student loading onto the bus, the use of seat belts for most students, and occupant positions throughout the bus trip. These continuous recordings helped establish an accurate seating chart, including occupant age and gender, preimpact position, and the level of restraint for most of the students.

### Injury Coding

Abbreviated Injury Scale (AIS) scores were assigned and injury descriptions were summarized for all occupants who received medical attention. Copies of medical records and digital radiographic images were reviewed to confirm injuries. Standard AIS coding rules were used based on the most recent AIS manual. [9] Injuries were summarized using several metrics: the traditional International Civil Aviation Organization (ICAO) code with categories of uninjured, minor, serious, or fatal; the comprehensive AIS score; and the total Injury Severity Score (ISS) ranging from 0-75. Individual injuries by ISS body region, AIS code, and injury description were listed for each school bus occupant that received treatment and for the fatally injured occupant. [10]

Given the availability of the on-board video system, observation of loss of consciousness (LOC) was used to help determine the concussion diagnoses. Occupants were given the diagnosis of concussion if there was probable or certain LOC on the bus and no intracranial hemorrhage, or if a final concussion diagnosis was confirmed in the medical record (regardless of whether the passenger experienced LOC). Concussions were not coded if the patient had LOC with any intracranial hemorrhage.

## RESULTS

### Qualitative Observations from Continuous Video System

The continuous video system confirmed that the bus driver was not distracted by a cell phone or other portable electronic device and that he had both hands on the steering wheel during the left turn maneuver just prior to the collision. The driver consistently used the turn signals to indicate a transition from one lane to another and to indicate motion into the left turn lane prior to the collision. The driver also applied braking in preparation for this left turn. Further, it was apparent that the driver perceived the impact threat, though too late, because he turned his head toward the oncoming truck. The onboard videos and associated audio recordings showed that the driver encouraged seat belt use at the beginning of the trip and that he did not appear to be distracted by students just prior to the collision.

The continuous recordings also documented student loading onto the bus, the use of seat belts for most students (some views were partially obscured, including the seating position of the fatally injured occupant), and occupant positions throughout the bus trip. These data helped investigators establish an accurate seating chart, pre-crash occupant positions, and the level of restraint for most of the occupants. Pre-crash video and audio documentation showed that the driver's attentiveness to passenger safety and seat belt rules was a factor in the number of students who properly wore and adjusted their seat belts.

The most beneficial data obtained from the onboard video system were related to the crash sequence and the post-crash environment. The four interior cameras remained in place and functional throughout the crash event and continued recording for over 15 minutes after the initial impact.

**Crash Sequence and Post-crash Events as Determined from Video Systems**

Impact occurred at 15:55:03 and the bus came to final rest almost 10 seconds later. During the motion to final rest, the bus yawed approximately 180 degrees and experienced two large roll events. The first non-occupant to enter the school bus was an adult female who entered the bus at time 15:55:28 through the open rear emergency exit door and provided assistance to occupant 10D about 15 seconds after the bus came to final rest. She continued to provide assistance to the bus occupants until the end of the video recording, which stopped at 16:10:07. The first uniformed officer boarded the school bus about 3 minutes and 22 seconds after the bus came to final rest and emergency medical services arrived about 8 minutes and 22 seconds after the bus came to final rest.

**Seating Chart and Injuries**

The seating chart established based on the continuous onboard video system is shown in ***Figure 3***. All occupants are marked with the ICAO code. For those occupants with medical records, the maximum AIS level and the ISS score are also documented. In addition, occupant gender and age are listed. Seating positions were labeled based on the seat row (1-11) and the seat position (A-F from left to right as viewed from the back). The area of impact (AOI) is shown on the chart. Additional details on the injury documentation are included in the NTSB's Highway Safety Report – Commercial Vehicle Onboard Video Systems. [11]

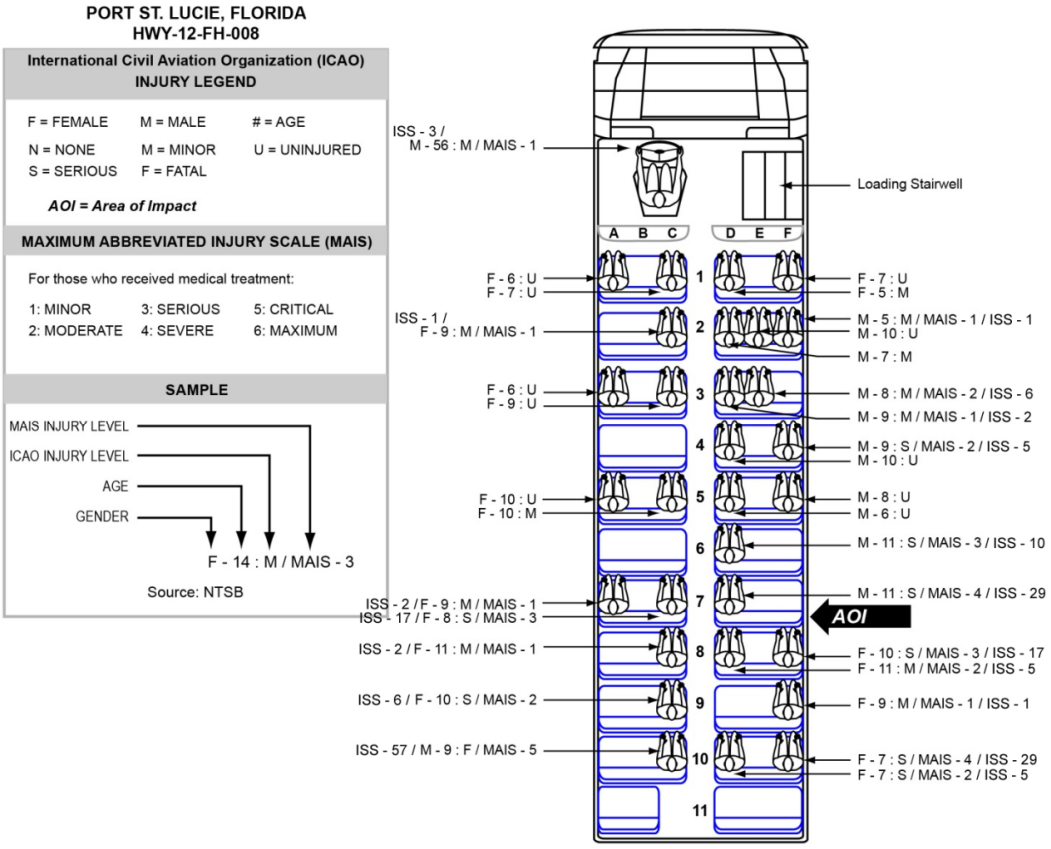


***Figure 3. The school bus passenger seating chart, with ICAO injury level, MAIS injury level, ISS score, and demographic information.***

**Belt Use**

Belt use was visible for twenty-two occupants and of those, seven appeared to wear the lap belt loosely or slightly loosely (1D, 2C, 4D, 5C, 7D, 8D, and 8F), as determined by the visible tension in the belt and the motion of the occupant during the crash sequence. There were no observations showing a lack of belt use, however, belt use was not visible for eight occupants (3D, 3E, 4F, 5A, 5F, 10C, 10D, and 10F) due to the obstructions of the seatbacks and the occupant's seating distance from the onboard cameras.

**Occupant Position Relative to Seat Compartment Post-crash**

Twelve occupants were ejected from their seat compartment during the crash sequence (1C, 1D, 2C, 2D, 3C, 3D, 4D, 5A, 5C, 9C, 10C, and 10D). All of these occupants, except occupant 5A, were initially seated along the aisle and most were ejected into the aisle post-crash despite wearing the lap belt. Occupant 5A was ejected into the aisle and then backward into seat row 6, on the driver side of the bus. Belt use was not visible for occupant 5A due to the camera positions and obstructions from the seatbacks. Other occupants (7C, 7D, 8C, and 8D) were not considered to be ejected from the seat compartment but it was noted that the occupants' heads and upper torsos flailed outside the seating compartment into the adjacent seating compartment across the aisle during the crash sequence.

**Occupant-to-Occupant and Occupant-to-Interior Impacts**

There were nineteen documented instances of occupant-to-occupant impacts, 16 of which involved an impact of an occupant's head with either another occupant's head or other part of their body. All of the documented occupant-to-occupant contacts occurred for occupants in rows 2, 3, 5, 6, 7, 8, and 9. Generally, the occupants impacted other occupants within the same seating row, but in rows 5/6 and 8/9, impacts occurred between occupants originally seated in different rows. For example, occupant 5A's right torso was impacted by occupant 6D's head as occupant 5A traveled into the seat row behind and occupant 6D flailed in that direction. In rows 8/9, occupant 8F's body was pushed upward and rotated backward over the seatback such that occupant 8F's head impacted the chest and pelvis of the occupant seated directly behind (9F). (Occupant 8F's head also continued back and contacted the seat pan near occupant 9F's seating position.) Occupant 8F was lap belted and observations from the video showed the belt visible on the occupant's thighs. Occupants in row 1 interacted with each other but specific impacts between occupants were not noted. Occupants in row 10 were generally not visible due to the camera positions and the obstruction from the high seatbacks.

There were also nineteen documented instances of occupant-to-interior impacts. Nine of these involved an impact of the occupant's head onto a passenger side window or sidewall structure (2F, 3E, 4F, 5F, 6D, 7D, 8D, 8F, and 9F) and one other involved an impact of the occupant's head with a driver side window and sidewall structure (3A). All of these occupant-to-interior impacts were sustained by occupants seated against the sidewall or in a position without other occupants between them and the sidewall, except in row 8 where both occupants on the right side of the bus impacted the sidewall. The other occupant-to-interior impacts involved impacts onto the seat pans and the aisle-side edges of the seatbacks.

**Loss of Consciousness and Head Injuries**

Loss of consciousness (LOC) was observed in seven occupants (3E, 6D, 7C, 7D, 8D, 8F, and 10C). The state of consciousness was unknown for three other occupants (8F, 10D, and 10F) who were not visible post-crash. The other twenty occupants were conscious post-crash. Of those occupants with an observed LOC, only occupant 6D remained unconscious at the end of the video recording. (Occupant 10C was documented with a LOC but was the fatally injured occupant.) In addition, recorded audio discussions between the adult female and emergency medical responders indicate that occupant 10F was conscious at the end of the recording.

Head injuries were documented on the medical records for twelve occupants (2F, 3E, 6D, 7A, 7C, 7D, 8D, 8F, 9C, 10C, 10D, and 10F) including six who were diagnosed with only a concussion (3E, 7A, 8D, 8F, 9C, and 10D). All seven occupants with an observed LOC had a documented head injury. As expected from the dynamics of the bus, the majority of the head injuries were seen in occupants seated in the back half of the bus. For the two front seated occupants with head injuries, the sustained injuries were less severe. For example, occupant 2F was diagnosed with a head injury that was not further specified and occupant 3E was diagnosed

with a concussion with LOC. In the back half of the bus, the head injuries were more severe, especially for occupants in rows 6, 7, and 10. Occupant 6D's head injuries included cerebral contusions, a cerebral hematoma, a subdural hemorrhage, a mastoid fracture, and a skull fracture. Head injuries to occupant 7C included a cerebral subarachnoid hemorrhage and left and right intraventricular hemorrhages. For occupant 7D, head injuries included comminuted basilar skull fractures on the left and right sides, a temporal bone fracture, and left and right cranial nerve VII palsy. Interestingly, the head injuries to occupants in rows 8 and 9 were limited to only concussions and minor lacerations. Yet occupants in row 10 again experienced severe head injuries. Occupant 10C, who was fatally injured in the crash, sustained bilateral cerebral edemas, multiple cerebral subarachnoid hemorrhages, and a skull fracture. Occupant 10F sustained a cerebral subdural hematoma.

**Evacuation**

Nineteen occupants self-evacuated out the front loading door (1A, 1C, 1D, 1F, 2C, 2D, 2E, 2F, 3A, 3C, 3D, 4D, 4F, 5A, 5C, 5D, 5F, 7A, and 9F). Eighteen of those self-evacuated in 60 seconds or less, from the time the bus came to final rest. Another four occupants were assisted out the rear emergency exit door (8C, 8D, 9C, and 10D). Occupants 3E, 6D, 7C, 7D, 8F, 10C, and 10F remained on the bus at the end of the video recording. Occupant 10D was the first occupant removed from the school bus with assistance by the adult female at 15:55:33, which was about 20 seconds after the bus came to final rest. Occupant 1D was the first to self-evacuate out the front loading door at 15:55:43, 30 seconds after final rest. Occupant 7A was the last to self-evacuate out the front loading door at 15:58:12, almost 3 minutes after final rest. Occupant 8C was the last occupant removed with assistance before the video recording ended, at 15:58:39, about 3.5 minutes after final rest.

**Injury Factors in Self-Evacuation**: None of the occupants with an observed LOC were able to self-evacuate. Most occupants with a LOC regained consciousness during the period of the video recording but only occupant 8D was evacuated off the bus with assistance. The remaining occupants with an observed LOC were on the bus at the end of the recording, which was almost 15 minutes after the bus came to final rest.

Five occupants sustained pelvis and/or lower extremity fractures as a result of the crash (4F, 7C, 7D, 8F, and 9C). The sustained pelvic/lower extremity fractures were a closed left ankle fracture for occupant 4F, a right pubic fracture for occupant 7C, a pelvic ring fracture at the anterior iliac spine for occupant 7D, a right talus fracture for occupant 8F, and pelvic fractures at the sacral spine and at the right ramus through the pubic symphysis for occupant 9F. Of the occupants that sustained a pelvic/lower extremity fracture, three also experienced a LOC and a documented head injury (7C, 7D, and 8F). In addition, occupant 9C sustained a concussion without LOC, as discussed above. Only occupant 4F sustained a lower extremity fracture without a head injury or LOC and this occupant was able to self-evacuate 48 seconds after the bus came to final rest.

Spinal injuries were rare. (The driver, although not a focus of this paper, sustained a cervical spine sprain, or whiplash, and a lumbo-sacral spine strain.) Occupant 3D sustained a cervical spine sprain (whiplash) and occupant 10D, the fatally injured occupant, sustained a cord laceration with fracture and dislocation at C7-T1. Except for the fatally injured occupant, the minor spinal injuries did not affect evacuation.

**Occupant Kinematics**

Using the "Front" camera, the head positions of occupants 2C, 3C, and 3E and the pelvis position of occupant 3C were tracked in the bus based coordinate system. The lateral position versus time history can be seen in *Figure 4*, where the lateral centerline of the bus is zero and motion toward the driver side is in the positive direction. The lateral distance from the bus centerline to the sidewall was 1.17m and is labeled on the graph.

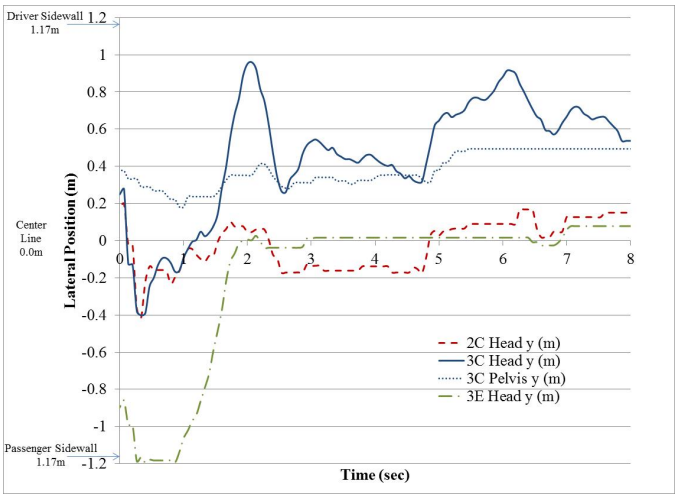


***Figure 4. The lateral (y axis) head position of occupant 2C, 3C, and 3E and the lateral pelvis position of occupant 3C.***

Using the "Mid" camera, the head positions of occupants 6D, 7A, 7C, and 7D and the pelvis position of occupant 6D and 7D were tracked. The lateral position versus time history can be seen in *Figure 5*.

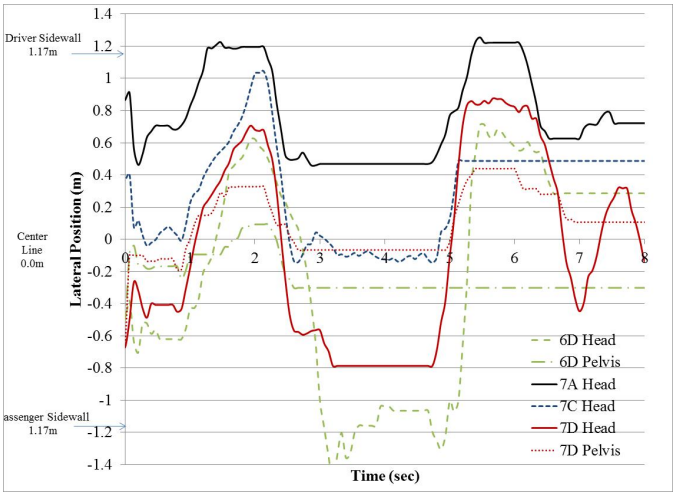


***Figure 5. The lateral (y axis) head position of occupant 6D, 7A, 7C, and 7D and the lateral pelvis position of occupant 6D and 7D.***

The position of the "Mid" camera did not remain stationary relative to the bus interior during the impact sequence. This relative motion between the camera and bus interior may have resulted from deformation at the floor and sidewall, camera orientation changes, or a combination of the two during the impact sequence. In an effort to document this relative velocity, four points fixed on the bus interior were tracked. The left sidewall experienced the least deformation and would, ideally, provide the best estimate of the camera velocity but since this sidewall moved out of the camera view for a portion of the impact sequence, points on the left sidewall were not tracked. Instead, the aisle-side position of seat 6C was used as a surrogate for the camera velocity since that seat was attached to the left sidewall and the floor underneath and experienced the least deformation of the interior points visible in the "Mid" camera.

Using this correction for the "Mid" camera, the maximum intrusion into row 7 was approximately 0.48m during the first 0.13 seconds with a recovery of 0.12m during the next 0.13 seconds. Similarly, the maximum velocity of the right sidewall in row 7 was 2.41 m/s and the maximum velocity of the aisle-side point on seat 7D was 3.50 m/s at 0.13 seconds. Note that these velocities are lower bounds on possible velocities because the calculation is limited by the video frame rate. Maximum displacement could have occurred between frames and not captured until the subsequent frame, 67 milliseconds later, which would reduce the calculated velocity.

Although the bus motion involved both translation and rotation, the initial occupant motion was predominantly lateral with some longitudinal components. Since the camera orientations were perpendicular to the lateral plane, motion in the lateral direction was well quantified. Table 1 summarizes the lateral head velocity at impact or immediately prior to impact along with a snap shot of the qualitative description of the occupant motion [12] at that time, during the initial motion toward the passenger sidewall. Note that all the velocities are negative indicating motion toward the passenger side of the bus.

**Table 1.**
**Lateral head velocity immediately prior to or at the estimated time of the head contact from the video observations.**

| Occupant | Time (sec) | Lateral Head Velocity (m/s) | Qualitative Description of Occupant Motion |
|---|---|---|---|
| 2C | 0.267 | -2.96 | Torso reaches maximum articulation onto seat 2D with back nearly horizontal across aisle, shoulders are completely obscured behind the seatback of row 1 |
| 3C | 0.133 | -3.04 | Upper body is fully articulated across aisle, occupant 3C's head on seat 3D (behind row 2 seatback) |
| 3E | 0.133 | -0.98 | Head shifts towards window and sidewall moves towards head due to the impact, face is either making contact or about to make contact with lower portion of window |
| 6D | 0.133 | -4.21 | Occupant 6D flails completely to the passenger side, head impacting sidewall below window (sidewall was deforming toward occupant 6D) |
| 7A | 0.133 | -5.43 | Head of occupant 7A impacts the posterior hips of occupant 7C |
| 7C | 0.133 | -5.34 | Occupant 7C's head near or in contact with left postero-lateral aspect of 7D's torso |
| 7D | 0.133 | -0.13 | Occupant 7D's head remains in essentially the same position relative to the camera as before the impact but due to the sidewall intrusion, the head and right shoulder are now in contact with the passenger side sidewall |

## DISCUSSION

This onboard video recording analysis utilized first of its kind data to describe the qualititative and quantitative kinematics of pediatric school bus occupants during a crash and related their movement to crash dynamics and injury outcomes. Being able to visualize living human movement in a crash setting provided insight into the magnitude of excursion capable from a restrained occupant, the flexibility without injury that children demonstrate, and the temporal nature of concussion.

Injury severity was highest for occupants in rows 6-8 and also in row 10. Likely, injuries were greatest in rows 6-8 because that was the region of impact and the area of maximum intrusion along the right passenger sidewall. In row 10, accelerations were the greatest in this region due to the dynamics of the bus as it pivoted about the front axle as a result of the side impact near the passenger side rear axle. These high accelerations likely resulted in the severe injuries for occupants in row 10.

The injury severity score (ISS) varied from 1 to 6 in the front of the bus. In the rear of the bus, the ISS ranged from 1 to 57 and included several mild to moderate traumatic brain injuries. Lateral head translations toward the point of impact in the front of the bus were similar to those in the rear during the initial impact, but the head translation for occupants in the rear of the bus was greater during the secondary and tertiary rebound motions toward each side of the bus. Lateral head velocities were generally higher in the rear of the bus except for occupant 7D who essentially did not move relative to the "Mid" camera. Instead, the sidewall intruded directly into his seating compartment and impacted his head and right shoulder before he began to flail toward the impact point. In the front of the bus, the lateral velocities of occupants' heads ranged between -0.98 and -3.04 m/s, but in the rear of the bus the maximum lateral velocities of occupants' heads were almost twice as high, ranging from -0.13 to -5.43 m/s.

Further, the magnitude of whole body pediatric occupant motion in the absence of injury was notable. For example, occupant 8F bent backward over the top of her seatback such that her head impacted the chest and pelvis of the occupant (9F) seated directly behind her. Her head continued downward, impacting the seat pan of seat 9F, as well. Her thighs were still restrained by the lap belt, which had slid down during her vertical translation and backward rotation. Despite this extreme hyper-extension, occupant 8F did not sustain any spinal injuries and her torso injuries consisted of only a lung contusion to the right middle and lower lobes and a right 7$^{th}$ rib fracture.

LOC had a noticeable effect on the ability for occupants to self-evacuate. Occupants with an observed LOC were not able to self-evacuate, even if they regained consciousness post-crash. Obviously, maintaining occupants' consciousness during the crash is critical to a timely evacuation, especially for post-crash environments that may involve water immersion or fire. Impact onto intruding sidewall and window surfaces, along with upper body flailing enabling occupant-to-occupant impacts, was likely the main cause for the occupants' LOC. Reducing the upper body flailing could be accomplished with greater upper body restraint, such as with a properly adjusted lap/shoulder belt. [13] Reducing the severity of impacts onto sidewall and window structures could be accomplished with school bus performance standards that address passenger protection for sidewalls, sidewall components, and seat frames, as first recommended by the NTSB in 2001. [14]

Other injuries, such as pelvic or lower extremity fractures, did not appear to negatively impact evacuation, if the injury was sustained by an occupant without a head injury or LOC. Spinal injuries, which may also reduce the ability to self-evacuate, were rare in this crash.

The study was limited by the resolution of the camera system and the frame rate, which was relatively low given the dynamics of the crash. The calculation of the vehicle dynamics was also limited due to the lack of a forward-facing camera. In addition, due to the high seatbacks on the school bus, occupants were not visible at all times during the crash sequence. Further, because concussions were not coded if the patient had LOC with any intracranial hemorrhage, the estimated number of concussions may be conservative. (For example, there may have been other occupants who had concussion and did not experience a visible LOC, but there was insufficient medical record documentation of symptoms or diagnosis). Additionally, there was variability in the available medical records for injured patients (for example, detail of radiographic imaging and reports and medical record documentation). As a result, some injuries may have not been captured. Similarly, there may have been occupants who did not seek medical attention, but who may have had minor injuries (for example, contusions, lacerations, and/or mild sprains).

The qualitative and quantitative descriptions represent the first time that lap-belted school bus pediatric occupant motion has been documented from onboard video recordings. The correlation of occupant kinematics with crash severity and injury outcomes was also unique. Ultimately, research using onboard video data from school buses can be a basis for a multidisciplinary approach to improving occupant safety.

## CONCLUSIONS

The documentation of real-world lap-belted pediatric occupant kinematics in a severe side impact crash based upon video and audio recordings combined with medical records provides unique information to evaluate realistic pediatric occupant kinematics and provide data unable to be found elsewhere to evaluate ATD biofidelity. This information also provides unique insight into injury mechanisms and outcomes.

The continuous video system offered the first such documentation of lap-belted children involved in a severe side impact collision. The videos further highlight differences in occupant kinematics across a range of collision severities, which were evident when contrasting occupant motion in the front of the bus with occupant motion in the rear of the bus. Because of the length of the school bus and the center of rotation at the front axle, the crash was much more severe for rear-seated occupants than for those seated in the front of the bus.

**REFERENCES**


[1] Partners for Child Passenger Safety. "The State of Child Occupant Protection Interim Report 2003", The Children's Hospital of Philadelphia Center for Injury Research and Prevention, 2003.

[2] Bohman, K, Stockman I, Jakobsson L., Osvalder A., Bostrom O., Arbogast K.B. 2011. "Kinematics and Shoulder Belt Position of Child Rear Seat Passengers during Vehicle Maneuvers." In Proceedings of the 2011 Association for the Advancement of Automotive Medicine, October 2011.

[3] Seacrist, T., Balasubramanian, S., García-España, T.F., Maltese, M.R., Arbogast, K.B., Lopez-Valdes, F.J., Kent, R.W., Tanji, H., Higuchi, K. 2011. "Kinematic Comparison of Pediatric Human Volunteers and the Hybrid III 6-Year-Old Anthropomorphic Test Device."
In Proceedings of the 2011 Association for the Advancement of Automotive Medicine, October 2011.

[4] Seacrist, T., Samuels, J., García-España, F., Arbogast, K.B., Mathews E.A., Balasubramanian, S., Maltese, M.R., Longhitano, D., St. Lawrence, S., 2012. "Kinematic Comparison of the Hybrid III and Q-Series Pediatric ATDs to Pediatric Volunteers in Low-Speed Frontal Crashes." In Proceedings of the 2012 Association for the Advancement of Automotive Medicine, October 2012.

[5] Seacrist, T., Locey, C.M., Mathews, E.A., Jones, D.L., Balasubramanian, S., Maltese, M.R., Arbogast, K.B., 2014. "Evaluation of Pediatric ATD Biofidelity as Compared to Child Volunteers in Low-Speed Far-Side Oblique and Lateral Impacts." Traffic Injury Prevention, 15, S206-S214, Taylor & Francis Group, LLC, June 2014.

[6] The SHRP 2 Naturalistic Driving Study (NDS), Strategic Highway Research Program, Transportation Research Board (TRB) of the National Academies, http://www.trb.org/StrategicHighwayResearchProgram2SHRP2/Pages/The-SHRP-2-Naturalistic-Driving-Study-472.aspx, accessed on March 9, 2015.

[7] Lopez-Valdes, F.J., Forman, J., Kent, R., Bostrom, O., Segui-Gomez, M. 2009. "A comparison between a child-size PMHS and the Hybrid III 6 YO in a sled frontal impact." In Proceedings of the 2009 Association for the Advancement of Automotive Medicine, October 2009.

[8] Horak, D. T. "Estimation of Vehicle Speed and Trajectory Based on Video from a Vehicle-Mounted Camera," Collision. The International Compendium for Crash Research, Volume 4, Issue 2, 2009, pp.18-25.

[9] Association for the Advancement of Automotive Medicine (AAAM). The Abbreviated Injury Scale (AIS) 2005-update 2008. Barrington, IL: Association for the Advancement of Automotive Medicine, 2008.

[10] NTSB (National Transportation Safety Board). 2013. "Injury Coding Factual Report." In NTSB: Docket Management System, HWY12FH008, http://dms.ntsb.gov/pubdms/, DC: NTSB.

[11] NTSB (National Transportation Safety Board). 2015. "Commercial Vehicle Onboard Video Systems", Safety Report NTSB/SR-15/01. Washington, DC: NTSB.

[12] NTSB (National Transportation Safety Board). 2013. "School Bus Video Documentation Group Factual Report." In NTSB: Docket Management System, HWY12FH008, http://dms.ntsb.gov/pubdms/, DC: NTSB.

[13] NTSB (National Transportation Safety Board). 2013. “School Bus and Truck Collision at Intersection Near Chesterfield, New Jersey, February 16, 2012”, NTSB/HAR-13/01. Washington, DC: NTSB.

[14] NTSB (National Transportation Safety Board). 2001. “Collision of CSXT Freight Train and Murray County School District School Bus at Railroad/Highway Grade Crossing, Conasauga, Tennessee, March 28, 2000”, NTSB/HAR-01/03. Washington, DC: NTSB.

**What is the Benefit of the Frontal Mobile Barrier Test Procedure?**

**Thorsten Adolph**
**Julian Ott**
Federal Highway Research Institute (BASt)
Germany

**Burkhard Eickhoff**
Autoliv B.V. & Co. KG Country
Germany

**Heiko Johannsen**
Medical School Hannover
Germany

Paper Number 15-0254

## ABSTRACT

Frontal impact is still the most relevant impact direction in terms of injury causation amongst car occupants. Especially for car-to-car frontal impacts the mass ratio between the involved vehicles has a significant impact on the injury risk (the heavier the opponent car the higher the injury risk). In order to address this issue frontal Mobile Deformable Barrier test procedures have been developed world-wide (for example the MPDB procedure that was fully described during the FIMCAR Project). The objective of this study was to investigate how vehicles of different weight classes perform in a mobile barrier test procedure compared to a fixed barrier test procedure (the full width rigid and offset deformable barrier test). Beyond that, the influence of vehicle mass and vehicle deformation on injuries was evaluated based on real world accident data.
Five vehicle types were selected and tested in a fixed offset test procedure (ODB), a full width rigid barrier test procedure (FWRB) and a mobile offset test procedure (MPDB). For the accident analyses data from the German In-Depth Accident Study (GIDAS) was evaluated with a focus on MAIS 2+ injured belted front row car (UN-R 94 compliant cars) occupants in frontal impact accidents.
Test data indicates higher dummy loadings, in particular for the head acceleration and chest acceleration, in the MPDB test for the vehicles with a mass lighter than the trolley (1,500 kg) compared to the FWRB test. The trend of increased vehicle stiffness (especially illustrated by tests with the MPDB and small cars) shows the need of a further improvement of passive restraint systems to reduce the occupant loading and with it the injury risk.
The analyzed GIDAS data confirm the higher injury risk for occupants in cars with an accident weight of less than 1,500 kg compared to those with a crash weight above 1,500 kg in car-to-car and car-to-object or car-to-HGV, respectively. Furthermore the injury risk increases with decreasing mass ratio (i.e., the opponent car is heavier) in car-to-car accidents. Independent from the higher injury risk, the risk for passenger compartment intrusion in frontal impact appears not to be independent on the crash weight of the car.

## INTRODUCTION

Frontal impact is still the most relevant impact direction in terms of injury causation [1]. While the stability of passenger compartments has been improved in Europe substantially in recent years, the performance of the restraint system becomes now even more important [2]. In the traditional restraint system test, the vehicle is crashed between 40 and 56 km/h against the rigid wall independent of the vehicle mass. This is a test procedure used in many countries all over the world. In real-world car-to-car impacts a light vehicle is more likely to be hit by a heavier vehicle and due to the principle of conservation of momentum, the lighter of the two vehicles has to withstand higher loading than the heavier vehicle. Higher loading not only affects cabin integrity, but also cabin acceleration as the lighter of the opponents suffer from a greater change of velocity (delta-v) due to the conservation of momentum. A test with a frontal mobile barrier would reflect these circumstances and was discussed several times in the past [3], [4] and [5]. For the present investigation the frontal mobile test procedure as defined by the FIMCAR

Project [5] was used, because the mass of the trolley and the stiffness of the barrier represents a European midsize car [6–8].
Current accident studies show that many injuries are caused by high vehicle acceleration in frontal impacts compared to injuries caused by intrusions into the passenger compartment [2]. It was also stated that the accidents with acceleration loading induced injuries had a high overlap. On the other hand crash tests with a low overlap at the corner of the vehicle are discussed in other consumer information programms or regulatory bodies [3, 9–11]. However in Europe, crash tests with a high overlap seem to have a higher priority [12].

With the analyses of real world accident data the following questions should be answered. Have occupants in smaller vehicles (less than 1,500 kg) a higher injury probability in frontal impacts compared to occupants in vehicles heavier than the crash trolley? And if so, is this due to the passenger compartment stability (intrusions) or due to higher occupant loads as a result of the crash pulse and the restraint system?
The different loading in terms of vehicle deformation, vehicle acceleration and injury assessment values for vehicles with a mass lighter and heavier than the mobile barrier should be investigated with the help of crash test data. It is assumed that lighter vehicles have a higher loading with a frontal mobile offset barrier compared to a fixed barrier test (FW / ODB) and that heavier vehicles have a lower loading.

## METHODS

### Methods Accident Data

For the accident analyses, data from the German in-depth accident study (GIDAS) was evaluated with a focus on MAIS 2+ injured belted front row car occupants[1] in frontal impact accidents. To ensure that only UN-R 94 [13] compliant vehicles were included, only vehicles with a date of first registration in 2003 or later were considered. Furthermore only completely coded and reconstructed accidents up to 2013 were included in the study to guarantee that not only EES but also delta-v was available. The GIDAS sampling method is explicitly explained in [14]. The final data set consisted of 98 cases including 112 front seat occupants with MAIS 2+ injuries.
The accident severity was evaluated using the reconstructed delta-v and EES values. The deformation of the vehicle was classified using the overlap and the CDC classification. The overlap is in percentage and it is important to note that the overlap is coded independently from the involvement of the vehicle corners (e.g., a center pole impact with a pole having a diameter of 20% of the vehicle width is coded as 20% overlap). That distinction was necessary to separate between accidents with a small overlap at the edge of the vehicle and pole impacts. For the analysis it was estimated which kind of frontal impact test procedure would cover best the accident scenario. Here the four possibilities pole, small overlap, half overlap and full frontal were considered. The accident scenarios were identified by separating between offset crash (30 % to 50 %) and large overlap crash (80% to 100%), see also Figure 2. All cases were manually checked in regard to the deformation classification with the help of the accidents pictures.
The collision opponents were classified, on the one hand, as vehicles and, on the other hand, as fixed structures (e.g. road side barriers, walls), poles (trees, traffic lights, street lamps) and others.
The injury severity was coded for the whole person by the official police classification (not injured, slightly injured, severe injured (hospitalization for more than 24 hours) and fatally injured (fatality as a direct result of the accident within 30 days after the accident). All injuries were separately analyzed using the AIS 2005 classification. The vehicle mass was described with the estimated crash weight of the specific vehicle at the time of the first impact.

### Methods Crash Test Data

Crash test data from different vehicle models were obtained in the test configurations: offset test according to the Euro NCAP test protocol (ODB), Full Width Rigid Barrier test (100% overlap, FWRB), and against a Mobile barrier with the Progressive Deformable Barrier attached (MPDB). To evaluate the injury risks Hybrid III

[1] MAIS = Maximum Abbreviated Injury Scale, injury severity classification according to AIS 2005

50% dummies on the driver seat were used. Table 1 is showing the vehicles used, including the acronyms, the test masses and the data source the test is obtained from.

**Table 1 Test vehicles, acronyms and data base used for the analyses**

| Vehicle acronym | DS | VU | SI | VT | VX |
|---|---|---|---|---|---|
| Test mass | 1164 kg | 1050 kg | 1181 kg | 1900 kg | 2400 kg |
| ODB | Euro NCAP | Euro NCAP | Euro NCAP | Euro NCAP | Euro NCAP |
| FWRB | BASt | BASt | BASt | n.a. | n.a. |
| MPDB | BASt | BASt | BASt | FIMCAR | FIMCAR |
| Description | Compact car, four doors, cheap | Super mini, two doors, new vehicle design | Compact car, two doors, popular | Midsize SUV | SUV |

The ODB test was conducted with a test speed of 64 km/h and an overlap of 40% using a deformable barrier face as defined in [13]. The FWRB had a test speed of 50 km/h, with 100% overlap and without a deformable barrier face [15]. The MPDB test procedure is explained in detail in [7] including the specifications for the test trolley. The closing speed was 100 km/h and the mass of the trolley was 1,500 kg. These values were not changed for the different vehicles. The progressive deformable barrier used for the MPDB is bigger and significantly stiffer compared to the ODB barrier. This makes barrier bottoming out much more unlikely. The barrier is specified in [16].

***Figure 1 Crash trolley used of the test with mobile barrier specified in [7] using the PDB v8.0 XT***

To analyze the loading on the vehicle the maximum acceleration measured at the b-pillar driver side was measured. Additionally the OLC (Occupant Loading Criterion, [17]) was calculated based on that acceleration signal. OLC predicts the relative motion of the dummy and vehicle and calculates the average acceleration experienced by the dummy when its relative position is in the interval between 65 mm and 235 mm. The structure of the vehicle was evaluated based on the a-pillar displacement (at waist line) measured after the test.
The restraint performance was evaluated using the following indices: belt forces measured at the upper shoulder belt between shoulder and the upper anchorage point (B3) and - if available - measured at the lap belt between the hip and the lower anchorage point (B6). Furthermore the airbag deployment time[2], the airbag contact time[3] and the seatbelt pretensioner time[4] was analysed. The time points were determined based on the high speed videos.

[2] Airbag deployment time = Timing correlating with first frame in the high speed film when the Airbag cover breaks
[3] Airbag contact time = Timing correlating with first frame in the high speed film when the dummy head contacts the airbag
[4] Seatbelt pretensioner time = Timing correlating with first frame in the high speed film when the seatbelt moves

For the analyses of the loading on the occupant the injury criteria from the HIII dummy were used. The focus was on the criteria which are sensitive to assess the loading from the vehicle acceleration: head acceleration (3ms value, HIC within 36ms), chest compression, chest acceleration (3ms value) and pelvis acceleration (peak). The injury criteria were scaled to the ratio of 100% injury assessment reference values (IARVs) to provide a better overview and to enable a better comparison according to UN-R 94 where possible [13, 18–20] [18]. For the chest and pelvis acceleration 60g as 100% were defined, see also Table 2.

***Table 2 Injury assessment reference values used for the analyses of the occupant loading***

| Injury Criteria | Pelvis acceleration | Thorax Acceleration | Thorax deflection | Head acceleration | Head injury criterion |
|---|---|---|---|---|---|
| Acronym | Pelvis Acc | Thorax Acc | Thorax Defl | Head a3ms | HIC 36 |
| IARV | 60g | 60g | 42mm | 80g | 1000 |
| Notes | peak value | 3ms value | max. value | 3ms value | within 36ms |

## RESULTS AND DISCUSSIONS

### Accident Data

The following picture (Figure 2) shows the distribution of the overlap crash scenarios for the 98 cases. Almost half of the accidents had a very large or a full overlap. The other three crash scenarios (offset, small overlap edge, small overlap in the middle) were almost equally distributed with values between 15% and 20%.

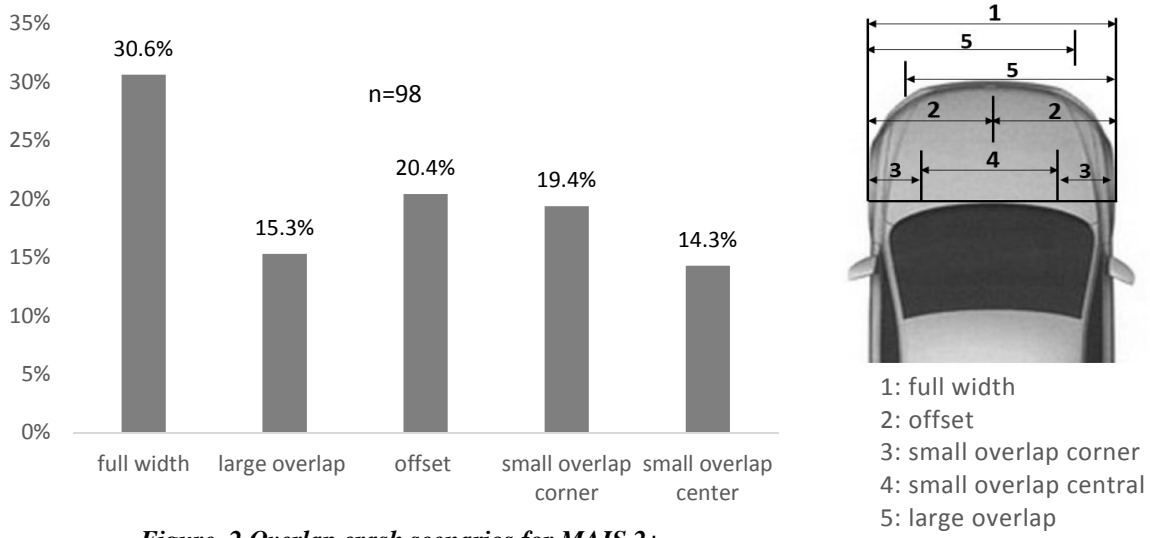


***Figure 2 Overlap crash scenarios for MAIS 2+***

Of the 98 cases, 52 accidents involved another vehicle and in the other cases the opponent was an object. Figure 3 shows the mass distribution (left) and mass ratio (right) of the vehicle opponents. The mass ratio was calculated by dividing the crash weight of the case vehicle by the crash weight of the opponent vehicle. Thus a mass ratio smaller than one indicates cases with the opponent being heavier than the case vehicle and vice versa. The mass was categorized in 300 kg steps starting with 800 kg. The mean value of the vehicle opponent mass was at 1,472 kg which is very close to the mass of the crash test trolley used (1,500 kg). With regard to the mass ratio it can be seen (Figure 3, right) that in the groups with a mass ratio around 1 (0.8 to 0.99 and 1.0 to 1.19) the injury risk was similar. However, there was a higher injury probability in vehicles with a mass ratio be-

tween 0.6 and 0.79 (the vehicle opponent was heavier) compared to the group with a mass ratio 1.2 to 1.39. It is believed that the numbers for the groups with a mass ratio beyond are too small.

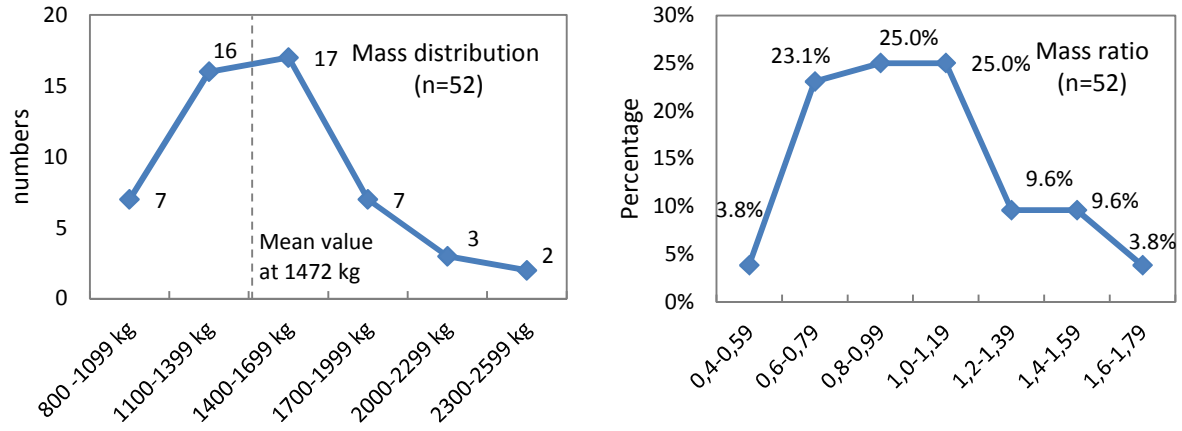


***Figure 3 Distribution (left) and ratio (right) of the mass for the vehicle opponents (n=52); vehicle opponent is heavier (ratio < 1), vehicle opponent is lighter (ratio >1)***

The influence of intrusion to the passenger compartment with regard to the mass ratio was evaluated and is illustrated in Figure 4. Intrusion is defined as stability loss in the a-pillar or the firewall. In general passenger compartment intrusion is observed in a small number of cases of car-to-car accidents only – when intrusion was observed it was mainly in accidents against objects and Heavy Goods Vehicles (HGV). Looking at the car-to-car impacts there were 4 cases in crashes with a mass ratio > 1 (the opponent vehicle was lighter) and 2 cases in crashes with a mass ratio < 1 (the opponent vehicle was heavier).

When looking at the 13 cases with a large weight difference between the accident vehicles (mass ratio between 0.6 and 0.79) in only one accident vehicle intrusion was observed. This indicates that intrusion seems not to be the major injury factor when a heavier vehicle crashes against a lighter vehicle as already postulated by Thompson et al. [2].

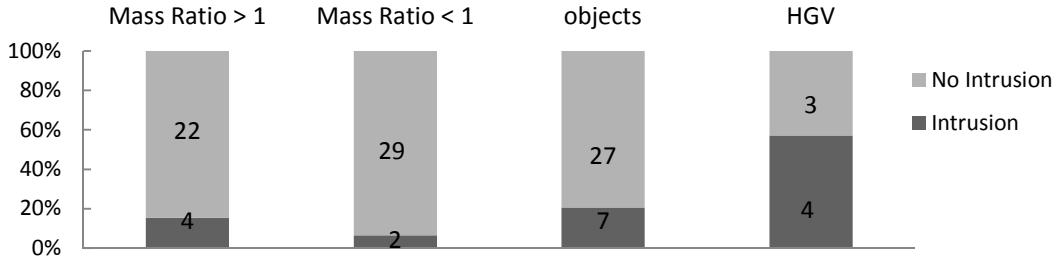


***Figure 4 Influence of Intrusion in regard of the passenger compartment identified for the vehicle to vehicle accidents with a certain mass ratio and the vehicle to object accidents***

Figure 5 illustrates the number of injured front seat occupants categorized in slightly injured, seriously injured and killed according to their own vehicle mass. As only cases with MAIS 2+ injuries were selected there were no uninjured occupants in this data set. On the left side there are crashes against all opponents (vehicles and objects). There were almost more than double of seriously injured occupants in lighter vehicles compared to heavier vehicles. While the left side of Figure 5 shows all accident scenarios the right side considers only car-to-vehicle accidents (including car-to-HGV). The data suggest that the injury risk is increasing when the vehicle is

lighter than the mean mass. However, there is a bias because heavier vehicles are more likely to be newer. Also, heavier vehicles are more likely to be a luxury vehicle having a more advanced restraint system.

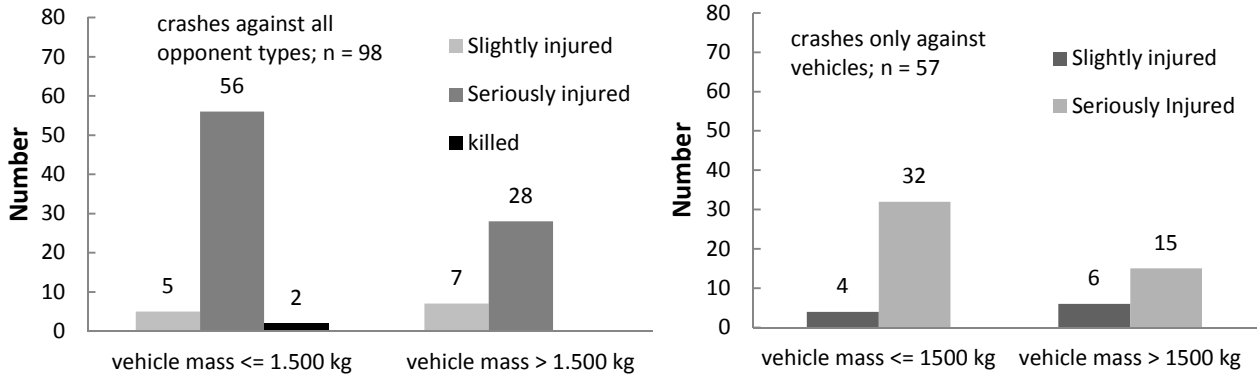


***Figure 5 Number of vehicles with MAIS2+ car occupants in regard to their injury categorization and their own vehicle mass; left: against all opponent types (n=98), right: only vehicle to vehicle crashes (n=57)***

The analyses of real world accident data suggests that occupants in smaller vehicles (less than 1,500 kg) have a higher probability on injuries in frontal impacts compared to occupants in vehicles heavier than the crash trolley. Although the numbers were low in regard to the mass ratio, the numbers were very clear when only the own vehicle mass was considered. The accident data also suggest that the higher injury probability is not due to the passenger compartment stability, but rather due to the occupant loading due to the crash pulse and the restraint system.

## Crash Test Data

To compare the loading on the vehicles in the different test configurations the maximum acceleration measured at the b-pillar driver side, the OLC and the maximal plastic deformation measured in x-direction at the upper a-pillar were evaluated.

Figure 6 shows the acceleration together with the OLC for the different crash tests. There is a strong linear correlation between OLC and maximum cabin b-pillar acceleration ($R^2$=0.93). It is important to note that the OLC was developed and is mainly valid for full frontal tests. However, for the MPDB tests, the maximum acceleration has a relatively higher increase compared to the OLC. The OLC values for the fixed barrier tests (FWRB and ODB) were in a range between 22.3 g and 32.4 g. The values were for lighter vehicles in the mobile barrier tests (MPDB) much higher 34.8 g and 46.6 g.

Eickhoff [21] has evaluated the OLC values for different vehicles using the NHTSA database. There, the majority of values were between 25 g and 38 g, which indicates that the OLC values for the lighter vehicles in the MDPB test are relatively high compared to conventional design levels.

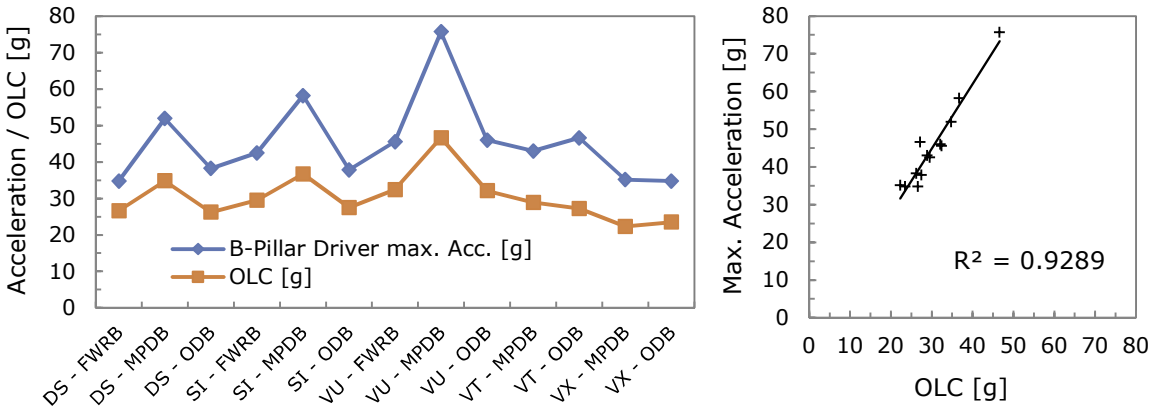


***Figure 6 Vehicle accelerations and occupant loading criterion (OLC)***

The maximum accelerations measured at the b-pillar driver side are shown in Figure 7. It is apparent that the maximum acceleration levels for vehicles lighter than 1,500 kg were much higher in the test against a mobile barrier (MPDB) compared to the test configurations with a fixed object (ODB, FWRB). Acceleration values for the vehicles in the ODB and FWRB test were in general between 30 and 40 g, while the acceleration values for the lighter vehicles in the MPDB test were over 50 g and in one case reaches up to 76 g. However, the acceleration values for the heavier vehicles were similar when comparing MPDB test and ODB tests for the same car. Previous research showed that the acceleration level for fixed PDB tests are considerable higher compared to ODB even for heavy vehicles [5]. The combination of PDB barrier face and mobile barrier with a fixed weight could explain why the acceleration of the heavy cars is similar between ODB and MPDB. This is most likely due to the different barrier stiffnesses (ODB vs PDB) and the fact that the vehicles are not optimized for the MPDB test procedure. The vehicle VX had a test mass of 2,400 kg and had almost no differences in the MPDB accelerations compared with the ODB test. The vehicles front structure is differently loaded by the PDB element comparing to the FWRB or the ODB tests. This counts in particular for vehicles with an inhomogeneous vehicles front (Figure 7, right).
Note: In previous projects it was criticized that the mobile barrier would not generate enough loading for the heavier vehicle which could potentially lead to insufficient compartment strength in single vehicle accidents [5].

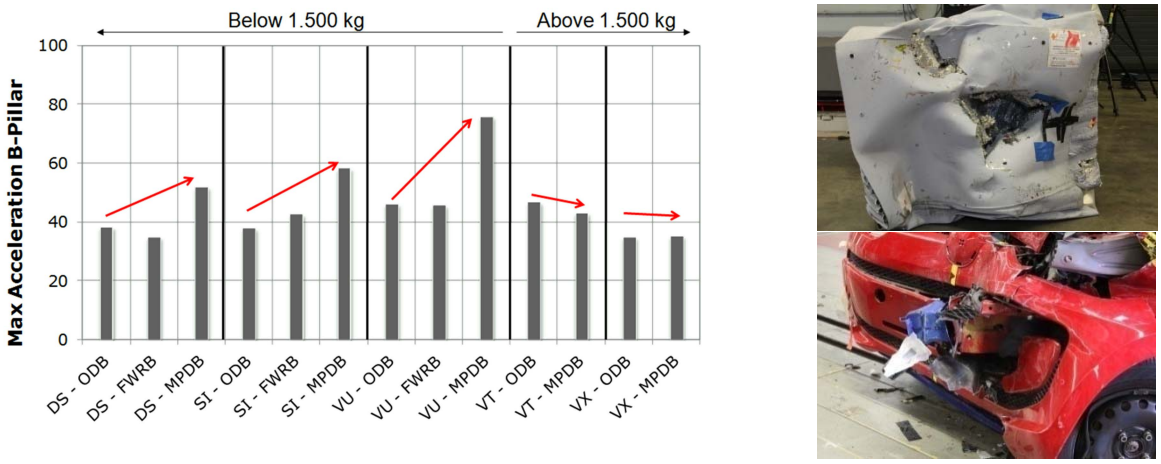


***Figure 7 Maximum vehicle accelerations for the vehicles measured at b-pillar driver side; right: example of the vehicle structure which is not optimized for the PDB barrier***

In Figure 8 the a-pillar displacement on the driver side measured at waist line is shown. Almost no deformation was measured for the vehicles in the FWRB tests. This was expected as the objective of this test is to generate a high acceleration pulse to assess the restraint systems. The vehicle's front structure is symmetrically loaded in the FWRB and the crash structures can deform in a perfect manner. Even for the other configurations the deformation was relatively small. The vehicle DS had the largest deformations between 40 mm (ODB) and 50 mm (MPDB). Generally there is no clear trend which test set-up (MPDB vs. ODB) results in higher compartment intrusions – for some tests larger intrusions were measured for the MPDB and for others in the ODB test. Previous research [5] furthermore indicated that the deformation patterns are different between ODB and PDB (i.e. the PDB appears to load the upper region of the car more than the ODB test). Therefore the intrusion depth might be influenced by the combination of deformation pattern and barrier stiffness.

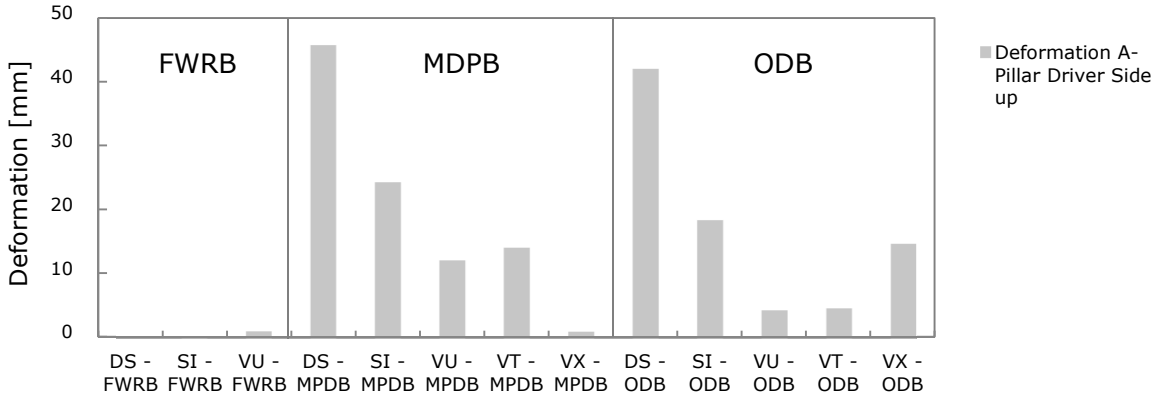


***Figure 8 Deformation of the vehicles measured in millimeter at the a-pillar of the driver side in the height of the waist line.***

The maximum vehicle acceleration was compared to the thorax acceleration [3ms], pelvis peak acceleration and the belt force measured at the outer lap belt (B6). As expected the acceleration measured at the dummy is similar to the vehicle acceleration and therefore a possible indicator for evaluating the loading on the dummy in the crash test. Nevertheless, the force measured on the belt had even a higher correlation ($R^2$=0.84) in regard to the vehicle acceleration.

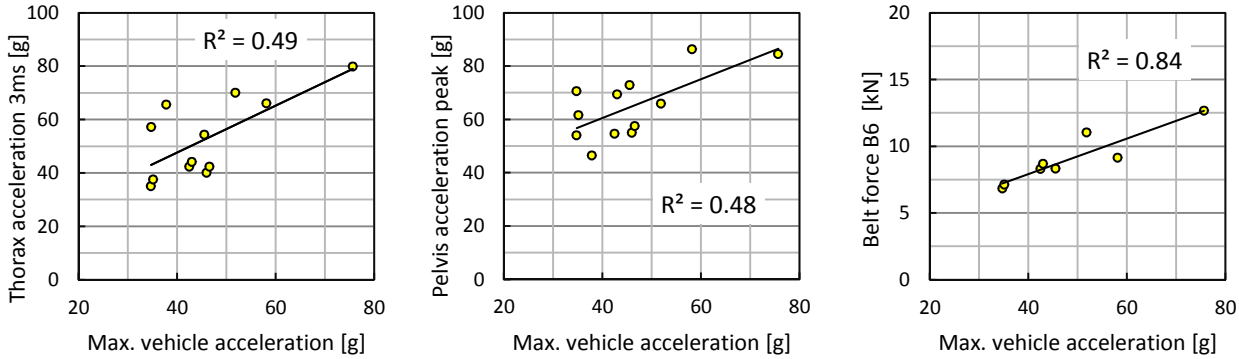


***Figure 9 Vehicle acceleration measured at a-pillar versus thorax acceleration, pelvis acceleration and lap belt force (B6).***

The injury criteria measured at the dummy are shown in Figure 10. In general the head acceleration was higher in the MPDB test procedure compared to the fixed barrier tests for all vehicles. It should be noted that the values in particular for the two lighter vehicles (VU and DS) were much higher, up to $a_{3ms}$ = 136 g. Nevertheless, head bottoming out and chest contact with the steering wheel was not observed. Also the thorax deflection was higher in the MPDB than in the FWRB test (approximately 10 to 20 %), while the thorax deflection in the ODB test was the lowest. The thorax and pelvis acceleration were much higher in the mobile barrier test and, in general, very close to or above the IARV.

For the heavier vehicles (VT and VX) the dummy values were equal or slightly higher in the MPDB test procedure. For the lighter vehicles the relevant IARVs in regard to UN-R 94 ($HIC_{36}$, $a_{3ms}$, thorax deflection) were slightly higher in the FWRB test, but still well below the limits. However, the pelvis and thorax acceleration were much closer or above the limits. The stronger loading on the lighter vehicles in the mobile barrier tests can be clearly seen in all IARVs. It has to be noted, that the restraint systems are optimized for Euro NCAP and are not adopting to the new crash pulse.

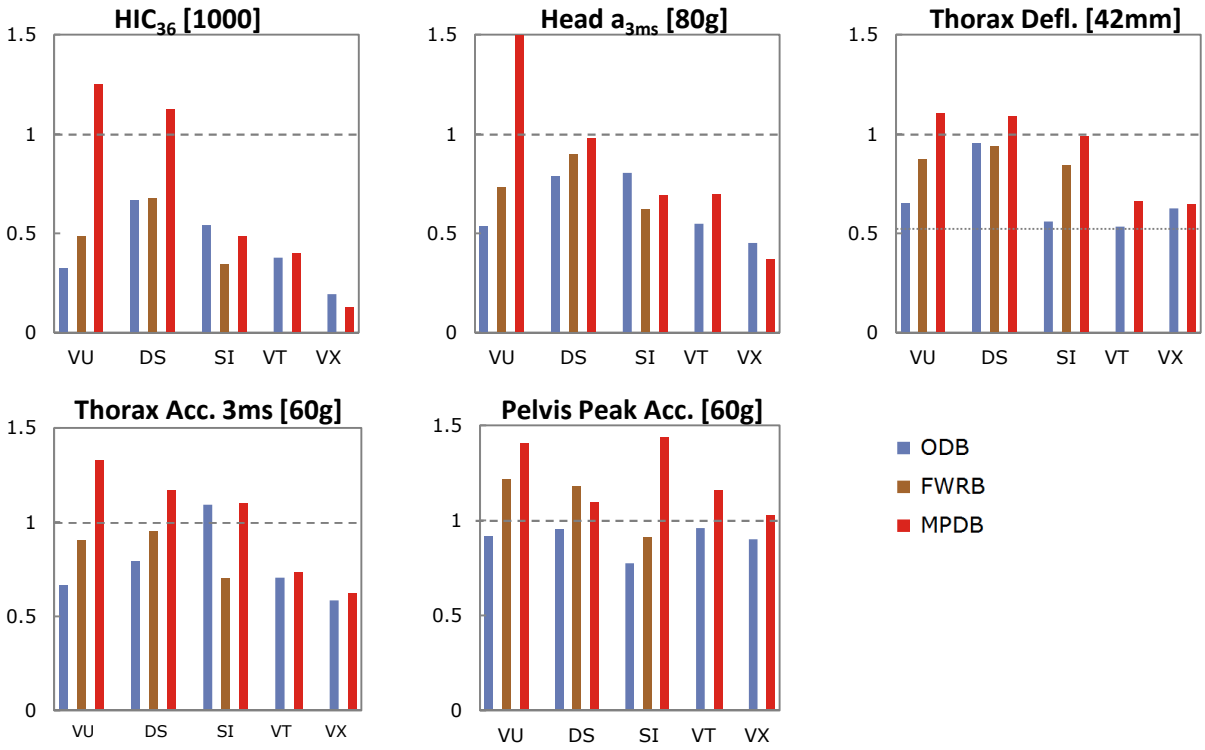


***Figure 10 Ratio of relevant injury assessment reference values for the vehicles in the test configurations ODB; FWRB and MPDB.***

The different loading in terms of vehicle structure, vehicle acceleration and injury assessment values for vehicles with a mass lighter and heavier than the mobile barrier should be investigated with the help of crash test data. It is assumed that lighter vehicles experience a higher loading with a frontal mobile offset barrier compared to a fixed barrier test (FW / ODB) and that heavier vehicles show a lower loading.

The vehicle crash test data with regard to vehicle deformation, vehicle acceleration and injury assessment values were analyzed. It has been shown that the assumption that lighter vehicles are subjected to a higher loading in a frontal mobile offset barrier test, compared to a fixed barrier test (FW / ODB), can be supported not only with regard to vehicle structural performance but also in regard to injury assessment values. On the other hand it has been that the vehicle acceleration and the injury assessment values were not substantially lower for the heavier vehicles. The delta-v is much lower for the heavier vehicles in MPDB tests but the PDB barrier is much stiffer and most of the vehicles are not designed for this test.

## LIMITATIONS

It has to be noted that the number of tested vehicles was limited. Furthermore, only one test per configuration was carried out.
It is important to note that not all vehicles were tested in the same test laboratory which could result in minor differences. However, the test configurations for the ODB test (Euro NCAP protocol) and the MDPB were among themselves the same.
With regard to the analyses of accident data, the data sample was carefully selected to address the appropriate accident configurations. However, this leads to a limited number of accident cases.

## CONCLUSIONS

The accident data show that the injury severity of car occupants is higher for lighter vehicles in car-to-car, car-to-HGV and car-to-object accidents. The influence of intrusion seems not to be the major factor for injuries in particular for car to car accidents. Accidents with large overlap are dominant. For impacts with a small overlap it is important to separate between impacts including one vehicle edge and centered impacts.

With the mobile deformable barrier test the loading conditions were seen more realistic in terms of real world car-to-car accidents. This was in particular true for the lighter vehicles. However, the loading on the light and stiff vehicles produces a very high acceleration pulse in the mobile barrier test procedure. The acceleration pulse was also influenced by the different deformation of the vehicle front structure when crashing against the PDB barrier. With regard to the IARVs, the vehicles had much higher head accelerations and thorax deflections in the mobile barrier test procedure. The data suggests that thorax and pelvis accelerations could be important and relevant indicators if the loading due to the vehicle pulse needs to be evaluated.

It was seen that the crash test with the mobile crash barrier induced a rotation to the vehicle which occurred relatively late in the impact. This motion induces high accelerations at the dummy head in the rebound phase, when the head hits the b-pillar. A dummy movement during the forward motion apart from the driver airbag due to the rotational effects of the MPDB test procedure has not been identified, though.

The benefit of the mobile deformable barrier test is the higher loading for smaller vehicles in particular in regard to the crash pulse. In addition, the PDB offers potential for the compatibility assessment of the vehicles structure. The trend of increased vehicle stiffness (especially illustrated by tests with the MPDB and small cars) shows the need of a further improvement of passive restraint systems to reduce the occupant loading and with it the injury risk.

As the measurement of the thorax loading with the chest deflection of the HIII dummy is not ideal, the evaluation of the loading in the mobile barrier test procedure with a more appropriate dummy is recommended.

## ACKNOWLEDGEMENTS

The authors would like to thank Euro NCAP for making the use of additional crash test data available.

## REFERENCES

[1] Richards, D.; Edwards, M.; Cookson, R. *Technical assistance and economic analysis in the field of legislation pertinent to the issue of automotive safety: provision of information and services on the subject of accident analysis for the development of legislation on frontal impact protection*, **2010**.
[2] Thompson, A.; Edwards, M.; Wisch, M.; Adolph, T.; Krusper, A.; Thomson, R. In: *FIMCAR*: *Frontal Impact and Compatibility Assessment Research*. Johannsen, H., Ed.; Universitätsverlag der TU Berlin: Berlin, **2013**; Vol. *D1.1*.
[3] Saunders, J.; Parent, D. *Assessment of an Oblique Moving Deformable Barrier Test Procedure:* Seoul, **2013**.
[4] Ratzek, A.; Sandner, V.; Kolke, R. Der ADAC-Kompatibilitätscrashtest 2013. *Verkehrsunfall und Fahrzeugtechnik*, **2014**, *1/2013*(5), 170–178.
[5] Johannsen, H., Ed. *FIMCAR: Frontal Impact and Compatibility Assessment Research;* Universitätsverlag der TU Berlin: Berlin, **2013**.
[6] Schram, R.; Versmissen, T. *The Development of a Mobile Deformable Barrier Test Procedure*, **2007**.
[7] Uittenbogaard, J.; Versmissen, T. In: *FIMCAR*: *Frontal Impact and Compatibility Assessment Research*. Johannsen, H., Ed.; Universitätsverlag der TU Berlin: Berlin, **2013**.
[8] Versmissen, T.; Welten, J.; Rodarius, C. In: *FIMCAR*: *Frontal Impact and Compatibility Assessment Research*. Johannsen, H., Ed.; Universitätsverlag der TU Berlin: Berlin, **2013**.
[9] Family Cars trump luxury models in rigorous new crash test. *IIHS Status Report*, **2012**, *47*(10).
[10] Murri, R.; Caviezel, S. Relevanz des IIHS-Small-Overlap-Crashtests in Europa. *Verkehrsunfall und Fahrzeugtechnik*, **2013**(6), 226–236.

[11]Bean, J.; Kahane, C.; Mynatt, M.; Rudd, R.; Rush, C.; Wiacek, C. *Fatalities in Frontal Crashes Despite Seat Belts and Air Bags:* Washington, DC 20590, **2009**.
[12]Adolph, T.; Eggers, A.; Pastor, C.; Damm, R. *New Requirements in Frontal Impact and Future Research for a Phase 2:* München, **April 08, 2014**.
[13]UN/ECE. *Regulation No 94 — Uniform provisions concerning the approval of vehicles with regard to the protection of the occupants in the event of a frontal collision;* Official Journal of the European Union, **January 26, 2012.** http://eur-lex.europa.eu/LexUriServ/LexUriServ.do?uri=OJ:L:2012:254:0077:0135:EN:PDF.
[14]Otte, D.; Krettek, C.; and Zwipp, H. *Scientific Approach and Methodology of a New In-Depth- Investigation Study in Germany so called GIDAS:* Japan, **2003**.
[15]Adolph, T.; Wisch, M.; Edwards, M.; Thomson, R.; Stein, M.; Puppini, R. In: *FIMCAR*: *Frontal Impact and Compatibility Assessment Research*. Johannsen, H., Ed.; Universitätsverlag der TU Berlin: Berlin, **2013**; Vol. *FIMCAR VIII*.
[16]Lazaro, I.; Vie, N.; Thomson, R.; Schwedhelm, H. In: *FIMCAR*: *Frontal Impact and Compatibility Assessment Research*. Johannsen, H., Ed.; Universitätsverlag der TU Berlin: Berlin, **2013**; Vol. *V*.
[17]Kübler, L.; Gargallo, S.; Elsäßer, K. In: *Airbag 2008*; Vol. *2008*.
[18]Adolph, T.; Eggers, A. *Full Width Test – ECE-R 94, Evaluation of test data, Proposal for injury criteria, Way forward:* Bergisch Gladbach, **2013**.
[19]Kramer, F.; Appel, H. In: *IRCOBI Conference 1990*.
[20]Mertz, H.; Irwin, A.; Prasad, P. In: *Stapp Car Crash Journal*; Vol. *47*; pp. 155–188.
[21]Eickhoff, B. Analyse, Mechanismen und Reduktion gurtinduzierter Thoraxbelastungen im Frontalcrash. Dissertatioin, Universitätsbibliothek der Helmut-Schmidt-Universität: Hamburg, **January 29, 2013**.

# EVALUATION OF MOTORCYCLE ANTILOCK BRAKING SYSTEMS

**Nicholas Basch**
**Matthew Moore**
**Laurie Hellinga**
Highway Loss Data Institute
United States

Paper Number 15-0256

## ABSTRACT

**Objective:** Previous studies have found lower crash rates for motorcycles equipped with antilock braking systems (ABS). Although prior studies controlled for a variety of personal factors related to motorcycle crashes, they did not control for the possibility that riders with similar demographics still can differ in the likelihood that they buy optional safety equipment and that this difference might be related to their crash likelihood. Specifically, motorcyclists who purchase ABS might be more likely to behave in a manner that makes them less likely to crash. The purpose of the current analysis was to examine the influence of individual crash risk on the frequency of insurance claims under collision coverage for ABS-equipped motorcycles. Auto collision claim histories were used as a proxy for the crash risk of individual riders, independent of the motorcycles they ride.

**Methods:** Coverage and loss data on nearly 2 million motorcycles by their unique vehicle identification numbers (VIN) were supplied by 13 insurers for model years 2003-14. The VINs were used to determine the ABS status of each motorcycle. Demographic characteristics including gender, marital status, date of birth, zip code, and insurance company were used to match the riders of these motorcycles to their auto insurance histories. Riders without any auto insurance history were excluded. Regression analysis was used to quantify the effect of ABS while controlling for auto claim frequency and other covariates including rider age and gender, garaging state, and collision deductible.

**Results:** Motorcycle riders with higher auto collision claim frequencies were associated with higher motorcycle collision claim frequencies. Riders with high auto claim frequencies (an average of more than two auto claims per 5 years insured) were associated with motorcycle claim frequencies that were 64 percent higher than those for riders with a history of zero auto claims. The percentage of motorcycles with ABS optionally equipped increased with the riders' auto claim frequencies. After controlling for auto claim frequency, motorcycles equipped with optional ABS were associated with a 21 percent reduction in claim frequency compared with similar motorcycles without ABS. Further analysis indicated that the reduction in motorcycle claim frequency associated with motorcycles equipped with ABS did not vary significantly depending on the auto claim frequency of the rider.

**Discussion:** Among motorcyclists with both auto and motorcycle collision insurance coverage, there was a strong relationship between motorcycle and auto claims experience. However, there was no evidence that safer riders, as measured by auto claim frequency, were more likely to purchase motorcycles with optional ABS. Rather, riders with higher auto claim frequencies were more likely to ride motorcycles with ABS. Most important, controlling for a rider's auto claim frequency did not substantively change the observed ABS effect, and the 21 percent estimated reduction in motorcycle collision claim frequency was consistent with prior research.

**Conclusion:** This analysis evaluated the real-world safety benefits of motorcycle ABS while also addressing the potential influence of self-selection by safer riders. Results indicate that all riders may be expected to benefit from ABS technology on their motorcycles. This study also confirms that auto crash risk is a reasonable proxy for a safety profile that may be applied to future research on other optional safety technologies.

## INTRODUCTION

According to the National Highway Traffic Safety Administration (NHTSA), motorcycle registrations more than doubled between 1997 and 2010 (NHTSA, 2012). Analysis by the Insurance Institute for Highway Safety of data from the Fatality Analysis Reporting System shows that, during the same time period, fatalities in motorcycle crashes increased by 110 percent. Motorcyclist deaths began to increase in 1998 and continued to increase and peaked in 2008. Motorcyclist deaths decreased by 16 percent in 2009 compared with 2008 and increased only slightly from 2010 through 2012. Motorcyclist deaths decreased again slightly in 2013. It is not known to what extent the overall decrease from 2008 is related to improvements in highway safety or due to the significant drop in new motorcycle sales from more than 1.1 million in 2008 to only 560,000 in 2010 (Motorcycle Industry Council, 2011). Compared with automobiles, motorcycles offer much less occupant protection in the event of a crash. Only 20 percent of automobile crashes result in injury or death, whereas 80 percent of motorcycle crashes do (NHTSA, 2005). Therefore, any countermeasure aimed at reducing the likelihood of motorcycle crashes should significantly reduce the risk of injury or death.

Improper braking was identified as a significant factor in causes of motorcycle crashes (Association of European Motorcycle Manufacturers, 2004; Hurt et al., 1981). Braking too hard and locking a wheel on a motorcycle can lead to loss of control resulting in a crash. Riders concerned with wheel lock may avoid applying full force to the brakes resulting in insufficient braking power to avoid or mitigate an impact. Antilock braking systems (ABS) were developed to help riders solve this dilemma by automatically adjusting braking pressure to avoid wheel lock. These systems allow a rider to brake with full force without fear of the wheels locking.

Evaluations of ABS have shown strong benefits for motorcyclists. Closed test track studies have shown that ABS improves the braking performance for both novice and experienced riders (Green, 2006; Vavryn and Winkelbauer, 2004). Other studies reconstructed real-world crashes to determine if ABS may have prevented the crash. Gwehenberger et al. (2006) estimated that approximately half of the crashes studied were relevant to ABS and, of those, between 17 and 38 percent could have been avoided if the motorcycle was equipped with ABS. Rizzi et al. (2009) and Roll et al. (2009) estimated that ABS had the potential to prevent 38 to 50 percent of motorcycle crashes. Teoh (2011, 2013) examined the motorcycle fatal crash rate per registrations for motorcycles with ABS compared with the rate for the same models without ABS. The author's most recent study estimated a statistically significant 31 percent reduction in the fatal crash rate for ABS-equipped motorcycles.

NHTSA (2010) conducted a study of motorcycle ABS effectiveness by defining a group of crashes likely to be affected by ABS. A comparison group comprised of crash types deemed not relevant to ABS was used as an alternative measure of exposure. The agency found that ABS had no statistically significant effect on motorcycle crash risk. However, the agency acknowledged the difficulty in identifying types of crashes for which ABS would not be relevant. Behavioral differences between the ABS and non-ABS groups of riders could also result in differing distributions of crash types causing selection bias.

The Highway Loss Data Institute (HLDI, 2009, 2013) examined the effects of ABS on insurance claim frequency. Its most recent results showed that ABS-equipped motorcycles were associated with a statistically significant 20 percent reduction in collision claims per insured vehicle year compared with the same model motorcycles without ABS. Another HLDI (2012) study found that ABS was more effective during the first 3 months of collision insurance policies. A new policy could represent a first time rider, an experienced rider on a new motorcycle, or a rider who changed their insurance company. Motorcycles with ABS were associated with a 30 percent reduction in collision claim frequency versus the non-ABS versions of the same motorcycle during the first 90 days of the policy. For policies in effect 91-720 days, ABS motorcycles were associated with a 19 percent reduction in collision claim frequency compared with the non-ABS versions.

Although the HLDI studies controlled for rated rider characteristics such as age, gender, marital status, and insurance risk group, one criticism is that there may still be a self-selection bias. People who place a greater value on safety may be more likely to purchase an optional safety feature and to ride in a manner that makes them less likely to crash. If primarily safer riders are the ones purchasing ABS-equipped motorcycles, then it is possible that a portion of the ABS benefit observed in prior research was attributable to safer crash risk.

The purpose of this study was to examine the relationship between ABS and insurance losses under collision coverage while controlling for self-selection. This study controls for the safer rider effect by using a motorcycle rider's available auto claim history as a measure of their crash risk. Doing so separates the effect on motorcycle collision claim frequency due to the ABS technology from that attributable to crash risk.

## METHODS

### Insurance Data

Automobile insurance covers damage to vehicles and property as well as injuries to people involved in crashes. Different insurance coverages pay for vehicle damage versus injuries, and different coverages may apply depending on who is at fault. The current study is based on collision coverage. Collision coverage insures against vehicle damage to an at-fault driver's vehicle sustained in a crash with an object or other vehicle; this coverage is common to all 50 states. HLDI has data on the vehicles insured by its member companies including the length of time those vehicles were insured as well as any claims filed for that vehicle under collision coverage. Using this information, HLDI calculates collision claim frequency as the number of collision claims divided by exposure, where exposure is defined as the number of insured vehicle years. One insured vehicle year can represent one motorcycle insured for 1 year, two motorcycles insured for 6 months, etc. HLDI also receives the vehicle identification numbers (VINs) of the vehicles on the insurance policy. The VIN for a motorcycle contains information about the manufacturer, model year, and model type. In some instances, the ABS status of a motorcycle may also be determined from the VIN.

Information about the garaging zip code of the vehicle, deductible amount, and rated rider are also provided. Rated rider characteristics include age, gender, marital status, and insurance risk group. Insurance risk group is a binary variable indicating whether the rated rider is considered to have standard or non-standard insurance risk. The rated rider is the one who typically is considered to represent the greatest loss potential for the insured vehicle. In a household with multiple vehicles and/or riders, the assignment of riders to vehicles can vary by insurance company and by state. The actual rider operating the motorcycle at the time of the claim is unknown.

### Motorcycle and Auto Loss Data

The HLDI database does not include a direct link between a given person's auto and motorcycle insurance policies. Therefore, it was necessary to match motorcycle and auto loss data using rated driver characteristics. The following multi-step process was used:

1. Rated rider/driver demographic data was used to create a mapping of a rated motorcycle rider's policy with their corresponding auto policy. An individual rated rider/driver was identified by their insurance company, gender, marital status, year of birth, date of birth, zip code, and state. Full date of birth data for some companies first became available to HLDI beginning in 2011.

2. In total, 505,864 unique combinations of insurance company, gender, marital status, year of birth, date of birth, zip code, and state existed in both auto and motorcycle databases concurrently. Approximately 13 percent of these combinations were associated with multiple auto or multiple motorcycle policies or both and were therefore excluded from the analysis. The remaining 87 percent had a one-to-one mapping of motorcycle and auto policies.

3. Once the mapping of policies was established, the motorcycle and auto loss data associated with the rated rider/driver were linked. Although a rider/driver's full date of birth was initially used to create the policy mappings, full date of birth data were only available beginning in 2011. Therefore, after motorcycle and auto policies were matched, year of birth was used as a substitute to track a rated rider/driver's motorcycle and auto loss data through years preceding 2011.

This procedure resulted in 949,551 years of motorcycle collision exposure and 16,605 motorcycle claims for model years 2003 to 2014, and calendar years 2006 to 2013. This was matched to 1,204,271 years of auto collision exposure and 62,742 auto claims.

**Analysis Methods**

The observed auto claim frequency for each rider, based on their total available matched auto history, was calculated as the total number of auto claims divided by the total years insured times 100. For example, a rider with one auto claim over 5 years with auto insurance would have an observed auto claim frequency of 1/5 * 100 = 20. The total years insured is the number of years the rider/driver had auto insurance. The observed auto claim frequencies were then categorized, as shown in Table 1.

**Table 1.**
**Categorization of auto claim frequencies.**

| Category | Auto claim frequency | Description |
|---|---|---|
| Zero | 0 | No auto claims |
| Low | 0-20 | An average of between 0 and 1 claims per 5 years insured |
| Medium | 20-40 | An average of between 1 and 2 claims per 5 years insured |
| High | 40+ | An average of more than 2 claims per 5 years insured |

Regression analysis was used to quantify the effect of ABS and/or auto claim frequency on motorcycle collision claim frequency while controlling for other covariates. Covariates included calendar year, vehicle age, garaging state, vehicle density (number of registered vehicles per square mile), rated driver age group, rated driver gender, rated driver marital status, deductible range, and insurance risk group. For analysis including only optional ABS vehicles, make and model was included as a covariate. For analysis including vehicles where ABS is standard or not available, motorcycle class and engine displacement were included as covariates. Claim frequency was modeled using a Poisson distribution using a logarithmic link function.

This study consisted of two main analyses to examine the effect of ABS on motorcycle crashes. The first compared the collision claim frequency of motorcycles with optional ABS to the same year\make\models without. For comparative purposes, the same study vehicles from the HLDI (2013) ABS-only study were chosen for this portion of the analysis. For a motorcycle to be included, its VIN had to have an ABS indicator. Only motorcycles with optional ABS and with loss data for both ABS and non-ABS versions were included. It should be noted that some motorcycles in this study population were also equipped with combined control braking systems (CCBS). However, both the ABS and non-ABS motorcycles had CCBS. Since CCBS was present in both the control and study group for those motorcycles, the estimated effect was for ABS only. Table 2 shows the exposure and percentage of exposure with and without ABS for the 17 models included in this portion of the analysis. In total there were 38,838 years of motorcycle exposure and 622 motorcycle claims, matched with 56,707 years of auto insurance with 2,638 auto claims. The effect of ABS with and without controlling for auto claim frequency was estimated and the results compared.

The second analysis examined a much broader range of motorcycles and included models where ABS was standard or not available, as well as motorcycles where ABS was optional and the presence of ABS was indicated by the VIN. The motorcycles were divided into two groups: with ABS and without ABS. Motorcycles where the ABS status

**Table 2.**
**Distribution of exposure of antilock braking systems for April 2013 study vehicles.**

| Make/Series | Exposure | Percent ABS | Percent no ABS |
|---|---|---|---|
| Aprilia Scarabeo 500 | 174 | 32% | 68% |
| Honda Gold Wing | 25,581 | 23% | 77% |
| Honda Interceptor 800 | 1,005 | 29% | 71% |
| Honda Reflex | 856 | 16% | 84% |
| Honda Silver Wing | 1,221 | 20% | 80% |
| Honda ST1300 | 2,448 | 31% | 69% |
| Kawasaki Ninja 650 | 90 | 36% | 64% |
| Kawasaki Ninja ZX-10R | 119 | 40% | 60% |
| Suzuki Bandit 1250 | 503 | 27% | 73% |
| Suzuki Burgman 400 | 181 | 42% | 58% |
| Suzuki Burgman 650 | 1,447 | 20% | 80% |
| Suzuki V-Strom 650 | 1,672 | 30% | 70% |
| Triumph Sprint ST | 587 | 41% | 59% |
| Triumph Thunderbird | 477 | 58% | 42% |
| Triumph Tiger | 672 | 34% | 66% |
| Triumph Tiger 800 | 310 | 89% | 11% |
| Yamaha FJR1300 | 1,496 | 48% | 52% |
| Total | 38,838 | 26% | 74% |

was unknown were excluded. Unlike the first analysis, the motorcycle models in the with-ABS and without-ABS groups were not the same. Therefore, in order to control for differences between models, motorcycle class and engine displacement were included as covariates. In addition, while only motorcycles with known ABS status are included in this analysis, the CCBS status is not always known. In the HLDI (2013) study of ABS with CCBS, an extensive review of publically available documentation was conducted on all motorcycles included in the analysis. However, information about the presence of CCBS for some motorcycles is not always available from public sources. This analysis includes more than 630 different motorcycle series over 12 model years. As a result, the effect of ABS in this study may be confounded with CCBS since some of the study motorcycles have ABS only while others may have both ABS and CCBS. Therefore the effect being measured may be attributable to "ABS and ABS/CCBS" as opposed to solely ABS. In addition, some of the motorcycles without ABS may have CCBS. However, this analysis assumes that CCBS in non-ABS motorcycles is a small part of the overall exposure.

Therefore, the second analysis is a less focused examination of the ABS effects but has the advantage of involving much more exposure. The addition of motorcycles with standard and not available ABS resulted in 842,487 years of motorcycle exposure and 14,311 motorcycle claims matched with 1,093,225 years of auto exposure and 57,193 auto claims. This was an increase of more than 21 times the motorcycle exposure of the optional ABS analysis. The effect of ABS and ABS/CCBS is estimated with and without controlling for auto claim frequency and the results compared. Finally, the interaction effect of ABS and ABS/CCBS with auto claim frequency category is also estimated.

**RESULTS**

Full regression results for the second analysis are shown in the Appendix. To further simplify the presentation here, the exponent of the parameter estimate was calculated, 1 was subtracted, and the result multiplied by 100. The resulting number corresponds to the effect of the feature on that loss measure. For example, the estimate of the effect for ABS and ABS/CCBS on motorcycle collision claim frequency was (-0.3268); thus, collision claim frequency for motorcycles with ABS and ABS/CCBS is expected to be 28 percent lower than for motorcycles without ABS ((exp(-0.3268) -1)*100 = -28).

Figure 1 shows the relationship between auto claim frequency category and motorcycle claim frequency. Riders with higher auto claim frequencies were associated with higher motorcycle claim frequency. The black bars correspond to the 95 percent confidence intervals. Riders in the high auto claim frequency category were associated with a statistically significant 64 percent increase in motorcycle collision claim frequency compared with riders with no history of auto claims. Riders in the medium auto claim frequency category were associated with a statistically significant 18 percent increase, while those categorized as having low auto claim frequency were associated with a 4 percent increase.

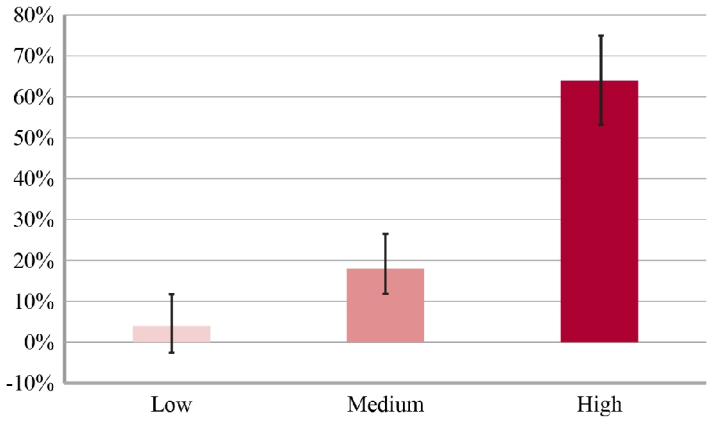


***Figure 1. Motorcycle collision claim frequency by auto claim frequency category relative to rider/drivers with no auto claims.***

Figures 2 and 3 show the results of the first analysis examining collision claim frequencies for motorcycles equipped with optional ABS relative to the same models without ABS. Figure 2 compares the estimated ABS effect in the present dataset, without controlling for auto claim frequency, with results from the full dataset used in the 2013 HLDI study. The ABS effect is essentially the same in both datasets — a 20 percent reduction in collision claim frequency compared with motorcycles not equipped with ABS.

Given that the ABS effect is present in the matched data set, the effect of additionally controlling for auto claim frequency was then analyzed. Table 3 shows the breakdown of motorcycle exposure with and without ABS by auto claim frequency category. Although the amount of the exposure is small, the percentage of exposure with ABS increases with auto claim frequency; 26 percent of the motorcycle exposure with zero auto claim frequency was for motorcycles with ABS compared with 32 percent of the exposure with high auto claim frequency.

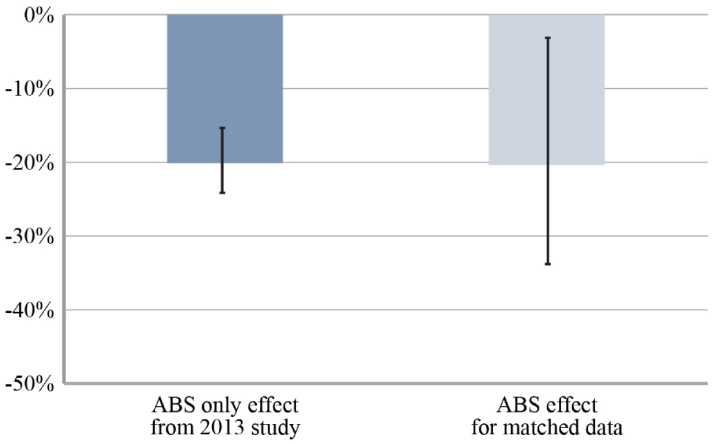


***Figure 2. Effect of optional ABS on motorcycle collision claim frequency without regard to auto claim frequency, HLDI (2013) study vehicles***

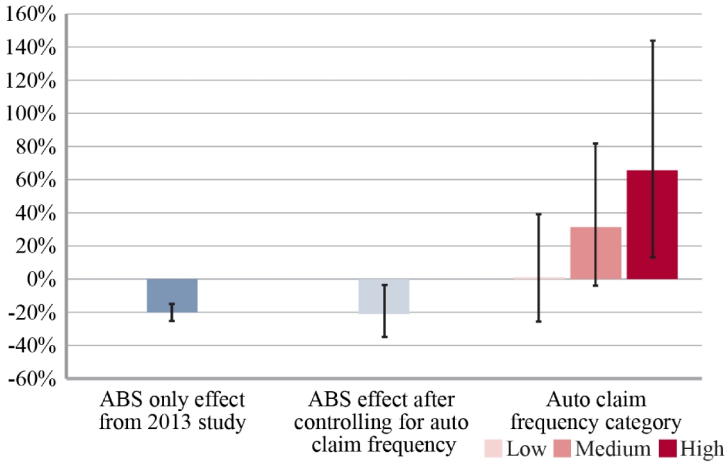


***Figure 3. Effect of optional ABS and auto collision claim frequency on motorcycle collision claim frequency, HLDI (2013) study vehicles***

**Table 3.**
**Distribution of exposure by auto claim frequency category for April 2013 study vehicles.**

| Auto claim frequency category | Exposure | Percent ABS | Percent no ABS |
|---|---|---|---|
| Zero | 33,279 | 26% | 74% |
| Low | 2,590 | 28% | 72% |
| Medium | 1,949 | 29% | 71% |
| High | 1,021 | 32% | 68% |

Figure 3 shows the results when both ABS status and the auto claim frequency categories are added as variables in the regression model. After controlling for auto claim frequency, the reduction in motorcycle collision claim frequency for ABS-equipped motorcycles increases slightly from 20 to 21 percent. Also shown in Figure 3 is the relationship between auto claim frequency category and motorcycle claim frequency using this subset of data. The results are consistent with Figure 1, although the confidence bounds are larger due to the reduced size of the dataset.

Figures 4 and 5 show the results of the second analysis that examines the effect of ABS and ABS/CCBS on motorcycles where ABS is standard or equipped with optional ABS versus motorcycles without ABS. Figure 4 compares the estimated ABS and ABS/CCBS effect in the present dataset, without controlling for auto claim frequency, with results from the 2013 HLDI study. The observed effect of 28 percent for ABS and ABS/CCBS falls between the 2013 study results of 20 percent for ABS only and 31 percent for ABS/CCBS.

Figure 5 shows that after controlling for auto claim frequency, the effect of ABS and ABS/CCBS was also a statistically significant 28 percent. The relationship between auto claim frequency category and motorcycle claim frequency using this subset of data is also shown. Again, the results for auto claim frequency are consistent with Figure 1. Full regression results for this model are shown in the Appendix.

Figure 6 shows the effect of ABS and ABS/CCBS by auto claim frequency category. The effect by auto claim frequency category is fairly consistent. Motorcycles with ABS and ABS/CCBS are associated with a 29 percent reduction in motorcycle claim frequency compared with motorcycles without ABS for riders with no history of auto claims. ABS and ABS/CCBS for riders categorized with a low auto claim frequency was associated with a 24 percent reduction. ABS and ABS/CCBS for riders categorized with medium or high auto claim frequencies was associated with 26 and 25 percent reductions, respectively. The differences between the effects of ABS and ABS/CCBS by rider auto claim frequency was not statistically significant.

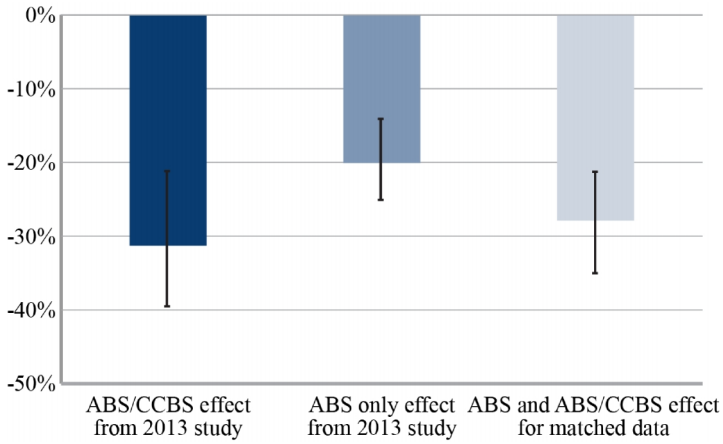


***Figure 4. Effect of ABS and ABS/CCBS on motorcycle collision claim frequency, no auto claim frequency***

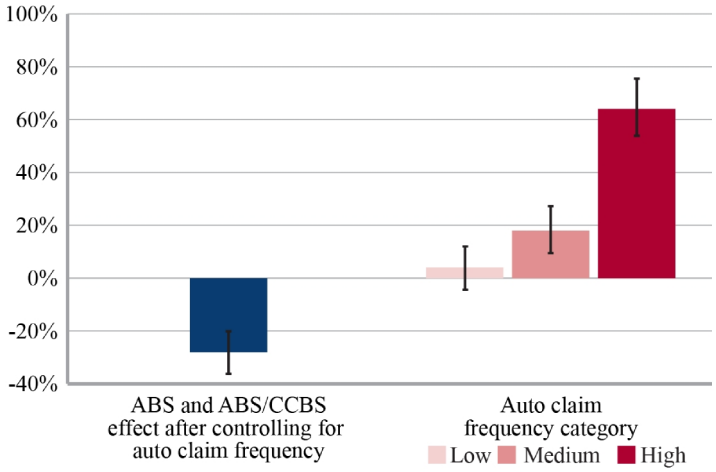


***Figure 5. Effect of ABS and ABS/CCBS and auto collision claim frequency on motorcycle collision claim frequency***

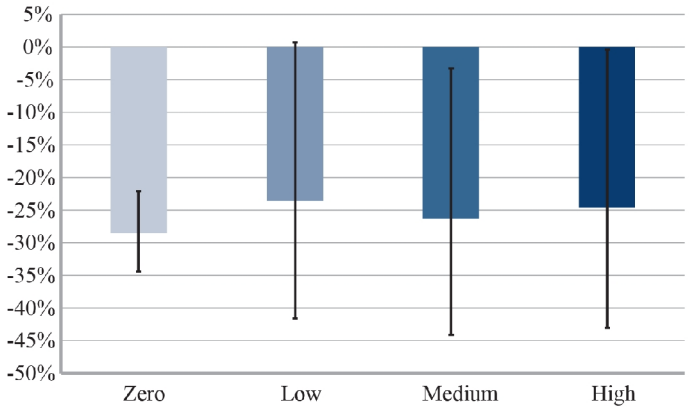


***Figure 6. Effect of ABS and ABS/CCBS by auto claim frequency category***

## DISCUSSION

Prior HLDI studies have shown that ABS on motorcycles is effective in reducing collision losses by 20 percent, and others have shown motorcycle ABS reduces fatal crashes by 31 percent (HLDI, 2013; Teoh, 2013). These studies were criticized because they did not control for the possibility that the crash reductions attributed to ABS were not instead the result of safer riders choosing ABS. The present study addresses this concern by using a rider's auto claim frequency as an independent measure of their crash risk. Regression analysis showed that riders with higher auto claim frequencies were associated with higher motorcycle collision claim frequencies and, after taking this into account, the ABS benefit persists.

European regulators have acted on the strong evidence of the benefits of ABS for motorcycles, Beginning in 2016 in the European Union, ABS will be mandatory for motorcycles that have an engine displacement greater than 125 cc. In contrast, motorcycle ABS is not required in the United States. Despite the lack of a requirement, manufacturers have taken the initiative to increase the availability of ABS on new motorcycles in the United States during the past few years.

Figure 7 shows the increase in ABS availability by model year as indicated in motorcycle VINs process by HLDI, which represents a large sample of the registered fleet. More than 90 percent of 2002 model year bikes were not available with ABS. In contrast, more than two-thirds of new bikes in the 2013 model year have either standard (22 percent) or optional (46 percent) ABS. Moreover, manufacturers such as BMW, KTM, and Ducati have begun fitting stability controls systems that promise to prevent even more loss of control crashes among motorcycles (Bosch, 2014)

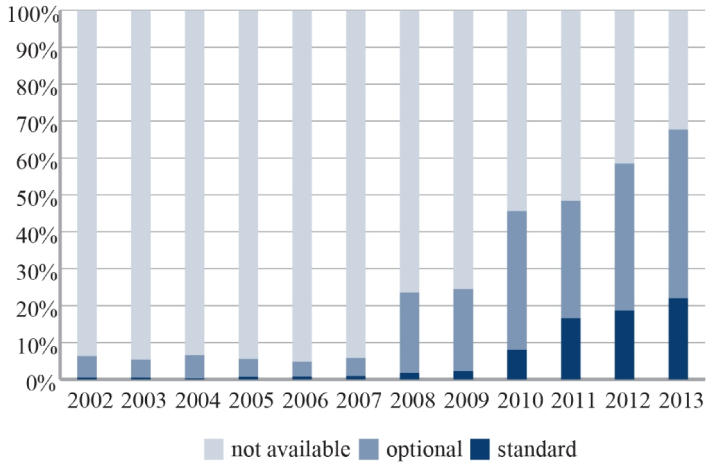


***Figure 7. Motorcycle ABS availability by model year***

### Limitations

There are limitations on the data used in this analysis. Using auto claim frequency as a covariate in the regression required matching data from two separate databases using demographic data. Although there is no way to be absolutely certain that a matched rider/driver is the same person, using the full date of birth, zip code, gender, and marital status limit the likelihood of erroneous matches. It is also possible that a particular person would have their auto and motorcycle policies with different companies. These individuals would be excluded from the analysis. In addition, motorcycle riders who do not have an auto policy would also be excluded from this analysis. It is unknown whether there are significant differences between riders who also have an auto policy and those with just a motorcycle policy.

**REFERENCES**


Association of European Motorcycle Manufacturers. 2004. MAIDS In-depth investigations of accidents involving powered two wheelers. Final report 1.2. Brussels, Belgium.

Bosch. 2014. MSC motorcycle stability control for all classes of bike. Mobility Solutions, Press Release. EICMA International Motorcycle Show 2014. Stuttgart, Germany. Retrieved from http://www.bosch-presse.de/presseforum/details.htm?txtID=7020&tk_id=108

Green D. 2006. A comparison of stopping distance performance for motorcycles equipped with ABS, CBS, and conventional hydraulic brake systems. Paper presented at the 2006 International Motorcycle Safety Conference, March 28-38, Long Beach, CA.

Gwehenberger J, Schwaben I, Sporner A, Kubitzki J. 2006. Schwerstunfälle mit Motorrädern – Analyse der Unfallstruktur und der Wirksamkeit von ABS. VKU Verkehrsunfall und Fahrzeugtechnik, Issue 1. Springer Automotive Media/GWV Fachverlage GmbH.

Highway Loss Data Institute. 2009. Motorcycle antilock braking system (ABS). Insurance special report A-81. Arlington, VA.

Highway Loss Data Institute. 2012. Motorcycle ABS and time to claim. *HLDI Bulletin* 29(4). Arlington, VA.

Highway Loss Data Institute. 2013. Evaluation of motorcycle antilock braking systems, alone and in conjunction with combined control braking systems. *HLDI Bulletin* 30(10). Arlington, VA.

Hurt HH, Ouellet JV, Thom DR. 1981. Motorcycle accident cause factors and identification of countermeasures; Volume 1: Technical report, Final report. Washington, DC: U.S. Department of Transportation.

Motorcycle Industry Council. 2011. Statistical annual. Irvine, CA.

National Highway Traffic Safety Administration. 2005. Without motorcycle helmets we all pay the price. Washington, DC: U.S. Department of Transportation.

National Highway Traffic Safety Administration. 2010. Motorcycle antilock braking systems and crash risk estimated from case-control comparisons. Submitted to Docket No. NHTSA-2002-11950. Washington, DC: U.S. Department of Transportation.

National Highway Traffic Safety Administration. 2012. Traffic safety facts, 2010. Report no. DOT HS-811-659. Washington, DC: U.S. Department of Transportation.

Rizzi M, Strandroth J, Tingball C. 2009. The effectiveness of antilock brake systems on motorcycles in reducing real-life crashes and injuries. *Traffic Injury Prevention* 10:479-87

Roll G, Hoffman O, König J. 2009. Effectiveness of antilock brake systems (ABS) for motorcycles in real-world accident scenarios. *Proceedings of the 21st International Technical Conference on the Enhanced Safety of Vehicles* (CD-ROM). Washington, DC: National Highway Traffic Safety Administration.

Teoh ER. 2011. Effectiveness of antilock braking systems in reducing motorcycle fatal crash rates. *Traffic Injury Prevention*. 12:169-73

Teoh ER. 2013. Effects of antilock braking systems on motorcycle fatal crash rates: an update. Insurance Institute for Highway Safety, Arlington, VA.

Vavryn K, Winkelbauer M. 2006. Braking performance of experienced and novice motorcycle rides: results of a field study. Paper presented at the 2004 International Conference on Transport and Traffic Psychology, Nottingham, United Kingdom.

**APPENDIX**

**Table A1**
**Illustrative regression results: Collision claim frequency for motorcycles with and without ABS or ABS/CCBS.**

| Parameter | Degrees of freedom | Estimate | Effect | Standard error | Wald 95% confidence limits | | Chi-square | p-value |
|---|---|---|---|---|---|---|---|---|
| Intercept | 1 | -9.2916 | | 0.4588 | -10.1908 | -8.3925 | 410.22 | <0.0001 |
| Calendar Year | | | | | | | | |
| 2006 | 1 | -0.3742 | -31.2% | 0.0961 | -0.5626 | -0.1857 | 15.15 | <0.0001 |
| 2007 | 1 | -0.4147 | -33.9% | 0.0571 | -0.5266 | -0.3029 | 52.83 | <0.0001 |
| 2008 | 1 | -0.4572 | -36.7% | 0.0428 | -0.5412 | -0.3732 | 113.87 | <0.0001 |
| 2009 | 1 | -0.5816 | -44.1% | 0.0389 | -0.6578 | -0.5053 | 223.49 | <0.0001 |
| 2010 | 1 | -0.5634 | -43.1% | 0.0332 | -0.6285 | -0.4982 | 287.54 | <0.0001 |
| 2011 | 1 | -0.3190 | -27.3% | 0.0249 | -0.3679 | -0.2701 | 163.45 | <0.0001 |
| 2012 | 1 | -0.2549 | -22.5% | 0.0230 | -0.3001 | -0.2098 | 122.37 | <0.0001 |
| 2013 | 0 | 0 | 0 | 0 | 0 | 0 | | |
| Vehicle age | 1 | -0.1087 | -10.3% | 0.0038 | -0.1161 | -0.1013 | 825.01 | <0.0001 |
| Rated driver age | | | | | | | | |
| 14-24 | 1 | 0.9486 | 158.2% | 0.0545 | 0.8417 | 1.0554 | 302.84 | <0.0001 |
| 25-39 | 1 | 0.3173 | 37.3% | 0.0383 | 0.2422 | 0.3923 | 68.65 | <0.0001 |
| 40-64 | 1 | 0.0105 | 1.1% | 0.0347 | -0.0575 | 0.0784 | 0.09 | 0.7629 |
| 65+ | 0 | 0 | 0 | 0 | 0 | 0 | | |
| Gender | | | | | | | | |
| Female | 1 | -0.1211 | -11.4% | 0.0266 | -0.1732 | -0.0691 | 20.79 | <0.0001 |
| Male | 0 | 0 | 0 | 0 | 0 | 0 | | |
| Marital status | | | | | | | | |
| Married | 1 | -0.1211 | -11.4% | 0.0978 | -0.3128 | 0.0706 | 1.53 | 0.2158 |
| Single | 1 | 0.0231 | 2.3% | 0.0988 | -0.1706 | 0.2168 | 0.05 | 0.8152 |
| Unknown | 0 | 0 | 0 | 0 | 0 | 0 | | |
| State | | | | | | | | |
| Alabama | 1 | 0.3570 | 42.9% | 0.1816 | 0.0011 | 0.7130 | 3.86 | 0.0493 |
| Arizona | 1 | 0.4653 | 59.2% | 0.1771 | 0.1182 | 0.8125 | 6.90 | 0.0086 |
| Arkansas | 1 | 0.2089 | 23.2% | 0.1995 | -0.1820 | 0.5999 | 1.10 | 0.2949 |
| California | 1 | 0.4862 | 62.6% | 0.1724 | 0.1484 | 0.8240 | 7.96 | 0.0048 |
| Colorado | 1 | 0.2029 | 22.5% | 0.1782 | -0.1463 | 0.5521 | 1.30 | 0.2548 |
| Connecticut | 1 | 0.2198 | 24.6% | 0.1846 | -0.1420 | 0.5817 | 1.42 | 0.2337 |
| Delaware | 1 | 0.8593 | 136.2% | 0.3354 | 0.2018 | 1.5167 | 6.56 | 0.0104 |
| District of Columbia | 1 | 0.6508 | 91.7% | 0.2285 | 0.2031 | 1.0986 | 8.12 | 0.0044 |
| Florida | 1 | 0.1984 | 21.9% | 0.1726 | -0.1398 | 0.5366 | 1.32 | 0.2502 |
| Georgia | 1 | 0.3296 | 39.0% | 0.1762 | -0.0157 | 0.6748 | 3.50 | 0.0614 |
| Hawaii | 1 | 0.2810 | 32.4% | 0.2000 | -0.1111 | 0.6730 | 1.97 | 0.1601 |
| Idaho | 1 | 0.1199 | 12.7% | 0.2018 | -0.2757 | 0.5155 | 0.35 | 0.5525 |
| Illinois | 1 | 0.0813 | 8.5% | 0.1768 | -0.2653 | 0.4279 | 0.21 | 0.6457 |
| Indiana | 1 | 0.2783 | 32.1% | 0.1842 | -0.0829 | 0.6394 | 2.28 | 0.1310 |
| Iowa | 1 | -0.0066 | -0.7% | 0.1868 | -0.3727 | 0.3594 | 0.00 | 0.9717 |
| Kansas | 1 | 0.1217 | 12.9% | 0.1895 | -0.2498 | 0.4931 | 0.41 | 0.5209 |
| Kentucky | 1 | 0.3797 | 46.2% | 0.1978 | -0.0080 | 0.7674 | 3.68 | 0.0549 |
| Louisiana | 1 | 0.4134 | 51.2% | 0.1817 | 0.0573 | 0.7695 | 5.18 | 0.0229 |
| Maine | 1 | 0.3473 | 41.5% | 0.2226 | -0.0890 | 0.7836 | 2.43 | 0.1187 |

| Parameter | Degrees of freedom | Estimate | Effect | Standard error | Wald 95% confidence limits | | Chi-square | p-value |
|---|---|---|---|---|---|---|---|---|
| Maryland | 1 | 0.3205 | 37.8% | 0.1769 | -0.0262 | 0.6673 | 3.28 | 0.0700 |
| Michigan | 1 | 0.3058 | 35.8% | 0.1845 | -0.0558 | 0.6674 | 2.75 | 0.0974 |
| Minnesota | 1 | 0.0431 | 4.4% | 0.1875 | -0.3243 | 0.4105 | 0.05 | 0.8181 |
| Mississippi | 1 | 0.2709 | 31.1% | 0.2041 | -0.1292 | 0.6710 | 1.76 | 0.1845 |
| Missouri | 1 | 0.2400 | 27.1% | 0.1890 | -0.1304 | 0.6105 | 1.61 | 0.2040 |
| Montana | 1 | -0.1582 | -14.6% | 0.3089 | -0.7637 | 0.4472 | 0.26 | 0.6085 |
| Nebraska | 1 | 0.0666 | 6.9% | 0.1946 | -0.3147 | 0.4479 | 0.12 | 0.7322 |
| Nevada | 1 | 0.6364 | 89.0% | 0.1901 | 0.2639 | 1.0090 | 11.21 | 0.0008 |
| New Hampshire | 1 | 0.2025 | 22.4% | 0.2255 | -0.2395 | 0.6446 | 0.81 | 0.3691 |
| New Jersey | 1 | 0.1643 | 17.9% | 0.1879 | -0.2039 | 0.5325 | 0.76 | 0.3818 |
| New Mexico | 1 | 0.2884 | 33.4% | 0.1846 | -0.0735 | 0.6502 | 2.44 | 0.1183 |
| New York | 1 | 0.3641 | 43.9% | 0.1733 | 0.0243 | 0.7038 | 4.41 | 0.0357 |
| North Carolina | 1 | 0.2203 | 24.6% | 0.1785 | -0.1295 | 0.5701 | 1.52 | 0.2171 |
| North Dakota | 1 | 0.1481 | 16.0% | 0.3090 | -0.4575 | 0.7536 | 0.23 | 0.6318 |
| Ohio | 1 | 0.0211 | 2.1% | 0.1763 | -0.3245 | 0.3667 | 0.01 | 0.9046 |
| Oklahoma | 1 | 0.2389 | 27.0% | 0.1851 | -0.1238 | 0.6016 | 1.67 | 0.1968 |
| Oregon | 1 | 0.3714 | 45.0% | 0.1877 | 0.0035 | 0.7394 | 3.92 | 0.0478 |
| Pennsylvania | 1 | 0.2132 | 23.8% | 0.1760 | -0.1318 | 0.5582 | 1.47 | 0.2258 |
| Rhode Island | 1 | 0.1529 | 16.5% | 0.2267 | -0.2914 | 0.5973 | 0.46 | 0.4999 |
| South Carolina | 1 | 0.2064 | 22.9% | 0.1838 | -0.1538 | 0.5667 | 1.26 | 0.2614 |
| South Dakota | 1 | 0.0033 | 0.3% | 0.2620 | -0.5102 | 0.5169 | 0.00 | 0.9898 |
| Tennessee | 1 | 0.3529 | 42.3% | 0.1738 | 0.0122 | 0.6935 | 4.12 | 0.0423 |
| Texas | 1 | 0.3324 | 39.4% | 0.1729 | -0.0064 | 0.6713 | 3.70 | 0.0545 |
| Utah | 1 | -0.0321 | -3.2% | 0.1852 | -0.3951 | 0.3309 | 0.03 | 0.8623 |
| Vermont | 1 | -0.0052 | -0.5% | 0.2690 | -0.5324 | 0.5220 | 0.00 | 0.9845 |
| Virginia | 1 | 0.2582 | 29.5% | 0.1750 | -0.0847 | 0.6012 | 2.18 | 0.1400 |
| Washington | 1 | 0.3058 | 35.8% | 0.1786 | -0.0443 | 0.6558 | 2.93 | 0.0869 |
| West Virginia | 1 | -0.0597 | -5.8% | 0.2119 | -0.4749 | 0.3556 | 0.08 | 0.7781 |
| Wisconsin | 1 | 0.0623 | 6.4% | 0.1917 | -0.3135 | 0.4380 | 0.11 | 0.7453 |
| Wyoming | 1 | 0.2364 | 26.7% | 0.2433 | -0.2404 | 0.7132 | 0.94 | 0.3313 |
| Alaska | 0 | 0 | 0 | 0 | 0 | 0 | | |
| Density | | | | | | | | |
| <50 | 1 | -0.4348 | -35.3% | 0.0380 | -0.5092 | -0.3603 | 130.95 | <0.0001 |
| 50-99 | 1 | -0.3254 | -27.8% | 0.0322 | -0.3884 | -0.2624 | 102.39 | <0.0001 |
| 100-249 | 1 | -0.2349 | -20.9% | 0.0277 | -0.2892 | -0.1806 | 71.87 | <0.0001 |
| 250-499 | 1 | -0.2269 | -20.3% | 0.0274 | -0.2806 | -0.1732 | 68.59 | <0.0001 |
| 599-999 | 1 | -0.1463 | -13.6% | 0.0277 | -0.2006 | -0.0920 | 27.86 | <0.0001 |
| >999 | 0 | 0 | 0 | 0 | 0 | 0 | | |
| Risk | | | | | | | | |
| Nonstandard | 1 | 0.0509 | 5.2% | 0.0202 | 0.0112 | 0.0905 | 6.32 | 0.0119 |
| Standard | 0 | 0 | 0 | 0 | 0 | 0 | | |
| Deductible range | | | | | | | | |
| 0 | 1 | -0.2403 | -21.4% | 0.4516 | -1.1254 | 0.6447 | 0.28 | 0.5946 |
| 1-50 | 1 | 0.6109 | 84.2% | 0.4142 | -0.2009 | 1.4228 | 2.18 | 0.1402 |
| 51-100 | 1 | -0.2555 | -22.5% | 0.4096 | -1.0583 | 0.5472 | 0.39 | 0.5327 |
| 101-200 | 1 | -0.1534 | -14.2% | 0.4106 | -0.9581 | 0.6513 | 0.14 | 0.7087 |
| 201-250 | 1 | -0.0151 | -1.5% | 0.4090 | -0.8167 | 0.7865 | 0.00 | 0.9706 |

| Parameter | Degrees of freedom | Estimate | Effect | Standard error | Wald 95% confidence limits | | Chi-square | p-value |
|---|---|---|---|---|---|---|---|---|
| 251-500 | 1 | -0.1875 | -17.1% | 0.4087 | -0.9884 | 0.6135 | 0.21 | 0.6464 |
| 501-1000 | 1 | -0.5987 | -45.0% | 0.4102 | -1.4028 | 0.2053 | 2.13 | 0.1444 |
| >1000 | 0 | 0 | 0 | 0 | 0 | 0 | | |
| Motorcycle class | | | | | | | | |
| Chopper | 1 | -0.8309 | -56.4% | 0.1007 | -1.0283 | -0.6335 | 68.07 | <0.0001 |
| Cruiser | 1 | -0.5776 | -43.9% | 0.0505 | -0.6765 | -0.4786 | 130.85 | <0.0001 |
| Dual purpose | 1 | -1.0269 | -64.2% | 0.0777 | -1.1792 | -0.8747 | 174.73 | <0.0001 |
| Scooter | 1 | -0.2698 | -23.6% | 0.0674 | -0.4018 | -0.1377 | 16.03 | <0.0001 |
| Sport | 1 | 0.2885 | 33.4% | 0.0584 | 0.1740 | 0.4030 | 24.39 | <0.0001 |
| Sport touring | 1 | -0.1931 | -17.6% | 0.0759 | -0.3419 | -0.0442 | 6.46 | 0.0110 |
| Standard | 1 | -0.2881 | -25.0% | 0.0841 | -0.4529 | -0.1233 | 11.74 | 0.0006 |
| Super sport | 1 | 0.5819 | 78.9% | 0.0535 | 0.4771 | 0.6868 | 118.31 | <0.0001 |
| Touring | 1 | -0.4736 | -37.7% | 0.0553 | -0.5820 | -0.3651 | 73.27 | <0.0001 |
| Unclad sport | 0 | 0 | 0 | 0 | 0 | 0 | | |
| Engine displacement | 1 | 0.0004 | 0.0% | 0.0000 | 0.0004 | 0.0005 | 235.58 | <0.0001 |
| Auto claim frequency category | | | | | | | | |
| Low | 1 | 0.0358 | 3.6% | 0.0377 | -0.0381 | 0.1098 | 0.90 | 0.3422 |
| Medium | 1 | 0.1661 | 18.1% | 0.0349 | 0.0976 | 0.2345 | 22.63 | <0.0001 |
| High | 1 | 0.4975 | 64.5% | 0.0358 | 0.4272 | 0.5677 | 192.65 | <0.0001 |
| Zero | 0 | 0 | 0 | 0 | 0 | 0 | | |
| ABS and ABS/CCBS | | | | | | | | |
| Equipped | 1 | -0.3268 | -27.9% | 0.0421 | -0.4092 | -0.2444 | 60.38 | <0.0001 |
| Not equipped | 0 | 0 | 0 | 0 | 0 | 0 | | |

# EVALUATION OF FRONTAL CRASH STIFFNESS MEASURES FROM THE U.S. NEW CAR ASSESSMENT PROGRAM

**Christopher Wiacek**
**Vinay Nagabhushana**
**Taryn Rockwell**
**Stephen Summers**
**Lixin Zhao**
National Highway Traffic Safety Administration
USA

**Lauren A. Collins**
Alpha Technology Associate, Inc.
USA

Paper Number 15-0257

## ABSTRACT

Over the years, vehicle manufacturers may have implemented structural changes to light vehicles to comply with upgraded Federal Motor Vehicle Safety Standards (FMVSS) such as advanced air bags (FMVSS No. 208), side impact protection (FMVSS No. 214), and roof crush (FMVSS No. 216), as well as to improve performance in tests conducted by consumer information programs such as NHTSA's New Car Assessment Program (NCAP) and the Insurance Institute for Highway Safety (IIHS). Both programs have undergone changes in recent years. The NCAP was updated in 2010 to include advanced test dummies, new injury criteria, and a side pole test, and the IIHS adopted side impact, small overlap, and roof crush test protocols. Furthermore, as fuel economy requirements become more stringent, vehicle manufacturers may choose to light-weight vehicles and incorporate materials such as advanced high-strength steel and aluminum. This paper will investigate what effect, if any, these changes have had on vehicle crash pulses, as measured under NCAP. Although more stiffness metrics and crash pulse characteristics have been examined, this study mainly updates the analysis from the 2003 ESV paper, *Evaluation of Stiffness Measures from the U.S. NCAP*. [Swanson, 2003]

This paper utilizes data from model year (MY) 2002 to MY 2014 frontal NCAP crash tests to compute vehicle stiffness using four different methods: linear "initial" stiffness, energy equivalent stiffness, dynamic stiffness and static stiffness. The data are averaged and examined historically for three light duty vehicle classes (light duty pickup trucks (PUs), multi-purpose vehicles (MPVs), and passenger cars (PCs)) to provide a fleet perspective on changes to frontal crash characteristics. In addition, various crash pulse characteristics such as duration and peak acceleration are investigated. Collectively, these metrics have been traditionally used to characterize a vehicle's crash behavior and can subsequently influence restraint design.

The Swanson study found that not only were the average stiffnesses of PCs increasing from MY 1982 to 2001, but there was also a large disparity between the average stiffnesses of PCs and those of MPVs and PUs. The current study identified different trends. The average stiffnesses of PCs and MPVs appear to be converging, indicating that these two vehicle classes may have become more structurally homogenous in this respect. This is also evidenced by the changes observed for the crash pulse characteristics. In recent years, the crash pulse durations for both PCs and MPVs have decreased (though MPVs slightly more than PCs) such that the pulse duration is now essentially equal, on average, for both vehicle classes. The average peak accelerations for PCs and MPVs also increased during the years in this study. PU data is presented for completeness, but no extensive conclusions were made on this vehicle class because no statistically significant trends could be identified.

## INTRODUCTION

Over the years, new or more stringent Federal Motor Vehicle Safety Standards (FMVSS) such as advanced air bags, side impact protection, and roof crush have been promulgated and implemented for the modern light vehicle fleet. In addition, NHTSA's NCAP consumer information program was updated in 2010 to include advanced test dummies, new injury criteria, and a side pole test, and the IIHS expanded its crash test information program to include not only a 40 percent frontal offset test, but also side impact, small overlap, and roof crush test protocols. As a result, vehicle manufacturers have implemented structural changes throughout their vehicles.

During a crash, the vehicle's front structure manages the crash forces by transferring the crash energy to structural elements throughout the vehicle. Intrusion and forces into the occupant compartment must be limited so that the restraints can manage the energy transferred to the occupant(s). Side impact and roof crush tests have driven vehicle manufacturers

to make additional improvements to the occupant compartment structure in an attempt to limit door and roof intrusion, respectively.

Concurrently, as fuel economy requirements became more stringent, vehicle manufacturers may have chosen to light-weight vehicles by incorporating materials such as advanced high-strength steel and aluminum while continuing to comply with FMVSS requirements and perform well in consumer information programs. Being successful in such an approach most likely requires optimization of the vehicle structure while giving consideration to the special material properties for these higher strength and lightweighted materials. This paper will explore what impact these additional tests and regulations may have had on vehicle front stiffness as measured in MY 2002 to MY 2014 frontal NCAP tests.

Stiffness is one factor studied to understand how vehicles interact with their collision partners in the real world. Stiffness, as well as other factors such as mass and geometry, provides insight into how energy is managed in crashes. It is also an important factor in understanding the energy that the frontal restraint systems will have to manage in crashes in order to protect the occupants.

Swanson examined three methods of evaluating vehicle front-end stiffness using passenger car data from NCAP tests conducted between MY 1982 and MY 2001. The methods included: initial stiffness, static stiffness, and dynamic stiffness. Two of these methods, initial stiffness and dynamic stiffness, showed a steady increase for PCs over the model years analyzed (21 percent and 34 percent, respectively). The static stiffness method predicted much greater increases (61 percent) in stiffness due to its reliance on static crush data that does not account for the elasticity in front-end structures like dynamic stiffness does.

Average force-deflection plots generated in the Swanson paper for the various PC classes (compact, midsize, full-size) confirmed the increasing stiffness trends predicted by the initial stiffness and dynamic stiffness methods. Similar plots were generated for three other vehicle classes, light trucks, vans, and sport utility vehicles (SUVs), known collectively as LTVs. While stiffness values for the LTV classes tended to be much higher than those for the PC classes, their stiffness characteristics had not changed as much over the same time period.

A recent study using full-frontal rigid-barrier tests data from the NHTSA and Transport Canada crash test databases was conducted to analyze the vehicle crash pulse. [Caitlin, 2012] The paper grouped the data by vehicle type (PC, PU, minivan, and SUV) and size (small, midsize, and large) using the Highway Loss Data Institute classification based upon size and weight. The authors examined crash pulse characteristics, such as peak acceleration and crash pulse duration, for tested MY 2000–2010 vehicles. The paper showed an overall increasing trend in peak acceleration and a decrease in pulse duration, by year, for most vehicle classes. The authors concluded that the shorter, more severe pulse is consistent with stiffening vehicle structure for the current vehicles within the fleet. However, they also found that for later model year vehicles, the crash pulse characteristics were becoming more homogeneous for different vehicle classes.

As with Swanson, this paper will investigate initial stiffness (now termed linear "initial" stiffness), and static and dynamic stiffness. In addition, energy-equivalent stiffness will be calculated using the Kw400 methodology. [Patel, 2007] To expand upon the findings of Caitlin, this paper will also investigate various crash pulse characteristics for severity and duration as measured by time-to-zero velocity and peak acceleration, and will study the characteristics of force-deflection profiles seen in the modern fleet. Though the earlier papers divided their data based on vehicle type and size, since there is not a standard definition for vehicle size classification, this paper will utilize only vehicle type (as identified on the FMVSS certification label) in an effort to gain a fleet perspective on changes to frontal crash characteristics.

## METHODOLOGY

Since 1979, NHTSA has been providing consumers with comparative frontal crashworthiness information on new passenger vehicles through NCAP. In the frontal NCAP test, vehicles are evaluated based on the crash protection they provide in a 56 km/h full-frontal rigid barrier crash. This is determined from injury readings recorded by Hybrid III test dummies positioned in the driver and right front passenger seats. Frontal NCAP test data can also be used to characterize a vehicle's crash behavior.

In this study, available frontal NCAP data collected for MY 2002-2014 test vehicles was used to compute vehicle stiffness using four different methodologies – linear "initial" stiffness, energy-equivalent stiffness, dynamic stiffness, and static stiffness – each of which will be detailed in the next section.

For the first two of these methodologies, linear "initial" stiffness and energy-equivalent stiffness, stiffness is derived using data from (1) accelerometers that are mounted onto the vehicle structure near the driver or front passenger's seating location, and (2) load cells that have been added to the rigid barrier face to measure the total force the vehicle exerts on the barrier. The data from the vehicle accelerometer is double-integrated to obtain the vehicle's dynamic displacement, or crush, and the outputs from all of the individual load cells on a barrier are summed to obtain the total barrier force. (All accelerometer and load cell data were filtered according to the Society of Automotive Engineers Recommended Practice J211/1 rev. Mar 95, "Instrumentation for Impact Test – Part 1 – Electronic Instrumentation.") Although the sizes and numbers of load cells varied among NCAP testing laboratories over the years under study, this should have negligible effect on the total force exerted on a barrier; therefore, it is appropriate to use data from the various arrays for this study.

To compute dynamic stiffness and static stiffness, a vehicle's mass and veloctiy are used in combination with dynamic displacement data (again, derived from the vehicle accelerometers in the occupant compartments) and post-test vehicle crush measurements, respectively. For this study, crush measurements were calculated to be the difference between pre- and post-test measurements of the vehicle length, as recorded in the NCAP final test reports. It should also be noted that test weight, not curb weight, was used for these calculations since test weight includes the weight of the two Hybrid III test dummies and the vehicle-rated cargo weight, and best reflects the weight of the vehicle at impact and the resulting forces on the load cells on the barrier.

Although the original data set was comprised of 611 passenger vehicles, the data set for a given metric has been reduced because either the required data was lost, or because the available data was deemed invalid. The final data sets for each of the four stiffness metrics were divided into three vehicle class categories – PCs, MPVs (comprised of SUVs and vans), and light PUs. SUVs and vans were combined into one class, MPVs, because only a small number of vans were tested by NCAP over the years studied. The class category for a given vehicle was dictated by the classification noted on the vehicle's certification label – PC, MPV, or truck (PU).

Additionally, vehicle crash pulse data such as peak acceleration and time to zero velocity were grouped by vehicle class to observe any changes during the model years considered.

The trends in vehicle dynamic and static stiffness from MY 1982-2014 were examined. In doing so, the MY 2002-2014 data is added to that from Swanson. For the trend analysis spanning from MY 1982-2014, the data was subdivided into model year clusters, with each cluster spanning two model years, and the computed stiffness values for each cluster were then averaged. Three-year intervals were used to present force-deflection profiles for each vehicle class.

As this study is limited to only those vehicles selected for NCAP testing during the given model years, and data was not weighted based on vehicle sales or registration volumes, findings are not necessarily representative of the vehicle fleet as a whole. Trends observed can only be inferred for those vehicles tested by NCAP for the model years under study. Further, no effort was made to relate occupant injury values collected in these tests to the stiffness metrics explored.

**RESULTS AND DISCUSSION**

For each of the stiffness metrics and the vehicle parameter analysis, the data was primarily analyzed by grouping the first four MY of the study (2002-2005) and the last four MY of the study (2011-2014) and comparing the averages found for each interval. For ease of discussion, these intervals will be referred to as the "first four years" and the "last four years."

**Linear "Initial" Stiffness**

For this first method, vehicle stiffness was defined to be the slope of a linear regression line fit to the early portion of a vehicle's force-deflection profile. A force-deflection profile reflects the total force exerted on the load cell barrier versus the dynamic deformation, or crush, that a vehicle experiences during the duration of a crash test. As mentioned above, this crush is calculated by double-integrating the acceleration recorded by vehicle accelerometers in the occupant compartments.

Force-deflection profiles were generated for the 611 passenger vehicles subjected to frontal NCAP testing spanning model years 2002 through 2014; however, 89 tests were ultimately eliminated because of errors in accelerometer or load cell data collection or because a linear fit of the data could not be achieved. This resulted in a final data set of 522 vehicles for this metric. In the absence of a standard technique, the authors developed a method for resolving differences in the data collected by load cell barriers and vehicle accelerometers. The data collected from the load cell wall and vehicle accelerometers were verified for accuracy by analyzing the momentum balance. Data was considered acceptable if the vehicle velocity (calculated by integrating the vehicle accelerometer data): (1) shared a similar slope to the momentum curve (determined by the force measured at the load cell wall) for the first 400 mm of crush, which was generally 30 ms or less into the crash event, and (2) reflected the actual delta-V. The data was visually inspected to ensure the force on the load cell wall (i.e., momentum curve) led the velocity response and did not diverge from the velocity response prior to the first 400 mm of crush.

For the 522 qualifying tests, linear "initial" stiffness was determined by applying the following criteria: (1) good correlation of linear fit ($R^2$ value greater than 0.95), (2) correlation begins within the first 200 millimeters of deflection to emphasize what is considered the "initial" deformation of the vehicle, (3) correlation is maintained for a minimum distance of 150 millimeters in order to reflect the overall slope, and (4) linear fit is not constrained to zero force at zero deflection to compensate for small variations in time zero data collection. For a given vehicle, the longest linear correlation that met all four criteria was estimated to be indicative of the vehicle's linear stiffness. [Summers, 2002], [Swanson, 2003] If a linear fit meeting the preceding criteria could not be achieved for a particular force-deflection profile, linear "initial" stiffness was not quantified for the corresponding vehicle. Figure 1 depicts the results for the three vehicle classes studied. The associated data is provided in the Appendix.

The average linear "initial" stiffness was 1,678 N/mm for all vehicles tested since MY 2002. By class, the average was 2,448 N/mm for PUs, 1,895 N/mm for MPVs, and 1,336 N/mm for PCs during this time period. As shown in Figure 1, average linear "initial" stiffness decreased for MPVs and slightly increased for PCs over the years studied. The average linear "initial" stiffness for the first four years was 1,292 N/mm for PCs, whereas for the last four years, the average was 1,431 N/mm. This was an increase of 10.7 percent, which was found to be significant at the 95% confidence level. MPVs, however, have shown a clear decrease in linear "initial" stiffness since MY 2002. For the first four years, MPVs had an average linear "initial" stiffness of 2,054 N/mm, while for the last four years, this average dropped 14.4 percent to 1,759 N/mm. This result was also significant at the 95% confidence level. It appears that linear "initial" stiffness values for MPVs and PCs are converging. The difference in the average linear "initial" stiffness for the first four years between MPVs and PCs was 45.5 percent. This difference has dropped to 20.6 percent for the last four years. This is consistent with the trend to construct MPVs on more car-like, unibody platforms instead of truck-based, body-on-frame construction. There are more unibody-based MPV offerings than there were during the time period studied in Swanson. Figure 1 shows that average linear "initial" stiffness values for PUs remained higher than those for PCs and MPVs. No statistically significant trend in linear "initial" stiffness could be identified for PUs.

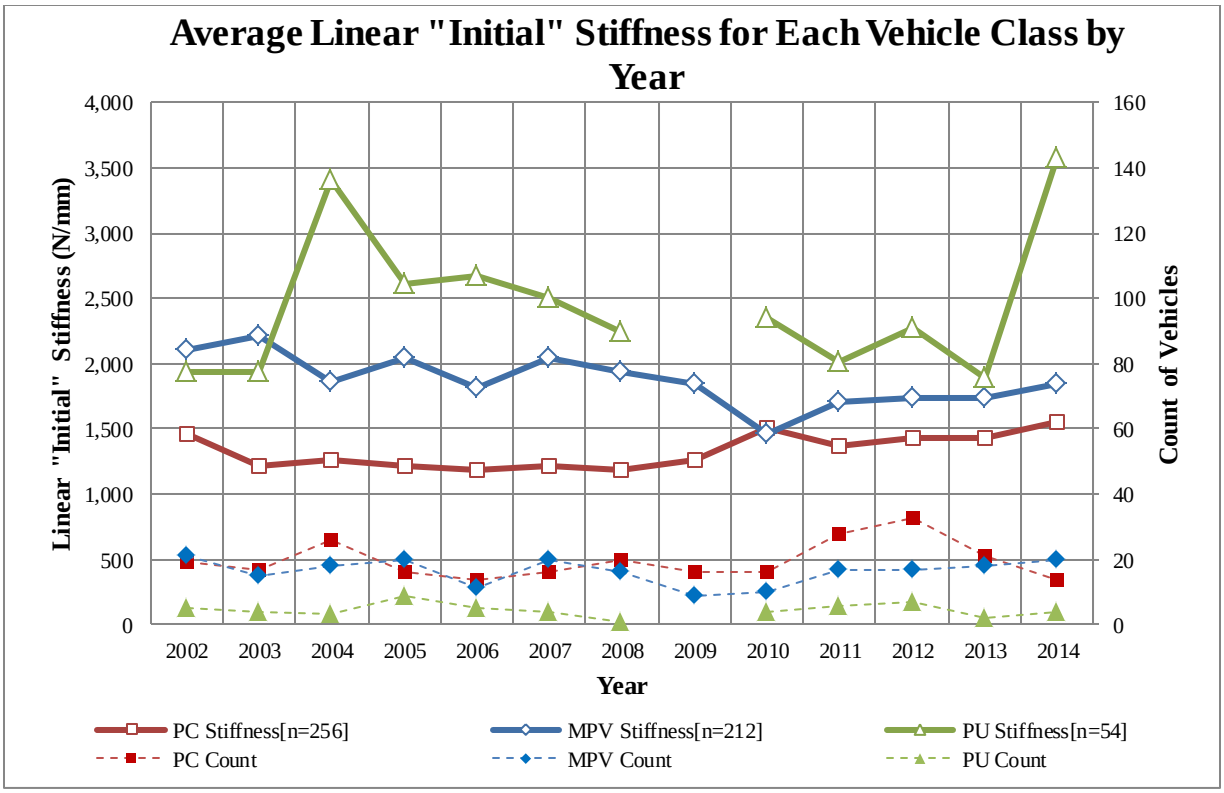


***Figure 1: Average linear "initial" stiffness values computed for MY 2002-2014 NCAP test vehicles.***

**Energy-Equivalent Stiffness: Kw400**

Like the linear "initial" stiffness method, this second method, energy-equivalent stiffness, is also designed to characterize a vehicle's stiffness based on its force-deflection profile. However, where the linear stiffness method approximates initial stiffness based on the slope of a line fit to the force-deflection curve over a given displacement range, this second method is based on the crash energy (or area under the force-deflection curve) over a given range.

One metric that can be used to approximate energy-equivalent stiffness is Kw400. Kw400 is derived from equating the energy stored in an ideal spring ($\frac{1}{2} Kx^2$) to the work of crushing the front end of a vehicle ($\int Fdx$). Contrary to the linear "initial" stiffness method, in which the displacement range is variable, the displacement range for the energy-equivalent stiffness method, as defined by Kw400, is fixed. To calculate energy-equivalent stiffness, the integral of the area under the force-deflection curve is evaluated between 25 and 400 mm of vehicle frontal crush. The equation for Kw400 is shown below. [Patel, 2007]

$$\mathrm{Kw400} = \frac{2\int_{25mm}^{400mm} Fdx}{\left(400^2 - 25^2\right)}$$

This equation was used to calculate energy-equivalent stiffness for the same 522 qualifying tests discussed in the linear "initial" stiffness section.

The average energy-equivalent stiffness was 1,362 N/mm for all vehicles tested from MY 2002 to MY 2014. By class, the average energy-equivalent stiffness was 1,720 N/mm for PUs, 1,502 N/mm for MPVs and 1,171 N/mm for PCs during this time period. More specifically, Figure 2 shows that PCs had an average energy-equivalent stiffness

of 1,106 N/mm during the first four years, and 1,245 N/mm for the last four years – a 12.6 percent increase that was statistically significant at the 95% confidence level. Conversely, the average energy-equivalent stiffness for MPVs was 1,561 N/mm for the first four years, and decreased 7.8 percent to 1,439 N/mm for the last four years. Again, this difference was found to be statistically significant at the 95% confident level. The difference in energy-equivalent stiffness between MPVs and PCs was 34.2 percent for the first four years of the data set. This difference dropped to 14.5 percent for during the last four years. Directionally, the results are consistent with those found for linear "initial" stiffness; however, the energy-equivalent stiffness metric identified a smaller difference in stiffness between PCs and MPVs than the linear "initial" stiffness metric. No statistically significant changes were identified for the PU fleet. Similar to that mentioned for linear "initial" stiffness, the average energy-equivalent stiffness for PUs is higher than that for PCs and MPVs as shown in Figure 2.

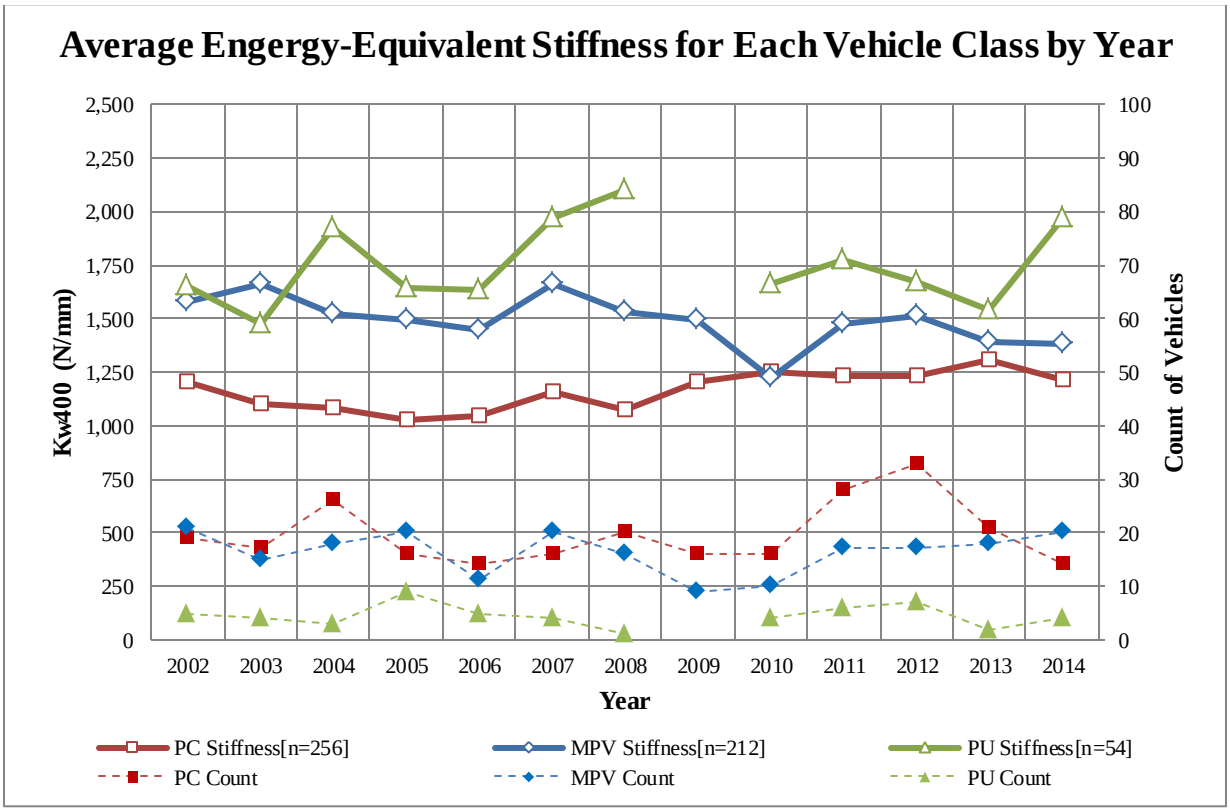


***Figure 2: Average energy-equivalent stiffness values computed for MY 2002-2014 NCAP test vehicles.***

**Dynamic Stiffness**

For the third method, dynamic stiffness, a vehicle's stiffness, $K$, is computed using the equation $K = mv^2/x^2$, where $m$ is the test weight of the vehicle, $v$ is the closing speed of the vehicle, and $x$ is the maximum dynamic displacement. This equation was derived using the approximation of the conservation of total energy, $E = ½\ mv^2 = ½\ Kx^2$. As mentioned previously, the maximum dynamic displacement (or crush) for a vehicle is found by taking the maximum of the double integral of the vehicle acceleration in the front occupant compartment. Dynamic displacement accounts for the elastic behavior often found in the vehicle front-end structure. [Swanson, 2003]

There were 611 passenger vehicles subjected to frontal NCAP testing from MY 2002 through MY 2014; however, 10 of the tests were ultimately eliminated because of errors in accelerometer data, resulting in a final data set of 601 for dynamic stiffness, static stiffness and vehicle acceleration data. The average dynamic stiffness from MY 2002 to MY 2014 for all vehicles was 1,101 N/mm. By class, the average dynamic stiffness for the model years studied was 1,409 N/mm for PUs, 1,191 N/mm for MPVs, and 959 N/mm for PCs. During the first four years, the average dynamic stiffness for PCs was 916 N/mm. For the last four years, the average dynamic stiffness for PCs was 980 N/mm – an increase of 7.0 percent over the earlier interval. This increase was statistically significant at the 95% confidence interval. When examining the same intervals, dynamic stiffness values decreased for MPVs. In the first

four years, the average dynamic stiffness for MPVs was 1,221 N/mm. This value decreased 6.7 percent to an average of 1,138 N/mm for the last four years. These results were also found to be statistically significant at the same level of confidence. The dynamic stiffness decrease for MPVs, again, likely corresponds to the trend of constructing MPVs on more car-like, unibody structures and not on pickup truck-based, body-on-frame structures. The difference in average dynamic stiffness between MPVs and PCs was 28.5 percent during the first four years. This difference dropped to 15.0 percent in the last four years. This converging trend is directionally consistent with the other stiffness metrics already discussed and very similar to the 14.5 percent difference found when using the Kw400 (energy-equivalent) approach. Again, although no significant differences could be identified for the PU data set, dynamic stiffness is higher, on average, for PUs than for PCs and MPVs.

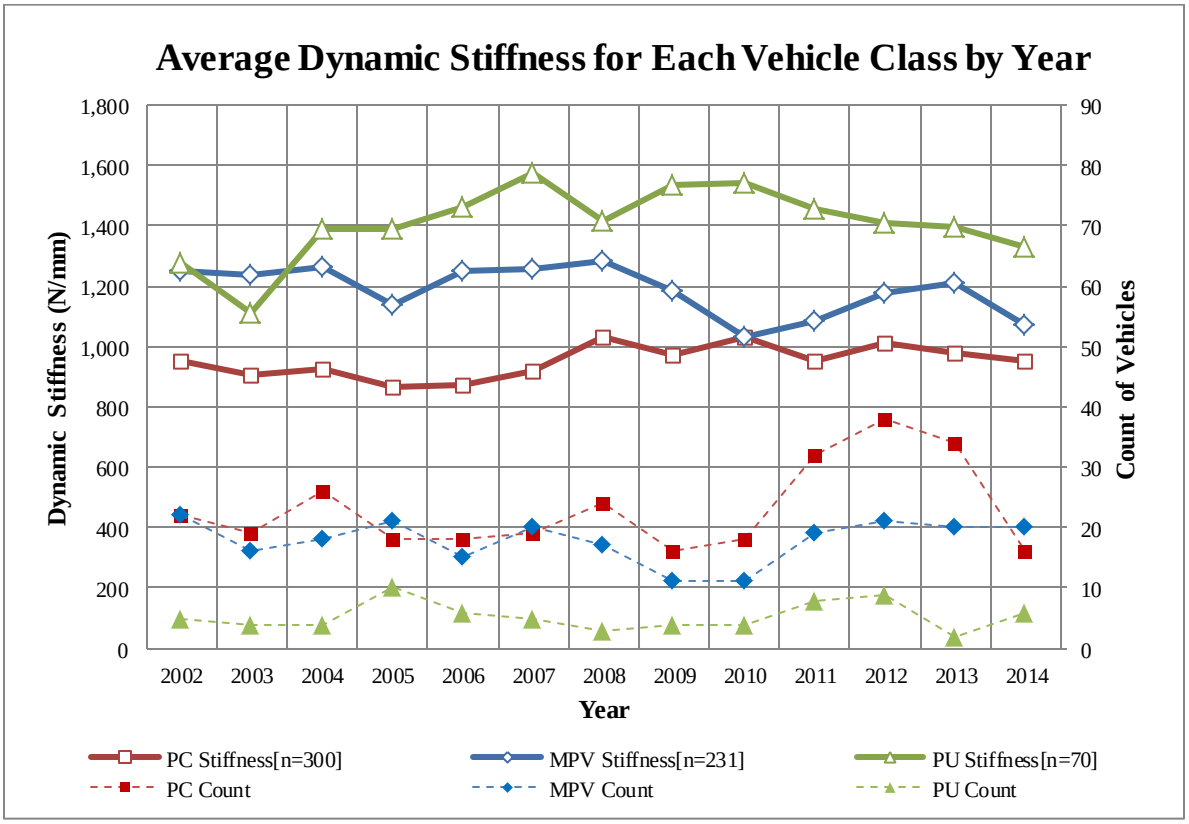


***Figure 3: Average dynamic stiffness values computed for MY 2002-2014 NCAP test vehicles.***

**Static Stiffness**

The fourth stiffness calculation method, static stiffness, is similar to dynamic stiffness in that it uses the same equation derived from the conservation of energy ($K = mv^2/x^2$); however, $x$ instead reflects the maximum static crush measured for the vehicle post-test. Unlike dynamic stiffness, static stiffness does not account for the elastic deformation of the vehicle front-end. [Swanson, 2003]

Static stiffness was computed for the same 601-vehicle data set used to calculate dynamic stiffness. The average static stiffness for all vehicles from MY 2002 to MY 2014 was 2,035 N/mm. By class, the average stiffness was 2,149 N/mm for PUs, 2,160 N/mm for MPVs, and 1,913 N/mm for PCs over this time period. As shown in Figure 4, the static stiffness for PCs has generally been increasing since MY 2002. In the first four years, the average static stiffness for PCs was 1,691 N/mm, which increased 24.0 percent to 2,097 N/mm in the last four years. This was a statistically significant increase at the 95% confidence level. Conversely, in the first four years, the average static stiffness for MPVs was 2,183 N/mm, which decreased 3.6 percent in the last four years to 2,104 N/mm. This difference was not found to have statistical significance at the 95% confidence interval. The difference in static stiffness between MPVs and PCs was 25.4 percent during the first four years; this difference dropped to 0.3 percent in the last four model years. In general, it also yielded the highest average values among the methods. As with the

other stiffness metrics discussed, there currently appears to be more homogeneity in stiffness between PCs and MPVs compared to earlier model years. As with the other stiffness metrics, no statistically significant changes could be identified for PUs. However, it should be noted that the magnitude of static stiffness values for PUs appears to be more comparable to those for MPVs and PCs when compared to results seen for the other three stiffness metrics.

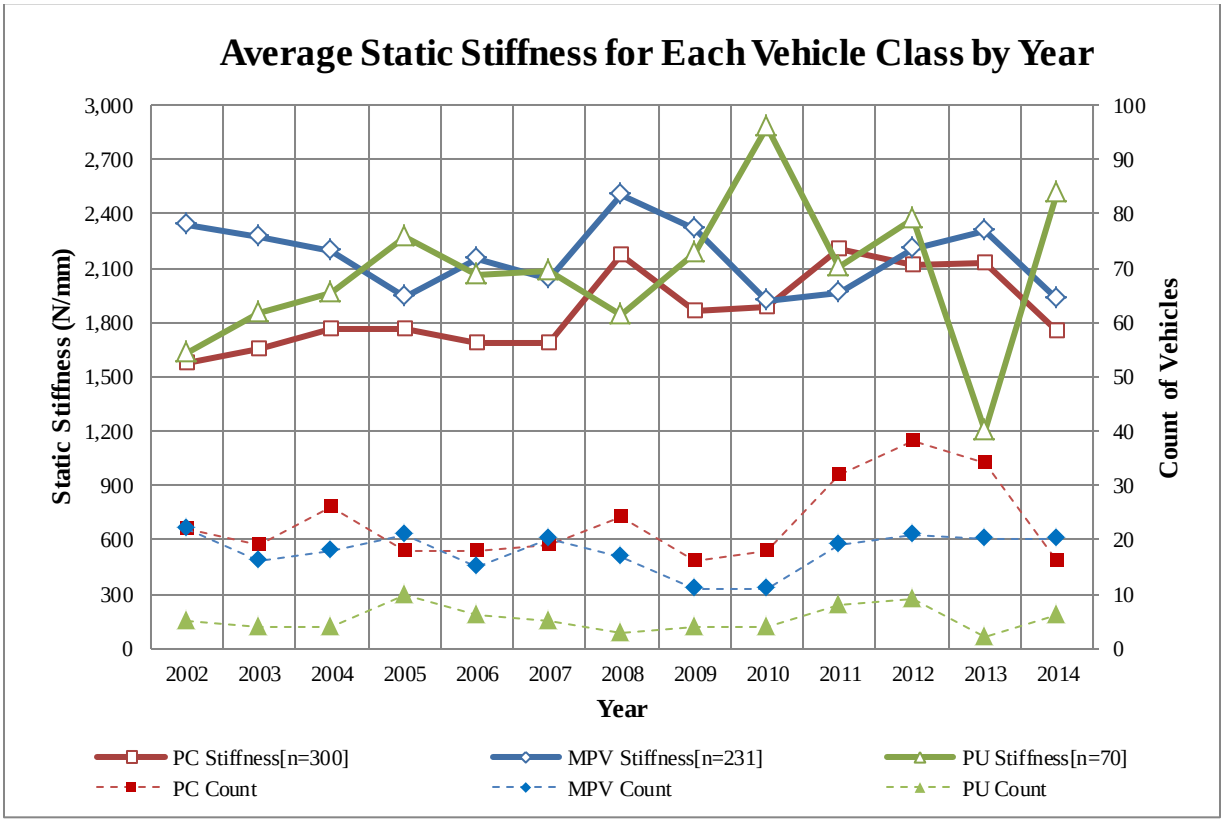


***Figure 4: Average static stiffness values computed for MY 2002-2014 NCAP test vehicles.***

Overall, the four methods of computing vehicle stiffness showed similar trends. They each showed a slight increasing trend in average stiffness for PCs, and a concurrent responding decreasing trend in average stiffness for MPVs, with both classes becoming more homogenous with respect to their front-end stiffnesses. When comparing the first four years to the last four, average percent increases in stiffnesses for PCs when compared to average percent decreases in stiffnesses for MPVs varied depending on the metric used. This is illustrated in Table 1. Table 2 shows, by stiffness metric, the percent difference between the average stiffnesses of PCs and MPVs when comparing the first four years to the last four. All of the metrics showed a decrease in the difference between PC average stiffnesses and MPV average stiffnesses, again supporting the notion that the two are converging. The metric that showed the least difference when comparing MPVs versus PCs for the first four years with the last four was static stiffness.

**Table 1.**
**Differences in average stiffnesses for PCs and MPVs between the first and last four years.**

| | PCs | MPVs |
|---|---|---|
| **Linear "Initial" Stiffness** | 10.7% | -14.4% |
| **Energy-Equivalent Stiffness** | 12.6% | -7.8% |
| **Dynamic Stiffness** | 7.0% | -6.7% |
| **Static Stiffness** | 24.0% | -3.6% |

**Table 2.**
**Differences in average stiffnesses, MPVs versus PCs, for the first and last four years.**

| | MY 2002-2005 | MY 2011-2014 |
|---|---|---|
| **Linear "Initial" Stiffness** | 45.5% | 20.6% |
| **Energy-Equivalent Stiffness** | 34.2% | 14.5% |
| **Dynamic Stiffness** | 28.5% | 15.0% |
| **Static Stiffness** | 25.4% | 0.3% |

Differences between static stiffness trends and the other three stiffness metrics may largely be due to the fact that the static stiffness metric relies upon post-test vehicle crush measurements for displacement rather than dynamic (accelerometer-based) measurements, which are used for the other three metrics. Unlike dynamic deformation, static post-test crush measurements cannot account for the elastic deformation that occurred during the crash. Instead, static measurements represent only the inelastic residual crush. As such, static crush measurements are inherently smaller than calculated values for dynamic displacement, and this translates into higher stiffness values for static stiffness compared to the other three metrics evaluated.

To better understand the role elastic vehicle components play in stiffness results for the metrics studied, it was of interest to compare static and dynamic stiffness results directly since the same equation is used to calculate both; the only difference between the two calculations is the source of displacement - either post-test vehicle measurements (for static stiffness) or vehicle accelerometer readings (for dynamic stiffness).

Figure 5 depicts the average calculated static stiffness and dynamic stiffness for PCs tested by NCAP since MY 1982. For this comparison, data from Swanson (MY 1982-2001) was added to that used for the current study (MY 2002-2014). The static and dynamic stiffness data was subdivided into two-year intervals and then averaged for each interval. This figure shows that there was a gradual upward trend in static and dynamic stiffness from MY 1982 to MY 2014. It is also of interest that the values for both seemed to stabilize just prior to the last four years in this study. It can also be seen that the difference between average dynamic and static stiffness values has grown larger over the years. This indicates an increase in elasticity of the front-end vehicle structure. Therefore, results using linear "initial" stiffness, energy-equivalent stiffness, and dynamic stiffness – the three methods that use dynamic displacement in their calculations – may more realistically approximate the stiffness of the current fleet, since dynamic deformation accounts for the elastic and energy-absorbing front-end components.

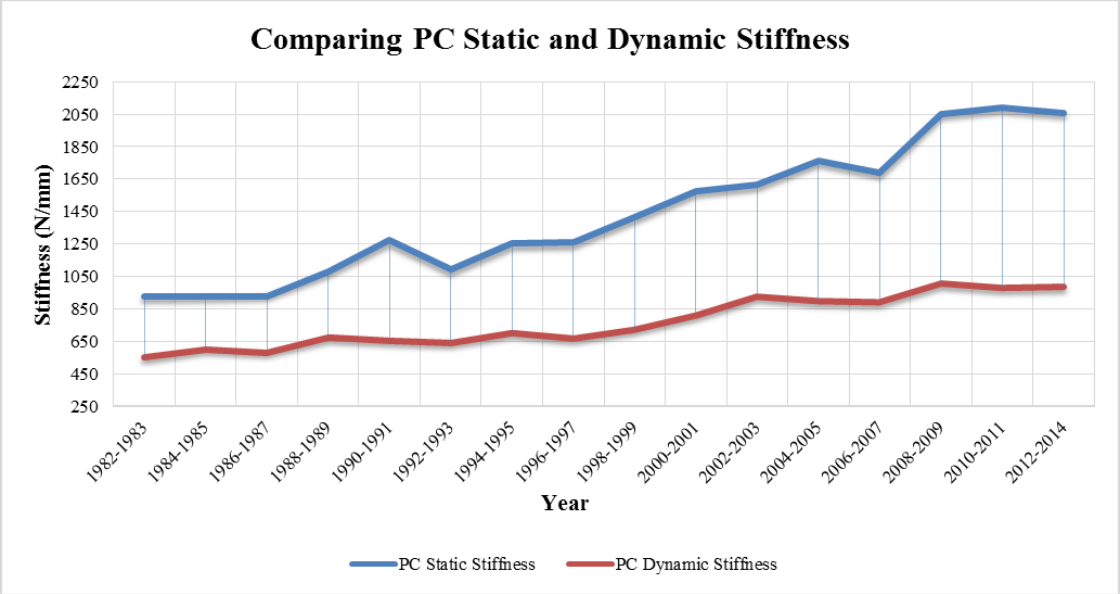


***Figure 5. Comparing static and dynamic stiffnesses for NCAP-tested vehicles.***

Considering the previous discussion, it is not surprising that a correlation was found between energy-equivalent and dynamic stiffness, which is shown in Figure 6. This is also demonstrated by a similar percent decrease in stiffness observed using the energy-equivalent and dynamic stiffness metrics. These metrics showed stiffness decreases of 14.5 percent and 15.0 percent, respectively, for the last four model year interval when compared to the first four model year interval. As both metrics rely on test instrumentation, and in particular, vehicle acceleration data, to calculate stiffness, both metrics may be more reliable than methods that do not take these into account. Although linear "initial" stiffness also relies on vehicle acceleration data to compute stiffness, a similar correlation to energy-equivalent stiffness and/or dynamic stiffness was not observed for this metric. This may be because of the potential error introduced by fitting a straight line to the force-deflection curve. Fitting a line slightly earlier or later in time along the curve, or over a longer stretch of time, could significantly influence the slope of the line, and therefore, the approximated stiffness.

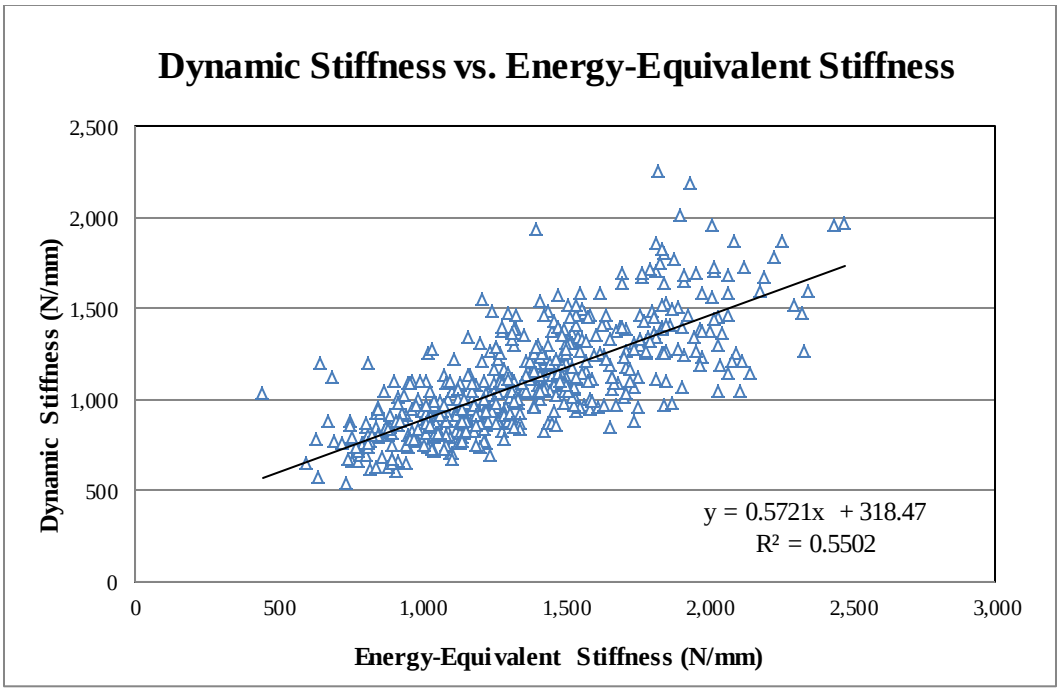


***Figure 6. Comparing energy-equivalent stiffness and dynamic stiffness for NCAP-tested vehicles.***

As an additional check, the force-deflection profiles used for the linear "initial" stiffness and energy-equivalent stiffness metrics were studied. Similar to that done for the comparison of static and dynamic stiffness, the force-deflection data was subdivided into three-year intervals and then averaged for each interval. The slope of each of the averaged force-deflection profiles was then examined for the first ~200 mm of deflection as an indicator of vehicle stiffness (i.e., the sharper the rise of the curve, the stiffer the vehicle front-end). Figure 7 illustrates the concept previously discussed, that the linear stiffnesses of PCs and MPVs are converging. This is shown by the similar amount of force required to crush each of these vehicle types 200 mm in the later model years. Furthermore, the stiffness of PUs, on average, is higher than that of both PCs and MPVs.

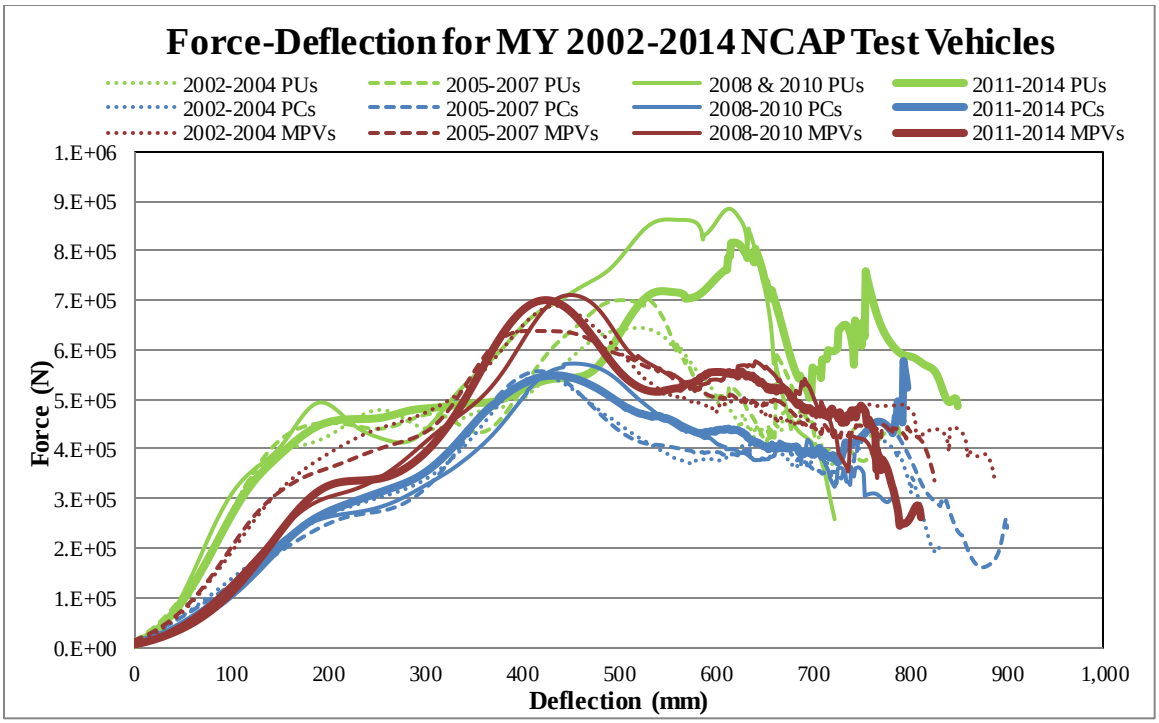


***Figure 7. Force-Deflection Plot for MY2002-2014 NCAP Test Vehicles.***

Changes to the fleet in response to things such as new regulatory requirements, revisions to consumer information programs, and shifting consumer preferences do not occur all at once and are generally phased in over time. This is evidenced by the steady increase in offerings of unibody-based MPVs compared to the prior (Swanson) study. However, the analysis of vehicle stiffness appears to support the notion that just prior to the last four years of this data set, a change affecting the front-end design of PCs and MPVs may have occurred in the fleet. To expand upon this finding, and build upon the Caitlin study, an additional analysis that focused on crash pulse characteristics was conducted. Specifically, peak acceleration and crash pulse duration for the vehicles tested during the model years under study were examined. With this analysis, there was a desire to see how vehicles designed to the latest regulatory and consumer information programs are managing crash forces. It was of particular interest to note any change in the amount of force translated to the occupant compartment over the years studied. It was also hoped that the trends observed for the stiffness metrics would correspond, in time, to any observations made for the crash pulse characteristics. To be consistent with the stiffness analysis, the same model year intervals were used for this analysis.

**Peak Acceleration**

The first crash pulse characteristic reviewed was the peak x-axis acceleration, measured in G's. Once again, this measurement is recorded by accelerometers that are mounted onto the vehicle structure near the driver or front passenger's seating location. Peak acceleration is typically indicative of the crash severity and correlates, in combination with the occupant's mass, to the amount of force the restraint system would need to manage during the crash. Effectively, this metric reflects how much of the crash forces are translated to the occupant compartment during the crash.

The average peak acceleration for all vehicles tested during the model years under study was 43G. By vehicle class, the average peak acceleration was 41G for PUs, 44G for MPVs, and 43G for PCs over this same time period. Averages for each model year by vehicle type are shown in Figure 8. Of interest is the relatively narrow range of average peak acceleration values calculated for the model years under study. The peak acceleration range for PUs was 36G to 49G; for MPVs, the range was 39G to 51G, and for PCs, the range was 39G to 48G. For the first four years, the average peak acceleration for PCs was 41G, and for the last four years, it increased 10.0 percent to 45G. This was a statistically significant increase at the 95% confidence interval. The average peak acceleration for MPVs from these same intervals increased 16.3 percent from 40 G to 47 G. This was also a significant finding at the 95% confidence level. Furthermore, for both PCs and MPVs, average peak accelerations have increased in the most recent

years, even though, when comparing the first four years to the last four years, the average stiffnesses of PCs were increasing while the average stiffnesses of MPVs were decreasing. A statistically significant trend was not identified for PUs.

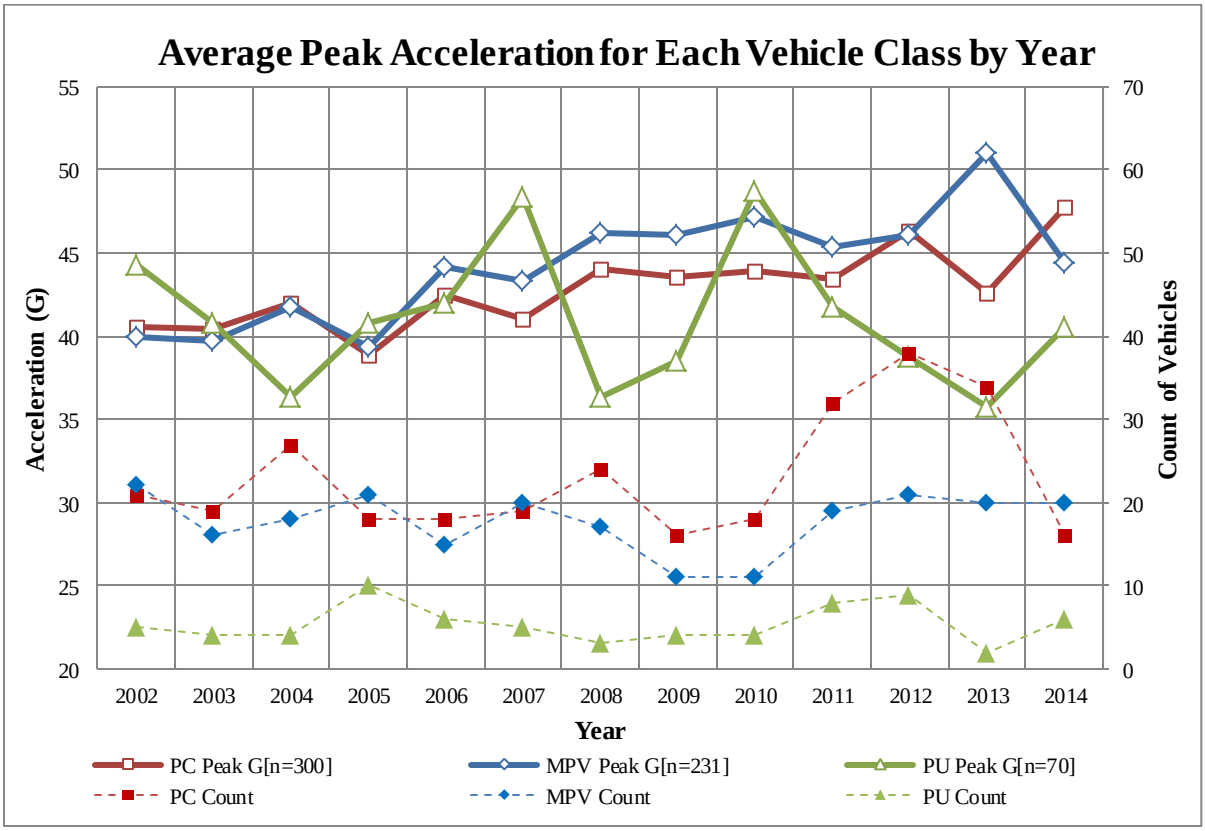


***Figure 8. Average peak acceleration.***

**Time-to-Zero Velocity**

The second pulse characteristic analyzed was the crash pulse duration, which is measured in milliseconds. This measurement is determined from single integration of the vehicle's x-axis acceleration and spans from the point of impact (t=0) until barrier separation, or when the vehicle velocity is equal to zero. Like peak acceleration, the crash pulse duration is also indicative of crash severity. If the duration of the crash event is shorter, the occupant and the restraint system may have to absorb the crash energy over a shorter period of time, which could make the event more severe.

For all MY 2002-2014 vehicles tested, the average time-to-zero velocity was 72 ms. By vehicle class, the time-to-zero velocity was 74 ms for PUs, 73 ms for MPVs, and 71 ms for PCs over this same time period. Figure 9 shows that there do not appear to be any significant trends overall; however, the results for PCs for the first four years show an average crash duration of 72 ms, which decreased by 3.8 percent to 70ms for the last four years. For MPVs, the average pulse duration for the first four years was 75 ms, and this decreased 5.7 percent to 71 ms during the last four years. For all practical purposes, on average the crash duration for both PCs and MPVs is now nearly the same.

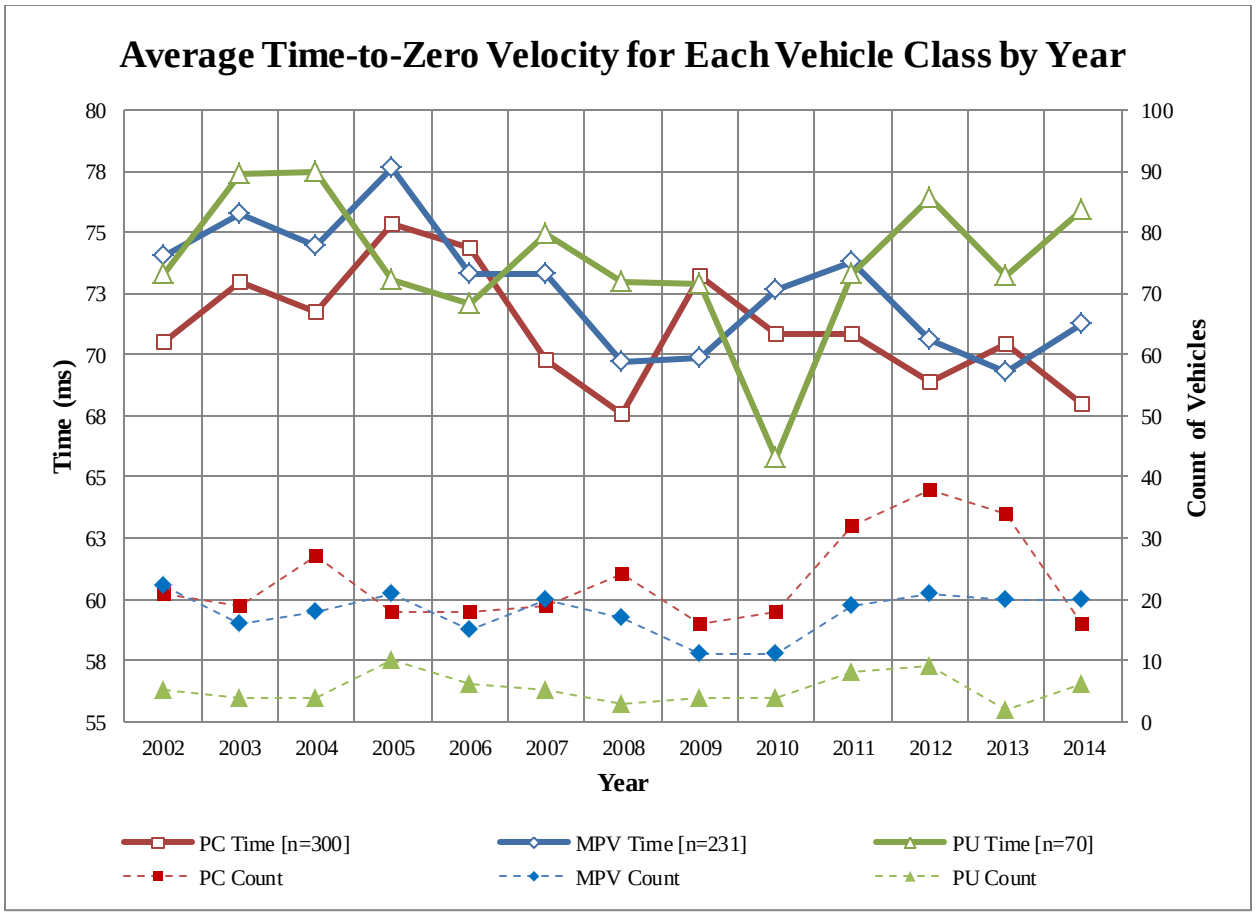


***Figure 9. Average time-to-zero velocity.***

The results for the pulse characteristics suggest that an increase in pulse severity (i.e., an increase in peak acceleration and/or a decrease in duration) does not necessarily equate to an increase in vehicle stiffness. This is evident from the stiffness trends previously discussed for MPVs during recent model years. Although average peak accelerations increased when comparing the last four years to the first four years, average MPV stiffness was shown to have decreased. The same phenomenon exists when looking at pulse durations: average MPV pulse durations decreased during the same time period in which a decrease in stiffness was observed. In sum, average traditional vehicle pulse characteristics may be in contrast to these front-end stiffness findings. This finding is also supported by Figure 10, which compares peak acceleration values to stiffness values computed using the energy-equivalent stiffness method. As shown, there is no correlation between peak acceleration and energy-equivalent stiffness. Comparisons of linear "initial," dynamic, and static stiffness to peak acceleration showed similar results..

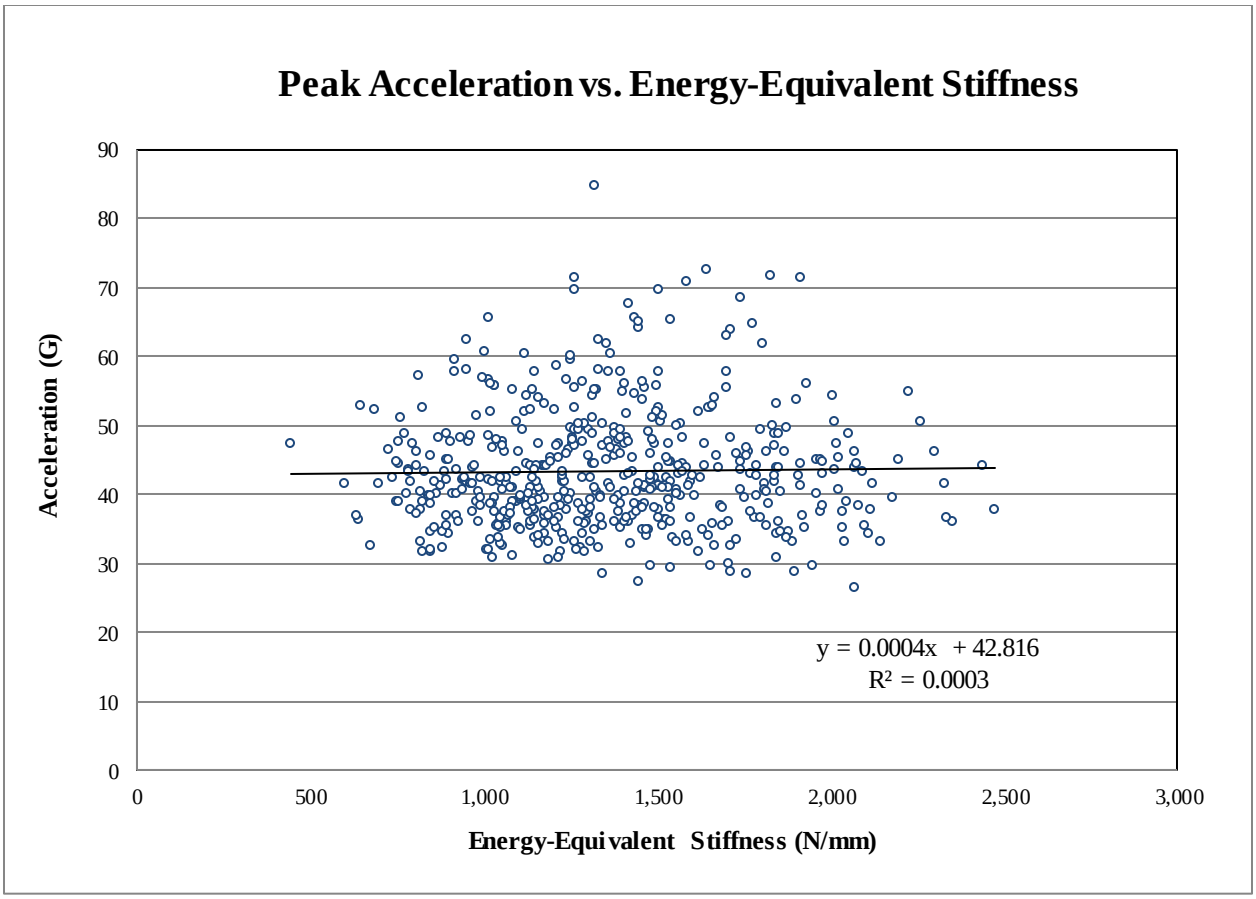


***Figure 10. Comparing peak acceleration and energy-equivalent stiffness for NCAP-tested vehicles.***

**CONCLUSIONS**

This study examined four methods of calculating front-end stiffness using vehicle crash data collected from NCAP tests conducted from MY 2002 through 2014. These methods included linear "initial" stiffness, energy-equivalent stiffness, dynamic stiffness, and static stiffness. This approach was similar to a study conducted by Swanson et al. that examined the MY 1982-2001 fleet. The Swanson study, which also used frontal NCAP data, found that not only were the average stiffnesses of PCs increasing over time, but there was also a large disparity between the average stiffnesses of PCs and that of MPVs and PUs. The results presented herein identified different trends. Generally, PCs continued to increase in average stiffness until stabilizing just prior to the last four years of this study, while MPVs decreased in average stiffness when considering the same time period. The average stiffnesses for PCs and MPVs appear to be converging, indicating that the fleet has become more homogenous with respect to these two vehicle classes. This is supported by the increase in MPV offerings utilizing unibody construction rather than traditional body-on-frame techniques. This study also examined the changes in crash pulse characteristics. While average peak accelerations generally increased for MPVs and PCs and pulse duration slightly decreased when comparing the first four years to the last four years of data, these findings do not appear to correlate to any of the stiffness metrics discussed. This analysis also further confirms the findings in Caitlin, which identified a slightly more severe, but homogeneous, crash pulse in the fleet.

**REFERENCES**

[1] Swanson, J., Rockwell, T., Beuse, N., Summers, L., Summers, S., Park, B., "Evaluation of Stiffness Measures from the U.S. New Car Assessment Program", Enhanced Safety of Vehicles Conference, Paper Number 527, 2003

[2] Caitlin M. Locey, BS, J. Felipe Garcia-Espana, PhD, Akira Toh, MS, Aditya Belwadi, PhD, Kristy B. Arbogast, PhD, and Matthew R. Maltese, PhD, Homogenization of Vehicle Fleet Frontal Crash Pulses from 2000–2010, Annals of Advances in Automotive Medicine/Annual Scientific Conference, 2012

[3] O'Reilly, Peter, "Status Report of IHRA Compatibility and Frontal Impact Working Group," Enhanced Safety of Vehicles Conference, Paper Number 402, 2003

[3] Summers, Stephen and Prasad, Aloke, "NHTSA's Recent Compatibility Test Program," Enhanced Safety of Vehicles Conference, Paper Number 05-027, 2005

[4] Summers, Stephen, Hollowell, W.T., and Prasad, A., "Design Considerations for a Compatibility Test Procedure," Society of Automotive Engineers Paper No. 02B-169, 2002

[5] Patel, S., Smith, D., Prasad, A., and Mohan, P., "NHTSA's Recent Vehicle Crash Test Program on Compatibility in Front-to-Front Impacts," Enhanced Safety of Vehicles Conference, Paper Number 07-0231, 2007

## Appendix

| *Linear "Initial" Stiffness (N/mm)* | | | | | | | | | | | | | | |
|---|---|---|---|---|---|---|---|---|---|---|---|---|---|---|
| *Year* | *MPV* | | | | *PC* | | | | *PU* | | | | *Avg of 3 Classes* | *Total Count* |
| | *Stiffness* | *Min* | *Max* | *Count* | *Stiffness* | *Min* | *Max* | *Count* | *Stiffness* | *Min* | *Max* | *Count* | | |
| ***2002*** | *2,111* | *1,053* | *3,375* | *21* | *1,468* | *985* | *2,848* | *19* | *1,936* | *1,473* | *2,732* | *5* | *1,820* | *45* |
| ***2003*** | *2,207* | *894* | *3,578* | *15* | *1,221* | *769* | *1,702* | *17* | *1,929* | *1,613* | *2,505* | *4* | *1,711* | *36* |
| ***2004*** | *1,866* | *962* | *3,601* | *18* | *1,261* | *803* | *1,761* | *26* | *3,402* | *2,828* | *4,456* | *3* | *1,630* | *47* |
| ***2005*** | *2,049* | *1,045* | *4,289* | *20* | *1,210* | *759* | *1,700* | *16* | *2,613* | *1,929* | *3,809* | *9* | *1,863* | *45* |
| ***2006*** | *1,806* | *952* | *4,276* | *11* | *1,189* | *723* | *1,608* | *14* | *2,673* | *1,921* | *3,444* | *5* | *1,663* | *30* |
| ***2007*** | *2,050* | *819* | *3,951* | *20* | *1,208* | *440* | *1,667* | *16* | *2,504* | *2,374* | *2,811* | *4* | *1,759* | *40* |
| ***2008*** | *1,939* | *857* | *3,041* | *16* | *1,188* | *577* | *2,439* | *20* | *2,240* | *2,240* | *2,240* | *1* | *1,541* | *37* |
| ***2009*** | *1,843* | *1,258* | *2,857* | *9* | *1,261* | *655* | *1,955* | *16* | - | - | - | - | *1,471* | *25* |
| ***2010*** | *1,457* | *838* | *2,683* | *10* | *1,506* | *599* | *2,308* | *16* | *2,344* | *916* | *3,039* | *4* | *1,602* | *30* |
| ***2011*** | *1,713* | *866* | *3,387* | *17* | *1,366* | *489* | *2,059* | *28* | *2,016* | *1,684* | *2,486* | *6* | *1,558* | *51* |
| ***2012*** | *1,741* | *942* | *3,373* | *17* | *1,426* | *761* | *2,631* | *33* | *2,277* | *1,041* | *3,206* | *7* | *1,624* | *57* |
| ***2013*** | *1,733* | *731* | *3,044* | *18* | *1,437* | *723* | *2,286* | *21* | *1,892* | *1,572* | *2,212* | *2* | *1,589* | *41* |
| ***2014*** | *1,836* | *816* | *2,745* | *20* | *1,560* | *943* | *2,774* | *14* | *3,570* | *1,520* | *5,381* | *4* | *1,917* | *38* |
| ***Avg/Total*** | *1,895* | *731* | *4,289* | *212* | *1,336* | *440* | *2,848* | *256* | *2,448* | *916* | *5,381* | *54* | *1,678* | *522* |

| **Energy-Equivalent Stiffness (Kw400) (N/mm)** | | | | | | | | | | | | | | |
|---|---|---|---|---|---|---|---|---|---|---|---|---|---|---|
| **Year** | **MPV** | | | | **PC** | | | | **PU** | | | | **Avg of 3 Classes** | **Total Count** |
| | **Stiffness** | **Min** | **Max** | **Count** | **Stiffness** | **Min** | **Max** | **Count** | **Stiffness** | **Min** | **Max** | **Count** | | |
| **2002** | 1,582 | 1,044 | 2,257 | 21 | 1,203 | 805 | 1,870 | 19 | 1,650 | 1,408 | 2,022 | 5 | 1,429 | 45 |
| **2003** | 1,667 | 752 | 2,441 | 15 | 1,104 | 639 | 1,635 | 17 | 1,474 | 1,395 | 1,619 | 4 | 1,380 | 36 |
| **2004** | 1,527 | 644 | 2,472 | 18 | 1,085 | 754 | 1,787 | 26 | 1,928 | 1,769 | 2,038 | 3 | 1,308 | 47 |
| **2005** | 1,491 | 1,008 | 2,181 | 20 | 1,024 | 747 | 1,376 | 16 | 1,645 | 1,336 | 1,913 | 9 | 1,356 | 45 |
| **2006** | 1,447 | 882 | 2,334 | 11 | 1,047 | 736 | 1,295 | 14 | 1,633 | 1,430 | 1,961 | 5 | 1,291 | 30 |
| **2007** | 1,660 | 859 | 2,331 | 20 | 1,158 | 756 | 1,566 | 16 | 1,973 | 1,901 | 2,051 | 4 | 1,490 | 40 |
| **2008** | 1,533 | 688 | 2,302 | 16 | 1,072 | 444 | 1,816 | 20 | 2,098 | 2,098 | 2,098 | 1 | 1,299 | 37 |
| **2009** | 1,492 | 1,101 | 1,851 | 9 | 1,204 | 597 | 1,909 | 16 | 0 | 0 | 0 | 0 | 1,307 | 25 |
| **2010** | 1,221 | 848 | 1,640 | 10 | 1,250 | 698 | 1,766 | 16 | 1,666 | 1,027 | 2,228 | 4 | 1,296 | 30 |
| **2011** | 1,478 | 760 | 2,084 | 17 | 1,231 | 727 | 2,072 | 28 | 1,771 | 1,413 | 1,917 | 6 | 1,377 | 51 |
| **2012** | 1,513 | 1,139 | 2,067 | 17 | 1,233 | 674 | 1,825 | 33 | 1,676 | 1,020 | 1,969 | 7 | 1,371 | 57 |
| **2013** | 1,396 | 917 | 1,712 | 18 | 1,305 | 895 | 1,753 | 21 | 1,542 | 1,539 | 1,544 | 2 | 1,356 | 41 |
| **2014** | 1,382 | 969 | 1,853 | 20 | 1,214 | 805 | 1,588 | 14 | 1,974 | 1,590 | 2,143 | 4 | 1,382 | 38 |
| **Avg/Total** | 1,502 | 644 | 2,472 | 212 | 1,171 | 444 | 2,072 | 256 | 1,720 | 1,020 | 2,228 | 54 | 1,362 | 522 |

| Static Stiffness (N/mm) | | | | | | | | | | | | | | |
|---|---|---|---|---|---|---|---|---|---|---|---|---|---|---|
| Year | MPV | | | | PC | | | | PU | | | | Avg of 3 Classes | Total Count |
| | Stiffness | Min | Max | Count | Stiffness | Min | Max | Count | Stiffness | Min | Max | Count | | |
| 2002 | 2,341 | 1,104 | 7,762 | 22 | 1,578 | 1,051 | 2,758 | 22 | 1,635 | 1,312 | 2,065 | 5 | 1,926 | 49 |
| 2003 | 2,267 | 1,585 | 4,927 | 16 | 1,657 | 1,035 | 4,230 | 19 | 1,850 | 1,359 | 2,615 | 4 | 1,927 | 39 |
| 2004 | 2,194 | 1,477 | 3,602 | 18 | 1,762 | 926 | 3,597 | 26 | 1,967 | 1,827 | 2,111 | 4 | 1,941 | 48 |
| 2005 | 1,944 | 1,156 | 3,041 | 21 | 1,762 | 979 | 4,113 | 18 | 2,271 | 1,330 | 3,474 | 10 | 1,944 | 49 |
| 2006 | 2,152 | 1,226 | 3,910 | 15 | 1,688 | 899 | 2,746 | 18 | 2,060 | 1,721 | 2,306 | 6 | 1,924 | 39 |
| 2007 | 2,045 | 1,294 | 3,252 | 20 | 1,687 | 1,024 | 2,477 | 19 | 2,081 | 1,439 | 3,143 | 5 | 1,895 | 44 |
| 2008 | 2,509 | 1,511 | 5,434 | 17 | 2,178 | 1,093 | 5,883 | 24 | 1,844 | 1,507 | 2,035 | 3 | 2,283 | 44 |
| 2009 | 2,312 | 1,259 | 5,689 | 11 | 1,864 | 1,108 | 3,613 | 16 | 2,189 | 1,693 | 3,144 | 4 | 2,065 | 31 |
| 2010 | 1,923 | 1,224 | 3,977 | 11 | 1,887 | 1,258 | 3,039 | 18 | 2,881 | 1,224 | 4,638 | 4 | 2,020 | 33 |
| 2011 | 1,960 | 1,304 | 2,941 | 19 | 2,203 | 912 | 9,679 | 32 | 2,103 | 1,588 | 3,039 | 8 | 2,111 | 59 |
| 2012 | 2,209 | 1,244 | 3,797 | 21 | 2,120 | 1,015 | 4,612 | 38 | 2,373 | 1,180 | 4,692 | 9 | 2,181 | 68 |
| 2013 | 2,305 | 1,392 | 4,567 | 20 | 2,133 | 1,027 | 4,617 | 34 | 1,199 | 562 | 1,835 | 2 | 2,161 | 56 |
| 2014 | 1,931 | 1,015 | 4,765 | 20 | 1,754 | 1,257 | 2,620 | 16 | 2,515 | 1,506 | 4,453 | 6 | 1,947 | 42 |
| Avg/Total | 2,160 | 1,015 | 7,762 | 231 | 1,913 | 899 | 9,679 | 300 | 2,149 | 562 | 4,692 | 70 | 2,035 | 601 |

| Dynamic Stiffness (N/mm) | | | | | | | | | | | | | | |
|---|---|---|---|---|---|---|---|---|---|---|---|---|---|---|
| Year | MPV | | | | PC | | | | PU | | | | Avg of 3 Classes | Total Count |
| | Stiffness | Min | Max | Count | Stiffness | Min | Max | Count | Stiffness | Min | Max | Count | | |
| 2002 | 1,253 | 798 | 1,867 | 22 | 953 | 731 | 1,407 | 22 | 1,277 | 1,027 | 1,704 | 5 | 1,121 | 49 |
| 2003 | 1,238 | 840 | 1,949 | 16 | 905 | 565 | 1,358 | 19 | 1,112 | 954 | 1,193 | 4 | 1,063 | 39 |
| 2004 | 1,263 | 799 | 1,965 | 18 | 926 | 624 | 1,380 | 26 | 1,391 | 1,224 | 1,672 | 4 | 1,091 | 48 |
| 2005 | 1,138 | 743 | 1,827 | 21 | 868 | 616 | 1,289 | 18 | 1,389 | 1,035 | 1,795 | 10 | 1,090 | 49 |
| 2006 | 1,250 | 755 | 1,746 | 15 | 871 | 537 | 1,304 | 18 | 1,460 | 1,016 | 1,715 | 6 | 1,107 | 39 |
| 2007 | 1,260 | 868 | 1,668 | 20 | 922 | 748 | 1,295 | 19 | 1,577 | 1,109 | 2,009 | 5 | 1,150 | 44 |
| 2008 | 1,282 | 832 | 1,851 | 17 | 1,033 | 672 | 1,706 | 24 | 1,418 | 1,250 | 1,568 | 3 | 1,156 | 44 |
| 2009 | 1,186 | 881 | 1,563 | 11 | 975 | 648 | 1,342 | 16 | 1,539 | 1,463 | 1,581 | 4 | 1,123 | 31 |
| 2010 | 1,031 | 812 | 1,576 | 11 | 1,034 | 732 | 1,479 | 18 | 1,541 | 889 | 1,933 | 4 | 1,094 | 33 |
| 2011 | 1,085 | 727 | 1,680 | 19 | 954 | 662 | 1,681 | 32 | 1,457 | 1,240 | 1,745 | 8 | 1,064 | 59 |
| 2012 | 1,180 | 870 | 1,638 | 21 | 1,012 | 605 | 2,250 | 38 | 1,409 | 915 | 2,184 | 9 | 1,117 | 68 |
| 2013 | 1,209 | 871 | 1,566 | 20 | 982 | 668 | 1,481 | 34 | 1,397 | 1,339 | 1,454 | 2 | 1,078 | 56 |
| 2014 | 1,075 | 858 | 1,397 | 20 | 951 | 650 | 1,219 | 16 | 1,333 | 939 | 1,771 | 6 | 1,065 | 42 |
| Avg/Total | 1,191 | 727 | 1,965 | 231 | 959 | 537 | 2,250 | 300 | 1,409 | 889 | 2,184 | 70 | 1,101 | 601 |

| Peak Acceleration (G's) | | | | | | | | | | | | | | |
|---|---|---|---|---|---|---|---|---|---|---|---|---|---|---|
| Year | MPV | | | | PC | | | | PU | | | | | |
| | Accl. | Min | Max | Count | Accel. | Min | Max | Count | Accel. | Min | Max | Count | Avg of 3 Classes | Total Count |
| 2002 | 40 | 58 | 30 | 22 | 41 | 55 | 29 | 21 | 44 | 54 | 40 | 5 | 41 | 48 |
| 2003 | 40 | 49 | 29 | 16 | 40 | 60 | 30 | 19 | 41 | 55 | 32 | 4 | 40 | 39 |
| 2004 | 42 | 55 | 28 | 18 | 42 | 62 | 32 | 27 | 36 | 43 | 32 | 4 | 41 | 49 |
| 2005 | 39 | 54 | 29 | 21 | 39 | 55 | 31 | 18 | 41 | 50 | 27 | 10 | 39 | 49 |
| 2006 | 44 | 65 | 32 | 15 | 42 | 70 | 32 | 18 | 42 | 49 | 35 | 6 | 43 | 39 |
| 2007 | 43 | 58 | 32 | 20 | 41 | 61 | 32 | 19 | 48 | 54 | 35 | 5 | 43 | 44 |
| 2008 | 46 | 58 | 33 | 17 | 44 | 71 | 32 | 24 | 36 | 38 | 36 | 3 | 44 | 44 |
| 2009 | 46 | 61 | 36 | 11 | 44 | 62 | 34 | 16 | 39 | 45 | 34 | 4 | 44 | 31 |
| 2010 | 47 | 56 | 34 | 11 | 44 | 68 | 29 | 18 | 49 | 58 | 39 | 4 | 46 | 33 |
| 2011 | 45 | 71 | 33 | 19 | 43 | 66 | 31 | 32 | 42 | 52 | 33 | 8 | 44 | 59 |
| 2012 | 46 | 60 | 26 | 21 | 46 | 72 | 32 | 38 | 39 | 56 | 27 | 9 | 45 | 68 |
| 2013 | 51 | 85 | 30 | 20 | 43 | 67 | 30 | 34 | 36 | 38 | 34 | 2 | 45 | 56 |
| 2014 | 44 | 63 | 35 | 20 | 48 | 71 | 33 | 16 | 41 | 51 | 33 | 6 | 45 | 42 |
| Avg/Total | 44 | 85 | 26 | 231 | 43 | 72 | 29 | 300 | 41 | 58 | 27 | 70 | 43 | 601 |

| Time to Zero Velocity (ms) | | | | | | | | | | | | | | |
|---|---|---|---|---|---|---|---|---|---|---|---|---|---|---|
| Year | MPV | | | | PC | | | | PU | | | | | |
| | Time | Min | Max | Count | Time | Min | Max | Count | Time | Min | Max | Count | Avg of 3 Classes | Total Count |
| 2002 | 74 | 63 | 98 | 22 | 70 | 58 | 84 | 21 | 73 | 69 | 79 | 5 | 72 | 48 |
| 2003 | 76 | 61 | 96 | 16 | 73 | 61 | 91 | 19 | 77 | 70 | 91 | 4 | 75 | 39 |
| 2004 | 74 | 62 | 91 | 18 | 72 | 61 | 91 | 27 | 78 | 70 | 85 | 4 | 73 | 49 |
| 2005 | 78 | 60 | 95 | 21 | 75 | 61 | 93 | 18 | 73 | 63 | 87 | 10 | 76 | 49 |
| 2006 | 73 | 64 | 97 | 15 | 74 | 60 | 93 | 18 | 72 | 62 | 82 | 6 | 74 | 39 |
| 2007 | 73 | 63 | 98 | 20 | 70 | 62 | 78 | 19 | 75 | 57 | 106 | 5 | 72 | 44 |
| 2008 | 70 | 59 | 80 | 17 | 68 | 46 | 84 | 24 | 73 | 68 | 78 | 3 | 69 | 44 |
| 2009 | 70 | 58 | 76 | 11 | 73 | 64 | 89 | 16 | 73 | 69 | 77 | 4 | 72 | 31 |
| 2010 | 73 | 60 | 84 | 11 | 71 | 60 | 82 | 18 | 66 | 56 | 79 | 4 | 71 | 33 |
| 2011 | 74 | 64 | 85 | 19 | 71 | 57 | 86 | 32 | 73 | 62 | 81 | 8 | 72 | 59 |
| 2012 | 71 | 61 | 96 | 21 | 69 | 42 | 85 | 38 | 76 | 57 | 98 | 9 | 70 | 68 |
| 2013 | 69 | 55 | 79 | 20 | 70 | 47 | 87 | 34 | 73 | 69 | 78 | 2 | 70 | 56 |
| 2014 | 71 | 60 | 79 | 20 | 68 | 61 | 78 | 16 | 76 | 62 | 92 | 6 | 71 | 42 |
| Avg/Total | 73 | 55 | 98 | 231 | 71 | 42 | 93 | 300 | 74 | 56 | 106 | 70 | 72 | 601 |

# BEYOND SAFETY LEGISLATION: CONTRIBUTION OF CONSUMER INFORMATION PROGRAMMES TO ENHANCED INJURY MITIGATION OF PEDESTRIANS DURING ACCIDENTS WITH MOTOR VEHICLES

**Oliver Zander**
Federal Highway Research Institute (BASt)
Germany

**Dirk-Uwe Gehring**
BGS Boehme & Gehring GmbH
Germany

**Michiel van Ratingen**
European New Car Assessment Programme (Euro NCAP)
Belgium

Paper Number 15-0258

## ABSTRACT

During the past five years, a Euro NCAP technical working group on pedestrian safety has been working on improving test and assessment procedures for enhanced passive pedestrian safety.

After harmonizing the tools and procedures as much as possible with legislation, the work was mainly focused on the development of grid procedures for the pedestrian body regions head, upper leg with pelvis and lower leg with knee. Furthermore, the test parameters for the head and the upper leg were revised, a new lower legform impactor was introduced and the injury thresholds were adjusted or, where necessary, the injury criteria were changed. Finally, the assessment limits and colour scheme were refined, widening the range and adding two more colours in order to provide a more detailed description of the pedestrian safety performance.

By abstaining from an assessment based on a worst point selection philosophy, the improved test point determination procedures that were introduced during the years 2013 and 2014 give a more homogeneous, high resolution picture of the pedestrian safety performance of the vehicle frontends. By using a uniform grid for each test zone approximately 200 test points, evenly distributed within each area, can now be assessed per vehicle.
The introduction of the flexible pedestrian legform impactor in 2014 enables a more realistic injury prediction of the knee and the tibia using a biofidelic test tool.

With the new upper legform test that has been launched in 2015 the assessment in that area is now focusing on the injured body region instead of the injury causing vehicle part and thus is aligned with the approach in the remaining body regions head and lower leg. At the same time, a monitoring test with the headform impactor against the bonnet leading edge is closing the possible gap between the test areas to identify injury causing vehicle parts that moved out of focus due to the introduction of the new upper legform test.

The paper describes the new test and assessment procedures with their underlying philosophy and gives an outlook in terms of open issues, specifying the needs for further improvement in the future.

In parallel to the work of the pedestrian subgroup, a Euro NCAP working group on heavy vehicles introduced a set of protocol changes in 2011 that were related to the assessment of M1 vehicles derived from commercial vehicles, with a gross vehicle weight between 2.5 and 3.5 tons and 8 or 9 seats. The paper also investigates the applicability of the new pedestrian test and assessment procedures to heavy vehicles.

## INTRODUCTION

A Euro NCAP technical working group on pedestrian safety has elaborated during the past five years updated protocols for testing and assessment of passive pedestrian protection systems of passenger cars. After harmonizing the test tools and procedures as much as possible with pedestrian legislation, the overall objective of the group was to make the assessment of the pedestrian protection offered by the vehicle front-end more robust, reproducible, accurate and realistic. The work was mainly focused on the improvement of test procedures for the body regions head, pelvis, upper leg and lower leg, also including a new impactor for the lower leg test as well as a vehicle grid markup, the adaptation of injury criteria and a modified visualization by introducing a five colour scheme for all rated test procedures.

In parallel to the activities undertaken by the pedestrian working group, an ad hoc group of Euro NCAP developed specific test procedures for active systems of passive pedestrian safety, in particular active bonnets, that were as from version 5.3 onwards included within the pedestrian testing protocol. Another working group dealt with issues related to heavy M1 vehicles derived from commercial vehicles and the applicability of the new pedestrian test and assessment procedures to this class of vehicles.

This paper describes the main results of work undertaken by the pedestrian safety working group of Euro NCAP with input from the ad hoc working group on active pedestrian protection systems and the working group on heavy commercial vehicles that were successively implemented within the Euro NCAP test and assessment protocols for pedestrian protection.

## EURO NCAP UNTIL 2012

The first phase of work performed by the pedestrian safety group was mainly focused on a harmonization with Comission Regulation (EC) No. 631/2009 prescribing the test and assessment procedures for M1 vehicle type approval in Europe (European Commission, 2009). The borderline of test areas for child and adult headform impactors that were previously, in principle, described by wrap around distances (WAD) between 1000 and 1500 for the child headform impactor and between 1500 and 2100 for the adult headform impactor, was changed from WAD 1500 to WAD 1700, following the technical prescriptions of the Commission Regulation. Different to a hard borderline between both headfrom impact zones in legislation, Euro NCAP defined a transitional area between WAD 1500 and WAD 1700 where to use the adult headform impactor in the windscreen and windscreen base area and the child headform impactor on the bonnet and its periphery. In 2010, by introducing testing protocol version 5.0, the headforms themselves were changed from a 4.8 kg adult headform impactor with 165 mm diameter to a 4.5 kg impactor with unchanged dimensions, and from a 2.8 kg child headform impactor with a diameter of 130 mm to a 3.5 kg impactor with a diameter of 165 mm.

The philosophy of a worst point selection remained unchanged within Euro NCAP until the end of 2012: Both, the adult and the child headform areas were divided into six sixths, each of them subdivided into four quarters. While Euro NCAP selected the potentially most injurious impact point within each of the twelve sixths, the vehicle manufacturer was allowed to nominate up to three quarters within each sixth where then Euro NCAP again picked the expected hardest impact point. Altogether between 12 and 24 head impact points were selected, each sixth scored with a maximum of 2 assessment points. Although being assessed entirely, not all of these points were actually tested, given that points located on certain structures were defaulted either red (no score, e.g. on the A-Pillar) or green (full score, e.g. on the centre of the windscreen), symmetry occurred or that previous tests on adjacent areas already indicated the performance in the area to be assessed. For the upper and lower legform area, the method of worst point selection remained unchanged as well: both areas were divided into three thirds, each of them subdivided into two halves. Again, Euro NCAP selected the most injurious point within each third, while the manufacturer was given the possibility to nominate the remaining half of each third, where afterwards Euro NCAP again selected the hardest point. Altogether, between 3 and 6 impact points were determined in both, the upper and the lower legform area, each third scored with a maximum of 2 assessment points. Like in the headform area not all of these points were tested, given that symmetry occurred or there was agreement between the manufacturer and Euro NCAP of particular points defaulted red (no score) without being tested.

The last version of the Euro NCAP test and assessment protocols applying the philosophy of worst impact point selection is still valid nowadays as fall back scenario when the manufacturer opposes to the grid procedure that will be described in the following. In that case, the five colour scheme has to be applied.

An overview of the Euro NCAP test and assessment procedure before 2013 is depicted in Figure 1:

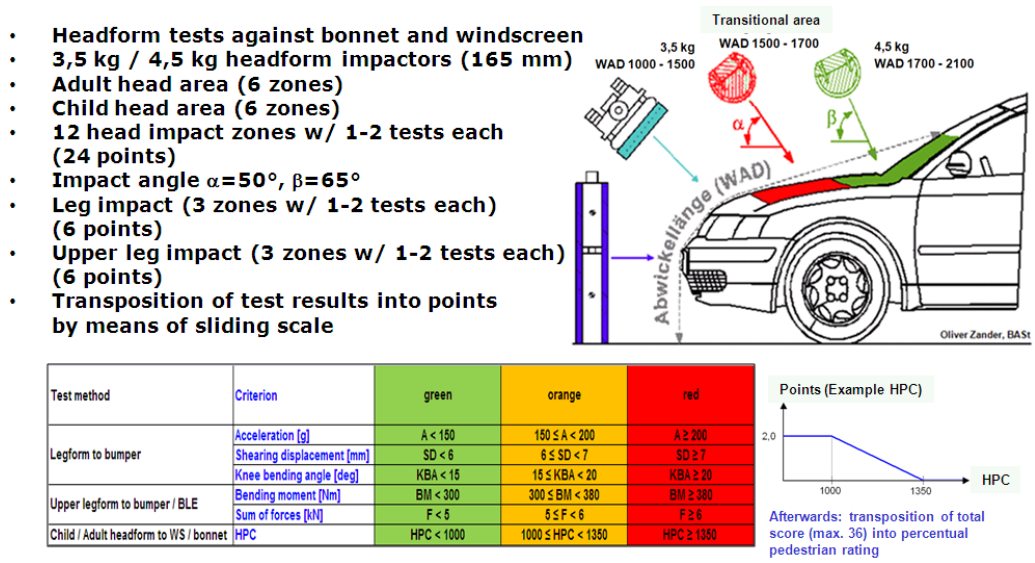


| Test method | Criterion | green | orange | red |
|---|---|---|---|---|
| Legform to bumper | Acceleration [g] | A < 150 | 150 ≤ A < 200 | A ≥ 200 |
| | Shearing displacement [mm] | SD < 6 | 6 ≤ SD < 7 | SD ≥ 7 |
| | Knee bending angle [deg] | KBA < 15 | 15 ≤ KBA < 20 | KBA ≥ 20 |
| Upper legform to bumper / BLE | Bending moment [Nm] | BM < 300 | 300 ≤ BM < 380 | BM ≥ 380 |
| | Sum of forces [kN] | F < 5 | 5 ≤ F < 6 | F ≥ 6 |
| Child / Adult headform to WS / bonnet | HPC | HPC < 1000 | 1000 ≤ HPC < 1350 | HPC ≥ 1350 |




Afterwards: transposition of total score (max. 36) into percentual pedestrian rating

***Figure 1. Euro NCAP test and assessment procedure before 2013.***

**EURO NCAP 2013**

The second phase of work performed by the pedestrian safety working group mainly concentrated on the grid procedure for the headform impactor tests. The principal idea of the new method was to abstain from a, to some extent, subjectively performed selection of worst case head impact points, towards an objective and homogeneous assessment of the entire headform area. By introducing the possibility of providing in-house simulation results by the vehicle manufacturer, the amount of tests was limited, keeping the testing effort in the previous range. At the same time, the sliding scale assessment procedure between HIC 1000 and HIC 1350 with three colours was changed to an incremental approach between HIC 650 and HIC 1700 and five color bands, the middle three of them having a range of HIC 350: HIC below 650 - green, 2 points; HIC between 650 and 1000 - yellow, 1.5 points; HIC between 1000 and 1350 - orange, 1 point; HIC between 1350 and 1700 - brown, 0.5 points; HIC over 1700 - red, no point.

According to the new method and starting from the intersection between the vehicle's vertical longitudinal centerplane and the WAD 1000 (C 0,0, see Figure 2) a grid with 100 mm * 100 mm resolution on the xy plane is vertically projected onto the headform area that is, in principle, described by the WAD 1000 and 2100 and the side reference lines, where all grid points within a distance of less than 50 mm to the side reference lines are deleted, and additional grid points are marked on the side reference lines on the A-pillar. After the provision of the safety performance by means of colour information for each of the determined grid points by the OEM, a default minimum of 10 and, on request of the vehicle manufacturer, a maximum of 20 verification points is generated randomly. Additionally, the manufacturer is given the opportunity to select a maximum of 8 blue zones, each consisting of 1 or 2 grid points, where the safety performance is unknown or previous tests have indicated instable results, and which are tested once on the point selected by Euro NCAP, unless symmetries are being applied. Thus, in total a minimum of 10 and a maximum of 28 head impact tests are to be performed according to the headform grid method. After testing, a correction factor is calculated by the quotient of the sum of actual verification test results and the sum of the points resulting from the colour predictions. The correction factor provides an indication of how accurate actual testing matches the prediction and should be between 0.75 and 1.25 for the predictions to be accepted by Euro NCAP. By multiplying the sum of points obtained by the colour predictions times the correction factor, the actual performance of the predicted grid points is calculated.

In a last step, the total head score is calculated by including the number of green defaulted points and the actual test result from the blue zones, and scaled to the 24 points that are available for the head performance in box 3 (pedestrian protection) of the Euro NCAP overall rating scheme. A visualization of the test results by applying a five colour code scheme defined by the underlying results to each individual grid point completes the head assessment.

A flowchart describing the principal markup, test and assessment procedures for the headform grid is illustrated in Figure 2:

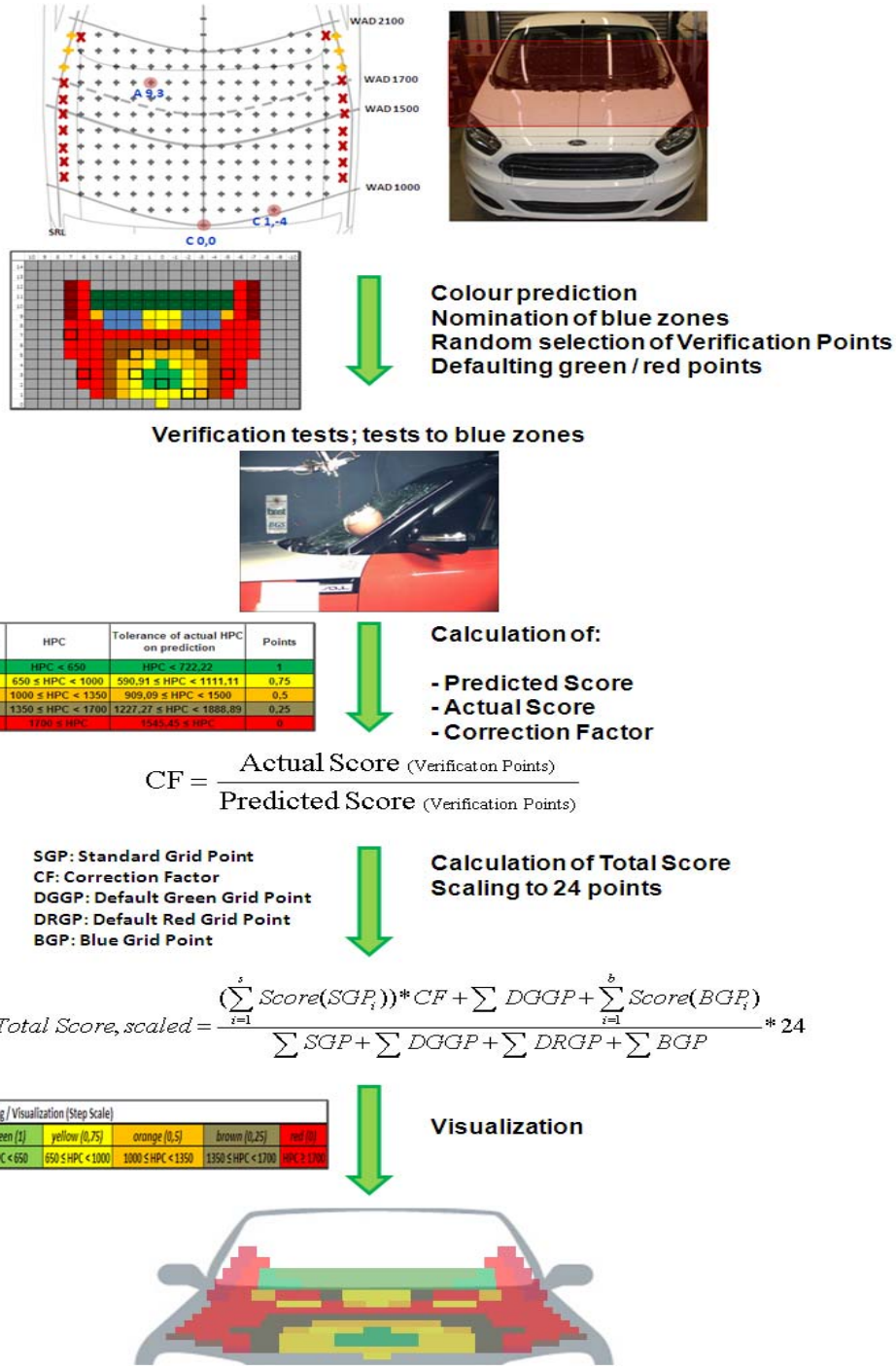


***Figure 2. Euro NCAP headform grid procedure.***

**EURO NCAP 2014**

The next big step in the further development of the Euro NCAP pedestrian test and assessment procedures was finalized with the introduction of the flexible pedestrian legform impactor (FlexPLI) from the beginning of the year 2014 on. The FlexPLI with enhanced biomechanical properties compared to those of the lower legform impactor according to EEVC, in particular in the knee and tibia area, was developed by the Japan Automobile Research Institute (JARI) as from the year 2000 onwards and evaluated by a technical evaluation group (TEG) under the umbrella of the Working Party on Passive Safety (GRSP) of the United Nations Economic Commission for Europe (UNECE) since 2005. Last issues with the impactor were dealt with by an Informal Working Group on Phase 2 of GTR9 before UNECE Working Party 29 finally adopted the FlexPLI, in a first step, for the 01 series of amendments of UN Regulation No. 127 on Pedestrian Safety (UNECE, 2015) that has become effective on 22 January 2015. Until the mandatory use of the FlexPLI as from 1 September 2017 onwards, the vehicle manufacturers are given the choice to either submit new vehicles to type approval using the new test tool or to alternatively use the lower legform impactor developed by Working Group 17 of the European Enhanced Vehicle-safety Committee (EEVC).

With the implementation of tests with the FlexPLI, the Euro NCAP markup and test procedures changed from the subdivision of the upper and lower legform test area into six subareas each to a grid markup, testing every second grid point and allocating the test result to the corresponding adjacent grid points; besides, where possible, application of symmetry.

For the lower legform tests with the FlexPLI, starting at $y_0$ (vehicle centreline), a grid with 100 mm resolution is marked in lateral direction onto the upper bumper reference line. If the distance between the last (outermost) grid point and the end of the test area is greater than 50 mm, an additional grid point is marked at a lateral distance of 50 mm to the last grid point onto the upper bumper reference line. After defining the starting point which is located either on $y_0$ or one of its adjacent points, every second grid point is selected and tested. Where possible, symmetries are to be applied. All asymmetrical grid points not being tested are awarded with the worse of the two results coming from both adjacent grid points. Prior to the determination of the starting point by Euro NCAP, the vehicle manufacturer is given the choice to nominate grid points to be exempted from being assessed by taking over the results from adjacent or symmetrical identical grid points, thus these grid points need to be tested.

Along with the introduction of the FlexPLI in Euro NCAP, Zander (2011) derived upper performance limits from the injury criteria of the FlexPLI as equivalents for 20% tibia fracture risk, 15 deg knee bending angle of the EEVC WG 17 pedestrian legform impactor and a transposition of the results of PMHS testing reported by Bhalla et al. (2003) to the FlexPLI. In terms of assessment of the lower legform test results, the pedestrian subgroup decided to equally balance the injury risks related to the medial collateral ligament (MCL) and the tibia segments, whereas points for the MCL are only awarded in case of not exceeding the identified risk of 10 mm elongation for cruciate ligament rupture (ACL/PCL). Furthermore, as far as the tibia is concerned, only the highest of the four bending moments is taken into account for the assessment. Between the defined upper and lower performance limits for MCL elongation and tibia bending moment, a sliding scale is applied to both criteria. The total score for the lower legform area is calculated by adding the points for the individual grid points and scaling the results to 6 points. For visualization, a five colour scheme is applied.

Figure 3 describes in principle the markup, test and assessment procedure for the tests with the FlexPLI:

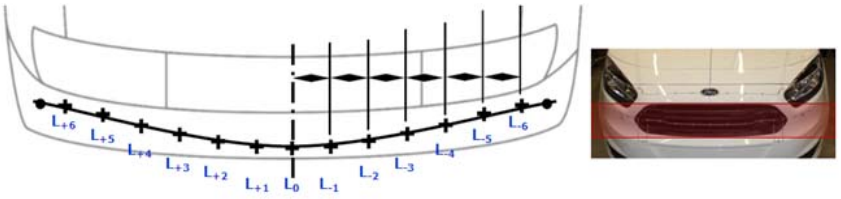


OEM to nominate points to be tested in either case
Definition of starting point ($L_0$ or $L_{+1}$)
Use of symmetry, where applicable
Testing of every second grid point
Allocation of results to adjacent points

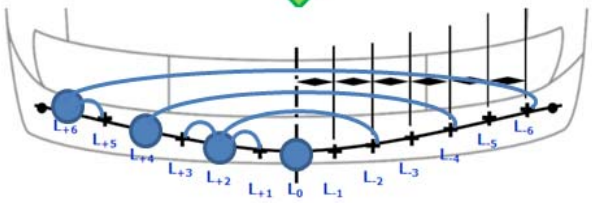


| Criterion | Full score | Sliding Scale | 0 | Points |
|---|---|---|---|---|
| Tibia BM [Nm] | $BM_{max} < 282$ | $282 \leq BM_{max} < 340$ | $BM_{max} \geq 340$ | 0 - 0,5 |
| MCL-EL [mm] | $EL_{MCL} < 19$ | $19 \leq EL_{MCL} < 22$ | $EL_{MCL} \geq 22$ | 0 - 0,5 |
| ACL/PCL-EL [mm] | $EL_{ACL/PCL} < 10$ | | $EL_{ACL/PCL} \geq 10$ | n/a |

Calculation of grid point score:

- Tibia BM & MCL (use 10 mm ACL/PCL switch)
- Use of sliding scale
- Weighting of tibia and knee (50%/50%)

$$Score(GP) = Score(TibiaBM_{max}) + Score(MCL)$$

Calculation of total score
Scaling to 6 points

$$\frac{\sum_{i=1}^{n} Score(GP_i)}{n} * 6$$

| Score (GP) | S=1 | 1>S>0,75 | 0,75≥S>0,5 | 0,5≥S>0,25 | 0,25≥S |
|---|---|---|---|---|---|

Visualization

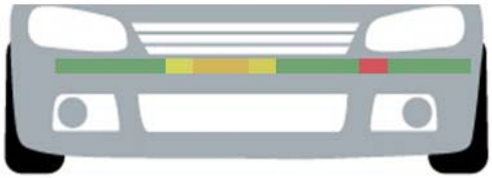

***Figure 3. Euro NCAP FlexPLI grid procedure.***

In 2014, the test procedure and the injury criteria for the upper legform impactor remained in principle unchanged. For the markup, however, a grid along with a five colour scheme based on grid point scores as for the headform and the lower legform tests was inroduced. Besides, in 2014 only, a requirement was applied that in case of the distance between the last (outermost) grid point and the corner reference point being greater than 75 mm, an additional grid point was to be marked at a lateral distance of 50 mm to the corner reference point onto the bonnet leading edge reference line.

**EURO NCAP 2015**

In 2015, Euro NCAP introduced two new pedestrian protection tests, namely the new upper legform test replacing the upper legform to bonnet leading edge test, and the headform to bonnet leading edge test.

**Upper legform test**

As from 2015 onwards, the test with the upper legform impactor was fundamentally changed. Main reason for the significant change was an analysis of accident data showing a decreasing number of upper leg injuries caused by the bonnet leading edge, mainly due to the development of passenger vehicle frontends away from the typical Sedan design with sharp and high leading edges towards rounded frontends with lower and significantly softened leading edges. Besides, a change of injury patterns could be observed. Thus, a test with the upper legform impactor against the bonnet leading edge was no longer seen as best representing present real world injury data. However, real world accident data also showed that injuries of femur and pelvis are still of a high importance and therefore need to be addressed. Therefore, since this point in time, the injured body regions (pelvis, femur) rather than the injury causing vehicle parts are in the focus of assessment. Thus, the new test procedure is in line with the assessment of head and lower leg injuries. The new upper legform test aims for a more realistic simulation of the correct impact height and position of the human thigh and pelvis during an impact. Therefore, the nominal impactor weight is standardized to 7.4 kg and the upper load cell of the impactor is approximately aligned with WAD 930 as the height of the human hip joint. As the impactor centerline always aims at WAD 775, the corresponding WAD line is used as markup line for the upper legform grid points. The angle of impact $\alpha$ depends on the outer vehicle contour and is perpendicular to a line on the same vehicle vertical longitudinal plane as the respective grid point, connecting the WAD 930 with the internal bumper reference line (IBRL). The IBRL is a connection line of the averaged grid point bumper beam heights (i.e. averaged height of the bumper beam at the lateral grid point position and its two adjacent markings at a distance of 33,3 mm from the grid point), marked on the bumper beam and projected onto the bumper fascia. The nominal vehicle speed $v_0$ at time of first pedestrian contact, the relative speed $v_c$ and the angle of impact $\alpha$ of the upper leg, both measured at time of mid femur contact with the vehicle front, are used for calculation of the test speed $v_t$ under application of a uniform impactor test mass of 10.5 kg (Figure 4). These calculations lead to possible impact angles of up to 44.7 degrees and maximum test speeds of 9.3m/s. As a comparison with the previous energy calculation procedure shows that the impact energy is reduced for many vehicles, the lower energy limit is reduced to 160 J, i.e. tests will now also be performed with energies below 200 J up to a minimum of 160 J. The upper energy limit of 700 J is not needed anymore because the results from the energy calculation are limited to 456 J.

For the upper legform test, starting at $y_{0,}$ a grid with 100 mm resolution is marked in lateral direction onto the WAD 775 reference line up to a distance of no less than 50 mm to the lateral projection of the corner reference point. After defining the starting point which is located either on $y_0$ or one of its adjacent points, every second grid point is selected and tested. Again, whereever possible, symmetries are to be applied. All asymmetrical grid points not being tested are awarded with the worse of the two results coming from both adjacent grid points. As for the lower legform tests, prior to the determination of the starting point by Euro NCAP, the vehicle manufacturer is given the opportunity to nominate grid points to be exempted from being assessed by taking over the results from adjacent or symmetrical identical grid points which thus must be tested.

Regarding the test evaluation, in contrary to the tests with the FlexPLI, no weighting of the maximum bending moments and the maximum sum of forces is done, but, as before, the worst of the two results is taken into account only. For the allocation of points to the particular test results, a sliding scale is applied between the upper and lower performance limits, which in terms of the maximum bending moments has been decreased to 285 or 350 Nm respectively.

The total score for the upper legform area is calculated by adding the points for the individual grid points and scaling the results to 6 points. For visualization, the five colour scheme that was already introduced in 2014 remains unchanged.

The flowchart of the upper legform markup, test and assessment procedure is shown in Figure 4:

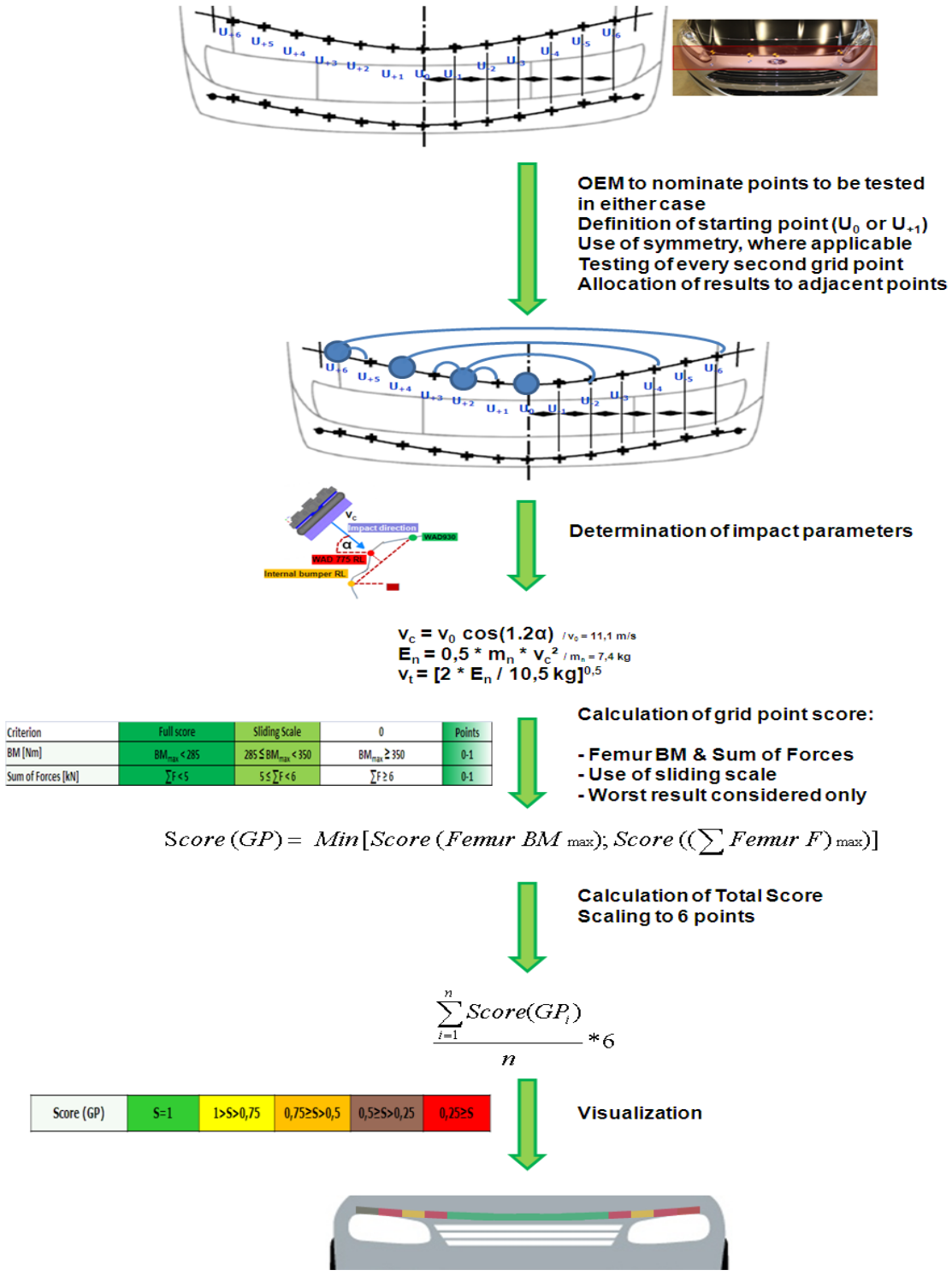


***Figure 4. Euro NCAP New Upper Legform grid procedure.***

**Headform to bonnet leading edge test**

With the introduction of the new upper legform test, the bonnet leading edge is not anymore in the focus of Euro NCAP passive pedestrian safety assessment. Longhitano et al. (2005) and Zander (2014) found the bonnet leading edge having a high relevance as injury causing part in real world accident data. While in most cases, the bonnet leading edge is to some extent also covered by the new upper legform test, in case of being located between WAD 930 and WAD 1000 the bonnet leading edge reference line (BLE-RL) is not assessed anymore, see Figure 5.

***Figure 5. Untested critical area after introduction of Euro NCAP New Upper Legform grid procedure.***

To encounter the injury risk for vulnerable road users, in particular head injuries of small children, that is related to the bonnet leading edge, BASt had proposed to the Euro NCAP pedestrian safety working group a supplementary test with the child headform impactor against the bonnet leading edge as illustrated in Figure 6. The proposal was adopted by Euro NCAP and is detailed in Technical Bulletin 019 (Euro NCAP, 2014). For the vertical longitudinal plane of any upper legform grid point where the bonnet leading edge reference line is located between WAD 930 mm and WAD 1000 mm, an additional test with the child headform impactor is performed at the intersection of the vertical longitudinal plane with the bonnet leading edge reference line at an impact speed of 40 km/h under an impact angle of 20° ±2° to the Ground Reference Level. The result of this test will be monitored against a HIC value of 650.

***Figure 6. Headform to bonnet leading edge test.***

**ACTIVE PEDESTRIAN PROTECTION SYSTEMS OF PASSIVE PEDESTRIAN SAFETY**

An ad hoc Euro NCAP working group on active pedestrian protection systems has developed test and assessment procedures for deployable (non-static) systems, in particular pop up bonnets. As the legal requirements in that area do not cover significant aspects related to a pedestrian impact on a deployable system, the working group defined additional test and assessment procedures such as requirements for sensor systems and actuators to detect the hardest to detect pedestrian, requirements in terms of the total response time (TRT) of the system (time between the first contact of the pedestrian and full deployment of the safety system), performance requirements below the deployment threshold as well as at higher speeds after initiation of the deployment. Furthermore, the bonnet deflection due to pedestrian torso contact at pedestrian head impact location at time of the impact is required to not exceed a certain extent. Finally, the grade of fulfillment of the requirements defines the ambient conditions and test parameters, i.e. whether a system is tested in closed position, in fully deployed position or dynamically. The active pedestrian protection test procedures have been implemented within the test protocol version 5.3 and are valid since January 2011.

## HEAVY VEHICLES

In 2011, the Euro NCAP working group on heavy vehicles finalized the development of a set of changes to the different protocols that were particularly related to the testing and assessment of M1 vehicles derived from commercial vehicles, with a gross vehicle weight between 2,5 and 3,5 tons and 8 or 9 seats. In terms of pedestrian safety, BASt investigated the main differences between passenger cars and heavy commercial vehicles and proposed to the working group a set of particular test parameters that were different to the ones related to the standard pedestrian tests (Zander 2010-1 and 2010-2). Essentially, as main differences, Euro NCAP concluded a uniform head impact angle of 50 degrees rearwards and of 20 degrees forward of the bonnet leading edge reference line. Besides, at impact points with a height of the bonnet leading ede reference line greater than 835 mm, no test with the upper legform impactor against the BLE was required. In terms of rating, a soft landing for heavy vehicles was introduced: while in 2011, a fufilment rate of 25 percent was required for 5 stars balancing criteria, the requirements were identical between commercial vehicles and passenger cars for four and five stars vehicles in 2014.

After finalization of the pedestrian test procedures for 2015, the Euro NCAP working group on pedestrian safety discussed the applicability of the modified tests to commercial vehices. Gehring et al. (2014) examined several heavy commercial vehicles in detail (see Figure 7) and found the general applicability of the pedestrian testing protocol also to heavy vehicles.

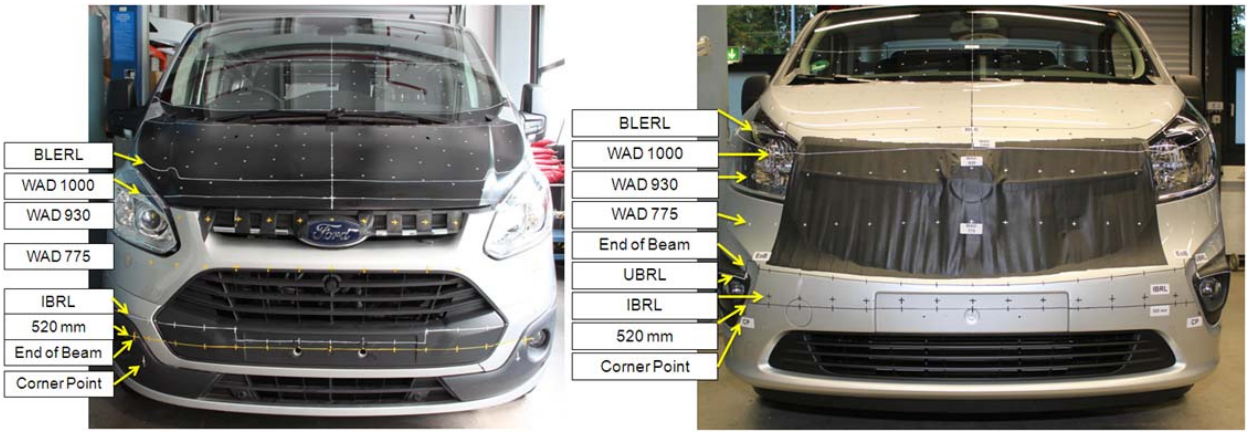


***Figure 7. Investigation on the applicability of pedestrian testing protocol to heavy vehicles.***

As in the meantime a head impact angle of 20 degrees for tests on or forward of the BLERL had already been introduced for passenger cars, the remaining main difference to the pedestrian testing protocol was the adult headform angle of 50 degrees instead of 65 degrees for the passenger cars. During the investigations, Gehring et al. also found some potential for improvement that was well applicable to the pedestrian testing protocol. For practical reasons they proposed for steeper parts of the outer contour of the vehicle to markup the grid using a horizontal instead of a vertical projection. This proposal was adopted by Euro NCAP for all areas forward of the BLERL where the angle of a line, connecting the BLE-RL and WAD 1000 on the vehicle's vertical longitudinal centerplane, is greater than 60 degrees to the ground reference level. For relevant gaps in the markup area, the outer contour of the vehicle is to be approximated with tape, whereas between the lower bumper reference line and the BLE, a wrap around is to be created.

Due to the fact that within the new upper legform test the impactor centreline is always aligned with WAD 775 and thus the grid point height is always below 835 mm, the test exemption that was valid for the first phase of the heavy vehicles protocol is not applicable anymore with the introduction of the new test.

## DISCUSSION

In the past five years, the work performed by the Euro NCAP pedestrian safety working group with input from the ad hoc working group on active pedestrian protection systems as well as the heavy vehicles working group was mainly focused on three topics related to pedestrian safety. The first topic concentrated on harmonization with the legal requirements. In this context, amongst other things, the headform impactors and impact areas as well as the lower performance limits were aligned with the impactors and with the pass/fail criterion for one third of the impact area detailed in Commisson Regulation (EC) No. 631/2009.

The second topic dealt with the objectification of the test procedures which was mainly done by introducing a high resolution grid over the entire front area to be assessed, resulting in detailed and homogeneous information in terms of the pedestrian safety performance. The grid approach has opened up the protocol to virtual testing predictions by vehicle manufacturers based on CAE. This way of combining physical testing and simulations is a first in consumer safety testing. The first two years of experience with the head grid method give evidence that the capability of predicting the safety performance is already at a high level. A study of the results of 70 vehicles tested and assessed according to the 2013 and 2014 protocols shows that the target of a correction factor between 0,75 and 1,25 was met in all but three cases. In most cases, the correction factor was significantly below the phase-in target of a deviation from the actual verification test results of no more than 25 percent. With the majority of cars having a positive correction factor above 1, the mean value was 1,05, meaning only a 5 percent underestimation by the given colour predictions, being well in line with the actual safety performance, proving the feasibility and applicability of the grid method using colour predictions.
Also testing active systems of passive pedestrian safety such as active bonnets is allowing human body model simulations as part of the evidence, what again is a new approach in the world of safety assessment and consumer testing.

The third topic was related to improved biomechanics of the test tools and procedures. With the introduction of the FlexPLI a biofidelic test tool with the capability of simulating the kinematic behaviour and human responses of the lower leg and knee area in an appropriate manner along with new injury criteria was introduced. Here, the first year of testing resulted in a majority of cars performing quite well in the lower leg area. A comparison of the 2013 and 2014 lower legform results gives evidence of the feasibility of the new test method using the FlexPLI. While in 2013 the 31 assessed vehicles resulted in an average of 5.7 points when tested with the EEVC WG 17 lower legform impactor, the mean value of the 39 vehicles tested in 2014 with FlexPLI and grid method was 5,9 points. In 2013, 87% of the vehicles scored full points in the lower legform area; in 2014, 76 % of vehicles had entire green bumper zones. None of the assessed vehicles scored less than 4.8 points.
The upper legform impactor remained, in principle, without further modification but with the focus on the injured body regions pelvis and femur rather than on the bonnet leading edge as injury causing part of the vehicle. To avoid crucial gaps in the assessment, the bonnet leading edge is covered by an additional test with the headform impactor, where necessary.

A fourth topic that has not yet been entirely covered by the work in the past years is the review of pedestrian injury patterns currently existing in real world accidents. Figure 8 depicts injury patterns occurring in vehicle to pedestrian collisions according to AIS98 code based on body parts (Zander et al., 2015):

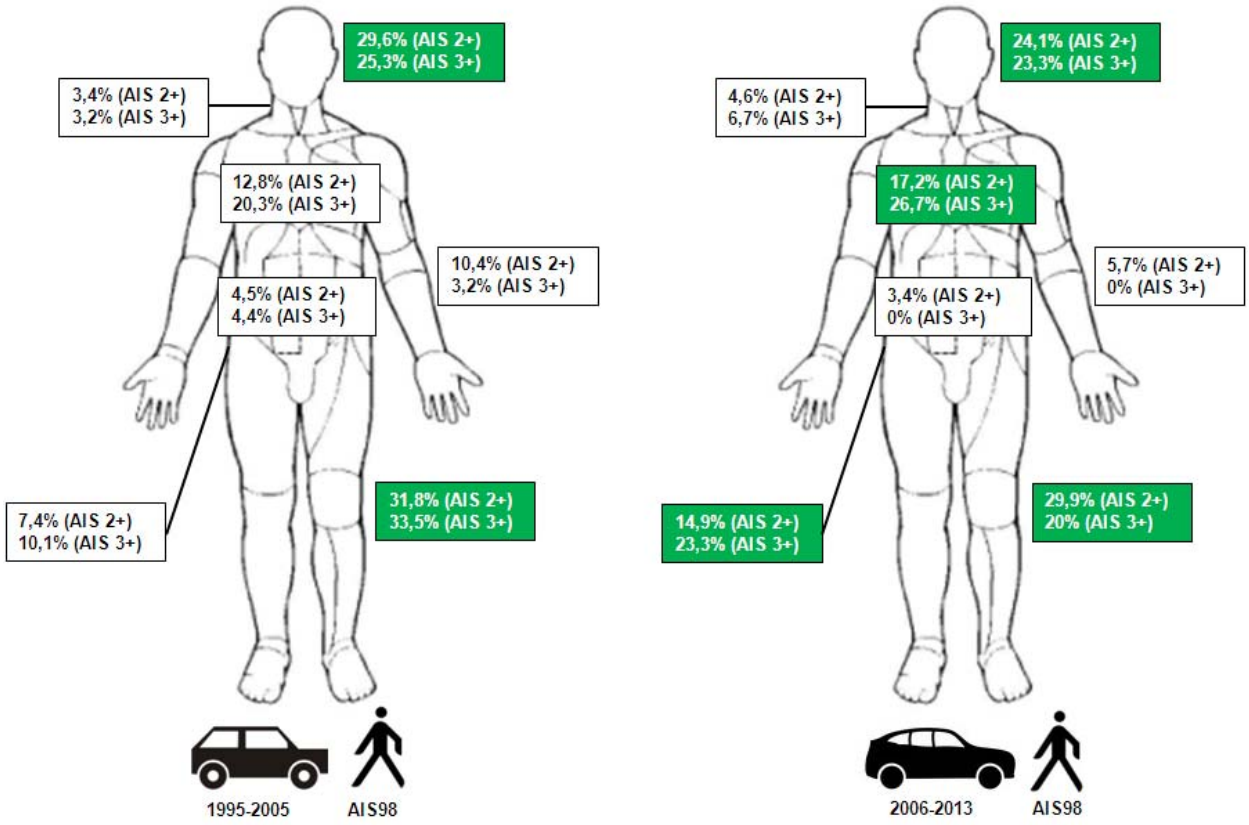


***Figure 8. Injury patterns occurring in vehicle to pedestrian collisions according to AIS98 code based on body parts. The Figure shows the relations between the injury severity from AIS 2 (or AIS 3 respectively) to AIS6 (i.e. AIS2+ or AIS3+ respectively) in the particular body region and AIS2+ (AIS3+) injury severities of all body regions.***

The in-depth investigation of road accidents in Germany shows the relevance of AIS2+ and AIS3+ head and leg injuries (approximately 30% each) in particular for pedestrians involved in accidents with passenger cars registered between 1995 and 2005, i.e. in the time when the pedestrian impactors have been developed by the pedestrian safety working groups of the European Enhanced Vehicle-safety Committee (EEVC), but still before application of the Framework Directive 2003/102/EC as predecessor of Commission Regulation (EC) No. 631/2009. During accidents with passenger cars registered from 2006 onwards, i.e. after application of the Framework Directive, the distribution especially of the AIS3+ coded injuries has been shifted towards the body regions thorax and pelvis while the relevance for the head and leg remains more or less unchanged. From this study it can be concluded that on the one hand, a test procedure covering the pelvis area as now introduced by Euro NCAP is addressing the real world accident scenarios, but also that an additional thorax test could be expected to significantly reduce thoracic injuries on the other hand.

Another point that has not yet been addressed is the safety of cyclists being the second big group of vulnerable road users besides pedestrians. Euro NCAP is planning to cover cyclist safety as from 2018 onwards by means of active safety. However, like for pedestrians, a baseline passive safety level also for cyclists should be ensured, especially as active safety systems are expected to mitigate rather than avoid crashes in most cases. A current research project at BASt dealing with the development of passive test and assessment procedures for cyclists aims at implementing modifications to the current pedestrian procedures to adequately cover both groups of vulnerable road users.

Finally, in the light of demographical change the procedures to-be should also focus on elderly as vulnerable road users. The upcoming European SENIORS (Safety-ENhancing Innovations for Older Road userS) project settled under the European HORIZON 2020 framework programme will in particular address the passive safety of the elderly.

## CONCLUSIONS

The Euro NCAP pedestrian test and assessment protocols have been substantially updated and, where necessary, amended. Where possible, the procedures were harmonized with legislation. The assessment has gained objectivity by introducing grid procedures for all assessed body regions. The tools and test procedures have been modified to better reflect impact kinematics as well as the biomechanical response that can be observed in real world accidents. However, there is room for further improvement in terms of real world injuries and their coverage by the latest test and assessment procedures. The linearly guided upper legform impactor is lacking biofidelic behavior that should be reflected in terms of pedestrians' pelvis and femur. While knee and tibia injuries can be reliably predicted with the FlexPLI, the readings for the femur cannot be used mainly due to the lack of the torso mass of the pedestrian. Studies by Zander et al. (2011) have shown a good correlation between full scale dummy tests and tests with the FlexPLI with applied upper body mass (UBM); however, for an implementation within the existing test procedures the generated database needs to be extended by more vehicle frontends and human body simulations, i.e. further research is needed. In depth accident studies show a redistribution of pedestrian injury patterns towards thoracic and pelvic injuries that need to be addressed by new or improved impactors and test procedures. Furthermore, the procedures need to also cover cyclists as the second big group of vulnerable road users. Finally, pedestrian safety should also take care of the elderly being the most vulnerable road users. Results in this context can be expected from the upcoming European SENIORS project.

## REFERENCES


Bhalla K., Bose D., Madeley N., Kerrigan J., Crandall J. 2003. „Evaluation of the response of mechanical pedestrian knee joint impactors in bending and shear loading." Paper no. 429 of ESV conference proceedings.

European Union. 2009. "COMMISSION REGULATION (EC) No 631/2009 of 22 July 2009 laying down detailed rules for the implementation of Annex I to Regulation (EC) No 78/2009 of the European Parliament and of the Council on the type-approval of motor vehicles with regard to the protection of pedestrians and other vulnerable road users, amending Directive 2007/46/EC and repealing Directives 2003/102/EC and 2005/66/EC." Official Journal of the European Union, 25 July 2009.

European Union. 2003. "Directive 2003/102/EC of the European Parliament and of the Council of 17 November 2013 relating to the protection of pedestrians and other vulnerable road users before and in the event of a collision with a motor vehicle and amending Council Directive 70/156/EEC." Official Journal of the European Union, 06. December 2003.

European New Car Assessment Programme. 2011. "Pedestrian Testing Protocol Version 5.3.1." Euro NCAP, November 2011.

European New Car Assessment Programme (Zander O., van Ratingen M.). 2014. "Headform to Bonnet Leading Edge Tests. Technical Bulletin TB 019 Version 1.0." Euro NCAP, May 2014.

Gehring D.-U., Zander O. 2014. "Application of the new Euro NCAP pedestrian test procedures to heavy vehicles." Presentation to the Euro NCAP Pedestrian Safety Working Group during their 30th meeting. 25 November 2014.

Longhitano D., Ivarsson J., Henary B., Crandall J. 2005. "Torso injury trends for pedestrians struck by cars and LTV's." Paper no. 05-0411 of 19th ESV conference proceedings. Washington DC, 2005.

United Nations Economic Commission for Europe. 2015. “Agreement Concerning the Adoption of Uniform Technical Prescriptions for Wheeled Vehicles, Equipment and Parts which can be Fitted and/or be Used on Wheeled Vehicles and the Conditions for Reciprocal Recognition of Approvals Granted on the Basis of these Prescriptions (Revision 2, including the amendments which entered into force on 16 October 1995). Addendum 126: Regulation No. 127 01 series of amendments to the Regulation – Date of entry into force: 22 January 2015. Uniform provisions concerning the approval of motor vehicles with regard to their pedestrian safety performance.” Website of the UNECE, Doc. ECE/TRANS/505/Rev.2/Add.126/Rev.1. 4 February 2015

Zander O. 2010-1. “Testing of heavy vehicles according to a draft pedestrian testing protocol.” Presentation to the Euro NCAP Heavy Vehicles Subgroup during their 6th meeting. Brussels, 9 September 2010.

Zander O. 2010-2. “Proposal for BLE testing of heavy vehicles.” Presentation to the Euro NCAP Heavy Vehicles Subgroup during their 7th meeting. Brussels, 8 October 2010.

Zander O. 2011. “Introduction of FlexPLI within Euro NCAP legform test procedure.” Presentation to the Euro NCAP Pedestrian Protocol Subgroup during their 13th meeting. Brussels, 6 May 2011.

Zander O., Gehring D., Leßmann P. 2011. “Improved assessment methods of lower extremity injuries in vehicle-to-pedestrian accidents using impactor tests and full scale dummy tests.” Paper no. 11-0079 of 22nd ESV conference proceedings.

Zander O. 2014. “Status of the Lower Extremity Test and Assessment Procedures for Vulnerable Road Users. Proceedings of the 9th Praxis Conference Pedestrian Protection, Bergisch Gladbach, 2014.

Zander O., Wisch M. 2015. “Kausalzusammenhänge bei Radfahrer-Pkw-Unfällen, Verletzungsmuster von Radaufsassen und Maßnahmen von Gesetzgebung und Verbraucherschutz zur Minderung der Verletzungsschwere.“ Annual Report 2013-2014 of the Federal Highway Research Institute (BASt). 2015

# AIR BAG RELATED INJURIES IN NHTSA'S CRASH DATABASES

**Augustus "Chip" Chidester**
**Mark Mynatt**
National Highway Traffic Safety Administration
United States of America
Paper Number 15-0259

## ABSTRACT

The National Highway Traffic Safety Administration (NHTSA) has been monitoring and gathering information on air bag related injuries and fatalities in its data collection programs since air bags were introduced. As frontal air bag technology has progressed from barrier certified (a.k.a. first generation) to sled certified (a.k.a redesigned) and to advanced certified air bag systems, there has been a drastic reduction in the number of injuries and fatalities attributed to these air bags. More recently developed air bags designed to protect occupants in side impacts and rollovers also do not appear to pose a serious threat. The purpose of this paper is to describe the evolution of air bag injuries in all types of air bags collected in NHTSA's in-depth investigation and crash report based programs. Additionally, the paper discusses future plans for collection of air bag and injury information as NHTSA's data collection programs are redesigned in the Data Modernization Project.

## INTRODUCTION

Investigation-based programs are the only source of detailed information required to research the injury outcomes related to air bag deployments. NHTSA currently operates three investigation-based data collection programs with detailed air bag information; the National Automotive Sampling System-Crashworthiness Data System (NASS-CDS), Special Crash Investigations (SCI) and the Crash Injury Research and Engineering Network (CIREN). Data from each of the programs has been critical in NHTSA's evaluation of air bag performance. These data collection programs have somewhat different focuses, but also complement one another in different ways.

NASS-CDS is a nationally representative sample of towed light vehicle crashes with an emphasis on the crashworthiness of the vehicle. The case selection algorithm is designed to give fatal and severe injury crashes a higher probability of selection. Data is collected at 24 sites across the country with a yearly average of 4,500 cases per year since 1999. NASS-CDS data can be viewed clinically at http://www.nhtsa.gov/NASS. The yearly SAS data sets are available for statistical use at ftp://ftp.nhtsa.dot.gov/NASS/.

SCI is a collection of approximately 125-150 targeted investigations each year that are utilized by NHTSA and the automotive safety community to understand the real-world performance of existing and emerging advanced safety systems. Both the SCI case viewers and Technical Reports can be accessed at http://www.nhtsa.gov/SCI.

CIREN is a hospital-based study operating at six centers across the country, collecting approximately 300 cases per year. The CIREN process combines prospective data collection with professional multidisciplinary analysis of medical and engineering evidence to determine injury causation in every crash investigation conducted. CIREN data is available at http://www.nhtsa.gov/CIREN.

Although the programs have different overall objectives they are all modeled on the same data collection practices, procedures, and data structures. This consistency allows for researchers to quantify the relationship between vehicle damage and the occupant injuries in the real-world crash environment across multiple programs. Investigations conducted in NHTSA's NASS-CDS, SCI and CIREN include:

- A vehicle inspection is conducted that involves detailed documentation including crush deformation, occupant compartment intrusion, occupant contacts, assessment of the safety systems, and photography.
- Additionally, the vehicle inspection includes an image of the Event Data Recorder (EDR) data when available.
- Medical records for injured occupants are evaluated, allowing trained injury coders to assign Abbreviated Injury Scale (AIS) codes and make a determination on the specific

vehicle component that was contacted to produce the injury.

The analysis in this paper is focused on the injury outcomes of the various air bag systems in real world crashes. This was especially important for looking at the injury outcomes that may be related to the advanced air bag occupant protection rulemaking.

## BACKGROUND

NHTSA has been collecting in-depth data utilized to study the effects of occupant protection devices since 1972. While the focus of the specific investigations has changed over the years the primary goal has remained to provide researchers the information necessary to protect occupants in crashes with little or no unintended consequences.

The air bag has been utilized as a supplemental form of occupant protection restraint since 1974. Air bag systems have evolved through the years, primarily to mitigate unintended injury consequences to occupants positioned too close to the air bag at the time of deployment. NHTSA initiated interim and long-term regulatory actions to reduce and eventually eliminate the adverse effect of frontal air bags for infants, children, and other high-risk occupants while retaining the benefits of air bags for most people.

These regulatory actions aimed at air bag systems were made based in part on the data collected from NHTSA's in-depth data collection programs. The data was also utilized to help evaluate the effectiveness of the regulatory actions in real-world crashes [1]. The details on the unintended injury consequences are documented in previous ESV papers [2].

NHTSA's interim action was to modify the occupant protection Federal Motor Vehicle Safety Standard No. 208 (FMVSS No. 208) to introduce a sled test option in lieu of the existing unbelted barrier crash test certification requirement on March 19, 1997. The sled test allowed air bags to be designed to deploy less forcefully. While some researchers felt this was sufficient, the real-world in-depth data was still reporting unintended consequences. While significantly less than first generation air bags, the undesirable outcome still existed in the sled certified air bags.

In 2000, NHTSA issued another upgrade to FMVSS No. 208 to fulfill its long-term effort to counter the adverse effects of frontal air bags. In this advanced air bag rule, significant changes were specified in the frontal occupant protection requirements for light passenger vehicles. These changes included adding requirements for protecting small adult female occupants, adding requirements to minimize the risk of deploying air bags to out-of-position (OOP) children and small adult occupants, increasing the requirements for belted occupants, and reducing the test speed for the unbelted 50th percentile male occupants. Manufacturers began phasing in the sale of vehicles meeting the advanced air bag requirements beginning with model year 2003 vehicles. All vehicles sold after August 31, 2006 must certify meeting the advanced air bag requirements. Details on the real-world results are included in a previous ESV paper [3].

As of the writing of this paper NHTSA's crash data systems have not identified or reported any fatality related to the air bag deployment involving a vehicle certified to the advanced air bag requirements.

## METHODS

The data used in this analysis were NASS-CDS, SCI, and CIREN cases from crash years 2000-2013 in which a 1990-2013 model year vehicle had a deployed air bag in an occupied seat. The air bags deployment location was not limited to upper instrument panel or steering wheel air bags which were most common. Any deployed air bag location was considered including air bags that deploy from the seat back, roof side rail, door, and mid or lower instrument panel. Especially in more recent model year vehicles, there could be more than one deployed air bag per occupied seating location.

Injuries in NHTSA's in-depth investigation programs are assigned by trained injury coders based upon the Abbreviated Injury Scale (AIS) developed by the Association for the Advancement of Automotive Medicine (AAAM). Crashes prior to 2010 were coded using AIS90 Update 98. Cases with a crash date 2010 and newer used AIS2005 Update 2008.

### NASS-CDS

NASS-CDS was the primary data analyzed for this paper due to the sheer volume of cases and nationally representative design of the program. In NASS-CDS (2000-2013 in which a 1990-2013 model year vehicle had a deployed air bag in an occupied seat) a total 42,691 deployed air bags fit the criteria as shown in Figure 1. Applying the NASS-CDS weights, these represent over 12.5 million deployed air bags as shown in Figure 2.

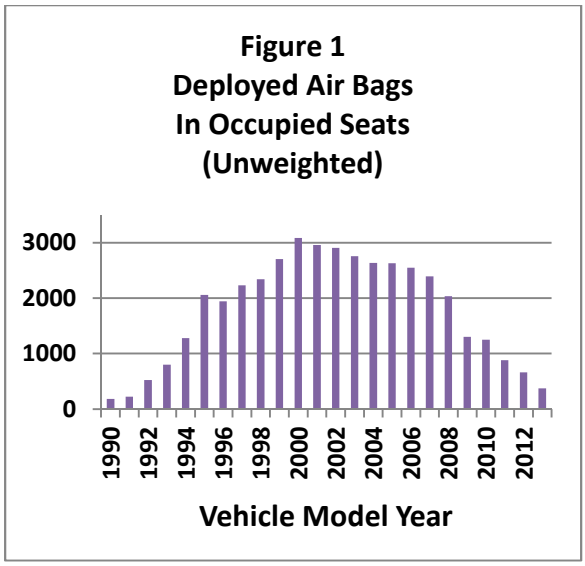


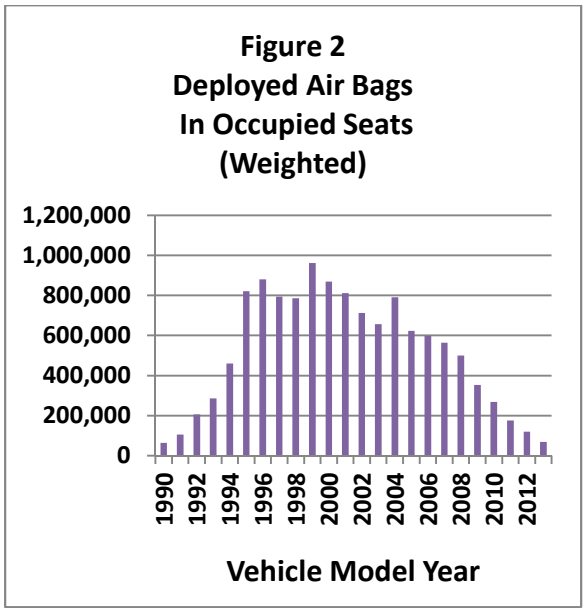


From the 42,691 deployed air bags in an occupied seat there were 16,776 instances where an air bag was identified as the source of an injury. These cases represent 4.4 million injuries nationwide during the 14-year period (2000-2013 in which a 1990-2013 model year vehicle had a deployed air bag in an occupied seat) using the weighted data. Though this may seem like a high number of injuries on the surface, Figure 3 shows over 96% of air bag injuries were minor (AIS-1) in severity and likely prevented more severe consequences in most instances. The analysis included all air bag associated injury sources which are listed in Appendix A. It should be noted that NASS and SCI refer to these as injury sources, while CIREN refers to them as involved physical component (IPC).

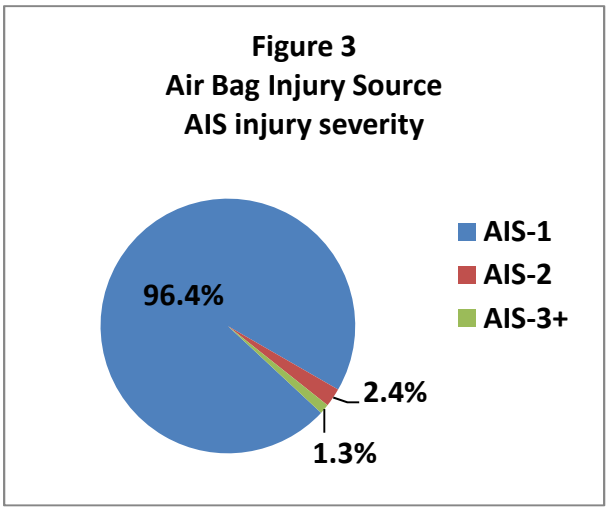


As the figures 1 and 2 show, the number of injuries attributed to air bags in NASS-CDS has decreased drastically as frontal air bag technology has progressed from first generation, to redesigned, and currently to advanced air bags systems.

Air bags designed to protect occupants in side impacts and rollovers also do not appear to pose a serious threat.

Although there is significant model year overlap in air bag generations due to phase-in periods the Figures 4 and 5 break down vehicle model years into 8-year ranges:

1990-1997 (first generation)
1998-2005 (redesigned)
2006-2013 (advanced)

Figure 4 shows the decrease in the number of total injuries sourced to the air bag in an injury per deployed air bag ratio. The unweighted raw counts as well as weighted values are included.

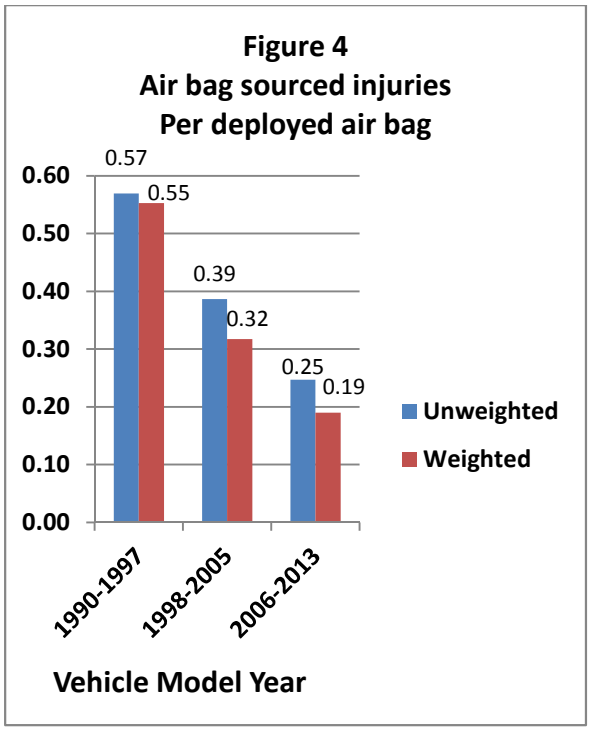


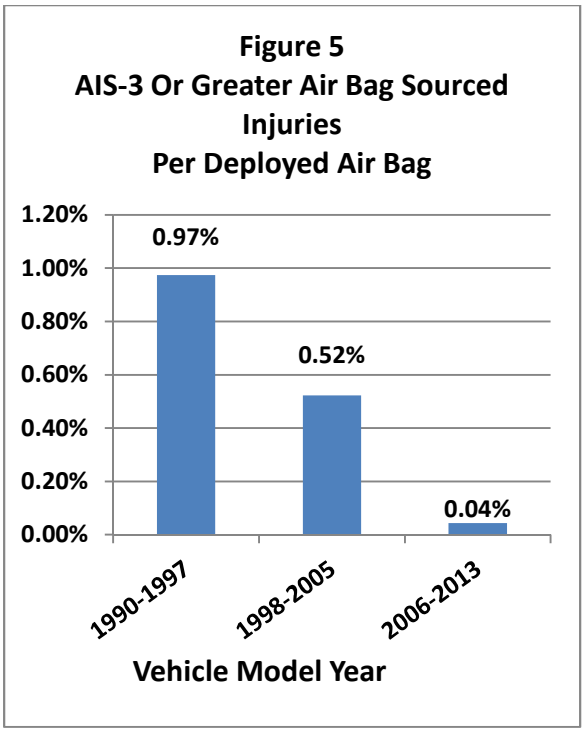


Figure 4 details vehicles from 1990-1997 averaging just over one coded injury for every two air bags deployed in an occupied seat. More recent air bags from 2006-2013 model year vehicles average less than half as many injuries. The severity of injuries in more recent air bags has also been greatly reduced. Figure 5 shows the decrease in AIS-3 (serious) or greater injuries where air bags were the injury source.

AIS-3+ injuries sourced to the air bag decreased from one in every 101 (.97%) deployed bags in first generation air bags to one in every 2,288 (.04%) deployed air bags in model years 2006-2013, a significant reduction.

Only five AIS-3+ injuries sourced to the air bag have been identified in NASS-CDS in the 2006 and newer model year vehicles . The data are summarized in Table 1. The cases reveal the five injuries involved extremity fractures and there were no indications of air bag malfunction.

**Table 1**
**NASS-CDS cases with AIS-3+ Injury**
**2006-2013 Model Year Vehicle**

| Case Number | Vehicle | Occupant | Air Bag Location | Injury Code | Injury Source |
|---|---|---|---|---|---|
| 2007-48-131 | 2006 Toyota Camry | 71-year-old Female Restrained Passenger | Top Instrument Panel | 7528043 Radius fracture open/displaced/comminuted | Air bag (Certain) |
| 2009-04-011 | 2008 Volkswagen Jetta | 26-year-old Female Restrained Driver | Steering Wheel | 7528043 Radius fracture open/displaced/comminuted | Air bag compartment cover (Probable) |
| 2008-75-116 | 2006 Toyota RAV4 | 90-year-old Female | Top Instrument Panel | 7528043 Radius fracture | Air bag (Certain) |

| | | | | | |
|---|---|---|---|---|---|
| | | Restrained Passenger | | open/displaced/comminuted | |
| 2008-75-116 | 2006 Toyota RAV4 | 90-year-old Female Restrained Passenger | Top Instrument Panel | 7532043 Ulna fracture open/displaced/comminuted | Air bag (Certain) |
| 2012-49-031 | 2009 Lexus ES | 96-year-old Female Restrained Driver | Lower Instrument Panel | 8541723 Tibia fracture, proximal, complete articular | Air bag compartment cover (Probable) |

**SCI**

SCI has actively sought out injuries and fatalities associated with air bags since their introduction into the fleet. It is important to remember that SCI cases are not nationally representative and the case selection criteria is very different from NASS-CDS. Table 2 shows the number of AIS-3+ injuries associated with air bags for SCI cases with a crash date 2000-2013. Similar to the NASS-CDS results, the number of AIS-3+ injuries has decreased dramatically in 2006-2013 model year vehicles and no fatalities have been confirmed due to air bag injury sources. Table 3 is a listing of the three AIS-3+ injuries in SCI. There were no indications of air bag malfunction in the cases.

**Table 2**
**SCI Air bag sourced AIS-3+ Injuries**

| Model Year Vehicle | AIS-3+ Injuries |
|---|---|
| 1990-1997 | 328 |
| 1998-2005 | 91 |
| 2006-2013 | 3 |

**Table 3**
**SCI cases with AIS-3+ Injury**
**2006-2013 Model Year Vehicle**

| Case Number | Vehicle | Occupant | Air Bag Location | Injury Code | Injury Source |
|---|---|---|---|---|---|
| DS13002 | 2012 Hyundai Sante Fe | 42-year-old Female Restrained Passenger | Roof Side Rail | 6402003 Cord contusion, cervical spine, NFS | Air bag Indirect (Probable) |
| DS07009 | 2006 Cadillac SRX | 81-year-old Male Unrestrained Driver | Steering Wheel | 4502524 Rib cage fracture open/displaced/comminuted with hemo-/pneumothorax | Air bag (Possible) |
| IN11016 | 2011 Buick Lucerne | 78-year-old Female Restrained Driver | Roof Side Rail | 6502283 Cervical Spine fracture odontoid (dens) | Air bag (Possible) |

**CIREN**

CIREN has six AIS-3+ injuries with an involved physical component (IPC) associated with an air bag in 2006-2013 model year vehicles. CIREN's ability to identify more air bag injuries than the other in-depth programs is likely due to the programs emphasis on newer model year vehicles, increased medical documentation detail and scrutiny, and biomechanics evaluation. It is important to note that CIREN cases are not nationally representative and the case selection criteria is different from NASS-CDS. Table 4 shows the number of AIS-3+ injuries associated with air bags for CIREN cases with a crash date 2000-2013. Similar to the NASS-CDS and SCI results, the number of AIS-3+ injuries has decreased dramatically in 2006-2013 model year vehicles and no fatalities have been noted due to air bag IPC's. The six AIS-3+ injuries in SCI are shown in Table 5. There were no indications of air bag malfunction in the cases.

**Table 4**
**CIREN Air bag sourced AIS-3+ Injuries**

| Model Year Vehicle | AIS-3+ Injuries |
|---|---|
| 1990-1997 | 250 |
| 1998-2005 | 196 |
| 2006-2013 | 6 |

**Table 5**
**CIREN cases with AIS-3+ Injury**
**2006-2013 Model Year Vehicle**

| Case Number | Vehicle | Occupant | Air Bag Location | Injury Code | Involved Physical Component |
|---|---|---|---|---|---|
| 857095509 | 2007 Hyundai Accent | 77-year-old Male Restrained Driver | Steering Wheel | 4502303 Rib cage fracture >3 ribs on one side and <=3 ribs on the other side, stable chest or NFS | Air bag (Possible) |
| 857095509 | 2007 Hyundai Accent | 77-year-old Male Restrained Driver | Steering Wheel | 7526043 Humerus fracture open/displaced/comminuted | Air bag (Probable) |
| 842012167 | 2006 Chrysler PT Cruiser | 63-year-old Female Restrained Driver | Steering Wheel | 6502223 Cervical Spine fracture facet | Air bag (Probable) |
| 842012167 | 2006 Chrysler PT Cruiser | 63-year-old Female Restrained Driver | Steering Wheel | 7532043 Ulna fracture open/displaced/comminuted | Air bag (Probable) |
| 842012167 | 2006 Chrysler PT Cruiser | 63-year-old Female Restrained Driver | Steering Wheel | 7528043 Radius fracture open/displaced/comminuted | Air bag (Probable) |
| 100108251 | 2006 Mercedes E-Class | 55-year-old Female Restrained Driver | Roof Side Rail | 1406063 Cerebrum contusion single small | Air bag (Probable) |

**DISCUSSION**

The first generation of frontal air bags saved the lives of thousands of drivers and right-front passengers. However, the first generation air bags harmed occupants positioned close to the air bag at the time of deployment, especially small statured females, infants and children. Air bag effectiveness analysis performed by NHTSA's Office of Regulatory Analysis and Evaluation (ORAE) using Fatality Analysis Reporting System (FARS) and SCI data have shown that as the fleet has moved from first generation to redesigned air bags, the fatality risk was reduced for children and the life-saving benefits of first-generation air bags was preserved for adults [4]. NASS-CDS data in Figures 4 and 5 show the high number of AIS-3+ injuries from air bags decreased over the progression of air bags.

The 2013 ORAE analysis using FARS and R.L. Polk National Vehicle Population Profile (NVPP) data concluded that the progression from redesigned frontal air bags to certified advanced systems showed no statistical significant difference in fatality rate [1]. Recent papers using FARS data through calendar year 2011 show statistically significant fatality reductions for all four types of curtain and side air bags in near-side impacts for drivers and right-front passengers of cars and LTVs [5].

Along with the fatality rate improvement as the fleet has moved from first generation to redesigned and finally to advanced air bags, the reduction in the number of AIS-3+ injuries sourced to the air bag in vehicle model years 2006-2013 has been substantial. These types of injuries have been significantly reduced with only fourteen AIS-3+ air bag injuries identified in all three of NHTSA's investigation-based programs. These cases were reviewed individually and revealed some common characteristics.

Older occupants were over-represented in the fourteen cases with AIS-3+ injuries sourced to the air bag in vehicle model years 2006-2013 as shown in Figure 6. The average age in the fourteen cases was over 69 years old. NHTSA's 5-year Traffic Safety Plan for Older People discusses the increased risk that older occupants face, primarily due to increased frailty, and potential measures that could attempt to address injury risks for older occupants [6].

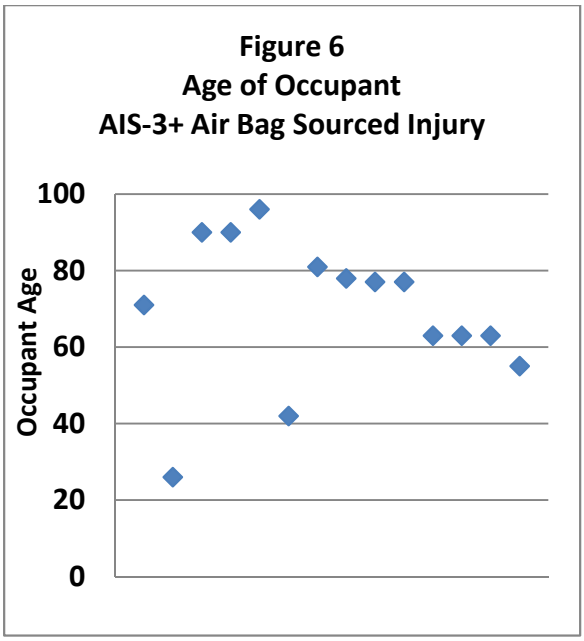


The AIS body regions involved for the AIS-3+ injuries are shown in Figure 7.

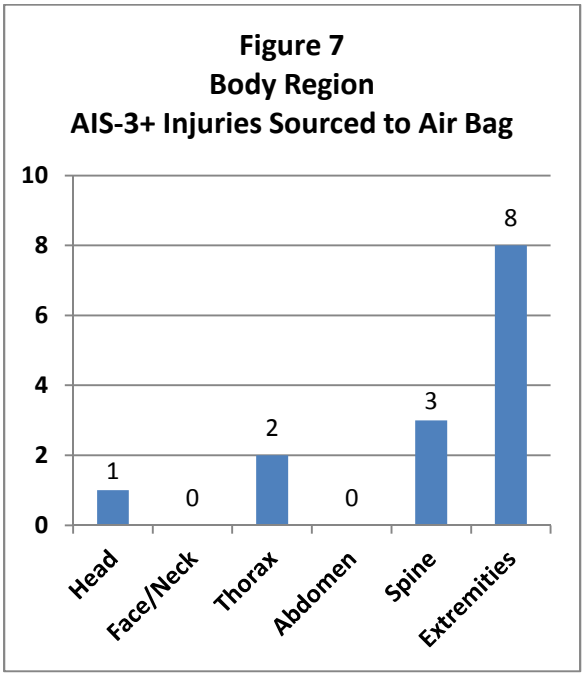


Half the AIS-3+ air bag injuries involved serious lower arm fractures to the radius or ulna. These injuries were identified with high confidence levels for the injury source/involved physical component. Primarily because of the physical evidence available. Identifying the air bag as the injury source to the other body regions are much more difficult, and often have a confidence level of only "possible." A

common situation is chest injuries to a driver in a severe frontal collision. The driver typically has interaction first with the seat belt, then loads through the air bag into the steering wheel. Determining which of the three components is the source of the specific injury is very challenging and ultimately relies on many factors including: crash scenario, exterior vehicle damage pattern, interior intrusion, occupant contact, interior component deformation, and injury patterns.

**Future Data Collection**

NHTSA currently collects data that can be used to evaluate injury sources in three crash investigation-based programs, NASS-CDS, SCI, and CIREN. In Fiscal Year 2012, Congress appropriated funds for NHTSA to modernize NASS. The formal project, known as the Data Modernization Project, was launched in January 2012. The goal of Data Modernization is to ensure that the agency is collecting quality data to keep pace with emerging technologies and policy needs, which will help affirm NHTSA's position as the leader in motor vehicle crash data collection and analysis. The multi-year project is set for implementation beginning in January 2016.

The replacement to NASS-CDS has been named the Crash Investigation Sampling System (CISS). New nationally representative data collection sites have been selected using a sample design approach similar to NASS-CDS. The new sites were chosen using the most recent census and vehicle registration data and hope to better reflect the nation's overall crash picture and improve upon the availability of newer model vehicles and severe crashes at the data collection sites.

NHTSA believes that collection of detailed injury data including medical record collection, AIS code assignment, contacted components, and injury causation must be a point of emphasis in CISS, as well as in the other field investigation-based data collection programs. Current plans include adopting the latest version of the Abbreviated Injury Scale (AIS 2015) and using the U.S. Army Research Laboratory (ARL) Visual Anatomical Injury Descriptor (VisualAID) software to enhance injury coding in all the NHTSA programs.

**CONCLUSION**

Unintended fatalities and serious injuries were a problem in barrier certified (a.k.a. first generation) air bags and to a lesser extent in sled certified (a.k.a. redesigned) air bags. No fatalities in a 2006-2013 model year vehicle have been reported in NHTSA's investigation-based data collection programs with an air bag attributed as injury source/involved physical component vehicle. The prevalence of AIS-3+ injuries has also been drastically reduced with the introduction of vehicles into the fleet that meet the advanced occupant protection rulemaking. NHTSA's future data collection efforts will continue to monitor for these types of injuries.

**REFERENCES**

[1] Greenwell, N. "*Evaluation of the Certified-Advanced Air Bags"*. National Highway Traffic Safety Administration, DOT HS 811 834, September 2013.

[2] Kindelberger, J. et al, "Air bag Crash Investigations". ESV 2003, Paper Number 03-0299.

[3] Brophy, J. et al, "INITIAL EVALUATION OF ADVANCED AIR BAGS IN REAL WORLD CRASHES". ESV 2005, Paper Number 05-0386.

[4] Kahane, C. J. "*AN EVALUATION OF THE 1998-1999 REDESIGN OF FRONTAL AIR BAGS"*. National Highway Traffic Safety Administration, DOT HS 810 685, August 2006.

[5] Kahane, C. J. "*Updated estimates of fatality reduction by curtain and side air bags in side impacts and preliminary analyses of rollover curtains"*. National Highway Traffic Safety Administration, DOT HS 811 882, January 2014.

[6] National Highway Traffic Safety Administration. "Traffic Safety for Older People- 5-Year Plan". DOT HS 811 837, December 2013.

**APPENDIX A**

**Air bag injury sources 2002-forward**

Air bag
Air bag and eyewear
Air bag and jewelry
Air bag and object held
Air bag and object in mouth
Air bag compartment cover
Air bag compartment cover and eyewear
Air bag compartment cover and jewelry
Air bag compartment cover and object held
Air bag compartment cover and object in mouth

NOTE: Beginning in 2002 air bag injuries were linked to a specific air bag

**Air bag injury sources 2000-2001**

Air bag-driver side
Air bag-driver side and eyewear
Air bag-driver side and jewelry
Air bag-driver side and object held
Air bag-driver side and object in mouth
Air bag compartment cover-driver side
Air bag compartment cover-driver side and eyewear
Air bag compartment cover-driver side and jewelry
Air bag compartment cover-driver side and object held
Air bag compartment cover-driver side and object in mouth
Air bag-passenger side
Air bag-passenger side and eyewear
Air bag-passenger side and jewelry
Air bag-passenger side and object held
Air bag-passenger side and object in mouth
Air bag compartment cover-passenger side
Air bag compartment cover-passenger side and eyewear
Air bag compartment cover-passenger side and jewelry
Air bag compartment cover-passenger side and object held
Air bag compartment cover-passenger side and object in mouth
Other air bag (specify)
Other air bag compartment cover (specify)

# EDR DATA COLLECTION IN NHTSA'S CRASH DATABASES

**Mark Mynatt**
**John Brophy**
**Augustus "Chip" Chidester**
National Highway Traffic Safety Administration
United States of America
Paper Number 15-0260

## ABSTRACT

The National Highway Traffic Safety Administration (NHTSA) has been gathering Event Data Recorder (EDR) information in its data collection programs since the late 1990s. The various EDR data elements collected in NHTSA's crash databases provide insight into the vehicles' safety systems and actions leading up to a crash. This EDR data will be a key source as focus on crash avoidance countermeasures increase and crashworthiness countermeasures are optimized in the automotive safety community. The purpose of this paper is to describe the evolution of EDR data collection in NHTSA's in-depth crash investigation programs leading up to the implementation of the Code of Federal Regulation (CFR) 49 Part 563. Additionally, the paper will discuss the techniques used to collect EDR data, and detail future plans for their coding in NHTSA's crash databases.

## INTRODUCTION

NHTSA is currently imaging EDR data using a commercially available tool in its three field investigation-based data collection programs: the National Automotive Sampling System-Crashworthiness Data System (NASS-CDS), Special Crash Investigations (SCI) and the Crash Injury Research and Engineering Network (CIREN).

NASS-CDS is a nationally representative sample of towed light vehicle crashes with an emphasis on the crashworthiness of the vehicle. The case selection algorithm is gives fatal and severe injury crashes a higher probability of selection than less severe crashes. Data is collected at 24 sites across the country with an annual average of 4,500 cases per year since 1999.

SCI is a collection of approximately 125-150 targeted investigations annually that are utilized by NHTSA and the automotive safety community to understand the real-world performance of existing and emerging advanced safety systems.

CIREN is a hospital-based study operating out of six centers across the country, collecting approximately 300 cases per year. The CIREN process combines prospective data collection with professional multidisciplinary analysis of medical and engineering evidence to determine injury causation in every crash investigation conducted.

EDR data was also collected by NHTSA in a special study using the NASS infrastructure from 2005-2007, the National Motor Vehicle Crash Causation Survey (NMVCCS). NMVCCS was a nationally representative survey of light vehicle crashes that used Emergency Medical Services (EMS) notifications as the primary case initiation criterion. Researchers conducted on-scene field investigations on nearly 7,000 crashes during the project, focusing on the pre-crash phase of the crash.

While the three active data collection programs NASS-CDS, SCI, and CIREN have distinct overall objectives they do share four key data collection areas:

- Examining the crash scene
- Interviewing involved occupants
- Reviewing occupant medical records
- Conducting detailed inspections of crash-involved vehicles

The vehicle inspection involves the documentation and photography of crush deformation, occupant compartment intrusion, occupant contacts, and assessment of the safety systems in the vehicle. Additionally, the vehicle inspections include an attempt to image the EDR if the vehicle is so equipped and supported by the commercially available Crash Data Retrieval (CDR) tool.

As of January 8, 2015 the four investigation-based programs have imaged 13,898 EDRs since 1999. Figure 1 outlines the breakdown of EDRs imaged by each of the NHTSA programs.

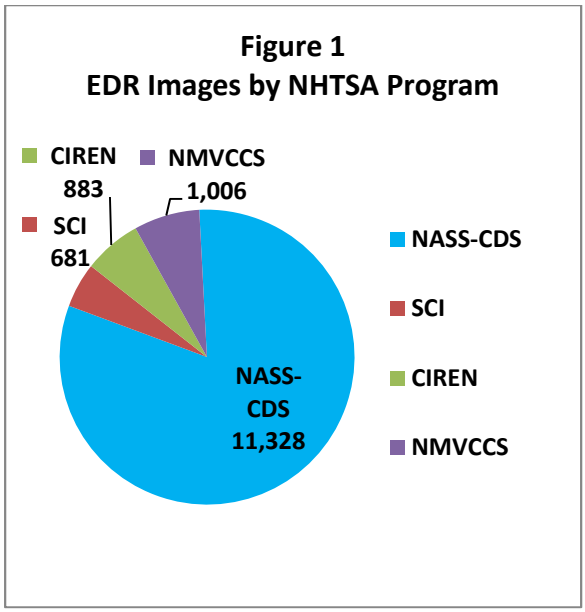


**BACKGROUND**

NHTSA began collection of very rudimentary EDR data in the 1970s. General Motors (GM) introduced the first regular production driver/passenger air bag systems as an option in selected 1974-76 production vehicles. They incorporated electromechanical g-level sensors, a diagnostic circuit that continually monitored the readiness of the air bag control circuits, and an instrument panel Readiness and Warning lamp that illuminated if a malfunction was detected. The data recording feature used fuses to indicate when a deployment command was given and stored the approximate time the vehicle had been operated with the warning lamp illuminated. This information was extracted by the SCI investigators with a GM proprietary tool.

In 1990, GM introduced a more complex air bag control module called the Diagnostic and Energy Reserve Module (DERM). The DERM was introduced with the added capability to record closure times for the multiple electromechanical switches for crash sensing, arming, and discriminating sensors as well as any fault codes present at the time of deployment. Beginning with the 1994 model year, GM introduced a single solid state analog accelerometer and a computer algorithm integrated in a Sensing & Diagnostic Module (SDM). The SDM also computed and stored the change in longitudinal vehicle velocity (deltaV) during the impact to provide an estimate of crash severity. This feature allowed GM engineers to obtain restraint system performance data when a vehicle was involved in a deployment event or experienced an impact-related change in longitudinal velocity, but did not command deployment (i.e. a near-deployment event). The SDM also added the capability to record the status of the driver's seat belt switch (buckled or unbuckled) for deployment and near-deployment events.

In certain GM vehicles beginning in the 1999 model year, the capability was added to record vehicle systems status information for a few seconds prior to an impact. Vehicle speed, engine RPM, throttle position, and brake switch on/off status are recorded for the five seconds preceding a deployment or near-deployment event.

At that time, the information in GM DERMs and SDMs could only be extracted by the manufacturer using a proprietary tool. Therefore, only a limited number of images were obtained by GM at the request of NHTSA to support air bag and EDR research from 1990 to 1999.

In 1999, NHTSA launched a research project with Ford on the real-world crash experience of advanced featured air bags equipped in 2000 Taurus/Sable fleet. For this research, Ford supplied the SCI teams a rudimentary EDR tool for extracting the basic air bag deployment data from the Restraint Control Module (RCM). The RCM also computed and stored a short duration (~80ms) of the change in longitudinal and lateral vehicle velocity during the impact sequence to provide an estimate of crash severity. This feature allowed Ford engineers to obtain restraint system performance data to help "tune" the deployment algorithms.

Beginning in 1999, the various NHTSA field data collection teams were equipped with a commercially available tool called the Crash Data Retrieval (CDR) system, produced by Vetronix Corporation to collect EDR data. Late in 2003, Vetronix, which was the only commercially available supplier of the CDR retrieval tool, was purchased by Robert Bosch GmbH. In the early years, only some GM vehicles were supported by the CDR hardware and software, but in 2003 and 2007, respectively, select Ford and Chrysler vehicles were added to the list of supported models. From 1999-2007, the number of models supported by the CDR tool continued to increase for these three major U.S. manufacturers. Therefore, by the beginning of 2008, roughly half of the vehicles sold in North America since model year 2004 were supported by the CDR system [1].

Based on the outputs from the early EDRs, the subsequent commercially available tool, and NHTSA's recognition of the safety benefits to the

driving public, a team of experts was formally organized to research the efficacy, collection, storage and imaging of the data. The Summary of Findings by the NHTSA EDR Working Group [2] was published in 2001 and included a recommended set of standardized results.

The final rule addressing EDRs, CFR 49 Part 563 was issued on August 6, 2006 [3] and on January 14, 2008 the response to petitions for reconsideration followed [4]. The regulation does not mandate that EDRs be installed in vehicles, but among other items, it specifies that if a vehicle is equipped with an EDR, the following conditions apply:

1. The EDR must capture crash data in a uniform format (detailed in Part 563)
2. There must be a standardized notification statement in the vehicle owner's manual
3. There must be a commercially available tool to access the data

CFR 49 Part 563 also defines an EDR as a device or function in a vehicle that records dynamic time-series data just prior to an event (speed versus time or delta V versus time) and the data is intended for retrieval after a crash event. It is important to note that EDR data does not include audio or video. If a vehicle is equipped with an EDR that records data, the following items are required:

- Delta V Longitudinal
- Max Delta V Longitudinal
- Time, Max Delta V
- Speed, vehicle indicated
- Engine throttle %
- Service brake on /off
- Ignition cycle, crash
- Ignition cycle, download
- Safety belt status, driver
- Frontal air bag warning lamp on/off
- Frontal air bag time to deploy – driver air bag
- Frontal air bag time to deploy – passenger air bag
- Multi-event – number of events
- Time from event 1 to 2
- Complete file recorded yes/no

The rule also specifies the interval/time and the sample rate for each element. There are also similar format requirements for additional data elements if they are recorded.

The regulation, which applied to vehicles manufactured after September 1, 2012, had a positive effect on the number of manufacturers standardizing their data and being supported by the Bosch CDR data retrieval tool. Several major Japanese and European manufacturers partnered with Bosch to make their EDR data retrievable using the CDR tool. By October 2014 the following manufacturers have some or all of their models supported:

- General Motors
- Ford
- Chrysler/Fiat
- Toyota
- Honda
- Mazda
- Nissan
- Volvo
- BMW
- Daimler
- Volkswagen
- Suzuki

The current Bosch CDR system (Version 14.1) costs about $11,400 and includes approximately seventy (70) different cables and connectors and a one-year subscription to the software. The software must be upgraded yearly at a cost of $900 per user. In addition to the equipment and software, extensive training for the field personnel is required for both the imaging and interpreting of the data.

Some manufacturers, Hyundai/Kia and Subaru for example, chose not to partner with Bosch and developed their own commercially available tool for EDR data collection in their vehicles. A few other manufacturers have elected to forego the recording of EDR data so they are not subject to Part 563. Although NHTSA has purchased some of the manufacturers proprietary EDR kits to image high interest cases, at the present time it is not cost effective to equip every field investigation team with those tools.

**Figure 2**
**Number of EDRs Imaged Yearly**

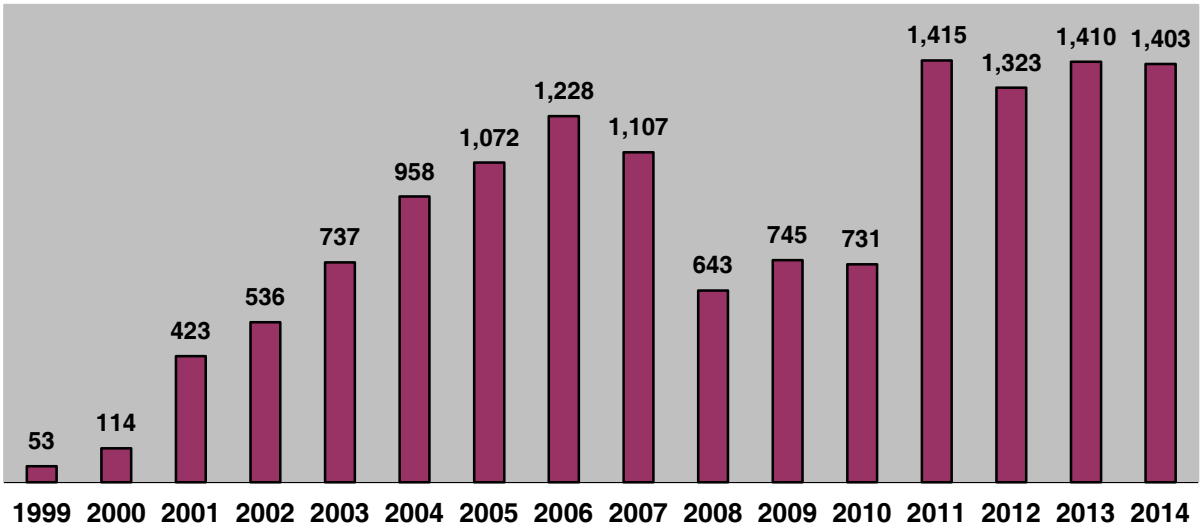


## HISTORICAL EDR DATA COLLECTION

Figure 2 shows the number of EDR's imaged yearly as of January 8, 2015, in the four NHTSA investigation-based programs (NASS-CDS, SCI, CIREN, and NMVCCS). In total they have imaged 13,898 EDRs since 1999.

As the number of vehicles supported by the CDR software has increased in the fleet, the number of EDRs imaged by the programs has generally increased yearly. However, the graph shown in Figure 2 has several fluctuations that require explanation. Aside from the general upward trend, a spike occurred from 2005-2007 due to the addition of the NMVCCS special study which was conducted during the time period. The sharp decrease from 2008-2010 was due to significant cuts that were made to the NASS system, eliminating the NMVCCS program and forcing significant cutbacks to the infrastructure. In an effort to reduce costs, NASS field offices were reduced in staff and EDR equipment was reduced to one complete CDR kit per field office.

Realizing the importance of EDR acquisitions as the effective date of CFR 49 Part 563 approached, late in 2010 NHTSA conducted a simple analysis to determine reasons NASS-CDS Technicians were unable to image the EDR data when the vehicle was supported by the CDR tool. Figure 3 depicts the reasons why the EDR data in supported vehicles could not be obtained in 2009-2010 NASS-CDS cases.

**Figure 3**
**Reasons EDR Not Obtained in Supported Vehicles NASS-CDS 2009-2010**

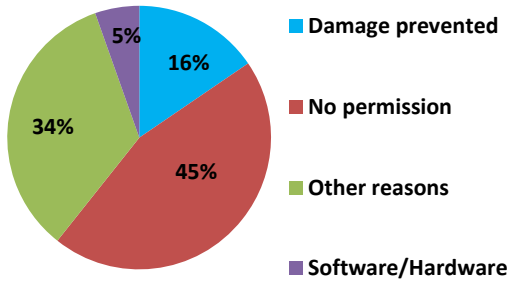


Among the reasons the EDR data could not be obtained, the largest percentage (45%) were because the vehicle owner denied permission to image the data. This included both outright owner refusals to the NASS-CDS Technician, and also the owner not wanting any additional damage to the vehicle to obtain the data. In cases where the On Board Diagnostic (OBD) plug was damaged, or there was no power to the vehicle, the Technician would need

to go direct to the module. This would include disassembling the vehicle's console or cutting the carpet to gain direct access to the EDR module. As Figure 3 indicates, damage prevented the Technician from obtaining the data in 16% of the cases. Vehicle damage included situations where the electrical system was compromised and the Technician could not access necessary connections and/or damage prevented access to the module.

"Other" reasons accounted for 34% of vehicles where the EDR data could not be obtained. These "other" reasons included:

- The Technician was allowed an exterior inspection only (evidentiary reasons) or the vehicle was locked and no keys were available
- The Technician only obtained photographs of the damaged vehicle
- The EDR was removed prior to the NASS-CDS vehicle inspection (usually by law enforcement)

A combination of software and hardware issues were cited as the reason the remaining 5% of supported vehicle downloads were unsuccessful. Software issues generally occurred when the Technician's CDR tool could not successfully communicate with the EDR module. Hardware issues were related to plugs, connectors, and laptop problems.

As mentioned earlier, owner permission was not limited to refusals to the NASS-CDS Technician to image the EDR data. "Refusal" also included a large percentage of owners who would not permit any additional damage to the vehicle in the process of imaging the EDR data. There are three basic ways to image an EDR:

- Through the On-Board Diagnostics (OBD) port
- Direct to the EDR module
- Removing the module and imaging later on a bench top

To successfully obtain an image of the EDR through the OBD port, generally the electrical system cannot be compromised and the OBD connection plug (usually located beneath steering wheel under instrument panel) port cannot be damaged. NASS-CDS cases are intentionally sampled at a higher rate for towed vehicles with severe damage and injuries. Therefore, the electrical system will sometimes be damaged either during the crash or during post-crash extrication activities.

Going direct to module is possible when the electrical system is compromised, however, this process involves:

- Determining module location
- Removing consoles, instrument panel parts, or seats
- Cutting the carpet

This process can be complicated by crash damage and in situations where power seats are obstructing access to the module and the vehicle has no power. Oftentimes, owners will not allow the additional damage to their vehicle that is required to access the EDR.

The final way to access the EDR data is to remove the module from the vehicle and image the data later at another location. This method is not permitted because strict NASS-CDS policies are in place forbidding retention of any vehicle component.

After NHTSA reviewed the results of the analysis it was apparent the number of EDR images in the programs could increase significantly if retrieval techniques could be employed that would:

- Cause no further damage to the vehicle
- Allow the EDR to be imaged when no keys are available
- Increase successful attempts on severely damage vehicles

A natural increase in the number of cases with EDR data would also be expected due to the greater penetration of EDRs into the fleet.

One advanced EDR imaging technique, commonly referred to as the Fuse Block Method (FBM), involves supplying power to the EDR through the vehicles fuse panel and imaging the data through the OBD port. Although not always successful, this method eliminates the need to dismantle consoles, disassemble vehicle components, and cut carpets. In addition, when vehicle keys are not available, powering the EDR through the fuse block allows for OBD download.

In December 2010 NHTSA conducted EDR update training and provided the necessary additional equipment for all field personnel to begin using the FBM when other data imaging techniques failed. The agency also instituted tighter quality control measures within the NASS software and placed additional emphasis on successful EDR retrieval. The field personnel began using the new

method of collection in 2011 and improved EDR acquisition results followed.

## CURRENT EDR DATA COLLECTION

The 2012-2013 NASS-CDS revealed that about 45% of the over 7,000 vehicles inspected were supported by the Bosch CDR retrieval tool. With CFR 49 Part 563 in place and the increased number of manufacturers supported by the commercially available tool, that percentage will likely continue to grow as EDRs become more widespread in the fleet.

The renewed emphasis on EDR data acquisition and implementation of the FBM had a major effect on the number of EDRs imaged by the NASS Technicians. Figure 4 shows the success rate roughly doubling the three years after the FBM EDR training compared to the two years prior. The two most recent years of data shows the NASS-CDS Technicians successfully imaged the EDR, when the vehicle was supported, 74% of the time.

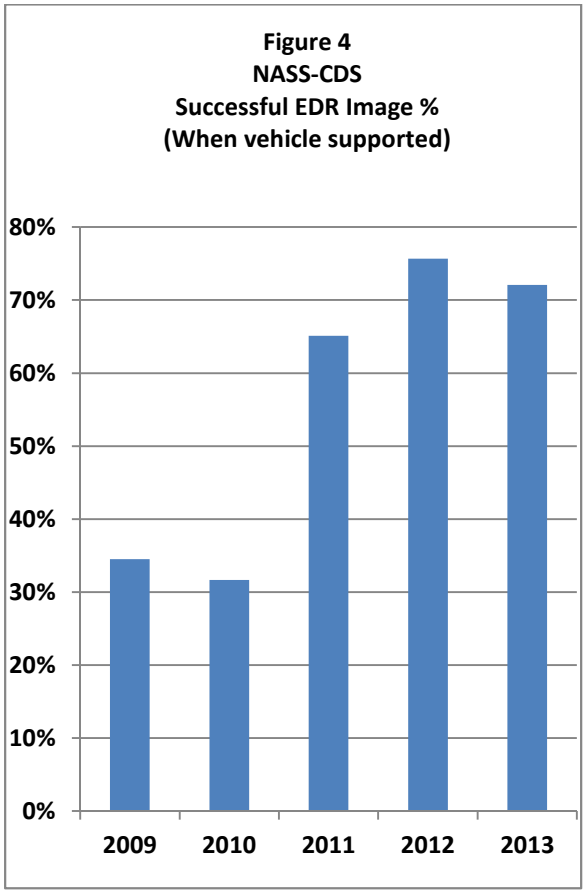


Figure 5 shows that after the training in late 2010 there was a decrease in unsuccessful EDR data retrieval. The figure also shows the associated reasons for lack of success by year. As discussed earlier, the FBM dramatically decreased the number of times damage prevented the EDR imaging, that permission was denied, and/or there were other reasons cited as the reason the EDR could not be imaged.

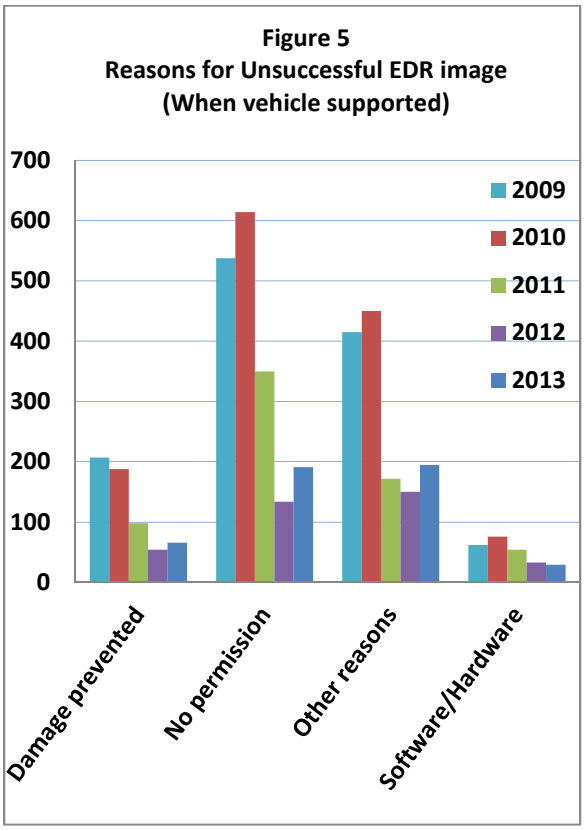


In the current NASS-CDS system EDR data is available to the public in two formats. An Acrobat .pdf of the CDR file is available for each vehicle with a successful image. The reports can be found at ftp://ftp.nhtsa.dot.gov/NASS/EDR_Reports/. Secondly, the coded EDR data is available for clinical review within each individual NASS-CDS case. The case viewer for 2004-2013 data year NASS cases is located at http://www-nass.nhtsa.dot.gov/nass/cds. 1999-2003 NASS-CDS cases are available at http://www-nass.nhtsa.dot.gov/BIN/NASSCaseList.exe/SETFILTER?CASETYPE=PUBLIC.

Query tools are also provided in the NASS-CDS case viewers to narrow areas of focus down to specific makes, models, delta V ranges, injuries, and deformation types, among many other filter criteria.

Figure 6 shows the final overall percentages of EDR acquisition in inspected NASS-CDS vehicles from

2012-2013. One third of inspected vehicles have imaged EDR data, 55% are not supported by the CDR tool, and the remainder are split among the various unsuccessful reasons. Those 55% that were not supported requires clarification. Although all light vehicles equipped with EDRs sold in the United States after September 1, 2012 are required to meet CFR 49 Part 563, and almost 2,500 year/make/models are supported in version 14.1 of the Bosch CDR software released in October of 2014 [5], one must keep in mind that NASS-CDS is not limited to late model year vehicles. Since it serves as a multi-purpose nationally representative database, a large percentage of the sample are older model year vehicles.

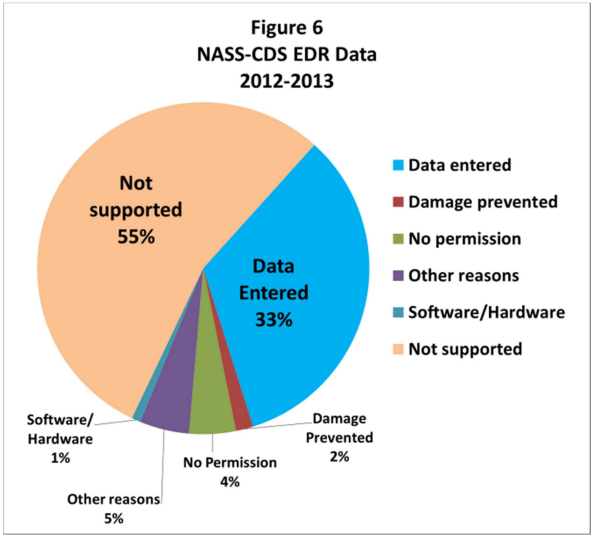


SCI cases are another valuable source of EDR data available to the public, and the cases can be viewed at http://www.nhtsa.gov/SCI. In addition to the data available in a NASS case, the SCI cases also feature a technical report which includes a detailed discussion of the EDR findings. The SCI investigators have attended EDR interpretation courses and are experts in advanced imaging techniques. In 2012-2013, the SCI investigators successfully imaged the EDR when the vehicle was supported 80% of the time.

## FUTURE EDR DATA COLLECTION

NASS was initially designed in the 1970s, and the system needed to be updated to meet the data needs of the transportation community that have increased and significantly changed over the last three decades. In Fiscal Year 2012, Congress appropriated funds for NHTSA to modernize NASS. The formal project, known as Data Modernization, was launched in January 2012. The goal of Data Modernization is to affirm NHTSA's position as the leader in motor vehicle crash data collection and analysis, by collecting quality data to keep pace with emerging technologies and policy needs. The multi-year project is set for implementation to begin in January 2016.

Congress was specific in their request to modernize NASS and NHTSA is looking to improve upon the following practices:

- Increase the sample size
- Expand the scope of its data collection to possibly include large trucks, motorcycles, and pedestrians
- Assess the need for more data from the pre-crash, crash, and post-crash phases of the crash sequence
- Review the crash data elements to be collected
- Solicit input from interested parties including suppliers, automakers, safety advocates, research organizations, and the medical community

The replacement to NASS-CDS has been named the Crash Investigation Sampling System (CISS). New nationally representative data collection sites have been selected using a sample design approach similar to NASS-CDS. The new sites were chosen using the most recent census and vehicle registration data and the goal is to better reflect the nation's overall crash picture and increase the availability of newer model vehicles and severe crashes at the data collection sites.

NHTSA believes that EDR data collection will continue to be a point of emphasis in CISS, as well as in the other field investigation-based data collection programs. Crash Technicians collecting data at the CISS sites will be trained on the various EDR imaging techniques and be equipped with the most current versions of the CDR software and connection cables.

Public access of EDR data in CISS will be an improvement from previous program. Current plans call for the original imaged .cdr file to be made available along with coded EDR data entered in the case viewers. Data from the Table 1 and Table 2 of CFR 49 Part 563 will also be available in SAS files and other analysis formats to enhance end user accessibility.

## CONCLUSION

EDRs will likely continue to be a important source of information as focus on crash avoidance countermeasures increase and crashworthiness countermeasures are optimized in the automotive safety community. Over the past 16 years, investigation-based data collection programs sponsored by NHTSA have accumulated one of the most extensive libraries of real-world crash EDR data in the world. Largely due to the implementation of CFR 49 Part 563, the vehicles in the fleet equipped with EDRs, and correspondingly the number of EDRs imaged by NHTSA, will increase even more rapidly in upcoming years.

Through the years EDR imaging acquisition rates in NHTSA's investigation-based programs have continually improved because of up-to-date equipment, the training of advanced imaging techniques, and the emphasis by the Agency to make the successful retrieval of EDR data a priority. The data collection programs are at the point now if the field personnel conduct an inspection of a vehicle equipped with an EDR, there is a high likelihood the data will be successfully imaged.

NHTSA's Data Modernization project should have a positive effect on EDR data collection, particularly in CISS which is set to begin in 2016. Plans are to equip each of the Crash Technicians with the CDR tool to image EDRs. The EDR data will be more accessible for end users through additional file formats, and the new data collection locations are projected to have increased percentages of EDR-equipped vehicles selected in the sample.

**References**

[1] Haight, Rusty. Spring 2010. "An Abbreviated History of CDR Technology," Collision Magazine, Volume 5, Issue 1.

[2] Summary of Findings by the NHTSA EDR Working Group, August 2001, Final Report (Docket No. NHTSA-1999-5218-9)

[3] National Highway Traffic Safety Administration. 2006. Federal Register Citation 71 FR 50998, Code of Federal Register 49 Part 563.

[4] National Highway Traffic Safety Administration. 2008. Federal Register Citation 73 FR 2168, Code of Federal Register 49 Part 563.

[5] Bosch Crash Data Retrieval Group. October 2014. "CDR version 14.1 Vehicle Coverage List."

# CONSIDERATION OF REPRESENTATIVENESS OF REAL-WORLD ACCIDENTS AND REPEATABILITY OF NEW NHTSA OBLIQUE OFFSET FRONTAL IMPACT TEST

**Ryuuji Ootani**
**Taisuke Watanabe**
**Tomosaburo Okabe**
Nissan Motor Co., Ltd.
Japan

**Dix Jeff**
**Lam Joyce**
Nissan Technical Center North America
USA

**Muthanandam Muthukumar**
Renault Nissan Technology and Business Center in India
India

Paper Number 15-0261

## ABSTRACT

The National Highway Traffic Safety Administration has been considering introducing an oblique frontal offset impact test (oblique test) as a new crash test procedure. By means of accident data analysis, it was examined whether this oblique test can represent real-world accidents. Tests were also conducted using two identical vehicles to examine the repeatability of the oblique test. Representativeness of real-world accidents was examined by using the National Automotive Sampling System Crash Worthiness Data System (NASS-CDS) to investigate frontal impact accidents from 2004 to 2008. Repeatability of the oblique test was investigated by conducting the same crash test twice using a midsize sedan. In terms of percentage of the total number of real-world accidents, the most frequent accident modes observed were Full-engagement and Offset frontal impacts, accounting for about 30%. Accidents similar to the oblique test accounted for about 10%. In terms of representativeness of severe injuries, the percentage of brain rotational injuries and lower extremity injuries differed from real-world accident statistics. Brain rotational injuries were considerably different from real-world accidents. With regard to repeatability, vehicle deceleration (G) was almost the same. However, the degree of cabin deformation differed because of a difference in the buckling mode of the front longitudinal member. Another notable point in the oblique test is that, as the test vehicle weight increases, the Delta-V decreases. However, this tendency is not observed in real-world accidents. To ensure the validity and significance of introducing this test procedure, more test data are required along with continued evaluation and analysis of occupant protection performance based on actual test results.

## INTRODUCTION

Occupant protection performance in frontal impacts is currently assessed in tests conducted under the New Car Assessment Program (NCAP) and by the Insurance Institute for Highway Safety (IIHS). The National Highway Traffic Safety Administration (NHTSA) has proposed introducing a frontal oblique offset impact test, which is different from the traditional test method. The NHTSA has been publishing results obtained from oblique tests and accident analysis. In 2011, Rudd et al. [1] conducted an analysis of small overlap and oblique accidents and also reported the factors causing injuries. In 2012, Saunders et al. [2] reported a small overlap and oblique test method and the results obtained for vehicle G and deformation. In 2013, Saunders and Parent [3] reported the results of additional oblique tests. Regarding the repeatability of the oblique test, the same authors [4] also published the results of a three-vehicle comparison using the same vehicle. For the THOR dummy, which is to be used in the oblique test, introduction of the Brain Injury Criteria (BrIC) is being considered. Saunders and Parent [5] discussed BrIC, and Dokko and Hasegawa [6] reported an evaluation of thoracic injuries using a human finite element model. Recent publications indicate that the studies related to the oblique test method and new THOR dummy have been increasing. In this study, attention was focused on analyzing the representativeness of real-world accidents and the repeatability of the oblique test.

## REPRESENTATIVENESS OF REAL-WORLD ACCIDENTS

### Method of accident analysis

The National Automotive Sampling System Crash Worthiness Data System (NASS-CDS) was used in this study to analyze injured occupants. Table 1 summarizes the extraction conditions of the accident analysis. The total number of MAIS3+ injured occupants was 3,214. The injured occupants were classified in nine types of crash configurations shown in Figure 1. In making this classification, "Small overlap" was classified based on the method proposed by the Medical College of Wisconsin [7]. "Offset", "Full-Engagement", "Narrow", "DYZ-NoRail", "Oblique", and "High/Low Vertical" were classified according to the taxonomy proposed by Sullivan et al. [8]. "Front-other" and "Side-other" were classified as other accident types.

**Table 1.**
**Summary of NASS-CDS data extraction conditions**

| | |
|---|---|
| Data years | 2004-2008 |
| Vehicle model years | 1959-2009 |
| Deformation location | Front, Left & Right |
| PDOF (Principal Direction of Force) [degrees] | Left & Right: 0-40, 320-360 |
| Rollover collisions | Not involved |
| MAIS | 3+ injuries |

### Results of Accident Analysis

Figure 1 shows a breakdown of the accidents by crash configuration. The most frequent accident types are the Full-Engagement and Offset frontal impact, each of them accounts for 27% of the total. The second most frequent accident type is the Small overlap impact, which accounts for 13%. The next frequent accident types are the Narrow, DYZ-NoRail, Oblique, and High/Low Vertical in decreasing order. Other accidents (Front-other and Side-other) are 15%.

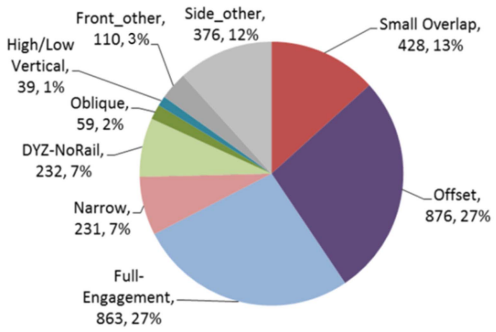


***Figure 1. Accident breakdown by crash configuration***

Among the results in Figure 1, Offset and Small overlap accidents were segmentalized in two directions: "Offset-Oblique" and "Offset-Colinear", "Small Overlap-Oblique" and "Small Overlap-Colinear". The results are shown in Figure 2. As a result of the segmentalization, the second most frequent accident type is "Offset-Oblique", which accounts for 15%. The next most frequent accident type is "Offset-Colinear", which accounts for 13%.

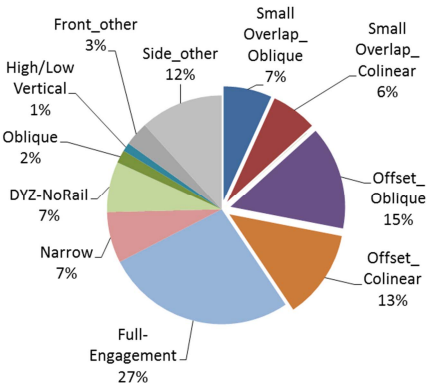


***Figure 2. Accident breakdown by crash configuration segmentalized by direction***

Among the results in Figure 2, Offset and Small overlap accidents were further segmentalized in terms of three types of collision partners: vehicle, pole and other object. The results are shown in Figure 3. As a result of the resegmentalization it is seen that the most frequent accident type is Full-Engagement, and the second most frequent type is "Offset-Oblique-Vehicle", which accounts for 12%. This "Offset-Oblique-Vehicle" is considered to be a crash configuration similar to the offset oblique impact test.

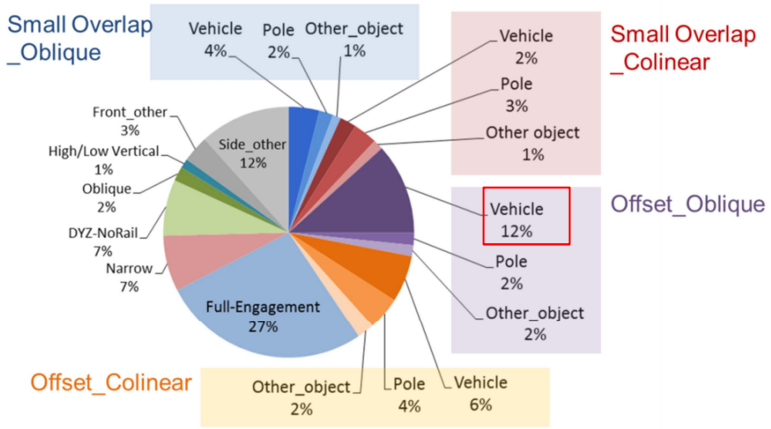


***Figure 3. Accident breakdown by crash configuration segmentalized by direction and collision partner***

Figure 4 shows the cumulative distribution of Delta-V of the "Offset-Oblique-Vehicle" type, and Figure 5 shows the frequency distribution. These data exclude unkown Delta-Vs. The number of seriously injured occupants (MAIS3+) was 256. The results indicate that Delta-V of 56 km/h covers 90% of the cases and the cumulative percentage of Delta-V less than 45 km/h was 75%.

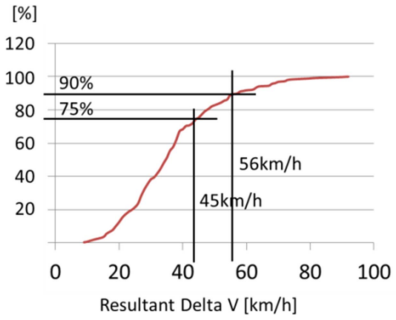


***Figure 4. Cumulative distribution of Delta-V***

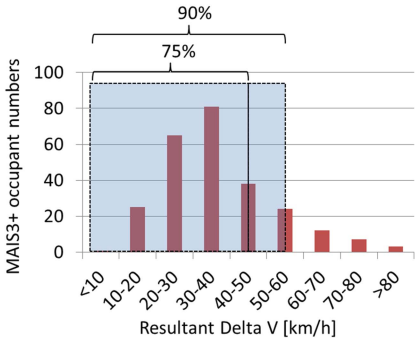


***Figure 5. Frequency distribution of Delta-V***

## Method of Detailed Accident Analysis

A more detailed accident analysis was then conducted using NASS-CDS data. The data sets were the same as those used in [1]. Table 2 shows the extraction conditions of this accident analysis. These conditions were applicable to 19 out of 117 number of total occupants used in [1]. The accidents involving these 19 occupants were analyzed.

**Table 2.**
**Summary of NASS-CDS data extraction conditions for detailed analysis**

| | |
|---|---|
| Data years | 1998-2009 |
| Vehicle model years | 1998-2005 |
| Deformation location | Left offset only |
| PDOF (Principal Direction of Force) [degrees] | 320-350 |
| Collision partner | Vehicle only |
| Rollover collisions and multiple crashes | Not involved |
| Occupants | Driver only |
| | Belted |
| | Not ejected |
| AIS | 3+ injuries |

## Comparison between NHTSA test results and detailed accident analysis results

The results of the accident analysis were compared with the results obtained for 16 vehicles in oblique frontal impact tests (Table 3) in a study conducted by NHTSA. Figure 6 shows the configuration of the oblique frontal impact test, and Table 3 is the list of vehicles used. In this oblique frontal impact test, the dolly with barrier impacts the target vehicle at 56mph (90 km/h) and the angle of the stationary vehicle is 15 degrees and the overlap is 35 percent on the driver side of the vehicle. In this paper, an oblique offset impact in real-world accidents is referred to as an Accident Oblique Offset Impact (AOOI) and an oblique offset imapct in the NHTSA research test is referred to as an Oblique Offset Impact (OOI).

**Table 3.**
**List of vehicles used in oblique frontal impact test conducted by NHTSA**

| Report No. | Name | Model Year | Test vehicle weight [kg] |
|---|---|---|---|
| 7458 | Smart For two | 2011 | 1034 |
| 7441 | Toyota Yaris | 2011 | 1331 |
| 8086 | Nissan Versa R | 2013 | 1438 |
| 8084 | Nissan Versa | 2013 | 1451 |
| 8089 | Hyundai Elantra | 2013 | 1590 |
| 7431 | Chevrolet Cruze | 2011 | 1662 |
| 7428 | Ford Fiesta | 2011 | 1671 |
| 8085 | Toyota Camry R | 2012 | 1752 |
| 8096 | Honda CRV | 2012 | 1757 |
| 8088 | Toyota Camry | 2012 | 1759 |
| 7467 | Buick Lacrosse | 2011 | 1944 |
| 8087 | Ford Taurus | 2013 | 2123 |
| 8097 | Honda Odyssey | 2012 | 2210 |
| 7476 | Ford Explorer | 2011 | 2363 |
| 7457 | Dodge Ram 1500 | 2011 | 2611 |
| 8099 | Chevrolet Silverado | 2012 | 2624 |

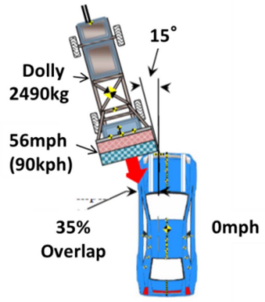


*Figure 6. NHTSA offset oblique impact test*

**Delta-V Direction** Figure 7 compares the results for the Delta-V direction, which is calculated with Eq. (I). Most of the Delta V-direction is within 10-20 degrees, and the average Delta-V direction of AOOI and OOI is almost the same.

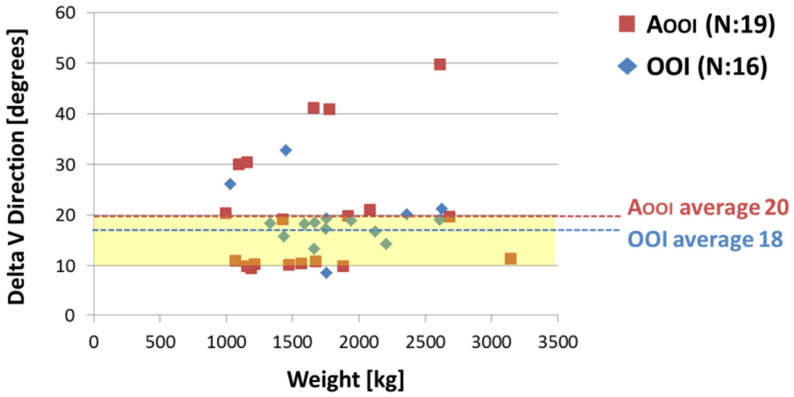


*Figure 7. Relationship between Delta-V direction and vehicle weight*

*Delta-V Direction = Tangent (longitudinal Delta-V / Lateral Delta-V)* *(I)*

**Relationship between Delta-V and Vehicle Weight** Figure 8 shows the relationship between the resultant Delta-V (longitudinal and lateral) and vehicle weight. In OOI, a strong correlation exists between the two. Delta-V of 41 km/h for the heaviest vehicle is the minimum velocity of all the Delta-V values; Delta-V of 67 km/h for the lightest vehicle is the maximum velocity and is approximately 1.6 times higher than that of the heaviest vehicle. On the other hand, weak correlation is observed between Delta-V and vehicle weight in AOOI. Delta-V in OOI is almost at the upper limit of Delta-V in AOOI.

Figure 9 shows the relationship between the resultant Delta-V and vehicle weight ratio. The vehicle weight ratio used in this study is explained here. The vehicle weight ratio in AOOI is found by dividing the weight of the impacted vehicle by the weight of the collision partner because the crash configuration is a car-to-car collision. In contrast, OOI is a research moving deformable barrier (RMDB)-into-stationary vehicle impact test. For this reason, the vehicle weight ratio cannot be calculated in the same way. For a better comparison between AOOI and OOI, as shown in Figure 10, the OOI test condition was translated into a car-to-car test at an initial velocity of 64 km/h and a vehicle weight of 1750 kg. The initial velocity and vehicle weight were derived using the law of conservation of momentum. The initial velocity was the same as in the offset deformable barrier (ODB) imapct test conducted by IIHS and EuroNCAP, and the vehicle weight was calculated with Eq. (II). For reference, the resultant Delta-V of the Toyota Camry R (1752 kg) and the Honda CRV (1757 kg), both of which weigh close to 1750 kg, was 52 km/h and 54 km/h, respectively. These values are similar to Delta-V of 56 km/h, having a cumulative composition ratio of

90% in Figure 4. The weight of the collision partner was 1750 kg, and the vehicle weight ratio was calculated by dividing the impacted vehicle weight by 1750 kg.

The results plotted in Figure 9 are almost the same as those in Figure 8. It is seen that the resultant Delta-V and vehicle weight ratio have a strong correlation in OOI but little correlation in AOOI.

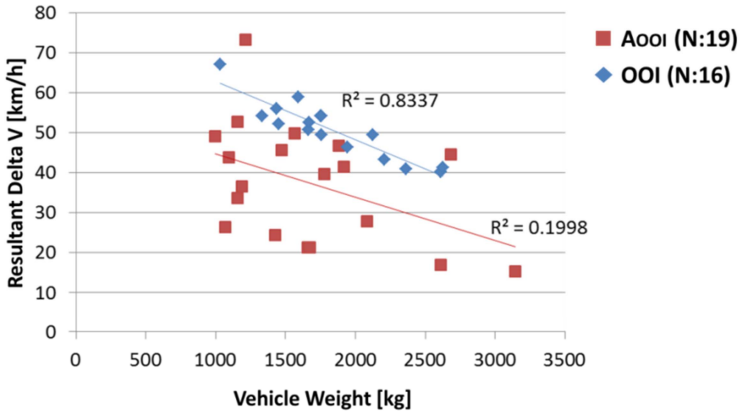


*Figure 8. Relationship between resultant Delta-V and vehicle weight*

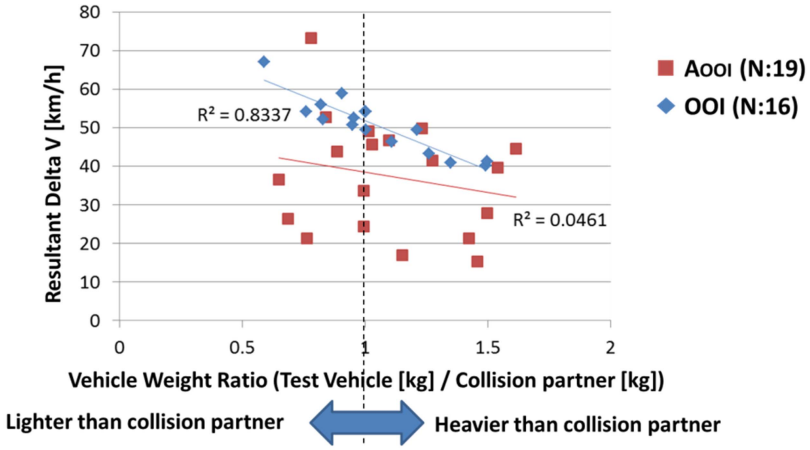


*Figure 9. Relationship between resultant Delta-V and vehicle weight ratio*

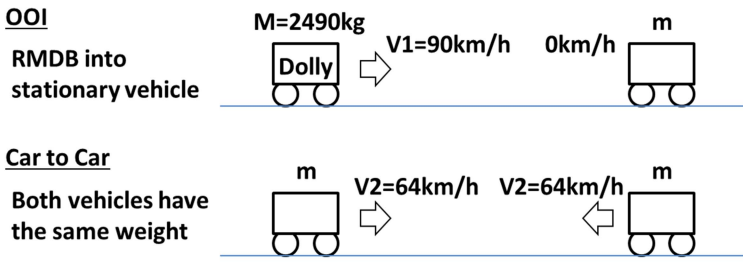


*Figure 10. Translation method to equivalent car-to-car impact*

$$2*m*V2 = M*V1 \qquad m=1750\ kg \qquad (II)$$

**Injuries in AOOI** Figure 11 shows the percentages of AIS3+ injuries by body region in AOOI. The most frequent type is knee, thigh, and hip (KTH) & lower leg (40%) injuries, followed by upper extremity (28%) and thorax (20%) injuries. Small percentages of injuries are seen for head (8%) and abdomen (2%).

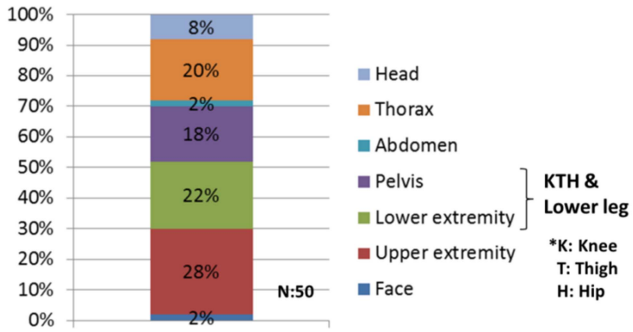


*Figure 11. AIS3+ injury percentages by body region*

Figures 12 and 13 show the details of AIS3+ head injuries and injury sources in AOOI. Number of injuries N:4 in Figure 12 is small and all of them involve brain damage. Injury sources are safety belt and left B-pillar.

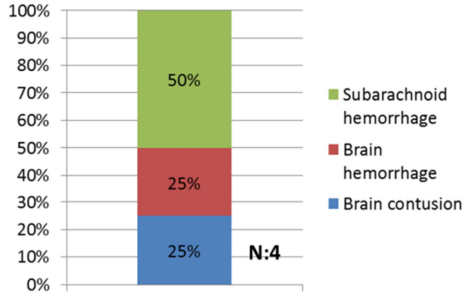


*Figure 12. Details of AIS3+ head injuries*

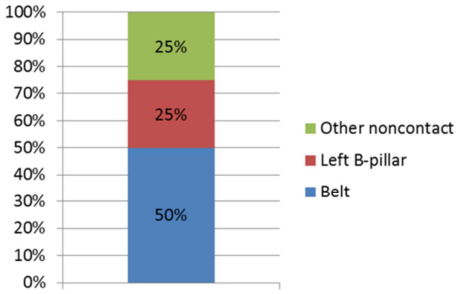


*Figure 13. Sources of head injuries*

Figures 14 and 15 show the details of AIS3+ thorax injuries and injury sources in AOOI. Thorax injuries comprise rib fracture, lung contusion, and thorax cavity damage. The main injury sources are left-side object and steering wheel.

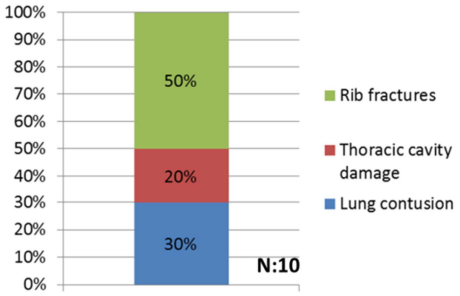


*Figure 14. Details of AIS3+ thorax injuries*

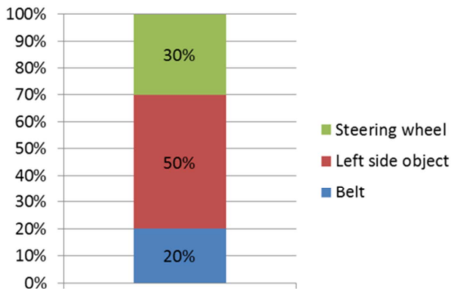


*Figure 15. Sources of thorax injuries*

Figures 16 and 17 show the details of AIS3+ KTH & lower leg injuries and injury sources in AOOI. All injuries are fractures, the most frequent of which are femur fractures, followed by acetabulum and tibia fractures. The main injury sources are the kneee bolster, the left-side object and the floor panel.

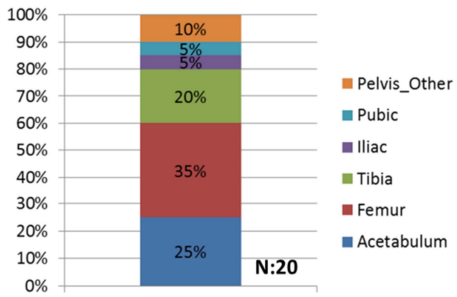


*Figure 16. Details of AIS3+ KTH & lower leg injuries*

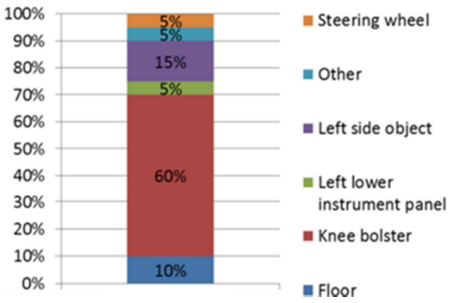


*Figure 17. Sources of KTH & lower leg injuries*

Figures 18 and 19 show the fracture points of AIS3+ KTH & lower leg injuries and injury sources for the femur, acetabulum and tibia in AOOI. Fracture occurs equally in both the right and left legs. Pelvis and upper leg fractures in particular occur frequently. Tibia fracture occurs in only the right leg. The injury sources for the acetabulum are the knee bolster, left lower instrument panel, and the steering wheel. The injury sources for the femur are the knee bolster and the left-side object, and for the tibia the knee bolster and the floor panel.

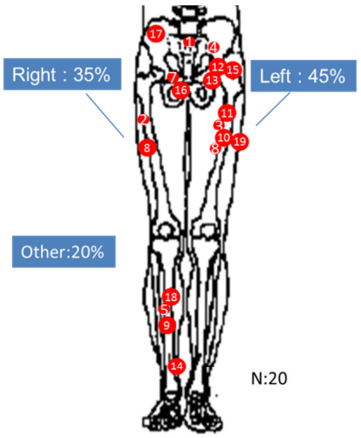


*Figure 18. Fracture points of KTH & lower leg*

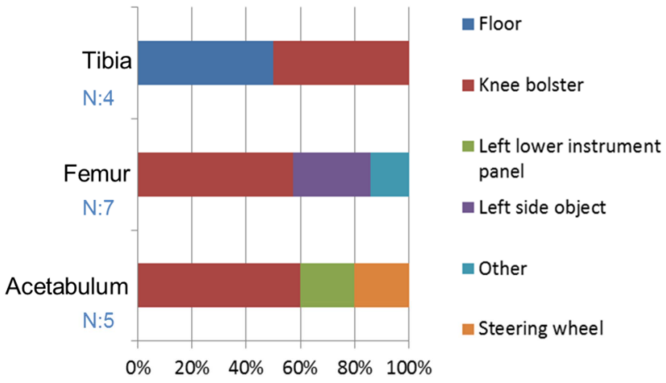


*Figure 19. Sources of acetabulum, femur, and tibia injuries*

**<u>Comparison of injuries between AOOI and OOI</u>** Figure 20 compares the percentages of serious injuries occurring in AOOI and OOI. In AOOI, AIS3+ injuries were treated as serious injuries, and the percentage of serious injuries was calculated in the following way: (a) at first, AIS3+ injury numbers of the driverside occupant were counted and (b) then it is diveded by the total number of injuries of the body region. For example, regarding the percentage of head serious injury, the percentage of serious injuries is 16% (3/19), where 3 was AIS 3+ and total numbers of injuries was 19. In OOI, the percentage of serious injuries was calculated in the following way: (a) at first, the injury numbers of the driverside dummy which exceeded the reference Injury Assessment Reference Value (IARV) were counted and (b) then it is diveded by the total number of injuries of the body region. For example, regarding the percentage of head serious injury, the percentage of serious injuries is 25% (4/16), where 4 exceeded IARV and total numbers of injuries was 16. It will be noted that the IARV of thorax injuries was not determined, so the upper deflection (53 mm) and lower deflection (46 mm) [2] were used as provisional values. The Brain Rotational Injury Criterion (BRIC) was also used as head injury value. As a result, the percentage of BRIC head injuries in OOI differed greatly from the percentage of AIS3+ head injuries in AOOI. As for KTH & lower leg injuries, the percentage of acetabulum and femur serious injuries differed between AOOI and OOI.

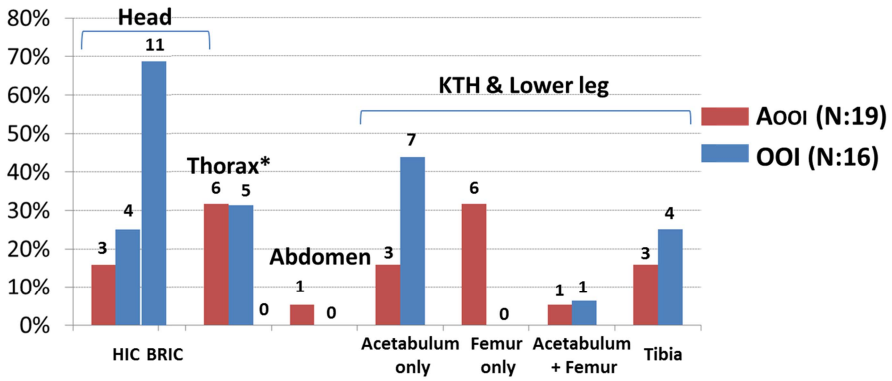


*Figure 20. Comparison of serious injury percentages between AOOI and OOI*

## REPEATABILITY OF OBLIQUE TEST

### Test Conditions

To examine the repeatability of the oblique offset impact test (OOI), a comparison was made for the vehicle deformation and G level in two tests conducted with the same vehicle. Table 4 shows the test conditons and vehicle specification for OOI. The vehicle used was a midsize sedan. The initial velocity and the test vehicle weight were almost the same in OOI#1 and OOI#2 tests. A 50th percentile male THOR-NT frontal impact test dummy was seated in the driver's seat. A Hybrid-III dummy was seated in the front passenger's seat. The THOR-NT dummy was a tentative version manufactured by GESAC and was different from the THOR dummies used in NHTSA's OOI research tests.

**Table 4.**
**Test conditions and vehicle specification of OOI test**

| No. | Vehicle | Weight [kg] | Velocity [km/h] |
|---|---|---|---|
| OOI #1 | V6 3.5L 2WD | 1868 | 90.1 |
| OOI #2 | | 1870 | 90.4 |

| Dummy | |
|---|---|
| Driver (Left) | THOR-NT (GESAC) |
| Passenger (Right) | Hybrid-III |

### Comparison results

**Summary** Figure 21 shows photographs of the post-test vehicles and barriers. The comparison did not show any significant difference for the vehicle and the barrier deformations between OOI#1 and OOI#2.

*Figure 21. Photographs of the post-test vehicles and barriers*

**Difference in Vehicle Deformation** Figures 22 and 23 compare the cabin deformation and floor deformation of the post-test vehicles, respectively. The cabin deformation around the front door opening was almost the same in OOI#1 and OOI#2; the maximum deformation point was the part of the door front near the lower A-Pillar, and the amount of deformation was 44 mm. On the other hand, floor deformation differed in the longitudinal and vertical directions. In the longitudinal direction, C2 and D2 showed large differences, with the maximum difference being 36 mm. In the vertical direction, B2, C2 and D2 showed large differences, with the maximum difference being 58 mm. Generally the vehicle deformation is greater in OOI#2 than in OOI#1.

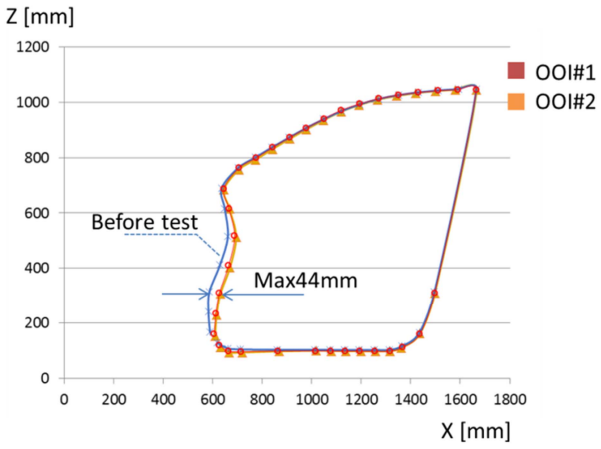


*Figure 22. Comparison of cabin deformation*

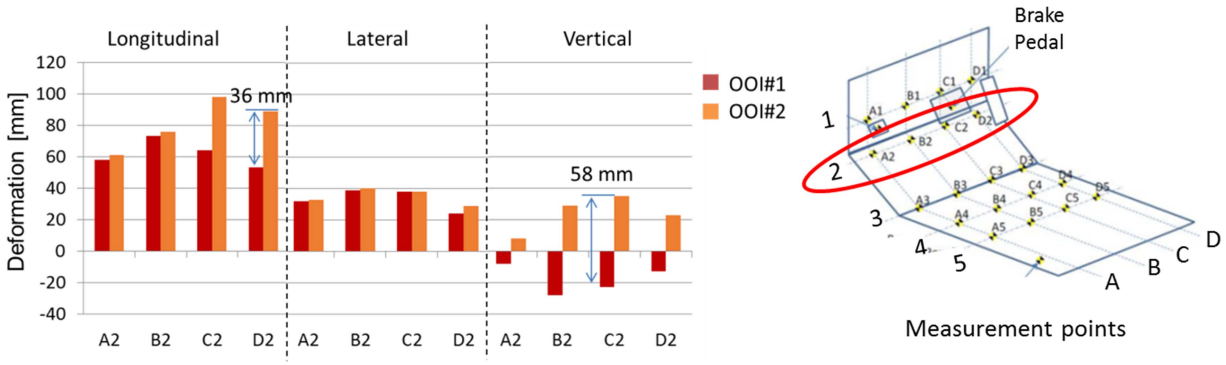


*Figure 23. Comparison of floor deformation*

The factors causing the difference in the floor deformation seen in Figure 23 were then examined. Figure 24 shows the deformation of Row 1 on the dash panel and mearument points 6, 7, 8 on the dash lower cross member. Figure 25 presents photographs of the post-test dash panels. The difference (52 mm) in the deformation at location 8 was especially large. In addition, as seen in Figure 25, the deformation mode of the dash panel near the dash lower cross member differed. In order to investigate the reason of these differences, the deformation of the front longitudinal member which is connected to the dash lower cross member in the engine compartment was then examined.

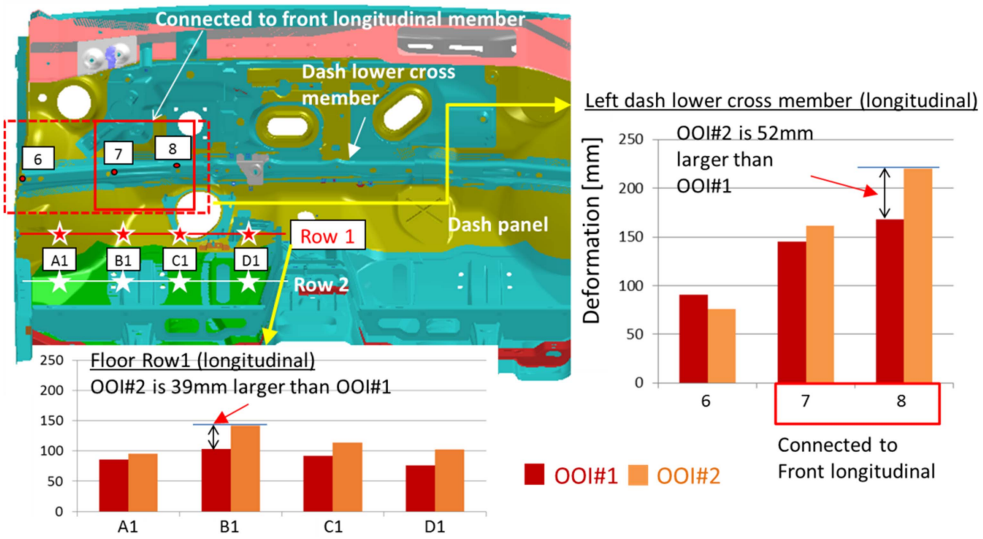


*Figure 24. Comparison of dash panel and dash lower cross member deformation*

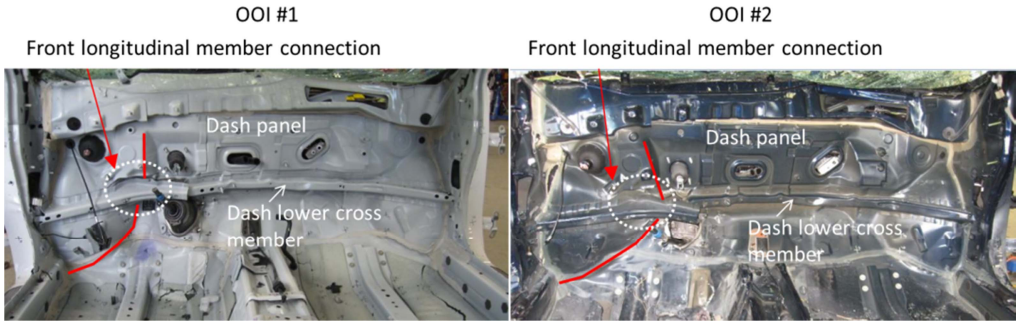


*Figure 25. Photographs of dash panel deformation*

Figures 26 and 27 show the measured deformation modes of the front longitudinal member. These results indicate that the deformation mode in OOI#1 differed from that in OOI#2 and that rearward displacement in OOI#2 was

larger than that in OOI#1. Two bending points occurred in the front longitudinal member and bumper reinforcement beam in OOI#1 and OOI#2, but the bending locations were different. The bending points in OOI#1 occurred only in the front longitudinal member, whereas in OOI#2, there were one bending point each on the front longitudinal member and the bumper reinforcement beam. Figures 28 and 29 show photographs of the post-test front longitudinal member and bumper reinforcement beam, respectively. It is seen in these photographs that the deformation mode and bending locations of the front longitudinal member and bumper reinforcement beam differed between the two tests.

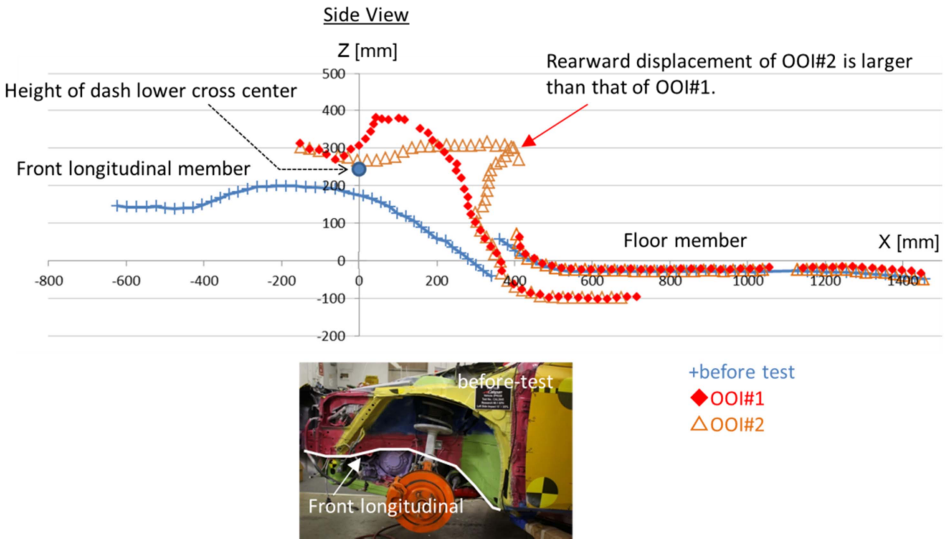


*Figure 26. Comparison of front longitudinal member deformation (side view)*

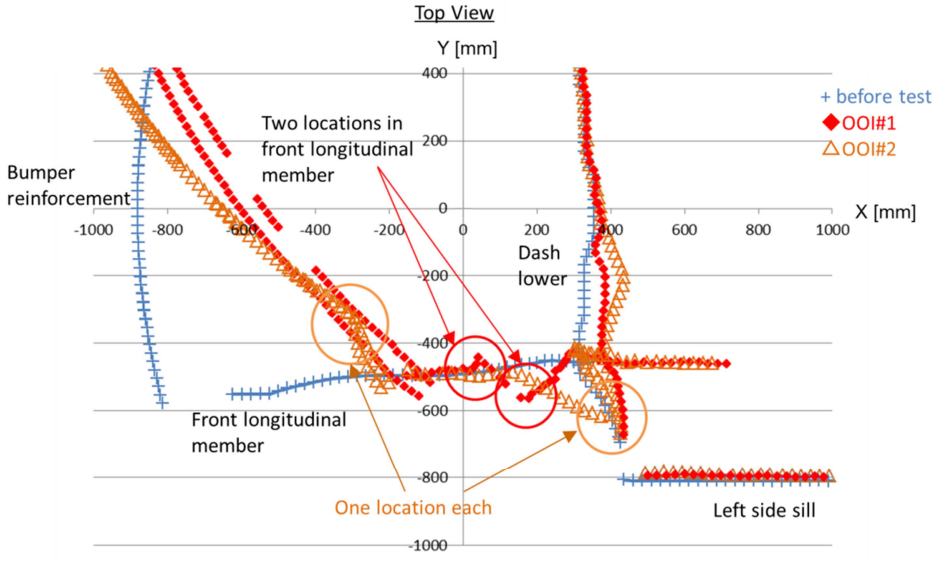


*Figure 27. Comparison of front longitudinal member deformation (top view)*

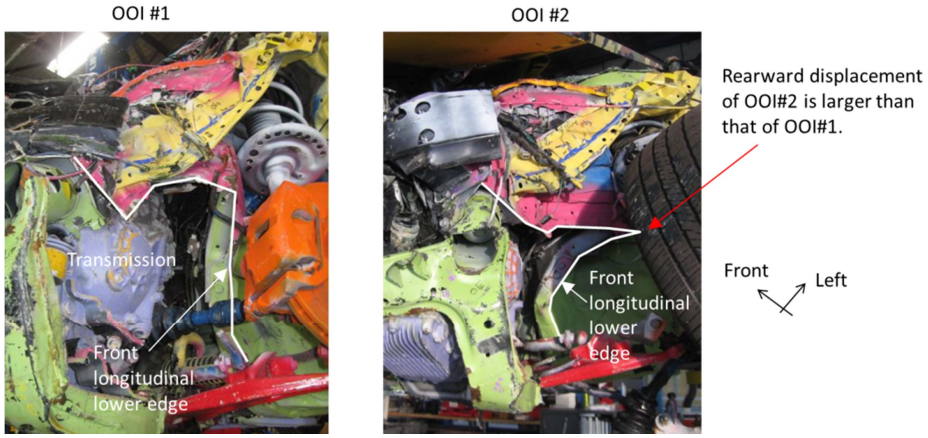


*Figure 28. Photographs of front longitudinal member deformation*

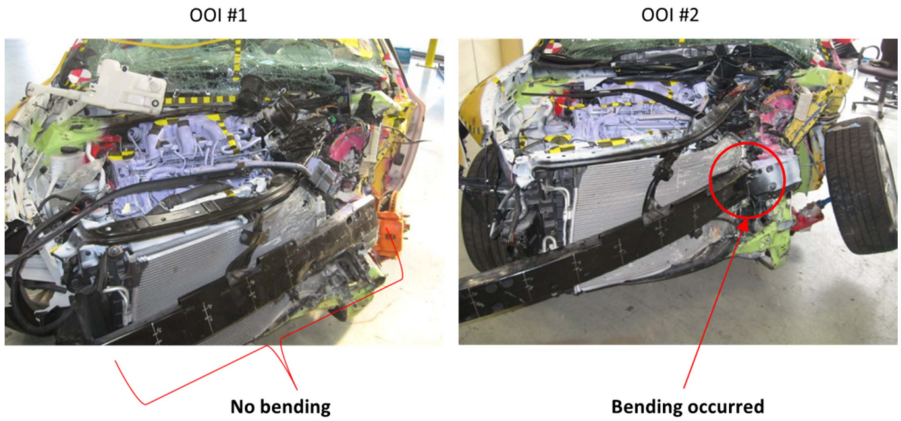


*Figure 29. Photographs of bumper reinforcement beam deformation*

The difference in floor deformation between OOI#1 and OOI#2 is presumed to be due to the following sequences. Initially, the deformation mode of the front longitudinal member differs, and larger rearward displacement occurs in OOI#2 than in OOI#1; then the dash lower cross member connected to the front longitudinal member undergoes large deformation toward the cabin side, this results in larger floor deformation in OOI#2 than in OOI#1. In a series of OOI research tests, NHTSA has conducted the repeatability evalluation using three same vehicles [4] (Figure 30). The variation of floor Row 1 deformation were at a similar level to the test results in this study as shown in Figure 24.

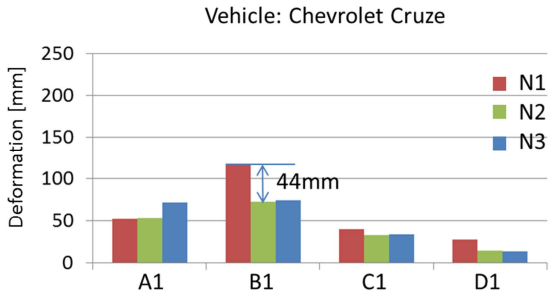


*Figure 30. Result of floor deformation in NHTSA research test*

**Difference in vehicle G and velocity** Figure 31 compares the vehicle deceleration (G) and Figure 32 compares the vehicle velocity. Deceleration was measured at the vehicle's center of gravity, and velocity was calculated by

integrating G. It is seen that the peak G values differed by a factor of 7G between the longitudinal direction and by a factor of 12G between the lateral direction. However the overall wave shapes and timing of the peaks were similar in both the longitudinal and lateral directions between OOI#1 and OOI#2. Longitudinal velocity differed by 2km/h, but lateral velocity was almost the same.

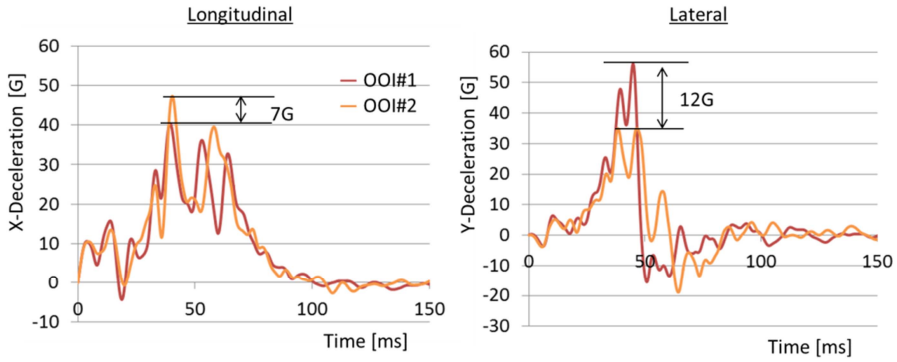


***Figure 31. Comparison of vehicle deceleration***

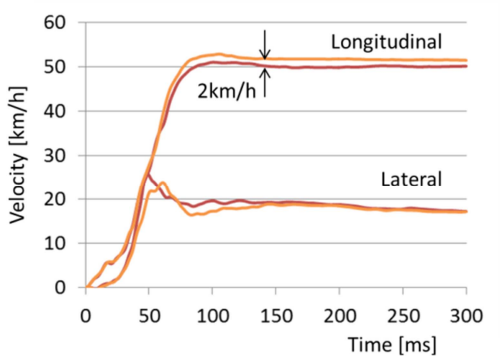


***Figure 32. Comparison of vehicle velocity***

## DISCUSSION AND CONCLUSION

Real-world frontal impact accidents were classified into 9 crash configurations based on the method in the literature [7], [8]. The most frequent accident types are Full-engagement and Offset, followed by Small overlap accidents in that order. Small overlap and Offset accidents were then reclassified in terms of two directions: Offset-Oblique, Offset-Colinear and Small Overlap-Oblique, Small Overlap-Colinear and three collision partners: vehicle, pole, and other object. It was found that an Offset-Oblique-Vehicle accident similar to the offset oblique impact (OOI) test was the second most frequent crash configuration next to Full-engagement. However, this Offset-Oblique-Vehicle accident accounts for only approximately 10% of all frontal impact accidents. Regarding crash severity, in the AOOI, the resultant Delta-V of approximately 56 km/h covers a cumulative accident coverage of 90%. In the OOI tests, a strong correlation was seen between the resultant Delta-V and vehicle weight and the resultant Delta-V of lighter vehicles tended to be higher than 56 km/h. The lightest vehicle is higher than 64km/h in the offset deformable barrier (ODB) imapct test. Therefore it is thought that additional vehicle structural countermeasure for lighter vehicles to address the current OOI test procedure may produce stiffer vehicles and shorter crash pulses and in consequence negatively affect the safety of vulnerable elderly drivers. As for the representativeness of the percentages of serious injuries, a large difference was seen between the accident data and the test results, especially for head injuries (BRIC). Differences between the accident data and the test results were also seen for lower extremity injuries, especially accetabulum and femur injuries.

Regarding repeatability of the OOI test, vehicle deformation, G values, and velocity were compared by conducting two tests using the same midsize sedan. The results showed that G values and velocity did not show any notable difference. However, floor deformation differed due to a difference in the deformation mode of the front

longitudinal member, which was caused by a difference in the bending location of the member and the bumper reinforcement beam. This difference in floor deformation was similar to the difference reported in a couple of OOI reserach tests previously carried out by NHTSA. The amount of this difference in floor deformation may affect the details and dimensions of countermeasures. These results suggest that further studies are required to validate the introduction of the OOI as a new crash test procedure in regulatory testing or NCAP.

## REFERENCES


[1] Rodney W. Rudd, Mark Scarboro, James Saunders, "Injury Analysis of Real-World Small Overlap and Oblique Frontal Crashes", 2011 ESV, Paper Number 11-0384.

[2] James Saunders, Matthew Craig and Daniel Parent, "Moving Deformable Barrier Test Procedure for Evaluating Small Overlap/Oblique Crashes", 2012 SAE, No 2012-01-0577.

[3] James Saunders and Dan Parent, "Assessment of an Oblique Moving Deformable Barrier Test Procedure", 2013 ESV, Paper Number 13-0402.

[4] James Saunders and Daniel Parent, "Repeatability of a Small Overlap and an Oblique Moving Deformable Barrier Test Procedure", 2013 SAE, No 2013-01-0762.

[5] James Saunders and Daniel Parent, "Repeatability of a Small Overlap and an Oblique Moving Deformable Barrier Test Procedure", 2013 SAE, No 2013-01-0762.

[6] Yasuhiro Dokko and Takahashi Hasegawa, "Evaluation of Thoracic Injury of the Occupants in Small Overlap/oblique Impact Using a Human FE Model", 2013 JSAE, No152-20135332.

[7] Erik G. Takhounts and Vikas Hasija, "An Operational Definition of Small Overlap Impact for Published NASS Data", 2013 STAPP, No 243-266.

[8] Kaye Sullivan, Scott Henry and Tony R. Laituri, "A Frontal Impact Taxonomy for USA Field Data", 2008 SAE, No 2008-01-0526.

[9] NHTSA, "NASS Analysis in Support of NHTSA's Frontal Small Overlap Program", 2011.


## GLOSSARY

AOOI: Accident Oblique Offset Impact

OOI: Oblique Offset Impact

PDOF: Principal Direction of Force

IARV: Injury Assessment Reference Value

KTH: Knee Thigh Hip

BRIC: Brain Rotational Injury Criterion

# INFLUENCE OF IMPACT TYPE AND RESTRAINT SYSTEM TRIGGERING TIME ON INJURY SEVERITY IN FRONTAL IMPACT CRASHES

**Heiko Johannsen**
**Dietmar Otte**
Medizinische Hochschule Hannover
Germany

Paper Number 15-0263

## ABSTRACT

The safety performance of cars is evaluated using standard tests. These standard tests are normally performed with full overlap or 40% overlap from the corner in different speed ranges. Analysis of accident data indicated that the injury severity of car occupants that were involved in accidents that are different compared to the standard tests (e.g., central pole impact) is considerably higher than for those that are similar to the standard tests. One of the discussed possible reasons for this observation is that the restraint system triggering might not be appropriate for these situations.

The combination of NASS CDS data with the NASS EDR data allows to analyse the accident circumstances, the restraint system triggering times and the injury situation in frontal impact accidents. The result of this analysis is a grouping of accident situations with corresponding injury severities and restraint system triggering times. These groups are rechecked using the GIDAS data to confirm the influence of the accident circumstances on the injury severity, as restraint system triggering time is not available in the GIDAS data sample.

The restraint system trigger time depends on several factors (e.g., delta-v, impact configuration (e.g., involving both long members, only one long member or no long member), impact angle etc.). While most of the differences appear to be sensible for optimal protection (e.g., at higher delta-v the airbag is needed earlier) the differences for the different impact configuration appears to be critical with respect to injury severity levels of the frontal occupants.

The shown correlation between crash configuration, restraint system triggering time and injury severity does not necessarily mean that there is a causative relation between triggering delay and increased injury severity. However, it is likely that there is a causative relation.

## INTRODUCTION

For the protection of car occupants the design of the vehicle structures, the restraint system that is composed of seat, bolster, belt system (including pretensioners and load limiters) and airbags as well as the appropriate timing of the active restraint system components (e.g., pretensioner and airbag) are important. The occupant protection system is assessed by standard tests (e.g., vehicle homologation and NCAP programmes). Although almost all cars are performing excellent in these standard tests, it might happen that individual cars are performing worse in real world conditions.

Reichert et al. [Reichert 2013] analysed thoracic and abdominal injury risks in NASS frontal impact accidents without front rail involvement (impact location between the rails to be more precise). While they observed an increased injury risk in the analysed accidents they were unable to replicate the increased injury risk in FE simulations. However, they used US NCAP trigger times for the restraint system triggering which might be the main cause for failing.

During the EU funded FIMCAR project airbag trigger times were analysed in order to define a frontal impact test procedure that is more representative of real world accidents than the Full Width Rigid Barrier (FWRB). For some cars considerably late restraint system triggering was observed in Full Width Deformable Barrier tests (FWDB) with important influence on the dummy readings [Johannsen 2012, Johannsen 2013a, Johannsen 2013b], see Figure 1 as an example.

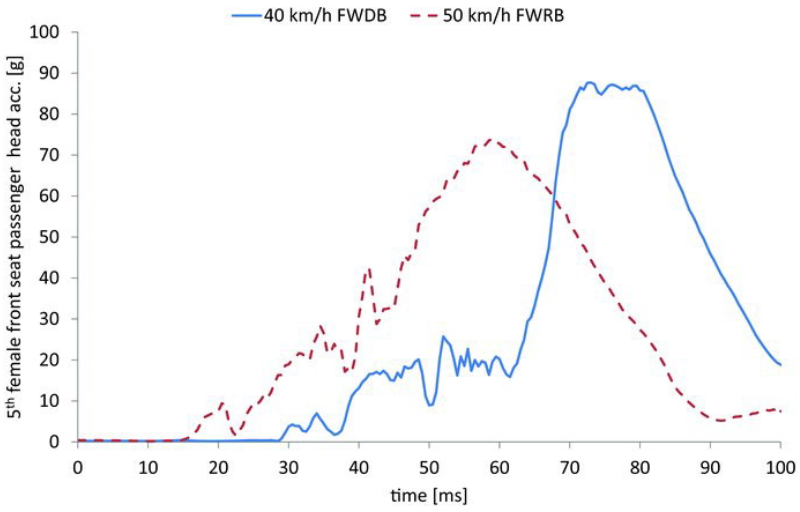


a

b c

***Figure 1. (a) Late air bag deployment in 40 km/h FWDB test and its consequences for head acceleration. (b) At approximately 30 ms the air bag starts to deploy and (c) at approximately 50 ms the head contacts the deploying air bag [Johannsen 2013a].***

In a physical reconstruction of a real world accident (approx. 35 km/h against a small object between the rails) the airbag was fired at approx. 90 ms by the ECU resulting in a contact between deploying airbag and the occupant in forward movement, see Figure 2 (note: in the original accident a rear facing CRS was positioned at the front passenger seat and the reconstruction was repeated to analyse the consequences for adults).

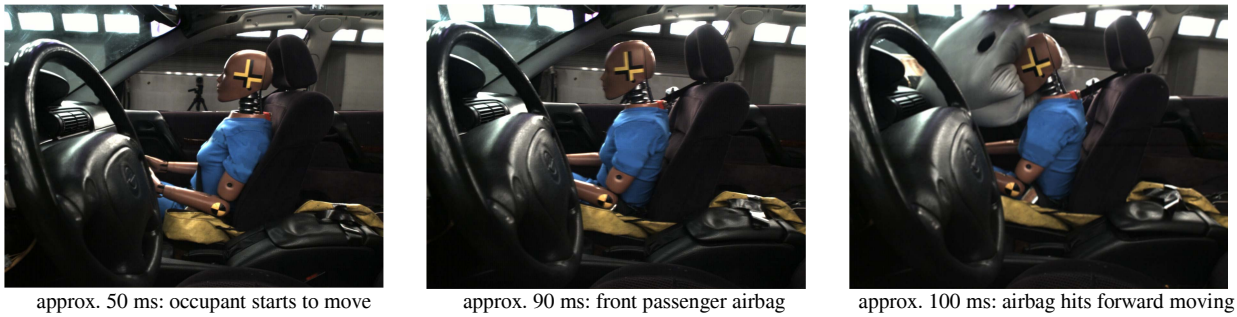

approx. 50 ms: occupant starts to move forward

approx. 90 ms: front passenger airbag deploys

approx. 100 ms: airbag hits forward moving occupant

***Figure 2. Front seat passenger airbag deployment in an accident reconstruction.***

In accident studies it is normally not possible to assess the restraint system firing time due to missing data insight into the control units. So it is normally only possible to assess whether or not an active restraint system was fired at all. The US NASS EDR data (Event Data Recorder) [Da Silva 2008; Dalmotas 2009; Gabler 2008] allows to also consider the firing time as it is normally recorded in the data sets.

## METHOD

For the EDR data analysis NASS CDS data for the accident years 2000 to 2012 were considered. Furthermore only MAIS 2+ injured belt restrained (according to NASS CDS data set) drivers that had a frontal impact and where EDR data are available were included. This selection resulted in 188 cases.

For some of the cases the restraint system trigger time was not recorded in the EDR spread sheet. These cases were excluded from the analysis. The same is true for most of the analyses for the cases without airbag deployment. These 19 cases were analysed seperately. Following this selection 155 cases with available restraint system triggering time were included.

In a last step roll-over cases were excluded as well as cases without pictures of the case car. Finally 148 MAIS 2+ injured car drivers using the seat belt that were involved in a frontal impact accident in the years 2000 to 2012 without roll-over and available restraint system triggering time were included in the study.

Because the structural interaction appears to be an important influencing factor for the restraint system triggering, all cases were categorised as good structural interaction, under- / overrun, between rails or small overlap (impact zone outside the rails) respectively by checking the images of the deformed cars.

The delta-v of the case cars was retrieved from the EDR data in most of the cases except for cases where the delta-v was not available or wrong without doubts. The latter one was for example true for cases with interruption of the data storage process before the end of the impact phase. In some other cases the recorded delta-v does not fit with the vehicle deformation. For those cases the reconstructed delta-v was considered.

The restraint system triggering time is recorded in the EDR data set as the time between the algorhythm enable signal (normally a vehicle acceleration exceeding 2 g) and the driver airbag system triggering signal (in case of multiple stage airbags the trigger time of the first stage). In some cases the accident was recorded as two or more events in the EDR spread sheets. For those cases the time between preceeding non-deployment events were added to the triggering time of the deployment event.

For the GIDAS analysis frontal impact accidents of ECE R94 compliant cars (i.e., for this study year of first registration after 2003) with MAIS 2+ injured front seat occupants in cars with a front airbag at the relevant seating position were considered. The data set includes 91 occupants meeting the criteria. Structural interaction issues were identified using the CDC and the information in the database whether or not over- / underrun occurred. Delta-v information was obtained from the reconstruction.

## DATA ANALYSIS

The data analysis is separated into the analysis of the NASS EDR data with airbag deployment, NASS EDR data without airbag deployment and the GIDAS data.

### NASS EDR Data with Airbag Deployment

The focus of this study is the analysis of the restraint system trigger time and to evaluate the restraint system trigger time influencing factors. The distribution of the restraint system trigger time dependending on the delta-v is shown in Figure 3. The trigger time varies between 2 and more than 600 ms. The average trigger time is 65 ms. When comparing this time with the average trigger time in FWRB tests of approx. 7 ms [Dalmotas 2009], it is obvious that the trigger time in real world accidents is normally later. However, in an accident with a lower crash severity (e.g., expressed by the delta-v) than in the test it might be sensible to trigger the restraint system later in order to provide optimal performance.

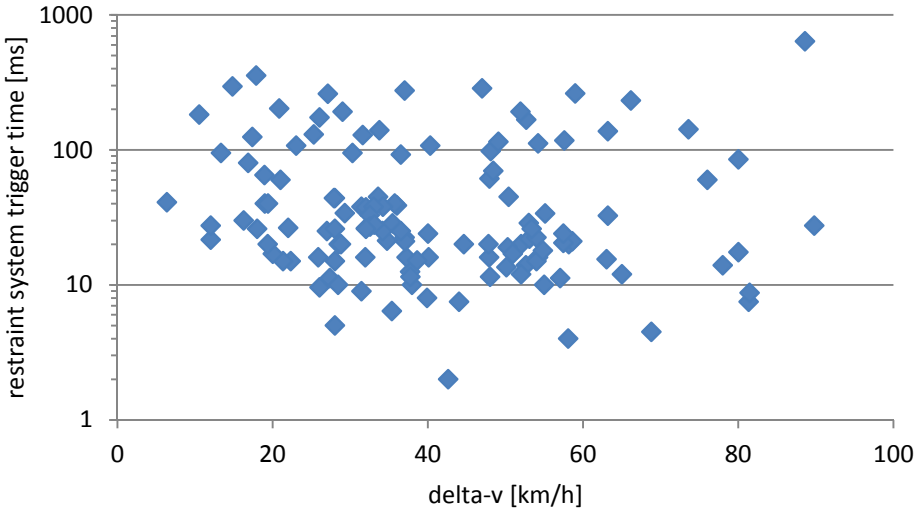


***Figure 3. Restraint system trigger time dependent on delta-v for all 129 car drivers.***

When dividing the accidents in groups with good structural interaction and those with poor structural interaction (i.e., small overlap, under- / overrun or between rails impact) the average trigger times are 48 ms in the good performing group and 89 ms in the group with poor structural interaction, respectively, see Figure 4.

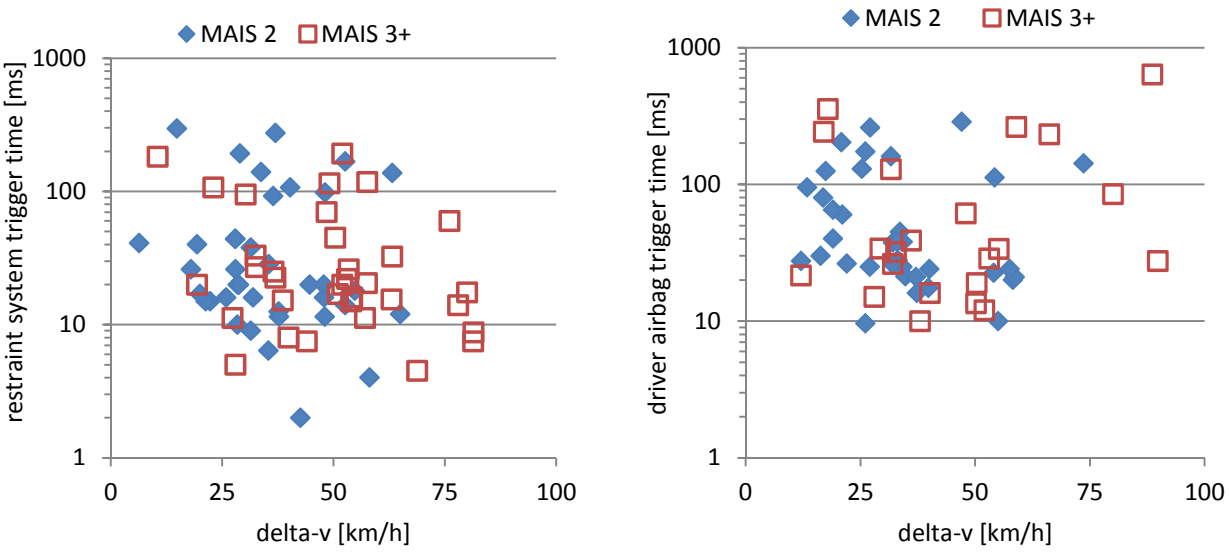


accidents with good structural interaction

accidents with small overlap, impact between rails or under- / overrun

***Figure 4. Injury severity depending on delta-v and restraint system trigger time for good and poor structural interaction.***

Although even in the accidents with good structural interactions relatively late timing of the airbag was observed there are more cases with long trigger times in the group with poor structural performance, Figure 4. The mean trigger time for the MAIS 2 cases with good structural interaction differs only slightly from the MAIS 3+ cases, 36 ms compared with 49 ms, respectively – see Figure 5.

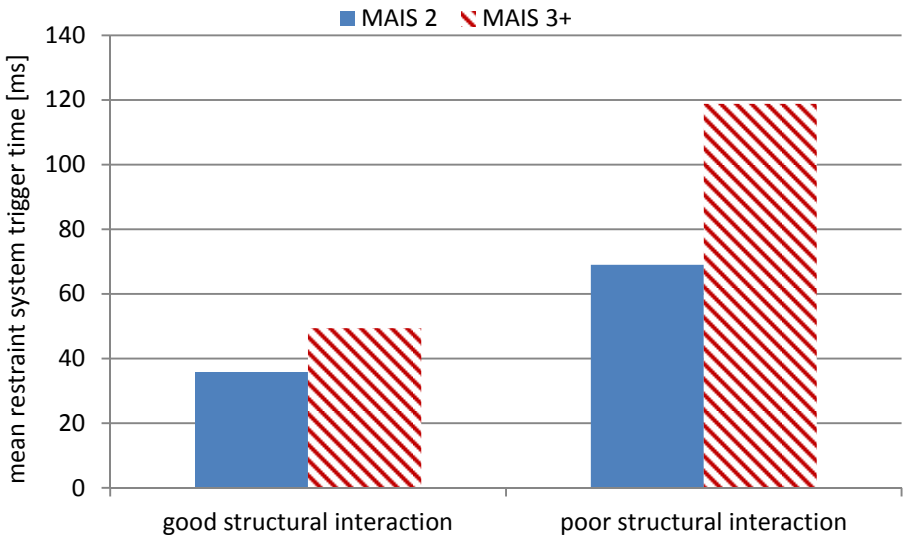


***Figure 5. Injury severity depending on delta-v and restraint system trigger time for good and poor structural interaction.***

For the cases with poor structural interaction the mean trigger time is much longer for both MAIS 2 and MAIS 3+ injured drivers compared to the cases with good structural interaction. Furthermore there is a large difference between MAIS 2 and MAIS 3+ cases in the group with poor structural interaction, 60 ms compared to 119 ms, respectively.

Further seperation of the group with poor structural interaction would lead to a too small sample size that would not allow further conclusions.

**NASS EDR Data without Airbag Deployment**

Looking at the cases without airbag deployment there are much more cases with poor structural interaction than with good structural interaction, see Figure 6. Furthermore 4 of the 5 non deployment cases with good structural interaction had a delta-v below 20 km/h, while this is true for only 3 of the 14 cases with poor structural interaction. In only one case with good structural interaction the non deployment resulted in MAIS 3 injuries while in 3 of the the cases with poor structural interaction the injury severity was MAIS 3, MAIS 4 and MAIS 5, respectively. The MAIS 3 case with good structural interaction was a multiple impact event – first with a small tree and approx. 30 m later with a wall – which could explain the MAIS 3 injuries.

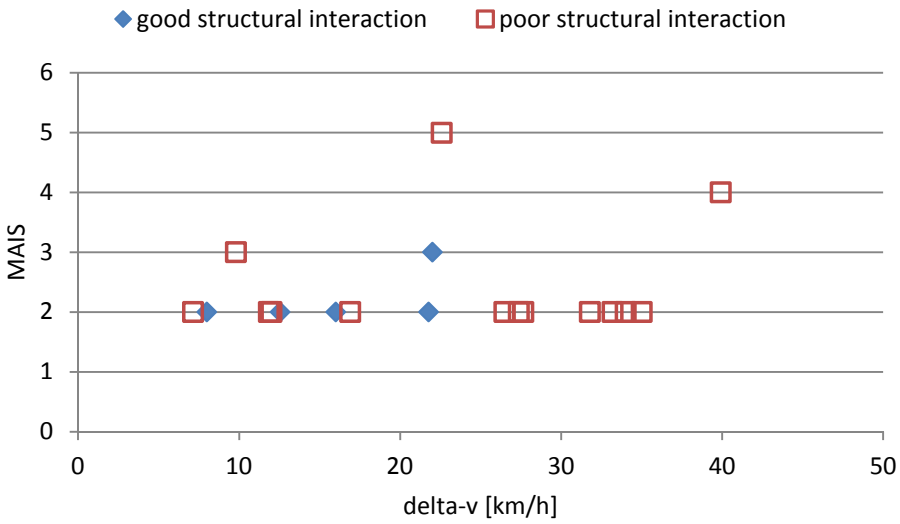


***Figure 6. Delta-v and injury severity in non deployment cases.***

**GIDAS Data**

The GIDAS data sample indicates that the injury severity for the head and chest is considerable higher in the cases with poor structural interaction. Especially for head, chest and abdomen it is expected that the injury risk is sensitive on the restraint system triggering time.For the arms and legs there appears to be no important difference between the accidents with and without good structural interaction. For the abdomen it is difficult to judge – the share of abdomen injuries is higher in the group with poor structural interaction while AIS 3+ injuries are only observed for the accidents with good structural interaction.

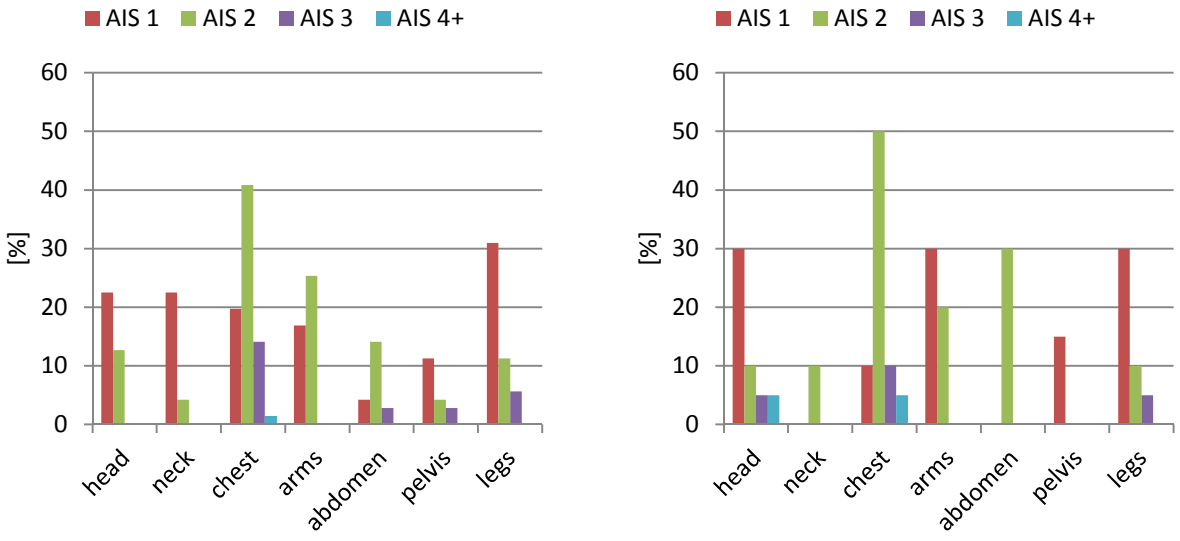


no poor structural interaction observed (n=71)

poor structural interaction observed (n=20)

***Figure 7. Injury severity depending on structural interaction assessment.***

## DISCUSSION AND CONCLUSION

The analysed accident data indicates that restraint system triggering time is much later than in the standard tests (e.g., FMVSS 208 full frontal test) in a large number of cases. While triggering times just being later does not necessarily mean that they are too late. For example accidents with light accident severity require a late triggering of restraint systems. However, in a small number of crash tests it was proven that the late ECU airbag triggering results in considerably higher dummy readings.

The NASS EDR data with airbag deployment indicates that the restraint system trigger time tends to be later in cases with poor structural interaction (i.e., small overlap, impact between rails and under- / overrun scenarios). It is expected that the firing decision is more difficult to safeguard in these condictions compared for example with a FWRB test.

Furthermore the injury severity appears to be higher in cases with high accident severity and late restraint system trigger time. Furthermore the analysed GIDAS data shows that the injury severity for those body regions that are expected to be sensitive to the restraint system trigger time (i.e., head and thorax) is higher in the cases with poor structural interaction. This is interesting because those cases are expected to mainly increase intrusion related injury risks. However, for accidents with high accident severity and poor structural interaction it is also expected that the acceleration history would have a more injury causing shape (i.e., back loaded pulse).

Unfortunately for approx. half of the analysed NASS EDR data (accident years 2011 nd 2012) the individual injuries were not yet coded at the NASS CDS web site. Therefore it is not yet possible to confirm the observation from the GIDAS data sample with EDR data. The EDR data set mainly contains newer accident years due to the introduction phase of EDR.

As a next step it would be sensible to run accident reconstructions with observed and modifed restraint system trigger time in order to verify whether or not the timing was wrong in individual cases.

## ACKNOWLEDGEMENTS

The NASS EDR data and NASS CDS data analysed for this study was collected during a Bachelor Thesis of Iryna Shevchenko [Shevchenko 2014].

## REFERENCES

DaSilva MP: “Analysis of Event Data Recorder Data for Vehicle Safety Improvement.” Report No. DOT HS 810 935; NHTSA; Washington, DC; April, 2008

Dalmotas DJ, German A and Comeau J-L; “Crash Pulse Analysis using Event Data Recorders”; Proceedings of the 19th Canadian Multidisciplinary Road Safety Conference, Saskatoon, Saskatchewan, June 8-10, 2009.

Gabler HC, Thor CP and Hinch J: “Preliminary Evaluation of Advanced Air Bag Field Performance using Event Data Recorders.” Report No. DOT HS 811 01; National Highway Traffic Safety Administration; Washington, DC; August, 2008

Johannsen, H.; Edwards, M.; Lazaro, I.; Adolph, T.; Versmissen, T.; Thomson, R.: “FIMCAR – Frontal Impact Assessment Approach”; Presentation of Project Results at 52nd GRSP Session, Geneva 2012 available online at http://www.unece.org/fileadmin/DAM/trans/doc/2012/wp29grsp/GRSP-52-24e.pdf.

Johannsen, H.; Adolph, T.; Edwards, M.; Lazaro, I.; Versmissen, T.; Thomson, R.: “Proposal for a Frontal Impact and Compatibility Assessment Approach Based on the European FIMCAR Project” Traffic Injury Prevention Volume 14 Supplement 1, 2013a.

Johannsen, H.: “I Summary Report”. In Johannsen, H. (Editor): “FIMCAR – Frontal Impact and Compatibility Assessment Research”. Universitätsverlag der TU Berlin, Berlin 2013b.

Reichert R, Morgan RM, Park CK, Digges K, & Kan CD: „Thoractic and Abdominal Injuries to Drivers in Between-rail Frontal Crashes." IRCOBI Conference 2013. Available online at http://www.ircobi.org/downloads/irc13/pdf_files/99.pdf.

Shevchenko I: "Auswertung von Rückhaltesystemauslösezeiten anhand von NASS EDR Daten." Bachelor Thesis at Department for Automotive Engineering at Technische Universität Berlin, 2014 (in German)

# VALIDATING VEHICLE SAFETY USING META-ANALYSIS: A NEW APPROACH TO EVALUATING NEW VEHICLE SAFETY TECHNOLOGIES

**Michiel van Ratingen**
Euro NCAP
Belgium

**Brian Fildes**
Monash University Accident Research Centre,
Australia

**Anders Lie**
Swedish Transport Administration (Trafikverket) and
Chalmers Technical University, Sweden

**Michael Keall**
Monash University Accident Research Centre,
Australia

**Claes Tingvall,**
Swedish Transport Administration (Trafikverket) and
Chalmers Technical University, Sweden

Paper Number 15-0267

## ABSTRACT

In a world of rapid developments in the field of vehicle safety, robust and reliable methods are essential to evaluate the safety effects in real traffic. Only with significant evidence-based findings can OEMs, governments and consumers act to encourage the most important systems. The Euro NCAP Validating Vehicle Safety using Meta-Analysis (VVSMA) consortium was assembled, comprising a collaboration of government, industry consumer organisations and researchers, using pooled data from a number of countries and the established MUNDS method. Technologies of immediate interest included low speed autonomous emergency braking (low speed AEB or AEB City), and Lane Departure Warning (LDW) technologies in current model passenger vehicles. Real-world crash data were assembled by 6 countries for the analyses and induced exposure methods were adopted to control for any extraneous effects. To date, the findings for AEB City technology found that while individual countries analyses failed to show significant reductions in crashes, robust statistically significant reductions were found overall from the meta-analysis due to the increase in the amount of data. The analysis for Lane Departure Warning technology is currently in process. Greater difficulty is experienced with evaluating this technology due to it only being available as optional equipment. The findings show how safety benefit analyses can be performed in a timely manner, using data from many countries in a meta-analysis procedure.

## INTRODUCTION

The safety of modern passenger cars has improved substantially in recent years. The reasons for this improvement include international vehicle regulations that specify minimum levels of occupant protection, and consumer tests that rate vehicle safety (Stucki, *et al*, 1996; Broughton *et al*, 2000; Ward, 2012; Newstead *et al*, 2013). Improvements have come from greatly improved vehicle structures and materials, as well as new safety technology to better restrain the occupant in a crash and to mitigate against serious injuries. This passive safety approach has focused on preventing injuries, rather than stopping the collision or mitigating injuries. More recently, industry and government initiatives have shifted their focus to improving active safety in vehicles (Giebel *et al*, 2008). In-vehicle safety technologies aimed at preventing the crash are developing fast across the world, driven by the market place, rather than in response to new regulations. However, there is only a limited understanding of the possible (and actual) benefits for most of these systems. An outline on how these technologies are expected to work is shown in Figure 1.

**The Crash Sequence (matching human error and crash protection)**

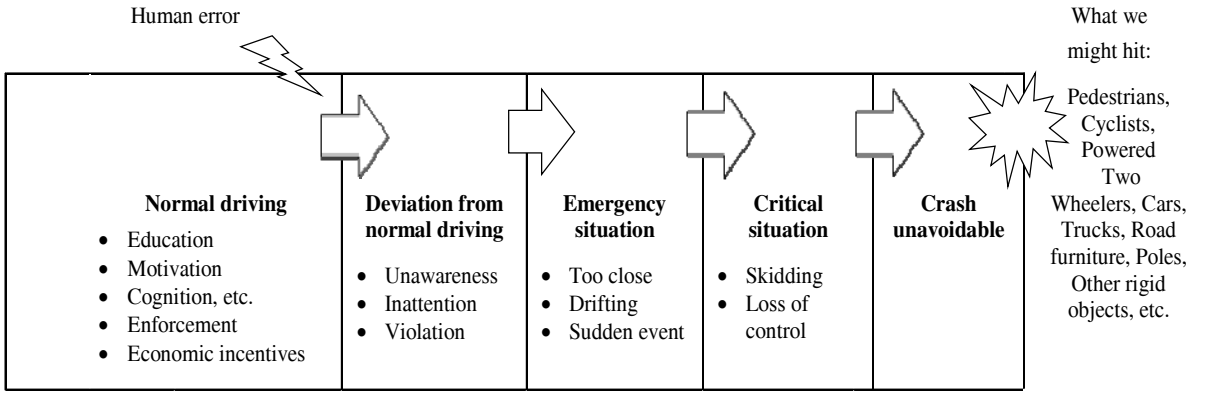


| | | | | | | |
|---|---|---|---|---|---|---|
| • Access to road transport system | • Comfort<br>• Economy<br>• Social conformity | • Warning system<br>• Supporting system | • Intervention in driving | • Immediate correction | • Preparation for crash | • Crash protection |
| **Vehicle** | Promote normal driving | ISA, SBR, Alcolock, … | AICC, LDW, … | ESC, LDA, AICC2, … | Pre-safe, emergency braking … | Seatbelt, airbag, whiplash protection, pedestrian protection, … |
| **Infrastructure** | Promote normal driving | | Tactile edge lines, … | High friction surface, … | | |
| **Others** | Promote normal driving | Enforcement, Insurance, Contracts | | | | Emergency service |

**Figure 1. The integrated safety chain**

For new systems there are often benefit analyses done based on target population estimates and laboratory verifications of these systems. However, in the hands of everyday drivers the systems may have a different performance. Real world benefits of active safety technologies, are often hampered by the lack of sufficient real-world crash and non-crash data to obtain early and reliable effects of new innovative safety systems in cars. There are simply not enough systems available in each market individually to conduct these analyses. One way of potentially speeding up this process would be to investigate the possibility of collecting and analysing crash data on a broader basis than one country can conduct from their limited crash numbers.

To address this problem, a new approach was developed using a meta-analysis approach, the so-called "MUNDS" method (Fildes *et al*, 2013) where those with suitable data from various countries, conduct their own analysis using a common strategy, and these are then pooled together to form a better estimate of effects of car technologies. The benefits with this approach are several. First, by pooling, a larger amount of data becomes available, allowing for early analysis of a new system performance, and much sooner than any one country can provide. Second, results can be generalized across countries, still allowing national variation and comparison. Moreover, no raw data needs to be given away from the national statistics of each country.

To help guide manufacturer, government, and consumer group judgments about which technologies ought to be encouraged, it is critical to establish their potential savings in crashes and injury mitigation. It is expected this will help encourage their introduction and ensure market penetration is optimized.

## THE VVSMA CONSORTIUM

To address this need, the Validating Vehicle Safety using Meta-Analysis (VVSMA) consortium was formed under the auspices of Euro NCAP to conduct analyses of the safety benefits of two emerging technologies, namely AEB City, and Lane Departure Warning (LDW) or Lane Keeping Assist (LKA) using the MUNDS approach. The VVSMA consortium involved a number of government, industry, consumer groups and research organisations from Sweden, France, Germany, UK, Italy, Netherlands, and Australia (Table 1) and commenced their activities in 2012. The European Automobile Manufacturer's Association ACEA maintained a watching brief on the consortium's deliberations.

**Table 1: Members of the VVSMA Consortium**

| Member | Organisation |
|---|---|
| Claes Tingvall - Founding Chair | Trafikverket, Sweden |
| Anders Lie - Chairman | Trafikverket, Sweden |
| Michiel Van Ratingen - Host | Euro NCAP, Belgium |
| Brian Fildes - Secretariat | ANCAP, Australia |
| Nils Bos | SWOV, Netherlands |
| David Brookes | Thatcham, UK |
| Sebastian Döering | VW, Germany (ACEA) |
| Michiel Keall | MUARC, Australia |
| Anders Kullgren | Folksam, Sweden |
| Olaf Jung | BMW, Germany (ACEA) |
| Yves Page | Renault (ACEA), France |
| Lucia Pennisi | ACI, Italy |
| Claus Pastor | BASt, Germany |
| Matteo Rizzi | Folksam, Sweden |
| Simon Sternlund | Trafikverket, Sweden |
| Johan Standroff | Trafikverket, Sweden |
| Pete Thomas | Loughborough, UK (DfT) |

Police data from six countries with a common analysis format were used in these analyses. Induced exposure was employed to control for extraneous factors across these databases. A major challenge with the approach was identifying crashed vehicles with and without the technology in each database and having the necessary analytic variables. Identifying the crashes that are potentially influenced by the safety system was also important. For reasons of maintaining confidentiality, it was agreed that the individual results for each country would not be identified in any subsequent analysis.

## METHODOLOGY

There were a number of steps involved in the MUNDS analysis process.

1. First, was the need to identify which vehicles in each country's database had the relevant technology on-board. Where the technology was offered as a standard feature on particular makes and models, it was possible to simply identify these vehicles by make and model year in the crash data which were then nominated as "case" vehicles. Where the technology was only fitted as optional, a different process was needed to identify the case vehicle. This is explained in more detail below.

2. For comparison, it was necessary to identify similar vehicles that did not contain the technology, and these were labelled as "control" vehicles. For an analysis involving a standard technology, controls consisted of a number of vehicles that embraced the range of case vehicle types (body designs, masses, similar market categories, and so on. For a technology only offered as "optional", the controls were then the same makes and model vehicles but those without the technology onboard.

3. As these technologies are designed to work on specific crash types, it was important to restrict the analyses to those "sensitive" crash types only. This was judged from the experience of the members of the consortium and other available sources. The induced exposure measure was determined from the control exposure that matched that of the case crashes. The appropriate formula for making the AEB City assessment in both sensitive and non-sensitive crash situations was:

$$E = 1 - (A/B) / (C/D)$$

where:

**A**= AEB fitted vehicles as **striking** vehicle

**B**= AEB fitted vehicles as **struck** vehicle

**C**= Non-AEB vehicles as **striking** vehicle

**D**= Non-AEB vehicles as **struck** vehicle

4. Once the parameters of the analysis were defined, the various data providers then conducted their own analyses and provided these for inclusion in the meta-analysis. Other factors that might have a bearing on the analysis such as the speed of the crash were also identified and adjusted for in the analysis procedure. Further factors such as driver age and sex can also be controlled for, as in an analysis of ESC effectiveness (Fildes et al., 2013).

Meta-analysis is a standard statistical procedure involving logistic regression and data merging techniques that estimate the relative rate of sensitive crashes for the case vehicles compared to that of the equivalent control vehicles. The meta-analysis was weighted by the inverse of the variance of the effectiveness measure for each jurisdiction (as is standard in meta-analysis) and tested for the homogeneity of the effect size. Where possible, separate analyses can be conducted for road type and speed zone if needed to further explain the range of effectiveness of the technology.

**RESULTS SO FAR**

The work of the consortium comenced late in 2012 and many of the early months involved identifying suitable data, defining the process, and understanding the method. As most of the members of the consortium were new to the approach, it required time for them to appreciate it and the techniques involved.

Of the two technologies nominated for the effectiveness analysis, (AEB City and Lane Departure Warning systems LDW and LKA), the analysis of AEB City has now been completed and LDW/LKA is currently under investigation. The analysis of AEB City was relatively simple to analyse, given that is was fitted to a number of production models dating back to 2008 as standard equipment and possible to identify case vehicles from each of the databases.

Lane Departure Warning systems on the other hand tends to be fitted by most OEMs as optional equipment which places a greater requirement on identifying crashed vehicles in each database that have the technology onboard. The consortium is currently working through processes to identify case vehicles for this analysis and expects to have the meta-analysis completed later in 2015.

**Low Speed AEB Effectiveness (AEB City)**

CarAdvice (2014) noted that Low Speed AEB or City Safe technologies are marketed under a variety of names, including City Brake Control (Fiat), Active City Stop (Ford), City Emergency Brake (Volkswagen) and City Safety (Volvo). As their names suggest, this type of AEB technology is geared towards low speed situations, generally under 30km/h. These systems rely on radar sensors detecting an emergency situation and apply the brakes as needed. They tend to work most effectively over short distances, usually 12m or less (CarAdvice, 2014).

A paper is currently in press on the full details of this analysis and should be available later this year (Fildes *et al*, 2015). Briefly, the findings show a strong and significant reduction in rear-end crashes for vehicles fitted with the technology over those that don't. While the benefits are mainly in low speed urban areas, there seemed to be a small, non-significant, benefit in rural areas too, although this needs further research, given there were very few cases and the likelihood that rural rear-end crashes are relatively rare.

Of importance, however, while the meta-analysis was highly significant, most of the individual countries analyses failed to reach significance in their own right. This further confirmed the need for, and advantage of, the meta-analysis approach used here. While the meta-analysis was able to show the effectiveness of the technology in a relatively short period of time, it would take considerably more years for any one country to report on the benefits of

the technology based on real-world crash data. In short, it confirms the need and advantage of the approach in conducting real-world evaluations of the benefits of emerging active safety technologies.

**Land Departure Warning Effectiveness (LDW/LKA)**

Lane Departure Warning and Lane Keeping Assistance system are designed to warn a driver when the vehicle begins to move out of its lane (unless a turn signal is on in that direction) on freeways and arterial roads or apply positive feedback to correct these encroachments. These systems are designed to minimize accidents by addressing the main causes of collisions: driver error, distractions and drowsiness. As noted earlier, it is difficult to identify vehicle makes and models that have the technology onboard due to optional fitment. In Europe this means, that there are very few cars where LDW/LKA is standard in Europe. There are other issues as well, e.g. unlike low speed AEB or ESC, the systems are often default off and cannot automatically assumed to be active when they should. The expected overall effectiveness is therefore lower and generally difficult to identify in these data.

As far as the fitment issue is concerned, this generally requires access to the Vehicle Identification Number (VIN) of the crashed vehicles that are known to offer the technology and then to match the particular VIN number with the presence or absence of the technology. This involves gaining access to VIN details of the individual make and models of each potential case vehicle to identify cases (fitted) as well as the controls (not fitted).

VIN is not freely available in most databases. As the VIN is uniquely linked to a car and its owner, there are privacy implications in use and hence, both industry and governments are sensitive to its use. This makes the analysis process difficult, but not impossible – some countries do list VIN and there are some data sources that can help identify the fitment of optional safety equipment from the VIN number. The VVSMA consortium is currently working towards overcoming these challenges and ensuring that the real-world effectiveness of LDW/LKA can be established using the meta-analysis approach.

**DISCUSSION**

There are various methods adopted to estimate the likely effectiveness of new safety technologies. The auto industry for instance invests considerable resources in developing forecasting (prospective) systems based on simulations of real accidents, using traffic, vehicle and driver models (Page *et al*, 2015). This pre-production "Prospective Effectiveness Assessment for Road Safety (PEARS)" approach relies on virtual analyses by means of simulation, assuming various driver behavioral characteristics. Alternative approaches, such as the MUNDS method used by the VVSMA consortium, analyses real-world crash data to assess the post-production safety benefits of these technologies. This is not to say that one method is superior to another as both methods are really complementary. It depends what purpose you have in mind whether one is more useful than the other.

Meta-analysis is a procedure that is frequently used by medical researchers in establishing the extent of medical conditions and successful treatments, using published randomised controlled trials and clinical controlled studies. The most well-known application of meta-analysis publications in the medical field is the Cochrane Reviews that through meta-analysis, provides evidence-based health care findings based on best available research evidence (Cochrane Collaboration (2014).

The medical approach, however, relies on published studies that fit their criteria, and hence is subject to long delays in evaluation time. The MUNDS approach adopted by the VVSMA consortium speeds up these evaluations by assembling multiple independent aggregate analyses from several countries using a common study design. This brings together a much larger pool of data than any one country has available and speeds-up the process of evaluating safety technologies.

The evaluation of Low Speed Autonomous Emergency Braking (AEB City) in rear-end collisions was a successful first attempt by the VVSMA Consortium using the meta-analysis approach. As noted earlier, the analysis revealed a significant reduction in rear-end crashes for vehicles fitted with the technology. It was facilitated by the relatively easy identification of target vehicles in these databases, given that the technology was standard equipment. The second analysis of Lane Departure Warning technology currently underway has additional challenges in that this

technology is only fitted to some vehicles as optional equipment. This was discussed in some detail in an earlier section.

The need for early evaluation of these technologies was noted. They promise substantial benefits in reduced crashes and mitigating injuries yet very few can support these claims using real-world crash data. In an earlier report by Fildes *et al* (2013), they noted that the evaluation period can be reduced by half, using the MUNDS approach which means that these evaluations can play an important role in demonstrating real reductions in road trauma and motivation for their widespread fitment to the whole vehicle fleet. Moreover, early findings may also highlight the need for modifications and/or fine tuning to improve their effectiveness. It is critical to establish their likely crash benefits to help guide manufacturer, government and community judgments about which technologies should be pursued to encourage their widespread introduction and ensure maximum market penetration.

Finally, the collaborative approach adopted in this work through Euro NCAP proved to be both positive and productive in achieving its aims. Bringing governments, OEMs, NCAP groups and researchers together to address a common objective led to a creative and innovative evaluation that otherwise would not have been possible.

**Limitations**

There are limitations with this meta-analysis approach that need to be noted. First, the databases used in this study inevitably differ in terms of the way and accuracy of data collection across each of the regions. Some data contain a higher proportion of minor collisions to others and the police attendance strategies at these crashes is likely to vary. Furthermore, the composition of the vehicle fleet and the crash patterns may differ from country to country. Indeed, in the Low Speed AEB analysis, there were observed differences in the ratio of striking and struck impacts. While this was unlikely to have affected the results, it does reveal national data differences across countries. To the extent that the focus crashes are subject to the same sorts of reporting errors as the control crashes, the effectiveness formula can be expected to adjust for any such biases at a country level.

As each database is inevitably structured around local definitions and variables, it can be difficult to undertake a range of additional analyses beyond the core analysis. Again in the low speed AEB analysis, the use of side impacts as an additional induced exposure approach was not possible as these crash types could not be identified in all databases.

As the vehicle fleets differed across countries, these findings may not be representative of the effectiveness in any one country. This is not necessarily a major problem for the analysis though as the findings probably have more relevance overall than a series of single studies from individual countries. This adds to decisions about the need for widespread international fitment of these technologies even stronger.

Finally, in conducting these meta-analyses, it is assumed that the benefits calculated in these univariate analyses are for the technology under examination. Yet, as vehicle safety technologies increase and become integrated with others, there is the potential for the benefits to be confounded. While the VVSMA approach is aware of this possibility and has taken this into account to some degree in the selection of sensitive crash types for the AEB City and LDW/LKA effectiveness studies, nevertheless, this will present an additional challenge as the extent of these integrated systems expands. The means of addressing these potential confounding effects in meta-analysis is beyond the scope of the work conducted to date and warrants further research.

## CONCLUSIONS & RECOMMENDATIONS

In conclusion, the use of the meta-analysis approach by the VVSMA consortium is seen as a valuable and important technique for evaluating new active safety technologies. The results showed that while individual country analyses were unable to show significant reductions in crashes for the AEB City technology, statistically significant reductions were obtained from the meta-analysis due to the increase in the amount of data. The approach to pool individual analyzes to achieve a common result worked well without the need to share data records. In addition, the collaborative approach between governments, industry, consumer groups, and researchers was successful with high levels of cooperation. The main challenge when evaluating new safety systems is to get an early and robust

indication of the real world performance in traffic. Often, the virtual predicted benefits of new technology can be influenced by human intervention. With a substantial increase in available data, statistically significant real-world findings can be obtained within much shorter timeframes using the meta-analysis approach. A major challenge is to identify vehicles with a specific safety feature when it is only offered as optional equipment. This paper has presented a bold new approach to evaluating the real-world crash benefits of safety technologies and recommends the approach for others to follow.

**ACKNOWLEDGEMENTS**

The authors acknowledge the contribution and valuable input to this study by all members of the VVSMA consortium and their organisations, namely Nils Bos, SWOV, Netherlands; David Brooks and Murray Doyle, Thatcham UK; Sebastian Döering, Volkswagen AG, Germany (and ACEA); Anders Kullgren and Matteo Rizzi, Folksam Insurance, Sweden; Olaf Jung, BMW Germany (and ACEA); Yves Page, Renault (and ACEA) France; Lucia Pennisi ACI Italy; Claus Pastor, BASt Germany; Simon Sternlund and Johan Standroth, Trafikverket, Sweden; Jim Hand at DfT, and Pete Thomas, Loughborough, University, UK (and DfT).

**REFERENCES**

Broughton J, Markey K A and Rowe Supt D (1998). A new system for recording contributory factors in road accidents. TRL Report 323. TRL Limited, Crowthorne.

CarAdvice (2014). Autonomous emergency braking explained, (downloaded December 2014) http://www.caradvice.com.au/293366/autonomous-emergency-braking-explained/

Cochrane Collaboration (2014). Cochrane Reviews, Evidence –based health care. http://community.cochrane.org/cochrane-reviews

Fildes B, Keall MD, Thomas P, Parkkari K, Pennisi L, Tingvall C (2013) Evaluation of the Benefits of Vehicle Safety Technology: The MUNDS Study, *Accident Analysis & Prevention* 55:pp. 274-281

Fildes B., Keall M., Bos N., Lie A., Page Y., Pastor C., Pennisi L. , Rizzi M., Thomas P., Tingvall C. (2015). Effectiveness of low speed Autonomous Emergency Braking in rear-end crashes. *Accident Analysis & Prevention*, (in Press).

Giebel T., Meinecke MM., Gonter M. & Widmann U. Current trends in vehicle active safety and driver assistance development, ATZAUTOTECHNOLOGY e-Magazine, 2008-09. http://www.atzonline.com

Newstead, S.V., Watson, L.M and Cameron, M.H. (2013). Vehicle Safety Ratings Estimated From Police Reported Crash Data: 2013 Update - Australian and New Zealand Crashes during 1987-2011, Report No. 318, Monash University Accident Research Centre, Clayton, Australia.

Page Y., Fahrenkrog, F., Fiorentino, A., Gwehenberger, J., Helmer, T., Lindman M., Op den Camp, O., van Rooij, L., Puch, S., Fränzle, M., Sander, U., Wimmer, P., (2015) A comprehensive and harmonized method for assessing the effectiveness of advanced driver assistance systems by virtual simulation: the PEARS Initiative, Paper Number 15-0370, 24th International Technical Conference on the Enhanced Safety of Vehicles (ESV) Gothenburg, Sweden, June 8-11, 2015.

Stucki SL, and Biss DJ (2000). A study of the NASS/CDS system for injury/fatality rates of occupants in various restraints and a discussion of alternative presentation methods, Presented at the 44th Annual Proceedings of the Association for the Advancement of Automotive Medicine (AAAM), Chicago, October 2-4, 2000.

Ward D. (2012). From Research to Global Policy and Action, 2012 Bertil Aldman Award Lecture, IRCOBI Conference, Dublin, Ireland.

.

# EVALUATION OF THE EURO NCAP WHIPLASH PROTOCOL USING REAL-WORLD CRASH DATA

**Anders Kullgren**
Folksam Research and Chalmers University of Technology
Sweden

**Brian Fildes**
MUARC, Monash University
Australia

**Michiel van Ratingen**

**James Ellway**
Euro NCAP, Belgium

**Michael Keall**
University of Otago
New Zealand

Paper Number 15- 0267

## ABSTRACT

Whiplash injuries account for the vast majority of casualties in road traffic crashes, leading to long-term consequences. The majority occur in rear-ends crashes. Consumer crash tests play an important role in promoting effective concepts to reduce the problem. The current Euro NCAP whiplash test protocol includes three sled tests at varying impact speeds and pulse shapes using a BioRID test dummy and 8 measures to assess whiplash potential based on previous best practice. Given the complexity of the test and with more experience, a real-world evaluation of the current protocol was undertaken. Three analyses were undertaken comprising an analysis of test outcome data, a logistic regression analysis, a ROC analysis, and a correlation analysis comparing crash and injury outcome. 13,389 drivers reporting whiplash injury symptoms to Folksam Insurance in Sweden were studied, of which 1,266 occurred in cars tested by Euro NCAP. For all occupants reporting initial symptoms, the risk of permanent medical impairment was followed up according to the procedure used by Swedish insurance companies. Test scores according to Euro NCAP, JNCAP and IIWPG protocols were calculated, as well as combinations of the three Euro NCAP pulses. For each combination or protocol, the test score was compared with the real-world outcome. A correlation analysis of the included injury criteria was also performed for the three crash pulses included.
The results showed that overall Euro NCAP, JNCAP and IIWPG all predict real-world whiplash injury outcome in terms of Permanent Medical Impairment (PMI). Based on limited data available, there was no statistical evidence using logistic regression and ROC analyses that any of the three tests performed better than any other. Correlations between the test scenarios of each of the three protocols, as well as the outcome associations with crash outcomes, suggested consistent improvements in the risk of permanent medical impairment. The main strength of the analyses conducted here was to show the validity of Euro NCAP, JNCAP and IIWPG whiplash test protocols when measured against real-world crash outcomes, which are the most important criteria showing that the tests are appropriately designed to help prevent injuries among the community. Some caution needs to be taken with these findings as many were not statistically significant because of the limited number of cases available. Further evaluation when additional data are available is warranted.

## INTRODUCTION

Soft tissue injuries to the neck and associated areas, so called whiplash associated disorders (WAD), in rear-end crashes are a major societal burden in terms of reported incidence, on-going disability, cost, and inability to return to work (Krafft 1998, Malm et al. 2008, Kullgren et al. 2013). These injuries account for half of all injuries leading to long-term or permanent medical impairment (Krafft 1998, Kullgren et al. 2013). WAD often occur in relatively low severity crashes, typically at a change of velocity below 25 km/h (Eichberger et al. 1996, Kullgren et al. 2003), and in all impact directions, although WAD in rear impacts are most frequent (Krafft 1998, Watanabe et al. 2000, Kullgren et al. 2013).

Since the late 1990s more advanced concepts aimed at reducing the risk of WAD have been introduced on the market (Jakobsson 1998, Wiklund and Larsson 1997, Lundell et al. 1998, Sekizuka 1998). Better protection is achieved through improved geometry and dynamic properties of the head restraint or by active devices that move in a crash as the body loads the seat. The main ways to lower the risk of WAD in rear impacts are to minimize the relative motion between head and torso, to control energy transfer between the seat and the human body and to absorb energy in the seatback. Studies have been presented showing the effect of the some seat concepts indicating a reducing effect in WAD of approximately 20-50% (Viano and Olsén 2001, Farmer et al. 2008, Jakobsson 2004, Jakobsson et al. 2008, Krafft et al. 2003, Kullgren et al. 2013).

In 2004 consumer test programmes were introduced (IIWPG and Folksam/SRA) (Thatcham 2013, Krafft et al. 2004). And since 2009 the European New Car Assessment Program (Euro NCAP) has introduced a test protocol for assessing the Whiplash potential of vehicle seats as part of its vehicle safety rating system in Europe. The protocol specifies 3-sled tests at varying impacts using a BioRID test dummy and 8-measures to assess whiplash potential based on previous best practice. To date, more than 200 make and model vehicles seats have been evaluated using the Euro NCAP protocol. JNCAP first conducted similar assessments of vehicles in Japan using other injury criteria and pulses around 2010 (JNCAP, 2014).

Given the complexity of the test and with greater knowledge, Euro NCAP decided to evaluate the current protocol to see if it was still appropriate and whether it could be improved and simplified without reducing its effectiveness. The objectives of the study was to evaluate the effectiveness of the current Euro NCAP whiplash assessment procedure and current assessment criteria to determining the real-world injury outcome and whether reduced tests and output measures would equally predict real-world performance.

## METHOD

Three analyses were undertaken comprising an analysis of Euro NCAP test outcome data, a logistic regression analysis, a ROC analysis, and a correlation analysis of whiplash injuries reported to Folksam Insurance, comparing crash test results and real-world injury outcome in crashes with car models tested by Euro NCAP.

Receiver Operating Characteristic curves (ROC) are a plot showing the comparative performance of systems across a varying threshold. Plotting the sensitivity and specificity of varying outcomes, in terms of true and false positives, the cumulative distribution function can then be found for each of the comparative relationships (the true positive rate against the false positive rate for the different possible cut-points of a diagnostic test). The area under the curve can then be used as a measure of the performance of the systems under test. Should one of the systems under examination score a larger area under the curve, it can be assumed to out-perform the others if the difference is statistically significant. ROC analysis is commonly used in association with a logistic regression analysis.

The Folksam material used in the correlation analysis consisted of 13,389 drivers (at least 18 years old) reporting symptoms of WAD to Folksam Insurance in Sweden between 1998 and 2013, of which 1,266 (55% females) occurred in cars tested by Euro NCAP (see Table 1). For all occupants reporting initial symptoms, the risk of permanent medical impairment was followed up according to a procedure used by Swedish insurance companies. In case an injured occupant is not recovered after approximately one year, a medical assessment is made by medical specialists to predict the impairment degree. The injured occupant is classified with a degree of medical impairment, between 1-100% depending on the injury type according to the Swedish manual for “Grading Medical Impairment” (Försäkringsförbundet 1996). All Swedish insurance companies use this manual. The manual consists of instructions of how to set the degree of medical impairment and table works for all injury types and their consequences. WAD often results in between 3-18% of medical impairment degree. The symptoms are regarded as permanent when no additional improvement in the injured patient’s mental or physical status has taken place, normally a maximum of three years after the crash.

It has been found that medical expertise in Sweden gradually has been classifying long-term consequences from whiplash associated disorders more restrictively (Kullgren et al. 2013). Therefore adjustments were made by weighting the number of occupants with long-term symptoms according to the year of impact. A reduction factor of 11% per accident year was used. In order not to change the total number of occupants with long-term symptoms the weighting was made based on accident year 2006, which is the mean accident year in the accident sample. All occupants with long-term symptoms in crashes occurring before 2006 were weighted lower and all after 2006 were weighted higher (Equation 1). By making an adjustment for accident year for each driver, the outcomes from all groups of cars under study could be compared with each other. In total 52 drivers sustained a permanent medical impairment and two out of three were females. The numbers are presented in Table 1.

$x_{pmi,adjusted} = x_{pmi}/1{,}11^{(2006- year_{accident})}$, $x_{pmi}$ = occupants with pmi Eq (1)

**Table 1: Number of drivers reporting whiplash symptoms and those with pmi in cars tested by Euro NCAP.**

| Gender | n | n pmi |
|---|---|---|
| Male | 547 | 17 |
| Female | 677 | 35 |
| Unknown | 42 | 0 |
| **Total** | **1266** | **52** |

Test scores according to Euro NCAP, JNCAP and IIWPG protocols were calculated based on the test performed by Euro NCAP. To increase the data available test results were also calculated based on non-official Euro NCAP test data from a test series performed before 2009. Also combinations of the three Euro NCAP pulses were calculated. For each combination or protocol, the test score was compared with the real-world outcome. The following comparisons were studied:

- Low, mid and high severity tests in Euro NCAP
- Combinations of tests (pulses) in Euro NCAP
- Individual injury criteria in each test
- Combinations of reduced criteria and reduced number of pulses

Test score expressed as per cent of maximum score versus proportion of occupants with pmi was plotted for the various combinations. For the injury criteria the abolute measured value was plotted against proportion of occupants with pmi. In each plot a linear line fit was added. The line fits were weighted for number of crashes in each point. Each point represent an average outcome in an interval. R-square values showing how well the line fits the points in each plot are calculated for each plot and p-values and 95% CI were added to each line fit.

## RESULTS

The results are presented in two forms. First, a statistical analysis was performed using logistic regression analysis and Receiver Operating Characteristics (ROC) curves. This was intended to provide a rigorous statistical analysis of the overall benefit of the three existing test protocols (Euro NCAP, IIWPG, and J-NCAP) as well as show if there were differences (improvements) between the individual findings. Second, a correlational analysis was also conducted both overall as well as on components of the test protocols to indicate opportunities for future improvement.

### Regression and ROC Analysis

An analysis was undertaken of the relationship between sensitivity and specificity of variations of the three test protocols that were plotted on ROC Curves. From earlier work, it was apparent that the sex and age of the victim had a substantial impact on the results in terms of risk and long term outcome, hence a regression analysis was also undertaken to control for these characteristics. The three test protocol combinations shown below were:

1. Euro NCAP comprising the median crash test (16km/h, 5.5g, with triangular pulse) and the seven test criteria (NIC, Nkm, Rebound velocity, Fx, Fz, T1 and THRC);
2. IIWPG with quantified scores, comprising a single crash pulse of 16km/h (5,5g) with triangular pulse, and four test criteria namely Time to head restraint (≤70 msec), T1 acceleration (≤ 9.5g), Fx and Fz; and
3. J-NCAP comprising a single triangular crash test pulse of 17.6km/h, and 7-injury criteria including NIC, Upper Fx (backward shear), Upper FZ (tension), Upper My (flexion), Upper My (extension), Lower Fx (backward shear) and Lower Fz (tension), and Lower My (flexion).

These data scores were all computed from Euro NCAP test data as sufficient factors are collected to create the three test protocols listed above. The ROC analysis for the 3-protocols with accompanying statistics are shown in Figure 1 and Table 2 below.

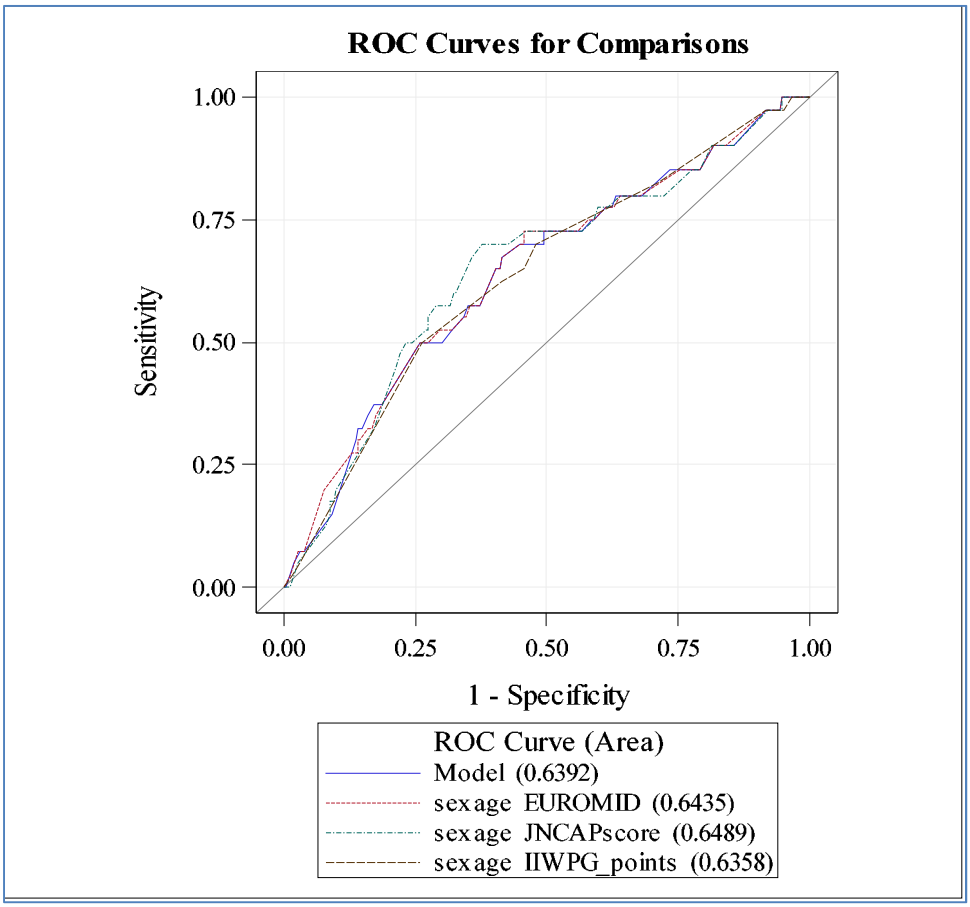


**Figure 1: Comparative ROC Curves for the three test protocols**

**Table 2: ROC associated statistics**

| ROC Association Statistics | | | | | | | |
|---|---|---|---|---|---|---|---|
| **ROC Model** | **Mann-Whitney** | | | | **Somers' D (Gini)** | **Gamma** | **Tau-a** |
| | **Area** | **Standard Error** | **95% Wald Confidence Limits** | | | | |
| **Model** | 0.6392 | 0.0461 | 0.5489 | 0.7295 | 0.2784 | 0.2882 | 0.0176 |
| **sex age EUROMID** | 0.6435 | 0.0464 | 0.5526 | 0.7344 | 0.2869 | 0.2978 | 0.0182 |
| **sex age JNCAPscore** | 0.6489 | 0.0462 | 0.5584 | 0.7394 | 0.2978 | 0.3084 | 0.0188 |
| **sex age IIWPG_points** | 0.6358 | 0.0442 | 0.5493 | 0.7224 | 0.2717 | 0.3339 | 0.0172 |

As noted above, the IIWPG subjective scale was converted into a numerical one for this comparison, which does lose a bit of information compared to the other test scores that use actual values. Nevertheless, this was necessary for the ROC analysis. The analysis showed that any apparent differences between the areas under the curves (the classic way of comparing tests) were indistinguishable from random variation. What these results do show is that any one of these tests has reasonable and statistically significant predictive value for real-world outcomes, but there was no apparent statistical difference observed between the 3-curves. It will take a considerable increase in data before apparent differences between tests will be detectable in the ROC analysis.

## Correlation Analysis

Euro NCAP was significantly correlated with the other two protocols. The match between the Euro NCAP and J-NCAP appeared to be slightly stronger (less variation) than between the others as shown in Fig. 2 to 4.

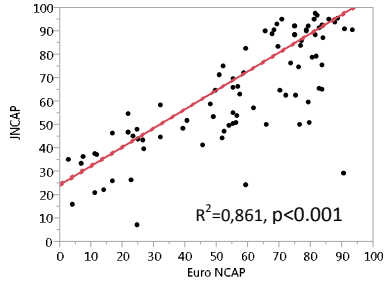


**Fig 2: Euro NCAP and JNCAP scores.**

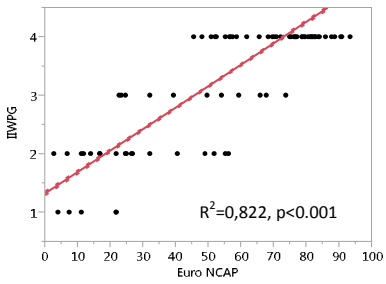


**Fig 3: Euro NCAP and IIWPG scores.**

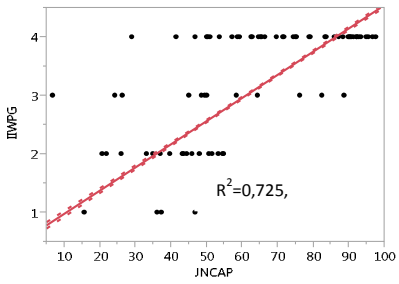


**Fig 4: JNCAP and IIWPG scores.**

Furthermore, all the test protocols were significantly correlated well with the risk for pmi as shown in Fig. 5 to 7.

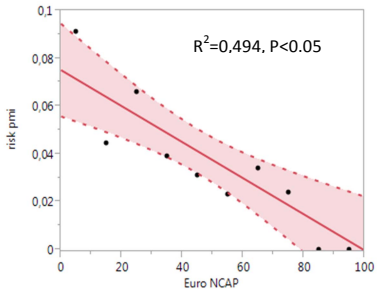


**Fig 5: Risk for pmi vs Euro NCAP score.**

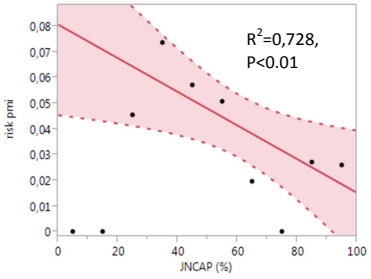


**Fig 6: Risk for pmi vs JNCAP score.**

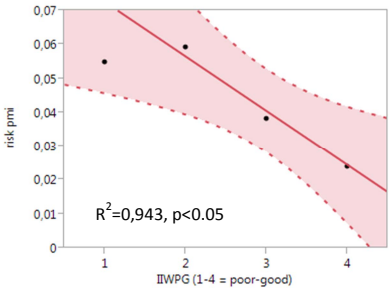


**Fig 7: Risk for pmi vs IIWPG score.**

## Risk of Permanent Medical Impairment by Euro NCAP Crash Pulse

Fig's 8 to 10 show the association between the risk of impairment (pmi) and the test pulse for the 3-Euro NCAP tests. All three pulses in Euro NCAP correlate with risk for pmi, but the correlation for the low and mid severity pulse was stronger than for the high severity pulse.

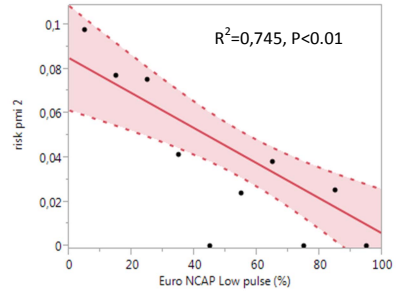


**Fig 8: PMI risk vs Euro NCAP low pulse.**

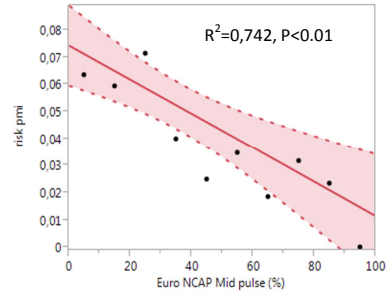


**Fig 9: PMI risk vs Euro NCAP mid pulse.**

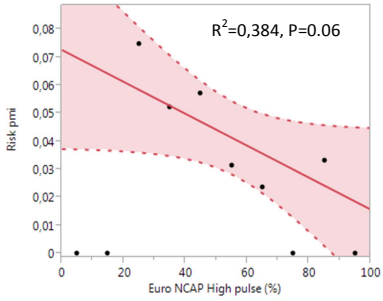


**Fig 10: PMI risk vs Euro NCAP high pulse.**

Further examination of the pmi risk between combinations of the three test pulses are shown in Fig's 11 to 13. The correlation between pmi risk for low and mid pulses and that for low and high pulses were significant, although the correlation between the mid and high pulse was not at the 5% probability level (around 6%).

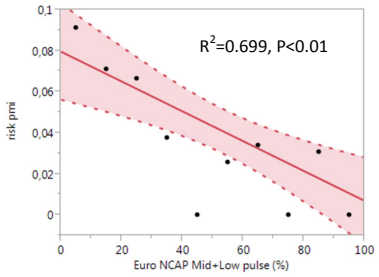


**Fig 11: PMI risk vs Euro NCAP Low and Mid test pulse.**

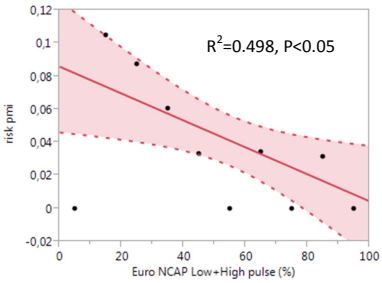


**Fig 12: PMI risk vs Euro NCAP Low and High test pulse.**

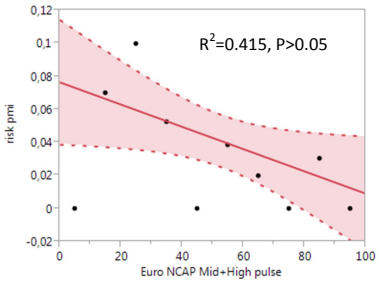


**Fig 13: PMI risk vs Euro NCAP Mid and High test pulse.**

## Injury Criteria

Examples of results of the correlation analyses undertaken between the risk of pmi and the test criteria are shown in Fig's 14 to 19 (plots for all criteria in all three pulses can be seen in the Appedix). The criteria that show correlation ($p<0.05$) to risk of pmi were NIC in all three pulses (p just above 0.05 in the low pulse), Fz in the high pulse and rebound velocity in the low pulse. Also the full geometry assessment explained risk for pmi while geometry did not. Fx had some outliers in the low and mid pulses, an example can be seen in Fig 17, where high Fx values were measured although the risk for pmi was low. If excluding these outliers a correlation could be verified for these pulses but not for the high pulse.

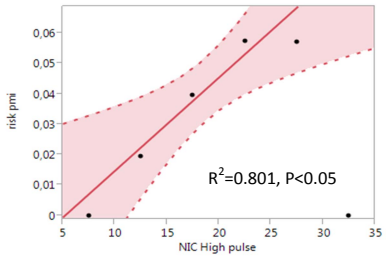


**Fig14: PMI risk vs Euro NCAP NIC measure with High test pulse**

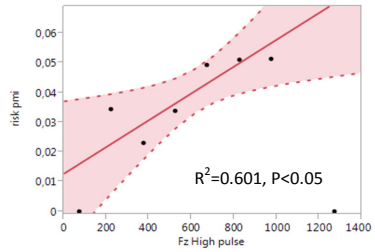


**Fig15: PMI risk vs Euro NCAP Fz measure with High test pulse**

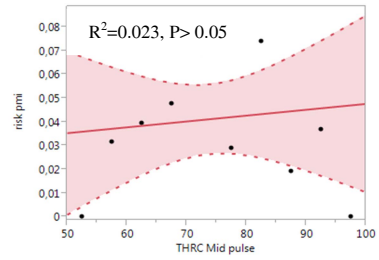


**Fig16: PMI risk vs Euro NCAP THRC measure with Mid pulse**

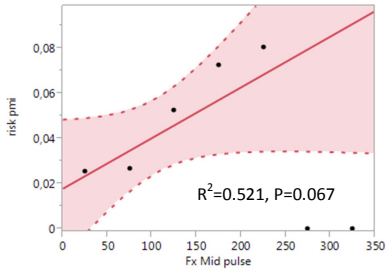


**Fig17: PMI risk vs Euro NCAP Fx measure with Mid test pulse**

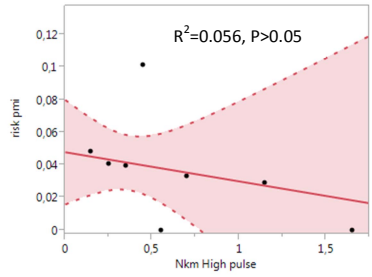


**Fig18: PMI risk vs Euro NCAP Nkm measure with High test pulse**

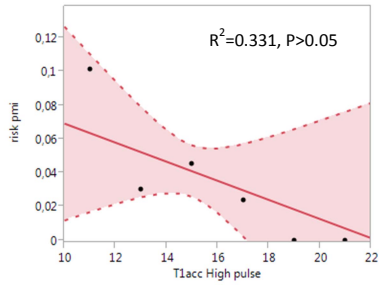


**Fig19: PMI risk vs Euro NCAP T1accel measure with High test pulse**

## Correlations with Modified Test Pulses and Criteria

The final set of analyses examined possibilities for fewer test pulses. And based on the correlation analysis of injury criteria an attempt to using a reduced number of criteria was made using; NIC, Fx, Fz and rebound velocity. Fig's 20 to 22 show the correlations for reduced combinations of Euro NCAP test pulses and test criteria. These should be read in conjunction with Fig 4 shown earlier for the 3 test pulses and the full set of criteria. All these combinations were significant (Euro NCAP 2 pulses and all criteria had a p value just avove 0.05). However, it could not be verified which of the combinations that best explained risk for pmi.

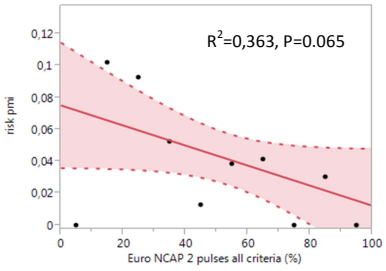


Fig 20: Two tests (Mid + High) with all criteria

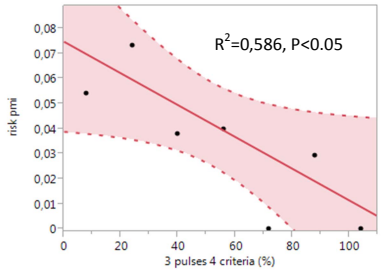


Fig 21: All tests with 4-test criteria

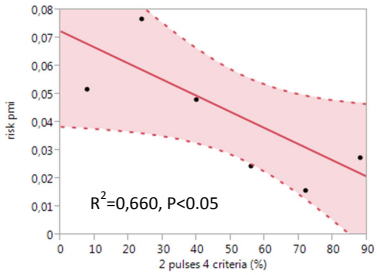


Fig 22: Two tests (Mid+High) with 4-test criteria

## DISCUSSION

Efforts to reduce the number of Whiplash Associated Disorders (WAD) are essential due to the societal burden in terms of costs and suffering from impairments (Krafft 1998, Malm et al. 2008, Kullgren et al. 2013). Consumer test programmes are important tools to reduce WAD in the way they promote cars with the most effective whiplash systems. Since the first consumer test programmes were introduced by IIWPG and Folksam/SRA in 2003 and 2004 the European New Car Assessment Program (Euro NCAP) in 2009 introduced a test protocol for assessing the whiplash potential of vehicle seats as part of its vehicle safety rating system in Europe. Also Japan NCAP has introduced whiplash tests as part of the Japanese consumer test programme (JNCAP 2014).

In conducting this study, two methods were adopted in an attempt to investigate associations between the variables and the outcome criteria. The first was a rigorous parametric statistical evaluation using logistic regression and Receiver Operating Curve (ROC) analysis, while the second was a correlation analysis between aspects of the tests and whiplash outcome. While the results suggested that all protocols examined (Euro NCAP, J-NCAP and IIWPG) appeared to have a strong meaningful association with the advent of Permanent Medical Impairment (pmi), there were no statistical differences between any of the three protocols for the data available. Moreover, as noted earlier, it will require a sizable increase in the available database before this could be expected.

In conducting the correlation analysis, there were two options available for measuring real-world outcome due to the injury data available. These included (i) the likelihood of sustaining a whiplash injury leading to symptoms lasting longer than 1 month after the crash event, and/or (ii) the likelihood of sustaining on-going impairment (most often classified as a chronic outcome). Previous research by for example Davidson and Kullgren (2011) showed that while early predictions of whiplash provided greater numbers of outcomes that could be assessed, the measurement of Permanent Medical Impairment (pmi) was a more stable measure.

It was positive to find that the 3 main consumer test programmes; Euro NCAP, JNCAP and IIWPG, were equally able to predict real-world whiplash injury outcome in terms of permanent medical impairment. Previous studies have shown that both IIWPG and Folksam/SRA test programmes correlate with real-world whiplash injury outcomes (Kullgren et al. 2007, Kullgren and Krafft 2008). But this is the first time it has been shown for the Euro NCAP consumer tests. The reader needs to be careful not to infer too much from these findings though. Given the sparseness of data available so far, this can only be considered as a preliminary analysis that needs further confirmation with a much larger data set.

The current Euro NCAP whiplash test protocol includes three crash pulses of various severity and all injury criteria included in the consumer tests developed by Folksam/SRA and IIWPG in 2002 to 2003. It is a mix of 7 injury criteria and a geometrical assessment of the head rest. One of the main reasons for this is to get a robustness of the rating procedure, in the sense that the tests cover a wide range in crash severity and that many possible injury causes are covered as long as we don't know the exact cause of the whiplash symptoms. Previous studies have shown correlations between various of the injury criteria used and real-world injury outcome (see for example Davidsson and Kullgren 2011). The results reported here showed that some of the criteria used were less able to predict with real-wold whiplash injury outcome. In particular, time to head rest contact (THRC) and the acceleration of the T1 vertebrae (T1acc) were not correlated with Permanent Medical Impairment as were Nkm and Fx (although Fx was significant however for the Mid pulse, although not for the Low and High pulses). In addition, for the car models with the highest measured Fx values the risk for pmi was very low. Note that the numbers of observations for these points in the plots involved only one or two crashes.

Even though the accident material covered 16 years (1998 to 2013) of crashes reported to Folksam Insurance, the number of available cases was too low to provide statistically robust results. Nevertheless, the findings reported here for reductions in the number of tests and outcome criteria were promising, suggesting possibile options for explaining the risk for pmi and as a basis for potentially developing the Euro NCAP protocol in the years ahead.

**Limitations**

By far the biggest limitation experienced with this analysis was in the number of suitable cases of Permanent Medical Impairment in the current Folksam database. While this could be overcome to some degree by using the outcome of whiplash injury with symptoms lasting longer than 1 month after the crash event, from previous studies, this may be offset by the degree of variation in the findings.

To increase the data avalable for analysis it was necessary to use non published Euro NCAP data nased on tests performed before 2009. It was not fully verified if these tests fully met all Euro NCAP protocol requeirements.

The ROC analysis is well-established as a means to compare the performance of test criteria against a gold-standard outcome measure (here, real-world injury). Substantially more data would be required before the tests studied can be distinguished using these criteria.

## SUMMARY AND CONCLUSIONS

The analyses conducted here were aimed at identifying real-world whiplash associations with existing test protocols used by Euro NCAP, J-NCAP, and IIWPG. Given the paucity in the data available, the finding here should be regarded as preliminary findings at this stage. Of interest, Euro NCAP, JNCAP and IIWPG were all found to be significanly correlated with each other and correlated to some degree with the risk for WAD leading to permanent medical impairment. There were signs that that there could be refinements in the number of test criteria. There was a suggestion that reductions in both the number of tests and criteria could still provide significant associations with Permanent Medical Impairment, but that further research is warranted to further test its robustness.

## REFERENCES


Davidsson J, Kullgren A (2011). Evaluation of Seat Performance Criteria for Rear-end Impact Testing. 22th International Conference on the Enhanced Safety Vehicles (ESV), Washington, DC, National Highway Traffic Safety Administration.

Eichberger A, Geigl B C, Moser A, Fachbach B, Steffan H, Hell W, Langwieder C (1996) Comparison of different car seats regarding head neck kinematics of volunteers during rear-end impact. Proc. of the Int. IRCOBI Conf. on the Biomechanics of Injury. Dublin, Ireland. pp153-164.

Farmer C, Zuby D, Well J, Hellinga L (2008). "Relationship of dynamic seat ratings to real-world neck injury rates." Traffic Inj Prev 9(6): 561-567.

Försäkringsförbundet (1996) Gadering av medicinsk invaliditet –96 (only in Swedish). IFU Utbildning AB, Stockholm Sweden.

Jakobsson L (1998). Automobile Design and Whiplash Prevention. Whiplash Injuries: Current Concepts in Prevention, Diagnoses and Treatment of the Cervical Whiplash Syndrome. R. Gunzberg and M. Szpalski. Philadelphia, Lippincott-Raven Publishers: 299-306.

Jakobsson L, Norin H, Svensson MY (2004) Parameters Influencing AIS 1 Neck Injury Outcome in Frontal Impacts, Traffic Injury Prevention, Vol. 5, No. 2, pp. 156–163.

Jakobsson L. Whiplash Associated Disorders in Frontal and Rear-End Car Impacts. Biomechanical. Thesis for the degree o doctor of philosophy. Crash Safety Dividson , Dep of Machine and Vehicle Systems. Chalmers University of Technology, Sweden 2004. Jakobsson et al. 2008

JNCAP (2014). Car Safety Performance Guidelines; New Car Assessments 2014.3, http://www.nasva.go.jp/mamoru/en/download/car_download.html

Krafft, M. (1998). Non-fatal injuries to car occupants, Injury assessment and analysis of impacts causing short- and long-term consequences with special reference to neck injuries. Karolinska Institutet, Institution of Clinical Neuroscience, Section for Personal Injury Prevention Stockholm, Sweden,

Krafft M, Kullgren A, Lie A, Tingvall C (2003) The Risk of Whiplash Injury in the Rear Seat Compared to the Front Seat in Rear Impacts, Traffic Injury Prevention, Vol. 4, No. 2, pp. 136–140

Krafft M, Kullgren A, Lie A, Tingvall C (2004). Assessment of Whiplash Protection in Rear Impacts - Crash Tests and Real-life Crashes. Test report of the Folksam/SRA consumer test program 2004. Folksam 10660 Stockholm, Sweden.

Eriksson L, Boström O, Krafft M (2003) Validation of neck injury criteria using reconstructed real-life rear-end crashes with recorded crash pulses. Proc. Of the 18 th Int. Techn. Conf. on ESV, paper 344.

Kullgren A, Krafft M, Lie A, Tingvall C (2007). The Effect of Whiplash Protection Systems in Real-Life Crashes and their Correlation to Consumer Crash Test Programmes. 20th International Technical Conference on the Enhanced Safety of Vehicles (ESV), Lyon, France.

Kullgren A, Krafft M (2008) Whiplash research in Sweden: results from real-life crashes. EVU conference, Nice

Kullgren A, Stigson H, Krafft M, (2013). Development of Whiplash Associated Disorders for Male and Female Car Occupants in Cars Launched Since the 80s in Different Impact Directions. Int. IRCOBI Conf. on the Biomechanics of Injury, Gothenburg, Sweden.

Lundell B, Jakobson L, Alfredsson B, Lindström M, Simonsson L (1998) The WHIPS seat – A car seat for improved protection against neck injuries in rear end impacts. Paper No 98-S7-O-08, Proc. 16th ESV Conf, 1998, pp. 1586-1596.

Malm S, Krafft M, Kullgren A, Ydenius A, Tingvall C. (2008). "Risk of permanent medical impairment (RPMI) in road traffic accidents." Annu Proc Assoc Adv Automot Med 52: 93-100.Proceedings of IRCOBI Conference, Berlin, Germany.

Sekizuka M (1998) Seat Designs for Whiplash Injury Lessening, Proc. 16th Int. Techn. Conf. on ESV, Windsor, Canada.

Thatcham (2013) www.thatcham.org

Viano D and Olsen S (2001) The Effectiveness of Active Head Restraint in Preventing Whiplash. Journal of Trauma 2001; Vol.51: 959-969

Watanabe Y, Ichikawa H, Kayama O, Ono, K, Kaneoka K, Inami S (2000) Influence of Seat Characteristics on Occupant Motion in Low-Velocity Rear-End Impacts, Accid. Anal. Prev. 32(2): 243–250.

Wiklund K, Larsson H (1997) SAAB Active Head Restraint (SAHR) - Seat Design to Reduce the Risk of Neck Injuries in Rear Impacts, SAE Paper 980297, Warrendale.

## APPENDIX

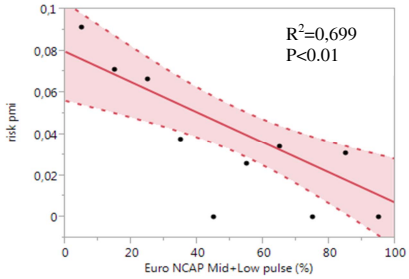


**Fig A1. Risk for pmi vs low+mid pulses.**

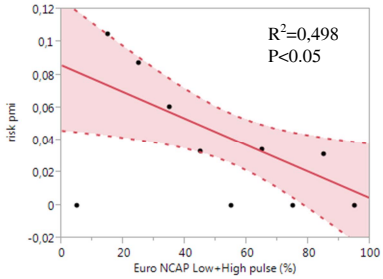


**Fig A2. Risk for pmi vs low+high pulses.**

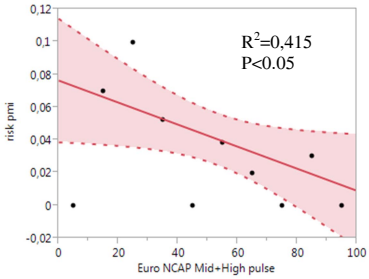


**Fig A3. Risk for pmi vs mid+high pulses.**

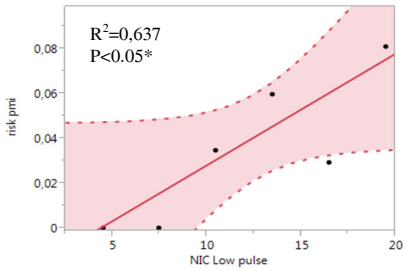


**Fig A4. Risk for pmi vs NIC low pulse.**

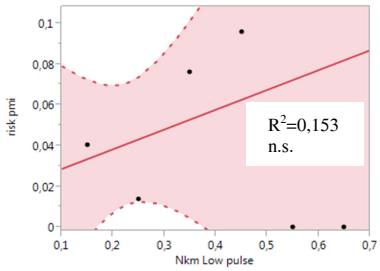


**Fig A5. Risk for pmi vs Nkm low pulse.**

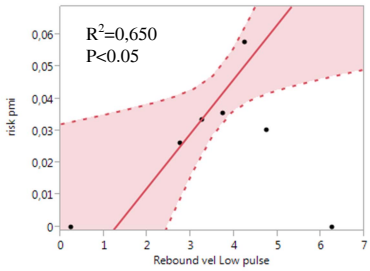


**Fig A6. Risk for pmi vs reb vel low pulse.**

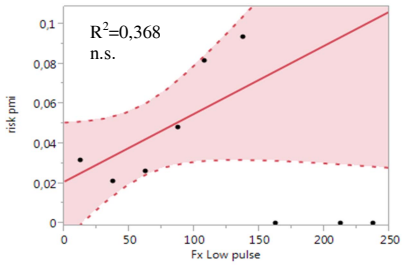


**Fig A7. Risk for pmi vs Fx low pulse.**

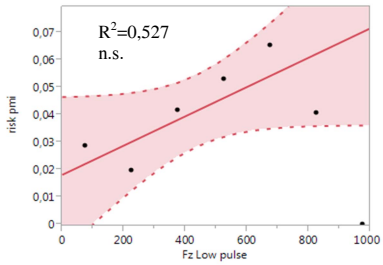


**Figure A8. Risk for pmi vs Fz low pulse.**

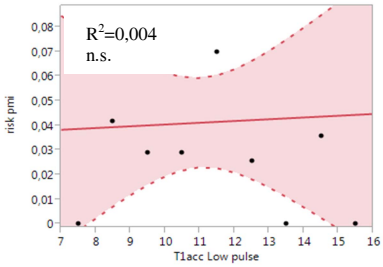


**Fig A9. Risk for pmi vs T1acc low pulse.**

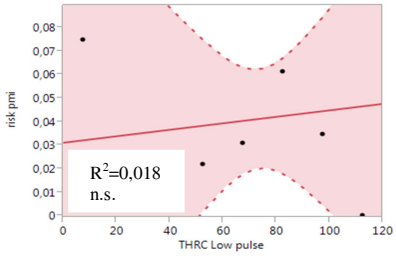


**Fig A10. Risk for pmi vs THRC low pulse.**

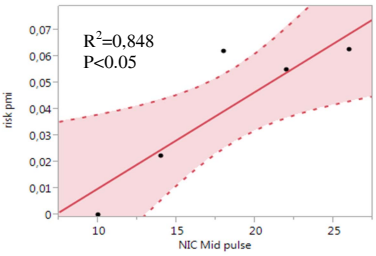


**Fig A11. Risk for pmi vs NIC mid pulse.**

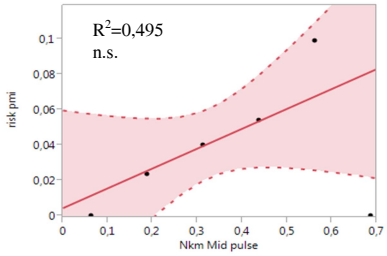


**Figure A12. Risk for pmi vs Nkm mid pulse.**

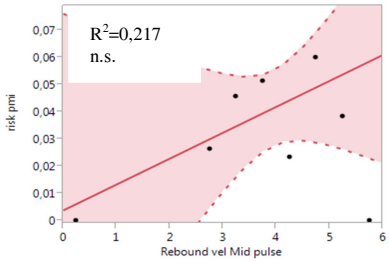


**Fig A13. Risk for pmi vs reb vel mid pulse.**

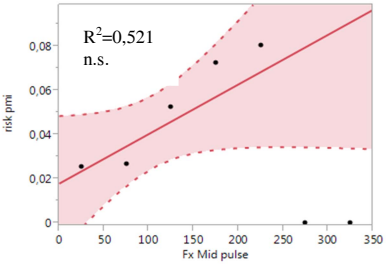


**Fig A13. Risk for pmi vs Fx (mid pulse).**

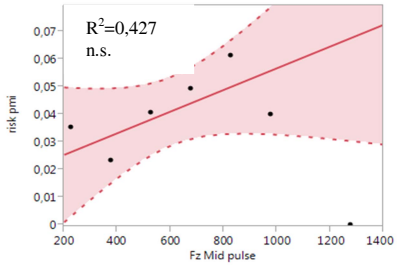


**Fig A14. Risk for pmi vs Fz mid pulse.**

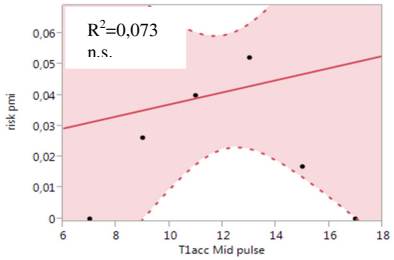


**Fig A15. Risk for pmi vs T1 acc mid pulse.**

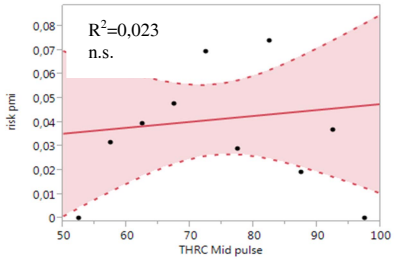


**Fig A16. Risk for pmi vs THRC mid pulse.**

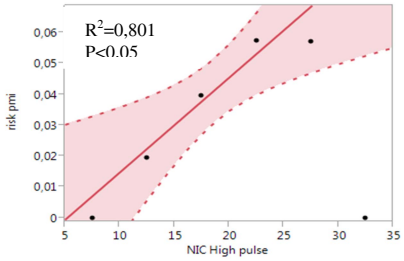


**Fig A17. Risk for pmi vs NIC high pulse.**

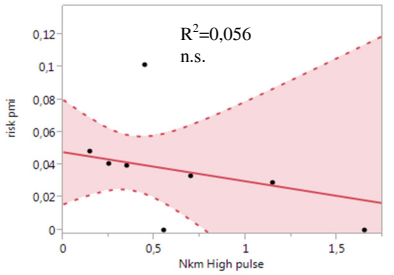


**Fig A18. Risk for pmi vs Nkm high pulse.**

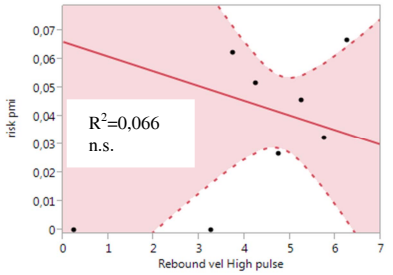


**Fig A19. Risk for pmi vs reb vel high pulse.**

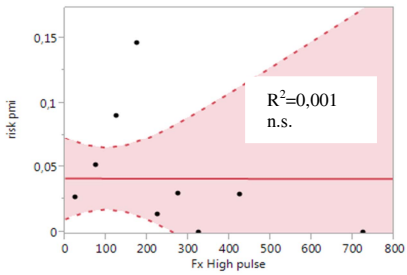


**Fig A20. Risk for pmi vs Fx high pulse.**

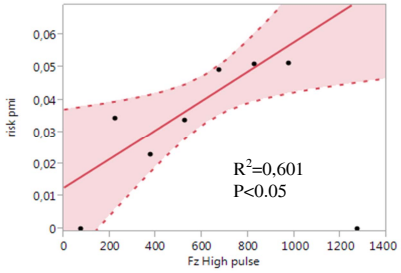


**Fig A21. Risk for pmi vs Fz high pulse.**

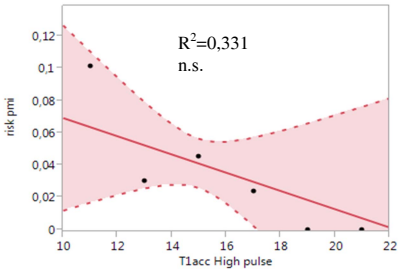


**Fig A22. Risk for pmi vs T1acc high pulse.**

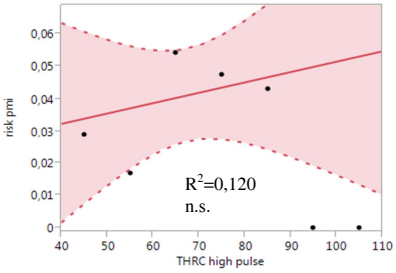


**Fig A23. Risk for pmi vs THRC (high pulse).**

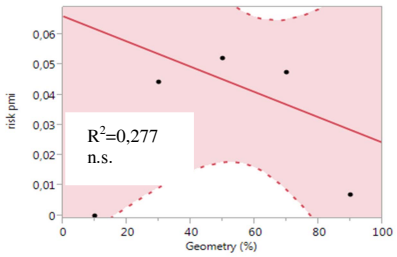


**Fig A24. Ris for pmi vs geometry.**

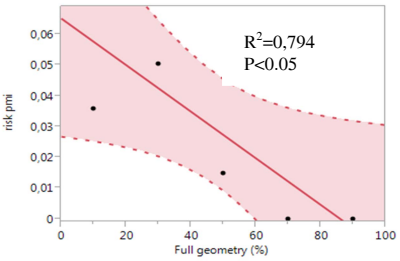


**Fig A25. Risk for pmi vs full geometry.**

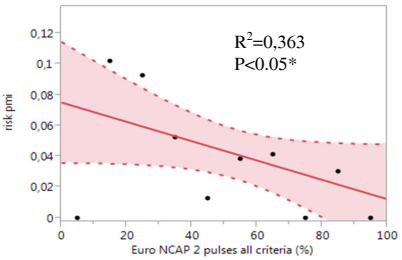


**Fig A26. Risk for pmi vs Euro NCAP 2 pulses (mid and high) and all criteria.**

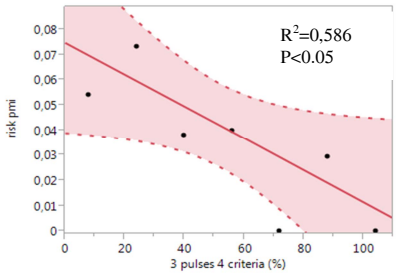


**Fig A27. Risk for pmi vs all Euro NCAP pulse and 4 criteria; NIC, Fx, Fz and reb vel.**

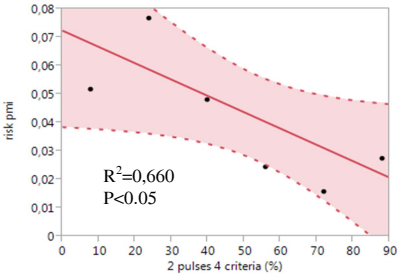


**Fig A28. Risk for pmi vs Euro NCAP 2 pulses mid and high and 4 criteria; NIC, Fx, Fz and reb vel.**

# AUTOMATED GENERATION OF VIRTUAL DRIVING SCENARIOS FROM TEST DRIVE DATA

**Robin, van der Made**
**Martijn, Tideman**
TASS International
The Netherlands

**Ulrich, Lages**
**Roman, Katz**
**Martin, Spencer**
Ibeo Automotive Systems GmbH
Germany

Paper Number 15-0268

## ABSTRACT

Intelligent vehicle systems such as ADAS, ITS and automated driving systems consist of increasing numbers of sensor technologies as well as increasingly advanced algorithms for sensor fusion, object tracking, object classification, risk estimation, driver status recognition and vehicle control. It is rapidly becoming infeasible to check the performance of each new (sensor) system in the traditional way: By performing test drives, storing data, manually labelling the data for reference, and manually evaluating the results. One of the approaches to address these difficulties is to install a reference sensor system on the test vehicle in addition to the prototype sensor system (device under test). The recorded data from the reference sensor system are processed – partly or fully - automatically to create reference scenarios, based on automatic object labelling and automatic event identification. Based on these reference data, the device under test can be automatically and objectively evaluated. The reference data from the reference sensor system can now be converted into a set of virtual scenarios which can be used within a CAE environment. These simulated "ground-truth reference scenarios" offer a platform for engineers to quickly check the consequences of design changes to the device under test, and allow engineers to subject the device under test to a wide variation of virtual traffic scenarios.

## INTRODUCTION

In recent years, automotive active safety systems have become more prevalent. Furthermore, these systems will be used as the foundation for the roll-out of autonomous vehicles. There are a variety of applications that encompass active safety including: Adaptive Cruise Control (ACC), Forward Collision Warning (FCW), Automatic Emergency Braking (AEB), Lane Departure Warning (LDW), Blind Spot Warning (BLSW), Lane Keeping Assistance (LKA), Pedestrian Avoidance (PA), Intelligent Headlight Systems (IHS) and Cooperative Driving Systems (CDS).
With the rising level of automation onboard vehicles, intelligent vehicle systems have to deal with an increasing amount of complex traffic scenarios. In turn, the intelligent systems themselves are also becoming more complicated. They consist of more and more different sensor technologies as well as increasingly advanced algorithms for sensor fusion, object tracking, classification, risk estimation, driver status recognition and vehicle control. As a result, it is rapidly becoming infeasible to check the performance of each new (sensor) system in the traditional way by driving around, storing data, manually labeling the data for reference, and manually evaluating the results.

## ADAS TESTING & REFERENCE SENSING

One of the approaches to address these difficulties is to install an additional reference sensor system (RSS) on the vehicle which is already equipped with the prototype sensor system that is going to be tested (DUT – device under test). The recorded data from the reference sensor system are processed to automatically create reference scenarios, based on automatic labeling of relevant road users and background environment description. Based on these reference data, the device-under-test can be automatically and objectively verified [1,2].

## Laser Scanner Advancements

Several advancements in the field of laser scanning [3] allow the sensor technology to be used as a reference sensor system for automatically generating reference scenarios from laser scan data. The current generation of laser scanners can detect objects with a high precision relative to the scanner. If a digital map is available which contains landmarks with centimeter accuracy, then the absolute position of the laser scanner can be determined to within a few centimeters, thus improving the accuracy of all tracked objects. The scanner is effectively used as a differential sensor, analogous to Differential GPS (DGPS), but without the need for a base station or for a clear view of the sky.

## Forward-Backward Tracking & Best Situation Classification

A further improvement is the use of offline processing to analyze the scenario. State of the art online tracking algorithms are inherently limited by the requirement to run in real time. If the data is reprocessed offline, it becomes possible to look ahead for all observations of an object and associate them with the first instant that the object is visible, which allows the system to be used as a true reference, since no online sensor can look into the future. This also allows the use of a Best Situation Classifier (BSC). The point in time where an object is most clearly visible can be used to classify the object, and this classification can be extended to the lifetime of the object. Additional benefits are improved robustness to occlusions, reduced uncertainty of the ego vehicle position between landmarks, and increased accuracy of object trajectories.

As an example, consider the scenario in Figure 1a. A sign and an oncoming vehicle are just visible by the laser scanner. Figure 1b and 1c show the results of two tracking approaches. In the online approach (Figure 1b), the approaching vehicle is initially detected, but it is not yet classified and the outline is not clear. As the vehicle gets closer, the outline can be clearly seen and it is classified as a car. In the offline approach (Figure 1c), this information is associated with the object in the first instant that it is visible, allowing a more accurate reconstruction of the scenario.

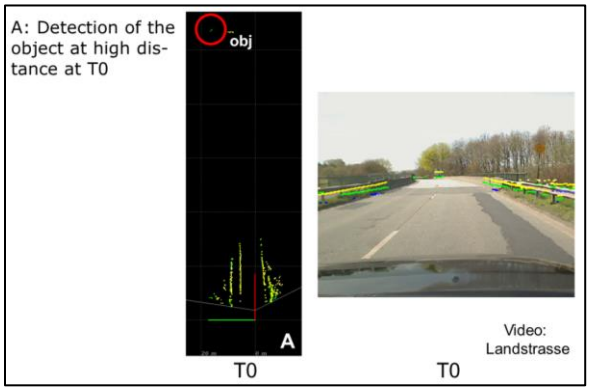


***Figure 1a: Online object tracking at time T0.***

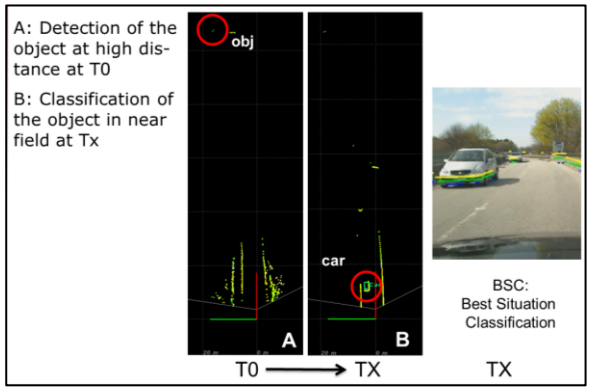


***Figure 1b: Online object tracking at time TX.***

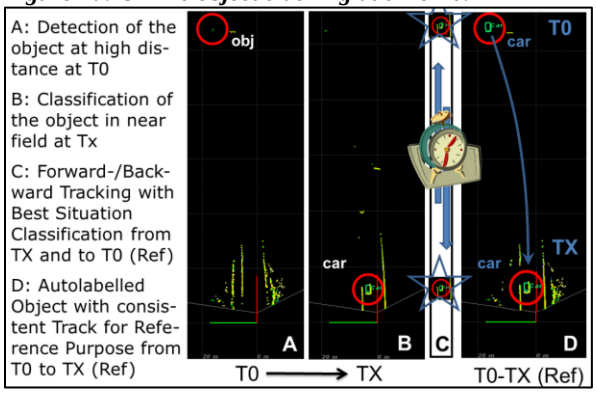


***Figure 1c: Forward-Backward Tracking principle.***

This process, which provides object information in full detail already at the time of the first detection of the object at high distance, is called Forward-Backward Tracking (FBT). This ensures that the laser scanners, used as a reference sensor system, provide detailed object information very early and with high precision at any time, as shown in the following example (Figure 2).

***Figure 2: Application example of post-processing using Best Situation Classification (BSC) and Forward Backward Tracking (FBT)***.

## VIRTUAL DRIVING SCENARIOS FROM REAL WORLD TEST DRIVES

While test driving is still the main method for ADAS system, the resulting data rarely contain events that would be truly tax the active safety system evaluation; even with a million miles driven. Crashes are rare and difficult to capture. Even near crashes are rare. Hence, we end up with much of the collected data being simple false alarm data (i.e. driving with no difficult decision to make). Many of the drawbacks of hardware testing of ADA systems [4] are not present for a virtual test environment. Virtual testing with simulation software provides an efficient and safe environment to design and evaluate ADA systems. Moreover, simulated scenarios are completely quantifiable, controllable and reproducible.
However, the creation of many virtual driving scenarios can be a time-consuming and laborious activity; in particular, when real testing scenarios and conditions must be manually converted into virtual scenarios for further testing. It is thus extremely valuable to be able to automatically obtain virtual scenarios from real world test drives.

The reference data from the reference sensor system as presented in previous section are well-suited to serve as basis for automatic creation of virtual scenarios. They can be converted into a set of simulated scenarios which can be used within a CAE environment. These simulated “ground-truth reference scenarios” offer a platform for engineers to quickly check the consequences of design changes to the device under test, or even to try out completely new system concepts.

## RESULTS

The concept of creation of virtual driving scenarios from real-world test drives was evaluated using an Ibeo laser scanner setup with two lasers scanners (see Figure 3).

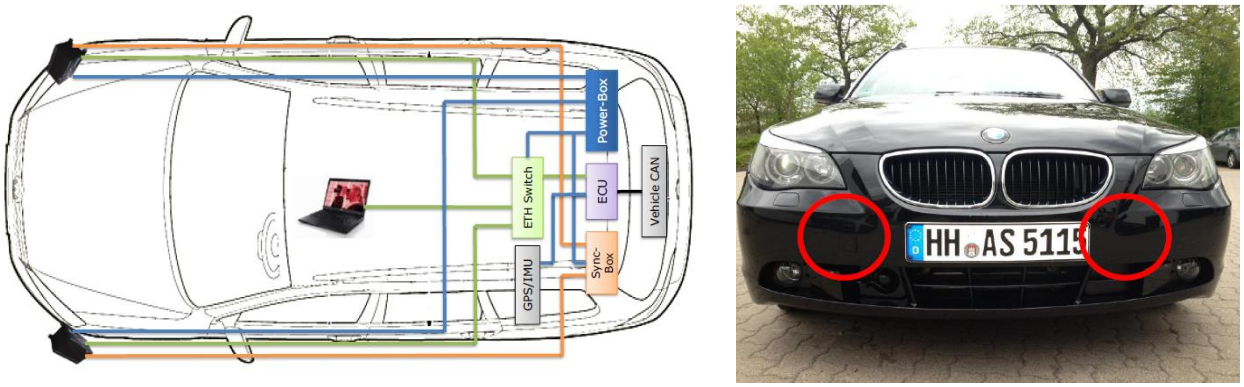


***Figure 3: Ibeo Sensor System mounted on a test vehicle. Red circles indicate two Lux scanners from a 2- Sensor fusion system mounted on the front bumper of the car.***

The recorded data is automatically labelled with a post-processing tool. These labels are then provided for the processing and evaluation of a device under test, and the conversion to virtual driving scenarios in the simulation software PreScan [5]. Figure 4a and 4b show a sample result in which a passenger car and pedestrians are detected, classified, and converted to a virtual environment. The applied laser system is able to classify passenger cars, trucks, motorcycles, bicyclists and pedestrians.

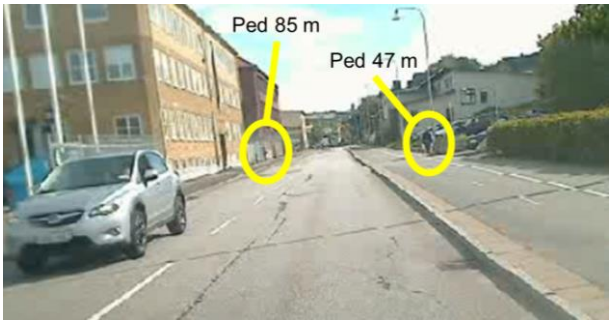


***Figure 4a: Reference scenario from real world test drive.***

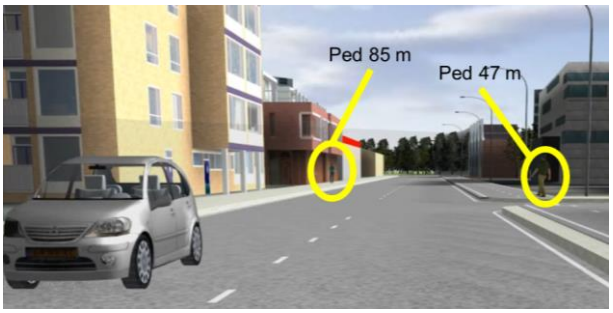


***Figure 4b: Virtual driving scenarios derived from real world test data.***

## CONCLUSIONS

This paper presented the use of advanced perception systems for obtaining reference data for the automated generation of simulated driving scenarios. We described our advances in the fields of laser scanning processing for reference generation, and illustrated the use of reference data for constructing simulated virtual scenarios that can be loaded, manipulated and used within a commercial simulator.

## REFERENCES

You can list your references in a numbered list in order of citation in text, or alphabetically by authors' names.

[1] Ulrich Lages, Martin Spencer, Roman Katz , "Automatic Scenario Generation based on Laserscanner Reference Data and Advanced Offline Processing", Proceedings of IEEE Intelligent Vehicle Conference, Gold Coast, Australia, June 2013.

[2] Martin Spencer, Roman Katz, Ulrich Lages, "Forward-Backward Object Tracking for Generation of Reference Scenarios Based on Laser Scan Data", Proceedings of ITS World Congress, Detroit, USA, 2014 [pending approval].

[3] http://www.ibeo-as.com, Ibeo Automotive Systems GmbH, 2014

[4] Roy Bours, Tino Schulze, Takahito Nakano, Eiji Teramura, Martijn Tideman, "Integral Simulation Toolset for ADAS Modeling", Proceedings of JSAE Conference, Yokohama, Japan, May 2012

[5] http://www.tassinternational.com/prescan, TASS International, 2014

# Updated Estimates of Potential Traffic Fatality Reductions With Automatic Collision Notification

Jingshu Wu, PhD, PE
Matthew Craig, PhD
Anders Longthorne

National Highway Traffic Safety Administration (NHTSA), Washington, DC

Paper Number 15-0269

## ABSTRACT

This paper updates the earlier work done by Wu, Craig, et al. (2013) that explored the effects of earlier emergency medical services (EMS) through Automatic Collision Notification (ACN) on passenger/driver survivability using Fatality Analysis Reporting System (FARS) 2005-09. In this continuing study the earlier results are updated using recent FARS 2009-2012 data, while additional factors together with ACN are also considered: such as EMS arrival, time to hospital, urban/rural location comparison, occupant age and correlation between EMS factors. Kaplan-Meier estimator is applied to compare the survival rates between two conditions (e.g., earlier versus late EMS notification); Proportional hazard model explores simultaneously multiple risk factors related to traffic mortality. Correlations between notification and EMS arrival are explored and especially in rural area. Based on FARS data from 2009-2012, Kaplan-Meier life curves clearly show the benefits associated with earlier notifications within 1-2 minutes (approximately 1.5-2.0% fatality reduction within a timeframe of 6 hours after crash) and earlier arrivals. The relative hazard ratio associated with collision notification, location and age are obtained from a multiple regression model, and the relatively higher fatality hazard (up to 4% higher) is associated the later notification of more than 2 minutes. This paper obtains the driver/passenger survival probability differences over time under different conditions of collision notifications, EMS arrivals, time to reach a hospital, and crash locations, furthermore, this analysis provides the estimations of lives that could potentially be saved (177 to 244 per year approximately) due to earlier crash notification, or Automatic Collision Notification (ACN).

## 1. INTRODUCTION

During 2009-2012, the Fatality Analysis Reporting System (FARS) data indicate that the traffic fatalities are approximately 33,000 per year in US (33,883 in 2009, 32,999 in 2010, 32,479 in 2011, and 33,561 in 2012, respectively), and approximately 83%~85% fatalities were from drivers and passengers each year. It has been a challenging effort to reduce the traffic fatalities, especially the target study population of drivers and passengers in light trucks and cars under 10, 000 lbs. by all possible means and new techniques. Automatic Collision Notification (ACN) system is one of such efforts and it has been available from some automobile manufacturers since the late 1990s. One benefit of these ACN systems may enable the injured occupants to inform the emergency response personnel quickly about location of a car crash.

Many prior publications have attempted to document the potential motor vehicle crash-related fatalities that could be reduced given ACN. Wu, Craig, et al. (2013) [1] explored the effects of earlier emergency medical services (EMS) through ACN on passenger/driver survivability. It was found that 154 to 290 additional lives per year (approximately 1.8% fatality reduction) could be saved by earlier collision notification times that could result from the presence of ACN systems in passenger vehicles and light trucks and vans. The earlier study used 2005 through 2009 Fatality Analytical Reporting System (FARS) data. The vehicle fleet, communication technologies, and other factors related to occupant safety may have changed in the past few years, and the potential fatality reduction estimates should be re-computed in the light of this changing vehicle fleet, communication technology, and mainly

notification status. This updates estimates for potential annual lives saved by ACN using FARS 2009-2012 data, and additional factors together with ACN are also including urban versus rural crash location and occupant age.

Earlier studies were carried out by various researchers. In one study with a relatively small fleet of vehicles equipped with ACN, Kanianthra et al. [2] documented that EMS providers received notifications within two minutes of the crash in all cases while 20% of non-equipped vehicles took over 5 minutes, their study estimated that 240 to 765 lives could be saved. Using similar survival analysis approach, Clark and Cushing [3] estimated the potential benefits of ACN through analysis of 1997 FARS data. One of their models matching FARS fatalities estimated a total annual reduction of 421 fatalities (1.5%). The European Commission's 'eCall' program [5] published a final report regarding its crash notification related efforts (European Commission, 2009). The estimated motor vehicle crash occupant fatality reduction with ACN in the cited studies ranged widely from 1% to 12%.

Existing research has not yet dealt with the relative comparisons of different conditions statistically with sufficiently larger data sizes and significant P-values, for instance, to compare earlier versus later notification outcomes or earlier versus later arrival outcomes. Some relatively older data (FARS 1997) may not reflect today's EMS call status well [3], and the work done by Toyota [6] have provided clear comparisons of notification and arrival times for scenarios with and without ACN, but also proposed prior assumptions of the possible correlations between EMS notification, timeliness of arrival, and survivability. Correlations among EMS factors were rarely mentioned. While the authors are inspired by the earlier research[2-6], efforts are still needed to understand the following:

- Impact of earlier or automatic collision notification on occupant survivability and the potential for fatality reduction with ACN if introduced across the passenger vehicle fleet;
- Survival rate comparisons of varied EMS arrival times including the impact of earlier EMS arrival on survivability, and the impact of shorter time to reach hospital;
- Comparison of EMS response time and survivability in rural versus urban areas;
- Correlations between EMS factors, such as notification time versus arrival time; and
- The relationship between the traffic fatality hazard with several risk factors, including later notification, rural area, and older age, simultaneously.

Earlier crash notification, with timely EMS and earlier hospitalization, may all play a significant role in mitigating the effects of the injuries suffered in a motor vehicle crash. Research [11] has also indicated that proximity to advanced trauma care (earlier EMS and shorter distance to hospital) may also be a key factor in mitigating injury outcome. Since time is of essence in EMS response to such situations, driver/passenger survival rates can vary significantly between different time conditions (e.g., time elapsed before or after the notification call). This could possibly be exacerbated in the case of single vehicle crashes in the remote rural areas where a lone occupant of a vehicle may have lower likelihood to call and receive emergency services, especially within a short time frame. In this paper, the techniques of 'time-to-event', such as Kaplan-Meier estimator and Cox proportional hazard model, are used to address the time effect. This study explores the relative comparisons between different conditions or groups, such as survival rates with earlier notification versus late notification, and survivability in rural areas versus urban areas.

## 2. DATA AND STUDY DESIGN

EMS is most helpful to the drivers and passengers of passenger cars and light trucks if received within 6 hours immediately following a crash.[1,2] Data was compiled using the 2009-2012 FARS data, with specific evaluation of the 6-hour post-crash timeframe (EMS notification/arrival within 6 hours after crashes; data with missing notification/arrival information was excluded). Data cleaning efforts (defining times of notification, arrival, death, and missing data, et. al) were made in FARS data verification, and all key time variable coding were defined by the authors of NHTSA. For each crash coded in FARS, the following times are recorded: *crash*, EMS *notification*, EMS *arrival at scene of crash*, EMS *arrival at hospital*, and *time of death* (in the event of a fatality, see Figure 1 for definitions of time events and time intervals).

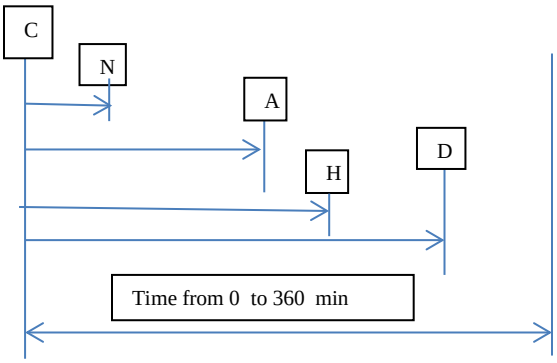


**Figure 1**: Crash time events and time elapsed between crash (C), notification (N), arrival (A), Hospital (H), and death (D).

These time-date values were used to generate the time intervals needed for the time-to-event or survival analysis. Note that only crashes with available notification and arrival times within six hour window after crashes were used. See Figure 2 for the data flow chart for this study: there were 88,703 fatalities and 29,916 incapacitating injuries under considerations (drivers and passengers in cars or light trucks), 68,043 of them died within 6 hours, and 33,125 fatalities were associated with known notification and arrival times (approximately 48.7% of the 68,043 fatalities within 6 hours, see Figure 3), and 9,873 of 33,125 people died instantly for whom ACN is of no help (crash to death time = 0), and the remaining 23,252 fatal cases are the research sample. They are matched with 24,812 cases of 'Incapacitating Injuries' within the same time frame of six hours as described as Table 2.

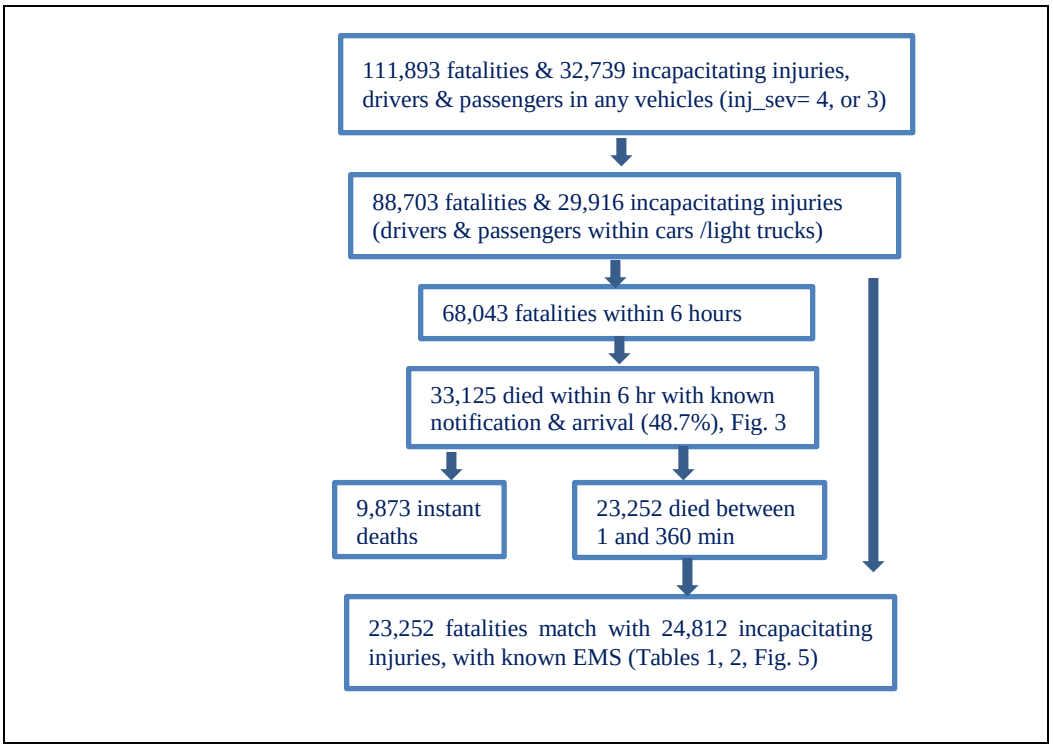


**Figure 2:** FARS 2009-2012 Population Study Sample

Table 1 shows the statistical descriptive summary for 23,252 fatalities that occurred from 1-360 minutes post-crash who were also associated with known notification and arrival time within six hours (overall, rural, and urban data). The definitions of rural and urban areas are from US Census Bureau.

**Table 1:** Overall, Rural and Urban EMS Response Times (minutes) Since Crash (FARS 2009-2012)

| **Overall** 23,252 Fatalities Within 6 Hours with Known Notification/Arrival info | | |
|---|---|---|
| **Time** | **Mean (min)** | **Std dev (min)** |
| Call | 6.24 | 17.33 |
| Arrival | 16.74 | 20.29 |
| Death | 66.21 | 67.99 |
| **Rural** 14,294 fatalities within 6 hours (61.5% of 23,252 fatalities) | | |
| Call | 7.25 | 19.16 |
| Arrival | 19.64 | 22.25 |
| Death | 66.46 | 67.05 |
| **Urban** 8,924 fatalities within 6 hours (38.4% of 23,252) | | |
| Call | 4.61 | 13.74 |
| Arrival | 12.10 | 15.63 |
| Death | 65.74 | 69.41 |

FARS database used the key injury variable of '*inj_SEV*' to indicate injury severity as follows: 0 = No Injury; 1 = Possible Injury; 2 = Non-Incapacitating Evident Injury; 3 = Incapacitating Injury; 4 = Fatal Injury; 5 = Injured, Severity Unknown; 6 = Died Prior to Crash; and 9 = Unknown. In this study, two groups of 'Incapacitating Injury, 3' and 'Fatal Injury, 4' are focused, since these two groups need EMS help immediately, and is compared with 'Fatal Injury' group within same time window, for example, within 6 hours after crashes.

Figure 3 shows the fatalities over time (inj_sev=4). This fatality curve, or survival probability curve over time, S(t), indicates that approximately *86.6%* of fatalities occurring within 6 hours occurred within 100 minutes of the crash (including 9,873 instant deaths at time = 0). More details of this life curve will be discussed later using Kaplan-Meier Estimator [7]. Additionally, 20,083 died within 40 minutes since crashes (approximately 61% of all fatalities within 6 hours).

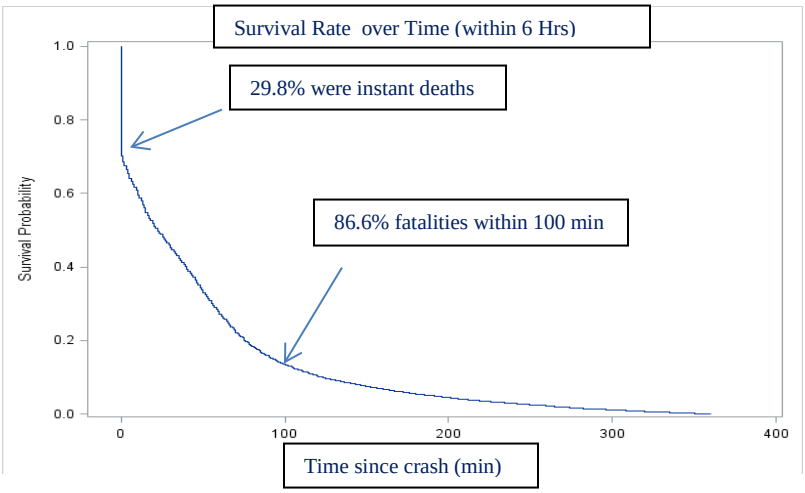


**Figure 3**: Survival rate, S(t), versus 'crash to death time' of fatalities within 6 hours (33,125 with known notification /arrival times, data from Figure 2).

For the purpose of analyzing the survival rate or proportion, the data set in this study includes the crashes that resulted in at least one fatality, and should not be generalized to the whole crash population. The values of 'inj_SEV=3, 4' are used as the study population, since these two categories need EMS help most while instant fatalities are excluded. There were 24,812 'Incapacitating Injury' cases (inj_Sev=3) that were matched with 23,252 fatalities (inj_SEV=4, within 6 hours after crashes and with known EMS information) in this *cohort study*, or

follow-up study [9] as described by Table 2, which compares the subsequent occurrence of traffic injury severities between two groups whose EMS status differs. Fatality rate of 'earlier group' is $R_e = A/(A+B)$, and $R_L = C/(C+D)$ for 'later group', and the fatality relative risk (RR) is ($R_L$ /$R_e$). The survival rate S(t) = (100% - Fatality Rate) over time, t.

**Table 2:** Cohort Study of Notification versus Traffic Severity within 6 Hours After Crash (inj_Sev = 3, 4)

| **Notification** | **Fatal, Inj_Sev=4** | **Inj_Sev= 3** | **Total** |
|---|---|---|---|
| **Earlier** | A | B | A+B |
| **Later** | C | D | C+D |
| **Total** | 23,252 | 24,812 | 48,604 |

## 3. SURVIVAL RATES WITH DIFFERENT EMS STATUSES

Various factors or EMS statuses may affect traffic fatalities: such as notification time, time of EMS arrival at the crash scene or time of EMS arrival at hospital. Furthermore, EMS services (notification, EMS arrival, et. al., as Table 1) in rural versus urban areas are also rather different. Time plays a very crucial role in life saving. All these issues will be explored in this section.

One of the most useful tools to compare the survival probability over time, S(t) (e.g. Figure 3), for each minute after crash, is a non-parametric method proposed by Kaplan and Meier that is used widely for medical research and reliability engineering [1 7]. The Kaplan-Meier estimator, or life curve, at any time is described by the following formula:

$$\hat{S}(t) = \prod_{t_i<=t}(1-\frac{d_i}{n_i}) = \prod_{t_i<=t}(\frac{s_i}{n_i}) \qquad (1)$$

where '$d_i$' is 'deceased' subjects or fatalities, and '$s_i$' is the 'survivor' subjects or alive ('censored') drivers/passengers, and '$n_i$' is total subject number (total persons in study). There were 360 equal intervals, with the length of one minute each since crash (i=1 to 360) if the survivability within 6 hours was focused in this analysis. The sign of 'Π $A_i$' stands for the product of "$A_1A_2A_3$" if i=1 to 3.

In order to compare the traffic fatality relative risk or differences between different blocks or groups (such as earlier calls versus late calls), the Log-Rank test, compares the Kaplan-Meir life curves and obtains the statistical significance with p-value. The SAS Proc LifeTest is used for the calculation, and Kaplan-Meier estimator is also termed as 'Product-Limit Survival Estimates'. [7, 8]

### 3.1 Effect of Earlier Notification

In order to study the survival rates within 6 hours (study or research time) immediately following a crash, Table 3 is used to show the correlation between survival status and notification time, when all data (inj_sev = 3,4) are divided into a few groups based on notification time**.**

**Table 3:** Notification Time (min) versus Survival Status Within 6 Hours After Crash

| Notification, N (minute) | Dead | Alive | Total | Alive % S(t) |
|---|---|---|---|---|
| **N<=1 min** | 8772 | 9635 | 18,408 | 52.35 |
| **1<N <=2** | 2817 | 3137 | 5,954 | 52.69 |
| 2<N<=3 | 2266 | 2210 | 4,476 | 49.37 |
| 3<N<=5 | 3062 | 2928 | 5,990 | 48.88 |
| 5<N<=8 | 2339 | 2372 | 4,711 | 50.35 |
| 8<N<=15 | 2223 | 2453 | 4,676 | 52.46 |
| 15< N<=360 | 1773 | 2077 | 3,850 | 53.95 |
| Total | 23,252 | 24,812 | 48,064 | 51.62 |

Table 3 indicates that approximately 51% injury and fatality cases (24,362 out of 48,065) occurred within notification time <=1, 2 minutes (top two rows), and occupants also need EMS helps more than any other moments

during these crucial two minutes. However, many risk factors, such as notification time, EMS arrival and EMS quality, crash severity, health condition and age, may all contribute to occupant survival status. Particularly, the earlier notification within 1-2 minutes would significantly improve survival rates compared with later notifications of '3-15 minutes'. Although Table 3 also shows that the survival rate is relatively high (53.95%) for the smaller group of '15 <N<=360 minutes', this smaller group might be associated with less severity crashes, better health conditions or other factors. This smaller group survived earlier crash time window and also happened to notify later than others, and more investigations may be needed for this survival status variation. Again Figure 3, together with Table 3, indicates the majority of fatalities happened very early and 86.6% fatalities occurred during 0-100 minutes, and 61% fatalities within early 40 minutes.

Based on the same format of Table 2 Cohort design, 24,812 'Incapacitating Injury' cases were matched, within same time frame of 6 hours with 23,252 fatalities, and the total sample was then statistically 'randomized' (each case had the same probability) and 'blocked' (divided into two groups based on EMS notification time). The people with survival times longer than 6 hours were regarded as 'censored' data or alive within the current study time.

The status of 'alive' or 'censored' is also relative and changing over time (Table 4 or Figure 4). The total study sample can be divided into two blocks or groups: the *preferred* or *earlier* group is 'Call <=1 min after crash and call time before death time'; the rest belong to a second, *un-preferred* group, for the purpose of understanding the effect of earlier notification on fatalities. The survival rate difference between the two groups with earlier (<=1 min) or late (>1 min) notifications is then compared using two Kaplan-Meier life curves and Log-Rank test. Table 4 displays the survival rates of the two groups within the study time (6 hours post-crash). The p-value from Log-Rank test is under 0.0001 (p-value<0.0001).

**Table 4:** Survivors and Fatalities within 6 Hours After Crash
(Notifications <=1 versus >1 min, inj_sev=3, 4, FARS 2009-12)

| Notification, (min) | Dead | Alive | Total | Alive % S(t) |
|---|---|---|---|---|
| **<=1 min** | 8,772 | 9,635 | 18,407 | 52.34 |
| **>1 min** | 14,480 | 15,177 | 29,657 | 51.18 |
| **Total** | 23,252 | 24,812 | 48,064 | 51.62 |

**Interpretation of Table 4:**
The earlier notified group (<=1 min) had a cumulative survival rate (alive/total) of 52.34%, which is 1.16% higher than the late notified group (>1 min, 51.18%) within 6 hours after crashes. Hence, if the late group had made the EMS calls within 1 minute like the earlier group did, then the possible additional lives saved from this late group would be approximately 1.16% x (29,657) =344, this reduction of 344 deaths represents 1.48% of original death numbers of 23,252 within a time frame of 6 hours after crash during four years between 2009-2012, or 86 fatality reductions per year (the earlier study using 2005-2009 had a fatality reduction of 1.84% [1]). Furthermore, data with known notification and arrival times within 6 hour window is only 48.7% of the sample population (Table 1 and Figure 2). If we assume all sample populations (with or without info of notification/arrival, all sample populations are 1/0.487=2.05 times of the sample with known notification/arrival info) would share similar trends, then additional lives potentially saved could have been 177 (2.05 times of 86) per year from 2009-2012. The fatality relative risk of later group versus earlier group is 1.024, or later group has 2.4% higher relative risk of death with a significant P-value under 5%.

Again, Table 3 indicates that earlier notification within 1-2 minutes is very helpful to life saving, and EMS notification cut-off time of '1 minute', or '2 minutes' may lead to slightly different estimations of lives saved, which is discussed as Table 5 (Figure 4), where notification time is divided as two groups of 'notification <=2 min and call time before death time' (*preferred* or *earlier* group), or otherwise. The notification group with 'N <=2 min and call time before death time' would have larger sample size compared with the group of 'N<=1 min.' earlier as Table 4, If notification <=2 min., there were 84 cases that were with notification time and death time being 2 minutes, and that were not treated as the preferred group but otherwise. The similar analysis of Kaplan-Meier life curves, comparing the survival rates of earlier group versus later group, was performed for two notification time divisions, as Table 4 or Table 5. It can be seen, from Table 5, that the preferred earlier notified group had a cumulative survival rate of 52.61%, which is approximately 2% higher than the late notified group (50.62%). Figure 4 came from the two

survival probability curves over time of two different notification times (Table 5), the earlier notification groups is assumed as 'notification <=2 min and call time prior to death'; if 'notification <=2 min' instead, the cumulative survival rate difference for earlier and later groups would be slightly smaller (1.63%).

**Table 5:** Survivors and Fatalities Within 6 Hours After Crash
(Notification<=2 or otherwise, inj_sev=3, 4 with FARS 2009-12**)**

| Notification, (min) | Dead | Alive | Total | Alive % S(t) |
|---|---|---|---|---|
| **<=2 min (preferred)** | 11,505 | 12,772 | 24,277 | 52.61 |
| **>2 min (non-preferred)** | 11,747 | 12,040 | 23,787 | 50.62 |
| **Total** | 23,252 | 24,812 | 48,064 | 51.62 |

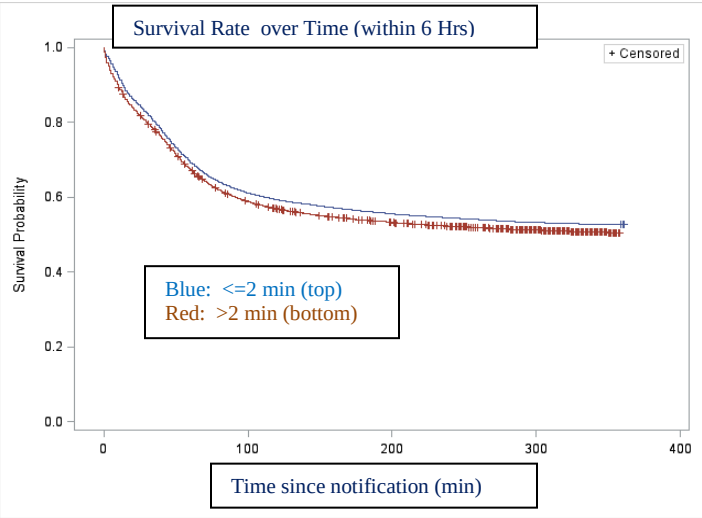


**Figure 4:** Notifications versus Survival Rate within 6 Hours after Crash (Notifications <=2 versus >2 min, inj_sev=3, 4)

**Interpretation of Table 5 and Figure 4:**
As seen in Table 5 and Figure 4, the preferred earlier notification group (<=2 min) had a cumulative survival rate (alive/total) of 52.61%, approximately 2% higher than the later notification group (>2 min) within 6 hours after crashes (P-value =0.0034). If the later notification group had made the EMS calls within 2 minutes as the earlier group, then the possible additional lives saved would be approximately 2% x (23,787) = 476 (approximately 2% reduction of original fatalities of 23,252) during 2009-12, or 119 fatality reductions per year. If all data with or without notification/arrival info are under consideration (the total population sample size is 1/0.487=2.05 times of the smaller sample with notification/arrival info), the additional lives saved due to earlier notification could be 244 annually during 2009-2012. The fatality relative risk of later group versus earlier group is 1.04, or later group has 4% higher fatality risk significantly.

Here are some discussions about the earlier notification effect and the analysis method:

- If the EMS cut-off time is longer than 6 hours in this study, the study population will be slightly larger than the population shown in Tables 4, 5. Although most people died within the first few hours as seen in Figures 3, 4, the proper EMS cutoff time depends on when the life curve becomes stabilized or flat after a crash.
- This method derived the fatality reductions or lives potentially saved due to ACN from crossing comparing the survival probabilities of two paired life curves at a specific time of 6 hours (360 minutes), and this comparison can also be made at any specific times chosen by researchers, 4, 5, or 6 hours, after a crash within the timeframe. Comparing survival rate difference of two paired groups at a specific time is a common approach used in clinical trials and public health research.
- The cut-off time of notifications <=1 or <=2 minutes also plays a role in determining the additional lives saved due to earlier notification (ACN), and Table 3 /Figure 4 show the notification within 1-2 minutes are most helpful.

## 3.2 Effect of Earlier EMS Arrival

Similarly, it is known that earlier EMS arrival may significantly improve occupant treatment and crash survivability, based on real-world data. The field-data also indicated that earlier notifications would not always guarantee either earlier arrivals or better survival chances, although there was a strong correlation between the EMS notification and EMS arrival (details to be discussed by using correlation coefficient). The EMS arrival was hence studied separately as one important variable for survival rate comparison.

Table 6 shows the correlation between the EMS arrival and survival status, and again Figure 3 life curve may be used together with Table 6: majority injuries and fatalities happened very early after crash (approximately 64% within 15 minutes after crashes as Table 6, top three rows). If EMS arrival is <= 5 minutes, the survival rate is 54.36%, which is 2.74% higher than the overall survival rate (51.62%). The smaller groups with '30< Arrival <=360 minutes', with approximately 11.7% of total occupants (bottom two rows), had a relatively high survival rate of 56% approximately, possibly due to less crash severity, better health conditions, or other unknown factors that are not explored in this study.

**Table 6:** Arrival Time versus Survival Status within 6 Hours After Crash

| Arrival, A (min.) | dead | alive | Total | Alive % S(t) |
|---|---|---|---|---|
| **A<=5** | 3063 | 3648 | 6,711 | 54.36 |
| **5<A<=10** | 6982 | 7180 | 14,162 | 50.70 |
| **10<A<=15** | 5074 | 4960 | 10,034 | 49.43 |
| 15<A<=30 | 5662 | 5878 | 11,540 | 50.94 |
| 30<A<=45 | 1467 | 1865 | 3,332 | 55.97 |
| 45<A<=360 | 1004 | 1281 | 2,285 | 56.06 |
| Total | 23,252 | 24,812 | 48,064 | 51.62 |

## 3.3 Effect of Earlier Arrival at Hospital

Similarly, an earlier arrival time to a hospital may significantly improve occupant medical treatment and crash survivability. Table 8 provides the correlation between the 'time-to-hospital' and 'survival status'. The survival rate with hospital arrival time (56.41%, Table 8) is approximately 5% higher than the overall survival rate, 51.62% (with and without hospital arrival information, as Table 3 or Table 6). Approximately 40% of occupants in this study, although with known notification and EMS arrival times within six hours, had no documented hospital arrival time. Table 8 does show the importance of reaching a hospital after crash overall, compared with Tables 3, 6.

**Table 8:** Time to Hospital versus Survival Status Within 6 Hours After Crash

| Time to Hospital, H | Dead | alive | Total | Alive % S(t) |
|---|---|---|---|---|
| H<=15 | 115 | 152 | 267 | 56.93 |
| 15<H <=30 | 2087 | 2407 | 4494 | 53.56 |
| 30<H<=45 | 3551 | 4432 | 7983 | 55.52 |
| 45<H<=60 | 2972 | 3821 | 6793 | 56.25 |
| 60<H<=90 | 2761 | 3815 | 6576 | 58.01 |
| 91 to 360 | 1039 | 1584 | 2623 | 60.39 |
| Total | 12,525 | 16,211 | 28,736 | 56.41 |

## 4. CORRELATIONS AND RURAL-URBAN COMPARISON

The statistical results yielded from Kaplan-Meier life curves and 2x2 correlation tables, are very useful when examining one single factor a time. However, many factors, such as time of notification, time of arrival, injury severities, person's age, rural/urban areas, etc., may contribute to the fatality status simultaneously. Hence, the focus here is on the correlation between various EMS factors.

### 4.1 Correlation between EMS Factors

Correlations between the factors are commonplace, and earlier notification would normally result in earlier EMS arrival (correlation coefficient of 0.69 from overall rural and urban data of Table 9), and following Table 9 indicates, with several notification time groups, the correlation between notification and arrival.

**Table 9:** Correlation between notification (N) & arrival (A) including urban/rural crashes, inj_sev = 3, 4
(Correlation Coefficient = **0.69**)

| A / N | A<=5 min | 6-10 min | 11-15 min | 16-30 min | 31-45 min | 46-360 min | Total |
|---|---|---|---|---|---|---|---|
| N<=1 | **5424** | **7493** | **3193** | 1991 | 222 | 84 | 18,407 |
| 1<N <=2 | **840** | **2688** | **1387** | 906 | 111 | 22 | 5,954 |
| 2<N<=3 | 306 | 1801 | 1341 | 878 | 109 | 41 | 4,476 |
| 3<N<=5 | 140 | 1641 | 2062 | 1845 | 249 | 53 | 5,990 |
| 5<N<=8 | 1 | 505 | 1508 | 2252 | 353 | 92 | 4,711 |
| 8<N<=15 | 0 | 30 | 543 | 2912 | 968 | 223 | 4,676 |
| 15 -360 | 0 | 4 | 0 | 756 | 1320 | 1770 | 3,850 |
| **Total** | 6711 | 14,162 | 10,034 | 11,540 | 3,332 | 2,285 | 48,064 |

Table 9 (or Figure 5) indicates that the earlier notifications (within 2 minutes) would normally result in EMS arrivals within 15 minutes for 21,025 people (bold number), or 44% of all 48,064 cases.

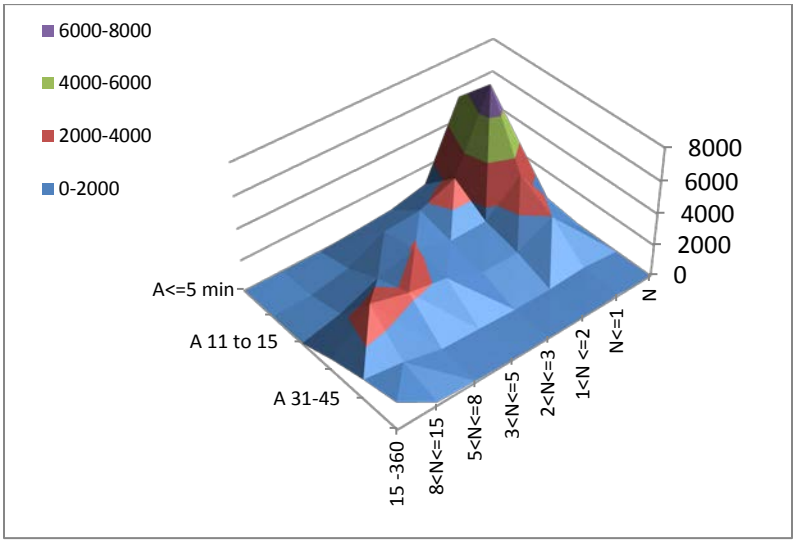


**Figure 5**: Correlation between notification (N) and arrival (A), and inj_sev=3,4

Urban areas, where over 61% of fatalities occurred, may differ in EMS responses, as shown in Table 1 (the average notification time is 7.25 minutes, and 4.61 minutes for rural and urban, respectively). The correlation between notification and arrival in rural area is different as following Table 10.

**Table 10:** Correlation between notification (N) and arrival (A) for rural cases (n=29,560)
(Correlation Coefficient = **0.67**)

| A / N | **A<=5 min** | **6-10 min** | **11-15 min** | 16-30 min | 31-45 min | 46-360 min | Total |
|---|---|---|---|---|---|---|---|
| **N<=1** | **2015** | **3831** | **2283** | 1641 | 204 | 72 | 10046 |
| **1<N <=2** | **311** | **1200** | **977** | 756 | 103 | 32 | 3379 |
| 2<N<=3 | 112 | 823 | 908 | 717 | 99 | 36 | 2695 |
| 3<N<=5 | 60 | 796 | 1332 | 1481 | 211 | 49 | 3929 |
| 5<N<=8 | 1 | 197 | 815 | 1758 | 317 | 89 | 3177 |
| 8<N<=15 | 0 | 12 | 270 | 2057 | 791 | 199 | 3329 |
| 16 -360 | 0 | 1 | 0 | 457 | 1075 | 1472 | 3005 |
| **Total** | 2499 | 6860 | 6585 | 8867 | 2800 | 1939 | **29560** |

Table 10 indicates that earlier notification times (within 2 minutes) would result in 10,617 EMS arrivals within 15 minutes, or approximately 36% of all rural cases of 29,560 (bold, top 2 rows and left three columns). Table 11, using urban area data, indicates that similar earlier notification times (N<=2 minutes) would result in 10,384 EMS arrivals within 15 minutes (approximately 56% of all 18,445 urban cases). Hence, the rate difference of EMS arrivals within 15 minutes is 20% between urban and rural areas from Table 10 and Table 11. The correlation coefficient is 0.70 in urban area and stronger than 0.67 of rural area, and the EMS arrivals in urban area are much quicker than the rural areas.

**Table 11:** Correlation between notification (N) and arrival (A) for urban cases (n=18,445)
(Correlation Coefficient = **0.70)**

| A / N | **A<=5 min** | **6-10 min** | **11-15 min** | 16-30 min | 31-45 min | 46-360 min | Total |
|---|---|---|---|---|---|---|---|
| **N<=1** | **3403** | **3652** | **908** | 345 | 16 | 12 | 8336 |
| **1<N <=2** | **527** | **1484** | **410** | 147 | 8 | 0 | 2576 |
| 2<N<=3 | 194 | 978 | 430 | 161 | 10 | 5 | 1778 |
| 3<N<=5 | 80 | 840 | 724 | 362 | 38 | 4 | 2048 |
| 5<N<=8 | 0 | 306 | 691 | 490 | 35 | 3 | 1525 |
| 8<N<=15 | 0 | 18 | 273 | 853 | 175 | 24 | 1343 |
| 15 -360 | 0 | 3 | 0 | 295 | 245 | 296 | 839 |
| **Total** | 4204 | 7281 | 3436 | 2653 | 527 | 344 | **18445** |

## 4.2 Multiple Relative Hazard Model

The goal of this aspect of the paper is to explore the relative comparison of passenger vehicle occupant survival rates with one risk factor alone or with several risk factors simultaneously. Cox [8] (1972) proposed a model to consider multiple risk factors simultaneously. The hazard function, *h(t)*, was introduced. Note, the hazard and survival probability functions, S(t) such as Figure 3, are closely related to each other, described by " *h(t) = - S'(t) / S(t)* ", where S'(t) is the derivative of S(t) [1 8]. It can be seen that *h(t)* provides the relative change rate of S(t) over time, and *h(t)* reaches a higher positive value when S(t) dropped rapidly during 0-100 minutes after crashes (Fig. 3 and Fig. 4), and *h(t)* remains zero approximately when S(t) changes little beyond 100 minutes after crashes. Cox proposed that the hazard function can be further expressed in Equation (2), known as the Cox Proportional Hazard Model.[8] This model is to establish a relationship between the hazard function with multiple risk factors simultaneously, while the previously discussed Kaplan-Meier curves, S(t), explore a single risk factor only.[7]

In the current study using same data and notification definitions as Table 5 or Figure 4, the Proportional Hazard Model is used to study the effects of EMS notification together with the effects of occupant age and crash location on crash survivability. It may be impossible to include all risk factors in the current study. SAS Proc *PHREG* is used for calculation.[8 10]

$$h(t) = h_0 \exp(\beta_1 Age + \beta_2 Call + \beta_3 Location) \qquad (2)$$

The model included three factors treated as binary variables: age (over 60 or younger), notification time (later than 2 minutes or earlier notification) and crash location (rural versus urban). The results indicate that age and location are not significant risk factor with P-values of 0.13 and 0.27, respectively. Similar to prior findings in this paper, later crash notification (>2 min) could carry a 4% relatively higher fatality hazard than earlier group of 'notification within 2 minutes and call time prior to death time' (Hazard Ratio=1.04, p-value=0.0028). The arrival variable was not used in the above modeling to avoid the collinearity issue, since it is strongly correlated with notification. Many other risk factors, such as crash severity, occupant health condition, EMS arrival and service quality, et. al., may all contribute to the survival status and hazard ratio. Future investigations are needed to explore these issues, as this study focuses mainly on the time-related issue and notification. Of special interest is that the EMS arrival time in rural area (19.64 minutes, Table 1) is approximately 7.5 minutes later than urban area (12.10 minutes), and the correlation coefficient in rural area (0.67) is also weaker than urban area (0.70), however, the mean time to death for both urban and rural areas remain approximately the same (66 minutes), and more investigations would be necessary to explore this rural/urban difference and hazard patterns.

## 5. CONCLUSIONS

EMS data is closely associated with time, and 'time to event' data analysis, or survival analysis, is a suitable approach than some other statistical approaches. While FARS 2009-2012 data had limited information about EMS notification, EMS arrival and time to reach a hospital, the data did suggest certain meaningful patterns and facts:

- Earlier crash notification associated with Automatic Crash Notification (ACN) systems could save approximately 177 to 244 motor vehicle occupant lives per year (approximately 1.5% - 2% fatality reduction) when a time window of six hours after crash is considered, and the research population is targeted at 'Incapacitating Injury' and 'Fatal Injury' only. Meanwhile, many other confounding factors may also contribute to occupant survival probabilities.
- Effective ACN and earlier EMS arrival significantly improve crash survivability, and earlier notification (<=1 or 2 minutes) would generally result in the sooner EMS arrival within 5-15 minutes. Kaplan-Meier curves clearly demonstrate the survival differences of two paired groups whose EMS status differs, for example, the benefits associated with earlier notifications within 1-2 minutes (approximately 1.5- 2% fatality reduction within a timeframe of 6 hours after crash). The fatality reductions or lives potentially saved due to ACN are estimated from cross comparing the survival probabilities of two paired life curves at one specific time after crash.
- We did not discover a significant difference in survivability between age groups, and between urban and rural areas overall. However, the results indicate that there is a strong need to improve the EMS arrivals in rural area where the rate of EMS arrival within 15 minutes is 20% lower than the similar rate in urban area, the correlation coefficient between the notification and arrival is 0.70 in urban area, and 0.67 in rural area. Approximately 61% of fatalities happened in rural areas. Earlier EMS arrival within 5-15 minutes would be desired in both rural and urban areas.
- Correlations among various factors, such as notification time, time of EMS arival, time to hospital, and survival status are commonplace. Most injuries and fatalities occurred within a short time window of 1-100 minutes after crash (86.6% fatalities occurred out of all fatalities within six hours). Earlier notification time within 1-2 minutes would significantly improve survival probability, although many other confounding risk factors may contribute to the occupant survival status. EMS arrival time is very desired as soon as possible (best within 5 minutes), reaching a hospital within 15 minutes is desired, although hospital time data are rather limited in this study, the occupants with hospital arrival have significantly higher survival rates than the other occupants.

## 6. REFERENCES


1. Wu, J., Subramanian, R., Craig, M., Longthorne, A., (August, 2013), The effect of earlier or automatic collision notification on traffic mortality by survival analysis, Traffic Injury Prevention (2013) 14, Taylor & Francis, London, UK.
2. Kanianthra, J., Carter, A., & Preziotti, G., (2001). Enhancing post-crash vehicle safety through an automatic collision notification system. Proceedings of the 17th International Technical Conference on the Enhanced Safety of Vehicles, Amsterdam, The Netherlands.
3. Clark, D. E. and Cushing, B. M. (2002). Predicted effect of automatic crash notification on traffic mortality. Accident Analysis & Prevention 34 (2002) 507-513, Elsevier Science Ltd.
4. Lahausse, J. A., Fildes, B. N., Page, Y., & Fitzharris, M. P., (2008). The potential for automatic crash notification systems to reduce road fatalities. Proceedings of the 52nd Annual Conference of the Association for the Advancement of Automotive Medicine, San Diego, CA.
5. European Commission,(2009). Impact assessment on the introduction of the eCall service in all new type-approved vehicles in Europe, including liability /legal issues. http://ec.europa.eu/information_society/activities/esafety/doc/studies/ecall/ecall_final_report.pdf
6. Toyota (2011). EMS and Notification Study, Centers for Disease Control and Prevention – AACN and Field Triage of Injury Patients Update Meeting, November, 2011, Atlanta, Georgia.
7. Kaplan, E. L. and Meier, P. (1958). Nonparametric estimation from incomplete observations. Journal of the American Statistical Association, 261, 719-724.
8. Cox, D.R. (1972). Regression models and life tables – with discussions. Journal of the Royal Statistical Society, 34, 187-220.
9. Breslow, N. and Day, N. (1987). *Statistical methods in cancer research II: Analysis of cohort studies.* International Agency of Cancer Study, Lyon.
10. Allison, P. (1999), *Applied Survival Analysis using SAS*, SAS Institute, Cary, North Carolina, US.
11. Anders Longthorne, NHTSA (2012), Analysis of the Proximity of Fatal Motor Vehicle Crash Locations to the Availability of Helicopter Emergency Medical Service Response, DOT HS 811 542.


## 7. ACKNOWLEDGEMENT


Review comments from Rajesh Subramanian, Ellen Lee, and Chou-Lin Chen of NHTSA co-workers are appreciated. This paper is a U.S. Government work and may be copied and distributed without permission.

# REAL-WORLD ANALYSIS OF FATAL REAR-END CRASHES

**Christopher Wiacek**
**James Bean**
**Dinesh Sharma**
National Highway Traffic Safety Administration
USA

Paper Number 15-0270

## ABSTRACT

In March 2011, the National Highway Traffic Safety Administration (NHTSA) published its Vehicle Safety Rulemaking and Research Priority Plan 2011 – 2013, which described the projects that are the agency's priority in the rulemaking and research areas in those calendar years. Programs that are priorities or will take significant agency resources included the development of performance criteria and objective tests to support the identification of effective advanced safety technologies that provide a warning of an impending forward collision and/or automatically brake the vehicle.

In support of the Forward Collision Avoidance and Mitigation project listed in the priority plan, an analysis of real-world crash data was conducted to determine the scope of the crash problem and examine the factors that contribute to rear-end crashes in light vehicles. A review of the 2003 – 2012 National Automotive Sampling System-Crashworthiness Data System (NASS-CDS) was conducted for rear-end crashes involving a fatal occupant.

For each crash identified, a review of the accompanying investigation was conducted using a methodology similar to that described by Bean, et al. [2009]. The authors were then able to identify crash characteristics associated with occupants sustaining fatal injuries in rear-end crashes. For each case, primary and secondary factors were assigned as crash attributes which contributed to the fatal injuries to an involved occupant. This review suggests that fatal rear-end crashes are generally attributed to excessive speed at the time of impact. In order to address these crashes with a forward collision avoidance system, a crash alert warning must be timely and any automatic emergency braking must be aggressive to significantly reduce the impact speed to mitigate the severity or prevent the crash from occurring.

## INTRODUCTION

According to NHTSA's Traffic Safety Facts 2012, fatal crashes increased by 3.1 percent from 2011 to 2012, and the fatality rate rose to 1.13 fatalities per 100 million vehicle miles of travel in 2012. The injury rate increased by 6.7 percent from 2011 to 2012, to 80 persons injured per 100 million vehicle miles of travel in 2012. However, the occupant fatality rate (including motorcyclists) per 100,000 population, which declined by 22.7 percent from 1975 to 1992, decreased by 31.1 percent from 1992 to 2012, and the occupant injury rate (including motorcyclists) per 100,000 population, which declined by 13.6 percent from 1988 to 1992, decreased by 37.8 percent from 1992 to 2012. Of the more than 5.6 million police-reported motor vehicle crashes that occurred in the United States in 2012, 29 percent of those crashes (1.63 million) resulted in an injury, and less than 1 percent (30,800) resulted in a death [NHTSA, 2014].

Rear-end type crashes (i.e., front of a motor vehicle striking the rear of another vehicle) are the most frequent first harmful event and account for approximately 33 percent of all crashes including collisions with a motor vehicle in transport, fixed object, non-fixed object and non-collisions such as rollovers. Specifically where the first harmful event was a rear-end crash there were 1,827 fatal, 518,000 injury and 1,327,000 property damage only crashes in 2012 [NHTSA, 2014].

Prior studies have focused on quantifying the size and the identification of trends in rear-ends crashes through the use of descriptive statistics. One study used NHTSA's 1992 – 1996 National Automotive Sampling System-General Estimates System (NASS-GES), which is a weighted sample database of police reported crashes, to identify the relative frequency of 10 major rear-end pre-crash scenarios [Najm, 1998]. Using the coded data, these scenarios identified the pre-crash dynamic state of the involved vehicles by roadway curvature. The rear-end crash data were sorted by injury severity, roadway surface condition and posted speed. The intent of the study was to define the crash problem from a dynamic crash scenario level for safety benefits estimation.

A follow up study analyzed the same NASS-GES years of data, and provided a statistical description of the scenarios discussed in the previous paper [Wiacek, 1999]. The statistics presented encompassed driver characteristics of the following vehicle, including avoidance maneuver attempted before impact, crash contributing factors, driver age, and gender; vehicle body types involved in these rear-end pre-crash scenarios; and initial travel speeds of the following vehicle under various posted speed limits. The results of the study were intended to be useful for estimating the safety benefits of rear-end crash avoidance technologies for crash number reduction and severity mitigation.

These studies have been used to assess the benefits of rear-end crash avoidance technologies, from field operational tests and also as the basis for evaluating these systems in a test environment. An independent evaluation of an Automotive Collision Avoidance System (ACAS) was conducted with vehicles equipped with forward collision warning and adaptive cruise control [Najm, 2006]. The goals of the independent evaluation were to characterize ACAS performance and capability; achieve a detailed understanding of ACAS safety benefits; and assess driver acceptance of ACAS. Utilizing data from the field tests and the crash scenarios defined above, the study estimated that ACAS, as an integrated system of forward collision warning and adaptive cruise control functions, has the potential to prevent about 6 to 15 percent of all rear-end crashes depending on the source of crash data used for safety benefits estimation.

A more recent study that used the NASS-GES data identified and described a new typology of pre-crash scenarios for crash avoidance research [Najm, 2007]. This new typology consists of pre-crash scenarios that depict vehicle movements and dynamics as well as the critical event occurring immediately prior to crashes involving at least one light vehicle. Specifically, the study identified the 37 most frequent crash scenarios; many of these crash types involved rear-end collision scenarios. Of the 37 groupings used to describe the overall distribution of pre-crash scenario types, the Lead-Vehicle-Stopped, Lead-Vehicle-Decelerating, and Lead-Vehicle-Moving-at-Lower-Constant-Speed crashes represented in the 2004 GES data were found to be the 2nd, 4th, and 12th most common crash scenarios overall, respectively, and were the top three rear-end pre-crash scenarios.

The prior studies have been instrumental in developing test procedures to evaluate the forward collision warning systems installed on late-model passenger vehicles. The test maneuvers described were designed to emulate the top three most common rear-end pre-crash scenarios reported in the 2004 NASS-GES data base. The test procedures continue to be the basis for evaluating advanced rear-end crash avoidance technologies, including those that automatically apply the foundation brakes to decelerate the vehicle to avoid or mitigate the severity of a potential crash.

The findings of the studies discussed primarily relied on NASS-GES police accident report based on coded data for high-level understanding of the frequency of rear-end crash specific characteristics. However, a detailed clinical analysis of the rear-end crash environment and injury causation using the NASS-CDS investigation data will help to provide a more thorough understanding and guide system performance to prevent or mitigate the severity of fatal crashes. This crash database is a nationally representative sample of tow-away crashes that occur on U.S. roads. Every year, detailed information on vehicle damage, injury, and injury mechanism is collected on about 4,500 of these light passenger motor vehicle crashes. The data consists of over 600 variables that describe crash events, damage to vehicle, crash forces involved, injuries to the victim and injury causation mechanisms for frontal, side, rear, and rollovers crashes. The work presented in this paper represents one of the steps necessary to better understand the rear-end crash problem.

## METHODOLOGY

Using a technique similar to Bean, et al. [2009], a detailed review of real-world rear-end crashes was conducted where an occupant sustained fatal injuries in an involved vehicle. The review focused on coded and non-coded data (photographs, summaries, crash diagrams, etc.), and resulted in the identification of critical factors contributing to the fatal injuries in rear-end crashes. The cases were selected from the NASS-CDS database for the years 2003 to 2012. The following parameters were required for a crash to be included in the data set:

- The crash was fatal (AIS level 6)
- The crash was coded as forward impact into a parked vehicle, rear-end, or forward impact of vehicles going in the same direction on the same trafficway (accident type 11 or 20-43)
- The subject vehicle (SV) was a passenger vehicle (bodytype 1-49)
- The SV general area of damage in the first crash event was frontal (General area of damage=F for accseq=1)
- The pre-impact location of the SV was "stayed in original travel lane" (preiloc=1)
- The SV pre-event movement was "going straight", "decelerating in traffic lane", "accelerating in traffic lane", "starting in traffic lane", or "passing or overtaking another vehicle" (premove=1,2,3,4, or 6)
- The lead vehicle (LV) preimpact location was "no driver present" or "stayed in original travel lane" (preiloc=0 or 1)
- The LV pre-event movement was "no driver present", "going straight", "decelerating in traffic lane", "accelerating in traffic lane", "starting in traffic lane", "stopped in traffic lane", "passing or overtaking another vehicle", or "disabled or parked in travel lane" (premove 0-7)
- There were no restrictions on restraint use or travel speed

Thirty eight cases that involved 39 fatalities were identified in the data set that met the above criteria. The cases were then divided amongst the authors, who summarized each case using a standard format. The authors then assessed the primary, secondary, and (if applicable) other factors associated with the fatal injury sustained by the vehicle occupant. A factor, in this context, is an event or condition present at or after the time of impact that probably and logically increased the likelihood that this specific impact would be fatal to an occupant. Factors related to the fatality were deemed primary or secondary, depending on the nature of their causative effects. The distinction between primary and secondary factors is similar to what was described by Rudd, et al. [2009].

The following section provides descriptions of the factors associated with injury causation assigned to the crashes in this data set:

**Improperly Restrained Occupant:** The occupant's injuries were directly associated with not utilizing the restraint system (i.e., seat belt) provided in the vehicle and/or the vehicle may not have been equipped with an air bag at the seating position in question. For nearly every occupant that was classified as being improperly restrained, the crash severity was deemed to be survivable.

**Medical Condition:** The driver of the subject vehicle lost consciousness just prior to the event because of an identified medical problem.

**Speed of Striking Vehicle:** The velocity of the subject vehicle at the time of impact (i.e., closing speed) was identified to have contributed to a high change in velocity and subsequent fatal injuries for an involved vehicle.

**Second Event the Most Harmful Event:** The primary source of the occupant's fatal injury was not directly attributed to the first event which was the rear-end impact. However, the fatal injury was attributed to a more harmful event that occurred directly after the initial rear-end impact.

**Multiple Vehicles Involved:** For an involved vehicle, the fatal injuries sustained by an occupant were attributed to the nature of the crash involving multiple impacts with multiple vehicles. For example, the subject vehicle was first involved in a minor rear-end crash by impacting a lead vehicle, however, it was subsequently impacted in the rear, which contributed to the fatal injuries.

**Post-Crash Fire:** The subject vehicle sustained a post-crash fire resulting from the rear-end impact, which caused or contributed to the fatal injuries. Generally, the crash severity as measured by rear-end crush was significant.

**Struck Vehicle Comparable Size or Smaller:** The NASS-CDS coded mass of the struck vehicle was either similar or less than the striking vehicle in the crash. This factor attempts to identify crashes where mass incompatibility between the striking and struck vehicle contributed to the severity of the crash outcome for the struck vehicle.

**Truck-Trailer Underride:** The striking subject vehicle experienced severe underride with intrusion extending generally into the greenhouse area of its occupant compartment, leading to fatal injuries. For the cases reviewed in this study, the type of rear-impact guards present on the trailers was unknown, and there was likewise no measure of their performance in the crash. The key is poor structural interaction with the crash partner.

**Alcohol Involvement:** The driver of an involved striking vehicle was determined to have had high Blood Alcohol Concentrations (BAC). This was only assigned as a factor if it was determined that alcohol consumption contributed to the cause of the crash, such as when the striking vehicle driver was under the influence of alcohol. When the BAC was known, it was well above the 0.08 legal limit.

Given the case-review nature of this work, no statistical analyses have been performed on the data, and no assessment of injury risk can be performed since case weights were not used.

## RESULTS

The cases were first grouped by common factors that were assessed to have been relevant to the severity of all the rear-end crashes reviewed. A high-level grouping of the factors for all the cases is presented in Table 1. For all the fatal cases analyzed, the primary factor associated with 27 of the 38 cases reviewed was the Speed of the Striking Vehicle. This was assessed to be the most frequent primary factor in the fatal crash event. For all the crashes, the most frequently occurring secondary factor was Struck Vehicle Comparable Size or Smaller followed by Truck-Trailer Underride. Lastly, alcohol involvement was identified in 14 of the cases.

**Table 1.**
**Summary of Rear-End Crashes by Factor.**

| Factor | Primary Factor | Secondary Factors | Other Factor | Totals |
|---|---|---|---|---|
| Improperly Restrained Occupant | 4 | 0 | 1 | 5 |
| Medical Condition | 1 | 0 | 0 | 1 |
| Speed of Striking Vehicle | 27 | 0 | 0 | 27 |
| Second Event the Most Harmful Event | 6 | 0 | 0 | 6 |
| Multiple Vehicles Involved | 0 | 0 | 4 | 4 |
| Post-Crash Fire | 0 | 0 | 3 | 3 |
| Struck Vehicle Comparable Size or Smaller | 0 | 18 | 0 | 18 |
| Truck-Trailer Underride | 0 | 13 | 1 | 14 |
| Alcohol Involvement | 0 | 3 | 11 | 14 |

What follows is a more detailed analysis of the primary and secondary factors, and the corresponding crash characteristics and associated injury. A summary of the data is presented in Table 2 and a summary of all of the factors associated with each individual case involved in this assessment is provided in the Appendix.

**Table 2.**
**Rear-End Crash Grouped by Common Primary and Secondary Factors.**

| Primary Factor | Secondary Factor | Cases |
|---|---|---|
| Speed of Striking Vehicle | Struck Vehicle Comparable Size or Smaller | 14 |
| Speed of Striking Vehicle | Truck-Trailer Underride | 13 |
| Second Event the Most Harmful Event | NA | 6 |
| Improperly Restrained Occupant | Struck Vehicle Comparable Size or Smaller | 4 |
| Medical Condition | NA | 1 |

**Fatal Occupant in Lead Vehicle Struck by a Similar or Larger Vehicle**

The most frequently occurring primary and secondary factor combination was the Speed of Striking Vehicle and Struck Vehicle Comparable Size or Smaller. This combination accounted for 14 of the cases reviewed. In these cases, the striking vehicle, impacted a vehicle with a similar mass or smaller at a high rate of speed. In this grouping, the fatal occupants were always in the struck vehicle. In these types of crashes the fatally injured occupant in the struck vehicle generally sustained head and/or neck injuries such as a brain stem laceration or cervical spine cord laceration sourced to the head restraint. In all but two crashes, the fatality was in the front seat. In Case Nos. 2006-9-168 and 2007-41-38 the fatal occupant was in the rear. It should be noted that in both of these crashes, the front occupants sustained moderate to minor injuries. The photos in Figure 1 illustrate the severity of the impacts.

***Figure1. NASS-CDS Case No. 2006-9-168 Struck Vehicle (left) and Case No. 2007-41-38 Struck Vehicle (right).***

For this type of crash, on average, the severity as measured by the NASS-CDS estimated Delta-V for the striking and struck vehicle was 46 km/h and 62 km/h, respectively. On average the striking vehicle was 400 kg heavier than the struck vehicle. The highest mass differential was 1,296 kg. The average maximum measured crush for the struck vehicle was 122 cm. It should also be noted that three cases involved a post-crash fire in the struck vehicle resulting in fatal burns. For the two crashes where the crush was measured, the maximum crush was 121 cm and 123 cm (Case Nos. 2006-2-12 and 2008-79-62).

The injuries for the striking vehicle were generally minor, especially when the occupant(s) were properly restrained and the vehicle was equipped with frontal air bags. Most occupants sustained minor bruising or abrasions. In five crashes there were no reported injuries in the striking vehicle. On average the Delta-V for the striking vehicle was 46 km/h, which is lower than the NHTSA's New Car Assessments Program's frontal crash test speed that results in a 56 km/h Delta-V.

In five cases, alcohol was involved for the driver of the striking vehicle, and it was also reported to be dark out in 11 cases. Lastly, for eight cases, it was reported that the lead vehicle was stopped prior to impact.

An example of this crash type is Case No. 2007-82-15. A 1994 Geo Prism (1,065 kg) was disabled and stopped in the same lane ahead of a 2002 Jeep Liberty (1,912 kg). The front of the Jeep impacted the back of the Geo resulting in 127 cm of crush in the rear (Figure 2.) For both of these vehicles the Delta-V was not computed. However, the maximum frontal crush measured on the Jeep was only 10 cm. The posted speed on the roadway was 97 km/h. The driver of Geo sustained a fatal brain stem laceration sourced to the head restraint, and the front passenger sustained a flailed chest sourced to the seat. The crash occurred at 03:44 with the conditions being coded as dark but lighted and with clear atmospheric conditions. The driver of the striking vehicle had a 0.08 BAC.

***Figure 2. NASS-CDS Case No. 2007-82-15 Struck Vehicle (left) and Striking Vehicle (right).***

**Fatal Occupant in Striking Vehicle Impacting Heavy Vehicle**

The second most frequently occurring primary and secondary factor combination was the Speed of Striking Vehicle and Truck-Trailer underride. This combination accounted for 13 of the 38 cases reviewed. In all of these cases, the striking vehicles were traveling at a high rate of speed and impacted the rear of a large truck and/or trailer where the driver of the striking vehicle sustained the fatal injuries. It was generally observed that speed along with insufficient structural interaction between the two vehicles resulted in underride and significant intrusion into the occupant compartment. For these crashes the severity as measured by the change in velocity (Delta-V) was not computed by NASS-CDS due to the crash being out of scope of the computing software. In this type of crash, the striking vehicle's driver sustained fatal injuries that were sourced to the intruding interior components or direct contact with the rear surface of the truck-trailer. Of the cases reviewed, it was found that for five of the 13 crashes the drivers of the striking vehicle had an elevated BAC. Seven cases occurred when it was dark. In eight of the cases, the struck vehicle was coded as stopped. In these cases, there was a significant speed differential between the vehicles at the time of impact.

For example, in Case No. 2003-73-129, a 1989 Chevrolet Cavalier impacted the rear of a 1998 International truck tractor pulling a trailer, which was slowing due to traffic congestion. The time of the crash was reported as 06:44 where it was dark and no adverse atmospheric-related driving conditions. The driver of the Chevrolet sustained a brain stem laceration sourced to direct contact with the rear of the struck vehicle. Figure 3 illustrates the severity of the damage to the striking vehicle.

***Figure 3. NASS-CDS Case No. 2003-73-129.***

**Second Event Was the Most Harmful Event**

Six cases were classified with a primary factor of the Second Event was the Most Harmful Event. For these cases the most harmful event that resulted in the fatal injuries was preceded by a minor rear-end impact. In five of the six cases, the most harmful event was a subsequent rollover, and one case resulted in a front-to-front head on impact with another vehicle. Of the five rollover crashes, three occupants were ejected. All but one crash occurred when it was dark out, and in two cases the driver of the striking vehicle had an elevated BAC. None of the struck vehicles was coded as stopped.

For two of the cases (Nos. 2006-81-79 and 2009-72-43), the striking vehicle was attempting to change lanes when it struck the rear of a lead vehicle resulting in a loss of control for an involved vehicle. The loss of control resulted in a rollover and ejection of an occupant causing fatal injuries. In Case No. 2006-81-79, the ejected occupant was the unrestrained driver of the striking vehicle and in Case No. 2009-72-43, the rear seat unrestrained occupant of the struck vehicle was ejected.

For example, in Case No. 2007-50-006, a 2007 Chevrolet Impala was traveling south on a urban roadway. A 2003 Mazda Pickup was traveling south in front of the Chevrolet on same roadway. The front of the Chevrolet contacted the back of the Mazda. The Chevrolet appeared to have lost control, departed the roadway, struck a utility pole, and rolled over. The crash occurred at 16:38. It was daylight but raining. The unrestrained driver of the striking vehicle (Figure 4) sustained a fatal brain stem laceration. It was unknown if the front seat passenger was restrained, but the occupant sustained only minor abrasions. The frontal air bags deployed in the event. No injuries were reported for the driver of the struck vehicle. As Figure 4 shows, there was negligible damage to the Mazda.

***Figure 4. NASS-CDS Case No. 2007-50-6 Striking Vehicle (left) and Struck Vehicle (right).***

Case No. 2006-49-23, was unique in that the fatal occupant was not involved in the initial rear-end impact. A 1998 Ford Windstar impacted the rear of a 2002 Toyota Corolla. The Ford, after impacting the Toyota, drove off of the roadway to the left and across the median into oncoming traffic. A 2003 Nissan Altima was traveling in the opposite direction. The front of the Ford impacted the front of the Nissan. The driver of the Nissan sustained fatal brain stem injuries (Figure 5). The driver of the Ford also sustained serious head injuries.

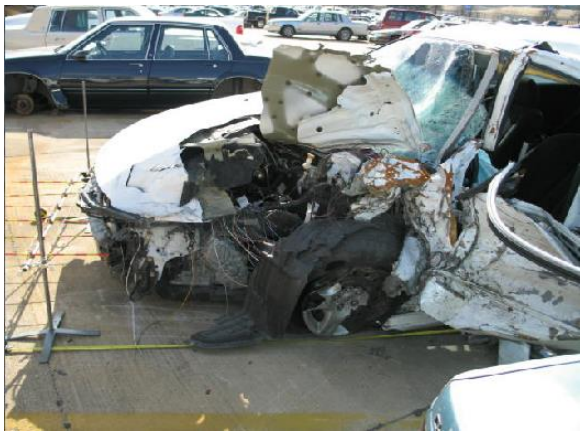

***Figure 5. NASS-CDS Case No. 2006-48-23 Other Vehicle.***

After assessing these cases, it was determined that if not for the rear-end impact, an involved vehicle would not have experienced the second event which resulted in the fatal injuries.

**Improperly Restrained Occupant**

Of the 38 cases analyzed, four were identified by the primary and secondary factors of Improperly Restrained Occupant and Struck Vehicle Comparable Size or Smaller. In these cases, the fatal occupant was in the striking vehicle. It was assessed that based upon the crash severity as measured by Delta-V and the crush on the striking vehicle, if the occupant was properly restrained with a lap and shoulder belt and the vehicle had frontal air bags the occupant would have likely survived the event. For all the crashes where it was computed, the estimated Delta-V for the striking vehicles was approximately 56 km/h or below. In all cases, the fatal front seat occupant sustained a severe brain stem injury. Three out of the four crashes occurred when it was dark out. Only one crash involved alcohol use for the driver of the striking vehicle.

In Case No. 2003-12-199, the fatal occupant was the front seat passenger and the vehicle was not equipped with a passenger side frontal air bag and the seat belt was not used. The passenger sustained fatal head injuries from contact with the windshield. However, the driver, who was restrained, only sustained minor skin abrasions. In Case No. 2003-49-133, the driver was wearing a seat belt at the time of the crash but the vehicle was not equipped with a frontal air bag. The driver sustained fatal head injuries from contact with the steering wheel.

Case No 2012-11-112, is an example of a multi-vehicle crash where the striking 2003 Dodge Ram impacted a stopped 2001 Hyundai Santa Fe, which then struck a stopped 2000 Freightliner. The crash occurred at 07:55 on a clear day. The severe impact resulted in a Delta-V of 60 km/h for the Dodge and 86 km/h for the Hyundai.

The unrestrained driver of the Dodge sustained brain stem injuries sourced to the steering wheel. The frontal air bags in the vehicle did not deploy. It should be noted that the 60 km/h Delta-V may overestimate the severity of the impact especially after observing the crush in Figure 6. Max crush was measured to be 34 cm but it was not uniform across the bumper.

The injuries for the Hyundai's front occupants were not coded. It is only noted in the case that they were incapacitating injuries. Given the severe nature of this crash for the Hyundai, even though the occupants did not sustain fatal injuries, the crash is consistent with the Fatal Occupant in Lead Vehicle Struck by a Larger Vehicle category discussed above. The severity was also aggravated by the Hyundai impacting the rear of a larger vehicle after being struck by the Dodge. It should be noted that in some multi-vehicle crashes the crash severity is

intensified because the struck vehicle is not pushed out of the way but is constrained by a vehicle it impacted. This leads to the vehicle having to absorb more of the crash forces.

***Figure 6. NASS-CDS Case No. 2012-11-112 Striking Vehicle (left) and Struck Vehicle (right).***

**Medical Condition**

In one relatively minor crash (Case No. 2009-79-44) an 84-year old unrestrained driver of a striking vehicle sustained fatal cervical spine injuries. However, according to the supplemental information associated with the case, there was a possibility that the driver of the striking vehicle suffered a stroke (cerebrovascular accident with infarct and hemorrhage) that led to the rear-end vehicle crash. There was no evidence of braking at the scene and no avoidance maneuver was attempted by the driver.

**DISCUSSION**

**Fatal Occupant in Lead Vehicle Struck by a Similar or Larger Vehicle**

Generally, in this rear-end crash type that resulted in a fatality in the struck vehicle, impact speed and mass were significant contributors to the amount of crush in the subject vehicle. The data showed on average the maximum measured crush for the struck vehicle was 122 cm and one case the vehicle experienced 155 cm of crush (Case No. 2011-49-41).

To understand the severity of these crashes, limited data was reviewed from crash tests that were conducted in accordance to the FMVSS No. 301 "Fuel system integrity" test procedure. NHTSA had conducted a number of crash tests on vehicles manufactured after 2005. The FMVSS No. 301 test specifies that the stationary test vehicle is impacted in the rear by a 1,367 kg deformable barrier, with a 70 percent overlap at, 80 km/h. The test does not specify that the maximum crush is measured post-impact. However, in 38 tests for which the vehicle crush was recorded for research purposes, the maximum crush varied from 11 cm for 2008 Volkswagen Touareg to 84.4 cm for 2013 Toyota Avalon Hybrid. The average maximum crush from all vehicles in the tests was 52.7 cm.

The crush in the rear-end fatal crashes on average is double the amount of maximum crush as measured in the FMVSS No. 301 test condition. It also should be mentioned that in eight of the 15 crashes the lead vehicle was stopped, which is consistent with FMVSS No. 301 test procedure. These crashes are thus exceedingly severe in nature, meaning that for a forward collision avoidance system to be effective, the alert would need to be timed to warn the driver early enough to significantly reduce the travel speed. Similarly, an automatic emergency braking system would need to be aggressive enough to reduce the travel speed to either prevent the crash from occurring or to reduce the impact severity well below the NASS-CDS estimated Delta-V of 62 km/h for the struck vehicle in this analysis.

**Fatal Occupant in Striking Vehicle Impacting Heavy Vehicle**

Rear-end crashes that involve a light vehicle striking a large tractor-trailer combination vehicle at a high rate of speed are generally characterized by the severity of the upper-body intrusion in the striking vehicle and serious head injury often attributed to direct contact with the struck vehicle. There also is an apparent lack of structural engagement between the two vehicles. It would also appear that in these crashes, if an underride guard was present, it could not withstand the force of the crash, leading to the rear of the heavy vehicle interacting with the A-pillar and upper compartment of the striking vehicle. This crash type has been identified in a prior analysis but not in the context of rear-end crashes (Bean, 2009). This crash type composed almost half of the cases analyzed.

There are a number of considerations to be examined from the perspective of utilizing rear-end crash avoidance technologies and determining the potential benefits. Five of the 13 drivers of the striking vehicle had an elevated BAC, seven cases occurred when it was dark and the struck vehicle was coded as stopped in eight of the cases. For intoxicated drivers, it is unknown how effective a warning may be. However, these systems would need to be robust enough to track a stopped or slowing vehicle in the night at a high rate of speed. In order to have changed the outcome of these particular crashes, automatic emergency braking systems would need to properly identify a stopped large truck sitting higher off the ground with a large rear overhang and underride guard, and have sufficient authority to mitigate or prevent the crash. The system would require enough braking authority to avoid the crash even if the driver is intoxicated; i.e., be able to intervene without driver action or involvement.

**Second Event was the Most Harmful Event**

These particular crashes were of interest because an initial rear-end impact set off a series of events that resulted in a fatality in an involved vehicle. Generally the rear-end crash was minor but still significant enough for an involved vehicle to lose control, which in turn led to a more harmful event. In five of the six cases, the initial rear-end impact led to a rollover. Whether the fatality was in the struck or striking vehicle was a matter of circumstance at the time of the crash. Of importance was the fact that, if not for the initial minor rear-end impact, the more harmful event would not have occurred. From a benefits standpoint, a rear-end crash avoidance system could be effective in preventing the initial rear-end crash, and thus the more harmful event.

**Improperly Restrained Occupant**

For all the crashes where it was assessed that the occupant sustained fatal injuries because the occupant was improperly restrained, the crash was likely survivable. In Case Nos. 2003-12-199 and 2003-49-133, because the vehicles were older and not designed to the current FMVSS, the occupants were not afforded the protection from frontal air bags. For occupants not wearing a lap and shoulder belt, it is not known how a rear-end crash avoidance warning and an automatic emergency braking system would have changed the outcome of the crash. A warning would have had to be extremely effective in causing the driver to react to prevent the crash from occurring as would an automatic emergency braking system. Even with an automatic emergency braking system that reduced the speed at impact, an occupant could still sustain serious injuries if not properly restrained. The estimated Delta-V for the striking vehicles was approximately 56 km/h or below for these crashes. For these reasons it is unknown how a crash avoidance system will predictably reduce injury levels unless the crash is avoided entirely.

**Medical Condition**

Only one case **(**Case No. 2009-79-44) was identified where a medical condition caused a minor crash where the occupant sustained fatal injuries. This case is noted only because this type of crash, though rare, does occur in the real-world. When assessing potential benefits of rear-end crash avoidance systems, various medical conditions can potentially cause a driver to lose consciousness and cause a crash, in which case a crash avoidance alert may be ineffective. However there may be some benefit for systems with automatic emergency braking that will prevent the crash or reduce the overall severity.

**EDR NASS-CDS Analysis**

A supplemental analysis of the NASS-CDS data was conducted to better understand the pre-crash dynamic states of the involved vehicles in rear-end crashes. Cases were selected where both the striking and struck vehicles were equipped with an Event Data Recorder (EDR). There were no other constraints placed on the case selection such as belt usage or injury severity. For the fatal cases, there was a very limited amount of EDR data available for the involved vehicles because they were generally not equipped with the device and the analysis had to rely on the coded or computed data from the investigation. This analysis attempts to better understand (1) pre-crash relative speed prior to impact, (2) if the striking vehicle's driver made any avoidance maneuver (such as braking), and (3) if the struck vehicle was stopped or decelerating to a stop prior to impact, and compares the data to how they were coded by the NASS-CDS investigator.

An EDR generally captures approximately five seconds of data prior to algorithm enable (AE) and approximately one hundred milliseconds or more during a crash. AE generally activates at the onset of a crash. An EDR reports AE as T-0 of a crash event and subsequently reports the pre-crash data such as vehicle speed and brake activation status from that reference and generally at one second increments prior to AE. After the crash, the EDR will capture the severity of the event as longitudinal Delta-V in the case of front-to-rear crashes.

The cases were analyzed using a common approach and similar format to the fatal cases. An initial cut of the 2003 through 2012 NASS-CDS data identified 29 cases with paired EDR data for both the striking and struck vehicles. A lot of focus was placed on assessing the EDR data for both vehicles to verify that the data were captured in the relevant crashes. For example, the air bags would likely not deploy in the struck vehicle. In this vehicle, the EDR may have captured data, but because the air bags did not deploy, the data were not locked and could have been overwritten by the time the investigation was conducted. The data captured needed to make sense in the context of the physical evidence from the investigation.

After an assessment of the EDR data, 19 cases were verified to have relevant data for both the struck and striking vehicles. The following is a summary of the results from the analysis:

- Average. Longitudinal Delta-V for striking vehicle was 19 km/h
    - Frontal air bag deployed in 10 crashes for the striking vehicle
- Average: Longitudinal Delta-V for struck vehicle, when known, was 17 km/h
- Average relative speed at T-1 with respect to AE prior to impact was 45 km/h
- In 8 cases the striking driver did not brake prior to impact, or AE
- In 7 cases the striking driver was braking prior to impact (longer than one second prior to AE)
- In 4 cases the striking driver applied the brakes at T-1 but not earlier
- In 1 case the struck lead vehicle was accelerating from a stop
- In 3 cases the struck lead vehicle was decelerating to a stop than impacted
    - NASS-CDS reported 2 cases where the struck vehicle was stopped
    - NASS-CDS reported 1 case where the struck vehicle was decelerating
- In 2 cases the struck lead vehicle was stopped
    - NASS-CDS reported both vehicles as stopped
- In 13 cases lead vehicle was decelerating
    - NASS-CDS reported 7 cases where the lead vehicle was stopped

The EDR vehicle speed and Delta-V data collected from these crashes suggest these were generally low severity events, which were further verified from the coded injury data. Almost all of the crashes occurred at a posted speed of 72 km/h or below. Only one AIS 3 wrist fracture injury was reported. For all other cases, injuries were either coded as unknown (not reported) or no injuries.

Of interest were the cases where the EDR data showed the struck lead vehicle was decelerating to a slower speed or decelerating to a stop at impact and NASS-CDS coded the vehicle as stopped. In a majority of the cases the driver of the striking vehicle did not brake or braked late prior to impact.

This analysis was conducted with the limited EDR data available. This analysis should be revisited when more paired EDR cases are available. Figure 7 plots the severity of the event for the struck vehicle. In 10 of the cases, the EDR did not record Delta-V. This is likely attributed to the way the EDR was designed, waking up from the impact but the crash was not severe enough to record Delta-V or of the type to deploy the frontal air bags since the vehicle was impact in the rear. Only pre-crash information was recorded. From the available data, the most frequent change in velocity range was between 9 km/h and 16 km/h, in four cases.

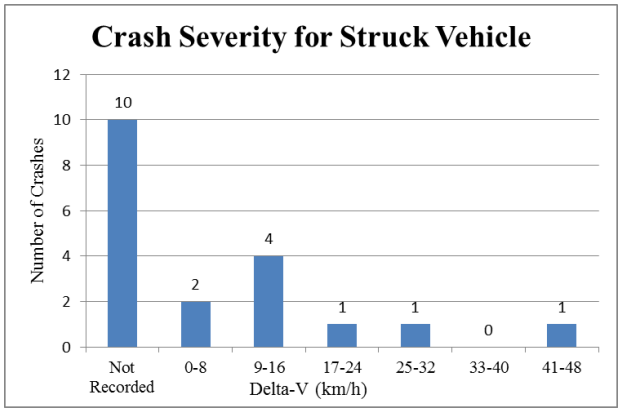


***Figure 7. EDR-Captured Crash Severity for Struck Vehicle.***

For the striking vehicle, all EDRs recorded a Delta-V (Figure 8). All the vehicles sustained a Delta-V at or below 56 km/h with 15 vehicles experiencing a Delta-V between 9 km/h and 40 km/h. When compared to the NCAP frontal crash Delta-V of 56 km/h, the crashes were of a low to moderate severity impact. This is also consistent with the low level of injuries experienced by the occupants.

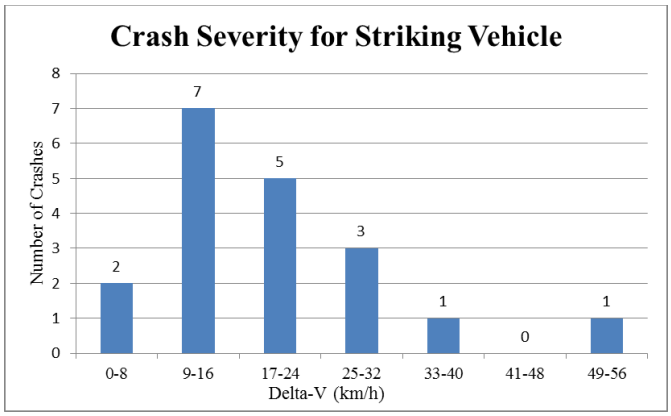


***Figure 8. EDR-Captured Crash Severity for Striking Vehicle.***

Of importance is the relative impact speed between the striking and struck vehicles (closing speed) when considering test conditions to measure the effectiveness of forward crash avoidance system with automatic emergency braking. The vehicle velocity used in this analysis was the vehicle speed captured by the EDR at T-1 second prior to AE. From Figure 9, all but one of the crashes occurred at closing speeds below 80 km/h. A majority of the crashes occurred with a relative impact speed of between 33 and 56 km/h. Again, this is limited data, but at these speeds, occupants in the vehicles were not injured. In Case No. 2006-12-123 where the relative impact speed was 102 km/h, the EDR captured Delta-V for the striking and struck vehicle were 51 and 48 km/h, respectively. The occupants of both vehicles sustained only minor injuries. To bound this discussion, in the crashes where the primary and secondary factor were the Speed of Striking Vehicle and Struck Vehicle Comparable Size or Smaller, on average the Delta-V resulting in the fatal injuries for the struck vehicle was 62 km/h.

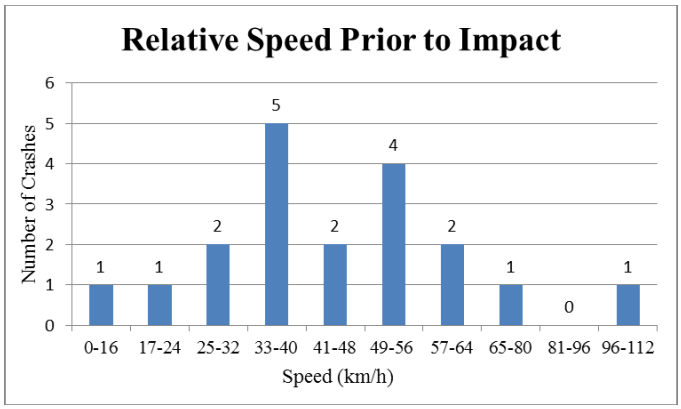


***Figure 9. EDR-Captured Relative Speed Prior to Impact.***

**CONCLUSION**

This paper did not focus on crash causation except to note alcohol involvement as a factor and the one case where a medical condition apparently caused the fatal crash. When reviewing these cases, it was initially concluded for every case except for those mentioned above, it appeared driver inattention or distraction was the likely cause of these fatal crashes. Given the frequency it was decided that the factors should focus on vehicle attributes and crash dynamics contributing to the fatal crash. This approach would also compliment the prior studies discussed earlier by providing a more detailed analysis of the fatal real-end crash problem.

This analysis showed, for a properly restrained occupant to sustain fatal injuries in a rear-end impact the striking vehicle must impact the struck vehicle at an excessive relative speed resulting in a high Delta-V. Which vehicle sustains the fatality is generally a factor of size and mass difference between the involved vehicles. The fatality was shown to occur in the striking vehicle when it impacts a large truck. Conversely the fatality is in a smaller struck vehicle when impacted by a larger vehicle at a high rate of speed. In general, for all of the crashes analyzed the fatal occupant sustained fatal head injuries in the smaller vehicle. It should also be noted that minor rear-end crashes can cause a loss of control for an involved vehicle resulting in a second, more harmful event such as a rollover.

The EDR data provided insight into the vehicle dynamics of rear-end crashes. The crashes were generally not severe and involved property damage only. It is recognized that the data analyzed was limited, but this analysis should be expanded as more paired EDR data is available. However, the data does provide some initial baseline conditions for an average rear-end crash and further evidence that the fatal rear-end crashes are extremely aggressive events. The results of this analysis could be used to assess the performance of vehicles equipped with advanced rear-end crash avoidance technologies and estimate the safety benefits in the real-world.

Lastly, what the analysis identified was fatal rear-end crashes are generally attributed to excessive speed at the time of impact. In order to address these crashes in the real-world, a forward collision avoidance system must provide a timely alert and automatic emergency braking must be aggressive to significantly reduce the impact speed to mitigate the severity or prevent the crash from occurring.

**REFERENCES**

1. NHTSA Vehicle Safety and Fuel Economy Rulemaking and Research Priority Plan 2011-2013, National Highway Traffic Safety Administration, March 2011
2. Bean, James D., et al., Fatalities in Frontal Crashes Despite Seat Belts and Air Bags, DOT HS 811 202, National Highway Traffic Safety Administration, Washington, DC, 2009.
3. Traffic Safety Facts 2012, National Highway Traffic Safety Administration, DOT HS 812 032, 2014
4. Najm, Wassim G., et al., Identification of Precrash Scenarios for Estimating The Safety Benefits of Rear-End Crash Collision Avoidance Systems, 5th World Congress on Intelligent Transportation Systems, Seoul Korea, 1998.
5. Wiacek, Christopher J., and Najm, Wassim G., Driver/Vehicle Characteristics in Rear-End Prescrash Scenarios Based on the General Estimates System (GES), Society of Automotive Engineers, 1999-01-0817, 1999
6. Najm, Wassim G., et al., Pre-Crash Scenario Typology for Crash Avoidance Research, DOT HS 810 767, April 2007
7. Najm, Wassim G., et al., Evaluation of an Automotive Rear-End Collision Avoidance System, DOT-VNTSC-NHTSA-06-01, March 2006
8. Forkenbrock, Garrick J. and O'Harra, Bryan C., A Forward Collision Warning (FCW) Performance Evaluation, 21st International Technical Conference on the Enhanced Safety of Vehicles, Paper No. 09-0561, 2009
9. Rudd, R.W., Bean, J., Cuentas, C., Kahane, C.J., Mynatt, M. and Wiacek, C., A Study of the Factors Affecting Fatalities of Air Bag and Belt-restrained Occupants in Frontal Crashes, 21st International Technical Conference on the Enhanced Safety of Vehicles, paper number 09-0555, 2009

## Appendix

| NASS-CDS Case No. | Primary Factor | Secondary Factor | Other Factor(s) |
|---|---|---|---|
| 2003-49-133 | Improperly Restrained Occupant | Struck Vehicle Comparble Size or Smaller | Alcohol Involved<br>Truck-Trailer Underride |
| 2003-12-199 | Improperly Restrained Occupant | Struck Vehicle Comparble Size or Smaller | |
| 2012-11-112 | Improperly Restrained Occupant | Struck Vehicle Comparble Size or Smaller | Multiple Vehicles Involved |
| 2012-49-36 | Improperly Restrained Occupant | Struck Vehicle Comparble Size or Smaller | |
| 2009-79-44 | Medical Condition | | |
| 2006-49-123 | Second Event the Most Harmful Event (Rollover) | Alcohol Involvement | |
| 2007-50-6 | Second Event the Most Harmful Event (Rollover) | Alcohol Involvement | |
| 2006-49-23 | Second Event the Most Harmful Event (Head on impact) | | |
| 2009-4-166 | Second Event the Most Harmful Event (Rollover) | | |
| 2009-72-43 | Second Event the Most Harmful Event (Rollover) | | |
| 2006-81-79 | Second Event the Most Harmful Event (Rollover) | Alcohol Involvement | |
| 2003-74-130 | Speed of Striking Vehicle | Struck Vehicle Comparble Size or Smaller | Alcohol Involvement |
| 2006-49-120 | Speed of Striking Vehicle | Struck Vehicle Comparble Size or Smaller | Alcohol Involvement |
| 2006-50-105 | Speed of Striking Vehicle | Struck Vehicle Comparble Size or Smaller | Alcohol Involvement |
| 2011-49-41 | Speed of Striking Vehicle | Struck Vehicle Comparble Size or Smaller | Muliple Vehicles Involved<br>Alcohol Involved |
| 2012-9-72 | Speed of Striking Vehicle | Struck Vehicle Comparble Size or Smaller | Alcohol Involvement |
| 2010-82-137 | Speed of Striking Vehicle | Struck Vehicle Comparble Size or Smaller | Multiple Vehicle Involved |
| 2006-2-12 | Speed of Striking Vehicle | Struck Vehicle Comparble Size or Smaller | Post Crash Fire |
| 2006-3-49 | Speed of Striking Vehicle | Struck Vehicle Comparble Size or Smaller | Post Crash Fire |
| 2008-79-62 | Speed of Striking Vehicle | Struck Vehicle Comparble Size or Smaller | Muliple Vehicles Involved<br>Post Crash Fire |
| 2006-9-168 | Speed of Striking Vehicle | Struck Vehicle Comparble Size or Smaller | |
| 2005-50-116 | Speed of Striking Vehicle | Struck Vehicle Comparble Size or Smaller | |
| 2007-41-38 | Speed of Striking Vehicle | Struck Vehicle Comparble Size or Smaller | |
| 2007-82-15 | Speed of Striking Vehicle | Struck Vehicle Comparble Size or Smaller | |
| 2010-79-89 | Speed of Striking Vehicle | Struck Vehicle Comparble Size or Smaller | |
| 2003-73-129 | Speed of Striking Vehicle | Truck-Trailer Underride | |
| 2005-72-129 | Speed of Striking Vehicle | Truck-Trailer Underride | |
| 2005-81-48 | Speed of Striking Vehicle | Truck-Trailer Underride | |
| 2005-9-189 | Speed of Striking Vehicle | Truck-Trailer Underride | |
| 2006-48-161 | Speed of Striking Vehicle | Truck-Trailer Underride | Alcohol Involved |
| 2007-50-108 | Speed of Striking Vehicle | Truck-Trailer Underride | Alcohol Involved |
| 2007-73-37 | Speed of Striking Vehicle | Truck-Trailer Underride | Alcohol Involved |
| 2009-49-178 | Speed of Striking Vehicle | Truck-Trailer Underride | Alcohol Involved |
| 2009-73-144 | Speed of Striking Vehicle | Truck-Trailer Underride | |
| 2009-9-99 | Speed of Striking Vehicle | Truck-Trailer Underride | |
| 2010-11-240 | Speed of Striking Vehicle | Truck-Trailer Underride | Alcohol Involved |
| 2012-49-160 | Speed of Striking Vehicle | Truck-Trailer Underride | |
| 2011-73-83 | Speed of Striking Vehicle | Truck-Trailer Underride | Improperly Restrained Occupant |

# COMPARISON OF HIC AND BrIC HEAD INJURY RISK IN IIHS FRONTAL CRASH TESTS TO REAL-WORLD HEAD INJURIES

**Becky Mueller**
**Anna MacAlister**
**Joe Nolan**
**David Zuby**
Insurance Institute for Highway Safety
United States

Paper Number 15-0272

## ABSTRACT

The Insurance Institute for Highway Safety (IIHS) has been measuring head injury criterion (HIC), a measure based on linear impact skull fracture data, to assess head injury risk in its front crash tests since 1995. In 2012, IIHS added instrumentation to measure brain injury criterion (BrIC), a rotationally based injury measure derived from animal data correlated to humans through computational modeling. BrIC is intended to complement HIC rather than replace it. Head injury risk associated with HIC and BrIC values measured with a Hybrid III dummy in 138 front crash tests was compared with real-world injury rates in similar frontal crash configurations calculated from the National Automotive Sampling System Crashworthiness Data System (NASS CDS) database.

NASS CDS identified 1.3-5 percent AIS3+ head injury rates in crashes similar to the test configurations. The mechanisms of injury represented by HIC and BrIC are a subset of all head injuries; therefore, the NASS-indicated head injury rates inherently may be an overprediction of injuries directly applicable to these formulas. In crash tests, HIC AIS3+ head injury risk ranged 0-22 percent and BrIC AIS3+ head injury risk ranged 3-85 percent. BrIC AIS3+ head injury risk greater than 50 percent was associated with a variety of head kinematic events including front airbag loading, head contact with instrument panel, and non-contact forward excursion.

The published injury risk curve for BrIC indicates that crash tests represent significantly higher serious head injury risk than observed in real-world crashes of similar configurations. Hybrid III may produce exaggerated measures of BrIC or, if accurate, the BrIC formula may need to be reexamined against the underlying animal test data to determine the limitations of BrIC, and the proposed injury risk curves need to be re-evaluated against real human injury risk. Despite its origins as an indicator of skull fracture risk, the range of HIC-based head injury risk observed in crash tests more closely reflects the real-world head injury rates than the range of BrIC-based head injury risk.

## INTRODUCTION

According to the U.S. Centers for Disease Control and Prevention, 17 percent of all traumatic brain injury (TBI) is caused by traffic crashes, and these have the highest proportion leading to death of all causes of TBI (Faul et al., 2010). Not only are motor vehicle crashes a frequent source of TBI, but TBI is a frequent outcome of crashes and the number of fatalities attributable to these injuries is second behind injuries of the chest (Eigen and Martin, 2005). This is the case despite great progress at reducing the risk of head injuries in crashes. Front airbags have been associated with a 29 percent reduction in the risk of head injury in front crashes (Kahane, 2015). Side airbags with head protection reduce the odds of dying in side crashes by 37 percent (McCartt and Kyrychenko, 2007). Nevertheless, it has been suggested that head injury risk in crashes has been increasing during the past decade (Takhounts et al., 2013).

In modern passenger vehicles, airbags provide the principal means of protecting the head from impacts with the vehicle interior because such impacts are possible even when seat belts are used. Canadian Motor Vehicle Safety Standard No. 208 limits linear acceleration of the head in crash tests with belted dummies as a way of ensuring that

passenger vehicles will be fit with airbags to protect a driver's head from impact against the steering wheel (Transport Canada, 2011). Similarly, linear accelerations of the head are limited in U.S. regulatory crash tests by requiring that the head injury criterion (HIC) remain below 1000 in unbelted front crash tests with both belted and unbelted dummies, in addition to side crashes against a rigid pole targeted at the dummy's head (Office of the Federal Register, 2011a, 2011b). HIC essentially is a measure of the linear impulse of the head's motion during a crash. It is largely based on the Wayne State Tolerance Curve (WSTC), which described a set of head impact experiments relating accelerations of cadaver skulls to the onset of skull fractures (Lissner et al., 1960, Society of Automotive Engineers, 1980). Skull fracture was used as an indicator of brain injury because a large proportion of people suffering fractures also are concussed (Melvin et al., 1993). Since its adoption as a regulatory limit in motor vehicle safety standards, HIC has been related to the risk of severe brains injuries — 4 and greater on the Abbreviated Injury Scale (AIS) — through the analyses of additional experiments with human surrogates (Mertz et al., 1996). Despite its widespread use for evaluating head injury risk in regulatory and consumer information crash tests, studies continue to reiterate that HIC was not developed as a comprehensive predictor of all head injuries, but rather an indication of translational-based skull fracture injuries involving impacts and not rotational-based injury mechanisms (Digges, 1998; Hess et al., 1980; Prasad and Mertz, 1985).

Head injuries remain a lingering concern to be addressed by further improvements in vehicle crashworthiness. Even among vehicle designs earning good ratings in the Insurance Institute for Highway Safety's (IIHS) moderate overlap front crash test, the head is the second most common seriously injured body region in front crashes (Brumbelow and Zuby, 2009). These head injuries often occurred in crashes with large deformations of the safety cage, but also were observed in crashes during which the safety cage remained largely intact, thereby suggesting a failure of the restraint system to protect the head from injury.

The IIHS small overlap front crash test illustrates one possible means by which occupants' heads are injured in front crashes of vehicles judged to provide good head protection. Especially in cases with large safety cage deformations, the dummy's head sometimes slides past the front airbag and impacts directly against the door, A-pillar, or instrument panel. This head injury mechanism also has been documented in real crashes (IIHS, 2012; Sherwood et al., 2009). HIC values in small overlap front crash tests with head impacts against the vehicle interior, however, indicate a relatively low risk of serious head injury, with values ranging from 82 to 651 and representing an AIS 3+ injury risk of essentially 0-14 percent. Observations like these raise the question about whether HIC is completely measuring TBI risk in crash tests.

Since the earliest studies of the biomechanics of brain injury, rotational motion of the head also has been hypothesized to create stresses and strains in the brain that manifest as the injuries observed in motor vehicle crashes (Melvin et al., 1993). Considerable effort has been expended on understanding the relationship between rotational movement of the head and TBI, but none have been widely employed in crash testing (Kimpara and Iwamoto, 2012; Kimpara et al., 2011, Newman et al., 2000). Recently, a measure of both linear and rotational accelerations has been developed for evaluating concussion risk in sports helmet testing (Rowson and Duma, 2012).

The National Highway Traffic Safety Administration (NHTSA) also has developed a brain injury criterion (BrIC) based on head rotational velocity that could be used in conjunction with HIC for a more complete evaluation of TBI risk in crash tests (Takhounts et al., 2011; Takhounts et al., 2013). The basis for BrIC is its correlation with measurements of strain in finite element (FE) brain models subjected to impacts. Specifically, maximum principal stress (MPS) and cumulative strain damage metric (CSDM) were highly correlated with BrIC when the measured head kinematics from head impact tests and crash tests were used as inputs to FE brain models. Both MPS and CSDM were related to AIS 4+ brain injury risk using data from animal experiments. The motions of the animals' head in these experiments were scaled to account for differences in size between the animal and human brains and then used as inputs to the FE brain models. Thus, the validity of BrIC as an indicator of human brain injury risk in crash tests depends on the validity of the scaling methods and the similarity of the head motions in the animal experiments to those experienced by occupants in motor vehicle crashes.

At least two studies have attempted to compare TBI risk predictions from crash tests with real-world injury experience. Prasad et al. (2014) found that BrIC values from NHTSA's oblique frontal crash tests estimate higher AIS 3+ brain injury risks compared with the actual rate of injury in similar real crashes. On average, BrIC values in NHTSA's crash tests suggest that the AIS 3+ injury risk was greater than 50 percent, compared with the real-world head injury rates in similar crashes of less than 2 percent. The Center for Applied Biomechanics at the University of Virginia has found that the correlations between BrIC and MPS and CSDM for various simulated tests are different from those reported by Takhounts et al. (2013) (Gabler et al., 2014). Of special concern is that these analyses show BrIC values from experimental pedestrian crashes indicate a 50 percent risk of AIS 2+ brain injury before the dummy's head impacts the vehicle, which seems an unrealistic assessment of pedestrian head injury risk.

## OBJECTIVE

The objective of this study is to expand the comparison of head injury risk predicted by BrIC in crash tests with real-world injury rates in similar crash configurations. In particular, injury risk based on HIC and BrIC measured with a Hybrid III dummy in IIHS moderate and small overlap front crash tests are compared with real-world head injury rates in similar frontal crashes. In addition, several crash tests with indications of possible head injury risks are examined in detail to ascertain the extent to which BrIC augments the evaluation of these risks provided by HIC.

## METHODS

### Crash Test Data

IIHS has conducted standardized moderate overlap front crash tests since 1995 and standardized small overlap front crash tests since 2012 as part of its crashworthiness evaluation program. The moderate overlap test involves crashing a new vehicle into a deformable barrier at 64 km/h with 40 percent of the vehicle's width on the driver side aligned with the barrier. The small overlap test also is conducted at 64 km/h but involves aligning 25 percent of the vehicle's width with a rigid barrier. In both tests, a midsize male Hybrid III dummy is seated in the driver seat. Detailed test protocols are available from the IIHS website (iihs.org).

Since 2012, driver dummies in IIHS moderate and small overlap tests have been equipped with sensors to measure the rotational movement of the head. Specifically, an orthogonal array of three angular rate sensors measures the rotational velocity about the head's center of gravity. The resulting dataset includes 17 moderate overlap and 121 small overlap crash tests of 2012-15 model year vehicles from which both HIC and BrIC can be calculated.

HIC is calculated according to Equation 1, where a(t) is the vector resultant linear acceleration at time t and $t_2 - t_1$ is the time interval during the crash that is no longer than 15 ms in duration and that maximizes the expression in brackets. HIC is related to the risk of AIS 4+ injury according to Equation 2 (Mertz et al., 1996) and to the risk of AIS 3+ injury according to Equation 3 (NHTSA, 1995).

(Equation 1): $$HIC_{15} = \left\{\left(\frac{1}{t_2-t_1}\int_{t_1}^{t_2} a(t)dt\right)^{2.5}(t_2-t_1)\right\}_{max}$$

(Equation 2): $$PR_{AIS4+} = Normal\left(\frac{HIC-1434}{430}\right)$$

(Equation 3): $$PR_{AIS3+} = \frac{1}{1+e^{\left(3.39+\frac{200}{HIC}\right)-0.00372*HIC}}$$

Angular velocity measurements are filtered to channel frequency class 60 according to Society of Automotive Engineers recommended practice J211 before calculating BrIC according to Equation 4, where $\omega_i$ is the single absolute value of the maximum magnitude velocity measurement about the $i^{th}$ axis

(x, y, z corresponding to posterior-anterior, laterally to the right, superior-inferior directions) during the test. BrIC is related to the risk of brain injury according to Equations 4 and 5 (Takhounts et al., 2013).

(Equation 3): $$BRIC = \sqrt{\left(\frac{\omega_x}{66.25_{rad}}\right)^2 + \left(\frac{\omega_y}{56.45_{rad}}\right)^2 + \left(\frac{\omega_z}{42.87_{rad}}\right)^2}$$

(Equation 4): $$PR_{AIS3+} = 1 - e^{-\left(\frac{BRIC}{0.987}\right)^{2.94}}$$

(Equation 5): $$PR_{AIS4+} = 1 - e^{-\left(\frac{BRIC}{1.204}\right)^{2.94}}$$

**Real-World Head Injuries**

Cases of real-world front crashes were obtained from the National Automotive Sampling System Crashworthiness Data System (NASS CDS) crash data collection program conducted and maintained by NHTSA. The NASS CDS sample contains more detail than is available from police crash reports because investigators visit the crash site, examine the vehicles involved, and collect injury data from hospital or coroner reports. The sample is intended to be representative of all tow-away crashes occurring in the United States. The total number of crashes investigated ranged from 4,000 to 5,600 during 2004-12, the years used in the study. Each case is assigned a sample weight, based on its likelihood of being investigated, that scale the individual crash observations to nationwide estimates.

The sample of NASS CDS crashes used in this study were intended to include damage and occupant patterns similar to IIHS small and moderate overlap test configurations. Consequently, only passenger vehicles (body type = 1-49) from model years 2000 and later that received a good rating in the IIHS moderate overlap test were included. Further restricting the case model year range to correspond exactly with the crash test model years (2012-15) likely would have yielded too few crashes for analysis. A broader group of front-damaged vehicles were chosen based on NASS classifications, and damage photographs were used to further categorize which cases reflect patterns similar to crash tests. Front crashes were identified as having damage to the frontal plane in the principal impact according to the crash deformation classification (CDC) as well as a principal direction of force (PDOF) between 30 degrees left of center and 30 degrees right of center. To further ensure the sample consisted of vehicles with damage similar to the crash tests, only vehicles with a vertical distribution of damage extending from the bumper to level of the hood were included. Thus, vehicles that underrode their crash partner or had significant damage to the undercarriage were excluded. Additionally, only vehicles with extent-of-damage classification of 3 or greater were included, as this is typical of the damage observed in the comparison crash tests. Vehicles involved in a rollover or fire were excluded because of the difficulty in identifying injury mechanisms. Finally, only drivers who were using lap/shoulder belts and not ejected from the vehicle were examined.

After obtaining the 880 cases meeting the NASS coding criteria, all remaining assessments of crash configurations and severity were based on photographs of vehicle damage. Vehicles with damage originating from the right side of the vehicle (right offset), both frame rails significantly engaged (full overlap), or narrow center damage were excluded because of their dissimilarity to comparison crash tests. Small or moderate overlap configurations were defined based on the extent to which the left longitudinal frame rail was engaged in the crash. If the left frame rail was not engaged or only minimally so, the subject vehicle was classified as having small overlap damage; if only the left frame rail was significantly

damaged, then the vehicle was classified as having moderate overlap damage. Severity, classified as less than, equal to, or greater than crash tests, was determined by comparing case photographs of exterior damage extent to example crash test photos of damage representing similar vehicles.

Crashes meeting the criteria for small and moderate overlap configurations, including an AIS 3+ head injured driver, were examined in detail to collect specific information about the injuries including their possible causation. Photographic evidence, medical records, and investigator notes were used to determine evidence of head contact with interior components.

## RESULTS

### Real-World Crashes

There were 880 frontal crashes involving good-rated passenger vehicles from model years 2000 and later. Of these, 343 cases (86,389 weighted) were determined to be small or moderate overlap configurations with damage offset to the driver side. There were no drivers with AIS 3+ head injuries in moderate and small overlap front crashes that were less severe than the IIHS tests in this sample; therefore, lower severity crashes were excluded from in-depth analysis. The final sample included 168 cases (17,276 weighted) of small or moderate overlap configurations with damage offset to the driver side at equal or greater severities. Most of the cases were of similar severity to the corresponding IIHS crash test, as the distribution of cases by severity and damage shows (Figure 1). Of these 168 cases, 51 drivers had a head injury of any severity. The distribution by AIS severity level of the most severe head injuries for these 51 drivers is shown in Figure 2. Among the crashes with driver head injuries at the AIS 3+ level, most were more severe than their corresponding IIHS crash test (Figure 3). Appendix A contains details about the head injuries for each of the 17 drivers injured at the AIS 3+ level.

Table 1 shows head injury rates (weighted data) for drivers exposed to front left offset crashes that were at least as severe as IIHS tests. The risk of sustaining a serious head injury is greater in front crashes with small overlap damage than those with moderate overlap damage. The AIS 4+ risk is lower than the AIS 3+ injury risk, but the difference is proportionally smaller among small overlap crashes. There were five drivers with skull fractures resulting in fracture rates (weighted data) of 0.2 and 0.9 percent for moderate and small overlap crashes, respectively. Two other drivers, both in moderate overlap crashes, had fractures limited to the facial bones.

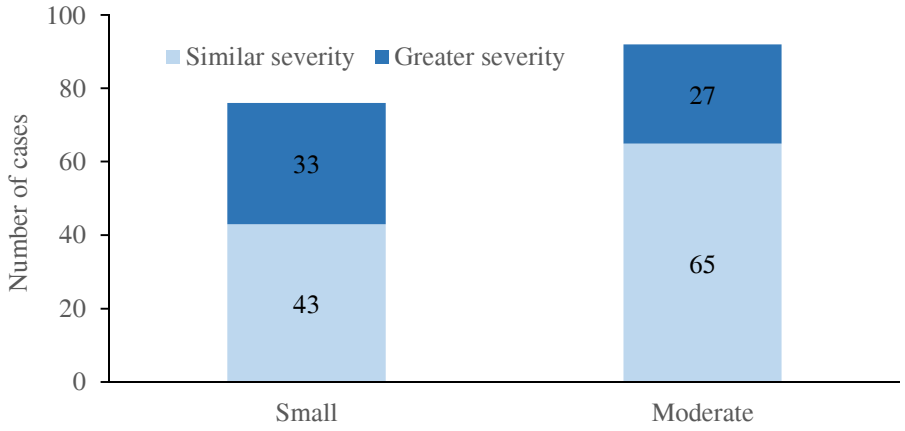


***Figure 1. Case distribution.***

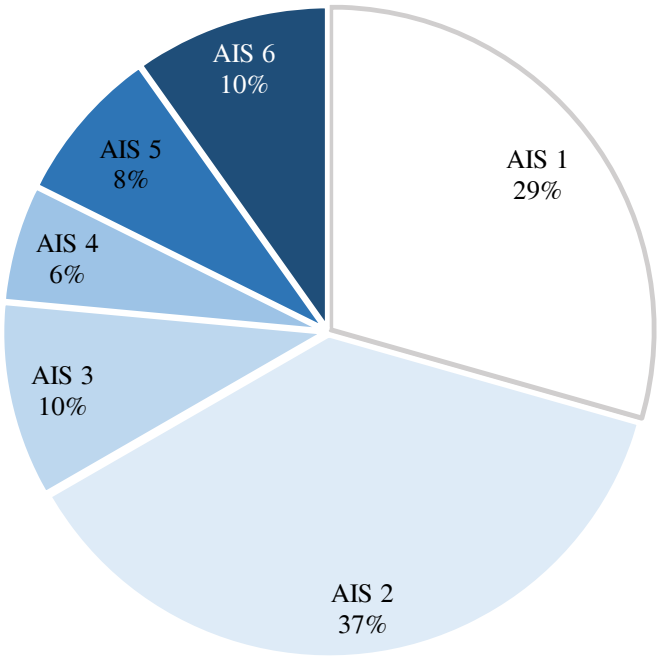


***Figure 2. Distribution of head injury severity for 51 head-injured drivers.***

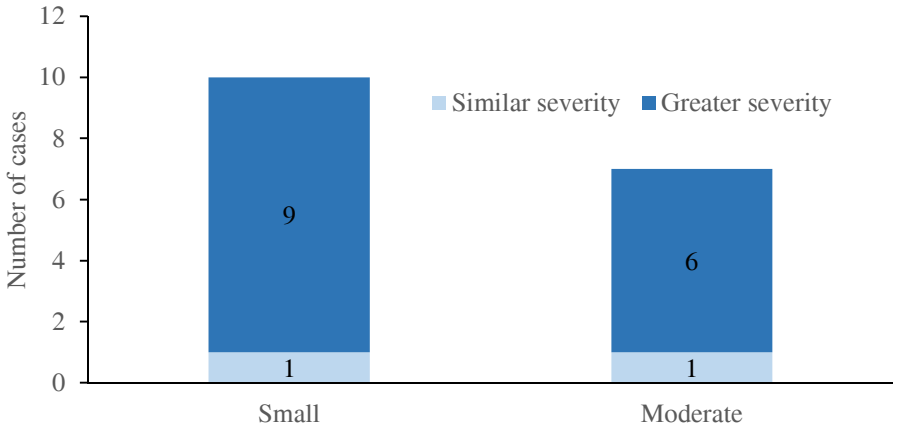


***Figure 3. Head injured cases.***

**Table 1.**
**Head injury rates for real-world crashes of equal or greater severity as IIHS tests.**

| | Moderate overlap (10,027) | Small overlap (7,249) |
|---|---|---|
| Skull fracture | | |
| Cases (weight) | 2 (21.84) | 3 (67.29) |
| Rate | 0.2% | 0.9% |
| AIS 3+ | | |
| Cases (weight) | 7 (117.21) | 10 (330.8) |
| Rate | 1.2% | 4.6% |
| AIS 4+ | | |
| Cases (weight) | 5 (67.11) | 7 (247) |
| Rate | 0.7% | 3.4% |

It is likely that the heads of all of the drivers injured at the AIS 3+ level made at least minimal contact with the driver airbag. Examination of the vehicle photographs, consideration of documented external injuries to the face and head, along with investigator-coded contact sources suggested that 10 of these drivers' heads also likely contacted some part of the vehicle interior other than the airbag — four in moderate overlap crashes and six in small overlap crashes. The other seven drivers' heads also may have contacted something besides the airbag, as the lack of contact evidence does not preclude its possibility.

## Crash Tests

Table 3 shows the range and the average of HIC and BrIC values for each sample of crash tests. Appendix B contains details about the HIC and BrIC values calculated for each of the 128 crash tests. On average, HIC values were greater in moderate overlap crashes, but the highest HIC values were measured in small overlap tests. The average BrIC values were similar from the two different crash tests and, again, the highest measures were recorded in small overlap tests. Table 4 shows the average estimated injury risks associated with these measures. For both injury severity levels and both crash types, BrIC indicates a much higher risk of brain injury than HIC. BrIC suggests that the AIS 3+ injury risk is 6.5-13 times greater than predicted by HIC, and the AIS 4+ injury risk is 40-67 times greater than indicated by HIC. BrIC suggests that serious brain injury risks are greater in small overlap than moderate overlap crashes, while HIC suggests the opposite. Not surprisingly, HIC and BrIC are not highly correlated, as shown in Figure 4, although they are more so in small overlap than moderate overlap crash tests.

**Table 3.**
**HIC and BrIC: Moderate (n=17) and small overlap (n=121) front crash tests at 64 km/h.**

| | HIC | | BrIC | |
|---|---|---|---|---|
| | Moderate | Small | Moderate | Small |
| Minimum | 116 | 39 | 0.43 | 0.3 |
| Average | 259 | 173 | 0.64 | 0.69 |
| Maximum | 459 | 651 | 0.88 | 1.24 |

**Table 4.**
**Average brain injury risk based on HIC and BrIC measured in crash tests at 64 km/h.**

| | Skull/facial fracture risk | AIS 3+ risk | | AIS 4+ risk | |
|---|---|---|---|---|---|
| | HIC | HIC | BrIC | HIC | BrIC |
| Moderate overlap crash test (n=17) | 0.6% | 4.1% | 27% | 0.4% | 16% |
| Small overlap crash test (n=121) | 0.1% | 2.5% | 32% | 0.3% | 20% |

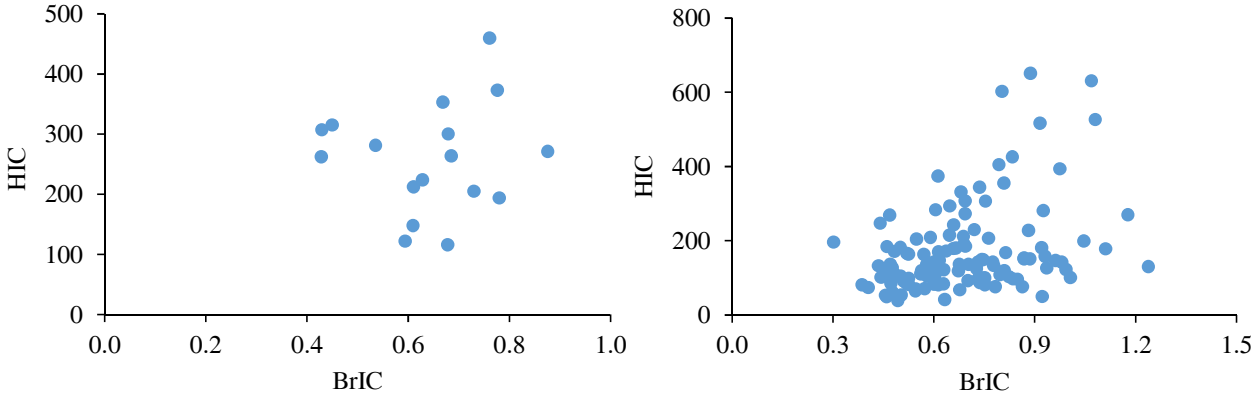


***Figure 4. HIC and BrIC values for moderate (left) and small overlap (right) crash tests.***

Associating HIC and BrIC with kinematic events provides some insight into the specific brain injury risks highlighted by each measure. Small overlap crash tests were used for this analysis because the moderate overlap tests lack the camera coverage necessary to identify kinematic events of the head. Three classes of events were defined for this analysis: airbag contact, hard contact, and unrestrained head motion. The HIC timeframe always encompassed the main contributing event, but choosing a contributing event for BrIC was not always straightforward, as each of the three peak rotational velocities may occur at different times during the crash. An approximate way of identifying the kinematic event most responsible for a particular BrIC value consists of using the event associated with the greatest peak. Ninety percent of tests had at least two components of BrIC occurring during the same event. Table 5 shows the HIC and BrIC values associated with three classes of kinematic events. The lowest values for HIC and BrIC were measured while the head was in contact with the airbag. The highest values for BrIC also occurred as a result of airbag contact, while the highest values for HIC occurred when the head impacted some interior surface other than the airbag. On average, HIC also was higher from hard contacts than the other classes of head motion. Free forward motion of the head after it slid off the airbag, on average, was associated with higher BrIC values than either contact with the airbag or hard interior surfaces.

**Table 5.**
**HIC and BrIC values for different kinematic events in 64km/h small overlap front crash tests.**

| | HIC | | | BrIC | | |
|---|---|---|---|---|---|---|
| | Airbag | Unrestrained motion | Hard contact | Airbag | Unrestrained motion | Hard contact |
| Minimum | 39 | 54 | 42 | 0.3 | 0.53 | 0.47 |
| Average | 163 | 172 | 205 | 0.66 | 0.77 | 0.72 |
| Maximum | 527 | 426 | 651 | 1.24 | 1.07 | 0.89 |

A close examination of 10 crash tests where the HIC timeframe included significant head impacts other than with the inflated airbag offers further insight into the ability of BrIC to augment the assessment of head injury risk based on crash tests. Table 6 shows the HIC and BrIC values, times associated with the three BrIC components, and non-airbag impacts between the dummy's head and vehicle interior. In all cases, the HIC time interval (not shown) includes the interior impact of interest. As before, HIC and BrIC are not highly correlated (0.24) (Figure 5) and, in every case, BrIC indicates a higher risk of AIS 3+ injury than HIC, with BrIC risk assessment ranging 2.4-58 times higher than HIC. In five tests, the greatest contributor (largest component peak) to BrIC occurs at a time greater than 4 ms from the impact highlighted within the HIC timeframe; therefore, BrIC cannot be associated with that impact. The correlation between HIC and BrIC among the remaining five tests is 0.60 (Figure 5), with BrIC indicating a risk ranging 2.2-23 times higher than HIC.

The sensitivity of HIC and BrIC to vehicle design changes was examined from comparison tests of three models that were redesigned or modified to improve small overlap front crashworthiness. The Mazda 6 was first evaluated for small overlap crashworthiness in model year 2012, and the full-model redesign was evaluated in model year 2014. In both tests, the Mazda 6 overall rating was acceptable. However, the earlier model received a restraints and kinematics score of marginal because the dummy's head slid off the driver airbag and impacted the door sill. The HIC in this test was 148, low enough that head protection was rated good. The full-model redesign in 2014 also received an acceptable overall rating even though the dummy's head remained in contact with the airbag during its forward excursion. Unfortunately, the head struck the steering wheel through the airbag, resulting in a HIC of 331, which was

**Table 6.**
**HIC and BrIC timing related to hard contacts.**

| Vehicle | Test ID | Hard contact source | Hard contact time | HIC | AIS 3+ | BrIC | AIS 3+ | BrIC peak component times x | y | z |
|---|---|---|---|---|---|---|---|---|---|---|
| 2012 Mazda 6 | CEN1220 | Door sill | 124 | 148 | 1% | 0.62 | 23% | 174 | **120*** | 135 |
| 2014 Mazda 6 | CEN1305 | Steering wheel through airbag | 122 | 331 | 6% | 0.68 | 29% | 139 | **124*** | 131 |
| 2014 Kia Forte | CEN1318 | Instrument panel | 122 | 355 | 7% | 0.81 | 43% | 176 | **110*** | 77 |
| 2013 Toyota RAV4 | CEN1319 | Instrument panel | 120 | 283 | 5% | 0.60 | 22% | 125 | **129*** | 132 |
| 2013 Toyota Prius C | CEN1328 | Instrument panel | 119 | 426 | 9% | 0.83 | 46% | 82 | **119*** | 84 |
| 2013 Toyota Yaris | CEN1331 | Instrument panel | 137 | 127 | 1% | 0.94 | 58% | 146 | **139*** | 122 |
| 2014 Ford Fiesta | CEN1343 | Instrument panel | 108 | 509 | 13% | 0.80 | 43% | 123 | **111*** | 87 |
| 2014 Fiat 500L | CEN1414 | A-pillar | 101 | 228 | 3% | 0.88 | 52% | 108 | 108 | **105*** |
| 2015 Hyundai Sonata | CEN1427 | Steering wheel through airbag | 105 | 405 | 8% | 0.79 | 42% | 123 | 109 | **115*** |
| 2015 Honda Fit | CEN1430 | Steering wheel through airbag | 87 | 651 | 22% | 0.89 | 52% | 102 | **92*** | 88 |

*Maximum individual component

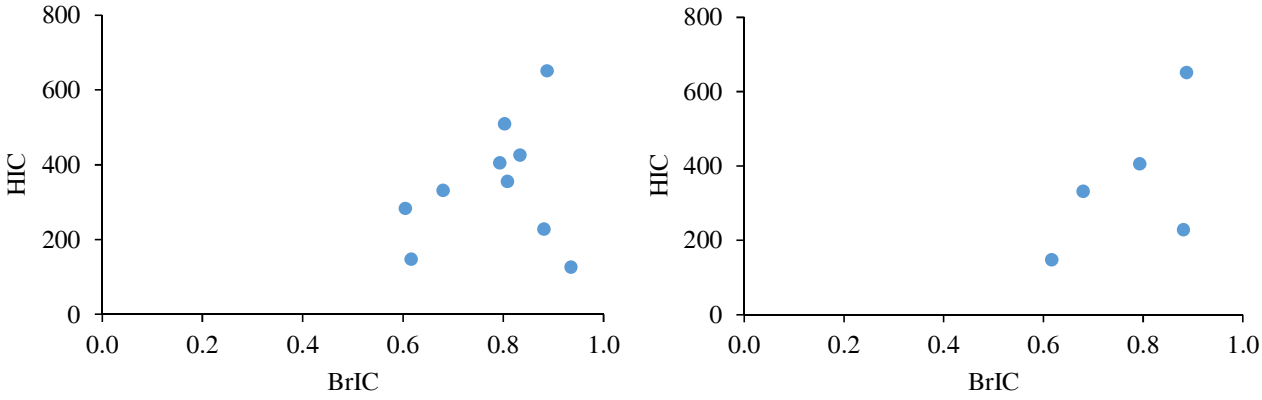


***Figure 5. Correlation of HIC and BrIC in all tests with head contacts (left) and tests where HID and BrIC both associated with hard contact (right).***

higher than in the test of the earlier design, and head protection was downgraded to acceptable because of a peak acceleration of 108 g despite the improved restraints and kinematics rating. The BrIC values for the two tests were similar, 0.62 and 0.68, despite differences in the head motions between tests.

The 2013 Honda Fit was rated poor overall because its safety cage collapsed in the small overlap test and the dummy's head struck the instrument panel after sliding off the airbag. This impact was associated with a HIC of 517, but the BrIC (0.92) recorded in this test was due to head motion occurring beforehand. The 2015 model was rated acceptable in the small overlap test, largely due to a greatly improved safety cage. However, the dummy's head struck the steering wheel through the airbag, resulting in a HIC of 651 and a BrIC of 0.89.

The Toyota RAV4 was first tested in model year 2013, receiving a poor overall rating, and then tested again in model year 2015 after it had been modified for better small overlap crashworthiness. In the test of the 2013 model, the dummy's head slid off the airbag and impacted against the instrument panel,

producing a HIC of 283 and a BrIC of 0.60. The modified design earned a good overall rating due largely to a stronger safety cage. In addition, the head impact against the instrument panel was eliminated, resulting in a lower HIC of 163 associated with the head's interaction with the airbag and a BrIC of 0.57.

Head impacts with the steering wheel through the airbag in tests of the 2015 Honda Fit and 2014 Mazda 6 were identified by HIC as more risky than impacts against the instrument panel and doorsill in the earlier models of each; however, the assessment of risk by BrIC was only slightly different between the newer and older designs. Similarly, HIC values suggest brain injury risk was halved with the modifications implemented in the 2015 RAV4 compared with the 2013 model, but the BrIC risk assessment was similar between the two designs.

**DISCUSSION**

BrIC values measured in IIHS frontal offset crash tests estimated a much larger risk of brain injury than observed in real crashes with similar offset crash damage and at least the same damage extent. This overestimation is larger for moderate overlap front crashes (18 times) than small overlap ones (6 times), and about the same for both AIS 3+ and AIS 4+ injury levels. Only 16 of these 139 tests resulted in the dummy's head impacting a hard surface inside the vehicle, indicating that BrIC predicts high levels of serious and severe brain injury risk as a result of contacting only the airbag. This is contrary to the NASS CDS cases examined in this study in which at least 70 percent of those drivers with AIS 3+ brain injuries apparently impacted a hard surface in the vehicle.

HIC values measured in IIHS frontal offset crash tests indicated a much lower risk of serious and severe brain injuries than BrIC (Table 4). With the exception of AIS 3+ injury risk in moderate overlap crashes, these measures suggest a lower risk of brain injury than observed in the NASS CDS crashes with frontal offset crash damage. The estimated AIS 4+ injury risk in small overlap crash tests is less than one-tenth of that observed in real crashes with this damage pattern and at least the same damage extent. Skull fracture risk based on HIC (Mertz et al., 1996) overestimates injury risk in moderate overlap crash tests (0.6 percent) compared with what was observed in the real crash sample (0.2 percent), but the risk in small overlap crash tests (0.4 percent) is lower than that seen in real crashes (0.9 percent), though neither deviates significantly. The underestimation of skull fracture and brain injury risks in these crash tests is understandable given that nearly all of the NASS CDS sample have more damage than the test vehicles. The source of overestimation by BrIC is unknown.

While both BrIC and HIC estimate quite different head injury risks in frontal offset crash tests than observed in similar real crashes, the estimates from HIC are closer to the real injury rates. However, HIC indicates moderate overlap crashes present a higher head injury risk than small overlap crashes, while real crash data indicated higher injury rates in small overlap crashes. The relative risks estimated by HIC may better align with a larger sample of real crashes more comparable with the crash tests; however, it seems unlikely that they would yield brain injury rates as high as the BrIC estimates, as this crash sample included generally more severe impacts than the crash tests.

Even though BrIC appears to correctly assess the relative brain injury risk between these two crash types, it is unknown whether BrIC correctly identifies why small overlap crashes are more injurious. Table 5 shows that the majority of BrIC values were associated with the head's contact with the inflated airbag

and free motion of the head following airbag contact. In contrast, the average and highest values of HIC in these tests were associated with head impacts against hard surfaces in the vehicle interior, which is more consistent with real crash observations. Eight of the 17 NASS CDS cases had drivers with face or skull injuries not likely caused by contacting the inflated airbag or as a result of post-airbag forward motion alone. An additional two drivers were injured in ways that suggest their head's contacted something other than the airbag. The remaining drivers also may have impacted against something hard despite the lack of evidence recorded in the investigation file. It is unclear why BrIC brain injury risk estimates would be higher for seemingly more benign events than the head impacts that produced strong linear accelerations.

The lack of correlation between HIC and BrIC in the full crash test dataset suggests BrIC may be providing different indications of brain injury risk than HIC alone. However, the observations of the kinematic events associated with BrIC raise questions about whether BrIC is accurately identifying injurious events in a given crash test. For the five tests in which both HIC and BrIC could be associated with the same head impacts against the vehicle interior, HIC estimated an AIS 3+ injury risk of 2-20 percent and BrIC estimated a risk of 23-53 percent. While the BrIC estimates of brain injury risk were high relative to real crash injury rates, they may correctly indicate that the head impacts observed in these tests posed a greater brain injury risk than indicated by HIC.

BrIC seems insensitive to changes in vehicle design, while HIC makes distinctions. This is problematic for the process of developing countermeasures that can reduce BrIC in frontal crashes. Some of this insensitivity stems from the possibility that BrIC may be based on measurements from different times and events during the test. Takhounts et al. (2013) state that a time-based calculation of vector resultant rotation velocity did not yield a better correlation with measures of strain in the FE brain models than the formulation used here. As long as the time-based calculation still exhibits a reasonably strong correlation, its use may prove to be a better tool for evaluating head injury risks in crash tests than the version currently considered by NHTSA.

## CONCLUSIONS

Serious and severe brain injury risk estimates from offset crash tests based on BrIC are much higher than injury rates observed in a sample of crashes with similar damage type but greater severity. HIC appropriately estimates lower brain injury risk in tests less severe than real crashes with similar offset damage patterns. When both HIC and BrIC can be associated with the same head impact, the higher risk estimate from BrIC may be an indication that a brain injury risk exists that is not identified by HIC. It is not clear why BrIC predicts such high brain injury risks with contact between the head and airbag or free motion of the head afterward. If accurate, the injuries indicated by BrIC may be difficult to prevent except by reducing crash severity through the application of crash avoidance technologies.

## REFERENCES

Brumbelow ML, Zuby DS. 2009. Impact and injury patterns in frontal crashes of vehicles with good ratings for frontal crash protection. *Proceedings of the 21st International ESV Technical Conference* (CD-ROM) Washington, DC: National Highway Traffic Safety Administration.

Digges KH. 1999. Injury measurements and criteria. Keynote address at the Specialists' Meeting of the RTO Human Factors and Medicine Panel. *RTO Meeting Proceedings 20: Models for Aircrew Safety Assessment: Uses, Limitations, and Requirements*, pp. K2-1-5. Report no. RTO-MP-20. Quebec, Canada: Canada Communications Group Inc.

Eigen AM, Martin PG. 2005. Identification of real world injury patterns in aid of dummy development. Paper no. 05-0219. *Proceedings of the 19th International Technical Conference on the Enhanced Safety of Vehicles*. Washington, DC: National Highway Traffic Safety Administration.

Faul M, Xu L, Wald MM, Coronado VG. 2010. Traumatic brain injury in the United States; Emergency department visits, hospitalizations, and deaths, 2002-2006. Atlanta, GA: Centers for Disease Control and Prevention.

Gabler LF, Panzer MB, Crandall JR. 2014. On the application of BrIC to the biomechanics of various automotive impact scenarios. Presented at the 42nd International Workshop on Human Subjects for Biomechanical Research. San Diego, California.

Hess RL, Weber K, Melvin JW. 1980. Review of literature and regulation relating to head impact tolerance and injury criteria. Report no. UM-HSRI-80-52-l. Ann Arbor, MI: University of Michigan Transportation Research Institute.

Hodgson V, Thomas L. 1972. Effect of long-duration impact on head. SAE Technical Paper 720956. Warrendale, PA: Society of Automotive Engineers.

Insurance Institute for Highway Safety. 2012. Small overlap crashes: New consumer-test program aims for even safer vehicles. *Status Report* 47(6). Arlington, VA.

Kahane CJ. 2015. Lives saved by vehicle safety technologies and associated Federal Motor Vehicle Safety Standards, 1960 to 2012, Passenger cars and LTVs, with reviews of 26 FMVSS and the effectiveness of their associated safety technologies in reducing fatalities, injuries, and crashes. Report no. DOT HS 812 069. Washington, DC: National Highway Traffic Safety Administration.

Kimpara H, Iwamoto M. 2012. Mild traumatic brain injury predictors based on angular accelerations during impacts. Ann Biomed Eng. 40(1):114-26.

Kimpara H, Nakahira Y, Iwamoto M, Rowson S, Duma S. 2011. Head injury prediction methods based on 6 degree of freedom head acceleration measurements during impact. Int J Automot Eng 2:13-19.

Lissner HR, Lebow M, Evans FG. 1960. Experimental studies on the relation between acceleration and intracranial pressure changes in man. Surg Gynecol Obstet. 111:329-38.

McCartt AT, Kyrychenko SY. 2007. Efficacy of side airbags in reducing driver deaths in driver-side car and SUV collisions. Traffic Injury Prevention 8(2):162-170.

Melvin JW, Lighthall JW, Ueno K. 1993. Ch 12. Brain injury biomechanics. *Accidental Injury: Biomechanics and Prevention* (eds Nahum AM, Melvin JW), pp 268-291. New York: Springer-Verlag.

Mertz H, Irwin A. 1994. Brain injury risk assessment of frontal crash test results. SAE Technical Paper 941056. Warrendale, PA: Society of Automotive Engineers.

Mertz H, Prasad P, Nusholtz G. 1996. Head injury risk assessment for forehead impacts. SAE Technical Paper 960099. Warrendale, PA: Society of Automotive Engineers.

National Highway Traffic Safety Administration. 1995. Final economic assessment; FMVSS No. 201 Upper interior head protection. Washington, DC: U.S. Department of Transportation.

National Highway Traffic Safety Administration. 2008. Consumer information; New Car Assessment Program. Docket no. NHTSA-2006-26555. Federal Register 73(134): 40016-40050. Washington, DC: National Archives and Records Administration.

Newman JA, Shewchenko N, Welbourne E. 2000. A proposed new biomechanical head injury assessment function - the maximum power index. Stapp Car Crash J. 44:215-47.

Office of the Federal Register. 2011a. *Code of Federal Regulations*; Title 49 Transportation, Part 571 Federal Motor Vehicle Safety Standards, Standard No. 208 Occupant Crash Protection. Washington, DC: National Archives and Records Administration.

Office of the Federal Register. 2011b. *Code of Federal Regulations*; Title 49 Transportation, Part 571 Federal Motor Vehicle Safety Standards, Standard No. 214 Side Impact Protection. Washington, DC: National Archives and Records Administration.

Prasad P, Dalmotas D, German A. The field relevance of NHTSA's oblique research moving deformable barrier tests. *Stapp Car Crash J*. 58:175-196. Ann Arbor, MI: The Stapp Association.

Prasad P, Mertz HJ. 1985. The position of the United States delegation to the ISO Working Group 6 on the use of HIC in the automotive environment. SAE Technical Paper 851246. Warrendale, PA: Society of Automotive Engineers.

Research and Technology Organization, North Atlantic Treaty Organization. 1999. *RTO Meeting Proceedings 20: Models for Aircrew Safety Assessment: Uses, Limitations, and Requirements*. Report no. RTO-MP-20. Quebec, Canada: Canada Communications Group Inc.

Rowson S, Duma SM. 2013. Brain injury prediction: assessing the combined probability of concussion using linear and rotational head acceleration. Ann Biomed Eng. 41(5):873-82.

Sherwood CP, Nolan JM, Zuby DS. 2009. Characteristics of small overlap crashes. Proceedings of the 21st International Technical Conference on the Enhanced Safety of Vehicles (CD-ROM). Washington, DC: National Highway Traffic Safety Administration.

Society of Automotive Engineers. 1980. Human Biomechanics and Simulations Standards Committee, Standard J885B 198004. Warrendale, PA.

Takhounts EG, Craig MJ, Moorhouse K, McFadden J, Hasija V. 2013. Development of brain injury criteria (BrIC). Stapp Car Crash J. 57:243-66.

Takhounts EG, Hasija V, Ridella SA, Rowson S, Duma SM. 2011. Kinematic rotational brain injury criterion (BrIC). Proceedings of the 22nd International Technical Conference on the Enhanced Safety of Vehicles. Paper No. 11-0263. Washington, DC: National Highway Traffic Safety Administration.

Transport Canada. 2014. Motor Vehicle Safety Regulations; Schedule III: Canada Motor Vehicle Safety Standard No. 208 Occupant Protection in Frontal Impacts. Ottawa, Ontario.

Versace J. 1971. A review of the severity index. SAE Technical Paper 710881. Warrendale, PA: Society of Automotive Engineers.

## Appendix A. Head Injuries

**Table A-1. Real-world head injuries.**

| NASS-CDS case ID | Occupant ID | NASS case weight | Type of overlap | Impact side | Impact severity | Head MAIS | Evidence of head impact | | | Number of AIS 3+ head injuries | List of AIS 3+ head injuries (AIS) |
|---|---|---|---|---|---|---|---|---|---|---|---|
| | | | | | | | External injuries | Facial/Skull fractures | Vehicle evidence | | |
| 200549156 | 58681 | 8.113 | Moderate | Near | Greater | 4 | — | — | Makeup on frontal airbag | 2 | R cerebrum hematoma (4), R cerebrum subarachnoid hemorrhage (3) |
| 200849138 | 90861 | 9.584 | Moderate | Near | Greater | 6 | Facial abrasions and contusions | Basilar skull, maxilla, mandible, nasal fractures | Steering wheel bent | 2 | Brain stem laceration (6), basilar skull fracture (4) |
| 200973074 | 102687 | 38.929 | Moderate | Near | Greater | 3 | Scalp and chin contusions | — | Bent steering wheel | 1 | Cerebrum brain swelling/edema (3) |
| 200981154 | 105483 | 27.983 | Moderate | Near | Greater | 4 | Chin laceration | Mandible fracture | Hair evidence on A-pillar | 2 | L cerebrum small hematoma (4), cerebrum brain swelling/edema (3) |
| 201149139 | | 12.26 | Moderate | Near | Greater | 6 | Forehead abrasions | Basilar skull, maxilla, mandible, zygoma fractures | — | 2 | Brain stem laceration (6), basilar fracture (3) |
| 201179125 | | 8.206 | Moderate | Near | Greater | 3 | — | Orbit, nasal fracture | — | 2 | L cerebrum hematoma (3), R cerebrum hematoma (3) |
| 201249063 | | 12.21 | Moderate | Near | Similar | 5 | Scalp contusions | — | — | 3 | Brain stem hemorrhage (5), cerebrum bilateral subdural small hematoma (4), R cerebrum contusion (3) |
| 200473241 | 49180 | 14.998 | Small | Near | Greater | 5 | Whole scalp contusions | Basilar and vault skull, maxilla, nasal, orbit fracture | Blood evidence on steering wheel and airbag | 12 | Multiple vault fractures (3), basilar skull fracture (4), multiple cerebrum hematoma (5,5,5), brain stem (5), cerebrum brain swelling/edema (5), cerebrum laceration (4), cerebrum contusion (3) |
| 200649023 | 68818 | 10.286 | Small | Near | Greater | 6 | Forehead, nose cheek abrasions | Basilar and vault skull | — | 3 | Brain stem laceration (6), basilar fracture (4), vault fracture (2) |
| 200705021 | 74218 | 118.769 | Small | Near | Greater | 6 | Whole face abrasions | Teeth fracture | — | 4 | L cerebrum subarachnoid hemorrhage (3), R cerebrum subdural hemorrhage (4), brain stem transection (6), cerebrum swelling (3) |
| 200943250 | 100508 | 42.007 | Small | Near | Greater | 4 | — | Basilar and vault skull, orbit and nasal fracture | Blood/bio evidence on frontal airbag | 13 | Multiple vault fractures (4), basilar fracture (4), multiple cerebrum subarachnoid hemorrhage (3), hematoma (4,5), contusion (3), brain swelling (5), R-L infarctions (3), brain stem laceration (5) |
| 200949089 | 101901 | 12.488 | Small | Near | Greater | 5 | — | — | Hair evidence on roof rail | 4 | Cerebrum hematoma (5), cerebrum brain swelling/edema (3), cerebrum contusion (3), L cerebrum subarachnoid hemorrhage (3) |
| 200975216 | 103812 | 29.106 | Small | Near | Greater | 3 | — | — | Bent steering wheel rim | 1 | Multiple L cerebrum contusion (3) |
| 200981007 | 105183 | 19.941 | Small | Near | Greater | 6 | — | — | — | 1 | Brain stem laceration associated with spinal cord laceration (6) |
| 200982010 | 105510 | 7.029 | Small | Near | Greater | 3 | — | — | Skin transfer evidence on frontal airbag | 2 | R cerebrum subarachnoid hemorrhage (3), L cerebrum subarachnoid hemorrhage (3) |
| 201206073 | | 28.992 | Small | Near | Greater | 4 | — | — | Bent steering wheel | 4 | R cerebrum subarachnoid hemorrhage (3), L cerebrum subarachnoid hemorrhage (3), cerebrum edema and compression (4), R cerebrum hematoma (3) |
| 200675096 | 71165 | 47.826 | Small | Near | Similar | 3 | Deep scalp laceration | — | Hair and blood evidence on A-pillar | 2 | L cerebrum contusion (3), R cerebrum subarachnoid hemorrhage (3) |

**Appendix B. Crash Test Data**

**Table B-1. Moderate overlap tests.**

| Vehicle model | Test ID | Class | BrIC | AIS 3 BrIC | AIS 4 BrIC | HIC | AIS 3 HIC | AIS 4 HIC | HIC contact source |
|---|---|---|---|---|---|---|---|---|---|
| 2013 Ford Escape | CEF1206 | Small SUV | 0.61 | 23% | 14% | 212 | 3% | 0.2% | Airbag |
| 2013 Dodge Dart | CEF1207 | Small car | 0.63 | 24% | 15% | 224 | 3% | 0.2% | Airbag |
| 2013 Nissan Altima | CEF1208 | Midsize car | 0.61 | 22% | 13% | 148 | 1% | 0.1% | Airbag |
| 2014 Mazda 6 | CEF1301 | Midsize car | 0.68 | 29% | 18% | 116 | 1% | 0.1% | Airbag |
| 2013 BMW X1 | CEF1302 | Small SUV | 0.88 | 51% | 33% | 271 | 4% | 0.3% | Airbag |
| 2013 Buick Encore | CEF1303 | Small SUV | 0.78 | 40% | 25% | 194 | 2% | 0.2% | Airbag |
| 2014 Fiat 500 L | CEF1304 | Small car | 0.68 | 29% | 18% | 300 | 5% | 0.4% | Airbag |
| 2014 Jeep Cherokee | CEF1305 | Midsize SUV | 0.73 | 35% | 21% | 205 | 3% | 0.2% | Airbag |
| 2013 Chevrolet Spark | CEF1306 | Minicar | 0.76 | 38% | 24% | 459 | 11% | 1.2% | Airbag |
| 2014 Maserati Ghibli | CEF1307 | Large car | 0.45 | 10% | 6% | 315 | 5% | 0.5% | Airbag |
| 2014 Mitsubishi Mirage | CEF1308 | Minicar | 0.69 | 30% | 18% | 264 | 4% | 0.3% | Airbag |
| 2014 BMW 2 Series | CEF1401 | Midsize car | 0.59 | 21% | 13% | 122 | 1% | 0.1% | Airbag |
| 2014 Nissan Rogue | CEF1402 | Small SUV | 0.67 | 28% | 17% | 353 | 7% | 0.6% | Airbag |
| 2015 Subaru WRX | CEF1403 | Small car | 0.78 | 40% | 25% | 373 | 7% | 0.7% | Airbag |
| 2014 Ford C-Max | CEF1404 | Small car | 0.43 | 9% | 5% | 307 | 5% | 0.4% | Airbag |
| 2014 Mazda 5 | CEF1405 | Small car | 0.43 | 9% | 5% | 262 | 4% | 0.3% | Airbag |
| 2014 Hyundai Veloster | CEF1406 | Small car | 0.54 | 16% | 10% | 281 | 4% | 0.4% | Airbag |

**Table B-2. Small overlap tests.**

| Vehicle model | Test ID | Class | Delta V | Peak Accel | Vehicle motion | BrIC | AIS 3 BrIC | AIS 4 BrIC | HIC | AIS 3 HIC | AIS 4 HIC | HIC contact source | BrIC contact source |
|---|---|---|---|---|---|---|---|---|---|---|---|---|---|
| 2012 Hyundai Sonata | CEN1219 | Midsize car | 47 | -34 | Translate | 0.99 | 64% | 44% | 123 | 1% | 0.1% | Airbag | Airbag |
| 2012 Mazda 6 | CEN1220 | Midsize car | 41 | -38 | Translate | 0.62 | 23% | 14% | 148 | 1% | 0.1% | IP | IP |
| 2012 Suzuki Kazashi | CEN1221 | Midsize car | 43 | -23 | Translate | 0.58 | 20% | 12% | 104 | 1% | 0.1% | Forward excursion | Forward excursion |
| 2013 Ford Escape | CEN1222 | Small SUV | 48 | -21 | Translate | 0.62 | 23% | 14% | 122 | 1% | 0.1% | Forward excursion | Forward excursion |
| 2012 Honda CR-V | CEN1223 | Small SUV | 44 | -26 | Translate | 0.73 | 35% | 22% | 102 | 1% | 0.1% | Forward excursion | Forward excursion |
| 2012 Nissan Rogue | CEN1224 | Small SUV | 50 | -27 | Translate | 0.39 | 7% | 4% | 82 | 0% | 0.1% | Airbag | Airbag |
| 2012 Kia Optima | CEN1225 | Midsize car | 44 | -32 | Translate | 0.46 | 11% | 6% | 53 | 0% | 0.1% | Airbag | Airbag |
| 2012 Jeep Patriot | CEN1226 | Small SUV | 48 | -24 | Translate | 0.75 | 37% | 23% | 81 | 0% | 0.1% | Forward excursion | Forward excursion |
| 2012 Mitsubishi Outlander Sport | CEN1227 | Small SUV | 48 | -34 | Translate | 0.52 | 15% | 9% | 84 | 0% | 0.1% | Airbag | Airbag |
| 2013 Subaru Legacy | CEN1228 | Midsize car | 56 | -28 | Rotate | 0.56 | 18% | 11% | 110 | 1% | 0.1% | Airbag | Airbag |
| 2012 Honda Accord | CEN1229 | Midsize car | 56 | -33 | Rotate | 1.11 | 75% | 55% | 178 | 2% | 0.2% | Airbag | Airbag |
| 2012 Nissan Maxima | CEN1230 | Midsize car | 61 | -23 | Translate | 0.54 | 17% | 10% | 65 | 0% | 0.1% | Airbag | Airbag |
| 2013 Nissan Altima | CEN1231 | Midsize car | 52 | -42 | Translate | 0.78 | 40% | 25% | 143 | 1% | 0.1% | Airbag | Airbag |
| 2012 Volkswagen Passat | CEN1232 | Midsize car | 56 | -37 | Rotate | 0.69 | 31% | 19% | 307 | 5% | 0.4% | Forward excursion | Forward excursion |
| 2012 Volkswagen Jetta | CEN1233 | Midsize car | 55 | -29 | Rotate | 0.69 | 30% | 19% | 191 | 2% | 0.2% | Forward excursion | Forward excursion |
| 2013 Honda Accord coupe | CEN1234 | Midsize car | 57 | -35 | Rotate | 0.98 | 62% | 43% | 142 | 1% | 0.1% | Airbag | Airbag |
| 2013 Jeep Wrangler | CEN1235 | Small SUV | 44 | -27 | Translate | 0.96 | 61% | 41% | 147 | 1% | 0.1% | Airbag | Airbag |
| 2013 Ford Fusion | CEN1236 | Midsize car | — | — | Translate | 0.50 | 14% | 8% | 54 | 0% | 0.1% | Forward excursion | Forward excursion |
| 2013 Hyundai Tucson | CEN1237 | Small SUV | 55 | -36 | Rotate | 0.93 | 57% | 38% | 158 | 2% | 0.2% | Forward excursion | Forward excursion |
| 2013 Honda Civic (coupe) | CEN1301 | Small car | 60 | -35 | Rotate | 0.76 | 38% | 24% | 207 | 3% | 0.2% | Airbag | Airbag |
| 2013 Honda Civic (sedan) | CEN1302 | Small car | 62 | -34 | Rotate | 0.97 | 62% | 42% | 394 | 8% | 0.8% | Airbag | Airbag |
| 2013 Subaru Forester | CEN1303 | Small SUV | 56 | -33 | Rotate | 0.48 | 12% | 7% | 127 | 1% | 0.1% | Airbag | Airbag |
| 2013 Volvo XC60 | CEN1304 | Midsize SUV | 43 | -21 | Translate | 0.51 | 14% | 8% | 91 | 1% | 0.1% | Airbag | Airbag |
| 2014 Mazda 6 | CEN1305 | Midsize car | 57 | -40 | Rotate | 0.68 | 29% | 18% | 331 | 6% | 0.5% | Airbag | SW through airbag |
| 2013 Mazda CX-5 | CEN1306 | Small SUV | 52 | -29 | Rotate | 0.73 | 35% | 21% | 95 | 1% | 0.1% | Airbag | Airbag |
| 2013 BMW X1 | CEN1307 | Small SUV | 51 | -26 | Rotate | 0.30 | 3% | 2% | 196 | 2% | 0.2% | Airbag | Airbag |
| 2013 Buick Encore | CEN1308 | Small SUV | 50 | -26 | Translate | 0.86 | 49% | 32% | 76 | 0% | 0.1% | Forward excursion | — |
| 2013 Volkswagen Tiguan | CEN1309 | Small SUV | 54 | -27 | Rotate | 0.74 | 35% | 22% | 87 | 0% | 0.1% | Forward excursion | Forward excursion |
| 2013 Hyundai Elantra | CEN1310 | Small car | 56 | -27 | Rotate | 0.65 | 26% | 16% | 215 | 3% | 0.2% | Airbag | Airbag |
| 2013 Buick Encore | CEN1311 | Small SUV | 53 | -31 | Rotate | 1.01 | 65% | 45% | 101 | 1% | 0.1% | Forward excursion | Forward excursion |
| 2013 Chevrolet Cruze | CEN1312 | Small car | 45 | -26 | Translate | 0.55 | 17% | 10% | 70 | 0% | 0.1% | Forward excursion | Forward excursion |
| 2013 Chevrolet Sonic | CEN1313 | Small car | 51 | -36 | Translate | 1.05 | 69% | 49% | 199 | 3% | 0.2% | Forward excursion | Forward excursion |
| 2013 Ford Focus | CEN1314 | Small car | 48 | -32 | Rotate | 0.78 | 40% | 25% | 133 | 1% | 0.1% | Airbag | Airbag |
| 2013 Nissan Sentra | CEN1315 | Small car | 47 | -28 | Rotate | 0.74 | 35% | 22% | 344 | 6% | 0.6% | Forward excursion | Forward excursion |
| 2013 Volkswagen Beetle | CEN1316 | Small car | 48 | -27 | Rotate | 0.65 | 26% | 16% | 294 | 5% | 0.4% | Forward excursion | Forward excursion |
| 2013 Kia Soul | CEN1317 | Small car | 40 | -25 | Translate | 0.60 | 22% | 13% | 83 | 0% | 0.1% | Forward excursion | Forward excursion |
| 2014 Kia Forte | CEN1318 | Small car | 47 | -27 | Rotate | 0.81 | 43% | 28% | 355 | 7% | 0.6% | IP | IP |
| 2013 Toyota RAV4 | CEN1319 | Small SUV | 45 | -24 | Translate | 0.60 | 22% | 13% | 283 | 5% | 0.4% | IP | IP |
| 2014 Scion tC | CEN1320 | Small car | 40 | -30 | Translate | 0.58 | 20% | 12% | 127 | 1% | 0.1% | Forward excursion | Forward excursion |
| 2013 Dodge Dart | CEN1321 | Small car | 36 | -33 | Translate | 0.63 | 24% | 15% | 84 | 0% | 0.1% | Airbag | — |
| 2013 Dodge Dart | CEN1322 | Small car | 42 | -43 | Translate | 0.46 | 11% | 6% | 184 | 2% | 0.2% | Airbag | Airbag |
| 2014 Mitsubishi Outlander | CEN1323 | Midsize SUV | 45 | -28 | Translate | 0.61 | 23% | 14% | 81 | 0% | 0.1% | Airbag | Airbag |
| 2013 Mazda 2 | CEN1324 | Minicar | 42 | -34 | Translate | 0.92 | 56% | 38% | 281 | 4% | 0.4% | Forward excursion | Forward excursion |

| Vehicle model | Test ID | Class | Delta V | Peak Accel | Vehicle motion | BrIC | AIS 3 BrIC | AIS 4 BrIC | HIC | AIS 3 HIC | AIS 4 HIC | HIC contact source | BrIC contact source |
|---|---|---|---|---|---|---|---|---|---|---|---|---|---|
| 2013 Fiat 500 | CEN1325 | Minicar | 46 | -29 | Rotate | 0.89 | 52% | 34% | 151 | 2% | 0.1% | IP | IP |
| 2014 Honda Odyssey | CEN1326 | Minivan | 54 | -31 | Rotate | 1.24 | 85% | 66% | 130 | 1% | 0.1% | Airbag | Airbag |
| 2013 Mercedes-Benz C class | CEN1327 | Midsize car | 51 | -28 | Rotate | 0.44 | 10% | 6% | 248 | 4% | 0.3% | Airbag | Airbag |
| 2013 Toyota Prius C | CEN1328 | Minicar | 50 | -31 | Rotate | 0.83 | 46% | 30% | 426 | 9% | 1.0% | IP | IP |
| 2013 Hyundai Accent | CEN1329 | Minicar | 44 | -24 | Translate | 0.80 | 42% | 27% | 108 | 1% | 0.1% | IP | IP |
| 2013 Kia Rio | CEN1330 | Minicar | 48 | -32 | Translate | 0.67 | 28% | 17% | 180 | 2% | 0.2% | Forward excursion | Forward excursion |
| 2013 Toyota Yaris | CEN1331 | Minicar | 54 | -27 | Rotate | 0.94 | 58% | 39% | 127 | 1% | 0.1% | IP | IP |
| 2014 Toyota Corolla | CEN1332 | Small car | 56 | -32 | Translate | 0.87 | 50% | 33% | 154 | 2% | 0.1% | Airbag | Airbag |
| 2014 Mercedes-Benz M class | CEN1333 | Midsize SUV | 55 | -27 | Rotate | 0.50 | 14% | 8% | 182 | 2% | 0.2% | Airbag | Airbag |
| 2014 Nissan Versa | CEN1334 | Minicar | 43 | -26 | Translate | 0.78 | 40% | 25% | 77 | 0% | 0.1% | Forward excursion | Forward excursion |
| 2013 Chevrolet Spark | CEN1335 | Minicar | 40 | -23 | Translate | 0.84 | 46% | 30% | 97 | 1% | 0.1% | Airbag | Airbag |
| 2014 Volvo XC90 | CEN1336 | Midsize SUV | 44 | -33 | Translate | 0.48 | 12% | 7% | 62 | 0% | 0.1% | Airbag | Airbag |
| 2014 Subaru Impreza | CEN1337 | Small car | 58 | -40 | Rotate | 0.44 | 9% | 5% | 133 | 1% | 0.1% | Airbag | Airbag |
| 2014 Infiniti Q50 | CEN1338 | Midsize car | 52 | -23 | Rotate | 0.55 | 17% | 10% | 204 | 3% | 0.2% | Airbag | Airbag |
| 2014 Acura MDX | CEN1339 | Midsize SUV | 60 | -28 | Rotate | 0.48 | 12% | 7% | 171 | 2% | 0.2% | Airbag | Airbag |
| 2013 Honda Fit | CEN1340 | Minicar | 53 | -26 | Rotate | 0.92 | 55% | 37% | 517 | 14% | 1.6% | IP | IP |
| 2014 Acura RLX | CEN1341 | Large car | 55 | -36 | Rotate | 0.87 | 50% | 33% | 151 | 2% | 0.1% | Airbag | Airbag |
| 2014 Mitsubishi Mirage | CEN1342 | Minicar | 43 | -31 | Rotate | 0.92 | 56% | 37% | 50 | 0% | 0.1% | Forward excursion | Forward excursion |
| 2014 Ford Fiesta | CEN1343 | Minicar | 48 | -31 | Rotate | 0.80 | 43% | 27% | 509 | 13% | 1.6% | IP | IP |
| 2014 Volvo S80 | CEN1344 | Large car | 43 | -20 | Translate | 0.44 | 10% | 6% | 102 | 1% | 0.1% | Airbag | Airbag |
| 2014 Mazda CX-5 | CEN1345 | Small SUV | 58 | -38 | Rotate | 0.92 | 56% | 37% | 181 | 2% | 0.2% | Airbag | Airbag |
| 2014 Mazda 3 | CEN1346 | Small car | 54 | -38 | Rotate | 0.59 | 21% | 12% | 209 | 3% | 0.2% | Airbag | Airbag |
| 2014 Toyota Prius | CEN1347 | Small car | 47 | -26 | Translate | 0.61 | 23% | 14% | 170 | 2% | 0.2% | Forward excursion | Forward excursion |
| 2014 Toyota Highlander | CEN1348 | Midsize SUV | 52 | -23 | Translate | 0.52 | 15% | 9% | 99 | 1% | 0.1% | Forward excursion | Forward excursion |
| 2014 Toyota Camry | CEN1349 | Midsize car | 46 | -28 | Translate | 0.73 | 34% | 21% | 125 | 1% | 0.1% | Airbag | Airbag |
| 2014 Chevrolet Equinox | CEN1401 | Midsize SUV | 33 | -19 | Translate | 0.46 | 11% | 6% | 49 | 0% | 0.1% | Airbag | Airbag |
| 2014 Ford Explorer | CEN1402 | Midsize SUV | 42 | -28 | Translate | 0.70 | 31% | 19% | 93 | 1% | 0.1% | Forward excursion | Forward excursion |
| 2014 Toyota 4 Runner | CEN1403 | Midsize SUV | 39 | -17 | Translate | 0.73 | 35% | 22% | 142 | 1% | 0.1% | Airbag | Airbag |
| 2014 Jeep Grand Cherokee | CEN1404 | Midsize SUV | 53 | -27 | Rotate | 0.64 | 25% | 15% | 172 | 2% | 0.2% | Airbag | Airbag |
| 2014 Honda Pilot | CEN1405 | Midsize SUV | 47 | -17 | Translate | 0.63 | 25% | 15% | 42 | 0% | 0.1% | Forward excursion | Forward excursion |
| 2014 Kia Sorento | CEN1406 | Midsize SUV | 43 | -23 | Translate | 0.66 | 27% | 16% | 179 | 2% | 0.2% | Forward excursion | Forward excursion |
| 2014 Nissan Rogue | CEN1407 | Small SUV | 46 | -24 | Translate | 0.69 | 31% | 19% | 185 | 2% | 0.2% | Airbag | Airbag |
| 2014 Mazda CX-9 | CEN1408 | Midsize SUV | 38 | -29 | Translate | 0.47 | 11% | 7% | 137 | 1% | 0.1% | Door sill | Doorsill |
| 2014 BMW 2 Series | CEN1409 | Midsize SUV | 51 | -23 | Translate | 0.47 | 11% | 7% | 269 | 4% | 0.3% | Airbag | Airbag |
| 2014 Mini Countryman | CEN1410 | Small car | 41 | -27 | Translate | 0.68 | 29% | 18% | 68 | 0% | 0.1% | Airbag | Airbag |
| 2014 Mitsubishi Lancer | CEN1411 | Small car | 48 | -34 | Rotate | 0.81 | 44% | 28% | 168 | 2% | 0.2% | Forward excursion | Forward excursion |
| 2014 Chevrolet Malibu | CEN1412 | Midsize car | 48 | -27 | Translate | 0.56 | 18% | 11% | 112 | 1% | 0.1% | Airbag | Airbag |
| 2015 Audi A3 | CEN1413 | Midsize car | 51 | -39 | Rotate | 0.82 | 45% | 29% | 103 | 1% | 0.1% | Airbag | Airbag |
| 2014 Fiat 500L | CEN1414 | Small car | 46 | -22 | Rotate | 0.88 | 52% | 34% | 228 | 3% | 0.3% | A-pillar | A-pillar |
| 2014 Hyundai Veloster | CEN1415 | Small car | 51 | -26 | Rotate | 0.75 | 37% | 23% | 100 | 1% | 0.1% | Forward excursion | Forward excursion |
| 2014 Nissan Juke | CEN1416 | Small car | 40 | -25 | Translate | 0.40 | 8% | 4% | 74 | 0% | 0.1% | Forward excursion | Forward excursion |
| 2015 Honda Fit | CEN1417 | Minicar | 51 | -36 | Rotate | 1.07 | 71% | 51% | 631 | 20% | 3.1% | Forward excursion | Forward excursion |
| 2015 Subaru WRX | CEN1418 | Small car | 52 | -27 | Rotate | 0.46 | 11% | 6% | 116 | 1% | 0.1% | Airbag | Airbag |
| 2015 Hyundai Genesis | CEN1419 | Large car | 61 | -32 | Rotate | 0.45 | 10% | 6% | 106 | 1% | 0.1% | Airbag | Airbag |

| Vehicle model | Test ID | Class | Delta V | Peak Accel | Vehicle motion | BrIC | AIS 3 BrIC | AIS 4 BrIC | HIC | AIS 3 HIC | AIS 4 HIC | HIC contact source | BrIC contact source |
|---|---|---|---|---|---|---|---|---|---|---|---|---|---|
| 2014 Ford C-Max | CEN1420 | Small car | 49 | -23 | Rotate | 0.69 | 30% | 18% | 212 | 3% | 0.2% | Forward excursion | Forward excursion |
| 2014 Mercedes-Benz E Class | CEN1421 | Large car | 60 | -38 | Rotate | 0.52 | 15% | 9% | 164 | 2% | 0.2% | A-pillar | A-pillar |
| 2015 Volkswagen GTI | CEN1422 | Small car | 55 | -27 | Rotate | 0.66 | 27% | 17% | 243 | 4% | 0.3% | Airbag | Airbag |
| 2014 Scion FR-S | CEN1423 | Small car | 50 | -32 | Translate | 0.57 | 19% | 11% | 71 | 0% | 0.1% | Airbag | Airbag |
| 2014 Mazda 5 | CEN1424 | Small car | 54 | -23 | Rotate | 0.63 | 24% | 15% | 122 | 1% | 0.1% | Forward excursion | Forward excursion |
| 2014 Chevrolet Volt | CEN1425 | Small car | 51 | -32 | Translate | 0.60 | 22% | 13% | 101 | 1% | 0.1% | Airbag | Airbag |
| 2014 Nissan Leaf | CEN1426 | Small car | 51 | -29 | Rotate | 0.85 | 48% | 31% | 96 | 1% | 0.1% | Forward excursion | Forward excursion |
| 2015 Hyundai Sonata | CEN1427 | Midsize car | 58 | -34 | Rotate | 0.79 | 42% | 26% | 405 | 8% | 0.8% | Airbag | SW through airbag |
| 2014 Scion xB | CEN1428 | Small car | 47 | -26 | Translate | 0.69 | 31% | 19% | 273 | 4% | 0.3% | Airbag | Airbag |
| 2014 BMW 5 Series | CEN1429 | Large car | 58 | -33 | Rotate | 0.47 | 12% | 7% | 86 | 0% | 0.1% | Airbag | Airbag |
| 2015 Honda Fit | CEN1430 | Minicar | 59 | -43 | Rotate | 0.89 | 52% | 34% | 651 | 22% | 3.4% | Airbag | SW through airbag |
| 2014 Infiniti Q70 | CEN1431 | Large car | 53 | -25 | Translate | 0.48 | 12% | 7% | 109 | 1% | 0.1% | Airbag | Airbag |
| 2015 Chrysler 200 | CEN1432 | Midsize car | 57 | -43 | Rotate | 0.67 | 29% | 17% | 119 | 1% | 0.1% | Airbag | Airbag |
| 2015 Subaru Legacy | CEN1433 | Midsize car | 58 | -31 | Rotate | 0.56 | 18% | 11% | 120 | 1% | 0.1% | Airbag | Airbag |
| 2015 Kia Soul | CEN1434 | Small car | 54 | -28 | Rotate | 0.61 | 23% | 14% | 374 | 7% | 0.7% | Airbag | Airbag |
| 2014 Lincoln MKS | CEN1435 | Large car | 44 | -26 | Translate | 0.53 | 15% | 9% | 82 | 0% | 0.1% | IP | IP |
| 2015 Kia Forte | CEN1436 | Small car | 56 | -44 | Rotate | 0.75 | 36% | 23% | 149 | 2% | 0.1% | IP | IP |
| 2015 Volkswagen Jetta | CEN1437 | Midsize car | 55 | -27 | Translate | 0.75 | 37% | 23% | 306 | 5% | 0.4% | Forward excursion | Forward excursion |
| 2014 Chrysler Town & Country | CEN1438 | Minivan | 48 | -23 | Translate | 0.72 | 34% | 21% | 230 | 3% | 0.3% | IP | IP |
| 2015 Toyota Sienna LE 4-door | CEN1439 | Minivan | 57 | -28 | Rotate | 0.57 | 19% | 11% | 118 | 1% | 0.1% | Forward excursion | Forward excursion |
| 2014 Mini Cooper | CEN1440 | Minicar | 43 | -33 | Translate | 0.52 | 15% | 9% | 166 | 2% | 0.2% | Airbag | Airbag |
| 2015 Kia Sedona | CEN1441 | Minivan | 59 | -26 | Rotate | 0.81 | 43% | 28% | 120 | 1% | 0.1% | Airbag | Airbag |
| 2015 Acura TLX | CEN1442 | Midsize car | 52 | -47 | Rotate | 0.70 | 32% | 19% | 136 | 1% | 0.1% | Airbag | Airbag |
| 2015 Honda Accord 2- door | CEN1443 | Midsize car | 55 | -23 | Rotate | 1.18 | 81% | 61% | 270 | 4% | 0.3% | Airbag | Airbag |
| 2015 Honda CR-V | CEN1444 | Small SUV | 49 | -25 | Translate | 0.68 | 29% | 18% | 137 | 1% | 0.1% | Airbag | Airbag |
| 2014 Nissan Quest | CEN1445 | Minivan | 53 | -17 | Rotate | 1.08 | 73% | 52% | 527 | 14% | 1.7% | Airbag | Airbag |
| 2015 Toyota Avalon | CEN1446 | Large car | 50 | -49 | Translate | 0.58 | 20% | 12% | 137 | 1% | 0.1% | Airbag | Airbag |
| 2015 Nissan Pathfinder | CEN1447 | Midsize SUV | 41 | -18 | Translate | 0.49 | 13% | 8% | 39 | 0% | 0.1% | Airbag | Airbag |
| 2015 Lexus RC | CEN1448 | Midsize car | 57 | -24 | Rotate | 0.50 | 14% | 8% | 105 | 1% | 0.1% | Airbag | Airbag |
| 2015 Lexus NX | CEN1449 | Small SUV | 48 | -25 | Translate | 0.74 | 36% | 22% | 150 | 2% | 0.1% | Airbag | Airbag |
| 2015 Lexus CT | CEN1450 | Small car | 45 | -30 | Translate | 0.60 | 22% | 13% | 142 | 1% | 0.1% | Airbag | Airbag |
| 2015 Toyota RAV4 | CEN1451 | Small SUV | 54 | -32 | Rotate | 0.57 | 19% | 11% | 163 | 2% | 0.2% | Airbag | Airbag |
| 2015 Toyota Prius V | CEN1452 | Midsize car | 58 | -41 | Translate | 0.62 | 23% | 14% | 193 | 2% | 0.2% | Airbag | Airbag |
| 2015 Kia Sedona | CEN1453 | Minivan | 61 | -25 | Rotate | 0.68 | 29% | 18% | 102 | 1% | 0.1% | Airbag | Airbag |

***The Assessment results of the Advanced Safety Technology in JNCAP and its future***

Hiroyuki Inomata,

Director of NCAP Management Department & Planning Department, National Agency for Automobile safety and Victim's Aid (NASVA),

Ms. Yoko Kishino,

International Adviser, NASVA

Mr. Souta Miyamoto,

Staff, NASVA

Japan

15-0275

**Abstract**

The Japanese government has set up the target of fatalities-from-traffic-accidents reduction. Its aim is to be at the safest traffic society in the world. However, the reduction rate of the death toll in Japan has declined but it's still in a severe situation. Moreover, we have a rapidly aging society. This is another problem.

On the other hand, with the rise of a national safety consciousness, many cars equipped with advanced technology are available on Japan's market including the small sized car, so called kei-car and it is in the most diffused situation in the world at a present stage. But more promotion is desired.

Nevertheless, an understanding about a difference of the performance and the characteristic of that technology are not yet understood efficiently.

Although NCAP has so far achieved big success by the technique of the information dissemination to a consumer for improvement in the safety performance of a car, extending this to the domain of advanced safety technology is called for.

JNCAP started advanced safety technology assessment from 2014 based on our roadmap. In 2014, we adjusted the protocol of the procedure of Autonomous Emergency Braking System (AEBS) test, Lane Departure Warning System (LDWS) test and an evaluation method.

In the protocol of an evaluation method, it is prescribed that an official announcement shows the overall points of several results of advanced safety technology assessment.

We are targeting the spread of technology by evaluating various advanced safety technology synthetically and thus more technical development is urged with the digitization technique of evaluating the reduction effect of a deaths and serious injury accidents based on the actual accident data from Japan.

We implemented the assessment according to these protocols and released the result of 37 models in FY2014.

So, various characteristics for every technology became clear as a result of the AEBS tests. Although various technologies, such as laser radar equipment, millimeter-wave radar equipment, mono-eye, dual-eye camera is used, we are able to discuss about the important information we should give to a consumer and the future course of the advanced safety technology depending on current test results.

Finally, I would also like to write about the future work of JNCAP based on the discussion taken in our steering committee meetings and the WGs.

Presently, NCAPs are taking places in every region in the world. In Japan, JNCAP have made a significant progress on road safety. This article includes advanced safety assessment, analysis and results which were started in fiscal year of 2014 and further developed.

## 1. Background

The number of road traffic deaths and serious injuries are declining recently. However, more can be done as the death toll in 2014 was 4,113 and 5,152 if it includes death within 30 days after the accident (data on 2012). NASVA (National Agency for Automotive Safety and Victim's Aid) acts to help those who are seriously injured from the road accidents. The government of Japan now sets the target of reducing death records to less than 2500. Its aim is to have the best road safety record in the world by 2018. MLIT has three measures linking each other on vehicle technical aspects for safety. JNCAP is one of them which is promoted by MLIT (Ministry of

Land, Infrastructure, Transport and Tourism), and NASVA. NASVA, as an exclusive organization, for supporting the seriously injured and their family members it carries out three types of activities; support, prevent and protect which are linked effectively. From fiscal year of 2014, JNCAP carried out passenger safety performance evaluation and pedestrian performance evaluation which prevent collision.

**2. Outline of advanced safety performance assessment**

To achieve the target that government sets, collision safety technologies are not quite enough. Also, older drivers directly involved in traffic accidents are increasing. Pedestrian death rate becomes over 50% is considerably high, thus clearly shows marked characteristic of an aging society. Meeting these problems, it is necessary to introduce a new safety technology such as AEBS which can avoid collision.

Under this circumstance, JNCAP steering committee has decided to enforce advanced safety technology assessment as one of measures which contributes to reducing deaths and severe injuries.

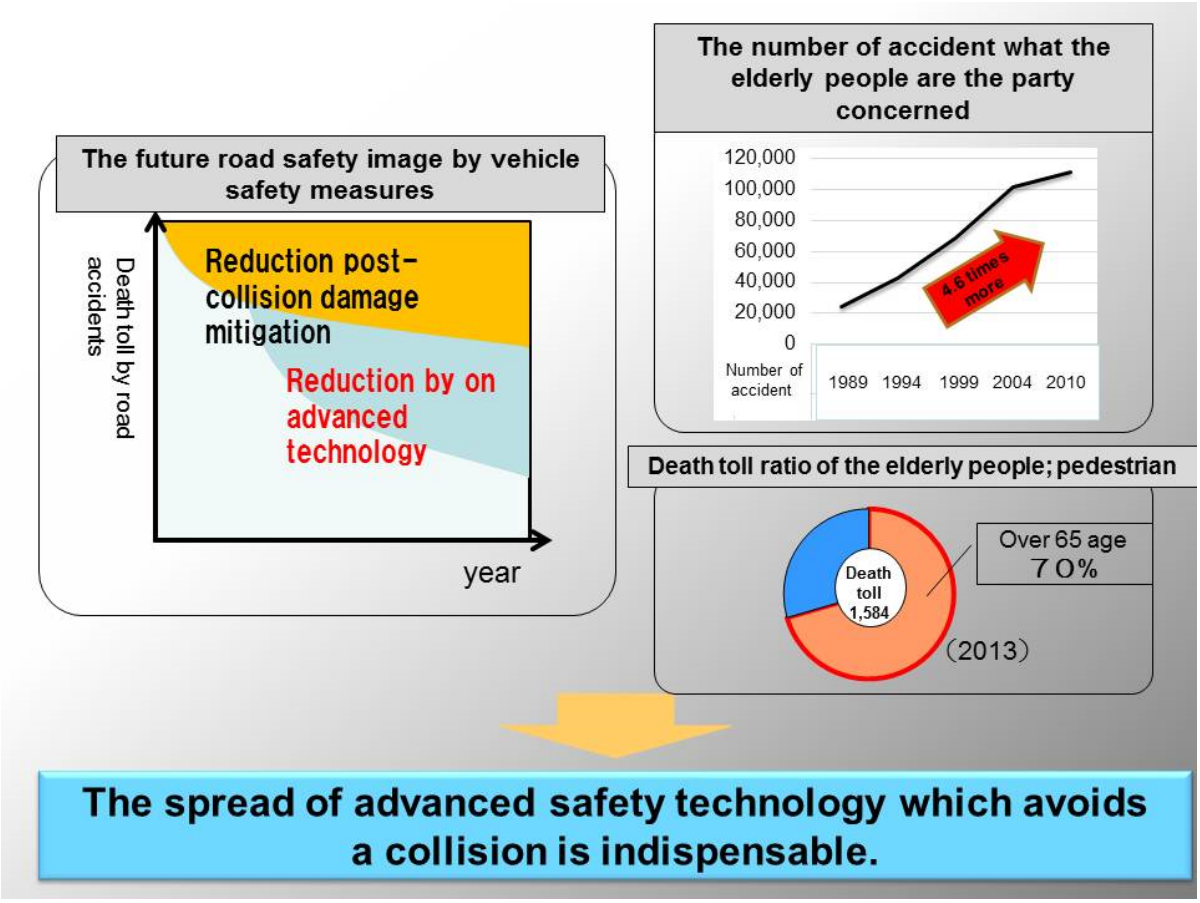


The steering committee refers to computed data of which the result of calculated the damage reduction effect is used in the ASV project which government promotes to make a roadmap for this technology. Digitization for reduction effects of deaths and injuries were calculated by multiplying relevance factor and safe contribution ratio at the time of system functioning and social loss ratio of death and severe injury is defined as 30:8. The total points of AEBS (car to car) and AEBS (car to pedestrian) refers as 100 points that is most effective.

## Evaluation points for advanced assessment
## （Forecast on accident reduction effect ）

| | ＡＳＶ technology | Estimated reduction numbers | | | | total of microdata | | | main cause |
|---|---|---|---|---|---|---|---|---|---|
| | | deaths | severe injuries | reduction effects | | deaths | severe injuries | injuries | |
| (1) | Autonoomous Emergency Brake System(AEBS) [car to car] | **59** | **1,649** | 33 | 100 | **59** | **1,664** | 164,453 | distracted driving Misoperation |
| (2) | Autonoomous Emergency Brake System(AEBS) [car to pedestrian] | **552** | **1,708** | 67 | | **700** | **2,287** | 14,639 | distracted driving |
| (3) | Lane Deoarture Warning System(LDWS) | **67** | **206** | 8 | | **168** | **516** | 1,274 | distracted driving・traffic condition |
| (4) | Lane Keep Asist system (LKAS) | **15** | **75** | 2 | | **15** | **75** | 260 | distracted driving・traffic condition |
| (5) | Rear View Monitoring System[rear] | **9** | **291** | 6 | | **13** | **415** | 3,638 | distracted driving |

Evaluation points

○The accident reduction effect of ASV technology is based on the macro accident statistical data for H 21（limiting to a passenger car/standard-sized car, and a minicar）

○Reductional effect score are calculated by multiplying the ratio of the social amount of a loss (3.75:1)and the number of and deaths and the serious injuries,then added each other.

○）making the numerical value into 100pt used as a standard by adding the accident reduction effect of car to car (1) car to pedestrian(2).

→Value of one point in the accident reduction effect of death and a serious injury for by system are calculated equarlly on 1 pt by each system

As it shows on our roadmap, we set 2 test protocols, allocation of the points, logo marks for AEBS (car to car) and LDWS and three policies for publication of test results, and started tests and evaluations in fiscal year of 2014.

### 3. Test procedures and evaluation methods for AEBS (car to car) and LDWS

1) Test procedures and evaluation methods for AEBS

We referred to Euro NCAP's test procedure and modified the evaluating methods for meeting a real Japanese accident condition.

Test scenarios are;

1. CCRs (Car to car rear collision stationery)

2. CCRm at constant speed (Car to car rear collision moving)

The function of each AEBS and Forward Collision Warning System (FCWS) are evaluated. We evaluate the damage mitigation effect by the combination of the alert to a driver, and the brake assisting function in each scenario. In order to examine impartially and properly, we use the steering robot and the accelerator brake robot. We use the same type of target as EuroNCAP representing vehicles back to sensing technology, such as radar and a camera. It is what can absorb a shock at the time of a collision.

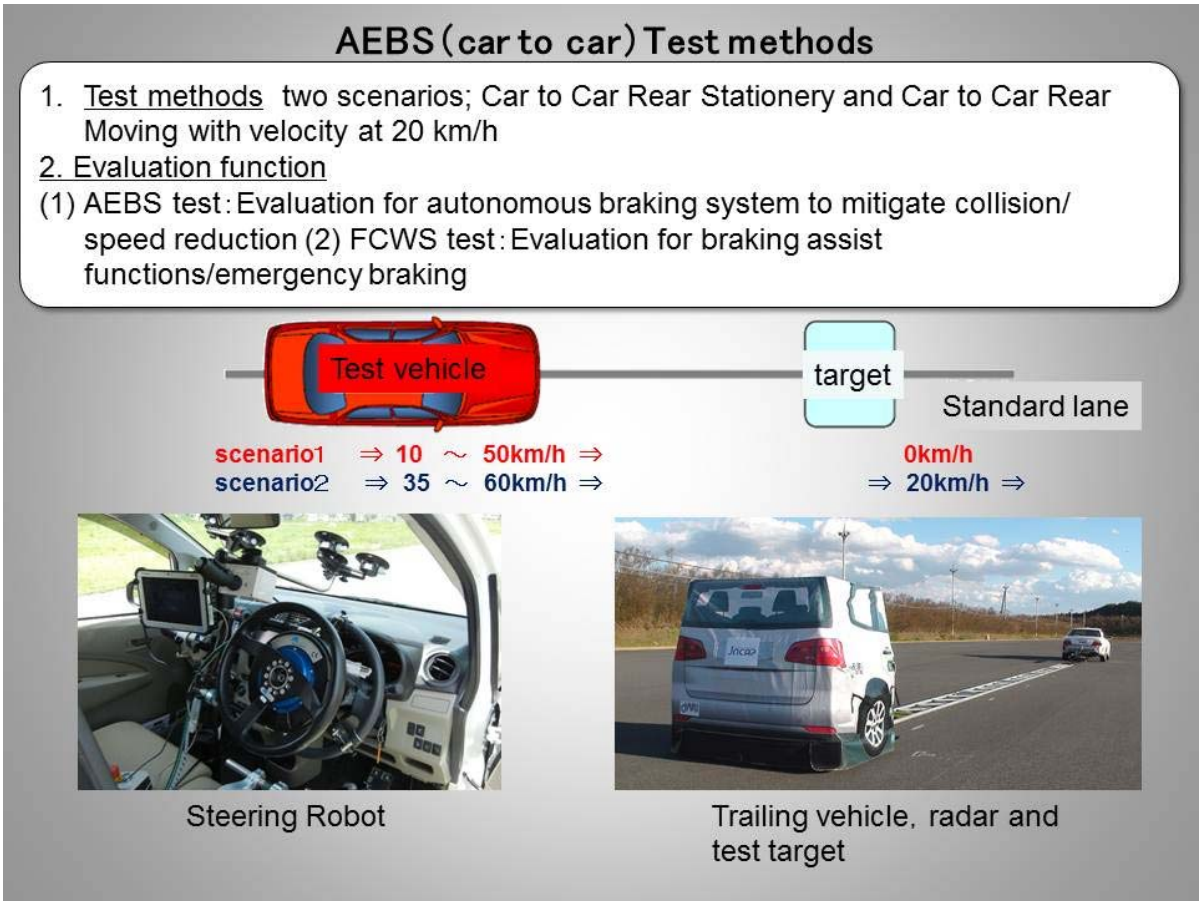


Each scenario, evaluating functions and speed reduction rate in each speed category are calculated with evaluation methods. (if collision is mitigated it refers as 1) are allocated this real accident data and adds up the total as for evaluation methods. All the marks are based on the forecast of the reduction effects of accidents by the government and the full marks for AEBS for car to car is 33 points. However, because of the safety reason, tests speed of 55km/h and 60 km/h are not carried out at the CCRs scenario, therefore total score at present is 32 points.

## AEBS test and evaluation

3. The index of evaluation
tested with each scenario speed by 5-km/h for every function (Max.34 conditions)
The speed reduction rate at the time of a collision is calculated for every test.

$$\text{The speed reduction rate} = \frac{\Delta V0 - \Delta Vc}{\Delta V0}$$

Vo: Initial relative velocity, Vc : relative velocity in case of collision is able to be avoided at the time of a collision, a speed reduction rate is set to "1."

4. Allocation of marks(points)
32 points are assigned about AEBS (car to car) according to the accident reduction
Calculated the reduction effect by a system functioning in death and a serious injury accident. An alarm function and a control facility is 1:1

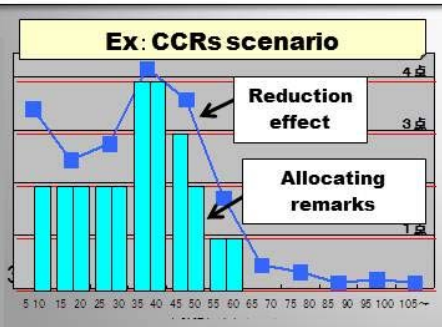


Score points based on effect

| condition | The reduction number of deaths and seriously injured per year | The effect of reducing the social loss (Evaluation points) |
|---|---|---|
| total | 3,968 | 100 |
| car to car | 1,708 | 33 |
| car to pedestrian | 2,260 | 67 |

For safety reason of test, 32 points are assigned instead of 33

2) Test procedures and evaluation methods for LDWS

We referred to US NCAP's test procedure and modified the evaluating methods for meeting a real Japanese accident condition. To be concrete, audible or visual; more than two different alert at a time should be confirmed in the test area when test vehicle runs with constant lateral velocity at 60km/h or 70km/h when approaching the lane line. This is repeated five times for both sides. Points should be calculated with the evaluation methods same as AEBS test. 8 points is given when it has started appropriately with velocity at 60km/h that is forecasted from the reduction effects of accidents.

**4. Publishing policy of advanced safety technology assessment**

The publication of the advanced safety technology assessment is held separately from other results of the assessments with the respect of enhancing its spread. We use a logo mark for exclusive use to gain more public interests.

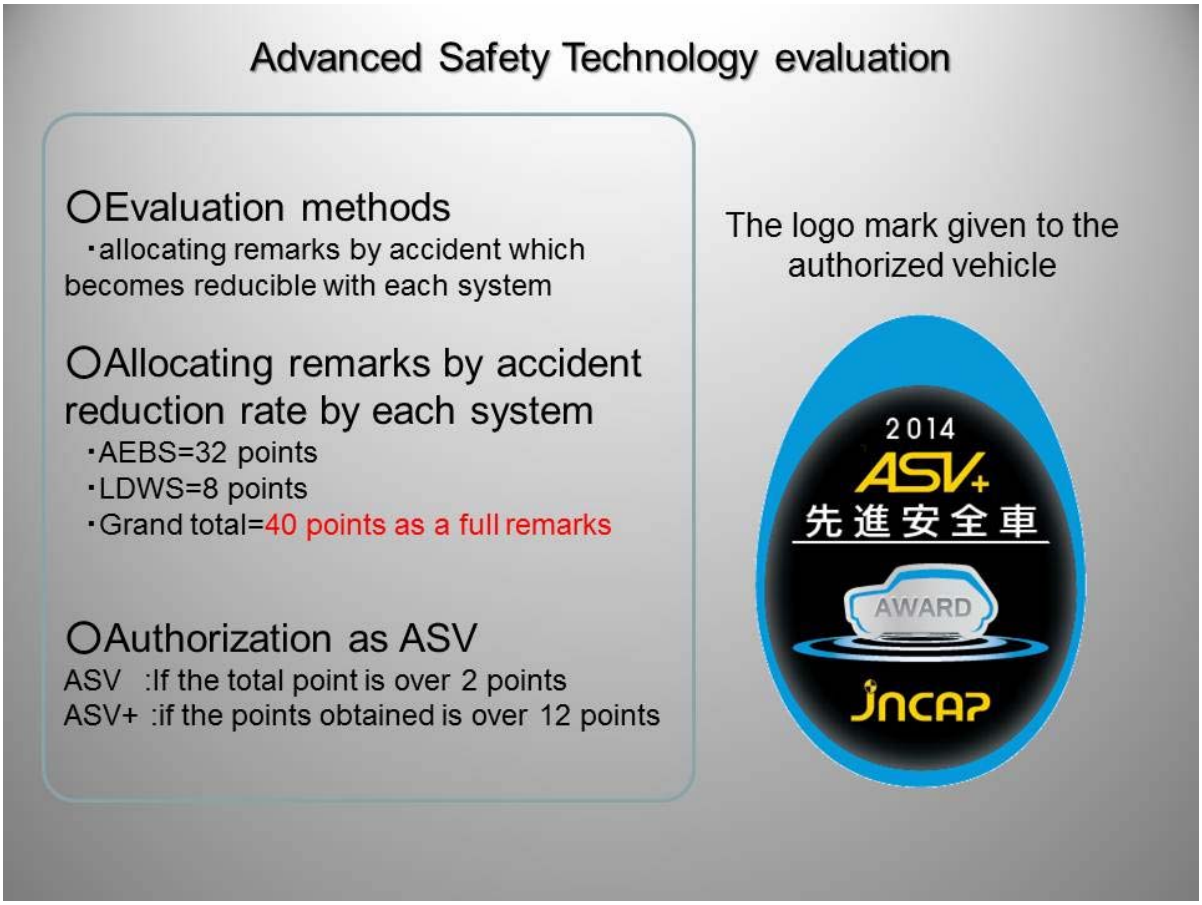


Moreover, we implement public relation activities including distribution of comprehensive leaflets and more than 500 thousands leaflets distributed among each manufacture's sales points. And logo mark stickers are indicated on their models.

**5. The results of advanced safety assessment in** fiscal year of **2014**

In fiscal year of 2014, we had 37 models tested as many devices are spreading rapidly to the market and it becomes competitive. As a result, all models had a definite safety performance. On the other hand, each of the technology which was used in AEBS had different characteristics and detection system to different speed range. We have found two characteristics; 1. AEBS using lazar radar mainly used in reasonable compact cars such as kei-cars, are spreading well. 2. AEBS using milli-wave or camera functioning well at middle speed range. This category aims at a higher level of safety. Combination with FCWS and assist braking system, combination of multi detectors, image detecting system with high resolution and coloring dual camera raises more safety. Considering the tests have many aspects in speeds and scenarios making a valiant effort should be important for stable controls and indispensable for forthcoming AEBS (car to pedestrian) tests. I believe that many manufacturers and suppliers cooporate to develop these technologies.

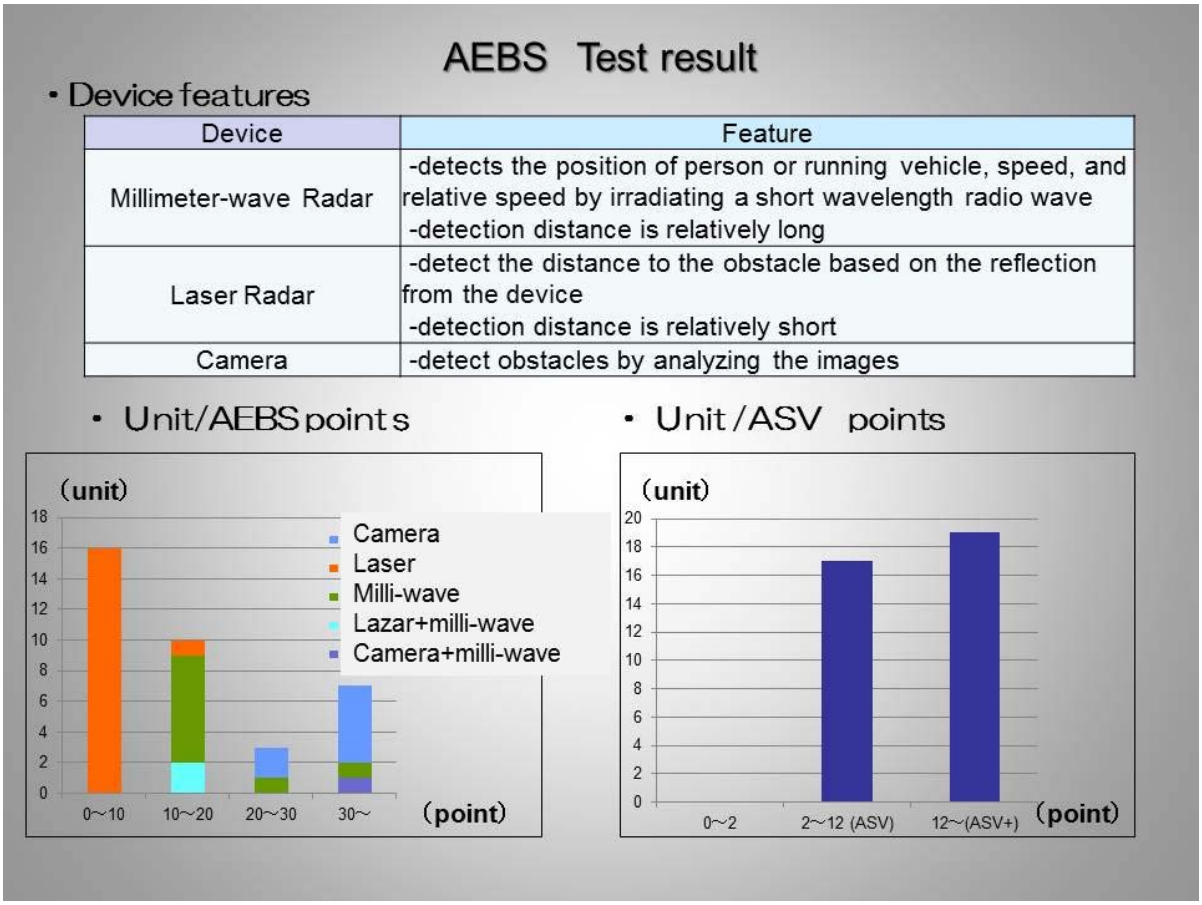


**6. Forthcoming events**

We are implementing for introduction of rear view monitoring test in fiscal year of 2015 and AEBS (car to pedestrian) tests and evaluations in fiscal year of 2016 in respect of needs from end users and victims of the traffic accident according to our roadmap. We have already started after setting up procedures and evaluation methods for around view camera with the research on accident data and simulations. Also for AEBS (car to pedestrian) tests, we need to determine procedures and evaluation methods with the making of test scenarios meeting real accident data and allocation of the points based on the reduction effects of accidents in 2015. Having been considering Japan's present circumstances, it is the key issue how we can focus to link with the assessment with increasing number of accidents that is often very severely involved by elderly people and accidents at night. We have been discussing many points at Task Force and Working Group under JNCAP steering committee.

**7. Conclusion**

We will have 30 to 40 models be tested in fiscal year of 2015 as manufactures became conscious of putting safer and innovative technology on the market. We need to maintain this trend continuously. NCAP operation bears a big power on its cooperation with the Japanese nation, industries, government and academics. And end users and manufactures need to take the results of NCAP assessments seriously moer than ever before. For those accounts we need more substantial work on test procedures and evaluation methods, also we regard international cooperation important to share experience and knowledge.

# DRIVER ALCOHOL DETECTION SYSTEM FOR SAFETY (DADSS) – A STATUS UPDATE.

**Abdullatif K. Zaouk**
**Michael Wills**
QinetiQ North America
U.S.A.
**Eric Traube**
National Highway Traffic Safety Administration
U.S.A.
**Robert Strassburger**
Alliance of Automobile Manufacturers
U.S.A.

Paper Number 15-0276

## ABSTRACT

The National Highway Traffic Safety Administration (NHTSA) and the Automotive Coalition for Traffic Safety (ACTS) began research in February 2008 to try to find potential in-vehicle approaches to the problem of alcohol-impaired driving. Members of ACTS comprise motor vehicle manufacturers representing approximately 99 percent of light vehicle sales in the U.S. This cooperative research partnership, known as the Driver Alcohol Detection System for Safety (DADSS) Program, is exploring the feasibility, the potential benefits of, and the public policy challenges associated with a more widespread use of non-invasive technology to prevent alcohol-impaired driving. The 2008 cooperative agreement between NHTSA and ACTS for Phases I and II outlined a program of research to assess the state of detection technologies that are capable of measuring blood alcohol concentration (BAC) or Breath Alcohol Concentration (BrAC) and to support the creation and testing of prototypes and subsequent hardware that could be installed in vehicles. This paper will outline the technological approaches and program status.

## INTRODUCTION

Alcohol-impaired driving (defined as driving at or above the legal limit in all states of 0.08 g/dL or 0.08 percent) is one of the primary causes of motor vehicle fatalities on U.S. roads every year and in 2011 alone resulted in almost 10,000 deaths. There are a variety of countermeasures that have been effective in reducing this excessive toll, many of which center around strong laws and visible enforcement. Separate from these successful countermeasures, the National Highway Traffic Safety Administration (NHTSA) and the Automotive Coalition for Traffic Safety (ACTS) began research in February 2008 aimed at identifying potential in-vehicle approaches to the problem of alcohol-impaired driving. Members of ACTS comprise motor vehicle manufacturers representing approximately 99 percent of light vehicle sales in the U.S. This cooperative research partnership, known as the Driver Alcohol Detection System for Safety (DADSS) Program, is exploring the feasibility, the potential benefits of, and the public policy challenges associated with a more widespread use of non-invasive technology to prevent alcohol-impaired driving. The 2008 cooperative agreement between NHTSA and ACTS (the "Initial Cooperative Agreement") for Phases I and II outlined a program of research to assess the state of detection technologies that are capable of measuring blood alcohol concentration (BAC) or Breath Alcohol Concentration (BrAC) and to support the creation and testing of prototypes and subsequent hardware that could be installed in vehicles.

Since the program's inception it has been clearly understood that for in-vehicle alcohol detection technologies to be acceptable for use among drivers, many of whom do not drink and drive, they must be seamless with the driving task, they must be non-intrusive, that is, accurate, fast, reliable, durable, and require little or no maintenance. To that end, the DADSS program is developing non-intrusive technologies that could prevent the vehicle from being driven when the device registers that the driver's blood alcohol concentration (BAC) exceeds the legal limit (currently 0.08 percent throughout the United States).

To achieve these challenging technology goals, very stringent performance specifications are required. These specifications have been formally documented in the DADSS Performance Specifications, which provide a template to guide the overall research effort. Another important challenge will be to ensure that the driving public will accept in-vehicle alcohol detection technology once it meets the stringent criteria for in-vehicle use. A parallel effort is underway to engage the driving public in discussions about the technologies being researched so that their feedback can be incorporated into the DADSS Performance Specifications as early as possible. The challenges to meet these

requirements are considerable, but the potential life-saving benefits are significant. An analysis of NHTSA's Fatality Analysis Reporting System (FARS) estimates that if driver BACs were no greater than 0.08 percent, 7,082 of the 10,228 alcohol–impaired road user fatalities occurring in 2010 would have been prevented.

The research effort that comprised the Initial Cooperative Agreement followed a phased process. The five-year Initial Cooperative Agreement began with a comprehensive review of emerging and existing state-of-the-art technologies for alcohol detection in order to identify promising technologies. Phase I, completed in early 2011, focused on the creation of proof-of-principle prototypes. The objective of Phase I was to determine whether there were any promising technologies on the horizon. Three prototypes were delivered and tested at the DADSS laboratory that yielded promising results for two of the three technologies.

The Phase II effort, begun in late 2011 and completed in late 2013, focused on the continued research of the technology to narrow gaps in performance against the DADSS Performance Specifications and meet the DADSS Performance Specifications within the needs of an in-vehicle environment.

Phase III and subsequent phases of research – the focus of the current Cooperative Agreement – will permit further refinement of the technology and test instruments as well as basic and applied research to understand human interaction with the sensors both physiologically and ergonomically – that is how these technologies might operate in a vehicle environment. At the culmination of this Agreement will be a device or devices that will allow a determination to be made regarding whether the DADSS technologies can ultimately be commercialized. If it is determined that one or more of these technologies can be commercialized, it is currently anticipated that the private sector will engage in additional product development and integration into motor vehicles.

The purpose of this paper is to outline the technological approaches taken in developing alcohol detection hardware. These approaches are founded on a clear understanding of the processes by which alcohol is absorbed into the blood stream, distributed within the human body, and eliminated from it. Not only must technologies under consideration quickly and accurately measure BAC, but the medium through which it is measured (e.g., breath, tissue, sweat, etc.) must provide a valid and reliable estimation of actual BAC levels. Alcohol absorption, distribution, and elimination measurement is a topic about which much has been written yet some large gaps in our understanding still remain. This paper will provide an overview of what is known regarding alcohol measurement via various methods and their implications for the decisions about which technologies deserve further study. The paper also will provide an overview of the current performance specifications developed to assess the in-vehicle advanced alcohol detection technologies and the rationale for them as well as an overall status of progress made to date.

## ALCOHOL ABSORPTION, DISTRIBUTION, AND ELIMINATION IN HUMANS

The science of pharmacokinetics is concerned with the ways in which drugs and their metabolites are absorbed, distributed, and eliminated from the body (Jones, 2008). This is separate from pharmacodynamics which is the study of the physiological effects of drugs and their actions on the body (Buxton, 2006 see Jones paper). Ethyl alcohol or ethanol, more commonly referred to as alcohol, is only one of a family of organic compounds known as alcohols. Ethanol, referred to hereafter as alcohol, is highly soluble in the body's water, which makes up 50-60 percent of body weight. Even though alcohol is a central nervous system depressant, people perceive it as a stimulant and in the early stages it can produce feelings of euphoria (Jones, 2008). With the consumption of larger amounts of alcohol, performance and behavior can be impaired resulting in reduced coordination, loss of motor control, lack of good judgment, and at very high concentrations (greater than 0.4 g/dL) loss of consciousness and death. Figure 1 portrays schematically the pathways by which alcohol is absorbed into the blood stream, is distributed throughout the body, and eliminated from it.

After ingestion, alcohol enters the stomach where it is partially absorbed through the stomach wall (about 20 percent), and then to the small intestines where most of the absorption takes place (about 80 percent). Alcohol is then transported to the liver and on to the heart before it is distributed by the arteries throughout all body fluids and tissues. Alcohol easily passes the blood-brain barrier where it affects central nervous system functioning. The time required for reaching equilibrium depends on the blood flow to the various organs and tissues, but over time alcohol mixes completely with all the water in the body and reaches into all fluid compartments within the body.

The characteristics of alcohol's distribution and elimination can point to potential ways in which BAC can be measured. There are two mechanisms by which alcohol is eliminated from the body, metabolism and excretion. The liver is the primary organ responsible for the elimination of alcohol and it is where about 95% of ingested alcohol is metabolized. The remainder of the alcohol, about 2-5 percent, is excreted unchanged wherever water is removed from the body; through the skin in sweat, from the lungs in breath, from the eyes in tears and from the

kidneys in urine. As noted above, alcohol distributes completely into all the body's compartments so alcohol can be measured in vivo in bodily tissue.

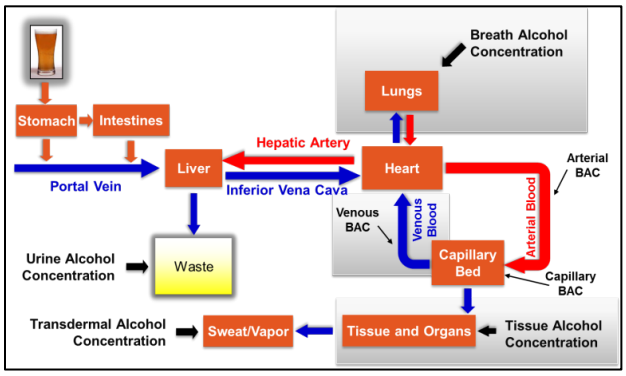


***Figure 1. Alcohol absorption, distribution and elimination though the body***

**Methods used to measure blood alcohol concentration**

For many years the only means to determine BAC was through blood and urine testing. As early as 1874 it was recognized that ingested alcohol can be measured in breath (Jones, 2008), and the smell of alcohol on breath is a well-known indication that someone has been drinking. Accurate measurement of alcohol in expired air has a physiological basis. Under normal lung function there is an efficient gas exchange between blood and gases, thus resulting in a close correlation between blood and gas concentrations of alcohol (Hök, 2006). Furthermore, a recent study (Lindberg et al., 2007) has established that the concentration of alcohol in breath is in very close agreement to that of alcohol in arterial blood (Figure 2), even though the gold standard for equating breath to blood alcohol is venous BAC. Of note is that arterial BAC is a better indication of brain alcohol and hence impairment than venous blood, so BrAC is particularly well suited as a measure of driver impairment.

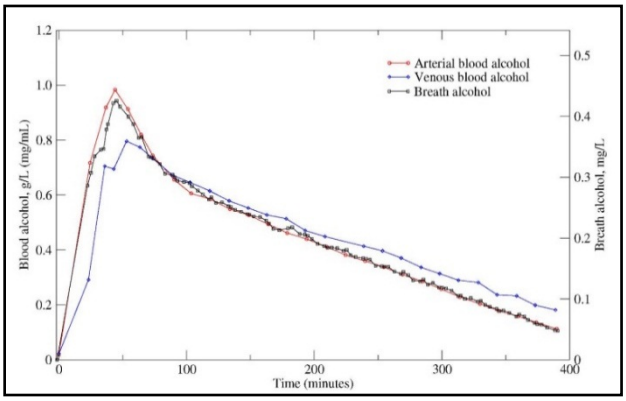


***Figure 2. Pharmacokinetic profile in one subject showing concentrations of alcohol in arterial blood (ABAC), venous blood (VBAC) and breath after oral ingestion of 0.6 g of alcohol per kg body weigh***

Dr. Robert Borkenstein is recognized as the inventor of the first system that measured alcohol on a person's breath. In 1954, he invented the first breath testing device, which used chemical oxidation and photometry to measure alcohol concentration. Subsequently physiochemical methods were developed for the measurement of alcohol in breath such as gas chromatography, electrochemical oxidation, and infra-red analysis. Breath testing has flourished because it is non-invasive and, in contrast to urine and blood samples that have to be sent away for testing, provides on-the-spot results. As a result most countries have adopted breath testing both for roadside screening and evidential purposes to establish BAC.

In recent years a number of other approaches have been identified that could be used to measure alcohol in perspiration (either vapor phase or liquid phase) or from measurements of alcohol in a person's tissue. As noted below, these techniques have not yet been widely used to measure to measure alcohol concentration.

## TECHNOLOGICAL APPROACHES

One of the first tasks of the project team was to perform a comprehensive review of emerging and existing state-of-the-art technologies for alcohol detection (Ferguson et. al., 2010). Technology scans were undertaken through patent and literature reviews. Based on these reviews four categories of technologies were identified with potential for measuring driver BAC within the vehicle environment:

### 1. Electrochemical/Transdermal Systems

Electrochemical Systems are chemical-reaction-based devices such as transdermal and breath-based systems. Alcohol in the presence of a reactant chemical will produce colorimetric changes measured by spectral analysis or a semi-conductor sensor. In fuel cell systems (typically used in current technology – breath-alcohol ignition interlocks), exhaled air containing alcohol passes over platinum electrodes which oxidize the alcohol and produce an electrical current; the more alcohol in the air sample, the greater the electrical current. The electrical current level permits accurate calculation of breath alcohol concentration (BrAC) which can be converted to blood alcohol concentration (BAC) using a standardized conversion factor.

### 2. Tissue Spectrometry Systems

Tissue Spectrometry Systems allow estimation of BAC by measuring the alcohol concentration in tissue. This is achieved through detection of light absorption at a particular wavelength from a beam of Near-Infrared (NIR) reflected from within the subject's tissue. As classified herein, they are touch-based systems and require skin contact. Variations of tissue spectrometry systems include Michelson, Raman, Fabry-Perot, Laser Diode and Light Emitting Diode (LED) based devices.

### 3. Distant/Offset Spectrometry Systems

Distant Spectrometry Systems use an approach that is similar to Tissue Spectrometry, except that no skin contact is required. Infrared (IR) is transmitted toward the subject from a source that also has a sensor to receive and analyze the reflected and absorbed spectrum to assess alcohol concentration in the subject's exhaled breath.

### 4. Behavioral Systems

Behavioral Systems detect impaired driving through objective behavioral measures. These include ocular indices such as gaze and eye movement, driving performance measures, as well as other performance measures believed to be related to driving performance.

In addition to the technology scans, a Request for Information (RFI) was published as a means by which the DADSS program was first communicated to potential technology developers . The goal of the RFI was to establish the level of interest among technology developers in taking part in the research, the kinds of technologies available, and their states of development relevant to in-vehicle applications. Based on information gleaned during the RFI process, a subset of technology companies were selected to receive a Request for Proposal. Detailed evaluation of the proposals that were received resulted in awards to technology companies based on two of the technological approaches outlined above; tissue spectroscopy and distant spectroscopy. The electrochemical/transdermal and behavioral approaches were not being pursued due their limitations for the DADSS application.

Current breath-based measurement systems as well as transdermal systems that measure alcohol in vapor or liquid phase perspiration, utilize electrochemically-based fuel-cell technology which has several limitations. Fuel cells must be warmed up to breath temperature to meet accuracy requirements, which in cold climates can take several minutes to accomplish. Furthermore, fuel cell alcohol measurements experience drift over time and require recalibration within one year or less. Both of these aspects render fuel cell technologies unsuitable for every-day use by the general public. Transdermal fuel-cell based devices suffer from the same disadvantages; however, there is an additional concern due to the long lag time of peak alcohol concentration in sweat versus blood. Various studies have identified the lag times to be on the order of two hours or more and it is not clear how future technological approaches to measuring TAC at a point in time can address this fundamental physiological difference.

Interest in behavioral-based approaches to measuring alcohol impairment dates back to the 1970s when the government and industry collaborated on possible vehicle-based measures of impairment (Ferguson et. al., 2010). There are a large number of measurable behaviors that have been identified that are affected by alcohol, including eye movements, reaction times, and vehicle-based measures of impairment such as lane position variability/lateral position, changes in driving speed and speed variability, pedal and steering control, distance from the car in front, and delay in motor actions and responses such as braking reaction times. Researchers have examined the

relationship of BAC to changes in these behaviors; however, close correlations between these measures have not yet been established. Another issue is that behavioral task performance may change as a result of a variety of impairments, whether from fatigue, illness, alcohol, medications, illegal drugs, or other sources. Furthermore, in order to measure impairment there has to be some measure of "normal" abilities on the specific task that can act as a baseline measurement for comparison. It should be noted that other sources of impairment can result in unsafe driving, and research continues to identify those risks and determine potential countermeasures. However, the limitations outlined above would be hard to deal with in an unobtrusive device to measure alcohol.

## PERFORMANCE SPECIFICATIONS

ACTS developed performance specifications to assess the in-vehicle advanced alcohol detection technologies that are being developed. The specifications are designed to focus the current and future development of relevant emerging and existing advanced alcohol detection technologies (Ferguson et. al., 2010). In addition to requirements for a high level of accuracy and very fast time to measurement, the influences of environment, issues related to user acceptance, long-term reliability, and system maintenance also will be assessed. The resulting list of specifications with definitions, measurement requirements, and acceptable performance levels are documented in the DADSS Subsystem Performance Specification Document. The accuracy and speed of measurement requirements adopted by the DADSS Program are much more stringent than currently available commercial alcohol measurement technologies are capable of achieving. As noted above, the devices would need to be seamless with the driving task and not inconvenience drivers. Translating that to appropriate performance specifications was approached by estimating the potential for inconvenience if reliability, accuracy, and time to measurement were set at various levels. Presented below are the processes used to derive them.

**Reliability** Developing an alcohol detection device as original equipment for the vehicle environment brings with it special challenges. Reliability is defined as the ability of a system or component to perform its required functions under stated conditions for a specified period of time. Levels of reliability that are too low would result in an unacceptable number of failures to operate the vehicle. It has been estimated that at the 3σ reliability (sigma - Greek letter σ - is used to represent the standard deviation of a statistical population) there could be the potential for 66,800 defects per million opportunities, where an opportunity is defined as a chance for nonconformance. The accepted level of reliability within the industry is 6σ. The term "six sigma process" comes from the notion that with six standard deviations between the process mean and the nearest specification limit, there will be practically no items that fail to meet specifications. In practice, 6σ is equivalent to 99.9997% efficiency. Processes that operate with "six sigma quality" over the short term are assumed to produce long-term defect levels below 3.4 defects per million opportunities.

**Accuracy and Precision** Accuracy is defined as the degree of closeness of a measured or calculated quantity to its actual (true) value (also referred to as the Systematic Error – SE). Precision is the degree of mutual agreement among a series of individual measurements or values (also referred to as the Standard Deviation – SD). To limit the number of misclassification errors, accuracy and precision must be very high, otherwise drivers may be incorrectly classified as being over the threshold (false positives), or below the legal limit (false negatives). To assure that drivers with BACs at or above the legal limit will not be able to drive, while at the same time allowing those below the limit to drive unhindered, SE and SD requirements at a BAC of 0.08 g/dL will need to achieve levels of 0.0003%. See Table 1 for the accuracy (SE) and precision (SD) requirements at other BACs.

***Table 1. DADSS Performance Specifications (% BAC or % BrAC)***

| Ethanol concentration | SE | SD |
|---|---|---|
| **0.020** | 0.0010 | 0.0010 |
| **0.040** | 0.0010 | 0.0010 |
| **0.060** | 0.0007 | 0.0007 |
| **0.080** | 0.0003 | 0.0003 |
| **0.120** | 0.0010 | 0.0010 |

**Speed of measurement** Another important performance requirement is that time to measurement be very short. Sober drivers should not be inconvenienced each and every time they drive their vehicle by having to wait for the

system to function. Current breath-based alcohol measurement devices can take 30 seconds or more to provide an estimate of BAC. However, it was determined that the DADSS device should take no longer to provide a measurement than the current industry standard time taken to activate the motive power of the vehicle. Thus, the subsystem should be capable of providing a reading of the current BAC and communicating the result within 325 msec. It should be capable of providing a second reading, if necessary, within 400 msec.

## THE DADSS SUBSYTEMS

### Tissue Spectrometry: Takata-TruTouch Touch-based Subsystem

Also known as near-infrared (NIR) spectrometry, this is a noninvasive approach that utilizes the near infrared region of the electromagnetic spectrum (from about 0.7 µm to 2.5 µm) to measure substances of interest in bodily tissue (Ferguson et. al., 2010). NIR spectroscopy is the science that characterizes the transfer of electromagnetic energy to vibrational energy in molecular bonds, referred to as absorption, which occurs when NIR light interacts with matter. Most molecules absorb infrared electromagnetic energy in this manner. The specific structure of a molecule dictates the energy levels, and therefore the wavelengths, at which electromagnetic energy will be transferred. As a result, the absorbance spectrum of each molecular species is unique. Better-known applications include use in medical diagnosis of blood oxygen and blood sugar, but devices have been developed more recently that can measure alcohol in tissue (Ridder et al., 2005).

Although the entire NIR spectrum spans the wavelengths from 0.7 – 2.5 µm, TruTouch has determined that the 1.25-2.5 µm portion provides the highest sensitivity and selectivity for alcohol measurement. The 0.7-1.25 µm portion of the NIR is limited by the presence of skin pigments such as melanin that can create large differences among people, particularly of different ethnicities. In contrast, the longer wavelength portion of the NIR, from 1.25-2.5 µm, is virtually unaffected by skin pigment (Anderson et al., 1981). One other advantage of using this part of the spectrum is that the alcohol signal in the 1.25-2.5 µm region is hundreds of times stronger than the signal in the 0.7-1.25 µm part of the NIR.

For the 1st generation prototype, as shown in Figure 2, the measurement begins by illuminating the user's skin with NIR light which propagates into the tissue (the skin has to be in contact with the device). A portion of the light is diffusely reflected back to the skin's surface and collected by an optical touch pad. The light contains information on the unique chemical information and tissue structure of the user. This light is analyzed to determine the alcohol concentration and, when applicable, verify the identity of the user. Because of the complex nature of tissue composition, the challenge is to measure the concentration of alcohol (sensitivity) while ignoring all the other interfering analytes or signals (selectivity).

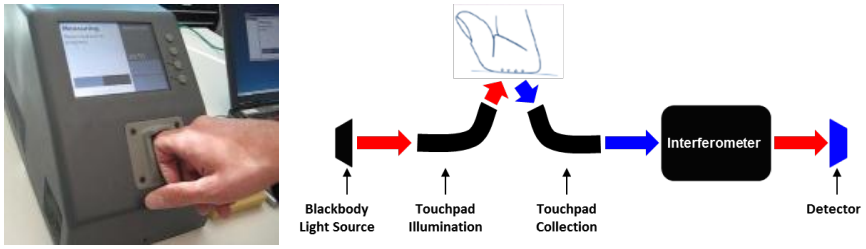


***Figure 2. Touch-based subsystem 1st generation sensor and block diagram***

Currently, the 2nd generation prototype is undergoing a fundamental change in system architecture; namely, a shift from a bulky spectrometer engine with moving parts to a fully solid-state sensor. This new approach, shown in Figure 3, requires extensive hardware and software research, the aims of which are to transform the touch-based sensor to improve suitability for long-term in-vehicle use and to improve the signal to noise ratio for better accuracy, precision, and shorter measurement times. The key enabling innovation is the ability to define an optimized subset of optical wavelengths which provide a high quality non-invasive alcohol measurement in humans. The 2nd generation uses modulated laser diodes to generate 40 unique wavelengths of light for alcohol measurement. The necessary laser diode target specifications were derived from an analysis of the human subject system data with accurate comparative reference data. The proposed design is also based on a Hadamard laser modulation scheme, a multiplexing technique, to improve signal to noise, along with re-design of the electronics, fiber-optical assembly, reference, touchpad and software controls to approach the necessary environmental and durability requirements for an automotive sensor device.

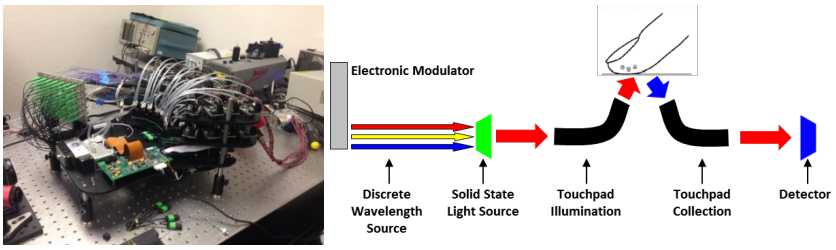


***Figure 3. Touch-based subsystem 2nd generation sensor and block diagram***

The focus of the current effort is to validate the new system architecture using 40 single laser packages with the goal of acquiring, verifying and integrating the full set of required multi-lasers packages into the 3rd generation benchtop system. Based on success of the 3rd generation sensor, the plan is to evolve and integrate into the DADSS research vehicle as show in Figure 4.

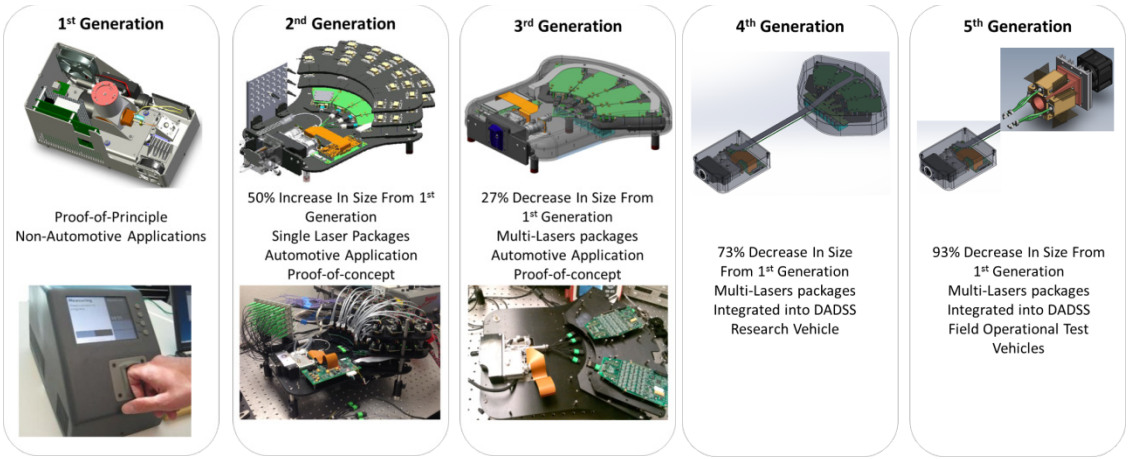


***Figure 4. Evolution of solid state touch-based DADSS subsystem***

**Autoliv Breath–based Subsystem**

Distant spectrometry systems use an approach similar to tissue spectrometry, in that they utilize the mid infrared (MIR) region of the electromagnetic spectrum (2.5-25 μm), except that no skin contact is required (Ferguson et. al., 2010). Infrared light is transmitted toward the subject from a source that receives and analyzes the reflected and absorbed spectrum to assess alcohol concentration in the subject's exhaled breath. There are a number of approaches under development that aim to remotely analyze alcohol in breath either within the vehicle cabin or around the driver's face without the driver having to provide a deep-lung breath sample.

As mentioned above, under normal lung function there is an efficient gas exchange between blood and gases, resulting in a close correlation between blood and breath alcohol concentrations (Hök, 2006) reflecting the very rapid equilibrium kinetics between pulmonary capillary blood and alveolar air (Opdam et al., 1986). In fact, as seen in Figure 2, BrAC measurements (converted to units of BAC) track arterial BACs throughout the blood alcohol time curve; only slightly below during the ascending curve, then virtually identical on the descending limb of the BAC time curve (Lindberg et al., 2007).

Current breath-based alcohol measurement techniques require direct access to undiluted deep-lung air, and therefore employ a mouthpiece. The challenge in measuring alcohol in breath from around the driver's face or within the vehicle cabin is that the breath is diluted with the cabin air. With funding from the Swedish Road Administration, Autoliv, Hök Instruments AB, and SenseAir AB have collaborated in the development of a non-contact method to measure alcohol in breath. The measuring principle of the sensor is to use measurements of expired carbon dioxide ($CO_2$) as an indication of the degree of dilution of the alcohol concentration in expired air. Normal concentration of $CO_2$ in ambient air is approximately 400 parts per million or 0.04%. Furthermore, $CO_2$ concentration in alveolar air is both known and predictable, and remarkably constant. Thus, by measuring $CO_2$ and alcohol at the same point, the degree of dilution can be compensated for using a mathematical algorithm. The ratio between the measured

concentrations of $CO_2$ and alcohol, together with the known value of $CO_2$ in alveolar air, can provide the alveolar air alcohol concentration.

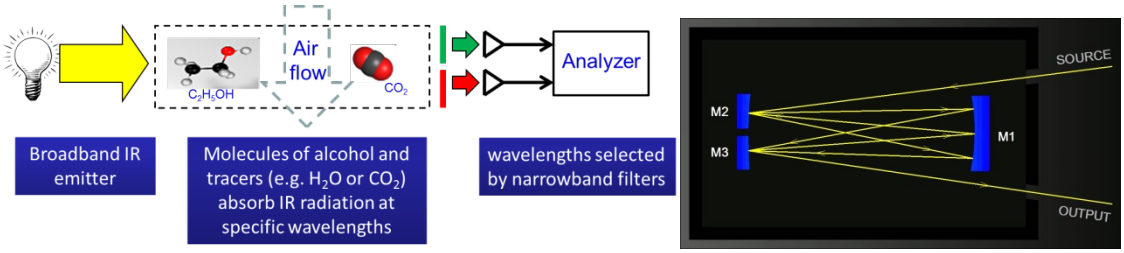


***Figure 5. Breath-based sensor block diagram***

The sensor technology under development by Autoliv and its partners uses infrared (IR) spectroscopy, which is superior to conventional fuel-cell devices in two ways. The IR-based sensors can be stable over the full product lifetime, eliminating the need for recurrent calibrations. Furthermore, the IR sensor is not as sensitive as the fuel-cell to major variations in ambient temperature. The 1st generation prototype uses a patented optical device in which multiple reflections of the IR beam within a closed space enables the calculation of alcohol concentration with high resolution. The expired breath from the driver is drawn into the optical module through the breathing cup. Once in the chamber, IR light is emitted from a light source and reflected by mirrors to increase the overall length of the IR optical path as shown in Figure 5, thus increasing the prototype's resolution. Detectors in the module then measure the ethanol and CO2 concentrations. For the purposes of human subject testing, the current device requires drivers to blow towards the sensor, which is positioned at a distance of 5 inches.

The 2nd generation sensor underwent incremental improvement that primarily involved a change in material composition of the sensor optical housing as well as significant improvements in mirror fabrication, coating, and integrated heaters designed to improve startup time, accuracy and precision. Significant progress was made in the 2nd generation with improvement to the startup time, dynamic accuracy and measurement performance at very low temperatures. The sensor underwent a series of Verification and Validation (V&V) tests as per the DADSS Performance Specification. The results from the V&V tests showed that there was no observed degradation or aging after these tests which simulated a vehicle life time of fifteen years.

The 2nd generation optical sensing element is too bulky and not suitable for vehicle integration. Further improvements are required to meet the DADSS specification. In addition, the improved sensor should be more robust when exposed to thermal gradients during the startup sequence. The focus of the current effort is to design, test, and validate a smaller, more robust optical sensor cavity that may be more easily packaged into a motor vehicle, with the objective remaining that the devices meet or exceed the DADSS Performance Specifications. Figure 6 shows the evolution of the Autoliv sensors.

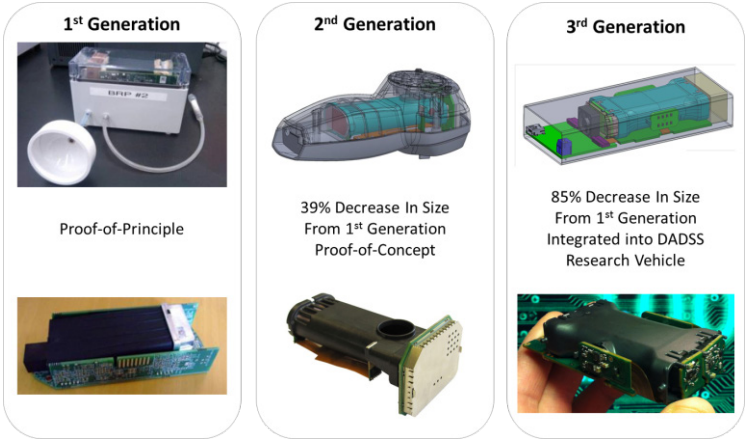


***Figure 6. Evolution of Breath-based DADSS Sensor***

## TECHNOLOGY & MANUFACTURING READINESS LEVELS

To manage, measure, and assess the progress and maturity of both technologies during the research and development phase, Technology Readiness Levels (TRL) and Manufacturing Readiness Levels (MRL) will be used throughout the program. These Readiness levels provide common terms to define technology from concept to commercial production, and have a proven effectiveness from the aerospace and defense sectors. Independently, readiness levels can also assist with self-assessment, monitoring progress and planning goals and actions. The advantages of using readiness levels are:

- provide a common understanding of technology and manufacturing readiness status
- risk management
- make decisions concerning technology funding
- make decisions concerning transition of both technologies to the automotive industry

The readiness levels used for the program are based on the "Automotive Technology and Manufacturing Readiness Levels, A guide to recognized stages of development within the Automotive Industry" by Professor Richard Parry-Jones CBE, Co-Chairman of the Automotive Council. These levels were revised and updated by the DADSS Technical Working Group (TWG) to incorporate DADSS specific milestones to achieve demonstrated commercial feasibility as shown in Figure 5.

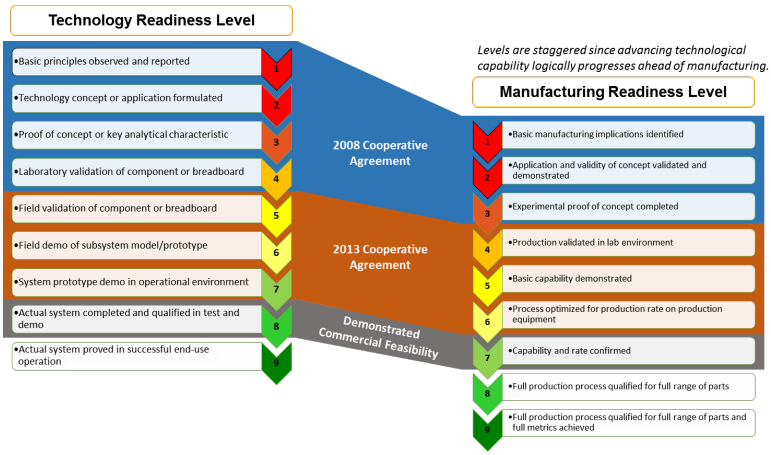


***Figure 7. TRL/MRL Demonstrated Commercial Feasibility***

Table 2 summarizes a preliminary evaluation of the "readiness" of the breath–based and touch–based technologies at the end of Phase II. As Figure 7 indicates, at the end of the 2008 cooperative agreement, the breath based technology achieved the expected TRL 4 level. The touch-based technology on the other hand was behind both TRL and MRL expectations. However, a number of technological challenges are ahead for the breath–based system relating to sampling in a vehicle cabin with the windows open and the air conditioning or heater on, which are not expected to be challenges that the touch–based system will need to surmount. Furthermore, the touch-based system readiness levels are anticipated to increase rapidly once development and integration of the full set of required multi-lasers packages is complete.

***Table 2. Technology and Manufacturing Readiness Levels by Technology Type***

| Technology | TRL | MRL |
|---|---|---|
| **Breath-based** | 4 | 4 |
| **Touch-based** | 3 | 2 |

## STANDARD CALIBRATION DEVICE (SCD) DEVELOPMENT

Standard Calibration Devices (SCD) were developed to assess and document the accuracy and precision of the Phase I prototypes. Two different SCDs were developed for prototype testing; one breath-based and one touch-

based. There are two aspects that were addressed (Ferguson et. al., 2010). First, samples of simulated "breath" and "tissue" were developed to provide a calibrated (known) and consistent ethanol concentration in vapor and/or liquid to the prototype. These samples also had to provide reasonable facsimiles of human breath and tissue. As noted above, the DADSS Performance Specifications for accuracy (SE) and precision (SD) are significantly more stringent than current evidential calibration instruments, thus the sample sources of breath and tissue had to exceed the DADSS specifications by an order of magnitude. The second requirement necessitated the development of delivery methods so that the targeted samples could be effectively delivered to the prototypes.

**Tissue Spectrometry SCD**

An SCD sample that simulates human tissue must produce a consistent ethanol response from the sensor at all concentrations of BAC, mimic the average optical scattering properties of human tissue over the target NIR wavelength range, and maintain the test material at normal human skin temperature (34 ºC). Figure 8 compares NIR reflectance of human versus simulated tissue and demonstrates the high level of concordance at the relevant wavenumbers. The system also must support varying concentrations of ethanol over the target BAC test range of 0.02% through 0.12 % BAC.

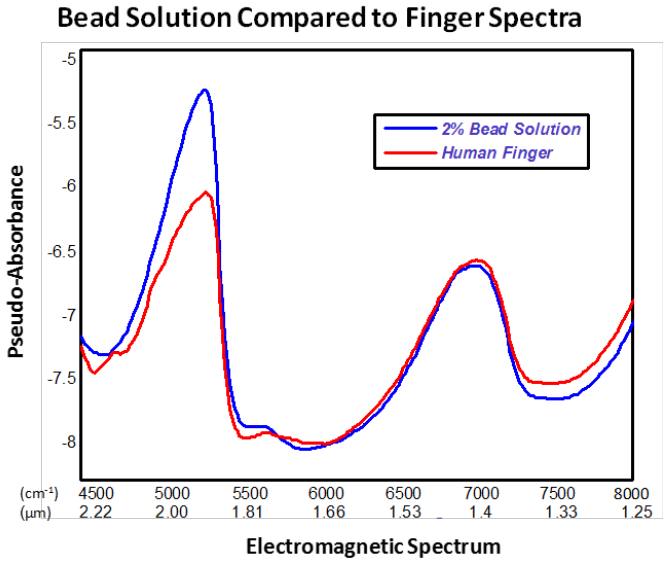


***Figure 8. Comparison of NIR reflectance of simulated tissue solution with human tissue***

Working with TruTouch Technologies, an SCD system was developed that comprised standardized aqueous test samples representative of human tissue and an electromechanical fluidic system for introducing the samples to the sensor. The standardized aqueous test samples are gravimetrically prepared solutions that use mono-dispersive polystyrene microspheres as an optical scattering agent. Quantities of ethanol in the solutions are certified by GC analysis to meet the required concentration levels after the beads are added. The simulated tissue solutions were stored in individual 15 mL vials. In addition to water and alcohol the "tissue" samples contain normal components of human blood such as urea, salt, and creatinine, as well as albumin that simulates blood density, microspheres that simulate the reflectance and scattering properties of collagen, and Triton that prevents the beads from clumping. An automated pipette delivery system made by Hamilton eliminates human error and operator variability, as well as improves accuracy and precision during gravimetric preparation of the solutions. The system consists of the Nimbus independent two channel work station, the pedestals and deckware custom containers, and a third party Mettler Toledo scale to accommodate 10, 20, 40, 100mL vials (Figure 9).

***Figure 9. Hamilton Nimbus Automated pipette delivery system***

The fluidic delivery system module was designed to easily attach to the TruTouch prototype sensor touch pad. The system module creates a liquid seal interface to support direct coupling between the optical sensor and the SCD test sample. The system also includes an agitation mechanism to prevent settling of the microspheres without introducing bubbles into the sample at the optical surface. The sealed system prevents evaporation loss, allows for sample removal, cleaning, and drying between sample measurements to prevent cross-contamination, and provides a reasonable degree of automation to avoid operator error. The prototype fluidics system is illustrated in Figure 9.

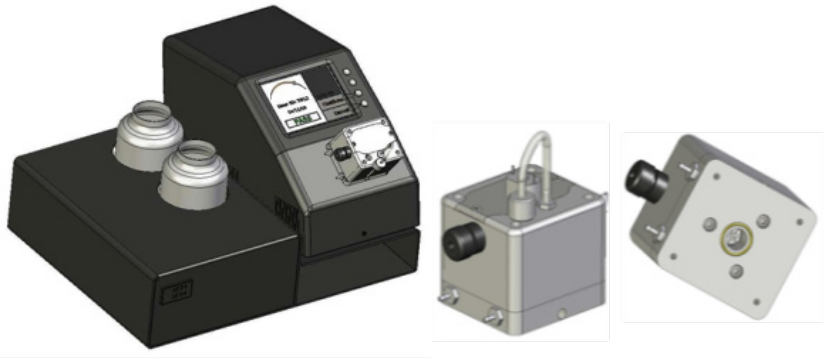

***Figure 10. Liquid coupling interface and prototype delivery system***

**Distant Spectrometry SCD**

The first step in the development of highly accurate breath samples was the production of standardized calibration dry gases (Ferguson et. al., 2010). Then the next step was to develop the DADSS dry gas mixture with the potential to exceed the DADSS Performance Specifications.

Two ethanol gas mixtures in 110 L pressurized bottles were developed in cooperation with ILMO Products Company:

1. Ethanol/Nitrogen (N2)
2. Ethanol/N2/5 % CO2/16 % oxygen (O2)

Each mixture was gravimetrically prepared at concentrations of 0.02, 0.04, 0.06, 0.08, 0.12 % BrAC. The mixtures were certified at ±0.5 ppm (±0.0002 % BrAC) by the vendor, exceeding the 0.0003 % BAC SE and SD when tested at 0.08 % BAC. In-house GC testing confirmed that the gas mixtures provided the levels of accuracy and precision for ethanol and other gases to the DADSS specifications over the complete range of gas concentrations. Additional testing verified acceptable shelf-life stability of the gas bottles.

Having validated that the dry gas mixtures complied with DADSS specifications, the next step was to humidify the gases to simulate human breath. Tests were conducted using a spirometer on a healthy male subject to measure the average flow rate and time of an exhaled breath. The ACTS team then developed a Wet Gas Breath Alcohol Simulator (WGBAS), shown in Figure 11, to add the necessary humidity.

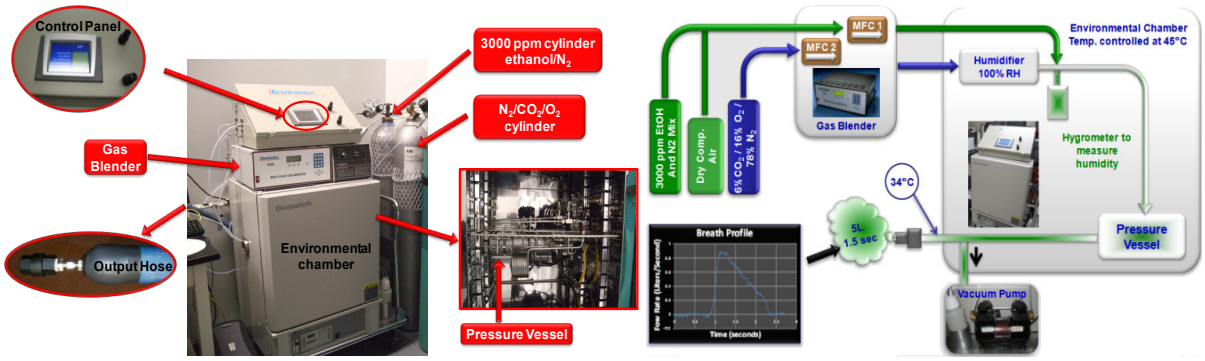


***Figure 11. WGBAS Configuration and principal of operation***

The WGBAS uses two dry gas sources: the first a mixture of N2/CO2/O2, and the second a 3000 ppm cylinder of ethanol, balanced with nitrogen. Mass flow controllers (MFC) generate the range of humidified ethanol from 0.02 % BAC to 0.12 % BAC. The gas in the premixed cylinder of N2/CO2/O2 enters the gas mixing module, flowing through humidifier metering valves located in an enclosure on top of the heated chamber. The proportional control of these valves allows the humidity to be adjusted. The ethanol/ N2 mixture flows out of the second MFC and into the bypass line that flows around the humidifier. The humidified N2/CO2/O2 mixture and the ethanol mixture meet before entering the hygrometer, which reports the dew point, humidity and gas temperature values, allowing for any necessary adjustments to obtain the required output of the humidifier. The humidified gas mixture then passes into the evacuated pressure vessel where it accumulates to a preset pressure, as monitored by an absolute pressure transmitter. When the preset pressure is met, the pressurized gas is expelled into the evacuated output tubing. As the gas leaves the system it is cooled to 34°C, the dew point temperature of the mixture, at a rate of approximately 1 liter in 2-3 seconds, thus simulating a humidified gas flow of breath. Figure 11 shows the WGBAS principle of operation described above.

The SCD dry gas, when passed directly through the WGBAS, was capable not only of meeting but also exceeding the DADSS SEs and SDs. In the second set of verification tests, humidity was added to the mixed gases with an output dew point of 34 °C. The addition of humidity resulted in much larger SE values than the DADSS specifications and the SD values were influenced by differences in the ethanol concentration, with only the lowest ethanol concentration being able to meet and exceed the specifications.

The WGBAS was not used in the Phase I evaluation process due to its current early development status. The system will undergo additional enhancements in Phase II to improve accuracy and precision through the introduction of a closed-loop feedback system to control the amount of ethanol concentration mixed into the gas stream. Therefore, the system is planned to be used for prototypes evaluation in Phase II.

**Verification Process**

An SCD qualification process was developed to document that the breath and tissue sample performance meet the requisite performance specifications. Initially, components of the breath and tissue SCD were measured with a Gas Chromatograph (GC) using a Flame Ionization Detector (FID) to verify that the critical SEs and SDs were achieved. The primary function of a GC is to separate and detect chemicals in a gas flow passing through a thin column lined with specific coatings that interact with the components in the flow. The FID ignites the gases flowing out of the column with hydrogen gas. The detector then generates an electrical signal corresponding to the amount of ionized products from the combustion. The area under the curve of the electrical signal is integrated to correspond to the concentration of the gases at the column exit. Temperature, flow rate, and column selection influence the retention time of gas flow components.

The tubing and connections to the GC and the mass flow controller are heated to 34 °C, the exit temperature of human breath, to ensure the incoming gases are uniform and to assure consistent results. Several variables were found to affect and improve the GC ethanol measurement, including:

- Operating at low temperature vs. high temperature;
- Obtaining a homogeneous system, with uniform equilibrium temperature for each part of the system;
- Passivating (ability to treat a surface (typically metal) so that it is less reactive chemically) the sample line and regulator;

- Reducing the surface area of the sample line;
- Creating a constant backpressure on the actuator valve exhaust line;
- Producing a purging process for the regulator and sample loop.

The influence of the variables were quantified and examined before an optimal operating condition was obtained for the ethanol gas measurement process. Once the optimal operating conditions were identified, the dry and wet gases were then measured using the improved system shown in Figure 12.

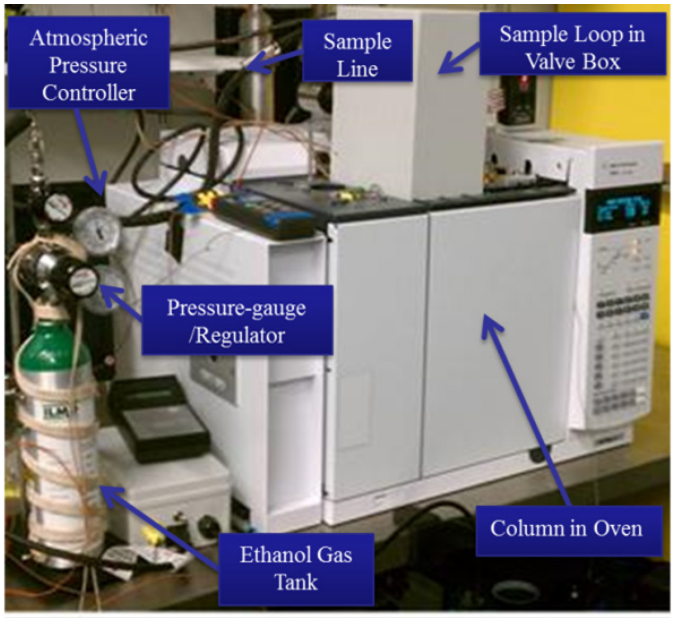


***Figure 12. GC system used to measure ethanol gas***

Figure 13 shows the dry gas ethanol gas measurement that is inaccurate and imprecise (left) compared with a measurement, using the developed measurement process, that shows accurate and precise measurements within the DADSS specification (right). Figure 14 shows the WGBAS measurements within the DADSS tolerance specification.

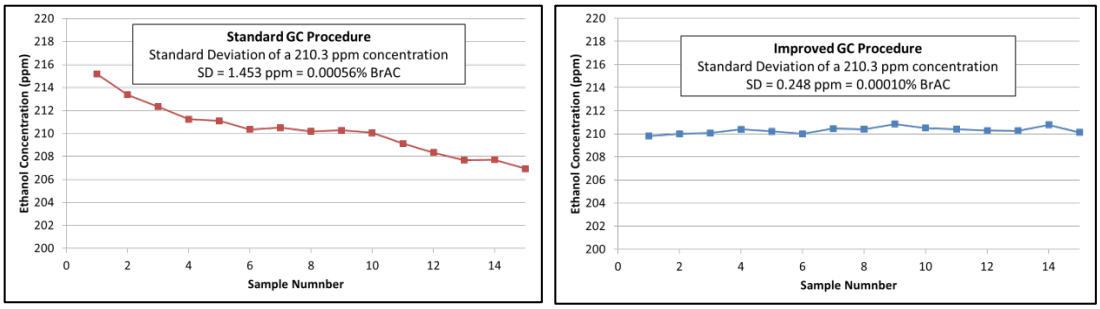


***Figure 13. Standard and improved dry gas measurements comparison***

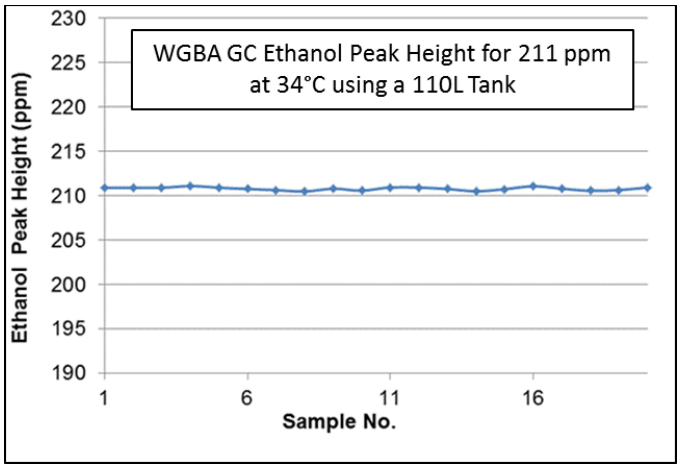


| GC Ethanol Gas Peak Height | BrAC GC Ethanol Tolerance (Precision) | BrAC GC Ethanol Tolerance (Accuracy) |
|---|---|---|
| % BrAC | % BrAC | % BrAC |
| 0.07996 | 0.000040268 | 0.000038566 |
| 0.07996 | 0.000033894 | 0.000044940 |
| 0.07997 | 0.000045174 | 0.000033660 |
| 0.08004 | 0.000115565 | 0.000036731 |
| 0.07997 | 0.000046275 | 0.000032559 |
| 0.07991 | 0.000013155 | 0.000091989 |
| 0.07986 | 0.000057380 | 0.000136214 |
| 0.07980 | 0.000117447 | 0.000196281 |
| 0.07992 | 0.000001654 | 0.000077180 |
| 0.07984 | 0.000081450 | 0.000160284 |
| 0.07998 | 0.000056851 | 0.000021983 |
| 0.07997 | 0.000049346 | 0.000029488 |
| 0.07991 | 0.000010844 | 0.000089678 |
| 0.07981 | 0.000107518 | 0.000186352 |
| 0.07990 | 0.000018249 | 0.000097083 |
| 0.08003 | 0.000107089 | 0.000028255 |
| 0.07992 | 0.000001586 | 0.000077248 |
| 0.07983 | 0.000089980 | 0.000168814 |
| 0.07986 | 0.000057055 | 0.000135889 |
| 0.07998 | 0.000055376 | 0.000023458 |
| Average | | |
| 0.07992 | | |

***Figure 14. WGBAS accuracy and precision using the improved GC system***

## CONCLUSIONS

Significant progress has been made to identify DADSS technologies that have the potential to be used on a more widespread basis in passenger vehicles. Two specific approaches have been chosen for further investigation; tissue spectrometry, or touch-based, and distant/offset spectrometry, or breath-based sensors. Proof-of-principle prototype DADSS sensors have been developed, one designed to remotely measure alcohol concentration in drivers' breath from the ambient air in the vehicle cabin, and the other is designed to measure alcohol in the driver's finger tissue through placement of a finger on the sensor.

Progress also has been made to develop calibration devices for both breath-and touch-based bench testing that will be able to measure whether the DADSS devices can meet the stringent criteria for accuracy and precision. Unique standard calibration devices have been developed for both the breath- and touch-based systems that go well beyond current alcohol-testing specifications.

In summary, the DADSS Program so far has accomplished the goals set at the onset of the program. Prototype testing has indicated that there are potential technologies that ultimately could function non-invasively in a vehicle environment to measure a driver's BAC. Furthermore, the DADSS Program is on track to develop research vehicles to demonstrate the technologies by the end of 2015.

## REFERENCES

Anderson, R.R., Parrish, J.A. 1981. The Optics of Human Skin. The Journal of Investigative Dermatology, 77, 13-19.

Ferguson, S.A., Traube, E, Zaouk, A, Strassburger, R. 2009. Driver Alcohol Detection System For Safety (DADSS) – A non-regulatory approach in the development and deployment of vehicle safety technology to reduce alcohol-impaired driving. Paper Number 09-0464. Proceedings of the 21st International Technical Conference on the Enhanced Safety of Vehicles.

Ferguson, S.A., Zaouk, A., Strohl, C. 2010. Driver Alcohol Detection System for Safety (DADSS). Background and Rationale for Technology Approaches. Society for Automotive Engineers Technical Paper, Paper No. 2010-01-1580, Warrendale, PA: Society of Automotive Engineers.

Ferguson, S.A.; Traube, E; Zaouk, A; Strassburger, R. 2011. Driver Alcohol Detection System For Safety (DADSS) – Phase I Prototype Testing And Finding. Paper Number 11-0230. Proceedings of the 22nd International Technical Conference on the Enhanced Safety of Vehicles.

Hök, B., Pettersson, H., Andersson, G. 2006. Contactless measurement of breath alcohol. Proceedings of the Micro Structure Workshop. May, 2006, Västerås, Sweden.

Jones, A.W. 2008 Biochemical and Physiological Research on the Disposition and Fate of Ethanol in the Body. Garriott's Medicological Aspects of Alcohol (Fifth Edition), 47.

Lindberg, L., Brauer, S, Wollmer, P., Goldberg, L., Jones, A.W., Olsson, S.G. 2007. Breath alcohol concentration determined with a new analyzer using free exhalation predicts almost precisely the arterial blood concentration. Forensic Science International. 168: 200-207.

Opdam, J.J., Smolders, J.F. 1986 Alveolar sampling and fast kinetics of tetrachloroethene in man. I Alveolar sampling. British Journal of Industrial Medicine, 43, 814-824.

Ridder, T.D., Hendee, S.P., Brown, C.D. 2005. Noninvasive alcohol testing using diffuse reflectance near-infrared spectroscopy. Applied Spectroscopy, 59, 181-189.

# EURO NCAP'S FIRST STEP TO ASSESS AUTONOMOUS EMERGENCY BRAKING (AEB) FOR VULNERABLE ROAD USERS

**Richard Schram**
**Aled Williams**
**Michiel van Ratingen**
European New Car Assessment Programme,
Belgium
**on behalf of the Euro NCAP P-NCAP Working Group**

**Stephan Ryrberg (Chairman of ACEA TF NCAP Expert Group AEB)**
Volvo Car Corporation
Sweden
**Raimondo Sferco (Chairman of ACEA TF NCAP)**
Ford Motor Company
Germany
**on behalf of the ACEA, JAMA and KAMA joint WG on AEB**

Paper Number: 15-0277

## ABSTRACT
Following the implementation of AEB City and AEB Inter-Urban systems in Euro NCAP's safety rating in 2014, a third type of AEB technology, Autonomous Emergency Braking for Vulnerable Road Users (AEB VRU), will be added to the overall assessment of new vehicles in 2016. The introduction of AEB VRU will be done in two phases where in 2016 AEB Pedestrian is implemented followed by AEB Cyclists in 2018.

AEB VRU will be awarded as part of the assessment of Pedestrian Protection and represents the next step to improve the protection of vulnerable road users, complimentary to the existing subsystem tests to the vehicle front end. Following system tests in common pedestrian accident scenarios, more challenging and demanding cyclist scenarios are planned in a subsequent phase.

In close corporation with the car industry represented by the ACEA, JAMA and KAMA associations, Euro NCAP has developed detailed test and assessment procedures for AEB Pedestrian. The procedures are based on the existing car to car AEB test and assessment protocols and validated and checked for repeatability and reproducibility at several Euro NCAP laboratories. This paper describes both the test and assessment protocols.

## BACKGROUND
In 2009, Euro NCAP introduced the overall rating scheme, which allows new technologies to be implemented in the safety assessment of a new vehicle. The new rating scheme consists of four areas of assessment, also called boxes, which together result in a single overall safety rating. The four areas of assessment are Adult Occupant Protection (AOP), Child Occupant Protection (COP), Pedestrian Protection (PP) and Safety Assist (SA).

Over the last few years, Euro NCAP has rapidly raised the requirements for better protection of vulnerable road users in the event of a crash which was seen to lag behind. After significant updates to the test and assessment protocols in the area of passive safety, the next logical step was to include the assessment of AEB systems. Due to the nature of pedestrian accidents with passenger cars, most AEB systems are only capable of mitigating these crashes and therefore, Euro NCAP considers these systems complementary to passive safety measures already in place.

At the moment different AEB Pedestrian systems are already available on the market, based on radar, (stereo) camera or a combination of these sensors. The performance of these systems vary significantly based on the sensors used. The first generation of camera based systems typically switch off during low ambient lighting conditions as classification of pedestrians in darkness is not reliable enough. Euro NCAP has based its requirements for AEB Pedestrian systems on best practice to push for further development of these lifesaving technologies.

## WORKING GROUP

As for all Euro NCAP protocols, the development of the test procedure and assessment criteria was done within a collaborative Working Group. The Primary NCAP working Group, P-NCAP TWG in short, involved Euro NCAP members and laboratories and was given the task to deliver AEB Pedestrian protocols by the end of 2014, for implementation in 2016. Although car makers and suppliers were not directly involved in the working group, several meetings were organised between representatives of both sides to review the procedures. More importantly, the work of the group took advantage of and brought together the results delivered by several main research initiatives in Europe that where looking into the development of AEB test and assessment procedures.

### Initiatives

In Europe, several initiatives have been running in parallel, all with the same goal of developing test procedures for assessing AEB systems in general and AEB Pedestrian systems in particular: "AEB", "AsPeCSS" and "vFSS". Besides this, ACEA started an internal project to develop so called *articulated* pedestrian targets.

The RCAR Autonomous Emergency Braking group, led by Thatcham aims at designing and implementing a testing and rating procedure for Autonomous Emergency Braking ("AEB") systems reflecting real world accident data. It is hoped that this will encourage the development of AEB systems that can avoid or mitigate the effects of car-to-pedestrian and car-to-car collisions seen in the most common crash types. The group mainly consists of insurance institutes, supported by Volvo Car Corporation, Subaru, Daimler and first-tier supplier Continental. The work of the RCAR AEB group is ongoing.

The European Commission sponsored FP7 project AsPeCSS (Assessment methodologies for forward looking Integrated Pedestrian and further extension to Cyclist Safety Systems) led by IDIADA had specific project goals to develop harmonised and standardised procedures for the assessment of forward looking integrated pedestrian safety systems. The project partners consisted of nine research institutes, three of which were Euro NCAP laboratories: BASt, IDIADA and TNO. From industry side, BMW, PSA and Toyota participated as car manufacturers and Autoliv, Bosch and TRW as first-tier suppliers. The AsPeCSS project ran from 2011 until 2014.

The third initiative was vFSS (Advanced Forward-Looking Safety Systems) led by DEKRA. The project was supported by the BASt as a Euro NCAP Test Lab. The Insurance Companies Allianz, GDV and KTI as well as the AUDI, BMW, Daimler, Ford, Honda, Opel, Porsche, Toyota and VW as industry partners. One of the main deliverable were the static pedestrian targets that were adopted in the Euro NCAP protocols. They will be described in further detail within this paper.

The outcome and deliverables of all the initiatives were extensively discussed within the working group and formed the basis for the decision on test scenarios and targets used.

## TEST SCENARIOS AND TARGETS

There was a large overlap of the proposed test scenarios from the different initiatives, based on an extensive analysis of real world car-to-pedestrian accidents mainly from Germany, Great-Britain and France. Overlaying the proposed test scenarios, the P-NCAP TWG agreed to focus on four test scenarios for AEB Pedestrian. In the Car-to-VRU Farside Adult (CVFA) scenario, the running pedestrian crosses the vehicle path from the farside. It represents the situation where a pedestrian first crosses another lane before entering the lane in which the vehicle is driving. The timing is set such that without any AEB reaction from the vehicle, the adult pedestrian target would end up contacting the centreline of the vehicle. The second adult pedestrian scenario represents a pedestrian stepping of the sidewalk into the lane the vehicle is driving in. There are two variants with different impact locations of 25 and 75% of the vehicles width (CVNA-25 & CVNA-75).
The final scenario is the most challenging one, where a child pedestrian appears from behind two parked vehicles and directly stepping into the lane the vehicle is in. Similar to the farside adult scenario, the impact location will be in the middle of the vehicle (CVNC).

**Car-to-VRU Farside Adult (CVFA)**

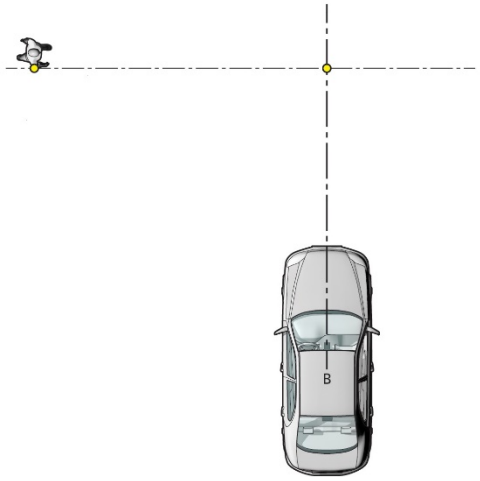


*Figure 1.* AEB Pedestrian scenario, CVFA

**Car-to-VRU Nearside Adult (CVNA-25 & CVNA-75)**

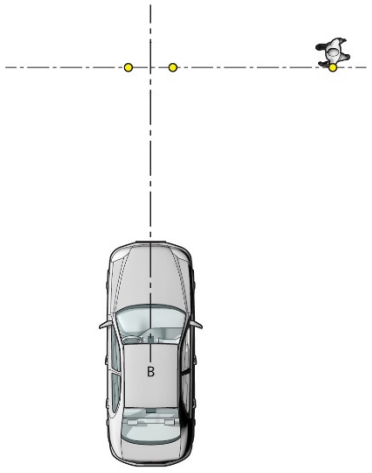


*Figure 2.* AEB Pedestrian scenario, CVNA-25 & 75

**Car-to-VRU Nearside Child (CVNC)**

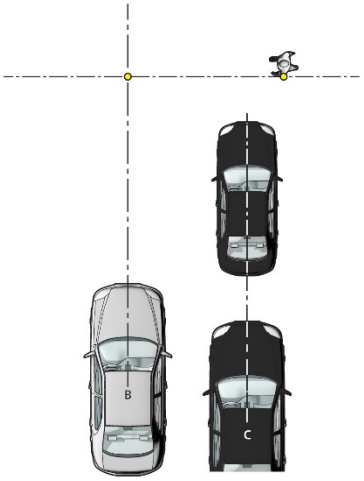


*Figure 3.* AEB Pedestrian scenario, CVNC

*Figure 4.* Euro NCAP Pedestrian Targets (EPTa & EPTc)

For the all of the above described AEB Pedestrian scenarios, only the AEB function (i.e. the vehicle braking without driver involvement) is tested and assessed. Possible Forward Collision Warning (FCW) functionality (the driver responding to a warning by applying the brakes) is not taken into account as it assumed that in this type of situations, there is generally not sufficient time to react to a warning.

**Incremental Speed Approach**

All of the scenarios will be tested with an incremental approach. Starting at a low speed of 20 km/h, the approach speed of the Vehicle Under Test (VUT) is stepwise increased by 5 km/h up to a maximum test speed of 60 km/h. For each run, the vehicle's speed reduction is recorded.

**Euro NCAP Pedestrian Targets**

A large number of different pedestrian targets have been developed over time. Following several workshops, it was decided to take the pedestrian targets as developed within vFSS as a basis. Further events to verify the radar cross section and infrared reflectivity were performed and it was confirmed that the static dummy was detectable by both radar and camera based systems. The figures 5 and 6 show the stance and statures of the adult and child pedestrian targets.

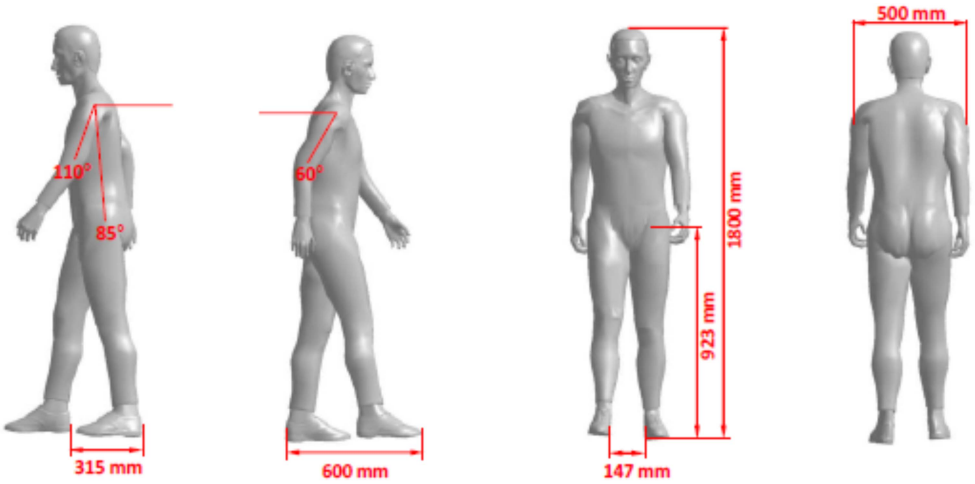


*Figure 5.* Euro NCAP adult Pedestrian Target stance and dimensions

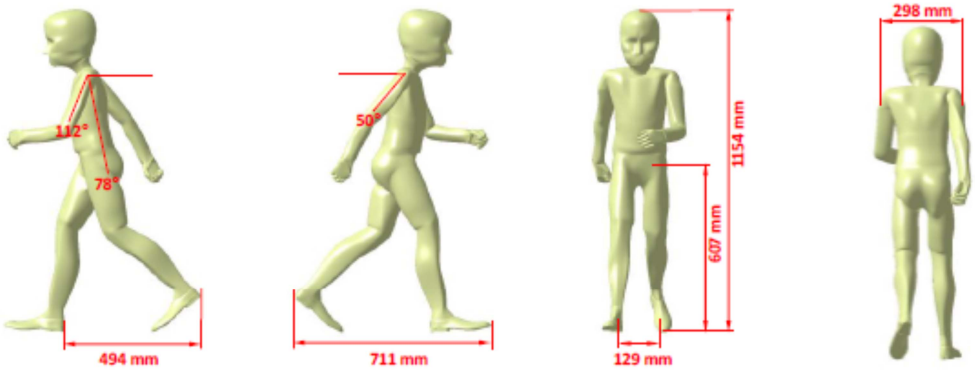


*Figure 6.* Euro NCAP child Pedestrian Target stance and dimensions

At a later stage, industry started the development of an articulated dummy with moving legs that would reflect a more realistic Doppler image, used by more advanced radar systems. Apart from the moving legs, the dummy radar cross section, clothing and stature are the same as for the static pedestrian targets. It was agreed by Euro NCAP to consider specifying this dummy as the pedestrian target in the protocols when all parties involved had verified and approved it. The evaluation and fine-tuning of this dummy is ongoing at the time of writing of this paper.

**Test equipment and test track**

Euro NCAP uses different facilities for all of its tests. To ensure repeatable and reproducible results now and in the future, the WG had already decided to set strict tolerances for testing all of the AEB systems, even though it was acknowledged that this may not always be necessary to evaluate the performance of these systems in the scenarios described earlier. The tolerances used for the AEB Pedestrian tests are listed below:

- Speed of VUT (GPS-speed) — Test speed + 0.5 km/h
- Lateral deviation from test path — 0 ± 0.05 m
- Yaw velocity — 0 ± 1.0 °/s
- Steering wheel velocity — 0 ± 15.0 °/s

- Speed of EPT during steady state
  - CVFA — 8 ± 0.2 km/h
  - CVNA — 5 ± 0.2 km/h
  - CVNC — 5 ± 0.2 km/h
- EPT Steady state
  - Nearside — 3.0 m from vehicle centerline
  - Farside — 4.5 m from vehicle centerline

Due to these strict tolerances, all of the Euro NCAP test facilities are using both steering and brake robots to control the vehicle during test.

Another, less controllable, influencing factor is weather condition. The tracks used for the assessment are spread over Europe with different climates. Although the weather may influence the performance of the systems, it is thought that in day-to-day use these systems also encounter various weather conditions and hence should be robust enough to deal with normal variations. To minimise test to test variability, limits are set to temperature (between 5 and 40°C) and wind (below 10 m/s). There may be no precipitation falling and horizontal visibility at ground level must be greater than 1km. Finally, the natural ambient illumination must be homogenous in the test area and in excess of 2000 lux for daylight testing. For practical reasons, Euro NCAP does not physically test the performance of these systems in low ambient lighting conditions even though accident data reveals this is relevant. It is also ensured that testing is not performed driving towards or away from the sun when there is direct sunlight.

**ASSESSMENT**

The assessment of AEB Pedestrian systems is based on two aspects: the Autonomous Emergency Braking function, i.e. how well the system reacts to an imminent pedestrian impact, and the Human Machine Interface. The latter assessment carries less weight but is important to promote the use of the system.

**Assessment of AEB function**

The only assessment criterion used is the impact speed reduction. For each run into the target at incremental speed, a full score is given when the impact is completely avoided. Where a contact occurs, the points are awarded on a sliding scale basis for speeds up to and including 40 km/h, where the proportion of speed reduction based on the relative test speed determines the proportion of available points scored.

$$Score_{\ test\ speed} = ((Vtest - Vimpact)/Vtest) \times points_{test\ speed}$$

For test speeds above 40km/h points are available on a pass/fail basis only. For each of these test speeds points are awarded when a speed reduction of at least 20 km/h is achieved related to actual test speed. It was acknowledged within the working group that at the moment it is not realistic to ask for full avoidance at speeds above 40 km/h as this would require a relatively early AEB activation at a point in time where the pedestrian has not yet entered the vehicle path. By requiring the impact speed to be reduced with at least 20 km/h, it brings the severity of the crash into the range where passive safety measures are designed to work.

The number of points available for the different test speeds is the same for each of the 4 scenarios based on exposure multiplied by injury levels coming from the accident data. The available point distributions for all scenarios are shown in the figure below.

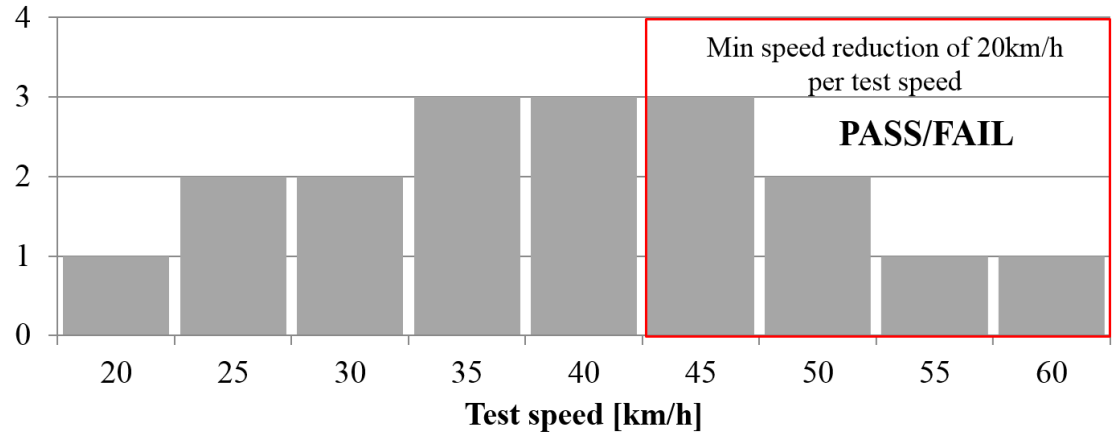


*Figure 6.* Maximum points per test speed

**Human Machine Interface**

The effectiveness of the whole system does not only depend on the speed reduction achieved. The ON/OFF rate of the system is highly influencing the actual performance. At this moment, Euro NCAP has not defined qualitative criteria for warning due to the limited knowledge available on this subject. However, points are

awarded to systems that encourage use, for instance making it less easy to switch the system off or avoiding the system to automatically switch off at low ambient lighting conditions.

**Scoring**
For AEB Pedestrian, only the autonomous emergency braking functionality is considered and HMI points will only be awarded if the AEB system is default ON at the start of every journey.

For the total score of these systems, the normalized sub-scores (as a percentage of the maximum points available) of AEB and HMI are weighted and summed.

$$AEB\ Pedestrian\ total\ score = (AEB\ score\ x\ 5) + (HMI\ score\ x\ 1)$$

A scoring example for an AEB Pedestrian system is provided below.

**Table 1**
**Example of AEB function test results in CVFA scenario**

| Vtest | $points_{test\ speed}$ | Vimpact | $Score_{test\ speed}$ |
|---|---|---|---|
| 20 km/h | 1.000 | 0 km/h | 1.000 |
| 25 km/h | 2.000 | 0 km/h | 2.000 |
| 30 km/h | 2.000 | 0 km/h | 2.000 |
| 35 km/h | 3.000 | 0 km/h | 3.000 |
| 40 km/h | 3.000 | 20 km/h | 1.500 |
| 45 km/h | 3.000 | 25 km/h | 3.000 |
| 50 km/h | 2.000 | 30 km/h | 2.000 |
| 55 km/h | 1.000 | 40 km/h | 0.000 |
| 60 km/h | 1.000 | Not tested | 0.000 |
| **Total** | **18.000** | | **14.500** |
| **Normalised score** | | | **80.6%** |

**Assumed normalized scored for this example in the other scenarios**
- Normalized score in CVNA-25 scenario: 76.7%
- Normalized score in CVNA-75 scenario: 100.0%
- Normalized score in CVNC scenario: 45.3%

Averaged AEB score for the four scenarios = 75.7%

**HMI score:**
- De-activation of the system not possible with a single push on a button **2 points**
- No FCW at speeds over 40 km/h **0 points**
- System switches off at low ambient lighting conditions **0 points**

Based on the above, the normalized HMI score = 50.0%

In total, the AEB Pedestrian total score will be:

$$AEB\ Pedestrian\ total\ score = (AEB\ score\ x\ 5) + (HMI\ score\ x\ 1)$$
$$= 5.0\ x\ 75.7\% + 1.0\ x\ 50.0\%$$
$$= 4.285\ points$$

Finally, the AEB Pedestrian score is included in the overall rating for the vehicle within the Pedestrian Protection box. It should be noted that Euro NCAP will only include the AEB Pedestrian score when the total passive safety protection score (headform, upper legform and lower legform) is 22 points or higher.

**DISCUSSION**
With the introduction of a relatively simple test to assess advanced systems like AEB, Euro NCAP would like to promote the introduction of these systems in the market. From the start of the development of the protocols, it was clear that the protocol would have to be reviewed and updated within a couple of years. For AEB VRU, additional cyclist scenarios will be included in 2018. On top of that, Euro NCAP will consider how and if it is

needed to also include other scenarios in daytime or obscure lighting conditions to the assessment of these systems.
The final decision whether the articulated pedestrian targets are to be used from 2016 onwards is yet to be made. As sensor systems get more advanced, the articulated dummy seems to support a more robust decision making process which improves system performance and acceptance.

All in all, Euro NCAP will continue to develop the requirements for AEB technologies to keep up with the development of these technologies and to ensure high quality systems for consumers.

## CONCLUSIONS

Almost half of European road deaths in urban areas are pedestrians and cyclists. Vehicle design and technology such as forgiving front-ends and avoidance systems can help address this problem. In recent years, a number of vehicle manufacturers have started to offer AEB Pedestrian systems that mitigate the consequence of a potential crash with pedestrians and/or cyclist. To promote and guide the further development of these systems, Euro NCAP will adopt AEB Pedestrian systems in the rating from 2016 onwards. Based on the expected performance of current systems and accident priorities, test scenarios and an assessment scheme have been agreed between the main stakeholders in Europe. The proposed procedures are considered a first step and will be updated and expanded upon in the coming years.

## ACKNOWLEDGEMENT

The P-NCAP working group was able to deliver the test and assessment protocols in time for implementation in 2016 due to all the valuable work done within and outside of the working group.

### P-NCAP WG members

ADAC, BASt, IDIADA, NL-MOT/RDW, Swedish Transport Administration (STA), Thatcham, TNO and UTAC.

The members of the P-NCAP WG have all put significant effort and resources into the development and verification of these protocols. OEMs and suppliers are acknowledged for their support and feedback on the protocols, and special thanks goes out to the OEMs represented in ACEA/JAMA/KAMA for supporting the development of the protocols by funding and supporting round robin test series.

# Preliminary Study of the Responses of Hybrid III 5th female, 50th male, Q6 and Hybrid III 5th pregnant female dummy seated in the 2nd row seats of passenger vehicles in sled tests

**SIWOO KIM, JAEWAN LEE, JONGSOO KIM, GYUHYUN KIM**
Korea Automobile Testing & Research Institute
KOREA

**MYUNGWON SUH**
School of mechanical Engineering, Sungkyunkwan Univ.,
KOREA

Paper Number 15-0282

## ABSTRACT

The objective of this study was a preliminary study of the responses of dummies seated in the 2nd row seat of passenger vehicles in frontal crashes using a sled system. Q6, Hybrid III 5th female, Hybrid III 5th pregnant female, and Hybrid III 50th male ATD were used in the tests. 8-tests were carried out according to a draft protocol for the 2nd row seat evaluation program. The vehicle type was a sedan and SUV's. The cut-body or jig was used to simulate the ATD in the 2nd row seat/belts of a passenger vehicle. The frontal crash pulse in sled tests was an average acceleration of about 30 vehicle acceleration pulses tested according the KNCAP FFRB test. ATD seating positions were set using the H-point machine. Injury criteria were considered among the $HIC_{15}$, upper neck tension force, chest deflection. The $HIC_{15}$ ranged from 350 to 800 for both a Hybrid III 5th female and a pregnant female. The upper neck tension forces of a 5th female dummy and a 5th pregnant female dummy were also higher than that in FMVSS 208. The kinematics was influenced by the seat and seatbelt characteristics. The sled test results were compared with those of the same vehicle KNCAP FFRB test results. The possibility of fatal injury of Hybrid III 5th female and 50th male ATD in the rear seat could have much higher than in the front seat, especially case of the chest deflection. In addition, the further consideration should be given regarding Y- axis in the regulation at the seat belt anchorage point.

## INTRODUCTION

The motor vehicle safety standard refers to a fundamental regulation that should be complied by all vehicles. It should be enacted to prevent traffic accidents and to reduce injuries among vehicle occupants and/or pedestrians at a traffic accident. The Korean government established the "Korea motor vehicle safety standard" in September 1987 under an ordinance of the Ministry of Transportation. For the safety standard regarding the occupant safety of a vehicle at a crash, parts of FMVSS 208 - Occupant Crash Protection, a U.S. motor vehicle safety standard, were introduced in 1993, and the safety standard for occupant safety was established for the FFRB (Full-width Frontal Rigid Barrier) test. Article 102 of the "Korea motor vehicle safety standard" specifies the standard for occupant safety in a head-on collision. The FFRB test is designed the injury criteria of a dummy, by using a Hybrid III 50th male ATD in the driver's seat and the front passenger seat of a vehicle during the impact speed at 48.3km/h.

Therefore, the KMVSS (Korea Motor Vehicle Safety Standard) to protect a vehicle occupant at the FFRB test is applied to the driver's seat and front passenger seat only. The KMVSS includes a standard for seat strength and seat belt anchorage strength for the protection of occupants seated on the second or other rows also. In other words, this can be interpreted in such a way that seats after the 2nd row does not have to meet the safety requirement during the FFRB test. We can see that the safety of the driver's seat and front passenger seat has been dramatically improved over the last ten years, largely as a result of the motor vehicle safety standard and the new car assessment system. KNCAP (Korea New Car Assessment System) introduced the FFRB test in 1999 and has used it ever since. The trend of a star rating shows that only three vehicles (18.8%) out of nineteen tested between 1999 and 2001 received

a five-star rating, whereas thirty-seven (97.4%) out of thirty-eight vehicles tested between 2011 and October 2014 received a five-star rating. As shown in Figure 1, a comparison of the 3-year-average AIS (Abbreviated Injury Scale) 4+ injury risk probability for head and chest injuries measured in a 56km/h FFRB test by the KNCAP. It shows that the probability of sustaining a AIS4+ injury risk probability of head injury was reduced from 12.2% to 4.7%, whereas the probability of a joint injury was reduced from 21.6% to 15.1%. This result shows that the probability of a joint injury has been reduced by 70%, compared with the initial stages.

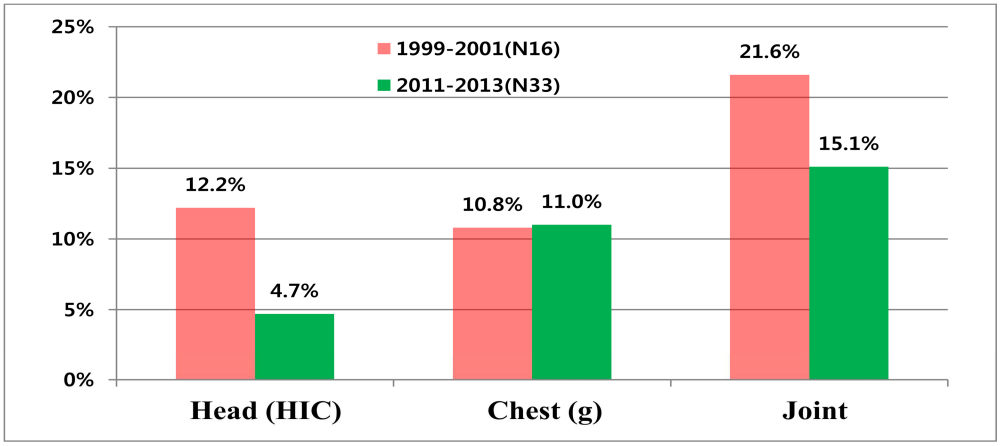


***Figure 1. Average Injury risk possibility (AIS 4+) of ATD in KNCAP FFRB test***

When we compared the effects of introducing the FFRB test in KNCAP, based on real accident analysis in Korea, vehicles with a higher star rating were found to be safer. Thus, the MAIS3+ (Maximum Abbreviated Injury Scale) occurrence rate of vehicles with a 4-star rating was found to be 34.2% lower than that of vehicles with from 1 to 3 stars in a frontal crash accident. As described above, the safety of the driver's seat and front passenger seat has been significantly improved owing to the considerable efforts made by car manufacturers, the government, and research institutes. Also, the rate of injury is now quite low. However, little attention has been paid to rear seats, because we can see that a motor vehicle safety standard for the rear seat passengers based on an FFRB test, offset test has not yet been established.

Evans (1987) analyzed that the rear seat lap belt reduces the likelihood of by 18±9 percent, whereas the 3-point seat belt has a 41±4 percent effect for the front passenger seat. Morgan (1999) found that the level of safety increased by 25%, compared with two-point seat belt, as the regulation for the rear seat had changed from the two-point seat belt to the three-point seat belt. Paranteau and Viano (2003) found that torso injuries generally occur due to the seat belt, according to data about frontal crash accidents suggesting that rear seat passengers wear the 3-point seat belt. They also found that abdominal injuries among rear seat occupants caused by the type 1 seat belt also occur when the type 2 seat belt is worn. Suzanne et al (2012) evaluated Hybrid III 5$^{th}$ female ATD and Hybrid III 10 years old on the rear seat. Even when the dummy wore a 3-point seat belt, the dummy in the rear seat was subjected to a more forward movement, compared with the occupant of the front seat. As movements become frequent, the measurement value has an important effect on the head, neck, chest, and lower spine. Sometimes, the head and neck injury value was likely to exceed the reference value. Chest displacement occurs more frequently when the seatbelt is well maintained from the center of the shoulder to the center of the torso.

When we reviewed the results of past studies, analysis was performed on the excellence of the 3-point safety belt, the abdominal injury when the 3-point safety belt is used, and the injury of the 5$^{th}$ female ATD. However, the possibility of injury did not much analyzed by comparing the front and rear seat occupant. The occupation rate of the rear seat in Korea is 21.1%, which is somewhat smaller than the front passenger seat (39.6%). However, we

cannot disregard the vehicle safety of the rear seat due to a low rear seat occupation rate, in order to reduce traffic casualties. Therefore, this study ran a frontal sled test by using a Hybrid III 50$^{th}$ male ATD, Hybrid III 5$^{th}$ female ATD, Hybrid III 5$^{th}$ pregnant female ATD, and a child Q6 on the rear seat, in order to stimulate greater interest in the safety of the rear seat occupant, which generally attracts little attention, and to compare the possibility of injury with the occupant of the front seat, which will require further studies.

## TEST METHOD

### DUMMY

The sled comparison test was performed by using a Hybrid III 50$^{th}$ male ATD, Hybrid III 5$^{th}$ female ATD, Hybrid III 5$^{th}$ female ATD pregnant, and child Q6 in the booster seat on the rear seat of a sedan and SUV type vehicles. The Hybrid III 5$^{th}$ female ATD and Q6 were seated in the rear seat for the test, while the Hybrid III 5$^{th}$ female ATD pregnant and Hybrid III 50$^{th}$ male ATD were seated in the same vehicle rear seat for another test (See Figure 2).

***Figure 2. Test set up of Hybrid III 5$^{th}$ & Q6, MAMA & Hybrid III 50$^{th}$ male ATD***

The new rear seat and safety belt were installed with each test. The rear seat cushion, seat backs, and safety belt D-ring points were set on the design point. The dummy was seated by checking the H-point machine. In particular, the seating reference point of the Hybrid III 5$^{th}$ female ATD was different from the H-point machine. Hybrid III 5$^{th}$ female ATD was lowered by 6mm below the H-point machine, and the H-point was reset by reducing the seat length rate by the same degree as the forward direction of the car. The Hybrid III 5$^{th}$ pregnant female ATD was seated in the same way as the Hybrid III 5$^{th}$ female ATD. The Hybrid III 50$^{th}$ male ATD was seated with the same seating method as the dummy used for the FFRB test in the motor vehicle safety standard. As there was no steering handle, the upper arm was placed on the seat back and the ring finger was placed on the outer thigh and seat cushion. The Q6 was seated in the booster seat, according to the child safety test method that is being prepared by KNCAP. The frontal sled test speed was 56km/h, and the average acceleration speed pulse was used, regarding the upper and lower limit of the KNCAP FFRB test acceleration speed conducted in 2013 (See Figure 3).

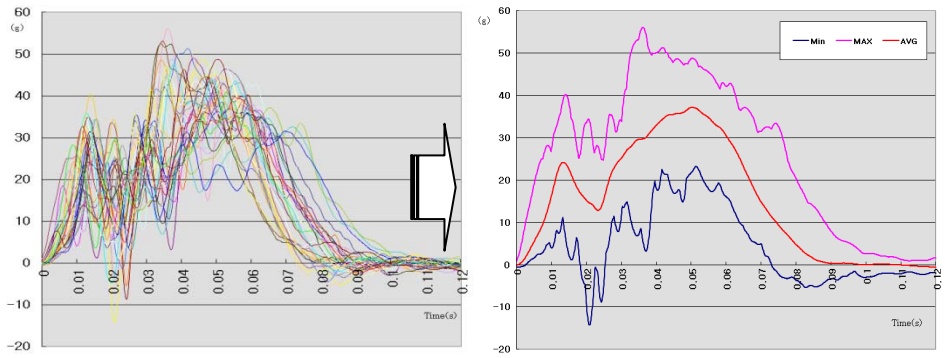


***Figure 3. FFRB test acceleration and mean acceleration***

## TEST EQUIPMENT

The test data was recorded in 10 kHz and filtered according to SAE J211. The scene was recorded from the left and right sides and the upper front, using a 1,000 frame high-speed digital camera. The parts needed for the rear seat test was cut from the actual car (sedan) and made in a jig form. For the SUV car, the second row seat and safety belt part were made in a jig form for the test. The baseline ATD instrumentation included a tri-axial accelerometer at the head CG; a 6-axis load cell at the upper and lower neck; tri-axial accelerometers at the chest and chest potentiometer at chest the Hybrid III 50$^{th}$ male, Hybrid III 5$^{th}$ female, and Hybrid III 5$^{th}$ pregnant female ATD. The same equipment was installed on the Q6 dummy, except that the IR-TRACCs were installed on the lower and upper sternum.

## TEST RESULTS

Total 4 vehicles were conducted using the sled system in KATRI (Korea Automobile Testing & Research Institute). The responses of the Hybrid III 50$^{th}$ male, Hybrid III 5$^{th}$ female, and Hybrid III 5$^{th}$ pregnant female ATD seated on the rear seat were compared. The $HIC_{15}$ of the Hybrid III 50$^{th}$ male ATD were 333, 356, 446 and 498. The $HIC_{15}$ of the Hybrid III 5$^{th}$ female ATD were 354, 705, 723 and 745. The $HIC_{15}$ of the Hybrid III 5$^{th}$ female pregnant ATD were 580, 698, 787 and 794. The $HIC_{15}$ of female ATD had higher than the male ATD, and either came close to or exceeded $HIC_{15}$ 700, which is the injury reference value in FFRB test in the regulation.

The upper neck tension force of the Hybrid III 5$^{th}$ pregnant female ATD were 2.42kN, 2.79 kN, 2.19kN and 1.93kN which is similar to the Hybrid III 5$^{th}$ female ATD (2.62kN, 2.12kN, 2.14kN, 1.52kN). The value for the Hybrid III 50$^{th}$ male ATD were 2.76kN, 2.31kN, 2.27kN and 1.75kN.

The chest displacement of the Hybrid III 5$^{th}$ female ATD were 42.76mm, 42.14mm, 40.3mm and 40.6mm respectively, while those of Hybrid III 50$^{th}$ male ATD were 43.76mm, 49.52mm, 44.8mm and 40.9mm. The chest acceleration 3msec clips of the Hybrid III 5$^{th}$ female ATD were 44.92g, 63g, 63.67g and 52.82g. The chest acceleration 3msec clips of the Hybrid III 5$^{th}$ pregnant female ATD were 41.1g, 51.14g, 58.5g and 61.5g. The female ATD chest acceleration 3msec clip of two vehicles was found to exceed the limits referenced in compliance. The chest acceleration 3msec clip observed for the Hybrid III 50$^{th}$ male ATD were 54.28g, 52.11g, 54.3g and 43.4g. The chest displacement of the Hybrid III 5$^{th}$ female ATD were 47.26mm, 42.14mm, 40.3mm and 40.6mm. The chest displacement of the Hybrid III 50$^{th}$ male ATD were 43.76mm, 49.52mm, 44.8mm and 40.9mm. When comparing the injury criteria between male and female ATD, the male ATD showed a higher value, with the exception of the $HIC_{15}$. The $HIC_{15}$ of the child Q5 seated on the booster seat were 502 and 491, and those for upper neck tension force were 2.23kN and 2.17kN, which exceeded the AIS3+20% reference value suggested by the EEVC.

## COMPARISON WITH THE RESPONSES OBTAINED FOR THE FRONT SWAR OF SAME VEHICLE FFRB TEST

The results of the FFRB test conducted by the KNCAP were compared with the ATD responses seated on the rear seat, by positioning a Hybrid III 50$^{th}$ male ATD on the driver's seat and a Hybrid III 5$^{th}$ female ATD on the front passenger seat. Figure 4 (left) compares the $HIC_{15}$ and upper neck tension force, which were both found to be lower than the ATD responses recorded for the rear seat, due to the influence of the load limiter in the airbag and the seat belt. Figure 4 (right) shows the comparison between the head acceleration 3m sec clip and the upper neck tension force. Head acceleration is similar to the front seat, but the upper neck tension force in the rear seat is higher than the front seat.

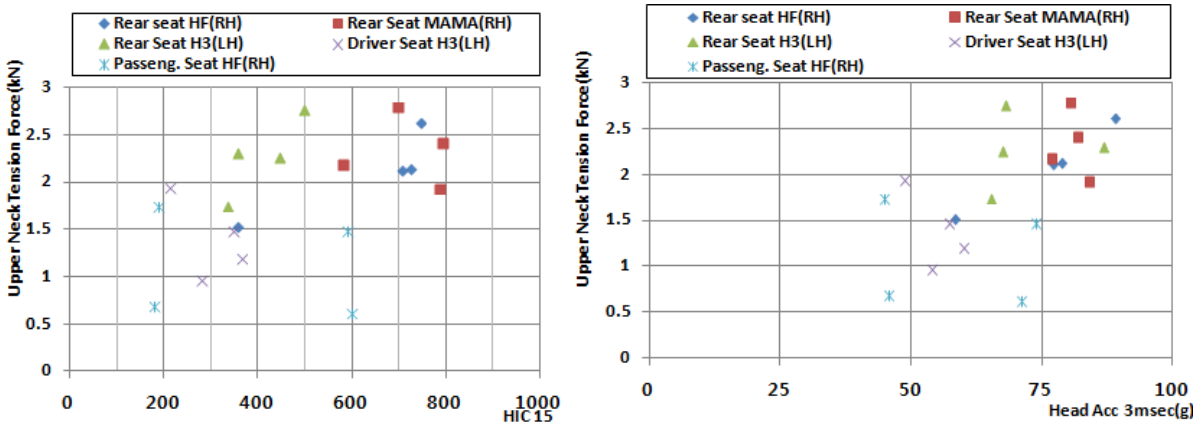


*Figure 4. Peak upper neck tension force and $HIC_{15}$ (left) / Peak upper neck tension force and peak resultant head acceleration of 3msec(right)*

Figure 5 shows the chest deflection of the comparison between shoulder belt load and lap belt load, respectively. The shoulder belt load of the front seat was under 4kN, whereas the lap belt load was distributed between 4.99kN and 11.25kN. The Hybrid III 50$^{th}$ male ATD has a greater lap belt load than the Hybrid III 5$^{th}$ female ATD on the front seat, because the former weighs more. However, the shoulder belt load was similar. It was found that the Hybrid III 50$^{th}$ male ATD received a greater lap belt load and shoulder belt load in the rear seat. When compared with the front seat, the shoulder belt load was applied to the torso more than three times in the rear seat, and chest deflection compared with the front seat was increased.

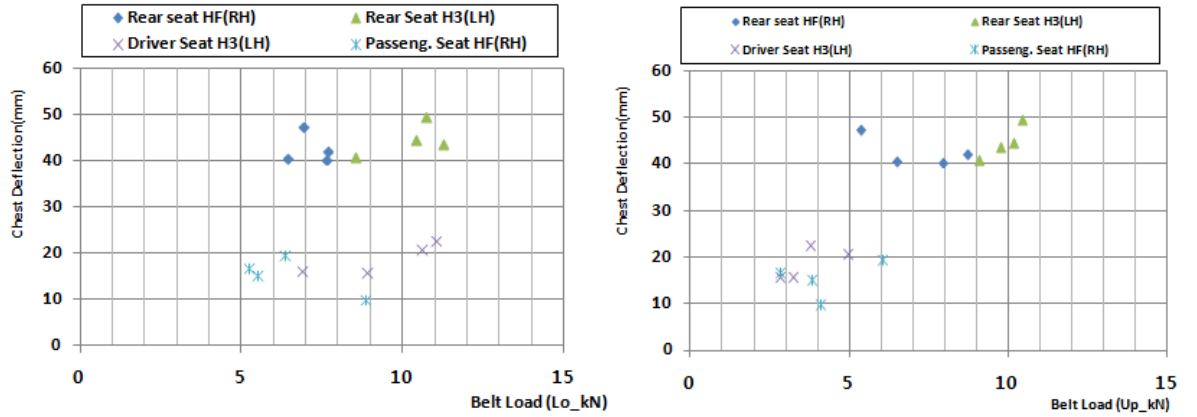


*Figure 5. Peak chest deflection and peak lap belt load (left) / Peak chest deflection and peak shoulder belt load (right)*

**COMPARISON WITH THE FFRB TEST IN KNCAP**

To compare our results with those of the KNCAP, 52 FFRB test results were reviewed among the test results of KNCAP from 2011 to 2014. The Hybrid III 50$^{th}$ male ATD was seated in the driver's seat and the front passenger seat in 2011 and 2012. The Hybrid III 50$^{th}$ male ATD was seated in the driver's seat but the Hybrid III 5$^{th}$ female ATD was seated in the front passenger seat for the evaluations conducted in 2013 and 2014. As a result, the rear seat and front passenger seat were compared for the Hybrid III 5$^{th}$ female ATD, and the test results of the driver's seat, front passenger seat, and rear seat were compared for the Hybrid III 50$^{th}$ male ATD.

The average $HIC_{15}$ of the Hybrid III 5$^{th}$ female ATD response of the front passenger seat was 452.72, while the average upper neck tension force was 0.911kN. On the other hand, the average of $HIC_{15}$ and upper neck tension force responses recorded for the rear seat were 631.75 and 2.1kN, respectively. The $HIC_{15}$ of the Hybrid III 5$^{th}$ female ATD in the rear seat was about 140% greater than that of the front seat, whereas the upper neck tension force was about 230% greater. On the contrary, the average $HIC_{15}$ among driver, front passenger and rear seat occupant did not show a big difference (i.e. driver's seat: 353.29; front passenger seat: 409.65; rear seat: 427). The average upper neck tension force of ATDs for the driver's seat, front passenger seat and rear seat was 1.42kN, 1.3kN, and 2.27kN, respectively. These results indicate that the female ATD in the rear seat could have sustained more injuries than the male ATD in the front and rear seats (See Figures 6).

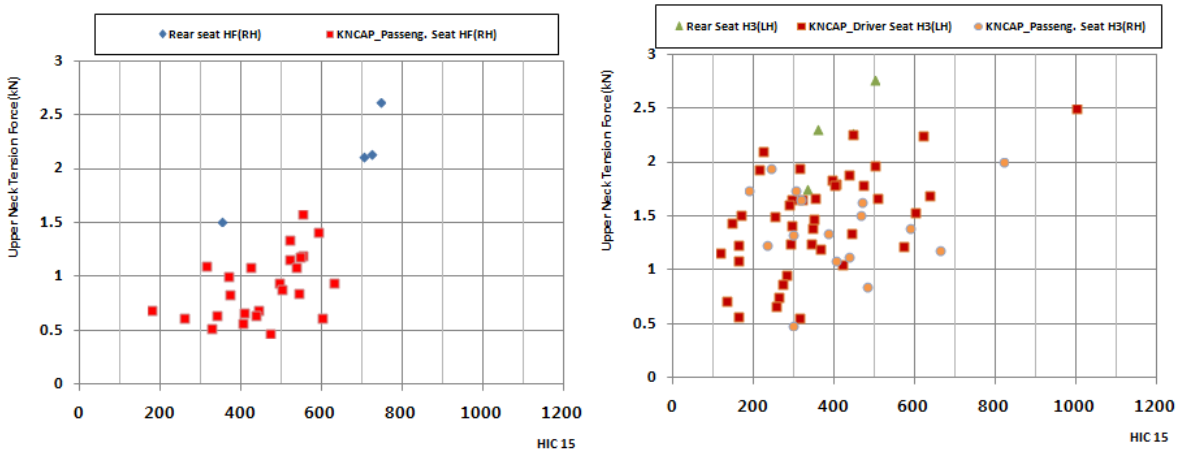


***Figure 6. Peak upper neck tension force and $HIC_{15}$ of 5$^{th}$ female ATD(left) / Peak upper neck tension force and $HIC_{15}$ of 50$^{th}$ male ATD(right)***

The chest deflection of both the driver's seat and the front passenger seat was under 30mm in the Hybrid III 50$^{th}$ male ATD and the Hybrid III 5$^{th}$ female ATD. However, that of the rear seat was 40 - 49mm. The chest deflection of the Hybrid III 5$^{th}$ female ATD was about 270% more compressed than the front seat average (See Figures 7). Furthermore, it was found that chest deflection in the driver's seat and front passenger seat is not as great as in the rear seat, even though the lap belt load and shoulder belt load increase, regardless of the type of ATD. Figure 8 (right) shows the comparison between shoulder belt load and chest deflection in KNCAP and rear seat frontal sled test. The ATDs of FFRB test in KNCAP is controlled by chest deflection of about 30mm and a shoulder belt load of about 7kN.

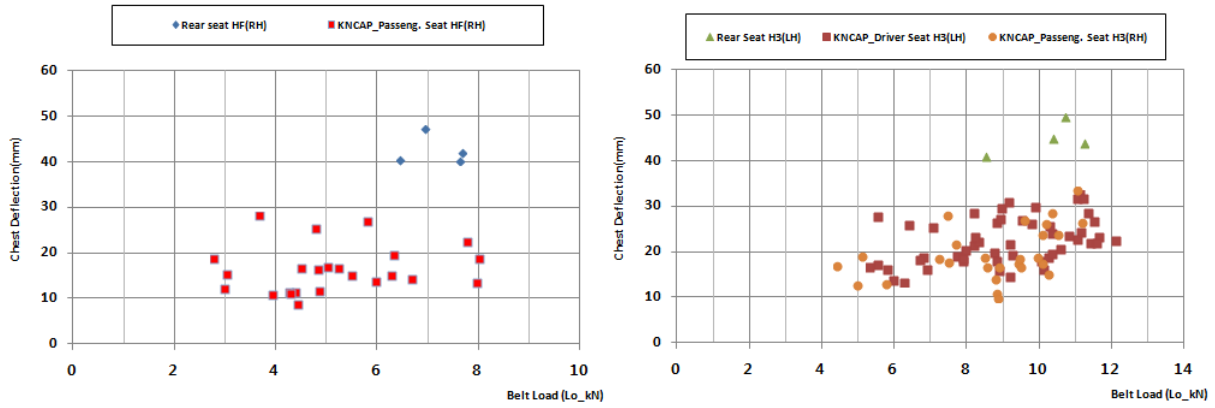


***Figure 7. Peak chest deflection and lap belt load of 5th female ATD(left) / Peak chest deflection and lap belt load of 50th male ATD(right)***

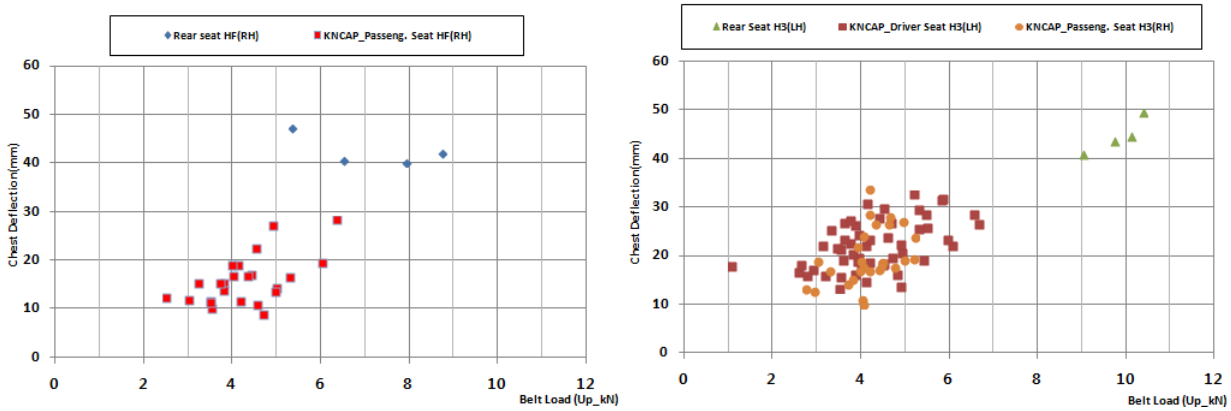


***Figure 8. Peak chest deflection and shoulder belt load of 5th female ATD(left) / Peak chest deflection and shoulder belt load of 50th male ATD(right)***

## KINEMATICS ANALYSIS

Figure 9 shows photos of the ATD prior to the frontal sled test. As the torso position of the seat belt for the Hybrid III 50th male ATD in the rear seat is correct, the seat belt is fastened from the center of the shoulder to the center of the chest. However, the seat belt did not protect the torso of the Hybrid III 5th pregnant female ATD properly in the test, because its sitting height is short and the shoulder belt leans toward the neck due to the presence of the fetus in the abdomen.

***Figure 9. 5th female pregnant ATD(left) and 50th male ATD(right) set up in the rear seats***

The ATD loaded onto the rear seat moves forward more strongly than that in the front seat. In particular, the test was performed without the front seat. Therefore, restriction of the ATD movement by the front seat could not be tested. It was also found that the seat belt could not control chest displacement at a proper position, due to the presence of the fetus in the lower abdomen of the Hybrid III 5$^{th}$ pregnant female ATD (See Figure 10). The frontal movement displacement of the Hybrid III 50$^{th}$ male ATD was the greatest followed by the 5$^{th}$ female ATD, pregnant female ATD and Q6.

***Figure 9. Examples of kinematic responses observed 5$^{th}$ female pregnant ATD and 50$^{th}$ male ATD in the rear seat***

**DISCUSSION**

This study presents the same conclusion as the data of Paranteau and Viano (2003) regarding frontal crash accidents in which rear seat passengers put on the 3-point seat belt, confirming that a torso injury generally occurs due to the safety seatbelt, and that abdominal injuries of the rear seat occupants caused by the 3-point seat belt also occur when the type-3 seat belt is worn. Even though the abdominal load on the dummy was not checked due to the lack of measurement system, the chest deflection of the female ATD in the rear seat was observed to increase by 270% greater than the front seat. Also, the shoulder belt load of the front passenger seat is 5.13kN, whereas rear seat was about 7kN, indicating that the possibility of abdominal injury increases. The test results suggest that we need to devise a method of reducing injuries in actual accidents, by taking into account the fact that the lap belt load on the abdominal area is high.

The percentage of injury risk possibility was analyzed according to the average values of injury criteria of the same vehicle FFRB test conducted by the KNCAP, and the results of the rear seat frontal sled test. For the Hybrid III 50$^{th}$ male ATD on the driver's seat, the injury risk possibility (AIS3+) of $HIC_{15}$ in the FFRB test was found to be 0.9%; that of chest deflection, 1.1%; and that of upper neck tension force, 0.05%. The joint possibility of an injury being caused by all three factors was 2.04%. Meanwhile, for the Hybrid III 50$^{th}$ male ATD, the injury risk possibility (AIS3+) of $HIC_{15}$ in the rear seat frontal sled test was 2.6%; that of chest deflection, 18.3%; and that of upper neck tension force, 0.4%. The joint possibility of an injury being caused by all three items was 20.74%. These results indicate that the joint possibility of an injury in a rear seat is greater than in the case of the driver's seat.

For the front passenger seat of the Hybrid III 5$^{th}$ female ATD, the injury risk possibility (AIS3+) of $HIC_{15}$ in the FFRB test conducted by the KNCAP was found to be 3.5%; that of chest deflection, 1.3%; and that of upper neck tension force, 0.1%. The joint possibility of an injury being caused by all three factors was 4.85%. However, for the Hybrid III 5$^{th}$ female ATD, the injury risk possibility (AIS3+) of $HIC_{15}$ in the rear seat frontal sled test was 8.7%; that of chest deflection, 30.2%; and that of upper neck tension force, 4.6%. The joint possibility of an injury being caused by all three factors was 39.2%. These results indicate that the joint possibility of injury is also greater than in the case of the front passenger seat. The Hybrid III 5$^{th}$ pregnant female ATD, the injury risk possibility (AIS3+) of

HIC15 in the rear seat frontal sled test was 11.7%, and that of upper neck tension force, 0.4%. As a result, the rear seat is concluded to be less safe than the front seat in the case of both the male and female ATDs.

The shoulder belt part was found to be inappropriate for each dummy, as it was pushed into the lower neck during the test, making it impossible for the chest to absorb the energy properly. As such, it seems that more regulation should be proposed regarding the adjustable Y-axis for short adults, besides the regulation on the X-axis and Z-axis, when defining the shoulder belt of the rear seat belt in the motor vehicle safety standard. It seems that the motor vehicle safety standard and NCAP for rear seat safety and new car safety assessment should be implemented immediately, as the possibility of a head, neck, or chest injury is higher in the rear seat than in the front seat.

## SUMMARY AND FUTURE WORKS

It was observed that the performance of safety for the rear seats and restraints was different compared with the front seat in a same vehicle. The possibility of fatal injury of Hybrid III $5^{th}$ female and $50^{th}$ male ATD in the rear seat could have greater than in the front seat, especially case of the chest deflection. For the Hybrid III $50^{th}$ male ATD on the driver's seat in FFRB test, the joint possibility of an injury risk (AIS3+) was 2.04%. But for the $50^{th}$ male ATD on rear seat, the joint possibility of an injury risk (AIS3+) was 20.74%.

For the Hybrid III $5^{th}$ female ATD on the front passenger seat in FFRB test, the joint possibility of an injury risk (AIS3+) was 4.85%. However, for the $5^{th}$ female ATD on rear seat, the joint possibility of an injury risk (AIS3+) was 39.2%. In case of the injury risk possibility (AIS3+) of chest deflection of passenger seat in the FFRB test was 1.3%, but rear seat frontal sled test was 30.2%. As a result, it was found that the rear seat was to be less safe than the front seat in the case of both the male and female ATDs. Also it was found that the possibility of injury risk for the female ATD on rear seat in frontal crash was greater than male ATD. In addition, the further consideration should be given regarding Y- axis in the regulation at the seat belt anchorage point.

**Acknowledgements**
This research was supported by the Korea Ministry of Land, Transport and Maritime Affairs. It was also supported by the Korea Institute of Construction and Transportation Evaluation and Planning (Project No.: 12PTSI-C054118-04).

## REFERENCES

[1] Evans, L., 1987. “Rear Compared to Front Seat Restraint System Effectiveness in Preventing Fatalities,” Society of Automotive Engineers, Warrendale, PA, SAE Paper No. 870485.
[2] Korea motor vehicle safety standard, 2014, http://www.law.go.kr/
[3] Korea Auto-vehicle Safety Association, 2014, “ A study on the introducing benefit and analysis of vehicle crash test protocols in KNCAP ”, Report.
[4] Morgan, C., 1999. “Effectiveness of Lap/Shoulder Belts in the Back Outboard Seating Positions,” NHTSA Report No. DOT HS 808 945.
[5] Paranteau, C., Viano, D., 2003. “Field Data Analysis of Rear Occupant Injuries Part 1: Adults and Teenagers,” SAE World Congress, Society of Automotive Engineers, Warrendale, PA, SAE Paper No. 2003-01-0153.
[6] Richard Kent1, Jason Forman1, Daniel P. Parent1, Shashi Kuppa2, 2007, "Rear seat occupant protection in fromtal crashes and its feasibility", 20th ESV conference, pp 07-0386
[7] Smith, K., Cummings, P., 2004. “Passenger Seating Position and the Risk of Passenger death or Injury in Traffic Crashes,” Accident Analysis and Prevention, Vol. 36, pp. 257-260.

[8] Shashi Kuppa1, James Saunders1, Osvaldo Fessahaie2, 2005, Rear seat occupant protection in frontal crashes", 19th ESV conference, pp 05-0212
[9] Suzanne Tylko1 , Alain Bussières2, 2012, "Responses of the Hybrid III 5th Female and 10- year-aold ATD", IRCOBI conference 2012, pp IRC-12-65
[10] YW Kim, 2013, “Korea NCAP status and future plan”, Seminar of Safest vehicle of year

# Tools and methods for current and future controllability assessment

**Andreas Pütz, Lutz Eckstein**
Institut für Kraftfahrzeuge (ika), RWTH Aachen University
Germany

**Adrian Zlocki**
Forschungsgesellschaft Kraftfahrwesen mbH Aachen
Germany

Paper Number 15-0283

**ABSTRACT**

Driver related evaluation of Advanced Driver Assistance Systems (ADAS) needs to address controllability, effectiveness and user acceptance, which are to some extend interfering with each other. The state of the art in the controllability assessment is currently defined by the Code of Practice of the RESPONSE 3 project which focuses on the driver-system-interaction with single assistance functions like ACC or LKA. However, the controllability evaluation of new assistance functionalities such as ADAS of automation level 2 or automated driving on level 3 (according to SAE definitions) requires a review of the existing methods and tools with regard to necessary adaptations and new developments.

For controllability evaluation of future ADAS and systems of higher automation levels the existing methodology needs to be adapted. Aspects to be considered in this context are the increasing amount of information with regards to the automation level. This information needs to be perceived and processed by the driver when interacting with multiple parallel operating assistance functions and complex information and communication systems.

The controllability of urban assistance functions and their failures is subject of discussion especially focusing on tools and methods for an urban controllability assessment. To that end, driving simulator experiments, vehicle-in-the-loop and real vehicle studies are conducted analyzing existing controllability methods on their suitability for urban assistance functions. The results show the specific advantages of each applied testing tools and suggest that an overall system evaluation addressing controllability, effectiveness and acceptance combines the advantages of the different testing environments.

Next to acceptance and effectiveness the controllability analysis is embedded in the overall evaluation process with focus on the driver and the interaction with the vehicle. The controllability analysis process for higher levels of automation is described. An overview of state of the art controllability evaluation is provided. The problem for future systems is analyzed and possible methods and tools are proposed. The necessary methods and tools are described focusing on next generation ADAS and higher levels of automated driving.

The results are limited to the driver interaction with assisted driving. For the assessment of the driver reaction to higher automation levels the use of a high-fidelity driving simulator seems reasonable to achieve a high reproducibility of the driving scenario and a good representation of the driving dynamics.

## INTRODUCTION

Recently, various national organizations have proposed classification levels for vehicle automation (BASt, VDA, SAE, NHTSA). Within this paper the degree of vehicle automation is defined according to SAE [1] into

6 different automation levels ranging from manual driving (level 0) to fully automated driving (level 5). Necessary legal adaptations for the use of assistance functonalities of higher automation level are currently ongoing to build up the legal framework for their implementation. Beside this basic legal adaption evaluation methods for these functions need to be adjusted or extended since level 2 and 3 systems require the human driver as a fallback solution. Thus, an interaction between system and driver is still necessary, but may differ from previously known systems with a limited scope of system actions and system limitations. Figure 1 shows the different interaction dimensions in the control loop driver - vehicle - environment according to [2]. These are to be taken into account for the evaluation of the system. Especially the controllability evaluation at system limitations and boundary conditions or technical failures needs to be considered in order to ensure safe operation.

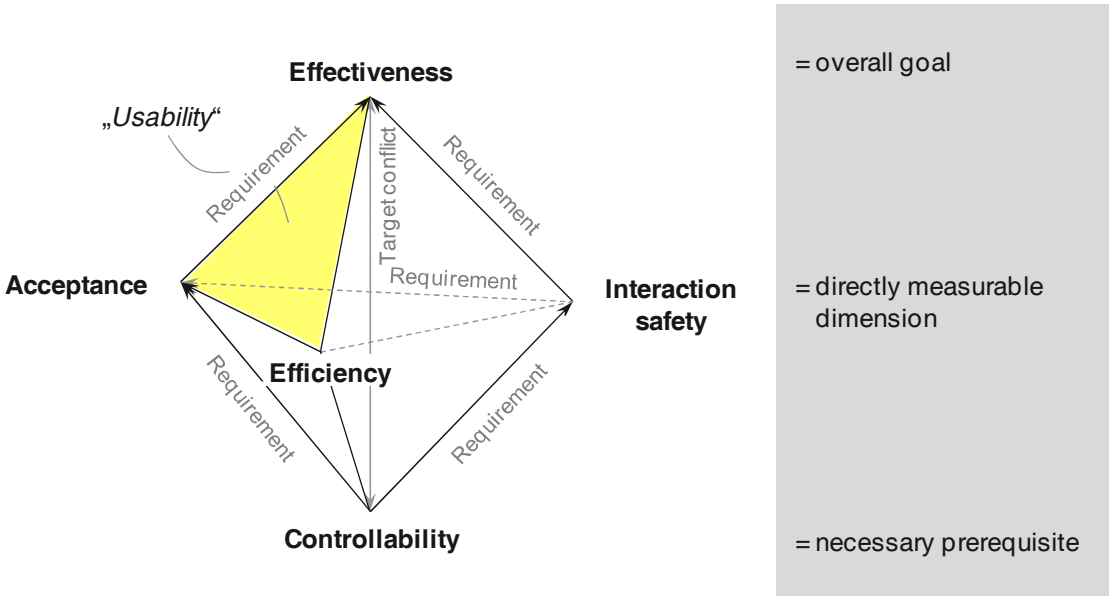


***Figure 1. Interaction dimensions for ADAS and automated driving function evaluation [2]***

In the following state of the art tools and methods for the controllability assessment are discussed with regards to their applicability for future assistance and automation functionalities. To that end, the current state of the art is highlighted and compared to the requirements arising from the wider operation scope of new functionalities. Necessary adaptations and new developments are highlighted and deduced to meet the new challenges.

## REQUIREMENTS DUE TO NEW ASSISTANCE FUNCTIONS AND HIGHER AUTOAMTION LEVELS

The increasing automation level in new production vehicles leads to a change in the role of the driver. The SAE definition of different automation levels is therefore closely related to the responsibilities of the human driver and the system in their (timely parallel) interaction which is necessary on level 1 to 3 (see *Figure 2*). Level 1 assistance systems are directly addressed by the current state of the art methodical framework. In level 2 and 3 the human driver is still considered for the fallback performance of the dynamic driving task in case of system errors, failures or system limitations. Thus, for these systems the controllability by average skilled drivers has still to be proven. Systems of even higher automation levels (4 and 5) do not require the human driver as fallback solution by definition and therefore necessitate a purely technical approach in terms of the controllability even in critical situations.

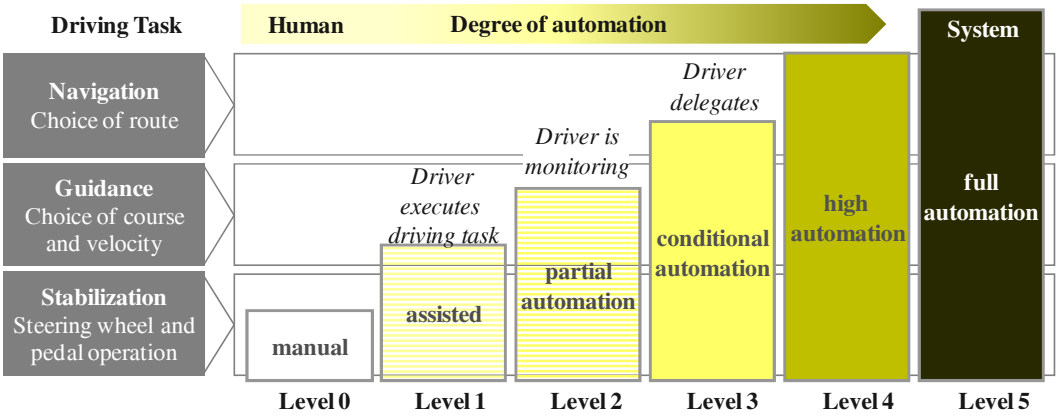


***Figure 2. Definition of different automation levels***

Even though the driver is still considered for the fallback performance of level 2 and 3 systems the system takes over more responsibilities which lead to a change in the driver role from an active element of the control loop to a passive supervisor. While systems of level 2 (combination of at least two ADAS such as LKS and ACC) expect the driver to constantly monitor the driving environment, level 3 systems also take over this task. In reverse, automated driving systems (level 3) provide a transition time between system and human driver so that the driver can resume to the driving task. Here, the questions arise if the driver is able to serve as a fallback solution in situations in which he is not continuously "in the loop" anymore and the overall duration necessary for a safe transition between system and driver. First insights on the necessary time frames for the takeover by the driver can be found in [3], [4], [5], [6] and indicate time spans in the range of 5 to 10 s. However, if the situation does not provide the required time for the driver to perceive and process all relevant information for a safe takeover, the driver may react inappropriately due to a panic reaction. From the human factors prospective it seems therefore doubtful, whether a safe transition between system and driver may be realizable in all conditions in automation level 3.

In addition, the increasing level of automation requires automated driving systems to cope with scenarios that require system actions in high dynamic driving situations. Thus, the system capabilities have to be widened with regard to intervention intensity and short time frames targeting an appropriate system behavior in emergency situations in which a transition time between system and driver cannot be realized. The enhanced capabilities on the other hand reduce the driver's controllability in case of a system failure resulting in a target conflict between system effectiveness and controllability. Controllability by the driver may therefore not be achievable at any time. In this case the applied controllability criteria and even the term "controllability" need to be chosen with care. In a worst case scenario a system failure may occur while driving in automated mode and therefore while the driver is inattentive. Even in a test environment such a situation may be critical since it cannot be estimated, if the driver will react in an inappropriate manner worsening the current situation. Hence, appropriate testing tools have to assure testing of automated driving scenarios without physical risk for test subjects and prototypes.

The requirements due to new assistance functions can be summarized to:

1. New role of the driver (especially for level 3 automation and higher)
    a. What are controllabilty criteria for a system that has to provide a transition time between system and driver? Is controllabilty by the driver achievable if the driver does not have to monitor the driving process?

   b. Driver do not have to monitor driving environment and therefore the driver might be inattentive. The current methodical framework for controllabilty assessment does not sufficiently consider the driver state.
   c. Testing with inattentive driver may lead to critical situations due to unexpected driver reactions and therefore test with inattentive drivers is necessary in a environment without physical risk.
2. Enhanced system capabilities
   a. Systems need to be able to act with higher dynamics and therefore a target conflict between effectiveness and controllabilty increases.
   b. Controllabilty by the driver may not be achievable at any time. Therefore criteria and definition for controllabilty have to be adapted.
3. Multiple parallel acting functions
   a. Driver has to consider lateral and longitudinal control at the same time which may cause difficulty for drivers to operate both parallel (especically in critical situations)
   b. Priorization of controllability criteria for lateral and longitudinal control

## STATE OF THE ART IN CONTROLLABILITY ASSESSMENT

In the following available tools as well as the methodical framework for controllability assessment are described. The objective is to provide an overview of state of the art controllability evaluation, analyze possible problems for future systems and higher automation levels and evaluate the methodical framework and applied tools on their suitability for these systems.

### Methods

The methodical state of the art in the controllability assessment of assistance functionalities is currently defined by the methods given in the ISO 26262 [7] for functional safety and the Code of Practice of the RESPONSE 3 project [8]. While the ISO 26262 has a wider scope with regards to functional safety, the CoP directly addresses the controllability evaluation of ADAS (level 2).

#### ISO 26262

The norm ISO 26262 addresses the functional safety of electrical and/or electronic (E/E) systems of series production passenger cars. Hence, assistance functionalities are also in the scope of the norm. In part 3 the hazard analysis and the risk assessment during the concept phase is elaborated giving methods for the identification and classification of potential hazard events. To that end, hazardous events are classified in automotive safety integrity levels (ASIL) by evaluating the severity of a potential harm, the probability of exposure regarding the operational situation and the controllability of the hazardous event.

Controllability is defined as “the probability that the driver or other persons potentially at risk are able to gain sufficient control of the hazardous event, such that they are able to avoid the specific harm” ([7]). Therefore, controllability classes are linked to the percentage of the driver collective that are able to “control” the specified situation based on pre-defined criteria (see Table 1). With regard to the content of the RESPONSE 3 Code of Practice the norm annotates that C2 classification can also be achieved by a controllability level of 85% in a practical testing experience with 20 valid data sets.

Important in context of this paper is that the norm considers the driver condition by assuming that the driver (a) is in an appropriate condition to drive (not tired), (b) has the appropriate driver training and (c) is complying with all applicable legal regulations, including due care requirements to avoid risks to other traffic participants.

*Table 1. Definition of controllability classes according to ISO 26262 [7]*

| Class of controllability | | | |
|---|---|---|---|
| **C0** | **C1** | **C2** | **C3** |
| Controllable in general | 99% or more of all drivers or other traffic participants are usually able to avoid harm | 90% or more of all drivers or other traffic participants are usually able to avoid harm | Less than 90% of all drivers or other traffic participants are usually able, or barely able, to avoid harm |

**RESPONSE 3 - Code of Practice**

Other than the ISO 26262 the RESPONSE 3 Code of Practice is not a mandatory norm but a guideline with principles that are considered by car manufactures on a voluntary basis. Also, its scope is tighter by referring only to Advanced Driver Assistance Systems (ADAS). By CoP-definition these systems "assist the driver and do not take over the driving task completely, thus the responsibility always remains with the driver" [8].

Key requirement of the CoP is the controllability which is stated to be dependent on (a) the possibility and driver's capability, to perceive the criticality of a situation, (b) the driver's capability to decide on appropriate countermeasures and (c) the driver's ability to perform the chosen countermeasure (see [8]). In contrast to the ISO 26262 the CoP gives three concrete approaches to proof the controllability of an ADAS (Proof by an interdisciplinary expert panel, by a test with naïve subjects or by direct recommendation by the ADAS development team). For the final proof by a test with naïve subjects the CoP states that "absolute controllability does not exist" [8]. Based on practical experience a test scenario is considered as passed if at least 85% of at least 20 test subjects meet the previously anticipated behavior or react in an adequate way to control the situation.

In the AdaptIVe project [9] the RESPONSE 4 subproject defines requirements and next steps for an adaptation of the Code of Practice towards higher automation levels. Especially the legal requirements and liability issues are in focus of RESPONSE 4. A new CoP for automated driving might be developed in a possible RESPONSE 5 project in the future.

**Tools / Test environments**

Different test tool / test environments are currently known to assess the controllability of assistance functions. They vary in their complexity of the representation of the vehicle and its environment and can contribute their specific advantages at different development stages of the function development. Generally, they can be subdivided into simulative testing which uses a virtual environment for the vehicle environment and the vehicle's movement and in real world testing that enables investigations in controlled test fields or even on public roads. Instead of a detailed description of the various types of simulative and real-world testing tools their specific advantages and disadvantages with regard to their suitability for the controllability evaluation for future assistance functions will be discussed in the following.

**Simulative testing**

Simulative testing tools (see Figure 3) provide the possibility to investigate the interaction between a human driver and the system especially at an early stage in the development process. Therefore, the function (or functional aspects) can be experienced by the driver even before the system is implemented in its final environment [10]. This is of high importance for system of level 3 since those systems are currently under development. At the same time, also the driver reaction to system actions can be analyzed in critical situations and critical driver behavior can be estimated without actual physical risk for test subjects and prototypes. In

addition, all types of simulative testing tools have the key advantage of high reproducibility regarding the scenario experienced by the test subjects.

The required complexity of the driver surrounding and the motion feedback suggests which type of simulative test environment is best suited for the investigation depending on the analyzed aspect. Choosing a test environment is therefore a trade-off between needed resources for the investigation and external validity. While results from laboratory studies are not directly transferable to the human behavior in real world driving they enable to estimate particular aspects of the driver reaction (e.g. reaction time in specific situations) and require only few resources. If however the aspect under investigation is influenced by the motion feedback from the vehicle dynamics the use of a dynamic or high-fidelity driving simulator becomes necessary.

***Figure 3. ika simulative tools for controllability assessment***

Main disadvantage of the simulative testing tools is the missing or lower validity of the motion cuing for investigations of scenarios in which the vehicle dynamics are important for the driver reaction or the evaluation of the resulting vehicle motion. This problem is addressed by the implementation of high-fidelity driving simulators (see Figure 3): With the help of a rail system on which a hexapod with the simulator dome is mounted the transversal motion of the vehicle can be realized more accurately than with a single fixed base hexapod as it commonly used in dynamic driving simulators.

In comparison to real world testing tools in driving simulators scenarios of automated driving are comparatively easy to realize because of the not necessary environment perception and the already integrated driver models. This is relevant for investigation of level 3 systems that have to proof their controllability also during automated driving.

**Real world testing**

Real world testing enables not just the qualitative evaluation of the driver behavior, but also the quantitative analysis of its outcome with a high validity. To that end, relevant driving scenarios are realized in controlled test fields. Figure 4 shows an example of a controllability assessment of an emergency steering assist that was conducted within the research project UR:BAN [11] with the ika test vehicle which is equipped with various sensors, actuators and processors on the ika test track. In this study the driver reaction to system initiated steering interventions in different use cases (erroneous interventions as well as normal system use) was investigated with regard to the influence of driving situation [12] [13]. Due to the triggering of the interventions by a high precision positioning a high reproducibility regarding the driving scenario was achieved.

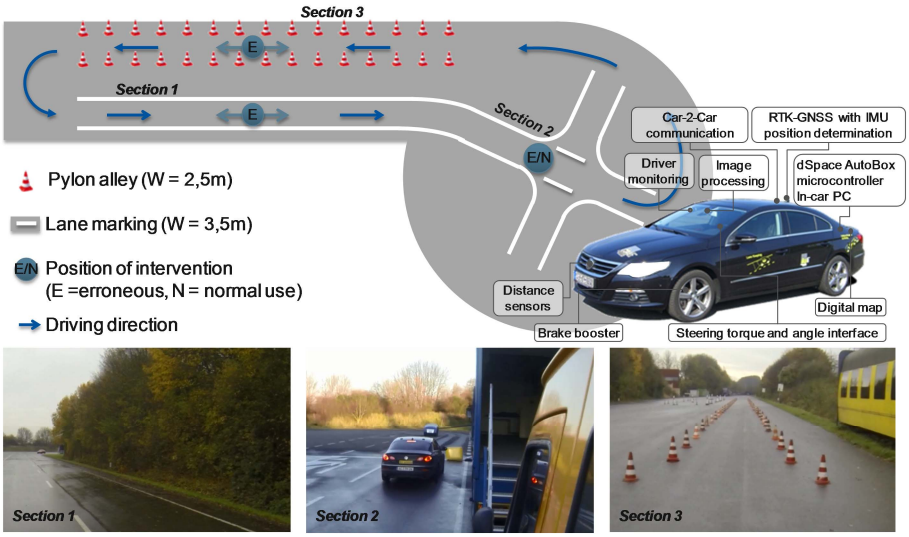


*Figure 4. ika real world testing for the controllability assessment in research project UR:BAN [13]*

While for most tests of systems operating on the assistance level also smaller test tracks are sufficient, controllability assessment of systems that enable automated driving require a larger test field on which these driving scenarios can be simulated without physical risk. One example for such a controlled test field is the Aldenhoven Testing Center which comprises a vehicle dynamics area, a high speed oval, a handling track and further elements (see Figure 5). Especially the high speed oval with its highway characteristic enables testing of automated systems (e.g. traffic jam assist or highway pilot) under controlled test conditions. Thus, also critical situations in automated driving scenarios can be investigated and controllability evaluation of level 3 systems can be conducted under realistic test conditions.

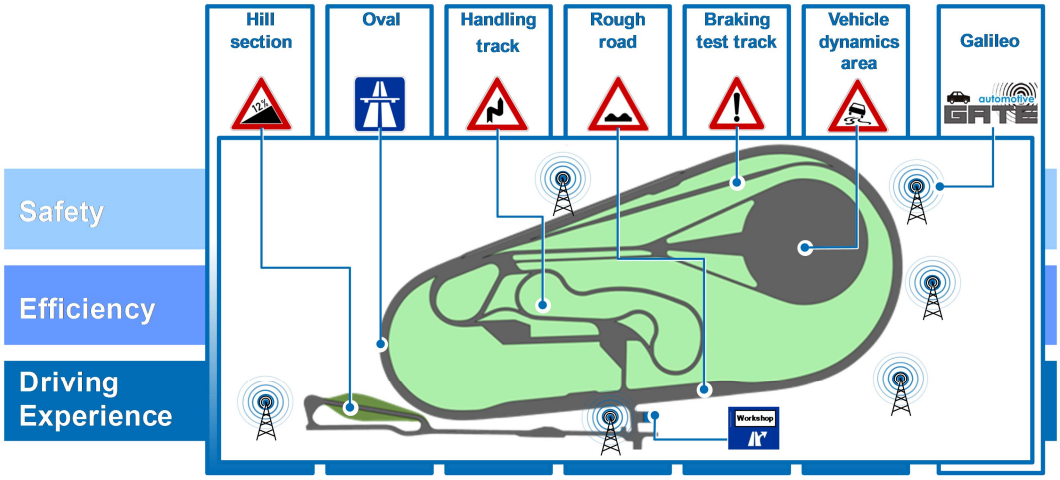


*Figure 5. ATC test track layout [14]*

## SPECIFICATION OF NECESSARY ADAPTATIONS / FUTURE TEST METHODS AND TOOLS

Introduction of systems of higher automation levels provides challenges regarding the methodical approach for the controllability assessment. Especially at the step between level 2 and level 3 there are currently open research questions concerning the capabilities of the driver to serve as fallback solution in situations when he is not continuously involved in the driving task. Those are mainly related to the required time for a safe

transition between system and driver and the consequences if this time cannot be provided due to a critical situation. Thus, the driver state and its impact for the driver performance in controllability situations need to be considered in the methodical framework. The current assumption of an attentive driver as in the ISO 26262 is conflicting with the definition of driver's role for level 3 systems.

Due to the fact that level 3 systems need to provide a certain transition time for the takeover to the driver the systems have to deal with (critical) situations that require system interventions with high vehicle dynamics in short time frames. The enhanced system capabilities (and the related increase in effectiveness) reduce on the other hand the controllability by the driver - in particular, if the driver is inattentive in this situation. If the driver is still ought to be a fallback solution the applied controllability criteria need to the adjusted to the changed driver role. Traditional controllability criteria will not be suited for evaluation of those scenarios.

Beside the methods also the tools for the controllability assessment of higher automation systems need to be reconsidered. Like for the previously discussed methodical aspects the role of the driver influences the suitability of the presented testing tools for controllability scenarios. One of the key factors is to enable the driver to experience automated driving situations and induced a realistic driving situation with regard to the driver state at the same time. Here, driving simulators show their advantage to offer the possibility to experience automated driving at a very early stage of the development when physical prototypes not yet exist. As mentioned before systems of level 3 require the representation of high vehicle dynamics which puts the focus on the motion system of the driving simulator. Since common driving simulators are somewhat limited in the implementation of translational motion this shortcoming has to be addressed by test tools for the controllability assessment of level 3 systems (e.g. by use of high-fidelity driving simulators). If however also the motion representation of a high-fidelity driving simulator is not sufficient or thresholds have to be defined, large test fields are required to build up realistic scenarios of automated driving.

## CONCLUSIONS

The increasing automation level of driving assistance functionalities suggest to review to currently applied methods and testing tools for the controllability assessment on their suitability for those systems. To that end, the paper summarized the state of the art methods and tools and compared them to the requirements for the valid evaluation of these systems. In doing so, the step from automation level 2 to 3 has been identified to provide the biggest challenges from the human factor prospective. While the methods and tools are mainly well suited for level 2 (beside system that intervene in time critical situations, e.g. automated steering in emergency situations) the change in the driver role between level 2 and 3 induces necessary adaptations, especially in the methodical framework. ISO 26262 and CoP were intended to scenarios in which the driver is actively involved in the driving task, either by fulfilling it himself or by constantly monitoring it. On level 3 the driver however can delegate the driving task to the system and has therefore not to be attentive at all times. The proposed transition time between system and driver may lead to situations in which the driver is not able to react in an adequate manner due to a critical situation.

In addition to the methods, also the testing tools for the controllability assessment were review. In general, driving simulators seem best suited for representation of automated driving scenarios since they provide the possibility to experience the automation system at an early stage in the development without physical risk for prototypes and test subjects. Here, the ability for a good representation of the vehicle dynamics was identified as one key factor since the systems capabilities have to be widened to handle also time critical driving scenarios. If a common motion system is not sufficient high-fidelity driving simulators enable to consider also scenarios that were previously only tested in controlled test fields.

**REFERENCES**


1. SAE Standard J 3016 (2014): Taxonomy and Definitions for Terms Related to On-Road Motor Vehicle Automated Driving Systems
2. Eckstein, L; Schwalm, M.; Zlocki, A.: Methodenbaukasten zur Bewertung der automatisierungsrelevanter Dimensionen der Fahrer-Fahrzeug Interaktion, Haus der Technik, RWTH Aachen, Essen, 2015
3. Petermann-Stock, I. et al. (2015): "Bitte übernehmen Sie das Fahren!" Ein multimodaler Vergleich von Übernahmestrategien. AAET 2015, Braunschweig, 2015
4. Gold, C. et al. (2013): "Take over!" How long does it take to get the driver back into the loop? Proceedings of the Human Factors and Ergonomics Society 57th Annual Meeting 2013
5. Willemsen, D., Stuiver, A. & Hogema, J. (2014): Transition of Control: Automation Giving Back Control to the Driver. Proceedings of the 5th International Conference on Applied Human Factors and Ergonomics 2014
6. Flemisch, F. et. al. (2009): Validation of preliminary design by simulation, Deliverable D33.3, Have-it project
7. ISO 26262 (2012): International Standard
8. Knapp, A. et al. (2006): Code of practice for the design and evaluation of ADAS, Response 3, Prevent Project
9. http://www.adaptive-ip.eu/ Adaptive project, European Comission, 2014
10. Schwalm, M.; Zlocki. A.; Eckstein, L. (2013): Idea to Product – A modular approach for the evaluation of ADAS. 22nd Aachen Colloquium Automobile and Engine Technology 2013
11. http://urban-online.org/de/urban.html (Stand 09.01.2015)
12. Pütz, A.; Zlocki, A.; Eckstein, L. (2014): Driver reaction to system initiated evasive manoeuvres. 10th ITS European Congress 2014
13. Pütz, A.; Josten, J.; Zlocki, A.; Eckstein, L. (2014): Driving situation influence in the controllability assessment. 21st ITS World Congress 2014
14. http://www.atc-aldenhoven.de (Stand 09.01.2015)

Opportunities for Injury Reduction in Rollover Crashes

Ana Maria Eigen, FHWA

Kennerly Digges, GWU

## ABSTRACT

The NASS/CDS remains the best US data source for understanding the magnitude of the opportunities for reducing rollover injuries to the various body regions. However, judicious analysis techniques are required to address the many confounding factors, including but not limited to the consequence of recent safety improvements such as electronic stability control and increased roof strength. To better assess the effect of recent safety improvements, the population of drivers in rollovers in light vehicles model year 2000 and later was examined. To address crash severity, the number of quarter-turns was used. Injuries were separated by body region and the HARM method of aggregating injuries was used to provide added weighting to the more severe injuries. For belted drivers in near-side rollovers, the fourth quarter-turn contained the most HARM and the highest injury risk, especially for chest injuries. For belted drivers in far-side rollovers, most of the chest injury HARM is fairly uniformly distributed between quarter-turns 2, 4, 6 and 8.

## INTRODUCTION

During the past 15 years there have been a number of changes in safety testing to encourage safety improvements in passenger vehicles. Improvements in the vehicle structure occurred in response to dynamic side impact testing and static roof testing for safety regulations and consumer information. Dynamic side impact testing was required by 1997 and the Insurance Institute for Highway Safety (IIHS) began consumer testing for side impacts in 2003. A continuing priority at NHTSA has been to increase the severity of the roof strength standard. The earlier standard required the roof to withstand a load of at least 1.5 times the vehicle weight when compressed 5 inches in a static test. In 2009, IIHS raised the requirement to 4 times the vehicle weight for a best score in their consumer information test that was based on the Federal Standard. The US Department of Transportation subsequently raised the standard to 3 times the vehicle weight. Electronic stability control (ESC) entered the market in 1995 and became standard on approximately 38% of the cars and SUV's by model year 2005. By MY 2009, the ESC was standard equipment on 100% of SUV's, 74% of cars and 38% of pickups (IIHS 2013). These structural and rollover avoidance countermeasures should result in improvements in rollover protection that will require continued monitoring and evaluation to determine what additional countermeasures may be effective and practical. In an earlier ESV paper, we examined the rollover safety performance of the passenger vehicle fleet documented in NASS years 1995-2005 (Digges 2007). A purpose of this paper is to examine how rollover injuries are occurring in recent models of vehicles, model year 2000 and later. Of particular interest is to determine the quarter-turns and the injuring contacts with the highest content of injury HARM in both near-side and far-side rollovers. Studies of this kind will assist in the search for the causes of rollover injuries and possible ways to mitigate them.

In an earlier paper, we examined safety changes in the vehicle fleet by model year (Eigen 2013). In that paper, we aggregated groups of vehicles my model year beginning with model year 1985 and examined how the injury rates had changed in all crash modes. The most recent model year grouping, model years 2000 to 2009, displayed a 40% reduction in serious injury rate compared with earlier model years. For that latest model year grouping, head and chest injuries each accounted for about 35% of the HARM to belted drivers in rollovers. The spine and upper extremities each accounted for about 10% and lower extremities about 5%. It is evident that head and chest protection offered the greatest opportunities for injury reduction and consequently they are a principal focus of this paper.

## METHODS

The source for exposure and injury data was the NASS/CDS (National Automotive Sampling System/Crashworthiness Data System) years 1999 to 2012. NASS/CDS is a weighted estimate of tow-away crashes occurring in the United States. The NASS/CDS weighted data contains approximately 23 million drivers of passenger cars, SUV's, passenger vans or light trucks (pickups) who were exposed to crashes. NASS/CDS data were disaggregated by vehicle model year and crash mode.

**Query Description**

The Statistical Analysis System (SAS) was used to merge and extract NASS CDS data. The accident, vehicle, occupant, and injury files were merged. The filters, applied to each of the files, appear in Table 1.

Table 1: NASS CDS Data Files and Filters Applied

| File Name | Variable with Filter | Rationale |
|---|---|---|
| Accident | 1999<=***Year***<=2012 | Crashes occurring in ***calendar years*** 1999 through 2012. |
| Vehicle | 1<=***Bodytype***<=49 | Passenger ***Vehicle body types***, including passenger cars, sport utility vehicles, pick up trucks, and vans |
| | Modelyr ge 2000 | Vehicle model years greater than or equal to 2000 were retained, with 2013 as latest model year. |
| | 1<=***Rollover***<=17 (pre-1998)<br>1<=***Rollover***<=21 (1998-onward) | ***Rollover crashes*** about the longitudinal axis, 1 through 16, aggregating 17+, later 1 through 20, aggregating 20+. |
| Occupant | Role = 1 | Occupant role was set to drivers only |
| | Manuse in(0,1,4) | Occupant restrained by a lap and shoulder belt (4) compared to unrestrained (0,1) |
| | 3<=MAIS<=6 | Maximum Abbreviated Injury Score serious (3), severe (4), critical (5), or maximum (6) |
| Injury | Region90=5 | Occupants sustaining thoracic injuries |
| | 3<=AIS<=6 | Abbreviated Injury Scores 3 – 6, maximum per body region (BMAIS) |

In order to capture all vehicles of model year 2000 and later, the calendar years1999 through 2012 were queried, resulting in vehicles through model year 2013. The vehicles were restricted to passenger vehicles, as the NASS CDS is a sample of tow-away passenger vehicle crashes. Larger vehicle types would fall outside the scope of NASS CDS and would not receive a full vehicle inspection, if impacting with a qualifying passenger vehicle.

The rollover quarter turn variable was modified in 1998. Previously, up to 16 quarter turns were quantified, aggregating 17 quarter turns and greater. In 1998, the quantified quarter turns were increased to 20, aggregating 21 quarter turns and greater. As this has been an on-going comparative study, the previous formatting was retained for comparative purposes. For future analyses, the 1998 rollover quarter turn formatting will be adopted.

Filters were applied to the occupant file. The occupant role was restricted to drivers. This has a normalizing effect, as vehicles inconsistently carried right front seat passengers. These drivers were further restricted to unrestrained,

those not using a factory-installed restraint or seated in a position without a factory-installed restraint, and restrained, those using lap and shoulder belt combination. Only occupants sustaining at least a serious injury were considered in this study. Additional review of drivers sustaining thoracic injuries suggested the need for additional future analyses. This review was based upon the severity of the maximum thoracic injury sustained, eliminating the possibility of double counting and misstating the effects of more pervasive, concomitant injury types.

**Interpretation of Queried Data**

There are a variety of ways to examine the frequency and rate of injuries in the available databases. Frequently, Maximum Abbreviated Injury Scale (MAIS) 3 and above injuries are combined. Alternatively, the HARM weighting scheme is applied to injuries of different severity. The latter has the advantage of weighting injuries in proportion to their cost (Malliaris 1982). The HARM method will be the primary method used in this paper to assess the magnitude of the injuries suffered by the populations under consideration.

The HARM calculations for the body regions were based on the approach introduced by Fildes and Digges [Fildes 1992]. This methodology applies a weighting factor to each AIS 2+ injury in the database. The weighting factor is proportional to the cost of the occupant's most serious injury. In general, minor injuries (AIS 1) are high frequency, events that tend to cloud the analysis of serious injury reduction by safety systems. For this reason, AIS 1 injuries were excluded from the HARM calculations. The AIS 2+ HARM, measured in equivalent fatalities, was based on NHTSA's data on average cost of injuries. The equivalent fatality measurement is obtained by normalizing the average cost of a given injury by the cost of a fatality. The average cost of each injury severity was obtained from a Table E-1 in the 1995-1997 NASS/CDS Summary (NHTSA 2001). The injury cost values are: MAIS 2, 3,600; MAIS 3, 98,011; MAIS 4, 221,494; MAIS 5, 697,533; and MAIS 6, 822,328. The Mean HARM for each category was calculated by dividing the HARM suffered by drivers by the number of drivers exposed to that category. The Mean HARM results were multiplied by 100 to simplify the presentation.

**RESULTS**

The distribution of drivers in model year 2000 and later light vehicles who were involved in NASS/CDS rollover crashes is displayed in Figure 1. This Figure also displays the distribution of AIS 2+HARM for the same population. The weighted driver population consisted of 318,376 belted and 29,781 unbelted drivers. The unbelted population suffered 37% of the AIS 2+ HARM. The unweighted population consisted of 926 of which 78.5% were belted. The unbelted sustained almost half of the unweighted AIS 2+ HARM.

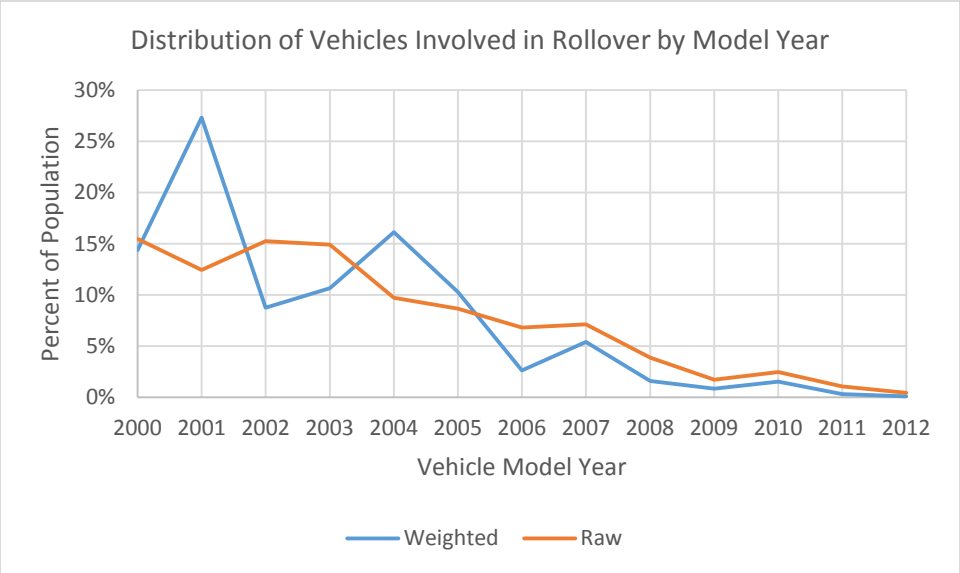


*Figure 1.* Distribution of rollover involved light vehicles in 2000-2012 NASS/CDS by model years

Figure 2 shows the exposure of rollover involved vehicles, model year 2000 and later, by vehicle type. The corresponding distributions of AIS 3+ injuries and AIS 2+ HARM are also shown. It may be noted that the HARM generally tracks the AIS 3+ injuries. However, HARM allows for the representation of AIS 2 injuries and gives additional weight to AIS 4+ injuries.

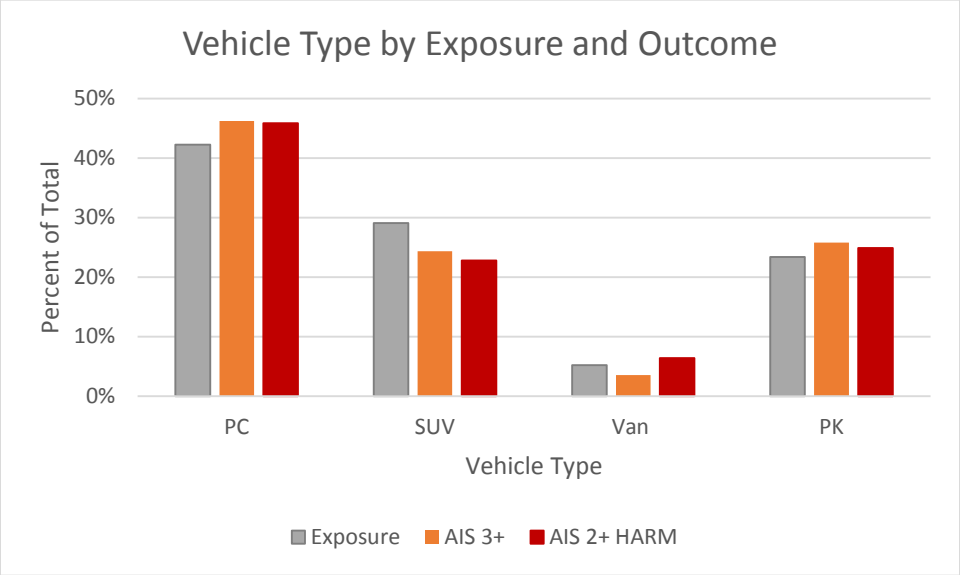


*Figure 2.* Distribution of rollover involved MY 2000+ light vehicles in 2000-2012 NASS/CDS by vehicle type

Figure 3 examines the distribution of vehicle quarter-turns and compares weighted and raw data. The weighting factors reduce the populations exposed to 2, 4 and 6 quarter-turns and increase the populations exposed to 1 and 5 quarter-turns.

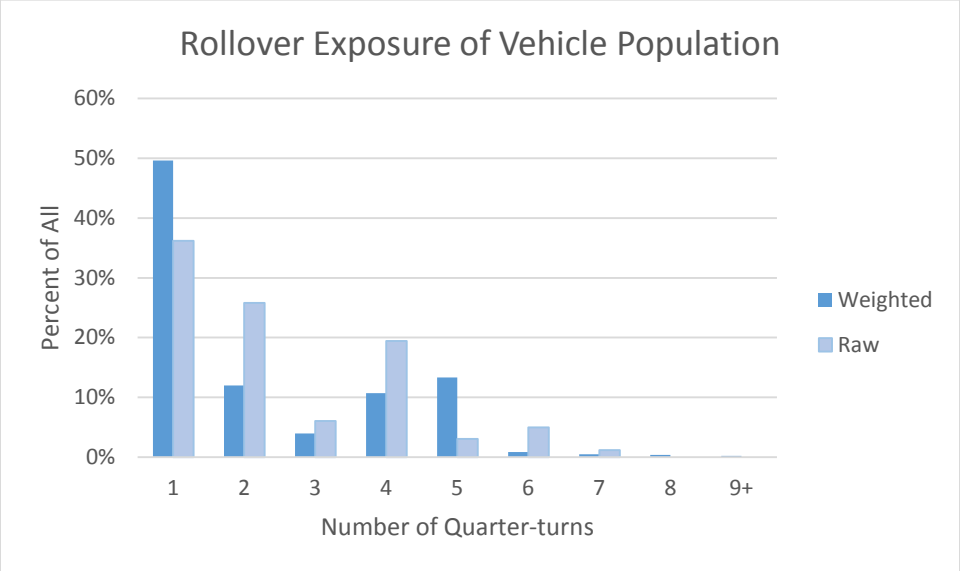


*Figure 3.* Distribution of rollover involved MY 2000+ light vehicles by number of quarter-turns

Figure 4 examines the distribution of AIS 2+ HARM by vehicle quarter-turns and compares weighted and raw data. Although the weighting factors reduced the populations exposed to 2 and 4 quarter-turns, the HARM level remained high for those quarter-turn groups.

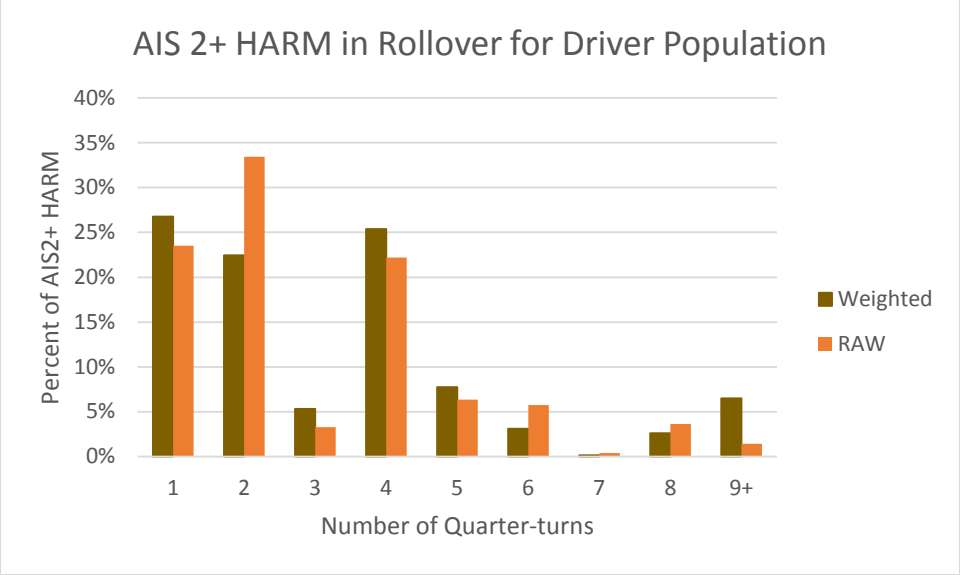


*Figure 4.* Distribution of driver AIS 2+ HARM in rollover involved MY 2000+ light vehicles by number of quarter-turns

Figure 5 focuses on belted drivers and displays their exposure and AIS 2+ HARM distributions by vehicle quarter-turns. It may be noted that 4 quarter-turns is especially harmful.

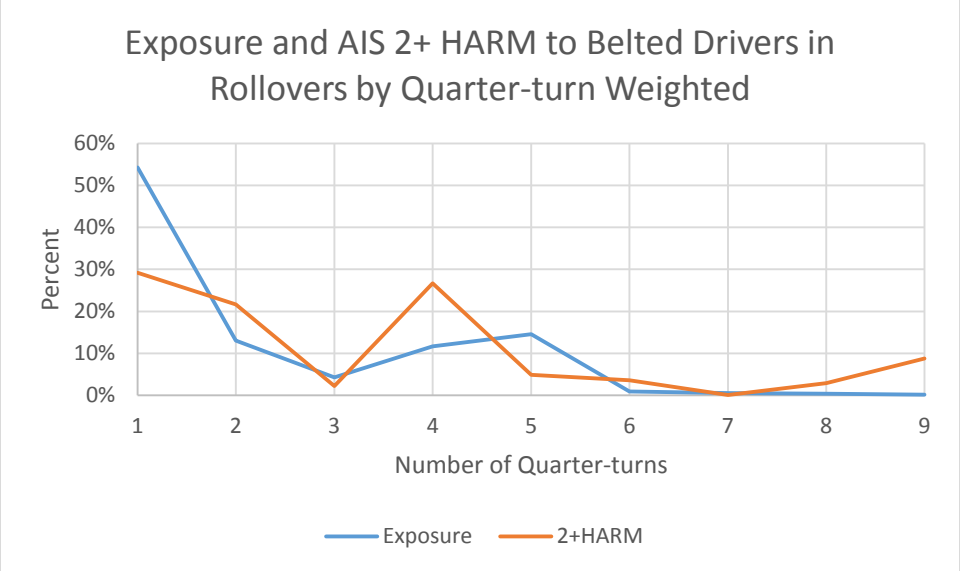


*Figure 5.* Distribution of rollovers and AIS 2+ HARM for belted drivers of rollover involved light vehicles in 2000-2012 NASS/CDS by number of quarter-turns (weighted)

Figure 6 examines the distribution of AIS 2+ HARM by vehicle quarter-turns and compares near-side and far-side rollovers. Populations exposed to 1, 2 and 4 quarter-turns sustain the largest percentage of HARM in both roll directions.

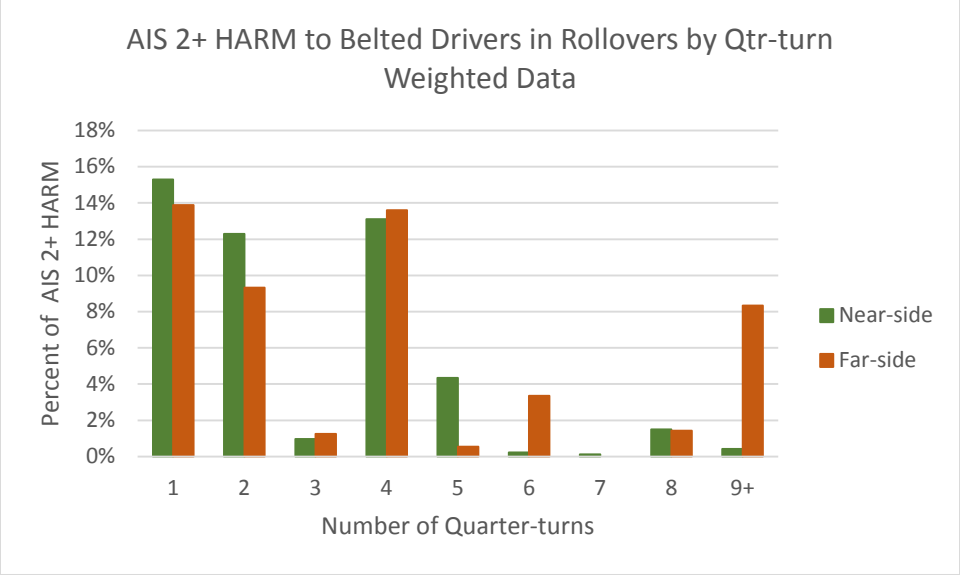


*Figure 6.* Distribution of belted driver AIS 2+ HARM in rollover involved MY 2000+ light vehicles by direction of rollover and number of quarter-turns (weighted data)

Figure 7 examines the distribution of AIS 2+ HARM from chest injuries by vehicle quarter-turns and compares near-side and far-side rollovers. For near-side rollovers, 1, 2 and 4 quarter-turns sustain the largest percentage of AIS 2+ HARM. Quarter-turn 4 appears to be particularly harmful, with about 30% of the total chest HARM. For the far-side rollover, the HARM is more uniformly distributed among the even number of quarter-turns – 2, 4, 6 and 8.

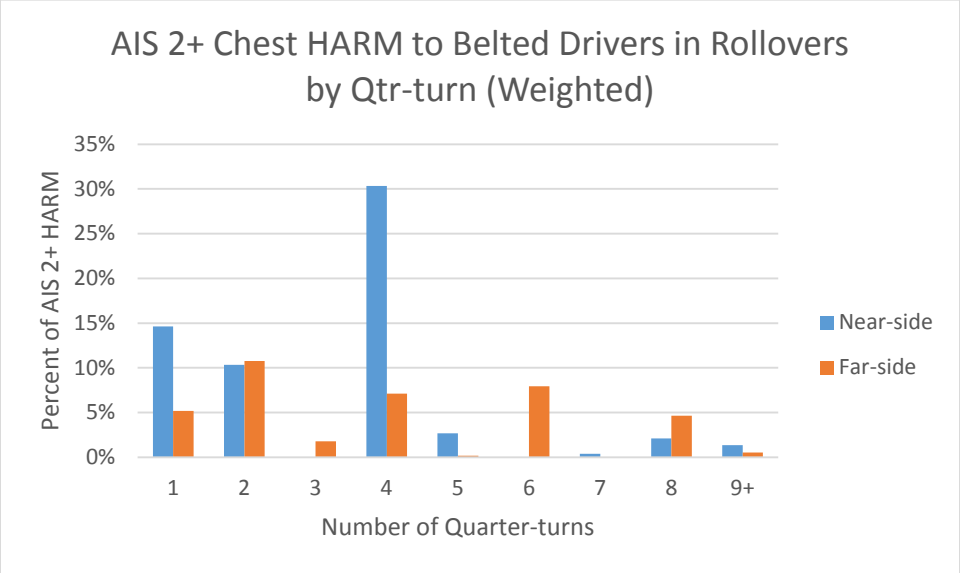


*Figure 7.* Distribution of belted driver AIS 2+ HARM from chest injuries in rollover involved MY 2000+ light vehicles by direction of rollover and number of quarter-turns (weighted data)

To better understand what parts of the vehicle are causing injuries in rollovers, an analysis of injuring contacts was conducted. NASS CDS allows the coding of more than 100 possible injuring contacts for occupant injuries. To clarify the location of occupant contacts in rollovers, it was necessary to aggregate the possible contacts according to location within the vehicle. The following contacts were included: roof, near-side compartment, far-side compartment, center compartment (including seat), frontal compartment, floor, other occupant and all other (including safety belt). The resulting distribution of contacts by injuring contacts by body region are shown in Tables 2 and 3. In Table, injuries at all AIS levels are included. In Table 3 only serious injuries (AIS 3+) are included. In both tables multiple injuries per occupant are allowed. Both near-side and far-side rollovers are included in these tables.

The number of injuring contacts were equally divided between near and far-side rollovers. The head and trunk contacts with the near-side compartment accounted for 59% of the contacts for near side-rollover compared to 27% for far-side rollovers. The all other contacts for head and chest injuries was much larger for far-side rollovers (52% vs 23%). Other contacts were generally similar.

Table 2. Distribution of injuring contacts in rollover crashes by injured body region (all injury levels)

| Contact Location | Head & Trunk | Upper Ex. | Lower Ex. |
|---|---|---|---|
| roof | 13% | 5% | 0% |
| near-side compartment | 27% | 62% | 57% |
| far-side compartment | 1% | 2% | 0% |
| center compartment | 3% | 1% | 3% |
| frontal compartment | 1% | 2% | 0% |
| floor | 2% | 0% | 22% |
| other occupant | 1% | 1% | 0% |
| all other | 52% | 25% | 17% |

Table 3. Distribution of injuring contacts in rollover crashes by injured body region (AIS 3+ injury levels)

| Contact Location | Head & Trunk | Upper Ex. | Lower Ex. |
|---|---|---|---|
| roof | 11% | 0% | 0% |
| near-side compartment | 66% | 90% | 93% |
| far-side compartment | 6% | 1% | 0% |
| center compartment | 2% | 2% | 1% |
| frontal compartment | 0% | 5% | 0% |
| floor | 3% | 0% | 7% |
| other occupant | 1% | 0% | 0% |
| other | 10% | 3% | 0% |

## DISCUSSION

The separation of NASS CDS data by vehicle model year 2000 and later, and the aggregation of injuries by the HARM weighting scheme provides new insights into the opportunities for further reducing injuries in rollovers. The historical method of analysis uses NASS data years for longitudinal studies and AIS 3+ injuries for measuring casualties. This approach obfuscates the presence of new vehicles in the fleet and inflates the effect of AIS 3 injuries. Separation of rollovers by crash severity (number of quarter-turns), rollover direction and injured body region is rarely done. This paper presents an innovative approach to rollover casualty analysis and highlights opportunities for further safety improvements.

Figures 3 and 4 show that the most frequent number of quarter-turns for both the exposure and the AIS 2+ HARM are 1, 2 and 4. The NASS weight factors for quarter-turn categories 5 and 9 may result in an unreliable prediction of the frequency of these events. Figure 5 shows that quarter-turns 2 and 4 carries the highest rate of AIS 2+ HARM.

A comparison of near-side and far-side rollover AIS 2+ HARM is displayed in Figures 6 and 7. Figure 6 addresses the HARM from all injuries and indicates that far-side rollovers have a higher percentage of HARM at the higher (6+) quarter-turns compared to near-side rollovers.

A further breakdown of HARM by the chest body region is displayed in Figure 7. The near-side chest HARM tends to track the overall HARM distribution with peaks at 1, 2 and 4 quarter-turns. However, the far-side chest harm is more uniformly distributed between quarter-turns 1, 2, 4, 6 and 8.

As shown in Table 2, the near-side compartment is the most frequent injuring contact for belted drivers. It accounts for 27% of the head and trunk injuries, 62% of the upper extremity injuries and 57% of the lower extremity injuries. When considering only AIS 3+ injuries these contact percentages are even higher (Table 3).

We need further study to better understand the causes of the high frequency of chest injury in near-side rollovers with 4 quarter-turns. For far-side rollover, chest injuries at 2 and 6 quarter-turns require further investigation. Explanations of chest injury causation in far-side rollovers with 4 and 8 quarter-turns were offered in an earlier ESV paper (Digges, 2013; Tahan, 2013).

## CONCLUSIONS

The number of rollover quarter-turns with the highest exposure and AIS 2+ HARM are 1, 2 and 4.

Far-side rollovers have a higher percentage of HARM at the higher (6+) quarter-turns compared to near-side rollovers.

The near-side chest HARM tends to track the overall HARM distribution with peaks at 1, 2 and 4 quarter-turns. However, the far-side chest harm is more uniformly distributed between quarter-turns 1, 2, 4, 6 and 8.

One cause of chest injuries in far-side rollovers with 4 and 8 quarter-turns has been proposed in earlier papers [Digges 2013, Tahan 2013]. Additional studies may be required to determine the high rate of chest injuries in four quarter-turn near-side rollovers.

REFERENCES

Digges, K., and Eigen, A., Injuries in Rollovers by Crash Severity, Enhanced Safety Vehicle Conference Paper, 07-0236, Lyon, France, June 2007.

Digges, K., Tahan, F., Grzebieta, R., Bambach, M., Mattos, G., McIntosh, A., Crash Damage Patterns Associated with Chest Injuries in Far-Side Rollovers, Enhanced Safety Vehicle Conference, Paper 13-0066W, Seoul, Korea, 2013.

Eigen, A, Digges, K., Safety Changes in the US Vehicle Fleet by Vehicle Model Year, Enhanced Safety Vehicle Conference, Paper 13-0062-O, ESV 2013.

Fildes, B., Cameron, M., Vulcan, A., and Digges, K., Injury Mitigation for a Range of Vehicle Safety Measures, 32nd Annual Proceedings of the Association for the Advancement of Automotive Medicine, p 93-108, 1992.

IIHS (2013) IIHS website www.iihs.org/ratings/esc, last accessed 03/14/15.

Malliaris AC, Hitchcock R, Hedlund J. (1982) A search for priorities in crash protection.SAE International paper #820242. Society of Automotive Engineers, Warrendale, PA.

National Highway Traffic Safety Administration (2001) National Automotive Sampling System Crashworthiness Data System 1995 – 1997, DOT HS 809 203, page 152, February 2001.

National Highway Traffic Safety Administration, National Automotive Sampling System Crashworthiness Data System, 1999 – 2013, ftp://ftp.nhtsa.dot.gov/NASS/, last accessed 11/17/2014.

National Highway Traffic Safety Administration, NASS CDS Coding and Editing Manual 1997, Washington, D.C., 1997.

National Highway Traffic Safety Administration, NASS CDS Coding and Editing Manual 2000 (Includes 1998 & 1999), Washington, D.C., 2000.

National Highway Traffic Safety Administration, NASS CDS Coding and Editing Manual 2013, Washington, D.C., 2014.

Tahan, F., Cohen, S., Digges, K., Kan, C.D., Assessment of a Dynamic Test Device to Evaluate Vehicle Rollover Safety, Paper 13-0398-O, Enhanced Safety Vehicle Conference, Seoul, 2013.

**Development of a Test Procedure for Driver Assist Systems Addressing Accidents Between Right Turning Trucks and Straight Driving Cyclists**

**Patrick Seiniger, Jost Gail, Benjamin Schreck**

Bundesanstalt für Straßenwesen (Federal Highway Research Institute) Bruederstraße 53, 51427 Bergisch Gladbach, Germany

**Paper ID#: 15-0286**

## ABSTRACT

Accidents between right turning trucks and straight riding cyclists often show massive consequences. Accident severity is much higher than in other accidents. The situation is critical especially due to the fact that, in spite of the six mirrors that are mandatory for ensuring a minimum field of sight for the truck drivers, cyclists in some situations cannot be seen or are not seen by the driver. Either the cyclist is overlooked or is in a blind spot area that results from the turning manoeuvre of the truck and its articulation if it is a truck trailer or truck semitrailer combination.
At present driver assistance systems are discussed that can support the driver in the turning situation by giving a warning when cyclists are riding parallel to the truck just before or in the turning manoeuvre. Such systems would generally bear a high potential to avoid accidents of right turning trucks and cyclists no matter if they ride on the road or on a parallel bicycle path. However, performance requirements for such turning assist systems or even test procedures do not exist yet. This paper describes the development of a testing method and requirements for turning assist systems for trucks.
The starting point of each development of test procedures is an analysis of accident data. A general study of accident figures determines the size of the problem. In-depth accident data is evaluated case by case in order to find out which are representative critical situations. These findings serve to determine characteristic parameters (e.g. boundary conditions, trajectories of truck and cyclist, speeds during the critical situation, impact points). Based on these parameters and technical feasibility by current sensor and actuator technology, representative test scenarios and pass/fail-criteria are defined.
The outcome of the study is an overview of the accident situation between right turning trucks and straight driving cyclists in Germany as well as a corresponding test procedure for driver assistance systems that at this first stage will be informing or warning the driver. This test procedure is meant to be the basis for an international discussion on introducing turning assist systems in vehicle regulations.

## INTRODUCTION

The share of accidents at crossings and intersections between right turning trucks and cyclists that move straight is rather low with regard to other accident types. However these accidents are particularly severe if the cyclist is hit and as a consequence overrun. Such cases always cause high public awareness due to the appalling implications for the victim as well as for the involved truck driver so that countermeasures are searched for a long time.
Already in the year 2004 the German Federal Highway Research Institute (BASt) published a study on the risk for pedestrians and cyclists at crossings due to right turning trucks [DEKRA (2004)] which was carried out by DEKRA accident research on behalf of BASt. This report especially depicted the lacking fields of vision for the truck driver to the front and to the right side (for left hand traffic).
In the meantime improvements for the direct field of vision and for the indirect vision via mirrors have been implemented with the aim to reduce blind spots to a minimum. With the European directive 2003/97/EC a larger field of vision became mandatory so that a truck normally has to be equipped with six mirrors in order to cover the required areas of the field of view. In addition the European directive 2007/38/EC was entered into force. Trucks above 3.5 t with their first registration in the year 2000 or later had to be retrofitted with corresponding mirrors on the right side until end of March 2009.
The mirrors however are only able to serve as useful remedy in eliminating blind spots if they are adjusted correctly if the driver looks into the mirror and if he, depending on what he has detected, takes the appropriate action with regard to the following driving manoeuvre.
Another project on behalf of BASt [TU BERLIN (2014)] (“Blind spot – conflict between right turning truck and straight driving cyclist”) considered, which issues in terms of the construction and operation of a junction are relevant if we look at blind spot accidents or road traffic safety. In addition it was examined in a simulator study if driver assistance systems could possibly contribute to alleviate the conflict in question. As main results, the regarded accidents were widely spread over built-up areas and both traffic participants (truck and cyclist) were mostly moving previous to the collision. Thus there was no standstill at the junction before the accident happened.
At present there is an ongoing discussion on turning assist systems, which warn the truck driver in the turning situation if a cyclist might be overlooked. Accident research of German insurers [HUMMEL et al. (2011)]

estimated ex-ante that a generic and best performing turning assist system (if the whole truck fleet is equipped) which scans the areas in front of and at the right side of the truck and which warns the driver or hinders the truck to move on would avoid about 40 % of the truck-pedestrian and truck-cyclist accidents.
However, there are no performance requirements for turning assist systems and on how they are supposed to operate yet. But the presence of such requirements would be a prerequisite for a possible promotion of systems and the basis for a possible mandatory installation by legislation.

**Starting Point**

Since there is no turning assist system on the market up to now it is on the one hand difficult to assess to which extent a system would be able to mitigate a certain critical turning situation and on the other hand to develop performance requirements which a system would have to fulfil. At least truck manufacturers revealed that systems are at stage of development.
The aim to avoid and mitigate the accidents with severe consequences between right turning trucks and cyclists is also pursued by the German Ministry of Transport and Digital Infrastructure (BMVI). How to tackle the problem of those blind spot accidents and if turning assist systems might help was also discussed with relevant stakeholders at round tables in April 2012 and May 2014 initiated by BMVI. It is planned to make a proposal for regulating a test procedure for turning assist systems on international level to introduce requirements in vehicle type approval regulations. For that purpose BASt was assigned by BMVI to develop a corresponding test procedure based on existing knowledge and taking in to account the state of the art technology, accident figures and circumstances of the accidents in question.
Thus BASt is actively developing a test method for turning assist systems for trucks since mid of the year 2014 addressing the following tasks:
At the beginning a thorough analysis of recorded accidents has to be carried out in order to identify the essential situations and accident constellations from which parameters for the test method have to be derived:

- Are vulnerable road users who become injured or killed by right turning trucks mostly cyclists or do pedestrians also have to be paid attention to?
- Is it allowed to restrict a testing procedure to daytime lighting conditions or do also accidents during night-time have to be taken into account?
- Initial speeds and collision speeds of cyclist and truck are of interest.
- How do cyclist and truck behave relatively with regard to their trajectory?
- Which typical turning radii are taken by trucks?
- What are typical lateral distances between truck and cyclist?
- Do obstructions for the view of the truck driver play any role?
- Should a testing procedure focus on trucks above 7.5 t or should lighter trucks be included as well?

The answers to these questions will deliver findings that allow to establish a few representative test cases for which boundary conditions, test parameters and criteria for pass/fail can be fixed.

**ACCIDENT ANALYSIS**

In 2010, 1,994 cyclists were killed in road accidents in the EU-24 countries, this represented 6.8 % of all road fatalities. For comparison: 381 cyclists were killed in road accidents in Germany in 2010 and 406 in 2012, which corresponds to 10.4 % (2010) and 11.3 % (2012) of all road fatalities, respectively [CANDAPPA N. et al. (2012)].

Road traffic accidents between heavy goods vehicles (HGVs over 3.5 tons maximum permissible gross vehicle weight) and cyclists resulted in 296 fatalities for 2010, as shown in Figure 1.

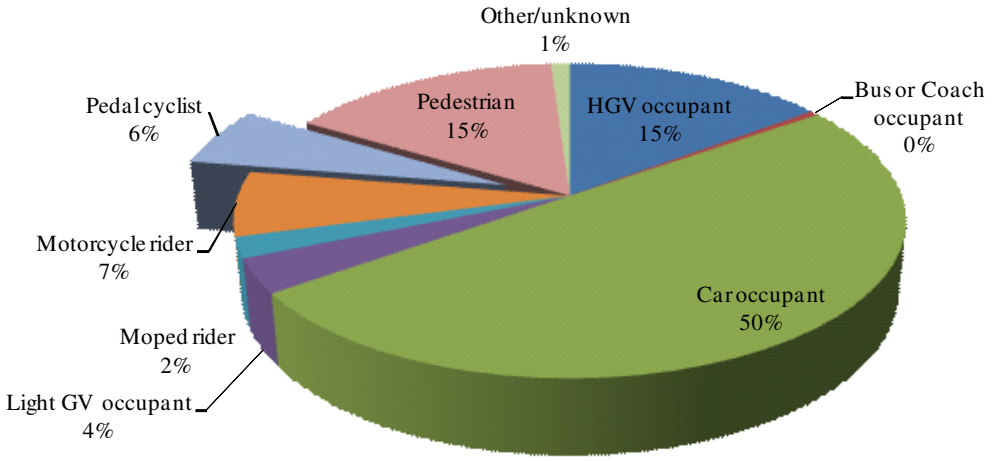


***Figure 1:*** **Fatalities in accidents involving HGVs and in accidents involving buses or coaches, by road user type (Data: EU-24; 2010 (for EE, NI, NL and SE from 2009); Source: CARE Database/EC)**

It is not possible to identify the exact number and severity of this accident situation in the German national road accident statistics because the conflict situation "blind spot" is not explicitly quantified. Therefore, an extrapolation [SCHRECK & PÖPPEL-DECKER (2014)] for the year 2012 was carried out to regarding the relevance of the conflict situation. The extrapolation shows that around 640 injury accidents resulting in 23 fatalities and another 118 seriously injured cyclists are due to the accident situation between right-turning trucks and driving straight cyclists. In the same configuration, the number of injured, severely injured and killed pedestrians is a magnitude lower (55 injured, 16 sesiously injured, 4 fatalities), so pedestrians will be neglected for the following considerations.

Thus, accidents involving right turning trucks represent 1 % of all bicycle accidents, and about 6 % of cyclists killed. It became clear that the "light" trucks, as defined as vehicles weighing less than 7.5 tones permissible gross weight, only slightly contribute to the serious accidents. In 549 collisions with "light" trucks, one cyclist was killed. 90 % of the accidents with killed cyclists in "blind spot" situations are accidents with "heavy" trucks (more than 7.5 tones permissible gross weight). So, in every 10 injury accidents between a “heavy” truck and a cyclist in a "blind spot" situation on average about one cyclist is killed. That shows the accident severity in terms of seriously or fatally injured cyclists that are involved are much higher than in accidents of other traffic participants in other accident situations.

Within the research project this paper is based on ([SCHRECK & SEINIGER (2014)]), accidents are analyzed in detail. The study uses police-reported accident data from the German Federal Statistical Office. Furthermore the German In-Depth Accident Study (GIDAS) and the German Insurers accident database (database UDV) was used. For the detailed analysis of accidents in GIDAS and in the database UDV, 120 accidents were available.

Accident databases GIDAS and UDV allowed for the detailed analysis of the speeds of the truck and bicycle, the driving behavior of the truck before and during the collision, the driving characteristics of the truck before the collision with respect to the infrastructure and the type of junction. The point of collision of the cyclist hitting the truck and potential visual obstructions in the infrastructure were available as well. Figure 2 shows as an example for the evaluation of accident data the difference in speed between trucks and cyclists, absolute speeds as well as relative speeds.

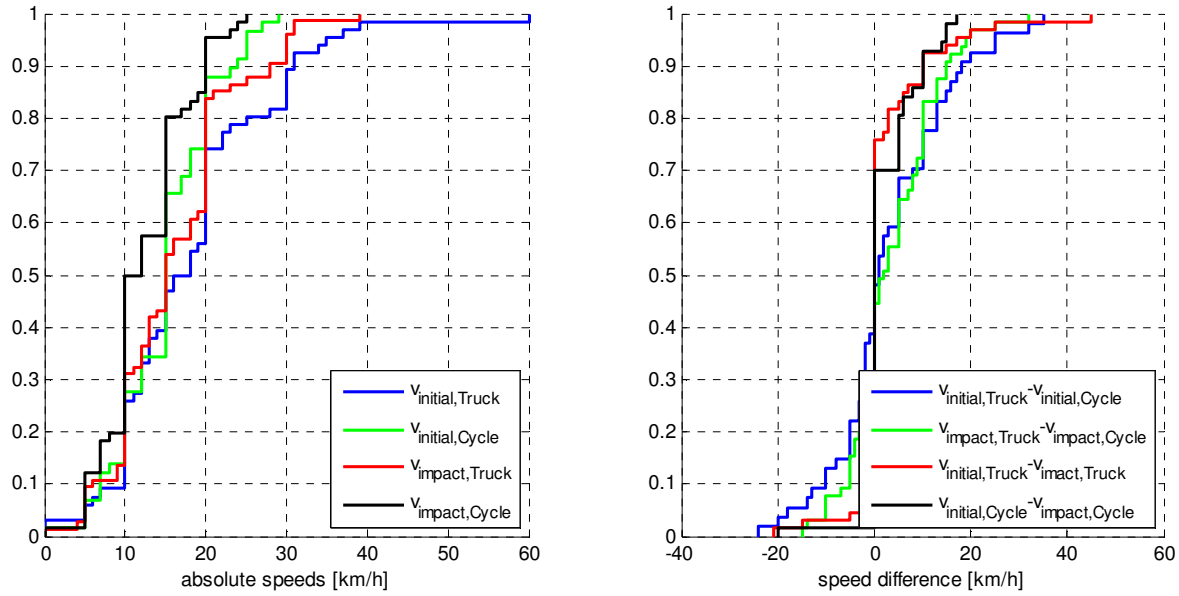


*Figure 2:* **Speeds and speed difference [km/h] between trucks and cyclists [SCHRECK & SEINIGER (2014)]**

Main findings from the accident analysis are:

- Truck speeds are below 30 km/h in more than 90% of all cases (as shown in Figure 2)
- Bicycle speeds are below 20 km/h in more than 80% of all cases (as shown in Figure 2)
- Bicycle and truck did not change their speeds during the accident in about two thirds of all cases.
- Visual obstruction and / or bad visibility due to weather (night, rain etc.) was not found to be an important factor.

With these results, it was possible to classify the accidents roughly into four scenarios. Figure 3 shows a sketch of this classification of the information collected, with the speed and track behavior of the truck and the lateral distance between truck and cyclist.

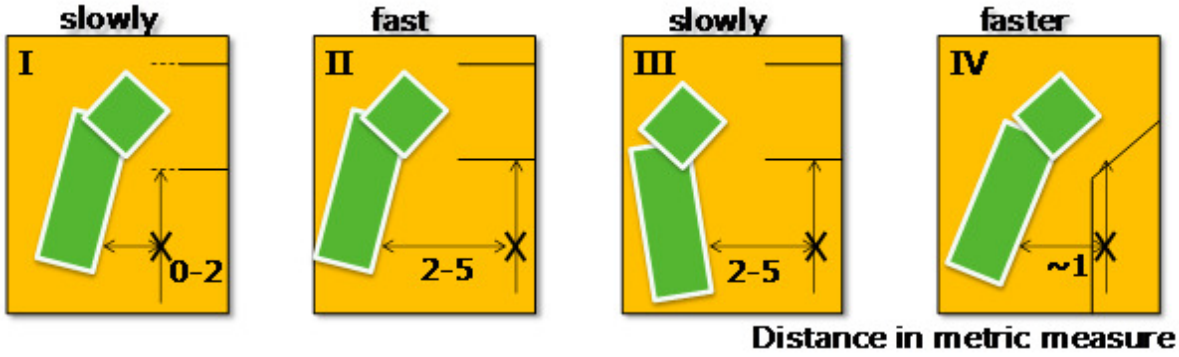


*Figure 3:* **Accident scenarios [SCHRECK & SEINIGER (2014)]**

## DEDUCTION OF TEST CASES

The benefits of a turning assistance system for trucks based on the accident increases with increasing overlap between the standards set by the requirements of the test method for the system and the conditions in the accident situations.

Once a parameter space for typical accidents between trucks and cyclists is outlined, the greatest possible coverage of this parameter space by as few as possible test cases needs to be achieved.

Due to the missing experience with a turning assistance, the use of emergency braking for safety reasons (possible false activations) is initially not advisable. High-intensity information (warnings) are in the course of a driving situation only justified if the probability for an accident is high - otherwise vehicle drivers tend to ignore or disable the system alerts.

In general, driver reactions to any information (high or low threshold / warning or information) can be expected only after a reaction time. This response time is much longer than the time required to avoid the accident in many situations - the accident cannot be avoided despite the warning.
A (low threshold) informational assistance system, however, can be activated sufficiently early, as it helps the driver rather than annoys him. Such an approach provides a useful solution if the information is made available to the driver in an appropriate manner. The identification of an appropriate transfer of information in terms of human machine interaction is not part of this work.
Since the information given by turning assistance systems needs to be reliable, effective recognition of the objects is required. Specifications for sensors, viewing angles, and detection times can be derived from this detection requirement.
The definition of relevant detection areas is done via a parametric kinematics model of the truck and bicycle trajectories during an accident, and taking into account the needed reaction times (of the driver) and stopping distances (of the truck). Test cases then are defined in such a manner that the whole detection area around the truck is covered by as little as possible test cases.
An accident between truck and bicycle happens when the collision partners are at a time in the same place, so the trajectories of bicycle and any give point of the truck intersect in space and time. In first approximation, the bicycle motion can be described by a straight line. The movement of the truck is divided into two basic movements: first, it is a straight line as well, parallel to bicycle movement line, which at a certain time changes towards a turn. The turn is considered to have a constant radius for reasons of simplicity. Both trajectories intersect at the theoretical collision. Accident analyses show that obstructions of sight, night and bad weather are not an essential factor for these accidents.
The following parameters have been derived from accidentology:

- Driving speed truck: $v_{Truck}$ = 10, 20, 30 km / h
- Driving speed bike: $v_{Cycle}$ ranges from 10 to 20 km / h
- Lateral distance of the initial trajectories (with respect to the right edge of the truck): A = 1.5 to 4.5 m
- Truck turning radius R = 5, 10, 25 m
- Maximum lateral acceleration of the truck: $a_y < 3{,}2$ m/s²
- Impact location of the bike onto the truck: L = 0 to 6 m
- Required reaction time after driver information: 1,4 s
- Braking performance of driver after reaction time: 6 m/s²

A sketch of the situation is shown in *Figure 4*.

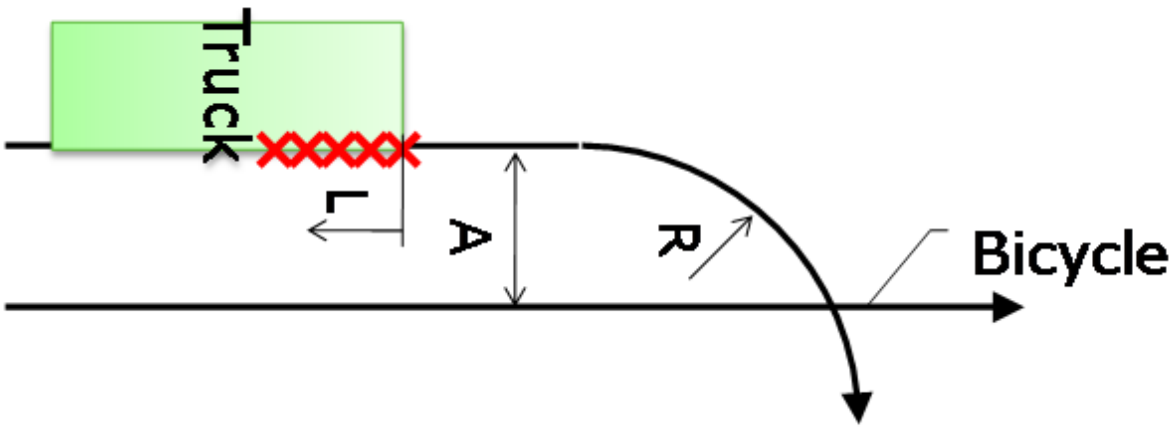


***Figure 4.*** **Sketch summarizing the relevant parameters describing the accident situation.**

The necessary viewing area of a sensor is the hull around all bicycle trajectories relative to the front inner corner of the truck. All bicycle trajectories are determined assuming a full combination of all parameters, until the time when warning or information is still feasible, and starting with for instance 4 s time to go for both vehicles up to the theoretical collision.

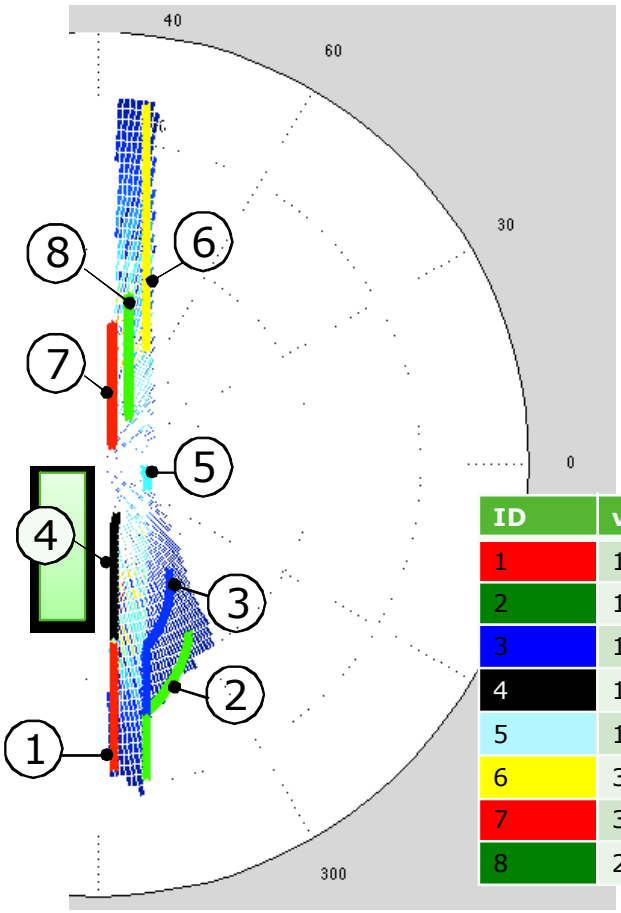


| ID | $v_{Truck}$ | $v_{Cycle}$ | R | A | L |
|---|---|---|---|---|---|
| 1 | 10 | 20 | 5 | 1,5 | 6 |
| 2 | 10 | 20 | 10 | 4,5 | 6 |
| 3 | 10 | 20 | 10 | 4,5 | 3 |
| 4 | 10 | 20 | 10 | 1,5 | 0 |
| 5 | 10 | 10 | 5 | 4,5 | 0 |
| 6 | 30 | 10 | 25 | 4,5 | 0 |
| 7 | 30 | 20 | 25 | 1,5 | 6 |
| 8 | 20 | 10 | 10 | 3 | 0 |

***Figure 5.*** **Bicycle trajectories relative to the front inner corner of the truck (=center of polar diagram), and proposed test cases (ID = 1 to 8). Field size in the polar diagram is 1m and 1°.**

The required viewing area as well as appropriate test cases to check bicycle detection in the viewing area are shown in Figure 5. Note that in theory a bicycle detection at the end of the nearer end of the trajectory satisfies the necessary detection criterion; it is not required to inform the driver already at the point where the bicycle is at the far end of the trajectory (which corresponds to 4 seconds TTC before the last possible information).

## TESTING

### Concept

Purpose of testing is to verify whether the system informs the driver, at least at the latest time at which avoidance is still possible, defined by the braking performance, driver reaction time and kinematics as laid out in the preceeding section.
This means that an object which sufficiently appears to any sensor technology as a cycle needs to be moved and synchronized to the truck according to the proposed test cases.
Since an information must be given at a time when the accident is still comfortably avoidable, all tests can be conducted without impacts, thus allowing for the use of a real bicycle (and possibly human dummy) rather than a specific bicycle dummy.

### Test Tools and Equipment

For tests of pedestrian emergency braking in cars using the Euro NCAP test procedure, a propulsion system for the pedestrian dummy is used. This system can determine the speed of a vehicle over several light barriers and thus synchronize the movement of the dummy very closely with the moving vehicle, so the development of test tools does not need to start from scratch. Measurement equipment in the truck is not required. For cost reasons, it may be useful to establish a simplified test tool and not to use the said motion system - but for feasibility studies and the identification of the tolerable error in testing it is a suitable tool.
While the propulsion system is commercially available, testing with parallel trajectories requires a few modifications, which have been prototypically established at BASt.

The bicycle is guided by the motion system, therefore a review of the trajectory is not required. For checking the trajectory of the truck itself, an alley from pylons or "Botts' Dots" can be used to visually determine whether the vehicle had maintained the required trajectory.
Video recording and time synchronizing equipment might be required to check whether the information was given at an appropriate time.

**Necessary Modifications to the Propulsion System**

In a first step, the use of a pedestrian propulsion system, for instance "4active systems surfboard" (see Figure 6) could be used. This system is state of the art and will be used by several test labs for Euro NCAP AEB pedestrian testing (starting in 2016).

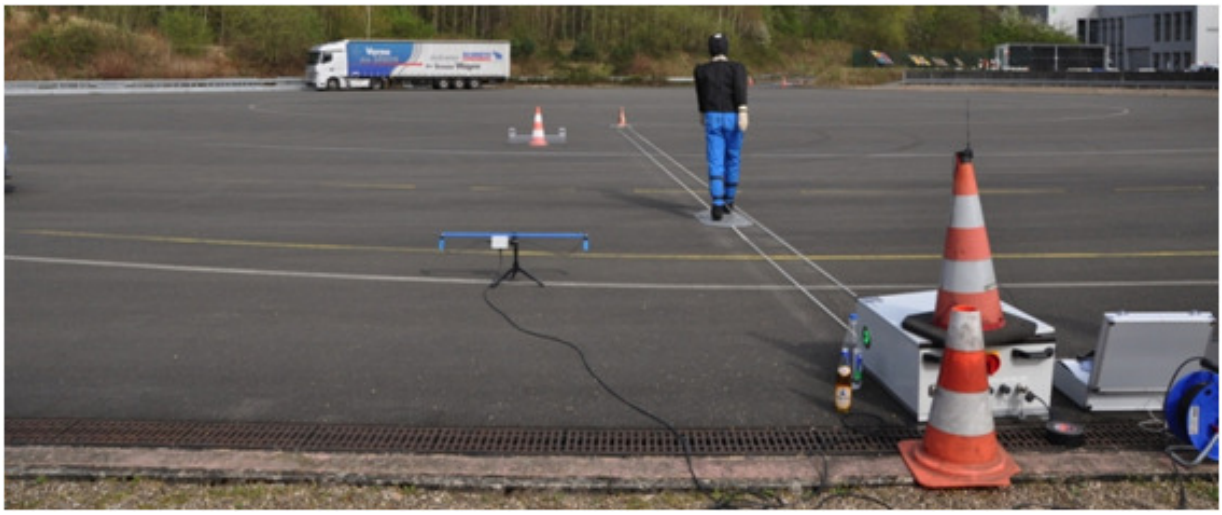

***Figure 6.*** **4active systems "Surfboard" dummy propulsion system.**

This propulsion system has been designed to test with a crossing pedestrian. Magnets fit the pedestrian dummy to a platform. The platform is driven by a circular timing belt that of course requires bearings on both sides. When testing longitudinal scenarios (as is the case for the turning assistance systems), counter bearing or drive mechanism might disturb the vehicle's sensors, and since the belt is used in a circle, the available dummy displacement is not sufficient.
BASt therefore developed a method to use the propulsion system with a linear belt. This removes any bearing out of the sight of the vehicle sensors and doubles the effective belt length but also takes away lateral positional accuracy and requires manual transportation of the dummy to its' origin during testing.
A mechanism to fit a bicycle to the propulsion system also required and currently under development.

**Test Track Requirements**

As for all testing, a test track is required; it needs to be sufficiently large to fit all test cases. A typical test will consist of an acceleration phase for the truck (phase 1), a phase where the truck is moving alone at a stabilized speed (phase 2), and a phase where the bicycle movement is synchronized to the truck speed (phase 3). The space demand on the test track for phase 3 can be calculated from the kinematics of test cases as defined in *Figure 5*: the maximum space requirement is 44 m x 4.5 m excluding the size of the truck. The proposed tests therefore can be conducted even on small test tracks.

**SUMMARY AND PERSPECTIVE**

Turning maneuvers with collisions between trucks turning right and cyclists usually have serious consequences for the vulnerable road user. In the past the safety of vulnerable road users was raised by an improvement of the truck driver's vision by increasing the number of mirrors and by equipping trucks with side underrun protection. Since turning accidents still happen and driver assistance systems have been introduced in a lot of vehicle segments it seems to be obvious to use such assistance to address turning accidents between trucks and cyclists.
In order to stimulate system development, e. g. by means of incentives or legislation, performance requirements and corresponding test procedures are necessary. Aim of the work carried out by BASt therefore was to develop such requirements and a possible test method.
Starting from an in depth analysis of accidents, parameters and circumstances being characteristic in accidents with cyclists and right turning trucks were identified. Data at hand shows that the velocity is up to 30 km/h for the truck and up to 20 km/h for the bicycle. At the beginning of the critical situation the truck and the cyclist move parallel with a lateral distance of 1.5 m up to 4.5 m. Although there is no precise information about curve

radii it can be assumed that the inner side of the truck propagates predominantly on a radius between 5 m and 10 m since accidents occur in built-up areas. However, there can be junctions with triangular traffic islands where the radius is up to 25 m. Obstructions for the view of the truck driver were present only in a few cases. Also bad weather conditions or darkness hold only for a small fraction of accidents.
Considering driving dynamics in terms of reaction time and stopping distance for the given initial conditions leads to the conclusion that only an early and not annoying driver information can serve as effective function that assists the driver avoiding the accidents. For automatic braking being a massive intervention too less experience has been gained so far. Well known high priority warnings that are given at a late point in time would have no effect since the driver reaction time lasts that long that an emergency braking manoeuvre would start too late. So those variables and parameters that allow for comfortable braking can be used in a kinematic model to calculate the areas around the truck that have to be covered by a sensing system which has to detect cyclists in such a way that the driver is informed about the cyclist in time. Within the parameter range those special parameter combinations can be selected as test cases which cover the necessary sensing area with as less test cases as possible. A method to identify these test cases and the resulting test cases that are proposed for the test procedure were described in detail. A proposal how to effectively execute driving tests by using existing test tools coming from testing of automatic emergency braking systems to protect crossing pedestrians was described as well.
After having fixed the set of test cases and parameters a validation phase has to follow. For that purpose trucks equipped with turning assist system have to be used. It has to be examined if the system is able to inform the driver when necessary and how far it is still annoying due to possibly given false warnings.
It can be expected that a turning assist system that fulfils the requirements and tests elaborated in this study will have a very positive influence on accident figures concerning right turning trucks and cyclists.

**Literature**

[CANDAPPA N. et al. (2012)] Candappa N. et al. :Basic Fact Sheet "Cyclists", Deliverable D3.9 of the EC FP7 project DaCoTA.]

[DEKRA (2004)] Niewöhner, W., Berg, A.F.: Gefährdung von Fußgängern und Radfahrern an Kreuzungen durch rechts abbiegende Lkw, Berichte der Bundesanstalt für Straßenwesen, Heft F54, Bergisch Gladbach, 2004.

[DEKRA (2014)] Ritter, Stefanie: Kollisionen zwischen rechts abbiegenden Lkw und Fahrrädern – ein Update nach zehn Jahren, p. 296-305, Verkehrsunfall und Fahrzeugtechnik, September 2014.

[HUMMEL et al. (2011)] Hummel, Thomas; Kühn, Matthias; Bende, Jenö; Lang,Antje: Ermittlung des Sicherheitspotenzials auf Basis des Schadengeschehens der Deutschen Versicherer, Forschungsbericht FS 03, Unfallforschung der Versicherer, Gesamtverband der deutschen Versicherungswirtschaft e.V., Berlin, 2011.

[SCHRECK & PÖPPEL-DECKER (2014)] Schreck, Benjamin & Pöppel-Decker, Martin: Unfallgeschehen zwischen rechtsabbiegenden Güterkraftfahrzeugen und geradeausfahrenden Radfahrern, p. 239-242, Zeitschrift für Verkehrssicherheit, 4.2014.

[SCHRECK & SEINIGER (2014)] Schreck, Benjamin & Seiniger, Patrick: Abbiege-Assistenzsystem für Lkw, Grundlagen für ein Testverfahren; Bericht, Bergisch Gladbach, 2014.

[SEINIGER (2013)] Seiniger, Patrick et al.: Anforderungen an das Testen von Fußgänger-Notbremssystemen - erste Ergebnisse von AsPeCSS und ADAC. 6. Tagung Fahrerassistenz, München, 28./29.11.2013.

[TU BERLIN (2014)] Richter, Thomas et al.: Toter Winkel - Konflikt zwischen rechtsabbiegenden Lkw und geradeausfahrendem Radverkehr (FE 82.512/2010), Schlussbericht, to be published, Berlin, 2014.

# IDENTIFYING AND PROVING AUTOMOTIVE ALGORITHM DEFECTS AND AFFECTING RECALLS

**Donald Friedman**
**Jacqueline G. Paver Ph.D.**
Center for Injury Research
United States
Paper Number 15-0287

## ABSTRACT

The societal cost in lives lost and injuries sustained from electronic defects, such as occupant size algorithm misclassification and ignition switch failure, was studied. In addition, the societal cost of ineffective production restraint systems in frontal and angled-frontal crashes was evaluated. Fatalities due to electronic defects were compared to the total fatalities from frontal and angled-frontal crashes.

Accident statistics show that, from 2001 to 2013, there were only 50 electronic algorithm defect deaths annually compared to 10,676 deaths annually from frontal and angled-frontal crashes involving vehicles that met the Federal Motor Vehicle Safety Standard (FMVSS) 208 test requirements. Our research indicates that many more deaths would have been prevented in a single year than electronic defects caused in 20 years if certain features of passive restraint systems proposed in the 1970's had been implemented. The same trend applies to injury mitigation.

The research question explored here is: Should "WE" prioritize identifying and repairing:

- algorithm defects that cause only 50 of the 10,676 fatalities annually, or
- ineffective production restraints systems in vehicles compliant with FMVSS 208 test requirements that cause 10,626 of the 10,676 fatalities annually.

Since NHTSA cannot specify design requirements, a simple solution is to substitute for the right and left angled barrier test a compartment angled at 20º to the right and then 20º degrees to the left on a sled simulating a 30 mph crash.

## BACKGROUND

Since the first Drive-by-Wire (DBW) systems, independent engineers, manufacturers, and government have been aware of algorithm defects in production vehicles. Unintended acceleration, occupant size algorithm misclassification, and ignition switch failures are newly-reported, not newly-identified defects. To affect a recall, complaints and accidents must occur. Then, the NHTSA directs research and testing to identify and prove a defect. Litigation often accelerates the research and testing phase of the recall process. However, crashworthiness testing does not prove causation. Electronic defects are proven by downloading and anaylyzing control module stored functional data for a specific crash; this stored data does prove causation. The population of affected vehicles are identified. The cost of the defect is assessed in terms of lives lost and injuries mitigated. Technical service bulletins are issued. Recalls are implemented. Today's media informs the public.

Automotive DBW systems interconnect at least 40 microprocessors, their algorithms, hundreds of sensors and millions of lines of software code. Industry has developed DBW systems to improve engine fuel efficiency and responsiveness, reduce emissions, enhance occupant comfort, improve injury protection, and streamline repair and service diagnostics. In spite of rigorous testing, the DBW system is so complicated that it still has previously-identified, but unfixed bugs. Those bugs are generally discovered in litigation and lead to millions of recalled vehicles to mitigate potential deaths and injuries.

In 2014, millions of vehicles were recalled for unintended acceleration, ignition switch engine cut off, and/or failed airbag inflator housings. Congressional oversight investigations urged NHTSA to penalize manufacturers for delaying notification of such defects for up to 10 years. Press coverage highlighted the potential for death and injury.

in this paper, the annual fatalities and injuries caused by automotive electronic defects are compared with the thousands of deaths that occur annually in vehicles that meet all applicable FMVSS test requirements due to ineffective restraint systems. An example of the cost in lives is presented here.

## METHODS

### Accidents Statistics Data

In 2013, the Fatality Analysis Reporting System (FARS) identified 27,051 vehicle fatalities categorized as frontal, side, rear and rollover. Of those, there were 10,676 fatalities in non-rollover frontal impacts and angled-frontal impacts between 11 o'clock and 1 o'clock. That amounts to an average of 29 deaths per day in the United States [1]. These deaths are valued at $9.1 billion in accordance with Department of Transportation Policy Guidance, amount to a societal loss of $96 billion in monetary terms , not moral terms.

An estimate of the distribution at 11 o'clock, 11:30 , 12 o'clock, 12:30 and 1 o'clock of the 10, 676 fatalities from frontal and angled-frontal crashes[2] is shown in Table 1:

**Table 1.**
**Estimated Frontal Fatalities by Clock Position**

| Clock Position | Angle | Total Fatalities |
|---|---|---|
| 11:00 | -30º | 843 |
| 11:30 | -15 º | Estimated 2,745 |
| 12:00 | 0 º | Estimated 3,850 |
| 12:30 | 15 º | Estimated 2,560 |
| 1:00 | 30 º | 679 |

It is important to note the large number of deaths attributed to angled impacts at 11:30 and 12:30 where the restraints are ineffective. In developing airbags for NHTSA in the 1970s, Minicars determined that the left and right frontal 30º angled barrier impacts corresponded to ±10º of real world angled impacts because corner friction between the vehicle and the barrier limits the equivalent real-world angle. In other words, compliance with the regulatory test only requires occupant protection in frontal and ±10º angled real-world impacts. Current supplemental airbags are sized to protect occupant head and neck from contact with interior components. The deployment algorithms preclude activation in angled impacts relying on the belts to limit motion. Therefore, occupants of real-world angled impacts greater than ±10º are virtually unprotected and account for the large number of fatalities at 11:30 and 12:30 clock positions. Apparently, NHTSA has not recognized this discrepancy in protection, where the industry can be in full compliance with the test requirements, but only protect less than half of the frontal fatality population.

**Algorithm Misclassification** An investigation of an essentially frontal crash in a 2008 sedan produced physical evidence of a defective occupant size algorithm misclassification defect. The Crash Data Retreival (CDR) record confirmed the driver airbag deployment and right front passenger airbag deployment suppression. A download of the stored data in the passive occupant detection system control module was conducted. The stored data showed that a 170-lb belted right front seat passenger, who lifted off the seat, was misclassified as a small adult 1.5 seconds prior to impact, resulting in suppressed passenger airbag deployment.

An Office of Defect Investigation (ODI) petition called for a response from the manufacturer, whose analysis refuted the defect claim. The manufacturer:

1. did not deny that the algorithm resulted in occupant size misclassification, and
2. claimed the right front passenger was out-of-position.

**Ignition Switch Defect** Studies show that, over the 10-year period from 2003 to 2013, the ignition switch defect accounts for the 338 fatalities of the 3,806 claims. Based on the probable resolution of many of these claims, the annual cost of this defect is unlikely to exceed 20 fatalities and 100 serious injuries annually.

**Safety Belts and Airbag Defects** In the 1960s, there were no safety belts in cars and the concept of passive protection by automatically deploying airbag was born. In 1973, GM produced about 10,000 Cadillacs and Oldsmobiles with driver and passenger airbag protection.

In the context of the 1974 amendment to FMVSS 208, occupant protection is specified in Paragraph S4.1 Frontal Barrier Crash. "When the vehicle impacts a fixed collision barrier perpendicularly or at any angle up to and including 30º in either direction from the perpendicular, under the applicable conditions of S6, while moving longitudinally forward at any speed up to and including 30 mph with test device at each designated testing position, it shall meet the injury criteria of S5."[3] A review of the latest post 2006 version of FMVSS 208 confirms this test procedure.

In spite of the amendment by 1981, the automotive industry drove the design of 3-point safety belts and associated supplemental airbags to perform in frontal and angle barrier impacts at the equivalent of ±10º of impact angle. This design strategy rendered occupants in crashes involving impact angles greater than 10º or 15º vulnerable to deaths and injuries. The annual cost of those impacts is in the range of 5,000 fatalities.

In the example frontal crash of the 2008 sedan presented above, the manufacturer claimed that there existed no proof that passenger airbag deployment would have mitigated the occupant's injuries. The manufacturer made the following statement:

> *"The Petitioner's suggestion that the occupant would have benefited from passenger airbag deployment is not supported in the Petition and is pure speculation. The Petitioner has not supplied – and the manufacturer is not aware of – any evidence or argument that supports the conclusion that a passenger-side airbag should deploy in the conditions recorded by the vehicle's AOS, or that the full deployment of the passenger-side airbag would have mitigated – and not exacerbated – the injuries allegedly sustained by the occupant during the accident.[4]*

The implication of this statement is that safety belts do not keep the occupant in close proximity to the seat and, if the passenger's airbag had deployed, it would not have mitigated the passenger's injuries as it did for the driver. In fact, the manufacturer claimed that deployment could exacerbate occupant injury.

An analysis of airbag effectiveness is tied to the frontal impact regulatory requirement test. The airbag is optimized to minimize head injury criteria in frontal ±10º impacts and sized accordingly. However, the slack in the safety belts is sufficient to put the occupant somewhat out-of-position, where the size of the airbag is insufficient to protect the occupant's head. This analysis suggests that fatalities and injuries are the result of ineffective safety belts and/or airbags.

As early as 1972, the NHTSA sponsored the 1975 Minicars Research Safety Vehicle (RSV) project aimed at airbag development to protect occupants from interior impact at up to 30º at 30 mph [5-6]. Minicars found that a large-diameter chambered airbag had a significant effect on mitigating fatality and injury without requiring a revised test standard. The requirements for the airbags included frontal protection at 50 mph and protection from 11 to 1 o'clock at 30 mph. The RSV driver dual airbag was incorporated into the steering wheel on a stroking steering column with a foam knee restraint. The inner bag deployed first and vented into an approximately 30-inch outer diameter bag tethered to each other. The passenger airbag was chambered to fill in the bottom half and vent into a multichambered head impact bag. This design provided 50 mph occupant protection without safety belts at up to 30º off-axis (at 30 mph). Projected to the 1985 vehicle population, this design results in a 75% reduction in frontal fatalities.

The frontal crashworthiness compliance test and its vehicle rating system is based on a barrier crash at ±10° of 12 o'clock. The vehicle rating system assigns 3 of 5 possible stars if dummy injury measures meet the injury criteria and up to 5 stars if the injury measures are 50% of the injury criteria. This is a powerful incentive for manufacturers to optimize safety belt and airbag design for the test at minimum size, cost and weight.

Since NHTSA can only require performance criteria, an equivalent simple solution is to substitute for the right and left angled barrier test a compartment angled at **20**º to the right and then **20**º degrees to the left on a sled simulating a 30 mph crash**.** A further modification within NHTSA's authority is to substitute a low durometer neck for the Hybrid III production neck to more appropriately represent current population of occupants. An experiment demonstrated the effect. Two identical sled tests of a restrained Hybrid III dummy, one with a production and the other a low durometer neck were tested a 15 mph. The low durometer neck allowed the head of the dummy to be extended forward approximately 4" further than the production neck as shown in Figure 1.

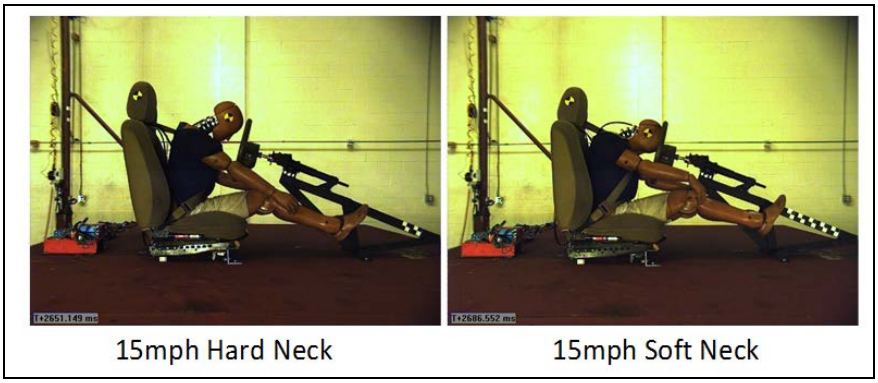

Figure 1. Production vs. Low Durometer Neck

**RESULTS**

The occupant size algorithm misclassification and the ignition switch defects account for only about 50 fatalities annually. In contrast, restraint systems that meet the regulatory requirements account for nearly 30 times the annual fatalities caused by electronic defects. The narrowly-defined FMVSS 208 requirements only protects occupants in direct frontal crashes. A variety of variables, each of which can account for several hundreds of fatalities in the real-world, are not adequately addressed in the existing standard. For example:

- the impact angle is greater than ±10º,
- occupants are frequently out-of-position,
- the dummy does not represent the current population,
- 30% of occupants do not wear their safety belts, and
- the DBW system fails.

**CONCLUSION**

Clearly, automotive safety efforts should prioritize reducing the 10,626 of 10,676 annual fatalities by improving safety belts for those occupants who wear them and expanding airbag passive protection for those who do not wear safety belts, instead of focusing on algorithm defects that cause only 50 of 10,676 fatalities annually.

Since FMVSS 208 is a performance, not design requirement, the most effective means of reducing fatalities and injuries is to substitute for the right and left angled barrier test a compartment angled at 20º to the right and then 20º degrees to the left on a sled simulating a 30 mph crash. A further modification would be to substitute a low durometer neck for the Hybrid III production dummy neck.

**REFERENCES**

[1] http://www-fars.nhtsa.dot.gov/main/index.aspx.
[2] *Ibid*.
[3] FMVSS 208 Amendement, Docket 69-7, Notice 7 Federal Register Vol 35, No. 214, 11/3/70.
[4] General Motors Response to Petitioner, DP14-001, 10/3/14.
[5] Advanced Air Bag Restraints for Standard Size Car Drivers, 1972, DOT-HS-113-2-441, $263,496.00.
[6] Advanced Air Bag Restraints for Subcompact Car Drivers, 1973, DOT- HS-1 13-3-742, $194,664.00.

**Instrumentation Technique for Measuring Six Degrees of Freedom Head Kinematics in Impact Conditions using Six-Accelerometers and Three-Angular Rate Sensors (6aω Configuration) on a Lightweight Tetrahedron Fixture**

**Yun-Seok Kang**
Injury Biomechanics Research Center, The Ohio State University
USA

**Kevin Moorhouse**
National Highway Traffic Safety Administration, Vehicle Research & Test Center
USA

**John H. Bolte IV**
Injury Biomechanics Research Center, The Ohio State University
USA

Paper Number 15-0288

## ABSTRACT

The ability to measure six degree of freedom head kinematics in impact conditions (i.e. motor vehicle crashes and sport activities) plays an important role in injury assessment of the head/neck complex. Potential accuracy of head instrumentation schemes have recently been improved by using advanced angular rate sensors, so in this study an instrumentation technique for obtaining accurate head kinematics in impact conditions using an external fixture is proposed and validated. The methodology proposed in this study utilizes six accelerometers and three angular rate sensors (6aω) on a lightweight tetrahedron fixture (t6aω) originally designed for measuring head kinematics of post mortem human surrogates (PMHS) in car crash scenarios using a nine accelerometer array package (NAAP) configuration (tNAAP). A Hybrid III 50th percentile male anthropomorphic test device (ATD) head containing an internal nine accelerometer array package (iNAAP) was used to validate the t6aω method proposed in this study. The t6aω instrumentation was installed on a tetrahedron fixture which was attached externally to the Hybrid III ATD head, tested in direct contact tests of various severities, and then compared to data measured from the iNAAP of the Hybrid III ATD head which provided the kinematics gold standard to validate the proposed technique. Results indicate that angular acceleration obtained from the t6aω scheme was comparable to that determined from the iNAAP scheme in the head impact conditions, showing normalized root mean squared deviation (NRMSD) values less than 5%. Transformed linear acceleration from the t6aω to the center of gravity (CG) of the Hybrid III ATD head was also comparable to acceleration measured directly from the accelerometers at the CG, exhibiting less than 5% NRMSD. Accurate angular acceleration and velocity are important to obtain accurate transformed acceleration. Since the t6aω angular acceleration component of the transformed linear acceleration at an inaccessible point was shown to have equivalent accuracy to iNAAP (less than 5% error), and the angular velocity component of t6aω instrumentation should be more accurate than the tNAAP scheme (since it is directly measured by the ARS as opposed to using numerical integration as in tNAAP), the t6aω scheme should yield more accurate transformed linear acceleration at an inaccessible location than the tNAAP scheme. The proposed instrumentation should aid in the development and evaluation of head, neck and brain injuries in future testing.

## INTRODUCTION

Numerous measurement techniques for head kinematics in motor vehicle crashes and sports activities have been developed and evaluated [1-9], and the accuracy of angular kinematics, in particular, has been a challenge in developing these instrumentation techniques [1-4, 7]. The most frequent method to obtain accurate six degrees of freedom (6DOF) head kinematics is to use the nine accelerometer array (3-2-2-2) package (NAAP), in which angular acceleration can be calculated from simple algebraic equations [1]. Although the NAAP is capable of measuring angular acceleration accurately, single and double numerical integrations are required to obtain angular

velocity and displacement, which can particularly cause issues with the accuracy of the resulting displacement [5, 7]. Therefore, with the advent and availability of more advanced angular rate sensors (ARS), ARS combined with accelerometers have been recently employed to provide even more accurate angular velocity and displacement [5], since angular acceleration can still be obtained from algebraic equations, while angular velocity is directly measured from the ARS [7]. Therefore, six accelerometers and three ARS (6aω) should theoretically be capable of measuring more accurate 6DOF kinematics than NAAP, and this has been demonstrated for sensors installed inside an ATD head (i6aω versus iNAAP where "i" stands for internal) [7].

In order to measure 6DOF kinematics of the head of post mortem human surrogates (PMHS), an external fixture is typically used, and should be lightweight and stable against structural vibration. Previous studies evaluating head and brain injuries have used various external fixtures with nine accelerometers (NAAP) installed, such as a triangular pyramidal fixture [10] and a tetrahedral fixture [11]. Although the i6aω scheme has been validated inside a Hybrid III iNAAP head [7], its integrity with a lightweight/small external fixture should also be validated. Therefore, the objective of this study is to propose and validate a 6aω scheme installed on a lightweight tetrahedron fixture (t6aω, where "t" stands for tetrahedron).

## METHODS

### 6aω Scheme on a Lightweight Tetrahedron Fixture

An external tetrahedron fixture, similar to the one developed and validated (including its structural integrity and stability) by Yoganandan et al. [10], was utilized in this study. The t6aω scheme was implemented as shown in Figure 1. The edge length of the tetrahedron is approximately 6 cm, while the mass of the fixture is 72 grams without sensors and 96 grams with sensors attached. In order to obtain algebraic equations for angular acceleration of the t6aω scheme, the acceleration at each corner point (points A-B-C shown in Figure 1b) with respect to a body fixed coordinate system on the tetrahedron fixture was derived as Eqs (1) – (3).

$$a_{az'} = a_{0z'} + \omega_{x'}\omega_{z'}\rho_{ax'} - \dot{\omega}_{y'}\rho_{ax'} \quad (1)$$

$$a_{bx'} = a_{0x'} + \omega_{x'}\omega_{y'}\rho_{by'} - \dot{\omega}_{z'}\rho_{by'} \quad (2)$$

$$a_{cy'} = a_{0y'} + \omega_{y'}\omega_{z'}\rho_{cz'} - \dot{\omega}_{x'}\rho_{cz'} \quad (3)$$

where,
$\dot{\omega}$ : angular acceleration in the body fixed frame
$a$ : acceleration measured from accelerometers at each location
$\omega$ : angular velocity measured from ARS
$\rho$ : distance between accelerometers at vertex and accelerometers at points A, B, and C

Eqs (1) – (3) can now be expressed in terms of the angular accelerations, which are the only unknown variables under the proposed t6aω configuration, as in Eqs (4) – (6):

$$\dot{\omega}_{x'} = (a_{0y'} - a_{cy'})/\rho_{cz'} + \omega_{ay'}\omega_{bz'} \quad (4)$$

$$\dot{\omega}_{y'} = (a_{0z'} - a_{az'})/\rho_{ax'} + \omega_{cx'}\omega_{bz'} \quad (5)$$

$$\dot{\omega}_{z'} = (a_{0x'} - a_{bx'})/\rho_{by'} + \omega_{cx'}\omega_{ay'} \quad (6)$$

The detailed procedure for deriving the kinematic equations with respect to the body fixed frame for the t6aω scheme is described in a previous study [7].

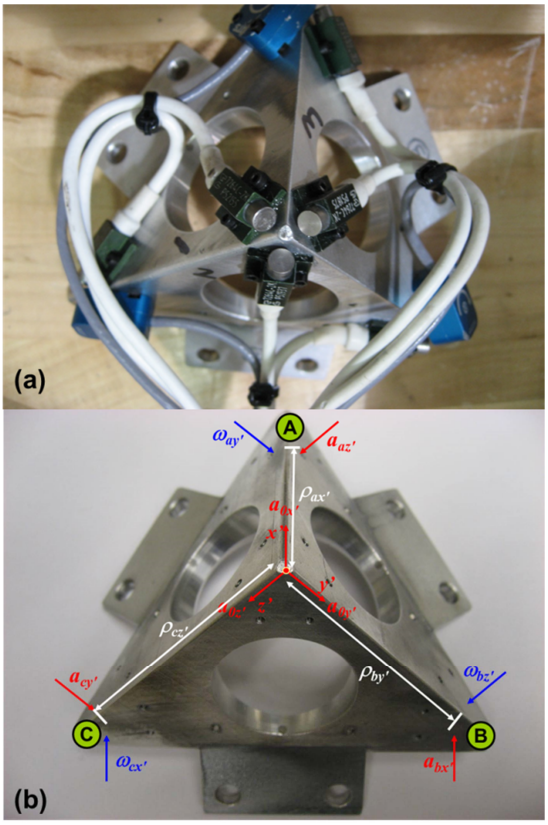


***Figure 1. (a) An external fixture with 6aω scheme and (b) body fixed coordinate system embedded on the tetrahedron fixture.***

**Test Configuration and Instrumentation**

Thirteen head impact tests were conducted to validate the proposed external instrumentation in a direct impact condition that usually yields high peak, short duration responses. The Hybrid III head/neck was fixed to an adjustable height table and a hydraulic ram impactor was used to deliver a severe head impact. The lower neck of the Hybrid III was fixed to the table after being rotated 30 degrees about the z direction according to SAE J211 (SAE, 2007), as shown in Figure 2, such that the impactor could collide with the head antero-laterally. The body fixed frame (x-y-z) on the Hybrid III head was defined as shown in Figure 2. In order to produce various severities and head injury criteria (HIC) values, the head was struck by the impactor without padding for five tests and with padding for eight tests. For the padded condition a one inch thick piece of gray "Ensolite SCC" foam was affixed to the head at the impact location. The Hybrid III iNAAP head was instrumented with nine accelerometers (Endevco 7264C 2K), while the t6aω scheme installed on the tetrahedron fixture was composed of six accelerometers (Endevco 7264C 2K) and three ARS (DTS ARS-18K). In addition to the t6aω scheme, a t3aω scheme on the tetrahedron fixture was also evaluated in this study. The t3aω scheme was composed of the three accelerometers at the origin (i.e. vertex of the fixture) and the three ARS at points A-B-C shown in Figure 1. Accuracy of the external instrumentation could be affected by any relative movement between the fixture and the head. To reduce the risk of relative motion, the tetrahedron fixture was screwed into the skull cap using six screws, as shown in Figure 2.

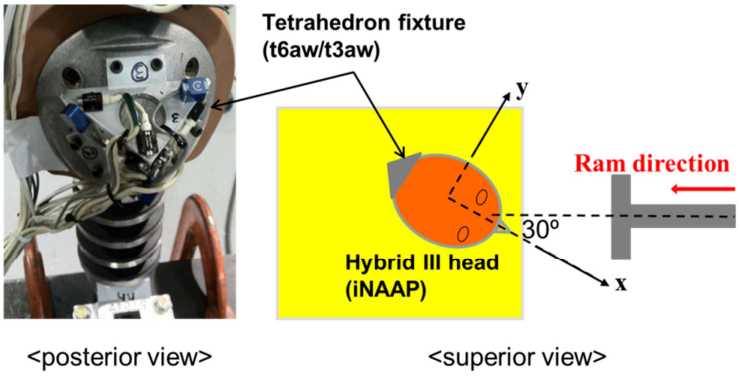


***Figure 2. Head impact test configuration***

**Data Analyses**

Data was sampled at 20,000 Hz. The consistency of the data measured from the accelerometers of the iNAAP was inspected by SIMon (version 4.0, NHTSA), which checked the integrity of the accelerometers, including instances of sensor malfunction and incorrect sensitivity [13, 14]. A 4th-order Butterworth low pass filter corresponding to appropriate SAE J211 channel filter classes (CFC) was applied to the data. For the iNAAP and t6aω schemes, the data recorded from the accelerometers and ARS were filtered at 1650 Hz (CFC1000). The angular velocity for the t3aω scheme was first filtered at 300 Hz (CFC180) and then numerically differentiated to obtain angular acceleration. Angular acceleration for the iNAAP was calculated by employing the procedure proposed by Padgaonkar et al. [1], while that for the t6aω was determined using Eqs (4) – (6). The kinematic data relative to the body fixed coordinate system on the external fixture was transformed to the body fixed coordinate system on the Hybrid III head using the procedure described by Kang et al. [7]. Origin locations and initial orientation of the body fixed coordinates for both the external fixture and the Hybrid III head were determined by digitizing points on the fixture and the head using a Faro arm device (Faro Arm Technologies, Lake Mary, FL). The normalized root mean squared deviation (NRMSD) shown in Eq (7) was used for quantitative evaluation of the proposed scheme. The NRMSD provided an average percent error over time between the iNAAP (i.e. gold standard) and kinematic data (linear acceleration and angular acceleration) obtained from the t6aω and t3aω. In addition to the NRMSD, percent differences of the peak values between the iNAAP and t6aω/t3aω schemes were also calculated since most injury criteria rely upon peak values.

$$NRMSD = \frac{\sqrt{\frac{1}{n}\sum_{i=0}^{n}(Y_i - Y_i')^2}}{Y'_{\max} - Y'_{\min}} \tag{7}$$

where:

- n is the total number of data points
- *Y'max* and *Y'min* represent the maximum and minimum values of the gold standard. *Yi* and *Y'i* are the $i^{th}$ data point obtained from the instrumentation scheme being evaluated and the
- $i^{th}$ data point obtained from the gold standard, respectively.

The angular velocity for the iNAAP was also computed using a single numerical integration, and then transformed to the coordinate system on the tetrahedron fixture so it could be compared to the angular velocity

directly measured on the tetrahedron by the ARS. For this evaluation the directly measured ARS were deemed as the gold standard for NRMSD calculation.

**RESULTS**

Three dimensional head motion was generated to validate the proposed instrumentation technique for measuring six degrees of freedom kinematics. Various impact severities were created randomly, ranging from HIC15 values of 319 to 1820. Many studies have looked at resultant linear and/or angular acceleration in their validation studies for instrumentation techniques [5, 6, 8, 10, 15, 16], likely due to the fact that transformation errors can be minimized by using the resultant acceleration. However, considering linear and angular kinematics in each component direction (x, y, and z) has been shown to be important in the prediction of brain injury [17]. Therefore, in this study linear and angular acceleration with respect to the body fixed frame on the tetrahedron fixture was transformed to the head coordinate system in x, y, and z axes at the center of gravity (CG) (Figure 2). When transforming the kinematics to the head CG coordinate system there can be some inherent transformation errors due to digitization of the tetrahedron fixture and ATD landmarks (e.g. OC joint and peripheral CG point). However, these transformation errors are likely to be small since both the tetrahedron and the ATD head have well-defined geometries. Figure 3 shows the linear and angular acceleration in x, y, and z axes for HImpact13, which resulted in a HIC15 value of 1820 (Table 1). NRMSD values were calculated for the first 40 ms after head contact for each test. Despite inherent transformation errors, the t6aω scheme yielded an average NRMSD of 1.8 ± 1.0% for the linear acceleration and 3.4 ± 0.9% for the angular acceleration, while the t3aω produced an average NRMSD of 5.6 ± 5.6% for the linear acceleration and 5.4 ± 1.4% for the angular acceleration for all thirteen tests (Tables 1 and 2). For the average peak value differences, the t6aω scheme yielded an average 5.3 ± 4.1% for the linear acceleration, 5.0 ± 4.8% for the angular acceleration and 2.4 ± 1.0% for $HIC_{15}$, while the t3aω produced an average 16.0 ± 21.7% for the linear acceleration, 14.0 ± 15.6% for the angular acceleration and 1.6 ± 1.3% for $HIC_{15}$ in all thirteen tests.

When evaluating the NRMSD values or peak value differences in Tables 1 and 2 it is important to consider the importance and/or magnitude of the signal being assessed, because in many cases the high percentage differences are simply a result of a low signal magnitude dominated by noise. Therefore, linear accelerations with a magnitude greater than 100g were highlighted in green in Table 1, and average NRMSD and peak value differences were calculated only using the highlighted linear accelerations with sufficient magnitude. Average NRMSD and peak value differences calculated in this manner were reduced for the t6aw configuration: 1.0 ± 0.8% for NRMSD and 2.9 ± 3.7% for peak value differences. The t3aw configuration showed even greater reduction in NRMSD and peak values differences: 1.4 ± 1.3% for NRMSD and 5.1 ± 6.6% for peak value differences.

Similarly in Table 2, angular accelerations with a magnitude greater than 3000 rad/s$^2$ were highlighted in yellow and the mean and standard deviation for only highlighted angular accelerations were calculated. Average NRMSD and peak value differences using only the highlighted angular accelerations were reduced to 3.1 ± 0.5% NRMSD and 3.7 ± 4.4% peak value differences for the t6aw, and 4.6 ± 1.2% NRMSD and 5.4 ± 6.5% peak value differences for the t3aw.

NRMSD and peak value differences for angular velocities are also shown in Table 2, and angular velocities with a magnitude greater than 1000 deg/s are highlighted in green. The average NRMSD for all thirteen tests was 4.6 ± 1.1%, while the average including only highlighted values was 5.0 ± 1.2%. For the average peak value differences in angular velocity, both mean values were less than 5% (4.7 ± 2.0% for all thirteen values and 4.3 ± 1.3% for only the highlighted values).

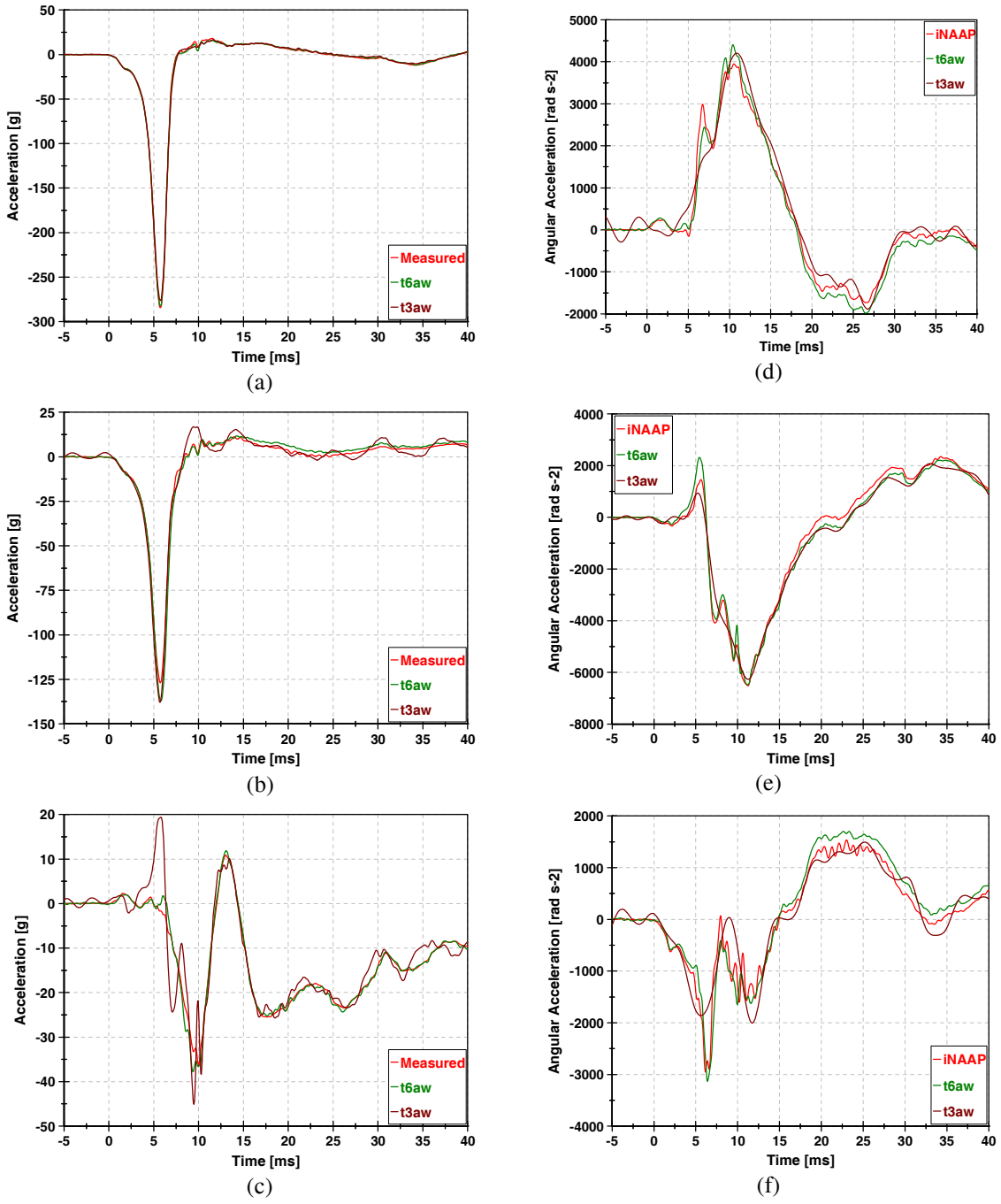


***Figure 3. Kinematics in HImpact13: linear acceleration in (a) x direction, (b) y direction, (c) z direction and angular acceleration in (d) x direction, (e) y direction, (f) z direction***
***Filter class: CFC1000 for accelerometers in all three schemes, CFC1000 for ARS in t6a$\omega$, and CFC180 for ARS in t3a$\omega$due to numerical differentiation***

**Table 1.**
**NRMSD and peak value percent differences (t6aω vs. NAAP and t3aω vs. NAAP) for linear acceleration at CG and $HIC_{15}$**
**Gold standard: measured acceleration at CG**
**Highlighted cells: Acceleration > 100g**

| | Pad | $HIC_{15}$ | $HIC_{15}$ Peak difference (%) | | Axes | Linear acceleration NRMSD (%) | | Linear acceleration Peak difference (%) | |
|---|---|---|---|---|---|---|---|---|---|
| | | | t6aω | t3aω | | t6aω | t3aω | t6aω | t3aω |
| HImpact01 | No | 381 | 2.9 | 3.7 | x | 0.4 | 0.7 | 1.4 | 1.1 |
| | | | | | y | 2.1 | 4.4 | 6.9 | 20.7 |
| | | | | | z | 3.1 | 21.3 | 4.3 | 6.7 |
| HImpact02 | No | 633 | 1.9 | 1.6 | x | 0.4 | 0.8 | 2.1 | 2.8 |
| | | | | | y | 2.0 | 4.1 | 11.1 | 22.5 |
| | | | | | z | 3.1 | 17.6 | 15.9 | 128.2 |
| HImpact03 | No | 934 | 0.7 | 0.3 | x | 0.4 | 0.7 | 0.2 | 1.4 |
| | | | | | y | 1.9 | 4.3 | 2.9 | 20.1 |
| | | | | | z | 2.5 | 15.8 | 9.3 | 21.2 |
| HImpact04 | No | 1001 | 1.7 | 2.8 | x | 0.5 | 0.5 | 0.4 | 1.0 |
| | | | | | y | 1.9 | 4.0 | 7.5 | 21.3 |
| | | | | | z | 2.5 | 12.6 | 10.0 | 51.6 |
| HImpact05 | No | 1059 | 2.2 | 2.6 | x | 0.6 | 0.8 | 0.2 | 0.7 |
| | | | | | y | 1.8 | 3.8 | 6.4 | 16.4 |
| | | | | | z | 1.8 | 13.1 | 4.1 | 32.2 |
| HImpact06 | Yes | 319 | 4.4 | 4.1 | x | 0.5 | 0.7 | 0.4 | 1.2 |
| | | | | | y | 3.0 | 4.5 | 9.7 | 14.6 |
| | | | | | z | 3.4 | 13.7 | 6.4 | 12.6 |
| HImpact07 | Yes | 543 | 2.9 | 0.2 | x | 0.6 | 0.7 | 0.4 | 0.9 |
| | | | | | y | 2.5 | 3.0 | 8.0 | 9.7 |
| | | | | | z | 2.1 | 10.3 | 4.9 | 9.8 |
| HImpact08 | Yes | 846 | 2.7 | 1.3 | x | 0.7 | 0.8 | 1.9 | 2.9 |
| | | | | | y | 2.3 | 2.6 | 7.6 | 8.2 |
| | | | | | z | 2.4 | 8.8 | 9.1 | 29.8 |
| HImpact09 | Yes | 1153 | 2.9 | 1.4 | x | 0.4 | 0.6 | 0.1 | 1.1 |
| | | | | | y | 2.2 | 2.8 | 8.2 | 9.7 |
| | | | | | z | 2.1 | 8.9 | 5.5 | 23.9 |
| HImpact10 | Yes | 1183 | 3.0 | 0.3 | x | 0.5 | 0.6 | 0.5 | 1.6 |
| | | | | | y | 2.4 | 3.0 | 8.1 | 8.2 |
| | | | | | z | 2.3 | 9.7 | 4.9 | 20.8 |
| HImpact11 | Yes | 1421 | 3.2 | 0.7 | x | 0.5 | 0.6 | 0.8 | 2.1 |
| | | | | | y | 2.4 | 2.5 | 9.9 | 10.5 |
| | | | | | z | 2.8 | 8.5 | 3.9 | 14.3 |
| HImpact12 | Yes | 1432 | 1.0 | 0.2 | x | 0.5 | 0.7 | 0.6 | 2.7 |
| | | | | | y | 2.3 | 4.9 | 10.4 | 24.7 |
| | | | | | z | 4.0 | 14.0 | 11.9 | 29.2 |
| HImpact13 | Yes | 1820 | 1.8 | 1.5 | x | 0.4 | 0.6 | 0.6 | 2.8 |
| | | | | | y | 2.0 | 2.4 | 8.0 | 8.7 |
| | | | | | z | 2.0 | 8.4 | 3.8 | 23.9 |
| Total mean (SD) | N/A | 979 (439) | 2.4 (1.0) | 1.6 (1.3) | N/A | 1.8 (1.0) | 5.6 (5.6) | 5.3 (4.1) | 16.0 (21.7) |
| Highlighted mean (SD) | N/A | N/A | N/A | N/A | N/A | 1.0 (0.8) | 1.4 (1.3) | 2.9 (3.7) | 5.1 (6.6) |

**Table 2.**
**NRMSD and peak value percent differences for angular velocity (NAAP vs. ARS) and angular acceleration (t6aω vs. NAAP and t3aω vs. NAAP)**
**Gold standards: ARS for angular velocity; NAAP for angular acceleration**
**Highlighted cells: angular velocity > 1000 deg/s; angular acceleration > 3000 rad/s$^2$**

| | Pad | $HIC_{15}$ | Axes | Angular velocity | | Angular acceleration | | | |
|---|---|---|---|---|---|---|---|---|---|
| | | | | NRMSD (%) | Peak difference (%) | NRMSD (%) | | Peak difference (%) | |
| | | | | iNAAP | iNAAP | t6aω | t3aω | t6aω | t3aω |
| HImpact01 | No | 381 | x | 3.5 | 4.7 | 3.5 | 8.2 | 3.4 | 9.9 |
| | | | y | 3.9 | 4.0 | 3.3 | 7.1 | 1.7 | 5.7 |
| | | | z | 5.2 | 12.1 | 2.2 | 5.9 | 2.5 | 40.0 |
| HImpact02 | No | 633 | x | 3.9 | 2.0 | 3.8 | 8.2 | 3.8 | 8.6 |
| | | | y | 3.7 | 3.6 | 3.0 | 4.9 | 0.1 | 3.6 |
| | | | z | 4.5 | 8.7 | 3.1 | 6.0 | 14.2 | 29.3 |
| HImpact03 | No | 934 | x | 3.6 | 3.8 | 2.5 | 5.5 | 10.7 | 9.6 |
| | | | y | 4.0 | 5.5 | 2.1 | 4.5 | 1.1 | 0.0 |
| | | | z | 3.6 | 6.0 | 3.1 | 6.3 | 6.1 | 41.6 |
| HImpact04 | No | 1001 | x | 3.8 | 3.9 | 3.7 | 6.8 | 2.1 | 1.5 |
| | | | y | 4.6 | 4.2 | 2.8 | 4.4 | 0.7 | 3.7 |
| | | | z | 3.9 | 7.0 | 3.2 | 6.7 | 24.0 | 30.9 |
| HImpact05 | No | 1059 | x | 4.0 | 3.2 | 3.4 | 7.3 | 4.2 | 2.3 |
| | | | y | 4.7 | 4.9 | 3.0 | 5.5 | 1.8 | 0.0 |
| | | | z | 3.9 | 8.5 | 3.1 | 5.8 | 3.1 | 50.5 |
| HImpact06 | Yes | 319 | x | 4.0 | 2.9 | 2.9 | 3.8 | 9.0 | 1.8 |
| | | | y | 5.2 | 4.3 | 4.6 | 7.6 | 1.6 | 4.1 |
| | | | z | 4.0 | 4.2 | 6.4 | 6.4 | 2.2 | 3.3 |
| HImpact07 | Yes | 543 | x | 3.9 | 4.0 | 3.2 | 5.5 | 6.2 | 1.2 |
| | | | y | 5.7 | 4.0 | 2.6 | 3.4 | 0.9 | 0.9 |
| | | | z | 3.2 | 4.2 | 4.5 | 5.4 | 5.0 | 36.3 |
| HImpact08 | Yes | 846 | x | 4.7 | 7.0 | 3.0 | 4.6 | 9.8 | 9.9 |
| | | | y | 5.9 | 5.4 | 2.5 | 3.4 | 0.8 | 1.2 |
| | | | z | 4.1 | 3.4 | 4.6 | 4.5 | 9.5 | 31.9 |
| HImpact09 | Yes | 1153 | x | 5.0 | 5.1 | 3.1 | 3.8 | 8.9 | 6.6 |
| | | | y | 6.3 | 3.8 | 2.8 | 3.4 | 0.7 | 1.2 |
| | | | z | 3.6 | 3.5 | 4.9 | 5.5 | 4.8 | 26.3 |
| HImpact10 | Yes | 1183 | x | 5.1 | 4.3 | 3.2 | 4.5 | 4.2 | 8.8 |
| | | | y | 6.7 | 6.8 | 2.9 | 3.5 | 1.0 | 3.0 |
| | | | z | 3.7 | 1.8 | 5.3 | 6.1 | 6.7 | 34.7 |
| HImpact11 | Yes | 1421 | x | 5.7 | 3.9 | 3.7 | 5.0 | 7.9 | 8.6 |
| | | | y | 7.3 | 5.6 | 3.1 | 3.6 | 0.4 | 0.5 |
| | | | z | 4.3 | 3.8 | 5.1 | 5.2 | 3.5 | 23.8 |
| HImpact12 | Yes | 1432 | x | 3.8 | 3.6 | 3.9 | 6.5 | 2.4 | 6.4 |
| | | | y | 4.3 | 4.1 | 3.0 | 4.2 | 1.6 | 5.5 |
| | | | z | 4.1 | 6.9 | 2.7 | 5.6 | 10.2 | 50.0 |
| HImpact13 | Yes | 1820 | x | 5.8 | 3.9 | 3.1 | 4.6 | 11.6 | 6.4 |
| | | | y | 7.3 | 4.5 | 2.6 | 3.5 | 0.5 | 3.8 |
| | | | z | 4.1 | 1.3 | 4.6 | 6.2 | 6.2 | 32.1 |
| Total mean (SD) | N/A | 979 (439) | N/A | 4.6 (1.1) | 4.7 (2.0) | 3.4 (0.9) | 5.4 (1.4) | 5.0 (4.8) | 14.0 (15.6) |
| Highlighted mean (SD) | N/A | N/A | N/A | 5.0 (1.2) | 4.3 (1.3) | 3.1 (0.5) | 4.6 (1.2) | 3.7 (4.4) | 5.4 (6.5) |

**DISCUSSION**

Various filtering classes for the instrumentation have been suggested to yield accurate head kinematics [2, 5, 7, 10, 11, 18]. The same filtering class (1650 Hz cutoff frequency, CFC1000) was applied to the accelerometers and ARS for both the t6aω (all six accelerometers and three ARS) and iNAAP (nine accelerometers) schemes. However, the t3aω scheme required a different filtering class due to numerical differentiation of the data measured from the angular rate sensors [2, 5, 7]. In order to determine the most appropriate filtering class for numerical differentiation in the t3aω scheme, different filtering cut-off frequencies were applied to the most severe impact tests: HImpact05 (with no padding and HIC15 value of 1059) and HImpact13 (with padding and HIC15 value of 1820) shown in Figure 4(a) and 4(b), respectively. Representative traces for both HImpact 05 and 13 are presented in Figure 4(c) and 4(d), respectively, where it can be seen that inaccuracies were inherent in the 100 Hz cut off frequency due to excessive signal attenuation, and also in the 500 Hz cut off frequency due to excessive noise. The NRMSD and peak value differences of the resultant angular acceleration between the iNAAP and t3aω were smallest at 300 Hz (CFC180) in the unpadded test (Figure 4a), consistent with what previous studies have used [4, 5]. Although the peak values were still smallest at 300 Hz in the padded test (Figure 4b), the NRMSD values were smallest at 400 Hz. For the most part, NRMSD and peak value differences in the padded test (HImpact13) were smaller than those in the unpadded test (HImpact05). Numerical differentiation errors in the t3aω scheme seem to be reduced in padded head impacts.

In a rigid body, the accuracy of the measured angular acceleration at a remote point affects the accuracy of the transformed linear acceleration at other locations which may be inaccessible (e.g., center of gravity of the head), because transformed linear acceleration is a function of both angular velocity and angular acceleration (Eqs 1 – 3). Therefore, accurate angular acceleration and velocity are important to obtain accurate transformed acceleration. Since the t6aω angular acceleration component of the transformed linear acceleration at an inaccessible point was shown to have equivalent accuracy to iNAAP, and the angular velocity component of t6aω instrumentation should be more accurate since it is directly measured by the ARS (as opposed to using numerical integration as in tNAAP), the t6aω should theoretically yield more accurate transformed linear acceleration at an inaccessible location than tNAAP.

Both 6aω and NAAP schemes use algebraic equations to compute angular acceleration [1, 7], which is numerically more stable and accurate than using nonlinear ordinary differential equations [19] and numerical differentiation of ARS [2, 5]. The NRMSD and peak value differences for the angular velocity determined from iNAAP were 4.6% and 4.7% (Table 2), which is generally acceptable, but the t6aω scheme should theoretically provide the most accurate six degrees of freedom head kinematics since the angular velocity is measured directly. The 6aω scheme should also provide more accurate angular displacement, and thus the most accurate six degrees of freedom head kinematics, both when installed inside an ATD head and when installed on an external fixture mounted to the outside of the head.

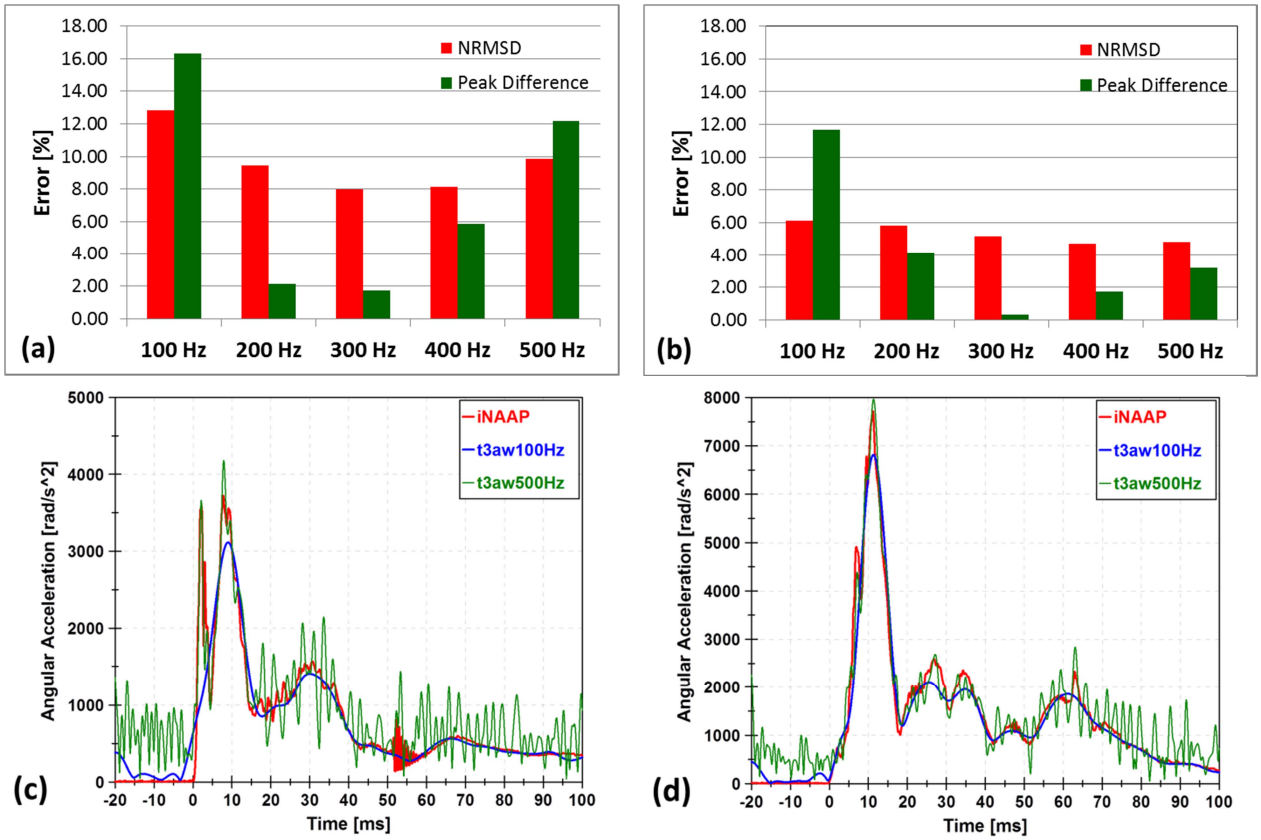


***Figure 4. NRMSD and peak difference of the angular acceleration between iNAAP and t3aω using different filtering classes: (a) HImpact05 (no pad impact), (b) HImpact13 (pad impact), (c) representative traces for HImpact05 (no pad impact), and (d) representative traces for HImpact13 (pad impact)***

## CONCLUSIONS

Six accelerometers and three angular rate sensors (6aω) installed on an external tetrahedron fixture (t6aω) were proposed and validated on a Hybrid III nine accelerometers array package (NAAP) head. Validation tests were conducted in various HIC15 levels (HIC15 of 319 to 1820). Quantitative comparison using the NRMSD and peak percent difference were made between each scheme evaluated (t6aω and t3aω) and the relevant gold standard (iNAAP). The proposed t6aω method appears to be capable of measuring accurate 6 DOF kinematics of the head in any severity of impact conditions. The results exhibited NRMSD less than 4% and peak percent difference less than 6% for both linear and angular acceleration. The proposed instrumentation should aid in the development and evaluation of head, neck and brain injuries in future testing.

## ACKNOWLEDGMENTS

The authors would like to thank Jim Stricklin and David Hyder from the Transportation Research Center, Inc. for their considerable support during test days.

**REFERENCES**


[1] Padgaonkar, A., Krieger, K., King, A., 1975. Measurement of angular acceleration of a rigid body using linear accelerometers. Journal of Applied Mechanics 42, 552–556.
[2] Laughlin, D.R., 1989. A magnetohydrodynamic angular motion sensor for anthropomorphic test device instrumentation. Stapp Car Crash Journal, 33, 43 – 77.
[3] Nusholtz, G.S., 1993. Geometric methods in determining rigid-body dynamics. Exp. Mech. 33, 153–158.
[4] Martin, P.G., Hall, G.W., Crandall, J.R., Pilkey, W.D., Chou, C.C., Fileta, B.B., 1997. Measurement Techniques for Angular Velocity and Acceleration in an Impact Environment. SAE Paper 970575.
[5] Martin, P.G., Hall, G.W., Crandall, J.R., Pilkey, W.D., 1998. Measuring the Acceleration of a Rigid Body. Shock and Vibration 5, 211-224.
[6] Hanlon, E., Bir, C., 2010. Validation of a wireless head acceleration measurement system for use in soccer play. J. Appl. Biomech. 26, 424–31.
[7] Kang, Y.-S., Moorhouse, K., Bolte, J.H., 2011. Measurement of six degrees of freedom head kinematics in impact conditions employing six accelerometers and three angular rate sensors (6aω configuration). J. Biomech. Eng. 133, 111007.
[8] Rowson, S., Beckwith, J.G., Chu, J.J., Leonard, D.S., Greenwald, R.M., Duma, S.M., 2011. A six degree of freedom head acceleration measurement device for use in football. J. Appl. Biomech. 27, 8–14.
[9] Allison, M., Kang, Y., Maltese, M., Bolte, J., 2013. Validation of a Helmet-Based System to Measure Head Impact Biomechanics in Ice Hockey. Medicine and Science in Sports and Exercise, DOI: 10.1249/MSS.0b013e3182a32d0d.
[10] Yoganandan, N., Zhang, J., Pintar, F. A, Liu, Y., 2006. Lightweight low-profile nine-accelerometer package to obtain head angular accelerations in short-duration impacts. J. Biomech. 39, 1347–54.
[11] Hardy, W.N., Foster, C., Mason, M., Yang, K., King, A., Tashman, S., 2001. Investigation of Head Injury Mechanism Using Neutral Density Technology and High-Speed Biplanar X-ray. Stapp Car Crash Journal, 45, 337-368.
[12] SAE, 2007. Instrumentation for impact test, Part 1: Electronic instrumentation, SAE J211/1, Society of Automotive Engineers.
[13] Takhounts, E.G., Eppinger, R.H., Campbell, J.Q., Tannous, R.E., Power, E.D., Shook, L.S., 2003. On the Development of the SIMon Finite Element Head Model. Stapp Car Crash Journal, 47, 107-33.
[14] Takhounts, E.G., Hasija, V., Eppinger, R. H., 2009. Analysis of 3D Rigid Body Motion Using The Nine Accelerometer Array and the Randomoly Distributed in-plane Accelerometer Systems. In Proceedings of International Technical Conference on the Enhanced Safety of Vehicle, Stuttgart, Germany.
[15] Crisco, J.J., Chu, J.J., Greenwald, R.M., 2004. An Algorithm for Estimating Acceleration Magnitude and Impact Location Using Multiple Nonorthogonal Single-Axis Accelerometers. J. Biomech. Eng. 126, 849.
[16] Duma, S.M., Manoogian, S.J., Bussone, W.R., Brolinson, P.G., Goforth, M.W., Donnenwerth, J.J., Greenwald, R.M., Chu, J.J., Crisco, J.J., 2005. Analysis of real-time head accelerations in collegiate football players. Clin. J. Sport Med. 15, 3–8.
[17] Takhounts, E.G., Craig, M.J., Moorhouse, K., McFadden, J., 2013. Development of Brain Injury Criteria (BrIC). Stapp Car Crash Journal, 57, 243-66.
[18] Hardy, W.N., Mason, M., Foster, C.D., Shah, C.S., Kopacz, J.M., Yang, K.H., King, A.I., 2007. A Study of the Response of the Human Cadaver Head to Impact. Stapp Car Crash Journal, 51, 17-80.
[19] Becker, E., Willems, G., 1975. An experimentally validated 3-D inertial tracking package for application in biodynamic research. Stapp Car Crash Journal 19, 899-930.

# Lives Saved by Vehicle Safety Technologies and Associated Federal Motor Vehicle Safety Standards, 1960 to 2012 – Passenger Cars and LTVs

**Charles J. Kahane**
National Highway Traffic Safety Administration (Retired)
United States

Paper Number 15-0291

## ABSTRACT

NHTSA began in 1975 to evaluate the effectiveness of vehicle safety technologies associated with the Federal Motor Vehicle Safety Standards (FMVSS). By June 2014, NHTSA had evaluated the effectiveness of virtually all the life-saving technologies introduced in passenger cars, pickup trucks, SUVs, and vans from about 1960 up through about 2010. A statistical model estimates the number of lives saved from 1960 to 2012 by the combination of these life-saving technologies. Fatality Analysis Reporting System (FARS) data for 1975 to 2012 documents the actual crash fatalities in vehicles that, especially in recent years, include many safety technologies. Using NHTSA's published effectiveness estimates, the model estimates how many people would have died if the vehicles had not been equipped with any of the safety technologies. In addition to equipment compliant with specific FMVSS in effect at that time, the model tallies lives saved by installations in advance of the FMVSS, back to 1960, and by non-compulsory improvements, such as pretensioners and load limiters for seat belts. FARS data has been available since 1975, but an extension of the model allows estimates of lives saved in 1960 to 1974. A previous NHTSA study using the same methods estimated that vehicle safety technologies had saved 328,551 lives from 1960 through 2002. The agency now estimates 613,501 lives saved from 1960 through 2012. The annual number of lives saved grew from 115 in 1960, when a small number of people used lap belts, to 27,621 in 2012, when most cars, light trucks, and vans were equipped with numerous modern safety technologies and belt use on the road achieved 86 percent.

## INTRODUCTION

The National Highway Traffic Safety Administration began in 1975 to evaluate the effectiveness of vehicle safety technologies associated with the Federal Motor Vehicle Safety Standards (FMVSS). By 2004, NHTSA had evaluated virtually all of the life-saving technologies introduced in passenger cars and in LTVs (light trucks and vans – i.e., pickup trucks, SUVs, minivans and full-size vans) from about 1960 through the mid-1990s. These were retrospective evaluations with estimates of fatality-reducing effectiveness based on statistical analyses of the actual crash experience of production vehicles equipped with the technologies. In October 2004, the agency issued a report estimating the number of lives saved from 1960 to 2002, year-by-year, by the combination of those life-saving technologies and by each individual technology; the estimates added up to 328,551 lives saved through 2002.[1]

Since 2004, NHTSA has evaluated nine additional life-saving technologies, such as electronic stability control (ESC) and curtain air bags and has acquired 10 additional years of crash data (through 2012). Although some of these technologies, including ESC and curtain air bags were already available in production vehicles by 2002, they could not be included in the previous report because the vehicles had not yet accumulated enough on-the-road experience for statistical analyses. NHTSA has issued a report updating the 2004 study and estimating 613,501 cumulative lives saved from CY 1960 through 2012. The update includes not only new estimates of 281,042 lives saved from CY 2003 through 2012 (the years not included in the earlier report), but also a slight upward revision from the previous report's estimate of 328,551 to 332,459 for CY 1960 through 2002 to account for the technologies that had begun to appear in production vehicles by 2002 but had not yet been evaluated by 2004.[2]

## METHOD

Past evaluation reports estimated the **effectiveness** of a safety technology – a percentage reduction of fatalities – by statistically analyzing crash data. An initial evaluation is based on production vehicles produced just before versus just after a make-model received that technology. Effectiveness might subsequently change over time if vehicles and/or the crash environment changes; when feasible, NHTSA tracks effectiveness with follow-up evaluations of crash data based on later vehicles. These follow-up analyses show that effectiveness has remained quite stable for key safety technologies such as seat belts, frontal air bags, and ESC. But the **benefits** of a technology – the absolute number of lives saved in a year – readily change from year to year depending on the number of vehicles equipped

with the technology, their vehicle miles travelled (VMT), and the crash-involvement rate of the driving population (exposure). NHTSA has:

- Reviewed the effectiveness estimates in past evaluations of safety technologies for cars and LTVs, describing how the technologies work and the history of the FMVSS that regulate them.[3]
- Developed a model that uses Fatality Analysis Reporting System (FARS) data and these past effectiveness estimates to calculate how many lives the following technologies have saved, individually and in combination, in each year from 1960 to 2012:[4]

| FMVSS: Safety Technologies | Cars | LTVs | Heavy Trucks |
|---|---|---|---|
| 105/135: Dual master cylinders & front disc brakes* | X | X | |
| 108: Conspicuity tape for heavy trailers | | | X† |
| 126: Electronic stability control‡ | X | X | |
| 201: Voluntary mid/lower instrument panel improvements | X | X | |
| Head-impact upgrade | X | X | |
| 203/204: Energy-absorbing steering assemblies | X | X | |
| 206: Improved door locks | X | X | |
| 208: Lap belts | X | X | |
| 3-point belts | X | X | |
| 2-point automatic belts** | X | | |
| Voluntary NCAP-related improvements for belted occupants†† | X | | |
| Belt pretensioners and load limiters | X | X | |
| Frontal air bags (barrier-certified, sled-certified, advanced) | X | X | |
| 212: Adhesive windshield bonding | X | X | |
| 213: Child safety seats | X | X | |
| 214: Side door beams | X | X | |
| Structure and padding to meet a dynamic side-impact test | X | | |
| Curtain and side air bags | X | X | |
| 216: Roof crush resistance (eliminate true hardtops) | X | | |
| 226: Ejection mitigation (rollover curtains) | X | X | |
| 301: Fuel system integrity: rear-impact upgrade | X | X | |

*Applies to cars and LTVs, but also saves pedestrians, bicyclists and motorcyclists not hit by these cars and LTVs.
†Applies to heavy trailers, but also saves occupants of cars and LTVs that avoid collisions with these trailers.
‡Applies to cars and LTVs, but also saves motorcyclists not hit by these cars and LTVs.
**LTVs were not equipped with 2-point automatic belts.
††NCAP testing, the dynamic side-impact test of FMVSS No. 214, and FMVSS No. 216 apply to LTVs as well as cars, but NHTSA evaluations have not identified a life-saving effectiveness for the LTVs.

In addition to safety equipment compliant with a specific FMVSS in effect at that time (and perhaps even excelling the performance requirements of that FMVSS), the model tallies lives saved by installations in advance of the FMVSS and by non-compulsory improvements shown in the preceding list, such as belt pretensioners and load limiters. The model includes car/LTV occupants saved by car/LTV technologies or child safety seats (99 percent of the total) plus pedestrians/bicyclists/motorcyclists saved by car/LTV brake improvements, motorcyclists saved by ESC, and car/LTV occupants saved by conspicuity tape on heavy trailers.

The model does not include technologies so recent that NHTSA has not yet evaluated them based on statistical analysis of crash data, such as tire pressure monitoring systems (phased in during MY 2006 to 2008). The study is limited to technologies in cars and LTVs or technologies that save lives of car/LTV occupants; for example, motorcycle helmets are not included. It is limited to vehicle technologies. It does not estimate the effects of behavioral safety programs such as the reduction of impaired driving – except to the extent that buckle-up programs have contributed greatly to the number of lives saved by belts and child safety seats. It does not include effects of roadway and traffic engineering improvements (such as rumble strips), shifts in the vehicle fleet – e.g., between large and small cars or between cars and LTVs, or improvements in EMS or follow-up medical care. The model is

limited to estimating fatality reduction by the safety technologies; NHTSA does not have sufficiently complete evaluation results to develop comparable estimates for the numbers of nonfatal injuries prevented.

Consider 1,000 cases of driver fatalities in directly frontal multivehicle crashes in cars with 1960 technology: no energy-absorbing steering columns, all drivers unbelted, and no air bags. A NHTSA evaluation estimates that energy-absorbing steering columns reduce fatalities of drivers in frontal crashes by 12.1 percent. Thus, if these cars had been equipped with them, there would have been only 879 fatalities, a saving of 121 lives. Another evaluation estimates that 3-point belts, in cars with energy-absorbing steering columns, reduce drivers' fatality risk by 42 percent in these types of crashes. If the cars had been equipped with 3-point belts in addition to energy-absorbing steering columns and the drivers had buckled up, the 879 fatalities would have diminished to 510, saving another 369 lives. A third evaluation estimates that frontal air bags reduce fatality risk by 25.3 percent for belted drivers in these types of crashes, in cars with energy-absorbing steering columns. Frontal air bags would have cut the 510 fatalities down to 381, saving another 129 lives.

The model uses 1975-to-2012 FARS data and performs the same calculations in reverse order: e.g., there might be 381 actual FARS cases of 3-point-belted driver fatalities in directly frontal multivehicle crashes in MY 1999 cars, all of which were equipped with frontal air bags and energy-absorbing steering columns. If frontal air bags, the most recent (1990s) of these three safety technologies, had been removed from the cars, fatalities would have increased to an estimated 510. In other words, we surmise there must have been 129 potentially fatal collisions of these MY 1999 cars that did not become FARS cases because frontal air bags saved the driver's life. If the 3-point belts, a 1970s technology, had also been removed from the cars and all the drivers had been unbelted, the fatalities would have increased to 879. Finally, if the energy-absorbing steering columns, a 1960s technology, had been replaced by rigid columns, downgrading these cars all the way back to a 1960 level of safety, fatalities would have increased to 1,000. The three technologies, in combination, saved an estimated 619 lives: 129 by air bags, 369 by 3-point belts and 121 by energy-absorbing columns. In summary, FARS cases of fatalities in vehicles equipped with modern safety technologies constitute evidence of an even larger hypothetical number of fatalities that would have occurred without those technologies. This approach "removes" the technologies in reverse chronological order; alternative approaches removing them in some different order would still have estimated 619 overall lives saved from 1960 to 2012, but might have allocated that total differently among the individual safety technologies. FARS data has been available since 1975, but the FMVSS date back to January 1, 1968, and some technologies were introduced even before that. An extension of the model allows estimates of lives saved from 1960 to 1974.

**FINDINGS: LIVES SAVED FROM 1960 TO 2012**

Safety technologies saved an estimated 613,501 lives from 1960 through 2012. Table 1 shows that the annual number of lives saved grew from 115 in 1960, when a small number of people used lap belts, to 27,621 in 2012, when most cars and LTVs were equipped with numerous modern safety technologies and belt use on the road achieved 86 percent. This is a large increase from the previous NHTSA study, which estimated 328,551 lives saved from 1960 through 2002. Table 1 shows that vehicle safety technologies had great benefits during the decade from 2003 through 2012, saving between 26,000 and 31,000 lives each year.

Fewer than 1,000 lives per year were saved during 1960 to 1967. Starting in 1968, vehicles incorporating most of the safety improvements of the 1960s superseded older vehicles; lives saved reached 4,000 in 1978, but remained at that level for 6 years as belt use temporarily declined. The greatest increase, from 4,835 in 1984 to 11,265 in 1988, came with buckle-up laws in the States. From 1988 until 2007, continued increases in belt use; air bags, ESC, and other recent technologies; and an expanding "base" of more vehicles and more VMT helped the fatality reduction grow, exceeding 15,000 in 1994 and 20,000 in 1999, reaching a peak of 30,312 in 2007. From 2007 until 2011, however, even though safety technologies continued to save a growing share of the potential fatalities, a shrinking "base" of VMT, especially the high-risk VMT, contributed to a decrease in the absolute number of lives saved, down to 26,098 in 2011, but then rebounding to 27,621 in 2012.[5]

***Table 1:*** **Lives Saved by Vehicle Safety Technologies, 1960 to 2012**
(Car and LTV Occupants Saved, Plus Non-Occupants and Motorcyclists Saved by Car/LTV Brake Improvements or ESC)

| CY | LIVES SAVED |
|---|---|
| 1960 | 115 |
| 1961 | 117 |
| 1962 | 135 |
| 1963 | 160 |
| 1964 | 203 |
| 1965 | 251 |
| 1966 | 339 |
| 1967 | 509 |
| 1968 | 816 |
| 1969 | 1,179 |
| 1970 | 1,447 |
| 1971 | 1,774 |
| 1972 | 2,226 |
| 1973 | 2,576 |
| 1974 | 2,518 |
| 1975 | 3,058 |
| 1976 | 3,240 |
| 1977 | 3,671 |
| 1978 | 4,040 |
| 1979 | 4,299 |
| 1980 | 4,540 |
| 1981 | 4,455 |
| 1982 | 4,057 |
| 1983 | 4,248 |
| 1984 | 4,835 |
| 1985 | 6,389 |
| 1986 | 8,531 |
| 1987 | 9,992 |
| 1988 | 11,292 |
| 1989 | 11,522 |
| 1990 | 11,761 |
| 1991 | 12,250 |
| 1992 | 12,573 |
| 1993 | 13,902 |
| 1994 | 15,263 |
| 1995 | 16,265 |
| 1996 | 17,956 |
| 1997 | 18,751 |
| 1998 | 19,613 |
| 1999 | 20,256 |
| 2000 | 22,280 |
| 2001 | 23,364 |
| 2002 | 25,691 |
| 2003 | 27,174 |
| 2004 | 28,253 |
| 2005 | 29,936 |
| 2006 | 30,242 |
| 2007 | 30,312 |
| 2008 | 27,941 |
| 2009 | 26,770 |
| 2010 | 26,695 |
| 2011 | 26,098 |
| 2012 | 27,621 |
| | ========== |
| | **613,501** |

**Car/LTV occupants: actual fatalities, potential fatalities and percent saved**
Among the 613,501 lives saved in 1960 to 2012, 610,566 were occupants of cars and LTVs. (The remaining 2,935 were pedestrians, bicyclists, and motorcyclists who avoided fatal impacts by cars or LTVs because dual master cylinders, front disc brakes, or ESC improved the car or LTV's braking or handling performance.) The sum of the

actual fatalities and the lives saved is the number of fatalities that potentially might have happened if cars and LTVs still had 1960 safety technology and nobody used seat belts. Table 2 shows 1,712,855 actual car/LTV occupant fatalities from 1960 through 2012; without the 610,566 lives saved, there would have been 2,323,421 potential fatalities. Actual car and LTV occupant fatalities decreased from 28,183 in 1960 to 21,696 in 2012. Without the vehicle safety technologies and increases in belt use, the model estimates that fatalities would not have declined but would have substantially increased, from 28,298 in 1960 to 49,214 in 2012.

Figure 1 compares the trends in actual and potential fatalities. Up to the early 1980s, both trend lines were fairly close together. Both moved up or down in response to the large cohort of baby boomers starting to drive in the 1960s; the same cohort in the 1970s turning 25, an age when fatal-crash involvement rates are already substantially lower than in adolescence; plus transient reductions in the mid-1970s and early 1980s, perhaps triggered by events such as an energy crisis, high fuel prices, or an economic slowdown. From the mid-1980s, vehicle safety made a big difference. Potential fatalities have historically continued to rise as the number of registered vehicles and VMT increased in an affluent society – with transient interruptions from 1989 to 1992 and 2006 to 2011. But increased belt use, air bags, ESC, and other vehicle safety technologies held the line on actual fatalities at about 32,000 a year during the two decades of generally rising potential fatalities and then helped bring them down to levels not seen since the 1940s, such as 21,331 in 2011 and 21,696 in 2012.[6]

***Table 2:*** **Actual Occupant Fatalities, Potential Fatalities without the Vehicle Safety Technologies, and Lives Saved in Cars/LTVs**

| | CAR+LTV OCCUPANT FATALITIES | | | |
|---|---|---|---|---|
| CY | ACTUAL | W/O SAFETY TECHS. | LIVES SAVED | PERCENT SAVED |
| 1960 | 28,183 | 28,298 | 115 | 0.40 |
| 1961 | 28,087 | 28,204 | 117 | 0.41 |
| 1962 | 30,544 | 30,679 | 135 | 0.44 |
| 1963 | 32,664 | 32,823 | 159 | 0.49 |
| 1964 | 35,603 | 35,805 | 202 | 0.56 |
| 1965 | 36,518 | 36,767 | 249 | 0.68 |
| 1966 | 39,130 | 39,465 | 334 | 0.85 |
| 1967 | 39,327 | 39,826 | 499 | 1.25 |
| 1968 | 41,019 | 41,818 | 799 | 1.91 |
| 1969 | 42,117 | 43,273 | 1,156 | 2.67 |
| 1970 | 39,556 | 40,972 | 1,415 | 3.45 |
| 1971 | 38,916 | 40,651 | 1,735 | 4.27 |
| 1972 | 40,103 | 42,281 | 2,178 | 5.15 |
| 1973 | 38,739 | 41,258 | 2,520 | 6.11 |
| 1974 | 31,145 | 33,608 | 2,463 | 7.33 |
| 1975 | 31,361 | 34,355 | 2,995 | 8.72 |
| 1976 | 32,222 | 35,398 | 3,176 | 8.97 |
| 1977 | 33,173 | 36,772 | 3,599 | 9.79 |
| 1978 | 34,988 | 38,951 | 3,964 | 10.18 |
| 1979 | 35,108 | 39,325 | 4,217 | 10.72 |
| 1980 | 35,097 | 39,554 | 4,456 | 11.27 |
| 1981 | 33,911 | 38,284 | 4,373 | 11.42 |
| 1982 | 29,855 | 33,834 | 3,979 | 11.76 |
| 1983 | 29,209 | 33,384 | 4,176 | 12.51 |
| 1984 | 30,177 | 34,935 | 4,758 | 13.62 |
| 1985 | 30,044 | 36,357 | 6,314 | 17.37 |
| 1986 | 32,394 | 40,849 | 8,454 | 20.70 |
| 1987 | 33,334 | 43,251 | 9,916 | 22.93 |
| 1988 | 34,245 | 45,461 | 11,216 | 24.67 |
| 1989 | 33,725 | 45,177 | 11,452 | 25.35 |
| 1990 | 32,844 | 44,534 | 11,690 | 26.25 |
| 1991 | 30,939 | 43,126 | 12,187 | 28.26 |
| 1992 | 29,557 | 42,071 | 12,514 | 29.75 |
| 1993 | 30,192 | 44,033 | 13,840 | 31.43 |
| 1994 | 30,995 | 46,200 | 15,204 | 32.91 |
| 1995 | 32,067 | 48,271 | 16,204 | 33.57 |
| 1996 | 32,541 | 50,438 | 17,897 | 35.48 |

| | | | | |
|---|---|---|---|---|
| 1997 | 32,515 | 51,208 | 18,693 | 36.50 |
| 1998 | 31,955 | 51,512 | 19,557 | 37.97 |
| 1999 | 32,171 | 52,373 | 20,202 | 38.57 |
| 2000 | 32,241 | 54,465 | 22,225 | 40.81 |
| 2001 | 32,021 | 55,327 | 23,306 | 42.12 |
| 2002 | 32,872 | 58,506 | 25,634 | 43.81 |
| 2003 | 32,297 | 59,411 | 27,114 | 45.64 |
| 2004 | 31,871 | 60,064 | 28,193 | 46.94 |
| 2005 | 31,539 | 61,408 | 29,869 | 48.64 |
| 2006 | 30,633 | 60,804 | 30,171 | 49.62 |
| 2007 | 29,009 | 59,246 | 30,236 | 51.04 |
| 2008 | 25,423 | 53,287 | 27,864 | 52.29 |
| 2009 | 23,417 | 50,115 | 26,698 | 53.27 |
| 2010 | 22,235 | 48,852 | 26,617 | 54.49 |
| 2011 | 21,331 | 47,342 | 26,011 | 54.94 |
| 2012 | 21,696 | 49,214 | 27,518 | 55.92 |
| | **1,712,855** | **2,323,421** | **610,566** | |

**FIGURE 1: ACTUAL VERSUS POTENTIAL CAR/LTV OCCUPANT FATALITIES, 1960 TO 2012**

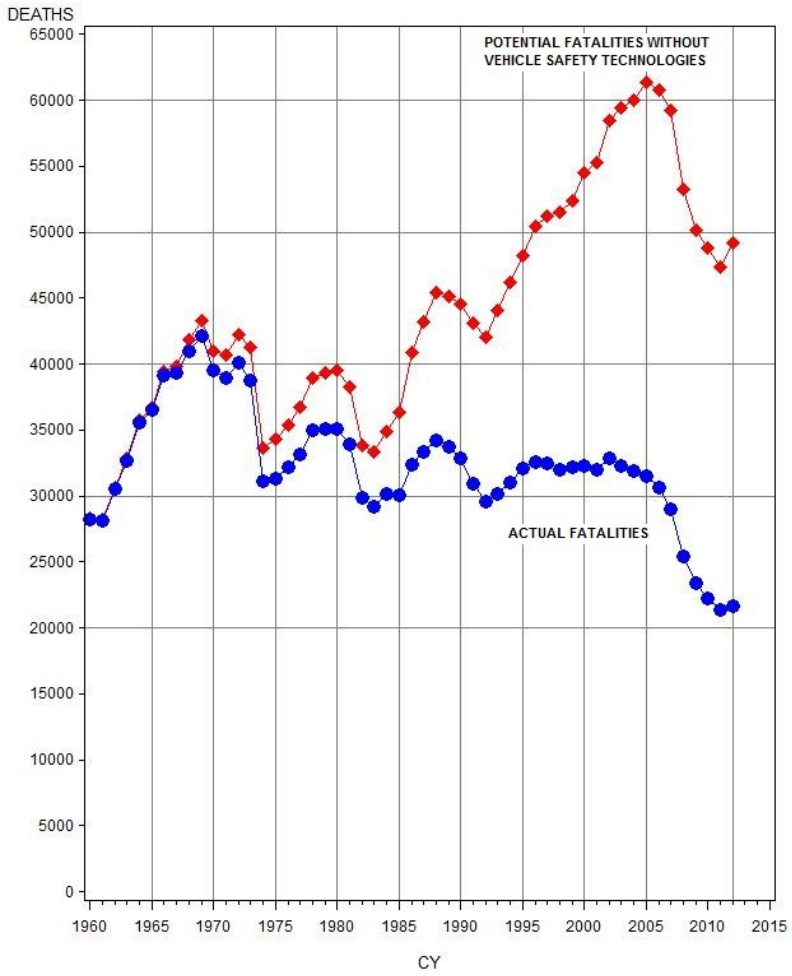


The overall, combined **effectiveness** of the vehicle safety technologies is the percentage of potential fatalities that were saved, as shown in the right column of Table 2. The effectiveness grew in **every** year from 1960 to 2012, from a humble 0.40 percent in 1960 to a very substantial 55.92-percent fatality reduction in 2012. The trend shows:

- Not much effect before the FMVSS;
- Steady growth in the early-to-mid 1970s as the early FMVSS phased in;
- A slowdown in 1978 to 1982, when belt use declined prior to national buckle-up campaigns;
- The largest gains coming with the buckle-up laws in the mid-to-late 1980s; and
- Steady progress since the late 1980s thanks to continued increases in belt use, air bags, ESC, and other recent technologies.

Figure 2 tracks a **vehicular fatality-risk index** for occupants of cars or LTVs that isolates the effects of vehicle safety improvements. The index is obtained by subtracting from 100 the percentage of potential fatalities saved. The index was 100 in 1955 and had declined to 44 by 2012. In other words, given the same mileage by the same driver on the same roads, the average vehicle on the road in 2012 would have 56 percent lower fatality risk for its occupants than the average vehicle on the road in 1955.

**FIGURE 2: VEHICULAR FATALITY-RISK INDEX BY CALENDAR YEAR (1955 = 100)**
BASED ON PERCENT OF POTENTIAL FATALITIES SAVED BY VEHICLE SAFETY TECHNOLOGIES

**Estimates of lives saved by individual technologies (grouped by FMVSS)**
Car/LTV safety technologies saved an estimated 27,621 lives in 2012. That total includes 14,018 car occupants and 13,500 LTV occupants. It also includes 103 pedestrians, bicyclists and motorcyclists saved by car/LTV braking improvements or by ESC. Table 3 apportions how many of those lives were saved by the various individual technologies and groups those technologies according to the FMVSS with which they appear to be most closely associated:[7]

***Table 3:*** **Estimates of Lives Saved by Safety Technologies in 2012**

| FMVSS & Associated Safety Technologies | Car Occupants | LTV Occupants | Pedestrians Bicyclists Motorcyclists | TOTAL |
|---|---|---|---|---|
| 105/135: Dual master cylinders & front disc brakes | 217 | 201 | 65 | 482 |
| 108: Conspicuity tape for heavy trailers | 90 | 70 | | 161 |
| 126: Electronic stability control for cars and LTVs | 500 | 824 | 38 | 1,362 |
| 201: Instrument panel improvements & head impact protection | 778 | 573 | | 1,350 |
| 203/204: Energy-absorbing steering assemblies | 1,323 | 1,084 | | 2,407 |
| 206: Improved door locks | 486 | 641 | | 1,127 |
| 208: Seat belts – all types, all seating positions* | 7,169 | 8,316 | | 15,485 |
| 208: Frontal air bags* | 1,738 | 1,193 | | 2,930 |
| 212: Adhesive windshield bonding | 177 | 95 | | 271 |
| 213: Child safety seats* | 213 | 145 | | 357 |
| 214: Side impact protection & curtain/side air bags | 1,196 | 315 | | 1,512 |
| 216: Roof crush resistance (eliminate true hardtops) | 122 | | | 122 |
| 226: Curtains that deploy in rollovers | 3 | 41 | | 43 |
| 301: Fuel system integrity – rear impact upgrade | 5 | 4 | | 9 |
| TOTAL | 14,018 | 13,500 | 103 | 27,621 |

* Estimates in this table for seat belts, frontal air bags, and child safety seats do not supersede NHTSA's official annual estimates in *Traffic Safety Facts 2012 Data – Occupant Protection* of the lives **directly** saved by those technologies. The estimates in this table, which also include estimates of lives **indirectly** saved by those technologies (discussed below), are meaningful primarily in this report's context of computing the overall effect of the FMVSS and the comparing the effects of various FMVSS.

- Seat belts are by far the most important occupant protection, saving an estimated 15,485 lives: over half the total of 27,621. The estimate includes seat belts of all types (3-point, lap-only, automatic), at all designated seating positions. Seat belts are designed to keep occupants within the vehicle and close to their original seating position, provide "ride-down" by gradually decelerating the occupant as the vehicle deforms and absorbs energy, and, if possible, prevent occupants from contacting harmful interior surfaces or one another (however, NHTSA recommends correctly-installed, age-appropriate safety or booster seats for child passengers until they are at least 8 years old, unless they are at least 4'9" tall). Seat belts are especially important in LTVs, where a large proportion of unrestrained fatalities are ejections and/or rollover crashes; belts saved 8,316 lives in LTVs, over 60 percent of the 13,500 LTV occupants saved.

  (NHTSA's official estimate is that belts directly saved 12,174 lives in 2012 – i.e., fatalities would have increased by 12,174 if nobody had buckled up, but otherwise the cars and LTVs on the road had remained unchanged.[8] This report's estimate, 15,485 lives saved in 2012, is higher because it also includes some indirect savings: this report estimates how many additional fatalities would have occurred if all safety technologies had been removed, not just the belts, and it then apportions the total among the various individual technologies. Accounting for the lives directly saved by recent technologies such as ESC, by this report's computational method, also indirectly augments the estimates of lives saved by earlier technologies such as seat belts.[9] The estimates here do not supersede the agency's official estimates of lives directly saved by seat belts, frontal air bags, and safety seats. They are primarily meaningful within the context of this report: estimation of the overall effect of all the vehicle safety technologies and apportionment of the overall effect among the individual technologies.)

- Frontal air bags saved 2,930 lives in 2012, when 95 percent of cars and 91 percent of LTVs on the road were equipped with dual or driver-only frontal air bags. (NHTSA's official estimate in *Traffic Safety Facts 2012 Data – Occupant Protection* is 2,213 lives saved directly by air bags in 2012.) Frontal air bags have significant benefits in frontal and partially frontal impacts for nearly all occupants 13 and older, including the oldest drivers and passengers, by providing energy absorption and ride-down and by preventing head contacts with the windshield or windshield header. However, a deployed frontal air bag, especially some of the pre-2007 designs without the advanced features of current models, can present risks to child passengers 12 and younger. The risk can be eliminated if the child rides in the rear seat, correctly restrained – or by

turning off the manual on-off switch in pickup trucks or other vehicles where children cannot ride in a rear seat correctly restrained.

- Energy-absorbing steering assemblies meeting FMVSS Nos. 203 and 204 are an important "built-in" safety technology that saved an estimated 2,407 lives in 2012. In the 1960s, they were the first basic protection for drivers in frontal crashes, designed to cushion their impact into the steering assembly. Today, the combination of energy-absorbing steering columns, seat belts and frontal air bags provides far better protection for the driver in frontal crashes.

- Three groups of technologies associated with FMVSS No. 214, "Side impact protection," saved an estimated 1,512 lives in 2012. The technologies are: (1) Side door beams in cars and LTVs meeting the original static crush test of FMVSS No. 214, which are primarily effective in side impacts with fixed objects, such as trees or poles; (2) Structures and padding added to passenger cars before or after FMVSS No. 214 was upgraded in the 1990s with a dynamic test requirement, which are primarily effective in near-side impacts by other vehicles (i.e., left-side impacts for drivers and right-side impacts for right front passengers); and (3) Curtain and side air bags, which further enhance protection in near-side impacts.

- Electronic stability control (now required in new cars and LTVs by FMVSS No. 126) saved 1,362 lives in 2012, the first year when all new cars and LTVs had ESC – but in 2012 only 20 percent of cars and 22 percent of LTVs on the road were ESC-equipped. Benefits can be expected to grow substantially in future years as the on-road fleet approaches 100 percent ESC-equipped. ESC detects when a vehicle is about to lose traction and automatically applies the brakes to individual wheels and/or reduces engine torque to help the driver stay on course. It is a highly effective crash avoidance technology.

- Two groups of technologies associated with FMVSS No. 201, "Occupant protection in interior impact" saved an estimated 1,350 lives in 2012. The technologies are: (1) Improvements to the materials and contours of middle and lower instrument panels in the late 1960s and 1970s, not specifically required by FMVSS No. 201 but historically and functionally associated with that standard to some extent; instrument panels were redesigned, using energy-absorbing materials, to decelerate occupants at a safe rate and keep them in an upright position during frontal crashes. (2) The head-impact upgrade of FMVSS No. 201, phased in during MY 1999 to 2003, which added energy-absorbing padding to pillars, roof headers, roof side rails, and other components that were sources of life-threatening head injuries.

- Improvements to door locks, latches, and hinges, generally implemented by manufacturers in the 1960s and regulated by industry standards subsequently incorporated into FMVSS No. 206, saved 1,127 lives in 2012. They reduce the risk of occupant ejection by keeping doors closed in rollover crashes.

- Car/LTV braking improvements directly or indirectly associated with FMVSS Nos. 105 and 135 include dual master cylinders and front disc brakes. By eliminating brake failure or helping cars and LTVs stop more effectively, they saved 482 lives in 2012, including 65 pedestrians, bicyclists or motorcyclists.

- Child safety seats or booster seats meeting FMVSS No. 213 saved an estimated 357 young passengers in 2012. (NHTSA's official estimate is 284 lives saved directly by child safety seats in 2012.) Child safety seats and booster seats are the basic protection system for passengers who are too small to obtain full benefits from seat belts. Newborns should start with rear-facing seats and stay in them until their weight or height reaches a point where they should graduate to forward-facing seats, subsequently to booster seats and, finally, when they are at least 9 years old or 4'9" tall, to adult seat belts.

- Adhesive windshield bonding saved 271 lives in 2012 by keeping the windshield attached to the vehicle in severe impacts and preventing occupant ejection via the windshield portal. FMVSS No. 212 regulates windshield retention for cars and LTVs.

- FMVSS No. 108 requires red-and-white conspicuity tape on heavy truck trailers. The tape reflects another vehicle's headlights strongly and it is highly visible in the dark. Although this device is furnished on heavy

trailers, not cars or LTVs, it is the occupants of cars and LTVs who primarily benefit by avoiding collisions with the trailers. The tape saved an estimated 161 car and LTV occupants in 2012.

- FMVSS No. 216, "Roof crush resistance" is associated with the redesign of true hardtops as pillared hardtops or sedans during the 1970s. True hardtops had no B-pillars to support the roof, making it more susceptible to crush in a rollover. If cars were still built that way there might have been 122 additional fatalities in 2012.

- FMVSS No. 226, "Ejection mitigation" began to phase in during MY2014. Curtain air bags that deploy in rollover crashes are the key technology for meeting the standard. Rollover curtains have already been available in some production vehicles since 2002. They are effective in preventing ejection and mitigating interior impact. They saved an estimated 43 lives in 2012.

- The rear-impact test of FMVSS No. 301, "Fuel system integrity" was substantially upgraded during the past decade. The upgrade saved an estimated 9 lives in 2012: people who otherwise would have died of burns in post-crash fires.

Table 4 shows cumulative lives saved from 1960 through 2012: 385,408 car occupants and 225,158 LTV occupants, plus 2,936 pedestrians, bicyclists and motorcyclists saved by car/LTV braking improvements or ESC, for an estimated total of 613,501. Seat belts (329,715) accounted for more than half the total. Frontal air bags had saved 42,856 lives by the end of 2012 and child safety seats, 9,891. The "built in" non-belt technologies regulated by or associated with the remaining 13 FMVSS in Table 4 (Nos. 105/135, 108, 126, 201, 203/204, 206, 212, 214, 216, 226, and 301) sum to 231,039 lives saved; energy-absorbing steering assemblies, improved door locks, occupant protection in interior impact, and side impact protection have cumulatively saved the most lives.

***Table 4:*** **Estimates of Cumulative Lives Saved by Safety Technologies from 1960 through 2012**

| FMVSS & Associated Safety Technologies | Car Occupants | LTV Occupants | Pedestrians Bicyclists Motorcyclists | TOTAL |
|---|---|---|---|---|
| 105/135: Dual master cylinders & front disc brakes | 10,559 | 5,001 | 2,790 | 18,350 |
| 108: Conspicuity tape for heavy trailers | 1,524 | 1,136 | | 2,660 |
| 126: Electronic stability control for cars and LTVs | 2,420 | 3,604 | 146 | 6,169 |
| 201: Instrument panel improvements & head impact protection | 24,779 | 9,698 | | 34,477 |
| 203/204: Energy-absorbing steering assemblies | 57,112 | 22,877 | | 79,989 |
| 206: Improved door locks | 25,377 | 16,758 | | 42,135 |
| 208: Seat belts – all types, all seating positions | 187,442 | 142,274 | | 329,715 |
| 208: Frontal air bags | 27,765 | 15,091 | | 42,856 |
| 212: Adhesive windshield bonding | 7,268 | 2,585 | | 9,853 |
| 213: Child safety seats | 7,257 | 2,634 | | 9,891 |
| 214: Side impact protection & curtain/side air bags | 28,971 | 3,317 | | 32,288 |
| 216: Roof crush resistance (eliminate true hardtops) | 4,913 | | | 4,913 |
| 226: Curtains that deploy in rollovers | 8 | 171 | | 178 |
| 301: Fuel system integrity – rear impact upgrade | 14 | 13 | ___ | 26 |
| TOTAL | 385,408 | 225,158 | 2,936 | 613,501 |

## DISCUSSION

The fatality-reducing effectiveness estimates used in the model are all derived from published NHTSA evaluation reports. The model includes a technology only if its estimate of fatality reduction in NHTSA evaluations is statistically significant. As stated above, the estimates are based on statistical analyses of crash data. An initial evaluation report usually compares fatality risk in vehicles built just before and just after make-models became equipped with the technology, statistically controlling for factors other than the technology by using double-pair comparison, control groups, logistic regression, or other techniques. For some technologies, including seat belts,

frontal air bags, ESC, and curtain and side air bags, the agency has performed follow-up evaluations of crash data involving later vehicles to see if effectiveness might have changed over time.

The basic assumption of the model is that any group of FARS fatality cases involving vehicles equipped with a safety technology known to be effective in that type of crash may be considered evidence that there were additional crashes where that technology saved lives: these additional crashes are not in FARS because the technology made them nonfatal crashes. For example, if there are 100 belted fatality cases in FARS in a type of crash where statistical analysis shows 50-percent belt effectiveness, we surmise that there must have been another 100 people in potentially fatal crashes who were saved by the belt. This is a leap of faith to the extent that we cannot identify those 100 specific occupants who were "saved by the belt" – we assume they must exist, based on our effectiveness estimate.

The model simulates "removing" safety equipment from a modern vehicle one piece at a time, starting with the most recent technology and working backward. Some of these technologies were introduced at about the same time, and it is not always obvious which was first: for some of the earliest ones, limited information is available about their introduction dates. Changing the order in which the technologies are "removed" would still produce the same estimate of overall lives saved, but the allocation among the individual technologies could change.

The model assumes that the belt use of **fatally injured** occupants (not survivors) in FARS is accurately reported. NHTSA has long believed this to be true, based on statistical analyses comparing FARS data with belt use observed in surveys. In the future, conceivably, event data recorders could provide additional evidence on belt use in crash data files.

Finally, when the model says vehicle safety technologies saved 613,501 lives, it estimates that this number of additional fatalities might have occurred from 1960 through 2012, without those technologies, if all other factors had stayed the same: the same increase in VMT from 1960 to 2012, the same driving behaviors. It is a hypothetical estimate. If seat belts and the other modern vehicle safety technologies had never been invented and if occupant fatalities had continued climbing toward 61,000 instead of remaining near 32,000, as shown in Table 2, the public might have demanded much stronger regulation of drivers (e.g., licensing) or the infrastructure (e.g., speed limits). Consumers might have purchased a different mix of vehicles and some people might have been more reluctant to travel during the riskiest hours (e.g., weekend nights). Those measures might have prevented at least some of the additional 613,501 fatalities – but surely not as efficiently and with as little impairment of driving enjoyment and mobility as the vehicle safety technologies.

## CONCLUSIONS

- Vehicle safety technologies and their associated FMVSS have greatly reduced fatality risk for car and LTV occupants over the past decades in the United States. Given the same mileage by the same drivers on the same roads, the average vehicle on the road in 2012 would have an estimated 56 percent lower fatality risk for its occupants than the average vehicle on the road in 1955 to 1960.

- These technologies have saved an estimated cumulative 613,501 lives since 1960, including 27,621 in calendar year 2012.

## REFERENCES

[1] Kahane, C. J. (2004, October). *Lives saved by the Federal Motor Vehicle Safety Standards and other vehicle safety technologies, 1960-2002*. (Report No. DOT HS 809 833). Washington, DC: National Highway Traffic Safety Administration.
[2] Kahane, C. J. (2014, September). *Lives saved by vehicle safety technologies and associated Federal Motor Vehicle Safety Standards, 1960 to 2012 – Passenger cars and LTVs – With reviews of 26 FMVSS and the effectiveness of their associated safety technologies in reducing fatalities, injuries, and crashes.* (Report No. DOT HS 812 069). Washington, DC: National Highway Traffic Safety Administration.
[3] *Ibid*., pp. 14-213.
[4] *Ibid*., pp. 1-13 and 214-226.
[5] *Ibid*., pp. 227-232.
[6] *Ibid*., pp. 233-244.
[7] *Ibid*., pp. 244-252.

[8] National Highway Traffic Safety Administration. (2014, March). *Traffic safety facts 2012 Data – Occupant protection*. (Report No. DOT HS 811 892). Washington, DC: Author.
[9] Kahane (2014, September), pp. 244-249.

# EVALUATION of MOTORCYCLE HELMET USABILITY and STABILITY in the CONSUMER SAFETY RATING PROGRAM 'CRASH'

**Andrew McIntosh**
McIntosh Consultancy and Research
Monash Injury Research Institute, Monash University
Australia

**Basuki Suratno**
Transport for NSW
Australia

**Jack Haley**
NRMA Motoring and Services
Australia

**Jessica Troung**
Transport Accident Commission
Australia

Paper Number 15-0292

## ABSTRACT

A review of certain aspects of the Consumer Rating and Assessment of Safety of Helmets (CRASH) for motorcyclists was undertaken. The paper examines the relationships between the assessment of helmet stability with volunteers and other usability assessments. The paper reports on how these assessments are incorporated into the Consumer Rating and Assessment of Safety Helmets (CRASH) and general relationships between Safety Scores and Ergonomic Scores. Ninety (90) motorcycle helmets were evaluated in the years 2011 to 2014 involving dynamic stability tests, dynamic strength of retention tests and usability tests with six participants. All helmets complied with AS/NZS 1698: 2006. The participants rated each helmet across ten items using a five point Likert scale. Forward, rearward and lateral pull tests were performed on each participant with each helmet. The force required to move the helmet with respect to the scalp was measured. The analysis revealed a number of important findings. First, safety performance tests are not correlated with ergonomic assessments of the helmets, including formal usability assessments. This observations highlights the importance of providing both safety and ergonomic information to motorcyclists. Helmet mass ranged between approximately 1 kg and 2 kg in the sample assessed. On the assumption that the total Safety Score reflects a helmet that offers greater protection in a crash, a heavier helmet within the sample assessed offers more protection to the motorcyclist. Full face helmet types also performed better on total Safety Score than the open face helmet. Full face helmets were heavier than open face styled helmets. Differences in the total Ergonomic Score by helmet type were fewer than those observed with Safety Scores. There were strong correlations between the rater responses between pairs of questions regarding comfort, fit, but not restraint adjusment. Although there is some overlap between these questions, each question appears to elicit a slightly different response across all helmet types and raters. Helmet mass is either not correlated or weak to moderately correlated with user ratings. This suggests that the raters are considering other factors, not simply mass, when rating helmet weight. The raters might be considering the mass distribution, for example. In general, helmet stability as measured quasi-statically on each rater was weakly associated with the raters' assessment of the helmet. This suggests that the motorcyclist's impression of fit is not a strong indicator of helmet stability. Ease of use of operation was only weakly associated, based on these results, with the forces required to displace the helmet on the rater's head. Correlations between the stability test forces by direction (front, rear and lateral) were strong.

## INTRODUCTION

Powered two wheeler (PTW), including motorcycle, safety is a major global issue. Although the incidence rates for motorcyclist injury and death have decreased over decades, the absolute number of cases has been increasing as a result of increased motorcyclist exposure.[1] Motorcycle helmets are one method for preventing head injury in motorcycle crashes.[2,3] Geographical regions and countries have unique systems in place that regulate the supply and use of motorcycle helmets. A central element of these systems are motorcycle helmet standards. Standards are referred to with regards to both sale and on-road use. Standards are critical in terms of providing motorcyclists with effective helmets. However, Standards do not assess all aspects of helmet use or performance.[4,5] Consumer rating programs can address a range of usability and performance issues that affect motorcyclist safety.[5] The paper assists in identifying how usability assessments can be applied in consumer information programs and what factors may be important in terms of helmet stability at the point of sale.

The 2011 IRTAD report highlighted that despite reductions in mortality rates for PTW operators, the relative risk remains much greater for PTW groups than passenger car occupants; in European countries the relative rate is between 17 and 20 times in some countries.[1] In the USA motorcycle fatalities comprised 14% of the total road fatalities in 2010. [1] In other regions, PTW fatalities represent the majority of road fatalities, e.g. 71% in Cambodia and 59% in Malaysia. [1] Helmet use has been shown to be effective in preventing head injury. A 2008 Cochrane review of motorcycle helmet estimated that helmets reduce the risk of head injury by 69% and death by 42%. [2] A study of trauma centre admissions found that helmets were associated with a significant reduction in intracranial injury likelihood of 66% amongst motorcyclists.[6] Therefore, an important element of a road safety system is helmet use.[1-6]

Helmets need to fit well and be comfortable.[7] Maintaining the positional stability of a motorcycle helmet in general use and a crash is a fundamental performance requirement. [7-10] Helmet stability is assessed in many helmet standards, but ergonomic surveys of motorcyclists have shown that helmet design and the user influence helmet stability.[4,7] A survey of 216 motorcyclists found that "the size of the in-use motorcycle helmets did not correspond well to the predicted size based on head dimensions, although motorcyclists were generally satisfied with comfort and fit."[7] The forces required to displace each wearer's helmet were also observed to be low, around 25 N. [7] The paper will examine the relationships between the assessment of helmet stability with volunteers and other usability assessments. The paper will report on how these assessments are incorporated into the Consumer Rating and Assessment of Safety Helmets (CRASH) and general relationships between Safety Scores and Ergonomic Scores.

## METHODS

Ninety (90) motorcycle helmets were evaluated in the years 2011 to 2014 involving a range of tests, including formal usability tests with six participants (raters). All helmets complied with AS/NZS 1698: 2006. The helmet sample was derived from advice from wholesalers, retailers and consumers, as well as historical trends and coverage of specific categories of helmet types. Over three CRASH rating periods Dual Sport, Full Face, Flip Up, Motocross, Open Face, and Open Face with Visor helmet types have been tested.

The test program methods were reported in 2013.[5] In short the total Safety Score reflects performance on: helmet coverage; dynamic stability; high level impact energy attenuation (2.5 m drop); low level impact energy attenuation (0.8 m drop); kerb anvil high level impact energy attenuation (2.5 m drop); and dynamic retention strength. The total Ergonomic Score reflects usability rater assessment and performance on visor fogging, splash resistance, aerodynamics, in-helmet noise, mass and field of view. The rater assessment comprises (i) a standard protocol with ten questions and (ii) in-situ force to commence helmet displacement measured. All participants had a head circumference equivalent to the ISO "J" headform (57-58 cm). The participants rated each helmet across ten items using a five point Likert scale. Forward, rearward and lateral pull tests were performed on each participant with each helmet.[5] The force required to move the helmet with respect to the scalp was measured.[5,7]

The following rating questions were considered in this analysis: Question 1. Does the helmet allocated to you fit your head comfortably; Question 2 From no pain or pressure points (score 5) to very uncomfortable (score 1) please rate the helmet with reference to your face, chin and head; Question 3 Please rate the weight of the helmet in terms

of its comfort from very comfortable (5) to very uncomfortable; Question 4 Please rate the helmet in terms of comfort and fit overall from very good (5) to very poor (1); and Question 10 How easy is it to adjust and tighten the chin strap or restraint system from very easy (5) to very difficult (1). Questions 5 to 9 were not considered relevant to the assessment as they dealt with other helmet features, e.g. the visor operation. The higher the score on the Likert scale the better the rating. Data were collated and analysed using the following statistical methods. Descriptive statistics for the total Safety and Ergonomic Scores and mass were prepared. Correlations between the total scores and mass were assessed, as were differenes in the mean total scores and mass by helmet type. Bivariate correlations between rater scores (1 to 5) and helmet mass, and pull forces were assessed.

**RESULTS**

Over three CRASH rating periods a total of ninety helmets were evaluated for safety and ergonomic performance. The total Safety and Ergonomic Scores and helmet masses are presented in figures 1 to 3. The helmets are de-identified. Helmets have been sorted by type (DS Dual Sport; FF Full Face; FU Flip Up; MC Motocross; OF Open Face; OFV Open Face with Visor). There were four Dual Sport helmets (4.4%), 51 Open Face (56.7%), 10 Flip Up (11.1%), 2 Motocross (2.2%), 12 Open Face (13.3%) and 11 Open Face with Visor helmets (12.2%). Table 1 presents descriptive statistics for total safety and ergonomic scores and helmet mass by helmet type. There are significant differences ($p<0.05$) in the mean helmet mass by type: DS, FF,FU and MC are heavier than OF and OFV; OFV is heavier than OF; and, FU is heavier than FF. There are significant differences ($p<0.05$) in the mean helmet total Safety Scores by type: DS, FF and FU have higher mean Safety Scores than OF. There are significant differences ($p<0.05$) in the mean helmet Ergonomic Scores by type: FF has a greater mean than OFV. Figure 4 shows that in terms of the total Safety and Ergonomic Scores, there is a strong correlation between total Safety Score ($r^2 = 0.275$) and mass and none between total Ergonomic Score and mass. Therefore, as helmet mass increases there is an increase in the safety rating as scored in the CRASH program. The analysis of total Ergonomic Score with respect to mass is confounded by the components in the total score. Total Ergonomic and Safety Scores were not correlated.

**Table 1.**
**Descriptive statistics for helmet total safety and ergonomic scores and mass by helmet type (n=90).**

| | | Count | Mean | Median | Standard Deviation | Minimum | Maximum |
|---|---|---|---|---|---|---|---|
| DS | Mass (kg) | 4 | 1.68 | 1.69 | 0.12 | 1.53 | 1.8 |
| | Safety | 4 | 62 | 61 | 8 | 54 | 72 |
| | Ergonomic | 4 | 54 | 53 | 10 | 44 | 68 |
| FF | Mass (kg) | 51 | 1.61 | 1.62 | 0.1 | 1.36 | 1.94 |
| | Safety | 51 | 58 | 59 | 11 | 35 | 76 |
| | Ergonomic | 51 | 57 | 55 | 10 | 43 | 77 |
| FU | Mass (kg) | 10 | 1.78 | 1.78 | 0.1 | 1.58 | 1.96 |
| | Safety | 10 | 57 | 58 | 13 | 35 | 74 |
| | Ergonomic | 10 | 49 | 49 | 8 | 32 | 62 |
| MC | Mass (kg) | 2 | 1.66 | 1.66 | 0.01 | 1.65 | 1.67 |
| | Safety | 2 | 59 | 59 | 17 | 47 | 71 |
| | Ergonomic | 2 | 44 | 44 | 2 | 42 | 45 |
| OF | Mass (kg) | 12 | 1.18 | 1.17 | 0.15 | 0.96 | 1.43 |
| | Safety | 12 | 38 | 36 | 12 | 21 | 58 |
| | Ergonomic | 12 | 50 | 49 | 8 | 37 | 62 |
| OFV | Mass (kg) | 11 | 1.34 | 1.34 | 0.11 | 1.17 | 1.51 |
| | Safety | 11 | 51 | 49 | 10 | 37 | 66 |
| | Ergonomic | 11 | 46 | 47 | 5 | 36 | 55 |

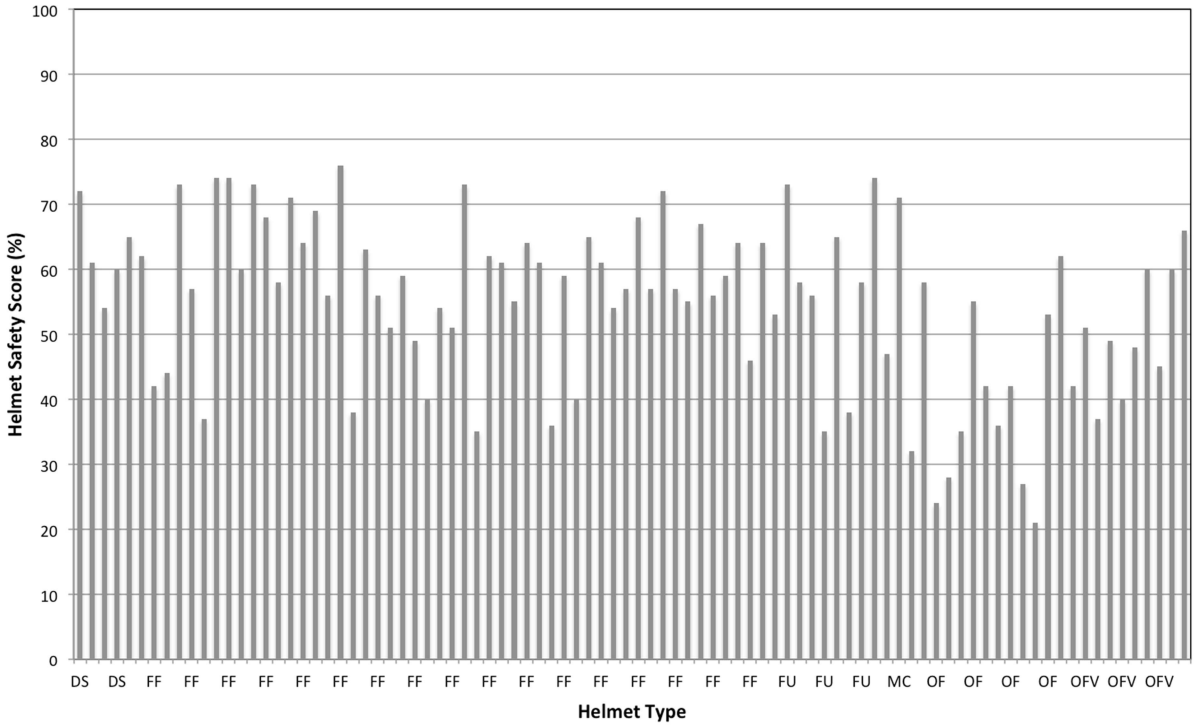


***Figure 1*. Final total safety score by helmet model grouped under type.**

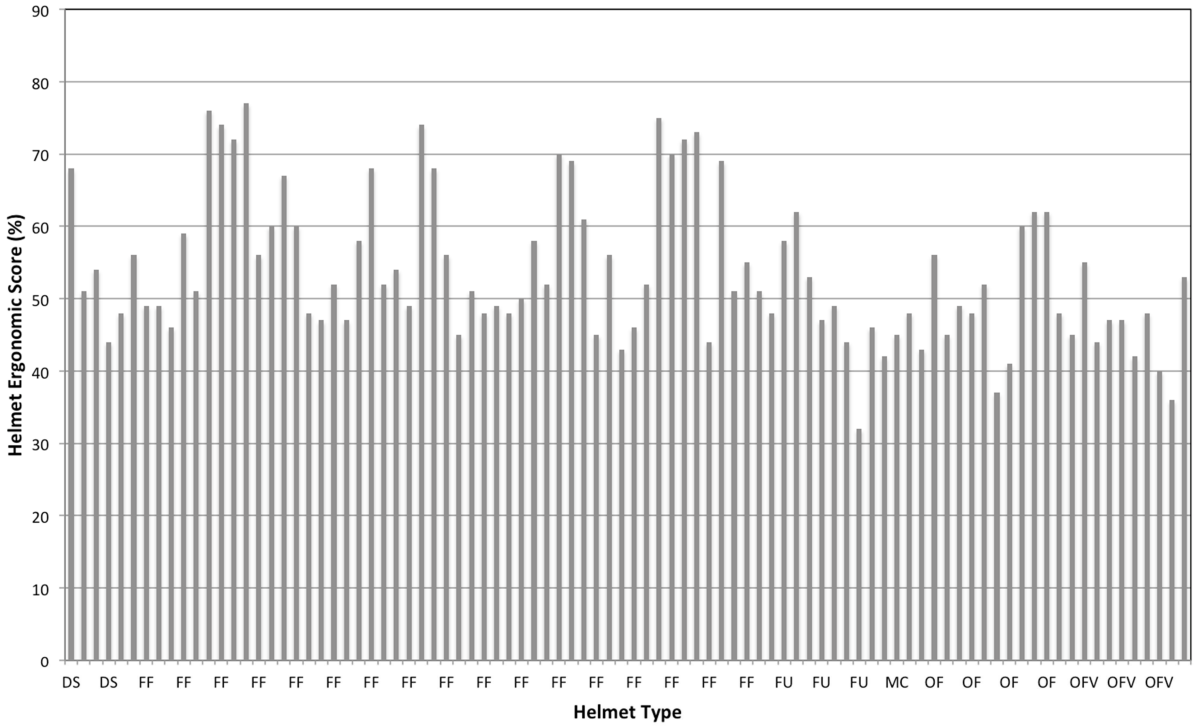


***Figure 2*. Final total ergonomic score by helmet model grouped under type.**

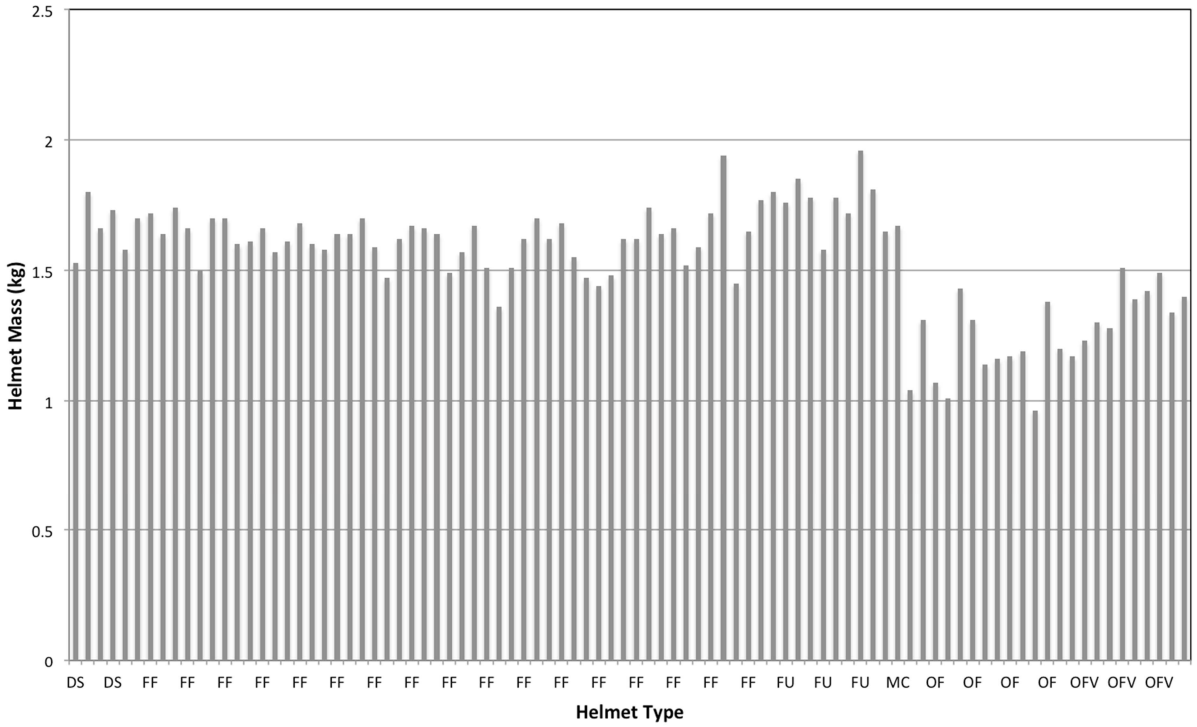


***Figure 3.*** **Helmet mass by helmet model grouped under type.**

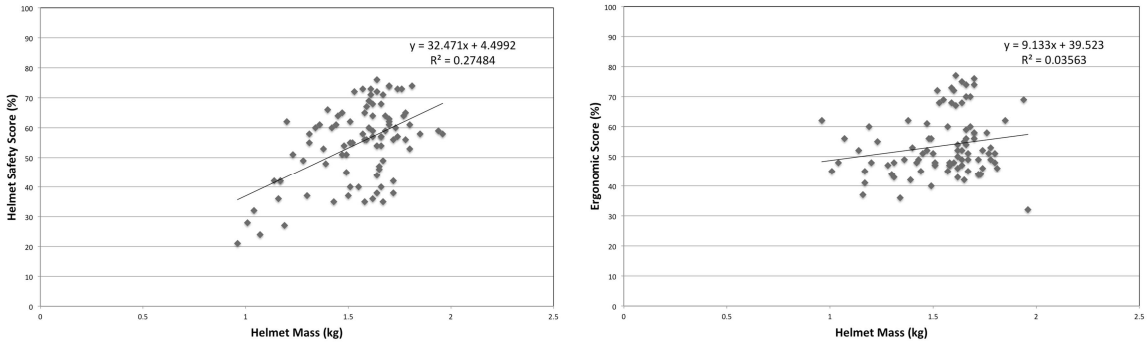


***Figure 4.*** **Helmet mass by total Safety Score (left) and Ergonomic Score (right).**

The component ergonomic scores were examined for relationships between individual ratings on specific questions, helmet mass and stability as measured quasi-statically on the rater (table 2). A number of significant correlations were observed. Analyses were not adjusted for potentially confounding factors, e.g. helmet type, rater experience and preference.

**Table 2.**
**Correlations between individual rater scores, helmet mass and forces measured in individual stability tests. The average force represents the average of three tests in each pull direction. PC is Pearson Correlation. Significance tests are two-tailed. ** Correlation is significant at the 0.01 level (2-tailed). *Correlation is significant at the 0.05 level (2-tailed).**

| | | Q1 | Q2 | Q3 | Q4 | Q10 | Mass (kg) | Rear (N) | For. (N) | Lat. (N) |
|---|---|---|---|---|---|---|---|---|---|---|
| | PC | 1 | .730** | .522** | .789** | .226** | -0.02 | -.172** | -.159** | -.097* |
| | Sig. | | 0 | 0 | 0 | 0 | 0.655 | 0 | 0 | 0.028 |
| Q1 | N | 509 | 509 | 509 | 509 | 509 | 509 | 509 | 509 | 509 |
| | PC | .730** | 1 | .607** | .811** | .121** | -.136** | -.208** | -.132** | -0.071 |
| | Sig. | 0 | | 0 | 0 | 0.006 | 0.002 | 0 | 0.003 | 0.11 |
| Q2 | N | 509 | 509 | 509 | 509 | 509 | 509 | 509 | 509 | 509 |
| | PC | .522** | .607** | 1 | .554** | 0.08 | -.243** | -.219** | -.206** | -.152** |
| | Sig. | 0 | 0 | | 0 | 0.072 | 0 | 0 | 0 | 0.001 |
| Q3 | N | 509 | 509 | 509 | 509 | 509 | 509 | 509 | 509 | 509 |
| | PC | .789** | .811** | .554** | 1 | .214** | -0.077 | -.155** | -.132** | -0.055 |
| | Sig. | 0 | 0 | 0 | | 0 | 0.083 | 0 | 0.003 | 0.214 |
| Q4 | N | 509 | 509 | 509 | 509 | 509 | 509 | 509 | 509 | 509 |
| | PC | .226** | .121** | 0.08 | .214** | 1 | .215** | .172** | 0.065 | .100* |
| | Sig. | 0 | 0.006 | 0.072 | 0 | | 0 | 0 | 0.144 | 0.024 |
| Q10 | N | 509 | 509 | 509 | 509 | 509 | 509 | 509 | 509 | 509 |
| | PC | -0.02 | -.136** | -.243** | -0.077 | .215** | 1 | .443** | .350** | .352** |
| | Sig. | 0.655 | 0.002 | 0 | 0.083 | 0 | | 0 | 0 | 0 |
| Helmet Mass (kg) | N | 509 | 509 | 509 | 509 | 509 | 509 | 509 | 509 | 509 |
| | PC | -.172** | -.208** | -.219** | -.155** | .172** | .443** | 1 | .643** | .616** |
| | Sig. | 0 | 0 | 0 | 0 | 0 | 0 | | 0 | 0 |
| Average Rear Pull Force (N) | N | 509 | 509 | 509 | 509 | 509 | 509 | 509 | 509 | 509 |
| | PC | -.159** | -.132** | -.206** | -.132** | 0.065 | .350** | .643** | 1 | .778** |
| | Sig. | 0 | 0.003 | 0 | 0.003 | 0.144 | 0 | 0 | | 0 |
| Average Forward Pull Force (N) | N | 509 | 509 | 509 | 509 | 509 | 509 | 509 | 509 | 509 |
| | PC | -.097* | -0.071 | -.152** | -0.055 | .100* | .352** | .616** | .778** | 1 |
| | Sig. | 0.028 | 0.11 | 0.001 | 0.214 | 0.024 | 0 | 0 | 0 | |
| Average Lateral Pull Force (N) | N | 509 | 509 | 509 | 509 | 509 | 509 | 509 | 509 | 509 |

## DISCUSSION

The analysis of ninety motorcycle helmets revealed a number of important findings. First, safety performance tests are not correlated with ergonomic assessments of the helmets, including formal usability assessments. This observations highlights the importance of providing both safety and ergonomic information to motorcyclists to assist in purchasing decisions that might influence long term helmet use. This underpins the rationale for the CRASH program. On one hand the helmet purchaser may select a helmet that is comfortable, for example, but this does not provide an indication of the helmet's potential safety performance in a crash. On the other hand, a focus on safety performance alone does not identify areas where improvements might be made to encourage helmet use and selection. Helmet mass was correlated with the total Safety Score. On the assumption that the total Safety Score reflects a helmet that offers greater protection in a crash, a heavier helmet within the sample assessed offers more protection to the motorcyclist. Helmet mass ranged between approximately 1 kg and 2 kg in the sample assessed. Full face helmets were heavier than open face styled helmets. Full face helmet types (DS, FU and FF) also performed better on total Safety Score than the open face helmet. Differences in the total Ergonomic Score by helmet type were fewer than those observed with Safety Scores. These analyses are very general, because they do not consider the individual elements that make up the total scores. For example, the total Ergonomic Score comprises aerodynamic and in helmet noise assessments that tend to favour full face type helmets and are less influenced by helmet mass.

The analysis of comfort and fit related usability test questions, helmet mass and user stability tests showed a number of significant correlations (table 2). There were generally strong correlations between the rater responses between pairs of questions 1, 2, 3 and 4. Correlations between questions 1 to 4 and 10 were weak. Further analyses are required to assess rater and helmet type effects on these associations. Although there is some overlap between these questions, each question appears to elicit a slightly different response across all helmet types and raters. Helmet mass is either not correlated or weak to moderately correlated with user ratings. Question 3 is a direct rating of helmet weight; there is a significant but weak association between Question 3 and measured helmet mass. This suggests that the users are considering other factors, not simply mass, in Question 3. The raters might be considering the mass distribution, for example. The experiences of each rater might also influence the assessment, e.g. a rater accustomed to wearing a 'heavy' helmet, might be comfortable with helmets in that mass range. Further analysis is required.

In general, helmet stability as measured quasi-statically on each rater was weakly associated with the raters' responses to questions 1, 2, 3, 4 and 10 (table 2). Therefore, the rater's assessment of fit and comfort are not subsitutes for stability as assessed in these tests. This requires further analysis. It does suggest that the motorcyclist's impression of fit is not a strong indicator of helmet stability. Therefore, a motorcyclist might purchase a helmet based on fit that does not offer the level of stability that they expect. Question 10 relates to the operation of the restraint system. Ease of use of operation was only weakly associated, based on these results, with the forces required to displace the helmet on the rater's head.

Correlations between the stability test forces by direction were strong. Further research is required to account for potential confounding factors, e.g. helmet type and head dimensions.[7]

## CONCLUSIONS

Research has identified the importance of helmet stability and retention in terms of usability and crash performance. An analysis of the CRASH helmet data provides a greater understanding of the user's perceptions of the helmet function and what needs to be assessed in a consumer safety rating program. This information can complement impact performance and standards compliance information to assist consumer decisions and helmet suppliers in improving helmet design.

The CRASH program is funded by Transport for NSW, NRMA Motoring and Services and Transport Accident Commission (Australia).

The opinions presented in this paper are those of the authors and do not represent those of the organisations they represent.

**REFERENCES**

[1] IRTAD. Road Safety Annual Report 2011: International Traffic Safety Data and Analysis Group IRTAD, OECD/ITF; 2012
[2] Liu BC, Ivers R, Norton R et al, (2008) Helmets for preventing injury in motorcycle riders, Cochrane Database Syst Rev. Jan 23;(1):CD004333
[3] Lin M-R & Krauss JF (2008) Methodological issues in motorcycle injury epidemiology; 40: 1653-1660
[4] McIntosh AS & Grzebieta R, (2013) Motorcycle helmet standards – harmonsation and specialisation ? 2013, 23rd International Technical Conference on the Enhanced Safety of Vehicles, May 27-30, Seoul, Paper Number 13-0160
[5] McIntosh AS, Suratno B, Haley J, Truoung J, (2013) Consumer rating and assessment of safety helmets for motorcyclists, 2013, 23rd International Technical Conference on the Enhanced Safety of Vehicles, May 27-30, Seoul, Paper Number 13-0157
[6] McIntosh AS, Curtis K, Rankin T, Cox M, Pang TY, McCrory P and Finch CF, (2013) Helmets prevent brain injuries in injured pedal- and motor-cyclists: A case series analysis of trauma centre presentations, Australian College of Road Safety Journal, 24: 11-20.
[7] Thai KT, McIntosh AS, Pang TY, Factors affecting motorcycle helmet use: Size selection, stability and position. Traffic Injury Prevention 2015 Apr 3;16(3):276-82. doi: 10.1080/15389588.2014.934366. Epub 2014 Nov 14
[8]. McIntosh AS & Lai A (2013) Motorcycle Helmets: Head and Neck Dynamics in Helmeted and Unhelmeted Oblique Impacts, Traffic Injury Prevention, 14:8, 835-844
[9] Hurt HH, Thom DR, Ouellet JV. (1998) Testing the positional stability of motorcycle helmets. Paper presented at: 16th International Technical Conference on the Enhanced Safety of Vehicles (ESV); 1998; Windsor, ON, Canada.
[10] Chinn B, Canaple B, Derler S, et al. (2001) COST 327: Motorcycle Safety Helmets. Brussels, Belgium: European Commission, Directorate General for Energy and Transport; 2001

# AUTOMATIC OPENING OF EMERGENCY WINDOW BY MAGNETIC RELEASE MECHANISM

**DINESH, RAMACHANDRAN**
Thiagarajar College of Engineering
INDIA

**KARTHIK, RAVISHANKAR**
St. Joseph's College Of Engineering
INDIA

Paper Number 15-0295

## ABSTRACT
The main objective is to facilitate quicker and safer evacuation of passengers in case of frontal and rear impact of bus by automatic opening of emergency windows. The integrated magnetic release mechanism controlled by various sensors like piezo sensor, accelerometer sensor, temperature sensor and poison gas sensor installed at various locations inside the bus, helps in releasing the emergency windows during an impact. This reduces the time the passenger takes to exile the bus as the need for break opening of the windows is avoided. This system also facilitates increased number of exit points for the passengers by changing all windows into exit windows. At normal situations, the metal beaded windows are held firmly in position by the magnet, whereas during impact it releases the windows without damaging them which increases the longevity of the system.

## INTRODUCTION
The present system of emergency exit consists of a breakable window with a provision of a hammer. However during impact the because of sudden G-force change and Post-Traumatic Stress Disorder, the normal human response time increases. This delay increases the time taken to come out of the bus which can dangerous in case of accidents involving fire or those involving spreading of poisonous gases. This can be reduced by using the proposed system

*Figure 1: emergency window with hammer to break open*

The proposed system consists of metal beaded windows, Piezo sensors, accelerometer sensor, poison gas detector and temperature sensor. These sensors when activated, sends signal which is used to drive the servo motor. The servo motor turns the diametrically magnetized cylindrical permanent magnet. This changes the magnetic field, causing the emergency windows to open. This is advantageous because in case of minor incident, then we can override the system and close the windows and operate the bus.

**BACKGROUND**

**Magnetic Setup** consists of a permanent cylindrical diametrically magnetized neodymium magnet. It is installed similar to a magnetic V- block (shown in *fig 2).*

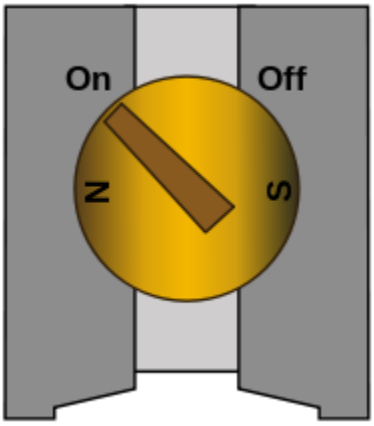


*Figure 2: Magnetic V-block*

The center permanent magnet, due to its field strength holds the metal piece firmly in its position. The magnetic strength of the permanent magnet on the metal strip at a distance is given by

$B_r (r, Ø) = \mu_o * M * a^2 * \cos (Ø) / 2 * r^2$
$B_Ø (r, Ø) = \mu_o * M * a^2 * \sin (Ø) / 2 * r^2$

Where,
M= magnetization of the magnet
r and Ø are cylindrical coordinates of the metal strip from poles of the magnet

From above equations, the magnetic strength is inversely proportional to the square of distance of the magnet, when the magnet is turned away using a servo motor, the distance of the poles from metal strip increases therefore causing the strength to decrease, thus resulting in opening of the windows.

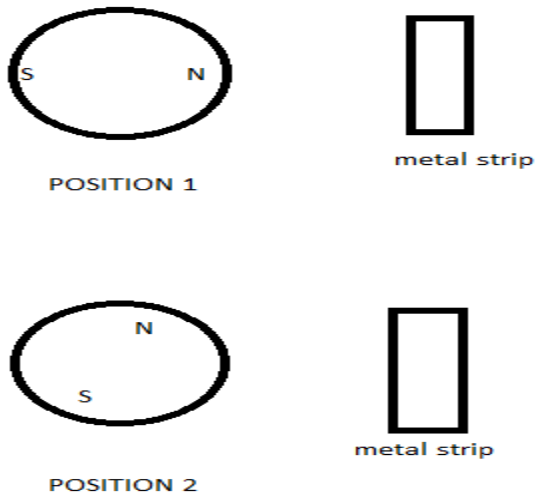


*Figure 3: Positions of the magnet*

The position 1 (in figure 3) shows the position of the magnet during normal working conditions of the bus. Position 2 shows the magnet being displaced by a motor which results in opening of the windows.

**The Poison Gas Detector** is installed inside the bus and it send signal to the central ECU when the gas concentration crosses the maximum ppm range tolerable by humans.

**Accelerometer sensor** detects the vibration level of the bus structure. During an event of accident where the structure undergoes vibration above the particular the standard WBV (whole Body Vibration), Then it send signal to the ECU. Also the Piezo sensors installed at various locations on the bus when impacted will send signal to the ECU.

**Temperature Sensor** monitors the temperature inside the bus and when it detects a sudden rise in temperature above the desirable limits, it send signal to the ECU.

**Electronic Control Unit** receives signal from sensors installed at different locations on the bus. When signal comes from the sensors, it activates the warning indicator present in the display unit present near to the driver and it also controls the servo motor to rotate the cylindrical magnet away from the metal strip ($90^{o}$).

The overall schemtic layout of the emergency system is shown in *figur 4*

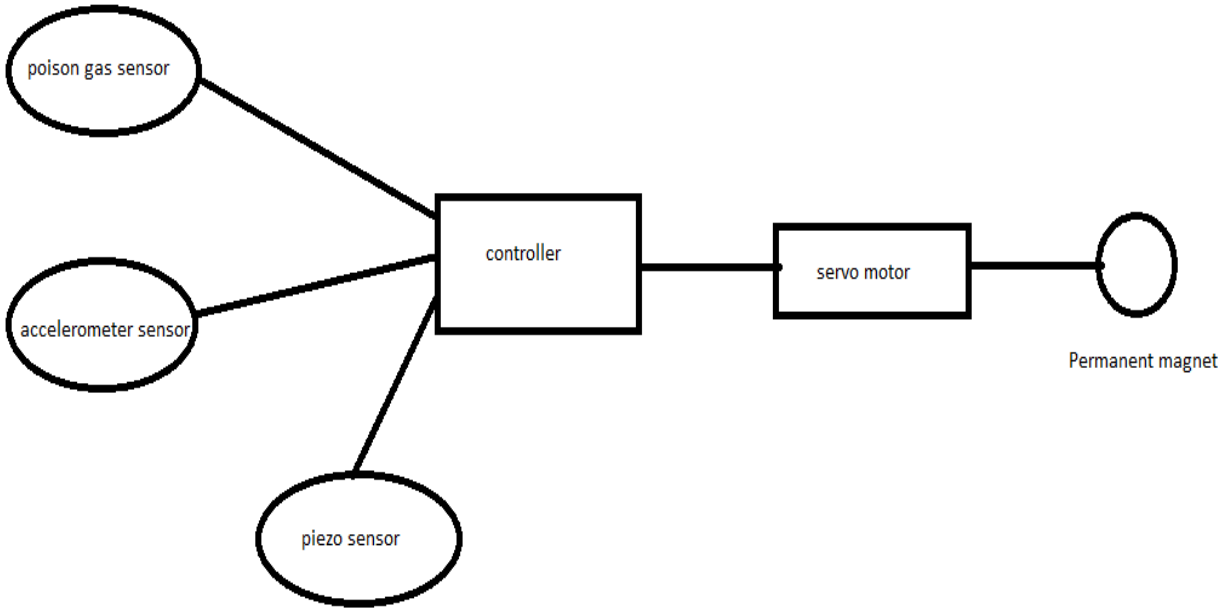


*Figure 4: Schematic Representation of the system*

**CONCLUSION AND RECOMMENDATION**

The proposed system can help in quicker evacuation of the passengers because of reducing the time required to open the emergency windows, in case of frontal impact, rear impact and fire accidents. Due to the increasing the number of accidents[1] involving buses, the need to improve the safety features of the existing buses is an ultimate requirement.
However the proposed system doesn't provide any advantage over the current system in case of rollovers.

1: Asia-Pacific road accident statistics

**REFERENCES:**

**1:** Edward P. Furlani. “Permanent magnet and electromechanical devices”

2: Dr. Matolacsy, Matyas. “New requirement to emergency exit of buses”

3: Whole body vibration Fact sheet.

**Sensitivity of Q10 and Q6 chest measurements to restraint and test parameters**

**Andre Eggers**
**Britta Schnottale**
**Julian Ott**
Federal Highway Research Institute (BASt)
Germany

Paper Number 15-0300

## ABSTRACT

Upcoming test procedures and regulations consider the use of Q-dummies. Especially Q6 and Q10 will be introduced to assess the safety of child occupants in vehicle rear seats. Therefore detailed knowledge of these dummies is important to improve safety. As recent studies have shown, chest deflection measurements of both dummies are influenced by parameters like belt geometry. This could lead to a non optimized design of child restraint systems (CRS) and belt systems. The objective of this study is to obtain a more detailed understanding of the sensitivity of chest measurements to restraint parameters and to investigate the possibilities of chest acceleration as an alternative for the assessment of chest injury risks.
A study of frontal impact sled tests was performed with Q6 and Q10 in a generic rear seat environment on a bench. Belt parameters like modified belt attachment locations were varied. For the Q6 dummy, different positioning settings of the CRS (booster with backrest) and of the dummy itself were investigated. The Q10 dummy was seated on a booster cushion. Here the position of the upper belt anchorage point was varied. To simulate the influence of vehicle rotation in the ODB crash configuration, the bench was pre-rotated on the sled in additional tests with the Q10. This configuration was tested with and without pretensioner and load limiter.
Chest deflection in Q6 showed a high sensitivity to changes in positioning of the CRS and the dummy itself. A more slouched position of the CRS or dummy resulted in a reduction of measured chest deflection, whereas chest acceleration increased for a more slouched position of the CRS. Chest deflection in Q10 is sensitive to belt geometry as already shown in other studies. In a more outboard position of the shoulder belt anchorage the measured chest deflection is higher. Chest acceleration shows the opposite tendency, which is highest for the rearmost location of the upper belt anchorage. On a pre-rotated bench the highest chest deflection within this test series was observed without load limiter/pretensioner and an outboard belt position. By optimizing the belt location and the use of pretensioner/load limier the chest deflection was significantly reduced.
For the Q6 a criterion based on chest acceleration as well as deflection measured at two locations might be the most reliable approach, which requires further research with an additional upper deflection sensor. In the Q10 the measured chest deflection does not always correctly reflect the severity of chest loading. The deflection is depending on initial belt position and restraint parameters as well as test conditions, which result in different directions of belt migration. A3ms chest acceleration might be a better indicator for severity of chest loading independent of different conditions like belt geometries. However, in some cases the benefit of an optimized restraint system could only be shown by deflection. These findings suggest that further research is needed to identify a chest injury assessment method, which could be based on deflection as well as acceleration or other parameters related to belt to occupant interaction.

## INTRODUCTION

To assess the safety of child occupants in the rear seat the dummies Q6 and Q10 are considered in upcoming test procedures (EEVC WG12 2015, EEVC WG12/18 2008). Recent studies with these dummies have shown sensitivity of chest deflection to parameters like belt path. Due to this, the design of protection systems for children based on chest deflection might be misguiding. An alternative to evaluate the chest injury risk could be the assessment of chest acceleration instead. Therefore, the objective of this study is to get a better and more detailed understanding of the sensitivity of chest measurements to test parameters.
Other studies with the Q10 have shown a high sensitivity of chest deflection to restraint parameters like belt geometry (Bohman et al. 2012, Croatto et al. 2013). However, chest acceleration was not discussed in these studies. The objective of this study was to investigate sensitivity of chest deflection and chest acceleration in dummies Q6 and Q10 to test conditions and restraint parameters. The main focus of the Q6 study was to investigate the influence of the position of the dummy in the CRS and position settings of the CRS itself. The focus of the Q10 study was the investigation of chest assessment parameters to belt geometry in a test configuration without backrest.

## METHODOLOGY

For this purpose a series of sled tests was conducted with the dummies Q6 and Q10. A generic rear seat environment was created represented by a bench with deformable cushion based on ECE-R 129 specifications, mounted on a

deceleration sled with a hydraulic deceleration system (Figure 1). The test environment included a three-point-belt system with a 4 kN load limiter and a retractor pretensioner in the baseline configuration. The upper belt anchorage attachment point was variable to investigate different belt geometries. The pulse used for testing was based on the x-component of a 64 km/h ODB Euro NCAP deceleration pulse of a midsize vehicle with a peak of 30g and duration of 125 ms. The two dummies could be tested in parallel on the sled on separate benches. The Q10 dummy was positioned on a booster without backrest. The Q6 dummy was placed in a booster with backrest.

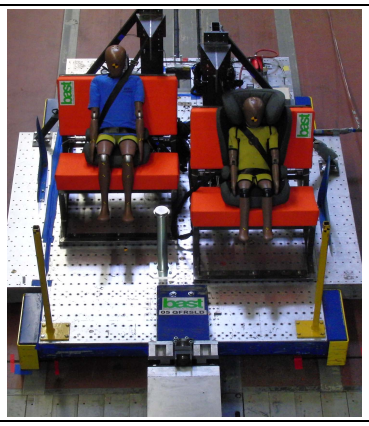

Test rig with Q10 and Q6

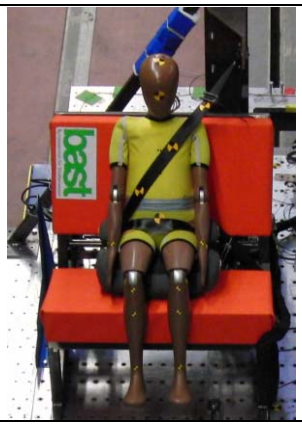

Test bench with Q10 in frontal position (0°)

Test bench with Q10 rotated 13°

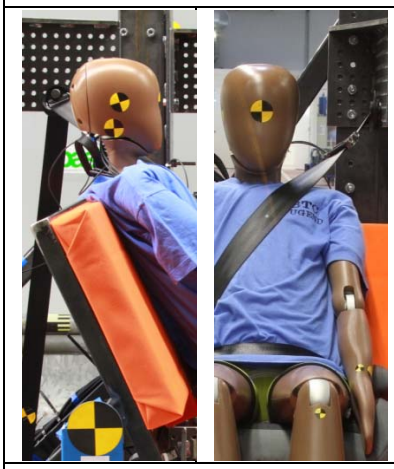

Belt Position **Standard**

Belt Position **Far** Y: +70mm outboard

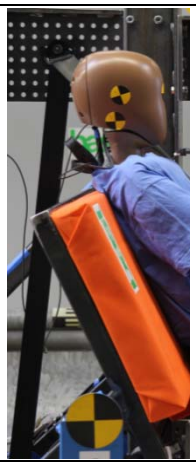

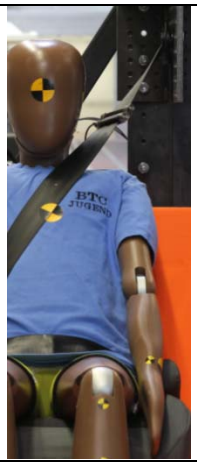

Belt Position **High** Z: +75 mm

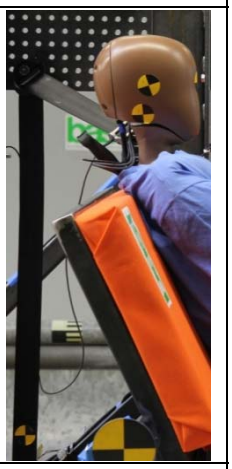

Belt Position **Rear** X: -100 mm

***Figure 1. Test rig for sled tests with Q6 and Q10 dummies.***

**Test parameters**

For the Q6 dummy a study of different positioning settings of the dummy and/or CRS was conducted, using a booster with backrest, a standard position of the upper belt anchorage point and a 4 kN load limiter with a pretensioner. Figure 2 shows the CRS and dummy in standard position (Setting 1). By placing a tube with a diameter of 70 mm behind the dummy in the CRS a slouched dummy position was defined (Position Setting 3). This led to a forward movement of the knees of 68 mm in x. The tube was removed before testing. When using the relax function of the CRS the backrest joint of the CRS was moved 72 mm in x direction, which was defined as slouched CRS position (Position Setting 2). The positioning of both, dummy in slouched position and CRS in slouched position resulted in a forward movement of the knees in comparison to the standard position of 134 mm in x-direction (see Figure 2 Setting 4). The parameters of all tests are shown in Table 1.

| | | | |
|---|---|---|---|
| | | | |
| Position Setting 1 | Position Setting 2 | Position Setting 3 | Position Setting 4 |
| | | | |
| CRS standard, Dummy standard | CRS slouched, Dummy standard | CRS standard, Dummy slouched | CRS slouched, Dummy slouched |
| | Backrest joint:<br>X: 72 mm forward | Knee joint:<br>X: 68 mm forward | Backrest joint:<br>X: 72 mm forward<br>Knee joint:<br>X: 134 mm forward |

***Figure 2. Different combinations of position setting of the Q6 dummy and CRS***

***Table 1: Test matrix***

| Test | Dummy | Load Limiter | Pretensioner | Orientation | CRS | ISOFix | Belt Position | CRS Setting | Dummy Setting |
|---|---|---|---|---|---|---|---|---|---|
| 1 | Q6 | 4 kN | Yes (20ms) | frontal (0°) | booster with backrest | no | standard | standard | standard |
| 2 | Q6 | 4 kN | Yes (20ms) | frontal (0°) | booster with backrest | no | standard | slouched | standard |
| 3 | Q6 | 4 kN | Yes (20ms) | frontal (0°) | booster with backrest | no | standard | standard | slouched |
| 4 | Q6 | 4 kN | Yes (20ms) | frontal (0°) | booster with backrest | no | standard | slouched | slouched |
| 5 | Q10 | 4 kN | Yes (20ms) | frontal (0°) | booster w/o backrest | no | high | standard | standard |
| 6 | Q10 | 4 kN | Yes (20ms) | frontal (0°) | booster w/o backrest | no | far | standard | standard |
| 7 | Q10 | 4 kN | Yes (20ms) | frontal (0°) | booster w/o backrest | no | rear | standard | standard |
| 8 | Q10 | No | No | frontal (13°) | booster w/o backrest | yes | far | standard | standard |
| 9 | Q10 | 4 kN | Yes (20ms) | frontal (13°) | booster w/o backrest | yes | far | standard | standard |
| 10 | Q10 | 4 kN | Yes (20ms) | frontal (13°) | booster w/o backrest | yes | standard | standard | standard |

In the tests with the Q10 dummy the effect of different belt geometry on dummy chest measurements were investigated by changing the upper belt anchorage point. Four different locations of the upper anchorage point were defined: “standard”, “far”, “high” and “rear” as indicated in Figure 1. The geometry of the belt, defined different attachment points of the upper anchorage and the location of buckle and lower belt anchorage, were based on average measurements taken from real vehicles confirmed by measurements of a study by Reed et al. (2008). From the standard position of the upper belt anchorage point position “far” is defined by moving the attachment plate 70 mm outboard. For position “high” the D-ring attachment screw was moved 75 mm upwards from the standard position and the “rear” position is defined as 100 mm behind the standard position keeping the same vertical height (see Figure 2)
To investigate the sensitivity of chest deflection measurement in oblique loading condition additional tests were conducted with the Q10 with a 13° pre-rotated bench to simulate the vehicle rotation in the ODB crash configuration. In these tests a backless booster with ISOFix attachment was used. Parameter variations in this test configuration include a modification of upper belt anchorage position. In addition the tests were conducted with and without load limiter and pretensioner. The test parameters are summarized in Table 1.

## RESULTS

### Q6 – position settings

The changes in the positioning settings of the Q6 led to different belt routings during the deceleration which are shown in Figure 3. Compared to the dummy and CRS in standard position the slouched position of the CRS supports an upward movement of the diagonal belt, in both cases the diagonal belt stays close to the IR-Tracc during impact. With the dummy in slouched position the diagonal belt shows a clear tendency to move toward the neck and away from the IR-Tracc. The slippage of the belt was also observed with the dummy and the CRS in slouched position. Here the diagonal belt moved up to the neck and under the arm of the dummy.

| 01 | 02 | 03 | 04 |
|---|---|---|---|
| CRS standard, Dummy standard | CRS slouched, Dummy standard | CRS standard, Dummy slouched | CRS slouched, Dummy slouched |

***Figure 3. Comparison of kinematics of Q6 relative to shoulder belt during deceleration phase at 60 ms after impact***

The chest deflection decreases when the diagonal belt moves away from the sensor towards the neck, especially with dummy and CRS in slouched position the deflection is low (Figure 4). The chest acceleration seems to be less sensitive for the belt position. Peak values for deflection and acceleration over the tests 1-4 showing the different positioning settings of the dummy and/or CRS are shown in (Figure 4). The chest deflection decreased with the distance of the belt from the IR-Tracc. Chest acceleration is only affected by the dummy position with an increase for the dummy in slouched position.

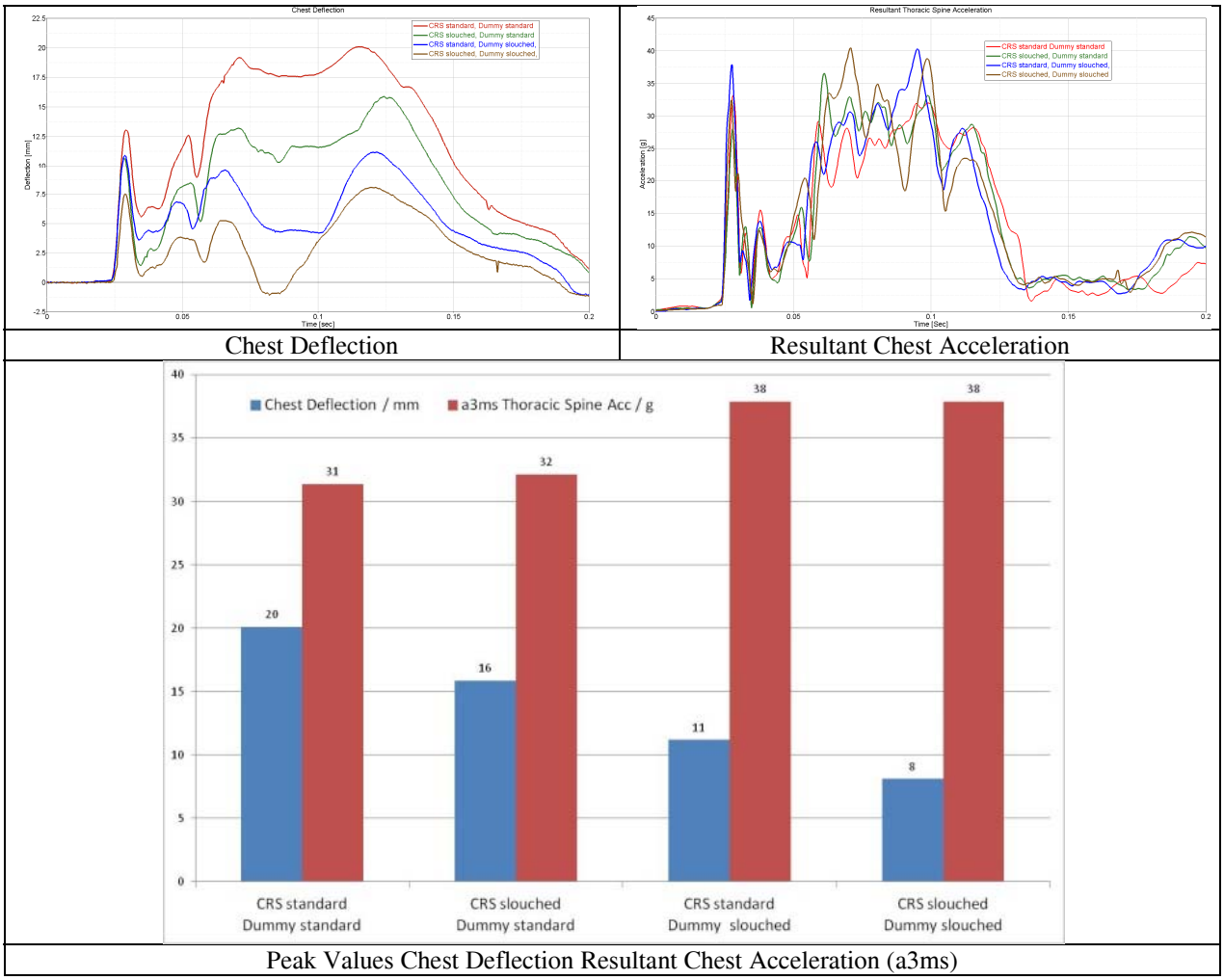


***Figure 4. Q6 – Time History and Peak Values for Chest Deflection and Chest Acceleration***

**Q10 – belt position variation**

For the Q10 in the tests 5-7 the upper belt anchorage was varied to “far”, “high” and “rear”. In the initial position the D-ring position “far” led to a belt routing close to the shoulder joint of the Q10 whereas the belt routings “high” and “rear” resulted in a belt position closer to the neck, especially for the position “high”. During impact (Figure 5), the belt in position “far” stays in the middle of the shoulder and on the chest close to the IR-Traccs. In both other positions the belt slides towards the neck during impact.

Looking at the chest deflection measured by the upper and the lower IR-Tracc, the deflection in the position “far” is nearly twice as high as in both other positions. For the chest acceleration differences are less, with the highest acceleration for the “rear” position (Figure 6). This tendency can also be seen in the peak values. Were the highest deflections are found for the D-ring position “far”, 44 mm (upper) and 49 mm (lower), the a3ms acceleration is the lowest in this test series (31 g). The peak values for both other belt position are only halve for deflection (23/ 25mm upper deflection; 21/ 21 lower deflection) while the resultant acceleration is slightly increasing (34 g for “high”; 39 g for “rear”).

06

Belt Position Far

05

Belt Position High

07

Belt Position Rear

***Figure 5. Kinematics of Q10 relative to shoulder belt at 90 ms start of deceleration***

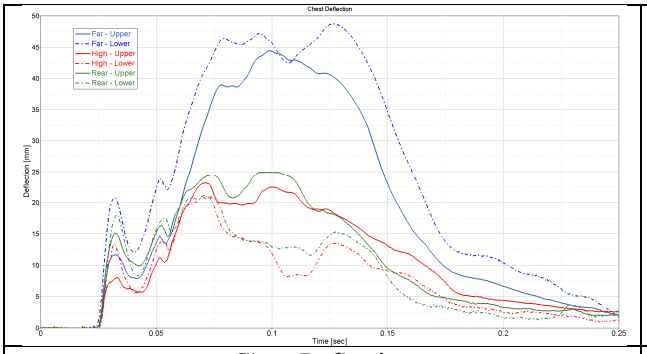


Chest Deflection

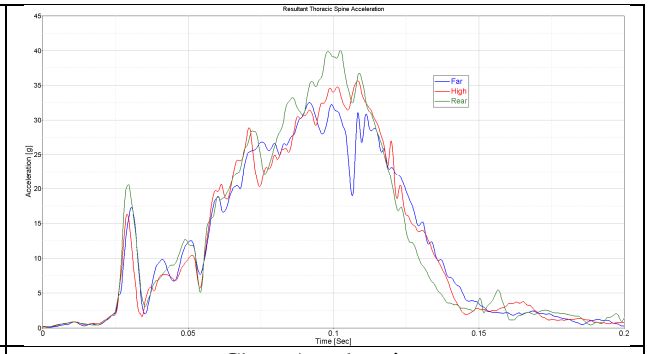


Chest Acceleration

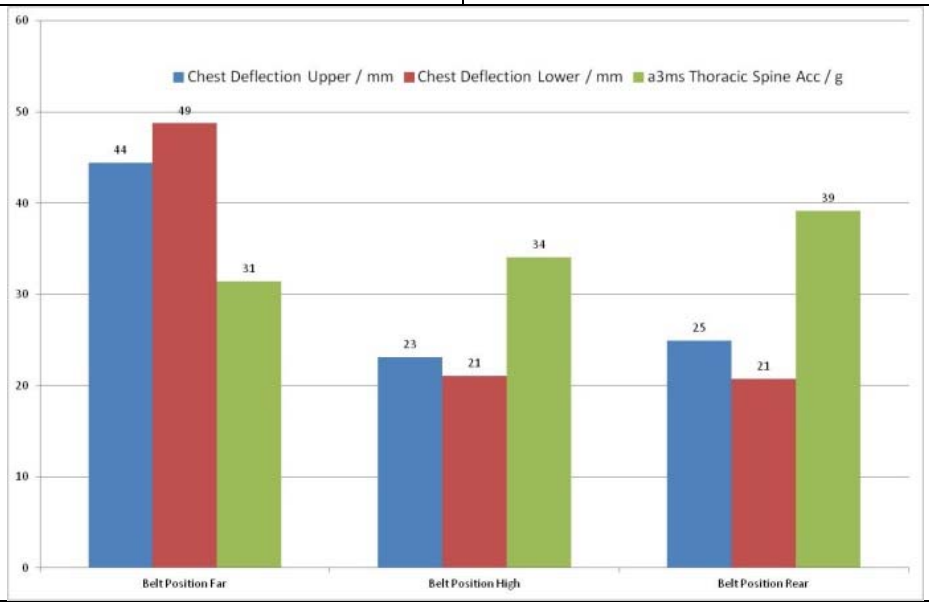


Peak Values Chest Deflection Resultant Chest Acceleration (a3ms)

***Figure 6. Q10 belt position variation – Time History and Peak Values for Chest Deflection and Chest Acceleration***

**Q10 – tests in 13° rotated bench**

The kinematics of the Q10 on the 13° rotated bench at 80 ms after impact are shown in Figure 7. With the D-ring in "far" position the dummy rotates around the diagonal belt and slippage from the shoulder was observed. The belt gets trapped in the shoulder joint between shoulder and arm. Without load limiter and pretensioner the rotation is even more. Here also the lower part of the diagonal belt intrudes below the rib cage.

| 08 | 09 | 10 |
|---|---|---|
| No Load Limiter, no Pretensioner, Belt Position Far (at 80 ms) | Load Limiter, Pretensioner, Belt Position Far (at 80 ms) | Load Limiter, Pretensioner, Belt Position Standard (at 80 ms) |

***Figure 7. Kinematics of Q10 relative to shoulder belt at 80 ms after beginning of deceleration***

With load limiter and pretensioner and especially in combination with the standard D-ring position the Q10 stayed within the belt system.
For the cases tested with pretensioner and load limiter the load limiter level was reached (see upper plot in Figure 8). Without load limiter and pretensioner very high chest deflections were observed, especially at the lower IR-Tracc. Also the chest acceleration was higher. Load limiter and pretensioner reduced the chest deflection for both sensors and also the chest acceleration. Additional reduction for the chest deflection was achieved by the use of the "standard" D-ring position. These observations are supported by the peak values of chest deflection and resultant chest acceleration a3ms. The deflection at the lower IR-Tracc was more than halved by the use of load limiter, pretensioner and standard D-ring position. The chest acceleration slightly increased using the standard D-ring position compared to the use of pretensioner and load limiter in the far position.

**DISCUSSION**

**Q6 – position settings**

The deflection measured in the Q6 by the IR-Tracc is sensitive the position of the dummy within the CRS as well as the CRS position setting itself. The highest deflection is observed for the dummy and CRS in standard position, which would correspond to the position that would be used in regulatory or consumer test procedures. In the other test configurations with the dummy and/or CRS in a slouched position the chest deflection decreases. The lowest deflection is measured in the configuration with both dummy and CRS in a slouched position.
The chest deflection decreases even though a CRS with backrest including belt guidance for the upper shoulder belt is used. Thus the effect of belt migration towards the neck, which was provided as an explanation for reduced chest deflection in other studies without backrest is not the reason in this test series.

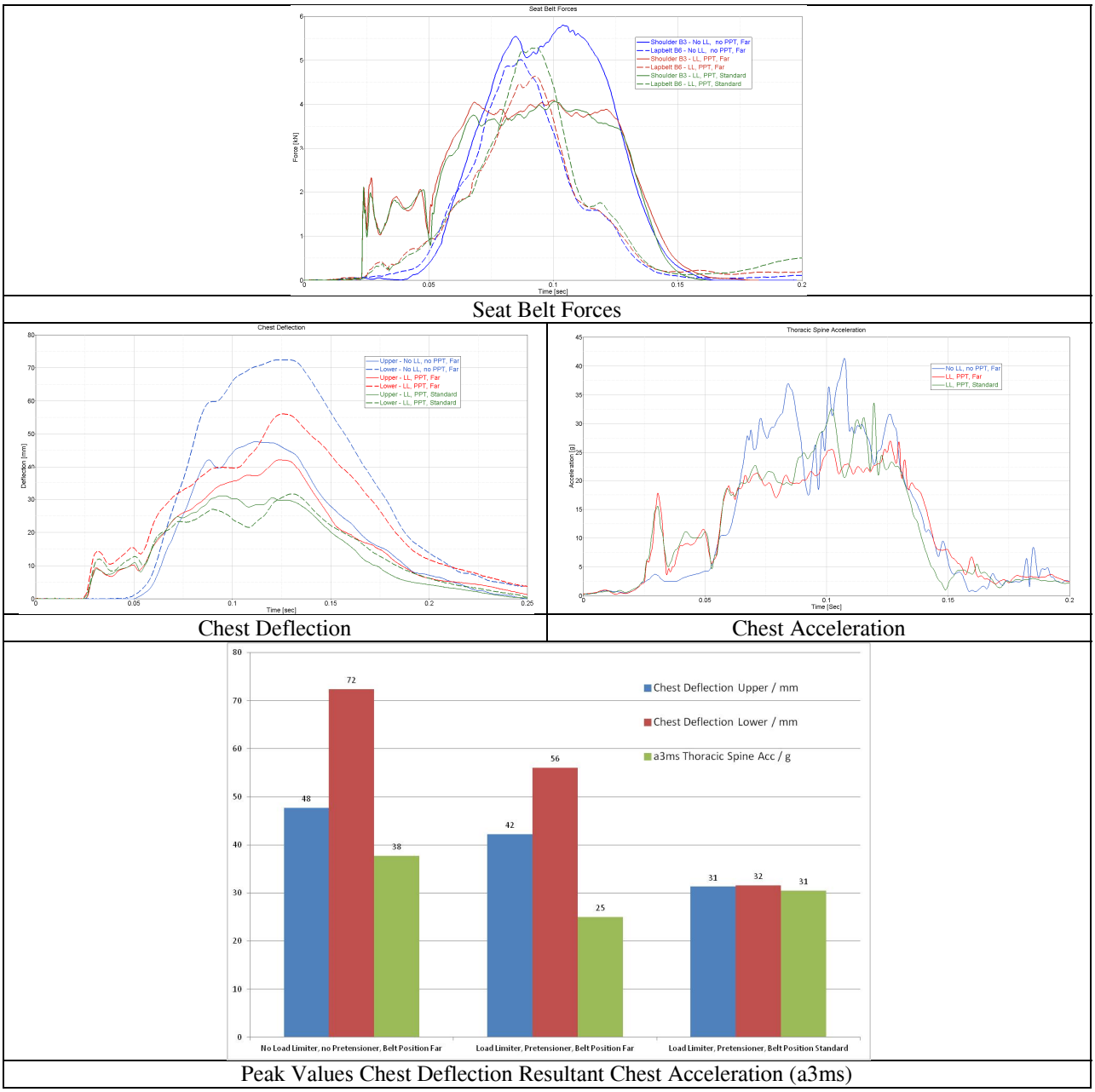


***Figure 8. Q10 tests in 13° rotated bench – Time History Seat Belt Forces, Time History and Peak Values for Chest Deflection and Chest Acceleration***

The decrease of measured chest deflection can be explained by the belt position relative to the IR-Tracc measurement location, which results from the dummy moving forward under the shoulder belt due to its inclined position. Due to this the belt moves up closer to the neck and does not apply direct load to the center of the chest where the IR-Tracc sensor is located. However, a slouched dummy position resulting in the observed belt kinematics could be realistic regarding the real world position of a real child in a CRS and should be considered for assessment of the CRS in a worst case scenario. On the other hand, the deflection sensor cannot assess the severity of this dummy to belt interaction, which seems to be worse compared to a standard position, correctly. A possible solution could be an additional upper deflection sensor in the Q6, which has already been proposed by other researchers. The a3ms value of chest resultant acceleration does not seem to be sensitive to dummy position in these tests. However, it increases with a more slouched CRS position setting. Based on this an acceleration based criterion seems to be more suitable than chest deflection measured only at the center of the chest.

**Q10 – belt position variation**

In the Q10 dummy the chest deflection shows a high sensitivity to changes in the position of the upper belt anchorage location. A more outboard location of the belt anchorage (position far) shows the highest chest deflection because the belt path is cloth to the location of the IR-Tracc sensors as shown in the photos during the deceleration event. Similar findings were also reported by (Bohman und Sunnevång 2012).
A higher belt anchorage location or a more rearward both lead to belt migration towards the dummy neck, which was also seen in the study by (Bohman und Sunnevång 2012). Belt migration towards the neck results in two effects. On the one hand part of the belt load will be transferred through the neck unloading the chest, which will lead to a reduction of actual chest compression. On the other hand a belt path close to the neck also leads to an increase of distance between the belt and the IR-Tracc measurement locations, which are in the centerline of the dummy. In this case the IR-Traccs will not measure the actual peak chest deflections and underestimate the maximum chest deflection. Due to this the observed sensitivity of deflection measurements to upper belt anchorage might not be biofidelic. Injury ratings based on chest deflection might underestimate the real injury risk.
Furthermore in studies with pediatric volunteers and child dummies by (Arbogast et al. 2013) an even higher magnitude of belt migration towards the neck was observed in volunteers compared to the Q10 dummy. If these finding would also be applicable to higher crash severities the possible above described underestimation of injury risk by chest deflection in the Q10 dummy might be even higher.
On the other hand a3ms values of peak chest acceleration shows the opposite trend for different upper belt anchorage locations. Chest a3ms is lowest for the "far" and the highest for the "rear" belt anchorage location. Based on this observation an acceleration based criterion might be more applicable to correctly rate the injury risk.

**Q10 – tests in 13° rotated bench**

In Q10 test with a test bench rotated by 13° without pretensioner and load limiter very high chest deflections were observed whereas the a3ms chest acceleration shows a comparable magnitude like in the 0° tests. The high deflections can be explained by the belt and dummy kinematics during the deceleration events. The shoulder belt completely slides of the shoulder and stays in the gap between arm and shoulder as can be observed in Figure 7. The lower part of the shoulder belt slides up the pelvis. As results the shoulder belt completely loads the thorax without any contact to the pelvis or shoulder structure.
Comparison to another test configurations shows that the dummy kinematics can be effectively controlled by introduction a pretensioner even this severe tests configuration with an oblique loading condition and a far position of the upper belt anchorage location. The belt still moves outboard during the deceleration event. However, the chest deflections are significantly reduced. A reduction of chest deflection by a belt load limiter was also found in a study by (Schnottale et al. 2013) with a Q10 in sled tests in a pre-rotated car body in white.
By an optimization of the location of the upper belt anchorage to an initial belt position in the middle of the shoulder the dummy kinematics can be further improved, which results in a further significant reduction of chest deflections at upper and lower IR-Tracc. The high importance of an optimized position of the upper belt anchorage in combination with a pretensioner and load limiter becomes clear by a comparison with the findings of a study by (Croatto und Masuda 2013). A sled test with the Q10 without backrest and a belt anchorage similar to the "rear" position was done as a base line test without pretensioner and load limiter. The shoulder belt was sliding towards the neck resulting in a low chest deflection. In another test with a pretensioner and load limiter the shoulder belt load was reduced. However, due to the pretensioner belt migration towards the neck was prevented, which resulted in increased chest deflection. Thus it highly depends on the belt geometry and the resulting direction of belt migration, whether a possible positive effect of a pretensioner to keep the belt in place and the positive effect of load limiter to reduce chest loading can be seen in a resulting reduction of chest deflection.
The a3ms value of the thorax acceleration shows a decrease by the introduction of pretensioner and load limiter in combination with the "far" belt location. However, an optimized belt anchorage location leads again to an increase of the a3ms value.
In summary in the tests with the rotated bench an optimization of the belt restraint system by introduction of a pretensioner/load limiter and adjustment of the belt anchorage location led to an improvement of dummy kinematics and dummy belt interaction. A chest deflection based assessment criterion would be able to show the benefit of this optimized restraint system. An assessment criterion only based on chest acceleration would not be able to show the benefit of an optimized restraint system in these test conditions.

## CONCLUSIONS

For the Q6 it would be recommendable to implement an additional upper chest deflection sensor. An acceleration based assessment criterion seems to be more suitable than chest deflection measured only at the center of the chest, until further research has been done with this kind of sensor. Finally a chest injury assessment based on chest acceleration as well as chest deflection measured at two location in the chest might be the most reliable approach.
Chest deflection measured in the Q10 dummy is highly influenced by initial belt geometry. Belt migration towards the neck was observed in previous studies and also in this study for certain initial belt geometries and test conditions. This leads to a reduction of measured chest deflection, which does not correctly reflect the severity of chest loading. For initial belt positions far from the neck and restraint parameters as well as test conditions that result in a shoulder belt sliding outboard or staying in place on the shoulder the measured deflection might be correctly representing the severity of chest loading by the belt. Thus, only a deflection based criterion would not be able to correctly indicate the severity of thoracic loading under certain conditions and due to this has limitations.
A3ms chest acceleration seems to be a better indicator of severity of chest loading for different belt geometries. However, in the tests with the rotated bench an acceleration based criterion would not be able to show the benefit of a restraint system optimized with pretensioner, load limiter and adjusted D-ring position. Thus, a chest assessment only based on acceleration is also not recommendable.
Further research on a meaningful use of a deflection based criterion is recommended. A possible solution could be a criterion taking into account both deflection as well as acceleration and/or assessment of interaction between dummy and belt system during the deceleration.

## REFERENCES

Arbogast, Kristy B.; Locey, Caitlin; Bohman, Katarina; Seacrist, Thomas (2013): Relative Kinematics of the Shoulder Belt and the Torso: Comparison of the Q10 ATD and Pediatric Human Volunteers. International Research Council on the Biomechanics of Injury. Gothenburg, Sweden, 2013.

Bohman, Katarina; Sunnevång, Cecilia (2012): Q10 child dummy performance in side and frontal sled tests. International Conference Protection of children in cars. Munich, Germany, 2012.

Croatto, Sandy; Masuda, Mitsutoshi (2013): Q10 and HIII-10 YO in Frontal Impact: Sensitivity to Restraint Systems. Papernumber: 13-0343-O. Enhanced Safety of Vehicles (ESV). Seoul, Korea, 2013.

EEVC WG12 (2015): Q10 dummy Report - Advanced Child Dummies and Injury Criteria for Frontal Impact. Document No. 642. Available at: www.eevc.org.

EEVC WG12/18 (2008): Q-dummies Report - Advanced Child Dummies and Injury Criteria for Frontal Impact. Document No. 514. Available at: www.eevc.org.

Schnottale, Britta; Lorenz, Bernd; Eggers, Andre; Eickhoff, Burkhard; Verheyen, Christian; Zellmer, Harald (2013): The influence of belt geometry and different booster cushions on main injury assessment values of the Q10 dummy in frontal crashes. International Conference Protection of children in cars. Munich, Germany, 2013.

Reed, M.P.; Ebert-Hamilton, S.M.; Klinich, K.D.; Manary, MA; Rupp, J.D. (2008): Assessing Child Belt Fit, Volume I: Effects of Vehicle Seat and Belt Geometry on Belt Fit for Children With and Without Belt Positioning Booster Seats. Ann Arbor, MI: University of Michigan Transportation Research Institute, 2008. UMTRI-2008-49

# HOWSAFEISYOURFIRSTCAR.COM.AU – A WEBSITE TO ASSIST YOUNG DRIVERS TO FIND A SAFE CAR, IN THEIR BUDGET.

**Samantha Collins**
**Jessica Truong**
**Samantha Cockfield**
Transport Accident Commission
Victoria, Australia

Paper Number 15-0306

## ABSTRACT

Young drivers constitute approximately 13% of all license holders, yet they represent around 25% of drivers killed each year. Although gains have been made in reducing the number of young people being killed and seriously injured on our roads, they continue to be overrepresented in fatal and serious injury crashes each year.

Research has demonstrated that young drivers are at greater risk because they are inexperienced and more likely to take risks on the road.

Some of the factors that increase the risks of crashing among young drivers include:

- Driving with peer aged passengers
- Night time driving
- Use of mobile phones
- Drink/drug driving
- Speeding
- Driving older and less safe cars

Research shows that young drivers tend to drive the least safe and oldest cars on our roads. Research from the Monash University Accident Research Centre (2009) demonstrated that:

- Both female and male young crash-involved drivers are driving older vehicles than their older counterparts.
- Young males are driving older vehicles than females.
- Young female drivers are driving smaller vehicles than their older counterparts.
- Crashworthiness of cars driven by younger drivers is poorer than for older drivers.
- Young female's cars are less crashworthy than young male's cars.

An annual survey from the Transport Accident Commission (TAC) demonstrates that 24% of 18-25 year olds intend to buy a new car, 51% intend to purchase a used car and 25% are undecided. Safety features rank second in importance for 18-25 year olds after condition of vehicle (and price). 67% of 18-25 year olds say they will consider crash test results or safety ratings before purchasing a car, compared to 71% of 26-39 year olds, 64% of 40-60 year olds and 87% of 61+ year olds. 23% of 18-25 year olds say they will not consider safety ratings, and 11% don't know.

In addition to other initiatives to improve young driver safety, including a graduated licensing scheme and school based road safety education, the TAC has now developed a website to make it easier for young drivers to find a safe car within their budget. The website allows users to search through a database of cars that have a 4 or 5 star Australasian New Car Assessment Program (ANCAP) rating or Used Car Safety Rating (UCSR) and are approved by the roads authority for probationary license holders to drive. Users can search by price ranges starting from as low as $2,500 to find a safe car, within their budget.

This paper will detail the background research, development of the website, including data used, marketing strategies and an early evaluation.

## INTRODUCTION

In Victoria, Australia, young drivers aged between 18 and 25 years old, constitute approximately 13% of all licence holders, yet they represent around 20-25% of drivers killed each year. This is a trend that is seen in many other jurisdictions globally. Although gains have been made in reducing the number of young people being killed and seriously injured on our roads, they continue to be overrepresented in fatal and serious injury crashes each year.

There are many factors that increase the risks of crashing among young drivers including:

- Driving with peer aged passengers
- Night time driving
- Fatigue
- Use of mobile phones and other distractions
- Drink and drug driving
- Speeding

Another important factor that plays a role in crash avoidance and injury severity is the car that a young person is driving. Research from the Monash University Accident Research Centre (MUARC) [1] demonstrates that:

- Both female and male young crash-involved drivers are driving older vehicles than their older counterparts.
- Young males are driving older vehicles than females.
- Young female drivers are driving smaller vehicles than their older counterparts.
- Crashworthiness of cars driven by younger drivers is poorer than for older drivers.
- Young female's cars are less crashworthy than young male's cars.

An annual survey by the Social Research Centre for the Transport Accident Commission (TAC) demonstrates that the majority of (51%) young people are looking to purchase a used car rather than new (24%) however 25% were undecided [2]. Safety features rank second in importance for 18-25 year olds after condition of vehicle (and price). 67% of 18-25 year olds say they will consider crash test results or safety ratings before purchasing a car, compared to 71% of 26-39 year olds, 64% of 40-60 year olds and 87% of 61+ year olds. 23% of 18-25 year olds say they will not consider safety ratings, and 11% don't know.

Based on research that indicated the low level of protection provided by the cars young people tend to drive, Victorian road safety organisations, the TAC, VicRoads and the Royal Automobile Club of Victoria (RACV), sought to promote awareness of the importance of vehicle safety for young drivers, and make it as easy as possible for young drivers and their parents to find a safe car. Safety ratings for used vehicles were already available as Used Car Safety Ratings (UCSR) which are calculated every year by MUARC [3]. However, a key consideration for young people who are purchasing a car is price. It was recognised that to make it as easy as possible for consumers to find a safe car, within their budget, pricing information would need to be provided along with safety ratings.

## FIRST CAR LIST

The Victorian road safety organisations engaged a vehicle specifications and pricing information supplier, Redbook, to match UCSR with their database to provide a list of safe (4 or 5 star rated) cars under $14,000. The list of cars was dveloped into a static document that was made available online. The document also included supporting information explaining the UCSR, prohibited vehicles for probationary drivers, crashworthiness ratings, harm to other road users ratings, pricing information. The list was promoted via schools, youth activations and events, and local community organisations.

While the list was very popular, it was difficult to keep up to date and it was recognised that it could be more interactive and useful for young drivers. The list also lacked Australasian New Car Assessment Program (ANCAP) rated vehicles and didn't clearly identify possible probationary prohibitied vehicles. Taking these barriers into consideration it was decided that an online searchable tool would be more useful, easier to update and promote.

**HOWSAFEISYOURFIRSTCAR.COM.AU**

Following the popularity of the First Car List, the partners investigated the possibility of turning it into a searchable online tool. The TAC managed the project and engaged Redbook to match the latest UCSR data to their database (which already includes VicRoads data on probationary approved vehicles) and develop a search tool to enable safe, probationary approved vehicles to be displayed easily. A website was developed which allowed the TAC to manage the homepage content and additional pages while Redbook managed the search tool and search results.

Essentially, the website and search tool allows users to search through a database of 4 and 5 star UCSR and ANCAP rated cars that are P plater approved, up to $35,000. The user is able to filter by different price ranges, and undertake make/model searches. Further information about the ratings and safety features is also available on the site.

**HOWSAFEISYOURCAR.COM.AU**

Howsafeisyourfirstcar.com.au is a complementary website to howsafeisyourcar.com.au. howsafeisyourcar.com.au is a broader website which the TAC uses to support its vehicle safety campaigns. Howsafeisyourcar.com.au includes all vehicles sold from 1990 until the present day and their safety feature specifications. Where available it also includes UCSR and ANCAP ratings. Further information is also provided about individual safety features, fleet policies, child restraints and other related vehicle safety information. This website has become quite successful and obtains an average of around 60,000 unique visitors per month when not supported by mass media but reaches around 120,000 unique visitors per month when supported by mass media. howsafeisyourcar.com.au does not currently include pricing information or probationary approved vehicle information.

**PROMOTION**

Howsafeisyourfirstcar.com.au was launched on October 19 2014. Initially the website was promoted via stakeholders, local community groups and social media. The website is also promoted via the TAC's young driver activation activities and events. The TAC manages a program aimed at young drivers which is based around a large bus, which has been converted into a chill out space for young people. The bus is named Vanessa and attends major festivals and events in Victoria, Australia that have a predominantly young patronage. Vanessa is manned by young people who have received road safety training and information, and have been trained to use police issue breathalyzer machines. The main function of Vanessa is to provide free breath tests to festival patrons to help them to get home safely. Vanessa also provides road safety information, free merchandise, competitions and games to engage with young people. Some competitions, merchandise and information include vehicle safety messages and the howsafeisyourfirstcar.com.au URL.

The TAC has also developed a postcard to be sent to all Learner drivers letting them know about the website. The first mailout will go out in early 2015. Further mailouts will be sent every quarter. Search engine optimization will also be used to promote the website.

**EVALUATION**

Despite the small amount of promotion the website has had a good amount of unique visitors and page views. Refer to Table 1 for exact numbers.

**Table1.**
**Number of Unique visits and page views by month for howsafeisyourfirstcar.com.au.**

| Month | Unique Visits | Page Views |
|---|---|---|
| October | 624 | 4149 |
| November | 527 | 2890 |

| | | |
|---|---|---|
| December | 251 | 1715 |
| January | 221 | 1597 |
| February | 342 | 1675 |

The TAC will continue to monitor the usage of the howsafeisyourfirstcar.com.au and make improvements.

## CONCLUSION

Young drivers are some of the most at risk drivers on Victorian roads, yet they often drive the least safe cars. The aim of howsafeisyourfirstcar.com.au is to provide young drivers and their parents an easy to use tool to easily identify safe cars within their budget. The website was launched in late 2014 and has attracted a good amount of unique visitors and page views. Work will continue to be undertaken by the road safety organisations to promote this website, in a bid to get more young drivers into safer cars.

## REFERENCES


1. Whelan, M., J. Scully, and S. Newstead, *Vehicle safety and young drivers: Stages 2 & 3 - Analysis of young driver crash types and vehicle choice optimisation*. 2009, Monash University Accident Research Centre: Melbourne, Australia.
2. Social Research Centre, *The Transport Accident Commission Road Safety Monitor*. 2014: Geelong, Australia.
3. Newstead, S., L. Watson, and M. Cameron, *Vehicle safety ratings estimated from police reported crash data: 2014 update. Australian and New Zealand crashes during 1987-2012*. 2014, Monash University Accident Research Centre: Melbourne, Australia.

**APPENDIX 1**

**Definition of probationary prohibited vehicle**

If the vehicle is manufactured before 1 January 2010:

- has an engine with eight cylinders or more, or
- has an engine that is turbocharged or supercharged.
- has an engine that has been modified to increase the vehicle's performance (other than a modification made by the manufacturer in the course of the manufacture of the vehicle, or
- is a nominated high performance six cylinder engine.

If the vehicle is manufactured after 1 January 2010

- has a power to mass ratio of greater than 130 kilowatts per tonne, or
- has an engine that has been modified to increase performance (other than a modification made by the manufacturer in the course of the manufacture of the vehicle)

Manufacture date

The date of manufacture is determined by the date on the vehicle's compliance plate or, in the case of a used import, the "Built" or "Built Date" recorded on a metal plate or component of the vehicle.

The vehicle compliance plate confirms that the vehicle complies with Australian design standards and emissions. The date shown on the compliance plate is the date that the compliance plate was fitted to the vehicle by the manufacturer. With some vehicles, there may be a significant difference between the build date and the date of compliance due to shipping and storage time. The compliance plate may even be fitted in a different year.

The compliance plate can be a silver metal plate or sticker that is attached to the vehicle, usually fitted to the firewall (between the passenger compartment and engine) or in the driver's door jam or boot area.

Exemptions

An exemption from VicRoads allows a probationary licence holder to drive a probationary prohibited vehicle.

# OCCUPANT PROTECTION PERFORMANCE IN SIDE IMPACT COLLISIONS PRECEDED BY PRE-CRASH DEPLOYMENT OF ON-BOARD SAFETY SYSTEMS

**Nicola Leone**
**Kajetan Kietlinski**
**Michiel Unger**
TASS International
Germany

**Martin Tijssens**
TASS International
The Netherlands

Paper Number 15-0310

## ABSTRACT

This paper presents a simulation methodology for developing new automotive safety systems in an integrated manner that ensures optimal exploitation of benefits of predictive sensing and occupant restraints.
The investigation was performed using the combination of available simulation techniques for modeling Advance Driver Assistance Systems (PreScan software) and simulating the behavior of dummies and real humans under certain load conditions (MADYMO software and Active Human Model (AHM)).
The methodology was applied to investigate the occupant protection in side impact collisions making use of pre-crash deployed safety systems, such as pre-crash thorax airbag, inflatable seat bolsters, movable seat and a combination of them. The impact load on the dummy was derived from the simulation of the full FE vehicle under Euro NCAP Side Impact Testing protocol conditions.
The results obtained showed the clear potential of adopting an integrated safety system for side impact protection applications. When the collision is detected in advance the time gained can be exploited to increase the overall occupant protection by deploying safety countermeasures prior to the crash. Keeping the occupant further from the intrusion zone, reducing the relative impact velocity and controlling the occupant motion when entering the in-crash phase were key to significantly reduce the injury risk.
To realize the above phenomena, different pre-crash concept occupant motion solutions were defined and investigated: pre-crash deployed thoracic airbag, pre-crash deployed side-bolsters and pre-crash deployed laterally moving seat. Additionally combinations of each solution were investigated. The simulation analysis showed the best protection is ensured by the system combined of side-bolsters and moving seat deployed before the collision, in which case the overall injury risk was lowered from 130% to 44%, when expressed as values normalized with respect to high performance Euro NCAP limits.

## INTRODUCTION

Worldwide, the number of people killed in road traffic crashes each year is estimated at almost 1.2 million, while the number of people injured could be as high as 50 million [1, 2, 3]. Without increased efforts and new initiatives, the total number of road traffic deaths worldwide and injuries is forecast to rise by some 65% between 2004 and 2030 becoming the fifth most likely cause of death [4].
Improving vehicle safety is a key strategy used in addressing international and national road casualty reduction targets and in leading to a safer road traffic system. It is also one of the major research areas in automotive engineering [5]. The safety of vehicle occupants has evolved recently due to the market implementation of new sensing technologies that enable to predict and identify hazardous road traffic situations and thus actively prevent or mitigate collisions. The upcoming safety developments lead to the potential future integration of these technologies with the conventional passive safety, where the safety systems are deployed based on crash sensing.
The integrated safety system proposed for the future focuses on managing the information from the predictive sensing about the imminent collision and communicating it to the on-board restraint systems to optimally protect the occupants and thus further reduce the injury risk in case of a collision. Developing an integrated safety system doesn't mean only to fuse together the active and passive systems. The work behind the fusion concerns the necessity of first developing the system in an integral manner and then studying and assessing what is its global effect on the injury mitigation.

Being at the beginning of the development of this new family of safety systems, at the moment there's lack of literature reference regarding this topic. New experimental methods and simulation tools for evaluating the efforts of pre-crash dynamics on the occupant injury risk during the crash phase are needed.
The present paper shows and proposes a simulation methodology created to support an integrated safety system development process for side collision application. Analyzing traffic accident statistics, it comes out that side impact is one of the car accident typologies and also one of the most critical sources of fatalities. According to the American Insurance Institute for Highway Safety (IIHS), side impact crashes accounted for 27 percent of passenger vehicle occupant deaths in the United States in 2009 [6].
The higher level of danger related to the side impact, if compared to the one caused by frontal crashes, lies in the considerably lower energy absorption capabilities of side structures and consequently larger intrusion and higher risk of injuries resulting from the contact with them [7]. The limitations of further improvements to vehicle safety for the side impact collisions motivate the development of innovative methods to lower the injuries and make the vehicle safer.
This paper presents the methodology for developing and testing the integrated safety system for side collision application and provides a safety performance overview of different pre-crash occupant protection countermeasures compared to a regular in-crash protection system used as a performance reference.

## METHODOLOGY

### Tools

The methodology used in the study follows the one illustrated in the paper published at SAE International in 2013 by M. Velardocchia at al. [8] in which a virtual integrated safety development platform was created and assessed. The methodology consists of the coupled and complementary use of two software packages: PreScan and Madymo [8]. PreScan was used for accident scenarios modeling and for designing the sensing and control systems for the side collision recognition, whereas Madymo was utilized for assessing the effects of pre-crash deployment of the thorax airbag.
In the Figure 1 the schematic illustration of the methodology and its tools derived from the previously published investigations [8] is presented. The analysis starts from the real world scenario that determines input boundary conditions for PreScan in which the vehicle maneuvering is being simulated. The results produced by PreScan simulation are then fed to MADYMO in order to simulate pre- and in-crash crash actions on the occupant motion. The consequent effects on the in-crash phase determine the injury values, thus the occupant response.

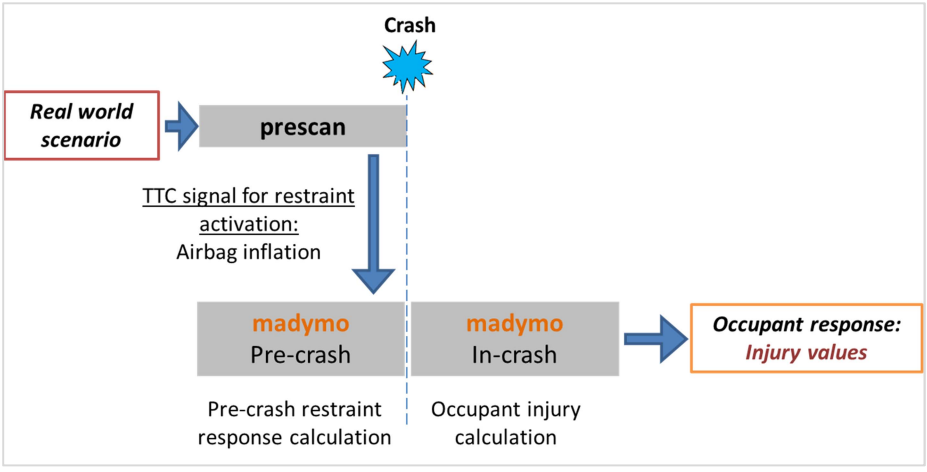


***Figure1. The methodology: combined usage of PreScan and Madymo.***

The parameters used to give a quantification of the injuries on the occupant in the EuroNCAP side impact test protocol refer to head, chest, abdomen and pelvis; more details about injuries parameters are available in the Appendix section. Since the Head Protection Criteria (HPC) is typically not significant in these crash conditions and has a low value when compared to the low performance limits, this was not used in the present study as protection performance parameter.

The focus of this study was then on the rib deflection, on the viscous criterion, on the abdomen peak force and on the pubic symphysis peak force. In particular, the protection system performance was based on the comparison with respect to the high performance limits (see Figure 2) of the EuroNCAP "Side Impact Test Protocol", version 5.2, from November 2011.

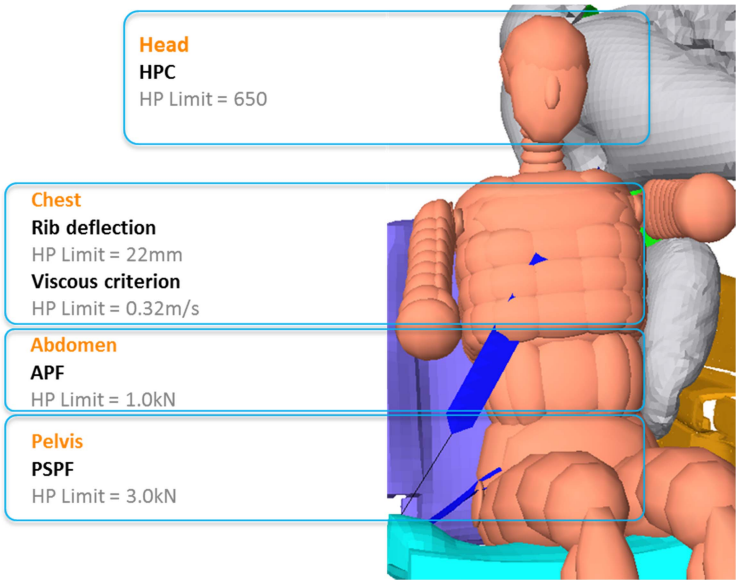


***Figure2. EuroNCAP high performance protection criteria in side impact.***

**Case study scenario**

The present study was carried out with the aim of modeling a side impact scenario which represents real accident data gathered by surveys. M. Velardocchia et al. [8] points out that typical side impacts occur in urban areas, when one of the two vehicles involved runs a red traffic light, other traffic control such as a stop or yield sign, or tries to perform an incorrect maneuver for turning and driving into another road.
Resting upon this information a representative scenario was selected as object of the investigation and modeled with PreScan. The scenario represents an urban intersection in daylight conditions, where a couple of generic compact cars are involved in a side impact (Figure 3).

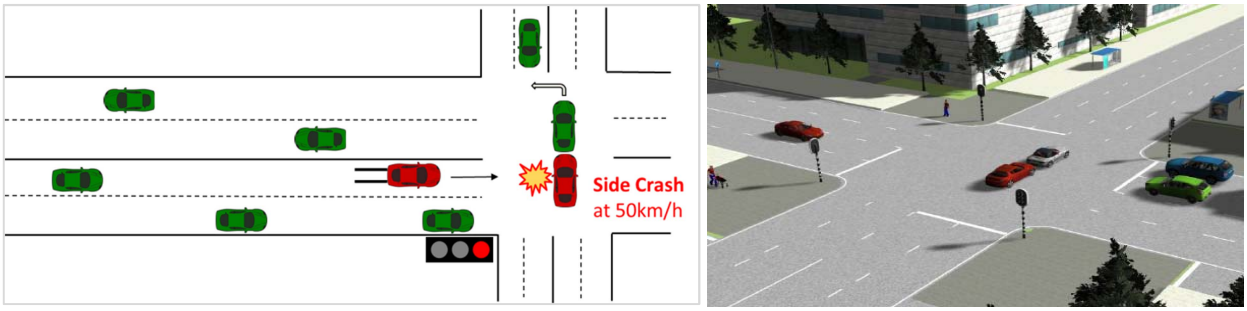


***Figure3. Studied side impact scenario.***

At the moment of impact the struck car (hosting the side impact pre-crash system) is stationary on the road crossing, queuing for a left turn. It is blocking the lane for the upcoming traffic from perpendicular direction. The striking car on the perpendicular lane is initially travelling at 60 km/h, fails to notice the red traffic light, and collides with the struck car at a velocity of 50 km/h, after an emergency braking performed by the driver.
The scenario represents the layout of a real life side impact and the resulting accident dynamics is in line with the one required by European regulatory [9] and consumer [10] side test protocols, where the car under examination is struck by a mobile deformable barrier (MDB) moving at 50 km/h and colliding at an angle of 90 degrees with respect to the tested vehicle.

The test condition parameters are as follows:
1. Impacted car speed: 0 km/h (stationary);
2. Impacting car speed: 50 km/h;
3. Angle of impact: 90 degrees;
4. Side of impact: driver side.

**Pre-Crash Detection System**

The vehicle that undergoes the side impact is equipped with two idealized surrounding sensors located on the impact side of the vehicle and at the same location in the vehicle longitudinal direction. The two sensors are:
1. Short Range Radar (SRR) with a single detecting beam;
2. SRR with 20 scanning beams.

Besides the different number of scanning beams, the other scan parameters are the same for both radars:
1. Horizontal scan;
2. Maximum range: 30[m];
3. Field of View (FoV) in Azimuth: 80[°];
4. Field of View in Elevation: 3.5[°];
5. Heading angle: 70[°];
6. Total scanning frequency: 100[Hz].

The two radars work constantly together although each one is assigned a specific task: the single beam radar detects the objects inside the field of view, pre-selects collidable ones and calculates the time to collision (TTC); in parallel the multiple beam radar is in charge of identifying vehicles among the collidable objects. Making use of the data from the two radars and fusing them, the detection algorithm is able to identify the presence of a collidable vehicle. When the TTC of a collidable vehicle is less than 0.6s, then the necessary condition to activate the desired on-board pre-crash device is satisfied.
A detection performance assessment of the algorithm was executed in [8]: results showed that the system could detect an impending side collision 150ms before this actually took place, in the worst case. Starting from this assumption and considering an additional margin of risk, all the studied pre-crash countermeasures that will be showed in the following paragraph were always triggered not more than100ms before the crash.

**Vehicle Model And Restraint Systems**

The side impact dynamics and the consequent injuries on a hypothetical occupant sitting in a vehicle equipped with collision detection system and pre-crash restraint systems were studied by building and using a virtual vehicle model with the tool MADYMO.
The side impact load on the driver was obtained by giving the side structure (B-pillar and door) and the seat a prescribed motion as obtained from the simulation of a Finite Element (FE) full vehicle system impacted by a Mobile Deformable Barrier (MDB) at the speed of 50 [km/h].
The vehicle model representation is simplified, as limited to the components relevant for the interaction with the occupant in the side impact collision load case: the seat, door and B-pillar. The door model is built using Multibody techniques and consists of several parts representing the elements of door structure and door trim. The external geometry of each element is represented by rigid FE models that are assigned to the corresponding door part and form together the entire door. The deformation of the door during the collision (door intrusion) is represented by prescribed motion of the bodies of appropriate door parts. The local deformability of the door trim that results from the interaction with the occupant is represented in a simplified manner using translational joints between the external trim geometry and underlying moving bodies. The compliance of the joints is restrained using distance-force characteristics that were tuned to represent the local deformability of each part of the door including the crushable and energy absorbing structures. The seat and the B-pillar motion resulting from the collision deformations is prescribed in a similar manner as for the door. The contact characteristics and material properties of the seat cushion were tuned in order to simulate accurate interactions with the dummy during its relative motion.
The base Madymo model also contains: a 3-point seat belt, a curtain airbag and a seat mounted thorax airbag.
The seat belt insertion points are attached to the B-pillar and the seat. The seat belt is equipped with a retractor and a pretensioner. The pretensioner was triggered at the time of 8ms after the crash in all considered cases; the curtain and the thorax airbags are also triggered 8ms after the crash.
The curtain airbag is a cushion of about 35liter in size. This is attached to nodes moving according to the deforming structure simulated in the full FE vehicle crash mentioned above.

The thorax airbag has a volume of about 10.5liter; the inflator used reaches 223kPa when inflated in a 10liter closed tank. Its permeability is set to 0.5% and vent hole diameter is 6.2mm.
The reference model so far described was then modified so that pre-crash protection systems could be implemented and studied. The three investigated restraint systems presented in this paper are:

1. Pre-crash thorax airbag

The pre-crash thorax airbag was already investigated and assessed in [8]. In the current study it is again mentioned for comparison with the other proposed solutions. The optimization study performed previously brought as result a thorax airbag model with the same cushion shape and material as in the reference model, which is deployed 100ms earlier than the reference thorax airbag (effectively 92ms before the crash). Furthermore, when the airbag deploys the vent hole (whose equivalent diameter is in this case 8.3mm) is still closed; only later, 15ms after the crash, the vent hole is opened.

2. Pre-crash inflatable seat bolsters

The solution with the inflatable seat bolsters was studied by Daimler-Benz AG for the Experimental Safety Vehicle program in 2009, called ESF 2009 [11, 12]. Following the information available about this study, two inflating bolsters located respectively in the seat cushion and in the seat back cushion (only on the impact side) were implemented in the base Madymo model. They have been modeled as two ellipsoids attached to their own translational joint. The countermeasure is triggered 92ms before the crash; when the system is deployed, the ellipsoids move 40mm towards the dummy, pushing it towards the center of the vehicle. In particular, one ellipsoid acts on the thorax and the abdomen of the dummy, whereas the other ellipsoid pushes its pelvis and its outer leg. The bolsters can move back to their initial position according to a load characteristic specifically tuned to minimize the chest deflection of the dummy in the phase preceding the contact with the thorax airbag. The thorax airbag is the same as in the reference model, therefore is deployed 8ms after the crash.

3. Pre-crash moving seat

Similar to the inflatable seat bolsters also the pre-crash moving seat was part of the ESF 2009 program [13]. The driver seat in the reference model is already attached to a joint and is moving with a prescribed motion during the in-crash phase. In the pre-crash phase it has been given an additional displacement of 50mm towards the center. The seat starts moving 92ms before the crash and stops at time t=0ms, whereas the thorax airbag is the same as in the reference model, therefore is deployed 8ms after the crash. The pre-crash seat travel was represented as prescribed motion following the S-shape displacement in time (see Figure 4). The resulting acceleration transmitted to the seat to execute the prescribed motion accordingly to the assumed seat motion, requires application of external force of 4.7kN, with the assumption that the total weight of the moving system (occupant and seat) amounts to 100kg. The plots illustrating the mechanics of the pre-crash seat motion are presented in the Figure 4.

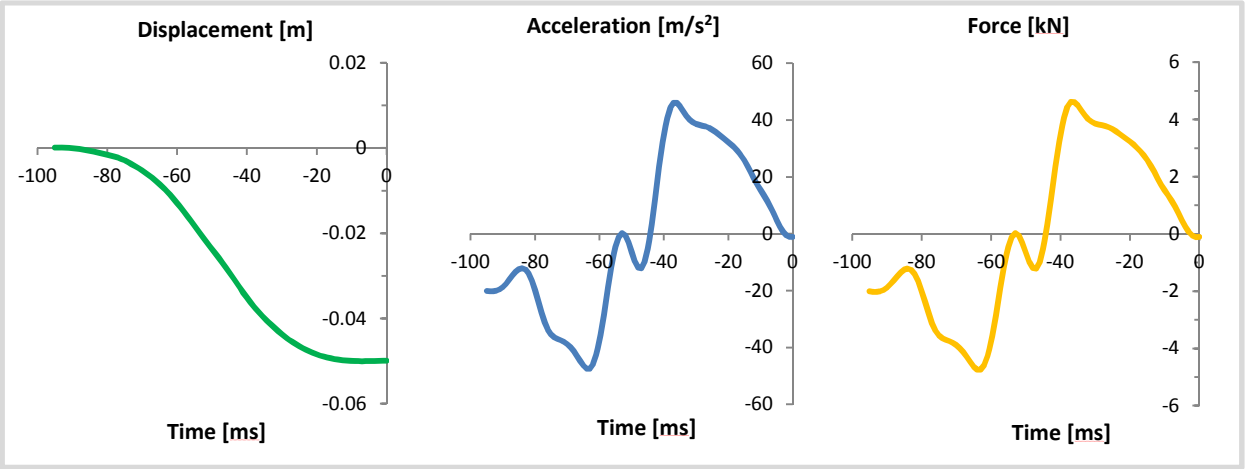


***Figure4. Pre-crash moving seat displacement, acceleration and force plots.***

An overview of the above-mentioned pre-crash safety systems is presented in Figure 5.

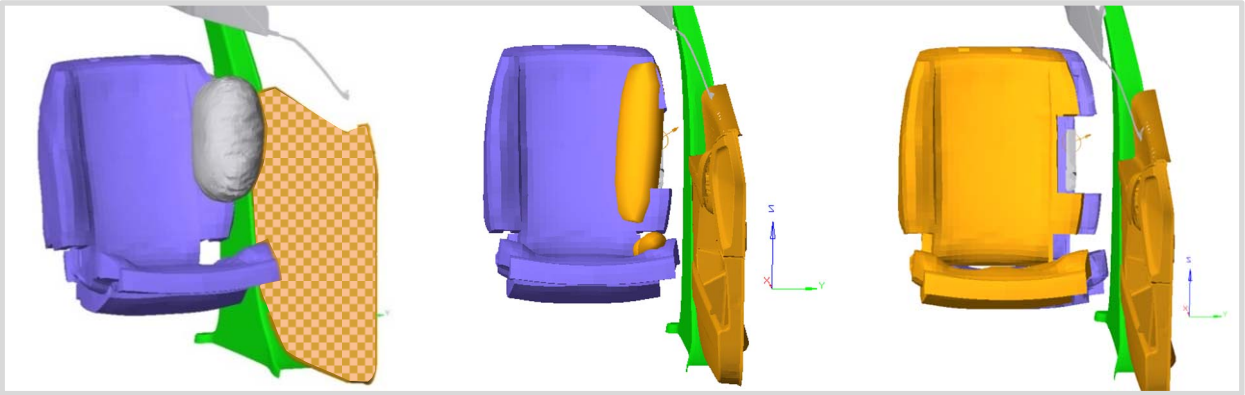

***Figure5. Pre-crash safety systems; from left: thorax airbag, inflatable seat bolsters and movable seat.***

The occupant dummy used throughout the complete investigation is the ES-2re Q Madymo ellipsoid dummy model.

## INVESTIGATION APPROACH

The need for the assessment of the potential of pre-crash activated protection systems arose directly from the results of the study [8] about the integrated safety potential in a side impact load case.
When using a pre-crash thorax airbag (with the specifics as described in the paragraph above), the chest deflection could be significantly improved. This confirmed the assumption that by pushing away the driver from the intrusion zone towards the center of the vehicle, it could be possible to significantly reduce the chest injuries. For rib deflection and rib VC parameters, the explained strategy led to reductions of about 20% and 50% respectively. Unfortunately a side effect was also observed, because APF and PSPF injury parameters showed a degradation of about 10 percent. The significance of the problem was related not only to the degradation of APF and PSPF injury parameters, but also to the fact that the APF, came dangerously close to the EuroNCAP protocol low performance limit, and thus could be considered as a significant limitation of the investigated system.
The analysis showed that the airbag, when deployed, interacts directly only with the thoracic and abdominal dummy regions, while the pelvic region is not loaded. This interaction generates the torque that causes lateral rotation of the dummy before the in-crash loading occurs. As a consequence, the pelvis and abdomen are not optimally restrained by the seat and by the thorax airbag respectively. In order to address the unwanted dummy rotation, and APF and PSPF deterioration, the dummy would need a more homogeneous push along the entire upper body region in the pre-crash phase.
Starting from these considerations, the first objective of the study was to find alternative solutions to the pre-crash thorax airbag which allow intervening more effectively on the occupant motion. The second objective was to quantify their potential as well as to make a comparison between the systems and with respect to the base model. The reference protection system together with the investigated pre-crash occupant protection systems whose results are presented in the following paragraph, are listed below:

1. In-crash thorax airbag
2. Pre-crash thorax airbag
3. Pre-crash inflatable seat bolsters
4. Pre-crash moving seat
5. Pre-crash moving seat together with pre-crash thorax airbag
6. Pre-crash moving seat together with pre-crash inflatable seat bolsters

## RESULTS

The injury values produced by the ES2-re dummy in the simulations are presented in Figure 6. Each value represents the ratio (expressed in percentage) between the calculated dummy injury value and the related high performance limit according to the EuroNCAP protocol (see Figure 2).

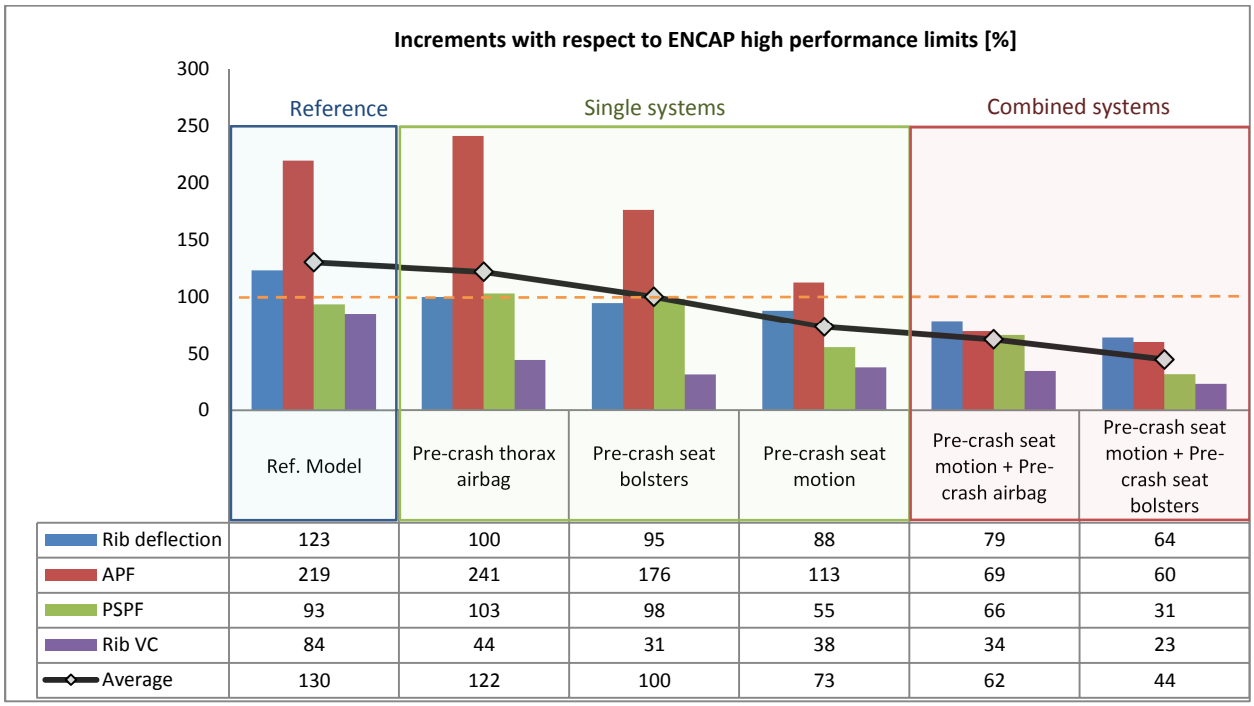


| | Ref. Model | Pre-crash thorax airbag | Pre-crash seat bolsters | Pre-crash seat motion | Pre-crash seat motion + Pre-crash airbag | Pre-crash seat motion + Pre-crash seat bolsters |
|---|---|---|---|---|---|---|
| Rib deflection | 123 | 100 | 95 | 88 | 79 | 64 |
| APF | 219 | 241 | 176 | 113 | 69 | 60 |
| PSPF | 93 | 103 | 98 | 55 | 66 | 31 |
| Rib VC | 84 | 44 | 31 | 38 | 34 | 23 |
| Average | 130 | 122 | 100 | 73 | 62 | 44 |

***Figure6. Result overview: protection performance comparison among the different investigated solutions.***

The safety performance of the reference model and of the pre-crash thorax airbag is the same as the one mentioned in the [8] and is here reported for a wider and more complete results analysis and discussion. As already mentioned in the Investigation Approach section, the most critical parameter for the dummy in the reference model is the APF, which is only 300N below the low performance limits and no less than 1.2kN above the high performance limits. Whereas the pre-crash thorax airbag showed good potential in the reduction of the chest related injuries, with no possibility to decrease the problematic APF, all the other investigated countermeasures provided an overall increased protection to the dummy, as this was observed for the chest, for the abdomen and for the pelvis.
The two single system solutions, namely the pre-crash inflatable seat bolsters and the pre-crash moving seat decreased the averaged injuries of the dummy from 130% to 100% and 73% respectively, with respect to the EuroNCAP high performance limits. Although the better protection of the chest area is comparable between the two systems, the main difference was encountered at the level of the abdomen and of the pelvis: the inflatable seat bolsters did not decrease the PSPF and could only reduce the APF by about 20%, whereas the moving seat could almost half both APF and PSPF. Therefore the overall protection performance of the moving seat was the best among the single system solutions.
Combining the pre-crash seat motion with the pre-crash airbag or pre-crash seat bolsters shows an increased potential in the dummy injury reduction when compared to both the reference model and the moving seat solution. The most important achievement is that all the injury peak values fall below the high performance threshold including APF. The model in which the pre-crash moving seat is combined with the inflatable seat bolsters could achieve an APF reduction of 73% with respect to the reference system, meaning about 1.6kN of less force acting on the abdominal area; the APF reduction for the other combined solution equals 68%. These results indicated that in case of fusion of two protection systems, no degradation of the overall injury performance occurred; rather there is potential for further improvements of injury levels. Only the PSPF peak value measured in the moving seat and pre-crash airbag combination increased slightly, although it remained safely below its reference value and below the high performance limits.

Besides the injury values, the simulations provided also other useful information necessary for the comprehension and the analysis of the results. Each system, as already highlighted in this paper, intends to give the dummy an initial impetus towards the center of the vehicle. The animation output shows the differences between how each investigated solution had acted on the dummy pre-crash motion and is presented in the Figure 7.

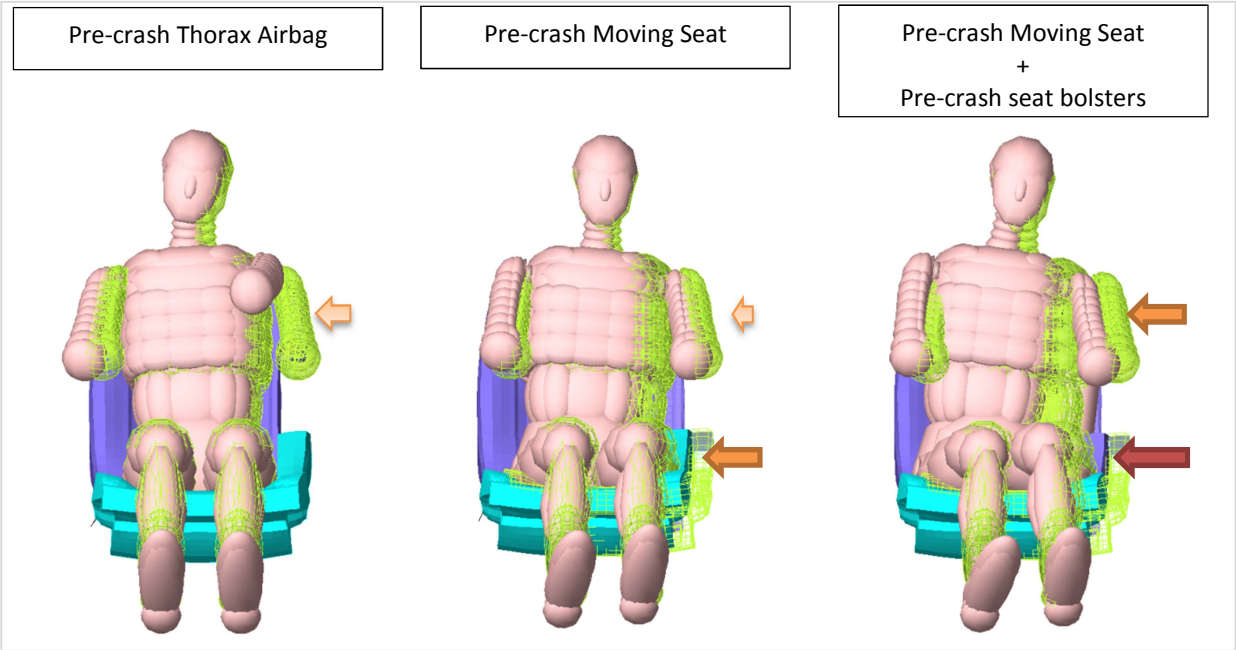


***Figure7. Dummy position at the crash time t = 0ms in three different models. Green coloring is used for reference dummy model position.***

The first investigated solution, the pre-crash thorax airbag, pushes the dummy directly on the rib cage, resulting in a rotation of the upper body around the pelvis which itself does not move significantly (see Figure 7). When the side structures start intruding into the vehicle, the first contacts occur with the pelvis and with the abdomen which are not protected by the airbag, causing a worsening of APF and PSPF. Only the thorax, which is already supported by the cushion, can be efficiently protected.
The direction of the upper body rotation observed for the other four studied solutions was different; two of them are taken as example and presented in Figure 7, in order to show and explain this different behavior.
In the pre-crash moving seat solution, the seat pushes the dummy mostly from the pelvis. Because of the inertia the upper part of the body tends to remain in the original position; the contact of shoulder and chest with the seat back cushion gives some additional support to the dummy during the desired pre-crash motion, although the dummy is clearly rotated outwards. Despite this, the effective relative distance of chest, abdomen and pelvis from the door is increased, whereas the head stays almost in the initial position.
Similar considerations can be made on the last pictured solution (see Figure 7), the combination of the moving seat and the inflatable seat bolsters. Also in this case the upper body is rotated outward as a result of the direct push of the seat cushion on the pelvis. There is however a difference, which consists in the higher overall force applied to the dummy and which is directly depending on the fact that during the pre-crash seat motion also the inflatable seat bolsters are deployed.
Each system performed differently from the other but the common factor was that, in all the cases, the effect of acting on the occupant motion before the crash was always beneficial. The injury curves showed a close and direct link between the injury peak values and the time when these were measured: the more significant push on the dummy, the faster it moved away and the bigger the gap from the intrusion zone. As a consequence the loads on the dummy body regions started later and less and less intensely, as the intrusion velocity and the related effect on the dummy decreases during the crash from the peak value (at crash time t=0ms) to zero, when the maximum intrusion is measured.
Besides the importance of giving the dummy more space and initial velocity at the moment of the crash, the results showed the importance of the upper body orientation. In particular, having the dummy upper body orientated outward was found to be consistently effective in the reduction of all the injury values, throughout all the

investigated solutions. The described position shows to work effectively in the distribution of the load on the dummy as it enters the in-crash phase with an angle which is very similar to the one that it will get throughout the loading phase: this prevents the 'pendulum' effect observed when using the pre-crash thorax airbag, thus allowing a more evenly distributed load on the dummy.

## CONCLUSIONS

The paper intends to present a methodology based on the coupled use of two software packages to simulate road accident scenarios by designing a side collision detection system (PreScan) and assessing the effects of pre-crash strategies on injury parameters on a virtual dummy model (Madymo).
The investigation into different pre-crash deployed injury conceptual countermeasures showed that the most effective occupant motion control system is the one in which the pre-crash inflatable seat bolsters system is coupled with the pre-crash moving seat solution. The two countermeasures are triggered simultaneously 92ms before the crash, while the thorax airbag and the seat belt pretensioner are trigger 8ms after the crash as in the reference model. With this proposed occupant protection it was possible to bring the peak values of rib deflection, APF, PSPF and VC, below the EuroNCAP high performance limits.
The most significant improvement were obtained on the APF, as this was lowered by 73% with respect to the reference system, meaning about 1.6kN of less force acting on the abdominal area. The rib deflection that in the reference model was above the high performance limits could be decreased by 48%. The average of the four injury parameters peak values dropped by about 65%.
The other investigated solutions showed also a significant potential in reducing injury values in all body regions and outlined the real potential of the integrated safety systems for side impact scenarios and which of the occupant motion control strategies are the most effective for injury risk reduction. It can be summarized that the key biomechanical phenomena that contribute most to the occupant protection for side impact loadings are:

a) increased distance between the occupant and parts of the vehicle that intrude during the side impact, that results in decreased contact speed between occupant and intruding parts
b) initial occupant velocity in the same direction as the impact direction, that additionally reduced the contact velocity between occuapnt and intruding parts
c) initial outward rotation of the lower body that results in a more equal distribution of the contact interaction between occupant nad intruding parts

Similar, conceptual level observations were previously published in [11].
Introduction of predictive sensing to the side collision protection and utilizing the information about the upcoming collision to take actions on the occupant pre-crash kinematics, results in the global occupant injury risk reduction. The aim was to demonstrate the potential of the new design concepts which are still not possible to implement in series production and/or are currently only mentioned in the literature, so as to stimulate discussion of the necessary technological developments.
The investigation was limited to the specific crash conditions and does not show the sensitivity of the proposed solutions to different load cases. In order to assess the total potential of predictive sensing for side impact collision application, future studies are needed to prove the usefulness of the proposed approach for other load cases, different occupant sizes and different vehicle types and sizes.
Integrated Safety is a new region of automotive safety and does not have established simulation methods in place. The combined use of PreScan and Madymo for side pre-crash study is one of the first applications of both software packages together for the Integrated Safety purposes. The use of this method requires expertise in both active and passive safety areas and additional effort from the user in terms of interface handling throughout the use of both software suits. It should be also noted that Madymo was originally designed for in-crash simulations, and its functionalities are not yet fully optimized for pre-crash problem analysis. One Madymo limitation is the lack of validated side impact dummy models for low-g loadings that occur during the pre-crash phase.
In conclusion, given the significant injury damage, typically accompanying side impact collisions and the yet limited understanding of the potential for integrated safety to address this issue, this paper intends to initiate the interest in further research that can exploit new predictive technologies to reduce the harm caused by side impact.

## REFERENCES


[1] Peden, M., & al. (2004). World report on road traffic injury prevention. *World Health Organization.*

[2] Kopits, E., & Cropper, M. (2003). Traffic fatalities and economic growth. *Policy Research Working Paper*, No. 3035.

[3] Murray, C., & Lopez, A. (1996). The global burden of disease: a comprehensive assessment of mortality and disability from diseases, injuries, and risk factors in 1990 and projected to 2020. *Global burden of disease and injury series*. Boston, MA: Harvard School of Public Health.

[4] Global status report on road safety: time for action. Geneva: World Health Organization, 2009. Retrieved from www.who.int/violence_injury_prevention/road_safety_status/2009

[5] Belingardi, G., & Obradovic, J. (2010). Design of the impact attenuator for a formula student racing car: numerical simulation of the impact crash test. *Journal of the Serbian Society for Computational Mechanics, 4(1),*52-65.

[6] Teoh, E., & Lund A. (2011). IIHS side crash test ratings and occupant death risk in real world crashes. Arlington, VA: Insurance Institute for Highway Safety.

[7] Guang, D., & al. (2007). Side structure sensitivity to passenger car crashworthiness during pole side impact. *Tsinghua Science and Technology*, 9(18), 290-295.

[8] Velardocchia, M., & al. (2013). Integrated active and passive systems for a side impact scenario. *SAE Technical Paper 2013-01-1162.*

[9] Uniform provisions concerning the approval of vehicles with regard to the protection of the occupants in the event of a lateral collision. Economic Commission for Europe (ECE). Regulation No.95. October 2003.

[10] Side Impact Test Protocol. EuroNCAP. Version 5.2. November 2011.

[11] Mellinghoff U., & al. (2009). The Mercedes Benz - Experimental Safety Vehicle ESF 2009. *ATZ Worldwide Magazine, 111*(07-08).

[12] Daimler. (2009). PRE-SAFE Pulse: an automatic nudge in the ribs. *Technology & Innovation, Safety*. Retrieved from: http://www.daimler.com/dccom/0-5-1214698-1-1214757-1-0-0-1214699-0-0-135-0-0-0-0-0-0-0-0.html

[13] Daimler. (2009, June). The ESF 2009 Experimental Safety Vehicle. *Technology & Innovation, Safety*. Retrieved from: http://www.daimler.com/dccom/0-5-1214698-1-1214703-1-0-0-1214699-0-0-135-7165-0-0-0-0-0-0-0.html


## APPENDIX

1. APF

The Abdominal Peak Force is a measure of injury to the abdomen: APF is the maximum side abdominal strain criterion and is expressed as the highest value of the sum of the three forces [N] measured at each abdominal load cell (front, middle and rear) on the impact side.

2. HPC

The Head Protection Criteria is the standardized maximum integral value of the head acceleration.

3. PSPF

PSPF is the criterion for pelvis strain during side impact and is determined by the maximum strain on the pubic symphysis, expressed in [kN].

4. RDC

The Rib Deflection Criteria is the criterion for the deflection of the ribs, expressed in millimeters [mm], in a side impact collision.

5. VC

Also called as Viscous Injury Response, VC is an injury criterion for the chest area. The VC value [m/s] is the maximum crush of the momentary product of the thorax deformation speed and the thorax deformation. Both quantities are determined by measuring the rib deflection.

# ABDOMINAL CHARACTERIZATION UNDER LAP BELT LOADING

**Taewung Kim**
**Gwansik Park**
**Salvador Montesinos**
**Damien Subit**
**James Bolton**
**Brian Overby**
**Jason Forman**
**Jeff Crandall**
University of Virginia Center for Applied Biomechanics
USA

**Hyungjoo Kim**
Hyundai Motor Group
South Korea

Paper Number 15-0312

## ABSTRACT

The phenomenon of submarining is of major interest in the design and optimization of restraint systems. A biofidelic finite element human body model can be more useful for investigating this phenomenon than the existing dummy. For the validation of finite element human body models, belt pull tests were performed to characterize thoracic and abdominal regions of the PMHS, and the 50%tile male Hybrid III dummy was tested for comparison with the PMHS. The spines of subjects were rigidly mounted to a test fixture through a mounting system to minimize the influence of the spinal motion during the test. The pelvis of the subjects were positioned close to the normal driving posture, but the torso angle was more reclined than the average driving posture due to the difficulty of adjusting the torso angle during the mounting process. This torso angle led to the belt being positioned more rearward with respect to anterior superior iliac spine (ASIS) in the longitudinal direction. The subjects were loaded under lap belt only configurations with two levels of load limits, 1 kN and 3 kN. The lap belt was positioned in various vertical offsets with respect to ASIS and belt angles. The vertical offset of the belt from ASIS was determined based on volunteer test data. Belt pulling distance, belt cable force, spine reaction force, and belt kinematics were documented for the human body model validation. During the lap belt tests, both belt sliding over the pelvis and belt staying in front of the pelvis were observed, and a large amount of abdominal compression was observed during the submarining cases. After finishing the test series, autopsies were performed on the PMHS, and both PMHS showed no injuries in the abdominal region. One of the PMHS also showed a pelvic fracture at the iliac crest, but the PMHS had a pre-existing healed pelvic fracture at the same location. It was believed that this pre-existing fracture had not healed completely prior to death. Note that its ASIS region was intact so it should not have affected the occurrence of the submarining-like belt kinematics. Although only two PMHS were tested, the biomechanical responses collected through the belt pull test can be used to validate the computational human body model for further investigation on the submarining phenomenon.

## INTRODUCTION

Submarining is one of the major concerns in restraint system design. Lamielle et al. (2006) showed grown relative importance of abdominal injury due to the greater reduction in severe or fatal injuries in head and thorax than in the abdominal region. Poplin et al. (2014) showed that increased speed and the resulting crash delta V increases risk of AIS 2+ injuries to the hollow organs of the abdomen and suggested that direct loading from lap belts into lower abdomen seems to be one of the mechanisms of the abdominal injuries. Adomeit and Hegar (1975) pointed out that the occurrence of submarining harmfult to an occupant during a vehicular crash not only because the belt directly loads the abdominal region but also it can increase the risk of the thoracic injury and the lower extremity injury due to greater pelvic motion and loading the lower torso by shoulder belt due to reclined posture of an occupant, respectivley.

Abdominal characterization tests have been performed focusing on the abdominal region but initial lap belt to pelvis interaction or the driving posture of PMHS were not given much consideration during those tests (Foster et al., 2006, Lamielle et al., 2008). The subjects were positioned the belt at mid-umbilicus and pulled horizontally by only engaging the abdominal region. While the biomechanical test data collected from these two studies provide rich information to validate the abdominal region, it does not provide information on the initial interaction between the belt and the pelvis.

Uriot et al. (2006) studied the interaction between the lap belt and the pelvic region using a component level belt pull test by rotating the pulling direction. This study characterized the behavior of the pelvic region under lap belt loading conditions, but the belt was initially positioned below the ASIS. Note that Reed et al. (2013) found that out-of-position belt fit, which means wearing the lap belt over the ASIS, was prevalent from their volunteer belt fit study. This suggests the importance of characterizing the lap belt to abdominal and pelvic region interation under out-of-position belt fit.

The finite element human body model has the potential to investigate the submarinig phenominon since the current anthropomorphic test devices showed substantial difference in behavior while interacting with a lap belt under submarining at risk conditions (Uriot et al., 2006, Luet et al., 2012).

In the current study, an abdomonial characterization test using a lap belt was performed with for the average pelvic angle of driving posture. The belt was positioned around and above the ASIS based on the volunteer belt fit study (Reed et al., 2013) The spine was fixed to isolate the chracteristics of the abdominal region from other body regions. Belt force, belt displacement, and belt kinematics in 3-dimensional space were documented to aid computational model validation.

## METHOD

### Specimen and Specimen Preparation

Two female PMHS with similar statures but different weights, a health weight and an obese, were subjected to lap belt loading (Table 1). It was hyphothesized that females has higher risk of submarining due to their lower pelvis height compared to males. In addition to the PMHS, the 50$^{th}$ percentile male Hybrid III dummy was tested for comparison.

**Table 1.**
**PMHS information**

| PMHS No. | 683 | 700 |
|---|---|---|
| Age | 83 | 67 |
| Gender | Female | Female |
| Height (cm) | 168 | 165 |
| Weight (kg) | 68.0 | 84.4 |
| Body Mass Index (BMI) | 24.1 (Normal range) | 31.0 (obese) |
| Spine mount location | Upper spine mount: C6, T2, T6, T8, T10, and T11-12<br>Lower spine mount: L2, L4, and sacrum | Upper: T1, T4, T7, T9, T11, and L1<br>Lower spine mount: L3, L5, sacrum |

All PMHS specimens were screened for Hepatitis A, B, C, and HIV, as well as for pre-existing pathologies with the potential to influence thoracic properties. Pre-test radiographs and CT scans were taken to verify that specimens with acute or healed rib fractures or other pre-existing thoracic trauma were excluded from this study. All test procedures were approved by the University of Virginia cadaver institutional review board.

**Test Rig**

The test rig consisted of seat and seat back to support a subject, which was mounted onto the upper and lower spine mounts, and belt pull system (Figure 1 and Table 2). The design objectives for the test rig were to consider the shape of the abdominal skin of a typical driving situation during the interaction between the lap belt and the skin and to isolate the characteristics of the abdomen and pelvis from spinal motion for model validation purposes. The test fixture had 3 degrees of freedom to accommodate various sizes of subjects and to control belt angles. To prevent a parallel path for the vertical component of the belt force, the seat plate was positioned forward so that it did not support the pelvis. Since the hip joints of the PMHS were compliant in flexion and extension of the thigh, the seat load cell did not experience a substantial amount of vertical force.

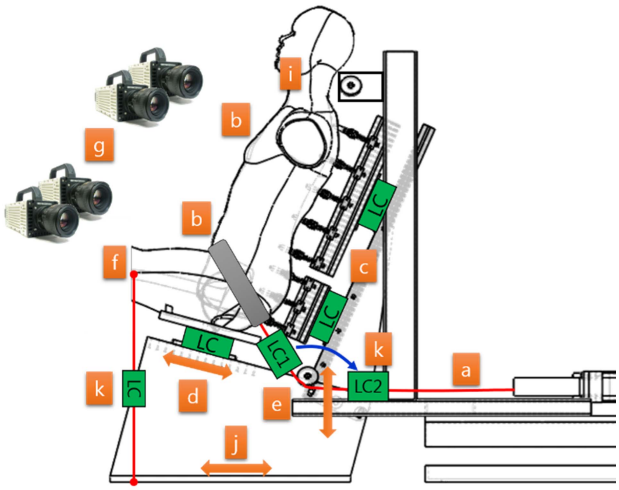


***Figure 1. Schematic of belt pull test rig***

**Table 2.**
**Description of a belt pull test set-up**

| Item | Description |
|---|---|
| a | The belt cables attached to the belt ends were pulled by a pneumatic cylinder. A honeycomb was used to prevent excessive force applied to the PMHS. |
| b | A custom rigidized belt was placed on the abdomen and connected to the steel belt cables (see Custom rigidized belt). |
| c | Almost every other vertebra were mounted onto the upper and lower spine mounts. Six-axis loadcells (Model 2554AJ) were installed between the upper and lower spine mounts and the seat base. (see Spine mount) |
| d | A five-axis load cell was mounted under the seat to measure the reaction forces and moments. |
| e | The height of the anchor was adjusted to control the angle of the belt. The belt cable goes through a pulley to transmit the tensile force from the pneumatic cylinder to the belt. The distance between the left and right pulley was 560 mm. |
| f | The femurs were amputated and constrained to the seat bottom to prevent any upward motion of them. |
| g | Two Aramis optical displacement and strain mapping systems were used to track the 3-dimensional motion of the belt and deformation of the skin. |
| h | A uniaxial loadcell was placed in the cable that connected the femur and the seat base to measure tensile force in the cable. |
| i | Neck support was used to support the head due to the inactivity of the neck muscle. |
| j | The distance between the seat and seat back was adjustable to accommodate different sizes of subjects. |
| k | Belt cable loadcells were installed in the steel belt cable. It was moved from LC1 location fo LC2 location for the PMHS700 and the dummy tests. |

Both ends of the belt was pulled by a pneumatic cylinder at the same speed (Figure 2), and the belt pulling force was measured using uniaxial belt cable loadcells on each end of the belt. Note that the belt cable loadcells were placed right next to the belt ends (LC1 in Figure 1) to exclude inertial and frictional force from pulleys for PMHS683 but it was moved to after the first pulley (LC2 in Figure 1) to resolve an initial slack problem in the belt. The belt pulling force was limited using a force limiting device by placing honeycomb between piston disk and belt pulling disk (Figure 2).

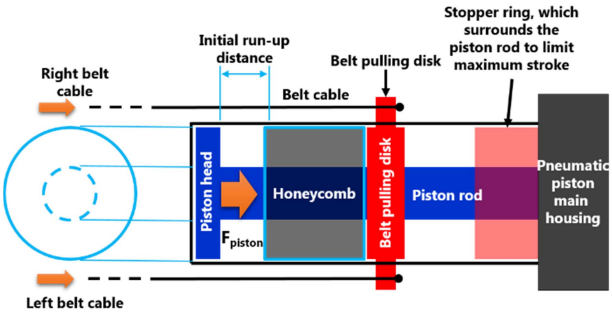


***Figure 2. Load limiting device (top view)***

**Spine mount** The spine mounts (Salzar et al., 2013), which were used for table-top tests, were installed to fix alternating vertebrae to the seat back (Figure 3). The thoracic spines were mounted to the upper spine mount column and the lumbar spine and sacrum, except L1 of PMHS700, were mounted to the lower spine mount column (Figure 1 and Table 2). Each spine mount had two degrees of freedom to adjust the pelvic angle and spine posture of the subject.

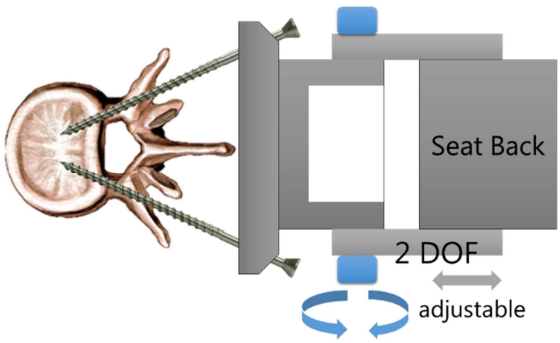


*Figure 3. Spine mount (top view)*

**Custom rigidized belt** The belt used in the current study was made of a polyethylene fiber-reinforced composite (Spectra®, E = 97 GPa) to minimize belt elongation (Salzar et al., 2013). The belt ends were clamped using metal plates and bolts (Figure 4), and steel belt cables were attached to each belt end to trasmit the pulling force from the pneumatic piston. The mass of the belt was tabulated to allow computational modeling of the belt since the inertial effect of the belt during the testing was not compensated in the belt pulling force in the Results section. There was belt slack during the PMHS683 tests due to the weights of the clamps and belt cable loadcell. To resolve this issue, another custom belt was built to lighten the weight, and the belt cable loadcell was moved from right next to the clamps to after the first pulley the belt cable went through.

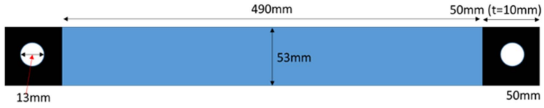


*(a) Belt used for PMHS683*

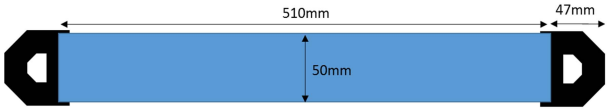


*(b) Belt used for PMHS700 and Dummy*

*Figure 4. Belt geometry*

**Table 3.**
**Mass of belt and belt loadcell**

| Part | Mass [g] | |
|---|---|---|
| | PMHS683 | PMHS700 and Dummy |
| belt | 55 | 38 |
| clamps | 335 | 33 |
| bolts on clamps | 48 | 6 |
| pins for the hole at belt ends | 13 | 13 |
| belt total (exc. loadcell) | 451 | 90 |
| belt loadcells | 83 | 83 |

**Instrumentation**

**Sensor data** The force and moments from loadcells were filtered using CFC180 filter, and the belt displacement and belt 3-dimensional kinematics data was not filtered (Table 4). The belt pulling forces and displacements were not scaled for PMHS responses. Instead, the flesh thickness around the pelvic region was provided (see Flesh Thickness).

**Table 4.**
**List of measurement for belt pull test**

| Measurement | Description | Filter |
|---|---|---|
| Belt force | belt cable loadcell (not inertially compensated for the mass of the belt, belt cable, and belt cable loadcells) | CFC180 |
| Belt displacement | laser displacement sensor and video analysis | None |
| Reaction force and moment | 6-axis spine mount loadcell | CFC180 |

**Belt kinematics and skin deformation** The Aramis optical displacement and strain mapping system (Aramis v6.2, GOM) was used to determine detailed kinematics of the belt, thorax, and abdomen of the subject during test. Note that the belt kinematics in the Results section was measured at the midline of the belt on the sagittal plane at the ASIS while the initial belt position in the Test matrix section was measured at the upper edge of the belt to follow Reed et al.'s method (2013). Lastly, a high speed x-ray system was used to record relative motion between belt and pelvis in sagittal plane during the lap belt test.

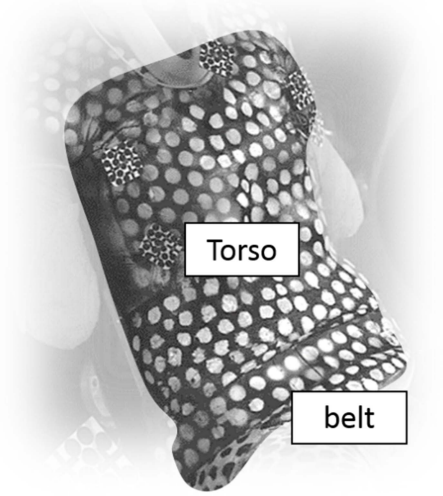


***Figure 5 Pattern on the skin and belt for tracking***

**Test Condition**

**Coordinate Systems** The SAE coordinate system was used to process the test data, and the upper right front corner of the seat was chosen as the origin for the global coordinate system (Figure 6). To obtain the desired belt position and angle, the seat was moved in X-direction and the D-ring and anchors were moved in Z-direction. Note that the positions of the D-ring and the anchors can be adjusted separately. Although the seat was moved during the positioning, the origin was attached to the front right corner of the top surface of the seat during data processing. In this way, only the positions of the anchors and the D-ring needed to be adjusted for the modeling.

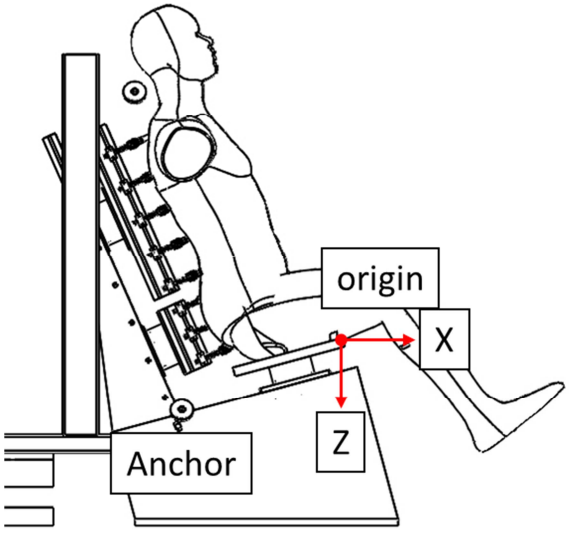


*Figure 6 Global coordinate system and d-ring and anchor locations (origin: right front corner of the top surface of the seat)*

**PMHS and dummy positioning** It was targetted to obtain 44 degrees of pelvic angle from vertical axis and C7 re ASIS X, which is a function of stature and BMI, was targeted to be around 265 mm. It was difficult to obtain the desired ASIS to C7 distance due to the range of adjustability of the spine mount system.

**Table 5.**
**PMHS and dummy position**

| Measurement | | PMHS683 | PMHS700 | Dummy |
|---|---|---|---|---|
| Pelvic angle [deg] | aft of vertical | 44 | 37 | 55 |
| | roll angle | -3 | -5 | 0 |
| ASIS to C7 (fore-aft) [mm] | | 304 | 347 | 285 (Upper and rearmost upper spine) |

**Definition of lap belt position** The belt location was measured following the method used by Reed et al. (2013). The location of the upper edge of the belt was calculated by taking an average of the location of the upper edge at left and right sides of ASIS (anterior superior iliac spine) in the sagittal plane (Figure 7). Note that while Belt Z was within a range of Reed et al.'s volunteer belt fit tests during the belt pull test, Belt X was located more rearward due to the more reclined torso angle during the spine mounting.

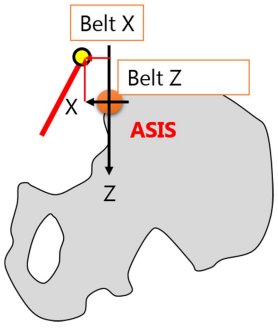


*Figure 7 Belt position measurement*

**Test matrix** Both the PMHS and the Hybrid III dummy were tested using a lap belt only condition by pulling both ends at the same time (Table 6). Although the belt was positioned to a target position based on the location of

ASIS from palpating on the skin during the tests, the calculated belt position, which was obtained by combining CT scan data of pelvis and spine mounts and belt position data from Aramis, were provided in Table 6. The lap belt angle was measured in the sagittal plane (XZ plane) using an inclinometer. Belt position, belt angle, belt force, and initial stroke rate were varied to see the effects of those on the responses of the abdominal area of the PMHS and the dummy. Note that the angles of belt and belt cable were different during PMHS683 tests due to relatively heavy weight of the belt clamps (Table 3) and the position of the belt cable loadcells.

**Table 6**
**Test Matrix for PMHS683 (angle: X to -Z)**

| Test Name | Belt Upper Edge Position w.r.t ASIS (X, Z), Belt and Belt Cable Angles | Load limit (initial loading rate) | run# |
|---|---|---|---|
| PMHS683 | (-8, -25) mm, belt cable: 52 deg, belt: 61 deg | 1 kN (0 m/s) | 3 |
| | (-17, -31) mm, belt cable: 35 deg, belt: 55 deg | 1 kN (0 m/s) | 5 |
| | (-16, -26) mm, belt cable: 44 deg, belt: 59 deg | 3 kN (2 m/s) | 7 |
| PMHS700 | (-12, -53) mm, 45 deg | 1 kN (3 m/s) | 3 |
| | (-16, -55) mm, 45 deg | 3 kN (4 m/s) | 4 |
| | (-46, -66) mm, 45 deg | 1 kN (3 m/s) | 5 |
| | (-35, -69) mm, 45 deg | 3 kN (4 m/s) | 6 |
| HybridIII | (22, -9) mm, 65 deg | 3 kN (4 m/s) | 6 |
| | (22, -7) mm, 65 deg | 1 kN (3 m/s) | 7 |
| | (15, -25) mm, 32 deg | 1 kN (3 m/s) | 8 |
| | (7, -43) mm, 35 deg | 1 kN (3 m/s) | 9 |
| | (7, -43) mm, 35 deg | 3 kN (4 m/s) | 10 |

## RESULTS

### Flesh Thickness

The flesh thickness of the the two PMHS and the dummy was measured on the sagittal plane at ASIS and mid-sagittal plane (Figure 8). The flesh thickness of PMHS683 was 15 mm and 38 mm on the sagittal plane at ASIS and the mid-point of ASIS of the subject, respectively. The flesh thickness of PMHS700 was 40 mm and 70 mm on the sagittal plane at ASIS and the mid-point of ASIS of the subject, respectively. The flesh thickness of the dummy was 25 mm and 63 mm on the sagittal planes at ASIS and at the mid-point of ASIS, respectively. Note that the geometry of the pelvis of the Hybrid III dummy is different from that of the PMHS. It does not have a protruded area at the tip of iliac wings like the PMHS.

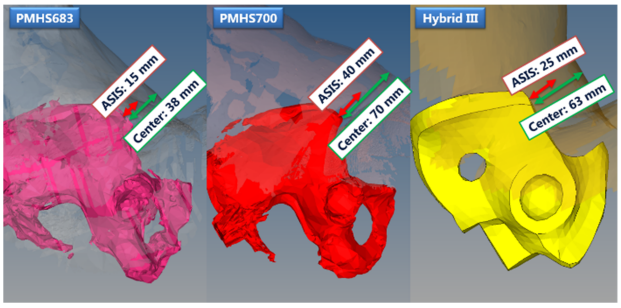


***Figure 8 Flesh thickness around ASIS***

### Belt Kinematics and Belt Force

**PMHS700** The time histories of belt pulling force and displacement and kinematics of the belt midline at ASIS were shown in Figure 9. The belt moved toward the pelvis at the beginning due to the initial belt angle and moved mostly horizontally afterwards. Although a honeycomb was used to limit the belt force, the belt pulling force exceeded the load limit in the beginning of the events as the belt loaded the pelvis through the flesh. Note that all

the honeycombs that were used in the testing were pre-crushed to ensure its limiting load. In the PMHS700-3 test, the belt slid over the iliac crest on the left side but caught near the ASIS on the right side. As the load limit increased and/or initial belt position heightened (Figure 9b-d), the belt completely slid over the pelvis in the end. Interestingly, once the belt completely slid over the iliac crest, the belt intrusion amounts into the abdomen were similar between low and high load limit cases (Figure 9c-d). The belt pulling force subsided after the belt slid over the iliac crest, and the belt stopped due to the limit of the range of motion of the pneumatic cylinder. The lower spine reaction force, which was the resultant force of $F_x$ and $F_z$, showed similar peak forces for the lower load limit cases and lower peak forces for the higher load limit cases with time delays compared to the belt pulling forces.

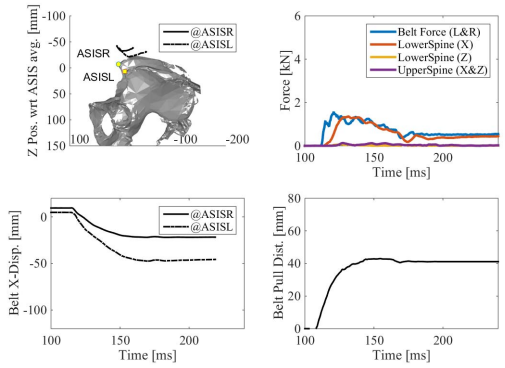


*(a) PMHS700-3 (load limit, 1kN)*

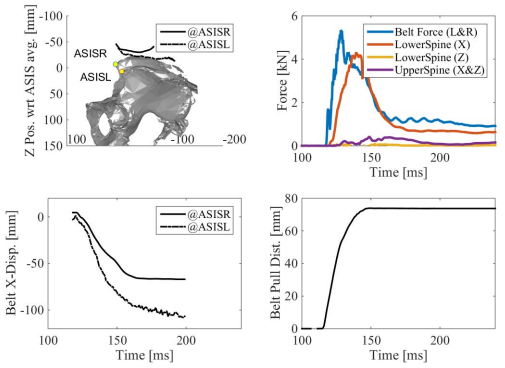


*(b) PMHS700-4 (load limit, 3kN)*

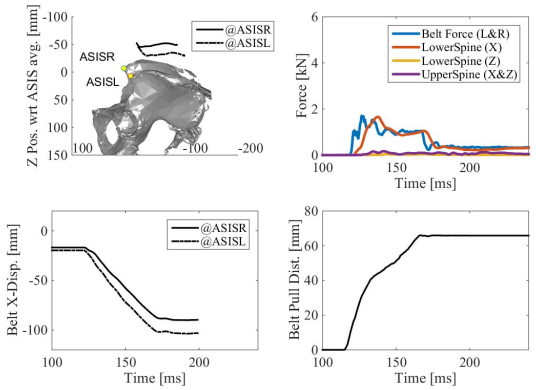


*(c) PMHS700-5 (load limit, 1kN)*

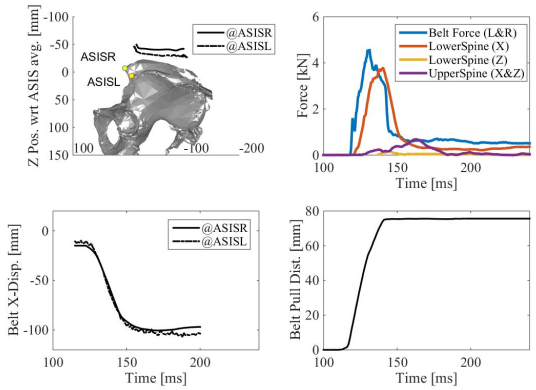


*(d) PMHS700-6 (load limit, 3kN)*

***Figure 9. Belt pulling displacement and force time histories (PMHS700)***

**PMHS683** Although the slack of the belt made the responses of the PMHS683 less desirable to use for model validation, the PMHS683 test provided belt kinematics both sliding over the pelvis (Figure 10a-b) and staying at the ASIS (Figure 10c). The belt showed downward motion when the belt stayed in front of the ASIS, and the maximum belt pulling distance was similar for the lower load limit (Figure 10a) and the higher load limit cases (Figure 10b). During the PMHS683-5 test, the belt moved toward the pelvis initially and slid over the pelvis in the end showing large amount of belt intrusion toward the abdomen (Figure 10c). The belt pulling force subsided to almost zero after the pneumatic piston reached its limit of range of motion. The belt was completely over the ASIS during the PMHS683-1 test (Figure 10d). The belt initially penetrated the abdomen due to 10 N of preload. With 1 kN of load limit, the belt intruded toward the abdomen more than 50 mm.

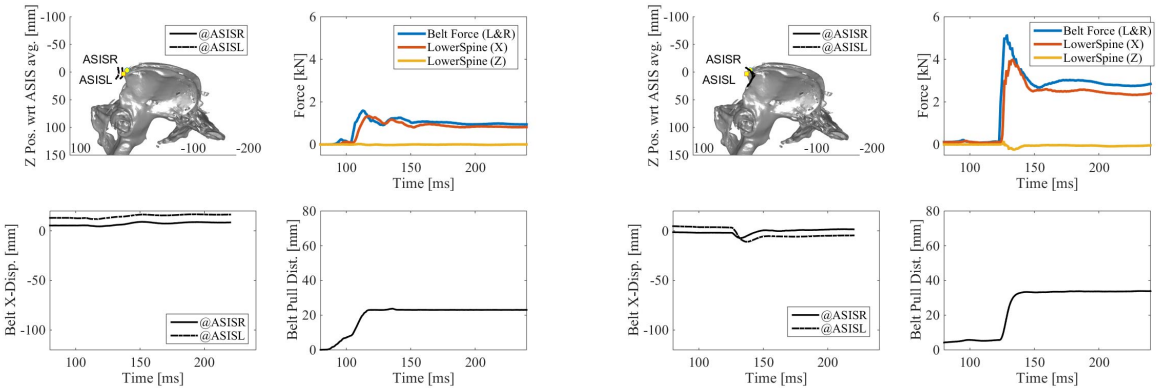


*(a) PMHS683-3 (load limit, 1kN)* *(b) PMHS683-7 (load limit, 3kN)*

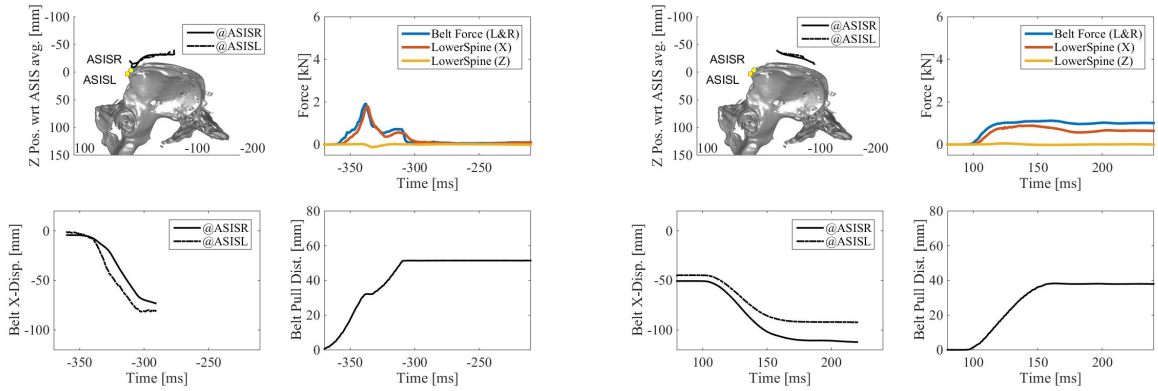


*(c)PMHS683-5 (load limit, 1kN)* *(d) PMHS683-1 (load limit, 1kN)*

***Figure 10. Belt pulling displacement and force time histories (PMHS683)***

**High speed X-ray** The high speed x-ray was used during the PMHS683 tests (Figure 11). The x-ray images confirmed that the belt stayed in front of the pelvis during the PMHS683-3 and PMHS683-7 tests and it slid over the pelvis during PMHS683-5 tests. It was difficult to see the ASIS due to the over exposure around ASIS from the high speed x-ray images.

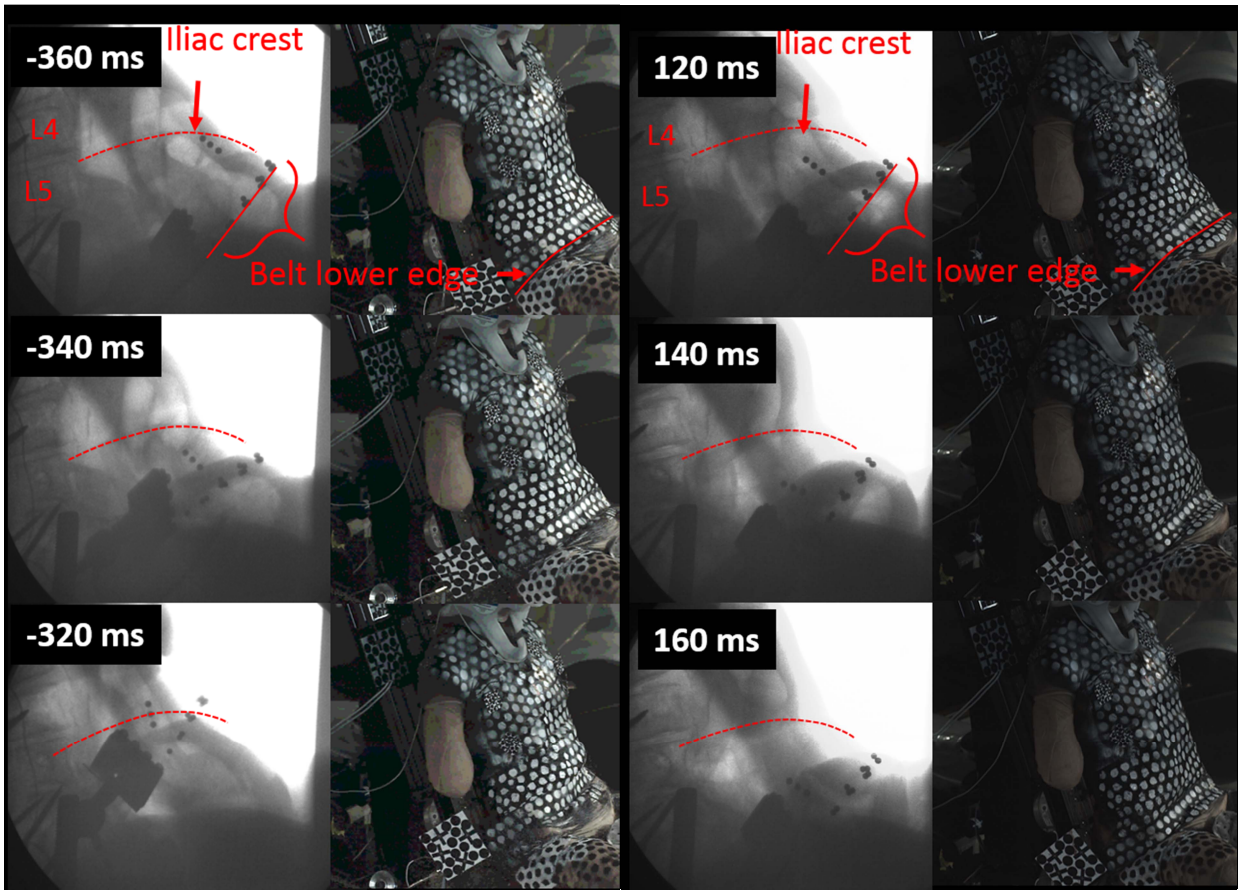


*(a) PMHS683-5* *(b) PMHS683-7*

***Figure 11 Snapshot of high speed x-ray***

**Hybrid III** The belt did not completely slide over the pelvis during either HybridIII-9 (Figure 12a) or HybridIII-10 (Figure 12b) tests but the belt did show slight upward motion during the HybridIII-10 test. The dummy showed less belt intrusion (Figure 12b) toward the abdomen compared to both PMHS700-4 (Figure 9b) and PMHS683-5 (Figure 10c). Note that PMHS683-5 was tested with the 1kN of load limit while HybridIII-10 was tested with the 3 kN of load limit. The HybridIII-8 test (Figure 12c) showed lower peak belt pulling displacement than that of PMHS683-3 but this difference may come from the initial belt slack during the PMHS683-3 test. The HybridIII-6 test (Figure 12d) showed similar peak belt pulling displacement as that of PMHS683-7 (Figure 10b).

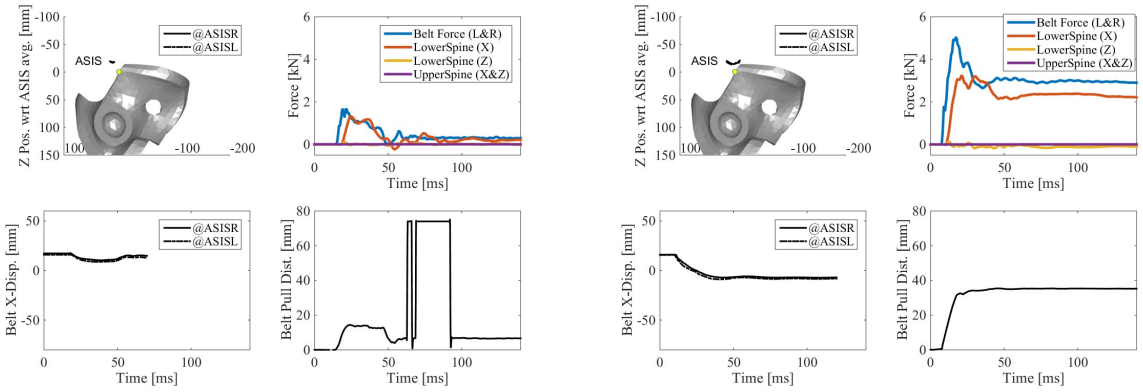


*(a) HybridIII-9 (load limit, 1kN) (b) HybridIII-10 (load limit, 3kN)*

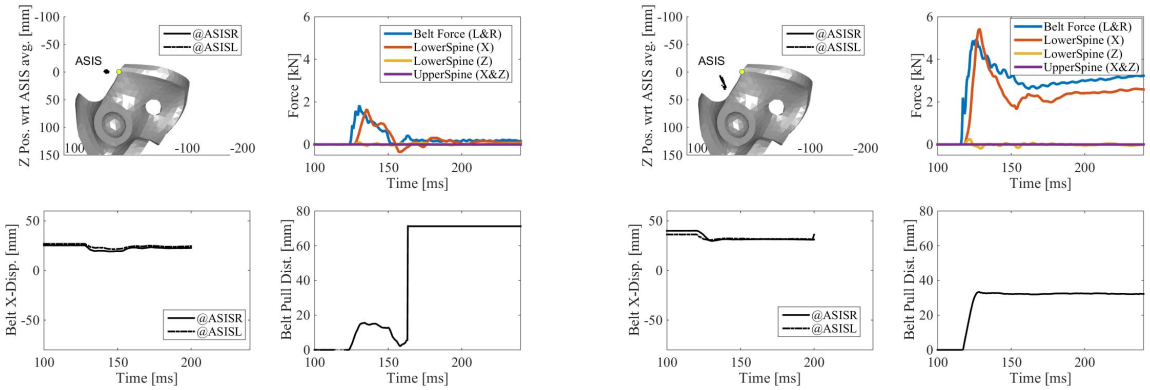


*(a) HybridIII-8 (load limit, 1kN) (b) HybridIII-6 (load limit, 3kN)*

***Figure 12. Belt pulling displacement and force time histories (Hybrid III)***

**Injury Summary**

Neither PMHS showed any signs of abdominal injury. PMHS683 showed a right iliac wing fracture and initially had a healed right iliac wing fracture. It seems that the right iliac wing of PMHS683 was not completely healed prior to death.

## DISCUSSION

A new test rig to investigate subject to lap belt interaction was developed in the current study. To measure the belt kinematics, 3-dimensional motion tracking was used and provided useful information for understanding belt kinematics when the belt slid over the pelvis and for future computational model validation. Through the testing, the weight of the custom belt was reduced and the location of the belt cable loadcell was changed to resolve the belt initial slack issue. There was no initial slack issue with the older design of the custom belt on the table-top configuration, which was tested on subjects in a supine posture, but there was a problem in a seated posture.

An obese (PMHS700) and a normal weight (PMHS683) PMHS were tested in a seated posture under lap belt loading conditions to chracterize abdominal region. The belt was positioned near the ASIS and either slid over the pelvis or stayed in front of ASIS. With the aid of 3-dimensional motion tracking, the belt kinematics was well documented for validation of a computational human body model. Due to the belt slack issue in the PMHS683 tests, it was decided to use PMHS700 test results for human body model validation. Although there was a belt slack problem during the PMHS683 tests, the high speed x-ray images taken during the test confirmed that the belt kinematics measured using the Aramis system was reasonable.

For the cases that the belt slid over the pelvis, the belt force peaked in the beginning of the events while the belt was compressing the pelvis, and subsided while the belt slid over the pelvis. The reaction force from the spine mount

loadcells showed time delay, which indicates the inertial forces from the soft tissue and/or pelvis (Figure 10 and Figure 12). The PMHS700 showed larger time delays in lower spine reaction forces compared to the belt pulling forces than those of the PMHS683, and it may have stemmed from the heavier soft tissue of the PMHS700 (obese) than that of the PMHS683 (normal weight) (Table 1). It should be noted that the spine mounts that were holding the lumbar spine and pelvis showed the downward motion about 10 mm during the PMHS700-4 test (Figure 9b) from 132 ms to 145 ms, but it was after the lower spine reaction force reached 3.5 kN.

For the cases that the belt stayed on the pelvis, the belt showed little motion in X direction while showing about 20 mm of downward motion for 1 kN of load limit (Figure 10a and 30 mm of downward motion for 3 kN of load limit (Figure 10b). Although the high speed x-ray images provided qualitative information about the belt kinematics, it showed that the belt was at almost the same locations with respect to ASIS to that of the initial location at the end of the event. Therefore, the downward motion observed from the Aramis system was due to the pelvic rotation in Y direction rather than the belt sliding downward relative to ASIS (Figure 10a and b).

PMHS683-5 had 9 mm more rearward and 6 mm higher initial belt position than that of PMHS683-3 (Table 6). The 11 mm of difference in initial belt position drastically changed the test outcome (Figure 10a and c).

For model validaiton, the belt displacement time histories can be used as an input condition, and belt pulling force, spine reaction force, and the kinematics of the midline of the belt can be used as an target response. It will be important for a computation model to show the sudden increase of the belt pulling force in the beginning and the decrease of the belt pulling force afterwards with similar belt intrusion toward the abdomen prior to investigation of the submarining phenomenon. In addition, the model should be able to capture the transition between the belt sliding over the pelvis and the belt staying in front of the pelvis, for use in submarining investigation.

Althougth the current study limited due to small number of the PMHS and issues in the test fixture during the PMHS683 tests, it provided detailed information on the belt kinematics during the lap belt to the subject interaction in simulated real world driving conditions. It should be noted that the torso of the PMHS was more reclined (C7 was located about 50 to 65 mm rearward than that of the normal driving posture).

**ACKNOWLEDGEMENTS**

The author would like to acknowledge and thank the Hyundai Motor Group for funding this research and providing valuable participation, review and feedback throughout the process. The opinions, findings, and conclusions expressed in this manuscript are those of the authors and do not necessarily reflect the views of the Hyundai Motor Group. Additionally, the author would like to acknowledge Rob Salzar, Dennis Roethlisberger and Sara Heltzel for helping the test, Joey White for manufacturing the test rig, and Tim Gillispie for the proofread.

**REFERENCES**

ADOMEIT, D. & HEGAR, A. 1975. Motion Sequence Criteria and Design Proposals for Restraint Devices in Order to Avoid Unfavorable Biomechanic Conditions and Submarining. *SAE Technical Paper 751146.* SAE International.

FOSTER, C. D., HARDY, W. N., YANG, K. H., KING, A. I. & HASHIMOTO, S. 2006. High-speed seatbelt pretensioner loading of the abdomen. *Stapp car crash journal,* 50**,** 27-51.

LAMIELLE, S., CUNY, S., FORET-BRUNO, J., PETIT, P., VEZIN, P., VERRIEST, J. & GUILLEMOT, H. 2006. Abdominal injury patterns in real frontal crashes: influence of crash conditions, occupant seat and restraint systems. *Annual proceedings / Association for the Advancement of Automotive Medicine. Association for the Advancement of Automotive Medicine,* 50**,** 109-24.

LAMIELLE, S., VEZIN, P., VERRIEST, J.-P., PETIT, P., TROSSEILLE, X. & VALLANCIEN, G. 2008. 3D deformation and dynamics of the human cadaver abdomen under seatbelt loading. *Stapp car crash journal,* 52**,** 267-94.

LUET, C., TROSSEILLE, X., DRAZETIC, P., POTIER, P. & VALLANCIEN, G. 2012. Kinematics and dynamics of the pelvis in the process of submarining using PMHS sled tests. *Stapp car crash journal,* 56**,** 411-42.

POPLIN, G. S., MCMURRY, T. L., FORMAN, J. L., HARTKA, T., PARK, G., SHAW, G., SHIN, J., KIM, H. J. & CRANDALL, J. 2015. Nature and etiology of hollow-organ abdominal injuries in frontal crahses. *Accident Analysis & Prevention,* (in press).

REED, M. P., EBERT, S. M. & HALLMAN, J. J. 2013. Effects of driver characteristics on seat belt fit. *Stapp car crash journal,* 57**,** 43-57.

SALZAR, R., LAU, S., LESSLEY, D., SOCHOR, M., SHAW, C., KENT, R. & CRANDALL, J. 2013. Thoracic response to shoulder belt loading: comparison of tabletop and frontal sled tests with PMHS. *Traffic Inj Prev. ,* 14**,** 159-67.

URIOT, J., BAUDRIT, P., POTIER, P., TROSSEILLE, X., PETIT, P., GUILLEMOT, H., GUERIN, L. & VALLANCIEN, G. 2006. Investigations on the belt-to-pelvis interaction in case of submarining. *Stapp car crash journal,* 50**,** 53-73.

# Rib length variation with age and sex - Measurements from high-resolution low-radiation X-ray images of volunteer subjects

**Damien, Subit**
Arts et Métiers ParisTech, LBM/Institut de Biomécanique Humaine Georges Charpak, 151 bd de l'Hôpital 75013 Paris
France

University of Virginia, Center for Applied Biomechanics, 4040 Lewis and Clark dr, Charlotesville VA 22902 USA

**Baptiste, Sandoz**
**Julie, Choisne**
**Célia, Amabile**
**Claudio, Vergari**
**Wafa, Skalli**
**Sébastien, Laporte**
Arts et Métiers ParisTech, LBM/Institut de Biomécanique Humaine Georges Charpak, 151 bd de l'Hôpital 75013 Paris
France

Paper Number 15-0313

## ABSTRACT

*Research Question*: Human surrogates such as anthropomorphic test devices and computational models are common tools used by the automotive industry to characterize injury mechanisms and design countermeasures. The surrogates currently available were designed to be representative of certain sex and percentile of the population, such as the 5$^{th}$- and 50$^{th}$-percentile females, and the 50$^{th}$- and 95$^{th}$-percentile males. Great improvements were achieved in crash protection thanks to these models, but there is a need for more refined models that take into account a greater variation of the human diversity, such as the geometric variation due to aging. Therefore, the objective of this study was to determine how the length of ribs varies with age and sex.
*Methods and Data Sources:* A total of 103 asymptomatic volunteer subjects aged 0 to 84 years old were included in the study. First, each volunteer was imaged either with a standard clinical CT-scan, or in a standing position with the EOS imaging system, a low-radiation X-ray system that acquired one frontal and one sagittal high resolution images of the ribcage. Second, a custom-made software toolbox was used to create a subject-specific geometrical 3D model of each subject bony ribcage by registration of a statistical parametric ribcage model. Third, the rib length and mean thoracic index were extracted from the 3D ribcage models.
*Results:* The two main results were that the thoracic index (depth to width ratio of the thorax) was found to be fairly age-independent, and that the ribs length increased linearly with age between 0 and 20 years old before reaching a plateau. The growth rate of the ribs increased between each rib level from rib 1 (4 mm/year) to rib 10 (10.5 mm/year). This indicates a change in the size and shape of the ribcage during growth.
*Conclusion and relevance:* The study provides a quantitative characterization of age and sex-induced variation in the ribcage geometry, based on asymptomatic adult volunteer data. This study addresses the need for the geometric data required to build a set of computational models that represent male and female subjects of various age.

## INTRODUCTION

A significant research effort has been undertaken in the last four decades to document motor vehicle crashes (MVC) such as vehicle speed, types of occupants, and injury outcomes, and develop typical scenarios for frontal, lateral and oblique impacts. In parallel, models of the human body were developed to estimate the severity of an impact, by determining the mechanical response and strength of the human body during a crash to describe the mechanisms of injury as well as the injury thresholds. Physical and computational human body models, or human surrogates, are used to achieve this goal. The surrogates currently available were designed to be representative of certain sex and percentile of the population, such as the 5$^{th}$- and 50$^{th}$-percentile females, and the 50$^{th}$- and 95$^{th}$-percentile males. Great improvements were achieved in crash protection thanks to these models, but there is a need for more refined models that take into account a greater variation of the human diversity, such as the geometric variation due to

aging, to create human surrogates that represent a larger spectrum of the population. In that effort, the ribcage is of particular interest: older drivers are more likely to die of a chest injury and less likely to die from a head injury compared to the youngest group (Morris et al., 2003). This is a direct consequence of the high rate of seat belt used in this population: in frontal crash, seat belts are designed to load the thorax to limit the forward excursion of the body and, in combination with airbags, prevent the impact of the head and thorax with the vehicle interior structures. However, determining the maximum load that can be safely applied to the thorax without fracturing ribs and how it varies with age has yet to be done. There is a need for geometric and morphologic data to develop a ribcage model that include age-dependent features. Several dataset are available in the published literature and provide valuable information about the age-related changes in the adult (Gayzik et al; 2008) and pediatric ribcage (Holcombe et al, 2013), however they all rely on computed tomography images obtained during routine trauma medical exams. Although, these studies included only subjects that were free of skeletal pathology, CT analysis obtained from hospital databases suffer two important limitations: the subjects are lying on the CT bed, and the resolution of the X-ray images is limited to minimize exposure for the subject for health concerns. Therefore, the goal of the present study was to measure the variations in the length of the ribs as a function of age and sex, based on high-resolution low-dose X-ray images obtained with the EOS system. The EOS system has been developed and used for several years now (Dubousset et al, 2010) to perform follow-up for spine deformity treatments for patients with scoliosis through the creation of subject-specific models of the spine (Humbert et al, 2009). The present study is the first step towards the description of age- and sex-induced variations in the ribcage geometry, and focused on the variation in the rib lengths for a wide range of age.

## MATERIALS AND METHDODS

This study uses pediatric data from the literature (Sandoz et al, 2013), and new data for the adult population obtained with the EOS system.

### The EOS imaging system

The EOS system is a system approved worldwide for clinical exam. Its main feature is to be a low-dose X-ray imaging system that allows the acquisition of the geometry of the musculoskeletal structure of volunteer subjects in a weight-bearing posture from two ‘head-to-toe’ X-ray images (Dubousset et al, 2010)(Figure 1). Furthermore, these images are high resolution (0.2 mm/pixel) compared to standard CT images of living patients (typically 2 to 5 mm/pixels). Several statistical models were developed to create subject geometry from the biplanar images obtained with EOS, in particular the spine (Humbert et al, 2009), and the ribcage (Aubert et al, 2014). The subject-specific geometry are created by registering a statistical parametric model of the spine and of the ribcage on the frontal and sagittal images obtained with EOS.

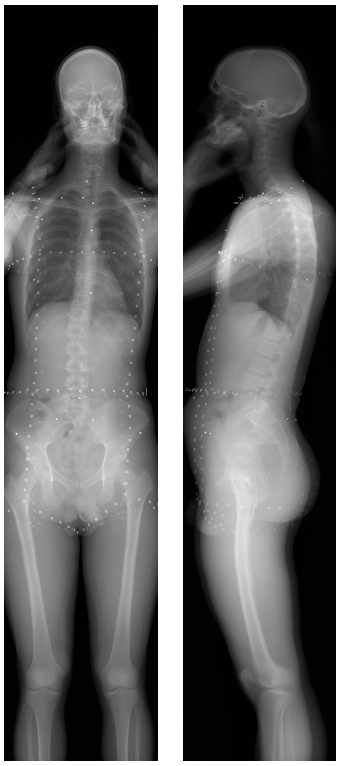

***Figure 1.Frontal and sagittal views obtained with EOS and used to create subject-specific spine and ribcage.***

**Adult morphological data**

Fifty five asymptomatic adult volunteers were included in this study (36 men, 19 women), aged 20 to 84 years (mean 38), with a body mass index ranging from 15.4 to 29.5 kg/m² (average: 22.9). Participants were confirmed to be free of spine pathologies or instrumentation anywhere in the upper body. Each participant completed and signed an informed consent form approved by the ethical committee at Hôpital Pitié Salpêtrière (Paris, France) (CPP 6001 and CPP 6036 Ile-de-France VI). The acquisition of the X-ray images took about 20 seconds. No specific instructions about breathing were given to the volunteers.

For each volunteer, a subject-specific geometric model was created: this model included the spine and the ribs 1 to 10. The length of each rib was calculated based on the method described in Aubert et al (2014): the rib length was defined as the length of the centroidal line from the costo-vertebral joint to the costo-chondral junction.

The rib cage morphometry was also described by the mean thorax index that is defined as the mean value of the thorax lateral width to thorax anteroposterior depth ratio calculated for eight horizontal slices equally distributed between the $2^{nd}$ and the $12^{th}$ thoracic vertebrae.

**Pediatric morphological data**

The pediatric data consisted of 960 ribs reconstructed from CT images from 48 children aged 4 months to 15 years (22 girls, 26 boys) (Sandoz et al., 2013). The pediatric data were organized in 16 age groups (less than 1 year-old, 1 year old, 2 years old, …, and 15 years old), and male and female data were combined in a single data set. Similar to the procedure used with the EOS images, the rib length was defined for ribs 1 to 10 as the length of the centroidal line from the costo-vertebral joint to the costo-chondral junction.

**RESULTS**

**Rib lengths**

The rib lengths were plotted for each rib level from 1 to 10. The data for the age 0 to 15 years old combine both sex, while the new data generated in this study separates male and female (figures 2 and 3).

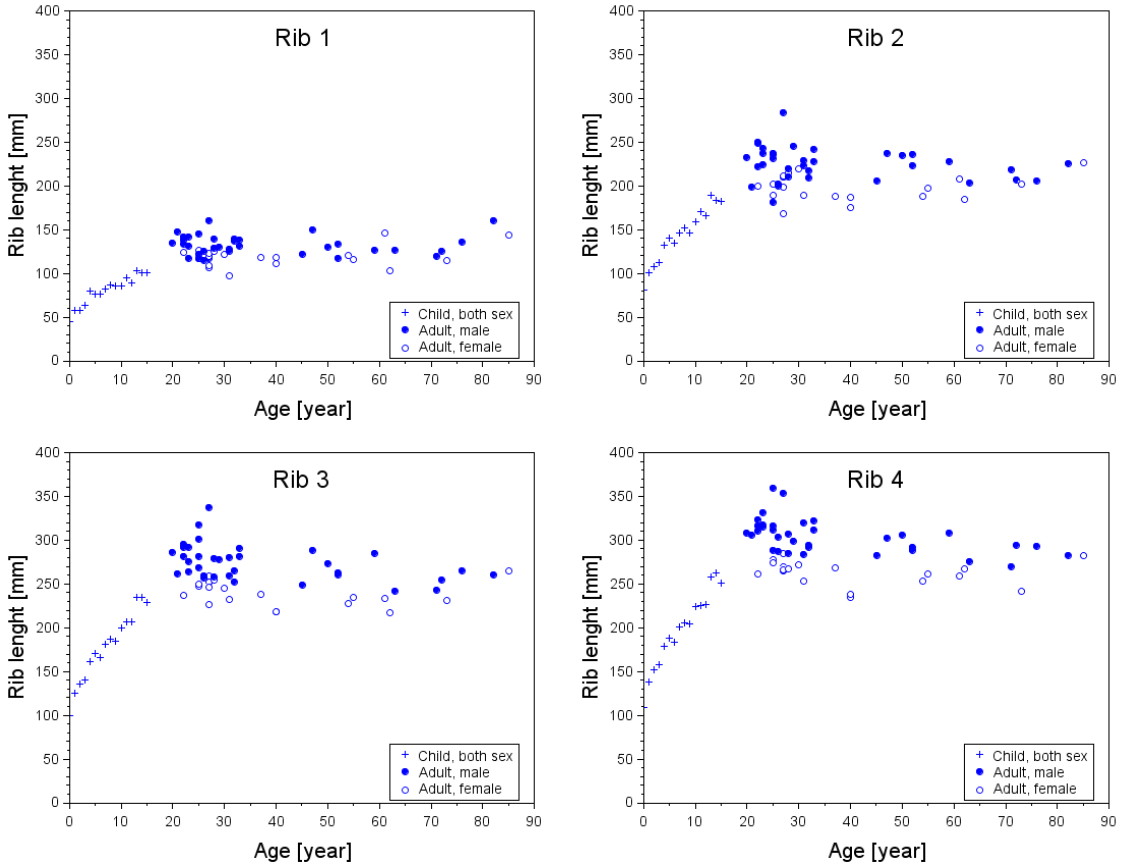


***Figure 2. Rib lengths from 0 to 84 years old (ribs 1 to 4).***

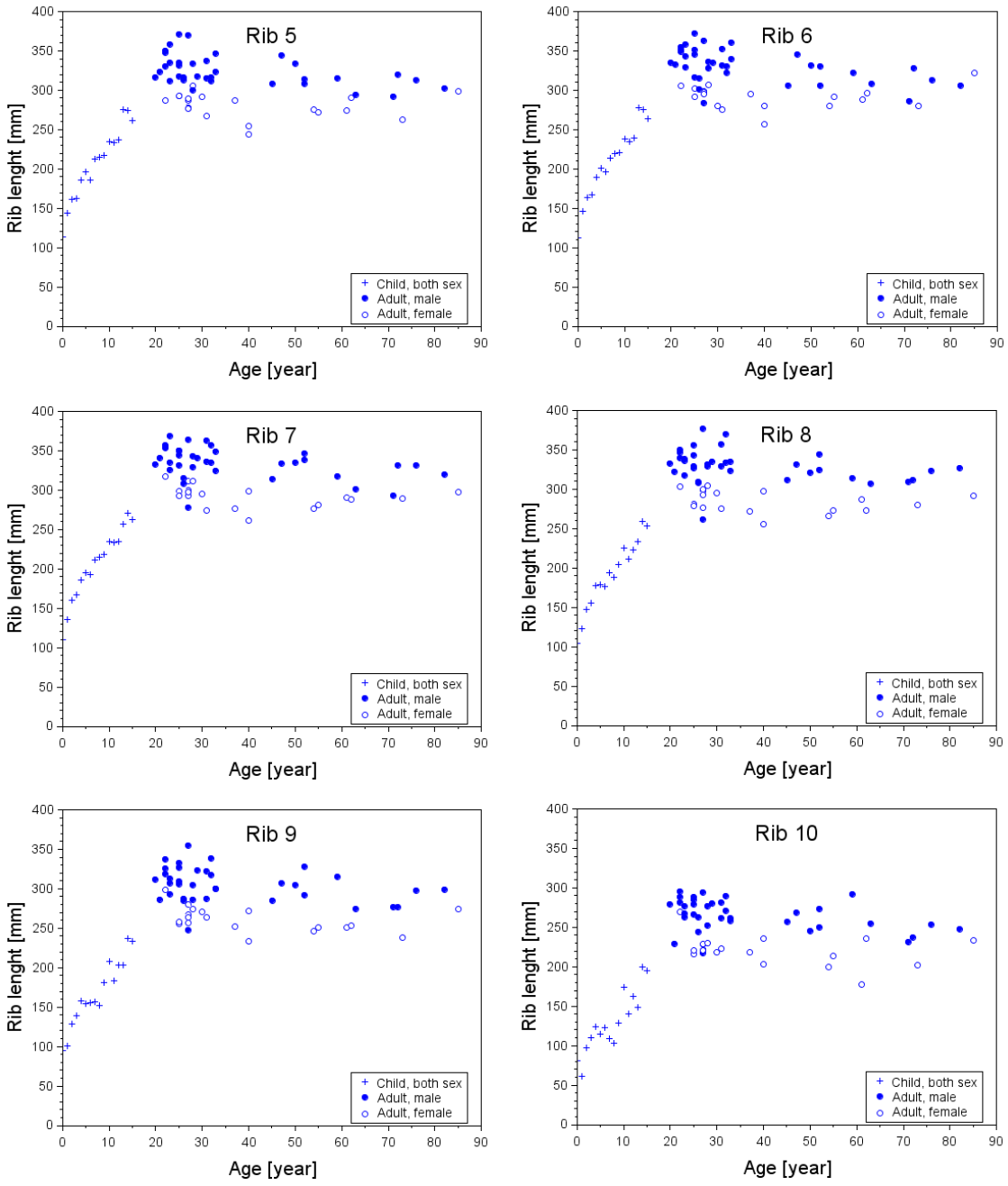


***Figure 3. Rib lengths from 0 to 84 years old (ribs 5 to 10).***

**Mean thoracic index**

The mean thoracic index was calculated for the male and female adult subjects (figure 4).

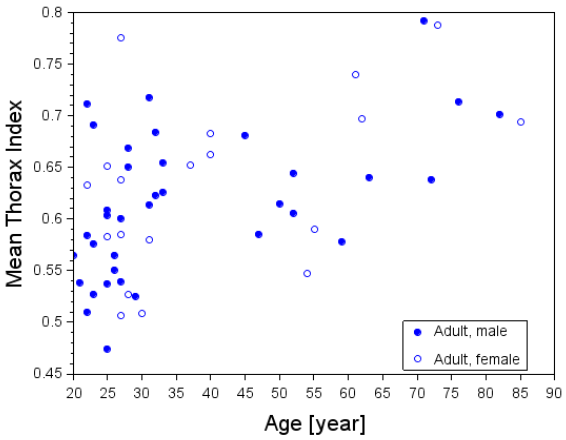


***Figure 4. Mean thoracic index.***

## DISCUSSION

### Effect of age

Both the rib length and mean thoracic index were found to vary with age. The rib length increased linearly with age between 0 and 20 years old before reaching a plateau; this trend was common to all rib levels. The growth rate of the ribs before age 20 increased between each rib level from rib 1 (4 mm/year) to rib 10 (10.5 mm/year). This indicates a change in the size and shape of the ribcage during growth. After 20 years of age, the rib length was nearly independent of age. One could have expected the rib to lengthen with age because of the calcification of the costal cartilage, but this trend was not obvious from the data presented in this study. As for the mean thoracic index, it was found to increase with age, indicating that the thorax widens to become 'rounder", which is consistent with the results from other study based on CT images (Kent et al, 2005; Weaver et al, 2014). The data provided in Sandoz et al (2013) for the range 0 to 15 years old are averaged (3 subjects in each 1-year age group), while the adult data was not.

### Effect of sex

The female ribs were found to be on average per rib level 10 to 17 % shorter than the male's ribs (figure 5). Conversely, the mean thoracic index was found to be rather insensitive to sex, which suggests that the female ribcage is similar is shape to the male ribcage, but potentially smaller. However, the orientation of the ribs was not reported in this study, although it could be a factor in the overall size and shape of the ribcage.

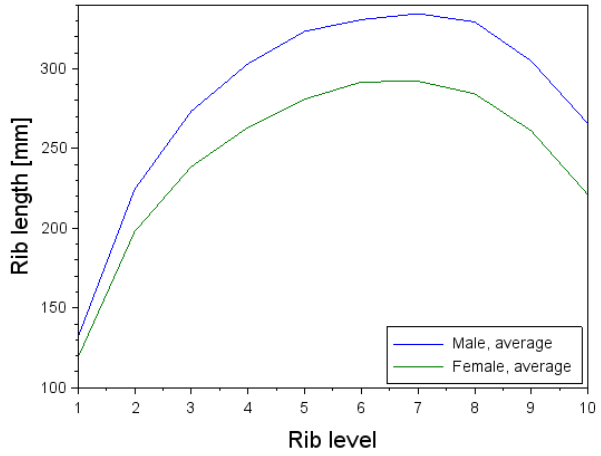


***Figure 5. Mean rib length for male and female volunteers.***

## LIMITATIONS

The analysis presented in this paper is based upon a transversal study, and therefore the inter-individual differences may contribute to the differences that are attributed to age. Furthermore, the data set is biased towards the young adults age group (20 to 35 years of age), and the male subjects.

## CONCLUSIONS

The study presented in this manuscript relies on a unique imaging system that can be used to image asymptomatic volunteer subjects with no pathology. In addition, subjects can be imaged in a standing or sitting position. The results presented in this paper focused on the variation of rib length with age and sex, for a relatively small data set. This manuscript provides a first set of results. The analysis is on-going to further established the morphological differences between male and female subjects, as a function of age, to elucidate the link between the geometry of the ribcage and the risk of injury during a motor vehicle crash.

## ACKNOWLEDGEMENT

The authors thank the Banque Public d'Investissement for financial support through the French Fonds unique interministériel program (FUI14, project dexEOS), and the ParisTech BiomecAM chair program on subject-specific musculoskeletal modelling, and in particular COVEA and Société Générale. D. Subit thanks the European Union for financial support through the Marie Curie International Incoming Fellowship (FP7-PEOPLE-2013-IIF, project BioAge # 622905). The views expressed in this article are those of the authors and do not necessarily represent the views of the funding bodies.

## REFERENCES

Aubert, B, Vergari, C, Ilharreborde, B, Courvoisier, A, Skalli, W. 2014. "3D reconstruction of rib cage geometry from biplanar radiographs using a statistical parametric model approach", Computer Methods in Biomechanics and Biomedical Engineering: Imaging & Visualization, in press.

Dubousset, J, Charpak, G, Skalli, W, Deguise, J, Kalifa, G. 2010. "EOS: a new imaging system with low dose radiation in standing position for spine and bone & joint disorders", Journal of Musculoskeletal Research, 13(1):1-12.

Gayzik F, Yin M, Danelson K, Slice D, Stitzel J. 2008. "Quantification of age-related shape change of the human rib cage through geometric morphometrics", Journal of Biomechanics, 41:1545–1554.

Holcombe S, Kindig M, Zhang P, Parenteau C, Rabban P, Hully L, Wang S. 2013. "Age-based predictive model of the pediatric ribcage", International Journal of Automotive Engineering 5:15-22.

Humbert, L, De Guise, JA, Aubert, B, Godbout, B, Skalli, W. 2009. "3D reconstruction of the spine from biplanar X-rays using parametric models based on transversal and longitudinal inferences", Medical Engineering & Physics, 31(6):681-687.

Kent R, Lee S, Darvish K, Wang S, Poster C, Lange A, Brede C, Lange D, Matsuoka F. 2005. "Structural and material changes in the aging thorax and their role in crash protection for older occupants", Stapp Car Crash Journal 49: 231-249.

Morris A, Welsh R, Hassan A (2003). Requirements for the crash protection of older vehicle passengers. Annual Proceedings of Association for the Advancement of Automotive Medicine (AAAM), 47:165-80.

Sandoz, B, Badina, A, Laporte, S, Lambot, K, Mitton, D, Skalli, W. 2013. "Quantitative geometric analysis of rib, costal cartilage and sternum from childhood to teenagehood", Med Biol Eng Comput.,51(9):971-9.

Weaver, A, Schoell, S, Stitzel, J. 2014. Morphometric analysis of variation in the ribs with age and sex, J Anat;225(2):246-61.

# THE ENHANCED U.S. NCAP: FIVE YEARS LATER

**Brian T. Park**
**Taryn E. Rockwell**
National Highway Traffic Safety Administration
United States of America

**Lauren A. Collins**
**Christina S. Smith**
**Mai Lan Aram**
Alpha Technology Associate, Inc.
United States of America

Paper Number 15-0314

## ABSTRACT

The U.S. New Car Assessment Program (NCAP) encourages vehicle manufacturers to make safety improvements to their vehicles through its award-winning consumer information-based 5-Star Safety Ratings Program. Occupant injury readings have decreased and star ratings have generally improved since the program was enhanced in the 2011 Model Year (MY). This paper summarizes vehicle crash test results for the five MYs since the program was last upgraded to demonstrate how quickly vehicles have been redesigned to achieve high ratings under the more stringent requirements. As a result, most vehicles are achieving 4- or 5-star ratings. Though there are still vehicles the agency has tested that do not achieve the highest ratings, the performance of the majority of vehicles tested under the enhanced program is excellent. This sets the stage for the agency to begin exploring the possibility of making additional changes to the current program to spur even further vehicle safety improvements through market forces and consumer demand. The NCAP's crash test data (specifically, occupant injury data) and star ratings derived from those data will be used throughout this study. Occupant performance from the first year of the enhanced program will be compared to more recent results. A comparative analysis of paired data for vehicles that have been tested and retested under the enhanced NCAP will also be shown. These analyses will serve to demonstrate the effectiveness of the program in encouraging vehicle manufacturers to make immediate design changes that improve the occupant protection afforded by their vehicles.

## LIMITATIONS OF THIS STUDY

The crash test data included in this study spans MYs 2011 to 2015; however, MY 2015 data is limited as testing was not completed in time for all results to be included in this publication. Also, the study is limited by the vehicles the NCAP selected each MY for testing. Though these tests encompass results from over 85% of the vehicles (by projected sales volume) in the U.S. fleet each MY they do not represent the composition of the entire fleet (NHTSA 2013d). Therefore, the authors do not make any further projections about overall fleet safety. Furthermore, this study also does not include an analysis of how the probabilities of injury risk measured in NCAP tests relate to the reduction of real-world injuries and fatalities.

## HISTORY OF THE U.S. NCAP

The National Highway Traffic Safety Administration (NHTSA) established the NCAP in 1978 in response to Title II of the Motor Vehicle Information and Cost Savings Act of 1972. At the time, the agency only assessed vehicles for their occupant protection in frontal impacts. Though stars were not used at the time, it has been estimated that less than 30% of those tested vehicles would have been able to achieve the highest possible ratings (4 or 5 stars) for the driver (2008a). After several years and the addition of a side moving deformable barrier (MDB) impact crash test for MY 1997 vehicles, and a rollover resistance test in MY 2001, the NCAP began soliciting comments for a program overhaul in 2007 (2007a). The agency began testing and rating vehicles under an enhanced program (NHTSA 2008a) in 2010 beginning with MY 2011 vehicles. Under the enhanced program, the agency continues to conduct a 35 mph (56 km/h) vehicle frontal impact rigid barrier test and a 38.5 mph (62 km/h) MDB side impact vehicle test, but now uses newer side-impact test dummies compared to the previous program. The enhanced program now also includes a 20 mph (32 km/h) vehicle side impact pole test. For each test type, injury data from each occupant is

collected from different body regions and is incorporated into a single combined probability of injury. An occupant's combined probability of injury is divided by a baseline risk of injury and the resulting relative risk score, or RRS, is converted to a star rating for that occupant. The results of all three crash tests are then merged with the results from a rollover resistance test, which remained unchanged from the previous version of the program, in order to provide consumers with a single, combined vehicle rating known as the Overall Vehicle Score (OVS) (NHTSA 2008a).

The agency examined the performance of vehicles tested soon after the enhanced program was initially launched and was encouraged that those results showed lower levels of injury when compared to the performance of vehicles tested under the previous version of the program (Park 2011). After five MYs, the agency believes that sufficient data has been collected to adequately assess occupant performance in modern vehicles under the NCAP. This paper will present the results of this analysis.

Since the rollover resistance test remained the same under the enhanced program and this paper focuses only on crashworthiness results, the authors will not explore the results of that testing mode over the past five MYs. Likewise, since rollover results are needed to calculate the OVS, this paper will not discuss how that particular metric has changed. Each section below will briefly describe the test setup and protocol for each crash test mode before describing the results of the study. If desired, additional procedural details can be obtained from the individual test protocols (NHTSA 2013a, b, and c), and more detailed information pertaining to the injury risk curves and ratings system can be found in the appendices of the "Final decision" notice (NHTSA 2008a).

## METHODOLOGY OF ANALYSES

The purpose of this study was to determine the effectiveness of the program over the five MYs since the enhancements were implemented, primarily by comparing crash test data from previous versions of make models selected and tested in the program with those of a later version. To accomplish this, NCAP test data was analyzed in two ways.

First, for each test mode, aggregate crash test results from the beginning of the enhanced NCAP were compared to the most recent data collected. Unpaired t-tests were conducted to determine whether occupant injury probability and star ratings from MY 2011vehicles were different from those collected for MY 2014-2015 vehicles. The last two years of test data were combined to ensure sufficient data points for analysis since the full set of 2015 data was not available at the time of publication. For ease of discussion, this analysis will be referred to as the unpaired analysis. Both star ratings and the occupant combined injury probabilities were analyzed because it was thought that the two could show different nuances in the data.

Second, vehicles that were tested more than once from the 2011 to 2015 MYs were identified and isolated to perform a similar analysis. At the beginning of each MY, the NCAP solicits information about light vehicle production from each vehicle manufacturer. In these requests, manufacturers are given the opportunity to inform the agency about the vehicles they plan to produce in the next MY. Some vehicle designs are considered identical from one MY to the next. When this is the case, the NCAP is able to "carry over" a given set of vehicle ratings to the next MY. In other cases, design changes are made that only affect the performance of a vehicle in one test mode. For example, changes may be made to the design of a frontal air bag which could result in retesting the vehicle for the frontal rigid barrier test, but not for the side impact test modes.

The authors examined data from the "first" and "last" times a make and model was tested under the enhanced NCAP and, using paired t-tests, tried to determine whether design changes between those two versions resulted in measurable improvements in the crash protection afforded to the vehicle occupants. Some vehicles may have been tested more than twice over this time period, such that other test data fell in the interim – either after the "first" test or before the "last" test. In these cases, manufacturers may have incorporated one or more interstitial design changes in vehicles that were not necessarily successful in achieving better star ratings, which resulted in retesting those vehicles several times during the course of the enhanced program. For ease of calculation and discussion, the authors decided to exclude this interim data and focus only on the first and last tests from the past five MYs. By selecting the latest version tested, it was expected that manufacturers' best efforts to date would be captured. This second

analysis will be referred to as the paired analysis. Test results from the first time a given vehicle model was tested under the enhanced program were compared to those from the most recent time that vehicle was retested.

In addition, data was analyzed based on changes to the ratings assigned, which may or may not be represented by the same vehicle make and model from year to year. This is due to several factors. For instance, vehicle manufacturers may change and/or rebrand particular vehicle names from one year to the next. A vehicle model may also be referred to as something new from a marketing perspective, but in actuality, it is identical to a model that was previously produced. In addition, vehicles that a manufacturer claims are corporate twins in one MY may not be designated as such in subsequent years.

Lastly, some vehicles demonstrated an increase in risk of occupant injuries (or a subsequent decrease in star ratings) after a redesign. No additional effort was made to determine how or why these vehicles performed more poorly after a redesign.

## RESULTS

### Frontal NCAP – Rigid Barrier Test

The NCAP's frontal star ratings are based on the performance of two Hybrid III dummies installed in the first row of a vehicle. The driver is a 50$^{th}$ percentile male and the right front passenger is a 5$^{th}$ percentile female. For this test, the vehicle impacts a rigid wall at 35 mph (56 km/h) (NHTSA 2013a). Readings from the dummies' heads, necks, chests, and legs are used to calculate combined probabilities of AIS3+ injury, which are then divided by a baseline risk of injury and converted to star ratings (NHTSA 2008a). For ease of discussion, this paper will primarily focus on the probabilities of injuries recorded by the test dummies and the star ratings assigned to them, and will not explain the calculations involved, as these are presented in detail in the 2008 "Final decision" notice (2008a).

A summary of the average probabilities of injury and star ratings over the years for the driver and front passenger dummies in the frontal NCAP test may also be found in the Appendix in Tables A1-A4.

**Comparison of unpaired vehicle data – 2011 versus 2014/2015 (unpaired analysis)** The average combined injury probabilities and star ratings for the driver dummy did not change much from MY 2011 to MY 2014/2015. There was no statistical difference found at the 95% confidence interval as evidenced by the P-value between the MY 2011 and MY 2014/2015 data sets when considering the occupants' combined injury probabilities and star ratings. However, differences between MY 2011 and MY 2014/2015 average combined injury probabilities and star ratings for the right front passenger were found to be statistically significant at the 95% confidence interval. The combined injury probabilities showed a significant decrease, and consequently, the star rating significantly increased. Table 1 details the results of this analysis.

***Table 1.***
***Results of Frontal NCAP Unpaired Analysis***

| | **Frontal NCAP Driver** | | | | **Frontal NCAP Front Passenger** | | | |
|---|---|---|---|---|---|---|---|---|
| | ***Comb. Injury Prob.*** | | ***Star Rating*** | | ***Comb. Injury Prob.*** | | ***Star Rating*** | |
| **Data Set** | **2011** | **2014/15** | **2011** | **2014/15** | **2011** | **2014/15** | **First Test** | **Last Test** |
| **t-stat** | 0.928 | | 0.386 | | 4.219 | | 4.532 | |
| **Two tailed P-value** | 0.355 | | 0.700 | | < 0.0001 | | < 0.0001 | |
| **Mean** | 0.117 | 0.111 | 4.28 | 4.33 | 0.151 | 0.117 | 3.55 | 4.24 |
| **Standard Deviation** | 0.036 | 0.036 | 0.81 | 0.73 | 0.051 | 0.042 | 0.92 | 0.82 |
| **N** | 64 | 66 | 64 | 66 | 64 | 66 | 64 | 66 |

**Comparison of paired vehicle data – 2011 versus most recent test (paired analysis)** While driver performance in frontal NCAP has not improved significantly on average from MY 2011, the paired analysis shows that when manufacturers make changes to specific vehicles, significant improvements are seen in both combined injury probabilities and star ratings. These differences were significant at the 95% confidence level. Likewise, differences in the most updated vehicles' right front passenger combined injury probabilities and star ratings were

also statistically significant at the 95% confidence level. Both the driver and right front passenger dummies' combined injury probabilities showed a significant decrease, and consequently, the star ratings significantly increased. Table 2 illustrates the results for this analysis.

***Table 2.***
***Results of Frontal NCAP Paired Analysis***

| | **Frontal NCAP Driver** | | | | **Frontal NCAP Front Passenger** | | | |
|---|---|---|---|---|---|---|---|---|
| | ***Comb. Injury Prob.*** | | ***Star Rating*** | | ***Comb. Injury Prob.*** | | ***Star Rating*** | |
| **Data Set** | **First Test** | **Last Test** | **First Test** | **Last Test** | **First Test** | **Last Test** | **First Test** | **Last Test** |
| **t-stat** | 4.443 | | 3.244 | | 7.889 | | 7.496 | |
| **Two tailed P-value** | < 0.0001 | | 0.0018 | | < 0.0001 | | < 0.0001 | |
| **Mean** | 0.121 | 0.103 | 4.19 | 4.49 | 0.158 | 0.118 | 3.41 | 4.18 |
| **Standard Deviation** | 0.040 | 0.023 | 0.84 | 0.58 | 0.054 | 0.038 | 0.93 | 0.71 |
| **N** | 73 | | 73 | | 73 | | 73 | |

**Side NCAP – MDB Test**

The side MDB NCAP test is conducted by towing an MDB into the driver's side of a stationary vehicle crabbed at a 27 degree angle at 38.5 mph (62 km/h) (NHTSA 2013b). An ES-2re 50$^{th}$ percentile male dummy is seated in the driver's seat, and a 5$^{th}$ percentile female SID-IIs dummy is seated in the rear seat behind the driver. Readings from the driver dummies' heads, chests, abdomens, and pelvises, and the rear passenger dummies' heads and pelvises, are used to calculate combined probabilities of AIS3+ injury, which are then divided by a baseline risk of injury and converted to star ratings (NHTSA 2008a).

A summary of the average injury probabilities over the years for the driver and rear passenger dummies in the side MDB test may be found in the Appendix in Tables A5-A8.

**Comparison of unpaired vehicle data – 2011 versus 2014/2015 (unpaired analysis)** As shown in Table 3, the differences between both the star ratings and the combined injury probabilities in the 2011 data and the 2014/2015 data were found to be statistically significant at the 95% confidence interval for both dummies in the side MDB test. Both the driver and rear passenger dummies' combined injury probabilities showed a significant decrease, and consequently, the star ratings significantly increased. Five-star ratings dominate the 2014/2015 data set; 89% of driver ratings and 96% of rear passenger ratings were five stars. These figures can be compared to 67% of driver ratings and 68% of rear passenger ratings that achieved five stars in the 2011 data set.

***Table 3.***
***Results of Side MDB NCAP Unpaired Analysis***

| | **Side MDB NCAP Driver** | | | | **Side MDB NCAP Rear Passenger** | | | |
|---|---|---|---|---|---|---|---|---|
| | ***Comb. Injury Prob.*** | | ***Star Rating*** | | ***Comb. Injury Prob.*** | | ***Star Rating*** | |
| **Data Set** | **2011** | **2014/15** | **2011** | **2014/15** | **2011** | **2014/15** | **2011** | **2014/15** |
| **t-stat** | 3.820 | | 3.518 | | 3.353 | | 3.585 | |
| **Two tailed P-value** | 0.0002 | | 0.0006 | | 0.0010 | | 0.0005 | |
| **Mean** | 0.099 | 0.057 | 4.44 | 4.87 | 0.087 | 0.047 | 4.37 | 4.88 |
| **Standard Deviation** | 0.088 | 0.034 | 0.96 | 0.41 | 0.089 | 0.051 | 1.04 | 0.59 |
| **N** | 64 | 75 | 64 | 75 | 62 | 75 | 62 | 75 |

**Comparison of paired vehicle data – 2011 versus most recent test (paired analysis)** For the paired analysis, Table 4 shows the differences between the combined injury probabilities and star ratings in the two sets of data ("first" test versus "last" test) were found to be significant at the 95% confidence interval. Both the driver and rear

passenger dummies' combined injury probabilities showed a significant decrease, and consequently, the star ratings significantly increased.

***Table 4.***
***Results of Side MDB NCAP Paired Analysis***

| | **Side MDB NCAP Driver** | | | | **Side MDB NCAP Rear Passenger** | | | |
|---|---|---|---|---|---|---|---|---|
| | ***Comb. Injury Prob.*** | | ***Star Rating*** | | ***Comb. Injury Prob.*** | | ***Star Rating*** | |
| **Data Set** | **First Test** | **Last Test** | **First Test** | **Last Test** | **First Test** | **Last Test** | **First Test** | **Last Test** |
| **t-stat** | 3.884 | | 4.323 | | 4.073 | | 3.915 | |
| **Two tailed P-value** | 0.0002 | | < 0.0001 | | 0.0001 | | 0.0002 | |
| **Mean** | 0.093 | 0.062 | 4.38 | 4.79 | 0.093 | 0.046 | 4.32 | 4.86 |
| **Standard Deviation** | 0.083 | 0.052 | 0.91 | 0.58 | 0.095 | 0.048 | 1.10 | 0.51 |
| **N** | 72 | | 72 | | 72 | | 72 | |

**Side NCAP – Pole Test**

The side impact pole test, which was new to the NCAP beginning with the enhanced program, is conducted by towing a test vehicle angled at 75 degrees sideways at 20 mph (32 km/h) into an 8 in. (20 cm) diameter rigid pole (NHTSA 2013c). To assess the maximum injury potential in this type of crash, the test protocol requires that the pole be aligned with the center of gravity (CG) of the SID-IIs 5$^{th}$ percentile female driver dummy's head. Readings from the dummies' heads and pelvises are used to calculate combined probabilities of AIS3+ injury, which are then divided by a baseline risk of injury and converted to star ratings (NHTSA 2008a).

A summary of the average injury probabilities and star ratings over the years for the driver dummy in the side pole test may be found in the Appendix as Tables A9 and A10.

**Comparison of unpaired vehicle data – 2011 versus 2014/2015 (unpaired analysis)** The driver dummy in the side NCAP pole test has seen a large increase in average star ratings since the beginning of the enhanced program in 2011. Both the dummy and the crash test type were completely new beginning with that MY. Despite the obvious increase in pole test driver star ratings over the past few years, a t-test to determine significance was performed comparing the first MY of data to the most recent. The results of this analysis proved statistical significance for the decrease in the combined probability of injury and for the increase in the star rating at the 95% confidence level.

***Table 5.***
***Results of Side Pole NCAP Unpaired Analysis***

| | **Side Pole NCAP Driver** | | | |
|---|---|---|---|---|
| | ***Comb. Injury Prob.*** | | ***Star Rating*** | |
| **Data Set** | **2011** | **2014/15** | **2011** | **2014/15** |
| **t-stat** | 4.229 | | 4.448 | |
| **Two tailed P-value** | < 0.0001 | | < 0.0001 | |
| **Mean** | 0.137 | 0.063 | 4.10 | 4.84 |
| **Standard Deviation** | 0.145 | 0.034 | 1.35 | 0.44 |
| **N** | 62 | 74 | 62 | 74 |

**Comparison of paired vehicle data – 2011 versus most recent test (paired analysis)** For the paired analysis, the data shows that manufacturers' efforts to improve performance were extremely successful. The t-test analysis shows that between the "first" and "last" vehicle tests, the reduction in probability of injury and the increase in star ratings are both significant at the 95% confidence level. The driver dummies' combined injury probabilities showed a significant decrease, and consequently, the star rating significantly increased.

***Table 6.***
***Results of Side Pole NCAP Paired Analysis***

| | Side Pole NCAP Driver | | | |
|---|---|---|---|---|
| | *Comb. Injury Prob.* | | *Star Rating* | |
| **Data Set** | **First Test** | **Last Test** | **First Test** | **Last Test** |
| **t-stat** | 4.518 | | 5.688 | |
| **Two tailed P-value** | < 0.0001 | | < 0.0001 | |
| **Mean** | 0.181 | 0.065 | 3.79 | 4.81 |
| **Standard Deviation** | 0.216 | 0.033 | 1.46 | 0.43 |
| **N** | 70 | | 70 | |

## DISCUSSION

Percentages listed in the below analyses are derived from the data found in the Appendix.

### Unpaired Analysis

It is expected that the driver data in the frontal NCAP test would not show significance when comparing the MY 2011 data to the most recent years' data because the dummy type and seating method remained the same in the enhanced program even though the method used to assess the driver dummy's injuries was changed. The 50$^{th}$ percentile Hybrid III dummy has been a fixture as the driver in the frontal NCAP test since 1986 (1995). These circumstances may have given manufacturers a head start in developing design strategies for vehicles tested under the requirements of the enhanced program.

When the enhanced program began (MY 2011), the right front occupant in the frontal crash test had a larger proportion of two- and three-star ratings than the frontal driver did; nearly 38% of right front passenger ratings were less than four stars as opposed to 16% of driver ratings. By MY 2014/2015, these percentages had decreased to 12% for the front passenger and 9% for the driver. The occupants that showed the greatest improvement since the enhanced program began in terms of average star ratings were the Hybrid III 5$^{th}$ percentile female in the right front passenger seat of the frontal test and the 5$^{th}$ percentile SID-IIs driver in the pole test. Since the enhanced program's inception, these occupants experienced a 19% and 18% increase in average star ratings, respectively. The use of 5$^{th}$ percentile female dummies was new to the NCAP in MY 2011. The pole test configuration itself was also completely new. Manufacturers have developed countermeasures to reduce injury risk in these crashes. For instance, the combined probability of injury for the 5$^{th}$ percentile female in the pole test has been reduced by more than half (54%) since MY 2011. For the side MDB test, the probability of injury in the 5$^{th}$ percentile female SID-IIs, seated in the rear seat, reduced by half – more or less (47%), and star ratings increased by 12% on average.

The 50$^{th}$ percentile male ES-2re dummy was also new for the enhanced program. Similar to the results of the SID-IIs in the side MDB test, the ES-2re dummy showed a marked decrease in the combined probability of injury (42%) with only a moderate increase in average star ratings (10%).

The NCAP also tests vehicles beyond the requirements of the Federal Motor Vehicle Safety Standards (FMVSSs), and this is accomplished in several ways. For instance, the NCAP tests vehicles that are beyond the weight requirements set forth in various FMVSSs. This allows the program to select and test vehicles with up to a 10,000 lb (4,536 kg) Gross Vehicle Weight Rating (GVWR) to ensure that some popular consumer vehicles are subject to full-scale crash testing when they may not have been otherwise. Hence, the NCAP test results of certain vehicles may highlight the need for further refinements perhaps in the restraint systems to achieve better NCAP performance. For instance, side air bags, particularly chest and pelvis air bags, are now seen more often in larger vehicles. Note that risk of head injury in the side MDB test is very low and has been, at least since the enhanced program's inception (Table A5). Prior to the enhanced program, side curtain air bags were not necessarily needed to achieve top ratings for these vehicles, but the addition of the side pole test has challenged manufacturers to include safety equipment for head and chest protection on vehicles, including those with GVWRs that exceed FMVSSs. In the MYs during which the enhanced program was formally announced (MY 2009), no vehicles with GVWR between 8,500 lb and 10,000 lb (3,856 kg to 4,536 kg) offered side air bags to protect the occupant's chest or pelvis, and only 38% of these

models offered head protection. Now, many more vehicle models in the MY 2015 heavy vehicle fleet offer side air bags, and all models offer head protection, with 47% of them having head air bags as standard equipment. Additionally, 73% of models offer chest and/or pelvis protection as either optional or standard equipment.

**Paired Analysis**

Injury probabilities and star ratings examined in the paired analysis showed promising results for all occupants in the NCAP's crash tests.

While the average combined injury probability for the frontal crash test driver decreased by only 5% in the unpaired analysis, it decreased by 15% when looking at the paired vehicle tests; the decrease was sufficient to achieve statistical significance. Accordingly, the average star ratings for the frontal crash test driver increased by 1% in the unpaired analysis versus an increase of 7% in the paired analysis. The frontal crash test passenger's combined injury probability decreased by 25% and the star ratings increased by 23% in the paired study. This provides evidence that manufacturers are responding to frontal NCAP crash test results and further support the hypothesis that manufacturers are making specific design changes to improve occupant performance in vehicles with lower NCAP star ratings even when the larger population of frontal NCAP vehicles shows generally good performance.

The side pole test driver in this paired analysis experienced the largest decrease (64%) in average combined probability of injury of any occupant in either analysis and a 27% increase in average star ratings, an average of greater than one whole star, which was the largest of any occupant's average star rating increase. In fact, a large number of pole test ratings increased by three (n=10, 14%) and even four (n=6, 9%) stars after redesign. In the same analysis, the driver in the side MDB test experienced a 33% reduction in average combined injury probability. The reductions in both MDB and pole test driver combined injury probabilities demonstrate that the driver's position in side impact tests is becoming safer for both the 50$^{th}$ percentile male and the 5$^{th}$ percentile female. Also, it appears countermeasures can be put in place to improve injury readings for both the 50$^{th}$ percentile male and the 5$^{th}$ percentile female. The rear passenger in the MDB test paired data set saw a decrease in average combined injury probability of 51% and star ratings increased 13%. No ratings increased by four stars, but unlike in the pole test, none of the rear passenger ratings were one-star initially, so a four-star increase would be unattainable. Of the ten vehicles in which the rear passenger received a two-star rating, eight vehicles were modified in the later version and achieved five-star ratings.

Though the specific details of a given vehicle's design changes are considered confidential information, there are some general trends in restraint and structural changes the authors can note that have occurred during the past five years of the enhanced program. To improve their vehicles' frontal crash performance, manufacturers made air bag design and deployment refinements, and modifications to advanced seat belt features such as load limiters and pretensioners. Manufacturers have also made front-end changes to better manage crash energy. Regarding the side impact crash mode, the presence of the 5$^{th}$ percentile female SID-IIs in the rear seat of each MDB test seems to have encouraged manufacturers to equip more rear seating positions with side torso air bags or larger torso-abdomen-pelvis (TAP) air bags. This equipment was not often seen prior to the enhanced program. Manufacturers have also opted to install TAP air bags in many front row seats to maximize vehicle performance in both side impact tests. Structural improvements to the side sills, pillars, and door trims have also been made to reduce intrusion into the occupant compartment and/or provide a load path through the vehicle, particularly for the pole test. Chamber locations in curtain air bags have been modified to protect both the 50$^{th}$ percentile male and the 5$^{th}$ percentile female in side crash scenarios.

Four of the vehicles included in the paired analysis had GVWRs between 8,500 lb and 10,000 lb (3,856 kg to 4,536 kg). In all four cases, the combined probabilities of injury substantially improved for the pole test between the first and last test. Three driver occupants experienced high head injury probabilities during the first test. In these cases, injury probabilities appeared to be later improved, in part by the addition of side curtain air bags. The fourth case involved a driver whose pelvic injury probability was high. Side torso air bags were added to this vehicle, among other improvements, and its star rating increased dramatically.

Occupant protection performance in vehicle crash tests is complex. There is no single way to reach a five-star rating, and vehicle manufacturers employ a variety of techniques to achieve the top ratings. In addition, manufacturers must take into account other factors such as vehicle weight, style, and comfort. However, because of improvements made to vehicles, most manufacturers were successful in their efforts to decrease probability of injury and therefore

increase star ratings. The paired analysis suggests that, in the majority of cases, when manufacturers choose to implement design changes, occupant safety is enhanced.

## CONCLUSIONS

Two methods of analysis were used to compare changes to occupant injury risk under the enhanced NCAP. An unpaired analysis was undertaken to generally assess the state of injury risk and vehicle ratings in both the first MY of the enhanced program and the most recent MYs, 2014 and 2015. A paired analysis was then run to investigate whether vehicle redesigns were successful in reducing injury risk. All differences were statistically evaluated using t-tests, and for these analyses, significance is defined using a 95% confidence interval.

Driver data in the frontal NCAP test does not show a significant difference overall when comparing MY 2011 to 2014/2015. Likely, manufacturers had already had a head start in designing strategies to protect this occupant in this test mode, as the dummy, seating procedure, and test itself did not change under the enhanced program. However, when considering the paired analysis, driver results from the first and last tests of a vehicle, when one was retested, showed that injury risk was significantly decreased and star ratings significantly increased.

Passenger data in the frontal NCAP test, as well as driver and passenger data from the side impact tests (MDB and pole), show significant decreases in injury risk and, subsequently, significant increases in star rating. This is true for both the unpaired and paired analyses and suggests that manufacturers are successfully responding to the enhanced NCAP crash tests.

Vehicles with GVWRs between 8,500 lb to 10,000 lb (3,856 kg to 4,536 kg) are, in general, being fitted with additional safety equipment in recent MYs. The additions protect body regions which are evaluated in the enhanced NCAP's crash tests, particularly those in the side pole test. When side impact safety equipment was added to the four heavier vehicles included in the paired study, side pole star ratings increased substantially.

## REFERENCES

"Consumer Information; New Car Assessment Program; Final decision notice," 73 Federal Register 134 (11 July 2008a), pp 40016- 40050.

"Consumer Information; New Car Assessment Program (NCAP); Notice of postponement of the implementation of enhancements to the New Car Assessment Program (NCAP)," 73 Federal Register 248 (24 December 2008b), pp 79206- 79207.

"Highway Safety: Reliability and Validity of DOT Crash Tests." GAO/PEMD-95-5. May 1995.

"Laboratory Test Procedure for New Car Assessment Program Frontal Impact Testing," Docket NHTSA-2013-0052, 18 September 2013a.

"Laboratory Test Procedure for New Car Assessment Program Side Impact Moving Deformable Barrier Testing." Docket NHTSA-2013-0052. 19 September 2013b.

"Laboratory Test Procedure for the New Car Assessment Program Side Impact Rigid Pole Test." Docket NHTSA- 2013-0052. 19 September 2013c.

National Highway Traffic Safety Administration. (2013d). NHTSA Announces Model Year 2014 Vehicles to be Rated Under Government 5-Star Safety Ratings Program [Press Release]. Retrieved from http://www.nhtsa.gov/About+NHTSA/Press+Releases/NHTSA+Announces+Model+Year+2014+Vehicles+to+be+Rated+Under+Government+5-Star+Safety+Ratings+Program.

"Opportunities Exist to Enhance NHTSA's New Car Assessment Program" GAO-05-370. April 2005.

Park, Brian T., et. al. “The Newly Enhanced U.S. NCAP: A First Look at Model Year 2011 Ratings.” Paper 11-0440, 22nd International Conference on the Enhanced Safety of Vehicles, Washington, D.C. June 13-16, 2011.

“The New Car Assessment Program; Suggested Approaches for Enhancements.” 72 Federal Register 16 (25 January 2007a), pp 3473-3477.

“The New Car Assessment Program Suggested Approaches for Future Program Enhancements.” DOT HS 810 698. January 2007b.

**APPENDIX**

***Table A1.***
***Frontal NCAP Driver Average Probability of Injury Readings and Number of Star Ratings by Model Year***

| | 2011 | 2012 | 2013 | 2014 | 2015 | 2014/2015 Combined | All Years |
|---|---|---|---|---|---|---|---|
| **Number of Ratings** | 64 | 69 | 57 | 42 | 24 | 66 | 256 |
| **Average Probability of Head Injury** | 0.005 | 0.005 | 0.006 | 0.008 | 0.006 | 0.008 | 0.006 |
| **Average Probability of Neck Injury** | 0.069 | 0.069 | 0.071 | 0.070 | 0.070 | 0.070 | 0.070 |
| **Average Probability of Chest Injury** | 0.029 | 0.032 | 0.021 | 0.026 | 0.024 | 0.025 | 0.027 |
| **Average Probability of Leg Injury** | 0.018 | 0.015 | 0.012 | 0.013 | 0.010 | 0.012 | 0.014 |
| **Average Occupant Combined Injury Probability** | 0.117 | 0.116 | 0.106 | 0.113 | 0.107 | 0.111 | 0.113 |
| **Average Star Rating** | 4.28 | 4.30 | 4.44 | 4.29 | 4.42 | 4.33 | 4.34 |

***Table A2.***
***Frontal NCAP Driver Star Ratings by Model Year***

| | 2 Star Rating | | 3 Star Rating | | 4 Star Rating | | 5 Star Rating | | Total |
|---|---|---|---|---|---|---|---|---|---|
| **Model Year** | **Count** | **% Total** | **Count** | **% Total** | **Count** | **% Total** | **Count** | **% Total** | |
| 2011 | 2 | 3.13% | 8 | 12.50% | 24 | 37.50% | 30 | 46.88% | 64 |
| 2012 | 2 | 2.90% | 4 | 5.80% | 34 | 49.28% | 29 | 42.03% | 69 |
| 2013 | 1 | 1.75% | 5 | 8.77% | 19 | 33.33% | 32 | 56.14% | 57 |
| 2014 | 1 | 2.38% | 4 | 9.52% | 19 | 45.24% | 18 | 42.86% | 42 |
| 2015 | 1 | 4.17% | 0 | 0.00% | 11 | 45.83% | 12 | 50.00% | 24 |
| 2014/2015 Combined | 2 | 3.03% | 4 | 6.06% | 30 | 45.45% | 30 | 45.45% | 66 |
| **Total** | **7** | **2.73%** | **21** | **8.20%** | **107** | **41.80%** | **121** | **47.27%** | **256** |

***Table A3.***
***Frontal NCAP Front Passenger Average Probability of Injury Readings and Number of Star Ratings by Model Year***

| | 2011 | 2012 | 2013 | 2014 | 2015 | 2014/2015 Combined | All Years |
|---|---|---|---|---|---|---|---|
| **Number of Ratings** | 64 | 69 | 57 | 42 | 24 | 66 | 256 |
| **Average Probability of Head Injury** | 0.015 | 0.013 | 0.012 | 0.008 | 0.011 | 0.009 | 0.012 |
| **Average Probability of Neck Injury** | 0.104 | 0.094 | 0.088 | 0.082 | 0.081 | 0.082 | 0.092 |
| **Average Probability of Chest Injury** | 0.018 | 0.016 | 0.014 | 0.014 | 0.018 | 0.015 | 0.016 |
| **Average Probability of Leg Injury** | 0.022 | 0.022 | 0.014 | 0.015 | 0.013 | 0.015 | 0.018 |
| **Average Occupant Combined Injury Probability** | 0.151 | 0.140 | 0.124 | 0.116 | 0.119 | 0.117 | 0.133 |
| **Average Star Rating** | 3.55 | 3.71 | 4.05 | 4.24 | 4.25 | 4.24 | 3.88 |

***Table A4.***
***Frontal NCAP Front Passenger Star Ratings by Model Year***

| | 2 Star Rating | | 3 Star Rating | | 4 Star Rating | | 5 Star Rating | | Total |
|---|---|---|---|---|---|---|---|---|---|
| **Model Year** | **Count** | **% Total** | **Count** | **% Total** | **Count** | **% Total** | **Count** | **% Total** | |
| 2011 | 12 | 18.75% | 12 | 18.75% | 33 | 51.56% | 7 | 10.94% | 64 |
| 2012 | 4 | 5.80% | 21 | 30.43% | 35 | 50.72% | 9 | 13.04% | 69 |
| 2013 | 2 | 3.51% | 9 | 15.79% | 30 | 52.63% | 16 | 28.07% | 57 |
| 2014 | 3 | 7.14% | 2 | 4.76% | 19 | 45.24% | 18 | 42.86% | 42 |
| 2015 | 1 | 4.17% | 2 | 8.33% | 11 | 45.83% | 10 | 41.67% | 24 |
| 2014/2015 Combined | 4 | 6.06% | 4 | 6.06% | 30 | 45.45% | 28 | 42.42% | 66 |
| **Total** | **22** | **8.59%** | **46** | **17.97%** | **128** | **50.00%** | **60** | **23.44%** | **256** |

***Table A5.***
***Side MDB NCAP Driver Average Probability of Injury Readings and Number of Star Ratings by Model Year***

| | **2011** | **2012** | **2013** | **2014** | **2015** | **2014/2015 Combined** | **All Years** |
|---|---|---|---|---|---|---|---|
| **Number of Ratings** | 64 | 66 | 52 | 46 | 29 | 75 | 257 |
| **Average Probability of Head Injury** | 0.001 | 0.001 | 0.001 | 0.001 | 0.000 | 0.001 | 0.001 |
| **Average Probability of Chest Injury** | 0.070 | 0.059 | 0.040 | 0.040 | 0.040 | 0.040 | 0.052 |
| **Average Probability of Abdomen Injury** | 0.027 | 0.023 | 0.018 | 0.014 | 0.013 | 0.014 | 0.020 |
| **Average Probability of Pelvis Injury** | 0.006 | 0.005 | 0.004 | 0.003 | 0.003 | 0.003 | 0.004 |
| **Average Occupant Combined Injury Probability** | 0.099 | 0.085 | 0.062 | 0.058 | 0.055 | 0.057 | 0.076 |
| **Average Star Rating** | 4.44 | 4.56 | 4.81 | 4.87 | 4.86 | 4.87 | 4.67 |

***Table A6.***
***Side MDB NCAP Driver Star Ratings by Model Year***

| | 1 Star Rating | | 2 Star Rating | | 3 Star Rating | | 4 Star Rating | | 5 Star Rating | | Total |
|---|---|---|---|---|---|---|---|---|---|---|---|
| **Model Year** | **Count** | **% Total** | **Count** | **% Total** | **Count** | **% Total** | **Count** | **% Total** | **Count** | **% Total** | |
| 2011 | 1 | 1.56% | 3 | 4.69% | 6 | 9.38% | 11 | 17.19% | 43 | 67.19% | 64 |
| 2012 | 0 | 0.00% | 2 | 3.03% | 7 | 10.61% | 9 | 13.64% | 48 | 72.73% | 66 |
| 2013 | 0 | 0.00% | 0 | 0.00% | 1 | 1.92% | 8 | 15.38% | 43 | 82.69% | 52 |
| 2014 | 0 | 0.00% | 0 | 0.00% | 1 | 2.17% | 4 | 8.70% | 41 | 89.13% | 46 |
| 2015 | 0 | 0.00% | 0 | 0.00% | 1 | 3.45% | 2 | 6.90% | 26 | 89.66% | 29 |
| 2014/2015 Combined | 0 | 0.00% | 0 | 0.00% | 2 | 2.67% | 6 | 8.00% | 67 | 89.33% | 75 |
| **Total** | **1** | **0.39%** | **5** | **1.95%** | **16** | **6.23%** | **34** | **13.23%** | **201** | **78.21%** | **257** |

***Table A7.***
***Side MDB NCAP Rear Passenger Average Probability of Injury Readings and Number of Star Ratings by Model Year***

| | 2011 | 2012 | 2013 | 2014 | 2015 | 2014/2015 Combined | All Years |
|---|---|---|---|---|---|---|---|
| **Number of Ratings** | 62 | 66 | 51 | 46 | 29 | 75 | 254 |
| **Average Probability of Head Injury** | 0.009 | 0.021 | 0.007 | 0.009 | 0.005 | 0.007 | 0.011 |
| **Average Probability of Pelvis Injury** | 0.079 | 0.073 | 0.041 | 0.044 | 0.033 | 0.040 | 0.058 |
| **Average Occupant Combined Injury Probability** | 0.087 | 0.092 | 0.047 | 0.052 | 0.038 | 0.047 | 0.068 |
| **Average Star Rating** | 4.37 | 4.38 | 4.86 | 4.80 | 5.00 | 4.88 | 4.62 |

***Table A8.***
***Side MDB NCAP Rear Passenger Star Ratings by Model Year***

| | 1 Star Rating | | 2 Star Rating | | 3 Star Rating | | 4 Star Rating | | 5 Star Rating | | Total |
|---|---|---|---|---|---|---|---|---|---|---|---|
| **Model Year** | **Count** | **% Total** | **Count** | **% Total** | **Count** | **% Total** | **Count** | **% Total** | **Count** | **% Total** | |
| 2011 | 0 | 0.00% | 7 | 11.29% | 5 | 8.06% | 8 | 12.90% | 42 | 67.74% | 62 |
| 2012 | 1 | 1.52% | 6 | 9.09% | 5 | 7.58% | 9 | 13.64% | 45 | 68.18% | 66 |
| 2013 | 0 | 0.00% | 1 | 1.96% | 1 | 1.96% | 2 | 3.92% | 47 | 92.16% | 51 |
| 2014 | 0 | 0.00% | 3 | 6.52% | 0 | 0.00% | 0 | 0.00% | 43 | 93.48% | 46 |
| 2015 | 0 | 0.00% | 0 | 0.00% | 0 | 0.00% | 0 | 0.00% | 29 | 100.00% | 29 |
| 2014/2015 Combined | 0 | 0.00% | 3 | 4.00% | 0 | 0.00% | 0 | 0.00% | 72 | 96.00% | 75 |
| **Total** | **1** | **0.39%** | **17** | **6.69%** | **11** | **4.33%** | **19** | **7.48%** | **206** | **81.10%** | **254** |

***Table A9.***
***Side Pole NCAP Driver Average Probability of Injury Readings and Number of Star Ratings by Model Year***

| | 2011 | 2012 | 2013 | 2014 | 2015 | 2014/2015 Combined | All Years |
|---|---|---|---|---|---|---|---|
| **Number of Ratings** | 62 | 64 | 48 | 46 | 28 | 74 | 248 |
| **Average Probability of Head Injury** | 0.024 | 0.064 | 0.036 | 0.015 | 0.012 | 0.014 | 0.034 |
| **Average Probability of Pelvis Injury** | 0.117 | 0.082 | 0.064 | 0.048 | 0.054 | 0.050 | 0.078 |
| **Average Occupant Combined Injury Probability** | 0.137 | 0.136 | 0.098 | 0.062 | 0.065 | 0.063 | 0.107 |
| **Average Star Rating** | 4.10 | 4.23 | 4.52 | 4.85 | 4.82 | 4.84 | 4.44 |

***Table A10.***
***Side Pole NCAP Driver Star Ratings by Model Year***

| | 1 Star Rating | | 2 Star Rating | | 3 Star Rating | | 4 Star Rating | | 5 Star Rating | | Total |
|---|---|---|---|---|---|---|---|---|---|---|---|
| **Model Year** | **Count** | **% Total** | **Count** | **% Total** | **Count** | **% Total** | **Count** | **% Total** | **Count** | **% Total** | |
| 2011 | 5 | 8.06% | 7 | 11.29% | 2 | 3.23% | 11 | 17.74% | 37 | 59.68% | 62 |
| 2012 | 4 | 6.25% | 5 | 7.81% | 6 | 9.38% | 6 | 9.38% | 43 | 67.19% | 64 |
| 2013 | 1 | 2.08% | 1 | 2.08% | 3 | 6.25% | 10 | 20.83% | 33 | 68.75% | 48 |
| 2014 | 0 | 0.00% | 0 | 0.00% | 1 | 2.17% | 5 | 10.87% | 40 | 86.96% | 46 |
| 2015 | 0 | 0.00% | 0 | 0.00% | 1 | 3.57% | 3 | 10.71% | 24 | 85.71% | 28 |
| 2014/2015 Combined | 0 | 0.00% | 0 | 0.00% | 2 | 2.70% | 8 | 10.81% | 64 | 86.49% | 74 |
| **Total** | **10** | **4.03%** | **13** | **5.24%** | **13** | **5.24%** | **35** | **14.11%** | **177** | **71.37%** | **248** |

For the star rating tables, percentages may not total 100 due to rounding.

# A METHODOLOGY TO DERIVE PRECISION REQUIREMENTS FOR AUTOMATIC EMERGENCY BRAKING (AEB) TEST PROCEDURES

**Patrick Seiniger, Jost Gail**

Bundesanstalt für Straßenwesen (Federal Highway Research Institute) Brüderstraße 53, 51427 Bergisch Gladbach, Germany

Phone: +49 2204 43619
Fax: +49 2204 43676
E-mail: seiniger@bast.de

**Paper ID#: 15-0315**

## ABSTRACT

AEB Systems are becoming important to increase traffic safety. Test procedures in testing for consumer information, manufacturer self-certification and technical regulations are used to ensure a certain minimum performance of these systems. Consequently, test robustness, test efficiency and finally test cost become increasingly important.
The key driver for testing effort and test costs is the required repeatable accuracy in a test design - the higher the accuracy, the higher effort and test costs. On the other hand, the performance of active safety systems depends on time discretization in the environment perception and other sub-systems: for instance, typical sensors supply information with a cycle time of 50 - 150 ms. Time discretization results in an inherent spread of system performance, even if the test conditions are perfectly equal.
The proposed paper shows a methodology to derive requirements for a test setup (e.g. test repeats, use of driving robots, ...) as function of AEB system generation and rating method (e.g. Euro NCAP points awarded, pass/fail, ...). While the methodology itself is applicable to AEB pedestrian and AEB Car-Car scenarios, due to the lack of sufficient test data for AEB Car-Car, the focus of this paper is on AEB pedestrian scenarios.
A simulation model for the performance of AEB Pedestrian systems allows for the systematic variation of the discretization time as well as test condition accuracy. This model is calibrated with test results of 4 production vehicles for AEB Pedestrian, all fully tested by BASt according to current Euro NCAP test protocols.
Selected parameters to observe the accuracy of the test setup in case of pedestrian AEB is the calculated impact position of pedestrian on the vehicle front (as if no braking would have occurred), and the test vehicle speed accuracy. These variable was shown in real tests to be repeatable in the range of ± 5 cm and ± 0,25 km/h, respectively, with a fully robotized state of the art test setup.
The sensitivity of AEB performance (measured in achieved speed reduction as well as overall rating result according to current Euro NCAP rating methods) towards discretization and the sensitivity of performance towards test accuracy then is compared to identify economic yet robust test concepts.
These comparisons show that the available repeatability accuracy of current test setups is more than sufficient for today's AEB system capabilities. Time discretization problems dominate the performance spread especially in test scenarios with a limited pedestrian dummy reveal time (e.g. child behind obstruction, running adult scenarios with low car speeds). This would allow to increase test tolerances to decrease test cost.
A methodology which allows to derive the required tolerances in active safety tests might be valuable especially for NCAPs of emerging countries that do not have the necessary equipment (e.g. driving robots, positioning units) available for the full-scale and high tolerance EuroNCAP active safety procedures yet still want to rate active safety systems, thus improving the global safety.

## INTRODUCTION

AEB Systems are becoming important to increase traffic safety. Test procedures in testing for consumer information, manufacturer self-certification and technical regulations are used to ensure a certain minimum performance of these systems. Consequently, test robustness, test efficiency and finally test cost become increasingly important.
One of the major discussion points during the implementation of AEB test procedures was the required precision of test execution. The initial scenarios (as implemented in 2014) had been longitudinal scenarios. Both vehicles (target as well as vehicle under test) move on parallel - ideally identical – tracks. The main parameters which drive test cost are the precision of both vehicles' speeds, and the lateral displacement between the vehicles at all times.

Things become more complicated for scenarios where the target brakes during the test conduction: the initial longitudinal displacement between both vehicles should ideally be constant, and the target deceleration process, characterized by brake ramp and target deceleration, needs to be repeatable.
Finally, lateral traffic accident situations such as the proposed pedestrian scenarios require an exact match between positions of both target and vehicle under test during the constant speed phase of the test execution; otherwise the AEB system is presented with a different situation. A parameter representing this match of positions is the theoretical impact position of the target on the vehicle-under-test's front, calculated for a situation without automatic braking.
Testing always introduces uncertainties into how good these parameters can be maintained. The more complex the equipment is, the lower become the tolerances, and the higher is the precision of testing. Goal of this paper is to identify the relation between tolerances and expected certainty of results (e.g. speed reduction for the pedestrian AEB systems).

**Research Questions and Methodology**

The goal of this paper is to identify the relation between precision in test execution and variability in test results for AEB pedestrian test setups. Variability is influenced by test execution precision, but also by limitations inside current AEB systems.

- How does the test execution precision in AEB pedestrian tests influence the variability in speed reduction and overall rating?
- How do technical limitations in pedestrian AEB systems influence the variability in speed reductions and overall rating?

These questions will be answered with a simulation model for AEB pedestrian tests. The model allows to introduce tolerances in the test execution and as well as technical limitations (e.g. sensor angles, processing times, time discretization). A model for AEB Car-Car braking scenarios is developed as well, however there is not sufficient data for model validation.
Model input besides the mentioned tolerances and technical simulations is the test condition, output is the achieved speed reduction This model is parameterized and validated using all possible test data. Validation is successful if the simulation results match the test track results sufficiently well. Sufficiently well in this case means that the observed effects (e.g. variations, peak avoidance speeds, tendencies of speed decrease) can be replicated.
Results of the sensitivity investigations then are presented as plots overall rating variation as function of the varied parameter.

**SIMULATION MODEL**

The simulation model is loosely based on the model presented in [Seiniger, 2013]. It simulates the braking process of a vehicle, including brake delay time, deceleration ramp and deceleration levels. In [Seiniger, 2013], the model determined the brake time using certain paradigms (e.g. when the accident cannot be avoided by driver or pedestrian). The updated model now determines the appropriate brake time using AEB logic, sensor and visibility characteristics. These parameters had been derived from test data, gained within the AsPeCSS project [ASPECSS, 2014] and in BASt tests for manufacturers. Brake time determination differs whether the simulated test is an AEB pedestrian test or an AEB Car-Car test.

**Generic Simulation Model Structure**

Main part of the simulation model is the calculation of speed reduction as function of brake parameters, brake time and vehicle initial speed. The brake time is determined either by brake strategy (in cases where target detection is not a limiting factor) or by the remaining time before the impact after sensor detection (in other cases). The target reveal time (only applicable for pedestrian AEB simulation) is not only limited due to obstructions, but in some situations also by the sensor field-of-view and / or additional processing time. The overall structure of the simulation model is shown in Figure 1.

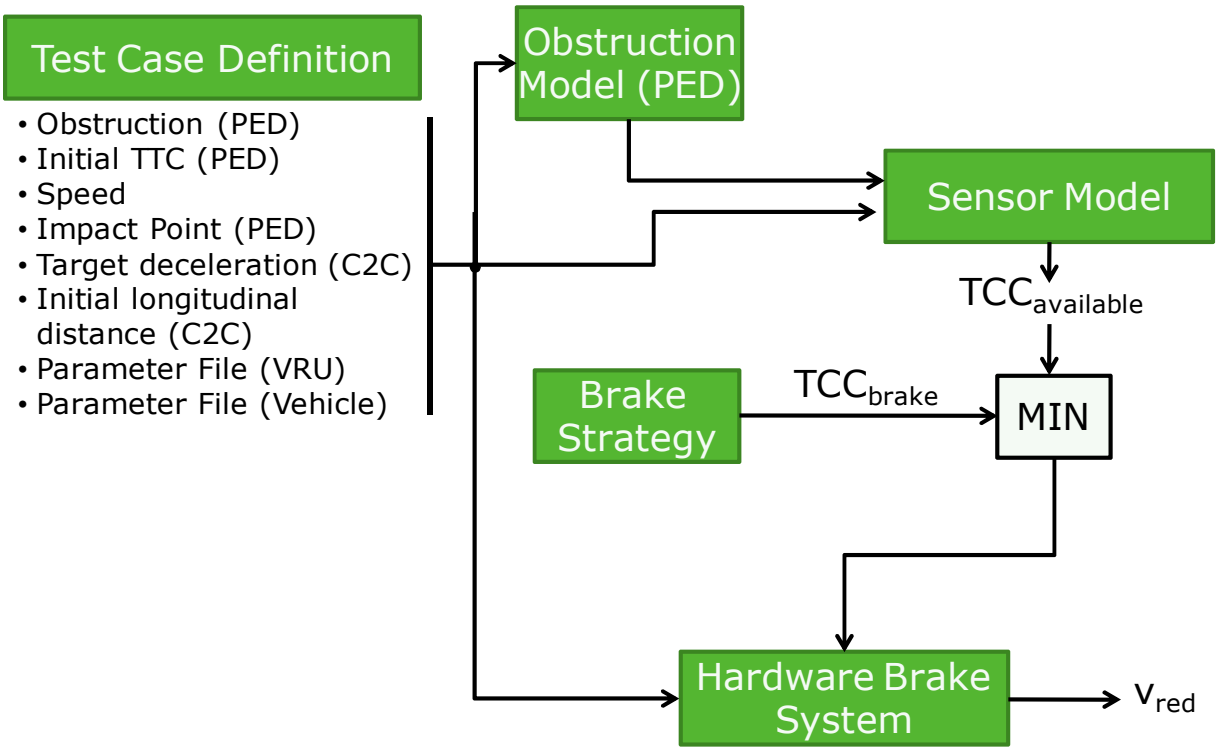


***Figure 1.*** **General structure of the simulation model (PED = pedestrian, C2C = Car-Car, MIN = minimum value of $TTC_{available}$ and $TTC_{brake}$ is selected)**

**Sensor and obstruction models for Pedestrian AEB tests**

The concept behind the obstruction and sensors model block in case of pedestrian AEB is depictured in Figure 2. For Field-of-view investigation, the angular position of the target towards the sensor is evaluated. The sensor model calculates the time at which the target enters the sensor field of view, if this is a limiting factor, and the obstruction model calculates the time at which the target appears from behind the obstruction, if this is a limiting factor. In both cases, the percentage of the target that is required for proper detection is a parameter of the simulation. Other parameters within the obstruction and sensor model block are the size and position of the obstruction with respect to target and vehicle-under-test, the sensor field-of-view angle, the sensor longitudinal position with respect to the vehicle front, and the required sensor processing time, after the target becomes visible.

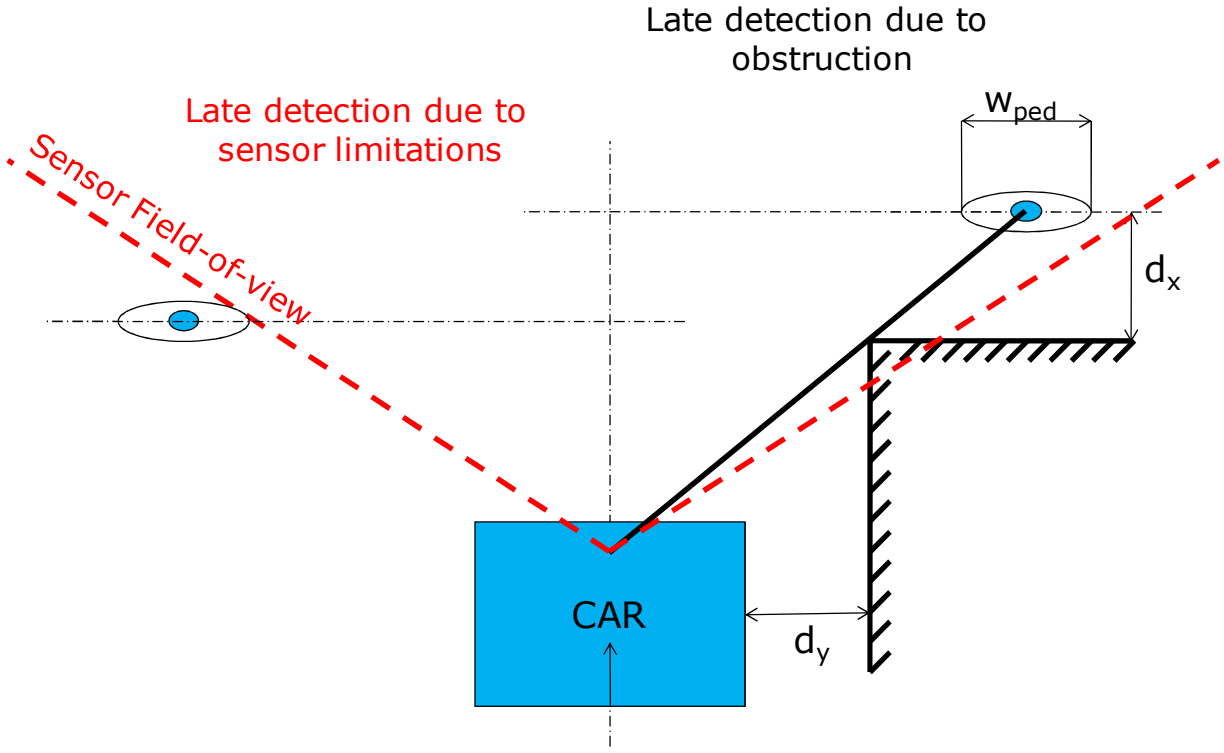


***Figure 2.*** **Concepts behind the sensor model and obstruction model blocks. Variables are the lateral position of obstruction with respect to the vehicle $d_y$, the longitudinal position of the obstruction with respect to the pedestrian target $d_x$, the size of the pedestrian target $w_{ped}$.**

An important parameter that is responsible for variations in measured speed reduction even with perfectly constant test parameters is the sensor sample rate. All sensors sample their data at discrete times, and usually the interval between sampling times is constant. Assuming that the AEB system brake decision requires at least one measurement (=sample) to verify that brake conditions exist, this final verification is available with a maximum variability equal to the sample rate, see Figure 3.

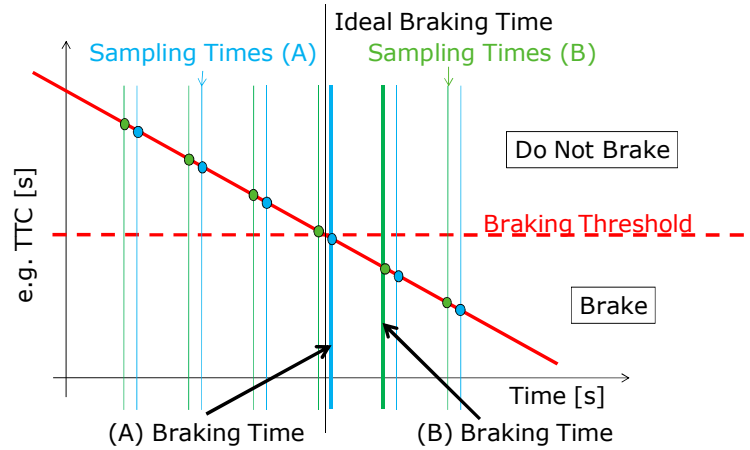


***Figure 3.*** **Sensor time discretization creates brake timing variations: an example using TTC as threshold for brake timing. The ideal brake timing would be at the point where TTC crosses the threshold. In case A, blue, a new measurement (dots on the TTC line, accompanied by vertical lines ) is available just after TTC crosses the threshold, so almost no additional time delay due to sensor time discretization is introduced. In case B, green, a measurement occured just before the TTC crossed the threshold, so the new measurement is**

**available almost one complete sample time after TTC has crossed the threshold - and thus, almost one complete sample time is introduced as the additional time delay. Since the sampling process starts at system start far before the test, the probability for any time delay between no delay and full sampling time should be equal.**

**Brake Strategy for Pedestrian AEB Systems**

Identification of brake strategy requires some system identification from the available test data. Various strategies are used by the in total 5 cars that were available for validation. An appropriate criterion to characterize the threat of collision is the value Time-To-Collision TTC [Winner, 2011]. TTC is the quotient of relative distance in direction of travel $\Delta x$ and relative speed $\Delta v$:

$$TTC = \frac{\Delta x}{\Delta v}.$$

The variable TTC describes the current time that is left until a collision occurs if speeds of target and vehicle-under-test do not change.
Test data shows that all vehicles use a threshold for the lateral position of the target, a threshold for the Time-To-Collision value (TTC), or both, and in some cases, different thresholds for different pedestrian speeds have been observed. Note that a collision will occur in all of the defined test cases, if no braking is initiated.

**Brake Strategy for Car-Car AEB Systems**

The most relevant and demanding Car-Car test scenario with respect to required accuracy is the braking scenario: two vehicles initially travel at an equal and constant speed, with a constant longitudinal distance, until the target vehicle decelerates. The target vehicles' deceleration level and the time until this fully developed deceleration is achieved are test parameters. In this case, the variable TTC as described above cannot be used, since it does not take the target deceleration into account. A more appropriate variable is the "enhanced TTC" ETTC [Winner, 2011]:

$$ETTC = \frac{\sqrt{\Delta v^2 + 2 \cdot D_{rel} \cdot \Delta x} - \Delta v}{D_{rel}},$$

introducing the relative deceleration between both vehicles $D_{\mathrm{rel}}$. Test data shows that ETTC characterizes the brake timing relatively well: start of braking consistently occurs at a constant ETTC threshold (only test data from one vehicle test series used).
The sampling time effect on time variability should be relevant for these tests as well, but sensor detection usually is not a limiting factor since the target vehicle is in full sensor field of view during the whole experiment.

**Hardware Brake System**

The model for the hardware brake system calculates the achieved speed reduction for a given TTC of commanded braking, relative velocity and initial conditions, taking a constant delay time after brake command, constant brake jerk and maximum deceleration into account. All calculations are numerical.
Additionally to calculation of speed reduction, this block also evaluates whether the accident is avoided or not: for pedestrian AEB tests, in some cases pedestrians gain enough time to clear the path due to the brake intervention, and these situations then are counted as avoided accidents.

**Model Parameter List**

Table 1 shows a full set of the available model parameters for AEB pedestrian as well as AEB Car-Car.

***Table 1.*** **Simulation model parameter list**

| Parameter | Category | Description | Typical value |
|---|---|---|---|
| TTC_AEB_DESIRED | Brake Strategy | TTC Threshold for brake onset | 1 s |
| DIST_PEDESTRIAN | Brake Strategy | Lateral distance threshold between pedestrian and vehicle center at brake onset | 2.2 m |

| | | | |
|---|---|---|---|
| ADJUST_DIST_RUNNING | Brake Strategy | Increase DIST_PEDESTRIAN by this factor for running pedestrians (8 km/h rather than 5 km/h) | 1.2 |
| ETTC_BRAKE | Brake Strategy | ETTC Threshold for brake onset in Car-Car scenarios | 1 |
| TTC_DELAY | Sensor Characteristics | Time that is required from first sensor measurement until proper target recognition | 0.2 s |
| ADJUST_T_DELAY_SPEED | Sensor Characteristics | Higher relative speeds will increase the detection time, because optical flux / differences between two images become to great. | YES (for camera) |
| T_DELAY_SPEED | Sensor Characteristics | Speed threshold after which detection time increases | 35 km/h |
| T_DELAY_HIGH_SPEED | Sensor Characteristics | Factor for detection time increase | 2 |
| ADJUST_T_DELAY_DISTANCE | Sensor Characteristics | Higher distance will increase the detection time for stereo cameras, because stereo effect vanishes for far objects | YES (stereo camera) |
| T_DELAY_DISTANCE | Sensor Characteristics | Distance | 15 m |
| T_DELAY_HIGH_DISTANCE | Sensor Characteristics | Factor for detection time increase at high distances | 2 |
| SENSOR_ANGLE | Sensor Characteristics | Field of view-angle of the most relevant sensor | 20° |
| TARGET_PROPORTION | Sensor Characteristics | What proportion of the target needs to be in sight for proper target recognition | 50% |
| SENSOR_X_POS | Sensor Characteristics | Most relevant sensor longitudinal position with respect to vehicle front | 0 m (for RADAR) |
| FRAMERATE | Sensor Characteristics | Most relevant sensor frame rate | 10 Hz |
| T_DEAD_AEB | Brake Hardware | Delay between brake command and brake onset | 0,35 s |
| JERK_AEB | Brake Hardware | Maximum rate of deceleration increase | 20 $m/s^3$ |
| A_MAX_AEB | Brake Hardware | Maximum achievable deceleration | 6 $m/s^2$ |
| W_VEHICLE | Vehicle | Width of vehicle | 1.85 m |
| W_PED | Target | Width of target (e.g. length of bicycle target, width of pedestrian dummy) | 0.6 m (Pedestrian Dummy) |

## MODEL VALIDATION

### AEB for Pedestrians

The quality of the simulation model can be estimated by comparing simulation results with test data. For the validation process of the pedestrian AEB model, test data from four different vehicles is available. All four vehicles have an own parameter set. Parameters have been identified from the test data as well.
Simulations and test results for four vehicles and four scenarios are shown in Figure 4.

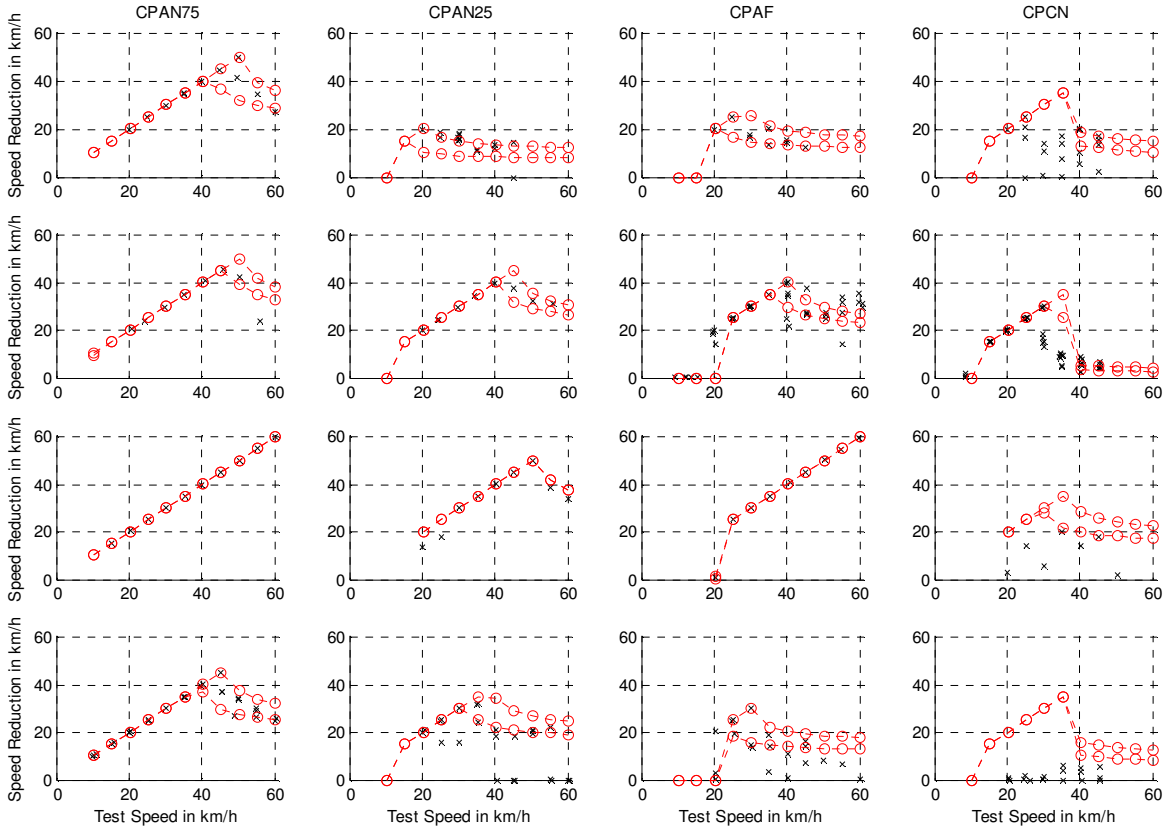


***Figure 4.*** **Comparison of measured speed reductions (black crosses) and simulation results (red circles) for pedestrian AEB tests. Scenarios according to Euro NCAP pedestrian scenarios, CPAN75=Car-Pedestrian-Adult-Near Side-75%, CPAN25=Car-Pedestrian-Adult-Near Side-25%, CPAF=Car-Pedestrian-Adult-Far Side, CPCN=Car-Pedestrian-Child-Nearside. Two different plots for simulation results are available: one for no time delay due to sensor sampling time (in general the upper line), and one for full time delay due to sensor sampling time.**

Simulation results match test data sufficiently well: they reproduce the general tendencies of the test data like peak avoidance speeds, minimum activation speeds, and result variability. This leads to the conclusion that the model structure is valid and the model can be used for the projected sensitivity studies.

## SENSITIVITY ANALYSIS

### Methodology for sensitivity analysis

The goal of this paper is to identify the influence of tolerances in test execution and variability in technical systems on the test result in AEB tests. A simulation model with parameter sets for four different real world vehicles is used to answer these questions. The baseline is ideal test execution according to current Euro NCAP scenarios for pedestrian AEB and a sensor processing factor of 0.5 (meaning additional delay of half the sensor sampling time). Based on this, selected parameters (one at a time) are modified to represent inaccuracies in test setup. The results are given in one combined plot per vehicle and scenario, resulting in an array of 16 plots.

These 16 plots in Figure 5 show much detail about the required test precision, but for an overview, an integral criterion is needed: Euro NCAP's assessment method is such an appropriate integral criterion.
Euro NCAP awards different points per test speed, corresponding to the real world relevance of that specific speed (for details, see [Seiniger 2015]). Full points for lower speeds are awarded for full speed reduction using a sliding scale. Full points for higher speeds (>45 km/h) are available if the speed reduction at the individual test is more than 20 km/h, and the test is conducted only if the preceding test was passed. The scoring is shown Table 2.

***Table 2.*** **Rating parameters.**

| **Index "k"** | **1** | **2** | **3** | **4** | **5** | **6** | **7** | **8** | **9** |
|---|---|---|---|---|---|---|---|---|---|
| **Test speed** | 20 | 25 | 30 | 35 | 40 | 45 | 50 | 55 | 60 |
| **Points** | 1 | 2 | 2 | 3 | 3 | 3 | 2 | 1 | 1 |
| **Sliding Scale** | 1 | 1 | 1 | 1 | 1 | 0 | 0 | 0 | 0 |
| **PassFail** | 0 | 0 | 0 | 0 | 0 | 1 | 1 | 1 | 1 |
| **Method** | • Sliding scale: ratio of speed reduction and initial speed | | | | | • Pass for speed reduction > 20 km/h<br>• Test only executed if previous test speed is passed | | | |

In a mathematical formulation, the rating result per scenario will become:

$$Rating = \sum_{k=1}^{k=n} \mathrm{SC}(k) \cdot \mathrm{Points}(k) \cdot \frac{v_{\mathrm{x,red,k}}}{v_{\mathrm{x,0,k}}} + \mathrm{PF}(k) \cdot \mathrm{Points}(k) \cdot < v_{\mathrm{x,red,k}} - v_{\mathrm{x,red,min}} >^{0},$$

with the vectors "Sliding scale SC", "PassFail PF", "Points" and "$v_{x,red,min}$ = minimum speed reduction = 20 km/h" as defined in Table 2, and using the Föppl-parenthesis "$< >^{0}$" which becomes 0 for results less than zero and 1 elsewise.

**Results**

Test case definition, color coding for the plots and rating results relative to each baseline condition per vehicle is shown in Table 3.

***Table 3.*** **Parameter variations, coding as shown in *Figure 5* and overall rating results compared to baseline in %, for vehicles A to D**

| Variant No. | Variation | Color | Marker | Rating A | B | C | D |
|---|---|---|---|---|---|---|---|
| 1 | Baseline | Black | . | 100% | 100% | 100% | 100 % |
| 2 | Earlier Detection, no influence of sampling time | Red | + | 107% | 101% | 104% | 104 % |
| 3 | Later Detection, full influence of sampling time | Red | O | 93% | 99% | 98% | 90% |
| 4 | Impact Point 5 cm towards Dummy | Blue | O | 96% | 99% | 99% | 95% |
| 5 | Impact Point 20 cm towards Dummy | Green | O | 84% | 91% | 99% | 75% |
| 6 | Impact Point 5 cm away from Dummy | Blue | + | 104% | 101% | 101% | 102 % |
| 7 | Impact Point 20 cm away from Dummy | Green | + | 133% | 101% | 102% | 120 % |
| 8 | Test speed 1 km/h below nominal speed | Cyan | + | 104% | 101% | 105% | 105 % |
| 9 | Test speed 1 km/h above nominal speed | Cyan | O | 98% | 96% | 102% | 101 % |

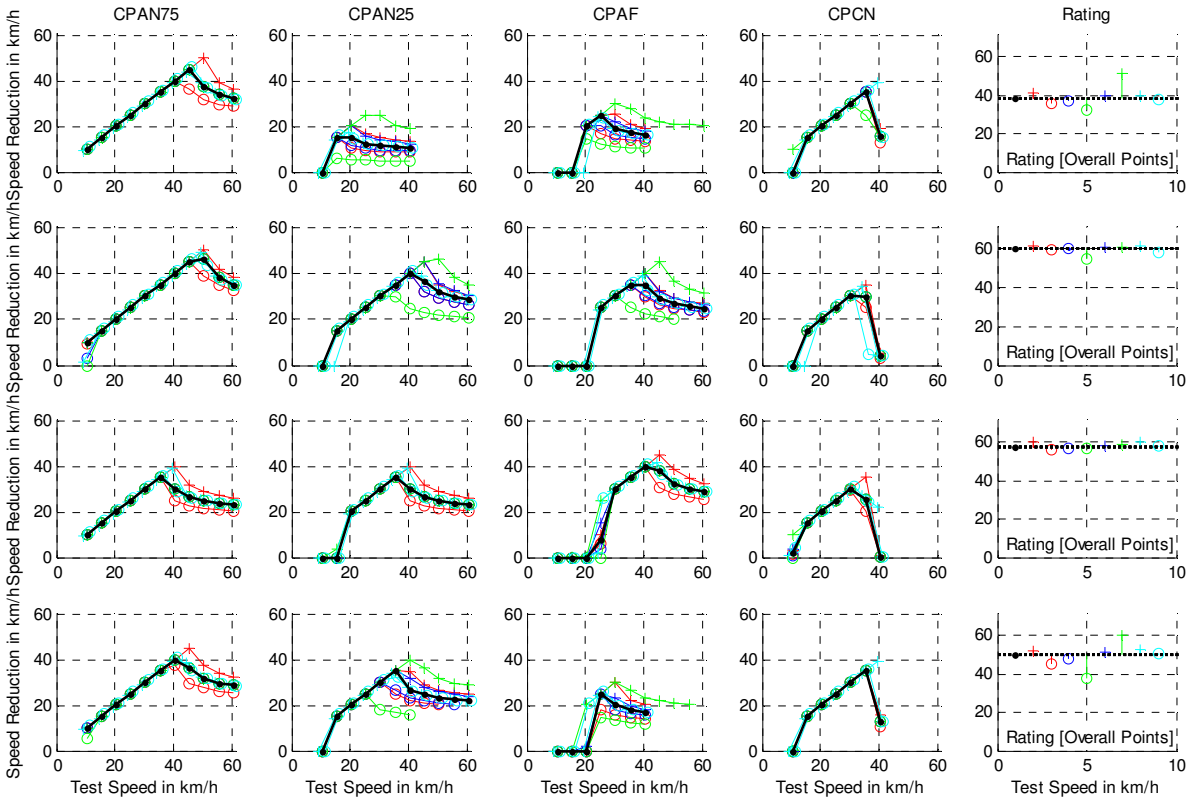


***Figure 5.*** **Results for parameter variations, one vehicle per row. Shown is the achieved speed reduction for each test case from *Table 3* with the appropriate color coding, as well as the overall test result using the Euro NCAP assessment method.**

These results show that the most relevant parameter with respect to test execution precision seems to be the variation in impact point location. While a shift in impact point of 5 cm (as required according to current Euro NCAP protocol) changes the overall results by maximum +4% and -5%, a shift by 20 cm affects the results by a tremendous +33% or -25%. Speed variations during the test, even up to 1 km/h plus or minus (which is four times the value allowed according to the current Euro NCAP protocol) have an effect comparable to the allowed 5 cm impact point shift. Assumed timing variations due to sensor sampling by ± half of sampling time affect the rating slightly more than the allowed 5 cm impact point shift.
These three parameters have been used for a further detailed study of their influence towards the overall rating result per vehicle, see Figure 6. All three plots are based on the baseline, only the selected parameter has been varied.
General tendencies are as expected:

- Moving the impact point away from the position where the pedestrian comes from generally gives AEB systems more time for detection, classification and braking, thus increasing the overall score. The score is more sensitive towards the impact shift for vehicles with generally lower score.
- Increasing the vehicle speed slightly allows for earlier pedestrian detection in critical scenarios for a given sensor angle, but also slightly takes away potential for speed reduction. Both effects seem to compensate each other in the overall rating result, and this is true for all four vehicles.
- Shifting the sensor detection time within an assumed sample rate to earlier values allows for an earlier target detection and thus braking decision which increases the overall rating. The effect of sensor time shift is different for the various vehicles.

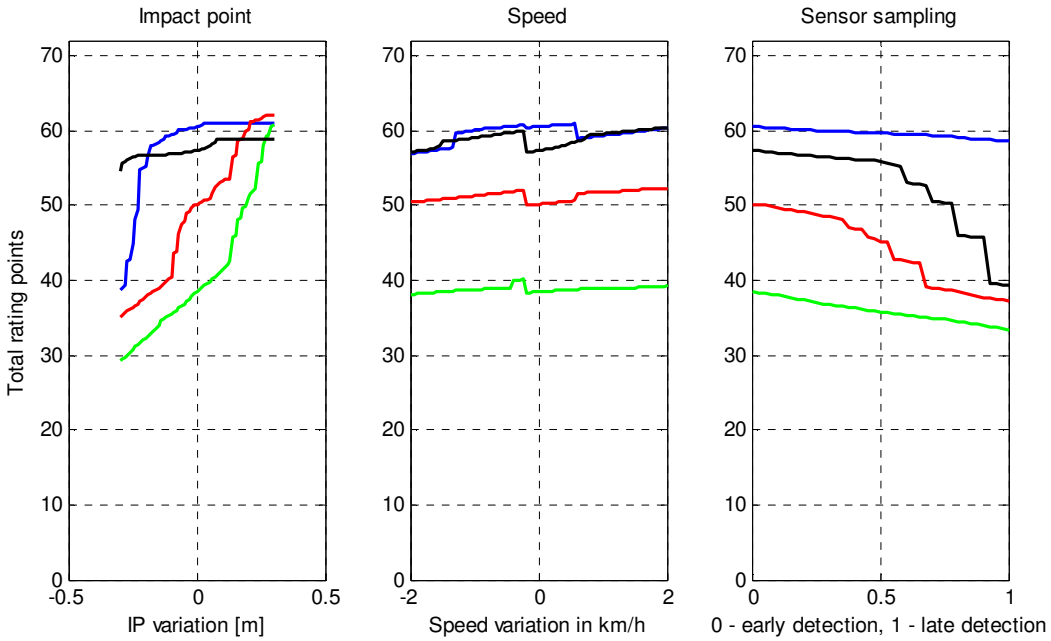


***Figure 6.*** **Sensitivity of overall rating result towards variations of impact point (with respect to the side where the pedestrian comes from), vehicle speed and sensor sampling timing.**

**Derivation of required test precision**

The most sensitive parameter that needs to be controlled by the test lab is the lateral variation of the impact point. If the test lab is able to maintain the impact point within a range of ± 5 cm, the results in the worst have a variability of ± 2 points of the Euro NCAP rating scheme. For ± 10 cm, this increases to ± 10 points. Note, however, that these values are worst case, assuming a systematic shift of the impact point in the direction of worse test results. In reality, the error will rather be stochastic and vary towards both directions - thus, the influence of the impact point error to overall test result will be much lower.
The other relevant parameter, the vehicle test speed, has a neglectable influence towards the overall score, even if it is varied by ± 2 km/h with respect to the desired test speed.

**Consequences**

Test experience shows that human drivers are able to maintain one variable (vehicle speed, lateral offset etc.) in acceptable ranges, but are not able to control two variables at the same time. If the test setup is able to synchronize the dummy movement with unprecise but constant vehicle speeds, the tests could be driven by human drivers alone and still allow for an acceptable accuracy with regards to the test result. The influence of vehicle sensor timing issues to the overall test result is then comparable to the error from test conduction.
Since in this case driving robots are not necessary anymore, the test cost can be greatly reduced.

**SUMMARY**

Goal of this paper was to show a methodology to derive accuracy requirements for a test setup for AEB systems, with focus on AEB pedestrian systems. A simulation model allows to vary relevant parameters and estimate the influence of the given parameters towards speed reduction and overall test result (according to the Euro NCAP assessment method).
The simulation model has been calibrated and validated against AEB pedestrian test data from four different production vehicles.
Sensitivity studies show that the most relevant parameter that needs to be controlled by the test lab is the lateral impact point of the pedestrian dummy on the vehicle-under-test's front. It should be in the range of ± 5 cm. Test vehicle speed variations in the range of ± 2 km/h have an neglectable influence towards test outcome.

Since test vehicle speed just needs to be held constant, but not exactly on a defined value, only one control channel for vehicle control is needed. In this case, it is anticipated that a combination of human driver and test setup (dummy propulsion system) with compensation for speeds and lateral offsets is sufficient to achieve an acceptable test execution precision.

**REFERENCES**


[AsPeCSS, 2014] Seiniger P, Bartels O, Kunert M, Schaller T: *Test procedure including test target and misuse tests, based on test results*. ASPECSS Deliverable D2.5, May 2014.Available for download at www.aspecss-project.eu.

[Seiniger, 2013]: Seiniger P, Bartels O, Wisch M, Pastor C.: *An Open Simulation Approach to Identify Chances and Limitations for Pedestrian Active Safety*. Paper presented at: 23nd Conference on the Enhancement of the Safety of Vehicles (ESV). May 27-30, 2013; Seoul, South Korea.

[Seiniger, 2015] Seiniger P, Hellmann A, Bartels O, Wisch M, Gail J: *Test Procedures and Results for Pedestrian AEB Systems*. Paper presented at: 24th Conference on the Enhancement of the Safety of Vehicles (ESV). June 8-11, 2015; Göteborg, Sweden.

[Winner, 2011]: Winner H. *Frontalkollisionsschutzsysteme*. In: Winner H, Hakuli S, Wolf G (Ed.).: *Handbuch Fahrerassistenzsysteme*. Wiesbaden: Vieweg + Teubner, 2012:S.522.

# CRASHWORTHINESS TESTING OF ELECTRIC AND HYBRID VEHICLES

**Sean O'Malley**
**David Zuby**
**Matthew Moore**
Insurance Institute for Highway Safety
United States

**Michael Paine**
**David Paine**
Australasian New Car Assessment Program (ANCAP)
Australia

Paper Number 15-0318

## ABSTRACT

Electric and hybrid vehicles are increasingly being offered as a means to provide personal transportation with less negative impact on the environment and lower operational cost. While still representing a small portion of fleets in industrialized countries, the availability of these types of vehicles is growing. Electric and hybrid vehicles comprised approximately 1 percent of new vehicle sales in the United States in 2004, and by 2013 this had grown to almost 4 percent. As a result, there is considerable interest in the crash safety of these vehicles and, in particular, potential hazards unique to their electrical drive systems such as electrocution, fire, and electrolyte spillage. This paper summarizes the crash test experience of electric/hybrid vehicle from the Australasian New Car Assessment Program (ANCAP) and Insurance Institute for Highway Safety (IIHS).

Since 2004, ANCAP and IIHS have subjected 42 hybrid and electric drivetrain vehicles to a variety of crashworthiness tests including both moderate and small overlap front crashes, side crashes, and roof strength tests. Crashworthiness results are summarized with special attention paid to the risk of electrical drive system hazards, and laboratory best practice related to electric vehicle testing is described.

The crashworthiness of hybrid and electric drive vehicles is typically similar to that of vehicles with internal combustion engines. IIHS has assigned eight good ratings, three acceptable ratings, and three poor ratings in frontal crash tests (both moderate and small overlap tests); 10 good ratings and one poor rating in side crash tests; and eight good ratings and one acceptable rating in roof strength tests. To date, ANCAP has assigned one 4-star rating and two 5-star ratings to electric vehicles in its evaluation program. Neither organization observed damage to the batteries or other portions of the electrical drive systems that indicated a potential risk.

Safety precautions and inspections of the electrical systems have evolved to include post-crash checks for isolation of high voltage from the chassis, leakage of volatile gases, and physical damage of the systems. In addition, vehicles are quarantined and observed after a test to ensure hidden damage does not result in fire risk developing over time.

Ten years of crash testing electric/hybrid vehicles by ANCAP and IIHS, covering a wide range of crash conditions, indicates the variation in crashworthiness performance of hybrid/electrical drive vehicles is comparable with the variation observed with conventionally powered vehicles. Neither ANCAP nor IIHS has observed problems associated with the electrical drive systems in tests of more than 40 hybrid and electrical vehicles. This observation suggests safety designers are providing good protection of the electrical drive systems in crashes represented by federal and consumer information tests.

While vehicles with high-voltage batteries present unique challenges to laboratory safety, ANCAP and IIHS experience suggests these potential hazards can be managed. Using appropriate tools and taking extra steps to ensure isolation of the battery from other parts of the vehicle has resulted in the successful execution of electric vehicle crash tests by both organizations without injury or other dangerous incident.

## INTRODUCTION

Tougher fuel economy standards have spurred automakers to make design changes to their vehicle fleets to meet new regulations. Making vehicles lighter, installing smaller engines, using alternative fuels, and manufacturing hybrid and electric vehicles are some of the strategies for increasing fuel economy.

A vehicle is considered a hybrid if it has more than one power source to propel the vehicle, typically an internal combustion engine and electric motor. An electric vehicle is equipped with one or more electric motors to propel the vehicle. Both hybrid and electric vehicles have high-voltage battery packs, often referred to as Rechargeable Electric Storage Systems (RESS).

In 1999, the Honda Insight was the only hybrid electric vehicle (HEV) available in the United States, with 17 vehicles sold. In 2000, the Toyota Prius was introduced, with more than 5,500 vehicles sold. In 2004, the Honda Civic hybrid was introduced, with sales of 13,700 units. Beginning in 2004, there have been at least two new HEV models introduced each year, with 11 introduced in 2012. A total of 47,600 HEVs were sold in the United States in 2003. By 2013, that number had grown to almost 500,000 units (Figure 1). In 2013, there were 46 HEV models available in the U.S. market [1].

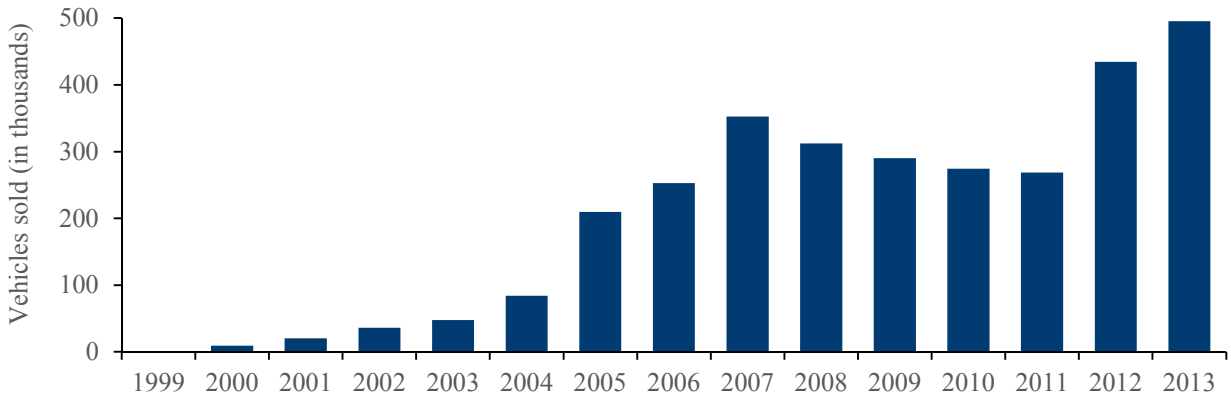


***Figure 1. Hybrid and electric vehicle sales, United States.***

The first mainstream plug-in electric vehicles (PEV) available in the United States were the Nissan Leaf and Chevrolet Volt, both introduced in December 2010, with sales of 19 and 326 units, respectively. Two additional PEV models were introduced in 2011, the Mitsubishi i-MiEV and Smart ED, with sales of 76 and 310 units, respectively. Nine PEVs were introduced in 2012, and six in 2013. By 2013, PEV sales totaled almost 100,000 units (Figure 2). There were 16 PEV models for sale in the United States in 2014 [1].

Sales of PEV and HEV vehicles in the United States have increased annually, from 17 vehicles in 1999 to 592,231 vehicles in 2013, approximately 3.5 percent of all passenger vehicles sold. The sales volume of electric/hybrid vehicles in Australia is smaller (Figure 3), but the same upward trend is evident [2][3][4][5][6][7][8][9][10][11][12].

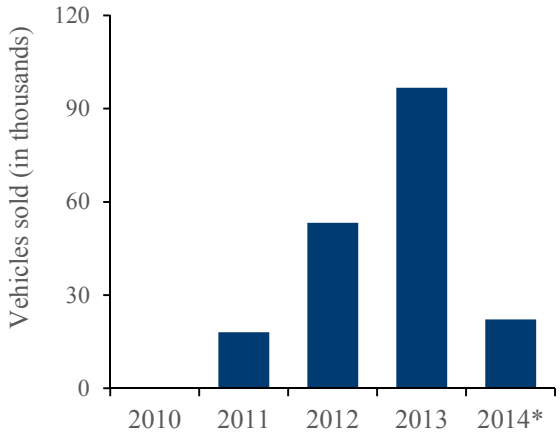


***Figure 2. Plug-in electric vehicle sales, United States (*2014 sales, through first quarter).***

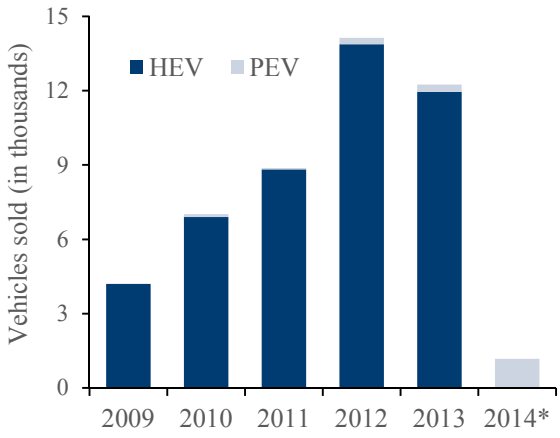


***Figure 3. Plug-in electric and hybrid vehicle sales, Australia (*HEV sales not available).***

**Real-World Safety Concerns**

Electric/hybrid vehicles have a number of safety concerns not associated with conventional vehicles including electrocution, explosion, electrolyte spillage, and/or fire. There have been numerous real-world examples of electric vehicles catching on fire after a crash and in the garages where they were being stored; in some cases, this may have been while the vehicle was being charged.

The most widely publicized fire incident involved a 2011 Chevrolet Volt after it was crash tested at MGA Research, in Burlington, Wisconsin, in June 2011. The Volt's lithium-ion battery caught on fire 3 weeks after being subjected to an 18 mi/h side pole test as part of the National Highway Traffic Safety Administration's (NHTSA) New Car Assessment Program (NCAP). The fire quickly spread to three adjacent vehicles. An extensive post-fire investigation later determined that a small amount of battery coolant penetrated the high-voltage battery case after the crash, causing the battery to short and eventually leading to a thermal runaway condition [13].

In 2012, 16 Fisker Karma electric vehicles caught fire and were destroyed at a port in New Jersey after Hurricane Sandy. It is believed that flooding caused a short circuit in one of the Karma's lithium-ion batteries, leading to a thermal runaway condition. The fire then spread, eventually igniting the 15 adjacent vehicles [14].

In 2013, two Tesla Model S sedans caught fire while being driven in the United States. The first, in Washington State, occurred after the car struck a metal object in the road. The second occurred after the car ran over a trailer hitch lying on the road in Tennessee. In both cases, road debris punctured the floor and battery pack, leading to battery failure and thermal runaway. Both drivers were able to pull over and exit the cars safely. Tesla said it would add underbody shielding to help protect the lithium-ion battery [15]. In 2014, a fire occurred when the driver, a car thief, crashed the car at high speed, tearing the vehicle in two. The battery pack was ejected and caught fire. The driver later died in the hospital from injuries sustained in the crash [16].

**Real-World Safety**

Due to the extra weight of RESS, hybrids are 10 percent heavier on average than their non-hybrid counterparts. Provided that the vehicle has good crashworthiness, this extra mass provides a slight safety advantage in some types of crashes, such as those involving other vehicles. A study by the Highway Loss Data Institute estimated the odds that a crash would result in injuries if people were riding in a hybrid vehicle versus the conventional version of the

same vehicle [17]. The analysis included more than 25 hybrid-conventional vehicle pairs, all 2003-11 models, with at least one collision claim and at least one related injury claim filed under personal injury protection (PIP) or medical payment (MedPay) coverage in 2002-10. Both PIP and MedPay are first-party insurance that cover the costs of injuries to drivers and their passengers in the insured vehicles. Figures 4 and 5 compare the injury odds of hybrids with their conventional counterparts under both types of insurance and show that the odds of injury are at least 25 percent lower in hybrids. The differences in injury odds may have been partly influenced by differences in how, when, and by whom hybrids are driven in comparison with their counterparts that are not completely captured by the covariates in the analysis. Nevertheless, these results indicate that electric drivetrains do not pose an overall increased risk of injury for their occupants.

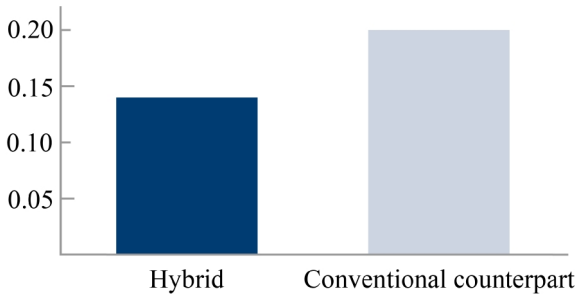


***Figure 4. Estimated injury odds under collision and personal injury protection coverage.***

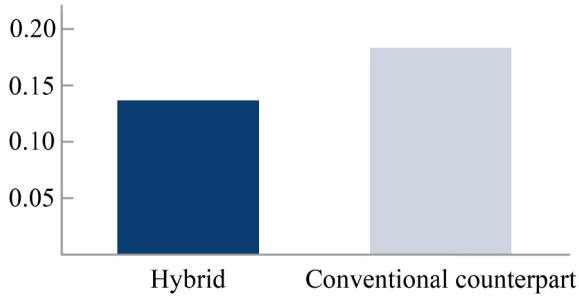


***Figure 5. Estimated injury odds under collision and medical payment coverage.***

Additionally, IIHS conducted a study of fatal vehicle crashes associated with a fire for model year 2009-14 vehicles [18]. The rate of fire incidences for electric and hybrid vehicles was comparable with those for conventionally powered vehicles.

## ELECTRIC/HYBRID VEHICLE TESTS

### Battery Testing Standards

There are numerous standards that address the safety of batteries and RESS at the component level such as the Society of Automotive Engineers (SAE J2464, J2929, and J2380), United Nations Economic Commission for Europe (ECE R.100), and draft Global Technical Regulation No.13 for RESS [19-20]. All prescribe tests that simulate various environmental, mechanical, and electrical conditions that batteries and RESS can be subjected to in the automotive environment including:

- Vibration
- Thermal shock and cycling
- Mechanical impact, integrity, and shock
- Fire resistance
- External short circuit protection
- Over- and under-charge protection
- Over-temperature protection

Generally, the standards specify that the battery or RESS shall not leak electrolyte, rupture, catch fire, or explode when subjected to the conditions of each test. The isolation resistance is measured between the positive and negative terminals and the battery case/ground to ensure the internal integrity of the battery or RESS has not been compromised. The isolation resistance should exceed 100 Ω/V, following procedures described in the standards.

In the United States, Federal Motor Vehicle Safety Standard (FMVSS) No. 305 [21] addresses the crash safety of RESS through full-vehicle crash tests. Specifically, FMVSS 305 requires that following regulatory compliance frontal barrier, rear moving barrier, and side moving deformable barrier crash tests:

- RESS shall remain attached and secured in the vehicle, with no intrusion into the occupant compartment
- Electrical isolation of the RESS must be no less than 500 Ω/V
- Any electolyte spillage shall not enter the occupant compartment nor exceed 5 liters outside the occupant compartment.

FMVSS 305 does not impose separate requirements for RESS internal integrity, as this is covered by the aforementioned standards.

**Laboratory Vehicle Tests**

The Insurance Institute for Highway Safety (IIHS) and Australasian New Car Assessment Program (ANCAP) have crash tested 42 hybrid and/or electric vehicles in various test scenarios. IIHS performs vehicle crashworthiness evaluations using the following tests:

1. Moderate overlap front crash test (64 km/h, 40 percent overlap on driver side, into deformable barrier)
2. Small overlap front crash test (64 km/h, 25 percent overlap on driver side, into rigid barrier with radius on the right edge)
3. Side crash test (50 km/h, deformable mobile barrier into driver side)
4. Roof strength (quasi-static loading on either driver or passenger side of vehicle)

Ratings of good, acceptable, marginal, or poor are awarded to the vehicle in each test mode. The crash test ratings are based not only on measurements made by sensors in the test dummy but also analysis of the dummy's observable motion and measurements of safety cage deformation. The roof crush test is evaluated by measures of crushing force and displacement of the crushing platen [22].

ANCAP performs similar tests as part of its 'Star' rating evaluation program that include:

1. 40 percent frontal offset test (64 km/h on driver side)
2. Side impact test (50 km/h, mobile deformable barrier crashing into driver side of vehicle)
3. Pole side impact test (29 km/h, driver side of vehicle into rigid pole)

The IIHS and ANCAP side impact tests differ in that the deformable barrier used in the IIHS side test has a mass of 1,500 kg and is shaped like an SUV, whereas the ANCAP side impact barrier is shaped like passenger car with a mass of 950 kg.

The results of the three vehicle crash test scenarios above contribute to the ANCAP overall star ratings, which range from 1 to 5 stars. In addition to the vehicle crash tests, ANCAP performs a pedestrian protection assessment, a whiplash protection assessment, and reviews the inclusion of safety assist technology on the vehicle in order to derive the ANCAP overall star rating for the vehicle. The ANCAP rating covers three vehicle safety areas: occupant protection, pedestrian protection, and safety assist technology [23].

Figures 6-9 compare the ratings of plug-in electric (PEV) and hybrid electric (HEV) vehicles with the ratings of conventional vehicles in the same vehicle classes and model years. The electric/hybrid vehicles have a higher proportion of good IIHS ratings in the moderate overlap front test, side impact test, and roof strength test than conventionally powered vehicles from the same vehicle classes and model years. In addition, several HEVs and PEVs have been awarded IIHS *Top Safety Pick* awards, indicating they have the highest level of overall safety according to IIHS guidelines (Table 1).

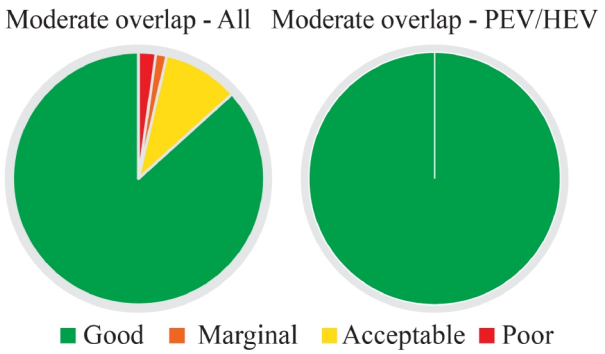


***Figure 6. IIHS moderate overlap test ratings.***

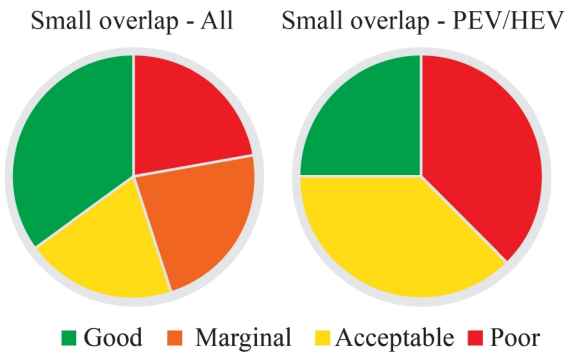


***Figure 7. IIHS small overlap test ratings.***

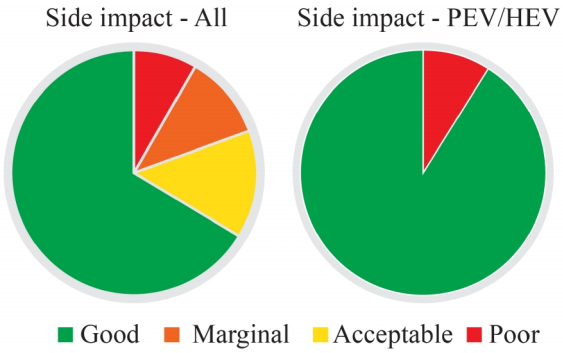


***Figure 8. IIHS side impact test ratings.***

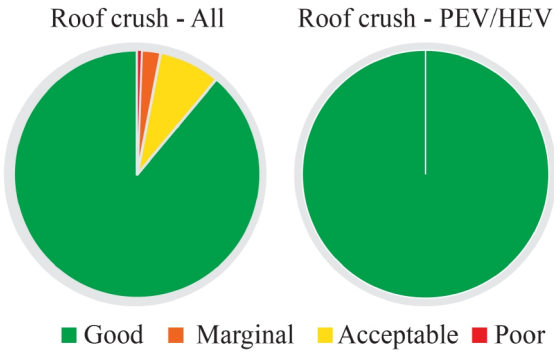


***Figure 9. IIHS roof crush test ratings.***

**Table1**
***Top Safety Pick* awards for PEV/HEV tested by IIHS.**

| | 2009 | 2010 | 2011 | 2012 | 2013 | 2014 | 2015 |
|---|---|---|---|---|---|---|---|
| Chevrolet Volt | | | x | x | x | x | x |
| Ford C-Max Hybrid | | | | | | x | x |
| Honda CRZ | | | | x | x | | |
| Honda Insight | | | | x | x | | |
| Lexus CT200h | | | x | x | x | | x |
| Nissan Leaf | | | x | x | | | |
| Toyota Prius | x | | x | x | x | x | x |
| Toyota Prius C | | | | x | | | |
| Toyota Prius V | | | | x | x | | x |

Three IIHS small overlap crash tests of electric/hybrid vehicles resulted in poor structural ratings, and six IIHS side impact tests resulted in acceptable structural ratings. However, the area surrounding the vehicle's high-voltage battery (RESS) was intact in all cases, with no electrical safety issues (Figures 10-12). Moreover, of the 12 HEV/ PEV models tested since IIHS incorporated a 2-week post-test observation period, none have caught fire like the Chevrolet Volt tested by NHTSA.

For the ANCAP tests, only the 2010 Mitsubishi i-MiEV scored lower than the maximum 5 star ANCAP rating, with a final rating of 4 stars. The rating was influenced by occupant injury risk, rather than structural performance of the vehicle, and no crashworthiness deficiencies related to electrical safety were identified as part of the usual assessment.

*Figure 10. RESS location in 2013 Toyota Prius C after IIHS small overlap test, side view.*

*Figure 11. RESS location in 2014 Nissan Leaf after IIHS small overlap test, bottom view.*

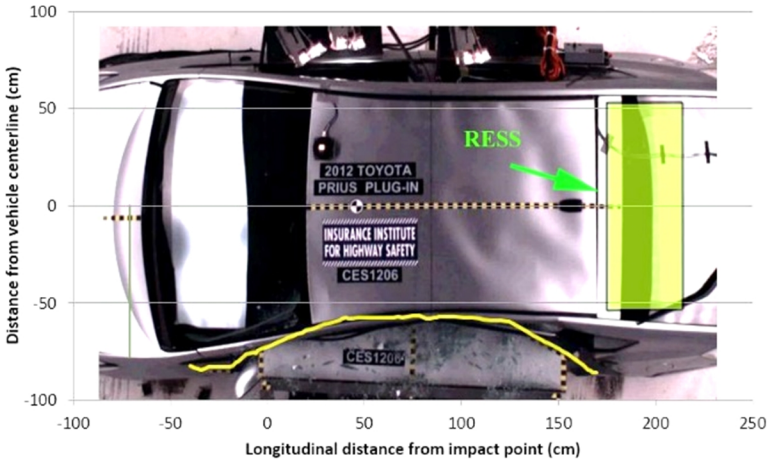


*Figure 12. RESS location in 2012 Toyota Prius Plug-In during IIHS small overlap test, overhead view with intrusion chart.*

**Laboratory Safety for HEV/PEV Crash Testing**

HEV/PEV crash test procedures utilized by IIHS and ANCAP have evolved since these vehicles were first introduced in the mass market. There are no specific SAE or other guidelines on crash testing such vehicles; instead, IIHS and ANCAP have evaluated the best practices utilized by automakers and other testing organizations and developed them into a single procedure. It is anticipated that these procedures will continue to evolve as new types of HEV/PEVs enter the market. This section describes the procedures adopted to evaluate the crashworthiness of HEV/PEV vehicles.

Test procedures include monitoring the battery temperature, electrical isolation of the RESS from the vehicle chassis, and verifying that automatic battery disconnection from the drive circuit has occurred after a crash. In addition, as fires caused by RESS damage may occur, a fire management plan has been implemented. Finally, proper discharging and disposal procedures are followed before discarding the vehicle.

Laboratory safety when working on vehicles that include a high-voltage RESS requires the use of protective gear and tools designed for high-voltage work. Eye protection (safety goggles) and insulated gloves and boots should be worn by personnel working with an HEV/PEV RESS. In addition, hand tools should be adequately insulated and, where applicable, include cross-guards to prevent hands from slipping on to any uninsulated part (Figure 13). Finally, high-voltage tool kits should include an insulated pole with a hook or loop that can be used by a second person to pull away a technician who may come in contact with the high-voltage source despite precautions (Figure 14). High-voltage work kits are available from major tool suppliers.

Safely preparing an HEV/PEV for an IIHS crash test requires gathering information about the electric drive system from the test vehicle manufacturer and having a detailed checklist of procedures to follow (Appendix A). The following information can facilitate safe installation of monitoring systems and post-crash disposal of the tested vehicle:

- Location of the manual service disconnect (MSD)
- Locations of the RESS and high-voltage wiring
- Recommended connection locations for monitoring RESS isolation
- Instructions for charging/discharing the RESS
- Information about the chemical properties of the battery coolant
- Information about the color and location of the battery coolant
- Copy of the Material Safety Data Sheet for the battery or its components
- Information about hazards unique to the test vehicle's partiular RESS

***Figure 13. Assortment of high-voltage tools.***

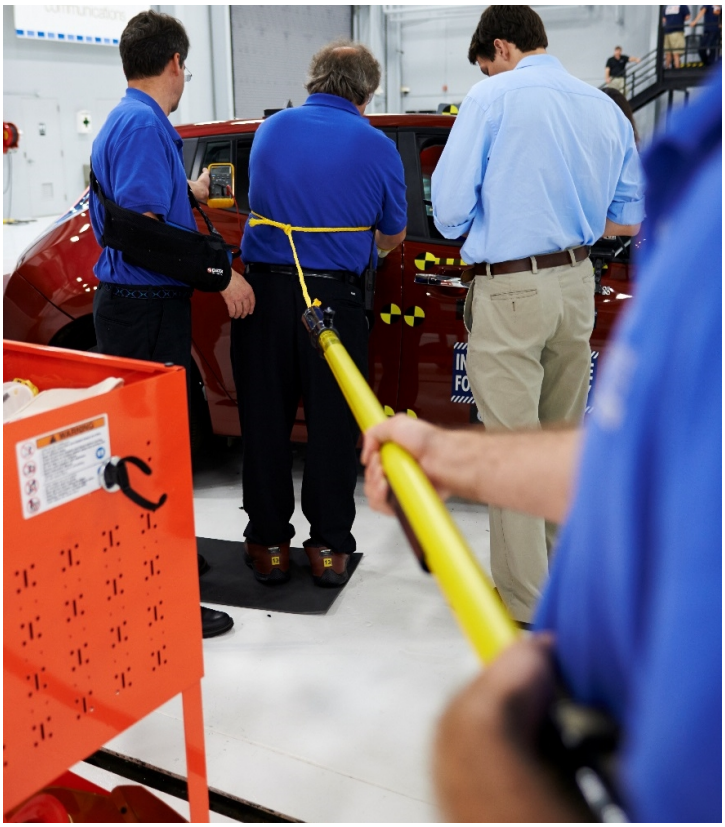

***Figure 14. Insulated pole, shown attached to technician measuring high-voltage battery isolation.***

Preparation of an HEV/PEV for a crash test begins with using the MSD to isolate the RESS from the vehicle chassis while test equipment is installed and pre-crash measurements are taken. Locations of the MSD are not standardized and vary considerably (Table 2 and Figures 15-16).

**Table2.**
**Examples of locations for manual service disconnects on HEV/PEV.**

| Model(s) | Location | Notes |
|---|---|---|
| Chevrolet Volt | Rear of center console | Accessed through panel inside console |
| Ford C-Max | Behind and under left rear seat | Rear seat must be folded fully forward |
| Lexus CT 200h (also Toyota Prius and Prius V) | Rear cargo area | Remove spare tire cover and foam tool bin |
| Mitsubishi i-MiEV | Under rear of front passenger seat | Move front passenger seat fully forward |
| Nissan Leaf | Center tunnel in rear seating area | Remove bolted cover |
| Toyota Prius C | Under rear seat cushion | Remove cushion and access panel |
| Toyota Prius V | Within center console | Remove center console fascia then remove plastic MSD cover |

A clear means of identifying the MSD status should be adopted so that all personnel can know when the vehicle is safe to work on. For example, IIHS practice is to secure the MSD key/plug to the roof of the test vehicle with orange tape (Figure 17). Personnel should consider the RESS to be connected to the drive system if this indicator is absent.

***Figure 15. Manual service disconnect in Lexus CT200h, shown in cutaway.***

***Figure 16. Manual service disconnect in Chevrolet Volt, shown in cutaway.***

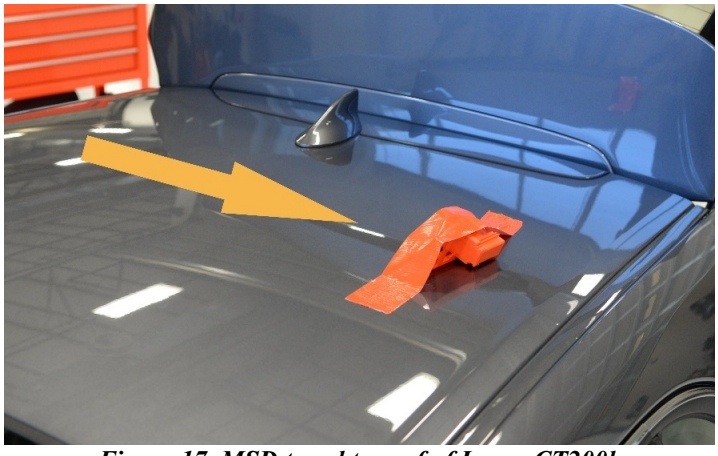

***Figure 17. MSD taped to roof of Lexus CT200h while work is conducted to battery system.***

For IIHS tests, a monitoring circuit, as described in FMVSS 305, is installed across the positive and negative leads on the drive side of the MSD. This attachment allows the post-crash measurements to ascertain whether the crash-initiated disconnection of the RESS from the drive system has occurred. The IIHS box that contains this circuit also contains circuitry to monitor a thermocouple that is attached to the RESS housing to help identify the potential for post-crash fire events. Figure 18 shows the schematic diagram of the IIHS RESS monitor. Figure 19 illustrates how test probe terminals are protected from accidental contact by technicians and test witnesses. Care should be taken not to interfere with the RESS of high-voltage wiring when installing other test equipment (e.g., data acquisition system, cameras, and related power supplies).

The first check after a crash test is to confirm isolation of the high-voltage power source from the vehicle chassis. This is done by measuring the voltage between the various test points on the monitor. If a non-zero potential is measured, then the isolation resistance is calculated by switching in the known resistors and using the re-measured voltages in the formulas shown in Figure 18.

An isolation resistance of more than 500 Ω/V is considered safe and would represent compliance with FMVSS 305 following regulatory tests. This measurement confirms the high-voltage battery is isolated from the vehicle body. Simultaneously and from a distance, other laboratory personnel visually check for signs of smoke or coolant leakage. Once electrical isolation of the RESS is established, collection of any leaking coolant may begin. Temperature of the RESS housing is monitored throughout post-crash procedures. As an extra precaution, the MSD should be removed as soon as it is accessible to test personnel.

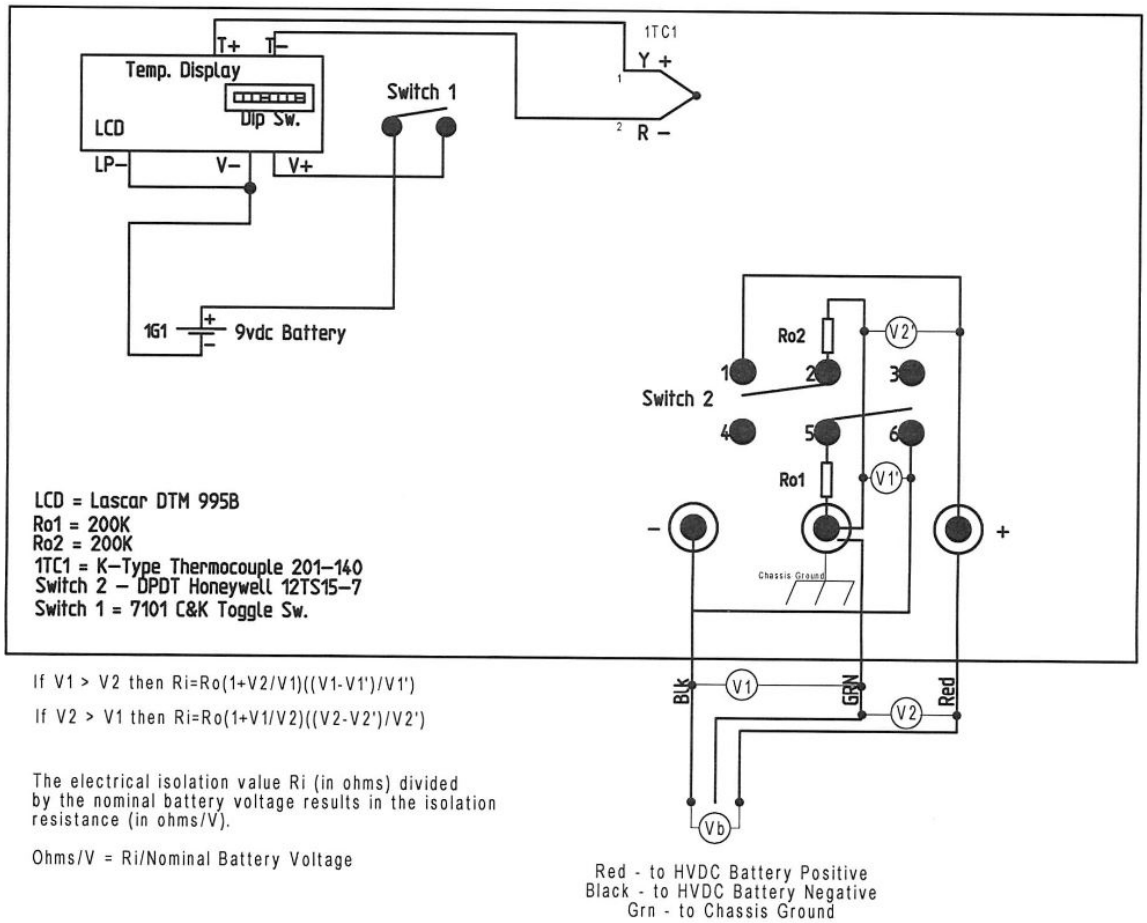


***Figure 18. Schematic of IIHS '305' box, including thermocouple circuit and isolation resistance formula.***

***Figure 19. IIHS '305' box, showing thermocouple readout, resistor switch, and terminal cover.***

In the event of any sign of fire or rising temperatures at the RESS housing, the vehicle should immediately be moved out of the laboratory if it is safe to do so. This can be managed with a lift truck equipped with insulating material on its forks to shield both the lift and its operator from potential electric shock. Fire extinguishing operations should commence immediately. Extinguishing fires associated with both nickel metal hydride (Ni-MH) and lithium-ion (Li-Ion) batteries typically involves applying copious amounts of water, although there is conflicting advice amongst some manufacturers regarding how to best handle a fire event; for example, instructions for the Toyota Prius C and Prius V are to let the battery burn itself out [24]. Regardless, as an additional precaution, it is good practice to arrange for the local fire department to be present during crash tests of HEV/PEV, especially those with Li-Ion batteries.

Another hazard associated with damage to high-voltage batteries is the possible release of carbon monoxide, hydrogen fluoride, and other harmful gases. Gas detection equipment can be used to check for their presence after a test, but this equipment is very expensive and the release of gases is unlikely in tests conducted by IIHS and ANCAP. The potential hazard may be managed by moving the vehicle to a well-ventilated area. A release of gas typically indicates a serious problem within the RESS.

Since the post-crash fire from the Chevrolet Volt test was reported by news media, IIHS has included an additional precaution and evaluation of this potential risk. Tested HEV/PEVs are stored for a period of 2 weeks in a metal storage shed located remote from the test laboratory (Figure 20). This minimizes the risk of collateral damage in the unlikely event of a fire. After this observation period, the vehicle's high-voltage battery is discharged per the manufacturer's recommended procedure.

***Figure 20. Electric/hybrid vehicle post-test storage.***

## CONCLUSIONS

Neither ANCAP nor IIHS crashworthiness testing has identified safety-related issues associated with the high-voltage RESS of electric and hybrid vehicles. In fact, test results suggest that, as a class, these vehicles are more crashworthy than their conventionally powered counterparts. However, the number of crash tests of vehicles with electric drive systems is small compared with ANCAP and IIHS experience with conventional vehicles, and there are crash test scenarios not covered by the crash tests conducted by ANCAP and IIHS. For example, higher speed narrow object impacts may intrude into the battery compartment. As the availability of these vehicles increases, it seems likely that crash testing may uncover problems unique to these vehicles.

Crash testing has been executed safely through careful attention to the unique hazards associated with high-voltage batteries. However, new types of electric powertrains (e.g., fuel-cells) are being introduced into the market, so laboratory safety practice will need to evolve. Current electric/hybrid safety procedures may be a good starting point when developing them.

Additional information regarding the safety precautions used when testing electric/hybrid vehicles can be found in "Safety Precautions and Assessments for Crashes Involving Electric Vehicles" [24].

## REFERENCES


[1] U.S. Department of Energy. 2014. Alternative fuels data center. Available: http://www.afdc.energy.gov/data/. Accessed: 2 Mar 2015.Washington, DC.

[2] Pontes, J. 2014. EV sales; Australia December 2013. EV-Sales.blogspot.ca, Jan 18. Available: http://www.ev-sales.blogspot.ca/2014/01/australia-december-2013.html. Accessed: 2 Mar 2015.

[3] Pontes, J. 2015. EV sales; Australia full year 2014 (updated). EV-Sales.blogspot.ca, Jan 15. Available: http://ev-sales.blogspot.com.br/2015/01/australia-full-year-2014.html. Accessed: 2 Mar 2015.

[4] Dowling J. 2011. Mitsubishi electric car back in stock. Carsales.com.au. Available: http://www.carsales.com.au/news/2011/small-passenger/mitsubishi/mitsubishi-electric-car-back-in-stock-26567. Accessed: 2 Mar 2015. Victoria, Australia.

[5] Pontes, J. 2013. EV sales; Australia full year 2012. EV-Sales.blogspot.ca, Jan 5. Available: http://www.ev-sales.blogspot.ca/2013/01/australia-full-year-2012.html. Accessed: 2 Mar 2015.

[6] Ottley S. 2013. Hybrid car sales make up 1 per cent of vehicle sales. *The Sydney Morning Herald*, Nov 30. Available: http://www.smh.com.au/national/hybrid-car-sales-make-up-1-per-cent-of-vehicle-sales-20131129-2ygw9.html. Accessed: 2 Mar 2015.

[7] Nicholson T. 2014. Toyota hits new hybrid high. GoAuto.com.au, Mar 27. Available: http://www.goauto.com.au/mellor/mellor.nsf/story2/A19B001FC141478ECA257CA800178264. Accessed: 2 Mar 2015.

[8] Bober I. 2014. Hybrid sales flopped in 2013. *Practical Motoring*, Jan 21. Available: http://practicalmotoring.com.au/car-news/hybrid-sales-flopped-2013/. Accessed: 2 Mar 2015. New South Wales, Australia: Practical Motoring.

[9] Pettendy M. 2014. New Mazda2 to plug in. Motoring.com.au, Jun 30. Available: http://www.motoring.com.au/news/2014/small-passenger/mazda/2/new-mazda2-to-plug-in-44423. Accessed: 2 Mar 2015. Victoria, Australia.

[10] TMR Team. 2013. Toyota's greenest Camry surpasses Prius in Australian hybrid sales. *The Motor Report*, Apr 10. Available: http://www.themotorreport.com.au/56320/toyotas-greenest-camry-surpasses-prius-in-australian-hybrid-sales. Accessed: 2 Mar 2015.

[11] Martin S. 2012. Cool and green hybrid car sales surge to Australian record. News.com.au, Aug 2. Available: http://www.news.com.au/finance/cool-and-green-hybrid-car-sales-surge-to-australian-record/story-e6frfm1i-1226441599395. Accessed: 2 Mar 2015. New South Wales, Australia.

[12] Australian Business Journal. 2015. Drivers going green as hybrid cars sales soar. TheAuBJ, Aug 2. Available: http://www.australianbusinessjournal.com.au/drivers-go-green-as-sales-of-hybrid-cars-soar/. Accessed: 2 Mar 2015. Victoria, Australia.

[13] Crawley J. 2012. Probe of Chevy Volt fires closed. Reuters, Jan 20. Available: http://www.reuters.com/article/2012/01/ 21/us-gm-volt-idUSTRE80J20X20120121. Accessed: 2 Mar 2015.

[14] Lienert A. 2012. Fisker reveals cause of Karma fires during Hurricane Sandy. Edmonds.com, Nov 6. Available: http://www.edmunds.com/car-news/fisker-reveals-cause-of-karma-fires-during-hurricane-sandy.html. Accessed: 2 Mar 2015.

[15] Ivory D. 2014. Federal safety agency ends its investigation of Tesla fires. *The New York Times*, Mar 28. Available: http://www.nytimes.com/2014/03/29/business/safety-agency-ends-investigation-of-tesla-fires.html. Accessed: 2 Mar 2015.

[16] Burke K. 2014. Driver of stolen Tesla that crashed, split in 2, dies. *Automotive News*, Jul 10. Available: http://www.autonews.com/article/20140710/OEM11/140719991/driver-of-stolen-tesla-that-crashed-split-in-2-dies. Accessed: 2 Mar 2015. Detroit, MI: Crain Communications Inc.

[17] Highway Loss Data Institute. 2011. Injury odds and vehicle weight comparison of hybrids and conventional counterparts. *HLDI Bulletin* 28(10). Arlington, VA.

[18] National Highway Traffic Safety Administrations. 2015. Fatality Analysis Report System. Available: http://www.nhtsa.gov/FARS. FARS data, February. Washington, DC: U.S. Department of Transportation.

[19] Society of Automotive Engineers. 2014. Safe handling of high-voltage battery systems. Classroom training, Course ID C1019. Available: http://training.sae.org/seminars/c1019/. Accessed: 2 Mar 2015. Warrendale, PA.

[20] Society of Automotive Engineers. 2015. Impact and Rollover Test Procedures Standards Committee meetings. Available: http://www.sae.org/works/committeeHome.do?comtID=TEVSSTS1. Accessed: 2 Mar 2015. Warrendale, PA.

[21] Office of the Federal Register. 2011. *Code of Federal Regulations*; Title 49 Transportation, Part 571 Federal Motor Vehicle Safety Standards, Standard No. 305 Electric-powered vehicles: electrolyte spillage and electrical shock protection. Washington, DC: National Archives and Records Administration.

[22] Insurance Institute for Highway Safety. 2015. About our tests. Available: http://www.iihs.org/iihs/ratings/ratings-info/frontal-crash-tests. Accessed: 2 Mar 2015. Arlington, VA.

[23] Australasian New Car Assessment Program. 2015. ANCAP safety ratings explained. Available: http://www.ancap.com.au/safety-ratings-explained. Accessed: 2 March 2015. Manuka, Australia.

[24] Paine M, Paine D, Ellway J, Newland C, Worden S. 2011. Safety precautions and assessments for crashes involving electric vehicles. Paper no. 11-0107. *Proceedings of the 11th International Technical Conference on Experimental Safety Vehicles*. Washington, DC: National Highway Traffic Safety Administration.

**Appendix A – Electric Vehicle Supplemental Checklist (IIHS)**

| INSURANCE INSTITUTE FOR HIGHWAY SAFETY VEHICLE RESEARCH CENTER | CHECKLIST | Page: 1 of 2 | Electric Vehicle Supplement | COORDINATOR |
|---|---|---|---|---|
| **Safety Measures and Tasks** | | | **CENXXXX** | |

| This checklist covers safety related tasks and pre and post-crash measurements. | Vehicle: | |
|---|---|---|
| **!! HIGH VOLTAGE SYSTEMS ARE NEVER SAFE, THEY CAN ONLY BE CONSIDERED SAFER !!** | VIN: | |

| Initial | Date | Checklist Items |
|---|---|---|
| **Pre-Test (before vehicle prep)** | | |
| | | Type of propulsion battery (e.g. Li-Ion, NiMH, etc.) _____. |
| | | Manufacturer instructions for installing '305' isolation box received and satisfactory |
| | | Copy/Paste 'Battery Isolation Worksheet' (Crashworthiness/ElectricVehicleInformation) into test Data folder |
| | | Nominal HV battery voltage _____V & resistor needed for '305' box (at least 500 times nominal battery voltage) _____ Ω |
| | | Verify propulsion battery is at full state of charge, per readout (varies by car; all but one 'bar' is typically sufficient) |
| | | Color of HV battery coolant (for leak detection, post-crash) |
| **Pre-Test Prep (Vehicle)** | | **!!! Appropriate Personal Protective Equipment to be worn at ALL TIMES !!** |
| | | **Remove positive cable from battery (12v) and then the HV service disconnect (MSD)** |
| | | Tape MSD to roof of vehicle with orange tape **!! MSD is to be taped to roof of vehicle whenever it is not installed in the HV battery!!** |
| | | Install '305' box, per manufacturer instructions **OR** request OEM to install if installation is deemed too hazardous **(Caution; the 305 box is now essentially part of the HV system)** |
| | | Install thermocouple on battery (or as close as possible to actual battery housing) |
| | | Photograph wiring hook-up and routing |
| | | Check voltage of + and – terminal to vehicle body; both should be zero. If not, STOP and contact manufacturer! |
| | | **Install service disconnect** |
| | | Check battery isolation, using Battery Isolation Worksheet. If results are more than 500 Ω/V, **remove service disconnect & tape to roof** and continue….. |
| | | Remove accelerator cable/connector |
| | | Fabricate a locking plate to hold transmission in 'Neutral' during crash |
| | | Verify area surrounding HV battery is clear of metal shavings, tools, loose cables, etc. |
| | | Schedule Fire Department to be on hand during test if vehicle contains Li-Ion battery |
| | | Verify all HV safety equipment is in Crash Hall and easily accessible, the emergency egress path for vehicle is clear, and forklift present (with fork isolators attached) |

| INSURANCE INSTITUTE FOR HIGHWAY SAFETY VEHICLE RESEARCH CENTER | CHECKLIST | Page: 2 of 2 | Electric Vehicle Supplement | COORDINATOR |
|---|---|---|---|---|

**Safety Measures and Tasks** **CEN1453**

| This checklist covers safety related tasks and pre and post-crash measurements. | Vehicle: | |
|---|---|---|
| **!! HIGH VOLTAGE SYSTEMS ARE NEVER SAFE, THEY CAN ONLY BE CONSIDERED SAFER !!** | VIN: | |

| Initial | Date | Checklist Items |
|---|---|---|
| **Pre-Test (Shed)** | | **!!! Appropriate Personal Protective Equipment to be worn at ALL TIMES !!** |
| | | Prior to Final Checklist, install the service disconnect |
| | | Record battery isolation, using Battery Isolation Worksheet in Excel (Pre-test). If results are more than 500 Ω/V, continue with final checklist |
| **Post-Test (Crash Hall)** | | *****Perform Steps Prior to Human Contact With Vehicle***** |
| | | INFORM PEOPLE ON FLOOR TO NOT TOUCH THE VEHICLE UNTIL THE ALL CLEAR IS GIVEN!! |
| | | Verify there is no toxic gas venting – visual |
| | | Verify there is no smoke or fire coming from battery |
| | | Verify there is no battery coolant leakage |
| | | Record battery temperature (thermocouple reading) _____°F. Continue to monitor for increase using thermal imager and by monitoring temperature readout |
| | | Check battery isolation, using Battery Isolation Worksheet in Excel (Post-test).<br>☐ Greater than 500 Ω/V, continue….<br>☐ Less than 500 Ω/V means a potential isolation loss; quarantine vehicle and continue to monitor……. |
| | | Continue to monitor battery temperature and isolation for 5 minutes. If stable ⇨ |
| | | Continue with typical post-crash analysis |
| | | **Remove service disconnect if possible & tape to roof** |
| | | DO NOT LEAVE VEHICLE IN BUILDING UNATTENDED AT ANY TIME! |
| **Post-Test (Photo Studio)** | | **!! Appropriate Personal Protective Equipment to be worn at ALL TIMES !!** |
| | | **Remove service disconnect as soon as possible & tape to roof** |
| | | Remove '305' box |
| | | If vehicle has Li-Ion propulsion battery, have observer present when the vehicle is in the building. Move vehicle to secure area outside at end of day (DO NOT LEAVE IN BUILDING UNATTENDED AT ANY TIME!). Vehicle will be quarantined in secure area, with fully charged battery, for at least 2 weeks before allowing manufacturer to discharge it |
| | | If vehicle propulsion battery is not Li-Ion, the battery should be discharged by manufacturer ASAP and before vehicle is sold for scrap (alternatively, the OE's can take possession of the battery) |

# GUIDELINES FOR PEDESTRIAN FRIENDLY WINDSCREEN DESIGNS CONSIDERING PROBABILISTIC FRACTURE BEHAVIOR

**Frederic Nuss**
**Lutz Eckstein**
Institut für Kraftfahrzeuge RWTH Aachen University
Germany

**Andreas Teibinger**
Virtual Vehicle Research Center
Austria

Paper Number 15-0319

## ABSTRACT

If adult pedestrians are being struck by passenger cars with short bonnets, head contact usually occurs in the windscreen area. In test procedures for regulation and consumer protection, this impact type is being assessed using so-called pedestrian head impactors. The head injury risk is being evaluated based on the acceleration signal using the so-called Head Injury Criterion (HIC). Corresponding experimental impactor tests in the windscreen center show large scatter. Main reason for the observed scatter is the fracture initiation of glass as already published in several studies [5]. Thus, for a head impact in the windscreen center an early fracture initiation results in a small head injury risk, while a late fracture initiation increases the injury risk significantly [14]. In the design of measures for the enhancement of vehicle sided pedestrian safety, this scatter is currently neglected.
Based on a theoretical description of the probabilistic fracture mechanics of glass, a methodology for designing pedestrian friendly windscreens considering the probabilistic fracture mechanics of glass will be described in the present paper. This methodology consists of two steps. First, the probability for certain fracture initiation times are assessed, considering probabilistic fracture mechanics and the tensile stress distribution on the glass surfaces during head impact. In a second step, the head injury risks for the different fracture initiation times are evaluated.
In order to show the potential impact of the described methodology, a windscreen of a vehicle model is being assessed and optimized. The findings of this optimization process are being used to derive guidelines for pedestrian friendly windscreens.

## INTRODUCTION

In case of a vehicle-pedestrian collision the impact location of the head of the pedestrian is being mainly influenced by the vehicle speed, by the pedestrian size and the vehicle shape. For a combination of an adult pedestrian and a passenger car with a short bonnet, head contact usually occurs in the windscreen area (e.g. [8, 9]). If a pedestrian head impactor is being shot against the windscreen center, large scatter can be observed for the acceleration signal of the head impactor as shown by [5] and [14] (see Figure 1).

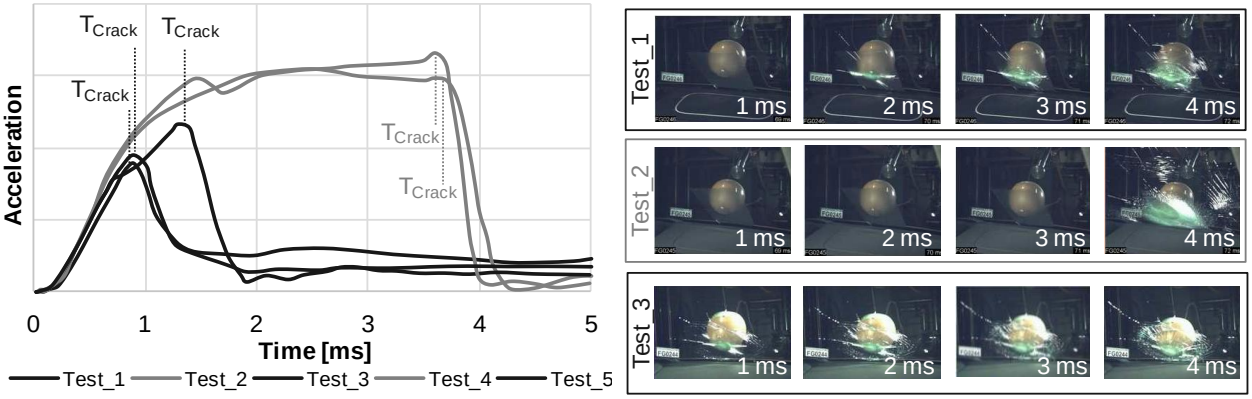


***Figure 1. Acceleration signal and crack initiation times for head impact in windscreen center [14].***

Since the boundary conditions are not changed and the windscreens are from the same batch, main reason for the scatter is the stochastic fracture behavior of the windscreen glass [14]. As can be seen in Figure 1, an early fracture initiation as in test 1, 3 and 5 results in lower accelerations and thus in lower head injury risks [14].
The stochastic fracture behavior of glass is a material dependent property, which cannot be changed easily. Due to the high viscosity of molten glass, the silicon dioxide molecules of glass cannot take the ordered structure of a crystal lattice during the cooling process, but solidify in a metastable order [4, 17]. Since the tensile stresses cannot be homogenized by plastic flow as within the elastic-plastic behavior of most metals [15], all glass components show a brittle fracture behavior.
Stochastically distributed material or surface defects influence the fracture behavior of glass [2]. In order to describe this stochastic behavior, the so-called Weibull-Distribution shown in Eq.1 is often used [10]. According to Eq.1 the fracture probability FP can be described by the current stress load $\sigma$, the characteristic strength $\sigma_c$ and the so-called Weibull-Module $m$. $\sigma_c$ and $m$ can be assessed using quasi-static experiments like the double-ring (also called ring-on-ring) bending test.

$$FP(\sigma) = 1 - \exp\left(-\left(\frac{\sigma}{\sigma_c}\right)^m\right) \qquad \text{Eq.1 [10]}$$

In an approach with the title GLASPROB, the Weibull-Distribution has already been used for the design of windscreens focusing on endurance strength loads [1]. In [1] the stress state of the windscreen for different load cases is assessed based on Finite-Element (FE) simulations. Since the size of the loaded area strongly influences the fracture probability [19], [1] extended Eq.1 to Eq.2 in order to assess the fracture probability based on the stress loads for a certain area A for different endurance strength loads.

$$FP = 1 - \exp\left(-\int_A \left(\left(\frac{\sigma}{\sigma_c}\right)^m\right) dA\right) \qquad \text{Eq.2 [1]}$$

By considering the increase of the tensile strength in case of dynamic loadings [7], [3] has further extended Eq.2 for dynamic load cases as well. As shown in Eq.3 the fracture probability depends now on a Dynamic Factor $DF$, a reference area $A_{ref}$ as well as the tensile stress and the size of the N FE-elements of the windscreen glass.

$$FP = 1 - \exp\left(-\frac{1}{A_{ref}}\sum_i \left(\frac{\sigma_i \cdot A_i}{\sigma_c \cdot DF}\right)^m\right) \quad \text{for i} = 1 \text{ to N} \qquad \text{Eq.3 [3]}$$

Scope of this study is to use the findings from [3] for the assessment of the probabilistic fracture mechanics of glass in order to design a pedestrian friendly windscreen geometry for a head impact against the windscreen center.

## METHODS

For the evaluation of the head injury risk for an impact against the vehicle windscreen, a method considering the probabilistic fracture mechanics is proposed (see Figure 2). This procedure consists of two steps.
In the first step, which in part is already be published in [3] and [11], the probability for certain fracture initiation times is assessed. Within this step, a FE simulation of a head impactor being shot against the center of a vehicle windscreen is calculated. The windscreen center is being chosen in order to minimize the influence of the windscreen adhesive and of the glass edges. For these impact simulations an adult head impactor with a mass of 4.5 kg is used. The impact conditions are chosen based on the latest Euro NCAP test procedure. Since vehicle windscreens are made of laminated safety glass, consisting of two 2.1 mm thick float glass plies being attached by a 0.76 mm thick intermediate layer of polyvinyl butyrale (PVB), a three layered approach is being chosen. For the windscreen model a so-called Shell-Solid-Shell-approach is being used. The material data for glass is chosen based on literature values for not-pre-stressed glass, which is usually the case for the windscreen center. During this first step, the glass is modeled without fracture. More detailed information about the validation of the glass model is given in [11]. The windscreen is modeled to be attached to an adhesive layer, while the degrees of freedom of the adhesive surface being usually attached to the vehicle body is being blocked in the global coordinate system.

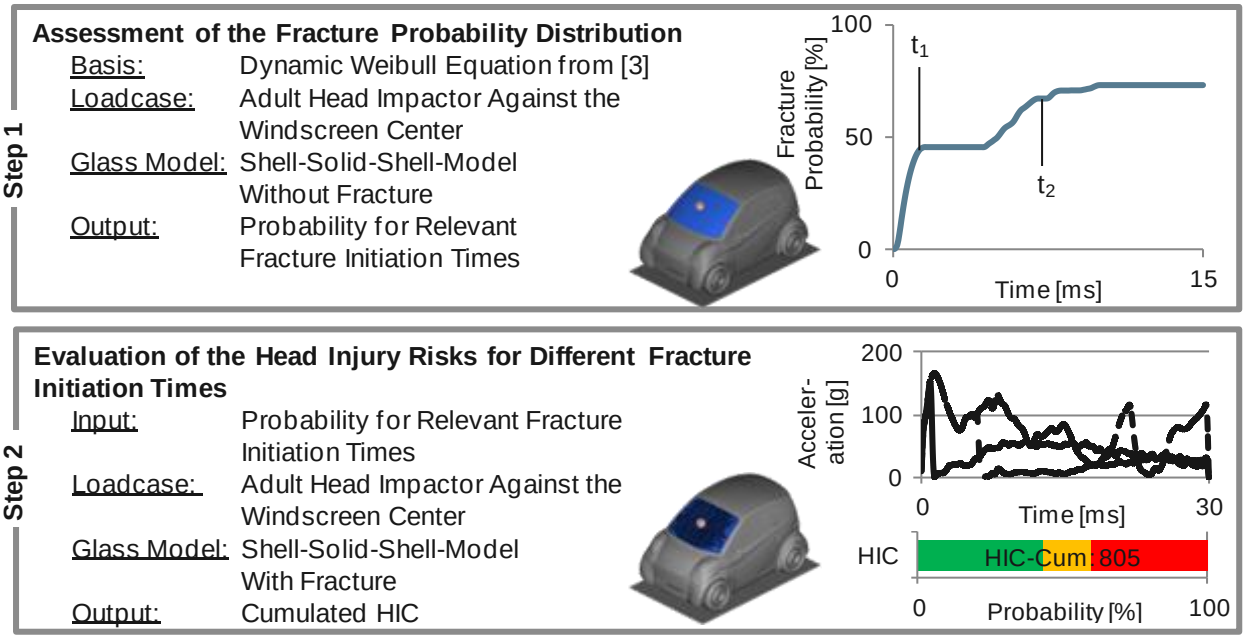


***Figure 2. Methodology for Evaluation of Head Injury Risk Considering Probabilistic Fracture Mechanics.***

As a result of the simulation the tensile stress over time distribution of each element on the glass surface is stored in a separate file. Due to the layered set-up of laminated safety glass, four glass surfaces have to be differentiated. The tensile stresses are combined with the test results from specimen tests using the Weibull-Distribution. Similar to windscreens of series vehicles, the windscreen is assumed to be in FTTF-design. This refers to the production process of float glass, in which the glass melt floats on a tin bath. The glass side floating on the tin bath is called tin side (T), while the other surfaces pointing to the atmosphere is called fire side (F). In an FTTF-design, for the outer and inner surface of the windscreen the fire (F) side of the float glass is chosen, while the surfaces attached to the PVB-foil are the tin (T) side of the float glass. In general, the fire side has a higher tensile strength than the tin side, since in the tin side some tin molecules are diffused in the glass structure. More specific information on the chosen material parameters as well as the dynamic factor is given in [3]. Result is a graph showing the fracture probability over time. In this graph, the probability for certain fracture initiation times can be assessed.
These fracture initiation times are used as input for the second step, which is not been published before. By integrating a failure criteria, the so-called 'non-local failure criterion' developed by [13], in the glass model, the head acceleration curve as well as the so-called Head Injury Criterion (HIC) can be determined. One simulation has to be conducted for each combination of fracture initiation time and fracture probability. Thus, the failure criterion parameters have to be adapted for each fracture initiation time. Further information on the validation of this failure criterion is given in [11]. Finally a cumulated HIC can be determined using Eq.4.

$$HIC_{cum} = \sum_{i} FP_i \cdot HIC_i \quad \text{for i} = 1 \text{ to N} \qquad \text{Eq.4}$$

A sequence of the further work being described in the present paper is shown in Figure 3. The methodology and results of this work is also not been published before. The work is being conducted within a European research project named 'SafeEV', which is co-funded by the European Commission within the Seventh Framework Programme (2007-2013) (see http://www.project-safeev.eu/).
In order to show the potential impact of the described methodology, the head injury risk during an impact on a windscreen of a vehicle model is being assessed using the methodology described above. For the vehicle model the so-called REVM1 is being used. A description of the vehicle model is included in [12]. The resulting cumulated HIC is being used as reference.

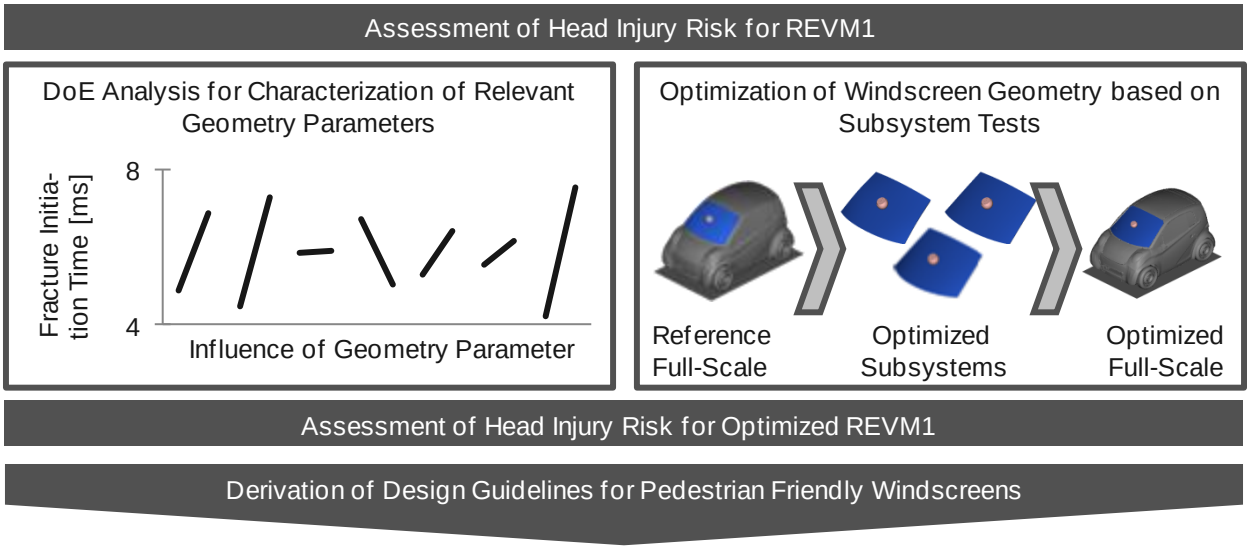


***Figure 3. Work Sequence of Present Investigation.***

Afterwards a "Design of Experiment" (DoE) analysis is conducted, in order to analyze the influence of the windscreen geometry on the fracture probability respectively the fracture initiation time. Seven of the eight geometry parameters shown in Figure 4 are included in the DoE analysis. Only the so-called end tangent angle is not included, since the windscreen side is assumed to have only a minor effect during an impact in the windscreen center. As a consequence a test plan including 64 windscreen designs is developed (see Figure 10). The according maximum and minimum values for the seven parameters are chosen based on series production vehicles (see Figure 11). In order to determine the fracture probability for certain fracture initiation times, the first step of the methodology shown in Figure 2 is being conducted for each of the 64 windscreens.

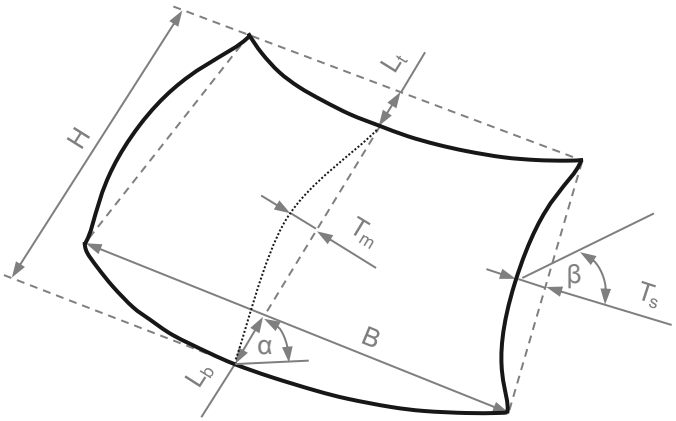


Legend:

| | |
|---|---|
| H | Height |
| B | Width |
| $L_b$ | Longitudinal Curvature Bottom |
| $L_t$ | Longitudinal Curvature Top |
| $T_m$ | Transverse Curvature Mid |
| $T_s$ | Transverse Curvature Side |
| α | Mounting Angle |
| β | End Tangent Angle |

***Figure4. Geometrical Characterization of Vehicle Windscreens.***

Assuming that during a head impact in the windscreen center an early fracture initiation time results in low injury risk, the windscreen geometry of REVM1 can be optimized using the results of the DoE analysis. Since the integration of a redesigned windscreen in an existing vehicle geometry is very time-consuming, the effect of the redesigned windscreen is first investigated in a subsystem environment. Thus, the redesigned windscreens are only attached to a constrained windscreen. Since this new constraint is stiffer, the original windscreen is also being investigated as a subsystem. After the optimization process results in a satisfactory change of the fracture probability distribution, the windscreen flanges of the vehicle model are being updated for the new windscreen geometry, so that a full-scale model is available.
This full-scale model is being assessed using the methodology described in Figure 2. By comparing the cumulated HIC of the reference and the optimized vehicle, the benefit can be shown.

Finally, design guidelines for pedestrian friendly windscreens considering the probabilistic fracture mechanics of glass are being derived.

## RESULTS

### Assessment of Head Injury Risk for REVM1

Figure 5 shows the fracture probability over time curve for REVM1. Using the graph shown in Figure 5 a probability for three fracture initiation time periods are determined. The number of different periods is set to three periods in order to limit further necessary calculations to a reasonable number. For a first period from first impact to 1.5 ms after first impact, the windscreen will fracture with a probability of 43%. In a second time period between 1.5 ms and 6 ms after first impact, the windscreen will fracture with a probability of 17% (relative probability being calculated by subtracting 43% from 60%). Considering a worst case approach and assuming the head injury risk will decrease with an earlier fracture, the third period is being defined from 6 ms until the end of the impact. During this period the windscreen will not fracture with a probability of 40%.

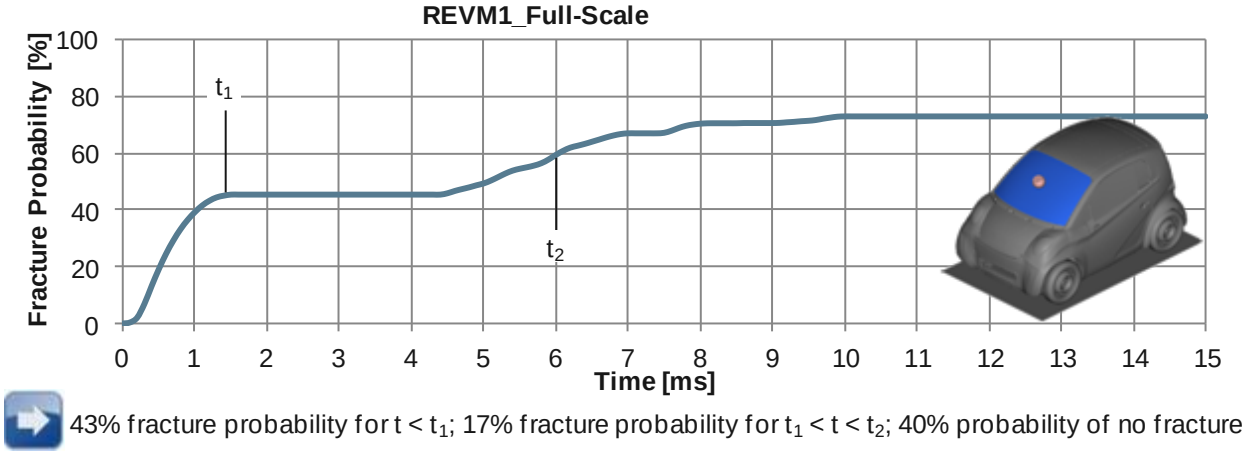


***Figure 5. Fracture Probability over Time Curve for Head Impact in the Windscreen Center of REVM1.***

By integrating a fracture criterion in the windscreen model, the head injury risk can be determined. The failure criterion is chosen in order to initiate the fracture at the end of the time period for the first two periods, while the windscreen should not fracture for the third period. Figure 6 shows the corresponding acceleration curves and the HIC-values. The cumulated HIC, which can be calculated using Eq.4, is 805.

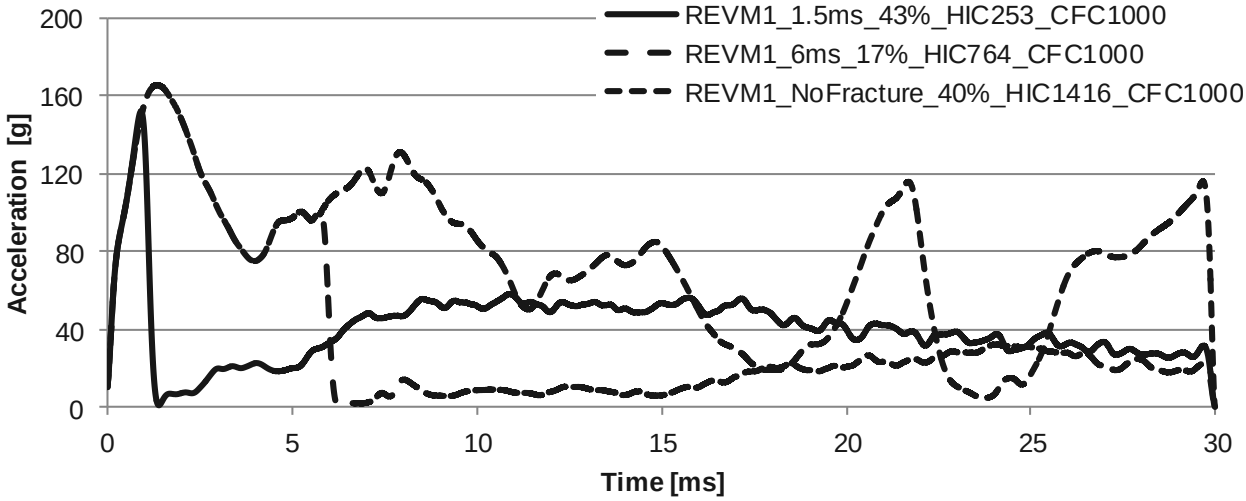


***Figure 6. Head Impactor Acceleration for REVM1 for Three Different Fracture Times.***

Similar to the results from [14], the head injury risk increases with later fracture times (see Figure 6). Since the stiffness of the windscreen strongly decreases after the fracture is being initiated, the acceleration signal rapidly decreases as well. After glass fracture, the head impactor is being further decelerated by the PVB-foil and attached glass fragments.

**DoE Analysis for Characterization of Relevant Geometry Parameters**

In Figure 7 the result of the DoE analysis is shown. The lines displayed in Figure 7 represent the influence of each windscreen parameter. A positive slope implies a small fracture initiation time for the corresponding minimum value of the parameter, while a negative slope implies a small fracture initiation time for a maximum value respectively. The absolute value of the slope gradient can be used to describe the impact of this parameter. According to this, the mounting angle, the windscreen width as well as the windscreen height have the largest influence on the fracture initiation time.

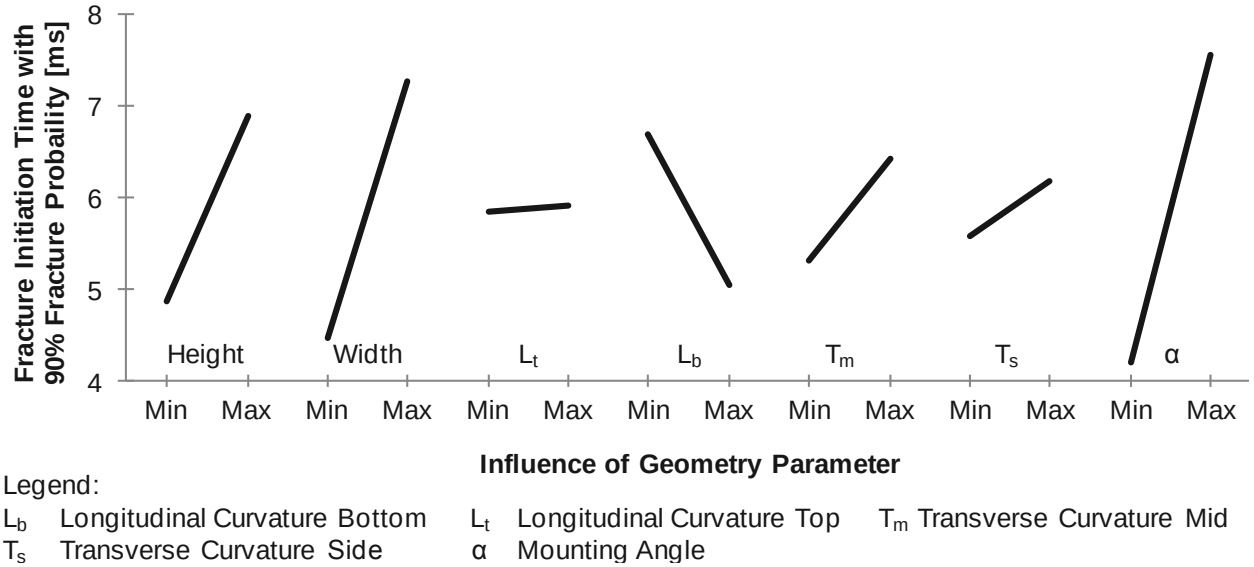


***Figure 7. Effect of Windscreen Characteristics on Fracture Initiation Time.***

**Optimization of Windscreen Geometry based on Subsystem Tests**

Assuming that during a head impact in the windscreen center an early fracture initiation time results in low injury risk, the windscreen geometry can be optimized using the results from the DoE analysis. According to the DoE analysis especially the windscreen mounting angle, height and width influence the fracture probability (see Figure 7). But since these parameters are usually defined by the vehicle designers, they were excluded from the optimization process in order to minimize the change of the vehicle design.
Other parameters influencing the fracture probability are the transverse curvature at the middle of the windscreen, the transverse curvature at the windscreen side as well as the longitudinal curvature at the bottom. In order to show the influence of these parameters, the windscreen geometry is changed. The fracture probability over time curves for the full-scale and subsystem tests are shown in Figure 8. As expected, the stiffer constraint influences the subsystem test of the original windscreen, so that the fracture probability for the subsystem test is being increased from 4 ms after first impact onwards. In the first optimization step (OPT1) only the transverse curvature at the middle of the windscreen is being reduced. In the second optimization step (OPT2) the transverse curvature at the middle of the windscreen as well as the transverse curvature at the windscreen side are reduced. In the third optimization step (OPT3) both transverse curvatures are reduced and the longitudinal curvature at the bottom is increased.

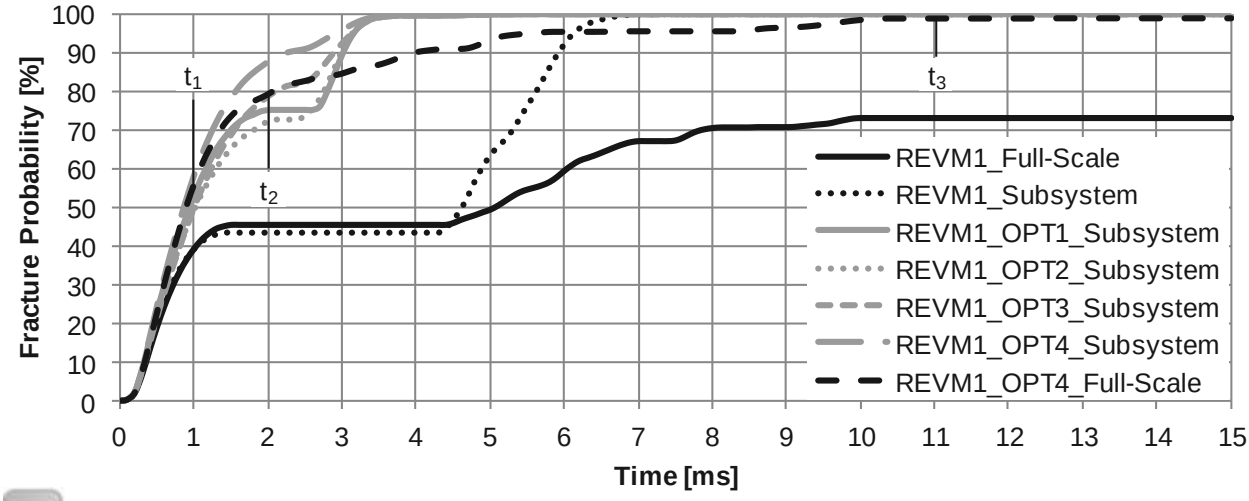


55% fracture prob. for $t < t_1$; 25% fracture prob. for $t_1 < t < t_2$; 20% fracture prob. for $t_2 < t < t_3$

***Figure 8. Fracture Probability over Time Curve for Optimized Windscreen Designs of REVM1.***

As can be seen in Figure 8, the fracture probability increases for OPT1, OPT2 and OPT3. Especially for the first 2 ms the fracture probability is larger compared to the original windscreen geometry. It seems that the influence of the transverse curvature at the side shows the largest effect, since either OPT2 as well as OPT3 show only a minor increase compared to OPT1.
In the fourth optimization step (OPT4), the effect of the positioning of the float glass within the laminated safety glass is considered. Thus, the windscreen geometry OPT3 is assessed in the so-called TFFT-design. Here, the inner and outer surface of the windscreen glass are chosen to be the tin side (T) of float glass, while the intermediate surfaces are made of the fire side (F). OPT4 shows a further increase of the fracture probability. By analyzing the corresponding tensile stress distribution, it seems that the combination of large tensile stresses and the corresponding area loaded by these stresses is especially for the glass surface directing to the vehicle compartment. The largest fracture probability results, if the tin-side is chosen for this surface. Thus, it is expected that a FTFT-design could lead to similar results. But this assumption is not further specified.
Since OPT4 shows the largest fracture probability, OPT4 is chosen to be integrated in the vehicle model. As can be seen in Figure 8, the fracture probability of OPT4 assessed in the Full-Scale model decreases due to the softer constraints as expected. But still, the improvement in comparison to the original windscreen is significant.
In order to calculate the head injury risk in the next step, three time periods have to be chosen based on the fracture probability curve for the Full-Scale model of the optimized windscreen geometry OPT4. Since the fracture probability curve changes due to the redesign, this step is necessary. The first period is defined to be between first impact and 1 ms after first impact with a probability of 55%. The second period with a probability of 25% is defined between 1 ms and 2 ms and the third period between 2 ms and 11 ms with a probability of 20% respectively.

**Assessment of Head Injury Risk for Optimized REVM1**

Figure 9 shows the resulting acceleration curves and the HIC-values for the optimized windscreen geometry. Similar to the results shown in Figure 6, the head injury risk increases with later fracture times due to the significant reduction of the windscreen stiffness after fracture initiation. Comparing Figure 6 and Figure 9 shows that the HIC values for the three periods of the original and the optimized windscreen are in a similar range. Due to the changes of the geometry design, the probability for the first two periods are increased for the optimized windscreen, which results in the reduction of the cumulated HIC from 805 to 577.
But Figure 9 reveals as well that a higher fracture probability for short fracture initiation times results in a higher acceleration peak. So, it seems that the windscreen stiffness has to be increased for a higher fracture probability.

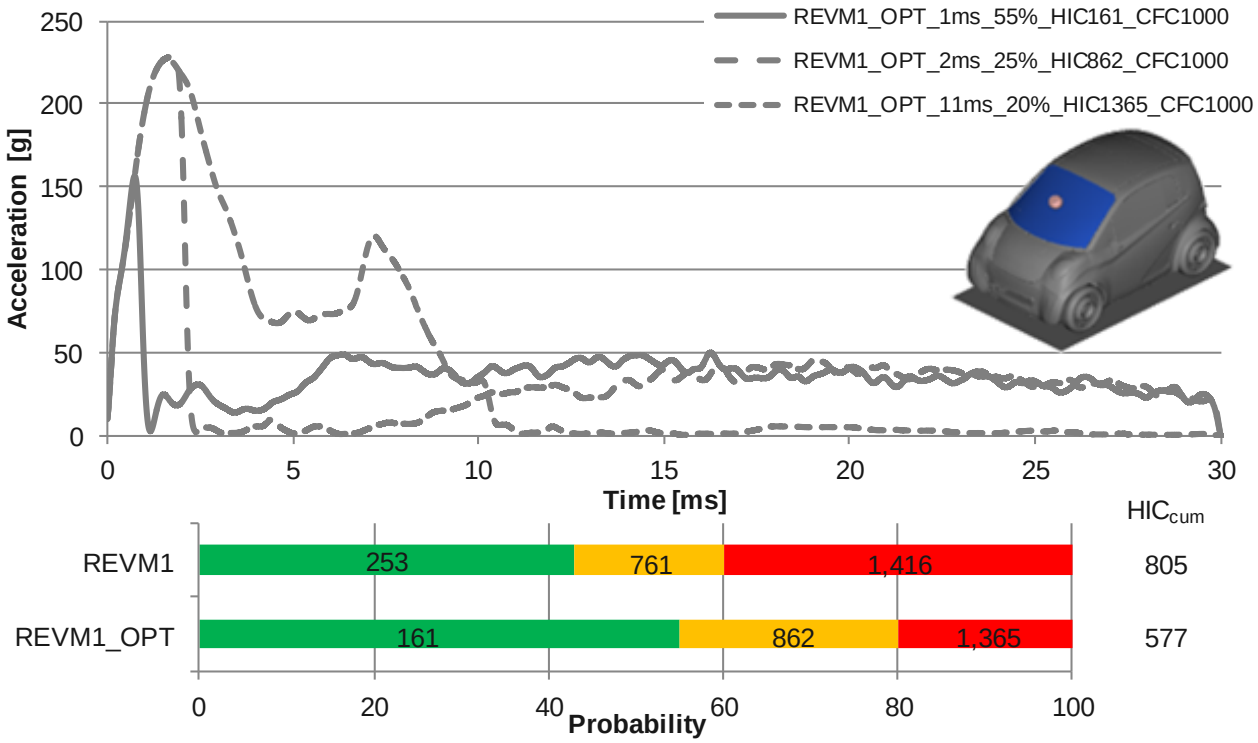


***Figure 9. Head Impactor Acceleration for REVM1 and Optimized Windscreen.***

**Derivation of Design Guidelines for Pedestrian Friendly Windscreens**

Based on the work described in the present paper some guidelines for a pedestrian friendly windscreen design can be derived. These guidelines are only valid for a head impact in the windscreen center and are based on an evaluation of the HIC using an adult head impactor.
First, probabilistic fracture mechanics shall be considered within the design process of the windscreen geometry and associated injury risks, since an early fracture initiation seems to result in low injury risks.
Second, in order to increase the fracture probability for an early fracture initiation time, the mounting angle, the windscreen width, the windscreen height, the transverse curvature at the middle of the windscreen as well as the transverse curvature at the windscreen side shall be reduced and the longitudinal curvature at the bottom increased.
Third, the positioning of the float glass influences the fracture probability as well. In the present case it seems that a TFFT- or a FTFT-design is more beneficial for pedestrian safety.

## LIMITATIONS

The presented study can be separated in two main sections. First the limitations of the methodology for the assessment of the fracture probability over time curve are discussed. Afterwards the limitations of the optimization process will be given.
Input for the fracture mechanical analysis are mainly material data based on a literature study. If this approach is being considered in the design phase of series vehicles, the material data should be updated in cooperation with the windscreen manufacturer. Thus, the specification sheet for the windscreen manufacturer should be expanded e.g. by Weibull-Module, characteristic tensile strength and Dynamic Factor.
Especially, the Dynamic Factor should be investigated in more detail. At the moment, the Dynamic Factor is defined based on Split Hopkinson Pressure Bar tests for laminated safety glass from [18] and the resulting strain rate during head impactor simulations in the windscreen center. Unfortunately, the analyzed strain rates in [18] show a large gap in the relevant strain rate field during head impact. Thus, the chosen Dynamic Factor is a rough approximation. In order to specify the Dynamic Factor further tests in the relevant strain rate field should be conducted.

Main input for the calculation of the fracture probability over time curve is the tensile stresses on the glass surfaces. These tensile stresses are being determined using FE simulations. An experimental verification of the resulting tensile stresses is according to the opinion of the authors not possible. Using polarization filters results only in a qualitative stress state, while instruments using the scattered light method cannot be conducted without contact to the glass surface and thus would influence the test results.
Nevertheless, the combination of stress state during head impact in the windscreen center and probabilistic fracture mechanics are verified using internally available test results. Thus, the authors are confident, that the effects and tendency shown in the present paper are reasonable.
The optimization steps currently focus on head impacts in the windscreen centre. In case of a head impact being close to the scuttle area, an early fracture initiation might result in a more severe impact with the instrument panel. This effect has to be investigated in future studies.
Furthermore, the pedestrian friendly windscreen design is evaluated using the HIC value. According to [16] the larger acceleration peak shown in Figure 8 can also result in a higher skull fracture risk. This risk will be integrated in the further course of the SafeEV-project. If the results from [16] are confirmed, further optimization criteria should be included in the optimization process.
For the validation of the windscreen model including failure, experimental tests of a middle class vehicle are used. Since no test results for the REVM1 are available, the windscreen model for the original and for the optimized windscreens could not be validated. Nevertheless based on the expertise of the authors, the calculated acceleration signals and fracture behavior seem reasonable. Main scope of the present paper is to show that the probabilistic fracture behavior of glass could be considered during the design of a pedestrian friendly windscreen. Thus, using reasonable, but not fully validated windscreen models is assumed to be acceptable. If this approach will be further evaluated, a broad experimental testing verification should be done.
The windscreen is optimized in order to minimize the head injury risk for pedestrians. In this context an early fracture is beneficial. Nevertheless, the windscreen shall fulfill further requirements as well. Main tasks for windscreen are protection against external events, optically faultless vision, prevention of serious injuries and sufficiently long service life [6]. None of these main tasks are negatively influenced by an early fracture initiation. In addition, the windscreen shall support the correct unfolding process and position of airbags for occupants. For this task a late fracture initiation is required. According to the opinion of the authors, the presented methodology could also be used to assess the corresponding effects.

## CONCLUSIONS

In the present paper a methodology for designing pedestrian friendly windscreens is described. Main advantage of this methodology is that the probabilistic fracture behavior of glass, which strongly influences the injury risk during head impact in the windscreen center, is considered within the design process. The methodology consists of two steps. In the first step, the probability for certain fracture initiation times is assessed. Therefore, a FE simulation of a head impactor being shot against a vehicle windscreen without fracture criteria is calculated. The resulting tensile stress over time distribution of each element on the glass surface is used to calculate the fracture probability. Result is a graph showing the fracture probability over time, in which the probability for certain fracture initiation times can be assessed. These fracture initiation times are used as input for the second step. By integrating a failure criteria, the so-called ‘non-local failure criterion’ developed by [13], in the glass model, the head acceleration curve as well as a so-called cumulated Head Injury Criterion (HIC) can be determined.
In order to show the potential impact of the described methodology, a windscreen of a vehicle model is being assessed and optimized assuming a short fracture initiation time results in a small injury risk. By changing the transverse curvature, the longitudinal curvature at the bottom of the windscreen and the set-up of the laminated safety glass of the windscreen, the cumulated HIC value could be significantly decreased from 805 to 577. This refers to a reduction by 28 %. Finally guidelines for pedestrian friendly windscreen designs are derived.

## ACKNOWLEDGEMENTS

Part of this study was conducted within a European research project with the title SafeEV (http://www.project-safeev.eu/). SafeEV has received funding from the European Community's Seventh Framework Programme (FP7/2007-2013) under grant agreement n° 314265. This publication solely reflects the author’s views. The European Community is not liable for any use that may be made of the information contained herein.

**REFERENCES**


[1] Geiss, M. and Sandoz, N. 1995. ‘GLASPROB – Ein Rechenprogramm zur Quantifizierung der Bruchbelastung von Automobilfrontscheiben.‘
ISBN: 3-8169-1250-8, In Proceedings of Fahrzeugverglasung – Kundennutzen im Spannungsfeld von Funktion, Design, Produktion, Publisher expert Verlag
[2] Griffith, A.A. 1920. ‘Fracture Behavior of Brittle Materials.’
Phil. Trans. Roy. Soc., A221, Page 163-198
[3] Herkenhoff, A., Nuss, F. and Eckstein, L. 2014. ‘Implementierung einer bruchstatistischen Methodik zur Prognose des Versagenszeitpunktes von spröden Werkstoffen bei Impaktbelastung für die explizite FEM.‘
In Proceedings of SIMVEC - Simulation und Erprobung in der Fahrzeugentwicklung, BadenBaden, Germany, 18.-19.November 2014
[4] Jebsen-Marwedel, H. and Brueckner, R. 2011. ‘Glastechnische Fabrikationsfehler.’
ISBN 978-3-642-16432-3, Publisher Springer Berlin Heidelberg 1936, 1959, 1980, 2011
[5] Kinsky, T. 2005. ‘Head Impact Tests in the Center of the Windscreen.’
Presentation at 9th GTR Pedestrian Protection Informal Group Meeting, INF GR / PS / 134
[6] Kramer, F. 2013. ‘Integrale Sicherheit von Kraftfahrzeugen - Biomechanik – Simulation – Sicherheit im Entwicklungsprozess.‘
ISBN 978-3-8348-2607-7, Publisher Springer Wiesbaden
[7] Krohn, M.H., Hellmann, J.R., Shelleman, D.L., Pantano, C.G. and Sakoske, G.E. 2002. ‘Effect of Enameling on the Strength and Dynamic Fatigue of Soda–Lime–Silica Float Glass.’
J. Am. Ceram. Soc., 85 [10], Page 2507–14.
[8] Kuehn, M., Froeming, R. and Schindler, V. 2007. ‘Fußgängerschutz – Unfallgeschehen, Fahrzeuggestaltung, Testverfahren.’
ISBN-10 3-540-34302-4, Publisher Springer Berlin, Heidelberg, Germany
[9] Mizuno, Y. 2005. ‘Summary of IHRA pedestrian safety working group activities – Proposed test methods to evaluate pedestrian protection offered by passenger cars.’
In Proceedings of the 2005 Experimental Safety Vehicles Conference (ESV) Washington, 05-0138-O
[10] Nattermann, K. and Habeck, A. 2001. ‘Bruchstatistik - Festigkeit von Glas, Grundlagen und Messverfahren.‘
Published in Hüttentechnische Vereinigung der Deutschen Glasindustrie, Publisher: Deutsche Glastechnische Gesellschaft, Offenbach/Main, 2nd Edition
[11] Nuss, F., Herkenhoff, A. and Eckstein, L. 2014. ‘Effect of the Non-Local Failure Criterion on the Acceleration Signal of Head Impactors at Impact in Windscreen Centre.’
In Proceedings of 13th LS-Dyna Forum, 6th to 8th October 2014, Bamberg, Germany
[12] Puppini, R., Puleo, G. and Hinc, K. 2013, ‘Reference Electric Vehicle Models.’
Deliverable D3.1 of European Research Project “Safe Small Electric Vehicles through Advanced Simulation Methodologies” (SafeEV)
[13] Pyttel, T., Liebertz, H. and Cai, J. 2011. ‘Failure criterion for laminated glass under impact loading and its application in finite element simulation.’
International Journal of Impact Engineering 38, Page 252-263
[14] Ries, O. 2005. ‘Observation of different windscreen glass fracture modes during headform impactor tests.’
Presentation at 9. GTR Pedestrian Protection Informal Group Meeting, INF GR / PS / 164
[15] Schaffer, H.A. and Langfeld, R. 2014. ‘Werkstoff Glas - Alter Werkstoff mit großer Zukunft.‘
ISBN 978-3-642-37230-8, Publisher Springer Berlin Heidelberg, Germany
[16] Schmitt, K.-U., Niederer, P.F., Muser, M.H. and Walz, F. 2007, ‘TraumaBiomechanics - Accidental injury in traffic and sports.’
ISBN 978-3-540-73872-5, Publisher Springer Berlin, Heidelberg, Germany
[17] Tammann, G. 1933. ‘Über die Gläser als unterkühlte Flüssigkeiten.‘
In Proceedings of Glastech. Bericht 3 Page. 73 (1925 /26), Der Glaszustand Leipzig
[18] Xu, J., Zhu, M., Liu, B., Sun, Y. and Li, Y. 2011. ‘Head Protection Characteristics of Windshield During Pedestrian-Vehicle Accident.’
SAE-Paper 2011-01-0082

[19] Zammit, K. and Overend, M. 2009. 'Increasing the design strength of glass – fractography and stress testing.'
Proceedings of the International Association for Shell and Spatial Structures (IASS) Symposium, Valencia

**APPENDIX**

| Windscreen Design | Height [mm] | Width [mm] | Longitudinal Curvature Bottom [mm] | Longitudinal Curvature Top [mm] | Transverse Curvature Mid [mm] | Transverse Curvature Side [mm] | Mounting Angle [°] |
|---|---|---|---|---|---|---|---|
| 1 | - | - | - | - | - | - | + |
| 2 | + | - | - | - | - | - | - |
| 3 | - | + | - | - | - | - | - |
| 4 | + | + | - | - | - | - | + |
| 5 | - | - | + | - | - | - | - |
| 6 | + | - | + | - | - | - | + |
| 7 | - | + | + | - | - | - | + |
| 8 | + | + | + | - | - | - | - |
| ……. | | | | | | | |
| 63 | - | + | + | + | + | + | - |
| 64 | + | + | + | + | + | + | + |

***Figure 10. Parameter Set-Up for DoE Analysis based on 64 Windscreen Designs.***

| Parameter | Maximum Value (+) | Minimum Value (-) |
|---|---|---|
| Height [mm] | 1,000 | 600 |
| Width [mm] | 1,600 | 1,100 |
| Longitudinal Curvature Bottom [mm] | 150 | 0 |
| Longitudinal Curvature Top [mm] | 75 | 0 |
| Transverse Curvature Mid [mm] | 100 | 0 |
| Transverse Curvature Side [mm] | 40 | 0 |
| Mounting Angle [°] | 70° | 25° |

***Figure 11. Maximum and Minimum Value for DoE Analysis.***

# The trolley test way of IIHS small overlap and side test

## - with minimized structure usage -

**Park Un-chin** **Song Ha-jong*** **Kim Hyun-chul***
**Florian Ganz**** **Sudar Sankar**** **Mario Wohlfahrt****

ABSTRACT

To develop a vehicle in low cost and early well-customized performance trolley test can be used efficiently. In this research, we will introduce how to make the trolley for the IIHS smalloverlap and side crash with substituting parts by CAE validation and show the good validation with real vehicle crash after the test

**Key Word** : Trolley, Buck. BIW, Vehicle Crash, Component Test, CAE, IIHS Small overlap, IIHS Side

## 1. Introduction

We use sled test often to tune the restraint system in the vehicle because of its repeatability and low cost. If we have something similar to this in structure performance test, it would be very useful to reduce the vehicle developing cost.

If we use the whole BIW that is useful way because we usually produce not the parts of front buck or side structure but the total of BIW to develop many kinds of performances and reduce the cost. But for the repeatability too many parts are used. For example at the IIHS small overlap test rear half part of the car can not be needed necessarily and at the IIHS side test right half and floor part not be needed so much. To see a certain point for some issues like lower arm dislocation, B-pillar breakage or door trim sharp edge, we should repeat the test several times.

If we use half structure it will be more useful to repeat and concentrate on that point. Also this way is more useful than one part component test like lower arm breakage test, B-pillar tensile test or door trim sharp edge test in the viewpoint of total structural test. [1)~4)]

So, in this research we will introduce how to make the front buck trolley for IIHS small overlap structure test and side structure trolley with CAE validation. We tried to minimize the cost of manufacturing by making the substitutes for many parts like the engine, cowl cross bar at the IIHS small overlap trolley test and using only the side structure and doors at the IIHS side trolley test. We will judge the validation of this trolley test by comparing the results with full car crash.

* Safety Performance Team 1 : Author or Co-Author
** Crash Simulation Team : Co-Author
*** ACTS (Advanced Car Technology System) : Co-Author

## 2. Main Subject

### 2.1 IIHS small overlap trolley test

#### 2.1.1 The concept of frontal small overlap trolley

To make the small overlap trolley we used ACTS Mobile barrier. The mobile modular crash device consists of four basic elements that can be combined in different configurations. This enables the fixing of bigger parts and has clear benefits regarding the matching of sizes, of CG positions and of weight of the tested vehicles. Also, different wheel and roller systems, as well as bushings can be adaptive. We use only rear half for the Forte IIHS small overlap test.

Fig.1 Configuration modular mobile crash cart

Table 1. The Spec of ACTS frontal mobile barrier

| Detail | Adjustability | Unit | | Length | | |
|---|---|---|---|---|---|---|
| | | | | 2.600 | 3.200 | 3.800 |
| Width | 50 mm steps | mm | from | 900 | 900 | 900 |
| | | | to | 1.300 | 1.300 | 1.300 |
| Mass | depending on width | kg | from | 708 | 875 | 939 |
| | | | to | 828 | 1.046 | 1.110 |
| Wheelbase | 50 mm steps | mm | from | 1.560 | 2.120 | 2.720 |
| | | | to | 2.160 | 2.720 | 3.320 |
| Width | 50 mm steps | mm | from | 1.295 | 1.295 | 1.295 |
| | | | to | 1.695 | 1.695 | 1.695 |
| Height | fix | mm | | 400 | 400 | 400 |
| Ground clearance | stepless | mm | from | 100 | 100 | 100 |
| | | | to | 300 | 300 | 300 |

Its frame mass can be adjusted from 700kg to 2,800kg and additional mass can be adaptive and adjusted. Statistic simulation can be done for a longitudinal beam with 600kN force and a cross beam with 400kN. Also crash panel and basic frame can be adjusted with step less.

With this barrier, we decided to use the front Forte BIW from the forward to right in front of b-pillar. If we use the door and B-pillar the validation would be better but for the future use to minimize the part we did it. The cut area will be Also, we decided to remove all the trim an chassis parts except the parts related to the moving and the connection of engine to reduce the cost and improve the repeatability. Those parts are front wheels, lower arms, suspensions, a roll rod, an engine mounting, a transmission mounting, etc. The engine, front doors, cowl cross beam, delta glass and the first roof cross beam will be substituted by appropriate designed material by CAE. In case of wind glass and front seat they are removed. We couldn't install the front seat because rear seat mounting is removed.

We selected the Forte vehicle is the US model of 1.8 Nu engine auto transmission. This vehicle's intrusion is poor grade which has some deformation on the roofrail of B-pillar and the worst case of the deformation among the Hyundai-Kia vehicles, we believe if we are successful for the validation that can be available for the most of vehicles.

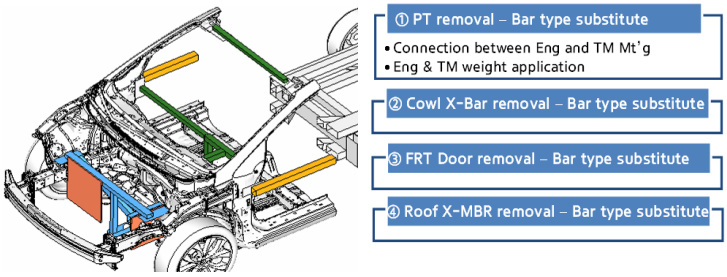


Fig.2 The concept of small overlap trolley

### 2.1.2 Substituting parts

In the IIHS small overlap test engine compartment doesn't influence so much as in frontal US NCAP test but during the crash the left hand front side member becomes to contact the transmission because it is bent by crash energy. So we designed substitution of transmission part side with the wall to block front side member bending at the same distance as real transmission.

Also the engine room weight distribution is important to fit the total vehicle weight distribution and determine the movement of powertrain. So we pick out the CG coordinates for engine and transmission each. And we added several 10 to 25kg weights to left and right positions of the upper beam to fit the CG. The Forte engine weight is 114kg and transmission 80kg. The powertrain coordinates is (x:236 y:22.8 z:212) and the coordinate measured from (x:236 y:17.9 z:211). So they are so close.

The links to the vehicles are designed same as a vehicle. Bolting is done at the left transmission mount, the engine mount and roll rod with same direction with the vehicle assembly.

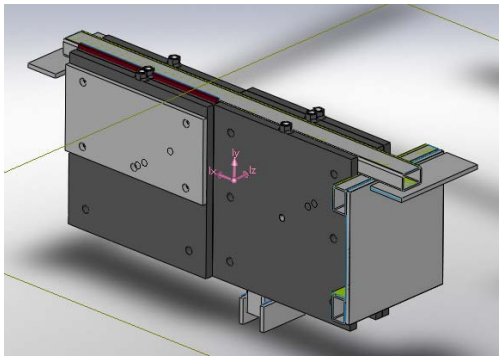

Fig.3 Powetrain substitute model

Fig.4 Powetrain mounting points

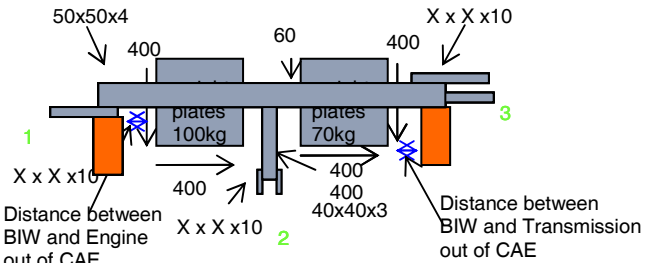


Fig.5 The concept of powertrain substitute

The links to the vehicles are designed same as a vehicle. Bolting is done at the left transmission mount, the engine mount and roll rod with same direction with the vehicle assembly.

For the front door we set the 2 bars instead of door assembly initially. But lower beam is removed at 2nd CAE validation. The links to the vehicles are designed same as a vehicle. Bolting is done at the 2 door hinge mountings.

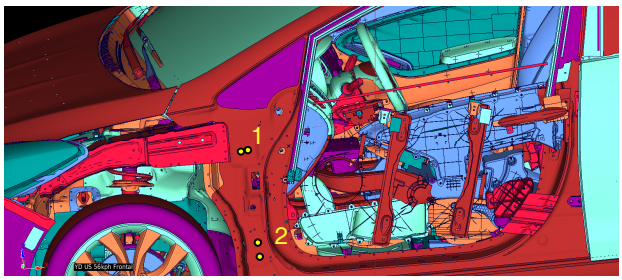


Fig.6 Front door mounting points

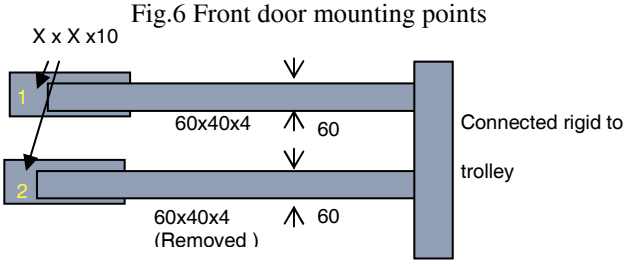


Fig.7 The concept of powertrain substitute

Also we designed the cowl crossbar substitute and 1st roof cross member to minimize the parts. When we get the structure assembly the cowl cross bar is not contained and the roof cross member is not the part of side structure like A-pillar and side sill.

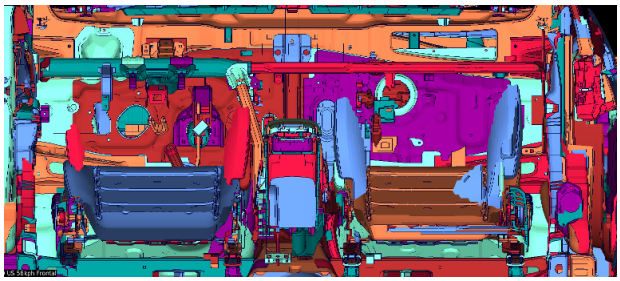

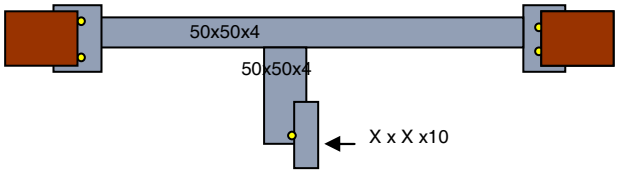


Fig.8 The concept of cowl crossbar substitute

All beams' material were S235 of plastic stress 235Mpa. And the surface area parts were welded to the trolley bracket

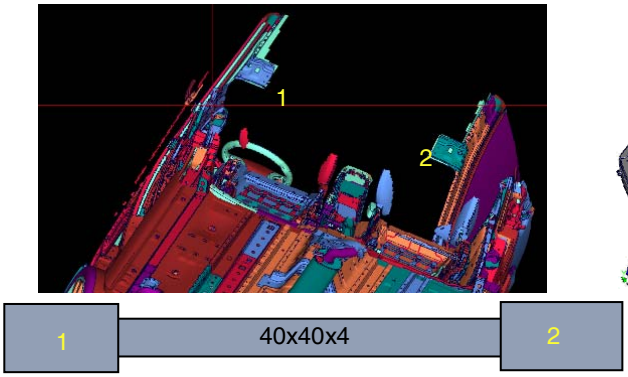


Fig.9 The concept of roof cross mebmer substitute

### 2.1.3 CAE validation

From the 1st to 7th CAE validation we set the wheel rims rigidity, door substitute lower beam removal and most of the section size with thickness. But there was front side member upper moving. But when we did apply very weak connecting condition to the most of welding points as a trial at 5th CAE, there was no front side member upper moving. We can also assume this in the comparison of vehicle CAE and vehicle crash because we know most small overlap welding points are failure in Forte correlation experience.

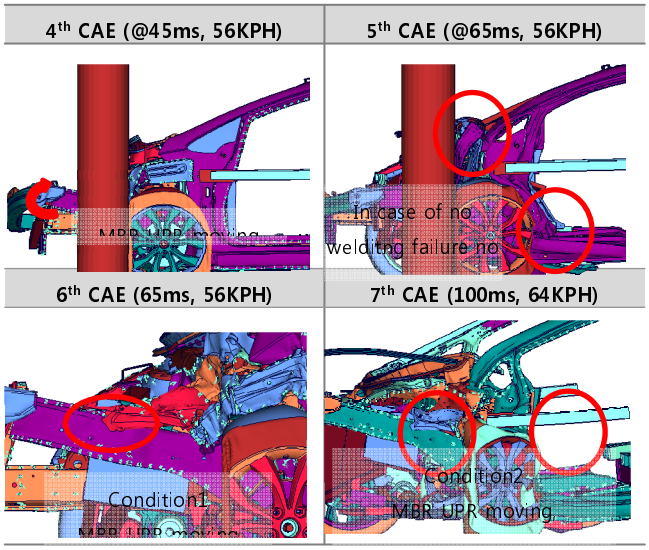


Fig.10 CAE validations from 4th to 7th

So we applied 3 times of welding condition adjustment. from 6th to 8th. Finally we weakened 27 welding points by engineering judgment the member upper going reduced enough. Also we set the final trolley test speed as not 64kph but 56kph, because in case of 64kph there was too much rotation of the vehicle. We also already knew the fact 56kph is better than 64kph in DM small overlap trolley tests research as an experience because there are many missing points like hood, chassis and trims.

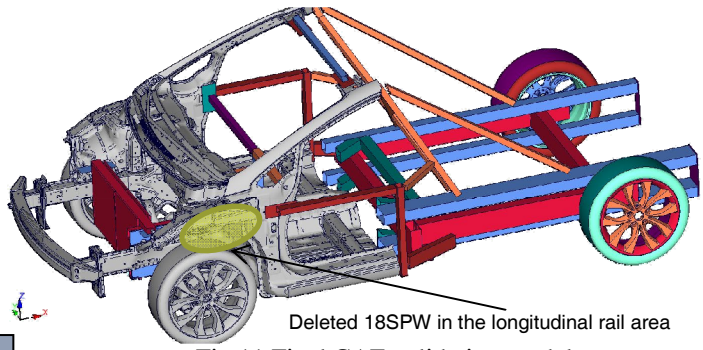


Fig.11 Final CAE validation model

### 2.1.4 Results of small overlap trolley test

We focused the validation on the contacting time of wheels, the dislocation time of lower arm A-point, the

rotation angle of vehicle and the structural deformation. As you see from table2 and fig11, the criteria matches very well. In case of structural deformation the result was closer to the full car than car CAE.

Table 2. Results summary of small overlap trolley

| Item | Full car | Trolley |
|---|---|---|
| Tire contact | 39ms | 39ms |
| A pt. dislocation | 42ms | 42ms |
| Car rotation@200ms | 19deg | 20deg |

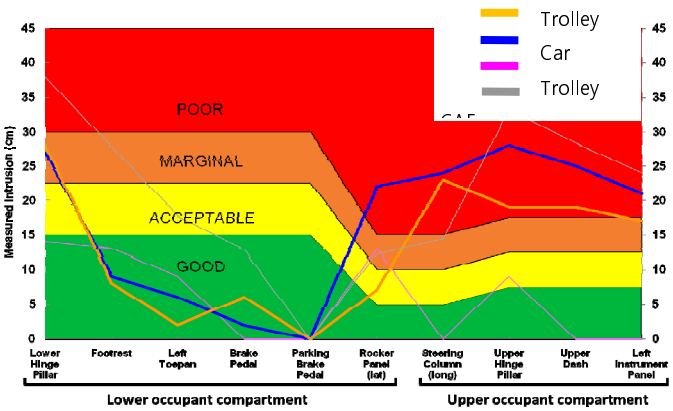


Fig.11 Structural deformation comparison

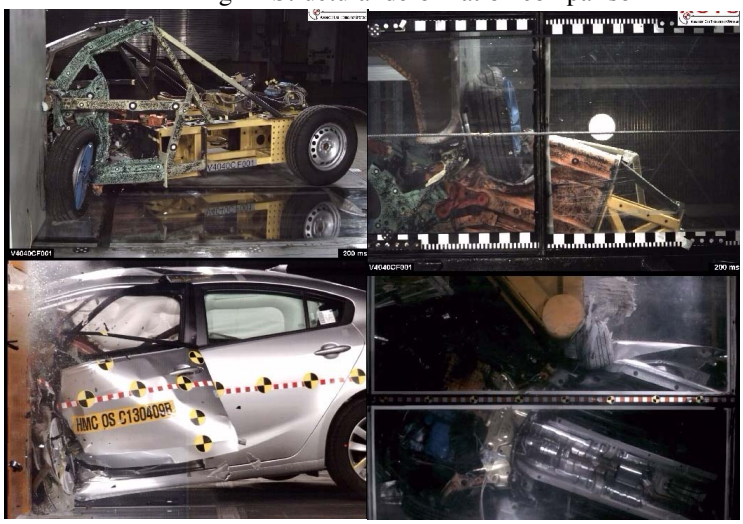

Fig.12 Video comparison with full car crash @ 200ms

As a result, this method for small overlap trolley test is valid. We can use this method for better crash performance developing with reduced developing cost. There were some points to be improved next time. Firstly, the wheel rotation for x-axis was different because we run the test without drive shaft. Secondly, the door substituting beam hinge mounting was broken and rear part was bended even it was indispensable. Next time we must invent better substituting system.

## 2.2 IIHS side trolley test

### 2.2.1 The concept of side trolley

To make the IIHS side trolley we used ACTS side trolley. The trolley device consists of many beams and 13 inch wheels to be adjusted wheel base and wheel tread distance but there is the limit for the wheel base adjustment of the minimum value 1630, because the left wheels are inside comparing with rear car this is needed to be supported in case of 1570 wheelbase length car Forte. So CG positions and weight distribution can be easily adjusted. This trolley usually

Fig.13 Configuration of ACTS side trolley

Table 3. Characteristics of ACTS side trolley

- Different adaptation (B-pillar, hinges, doors, trims)
- Speed max = 65 km/h
- Angle max = ± 45°
- Weight max = 2500kg
- Different configurations (Buck vs. pole or barrier)

In this research our purpose is the total test of side structure. So we decide to attach the whole side structure with doors of none glass and whole inner parts. Because there was severe deformation at the roof rail and side sill area in the 1st CAE with just rigid connection between side structure and trolley we decide to attach bending bar with some distance for roof rail and "V" shape struts with several rectangular brackets. Also almost-none deformable area like A-pillar and C-Pillar we will make 3 rigid bars connection for each. All the supporting bars are changed for the size and shape through 8 CAE validations. Crash speed 50kph is same as vehicle's.

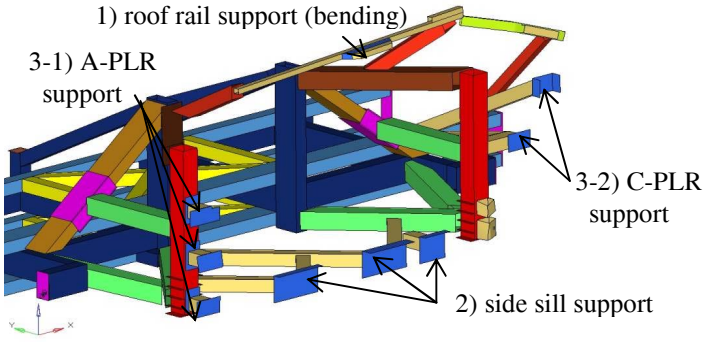


Fig.14 The connecting parts concept

### 2.2.2 CAE validation

At the first CAE validation, Vehicle side structure including roof and roof cross members are connected to trolley by rigid elements at A and C pillar and roof. As a result there was severe deformation at the roof rail and

side sill area because there was no support for them.

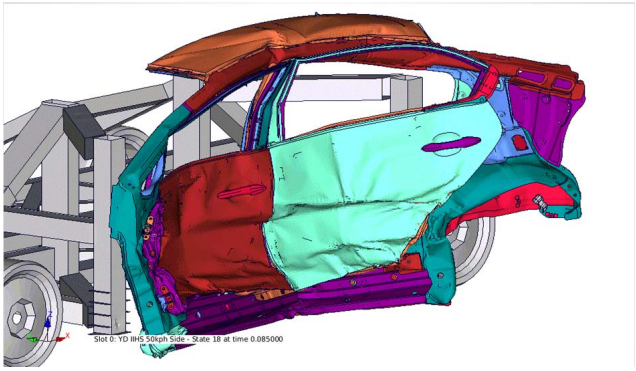

Fig.15 The 1st CAE result of side trolley

So we deleted roof and roof-beams at 2nd CAE, added trolley beams on the upper and lower area. Spec are like Fig.16. But as a result the roof rail have passed away over the trolley supporting beams and side sill rotation was too much.

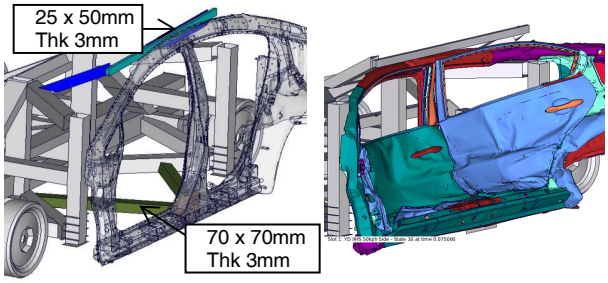


Fig.16 The 2nd CAE model and result

At the 3rd CAE, lower B-pillar support defined roof support with deformable profile between A and C pillar. Even there was still big rotation on the side sill and drop down of roof rail, the B-pillar profile became much closer to full car CAE.

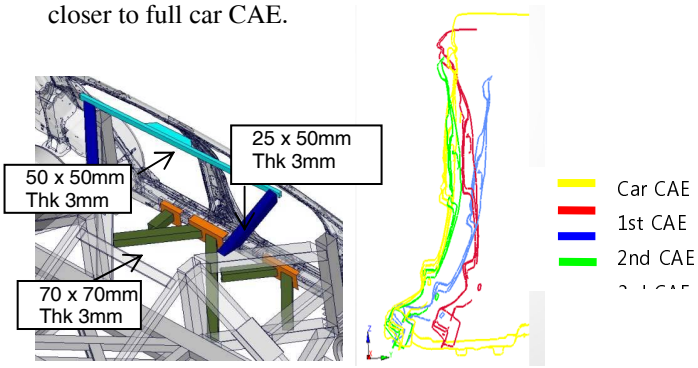


Fig.17 The 3rd CAE model and B-PLR profile (1,2,3rd)

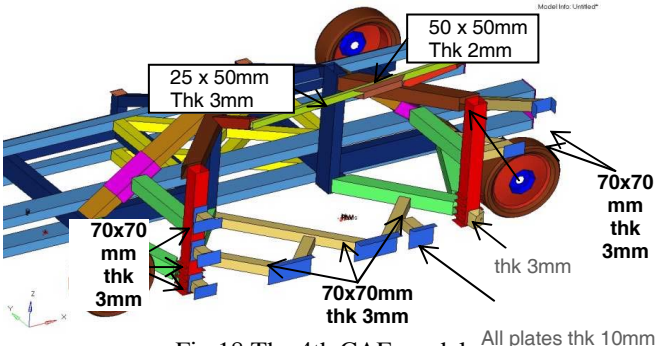


Fig.18 The 4th CAE model

At the 4th CAE, we added connections between trolley and vehicle at A & C-pillar to resist too much Z-axis rotation of them. As a result it is improved. Also we changed roof support beam thickness from 3 to 2mm to make more intrusion like full car CAE.

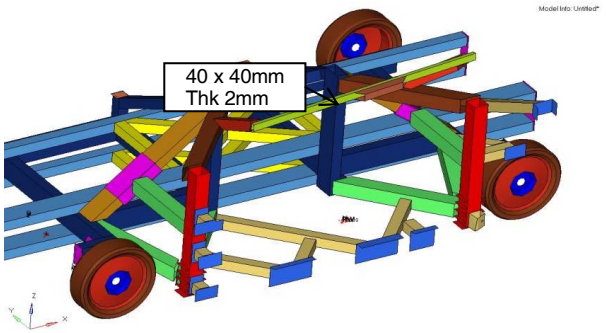


Fig.19 The 5th CAE model

At the 5th CAE, we weakened roof beam to prevent too fast spring back. as a result spring back was improved but the initial intrusion was too high.

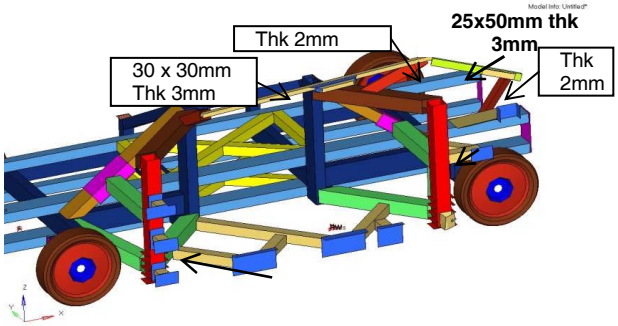


Fig.20 The 6th CAE model

So at the 6th CAE, we modified C-pillar support because we thought the rear part deformation of roof rail support makes too fast initial intrusion. Then we weakened roof beam more to prevent too fast spring back. As a result upper b-pillar intrusion became closer than 5th CAE.

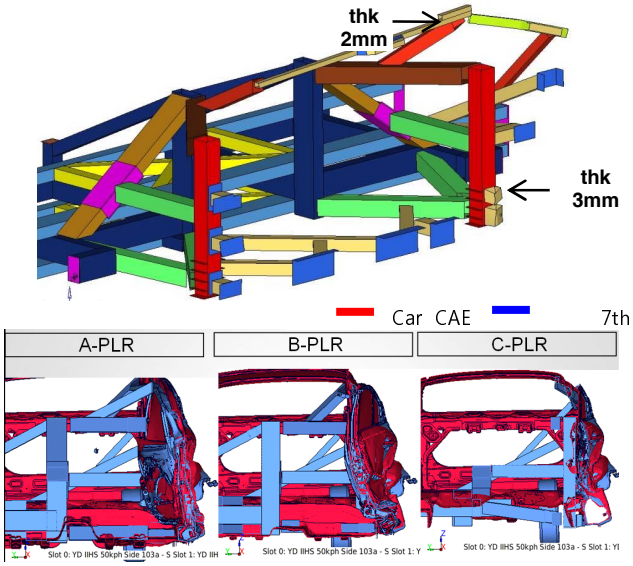


Fig.21 The 7th CAE model & A,B,C-PLR comparison

At the 7th CAE, we strengthen the rear of roof beam by adding one box and also added new box between trolley and sill at C-pillar to prevent C-pillar partial intrusion. As a result we got the successful validation to make the trolley. There were still some points not validated partially like front & rear door beltline bending point and B-pillar upper & lower rotation but even the full CAE is not

At the 8th CAE, we changed all the beams material from S355 to S235 because we cannot get the S355 soon. Also we changed some rigid parts to real modeling. As a result the intruding speed and permanent deformation was closer to the full car CAE than 7th CAE. [5)~6)]

### 2.2.3 Results of IIHS side trolley test

Through the comparison of intruding speed, we've come to know this trolley has really close structural performance. In case of upper and lower part the intruding speed correlation was not so good as beltline height but the modes are clearly same.

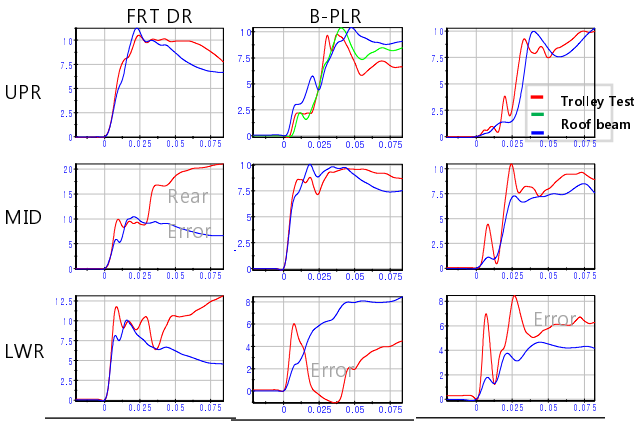


Fig.22 Comparison of UPR/MID/LWR intruding speed

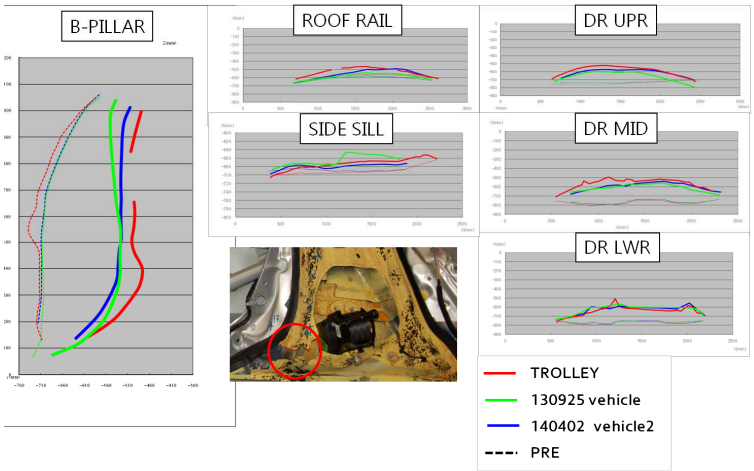


Fig.23 Comparison of static deformation

For the static deformation comparison, there were 50mm difference on the B-pillar lower, roof rail front and door upper/middle front. When we inspect the trolley, there was crack on the B-pillar lower inner panel. The reason was thought there was no front seat support in this trolley. So we added seat support substitute (inner 10t thickness, outer 5t thickness) and run the CAE again. As a result B-pillar and front door deformation was much closer to the real vehicle and the high strain area of B-pillar disconnected place was reduced. This means the probability of B-pillar disconnection became lowered.

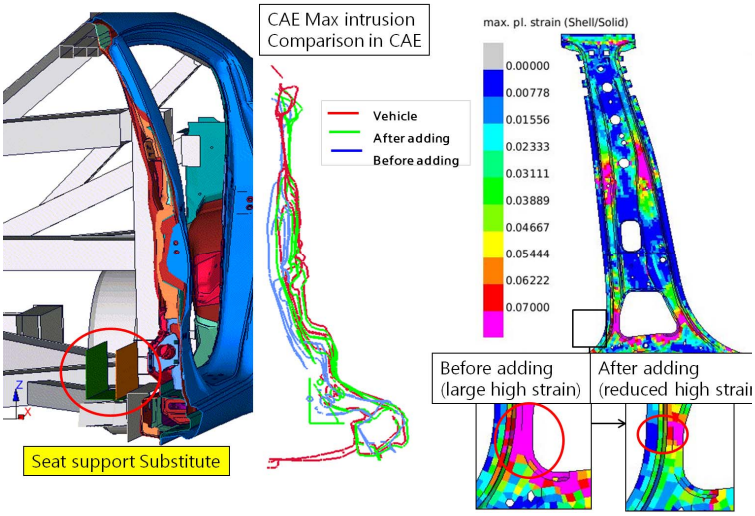


Fig.24 Seat support substitute CAE result

## 3. Conclusion

We made 2 kinds of trolley- IIHS small overlap and IIHS side, by using CAE validation for the Kia Forte vehicle. The correlation was very good even it's just made once and minimized parts because we concentrated on the important parts.

In case of small overlap trolley, we deleted many parts but we substitute powertrain, door, cowl cross bar and roof rall cross beam by creative ideas. All the strengths are tuned by CAE and CG points of powertrain and vehicle was set very accurately. As a result the trolley test many event time and structural values are really close to the vehicle test.

In case of side trolley, we designed many supporting beams and tuned them by CAE. Even if side structure deformation is complicated, there was not a big deformation in the roots like A/C pillar we install the beam by welding. Only the roof rail and side sill we applied very smart idea-making space and supporting by bending beams or rectangular brackets to realize the deformation better. As a result the trolley test many event time and structural values are really close to the vehicle test.

Now if we use these skills to develop a vehicle structure we can solve the main issue faster and with low cost because we can repeat the tests more easily. We expect test numbers side and smalloverlap could be reduced half. For one vehicle development the developing cost saving would be over $210,000. We are planning this methodology adaptation from PD project.

■ Patent: Be submitted "Efficient IIHS smalloverlap structure trolley", "Efficient IIHS side structure trolley"

## References


1. Jason R. Kerrigan "Design of a Dynamic Rollover Test System" UVA Center for Applied Biomechanics, 2011
2. Jeff R. Crandall, "Reproducing the Structural Intrusion of Frontal Offset Crashes in the Laboratory Sled Test Environment" University of Virginia, 2014
3. P. Michael Miller II, "A Compact Sled System for Linear Impact, Pole Impact, and Side Impact Testing" MGA Research Corp.,2002
4. Patrick M. Miller, "Evaluation Methodologies for Automobile Side Impact DevelopmentMGA Research Corp. ",1993
5. Karl Hoffmann, "Eine Einfüfrung in die Technik des Messens mit Dehnungsmeßstreifen", Herausgeber: Hottinger Baldwin Messtechnik GmbH, Sarmtadt
6. Herausgegeben von W.Beitz und K.-H., "DUBBEL TASCHENBUCH FÜR DEN MASCHINENBAU" 20. AUFLAGE


## ■ Author ■

Park Un-chin

Song Ha-jong

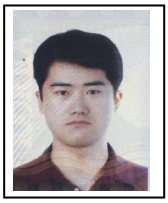
Kim Hyun-chul

Florian Ganz

Sudar Sankar

Mario Wohlfahrt

# IMPROVING THE SWISS NATIONAL ACCIDENT STATISTICS BY PROVIDING AIS DATA TO CLASSIFY INJURY SEVERITY

**Kai-Uwe Schmitt**
AGU Zurich / University and ETH Zurich, Institute for Biomedical Engineering
Switzerland

**Laura Baumgartner, Markus Muser**
AGU Zurich
Switzerland

**Mathias Baudenbacher, Anja Simma**
FEDRO – Federal Roads Office
Switzerland

Paper Number 15-0323

## ABSTRACT

To provide more detailed data on the injury severity of persons involved in a traffic accident, Switzerland has implemented various measures. The key component was the establishment of AIS coded injury severity data. Linking the national hospital statistics to the national traffic accident statistics allowed identifying persons that were injured in a police recorded traffic accident. Using information on the diagnosis given in the hospital statistics (ICD code) the corresponding AIS code was derived. An ICD-to-AIS translator was developed, mapping the medical information to corresponding AIS codes. Since not all ICD codes correspond to a unique AIS code the translator made use of additional medical information in order to map as many cases as possible. Applying the translator to the data sets of 2011 and 2012, a MAIS could be derived for approximately 95% of all cases. Using the newly implemented procedures, it is now possible to report the share of MAIS3+ injuries sustained on Swiss roads.

## INTRODUCTION

Information on the severity of injuries sustained in traffic accidents is a key factor for policy making. To develop strategies for road safety such basic data is required. While the number of traffic fatalities is usually very reliable, information on the number of surviving casualties and the severity of their injuries is of a lesser quality. To date, many countries rely on police-recorded data on the injury severity. In Switzerland and various other countries the police coarsely classifies injury severity as “not injured”, “minor injuries”, “severe injuries”, “died on the spot”, “died within 30 days” or “unknown”, respectively. The definitions when an injury is to be regarded as minor or severe are often not very precise and /or the application of the definitions is not particularly strict. In Switzerland, a person was by definition regarded as severely injured when he/she sustained an impairment that prohibits normal activity at home for at least 24h, for example, due to a stay in hospital. Practically every person that was admitted to hospital was thus regarded as severely injured independent of the duration of hospitalization which could range from a day to several weeks. Analysis of the data showed that injuries classified as severe include fairly simple fractures as well as life-threatening brain injury. With politics currently shifting their focus from road fatalities to addressing severely injured persons, more detailed information on injury severity is needed to be able to appropriately analyze this group.
To improve the data basis, the use of the Abbreviated Injury Scale (AIS) is recommended [1, 2] where "serious" injuries are generally regarded as injuries with a maximum AIS of 3 or greater (MAIS3+). Currently there is no general agreement on how such AIS data should be derived. Depending on the national data available, different approaches are pursued.
This study presents the different measures that Switzerland has implemented to improve injury severity data. The key component of this approach is the establishment of AIS coded data based on hospital statistics. The strategy how to derive AIS data along with first results is presented.

## METHODS

To improve the Swiss national accident statistics, data acquisition was addressed on two levels. Generally the police will continue to record injury severity when reporting a traffic accident. Gathering all relevant information needed to investigate an accident is a responsibility of public administration. However, to improve data collection a slightly altered scheme was introduced. Furthermore, these efforts were complemented by retrospectively deriving AIS data based on the hospital statistics. An algorithm mapping ICD to AIS codes was developed and implemented.

### Improved police reports

The classification of the injury severity that was used in the national police reports until the end of 2014 was coarse. It allowed differentiating the injury outcome of a person as “not injured”, “minor injuries”, “severe injuries”, “died on the spot”, “died within 30 days” or “unknown”, respectively. Given the prerequisite that injury severity data must be reported by the police, complex medical schemes are not applicable. Furthermore, practical aspects must be considered in order not to increase the administrative work load of police officers too much. Therefore it was decided to change the currently used classification scheme in police reports such that a further category was introduced. The classification “severe injuries” was replaced by the two categories “life-threatening injuries” and “serious injuries”. Similarly to countries like, for instance, Norway, life-threatening injuries should be recorded separately from all other injuries requiring medical treatment in a hospital (i.e. “serious injuries”). All other categories remain unchanged. Detailed guidelines were provided to the police, and the new national reporting system became effective on 1 Jan 2015. Based on this concept the current scheme of police reporting was slightly changed with the benefit of identifying life-threatening injuries.

### ICD-AIS-Mapping

Every in-patient in a Swiss hospital is registered and the medical data related to this stay in hospital is recorded in the national hospital statistics. For each patient, the relevant data includes the main diagnosis and up to eight further diagnoses. All diagnoses are coded using ICD-10-GM, i.e. the German version of the International Statistical Classification of Diseases and Related Health Problems issued in 2008. It was decided to use the ICD codes as a basis to derive AIS codes for each person injured in a traffic accident. An ICD-to-AIS translator was therefore developed and applied to the data sample to generate a better assessment of the injury severity. Figure 1 illustrates the decision tree model that forms the basis for the translator.

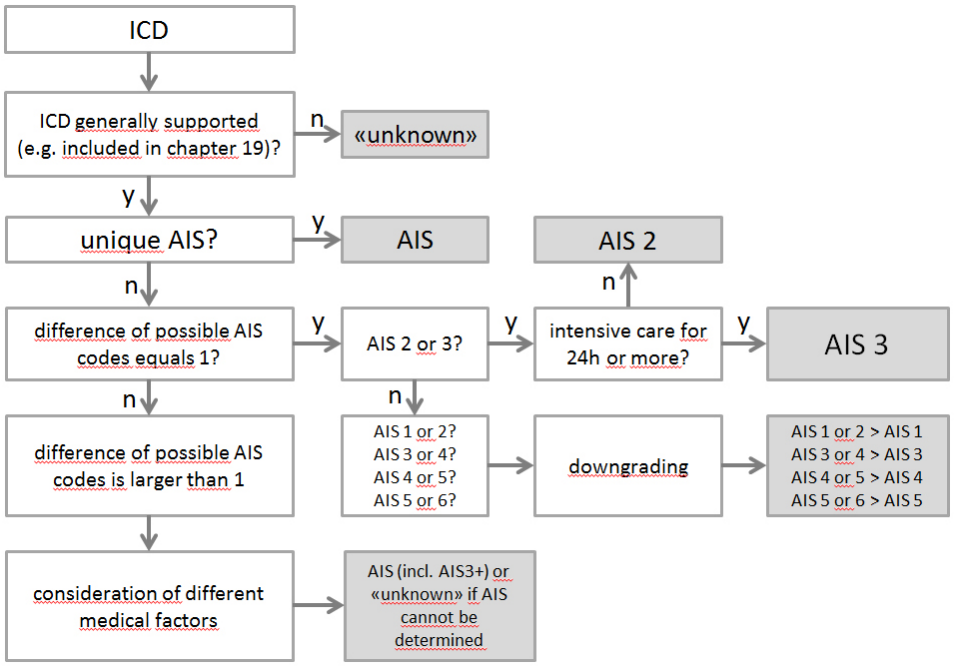


***Figure1. Simplified schematic of the decision tree model used to derive AIS codes based on ICD.***

Only ICD codes of chapter 19 (injuries) were considered. The translator automatically derives AIS codes for given ICD codes and then determines the patient's maximum AIS (MAIS) and the body region(s) that correspond to the MAIS. Since not all ICD codes correspond to a unique AIS code, a decision scheme also considering further medical information was developed and implemented. The most important of these additional parameters was the information whether a patient required intensive care and the duration (in hours) which a patient spent in an intensive care unit. Generally, a conservative approach was implemented; in cases where one ICD code corresponded to two possible AIS codes differing only by 1, the lower AIS code was chosen, i.e. the true injury severity was at least the chosen AIS code.

ICD chapter 19 consists of 2026 diagnoses of which 1204 were regarded relevant in the context of traffic accidents. Of these 1204 entries only 480 correspond to a unique AIS code. 215 diagnoses can be transferred to a set of AIS codes of the same severity (e.g. an ICD describing a fracture can correspond to several entries in the AIS dictionary all having the same code). Consequently these 215 diagnoses result in the same AIS. For a further 229 ICD codes several options of AIS coding exist where the difference of these AIS codes is only 1. Using a conservative approach, the lower of two possible codes was chosen. The remaining 280 ICD codes can be mapped to AIS codes of different severity. The ICD code for concussion, for instance, can correspond to AIS codes ranging from 1 to 5 depending on the duration of unconsciousness, whereas this duration is mostly unknown in the available medical data set.

Based on (a) the official handbook for hospitals how to record data for the national hospital statistics, (b) the results of a first correlation between injury severity and the length-of-stay in hospital [3] and (c) considering the characteristics of the Swiss health system it was assumed that a more severe injury most likely results in a longer stay in intensive care. Hence, cases in which an ICD code can correspond to a range of AIS codes and in which the patient did stay in intensive care for more than 24h, the AIS is most likely AIS3 or more. These cases were therefore translated into a code called AIS3+, i.e. the AIS is expected to be at least AIS3. If the duration on an intensive care unit was below 24h, the AIS code was downgraded. The introduction of the code "3+" also reflects the fact that there is a particular political interest in identifying the number of MAIS3+ victims.

**Data sources**

The Swiss national hospital statistics and the national traffic accident database were used. While the accident data base is continuously updated, unfortunately the hospital statistics linked to the accident data can only be provided annually and – due to administrative processes – it is only available with a delay of two years, i.e. in 2014 the hospital data of 2012 were made available. To improve injury severity data for road traffic accidents, it is necessary to match both available databases. The accident data formed the basis of this approach such that the hospital statistics was checked whether it included a person registered in the accident statistics. As there is no unique identifier that allows matching personal data, different criteria (such as age and postal code) were used to link the two data sets. Matching of the data was performed by the Swiss Federal Statistical Office. For this study the data sets of 2011 and 2012 were made available.

## RESULTS

The national traffic accident statistics for 2011 and 2012 include a total of 113’240 and 112’598 cases, respectively. In the corresponding hospital statistics 4’277 and 4’123 cases, respectively, were identified that could be matched with traffic accident data (Table 1), i.e. these persons received treatment as in-patients in a hospital after being injured in a road traffic accident. As can be seen from Table 1, the police-reported injury severity does not match well with the cases identified in the hospital statistics. There are, for example, some cases in which the police records indicated that a person was not injured, although the person was actually treated as in-patient in hospital.

**Table1.**
**Number of cases available in the accident and hospital statistics.**

| | 2011 | | 2012 | |
|---|---|---|---|---|
| **Injury severity according to police reported accident data** | **Number of cases in traffic accident data base** | **Number of these cases identified in hospital data (ICD available)** | **Number of cases in traffic accident data base** | **Number of these cases identified in hospital data (ICD available)** |
| not injured | 83'510 | 321 | 83'647 | 301 |
| minor injuries | 18'805 | 1'898 | 18'016 | 1'780 |
| severe injuries | 4'437 | 2'022 | 4'202 | 1'998 |
| died on the spot | 195 | 0 | 217 | 4 |
| died within 30 days | 125 | 35 | 122 | 33 |
| unknown | 6'168 | 1 | 6'394 | 7 |
| **total** | **113'240** | **4'277** | **112'598** | **4'123** |

The ICD-to-AIS translator was applied to determine the MAIS code for all cases identified in the hospital statistics. Table 2 summarizes the results, i.e. it shows the distribution of AIS code for cases which could be considered by the ICD-to-AIS translator. The score 3+ indicates cases in which the MAIS could not be established clearly, but the medical data suggests that the injury severity was at least MAIS 3. Using the translator it was possible to assign a MAIS code to approximately 95% of the cases for which ICD codes were available; for the remaining cases no MAIS was derived.

**Table2.**
**MAIS codes that were derived based on ICD data.**

| | 2011 | 2012 |
|---|---|---|
| **MAIS** | **Number of cases** | **Number of cases** |
| 0 | 14 (0.3%) | 19 (0.5%) |
| 1 | 610 (15.0%) | 587 (15.0%) |
| 2 | 2'523 (61.9%) | 2'355 (60.1%) |
| 3 | 362 (8.9%) | 349 (8.9%) |
| 3+ | 521 (12.8%) | 563 (14.4%) |
| 4 | 5 (0.1%) | 8 (0.2%) |
| 5 | 19 (0.5%) | 20 (0.5%) |
| 6 | 1 (0.0%) | 0 (0%) |
| unknown | 22 (0.5%) | 18 (0.5%) |
| **total** | **4'077 (100%)** | **3'919 (100%)** |

As shown in Table 2, the distribution of MAIS codes is very similar for both years investigated here. Approximately 76% of the persons injured in traffic accidents sustained an MAIS1 or MAIS2 injury while approximately 23% sustained in MAIS3+ injury.

The potential of the improved injury severity data is illustrated in the following example. In Table 3 the injury severity for different kinds of two-wheelers is compared (inclusion criteria: injured person was driver, ICD diagnosis was available). The example demonstrates that more detailed information is now available thanks to AIS-based injury severity data. It can be observed that the number of injured e-bikers increased between 2011 and 2012, but the MAIS distribution of injured e-bike users seems very similar to injured cyclists. Also the MAIS distribution for motorbike users is similar to the bicyclists and e-bikers, but there are clearly more cases with MAIS 4 and MAIS 5 injuries.

This data can now be used as a basis for a more detailed analysis of the injury outcome and thus provides a better foundation for policy making. In addition the newly established data provides details such as injured body regions. Depending on the research question, it can, for example, be analyzed which body region is responsible for the corresponding MAIS. While it seems not particularly helpful to present a summary table simply counting all injured body regions, it can be interesting to define specific research questions and investigate possible correlations between injury severity and injured body regions. With more data becoming available in future, such an analysis seems highly promising with respect to investigating a possible shift in injury outcome due to various measures to reduce the accident or injury risk, respectively.

**Table3.**
**Example: MAIS data for different kind of two-wheelers.**

| MAIS | bicycle | | | | e-bike | | | | motorbike | | | |
|---|---|---|---|---|---|---|---|---|---|---|---|---|
| | 2011 | | 2012 | | 2011 | | 2012 | | 2011 | | 2012 | |
| | n | % | n | % | n | % | n | % | n | % | n | % |
| 0 | 1 | 0.2 | 1 | 0.2 | 0 | 0.0 | 0 | 0.0 | 3 | 0.3 | 0 | 0.0 |
| 1 | 47 | 7.5 | 33 | 5.1 | 3 | 5.1 | 4 | 5.4 | 102 | 8.9 | 113 | 10.3 |
| 2 | 435 | 69.2 | 428 | 66.5 | 43 | 72.9 | 50 | 67.6 | 722 | 62.9 | 664 | 60.6 |
| 3 | 58 | 9.2 | 66 | 10.2 | 4 | 6.8 | 7 | 9.5 | 147 | 12.8 | 134 | 12.2 |
| 3+ | 85 | 13.5 | 111 | 17.2 | 9 | 15.3 | 12 | 16.2 | 149 | 13.0 | 171 | 15.6 |
| 4 | 1 | 0.2 | 2 | 0.3 | 0 | 0.0 | 0 | 0.0 | 2 | 0.2 | 2 | 0.2 |
| 5 | 0 | 0.0 | 2 | 0.3 | 0 | 0.0 | 0 | 0.0 | 13 | 1.1 | 10 | 0.9 |
| 6 | 0 | 0.0 | 0 | 0.0 | 0 | 0.0 | 0 | 0.0 | 0 | 0.0 | 0 | 0.0 |
| unknown | 2 | 0.3 | 1 | 0.2 | 0 | 0.0 | 1 | 1.4 | 10 | 0.9 | 1 | 0.1 |
| **total** | **629** | **100.0** | **644** | **100.0** | **59** | **100.0** | **74** | **100.0** | **1148** | **100.0** | **1095** | **100.0** |

## DISCUSSION

To obtain more information on the injury severity of persons injured in traffic accidents, the Swiss national accident statistics were improved by establishing MAIS data. Today Switzerland is thus one of the few European countries providing AIS-based information on the injury severity of road traffic victims. This represents a significant improvement as such data allows a more detailed analysis of the outcome of traffic accidents.

The ICD-to-AIS translator that was developed for this purpose worked well. Besides ICD codes, also information such as the duration of intensive care was used to map the codes. Eventually the algorithm allowed assigning a MAIS code to approximately 95% of all cases. Limitations of this process include the fact that hospital statistics cover in-patients only. Currently this limitation seems acceptable as the focus is on MAIS3+ injuries which generally require treatment at a hospital. For research purposes it would, however, be interesting to add AIS based information for other patients. Mapping data from a national accident insurance database could be one option to obtain this additional data.
Furthermore it must be noted that not all ICD codes can be uniquely mapped to AIS codes. This requires implementation of certain strategies in the ICD-to-AIS translator. Of course, general strategies such as downgrading a code introduce a bias towards a more conservative estimation. Applying such rules consistently also ensures comparability of data from different years.
The introduction of MAIS3+ as a further category could be regarded as a further limitation. However, given the general interest in MAIS3+ injuries, this procedure resolved the problem of not being able to assign a unique AIS code in some cases without having to make use of further assumptions in the medical data.

A more general problem is the fact that the hospital data is currently only available with a time delay of two years. Procedures should be improved such that the medical information becomes available more rapidly. On the other hand, this highlights the necessity to also improve the police-recorded injury severity data since this data is continuously available. The introduction of a further category “life-threatening injury”, which became effective in 2015, is considered to represent an important step in this context. Future analysis will investigate how well this

category matches with AIS-based data and to which extent the police-recorded data correlates to ICD-derived AIS data.

In addition to the injury severity, the MAIS derived from ICD codes also offers the possibility to locate the body regions that were injured. This represents an interesting information which was not available in the past. Depending on the research questions, additional information with respect to changes in injury patterns can thus be retrieved.

In summary, it was shown that the implementation of an ICD-to-AIS translator allows generating injury severity data with a high relevance for policy making and research. Switzerland has established a national scheme to derive detailed injury severity data and has thus set a well-founded basis for future accident statistics.

## CONCLUSIONS

ICD-to-AIS mapping was introduced on a national level which improves the available information on injury severity significantly. Injury severity data is essential to evaluate the performance of measures to improve traffic safety. Estimates of the potential benefit of safety technologies or any other preventive measure can thus be improved.

## REFERENCES

[1] Tingvall C, Ifver J, Krafft M, Kullgren A, Lie A, Rizzi M, Sternlund S, Stigson H, Strandroth J. 2013. "The consequences of adopting a MAIS3 injury target for road safety in the EU: a comparison with targets based on fatalities and long-term consequences", Proc. IRCOBI Conf., paper no. IRC-13-10, www.ircobi.org, last accessed 04 February 2015
[2] OECD. International Road Traffic and Accident Database (IRTAD), International Traffic Safety and Analysis Group, www.irtad.net, last accessed 09 January 2015
[3] Schmitt KU, Baumgartner L, Muser M, Furter K, Scholz St, Lüber B, Thomas P, Simma A. 2014. „Developing a scheme to report AIS-coded injury severity for Swiss traffic accident data". Proc. IRCOBI Conf., paper no. IRC-14-50, www.ircobi.org, last accessed 04 February 2015

# FIRST GENERATION OBESE ATD (FGOA)

**Breanna, Beahlen**
**Michael, Beebe**
Humanetics Innovative Solutions
United States

**Jeff, Crandell**
**Jason, Forman**
**Hamed, Joodaki**
University of Virginia, Center for Applied Biomechanics
United States

Paper Number 15-0325

## ABSTRACT

This paper sets forth the need for an Obese ATD. The goal of this study was to build a prototype that accurately represents an obese subject with a BMI of 35 kg/m$^2$, and also to explore new ATD flesh material options.

The prototype ATD was designed using a THOR-M platform and a 35 kg/m$^2$ BMI target. The finished prototype was then tested on a rear seat buck at 29 km/h and 48 km/h. The kinematic data from these tests was compared to the kinematic data from previous tests ran at the University of Virginia using a 35 kg/m$^2$ BMI PMHS. This comparison was used to evaluate the existing prototype and reform the next iteration of the ATD.

## INTRODUCTION

The obesity rate has increased dramatically in the U.S. and many places in the world in recent years. From 1980 to 2000, the prevalence of obesity in Americans increased from 14.4% to 30.5% [1]. In 2009-2010, approximately 78 million adult Americans – over 35% of the adult U.S. population - were obese (defined as a Body Mass Index, BMI, greater than or equal to 30 kg/m2) [2].

Obese occupants pose unique challenges for restraint systems. In addition to the increased mass of the occupant, the increased amount of centrally-located subcutaneous tissue associated with obesity limits the ability of the lap belt to properly engage the pelvis. Depending on the anthropometry of the occupant, the increased depth of the subcutaneous tissue can result in the lap belt being located more anterior and more superior relative to the pelvis than would be observed in a non-obese occupant [3]. In many cases, the depth of tissue around the waist, thighs, buttocks, and abdomen may result in the lap belt being placed above the level of the anterior superior iliac spines. This sub-optimal belt position may result in limited-to-no engagement of the pelvis in frontal impacts, resulting in excessive forward motion of the occupants and direct loading of the lap belt into the abdomen [4][5]. In addition to the effect on abdominal injury risk, this may lead to increased injury risk to the lower extremities through striking the knee bolster [6][7], and increased risk of injury to the chest due to a greater portion of the restraining load being applied to the torso [8][9].

Current anthropomorphic test devices lack the ability to assess restraint interactions with obese occupants. The Hybrid III 95% male dummy – the only current ATD representation of a “large male” – has a height of 188 cm and a weight of 101 kg. This corresponds to a BMI of 28.6 kg/m$^2$. This is less than the 65th percentile BMI in U.S. adults (ages 20+) [2]. In addition, the Hybrid III 95th does not take into account changes in body mass distribution or increases in superficial soft tissue depth associated with obesity.

## METHODOLOGY

### ATD Development

The First Generation Obese ATD (FGOA) is built on an existing platform of the THOR 50th percentile male ATD. The conversion to an obese ATD is accomplished through a flesh jacket representing the superficial tissue of an obese male. The FGOA flesh jacket consists of chest, pelvis, and upper thigh fleshes. The flesh jacket is constructed from different molded materials that allow the flesh to be pliable enough so that the dummy buttock and thighs would fit and conform into a seat. The legs and arms were ballasted to meet their target weights (Table 1).

The external geometry of the current prototype of the FGOA jacket is based on the anthropometry of a selected obese male post mortem human surrogate (PMHS) previously reported in a series of frontal impact restraint sled tests [4][5]. That subject had a height of 189 cm, mass of 124 kg, and BMI of 35 kg/$m^2$. The internal skeletal dimensions of that subject (e.g., the internal diameter of the ribcage) were similar to those of a 50th percentile male PMHS [4]. Thus, the majority of the difference in the mass and exterior dimensions between this particular obese subject and a 50th percentile male occurred as a result of increased superficial tissue and abdominal fat. The finished ATD can be shown in Figure 1.

***Figure1. Completed Obese ATD prototype***

Once the Obese ATD prototype was complete, the external dimensions were measured and compared to the external dimensions of the PMHS (See Table 1). Furthermore an overlay picture of the 35BMI PMHS and Obese ATD is shown in Figure 1. Minor dimensional differences were noticed between the flesh jacket and PMHS, and will be corrected in the next version of the ATD. Also, differences in the seated height can be improved by using a slightly stiffer pelvic flesh material. Table 2 below indicates the target mass distribution weights; these distributions were based on a the THOR-M ATD.

**Table1.**
**ATD VS. PMHS External Measurements**

| Location | ATD measurements (cm) | PMHS measurements (cm) |
|---|---|---|
| Chest Breadth - 4th Rib | 42 | 40 |
| Chest Breadth - 8th Rib | 41 | 36 |
| Chest Depth - 4th Rib | 29 | 23.5 |
| Chest Depth - 8th Rib | 30 | 25.5 |
| Hip Breadth | 44.5 | 39.1 |
| Chest Circumference - 4th Rib | 130 | 110.7 |
| Chest Circumference - 8th Rib | 119 | 114.3 |
| Waist Circumference - At Umbilicus | 123.5 | 120 |
| Waist Circumference - 8cm above Umbilicus | 120 | 119.7 |
| Waist Circumference - 8cm below Umbilicus | 126 | 116.9 |
| Thigh Circumference | 65 | 68.6 |
| Shoulder Breadth (Biacromial) | 49 | 43 |
| Seated Height | 93.5 | 98 |

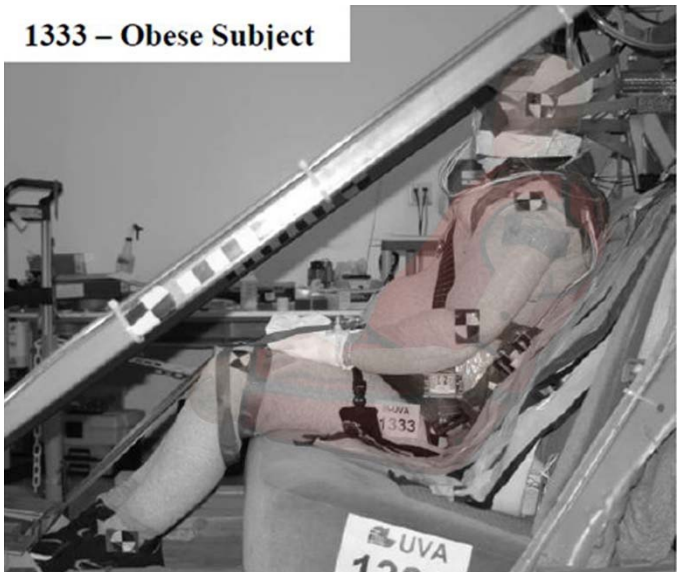


***Figure2. Overlay of Obese ATD with 35BMI PMHS.***

**Table2.**
**Body Mass Distribution Targets**

| Segment | Hybrid III (lbs) | THOR (lbs) | Obese Design Targets (lbs) |
|---|---|---|---|
| Head | 10 (5.8%) | 10.2 (6.1%) | 10.2 |
| Neck | 3.4 (1.9%) | 3.64 (2.2%) | 3.64 |
| Upper Torso | 37.9 (22.1%) | 29.59 (17.9%) | 49 |
| Lower Torso | 50.8 (29.7%) | 62.3 (37.7%) | 112 |
| Upper Arm (each) | 4.4 (5.1%) | 4.4 (5.3%) | 7.25 |
| Lower Arm + Hand (each) | 5 (5.8%) | 5 (6.05%) | 8.25 |
| Upper leg (each) | 13.2 (15.4%) | 9.81 (11.9%) | 16.2 |
| Lower leg + feet (each) | 12 (14%) | 10.47 (12.7%) | 17.4 |
| Total Weight | 171.3 | 165.15 | 273 |

## Testing

Four tests, including two 48 km/h and two 29 km/h were performed with a sled buck representing the rear seat occupant component of a 2004 mid-sized sedan (See Figure 2.) Data was collected from accelerometers located in the head, neck and pelvis as well as angular rate sensors located in the head and T1 position. The tests were performed based on the test conditions of the obese PMHS test completed at the University of Virginia.

***Figure3. Dummy sled test set-up, right side view.***

## RESULTS AND DATA

The trajectories shown below illustrate the trajectories from the 48km/h testing completed on a 23 kg/m$^2$ BMI PMHS (Figure 3), a 35 kg/m$^2$ BMI PMHS (Figure 4), and the obese ATD (Figure 5). As you can see from these comparisons, the ATD mimicked the substantially greater forward pelvis and knee motion caused by increased mass of the lower body and limited-to-no interaction between the pelvis (bone) and the lap belt that was seen in the 35 kg/m$^2$ PMHS.

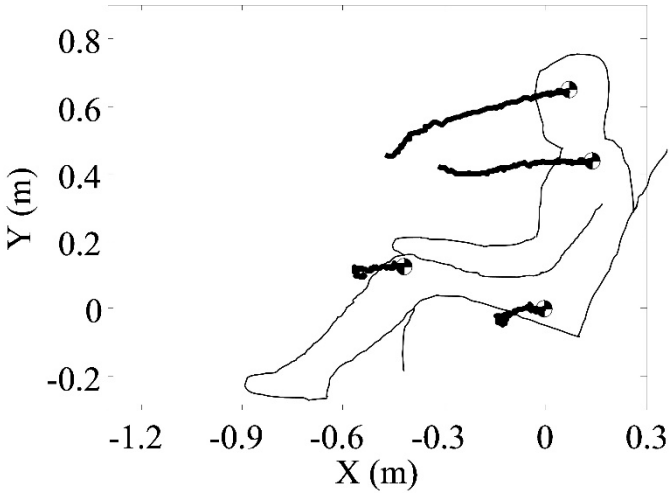


***Figure4. Trajectory of the 23BMI PMHS [4].***

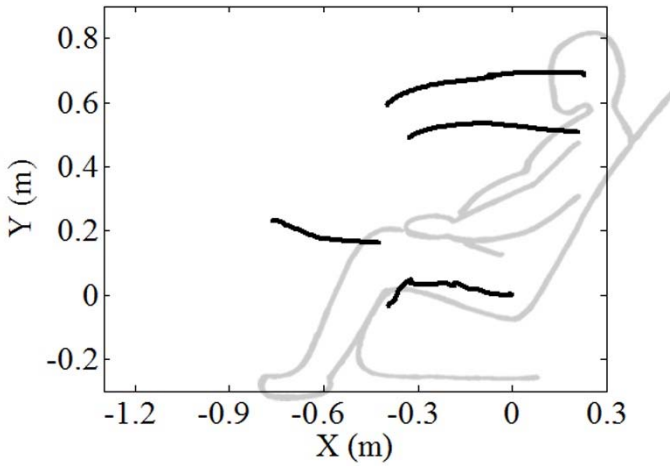


***Figure5. Trajectory of the 35BMI PMHS [4].***

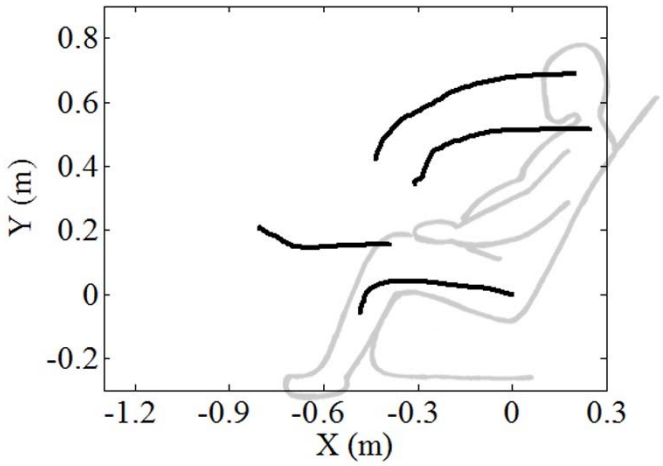


***Figure6. Trajectory of the 35BMI Obese ATD.***

Forward motion of head and knee of the dummy were 14 cm and 4 cm less than those of PMHS, and forward motion of pelvis of the dummy was 7 cm greater than PMHS. The mean peak of upper shoulder belt, lower shoulder belt, and lap belt tension in dummy tests were 6.5 kN, 6.7 kN, and 8.8 kN, and in PMHS tests, they were 6.4kN, 6.3 kN, and 8.3kN. Peak head, chest, and pelvis accelerations also tended to be greater with the dummy than with the PMHS.

## CONCLUSIONS

The results suggest some differences in the kinematics and dynamics of the dummy compared to the PMHS that may be indicative of differences in the interaction of the posterior pelvis flesh and the seat, and a difference in mass distribution affecting relative loads on the various portions of the seatbelt. The differences in the head trajectories most likely stem from differences that already existed between the THOR ATD and the PMHS.

To correct the differences, next steps will be to create new flesh components for the arms and lower legs rather than ballasting the bones. More evaluation will be conducted on the stiffness of the material used for the flesh components as well.

Despite these differences, the obese dummy still exhibited the same kinematic characteristics that were highlighted as potentially challenging for restraint systems by the PMHS tests – most notably, both exhibited substantial forward motion of lower body and subsequent backwards rotation of the torso affected by limited engagement of the lap belt with the pelvis. This suggests that although further refinement may be warranted, this dummy may prove useful as a research tool to begin investigating the challenges of, and potential strategies for, the safe restraint of obese occupants.

**REFERENCES**

[1] Flegal KM, Carroll MD, Ogden CL, Johnson CL. Prevalence and trends in obesity among US adults, 1999–2000. JAMA. 2002;288:1723–7.
[2] Cynthia L. Ogden, Margaret D. Carroll, Brian K. Kit, Katherine M. Flegal. Prevalence of Obesity in the United States, 2009–2010, NCHS Data Brief, No. 82, January 2012
[3] Matthew P. Reed, Sheila M. Ebert, Jason J.Hallman. Effects of Driver Characteristics on Seat Belt Fit, Stapp Car Crash Journal, Vol 57 , pp. 43-57, November 2013
[4] Foreman, J. 2009. "The Effect of Obesity on the Restraint of Automobile Occupants." In AAAM's Vol 53, 2009.
[5]Richard W Kent, Jason L. Forman, Ola Bostrom. Is there really a "cushion effect"? : A biomechanical investigation of crash injury mechanisms in the obese, Obesity (Silver Spring), Vol 18, pp. 749-753, April 2010
[6] Boulanger BR, Milzman D, Mitchell K, Rodriguez A. Body Habitus as a Predictor of Injury Pattern After Blunt Trauma. Journal of Trauma Vol. 33, No. 4,pp 228-232, August 1992.
[7] Neville, A.L. 2004. "Obesity is an Independent Risk Factor of Mortality." Communications of the Arch Surg, Volume 139
[8] Mock, C. N. 2002. "The Relationship between Body Weight and Risk of Death and Serious Injury in Motor Vehicle Crashes." Communications of the Accident Analysis and Prevention, 34, 221-228
[9] Jakobsson L, Lindman M. Does BMI (Body Mass Index) Influence the Occupant Injury Risk Pattern in Car Crashes? Proceedings of the International Research Council on the Biomechanics of Impact, pp 427-430, September 2005.

ID#: 15-0326
Title: Failure Analysis of Compressed Natural Gas Containers for Automotive Use
Session: Advanced Fuels Crash Safety

Barbara Hennessey NHTSA, Nathanael Greene NASA, Darren Cone NASA, Tommy Yoder NASA, Daniel Wentzel NASA, David McColskey NIST

## ABSTRACT

In 2009, the National Highway Traffic Safety Administration's (NHTSA's) Office of Defects Investigation made site visits to two different companies that utilized compressed natural gas (CNG) to fuel their vehicle fleets. The purpose of these site visits was to obtain information concerning two independent incidents where high pressure CNG fuel containers on fleet vehicles ruptured during or shortly after refueling. These containers were represented as conforming to industry standard ANSI/NGV2 [1], and were still within their 15 year manufacturer recommended service life (although they had experienced several years of on-road use). Further, the newer model containers were self-certified by the manufacturer as compliant with Federal Motor Vehicle Safety Standard (FMVSS) 304 [2].
After the container ruptures occurred, each of the companies, for reasons of safety, retired the sister vehicles in their fleets. The decommissioning of these fleets offered an opportunity to NHTSA to obtain some of the retired CNG containers, which experienced similar service conditions to those that ruptured during refueling, and to subject them to both nondestructive (NDE) and destructive evaluation (DE) to document in-service wear, damage and residual life. To this end, NHTSA entered into an Interagency Agreement with the National Aeronautics and Space Administration (NASA) White Sands Test Facility (WSTF), to conduct the evaluation of the used containers and compare them to unused containers of similar design. NASA has been performing test and evaluation of composite pressure vessels, similar to those designed for automotive use, since 1978. The objective of the evaluation is to gain valuable insight into the construction and deterioration elements that could suggest potential improvements in the existing standards. Destructive and nondestructive evaluation of the aged and new containers is on-going. This paper presents the results of the evaluation to date and potential future steps in the program.

## INTRODUCTION

In 2009, the National Highway Traffic Safety Administration (NHTSA's) Office of Defects Investigation made site visits to two different companies that utilized compressed natural gas (CNG) to fuel their vehicle fleets. The purpose of these site visits was to obtain information concerning two independent incidents where high pressure CNG fuel containers on-board fleet vehicles ruptured shortly after refueling. After the container ruptures occurred, each of the companies, for reasons of safety, retired the sister vehicles in their fleets. The decommissioning of these fleets offered an opportunity to NHTSA to obtain retired CNG containers which experienced similar service conditions to those that ruptured during refueling, and to subject them to both nondestructive (NDE) and destructive evaluation (DE) to document in-service wear, damage and residual life. To this end, NHTSA entered into an Interagency Agreement with the NASA/WSTF, to conduct the evaluation of the used containers and compare them to unused containers of similar design.
NHTSA had sister containers from each of the retired fleets shipped to NASA/WSTF for evaluation. The shipments included twenty-three Brunswick Type-4 CNG containers from one fleet and thirty-six Lucas Aerospace Type-2 containers from the other. The "Type" designation refers to the construction of the container. Type-1 containers are all metal – e.g., aluminum alloy or steel. Type-2 containers have a load bearing metal liner that is reinforced with composite (glass, aramid, carbon fiber or combinations thereof) hoop wrap around the parallel length of the container. Type-3 containers are fully wrapped by composite fiber and have a thin metal liner with most of the stress on the composite wrap. Type-4 containers have a non-metallic liner fully wrapped with composite fiber, which provides all of the container strength. The Brunswick containers were manufactured in 1994, and certified to ANSI/NGV2 for 15 years. The Lucas containers were manufactured in 1998 and certified for 15 years to ANSI/NGV2. They were also self-certified as compliant with FMVSS 304, which went into effect in 1995.
Federal Motor Vehicle Safety Standard 304*, Compressed Natural Gas Fuel Container Integrity*, is based on a subset of recommendations in the industry standard NGV2, and specifies performance and labeling requirements for the integrity of CNG motor vehicle fuel containers. Specifically, FMVSS 304 requires that non-welded containers (such as those evaluated in this study) do not leak or rupture in a hydrostatic burst test, when held at not less than 2.25 times the service pressure (SP) for 10 seconds. Containers must

also undergo a hydraulic pressure cycling test without leakage, and are subjected to bonfire tests per FMVSS 304. They must be labeled with information specified in the standard, and the label must remain affixed and legible for the manufacturer's recommended service life of the container. The FMVSS 304 labeling requirements are shown in Figure 1.

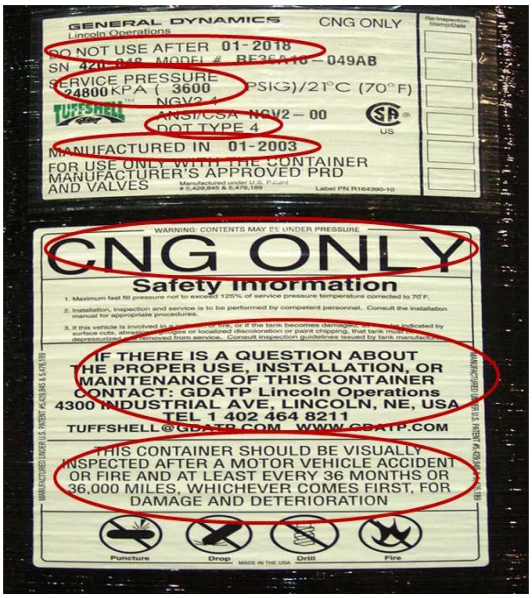


***Figure 1. Labeling Requirements in FMVSS 304, CNG Fuel Container integrity***

**PURPOSE**

The purpose of this effort is to document in-service wear, damage and residual life in CNG containers that have seen real world service, through nondestructive and destructive evaluation techniques. New containers are certified to the strength (i.e., burst) and durability (i.e., cycling) test requirements in standards and regulations such as ANSI/NGV2 and FMVSS 304, but (in this study) we seek additional data about the effects of the real world service environment on container life. While this study may not determine the root cause of the failures that occurred in the aforementioned two fleet vehicles, internal/external examination and residual strength tests may reveal weaknesses that can be addressed through improved tests, periodic inspection, and/or installation guidelines.

**Synopsis of the CNG Container Failures**

On June 9, 2008 a Type-2 Lucas Aerospace CNG container in a 1998 dedicated CNG Ford E350 van ruptured shorty after refueling at a Philadelphia Gas Works facility. The vehicle was equipped with three 3,000 psi rated containers that had a manufacturer recommended service life of 15 years and were manufactured in March 1998. Two 14" x 34" containers were mounted transversely in the rear of the vehicle. The third 12"x72" container, which ruptured, was mounted alongside the driveshaft inside the frame rail on the driver's side. The glass fiber overwrap failure was the result of stress corrosion cracking caused by an unidentified corrosive agent between the overwrap and the steel liner [3,4]. Over-pressurization of the steel liner during fueling also may have contributed to the failure. This may have been caused by a failure to close condition of the tank mounted solenoid valve and/or an improperly set relief valve on the fueling station [5]. Figure 2 shows the failed container.

***Figure 2. Failed Type-2 Lucas Aerospace Container (portions of overwrap and steel liner missing)***

On March 16, 2009 two Brunswick Type-4 containers ruptured during refueling of a laundry truck (i.e., conversion step van) in Pasadena CA. For the 3,000 psi rated containers, the manufacturer stated that the service life is 15 years and these containers were manufactured in 1994. They would have been at the end of their manufacturer recommended service life in October 2009. One of the containers was mounted vertically inside the back of the van onto a rubber padded steel ring with the shut off valve, pressure relief device (PRD), and piping exposed under the vehicle. The second ruptured container was mounted longitudinally under the vehicle, unshielded, and with its valve end dome directly beneath the vertical container [5]. The containers ruptured sequentially. The order and exact cause of rupture is unknown. Possible scenarios are that either the horizontal or vertical container failed first, due respectively to possible road damage or damage caused by the vertical mounting. The second container failed from fragmentation caused by the first rupture. Figure 3 shows some of the damage to the vehicle.

***Figure3. Step Van Damaged by Type-4 Container Ruptures on Driver's side***

**Program Plan Overview/Status**

The objective of the test program is to employ destructive and nondestructive evaluations on intact containers removed from service, and new containers. The goal is to ascertain if there are gaps in codes, standards and regulations which could be addressed to improve safety performance of future container designs.

The Test Plan consists of the following major components shown in Table 1.

**Table 1.**
**Overview of Phased Evaluation of Type-2 and Type-4 CNG Containers**

| | Test Plan Phase | Status |
|---|---|---|
| 1.1 | Type-4 Nondestructive Service Evaluation | Complete |
| 1.2 | Type-4 Destructive Evaluation | Complete* |
| 1.3 | Type-4 Mechanical Sectioning and Materials Analysis | Complete |
| 1.4 | Type-2 Nondestructive Service Evaluation | Underway |
| 1.5 | Type-2 Destructive Evaluation | Planned |

*One additional pneumatic burst test of an aged Type-4 container will be conducted in 2015

**Type-4 Test Articles**
Twenty-three Type-4 containers were removed from service and shipped to WSTF for testing. The WSTF numbers assigned to the containers for testing are WSTF# 11-45269 through 11-45291. These control numbers provide traceability to historic records and to each test that is performed. The containers were individually packaged in cardboard boxes for shipment from California. Once received at NASA/WSTF the containers were locked inside controlled access facilities.

**Type-4 Containers - Nondestructive Service Evaluation Methods**
Each of the containers was subjected to the following nondestructive examination techniques, the results of which are documented in individual data packages.

- Shipping containers, packing materials, and all accessible exterior surfaces were inspected in the as-received condition. Digital photographs of the container, packaging arrangement, and exposed surfaces were taken.
- An as-packed coordinate system was registered to the exposed features on the test article, enabling subsequent registration with a fully-exposed-article grid coordinate system to be referenced and remain consistent throughout the examination.
- Once the CNG containers were removed from the shipping containers, visual inspections of the remaining exterior surfaces were completed and documented through a combination of near and far field photography. Visual indications were recorded and documented per the manufacturer's criteria.
- Physical dimensions such as weight, length, and circumference at several distances from the top dead center (TDC) reference boss (A-end or valve end boss), were measured and recorded.
- A detailed visual inspection damage log and high magnification photography, recorded damage indications mapped to the coordinate system on the exterior upper dome (A-end), hoop region and lower dome (B-end plug) of each container.
- Prior to internal inspection, the break-away torque of the manual valve and plugs were measured.
- Internal visual inspection and boroscopic images recorded presence of contaminants (e.g., compressor oil), bubbles, voids, staining, and other indications on the container interior.
- Radiographic images of the interior documented internal interfaces such as boss-to-liner and liner-to-overwrap.
- Flash thermography was used to reveal infrared transfer of heat into wall surface fiber layers, useful for identifying subsurface areas of delamination.
- Laser shearography was used to detect non-visible internal flaws (two containers only).
- Samples of interior and exterior contaminants and foreign debris were collected, analyzed, and archived (twenty-three samples of each collected and archived, 2 analyzed).
- Samples of residual gas in containers that arrived with valve closed were collected and analyzed (three containers only).

**Type-4 Containers - Nondestructive Evaluation Results**

Appendix A provides an inventory of the Type-4 containers and a summary of the NDE results. The following general observations were made.

- Some damage was observed on several shipping containers, including mechanical damage and oil contamination.
- Inconsistent and/or variable debris buildup was observed on test article exteriors.
- Some labels were missing, illegible, or obscured by container mounting straps in service.
- Some labels were wrinkled in such a way to imply containers were shifting within vehicle mounts during service.
- Paint transfer was observed on numerous test articles. Primers, paints, or other "incidental contact" chemicals not addressed in testing may not be compatible with container overwrap materials.
- Break-away torque of the pressure fittings on containers varied from below 5 ft-lb to 170 ft-lb, with oil on the outside of some containers which was chemically similar to oil found on the inside, possibly indicating a chemical/flammability hazard.
- The largest average container circumference was near the dome regions. The smallest circumference was near the center of the container length.
- No provisions for proper torque of the pressure fittings (wrench flats) are available. Over torque may cause damage to boss-to-liner or boss-to-overwrap interface.
- Mechanical damage was present up to Level 2 per CGA Pamphlet C-6.4-2007 and Level 2b per OEM technical inspection manual. Level 1 damage does not require repair. Level 2 damage requires the manufacturer's recommendation in writing for disposition or repair of the container. Level 3 damage requires the container to be condemned.
- Rubber hose mounting ring and adhesive material was observed on containers that were mounted vertically in vehicles which may not be compatible with overwrap.
- Vertical dome mounting configuration was not addressed by the container manufacturer, which recommends horizontal strap mounting with guidance on strap locations. There may be potential for direct dome mounting to damage the structural composite.
- Circumferential witness marks were unevenly spaced from boss to boss with a variation in witness mark width. This provides evidence of shifting during service. Torque and pre-load specifications on container straps should preclude structural damage and limit lateral translation.
- Oil was observed on the interior and exterior of the test articles, internally as much as half a gallon of compressor oil was measured in a container used in the horizontal mounting configuration.
- Liner visual indications such as blistering were observed in the dome regions of almost all test articles. Significance of blistering, whether from manufacture or use, is unknown.
- Evidence of severe liner separation from overwrap and boss was observed in one container via computed radiography.
- Laser shearography data was of little value and excessively noisy due to as-received surface condition of containers. The "Tuffshell" sacrificial glass layer distorts data in the hoop transition and dome regions. Application of a dulling developer solution improved readings slightly.
- Thermography data was of little value. The overall composite wall thickness and sacrificial glass layer distorts heat transfer characteristics. The addition of impact protection in hoop transition and dome regions confounded useful data from the load bearing surface underneath.
- Three containers with closed valves had 1 – 5 psi residual gaseous contents composed of approximately 94% air, 3.5% ethane, 1.5% propane, 0.6% butane and a trace amount of methane.
- Exterior contaminants consisted of kaolin (clay), aliphatic hydrocarbon (oil), and silicon dioxide (sand) – all expected road contaminants.
- Interior contaminants were a two phase oil residue/paste consisting of aliphatic hydrocarbon and polypropylene glycol, white crystalline carboxylic acid and cellulose acetate butyrate.

**Type-4 Containers - Destructive Evaluation Methods**

Seven of the twenty-three containers that were examined nondestructively were selected for destructive evaluation under this test plan. The NDE served as the basis for selection of six test vessels to undergo

hydraulic cycling and burst, based on the test methods in certification standards. One container was selected for pneumatic burst testing, as pneumatic burst was the failure mode in the delivery vehicles. For comparison, two new vessels of similar design were also selected for hydraulic burst testing. Unfortunately the new containers are not the exact configuration of the service containers, but they do share many of the same features of construction and materials, giving them some limited value as reference test articles. A comparison of the containers is provided in Table 2.

**Table 2.**
**Typical Dimensions of Type-4 Service and New Containers**

| Description | Service Containers | New Containers |
|---|---|---|
| Manufacturer | Brunswick Composites (now Lincoln) | Lincoln Composites |
| Mfgr Part Number | RA30A16-055AB | 240172-030 |
| Service Pressure (SP) | 3000 psig | 3600 psig |
| Standard | NGV2-4 | ANSI/CSA NGV2 |
| Volume | 124 L | 54 L |
| Length (typical) | 55 in. | 35 in. |
| Weight | 114 lb | 65 lb |
| Diameter (typical) | 16 in. | 13.8 in. |
| Shell Construction | Glass/C/epoxy hybrid with TuffShell®[a] protective shoulder | Glass/C/epoxy hybrid with TuffShell protective shoulder |
| Liner Material | HDPE | HDPE |
| Resin | Epoxy | Epoxy |
| Fiber Reinforcement | Carbon and glass fiber hybrid | Carbon and glass fiber hybrid |

[a] TuffShell® is a registered trademark of General Dynamics Armament and Technical Products, Inc., Charlotte, North Carolina.

Selection of the containers for cycling and burst testing sought to provide data representative from as broad a sample of container use-conditions as possible. Therefore, containers selected were as follows in Table 3.

**Table 3.**
**Type-4 Container Cycling and Burst Tests**

| Hydraulic Cycling and Burst |
|---|
| New Test Articles:<br>WSTF ID #12-45898<br>WSTF ID #12-45894 - Previously pressure cycled : (15,000 cycles to 1.25*SP)<br><br>Service Test Articles (Unconstrained during Testing)<br>Vertically-Mounted: WSTF ID#11-45272<br>Horizontally-Mounted: WSTF ID# 11-45276<br><br>Service Test Articles (Constrained in OEM Mounting Straps):<br>Vertically-Mounted: WSTF ID#11-45278<br>Horizontally-Mounted: WSTF ID# 11-45273<br><br>Service Test Articles (Unconstrained, Tuffshell Removed from Dome):<br>Vertically-Mounted: WSTF ID#11-45281 |

Horizontally-Mounted: WSTF ID#11-45282

Pneumatic Burst (Nitrogen Fill Gas)

Service Test Article (Unconstrained during Testing)
Vertically-Mounted WSTF ID#11-45269

Pressure data, volumetric response, dome response, strain response (sixteen strain gauges) and high speed video was collected for each of the tests and archived in data packages.

Hydraulic testing on eight containers consisted of seven pressure cycles, each with a dwell time of sixty seconds, and then ramp at <50 psi/sec to burst. These pressurization rates are in family with existing limits. Cycle 1 had a dwell pressure of 1000 psi and was performed as an instrumentation check-out cycle. Cycles 2, 4 and 6 were to service pressure, and cycles 3, 5, and 7 were to 1.25 times service pressure.

**Type-4 Containers - Destructive Evaluation Results**

Observations and results of hydraulic cycling and burst tests are as follows:

- All Type-4 service test containers demonstrated repeatable response during cycling.
- Strain response was consistent in each respective gage location across the population of containers tested.
- Compressive/negative strain was observed in the transition regions.
- Volumetric change (mass of water put into the container) remained consistent.
- Containers grew axially (0.5 – 0.75 inches) between ambient and full fill pressure.
- Radial growth was minimal to 1.25 SP
- No significant difference in response was observed between unconstrained vs. constrained pressurization test conditions (OEM-supplied mounts were installed on constrained containers per OEM guidelines and in locations consistent with “witness marks” on service containers.)
- All containers exceeded minimum allowable burst pressure of 2.25 SP.
- No significant difference in response was observed between the new test container and the sister new container that had been previously cycled 15,000 times to 1.25 SP.
- All containers demonstrated the same failure mode. Split/rupture in the cylindrical section of the container. This was a different failure mode from that observed in the field.

Table 4 shows the burst pressures for each container.

**Table 4.**
**Hydraulic Burst Test Results**

| WSTF ID | Burst Pressure (psi) | Service Pressure (psi) | Ratio Burst to Service Pressure |
|---|---|---|---|
| 11-45898 | 12015 | 3600 | 3.34 |
| 11-45894 | 12521 | 3600 | 3.48 |
| 11-45272 | 8511 | 3000 | 2.84 |
| 11-45276 | 8166 | 3000 | 2.72 |
| 11-45278 | 8553 | 3000 | 2.85 |
| 11-45273 | 8246 | 3000 | 2.75 |
| 11-45281 | 8395 | 3000 | 2.80 |
| 11-45282 | 8358 | 3000 | 2.79 |

Observations and results of the pneumatic burst test are as follows:

- The final burst pressure was 7904 psi. Ratio of burst to service pressure (3000 psi) was 2.63.
- Rupture pressure was approximately 500 psi lower than the average hydraulic burst pressure of other test articles. This may be a temperature effect (adiabatic compression). One or more additional pneumatic burst tests for comparison are desirable.

- The failure mode resulted in total destruction of the container.
- Apparent rupture initiation location was in the mid-hoop region, similar to the hydraulic burst tests. Again, this was a different failure mode from that observed in the field.
- Rupture spiraled axially simultaneously toward both A and B-Ends.
- B-End remnants were found 220 feet from "ground zero".

**Type-4 Containers - Mechanical Sectioning and Materials Analysis Methods**
NASA/WSTF entered into an agreement with the Materials Science and Engineering Laboratory of the National Institute of Standards and Technology (NIST) to conduct complementary evaluation of mechanical and physical properties of coupon samples that were sectioned from the composite overwrap layer of two of the service containers (WSTF #11-45284 and 11-45290). Sections were examined microscopically for voids, porosity, matrix and ply cracking, and delamination. Specimens were tested for tensile and fatigue strength.

**Type-4 Containers – Mechanical Sectioning and Materials Analysis Results**
- There was significant void percentage throughout the dome/body transition region and body region of the container.
- Multiple cracks and ply delamination were found throughout the transition region.
- Ultimate tensile strength of straight-sided specimens had little data scatter.
- Fatigue of specimens at normal operating strains for 20,000 cycles had no effect on specimen residual strength.
- The Glass Transition Temperature (Tg) of samples compared to historical reference data increased with container use and age. This result may indicate an increase in brittleness.

**Type-2 Test Articles**
Thirty-six Type-2 containers were removed from service at Philadelphia Gas Works and shipped to WSTF for testing. In addition to these containers, WSTF maintains an inventory of thirty-one Pressed Steel Type-2 containers, which have seen real world service, and are available for comparative testing in this program. All containers are locked inside controlled access storage in the original shipping configuration. These containers are banded to pallets.

**Type-2 Containers – Nondestructive Evaluation Methods**
The nondestructive evaluation of the Lucas Aerospace and Pressed Steel containers employs the same techniques as those used for the Type-4 containers. Including the Pressed Steel containers in the evaluation provides a good representation from an additional vendor. These evaluations are scheduled to be completed in July 2015.

**Type-2 Containers - Destructive Evaluation**
In general, the destructive evaluation will follow the test plan developed for the Type-4 containers. However, since there are major differences in construction and failure modes between the two container designs, some modifications are planned, and others may develop over the course of the nondestructive evaluation.
For example, unlike the plastic liner of the Type-4 container, we believe the steel liner of the Type-2 container would be capable of withstanding at least 50% of the design burst pressure. Therefore, it is planned to conduct burst tests on containers, as received, and with the composite overwrap removed, to determine residual strength in the liner alone. These evaluations are scheduled to be completed in July 2015.

**CONCLUSIONS AND RECOMMENDATIONS**

NDE revealed mechanical damage and chemical exposure, which could be reduced through improved installation considerations. This damage was evidenced by missing and wrinkled labels, debris buildup, and "witness marks" left by container straps that indicated shifting during service, which may induce surface damage or stress on container valves and fittings. A large amount of compressor oil and other contaminants were drained from the interior of some containers. The effects of these contaminants on the container interior are unknown and could be assessed in further research. CGA Pamphlet C6.4 Level 2+ damage was observed on the exterior of two of the containers. It is not known whether this damage could have been detected in a periodic inspection with the container in situ, but CGA inspection requires the manufacturer's recommendation in writing for repair or disposal for Level 2 damage. No inspection records for the Type-4 containers were available. Labeling should remain on

the containers for life, in order to provide safety and tracking information like manufacturer contact information, service pressure rating, and end of life date for the containers.
The new and used Type-4 containers all exceeded the minimum hydrostatic burst strength requirement in FMVSS 304 of 2.25*SP. The container that was pneumatically burst exceeded the minimum burst strength as well, although at a lower margin. Running additional pneumatic burst tests of a Type-4 container would help to determine whether this result is consistent.
Microscopic inspection of composite coupon sections revealed voids, cracks, and ply delamination. Additional evaluation of new and used construction materials could provide insight into the relationship between physical and mechanical properties of samples and container performance and to provide comparison of what typical void and micro-cracking of unused containers looks like.

**REFERENCES**

[1] ANSI NGV2 (1992) Basic Requirements for Compressed Natural Gas Vehicle (NGV) Fuel Containers
[2] 49 CFR Part 571, FMVSS 304, Compressed Natural Gas Container Integrity, Effective Date March 27, 1995
[3] Brown, C., (2008) Metallurgical Evaluation of a Compressed Natural Gas Tank Cylinder Liner From PGW #3436, Report No. 0809-25278, Stork Technimet, Inc.

[4] Stenmark, N., (2008) Failure Analysis of a Composite Wrap on a Compressed Natural Gas Tank from PGW #3436, Report No. 0810-25584, Stork Technimet, Inc.
[5] Horne, D., (2010) CNG Cylinder Safety Issues & Opportunities, Natural Gas Vehicle Technologies Forum, October 12, 2010, Clean Vehicle Education Foundation

**Appendix A**

**Table A1: NDE Summary of Service Containers (Horizontally Mounted**

| | | Breakaway Torque | | Weight [2] | Visual Inspection | | | | | Chemical Sampling | | | Radiography | | |
|---|---|---|---|---|---|---|---|---|---|---|---|---|---|---|---|
| WSTF ID | S/N | Manual Valve | Plug | | Internal | | External (# of indications) | | | External | Internal | Gas Sampling | A-End | Hoop | B-End |
| | | (ft/lb) | (ft/lb) | (lb) | Oil Present | Blister/wrinkle Indications | General [4] | CGA Level 1 | CGA Level 2 | | | | | | |
| 11-45271 | 43-3 | 105 | < 5 | 118.7 | Pooling | YES | 6 | 3 | 1 | Archived | Archived | N/A | Boss fitting delamination | Deformed Liner | Boss fitting delamination |
| 11-45273 | 35-191 | 105 | < 5 | 118.2 | Trace | YES | 4 | 5 | 0 | Archived | Archived | N/A | Boss fitting delamination | No anomalies observed | Boss fitting delamination |
| 11-45274 | 35-190 | 110 | < 5 | 119.2 | Trace | YES | 7 | 4 | 0 | Archived | Archived | N/A | Boss fitting delamination | No anomalies observed | Boss fitting delamination |
| 11-45276 | 35-106 | 90 | < 5 | 118.9 | Pooling | YES | 2 | 3 | 0 | Archived | Archived | N/A | Boss fitting delamination | No anomalies observed | Boss fitting delamination |
| 11-45277 | 35-107 | 105 | < 5 | 120 | Pooling | YES | 5 | 6 | 0 | Archived | Archived | N/A | No anomalies observed | No anomalies observed | No anomalies observed |
| 11-45279 | 35-079 | 105 | < 5 | 119.5 | Pooling | YES | 1 | 8 | 1 | Archived | Archived | N/A | Boss fitting delamination | No anomalies observed | Boss fitting delamination |
| 11-45280 | 35-078 | 105 | < 5 | 119.7 | Pooling | YES | 3 | 4 | 0 | Archived | Archived | N/A | Boss fitting delamination | No anomalies observed | Boss fitting delamination |
| 11-45282 | 35-109 | 110 | < 5 | 119.5 | Trace | NO | 2 | 6 | 0 | Archived | Archived | N/A | Boss fitting delamination | No anomalies observed | Boss fitting delamination |
| 11-45283 | 35-111 [1] | N/A | N/A | 120.0 | Pooling | YES | 6 | 5 | 0 | LWO# 726585 | LWO# 726475 | N/A | No anomalies observed | No anomalies observed | No anomalies observed |
| 11-45285 | 35-042 | 40 | < 5 | 118.7 | Trace | YES | 3 | 6 | 3 | Archived | Archived | N/A | Boss fitting delamination | No anomalies observed | Boss fitting delamination |
| 11-45286 | 35-039 | 100 | < 5 | 117.7 | Trace | YES | 2 | 3 | 0 | Archived | Archived | N/A | Boss fitting delamination | No anomalies observed | Boss fitting delamination |
| 11-45289 | 35-123 | 130 | < 5 | 121.2 [3] | Pooling | YES | 3 | 1 | 1 | Archived | Archived | Archived ( ~5 psig) | Boss fitting delamination | No anomalies observed | No anomalies observed |
| 11-45290 | 35-121 | 115 | < 5 | 121.4 [3] | Pooling | YES | 3 | 0 | 0 | Archived | Archived | Archived ( ~5 psig) | Boss fitting delamination | No anomalies observed | No anomalies observed |

Notes:

1 Label detached and found loose within shipping container
2 Weight obtained after removal of boss fittings, includes residual oil
3 Weight includes closed boss fittings and residual gas contents
4 General indications, not assigned a classification level per CGA inspection criteria

**Table A2: NDE Summary of Service Containers (Vertically Mounted)**

| WSTF ID | S/N | Breakaway Torque | | Weight [2] | Visual Inspection | | | | | Chemical Sampling | | | Radiography | | |
|---|---|---|---|---|---|---|---|---|---|---|---|---|---|---|---|
| | | Manual Valve | Plug | | Internal | | External (# of indications) | | | External | Internal | Gas Sampling | A-End | Hoop | B-End |
| | | (ft/lb) | (ft/lb) | (lb) | Oil Present | Blister/wrinkle Indications | General [4] | CGA Level 1 | CGA Level 2 | | | | | | |
| 11-45269 | 35-119 | 20 | < 5 | 119.0 | NO | YES | 4 | 7 | 1 | Archived | Archived | N/A | Boss fitting delamination | No anomalies observed | Boss fitting delamination |
| 11-45270 | 43-2 | 110 | < 5 | 117.8 | NO | YES | 4 | 6 | 0 | Archived | Archived | N/A | Boss fitting delamination | No anomalies observed | Boss fitting delamination |
| 11-45272 | 35-189 | 120 | 170 | 117.1 | Trace | YES | 2 | 7 | 0 | Archived | Archived | N/A | Boss fitting delamination | No anomalies observed | Boss fitting delamination |
| 11-45275 | 35-041 | 110 | < 5 | 117.8 | NO | YES | 7 | 8 | 0 | Archived | Archived | N/A | Boss fitting delamination | No anomalies observed | Boss fitting delamination |
| 11-45278 | 35-074 | 100 | < 5 | 120.1 [3] | NO | YES | 2 | 7 | 0 | Archived | Archived | Archived ( ~1 psig) | No anomalies observed | No anomalies observed | No anomalies observed |
| 11-45281 | 35-108 | 105 | 170 | 117.6 | Trace | YES | 2 | 6 | 0 | Archived | Archived | N/A | Boss fitting delamination | No anomalies observed | Boss fitting delamination |
| 11-45284 | 35-040 | 120 | 160 | 117.8 | Trace | YES | 2 | 7 | 1 | Archived | Archived | N/A | Boss fitting delamination | No anomalies observed | Boss fitting delamination |
| 11-45287 | 35-122 | 105 | < 5 | 118.1 | Trace | YES | 3 | 6 | 1 | Archived | Archived | N/A | No anomalies observed | No anomalies observed | No anomalies observed |
| 11-45288 | 35-120 | 115 | < 5 | 118.9 | Trace | YES | 3 | 8 | 2 | Archived | Archived | N/A | No anomalies observed | No anomalies observed | No anomalies observed |
| 11-45291 | 35-038 | N/A | N/A | 117.4 | Trace | YES | 2 | 11 | 1 | LWO# 726585 | LWO# 726475 | N/A | Boss fitting delamination | No anomalies observed | No anomalies observed |

Notes:

1 Label detached and found loose within shipping container
2 Weight obtained after removal of boss fittings, includes residual oil
3 Weight includes closed boss fittings and residual gas contents
4 General indications, not assigned a classification level per CGA inspection criteria

# VEHICLE SAFETY TRENDS AND THE INFLUENCE OF NCAP SAFETY RATINGS

**Michael Paine**
**David Paine**
**Jason Smith**
Australasian NCAP, Australia
**Michael Case**
RACV, Australia
**Jack Haley**
NRMA Motoring & Services, Australia
**Stuart Worden**
New Zealand Transport Agency, New Zealand

Paper Number 15-0328

## ABSTRACT

In 1999 the Australasian New Car Assessment Program (ANCAP) aligned its test and assessment protocols with Euro NCAP and began issuing safety ratings, with a maximum rating of 5 stars. In effect, to achieve 5 stars, the vehicle needed good frontal offset crash test performance and good head protection in intrusive side impacts. The rating system awards bonus points for intelligent seat belt reminders and, recently, requires certain safety features such electronic stability control (ESC) and emergency brake assist (EBA).

The proportion of models achieving a 5-star safety rating has gradually increased from zero in 2002 to an estimated 75% of models on sale in 2014. This paper presents an analysis of trends with safety ratings and the uptake of key safety features during this period.

This paper also provides estimates of future savings due to the penetration of 5-star vehicles into the Australian vehicle fleet.

## INTRODUCTION

The Australasian New Car Assessment Program has conducted consumer crash tests since the early 1990s. These tests cover passenger cars and light commercial vehicles. In 1999 ANCAP aligned its test and assessment protocols with Euro NCAP and began publishing safety ratings with a maximum rating of 5 stars. About half of ANCAP's ratings since then have been based on crash tests conducted by Euro NCAP.

Under these protocols a vehicle needed to perform exceptionally well in three crash tests: frontal offset at 64km/h (maximum 16 points), mobile barrier side impact at 50km/h (maximum 16 points) and side pole impact at 29km/h (maximum 2 points). To score the maximum 5 star rating the combined score also needed to be at least 32.5. The Renault Laguna became the first ANCAP 5-star model in 2001. In 2003 Euro NCAP introduced up to 3 bonus points for intelligent seat belt reminders (SBR). In that year the Mercedes-Benz C-Class achieved a 5-star rating by including driver and front passenger SBR.

It became evident to ANCAP that a vehicle could achieve a 5-star rating without the need for a pole test (and therefore without head-protecting side airbags - head protection technology or HPT). Therefore in 2004 it was made a 5-star requirement that, to be eligible for a 5 star rating, a vehicle must score at least one point (out of 2) in the pole test.

In 2008 ANCAP made it a 5-star requirement that a vehicle has ESC as standard. In 2011 ANCAP published its 2011-2017 Road Map which required minimum performance in pedestrian protection and whiplash protection as well as a range of safety assist technologies (SAT). For example, for a 5-star safety rating in 2013 the vehicle needed driver and front passenger SBR and EBA. In 2014 the side head protection needed to cover the 2nd row outboard seats and in 2015 any 2$^{nd}$ row fixed (non-removable) seats required SBR. The Road Map also requires a minimum number of additional (non-mandatory) SAT and manufacturers are able to choose from a list of more than forty SAT for this purpose.

In Australasia there is a strong demand for vehicles with a 5-star safety rating. For example many fleet buyers now set this as a purchasing requirement. This demand for 5-star vehicles, combined with the increasingly higher requirements for a 5-star rating means that ANCAP has likely accelerated the uptake of safer vehicles and key safety technologies.

This paper sets out the results of an analysis of the trends with safety ratings and the uptake of key safety features during the period 2001-2014. These trends are also projected to 2020 to provide an estimate of the

road trauma savings that can be expected from increasing use of 5-star rated vehicles.

## SOURCES OF DATA

ANCAP maintains a database of safety ratings for vehicle models and the key safety features that are available for these models. The database was analysed to provide an estimate of the number of vehicle models available for sale in a particular year that were 5-star rated or not.

It took several years for ANCAP to assign star ratings to a large proportion of all models for sale in Australia and New Zealand. During the period 2001 to 2004 the ratings were dominated by models tested by Euro NCAP. These tended to be luxury models and so the estimates of the uptake of safety features, and star rating are likely to be higher than the actual numbers.

Using data from the VFACTS service, an estimate was also made of the annual sales of each model. From this an estimate was made of the proportion of annual sales that were 5-star models. Note that this is not the same as the proportion of new ANCAP ratings that were 5-stars in any particular year. There are many older models that are still on sale as new vehicles and these are less likely to be 5-stars than new models to the market.

A desirable aim for safer vehicles is to increase the proportion of 5-star rated models in the total annual kilometres travelled by light passenger vehicles (vehicle kilometres travelled or VKT). Newer vehicles tend to travel higher annual kilometres than older vehicles and so data published by the Environmental Protection Agency of NSW on VKT by vehicle age for the 2008 calendar year was utilised in the analysis (EPA 2012). A key assumption is that these proportions do not change greatly in earlier or subsequent years. In other words, a 3 year old vehicle in 2008 has the same proportion (8%) of annual light passenger vehicle VKT as a 3 year old vehicle in 2001 or 2014. The VKT data is listed as an appendix.

## RESULTS

Figure 1 shows the uptake of key safety features of models rated by ANCAP in the period 2001 to 2014. The figure also shows milestones in ANCAP-related policy that likely had an influence on this uptake.

Table 1. Estimated uptake of safety features

| Safety Feature | 2001* | 2007 | 2014 |
|---|---|---|---|
| HPT | 35% | 46% | 85% |
| ESC | 20% | 41% | 85% |
| Front Passenger SBR | 0% | 46% | 79% |
| 2nd row SBR | 0% | 9% | 35% |
| AEB | 0% | 0% | 2% |

* Biased towards European models

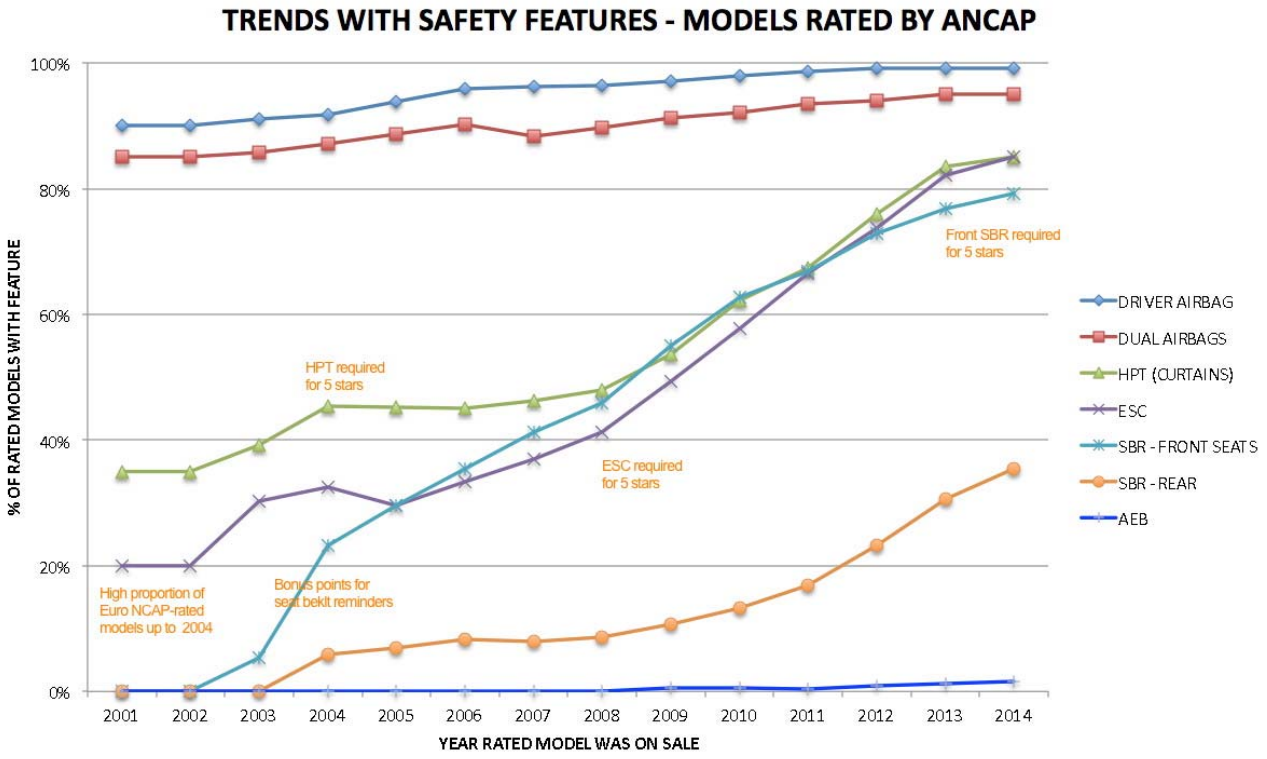

## DISCUSSION - SAFETY FEATURES

### Frontal airbags

By 2001 most popular cars already had frontal airbags for the driver and passenger. The 10% of models without a driver airbag in 2001 were mostly light commercial vehicles such as pickups and vans. It is likely that during the following decade ANCAP contributed to the uptake of frontal airbags on these remaining models, or their withdrawal from the market. There were no regulation changes during this period that might have influenced this trend.

### Head-protecting side airbags

A new Global Technical Regulation on Pole Side Impact will be introduced under the Australian Design Rules (ADR) in the next few years. This will be the first global regulation that requires head protection in severe side impact crashes.

Since 2001 the Euro NCAP/ANCAP protocols strongly encourage head-protecting side airbags through the side pole test. About one third of the models rated by these organisations in 2001 had HPT. This improved steadily to 46% by 2007 and then uptake increased, with 85% of rated models having the technology by 2014. The demand for 5-star rated models is likely to have contributed to the improved uptake.

### Electronic stability control

Subject to the over-representation of prestige European models between 2001 and 2004, there was a gradual uptake of ESC on models rated by ANCAP. Increased uptake is evident from 2008 when ANCAP made ESC a mandatory requirement for the 5-star safety rating. This was at a time when the demand for 5-star rated models increased. Other factors at this time were an industry-based voluntary code for fitting ESC and the announcement of amendments to the Australian Design Rules to require ESC on new models from November 2011.

Despite these regulatory changes there are some models being offered for sale without ESC. To address this ANCAP has made ESC mandatory for a 2-star safety rating from 2014. A vehicle without ESC cannot do better than a 1-star safety rating.

### Seat belt reminders - front seats

The Australian Design Rules require a basic warning system for the driver's seat belt but there are no regulations that encourage the fitting of advanced seat belt reminders to vehicles. These devices were only available on a handful of models prior to 2003.

ANCAP and Euro NCAP introduced bonus points for seat belt reminders in 2003 and the uptake was quite dramatic from that time, improving from 20% to 80% of rated models between 2004 and 2014. The bonus points enabled many models to reach a total score sufficient for a 5-star safety rating.

ANCAP made front seat belt reminders mandatory for 5-stars from 2013 and for 4-stars from 2015.

### Seat belt reminders - rear seats

Under the protocols a vehicle with seat belt reminders for all rear seats can earn a bonus point. It is apparent that this was not strong incentive for uptake of this technology, despite the protocol only requiring a warning if there was a change in state of the seat belt use (the front passenger seat requires occupant detection). By 2014 only one third of rated models had rear seat belt reminders.

To address the low uptake of rear seat belt reminders the ANCAP Road Map includes them as a mandatory 5-star requirement for 2nd row fixed (non-removable) seats from 2015. The Euro NCAP protocols also strongly encourage seat belt reminders for all seats through the Safety Assist component of the rating system.

### Autonomous emergency braking

AEB is a relatively new technology that has excellent potential for reducing road trauma (Anderson 2012).

Less than 2% of the models rated by ANCAP in 2014 had AEB as standard. Several Australasian models had AEB available on higher-priced variants but not on the base variant.

The situation is different in Europe. For example about half of the models rated by Euro NCAP in 2014 earned points for AEB. Since 2013 the Euro NCAP rating system has encouraged the uptake of AEB. The ANCAP Road Map 2011-2017 includes AEB in the list of additional SAT but it is evident that stronger encouragement is needed to reach the levels of uptake seen in Europe.

From 2018 ANCAP will be aligning its protocols with Euro NCAP and this is expected to focus attention on AEB. In the meantime, through media releases and other communications strategies, ANCAP is encouraging consumers to ask for AEB. For example, ANCAP datasheets now indicate if AEB is available in Europe but is not available on any Australasian variant - a measure intended to put pressure on the Australian distributors.

### Speed assist systems

The Euro NCAP Safety Assist protocol also encourages manufacturers to fit speed assist systems (Schram 2013). 85% of models rated by Euro NCAP in 2014 earned points for Speed Assist Systems (SAS).

Most of these had a manual speed assist (MSA) function, where the driver sets an upper limit to the vehicle speed. This is similar to the operation of cruise control and many recent MSA systems utilise the same driver controls as cruise control (set, cancel, resume etc).

From a safety perspective the use of MSA is preferred to cruise control because driver intervention (such as pressing the cancel button) is required in order to slow down a vehicle that is operating under cruise control. This can take several seconds. With MSA the driver simply reduces throttle to slow down and driver intervention is only necessary when the driver wishes to exceed the set speed. This is more practical for typical motorways and busy rural roads where slower moving traffic is frequently encountered but the driver wishes to not exceed a certain speed (preferably the posted speed limit) at other times. It is less complex and much less costly than adaptive cruise control, which is intended to achieve similar outcomes without driver intervention.

The other SAS function rewarded by the Euro NCAP protocols is a Speed Limit Information Function (SLIF). The driver is provided with information about the posted speed limit. This can be done through digital mapping of speed limits, through the recognition of speed limit signs or a combination of these systems. Several models rated by Euro NCAP in 2014 had digital maps or optical sign recognition.

There is good potential for SAS to reduce road trauma (Paine 2013a). The next step is Intelligent Speed Assistance (ISA) where, in effect, the SLIF and MSA are combined so that the maximum vehicle speed is automatically set according to the posted speed limit, unless the driver intervenes. The Euro NCAP SAS protocol awards additional points for ISA but, so far, no models have received these bonus points. This is expected to change as the coverage and reliability of digital mapping improves. For example, during 2014 the New South Wales government released a smartphone application which alerted drivers to speeding throughout NSW, including time-based 40km/h school zones. The government also made the data on posted speed limits available to the private sector for use in navigator applications and other uses.

The ANCAP Road Map 2011-2017 includes SAS as an additional SAT. Historical data about the uptake of SAS is not readily available and so SAS has not been included in Figure 1. However it is expected that manufacturers, fleets and consumers will give greater attention to SAS when ANCAP aligns its protocols with Euro NCAP in 2018.

**Fleet purchasing policies**

In 2011 the Australian government amended its fleet purchasing policy to require cars to have a 5-star ANCAP safety rating and for light commercials to have a 4-star rating.

In 2012 BHP Billiton, introduced a 5 star NCAP safety rating requirement across its worldwide vehicle fleet. This included light commercial vehicles and followed the release of the 5-star Ford Ranger pickup in late 2011. This generated substantial interest from other pickup manufactures and most popular brands are now available with 5 stars safety ratings.

## PROJECTED BENEFITS OF SAFER VEHICLES

Paine (2013b) analysed data from Australasian real-world crashes to track the improvement in occupant safety as vehicle models improve in star ratings. That analysis found that the risk of serious injury to drivers of 5-star models was half of that for drivers of vehicles with the same model name when it was 3-stars or less.

That analysis is considered to be a reasonable approximation for dividing the Australian light vehicle fleet into "5-stars" and "not 5-stars" for the purpose of determining benefits for all light vehicle occupants. The following analysis therefore assumes that if all non 5-star models were replaced by 5-star models then light occupant fatalities and serious injuries would reduce by 50%. This is in the range of values from analysis of real-world crashes in Europe: a reduction of 23% (+/-8%) for serious injuries and 68% (+/-32%) for fatalities (Kullgren 2010). Furthermore, Newstead (2014) reported that a typical 2010 Australian car had 40% lower risk of serious injury to the driver than a 2001 model (based on his Fig 20). It is estimated that 56% of sales in 2010 were 5-star models and that the relative savings from these was around 30%.

It is expected that the sales of 5-star models will level out during the next 5 years. It is assumed that by 2020 95% of sales will be in 5-star models and that two-thirds of VKT will be in 5-star models.

## RESULTS

Table 2. Estimated benefits from 5-star models

| Parameter | 2001 | 2007 | 2014 | 2020 |
|---|---|---|---|---|
| 5-star sales | 0% | 18% | 86% | 95% |
| 5-star models on the market | 0% | 33% | 75% | 82% |
| % of fleet 5-stars | 0% | 4% | 31% | 61% |
| Annual VKT in 5-stars | 0% | 5% | 34% | 67% |
| KSI relative to 2001 | 100% | 98% | 83% | 66% |

The results are set out in Figure 2.

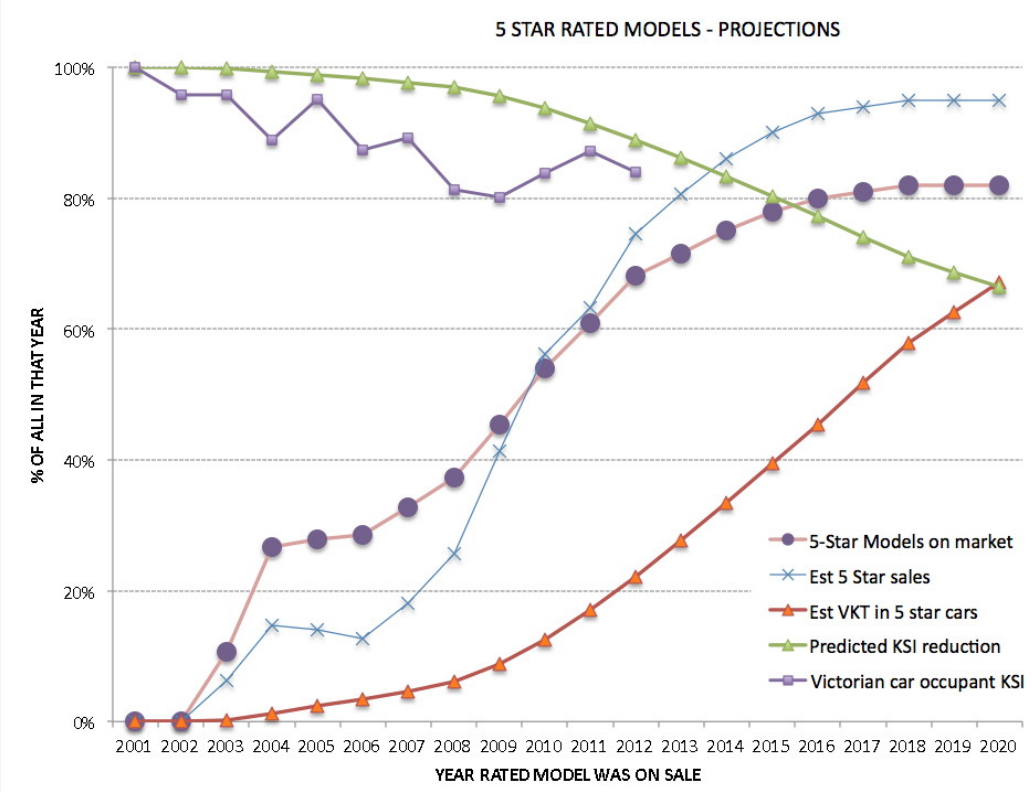


Figure 2. Trends will 5-star models and projected savings

## DISCUSSION OF POTENTIAL BENEFITS

Light vehicle occupant casualties (killed and seriously injured) are likely to have dropped by 17% between 2001 and 2014 due to the uptake of 5-star rated vehicles.

There are very few sources of data about actual occupant casualties in Australia during this period. Once source is the TAC online database for Victoria for the period 2001-2012 (see appendix). These data are also shown in Figure 2. The Victorian data show that light vehicle occupant KSI reduced by 16% during this period. The estimated reduction due to VKT in 5-star vehicles in 2012 is 11%.

There were many other road-safety initiatives that contributed to the reduction in overall road crash casualties during the period studied. However an indication of the benefits of 5-star models can be obtained by applying the 2014 fleet composition to the 2001 Australian road toll. Extrapolating the TAC data for Victoria, it is estimated that there were 1200 fatalities and 17400 serious injuries to *occupants of light vehicles* in 2001(when no vehicles were 5-stars). If 34% of VKT (the 2014 estimate) had been in 5-star models during 2001 then there would have been 200 fewer fatalities and 2900 fewer serious injuries to light vehicle occupants. The societal cost savings would have been in excess of one billion dollars (based on BITRE 2009).

The forward projections are somewhat speculative but it is evident that the benefits from the increase in sales of 5-star models over the past 5 years are resulting a replacement of older models with newer, safer vehicles. It is estimated that in 2014 34% of VKT were in 5 star models and that this will double by 2020. As a result it is predicted that light vehicle occupant KSI will have reduced to 66% of the 2001 value.

## LIMITATIONS

Reliable information about the availability of safety features during the study period is not available. This analysis is based on ANCAP historical data and the assumption that there is very little uptake of optional safety features. Additionally it is difficult to determine when some safety features became standard on certain models. This uncertainty will also affect the estimate of 5-star models sold.

Assumptions about VKT by age of vehicle are based on EPA estimates for 2008 and may have changed by 2014.

There is limited information about the number of serious injuries to light vehicle occupants in Australia during the study period.

## CONCLUSIONS

Since 2001 ANCAP made a major contribution to the uptake of several important safety features on light vehicles. Regulation initiatives for these safety features either do not exist or lag ANCAP initiatives by five years or more.

The proportion of the light vehicle sales with a 5-star ANCAP safety rating has increased strongly from 2008. As a result older vehicles are being replaced by safer 5-star vehicles at an increasing rate. It is predicted that, by 2020, this effect will result in a saving of approximately 34% in light vehicle occupants killed and seriously injured, compared with a vehicle fleet that had the same crashworthiness as that in 2001. Societal cost savings are estimated to be more than AU$2 billion per year (that is, twice that estimated for 2014).

NCAPs are now encouraging the uptake of the latest crash avoidance technologies, such as autonomous emergency braking and improved protection for vulnerable road users struck by light vehicles. These should result in further casualty savings for a wider range of road users.

This analysis shows that NCAP programs are highly cost-effective.

## REFERENCES


Anderson R, Doecke S, Searson D (2009) *Vehicle age-related crashworthiness of the South Australian passenger fleet* , Centre For Automotive Safety Research, CASR0106 April 2012

Anderson R, Doecke S, Mackenzie J , Ponte G, Paine D & Paine M (2012) Potential benefits of forward collision avoidance technology, Centre For Automotive Safety Research, CASR0106 April 2012

BITRE (2009) *Cost of Road Crashes in Australia in 2006,* Dept Infrastructure and Transport, Canberra

EPA NSW (2012) *Air Emissions Inventory for the Greater Metropolitan Region in New South Wales 2008 Calendar Year - On-Road Mobile Emissions: Results*, Technical Report 7, Environment Protection Authority of NSW, Sydney

Kullgren A., Lie A. and Tingvall C. (2010) *Comparison between Euro NCAP test results and real-world crash data*, Traffic Injury Prevention, 11:587-593, 2010

Lie A., Kullgren A. and Tingvall C (2001) *Comparison of Euro NCAP test results with Folksam car model safety ratings*, *Proceedings of 17th ESV,* Netherlands

Newstead S, Watson L and Cameron M (2014) *Vehicle safety ratings estimated from police reported crash data: 2014 update Australian and New Zealand crashes during 1987-2012,* Report 323, Monash University Accident Research Centre, Australia

Paine M., Griffiths M., Haley J and Newland C. (2009) *Injury and structural trends during 12 years of NCAP frontal offset crash tests*, Proceedings of 19th ESV, Washington

Paine D, Paine M, Wall J & Faulks I (2013a) *Development of an assessment protocol for after-market speed limit advisory devices*, Proceedings of 23rd ESV, Seoul

Paine D, Paine M, Case M, Haley J, Newland C and Worden A (2013b) *Trends with ANCAP safety ratings and real-world crash performance for vehicle models in Australia*, Proceedings of 23rd ESV, Seoul

Schram R, Williams R, van Ratingen M, Strandroth J, Lie A & Paine M (2013) *NCAP Test and Assessment Protocols for Speed Assistance Systems, a first in many ways*, Proceedings of 23rd ESV, Seoul

**APPENDIX**

Estimated Vehicle Kilometres Travelled by Vehicle Age in 2008 (EPA 2012).

| Vehicle Age (Years) | % of light vehicle fleet | % of total annual light vehicle VKT |
|---|---|---|
| New | 6.25% | 4% |
| 1 | 6.34% | 8% |
| 2 | 6.77% | 8% |
| 3 | 6.88% | 8% |
| 4 | 7.05% | 7% |
| 5 | 6.77% | 7% |
| 6 | 5.56% | 6% |
| 7 | 5.03% | 6% |
| 8 | 5.25% | 6% |
| 9 | 5.78% | 6% |
| 10 | 4.93% | 5% |
| 11 | 3.98% | 5% |
| 12 | 3.75% | 5% |
| 13 | 3.46% | 5% |
| >13 | 27% | 13% |

Notes

These values reflect changes in the total number of vehicle sales each year, due mainly to economic issues. This is not expected to have major effect on the analysis since the contribution of any one year is relatively small.

The mean age of the Australian light vehicle fleet in 2008 was 10 years (Anderson 2009)

Victorian car occupant casualties 2001-2012

( http://www.tac.vic.gov.au/road-safety/statistics/online-crash-database )

| Year | Killed or seriously injured | % of 2001 |
|---|---|---|
| 2001 | 4525 | 100% |
| 2002 | 4337 | 96% |
| 2003 | 4332 | 96% |
| 2004 | 4025 | 89% |
| 2005 | 4307 | 95% |
| 2006 | 3951 | 87% |
| 2007 | 4035 | 89% |
| 2008 | 3677 | 81% |
| 2009 | 3627 | 80% |
| 2010 | 3792 | 84% |
| 2011 | 3948 | 87% |
| 2012 | 3799 | 84% |

Notes

There is no adjustment for exposure in these data

---

Used Car Safety Ratings (Newstead 2014 Fig 20)

Risk of serious injury to driver

| Vehicle type | 1997-2001 | 2002-2006 | 2007-2012 |
|---|---|---|---|
| Large car * | 66% | 53% | 35% |
| Small car* | 77% | 54% | 48% |
| Utility* | 63% | 50% | 40% |
| Large car # | 100% | 80% | 53% |
| Small car# | 100% | 70% | 62% |
| Utility# | 100% | 79%% | 63% |
| Average# | 100% | 76% | 60% |

* Relative to 1982-86

# Relative to 2001

# A METHODOLOGY AND TOOL CHAIN TO DEVELOP INTEGRATED SAFETY SYSTEMS

**Tijssens, Martin**
**Bosma, Freerk**
TASS International
The Netherlands

**Kietlinski, Kajetan**
TASS International
Germany

Paper Number 15-0329

## ABSTRACT

This paper presents a methodology that enables designing integrated safety systems. The advantages of the methodology are demonstrated by applying it to a passive safety system that is supplemented by an AEB active safety system. The passive and integrated safety systems are compared through simulations with a set of vehicles and occupants subjected to load cases obtained from regulations. The methodology reveals changes in injury mechanisms and advantages of the addition of AEB.

## INTRODUCTION

Road vehicles are increasingly equipped with active safety systems that aid the driver in preventing frontal collisions (for example collision imminent braking (CIB), autonomous emergency braking (AEB) systems) as well as lateral collisions (for example lane departure warning (LDW) and lane keeping assistance (LKA) systems). These systems use sensing technologies like radar, lidar and cameras and are designed and introduced as safety systems that help avoid crashes or mitigate injuries when crashes are unavoidable.
Previous investigations on the effect of autonomous braking and evasive steering on the occupant's position have shown, that the occupant being out of position may result in an altered injury mechanism during the crash [1,2]. Furthermore, countermeasures like PRE-SAFE ® [3] or predictive pre-pretensioning are effective in reducing the occupant's out-of-position situation provided that the timing of the pre-tensioning of the belt is well-chosen.
In order to develop innovative restraint systems that provide an increased occupant protection, it is important that engineers are able to analyse the effects on the occupants of active systems that take over the control over the vehicle from the driver and understand why and how injury mechanism are altered.
This paper presents a methodology that enables an engineer to simulate various accident scenarios and to develop countermeasures to avoid adverse effects of increased injuries due to active safety system deployment. The methodology is demonstrated in the example case study of a frontal collision preceded by the activation of the AEB.

## METHODOLOGY

The Integrated Safety System is a holistic vehicle safety system in which active safety systems and passive safety systems continuously exchange information regarding occupant state and vehicle state to provide the maximum protection to the occupants. Integrated Safety is a relatively new domain in the automotive safety landscape and production-level design processes are starting to be adapted to account for a further integration of passive and active safety system design. The methodology is illustrated in Figure 1.

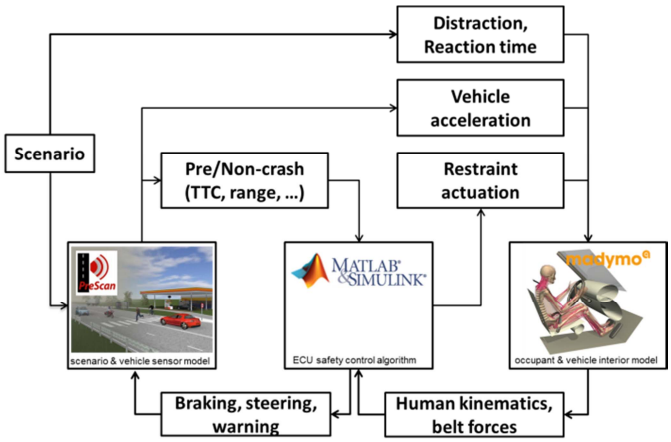


***Figure 1. Integrated Safety Methodology***

The accident scenario prescribes all boundary and initial conditions with respect to the participating vehicles and the human actors. Traditionally, when active safety system development and passive occupant restraint system development are separated, the scenario delivers information to both designs separately. In Figure 1 this is illustrated with the scenario that is described in an ADA development tool which feeds pre/non-crash information like time to collision, distance to preceding vehicle, etc. into the ECU safety control algorithm. In turn this algorithm provides modifications to the scenario like warnings to be given to the driver or interventions like braking or steering. Separately from this, the scenario provides occupant information like distraction and reaction time as well as vehicle information like its acceleration to enable an in-crash simulation to evaluate occupant safety.
When the ADA system influences the vehicle motion, be it pre- or in-crash, the vehicle motion no longer comes directly from a predefined scenario, but is to be communicated from the evolving scenario in the ADA tool to the occupant simulation to allow the simulation of pre-crash motion of the occupants as well as to determine initial conditions for the in-crash phase. Similarly, when the ADA system influences the restraint actuation, the conditions of the restraint system are to be communicated to the occupant safety simulation to start the in-crash simulation with the proper initial conditions.
Finally, the influence of the occupant restraint system on the occupant and visa versa is to be communicated back to the ECU safety control algorithm to allow for a feedback loop on the restraint actuation. This information can also be used to allow for a feedback loop on the vehicle parameters, i.e. the occupant state influences the strategy chosen to avoid or mitigate the collision.
The following simulation tools are used in this methodology [4]:

- PreScan: This tool allows to build scenarios, to design active safety systems using the tool's sensor models or by using users' own sensor data to develop and test algorithms of the ECUs. The tool also produces the vehicle's linear and angular velocity and acceleration data when the tool's or third-party vehicle dynamics models are used.
- Active Human Model (AHM): This tool allows to represent real human motion during pre-crash maneuvers with low acceleration levels [5,6,7]. Volunteer testing confirmed that the actual human being (50th %ile male volunteer) behaves differently compared to the Hybrid-III dummy during pre-crash manouvers with low acceleration levels. Hybrid-III dummies were mainly developed for high speed crashes and for in-position crash tests. Therefore Hybrid-III dummies are not adequate to predict human behavior during the pre-crash braking phase.
- MADYMO: MADYMO is a simulation tool to help analyze occupant behavior and calculate injuries during the crash.

## APPLICATION

Here the strength of the methodology is illustrated by focussing on a pre-defined frontal collision accident in which an existing passive safety design is supplemented with an AEB system. It is analysed how this modification affects the occupant's safety by focussing on the human kinematics and the resulting changes in injury mechanisms.

**Accident sequence**

The frontal crash is divided in several phases, illustrated in Figure 2.

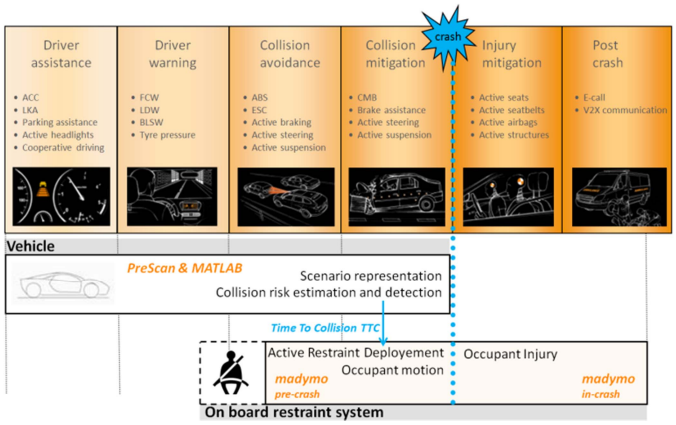


***Figure 2. Sequence of the pre-collision and post-collision events***

1. Driver warning phase: the radar / camera system detects an object in the path of the vehicle and sends a warning to the driver.
2. Collision avoidance phase: the ECU safety control algorithm determines that under the given circumstances a collision is likely and decides that the AEB system must be activated. The vehicle starts to decelerate with a given moderate deceleration level.
3. Collision mitigation phase: the ECU safety control algorithm determines that a collision can no longer be avoided and decides to apply a more aggressive decelleration strategy as well as to prepare the occupant restraint system for the imminent collision.
4. Injury mitigation phase: the AEB system does not stop the vehicle completely and the vehicle collides, the (activated) restraint system (seatbelts, airbags, etc.) provides protection to mitigate occupant injuries.

**Assumptions and limitations**

In this study we start from a traditional passive safety restraint system (containing dual stage inflated airbags, belts, belt load-limiters and belt pre-tensioners), used in the injury mitigation phase and wish to extend the safety system into the collision avoidance phase. Validated models for motorized seatbelt pretensioners or other types of OOP countermeasures were not available therefore not used in the analysis.
Furthermore, it is assumed that the crash speed is higher than the airbag deployment threshold speed and consequently the airbags still deploy.
This study is limited to one idealized braking profile, having moderate decelleration in the collision avoidance phase and aggressive decelleration in the collision mitigation phase, illustrated in Figure 3.

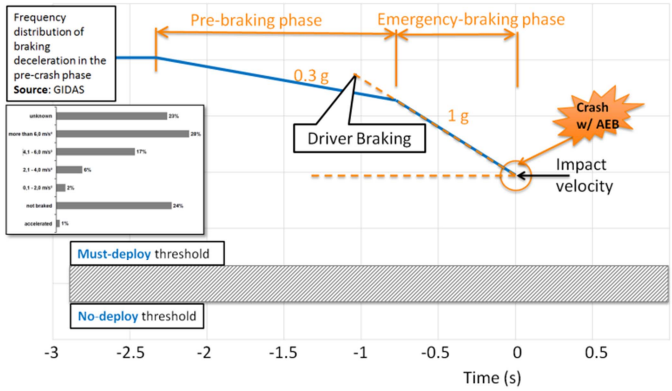


***Figure 3. Pre-crash velocity profile***

The braking profile contains two distinct phases, i.e. 0.3 g for 1 sec followed by 1 g's for 0.6 seconds. Many automakers use different braking strategies therefore produce different braking profiles. Although the profile is based on those considered by some of our customers, we realize it may not represent real-life braking performance of actual AEB systems currently in production.
In the study 3 MADYMO models are used that represent various vehicle types, i.e. a sports car (vehicle 1), a A/B-class vehicle (vehicle 5) and a C-class vehicle (vehicle 4). All vehicle models were fully validated against actual crash tests. Special attention was given to the models to make sure all occupants remain in an exact equilibrium when no load was applied to make them suitable for use in pre-crash simulations.
Three impact speeds were used in the analysis, i.e. protocol speeds from FMVSS 208 (25 mph, unbelted), US NCAP (35 mph) and Euro NCAP (64 km/h). To ensure that the impact simulations are all done at crash speeds for which the MADYMO models are validated and to exclude any effects on the injury levels from the reduced impact speed, the initial speeds for the AEB simulations were chosen to be 31.8 km/h (19.7 mph) higher as the non-AEB simulations which corresponds to the total reduction of speed of the chosen braking profile.
Besides this technical limitation of our analysis, we believe that although the goal of AEB is to reduce the impact speed, future accident statistics still have to confirm that impact speeds have indeed reduced due to the introduction of AEB. Until then, it seems wise to continue to adopt the accepted protocol speeds for the in-crash scenarios.

**Simulation set-up**

For each vehicle, 3 occupant models are used, i.e. the Hybrid-III 5%ile ATD, Hybrid-III 50%ile ATD and the Active Human Model 50%. All occupant models were used in both the driver as well as the passenger configuration and each was subjected to three impact configurations, i.e. a rigid wall belted, a rigid wall unbelted and an ODB condition, conforming to the choice of impact speeds. The simulation matrix is illustrated in Figure 4.
For all these 54 combinations a standard impact scenario as well as an impact scenario preceded by AEB was analysed. Note that for vehicle 1 the ODB validation of the model was not available, i.e. in the end 48 different load cases were analysed.

| | | | Impact speeds [km/h] | | | | | |
|---|---|---|---|---|---|---|---|---|
| | | | RW -B | | RW - UB | | ODB | |
| | | | std | AEB | std | AEB | std | AEB |
| Driver | 5 % Hybrid-III | Vehicle 01 | 56 | 56 | 40 | 40 | *na* | *na* |
| | | Vehicle 04 | 56 | 56 | 40 | 40 | 64 | 64 |
| | | Vehicle 05 | 56 | 56 | 40 | 40 | 64 | 64 |
| | 50 % Hybrid-III | Vehicle 01 | 56 | 56 | 40 | 40 | *na* | *na* |
| | | Vehicle 04 | 56 | 56 | 40 | 40 | 64 | 64 |
| | | Vehicle 05 | 56 | 56 | 40 | 40 | 64 | 64 |
| | 50 % AHM | Vehicle 01 | 56 | 56 | 40 | 40 | *na* | *na* |
| | | Vehicle 04 | 56 | 56 | 40 | 40 | 64 | 64 |
| | | Vehicle 05 | 56 | 56 | 40 | 40 | 64 | 64 |
| Passenger | 5 % Hybrid-III | Vehicle 01 | 56 | 56 | 40 | 40 | *na* | *na* |
| | | Vehicle 04 | 56 | 56 | 40 | 40 | 64 | 64 |
| | | Vehicle 05 | 56 | 56 | 40 | 40 | 64 | 64 |
| | 50 % Hybrid-III | Vehicle 01 | 56 | 56 | 40 | 40 | *na* | *na* |
| | | Vehicle 04 | 56 | 56 | 40 | 40 | 64 | 64 |
| | | Vehicle 05 | 56 | 56 | 40 | 40 | 64 | 64 |
| | 50 % AHM | Vehicle 01 | 56 | 56 | 40 | 40 | *na* | *na* |
| | | Vehicle 04 | 56 | 56 | 40 | 40 | 64 | 64 |
| | | Vehicle 05 | 56 | 56 | 40 | 40 | 64 | 64 |

| | |
|---|---|
| 64 | Impact speed of model used for study [km/h] |
| *na* | No material available for study |
| std | Standard Loadcase as defined per protocol |
| AEB | With braking, scenario (impact speed = protocol impact speed) |
| RW - B | Rigid Wall Belted - FMVSS208/USNCAP 35 mph test |
| RW - UB | Rigid Wall Un-Belted - USNCAP 25 mph test |
| ODB | Offset Deformable Barrier - EuroNCAP 64 km/h |

***Figure 4. Simulation Matrix 2***

**Belt retractor model**

In order to mimic real life situations as closely as possibly, the belt retractor model, including a detailed locking mechanism was used in the simulations. Similar to a real-world example, a small ball triggers the locking mechanism after it has travelled 2 mm of distance against a sloped surface. The angle of this surface represents the acceleration level at which the locking device should trigger. The mechanism is designed to trigger only when subjected to accelerations of more than 0.30 g, see Figure 5 for an illustration.
In order to prevent seat belts from slipping down on the occupant during the pre-braking phase, a continuous retraction force of 5N is applied to the retractor belt output, until the locking mechanism is triggered.

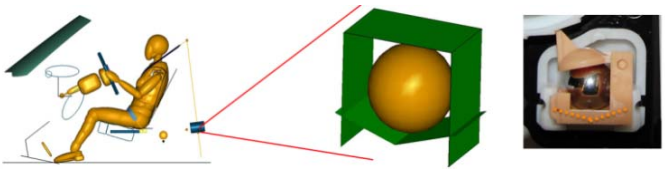

***Figure 5. Simulation model of the belt locking mechanism***

Using these models, a series of simulations were run to assess injuries and injury mechanisms of occupants by intentionally introducing the braking effect before the crash. In this study, the simulation was done as follows:

1. The pre-defined vehicle acceleration illustrated in Figure 3 was applied to the MADYMO model with occupants to predict the position of the occupants;
2. Subsequently, the occupant was subjected to the crash pulse belonging to the specific load case being analysed, see Figure 4;
3. Injury numbers from MADYMO models were obtained and normalized to the injury targets specified in Table 1. The new injury numbers were compared to the baseline injury numbers from models without braking effect.

## RESULTS

The objective of this study is to identify any changes affecting the occupant safety level from the activation of AEB, for example changes in injury mechanisms. In order to compare all simulation results, a selection of injuries is made based on what is common for US and EU regulations such that the four main areas (Head, Neck, Chest and Femurs) of an occupant are covered in the comparison. For each of the areas a target performance was selected based on maximum values allowed in various protocols. These target performances, see Table 1, are only used to calculate the relative improvement or degradation of a "crash situation with AEB" compared to the standard crash situation without AEB, i.e. the calculated percentage is a percentage of the Target Performance. For the Active Human Model the injury target values for the Hybrid-III 50%ile dummy are used.

***Table 1.***
***Summary of the target injury performances***

| Type | Region | Injury | Unit | Target | Ref. |
|---|---|---|---|---|---|
| Hybrid-III 5%ile | Head | HIC15 | - | 700 | 3 |
| | | a 3ms | g | 80 | 1 |
| | Neck | Nij | - | 1 | 3 |
| | Chest | Chest deflection | mm | 52 | 3 |
| | | a 3ms | g | 60 | 3 |
| | Femur | Load LHS/RHS | kN | 6.805 | 3 |
| Hybrid-III 50%ile | Head | HIC36 | - | 1000 | 1 |
| | | a 3ms | g | 80 | 1 |
| | Neck | Nij | - | 1 | 2 |
| | Chest | Chest deflection | mm | 50 | 1 |
| | | a 3ms | g | 60 | 2 |
| | Femur | Load LHS/RHS | kN | 9.070 | 1 |
| Active Human Model 50%ile | Head | HIC36 | - | 1000 | 1 |
| | | a 3ms | g | 80 | 1 |
| | Neck | Nij | - | 1 | 2 |
| | Chest | Rib deflections | mm | 50 | 1 |
| | | Rib 3ms | g | 60 | 2 |
| | | a 3ms | g | 60 | 2 |
| | Femur | Load LHS/RHS | kN | 9.070 | 1 |
| *1 ECE R95 - injury limit values for a Hybrid-III 50%ile | | | | | |
| *2 FMVSS 208 - injury limit values for a Hybrid-III 50%ile | | | | | |
| *3 FMVSS 208 - injury limit values for a Hybrid-III 5%ile | | | | | |

The comparison between the injuries calculated from the 48 standard and 48 AEB load cases shows that the majority of the injuries *improves* due to pre-crash braking even though the impact velocities for standard and AEB load cases are the same, see Figure 6. The comparison also shows that injury mechanisms may change due to the pre-crash braking which results in an increase of some injuries. In the next section we will investigate the mechanisms responsible for these changes in more detail, using two cases for which an injury becomes worse by more than 20% and for which the injury value is close to the target value.

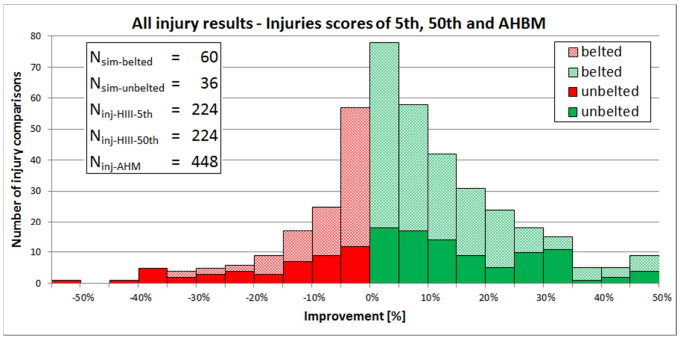


*Figure 5. Distribution of injury scores comparisons between the collisions with and without AEB activation*

## Changed belt loading

Generally, it was observed that the pre-crash braking pulse causes the Hybrid-III 5%ile, 50%ile and Active Human to slide forward on the seat due to the pre-crash braking decelleration. For the Hybrid-III 5%ile this results in a change in injury mechanism observed in vehicle 1.

Compared to the standard case, the occupant loads the restraint system differently in the AEB case which causes the lap belt to slip off the illiac wings of the Hybrid-III 5%ile and submarining occurs. This results in an increased risk of abdominal injuries. The submarining additionally results in a further increased forward motion of the pelvis, i.e. the lapbelt is less effective in restraining the pelvis. Subsequently this results in a heavier impact of the femurs on the IP and consequently higher femur forces (see Figure 7).

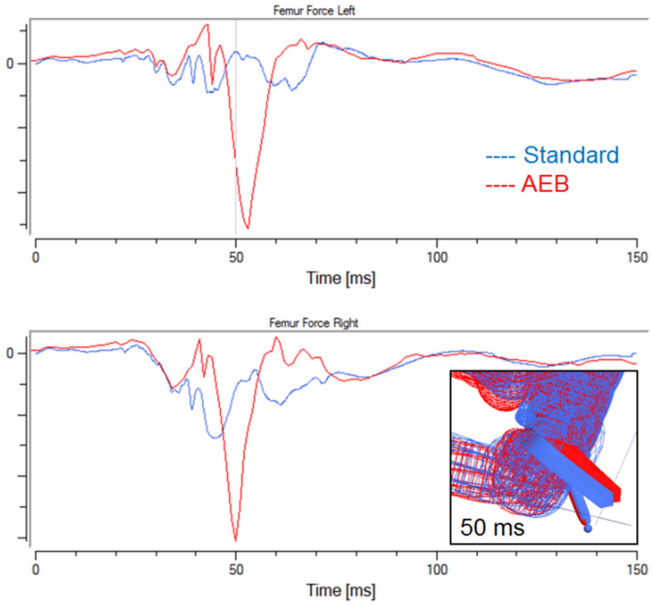


*Figure 6. Illustration of the different belt loading causing higher femur forces and possible abdominal injuries.*

**Out-of-position effect**

Another general observation is that due to the pre-crash braking the occupants bend forward. Although this was observed for the Hybrid-III's as well as the Active Human, the Hybrid-III dummy does not represent the human behaviour accurately enough under low acceleration loading conditions [6,8].
In all belted cases the Active Human Model shows a more forward motion for both driver and passenger than the standard Hybrid-III dummy, see Figure 8. The increased forward motion is mainly present in the neck and head region due to the higher flexibility of the human compared to the Hybrid-III dummy. The unbelted load cases show that the occupants bend forward significantly and that, whereas the Hybrid-III dummy falls forward onto the IP, the Active Human model is able to withstand the out-of-position effect due to the braking decelleration by active muscle tensioning and predicts a more realistic (initial) position prior to the crash, see Figure 9.
The change in injury mechanisms for all these cases result either in different neck or different head injury values and in all cases this is related to the airbag hitting the occupant (bag slap).

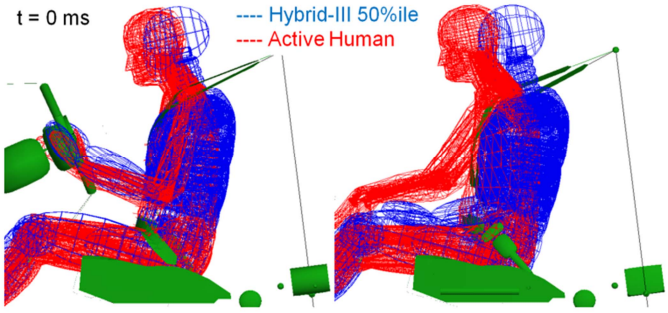


***Figure 7 Forward motion of the Hybrid-III 50%ile compared to the Active Human driver (left) and passenger (right) for vehicle 05***

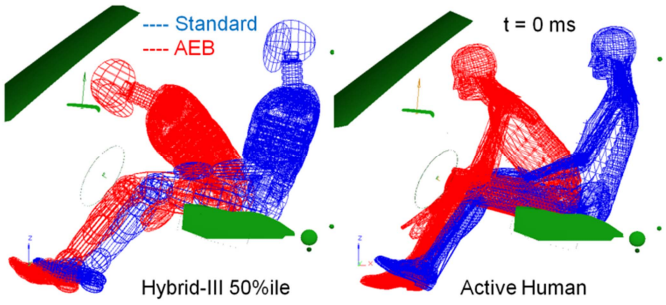


***Figure 8 Illustration of the FMVSS 208 unbelted load case for the Hybrid-III 50%ile and Active Human passenger for vehicle 05***

**Ride-down effect**

The analysis also revealed an improvement of the occupant injuries when AEB was activated. To understand the mechanism that gives this positive effect the ride down velocities of the occupant's head, thorax and pelvis were calculated and compared for all simulations. The comparison shows that activation of AEB results in an earlier and softer "Ride Down" compared to the standard crash case. This effect is visible for most of the simulated cases and is expected to have a positive effect on the occupant injuries.

To illustrate the ride-down effect, Figure 10 shows the ride-down velocities and the femur forces for the Hybrid-III 5%ile dummy in the FMVSS208 unbelted loadcase for both the standard crash condition as well as the case where AEB was activated. In the standard case the knees have an initial distance to the kneebolster which results in an almost constant forward velocity of the occupant's pelvis until the knees impact the knee bolster. From that moment (around 70ms) the pelvis velocity drops and the "ride down" of the pelvis is much steeper compared to the vehicle deceleration. In the situation where AEB is activated the occupant slides forward during the pre-crash braking phase which causes the knees to touch the kneebolster prior to impact. As a result the ride-down of the occupant's pelvis follows the ride-down of the vehicle much more closely which in turn results in lower femur forces.

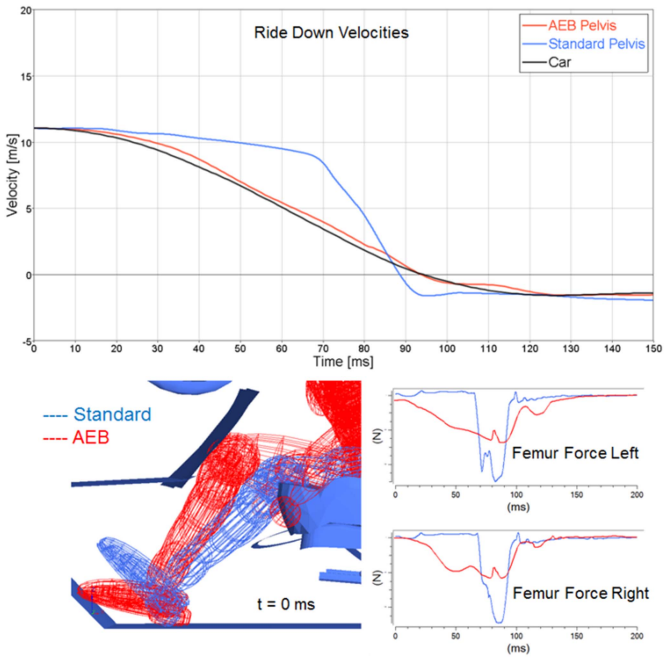


***Figure 9. Ride down example femur forces and pelvis ride down velocities of the Hybrid-III 5%ile in vehicle 04 for FMVSS208 unbelted***

Figure 11 shows an example of a (belted) USNCAP case with a Hybrid-III 50%ile passenger dummy. It is observed that in the AEB case there is an earlier and softer ride down for the head, thorax and pelvis, which improves the head acceleration and chest deflection. Additionally a slight improvement of the femur loads is observed.

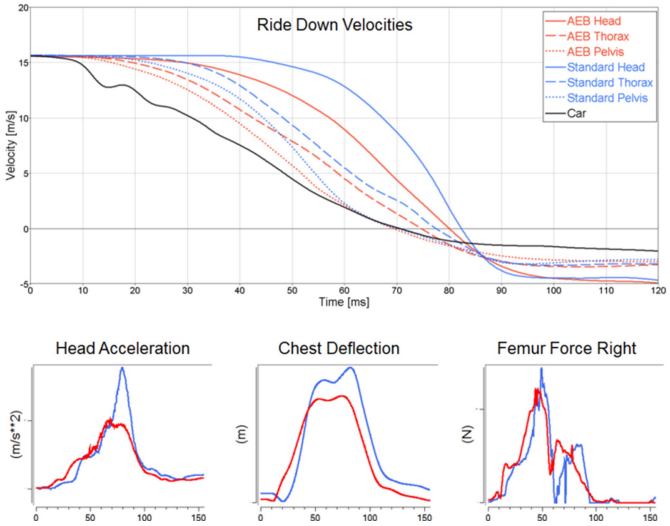


***Figure 10. Comparison of the "ride down" effect during the in-crash phases with and without AEB activation in 35 MPH US NCAP crash simulation for vehicle 05 Hybrid-III 50%ile passenger***

Although we expect that the earlier ride down generally has a positive contribution to the improvement of injuries, this is not confirmed in all simulations with actually improved injuries. In Figure 12 this is illustrated with the results for the Hybrid-III-50%ile driver of vehicle 01 in which differences for the chest deflection are observed. In this situation the chest deflection is increased for the AEB case. The reason for this increased chest deflection is mainly attributed to a changed belt routing caused by the AEB activation. Referring back to the feedback loop in Figure 1, the occupant restraint system may be adapted to prevent this change in belt routing in the pre-crash phase.

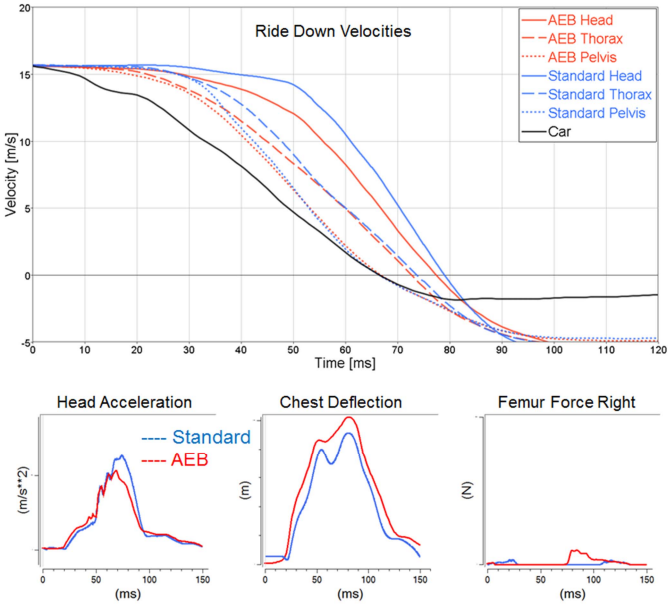


***Figure 11. Comparison of the "ride down" effect during the in-crash phases with and without AEB activation in 35 MPH USNCAP crash simulation for vehicle 01 Hybrid-III 50%ile driver***

However from our studies we noted that developing a restraint system for only the standard crash conditions can result in a sub optimal solution. An additional verification of the restraint system in cases where AEB is activated is recommended.

## CONCLUSIONS

This paper presents a methodology and tool chain that allows to design Integrated Safety systems, i.e. safety systems in which the active safety systems and passive safety systems are designed as one system aiming to protect the occupant. The tool chain's effectiveness is illustrated by analysing the changes in injuries and injury mechanisms for a traditional passive safety system which is supplemented with active pre-crash braking.
The study shows the effect of altered pre-collision conditions on the injuries as a result of activation of AEB. In most cases the pre-tensioning of the safety belts due to the occupant's pre-crash ride-down results in a reduced injury risk in the subsequent crash. In some cases, the earlier and softer ride-down is compromised by, for example, a changed belt routing or an out of position situation prior to the crash. The more accurate representation of human motion with the Active Human Model helps to predict the initial occupant position before the crash and therefore helps to identify countermeasures for these situations.

***Figure 13. Current situation where Active and Passive safety systems work independently***

At present passive safety systems and active safety systems are often designed independently from each other and countermeasures may often be identified "off-line", i.e. without a further integration of the passive and active systems. We advocate that the Integrated Safety System is a total vehicle safety system in which active safety systems and passive safety systems communicate and collaborate with each other all the time and exchange information such as occupant status, vehicle speed, braking status, etc. in order to provide the maximum protection to the occupants. The methodology described here allows to analyse potential benefits as well as address potential risks of unexpected increased occupant injuries from the (un-)coordinated activation of active and passive safety systems.

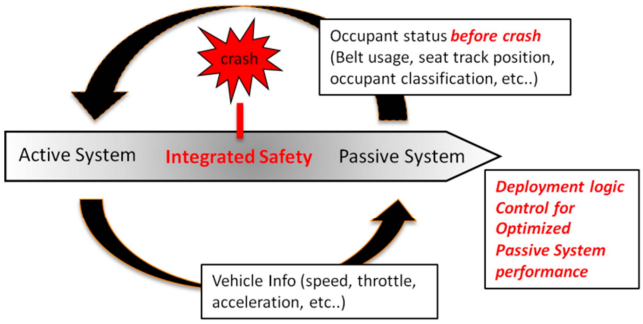


***Figure 14. Integrated Safety System Development concept of TASS International.***

## REFERENCES

[1] Markus Woldrich, Movement in the PRE-Crash situation - A simulation research with a reversible PRE-SAFE® Pulse system, Abstract for the poster session (P24) Airbag 2010

[2] Mages M., et al., " Benefit of reversible belt pre-pretensioning for different pre-crash scenarios – reduction of occupant displacement and the effect on injury severity", in Proceedings of Airbag 2010 (Karlsruhe, Germany, December 6-8, 2010)

[3] Prof. Dr. Rodolfo Schoeneburg, Karl-Heinz Baumann, Michael Fehring – Daimler AG "The Efficiency of PRE-SAFE Systems in Pre-braked Frontal Collision Situations" ESV paper 11-0207

[4] https://www.tassinternational.com/integrated-safety

[5] Happee R., et al., “Mathematical human body models representing a mid size male and a small female for frontal, lateral and rearward impact loading”, IRCOBI, Sept. 20-22, 2000; Montpellier, France

[6] Meijer, R. et al., “Development of a Multi-body Human Model that Predicts Active and Passive Human Behaviour.” In Proceedings of the IRCOBI Conference, Dublin, Ireland, September 12-14, 2012

[7] Meijer, R. et al., “Modelling of Bracing in a Multi-Body Active Human Model” In Proceedings of the IRCOBI Conference, Gothenburg, Sweden, September 11-13, 2013

[8] Sunnevång, C., et al., “Comparison of the THORAX Demonstrator and HIII sensitivity to crash severity and occupant restraint variation” In Proceedings of the IRCOBI Conference, Berlin, Germany, September 10-12, 2014

# IS COMFORT IMPORTANT FOR OPTIMAL USE OF CHILD RESTRAINTS?

**Cameron K. Fong**
Neuroscience Research Australia and School of Medical Science, UNSW
Australia

**Lynne E. Bilston**
Neuroscience Research Australia and Prince of Wales Clinical School, UNSW
Australia

**Gunther Paul**
School of Public Health and Social Work, QUT
Australia

**Julie Brown**
Neuroscience Research Australia and School of Medical Science, UNSW
Australia

Paper Number 15-0330

## ABSTRACT

Suboptimal restraint use, particularly the incorrect use of restraints, is a significant and widespread problem among child vehicle occupants, and increases the risk of injury. Previous research has identified comfort as a potential factor influencing suboptimal restraint use.

Both the real comfort experienced by the child and the parent's perception of the child's comfort are reported to influence the optimal use of restraints. Problems with real comfort may lead the child to misuse the restraint in their attempt to achieve better comfort whilst parent-perceived discomfort has been reported as a driver for premature graduation and inappropriate restraint choice. However, this work has largely been qualitative. There has been no research that objectively studies either the association between real and parental perceived comfort, or any association between comfort and suboptimal restraint use. One barrier to such studies is the absence of validated tools for quantifying real comfort in children.

We aimed to develop methods to examine both real and parent-perceived comfort and examine their effects on suboptimal restraint use.

We conducted online parent surveys (n=470) to explore what drives parental perceptions of their child's comfort in restraint systems (study 1) and used data from field observation studies (n=497) to examine parent-perceived comfort and its relationship with observed restraint use (study 2). We developed methods to measure comfort in children in a laboratory setting (n=14) using video analysis to estimate a Discomfort Avoidance Behaviour (DAB) score, pressure mapping and adapted survey tools to differentiate between comfortable and induced discomfort conditions (study 3).

Preliminary analysis of our recent online survey of Australian parents (study 1) indicates that 23% of parents report comfort as a consideration when making a decision to change restraints. Logistic regression modelling of data collected during the field observation study (study 2) revealed that parent-perceived discomfort was not significantly associated with premature graduation. Contrary to expectation, children of parents who reported that their child was comfortable were almost twice as likely to have been incorrectly restrained ($p<0.01$, 95% CI 1.24 - 2.77).

In the laboratory study (study 3) we found our adapted survey tools did not provide a reliable measurement of real comfort among children. However our DAB score was able to differentiate between comfortable and induced discomfort conditions and correlated well with pressure mapping.

Our results suggest that while some parents report concern about their child's comfort, parent-reported comfort levels were not associated with restraint choice. If comfort is important for optimal restraint use, it is likely to be the real comfort of the child rather than that reported by the parent. The method we have developed for studying real comfort can be used in naturalistic studies involving child occupants to further understand this relationship.

This work will be of interest to vehicle and child restraint manufacturers interested in improving restraint design for young occupants as well as researchers and other stakeholders interested in reducing the incidence of restraint misuse among children.

## INTRODUCTION

One of the leading causes of death among children in Australia is traffic crashes. On average 70 children are killed per year (10 year average, 2002-2011, (BITRE 2012)), and 3000 are seriously injured as vehicle passengers (Brown and Bilston 2012) despite greater than 99% child restraint system (CRS) use (Brown et al. 2010). These statistics have not changed greatly over the last two decades (Brown and Bilston 2012).

Incorrect and inappropriate CRS use or suboptimal CRS use is a widespread problem that reduces the protection offered by a child restraint and increases the risk of injury (Brown and Bilston 2007; Bull et al. 1988; Jakobsson et al. 2005). Incorrect restraint use includes both the errors in installation as well as incorrect adjustment and securing of the child into the restraint. Inappropriate restraint use is the use of a restraint that does not match the age and size of the child, this usually manifests in using a restraint designed for an older/larger child. Incorrect restraint use is as common as inappropriate restraint choice (Brown et al. 2010) and carries a higher risk of injury than inappropriate choice (Brown and Bilston 2007; Du et al. 2008).

There have been some indications that child comfort and/or the parental perception of child comfor plays a role in the choice of CRS and/or the correctness of use of a child restraint (Bilston et al. 2011; Pettersson and Osvalder 2005; Simpson et al. 2002). Studies have suggested that children prefer restraints that are comfortable for them (Bohman et al. 2007; Osvalder et al. 2013; Pettersson and Osvalder 2005). While Bingham et al. (2006) reported that parental perception of increased comfort motivated parents to use boosters for their children rather than adult seat belts, other studies report perceived discomfort in a booster seat as a reason for parents to prematurely move their child to an adult seat belt (Charlton et al. 2006; Simpson et al. 2002).

Discomfort has also been associated with incorrect child restraint use (Klinich et al. 1994; Osvalder et al. 2013). Bohman et al. (2007) suggested that poor restraint fit caused discomfort in children, and the avoidance of discomfort resulted in severe misuse of restraints.

The lack of validated methods for studying seating comfort in children is a barrier to the study of comfort among children in child restraints. While there are accepted methods such as the use of self-report survey tools (Chae et al. 2011; Donnelly et al. 2009; Gyi and Porter 1999; Smith et al. 2006) and pressure distribution mapping (Chae et al. 2011; Gyi and Porter 1999; Kyung and Nussbaum 2008; Kyung et al. 2008; Paul, Daniell, et al. 2012; Paul, Pendlebury, et al. 2012; Porter et al. 2003) for studying the comfort of adults in vehicles there has been almost no use of these methods for child occupants. The exception is a recent study by Osvalder et al. (2013) who used a self-report survey tool to capture comfort of children in a naturalistic study of children in booster seats. However, the validity of this self-report tool is untested. Earlier studies examined the comfort and usability of different CRS through the observation of parental handling and interaction with the CRS, parental surveys and observations of the child in the CRS during a drive (Pettersson and Osvalder 2005). This study did not interview the child, noting that incoherent answers are often provided by children under the age of 10. Nilsson and Wolstedt (2007) combined anthropometric data, ergonomic modelling and child opinions to develop an ergonomic booster seat however they did not describe the process in detail.

Over the last three years, we have undertaken a number of studies in an attempt to study comfort and its association with sub-optimal restraint use. This paper presents an overview of the work conducted to date.

## METHODS

The work presented here relates to preliminary findings from three independent studies conducted as part of a large program of work aimed at providing a wider understanding of the factors underpinning optimal restraint use and the role that comfort might play. All studies have been approved by the UNSW Human Research Ethics Committee.

### Online Parent Survey

This study used data collected during an online survey of a cohort of Australian parents and carers, designed to examine and evaluate barriers to appropriate and correct restraint use. Data was collected between May and

July, 2014. Participants had to be over the age of 18, own their own vehicle, have a child between the ages of 0 and 7 years who they transport at least once a week, and regularly use some sort of child restraint. Three questions related to comfort were extracted for this analysis.

One question asked parents to report which of the following factors they would take into account when making a decision to move their child into a different type of restraint: "My child is too big for the restraint; The new restraint is more convenient that than my current restraint; The restraint is easier to use than my current restraint; My child is not comfortable in the current restraint; My child is too old for the restraint; My child does not want to use the current restraint any longer; I need the restraint for a younger child". This data was used to examine how often parents take comfort into account when making transition decisions.

The second question asked whether parents thought that the child restraint their child was using looked comfortable using a five level Likert scale.

The third question asked parents directly if their child was comfortable in the restraint and if so they were asked to provide reasons why. This was an open ended question. The reasons provided by parents were qualitatively explored. This involved reading through the responses and identifying commonly reported reasons why parents thought the child was comfortable using content analysis techniques.

**Field Observation Study**

This analysis used data collected during a 2008 cross-sectional population representative observational study of child restraint practices among children aged 0-12 years across NSW (see Brown et al. (2010) for more details). Children aged 0-12 arriving in vehicles were observed at randomly selected early childhood health clinics, day care centres, pre-schools and primary schools within randomly selected local government areas across NSW. Trained researchers made in situ observations of the child within the restraint, conducted a detailed examination of the restraint installation, and conducted a structured interview with the driver. Only one child per vehicle was selected for observation.

Variables related to parent perceived comfort issues and other known risk factors of inappropriate and incorrect use, together with the observed appropriate and correct use of restraints was extracted for this analysis and this has been reported elsewhere (Fong et al, manuscript under review). In summary, logistic regression modelling was used to examine 1. the relationship between age appropriate restraint use and parent reported comfort issues while controlling for parent education levels, language spoken at home, parent income and the restraint type (seat belt vs child restraint), and 2. The relationship between correct restraint use and parent reported comfort issues while controlling for parent education levels, language spoken at home, parent income and the restraint type (convertible restraint, yes/no).

All analysis was performed using SAS Version 9.4 (SAS Institute, 2013). The SURVEYLOGISTIC procedure was used to account for the complex sample design.

**Laboratory Comfort Measuring Study**

This study compared anthropometrically comfortable seating positions to induced discomfort seating positions using a specially designed seating rig that allowed for the adjustment of cushion length and seat belt height. Children aged 4- 8yrs were recruited through social media and advertisements on public noticeboards. Prior to the sitting trial, stature, weight and buttock-to-popliteal length (BPL) were measured.

The comfortable (Fit) position of the seat was determined for each child using (i) a seat cushion length that corresponded to the BPL, and (ii) adjusting the seatbelt D-ring so that the sash belt was placed in the optimum position running midway across the shoulder, crossing the centre of the chest without contacting the neck. The seat back angle remained at a constant 10 degree recline.

Children were then asked to sit sequentially in the four conditions listed in Table 1. The order of these conditions was randomised. Each child was required to sit, correctly restrained, in each condition for 10

minutes. At the end of the 10 minutes, while the child was still restrained, the self-report survey tool was administered. There was a 10 minute break between each trial.

For the majority of the trials, the child watched children's TV shows throughout the 10 minute trial interval. In four participants, this was removed to provide the 'no stimulus' (NS) condition.

Each trial was video recorded for later analysis.

**Table 1**

**Laboratory study experimental conditions, presented randomly**

| ***Condition*** | ***n*** | ***Description*** |
|---|---|---|
| Fit | 14 | Anthropometric fit based of stature and buttocks to popliteal length (comfortable) |
| Fit+Footrest | 14 | As above with the introduction of a footrest (comfortable) |
| Cushion Long | 14 | As above but with the cushion length 10cm too long (uncomfortable) |
| Seat Belt High | 14 | As Fit+Footrest but with the seatbelt height adjusted to create sash belt contact with neck (uncomfortable) |
| No Stimulus | 4 | As Fit but without video stimulus |

Three different methods of measuring comfort were compared in order to find a method that can reliably differentiate between comfortable and uncomfortable seating positions among children. This is also presented in more detail elsewhere (Fong et al, manuscript in preparation). In summary, the methods used to measure comfort were (i) a self-report questionnaire, (ii) pressure distribution mapping, and (iii) a newly developed analysis method.

For the self-report survey tool, we looked at established and validated pain research protocols (Bieri et al. 1990; Hicks et al. 2001; Wong and Baker 1988) and guidelines for constructing surveys for children (Borgers et al. 2000, 2004) as well as some tools used to study comfort in adults (Gyi and Porter 1999). Taking all these into account we modified the body discomfort chart (Gyi and Porter 1999) and paired it with a modified form of the Wong-Baker FACES Pain (Wong and Baker 1988) in an effort to create a survey instrument that can be used with children.

Two different survey tools were used. Survey Tool 1 included the FACES Pain Scale with one mid-range face removed (7 point scale modified to 6 point scale) and the full 20 point Body Part Discomfort Chart, with the scale reduced from 1-7 to 0-5. The mid-range face was removed as it did not appear to provide much discrimination between the two adjacent faces, and the Body part Discomfort Chart scale was reduced in line with Borgers et al. (2000, 2004)'s guidelines. Survey Tool 2 used the same components of the FACES Pain Scale with the 20 Body Part Discomfort Chart summarised to six body regions. See Figure 1.

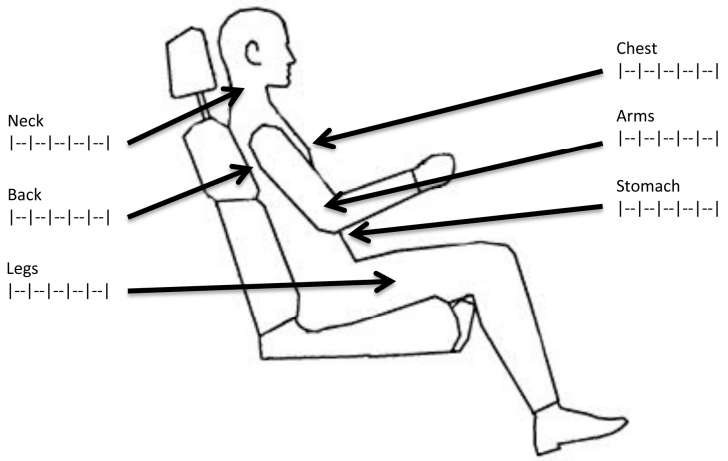


*Figure 1: Six Point Scale*

Pressure distribution data were collected using a CONFORMat (Tekscan, Inc South Boston MA, USA) which consists of two pressure mats, one for the seat base and one for the seat back. Recordings from the CONFORMat system was analysed in three ways; change in centre of force (ΔCOF - distance), contact area (CA - area) and peak pressure (PP - force).

Video footage was recorded using a 720p camcorder placed at a 45 degree angle to the left of the testing rig to record wide angle front left quarter view. Still images were also captured using a 12MP digital camera for reference. A video analysis protocol was developed to calculate the rate of Discomfort Avoidance Behaviours (DAB) observed. Video footage was analysed using Kinovea (Kinovea 0.8.15, Kinovea.org 2012) video analysis software. DAB was defined as any shift in seating position, playing with the seat belt, and child stretching. To score the footage, each clip was watched and any instance of these behaviours was marked with a reference frame in the software. These behaviours were then tallied for each condition before being divided by the video clip duration to calculate the average number of discomfort avoidance behaviours per minute (the DAB score or DAB rate).

The reliability of the DAB rate was measured by having a second researcher repeat the scoring. Differences between the two researcher scores were examined using the intraclass correlation coefficient (ICC).

The overall analysis involved paired samples T-tests to examine differences between seating conditions for the DAB, pressure and survey protocols. Correlation between the three measures of comfort was examined using Pearson's r. Normal distribution of data was also tested.

**RESULTS**

**Online Survey**

Data was collected from 470 parents or carers across Australia. Figure 2 provides the responses obtained to the question about what factors parents consider in making restraint transitions.

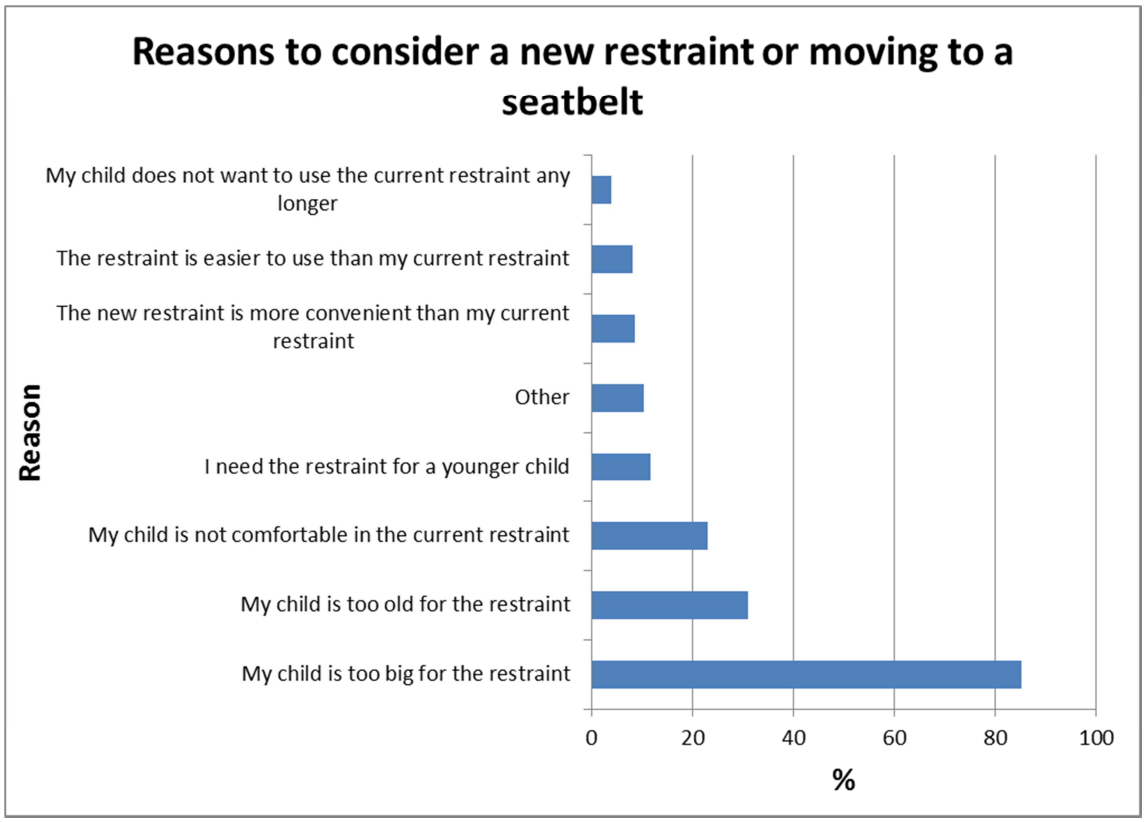


*Figure 2: Relative importance of reasons provided by parents for considering a new restraint or moving their child into a seat belt (multiple responses were allowed)*

Almost one quarter of parents (23%) reported that they would consider transitioning their child if they thought their child was not comfortable in their current restraint.

Most parents (86.4%) agreed that the restraint their child was using looked comfortable (39.4% strongly agree, and a further 47% agree).

Three quarters (75%) of parents also indicated they perceived their child was comfortable in the restraint. The most common reasons given related to a lack of complaint from the child (26% of those reporting the child was comfortable), the ability of the child to sleep in the restraint (22% of those reporting the child was comfortable) and the presence of padding and support in the restraints (22% of those reporting the child was comfortable).

**Field Observation Study**

Results from the logistic regression modelling are presented in Table 2 and Table 3.

As shown in Table 2 there was a significant increase in the odds of child restraint misuse when there were no comfort problems reported by the parent (OR 1.85, 95% CI 1.24-2.77). There was also an increased odds of restraint misuse when a convertible restraint (rearward facing/forward facing or forward facing/booster) was used, irrespective of a reported comfort problem (OR 13.47, 95% CI 5.66-32.03).

**Table 2**

**Logistic regression results for incorrect use vs correct use (** = significant)**

| *Misuse* | | | | | | | | | | | |
|---|---|---|---|---|---|---|---|---|---|---|---|
| ***Variable*** | ***Category*** | ***Unweighted Frequency*** | ***Weighted %*** | ***Unweighted*** | | | | ***Weighted*** | | | |
| | | | | ***OR*** | ***CI 95%*** | | | ***OR*** | ***CI 95%*** | | |
| *ComfortProblem*** | Yes | 60 | 61.7% | Reference | | | | Reference | | | |
| | No | 374 | 58.3% | 0.87 | 0.57 | - | 1.32 | 1.85 | 1.24 | - | 2.77 |
| Education | Tertiary Education | 288 | 56.9% | Reference | | | | Reference | | | |
| | Secondary or Lower | 155 | 61.9% | 1.24 | 0.81 | - | 1.91 | 0.98 | 0.46 | - | 2.10 |
| LanguageAtHome | Other | 20 | 60.0% | Reference | | | | Reference | | | |
| | English | 444 | 58.6% | 1.24 | 0.35 | - | 4.36 | 2.15 | 0.69 | - | 6.67 |
| Income | Over $100,000 | 112 | 60.7% | Reference | | | | Reference | | | |
| | $50,000-$100,000 | 191 | 56.5% | 0.91 | 0.52 | - | 1.60 | 0.99 | 0.36 | - | 2.71 |
| | Less than $50,000 | 132 | 59.8% | 1.13 | 0.71 | - | 1.78 | 1.45 | 0.42 | - | 4.99 |
| Convertible** | No | 350 | 46.0% | Reference | | | | Reference | | | |
| | Yes | 147 | 90.5% | 11.88 | 6.73 | - | 20.97 | 13.47 | 5.66 | - | 32.03 |

As shown in Table 3 there was no significant association between parent reported comfort problems and the use of age appropriate child restraints. However, there was a significant decrease in the odds of using a non-age appropriate restraint when the parents education level was higher, irrespective of a parent reported comfort problem (OR 0.33, 95% CI 0.21-.53). Furthermore, the likelihood that an age appropriate restraint was used was increased when a child restraint was used as opposed to a seatbelt, irrespective of a parent reported comfort problem (OR 2.75, 95% CI 1.29-5.12).

**Table 3**

**Logistic regression results showing age appropriate restraint use versus inappropriate use (** = significant)**

| *Age Appropriate* | | | | | | | | | | | |
|---|---|---|---|---|---|---|---|---|---|---|---|
| ***Variable*** | ***Category*** | ***Unweighted Frequency*** | ***Weighted %*** | ***Unweighted*** | | | | ***Weighted*** | | | |
| | | | | ***OR*** | ***CI 95%*** | | | ***OR*** | ***CI 95%*** | | |
| *ComfortProblem* | Yes | 60 | 73.3% | Reference | | | | Reference | | | |
| | No | 374 | 80.7% | 1.42 | 0.80 | - | 2.54 | 1.11 | 0.34 | - | 3.59 |
| Education** | Tertiary Education | 288 | 80.2% | Reference | | | | Reference | | | |
| | Secondary or Lower | 155 | 76.1% | 0.78 | 0.59 | - | 1.03 | 0.33 | 0.21 | - | 0.53 |
| LanguageAtHome | Other | 20 | 60.0% | Reference | | | | Reference | | | |
| | English | 444 | 80.2% | 1.75 | 0.51 | - | 6.03 | 1.90 | 0.88 | - | 4.12 |
| Income | Over $100,000 | 112 | 83.0% | Reference | | | | Reference | | | |
| | $50,000-$100,000 | 191 | 78.0% | 0.80 | 0.50 | - | 1.28 | 0.81 | 0.31 | - | 2.15 |
| | Less than $50,000 | 132 | 78.8% | 0.88 | 0.49 | - | 1.61 | 1.03 | 0.40 | - | 2.67 |
| RestraintType** | Seatbelt | 196 | 63.8% | Reference | | | | Reference | | | |
| | Restraint | 301 | 89.7% | 3.99 | 2.40 | - | 6.64 | 2.57 | 1.29 | - | 5.12 |

## Laboratory Comfort Study

Data was collected from 14 participants aged 4-8yrs (M=5.4yrs, SD=1.5yrs), 3 males and 11 females.

We found our adapted survey tools did not provide a reliable measurement of real comfort among the children within our sample. There were no significant differences in survey scores between seating conditions with the

children reporting comfort even in induced discomfort seating conditions. Survey Tool 1 was used with the first 10 participants but we found it was impractical with the young children that we were working with because they appeared to lose concentration due to the number of items in the tool. Survey Tool 2 was used with the remaining 4 participants but did not seem to be any more useful than Survey Tool 1 because the children did not provide answers that could be used to discriminate between seating conditions.

The seat base and the seat back pressure distributions were analysed separately. There was a significant increase in the ΔCOF between Fit and Fit+Footrest conditions for the seat base ($p=0.033$, $n=13$) and a non-significant trend towards an increase ΔCOF for the seat base between Fit and No Stimulus ($p=0.056$, $n=4$). For the seat back there was a non-significant trend toward an increase in ΔCOF between Fit and No Stimulus ($p=0.058$, $n=4$).

There was a significantly higher average seat base contact area for the Fit condition compared to the Fit+Footrest condition ($p=0.007$, $n=14$) and a significantly lower average seat base contact area for the Fit condition compared to the Cushion Long condition ($p=0.000$, $n=14$). For the seat back there was a significantly higher contact area for the F condition compared to the CL condition ($p=0.023$, $n=14$).

There were no significant differences for either the seat back or seat base for peak pressure.

Analysis of the video footage for discomfort avoidance behaviours allowed us to calculate a DAB rate. We observed a significant increase in the DAB rate for the Seat Belt High condition over the baseline F condition ($p<0.01$, $n=13$). No other significant differences were observed between any conditions (Figure 4). However the difference in the DAB rate between Fit and the No Stimulus condition could be significant if there was a larger sample ($p=0.087$, $n=4$).

Significant correlations between DAB rate and ΔCOF were observed for the seat base ($r(10)=0.763$, $p<0.01$) and seat back ($r(11)=0.584$, $p<0.05$) in the Cushion Long condition and in the seat base ($r(11)=0.679$, $p<0.05$) of the Fit condition.

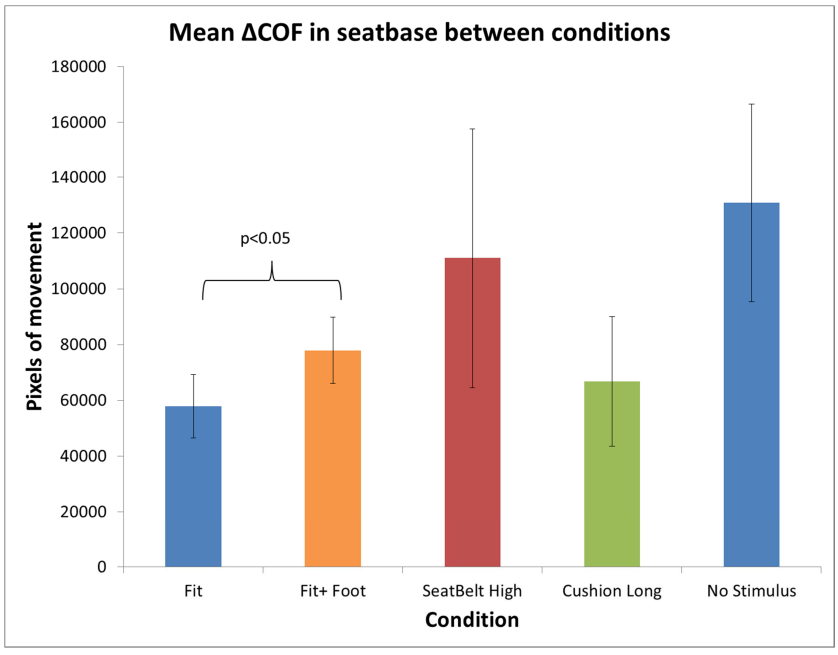


*Figure 3: Comparison of ΔCOF for the seat base between conditions (No Stimulus, n=4, for all other conditions n=14). A statistically significant difference was observed between the Fit and Fit+Footrest conditions ($p<0.05$).*

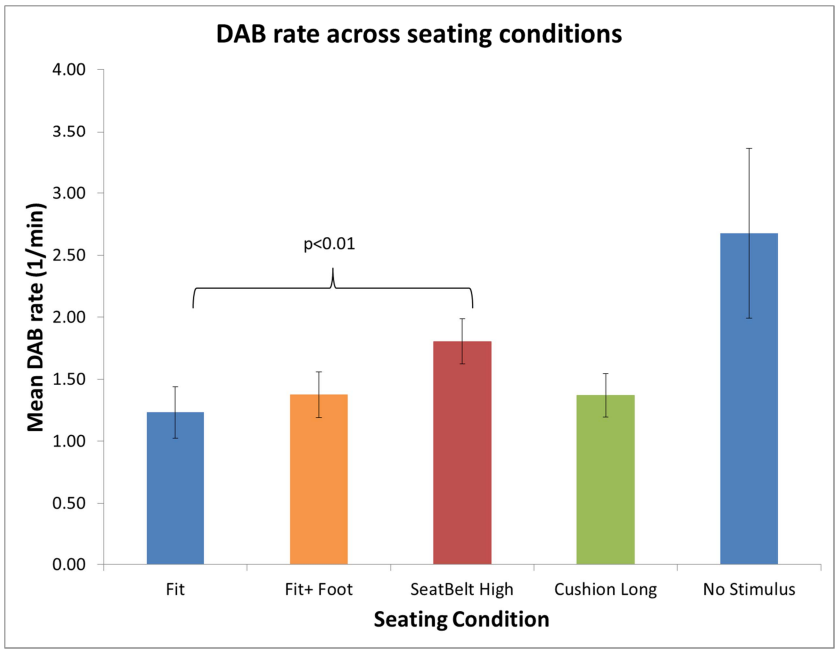


*Figure 4: Comparison of DAB rate across tested seating conditions (No Stimulus, n=4, for all other conditions n=14)*

The DAB scoring method also proved to be repeatable with average intra class correlation coefficient (ICC) was 0.98 (95% CI 0.954-0.991, $F(31,31)=61.425$, $p<0.001$) which indicates a high degree of agreement between the two raters used to assess the DAB rate, indicating the repeatability of this measurement

## DISCUSSION

Our key results from the online survey were that parents continue to report comfort as a factor in their transition decisions but most parents feel that their child is comfortable in their current restraint. In the field observation study we saw that parent perceived comfort is not a predictor of age appropriate restraint use, but contrary to expectation the lack of reported comfort problems increased the odds of restraint misuse. The laboratory comfort study demonstrated that the most useful tool for studying comfort of children in child restraints is likely to be the DAB score.

### Parent perception of child comfort in restraints

From the combined field observation study and parental survey we observed an overall low rate of parent reported comfort problems, suggesting that most parents do not believe that their child is experiencing issues with comfort in their CRS. Despite this, comfort was the third most common factor reported as a consideration when making decisions about restraint transitions. This suggests some disconnect in how parents perceive the comfort of their children 'now' i.e. the restraint they are using now looks comfortable, and they are comfortable in the restraint they are using now, compared to how parents think they might act in the future e.g. if the child becomes uncomfortable in the future they would change restraints. Yet in the logistic regression models, there was no significant association between parent reported comfort and appropriate/inappropriate restraint status of the child, indicating this 'future' concern is not actually driving inappropriate restraint choices. Future analysis could explore this in more detail to examine any possible difference in parent reported comfort for children at transition margins compared to other children.

In our open-ended questions asking why parents thought their child was comfortable; the most common reasons were a lack of complaint from the child, and the child's ability to sleep in the restraint. While these would appear to be indicators of the child's actual comfort in the restraint, there is no available data linking child behaviour to comfort. Therefore while this provides some understanding of how the parent perception of child comfort is built, it still does not tell us anything concrete about the actual comfort of the child.

Our finding that child restraint misuse is almost twice as more likely in children where parents do not report comfort problems is contrary to expectations. Considering the above discussion it suggests that when children are not complaining, or are sleeping, or are otherwise indicating to their parents that they are not uncomfortable there is an increased risk of misuse. This anomaly requires further study. It may be that children have incorrectly positioned themselves to achieve a level of comfort or that there is some problem with the factors parents use in making decisions about their child's level of comfort. Either way it highlights the need to educate parents to be alert for errors in use. Furthermore, this indicates that as suggested by other researchers (Bilston et al. 2011; Pettersson and Osvalder 2005; Simpson et al. 2002), there may be a relationship between the actual comfort of children and incorrect use. While there have been few studies examining comfort experienced by children in child restraint systems and the influence this might have on misuse this remains untested. One study which examined the subjective comfort experienced by a small sample of children using different types of boosters suggested a potential interaction between comfort and the seated posture adopted by a child (Osvalder et al. 2013). There may also be a link between the posture adopted by the child and incorrect use, and this also requires further study.

**Measuring the actual comfort of the child**

A major barrier to the study of the actual comfort of the child is the lack of available validated measures of comfort in children in child restraint systems. Comfort in general is difficult to study, and young children offer a particular challenge. While there have been a number of studies examining comfort in adults, including in vehicles (Chae et al. 2011; Kyung and Nussbaum 2008; Kyung et al. 2008; Paul, Pendlebury, et al. 2012), there are few validated methods for assessing comfort that could easily be adapted for use with young children. Self-report surveys, questionnaires and pressure distribution mapping (Chae et al. 2011; Gyi and Porter 1999; Porter et al. 2003; Smith et al. 2006) appear to be the most common methods employed. Notable examples of survey instruments include the Automotive Seating Discomfort Questionnaire (ASDQ) (Smith et al. 2006) and the body discomfort chart used by Gyi and Porter (1999). However as noted by other researchers (Pettersson and Osvalder 2005), survey and interview measures may not be reliable in children as unreliable answers are often provided by children under age 10. To counter this, we attempted to combine a method commonly used to capture self-reported pain data in young children, with survey and interview methods. However, as reported here, we found this to be an unsuccessful approach. Interestingly, Osvalder et al. (2013) reported the successful use of a survey tool developed using a combination of faces paired with questions in their battery of survey tools to collect information about comfort from children in vehicles. It may be that the difference in child age range between our study and their study might explain this discrepancy. In our study the majority of our participants were less than the age of 6, while in the (Osvalder et al. 2013) study they studied children aged 7-9 years. However it is important to note that our laboratory study aimed to validate the responses of the children with anthropometrically predicted comfortable and uncomfortable seating positions while no validation data for the survey used by other researchers has been presented.

In our laboratory comfort study we attempted to provide each participant with a personalised baseline anthropometric fit using our adjustable testing rig which was constructed from the rear seat of a car as a baseline "comfort" seating condition. This rig was constructed to allow the adjustment of cushion length and height of the D-ring for the seat belt. The angle of the seat back was fixed. For children it has been suggested that a seat base length of 80-95% of the buttocks to popliteal length is required for good fit (Parcells et al. 1999). Our rig allowed us to achieve this seat base length. We have assumed that this will equate to a comfortable seating situation as providing sufficient cushion length would avoid discomfort caused by uneven pressure distribution due to increased flexion of the hips and knees as seen by Le et al. (2014) in taller people; and discouraging a slouched posture since the knees can bend over the front edge of the seat (Parcells et al. 1999). We have also assumed that having an appropriate sash belt fit that does contact the neck and passes over the mid line of the shoulder would also equate to a comfortable condition. However, to date there is no data to support or refute this assumption. Our DAB results do however indicate that children were more likely to fidget in seating conditions where the seatbelt D-ring was high indicating that our assumption about sash belt fit comfort may be correct.

Pressure distribution mapping is another method commonly used to study comfort of adults in vehicle seats. Pressure data has been reported to be strongly associated with comfort (Kolich and Taboun 2004; Kyung and Nussbaum 2008) and static pressure distribution measurements have been shown to be repeatable and sensitive to different seating characteristics (Kolich and Taboun 2004). However, at least two studies have reported no clear relationship between interface pressure and comfort (Chae et al. 2011; Gyi and Porter 1999; Porter et al. 2003). Furthermore, Porter et al. (2003) reported pressure measurements lacked enough sensitivity to distinguish between four different seats. Despite the contentiousness of this issue, pressure mapping continues to be a reasonable objective measure of comfort/discomfort and pressure variables are still commonly used for this purpose in ergonomic seat design. Chae et al. (2011) and Kyung and Nussbaum (2008; 2008) argue that pressure data such as the total contact area, average pressure ratio and peak pressure still provide useful data for seat. In our laboratory study we did observe some significant variations between change in centre of force and average contact area between different seating conditions, indicating some sensitivity of this method to postural changes at least, when used with child occupants. However the relationship between changes in pressure distribution and the association between anthropometrically predicted fit and comfort remains unclear.

We also saw significant correlations between pressure distribution measurements and our newly developed DAB score. The DAB rate proved to be the most sensitive measure of discomfort between the three different methods that we tested. Furthermore, this is a relatively easy method to implement and may prove a useful tool in naturalistic studies.

Osvalder et al. (2013) used video analysis in their naturalistic study to monitor the child's behaviour and body language. Our work takes this further and employs video recordings and subsequent analysis to quantify the child behaviours in a repeatable form, the DAB rate. Forman et al. (2011) extracted frames from video recordings to evaluate seat belt fit and posture, whilst this is a good compromise for seat belt fit analysis we felt that we would lose too much data and we were using much shorter video recordings which made a full video analysis much more manageable.

**Limitations**

It should be noted that each of the three studies has its own limitations. Firstly, the online parental survey was distributed primarily through social media with the aid of a motoring services company, NRMA, and targeted parents who were currently using a child restraint. This delivery method leads to a sample bias towards those parents who are interested or concerned about child restraints and currently using a child restraint and consequently likely to be better informed about child restraints. It also targets parents with existing links to the motoring services organization. While the data extracted from the observation study came from a study that originally had a robust population referenced sample, the comfort variable used in this analysis had a lot of missing data (24.7%). Therefore weightings used may not accurately reflect the population, so results cannot be generalised to the wider population. Finally, the laboratory study was conducted as a pilot study to develop methods for later work. The sample size, particularly for some aspects of the analysis, was very small. Non-significant results may reflect low power, particularly those related to trials involving the 'NFS' condition. Further, the sample size was also biased towards younger children, and it may be fruitful to repeat this work with a larger sample and greater age range of children.

**Conclusion**

Our results suggest that whilst some parents report that child comfort is a contributor to their restraint transition decisions, in reality parent reported comfort is not associated with appropriate or inappropriate restraint use by their children. If comfort is important for optimal restraint, it is likely to be the real comfort of the child rather than that reported by the parent. The method we have developed for studying real comfort can be used to further understand this relationship.

**ACKNOWLEDGEMENTS**

Cameron Fong is supported by an Australian Postgraduate Award. Lynne Bilston and Julie Brown are supported by National Health and Medical Research Fellowships. The authors would also like to acknowledge the funders of the different studies included in this paper. The field observation study data was collected as part of An ARC Linkage funded project with partner funding from Transport NSW (formally known as the NSW Roads and Traffic Authority) and the NSW Motor Accidents Authority. The other studies were supported by NSW Centre for Road Safety, VicRoads, and NRMA. The pressure distribution mapping system was provided by Futuris Automotive Interiors Pty Ltd.

**REFERENCES**


Bieri D, Reeve RA, Champion GD, Addicoat L, Ziegler JB. The Faces Pain Scale for the self-assessment of the severity of pain experienced by children: development, initial validation, and preliminary investigation for ratio scale properties. *Pain*. 1990;41(2):139–150.

Bilston LE, Du W, Brown J. Factors predicting incorrect use of restraints by children travelling in cars: a cluster randomised observational study. *Injury prevention*. 2011;17(2):91–96.

Bingham CR, Eby DW, Hockanson HM, Greenspan AI. Factors influencing the use of booster seats: a state-wide survey of parents. *Accident Analysis & Prevention*. 2006;38(5):1028–1037.

BITRE. Road Deaths Australia, 2011 Statistical Summary. 2012.

Bohman K, Boström O, Osvalder AL, Eriksson M. Rear seat frontal impact protection for children seated on booster cushions-an attitude, handling and safety approach. In: *Proc 20th Int ESV Conf., paper no. 07-0268, June, Paris*.; 2007.

Borgers N, de Leeuw E, Hox J. Children as respondents in survey research: Cognitive development and response quality 1. *Bulletin de Methodologie Sociologique*. 2000;66(1):60–75.

Borgers N, Sikkel D, Hox J. Response effects in surveys on children and adolescents: the effect of number of response options, negative wording, and neutral mid-point. *Quality & Quantity*. 2004;38(1):17–33.

Brown J, Bilston L. Child restraint misuse: incorrect and inappropriate use of restraints by children reduces their effectiveness in crashes. *Journal of the Australasian College of Road Safety*. 2007;18(3).

Brown J, Bilston LE. Child Occupant Protection in Australia. *Journal of Australasian College of Road Safety*. 2012;23:37–45.

Brown J, Hatfield J, Du W, Finch CF, Bilston LE. Population-level estimates of child restraint practices among children aged 0-12 years in NSW, Australia. *Accident Analysis & Prevention*. 2010;42(6):2144–2148.

Bull MJ, Stroup KB, Gerhart S. Misuse of car safety seats. *Pediatrics*. 1988;81(1):98–101.

Chae S, Kyung G, Nam K. Measuring Drivers' Dynamic Seating Experience Using Pressure Mats. *Design, User Experience, and Usability. Theory, Methods, Tools and Practice*. 2011:368–375.

Charlton JL, Wales NS, Authority MA. *Factors that Influence Children's Booster Seat Use*. Monash University Accident Research Centre; 2006.

Donnelly CJ, Callaghan JP, Durkin JL. The effect of an active lumbar system on the seating comfort of officers in police fleet vehicles. *International Journal of Occupational Safety and Ergonomics*. 2009;15(3):295–307.

Du W, Hayen A, Bilston L, Hatfield J, Finch C, Brown J. Association between different restraint use and rear-seated child passenger fatalities: a matched cohort study. *Archives of Pediatrics and Adolescent Medicine*. 2008;162(11):1085.

Forman JL, Segui-Gomez M, Ash JH, Lopez-Valdes FJ. Child posture and shoulder belt fit during extended night-time traveling: an in-transit observational study. *Ann Adv Automot Med*. 2011;55:3–14.

Gyi DE, Porter JM. Interface pressure and the prediction of car seat discomfort. *Applied Ergonomics*. 1999;30(2):99–107.

Hicks CL, von Baeyer CL, Spafford PA, van Korlaar I, Goodenough B, others. The Faces Pain Scale-Revised: toward a common metric in pediatric pain measurement. *Pain*. 2001;93(2):173.

Jakobsson L, Isaksson-Hellman I, Lundell B. Safety for the growing child: experiences from Swedish accident data. In: *Proceedings of the 19th International Technical Conference on the Enhanced Safety of Vehicles.*

*Washington, DC: National Highway Traffic Safety Administration*.; 2005.

Klinich KD, Pritz HB, Beebe MS, Welty KE. Survey of older children in automotive restraints. In: *SAE PUBLICATION P-279. PROCEEDINGS OF THE 38TH STAPP CAR CRASH CONFERENCE, OCTOBER 31-NOVEMBER 4, 1994, FORT LAUDERDALE, FLORIDA, USA (SAE TECHNICAL PAPER 942222)*.; 1994.

Kolich M, Taboun S. Ergonomics modelling and evaluation of automobile seat comfort. *Ergonomics*. 2004;47(8):841–863.

Kyung G, Nussbaum MA, Babski-Reeves K. Driver Sitting Comfort and Discomfort (Part I): Use of Subjective Ratings in Discriminating Car Seats and Correspondence Among Ratings. *International Journal of Industrial Ergonomics*. 2008;38(5):516–525.

Kyung G, Nussbaum MA. Driver Sitting Comfort and Discomfort (Part II): Relationships With and Prediction From Interface Pressure. *International Journal of Industrial Ergonomics*. 2008;38(5):526–538.

Le P, Rose J, Knapik G, Marras WS. Objective classification of vehicle seat discomfort. *Ergonomics*. 2014;57(4):536–544.

Nilsson E, Wolstedt V. Concept and Development of an Ergonomic Booster Seat. In: ; 2007.

Osvalder A-L, Hansson I, Stockman I, Carlsson A, Bohman K, Jakobsson L. Older children's sitting postures, behavior and comfort experience during ride-A comparison between an integrated booster cushion and a high-back booster. In: *Submitted to International Research Conference on the Biomechanics of Impact (IRCOBI)*.; 2013.

Parcells C, Stommel M, Hubbard RP. Mismatch of classroom furniture and student body dimensions: empirical findings and health implications. *Journal of Adolescent Health*. 1999;24(4):265–273.

Paul G, Daniell N, Fraysse F. Patterns of correlation between vehicle occupant seat pressure and anthropometry. *Work: A Journal of Prevention, Assessment and Rehabilitation*. 2012;41:2226–2231.

Paul G, Pendlebury J, Miller J. The contribution of seat components to seat hardness and the interface between human occupant and a driver seat. *International Journal of Human Factors Modelling and Simulation*. 2012;3(3):378–397.

Pettersson I, Osvalder AL. Ergonomic Evaluation of Child Car Seats Comfort and Usability. In: *Proceedings of the Nordic Ergonomic Society (NES) Conference, Oslo, Norway, 9-11 October, 2005.*; 2005.

Porter JM, Gyi DE, Tait HA. Interface pressure data and the prediction of driver discomfort in road trials. *Applied Ergonomics*. 2003;34(3):207–214.

Simpson EM, Moll EK, Kassam-Adams N, Miller GJ, Winston FK. Barriers to booster seat use and strategies to increase their use. *Pediatrics*. 2002;110(4):729–736.

Smith DR, Andrews DM, Wawrow PT. Development and evaluation of the automotive seating discomfort questionnaire (ASDQ). *International Journal of Industrial Ergonomics*. 2006;36(2):141–149.

Wong D, Baker C. Pain in children: comparison of assessment scales. *IJI*. 1988;50:7.

**Mechanisms of head and neck injuries sustained by helmeted motorcyclists in NSW, Australia.**

**Thomas Whyte**
University of Technology, Sydney, Human Impact Engineering
Australia

**Tom Gibson**
Human Impact Engineering
Australia

**Julie Brown**
Neuroscience Research Australia
Australia

**Bruce Milthorpe**
**David Eager**
University of Technology, Sydney
Australia

Paper Number 15-0332

## ABSTRACT

The wearing of a standard-approved motorcycle helmet has been the most significant step in reducing fatal and serious injury among motorcyclists worldwide. Mandatory helmet use for motorcyclists is now in place in many parts of the world. Nevertheless, some researchers have observed a high percentage and duration of hospitalisations in helmet-protected motorcyclists with the long-term outcome considerably influenced by head injury severity. The objective of this study was to investigate head and neck injuries sustained by helmeted motorcyclists in real world crashes and define the circumstances which result in injury.

Data were collected by in-depth crash investigations of motorcyclist crashes in NSW, Australia. The crash investigations included inspections of the accident scene, the crash involved motorcycle and the helmet. Where possible, detailed helmet examination including helmet disassembly was performed to identify all crash related damage. The type of damage, damage location and damage severity on the helmets were recorded. The major head and neck injury types sustained by these helmeted riders were analysed for crash and helmet damage related factors which influenced the incidence of injury.

Due to the recruitment procedures used, participants in this study were biased towards lower severity head injuries. A head injury was sustained in 23.9% of cases but serious (AIS 3+) head injury was sustained in only 2.3%. There was neck injury in 9.1% of cases but no serious (AIS 3+) neck injuries. The main head and neck injury types by frequency were superficial injury (13.6%), “diffuse” type brain injury (13.6%), facial/dental fracture (4.5%) and cervical spine fracture (4.5%).

Helmet damage was observed in the majority of cases (86.4%) suggesting successful injury prevention in many instances. A high proportion of observed impact damage was to the front of the helmet (78.5% of cases), particularly the chin bar and visor of full-face helmets. Impact damage associated with a predominantly tangential force onto the head was more common than radially directed force damage.

Superficial head injury and facial/dental fractures was significantly more common ($p < 0.01$) in riders who were wearing open face helmets, where the face and chin are exposed to direct impact, compared to full face protected riders. There were significantly more cervical spine fractures in cases with damage indicative of a radially directed force ($p = 0.036$) than where damage indicated a tangentially applied force. The circumstances resulting in “diffuse” brain injuries could not be clearly defined by the data in this study due to the small number of riders with this injury.

The results highlight potential areas for improving the head and neck protection offered to motorcyclists including extending the required region of coverage, particularly to the face, and through mitigating the effect of tangential

impacts on the helmet. Given the high frequency of diffuse intracranial injury even in lower severity head injury cases, assessment of helmet effectiveness should use performance criteria reflecting the mechanisms of this type of injury.

## INTRODUCTION

The effectiveness of motorcycle helmets in reducing fatal and serious injury among motorcyclists is well known [1–3]. Mandatory helmet use is now required by motorcyclists in many countries including Australia and throughout Europe. Nevertheless, a high percentage and duration of hospitalisations have been observed even in helmet protected motorcyclists [5] and injuries to the head are still the most common cause of death in fatally injured helmeted motorcyclists [6].

Current motorcycle helmet designs are largely shaped by helmet performance standards which are in force in most countries. Standards define how a helmet must perform in an impact consisting of dropping an instrumented rigid headform, fitted with the test helmet, onto a rigid anvil. The helmet is assessed based on the linear acceleration experienced by the headform centre of gravity. This test and helmet assessment criteria were originally developed in the late 1960's [7] using some of the earliest and most widely used biomechanical head injury tolerance data, the Wayne State University Concussion Tolerance Curve [8], which despite its name, was originally based on the level of linear acceleration producing a linear skull fracture in an adult. The simplified loading conditions of the impact attenuation tests were chosen to ensure the test results were repeatable and reproducible, both necessary and appropriate for ensuring the consistent performance of a mass produced product such as helmets. However the drop test may not reflect what occurs to the head of a motorcyclist in a real crash. Furthermore the response criteria measured during these tests cannot assess the potential for all types of head and neck injury.

The aim of the present study was to investigate the types of head and neck injury sustained by helmeted motorcyclists in real crashes and common loading conditions to the helmet that result in injury to the rider. Hence indicating areas of helmet protection where further research effort can be applied to reduce the frequency and severity of head and neck injuries to helmeted riders in crashes.

## METHODS

The data used for this study were collected by Neuroscience Research Australia as part of an in-depth case-control study of motorcycle crashes. 91 cases of injured motorcyclists over the age of 14, admitted to a NSW hospital, were recruited by research nurses. The participant then completed a face-to-face interview, self-reporting various details regarding the crash. The crash related injuries were recorded from the medical records of the patient. The crash involved motorcycle and the crash scene were inspected noting all evidence of the incident. The clothing and helmet worn by the rider at the time of the crash were also inspected. Where authorised by the study participant the clothing and helmet were collected for subsequent analysis. A subset of these cases has been previously presented assessing the effectiveness of the motorcycle protective clothing worn by the rider [9].

To address the aims of the current study, three of the cases were excluded from the analysis because there was either no helmet worn in the crash or the helmet was ejected sometime during the crash sequence. Helmets that were retained from the study participants were disassembled and any internal or external evidence of crash related damage was also recorded.

The data were analysed using the Statistical Package for Social Sciences, version 21. Pearson's Chi-square tests and Fisher Exact tests were used to analyse any differences in the proportion of injured riders with respect to variables of crash characteristics, helmet characteristics, helmet damage and damage location. A p-value of $< 0.05$ was considered significant.

## RESULTS

The 88 helmeted riders had an average age of 36.9 ± 15.6 years with a range of 16 to 80 years. 82 riders were male (93.2%) and six (6) were female (6.8%). The following sections outline the injuries sustained by these riders, the general crash characteristics and details regarding the helmets.

**Incidence of Head and Neck Injury**

Head injury was sustained in 21 of the 88 cases (23.9%), see Table1. but serious (AIS 3+) head injury was sustained in only 2 (2.3%). Based on the frequency and severity of the injuries, the major injury types sustained in this set of riders were superficial head injury, diffuse intracranial brain injury, facial/dental fractures and cervical spine fractures.

Superficial head injury was most common with the face sustaining the majority (80.8%) of these injuries. Of the 9 fractures to the head 1 (11.1%) involved the skull vault and the remaining 8 (88.9%) involved the facial bones or teeth. The intracranial injuries seen in this study were predominantly "diffuse" type brain injuries which included closed head injury/loss of consciousness, concussion or change in cranial pressure which was sustained by all 12 riders with intracranial injury. Neck injury was sustained in 8 cases (9.1%), see Table1., but there were no serious (AIS 3+) neck injuries. Cervical spine fractures occurred in 4 cases (5%) and minor injuries to the skin and soft tissues occurred in a further 4 cases (5%).

**Table1.**
**Head and neck injury cases**

| Injury type | | Number of cases (% of total cases) | Total no. of injuries | Frequency of injury severity (% of injuries) | | | |
|---|---|---|---|---|---|---|---|
| | | | | AIS 1 | AIS 2 | AIS 3 | AIS 4 |
| **Head injuries** | Superficial | 12 (14%) | 26 | 26 (100%) | 0 | 0 | 0 |
| | Fracture | 4 (5%) | 9 | 2 (22%) | 6 (67%) | 1 (11%) | 0 |
| | Intracranial | 12 (14%) | 17 | 6 (35%) | 7 (41%) | 3 (18%) | 1 (6%) |
| | All Head Injury | 21 (24%) | 52 | 38 (68%) | 13 (23%) | 4 (7%) | 1 (2%) |
| **Neck injuries** | Superficial | 2 (2%) | 4 | 4 (100%) | 0 | 0 | 0 |
| | Fracture | 4 (5%) | 4 | 0 | 4 (100%) | 0 | 0 |
| | Soft Tissue | 2 (2%) | 2 | 2 (100%) | 0 | 0 | 0 |
| | All Neck Injury | 8 (9%) | 10 | 6 (60%) | 4 (40%) | 0 | 0 |

**Crash Characteristics**

The estimated speed prior to crashing was recorded for 91.2% of cases, with a median estimated pre-crash speed of 52.5 km/h and a mean of 52.3 ± 23.9 km/h.

In the majority of cases (75%), the crashed motorcyclist was involved in a collision with another vehicle. The predominant collision opponent was a passenger car (58%) followed by the roadway/kerb only (13.6%) and then poles/trees (6.8%).

Table2. shows the distribution of crash configurations based on the classification used in the COST 327 study of European motorcycle in-depth crash investigations [1]. Type 7 crashes (at 29.5%) were most common, which included 22 cases of single vehicle loss of control crashes (25% of all cases). Circumstances where the front of the motorcycle collided with the rear (Type 5) or side (Types 3 and 4) of a passenger car were also common.

**Helmet Type**

The majority of riders (86.4%) wore a full face type motorcycle helmet which included a chin bar and the remainder wore an open face "jet" style helmet (13.6%).

There was a statistically higher proportion of open face helmeted riders who sustained superficial head injuries ($p=0.009$, FET) and facial/dental fractures ($p=0.007$, FET) compared to full face protected riders.

**Table2.**
**Distribution of crash configurations**

| Collision Types | Description | Diagram | Number of Cases (% of cases) |
|---|---|---|---|
| Type 1 | Side collision against the front of a four wheel vehicle | | 4 (4.5%) |
| Type 2 | Head-on collision against the front of a four wheel vehicle | | 7 (8.0%) |
| Type 3 | Head-on against the side of a four wheel vehicle | | 12 (13.6%) |
| Type 4 | Oblique collision against the side of a four wheel vehicle | | 13 (14.8%) |
| Type 5 | Head-on collision against the rear-end of a four wheel vehicle | 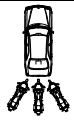 | 14 (15.9%) |
| Type 6 | Rear-end collision against the front of a four wheel vehicle | | 12 (13.6%) |
| Type 7 | Collision against pedestrians, bicycles, non-moving objects | | 26 (29.5%) |
| Total | | | 88 |

**Helmet Damage Type**

There was observed or reported damage to the helmet in 76 cases (86.4%), 10 helmets (11.4%) were undamaged and the condition was not known for 2 (2.2%). Scratches were most common, observed in 72 cases, followed by cracks to the shell (16) and observable liner damage (10).

The type of helmet damage was assessed in 69 cases as either associated with a tangentially directed force or radially directed force to the head. Tangentially directed force damage was more common (62.5%) than radially directed force damage (44.9%) and 24.6% of cases had areas of both types of damage.
Cases with radially directed impacts had a significantly higher incidence of cervical spine fracture than cases without normal impacts ($p = 0.036$, FET).

**Helmet Damage Location**

The location of the damage on 65 inspected helmets was mapped on a schematic of the helmet divided into zones based on the crown, front, sides and rear of the helmet at varying levels of elevation from the helmet rim. Figure1. shows that the majority of helmet damage was to the face, despite 11 open face helmets without a chin bar and 5 of these without a face shield (visor) that could not sustain damage in these areas. The remainder of the damage was concentrated in a band around the sides and the rear of the mid-level of the helmet with relatively infrequent damage to the crown. The proportion of cases sustaining damage to each area of the helmet is shown in Table3.

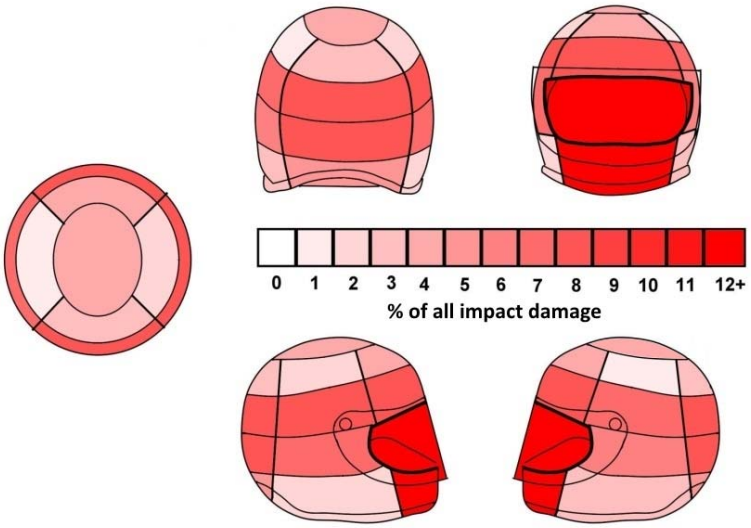


***Figure1. Distribution of impact damage on the 65 inspected helmets.***

**Table3.**
**Location of helmet damage for 65 inspected helmets**

| Location on helmet | Frequency of cases | Percentage of cases |
|---|---|---|
| **Chin bar** | 34 | 63.0 (of full-face type helmets) |
| **Visor/Facial** | 39 | 65.0 (of visor equipped helmets) |
| **Frontal** | 19 | 29.2 |
| **Any frontal impact damage** | 51 | 78.5 |
| **Left** | 30 | 46.2 |
| **Right** | 32 | 49.2 |
| **Rear** | 40 | 61.5 |
| **Crown** | 8 | 12.3 |
| **Total helmets with recorded damage location** | 65 | 100.0 |

**Devices attached to the Helmet Shell**

11 (12.5%) of the crashed riders in this study had a Bluetooth headset attached to the exterior of the outer shell of the helmet. The devices allow the motorcyclist to communicate with other riders, make phone calls and listen to audio while riding and typically consist of a set of speakers and a microphone placed inside the helmet, and a small box of electronics mounted on the outside of the helmet, as shown in Figure 2. In one of these 11 cases, the helmet also had an attachment for a video camera device.

When an attachment to the external shell was present, 27.3% of riders sustained a diffuse type intracranial injury compared to only 7.4% of riders sustaining intracranial injury when there was no attachment. However, this difference was not statistically significant ($p = 0.088$, FET).

***Figure2. Bluetooth device (left) and attachment point indicated by spots of glue (right).***

## DISCUSSION

In-depth crash investigations of the 88 helmeted motorcyclists attending an emergency room were used to identify the injuries being sustained by helmeted riders and to define the common and injurious loading conditions being applied to the helmet in real crashes. The collected cases demonstrate the effectiveness of motorcycle helmets in preventing injury as damage was present in over 85% of helmets while less than 25% of riders sustained a head or neck injury. However, the collected cases appear to be biased towards low severity head and neck injury as the proportion of serious (AIS 3+) head injury sustained by helmeted riders in this study (2.3%) is lower than that reported in European data [5] (9.7%) and in the Hurt data of crashes in the US [3] (17.9%). Exclusion of helmet ejected cases, which were classified as helmeted riders by both Richter et al. and Hurt et al., was not the reason for the difference with the two excluded cases in this study sustaining only AIS 1 superficial head injury. Nevertheless, the major injuries sustained by helmeted riders in these crashes in terms of frequency and severity were identified as intracranial injury, facial/dental fractures, superficial head injury and cervical spine fractures.

Superficial head injury (mostly comprising superficial facial injury) and facial and dental fractures were significantly more common when an open face helmet was worn compared to full-face helmet protection in this study. This result confirms the almost identical findings reported by Cannell et al. [10], although the relationship was not significant in their study, and is not surprising given the face of the rider is exposed to direct impact while wearing an open face helmet. Furthermore, inspection of the location of helmet damage demonstrates that the face region is the most commonly impacted region of the rider's head. Data reflecting a more severe group of fatal crashes is currently being investigated and will be able to determine whether this trend is also true for more seriously head injured riders.

Cervical spine fractures were sustained in only 4.5% of cases in this study. The cases indicated that cervical spine fracture tended to result from radially direct impacts to the helmet. This outcome relates to the clinical cadaver experiments performed by Hodgson and Thomas [11]. These researchers found that excessive strain on the cervical spine was produced in flat (radial) impacts to the crown and impacts inducing hyperextension on the neck. Hodgson and Thomas found that the effect of the helmet in preventing this type of injury was limited however considerable research effort has shown that the motorcycle helmet at least does not contribute to producing additional neck injury [12,13].

Diffuse intracranial injury was the most common and most severe head or neck injury sustained by the helmeted riders collected in this study but there were no clear circumstances that produced a significantly higher proportion of cases with this injury. The majority of these diffuse injuries were concussions and losses of consciousness. Such injuries have received considerable attention in sports such as American football. It is now understood that rotation of the head is the primary contributor to diffuse brain injury based on the pioneering experiments of Gennarelli et al. [14–16]. As a result, football helmets have undergone significant design improvements by using rotational head injury criteria specifically related to concussion. Assessment of motorcycle helmets to these criteria is ongoing[17–19] but it is important to note the concern that the stiffness of some helmets is such that they are ineffective in reducing brain injury risk at low impact speeds [20]. Given the severity and frequency of the diffuse brain injuries observed in real motorcycle crashes, there is a demonstrated need for helmet design to be assessed in a manner relevant to the known mechanism of this type of injury.

Examination of the crashed helmets in this study was performed to obtain data on the likely loading conditions experienced by the head and neck of riders in real crashes. In the distribution of impacts shown in Figure1., a high frequency of impacts occurred to the front and facial area of the helmets of crashed riders. This is in agreement with previous major crash investigation studies in Europe [5], the US [3] and Australia [21,22]. Despite this, the chin and facial region is outside the require region of protective coverage required by many motorcycle helmet standards, including the Australian Standard AS 1698 and the US regulation FMVSS 218. Further the distribution of impacts around the circumference of the crash damaged helmets, shown in Figure1., coincides with the edge of the region of protective coverage in AS/NZS 1698 and FMVSS 218. Previous Australian motorcycle crash studies recommended extending the area of impact protection to these areas to improve the protection of helmets in frontal and lateral impacts [21,22].

The specification of performance requirements for a helmet able to protect the rider in a frontal impact to the head is a complex task. This is due to the multiple types of injuries that can result from an impact to the face which include local focal injuries (face and skull fractures), remote focal injuries (basilar skull fracture) and head and neck motion induced injuries (brain and cervical spine injuries) [23]. Helmet design for facial impacts remains a critical area where further research could improve protection from injury for a motorcyclist.

The helmets in this study also predominantly showed damage indicating a tangentially directed force, or a rotation of the head. This has also been observed in real crash investigation studies by Otte et al. [24] and Hurt et al. [12]. Oblique impacts to the head have been the subject of ongoing research for two main reasons: First, current knowledge of head injury biomechanics recognizes the importance of head rotation in the production of brain injury; and second, most motorcycle helmet standards do not attempt to measure or produce this type of impact or rotation. A number of laboratory test methods [25,26] have demonstrated a reduction in angular head acceleration from current and new helmet designs but the relevance of these in real crash circumstances remains unknown.

The attachment of Bluetooth and video camera devices to the outside of the helmet shell is a relatively new issue. This tends to go against what is prescribed in motorcycle performance standards, such as in AS 1698 which requires a smooth outer helmet shell to minimize friction or snagging that may promote helmet rotation [27]. This study found a higher proportion of cases sustaining diffuse type intracranial injury when these devices were attached than when they were absent, although the difference was not significant. The fitment of such devices is becoming increasingly popular and accessible as they become cheaper and more reliable. The effect on head injury risk requires further investigation. At present there are no regulations in Australia regarding attaching these devices to helmets.

## DIRECTIONS OF FUTURE RESEARCH

This crash investigation study has highlighted a number of areas where further research has the potential to improve the head and neck protection for helmeted motorcyclists in real crashes.

1. Diffuse type intracranial injury was the predominant injury type in terms of frequency and severity sustained by the riders in these crashes indicating the need to be able to assess the capability of the helmet to ameliorate the risk of this type of injury.
2. Impacts to the front and face of the helmet were common and injurious, particularly to open face helmeted riders. Given the existing lack of impact protection required in this area of the helmet by many current motorcycle helmet standards, there is a need to examine the optimal design of full facial protection for the lowest risk of injury to the face, the skull, the brain and the neck.
3. Tangential impacts to the helmet were the predominant damage type to the crashed riders in this study. Further assessment of these types of impacts in the laboratory is required to match a test methodology to the loads and injuries experienced by riders in real crashes.

## ACKNOWLEDGEMENTS

The authors acknowledge Austroads and the Centre for Road Safety, Transport for NSW for funding and access to the materials used in this review.
The authors also acknowledge the crash investigation team at Neuroscience Research Australia, Mark Kazzi, Bianca Albanese and Lauren Meredith.

**REFERENCES**


[1] B. Chinn, B. Canaple, S. Derler, D. Doyle, D. Otte, E. Schuller, et al., COST 327 Motorcycle Safety Helmets, COST Transport, Luxembourg, 2001.

[2] MAIDS, In-depth investigations of accidents involving powered two wheelers. Final report 2.0, Assoc. Fo Eur. Mot. Manuf. (2009).

[3] H.H. Hurt, J. V Ouellet, D.R. Thom, Motorcycle accident cause factors and identification of countermeasures. Volume 1: Technical report, U.S. Department of Transport. NHTSA, 1981.

[4] N. Haworth, R. Smith, I. Brumen, N. Pronk, Case-Control Study of Motorcycle Crashes, 1997. http://trid.trb.org/view.aspx?id=579064 (accessed October 06, 2014).

[5] M. Richter, D. Otte, U. Lehmann, B. Chinn, E. Schuller, D. Doyle, et al., Head injury mechanisms in helmet-protected motorcyclists: prospective multicenter study, J. Trauma Inj. Infect. Crit. Care. 51 (2001) 949–958.

[6] P. Johnston, C. Brooks, H. Savage, Fatal and serious road crashes involving motorcyclists, Department of Infrastructure, Transport, Regional Development and Local Government, 2008.

[7] E.B. Becker, Helmet Development and Standards, in: N. Yoganandan (Ed.), Front. Head Neck Trauma. Clin. Biomech., 1998.

[8] H.R. Lissner, M. Lebow, F.G. Evans, Experimental studies on the relation between acceleration and intracranial pressure changes in man, Surgery, Gynecol. Obstet. 111 (1960) 329–338.

[9] L. Meredith, L. de Rome, M. Fitzharris, M. Baldock, J. Brown, Validation of test protocols for assessing motorcycle protective clothing using real world crash investigation, in: Proc. 2013 Australas. Road Saf. Res. Polic. Educ. Conf., Brisbane, Queensland, 2013: p. 12. http://trid.trb.org/view.aspx?id=1286898 (accessed October 02, 2014).

[10] H. Cannell, J.B. King, R.D. Winch, Head and facial injuries after low-speed motor-cycle accidents, Br. J. Oral Surg. 20 (1982) 183–191.

[11] V.R. Hodgson, L. Thomas, Mechanisms of Cervical Spine Injury During Impact to the Protected Head, SAE Tech. Pap. 801300. (1980).

[12] H.H. Hurt, J. V Ouellet, I. Rehman, Epidemiology of head and neck injuries in motorcycle fatalities., in: A. Sances, D.J. Thomas, C.L. Ewing (Eds.), Mech. Head Spine Trauma, 1986.

[13] J. V Ouellet, D.R. Thom, T. Smith, H.H. Hurt, Helmets and Neck Injuries in Fatal Motorcycle Crashes, in: Int. Mot. Saf. Conf., 2013.

[14] T.A. Gennarelli, L.E. Thibault, Biomechanics of acute subdural hematoma, J. Trauma. 22 (1982) 680–686.

[15] T.A. Gennarelli, Cerebral concussion and diffuse brain injuries, in: Head Inj., Williams and Wilkins, Baltimore/London, 1982: pp. 83–88.

[16] T.A. Gennarelli, L.E. Thibault, J.H. Adams, D.I. Graham, C.J. Thompson, R.P. Marcincin, Diffuse axonal injury and traumatic coma in the primate, Ann. Neurol. 12 (1982) 564–574.

[17] N. Bourdet, C. Deck, V. Tinard, R. Willinger, Behaviour of helmets during head impact in real accident cases of motorcyclists, Int. J. Crashworthiness. 17 (2012) 51–61.

[18] N.J. Mills, S. Wilkes, S. Derler, A. Flisch, FEA of oblique impact tests on a motorcycle helmet, Int. J. Impact Eng. 36 (2009) 913–925.

[19] M. Aare, S. Kleiven, P. Halldin, Injury tolerances for oblique impact helmet testing, Int. J. Crashworthiness. 9 (2004) 15–23.

[20] H. Fenner, D.J. Thomas, T. Gennarelli, F.A. Pintar, E.B. Becker, J.A. Newman, et al., Final Report of Workshop on Criteria for Head Injury and Helmet Standards, in: Med. Coll. Wisconsin Snell Meml. Found. Inc., Milwaukee,Wisconsin, 2005.

[21] J.P. Corner, C.W. Whitney, N. O'Rourke, D.E. Morgan, Motorcycle and bicycle protective helmets: Requirements resulting from a post crash study and experimental research, Department of Trasnport. Federal Office of Road Safety, 1987.

[22] B. Dowdell, G.J. Long, J. Ward, M. Griffiths, A study of helmet damage and rider head/neck injuries for crash involved motorcyclists, Road Safety Bureau. Crashlab, 1988.

[23] T. Gibson, K. Thai, Helmet protection against basilar skull fracture, Report to the Federal Office of Road Safety, Canberra, 2007.

[24] D. Otte, B. Chinn, D. Doyle, S. Makitupa, K. Sturrock, E. Schuller, Contribution to Final Report of COST 327 Project, Univ. Hann. (1999).

[25] A.S. McIntosh, A. Lai, Motorcycle helmets: Head and neck dynamics in helmeted and unhelmeted oblique impacts, Traffic Inj. Prev. (2013).

[26] P. Halldin, A. Gilchrist, N.J. Mills, A new oblique impact test for motorcycle helmets, Int. J. Crashworthiness. 6 (2001) 53–64.

[27] Standards Australia, AS/NZS 1698:2006 Australian / New Zealand Standard™ Protective helmets for vehicle users, 2006 (2006).

# THE AEB SYSTEM WITH ACTIVE AND PASSIVE SAFETY INTEGRATION FOR REDUCING OCCUPANTS' INJURIES IN HIGH-VELOCITY REGION

**Eung-Seo, Kim**
HYUNDAI MOTOR COMPANY
Korea

**Suk-Ki, Min**
**Dong-Hyun, Sung**
**Sang-Min, Lee**
**Chang-Bong, Hong**
HYUNDAI MOTOR COMPANY
Korea

Paper Number 15-0335

## ABSTRACT

AEB(Autonomous Emergency Braking) is a representative safety system that assists a driver to avoid forward collision or mitigate crash velocity resulting in reduction of occupant's injury risk using ADAS sensor. This paper focuses on establishing appropriate PSB activation time in order to minimize occupant forward movement and head & neck injuries in the event of collision when it is unavoidable in the aspect of active and passive safety system integration. And also, it is the other goal that decreases the collision velocity by applying more efficient pre-braking profile. For this, AEB test is performed with H-3 5% & 50% human dummy seated in the passenger side. The test vehicle is equipped with Lidar and camera sensor fusion AEB system, PSB(Pre-Safety seatBelt) and a premium ESC module. From this study, the last time to activate PSB considering occupant's injury and the improved pre-brake profile beneficial to collision velocity reduction and occupant's behavior were verified.

## INTRODUCTION

AEB(Autonomous Emergency Braking) is a active safety system that can make a vehicle to avoid collision or mitigate the damage by urgently reducing velocity with the informations obtained using ADAS(Advanced Driver Assist System) sensors such as camera or radar. Camera and radar fusion as shown in ***Figure1*** is typically applied to AEB system due to the system's reliablity in recognition performance and it is expected that single sensor is increaingly adopted to the system for general use.

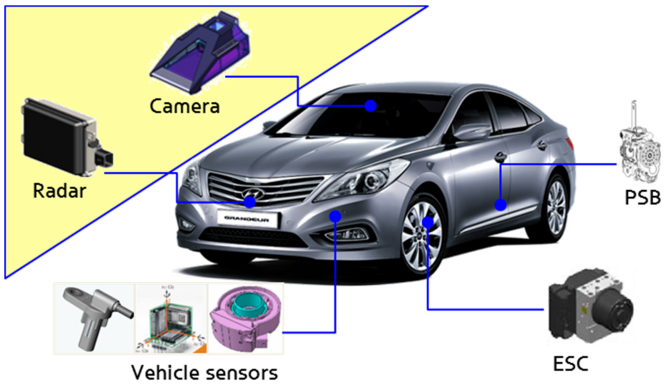


***Figure1. Typical AEB system configuration.***

From the Thatcham's research report[1] in ***Figure2*** , if the system is applied to the market satisfying the fitmet rate Euro NCAP suggets, it is predicted that the fatalities will be decreased by the 50% of current number. Due to this benefit of the system, Euro NCAP is planning to add AEB-VRU(AEB- Vulnerable Road Users) test to current assesment program with AEB-City/Urban in 2016 and IIHS already evaluate the system for TSP+ requirement in their test protocol.NHTSA is preparing for CIB/DBS tests. AEB system become a most important active safety sytem such as airbag became a essential passive one now after it was firstly adopted and then have made a great contribution to reducing fatalities.

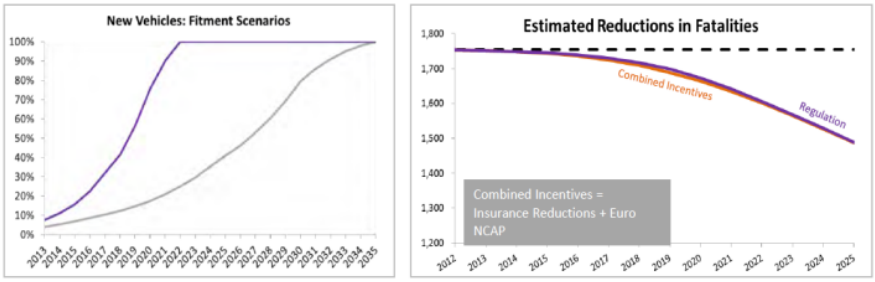


***Figure2. Expected reduction of fatalities with the fitment of Euro NCAP AEB.***

Now, Euro NCAP AEB test aims that collision is avoided under the relative velocity of 50kph, and IIHS performs their AEB test by 40kph.The AEB system in current test condition is more efficient in reducing occupans' neck injuries in target vehicle by crash avoidance or mitigation in low speed than the one in host vehicle. But it is more important to maximize it's efficiency in high velocity region in order to save more lives and reduce occupants' severe injury, because the relative risk increases rapidly in high velocity region over 60kph resulting in twice the risk per 5kph as shown in ***Figure3.*** And also the increase of head and neck injuries should be seiously considered when conventional driver or passenger airbags are deployed just after occupant's forward movement is produced by AEB system activation in high velocity crash from the viewpoint of passive and active safety system integration.

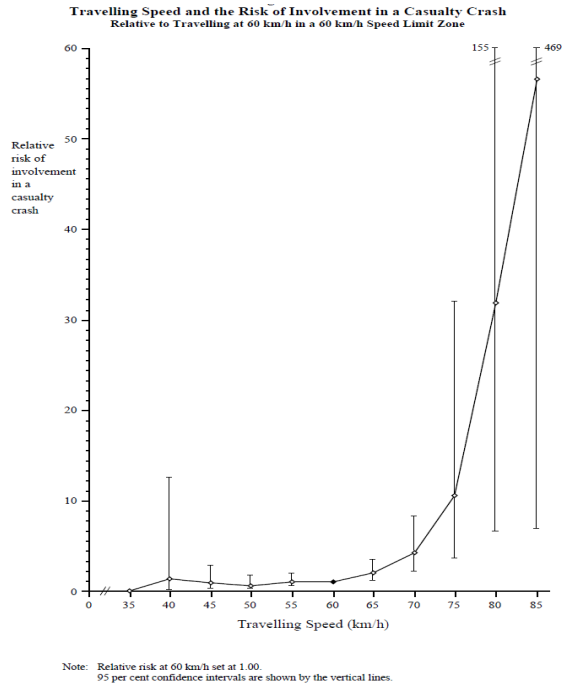


***Figure3. Traveling speed and the risk of involvement in a casualty crash.***

The main purpose of this paper is to improve both AEB and passive safety system to minimize the occupants' severe injury in the high velocity crash when the collision is unavoidble. The situation is assumed that a driver is in distraction, a vehicle is running in a sigle lane, there are another on-coming or rear lateral vehicles, etc. And the condition of the AEB activation is limited in the range of yaw rate so that the stability of vehiclecan be ensured. From this research, the appripriate PSB(Pre-Safety seatBelt) activation time was founded for reducing occupant's forward motion that affects head&neck injuries when AEB is working. Also, the reduction of crash speed and passenger behaviors are respectively compared according to different braking profile.

## THE AEB SYSTEM IMPREMENTATION WITH ACTIVE AND PASSIVE SAFETY INTEGRATION

### The Relation between active and passive safety system regarding AEB

AEB system primarilly helps decreasing occupants' injuries because of speed reduction in high velocity region. On the contrary, the increase of injury can be also accompanied due to the combination of occupants' faster behavior and airbag's high pressure deployment when AEB activated and then vehicle proceeded to crash, which is similar with OOP(Out of Position) situation. And if the vehicle's pitching motion is added, the injury can be amplified. Conventional airbags are not designed to cope with this situation, even though they satisfy LRD(Low Lisk Deployment) regulation in the US market. Some kinds of those airbags may give more harmful effect to occupants with their specific deployment mechanism.So, the tests and analisys were performed mainly to minimize the effect to occupants from AEB system and to reduce collision velocity more.

### AEB System Configuration and Behavior Measurement Test of Dummy

In this tests, human dummy's behavior was mesured when AEB is activated. The test vehicle consists of Camera and Lidar sensor fusion AEB system, a ESC module of premium level and PSB module. When high speed test is conducted, DGPS device replaces the Lidar sensor because or it's short detecting range.Hybrid-3 5% and 50% dummies were used considering the coditions of US-NCAP frontal and Euro NCAP offset crash test mode. There are much difference on the behavior between dummy and human body when the acceleration under 1g occurs. THOR dummy would be better for this test, if possible. Thus, the timing and relative motion of dummy were focused on when AEB is working with different parameters. Dummy is seated in passenger seat because the motion of dummy in driver seat is smaller with the driver grabing steering wheel in the real situation. The PAB(Passenger Air Bag) deployment area is marked with vertical line and the movement is visually verified by video records as shown in ***Figure4***.

***Figure4. System configuration, dummy seating and PAB deployment area.***

**The PSB Activation Condition for Reducing Occupants' injuries**

**The Occupants' Injuries from Air bag Deployment** In the US NCAP and Euro NCAP crash test protocol, the test is carried out in the constant speed, 56kph and 64kph, respectively. Thus, the dummies are seated statically and there's no relative behavior of dummies with vehicle to the blink of crash. However, the deceleration of vehicle by 1g is generated by emergency braking in case of the AEB equipped one when the collision is expected, and therefore, dummy can get the relative acceleration and moves forward in the vehicle. Also, the vehicle can get pitching motion by the braking and if it collide with frontal car in this situation, the airbag can directly impact the passenger's head and chest causing more amplified effect as shown in ***Figure5***. Even if there's no direct impact due to the small airbag size or a passenger seated in the rear position on the seat track(i.e. H-3 50%), the head and neck injury can be increased by the combination of pitching motion and accelerated head loading on airbag cushion. Especially, PAB modules for US market tend to be designed bigger and closer to the passenger in order to satisfy H-3 50% unbelted frontal test mode. In this case, the distance between airbag deployment region and H-3 5% dummy becomes closer and the bad effect on the passenger's injury also increases.

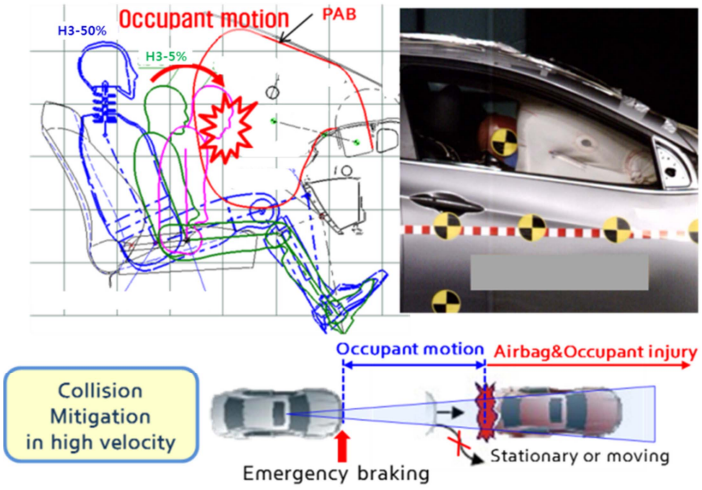


***Figure5. AEB activation and the mechanism of head & neck injuries generation.***

**The Dummy's Behavioral Characteristic according to PSB Activation Time** The tests are carried out to study the dummy's behavioral characteristic and to find the last PSB full retraction time so that the dummy's forward motion can be minimized. The test conditions are vehicle's running speed of 85kph and collision velocity of 50kph against stationary target. Firstly, dummy's behaviors were compared in cases of no retraction, the same PSB activation time with full brake by AEB. From the results, dummy was not effectively restrained due to the PSB actuator delay and increased load by relative acceleration. The PSB trigger time and PSB belt tension graph shows this in ***Figure6.*** Also, the time interval between full brake and maximum forward movement of dummy was measured by video and travel calculation. In the next tests, the PSB trigger time was advanced by the time gap considering the maximum forward movement time expressed as below:

Maximum forward movement time

= Signal transfer time (CAN delay) + PSB actuation delay + Dummy's behavioral moving time (1).

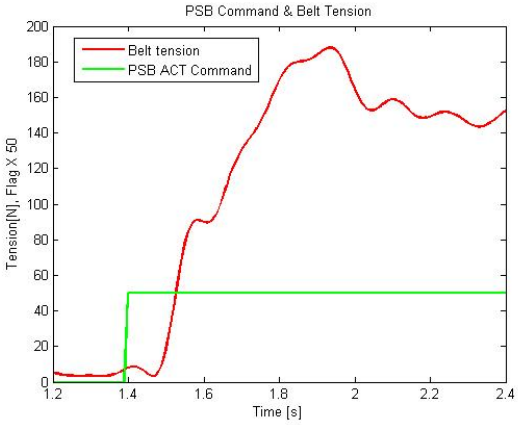


***Figure6. The belt tension of PSB in Shoulder and Maximum forward movement time.***

PSB actuation delay is defined that the time from it's trigger to reaching to maximum load of belt tension in static test and was measure 250ms. Dummy's behavioral moving time was 400ms, which is almost the same with the belt load reached maximum value shown in ***Figure6.*** Thus, PSB activation time was set 400ms advanced to full brake time. Additionally, the AEB tests were done in conditions of varying PSB activation time by 750ms prior to full brake, same time with pre-brake and 300ms prior to pre-brake.

From the test results in ***Figure7***, there's not much differences on dummy's forward movement when PSB is triggered before the 400ms prior to full brake. Dummy's head moves forward by 120mm with no PSB retraction, whereas, it moves about 50mm and 30mm with the trigger time of full brake and 400ms in-advance test case, respectively. If PSB is activated in the same time of full brake, dummy's head invades the PAB deployment area and then it can additionally goes further by crash impulse before airbag is fully deployed. It can be clearly expected that airbag impacts occupant's head resulting in head & neck injury increase. In case of real crash in the field, human's head would have more forward motion.

***(a) Position of dummy at the moment of collision in different PSB activation time(video capture).***

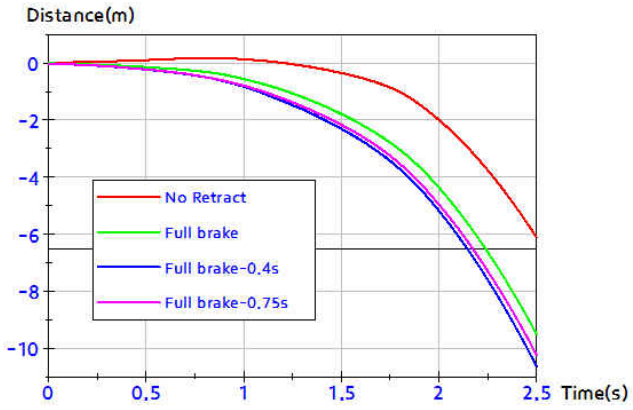


***(b) Relative displacement of dummy's head from the AEB activation time.***

***Figure7. Dummy's behavior according to PSB activation time.***

***Figure8*** shows the belt tensions in different cases, such as no retraction, various PSB activation time and pre-bre-brake profile(explained in next section).All of the belt load reach their peak almost same time which is caused by full brake, not by the first trigger time. It would be effective to reduce the forward motion of dummy befor the belt load rise up to it's peak.

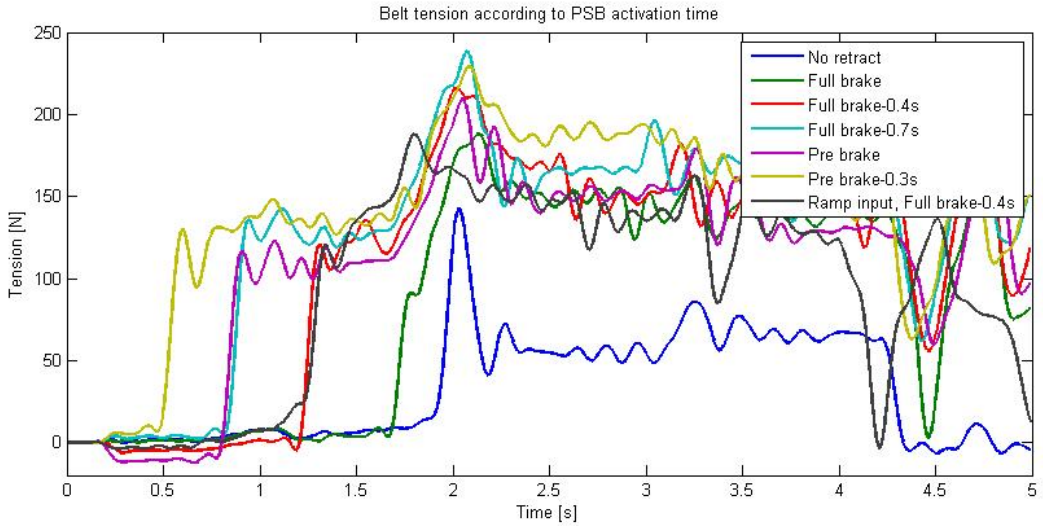


***Figure8. Seatbelt tension with various PSB activation time.***

It can be concluded that PSB can efficiently help preventing PAB from giving direct impact to occupant's head or reducing head & neck injury if it is triggered at least 0.4s before full brake is engaged. This can be applied to all range of vehicle velocity because there're similar dummy's behavioral characteristics according to different vehicle speed with the same amount of full brake.

**The AEB Braking Profile for Reducing collision velocity**

**AEB Control Logic** LPB(Last Point to Brake) and LPS(Last Point to Steer) are the time or relative distance to avoid collision about forward target vehicle by emergency braking and by steering control, respectively. Those physical quantities are illustrated in ***Figure9 (a)*** and the equations are Eqs. (2~4). Eq. (4) stands for the TTC at each collision avoidable distance and AEB system transmits the command signals to ESC following the control logic in ***Figure9 (b).***

As shown in ***Figure10,*** the collision avoidable distance by braking is shorter than the one by steering control in low velocity region and vice versa in high velocity region. The AEB control login in the test uses only full breke in low speed. In high speed, pre-brake is applied from LPB to LPS and, full brake after passing through LPS.This is for reducing frequent AEB system activation in the field by making the maximum braking at the final moment of collision avoidance by lateral control.

$$d_{brake} = -\frac{v_{rel}^2}{2a_x} \quad (2).$$

$$d_{steer} = -v_{rel}\sqrt{\frac{2s_y}{a_y}} \tag{3}$$

$$d_{brake} = -\frac{v_{rel}^2}{2a_x} \Rightarrow t_{LPB} = \frac{d_{brake}}{-v_{rel}} = -\frac{v_{rel}}{2\mu g}$$
$$d_{steer} = -v_{rel}\sqrt{\frac{2s_y}{a_y}} \Rightarrow t_{LPS} = \frac{d_{steer}}{-v_{rel}} = \sqrt{\frac{2s_y}{\mu g}} \tag{4}$$

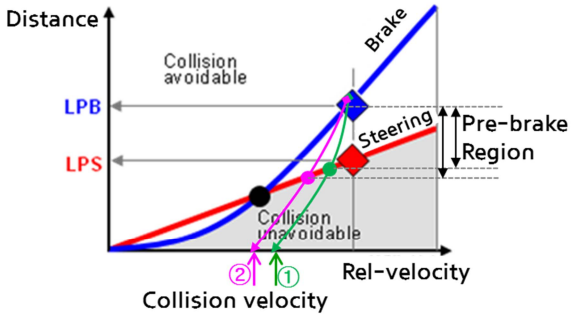


| Velocity region | Collision level | Brake profile | |
|---|---|---|---|
| Low | Avoidance | TTC < $t_{LPB}$ | Full brake |
| High | Mitigation | $t_{LPS}$< TTC < $t_{LPB}$ | Pre brake |
| | | TTC < $t_{LPB}$ | Full brake |

*(a)LPB, LPS graph* *(b) Control logic*

***Figure9. Braking time and AEB Control logic***

**Collision Velocity Reduction According to Pre-braking Profile** Generally, pre-brake with low deceleration is used in AEB system in order to raise the initial cylinder pressure of ESC and to make it easy for driver to avoid front obstacles by string control as the collision risk increases after ADAS sensors detect them. After that, full brake is engaged at the TTC condition when collision is unavoidable. With this scenario, the collision speed is mitigated in high velocity region. In this study, two kind of pre-brake profiles are applied without the change of pre and full braking time. One is step input with0.2g and the other is ramp input from 0g to 1g which is expressed by Eq.(5):

$$A_{brake} = \frac{1}{t_{LPS} - t_{LPB}}(t - t_{LPB}) \tag{5}$$

It seems to be obvious that the crash speed would decrease and the braking distance become shorter in the case of ramp input as shown in ***Figure11.***

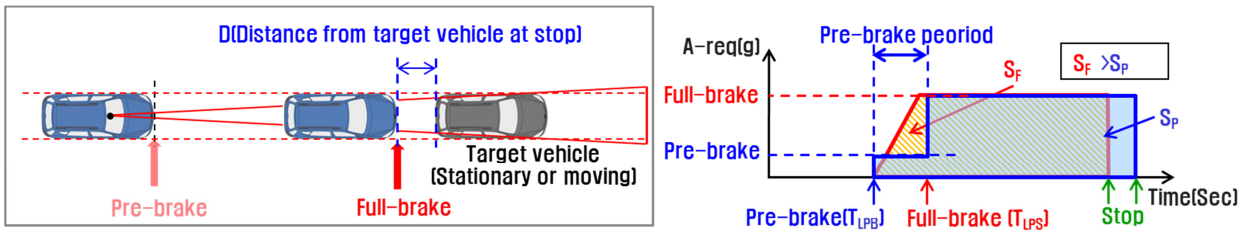


***Figure11. Braking point and the concept of braking profile.***

In this tests, the DGPS device is used for mesuring distance to crash point becase of the short detecting rage of Lidar sensor. With the same pre-braking time, the crash speed of ramp input decreases by 15kph in comparison to the step input case as shown in ***Table1***.When the crash occurs in those two conditions, whether PAB is deployed or not can be changed according to collision velocity. And the faster the the initial velocity is, the more the reduction of velocity beome because pre-brake time lasts longer. If this ramp input braking profile is applied to AEB logic, the collision avoidable vehicle speed can be raised maintaing the marketability same as step input. And also the probability of quality problem like frequent or unnecessary emergency braking activation can be reduced because the initial braking time can be set to later time if the collision speed is tuned same each other. This priciple is explained well in ***Figure9(a)*** with the line number ① and ②. In the ② case with ramp input, the reduction of velocuty increase between LPB and LPS, and finally drash speed goes down.

***Table1.***

***Collision velocity according to pre-braking profile.***

| Braking profile | Initial velocity | Collision velocity | Reduction of crash velocity |
|---|---|---|---|
| Pre-brake 0.2g | 85kph | 50kph | 35kph |
| Ramp input | 85kph | 35kph | 50kph |

Pre-fill and pre-brake input play a roll to make the cylinder pressure of ESC raise faster to full brake level. There's about 450ms delay of full deceleration after the moment when 1g step input command is transferred to ESC, whereas the vehicle deceleration follows the ramp input and full brake signals well in ***Figure12***. This mechnism mainly contributes to decreasing more collision velocity with ramp input. If ADAS sensors and communication performance in vehicle is improved in the future, the collision velocity would be minimized by using feedbak control.

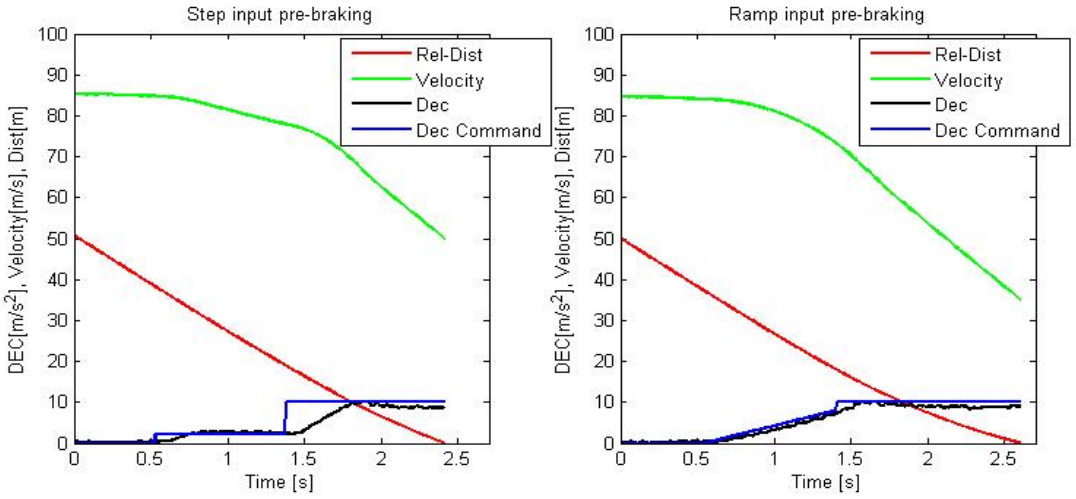


***(a) Pre brake : 0.2g Step input*** ***(b) Pre brake : Ramp input***

***Figure12. Vehicle behavior according to pre-braking profile.***

**Head Acceleration According to Pre-braking Profile** The relative acceleration at crash moment affects the occupant's head & neck injuries. In the NCAP frontal crash test, dummy has almost zero acceleration when the test vehicle impacts the barrier, but it gets relative acceleration at the moment with the AEB activation, which varies depending on braking performance and control level. When ramp type of pre-braking profile is used, the rise rate of acceleration and it's peak value are small compared with step input as verified in ***Figure13***. The passenger can also has soft feeling with small jerk. Ramp input signal can be expected to decrease occupant's head & neck injuries.

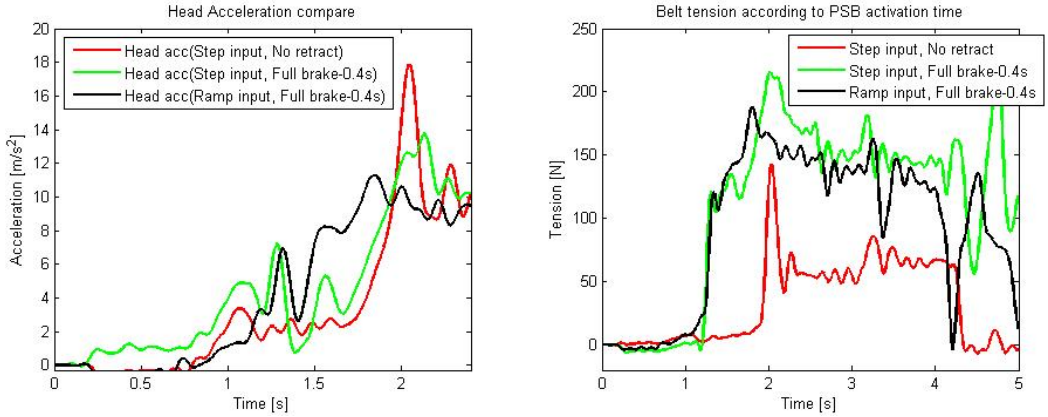


***Figure13. Head acceleration and belt tension according t pre-braking profile.***

## CONCLUSIONS

In the viewpoint of active and passive safety integration, this study aims to find appropriate PSB activation time so that the bad effect by AEB system can be removed and to reduce the final crash speed after AEB is activated by enhance the pre-braking profile. As a result, it was found out that dummy's forward motion is sufficiently decreased when PSB is activated at least 0.4s before full brake time, which can be changed by PSB and ESC performances. As well as this, the pre-brake profile of ramp input is more efficient in reducing crash speed and head's acceleration rather than constant one.

H-3 dummies used in this research have much difference with human body in behavioral aspects. The same tests targeting human or THOR dummy should be carried out to get more accurate data. And the research about various braking profile and feedback control logic to improve AEB performance considering occupants' injuries and marketability is needed in the future.

## REFERENCES

**[1]** Matthew Avery ,The Development of Euro NCAP AEB Test procedures-Car and Pedestrian. June, 2014

[2] Kloeden, et. al. "Travelling Speed and the Risk of Crash Involvement" NHMRC Road Accident Research Unit The University of Adelaide, November 1997

[3] Dae-seok, Jeon, et. Al. “The development of emergency driving assistant system by steering and braking integrated control”, KSAE, 2013

[4] R. Isermann, M. Schorn, U. Stahlin, “Anticollision system PRORETA with automatic braking and steering”, VSD, Vol.46, pp. 683-694, 2008.

[5] Cyril Chauvel, et. al. “Automatic emergency braking for pedestrians effective target population and expected safety benefits”, 23th International Technical Conference on the Enhanced Safety of Vehicles (ESV), paper 13-0008, United States Department of Transportation, National Highway Traffic Safety Administration, 2013

[6] Rodolfo Schoeneburg, Karl-Heinz Baumann, Michael Fehring, “The Efficiency of PRE-CRASH Systems in Pre-braked Frontal Collision Situations. ” ESV paper No. 11-0207, 2011

[7] Mark Mages, Martin Seyffert, Uwe Class, “Analysis of the pre-crash benefit of reversible belt pre-pretensoning in different accident senarios.” ESV Paper No. 11-0442,2011

# DYNAMIC VALIDATION OF ROLLOVER BUCK ROOF STRUCTURE

**Jacek Toczyski**
**Qi Zhang**
**Patrick Foltz**
**Brian Overby**
**Jim Bolton**
**Joey White**
**John Moors**
**Jack Cochran**
**Carolyn Roberts**
**Jeff Crandall**
**Jason Kerrigan**
Center for Applied Biomechanics, University of Virginia
United States

Paper Number 15-0336

## ABSTRACT

Effective passive countermeasure design for rollover injury prevention requires thorough understanding of the occupant response in rollover impact. Thus, the dummy biofidelity in rollover crashes is important. To evaluate the dummy biofidelity a test buck was developed for a variety of surrogate biofidelity analyses. The buck was designed to mimic the geometry and inertial properties of a modern strong-roof vehicle. It consisted of two major parts: a deformable, replaceable greenhouse and a rigid base. The goal of this study was to show that the greenhouse structure proposed in this paper, when loaded in a static roof crush test (similar to FMVSS 216) reaches the strength-to-weight ratio level of real vehicles and when loaded in a dynamic rollover test, the roof deformation matches deformation magnitude and shapes observed in the vehicles from the current United States (US) fleet. To achieve this goal a multi-step design approach was used, including a quasi-static roof crush test and a rollover test on fabricated prototypes of the buck roof structure. Based on the gathered data, modifications were introduced to the roof design to improve the greenhouse mechanical response, both dynamically and quasi-statically. Once the design was fixed, one additional static and twelve dynamic rollover tests were performed and roof structure deformation was compared to the measurements made on two late-model US-market vehicles (an SUV and a mini-van), tested in similar conditions. The roof exhibited a desired response under the quasi-static loading with the peak value (61.1 kN) within first 127 mm of platen motion, which resulted in the strength-to-weight ratio of 3.76. During the twelve rollover tests the magnitude and shape of the buck roof deformation were consistent with those measured on the two test vehicles. In the twelve tests the maximum resultant displacements of the trailing side A- and B-pillar (after excluding three outlier tests due to welding defects) were as follows: 189-223 mm and 183-222 mm, respectively. The component displacements of the B-pillar were: between 165-198 mm in SAE Y and between 84-106 mm in SAE Z. The results of this study showed that the designed roof structure can match the deformation magnitude and shapes, including the prevalence of greater lateral than vertical displacement, seen in the current US fleet vehicles. The roof developed in this study has a quasi-static response similar to that of real vehicles loaded in a FMVSS 216-like test. It mimics the stiffness of real vehicle roofs under static and dynamic roof crush loading, and thus it can be used with the test buck to simulate real vehicle rollover crashes to perform parametric analyses and evaluate dummy biofidelity.

## INTRODUCTION

Rollover crashes present a challenge to improve occupant safety. Effective passive countermeasure design for rollover injury prevention requires thorough understanding of the occupant response in rollover impact. NHTSA showed in one of its research notes that higher roof strength results in lower roof deformation during a rollover crash (NHTSA 2010). The lower roof deformation was previously correlated to reduction in injury risk to the head, neck, or face (Austin et al. 2005).

Currently in the United States (US), the only Federal Motor Vehicle Safety Standard (FMVSS) used for evaluating vehicle crashworthiness in rollover is FMVSS 216 that assesses the stiffness of the vehicle greenhouse structure in a quasi-static roof crush test. While numerous dynamic test methods (e.g. ramp test, curb-trip rollover test, dolly test, etc.) were developed and used to evaluate rollover crash dynamics, vehicle crashworthiness, and occupant injury risk, these methods were criticized for their lack of repeatability. To investigate the crash test dummy biofidelity in rollover-like scenarios, the University of Virginia Center for Applied Biomechanics is planning to compare crash dummy response to post-mortem human surrogate (PMHS) response in a series of experimental rollover investigations. To perform these tests, a vehicle-like test buck was developed. The buck was designed to mimic the geometric and inertial properties of twelve late-model full-size crossover vehicles or mid-size sport utility vehicles (SUV) from the US fleet, including BMW X5, Ford Explorer, Volkswagen Touareg and Volvo XC90. The buck is to be used in the biofidelity tests for a variety of reasons. Primarily, with the use of the test buck exact tests without relying upon a particular vehicle design can be repeated, even after several years from now. Secondly, the simplified buck allows for utilizing 3-d optical motion capture systems that have been used to characterize occupant surrogate motion in simulated crash tests (cf. Lessley et al. 2010). Using such a system provides detailed 3-d kinematics data that can be used to make intricate comparisons between crash test dummies and PMHS.

To evaluate dummy biofidelity during the injury causing parts of the rollover crash, a buck roof structure that matches modern vehicle deformations seen in real-world rollover accidents would be beneficial. Hence, the goal of this study was to show that the greenhouse structure described in this paper, when loaded in a static roof crush test (similar to FMVSS 216) meets the strength-to-weight ratio (SWR) level of cars with strong roofs and when loaded in a dynamic rollover test, the roof deformation matches deformation magnitude and shapes, including the prevalence of greater lateral than vertical displacement, observed in late-model US-market vehicles.

## STEP 1 – 1$^{st}$ ROOF DESIGN FABRICATION

The current study is a continuation of the study presented by Toczyski et al. in 2013. The previous study was carried out using finite element (FE) analyses to facilitate computationally and monetarily inexpensive evaluations of iterative changes to the roof structure design. Each of the roof component sections were sized by performing a detailed computational investigation using a commercial implicit FE code. A multi-tiered design approach was used, consisting of different – in terms of complexity – FE models of the roof, to better understand the quasi-static response of the structure in a 216-like roof crush test. Variations in an initial design of the greenhouse and computational analyses yielded a model that had a loading response representative of a modern full-size crossover vehicle. Based on that work the design of the roof was fixed. It was accomplished by modeling off-the-shelf parts in a way that made the roof easily fabricated. The next step was to manufacture the roof and examine its response in real tests (both, statically and dynamically).

## STEP 2 – 1$^{ST}$ QUASI-STATIC ROOF CRUSH TEST

The fabricated greenhouse structure was tested first in a static roof crush test similar to the roof resistance test described in the FMVSS No. 216 (NHTSA 2012). The roof was attached to the parametric buck rigid base (cf. Zhang et al. 2013). The structure was then loaded at a 25 degree roll and a 5 degree pitch angle, with a rigid platen. The platen was driven into the buck for a distance of 254 mm, and the peak reaction force on the platen generated in the first 127 mm of deformation was normalized by the test buck weight to determine the strength-to-weight ratio. SWR was calculated using two different buck masses: (1) the mass including the base and the greenhouse structure, all the instrumentation, high speed camera equipment, weight ballast, etc. needed to run a rollover test, but without occupants; (2) the mass with all needed equipment and one 80 kg occupant. The mass was found to be 1657 kg and 1737 kg, respectively. After the test all components and connections which fractured within the first 127 mm of platen motion were documented.

In the roof design the connections between the pillars, roof rails and the buck base utilized plastic joints, consisting of a round bar set into the tube ends (Figure 1a). One straight round bar was used to connect the AB to the BC roof rail. The round bar coming out of the B-pillar was then welded to the bar connecting the rails creating a "T-like" shape (Figure 1a). The C-pillars and the BC and CD rails were linked in the same way. During the first quasi-static roof test the four welds between the pillars and the rails fractured. The first weld broke after 48 mm of

platen displacement. After that point the load-bearing capabilities of the greenhouse structure were significantly reduced, which resulted in a peak force of 23.3 kN within first 127 mm of platen motion (Figure 1b; blue dotted curve) and SWR equaled to 1.43 (without including the occupant's weight in the overall buck weight) and 1.37 after including an 80 kg occupant. Based on the test data it was determined that the friction coefficient between the roof structure and the platen was between 0.2 and 0.3.

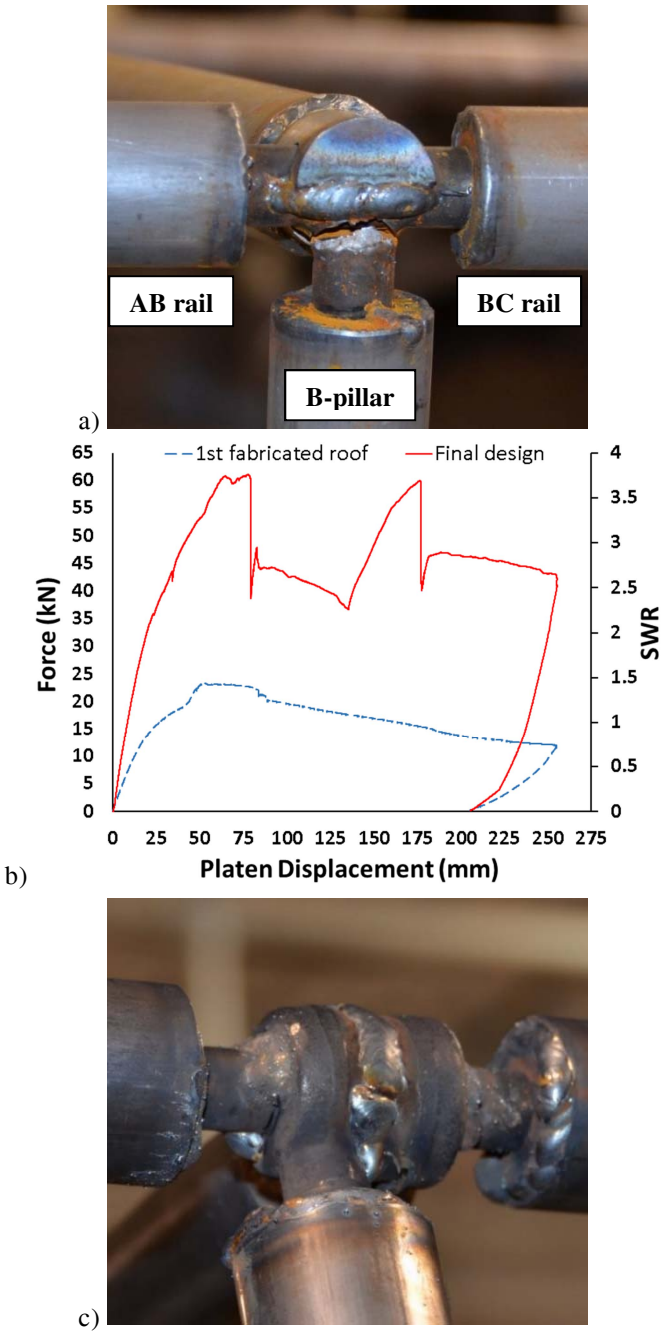


***Figure1. a) Fracture of one of the "T-like" top joints; b) 216 test-like results for the 1st and the final design of the roof structure; c) one of the modified top joints (eye bot used).***

In the next design the connections between the pillars and the roof rails were modified. Instead of a bar coming out of the pillar an eye bolt was used (Figure 1c). A straight bar coming out of the roof rail went through an

eye bolt and was welded to it on both sides around the bar circumference. This created much stronger connections between the components and let the load be distributed more equally in the greenhouse structure. To stiffen up the structure and to simplify the manufacturing process of further roofs it was also decided to uniform the diameter of plastic joints at the interface between the roof and the rigid base (all of them were set to 19 mm) as well as all of the top joints (set to 16 mm). Additionally, a cross bracing (steel bar of diameter of 5.6 mm, working in tension, Figure 3e) between A-, C- and D-pillars was added to increase the structure energy dissipation compatibility under quasi-static loading.

## STEP 3 – 1$^{ST}$ ROLLOVER TEST

After the quasi-static test the roof design was modified, the new greenhouse was fabricated, attached to the buck base and then subjected to a passenger-side leading rollover test, with the use of the Dynamic Rollover Test System (DRoTS) fixture (Kerrigan et al. 2011).

To minimize any potential risk of equipment damage during the test, minimal instrumentation was installed on the buck. To ensure the repeatability of the buck response from test to test, ballast was added onto the buck base to account for additional test instrumentation (data acquisition system, cameras, lights, imaging system components, etc.) that might be used in future tests. Two water dummies were also positioned in the driver and passenger seat, respectively. In addition, the buck was instrumented with nine string potentiometers (model 62-60, Firstmark Controls, Creedmoor, NC) to capture and resolve time histories of single point greenhouse deformations into local coordinate system components (cf. Lockerby et al. 2013). Local axes were defined using the Society of Automotive Engineers standard for vehicles (SAE 1995). The cables from three of the potentiometers were joined together and attached to hooks that were welded on the pillars. The time histories were captured for the top of the driver A- and B-pillars, as well as for the passenger B-pillar.

### Touchdown conditions for the first rollover buck roof test

To evaluate dummy biofidelity during the rollover crash, a buck roof structure matching modern vehicle deformations (in terms of the magnitude and the shape) seen in real-world rollover accidents was needed. To access the buck roof response in such an event deformation data gathered on real vehicles loaded dynamically in rollover-like scenarios was necessary as a reference point. For the purpose of this study, using the DRoTS fixture, two late-model US-market vehicles (a mid-size SUV and a mini-van) were tested in controlled rollover impact with slightly different test parameters (see Table 1). The vehicles were instrumented either with string potentiometers or an optical measurement system to capture and resolve time histories of single point greenhouse deformations into local vehicle coordinate system components. The touchdown conditions for both of the vehicles were obtained from crash reconstructions of actual crashes:

1) for the SUV they were the result of a reconstruction of a CIREN rollover case (Case 781125527) with an ADAMS multi-body model of the same mid-size SUV (cf. Kim et al. 2014),
2) for the mini-van they were the result of a crash reconstruction of National Automotive Sampling System Crashworthiness Data System (NASS-CDS) case number 2008-03-108.

Both vehicle tests simulated a driver-side leading rollover crash. However, to be consistent with the previous rollover buck kinematic tests (Zhang et al. 2014, Lessley et al. 2014), the rollover buck roof test was intended to simulate a passenger-side leading roll. Because the SUV happened to be one of the late-model full-size crossover or mid-size sport utility vehicles that were used for designing the rollover parametric buck base, for the first buck roof rollover test the SUV touchdown conditions were selected as the test parameters. Therefore, the roll angle and roll rate direction were changed accordingly to be 248 deg/s at a leading-side touchdown at 155 degree roll angle. The vertical velocity 1.1 m/s remained the same as in the vehicle test. In addition, the vehicle touchdown pitch angle was changed to -1.5 degree (pitched forward) to focus more on the A-B pillar responses of the buck roof.

**Table1.**
**Summary of the touchdown conditions for vehicle tests and the rollover buck test goals.**

| Vehicle | Mid-size SUV | Mini-Van | 1st Buck Roof Test | Other Buck Roof Tests (Goals) |
|---|---|---|---|---|
| Pitch Angle (deg)* | 1.4 | -7.7 | -1.5 | -1.5 |
| Roll Angle (deg)** | -155.3 | -143.2 | 155 | 145 |
| Roll Rate (deg/s)** | -248.2 | -245 | 248 | 248 |
| Vertical Velocity (m/s) | 1.1 | 1.67 | 1.1 | 1.1 |

* Negative means pitched forward
** Negative means driver-side leading roll

**Results from the first rollover buck roof test**

The roof deformation data measured by the string potentiometers were processed and presented in the buck local coordinate system (cf. Lockerby et al. 2013). The driver A-pillar recorded peak deformation of 291 mm in Y direction, 237 mm in Z direction and 376 mm resultant deformation. The driver B-pillar recorded peak deformation of 277 mm in Y direction, 184 mm in Z direction and 329 mm resultant deformation. Based on the tested vehicles the maximum deformation goals for the trailing side B-pillar for Y and Z directions were set to be: 166 mm and 94 mm, respectively (Figure 4). In the first buck rollover test the recorded trailing (driver) B-pillar peak deformation in Y direction was approx. 67% higher than the displacement goal and approx. 96% higher than the goal in Z direction.

During the test several components of the structure were broken. The top end (eye bolt) of the passenger B-pillar as well as the driver C-pillar fractured (sheared) at the intersection with the pillar tube (Figure 2a). On both sides of the buck the top of the stands in the B-pillar area were also fractured. The tubes broke close to the welds. In case of the bars, the welds were broken (Figure 2b). To prevent these fractures from happening again several changes were introduced to the structure before fixing the final design:

- material used for the rod ends (eye bolts) was changed from low carbon steel (more brittle) to stainless steel (more ductile),
- without affecting the overall geometry of the roof, the pillar tubes were shortened from the top (for B-, C- and D-pillars) to give the joints more room for bending,
- the top shelves for the B-pillar bar stands were drilled and the bars were put through the shelves to unload the welds and give the stands more support in bending,
- the diameter of the bottom joints of the B- and C-pillars was increased from 19 mm to 22 mm to stiffen up the overall greenhouse response in bending.

a)

b)

***Figure2. Joint fracture: a) passenger B-pillar, b) top connections of the B-pillar stands.***

After the test, it was determined that the leading-side roof either missed the roadbed or just barely touched it resulting in no sensor response from the roadbed load cells. This problem was partially caused by the fact that the target touchdown angle (155 degrees) was difficult to achieve. Even a small variation in the relative timing between the vehicle roll angle and vertical travel distance could result in a large variation in the touchdown conditions, or even totally missed the leading-side roof touchdown, making these touchdown conditions difficult to be repeatable from test to test. Hence, it was decided to change – in future tests – the touchdown roll angle to 145 degrees to ensure a more repeatable response of both, the buck and the occupants. To be consistent with the vehicle tests, the new touchdown roll angle was set based on the mini-van test (see Table 1).

## STEP 5 – FINAL DESIGN OF THE GREENHOUSE STRUCTURE

### Quasi-static roof crush test

Once the roof design was fixed (Figure 3), its structure was again subjected to a 216-like roof crush resistance test. The force-displacement response of the new design can be divided into several phases (Figure 1b, red solid curve). During the first phase (0-65 mm) the platen pushed the A-pillar, the head rail and the AB-roof rail inwards, engaging most of the plastic joints as well as putting the cross bracing between the bottom of the driver-side A-pillar and the top of the passenger-side A-pillar in uniaxial tension. During that phase the force increased monotonically and then – after 65 mm of platen displacement – plateaued around 60 kN. The force reached its maximum value

(61.1 kN) at 78 mm of platen motion. Just after 78 mm the A-pillar cross bracing fractured causing a drop in the force by approx. 30%. In the following phase the force started decreasing nonlinearly until 135 mm of deformation when the C-pillar was engaged. By engaging the pillar the cross bracing between the C-pillars was also engaged, what resulted in a large increase in global roof stiffness. The second peak of the force (60 kN at 177 mm) was observed just before the fracture of the C-pillar bracing. After the bracing breakage the force dropped to approx. 46 kN and started decreasing slightly till the end of the test, when it reached 40 kN. For the maximum force of 61.1 kN recorded on the platen within first 127 mm of its movement the calculated SWR equaled to 3.76 (without including the occupant's weight in the overall buck weight) and 3.59 after including an 80 kg occupant. By implementation of all the changes suggested after the first quasi-static and rollover tests, the SWR increased by approx. 160%.

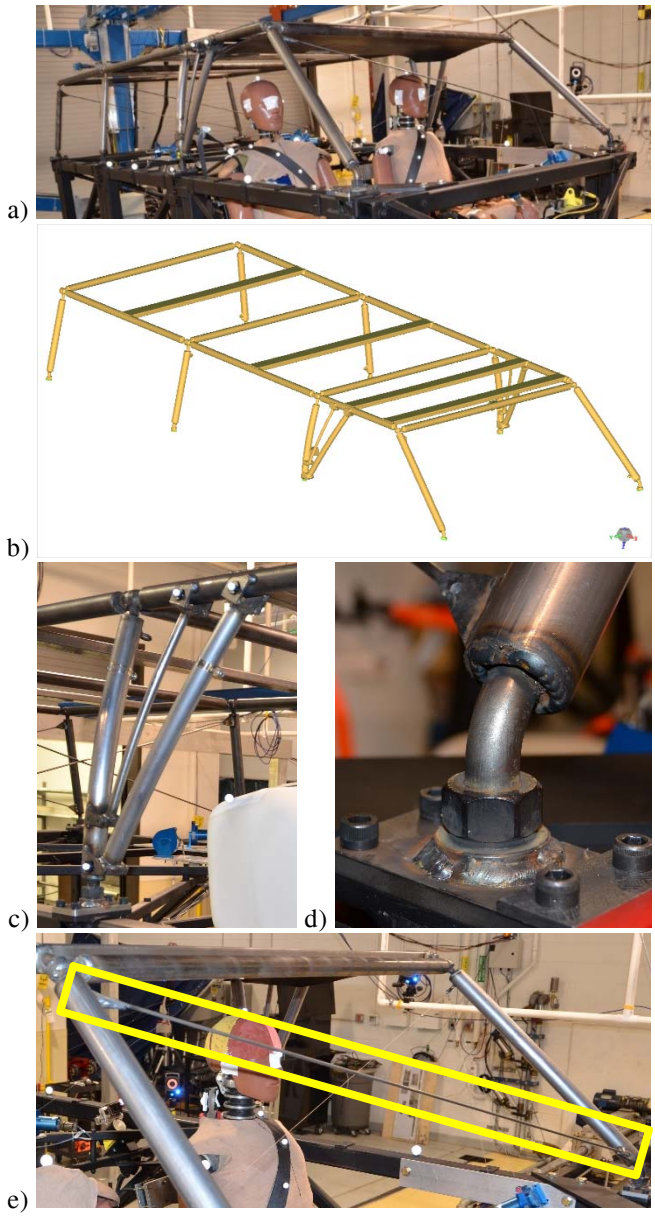


***Figure3. The final design of the roof structure: a) isometric view, b) pre-test scan of roof structure (cross bracing between A-, C- and D-pillars not shown), c) steel stands in B-pillar area, d) plastic joint, e) cross bracing between A-pillars.***

**Twelve rollover tests**

With the fixed roof design twelve passenger-side leading rollovers were performed. The actual touchdown parameters achieved in the tests did not varied much and were very close to the goal parameters presented in Table 1, in the "Other Buck Roof Tests" column. The average touchdown angle was 143.4 deg (standard deviation: 1.34 deg; median: 143.4 deg), the average roll rate was 244.6 deg/s (standard deviation: 3.86 deg/s; median: 244.7 deg/s) and the average buck vertical velocity was 1.14 m/s (standard deviation: 0.09 m/s; median: 1.13 m/s).

During the tests the buck was equipped with nine string potentiometers attached to the same points as in the first rollover test. The roof deformation data measured by the string potentiometers were processed and presented (for the driver-side B-pillar; Figure 4) in the buck local coordinate system. After the leading-side touchdown the whole roof structure moved slightly in the negative Y direction and after the trailing-side impact the driver-side pillars and roof rails moved inboard (positive SAE Y) and downward (positive SAE Z). When the roof-to-roadbed interaction ended approx. 0.15 sec after the trailing-side touchdown, elastic unloading of the greenhouse structure occurred.

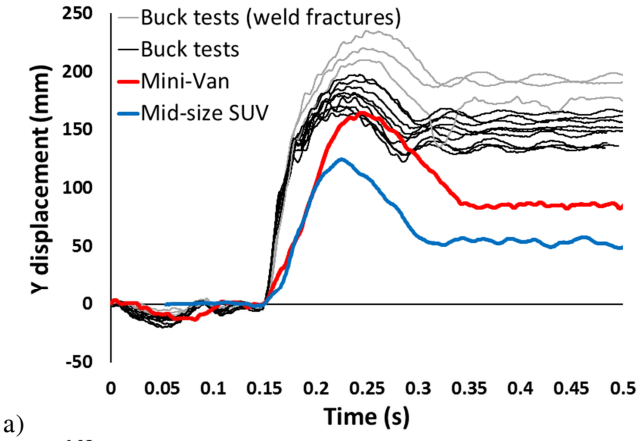


a)

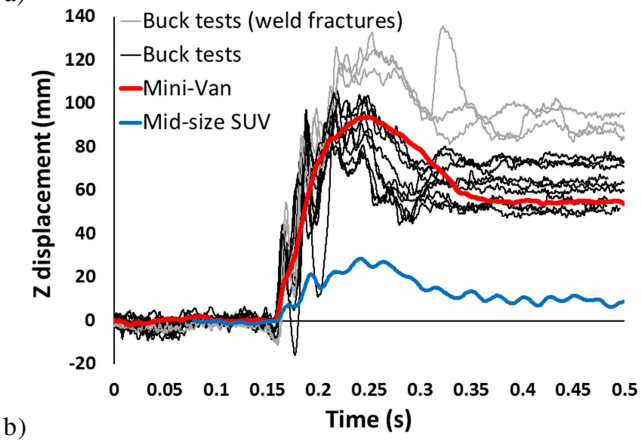


b)

c)

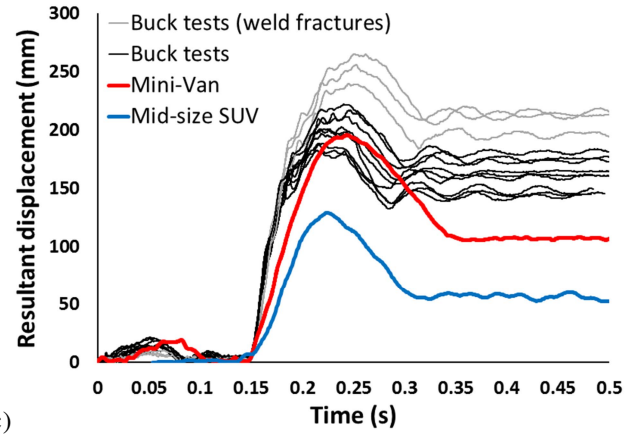


***Figure4. Driver B-pillar deformation versus the two test vehicles: a) Y displacement, b) Z displacement, c) resultant displacement.***

The driver A-pillar recorded average peak deformation of 205 mm in Y direction (standard deviation: 26 mm; median: 197 mm), 101 mm in Z direction (standard deviation: 15 mm; median: 100 mm) and 229 mm resultant deformation (standard deviation: 30 mm; median: 221 mm). The driver B-pillar recorded average peak deformation of 191 mm in Y direction (standard deviation: 22 mm; median: 185 mm), 103 mm in Z direction (standard deviation: 15 mm; median: 103 mm) and 214 mm resultant deformation (standard deviation: 27 mm; median: 207 mm). It was found that in three out of twelve tests the roof deformation was noticeable larger than in the remaining nine tests. These three tests were marked in gray in Figure 4. After analyzing the post-deformation structure it was determined that in the three tests several connections (mostly at the interface between the roof and the base but also for the stands in the B-pillar area; Figure 5) broke due to welding defects – i.e. the weld did not penetrate the material enough to ensure a proper bond. After excluding these tests from the average deformation calculations the results for the driver A-pillar were as follows: average peak deformation of 188 mm in Y direction (standard deviation: 11 mm; median: 194 mm), 92 mm in Z direction (standard deviation: 10 mm; median: 95 mm) and 209 mm resultant deformation (standard deviation: 14 mm; median: 216 mm). The driver B-pillar average peak deformation was: 180 mm in Y direction (standard deviation: 11 mm; median: 182 mm), 96 mm in Z direction (standard deviation: 9 mm; median: 95 mm) and 201 mm resultant deformation (standard deviation: 14 mm; median: 201 mm). It should be stated here that in all of the performed tests the maximum X displacement component of roof deformation (for all measurement points) varied between ±20 mm from test to test.

a)

b)

***Figure5. Weld fractures: a) bottom joint of Driver B-pillar, b) top joint of one of the B-pillar stands.***

Before and after one of the twelve rollover tests the greenhouse structure was scanned using a portable measuring arm equipped with a 3D laser scanner (ROMER Absolute Arm Scanner 7330Sl-2, Hexagon Metrology, North Kingstown, RI). After processing the scans, they were aligned together for post-test deformation comparison. It can be observed from the scans that the lateral deformation of the roof was larger than its vertical displacement (Figure 6). Additionally, it can be seen in Figure 6b, that the post deformation in the SAE X direction was much smaller (almost negligible) in comparison with the two other deformation components.

a)

b) 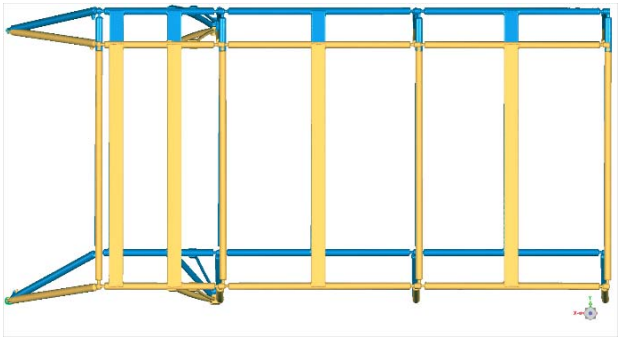

c) 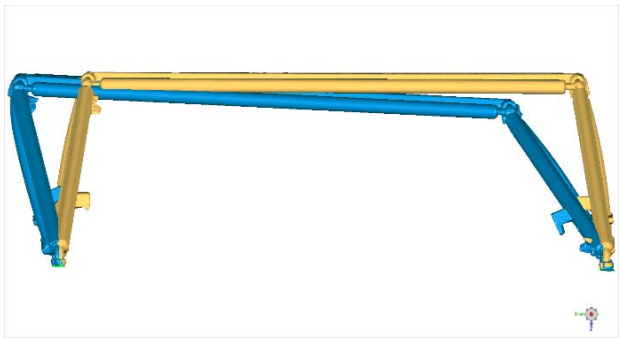

***Figure6. Roof deformation for one of the tests (yellow: undeformed; blue: deformed): a) 3D scan isometric view, b) 3D scan top view, c) 3D scan front view.***

The roof deformation time histories from the rollover buck tests (for the final roof design) were compared with the vehicle tests at the trailing side B-pillar (Figure 4). It should be noted here that the buck roof tests simulated a passenger-side leading roll crash, while the vehicle tests simulated a driver-side leading roll crash. Therefore the trailing-side B-pillar deformed in the negative Y direction (SAE vehicle local coordinate system) in the vehicle tests, while the trailing-side B-pillar in the buck roof tests deformed in the positive Y direction. The sign of the Y component of the vehicles B-pillar deformation time histories was flipped to facilitate the comparison. In general, the deformation time histories among the buck tests were either in-between or higher than for the tested vehicles. The buck roof structure had less elastic unloading than the vehicles in general. For all the displacement components the roof structure deformation was much closer to the deformation seen in the mini-van test, although in this test the vehicle vertical velocity and the vehicle mass were higher than in the UVA buck roof tests. A direct comparison between the buck roof response and the SUV response created a challenge due to the fact that at touchdown the SUV was pitched backward and the test buck forward. Based on the comparison of the buck results with the two tested vehicles it can be stated that the greenhouse response was softer than the response of the roof structure in the SUV or the mini-van, but still on the same order of magnitude. It can be also seen that the test roof structure matched deformation shapes, including the prevalence of greater lateral than vertical displacement, observed in modern strong-roof cars.

## CONCLUSIONS

The roof developed in this study has a quasi-static response similar to that of real vehicles loaded in a FMVSS 216-like test. It mimics the stiffness of real vehicle roofs also under dynamic roof crush loading. The tested roof structure can match the magnitude and shapes of deformation modes seen in the current US fleet vehicles and thus it can be used with the test buck to simulate real vehicle rollover crashes to perform parametric analyses and evaluate dummy biofidelity.

## ACKNOWLEDGMENTS

This study was partially supported by the National Highway Traffic Safety Administration (NHTSA) under Cooperative Agreement No. DTNH22-09-H-00247. Views or opinions expressed or implied are those of the authors and are not necessarily representative of the views or opinions of the NHTSA.

## REFERENCES

[1] Austin, R., Hicks, M. and Summers, S. 2005. “The Role of Post-Crash Headroom in Predicting Roof Contact Injuries to the Head, Neck, or Face during FMVSS No. 216 Rollovers.” Docket nos. NHTSA-2005-22143 and NHTSA-2005-22154, August 30. Washington, DC: National Highway Traffic Safety Administration.

[2] Kerrigan, J., Jordan, A., Parent, D., Zhang, Q., Funk, J., Dennis, N., Overby, B., Bolton, J. and Crandall, J. 2011. "Design of a dynamic rollover test system." Society of Automotive Engineers (SAE). Paper Number 2011-01-1116. Warrendale, PA
[3] Kim, T., Kerrigan, J., Bollapragada, V., Crandall, J. et al., "Rollover Initiation Simulations for Designing Rollover Initiation Test System (RITS)." SAE Technical Paper 2014-01-0530, 2014, doi: 10.4271/2014-01-0530.
[4] Lessley, D., Shaw, G., Parent, D., Arregui-Dalmases, C., Kindig, M., Riley, P., Purtsezov, S., Sochor, M., Gochenour, T., Bolton, J., Subit, D., Crandall, J.R., Takayama, S., Ono, K., Kamiji, K. and Yasuki, T. 2010. "Whole-body response to pure lateral impact." Stapp Car Crash Journal, Vol. 54, pp. 289-336
[5] Lessley, D., Riley, P., Zhang, Q., Foltz, P., Overby, B., Heltzel, S., Sochor, M., Crandall, J. and Kerrigan, J. 2014. "Occupant Kinematics in Laboratory Rollover Tests: PMHS Response." Stapp Car Crash Journal, Vol. 58, pp. 251-316
[6] Lockerby, J., Kerrigan, J., Seppi, J. and Crandall, J. 2013. "Optical Measurement of High-Rate Dynamic Vehicle Roof Deformation during Rollover," SAE Technical Paper 2013-01-0470, 2013, doi:10.4271/2013-01-0470.
[7] National Highway Traffic Safety Administration (NHTSA). 2010. "Trafic Safety Facts - Roof Strength Testing and Real-World Roof Intrusion in Rollovers." DOT HS 811 365. http://www-nrd.nhtsa.dot.gov/Pubs/811365.pdf
[8] National Highway Traffic Safety Administration (NHTSA). 2012. "Federal Motor Vehicle Safety Standards and Regulations." DOT HS 808 878. http://www.nhtsa.gov/cars/rules/import/fmvss/index.html
[9] Society of Automotive Engineers (SAE). 1995. "Instrumentation for Impact Tests. SAE J211/1 MAR95"
[10] Toczyski, J., Kerrigan, J., Mohan, P. and Crandall, J. 2013. "Design of a deformable vehicle roof structure for rollover crash testing with a test buck." Paper 13-0203, 23rd International Conference on the Enhanced Safety of Vehicles (ESV), Seoul, Korea
[11] Zhang, Q., Kerrigan, J., Lessley, D., Seppi, J., Riley, P., Foltz, P., Lockerby, J., Overby, B., Sowers, C. and Crandall, J. 2013. "Whole-body Kinematics: Response Comparison of the Hybrid III and Hybrid III Pedestrian ATD in DRoTS Rollover Tests." Paper IRC-13-40. 2013 IRCOBI Conference Proceedings, Gothenburg, Sweden
[12] Zhang, Q., Lessley, D., Riley, P., Toczyski, J., Lockerby, J., Foltz, P., Overby, B., Seppi, J., Crandall, J. and Kerrigan, J. 2014. "Occupant Kinematics in Laboratory Rollover Tests: ATD Response and Biofidelity." Stapp Car Crash Journal, Vol. 58, pp. 317-360

# CRASH PROTECTION OFFERED TO SMALL OCCUPANTS IN AN OFFSET FRONTAL CRASH

**David Paine, Michael Paine, Jason Smith,**
*ANCAP, Australia*
**Dan Leavy, Basuki Suratno,**
*TransportNSW, Australia*
**Simon Mclean**
*General Motors, Australia*
**Julie Brown**
*NEURA, Australia*
**Craig Newland**
*Australian Automobile Association, Australia*
**Jack Haley**
*NRMA, Australia*
**Michael Case,**
*RACV, Australia*

PAPER 15-0337

## ABSTRACT

**ANCAP crash tests are conducted to well-established protocols and use driver and front passenger anthropomorphic test devices (ATDs) that represent 50 percentile (%ile) adult males. Most modern vehicles do well in these crash tests. However, concerns have been raised about the protection provided to smaller occupants.**

**In 2013 ANCAP conducted a 64km/h frontal offset crash test of a Holden Commodore VF Ute (single-cab pick-up) with two Hybrid III 50%ile male ATDs (AM50). In 2014 the opportunity arose to conduct a further research crash test of a Commodore VF Ute using a small adult female driver ATD (5%ile adult female) and a 6 year old child ATD (Hybrid III 6) in a booster seat in the front passenger seating position.**

**The purpose of the research test was to determine whether the two occupants had an increased risk of injury, compared with the adult male ATDs.**

**The occupant injury measures for the smaller occupants were compared to the results of the previous vehicle crash test (with 50%ile adult male front occupants) in order to make comparisons between the level of protection offered to occupants of different sizes for this type of crash. Furthermore, the authors examined whether the restraint and airbag systems that perform well for 50%ile adult male occupants provide comparable protection for smaller occupants and whether there are any additional hazards for smaller occupants.**

**The outcome of the research was that for the case examined, with the available methods for assessing injury risk, smaller occupants appear to be offered comparative protection in a frontal offset impact for this particular vehicle model. It is apparent that the test vehicle manufacturer included consideration of smaller occupants in the design and development of this vehicle model.**

## INTRODUCTION AND BACKGROUND

In accordance with long-established protocols, ANCAP crash tests focus on average sized male occupants for the front seating positions (EuroNCAP 2011). Since 1993 Hybrid III 50$^{th}$ %ile adult male (AM50) ATDs have been used as driver and front passenger occupants for the ANCAP frontal offset crash test.

In 2014 a research test was conducted to examine the injury risk and occupant dynamics in a 64 km/h offset frontal crash, tested with a Hybrid III 5$^{th}$ %ile adult female driver (AF5) and a Hybrid III 6 year old (H6) child ATD restrained in a high back booster seat with a top-tether.

Front seat positions do not normally have an anchorage point for CRS because they are provided for rear seats, where available. This test was feasible because the Commodore Ute has an upper anchorage for the child restraint system (CRS) top-tether in this seat position and many Australian booster seats are provided with top-tethers. Where a top-tether anchorage is provided for a front passenger seat in a vehicle with one row of seats, a

child in a forward facing CRS or booster seat may occupy this position, even if a passenger frontal airbag is fitted. The Commodore Ute does not have provision for disabling the frontal passenger airbag when a CRS is installed in the front seat.

***Figure 1.*** **Research test vehicle impact with deformable barrier.**

The *possible* safety concerns with a small driver are:

a) that they are close to the deploying airbag and might be at risk of injury from the airbag
b) that because they are closer to the steering wheel there might be an increased risk of contact with the steering wheel
c) that the restraint system (seat belt, airbag and seat) is not optimised for this size occupant and so does not provide the same protection as the 50%ile male occupant (in particular the potential for an increased risk of chest injury)
d) that with the seat fully forward the knees are more likely to contact the instrument panel and/or steering column, with consequent extra risk of injury

In the case of a child in a booster seat, the *possible* concerns are:

e) interaction with the airbag might pose an injury risk
f) the lap portion of the seat belt might ride up and penetrate into the abdomen, increasing injury risk - seat belt pretensioners have been observed contributing to this effect (in rear seats - Tylko 2012)
g) the child starts to slide under the seat belt, particularly if there is excessive movement of the booster seat
h) the sash portion of the belt may not retained on the ATD shoulder up to the peak of the crash

**SELECTION OF TEST VEHCILE**

A fairly unique feature of the Australian vehicle population is the utility, or "ute" - a small pick-up with a single row of seats. Many Australian pick-ups are based on popular sedan models where the rear row of seats and luggage area of the sedan are replaced by a utility tray. Over the years the Holden Commodore Ute and Ford Falcon Ute have been popular vehicles. To meet a demand from families both Holden and Ford have provided a top tether anchorage for the front passenger seat of these models. Manufacturers instructions state that this seating position must not be used for a rearward facing CRS (in effect an infant restraint) and to slide the seat back as far as possible for forward facing CRS and booster seats.

A 2014 model year Holden Commodore Ute (VF variant) was chosen for the research test, partly because data from an ANCAP crash test with AM50 ATDs were available for comparison.

**SELECTION OF DRIVER (AF5)**

Vehicle regulations and NCAP protocols generally use AM50 ATDs as front occupants in frontal crashes tests.

Vehicle manufacturers design vehicles to provide protection to a wide size range of occupants however information about how well smaller occupants are protected is not commonly available.

In 2015 EuroNCAP introduced a 50km/h full-width frontal crash test with AF5 ATDs in the driver and kerbside rear seat. Other crash-test organisations, such as Japan NCAP, and China NCAP, also use the AF5 ATD in some seating positions. It was therefore decided to use the AF5 in the research test.

The injury limits specified in the Euro NCAP adult occupant protection protocol (EuroNCAP, July 2014) were used for assessing the research test outcomes for the AF5.

**SELECTION OF FRONT PASSENGER (H6 restrained in booster seat)**

Australian Research in the late 1970s led to the development of an Australian Standard (AS/NZS 1754) for child restraints that required dedicated child restraint systems (CRS) to have a top tether to control pitch rotation of the CRS. Since then all Australian CRS with an in-built harness have had the top tether system and (under Australian Design Rule 34/02 - Child Restraint Anchorages and Child Restraint Anchor Fittings) all light passenger vehicles that have two or more rows of seats have to be fitted with top tether anchorages for some rear seats (Paine 2003). In 2004 the standard was updated to encourage all booster seats (that utilise the adult seat belt to restrain the occupant) to have a top tether (AS/NZS 1754:2004).

For more than a decade the Commodore Ute and Falcon Ute have had top tether anchorage available for the front passenger seat. This was mainly to meet a demand from consumers to carry young children in this seating position because no rear seat was available.

Since the 1980s Australian researchers have monitored injuries to children in car crashes and have not come across any cases of injuries to correctly restrained children in this front seating position due to airbag deployment (Brown 2013). Nevertheless there remain concerns within the community due to tragic experiences in the USA with children and airbags - due mainly to children being unrestrained, out of position, and/or early aggressive designs of airbags (Child Passenger Safety Committee on Injury, Violence, and Poison Prevention, 2011).

A Hybrid III 6 year old child ATD was selected to occupy the front passenger seating position using a booster seat with a top tether. Since the ATD is restrained by the adult seat belt and not a dedicated harness this was considered to be a worse case for issues such as restraint geometry, submarining and head excursion. A 6 year old child in a booster seat was considered the most likely configuration to reveal the above problems. A smaller child in a forward facing child seat may not have reveal seat belt-related problems since forward facing restraints for smaller children use an in built harness, rather than the seat belt, to restrain the occupant. An infant in a rearward facing child seat is not recommended for the front passenger seating position, although Suratno and others (Suratno et al, 2009) concluded that there was unlikely to be additional injury risk with this configuration with modern designs of passenger airbags.

The H6 was restrained in a Hipod Boston Booster child seat. This booster performed well in the Australian Child Restraint Evaluation Program (CREP) and had a top tether.

**SET UP AND SEAT POSITIONING**

The vehicle was set up according to EuroNCAP frontal offset protocol version 5.1 (EuroNCAP, 2011) with the following changes:

- An AF5 replaced the AM50 in the driver position
- A H6 restrained in a booster seat replaced the AM50 in the front passenger position
- Driver seat and steering wheel were set to the following positions
    - The driver's seat was fully forward
    - The driver’s seat was set in the mid height setting.
    - The steering wheel was set in the most forward and mid height setting.
    - The driver’s head restraint was set in the lowest and fully forward tilt setting.
- The front passenger seat was set in the rearmost locking position
- The front passenger seat head restraint was removed as it obstructed installation of the booster seat.
- In addition to the standard ANCAP camera positions three cameras were mounted within the vehicle cabin. One roof camera was positioned to capture the left side of the driver ATD and another roof camera was positioned to capture the right side of the front passenger ATD. A third camera was mounted on the dashboard and was positioned to capture the right side of the front passenger ATD. These on-board cameras were positioned to capture views that would assist in the assessments, including lap belt performance and frontal airbag interaction. Footage was obtained from both roof mounted cameras but the dashboard mounted camera failed to record usable footage.

**OBSERVATIONS AND TEST DATA**

Injury scoring scales and limits for the EuroNCAP full-width frontal impact were used for the AF5 driver ATD. The AF5 scales are not necessarily the same as the AM50 scales because they reflect the risk of serious injury for a person of that size.

NHTSA has proposed Hybrid III 6 year old injury limits for US federal regulation FMVSS208 (Kleinberger, et al, 1998) and FMVSS 213 (NHTSA 2002). These injury limits were used for the H6 ATD because injury limits are not defined for this ATD in ANCAP and EuroNCAP protocols.

Injury data for the AF5 and H6 ATDs are shown below in Table 1 and Table 2 respectively.

**Driver Outcomes**
The calculated points score for the AF5 driver (13.42pts) was similar to the ANCAP points score for the AM50 driver (13.52pts) in the official ANCAP test.

The driver injury readings that exceeded the NCAP lower injury limits were the chest compression and tibia index. The AF5 chest compression of 20.7mm resulted in a score of 3.55 points compared to the official test (AM50) of 26.4mm for a score of 3.37 points indicating an 'acceptable' level of risk to the chest in both tests (using the NCAP injury risk scales - which are different for AM50 and AF5).

The AF5 tibia index of 0.88 returned a points score of 1.87 compared to the official test (AF50) tibia index of 0.82 for a score of 2.15 points. However the Euro NCAP full-width frontal crash test does not make use of the tibia readings for scoring due to uncertainty in the AF5 risk values for tibia and so caution should be exercised in interpreting the lower leg injury risk in the research test.

Although twisting of the driver neck was observed upon rebound from the airbag (a peak neck moment of 28.45Nm at 196ms) the twisting of the AF5 neck in this research test was not sufficient to warrant a modifier under the ANCAP protocols. No estimation of injury risk is carried out after the peak of the impact due to limited biofidelity of the H3 neck for this type of movement.

***Figure 2.*** **Twisting of the driver neck.**

The driver airbag contacted the driver ATD's face while the airbag was inflating (at approx. t= 35ms) and this may have contributed to the neck twisting. However the estimated airbag deployment speed at the time of contact was below the 90m/s limit used by Euro NCAP to determine whether the airbag deployment is potentially hazardous. It should be noted, however that although the hazardous airbag deployment modifier is used by EuroNCAP is it generally not applied by ANCAP. Airbag contact was judged to be stable and no undesirable interactions between the driver and airbag were observed.

*Table 1.* **AF5 Driver ATD injury data**

| | **Driver ATD (AF5)** | **Limits for scoring purposes*** | **Comment on injury outcomes** |
|---|---|---|---|
| Head G (Res) (g) | 46.8 | 80 | Good |
| 3ms Head G (g) | 42.8 | 80 - 72 | Good |
| HIC (36ms) | 243 | 700 - 500 | Good |
| Neck Shear (kN) | 0.30 | 1.95 - 1.2 | Good |
| Neck Tension (kN) | 1.15 | 2.62 - 1.7 | Good |
| Neck Extension (Nm) | 10.0 | 49 - 36 | Good |
| Chest compression (mm) | 20.7 | 42 - 18 | Acceptable |
| Chest viscous criterion (m/s) | 0.07 | 1 - 0.5 | Good |
| Femur compression (kN) (L/R) | 1.51/2.38 | 6.2 - 2.6 | Good |
| Knee slider (mm) (L/R) | 0.0/0.03 | 15 -6 # | Good |
| Tibia index, upper (L/R) | 0.56/0.47 | 1.3 - 0.4 # | Acceptable # |
| Tibia index, lower (L/R) | 0.88/0.37 | 1.3 - 0.4 # | Marginal # |
| Tibia compression (L/R) | 1.69/1.08 | 8 - 2 # | Good # |

* Zero if more than first value, maximum (4) if less than second value (based on Euro NCAP protocol for full frontal crash with AF5 driver)
# Not assessed by Euro NCAP for AF5. AM50 limit shown in this table

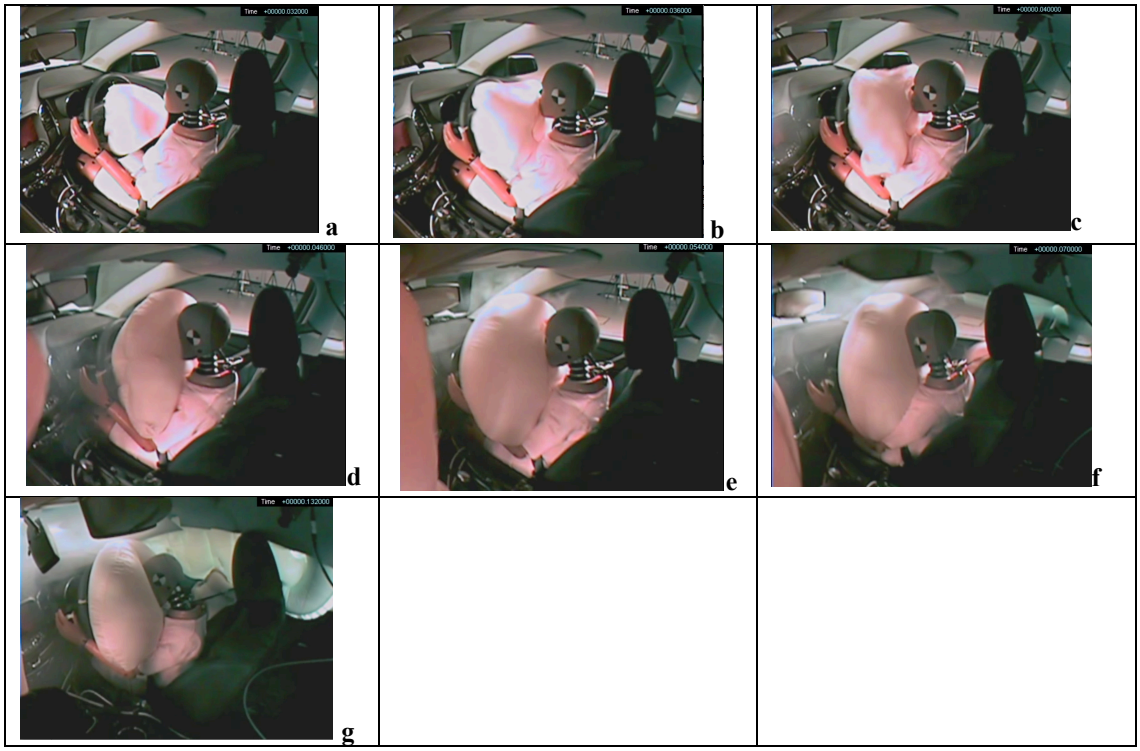


**Figure 3 a-g. Sequence of snapshots from on-board camera - driver**

**Front Passenger Outcomes**

The H6 passenger in the booster seat appeared to be well restrained with a relatively low likelihood of serious injury. The measured injury values were well below the limits for scoring purposes. The H6 injury data is provided in Table 2.

The passenger airbag fully inflated prior to contact with the H6 (contact occurs around t = 74ms when the crown of the ATD head contacts the bag. After contact with the airbag (upon rebound) the top of the H6 head slides across the surface of the airbag.

The child ATD forward head excursion was estimated by analysing the test footage and observing the maximum forward position of the head against reference markings on the vehicle. The maximum forward head excursion for the H6 ATD was estimated to be 300mm and no hard contacts were observed.

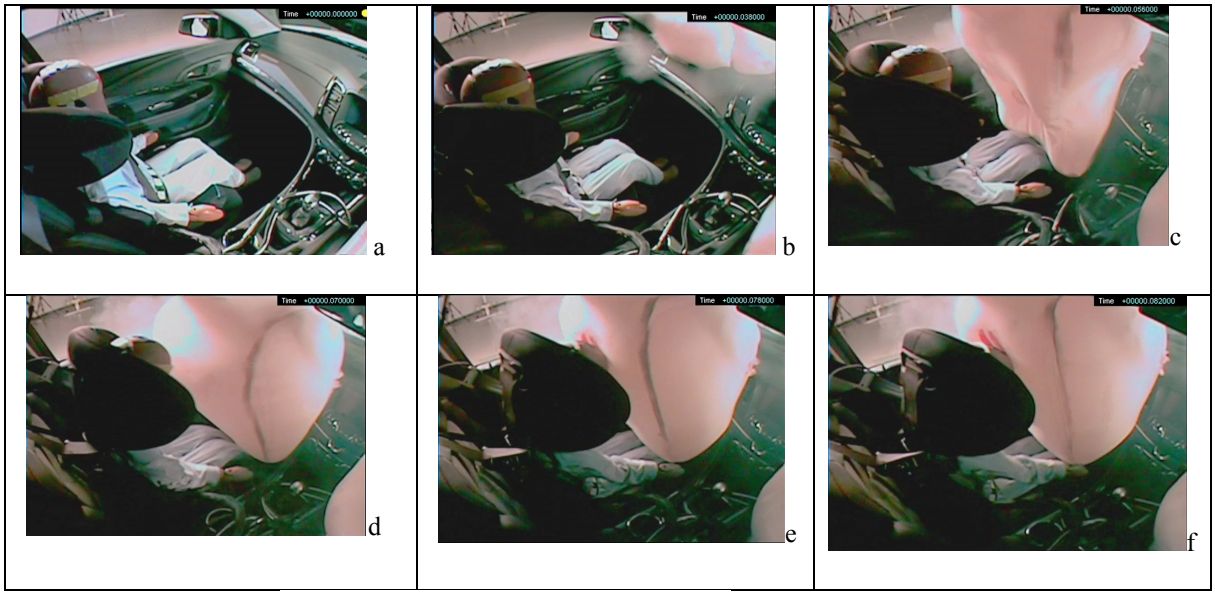


**Figure 5 a-f. Sequence of snapshots from on-board camera – H6 ATD**

***Table 2.*** **H6 Passenger ATD injury data**

| | **Passenger ATD (H6) Injury value** | **Failure limit for scoring purposes** | **Comment on injury outcomes** |
|---|---|---|---|
| $HIC_{36}$ | 350 | >1000* | Pass |
| $HIC_{15}$ | 191 | ≥ 700^ | Pass |
| Nij | 0.61 | > 1^ | Pass |
| Chest compression (mm) | 20.7 | >40^ | Pass |
| Chest acceleration (3ms) (g) | 40.8 | >60^ | Pass |
| Head excursion (mm) | 300 | >720^ | Pass |

* Proposed FMVSS 208 limit (Kleinberger, et al, 1998)
^ Proposed FMVSS 213 limit (NHTSA, 2002)

***Table 3.*** **Comparison between research test vs ANCAP test occupant injury data#**

| | **Research test Driver (AF5)** | **ANCAP test Driver (AM50)** | **Research test Passenger (H6)** | **ANCAP test Passenger (AM50)** |
|---|---|---|---|---|
| Head G (Res) (g) | 46.8 | 35.8 | 45.0 | 33.5 |
| 3ms Head G (g) | 42.8 | 35.5 | 44.4 | 31.6 |
| HIC (36ms) | 243 | 189 | 350 | 159 |
| Neck Shear (kN) | 0.30 | 0.46 | * | 0.50 |
| Neck Tension (kN) | 1.15 | 0.37 | * | 0.47 |
| Neck Extension (Nm) | 10.0 | 8.2 | * | 21.40 |
| Chest compression (mm) | 20.7 | 26.4 | 20.7 | 17.90 |
| Chest viscous criterion (m/s) | 0.07 | 0.07 | * | 0.05 |
| Femur compression (kN) (L/R) | 1.51/2.38 | 2.04/0.08 | * | 0.28/0.27 |
| Knee slider (mm) (L/R) | 0.0/0.03 | 0/46/0.00 | * | 0.38/0.30 |
| Tibia index, upper (L/R) | 0.56/0.47 | 0.58/0.39 | * | 0.28/0.16 |
| Tibia index, lower (L/R) | 0.88/0.37 | 0.82/0.31 | * | 0.39/0.18 |
| Tibia compression (L/R) | 1.69/1.08 | 3.89/1.82 | * | 1.33/2.12 |

# Note: Different injury scales are applied to each ATD. Direct comparison of injury data between ATDs is not possible.
* Not recorded for this ATD

**Restraint System Performance**

In addition to injury measurements, the ANCAP/EuroNCAP scoring system provides for "modifiers" that reduce the score if there is a further risk of injury that is not captured by the ATD injury measurements. These modifiers include steering column movement, structural integrity of the cabin, pedal movement, unstable head contact with the airbag, airbag bottoming out (resulting in head or chest contact with the steering column) and facial injury risk due to the manner in which the airbag deploys. The latter assessment is not currently applied by ANCAP.

In addition to these modifier assessments a preliminary assessment of the dynamic performance of the seat belts in accordance with observations by Suzanne Tylko from Transport Canada (Tylko & Bussières 2012) was carried out:

a) the sash portion should be retained on the shoulder up to the peak of the crash. It should not fall off the shoulder or load the neck

b) the lap portion should load the pelvis and not ride up and into the abdomen

c) there should be no tendency for submarining, where the ATD tends to slide down and forward

From analysis of the video footage there was no evidence of the lap portion of the seat belt riding up and loading the abdomen of the child ATD, nor was there evidence of the child ATD submarining. The sash portion of the seat belt appeared to be retained on the child ATD shoulder until after the peak of the crash (evidence of retention until 150ms) and there was no evidence that the seat belt loaded the neck of the ATD.

Pretensioners deployed for both occupant positions and no evidence of poor belt geometry caused by pretensioner deployment was observed.

## LIMITATIONS OF THE RESEARCH TEST

The findings are based on one crash test with two occupants. However, the research draws on experience with a wide range of vehicles and compares directly with a crash test of the same vehicle model.

Due to the different ATDs used, direct comparison between occupant injury readings is not possible but the scaled Euro NCAP scores do relate to the risk of serious injury for both types of adult ATDs.

Although tibia values are not used for the EuroNCAP full-width frontal test the values have been recorded here and compared to AM50 limits. Caution should be exercised in interpreting the lower leg injury risk in the research test. Direct comparison to AM50 values is not possible but the values provide an indication of injury risk for this body region.

The H6 ATD is only instrumented for head acceleration (3 axis), neck shear force and bending moment (3 axis) chest acceleration (3 axis) and displacement (x axis) and pelvis acceleration (3 axis). Injury outcomes for other body regions are not measured.

Child forward head excursion is approximate only, using external cameras and reference marks on the vehicle. This method is susceptible to parallax error. Strategically positioned on-board cameras would provide greater accuracy.

Additional on-board cameras could have provided an improved view of the seat belt buckles, retention of the sash portion of the seat belts on the ATD's shoulders and interaction of the lap portion of the seat belts with occupant abdomens.

## CONCLUSIONS

A successful research crash test was conducted to determine the crash protection provided to a small female driver and a 6 year old child restrained in a booster seat in the front seat of a utility style vehicle.

The 5%ile female driver ATD injury measurements indicated that the risk of serious injury was no worse than that of a 50%ile male driver in the same model vehicle and same type of crash test. The restraint system appeared to work well with no sign of submarining or lap-belt penetration into the abdomen. This test was conducted with the driver seat in its most forward position, which is considered to be a worst-case scenario for risk of airbag injury.

The child ATD injury measurements also indicated a low risk of serious injury. The restraint system appeared to work well with no sign of submarining or lap-belt penetration into the abdomen. It is likely that the head contact with the airbag would reduce head, neck and chest loads, compared with no airbag.

This test was conducted with the passenger seat in its rearmost position, as recommended by the manufacturer. Although this is considered to be the best-case scenario there is unlikely to be an elevated risk of serious injury from the airbag when the seat is located further forward.

It is concluded that, for the case examined, with the available methods for assessing injury risk, smaller occupants appear to be offered comparative protection in a frontal offset impact for this particular vehicle model. It is apparent that the vehicle manufacturer included consideration of smaller occupants in the design and development of this vehicle model.

## REFERENCES

Brown J, Kelly P, Suratno B, Paine M and Griffiths M (2009) 'The Need for Enhanced Protocols for Assessing the Dynamic Performance of Booster Seats in Frontal Impacts', Traffic Injury Prevention,10:1,58-69

Brown J, Paine D, Paine M and Bilston L (2013) 'Child Restraints and Airbags', Research report 13/02 prepared for Royal Automobile Club of Victoria (RACV) Ltd, Noble Park.

Child Passenger Safety Committee on Injury, Violence, and Poison Prevention *Pediatrics* 2011;127;e1050; originally published online March 21, 2011; DOI: 10.1542/peds.2011-0215

European New Car Assessment Program (EuroNCAP) (2011) ‘Frontal Impact Testing Protocol Version 5.1, June 2011’. EuroNCAP

European New Car Assessment Program (EuroNCAP) (2014) ‘Full Width Frontal Impact Testing Protocol, version 1.0, June 2014’. EuroNCAP

European New Car Assessment Program (EuroNCAP) (2014) ‘Assessment Protocol – Adult Occupant Protection, version 7.0.1, July 2014’. EuroNCAP

European New Car Assessment Program (EuroNCAP) (2014) ‘Assessment Protocol – Child Occupant Protection, version 6.5.1, December 2014’. EuroNCAP

Kleinberger M, Sun E, Eppinger R, Kuppa S and Saul R (1998) ‘Development of Improved Injury Criteria for the Assessment of Advanced Automotive Restraint Systems’. National Highway Traffic Safety Administration (NHTSA)

National Highway Traffic Safety Administration (NHTSA) Office of Regulatory Analysis and Evaluation (2002) ‘Proposed Amendment to FMVSS No 213 Frontal Test Procedure Chapter 3: Proposed Dummies, Injury Criteria, and Other Changes’
http://www.nhtsa.gov/cars/rules/rulings/CPSUpgrade/CPSRevise/PRE/chapter3.html Accessed 11/09/2014

Office of the Federal Register. ‘Code of Federal Regulations; Title 49 Transportation, Part 571 Federal Motor Vehicle Safety Standards, Standard No. 213; Child Restraint Systems’. Washington, DC: National Archives and Records Administration.

Office of the Federal Register. ‘Code of Federal Regulations; Title 49 Transportation, Part 571 Federal Motor Vehicle Safety Standards, Standard No 208; Occupant crash protection’. Washington, DC: National Archives and Records Administration.

Paine M, Griffiths M, Brown J, Case M and Johnstone O (2003) 'Protecting children in car crashes: the Australian experience', paper 193, Proceedings of 18th Conference on the Enhanced Safety of Vehicles, Nagoya.

Standards Australia (2004) 'Child Restraint Systems for Motor Vehicles' (AS/NZS 1754:2004) Standard Australia, Sydney.

Suratno B, Aquilina P, Wainohu D, Dal Nevo R and McIntosh A (2009) 'Are Airbags and Child Restraints Lethal Combinations?', Proceedings of 2009 Australasian Road Safety Research, Policing and Education Conference, Sydney

Tylko S and Bussières A (2012) ‘Responses of the Hybrid III 5$^{th}$ Female and 10-year-old ATD Seated in the Rear Seats of Passenger Vehicles in Frontal Crash Tests’. IRCOBI Conference 2012

# IMPACT RESPONSES OF THOR MOD KIT UNDER DIFFERENT CONDITIONS IN SLED TESTS AND VEHICLE CRASH TESTS

**Masayuki Yaguchi**
**Koshiro Ono**
Japan Automobile Research Institute
Japan

**Mitsutoshi Masuda**
**Hidetoshi Sokusai**
**Yoshinao Kusayama**
**Kazunobu Ogaki**
Japan Automobile Manufacturers Association, Inc.
Japan

Paper Number 15-0339

## ABSTRACT

In order to contribute to the development and improvement of the THOR dummies, the impact responses of the THOR Mod Kit were compared with the THOR-NT and the Hybrid III, based on the kinematic and dynamic responses to different conditions in the frontal sled and vehicle crash tests. In a 56 km/h frontal sled test where a dummy was installed on the driver seat of a white body, the responses of the THOR Mod Kit with SD3 shoulder to the differences of the seating procedures and restraint conditions were evaluated comparing with the THOR-NT and the Hybrid III. Moreover, two crash tests using a small passenger car at 55 km/h FWRB and 64 km/h ODB corresponding to JNCAP conditions were conducted, and the responses of the THOR Mod Kit were compared with that of the Hybrid III.
Difference of seating procedure affected the responses of the thoracic deflection, abdominal deflection, and iliac force, etc. Compared with the THOR-NT, the THOR Mod Kit clearly showed difference on each measurement location and the forward displacement of its shoulder on the unrestrained side was more pronounced. Regardless of the D-ring positions, the shoulder belt slippage didn't occur in the Hybrid III, whereas belt slippage occurred in the THOR Mod Kit when the D-ring was at the lowest position. When the load limiter force of the seatbelt was higher, forward displacements of the thorax became smaller in both the THOR Mod Kit and the Hybrid III and the neck flexion of the THOR Mod Kit became larger. Accompanying the difference of kinematics, the responses of the head acceleration, neck force and thoracic deflection also differed. In both the FWRB and ODB tests, the maximum rotation angle of the ankle eversion exceeded the preliminary IARV for the THOR at the rebound phase, not at the intrusion phase.
From the results above, it turned out, that the THOR Mod Kit response to the difference in seating procedure was more sensitive than that of the THOR-NT. The sensitivity of the THOR Mod Kit to the D-ring position was higher than that of the Hybrid III, and that the difference of load limiter affected the difference of kinematics and dynamic responses of the upper body in both the THOR Mod Kit and the Hybrid III.

## INTRODUCTION

While the Hybrid III is widely used in regulation and assessment in various countries, it has been expected that a more advanced dummy with higher biofidelity and higher measurement ability will be developed to advance the occupant protection performance of vehicles. From this background, the advanced frontal crash test dummy – THOR (Test device for Human Occupant Restraint), was developed. In 2001, the THOR-Alpha was released [1], and the THOR-NT, which had improved biofidelity, anthropometry, and durability from the THOR-Alpha, was introduced in 2005 [2].
Many researchers had a great interest in the THOR dummy, and further improvements on the biofidelity, repeatability, reproducibility, durability and usability of the THOR-NT were discussed under the SAE THOR Evaluation Task Force Group. Based on discussions in the THOR Task Force, the THOR Task Force Design Team investigated necessary improvements on the specifications of the THOR, drafted a development plan for a short-

term improvement of the THOR, and in 2010 the THOR Mod Kit, which added modifications to each component of the THOR-NT by utilizing the latest biomechanical data was manufactured [3]. At about the same time in Europe, the THORAX Project, the seventh framework program of the European Union, was initiated to perform studies on thoracic injury mechanisms considering the diversity of factors such as age, gender and the physique of the occupants in traffic accidents. In order to reflect the project's efforts to improve the THOR, research and development for the THOR's thorax were performed. The NHTSA had evaluated the THOR Mod Kit in collaboration with individual organizations from the U.S., Europe, and Japan, and they also developed the THOR Metric which redesigned all components based on the metric system.
Under these circumstances, JAMA/JARI has continuously conducted evaluation tests and proposed activities aimed at contributing to the development and improvement of the THOR dummies. In this study, the impact responses of the THOR Mod Kit were compared with the THOR-NT and the Hybrid III, based on the kinematic and dynamic responses to different conditions in the frontal sled and vehicle crash tests.

## THOR MOD KIT DUMMY

The THOR Mod Kit is a dummy which has added modifications to each component of the THOR-NT by utilizing the latest biomechanical data in order to further improve the biofidelity, repeatability, reproducibility, durability and usability of the THOR-NT. The SD3 shoulder, upgraded by the EU THORAX project from the original SD2 shoulder developed by Chalmers University of Technology, had been installed onto this dummy [4][5].

## SLED TEST

In order to contribute to the research and development of the THOR, sled tests of the THOR Mod Kit were conducted in different test conditions and its performance was evaluated. This included a comparison between its responses and that of the THOR-NT and the Hybrid III. In the test, a dummy was installed on the driver seat of a white body of sedan-type vehicle fixed on a sled. The sled was launched rearward so as to reach the maximum speed of 56 km/h. For the restraint system, the front air bag, seatbelt with force limiter and a double pretensioner at the retractor and outer lap belt anchorage were used.

### Comparative Conditions for Evaluation of the Dummy Dynamic Responses

To evaluate the influences on kinematic and dynamic responses of the THOR Mod Kit in different test conditions, the following three comparative conditions were considered and five sled tests were conducted. The data of the THOR Mod Kit from these tests are placed in the NHTSA biomechanics database. The NHTSA test numbers which correspond to these tests are shown in Table 1. Furthermore, the test results of the THOR Mod Kit were compared with those of the THOR-NT and the Hybrid III.

(1) Difference of the seating procedure

(2) Difference of the D-ring position

(3) Difference of the seatbelt load limiter

**Table1. Matrix of the sled tests.**

| NHTSA Biomechanics Database Test No. | Test Parameter for THOR Mod Kit | | | | Other Dummy Data | |
|---|---|---|---|---|---|---|
| | Sled G Pulse | Seat Belt | | Seating Procedure | THOR-NT | Hybrid III |
| | | D-ring Position | Load Limiter | | | |
| 11185 | 35 mph | Highest | N | FMVSS 208 | □ | □ |
| 11186 | 35 mph | Highest | N | UMTRI | □ | □ |
| 11187 | 35 mph | Highest | N | MP-30 | □ | □ |
| 11188 | 35 mph | Lowest | N | UMTRI | | □ |
| 11190 | 35 mph | Highest | N＋α(2kN) | UMTRI | | □ |

**Dummy Seating Procedure**

The dummy positioning was subject to the following three seating procedures:

(1) FMVSS 208; specified for the Hybrid III,

(2) UMTRI (the University of Michigan Transportation Research Institute); the seat position depends on the driver occupant size, geometry of steering wheel and accelerator pedal, and range of seat adjustment [6],

(3) MP-30; according to the FMVSS 208 procedure basically, only the seat slide was adjusted 30 mm forward from the mid position.

With respect to the seating posture of the THOR Mod Kit in different seating procedures, the right view photographs and the position plot of each body region in the X-axis (horizontal) and Z-axis (vertical) coordinate are shown in Figure 1. As the seat position differs among the three seating procedures, the positions of the head C.G., shoulder, H-point and knee in each procedure varied accordingly.

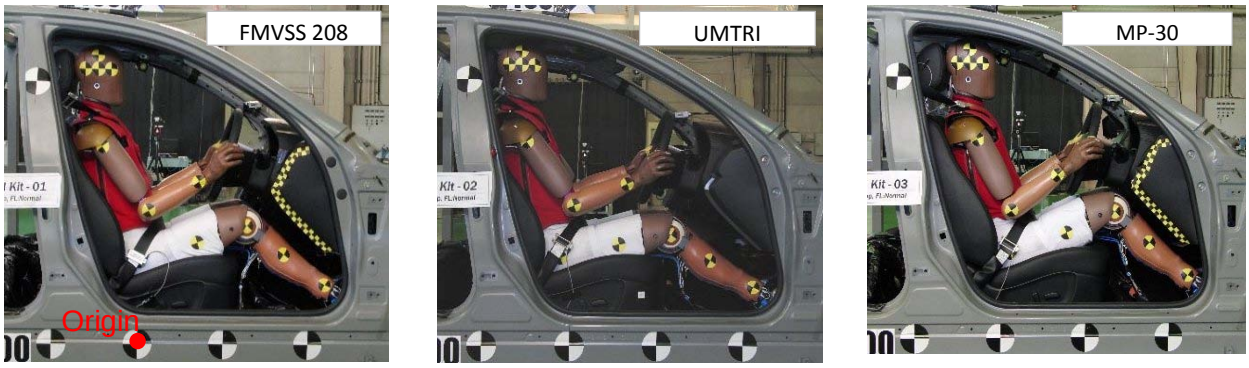


Seat Slide: Mid

Seat Lifter: Lowest

Seat Slide: 49 mm rearward*

Seat Lifter: 16 mm upward*

Seat Slide: 30mm forward*

Seat Lifter: Lowest

* Relative Positions to FMVSS 208

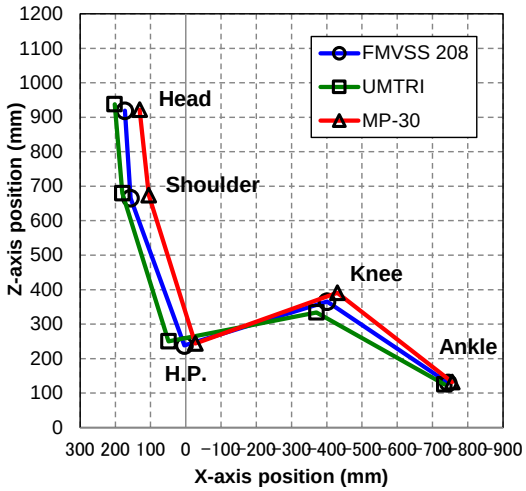


***Figure 1. Seat positions and THOR Mod Kit's seating posture in the three seating procedures.***

## VEHICLE CRASH TEST

In order to evaluate the performance of the THOR Mod Kit, two high-speed frontal crash tests corresponding to JNCAP condition were conducted using a small passenger car as the representative of Japanese cars. One was a 55 km/h Full Width Rigid Barrier (FWRB) test. Another was a 64 km/h Offset Deformable Barrier (ODB) test. The data from these crash tests are placed in the NHTSA biomechanics database. The NHTSA test numbers which correspond to these tests are shown in Table 2. Based on these test results, the response, measurement ability, and durability were compared between the THOR Mod Kit and the Hybrid III. The THOR Mod Kit and the Hybrid III were installed on the driver seat and front passenger seat of the small passenger car. Since the Hybrid III was seated in the front passenger seat merely as a weight dummy, the measurements for the Hybrid III were not taken. Take note that the Hybrid III measurements used in this paper are from JNCAP tests. For the restraint system, the test vehicle was equipped with airbag and the seat belt had pretensioner and load limiter.

**Table2. Vehicle crash tests in this study.**

| NHTSA Biomechanics Database | Test Condition |
|---|---|
| 11204 | 55 km/h FWRB |
| 11205 | 64 km/h ODB |

### Dummy Positioning

Figure 2 shows the comparison of the seating posture between the THOR Mod Kit and the Hybrid III in the FWRB and ODB tests. Since the THOR Mod Kit and the Hybrid III differ in structure and in dimension, the position coordinates of each body region differed in each dummy. Compared with the Hybrid III, the THOR Mod Kit was positioned more rearward and upward in the head, more forward and upward in the shoulders, more upward in the Hip-Point (H.P.), and more forward and upward in the knees. Although the H.P. of THOR Mod Kit could be placed at almost the same position as the H.P. of the Hybrid III in the X-axis, it was not possible to lower the H.P. of the THOR Mod Kit to the HP level of Hybrid III in the Z-axis due to the difference in length of the lower legs.

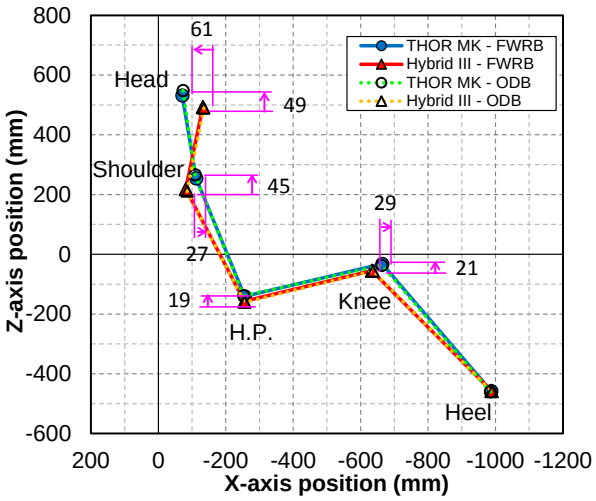


***Figure 2. Seating posture of the THOR Mod Kit and the Hybrid III.***

## RESULTS

### Comparison of Dummy Responses with Different Seating Procedures in Sled Test

Figures 3 shows the comparison of the thoracic deflections, lower abdomen deflections and iliac forces between the THOR Mod Kit and the THOR-NT. With respect to the four point thoracic deflections of the THOR-NT, there was little difference among the three seating procedures, whereas for the THOR Mod Kit, the upper right and lower left deflections in the FMVSS 208, which the seat belt had passed through a closer point to the dummy centerline, indicated smaller responses than those from the other two seating procedures. Because both the lower abdomen deflections (left and right) and the iliac forces (left and right) of the THOR Mod Kit indicated larger responses than those of the THOR-NT, it appears that the THOR Mod Kit improved with regard to sensitivity to seat belt compression compared with the THOR-NT. These differences in dummy responses are believed to be because of the following reasons: the thoracic and abdominal deflection measurement systems of the THOR Mod Kit were changed from the CRUX and the DGSP in the THOR-NT, respectively, to the IR-TRACC systems, and the iliac load cells were also redesigned.

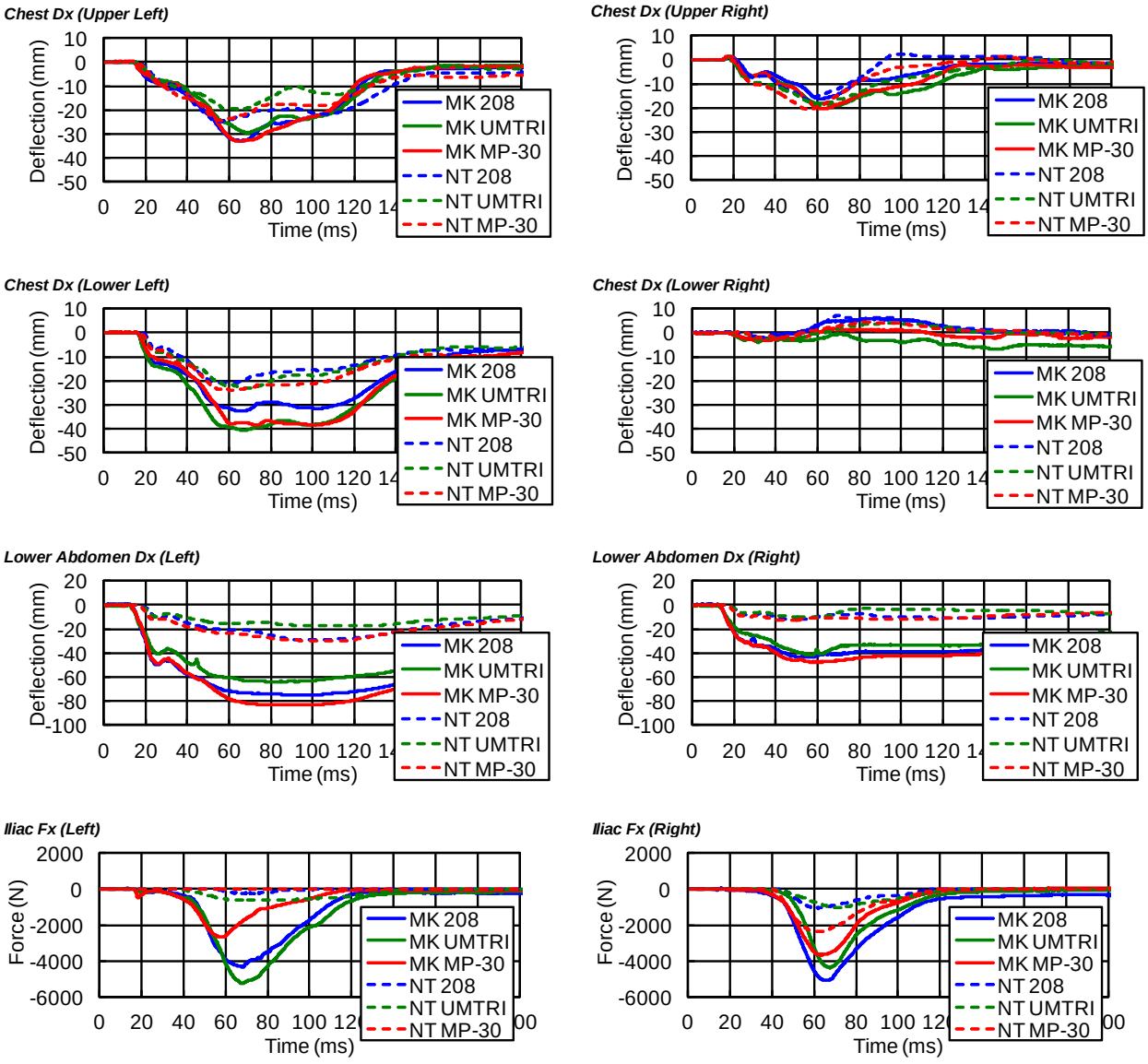


***Figure 3. Thoracic deflections, lower abdomen deflections, and iliac forces of the THOR Mod Kit and the THOR-NT.***

Figure 4 shows the difference in forward movement of the shoulder between the THOR Mod Kit and the THOR-NT in FMVSS 208. The forward movement of the right shoulder was approximately equivalent between the two dummies, whereas the left shoulder of the THOR Mod Kit indicated a larger forward movement than that of the THOR-NT. The left shoulder of the THOR Mod Kit moved forward more than its thorax after approximately 60 ms, and the forward movement at 100 ms was considerably large.

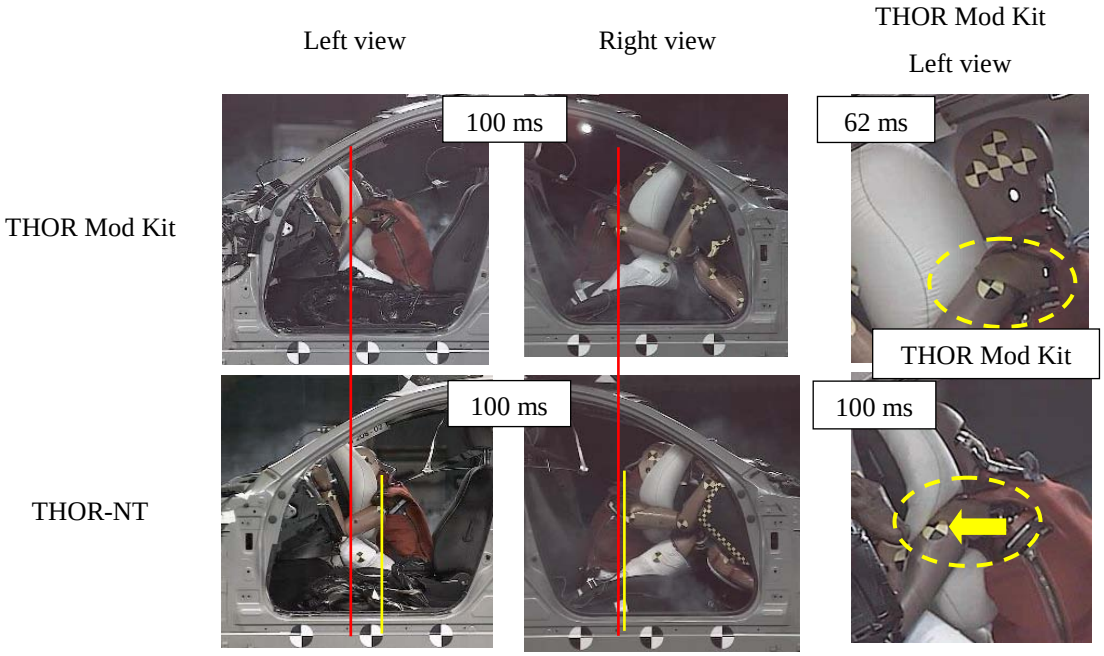


***Figure 4. Difference of shoulder forward displacements between the THOR Mod Kit and the THOR-NT in the FMVSS 208 seating procedure.***

**Comparison of Dummy Responses at Different D-ring Positions in Sled Test**

Based on the captured images from the high-speed video camera, the comparison of the kinematics for the THOR Mod Kit and the Hybrid III at different D-ring positions (load limiter - normal) is shown in Figure 5. Regardless of the D-ring position, shoulder belt slippage didn't occur in the Hybrid III, whereas belt slippage occurred in the THOR Mod Kit when the D-ring was at the lowest position. The belt path on the shoulder of the THOR Mod Kit had passed outward compared with that of the Hybrid III because of the difference in shoulder height between the dummies. Furthermore, the shoulder structure of the THOR Mod Kit with SD3 differs from that of the Hybrid III. These differences are presumed to bring about this phenomenon of slippage or non-slippage of the shoulder belt between the dummies.

Figure 6 shows the comparison of the head accelerations and thoracic deflections respectively of the THOR Mod Kit with respect to difference of the D-ring position (load limiter - normal). The peak acceleration in the X-axis indicated a higher value in the highest D-ring position than in the lowest D-ring position, whereas the peak acceleration in the Y-axis indicated the opposite result to that of the result in the X-axis. Since the seat belt slippage from the shoulder occurred in the case of the lowest D-ring position, the torsion of the dummy upper body about the Z-axis became large and the head lateral acceleration increased. Therefore, it seems that the head acceleration measurements of the THOR Mod Kit are able to sensitively respond to the difference of its own kinematics. Since in the lowest D-ring position the seat belt slippage occurred due to the effect of the seat belt path and the belt strongly compressed the right side of the thorax, the deflection on the thoracic upper right indicated larger values than in the highest D-ring position. It demonstrated that the THOR Mod Kit has high sensitivity to the seat belt path and has a high measurement ability utilizing the multi-point deflection measurements.

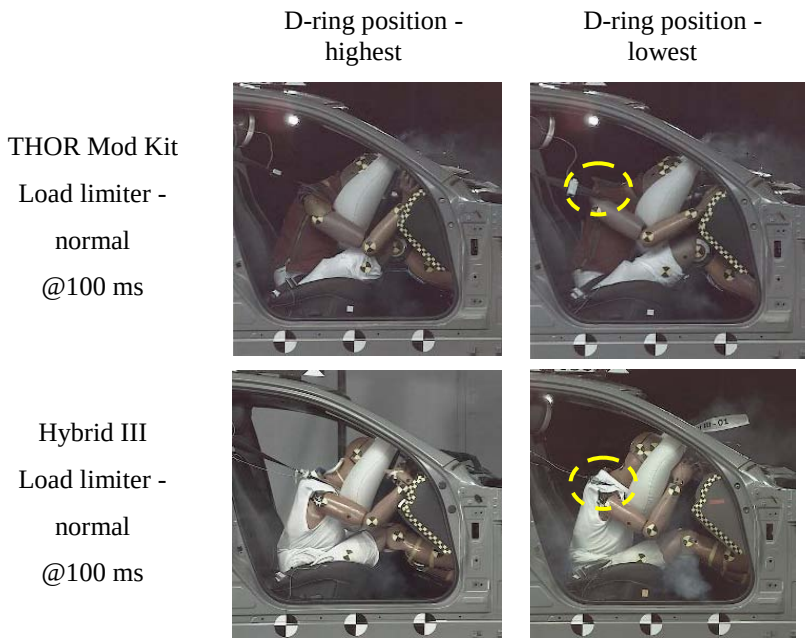


***Figure 5. Comparison of kinematics for the THOR Mod Kit and the Hybrid III at different D-ring positions.***

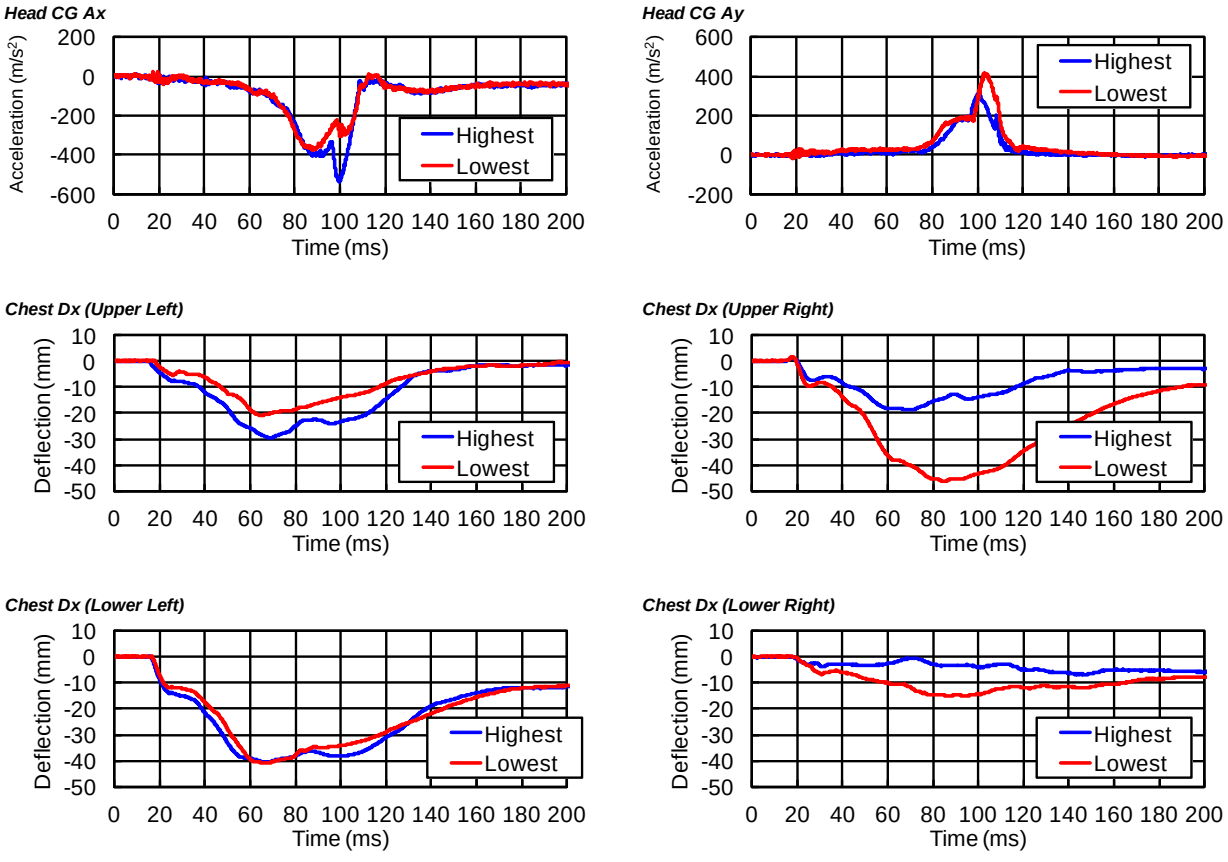


***Figure 6. Head accelerations (X- and Y-axes) and thoracic deflections (UL, UR, LL, LR) of the THOR Mod Kit.***

**Comparison of Dummy Responses with Different Seat Belt Load Limiter in Sled Test**

Comparison of the kinematics for the THOR Mod Kit and the Hybrid III with different load limiter forces (where the D-ring position was at the highest position) is shown in Figure 7. When the load limiter force was higher, the forward movement of the upper body of both the THOR Mod Kit and the Hybrid III was smaller than with a normal load limiter.

Figure 8 shows the comparison of the head resultant acceleration and Figure 9 shows the neck tensile force and the thoracic deflection, respectively, for the THOR Mod Kit and the Hybrid III with different load limiter forces (D-ring position was at the highest position). When the load limiter force was higher, the head accelerations of both dummies indicated lower values, while their thoracic deflections indicated larger values, compared with a normal load limiter. For the neck tensile force, the THOR Mod Kit indicated a higher value with a higher load limiter force than with a normal load limiter but there was little difference in the Hybrid III, because the neck flexion of the THOR Mod Kit became larger but that of the Hybrid III differed only slightly when the load limiter force was higher.

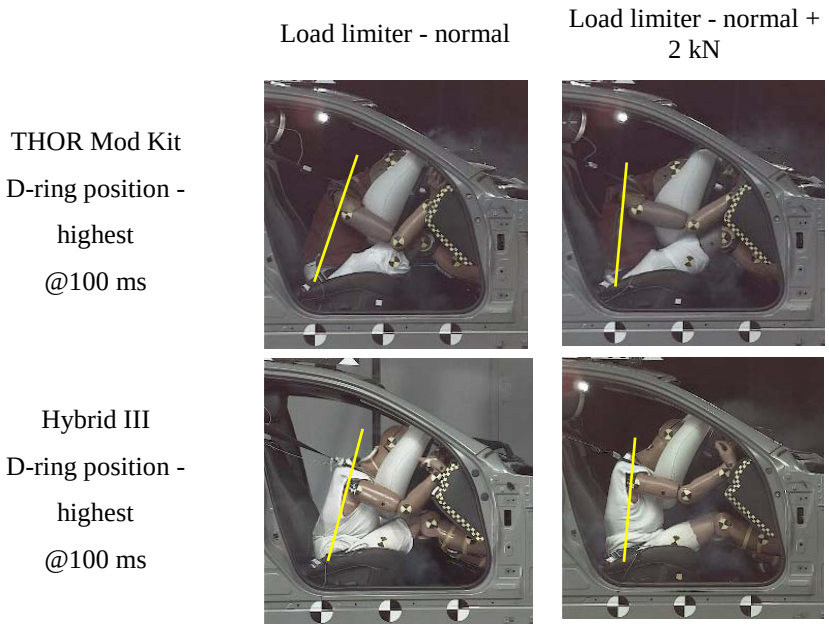


***Figure 7. Comparison of kinematics for the THOR Mod Kit and the Hybrid III with different load limiter forces.***

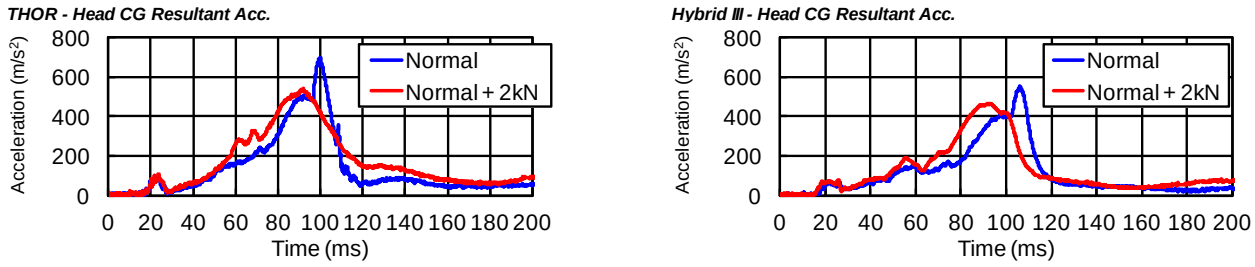


***Figure 8. Head accelerations of the THOR Mod Kit and the Hybrid III.***

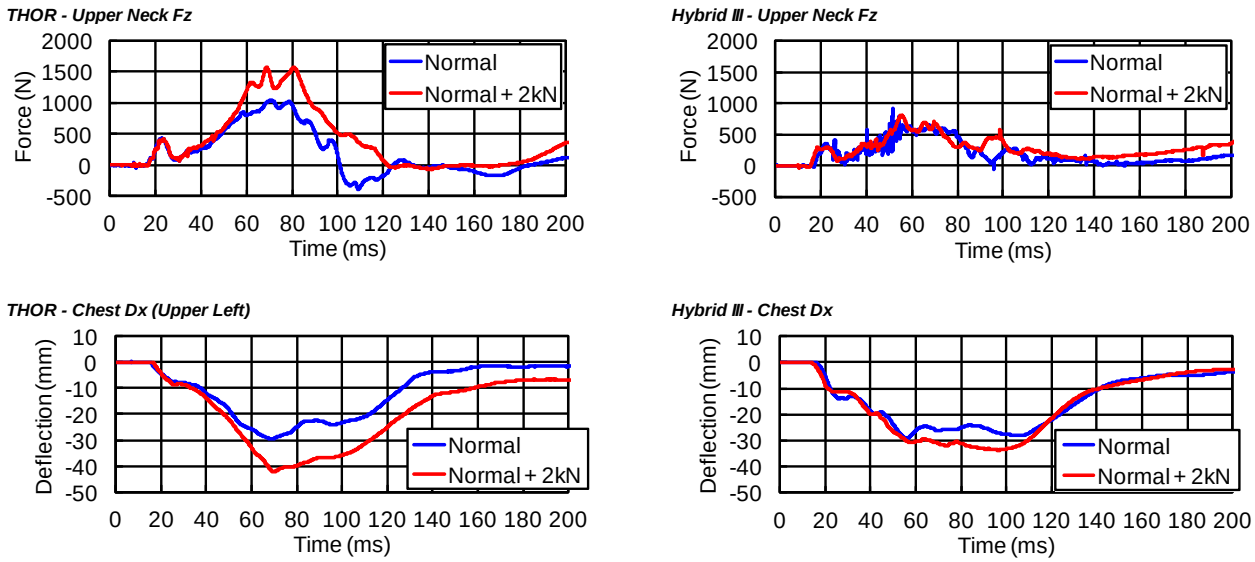


***Figure 9. Neck forces and thoracic deflections of the THOR Mod Kit and the Hybrid III.***

**Kinematics of the THOR Mod Kit with SD3 Shoulder in ODB Test**

Figure 10 shows the captured images from a high speed camera behind the dummies and Figure 11 shows some measurement curves of the THOR Mod Kit. After the left elbow of the THOR Mod Kit came in contact with the instrument panel at approximately 90 ms, its left shoulder moved rearward and upward because of the rebound of its upper body after 100 ms. At 120 ms, the right shoulder moved forward and torsion of the upper body occurred. T1 acceleration rapidly increased at 90 ms because the force was transmitted to the spine by the contact between the left elbow and the instrument panel. Furthermore, the force in Y-axis and moment about X-axis on the spine and the head angular velocity about Z-axis rapidly varied at 100 ms because of the upper body torsion.

| 80 ms | 90 ms | 100 ms | 120 ms |
|---|---|---|---|
| | Left elbow hit to dashboard | Left shoulder is pushed to rearward and upward | Right shoulder (belted side) move forward and torso is twisted |

***Figure 10. Kinematics of the upper body of the THOR Mod Kit in the ODB test.***

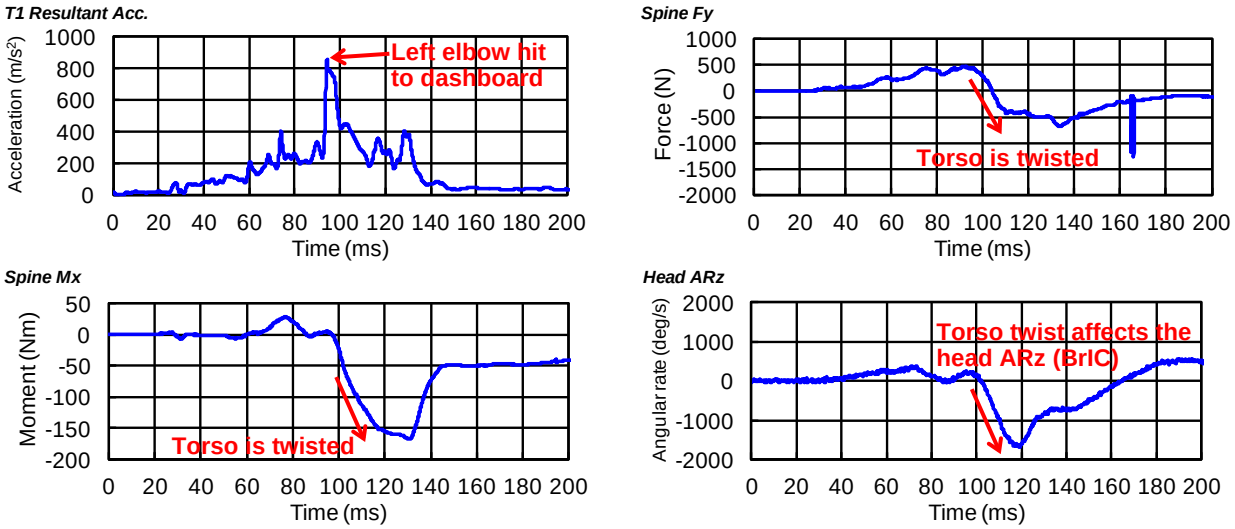


***Figure 11. Measurement curves of the THOR Mod Kit in the ODB test.***

**Ankle Rotation Responses of the THOR Mod Kit in the FWRB and ODB Tests**

Figure 12 shows the kinematics of the ankles of the THOR Mod Kit from a high speed camera on the floor of the driver side and Figure 13 shows the measurement curves of the right ankle rotation. In both the FWRB and ODB tests, the ankles of the THOR Mod Kit indicated eversion responses. A angle of the ankles in the FWRB test reached the maximum at about 80 ms, while in the ODB tests it reached the maximum at about 100 ms, and their values exceeded the preliminary reference value of 35 degrees. They were in the rebound phase of the vehicle after 63 ms in the FWRB test and in that after 90 ms in the ODB test.

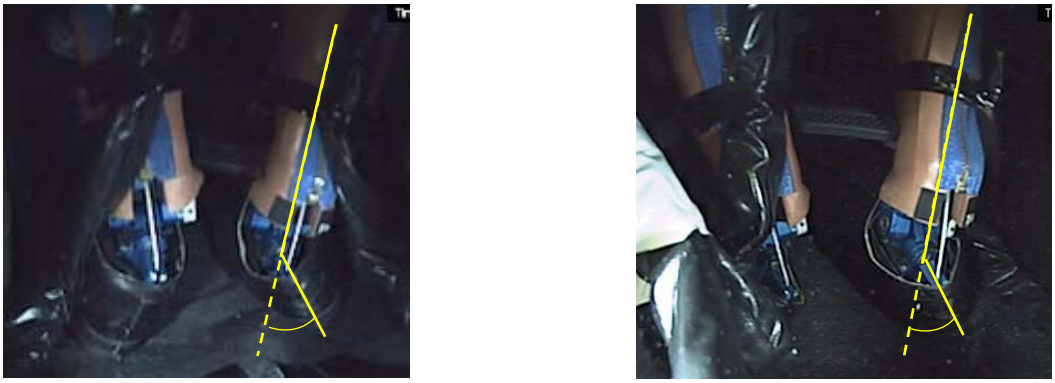

***Figure 12. Kinematics of the ankles of the THOR Mod Kit in the FWRB and ODB tests.***

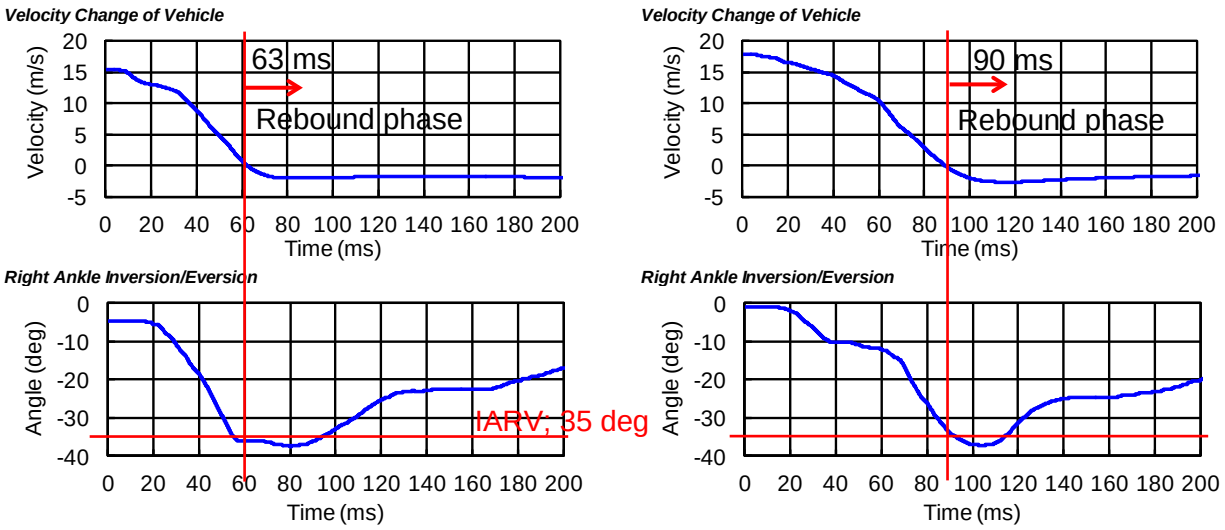


(a) FWRB test (b) ODB test

***Figure 13. Measurement curves of the right ankle of the THOR Mod Kit in the FWRB and ODB tests.***

**Comparison of the Injury Measures in the FWRB and ODB Tests**

The preliminary injury assessment reference values (IARVs) for the THOR [7][8] and the injury measures of the THOR Mod Kit and the Hybrid III obtained from the FWRB and ODB tests are shown in the APPENDIX. In the preliminary IARVs for the THOR, the kinematic rotational brain injury criterion (BRIC), abdominal deflection, acetabulum force, and ankle rotation are newly proposed, compared with the IARVs for the Hybrid III specified in FMVSS 208 and UN/R94. BRIC has been developed to estimate the risk of brain injury due to the rotation of the skull and is calculated by angular velocity and angular acceleration of the head center of gravity as shown in Eq. (1). The IARV of BRIC is 0.89, which corresponds to a 30% risk of AIS 3+ traumatic brain injury [9]. Furthermore, in 2013, the updated BrIC was developed [10]. As shown in Eq. (2), although the new BrIC is calculated only by angular velocity of the head center of gravity, the IARV has not been proposed yet as the study still in progress.

In the FWRB test, most of the injury measures of both dummies were less than the preliminary IARVs, however, the eversion on the right ankle of the THOR Mod Kit exceeded the reference value of 35 degrees. The moment My on the left upper tibia of the THOR Mod Kit was not measured because there was a disconnected wire problem on the load cell sensor (moment My) of the left upper tibia before the test. Due to that problem, calculating the tibia index was not done. In the ODB test, most of the injury measures of both dummies were less than the preliminary IARVs, however, the eversion on the right ankle of the THOR Mod Kit exceeded the reference value of 35 degrees.

Figure 14 shows a ratio of the injury measures of the THOR Mod Kit and the Hybrid III relative to the provisional IARVs in the FWRB and ODB tests. In the FWRB test, although the HIC 36 of both dummies were less than the reference value, the value of the Hybrid III was 285, whereas that of the THOR Mod Kit was 521. The THOR Mod Kit was approximately 1.8 times higher than the Hybrid III. For the neck tensile force, the THOR Mod Kit also indicated higher values than the Hybrid III. It is presumed that the contact force between the head and the steering wheel was larger because the upper body forward displacement and neck flexion of the THOR Mod Kit were larger than those of the Hybrid III. Among the four thoracic points of the THOR Mod Kit, the deflection at the upper left was the largest, which was approximately 1.4 times of the deflection at the chest center of the Hybrid III. The chest 3 ms clip G was almost the same between the two dummies. Compressive forces on the left and right femurs indicated higher values in the THOR Mod Kit than in the Hybrid III. The tibia index for the left tibia of the THOR Mod Kit was lower but that of its right tibia was higher than those of the Hybrid III. Particularly, on the right-lower tibia, the THOR Mod Kit indicated a tibia index of 0.56, which was 2 times over compared with a tibia index of 0.2 in the Hybrid III. In the ODB test, although the HIC 36 of both dummies were less than the reference value, the value of the Hybrid III was 263, whereas that of the THOR Mod Kit was 510. The THOR Mod Kit was approximately 1.9 times higher than the

Hybrid III. For the neck tensile force, the THOR Mod Kit also indicated higher values than the Hybrid III. Among the four thoracic points of the THOR Mod Kit, the deflection at the upper left was the largest, which was approximately 1.4 times of the deflection at the chest center of the Hybrid III. The chest 3 ms clip G was almost the same between the two dummies. Compressive forces on the left and right femurs indicated higher values in the THOR Mod Kit than in the Hybrid III. The tibia index for the left and right tibias of the THOR Mod Kit indicated higher values than those of the Hybrid III. Particularly, on the right-lower tibia, the THOR Mod Kit indicated a tibia index of 0.83, which was about 4 times higher compared with the tibia index of 0.2 in the Hybrid III.

$$BRIC = \frac{\omega_{max}}{\omega_{cr}} + \frac{\alpha_{max}}{\alpha_{cr}} \qquad \textbf{(1)}$$

$\omega$ = angular velocity at head CG , $\alpha$ = angular acceleration at head CG , max = maximum resultant value

cr = critical value for THOR, $\omega_{cr} = 63.5\ rad/s,\ \alpha_{cr} = 19501\ rad/s^2$

$$BrIC = \sqrt{\left(\frac{\omega_x}{\omega_{xC}}\right)^2 + \left(\frac{\omega_y}{\omega_{yC}}\right)^2 + \left(\frac{\omega_z}{\omega_{zC}}\right)^2} \qquad \textbf{(2)}$$

$\omega_x, \omega_y, \omega_z$ = maximum angular velocities about X-, Y-, Z-axes, $\omega_{xC}, \omega_{yC}, \omega_{zC}$ = critical angular velocities

$\omega_{xC} = 66.25\ rad/s$ (Average of CSDM and MPS), $\omega_{yC} = 56.45\ rad/s$ (Average of CSDM and MPS )

$\omega_{zC} = 42.87\ rad/s$ (Average of CSDM and MPS )

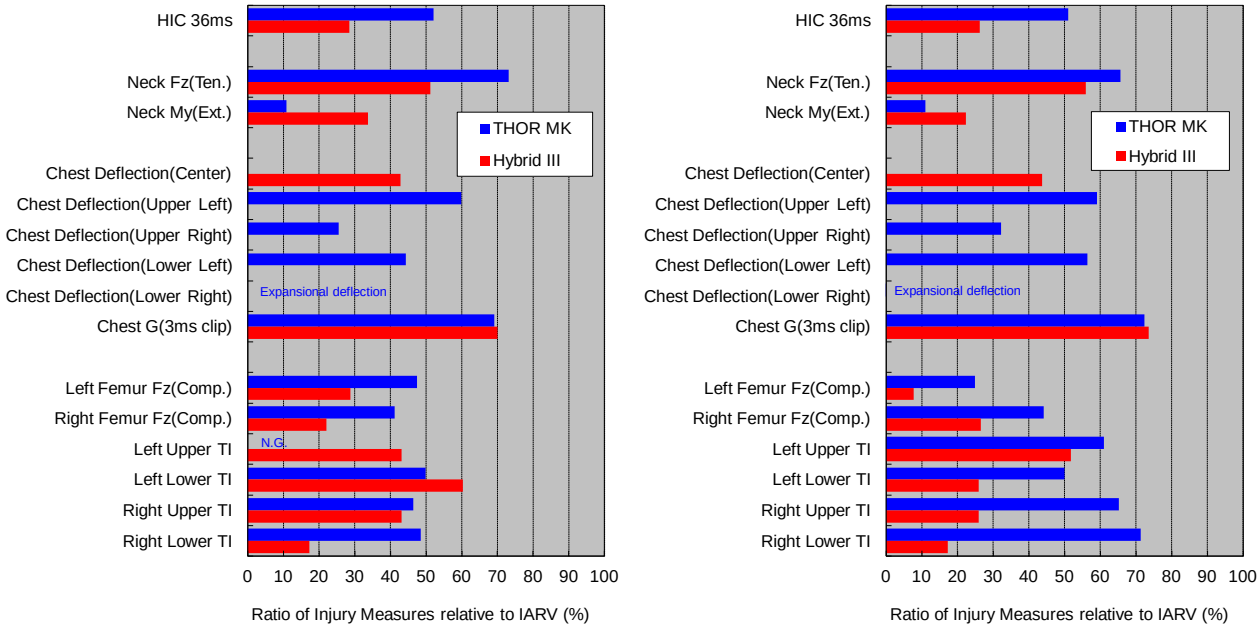


(a) FWRB (b) ODB

***Figure 14. Ratio of the injury measures of the THOR Mod Kit and the Hybrid III in the FWRB and ODB tests relative to preliminary IARVs.***

## DISCUSSION

### Shoulder Belt Slippage with Difference of D-ring Position in Sled Test

Regardless of the D-ring positions, the shoulder belt slippage didn't occur in the Hybrid III, whereas belt slippage occurred in the THOR Mod Kit when the D-ring was at the lowest position. Further verification of the biofidelity of the shoulder kinematics between the Post-Mortem Human Subjects (PMHS) and the ATD (Anthropomorphic Test Device) is needed.

### Difference between the Left and Right Shoulder Movements in Sled Test

From the image of the high speed camera, it was observed that the difference between the left and right shoulder movements of the THOR Mod Kit was large. How the seat belt restrains the shoulder, which is an important to design the specification of the seat belt and its location. Since the sensitivity of the shoulder restraint performance to the D-ring position was high in a series of tests, further verification for the shoulder motion is needed.

### Kinematics of the THOR Mod Kit with SD3 Shoulder in ODB Test

From the image of the high speed camera and some measurement curves of the dummy, it was presumed that the torsion of the upper body of the THOR Mod Kit occurred because its left elbow came in contact with the instrument panel, and this kinematics affected some measurement curves of the dummy. However, as for that, in the future, it needs to verify by comparing the dummy responses under the different condition, for instance, with and without the instrument panel. Furthermore, it is necessary to verify whether this dummy kinematics is human like in this test mode.

## CONCLUSIONS

In order to contribute to the development and improvement of the THOR dummies, the impact responses of the THOR Mod Kit were compared with those of the THOR-NT and the Hybrid III, based on the kinematic and dynamic responses to different conditions in the frontal sled and vehicle crash tests. From the results of this research, it turns out that:

- The response of the THOR Mod Kit to the difference of seating procedure was more sensitive than that of the THOR-NT
- The sensitivity of the THOR Mod Kit to the D-ring position was higher than that of the Hybrid III
- The difference of load limiter affected the difference of kinematics and dynamic responses of the upper body in both the THOR Mod Kit and the Hybrid III
- As for durability of the THOR in two JNCAP test conditions, there was no dummy failure and unusual mode.
- As for the relation between the contact between the elbow of dummy and the instrument panel and the increase of the spine moment about the X-axis in the ODB test, further verification by re-testing etc is needed.
- In both the FWRB and ODB tests, the eversion on the ankle of the THOR Mod Kit exceeded IARV at the rebound phase of the vehicle.

**REFERENCES**

[1] Haffner M., et al. “Foundations and Elements of the NHTSA THOR Alpha ATD Design,” Proceedings of the 17th International Technical Conference on the Enhanced Safety of Vehicles, 2001

[2] Shams T., et al. “Development of THOR-NT: Enhancement of THOR Alpha-the NHTSA Advanced Frontal Dummy,” Proceedings of the 19th International Technical Conference on the Enhanced Safety of Vehicles, 2005

[3] Ridella S., et al. “Modifications to Improve the Durability, Usability and Biofidelity of the THOR-NT Dummy,” Proceedings of the 22nd International Technical Conference on the Enhanced Safety of Vehicles, 2011

[4] Törnvall F., “A New Shoulder for the THOR Dummy Intended for Oblique Collision,” Chalmers University of Technology, 2008

[5] Lemmen P., et al. “An Advanced Thorax-Shoulder Design for the THOR Dummy,” Proceedings of the 23rd International Technical Conference on the Enhanced Safety of Vehicles, 2013

[6] IIHS “Guidelines for Using the UMTRI ATD Positioning Procedure for ATD and Seat Positioning (Version V)”, 2004

[7] Saunders J., et al. "NHTSA’s Test Procedure Evaluations for Small Overlap/Oblique Crashes," Proceedings of the 22nd International Technical Conference on the Enhanced Safety of Vehicles, 2011

[8] Saunders J., et al. "Assessment of An Oblique Moving Deformable Barrier Test Procedure,” Proceedings of the 23rd International Technical Conference on the Enhanced Safety of Vehicles, 2013

[9] Takhounts E., et al. “Kinematic Rotational Brain Injury Criterion (BRIC),” Proceedings of the 22nd International Technical Conference on the Enhanced Safety of Vehicles, 2011

[10] Takhounts E., et al. “Development of Brain Injury Criteria (BrIC),” Stapp Car Crash Journal, Vol. 57 (November 2013), pp. 243-266

## APPENDIX

### Table A1. Preliminary IARVs for the THOR and the injury measures in the FWRB test.

| | | IARV | Ref | THOR Mod Kit | Hybrid III |
|---|---|---|---|---|---|
| Head | BRIC(Previous Version) | 0.89 | [8] | 0.54 | No sensor |
| | BrIC(Latest Version) | TBD | [10] | 0.50 | |
| | HIC 36ms | 1000 | [8] | 520.8 | 284.8 |
| | HIC 15ms | 700 | [8] | 376.4 | - |
| | 3ms clip (G) | 80 | [7] | 59.7 | - |
| Upper Neck | Tension Force (N) | 2520 | [8] | 1842.1 | 1290 |
| | Compression Force (N) | 3640 | [8] | 234.9 | - |
| | Flexion at OC (Nm) | 48 | [7] | 1.5 | - |
| | Extension at OC (Nm) | 72 | [7] | 7.8 | 24.3 |
| Chest | Deflection(Center) | 63 | [8] | No sensor | 27.0 |
| | Deflection(Upper Left) (mm) | | | 37.7 | No sensor |
| | Deflection(Upper Right) (mm) | | | 16.1 | |
| | Deflection(Lower Left) (mm) | | | 27.9 | |
| | Deflection(Lower Right) (mm) | | | -9.5 | |
| | 3ms clip (G) | 60 | [8] | 41.5 | 42.0 |
| Abdomen | Deflection (mm) | 90 | [8] | 69.6 | No sensor |
| Acetabulum | Left Resultant Force (N) | 3316 | [8] | 1486 | No sensor |
| | Right Resultant Force (N) | | | 1042 | |
| Femur | Left Femur Force (N) | 9040 | [8] | 4288 | 2600 |
| | Right Femur Force (N) | | | 3725 | 2000 |
| Tibia | Left Upper Tibia Index | 1.16 | [8] | Sensor N.G. | 0.5 |
| | Left Lower Tibia Index | | | 0.58 | 0.7 |
| | Right Upper Tibia Index | | | 0.54 | 0.5 |
| | Right Lower Tibia Index | | | 0.56 | 0.2 |
| Ankle | Left Inversion/Eversion (deg) | 35/35 | [8] | 26.6 | No sensor |
| | Left Dorsiflexion/Plantarflexion (deg) | | | 16.1 | |
| | Right Inversion/Eversion (deg) | | | 37.4 | |
| | Right Dorsiflexion/Plantarflexion (deg) | | | 14.8 | |

**Note**
**Currently all IARVs are preliminary.**
**Negative value in chest deflection means chest expansion.**
**Hybrid III measurements are from JNCAP tests.**

### Table A2. Preliminary IARVs for the THOR and the injury measures in the ODB test.

| | | IARV | Ref | THOR Mod Kit | Hybrid III |
|---|---|---|---|---|---|
| Head | BRIC(Previous Version) | 0.89 | [8] | 0.60 | No sensor |
| | BrIC(Latest Version) | TBD | [10] | 0.72 | |
| | HIC 36ms | 1000 | [8] | 510.1 | 262.7 |
| | HIC 15ms | 700 | [8] | 291.5 | - |
| | 3ms clip (G) | 80 | [7] | 53.0 | - |
| Upper Neck | Tension Force (N) | 2520 | [8] | 1653.5 | 1410 |
| | Compression Force (N) | 3640 | [8] | 803.3 | - |
| | Flexion at OC (Nm) | 48 | [7] | 1.6 | - |
| | Extension at OC (Nm) | 72 | [7] | 7.9 | 16.1 |
| Chest | Deflection(Center) | 63 | [8] | No sensor | 27.5 |
| | Deflection(Upper Left) (mm) | | | 37.2 | No sensor |
| | Deflection(Upper Right) (mm) | | | 20.3 | |
| | Deflection(Lower Left) (mm) | | | 35.5 | |
| | Deflection(Lower Right) (mm) | | | -17.8 | |
| | 3ms clip (G) | 60 | [8] | 43.4 | 44.1 |
| Abdomen | Deflection (mm) | 90 | [8] | 68.7 | No sensor |
| Acetabulum | Left Resultant Force (N) | 3316 | [8] | 1121 | No sensor |
| | Right Resultant Force (N) | | | 1485 | |
| Femur | Left Femur Force (N) | 9040 | [8] | 2247 | 700 |
| | Right Femur Force (N) | | | 3995 | 2400 |
| Tibia | Left Upper Tibia Index | 1.16 | [8] | 0.71 | 0.6 |
| | Left Lower Tibia Index | | | 0.58 | 0.3 |
| | Right Upper Tibia Index | | | 0.76 | 0.3 |
| | Right Lower Tibia Index | | | 0.83 | 0.2 |
| Ankle | Left Inversion/Eversion (deg) | 35/35 | [8] | 33.5 | No sensor |
| | Left Dorsiflexion/Plantarflexion (deg) | | | 23.2 | |
| | Right Inversion/Eversion (deg) | | | 37.2 | |
| | Right Dorsiflexion/Plantarflexion (deg) | | | 21.5 | |

**Note**
**Currently all IARVs are preliminary.**
**Negative value in chest deflection means chest expansion.**
**Hybrid III measurements are from JNCAP tests.**

# LIMITATIONS OF USE OF AN INERTIAL POSITIONING SYSTEM IN A TRUCK DURING A MANEUVER OF AVOIDING A SUDDENLY APPEARING OBSTACLE

**Michał Dziewiecki**
Warsaw University of Technology, Institute of Radioelectronics
Poland

**Mirosław Gidlewski**
University of Technology and Humanities in Radom,
Poland

Paper Number 15-0341

## ABSTRACT

The objective of this work is to find limitations of using MEMS-type accelerometers and gyroscopes for finding position of a vehicle in short time prospective (few seconds). Such a system could be helpful for automated vehicle driving in some situations, like bypassing a suddenly appearing obstacle. A Monte-Carlo analysis was performed to find introduced position and direction errors for various trajectories of the vehicle. Transducer noise, offset and calibration errors were taken into account as possible error sources. Also, the influence of limited data sampling rate was checked. The results are presented in form of difference statistics between real and calculated vehicle position and orientation at the end of the track as function of various parameters, including the trajectory and performance of the used sensors. The Monte-Carlo simulation accuracy was checked by bootstrap method and the errors were shown in resulting plots. Presented results show that an inertial system can be used for determining the vehicle's position with accuracy reaching centimeters. Also, it is shown that compensation of the sensor offsets, as well as knowing the initial conditions are critical for the quality of the track reconstruction.

## INTRODUCTION

For a suddenly appearing obstacle partly blocking the road, an attempt to bypass it can be a more efficient maneuver than braking, at least for certain velocities and track geometry [1,2]. This maneuver can be performed automatically if the vehicle is equipped with appropriate position sensors, like laser scanners, radars and cameras. However, such kind of sensors may be vulnerable to external disturbances like flashes of light, water splashes, fog, smoke or momentary electromagnetic interference. Also, their accuracy, sampling frequency and latency may not meet the requirements for rapid movements. This makes a need to provide a system which is free of aforementioned drawbacks. It should provide vehicle position data in a time period of few seconds needed for maneuver completion, with good-enough accuracy, immunity to external interference and low latency. Modern MEMS-type inertial sensors (linear accelerometers and gyroscopes, i.e. angular speed sensors) seem to be a good candidate to be used for this purpose.
The aim of this work is to find limitations of use of these sensors due to their noise, miscalibration and generally ill-conditioned integration-based method of vehicle position reconstruction. To achieve this goal, a number of Monte-Carlo simulations were performed for different conditions, including noise of the sensors, sampling frequency, miscalibration, track geometry, initial vehicle velocity and deceleration during the maneuver.

## MARKET-AVAILABLE SENSORS

The manufacturers offer a variety of MEMS-based sensors for acceleration and angular velocity. Their performance is closely related to their intended application and related customer's budget, ranging from simple orientation sensors used for mobile phones, through sensors for game-console controllers, up to professional sensors which can be used in so demanding applications as autonomous control of drones or even 'big' aviation. Several sensors (including high-performance devices) are listed in Table 1. One of them – namely LSM330DL – contains both accelerometer and gyroscope in a single chip. Its parameters were used as base values for a number of performed simulations.
At this point, it's worth noting that also chip-integrated magnetometers are available which can provide absolute information on vehicle orientation, however their use for our purpose is generally pointless. This is due to their non-

negligible latency, relatively low sampling rate and – last but not least – vulnerability to interference from external sources of magnetic fields.

**Table1.**
**Several types of MEMS accelerometers and gyroscopes and their main parameters.**

| Type | Accelerometer | | | Gyroscope | | |
|---|---|---|---|---|---|---|
| | **Range [m/s$^2$]** | **Noise density** $\left[\frac{\mathrm{m/s^2}}{\sqrt{\mathrm{Hz}}}\right]$ | **Sample rate [Hz]** | **Range [$^o$/s]** | **Noise density** $\left[\frac{^o/\mathrm{s}}{\sqrt{\mathrm{Hz}}}\right]$ | **Sample rate [Hz]** |
| LIS3DH [1] | 20-160 | $2.2\cdot10^{-3}$ | 5000 | *n/a* | *n/a* | *n/a* |
| LIS33DE | 20-80 | *not specified* | 400 | *n/a* | *n/a* | *n/a* |
| LSM330DL [2] | 20-160 | $2.2\cdot10^{-3}$ | 5000 | 250-2000 | $3.0\cdot10^{-2}$ | 1344 |
| L3G4200D [3] | *n/a* | *n/a* | *n/a* | 250-2000 | $3.0\cdot10^{-2}$ | 800 |
| CMR3000-D01 | *n/a* | *n/a* | *n/a* | 2000 | $2.0\cdot10^{-1}$ | 160 |

## MONTE CARLO SIMULATION PROCESS

The basic simulation process consisted of few steps:

- calculating the position of the vehicle along a defined track over time with dense time step (typ. 1 ms);
- calculating the data for sensors, i.e. the values of acceleration (tangential and normal component related to the vehicle trajectory) and angular velocity over the vertical axis;
- decimating the above data to get undisturbed sensor data at real sampling frequency of the sensor;
- disturbing the data to get simulated data of a real sensor;
- track reconstruction basing on disturbed data;
- finding the reconstruction errors.

Last three steps were performed multiple times (typically 1000) to get statistical information on errors. Basing on acquired data, the mean value of the error, its standard deviation and RMS (root-mean-square) value were calculated.
The whole procedure was performed for various conditions, e.g. varying noise of the sensors, vehicle speed or track length. Following further assumptions were made in order to perform the simulations:

### The shape of the track

It is assumed that the vehicle moves along a straight road with a constant velocity as the maneuver begins. Then it changes its position across the road by a certain displacement (denoted as $D$) while moving forward. The total distance along the road during this movement (denoted as $L$) is generally longer than $D$. The track has a shape of half-cosine, according to Equation 1:

$$d(l) = \frac{1}{2} D \cdot \left(1 - \cos\frac{\pi \cdot l}{L}\right) \tag{1}$$

where $l$ and $d$ denote actual vehicle position along and across the road, respectively. One must note that $l$ can not be treated as linearly changing with time, as the velocity of the vehicle is calculated along its trajectory and not along the road.
For the purpose of simulation, two short segments of straight track (parallel to the road) are added at the beginning and the end of the track. Their length is determined according to the vehicle's velocity so that their duration is about 100 ms. The aim of inserting these segments is purely technical – an amount of data is to be generated to feed digital filters for data decimation, so that no oscillations at the beginning and the end of the track occur.

It's obvious that discontinuities in acceleration and angular velocity are present at the beginning and the end of the proposed half-cosine track. Despite that such kind of track is impossible to be followed in reality, these discontinuities are not an obstacle for the track reconstruction algorithm. Thus, the assumed model of the track is acceptable for our purpose.
Last but not least, it must be noted that our model is two-dimensional. This means that possible vehicle tilting is not taken into account. The consequence of this assumption is that only two acceleration sensors among three (one for each axis) are used in the track reconstruction procedure – a sensor for vertical acceleration is not used. Accordingly, only one rotation sensor is used – this is the one to measure angular speed over the vertical axis.

**Sensor models**

The sensors are outputting data with a defined sample rate. It's assumed that the data acquisition time is zero (i.e. the value of the sample refers to a certain moment and is not an effect of averaging of the input value over a period of time).
It was assumed that the sensors have following errors:

- Sensor noise, which is stationary, white in spectrum and has Gaussian probability density function (PDF). During simulation, a random value of noise is added to each sample of the sensor data. The input data for the simulation is the power spectral density of the noise, which is re-calculated to variance of a single sample.
- Sensor miscalibration, which has also Gaussian PDF. Sensor miscalibration is a constant value added to the sensor data for the whole realization, i.e. single MC attempt. However, it's determined independently for each realization, giving a spectrum of different results after a number of MC loops.

**Track reconstruction algorithm**

The aim of this algorithm is to calculate vehicle position and orientation (the angle between the vehicle's axis and initial movement direction) basing on the sensor data. The calculation is performed with a defined timestamp, which is identical with sampling period of the sensors. Actually, two main activities are performed for each time point: calculation of the vehicle orientation (i.e. the angle between the axis of the vehicle and the axis of the road) and position.
The vehicle orientation calculation is performed using only the data from the angular velocity sensor. For a given time point $t_n$, the vehicle's orientation $\psi$ is calculated as:

$$\psi(t_n) = \psi(t_{n-1}) + T_s \cdot \Omega(t_n) \tag{2}$$

where $\psi\ (t_{n-1})$ denotes vehicle orientation for the previous time point, $\Omega(t_n)$ the measured angular velocity and $T_s$ the sampling period.
The position reconstruction requires three consecutive steps: acceleration measurement, velocity calculation and position calculation.
For the first step, the sensor data is re-calculated from vehicle coordinates to road-related *l*-*d* coordinates, as it's presented in Equation 3:

$$\begin{aligned} a_l &= a_{par} \cdot \cos\psi - a_{perp} \cdot \sin\psi \\ a_d &= a_{par} \cdot \sin\psi + a_{perp} \cdot \cos\psi \end{aligned} \tag{3}$$

where $a_{par}$ and $a_{perp}$ are acceleration values measured with respect to the vehicle's axis (parallel and perpendicular, respectively) and $\psi$ is the calculated current vehicle orientation. The $a_l$ and $a_d$ denote the acceleration values in along *l* and *d* axis.
The velocity is calculated by integrating the acceleration values, basically the same way as it was done for vehicle orientation. Then, one more integration step is performed to get the position values.

**Dependencies to check**

The influence of the following factors on the achievable accuracy was checked:

- noise spectral density of the accelerometers and gyroscopes,
- miscalibration of the sensors (constant offset of the sensor readout),
- limited sampling rate of the sensors,
- length of the track along initial movement direction,
- initial vehicle velocity,
- vehicle deceleration during the maneuver.

Witch such a number of variables, performing simulations for all parameter combinations was virtually impossible. Thus, only 2-dimensional maps were calculated (i.e. the dependence on two selected parameters) with remaining parameters fixed at a constant value.

The basic parameter set was as follows:

- track length (L): 50 m (20 m for sample rate tests),
- track width (D): 5 m,
- initial velocity: 20 m/s
- vehicle deceleration: 0 $m/s^2$
- sample rate of the sensors: 100 Hz
- spectral noise density of the accelerometer: $2.2 \cdot 10^{-3}$ $m/s^2/\sqrt{Hz}$ ,
- spectral noise density of the gyroscope: $3.0 \cdot 10^{-2}$ $^o/s/\sqrt{Hz}$ ,
- accelerometer miscalibration: 0 $m/s^2$,
- gyroscope miscalibration: 0 $^o/s$.

**Error calculation**

The errors are present in each sample of the reconstructed data. However, they generally grow with time due to integration-based method of the track reconstruction – the error of any data sample is a result of the error of previous sample and new errors introduced by the sensors. Thus, the errors at the end of the track are statistically the biggest ones. For this reason, we used these 'final' errors as a gauge of the reconstruction quality.

Following errors were checked:

- misalignment in vehicle position at the end of the simulation, calculated independently in *d* and *l* axis, as well as combined position error;
- vehicle orientation error;
- the error of final movement direction.

The vehicle orientation and movement direction must be distinguished, as it is not an assumption that the vehicle is always moving along its axis. Even if we neglect small differences due to vehicle's chassis geometry, also huge discrepancies may occur if the vehicle gets into a skid. The reconstruction algorithm must take such a situation into account.

Basing on MC simulations, error statistics were gathered, giving following values:

- Error mean value. Generally, for 'input' errors with zero mean value, the mean value of the 'output' error should be also zero for a linear model. However, as our model is not linear, non-zero values may occur. It this controversial if this error can be suppressed in practice (despite it's theoretically deterministic), as its value may be strongly dependent on track parameters. Thus, we treat this error as incorrectable.
- Standard deviation of the error values. Only error spread is taken into account and not its mean value.
- Root Mean Square (RMS) value of an error. Both above components are incorporated in this value. It was used as a basic gauge during simulations.

**BASIC RESULTS**

In the following sections, basic results were presented in form of plots showing error RMS value as a function of various factors. Typically, each plot presents a family of curves showing the error dependence on two parameters. For each plot, 3σ error bars are plotted to show Monte-Carlo simulation accuracy.

**Influence of the sensor noise**

Figure 1 presents a set of plots showing the dependence of the errors on the noise of the sensors. Upper plots show the position reconstruction accuracy in two axes. Lower plots show movement direction error (left) and vehicle orientation error (right).

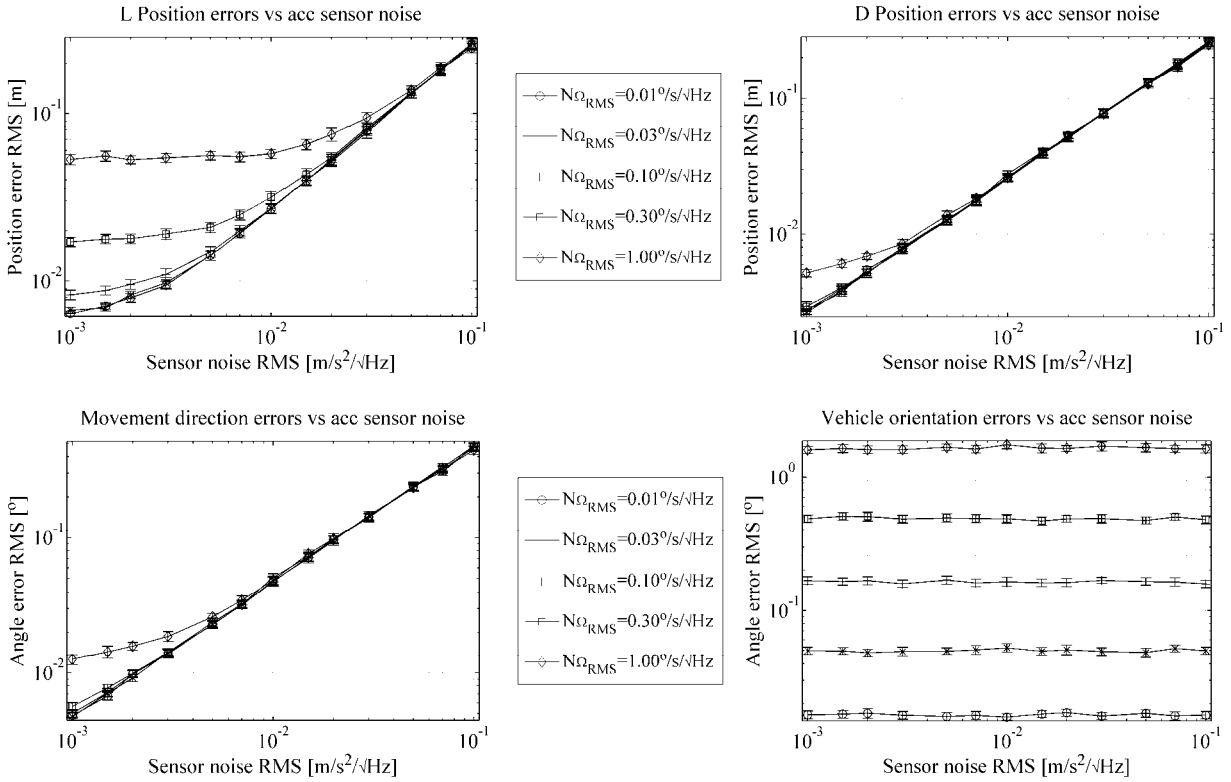


***Figure 1. The influence of the sensor noise on the track reconstruction. Upper plots present position reconstruction error, while lower ones show angle reconstruction errors.***

At this point, it should be noted that:

- For a given track geometry, the position reconstruction error is dependent mainly on the noise of the acceleration sensor. The influence of the gyroscope noise is visible mainly for the longitudinal component and only for high noise levels.
- The vehicle orientation reconstruction accuracy is dependent only on the noise of the angular velocity sensor, which is obvious given the reconstruction method described previously (see Equation 2).
- The accuracy of movement direction reconstruction is dependent mainly on the noise of the angular velocity sensor, but also an influence of the accelerometers can be observed for high noise amplitude.

Generally, the error values are small for expected noise levels of real sensors. For LSM330DL, the total position error should be below 1 cm for given track geometry and vehicle velocity of 20 m/s. Also, the vehicle orientation and movement direction accuracy should be well within 1°, which is more than satisfactory. Of course, these promising results should not be treated too seriously before analyzing the influence of track geometry, initial speed, sensor miscalibration etc.

**Influence of the sensor miscalibration**

Generally, the influence of sensor miscalibration is close (in its character) to the one of sensor noise, as Figure 2 shows. The main difference in the character of the curves is that no influence of miscalibration of the angular velocity sensor on position accuracy was observed.
If we define maximum errors as 0.1 m and 1° RMS, the allowable miscalibration values for given default conditions (see *Simulation Process, Dependencies to check*) are $3 \cdot 10^{-2}$ m/s$^2$ and $3 \cdot 10^{-1}$ °/s. One can see that assuring good sensor offset compensation is critical. Thus, an on-line algorithm is required to compensate slowly varying offsets of the sensors.

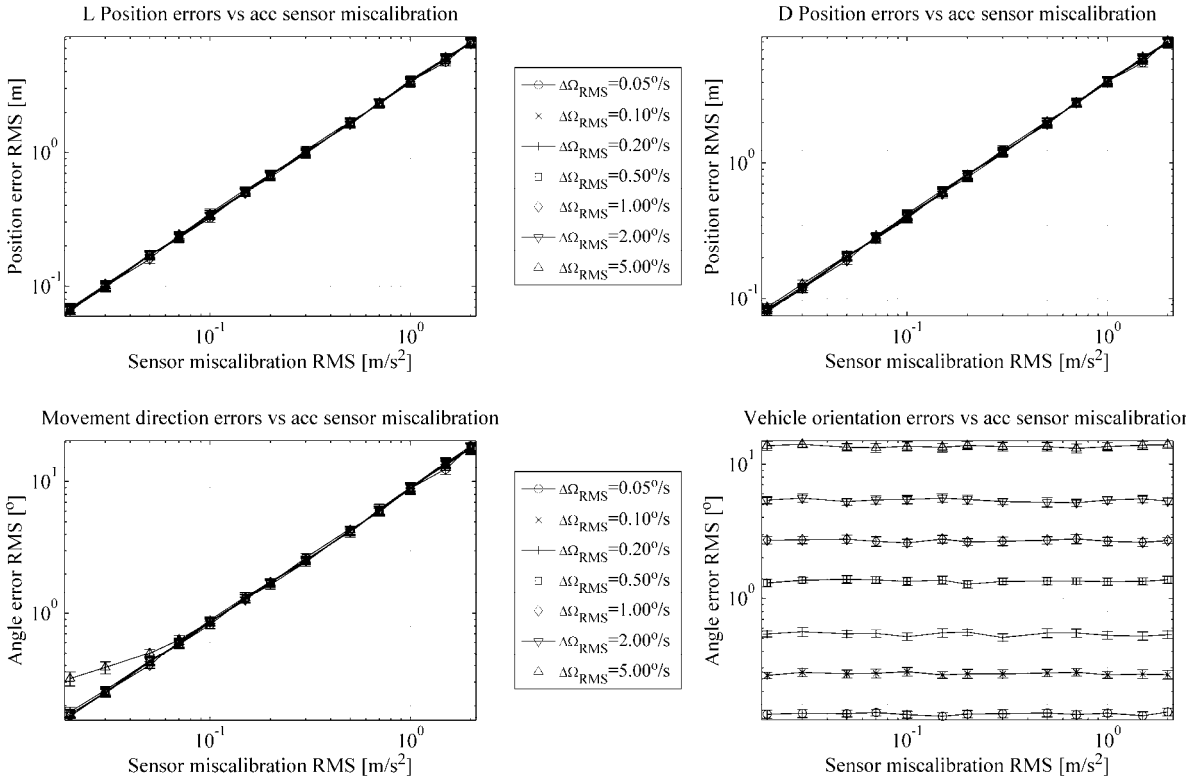


***Figure 2. The influence of the sensor miscalibration on the track reconstruction.***

**Influence of uncertainties in initial conditions**

The next possible error source is the uncertainty in initial conditions, i.e. vehicle velocity and movement direction. According to Figure 3, the simulations have shown that:

- The position reconstruction accuracy is dependent on errors both in initial velocity and movement direction. However, the influence of both parameters is different for longitudinal and perpendicular component of the displacement. As for the errors along the road, both error sources are sigificant. However, the influence on position across the road is dominated by initial direction errors.
- The accuracy of reconstruction of final movement direction and vehicle orientation is dependent only on initial direction error (it was checked that the influence of errors in initial velocity can be seen only for huge errors, which are comparable with the real value of the initial velocity).
- Achieving tolerable errors (0.1m / 1°) require that the initial velocity error is lower than ≈0.02 m/s and the initial movement direction is defined with an accuracy of 0.1°. These requirements are very demanding, especially for the velocity measurement. However, one can see that mainly the longitudinal position is vulnerable to initial velocity (see Figure 3, upper left plot). Thus if we decrease our requirements for this

axis (it's less critical than the perpendicular component of the position), also the requirements on initial velocity requirement will become less tight.

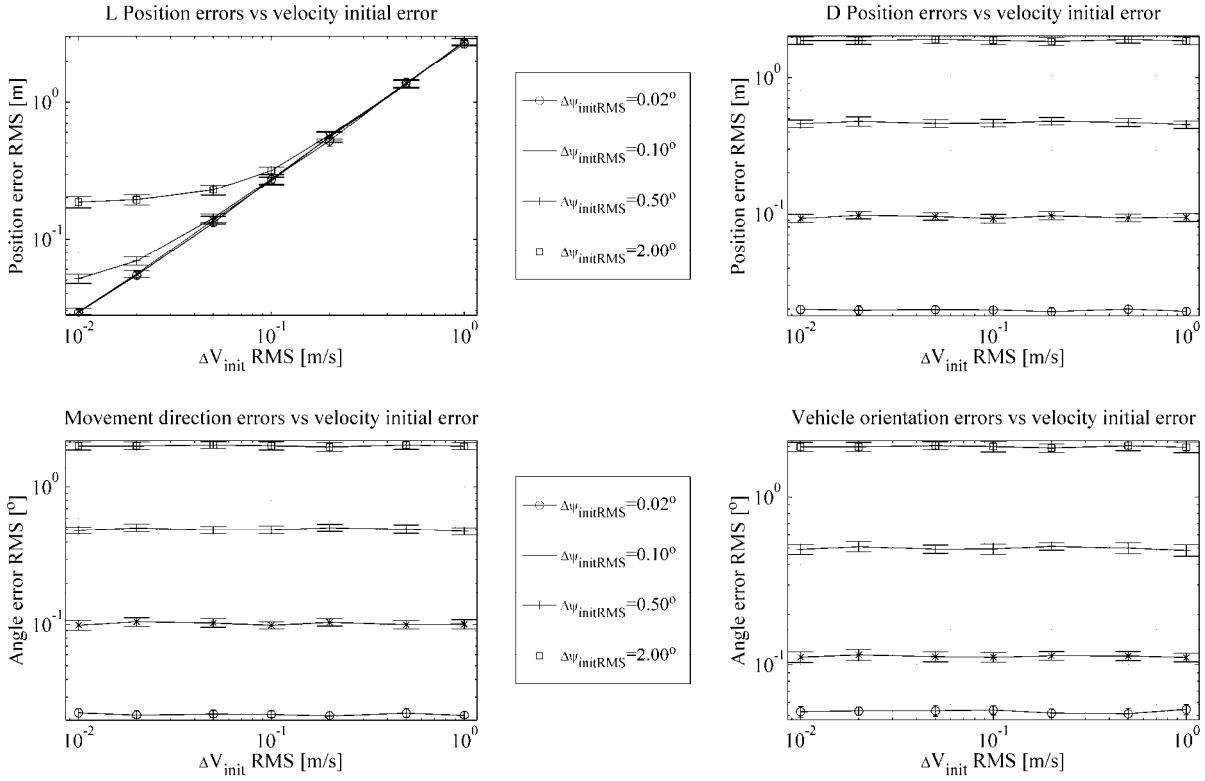


***Figure 3. The influence of errors in initial velocity and angle measurement on the track reconstruction.***

**Influence of varying trajectory, vehicle velocity and deceleration**

All presented results were obtained with a fixed track geometry (i.e. its length *L* and width *D*) and constant speed of 20 m/s. The question is, how these results change with the length of the track, initial speed and possible deceleration during the manoeuver.

For following simulations, all possible error sources were included. The simulation parameters were as follows:

- Spectral noise density of the accelerometers: $2.2 \cdot 10^{-3}$ $m/s^2/\sqrt{Hz}$ ,
- Spectral noise density of the angular velocity sensor: $3.0 \cdot 10^{-3}$ $^o/s/\sqrt{Hz}$ ,
- Miscalibration of the accelerometers: 0.01 $m/s^2$ RMS
- Miscalibration of the angular velocity sensor: 0.1 $^o$/s RMS
- Error in initial velocity: 0.01 m/s RMS
- Error in initial vehicle orienttion: 0.1 $^o$ RMS
- Sampling frequency of the sensors: 100 Hz

The distance along the road for deceleration-dependent plots was 50 m.

The results are presented in Figure 4. One can see that a combination of all disturbing factors may cause position errors exceeding 1m, especially for long distances and small vehicle velocity. Mostly sensor miscalibration and errors in initial conditions are responsible for this value. It was checked, that the accuracy in both axes is influenced. The distinctive peaks on the deceleration-related plots (right side of Figure 4) are related to a situation where the deceleration causes the vehicle to stop at the end of the maneuver.

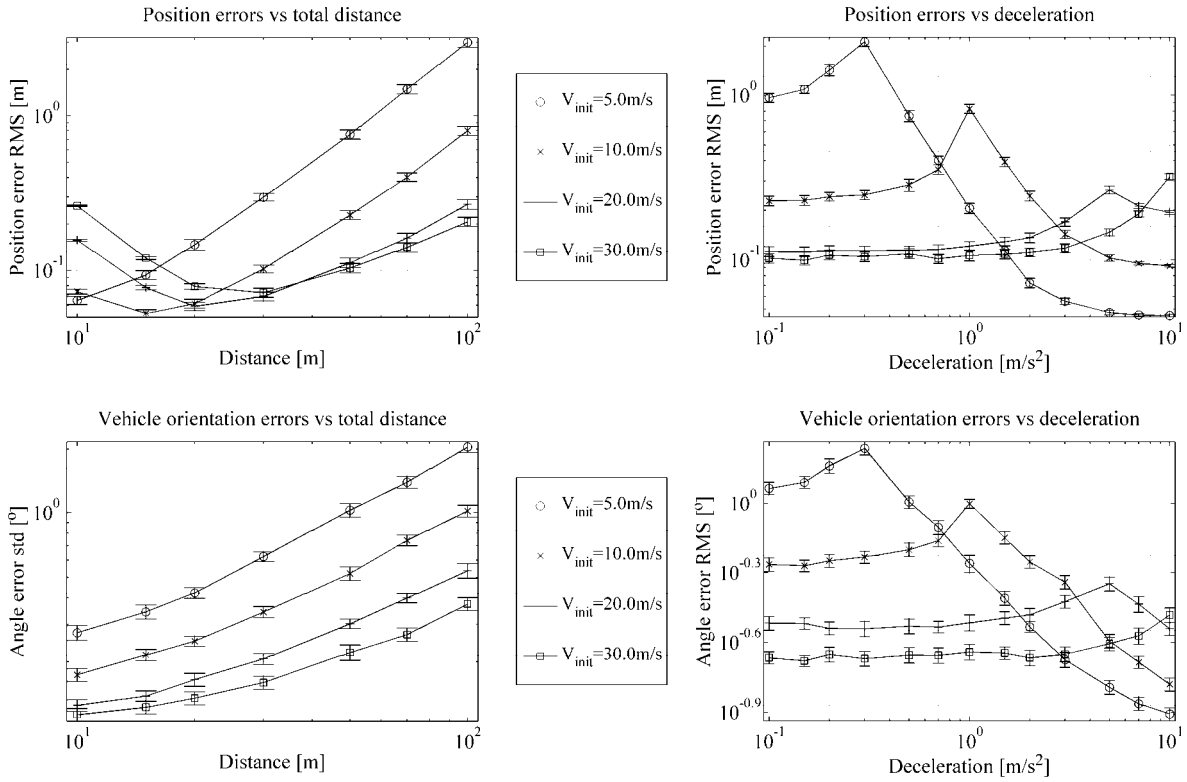


***Figure 4. The influence of the track geometry, initial velocity and deceleration on the track reconstruction.***

**Influence of the sampling rate**

The last simulation was performed to check the influence of the sampling rate of the converters on the results (Figure 5). The general outcome is that:

- the sampling frequency is more important for high velocities and narrow track shapes;
- for typical conditions, the sampling frequency in range of 100-400 Hz is sufficient.

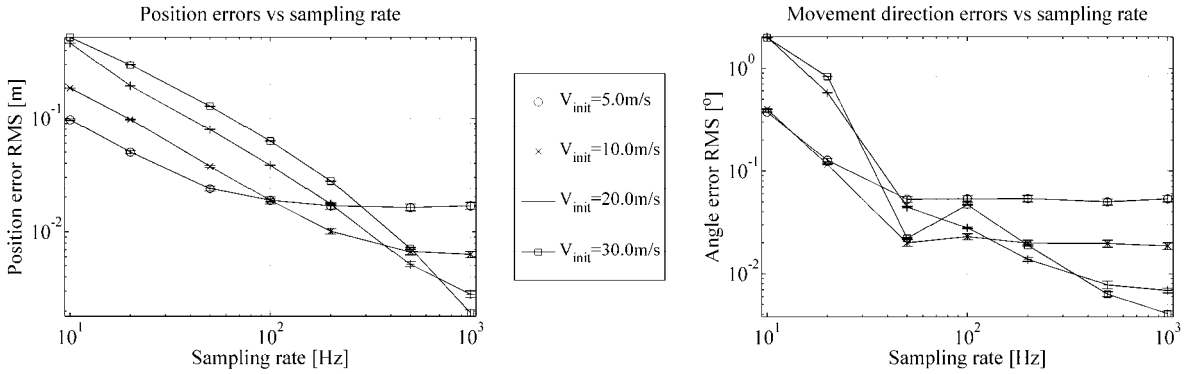


***Figure 5. The influence of the sampling rate of the converters on the track reconstruction. Track length along the road is 20 m.***

## CONCLUSIONS AND DISCUSSION

The presented research included an analysis of achievable accuracy of a system of inertial sensors intended for automated driving of a vehicle. The results show that driving a vehicle using only inertial sensors (accelerometers and gyroscopes) is possible over short distances reaching few dozens of meters.
The crucial factors determining the accuracy of position reconstruction are good calibration of the sensors, proper offset compensation and undisturbed information on initial conditions (vehicle's velocity vector and position). It was checked that the noise of the sensors is not a foreground component determining the accuracy. The requirements regarding the noise are easy to fulfill using modern MEMS-type sensors.
The simulations have shown that lowest errors are achievable for short times, i.e. for short track lengths and high velocities. However, some issues concerning the sample rate of the sensors may influence the accuracy for very rapid movements. Proper data interpolation may partly compensate this effect, but it will never be fully eliminated.

One must take into account the limitations of the simulations. First, all of them were performed using the same track shape – half-sine. Second, the used model is only two-dimensional, while vehicle tilting may require 3-dimensional reconstruction in real applications.
The aforementioned restrictions are not an effect of limited capabilities of the developed simulation engine. They were introduced intentionally to reduce the number of possible combinations of factors influencing the results. We believe that, for such a generic research, clear representation of the results is more important that covering the full area of possible input parameters. The obtained results should be representative and easily extendable over different track geometries and switching to a 3-dimensional model should cause only moderate accuracy degradation.

The tests reported herein were carried out and their results were analysed within an authors' own research project No. N N509 568439.

## REFERENCES

[1] Gidlewski, M.: Opportunities to investigate the steering system for improvement of truck driving properties under critical road conditions. Archives of Transport No. 3/2011.
[2] Gidlewski, M., Kochanek, H., Posuniak, P.: Methods of driver's support at the critical road situations. TTS Technika Transportu Szynowego 9/2012
[3] "LIS3DH, MEMS digital output motion sensor, ultra low-power high performance 3-axes 'nano' accelerometer", ST Microelectronics, Doc ID 17530 Rev 1, May 2010, www.st.com
[4] "LSM330, iNEMO inertial module: 3D accelerometer and 3D gyroscope", ST Microelectronics, Doc ID 023426 Rev 3, Dec 2013, www.st.com
[5] "L3G4200D, MEMS motion sensor: ultra-stable three-axis digital output gyroscope", ST Microelectronics, Doc ID 17116 Rev 3, Dec 2019, www.st.com

# A Mobile Deformable Barrier Test for the Front Crash Assessment of Future Urban Microcars

**Ernö Dux, Lutz Eckstein**
Institut für Kraftfahrzeuge, RWTH Aachen University
Germany

**Maja Wolkenstein, Gian Antonio d'Addetta**
Robert Bosch GmbH
Germany

**Peter Luttenberger**
Institut für Fahrzeugsicherheit, Graz University of Technology
Austria

Paper Number 15-0343

## ABSTRACT

A rising share of electric microcars (with mass well below 800kg) is predicted for the future urban vehicle fleet. Therefore the relevance of safety hazards due to mass incompatibility in case of front crashes will increase significantly. The front crash test according to ECE regulation no.94 initially defined for M class vehicles does not allow to reproduce the predicted real-world crash severity for light vehicles. This paper describes an alternative test for front crash assessment of microcars using a mobile progressive deformable barrier (MPDB) with adjusted mass properties. Since the long term development of the vehicle fleet is unclear, a test set-up with parameterized barrier mass properties having the potential to reproduce variable car-to-car front crash constellations is proposed.

The relevant test parameters for a microcar front crash test are chosen based on predicted future trends from literature, expert surveys and car-to-car crash sensitivity tests. Based on that, a finite element (FE) model of a parametric MPDB is proposed, reproducing the mass properties of various possible front crash opponents. To quantify the use potential of the test, a comparison of MPDB test outputs for three types of possible microcar concepts with car-to-car crash outputs using FE Generic Car Models from the FIMCAR project as opponents is carried out. The main focus of this comparison is on structural crash performance and occupant injury. In order to bridge these two, an adequate crash restraint system triggering based on the acceleration sensing system is proposed.

As conclusion general use recommendations for the parametric MPDB test configuration are formulated.

The study presented within this document was executed within the EC co-financed project SafeEV (Safe Small Electric Vehicles through Advanced Simulation Methodologies) – www.project-safeev.eu

## INTRODUCTION

The small cars segments (A/B) are predicted to show highest global growth rates in a mid-term perspective (*Kalmbach et al., 2011*). In an urban environment cars showing special features globally attributed to the term microcar – such as reduced overall dimensions, low fuel consumption due to reduced engine capacity, limited seating and storage space and in case of electric powering also local emission free usage – can become especially attractive.

Until now cars showing these properties can either be classified as M class vehicles (*Directive 2007/46/EC*) or as heavy quadricycles belonging to the category L7e-CP (*Regulation (EU) No 168/2013*) on the European market. The main distinction between these classifications with respect to passive safety is the lack of crash test assessment, that a L7e-CP vehicle has to fulfil for homologation, while M class vehicles are required to pass several crash tests. In addition, there is an upper speed limit of 90 km/h and an upper weight limit of 450 kg (without battery system) set to vehicles attributed to the L7e-CP class. M class listing is not related to a lower weight limit. Nevertheless current M class vehicles weight generally more than approximately 800 kg, due to the weight-increasing fulfilment of comfort and functionality requirements, partly not relevant in an urban use environment. The present study is focussing on future urban microcars defined as being placed in the weight gap between L7e-CP class and the virtual lower limit of 800 kg for current M class vehicles.

The main front crash passive safety hazard identified for light vehicles is the potential crash against heavier opponent vehicles (*O'Brien, 2010*) due to the high significance of mass incompatibility. This results in higher velocity change for the lighter crash partner and therefore in higher crash severity. Current European front crash testing procedures, either related to M class according to *UN-ECE Regulation No. 94* or related to L7e-C vehicles as seen in Euro NCAP's most recent test series for heavy quadricycles (*Euro NCAP, 2014*), are not addressing the issues of mass incompatibility by testing against fixed crash barriers. These test conditions do not reproduce the energy balance of a vehicle-to-vehicle crash and the possible influence of the mass ratio on crash severity for the assessed vehicle. Higher reproduction potential is attributed to mobile deformable barrier (MDB) tests according to different studies (e.g. *O'Brien, 2010 or Uittenbogaard and Versmissen, 2013*), due to the more realistic energy balance.
The use profile of these future urban microcars is not yet clear on midterm forecasting level: Will their use be restricted to urban areas? With what kind of possible crash opponents will they share the traffic environment and what developments will influence closing speed and impact direction in case of front crash? Resulting from that, precise parameters of the relevant real world safety hazard related to vehicle-to-vehicle front crash cannot yet be defined. Fixed testing conditions with a static logic behind the crash severity definition do not have the flexibility to respond to changes in the target crash scenario.

## USE POTENTIAL OF THE MOBILE PROGRESSIVE DEFORMABLE BARRIER (MPDB)

Previous studies have identified the high use potential of MDBs for the front crash assessment of light vehicles. MDB tests show good reproduction potential of the real world crash kinematic. In addition, the structural interaction between crash partners is also suitably reproduced, when a deformable barrier element is chosen with stiffness properties that are comparable to those of a crash opponent's vehicle front.

The MPDB, introduced by *Bosch-Rekveldt et al., 2006* and further developed during the 'Frontal Impact and Compatibility Assessment Research (FIMCAR)' project is the most recent European development in the field of MDBs for front crash assessment. The weight is adjusted to represent the European fleet average with inertia properties according to US vehicle fleet mass properties. The progressive deformable barrier (PDB) as energy absorption element has stiffness properties that are comparable the those of recent vehicles tested in EuroNCAP's offset front crash configuration (*Uittenbogaard and Versmissen, 2013*). First analysis of the influence of the barrier weight on crash severity was already executed by *Bosch-Rekveldt et al., 2006*, identifying a mayor influence on crash pulse and energy dissipation level of the tested vehicle. The test set-up investigated during the FIMCAR project for the 1,500 kg MPDB has the following parameters: 50 % overlap, 50 km/h-50 km/h impact speed, 0 ° impact angle.
Test configurations using a mobile test barrier offer the highest number of crash configuration parameters, therefore being most suitable for a flexible adjustment of the test in case of target scenario shift. In this way the current MPDB test set-up can easily be adapted to a configuration relevant for microcar assessment.

## DEFINITION OF A PARAMETRIC MOBILE PROGRESSIVE DEFORMABLE BARRIER (P-MPDB)

Concerning the future real-world vehicle-to-vehicle crash target scenario for microcars, only general trends can be discussed:

- Relevant crash opponent mass: The arguments related to fuel saving and emission reductions specially in urban traffic environment lead to significant lightweighting efforts in vehicle development, possibly leading to lower average vehicle weight (*Luttenberger et al., 2013*). *Wismans et al. 2013* identify 1,150 kg curb weight as average front crash opponent weight for possible future urban microcars.
- Impact speed: It is unclear, how far the use profile of future urban microcars will be restricted to urban traffic environment, resulting in lower relevant crash speeds. In the same form the future penetration of advanced driver assistance systems related to collision mitigation into the vehicle fleet might have an impact speed reducing effect.
- Impact angle: with a possible use concentration of microcars to urban areas, the relevance of accidents with oblique impact direction in turning and crossing traffic is supposed to grow in relation to conventional head-on collisions (*Wismans et al., 2013*).

The current MDPB test configuration requires a parametric adaptation to fit more to the possible traffic scenario developments and the resulting real world vehicle-to-vehicle front crashes involving microcars.
For a better understanding of the relevance of different vehicle-to-vehicle crash parameters (opponent vehicle mass properties and configuration parameters like impact speed and angle) on the resulting crash severity for the lighter crash partner, vehicle-to-vehicle crash sensitivity tests are executed on a virtual level. To eliminate the influence of specific structural properties of exemplary vehicle models on crash severity output parameters, vehicles with idealized form and force compatibility properties are used for these tests. For this purpose vehicle models with homogeneous energy absorbing honeycomb structures filling the front vehicle are defined (c.f. *Figure 1*, *left*). These idealized front vehicles show progressive stiffness comparable to the lower load path within the PDB. The only remaining incompatibility property within the sensitivity test set is related to mass, representing different vehicle-to-vehicle crashes with mass ratio between 1:1 and 1:2.8.

The executed sensitivity testing allows the formulation of approximately linear dependencies between crash configuration parameters and the crash severity output. Based on this assessment, the implementation of the following parameters into a parametric model of the MPDB FE model is decided (c.f. *Figure 1*, *right*):

- Centre-of gravity in x-direction (driving direction),
- Total barrier mass and
- Inertia properties of barrier (defined as dependent on total barrier mass).

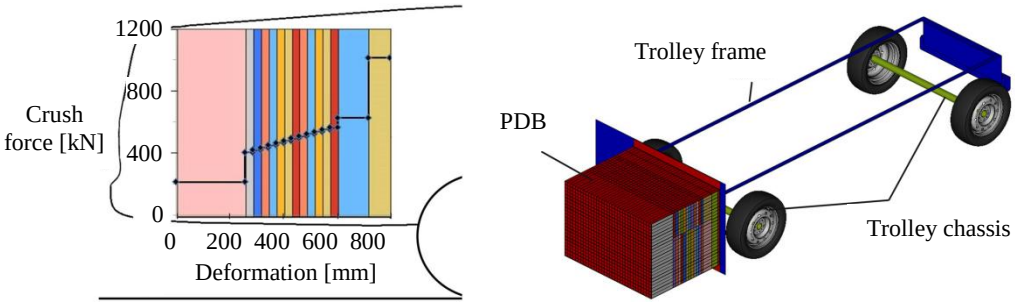


***Figure 1*** ***Idealized vehicle front model (left) and its correspondence to the P-MPDB FE model (right)***

The barrier model's main property is to represent real front crash opponent vehicles of different possible total mass. To model the mass-dependent inertia properties of a broad range of vehicles, the inertia values expressed as function of mass are implemented into the FE model of the barrier, based on fleet measurements as discussed by *Bosch-Rekveldt et al., 2006* (c.f. Equations 1-3).

$$I_{XY} = 0.0497 \cdot m^{1.4879} \quad (1.)$$

$$I_{XZ} = 0.0289 \cdot m^{1.5572} \quad (2.)$$

$$I_{YZ} = 0.0256 \cdot m^{1.3644} \quad (3.)$$

with m [kg]; $I_{ij}$ [kg·m$^2$]

Besides this adjustability of the barrier itself, also the influence of change of crash configuration parameters is to be analyzed. Therefore a range of impact speeds and angles are to be considered to represent different possible front crash scenarios. The barrier overlap is fixed to 50 % of the vehicle width, to allow a meaningful assessment of microcars structural performance in case of one sided loading of its energy absorbing structures.

## DEMONSTRATION OF P-MPDB USE POTENTIAL - STRUCTURAL CRASH BEHAVIOUR

In a next step, the use potential of the P-MPDB test configuration is to be quantified. The focus of this analysis is double:

- Show the advantages of this test set-up for microcar assessment in comparison to conventional offset crash test procedures.
- Identify the capacities and limitations of the test set-up to reproduce different crash severity aspects of vehicle-to-vehicle crash in different possible crash configurations.

For this assessment, three reference electric vehicle examples, being potential representatives of future urban microcars, are analysed in FE modelling environment concerning relevant structural crash severity output parameters in front crash situations:

Reference electric vehicle model 1 (REVM1) represents a light weight vehicle (curb weight = 685 kg), designed according to M class vehicle standards and therefore dimensioned to fulfil M class front crash regulation targets (*Puppini et al., 2013*).

Reference electric vehicle model 2 subversion 8 (REVM2_V8) is representative for vehicles situated at the borderline of the L7e-CP vehicle category (curb weight = 513 kg, including battery system weight), using conventional design tools and materials not considering any structural passive safety requirement. This design strategy results in a behaviour comparable to the ones of current heavy quadricycles (*c.f. Euro NCAP, 2014*), showing weak structures resulting in high crash deformations but soft deceleration pulses. Reference electric vehicle model 2 subversion 9 (REVM2_V9) shows the same structure and weight properties as REVM2_V8, but applies high performance materials, therefore showing stiff structural design resulting in low crash deformations but hard deceleration pulses. (*Hinc, 2015*)

Possible M class crash opponent vehicles to simulate real world vehicle-to-vehicle front crash are taken from the FE vehicle model pool of generic car models (GCM) (*Stein et al., 2012*).

### P-MPDB use benefit in baseline crash configuration

The first step of the use potential assessment of the P-MPDB consists of a comparison between a chosen baseline vehicle-to-vehicle front crash, different standard barrier front crash tests and front crash against P-MPDB in a mass property version adjusted to the chosen crash opponent vehicle. This assessment step allows to proof whether the defined test set-up shows a higher potential to reproduce the baseline real-world front crash than known standard laboratory tests. For this purpose the baseline vehicle-to-vehicle front crash configuration is chosen to be the same as the reference for the definition of the 56 km/h ODB front crash according to ECE regulation No. 94 (*Lowne, 1994*):

- 50 % horizontal overlap
- 50 km/h impact speed (100 km/h closing speed)
- 0 deg impact (in-line impacting)

The generic car model 2A (GCM2A) is selected as reference opponent (curb weight: 1,186 kg), at is has a weight comparable to the average front crash opponent weight for future urban microcars identified above. Standard front crash tests (ODB front crash test, according to *UN-ECE Regulation No. 94* and the PDB front crash test as described in *Regulation No. 94 – Proposal for draft amendments*) and the MPDB test are compared to the P-MPDB test (c.f. Table 1). For every assessed microcar in each barrier crash configuration the percentile variation of the structural crash severity parameters is calculated in comparison to the vehicle-to-vehicle reference crash output according to Equation 4.

$$Variation = \frac{(parameter_{veh-to-barrier} - parameter_{veh-to-veh})}{parameter_{veh-to-veh}} \cdot 100 \qquad (4.)$$

To condense the percentile variation for the three used microcar types into one index value per crash severity parameter, the root mean square (RMS) of the percentile variation of each parameter is calculated (c.f. Table 1). The RMS was chosen because it penalizes big differences with few occurrences over small differences with many occurrences and prevents that positive and negative values may compensate each other leading into unrealistic interpretations. The test set-up with the smallest parameter variation with respect to the vehicle-to-vehicle crash reference is highlighted in blue.

**Table 1**
**RMS of crash severity parameter deviation between baseline vehicle-to-vehicle crash (opponent: GCM2A) and examined vehicle-to-barrier tests**

| REVMx vs. | P-MPDB | MPDB | ODB | PDB |
|---|---|---|---|---|
| Barrier properties | MDB- 1,336 kg | MDB - 1,500 kg | Fixed barrier | Fixed barrier |
| Test configuration parameters | 50 - 50 km/h 50 % overlap | 50 - 50 km/h 50 % overlap | 0 - 56 km/h 40% overlap | 0 - 60 km/h 50% overlap |
| Passenger compartment intrusions | | | | |
| Max. intrusion | 20 % | 21 % | 70 % | 37 % |
| Kinematic behavior | | | | |
| $a_{x,max}$ | 10 % | 10 % | 36 % | 29 % |
| $\Delta v_x$ | 3 % | 6 % | 6 % | 6 % |
| Average z-rotation speed | 10 % | 28 % | 25 % | 26 % |
| Crash energy balance | | | | |
| Deformation energy | 12 % | 17 % | 64 % | 45 % |
| Energy Equivalent Speed (EES) | 6 % | 8 % | 40 % | 26 % |

Both fixed barrier tests show high deviation from the reference vehicle-to-vehicle crash behaviour, while the MDB tests show a good reproduction capacity. These high deviations are clearly related to the incapacity to reproduce the crash mechanic behaviour of a moving crash opponent vehicle with a fixed barrier test. Meanwhile, the reduction of the moving barrier's total mass from the MPDB mass level (1,500 kg) to the mass of the reference crash opponent GCM2A explains the highest reproduction accuracy of the P-MPDB test.

The calculations leading to the impact speed of 56 km/h in the ODB test (c.f. *Lowne, 1994*) to reproduce a 100 km/h closing speed reference crash between two vehicles assume that the involved vehicles are identical. This is no longer valid when the reference crash shows a high mass ratio between the crash partners. To overcome the intrinsic deficit of fixed barrier crash, not being able to reproduce the kinetic behaviour of a moving crash opponent, the impact speed for light vehicles could be increased. In accordance with this argument additional fixed barrier tests at higher impact speeds are executed for REVM2_V8 and REVM2_V9, representing the lightest microcars in the assessment, therefore showing the highest mass ratio in a crash against the GCM2A.

With increasing impact speed the crash severity is increasing for different types of microcars, as REVM2_v8 represents a weak SEV structure, while REVM2_v9 represents stiff structural response. Nevertheless, the severity increase is not proportional, resulting in improved reproduction capacity for energetic output parameters but only weak change to the kinematic outputs. Therefore no clear speed value can be identified, that would allow to overcome the intrinsic deficits of fixed barriers, not being able to reproduce the kinematic behaviour of a moving crash opponent.

**Reproduction limitations for alternative vehicle-to-vehicle crash configurations**

Having identified the use benefit of a P-MPDB test to reproduce vehicle-to-vehicle crashes in baseline configuration, the next step of the examination addresses the oblique crash configuration identified as representative for accident scenarios in turning and crossing traffic within an urban environment (c.f. *Wismans et al., 2013*). It is to quantify how far a P-MPDB based oblique test set-up can reproduce the crash severities occurring for different microcar structures in an oblique crash against the selected crash GCM2A. Table 2 shows the comparison of crash severity output parameters between the two oblique impact configurations for the three examined microcars.
The P-MPDB is capable of producing crash severities that are very well comparable (max. 15 % deviation) or higher than within the comparable vehicle-to-vehicle crash for different types of microcars also under oblique impact direction. Even though the barrier front shows better structural interaction possibilities for the assessed vehicles, the resulting severities in the field of intrusion and deceleration are higher than in the vehicle-to-vehicle crash. This is a result of the large size of the loaded surface of the barrier front under oblique impact angle in comparison to the interacting structures of a crash opponent's vehicle front. The difference between the interacting structures of a homogeneously deforming barrier and any given vehicle front geometry represents the intrinsic deficit of a MDB

test to reproduce a vehicle-to-vehicle crash. The relevance of this limitation is dependent on the impact angle, as the relative position of the interacting structures is influenced by the orientation of the crash partners.

**Table 2**
**Comparison of crash severity indicators: vehicle-to-vehicle and vehicle-to-P-MPDB crash**

| **Assessed microcar** | **REVM1** | | **REVM2_V8** | | **REVM2_V9** | |
|---|---|---|---|---|---|---|
| Crash opponent | GCM2A 1,336 kg | P-MPDB 1,336 kg | GCM2A 1,336 kg | P-MPDB 1,336 kg | GCM2A 1,336 kg | P-MPDB 1,336 kg |
| Crash configuration parameters: Overlap 50 %, impact speed 35 – 35 km/h, opponent impact angle 30 deg | | | | | | |
| Passenger compartment intrusions | | | | | | |
| Max. intrusion [mm] | 67.2 | 170 | 197 | 270 | 53.1 | 51.8 |
| Kinematic behaviour | | | | | | |
| $a_{x,max}$ [g] | 28.7 | 30.7 | 25.9 | 30.8 | 34.0 | 42.0 |
| $\Delta v_x$ [m/s] | 11.5 | 13.2 | 10.97 | 11.75 | 10.72 | 10.92 |
| $\Delta v_y$ [m/s] | 6.25 | 5.5 | 5.7 | 5.15 | 5.82 | 5.02 |
| Crash energy balance | | | | | | |
| Deformation energy [kJ] | 28.3 | 38.6 | 41.0 | 43.9 | 30.8 | 24.6 |
| EES [m/s] | 8.22 | 9.61 | 11.1 | 11.5 | 9.59 | 8.58 |
| Legend: green = deviation from reference <15 %; red = severity is > 15 % higher than in vehicle-to-vehicle crash; yellow = severity is > 15 % lower than in vehicle-to-vehicle crash | | | | | | |

## CRASH RESTRAINT SYSTEM TRIGGERING

Overall goal of vehicle to barrier tests is the reproduction of a real world vehicle to vehicle crash situation. Besides the right deformation of the vehicle it is also important to predict or rather assess the passive safety sensors and the restraint system of the tested vehicle. Comparable to a state-of-the-art vehicle development process the virtual sensor evaluation for front crash safety represents one key part within the SafeEV project development of an advanced simulation methodology for consistent safety analysis of electric microcars.

First step within the virtual sensor evaluation process is to define the sensor layout for the microcar. Therefore sensors have to be positioned at suitable areas within the vehicle. The typical sensor layout for small state-of-the-art vehicles is shown in *Figure 2*.

For accurate detection of frontal crashes at least one acceleration sensor for detection and one for the plausibility verification are used. The external satellite sensors (green in *Figure 2*) can be damaged or switched off during crash after the restraint system has been triggered. The electronic control unit (ECU) must remain intact even after the crash event because of crash data recording. The acceleration sensor should be mounted on a stiff structure within the vehicle. Regular driving mode and misuse crashes like driving trough a pothole should not cause a high excitation at the sensor position. In state-of-the-art vehicles the sensors are typically mounted at the vehicle tunnel or the pillars. If the vehicle structure of microcars changes strongly compared to these types of vehicles, a sensor on the left and right rocker sill can be placed instead of a central sensor at the tunnel.

The most important requirement for the virtual application of the sensor system is a good matching of acceleration crash signals between the real-world vehicle and the virtual model. Therefore the crash signals should be compared with state-of-the-art vehicles to check the plausibility of the virtual crash data. After defining the sensor position within the vehicle a crash set of different crash types must be generated including fire (e.g. ODB 40%, 64kph), no-fire (e.g. RCAR Bumper Test) and misuse (e.g. driving through a pothole) crashes. Via a simplified application procedure the trigger times for the restraint system are determined. The applied algorithm procedure consists of a standalone core part, which provides a capable base performance, and support functions, which consider the vehicle specific characteristics *(c.f. Kärner et al., 2008)*.

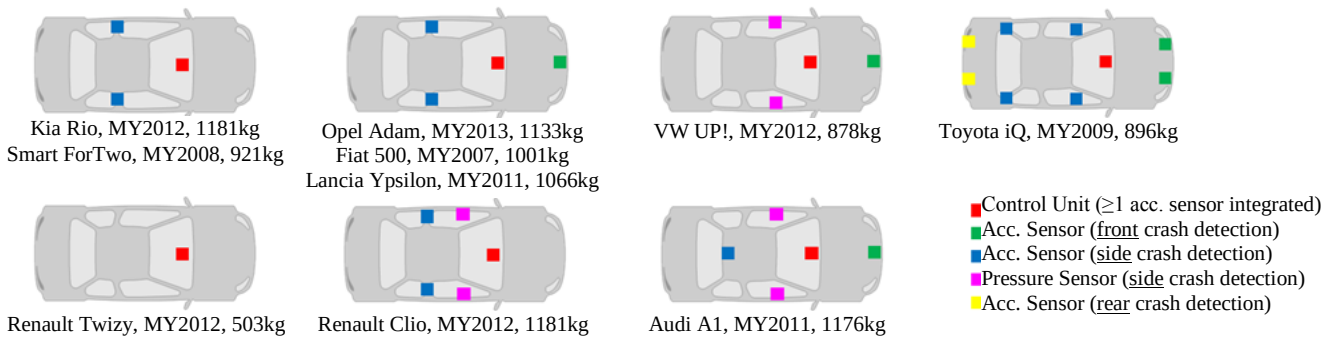


***Figure 2 Sensor layout in small state-of-the-art vehicles according to A2Mac1 database***

Since the used vehicle FE models in the SafeEV project are not suitable for the simulation of certain misuse cases only fire and nofire crash types are taken into account for the simplified application procedure. The advantage of the used algorithm application procedure is that the calibration of the use crashes is independent of the misuse crashes. Thus trigger times can be estimated by using the fire and no fire crash signals in the application procedure. However for the final determination of the trigger times the misuse crash signals are absolutely necessary. If misuse crash signals are included in the application procedure, a later triggering of restraint system may be obtained.

The application process in today's series algorithm calibration works contrary to the above described procedure. Generally the vehicle manufacturer first performs occupant simulations, defines the necessary triggering times for belt pretensioner and airbag for each crash and delivers the trigger times to the airbag control unit supplier. Afterwards the supplier adapts his algorithm to the customer needs. Through in-depth analysis of the vehicle crash pulses according to an extended and customer defined crash set the required trigger times are realized though an advanced version of the described application procedure.

The determined trigger times for the belt pretensioner and the first and second deployment stage of the airbag are shown in the Table 3 for REVM2_V9 as a result of the simplified crash signal calibration. The determined trigger times are compared with publicly available trigger times from state-of-the-art small vehicles like the Smart Fortwo and Fiat 500 (IIHS database) and Renault Twizy (EuroNCAP database). The determined trigger times for SafeEV's microcars are lower than the trigger times of above small vehicles. The main reason for this effect is the combination of REVM2_V9 low weight and high stiffness. High acceleration signals are measured earlier at the vehicle tunnel during the crash process resulting in an earlier triggering of the restraint systems. Nevertheless it should be verified if available in-crash sensors are capable to generate adequate crash signals in order to realize such an earlier triggering. Additional possible solutions would be more sensors in the vehicle front (upfront sensors) or environment sensing coupled with reversible or irreversible restraint systems, like electronic belt tensioner. Another alternative is to adapt the restraint systems, i.e. overall shorter deployment times.

**Table 3**
**Crash set for REVM2_V9 for assessment of restraint system triggering time for front crashes**

| Vehicle | Crash Type (Opponent) | Impact Velocity [km/h] | Belt Pretensioner / Airbag 1st Stage [ms] | Airbag 2nd Stage [ms] |
|---|---|---|---|---|
| Smart ForTwo | ODB 40% | 64 | 22 | - |
| Fiat 500 | ODB 40% | 64 | 20 | - |
| Renault Twizy | FWDB, 0° | 50 | 24 | - |
| REVM2_V9 | ODB 40% | 64 | 16.6 - 17.6 | 21.6 - 22.6 |
| REVM2_V9 | P-MPDB 50%, 0° | 50 / 50 | 8.8 - 9.3 | 13.8 - 14.3 |
| REVM2_V9 | P-MPDB 50%, 30° | 35 / 35 | 20.3 - 20.8 | 25.3 - 25.8 |
| REVM2_V9 | GCM2A 50%, 0° | 50 / 50 | 23.2 - 24.1 | 28.2 - 29.1 |

The analysis of the use potential of the P-MPDB has shown that the reproduction of a vehicle-to-vehicle crash is generally possible. Although a good correlation in vehicle deformation between REVM2_V9 vs. P-MPDB and REVM2_V9 vs. GCM2A can be shown (see section "P-MPDB use benefit in baseline crash configuration"), the obtained trigger times for the P-MPDB crash (cf. Table 3) are much lower than for the vehicle-to-vehicle crash. This can be attributed to the higher crash signal of the P-MPDB crash in the early stage of the crash (see *Figure 3*).

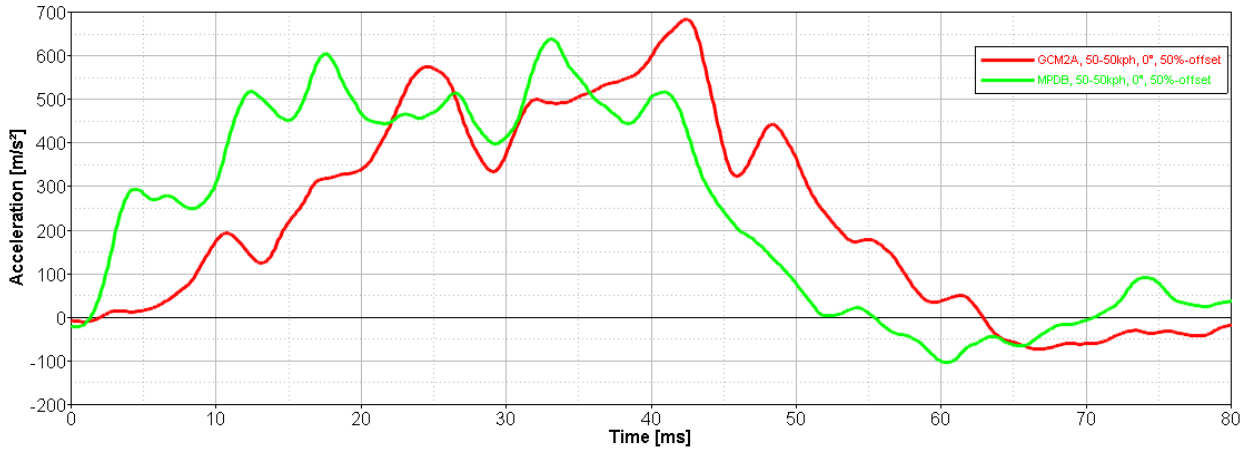


***Figure 3 Comparison of acceleration signal from REVM2_V9 vs. GCM2A / P-MPDB***

The estimated occupant forward displacements at the calculated trigger times for both crash types can be shown to be almost in the same range. In case of the REVM2_V9 vs. GCM2A crash the triggering of the restraint system occurs later but the occupant forward displacement is also slower than in the P-MPDB crash. Thus the same safety level for the occupant can be realized. The vehicle deformation and occupant safety of vehicle to vehicle crashes can be well reproduced by vehicle to P-MPDB barrier crash. However for the calibration of the restraint system triggering algorithm it makes a difference, since the signals must be processed differently.

## MICROCAR OCCUPANT INJURY PREDICTION IN OBLIQUE CRASH CONFIGURATION

For the assessment of the crash severity for the occupant a reduced sled model and the Human Body Model (HBM) "THUMSv4.0" was used. The results are then assessed with an injury prediction tool developed at the Vehicle Safety Institute in Graz. First a short summary of the models will be given. Secondly a review of energy, strain and stress based prediction for injuries is shown for the oblique crash configuration identified as representative for accident scenarios in turning and crossing traffic within an urban environment (c.f. *Wismans et al., 2013*).

The THUMSv4.0 was introduced in 2010 and is the latest version of Toyota´s HBM research activities in this field. The geometric data was obtained from computed tomography scans of a human male (173 cm, 77.3 kg) and scaled to a 50 percentile human. Due to the more detailed model and improved bio-fidelity injuries and injury criteria can be assessed. The validation of the model was done by running different loading situations on the human body regions (i.e. head or abdomen) and parts. For example, translational impacts, belt loading, 3-point bending, dynamic and quasi static tests, etc. were simulated (*Toyota Motor Company, 2011*). The sled model was derived from the microcar REVM2_V9 and was reduced to the most important components for occupant safety analysis. As the original vehicle model has no interior parts the used parts were extracted from a Ford Taurus, available at the *NCAC download area*.

The used restrain system within the model was implemented by a project partner. This system was not well optimized for the oblique crash configuration itself, but delivers sufficient response quality on injury severity to assess the output sensitivity on crash configuration parameter change. The usual restraint system models within the solver are used and the values for the numerical simulation runs were set to:

- Airbag Fire Time = 20.0 ms
- Pretensioner Fire Time = 20.0 ms
- Force Pretensioner = 1.5 kN
- Force Load Limiter = 4 kN

The assessment of the simulation results was performed with the injury tool. The development of the tool was necessary as already available post-processors are not capable of handling the amount of data caused by a detailed HBM and the evaluation procedure and injury criteria cannot be implemented easily. The injury tool includes following assessment groups in the latest version:

- Rib Fractures, Organ Damage, Bone Fractures, Head Injury, Ligament Elongation.

For the analyzed oblique front crash configuration the Strasbourg University Finite Elements Head Model (SUFEHM) criteria level is very low (probability of injury ~1 %). The Cumulative Strain Damage Measure (CSDM) criterion has an AIS3+ probability of 10 % for the load case. The probability for rib fracture was calculated with 83.6 % for 4 fractures and 16.4 % for 3 fractures. From the Abbreviated Injury Scale (AIS) codebook it is known that 4 fractured ribs would be classified as AIS3. The fractures occur in the shoulder area and next to the sternum. For the assessment of organ injuries the selected thresholds predict a probability of a possible damage varying from 38 % to ≥ 100 %.

In *Figure 4* the head and lower extremity assessment is shown. For the CSDM an injury risk curve is already available.

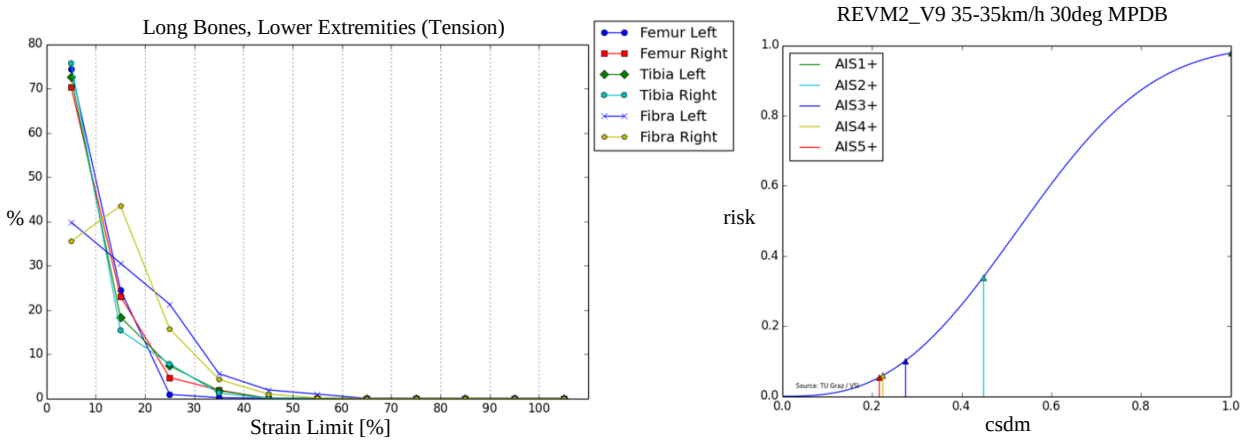


***Figure 4*** ***Head and lower extremity assessment for REVM2_V9***

In case of the long bones and strain-stress based injury prediction no risk curve was found. For the bones only the cortical volume was used. 100 % of strain limit in the diagram is the predefined threshold for long bones. The ordinate shows the fraction of elements of the cortical parts reaching a certain value based on the threshold.

## GENERAL USE RECOMMENDATIONS FOR THE P-MPDB TEST CONFIGURATION

The proposed virtual test shows good ability to reproduce the hazards arising for microcars within a car-to-car front crash and exceeds the use potential of common tests using fixed deformable barriers as crash targets. The advantage of the defined set-up in comparison to conventional tests is growing with shrinking mass of the assessed microcar. All configuration parameters of a vehicle-to-vehicle crash can be implemented directly into the P-MPDB crash set-up.

The comparison between the P-MPDB test and vehicle-to-vehicle front crashes quantifies the capacities of barriers to reproduce vehicle crash opponents. Visible limitation appears due to the barrier's homogeneous energy absorption properties in planar direction in comparison to exemplary crash opponent front structures. The relevance of this limitation is dependent on the impact angle, as the relative position of the interacting structures is influenced by the orientation of the crash partners. This effect cannot be overcome as long as a neutral assessment of the vehicle

should be assured, inhibiting optimization related to single selected opponent structures. Furthermore the resulting higher structural crash severities in a P-MPDB test are supposed to be beneficial to the crashworthy development of future microcars.

Through a simplified algorithm procedure plausible trigger times for an adequate in-crash triggering of the restraint systems could be achieved for the proposed test set-up. In comparison to a vehicle-to-vehicle crash against M class opponents, a microcar's restraint system triggering has to occur earlier as the occupant's forward displacement is faster during a P-MPDB crash.

The deceleration based occupant injury predicted for the oblique impact crash appears to be well controlled with common restraint system functioning also for microcars showing stiff structural response. The lateral displacement and rotation effect of an oblique impact on the microcar nevertheless is challenging for the effective interaction between occupant and front airbag.

## REFERENCES


A2Mac1 database https://www.a2mac1.com

Bosch-Rekveldt, M.; Versmissen, T.; van der Zweep, C.; Mooi, H.; McEvoy, S., 2006. "The Development of a Load Sensing Trolley for Frontal Offset Testing". Conference ICrash 2006. Athens / Greece

Directive 2007/46/EC of the European Parliament and of the Council of 5 September 2007 establishing a framework for the approval of motor vehicles and their trailers, and of systems, components and separate technical units intended for such vehicles

EURO NCAP, 2014. Euro NCAP tests on Heavy Quadricycles, www.euroncap.com

Hinc, K., 2015. „SafeEV Deliverable No. 3.7 – Report on final test configuration and evaluation criteria". Graz/Austria

Kalmbach, R.; Bernhart, W.; Grosse Kleinmann, P.; Hoffmann, M., 2011. „Automotive landscape 2025 – Opportunities and challenges ahead". Roland Berger Strategy Consultants, 03/2011

Kärner, C.; Körner,O.; Kolatschek,J., 2008. „Usage of FEA methods in order to ensure integration and appliaction in the restraint system control in early development phase". 9th International Symposium and Exhibition on Sophisticated Car Occupant Safety Systems. Karlsruhe/Germany

Lowne, R., 1994. "EEVC Working Group 11 report on the development of a frontal impact test procedure". 14th international technical conference on Enhanced Safety of Vehicles. Munich/Germany

Luttenberger, P.; Tomasch, E.; Willinger, R.; Bourdet, N.; Mayer, C.; Ewald, C., 2013. "SafeEV Deliverable No.1.1 – Methodical analysis on future accident scenarios involving SEVs". Graz/Austria

NCAC download area - http://www.ncac.gwu.edu/

O'Brien, S., 2010. "Measurement and Assessment of Passenger Vehicle Compatibility in Front and Side Collisions". Faculty of Engineering, RMIT University, Melbourne / Australia

Puppini, R.; Puleo, G.; Hinc, K. M., 2013. "SafeEV Deliverable No.3.1 – Reference Electric Vehicle Models". Graz/Austria

Regulation (EU) No 168/2013 of 15 January 2013 on the approval and market surveillance of two- or three-wheel vehicles and quadricycles

Regulation No. 94 – Proposal for draft amendments, 2007. Proposal submitted by France. Working Party on Passive Safety of GRSP, 42. Session. Geneva/Switzerland.

Safe Small Electric Vehicles through Advanced Simulation Methodologies – www.project-safeev.eu

Stein, M.; Johannsen, H.; Puppini, R., 2012. „FIMCAR Models for the Assessment of Frontal Impact Compatibility" iCrash Conference 2012. Milan/Italy

Toyota Motor Company, Toyota Central R&D Labs, Inc. 2011. Documentation – AM50 Occupant Model: Academic Version 4.0

Uittenbogaard, J.; Versmissen, T., 2013. "FIMCAR-Frontal Impact and Compatibility Assessment Research, Part IX - MDB Test Procedure: Initial Test Protocol". Technische Universität Berlin, Institut für Land- und Seeverkehr, Universitätsverlag der TU Berlin

UN-ECE Regulation No. 94, Revision 1, Uniform provisions concerning the approval of vehicles with regard to the protection of the occupants in the event of a frontal collision

Wismans, J.; Davidsson, J.; Carlsson, A.; Mayer, C.; Luttenberger, P.; D'Addetta, G. A.; Hinc, K. M.; Dux, E.; Nuss, F.; Willinger, R., 2013. "SafeEV Deliverable No.2 - Report on test conditions and evaluation criteria for occupant and vulnerable road user protection of small electric vehicles". Graz/Austria

# MUSCLE ACTIVATION STRATEGIES IN HUMAN BODY MODELS FOR THE DEVELOPMENT OF INTEGRATED SAFETY

**Jonas Östh**
**Karin Brolin**
**Jóna Marín Ólafsdóttir**
**Johan Davidsson**
Chalmers University of Technology
**Bengt Pipkorn**
Autoliv Research
**Lotta Jakobsson**
Volvo Car Corporation and Chalmers University of Technology
**Fredrik Törnvall**
Volvo Group Trucks Technology
**Mats Lindkvist**
Umeå University
Sweden

Paper Number 15-0345

## ABSTRACT

Human Body Models (HBMs) have been used in crash safety research for some time, and are now emerging as tools for the development of restraints systems. One important challenge in the development of advanced restraint systems is to integrate sensory information about the pre-crash phase (time to collision, impact speed and direction, occupant position) to alter restraint activation parameters. Restraint activation can begin even before the beginning of an impact, providing additional time to reposition or restrain the occupant. However, any such pre-crash intervention would invoke a muscle response that needs to be taken into account in HBMs used in simulation of integrated restraints.

The objective of this paper is to provide an update on state-of-the-art modeling techniques for active musculature in HBMs. Examples of applications are presented, to illustrate future challenges in modeling of car occupants muscle responses to restraint activation.

The most common approach for modeling active muscle force in HBMs is to use Hill-type models, in which the force produced is a function of muscle length, shortening velocity, and activation level. Active musculature was first implemented in cervical spine models. These models were applied to study occupant kinematic responses and injury outcome in rear-end, lateral, and frontal impacts; it was found that active musculature is essential for studying the response of the cervical spine. One approach utilized to represent muscle activity in HBMs is to use experimentally recorded muscle activities or activity levels acquired through inverse optimization in open-loop. More recently, in order to represent car occupant muscle responses in pre-crash situations, closed-loop control has been implemented for multibody and finite element HBMs, allowing the models to maintain their posture and simulate reflexive responses. Studies with these models showed that in addition to feedback control, anticipatory postural responses needs to be included to represent driver actions such as voluntary braking.

Current HBMs have the capacity to model (utilizing closed-loop control) active muscle responses of car occupants in longitudinal pre-crash events. However, models have only been validated for limited sets of data since as high quality volunteer data, although it exists, is scarce. Omni-directional muscle responses have been implemented to some extent, but biofidelity of the simulated muscle activation schemes has not been assessed. Additional experimental volunteer muscle activity measurements (with normalized electromyogram recordings) in complex 3D-loading scenarios are needed for validation and to investigate how muscle recruitment depends on occupant awareness and varies between individuals. Further model development and validation of muscle activations schemes are necessary, for instance startle responses, and individual muscle control. This could improve assessment of restraint performance in complex accident scenarios, such as multiple impacts, far-side impacts and roll-over situations.

## INTRODUCTION

Human Body Models (HBMs) have been used in crash safety research for some time. Compared to Anthropomorphic Test Devices (ATDs) they can be made more humanlike, and usually incorporates an omnidirectional design; which makes them suitable for a wider range of crash situations. Future safety development challenges include more oblique and complex crash scenarios, in contrast to standardized crash test scenarios (usually pure lateral, frontal, or rear-end impacts) with ATDs in upright seated postures. Recently, small overlap

frontal crashes have been included in the standardized test procedures (IIHS 2012) and one of the challenges identified is the ATDs' limitations in recreating occupant kinematics within these crashes, with a combination of longitudinal and lateral movement (Jakobson et al. 2013). Small overlap frontal crashes are an example of crash situations where the benefit of an omnidirectional HBM is clear. Other situations include oblique or angled impacts, multiple events, rollover, and run off road events. In a run off road event, the vehicle kinematics is complex and posing significant challenges for occupant simulation (Jakobsson et al. 2014). During run off road events not only the directions of impact can vary, but also the occurrence of multiple impacts connected with low acceleration amplitude events influencing occupant posture during the events. Such scenarios could perhaps be viewed as the ultimate challenge from an occupant simulation perspective. Developing HBMs to address this challenge would be beneficial from a real world safety perspective.

Pre-crash maneuvers can influence occupant posture prior to an impact (Heiter et al. 2005; Hault-Dubrulle et al. 2011). In an analysis of accident data in Japan for 1993–2004, Ejima et al. (2009) reported that approximately 50% of drivers made an evasive maneuver in the form of braking or combined braking and steering before an impact. The development of Collision Avoidance Systems (CASs) is likely to increase the occurrence of pre-crash braking, by adding autonomous braking to the cases where drivers did not brake prior to the accident. CASs help drivers avoid or mitigate collisions through warnings and/or interventions, based on information about the traffic environment (Ljung-Aust et al. 2015). This information can be obtained by radar, laser, camera and other sensors. Intervention can include automatic braking and/or steering as well as means for improving occupant protection by triggering/adapting restraints. The development of CAS has been rapid over the last decade. While quite exotic 10 years ago, today most vehicle manufacturers offer some form of CAS in their vehicles, at least as an extra option. This has been made possible through developments in sensing and threat assessment, as well as improved actuators in production vehicles like steering control and differential wheel braking. The first generation systems were introduced in early 2000 with functionality restricted to provide brake support by tracking objects moving in the same direction as the host vehicle (Coelingh et al. 2006). In 2015, the state of the art systems includes tracking of cyclists, pedestrians and vehicles in front of the host vehicle as well as a first step into addressing intersection situations (when turning in front of an oncoming vehicle) (Ljung-Aust et al. 2015). The results from the few available real world follow-up studies indicate that CAS provide a substantial safety benefit (IIHS 2011; Isaksson-Hellman and Lindman 2012; IIHS 2013; Rizzi et al. 2014). The development of CAS creates a need for tools to evaluate the occupant response during the pre-crash phase, combined with possible subsequent impacts.

To improve restraint functionality, and prepare occupants for impact, reversible pre-tension systems have also been used together with CAS (Schöneburg et al. 2011); this allows the occupant to be more tightly coupled to the seat during autonomous braking, and has the potential to reduce forward displacement of occupants as a result of the pre-crash braking (Antona et al. 2010). Advanced restraint systems, that utilize reversible pre-tensioning of seat belts during the pre-crash phase, are emerging and some studies on the effect of pre-tensioning on occupant kinematics have been published, using either volunteers (Mages et al. 2003; Good et al. 2008a; Schöneburg et al. 2011; Östh et al. 2013; Ólafsdottir et al. 2013; Develet et al. 2013; Ito et al. 2013) or ATDs (Good et al. 2008b; Woitsch and Sinz 2014). However, extending these studies to also assess the injury reduction potential of restraints active in both the pre- and in-crash phase is difficult. Volunteers cannot be subjected to injurious loads while ATDs, developed to predict injury in high energy impacts, are too stiff to represent relaxed vehicle occupants under low loading conditions (Beeman et al. 2012).

The limitations associated with ATD and volunteer testing can be addressed with mathematical HBMs that can represent occupant responses in pre-crash as well as crash loading conditions (Schöneburg et al. 2011, Mages et al. 2011). To represent an attentive occupant and the influence of the occupant's muscle reaction on the kinematic response during the pre-crash phase, active muscle response and a human-like control strategy of the muscles must be included in future HBMs. In the past, several models with one dimensional or solid elements only representing the passive elastic and damping response of the neck musculature have been developed (Jost and Nurick 2000; Robin 2001; Ejima et al. 2005; Toyota 2008). However, the active force generated by muscles has a different order of magnitude than the passive muscle stiffness and damping at physiological muscle lengths. Early implementation of active muscle properties in HBMs were made in cervical spine models (Deng and Goldsmith 1987; de Jager 1996; Wittek 2000; Brolin et al. 2005). Since then, models with active musculature have been included in numerous HBMs, summarized in Table 1. The most common method for implementing active muscle properties in HBMs is to utilize 1D Hill-type muscle elements. In some models 1D Hill-type elements have been super-positioned with a passive bulk material to provide 3D muscles geometry with existing material models in the FE solvers (Behr et al.

2006; Hedenstierna et al. 2008; Iwamoto et al. 2009; 2011; 2012). Another study implemented the Hill-model with local fiber directions in a continuum FE material model (Khodaei et al. 2013).

The aim of this paper is to provide an update on state-of-the-art modeling techniques for simulation of muscle activity in HBMs, and to highlight future challenges and benefits with modeling of car occupants muscle responses to restraint activation.

## REVIEW OF ACTIVE MUSCLE CONTROL IN HBM

Several methods for regulating muscle activity in HBMs have been proposed. These methods can be divided into two main categories: open-loop control, where muscle activation functions are defined prior to simulation, and closed-loop control, where muscle activities are regulated based on sensory information about the current state of the model, for instance the position of a limb.

**Table 1. Summary of HBM studies that have included active musculature. MB = Multibody; FE = Finite Element; 1D = 1 dimensional; 3D = 3 dimensional. EMG = Electromyogram; PID = Proportional, Integral, and Derivative; T1 = First thoracic vertebra.**

| ***Model*** **Type / Solver** | **Reference** | **Body part** | **Actuators**[1] | **Control** | **Activation scheme** | **Application** |
|---|---|---|---|---|---|---|
| *TNO Active Human Model* | Cappon et al. 2007 | Spine | Torque actuators | Closed-loop | PID controllers | Reversible belt pre-tension, roll-over |
| | Budziszewski et al. 2008 | Upper extremity | 1D muscles | Closed-loop | PID controllers | Elbow flexion |
| MB / MADYMO | Meijer et al. 2008 | Spine, left arm and legs | Torque actuators, 1D muscles | Open and closed-loop | PID controllers, engineering judgment | Far-side impact |
| | Fraga et al. 2009 | Cervical spine | 1D muscles | Closed-loop | PID controllers | Motorcycle braking and cornering |
| | Nemirovsky and van Rooij 2010 | Cervical spine | 1D muscles | Closed-loop | PID controllers | Rear-end impacts |
| | van Rooij 2011 | Spine | Torque actuators, 1D muscles | Closed-loop | PID controllers | Autonomous braking |
| | Meijer et al. 2012 | Whole body | 1D muscles, torque actuators | Closed- and open-loop co-contraction | PID controllers, variable co-contraction | Autonomous braking, frontal, lateral, and rear-end impact |
| | Meijer et al. 2013b | Whole body, hip and elbow added | 1D muscles, torque actuators | Closed- and open-loop (co-contraction) | PID controllers, variable co-contraction and reaction time | Pendulum impacts, car braking, sled impacts |
| | Meijer et al. 2013a | Whole body, new neck and elbow | 1D muscles, torque actuators | Closed- and open-loop (co-contraction) | PID controllers, varied levels of co-contraction | Anterior-posterior T1 perturbations, elbow flexion impulses, and autonomous braking. |
| | de Bruijn 2014 | Cervical spine | 1D muscles | Closed-loop | Vestibular and muscle spindle feedback | Anterior-posterior T1 perturbations |

**Table 1. Continued.**

| *Model* Type / Solver | Reference | Body part | Actuators[1] | Control | Activation scheme | Application |
|---|---|---|---|---|---|---|
| *SAFER A-HBM* | Östh et al. 2012b | Upper extremity | 1D muscles | Closed-loop | PID controller | Elbow flexion-extension impulse load and posture maintenance |
| FE / LS-DYNA | Östh et al. 2012a | Cervical and lumbar spine | 1D muscles | Closed-loop | PID controllers | Autonomous braking for car passengers |
| | Östh et al. 2014a | Cervical and lumbar spine, upper extremities | 1D muscles | Closed-loop | PID controllers | Autonomous braking with reversible pre-tension |
| | Östh et al. 2014b | Cervical and lumbar spine, upper and lower extremities | 1D muscles | Closed-loop with anticipatory component, and open-loop | PID controllers and based on normalized EMG (lower extremities) | Driver maximal emergency braking postural response |
| *Active THUMS* | Sugiyama et al. 2007 | Lower extremity | 1D muscles | Open-loop | Inverse dynamics model | Brake pedal impacts |
| FE / LS-DYNA | Iwamoto et al. 2009 | Upper extremity | 3D muscles | Open-loop | engineering judgment | Lateral impact to elbow |
| | Iwamoto et al. 2011 | Whole body | 3D muscles | Open-loop | Normalized EMG | Frontal impact |
| | Iwamoto et al. 2012 | Whole body | 3D muscles | Open-loop | Reinforcement learning model | Frontal and rear-end impacts |
| | Iwamoto and Nakahira 2014 | Whole body | 3D muscles | Open-loop | Normalized EMG, engineering judgment | Pedestrian impacts |
| FE /PAM-CRASH | Wittek 2000 | Cervical spine | 1D muscles | Open-loop | Reflex activation | Rear-end impacts |
| FE / LS-DYNA | Brolin et al. 2005; 2008 | Cervical spine | 1D muscles | Open-loop | Reflex activation, optimization | Frontal and lateral impact, helicopter crash |
| FE / LS-DYNA | Hedenstierna 2008 | Cervical spine | 3D muscles | Open-loop | Reflex activation, Optimization | Frontal, lateral and rear-end impacts |
| MB / LS-DYNA | Chancey et al. 2003; Dibb et al. 2013 | Cervical spine | 1D muscles | Open-loop | optimization | Tensile neck loading, frontal impact, child HBM |
| FE/LS-DYNA | Chang et al.2008; Chang et al. 2009 | Lower extremity | 1D muscles | Open-loop | Normalized EMG | Knee impacts |

[1] In all HBMs which used muscle elements as actuators, the active behavior was modeled with a Hill-type material model. All models with 3D muscles employ the super-position of a passive continuum bulk material and Hill-type line muscle elements (Hedenstierna et al. 2008).

**Muscle Models with Open-loop Control**

In models that use open-loop control, muscle activities are defined as a function of time prior to the simulation, based on know-how from previous simulations, experimental data, or optimization in static load cases. The outcome is observed afterwards, and the activation function may be iteratively adjusted to achieve a more biofidelic model response in upcoming simulations.

**Reflex Activation**

Several cervical spine models (de Jager 1996; Wittek 2000; van der Horst 2002; Brolin et al. 2005; Stemper et al. 2006) have accounted for the influence of active behavior by the application of a maximum activity starting at a specified time in the simulation. With this approach in a multibody (MB) neck model, de Jager (1996) showed the importance of active muscles to capture the human head-neck response in frontal and lateral impacts; the same model was later refined and employed in rear-end impacts, and yet again the importance of active muscles was shown by van der Horst (2002). Brolin et al. (2005) found that including muscle activity for an FE neck model, with 1D Hill-type muscle elements, improved the kinematic correlation with volunteer data for frontal and lateral impacts. The muscle activation properties, i.e. the shape of the curve defining muscle activity, were varied and the best correlation with experimental data was found when neck flexors and extensors were assigned different activity levels. In addition, Brolin et al. (2005) also found altered injury patterns as an effect of neck muscle activity with respect to cervical ligament strain.

Maximum muscle activation at a specified time in the simulation is a straightforward way to introduce the effect of reflexive muscle responses and that of eccentric muscle lengthening. If simultaneous activation of all muscles is modeled, the implicit assumption is that a reflexive startle response is present. A startle response is a rapid response to stimulation of mechanoreceptors, acoustic stimuli, visual stimuli, or a combination thereof. It is characterized as a bilateral response which includes closing of the eyes, extension of the neck, elevation of the shoulders, and extension of the lumbar back (Yeomans et al. 2002). This might very well be present in many impact-like scenarios, and this method may suffice for short duration impacts with a clear loading direction, but not for more complex scenarios or for scenarios in which posture must be maintained for a period of time (Brolin et al. 2008).

**Optimization of Static Posture-Maintaining Activities**

Chancey et al. (2003) developed an MB neck model with detailed muscles and studied the effect of muscle activity on tensile loading of the neck for two sets of muscle activities. The muscle activities evaluated were determined with an optimization scheme that gave initial stable postures for low-level and maximal muscle activation. More recently the same method was applied to find posture maintaining muscle activation schemes for six and ten-year-old pediatric cervical spine models (Dibb et al. 2013). The neck stabilizing muscle activity levels reported by Chancey et al. (2003) were used as a starting point to find load case specific stabilizing activities in a study with an FE neck model conducted by Brolin et al. (2008). The model was thereafter applied to evaluate the influence of tensed muscles on spinal injuries for helicopter pilots, and it was found that stabilizing neck muscle activation reduced the risk of ligamentous injuries. Bose and Crandall (2008) and Bose et al. (2010) used an MB HBM which was varied in size from the approximate $20^{th}$ to $80^{th}$ percentile male anthropometry, nine different initial postures, and 0–100% muscle co-contraction activity in 1D Hill-type elements. They performed optimization simulations to generate static stabilizing co-contraction activity levels and evaluated the influence of initial muscle co-contraction on a whole body injury metric in a simulated 57 km/h impact. They found that the initial posture was the most significant factor in determining the injury outcome, although the initial muscle co-contraction also had some influence. In particular, an increased risk for injury in the lower extremities with increasing muscle co-contraction was reported.

In open-loop control, optimization is a systematic way to balance a set of muscle activity levels. However, actual stabilizing activity levels are difficult to achieve. For instance, Chancey et al. (2003) defined posture maintenance as less than 5° rotation or 10 mm translation of the head over a period of 100 ms and Brolin et al. (2008) used a similar criteria in combination with a threshold of ±1 mm and 0.01 radians head motion for the subsequent 300 ms as a requirement for postural stability. In addition, any reflex responses due to the perturbation are not accounted for in an impact scenario.

**Optimization of Dynamic Activities**

Iwamoto et al. (2012) presented a version of the THUMS HBM with a detailed 3D representation of muscles for all body parts. For the head and neck, a simplified model using 1D Hill-type elements was also developed. Using the simplified neck model and an optimization process called reinforcement learning, tabulated muscle control functions that account for both joint angles and velocities were derived. The optimization provided individual muscle activation functions that were applied in the detailed model in a rear-end impact test case. With the reinforcement learning muscle activities the THUMS with 3D muscles appeared to perform better than with deactivated muscles in the initial phase of the impacts compared with volunteer data, but then it overestimated the effect of the muscle activity on kinematics.

Multi-dimensional, pre-determined, activity tables can resemble actual human motor control, as the joint angles and velocities would correspond to stretch and rate of change of muscle lengths and correlate with input to the vestibular organs. If the model is accurate in reproducing the muscle activity for a wide range of combinations of angles and velocities, the resulting activation patterns could be compared with experimental data and the muscle response of the model would be human-like. However, a drawback of the study performed by Iwamoto et al. (2012) appears to be the large number of simulations (660) needed to generate the dynamic activity tables, and that these tables were derived for a simplified model, that potentially have different dynamic properties than the actual active HBM.

**Estimation based on Experimental Data**

Behr et al. (2006), Sugiyama et al. (2007), and Chang et al. (2008; 2009) all modeled emergency braking with active muscles in the lower extremities. The muscle activity levels were taken from normalized electromyogram (EMG) measurements in emergency braking experiments. They studied the injury risk in frontal impacts (Behr et al. 2006), brake pedal impacts (Sugiyama et al. 2007) and knee impacts (Chang et al. 2008), and concluded that the inclusion of active musculature changes the injury risk in these situations. Chang et al. (2008) predicted that the external force producing a fracture in the knee-thigh-hip area decreases when muscle tension is taken into account, although a limitation of the study was the lack of detailed muscle activity data for the lower extremities. Therefore, a second study was made (Chang et al. 2009), in which an inverse dynamics musculoskeletal model was used to derive detailed individual muscle activity levels from experimental data. The same approach applying inverse optimization was used by Choi et al. (2005), i.e. an optimization in which muscle activity levels are derived using a musculoskeletal model, measured forces, and limb positions, together with hypothesized optimization constraints. They simulated occupant bracing in sled impacts with active muscles in the upper and lower extremities. Iwamoto and Nakahira (2014) simulated pedestrian impacts with a whole body HBM with 3D musculature without muscle activity, with relaxed activity and 20% activity in all muscles, as well as only neck muscle activity based on volunteer data. They concluded that muscle activity affected pedestrian kinematics and could have an influence on the injury outcome predicted in such simulations.

If maximum voluntary contractions are performed for the specific experimental setup, it is possible to derive muscle activity levels for measured muscles under experimental conditions. These levels can then be used in simulations, such as in the studies summarized in the present section, either directly or through optimization with inverse dynamics models. This approach will generate muscle activities in the model which are in good temporal agreement and of the right magnitude, if the EMG is appropriately processed. However, for each scenario simulated, volunteer experiments must be performed and the models would not be able to predict occupant responses in other conditions. Therefore, this practical approach has limited applicability for safety restraint development, since interaction with new restraint systems may change muscle activity, as will more severe loading than what can be used in volunteer experiments.

**Muscle Models with Closed-loop Control**

In closed-loop applications the response of the controlled system is continuously monitored and the control signal is adjusted in accordance with the actual model response. In the human body the reflex arc, is the simplest closed-loop structure in the neuromuscular control system. In current active HBMs, closed-loop control has mainly been implemented with proportional, integral, and derivative (PID) controllers defined as:

$$e(t) = r(t) - y(t) \tag{1}$$

$$u(t) = k_p \cdot e(t) + k_i \cdot \int_0^t e(\tau)d\tau + k_d \cdot \frac{de(t)}{dt}. \tag{2}$$

The current state of the system, $y(t)$, is compared with the reference, $r(t)$, and the control signal, $u(t)$, is proportional to the difference between the two according to Equation (2). The characteristics of the PID controller are determined by the proportional gain, $k_p$, integral gain, $k_i$, and derivative gain, $k_d$. The PID feedback control can be applied to model human postural responses; the proportional and derivative feedback then models the effect of muscle spindle and vestibular reflexive stabilization, while the integrative controller removes any steady state error due to constant loads such as gravity.

**Closed-Loop Postural Control with Torque Actuators**

One of the first implementations of closed-loop control to model occupant postural responses was realized by Cappon et al. (2007) who utilized PID controllers to apply torque at each individual vertebral joint in a MB HBM.

The model was applied to study the phase preceding a roll-over accident and a static application of a reversible pre-tensioned restraint. The addition of the active spine improved the model kinematics in the roll-over scenario but was less successful in capturing the volunteer response to the reversible pre-tensioned restraint. The spine with active torque actuators was later utilized in several publications on the *TNO Active Human Model* (Meijer et al. 2008; van Rooij 2011; Meijer et al. 2012; Meijer et al. 2013a; 2013b). In addition, the torque actuator approach was used to simulate child kinematics with a 6-year old MB child model (Brolin et al. 2014). Torque actuators with closed-loop control are suitable for modeling scenarios where kinematic responses are of primary interest, but less so for crash events or study of injury outcome.

**Closed-loop Postural Control with 1D Muscle Elements**

Budziszewski et al. (2008) implemented closed-loop control of 1D Hill-type elbow flexor and extensor muscles in a MB arm model. A PID controller was implemented for the elbow joint angle and the muscles were grouped into flexors and extensors and assigned equal activity levels from the controller. The model was tested and compared with experimental data of voluntary elbow flexion and extension; it was concluded that the kinematic performance of the model matched that of the volunteers but that predicted muscle activity levels were over-estimated. Fraga et al. (2009) used feedback PID control of line muscle elements to stabilize the head of a motorcycle rider in lateral and longitudinal maneuvers for MB simulations. They concluded that their model appeared to capture resulting head kinematics of a volunteer with average awareness who applied the brakes on a motorcycle. Furthermore, they stated that the model was promising for the development of advanced restraint systems for motorcycle riders, and that it was a step towards active whole body HBMs.

The head-neck model used by Fraga et al. (2009) was further developed by Nemirovsky and van Rooij (2010) by the implementation of a postural controller for the head-neck complex, with the aim of regulating flexion-extension, lateral flexion, and rotation of the head. The motions were decoupled by a muscle recruitment strategy, which would ensure that only one degree of freedom was influenced by each controller; however, only the model response in flexion-extension was evaluated. Along with three PID controllers for the three head rotational degrees of freedom, a variable co-contraction ratio was implemented. The co-contraction ratio was important for the resulting closed-loop response, as muscular co-contraction makes a significant contribution to the damping of the closed-loop system. The model was later used by van Rooij (2011), who hypothesized that the attentiveness of drivers is reflected by the gains used in the control model. He simulated the influence of different levels of awareness on driver kinematics in autonomous braking interventions.

Meijer et al. (2012) combined and extended the work presented in the previous publications on the *TNO Active Human Model* (Cappon et al. 2007; Meijer et al. 2008; Fraga et al. 2009; Nemirovsky and van Rooij 2010; van Rooij 2011) to form an active whole body model. The feedback loop was complemented with a reaction time for events that produce a larger controller error than the preceding ones in the simulation. A low-pass filter function representing the neural transmission time from the CNS to the distal muscles was also added. The signal from each controller was converted to the muscles or torque actuators through multiplication by a constant defined in a recruitment table, to ensure that only the degree of freedom being regulated was affected (Nemirovsky and van Rooij 2010). Furthermore, muscle co-contraction was defined prior to the simulations, i.e. open-loop control, to generate muscle tension without any net moment around the joints, contributing to the intrinsic stiffness. Kinematic responses of the model were evaluated for autonomous braking, frontal, lateral, and rear-end impacts. It was concluded that both feedback control and muscle co-contraction is needed to predict volunteer responses in these types of events.

In Meijer et al. (2013b), feedback controlled elbow and hip muscles were introduced and a muscle recruitment approach similar to that described by Nemirovsky and van Rooij (2010) was used to decouple hip flexion-extension, medial-lateral rotation and abduction-adduction. Utilizing 50% co-contraction of the muscle actuators, the model was reasonably well able to capture forward displacements of the chest and neck in 1 g driver braking events, and in 3.8 g, and 15 g volunteer impact tests. Meijer et al. (2013a) introduced new and more biofidelic neck muscle geometry in the TNO Active Human Model, and evaluated the response of the head-neck complex to low level random perturbations of the T1 vertebra. Furthermore, force pulse perturbations were applied to the hand, inducing flexion and extension of the elbow and the model response was compared with that of one volunteer. Finally, the difference between a braced state and a relaxed state for the model was evaluated by simulating a braking event. It was concluded that the model response for the relaxed condition is different from the braced condition.

The head-neck complex from *TNO Active Human Model* was taken a step further by modeling muscle spindle and vestibular feedback in more detail (de Bruijn 2014). The controller included a model of the dynamics of each reflex loop and their respective neural delays. Muscle activity regulation was based on inputs on muscle length and lengthening velocity (spindle feedback) and head angular velocity and gravitational force (vestibular feedback). Each muscle was activated individually based on a muscle recruitment scheme obtained from isometric optimization simulations. Although the model was not used to simulate the head-neck response in vehicle impact scenarios it has potential to be applied in such studies in the future.

Östh et al. (2012b) implemented PID control for the elbow joint of the THUMS v3 (Toyota 2008) FE HBM, actuated by 1D Hill-type muscles. This study showed the feasibility of using closed loop muscle activation with FE HBM. In this particular case the PID controller was implemented in LS-DYNA with use of the solution control subroutine (Erhart 2010) in LS-DYNA, which allows for users to program their own material models and element formulations, Figure 1. The model was able to maintain its posture in a field of gravity. With 5 % extensor and 3 % flexor co-contraction and experimentally determined controller gains the model was able to reproduce the response of one volunteer to a 15 N force impulse. Furthermore, it was concluded that the detail of the original contact based joints in the THUMS v3 did not provide biofidelic passive joint properties and had to be replaced with revolute joints. An alternative approach for performing feedback control in LS-DYNA was presented by Prüggler et al. (2011), who used external software for the feedback control algorithm coupled to the FE solver for simulations with a simplified FE HBM.

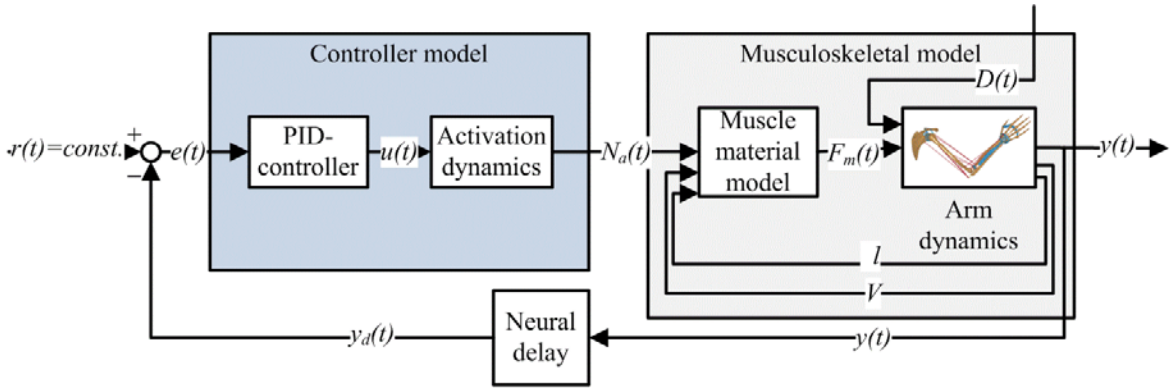


**Figure 1. Illustration of the neuromuscular feedback control loop used for the elbow joint by Östh et al. (2012b). Reprinted with permission from Taylor and Francis.**

The work by Östh et al. (2012b) was continued by adding 1D Hill-type muscles to the cervical and lumbar region and three PID controllers for the angles of the head, neck, and lumbar spine relative to the vertical axis. The model was used to study passenger forward head displacements in autonomous brake interventions of 6 m/s$^2$ compared with volunteer data (Östh et al. 2012a). It was reported that for passengers wearing a three-point seat belt, the support of the belt reduced the importance of the lumbar controller to match volunteer kinematics. Hence, to validate a lumbar controller experimental data from volunteers not wearing a shoulder belt is needed; instead wearing a lap belt or travelling unrestrained is needed. Moreover, in order to be able to simulate driver postural responses to autonomous braking, feedback control and linked 1D Hill-type muscles were added to the shoulders and combined with the previously developed elbow, trunk, and neck controllers (Östh et al. 2014b). This version of the model, denoted the *SAFER A-HBM* (Table 1), was then validated for four loading conditions: in driver and passenger positions for autonomous braking of 11 m/s$^2$ with two different three-point seat belt configurations. A seat belt with a reversible pre-tensioned retractor that provided 170 N of pre-tension to the shoulder belt prior to the braking was compared to a belt with a standard inertia reel retractor. The model compared well for kinematics, timing, and boundary forces between the occupant and vehicle, and reasonably for muscle activity levels. The validated model was employed in a parameter study of belt activation parameters, which showed that the largest reduction of peak head displacement was found for 570N pre-tension 0.15 s before deceleration onset, for both the driver and passenger positions.

Lastly, lower extremity muscles were added to the *SAFER A-HBM* (Östh et al. 2014a) and maximum driver braking was simulated. Based on experimental observations, an anticipatory postural response was hypothesized and implemented by changing the reference angles of the PID controllers for the head, neck, elbows and lumbar spine proportionally to the deceleration pulse. In general, most drivers will have extensive experience from braking events of varying magnitude, and, hence, will have inherent knowledge of the acceleration pulse that will follow after voluntary brake application. Without the anticipatory postural response the model predicted 100 mm longer forward displacements and 16° greater head rotations than were measured for braking volunteer drivers. With the anticipatory postural response, the model head displacement was within the volunteer corridors. Therefore, the hypothesized approach seems feasible and has the potential to be enhanced for other loading modes.

## DISCUSSION

HBMs will play an important role in future safety development of vehicles. Although certification procedures most likely will take a number of years to include virtual testing, it is not unlikely that it will become part of consumer information testing to a greater extent than today. Robustness and repeatability are important requirements for HBMs to be used for verification, with or without simulated muscle activity. This will be a challenge for HBMs with muscle control that changes their response with the level and direction of loading. From a real world safety development perspective there is a considerable need for active HBMs. Maneuvers prior to an impact are a reality (Ejima et al. 2009; Bohman et al. 2011) and are necessary to simulate in order develop protective systems for these situations. Evasive braking as well as steering maneuvers, represent the first priorities. However, ultimately HBMs should be designed to simulate a whole event of combined intensity, such as multiple impacts or run off road events. We would like to stress the importance of developing active HBMs that can be used to study both the pre-crash and crash in one or coupled simulations in a straight forward and simple methodology, preferably with the same HBM.

To date, one FE (Östh et al. 2014b) and one MB (Meijer et al. 2013b) whole body occupant HBM with muscle activity regulated by closed loop control, have been developed to simulate driver and passenger kinematics in pre-crash and emergency events. Both of these models are of average male anthropometry. They have been evaluated with respect to volunteer data in longitudinal loading situations. Future needs for safety development require HBMs with omnidirectional biofidelity and therefore there is a need to further enhance and validate these HBMs for oblique loading with lateral components. Also, to study long duration and complex crash scenarios FE HBMs are particularly needed for the crash simulations, as explicit FE is the industry standard. Furthermore, FE HBMs have the ability to predict injuries in more detail than MB HBMs. MB HBMs have the main strength for kinematics simulation, which is why they can have a benefit for applications like motorcycle events, pedestrian impacts, and for studying how design of sensors and signals and their systems will influence occupant kinematics in autonomous events without subsequent impacts. To conclude, FE HBMs are needed to study small overlap frontal crashes, oblique/angled impacts, multiple events, rollover, and run off road events, for example.

### Future Development of the *SAFER A-HBM*

The next step in the development of the *SAFER A-HBM* (Östh 2014a; 2014b) will be to implement muscle activity control for lateral and oblique load cases. The muscle activity varies between individual muscles and with the direction of loading (Ólafsdóttir et al. 2015). Therefore, refined recruitment strategies are needed, especially for the head-neck complex to capture head motion in various loading events. This means regulating the activity of each muscle individually. One of the major challenges in developing a controller for individual neck muscle regulation is the definition of load sharing and muscle recruitment patterns. So far this has been based on optimization in simulation of isometric conditions (Nemirovsky and van Rooij 2010, de Bruijn 2014) and not based on in vivo data from dynamic events, because such data has not been available previously. This year, Ólafsdóttir et al. (2015) published the first study providing such data by analyzing volunteer neck EMG data during seated perturbations and presenting spatial patterns of muscle recruitment for acceleration pulses in 45 degree intervals from 0 to 315 degrees.

More physiological muscle activity control in HBMs can be developed for many reasons; which are to be prioritized based on the simulation requirements for development of safety systems. Postural control by the central nervous system, for example of the head on the torso, can either be relative to space or relative to the torso depending on the loading conditions, low and high frequency perturbations respectively (de Bruijn 2014). We speculate that muscle control is modulated differently during driving (high frequency) and in autonomous interventions (low frequency). With these two postural control strategies muscle activity can be triggered by feedback from either muscle spindle, i.e. either stretch of the muscle, or from the vestibular system, i.e. balance in space. For vehicle occupants both

systems are likely important and should ideally be implemented in active HBMs. For instance, during an emergency event or a long-duration crash, where an occupant tries to maintain a posture while interacting with advanced restraint systems that may cause local high muscle stretch (repositioning for example), both control loops are likely triggered. Future active HBMs might therefore benefit from including both reflex loops. Furthermore, as the contribution of the two control strategies varies with perturbation bandwidth (de Bruijn 2014) the controller parameters in the HBM need to be modulated depending on the simulated loading condition. In addition, safety systems activated before the event, whether by a crash or avoidance maneuver, can trigger startle-like responses (Östh et al. 2013; Ólafsdóttir et al. 2013). Omnidirectional HBMs with detailed neuromuscular control models that can simulate the startle reflex would be useful to further study how increased muscle activity due to startle affects the injury risk. Further, enhanced models for anticipatory postural response for driver initiated maneuvers, provide the potential to study how drivers interact with autonomous systems and how that changes the occupant response.

**Validation Data for Future Active HBM**

The evaluation of the biofidelity of active HBMs requires experimental data from volunteers in scenarios that replicate pre-crash conditions. In these tests a non-injurious, but representative, acceleration pulse is applied to seated volunteers whose muscle activity can be measured through EMG, the kinematics can be recorded with a camera, a motion capturing system, and/or accelerometers, and the boundary conditions can be recorded with load cells mounted to the steering wheel, seat, pedals, etc. The experimental data obtained in these experiments can also provide an estimate of the muscle activation schemes adopted by occupants in actual pre-crash events, aiding the development of methods for simulating muscle recruitment strategies, as outlined in the previous section. Hence, future volunteer experiments should be prepared and carried out carefully in order to generate useful data on muscle activity, the kinematic response, and boundary conditions.

**Scenarios**

Volunteer data that represent the effect of autonomous braking are readily available. Ejima et al. (2007; 2008) measured EMG, kinematics, and boundary conditions in volunteers in frontal loading conditions with a sled configuration and accelerations ranging from 0.2 – 1.0 g. In addition, a number of volunteer experiments with autonomous braking events using passenger cars and driving in regular traffic are available (Carlsson and Davidsson 2011; Östh et al. 2013; Ólafsdóttir et al. 2013). By driving or riding in a regular vehicle on regular roads the experimental conditions mimicked the targeted scenario to a higher degree than sled tests conditions; it was expected that these experiments provided data more representative of a scenario for which brake systems are autonomously activated.

Systems that avoid a collision by steering are being researched (e.g. Eidehall et al. 2007) and therefore there is an urgent need for validated omnidirectional active HBMs that can mimic the human response in these scenarios. Volunteer experiments with lateral and oblique loading have so far received less attention than longitudinal loading. Volunteer kinematic responses and EMG data during pure lateral and lane change type loading have been provided by van Rooij et al. (2013) and Ejima et al. (2012). In both these studies the volunteers were seated in a rigid seat and the experiments were carried out inside a laboratory. Huber et al. (2012) presented upper torso, arm and head kinematics, activation timings and absolute EMG levels during 1 g lane change maneuvers for front row vehicle passengers. Future volunteer experiments are to be carried out in conditions that more closely resemble an actual driving event.

Other scenarios for which volunteer test data will be required are multiple events, rollover, and run off road events. These scenarios include complex vehicle kinematics and are difficult to simulate on a test track using a regular passenger car. Instead they could be replicated in advanced vehicle simulators or robot test rigs

**EMG**

EMG signals from various muscle groups were recorded and normalized to the maximum EMG value recorded during the event for several muscle groups in the experiments conducted by Ejima et al. (2007; 2008) and van Rooij et al. (2013). These experiments provided a valuable insight into which muscle group is activated during pre-crash braking and steering events, the respective activation timings and overall kinematics. The magnitude of the EMG signals, however, cannot be used to directly compare the level of muscle activity between different muscles or volunteers nor with the simulated muscle activity in active HBMs; hence, their applicability for model development are limited. EMG signals normalized to maximum voluntary contractions (MVCs), as were provided by Östh et al. (2013) and Ólafsdóttir et al. (2013), are more appropriate for active HBM development and validation where the signals are represented as a percentage of a maximum activation, which can more easily be compared to or defined

in an active HBM. For the simulation of test scenarios that result in lateral occupant motions there is a need for muscle data for the muscles surrounding the pelvis, legs and for the muscles stabilizing the lower spine. Few studies have yet presented such data; one study has presented leg muscle activations when the volunteer was performing emergency braking (Behr et al. 2010).

Several studies have measured the activation levels of deep muscles in the spine using intra-muscular EMG when the volunteer were subjected to perturbations (Siegmund et al. 2007; Ólafsdóttir et al. 2015). Such data provide neuromuscular parameters, muscle synergies and an understanding of neck stabilization in dynamic events and are essential for the development of muscle recruitment models for the head-neck complex. However, additional data is required for loading conditions matching those that would occur in vehicles fitted with systems that employ active steering.

In conclusion, access to MVC normalized EMG data from various loading conditions is imperative for development of muscle recruitment strategies and as validation data for active HBMs. Future studies should preferably include measurements of deep muscles activity and include muscles that stabilize the trunk.

**Kinematic response**

Proper recording of kinematics in volunteer experiments are a necessity for the development and evaluation of active HBMs. Recording volunteer kinematics with traditional video recordings in regular passenger vehicles when longitudinal acceleration is deployed have been carried out successfully (Carlsson and Davidsson 2011; Östh et al. 2013; Ólafsdóttir et al. 2013). The visibility of targets has sometimes been limited; targets mounted to the lower neck region can be obstructed by the seat and chest targets can be obstructed by clothing and other occupants. Motion capturing systems have also been successfully adopted (Huber et al. 2012) although these systems encounter similar visibility limitations as traditional video recordings. For scenarios including lateral vehicle acceleration, the volunteer response would be more complex and would require multiple video cameras or other systems to capture occupant kinematics. Although traditional video system and motion capturing systems can be adopted and installed we encourage the development of new methods to measure occupant kinematics during dynamic events.

**Boundary conditions**

It is important to measure boundary conditions, such as restraint, pedal, and steering wheel forces and seat contacts, as the occupants will be interacting with their environment. In past volunteer studies the boundary conditions have been recorded (Ejima et al. 2007; 2008; 2012 Östh et al. 2013; Ólafsdóttir et al. 2013) while in others the main purpose of volunteer studies has not been to provide validation data (Carlsson and Davidsson 2011) and boundary conditions have thus been omitted. Such boundary conditions are important in validations of active HBMs and should be recorded in future studies.

**ACKNOWLEDGEMENT**

The work presented in this paper was carried out at SAFER, the Vehicle and Traffic Safety Centre, at Chalmers, Gothenburg, Sweden. It was funded by VINNOVA, the Swedish Governmental Agency for Innovation Systems, as part of the FFI Vehicle and Traffic Safety research program and by the industrial partners. The authors would like to thank Elisabet Agar for language editing of the manuscript.

**REFERENCES**

Antona J, Ejima S, Zama Y (2010) Influence of the Driver Conditions on the Injury Outcome in Front Impact Collisions. *Proceedings of the JSAE Conference*; Tokyo, Japan.

Beeman SM, Kemper AR, Madigan ML, Franck CT, Loftus SC (2012) Occupant Kinematics in Low-speed Frontal Sled Tests: Human Volunteers, Hybrid III ATD, and PMHS. *Accident Analysis and Prevention* 47:128–139.

Behr M, Arnoux PJ, Serre T, Thollon L, Brunet C (2006) Tonic Finite Element Model of the Lower Limb. *Journal of Biomechanical Engineering* 128:223–228.

Bohman K, Arbogast KB, Boström O (2011) Head Injury Causation Scenarios for Belted, Rear-Seated Children in Frontal Impacts. *Traffic Injury Prevention* 12:62–70.

Bose D, Crandall JR (2008) Influence of Active Muscle Contribution on the Injury Response of Restrained Car Occupants. *Proceedings of the Annals of Advances in Automotive Medicine Conference*.

Bose D, Crandall JR, Untaroiu CD, Maslen EH (2010) Influence of Pre-Collision Occupant Parameters on Injury Outcome in a Frontal Collision. *Accident Analysis and Prevention* 42:1398–1407.

Brolin K, Gras L, Stockman I (2014) Active Spine Modeling Representing a 6 Year-Old Child. Presentation at the 7th World Congress of Biomechanics; Boston, USA.

Brolin K, Halldin P, Leijonhufvud I (2005) The Effect of Muscle Activation on Neck Response. *Traffic Injury Prevention* 6:67–76.

Brolin K, Hedenstierna S, Halldin P, Bass C, Alem N (2008) The Importance of Muscle Tension on the Outcome of Impacts with a Major Vertical Component. *International Journal of Crashworthiness* 13(5):487–498.

Budziszewski P, van Nunen E, Mordaka JK, Kędzior K (2008) Active Controlled Muscles in Numerical Model of Human Arm for Movement in Two Degrees of Freedom. *Proceedings of the IRCOBI Conference*; Bern, Switzerland.

Cappon H, Mordaka J, van Rooij L, Adamec J, Praxl N, Muggenthaler H (2007) A Computational Human Model with Stabilizing Spine: A Step Towards Active Safety. SAE Technical Paper No. 2007–01–1171; SAE International. Warrendale, PA, USA.

Carlsson S and Davidsson J (2011) Volunteer Occupant Kinematics during Driver Initiated and Autonomous Braking when Driving in Real Traffic Environments. *Proceedings of the IRCOBI Conference*; Krakow, Poland.

Chancey VC, Nightingale RW, Van Ee CA, Knaub KE, Myers BS (2003) Improved Estimation of Human Neck Tensile Tolerance: Reducing the Range of Reported Tolerance using Anthropometrically Correct Muscles and Optimized Physiologic Initial Conditions. *Stapp Car Crash Journal* 47:135–153.

Chang CY, Rupp JD, Kikuchi N, Schneider LW (2008) Development of a Finite Element Model to Study the Effects of Muscle Forces on Knee-Thigh-Hip Injuries in Frontal Crashes. *Stapp Car Crash Journal* 52:475–504.

Chang CY, Rupp JD, Kikuchi N, Schneider LW (2009) Predicting the Effects of Muscle Activation on Knee, Thigh, and Hip Injuries in Frontal Crashes Using a Finite-Element Model with Muscle Forces from Subject Testing and Musculoskeletal Modeling. *Stapp Car Crash Journal* 53:291–328.

Choi HY, Sah SJ, Lee B, Cho HS, Kang SJ, Mun MS, Lee I, Lee J (2005) Experimental and Numerical Studies of Muscular Activations of Bracing Occupant. *Proceedings of the 19th ESV Conference*; Washington, D.C., USA. Paper no. 05–0139.

Coelingh E, Lind H, Wolfgang B, Wetterberg D (2006) Collision Warning with Auto Brake, *FISITA World Congress*; Yokohama, Japan. Paper No. F2006V130.

de Bruijn E (2014) *Isometric and Dynamic Control of Neck Muscles*. Ph.D. Thesis; Delft University of Technology, Delft, the Netherlands.

de Jager MKJ (1996) *Mathematical Head-Neck Models for Acceleration Impacts*. Ph.D. Thesis; Eindhoven University of Technology, Eindhoven, the Netherlands.

Deng YC, Goldsmith W (1987) Response of a Human Head/Neck/Upper-Torso Replica to Dynamic Loading – II. Analytical/Numerical Model. *Journal of Biomechanics* 20(5):487–497.

Develet J-A, Carlsson A, Svensson M, Fredriksson R, Bråse D, Holcombe S (2013) Evaluation of the Biofidelity of the BioRID-II and THOR-NT Anthropometric Test Devices under Seatbelt Pre-Pretensioner Loading in Stationary Conditions. *Proceedings of the Ohio State University Injury Biomechanics Seminar*; Columbus, OH, USA.

Dibb AT, Cox CA, Nightingale RW, Luck JF, Cutcliffe HC, Myers BS, Arbogast KB, Seacrist T, Bass CR (2013) Importance of Muscle Activations for Biofidelic Pediatric Neck Response in Computational Models. *Traffic Injury Prevention* 14(Sup1):S116–S127.

Eidehall A, Pohl J, Gustafsson F, Ekmark J (2007) Toward Autonomous Collision Avoidance by Steering. *IEEE Transactions on Intelligent Transportation Systems* 8(1):84–94.

Ejima S, Ito D, Satou F, Mikami K, Ono K, Kaneoka K, Shiina I (2012) Effects of Pre-Impact Swerving/Steering on Physical Motion of the Volunteer in the Low-Speed Side-Impact Sled Test. *Proceedings of the IRCOBI Conference*; Dublin, Republic of Ireland.

Ejima S, Ono K, Holcombe S, Kaneoka K, Fukushima M (2007) A Study on Occupant Kinematics Behaviour and Muscle Activities during Pre-Impact Braking based on Volunteer Tests. *Proceedings of the IRCOBI Conference*; Maastricht, the Netherlands.

Ejima S, Ono K, Kaneoka K, Fukushima M (2005) Development and Validation of the Human Neck Muscle Model under Impact Loading. *Proceedings of the IRCOBI Conference*; Prague, Czech Republic.

Ejima S, Zama Y, Ono K, Kaneoka K, Shiina I, Asada H (2009) Prediction of Pre-Impact Occupant Kinematic behavior Based on the Muscle Activity during Frontal Collision. *Proceedings of the 21st ESV Conference*; Stuttgart, Germany. Paper no. 09–0913.

Ejima S, Zama Y, Satou F, Holcombe S, Ono K, Kaneoka K, Shiina I (2008) Prediction of the Physical Motion of the Human Body based on Muscle Activity during Pre-Impact Braking. *Proceedings of the IRCOBI Conference*; Bern, Switzerland.

Erhart T (2010) An Overview of User Defined Interfaces in LS-DYNA. Paper presented at the LS-DYNA Forum; Bamberg, Germany.

Fraga F, van Rooj L, Symeonidis I, Peldschus S, Happee R, Wismans J (2009) Development and Preliminary Validation of a Motorcycle Rider Model with Focus on Head and Neck Biofidelity, Recurring to Line Element Muscle Models and Feedback Control. *Proceedings of the 21st ESV Conference*; Stuttgart, Germany. Paper no. 09–0244.

Good CA, Viano DC, Ronsky JL (2008a) Biomechanics of Volunteers Subject to Loading by a Motorized Shoulder Belt Tensioner. *Spine* 33:E225–E235.

Good CA, Viano DC, Ronsky JL (2008b) The Hybrid III Dummy Family Subject to Loading by a Motorized Shoulder Belt Tensioner. *SAE International Journal of Passenger Cars-Mechanical Systems* 1(1):383–395.

Hault-Dubrulle A, Robach F, Pacaux M-P, Morvan, H (2011) Determination of Pre-Impact Occupant Postures and Analysis of Consequences on Injury Outcome. Part I: A Driving Simulator Study. *Accident Analysis and Prevention* 43:66–74.

Hedenstierna S (2008) *3D Finite Element Modeling of Cervical Musculature and its Effect on Neck Injury Prevention*. Ph.D. Thesis; Royal Institute of Technology, Stockholm, Sweden.

Hedenstierna S, Halldin P, Brolin K (2008) Evaluation of a Combination of Continuum and Truss Finite Elements in a Model of Passive and Active Muscle Tissue. *Computer Methods in Biomechanics and Biomedical Engineering* 11(6):627–639.

Hetier M, Wang X, Robache F, Autuori B, Morvan H (2005) Experimental Investigation and Modeling of Driver's Frontal Pre-crash Postural Anticipation. *Proceedings of the Digital Human Modeling for Design and Engineering Symposium*; Iowa City, Iowa, USA.

IIHS (2011) Status Report. *Insurance Institute for Highway Safety Status Report* 46(6).

IIHS (2012) Status Report – Small Overlap Crashes: New Consumer-test Program Aims for Even Safer Vehicles. *Insurance Institute for Highway Safety Status Report* 47(6).

IIHS (2013) Status Report. *Insurance Institute for Highway Safety Status Report* 48(3).

Isaksson-Hellman I, Lindman M (2012) The Effect of a Low-speed Automatic Brake System Estimated from Real Life Data. *Annals of Advances in Automotive Medicine* 56:231–240.

Ito D, Ejima S, Kitajima S, Katoh R, Ito H, Sakane M, Nishino T, Nakayama K, Ato T, Kimura T (2013) Occupant Kinematic Behavior and Effects of a Motorized Seatbelt on Occupant Restraint of Human Volunteers during Low Speed Frontal Impact: Mini-sled Tests with Mass Production Car Seat. *Proceedings of the IRCOBI Conference*; Gothenburg, Sweden.

Iwamoto M, and Nakahira Y (2014) A Preliminary Study to Investigate Muscular Effects for Pedestrian Kinematics and Injuries Using Active THUMS. *Proceedings of the IRCOBI Conference*; Berlin, Germany.

Iwamoto M, Nakahira Y, Kimpara H, Sugiyama T (2009) Development of a Human FE Model with 3-D Geometry of Muscles and Lateral Impact Analysis for the Arm with Muscle Activity. SAE Technical Paper No. 2009–01–226; Society of Automotive Engineers, Warrendale, PA, USA.

Iwamoto M, Nakahira Y, Kimpara H, Sugiyama T (2012) Development of a Human Body Finite Element Model with Multiple Muscles and their Controller for Estimating Occupant Motions and Impact Responses in Frontal Crash Situations. *Stapp Car Crash Journal* 56:231–268.

Iwamoto M, Nakahira Y, Sugiyama T (2011) Investigation of Pre-impact Bracing Effects for Injury Outcome using an Active Human FE Model with 3D Geometry of Muscles. *Proceedings of the 22nd ESV Conference*; Washington, D.C., USA. Paper no. 11–0150.

Jakobsson L, Kling A, Lindman M, Wågström L, Axelson A, Broberg T, McInally G (2013) Severe Partial Overlap Crashes – A Methodology Representative of Car to Car Real World Frontal Crash Situations. *Proceedings of the 23rd ESV Conference*; Seoul, South Korea. Paper no. 13-0294.

Jakobsson L, Lindman M, Axelson A, Lokensgard B, Petersson M, Svanberg B, Kovaceva J (2014) Addressing Run Off Road Safety. *Proceedings of the SAE Congress*; Detroit, MI. SAE Technical Paper 2014–01–0554.

Jost R, Nurick GN (2000) Development of a Finite Element Model of the Human Neck Subjected to High g-Level Lateral Deceleration. *International Journal of Crashworthiness* 5(3):259–270.

Khodaei H, Mostofizadeh S, Brolin K, Johansson H, Östh J (2013) Simulation of Active Skeletal Muscle Tissue with a Transversly Isotropic Viscohyperelastic Continuum Material Model. *Journal of Engineering in Medicine* 227(5):571–580.

Ljung-Aust M, Jakobsson L, Lindman M, Coelingh E (2015) Collision Avoidance Systems – Advancements and Efficiency. *Proceedings of the SAE Congress*; Detroit, MI. SAE Technical Paper 2015–01–1406.

Mages M, Seyffert M, Class U (2011) Analysis of the Pre-Crash Benefit of Reversible Belt Pre-pretensioning in Different Accident Scenarios. *Proceedings of the 22nd ESV Conference*; Washington, D.C., USA. Paper no. 11–0442.

Meijer R, Broos J, Elrofai H, de Bruijn E, Forbes P, Happee R (2013a) Modelling of Bracing in a Multi-Body Active Human Model. *Proceedings of the IRCOBI Conference*; Gothenburg, Sweden.

Meijer R, Elrofai H, Broos J, van Hassel E (2013b) Evaluation of an Active Multi-Body Human Model for Braking and Frontal Crash Events. *Proceedings of the 23rd ESV Conference*; Seoul, South Korea. Paper no. 13–0163.

Meijer R, Rodarius C, Adamec J, van Nunen E, van Rooij L (2008) A First Step in Computer Modelling of the Active Human Response in a Far-side Impact. *International Journal of Crashworthiness* 13(6):643–652.

Meijer R, van Hassel E, Broos J, Elrofai H, van Rooij L, van Hooijdonk P (2012) Development of a Multi-Body Human Model that Predicts Active and Passive Human Behavior. *Proceedings of the IRCOBI Conference*; Dublin, Republic of Ireland.

Nemirovsky N, van Rooij L (2010) A New Methodology for Biofidelic Head-Neck Postural Control. *Proceedings of the IRCOBI Conference*; Hannover, Germany.

Olafsdottir J, Brolin K, Blouin J, Siegmund G (2015) Dynamic Spatial Tuning of Cervical Muscle Reflexes to Multidirectional Seated Perturbations. *Spine* 40(4):E211–E219.

Ólafsdóttir JM, Östh JKH, Davidsson J, Brolin K (2013) Passenger Kinematics and Muscle Responses in Autonomous Braking Events with Standard and Reversible Pre-tensioned Restraints. Proceedings of the IRCOBI Conference; Gothenburg, Sweden, pp. 602–617.

Östh J, Brolin K, Bråse D (2014a) A Human Body Model with Active Muscles for Simulation of Pre-Tensioned Restraints in Autonomous Braking Interventions. *Traffic Injury Prevention* 16(3):304–313.

Östh J, Brolin K, Carlsson S, Wismans J, Davidsson J (2012a) The Occupant Response to Autonomous Braking: A Modeling Approach that Accounts for Active Musculature. *Traffic Injury Prevention* 13(3):265–277.

Östh J, Brolin K, Happee R (2012b) Active Muscle Response using Feedback Control of a Finite Element Human Arm Model. *Computer Methods in Biomechanics and Biomedical Engineering* 15(4):347–361.

Östh J, Eliasson E, Happee R, Brolin K (2014b) A Method to Model Anticipatory Postural Control in Driver Braking Events. *Gait and Posture* 40(4):664–669.

Östh J, Ólafsdóttir JM, Davidsson J, Brolin K (2013) Driver Kinematic and Muscle Responses in Braking Events with Standard and Reversible Pre-tensioned Restraints: Validation Data for Human Models. Stapp Car Crash Journal 57:1–41.

Prüggler A, Huber P, Rieser A, Steiner K, Kirschbichler S, Eichberger A (2011) Implementation of Reactive Human Behavior in a Numerical Human Body Model using Controlled Beam Elements as Muscle Element Substitutes. *Proceedings of the 22nd ESV Conference*; Washington, D.C., USA. Paper no. 11–0154.

Rizzi M, Kullgren A, Tingvall C (2014) The Injury Crash Reduction of Low-Speed Autonomous Emergency Braking (AEB) on Passenger Cars. *Proceedings of the IRCOBI Conference;* Berlin, Germany.

Robin S (2001) Humos: Human Model for Safety – A Joint Effort Towards the Development of Refined Human-like Car Occupant Models. *Proceedings of the 17th ESV Conference*; Amsterdam, the Netherlands. Paper no. 291.

Schöneburg R, Baumann K-H, and Fehring M (2011) The Efficiency of PRE-SAFE® Systems in Pre-braked Frontal Collision Situations. *Proceedings of the 22nd ESV Conference*; Washington, D.C., USA. Paper no. 11–0207.

Siegmund GP, Blouin J-S, Brault JR, Hedenstierna S, Inglis JT (2007) Electromyography of Superficial and Deep Neck Muscles during Isometric, Voluntary, and Reflex Contractions. *Journal of Biomechanical Engineering* 129(1): 66–77.

Stemper BD, Yoganandan N, Pintar FA, Rao RD (2006) Anterior Longitudinal Ligament Injuries in Whiplash May Lead to Cervical Instability. *Medical Engineering & Physics* 28:515–524.

Sugiyama T, Kimpara H, Iwamoto M, Yamada D, Nakahira Y, Masatoshi H (2007) Effects of Muscle Tense on Impact Responses of Lower Extremity. *Proceedings of the IRCOBI Conference*; Maastricht, the Netherlands.

Toyota (2008) *Users' Guide of Computational Human Model THUMS® – AM50 Occupant Model: Version 3.0–080225*. Toyota Motor Corporation, Toyota Central Labs Inc, Toyota City, Aichi, Japan.

van der Horst M (2002) *Human Head Neck Response in Frontal, Lateral and Rear End Impact Loading – Modeling and Validation*. Ph.D. Thesis; Eindhoven University of Technology, Eindhoven, the Netherlands.

van Rooij L (2011) Effect of Various Pre-Crash Braking Strategies on Simulated Human Kinematic Response with Varying Levels of Driver Attention. *Proceedings of the 22nd ESV Conference*; Washington, D.C., USA. Paper no. 11–0306.

van Rooij L, H Elrofai M, Philippens MGM, Daanen HAM (2013) Volunteer Kinematics and Reaction in Lateral Emergency Maneuver Tests. *Stapp Car Crash Journal* 57:313–42.

Wittek A (2000) *Mathematical Modeling of the Muscle Effects on the Human Body Responses under Transient Loads – Example of Head-Neck Complex*. Ph.D. Thesis; Chalmers University of Technology, Gothenburg, Sweden.

Woitsch G, Sinz W (2014) Influences of Pre-Crash Braking Induced Dummy – Forward Displacements on Dummy Behaviour during EuroNCAP Frontal Crashtest. *Accident Analysis and Prevention* 62:268–275.

Yeomans JS, Li L, Scott BW, Frankland PW (2002) Tactile, Acoustic and Vestibular Systems Sum to Elicit the Startle Reflex. *Neuroscience and Biobehavioural Reviews* 26: 1–11.

# PARKING CRASHES: THE RATIONALE FOR ACTION AND THE DEVELOPMENT OF TEST PROCEDURES

**Colin, Grover**
**Matthew, Avery**
Thatcham Research
UK

**Iain, Knight**
Apollo Vehicle Safety Limited
UK

Paper Number 15-0348

## INTRODUCTION

During the last decade parking and manoeuvring accidents appear to be increasingly relevant in third party damage liability and first party or motor own damage claims; a trend evident in many countries around the world. At the same time, vehicle manufacturers have offered a rapidly increasing variety of advanced driver assist systems such that there is greater scope for the avoidance of collisions than ever before. The low speed nature of parking and manoeuvring crashes strongly suggests that this problem should be solvable using technologies similar to those already used in other applications. In fact, several systems directly influencing parking crashes already exist, including proximity based warning systems, systems that will detect parking spaces and park semi-automatically and automatic braking systems similar to AEB that function in reverse.

This paper aims to assess the scale of the problem with low speed manoevring crashes, identify the most common collision mechanisms, assess the potential of the different technologies to solve the problem and to describe the development of test procedures capable of characterising system performance in relation to real world crashes.

## CHARACTERISING PARKING CRASHES

### Objectives

The objective of this element of the work was to quantify the scale of parking crashes around the world in terms of their frequency and cost and to investigate the common crash mechanisms such that a detailed understanding could be developed of what would be required of a really effective avoidance system for such crashes.

### Methods

Several Members of the RCAR network of insurance research centres analysed their individual data sets in order to answer the questions set out in the objectives. Crashes are classified differently in each data set but wherever possible the data have been compared on a consistent basis. The data sets included:

- Thatcham Research, UK: Analysis of 12,565 claims from a First Notification of Loss (FNOL) dataset involving collisions occurring in the UK in 2010. The data includes 1st and 3rd party claims, of which 7,687 (61%) are 1st party and single vehicle at fault cases. Crash categorisation was based on text analytics studies of collision descriptions.
- Allianz Centre for Technology, Germany: Analysis of 1,000 Third Party Liability (TPL) claims with material damage only and 983 Motor own Damage (MoD) claims from collisions occurring in Germany in 2011.
- German Insurers Accident Research (UDV), Germany: 345 Third Party Liability (TPL) claims with material damage and 219 Motor own Damage (MoD) claims with collisions only in Germany in 2004 to 2006 and 2012.

- Insurance Institute for Highway Safety, US: IIHS based their analysis on a retrospective analysis of data accumulated through a survey of 509 vehicles brought to drive-in insurance claims centers in the Washington D.C. metropolitan area in 2001 to 2002. The study examined the types and amounts of vehicle damage sustained in relatively minor front and rear crashes.
- Korea Insurance Development Institute, South Korea: 45,153 Third Party Liability claims (bodily injury & property damage) from 2007 to 2012 in Korea; Analysis was based on automatic extraction of parking related claims by using keywords such as 'parking' and 'reversing' etc.
- Jiken Centre, Japan: Analyses of insurance payment data from 2011.
- Insurance Australia Group, Australia: Data from in excess of 1million 1st and 3rd party insurance claims from 2010 to 2014 in Australia. Analysis was based on automatic extraction of parking related claims by using keywords such as 'parking' and 'reversing' etc.

**Results**

Despite the differences in data classification and analytical techniques used by the various RCAR partners in their independent analyses, the findings were remarkably consistent in the UK, Germany, US, Australia, Korea and Japan. Based on these analysis it can be confidently concluded that crashes while parking and manoeuvring at low speed:

- Represent a high proportion of all claims frequency, representing between approximately 15% and 40% of all claims;
- Are responsible for a large proportion (10% to 30%) of all motor insurance claims costs;
- Mostly (60% to 80 % of parking claims) result from reversing manoeuvres;
- Mainly involve collision with 3rd party vehicles (approximately 55% to 80%), poles and walls;
- Typically occur in car parks, and on private property and urban roads.

The findings above are valid internationally. More details were available in some of the individual national data sets. Although these cannot be strictly considered to be internationally valid, the high level of agreement where comparable data is available suggests that there is a good chance that results will be similar in other countries.

Analysis of the German data by Allianz and UDV shows that the main problem is not entering a parking space, but moving out of a parking space and manoeuvring (70% to 85%). Analysis of the UK data by Thatcham showed a comprehensive breakdown of the types of collision, as shown in **Table 1** below.

*Table 1: Distribution of UK parking crashes by 1st party manoeuvre and collision object*

| | | | | |
|---|---|---|---|---|
| All cases 1836 100% | Forward 382 21% | Parked vehicle 174 9% | Pole-like object 89 5% | Barrier/wall 87 5% |
| | | Moving vehicle 6 0% | Pedestrian 0 0% | Low object 17 1% |
| | | Motorcycle 1 0% | Cyclist 3 0% | Unknown 5 0% |
| | Reverse 1277 70% | Parked vehicle 828 45% | Pole-like object 199 11% | Barrier/wall 156 8% |
| | | Moving vehicle 48 3% | Pedestrian 2 0% | Low object 26 1% |
| | | Motorcycle 13 1% | Cyclist 0 0% | Unknown 5 0% |
| | Pedal misapplication 14 1% | Parked vehicle 6 0% | Pole-like object 1 0% | Barrier/wall 7 0% |
| | Unknown 163 9% | Parked vehicle 66 4% | Pole-like object 51 3% | Barrier/wall 39 2% |
| | | Motorcycle 1 0% | Low object 5 0% | Unknown 1 0% |

In addition to this, the Thatcham analysis was able to identify the areas of damage on the vehicle more specifically for the main crash types:

- Cases where the 1st party reverses and collides with another stationary vehicle (approx. 45% of all parking crashes)
  - 1st party damage predominantly to the rear corners (>80% of rear damage with known location)
  - 3rd party damage distributed between all corners and the sides of the vehicle
  - Central damage to the front or rear of the vehicle was infrequent for both 1st and 3rd party vehicles
- Cases where the 1st party reverses and collides with a "pole-like" object (approx 11% of all parking crashes)
  - 56% of damage is to the rear of the vehicle
  - 28% to the sides of the vehicle
  - 16% to the front of the vehicle
- Cases where the 1st party reverses and collides with a barrier or wall (8% of all parking crashes).
  - 61% of damage is to the rear of the vehicle, corner damage slightly more common than central or distributed damage
  - 16% to the sides of the vehicle
  - 16% to the front of the vehicle
  - 3% unknown

One substantial difference between the countries was in relation to reversing and collisions with pedestrians. As can be seen from **Table 1**, UK collisions where cars reversed into pedestrians were rare, representing just 0.1% of all parking crashes. The US data available does not directly quantify the total number of parking and

low speed manoeuvring crashes so it is not possible to produce a directly comparable percentage. However, it has been found (NHTSA, 2014) that on average there are 210 pedestrian fatalities as a result of "backover" accidents each year and a further 15,000 injuries. Of those killed, almost one third are children and just over a quarter are elderly adults of 70 years of age or more.

## ASSESSING THE POTENTIAL EFFECTIVENESS OF PARKING SYSTEMS

### Objectives

Having quantified the scale of the problem represented by parking crashes and characterised those crashes in a way that allows an understanding to be gained of what would be required to prevent them, the objective of this element of the work was to identify the different parking systems available and to try to quantify how effective they might be at preventing crashes.

### Methods

A variety of different methods were used to try to provide the answers required to achieve the objectives:

- Consultation with vehicle manufacturers and a review of vehicle specification data was undertaken in order to identify available parking assistance systems. A comparison was undertaken of their specifications and functions as an initial indicator of their ability to prevent the common types of crashes identified;
- A literature search and, where possible, an analysis of RCAR members insurer data was undertaken in order to identify measurements of the effect of parking assist systems on insurance claims and these were reviewed;
- A short, subjective benchmarking study was undertaken to gain an initial overview of the capabilities of different vehicle technologies;
- A comprehensive and objective test procedure was developed and then used to assess the performance of one type of technology.

### Results

#### Parking assistance availability and specification

The research showed that a wide variety of different driver support systems that could be classified as "parking assistance" were available. These have been grouped into the categories shown below:

- Parking sensors, or Park Distance Warning (PDW), provides proximity-based acoustic warnings to a driver during low speed manouvring and may also offer a visual display. This technology is widely available in the market and has been for many years, though it often remains an optional extra at additional cost or only available as standard on higher specification models.
- Rear view cameras: an in-vehicle screen shows the view from a camera mounted at the rear of the vehicle
- Surround view cameras: an in-vehicle screen shows a composite view derived from multiple cameras around the vehicle which shows a plan view of the vehicle and surrounding objects, sometimes combined with a direct rear view while reversing. Available on a few high specification models, such as Mercedes E and S class.
- Semi-automated parking: These systems can identify appropriate parking spaces and provide automated inputs to help manoeuver the vehicle into the space. System specification varies considerably, some will detect only parallel spaces, some both parallel and perpendicular, some will only steer and some will control steering, throttle and brake. Where systems do brake, this function is typically not active unless the semi-automated parking function is used. Many manufacturers now offer this type of system, usually as an option, including Mercedes, Volvo, Ford, and VW.

- Reverse auto-brake is similar to Autonomous Emergency Braking (AEB) for front-to-rear crashes. This technology detects potential crashes behind a reversing vehicle and automatically applies the brakes to slow or stop the vehicle thus mitigating or preventing the crash. Unlike the semi-automated parking systems, this system is always active unless de-activated by the driver. Only a small number of manufacturers offer this type of system, at the time of writing, understood to be Infinti, Mazda and Cadillac.
- Driverless parking: This is an autonomous valet parking function where the driver can leave the vehicle and use a phone app or other control to send the vehicle to find a parking space by itself and summon it again when needed. A small number of manufacturers have suggested this will become available on high specification models this year or next year.

**Existing evidence of effectiveness**

Although parking sensors, or Park Distance Warnings have been in production for a long time, there have been relatively few studies of their effectiveness. Since the introduction of rear view cameras there have been a few studies that have attempted to quantify the relative benefits of the different technologies experimentally by studying the responses of normal drivers with and without each technology when confronted by the unexpected presence of obstacles behind them while reversing. Kidd et al (2014) created an experiment where a child dummy was either positioned stationary, or moved into, the path of a reversing vehicle when the driver was not expecting it. It was found that when the child dummy was moving, most drivers (90%) avoided a collision even when they had no technology to support them and that there was no statistically significant difference to this when the drivers had any of the technologies available to them.

When the child dummy was stationary in the path of the vehicle, all of the drivers without technology collided with it. The addition of sensor systems giving a proximity warning reduced this very slightly to around 93% of drivers having a collision but this difference was not statistically significant. The use of a camera system reduced the incidence of collision to 56% and this was statistically significant. It was found that the effectiveness of the camera system was substantially reduced when the obstruction was in the shade. Counter intuitively, combining a sensor system with a rearview camera was found to be less effective than a camera alone. One explanation for this was that the participants looked at the in-vehicle screen less frequently when they also had the sensor system.

Although experimental studies of this are an extremely useful mechanism for predicting the potential of a system, operational factors such as the effects of shade, cited by Kidd et al (2014), as well as the possible effect of dirt on the camera lens etc., will affect the extent to which the systems are beneficial in real service. This can only really be measured by statistical comparison of collision or claims records of vehicles with and without the technology and, even then, the conclusions can be confounded by the wide range of interacting variables that affect crash frequency and severity. For example, the effect of a parking aid could be masked if parking aids were fitted only to vehicles with a very poor field of view or exaggerated if they were only selected as an option by very cautious and safe drivers. These factors can be hard to control for.

Statistical analysis of the effects on insurance claims of several parking systems has been undertaken for models of Toyota (Ydenius & Rizzi, undated) Mazda (HLDI, 2011a), Buick (HLDI, 2011b) and Mercedes (HLDI, 2012). The results of these analyses have been mixed:

- Ultrasonic parking sensors fitted to Toyota and Lexus Vehicles (model years 1999 to 2012) in Sweden were found to reduce the cost of damage while reversing by 27%;
- Ultrasonic parking sensors were found to be very effective for the Buick, reducing collision damage claims (insured vehicle) by 5% and property damage liability (typically 3$^{rd}$ party vehicle) claims by almost 17%. However, for the Mercedes version of the same system, the data suggested that collision claims were actually increased by 0.8% and property damage claims decreased by 1.8%, neither result being statistically significant;
- Rearview cameras fitted to Mercedes Vehicles were not found to have any statistically significant effect, while for Mazda vehicles they were found to produce a statistically significant 3.1% increase in collision claims and a non-significant 2.3% decrease in property damage liability claims;

- Semi-automated parking systems, in the form of the Mercedes Active Parking Assist system, was found to produce non-significant increases in claims frequency (6.3% collision, 5.0% PDL

It is not known whether the differences observed between experimental results and the various statistical analyses are the results of technical differences between systems, operational factors not replicated in the experimental environment, or confounding factors that could not be accounted for in the statistical analysis of claims rates. No effectiveness studies were identified that considered auto-brake systems for reversing.

**Technology Benchmarking**

An initial benchmarking exercise was undertaken by Thatcham in conjunction with Continental and Allianz. Three exemplary vehicles were selected, with a variety of technologies fitted, as defined below:

- Infiniti Q50
  - 360˚ Surround View
  - "Semi-guided" parking (scans for space and when driver selects a space provides the driver with instructions on movements and steering inputs required to get there)
  - Auto-brake while reversing
- Mercedes E Class
  - 360˚ Surround View
  - Semi-automated parking (steer, throttle and brake control, driver has to initiate system, initiate each movement and operate gear lever)
  - Auto-brake while semi-automated parking is in progress
- Skoda Octavia
  - Semi-automated parking (steering control automated, driver has to initiate system and operate accelerator, brake and gear lever)
  - Auto-brake while semi-automated parking is in progress

The tests undertaken were focused on the main needs identified by the data analysis rather than on a full exploration of the capabilities of different systems. As such, the test vehicle manoeuvres involved reversing in a straight line and reversing with full steering lock applied. The hazard objects considered were a stationary and moving vehicle target, a stationary and moving child pedestrian dummy, a traffic cone and a metal pole. The principle difference between the systems was that the Infiniti auto-brake system was always on, whereas for the Mercedes and Skoda it was active only when the semi-automated parking was activated. The claims data analysis reported in this paper showed that more than three-quarters of the reversing claims occurred when the vehicle was reversing out of a parking space, not reversing in. Neither of the semi-automated parking systems offer a function for reversing out of a space. While the presence of such a system may encourage more people to reverse into spaces, thus reducing the proportion that need to reverse out, the extent to which drivers will use the system in the long term is unknown. It is, therefore, likely that restricting the auto-brake function to only those times where the semi-automated parking is engaged will substantially reduce the potential benefit in the real world compared to a system that is "always on".

The main findings of the exercise have been summarized below:

- Infiniti Q50
  - Always on
  - Impressive performance with all static objects
  - Some reduced performance with moving objects, particularly a crossing pedestrian
  - No false positive with grass or small bush
  - Effective at reversing speeds of up to approximately 8 km/h
- Mercedes E class
  - Only active with semi-automated parking
  - Impressive performance with both stationary and moving targets
  - False positive tests led to additional manoeuvring and delay but final decision was always correct
  - Effective at all reversing speeds permitted by the active park assist.

- Skoda Octavia
    - Only active with semi-automated parking
    - Avoided less collisions with static objects than the other systems, smaller objects in particular
    - Further reductions in performance with moving objects
    - No false positive with grass or small bush
    - Effective at reversing speeds of up to around 4 km/h, though with some inconsistency.

**Developing a parking test procedure**

A comprehensive parking test procedure was designed, based on the results of the claims data analyses, the effectiveness studies and the initial benchmarking tests. The test scenarios defined were intended to cover the most frequent claims type, including a car reversing into another car and reversing into a post. In each of the scenarios, reversing straight and with full steering in either direction was considered as well as different overlaps, and different configurations of corner impact.

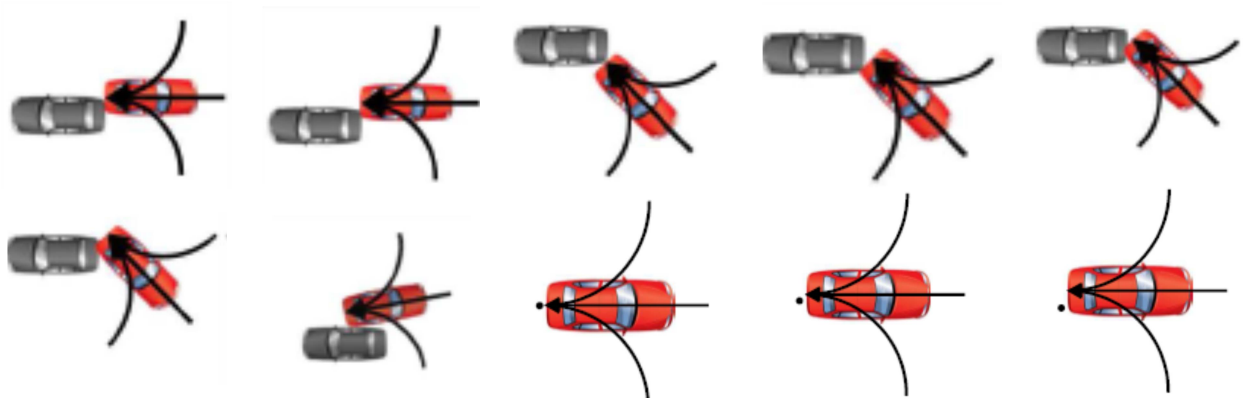

***Figure 1: Illustration of the 30 different crash configurations defined.***

For each of these configurations it was considered important to consider the ability of systems to detect and respond both at short range (c. 2m) and when approaches were at higher speed (c. 6 km/h). In practice, this is likely to be achieved by an approach procedure that constantly relies on moving away from rest, in reverse gear and using only engine idle speed (or small throttle in the case of hybrid/electric drivetrains). Thus the higher speed objective is achieved with the same vehicle inputs but just starting from further away from the object.

The tests were designed such that the correct impact configuration was achieved by positioning the vehicle at the impact point and applying the appropriate steering lock. The vehicle would then be moved slowly forward the prescribed distance and stopped. While maintaining the exact same steering input, the vehicle would then be reversed at engine idle speed.

For the tests, the collision objects need to be representative of real world collisions as far as the sensor systems are concerned, currently these are predominantly ultrasonic, camera or radar sensors. However, it also needs to be soft or collapsible so as not to cause damage to the test vehicle. For the initial vehicle-to-vehicle test configurations, the Euro NCAP Vehicle Target was defined. This represents the rear end of a vehicle and was designed to be representative for in-line crashes seen through the “eyes” of lidar, radar and camera sensors. It was considered likely to be effective for ultrasonic sensors, possibly OK for camera sensors but unlikely to be realistic for radar sensors when approached from an angle or with an offset. Further development of a three dimensional target is likely to be required before the test procedure could be reliably implemented in a technology neutral rating scheme.

The collisions with a “post” are actually intended to represent a broad range of collision objects found in the insurance claims data, including metal and plastic bollards, concrete posts, trees etc. A brief exercise was undertaken to measure a sample of 38 different “post-like” objects. It was found that heights ranged from 0.4m to 1m, with a median of 0.9m and the diameter ranged from 76mm to 275mm, with a median of 150mm. For

the purposes of the initial test programme a bespoke post was used, which was 110mm in diameter, 900mm tall and constructed from plastic drain fittings and ballasted with gravel.

**Test results: Infiniti Q50 with Back-up Collision Intervention**

The test results for the car to car scenarios are shown in **Figure 2**, below.

| | Range | | | | | | | |
|---|---|---|---|---|---|---|---|---|
| Straight | 1.0m | Avoid | Avoid | Avoid | Avoid | Avoid | Avoid | Avoid |
| | 2.0m | Avoid | Avoid | Avoid | Avoid | Avoid | Avoid | Avoid |
| | 3.0m | Avoid | Avoid | Avoid | Avoid | Avoid | Avoid | Avoid |
| Left lock | 10° | Avoid | Avoid | Avoid | Avoid | Avoid | Avoid | No effect |
| | 20° | Avoid | Avoid | Avoid | Avoid | Avoid | Avoid | Avoid |
| | 30° | Avoid | Avoid | Avoid | Avoid | Avoid | Avoid | Avoid |
| Right lock | 10° | Avoid | Avoid | Avoid | Avoid | Avoid | Avoid | No effect |
| | 20° | Avoid | Avoid | Avoid | Avoid | Avoid | Avoid | Avoid |
| | 30° | Avoid | Avoid | Avoid | Avoid | Avoid | Avoid | No effect |
| | Range | | | | | | | |
| Straight | 6.0m | Avoid | Avoid | Avoid | Avoid | Mitigation | Avoid | Avoid |
| | 8.0m | Mitigation | Avoid | Avoid | Avoid | Mitigation | Avoid | Mitigation |
| Left lock | 60° | Avoid | Avoid | Avoid | Avoid | Avoid | Avoid | Avoid |
| | 90° | Avoid | Avoid | Avoid | Avoid | Avoid | Avoid | Avoid |
| Right lock | 60° | Avoid | No effect | Avoid | Avoid | Mitigation | Mitigation | No effect |
| | 90° | Avoid | No effect | Mitigation | Avoid | Mitigation | Mitigation | No effect |

***Figure 2: Car to Car Results of Short Range Tests (Top) and Higher Speed Tests (Bottom) for Infiniti Q50***

It can be seen that performance is generally lower at the higher speeds and on the inside of the curve when turning. The performance in the tests against a bollard are shown below.

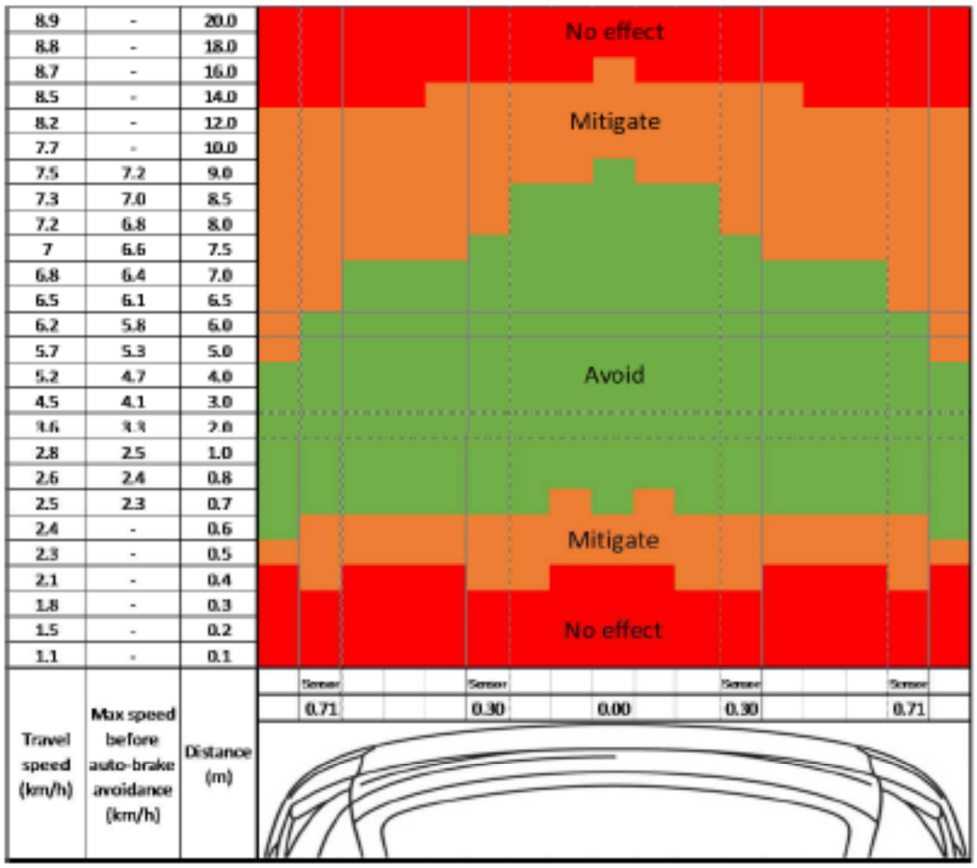


***Figure 3: Results of straight line tests against a post.***

It can be seen that performance was strong in the centre of the vehicle, avoiding collisions at up to around 7 km/h but that this dropped away slightly towards the corners of the vehicle (which is important because claims data shows the corners are frequently damaged). It is worth noting that the effectiveness is reduced or eliminated if starting from rest at very short distances to the collision partner.

One observational result of this range of tests was that when the auto-brake was activated and avoided a crash, the brake was only held on automatically for a period of around half a second and was then released. In the automatic vehicle to which this was fitted, this meant that the vehicle started to move backward again after a short period of time, if the driver had taken no action to brake themselves or place the vehicle in neutral. Subjectively, it was considered that some drivers, in real situations, may not react sufficiently quickly, potentially eroding some of the benefit.

## DISCUSSION

The evidence shows that parking and low speed manoeuvring crashes represent a very substantial cost in terms of damage, representing up to 30% of all insurer claims cost. In some jurisdictions, they also represent a substantial cause of death and serious injury to some of the most vulnerable people in society, those aged less than 5 and more than 70. This does, therefore, represent a significant problem to solve.

A range of semi-automated parking systems are available but these are offered as a convenience feature and by focusing on assisting the driver to get into spaces, do not directly affect the mechanism (reversing out of parking spaces) that is responsible for the most claims. In addition to this, they rely on the driver deciding to use the system. It is not known how often drivers will choose to use the system in practice.

Technologies intended to more directly prevent or mitigate this type of crash have already been implemented. Simple proximity warnings have been widely available for many years and, in the US, rear view cameras have

been made mandatory for certain vehicle types. However, the evidence regarding their effectiveness is very mixed. Experimental studies suggest that camera systems will substantially reduce the incidence of reversing crashes but that proximity warnings do not (and lessen the effectiveness of cameras when used in combination). Statistical analyses of claims rates has found proximity warnings to be effective on some cars but not others and has found little evidence of the effectiveness of cameras.

There are a range of possible reasons for the mixed results, including the possibility that the effectiveness:

- relies on driver action to achieve its results;
- will be influenced by the way in which warnings are delivered;
- will be affected by the positioning and quality of screens, the cleanliness of camera lenses, and the external lighting conditions, where mixtures of light and shade can obscure objects.

Linking these detection systems automatically to the braking system such that the vehicle can be stopped without driver intervention would be expected to avoid many of these human factors difficulties and improve effectiveness. Such systems have been fitted to a very small range of vehicles and are similar to AEB systems. Although no post-hoc studies of effectiveness are yet available the analogous comparison that showed AEB systems were more effective than forward collision warning systems suggests that reverse auto-brakes should be an improvement on both cameras and sensors alone.

A comprehensive test programme has been developed to assess performance in situations that have been demonstrated to be highly relevant to real world insurance claims and it has been seen that one reverse auto-brake technology (Back-up Collision Intervention on the Infiniti Q50) proves highly effective in those tests. It is, therefore, considered that there is a compelling case for using this test programme as the basis of a scheme to incentivize the fitment of systems that perform well in situations representing real crashes. In order to achieve this, the test programme is likely to require:

- Rationalisation, to reduce the burden of testing while still promoting good performance
- Refinement to the methods to ensure accurate and repeatable results, in particular the methods for achieving consistent impact points.
- The development of a new car target providing an accurate, 3 dimensional visual and radar signature.

## CONCLUSIONS

1. Parking and low speed manoeuvring crashes represent a significant cost to societies across the world, representing up to 30% of the cost of all insurance claims. Claims involving reversing out of parking spaces and colliding with other vehicles or fixed objects are the most common.
2. Existing measures to reduce the frequency of this type of crash show mixed results, with some promising signs of effectiveness but other evidence suggesting little evidence of effectiveness.
3. Many of the possible explanatory factors for the lower than expected effectiveness results are associated with human factors. These could be bypassed if the detection systems were linked to an autonomous braking function.
4. A handful of reversing auto-brake systems are already in production and tests undertaken during this research suggest they are capable of avoiding a large proportion of the the most common types of parking crash identified in the insurance data.
5. An initial test programme has been developed that is capable of assessing the performance of such systems in scenarios highly relevant to real world claims. Further refinements to this programme have been proposed to ensure it will be sufficiently robust to allow it to be implemented in suitable incentive schemes around the world.

**REFERENCES**

HLDI (2011a). 'Mazda collision avoidance features: initial results.' Highways Loss Data Institute Bulletin Vol. 28, No. 13: December 2011

HLDI (2011b). 'Buick collision avoidance features: initial results.' Highways Loss Data Institute Bulletin Vol. 28, No. 22: December 2011

HLDI (2012). 'Mercedes-Benz collision avoidance features: initial results.' Highways Loss Data Institute Bulletin Vol. 29, No. 7: April 2012

Kidd, Hagoski, Tucker and Chiang (2014). 'The effectiveness of a rearview camera and parking sensor system alone and combined for preventing a collision with an unexpected stationary or moving object'. Human Factors: The Journal of the Human Factors and Ergonomics Society **October 1, 2014.**

NHTSA (2014). "NHTSA announces final rule requiring rear visibility technology." NHTSA Press Release NHTSA 09-14.

Ydenius & Rizzi. "The effect of Ultrasonic sensors" Folksam powerpoint presentation, undated.

# THE EFFECTS OF ROAD CONTACT ANGLES AND PITCH/YAW ANGLES ON THE INJURIES OF DRIVERS IN CRIS TEST

**Byoungkee, Han**
**Youkeun, Oh**
Department of Mechanical Engineering, Hongik University
Republic of Korea

**Eundok, Lee**
**Jaewan, Lee**
**Gyuhyun, Kim**
Korea Automobile Testing & Research Institute
Republic of Korea

Paper Number 15-0350

## ABSTRACT

This paper shows the effect of the roof contact angle with ground and pitch/yaw angle on head and neck injuries in CRIS tests. In this study the effect of these conditions on injury in a rollover is simulated and analyzed by using a commercial multi-body software (ADAMS). The vehicle model consists of a rigid lower body and deformable upper body. Each member of the upper body is characterized to get the similar behavior to the results obtained from an equivalent finite element model. To evaluate the severity of driver's injuries in a CRIS test, a computer simulation to replicate the dynamic CRIS test is developed. The angular velocity of vehicle is set to a constant value of 270 degree/sec and the lateral velocity is varied to be 28.8kph or 35kph so that it can roll 2 or 3 turns. The roof contact angle with ground is selected to be 135, 145 and 155 degrees. The pitch and yaw angles of the vehicle is also varied to be 2 or 5 degrees and 0, 10, or 20 degrees, respectively. In addition to the peak acceleration of the dummy head, the maximum shear force, compressive force, and bending moment acting on the dummy neck are calculated to evaluate the rollover safety for various conditions. The simulation results are then compared to the KNCAP evaluation criteria. Considering the fact that the rollover accidents with less than 2 full turns account for about 90% of the entire rollover accidents, this study suggests that the 2-turn condition would be appropriate for a protocol of the dynamic rollover test.

## INTRODUCTION

Rollover accident mortality, which represents the number of deaths per 100 automobile accidents, is high compared to other types of car accidents. In Fig 1. the occurrence rate and mortality rate for each type of vehicle accidents in Korea compared to the European data are shown. The two regions show the significant difference in the occurrence rate and mortality rate. In particular, the vehicle-only-accidents in Korea are significantly smaller than the corresponding data in Europe. This difference might be considered to be due to the road condition, behavioral characteristics of drivers and pedestrians, and composition of vehicles. (Korea National Police Agency 2011; European Commission, 2008; UNECE, 2007; NHTSA, 2007)

Although the occurrence rate of the rollover accidents is relatively smaller than other types of accidents, the mortality rate related to the rollover accidents is significantly high. According to the Korean data set, the rollover accidents appear to be rare with the rate of 0.5%. But, as shown in Fig. 1, when considering the vehicle-only-accidents, which also include the accidents that can secondarily cause the rollover such as falls and veering due to breakaway, the mortality rate becomes significantly high with a 13.8 person compared to other types of accidents. (Korea National Police Agency 2011)

This observation is also supported by the data set in U.S. In contrast to the fact that the incident rate of the rollover in U.S. is approximately 3% out of the entire vehicle accidents, the 35% of automobile fatalities occur due to the rollover. Similarly, this trend can be found in the Australian data set. (NHSTA Traffic Safety Facts 2009)

There have been various efforts to reduce the fatality due to rollover by improving the vehicle stability performance with the equipped ESC (Electrical Stability Controller), securing the passenger compartment or occupant survival space with the enhanced roof crush resistance, and mitigating the passenger's ejection during a rollover. To encourage these efforts, the NHTSA has implemented the FMVSS 126 (i.e., mandatory installation of ESC) since 2011 and phased in the enhanced FMVSS 216a (i.e., roof crush resistance) and FMVSS 226 (i.e., ejection mitigation) since 2012 and 2014, respectively. In addition, the IIHS has also implemented the new roof strength rating system.

The rollover tests are developed in an effort to replicate what happens in real world collisions: Dolly test (FMVSS 208), CRIS (Controlled Rollover Impact System), and JRS (Jordan Rollover System). The Dolly test is not used as a mandatory requirement because it cannot test various conditions such as the pitch and yaw angle and lacks the repeatability. For the other two testing methods, researchers in the U.S. and Australia have actively worked on the test protocol to ensure the practicality of safety related regulations.

In real-world rollovers, the driver's injury is affected by not only the strength of vehicle's body structure (or chassis strength?), but also the posture of drivers. (Ridella et al. 2009; Cooper et al. 2001; Moffatt et al. 2003; Friedman et al. 2003) Seat belts prevent a driver to be ejected, thereby contributing to reducing fatal injuries. In the analyses of the CFIR data set, Huelke et al. have reported that seat belts reduce the severe injuries and fatalities by 91% under the roof crush of less than 6 inches (152mm). Evans et al. have reported that according to the FARS data, lap/shoulder belts can be effective to reduce fatalities by 82% and thus significantly contribute to the ejection prevention. (Huelke et al. 1973; Huelke et al. 1977; Evans, L. 1988)

Therefore, this study replicates the CRIS test using a dummy seated with a seat belt in order to prevent it from being ejected. As measured in the KNCAP (Korean New Car Assessment Programme) crash-test, the HIC15 induced to the dummy head and shear force, compressive force, and bending moment acting on the dummy neck are calculated and used to evaluate the safety under a rollover scenario.

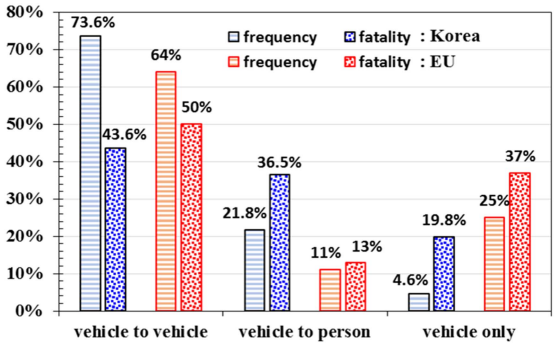


Fig. 1 Vehicle Crash Occurrence and Fatalities in South Korea and EU (Source: Korea National Police Agency 2011 and UNECE 2007)

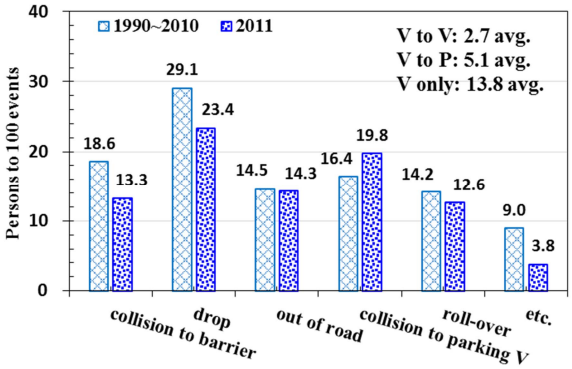


Fig. 2 Fatality of vehicle only accidents in Korea (Source: Korea National Police Agency 2011)

## CRIS TEST

It is required to maintain the ceiling strength at a certain level in order to ensure the survival space for passengers during a rollover. However, according to SNPRM (Supplemental Notice of Proposed Rulemaking), most of vehicle produced prior to the year 2008 have failed to satisfy the regulation of SWR $\geq$ 3.0 and resulted in serious casualties. Hence, the NHTSA has enhanced the regulations related to the ceiling strength.

It is, however, questionable if the static test would be appropriate for evaluating the ceiling strength. Currently, many researchers investigate how to better simulate a dynamic rollover accident, rather than replicating the Dolly rollover test (FMVSS 208). (Friedman, D., et al. 2009; Chirwa, E.C., et al., 2010; B. K. Han, et al. 2013)

Although the CRIS test is problematic in terms of the repeatability, it allows one to investigate the effect of the pitch and yaw angle for various road conditions and the behavior of the dummy as the roll progresses. (Linstromberf et al. 2005) The JRS test is actively used by the researchers in the CFIR(Center for Injury Research), University of Virginia, and University of New South Wales because it shows a high level of repeatability. (Grzebieta, R., et al. 2007; Kerrigan, J.R., et al. 2011; Mattos G.A., et al. 2013) This study constructs a simulation model to replicate the CRIS test and thus investigates the effect of the initial contact angle with ground, pitch/yaw angle on the safety during a rollover.

**Table 1. Estimated Fleet Failure Rates Based on GVWR reported (SNPRM in January 2008).**

| Two-Sided Testing | | | |
|---|---|---|---|
| GVWR : | 2.5 SWR | 3.0 SWR | 3.5 SWR |
| <2,722 kg | 67.2% | 78.6% | 85.0% |
| >2,722 kg | 100.0% | 100.0% | 100.0% |
| Total | 75.1% | 83.7% | 88.6% |
| Single-Sided Testing | | | |
| GVWR : | 2.5 SWR | 3.0 SWR | 3.5 SWR |
| <2,722 kg | 44.5% | 76.9% | 80.9% |
| >2,722 kg | 98.9% | 100.0% | 100.0% |
| Total | 57.6% | 82.5% | 85.5% |

## METHODS

### Protocol and Analysis Conditions for Simulated CRIS Test

As shown in Fig.5, in CRIS test device a vehicle is fixed to a trailer with the selected pitch and yaw angles. While the trailer moves forward at a constant speed, the vehicle falls apart from the trailer when the vehicle rotates at a desired angular velocity. As shown in Fig.6, the initial contact angles between the vehicle and the ground are varied to be 135, 135, and 155 degrees. The pitch and yaw angles are set to be 2 or 5 degrees and 0, 10, or 20 degrees, respectively.

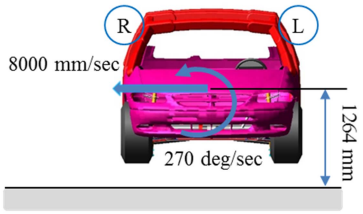


**Fig.5 Layout of CRIS test protocol**

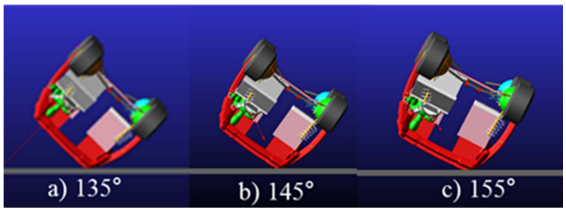


**Fig.6 Seat belted Hybrid 3 dummy model**

The analysis conditions for the simulated CRIS test are selected as in Table 2 so that the 2 turns and 3 turns of the rollover can be simulated. The drop height of the vehicle was set to be 0.3 m.

To assess the severity of injury for driver, a 50$^{th}$ percentile Hybrid III anthropomorphic test dummy (ATD) is seated in the driver's seat. The ATD is modeled to calculate the 3-dimensional forces and moments induced to its neck during the impact.

**Table 2 Analysis Conditions for the Simulated CRIS Test**

| | 2-turn condition | 3-turn condition |
|---|---|---|
| Roll rate (deg./sec) | 270 | 270 |

| | | |
|---|---|---|
| Velocity (kph) | 28(8 m/s) | 35(9.7 m/s) |
| Pitch angle (deg.) | 2, 5 | 2, 5 |
| Yaw angle (deg.) | 0, 10, 20 | 0, 10, 20 |

**Multibody Model for Base Vehicle**

A medium-sized passenger vehicle is used for the base vehicle of this study as shown in Fig. 6. The specifications for the base vehicle used are as follows: 2,000cc for the total engine displacement, 2,700 mm for the wheelbase, 4,400 mm for the overall length, 1,861 mm for the tread distance, 1,901 mm for the overall width, 1,610 mm for the overall height, 2,000 kg for the curb weight. The roof strength of the vehicle is modeled to have a strength-to-vehicle weight ratio (SWR) of 4.5, which exceeds the IIHS requirement for the static roof strength test (i.e., a SWR of 4.0).

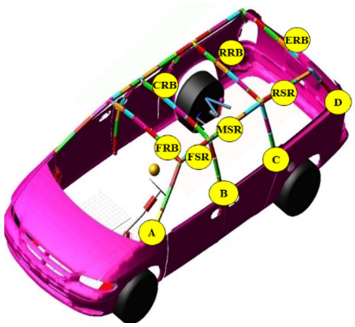


**Fig.6 Full Car model for multi-dynamics analysis**

The multibody vehicle model consists of the rigid lower body and the deformable upper body as shown in Fig. 5. The lower body is modeled to be rigid. The pillars, side rails, and roof bow members of the upper body are divided in 3~5 mass elements each. And the two adjacent elements are connected using the torsional and the bending spring. The characteristics of these springs are obtained using a finite element analysis (FEA), thereby mimicking the deformation of the upper body. (B. K. Han, et al. 2015)

**RESULTS**

Using the analysis conditions described in the Table 2, the model simulations are performed. In Fig. 7 to Fig. 12, the results for the 2-turn and 3-turn conditions are plotted. The p2 and p5 represent the pitch angles of 2 and 5 degrees and the y0, y10, and y20 represent the yaw angles of 0, 10, and 20 degrees, respectively. The effect of the initial contact angle (β) between the vehicle and ground is compared for the 2-turn and 3-turn conditions.

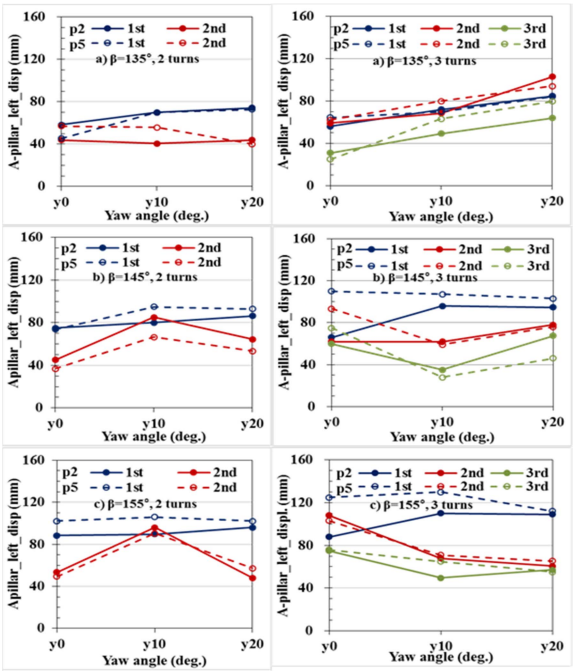


Fig.7 Maximum displacement of left A-pillar top-end; Left side for the 2 turns condition and right side

for the 3 turns condition. And β is the first contact angle of vehicle with ground.

**Displacement of Far-Side A-Pillar**

In Fig. 5, the maximum displacement of the left A-pillar for each roll is shown. Overall, as the pitch angle increases, the displacement of the left A-pillar increases, while it is not significantly affected by the changes in the yaw angle. In addition, as the initial contact angle (β) between the vehicle and ground increased, the maximum displacement of the left A-pillar increases.

As expected, the displacement for the 3-turn condition is greater than the one for the 2-turn condition. Under the 3-turn condition, the displacement for the second turn is dramatically decreased because the collision between the ground and the side of the vehicle, not the roof of the vehicle, is made. Instead, the large displacement consequently occurs in the third turn.

The maximum displacement of the left A-pillar of the vehicle indicates how much the roof penetrated the cabin, which is closely related to the passengers' survival. In other words, when the value gets large, a driver's head can get injured due to the contact with the roof. The overall resultant maximum displacement is smaller than 5 inches (127mm). This is because the roof strength of the vehicle has a SWR of 4.5.

**Variation in Head Acceleration**

The driver's head acceleration when the far-side of the vehicle collides with the ground is greater than the corresponding value when the far-side of the vehicle collides with the ground. When the roof is collapsed and thus the head contacted with the roof or front side rail, the acceleration reaches its maximum. In Fig. 8, the head accelerations are shown for the 2-turn and 3-turn conditions. The maximum head acceleration occurs during the first turn and it tends to decrease as the yaw angle increases. As the initial contact angle (β) increases, the peak head acceleration for each turn increases. Under the 3-turn condition, the peak head acceleration are greater than the one under the 2-turn condition. In addition, as the yaw angle increases, the peak head acceleration decreases. The peak head acceleration is not significantly affected by the pitch angle.

In Fig. 9 the values for HIC36 and HIC15, which are calculated from the line diagram of the head acceleration, are plotted. When the initial contact angle (β) between the vehicle and ground is 135 degrees, the values for HIC36 and HIC15 are significantly small. However, when either the contact angle (β) or the number of turns increase, the values significantly increase. The difference between the HIC15 and HIC 36 decreases as the yaw angle increases. The results suggest that it would be appropriate to use the HIC15 for a rollover evaluation criterion because the duration when the peak acceleration is maintained is short during a rollover in contrast to a frontal impact. Considering that the head acceleration is significantly high compared to the value of HIC15, it is recommended that the head acceleration would be included in the evaluation criteria for the vehicle's safety performance. Currently, the KNCAP adopts only the HIC36 to assess the risk for head injury during the frontal impact testing. For example, according to KNCAP, the HIC36 value exceeding 1000 indicates a higher probability of the head injury, while the HIC36 value below 650 represents less likelihood of the head injury.

**Shear/normal force of neck**

Compared to frontal impact tests, a rollover test induces greater values for the frontal shear force (i.e., Fx) and lateral shear force (i.e., Fy) in the dummy neck. The values for the frontal shear force are calculated to be less than or equal to 800 N under the loading conditions used in this study, except for when the initial contact angle (β) is equal to 135° and the yaw

angle is equal to 10°. As shown in Fig. 10, the frontal shear force (Fx) is not significantly affected by the pitch angle (α), initial contact angle with ground (β), and turn condition.

According to KNCAP criteria for frontal impact tests, the results of shear forces are included in the safe region for all testing conditions as shown in Fig. 10: the Fx values below 1.9kN and exceeding 3.1 kN indicate a higher probability or less likelihood to be safe, respectively. In Fig. 11, it is shown that the lateral shear force (Fy) is greater than the frontal shear force (Fx). In addition, it is the lateral shear force (Fy) that is significantly affected by the turn condition, rather than the frontal shear force (Fx). When compared to the KNCAP shear force criteria for frontal impact testing, the lateral shear force, Fy is also included in the safe region. However, the resultant force of the frontal and lateral shear forces may exceed the KNCAP shear force criteria. In case of the 3-turn condition, in order to satisfy the KNCAP criteria, additional constraining devices such as a curtain airbag would be required to reduce the impact with the front side rail.

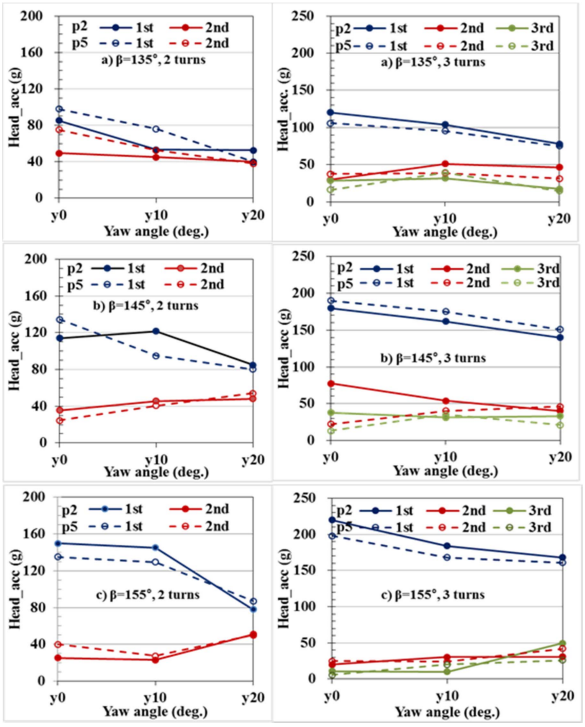


Fig.8 Maximum value of head acceleration at each roll; Left side for 2 rolls condition and right side for 3 rolls condition.

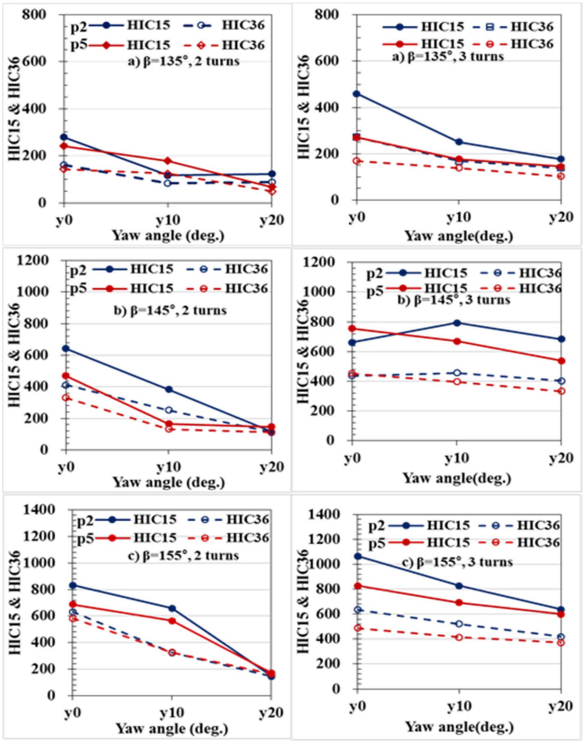


Fig.9 Maximum HIC value of head; Left side for 2 rolls condition and right side for 3 rolls condition.

The compressive force (i.e., Fz) on the neck will occur when the vehicle's chassis is collapsed and the dummy dives toward the roof, thereby impacting the roof or front side rail. The compressive forces on the neck (Fz) for each test conditions are shown in Fig.12. In the current model, the distance between the dummy head and roof ceiling is set to δ=80 mm. When the initial contact angle with ground (β) increases, a large displacement at the A-pillar is induced and thus the contact between the dummy head and the roof ceiling occurs thereby producing the compressive force on the dummy's neck. In real situation, the dummy also dives toward the roof ceiling augmenting the compressive force on the neck. The effect of the constraining devices such as a seat belt cannot be excluded. However, instead of considering the complicated dynamics of a seat belt, in this simulation the seat belt is simplified by maintaining the tension on it at a constant level. In the 2-turn condition, the largest compressive force acting on the neck occurs when the far side of vehicle contacts with the ground during the first roll.

Comparing to the criteria for the compressive force in a frontal impact, when the space between the roof ceiling and head is enough and seat belt works properly thereby minimizing the diving effect, the compressive force acting on the neck, Fz is included in the safe region.

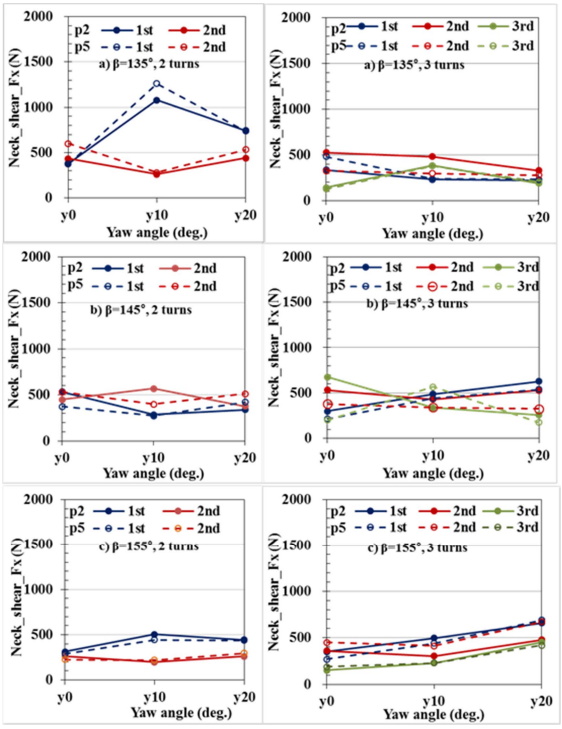


Fig. 10 Max. frontal shear-force acting on the neck (Fx) at each roll; Left side for 2 rolls condition and right side for 3 rolls condition.

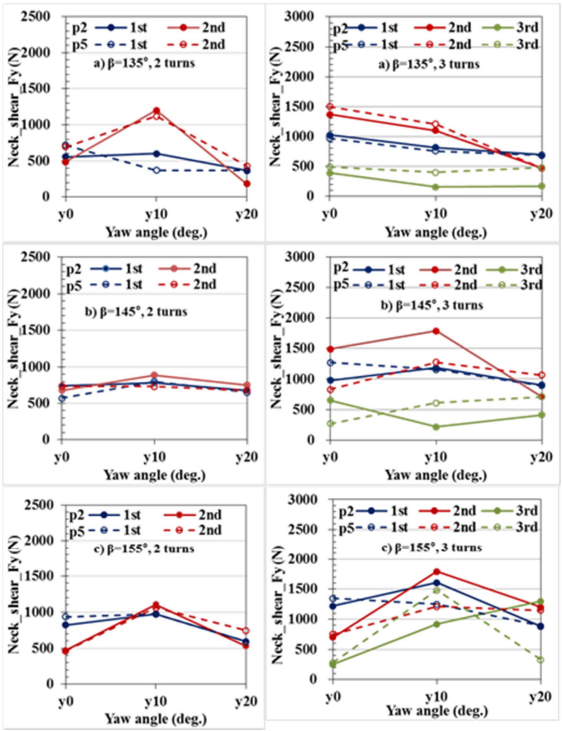


Fig. 11 Max. lateral shear-force acting on the neck (Fy) at each roll; Left side for 2 turns condition and right side for 3 turns condition

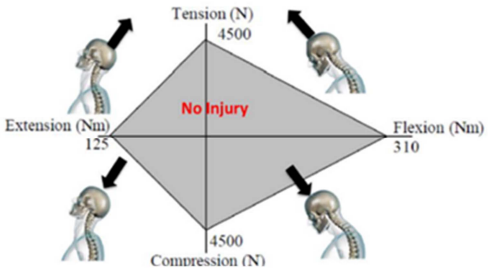


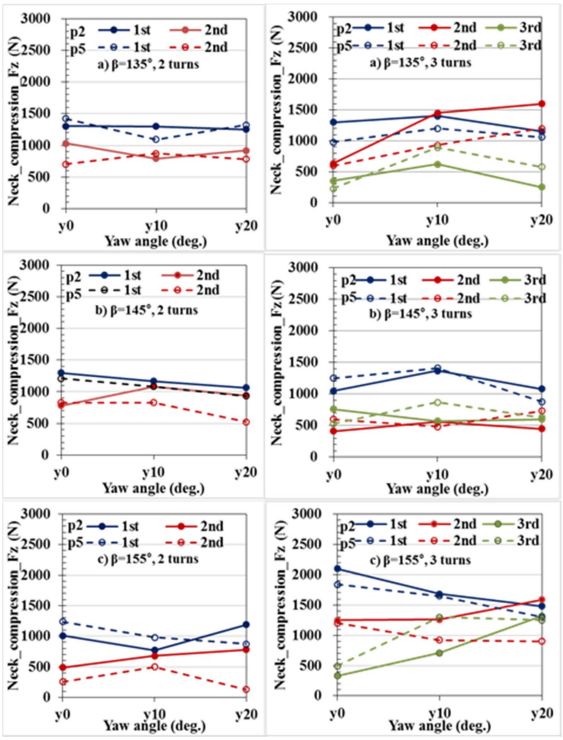


Fig. 12 Axial force acting on the neck (Fz) at each roll; Left side for 2 roll condition and right side for 3 roll condition.

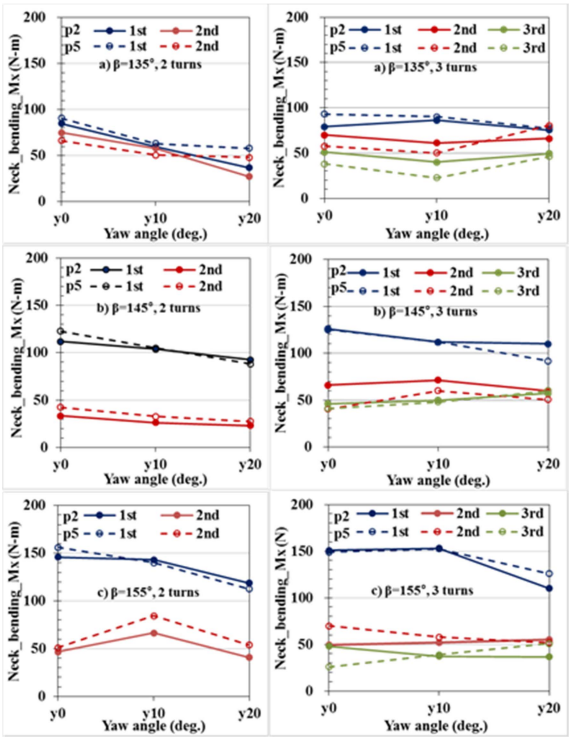


Fig. 13 Lateral bending moment (Mx) at each roll; Left side for 2 roll condition and right side for 3 roll condition

**Bending moment of neck**

The moment induced to the dummy neck can be decomposed into the lateral bending moment (Mx) and the extension/flexion moment (My). The lateral bending moment (Mx) under the 3-turn condition is significantly greater than the one under the 2-turn condition as shown in Fig. 13. It also increases as the initial contact angle (β) increases while it decreases as the yaw angle (θ) increases.

Fig. 14. Criteria for the neck injury suggested by Kleinberger et al.

It is difficult to evaluate the safety of the obtained results because the injury criteria related to the lateral bending moment (Mx) has not been in agreement. Thus, referring to the injury criteria of neck shown in Fig. 14, which has been proposed by Kleinberger et al., the lateral moment (Mx) should be evaluated based on the flexion moment rather than the extension moment. (Kleinberger et al. 1998)

Similarly to the injury criteria suggested by Kleinberger et al., the safety in the lateral direction is evaluated within the range between a third and half of the safety threshold for the flexion moment (i.e., 310 N·m): the lateral bending moment below 100 N·m is higher likelihood to be safe while the corresponding value above 150 N·m indicates a higher probability to be unsafe. Based on this injury criteria, the lateral bending moment calculated from the simulation is shown to be safe when the initial contact angle with the ground (β) is equal to 135°, but as the initial contact angle (β) increases, the level of safety decreases approaching the upper limit for the injury threshold.

Lastly, the bending moment (My) acting in the sagittal plane can be divided in two parts: the flexion moment (+My) to bend the neck forward and the extension moment (-My) to bend the neck backward. In general, the flexion moment is slightly greater than the extension moment, but, as shown in Fig. 14, in terms of the injury threshold, the flexion moment is approximately 2.5 times greater than the extension moment. Thus, the extension moment (-My) is used to define the injury criteria.

The extension moment (-My) is induced more frequently during either the 2nd or 3rd roll than the 1st roll. This suggests that as the roll of the vehicle progresses, how the constraining devices can exhibit the significant effects on the magnitude of the extension moment.

The results show that the extension moment obtained from the simulation is approximately within the KNCAP criteria (for the frontal impact testing where the extension moment below 42 N·m is considered to be highly safe and the value exceeding 57 N·m indicates high likelihood of the injury). In addition, the range for the KNCAP injury criteria corresponds to a third to half of the injury threshold (i.e., 125 N·m) that Kleinberger et al. have suggested.

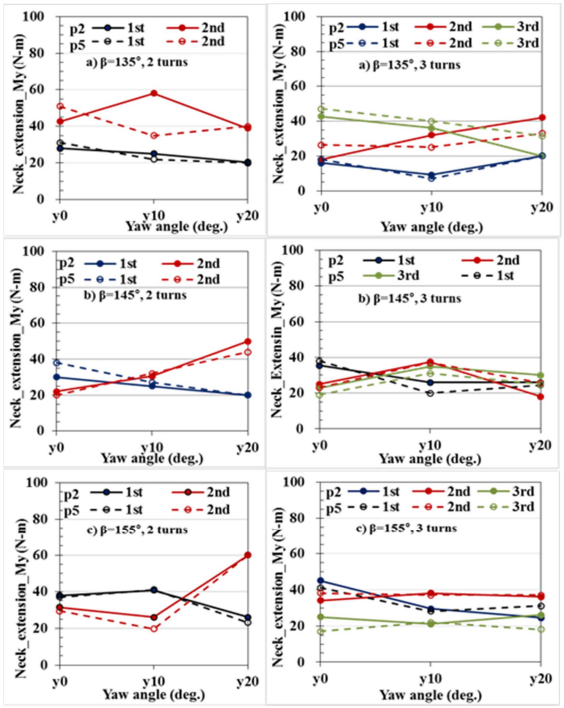


Fig. 15 Extension/flexion moment (My) at each roll; Left side for 3 roll condition and right side for 2 roll condition

## DISCUSSION

This stud investigates the relationship between the risk for driver's injury and the conditions for a vehicle's rollover. In addition, to establish the appropriate criteria for vehicle's safety, the conditions for the 2-turn and 3-turn rollover are compared.

The contact angle with ground, not the pitch and yaw angle, is the dominant factor that causes the increase in the magnitude of the A-pillar displacement. In addition, the head acceleration of the dummy seating on the driver's seat and the HIC value increase as the initial contact angle with the ground and the number of the turn increase. On the other hand, the corresponding values decrease as the yaw angle increases.

Considering the shear force induced on the neck, the shear force component in the lateral direction (Fy) is greater than the longitudinal shear force, Fx. Each shear force component independently satisfy the KNCAP criteria. However, the vector sum of the shear force components in both directions (can fail, may fail, or fails) to satisfy the KNCAP criteria. The results estimate that the compressive force (Fz) is significantly affected by not only the initial contact angle with the ground and the turn condition, but also the stiffness of roof interior and the constraining device, which is related to the diving effect.

The lateral bending moment induced on the neck (Mx) increases as the initial contact angle with the ground or the number of the turn increase. As the yaw angle increases, the corresponding value decreases. In contrast, the extension bending moment (My) is more affected by the yaw angle than either the initial contact angle with the ground or the number of turn.

Combining with the analysis that the rollovers with less than 2 turns account for 90% of the entire rollover accidents (Digges K and Eigen A. 2003), this study suggests that the 2-turn condition with the initial contact angle with the ground of either 145° or 155° would be appropriate for the evaluation criteria to assess the vehicle's safety performance.

## CONCLUSIONS

This study investigates the relationship between the risk for driver's injury and the conditions for a vehicle's rollover. For this purpose, the multi-body model for the vehicle's chassis is constructed using ADAMS multi-body dynamics software. The injury severity for the 2-turn and 3-turn conditions is investigated in order to propose pertinent criteria for assessing the vehicle's safety performance. To systematically simulate the various vehicle conditions, a three-level L27 orthogonal array for the 5 members of the upper body, which significantly affect the deformation at the top portion of the A-pillar, is used. Through the DOE analysis, the following conclusions are obtained.

1) In a rollover accident, it would be appropriate to use the HIC15 for the evaluation criterion of head injury, rather than the HIC36.

2) In contrast to a frontal impact testing where only Fx component acting on the neck is considered, when assessing a rollover safety, both Fx and Fy components should be considered. In general, the Fy component is greater than Fx component in a rollover.

3) In terms of the moment acting on the neck, the extension moment (-My) should be considered as an evaluation criterion in conjunction with the lateral bending moment.

4) The compressive force (Fz) is significantly affected by the chassis strength and the effect of constraining devices. Therefore, pertinent regulations related to the ceiling strength (SWR), which represents the chassis strength, would be warranted. To minimize the diving effect during a rollover, the constraining devices should be improved.

The contact angle with ground, not the pitch and yaw angle, is the dominant factor for the increase in the A-pillar displacement.

## ACKNOWLEDMENTS

This research was supported by the Korea Ministry of Land, Infrastructure, and Transport. It was also supported by the Korea Agency for Infrastructure Technology Advancement (Project No.: 14PTSI-C054118-06).

**REFERENCES**

[1] B. K. Han, E. D. Lee, J. S Shim, J. H. Jung (2013), Evaluation of the Dynamic Rollover Characteristics of Trip-over Vehicles through Multi-Body Dynamics Simulation, 23th Int. Tech. Conference on the ESV, Paper No. 13-0243-O.
[2] B. K. Han, E. D. Lee, J. H. Jung, S. M. Jang (2015), A Relationship of the Roof Strength Resistance with the Displacement of Top-end of A-pillar in CRIS Test, will be published in IJAT.
[3] Chirwa, E.C., et al. (2010), Review of the Jordan Rollover System (JRS) vis-a-vis other dynamic crash test devices. International Journal of Crashworthiness, 15(5): p. 553-569.
[4] Cooper ER, Moffatt EA, Curzon AM, Smyth BJ, Orlowski KF. (2001), Repeatable dynamic rollover test procedure with controlled roof impact. Society of Automotive Engineers, Warrendale, PA.
[5] Digges K and Eigen A. (2003), Crash Attributes that Influence the Severity of Rollover Crashes. Proceedings of the 18th International Technical Conference on the Enhanced Safety of Vehicles, Nagoya, Japan, May 2003. Paper 231
[6] Evans, L. (1988), "Restraint Effectiveness, Occupant Ejection from Cars, and Fatality Reductions." General Motors Research Laboratories, GMR-6398, September 1.
[7] Friedman D, Nash CE. (2003), Measuring rollover roof strength for occupant protection. IJCrash. 8, 97–105.
[8] Friedman, D. and R. Grzebieta (2009), A Proposed Rollover and Comprehensive Rating System, in 21st Int. Tech. Conference on the ESV.
[9] Grzebieta, R., et al. (2007), “Rollover Crashes: Diving Versus Roof Crush”, in 20th Int. Tech. Conference on the ESV, Lyon, France.
[10] Huelke. D. F., Marsh, J. C., Dimento, L J., Sherman, H. W., and Ballard, W. J. (1973), "Injury Causation in Rollover Accidents." Proceedings of the 17th Conference of the American Association for Automotive Medicine.
[11] Huelke, D. F., Lawson, T. E, Marsh, J. C. (1977), "Injuries, Restraints and Vehicle Factors in Rollover Car Crashes." Accid. Anal. & Prev., Vol. 9, pp. 93-107.
[12] Kerrigan, J.R., et al. (2011), “Design of a Dynamic Rollover Test System”, SAE International Journal of Passenger Cars - Mechanical Systems, 4(1): p. 870-903.
[13] Linstromberf, G. Scholpp, O. Scherf (2005), Test and Simulation Tools in Rollover Protection Development Process, 19th Int. Tech. Conference on the ESV, Paper No.05-0122-O.
[14] Mattos G.A., Grzebieta R.H., Bambach M.R., and McIntosh A.S. (2013), Validation of a Dynamic Rollover Test Device, 23th Int. Tech. Conference on the ESV.
[15] Moffat EA, Cooper ER, Croteau JJ. (2003), Matched-pair rollover impacts of rollcaged and production roof cars using the controlled rollover impact system (CRIS). Society of Automotive Engineers World Congress.
[16] Ridella SA, Eigen AM, Kerrigan JR, Crandall JR. (2009), An analysis of injury type and distribution of belted, non-ejected occupants involved in rollover crashes. Annals of Advances in Automotive Medicine, 53.
[17] European Commission (2008). “European Road Statistics”
[18] Korea National Police Agency (2011). “Statistics of Road Traffic Accidents 2011”
[19] NHTSA (2009). “NHTSA Traffic Safety Facts”
[20] SNPRM (2008). “Estimated Fleet Failure Rates Based on GVWR”
[21] UNECE (2007). "Statistics of Road Traffic Accidents"

# TECHNOLOGIES FOR THE PREVENTION OF RUN OFF ROAD AND LOW OVERLAP HEAD-ON COLLISIONS

**Colin, Grover**
**Matthew, Avery**
Thatcham Research
UK

**Iain, Knight**
Apollo Vehicle Safety Limited
UK

Paper Number 15-0351

## INTRODUCTION

A substantial number of serious collisions occur when a vehicle:

- Runs off the edge of the road way and collides with roadside furniture such as trees; and
- Crosses the centre line of the road and collides head-on with an oncoming vehicle.

A proportion of these are very likely to be caused by some form of inattention and/or distraction and several new technologies have been introduced into the market with the intention of preventing these crashes. Actions to promote the fitment of "lateral assist" systems are included within the Euro NCAP programme (Euro NCAP, 2014):

- Lane Keep Assist Test and Assesment Procedure for the 2016 rating scheme
- Advanced Lateral Support System Test and Assessment Procedure for 2018 rating scheme.

The aim of this research was to:

- Analyse the frequency and severity of relevant collisions in order to understand the potential impact of lateral control technologies
- Characterise crashes to inform the development of performance criteria that will be relevant to the real world
- Undertake initial research to explore the capability of different technologies
- Investigate the potential of candidate test procedures that could form part of future assessments.

## LATERAL ASSIST TECHNOLOGIES

A wide range of lateral assist technologies have been developed and put into production since the beginning of the 21st century. These include blind spot monitoring systems but these have not been considered in-depth in this paper because they are intended to be of benefit in crashes that occur during deliberate lane changes rather than crashes that occur because of unintended departure from the lane or road. The main characteristics of the different types of technology are briefly reviewed below.

### Lane Departure Warning

Lane Departure Warning (LDW) systems are now widely available on many production models, including high volume models. When the system detects that the vehicle has left the lane, or is just about to, without the activation of the direction indicator, then it provides a warning to the driver. Warning types have historically varied between different makes and models of vehicle (e.g. directional audible warnings, visual warnings on the multi-function display, steering wheel vibrations and even haptic seat vibrations) however at the time of writing warnings are generally converging to a visual multi-function display warning and/or haptic steering wheel vibration.

**Lane Keep Assist**

Lane Keep Assist (LKA) works on exactly the same principles as lane departure warning, except that when the system detects that the vehicle has left, or is leaving, the lane, a small heading correction is applied automatically in the form of steering torque or by differential braking in order to at least prevent further departure from the lane and, depending on exact circumstances, to re-direct the vehicle back into its lane. The intervention is deliberately kept relatively low such that it can be easily overcome by the driver, if they are deliberately changing lane and have simply forgotten to use the direction indicator.

Lane Keep Assist is now offered by many manufacturers, including Volvo, Volkswagen, Mercedes, Toyota, Subaru etc. but it tends to be offered on the higher end models.

**Lane Centering Assist**

Lane Centering Assist uses exactly the same technologies as a lane keeping assist. However, a lane keep assist only reacts to the vehicle passing over a road marking. Thus, in the absence of driver input it is possible that the vehicle would proceed along the road in a zig zag fashion "bouncing" from one lane boundary to the other. A lane centering system will autonomously apply steering inputs to keep the vehicle positioned as centrally in the lane as possible at all times.

This variation of the technology is less common than the systems based on crossing lane boundaries but Honda, Mercedes, Volkswagen and Infiniti have been early adopters of this strategy.

**Autonomous Emergency Steer**

All of the systems previously described react according to a relatively simple set of criteria, regardless of the extent of collision risk. If the speed is in excess of the threshold (typically 37 to 45 mile/h), a lane marking is detected and may be crossed, and the indicator is not activated, then the warning and/or corrective torque will be applied. Thus, the system will take the same action in normal driving with no other vehicles around, as it will in a critical incident where a head-on collision is imminent. The category of Autonomous Emergency Steer has been created to consider systems with two key differences:

- The activation criteria are combined with an assessment of the risk of collision. For example, if on a country road, in the absence of any other traffic, a driver takes a straight line path through a bend and cuts across the road centre marking, then the system may not activate at all, in other circumstances it may warn the driver but not intervene
- The range of actions available to the system is increased such that a relatively severe correctional steering input can be applied if a lane departure is detected and the sensors detect an imminent risk of collision with an overtaking or oncoming vehicle. While this could be applied via a higher steering torque, the first example of such a system used the electronic stability control system to generate the correcting moment via differential braking, with the added advantage that this also slows the vehicle down.

The aim of this system is to both reduce the chances of the system intruding on normal driving thus boosting driver acceptance and increase its effectiveness in terms of the ability to avoid critical incidents. This type of system has been introduced by Mercedes but, at the time of writing, was not known to have been introduced by other manufacturers.

**Features common to different systems**

Most lateral assist systems now use forward facing camera sensors to detect lane markings. It is therefore, a fundamental requirement of the system that lane markings are present and clearly visible. Effectiveness would be expected to be high on main highways and motorways where good quality markings are typically present. However, rural roads could be more challenging. For example, in the UK many rural roads may have only a centre line and not a road edge marking. Some systems can detect a road edge even without markings but the

accuracy and consistency of detection is thought to be lower, as is the level at which the system will intervene (e.g. warning only rather than corrective heading control).

In addition to this, some drivers have reported that false interventions of both warning and intervention systems. These can commonly occur where the vehicle crosses road features that appear somewhat like lane markings but are not. For example, where road works have taken place and temporary lane markings have been installed and then imperfectly removed.

The time at which warnings and interventions occur can vary considerably. For example, ISO 17361, permits a lane departure warning system to issue the warning at any point from when the vehicle remains 1.5m inside the lane boundary to a point where the vehicle is already 0.3m past the lane boundary. Given typical human reaction times, then the vehicle could be very significantly past the boundary by the time the driver reacts and the range of warning times would, therefore, be expected to substantially influence the overall effectiveness of the system.

## CHARACTERISING LANE DEPARTURE CRASHES

The objective of this element of work was to understand the quantity of crashes that lane keeping technologies might have the potential to prevent and to characterise those crashes in order to inform the development of test procedures that would promote the design of systems with the best real-world effects. The analysis was based on:

- Analysis of 12,565 insurance claims from a First Notification of Loss (FNOL) dataset involving collisions occurring in the UK in 2010. The data includes 1st and 3rd party claims and crash categorisation was based on text analytics of collision descriptions.
- Analysis of crash data from the German In-Depth Accident Study (GIDAS).
- Review of published effectiveness studies

Analysis of the crash types found in UK insurance claims showed that in combination, single vehicle collisions and head on collision represented approximately 21% of both damage and personal injury claims (see **Figure 1**).

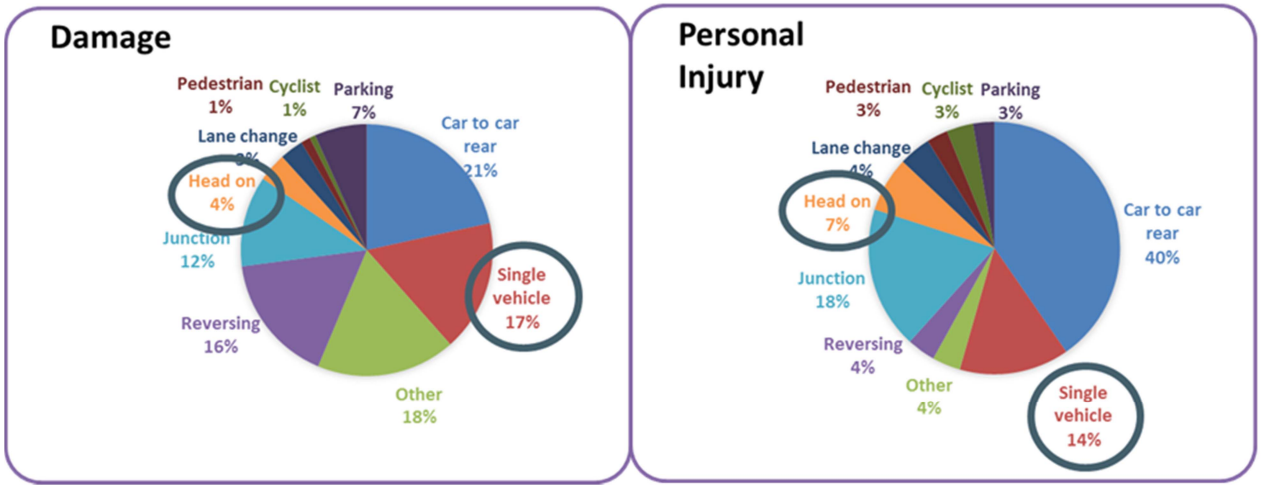


***Figure 1: Crash Type Analysis, UK insurance claims 2010***

Data provided to Thatcham from the GIDAS database characterised lane/road departure crashes as follows:

- Collision Mechanism
  - 44% straight road, 30% gentle left bend, 22% gentle right bend
  - 46% left departure, 40% right departure, 12% collision with other vehicle
  - Higher speeds typically 60-80km/h+

- Road Markings
  - 76% continuous white line, 12% dashed, 9% no marking
  - 72% well visible, 15% worn, 9% no marking
- Lighting & Weather conditions
  - 55% dry, 34% wet, 11% ice/snow
  - 61% daylight, 5% twilight, 34% darkness
  - 97% no fog
- Causation factors
  - Inattention
  - Fatigue
  - Failure to apply sufficient steering

It should be noted that this data is based on Germany. While this may well be representative of Europe in some respects, it may not be in all respects. Anecdotally, it would be expected that the presence, type and condition of road markings would be a feature that varied for road networks in different jurisdictions. Given that many lateral assist systems rely on cameras identifying road markings, this would be expected to have a strong influence on their overall effectiveness.

Concerns over roadmarkings notwithstanding, when combined with the data on the specification and intention of the technologies developed so far, the accident data suggests that there is strong potential for lateral assist systems to be effective. This is consistent with earlier predictive studies such as Visvikis et al (2008), which also showed strong potential (15% to 60% of lane departure crashes). However, the effects actually measured in terms of collision rates of vehicles with and without lane departure warnings have been much more ambiguous.

A US study (IIHS, 2012) found that lane departure warning systems fitted to Buick and Mercedes models were actually having a small adverse effect on claims rate for both collision (1st party) and property damage liability (3rd party) claims, although this was not statistically significant. A Volvo system appeared to be beneficial but the effect could not be separated from the fitment of a comprehensive AEB system for frontal crashes.

A more recent study (IIHS, 2014) has found that in combination a forward collision warning and lane departure warning has proved to be more effective than would have been expected based on earlier studies of both systems fitted to other vehicles. A reduction of 14% in the frequency of property damage liability claims was found, which compared to just 7% for earlier studies of forward collision warning systems. However, the effects of the FCW and LDW technologies could not be separated in the analysis of the Honda system so it remains unknown just how much the lane departure warning system has contributed to this benefit.

No studies have been identified that have yet attempted to measure the acutal claims reduction effect of a lane keeping system or other more advanced lateral assist system. Comparison of the typical results for forward collision warnings compared to autonomous braking systems suggests that the additional physical intervention should be beneficial but, as yet, this remains hypothetical.

## CANDIDATE TEST PROCEDURES

### Straight roads

The accident data suggests that a large proportion of lane departure crashes occur on straight roads. The type of crash most likely to be influenced by lateral assist systems is that where the driver is distracted, tired or otherwise impaired. The data suggests these crashes are characterised by relatively low lateral velocities (i.e. the vehicle leaves its lane relatively slowly.). Straight roads are thus likely to represent the simplest test procedure, and the circumstance where technology would be most capable. It is, thus considered that a straight road test would be well justified and will be the first scenario evaluated.

Any test procedure will need to define a series of standardised road markings, perhaps regionally adjusted, for which the system must be effective.

**Curves**

According to the data, an even larger proportion of lane departure crashes occur on gentle curves (c.52%). However, gentle bends could be interpreted as very large radius e.g. 300m plus. On these roads, the required sensor field of view and the rate of road departure (lateral velocity) may not be much greater than for straight roads. Conversely, executing tests may be more difficult because very large test areas could be required. Research tests will therefore focus on establishing whether testing on large radius curves is required by assessing whether it highlights any performance advantages or disadvantages of different lateral assist systems.

Testing on tighter bends represents a smaller proportion of all crashes, though potentially a higher proportion of severe crashes. It also represents a much greater technical challenge with much higher lateral velocities and much greater correctional steering inputs required to maintain the path. Investigation of small radius curves will therefore focus on the potential for systems to prevent this type of crash and the technical feasibility of developing appropriate tests.

Another consideration is how long lateral support should be continued for when negoatiating a curve and what mechanism should be employed to advise the driver of the support and the driving condition in which the vehicle should be left in if/when the support is terminated.

**Sensitivity to hazards**

One of the key factors distinghuishing between the systems described as lane keep (or lane centring) asssist and autonomous emergency steering is the ability to adapt the type or magnitude of autonomous intervention depending on the risk of collision. Thus, in order to distinghuish between such systems then tests on either straight roads or curves need to be repeated with and without the presence of a collision threat. For obvious safety and cost reasons the simulated collision risk must present minimal actual risk of equipment damage or injury.

The development of a suitable collision target for this type of testing has been the subject of much international discussion. There is an emerging concensus that the likely solution would be to define a harmonised world soft-car target which was an accurate 3D representation of a common world car in terms of radar, lidar, and visual signatures. Such a target also needs to be fully impactable at high relative speeds (100km/h+) without damaging the test vehicle. The target itself either needs to be a low cost, test consumable or it needs to be very durable such that it can be quickly re-built after impact, ready for the next test. The target could then sit on top of any low profile platform based delivery system that complied with an agreed set of performance criteria (e.g. radar signature, speed, acceleration capability etc.). Currently, a range of solutions have been proposed by various stakeholders, as illustrated in **Figure 2**, below.

***Figure 2: Candidate car target and propulsion systems for testing lateral assist systems (ABD top left, 4A top right, DSD bottom left & Perrone bottom right)***

**INITIAL TEST RESULTS**

Thatcham's initial test programme has focussed on assessing the capability of the Mercedes E Class, which is fitted with a system that corresponds with the earlier definition of Autonomous Emergency Steer (AES). The vehicle was equipped with path following robotic driving control to ensure repeatable testing. The test scenarios initially considered are based largely on the existing NHTSA standards for Lane Departure Warning confirmation on straight roads. The aim is to assess not only how the car responds to the different circumstances defined (e.g. solid lines, dashed lines, different lateral velocities etc) but also how the test procedure requires developing to allow more sophisticated systems to be fairly assessed.

For lane departure warning, the test procedure prescribes that the vehicle must simply pass through two geometrically defined "gates" that will create a lateral velocity within an acceptable range on approach to the lane boundary. The steering is applied manually and maintained as the vehicle crosses the lane boundary and the proximity to the lane boundary when the warning is isued is measured. The test procedure recommends this is achieved using a human driven open-loop steering input. The NHTSA procedure also offers a recommendation to assess lane keeping systems over a range of lateral velocities for reference purposes only where fitted, however no defined method is provided. On review of these procedures, Thatcham investigated two concerns:

- Repeatability, it was considered that the range of lateral velocities achieved in testing could possibly affect the performance of the vehicle
- If the test was controlled by robotic driving aids to improve accuracy and repeatability, a method would need to be defined to avoid the steering robot over-riding the lane keeping heading correction during the test.

Within the test procedure permitted by the NHTSA confirmation test there are a range of possible variables. If the lane boundary is to be approached at a constant lateral velocity, then the vehicle will initially travel in a straight line, be steered towards the lane boundary and then the path would be straightened. In this process, the initial steer input could be applied slowly (large radius curve) or fast (small radius curve). A range of different radii of initial turn-in were tested for the same resultant lateral velocity. Larger radii of turn required the vehicle to be initially positioned further away from the lane boundary to be crossed. Path controlled robotic steering was used to provide accurate inputs. In all cases, the steering was staightened and released by a distance 0.3m from the lane boundary and any heading control effect after that point was applied by the vehicle autonomously.

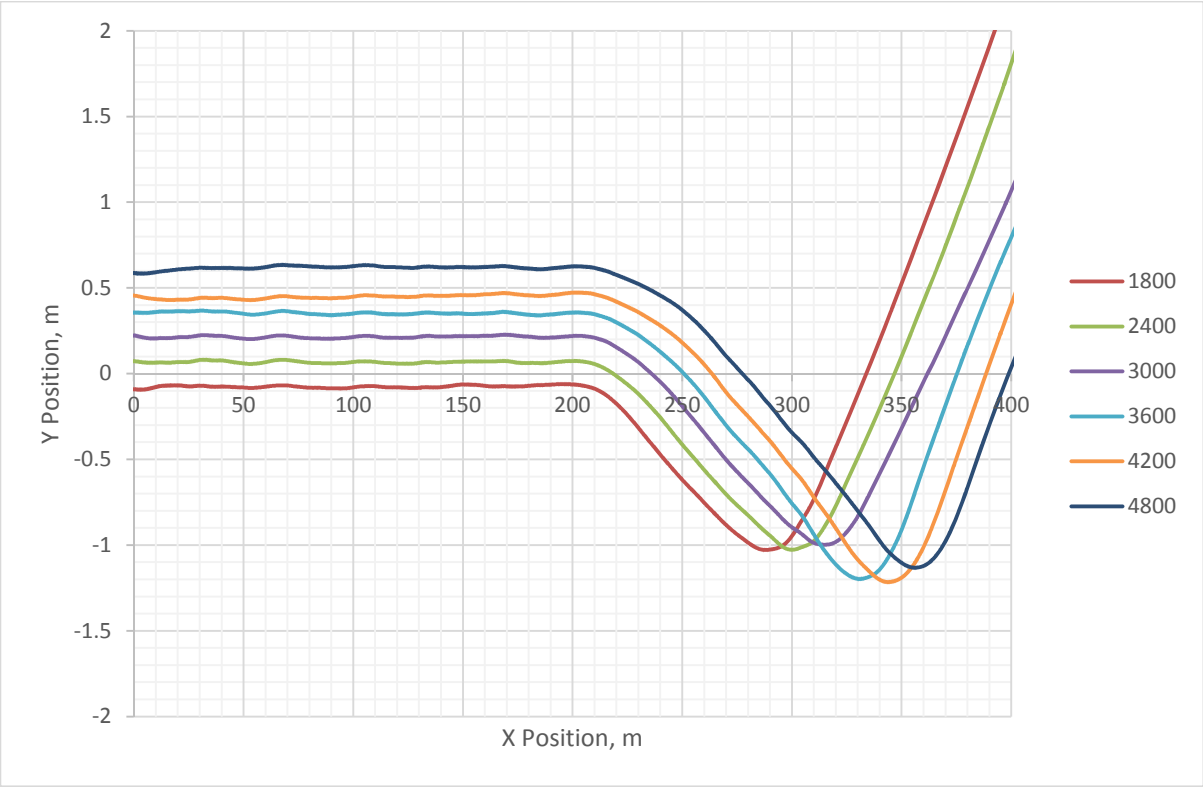


***Figure 3. Effect of initial turn radius on lane keep assist function and change in vehicle heading***

In this figure, the lane is centred on a y-position of zero and each trace represents the x-y position of the centre of gravity of the test vehicle. Thus, the lane boundaries would be at ± 1.75m and the edges of the vehicle will be at approximately ± 0.9m of the trace. Each trace represents the path of a test with a different radius of the initial curve. It can be seen that this variable has relatively little effect on the extent to which the edge of the vehicle crosses the lane boundary at y= – 1.75m (approximately 0.3m) or on the heading of the vehicle after the lane keep system has intervened.

It is worth noting that the lane markings during this test were such that the boundary at +1.75m was a dashed white line and the one at -1.75m was a solid white line. This graph also, therefore confirms that the Mercedes system adapts it's response according to the circumstances. Where it detected the solid white line (which in the centre of a UK road prohibits overtaking) the system intervened to correct the path. When it crossed the dashed white line it provided the driver with a lane departure waraning but did not actively steer the vehicle to correct the path. A Volvo V40 with lane keep assist tested in the same manner corrected the heading in response to both lane boundaries, such that the path of the vehicle zig-zagged from one lane boundary to the other and back again.

Subsequently, the effect of variation in the lateral velocity with which the lane boundary was approached was investigated, within a range of 0.1 to 0.6 m/s, all with the same initial radius of turn. The results are shown in **Figure 4**.

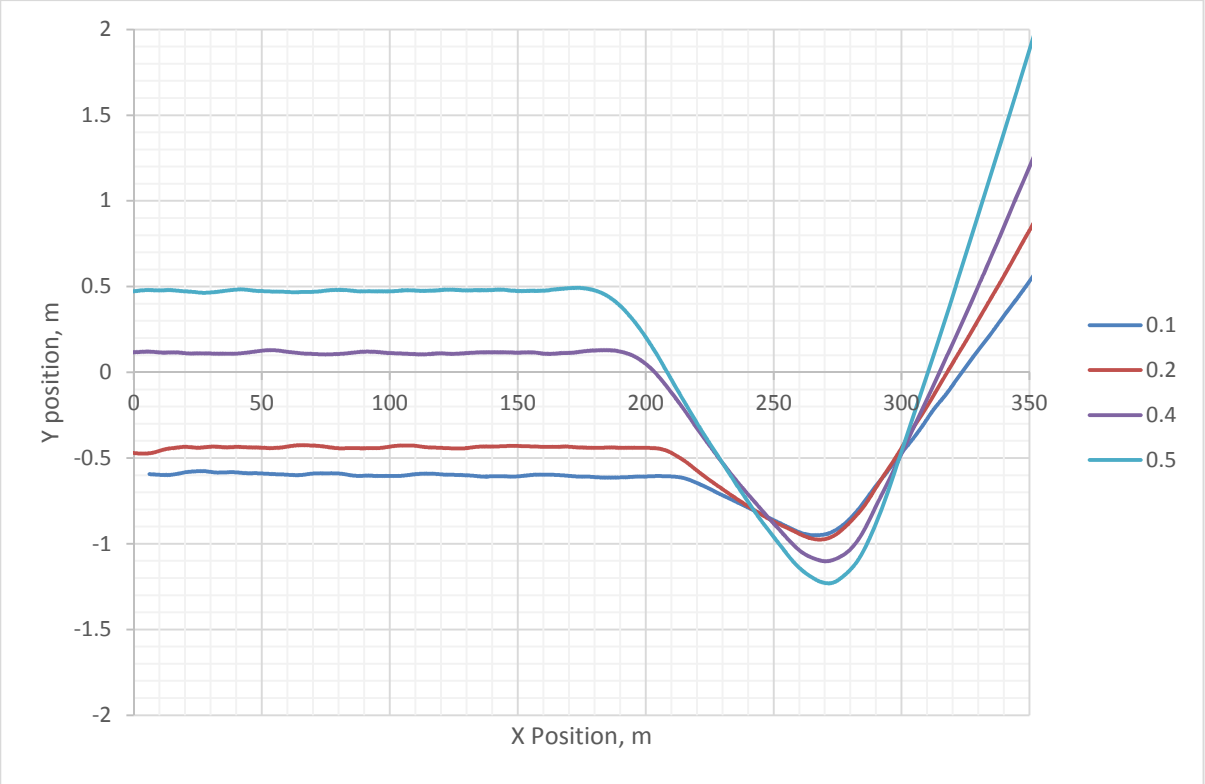


***Figure 4: Effect of lateral velocity on lane keep assist function and change in vehicle heading.***

It can be seen that higher lateral velocities could only be achieved by initially positioning the vehicle at the far side of the lane boundary to be crossed. However, in this case, it can also be seen that higher lateral velocities tended to result in the vehicle crossing the lane boundary by a greater margin before the active steering assist could correct the path. It also resulted in the correction of heading being applied with a greater yaw velocity, which in turn translated to the vehicle approaching the opposite lane boundary with a higher yaw velocity. The exact actions of the test inputs and vehicle response can be seen in the results of a single test at a lateral velocity of 0.6m/s.

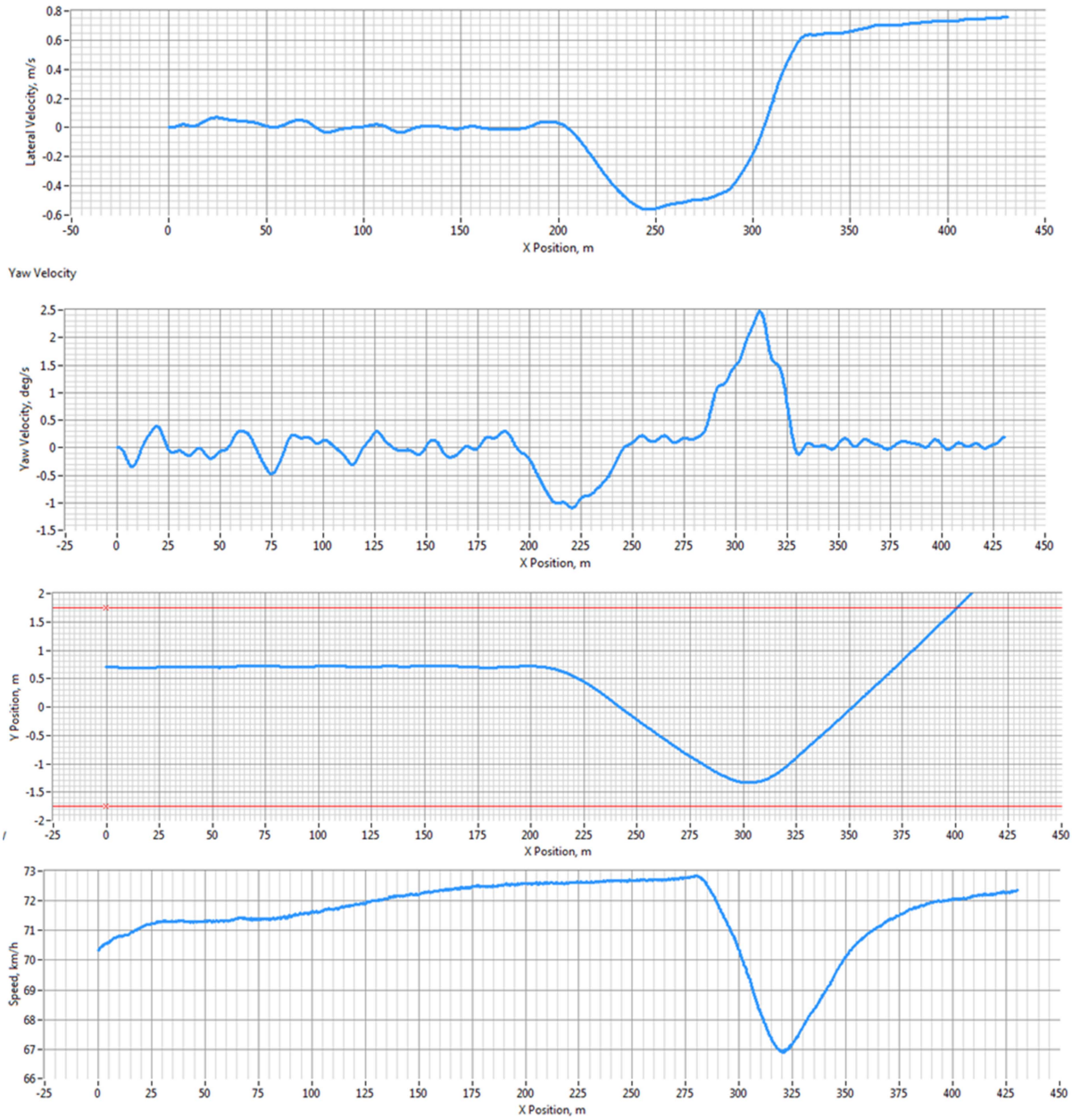


***Figure 5. Example of detailed results from a single test at a lateral velocity of 0.6m/s***

## DISCUSSION

It is clear that lane departures that result in run-off-road or head on collisions represent a substantial safety problems and that lateral assist systems have strong potential to prevent a substantial proportion of them. However, it is considerably less clear as to whether such systems are actually being effective in-service with some evidence suggesting that lane departure warning systems have little effect, or even an adverse effect. If forward collision warning and AEB are considered as a valid analogy, then it seems very likely that that lane keeping systems and autonomous emergency steering should be considerably more effective than a simple lane departure warning. However, further research is required to quantify the actual benefits of such systems as the available sample size increases with greater market penetration of the systems.

The capability of the lateral assist technology available is also evolving rapidly. The first lane keep assist systems only became widely available in the last few years but already the first examples of the next generation of AES is available from Mercedes. Thus performance ranges from a simple audible warning every time any kind of lane marking is crossed, to a system that varies its action in response to different situations and can provide a more abrupt correction in the heading when the threat of a collision is detected as a result of lane departure.

Test procedures already exist for the simpler systems but preliminary research has suggested that these require further development for assessing more advanced systems in a repeatable manner suitably for consumer testing. One essential requirement of a successful test programme will be the development of a lane departure test that occurs in the presence of an imminent collision threat with an oncoming vehicle. A range of different vehicle target and mobile platform systems is in existence to allow such testing. However, creating a harmonised 3-D vehicle target for use throughout the world would offer considerable benefits to both test authorities and industry and could also be used in a wide range of different test scenarios, including the existing car-to-car rear tests.

Actual testing of vehicles and the consequent refinement of test procedures remain at an early stage. However, the initial results are encouraging. They suggest that the vehicle performance offered is considerable and that accurate, representative and repeatable test procedures can be developed.

## CONCLUSIONS

1. Head on and single vehicle crashes represent approximately 21% of all UK motor insurance claims and a much greater proportion of fatal collisions. There is, therefore, a substantial problem to solve.
2. Lateral Assist Systems, including lane departure warning, lane keep assist, lane centering and autonomnous emergency steering, have been developed and are on the Euro NCAP roadmap for implementation within their rating scheme.
3. While the evidence regarding the effectiveness of lane departure warning systems is ambiguous, it is expected that systems that intervene on behalf of the driver would prove more effective. AES systems would be expected to both increase effectiveness and driver acceptance of the systems in normal driving.
4. Testing the more advanced lateral assist systems also requires more sophisticated test procedures. Development of these procedures is at an early stage but shows promising results.

## REFERENCES

Euro NCAP (2014). “European New Car Assessment Programme: 2020 RoadMap”. Available from www.euroncap.com

IIHS (2012). “They’re working: Insurance claims data show which new technologies are preventing crashes”. Insurance Institute for Highways Safety Status Report, Vol. 47, No. 5 July 3, 2012.

IIHS (2014). “Honda Warning System Trims Insurance Claims”. Insurance Institute for Highways Safety Status Report, Vol. 49, No. 4 May 29, 2014.

Visvikis C, Smith T, Pitcher M, & Smith R (2008). “Study on lane departure warning and lane change assistant systems”. TRL published project report PPR374, Crowthorne, UK.

# ASPECTS OF AGE RELATED ACCIDENT CAUSATION FACTORS AND IMPLICATION OF SAFETY MEASURES

**Michael Jänsch**
**Heiko Johannsen**
**Dietmar Otte**
Accident Research Unit of Hanover Medical School, Germany

**Bernd Pund**
TÜV Hessen, Germany

Paper Number 15-0354

## ABSTRACT

**Research Question/Objective**
The ageing society increases the requirements to focus on safe mobility for elderlies. It is expected that in Germany the population with an age above 65 years will reach more than 30% of the total population by 2060. In the same time the number of people above 80 years will double. In addition the relative share of driving license holder amongst the elderly will increase. In order to maintain the active role in mobility it is essential to identify specific risk factors of elderly and to develop countermeasures. The objective of this paper is to analyse specific accidents causes of elderly car drivers and to assess different measures such as improvement of the infrastructure, training measures, driver assistance systems etc.

**Methods and Data Sources**

For this study accident data of the Accident Research Unit Hannover (part of the GIDAS data sample) were used. The analysis focuses on the detailed 3 digit accident type and the Accident Causation Analysis System (ACAS) to identify functional problems in traffic situations with high accident risk for elderly. The driving task is derived from the detailed accident type, which describes the conflict that caused the accident and in more detail the positions and intended directions of the opponents.
ACAS as a hierarchic classification system and a sequence model is based on an in-depth data collection of predominantly directly event-related causation factors which were crucial in the accident emergence as situational resulting events and influences. The paradigm underlying this method refers to the findings of the psychological traffic accident research that most causally relevant features of the system components human, infrastructure and vehicle technology are found directly in the situation shortly before the accident. The focus in the immediate pre-crashphase lies on the human failures which are classified into five categories of basic human functions which are necessary to perform the driving task. With the detailed knowledge of the causes of the accident the causation factors are further specified into criteria of the categories and indicators of these criteria.

**Results**
The analyzed data shows that there are considerable age related deficits in the assessment of multiple information, e.g., reorientation after entering a crossing, observation of road users approaching from bypasses (e.g., cyclists) etc. Most of these deficits can be compensated by improved infrastructure, specific training modules and driver assistance systems. Predominantly information systems and active assistance systems for elderly drivers with the driving task "turning in intersections" can be useful.

**Discussion and Limitations**
Due to a limited number of elderly car drivers with ACAS codes in the GIDAS data set for most of the scenarios the number of cases is too low to analyse the data without grouping similar accident types and using main categories of the ACAS code. However, the data is consistent with knowledge from literature.

**Conclusion and Relevance to session submitted**

The paper presents data that judges which safety measures (mainly focusing on driver assistance systems) are beneficial for elderly car drivers on the one hand and describes relevant scenarios for the assessment of these safety measures on the other hand.

## INTRODUCTION

The demographic change in Germany is a well-known phenomenon which is leading to a distribution of population, where the share of older people in society is continuously increasing [1]. On the other hand human life expectancy is continuously increasing in Germany but the appearance of age related diseases such as dementia or poor eye sight is not delayed in the same manner. In contrast to other age groups accidents caused by elderly traffic participants have specific features that have been identified e.g. for car drivers in the past by means of accident research [2]. To preserve the ability for the elderly traffic participants to use a car it is sensible to provide cars with technical assistance systems to allow for a safe use even for eldery car drivers.

The research methodology (ACAS Accident Causation Analysis System) used in this study revealed that drivers aged 65+ have particular difficulties in reliably collecting relevant traffic information, especially if there are multiple simultaneously recorded external stimuli. For faster reaction sequences, such as those required in complex traffic situations, older drivers are more stressed than their younger counterparts. Between individuals the compensation for this loss of performance are widely scattered [3].

Therefore the question is, on the one hand what training and support measures for safe mobility of aged drivers are useful and on the other hand which technical assistance systems for the specific problems of older drivers are available.

## RELEVANCE OF THE STUDY

The study focuses on elderly car drivers that were involved in an accident with at least one person injured. To evaluate the relevance of the study on the accident situation of elderly car drivers in Germany, in a first step the German National Data was analyzed to display the occurrence of accidents with elderly car drivers in Germany. This analysis revealed that older drivers in fact are not more often involved in traffic accidents, which is assumed to be a result of the fact that older drivers use their car less and for shorter trips than younger drivers.

Therefore from the statistical data the share of drivers that caused an accident was compared to the share of drivers that where involved in an accident (being the causer or not), see Figure 1.

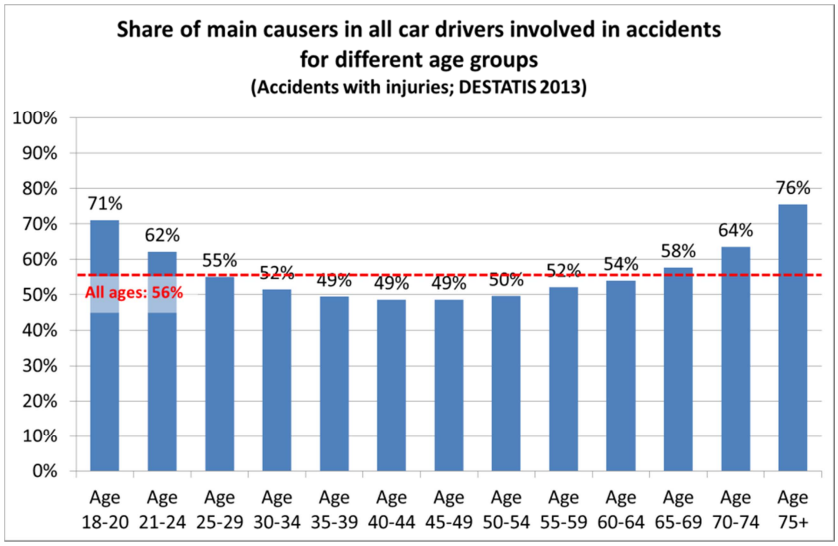


*Figure 1: Share of accident causers in the group of all car drivers involved in an accident for different age groups in Germany.*

It was then presumed, that if the share of causers in a certain age group is higher than in another age group, this indicates that the accent rate in this age group is higher. In general 56% of the car drivers involved in an accident were the main causers of the accident. When looking at different age groups however, the frequency of being an accident causer varies significantly. In the group of novice drivers (aged 18-20), which are known to have little experience and a high acceptance for taking risks in traffic, 71% involved in an accident had caused the accident. This portion drops to 62% in the age group 21-24 but is still over the portion of all age groups. Experienced drivers aged between 30 and 60 less often cause an accident compared to the average of 56%. However at the age group 65 to 69 the share of causers starts to rise again above the average of all age groups. With older ages the amount of drivers that had caused an accident compared to the amount of involved drivers constantly rises with 76% for the drivers aged 75 years or older to a point where this share is even higher than in the group of novice drivers.
Thus the analysis of the German national data shows that older drivers are at higher risk of causing an accident than the experienced younger drivers.

## DATA ANALYSIS

To analyze the accident situation and of older car drivers, The data collected by the accident research unit of the Hanover Medical School (MHH) was analyzed for the years 2008-2013, including available cases from 2014 (Figure 2).

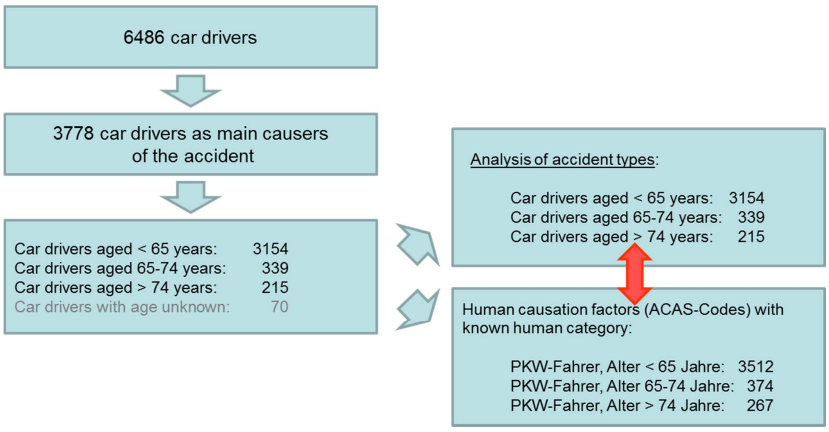


*Figure 2: Case numbers available for the in-depth accident analysis of older car drivers*

6486 car drivers were available in the database for analysis from the above mentioned space of time. To analyze the accident situation only the main causers of the accidents were included in the analysis, which led to 3778 drivers. Of these 339 were aged 65-74 years and 215 were aged over 75 years. Due to the rather low number of cases of older drivers the age groups “65-74 years” and “over 75 years” were merged to one group of older drivers aged 65+, containing 554 drivers.

### Analysis of the Accident Type

In a first step the accident type according to the GDV was evaluated. The accidents type is classified by the initial conflict situation which led to the crash. There are 7 main categories of accident types (driving accidents, accidents caused by turning-off the road, accident caused by turning into a road or by crossing it, accident caused by crossing pedestrian, accidents involving stationary vehicles, Accident between vehicles moving along in carriageway and “other” accidents) which are further specified by nearly 300 subtypes in those categories.
To display specific accident features of older car drivers the distribution of the main categories of accident types of older drivers is compared to the distribution of car drivers younger than 65 years in Figure 3.

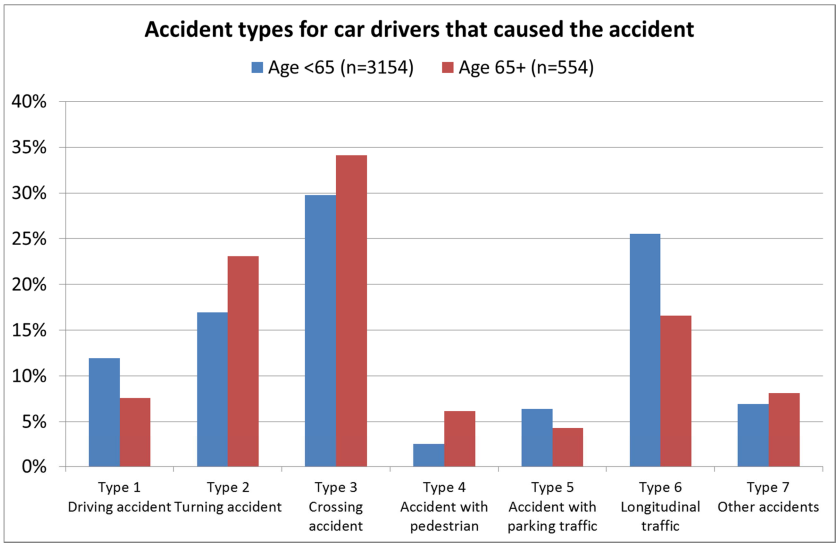


*Figure 3: Distribution of accidents types (main categories) for younger and older car drivers.*

For the age group comparison of the accident types the following criteria was determined:

- The frequency of each type of accident should be higher for the group of older drivers than for the drivers aged less than 65 years in order to consider specific accident characteristics for this age group
- These differences must be at least statistically significant to be included in the analysis process.

These criteria were met for the accident types 2, 3 and 4.

**Accident type 2** includes accidents which occurred due to a conflict between a road user turning off from a priority road and a road user coming from the same direction or the opposite direction (pedestrians included!) at crossings, junctions, access to properties or parking lots. 23% of accidents caused by older car drivers aged 65+ are of this accidents type in contrast to only 17% from younger control group. The most common sub types in this category for the drivers aged 65+ are displayed in Figure 4 together with the subgroup of drivers aged 75 years or older. For the drivers aged 65 years or older 31% of the turning-off-accidents are accidents where the driver collides with oncoming traffic on his road when turning left and in 13% of the turning off accidents the older car drivers has a conflict with a road user coming from ahead on a sidewalk or bicycle path respectively. Interestingly, the drivers which are even older (age 75+) show a very similar distribution of most frequent accident-subtypes.

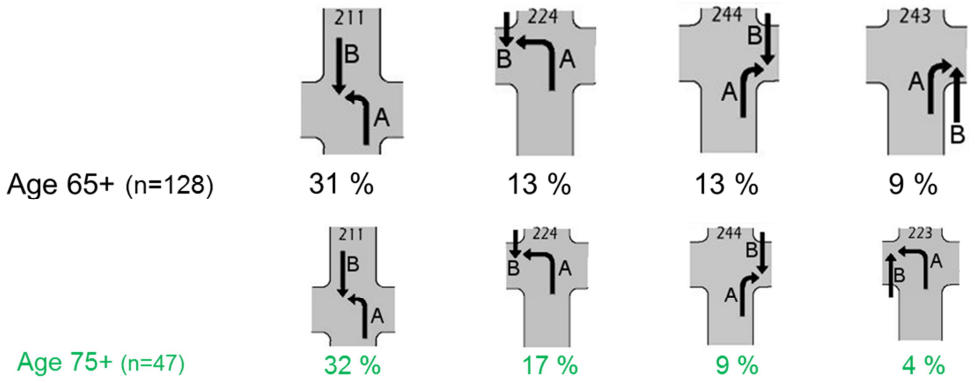


*Figure 4: Most common accident types of older car drivers aged 65+ in category 2 (turning accidents) and of car drivers aged 75+*

**Accident type 3** describes accidents that occurred due to a conflict between a turning in or a crossing road user without priority and a vehicle with priority at crossings, junctions, access to properties or parking lots. In contrast to younger car drivers with only under 30% the elderly car drivers cause accidents of this type in 34% of

the cases and therefore these accidents are the most common type of accidents caused by elderly car drivers for both age groups 65+ and 75+. Figure 5 shows that within this category again no major differences are found between the age groups 65+ and 75+ concerning the most frequent specific accident types. The small differences in the percentages can well be explained with the low numbers of cases. So for the eldery car drivers the most common subtypes are accidents with cyclists coming from the right when entering a crossing as a non-priority vehicle in 24% of cases and in 22% of cases respectively. Also frequent are accidents based on the conflict with traffic from the left when entering the priority road either to go straight (type 301 in 12% of cases for the drivers aged 65+) or to turn in to the left (type 302 in 20% of cases for the drivers aged 65+) or with traffic from the right when crossing the priority road (accident type 321).

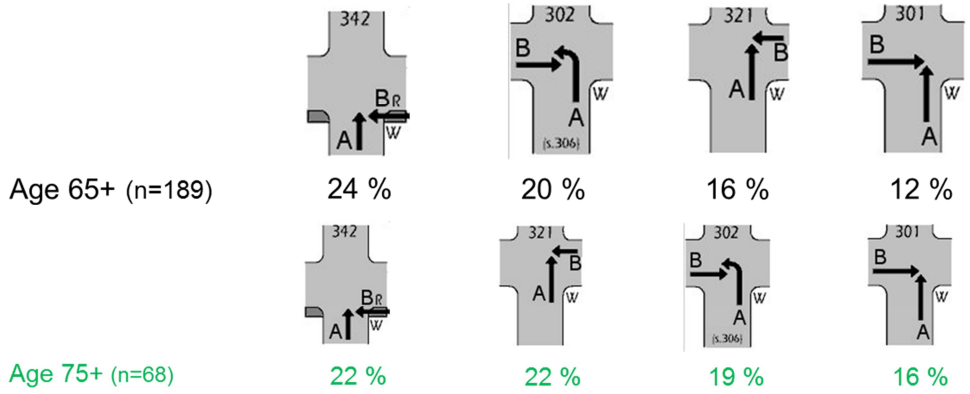


*Figure 5: Most common accident types of older car drivers in category 3 (crossing accidents)*

**Accident type 4** includes accidents which occurred due to a conflict between a vehicle and a pedestrian crossing the road (not applicable if he was walking in lateral direction and if the vehicle was turning in). This type is also applicable if the pedestrian was not hit. Even tough, these types of accidents are not the most common accident types, this category is relevant for describing the accidents situation of older car drivers because the incidence is more than double among the older car drivers aged 65+ with 6% in comparison to the car drivers younger than 65 years with only 2.5%. As seen in Figure 6, in this category the most frequent sub-types are accidents with a pedestrian crossing a road from the left or from the right without obstruction of sight either on a straight stretch of road (24% respectively 15%) or before a crossing (18% respectively 15%). Even though there are only 14 pedestrian accidents in the sub-group of drivers aged 75 years or older, the most frequent types also have a very similar distribution like the drivers aged 65+.

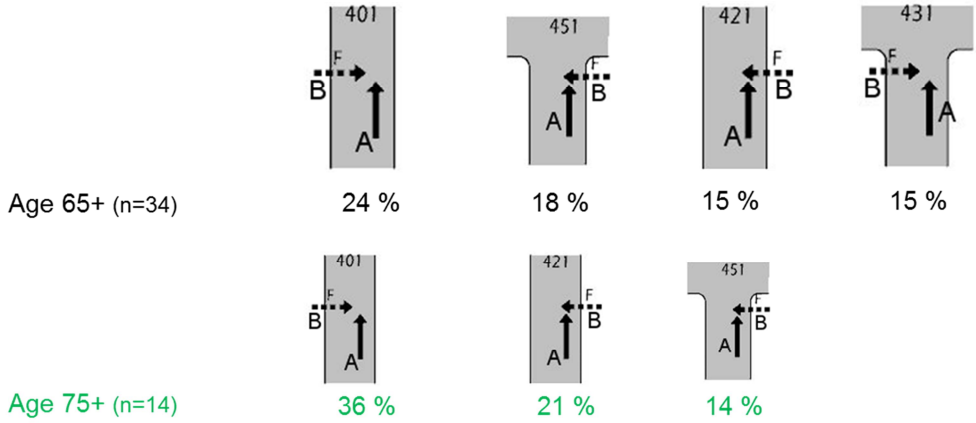


*Figure 6: Most common accident types of older car drivers in category 4 (pedestrian crossing the road)*

**Analysis of human causation factors**

The theoretical framework for the analysis of human causes is given with ACAS (Accident Causation Analysis System) which is a hierarchical classification scheme of five categories of basic human functions and errors in those that were effective in the emergence of an accident [4]. Except for the first step, information access, the next steps refer to human functional qualities in a sequential manner, which were active during the accident emergence either individually or in combination and contributed to the causation. These following steps are: Information admission, information processing, goal setting/planning and operation (see Table 1).
It has to be noted that, if relevant, multiple causation factors can be assigned to one accident participant. In addition accident participants which are not the main causers may also have been assigned with causation factors. For the present study however the focus lays the main causers of the accident, therefore only causation factors of the main accident causers were analyzed.

| Category | Examples |
|---|---|
| **1. Information access** | **…limited or hindered**<br>• Human influences (diseases)<br>• Information hidden due to obstruction of sight<br>• Information masking due to darkness or fog |
| **2. Information admission** | **… inattentive or recognition failure**<br>• Distraction (internal/external)<br>• Activation (too high/too low e.g. stress, fatigue)<br>• Alcohol/drugs<br>• Wrong focus of attention |
| **3. Information processing/evaluation** | **… misjudgment or wrong expectation**<br>• Insufficient ability to judge a situation<br>• Communication error<br>• Misjudgment of speed or distance |
| **4. Planning** | **…decision error / intentional breach of rules**<br>• Wrong maneuver planned<br>• Driving above speed limit |
| **5. Operation** | **…errors while executing the planned action**<br>• Overreaction while steering<br>• Mix-up of pedals |

**Table 1: Human failure categories according to ACAS**

In the next step the categories of human failures of older car drivers were analyzed for the 3 relevant categories of the accident types which were identified in the previous step. Due to relatively low case numbers of causation factors it has to be noted that for the very specific accident types, this analysis can only be conducted as a qualitative description of the accident situation of older car drivers aged 65+ instead of a quantitative statistical analysis. For this reason, no distinction could be made between the drivers aged 75 years or older from the drivers aged 65+.

The **Human failures at turning accidents (accident type 2)** can be divided into two groups of turning accidents: There are the accidents when turning left and having a conflict with oncoming traffic, accidents types 211 and 224, and there are the accidents when turning right and having a conflict with a participant from a parallel path such as a bicycle path (accident types 243 and 244). The distribution of human failure categories for those two groups of accident types is displayed in Table 2. In both cases common causes of those accidents were human failures from the category “information admission” (causation factors 36 and 17 respectively). These were mostly from the field of a wrong strategy of observation e.g. a failed reorientation or a missed reassuring view. Additionally for conflicts while turning left (accident types 211 and 224) a relative high number of failures due to visual sight obstruction due to other vehicles was reported.

| | Frequency distribution at accident types 211 and 224 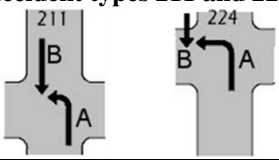  | Frequency distribution at accident types 243 and 244 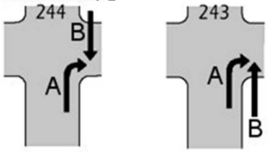  |
|---|---|---|
| **1. Information access** | 12 | 8 |
| **2. Information admission** | 36 | 17 |
| **3. Information evaluation** | 12 | 3 |
| **4. Planning** | 3 | 1 |
| **5. Operation** | 0 | 0 |

**Table 2: Distribution of categories of human failures for frequent types of turning accidents of older car drivers**

The **Human failures at crossing accidents (accident type 3)** are also divided into two groups: The accident type 342 where the car driver has a conflict with a cyclist from the right, travelling on the priority road and where the car driver has a conflict with a road user travelling on the priority road (accident types 302, 321, 301). The distribution of human failure categories here also shows a maximum of causation factors from the information admission (36 respectively 57 factors – see Table 3). The key aspects for the accident type 342 are a "focus on the other road user" (missing the relevant road user – in this case the cyclist) and a wrong strategy of observation e.g. a failed reorientation or a missed reassuring view for the accidents types 302, 321 and 301. Problems with the information access seem to be relevant as well for the older car drivers which often stated that they were dazzled by the sun in 21 cases when entering a crossing.

| | Frequency distribution at accident type 342 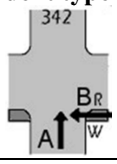  | Frequency distribution at accident types 302, 321 and 301 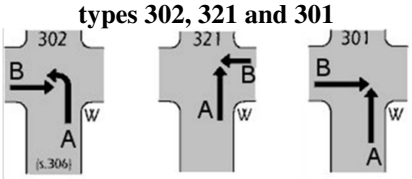  |
|---|---|---|
| **1. Information access** | 7 | 21 |
| **2. Information admission** | 36 | 57 |
| **3. Information evaluation** | 3 | 18 |
| **4. Planning** | 0 | 10 |
| **5. Operation** | 1 | 1 |

**Table 3: Distribution of categories of human failures for frequent types of crossing accidents of older car drivers**

The **Human failures at pedestrian accidents (accident type 5)** when pedestrians cross a road for older car drivers are categorized by the accidents where a pedestrian crosses the road on a straight stretch of road (types 401 and 421) and by the accidents where the pedestrians crosses the road just before an intersection (431 and 451). Again both groups of accident types were mostly caused by information access failures with 8 respectively 9 causation factors (see Table 4). While on the straight stretch of road the causes of the accidents were often distraction (external or internal), those accidents that happened just before an intersection were often caused by a wrong focus of attention.

| | Frequency distribution at accident types 401 and 421 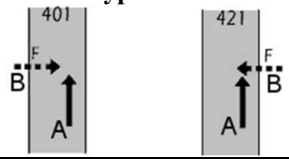  | Frequency distribution at accident types 431 and 451 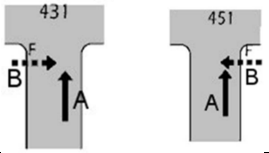  |
|---|---|---|
| **1. Information access** | 4 | 1 |
| **2. Information admission** | 8 | 9 |
| **3. Information evaluation** | 2 | 1 |
| **4. Planning** | 0 | 0 |
| **5. Operation** | 1 | 0 |

**Table 4: Distribution of categories of human failures for frequent types of pedestrian accidents of older car drivers**

## CONCLUSION

With older car drivers accidents at intersections seem to be represented more often than with younger drivers. This suggests that driving assistance systems should primarily focus on providing information about vehicles with priority and cyclists on bicycle lanes crossing the intended path of the older driver. Camera systems in the peripheral area or lateral short-range radar systems with blind-spot detection can be integrated into an intersection assistance system. An accident avoidance potential for the turning accidents at intersections can be expected from the detection oncoming traffic in combination with a brake assistance system (e.g. building up brake pressure when leaving the accelerator pedal). A closer look into the accidents caused by the older drivers aged 75 years or older in comparison to the drivers aged 65 years older revealed no significant differences for all three analysed types of accidents

Specific training for elderly drivers should be aimed at raising awareness of risks from side roads such as bicycle paths just before and at intersections including corresponding visual behavior training. Specific requirements of the "information collection/admission strategy" (e.g. frequency of attention towards different relevant road users) or the chosen speed when turning at an intersection could represent appropriate training modules.
Infrastructural improvements refer to the availability of clearly identifiable stop lines for turning maneuvers at intersections. But also conventional solutions such as the installation of mirrors for enhanced observability during turning maneuvers to the right (better recognition of cyclists approaching from behind) can prevent "overlooked" road users with priority. Especially when turning right, adaptive rear view mirrors of the car could provide an appropriate sight towards relevant road users on a parallel bicycle/pedestrian path.

The most common types of accidents with pedestrians crossing the road are on a straight stretch of road with conflicts with pedestrians coming from the left (24%) and right (15%). Here again the lack of information acquisition plays the biggest role. The combination of pedestrian detection using, for example, camera- or radar-based systems with an engaging brake assistant promises to be useful to prevent such accidents from happening. Since the driver distraction is a problem with this type of traffic conflicts, means to detect the attention condition of drivers (such as camera-based detection of lost sight of relevant objects) should be implemented. Training for older drivers should consider a specific module "dealing with and preventing distractions".
Innovative technical developments go towards a recognition of pedestrian intention via camera systems with a probability calculation for pedestrians crossing the path.

**REFERENCES**


[1] Statistisches Bundesamt: 11. Koordinierte Bevölkerungsvorausberechnung. Annahmen und Ergebnisse, Wiesbaden 2006, S. 28

[2] Jänsch, M., Otte, D., Pund, B.: Specific features of accidents caused by Elderly traffic participants. Reports on the ESAR Conference on 7th/8th September 2012, Berichte der Bundesanstalt für Straßenwesen, Fahrzeugtechnik, Heft F 87.

[3] Johannsen, H. & Müller, G. (2014): Anpassung von Kraftfahrzeugen an die Anforderungen älterer Menschen auf Basis von Unfalldaten. In: Schlag, B. & Beckmann, K. J. (Hrsg.): Mobilität und demographische Entwicklung. Eugen-Otto-Butz-Stiftung, TÜV Media GmbH, Köln.

[4] Otte, D., Pund, B., Jänsch, M. (2009): Unfallursachen-Analyse ACASS für Erhebungen am Unfallort. In: Zeitschrift für Verkehrssicherheit 3, 122-128.

# THE DEVELOPMENT OF ASSESSMENT TECHNOLOGIES FOR ADVANCED SAFETY VEHICLES

**Eun Dok, Lee**
**Jae Wan, Lee**
**Byung Do, Kang**
**Jong Soo, Kim**
Korea Automobile Testing & Research Institute
Republic of Korea

**Myung Won, Seo**
Korea Agency for Infrastructure Technology Advancement
Republic of Korea

Paper Number 15-0355

## ABSTRACT

Like many industrialized countries, the Republic of Korea (ROK) has implemented policy and research aimed at reducing the number of casualties caused by traffic accidents. For example, ROK launched the project titled "Reduce traffic casualties by half in 10 years" in 2008, Sweden introduced the Vision Zero Policy in the late 1990s, and other European Union members have launched similar projects aimed at reducing traffic accident fatalities by between 30 to 50 percent.

To reduce the number of casualties from road accidents requires improvements to vehicles, road and traffic managements systems. To expedite this process Intelligent Transport System has been adapted and implemented to the vehicles and road systems.

Vehicles with advanced safety features will be expected to reduce or prevent accidents which drivers cannot not respond to or perceive.

To date, there has been insignificant research into the effective performance of vehicles with advanced safety features. The lack of assessment procedures has impeded the public acceptance of vehicles with advanced safety features.

The Development of Assessment Technologies for Advanced Safety Vehicles has been introduced for the promotion of advanced safety vehicles. The project involves the development of assessment technologies for advanced safety vehicles.

This paper shows the development of assessment methods for passive and active safety technologies. These technologies primarily address active protection for pedestrians, rear passenger safety, lane keeping assistance system, and automatic emergency braking system.

## INTRODUCTION

Industrialized countries around the world, including the Republic of Korea (ROK), have implemented policies and research aimed at reducing traffic casualties. The goal has been to reduce traffic casualties by between 30 to 50 percent within ten years through policies that include ROK's "Reduce Traffic Casualties by Half" campaign and Europe's "Vision Zero" policy.

To attain such goals, it is necessary to complement and improve road and traffic systems including automobiles. Technologies utilizing Intelligent Transport System (ITS) in automobiles and road systems are actively being studied and disseminated as a way to expedite such improvements to road and traffic systems.

It is expected that the prevention of traffic accidents and improvements to traffic flow can be achieved by strengthening traffic infrastructure on roads that will enable communication between a vehicle and a road or between vehicles. In addition, vehicles themselves can be fitted with advanced safety features through convergence with IT technology, which can contribute to reducing traffic accidents through avoiding or preventing possible accidents by perceiving, assessing and responding to accident situations or by minimizing damage in the event of an unavoidable accident.

These state-of-the-art safety features can help prevent or reduce accidents by effectively responding to traffic situations to which a driver is unable to respond or perceive. For this reason, it is critical to develop and disseminate advanced safety features to reduce the number and severity of road traffic accidents.

However, it is not easy to disseminate and promote either advanced safety features or automobiles with advanced safety vehicles. This is because there has been insufficient research into the effective safety performance of those cutting-edge safety features and no technology has yet been developed to assess their safety performance.

Accordingly, this paper will assess the Advanced Safety Vehicle Project (hereinafter referred to as ASV Project), which aims to secure the safety performance of advanced safety vehicles. This research is thus designed to encourage the dissemination of advanced safety vehicles by providing independent justification for the development and application of advanced vehicle safety technologies.

## ABOUT THE PROJECT

### Implementation System

The ASV Project is a project funded by the Ministry of Land, Infrastructure and Transport and the Korea Agency for Infrastructure Technology Advancement. The lead research institute of the project is the Korea Automobile Testing and Research Institute under the Korea Transportation Safety Authority, and thirteen co-research institutes include Hyundai MOBIS and Seoul National University (Figure1).

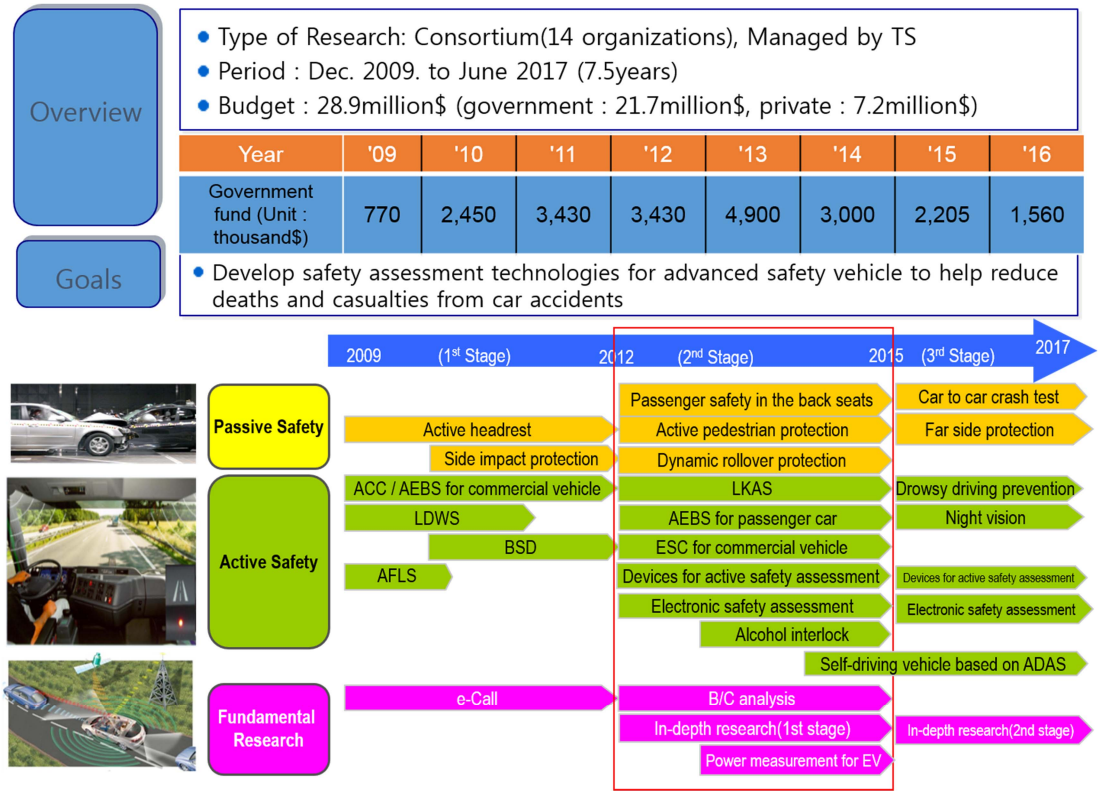


*Figure1. Roadmap for the development of assessment technologies for advanced safety vehicles*

The total project duration is eight years from December 2009 to July 2017 and consists of three phases (Phase I - 3 years, Phase II - 3 years, and Phase III - 2 years). The total research budget is 28.9 billion dollars. At present, the project is in the third year of Phase II, and Phase II research is scheduled to end in June, 2015.

**Research Roadmap**

The research area of the ASV Project is largely divided into three parts: crash safety technology, preventive safety technology and base technology. Research on crash safety technology is dedicated to examining the technologies required to improve the safety performance of passive safety technologies for pedestrians, as well as vehicle occupants in the event of a road traffic accident. By contrast, research into preventive safety technology is designed to develop the assessment technologies required to verify the safety performance of advanced safety features equipped with various active safety technologies to prevent traffic accidents. Lastly, research into base technology is designed to conduct research on the technologies required to support the development of passive and active safety technologies.

The following is a brief introduction to the main assessment technologies, starting with the Phase II research currently in progress.

**SPECIFIC SAFETY ASSESSMENT TECHNOLOGIES**

**Protection of Rear Seat Passengers**

The development of technologies for rear seat passenger protection involves the development of assessment technologies designed to improve the performance of crash safety for rear seat passengers, regardless of whether children or adults, in the event of a road traffic accident.

To this end, research is ongoing into the impact on rear seat passengers of road traffic accidents, through data analysis of the mechanism of injuries on children and adult passengers in the rear seats and the strengthening of rear seat passenger crash safety assessment methodology. The proposed criteria for assessment of crash safety for rear seat passengers are based on this analysis.

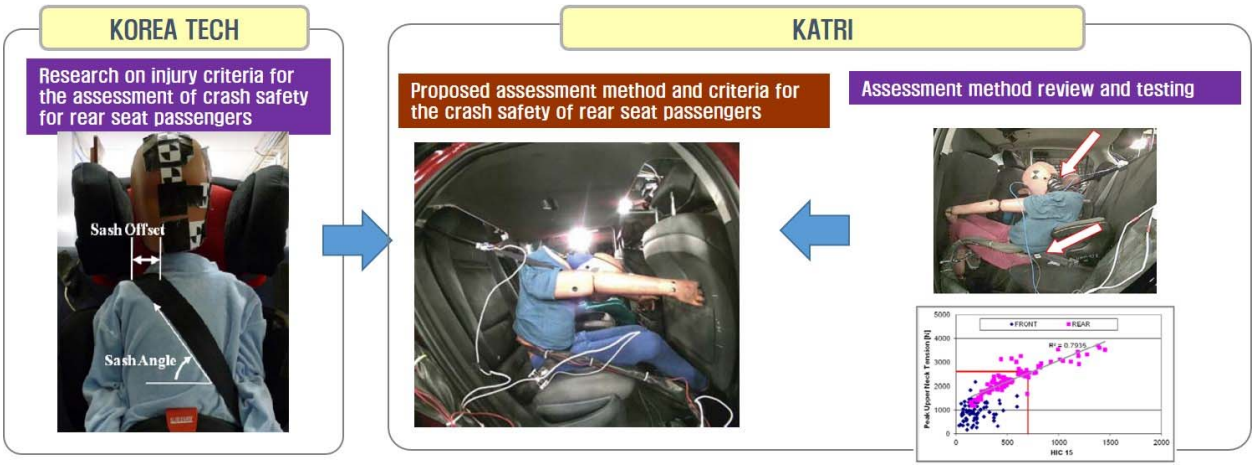


**Active Pedestrian Protection**

The development of technologies for active pedestrian protection assessment involves the development of assessment technologies for active hoods and pedestrian airbags, as well as technologies designed to reduce the casualties caused by traffic accidents, particularly given the relatively high frequency of pedestrian injuries in Korea that are caused by road traffic accidents.

To this end, there is ongoing design and fabrication work for safety systems that can be fitted to passenger cars and SUVs, with testing carried out using actual vehicles. Related interpretation models have been developed to support the establishment of proposed criteria for the assessment of crash safety for pedestrians.

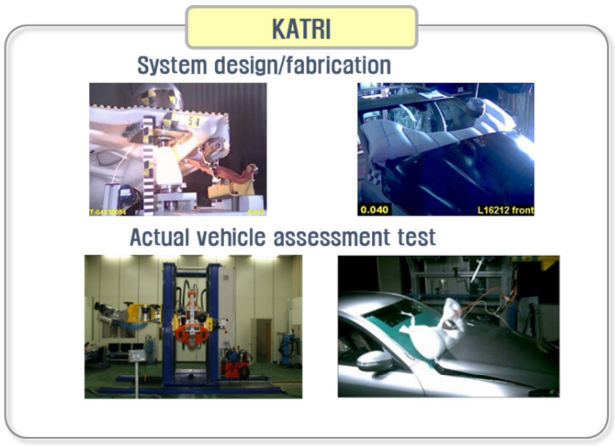


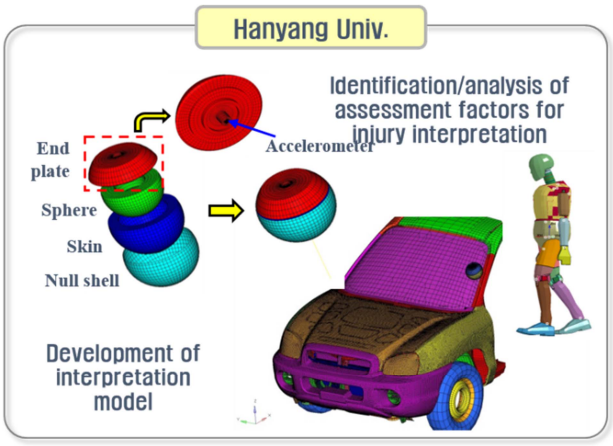


**AEBS for Passenger Cars**

Development of Advanced Emergency Braking System (AEBS) for passenger cars aims to develop technologies for safety assessment of AEBS, a technology designed to prevent or minimize traffic accidents when a driver is unable to perceive front traffic situations or properly brake the vehicle in emergency.

For this, this research develops assessment technologies for AEBS for passenger cars by studying international automotive criteria, implementing AEBS algorithm based on actual vehicles, developing assessment scenarios and fabricating vehicles for AEBS assessment and prototypes.

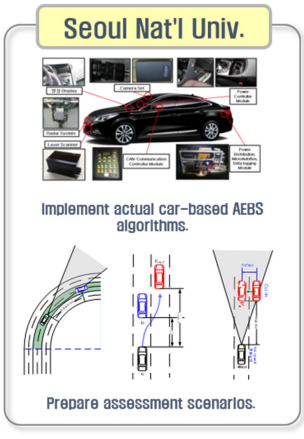

**Development of Assessment Technologies for the Safety Performance of LKAS for Passenger Cars**

The development of Lane Keeping Assistance System (LKAS) for passenger cars involves the development of technologies to assess the Lane Keeping Assistance System. LKAS is used to prevent possible accidents by

automatically operating the vehicle's steering system to keep the vehicle in the correct lane in the event of possible driver error or carelessness causing it to otherwise veer into another lane or off the road.

This research includes establishing a proper environment for LKAS assessment, analyzing and developing technologies for fail-safety assessment, developing universal LKAS assessment modules, identifying LKAS assessment factors and developing assessment scenarios.

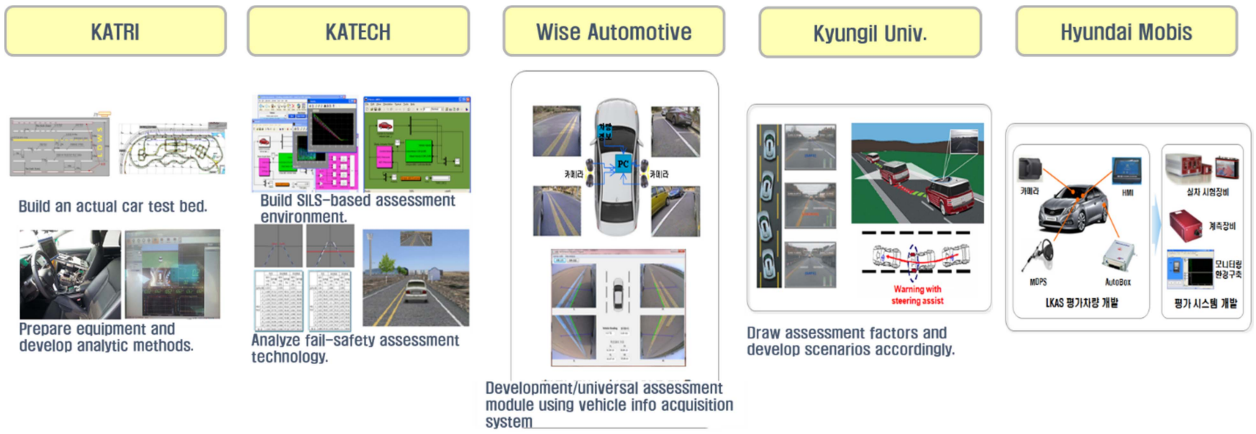


**Development of Assessment Technologies for the Safety Performance of ESC for Commercial Vehicles**

The development of assessment technologies for the safety performance of ESC for commercial vehicles involves the development of assessment technologies for the safety performance of Electronic Stability Control (ESC) equipped to vans and trucks to prevent rollover or slipping accidents.

This research includes verifying the assessment of the safety performance of the ESC of commercial vehicles (vans and trucks), developing simulation models and algorithms, analyzing assessment technologies for the performance of ESC and developing technologies for fail-safe assessment.

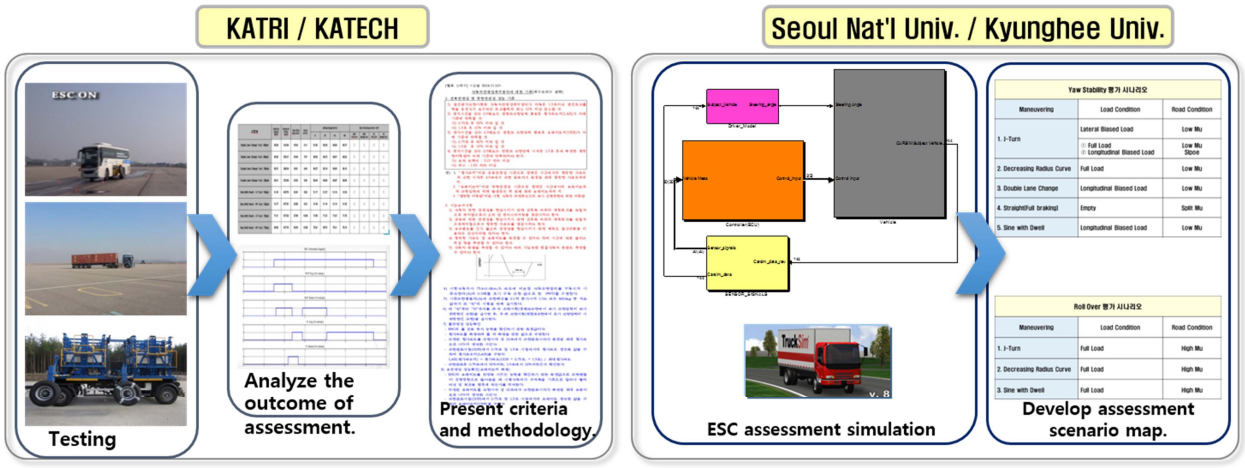

**Development of Active Safety Crash Assessment Systems**

This involves the development of systems for assessing the safety of vehicles equipped with advanced safety features such as Advanced Emergency Braking System (AEBS) and Electronic Stability Control (ESC).

This includes fabricating target vehicles for low/high speed driving, stabilizing them, and developing operating software.

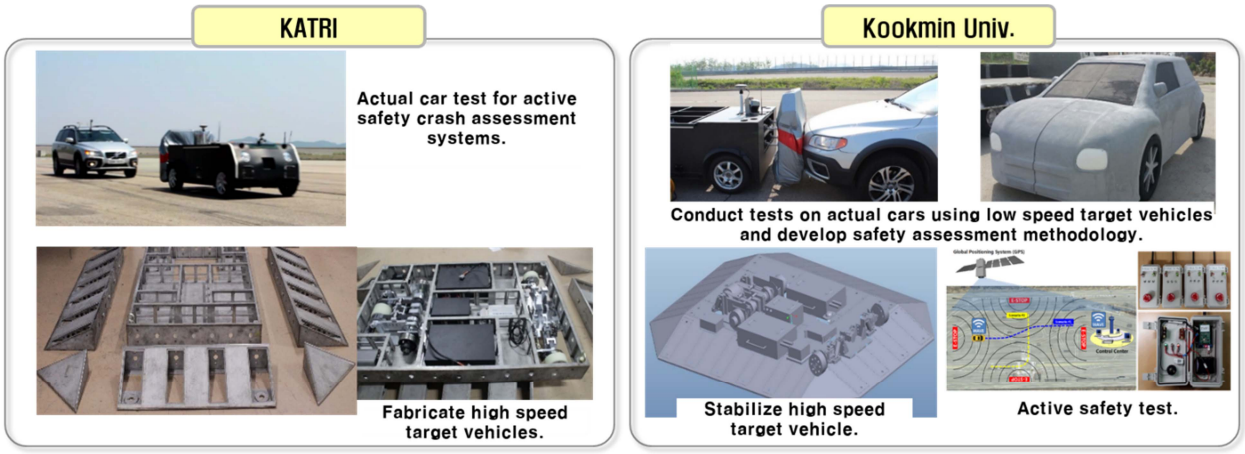


**Self-driving Vehicles**

The development of assessment technologies for the safety performance of self-driving vehicles involves the development of technologies for assessing the safety performance of self-driving vehicles equipped with sensor-based Advanced Driver Assistance System (ADAS).

This includes building self-driving assessment systems and test beds by integrating ADAS element technologies, developing algorithms for self-driving assessment systems, and conducting studies on the assessment criteria for the structural safety and driving safety of self-driving vehicles equipped with ADAS.

**KATRI**

- Conduct research on international technologies and standards (selection of items requiring establishment/amendment of safety standards)
- Decide assessment factors for safety assessment (proposed structure and criteria)
- Define test bed and assessment system (assessment procedures)

**Seoul Nat'l Univ.**

- Establish criteria for the safety assessment of self-driving systems (motorway)
- Develop algorithms for the control of self-driving system.

**MOBIS**

- Define specifications of ADAS-based self-driving vehicles.
- Configure ADAS-based self-driving vehicles for assessment.
- Configure control logic and systems by ADAS element.

**Wise Automotive**

- Build actual car-based test bed for V2V integrated system safety.
- Conduct actual car assessment based on V2V scenarios.
- Improve V2V assessment scenarios.

## CONCLUSIONS

This paper presented an introduction to the project for the Development of Assessment Technologies for Advanced Technology Vehicles, which is funded by the Ministry of Land, Infrastructure and Transport and the Korea Agency for Infrastructure Technology Advancement and conducted by the Korea Automobile Testing and Research Institute under the Korea Transportation Safety Authority and other partner research institutes.

The goal of this research is to develop the assessment technologies required to verify the safety performance of both advanced safety features utilizing IT convergence technology as well as advanced safety vehicles utilizing such features to reduce casualties from traffic accidents. More specifically, it involves the development of assessment technologies for the fields of crash safety technologies, preventive safety technologies and relevant supporting technologies.

The subjects for each phase of the project were selected by comprehensively taking into account the technology level, market environment and accident reduction effects of element technologies. Research on them is currently being conducted in three different phases.

This paper has introduced the high-level outline and detailed contents of the research on specific safety assessment technologies conducted in the Phase II research project (2012-2015).

The safety performance of vehicles around the world can be improved if automotive safety standards and New Car Assessment Program (NCAP) are updated to reflect the safety assessment technologies developed by the ASV Project. This research project, by contributing to the establishment and amendment of international vehicle safety standards, will also help to raise the prestige of Korea.
Moreover, it is expected that the international technical and market competitiveness of carmakers and parts makers can be improved through the more rigorous assessment of both advanced safety features and the vehicles equipped with such features.

## ACKNOWLEDMENTS

This research was supported by the Korea Ministry of Land, Infrastructure, and Transport. It was also supported by the Korea Agency for Infrastructure Technology Advancement (Project No.: 14PTSI-C054118-06).

## REFERENCES

[1] John Whitelegg, Gary Haq., “Vision Zero : Adopting a target of zero for road traffic fatalities and serious injuries”, Stockholm environment institute, 2006.
[2] TAAS, Road traffic accident statistics, 2011.
[3] NHTSA, FARS and NASS Data on vehicles and fatalities by collision type, 2003.
[4] Michael Paine M., Newland C., "Roof strength and occupant protection in rollover crashes", Australasian road safety research and policing and education conference, 2009.
[5] Korea Automobile Testing and Research Institute under Korea Transportation Safety Authority, et al., "Report on the Development of Assessment Technologies for Safety Performance of Advanced Safety Vehicles (Third Year)", Korea Agency for Infrastructure Technology Advancement, 2012.
[6] Korea Automobile Testing and Research Institute under the Korea Transportation Safety Authority, et al., "Report on the Development of Assessment Technologies for Safety Performance of Advanced Safety Vehicles (Fourth Year)", Korea Agency for Infrastructure Technology Advancement, 2013.
[7] Korea Automobile Testing and Research Institute under the Korea Transportation Safety Authority, et al., "Report on the Development of Assessment Technologies for Safety Performance of Advanced Safety Vehicles (Fifth Year)", Korea Agency for Infrastructure Technology Advancement, 2014.

# TEST PROCEDURES AND RESULTS FOR PEDESTRIAN AEB SYSTEMS

**Patrick Seiniger, Adrian Hellmann, Oliver Bartels, Marcus Wisch, Jost Gail**

Bundesanstalt für Straßenwesen (Federal Highway Research Institute) Bruederstraße 53, 51427 Bergisch Gladbach, Germany

Phone: +49 2204 43619

Fax: +49 2204 43676

E-mail: seiniger@bast.de

**Paper ID#: 15-0358**

## ABSTRACT

Euro NCAP will start to test pedestrian Automatic Emergency Braking Systems (AEB) from 2016 on. Test procedures for these tests had been developed by and discussed between the AsPeCSS project and other initiatives (e.g. the AEB group with Thatcham Research from the UK). This paper gives an overview on the development process from the AsPeCSS side, summarizes the current test and assessment procedures as of March 2015 and shows test and assessment results of five cars that had been tested by BASt for AsPeCSS and the respective manufacturer.
The test and assessment methodology seems appropriate to rate the performance of different vehicles. The best test result - still one year ahead of the test implementation - is around 80%, while the worst rating result is around 10%. Other vehicles are between these boundaries.

## INTRODUCTION

Automatic emergency braking systems for vehicle-to-rear-end-vehicle accidents are already in production since 2003 and have been considered in consumer testing by Euro NCAP since 2014. These look-ahead systems assess the risk of a collision with another vehicle and brake automatically if needed to mitigate or even avoid an accident.

Technology has made great progress in the last decade, and today also systems for avoiding or mitigating vehicle-to-pedestrian-accidents are within reach with first systems already on the market.

Systems that address pedestrian accidents are more challenging from a technology point of view due to three main reasons: pedestrians are able to change their heading almost immediately, making it difficult to correctly predict their movement; pedestrians are relatively small with only a little amount of metal, making it hard to detect and classify them with radar sensors, and last but not least, the majority of pedestrian accidents happen in cross-traffic situations. In longitudinal-traffic situations, directions of travel for both partners are parallel, while in cross-traffic they are perpendicular. Therefore, longitudinal accidents do happen as a function of velocity difference only. For cross-traffic accidents speed and starting position of the accident opponents have to match within small boundaries.

Pedestrian AEB[1] systems are being introduced into lower budget vehicle segments, but the technology is still relatively new. This poses the problem to define test and assessment criteria without knowing what the expected performance at the time of introduction will be. For a valid assessment methodology that also reflects real world accidentology it is of high importance to involve all stakeholders at an early state.

[1] Automatic Emergency Braking

Proposed requirements for pedestrian AEB systems (and corresponding test procedures) were developed mainly by three initiatives: the seventh-framework-program-founded research consortium AsPeCSS[2], the initiative vFSS[3] with German, Japanese and US-American manufacturers as well as independent research institutes) and the AEB-group (Thatcham Research, various manufacturers and suppliers, amongst others). The proposals then were considered by and discussed within Euro NCAP. A final set of test scenarios had been selected by the end of 2013, for extensive validation testing of the procedure (including repeatability and reproducibility considerations) in 2014. Pedestrian AEB systems will be rated from 2016 on.

This paper summarizes the proposals and concepts of the AsPeCSS-project and shows the scenarios that had been selected by Euro NCAP. An overview of the achieved rating according to Euro NCAP's preliminary rating scheme as of March 2015 will be given.

## ACCIDENTOLOGY AND BOUNDARY CONDITIONS

### Accidents involving passenger cars and pedestrians

Within the AsPeCSS project different European accident data sources (especially high level national data and in-depth accident data from Germany and Great Britain) were used to investigate the causations and backgrounds of road traffic accidents with pedestrians [Wisch 2013].

Results of the initiatives vFSS und AEB were reviewed and further extensive analysis was performed within AsPeCSS, focusing on the following topics:

- Aggregation of traffic accident data involving one passenger car and one pedestrian by accident type and impact configuration to Accident Scenarios
- Proportions of pedestrians by injury severity
- Darkness (i.e. frequency; accompanied visibility constraints due to weather conditions)
- Investigation of considerable accident parameters (i.e. pedestrian age; pedestrian impact points; crash reconstruction details such as driving and collision speeds of passenger cars, braking behaviour)
-

As result of the accident data analysis seven accident scenarios have been identified which are shown in Table 1. This data does show that most collisions between one pedestrian and one passenger car are crossing conflict situations. Smaller proportions could be assigned to crash situations with obstructed view as well as to collisions where the pedestrian went along the road. Crashes while reversing or parking have been excluded from the dataset due to their minor relevance regarding current ahead looking and thus front mounted pedestrian protection systems.

Table 1 shows the proportions of the AsPeCSS accident scenarios (crashes between one passenger car and one pedestrian) for killed pedestrians only again based on national accident data from Great Britain and Germany. For the killed or seriously injured the highest average shares were established for scenario 1 (25%; crossing straight road, **near side**, no obstruction), followed by scenario 2 (20%; crossing straight road, **far side**, no obstruction), other scenarios (16%) and scenario 7 (15%, along straight road, no obstruction). For the total fatalities the highest average shares were established for scenario 2 (30%; crossing straight road, offside, no obstruction), followed by scenario 1 (23%; crossing straight road, nearside, no obstruction), scenario 7 (19%, along straight road, no obstruction) and other scenarios (17%).

In summary, accident scenarios 1, 2 and 7 were found as the three most important scenarios for car-to-pedestrian crash configurations (sum of weights concerning KSI[4] is 60% and concerning fatalities is 72%) that may potentially be addressed by forward-looking integrated pedestrian safety systems. However, accident scenarios 3&4, 5 and 6 (KSI: 24%, Fatalities: 11%) also have a significant potential regarding future active pedestrian protection systems. Further, it was seen that more than half of the crashes which led to seriously injured pedestrians were assigned to darkness or low light conditions. This proportion increased to around three-quarters in case of killed pedestrians.

---

[2] including partners such as BMW, Toyota, PSA, TRW, Bosch, Autoliv, IDIADA, TNO, BASt
[3] advanced forward-looking safety systems
[4] KSI = killed or seriously injured

***Table 1.*** **AsPeCSS Accident Scenarios (A and B classify day (including twilight) and night times).**

| ID | Accident Scenario | % KSI Total (Day/Night) | % Fatalities Total (Day/Night) |
|---|---|---|---|
| 1 | Crossing straight road, near side, no obstruction | 25 (15/10) | 23 (8/15) |
| 2 | Crossing straight road, offside, no obstruction | 20 (8/12) | 30 (7/23) |
| 3 | Crossing at junction, near- or offside, vehicle turning across traffic | 8 (5/3) | 4 (3/1) |
| 4 | Crossing at junction, near- or offside, vehicle not turning across traffic | | |
| 5 | Crossing straight road, near side, obstruction | 9 (7/2) | 4 (1/3) |
| 6 | Crossing straight road, offside, obstruction | 7 (5/2) | 3 (1/2) |
| 7 | Along straight road, no obstruction | 15 (8/7) | 19 (5/14) |
| Total | | 84 (48/36) | 83 (25/58) |

In addition, the following conclusion could be drawn from the analysis of the accident data:

- Higher count of car-to-pedestrian crashes in urban areas, but higher injury severity on rural roads,
- Elderly (65+ years) record the highest percentage of casualties killed or seriously injured,
- Winter months November, December and January show higher number of car-to-pedestrian crashes compared to other months.

**Impact point**

The impact point of the pedestrian on the front of the hitting vehicle is a key factor for the expected AEB system performance.

An evaluation of in-depth data from GIDAS[5] shows that the impact point is actually distributed on the vehicle front, rather than being only in the vehicle center. In fact the occurrence of impacts at the outer regions of the vehicle front is higher than in the center. Impact point as function of vehicle velocity is shown in Figure 1 for running pedestrians that come from behind an obstruction. The lateral displacement of the impact point on the vehicle front is given in m, with 0 m corresponding to the vehicle centerline and with positive values towards the driverside. It can be seen that the impact is more likely to occur near the edge on that side where the pedestrian is coming from. Concluding from these observations, the impact point is a parameter that needs to be considered in the definition of test scenarios.

[5] German In-Depth Accident Study, see www.gidas.org

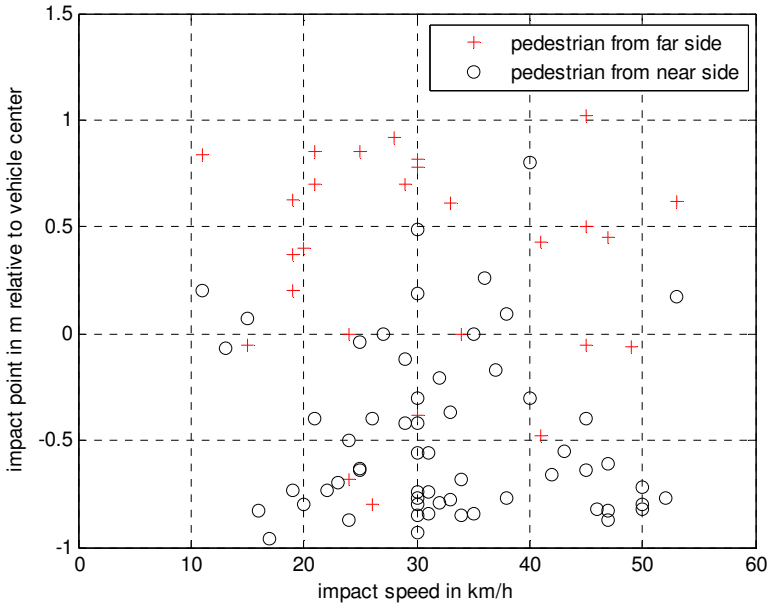


*Figure 1:* **Impact point as function of vehicle travelling speed for running pedestrians appearing from behind an obstruction.**

## DEFINITION OF TEST SCENARIOS

### Accident scenarios

Accident scenarios need to reflect real accident situations as good as possible. Since the accurate simulation of real accident situations in lab-testing is difficult and complex, characteristic parameters that have a significant impact on system performance have to be identified. Test scenarios then are defined using these characteristics.

For scenario definition, an accident kinematics model is developed using physical parameters like velocities, positions and starting times. In a first step, velocities are assumed to be constant, and in a second step, pedestrian detection timing and a brake logic were integrated. Using this model, the following parameters have been identified as most important for scenario definition:

- initial velocity of pedestrian and passenger car,
- impact point of pedestrian on the car front,
- start of pedestrian movement (timing) and total travel distance to impact point
- distance of obscuration (if applicable) to the passenger car path.

In addition, the following aspects need to be taken into account:

- test scenarios should reflect realistic accident situations as good as possible,
- test scenarios should be able to simulate various accident scenarios and not only those occurring most frequently,
- test scenarios should take estimated abilities of current and near-future AEB systems as well as current test tools (e.g. repeatability, contrast, light conditions) into account.

### Test scenarios

Theoretical considerations and first test results showed that initial scenario definitions, especially a running child from behind an obstruction, are far too difficult for current and expected AEB systems.

In collaboration with other European initiatives, AsPeCSS developed the idea of distributing these difficulties (small child dummy, obstruction and running dummy) into more than one scenario in order to be able to better assess and compare system performances.

The test scenarios have been improved based on the AsPeCSS test results shown in this paper and on the test results generated within the AEB group and together with Euro NCAP for better comparability of vehicles, see Table 2. The dummy speed in the child scenario has been decreased to 5 km/h, and the different impact points (a fact that is quite important according to accident figures) are tested with a walking, unobscured adult dummy. Higher pedestrian walking speeds are transferred to a scenario with an adult dummy coming from the far side - the dummy will be easily visible long before the impact in this case. Low dummy speeds might be difficult for certain sensor systems and will be tested in the form of an entrance test; the same goes for low vehicle speeds (10; 15 km/h) since the required sensor viewing angle becomes rather large for high ratios of dummy speed to vehicle speed.

***Table 2.*** **Current scenario definitions for Euro NCAP pedestrian tests.**

| Scenario / Parameter | Running adult | Walking adult | Walking adult | Walking child |
|---|---|---|---|---|
| Denomination | CPAF | CPAN25 | CPAN75 | CPCN |
| Pedestrian speed | 8 km/h | 5 km/h | 5 km/h | 5 km/h |
| Dummy type | Adult | Adult | Adult | Child |
| Dummy initial position | Far side | Near side | Near side | Near side |
| Vehicle speeds | 20-60 km/h | 20-60 km/h | 20-60 km/h | 20-60 km/h |
| Obscuration | No | No | No | Yes |
| Impact point | 50 % (Center) | 25% (Nearside) | 75% (Nearside) | 50 % (Center) |
| Weighting | 1 | 1 | 1 | 1 |

## ASSESSMENT METHODOLOGY

### Boundary conditions

Pedestrian travel speeds are generally much lower than car speeds [Tiemann, 2010]. But pedestrians can still comfortably avoid passenger car accidents just fractions of a second prior the collision. This is particularly true for accidents with impact on the near-side edge of the vehicle front and is less critical for impact points near the far-side edge. Determining for the achieved speed reductions is the time when full braking commences (which corresponds to a lateral distance of the pedestrian to the vehicle path). This brake timing limits the achievable speed reduction (which is a function of initial speed and deceleration). The ability of the brake system to increase the brake pressure and deceleration (maximum brake jerk) is another factor, as well as is the delay time between brake command and brake actuation.

If the pedestrian is hidden behind an obscuration and therefore is at first not freely visible for the vehicle's sensor system, the detection and classification time has a major impact on the entire system performance.

The derivation of performance boundaries in this paper is done based on an ideal braking system and a point-shaped pedestrian. A full investigation of the effects of real brake systems (e.g. increase of brake force) and finite size of pedestrians is published in [Seiniger, 2013].

The selected scenario configuration reflects the frequent case of a pedestrian crossing perpendicular to the vehicle. For full avoidance, the stopping distance $s_{\mathrm{Stop}}$ of an ideal vehicle is a function of initial velocity $v_{\mathrm{Vehicle}}$ and deceleration $a_{\mathrm{x}}$

$$s_{\text{Stop}} = \frac{v_{\text{Vehicle}}^2}{2 \cdot a_x}. \quad (1)$$

The quantity "Time-To-Collision" [Winner, 2011] is more reasonable for describing these situations than the stopping distance since it depends on the brake timing rather than a fixed distance. For the crossing pedestrian, is can be simplified to:

$$TTC = \frac{x_{\text{Vehicle}}}{v_{\text{Vehicle}}}. \quad (2)$$

The unit of TTC is the second. TTC is the time until the collision occurs if all speeds were held constant and in this case it is used to describe discrete points in time.

The TTC (when braking needs to start) for full avoidance is the combination of (1) and (2):

$$TTC_{\text{Stop}} = \frac{v_{\text{Vehicle}}}{2 \cdot a_{\text{x,Vehicle}}} \quad (3)$$

The essential quantity for speed reduction in pedestrian AEB systems is the time available for braking - which is in general the TTC at which the pedestrian is considered "critical". Real AEB systems will consider a pedestrian critical when it is near to the vehicle path (e.g. within a second) and on collision course.

The pedestrian's impact point on the vehicle front is the second essential quantity determining possible speed reduction. Pedestrians with a high probability for an impact on the near-side of the vehicle will become critical much later than those with an impact on the far-side of the vehicle, because those latter ones do travel within the path of the vehicle for a significant amount of time.

Balancing these criteria with the acceptable rate of false-positives then is the task of the vehicle manufacturer's philosophy, considering also product liability, customer acceptance and the likes, see for instance [Lübbe, 2013].

A real challenge for any AEB system are pedestrians coming from behind an obscuration near the side of the road. In this case, the total time available for detection, classification, decision and braking is limited by the time the pedestrian is visible.

**Relevance of test speed for traffic safety**

The assessment methodology for pedestrian AEBs needs to be in line with that established already for vehicle-vehicle AEB systems [Euro NCAP 2013]. For each scenario, tests with increasing test speeds are proposed.

In principle a linear assessment of speed reductions as measured in the individual test cases seems to be reasonable: 0% of "assessment units" for no speed reduction, 100% assessment units for full avoidance. The unified result of a test suite then depends on the weighting of the individual test speeds (within a test scenario) and the weighting in-between the scenarios.

The dose-response-model [Wisch 2013] is an established methodology for the weighting of speed reduction within a test scenario (= for different tested speeds). This methodology defines weighting factors by multiplying injury probability and accident occurrence frequency for all speeds. The factors then correspond to the "risk" and measure the relevance of a given test speed. Due to practicality reasons, the risk curve is approximated with 1 to 3 points, see Figure 2.

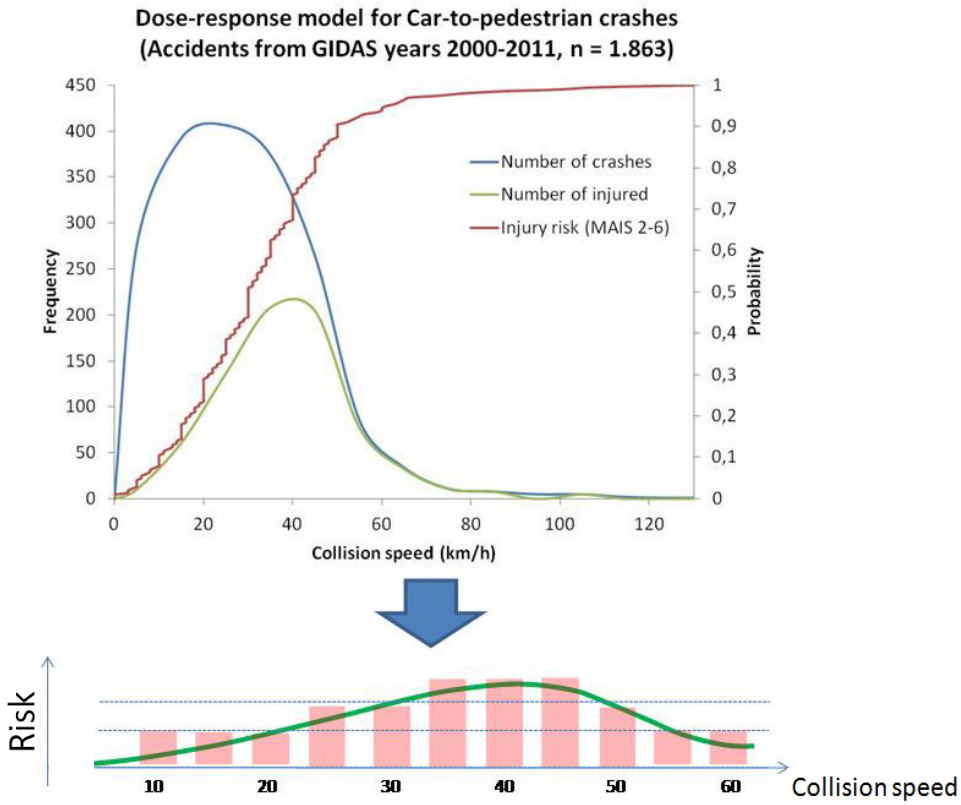


*Figure 2:* **Derivation of in-scenario weighting from accident velocity and injury risk.**

While the vehicle speed scale as defined from the AsPeCSS consortium runs from 10 to 60 km/h, tests and theoretical considerations have shown that an AEB intervention for low vehicle speeds is difficult to achieve due to the required high sensor viewing angle. Since additionally the risk level up to 20 km/h is still relatively low, Euro NCAP selected to exclude 10 and 15 km/h vehicle speed from performance testing; however it is necessary that the vehicle does at least show an AEB activation in these test speeds, in the form of an entrance test that needs to be passed for further assessment. The same goes for slower dummy speeds of less than 5 km/h.

In the previous section it has been laid out that full avoidance for high vehicle speeds is not possible: the pedestrian becomes a critical target so late that the time available for braking is not sufficient for the vehicle to come to a complete stop. Due to this, Euro NCAP has selected to award full score for high speeds (>45 km/h) if the speed reduction at the individual test is more than 20 km/h, and the test is conducted only if the preceding test was passed. The scoring is shown Table 3.

***Table 3.*** **Rating parameters.**

| **Index "k"** | **1** | **2** | **3** | **4** | **5** | **6** | **7** | **8** | **9** |
|---|---|---|---|---|---|---|---|---|---|
| **Test speed** | 20 | 25 | 30 | 35 | 40 | 45 | 50 | 55 | 60 |
| **Points** | 1 | 2 | 2 | 3 | 3 | 3 | 2 | 1 | 1 |
| **Sliding Scale** | 1 | 1 | 1 | 1 | 1 | 0 | 0 | 0 | 0 |
| **PassFail** | 0 | 0 | 0 | 0 | 0 | 1 | 1 | 1 | 1 |
| **Method** | • Sliding scale: ratio of speed reduction and initial speed | | | | | • Pass for speed reduction > 20 km/h<br>• Test only executed if previous test speed is passed | | | |

In a mathematical formulation, the rating result per scenario will become:

$$Rating = \sum_{k=1}^{k=n} \mathrm{SC}(k) \cdot \mathrm{Points}(k) \cdot \frac{v_{\mathrm{x,red,k}}}{v_{\mathrm{x,0,k}}} + \mathrm{PF}(k) \cdot \mathrm{Points}(k) \cdot < v_{\mathrm{x,red,k}} - v_{\mathrm{x,red,min}} >^{0} ,$$

with the vectors “Sliding scale SC”, “PassFail PF”, “Points” and “$v_{x,red,min}$ = minimum speed reduction = 20 km/h” as defined in *Table 3*, and using the Föppl-parenthesis "$< >^{0}$" which becomes 0 for results less than zero and 1 elsewise.

**TEST TOOLS**

Testing pedestrian AEB systems requires a pedestrian dummy as well as an apparatus that is able to move the dummy with a necessary accuracy.

Requirements for the dummy are as follows:

- appears like a human for the vehicle sensor system,
- impactable without significant damage to the vehicle under test (especially damage to the AEB system's sensors),
- durability: the possibility to conduct a high number of tests with impacts without significant change in the physical properties.

AsPeCSS uses a dummy as specified by the vFSS group. A detailed description of the dummy characteristics can be found in [Lemmen, 2013]. This dummy proved to appear close to a human in extensive verification testing with various test vehicles, and the current version is able to take over 100 impacts and does not damage the vehicle under test. This dummy has also been selected by Euro NCAP as an appropriate static dummy. A dummy with animated legs is currently developed by industry and might be selected as the official test dummy; this decision was not taken as of March 2015.

Dummy movement is achieved using a transportable platform system which has sufficient position accuracy due to its tooth belt drive (Figure 3) and that carries the dummy by means of magnets. Driving robots for accurate longitudinal and lateral vehicle control were used in all experiments in this paper. The specifications of the dummy propulsion system meet the requirements set by Euro NCAP in their preliminary test protocol at the time of writing.

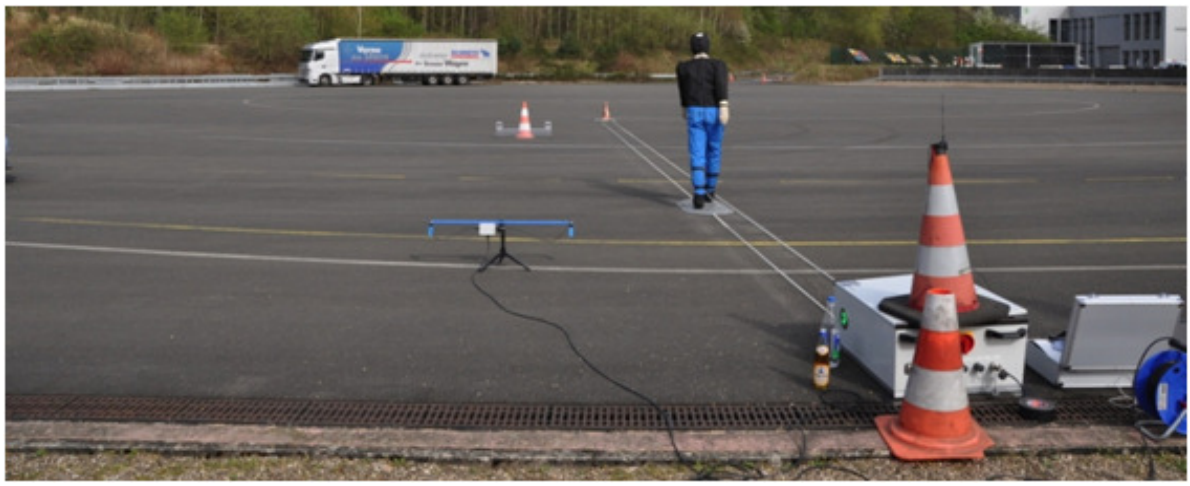

***Figure 3:*** **Test setup with adult dummy, platform, belt drive and light switch system.**

## DRIVING EXPERIMENTS AND RESULTS

Figure 4 shows speed reductions for vehicles A to D, distinguished between dummy type (child/adult), dummy speed, obstruction, propulsion system and desired impact point. All tests were conducted by BASt. Vehicles A, B and C were tested for the AsPeCSS project; vehicles D and E were tested in cooperation with the respective manufacturer.

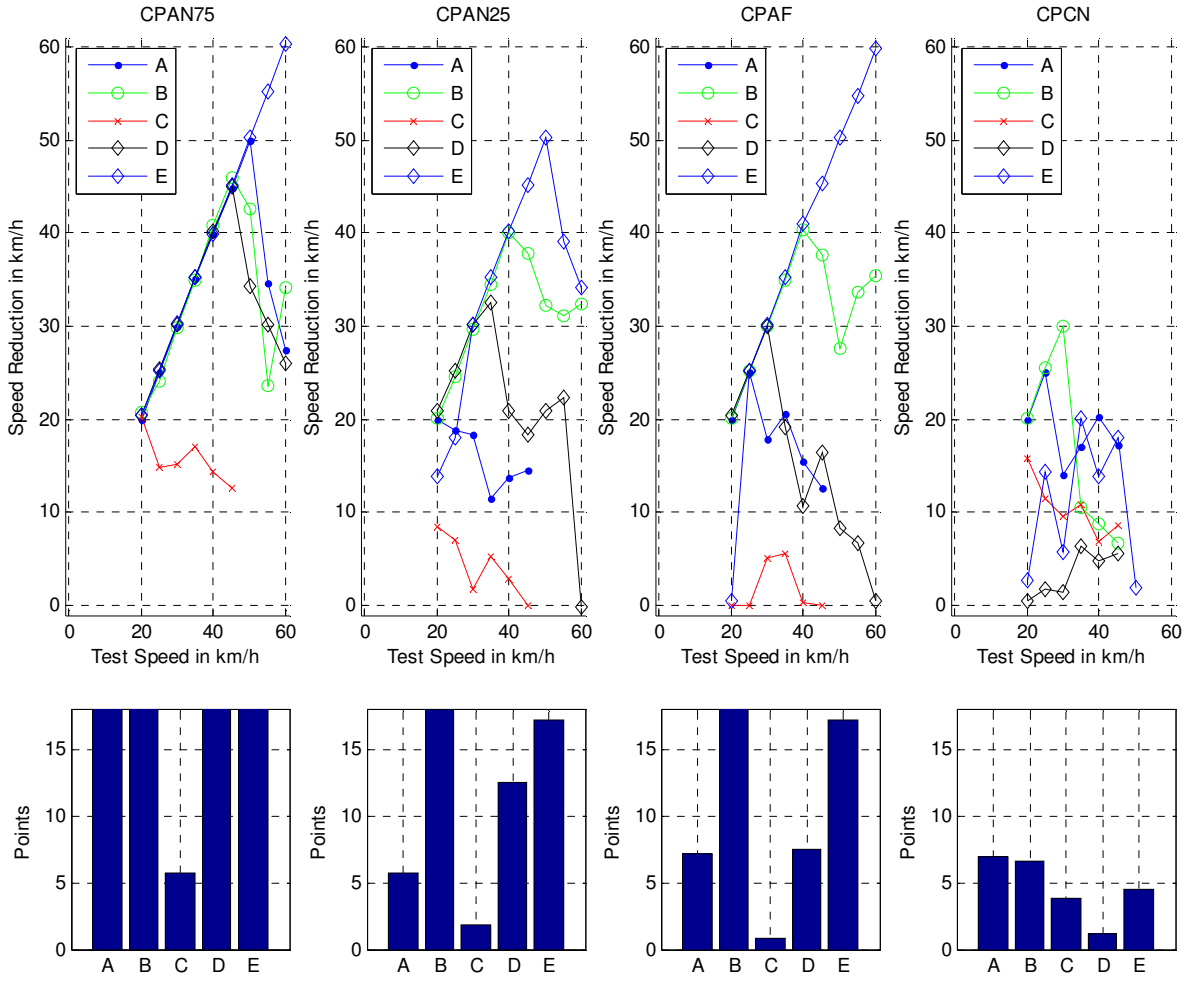


***Figure 4:*** **Speed reduction (upper diagrams) and points awarded (lower diagrams) per vehicle and scenario. CPAN75/25= Car-to-Pedestrian Adult Near side, impact point 25% or 75%, CPAF= Car-to-Pedestrian Adult Far side, CPCN= Car-to-Pedestrian Child Near side.**

Note that the vehicles A to D were tested more than once per test speed. For this analysis, the highest speed reduction per test speed has been picked. Vehicle E was a prototype vehicle, all others are production vehicles.

This overview gives an impression on the range of results to be expected for the first tests in 2016. All but one vehicle do achieve maximum rating in the Adult near-side 75%-scenario, which is from a technical perspective considered to be the easiest. The same setup with a 25% impact point is more difficult: since the dummy is located more to the right[6] throughout the whole experiment, the required sensor viewing angle is higher. The

[6] For right hand traffic

dummy will also enter the zone where a braking intervention is justified at a later time. Two of the vehicles still achieve almost full score in this scenario.

An adult approaching from the far side at running speed is difficult as well: for lower speeds, the required viewing angle becomes relatively large, and the dummy enters the zone where braking is justified at a late time as well. Results for this scenario are comparable: vehicles B and E again achieve almost full score.

The most critical scenario from a technical perspective is the obstructed child: the dummy appears relatively late, so there is little time available for detection, classification and braking. The results show that none of the tested vehicles is able to achieve a rating of more than 7 points. This might change when vehicles will be equipped with quicker brake systems.

## SUMMARY

The AsPeCSS project did define accident scenarios for pedestrian AEB systems. These scenario proposals then were discussed with other initiatives, the outcome of these discussions was the basis for Euro NCAP pedestrian test scenarios and assessment method.

Several vehicles have been tested and rated according to the Euro NCAP test and assessment method, within the AsPeCSS project and by BASt in cooperation with the respective vehicle manufacturer. While the 75% near-side adult scenario does not pose much difficulty to most of the systems, the near-side 25% and far-side running adult scenarios are far more difficult. Only two out of the five vehicles achieve almost full score.

None of the tested vehicles is able to achieve more than 7 points (=40% of the available points) in the running child scenario - a major technology innovation might be required before vehicles are able to perform equally well in this scenario.

## LITERATURE

[Euro NCAP, 2013]: *Euro NCAP: Assessment Protocol - Adult Occupant Protection, Version 6.0*. July 2013, S.30. Download available at http://www.euroncap.com/files/Euro-NCAP-Assessment-Protocol---AOP---v6.0---0-6da8ddb2-ac3e-4115-927d-180de4eb8d18.pdf.

[Lübbe, 2014]: Lübbe N, Rosén E.: *Pedestrian crossing situations: Quantification of comfort boundaries to guide intervention timing*. Accident Analysis and Prevention 71 (2014) 261-266

[Lemmen, 2013]: Lemmen P et al: *Evaluation of Pedestrian Targets for Use in Autonomous Emergency Brake System Testing - A Report from the Harmonisation Platform 2 Dealing With Test Equipment*. Paper presented at: 23nd Conference on the Enhancement of the Safety of Vehicles (ESV). May 27-30, 2013; Seoul, South Korea.

[Rigling, 2013]: ADAC press release, published November 14, 2013

[Seiniger, 2013]: Seiniger P, Bartels O, Wisch M, Pastor C.: *An Open Simulation Approach to Identify Chances and Limitations for Pedestrian Active Safety*. Paper presented at: 23nd Conference on the Enhancement of the Safety of Vehicles (ESV). May 27-30, 2013; Seoul, South Korea.

[Tiemann, 2010]: Tiemann N, Branz W, Schramm D.: *Predictive Pedestrian Protection – Situation Analysis with a Pedestrian Motion Model* Paper presented at: 10th International Symposium on Advanced Vehicle Control. August 22-26, 2010; Loughborough, UK.

[Winner, 2011]: Winner H. Frontalkollisionsschutzsysteme. In: Winner H, Hakuli S, Wolf G (Ed.).: *Handbuch Fahrerassistenzsysteme*. Wiesbaden: Vieweg + Teubner, 2012:S.522.

[Wisch, 2013]: Wisch M, Seiniger P, Pastor C, Edwards M, Visvikis C.: *Scenarios and weighting factors for pre-crash assessment of integrated pedestrian safety systems*.AsPeCSS D1.1, download available at www.AsPeCSS -project.eu, 2013.

# FIGHTING DRIVER DISTRACTION – RECENT DEVELOPMENTS 2013 - 2015

**Christian Heinrich**
Daimler AG
Germany

Paper Number 15-0359

## ABSTRACT

Research on driver distraction has a long history and attracts the attention of the scientific community, the public and the authorities. This resulted in a great number of activities. This article will summarize the main developments since the last ESV in 2013 from the perspective of an automotive manufacturer.

**Guidelines and standards:** In 2013 the National Highway Transport and Safety Agency (NHTSA) published a guideline for visual manual HMI . While basically following the structure of the European Statement of Principles (ESoP) [2] and the AAM guideline [1], the NHTSA guideline is much more restrictive, which means that more functions need to be blocked while driving. So the concern is that drivers will be inclined to use nomadic devices which have no restrictions at all (i.e. smartphones). Thus the overall impact of that guideline on safety may be negative.
The last version of the ESoP was published in 2008. In the framework of the iMobility Forum an HMI group was installed with the objective to check whether any changes, updates or additions are needed. The final report is expected for 2015. Some statements can be expected from the current draft which contains some recommendations and explicitly states to keep the ESoP as a design guideline, based on ISO standards, but not to include overall acceptance criteria. Due to the growing importance of applications that are being developed independently from hardware, another group was established within iMobility Forum, SafeAPP, in order to cover this specific topic.
On international level OICA (Organisation Internationale des Constructeurs d'Automobiles) published a white paper with recommendations for guidelines.

**Naturalistic driving studies (NDS):** Most experiments in simulators or on test tracks measure driving performance or glance behavior to determine mental workload. For using the telephone they usually report an odd ratio of four (The probability of a crash is four times higher compared to normal driving). It was quite a surprise when the 100 car study in 2013 presented odd ratios below one. Recent data from SHRP 2 give even lower values. NDS seem to be a powerful tool to identify actions and behavior that cause crashes. Detailed methods are under development and handling of great amounts of data is a challenging task.

**Tethering:** Nomadic devices can cause a problem since neither their displays nor their controls are developed for automotive use. Also they do not block functions that are not intended to be used while driving. One way to overcome this problem is to tether the telephone with the display and the controls of the car. This also makes it possible to apply existing guidelines (AAM, JAMA, ESoP). The Car Connectivity Consortium (CCC) has rephrased the existing guidelines so that they are better understandable by app developers. The CCC also established a process that will be run by certified labs to verify that the applications are in line with the guidelines.
Similar approaches are done be Google (Android auto) and Apple (Car play).

## INTRODUCTION

Research on telematics applications started in the eighties. The experts realized already at that time the need for appropriate means to reduce driver distraction. Since then the awareness of the scientific community, the public and the policy maker has ever increased. Two facts are the main driving forces for recent developments. One is the

increased connectivity with smartphones whose computing power compares desktop PC. Drivers increasingly use these devices for some reasons: Some applications are relevant for driving like navigation or warning of speed cameras, some allow some work during commuting time and some allow the driver stay connected with friends and relatives also during the ride. Of course not all of these activities are compatible with driving. This raised great concern in the public and at authorities.

Another driving force are new research activities. In the past a number of measured variables has been used which are assumed to be an indicator of driving safety, like maintaining speed, keeping lane position, biometrical data etc. But the proof was still missing that these parameters describe driving safety, it was just a consensus in the scientific community. This changed with the naturalistic driving studies. This method allows observing the relation between driver behavior and crash risk in real traffic.

## GUIDELINES

Based on the research done, guidelines have been developed in Europe, Japan and the US. A team of experts tasked by the European Commission developed the European Statement of Principles (ESoP) published in 2000 and revised in 2006. In Japan, the Japanese Automotive Manufacturers Association (JAMA) [4] published their guideline in 1990 with revisions in 2000 and 2004. In US the Alliance of Automotive Manufacturers (AAM) developed a guideline which was published in 2003 and revised in 2006. In 2013 the National Highway Traffic Safety Agency (NHTSA) in the US published a guideline. Since JAMA and AAM have not been updated in the last two years, the following focuses on ESoP and NHTSA Guideline.

### NHTSA Guideline

In 2010 the NHTSA (National Highway Traffic Safety Administration) presented a project to fight driver distraction [5]. One objective was to develop guidelines for visual manual interactions. A draft for public discussion [6] was published in 2012. This draft based to great extent on the AAM Guideline, but introduced very detailed seven methods to assess driver workload [3].

| | |
|---|---|
| EGDS | Eye glance testing |
| OCC | Occlusion testing |
| STEP | Step counting |
| DS-BM | Driving test protocol with benchmark |
| DS-FC | Driving test protocol with fixed acceptance criteria |
| DFD-BM | Dynamic following and detection protocol with benchmark |
| DFD-FC | Dynamic following and detection protocol with fixed acceptance criteria |

After publication of the draft NHTSA faced strong opposition from the automotive industry. The main concerns were:

- NHTSA tightens the criteria very much without a basis of scientific data.
- If, as a consequence of these restrictions, functions of integrated devices are further restricted, users will be inclined to use handheld devices that do not have a user interface developed for use while driving and thus increase the amount of distraction and hence the probability of an accident.

Beside that there were a number of minor inconsistencies.

In 2013 the final version of the guideline was published. Some inconsistencies have been removed (e.g. 30 letter requirement which came from Japanese writing). The requirements for the test equipment give more

freedom now. However the basic restrictive approach persisted. The possible tests were limited to eye glance measurement and occlusion with slightly modified criteria.

By measuring eye glance time in a driving simulator each of the following criteria has to be met by at least 21 of 24 participants

1) Glance time (85. percentil): < 2sec
2) Mean glance: < 2.0 sec
3) Total glance time:< 12.0

For occlusion testing: 12 sec TSOT (Total shutter open time) for at least participants 21 of 24 has to be reached.

The consequences are demonstrated with the following example: Phoning will be impossible, because dialing will not pass the above criteria. For Total Off-Road Glance Time Mehler et al. reported mean values for selecting a contact from a directory between 12.12 and 16.86 seconds [F]. So this will never meet the above limit of 12 seconds for the 85 percentile.

This means that the above mentioned concerns still exist. If too many functions have to be blocked the driver may be inclined to use handheld devices that have no restrictions of complex functions and no displays and controls appropriate for automotive use. Up to now no automotive OEM is committed to the guideline.

**European Statement of Principles**

The last version of the ESoP was published in 2008. Due to the changes in HMI technologies and the rapid development of connectivity there was the need to review the guideline. In the framework of the iMobility Forum an HMI group was installed with the objective to check whether any changes, updates or additions are needed. This group started its work in August 2013 and the final report is expected for 2015. Some recommendations can be concluded from the current draft. Most parts of the ESoP have been confirmed after careful review. Proposed changes are:

- Revising the scope
- Taking into account the consequences of automated driving
- The grey area regarding time critical and not time critical warnings should be covered by examples

A special focus of the discussions was the question whether a pass/fail criterion for overall workload should be introduced. This was especially careful examined in the light of the recent NHTSA developments and the JAMA guideline. The conclusion of the group was, to keep the ESoP as a design guideline with reference to ISO standards.

The ESoP should be reviewed at least every three years and approaches in other countries should be monitored. Also there should be an ongoing process of dissemination and publicity since the ESoP addresses multiple stakeholders (e.g. service provider, radio stations) but only the OEM are aware of the ESoP.

Parallel to the HMI group another working group , Safe APP started a document that focusses on the adaption of the ESoP to application programs. It references the generic principles and the application design principles of the ESoP as far as they are relevant for application development. The paper also will deal with standards that work as an interface between different applications and applications and service provider.

**OICA White Paper**

End of 2013 OICA (Organisation Internationale des Constructeurs d'Automobiles) started a white paper with the title "Recommended OICA Worldwide Distraction Guideline Policy Position". The basic statements of this paper are:

- Vehicle manufacturers have long recognized the importance of supporting the driver's ability to maintain proper awareness of the driving situation.
- OICA members have worked to develop and adhere to regionally appropriate distraction guidelines for integrated systems.
- Since the introduction of these guidelines no significant increase of accidents caused by distraction from integtrated devices has been observed.
- The overly restrictive NHTSA guidelines for integrated vehicle systems are expected to push drivers toward the use of nomadic devices and thus reduce driving safety.
- OICA recommends not to develop additional guidelines, but that countries wishing to adopt distraction guidelines should follow one of the existing guidelines, namely, Japanese (JAMA)/ United States (Alliance)/European (ESoP) guidelines, in order to avoid unnecessary divergence among individual countries. The ESoP is a cultural independent approach.
- OICA supports efforts to develop and implement standards for automatic pairing of portable devices to vehicle integrated systems. This makes the use of in car input devices and displays possible and also allows to disable certain functions while driving.

## NOMADIC DEVICES

Nomadic devices are personal electronic devices that can be brought into the car and have defined functionality including a user interface to control those functions. This definition includes smartphones, personal navigation devices (PND) or MP3 player. As pointed out in the introduction smart phones are the biggest concern because they are often used while driving in spite of the inappropriate user interface. Therefore this chapter focuses on smartphones. One possible way to reduce the distraction potential of smartphones is to connect them to the car: This has two advantages:

- The smartphone can use the large display and the automotive controls
- Certain functions can be disabled while driving

There are several realization of this concept by different organizations and companies.

### OEM Integration

Nearly every car manufacturer has its own solution for integrating apps into the car e.g. Audi connect, BMW connected drive, Ford sync, Mercedes drive style, Volkswagen car net, Volvo Sensus Connected Touch. Besides the mirror technology (running the app on the smart phone while using input and output devices of the car) also other approaches are used. Some alternatives are: the car has its own communication device and does not need a phone. The software then can run on the head unit a server. In other cases the touchscreen of the smartphone is used and the HMI is adopted in a way that it fulfills the relevant guidelines even with a smaller display. From the view of an app developer this is a highly fragmented market place so most applications are developed by the car manufacturers themselves.

### Apple CarPlay

Apple has defined a connection between the iPhone and the head unit of the cars with the brand name CarPlay. It uses different types of input devices like touchscreens, buttons or rotary knobs. A voice control (Siri) is implemented and can be activated by a button on the steering wheel. Of course all these features only work if the car makes these controls available to the iPhone. The applications within CarPlay are optimized for automotive use to reduce driver distraction.

**Android Auto**

Google has developed a similar interface for the connection of android phones to the car. They worked together with car manufacturers but also established their own HMI labs. Their guidelines regarding driver distraction followed the same general principles like ESoP, AAM and NHTSA guideline. Their interface to the app developer is template based. That means that templates are defined (e.g. selection from a list) that the app developer has to use. These templates can be tested regarding certain properties that have an influence on driver workload, especially font size and contrast. Together with rules about menue depth and list length the main factors regarding driver distraction are under control.

**MirrorLink**

The Car Connectivity Consortium (CCC) is a cross-industry collaboration to develop MirrorLink, an OS agnostic solution for smartphone and in-vehicle connectivity. The organization's more than 100 members represent more than 80 percent of the world's auto market, more than 70 percent of the global smartphone market and quite a number of aftermarket consumer electronics vendors.
The philosophy of MirrorLink was just to apply the existing guidelines (ESoP, JAMA and AAM) in the respective regions. But nevertheless it was necessary to compile new documents for the app developer for some reasons: The existing guidelines are written for experts of automotive HMI. For app developer with less experience of this topic some additional explanations are necessary. On the other hand the guidelines contain some parts (e.g. position of a display) that are important for automotive ergonomics but irrelevant for an app developer.
In addition to the guidelines CCC establishes two certification processes that cover both technical issues and driver distraction compliance. This means to authorize test labs and to select Subject Matter Experts. It is a challenging task to establish this process with many different stakeholders.

**NATURALISTIC DRIVING STUDIES**

During the last years there was significant progress in measurement technics. Storage media became smaller and cheaper. The same holds for cameras and sensors. Many physical data of the car are available via CAN (Car Area Network). This made a new type of experiment possible: Naturalistic Driving Studies (NDS). The basic idea is that the test persons drive a long time in their own cars which are equipped with cameras and sensors. The sensors typically include speed, acceleration yaw rate and distance to preceding cars. The cameras observe the traffic in all directions but also the face of the driver to determine glance behavior and the center stack to monitor the engagement in secondary tasks. While it has become easier to acquire all these data the processing is still a challenge especially since much of the work has to be done manually. If the objective is to analyze crash risk the statistic is still not very good since crashes and near crashes do not occur very often. So the results have to be taken with some caution. On the other hand the new method offers the opportunity to determine the relation between driver behavior including glance behavior and crash risk. All previous methods like determing driving quality or glance behavior just assumed based on the consensus of the scientific community that these are good indicators for crash risk.
Figure 1 shows the result for different secondary tasks. While previous measurements in simulators showed an Odd Ratio of around 4 for talking/listening on a phone we see here an Odd Ratio at or below 1. This means that the crash risk is lower than just driving. There are some hypothesis to explain that: 1) The influence of cognitive load on crash risk is overestimated 2) Glance behavior plays an important role and a person engaged in a phone call is less inclined to look around but always looks to the forward road. 3) The driver engages in a phone call only when the driving situation is less demanding. This means that the baseline risk is too high.

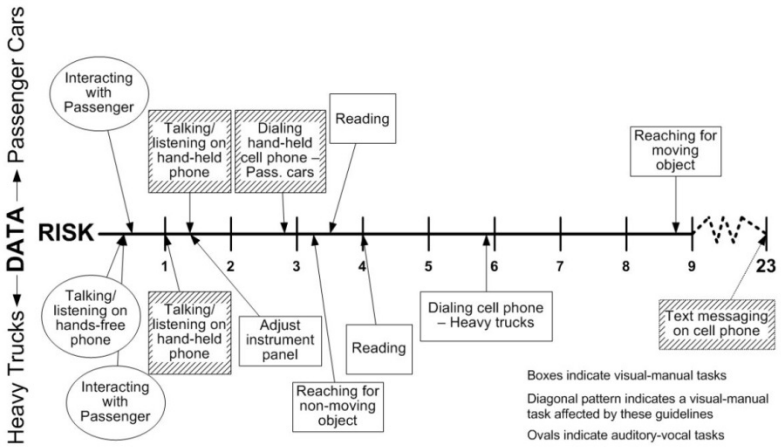


***Figure 1 gives a graphical representation of some of the secondary task risk odds ratios determined by the 100-Car Naturalistic Driving Study and the Two Study FMCSA Analyses. [6]***

Recently a evaluation of SHRP2 data was published [10]. This is a much bigger database than the 100 car study. It includes 3000 drivers and nearly 4000 vehicle years. Some results are shown in fig 2.

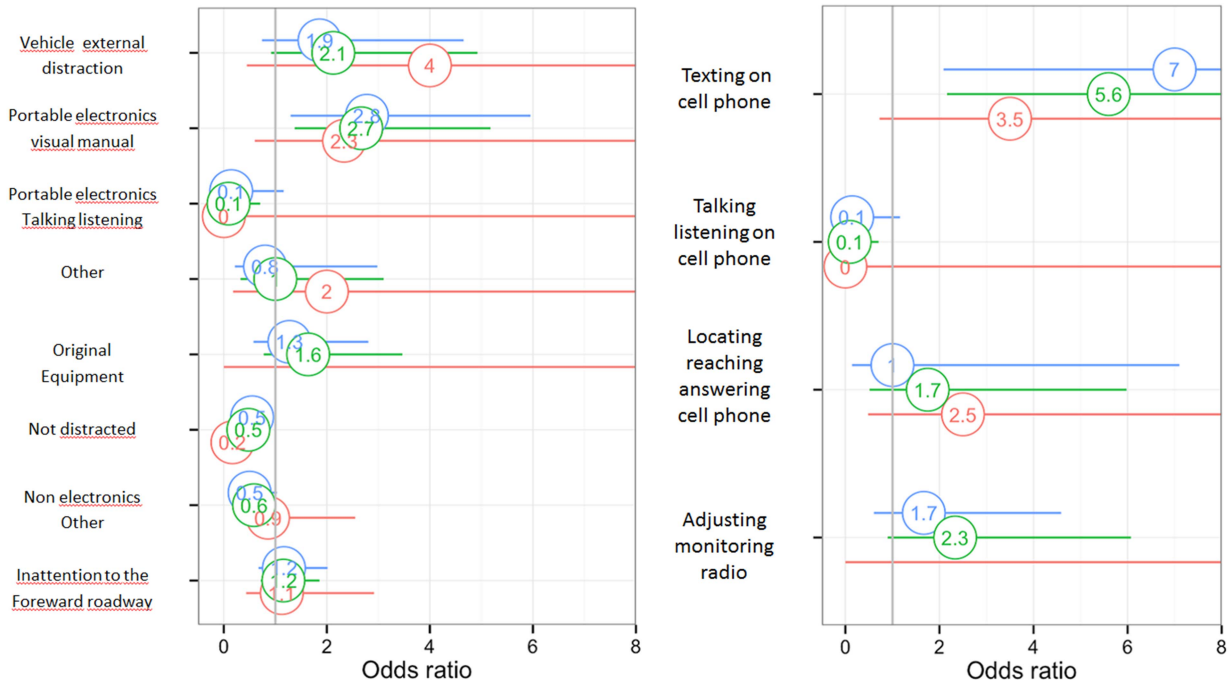


***Figure 2. Odds Ratios (numbers inside circles) and confidence intervals (as horizontal lines) for classes of distracting activities in crashes (C) (red), near crashes (NC)(blue) and crashes and near crashes combined (CNC)(green). Presence of a distracting activity was coded between 5 seconds before and one second after the precipitating event.***

Since not all data have been included in the evaluation statistic is still poor. Note that an odds ratio is significant only when the confidence intervals are fully above or below 1 (does not cross the vertical line at 1). Nevertheless the data give some indications what results can be expected in future evaluations with better statistics and some conclusions can be drawn for future standardization work.
Not surprisingly texting on cell phone and visual manual operation of portable electronic devices show high odd ratios. But also external distraction has comparably high values. It would be an interesting topic for future research

to have a more detailed description of these information and events. Outside information is never driver paced, i.e. the driver has only a short time slot to acquire that information If there is a chance to deliver part of that information inside the car, the driver can look at it when the driving situation is less demanding.
On the other hand it can be seen that talking and listening has only a very low odd ratio, even when it is done with a handheld device. The problems arise with locating, reaching and answering a cell phone.

## VOICE INTERFACES

Since a long time there are also approaches develop guidelines for speech interfaces. Some give recommendations on dialog level. SAE J2988 [8] as an example claims to be "a technology-neutral approach to voice user interface principles and guidelines applicable in an automotive environment".

But there is also the objective to measure the effective workload of speech interfaces. Additional methods to measure cognitive load are under development. An example is the Driver Response Test, which is just standardized in the ISO committee (ISO DIS 17488).

But there is a specific problem to measure the overall quality and workload of a speech interface. This is the great influence of the quality of the voice recognition. If an utterance is misrecognized by the speech engine this will irritate the user and result in additional steps in the dialog. Whatever method is used to measure driver workload the results will become worse. On the other hand recognition quality cannot be considered a constant for a specific recognition engine. Some influences are quite obvious like ambient noise or reflection in the surrounding. Some are more difficult to determine. Details of the training material are generally unknown and so is the influence of the dialect coloration of the subject group. Also speech engines may have some adaption algorithms. The influence of those should be known to the experimenter. All effects of the speech recognition should be carefully monitored. The author is not aware of measurements in the automotive field that took care of this issue.

Another observation is the fact that speech control shows a much better glance behavior than manual operation [9]. From that can be concluded that guidelines with performance parameters are not appropriate for the time being. More research both regarding Naturalistic Driving Studies and detailed analysis of speech control is needed.

## CONCLUSIONS

From the developments and research of the last two years the following conclusions can be drawn:

- The existing guidelines have proved to be efficient. For the time being the need for only slight corrections has been identified.
- Further improvement can only base on additional scientific findings. The Naturalistic Driving Studies seem to be a promising approach.
- Guidelines with too much restrictions will be contraproductive. The more the functionality of a well integrated OEM device is restricted the more the driver will be inclined to use a nomadic device. Thus reducing the functionality (i.e. making guidelines more stringent) will reduce the overall safety and should be avoided.
- Speech recognition seems to reduces the crash risk significantly. More and better speech systems should be offered to the driver
- To reduce the use of handheld devices the facility co pair the HMI of these devices to the car should be offered to a greater extend

## ACKNOWLEDGEMENT

The author thanks all experts who work in the different organizations and committees in this field for their contribution to driving safety

## REFERENCES


[1] Alliance of Automotive Manufacturers, "Statement of Principles, Criteria and Verification Procedures on Driver Interactions with Advanced In-Vehicle Information and Communication Systems" accessed February 9, 2012 http://www.autoalliance.org/files/DriverFocus.pdf

[2] European Commission "European Statement of Principles on the Design of Human Machine Interaction", 2006, accessed February 9, 2012. http://eur-lex.europa.eu/ Lex UriServ/ site/en/oj/ 2007/l_032/l_03220070206 en02000241.pdf

[3] Heinrich, C. "Fighting driver distraction: worldwide approaches", Proceedings of the 23rd International Technical Conference on the Enhanced Safety of Vehicles (ESV)

[4] Japanese Automotive Manufacturers Association , 2004 "JAMA Guideline" http://www.umich.edu/~driving/documents/ JAMA_guidelines_v30.pdf

[5] National Highway Traffic Safety Administration, "Driver Distraction Program", DOT HS 811 229, April 2012

[6] National Highway Traffic Safety Administration, "Visual-Manual NHTSA Driver Distraction Guidelines for In-Vehicle Electronic Devices" Docket No. NHTSA-2010-0053, Draft

[7] National Highway Traffic Safety Administration, "Visual-Manual NHTSA Driver Distraction Guidelines for In-Vehicle Electronic Devices" Docket No. NHTSA-2010-0053, Guideline

[8] SAE J2988 Society of Automotive Engineers, to be published

[9] Mehler, B, D. Kidd, B. Reimer, I. Reagan, J. Dobres and A. McCartt „Multi-Modal Assessment of On-Road Demand of Voice and Manual Phone Calling and Voice Navigation Entry across Two Embedded Vehicle Systems" Embedded Vehicle Voice Systems (2014-12-20 submission)

[10] Trent Victor, J. Bärgman, C.-N. Boda, M. Dozza J. Engström, C. Flannagan, J. D. Lee, G. Markkula. "Analysis of Naturalistic Driving Study Data: Safer Glances, Driver Inattention, and Crash Risk"

# RECOMMENDATIONS FOR SAFE HANDLING OF ELECTRIC VEHICLES AFTER SEVERE ROAD TRAFFIC ACCIDENTS

**Marcus Wisch**
**Julian Ott**
Federal Highway Research Institute (BASt), Germany
**Robert Thomson**
Chalmers University, Sweden
**Michael Abert**
Fraunhofer Institute for Chemical Technology ICT, Germany

Paper Number 15-0361

## ABSTRACT

The EVERSAFE project addressed many safety issues for electric vehicles including the crash and post-crash safety. The project reviewed the market shares of full electric and hybrid vehicles, latest road traffic accident data involving severely damaged electric vehicles in Europe, and identified critical scenarios that may be particular for electric vehicles. Also, recent results from international research on the safety of electric vehicles were included in this paper such as results from performed experimental abuse cell and vehicle crash tests (incl. non-standardized tests with the Mitsubishi i-MiEV and the BMW i3), from discussions in the UN IG REESS and the GTR EVS as well as guidelines (handling procedures) for fire brigades from Germany, Sweden and the United States of America. Potential hazards that might arise from damaged electric vehicles after severe traffic accidents are an emerging issue for modern vehicles and were summarized from the perspective of different national approaches and discussed from the practical view of fire fighters. Recent rescue guidelines were reviewed and used as the basis for a newly developed rescue procedure. The paper gives recommendations in particular towards fire fighters, but also to vehicle manufacturers and first-aiders.

## INTRODUCTION

This paper is based on work performed in the EVERSAFE project which, among other research topics, dealt with the crash and post-crash safety of electric vehicles (EVs) aiming to provide safety requirements and research needs for these (Wisch, et al., 2014). The project ran from 2012-2014 and was a collaborative project in the ERA-NET Electromobility+ programme.

EVs can be categorized into first (1GEV) and into second generation electric vehicles (2GEV), respectively. While 1GEV were defined as being solutions of electric vehicles based on existing chassis, vehicle geometries and established materials; 2GEV were defined as being developed and fabricated specifically by the car manufacturers and suppliers to best fit the users' demands of electric vehicles considering new vehicle construction concepts (including mass compensation measures regarding heavier battery weights), safety technologies and functionalities.

Motor vehicles with partial or full electric drivetrains are a small but growing component of the European vehicle fleet. An analysis of the current stock (end of year 2013) for different vehicle segments with electric drivetrains was performed based on figures for Germany (from the German Federal Motor Transport Authority) and Sweden (Trafikanalys, 2014). In both countries these vehicle types represent less than 1% of the vehicle fleet. Even in countries where government incentives are available, like Norway, the EV type is increasing faster but still is at only 1% of total vehicles (Statistics Norway, 2014). In terms of vehicle segments, in Germany around 81% of all registered passenger cars classified as battery (full) electric vehicles (BEV), range extender electric vehicles (REEV), fuel cell electric vehicles (FCEV) and plug-in hybrids have been assigned to the segments "mini" (56.7%), "small vehicle" (18.7%) and "compact class" (24.6%). The remaining share of around 19% contains larger vehicles. Due to this bias towards smaller vehicle sizes the target vehicles for investigating safety issues in EVERSAFE (and in this paper) were superminis and small family cars.

### Accident Data

The penetration of electric vehicles in the vehicle fleet is still low and this is reflected in the number of available analyses of electric vehicle crashes based on national data sources such as police reports. The most relevant report describing electric vehicle crash risks was that provided by Daimler (Justen & Schöneburg, 2011). Although electric vehicles could not be directly analyzed, they used conventional vehicles as a surrogate and identified deformation maps that could identify the most risky areas for battery placement in real crashes which were compared to deformation from standard crash tests. Also, given that electric vehicles will tend to operate in

a similar manner in the road system, the accident configurations most commonly observed should also be relevant for the near future.

Marschner and Liers also discussed potential road traffic accidents involving electric vehicles based on assumptions of similarity to existing vehicles types (Marschner & Liers, 2013). For that reason, a GIDAS (German In-Depth Accident Study) analysis was carried out focusing on microcars and similar. More than 22,000 accidents were used to identify all vehicles with usage patterns close to future electric vehicles. Afterwards, numerous parameters of anticipated electric vehicles and conventional M1 vehicles were compared from which safety requirements have been derived. To characterize the expected accident scenario of urban electric vehicles, typical collision constellations, collision parameters and injury mechanisms were analyzed. Even though the analyzed vehicles were mostly small and compact cars, a significant mass difference for future urban cars was foreseen. Since the majority of the electric vehicles will be used in urban areas, it was concluded that there will be a change in the future accident occurrence. In general, lower accident severities were expected including less crashes in the longitudinal direction but with an increase in crashes at junctions while crossing and turning conflicts result in a higher proportion of side crashes. The severity of such an accident is influenced greatly by the vehicle mass and speed of the striking vehicle but the proportion of crashes with heavier vehicles was expected to remain similar to today's situation with conventional passenger cars.

The Swedish Project "Räddningskedjan- EV Safe Rescue" reviewed 165 crashes involving hybrid vehicles based on the accident data from NASS-CDS database, the majority being the Toyota Prius and followed by Honda Civic Hybrid (Vinnova, 2014). The accident investigation team identified the primary impact direction and damage location. Of 110 hybrid vehicles with identified impact directions, 65% had a frontal impact followed by 20% with rear impacts. The car front and rear were also the two most frequently damaged areas (Vinnova, 2014), which accounted for 61% and 18% of identified damaged locations. In these 165 cases there were no fire accidents reported directly after the crash.

**Lithium-ion Batteries and Potential Hazards after Crash Loads**

Current Lithium-ion (Li-ion) batteries are highly developed, well balanced chemical systems. These batteries are comprised of two highly lithiated contrary charged electrodes commonly separated by an olefinic separator and filled with flammable organic solvents. The formation of a Solid Electrolyte Interface (SEI) during the first cycling of a Li-ion battery after assembly is an essential step for the function of the battery. SEI is composed of stable compounds like $Li_2CO_3$ and meta-stable compounds like e.g. $(CH_2OCO_2Li)_2$. The SEI becomes unstable when the cell temperature rises above 70 °C – 100 °C with an exothermic decomposition according to Equations (1-2):

$$(CH_2OCO_2Li)_2 \rightarrow Li_2CO_3 + C_2H_4 + CO_2 + ½\ O_2 \quad \text{(Eq.1)}$$
$$2\ Li + (CH_2OCO_2Li)_2 \rightarrow 2\ Li_2CO_3 + C_2H_4 \quad \text{(Eq.2)}$$

These reactions lead to the formation of ethene ($C_2H_4$) and carbon dioxide ($CO_2$). As a result, Li-ion batteries are very damageable by elevated temperatures. For example, an internal or external short circuit will raise the temperature inside the cell. An internal short circuit could arise when an external metallic part intrudes into the cell or by direct contact of battery electrodes after excessive compression of the separator. These examples may occur as a result of a car crash. Particles may also be introduced inside the cell during manufacturing process and cause an internal short circuit. Thermal and/or mechanical impact leads to the destruction of the SEI. After SEI decomposition, lithium reacts with organic electrolytes. Depending on the organic carbonates used as electrolyte components, different gaseous unsaturated hydrocarbons according to the reactions above are generated: ethene ($C_2H_4$), propene ($C_3H_6$), ethane ($C_2H_6$) and/or propane ($C_3H_8$). All these compounds are flammable and may form an explosive mixture depending on its concentration. An additional gas, hydrogen fluoride (HF), may also be produced due to reactions involving the conducting salts within the battery. Li-ion batteries can be provoked by internal or external heat sources and produce different gases that can be combustible or poisonous. The source of the heat can be fires surrounding the battery or internal short circuits of the battery cells caused by mechanical damage. High temperatures at one cell may affect adjacent cells and cause a chain reaction. With the organic solvent the conducting salt, $LiPF_6$, is also emitted and reacts in contact with water/air moisture according to Equations (3-4):

$$LiPF_6 + 4\ H_2O \rightarrow LiF\ (s) + H_3PO_4\ (l) + 5\ HF\ (g)\uparrow \quad \text{(Eq. 3)}$$
$$PF_5 + H_2O \rightarrow POF_3 + 2\ HF\ (g)\uparrow \quad \text{(Eq. 4)}$$

If a thermal runaway occurs a large number of different kinds of chemicals are generated. Combustion reactions evolve mainly the gases CO, $CO_2$ from organic materials, $NO_x$, HF as well as low molecular weight organic acids, aldehydes, ketones etc.

**Crash Safety by Regulation**

Electric vehicles shall fulfill all crash safety requirements as for conventional vehicles. Thus the current prevailing homologation tests regarding crash safety are applicable to electric vehicles as well. Depending on the market, different homologation tests are required for new vehicles to be type approved. It is necessary to address potential safety risks of EVs while in use and after a crash event, including electrical shocks associated with the high voltage (HV) circuits of EVs and potential hazards associated with Li-ion batteries and/or other rechargeable energy storage systems (REESS) (UNECE, 2012). In principal, the tests shall address safety considerations regarding the HV electrical safety, safety of electrical components, and REESS whereby there shall be no evidence of electrolyte leakage, fire, or explosion.

In Europe, all new vehicles should pass crash tests as specified by the United Nations Economic Commission for Europe (UNECE). With respect to complete vehicle crash tests, required tests include UN-R94 for frontal crash, UN-R95 for side crash, UN-R12 for steering mechanisms, and UN-R32 for rear end crash. For new vehicles to be sold in USA, they need to pass crash tests specified by the Federal Motor Vehicle Safety Standards (FMVSS). With respect to complete vehicle crash tests, they should pass FMVSS 208 (frontal crash, rollover, side crash), FMVSS 214 (side crash), and FMVSS 301 (rear end crash). The homologation tests in other regions such as in China, Japan, Australia and Canada are similar to those devised by UNECE and FMVSS.

Due to the introduction of HV system and traction battery system in electric vehicles, extra demands were raised concerning high voltage safety and battery safety in crash accidents. In Europe (and especially the 1958 agreement affiliated countries), UN-R100 sets requirements for the electric powered vehicles (classes M and N) and their REESS. In UN-R100, specific requirements on the REESS performance are defined concerning vibration, thermal shock and cycling, mechanical impact, fire resistance, external short circuit protection, overcharge/discharge protection, over-temperature protection and emissions. The date of entry into force of its latest series of amendments was 15 July 2013. Basic post-crash requirements regarding the safety of electric vehicles have also been added to UN-R94 and UN-R95 (e.g. regarding the releasing of electrolyte). In USA, FMVSS 305 specifies performance requirements that specify the: allowable electrolyte spillage, retention of propulsion batteries, and electrical isolation of the chassis from the high-voltage system during the crash event. This regulation is used in conjunction with FMVSS 208 (frontal rigid barrier crash tests), FMVSS 214 (side impact), and FMVSS 301 (rear, rigid barrier and deformable barrier impact tests).

Besides these crash regulations another Global Technical Regulation (GTR) is under development which addresses the safety of EVs. The Executive Committee of the 1998 Agreement (AC.3) gave, in November 2011, its general support to a joint proposal by the United States of America, Japan and the European Union to establish two working groups to address the safety and environmental issues associated with electric vehicles (EVs). That proposal (ECE/TRANS/WP.29/2012/36 and its Corr.1) was submitted to the World Forum for Harmonization of Vehicle Regulations (WP.29) at its March 2012 session for further consideration and formal adoption. The WP29 Committee has adopted this proposal with China as one of the co-sponsors together with the United States, Japan, and European Union (UNECE, 2012). The purpose of this regulation is to avoid human harm that may occur from the electric power train. The crash and post-crash phase are addressed by measures for the protection against electrical shock; REESS crashworthiness, including the limitation of electrolyte leakage, physical battery retention, and the maintenance of essential safety performance; and REESS safety assessment and stabilization procedures (UNECE, 2014). Major results from the GTR EVS are expected in 1-2 years.

## METHODS AND DATA SOURCES

**Abuse Cell Tests**

To study the performance of batteries under crash type loading a set of experimental abuse tests on cell level were conducted in the EVERSAFE project aiming to understand the deformation tolerance and potential thermal and gas generated by batteries (Wisch, et al., 2014). Nail penetration is part of the standard tests being conducted on cells. In EVERSAFE two different nail penetration test setups were conducted using pouch cells. Test setup 1 used a nail (rounded plastic punch) that had penetrations limited by the fixture back plate and did not fully penetrate the cell as specified in the standard procedures while test setup 2 had a nail penetrator according to the SAE J2464 standard (tapered conductive metallic nail) to promote internal short circuits that passed through a hole in the back plate allowing full penetration. The first case test can be considered more of a localized crush test. Another abuse test, a shear test, cleanly sliced the cells with metallic knives. Again, two different test configurations were applied. On the one hand a support plate for the pouch cell was used (test setup 3) and on the other hand the pouch cell had no support structure at the cut edge (test setup 4).

**Non-standardized Vehicle Crash Tests**

To study the performance of electric vehicles under crash type loading, and in particular their HV batteries, as well as and to evaluate the current protection levels of EVs and safe handling procedures for rescue services, two crash tests were conducted. Since both vehicles to be tested were already cars in serial production on the market

and successfully passed regulation and consumer program (Euro NCAP) tests, non-standardized crash test configurations have been developed to study other realistic impact conditions that are challenging for the HV battery system and which allowed studying existing and updated safe handling procedures for rescue services.

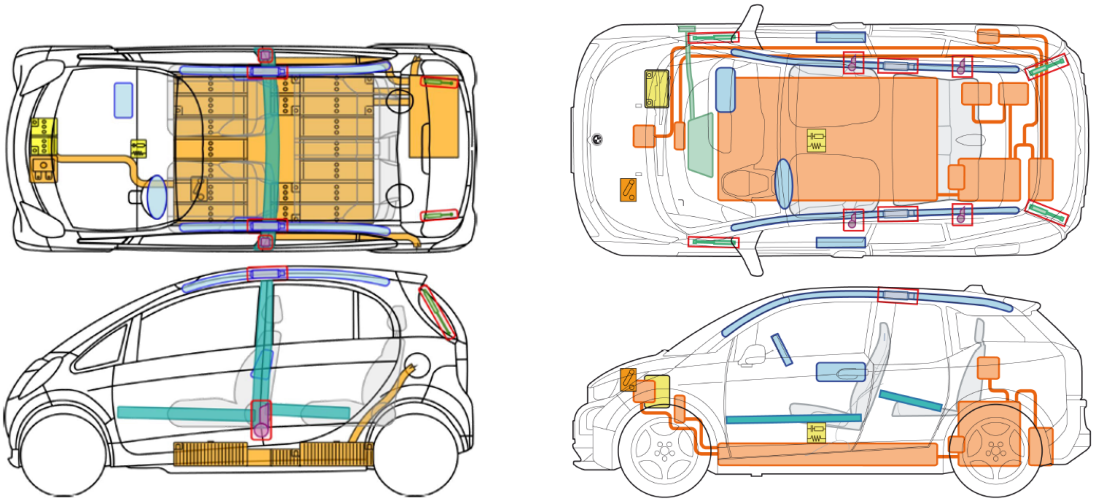

***Figure 1: Left: schematic Mitsubishi i-MiEV (source: Rescue data sheet Mitsubishi) and Right: schematic BMW i3 (source: Rescue data sheet BMW)***

Non-standardized Vehicle Crash Test #1 – Mitsubishi i-MiEV

As a first vehicle under test, the Mitsubishi i-MiEV (1GEV) was chosen representing a full electric vehicle with a Li-ion battery (330 V, 88 Li-ion cells, 16 kWh) that is located beneath both seat rows (see Figure 1) and two charging devices in the rear, a service-disconnect device beneath the driver seat and power electronics in the rear. As the test configuration, a 90 degree side pole impact was chosen whereby the i-MiEV was stationary (but not braked and with activated HV system) and a moving crash barrier (trolley) carried a rigid pole at its front (total mass ~2 t) approaching with 35 km/h, see Figure 2.

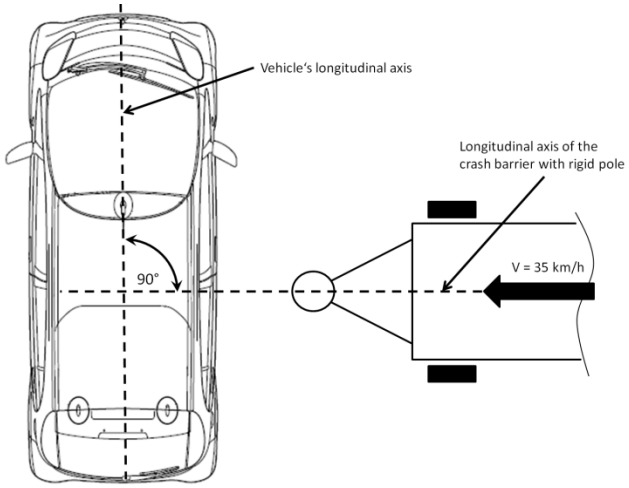


***Figure 2: Scheme of test configuration side pole impact Mitsubishi i-MiEV***

Non-standardized Vehicle Crash Test #2 – BMW i3

The second vehicle tested, the BMW i3 (2GEV), was chosen representing a full electric vehicle with a Li-ion battery (380 V, 96 Li-ion cells, 21.6 kWh thereof 18.8 kWh usable) that is located beneath both seat rows, see Figure 1. Further, it has one charging device in the rear, a service-disconnect device (executed as 12 V cutting line) in the car's front part and power electronics in the rear. Another peculiarity of the BMW i3 is that carbon fiber reinforced plastic (CFK) is primarily used as chassis material. However, the material used for front and rear crash structures are steel and aluminum. A crash configuration that represents both a frontal and a rear-end crash, as might occur in a traffic jam situation, was selected see Figure 3. A stationary, braked truck (weight ~10 t) was placed 2 m in front of the stationary BMW i3 test vehicle. The HV system was active and in driving readiness mode (with gear in neutral). A crash trolley fitted with a deformable barrier (total mass ~2 t) crashed then into the rear of the test vehicle BMW i3. All vehicles were centered along a common longitudinal axis. The trolley had a speed of 80 km/h. This test configuration exceeded standard crash requirements due to the fact that multiple impacts to the same vehicle were conducted.

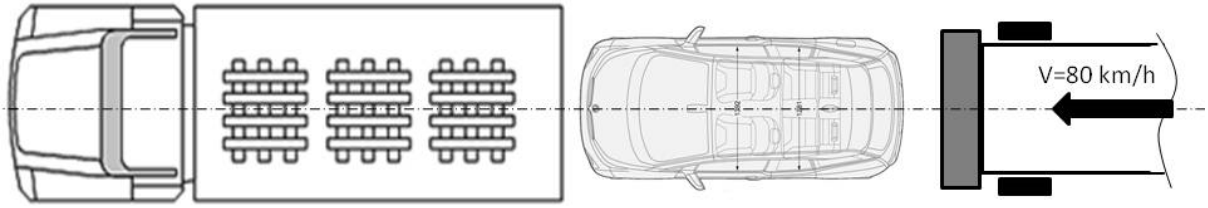


*Figure 3: Scheme of test configuration front and rear-end crash with BMW i3*

**Rescue Procedures / Guidelines, Rescue Data Sheets and Technical Solutions**

Rescue procedures vary within and between countries depending on the national, regional, and local organization of rescue services (Wisch, et al., 2014). Regardless of the location, firefighting and rescue services share common themes and technologies but there are local requirements that prohibit rigorous definition of rescue procedures. Due to the diversity of vehicles, occupants, and road conditions that will define a rescue operation, it is desirable that rescue personnel have a fundamental training that they can adapt to all possible conditions that they may encounter during their working career.

A study was performed to obtain an overview of existing rescue guidelines in Germany with special focus on information regarding the dealing with crashed electric vehicles (Wisch, et al., 2014). The information gained from the document "Accident Assistance & Recovery vehicles with high voltage systems" (German Association of the Automotive Industry (VDA), 2013) was considered to be most current and applicable. Other guidelines, as published by professional associations, do not focus sufficiently on the complete picture which is seen at a crash scene nor focused already on Li-ion battery technologies, but on organizational (mostly educational) aspects such as qualification levels or protection clothes.

Rescue data sheets have been developed to provide most important vehicle information for rescue teams in a clear and standardized way as well as in shortest time to ensure best rescue conditions for injured occupants. In Germany, the ADAC (General German Automobile Association) appealed in 2009 to the vehicle manufacturers to provide rescue data sheets for all new cars and to position them under the sun visor to provide information about cutting and pressure points, airbag zones and the location of the battery (Deutscher Feuerwehrverband e.V. (DFV), 2009). In addition to these data, rescue data sheets now include information regarding type of drive and the location of high-voltage components. Meanwhile several associations from the automobile sector and firefighting/rescue as well as vehicle manufacturers themselves and governmental entities promote the usage of these sheets in Europe. However, a legal obligation to carry a rescue card currently does not exist. The International Organization for Standardization (ISO) is developing a standard for rescue sheets (ISO, 2014). To ensure the availability of a rescue data sheet, Mercedes-Benz has introduced to the inside of the gas cap and on the opposite b-pillar QR codes that enables emergency services to access the individual sheet with a smartphone or tablet (Daimler AG, 2013).

In Germany in 2013, the Federal Ministry of Transport has set the basis to retrieve vehicle-related information directly from the database of the Federal Motor Transport Authority on software solutions on a tablet or laptop (Joint press release from von VDA, VDIK, ADAC, DAT and BMVBS, 2013). Two software solutions similar in functionality, the SilverDAT® - FRS (DAT group, 2013) from DAT (Deutsche Automobil Treuhand GmbH), and the Crash Recovery System® (Moditech Rescue Solutions BV, 2014) from Moditech Rescue Solutions use this option in the form of a license number query. Thus, it is possible to obtain directly by means of the license plate number at the accident scene information about the type of vehicle or drive and the access to the vehicle-related, digitized rescue data sheet.

In the United States, the National Fire Protection Association conducts diverse research on the handling of crashed electric vehicles and offers safety trainings as well as produces comprehensive material to be studied by firefighters. One of the basic documents, the Electric Vehicle Emergency Field Guide, provides an intuitive, quick reference guide, covering all current makes and models of hybrid and electric passenger cars drawn from manufacturer Emergency Response Guides (NFPA, 2012). Regarding the approach to a crashed vehicle, this document refers to always assume that the vehicle is some type of hybrid, electric or alternative fueled until proven otherwise.

The emergency call (eCall) is a system that in the event of a car accident automatically informs the locally responsible Public Safety Answering Point (PSAP). Technically, often the triggering of the airbag sensors initiates this automatic emergency call over the mobile network to the nearest PSAP. In addition to the position of the crashed car, vehicle-related data is transmitted, which are thus available to the emergency services even during the travel to the scene (German Federal Ministry of Transport and Digital Infrastructure, 2014). “The EC proposals for legislative acts foresaw that eCall would be seamlessly functioning throughout Europe by end of

2015. As the adoption procedure of these legislative acts by the European Parliament and the Council is still ongoing, the deadlines for implementation will most likely be the end of 2017 or early 2018." (European Commission - Digital Agenda for Europe - A Europe 2020 Initiative, 2014)

**RESULTS**

In general the tested pouch cells in the EVERSAFE project were quite resistant to the abuse. Only 1 of 19 cell tests resulted in thermal events. One cell was provoked by an overloading of the cell, after an external short circuit before testing and showed no negative effect on cell integrity. Shear tests gave comparable good results with no significant thermal activity (under 30°C) but with some toxic substance release. Even after the cells had been cut, there was a stable voltage developed by the cell. The lack of reaction in these tests could confirm that a clean cut of the cell will not lead to a failure of the separator and thus no direct contact appears between the cathode and anode. Results of nail penetration tests differ according to different types of nail (test setup 1 with rounded plastic punch and test setup 2 with thin metallic nail). None of the test setup 2 nail tests produced any significant cell swelling although there were traces of toxic substances. Temperatures did not exceed 60 °C. However, test setup 1 nail penetration tests produced some cell swelling and thermal activity was observed where temperatures up to 300 °C were recorded. The nail used at test setup 1 was made of plastic and could expand during the test, resulting in a local compression of the cell compared to the full nail penetration of the cell at test setup 2. The comparison of these tests shows that a clean penetration with a thin metallic, electrical conducting nail didn't lead to a reaction of the cell, whereas an intrusion with a wider object leads to a local compression and an internal short-circuit which deems to be more realistic in road traffic accidents. A special area of concern was also the reproducibility and the robustness of these tests since it could be shown that the results of cell tests might strongly differ already due to small differences of the test conditions and test scenarios applied. Pouch cells were also tested for external short circuit and overcharge of cells. External short circuit of cells has led to a tremendous evolution of gas inside the pouch cell, resulting in an inflating of the pouch like a balloon, but did not lead to bursting. After the temperature decreases, swelling was reduced and the pouch returned to its original flat profile but with wrinkles. Even a pouch cell rigidly held to the fixture by covering with non-flammable material has shown no bursting after inflating due to external short circuit. A consecutive overcharge with 5 V led to a thermal runaway with fire. It has to be pointed out that these tests should be referred to as extreme and demonstrate the high safety level of the device under test.

The crash tests with the two electric vehicles (Mitsubishi i-MiEV and BMW i3) produced no significant battery reactions (no new or unexpected risks such as electrical hazards, chemical reactions, thermal events, release of toxic substances battery, fire or explosion) and vehicle damage was as expected for current vehicle safety levels. Figure 4 shows the BMW i3 detached from the ground shortly after crashing into the rear of the truck indicating the high crash severity. Full test reports are provided in the EVERSAFE Deliverable 3.1 (Wisch, et al., 2014). Thus, both test vehicles exhibited high levels of safety in non-standardized, but realistic experimental configurations which were shown by:

- Good mechanical protection of the battery system.
- High-voltage system disconnected automatically to safe condition.
- Shut-down times of the HV systems much quicker (< 2s) than required by crash regulations (< 60s).
- No incidents (no undue temperature increase, no release of toxic / flammable gases or liquids).
- Intact cabin; a few bruised HV wirings and small deformations to the outer battery casing but without negative consequences.
- Newer chassis materials can produce stiff structures that increase the vehicle accelerations but can provide easier access to injured occupants as the doors may not bind due to distortions of the structure.

***Figure 4: BMW i3 and crash trolley have fully left the contact to the ground at ~494 ms after the first impact***

The main battery requirement from vehicle safety regulations was that the high-voltage outside the HV battery should drop down quickly (below 60 V) in a crash and this situation was fulfilled. As example, Figure 5 shows the HV network shut-off of the Mitsubishi i-MiEV after crash. There was no evidence of any danger after both crash tests that could be hazardous to occupants or rescue teams, neither with regard to electrical, thermal, nor chemical hazards. However, it could not be shown which effects further handling of this crashed vehicle might have (e.g., due to pulling, cutting or distorting the vehicle) during recovery operations.

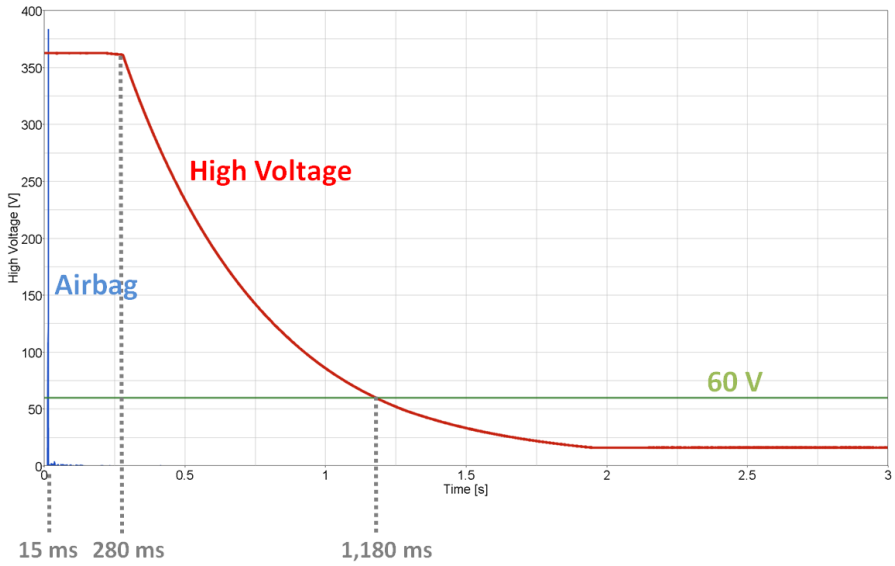


***Figure 5: Airbag ignition and high-voltage network shut-off of the Mitsubishi i-MiEV after side pole impact***

The severity of the full scale crash tests was chosen to be more challenging than required by the UN regulations or Euro NCAP tests, respectively. This decision was made because both test vehicles (Mitsubishi i-MiEV and BMW i3) have already successfully passed regulation and Euro NCAP crash tests and thus demonstrate a certain level of crash safety even with their new drive trains. The particular test configurations have been selected to reflect worst case, but realistic scenarios where potential hazards might occur.

Potential hazards originated from the high-voltage battery in severe crashes due to mechanical loading or fire close by during a crash are electrical shock risks, thermal events, chemical reactions and release of emissions of flammable, ignitable and/or toxic battery substances as well as fire or explosion. The main substances that can be expected from a Li-ion cell and their potential consequences are presented in Table 1.

Table 1: Table of critical emitted gases

| Substance | Chemical formula | Health Risk | Toxic Concentration/ exposure time | Flammable |
|---|---|---|---|---|
| Hydrogen | $H_2$ | No | | Yes |
| Carbon monoxide | CO | Yes | 6,400 ppm / 30 minutes | No |
| Carbon dioxide | $CO_2$ | No | 30,000 ppm | No |
| Methane | $CH_4$ | No | | Yes |
| Hydrogen fluoride | HF | Yes | 50-250 ppm / 5 minutes | No |
| Phosphor pentafluoride | $PF_5$ | Yes | 3 ppm / 8 hours | No |
| Electrolyte fumes | $LiPF_6$ | unknown | | Yes |

Portable multi-gas detectors are diffusiometers by default and are appropriated to detect critical emitted gases at a crash scene. Specialized rescue vehicles have addition measurement devices with active intake (integrated pump). In general, the multi-gas detectors allow directly measuring CO, $H_2S$ and $O_2$. Further the available Ex-sensor (explosion sensor) only measures combustible gases and hereby only measures exactly, when calibrated on these substances (often methane ($CH_4$) and nonane ($C_9H_{20}$)). However, gases such as $H_2$ can be calculated qualitatively using the explosion limit. As identified for Germany, in case of volunteer fire brigades a multi-gas detector is equipped on a vehicle specialized for measurements with a standardized configuration of the sensors and would be called subsequent to the initial vehicle arriving at the scene, whereas in case of a professional fire department this multi-gas detector is carried as standard in a vehicle of the first squad team.

A non-representative survey for available multi-gas detectors in Germany was performed in 2014 (Wisch, et al., 2014). Results have been summarized in Table 2. Although no longer commercially available the MSA “Solaris”

is still in use. There are other suppliers of portable gas detectors, but the companies MSA Auer and Dräger have largely prevailed in the fire service in Germany as standard.

Table 2: Typical multi-gas detectors used by German firefighters

| Gas detector class | Label |
|---|---|
| 1-5 | Dräger "X-am® 5000" |
| | MSA Auer "ALTAIR 5X" |
| 1-4 | Dräger "X-am® 2500" |
| | Honeywell/ Compur Monitors "Impact (Pro)" |
| | MSA Auer "ALTAIR 4X" |

To determine unknown liquids, a litmus paper test is standard for both volunteer and professional fire brigades. The same is true for thermal imaging cameras. In contrast, only specialized vehicles (e.g. the ABC-explorer) are typically equipped with short-time measurement tubules and need to be called subsequently by the incident commander. Water is still the standard extinguishing agent. However, additives are also used such as fire fighting foams which increase the impact of smothering a fire and cooling. Electrical measurements will be performed in most cases with a voltage tester that is present in the appropriate standardized toolbox.

An extended personal protective equipment (PPE) includes a chemical splash suit is available in several types ranging from part to full body protection in contrast to the standard PPE which contains of heat and (shortly) flame resistant jacket and trousers, helmet, leather boots (security class S3), respirator mask, special harness (incl. abseiling eyelet and hatchet).

**Recommendations for Rescue Teams**

In order to support rescue services when approaching road traffic accident scenes involving severely damaged electric and/or hybrid vehicles, a procedure for handling these vehicles with Li-ion traction batteries has been developed considering best practices and realistic resources. Inputs for the proposed rescue guideline (in the flow chart format of Figure 6) have come from several sources:

- Review of existing handling procedures for firefighters in particular from Germany and Sweden.
- Exchange of information and experiences with local firefighters around the crash tests conducted.
- Discussions within the EVERSAFE consortium and external experts.
- Survey regarding gas measurement devices available at German fire departments.

The flow chart in Figure 6 is divided into three columns identified with color. The middle, light blue column represents the decision path; the left, green column gives explanations and advice for the decision path; while the right, red column gives advice for measurement devices or special personal protection equipment. In addition to the explanations, information or user warnings are provided, partly by color or pictograms.

In addition to the measures for vehicle drivetrain identification, securing and deactivation of electric vehicles and the technical possibilities of monitoring the work site, the patient's health condition plays a decisive role in the flow chart. This results in a quick assessment of the accident and selection of the three approved types of rescue "Gentle rescue", "Fast rescue" and "Immediate rescue" as made use of in Germany. This approach uses procedures familiar for accidents involving conventional vehicles and reduces additional training requirements. The monitoring of the patient and the applied measurement technology must continue following the initial patient assessment and needs to follow the procedures identified in the flowchart until the patient is rescued from the vehicle. The ‘immediate rescue’ is the fastest possible rescue, tolerating a possible further deterioration of the patient from immediate danger or due to medical conditions. ‘Fast rescue’ is the fastest possible rescue of the patient with respect to time, tactical and medical aspects. In order to minimize the travel time to the hospital, transport is to be aimed at the ‘fast rescue’ time window of 20 to 30 minutes. ‘Gentle rescue’ is a rescue, in which the time aspect moves into the background because the diagnosed injury is not sensitive to time and the time window for medical consultation may in some cases be even greater than that of ‘fast recovery’) (Vereinigung zur Förderung des deutschen Brandschutzes e.V., November 2011).

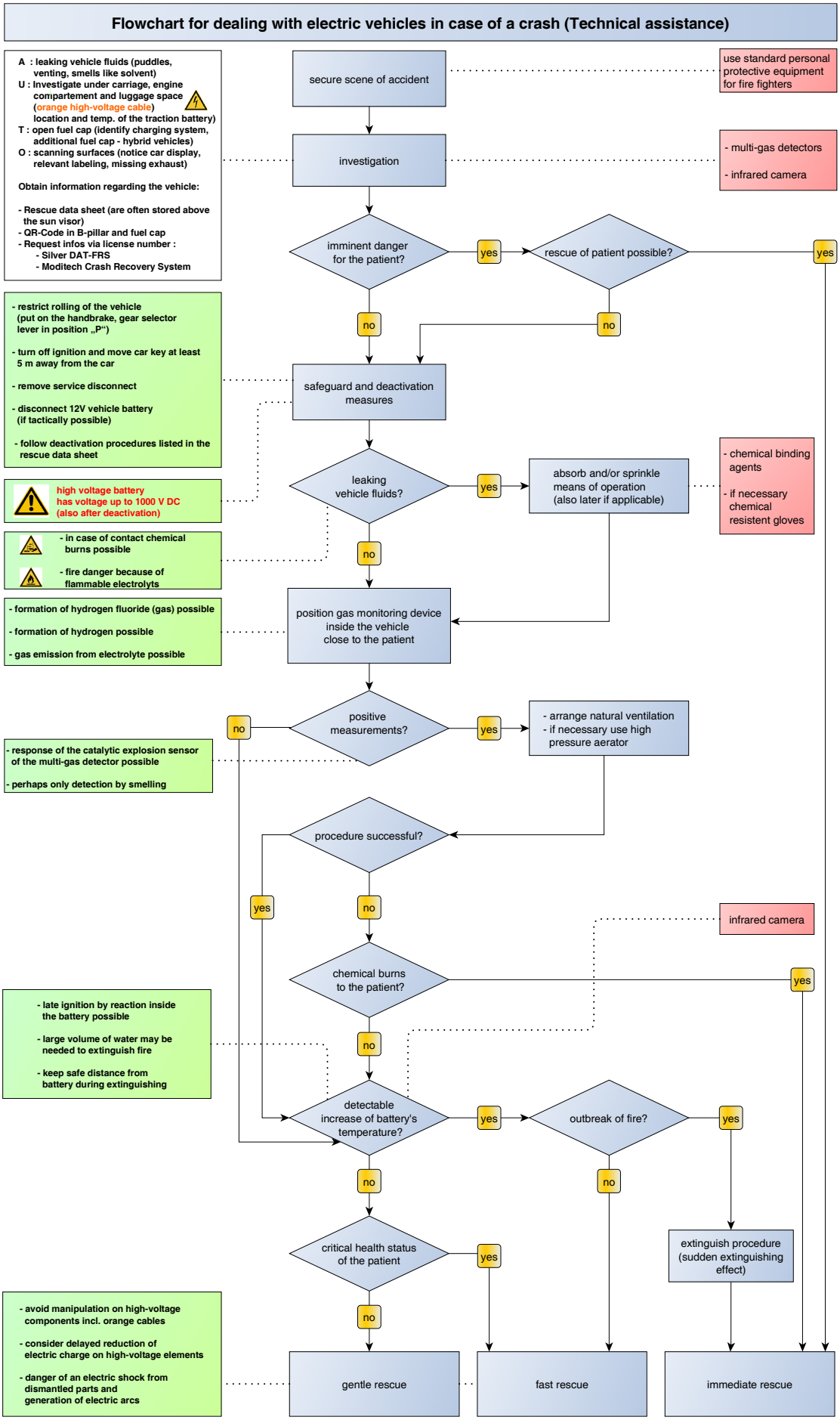


*Figure 6: Updated rescue guideline*

A summary of the features of the new handling procedure (see Figure 6) is provided below:

- Flow chart layout similar to best practices documentation but specialized for crashed vehicles with electric drive. The flowchart is focused on Li-ion battery technologies and not fuel cell drives.
- Clarity by three-column principle and color highlighting
- Flow chart can be used properly printed in an A4 format for use on scene
- Clear depiction that flammable, irritant and corrosive materials may be released by the HV battery and proposals for how to deal with them. For example, the explicit naming of the possible development of hydrogen fluoride (HF) could not be found in literature reviews of handling procedures.
- Procedure was optimized to maintain existing standard procedures used by (German) firefighters regarding their activities based on the patients' health states ("Gentle rescue", "Fast rescue" and "Immediate rescue") and if possible, to return rapidly to these three approved types of rescue
- Inclusion of relevant indicators for possible hazards (monitoring electrical and chemical conditions as well as temperature)
- Common measures to disable the HV system as replacement if specific rescue data sheet is not at hand.

With regard to the potential dangers that may arise due to a highly damaged electric vehicle, further recommendations and advice are provided below to complement the proposed updated rescue guidelines.

With focus on chemical hazards and fire:

- Chemical hazards exist and must be considered.
- The carbonates dimethyl carbonate (DMC), diethyl carbonate (DEC), ethylene carbonate (EC) and propylene carbonate (PC) are typical chemical substances used as electrolyte (also in mixed forms) in high-voltage traction batteries that possibly being released in case of mechanical damage to the HV battery or a cell. Therefore, these substances should be monitored using the gas detectors.
    - If released, then check the patient's condition (see also Figure 6).
    - In case patient should react to these carbonates (e.g. noticeable by sore throat or cough) cancel 'gentle rescue' and change to 'immediate rescue'
- Depending on the organic carbonates used as electrolyte components (see previous bullet point) and temperatures around 110 °C, different gaseous unsaturated hydrocarbons may be generated due to battery decomposition: ethene ($C_2H_4$), propene ($C_3H_6$), ethane ($C_2H_6$) and/or propane ($C_3H_8$). All these compounds are flammable and may form an explosive mixture depending on its concentration. A spark may ignite flammable gases or gas mixture.
- Hydrogen fluoride (HF) is difficult to measure on site (also costly due to required specialized gas detectors), therefore measurement of combustible gases is a suitable indicator (see previous bullet points) and is proposed by means of standard multi-gas detectors
- Multi-gas detectors should continuously measure the accident scene instead of using short-time measurement tubules which only provide a value per initiated measurement.
- Released substances are problematic in the case of Li-ion batteries because these would indicate opened (compromised) battery cells and packs which could increase the risk for gas development and resulting fire hazard.
    - The coolant may also be hazardous (not investigated here)
    - In case of Ni-MH traction batteries, alkaline solutions (pH 14) are used as electrolyte which leads to a risk of skin burns (not investigated here)

With focus on electrical hazards:

- Electrical hazards play a minor role due to multiple safety measures implemented by the vehicle manufacturers (no electrical hazards reported in the field known to date). However, in case of a severely damaged traction battery, extreme caution is appropriate.
- Difficulties at the scene:
    - The voltage tester or similar equipment / measurements must be used and assessed only by authorized personnel (electrically instructed person).
    - Difficult to determine measurement points on the vehicle as this is not described in rescue data sheets.
    - Possibly poor accessibility
- *Important to note:* Car manufacturers have not harmonized their recommendations with regards to the mandatory or voluntary usage of high-voltage gloves for rescue services during the de-activation process of the electric vehicle's high-voltage system. Some rescue data sheets (e.g. from Nissan or from Citroen) dictate wearing high-voltage gloves. Since no electrical issues in case of crashed electric vehicles were known from the field and any research project, and even the highly-challenging crash tests conducted in EVERSAFE did not lead to any safety issues, it is recommended that the use of HV

gloves is only warranted in case of a severely damaged traction battery and availability of specialized personnel. Latest news from the media need to be considered on this topic.

With focus on explosion:

- The risk of an explosion of the HV battery is very low.
- Ignition only occurs for high concentrations of chemical degraded products and only at high temperatures.

Monitoring the temperature change (in particular the increase of the temperature over time) of the Li-ion traction battery is probably the safest indicator for potential hazards in case of damaged electric vehicles.

- Due to available resources (in most cases only a thermal imaging camera is available) accurate measurement of the vehicle temperature is not possible and only a large increase of the temperature inside the battery is measurable from outside. The battery is often well insulated and might be difficult to be accessed for temperature measurements. Environmental influences such as high winds may exacerbate the measurement.
- If a traction battery is located below the passenger compartment, it is recommended to measure underneath the vehicle with a thermal imaging camera.
- As the temperature rises, the off gassing is amplified, which results in an increased concentration of carbonates.

Further general recommendations and advice for safe handling of EVs:

- Firefighters can approach the electric vehicle with standard PPE as approved for approaching conventional vehicles after crash. In case of any hazard (e.g. release of combustible gases) additional protection measures should be considered (e.g. wearing the respirator mask or the chemical protective clothing).
- The United States (NFPA) recommends the approach to always assume that it could be an alternatively powered vehicle (NFPA, 2012).
- The location of a vehicle's rescue data sheet may be changed and is recommended to be behind the driver's sun visor due to the severity of the crash sustained.

After the development of the new rescue guidelines, possibilities and proposals for further information and consolidation on knowledge regarding the handling of highly damaged electric vehicles involved in a crash include:

- Information and experiences with electric vehicles (and other alternatively powered vehicles) should be part of the basic training for firefighters
- Careful review of reports such as the VDA document (German Association of the Automotive Industry (VDA), 2013), from firefighting associations, research projects, service providers such as Dekra, articles in the magazine "Fire protection", etc.
- Create experience exchange forums (possibly on the Internet or in conferences)
- Firefighters are recommended to continuously browse through rescue data sheets
- Monitor current vehicle propulsion technologies and market shares

Technical solutions promising to provide important information about the vehicle in crash:

- Automatic Emergency Call (eCall) should include drivetrain information
- Query by vehicle's license number using the Crash Recovery System® of the Moditech Rescue Solutions or SilverDAT® - FRS
- QR-Codes applied to the vehicle

Finally, it should not be forgotten to ask the driver, when possible, about the type of drive and that all senses should be used in a careful manner when dealing with a crashed electric vehicle:

- Smell (e.g. released gases)
- Hear (e.g. opening of battery's safety relief valves)
- Feel (e.g. temperature increase)
- See (e.g. disrupted traction battery)

**Recommendations for Vehicle Manufacturers**

Vehicle manufacturers are requested to update rescue data sheets with information about chemical substances used in HV battery and possible reactions, to grant firefighters fast and simple access to (different) locations where the HV system can be shut down manually and to provide convenient, harmonized storage (positioning and attachment) for rescue data sheets inside the vehicle. Further, harmonization processes shall be reinforced with other manufacturers, automotive associations and governmental entities, e.g., to agree or not agree on the

mandatory usage of high-voltage gloves for rescue teams. Vehicle manufacturers should also promote eCall to their customers and provide as much useful information as possible within the emergency message. Finally, the communication with rescue team associations and fire brigades shall be continued and expanded.

**Recommendations for First-Aiders**
Based on the current results from crash tests and field experiences, persons arriving the crash scene first do not need to have specific concerns about their own safety when approaching a crashed electric vehicle in order to apply first aid to occupants. However, common sense should be applied all the times and news about this topic in media should be monitored. It is also recommended to inform other people close by about the presence of an electric vehicle if identified, including professional emergency workers. For first-aiders it is strongly prohibited to touch or modify any HV related vehicle components which are e.g. marked by an orange color or by figures.

**DISCUSSION**
In general and to the current state of the art technology, the batteries of electrically propelled mass production cars of the M1 category are well protected on standardized tests (e.g. according to UN-ECE R 94/95, Euro NCAP etc.) and even beyond. Nevertheless, in very severe crashes or unfortunate circumstances, the battery can be damaged severely causing hazards. Simulations in the EVERSAFE project and electric vehicle crash results showed that some current cell abuse tests, e.g. SAE J2464, might not be representative of what may happen in a vehicle crash as the intruding object would probably be wider as a thin nail.

Fuel sources for vehicles are becoming more individualized to the vehicle type and manufacturer. Additionally, the diversity of fuel types for vehicles sharing the same platform can lead to different rescue operations for vehicles with identical appearances. It is in regards to this point that electric vehicles impose new, and currently undefined, training needs for firefighters. Manufacturers can offer internal combustion, hybrid, or fully electric variants of the same vehicle model. Each has specific features that influence the rescue procedures. The documented rescue training materials for Swedish and German firefighters were summarized and compared in (Wisch, et al., 2014). Information provided is based on basic instructions that is under constant review and not every document is covered. Interviews with fire fighters were also conducted to capture the formal and informal knowledge of electric vehicles. A general outline of rescue operations for crashes involving electric vehicles was identified to facilitate the analysis. A general approach to rescue operations can be considered as:

1) Information on the way to the scene
2) Appraisal of the vehicle on the scene, identification of vehicle
3) Securing/stabilizing the vehicle
4) Fire control
5) Chemical hazard control
6) Shut-down electrical systems (to cut the vehicle)
7) Occupant extraction
8) Post crash issues

The review of Swedish and German rescue procedures and training materials indicate that there are many similarities that can be exploited when adapting existing methods for new vehicle technologies. The main point to be aware of is that the basic structure for approaching and acting at a accident scene are similar between countries and that the only issues that need to be addressed are related to the battery and its connections to the electric drivetrain. From the testing and simulation activities in the EVERSAFE project, there does not seem to be significant differences between EV and conventional vehicles in terms of fire and occupant extraction procedures.

The crash tests have also been used as training for firefighters. In particular, existing and alternative post-crash guidelines were considered and checked for their viability under realistic conditions. Different portable multi-gas detectors have been utilized to identify combustible gases (diffusion devices MSA Auer Altair 4X and devices with active intake MSA Auer Altair 5X and MSA Auer Sirius PID). Since hydrogen fluoride (HF) is the worst case result of possible chemical reactions, a special gas detector (Dräger X-am 5100 with HF/HCL sensor) was rented to directly measure HF (which did not emerge). Due to the high acquisition costs (around 1,500€) and maintenance costs of such a specialized gas detector it was considered to be not economical to propose the purchase for general application by rescue services. This conclusion was strengthened by consideration of the difficulties to measure under real conditions (e.g. wind) and the order of emergence of combustible gases due to a damage of the HV battery which can be detected with usual multi-gas detectors.

Following the crash test of the BMW i3, the work of the fire brigade was analyzed and discovered the following:

- Finding the rescue datasheet proved difficult, as this was thrown by the impact from the original position behind the sun visor in the back seat area and was discovered only in the further course of the training by the fire department. The firefighters were then able to act purposefully.
- The orange color of the 12 V rescue disconnect point and the resulting suspected high voltage danger were misleading so that the deactivation measures were carried out with high voltage gloves. Since the pulling of the plug required a detailed manipulation and took too long, the decision was taken to cut all connecting wires. However, it has to be noted that an adaptation of the color of the rescue disconnecting point was already provided at the time by BMW.
- Subsequent to the firefighter training performed at the BMW i3 crash test, the firefighters indicated that it is of high importance for them to recognize early in time the presence of an alternatively propelled vehicle. Therefore, the firefighters considered it advisable to consistently mark electric vehicles, e.g., similar to the license plate marking used in Norway (Balzter, 2013).

The training also confirmed the theoretical assumption that many firefighters are not yet adapted to the dangers of electric cars. Further, flowcharts of the procedure for accidents involving electric vehicles are largely unknown in the fire service. There is little distinction in the use of measures between conventional and electric vehicles.

There are some common actions observed in the rescue guidelines that need to be developed into rescue service education programs or better information is needed for rescue workers. The main points of interest are:

- How can EVs be readily identified at a crash or rescue scene? It is desirable that the vehicle identifies itself by eCall information or are there standardized identifications visible on the vehicle itself?
- How can a high-voltage system disconnect be confirmed? There is no visible indicator on the vehicle exterior that readily shows the high voltage circuit has been disconnected. This information can remove one step (Item 6) in the rescue process.
- Can there be a requirement (such as a UNECE regulation) that requires the HV system to disconnect when the 12V is disconnected? As rescue services routinely disconnect the 12 V system to eliminate pyrotechnical safety systems from inadvertently deploying, this interlock would also eliminate one step (Item 6) in the rescue process.
- How are batteries affected during extreme manipulation of the vehicle during occupant extrication? For example, the extension of the car from two winch points involves tension and bending loads on the vehicle floor, particularly if any of the pillars have been cut. This may induce internal deformation in the battery that may not have arose in the original crash, or accentuate existing damage in the battery caused prior to the extrication procedure.

In addition to the need to address the issues raised above, there is a lack of standardized or legislated procedures outlining the towing and storage of electric vehicles after a crash. Vehicle manufacturers develop their own product recommendations but there should be universal procedures to eliminate the risk of mistreatment of an EV due to a diversity of handling procedures.

The need for firefighters and other rescue workers to use specific protective equipment for EVs needs further investigation. Rescue operations should not require high voltage electrical repairs or investigation by individuals without appropriate training. It is desirable that standard protective equipment is sufficient and the vehicle systems are designed to ensure electrical isolation from rescue workers under foreseeable rescue operations.

One additional issue that requires further investigation is the influence of battery aging. Li-ion batteries are still a new technology with few years of service and thus experience with older batteries is lacking. There is a need to monitor EVs and identify if batteries and their structures exhibit degradation in their mechanical tolerance to failure.

The battery protection was achieved by very stiff protective structures using new materials as carbon fiber reinforced carbon (especially in 2GEV). This may lead to less overall vehicle deformations and higher acceleration loadings for occupants during crashes and thus increases the risk for severe, internal injuries. With regard to future user patterns, it has to be noted that other vehicle categories than the often discussed passenger vehicles (M1) will enter the markets. Especially in urban areas, smaller electric vehicles such as quadricycles and microcars are alternatives. Many of these small electric vehicles will be certified as vehicles of categories L6e or L7e which do not have to fulfill any legal crash requirements in Europe by now. This may result in less performing vehicle crash structures and other safety issues as tests of Euro NCAP have shown in 2014 (Euro NCAP, 2014). However, it has to be noted that most of the full-electrified small vehicles will run on low voltage networks that reduce the electrical hazards but depending on the cell chemistry thermal and chemical potential hazards may remain existent.

One final point regarding the risks from traction batteries is the influence of state of charge (SOC). The energy content of the battery is a function of its SOC. If a battery with a high SOC is disconnected from the external cables, the battery still has the potential to react internally and the safest condition would be to discharge or neutralize the battery immediately after the crash event. The former action is not feasible without developing extreme heat and electric shock hazards and there are no published methods yet to safely neutralize a fully charged battery. This is an area for new investigations.

**REFERENCES**


Balzter, S. (2013). Förderung von Elektromobilität: In Norwegen ist für Elektroautos sogar der Strom gratis. *Frankfurter Allgemeine*.

Daimler AG. (2013). Neue Mercedes-Benz Initiative: QR-Code kann Leben retten. http://www.daimler.com/dccom/0-5-7153-49-1601547-1-0-0-0-0-0-0-0-0-0-0-0-0-0-0.html.

DAT group. (2013). SilverDAT® - FRS Fire rescue brigade data sheet system. http://www.dat.de/en/offers/information-services/silverdatr-frs-fire-brigade-rescue-data-sheet-system.html.

Deutscher Feuerwehrverband e.V. (DFV). (2009). Rettungskarte soll Feuerwehr bei Unfällen helfen / Deutscher Feuerwehrverband begrüßt ADAC-Initiative für mehr Informationen. Press Portal - URL: http://www.presseportal.de/pm/50093/1404957/rettungskarte-soll-feuerwehr-bei-unfaellen-helfen-deutscher-feuerwehrverband-begruesst-adac.

Euro NCAP. (2014). *2014 Safety of Quadricycles*. http://www.euroncap.com/en/vehicle-safety/safety-campaigns/2014-quadricycles-tests/

European Commission - Digital Agenda for Europe - A Europe 2020 Initiative. (2014). eCall: Time saved = lives saved. http://ec.europa.eu/digital-agenda/en/ecall-time-saved-lives-saved.

German Association of the Automotive Industry (VDA). (2013). *Accident Assistance and Recovery of Vehicles with High-voltage Systems - Frequently asked questions.* Berlin.

German Federal Ministry of Transport and Digital Infrastructure. (2014). eCall für mehr Sicherheit im Straßenverkehr. http://www.bmvi.de/SharedDocs/DE/Artikel/LA/ecall-fuer-mehr-sicherheit-im-strassenverkehr.html.

ISO. (2014). *Road vehicles - Information for first and second responders - Rescue sheet for passenger cars and light commercial vehicles.* ISO/TC 22/SC 36: ISO 17840-1.

Joint press release from von VDA, VDIK, ADAC, DAT and BMVBS. (2013). Schnellere Hilfe mit dem digitalen Rettungsdatenblatt. http://www.dat.de/aktuell/news/schnellere-hilfe-mit-dem-digitalen-rettungsdatenblatt-156.html.

Justen, R., & Schöneburg, R. (2011). Crash Safety Of Hybrid- And Battery Electric Vehicles. *22nd ESV Conference.* Washington D.C.

Marschner, M., & Liers, H. (2013). Untersuchung des potentiellen Unfallgeschehens eineszukünftigen urbanen Elektrofahrzeuges auf Basis von Realunfalldaten. *9. VDI-Tagung mit Fachausstellung Fahrzeugsicherheit 2.0 - Wie viel passive Sicherheit benötigen zukünftige Fahrzeuggenerationen?* Berlin.

Moditech Rescue Solutions BV. (2014). The Mobile Vehicle Information System For Rescue Workers. http://www.moditech.com/en.

NFPA. (2012). *Electric Vehicle Emergency Field Guide - Classroom Edition.* Electric Vehicle Safety Training of the Naitonal Fire Protection Association (NFPA).

Statistics Norway. (2014). *Registered Vehicles*. URL: www.ssb.no/

Trafikanalys. (2014). URL: www.trafikanalys.se

UNECE. (2012). *Terms of Reference of the Informal Working Group on Electric Vehicle Safety.* ECE/TRANS/WP.29/2012/121, Paragraphs 1-6.

UNECE. (2014). *EVS GTR Draft protocol ver.4 (EVS-06-14e Rev.1.doc).* https://www2.unece.org/wiki/display/trans/EVS+6th+session.

Vereinigung zur Förderung des deutschen Brandschutzes e.V. (November 2011). *Merkblatt: Technisch-medizinische Rettung nach Verkehrsunfällen.*

Vinnova. (2014). *Räddningskedjan (E-Vehicle Safe Rescue).* www.vinnova.se/sv/Resultat/Projekt/Effekta/Raddningskedjan-Utformning-av-raddningstjanststrategi-baserad-pa-E-fordons-riskfaktorer/

Wisch, M., Ott, J., Thomson, R., Léost, Y., Abert, M., & Yao, J. (2014). *EVERSAFE - Deliverable 3.1 Recommendations and Guidelines for Battery Crash Safety and Post-Crash Safe Handling*. www.eversafe-project.eu, EC FP7 ERA-Net Electromobility+.

# DEVELOPMENT OF HIGH EFFFICIENCY LOAD PATH STRUCTURE TO ENHANCE SIDE IMPACT SAFETY PERFORMANCE

**Chinmoy Pal**
**Tomosaburo Okabe**
**Masato Sakurai**
**Makita Masashi**
Nissan Motor Co., Ltd.
Japan

**Kulothungan, Vimalathithan**
RNTBCI
India

Paper Number 15-0363

## ABSTRACT

In order to protect the occupants effectively in side impact crashes, the main tasks are (a) to minimize the intrusion of the deformed body structure after the impact in order to reduce direct contact force with the occupant and (b) to reduce the relative impact velocity of the intruding structure at the start of contact with the occupant. The existing concepts similar to SIPS (Side Impact Protection) system are basically based on good structural integrity with seat-mounted side air bags and roof-mounted curtain air bags for overall protection of the occupant in side impact crashes. However, for higher level of external input load at an inclined angle from high front-end SUVs acting on the side of an ordinary PV in case of SUV-to-PV side impact crashes, there is a room to have more efficient structural load-path system layout. A new inclined L-shaped High Efficiency Load Path System (HELPS) was developed and incorporated at the back of the existing seat back frame to bypass a part of the incoming load to the central console through the seatback frame. At first, a number of full vehicle FE-simulation studies were carried out to verify the performance in IIHS and SINCAP tests to assure the effectiveness of the concept. Finally, it is tuned to a feasible optimized structure in order to ensure other functional aspects, such as, seating comfort of the front passenger, leg-room of the rear occupants, etc. Its performance was calculated assuming various seating positions of the frontal occupant to examine the robustness of the concept in real world safety. Human Body Model (HBM) simulations were also carried out to compare two systems, one with HELPS and the other without HELPS concept. Similar to the results of the dummy response in IIHS and SINCAP tests, reductions in occupant injury level were observed in HBM simulations.

## INTRODUCTION

Side collisions remain a frequent cause of fatal and serious injury. From accident analysis, it is found that 60% of the fatal and serious injuries to front seat occupants in side collisions were to the struck side occupants, and 40% were to the non-struck side occupants [3], [4]. In lateral impact at the intersection of roads, the distance of occupant's chest and the front end of the colliding car is only few hundred millimeters. The advanced safety cage of recent vehicles is designed with careful mix of different steel grades of various strength and thickness to provide carefully controlled lateral deformation of the whole body structure in order to minimize the injuries of the occupant inside the vehicle compartment. The side airbag and roof curtain airbag provide additional protection of the pelvis, abdomen, thorax and head for both the front seat occupants as well as to the rear passengers. Strong rigid steel tubes of Volvo's SIPS concept across the seat frame help to transfer loads to the center console to maintain the seating space after the impact. It is very effective for a lateral input at a lower height when colliding with passenger vehicles. However, in case of collision with SUVs having higher front-end stiffness, it may not be that effective in an inclined lateral input load at a higher height from the ground. It is known that occupants in cars will encounter serious chest injuries when struck by vehicles with high front-end stiffness and high ground clearance such as sport utility vehicles (SUVs), multi-purpose vehicles (MPVs) and 1-box type of vehicles [3],[6],[7]. As these types of vehicles become increasingly more prevalent, consideration should be given to the vehicle structural design in light of the changing and mixed vehicle fleet [2], [5].

## BASIC INITIAL DESIGN CONCEPT

The Figure1 shows the basic concept of HELPS. The system consists of four main elements: 1) an outer contact element, 2) an inclined and curved seatback cross-reinforce member 3) an inner contact element and 4) a strong center console. The outer contact element facilitates an early contact of the seat frame to intruding door deformed by the moving barrier or a vehicle at the level of the bumper height. The input load to the seat is then transferred diagonally to the opposite side of the seat through the inclined cross-reinforce member which is located at the back of the seat and connects the two sides of the seat frames to secure a higher level of structural integrity of the whole seat frame (Figure2). It also enables more space between the pelvis of the occupant and the inner door panel for proper deployment of lower chamber of the side air bag to have a better coverage of the whole pelvis as shown in Figure3(a, b).

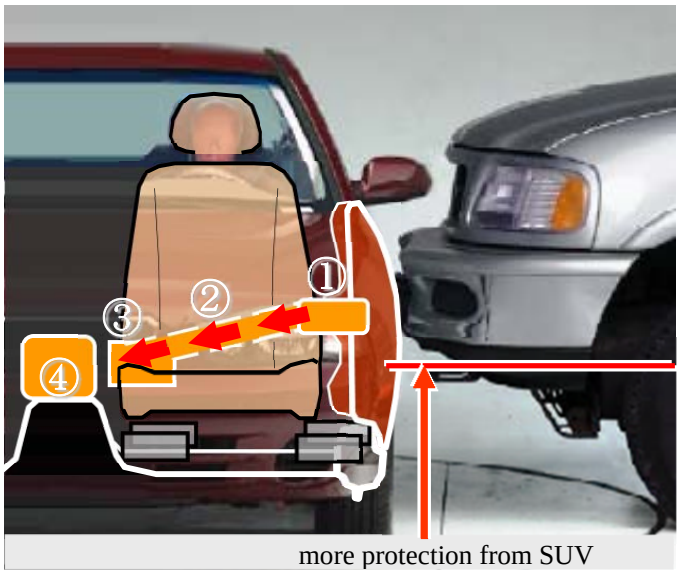


***Figure1. Basic concept of High Efficiency Load Path Structure (HELPS).***

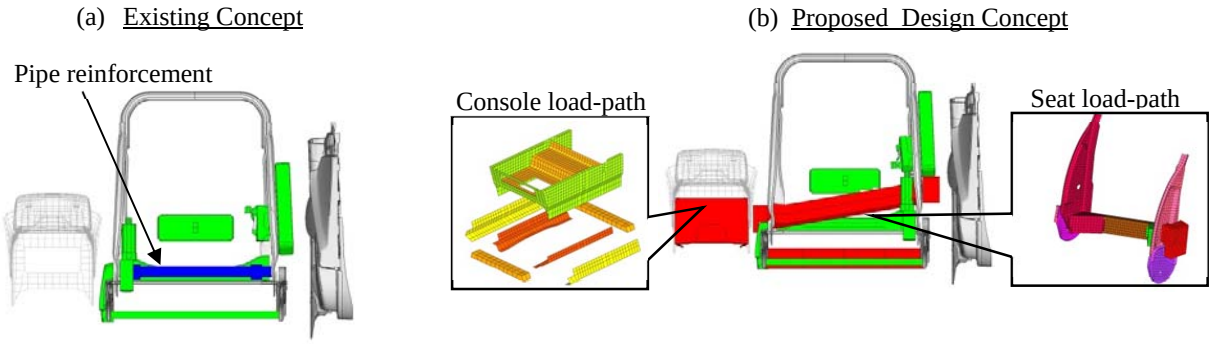


***Figure2. FEM model of the initial concept design level. (a) Existing system (b) Proposed design concept.***

As shown in Figure2, an initial design concept was made and consequently the safety performance was evaluated with help of a detail FEM model to study the feasibility of the concept in full vehicle side impact crash simulations for IIHS and SINCAP test conditions. With more deployment space for the inflating side airbag, it can absorb more input energy of the incoming deformed door as shown in Figure3. Consequently it becomes easier to decide the crash performance specification of door trims for better energy management. The inner contact element comes in contact with the center console which is properly reinforced to evenly distribute the load to over a large area of the vehicle floor and the propeller shaft tunnel.

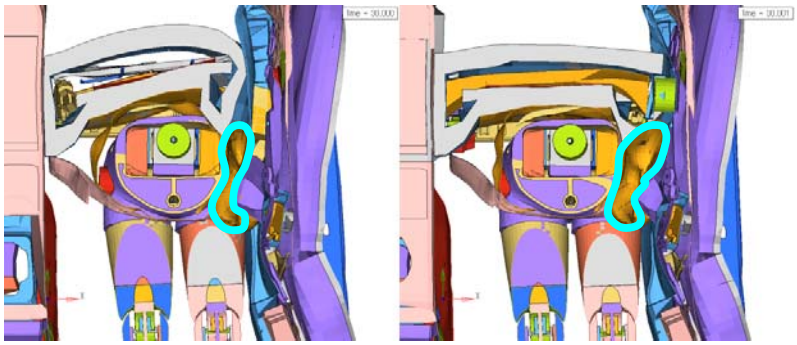

(a) without HELPS concept (30msec) (b) with HELPS concept (30msec)

***Figure3. Comparison of cross-sectional views of side airbag during deployment phase at abdomen level.***

There are other advantages of this concept, such as, better and more flexible design layout of door pockets.

## RESULTS OF INITIAL DESIGN CONCEPT

Figure4 shows the comparison of cross sectional views of the deformation patterns with von-misses stress distribution for (a) without-HELPS concept and (b) with-HELPS concept in IIHS side impact test conditions. It is very clear that a large amount of force can be transferred from the body side to the center console through the inclined seat reinforcement structure which absorbs some amount of external input energy. It also constraints the amount of total intrusion of the B-pillar and door with respect to the center line of the vehicle denoted by arrows.

(a) without HELPS concept (b) with HELPS concept

***Figure4. Comparison of deformation and stress at B-pillar, door and seat in full vehicle simulations.***

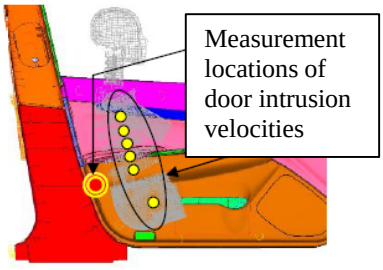


***Figure5. Location of evaluation points on interior door trim at different heights of ES2 dummy.***

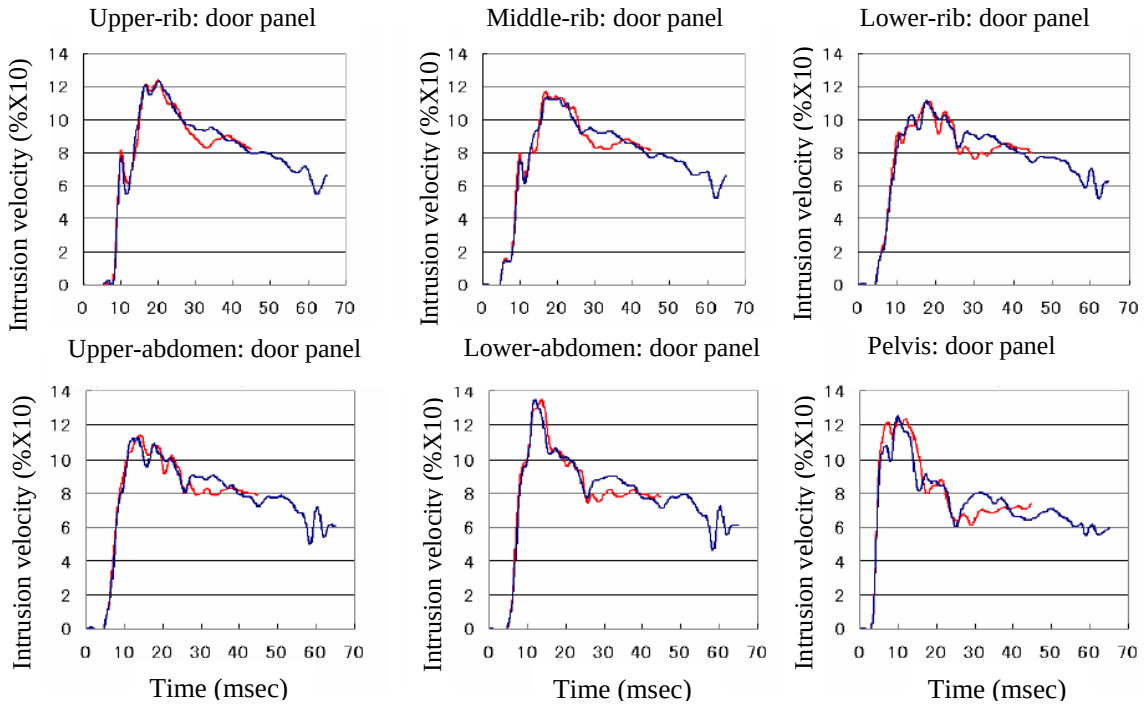


***Figure6. Comparison of door intrusion velocities of interior door trim corresponding to different locations of ES2 dummy. (blue line: without HELPS concept and red line: with HELPS concept).***

Figure6 shows the comparison of door intrusion velocities corresponding to different locations on the dummy as indicated by yellow circles in Figure5. After 25msec, the intrusion velocities dropped due to the load transfer from the body side to the center console through the inclined reinforcement structure of the seat. It is also effective in reducing the cumulative impact load on the dummy at the later phase of the structural deformation of the B-pillar intruding inside the vehicle compartment. The rib displacement will be reduced by 3 to 4 mm or more depending on the level and position of reinforcement. In this specific CAE result, the effect of outer contact element is omitted. Inclusion of outer contact element will make the starting time of the reduction of intrusion velocity a little earlier than 25msec and it will also change the initial phase of velocity profile before 25msec. Refer to the comparison of intrusion velocity time history plot (base vs final prototype) of a physical test as shown in Figure8.

**RESULTS OF FINAL DESIGN CONCEPT**

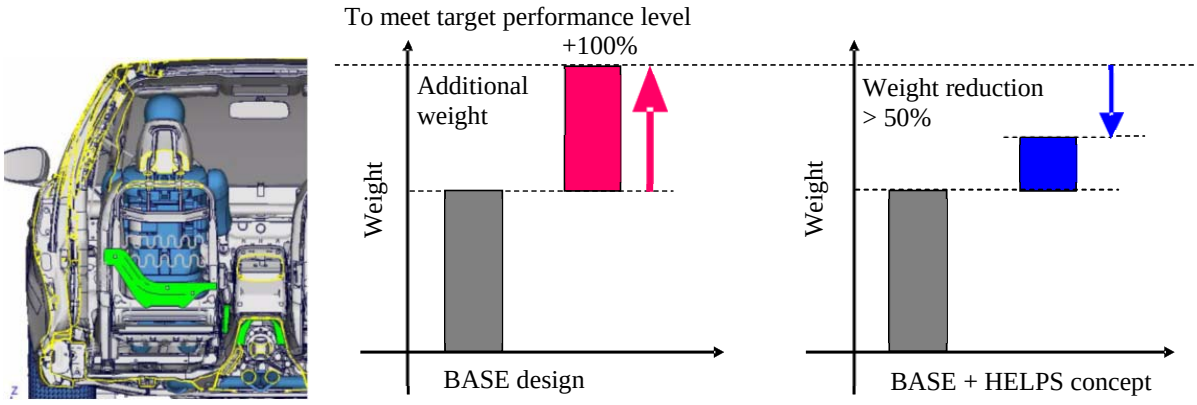


***(a) Final prototype*** ***(b) Performace chart to meet target safety performace.***

***Figure7. Final concept and weight reduction chart to meet required target performance.***

Figure7 indicates a considerable amount of reduction in weight due to increased structural integrity of the system in which one will be able to reduce the maximum intrusion and also the intrusion velocity of the surrounding intruding structures at different heights starting from pelvis to chest level of the dummy as illustrated in the intrusion velocity diagram (Figure8) and the deformation pattern diagram (Figure9), respectively.

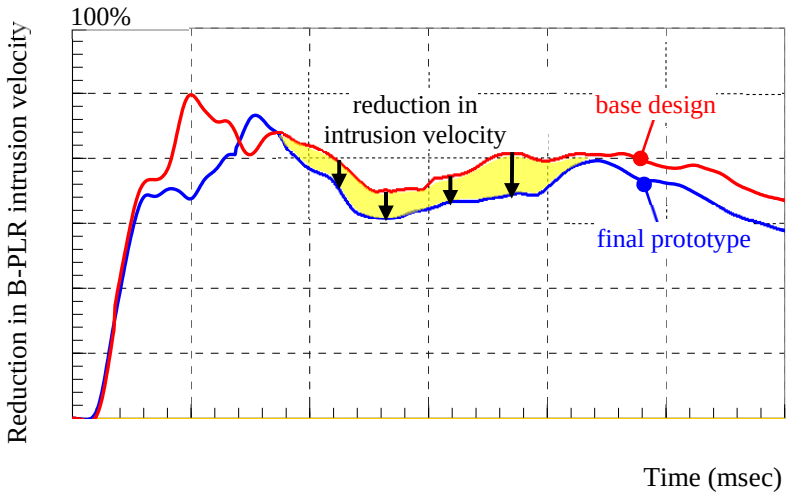


***Figure8. Maximum change in intrusion velocity of the surrounding structures around the occupant in physical test (red line: base design without HELPS and blue line: final prototype with HELPS concept).***

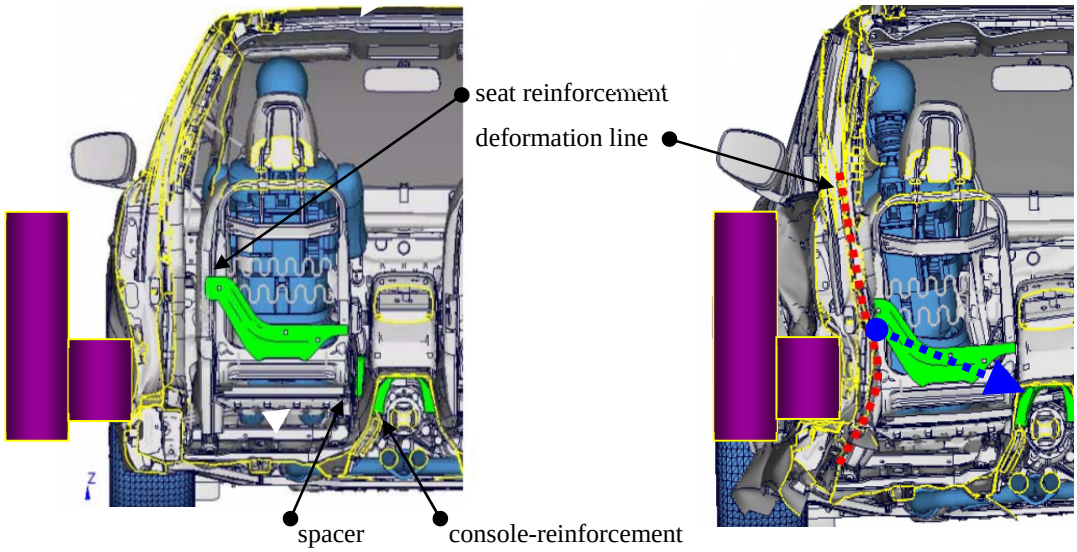


***Figure9. Deformation mode of the final prototype***

**RESULTS OF HBM SIMULATION**

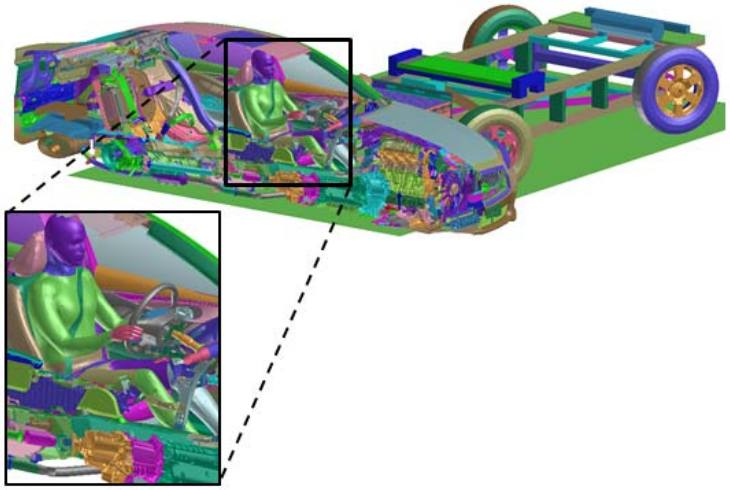

***Figure10. Full vehicle FE simulation with HBM.***

Figure10 shows a typical FE simulation set-up of a human body model (HBM: GHBMC, AM50 model, [8]) in SINCAP condition. By this simulation, a comparative study was carried out (i) with HELPS and (ii) without HELPS concepts to estimate the efficacy of the proposed system in real world. Comparison of (i) and (ii) was carried out on the amount of plastic strain distribution of chest rib and lower leg bones (pelvis and femur regions). The quantity of plastic strained regions across different bones was used as a comparative estimate for studying injury pattern. Bones will sustain plastic strain until a certain limit without failure and beyond certain threshold value of plastic strain, fracture will be initiated. Hence, a threshold of T* (T*=one-tenth of GHBMC reference value for fracture) was assigned for plastic strain and the total volume of elements crossing the threshold was calculated. By comparing the volumes of threshold elements across different bones, the injury pattern was estimated. The percentages of plastic strain>T* in chest ribs, pelvis and femur bones are shown in Figure11a,b. Detail of this plastic strain estimation method can be found in reference [1] where a detail description was given in female pedestrian human FE model development and its validation procedure based on PCDS pedestrian accident database combined with detail FE simulations.

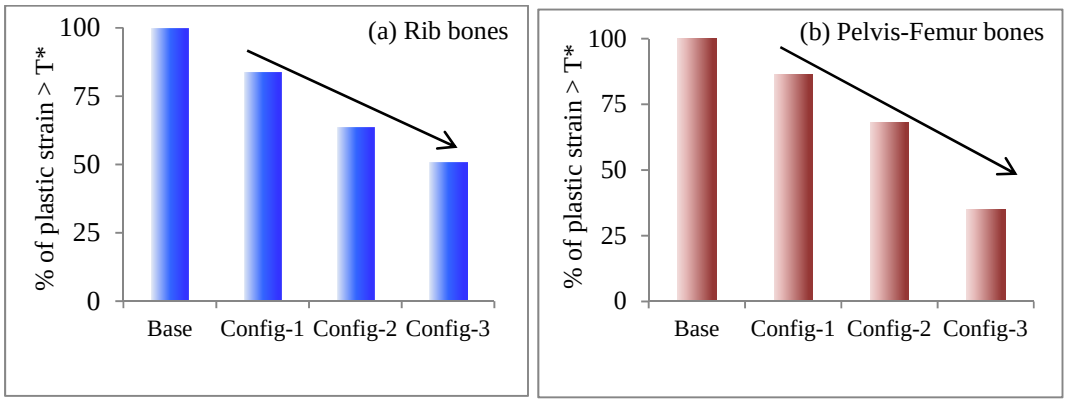


***Figure11. Comparison of relative plastic strain in bones for AM50 driver HBM simulation (Base: without HELPS; with HELPS in three different design configurations (i) Config-1: -0.3m.sec, (ii) Config-2: -0.6m/sec and (iii) Config-3: -1.0m/sec average reduction of intrusion velocities)***

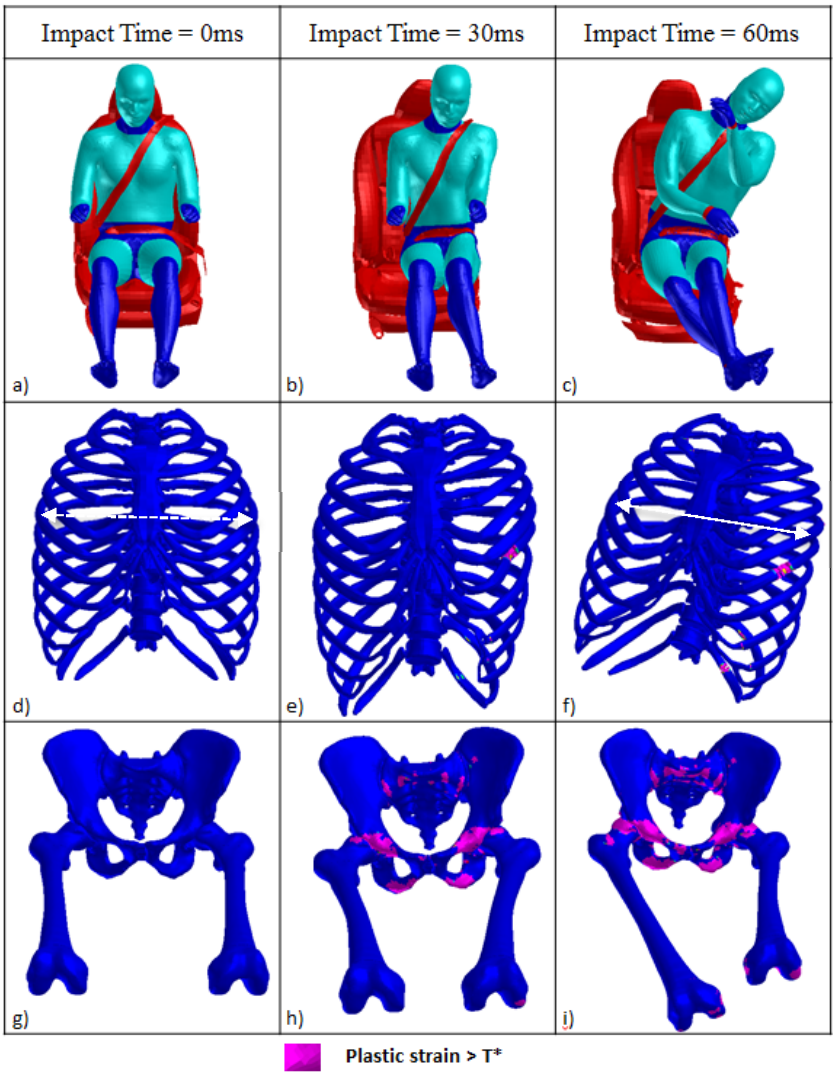


***Figure12. Kinematics of AM50 driver occupant (HBM) and plastic strain distribution of bones with a plastic strain threshold T* (T*= 1/10th of GHBMC reference value for bone fracture criteria)***

Figure11 shows the degree of effectiveness of the HELPS system based on the above mentioned plastic strain criterion of the bones with various levels of HELPS reinforcements related to (a) base design without HELPS concept, (b) low level of reinforcement with an average reduction of intrusion velocity of 0.3m/sec and (c) medium level of reinforcement with an average reduction of intrusion velocity of 0.6m/sec and (d) high level of reinforcement with an average reduction of intrusion velocity of 1.0m/sec. The higher is the level of reinforcement, the more is the effectiveness to reduce occupant injury, especially at the abdomen level of the dummy corresponding to the lower most ribs of the thorax of the human model. In case of human, unlike the upper and middle ribs which form a closed ring structure, the last few ribs are open and not connected to the sternum.

Figure12(a,b,c) show the occupant kinematics at 0msec, 30msec and 60msec. The level plastic strain of the chest ribs (Figure12d,e,f) and the lower leg region (pelvis and femur, Figure12g,h,i) are shown in second and third rows, respectively. It is clear that the amount of plastic strain volume of bones in the ribs and the lower leg regions are increasing with the increase of external load and deformation from the start 0msec to the end 60msec.

Figure13 shows the degree of effectiveness of the proposed system in reducing the thorax rib displacements corresponding to various levels of reinforcements of the HELPS concept with respect to the base design in (a)

base design without HELPS concept having no reduction of intrusion velocity, (b) lower level of reinforcement with an average reduction of intrusion velocity of -0.3m/sec, (c) medium level of reinforcement with an average reduction of intrusion velocity of -0.6m/sec and (d) high level of reinforcement with an average reduction of intrusion velocity of -1.0m/sec. It is clear that the amount of rib displacement starts decreasing with the increase of reinforcement level in HELPS concept. The rib displacement at each individual rib is the deformation measured between the outermost points of the left and right side of the corresponding rib. They are indicated by two white lines (i) dotted line (initial state) and (ii) solid line (deformed state) at the 5$^{th}$ rib from top as shown in Figure12d and Figure12f, respectively. Maximum amount of reductions in rib deflections occurred around the ribs 8-12. These three ribs (8, 9, and 10) are located at the similar position and height of the lower chest rib of ES2 dummy. There were also reductions in rib displacements in rib 11 and rib 12 which correspond to the abdomen region of a side impact dummy. Similar trends in injury reduction were also observed in ES2 dummy response of actual vehicle tests.

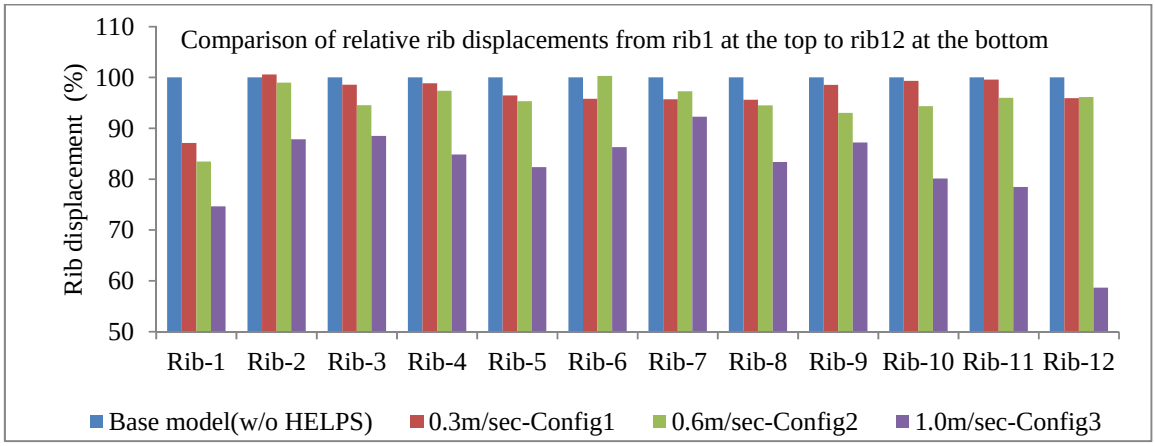


***Figure13. Comparison of relative rib displacements for AM50 driver HBM simulation (Base: without HELPS; in three different design configurations Config-1: -0.3m.sec, Config-2: -0.6m/sec and Config-3: -1.0m/sec average reduction of intrusion velocities)***

## CONCLUSIONS

The following are the main conclusions of this study.

A new concept of side impact occupant protection system is proposed by using the concept of a high efficiency load path system (HELPS) which consists of a combination of reinforced seat, center console and floor-tunnel structure. The system consists of four main elements: 1) an outer contact element, 2) an inclined and curved seatback cross-reinforce member, 3) an inner contact element and 4) a strong center console.

A two-step design development approach was performed to evaluate the feasibility of the present system. The first step is the basic feasibility study phase of the proposed concept to estimate the benefits based on safety performance requirements using extensive CAE simulations. The second step is the final prototype design phase by CAE together with verifications of safety performance in actual crash tests. All the necessary design constraints to meet other functional requirements, such as, seating comfort, minimum leg room space and size of the center console box etc. were also taken into account in determining the final design specifications.

Apart from the verification of the effectiveness of the proposed system using side impact dummy ES2, the human body model (GHBMC, AM50 occupant) was also used to estimate its effectiveness in real world accident. Similar to dummy response, the results of AM50 human model simulation also showed similar trend regarding the level of effectiveness of the system. Even though the numbers of simulation cases performed with HBM were very limited in number and related to certain specific test conditions, one can expect some benefits in real world accidents if HELPS concept is incorporated in conventional design.

The key essence of the present system HELPS is to effectively reduce the average intrusion velocity and the amount of intrusion of the deformed B-pillar, the surrounding door structures etc. to further decrease the level

of front seat occupant injuries in severe side impact crashes. However, the level of effective of this system will vary depending on the size, the category and the type of upper body structure of vehicles under consideration. Hence, to incorporate the proposed HELPS system in the existing vehicle design process, additional merits and demerits should be evaluated and judged carefully in order to get maximum benefits based on total vehicle system performance.

## REFERENCES


[1] C. Pal, et al, "Estimation of Pelvis Injuries and Head Impact Time using Different Pedestrian Human FE Models", SAE international conference, Paper Number 2014-01-0522, DOI: 10.4271/2014-01-0522 (2014).

[2] Helena Stigson, et al, "Effect of Side Impact Protection in Reducing Injuries", 22nd ESV, Paper No.11-0319.

[3] Hideki Yonezawa, et al, "Investigation for New Side Impact Test Procedures in Japan", 21st ESV, Paper Number 09-0369 (2009).

[4] Laberge-Nadeau, et al, "Occupant injury severity from lateral collisions: a literature review", Journal of Safety Research, 40, 427-35, 2009.

[5] Mark Scarboro et al, "Nearside Occupants in Low Delta-V Side Impact Crashes: Analysis of Injury and Vehicle Damage Patterns", 20th ESV, Paper Number 07-0225 (2007).

[6] Newland C., et al, "International Harmonized Research Activities Side Impact Working Group Status Report" 19th ESV, Paper Number 05-0460 (2005).

[7] Seyer K., et al, "International Harmonized Research Activities Side Impact Working Group Status report," 18th ESV, Paper Number 579 (2003).

[8] Updated version of GHBMC human FE model, 2012 release.


## GLOSSARY

AM50: 50th percentile American male

ES2: Side impact dummy; the next generation of the EuroSID1 dummy

GHBMC: Global Human Body Model Consortium

HBM: Human Body Model

HELPS: High Efficiency Load Path System

PCDS: Pedestrian Crash Data Study

SINCAP: Side Impact New Car Assessment Program (US motor vehicle safety standard)

IIHS: Insurance Institute for Highway Safety

## ACKNOWLEDGMENTS


The authors would like to acknowledge the support group of ESI Japan for PAM-CRASH and the members of GHBMC for the development of the 50th-%ile adult FE HBM.

# IMPROVEMENT OF THE PROTECTION OF LOWER EXTREMITIES OF VULNERABLE ROAD USERS IN THE EVENT OF A COLLISION WITH MOTOR VEHICLES

**Oliver Zander**
**Marcus Wisch**
Federal Highway Research Institute (BASt)
Germany

**Dirk-Uwe Gehring**
BGS Boehme & Gehring GmbH
Germany

Paper Number 15-0366

## ABSTRACT

Since the beginning of the testing activities related to passive pedestrian safety, the width of the test area being assessed regarding its protection level for the lower extremities of vulnerable road users has been determined by geometrical measurements at the outer contour of the vehicle. During the past years, the trend of a decreased width of the lower extremity test and assessment area realized by special features of the outer vehicle frontend design could be observed. This study discusses different possibilities for counteracting this development and thus finding a robust definition for this area including all structures with high injury risk for the lower extremities of vulnerable road users in the event of a collision with a motor vehicle.

While Euro NCAP[1] is addressing the described problem by defining a test area under consideration of the stiff structures underneath the bumper fascia, a detailed study was carried out on behalf of the European Commission, aiming at a robust, world wide harmonized definition of the bumper test area for legislation, taking into account the specific requirements of different certification procedures of the contracting parties of the UN/ECE[2] agreements from 1958[3] and 1998[4].

This paper details the work undertaken by BASt, also serving as a contribution to the TF-BTA[5] of the UN/ECE GRSP[6], towards a harmonized test area in order to better protect the lower extremities of vulnerable road users. The German In-Depth Accident Database GIDAS is studied with respect to the potential benefit of a revised test area. Several practical options are discussed and applied to actual vehicles, investigating the differences and possible effects. Tests are carried out and the results studied in detail. Finally, a proposal for a feasible definition is given and a suggestion is made for solving possible open issues at angled surfaces due to rotation of the impactor.

The study shows that, in principle, there is a need for the entire vehicle width being assessed with regard to the protection potential for lower extremities of vulnerable road users. It gives evidence on the necessity for a robust definition of the lower extremity test area including stiff and thus injurious structures at the vehicle frontend, especially underneath the bumper fascia.

The legal definition of the lower extremity test area will shortly be almost harmonized with the robust Euro NCAP requirements, as already endorsed by GRSP, taking into account injurious structures and thus contributing to the enhanced protection of vulnerable road users.

---

[1] Euro NCAP: European New Car Assessment Programme
[2] UN/ECE: United Nations Economic Commission for Europe
[3] Agreement concerning the adoption of uniform technical prescriptions for wheeled vehicles, equipment and parts which can be fitted and/or be used on wheeled vehicles and the conditions for reciprocal recognition of approvals granted on the basis of these prescriptions
[4] Agreement concerning the establishing of global technical regulations for wheeled vehicles, equipment and parts which can be fitted and/or be used on wheeled vehicles
[5] TF-BTA: Task Force Bumper Test Area
[6] GRSP: Working Party on Passive Safety

After finalization of the development of a torso mass for the flexible pedestrian legform impactor (FlexPLI) it is recommended to consider again the additional benefit of assessing the entire vehicle width.

## INTRODUCTION

Since the year 2000, the Japan Automobile Research Institute (JARI) has been developing a new flexible pedestrian legform impactor (FlexPLI) with the purpose of properly assessing the protection potential of vehicle frontends in terms of passive pedestrian safety. From the year 2005 on a Technical Evaluation Group[7] had evaluated the impactor towards introduction within legislation related to pedestrian safety. Subsequently, since 2011 an Informal Group[8] of the Working Party on Passive Safety has been working on a framework and the preconditions for including the flexible pedestrian legform impactor within the global technical regulation on pedestrian safety (GTR No. 9) as well as the UN regulation on pedestrian safety (UN-R 127). The impactor with humanlike kinematic behaviour and biofidelic human responses in the knee and the tibia area has been found ready for legislation by working party 29[9] of UN/ECE. Subsequently, the FlexPLI has been introduced within the 01 series of amendments of UN-R127 (UN/ECE, 2015). Due to an amendment of framework Directive 2007/46/EC of the European Parliament and of the Council (European Union, 2007), pedestrian protection requirements for the purpose of european type approval can be either tested according to Regulation (EC) No. 78/2009 in conjunction with Commission Regulation (EC) No. 631/2009 (European Union, 2009) or according to UN-R 127 in conjunction with UN-R 13H, latter one ruling the type approval provisions of passenger cars with regard to braking. Therefore, since 22 January 2015 and during a transitional period that lasts until 1 September 2017 all new vehicles to be type approved according to UN-R127 can be subjected to tests with the FlexPLI instead of the lower legform impactor according to EEVC[10] (UN/ECE, 2015). After the expiration of this transition period the FlexPLI is to be used mandatorily for type approval tests according to UN-R 127.

In parallel to the work performed by the Informal Group, the Task Force Bumper Test Area, chaired by the European Commission, was established under the umbrella of the Informal Group. Aim of this Task Force was to re-define the bumper area that is subjected to tests with the lower legform impactor according to UN-GTR 9 or UN-R 127 respectively, in order to avoid small bumper test areas that prevent large zones of the bumper from being tested, and to counteract some manufacturer's practice of downsizing the width by design means of the outer vehicle contour.

This paper details the investigations performed by the Task Force and in particular the contributions of BASt that finally led to the proposal for the supplement 1 of the 01 series of amendments to UN-R 127 (UN/ECE, 2014) that was endorsed by GRSP at its December 2014 session.

In case of angled test areas a rotation of the lower legform impactor may occur which is, to some extent, not always coincident with the behavior of the human leg, possibly leading to unrealistic test results. In order to limit this possible rotation a pedestrian torso mass may be applied to the lower legform impactor. However, the ongoing validation of the torso mass still needs to be finalized, including tests to a broad variety of vehicle frontend designs.

## PROBLEMS RELATED TO UN-GTR9 (PHASE 1) AND UN-R 127 (00)

The UN Regulation on pedestrian safety as transposition of the Global Technical Regulation No. 9 into national legislation entered into force in November 2012 (UN/ECE, 2013). The Regulation defines performance requirements for passenger cars with regard to the protection potential of their frontends when subjected to impactor tests with the adult and child headform impactors against the bonnet and the upper or lower legform impactor against the bumper fascia.

[7] Flex-TEG: Flexible Pedestrian Legform Impactor Technical Evaluation Group
[8] IG GTR9-PH2: Informal Group on phase 2 of GTR No. 9
[9] WP.29: Working Party 29 / World Forum for Harmonization of Vehicle Regulations
[10] EEVC: European Enhanced Vehicle-safety Committee

The test area defined for the legform to bumper test is described by the part of the bumper fascia that is limited by two points 66 mm laterally inboard of the corners of bumper, see Figure 1a. The corners of bumper are defined as the vehicle's points of contact with a vertical plane making an angle of 60 degrees with the vehicle vertical longitudinal centerplane.

In the past years, the application of specific vehicle design features resulted in a limitation of the bumper test area defined by legislation, as can be seen in Figure 1b. It is obvious that the definition of the corner of bumper which in the end defines the bumper test area rather depends on the outer contour of the vehicle than on the underlying hard structure that is responsible for the ocurrence of lower leg injuries that should be mitigated by fulfilling the requirements described in the Regulation.

***Figures 1a (left) and b (middle and right). Bumper test area according to GTR9 / UN-R 127 and its limitation by design means.***

To counteract the phenomenon of misrepresenting the bumper test area by means of the current procedure, based on the outer vehicle design, the task force bumper test area elaborated different options for an appropriate revision that will be described in the following.

## EURO NCAP MARKUP PROCEDURE

The problem of defining the bumper test area using vertical contact planes was already recognized by the technical working group of the European New Car Assessment Programme (Euro NCAP) in 2008. Until version 4.2 of the pedestrian testing protocol the width of the bumper test area was, also in line with the european legislation, in principle limited by the corners of bumper. Only in case of potentially injurious structures outboard of the described area Euro NCAP reserved the right of performing tests to those structures (Euro NCAP, 2008). However, an assessment of the results was not explicitly foreseen. An ad hoc group of Euro NCAP discussed the problems related to this procedure and concluded that, in principle, injurious structures outboard the corners of bumper shall be tested and the results shall be used for the final vehicle assessment. Additionally, the minimum distance requirements of 66 mm from the corners of bumper to define the bumper test area were removed from the protocol from its version 4.3 onwards (Euro NCAP, 2009). The bumper test area was then defined as the area limited by the corners of bumper or the outermost ends of the bumper beam/lower rails/cross beam structures, whichever area was wider. Figure 2a illustrates the markup of the bumper test area that was further divided into thirds, each of them subdivided into halves, until the end of 2013. As from 2014 onwards, along with the introduction of the FlexPLI, a homogeneous grid markup procedure for the legform area was introduced. However, the width of the test area basically remained unchanged. Additionally, since the introduction of the grid markup, in case of the distance between the outermost grid points and the end of the test area being greater than 50 mm, an additional grid point is to be marked at a lateral distance of 50 mm to the last grid point onto the upper bumper reference line. One example for the current Euro NCAP lower legform markup is depicted in Figure 2b.

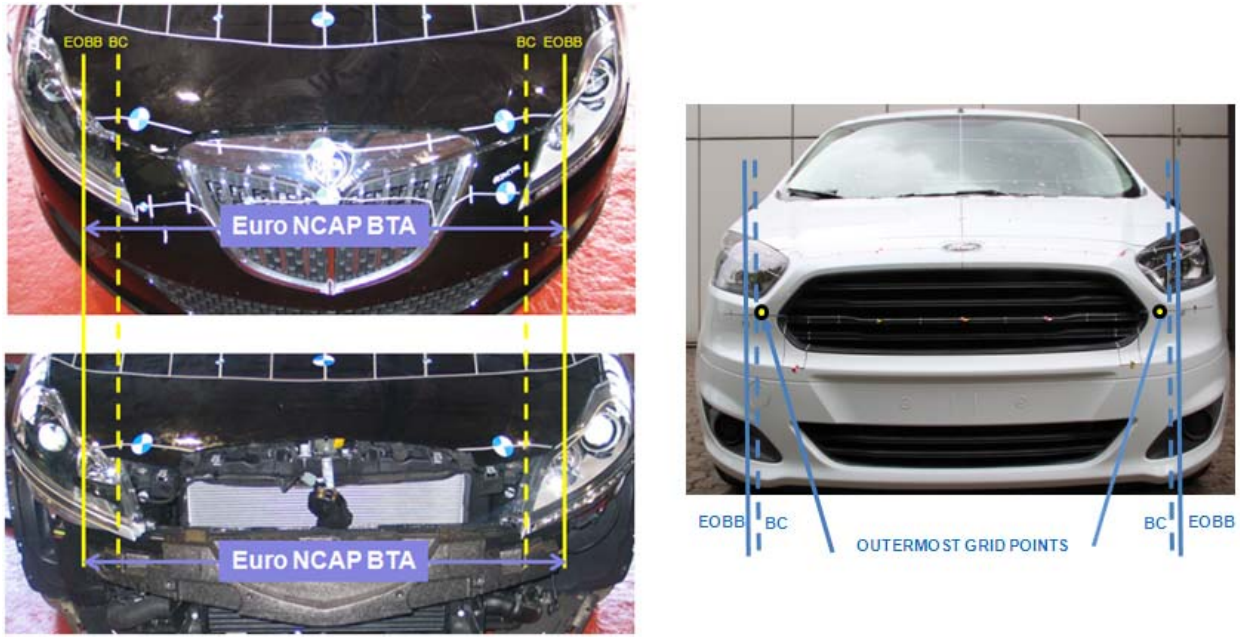


***Figures 2a (left) and b (right). Euro NCAP worst point and grid markup.***

**USE OF WHOLE VEHICLE WIDTH**

Already during the discussions within the Euro NCAP ad hoc working group, BASt brought up a proposal to modify the bumper test area in a way that, in principle, the possibility is given to test, where appropriate, the entire width of the vehicle frontend. At that point in time, passenger cars were still tested according to the principle of worst point selection. Therefore, despite the provisions changed according to protocol version 4.3, the selection procedure of injurious points outside the bumper corners remained unclear. It was not further defined how far outboard a point was allowed to be selected; furthermore, no advice was given which point finally to be selected in case of the outermost point being equally but not more injurious as the remaining points. Also, the assessment procedure in case of selecting impact points outside the corners of bumper was not yet further specified, e.g. whether these points to be additionally assessed or to replace adjacent points, whether manufacturers were given the option to additionally nominate the adjacent sixths or whether the maximum number of points would increase. BASt concluded that an extension of the test area using the entire vehicle width (without mirrors) while sustaining the remaining markup procedure would be the most pragmatic way forward. The proposal would give Euro NCAP the possibility of testing, where appropriate, outside a test area described by the outer vehicle contour without further essential changes to the test and assessment procedure. However, it was also suggested that in cases where the tangential vertical plane making an angle of less than 60 degrees to the vehicle longitudinal centerplane a test could possibly lead to unrealistic test results due to a high rotation around the yaw axis and the physical limitations of the impactor.

In the course of the work performed by the TF-BTA, the description of the bumper test area based on the entire width of the vehicle was examined again in detail by Zander et al (2014).

**Accident data**

Passenger car to pedestrian accidents with maximum two parties involved were the starting point for a study of German in-depth road accident data from the years 2000 until 2012 using GIDAS. The study focused on accidents with pedestrian impact locations between the most forward vehicle part and 20 percent of the total vehicle length rearward under consideration of injury causing vehicle parts being located on the vehicle frontend only, i.e. bumpers, grilles, headlamps, front spoilers, license plates and indicators. In total, 567 cases were found fulfilling the given prerequisites, with an equal distribution of first pedestrian contact along the passenger car front in crashes with at least one injury suffered from contact with a part of the vehicle frontend, as depicted in Figure 3:

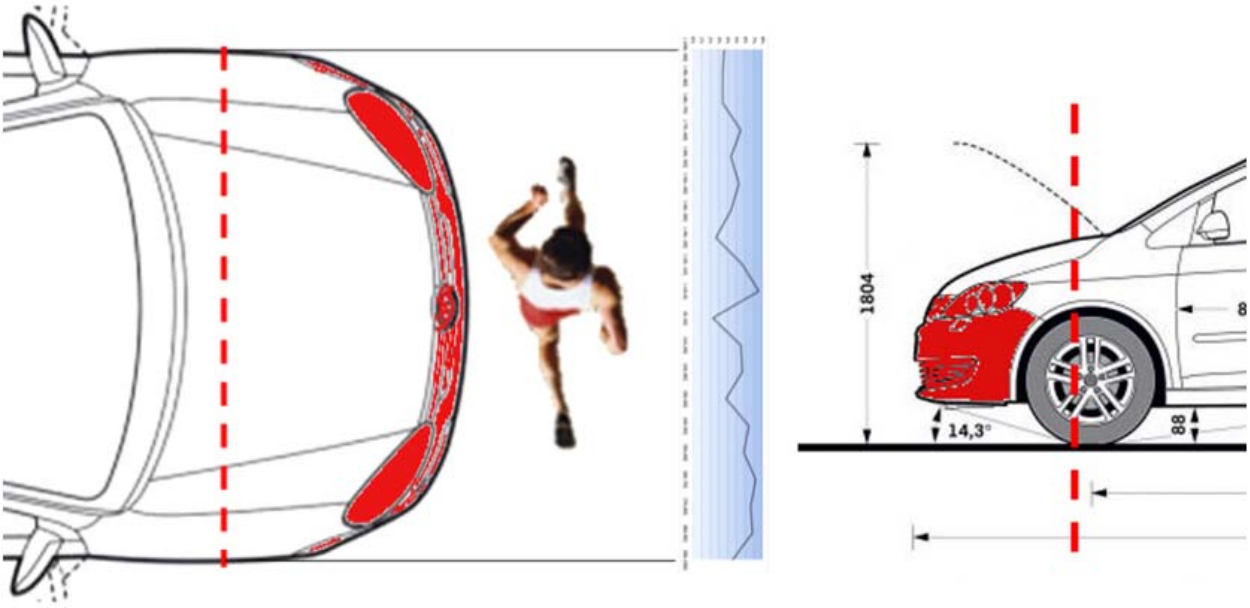


***Figure 3. Passenger car to pedestrian impact distribution (2000-2012) extracted from GIDAS database.***

Altogether, the study gives no indication for neglecting outboard areas of passenger cars being less impacted by pedestrians during accidents.

**Test data**

Besides the impact distribution in real world accidents, the significance of the impacted areas in terms of injury causation was examined in more detail. Within the Euro NCAP test programme, injurious points, reflected by impactor readings beyond the limits for the introduced injury criteria, have been continously found outside the test area described by the corners of bumper. It was thus concluded that the area to be considered should include all injurious structures underneath the bumper cover which are in most cases not indicated by the outer design. Therefore, a consideration of those structures, e.g. by dismantling of the fascia was found indispensable for a detection of hard structures.

Furthermore, a comparative test that was conducted outside the corners of bumper was examined with respect to the validity of the kinematics, see Figure 4. High speed film analysis revealed that until the timing of maximum readings the kinematic behaviour was comparable to the one during the baseline test on a location inside the corners of bumper.

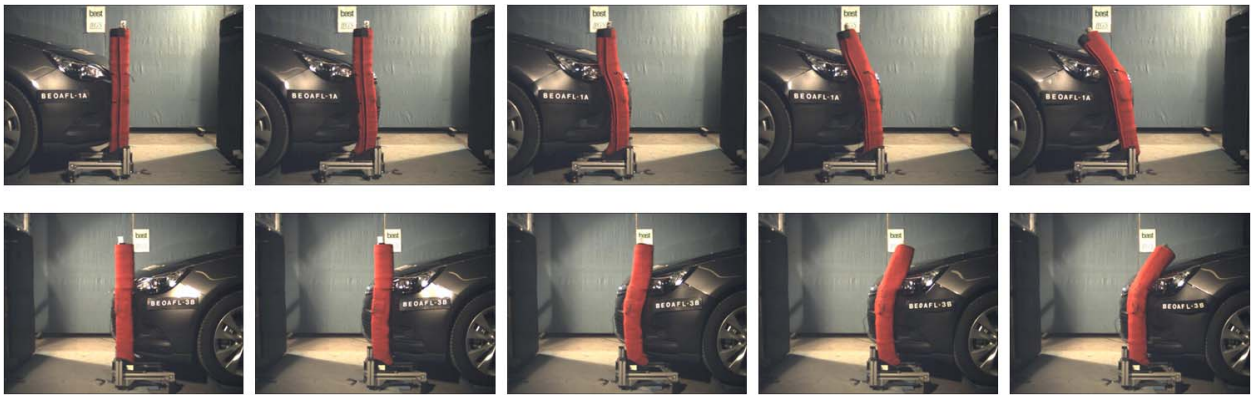

***Figure 4. FlexPLI kinematics during biofidelic impact phase inside (above) and outside (below) corners of bumper.***

## MODIFICATION OF DEFINITION OF CORNERS OF BUMPER

Apart from assessing the entire vehicle width by testing injurious structures of the vehicle frontend, TF-BTA discussed possibilities for modifying the corners of bumper definition.

The first option investigated was related to changing the angle between the vertical tangential planes and the vehicle vertical longitudinal centerplane from 60 to 45 degrees and thus enlarging the test area to a certain extent. This option that was investigated in detail within a study on behalf of the European Commission by Carroll et al. (2014) was already brought forward by the Transport Research Laboratory TRL during their studies for the Working Group on Pedestrian Safety (WG 17) of the European Enhanced Vehicle-Safety Committee in 2002. At that point in time, the proposal was justified with actual vehicles partly having very small bumper test widths, just between the inner ends of the headlights. It was noted that the performance of the legform at impact points with these tangential surface angles could be limited due to spinning of the impactor; however, the legform was expected to still be able to indicate particularly dangerous structures. Not testing these areas would open the door for putting bumper supports, longitudinal members or other hard structures in a non-evaluated area. (TRL, 2002)

The second option was evolved from the current corner of bumper definition described in US bumper standard 49 CFR part 581 (NHTSA, 2011). Instead of a vertical plane, a vertical corner gauge with the dimensions of the face of the impact device as described in part 581, making an angle of 60 degrees to the vehicle vertical longitudinal centerplane, is contacting the vehicle frontend with its vertical centerline while its horizontal centerline is moved between heights of 75 mm and 1003 mm above ground level, representing the lower and upper end of the FlexPLI during an impact, but not falling below the lower bumper reference line and not exceeding the upper bumper reference line. The outermost contact point between the corner gauge and the fascia is then defining the corner of bumper. In the end, the test area is limited by the corners of bumper minus a lateral distance of 42 mm on both sides of the car, taking into account half of the width of the FlexPLI femur and tibia section. This distance requirement was meant to avoid as far as possible any rotation or sliding of the impactor possibly leading to unrealistic test results during an impact against angled surfaces.

In a final stage, the second option was further modified, changing the original corner gauge dimensions to a 236 mm * 236 mm square.

BASt investigated the consequences in case of modifying the markup procedure by just using the corners of bumper defined by the modified corner gauges. When checking the robustness of the procedure against any changes in the outer contour, BASt found that by simple design features the test area could still be narrowed in future design concepts, as illustrated in Figure 5:

***Figure 5. Corner point due to gauge contact with daytime running light intake.***

Although the example given shows a comparatively small difference between the definition using the end of the bumper beam and the corner of bumper (12 mm plus 42 mm as distance requirement on each side), this design exemplarily demonstrates that in case of an inboard movement of the intake for the daytime running lights (DRL) the width of the test area could be easily minimized significantly. BASt concluded again the indispensability of defining the bumper test area using the underlying injurious structures. In a first step, addressing nowadays vehicle frontends, it seems reasonable to define the test area using the width of the bumper beam. A robust definition of the bumper beam is given by the Research Council for Automobile Repairs (RCAR). In the RCAR bumper test procedures it is described as the structural cross member under the bumper fascia protecting the front or rear of the vehicle, not including foam, cover support or pedestrian protection devices. The bumper beam width is to be measured from the outermost left to the outermost right section of the bumper beam, but only taking into account outer ends meeting the qualifying bumper beam heights. Latter ones are to be measured from a vertical plane contacting the beam up to a distance of 10 mm in direction of the profile (RCAR, 2010):

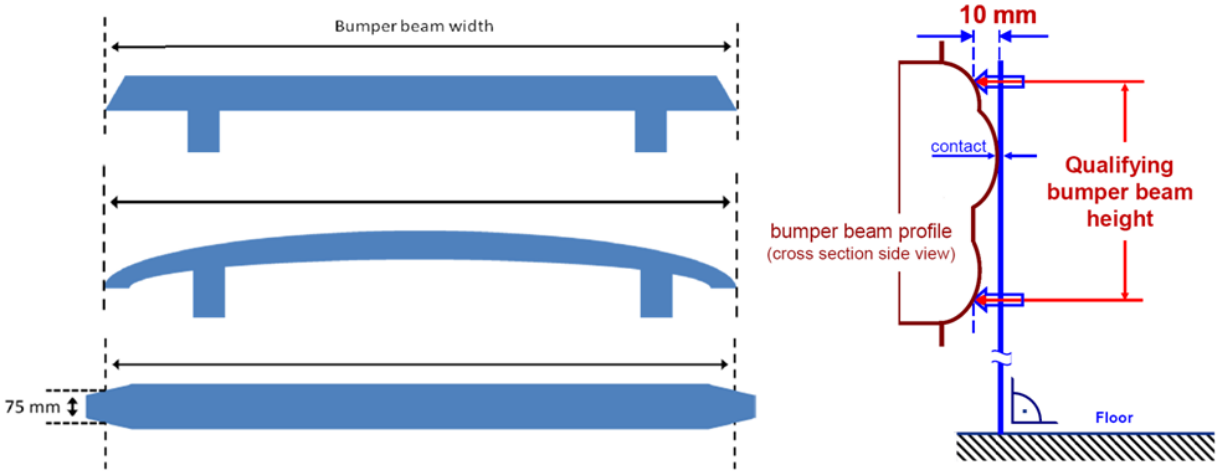


***Figure 6. Definition of the bumper beam width (RCAR, 2010).***

## COMBINATION OF MARKUP REQUIREMENTS

BASt examined the test areas resulting from the different markup procedures and compared them with the markup according to GTR9 (Phase 1) or UN-R 127 (00) respectively. Figure 7 exemplarily illustrates the differences in width of test areas:

***Figure 7. Comparison of different markup procedures and resulting test area widths.***

The example given in Figure 7 results in the different markups having a range of 530 mm just between the corners of bumper defined by 45 degree planes and the GTR9 (Phase 1) / UN-R 127 (00) markup. The difference between the bumper beam width and the markup with corner gauges is still 159 mm.

The Task Force Bumper Test Area concluded its work in forwarding two different proposals to GRSP for an amendment of GTR9 (Phase 2) and a supplement of UN-R 127.01. The first proposal reflects, while keeping the angle between vertical tangential plane and vehicle vertical longitudinal centerplane unchanged, the idea of defining the bumper test area by a revision of the bumper of corner definition only, using vertical 236 mm * 236 mm corner gauges and laterally moving 42 mm inboard on both sides, see Figure 8. The second proposal adds to the corner gauge definition a second definition of the bumper test area described by the width of the bumper beam. The maximum of both definitions is then to be used to describe the bumper test area:

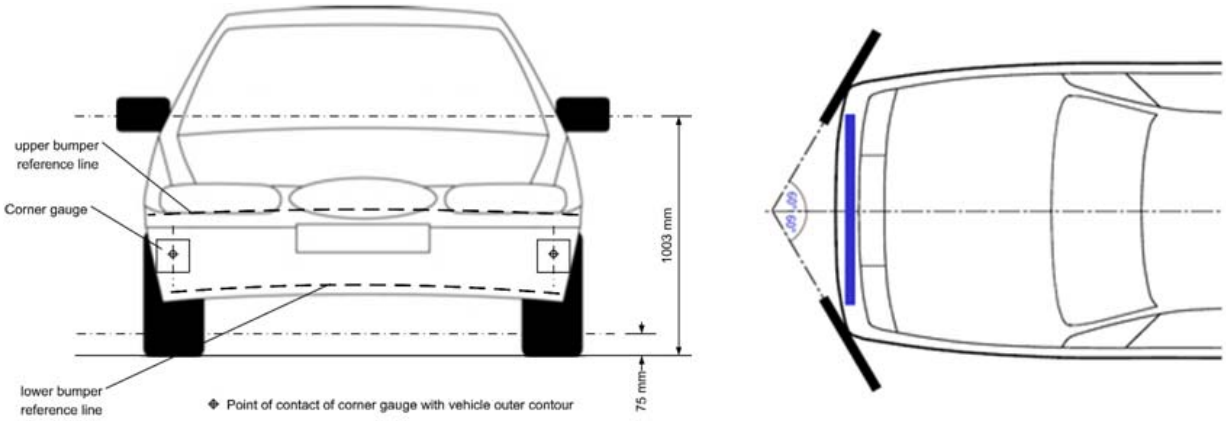


***Figure 8. Definition of bumper test area endorsed by GRSP in December 2014 (UN/ECE, 2014).***

It has to be noted that supplement 1 to the 01 series of amendments to UN-R127 relates to the FlexPLI only. Therefore, if tested in accordance with UN-R 127 in its original version, the tests conducted with the EEVC lower legform impactor will be limited to the bumper test area defined by the vertical 60 degree planes, whose contact points afterwards laterally moving 66 mm inboard on each side of the vehicle.

## OUTLOOK

Real world accident data has shown that pedestrians are generally impacted by locations along the entire vehicle width. Test results with the FlexPLI have proven that in many cases injurious impact locations occur outside the test area described by the corners of bumper. However, technical services need to take care of the fact that on angled surfaces a rotation of the impactor can lead to sometimes unrealistic test results. The rotation of the impactor that is not reflected to that extent by lower extremity rotation as seen in road traffic accidents, is expected to be compensated by the application of an upper body mass, representing the mass of the pedestrians' torso during an accident. An upper body mass for the FlexPLI has been developed within the European FP6 project APROSYS (Advanced PROtection SYStems) by Bovenkerk et al. (2009) and is being evaluated by Zander et al. (2011 and 2013). Subsequently, amongst other things, during the European FP 7 project AsPeCSS (Assessment methodologies for forward looking Integrated Pedestrian and further extension to Cyclist Safety Systems), BASt carried out comparative tests conducted with baseline FlexPLI and FlexPLI with applied UBM on angled vehicle frontend surfaces (Ferrer et al., 2014), see Figure 9:

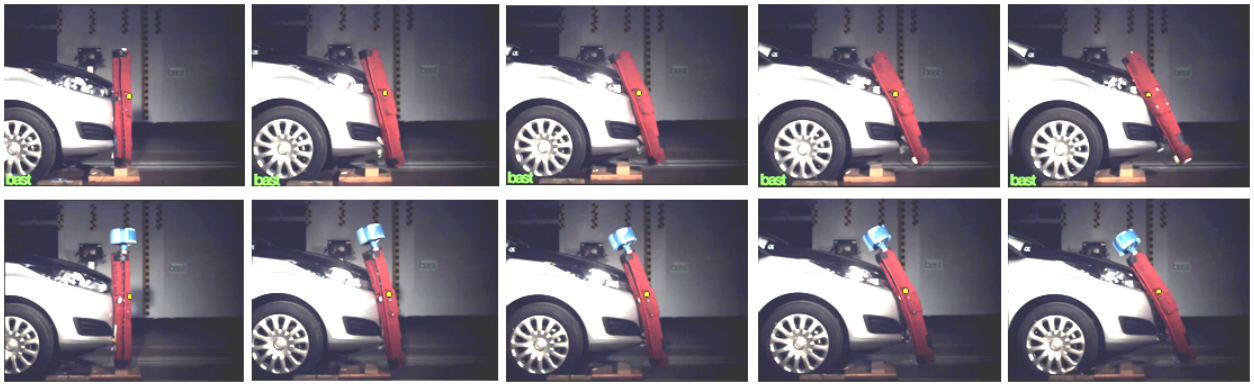

***Figure 9. Influence of applied upper body mass during impact on oblique surface.***

The depicted screenshots demonstrate that the application of an upper pedestrian mass can significantly reduce the rotation around its yaw axis as well as the sliding of the FlexPLI during impacts on angled areas, leading to an improved simulation of the lower extremity kinematics of a pedestrian. This observation can be underlined by the test results especially in the knee area:

**Table1.**
**Comparative test with Flex PLI baseline and with applied UBM on oblique surface.**

| y = 505 mm | **Impactor** | **Impact speed [m/s]** | **Tibia-1 BM [Nm]** | **Tibia-2 BM [Nm]** | **Tibia-3 BM [Nm]** | **Tibia-4 BM [Nm]** | **ACL-EL [mm]** | **PCL-EL [mm]** | **MCL-EL [mm]** |
|---|---|---|---|---|---|---|---|---|---|
| | FlexPLI | 9,58 | 111,5 | 79,8 | 132,8 | 86,0 | 2,5 | 6,5 | 10,8 |
| | FlexPLI-UBM | 9,69 | 206 | 154,4 | 136,9 | 65,0 | 7,1 | 7,1 | 22,1 |

## DISCUSSION

In depth accident data gives evidence of an equal distribution of first pedestrian contact at the front of passenger cars in crashes with at least one injury suffered from contact with a part of the vehicle frontend (Zander et al., 2014). For vehicles with market launch after 2006, a further study of the German In Depth Accident Data (GIDAS) showed an even distribution of the injury severities outside the current bumper test area while having a higher portion of uninjured or slightly injured pedestrians inside the current bumper test area. (Fries et al., 2014). Thus it can be concluded that vulnerable road user safety improvements are focused on the currently assessed areas. Also several stakeholders state the potentially injurious nature of hard structures outside the current bumper test area as defined in UN Regulation No. 127 and consequently confirm the need to assess the structural parts behind the bumper cover (Carroll et al., 2014).

During testing, injurious points have been continuously found outside test areas defined by measurements depending on the outer contour, especially at the ends of the bumper beam (Euro NCAP, 2012). Thus, the assessment of injury risks for vulnerable road users should basically consider the entire vehicle width. However, if a limitation of the test area is necessary, at least no potentially injurious structures should be prematurely excluded from the test area.

The contractor of the European Union states that it would be entirely reasonable to expect that vehicle front-end designs would react to any definition only related to the outer contour and in the future the bumper test area widths return to something similar as todays. Thus, it could be imagined that the same issue may occur again in several months or years (Carroll et al., 2014). The presented study already gives an example of an actual vehicle where outer design features could be easily used for downsizing the bumper test area, see Figure 5.

As procedures based on the outer vehicle contour do not necessarily include the relevant injurious vehicle structures (e.g. bumper beam), at least the entire bumper beam should be included within the test area.

It has been proven that the flexible pedestrian legform impactor works outside the current bumper test area as defined in UN Regulation No. 127, e.g. within the width of the bumper beam (Zander et al., 2014-2). A robust definition for the bumper beam is provided by RCAR (2010).

The above mentioned issues show that the use of the bumper beam for defining the BTA is inevitable.

The work undertaken within the TF-BTA resulted in different options on how to define the vehicle bumper area to be subjected to tests with the lower legform impactor. All options are basically following two different philosophies, either describing the test area by means of the outer vehicle contour or by elements of the underlying stiff structures. Starting from leaving the area as it is described within current legislation, the consequences of a modification of the angles between the tangential vertical planes and the vertical longitudinal vehicle centerplane from 60 degrees to 45 degrees as well as the modificaton of the markup tool for the corner of bumper definition from planes to gauges were investigated as means of leaving the test area definition depending on individual single details of the outer vehicle contour. A new definition of the test area using the ends of the bumper beam, following and harmonizing with the procedure that had been already introduced within Euro NCAP in 2009, reflects the philosophy of assessing the underlying injurious structures rather than the bumper fascia. A third philosophy aims at addressing the real world accident data which results in a homogeneous lateral impact distribution of pedestrians over the entire vehicle width, which therefore is suggested to be assessed. It thus should be, in principle, left to the testing authority to test over the entire width, considering the applicability of tests on angled structures.

## CONCLUSIONS

The present study gives evidence of the bumper test area of passenger cars currently assessed within the type approval procedures in terms of pedestrian safety not anymore adequatly addressing the purpose of protecting the lower extremities of pedestrians involved in accidents with passenger cars, mainly due to the downsizing of the test area width by means of outer vehicle design in many cases. It was demonstrated that any proposed method for a revision of the test area using tools related to the outer contour will most unlikely be of a permanent effect in terms of avoiding small test areas. Requirements for passive pedestrian safety unconditionally need to include the stiff structures, mainly located under the bumper fascia, which are responsible for injuries to the lower extremities. Therefore, for the time being, the test area definition using the bumper beam is indispensable. However, in the long run, giving consideration to current accident data which shows an equal distribution of pedestrian impacts along the entire vehicle width, the technical services should be given the opportunity to assess the complete vehicle width. Following this procedure, in case of angled test areas a rotation of the lower legform impactor may occur which is, to some extent, not always coincident with the behavior of the human leg, possibly leading to unrealistic test results. In order to limit this possible rotation a pedestrian torso mass may be applied to the FlexPLI. However, further research is needed and the ongoing validation of the torso mass still needs to be finalized, including tests to a broad variety of vehicle frontend designs. It is recommended to introduce the test and assessment procedure for the entire vehicle width after final validation and evaluation of the upper body mass, limiting impactor rotation during impacts on angled surfaces.

## REFERENCES

Bovenkerk J., Zander O. 2009. “Evaluation of the extended scope for FlexPLI obtained by adding an upper body mass.” Deliverable D333H of the European FP6 research project on Advanced Protection Systems (APROSYS).

Carroll J A., Barrow A., Hardy B J., Robinson B. 2014. “Pedestrian legform test area assessment. Final Report. ” Client Project Report CPR 1825 of the Transport Research Laboratory on behalf of the European Commission. Framework Contract Number 121/PP/2011/FC. 2014.

European New Car Assessment Programme. 2008. “Pedestrian Testing Protocol Version 4.2.” Euro NCAP, June 2008.

European New Car Assessment Programme. 2009. “Pedestrian Testing Protocol Version 4.3.” Euro NCAP, February 2009.

European New Car Assessment Programme (Ellway J.). 2012. “EC Task Force Legform Test Procedure” Doc TF-BTA-1-04 of 1st Meeting of the TF-BTA. 4 September 2012.

European Union. 2007. “Directive 2007/46/EC of the European Parliament and of the Council of 5 September 2007 establishing a framework for the approval of motor vehicles and their trailers, and of systems, components and separate technical units intended for such vehicles (Framework Directive).” Official Journal of the European Union, 09. October 2007.

European Union. 2009. “Regulation (EC) No 78/2009 of the European Parliament and of the Council of 14 January 2009 on the type-approval of motor vehicles with regard to the protection of pedestrians and other vulnerable road users, amending Directive 2007/46/EC and repealing Directives 2003/102/EC and 2005/66/EC.” Official Journal of the European Union, 04. February 2009.

European Union. 2009. “Commission Regulation (EC) No 631/2009 of 22 July 2009 laying down detailed rules for the implementation of Annex I to Regulation (EC) No 78/2009 of the European Parliament and of the Council on the type-approval of motor vehicles with regard to the protection of pedestrians and other vulnerable road users, amending Directive 2007/46/EC and repealing Directives 2003/102/EC and 2005/66/EC.” Official Journal of the European Union, 25 July 2009.

Ferrer A., del Pozo E., Rodarius C., Ott J., Zander O., Schaub S., Caspar M., Fredriksson R., Nuß F. 2014. „Experimental and virtual testing.“ Deliverable D3.2 of the European FP7 research project on Assessment methodologies for forward looking Integrated Pedestrian and further extension to Cyclist Safety Systems (AsPeCSS).

Fries A., Schenk T., Roth F. 2014. “Injury risk of lower leg outside of 30° tangent-area.” Doc TF-BTA-7-09 of 7th Meeting of the TF-BTA. 29 August 2014.

National Highway Traffic Safety Administration (NHTSA). 2011. “49 CFR 581 – Bumper Standard.” Code of Federal Regulations (annual edition), Title 49 – Transportation, Part 581 – Bumper Standard, 2011.

Research Council for Automobile Repairs (RCAR). 2010. “RCAR Bumper Test, Issue 2.0.” Issue 2.0, September 2010, available on www.rcar.org.

Transport Research Laboratory (TRL). 2002. “Suggestions for EEVC WG 17 test procedures and for EC Draft Directive.” EEVC WG 17 Doc 186. 20 May 2002.

United Nations Economic Commission for Europe. 2013. “Agreement Concerning the Adoption of Uniform Technical Prescriptions for Wheeled Vehicles, Equipment and Parts which can be Fitted and/or be Used on Wheeled Vehicles and the Conditions for Reciprocal Recognition of Approvals Granted on the Basis of these Prescriptions (Revision 2, including the amendments which entered into force on 16 October 1995). Addendum 126: Regulation No. 127 – Entry into force: 17 November 2012. Uniform provisions concerning the approval of motor vehicles with regard to their pedestrian safety performance.” Website of the UN/ECE, Doc. ECE/TRANS/505/Rev.2/Add.126. 7 January 2013

United Nations Economic Commission for Europe. 2014. “Proposal for amendments to global technical regulation No. 9 (Pedestrian safety)” Website of the UN/ECE, 56th session of GRSP, 9-12 December 2014, Doc. GRSP-56-39.

United Nations Economic Commission for Europe. 2014. “Proposal for Supplement 1 to the 01 series of amendments to Regulation No. 127 (Pedestrian safety)” Website of the UN/ECE, 56th session of GRSP, 9-12 December 2014, Doc. GRSP-56-41.

United Nations Economic Commission for Europe. 2015. “Agreement Concerning the Adoption of Uniform Technical Prescriptions for Wheeled Vehicles, Equipment and Parts which can be Fitted and/or be Used on Wheeled Vehicles and the Conditions for Reciprocal Recognition of Approvals Granted on the Basis of these Prescriptions (Revision 2, including the amendments which entered into force on 16 October 1995). Addendum 126: Regulation No. 127 01 series of amendments to the Regulation – Date of entry into force: 22 January 2015. Uniform provisions concerning the approval of motor vehicles with regard to their pedestrian safety performance.” Website of the UN/ECE, Doc. ECE/TRANS/505/Rev.2/Add.126/Rev.1. 4 February 2015

Zander O., Gehring D., Leßmann P. 2011. “Improved assessment methods of lower extremity injuries in vehicle-to-pedestrian accidents using impactor tests and full scale dummy tests.” Paper no. 11-0079 of 22nd ESV conference proceedings.

Zander O., Pastor C., Leßmann P., Gehring D. 2013. “Towards a world-wide harmonized pedestrian legform to vehicle bumper test procedure.” Paper no. 13-0175 of 23rd ESV conference proceedings.

Zander O., Wisch M., Gehring D.-U. 2014. “Proposal for a modification of the lower/upper legform to bumper test area in GTR9-PH2 and UN-R 127 01 series of amendments.” Doc TF-BTA-6-07 of 6th Meeting of the TF-BTA. Paris, France, 15 May 2014.

Zander O., Gehring D.-U. 2014. “Testing outside bumper corners.” Doc TF-BTA-7-11 of 7th Meeting of the TF-BTA. 9 September 2014.

# EFFECT OF FMVSS 226 COMPLIANT CURTAIN AIRBAGS ON THE BRIC RESULT OF A HYBRID III 50$^{TH}$% DUMMY DURING AN OBLIQUE IMPACT

**John Cadwell**
**Eugene Lee**
**Aviral Shrivatri**
**Shiro Ohara**
Toyoda Gosei North America Corporation
United States of America
**Hiroaki Yamada**
**Michihisa Asaoka**
Toyoda Gosei Co., Ltd.
Japan

Paper Number 15-0367

## ABSTRACT

The proposed oblique impact test with a Research Moving Deformable Barrier (RMDB) by the National Highway Traffic Safety Administration (NHTSA) is designed to represent crashes involving partial longitudinal structural engagement between vehicles. The RMDB moves at a speed of 56mph (90kph), with a small overlap of 35% and an impact angle of 15°, into a stationary vehicle. In addition, the newly developed Test Device for Human Occupant Restraint (THOR) dummy and the Brain Injury Criterion (BrIC) are used to evaluate the injury risk. The implementation of these test modes and measurement techniques will raise the bar for performance of passive safety systems.
Meanwhile, the introduction of the Federal Motor Vehicle Safety Standard 226 (FMVSS 226) as a countermeasure for ejection mitigation during a rollover has increased the occupant protection area of side curtain airbags (SCAB). As a result, SCAB designs have incorporated increases in height, width, and depth, depending on the interaction of the airbag with the vehicle's interior. This dimensional change in FMVSS 226 compliant SCAB, while yielding positive results in side impact and rollover crashes, may also play a critical role in the prevention of injury for the NHTSA oblique test mode. This study examines the effect of the expanded occupant protection coverage of FMVSS 226 compliant SCAB on BrIC results during an oblique impact.
This study used publicly available oblique pulse data (published by NHTSA) in a Finite Element (FE) model with a Hybrid III 50$^{th}$% dummy to perform an oblique impact test. The interior environment of the FE model was obtained by digitizing a generic buck and morphing available FE models from the National Crash Analysis Center (NCAC) database. The FE model was validated with a belted 35mph frontal impact test (FMVSS 208) and then used for the oblique impact analysis. This study examines three oblique FE models, each consisting of a different configuration of restraint systems. The first configuration did not utilize a SCAB; the second configuration had a non-FMVSS 226 compliant SCAB; and the third configuration had a FMVSS 226 compliant SCAB. In order to assess the effect of SCAB design, only the upper body results of the dummy were compared and analyzed. Differences in injury response were observed between the three configurations when evaluating the head acceleration, head rotation, and chest deflection. A significant improvement was observed in the BrIC result for the FMVSS 226 compliant SCAB when compared with the other two restraint system configurations tested. Though this study is design-specific, appropriate explanations are provided to support the study.

## INTRODUCTION

Despite continuous improvement to passive restraint systems, serious injuries and fatalities still occur during a crash event, even when all restraint systems operate as designed. Recently, oblique vehicle-to-vehicle impacts have been identified as a high risk scenario for occupants by the National Highway Traffic Safety Administration (NHTSA), and further supported by Rudd *et al*, [2011][1], wherein the vehicle's longitudinal structural members are only partially engaged. NHTSA has developed a test procedure to address this crash mode, refining the criteria for an oblique test method as a 35% overlap, at an angle of 15° (345 Degrees PDOF), impacting a stationary vehicle with a newly developed (Research Moving Deformable Barrier) RMDB that travels at 56mph (90kph)[2]. This test mode has

introduced new challenges in occupant safety system design, as the resulting kinematics cause limited engagement of the frontal and side restraint systems by the occupant. This has led to an increased focus in the automotive industry on the protection of the occupant by the side and curtain airbags during these types of crash modes.
Early research of the occupant kinematics and resulting injury modes in the oblique condition led to the creation of the Brain Injury Criterion (BrIC), presented in its most current form by Takhounts *et al.* [2013][3]. The BrIC is measured using the X-, Y-, and Z-axis angular velocities of the head, and is intended to capture the risk of brain injuries as a supplement to the translational acceleration measurement used to calculate the Head Injury Criterion (HIC). Due to the occupant kinematics found in oblique crash conditions, a high level of head and torso rotation and excursion may result, making BrIC a critical measurement for establishing safety system performance.
The FMVSS 226 test protocol was formally introduced in 2013 to prevent the ejection of occupants during a rollover crash, and has led to improved SCAB coverage in the X-, Y-, and Z-directions in-vehicle. This study will examine the effect of the utilization of an FMVSS 226 compliant side curtain airbag (SCAB) as it relates to occupant kinematics and BrIC results during an oblique test.

## METHODS

*Background*
The newly developed NHTSA oblique test condition is specified as a Near-Side collision, wherein the RMDB impacts a stationary vehicle at 90kph, with a 35% overlap and an impact angle of 15° (Figure 1).

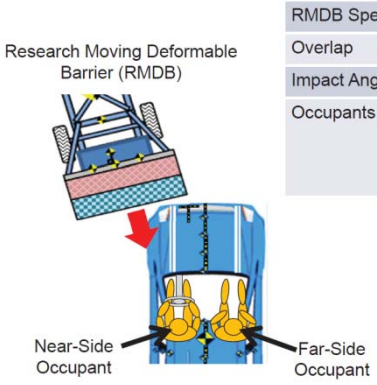


| | | |
|---|---|---|
| RMDB Speed | 56 mph (90 kph) | |
| Overlap | 35 percent | |
| Impact Angle | 15 degrees (PDOF = 345) | |
| Occupants | Near-side (Driver) | THOR Mod Kit 50th Male |
| | Far-side (Passenger) | THOR Mod Kit 50th Male |

**Figure 1. NHTSA Oblique RMDB Test Configuration.**

Previous research has found that the new NHTSA oblique test mode introduces an increase in injury risk primarily to the Head, Chest, and Lower Legs, due to the angle of impact and intrusion levels observed in testing[4]. BrIC is a recently established head injury metric developed by Takhounts *et al.* [2013] which uses the maximum angular velocity (ω) measured about the X-, Y-, and Z-axes to determine the risk of injury to the brain due to rotational velocity of the head. For this study, BrIC was calculated using the equation in Figure 2.

| Critical Angular Velocity | Rad/s |
|---|---|
| $\omega_{xC}$ | 66.25 |
| $\omega_{yC}$ | 56.45 |
| $\omega_{zC}$ | 42.87 |

Where $\omega_x$, $\omega_y$, and $\omega_z$ are maximum angular velocities about X-, Y-, and Z-axes respectively, and $\omega_{xC}$, $\omega_{yC}$, and $\omega_{zC}$ are the critical angular velocities in their respective directions.

$$BrIC = \sqrt{\left(\frac{\omega_x}{\omega_{xC}}\right)^2 + \left(\frac{\omega_y}{\omega_{yC}}\right)^2 + \left(\frac{\omega_z}{\omega_{zC}}\right)^2}$$

**Figure 2. BrIC Calculation based on Takhounts *et al* [2013].**

This study is concerned with the design and presence of installed SCABs, and their effect on both the BrIC value, and the overall reduction in head rotation.

*Model Development and Validation*

Before developing an oblique test method in computer-aided engineering (CAE), dummy kinematics and injury performance for an NCAP frontal crash were examined and validated using data from (3) developmental sled tests performed in-house. In order to correlate with the frontal NCAP sled testing, a Hybrid III dummy was used in the CAE environment.

For the frontal model validation, safety system components were chosen to match those used in the developmental sled program, and demonstrated good stability. The components used included a driver airbag (DAB), knee bolster airbag (KAB), and a 3-point seatbelt utilizing a pre-tensioner and load limiter. Simulations were then performed in CAE using the acceleration data used in the sled environment, and the results were analyzed. Upon reviewing the results, the CAE tests showed good correlation in Head, Chest, and Pelvis acceleration in both magnitude and phase, while Chest Deflection showed good correlation during loading, but exhibited a shorter duration than was observed on sled. Femur force was measured for both left and right femurs, and while the right femur showed good correlation to NCAP sled test data, the left femur exhibited higher magnitude and duration of loading than the physical tests (Figure 3). After evaluating the injury response by the upper body, it was decided to move forward with development of an oblique test setup in CAE, as the correlation to physical sled testing for occupant response in a frontal impact was good.

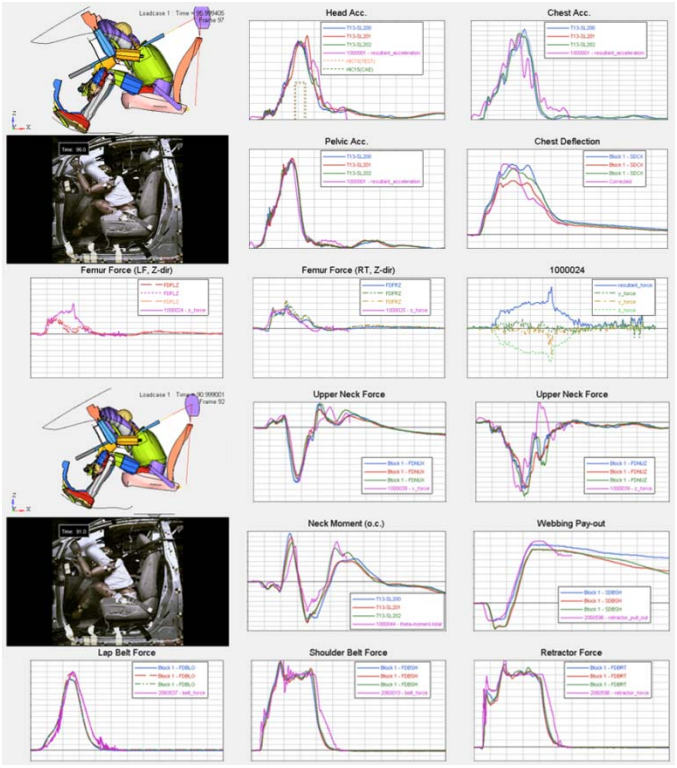


**Figure 3. Frontal Impact Validation with Sled Series.**

Three test conditions were chosen for examination of the SCAB effect on occupant kinematics in the oblique test condition. The first condition consisted of running the simulation with no SCAB present, utilizing only the DAB, KAB, and a pre-tensioning seatbelt with load limiter. In order to examine the benefit of an FMVSS 226 compliant SCAB, two SCAB models were used for the two subsequent tests. The first SCAB was a non-FMVSS 226 compliant, 2-row airbag, with a 50L capacity and an inflator whose output was 230kPA. Meanwhile, the FMVSS 226 compliant SCAB that was used in this experiment had a volume of 62L, and an inflator output of 350kPa. In the FMVSS 226 compliant SCAB, additional cells were added (Figure 4), and the airbag coverage was expanded in both the X- and Y-directions, relative to the vehicle coordinate system.

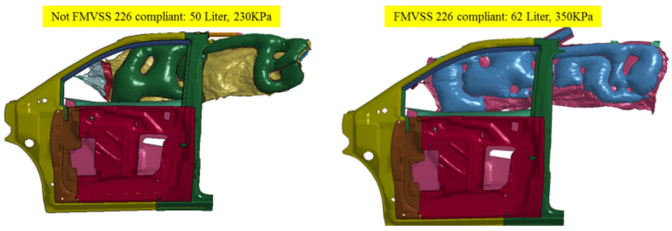


**Figure 4. Comparison of Non-FMVSS 226 compliant, and FMVSS 226 compliant SCAB.**

In order to establish an oblique acceleration to be used in the CAE model, a desktop review of NHTSA-published oblique pulse data was performed in order to find a pulse representing a stiff vehicle response. The acceleration data from the NHTSA database was selected[5], and the X- and Y-direction accelerations were input into CAE, with an impact location at the front left corner of the vehicle. This allowed the model to experience the same vector of acceleration as the NHTSA test, without incorporating vehicle rotation into the study.
A Hybrid III 50$^{th}$% male dummy was used for the CAE oblique testing. The Hybrid III exhibits a slightly different kinematic response and lower injury values than the THOR in physical testing when a significant vehicle Y-displacement is observed[6]. However, the Hybrid III model is very stable, and since the physical dummies are readily available, CAE oblique test results could be more easily confirmed at a later time through sled testing. The dummy was positioned using the setup numbers from the frontal sled tests, providing a uniform starting point for each simulation. SCAB modeling utilized a roll fold, and was then inflated at a time-to-fire (TTF) consistent with the published data, using the corpuscular particle method available in LS-DYNA to achieve full and representative deployment.

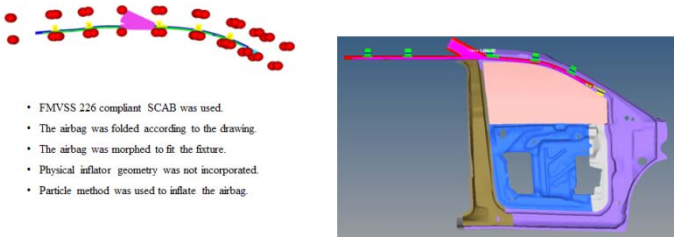


**Figure 5. SCAB Morphing and Inflation.**

Once the variables for the simulation were set, tests were performed for each of the three SCAB conditions, and results were compared.

## RESULTS

The simulation results for the SCAB performance and occupant behavior are presented and discussed below. Each of the three conditions simulated created marked differences in occupant kinematics as well as occupant injury response. The BrIC value, which is the injury factor of interest in this study, is evaluated in relation to the presence and design of the SCAB for each simulation.

*Occupant Kinematics*

For all three CAE simulations, the occupant exhibited forward and outboard movement consistent with that found during NHTSA oblique testing. The overall occupant kinematics were very similar in each test, as the seatbelt response was consistent throughout the experiment. However, in the absence of the SCAB, the occupant's head showed the greatest lateral movement of any configuration, as the head was unrestrained in its movement in the Y-direction (Figure 6).

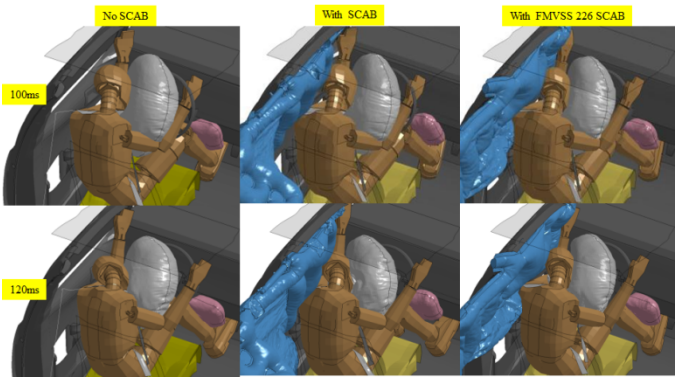


**Figure 6. Simulation Results - Occupant Kinematics Comparison.**

The head angular velocities for CAE were compared to the published data for the NHTSA oblique test[5] (Figure 7). The magnitude of the velocity for each direction of rotation was exhibited slight differences, but the location and timing of each peak were consistent between CAE results and the published data. This comparison demonstrated that kinematically, the CAE model was representative of the motion seen by the occupants in the NHTSA oblique test method.

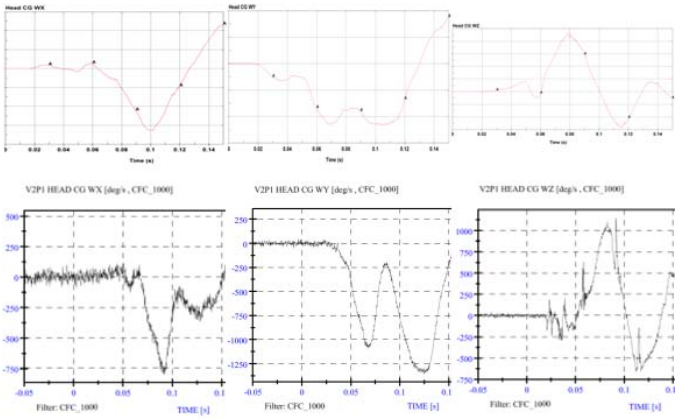


**Figure 7. Head Angular Velocity - CAE vs NHTSA Results.**

As seen in Figure 8, the increased chamber size in the Y-direction of the FMVSS 226 compliant SCAB creates contact with the occupant's head sooner in the crash event, limiting lateral movement and minimizing rotation. The early contact creates a counter- rotation effect that reduces the overall angular velocity for the event.

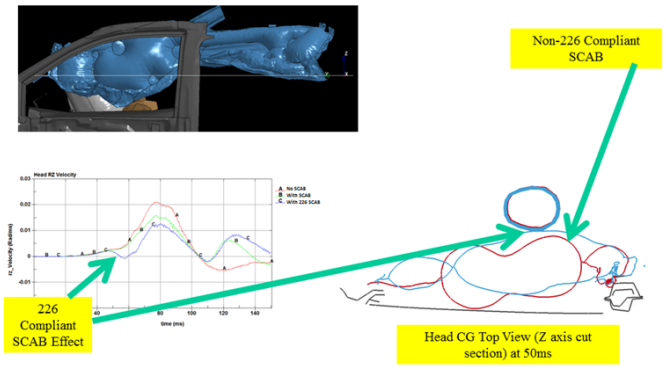


**Figure 8. Head Rotation about Z-axis - 226 SCAB Reduction Effect.**

*BrIC Performance*

In the baseline study, with no SCAB present in the simulation, the occupant exhibited forward and outboard movement. The DAB was contacted left-of-center, and the occupant's head proceeded to move outboard toward the door trim; however, the occupant's head made no contact with the door. The head experienced significant angular velocity about the X-axis (41.124 rad/s), as well as an elevated $\omega_z$ (21.163 rad/s), resulting in a BrIC score of 0.8725. Of the three CAE simulations, the baseline test resulted in the highest BrIC score. The second test incorporated a SCAB into the safety system design, yielding changes in the kinematics of the occupant. In this simulation, the occupant trajectory was similar to the baseline study; however the presence of the SCAB guided the head during forward movement, reducing the $\omega_z$ to 15.931 rad/s, while the $\omega_x$ result (41.552 rad/s) matched the baseline, and a reduction of 5.517 rad/s was seen in $\omega_y$. The BrIC score for the second simulation was 0.8647.

In the final simulation, a change in occupant head kinematics was observed during interaction with the DAB and SCAB. The FMVSS 226 SCAB contacts the occupant's head earlier in the crash event, inducing a counter-rotation that limits the magnitude of the peak angular velocity (Figure 8). As a result, $\omega_z$ was reduced to 12.772 rad/s, the lowest of all three of the simulations, while $\omega_x$ saw a reduction as well, showing a peak angular velocity of 25.519 rad/s. These reductions in angular velocity resulted in the lowest BrIC score for all three scenarios, at 0.655, representing a 24.2% reduction in BrIC when compared to the non-FMVSS 226 compliant SCAB. The BrIC values for each test are shown in Figure 9 and Table A1 in Appendix A.

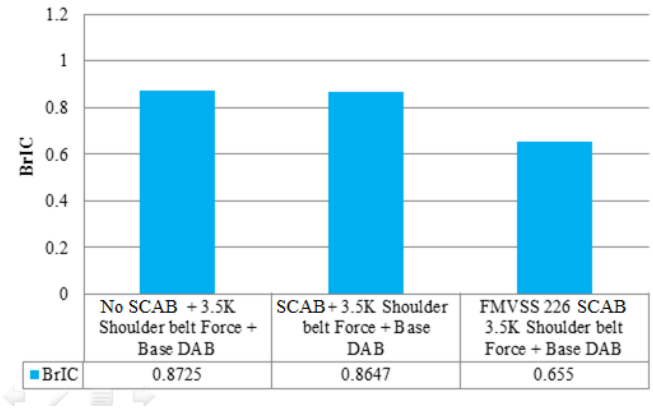


**Figure 9. BrIC Review for SCAB Configurations.**

Figure 10 shows the head angular velocity characteristics for each direction of rotation. Of note within this data is the reduction in magnitude of rotation about the X- and Z-axes for the FMVSS 226 compliant SCAB.

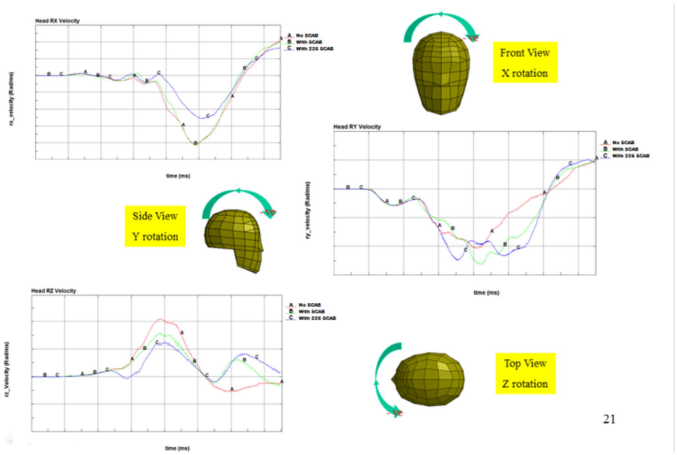


**Figure 10. Head Angular Velocity Comparison.**

## CONCLUSIONS

This study has demonstrated that early engagement of a driver side occupant's head in an oblique impact using an FMVSS 226 compliant SCAB can reduce the rotation and angular velocity about the X- and Z-axes, thus reducing the overall BrIC score in a CAE test environment. This study acknowledges several limitations, including, but not limited to, the following:

- This study shows vehicle- and design-specific results using CAE. An analysis of a broad range of vehicle platforms and SCAB designs would be beneficial to reinforce the results reported herein.
- Using the Hybrid III CAE model may underrepresent injury risk in certain body regions. Additional CAE research using the THOR model may provide further insight into the effect of the FMVSS 226 compliant SCAB on BrIC.

Further CAE and sled testing is recommended to verify the performance of different FMVSS 226 compliant SCAB designs in different vehicle environments.

## REFERENCES

[1] Rudd, R., Scarboro, M., and Saunders, J., "Injury Analysis of Real-World Small Overlap And Oblique Frontal Crashes." 22nd International Technical Conference on the Enhanced Safety of Vehicles, Paper number 11-0384, (2011)

[2] Saunders, J., Craig, M., and Parent, D., "Moving Deformable Barrier Test Procedure for Evaluating Small Overlap/Oblique Crashes." SAE Paper 2012-01-0577, (2012)

[3] Takhounts, E., Craig, M., Moorhouse, K., McFadden, J., and Hasija, V., "Development of Brain Injury Criterion (BrIC)." Stapp Car Crash Journal, Vol. 57, (2013)

[4] Saunders, J., and Parent, D., "Repeatability of a Small Overlap and an Oblique Moving Deformable Barrier Test Procedure" SAE Paper 2013-01-0762, (2013)

[5] National Highway Traffic Safety Administration, Vehicle Crash Test Database, Test No. 8097 (http://www-nrd.nhtsa.dot.gov/database/VSR/veh/VehicleInfo.aspx?LJC=8097)

[6] Guerrero, M., Butala, K., Tangirala, R., and Klinkenberger, A., "Comparison of the THOR and Hybrid III Responses in Oblique Impacts," SAE Technical Paper 2014-01-0559, (2014)

## APPENDIX A

| Angular Velocity (Rad/s) | No SCAB – CAE Result | With SCAB – CAE Result | With FMVSS 226 SCAB – CAE Result |
|---|---|---|---|
| $\omega_x$ | 41.124 | 41.553 | 25.519 |
| $\omega_y$ | 20.539 | 26.253 | 24.784 |
| $\omega_z$ | 21.163 | 15.931 | 12.772 |
| BrIC | 0.8725 | 0.8647 | 0.655 |
| HIC15 | 280.9 | 311.7 | 492.5 |

**Table A1. BrIC & Angular Velocity Detailed Results.**

# ANALYSIS OF DIFFERENT TYPES OF WINTER TYRES IN REAR-END INJURY CRASHES AND FATAL LOSS-OF-CONTROL CRASHES WITH ESC

**Johan Strandroth**
Swedish Transport Administration and Chalmers University
Sweden

**Matteo Rizzi**
Folksam Research and Chalmers University
Sweden

**Maria Ohlin**
University of Gothenburg and Chalmers University
Sweden

**Jenny Eriksson**
Swedish National Road and Transport Research Institute
Sweden

**Anders Lie**
Swedish Transport Administration and Chalmers University
Sweden

Paper Number 15-0368

## ABSTRACT

This study aimed to compare studded and non-studded winter tyres with regard to the risk of being the striking car in rear-end injury crashes with passenger cars. A further aim was to evaluate the risk for a passenger car equipped with Electronic Stability Control (ESC) to be involved in a fatal loss-of-control (LOC) crash with studded and non-studded winter tyres. This research was based on two different materials. The study on rear-end crashes used police reports from crashes in Sweden between 2008 and 2014. The study was limited to crashes occurring in the winter period, in this study defined as October through to March. Only car-to-car two vehicle crashes were included (n=4239). As tyre information was not included in the police reports, a survey form was sent to all drivers asking which type of tyres was fitted on their car at the time of the crash. In total, 717 drivers (17%) responded. The relative risk for being the striking or struck vehicle, depending on winter tyres, was calculated using an induced exposure approach. The analysis of fatal crashes in the winter period used in-depth studies of fatal crashes collected by the Swedish and Norwegian Transport Administrations in the winter period between 2003 and 2014. Cars fitted with ESC (n=44) were compared with cars without ESC (n=260). The odds ratio for being involved in a LOC-crash was calculated depending on the ESC fitment and fitment of different winter tyres. The findings showed that the risk for being the striking vehicle in a rear-end injury crash on ice or snow was at least 27% higher for non-studded winter tyres, compared to studded tyres. With regard to all road conditions, no significant difference between winter tyres with or without studs were found. As the proportion of ice and snow differs greatly in different parts of Sweden, the overall estimated effect was significant in northern Sweden but not in mid or southern Sweden. The risk of a fatal LOC-crash was 65% lower with studded tyres compared with non-studded winter tyres for cars without ESC. In ESC cars, the risk reduction, compared to cars without ESC, was 92% including all types of winter tyres, which were grouped together due to the limited size of the material. The rear-end crash analysis was based on a material with a rather limited response frequency. Hence, the representativeness of the results should be treated with caution. Regarding the fatal crashes it could be concluded that ESC is very effective in reducing LOC-crashes regardless of type of winter tyres. This is the first study that shows the effect of studded tyres related to specific crash types and to different geographical regions in Sweden. Hence, the findings in this study can contribute to the ongoing discussion on reducing the proportion of studded tyres in Sweden due to environmental and health issues.

## INTRODUCTION

Injury crashes on slippery roads are a common issue during the winter period in Sweden. Of all injury crashes with passenger cars during the Swedish winter, approximately 50% occur on ice and snow (Folksam, 2015). The proportion of crashes on ice and snow in fatal crashes is similar. Amongst fatalities on ice and snow, LOC crashes account for the majority of crashes (64%) as reported by Strandroth et al., (2012). However, in many parts of Sweden the majority of winter traffic runs on dry or wet roads.

Testing of studded winter tyres has shown increased braking performance and increased stability on road surfaces covered with ice and snow, compared to non-studded winter tires (Auto Motor & Sport, 2008). However, the performance of studded tyres has been shown to drop substantially over time when the studs become worn, while the non-studded winter tyre has a more consistent performance (Auto Motor & Sport, 2010). The effectiveness of winter tyres in reducing real-life crashes has been studied since the early 1970´s. Also, the benefit of studded winter tyres compared to non-studded winter tyres has been evaluated. In a meta-analysis, Elvik (1999) found that use of studded tyres was associated with a reduction of crashes by 5% on roads covered with ice or snow, however the result was not statistically significant. On dry or wet roads the effect of studded tyres was 2%, also non-significant. Later studies have been done in response to the issue of air quality problems related to the use of studded tyres. Gustafsson et al. (2006) estimated the typical added safety effect of studded tyres compared to non-studded winter tyres to 0–10% reduction of passenger car crashes over a winter period and 20-25% crash reduction on roads covered with ice and snow. In a study by Strandroth et al. (2012) including cars not fitted with Electronic Stability Control (ESC), studded tyres were found to reduce fatal crashes with passenger cars on roads covered with ice or snow by 42%, compared to non-studded winter tyres. The effect on LOC crashes was 65%. ESC has been shown to have a superior effect on injury reduction on low friction roads. In a literature review by Ferguson (2007) fatal single-vehicle car crashes were found to be reduced by about 30–50% and Lie (2012) estimated a 98% reduction of fatal LOC-crashes on ice and snow. While ESC has been proven to reduce the risk for severe crashes on ice and snow, Strandroth et al (2012) could not, due to a too limited number of cases of fatal crashes with ESC equipped cars, investigate in detail how the risk of LOC crashes may be affected by different winter tyres on ESC equipped cars.

One problem associated with the use of studded tyres is the wear on roads leading to emissions of particles. In Sweden, studded tyres are estimated to account for around 80 % of the emissions of particles from roads (Johansson et al., 2004). During the last years, the issues of air quality have forced municipalities to focus on reducing the proportion of studded tyres on the urban road network (Stockholm Municipality, 2015). This change in proportion of studded tyres could have an effect on the polishing of the road surface resulting in a lower friction. Findings from a Finnish study that investigated the effect of the proportion of studded tyres in the traffic flow on the tyre-ice friction coefficient concluded that ”the stud flow could be reduced to 25-50 % without any risk of severe polishing of the icy road” (Tuononen & Sainio, 2014). Similar conclusions were drawn in a Norwegian study based on accident statistics. It was found that the number of accidents would increase if the use of studded tyres decreased below 20-25 %, compared to usage above this level (Elvik et al, 2013). In the same study, results showed an increase in the number of injury accidents when the usage of studded tyres were reduced, and also vice versa, if the usage of studded tyres increased it was associated with a reduction in the number of injury accidents. However, this analysis was performed on a macro level and did not set out to investigate what types of crashes would be affected by changes in the studded tyre usage rate.

Due to the increased grip with studded tyres shown in winter tyre tests, it could be assumed that studded tyres would reduce the risk of low friction crashes like rear-end crashes and other stability-related crashes. However, no study has yet managed to calculate the effects of studded tyres in a specific scenario in real-life crashes.

The aims of this study were to firstly compare studded and non-studded winter tyres with regard to the risk of being the striking car in rear-end injury crashes during the winter period with passenger car. A second aim was to evaluate the risk for a passenger car to be involved in a fatal loss-of-control (LOC) crash on ice and snow with different type of winter tyres and with or without Electronic Stability Control (ESC).

## METHODS

This study was carried out in two separate analyses. Rear-end injury crashes were analysed to evaluate the risk of rear-end crashes in the winter period with different kind of winter tyres, also a case-by-case analysis was conducted based on in-depth studies of fatal crashes on ice and snow in order to evaluate the risk for a passenger car equipped with ESC of being involved in LOC crashes.

Both analyses were case and control studies. In the first one, an induced exposure approach was used, as the true exposure (e.g. vehicle mileage or number of registered vehicles) related to different kind of tyres was not available. With this approach, the number of crashes in which a safety measure is expected to be effective (i.e. sensitive crashes) is divided by the number of crashes where the same technology is expected to have no or limited effect (non-sensitive crashes). The basic assumption is that the non-sensitive crashes in the same way as the cases will vary with changes in vehicle miles traveled, driver characteristics, numbers of vehicles on the road, among other factors. However, these control crashes should be unaffected by the presence of the technology. Therefore, they can serve as a proxy for the true exposure (Ferguson, 2007) and the effect is given by the relative difference in crash rates between the case and control group.

### Rear-end injury crashes

In order to estimate the risk of being the striking vehicle in a rear-end crash, this analysis used police-reported rear-end injury crashes with passenger cars. These were acquired from the Swedish National Accident Database, STRADA. The STRADA database contains information from police records and hospital data. In STRADA no information is given on type of tyres, therefore additional information was collected from a sample of drivers involved in these accidents, using a questionnaire (see material section). The assumption was made that the positive effect of studded tyres would be relevant in a crash situation that involves braking, where the braking performance would be dependent by the friction. Being the striking part in a rear-end crash was assumed to be the sensitive event, while being the striking part in a rear-end crash was considered to be the non-sensitive event. The calculations were performed according to Equation 1 below.

$$R = \frac{striking_{studded}}{struck_{studded}} \div \frac{striking_{non-studded}}{struck_{non-studded}} \quad (1)$$

Thus, the effectiveness in reducing the risk of being the striking part in a rear-end crash with studded tyres can be expressed as:

$$E = 100 \times (1 - R)\% \quad (2)$$

The standard deviation of the effectiveness was calculated on the basis of a simplified odds ratio variance, according to Equation 3. This method gives symmetric confidence limits but the variance estimate is conservative.

$$Sd = \sqrt{\sum_{i=1}^{4} \frac{1}{n_i}} \quad (3)$$

Where n is the number of crashes of each crash type. The 95% confidence limits (CI95) are given according to:

$$\Delta E = 100 \times R \times Sd \times 1{,}96 \quad (4)$$

An important factor was to ensure that the only dissimilarities between the case and control groups were types of tyres. In Appendix 1, controls were made with regards to possible confounding factors influencing crash or injury risk.

These calculations were performed on all road conditions (ice and snow as well as dry and wet roads) and in crashes in different Swedish regions (southern, mid and northern Sweden, see Figure 2).

**Fatal crashes**

Data from in-depth studies of fatal crashes with passenger cars collected by the Swedish and Norwegian Transport Administrations were analysed to determine whether a crash should be classified as LOC or non-LOC and whether or not LOC had been a critical event in causing the crash. If more than one vehicle was involved in the crash (i.e. a head-on collision between the car and a heavy goods vehicle) it was determined which part initiated the chain of events (active part) leading to the crash and then whether LOC were a major contributing event or not (Figure 1). These parameters were in first hand vehicle trajectories, skid marks, impact location and direction, tyre and steering wheel angles in impact and other circumstances recorded in the in-depth studies. Only cases where a passenger car had been the active part were included.

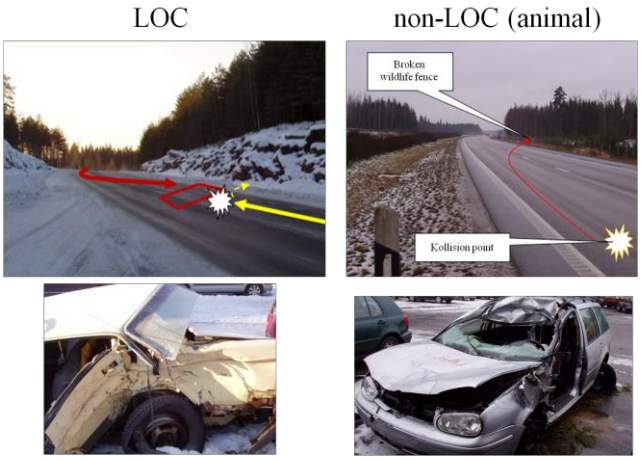


***Figure 1. An example of LOC and non-LOC crashes.***

Calculations were made using induced exposure, were the non-LOC crashes were considered to be non-sensitive to the effect of ESC and types of tyres. The odds-ratio (OR) for being involved in a LOC crash depending on types of tyres was calculated for both ESC and non-ESC equipped cars according to Equations 5, 6, 7 and 8.

$$OR_{non-ESC_1} = \frac{LOC_{non-studded}}{non-LOC_{non-studded}} \quad (5)$$

$$OR_{non-ESC_2} = \frac{LOC_{studded}}{non-LOC_{studded}} \quad (6)$$

$$OR_{ESC_1} = \frac{LOC_{non-studded}}{non-LOC_{non-studded}} \quad (7)$$

$$OR_{ESC_2} = \frac{LOC_{studded}}{non-LOC_{studded}} \quad (8)$$

## MATERIALS

### Rear-end injury crashes

Rear-end injury crashes involving passenger cars during 2008-jan 2014 were selected. The study was limited to crashes occurring in the winter period, in this study defined as October through to March. In this period studded tyres are allowed in Sweden. Only crashes involving two cars were included (n=4239).

In the accident database STRADA no information is given on type of tyres, therefore additional information was collected from a sample of drivers involved in rear-end crashes during the winter period, using a questionnaire. The questionnaire was designed as a postcard (A5-size) with four questions (Appendix 2). The first dispatch included the postcard and a missive, which were both put in an envelope. Two weeks later a reminder was sent out on a postcard and the respondents were informed about the option to answer a web-based questionnaire. The survey data collection period was May– June 2014.

In total, 4239 car drivers were identified to have been involved in winter period rear-end crashes, but the addresses were only available for 3945 of them, due to incomplete personal identification in the register or people living abroad, being deceased or having unknown/confidential address. A number of 31 questionnaires were returned to the sender, which indicated that the driver had moved from the address. Three of the respondents actively refused to answer the questionnaire. In all, 23 of the crashes appeared not to be rear-end collisions according to the accident descriptions given by the respondents. The overall response rate was 17 % (Table 1).

**Table 1.**
**Response rate and number of survey non-respondents.**

| **Total sample** | **No. of cases** |
|---|---|
| Total sample from STRADA | 4239 |
| Total posted questionnaires | 3945 |
| **Respondents** | |
| Total answers | 728 |
| **Non response** | |
| Refusals | 3 |
| Address known, but no response | 316 |
| Personal ID incomplete | 211 |
| Respondent living abroad, deceased or unknown | 83 |
| Return to sender | 31 |
| **Over coverage** | |
| Not a rear-end collision | 23 |
| **The response rate** | 17% |

Out of the 728 respondents, eleven cases were not possible to include in the analysis due to incomplete data. In total, 717 cases were further investigated. Table 2 shows the number and proportion of striking and struck cases.

**Table 2.**
**Proportion of striking and struck vehicles in the respondent group.**

| | **No. of cases** | **Proportion** |
|---|---|---|
| Striking | 265 | 37% |
| Struck | 452 | 63% |
| Total | 717 | 100% |

In Table 3, type of tyre is illustrated. As the purpose of this study was to examine the difference between studded (n=379) and non-studded (n=207) winter tyres, only these types of tyres were included in the final dataset and used in the induced exposure calculations.

**Table 3.**
**Type of tyre in the respondent group.**

| Type of tyre | No. of cases | Proportion |
|---|---|---|
| Studded | 379 | 53% |
| Non-studded | 207 | 29% |
| Summer | 111 | 15% |
| Unknown | 20 | 3% |
| Total | 717 | 100% |

**Fatal crashes**

The Swedish Transport Administration (STA) has been carrying out in-depth studies for each fatal road crash since 1997. At STA, crash investigators systematically collect information from the crash site as well as inspect the vehicles involved in fatal crashes and record direction of impact, vehicular intrusion, seat belt use, airbag deployment, tyre properties, etc. Information collected from the crash site is for example road characteristics, collision objects, etc. Information about injuries is provided by forensic examinations and emergency services. Also questioning and witness statements from the police are included in the in-depth studies. The Norwegian Public Roads Administration (NPRA) has been conducted in-depth investigations based on a similar process.

The analysis of fatal crashes used in-depth studies of fatal crashes collected by STA and NPRA in all winter period (Nov-March) between 2003 and March 2014. Crashes on dry or wet roads were excluded from the analysis since these crashes were assumed to be non-sensitive to studded tyres. Cases in which the cars were not fitted with approved winter tyres (i.e. thread depth below legal requirement of a minimum 3 mm or majority of studs missing) were excluded from the analysis. Also cases with documented suicide or death of natural causes. Two datasets were acquired. One including cars fitted with ESC (n=44) and one with cars not fitted with ESC (n=260). All crashes were analysed with regard to crash characteristics and type of winter tyres.

## RESULTS

### Rear-end injury crashes

In Table 5, the result from the odds ratio calculations for striking/struck cars in rear-end injury crashes are shown for all road conditions, ice and snow as well as dry conditions. Overall, on all road conditions, no significant difference was found between studded and non-studded winter tyres. In the specific case with braking applied by the striking car no significant difference was found on dry roads. However, on ice or snow, a 51% risk reduction for being the striking car was observed on cars fitted with studded tyres (CI95, 51%±24%).

**Table 4.**
**Number of striking/struck cars in rear-end injury crashes with studded and non-studded winter tyres.**

| | Striking | Struck | Odds ratio |
|---|---|---|---|
| **All road conditions** | | | |
| Studded | 142 | 237 | 0.6 |
| Non-studded | 85 | 122 | 0.7 |
| **Ice and snow** | | | |
| Studded | 81 | 163 | 0.5 |
| Non-studded | 47 | 46 | 1.02 |
| **Dry** | | | |
| Studded | 40 | 57 | 0.7 |
| Non-studded | 33 | 58 | 0.6 |

**Table 5.**
**The effect of studded tyres in reducing the risk of being the striking car in a rear-end injury crash.**

| | Effect | CI95 |
|---|---|---|
| All road conditions | 14% | ± 30% |
| Ice and snow | 51% | ± 24% |
| Dry | -23% | ± 73% |

The overall non-significant result for all road conditions was based on a proportion of 60% ice and snow and 40% dry or wet roads. Naturally, this proportion varies in different parts of Sweden. The overall results for northern, mid and southern parts of Sweden were therefore calculated (Table 6). In the northern part of Sweden, cars with studded tyres had a significantly lower risk for being the striking vehicle in a rear-end injury crash. No significant results was found in the mid or southern regions.

**Table 6.**
**The effect of studded tyres in northern, mid and southern Sweden.**

| | Striking | Struck | Effect | CI95 |
|---|---|---|---|---|
| **Northern Sweden** | | | 55% | ± 50% |
| Studded | 32 | 62 | | |
| Non-studded | 8 | 7 | | |
| **Mid Sweden** | | | -1% | ± 45% |
| Studded | 93 | 145 | | |
| Non-studded | 47 | 74 | | |
| **Southern Sweden** | | | 10% | ± 68% |
| Studded | 18 | 29 | | |
| Non-studded | 29 | 42 | | |

**Fatal crashes**

Regarding fatal crashes, the relative risk of being involved in a LOC crash depending on studded on non-studded tyres in non-ESC cars are shown in Table 8. Based on these results, it was calculated that the risk reduction with studded tyres on non-ESC cars was 65%. As the proportion of LOC crashes on ice and snow was 64%, the total risk reduction with studded tyres on non-ESC cars was 42% (CI95, 42%±16%). The total number of LOC crashes with ESC cars was only 10 cases. For that reason, all ESC cars were grouped together, regardless of type of winter tyres. Out of the 44 ESC cars, 30 were fitted with studded tyres and 14 were fitted with non-studded tyres. The LOC/non-LOC odds ratio for all ESC cars was 0.29, compared to 3.5 for non-studded non-ESC cars and 1.22 for studded non-ESC cars (1.78 for all non-ESC cars).

**Table 7.**
**Relative risk for loss-of-control in ESC and non-ESC cars with studded and non-studded tyres.**

| | LOC | Non-LOC | Odds ratio | Risk index |
|---|---|---|---|---|
| **Non-ESC cars (n=260)** | | | | |
| Non-studded | 42 | 12 | 3.5 | 1 |
| Studded | 113 | 93 | 1.22 | 0.35 |
| **ESC cars (n=44)** | 10 | 34 | 0.29 | 0.08 |

In non-ESC cars the risk reduction of LOC for studded tyres compared to non-studded was 65%. In ESC cars, the risk reduction, compared with non-ESC cars, was 92% including all types of winter tyres. In a similar way as for rear-end crashes, the effect of studded tyres depends on the proportion of traffic on ice and snow, which differs greatly between the different regions in Sweden. With non-ESC cars fitted with non-studded tyres, the risk for a fatal crash during the winter period increases in Southern Sweden by 9% compared to non-ESC cars with studded tyres. In the Middle and Northern part the same risk increase was 16 and 32%, respectively.

***Figure 2. Fatal crash risk increase with non-studded tyres on non-ESC cars compared to studded tyres.***

## DISCUSSION

### Rear-end injury crashes

In the first part of this study, studded winter tyres were found to reduce the risk of being the striking car in a rear-end injury crash on ice and snow by at least 27% (CI95, 51%±24%). Since the proportion of crashes on ice and snow differs greatly between different geographical regions, the overall effect of studded tyres in rear-end crashes also varies. On a national level, and in the mid and southern regions, no significant benefits were found. On the other hand, the effect on all road conditions was at least 5% in the northern regions (CI95, 55%±50%).

This was the first study to evaluate the benefit of studded tyres on a specific crash type such as rear-end injury crashes. This is a crash type in which better braking performance may play an important role. While the effects were large and significant, it should be noted that this particular crash type accounts for a small proportion of the total crashes during a winter period. Therefore, it is not surprising that earlier studies (Elvik 1999; Elvik 2013) only found small benefits on a macro level. As an example, rear-end crashes on ice and snow accounted for 4% of all injury crashes in the Stockholm region during 2010-2013. Under the assumption that 50% of the cars in that region are fitted with studded tyres, the overall effect of changing those tyres to non-studded winter tyres would be 1% increased risk of injury crashes (50%*50%*4%=1%), given that no other changes in the road environment occur (i.e. improved road maintenance).

One limitation in this study was the missing information on tyres in STRADA and the low response rate in the questionnaires (17%). The low response rate could depend on a number of reasons. One reason could be the fact that drivers may be ashamed, or just unwilling, to answer questions about their involvement in a crash were they are to blame as the striking part. This was also suggested by the high proportion (67%) of struck cars in the respondent group. The low response rate could naturally affect the representativeness and reliability of the result on a national level. However, the result could still be assumed as valid as the calculations were based on relative risk. Also, there is no reason to believe that the striking/struck proportion would vary in the respondent group dependent on the type of tyre.

In a case and control study with an induced exposure approach it is important to ensure that no confounding factors could influence the crash or injury risk. One obvious confounder could be the presence of Anti-lock Brake System (ABS) that is more prevalent on modern cars. However, the group fitted with non-studded tires involved newer cars making the result conservative. Control calculations with regards to other road, vehicle and driver characteristics are shown in Appendix 1. No significant differences between the case and control group were found. It could also be discussed weather being the struck part in a rear-end crash is a non-sensitive event related to studded tyres. Naturally, better braking performance could lead to a higher risk of being the struck vehicle. Thus, the result of this study could possibly also be influenced by a higher risk of the vehicles with studded tires of being the struck part in a rear-end crash.

### Fatal LOC crashes

Loss-of-control is the most common crash scenario in fatal crashes in Sweden during the winter period and since these account for 64% of all fatalities (Strandroth et al., 2012), interventions addressing stability could be assumed to have great benefits on roads covered with ice and snow. In this study, the effect of studded tyres and ESC were analysed based on in-depth studies of fatal crashes that occurred in the period 2003-2014. On cars without ESC, studded tyres were found to reduce the risk of a fatal LOC crash by 65%, compared to non-studded winter tyres. That corresponded to an overall risk reduction of fatal crashes by 42% during the winter period.

ESC has been proven to be very effective in reducing LOC crashes (Ferguson, 2007). In fatal LOC crashes, excluded non-conformities (i.e. crashes where ESC is basically not expected to have any benefits), Lie (2012) estimated the effect to be 98%. The results of the present study were found to be in line with previous research, showing large benefits of ESC, independent of type of winter tyre. The number of LOC crashes with ESC cars were very few, 5 fatalities in Sweden 2003-2014 (further 5 when including data from Norway), which made it difficult to analyse studded and non-studded winter tyres separately. However, when ESC cars with studded (n=30) and non-studded (n=14) winter tyres were grouped and compared to non-ESC cars, the risk reduction of LOC crashes were 83%. If ESC cars were compared to non-ESC cars with non-studded winter tyres the risk reduction was 92%.

The very low number of LOC crashes with ESC cars and the consequent result in risk reduction suggested that ESC may be effective in reducing LOC crashes regardless of type of winter tyres fitted on the car. However, due to the small number of LOC crashes with ESC cars these results should also be taken with some caution; further studies are also needed on a population with a higher proportion of non-studded winter tyres.

It should also be noted that calculations based on in-depth data could be subject to subjectivity and thereby somewhat biased. In this study, the parameters subject to the analysis were clearly specified a-priori and precise guidelines were developed to classify LOC-crashes. Regarding the classification of different winter tyres, experts were sometimes consulted to distinguish between summer tyres and non-studded winter tyres. While studded tyres are fairly easy to recognize, it may be more difficult to determine whether a non-studded winter tyre is of Nordic or Central European type. There are mainly two types of non-studded winter tyres on the Swedish market, one suited for Nordic conditions and one for Central European conditions. Nordic non-studded winter tyres are mostly designed for roads covered with ice and snow and Central European non-studded winter tyres are designed for milder conditions and higher speeds (STRO, 2010). In this study, they were both grouped together as non-studded winter tyres.

## CONCLUSIONS

There were a number of important findings in this research.

- ESC in combination with approved winter tyres reduces fatal LOC-crashes on ice and snow by 92%.
- One fatal LOC-crash on ice and snow occurs in Sweden every two years.
- Overall, similar results were found in the Norwegian in-depth dataset.
- Studded tyres on non-ESC cars reduce fatal crashes during the winter period by 9% in southern Sweden and by 32% in northern Sweden.
- Rear-end crashes on ice and snow account for 2-8% of all injury crashes annually in Sweden. In these crashes, studded tyres reduce the risk of being the striking part in a rear-end crash on ice or snow by at least 27%. A statistically significant result was found for northern Sweden, but not for mid or southern Sweden.

## ACKNOWLEDGMENTS

The authors gratefully acknowledge Magnus Larsson at the Norwegian Public Roads Administration (NPRA) for providing in-depth data and valuable input on this research.

**REFERENCES**


Auto Motor & Sport (Swedish variant), 2008. Test of non-studded winter tyres. Nr. 22, 2008, Stockholm, Sweden.

Auto Motor & Sport (Swedish variant), 2010. Test of winter tyres. Nr. 22, 2010, Stockholm, Sweden.

Elvik R, 1999. The effects on accidents of studded tyres and laws banning their use: a meta-analysis of evaluation studies. Accident Analysis & Prevention 31, 125-134.

Elvik R, Fridstrøm L, Kaminska J, Meyer SF, 2013. Effects on accidents of changes in the use of studded tyres in major cities in Norway: a long-term investigation. Accident Analysis & Prevention 2013 May;54:15-25.

Ferguson SA, 2007. The Effectiveness of Electronic Stability Control in Reducing Real-World Crashes: A Literature Review. Traffic Injury Prevention 8, 329-338.

Folksam, 2015. Customer Guidance for Choosing Winter Tyres. http://www.folksam.se/testergodarad/sakeritrafiken/bilsakerhet/1.91156 (2015-03-06).

Gustafsson M, Berglund CM, Forsberg B, Forsberg I, Forward S, Grudemo S, Hammarström U, Hjort M, Jacobson T, Johansson C, Ljungman A, Nordström O, Sandberg U, Wiklund M, Öberg G, 2006. Effects of winter tyres – state of the art. VTI-rapport 543. Swedish National Road and Transport Research Institute, Linköping, Sweden.

Johansson, C., M. Norman, G. Omstedt, and E. Swietlicki. Partiklar i stadsmiljö – källor, halter och olika åtgärders effekt på halterna mätt som PM10. SLB Analysis Report 4:2004.

Lie A, Tingvall C, Krafft M, Kullgren A, 2006. The Effectiveness of Electronic Stability Control (ESC) in Reducing Real Life Crashes and Injuries. Traffic Injury Prevention 7, 38-43.

Lie A, 2012. Nonconformities in Real-World Fatal Crashes – Electronic Stability Control and Seat Belt Reminders, Traffic Injury Prevention, 13:308–314.

Scandinavian Tyre and Rim Organization, 2010. Different winter tyres are good at different things. http://www.dackinfo.se/ (2010-09-28).

Stockholm Municipality, 2015. Banning studded tyres on Hörnsgatan. http://www.stockholm.se/Fristaende-webbplatser/Fackforvaltningssajter/Trafikkontoret/vinterdack/Dubbdacksforbud-pa-Hornsgatan/ (2015-03-06).

Strandroth J, Rizzi M, Olai M, Lie A, Tingvall C. The effects of studded tyres on fatal crashes with passenger cars and the benefits of Electronic Stability Control (ESC) in Swedish winter driving. Accident Analysis & Prevention 2012;45:50–60.

Tuononen A, Sainio P. 2014. Optimal proportion of studded tyres in traffic flow to prevent polishing of an icy road. Accident Analysis & Prevention, 2014. Nro 65, 53-62.

**APPENDIX 1**

**Table A.**
**Controls for the study on rear-end injury crashes.**

| | Studded tyres | Non-studded tyres |
|---|---|---|
| ***Injury severity*** | | |
| Severely injured | 5 % | 4 % |
| Slightly injured | 57 % | 53 % |
| Uninjured | 34 % | 40 % |
| Unknown | 5 % | 4 % |
| Sum | 100 % | 100 % |
| ***Road conditions*** | | |
| Snow | 20 % | 15 % |
| Dry | 33 % | 54 % |
| Thin ice | 32 % | 20 % |
| Thick ice/packed snow | 15 % | 11 % |
| Sum | 100 % | 100 % |
| ***Driver age*** | | |
| 18-24 y | 9 % | 9 % |
| 25-65 y | 75 % | 80 % |
| 65< y | 15 % | 11 % |
| Sum | 100 % | 100 % |
| ***Driver gender*** | | |
| Male | 55 % | 61 % |
| Female | 45 % | 39 % |
| Sum | 100 % | 100 % |
| ***Speed restriction*** | | |
| 30-60 km/h | 38 % | 39 % |
| 70-90 km/h | 33 % | 29 % |
| 100-120 km/h | 21 % | 23 % |
| Unknown | 8 % | 9 % |
| Sum | 100 % | 100 % |
| ***Car Model Year (MY)*** | | |
| Mean MY | 2002 | 2004 |

**APPENDIX 2**

## Frågor om däck vid olycka

1. Var du förare av:

☐ Den bil som körde på bilen framför

☐ Den bil som blev påkörd bakifrån

2. Om du var förare av den bil som körde på bilen framför, hann du bromsa innan kollisionen:

☐ Ja

☐ Nej

☐ Vet ej

3. Den bil du körde när olyckan inträffade, hade den

☐ dubbade vinterdäck

☐ dubbfria vinterdäck

☐ sommardäck

☐ vet ej

4. Om du körde med dubbfria vinterdäck, var de

☐ dubbfria vinterdäck gjorda för nordiska förhållande

☐ dubbfria vinterdäck gjorda för centraleuropeiska förhållande

☐ vet ej

5. Övriga kommentater

.....

.....

vti TRAFIKVERKET

***Figure A. Questionnaire sent to retrieve information on type of tyre (in Swedish).***

# INTELLIGENT VEHICLES + INFRASTRUCTURE TO ADDRESS TRANSPORTATION PROBLEMS – A STRATEGIC APPROACH

**John Maddox**
University of Michigan Mobility Transformation Center
Ann Arbor, Michigan
United States

**Dr. Peter Sweatman**
University of Michigan Mobility Transformation Center
Ann Arbor, Michigan

**Dr. Jim Sayer**
University of Michigan Transportation Research Institute
Ann Arbor, Michigan

Paper Number 15-0369

## ABSTRACT

Transportation systems around the world are showing signs of strain, and safety, congestion, and energy usage are significant societal problems. In the past, transportation professionals have attempted to solve these problems through largely "siloed" approaches focused on vehicle crashworthiness, infrastructure design, or energy efficiency. These separate approaches have had success, however transportation problems continue to grow.

The University of Michigan has formed the Mobility Transformation Center (MTC) to create a consortium of industrial, government, and academic partners who comprise an ecosystem for enabling a future transportation system that leverages connected and automated technologies. This group has convened to define a potential ecosystem, identify and prioritize key research needs for enabling a holistic approach, identify key technology and policy hurdles with paths forward, identify business drivers and opportunities, as well as identify gaps in standards, testing, facilities, and risk management schemes. A key goal is to lay a foundation for, and demonstrate, a commercially viable connected and automated transportation system in Ann Arbor by 2021.

To achieve these goals, MTC is designing, building, and deploying significant test beds, facilities, and deployments so that real-world results can be incorporated into this process in a rapid fashion.

This paper presents a summary of current status and early results of this effort, to the extent that they are ready for dissemination. This includes a description of the role various industrial sectors may play in a future transportation system, as well as identified first-level research gaps.

Included is a high-level description of strengths and weaknesses of various technologies (vehicle sensors and communication, infrastructure sensors and communication, infrastructure operating systems, data systems, etc.) and their ability to address key transportation problems and opportunities.

Lastly, a summary of the current status of the physical test beds and deployments will be included.

The authors seek to further the discussion of the potential roles various transportation system components and industrial sectors, as well as the roles for government and academia. Additionally, the authors hope to generate meaningful discussion on the importance of a systems approach to solving key transportation problems, including proper technology planning, evaluation and deployment to ensure that results address the widest range of societal needs as possible.

## INTRODUCTION

Transportation systems around the world are showing signs of strain, and safety, congestion, and energy usage are significant societal problems. In the United States 32,719 people were killed in motor vehicle crashes in 2013, and 2,313,000 were injured [1]. While these were decreased from 2012, motor vehicle crashes remain as a significant and persistent societal problem.

Similarly, traffic congestion is a well-known persistent problem in many U.S., and international cities, with significant impact on national economy and quality of life. It is estimated that congestion costs the U.S. over $120B annually, and causes 2.9B gallons of wasted fuel [2]. Unless unchecked, there are expectations that these costs and negative effects will increase as the population rises in the next 50 years.

In the past, transportation professionals have attempted to solve these problems through largely "siloed" approaches focused either on vehicle crashworthiness, infrastructure design, or energy efficiency. These separate approaches have had success, however transportation problems continue to grow.

New technologies including communication systems, automation, and "big" transportation data systems are being developed to address various problems. For the high-level strategic purposes of this paper, the following definitions are employed:

Connected – technologies that enable direct or indirect communication to and between transportation agents including vehicles, infrastructure, pedestrians, operation centers, and other entities. These include DSRC, cellular, Wi-Fi, satellite, and other media, and enable many applications and functions including navigation, driving information, infotainment, V2V, V2I, I2I, V2P (pedestrian), mapping, amongst others.

Automated Vehicles – technologies that enable automatic operation of some or all safety-critical control functions, including steering, throttle, braking, and motive power selection (forward, reverse, and other), and at various levels of occupant involvement or monitoring. Generally, the NHTSA-defined levels of automation will be used [3].

"Big" Transportation Data – data systems and technologies that gather, amalgamate, analyze, and report on numerous significant transportation and related data streams, such as vehicle-based data, telemetric data, fleet data, location data (to the extent that privacy is appropriately protected), operations data, maps, video data, weather, crash data, fuel usage data, amongst others. These systems must also address key components of cybersecurity and privacy.

The overarching premise is that a systems approach, encompassing all three technologies listed above, must be employed to ensure that society receives the maximum benefit from these technologies. Each of these are extremely complicated technologies, especially when applied to the very large scale of a national transportation system. If any of these are developed in isolation, we will not fully address the key needs of a future transportation system: safety, mobility, and energy efficiency.

As an example of this systems approach philosophy, MTC embraces the idea that these Connected and Automated vehicle technologies will not only function well together, but will developed simultaneously and be very complementary to maximize the functionality and benefit of each. MTC has subjectively considered the relative pros and cons of various applications of these technologies, and the results are shown in Table 1. Generally connected technology is relatively inexpensive, provides otherwise unavailable information on road partners and conditions, and provides a longer range "sensor" data compared to typical radar, camera, and lidar sensors. On the other hand, connected technology requires a

significant concentration of equipped vehicles/infrastructure, still relies ultimately on actions of human drivers, and can be perceived as a relinquishment of privacy.

Generally, automated technology can reduce dependencies on human action (and presumably error), doesn't rely on equipage of other vehicles, and has a high consumer interest. On the other hand for the highest levels of automation, the cost of sensors and onboard computing is quite high (which may limit broad adoption), the technology is not easily retrofitable and is not proven, and requires significant policy decisions and potentially changes for licensing, insurance, enforcement, etc.

| | pros | cons |
|---|---|---|
| Connected | | |
| V2V | proven effective for safety - avoiding collisions | relies on driver reaction |
| | inexpensive - can be applied on many vehicles | relies on other vehicles (critical mass) |
| | retrofittable | requires security system |
| | sees around corners | perception of privacy loss |
| | sees through fog/rain/snow | |
| | sees at longest sensor range | |
| | sees multiple vehicles ahead | |
| | knows much more about road partners | |
| | | |
| + V2I | enhances mobility thru adpative signal control | requires infrastructure investment |
| | enhances energy-use through eco routing/timing | requires added security system |
| | enables weather apps | further perception of privacy loss |
| | enables 0/1st level eco-driving | |
| | enables pedestrian detection in crosswalk | |
| | enables smart parking | |
| Automated | | |
| AV | relies less on human intervention | expensive - can't be applied on many vehicles |
| | doesn't rely on other vehicles | technology not fully ready |
| | added driver convenience | not yet proven reliability |
| | high customer interest | not retrofitatable |
| | potential for improved safety, unproven | requires security system |
| | potential for improved eco-driving | requires policy decisions/changes |
| | | unclear if all veh data can remain private/anonymous |
| | | may add VMT due to convenience |
| Automated + Connected | | |
| AV + V2V + V2I | all advantages above | most disadvantages above |
| | adds reliability to sensing & decision making | added cost |
| | enables platooning at close following distance | added proveout requirements |
| | enables safer lane changing and passing | requires comprehensive security system |
| | communicates locations of map changes/updates | |
| | communicates road construction / maintainence | |
| | enables 2/3/4th level eco-driving | |
| | enables L4 driverless (on most roads) | |
| | | |
| all + V2P | enables safe urban operation around pedestrians | requires smart phone/device solution |
| | enables rapid retrofit system | |
| | | |

**Table1.**
**Comparison of relative pros and cons of various applications of technologies.**

MTC has also considered, albeit subjectively, the relative future potential capabilities for these technologies to deliver key benefits in the form of core transportation metrics, namely safety, mobility, environment, and convenience, shown in Table 2. Generally, both technologies provide some potential benefit in all of these categories, though primarily to lower costs and greater penetration, connected technology provides a greater portion of safety and mobility benefits. While automation, primarily due to

the ability to relieve the driver provides significant convenience, especially at the highest levels of automation. Both technologies may play an equal role in delivering environmental benefits, and future research programs should strongly consider inclusion of a focus on environmental and energy saving opportunities for these technologies.

Because of these significant benefits, and in spite of the challenges, MTC has concluded that it is very likely, perhaps necessary that both technologies continue to be developed and deployed, along with accompanying data systems. This dual development will take advantage of significant synergies between the technologies and provide significant opportunities for benefit in key transportation metrics. Ultimately the expectation is that the benefit will outweigh the investment costs in both vehicles and infrastructure.

| | | Safety | Mobility | Environment | Convenience |
|---|---|---|---|---|---|
| Connected | | | | | |
| V2V | | 5 | 2 | 2 | 1 |
| V2I | | 1 | 5 | 3 | 2 |
| | | | | | |
| Automated | | | | | |
| L2 | | 2 | 1 | 2 | 1 |
| L3 | | 0 | 0 | 1 | 2 |
| L4 | | 2 | 2 | 2 | 4 |
| | | | | | |
| Con+Auto | | 10 | 10 | 10 | 10 |

**Table 2.**
**Relative benefit levels for Connected and Automated technologies.**
**(Higher number indicates increased benefit)**

## ESTABLISHING an ECO-SYSTEM

The University of Michigan has formed the Mobility Transformation Center (MTC) to create a consortium of industrial, government, and academic partners who represent a potential ecosystem for enabling a future transportation system. This group has convened to define a potential ecosystem, identify and prioritize key research needs for enabling a holistic approach, identify key technology and policy hurdles with ways forward, identify business drivers and opportunities, as well as identify gaps in standards, testing, facilities, and risk management schemes, all with the goal of fielding a significant demonstration of a working system in the next 6 years.

After surveying the current state of development of the above technologies, the following industries were identified as critical to a future transportation system:

- Auto and truck manufacturers
- Auto components and systems
- Telecommunications & communication services
- Consumer electronic devices

- Big data management and mapping
- Freight movement and logistics
- Traffic control systems
- Insurance
- Public transportation
- Payment systems
- Parking operations and systems

In parallel with industrial efforts, governmental bodies that have operational and jurisdictional roles at the national, state, city, and local levels are critical stakeholders. Lastly, academia must play a critical role in identifying, developing, and evaluating key technologies and as agents of change. Together, by including stakeholders from all of these realms, MTC has formed a true public-private partnership to further the technology, identify policy issues, and where needed, changes, spur innovation, provide living laboratories to test and evaluate technologies, and prototype an entire working system to identify at least one path forward to large-scale deployment.

## KEY RESEARCH NEEDS

The MTC has undertaken an extensive effort to identify, understand, categorize, and prioritize the state of art of the three key technologies from the viewpoint of members and stakeholders. Based on this effort and the resulting state-of-art assessment, a number of research thrusts were identifed in two different categories:

Technology

- Connectivity (V2X)
- Automation
- Cybersecurity
- ITS Interoperability
- Data Analytics
- Human Factors
- Energy Use & Emissions
- Standards
- Regulatory Issues
- Compliance

Policy

- Congestion Management
- Consumer Acceptance
- Public Policy
- Urban Planning
- Infrastructure Design
- Social Implications
- Legal Issues
- Business Models
- Payment Methods

Based on the above research thrusts, MTC has collected, brainstormed, and refined a number of research questions that need to be addressed to enable an accelerated and meaningful step towards significant demonstration. This full list of research questions is too long to reproduce fully in this report. And of course not all of these research topics can be addressed at one time, or in the context of pre-competitive research. Therefore MTC, along with its Leadership Circle Members, has undertaken a prioritization effort to identify the first and most critcal research thrusts and research questions. These are shown below, in appropriate categories.

Connected Technologies

- What applications, beyond safety, bring day-one value to the users and stakeholders?
- How are safety benefits extended to all road users including pedestrians?
- What is the business model of connected infrastructure deployment?
- How will a full-scale Security Credential Management System (SCMS) function?

Vehicle Automation

- How can automated vehicle technology be tested and validated to determine readiness for deployment?
- What role does the built roadside infrastructure play in a connected + automated environment and specifically what upgrades or updates, if any, would be required?
- What role does the data and mapping infrastructure play in a connected + automated environment and specifically what upgrades or updates would be required?
- What is the process to achieve broad accepatnce and engagement with the community?

"Big" Transportation Data

- What are the key cybersecurity risks and needs for automated vehicles?
- What data sets are required for connected + automated vehicles and what will be the tools and analytical approach?
- What data should be collected, and how are they useful for different purposes?
- How can the data drive entrepreneurship and new business models?
- How can the data support product development?

Policy

- What any changes if any are required to our legal system to maximize the value to connected + automated? State vs. Federal, Shared liability regimes, etc.
- How will fault be assessed in Automated Vehicle (AV) crashes?
- What are the key privacy impacts of automated vehicles?
- Do we need an ethics decision-making model for vehicle automation?

Customer Acceptance

- How do you define and measure value & customer acceptance?
- How do you define and measure value for all stakeholders (municipalities, etc)?

Standards

- What are the gaps in standards gaps for CAVs? which are a priority?
- Are existing regulations impediments to testing of connected and automated vehicles?
- What is the role of simulation in the prove-out of automated vehicle standards?
- Is a new testing methodology required to test the safety of connected and automated vehicles (confirmation of good events)?

Societal Impacts

- What is the implication of AVs on traffic congestion and VMT?
- How does a fully evolved connected and automated environment impact congestion, mobility, energy, public health, etc?
- What is the behavioral and economic impact of automated transportation?
- How will AVs impact urban transportation and design?
- What are implications for AVs on the aging population?

MTC has begun conducting internally-funded research projects on some of these, and other, questions and topics. The first round of research results and tools will be available in the August 2015 timeframe, and the second round was kicked off in April 2015. Results will discussed at MTC Annual Congress, currently being scheduled for September 2015 in Michigan.

## DEVELOPMENT and DEMONSTRATION PLANS

MTC believes that there are a number of significant, complex, and often intertwined questions and unknowns that need to be addressed to develop and deploy these technologies. These questions include those listed above, as well as many others. If left to standard, and individual, product research and development processes, these questions would likely require a decades-long product rollout. But given the significant potential benefits for transportation, MTC believes that these processes should be accelerated. MTC is promoting acceleration through collaborative efforts, and by fielding meaningful and ambitious model deployments to provide "living laboratories" and by creating unique purpose-built test facilities. MTC has undertaken work to build three "pillar" model deployments and one test facility.

Pillar 1: Connected Ann Arbor

MTC, with the collaboration of the City of Ann Arbor, will build on the success of the USDOT-funded Connected Vehicle Safety Pilot Model Deployment and expand that deployment up to 9,000 connected vehicles, and over 65 infrastructure nodes. This deployment will shift focus towards V2I applications, specifically those that can provide "day-one" benefits to drivers, road operators, cities, and importantly, vulnerable road users including motorcyclists, pedestrians and bicyclists. Figure 1 shows the geographic layout of this concept.

Pillar 2: Connected Southeast Michigan Initial Deployment

MTC, in a partnership with Michigan Department of Transportation (MDOT), member companies, and others, taking advantage of the region's uniquely large number of V2X activities and stakeholders, will create the first large scale connected transportation deployment in the United States. This deployment will leverage the MDOT Connected Corridor Program, as well as encompass the four existing test beds in the region, including Ann Arbor, Novi/Farmington, Telegraph Road, and City of Detroit. This deployment will focus also on V2I applications, especially to quantify benefit for road operators and municipalities for future investment decisions. Additionally, this deployment will support the auto industry by provding a dense connected environment to finalize development of V2V technology ahead of a NHTSA mandate. This deployment will also provide a unique opportunity to prototype and test a fully functional SCMS that can be scaled nationally. Lastly, this deployment will support early research and product development of AVs. Figure 2 shows the geographic layout of this concept.

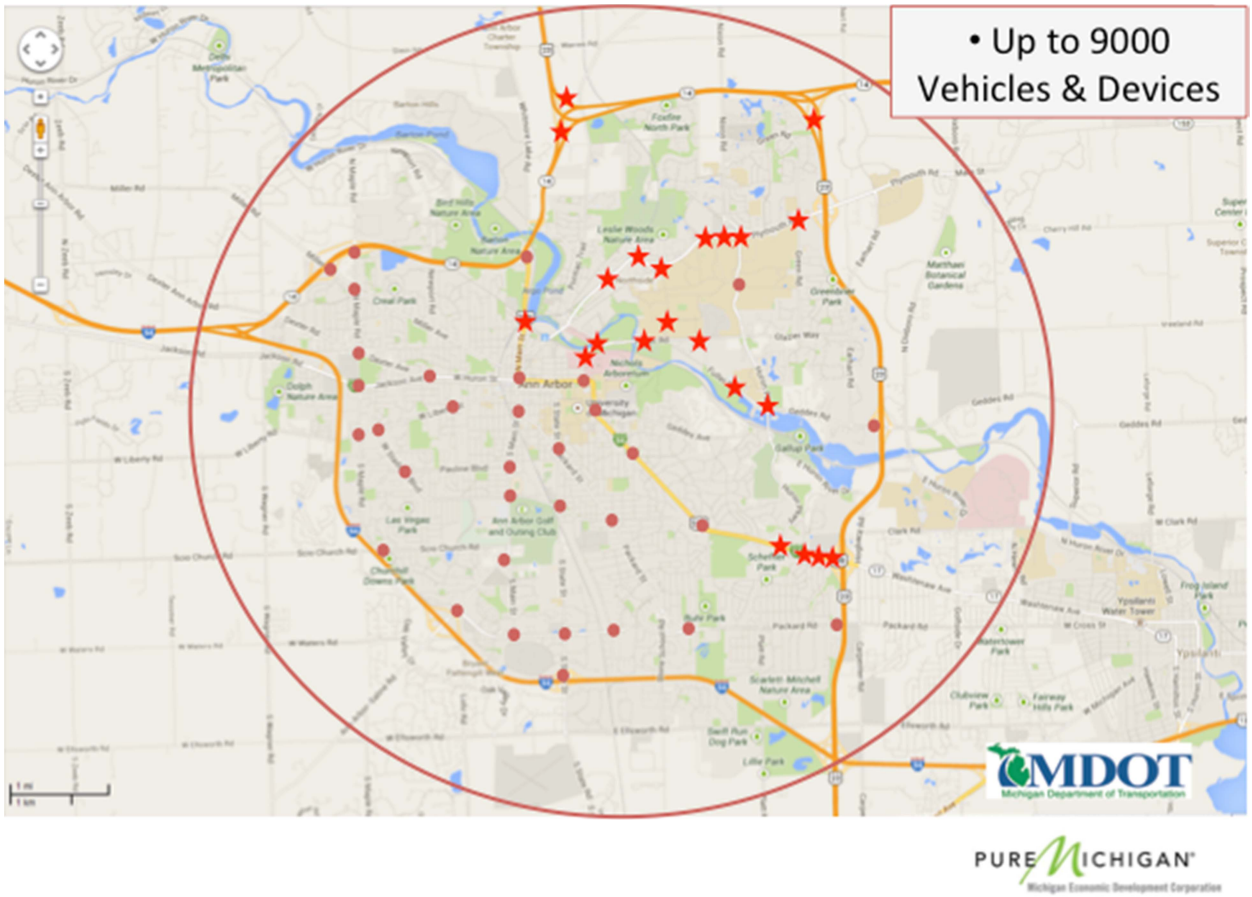


- 60 Intersections • 3 Curve-related sites • 12 Freeway sites
- Over-the-air security • All DSRC communications logged
- Backhaul communication network • Back-end data

**Figure 1.**
**Pillar 1: Connected Ann Arbor, MI**

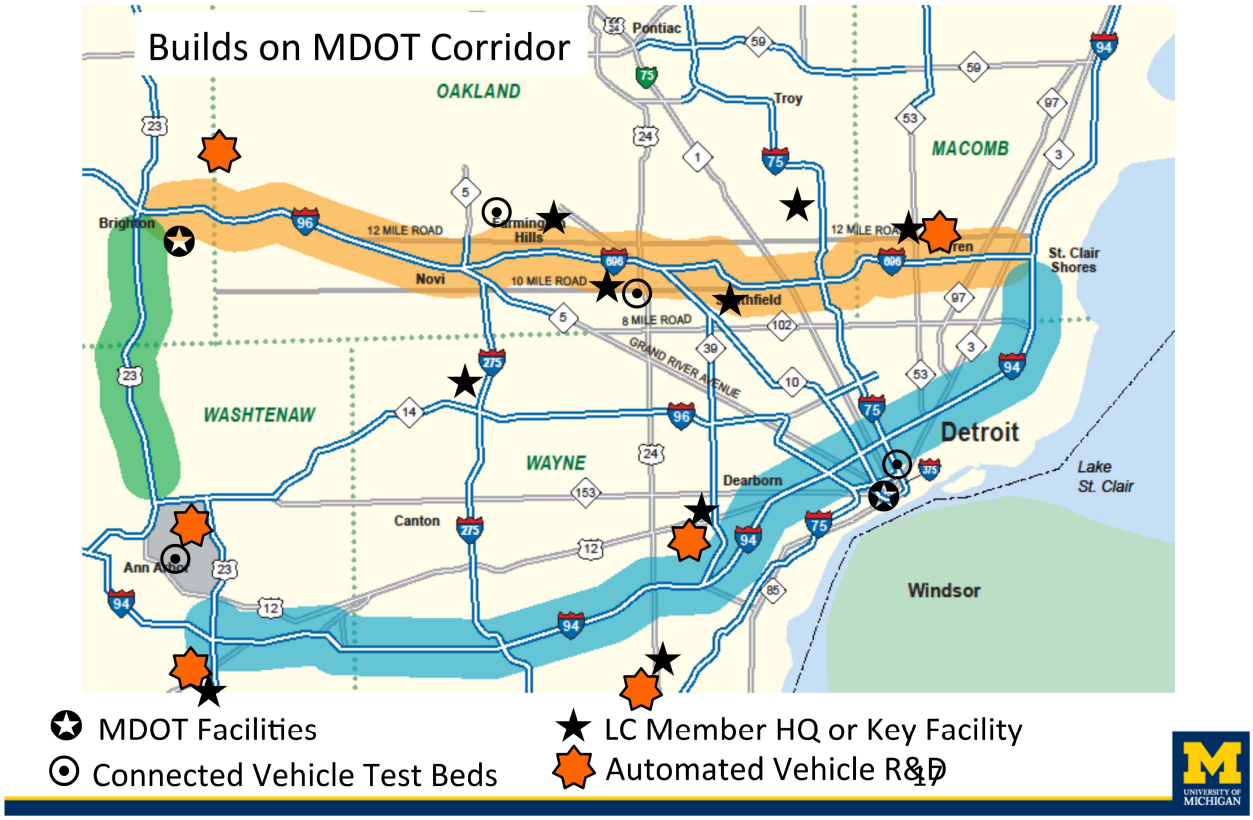


**Figure 2.**
**Pillar 2: Connected Southeast Michigan Initial Deployment**

Pillar 3: Automated Ann Arbor

MTC, in collaboration with the Leadership Circle of Companies, MDOT, and with the City of Ann Arbor, will utilize the dense connected Ann Arbor deployment to deploy an on-demand transportation service including 2,000 automated vehicles (AVs), including some number of levels 2, 3, and 4 vehicles. This transportation service will include the movement of people and goods, and will serve as a prototype for a future transportation system that will provide significant transportation benefits to the city and community. This deployment will include a fully-developed simulation platform (sensor, vehicle, driver, communications, infrastructure, environment) to complement the on-road environment. This deployment will leverage a to-be-developed "smart city" data and digital infrastructure, including backhaul and functions. It is expected that this deployment will also provide

an incredibly rich environment for product research and development, as well as addressing both technical and policy issues and questions.

Purpose-Built Test Facility: M City

MTC believes that a combination of both test track and on-road testing will be required for full development of high level AVs. Test tracks can provide a safe, controlled, and repeatable environment for early development without putting an unknowing public, especially pedestrians, at risk. And on-road testing is required because no track or simulation can anticipate the full plethora of conditions and scenarios that human drivers negotiate in the real world.

Therefore, MTC has designed and constructed a new, one-of-a-kind purpose built test facility for connected + and automated vehicles, named M City. This facility is designed to be a condensed, built to standard, simulation of a US city that will appear as a real environment to AV sensors. It is located directly adjacent to the Pillar 1 Connected Ann Arbor environment. Figure 3 shows the concept model of M City.

***Figure 3. Conceptual model of M City.***

M City includes an urban area with 13 intersection of various geometric designs, various road surfaces, curves of varying radii and elevation, round-about, traffic circle, building facades of varying geometry and materials, various traffic control devices and signage, pedestrian crossings and

bike lanes, street lighting, and mechanized pedestrians and bicyclists, amongst other features. It also includes a simulated highway stretch with on and off-ramps, multiple surface materials and markings, overhead and post-mounted signage, etc. Additionally, like the Automated Ann Arbor deployment, a full complement of simulations and tools will accompany the physical test facility.

Civil works and construction for this facility were completed in November 2014, with equipage of traffic control devices, lighting, and building facades scheduled at the time of this writing. The facility is expected to be fully operational by July 2015. Figure 4 shows an aerial photograph and layout of M City.

***Figure 4. Aerial photograph of M City.***

MTC and its private and public partners intend to utilize these deployments and this facility, and any others like it around the world, to conduct research and aid development of harmonized testing regimes, criteria, standards, and even future regulations that can speed the deployment of AV technology. MTC welcomes collaborations with other research and development stakeholders to achieve this goal.

## CONCLUSIONS

MTC has been formed to accelerate the development and deployment of connected and automated vehicle technologies, and believes both will be needed, and are largely complementary, to achieve significant improvements in our future transportation system. Many significant technical and policy questions remain to be answered, and model deployments will be a powerful, and likely necessary, tool to address these questions and find a way forward.

## REFERENCES

[1] Shankar, U. "2013 Crash Overview."
NHTSA, January 2015
[2] Lomax, Shrank, Eisele. « Urban Mobility Report »
Texas A&M Transportation Institute, 2013,
[3] Various NHTSA authors. "Preliminary Statement of Policy Concerning Automated Vehicles".
NHTSA 2013

# A COMPREHENSIVE AND HARMONIZED METHOD FOR ASSESSING THE EFFECTIVENESS OF ADVANCED DRIVER ASSISTANCE SYSTEMS BY VIRTUAL SIMULATION: THE P.E.A.R.S. INITIATIVE

**Yves, Page**
RENAULT
France
**Felix, Fahrenkrog**
Institut für Kraftfahrzeuge, RWTH Aachen University
Germany
**Anita, Fiorentino**
FCA
Italy
**Johann, Gwehenberger**
Allianz Center for Technology
Germany
**Thomas, Helmer**
BMW AG
Germany
**Magdalena, Lindman**
Volvo Cars
Sweden
**Olaf, op den Camp, Lex van Rooij**
TNO
The Netherlands
**Stefan, Puch, Martin Fränzle**
University of Oldenburg
Germany
**Ulrich, Sander**
Autoliv Research
Sweden
**Peter, Wimmer**
Virtual Vehicle Research Center
Austria

Paper Number 15-0370

## ABSTRACT

The assessment of real-world effectiveness of advanced driver assistance systems (ADAS) is gaining importance as more and more systems enter the market. Many different approaches have been developed. Therefore, the automobile industry, universities, and automotive research institutes in Europe have started an initiative for cooperative research. A 'Harmonization Group' was established in 2012 whose motivation is the development of a comprehensive, reliable, transparent, and thus accepted methodology for quantitative assessment of these systems by virtual simulation.

The harmonization group focuses on prospective analysis, which has the objective to estimate the expected safety benefits of current and beyond-state-of-the-art applications. Commonly used methods for prospective analyses are FOT's, subject studies in driving simulators, on closed test tracks or on open roads, and virtual analyses by means of simulation. Currently, the basis for an assessment by virtual simulation can be obtained either from reconstructed real-world crashes or from generic synthetic scenarios derived from realistic distributions of pre-crash conditions and traffic. Simulations allow for large number of cases and thus are capable of fulfilling the requirements posed by a sound sample size calculation. Simulation is certainly not a sole generic solution for all kinds of research questions, but it represents an integrative method to combine different knowledge areas in order to achieve an overall effectiveness result. It offers a promising combination of speed, flexibility, reproducibility, and experimental control.

The expected outputs of the group activities are the following:

- Identification of research questions (e.g. what changes in traffic safety can be expected due to the introduction of system X in country Y?);
- Definitions and metrics of the effectiveness (e.g. % reduction in fatal/injury crashes in a specific country/Europe; total reduction in fatalities over a period depending on a penetration rate);
- Structure for the assessment procedures including a description of the required sub-processes and the procedures to be followed;
- Description of the basic abstract models that are used in the simulation: driver, vehicle, road, traffic, and safety systems. The driver model is used to simulate various driver responses to inputs from the environment and the signals of the ADAS in various driving situations, traffic conditions, cars, and environments;
- Examples of the assessment of several ADAS (e.g. Lane Departure Warning, Advanced Cruise Control, Automated Emergency Braking).

The paper is a methodological paper presenting on-going activities of the Harmonization Group, so-called P.E.A.R.S. (Prospective Effectiveness Assessment for Road Safety), that involves more than 30 institutions in

Europe. Applied results will come once the harmonized framework is completed and the validation tests on several driving assistance systems have been shown successful. Further the document is set up to deliver the appropriate input for a draft proposal of an ISO or SAE standard.
This activity is an opportunity to harmonize methodologies used for assessment of ADAS in Europe. The involvement of non-European based stakeholders allows for a worldwide harmonization impact. A comprehensive assessment theoretical framework as well as concrete techniques should become available for wide usage by all stakeholders involved in ADAS effectiveness assessment.

## INTRODUCTION

Improved automobile sensor and inter-vehicle communication technologies are spurring the conception and development of novel **A**dvanced **D**river **A**ssistance **S**ystems (ADAS) including functions of active safety. Those possibly influence road safety. However, deploying such systems based purely on "engineering intuition" (without prior impact assessment) is neither risk-free nor cost-effective: Risks are associated with unintended system behavior (classically: false-positive system actions, i.e., if the system reacts, but ideally should not have reacted) or misuse by end-users, for example. Thus, in order to design assistance systems that will most effectively reduce the number of crashes and their severity, there is an urgent need for reliable safety performance assessment during development, prior to deployment, as well as assessment after market introduction. In addition to automobile manufacturers and suppliers, academia and research organizations, public policy makers, consumer organizations, as well as regulatory agencies and insurance institutions are key stakeholders in safety assessment. Assessment techniques likely to be accepted by all stakeholders should provide targeted, quantified, and verified safety performance prediction.
Ideally, a "gold standard" to quantify potential safety benefits of ADAS would be direct estimation of mortality and injury impacts in the field and direct measurement of unintended system behavior including their consequences. But estimation of ADAS safety benefits from, e.g., accident statistics, requires long observation periods (due to slowly increasing penetration) and is confounded by multiple parallel influences on these statistics; unintended actions need to be measured not just once, but for each algorithmic threshold setting. The main application for retrospective analysis is assessment of existing solutions. Development of new functions requires prospective analysis.
Hence, a methodology is required that can predict mortality and injury reduction as well as newly induced risks in traffic. Furthermore, the prediction of the effect on near crashes and crashes with material damage will be increasingly relevant for highly automated driving applications (e.g., with regards to acceptance, liability aspects).
Many recent projects, initiatives, and organizations have been working on aspects of safety assessment for various kinds of systems (e.g., TRACE [1], eIMPACT [2], EuroFOT [3]). Research activities on the field of traffic safety and safety impact have been conducted in the recent years as a result of the introduction of the ADAS into the market, e.g., ADVISORS [4], DaCoTA [5], IMVITER [6], interactIVe [7], PReVENT [8]. Although major steps have been taken in the assessment of safety systems, none of these projects describe a comprehensive methodology (ranging from the effectiveness in crashes via the interaction impact in traffic up to economic costs) in order to determine the real life impact of technology-based safety solutions. However, most of the projects focus either on the calculation of the safety impact on a general level, e.g., the number of a particular accident type addressed by the safety solution, or provide a methodology for the detailed analysis of specific crashes, e.g., car-to-car crashes. For development as well as assessment, a worldwide consensus and acceptance regarding methodological questions is required. Harmonization and standardization are essential for stakeholders and decision-makers for fundamental decisions.
This paper describes the objectives and recent progresses in the international P.E.A.R.S. (Prospective Effectiveness Assessment for Road Safety) group consisting of different kinds of stakeholders. The basic motivation is the creation of a generally accepted and applied methodology for quantitative assessment of road safety as a result of ADAS in vehicles. The joint effort of many stakeholders in early stages gives a chance to concentrate and discuss the state of the art, join forces for further research, and enable acceptance before standards are finally defined. History in vehicle safety strongly suggests worldwide standards instead of regional initiatives for assessment. P.E.A.R.S. thus is an open platform focusing especially on the following issues:

- Definition of research questions regarding assessment of ADAS;
- Evaluation of current methods regarding their potential to answer those research questions;
- Definition and agreement on a suitable assessment methodology and process;
- Practical description of the process steps and hints for implementation;
- Worldwide communication and standardization.

## METHOD

Development of a sound method for predicting the safety impact of ADAS functions requires three major steps (Figure 1. Top):

A. Identification of relevant analysis goals and related safety metrics precisely capturing the safety impact of ADAS functions while being amenable to model-based assessment in the function development phase;
B. Development and validation of a model-based assessment method quantitatively evaluating a functional design with respect to the metrics identified, where the term "model-based" is taken in a broad sense, covering the full range from statistical models to executable specifications and arbitrary blends thereof;
C. Definition of reporting standards for conveying the findings obtained to all kinds of stakeholders.

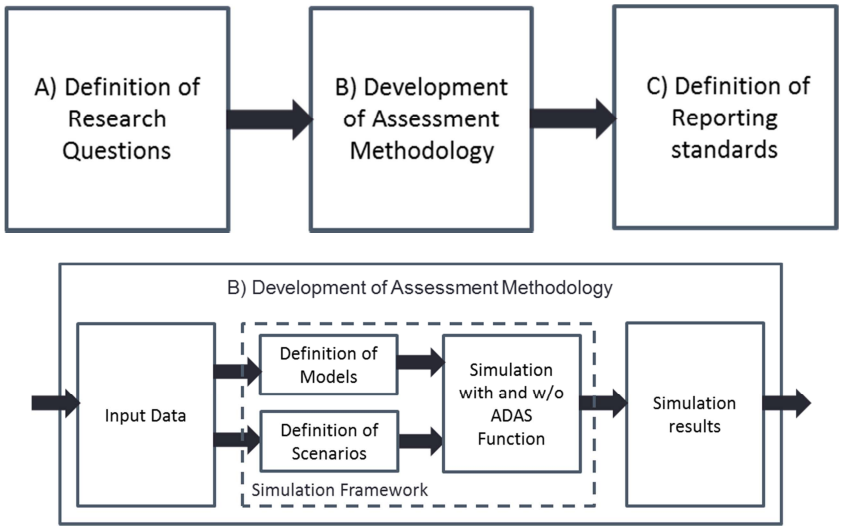


***Figure 1. Overall process for developing a methodology for prospective assessment of ADAS.***

In addressing these questions, P.E.A.R.S. takes advantage of the broad expertise provided by its assembly of relevant stakeholders featuring diverse backgrounds. Particularly, in addition to the regular exchange on working group meetings and the General Assembly, an inquiry was sent out to over 30 organizations that had so far contributed to the P.E.A.R.S. project. The objective of the inquiry was to gain feedback through all participants on general topics like relevance of certain research questions, applied methods and tools, and data utilized. Further specific questions were formulated on the currently used simulation setup (if available), previous assessments for specific ADAS functions, and interpretation of the results for certain operational regions. In a conclusive question, the participants were asked about their expectations on the P.E.A.R.S. project.

### Precise Definition of Research Questions by Means of Pertinent Analysis Goals and Metrics

The precise definition of Research Questions covers the work of identifying a terminology for efficient communication on prospective assessment of ADAS functions, followed by detailed definitions and delimitations of the possible assessment scopes. Also, metrics to be used in the Reporting as well as assessment targets are defined.
The P.E.A.R.S. group hereby follows a combined top-down and bottom-up approach. The aforementioned inquiry provided valuable input to ongoing research questions, but still they are also derived by a top-down-approach in a more general way. By the comparison of both approaches, what is used today and what could be applied in the future, missing scopes are identified and taken into account in present and further research.

### Development of an Assessment Methodology

The development of the Assessment Methodology is by far the most comprehensive task in the project covering a number of subtasks as illustrated in Figure 1(Bottom).

As a means of coordinating work within P.E.A.R.S., thereby also fostering cross-fertilization between different working groups, experiences from work in the different subtasks were compiled by means of the inquiry. From this together with a literature review, a state-of-the-art concerning the Assessment Methodology can be identified, forming the basis of a plan for further research effectuated by the joint program.
The general approach is to join models of traffic scenarios including road layouts, behavioral models for the traffic participants, and models for vehicles and their embedded safety functions in a heterogeneous co-simulation of their joint dynamics. To avoid investing computational and analytical efforts, for example, into situations unaffected by an ADAS function, the dynamic simulation focuses on potentially hazardous situations, called a *Scenario*, until the moment of collision or the moment that the collision has been avoided or mitigated thanks to an ADAS function. For a number of scenarios, the results of simulations with and without ADAS function can then be compared on different metrics as previously defined, providing a *conditional* assessment of the safety impact conditioned on the scenarios. Statistical background quantifying exposure and coverage, among related figures, can then be exploited for assessing the overall safety impact of the suggested safety function.
Soundness of the method hinges on identification of *Input Data* for both creation of scenarios and for development of dynamic models (e.g., driver-vehicle) combining tractable simulation with empirical validity for the research questions at hand. P.E.A.R.S. addresses that problem by comprehensively listing possible data sources and evaluating them in terms of quality, representativeness, scalability, and real-world relevance. As for the scenarios definitions, both current and future ADAS functions are taken into consideration, aiming at scenarios able to rigorously assess both their possible positive and negative effects.
For the dynamic simulation, the simulation framework, its sub-models, and required distributions for (input) parameters, have to be defined. This includes research on state-of-the-art simulation tools for pre-crash simulation and investigations on the respective strengths and limitations. A generic structure for such a framework has been defined. This structure comprises the required sub-models like vehicle model, safety system model, environment model, etc.
Additionally, possibilities for coupling the models have been looked at like High Level Architecture [24] and Co-Simulation. Different modeling depths including required parameters for each modeling depth were defined. Activities for defining requirements on different models have been started. Finally, research on state-of-the art processes to generate required distributions and parameterizations has been undertaken.
The simulation results have to contain the pre-defined metrics addressing the research question, either as a direct output or after post-processing. P.E.A.R.S. puts a strong focus on the processes to document the validity and accurateness of the applied framework and simulation models.

**Definition of Reporting Standards**

Different kinds of stakeholders will need different information for strategic decisions on traffic safety concepts. The number of avoided or mitigated accidents is a resulting metric close at hand, but further analyses can provide estimations of the number of avoided injuries of different severities. Also, a fleet penetration model can be considered for the assessment of the total effectiveness of ADAS functions. The P.E.A.R.S. approach will provide methods for generating such focused reports as well as for characterizing their confidence.
The definition of reporting metrics and standards is aligned with P.E.A.R.S. definition of research questions.

## EXPECTED OUTCOMES

This section deals with the expected outcomes of P.E.A.R.S. Therefore, the results achieved so far are presented as well as the results that can be expected from the group in the future. The section is divided into four sub-parts dealing with the main steps within an effectiveness assessment of ADAS: definitions of the addressed research questions, selection of appropriate metrics, conduction of the effectiveness analysis as well as the specification of the used simulation models. However, before the different steps are discussed first let's have a closer look on P.E.A.R.S. targeted applications.

**Outcome 1: The ADAS covered by P.E.A.R.S.**

In the recent years, different ADAS functions have been developed and introduced in the market. Examples are Adaptive Cruise Control (ACC), Advanced Emergency Braking Systems (AEB) or Lane Keeping Assist (LKA). Within the group of ADAS functions, different types of ADAS functions can be identified. One distinction that

can be made is that some ADAS aim to improve comfort, while others aim to improve safety, for example ACC and AEB, respectively. However, all functions have an impact on traffic and by this also on road safety. This applies also to comfort-oriented ADAS, although this is not their main objective, as indicated by [9] [10].
Next to the ongoing development of ADAS functions, also functions addressing a higher level of automation are developed. These functions are capable of taking over both the longitudinal and lateral driving task from the driver. First applications have already been introduced to the market for specific driving modes, e.g., traffic jam assist, e.g. [11] or [12]. For these functions, the driver still needs to monitor the function and take over in case the function reaches its functional limits. These functions are classified by the SAE definition [13] as partial automated. Demonstrations by, e.g., Google [14] have already provided an outlook on functions addressing higher levels of automation, which can be expected in the future. For these functions the driver does not need to monitor the driving task any longer.
Since all functions cover different driving scenarios and situations, it needs to be decided on which set of functions the P.E.A.R.S. harmonization group focuses. Within the group it has been decided to focus on ADAS including active safety functions as well as automated driving functions. Active safety functions act shortly before an imminent collision and aim to either avoid or mitigate the consequences of an accident. This decision was also reflected by the results of the inquiry which shows the interest in effectiveness assessment for different ADAS (highest interest for effectiveness assessment were detected for AEB Warning function, in particular AEB function addressing conflicts with Pedestrian or Bicyclist and rear-end conflict with other vehicles) and automated driving functions (Table 1).

**Table 1.**
**Interest in effectiveness assessment of different ADAS and automated driving functions according to the inquiry (6: high interest; 1: low interest; n = 26).**

| Function | Mean Rating | Function | Mean Rating |
|---|---|---|---|
| Pedestrian AEB/Warning | 5.4 | Lateral lane keeping | 4.0 |
| Bicyclist AEB/Warning | 5.3 | Active cruise control | 3.9 |
| Vehicle rear-end AEB/Warning | 5.0 | Active headlamps | 3.1 |
| Vehicle turning / crossing AEB/Warning | 4.9 | Other DAS | 3.6 |
| Lane departure warning / lane keeping system | 4.8 | Partial automated driving (SAE level 2) | 4.7 |
| Lane change warning / assistant | 4.8 | Conditional automated driving (SAE level 3) | 5.0 |
| Overtaking assistant function | 4.7 | Highly automated driving (SAE level 4) | 5.0 |
| Blind spot detection function | 4.2 | Full automated driving (SAE level 5) | 4.9 |
| Other ADAS | 3.7 | | |

**Outcome 2: A structuration of the Research Questions underlying the effectiveness assessments**

The typical start of an assessment process of an ADAS function is the definition of the relevant research questions [15] which defines what and why should be assessed within the assessment beforehand. Since P.E.A.R.S. aims at a standardization of effectiveness assessment, all research questions by all contributors must be taken into consideration before the harmonized method developed in P.E.A.R.S. can tackle them.
Five main objectives to conduct effectiveness assessment have been identified:

- Quantification of safety effects (positive and negative);
- Prioritization of systems / functions during development;
- Optimization of system design regarding components / sub-functions / parameterization;
- Detection of design issues in early stages to improve the benefits by respecting possible side effects;
- Argumentation of business case and anticipation of regulations / consumer testing.

Investigation on the research questions showed that many of the initial ones were formulated in a short way, not very precise. Thus, the actual meaning of the research question can only be interpreted. Examples for such research questions are “What is the effectiveness of AEB?” or “How many lives can be saved by function XY?”.
If results between different studies should be comparable, the research question needs to be more precise and already describe what should be assessed, how the effect is measured, which region and time horizon of prediction is

considered for the assessment. Therefore, a second round of investigations made the research questions more precise and some of them could be formulated the following way:

1. What are the potential safety benefits of driver assistance systems (ADAS) in the short term, mid-term, long-term, considering that there are a lot of other road safety actions not engineering-related :

- for each sub categories of ADAS modes (information, assistance, delegation, partially automated, automated) whether they are automated and/or cooperative;
- for each sub categories of ADAS functions (braking, speed management, lateral control, lighting, parking, etc.) whether they are automated and/or cooperative;
- for an optimized selection of ADAS functions (package or combination of ADAS).

Safety benefits could for example be defined the following way :

- How many lives could be saved if x% of the fleet is equipped with the y safety package compared to a baseline fleet;
- How many injuries of AIS "i" or ISS "j" could be mitigated if x% of the fleet is equipped with the y safety package compared to a baseline fleet;
- Reduction in risk to be fatally injured if x% of the fleet is equipped with the y safety package compared to a baseline fleet.

Reduction in risk to be injured AIS "i" or ISS "j" if x% of the fleet is equipped with the y safety package compared to a baseline fleet over n years,

… in each country and in all Europe, for different road users, categories, for different crash types, on different conditions (night / day ; road use ; urban / rural),

...considering a certain level of passive safety in cars (to be defined in the baseline)

2. What are the societal and economic benefits of driver assistance systems in the short term, mid-term and long-term? What are the externalities (side effects) linked to the development of driver assistance systems? What are the optimized parameterizations of technical aspects of safety functions if one wishes to reach the maximum safety benefit?

In order to standardize the research questions for the effectiveness assessment, the inquiry proposed all contributors to fill in table 2.

**Table 2.**
**Research questions for the effectiveness assessment (6: high interest; 1: low interest; N = 26).**

| Research questions | Mean Rating |
|---|---|
| What are the potential safety benefits of driver assistance systems (ADAS) in short term (<5yrs) considering that there are a lot of other road safety actions | 5.0 |
| What are the optimal parameterizations of technical aspects of safety functions if we wish to reach the maximum safety benefits? | 4.9 |
| What are the potential safety benefits of driver assistance systems (ADAS) in mid-term (5-10yrs) considering that there are a lot of other road safety actions | 4.8 |
| What are the externalities (side effects) linked to the development of driving assistance systems? | 4.2 |
| What are the potential safety benefits of driver assistance systems (ADAS) in long-term (>10yrs) considering that there are a lot of other road safety actions | 4.1 |
| What are the societal and economic benefits of driver assistance systems in short term (<5yrs)? | 3.6 |
| What are the societal and economic benefits of driver assistance systems in mid-term (5-10yrs)? | 3.3 |
| What are the societal and economic benefits of driver assistance systems in long term (>10yrs)? | 2.9 |

The results indicated there seem to be a higher interest in short term effects compared to long term effects. Furthermore, economic aspects seem to play a minor role in the effectiveness assessment compared to the quantification of the safety effects. However, this could be due to the current composition of members in P.E.A.R.S. The second most important aspect of the effectiveness assessment is the parameterization of functions.
Furthermore, the research questions will be clustered into different categories:

- the kind of effect that is quantified by used metric;
- the function, respectively the type of functionality under study. Here, also the penetration rate of the considered function must be mentioned;
- the considered scenario (e.g., maneuver, accident types, traffic participants, type of road…);
- the considered region and time horizon of prediction.

By combining these different categories, various but harmonized research questions can be generated. Examples of precise research questions defined by the construction kit are:

- Relative change in accidents due to pedestrian AEB (100% penetration rate in passenger vehicles) in urban pedestrian situations in Germany (short term = 2 years in the future);
- Absolute reduction of MAIS3+ injuries due to AEB (50% penetration rate in cargo vehicles) in highway rear-end accidents (excluding two-wheelers) in EU28 (midterm = 5 years in the future).

**Outcome 3: Harmonization of the Assessment Metrics**

The effect of an ADAS function can be analyzed in different ways. In order to come to a standardized assessment for the effectiveness of functions also the metric used for this assessment needs to be harmonized. Similar to the research questions also here P.E.A.R.S. has taken a bottom-up approach. Different available metrics that have been used by the different partners have been collected and clustered. The effect of a function can be described - independent of the metric used - in two ways: in absolute numbers or in relative change compared to a baseline scenario. An overview on the different metrics is given in Table 3. In the second step it has been determined by means of the inquiry how often a certain metric is used by the different partners, see also Table 3.

**Table 3.**
**Overview on metrics to determine the effectiveness of in-vehicle safety function (N=26).**

| Method | Type of metric | How often is the metric used by partners? (Mean value;1: never used … 5: 6 always used) |
|---|---|---|
| Avoidance of accidents | Absolute | 5.2 |
| Avoidance of injuries | Absolute | 4.9 |
| Avoidance of critical situations | Absolute | 3.9 |
| Changes in injury severity distributions (MAIS, fatality, ISS, etc.) | Relative | 4.8 |
| Changes in health aspects (functional years lost, etc.) | Relative | 2.2 |
| Changes in economic aspects (property damage, economic costs, etc.) | Relative | 2.1 |
| Percentage of triggered (critical) events | Relative | 3.3 |

The most frequently used metrics are the absolute number of avoided accidents and the number of avoided injuries. For the relative indicators the change in injury severity is analyzed most often. Health aspects, like functional years lost as well as economic aspects are more seldom used so far.

**Outcome 4. A harmonized assessment process**

Today different approaches for the effectiveness assessment of in-vehicle safety functions or ADAS functions are known. Table 4 provides an overview of different methods that have been applied in the past. Each approach has advantages as well as disadvantages with respect to the required effort, the appropriateness to answer the research questions, and the accuracy of the results. They will be investigated during the P.E.A.R.S. initiative. In order to get to a standardized approach for the effectiveness assessment of ADAS, P.E.A.R.S. collected different known assessment approaches, and, by means of the inquiry, assessed how often the different approaches are currently used for effectiveness assessment and which are the most common approaches for this purpose. The results are given in Table 4.
The results indicated that the most common approach is simulation, combining different techniques. Therefore, in P.E.A.R.S. it has been agreed to choose the general approach ‘virtual simulation’ as the basis for a harmonized approach for effectiveness calculation. A basic concept of a virtual simulation approach is given in Figure 2. P.E.A.R.S. seeks for a more detailed specification of the different steps. This includes the definition of minimum requirements for input data as well as the description of requirement for the used simulation models.

**Table 4.**
**Overview on method to determine the effectiveness of in-vehicle safety function (n = 26).**

| Method | Examples application | How often is the method used by partners? (1: never used … 5: always used) |
|---|---|---|
| Prospective statistical analysis based on crash data | TRACE [17] | 4.4 |
| Retrospective statistical analysis based on crash data | Effect of ESC [16] | 4.3 |
| Physical test | Assessing Forward Collision Warning [22], | 3.7 |
| Driving simulator | Daimler brake assist [21] | 3.2 |
| Field test | euroFOT [10] | 3.2 |

| | Examples application | Yes | No |
|---|---|---|---|
| Do you make use of virtual simulation in your assessment of system effectiveness? | rateEFFECT [18], Effectiveness Assessment of active Safety Systems [19], interactIVe SIMPATO [20], | 21 | 6 |

**Outcome 5: Description of the conceptual simulation models**

The conduction of simulation of certain driving situations requires a reproduction of the real world in the virtual simulation environment. This is typically done by different models that aim to represent the influencing parts of the reality under consideration and that run within a simulation framework.
Thus the first question is: what aspects of driving situations need to be modeled in order to simulate the function behavior for the effectiveness assessment. Also here a bottom-up approach has been taken by P.E.A.R.S. State-of-the-art simulation frameworks and models have been identified and their strengths and limitations have been listed.
As shown in Figure 2, the observer model and guiding model are required in order to run the simulation and to ensure at each point of time the appropriated simulation model is used as well as to ensure that the simulation models are used in the correct order. The scenario model describes, as the name already indicates, the scenario that should be analyzed. This description includes longitudinal and lateral controls (e.g., velocity, steering) of the involved traffic participants. It is linked to the traffic model that describes the characteristics and behavior of the other involved road participants and the environment model that describes the characteristic (road characteristics, traffic regulations, (temporarily) static objects, illumination, and weather). Traffic models were classified by on structure, included components, validity, and their nano-, micro-, meso-, or macroscopic modelling approach.

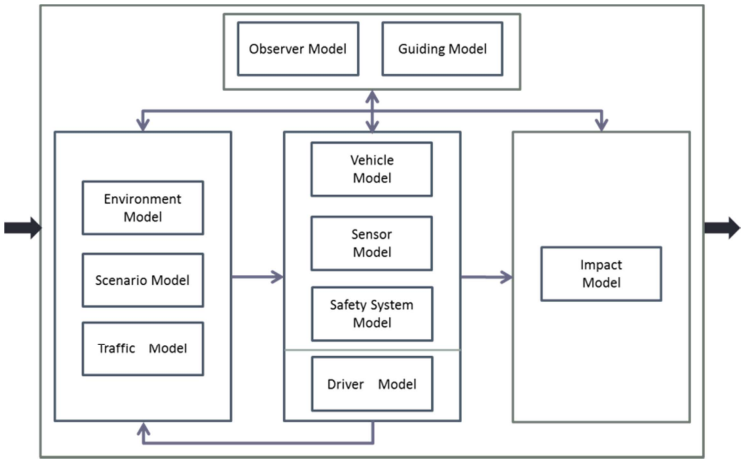


***Figure 2: Setup of Simulation Framework***

Further important models next to the scenario model are the driver, the vehicle as well as function models. If required, a driver or vulnerable road user model for other traffic participants can also be used. The behavioral models are used to represent how a driver reacts to the stimuli that he / she receives from the environment, other vehicles, traffic participants, and traffic signals in the traffic stream, or from inside a vehicle. The classification for behavioral models includes characteristics such as model structure, requirements, validity, and usability for different driving tasks. Based on the required complexity of the assessment, the driver model can include a description of driver behavior in critical situations, driver recognition (e.g., HMI, warnings), and driver response (e.g., latency times, steering, braking). Models should consider statistical distributions in intra- and inter-personal behavior, representing temporal driver state and preferred driving style, respectively.
The vehicle model describes all relevant parameters of the vehicle under test in the required degree-of-freedom. This model can include parameters for the chassis, suspension, tire, steering, and vehicle dimensions, depending on the degree-of-freedom used. Within the vehicle also the safety function needs to be modeled. The model for the function should describe the characteristics of the tested function including the system response as well as the operation regimen. The model of a function is typically a combination of one or more sensor models, a decision model (algorithm), and an actuation model (braking, steering, brake pulse, etc.), as well as - if required - communication model. Independent of the degree-of-freedom chosen for the different models, a vehicle model and function model is mandatory for the effectiveness assessment.
In case an accident occurs with the simulation also an impact model might be required, which defines an impact between two or more participants (e.g., cars, pedestrians, objects) as well as the behavior of occupants and their expected injuries. The model can contain a structure based crash model (e.g., the conventional impact model, force based models, multi-body models, and finite element models), kinematic and kinetic injury model (biomechanics) as well as statistical injury data. Depending on the metric used such a model is mandatory for the assessment.
In the next step, P.E.A.R.S. will take a top-down approach in order to specify the different models in more detail. This step includes 4 different tasks:

- Define the required input to the framework (direct or from pre-processing);
- Define the necessary output of the framework for the post-processing of simulation results;
- Describe the initialization (start condition) of a scenario simulation;
- Describe the termination criteria of a scenario simulation.

All models should not only be developed but also validated. The work is currently ongoing and a detailed description of the models is expected for end of 2015. The level of ‘granularity’ of each of the models will depend on the research questions, the degree of accuracy of the expected outcomes, and of course on the degree of availability of the data required for each model.

## DISCUSSION

The P.E.A.R.S. project is an important step towards a harmonized approach on the assessment of the effectiveness of road safety measures, especially for ADAS. Input to the assessment methodology is gathered from different types of stakeholders and the project is defined as an open platform for exchange and cooperation for all interested organizations.
Within the last three years of project existence, working groups have been established covering research questions, assessment metrics, data availability and requirements, simulation framework, and model requirements and verification. Within each working group objectives were defined, appropriate actions were derived and results were presented and exchanged on the General Assembly. A constructive working flow has been established in this way.
Elaborated output from the working groups is implemented into a working document that is designed as a ‘recipe-book’. Further the document is set up to deliver the appropriate input for a draft proposal of an ISO or SAE standard. A first public available version of the ‘recipe-book’ is planned for the end of 2015.
So far, results from working group activities and an internal inquiry are available. All of the P.E.A.R.S. project participating organizations (N=32; 44% industry, 28% university, 19% research institutes, one governmental organization) responded to the inquiry. Main reasons for participation in the harmonization group are being informed about ongoing work and contribution to a common methodology. Further important is the contribution to an ISO/SAE draft proposal and a framework development. Half of the responders within P.E.A.R.S. have less interest in model development itself. For the outcome of the project all participants of the enquiry have high

expectations on a common methodology and most of them have the expectation that the working document will lead to an ISO/SAE draft.
As mentioned before, near-term effectiveness is currently more in focus than mid- or long-term effectiveness. But future research will involve benefit of ADAS functions in mid-term, whereas long term evaluations becomes similar important than short term. Optimal parameterization of ADAS systems remains a key point. As for the objectives, the understanding of future accident situations and validation of systems is relevant. To date, most applied methods for evaluation of active safety-systems are prospective and retrospective statistical analysis. The majority of toolboxes for virtual simulation are own developments or based on the commercial tools Matlab/Simulink. For ADAS specific commercial tools, CarMaker is most frequently used. The majority of the responders make use of real accident data in their virtual simulations, a smaller group of users generate data stochastically themselves. Half of responders evaluate also 'avoidance of critical situations'. Most investigated events are crashes, near-crashes, and crash-relevant conflicts, only a minority consider normal driving, but putting this data as highly important.
Just now evaluations are done for (in this order) specific European country, EU in total, USA, Japan, China and North America. In the future evaluations are desired for EU in total, specific European country, USA, China, Japan, Asia, and North America, which means that China and Asia will come more into focus.
Changes in vehicle fleet, market penetration, and driver behavior are regularly considered by half of the responders.
Except of in-car modification, the 9-safety mechanisms [23] are not much considered by half of the responders. In the future analyses focus remains on the first point of nine safety mechanisms, the direct in-car modifications. Slight increase can be seen for influence by road side application and modification of driver behavior.
At the current state most detailed models are for passenger cars, ADAS algorithms, and sensors, followed by models for driver/VRU. Highest need in increase for level of detail is seen in the environment model, driver model, and sensor model, whereas the last two have given highest priority. Over 90% of the responders see a relevant barrier in the simulation of driver behavior. Two-third of responders regularly uses robustness analysis for the evaluation of the results. More than half of the participants conduct a verification by reviewing mathematical-physical equations and by comparison against physical tests or other secondary data.
All participants conducting virtual simulation agree on the importance to implement a harmonized methodology into their own framework with specific focus on the implementation of a scenario description, driver/VRU models, and usage of high quality data.
A standardized approach for the effectiveness assessment as proposed by P.E.A.R.S. provides the opportunity to deliver a widely accepted methodology, to define requirements to input data, and thus to establish the boundary conditions for reliable and repeatable estimations of the impact of new ADAS functions. This is important for the initial step to introduce effective ADAS functions to a market and further to accelerate their market penetration. This approach will also support the comparison of different studies in the same field and provide a better understanding of traffic safety in general. Additionally, this can lead to standardization of consumer oriented assessment of ADAS functions (e.g., in Euro NCAP), since virtual simulation can deliver more distinct results on the real life effect than only a limited set of physical test scenarios.
Next to the advantages all approaches for effectiveness assessment have their limitations. This applies for the harmonized approaches itself, as defined by P.E.A.R.S., and to the generated results. First of all, the effectiveness assessment relies on the input data. Therefore, reliable results can only be determined, if the quality, which means accuracy and representativeness, of input data is ensured.
The same applies with respect to the used models. It needs to be ensured that the models describe the real behavior in a sufficient manner. The definition of 'sufficient' depends on the function under study, the investigated scenario, as well as the aimed quality of the results. This is, verification and validation of the simulation environment has to be considered in high priority.
Although the P.E.A.R.S. approach focuses mainly on ADAS functions operating in critical driving situations, driver assistance systems that support the driver during the normal driving process (ACC, lateral lane support), connected ADAS or automated driving functionalities can be assessed in the same framework with regard to content extension, but based on the same methodology.
As the project does not have any external funding the progress of the project is currently depending on individual contribution of the stakeholders.

## OUTLOOK

So far the P.E.A.R.S. group consists of more than 30 stakeholders from the automotive industry, academia, private, and governmental research organizations in Europe. For a global harmonization approach and a

worldwide standard it is necessary to involve stakeholders from all parts of the world. This would support even more the consideration of differences in environment, traffic participant mode, vehicle fleet, and road user behavior in the methodology. Additionally, the input from a broader group of stakeholders would lead to a higher acceptance and thus, spread of the methodology.
Each stakeholder has its own individual objectives and own research questions that need to be answered. Results of assessments are most easily explained, discussed and understood, when a harmonized approach is followed, and the steps that have been taken in the assessment process are well-known and agreed upon. For the common understanding, it is important that the stakeholders represent different sectors in the automotive safety arena such as vehicle industry, academia, research institutes, consumer organizations, road authorities, policy makers, and insurance companies.
Although currently a focus is taken on developing a methodology for ADAS functions which are typically automation level 1 (assisted driving), the process should not be essentially different for higher levels of automation [13]. This explains the ambition, to provide results on the short term by developing a methodology dedicated to ADAS, with the requirement that the developed process is generally applicable and easily adaptable for higher levels of automation.
The partners in P.E.A.R.S. invite organizations that are interested in contribution to the development of a harmonized effectiveness assessment methodology to contact any of the authors for more information and participation in the General Assembly and working groups.

## REFERENCES


[1] Page Y, et al. Reconsidering accident causation analysis and evaluating the safety benefits of technology: final results of the TRACE Project ESV Conference. Stuttgart, June 2009
[2] eIMPACT, EU project on Methodology for assessing the socio-economic effect of safety systems. Web-page: http://www.eimpact.info/
[3] euroFOT, EU project on Field tests of ADAS functions. Web-page: http://www.eurofot-ip.eu/
[4] ADVISORS, EU project on Method to assess the impact of ADAS w.r.t. safety & environmental performance. Web-page: http://www.advisors.iao.fraunhofer.de/
[5] DaCoTA, EU project on Analysis of data from 30 European countries as input for decision-making tools. Web-page: http://www.dacota-project.eu/
[6] IMVITER, EU project on Implementation of Virtual Testing procedures in existing (passive) safety standards. Web-page: http://www.imviter.com/
[7] InteractIVe, EU project on Impact assessment for active safety systems by accident re-simulation. Web-page: http://www.interactive-ip.eu/
[8] PReVENT, EU project on General methodology on assessment of ADAS function. Web-page: http://www.prevent-ip.org/
[9]Schittenhelm H, The Vision of Accident Free Driving – How Efficient are we Actually in Avoiding or Mitigating Longitudinal Real World Accidents, ESV conference, Stuttgart, June 2009. Paper can be found at: http://www-nrd.nhtsa.dot.gov/pdf/esv/esv21/09-0510.pdf.
[10] Benmimoun, M.; Zlocki, A.; Eckstein, L., Advanced driver assistance systems: Benefit evaluation method and user acceptance for adaptive cruise control and collision warning system, TRB 92nd Annual Meeting and Transportation Research Record, Washington, USA, 2014
[11] N.N., Traffic jam assistant, internet: http://www.bmw.com/com/en/newvehicles/5series-/sedan/2013/showroom/driver_assistance/traffic_jam_assistant.html, BMW, 2015
[12] N.N., Mercedes-Benz Intelligent Drive, internet: http://www.mercedes-benz.com/en/mercedes-benz/innovation/mercedes-benz-intelligent-drive/, Daimler, 2015
[13] N.N.: Taxonomy and Definitions for Terms Related to On-Road Motor Vehicle Automated Driving Systems, SAE Standard J3016, USA, 2014.
[14] Lutin, J. M.; Kornhauser, A.; Lerner-Lam, E., The Revolutionary Development of Self-Driving Vehicles and Implications for the Transportation Engineering Profession, ITE Journal, July 2013.
[15] Scholliers, J. et al., PReVAL - Project final report and recommendations for future assessments, deliverable D12/D16.4, PReVENT project, 2008
[16] Unselt, T.; Breuer, J.; Eckstein, L.; Frank, P., Avoidance of "loss of control crashes" through the benefit of ESP, FISITA Conference paper no. F2004V295, Barcelona, Spain 20014

[17] Page, Y., Riviere, C., Cuny, S., A posteriori evaluation of Safety Functions effectiveness – Methodologies,TRACE Projekt, Deliverable 4.2.1, 2007
[18] Wille, J. M.; Jungbluth, A.; Kohsiek, A.; et al., rateEFFECT – Entwicklung eines Werkzeugs zur Effizienzbewertung aktiver Sicherheitssysteme, 5. Tagung Fahrerassistenz, München, 2012
[19] Wisselmann, D., Effectiveness Evaluation of active Safety Systems, Workshop on Connected and Automated Driving systems, Tokyo, 2014
[20] Van Noort, M.; Bakri, T.; Fahrenkrog, F.; et al., SIMPATO – the Safety Impact Assessment Tool of Interactive, 16th International IEEE Conference on Intelligent Transportation Systems (ITSC), Den Haag, 2013
[21] Unselt, T.; Breuer, J.; Eckstein, L, Fußgängerschutz durch Bremsassistenz, Aktive Sicherheit durch Fahrerassistenzsystem, Präsentation, München, 2004
[22] Forkenbrock, G.; Snyder, A.,; Heitz, M.; et al.; A Test Track Protocol for Assessing Forward Collision Warning Driver-Vehicle Interface Effectiveness, NHTSA Report, DOT HS 811 501, 2011
[23] Draskóczy, M., Carsten, O.M.J., Kulmala, R. (Eds.), 1998. Road Safety Guidelines. CODE Project, Telematics Application Programme, Deliverable B5.2.
[24] IEEE Computer Society. 1516-2010 IEEE Standard for Modeling and Simulation (M&S) High Level Architecture (HLA). Institute of Electrical and Electronics Engineers, Inc., August 2010

# Innovative Seat Belt System for Reduced Chest Deflection

**Bengt Pipkorn**
Autoliv Research
Sweden

**Francisco J. Lopez-Valdes**
University of Zaragoza
Spain

**Christer Lundgren**
**Dan Bråse**
**Cecilia Sunnevång**
Autoliv Research
Sweden

Paper Number 15-0371

## ABSTRACT

An innovative seat belt concept aimed at reducing chest injuries was evaluated by means of mechanical tests and mathematical modelling. The tools used were mechanical THOR dummy, mathematical THOR dummy model, THUMS human body model and (Post Mortem Human Surrogates) PMHS. The potenital chest injury reducing benfits with a innovative seat belt concept relative to a state of the art belt system was evaluated in sled tests. The reference belt system was a state of the art belt system with a pretensioning of 2kN at the retractor, a force limiter of 4.5kN and an outer lapbelt pretensioner with a pretensioning force of 3.5kN. The innovative seat belt concept was consisting of a retractor equipped with a 2kN pretensioner at the retractor, a force limiter of 6kN and two 3.5kN pretensioners at the buckle and outer lap belt anchorage. The belt was split at the buckle and the lower end of the diagonal belt was moved 50mm forward. With the altered belt geometry the load on the lower part of the chest was reduced and the peak chest deflection was reduced relative to a state of the art belt system. In mechanical sled tests with rigid seat and an impact velocity of 35 and 30kph with the THOR dummy peak chest deflection was reduced by 8.0mm compared to a state of the art belt system. In the corresponding sled model with the THOR dummy model peak chest deflection was reduced by 13mm. Head x-displacement was increased by 26mm for the mechanical THOR dummy and 24mm for the THOR dummy model. For the THUMS model pleak chest deflection was reduced by 10mm with the split buckle system.

Generally for the mechanical THOR dummy, the THOR dummy model and the Autoliv THUMS model peak chest deflection was reduced by approximately 8-13mm with the split buckle belt system while only a minor increase in head x-displacement was observed relative to a state of the art belt system.

## INTRODUCTION

Occupant fatalities and injuries in car crashes remains a global health issue. World Health Organization (WHO) found road injuries to be the 9th leading cause of death in the world after diseases such as stroke and heart disease [1]. Restraint systems have been developed and improved and have contributed to reduce the number of seriously and fatally injured occupants in vehicle crashes. However people are still being injured and killed in traffic. In Europe, frontal crashes still account 40% of all fatalities in car accidents [2]. In these accidents, injuries to the thorax are common and account for 13% of all moderate injuries and 29% of all severe injuries [3]. Statistics also show that the most frequent severe thoracic injuries are rib fractures [4]. Furthermore, the number of rib fractures is a good indicator of injuries to the thoracic and abdominal organs [5].

In testing with post mortem human subjects (PMHS) it was found that the injury threshold for chest deflection is strongly dependent upon the age of the subject [6]. This is true regardless of whether injury onset or severe injury is considered. A 30-year-old has a 50% risk of sustaining one rib fracture at a chest deflection level of 35% (of the

total width of the chest). A 70- year-old has a 50% risk of more than 6 rib fractures at 33% deflection. The age-fragility correlation is particularly important while in 2012 about 17% of all Europeans were aged 65 and older, the share of those above age 65 will rise to 28% in 2020 [7]. Due to their greater frailty and fragility, there is a need to develop restraint systems that reduces the load on the chest of the elderly occupants.

The use of mathematical human body models for restraint evaluation is increasing. One advantage with the human body models is that injuries can be assessed based on physical parameters such as strain for fracture analysis. A strain-based probabilistic method to predict rib fractures with finite element human body models was developed based on data from cortical bone coupon tests [8]. The method combined the results with collision exposure information to predict injury risk and potential intervention effectiveness in the field. An age-adjusted ultimate strain distribution was used to estimate local rib fracture probabilities within an FE model. These local probabilities were combined to predict injury risk and severity within the whole ribcage.

The Autoliv THUMS model was derived from the THUMS model (Total Human Body Model for Safety, version 1.4). The THUMS model was updated with a number of in-house modifications to improve its biofidelity in frontal impacts using table top and sled PMHS tests [9, 10]. The rhomboids major and rhomboids minor muscles that connect the medial border of the scapula to the spine were missing in the original THUMS and were added to the Autoliv THUMS. The aim of the study is to evaluate the potential injury reducing benefits of an innovative belt system, which alters the load distribution of the seat belt on the chest, relative to a state of the art 3-point belt system.

## METHOD

The evaluation of the innovative seat belt system was carried out by combining mathematical modelling with mechanical testing [11]. The sled test fixture (Gold Standard) consisted of a rigid metallic frame allowing complete visual access to the occupant while preserving the basic geometry of a standard seating position of a passenger car. This test fixture was used elsewhere as a reasonable approximation to the passenger posture in the study of ATD biofidelity and in the development of thoracic injury criteria [12, 13]. The 50%-ile THOR model (THOR-M version 0.6) was used to validate the test environment (seat and seatbelt) by matching predictions from the model to experimentally measured THOR test responses (Figure 1). The impact velocity was 35 km/h and peak acceleration 20g and a duration of approximately 80ms. The reference belt system was a state of the art belt system with a pretensioning of 2kN at the retractor, a force limiter of 4.5kN of the diagonal belt and a 3.5kN outboard lap belt pretensioner.

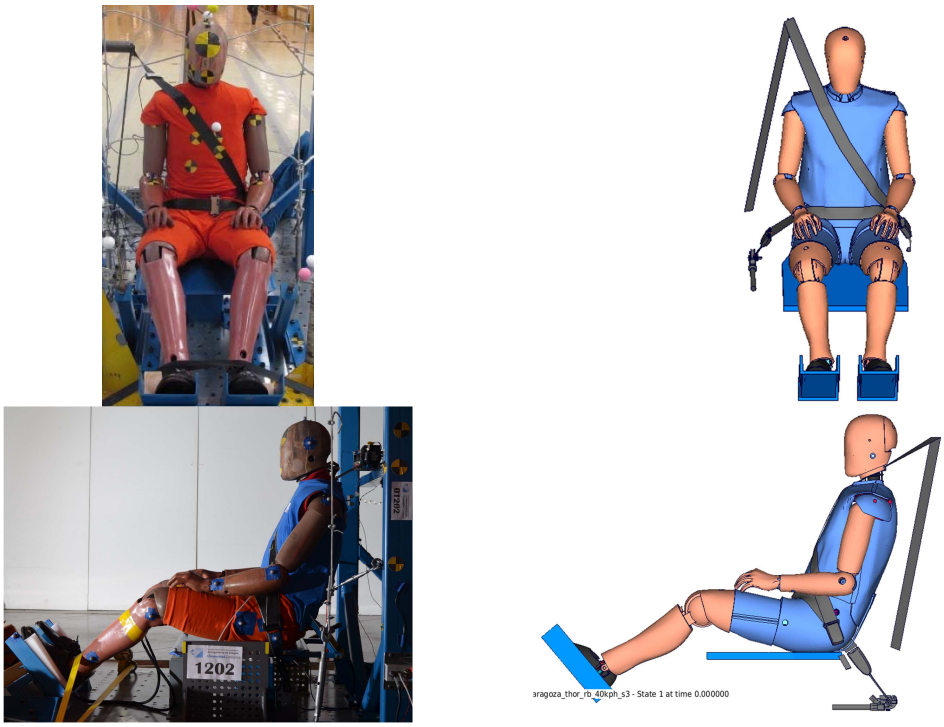


***Figure 1. THOR in Gold Standard***

When satisfactorily agreement between mechanical test results and mathematical model predictions was obtained for the reference belt system, the model of the restraint system was considered to be validated. The reference belt system was replaced with an innovative belt system (split buckle). The split buckle system consisted of a retractor equipped with a 3kN pretensioner at the retractor, a force limiter of 6kN at the diagonal belt and two 3.5kN pretensioners, one at the buckle and one at the outer lap belt anchorage. The belt was split at the buckle and the lower end of the diagonal belt was moved 50mm forward (Figure 2). THOR simulations were carried out with the advanced belt system, and thereafter corresponding mechanical tests with the THOR dummy were run to confirm the model predictions.

***Figure 2. Split buckle***

For both belt systems, standard and split buckle, chest loading in terms of mutlipoint deflection and strain were evaluated. The deflection measurement in the THOR consists of four 3D IR-Traccs (3D Infra-Red Telescoping Rod for the Assessment of Chest Compression) and their location was replicated in the THUMS model by deflection measurement at the level of the 4th rib for upper thorax, and between rib 6 and 7 for the lower thorax (Figure 3). In addition for THUMS rib strain was assessed. Head displacement (x-direction) and belt forces were also evaluated for the two systems.

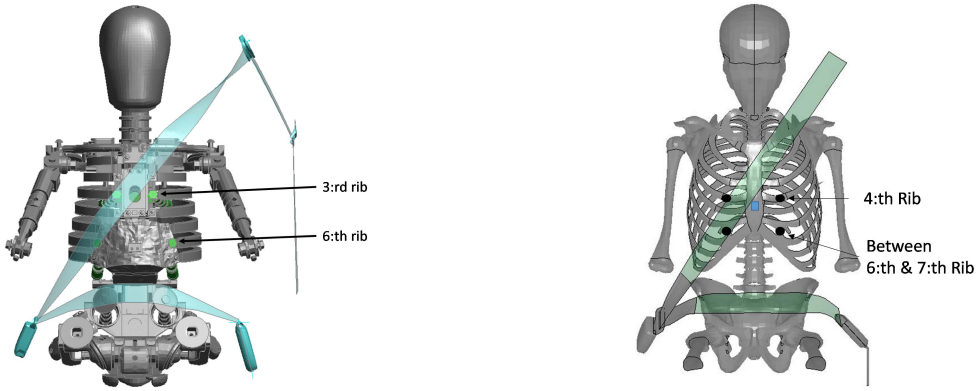


***Figure 3.Upper Left, Lower Left, Upper Right, Lower Right Chest Deflection Transducers THOR and THUMS***

The THOR dummy model was replaced with the human body model Autoliv THUMS. Both the reference belt system and the split buckle system were analyzed with the Autoliv THUMS model. Post Mortem Human Subject (PMHS) tests were previously carried out in the same test set-up using both the reference belt system and the split buckle system, and the results were to some extent compared to the Autoliv THUMS model results in this study [11]. The PMHS were of approximately the same age (reference: 42 YO, 60 kg, 159 cm; advanced: 39 YO, 62 kg; 175 cm). The predicted head x-displacement and belt forces were compared to the corresponding measurements in the PMHS tests, and the predicted risk to sustain rib fractures were compared to the number of fractured ribs in the post mortem human subject (PMHS) tests.

A parameter study, to evaluate the influence on chest deflection on diagonal belt lower attachment point, was carried out. The lower attachment point of the diagonal belt was moved in steps of 50mm horizontally (Figure 4). The buckle was moved 50mm rearwards, 50mm forward and 100mm forward relative to the test position.

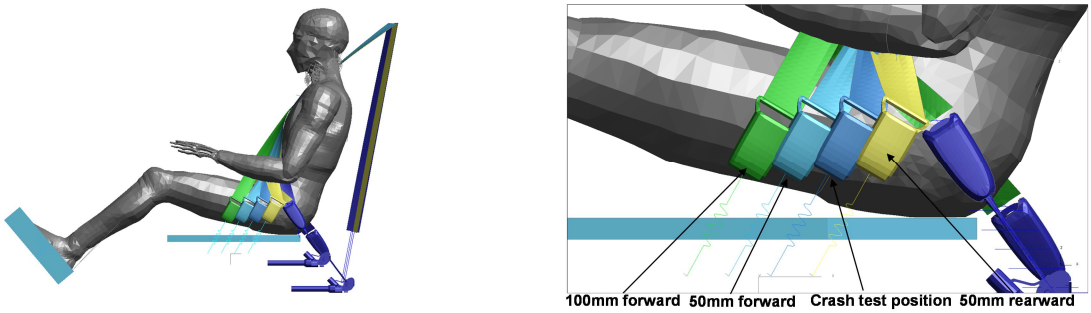


***Figure 4. Lower attachment point in parameter study***

## RESULTS

### Model Benchmark

The average peak chest x-deflection in the mechanical reference test with a state of the art belt system was for the mechanical THOR dummy 32mm in upper left IR-Tracc (Figure 5). The predicted peak chest deflection with THOR dummy model was 33mm in the upper left IR-Tracc. For the split buckle system the chest deflection in the mechanical THOR test was 25mm. For the model the predicted peak chest deflection was 20mm.

For the mechanical reference test with the THOR dummy head x-displacement was 397mm. The predicted head x-displacement was 343mm (Figure 5). For the split buckle system the x-displacement in the mechanical reference test was 405mm while for the model the head x-displacement was 367mm.

Peak belt force in the mechanical reference test was 5582N (Figure 5). While the predicted force was 4770N. In the mechanical split buckle belt system test the average diagonal belt force was 6085N. The predicted force for the split buckle system was 5606N.

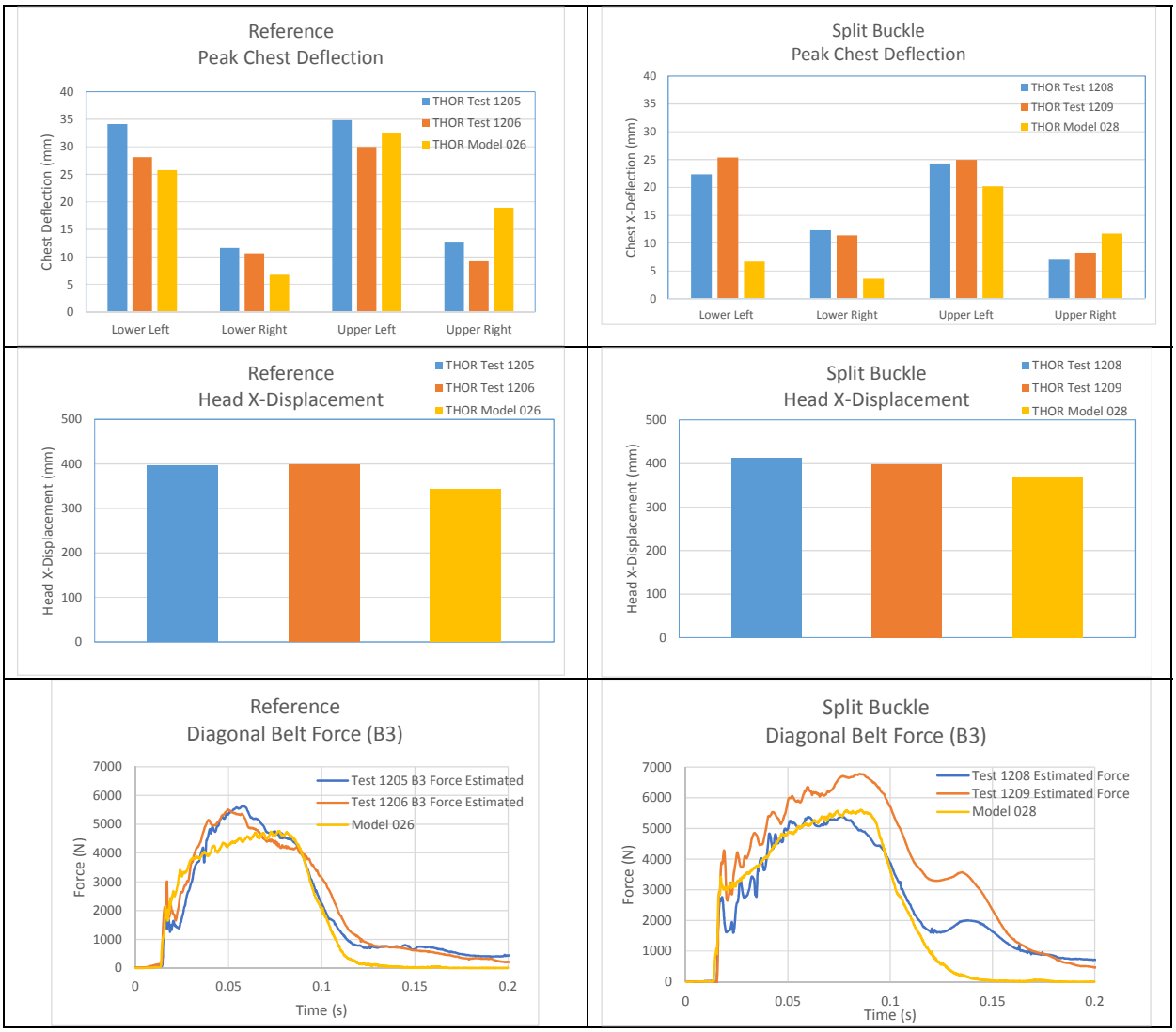


***Figure 5. THOR Test Results and Model Predictions, Chest Deflection, Head X-Displacement, Diagonal Belt Force***

For the THUMS model the predicted chest deflection for the reference belt system was 30mm in the upper left transducer and for the split buckle system the predicted chest deflection was 20mm (Figure 6).

The max head x-displacement in the reference test for the PMHS was 189mm while for THUMS the predicted head x-displacement was 378mm (Figure 6). For the split buckle system the max head x-displacement for the PMHS was 306mm while for THUMS the predicted x-displacement was 409mm.

The diagonal belt force in the reference PMHS test was 4000N. The predicted force with THUMS was 3900N. For the split buckle system the diagonal belt force in the PMHS test was 6000N while the predicted force was 5500kN.

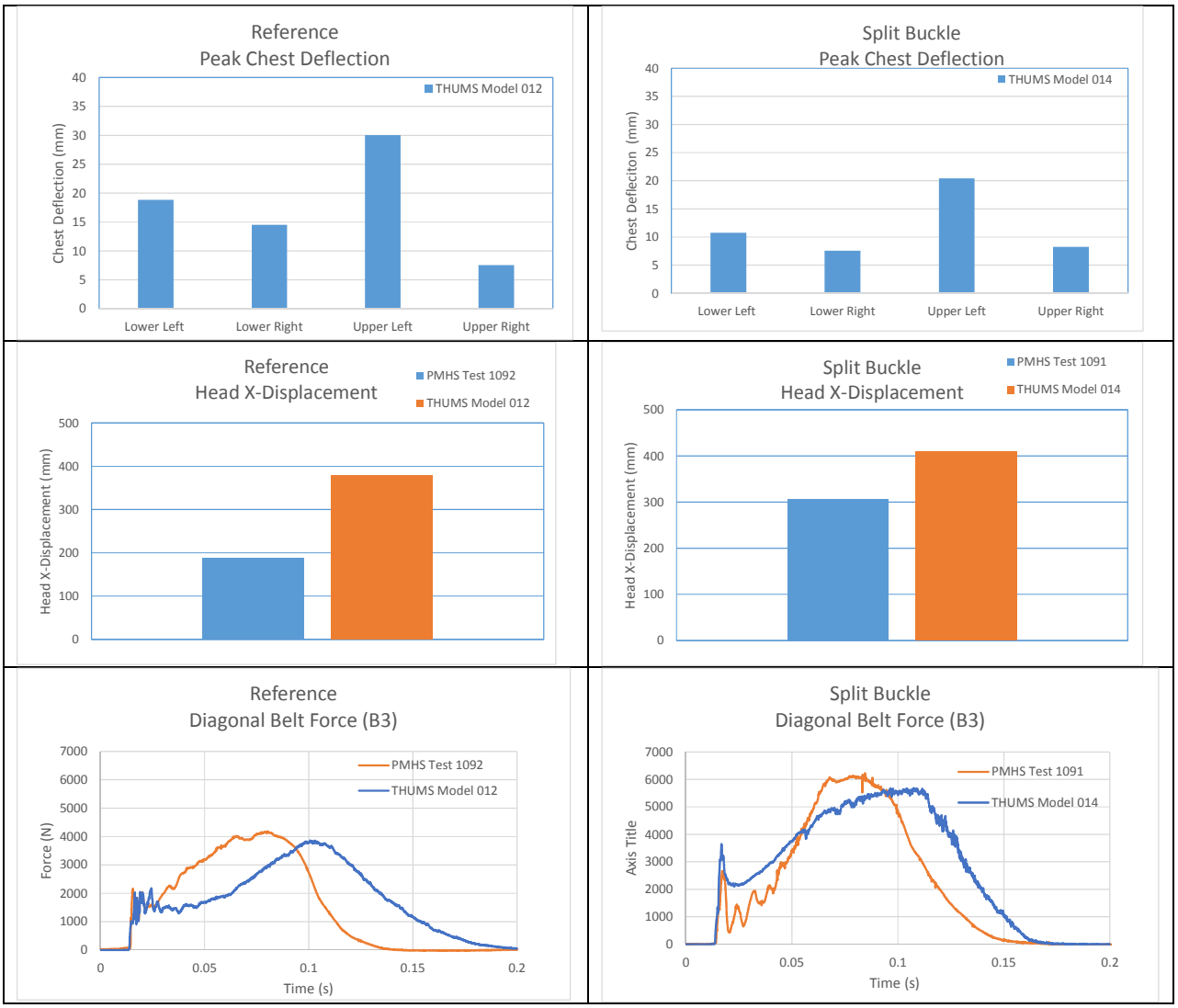


***Figure 6. PMHS Test Results and THUMS Model Predictions Chest Deflection, Head X-Displacement, Diagonal Belt Force***

**Split Buckle Parameter Study**

In the parameter study carried out for the split buckle system the lower attachment point for the diagonal point was moved in steps of 50mm. The predicted peak chest deflection for THOR was obtained at the upper left IR-Tracc for all locations of the lower attachment point (Figure 7). By moving the attachment point 150mm forward in the vehicle the chest deflection was reduced from 22mm to 15mm while ead x-displacement was increased by 41mm, from 357mm to 398mm.

For THUMS the peak chest deflection was for the upper left IR-Tracc (Figure 7). By moving the lower attachment point 150mm forward peak chest deflection was reduced from 24mm to 15mm while the head x-displacement was increased by 95mm, from 376mm to 471mm.

Peak belt forces for both the THOR dummy model and THUMS were 5500N. The belt forces were not altered when the attachment point was moved forward in the vehicle.

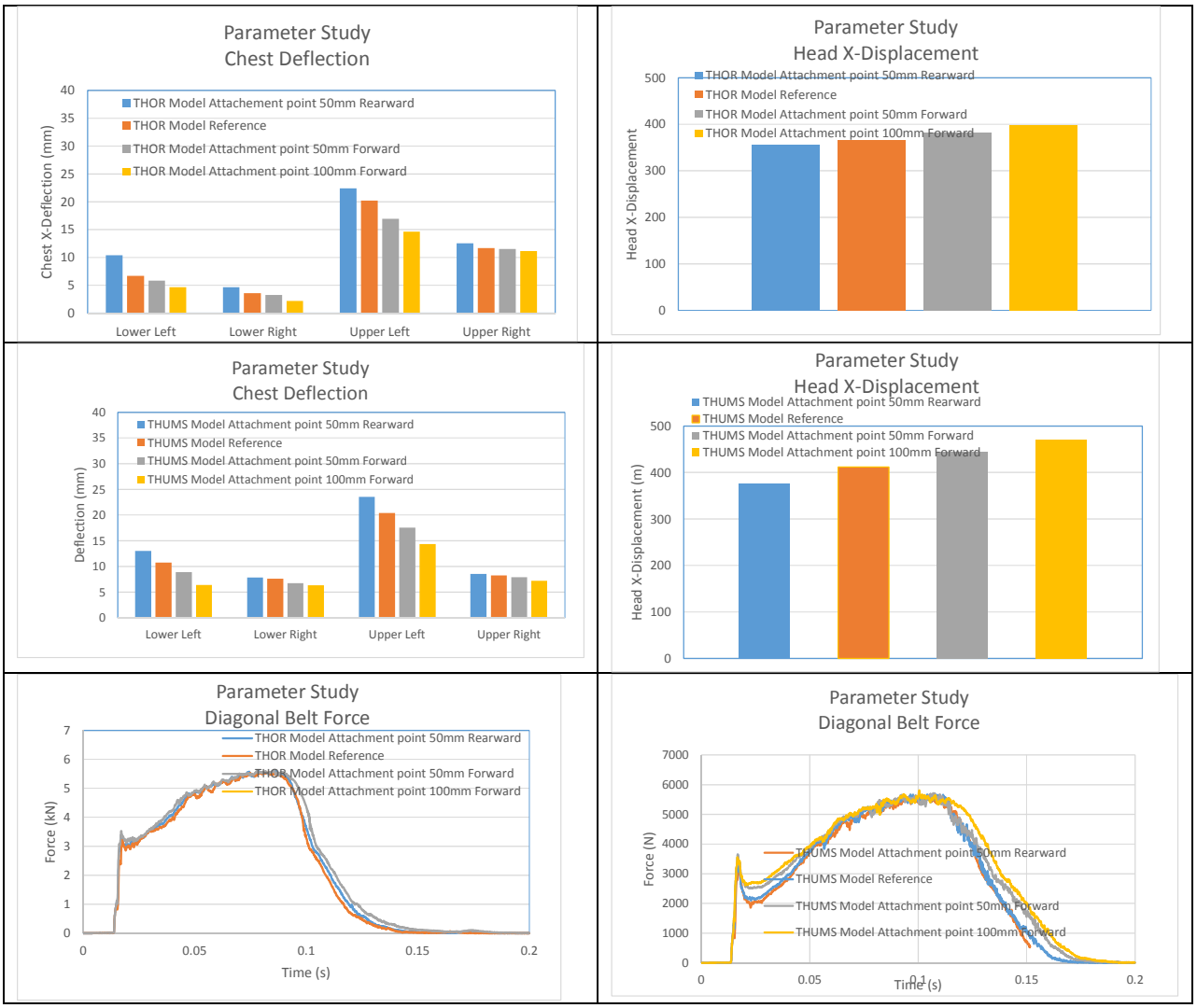


***Figure 7. THOR model & THUMS Chest Deflection, Head-Displacement and Belt Forces for Altered Lower Attachment Point***

For the Autoliv THUMS 0 fractured ribs were predicted for 39 and 60 year old occupants for both the reference belt system and the split buckle system.

## DISCUSSION

By splitting the belt system and moving the lower attachment point of the diagonal belt forward in the vehicle, increasing the pretensioning force and adding a lap belt pretensioner peak chest deflection was reduced. By moving the lower attachment point forward the load from the belt is reduced in the lower part of the chest. By increasing the level of the load limiter the excursion of the body was kept at the same level as for the reference belt system while the chest deflection was reduced. There is a potentially increased risk of clavicle injuries due to the increased force at the shoulder level. However, in the PMHS tests no clavicle injuries were observed [11]. In addition, the influence on pelvis kinematics of the split buckle system will be evaluated in future analysis.

A split buckle in vehicle system can consists of one buckle that splits in a crash (Figure 8). The occupant buckles up in the same way as a state-of-the-art belt system today. Both the diagonal belt and the lap belt are pretensioned by moving the buckle downwards. In a crash the lower point of the diagonal belt is moved forward while the lap portion of the belt remains at the initial location.

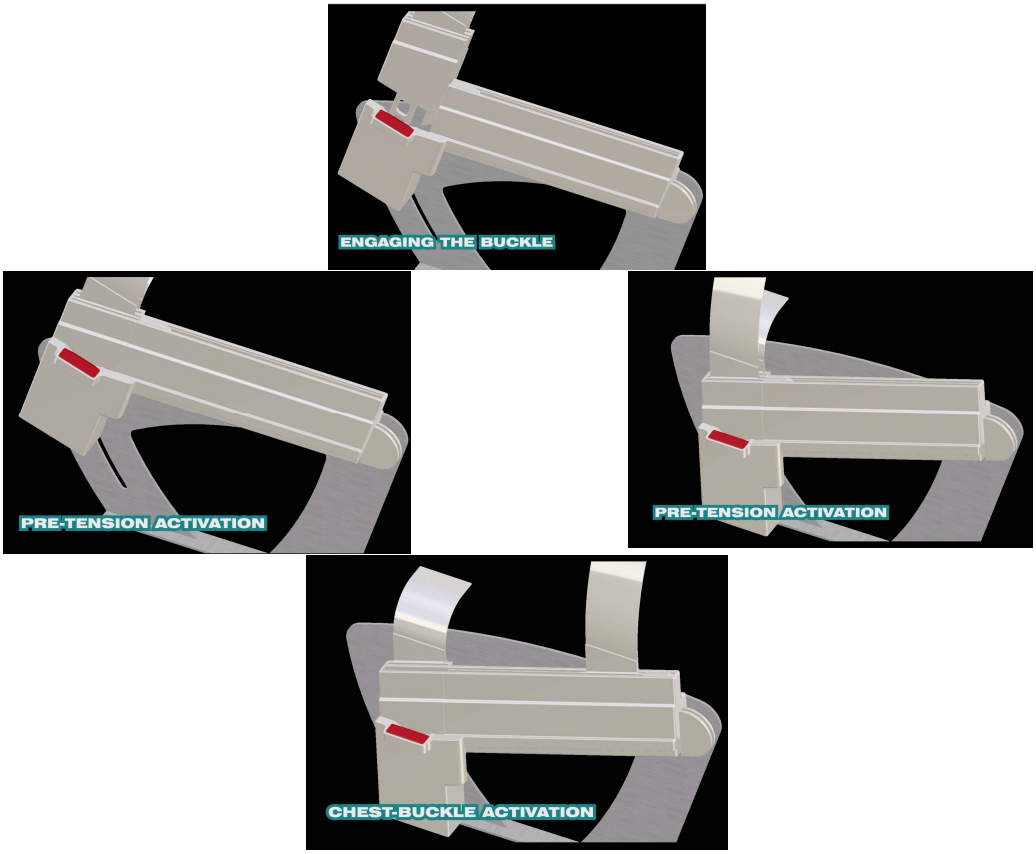


***Figure 8. Split buckle activation***

Generally there was agreement between the predictions from the model and the results from the mechanical sled tests. However, there were some discrepancies between predicted and measured chest deflections. However, for the reference test there was agreement for the two IR-Traccs with the greatest deflections (Figure 5). For the split buckle test there was agreement between the predicted and measured upper left and upper right deflections. The reason for the poor agreement for some of the chest deflection predictions can be that the model of the THOR dummy used was a beta version of the model and not fully validated. Due to the fact that the THOR model predicted the same reduction in chest deflection as was observed in the mechanical tests the model was considered sufficiently valid for the intentions of this study.

For the PMHS there was a significant (over 100mm) increase in head x-displacement with the split buckle system relative to the excursion with the reference belt system. Such increase was not observed for neither the mechanical THOR dummy, the mathematical THOR dummy model or for THUMS. For the mechanical THOR dummy there was an increase of 37mm in head x-displacement for the THOR dummy model and THUMS there were an increase in head x-displacement of 71mm and 31mm respectively. The reason for the significant increase in head x-displacement for the PMHS in the split buckle system compared to the reference system was an increased forward motion of the pelvis that resulted in reduced torso pitch. This finding is discussed in [11] in detail. However, it is important to point out that just one PMHS test is not enough to assess the performance of both systems. In future analyses, the reason for the increase for the PMHS will be investigated in more detail.

## CONCLUSION

The split buckle system:

- can reduce chest deflection for a belted occupant
- can have a minor increase in head x-displacement
- can reduce the number of fractured ribs for an elderly occupant
- can be made with one buckle for identical buckle up proceedure as today

**REFERENCES**

[1] WHO. (2013) "WHO methods and data sources for global causes of death 2000-2011". Department of Health Statistics and Information Systems WHO, 2013: Geneva.
[2] Klanner, W. (2001) "Status Report and Future Development of the EuroNCAP programme". in 23:rd International Conference on the Enhanced Safety of Vehicles. 2001. Amsterdam.
[3] Ruan, J., (2003) "Prediction and Analysis of Human Thoracic Impact Responses and Injuries in Cadaver Impacts Using a Full Human Body Finite Elment Model". Stapp Car Crash Journal, 47, 2003.
[4] Carroll, J. (2010) "Overview of Serious Throax Injuries in European Frontal Car Crash Accidents adn Implications for Crash Accidents and Implications for Crash Test Dummy Development". Proceedings of the IRCOBI Conference, 2010: p. 217-234.
[5] Wanek, S.M. (2004) "Blunt Thoracic Trauma: Flail Chest, Pulmonary Contousion, and Blast Injury". Crit Care Clin 20, 2004: p. 71-81.
[6] Kent, R., Patrie, J., Poteau, F., Matsuoka, F., Mullen, C. (2003) "Development of an Age Dependent Thoracic Injury Criterion for Frontal Impact Restraint Loading". in 18:th International Technial Conference on the Enhanced Safety of Vehicles. 2003.
[7] European Commission. (2011) "Demography Report 2010". Commission staff working document, Luxembourg.
[8] Forman, J.L., Kent, R., Morz, K., Pipkorn, B., Boström, O., Segui-Gomez, M. (2012) "Predicting Rib Fracture Risk with Whole-body Finite Element Models: Development and Preliminary Evaluation of a Probabilistic Analytical Framework". Annual Proceedings of the Association of the Advancement of Automotive Medicine (AAAM) 2012:56, 2012.
[9] Pipkorn, B. and K. Mroz. (2008) "Validation of a Human Body Model for Frontal Crash and its Use for Chest Injury Prediction". SAE Digital Human Modeling for Design and Engineering Conference. 2008. Pittsburgh, Pennsylvania.
[10] Pipkorn, B., Kent, R. (2011) "Validation of a Human Body Thorax Model and its use for Force, Energy and Strain analysis in Various Loading Conditions". International Research Council On Biomechanics Of Injury (IRCOBI). 2011.
[11] Lopez-Valdes, F., Juste-Lorente, O. (2015) "Innovative Restraints to Prevent Chest Injuries in Frontal Impacts". 24:th Technical Conference on the Enhanced Safety of Vehicles. 2015. Gothenburg.
[12] Lopez-Valdes, F., Lau, J.J., Lamp, J. (2010) "Analysis of Spinal Motion and Loads During Frontal Impacts, Comparison between PMHS and ATD". in Annual Proceedings of the Association of the Advancement of Automotive Medicine (AAAM) 2010:54. 2010.
[13] Shaw, G., Parent, D., Purtsezov, S. (2009) "Impact Response of Restrained PMHS in Frontal Sled Tests: Skeletal Deformation Patterns Under Seat Belt Loading". Stapp Car Crash Journal 2009, 53:1-48, 2009.

# EXTRAPOLATION OF GIDAS ACCIDENT DATA TO EUROPE

**Jens-Peter Kreiss**
**Gang Feng**
**Jonas Krampe**
**Marco Meyer**
**Tobias Niebuhr**
Technische Universität Braunschweig
Germany

**Claus Pastor**
**Jan Dobberstein**
Bundesanstalt für Straßenwesen

Paper Number 15-0372

## ABSTRACT

In the paper it is investigated to what extend one can extrapolate the detailed accident database GIDAS (German In-Depth Accident Study), with survey area Hanover and Dresden region, to accident behavior in other regions and countries within Europe and how such an extrapolation can be implemented and evaluated. Moreover, it is explored what extent of accident data for the target country is necessary for such an extrapolation and what can be done in situations with sparse and low accident information in a target region.
It will be shown that a direct transfer of GIDAS injury outcomes to other regions does not lead to satisfactory results. But based on GIDAS and using statistical decision tree methods, an extrapolation methodology will be presented which allows for an adequate prediction of the distribution of injury severity in severe traffic accidents for European countries. The method consists essentially of a separation of accidents into well-described subgroups of accidents within which the accident severity distribution does not vary much over different regions. In contrast the distribution over the various subgroups of accidents typically is rather different between GIDAS and the target. For the separation into the subgroups meaningful accident parameters (like accident type, traffic environment, type of road etc.) have been selected. The developed methodology is applied to GIDAS data for the years 1999-2012 and is evaluated with police accident data for Sweden (2002 to 2012) and the United Kingdom (2004 to 2010). It is obtained that the extrapolation proposal has good to very good predictive power in the category of severe traffic accidents.
Moreover, it is shown that iterative proportional fitting enables the developed extrapolation method to lead to a satisfactory extrapolation of accident outcomes even to target regions with sparse accident information. As an important potential application of the developed methodology the a priori extrapolation of effects of (future) safety systems, the operation of which can only be well assessed on the basis of very detailed GIDAS accident data, is presented.
Based on the evaluation of the presented extrapolation method it will be shown that GIDAS very well represents severe accidents, i.e. accidents with at least one severely or fatally injured person involved, for other countries in Europe. The developed extrapolation method reaches its limits in cases for which only very little accident information is available for the target region.

## INTRODUCTION

In this paper we present a methodology which allows for an extrapolation of the detailed German accident database GIDAS (German In-Depth Accident Study) to other regions or countries within Europe. The great advantage of GIDAS is that due to (in the regions of the German cities Hanover and Dresden) accident parameters are recorded in fine detail. However, the accident information within GIDAS is regionally restricted and cannot be transferred in a one-to-one manner directly to other regions or countries (even not in Germany). We suggest to apply well-developed statistical decision tree methods to achieve this goal. In [8] a different so-called weighting methodology has been developed and applied to GIDAS in order to extrapolate GIDAS to other regions in Germany.

To evaluate the proposed methodology we obtained rather detailed police recorded accident material for Sweden and the United Kingdom (UK) from the Swedish Transport Agency and the Bundesanstalt für Straßenwesen.

In the next section we briefly describe the accident data we used in this study. Then we describe in full detail the suggested decision tree method and the way of obtaining extrapolations for other regions or countries (target regions) within Europe. In order to see how the proposed methodology works for real accident data we report on applications to Swedish and British accident data. Since we have detailed accident data for these two countries at

hand we can even evaluate the proposed methodology. It will be seen that the proposed methodology works well for injured people in severe accidents, i.e. not taking uninjured participants into account.

As an example for application of such an extrapolation we present how the effectiveness of a fictional future safety system in vehicles can be predicted for regions or countries in Europe. The term "future safety system" refers to a system with no or low market penetration. For such systems an evaluation of the effectiveness cannot be carried through on the basis of recorded accident data. For complex systems even police recorded data may not be detailed enough to be able to measure effectiveness. Furthermore, we consider in a further section the situation when only low and aggregated accident information in the target country is available. Here we suggest to combine the proposed extrapolation method with the so-called iterative proportional fitting method (IPF). Finally, we will also discuss extrapolation possibilities for countries for which we only have number of fatalities broken down to very few accident parameters like type of vehicle and location of accident (rural versus urban). As an example in this section we have taken Austria. The paper is concluded by a summary of the obtained results.

## DATA SETS USED

For the evaluation and application of the proposed extrapolation of injury outcomes in accidents we make use of accident data from GIDAS the database for the period 1999 until 2012. These data contain detailed accident information of 24,341 injury accidents with 32,312 at least slightly injured people. As is discussed later we restricted ourselves to *severe accidents* (accidents with at least one severely or fatally injured person). This restriction leads within GIDAS to 7,474 severe accidents with 10,982 at least slightly injured people.

Based on this accident data we exemplarily extrapolate to severe accidents in Sweden and United Kingdom. To evaluate the obtained extrapolations we make use of Swedish accident data, which we have received from STRADA for the period 2002 until 2012 and make use of STATS19 accident data for UK for the period 2004 until 2010. The STRADA data set for Sweden contains 36,320 severe accidents with 60,999 injured people and the STATS19 data set for UK contains 184,263 severe accidents with 283,201 injured people.

Finally we present an application making use of accident data from CARE for the period 2008 until 2013. A special feature of this accident data set is, that it contains numbers of fatalities in road accidents for European countries, only, but not numbers of injured/uninjured persons involved.

## DECISION TREE BASED EXTRAPOLATION OF ACCIDENT BEHAVIOR

The main idea for accident extrapolation of GIDAS injury outcomes in road accidents to various target regions is to apply the well-established statistical method of decision trees (cf. [2], [9] and tailored for accident data [10]). The target variable, which we intend to predict for different countries or areas, is injury severity of people involved in road accidents. In order to obtain a widely applicable procedure we choose a rather simple categorization of injury severity, namely only the four categories *not injured*, *slightly injured*, *severely injured* and *fatally injured*. In GIDAS a person is referred to *severely injured*, if it has been hospitalized. In most European countries police recorded accidents contain some information about the injury severity of people involved in the accidents. Many countries also make use of the above categorization. However, the distinction especially between *slightly* and *severely injured* varies with different countries. Concerning Sweden and United Kingdom and also Austria, to which we exemplarily apply our method, the definition of injury severity is quite similar to that of Germany.

Proper application of decision tree methodology moreover needs decision variables in order to create a set of disjoint accident categories with their own and specific injury severity distributions. We applied a detection of relevant variables assisted by so-called iterated decision trees or bootstrap aggregation (cf. [3], [4], [5] and [14]). It is obtained that essential variables for this accident segmentation are

- ACCIDENT TYPE (UART in GIDAS)
- TRAFFIC ENVIRONMENT/LOCATION OF ACCIDENT (ORTSL in GIDAS)
- VEHICLE TYPE (FART in GIDAS)
- TYPE OF ROAD (STRART in GIDAS)
- NUMBER OF INVOLVED PARTIES (ANZBET in GIDAS)

- SPEED LIMIT (VZUL in GIDAS)
- LIGHTCONDITIONS (TZEIT in GIDAS)
- SEX (GESCHL in GIDAS)
- AGE OF CASUALTY (ALTER1 in GIDAS)
- PEDESTRIAN
- DIRECTION OF FIRST IMPACT (VDI1 in GIDAS).

For practical application it is of course most important to know which accident variables are available for the target region or country. We consider as a case a person involved in an accident. Persons involved in one and the same accident can be grouped into different categories depending on their accident parameters. So the method can take into account that passengers of a vehicle typically suffer different types of injuries as pedestrians or bicycle riders in accidents with each other.

Extensive investigations of extrapolation of GIDAS accidents to other European regions or countries clearly showed that reliable results can only be obtained if the consideration is restricted to at least slightly injured people in *severe accidents*, where the definition of a severe accident is, that at least one severely or fatally injured person is involved in that accident. However, within the category of *severe accidents* all involved injured people are taken into account and not only severely and fatally injured people.

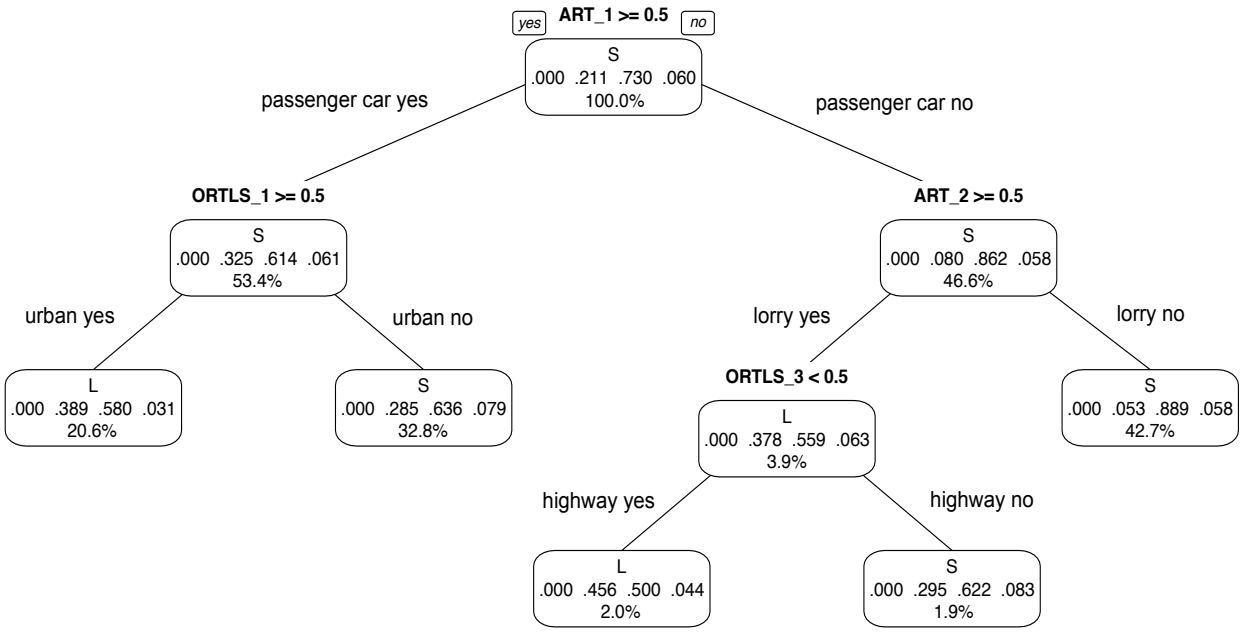


***Figure 1: Example of a decision tree based on GIDAS (1999-2012), which can only make use of a very limited number of variables related to traffic participation and accident location.***

Based on the selected and available variables a segmentation of injured people involved in severe accidents from GIDAS based on a decision tree method is constructed in a first step. Decision trees have the advantage that the segmentation results are very well visualized. For the application to Swedish accident data a part of such a decision tree is displayed in Figure 2. A decision tree is a kind of flowchart-like structure in which each path from the root to the various leaf nodes is represented by a sequence of classification rules. Each leaf node represents a selected category of injured people in accidents.

A resulting decision tree for accident data is explained in the following for a clear and limited example where only two variables (type of traffic participation and accident location) for each injured person in a severe accident are available (cf. Figure 1). According to the possible expressions of these two characteristics, eight

0-1-variables, namely

- Passenger car (ART_1)
- Lorry or Truck (ART_2)
- Motorized two-wheelers (ART_3)
- Pedal cycle (ART_4)
- Pedestrian (ART_5)

and

- Urban (ORTLS_1)
- Rural (ORTLS_2)
- Highway (ORTLS_3),

may be used in order to set up a decision tree. Put simply, the routine rpart now searches for the one of these variables which (according to their values yes/no) best splits the set of all injured people involved in severe accidents within GIDAS into two subgroups (internal nodes). More precisely rpart minimizes a specific measure of impurity or diversity (Gini index or information index) of a node (subgroup) in order to obtain a best split. A node is called completely pure if all persons within this node fall into the same injury category, i.e. the injury distribution is degenerate. In the considered example rpart selected the variable ART_1, which means "people seated in a passenger car: yes or no". The internal node *people seated in a passenger car 'yes'* in a second step is separated according to the variable ORTLS_1, which means "urban accident location: yes or no". After this step no further separation is suggested and two leaf nodes of the decision tree are obtained. The internal node *people seated in a passenger car 'no'* is separated according to the variable ART_2, which means "people seated in a lorry or truck: yes or no". If 'yes' a further separation is done depending on whether the accident happened on a highway or not. At the end five leaf nodes (endpoints of the branching) are obtained. Each leaf node contains the injury distribution (uninjured, slightly injured, severely injured and fatally injured). Since we have not included uninjured people the corresponding share always is zero. Above the injury distribution a letter indicates the predicted injury category for this specific leaf node. *L* stands for *slightly injured* and *S* stands for *severely injured*. Below the various injury distributions the share of all injured people in severe accidents who fall into the corresponding leaf node are displayed.

The decision tree, which is completely based on GIDAS data, provides a complete segmentation of all injured persons in severe accidents into so-called leaf nodes. From the injury outcomes of all cases within a leaf node we calculate an injury distribution, which typically varies substantially over the various leaf nodes. As a further and more realistic example consider in Figure 2 (decision tree making use of variables available for Sweden) the leaf node labeled number 6. This leaf node contains all injured people in accidents for which FART_3=0 and FART_5=1. The coding FART_3=0 and FART_6=1 means that this leaf node contains all injured persons which have been involved in severe accidents, have not been passengers of a passenger car (FART_3=0) but have been passengers of a bus (FART_5=1). Within this subgroup of injured people the injury severity distribution is as follows: 67.1% of the involved injured people are slightly injured, 30.3% are severely injured and 2.6% are killed. As a further example consider leaf node number 5. The coding FART_3=1 and ANZBET=1 means that within this subgroup injured people sitting in a passenger car and involved in a single vehicle accident are collected. The injury severity distribution for this subgroup reads rather different, namely: 15.1% of the involved people are slightly injured, 74.5% are severely injured and 10.4% are killed.

In order to apply a decision tree method to a target region (specific European region or country) an essential point to be clarified is, which accident variables for this region are available and whether they can be harmonized with accident information within GIDAS. As an example assume that for the target region we only know for each injured person in a severe accident the ACCIDENT TYPE, TRAFFIC ENVIRONMENT and VEHICLE TYPE and that the values each of the three variables can take are similarly defined in the target region compared to GIDAS. Then the calculation of a decision tree has to be based on these variables.

For the target region or country it is assumed that we do not have any information on the injury outcomes of people involved in the accidents.

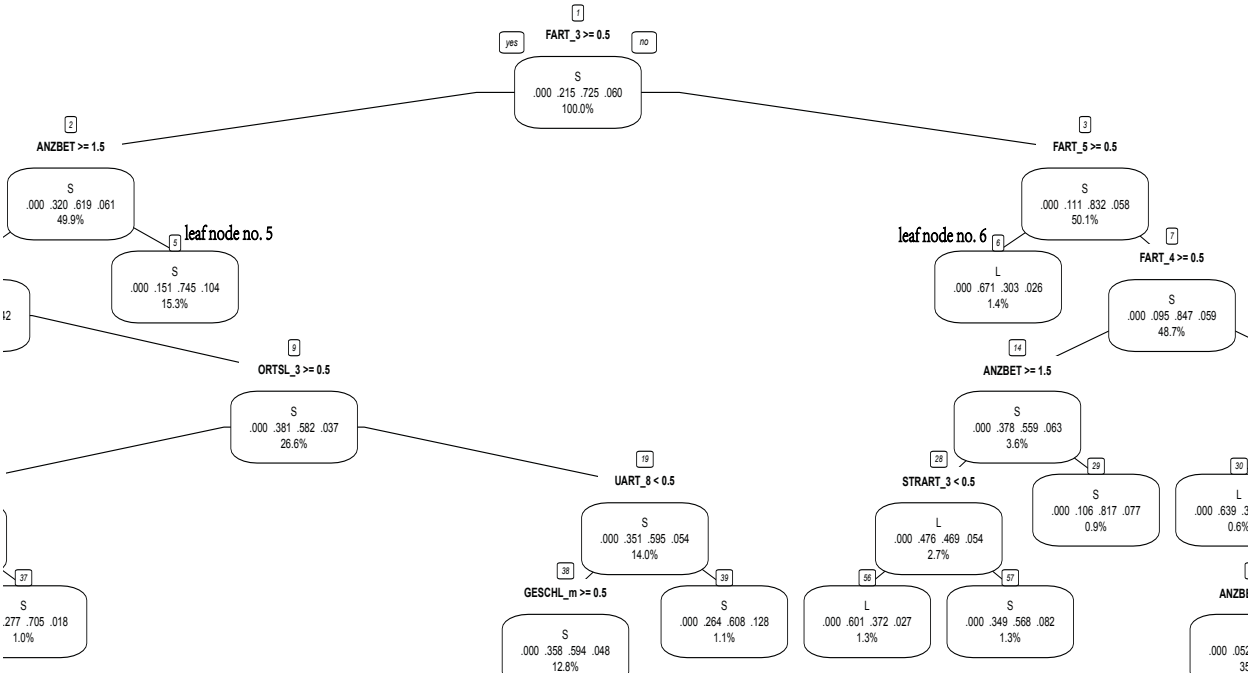


***Figure 2. Decision Tree (part) based on GIDAS (1999-2012) and based on variables available for Swedish accidents.***

From our experience it is advantageous to *binarize* nominal variables like `VEHICLE TYPE (FART in GIDAS)` or `ACCIDENT TYPE (UART in GIDAS)`, i.e. to create for any value the variable can take a derivative variable, which only takes the values yes (1) or no (0). For `FART` this would lead to binary variables `FART_1`, `FART_2`, … , `FART_K`, indicating for example by `FART_3=1` that the vehicle of the injured person is a passenger car. A freely available software to create such a decision tree is the `rpart` package in `R` (cf. [11], [12] and [14]).

Having such a decision tree, based on GIDAS accident data, at hand, the extrapolation now is as follows. Any person involved in a severe accident in the target region will be sorted according to the classification rules of the decision tree to a specific leaf node. Since we do not know the injury outcome of the cases for the target region we replace the injury outcome for the target by the injury distribution of the corresponding leaf node obtained from GIDAS accidents. Having done so we finally obtain the overall injury distribution for the target region as a weighted sum over the injury distributions within all leaf nodes. The distribution within a leaf node stems completely from GIDAS accidents, but the weights over the set of various leaf nodes stem from the target region. In order to obtain sound results it has to be assumed, that the injury distributions within a leaf node (for example single vehicle accidents in a rural area by night happened not on a motorway) does not vary much between GIDAS and the target region. In contrast, the relative frequencies of accidents belonging to the various leaf nodes (relative frequency of leaf nodes) may vary substantially between GIDAS and the target region. As already stated it has for example to be assumed, that the injury outcome for a person seated in a passenger car, which leaves the road by night in a rural area is comparable between GIDAS accidents and accidents in the target region, but the share of such accidents may be much higher or lower in the target region or country compared to GIDAS by what reason ever.

In the following we describe the decision tree methodology a bit more formally. As already said our investigations have shown that a reliable extrapolation via decision trees is only possible if we restrict to severe accidents and exclude non-injured people. For the extrapolation we therefore are interested to predict,

for a given target region or country, the conditional probability that a person in an accident suffers a specific injury severity given that the person is hurt at all and is involved in a severe accident. This probability is stated in equation (1).

$$P(\{PVERL = x\}|\{PVERL \geq 1, UKAT \geq 2\}) \quad , \quad x = 1,2,3 \tag{1}.$$

Here and in the following we follow the German accident coding. `PVERL` stands for the injury severity of a person involved in an accident and `PVERL` can take the values *0=not injured, 1=slightly injured*, *2=severely injured* and *3=fatally injured*. `UKAT` stands for the accident category. `UKAT≥2` indicates that the accident the person is involved in is *severe*, meaning that at least one person in this accident suffered a severe or fatal injury. Decision tree methods now lead to a decomposition of the conditional probability given in equation (1). Let us denote the leaf nodes of a decision tree by $B_i$, i=1,…,I, in which $B_i$ stands for a specific subgroup of injured persons (e.g. injured persons in passenger cars involved in a severe single vehicle accident by night in a rural environment). Then we consider on the one hand the injury severity distributions within each $B_i$ (each subgroup) $P(\{PVERL = x\}|\{PVERL \geq 1, UKAT \geq 2\}\ and\ B_i)$ and on the other hand the distribution of injured people in severe accidents over the $B_i$, namely $P(B_i|\{PVERL \geq 1, UKAT \geq 2\})$. This immediately leads to the decomposition of the aforementioned conditional probability given in equation (2).

$$P(\{PVERL = x\}|\{PVERL \geq 1, UKAT \geq 2\})$$

$$= \sum_{i=1}^{I} P(\{PVERL = x\}|\{PVERL \geq 1, UKAT \geq 2\}\ and\ B_i) \cdot P(B_i|\{PVERL \geq 1, UKAT \geq 2\}) \tag{2}.$$

The first factor in equation (2), namely $P(\{PVERL = x\}|\{PVERL \geq 1, UKAT \geq 2\}\ and\ B_i)$, is computed from the decision tree using GIDAS data only. The second factor, namely $P(B_i|\{PVERL \geq 1, UKAT \geq 2\})$, which is the distribution over the various leaf nodes of the decision tree, has to be derived from accident information of the target region or country. An essential assumption for the proposed method to work is that the injury severity distributions within the leaf nodes (subgroups) $B_i$ do not differ much between GIDAS and the target region or country. However, the distributions over the set of leaf nodes (subgroups) may differ substantially between GIDAS and the target.

Now we are ready to apply and to evaluate the proposed extrapolation method for two European countries.

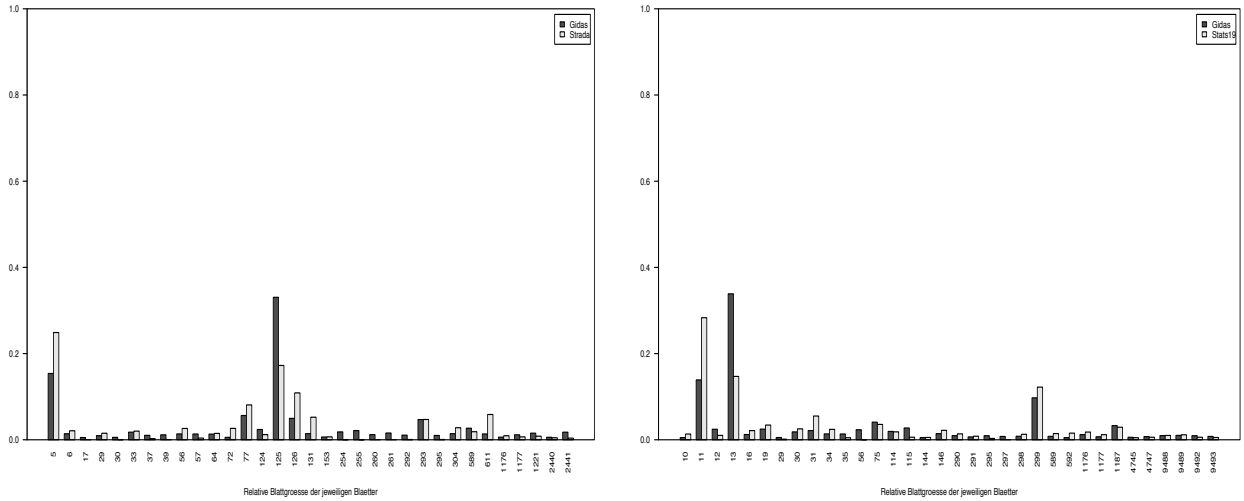


***Figure 3: Relative Frequencies of the leaf nodes of the decision tree for GIDAS (1999-2012) (dark) and Sweden (2002-2012) (light) on the left-hand chart and for GIDAS (1999-2012) (dark) and UK (2004-2010) (light) on the right-hand chart.***

## EXTRAPOLATION RESULTS FOR SWEDEN

For the extrapolation to Swedish accident behavior we have made use of the following variables, which are provided by STRADA and successfully have been harmonized with variables within GIDAS.

- ACCIDENT TYPE (UART)
- TRAFFIC ENVIRONMENT (ORTSL)
- TYPE OF ROAD (STRART)
- TYPE OF VEHICLE (FART)
- NUMBER OF INVOLVED PARTIES (ANZBET)
- LIGHT CONDITIONS (TZEIT)
- SPEED RESTRICTIONS (VZUL)
- SEX (GESCHL)

A part of the obtained decision tree is given in Figure 2. A comparison of the distribution over the set of leaf nodes of the decision tree is displayed in Figure 3. It can be seen that for some leaf nodes the differences are quite substantial. Examples of leaf nodes with big differences are the leaf nodes with number 5, 125 and 126. Leaf node number 5 represents injured passengers in single vehicle accidents of passenger cars, while leaf node number 125 represents people not in passenger cars, lorries, busses or streetcars and injured in accidents that happened in urban areas with one or two parties involved in the accident. Finally leaf node number 126 represents injured people not in passenger cars, lorries, busses, streetcars or motorbikes and injured in accidents that happened not in urban areas. A typical case in the last two leaf nodes could be an injured pedestrian or bicycle rider in urban areas (leaf node 125) or in rural areas (leaf node 126). From Figure 3 it can be seen that in Sweden a significantly higher share of people is involved in single vehicle accidents of passenger cars. In contrast to these substantial differences a closer look at the injury distributions within the leaf nodes shows very slight differences between GIDAS and Sweden for leaf node number 5 and 125 and still acceptable differences for leaf node number 126.

The final extrapolation to Sweden can be seen in the left plot in Figure 4. The plot shows for each of the injury categories *slight, severe and fatal* three column-charts. The left-hand column represents the relative frequencies of GIDAS to the injury categories *slight, severe and fatal.* The differently colored segments of the columns show the corresponding contributions of the various leaf nodes. It can be easily seen for example that within GIDAS the largest leaf node, which has number 125 (cf. Figure 3) contributes much more to the category of severely injured people compared to the other two columns. The columns on the right-hand side display the obtained extrapolation for Sweden and the columns in the middle show for evaluation the true injury distribution in Sweden for the categories *slight, severe and fatal*. It can be seen that the obtained extrapolation matches the true situation in Sweden to a large extent and performs much better than a one-to-one extrapolation directly from GIDAS (left-hand columns) without adaptation to the different distribution over the set of leaf nodes in the decision tree.

It is emphasized that the proposed extrapolation not only performs well in representing the overall distribution over the injury categories *slight, severe and fatal* in Sweden, which corresponds to the total height of the columns in Figure 4, but that also the breakdown to the leaf nodes (subgroups) within the three injury categories, for example severe injuries, is close to the reality. Of course from this result it cannot be concluded that the same holds true for a further and deeper breakdown of the leaf nodes.

## EXTRAPOLATION RESULTS FOR UNITED KINGDOM

For the extrapolation to accident behavior in UK we have made use of the following variables, which successfully have been harmonized with variables within GIDAS.

- TRAFFIC ENVIRONMENT (ORTSL)
- TYPE OF ROAD (STRART)
- TYPE OF VEHICLE (FART)
- NUMBER OF INVOLVED PARTIES (ANZBET)
- DIRECTION OF FIRST IMPACT (VDI 1)

- PEDESTRIAN
- SPEED RESTRICTIONS (VZUL)
- SEX (GESCHL)
- AGE OF CASUALTY (ALTER1)

A comparison of the distribution over the set of leaf nodes of the decision tree is displayed in Figure 3 (right-hand plot). It can be seen again that for some leaf nodes substantial differences occur. A look at the corresponding injury distributions within these leaf nodes does not show any relevant difference.

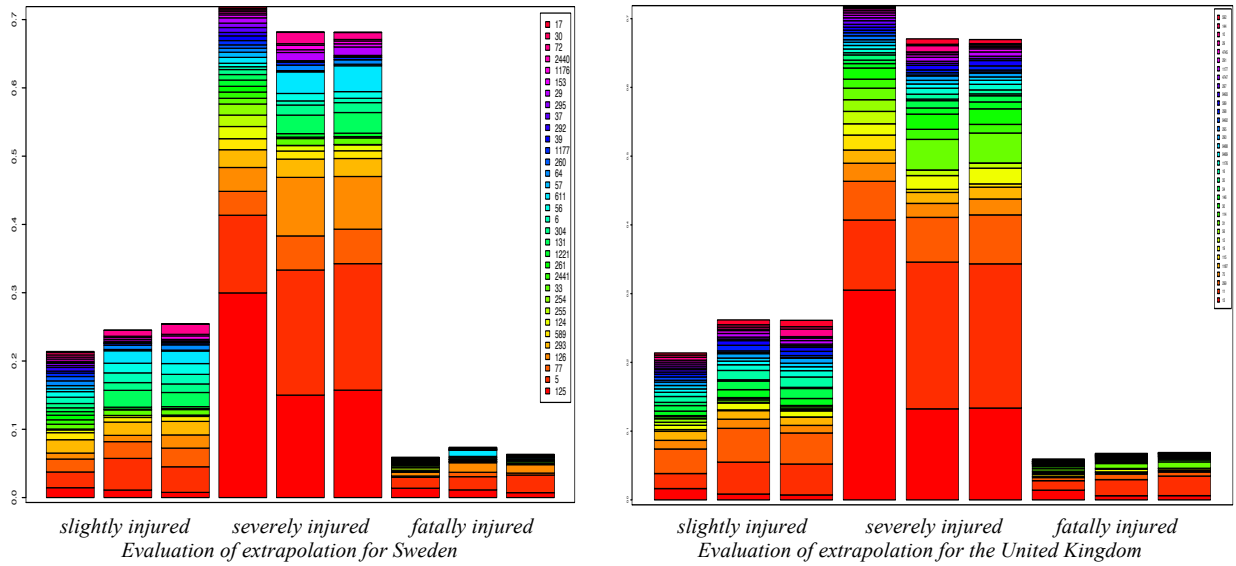


***Figure 4: Column-chart of obtained extrapolation for Sweden (left) and for UK (right). Only injured people in severe accidents are considered. The three columns on the left in each chart refer to slightly injured people, the three columns in the middle refer to severely injured people and the three columns on the right refer to fatalities. Within each group of three columns the leftmost column represents the situation within GIDAS (1999-2012) (slightly, severely and fatally injured people in severe accidents within GIDAS), the column in the middle represents the actual situation within Sweden (2002-2012) (left-hand plot) and UK (2004-2010) (right-hand-plot), while the rightmost column represents the obtained extrapolation from GIDAS to Sweden or UK. The break-down in each of the columns indicates the shares of the various leaf nodes of the decision tree to the specific injury severity. For example, the lowest segment in each of the columns for Sweden (left-hand plot) represents the contribution of the aforementioned leaf node 125 to the injury categories (slight, severe and fatal).***

The final extrapolation to UK can be seen in the right-hand plot in Figure 4. The rationale behind the plot is the same as for Sweden. It again can be seen that the obtained extrapolation matches the true situation to UK to a large extent and again performs much better than a one-to-one extrapolation directly from GIDAS (left-hand columns) without adaptation to the different distribution over the set of leaf nodes in the decision tree. It is worth mentioning that again the break down to the leaf nodes (subgroups) within the three injury categories, for example severe injuries, is very close to the reality in UK. Of course from this result it cannot be concluded that the same holds true for a further and deeper breakdown of the leaf nodes.

## EXTRAPOLATION OF EFFECTS OF FUTURE SAFETY SYSTEMS

This section is devoted to the application of the developed extrapolation methodology in order to get estimates for the effectiveness of future safety systems in vehicles. These are safety systems, which are either not yet on

the market or only have a small market penetration that effectiveness cannot be quantified from police recorded accidents. The specific question might be to estimate the number of fatalities, which possibly could be avoided if a particular safety system is on board of all vehicles on the roads. The idea is to take advantage out of the fact that for the detailed recorded accidents within the GIDAS database the effects of the safety system of interest can be quantified very well. This means, having the abilities of a safety system in mind, we evaluate all accidents within GIDAS once again and with respect to the injury outcomes for the involved people. In a next step we sort the newly evaluated accidents to the decision tree, which has been set up with the original GIDAS accident data. The following consequences may arise

1. An accident may completely drop out of the category of severe accidents because severe injuries for all involved people would have been prevented by the new safety system. All involved people drop out.
2. An accident stays within the category of severe accidents but part of the involved persons drop out because injuries would have been prevented by the safety system. This might change the injury distribution within some leaf nodes.
3. Injury severities of persons involved in an accident mitigate between the categories slight, severe and fatal.
4. All injury severities of all people involved in an accident stay unchanged.

Because of this, both the injury severity distributions within some leaf nodes of the decision tree as well as the distribution over the set of leaf nodes may change as a result of the safety system.

Based on a precise calculation of the effectiveness of a safety system for GIDAS accidents the extrapolation of the effectiveness to a target region is as follows:

1. For all leaf nodes, new injury distributions obtained from a safety system investigation in GIDAS have to be calculated.
2. The accidents from the target region will be sorted into the decision tree.
3. The change in the absolute case numbers over the set of leaf nodes in GIDAS caused by the safety systems will be extrapolated to the target and lead to adapted absolute case numbers over the set of leaf nodes.
4. As before, for each leaf node, we obtain changed absolute case numbers of slight, severe and fatally injured people. Accumulation leads to an overall extrapolation for the target.

**A fictional example of extrapolation**

Let us consider a single leaf node obtained from a GIDAS decision tree for which the absolute and relative injury severity distribution is given in the first two rows of Table 1. Let us fictitiously assume that a new safety function reduces the absolute number of injured people in this subgroup by 273 and that the reduction breaks down to the injury categories as given in the third row of Table 1. It is worth mentioning that on the one hand we observe a reduction of fatalities by 13 and on the second hand an increase of the relative frequency of fatalities among the group of injured people from 8.7% to 9.6%. Finally assume that for the target country we have 350 injured people within the considered leaf node (subgroup). As described before the extrapolation to the target is done by transferring the injury distribution within the considered leaf node from GIDAS to the target. This is of course done for the GIDAS injury distribution without and with the new safety system.

It is seen from Table 1 that we extrapolate that the future safety system reduces the number of fatalities within the considered subgroup (leaf node) by three. However, as in GIDAS, the relative frequency of fatalities increases. This phenomenon makes clear that in order to assess a safety function correctly absolute figures are vital.

If one carries through such an extrapolation for all leaf nodes of the decision tree one will receive an extrapolation of the effectiveness of the new safety system for the entire target region or country.

**Table 1.**
**Injury distribution for a single leaf node of a GIDAS decision tree and an extrapolation of a fictional future safety system.**

| | Slightly Injured | Severely Injured | Fatally Injured | Sum |
|---|---|---|---|---|
| Injury distribution GIDAS without new safety system | 95 | 1,147 | **118** | 1,363 |
| | 7.0% | 84.2% | **8.7%** | 100% |
| Injury distribution GIDAS with new safety system | 135 | 850 | **105** | 1,090 |
| | 12.4% | 78.0% | **9.6%** | 100% |
| | | | | |
| Extrapolation of injury distribution without new safety system to target | 25 | 295 | **30** | 350 |
| | 7.0% | 84.2% | **8.7%** | 100% |
| Extrapolation of injury distribution with new safety system to target | 35 | 218 | **27** | 280 |
| | 12.4% | 78.0% | **9.6%** | 100% |

## ITERATIVE PROPORTIONAL FITTING

For target countries with only sparse accident information the method of iterative proportion fitting (IPF) successfully can be used. Assume that for the target region only marginal distributions from accident databases are available. In contrast, for GIDAS, the full cross tables are available. The goal of IPF is to transfer the cross tables from GIDAS to the target taking into account all available accident information from the target country. For the validity of such an approach it is vital that the inner structure of GIDAS cross tables to a sufficient extent is close to the corresponding structure of the target country. The following subsection illustrates the situation for German accident data.

### IPF: An example

Assume that only accident information for Germany as given in the margins (blue background) in Table 2 is available. The variable `ANZBET` denotes the number of involved parties (`ANZBET=1,2,3` stands for one, two or three involved parties and `ANZBET=4` stands for four or more involved parties in the corresponding accident). The variable `ORTSL` denotes the location of the accident (`ORTSL=3` stands for urban areas and `ORTSL=4` stands for rural areas). Finally `UART` denotes the accident type according to the German coding (e.g. `UART=8` denotes an accident where the vehicle has left the road to the right hand side).

**Table 2.**
**Accident information available from target (margins, blue) and extrapolated via IPF from GIDAS (yellow).**

| ORTSL, ANZBET / UART | 3,1 | 3,2 | 3,3 | 3,4 | 4,1 | 4,2 | 4,3 | 4,4 | |
|---|---|---|---|---|---|---|---|---|---|
| **0** | 4.26% | 1.77% | 0.22% | 0.06% | 1.58% | 1.45% | 0.57% | 0.27% | **10.19%** |
| **1** | 0.04% | 1.70% | 0.44% | 0.26% | 0.05% | 0.53% | 0.06% | 0.13% | **3.21%** |
| **2** | 0.01% | 1.23% | 0.44% | 0.18% | 0.05% | 3.69% | 1.54% | 1.47% | **8.62%** |
| **3** | 0.02% | 0.92% | 0.19% | 0.02% | 0.02% | 1.69% | 0.38% | 0.27% | **3.50%** |
| **4** | 0.00% | 3.60% | 0.60% | 0.12% | 0.02% | 9.77% | 1.60% | 0.45% | **16.16%** |
| **5** | 0.11% | 15.68% | 1.00% | 0.32% | 0.02% | 6.42% | 0.89% | 0.04% | **24.49%** |
| **6** | 0.01% | 8.54% | 0.87% | 0.09% | 0.02% | 0.70% | 0.14% | 0.03% | **10.39%** |
| **7** | 0.29% | 0.04% | 0.00% | 0.00% | 0.27% | 0.03% | 0.03% | 0.00% | **0.66%** |
| **8** | 2.74% | 0.28% | 0.01% | 0.06% | 9.36% | 0.91% | 0.12% | 0.06% | **13.53%** |
| **9** | 1.63% | 0.19% | 0.01% | 0.03% | 5.83% | 0.98% | 0.47% | 0.12% | **9.24%** |
| | **9.10%** | **33.95%** | **3.79%** | **1.14%** | **17.22%** | **26.17%** | **5.81%** | **2.82%** | 100.00% |

The method IPF allows to transfer the inner structure from the GIDAS cross-table, which is completely available, to the target region, taking into account the accident information contained in the margins of Table 2. The margins of GIDAS and the target may and typically will be different. The IPF algorithm is described in detail in [1], [6], [7] and [13]. For the validity of IPF it is vital that the interaction-effects or, equivalently, the cross product ratios (cf. [1]) between GIDAS and the target are similar.

Having the full Table 2 at hand a decision tree method based on the accident variables accident location, number of involved parties and accident type can be set up. It has been obtained that the extrapolation for Germany (for which all injury information is available) in the described example works very well and leads to reliable extrapolation.

## EXTRAPOLATION TO EU COUNTRIES IN CASE OF LOW ACCIDENT INFORMATION

We present in this section an extrapolation from CARE accident records to the target country Austria for the year of 2008. Note that in this example only fatalities (broken down to accident location and vehicle type) for Austria are available. The final goal is to set up an accident decision tree which allows for extrapolation of GIDAS to Austria and applications as described in the section on extrapolation of the effects of future safety systems.

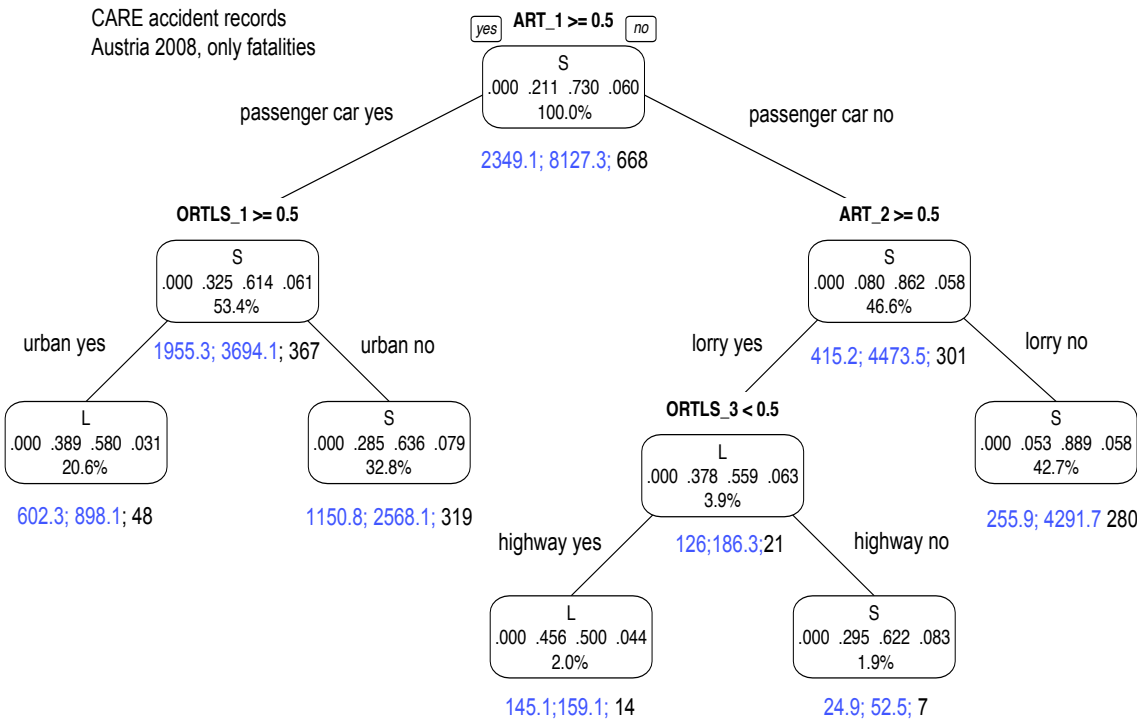


***Figure 5: Accident decision tree based on GIDAS (1999-2012) with adaption to Austria and based on fatalities, only. Below every box the fatalities for Austria (2008) (from CARE database (in black) and the extrapolated numbers of slightly and severely injured people (in blue) are displayed.***

Based on GIDAS and the two variables (accident location and vehicle type) we can set up a decision tree, which is given in Figure 5. Below every box the known fatalities for Austria (in black) are given. According to the relative frequencies of fatalities (calculated from GIDAS) within each box one can extrapolate the absolute numbers of slightly and severely injured people involved in the accidents of each group. These extrapolations are given in blue color below each box. From this we obtain an estimate of the unknown distribution of injured people over the set of

leaf nodes for Austria. This information is necessary in order to extrapolate the distribution of injury severity within Austria. Recall that for such an extrapolation we make use of the injury distributions within the leaf nodes (they can be calculated from GIDAS only) and the distribution over the set of leaf nodes, which necessarily has to be calculated from accident data of the target country. Of course the low depth of data affects the extrapolation methodology in the form that the resulting decision tree is less complex than for more detailed accident information within the target country. Compare with the extrapolations for Sweden and UK described above.

## CONCLUSIONS

Based on the extensive and detailed GIDAS accident database we have discussed in detail the decision tree method, a method for extrapolation from the GIDAS accident database to European regions or countries. It has been shown that in particular for severe accidents, that is, accidents with at least one severely or fatally injured person, GIDAS has good predictive power. The proposed methodology is able to take into account differences in the accidents between the survey area of GIDAS (Hanover region and Dresden region) and the target region, caused by different distributions of accidents over the various leaf nodes. For not severe accidents, i.e. accidents with uninjured or slightly injured persons, only, the proposed decision tree method reaches not the same quality as it does for severe accidents. This is to a substantial degree due to the fact that the category *slightly injured* in Germany, and probably in other countries as well, has a very soft and partially even diffuse definition. However, evaluation of the developed methodology with police recorded accident data for Sweden and the United Kingdom yields that the method successfully can be applied as long as only severe accidents are taken into account.

The key assumption for validity of the developed extrapolation methodology is that, with sufficient breakdown of accident scenarios, the injury severity distribution within each scenario no longer depends very strongly on the region, i.e. the injury severity distributions within a scenario for GIDAS and the target region are similar.

If a specific target region, for which one wants to extrapolate the injury outcomes from GIDAS, only a low data-depth of accident data is available, the proposed extrapolation methodology typically cannot be directly carried out. This is particularly the case, if for the target region only so-called marginal distributions from accident data are available. For this situation, a combination of the suggested methodology and the so-called iterative proportional fitting (IPF) leads to a reasonable extrapolation concept.

An important application of the proposed extrapolation methodology is, that an a priori assessment of effects of future safety systems can be carried out. Effects of future safety systems often can reliably be quantified for accidents reported in detail in GIDAS. The methodology developed then allows extrapolation of such a quantification of effects of future safety systems to target regions with possibly different accident behavior.

Finally, it is discussed to what extent an extrapolation is possible to target regions or countries with (very) low accident information. As an example this refers to regions or countries in which only fatalities broken down according to very few accident parameters (e.g. only accident location (rural/urban) and type of vehicle (passenger car, …)) are present. It is shown that even in such a situation the decision tree method can be applied to estimate the effectiveness of (future) safety systems.

Summarizing, it has been shown that advantage can be taken out of a very detailed in-depth accident database within a limited survey area (like GIDAS) for extrapolating accident outcomes to other regions and countries. Thus GIDAS in a sense successfully can be enabled to describe severe accidents in other regions of Europe. Further it is shown that the developed extrapolation method based on field accident data leads to benefits in assessment methods for safety systems in vehicles.

## ACKNOWLEDGEMENTS

We are grateful to Swedish Transport Agency for providing a very extensive database of police recorded accidents in Sweden. From the Federal Highway Research Institute we have received an accident database for the United Kingdom and access to CARE accident data.

We benefitted a lot from numerous discussions and suggestions from various colleagues obtained on a sequence of extrapolation workshops to be held at various places in Germany.

**REFERENCES**


[1] Agresti (2013). „Categorical Data Analysis.“ 3rd edition. John Wiley & Sons, NJ: Hoboken.
[2] Breiman, L., Friedman, J. H., Olshen, R. A., and Stone, C. J. (1984). „Classification and Regression Trees.“ Belmont, CA: Wadsworth.
[3] Breiman, L. (1996). „Bagging predictors.“ Machine Learning 24, 123–140.
[4] Breiman, L. (2001). „Random Forests.“ Machine Learning 45, 5–32.
[5] Bühlmann, P. (2004). „Bagging, Boosting and Ensemble Methods.“ In Handbook of Computational Statistics: Concepts and Methods (Eds.: Gentle, J., Härdle, W. and Mori, Y.), 877–907. Springer, New York.
[6] Deming, W.E. and Stephan, F.F. (1940). „On a least squares adjustment of a sampled frequency table when the expected marginal total are known.“ The Annals of Mathematical Statistics. 11, No. 4, 427–444.
[7] Fienberg, S.E. (1970). „An iterative procedure for estimation in contingency tables.“ The Annals of Mathematical Statistics. 41, No. 3, 907–917.
[8] Hautzinger, H., Pfeiffer, M. und Schmidt, J. (2006). „Hochrechnungen von Daten aus Erhebungen am Unfallort. Berichte der Bundesanstalt für Straßenwesen.“ Fahrzeugtechnik, Heft F 59.
[9] Hothorn, T., Hornik, K. and Zeileis, A. (2006). „Unbiased Recursive Partitioning: A Conditional Inference Framework.“ Journal of Computational and Graphical Statistics 15, 651–674.
[10] Kreiss, J.-P., Feng, G., Krampe, J. Meyer, M. and Niebuhr, T. (2014). „Methodik zur Hochrechnung von GIDAS-Daten auf Europa“, Bericht Bundesanstalt für Straßenwesen.
[11] Milborrow, S. (2014). rpart.plot: Plot rpart models. An enhanced version of plot.rpart. R package version 1.4-4. http://CRAN.R-project.org/package=rpart.plot.
[12] R Core Team (2014). „R: A language and environment for statistical computing.“ R Foundation for Statistical Computing, Vienna, Austria. URL http://www.R-project.org/.
[13] Stephan, F.F. (1942). „An iterative method of adjusting sample frequency tables when expected marginal totals are know.“ The Annals of Mathematical Statistics 13, 166–178.
[14] Therneau, T., Atkinson, B. and Ripley, B. (2014). rpart: Recursive Partitioning and Regression Trees. R package version 4.1-8. http://CRAN.R-project.org/package=rpart.

# IMPLEMENTATION OF NEW RIB MATERIAL MODELS TO A FE-HUMAN BODY MODEL FOR EVALUATION OF THE PRE-SAFE® IMPULSE SIDE RESTRAINT SYSTEM FOR SIDE IMPACT PROTECTION

**Markus Hartlieb**
**Christian Mayer**
**Julien Richert**
**Abdulkadir Öztürk**
**Florian Mayer**
Daimler AG
Germany

**Satyajit Pal**
**Ravikiran Chitteti**
Mercedes-Benz Research and Development India Pvt. Ltd
India

Paper Number 15-0373

## ABSTRACT

„Integrated“, „Smart“ and „Individual“ are new characteristics of future safety systems. Furthermore, side crashes are still dominant in terms of high injury risk for car occupants and are predicted to become even more relevant in future. Earlier studies on pre-conditioning the occupant during pre-crash phase have shown the potential to reduce injury risk in such accident scenarios. To evaluate and optimize such advanced safety systems to provide a high safety level for the occupant, finite element human body models were used. Especially integrated safety systems which interact with the occupant in the pre-crash phase require these new and supplementary evaluation tools.
With specific focus on the use case, the thorax and rib material of the FE human body model THUMS-D were modified and validated. Two different rib material properties have been defined for two different age groups, one for the young population and one for the elder population based on quasi static and dynamic 3-point bending test set-up. Furthermore, a damage model for the rib fracture was created and implemented to the THUMS-D model. The validation process of the complete thorax followed pendulum impact standards set by GESAC 2005 and ISO/TR 9790:1999.
Finally the PRE-SAFE® Impulse Side system was evaluated and optimized applying this upgraded THUMS-D model in FE car crash environment.

## INTRODUCTION

As a tool for the development and also the assessment of particularly secondary safety systems, dummies have been used over the last 50 years – successively updated in terms of mechanical design, injury criteria and, slightly with respect to “individual” characters (5th female, child dummies, etc.)

As of today, numerical models of these dummies are a common technology. As a next step in the field of numerical simulation, validated human models will be used as a supplemental tool to investigate the biomechanical impact of restraint systems more in detail. Those models offer the opportunity to study effects in body parts that are currently not addressed by common anthropomorphic dummy technology, especially if the pre-crash phase has to be considered.

Analyses of the injury patterns in real crashes reveal that there is still potential to improve loads on the thorax. In order to better understand mechanisms leading to a certain injury risk, a valid representation and

characterization of material properties and injury mechanisms in this development tool is necessary to assess and optimize new restraint systems. Especially improvements in the prediction capability for risk of rib fractures in elderly population with THUMS-D motivated the experimental and simulation work, which is described in the following sections. Finally, this modified THUMS-D was used to optimize an advanced pre-crash side protection system.

## METHODS

### Human Body Model

Mercedes-Benz is already using this integral simulation tool in the standard development process. In this study, a modified THUMS (Total Human Model for Safety) model was used. THUMS (AM50) was originally developed by Toyota Motor Corporation & Toyota Central R&D Labs, Inc. and meanwhile several THUMS base models (AF05, AM50, AM95) and derivatives are released respectively published [1]. The model used within Mercedes–Benz is based on the original THUMS versions V1.X and V3 and was continuously improved on several body parts in recent years and is therefore referred to as "THUMS-D" [2,3].

### Experimental work

The entire thorax shape, bone structure and material properties of the ribs are changing over the lifespan. Several studies and research activities were published or initiated in recent years whitin this topic [4, 5]. Almost all authors agree that the stiffness of ribs decrease the older the person is. In other words, the risk for a rib fracture is increasing.

Nevertheless, age specific models which allow also a realistic modeling of a fracture behavior are currently not existing. Therefore, an experimental study was initiated in collaboration with our scientific partner Technical University Graz to investigate and discuss relevant material properties and characteristics of human ribs for the derivation of constitutive laws and fracture modeling under FE code respectively for implemetation to THUMS-D.

#### 1st test phase - 3-point bending – correlation bone density, age and geometrical parameters

Within a first series of experiments to derive biomechanical charcteristics of young and elderly car occupants, force-displacement curves were determined for human ribs in different areas (anterior, lateral and posterior).

Rib samples were obtained from four female and three male Post-Mortem Human Subjects (PMHS) respectively bodies donated for research. One female PMHS was at the age of 32 – the male PMHS was 37 years old. All other subjects in the sample were in age range of 58 – 78 years. In this first series of experiments, the rib samples with a length of approximately 70 mm were taken from the anterior, lateral and posterior region of a rib. For each sample, the geometric dimensions (width, height, curvature height, cross sectional area) and the bone density was determined. Within this study the DXA method (Dual-X-Ray absorptiometry) was applied. It has to be stated, that the DXA method provides an "areal density" (mass / area, e.g g / $cm^2$ ) and does not destinguish between cortical and trabecular bone structures.

The rib ends were potted in a 30mm x 30mm cylindrical sleeve (aluminum) and then tested in 3-point bending set-up. Quasistatic load was applied in max. 11 cycles (hysteresis mode) starting with 30 N and complete unloading after each cycle. Results were discussed with specific focus on correlation of the geometic parameters, the bone density and age of the PMHS.

The following general findings and correlations were derived in this 1st test series. More details and an extensive discussion of the results could be found in the publication of Tomasch et.al. [6]:

- The bone density (BMD – Bone Mineral Density – g/$cm^2$ ) increases from sternum to vertebra region. (within sample a 1.39-fold increase was found on average).
- Ribs from younger PMHS showing 1.8 times higher density compared with rib samples from elderly persons on average.

- Gender specific differences are also observed: Measured bone density of male ribs were consistently higher compared with density of female ribs – but both sexes showing comparable increase of bone density values from sternum to vertebra.
- The height and cross sectional area of the ribs also increases from anterior to posterior. These parameters decrease with age.
- Rib samples from young, male PMHS could withstand approximately three times higher loads compared to rib samples from elderly, female persons.
- All tested specimen (young and elderly) showed a distinctive post-cracking behavior. Force remains on more or less constant level until load was reduced (approximately up to fourfold of the displacement of failure load).

## 2nd test phase - 3-point bending for failure modelling and dynamic impactor testing

28 middle ribs (mainly 3 – 6, partly 2 and 10-11) were obtained from four female PMHS. Three of them between ages of 59 and 65 – one 32 years old. Within the second series of experiments, the quasi-static 3-point bending test set-up was slightly modified with regard to the length (now approximately 100 mm) of the rib specimen and its support condition (now clamped firmly). The main focus of these experiments and especially of the further processing of the results was among the determination of the material properties on the faithful reproduction of the behavior at rupture and also the observed post-cracking mechanism of rib bones.

For the quasi-static test set-up the movement speed was 100 mm/min with a total displacement range of 30mm to generate a loading on the rib until fracture. The force vs. deflection curve was collected and the test itself was recorded by a camera.

The force-deflection diagram in Figure 1 shows typical behavior of elder and younger rib specimen. In principle the main characteristics of the curves are comparable with the 1st test phase. The rib bone shows a kind of elastic stiffness at the beginning of test. The curves of the younger rib specimen are consistently steeper and therefore indicate higher stiffness. Also in this test series rib samples from younger PMHS show failure at approximately three times higher load level compared with the sample from the elderly. Similar post-cracking behavior was observed in both tests.

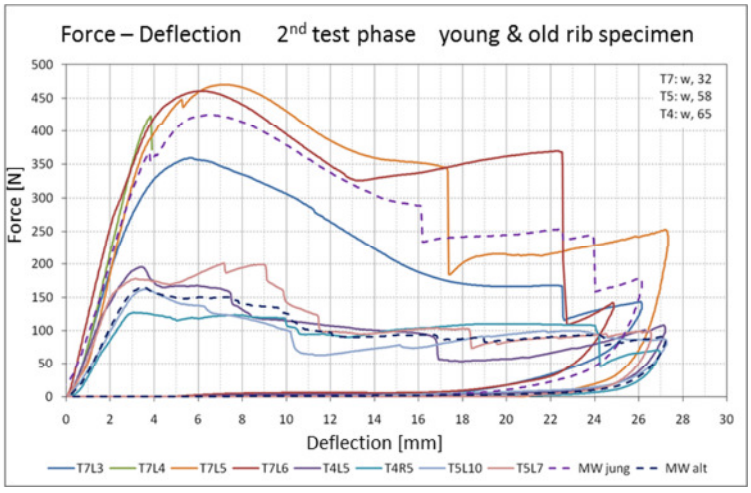


***Figure 1: Typical Force-Deflection of elder and younger rib specimen observed in this load case.***

The findings of the 2nd series of experiments (quasi-static) could be summarized as follows:

- Rib specimen with similar dimensions showing quite comparable elastic behavior – this applies for rib sample from younger and elderly.
- Rib samples from young PMHS (female) withstand approximately two to three times higher loads compared to rib samples from elderly (female) .
- Stiffness (elastic curve section) of younger ribs is significantly higher

The material model validated against this quasi-static testing was also assessed under dynamic loading conditions. Focus of this study was to confirm the material model and parameters for the elastic behavior on the one hand and for fracture on the other hand. For this, a DOE (Design Of Experiment) study was carried out based on FE-Simulation of the dynamic 3-point bending test set-up. The fracture or no-fracture behavior of a rib specimen was predicted for a certain combination of test parameters such as impactor mass and velocity. The rib samples were as well potted on both ends and clamped firmly in a test rig. The results were finally plotted into the DOE diagram and correlate well (final material properties) with the predicted behavior. Nevertheless, it has to be stated, that for this additional dynamic study only ribs from the elderly (59), female PMHS were available.

**Rib material model and failure modelling of rib fracture**

The results respectively force-deflection curves from mainly the second test series were now discussed to be transferred into a constitutive law and finally a material description to be used within the LS-Dyna code. As already described in previous paragraph, the rib bone shows an elastic stiffness at the beginning of test (Figure 2). At the end of the elastic material behavior the rib starts to get locally deformed while the test curve shows an elasto-plastic material behavior attended with a material hardening. At this point the bone starts to get a fibrous fracture at the force application point followed by an extension of the fracture along the rib in the closer area. The test curve shows a continuous elasto-plastic fracture behavior with steady reduction of the stiffness.

To regulate the elastic range of a response curve (section a in figure 2), the Young's modulus as contributing factor has to be adjusted to the test results in terms of the Hooke's law. The parameters to control the adjustment of non-linear hardening in the elastic-plastic range (section b in figure 2) are the effective plastic strain values (EPS) and the corresponding yield stress (ES). The third part of the response curve (section c in figure 2) shows an elastic-plastic behavior combined with a softening of the bone. This softening is now realized and controlled by a modulated failure flag in the material properties which limits the maximum plastic strain at 6.8% and conduct elements deletion of the shell elements (cortical bone). It has to be noted, that the threshold respectively failure flag of 6.8% is strictly model dependant. In case of any modification in mesh or use in other models, this threshold is not valid and has to be refined against the original test data. The material properties of the cortical rib bone are defined in MAT_24 similar to the current THUMS-D v3.2 but with different parameter values. One of the most essential adjustments was the change of the Young's modulus from 18 GPa to 3.5 GPa (Young Rib Material) and 1.5 GPa (Old Rib Material). Also the definition of the trabecular bone has been changed from MAT_12 to MAT_1 what is defined as elastic material behavior.

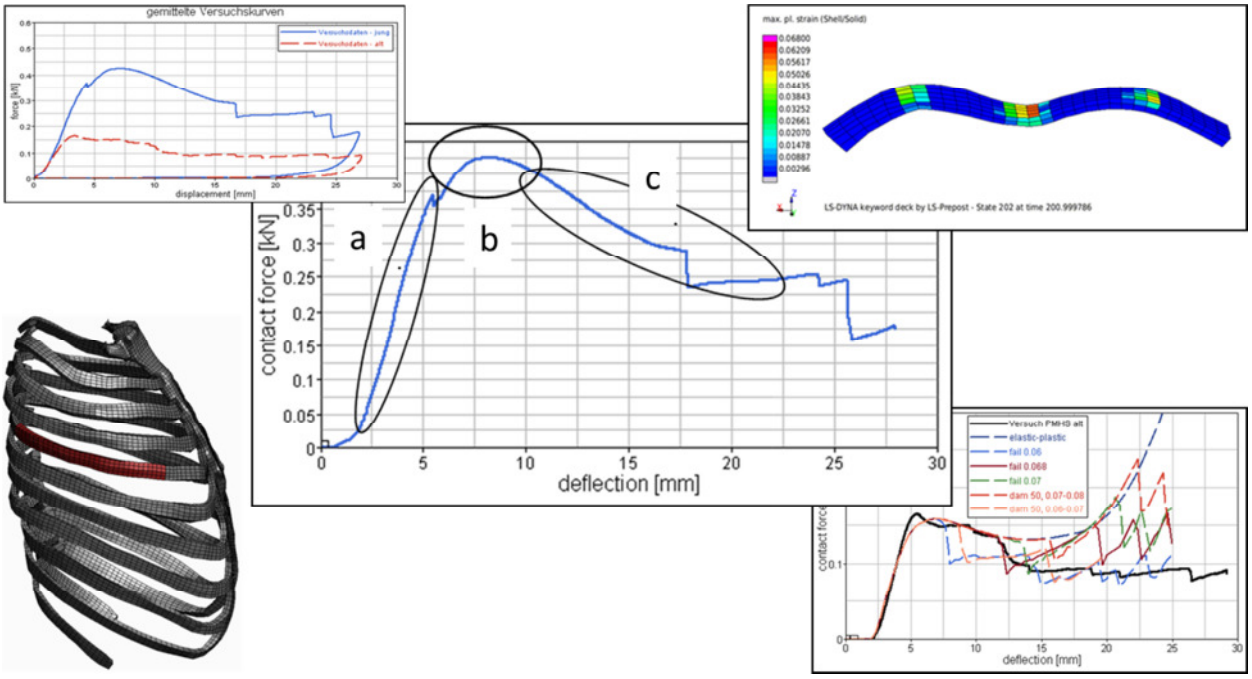


***Figure 2: Rib material model and failure modelling of rib fracture – Top Left: averaged test data of elder and younger rib specimen – Centre: characterization of test curve segments; elastic (a), elastic-plastic/hardening (b), elastic-plastic/softening (c) – Bottom Right: determination of damage parameter.***

**Validation against GESAC 2005 & ISO/TR 9790**

The validation of the complete THUMS-D with new rib materials comprises the frontal pendulum impact tests defined by GESAC 2005 [7] and the lateral and oblique-lateral pendulum impact tests defined by ISO/TR 9790 [8].

The study on fracture mechanism showed a significant difference between the Young Rib Material (NRy) and the Old Rib Material (NRo) in terms of material behavior and predicted risk of rib fractures. The NRy performs considerably more elastic than the NRo what reflects the embrittled bone material of the elderly population. A comparison with the Number of Fractured Ribs (NFR), documented in ISO/TR 9790 for lateral, low speed oblique-lateral and high speed oblique-lateral PMHS tests shows a good correlation to the predicted rib fractures given by simulations with NRy and NRo (Figure 3).

- The NFR in 4.3 m/s lateral impact PMHS tests have a range of 0 to 7. The model with NRy predicts no risk on any rib while NRo predicts a risk on 6 ribs including 2 of them with a high fracture risk.
- For the low speed oblique-lateral impact tests on PMHS showing 0 to 2 fractured ribs on impact side and 0 fractured ribs on the opposite side. THUMS-D with NRy predicts a relatively low risk for 1 rib on impact side. The model with NRo predicts 6 ribs with a risk thereof 2 to 3 with an advanced risk.
- The high speed oblique-lateral impact tests on PMHS showing 2 to 7 fractured ribs on impact side and 0 to 3 on the opposite side. The model with NRy predicts 6 ribs thereof 2 with advanced risk on the impact side. The model with NRo predicts 8 ribs thereof 6 multiple and 4 with critical risk on the impact side, additional 1 rib with an advanced risk on the opposite side.

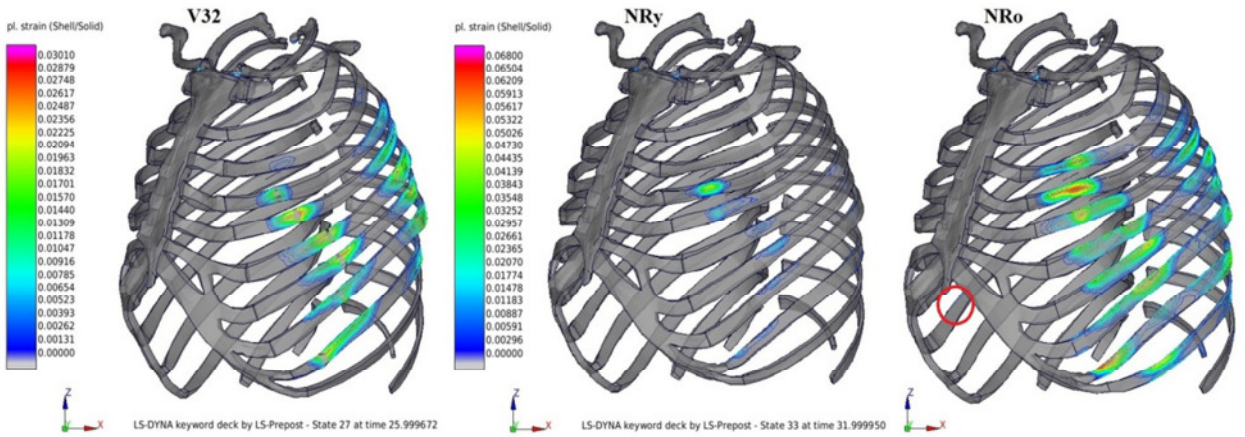


***Figure 3: Fringe plots / results ISO/TR 9790 load case oblique pendulum impact 6.7 m/s; plastic strains; From left: Rib material original THUMS-D (V32), Young rib material (NRy), Old rib material (NRo).***

**Discussion**

Two new rib material models and properties, for younger population (NRy) and for elder population (NRo), were defined for the use with LS-Dyna code based on human rib specimen tests by TU Graz. With reference to the pendulum impact results for validation, NRy and NRo are showing an improved chest response of the entire THUMS-D. The outcome of this is an improved but still amendable chest response on frontal pendulum impacts, an acceptable performance on lateral pendulum impacts and a good performance in the oblique-lateral impact tests which motivated finally the application within the loadcase and system development which will be presented in the following paragraphes.

Nevertheless, it is important to note, that several limitations arise from the biomechanical testing and modelling. The biomechanical test data is limited to three elderly female and two elderly male PMHS. The data for the younger population is just based on one male and one female subject. Within the modelling and validation part no change of the thorax shape and its changes over lifespan was realised. Also the modeled fracture mechanism just reflects the results of the 3-point bending test set-up.

## APPLICATION PRE-SAFE® IMPULSE SIDE:

In this chapter, the newly validated Human Body Model will be used for the development of a new generation of integral safety restraint systems: PRE-SAFE® Impulse Side.

### System description PRE-SAFE® Impulse Side

**Theory** PRE-SAFE® Impulse Side is the very first of a new generation of pre-impacting restraint systems whose field of action will be extended prior to the collision thanks to the integration of active and passive safety [9].

The specifics of the vehicle structure in a lateral impact make it necessary to use all the available space to reduce the loads to the occupants. Structural measures, the right material choice and the use of tailored side impact restraint systems like side airbags or curtain airbags describe the state of the art protection measures. But what if there were more space available to take efficient mitigation countermeasures without increasing the car body dimensions? That is the idea of PRE-SAFE® Impulse Side.

The new PRE-SAFE® Impulse Side restraint system aims at creating more space between occupant and car interior/structure only when needed i.e. right before a crash event occurs. As a result, the side airbag could better deploy, the contact with the intruding structure might occur later, so that more crash energy could be dissipated by the vehicle structure deformation before the gap between structure and airbag is being closed.

But PRE-SAFE® Impulse Side is not only increasing the space between occupant and side structure. Indeed, PRE-SAFE® Impulse Side also actively pre-accelerates the occupant toward the center of the car. As a result, the occupant has already been set in motion when the collision begins, in other words the relative velocity between occupant and intruding structure has been reduced.

Maximizing the distance and reducing the relative velocity between occupant and intruding structure can significantly reduce the occupant loads especially in the thorax region.

**Functional implementation** Inflating a specifically designed air bladder in the seat rest side bolster creates the impulse needed to move the occupant. The activation time has to be precisely calculated using information of the car surroundings gathered by camera and/or radar sensors [9].

Through the light impulse, the occupant is being moved towards the center of the vehicle prior to the predicted impact (Figure 4).

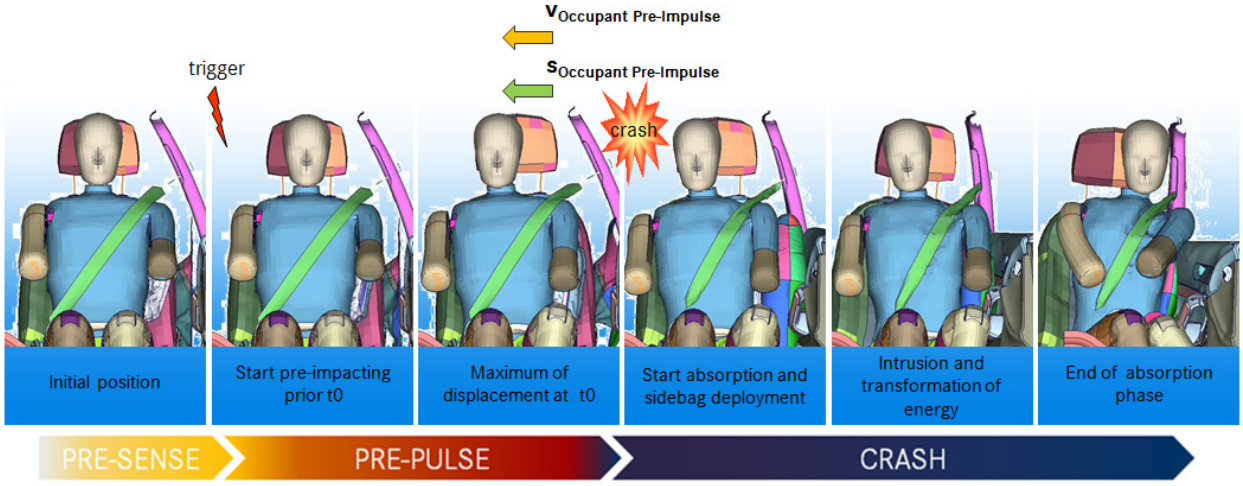


*Figure 4: PRE-SAFE® Impulse Side way of action*

## PRE-SAFE® Impulse Side safeguarding

In contrast to traditional irreversible restraint systems, the deployment decision for the PRE- SAFE® Impulse Side bladder is based on situation analysis of the vehicle surroundings before crash. As a result, there is a minimal chance of system activation remaining even though the collision could be avoided in the last moment. Therefore, the system characteristics were designed to meet the conflicting targets of both providing the required impulse to the occupant and being gentle enough in the deployment not to harm anyone.

The safeguarding assessment of the system was done by simulating a static deployment of PRE-SAFE® Impulse Side using THUMS-D with modified rib material representing elderly persons. After triggering PRE-SAFE® Impulse Side, the HBM displacement as well as rib compression, stress and strain were measured (Figure 5).

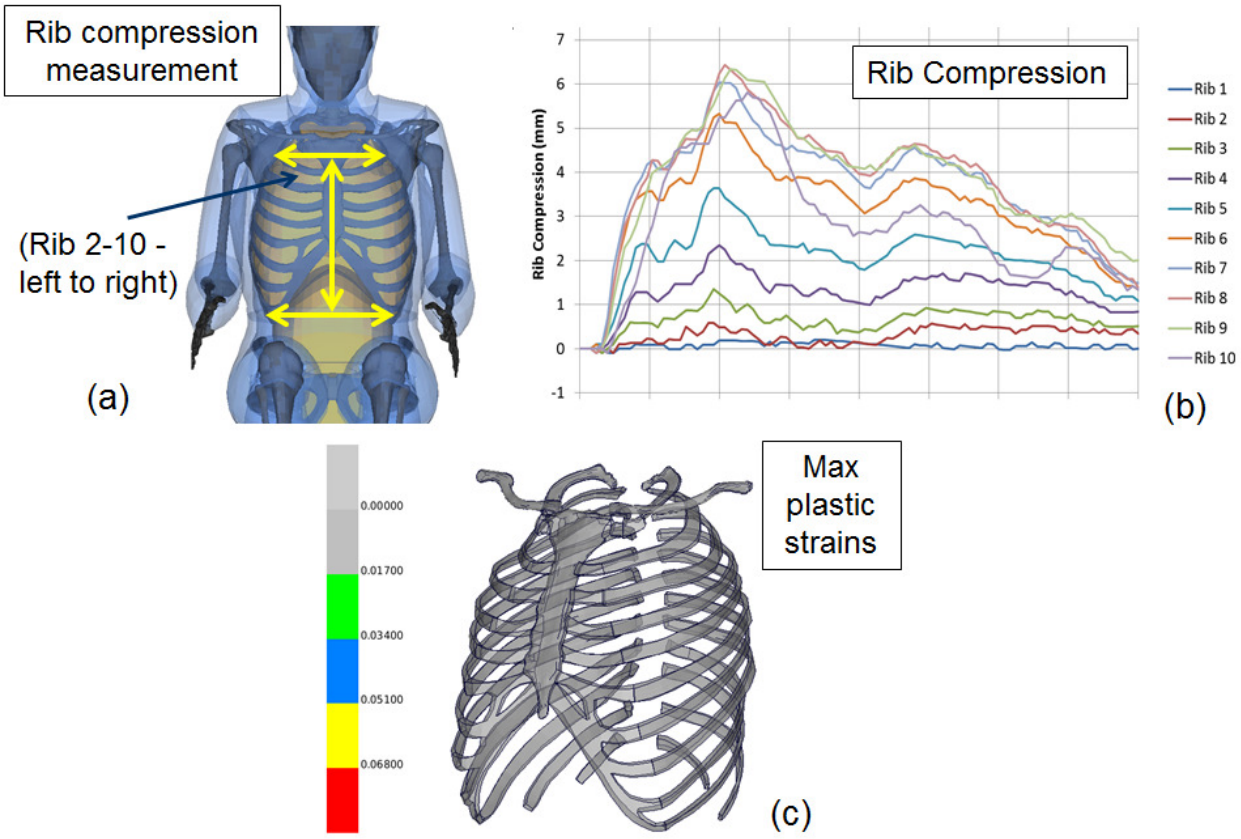


***Figure 5: Definition of relative rib compression (a) relative rib compression measurement (b) and fringe plot of plastic strains(c) of the ribs***

The rib compression is evaluated by monitoring the relative displacement of two outer nodes of each rib as shown in Fig. 5a. Fig. 5b shows the highest compression which takes place at the lower ribs (7, 8, 9) exactly at the height of the PRE-SAFE® Impulse Side air bladder. As can be seen on the diagram, the maximal compression does not exceed 6,5mm. Analysis of the maximal rib strains shows almost no plastic strains (c). As the fracture limit of the rib model is set to 6,8% plastic strain, the THUMS-D model is not predicting any fracture risk by an activation of PRE-SAFE® Impulse Side.

**Dynamic Results**

After having assessed the safeguarding of the system in a given static case, the following section describes its protection potential in a barrier load case using a full scale car crash simulation model. HBM was used to configure the system by determining the optimal time to deploy – frequently referred to as ttf (time to fire). The baseline simulation model was built using a carline achieving very good results in both European and US side crash ratings. The simulation was run with THUMS-D model with newly validated rib material (NRo).

In full scale vehicle crash tests using side impact dummy, the PRE-SAFE® Impulse Side system has already shown the potential to reduce the measurements of the rib cage significantly with up to 20-30% decreased rib deflection values. The goal of the following CAE activity was to confirm this result using HBM. It is commonly accepted that absolute values of measurements obtained by anthropomorphic test devices cannot be directly compared to calculation results derived from HBMs. In addition to the rib compression, maximal plastic strains of the ribs were estimated in order to assess the risk of rib fracture in a lateral collision with and without PRE-SAFE® Impulse Side. The results concerning rib compression and thorax strains are plotted in Fig. 6.

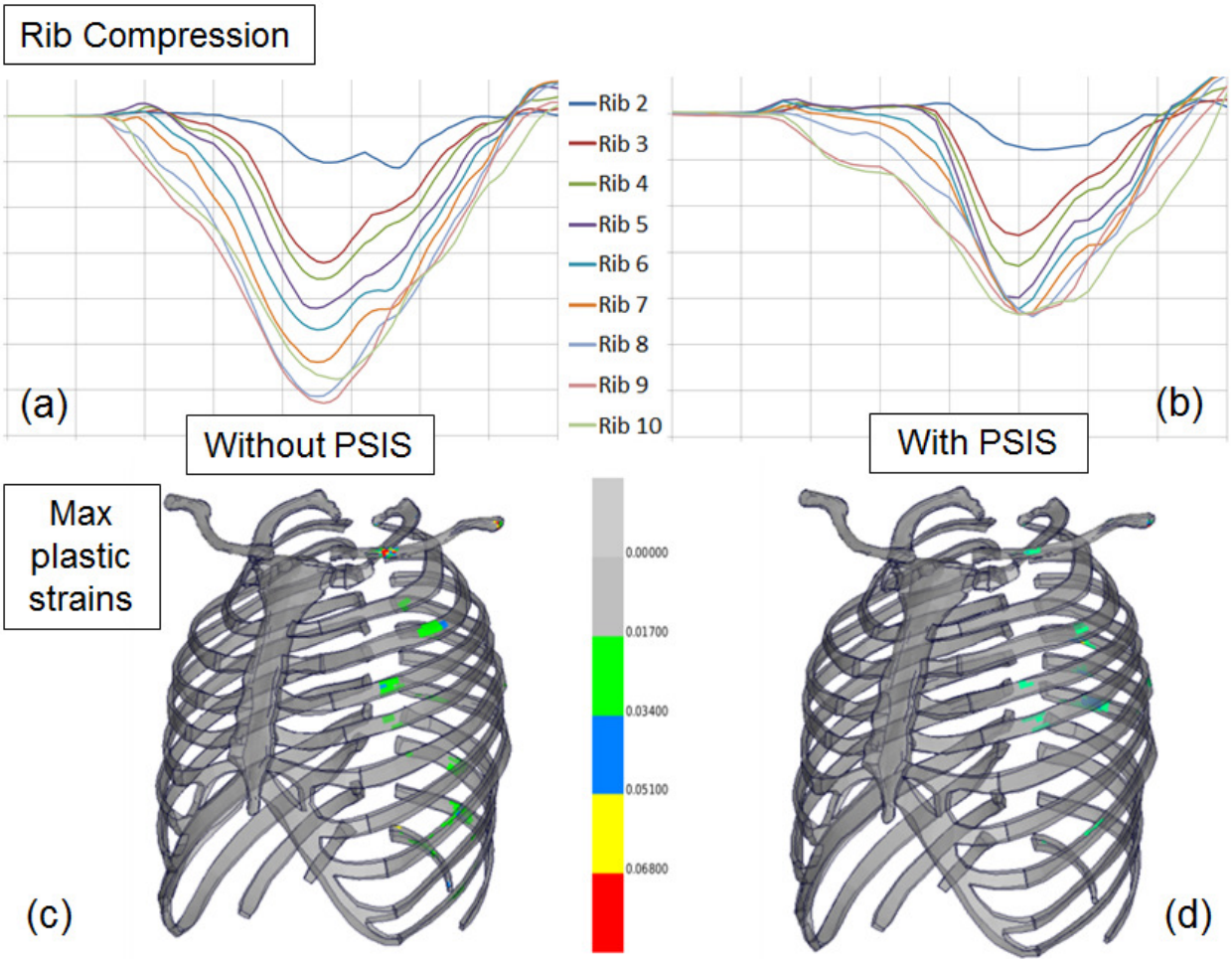


***Figure 6: Rib compression measurement without (a) and with PRE-SAFE® Impulse Side (PSIS) (b), maximum plastic strains without (c) and with (d) PSIS.***

The calculated rib compression shows a significant reduction of the thorax load when the PRE-SAFE® Impulse Side system is used, especially for ribs situated directly next to the air bladder. An average reduction of the rib compression by 20% was achieved.

As stated earlier in the paper, the new rib material was implemented with a failure flag when plastic strain exceeds 6,8%. Using this limit, the simulation without PRE-SAFE® Impulse Side indicates a possible rib fracture (red flag on Fig. 6c). A reduction of the calculated maximal plastic strain can be achieved while triggering PRE-SAFE® Impulse Side. Maximal plastic strain is not exceeding 4%, leading to a significant decrease of the rib fracture risk when PRE-SAFE® Impulse Side is used.

## CONCLUSIONS

It is challenging to verify the effects and to show the whole potential of advanced restraint systems with traditional CAE tools. Therefore, the methodology shown in this paper was developed to assess the effects of a new generation of pre-impacting restraint systems. Regarding safeguarding and system optimization, a newly validated HBM with improved prediction capability for risk of rib fractures in elderly population was used to assess the PRE-SAFE Impulse Side system. The use of this new THUMS-D was important toward the

development of the system showing that it remains harmless in case of unmotivated activation. Furthermore, the optimal triggering time of the PRE-SAFE® Impulse Side System, found using anthropomorphic test devices, has been confirmed by HBM simulations. In the investigated load case, both hardware tests and HBM simulations show a significant reduction of thorax load by using PRE-SAFE® Impulse Side.

## ACKNOWLEDGEMENTS

The authors wish to acknowledge our scientific partners of the Technical University Graz and the DYNAmore GmbH, which contributed to this research with their specific expertise.

## REFERENCES

[1] Kitagawa, Y. and Yasuki T. "Development and Application of THUMS Version 4".
Proceedings of CARHS 5th International Symposium Human Modeling and Simulation in Automotive Engineering; Oct 16th-17th, 2014; Munich.
[2] Gupta A.K., Sharma G., Shah P., Ageorges C., Mayer C. "Development of an anatomically-correct finite element model of the human shoulder".
Proceedings of IRCOBI Conf. , IRC-11-58, 2011, Krakow.
[3] Doerfel S., Zhou K., Sharma G., Mayer C., Peldschus S. "Development of FE models of clavicular ligaments: quasi-static tensile test and FE simulation".
Proceedings of IRCOBI Conf. , IRC-12-71, 2012, Dublin.
[4] Reporting THORAX project, "Thoracic Injury Assessment for Improved Vehicle Safety", www.thorax-project, 2009-2012, European Commission DG RTD, FP7 Theme 7,Transport-SST.2007.4.1.2.
[5] Agnew A.M., Moorhouse K., Murach M., White S.E., Kang Y-S, "Tensile Stress in Human Ribs throughout the Lifespan".
Proceedings of IRCOBI Conf. , IRC-14-44, 2014, Berlin.
[6] Tomasch E., Sinz W., Kirschbichler S., Steffan H., Darok M., Patsch J., Dimai H.P., "Korrelation von Knochendichte und Rippenfrakturen"; EVU 2011-8 ; 20th EVU Conference, 2011, Graz.
[7] GESAC, Biomechanical Response Requirements of the THOR NHTSA advanced frontal Dummy. Trauma assessment device development program. 2005.1 ed: GESAC - Gerneral Engineering and Systems Analysis Company; 2005.
[8] ISO, ISO TR 9790 - Road Vehicle - Anthropomorphic side impact dummy - Lateral impact response requirements to assess the biofidelity of the dummy. vol. ISO/TR 9790:1999(E) Geneva (CH)1999. p. 145.
[9] Marica Paurevic, Prof. Dr. Rodolfo Schöneburg, Dr. Julien Richert, Ralf Bogenrieder - Daimler AG, 2014. "PRE-SAFE® IMPULSE SIDE: A PREVENTIVE PRE-IMPACTING RESTRAINT SYSTEM" In Proceedings of the 12th International Symposium and Exhibition on Sophisticated Car Occupant Safety Systems, Airbag 2014 (Karlsruhe Dec. 1-3), #14

**Evaluation of Occupant Protection Systems:**
**FROM A PREVENTIVE TO A PRE-IMPACTING RESTRAINT SYSTEM**

**Prof. Dr. Rodolfo, Schöneburg**
**Marica, Paurevic**
**Michael, Fehring**
**Dr. Julien, Richert**
**Ralf, Bogenrieder**
Daimler AG
Germany

Paper Number 15-0374

## ABSTRACT

The safety of modern vehicles has reached such a high standard that experts view the remaining potential for improvement of conventional restraint systems as nothing more than minimal. However the use of information gathered during the pre-crash phase added to the combination of preventive and conventional restraint systems can reveal additional potential.
One example of this is the reversible pretensioner of the PRE-SAFE® system, launched in 2002, which can hold occupants in their position shortly before a potential collision and thus reduce forward displacement to offer improved protection in an accident.
This approach was further developed with the introduction of PRE-SAFE® Impulse, which debuts in the current S-Class of MJ 2013. PRE-SAFE® Impulse systems rapidly accelerate occupants at an early phase of the crash by moving them in the direction of the impact force so that the difference in kinetic energy between the vehicle and occupants can start to be reduced as early as possible. As a consequence the total energy does not have to be dissipated entirely during the crash itself, but is distributed over a minor initial impact and a major impact whose intensity is reduced accordingly.
The new PRE-SAFE® Impulse Side System, a pre-impacting restraint system, does not only applies this idea for side crash but brings the concept one step further. Previous measures for improving side impact protection were primarily implemented on the vehicle itself and did not directly influence the occupants prior to the crash. With PRE-SAFE® Impulse Side, a defined energy, is transferred to the occupant, who is set in motion already before the collision occurs. Therefore PRE-SAFE® Impulse Side is the very first of a new generation of pre-impacting restraint system whose field of action will be extended prior to the collision due to the integration of active and passive safety.
To this end, the PRE-SAFE® Impulse Side system uses a 360-degree sensor system, which permanently senses the car surroundings, to anticipate an unavoidable collision.
Using numerical simulation as well as sled and vehicle testing, relevant occupant loads have been shown to be reduced by 30 percent on average with the use of PRE-SAFE® Impulse Side.

## INTRODUCTION

Due to improved structure, seat belts and airbags the safety level of modern vehicles has reached a very high standard. Even small cars offer an impressive degree of protection.
Further improvement of occupant protection, even implementing modern restraint systems such as adaptive airbags and switchable belt force, is only possible to a certain extent.

To date, occupant protection systems have only been actively deployed after the accident has started to transpire. The enhancement of driver assistant systems offer opportunities to reliably detect accidents in advance, the time window in which restraint systems can offer protection increases dramatically. This, in turn, leads to great potential for further improving occupant protection in a passenger car.

In the future Advanced Driver Assistance Systems will largely contribute to reduce the number of injured occupant by avoiding crashes or mitigating their consequences. However side crashes remain very challenging for sensors to detect. Indeed potential collision partners are often hidden and cannot be properly seen i.e. tracked by the car sensors until the collision is unavoidable. At least when our own car is standing on-board driver assistance systems are incapable of minimize the intensity of the accident or avoid the accident. In that case, the severity of the impact at the side of the vehicle is directly linked to the proactive measures undertaken by the colliding vehicle partner.

Nevertheless if restraint systems (passive safety) and driver assistance systems (active safety) taken individually cannot offers great improvement for side crash scenarios, the integral safety approach, combining both active and passive safety components in one system appears extremely promising.

In this paper a solution will be proposed that shows to what extent the pre-accident phase can be taken into account to prepare the occupant for a side collision impact.

## OPERATIVE MECHANISMUS

### Side Impact

Mechanisms of action in a side impact depend on the distance between occupant and vehicle structure as well as on the intrusion or contact speed of the vehicle structure to the occupant.

Compared to frontal impact there is less absorption way and time to protect the occupant in side impacts. There are only limited distance between the occupant and the struck side of the vehicle as well as short time between the beginning of the collision and the moment when the occupant is loaded by the impact of the door.

The vehicle's dimensional design usually limits the distance between the occupant and the vehicle structure. Potentials to reduce the intrusion velocity have been primarily achieved through structural measures. Present airbags for side protection are designed and dimensioned to be activated shortly after the beginning of the impact. Those conditions limit the performance of possible passive safety countermeasures.

Involving the occupant in the sequence of an accident event earlier or even prior to a collision has not been considered till now.

### PRE-SAFE® Impulse

Today, occupant restraint systems are classified as reactive systems. The downside of these occupant protection systems is that they only take effect once the accident has already started. Occupants are then decelerated with a considerable time delay with respect to the initial collision sequence. Energy only begins to be dissipated once the

occupant has traveled a required distance within a specific time as a result of his or her forward excursion. In this time window, valuable deformation space has already been used to decelerate the vehicle but not the occupant.

The aim of PRE-SAFE® Impulse restraint systems is to couple the occupant as early as possible to the vehicle deceleration by distributing the total impact energy over a minor initial impact and a major impact whose intensity is reduced accordingly.

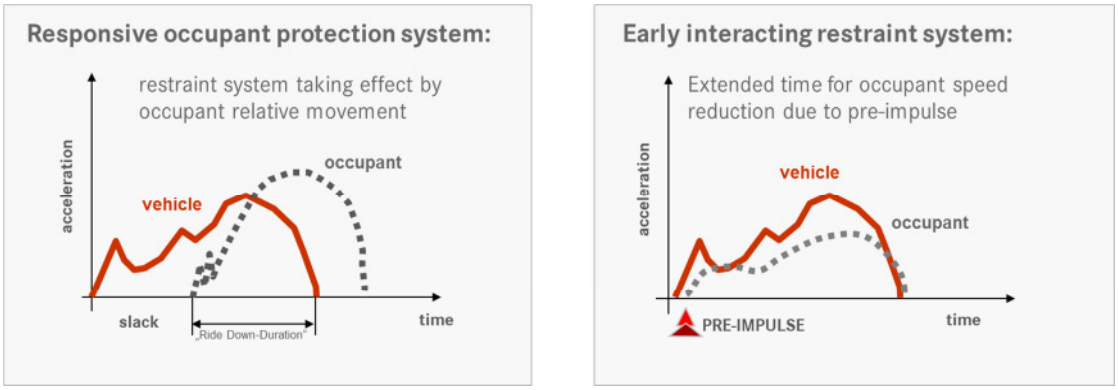


***Figure 1: Comparison of responsive and early interacting occupant restraint system***

Figure 1 shows a reactive and an early interacting restraint system. With an early interacting restraint system, the occupant is jolted in a very early phase of the accident, when the vehicle deceleration has not yet acted on him. The occupant perceives this as an acceleration impulse. This results in occupant deceleration, the occupant is briefly slower than the vehicle in which he is seated. The occupant is moved opposite the impact direction. The displacement path gained by the relative speed can be released again over the course of the accident via energy dissipation.

Such a restraint system influences the ride-down effect and occupant kinematics and can reduce the occupant load values via the longer deceleration period.

Assuming that the impact is known properly, the principle of reactivity can be augmented by actively moving the occupant in a defined direction. Prior to the impact occupants are not yet subjected to impact-specific inertial forces and can therefore be moved using little energy reaching comparable improvement with a lower pre-loading of the occupants (Figure 2).

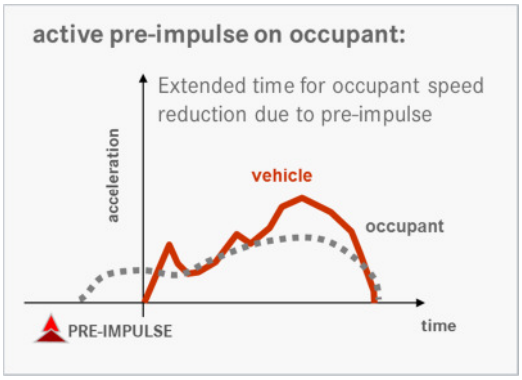


***Figure 2: Active pre-impulse on occupant enable the change of velocity over the maximum of time***

## PRE-SAFE® IMPULSE SIDE - occupant protection system for side impacts

The PRE-SAFE® Impulse Side protection system demonstrates how a pre-impacting system could work. PRE-SAFE® Impulse Side is the very first of a new generation of pre-impacting restraint system whose field of action will be extended prior to the collision due to the integration of active and passive safety.

### Occupant Impact as Operative Mechanism

At a precisely calculated time prior to the side impact, the occupant of a vehicle is laterally displaced by a movement of the backrest side bolster. This small impulse moves the occupant toward the center of the vehicle before the impact occurs.

Actively moving the occupant toward the center of the vehicle increases the distance between the upper body of the occupant and the door panel so that the side airbag can be safely and efficiently deployed.

The contact time between intruding structure and occupant also occurs later and therefore with reduced intrusion speed. In addition, the occupant is already moving at a certain speed in the direction of the impact. His/her relative velocity regarding to the intruding structure is smaller thus less kinetic energy has to be dissipated by the contact with the restraint system and/or the car structure.

PRE-SAFE® Impulse Side, like all other PRE-SAFE® systems, acts as an additional measure that does not replace the conventional restraint system, but enhance it.

### PRE-SAFE® Impulse Side Actuator

The seat was equipped with a dynamic multi contour seat component. There, in the side bolster of the driver and passenger seat backrests, an air bladder is inserted that can be filled to improve lateral support during cornering.

To generate the impulse on the occupant, this air bladder was modified in terms of their size and filling characteristics so that they are strong enough to initiate the movement of the occupants toward the center of the vehicle. This process takes place within the seat without any damage and can therefore be repeated. The challenge with this setup is to create an upholstery concept, which on the one hand must allow sufficient movement, but on the other hand has to meet customer requirements in term of design and comfort.

### Methods and Tools

The methodology for the assessment of the benefit of the PRE-SAFE® Impulse Side airbag is based on three tools: FEM crash simulation, sled tests and vehicle tests. In a first step FEM simulation was done to identify the optimal parameters of the airbag (pressure, geometry, volume) to reach the expected benefit. In static tests, the airbag design and deployment characteristic were performed and optimized. Sled tests were conducted to assess the reduction of the occupant injuries using PRE-SAFE® Impulse Side during a side impact. As final step the performance of the pre-impacting actor was ensured by vehicle tests.

Once a first prototype seat was available, the first step was to take some measurements of lateral excursion using different dummies in order to define a first set of parameter for the system and so insure the feasibility of the system. At each step, the data collected on dummies were validated against tests persons, both in static tests. For dynamic test validations, sled and car tests were compared to numerical simulation using Human Body Model to make sure that pre-impacting restraint systems do not induce any unwanted side effects.

## Results

Like every PRE-SAFE® system, PRE-SAFE® Impulse Side unfolds its fully potential in real life accident scenarios. To show the benefit of the system in this paper two common side crash scenarios have been chosen: a pole and a barrier test.

**Pole test** The pole test has following configuration: impact speed: 29 km/h, angle: 90°, ES2re-Dummy. Compared to conventional restraint systems, the benefit of PRE-SAFE® Impulse Side vary between 25% in lower rib up to 35% in middle and upper rib (Figure 3). The potential in the upper area is the highest and decreases slightly with respect to the lower rib. The effect of the displacement is at its greatest in the upper thorax region and corresponds to the acceleration of the occupants.

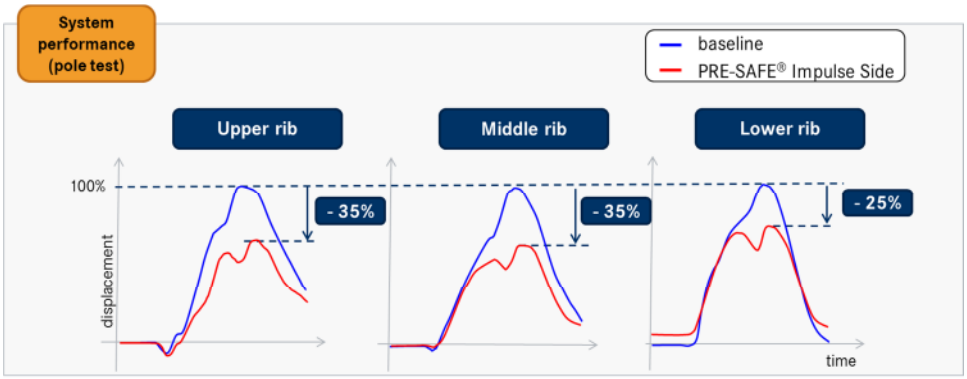


*Figure 3: Benefit of PRE-SAFE® Impulse Side in pole test with ES2re dummy*

**Barrier test** The barrier test was done according following configuration: impact speed: 50 km/h, movable deformable barrier with a mass of 1450 kg, SID2s-Dummy.
The PRE-SAFE® Impulse Side effect can also be seen in the barrier load case. Due to the lateral excursion, the loading of the shoulder begins later as it can be seen on the shoulder force curve in Figure 4. As a consequence, the rib intrusion value is also significantly reduced.

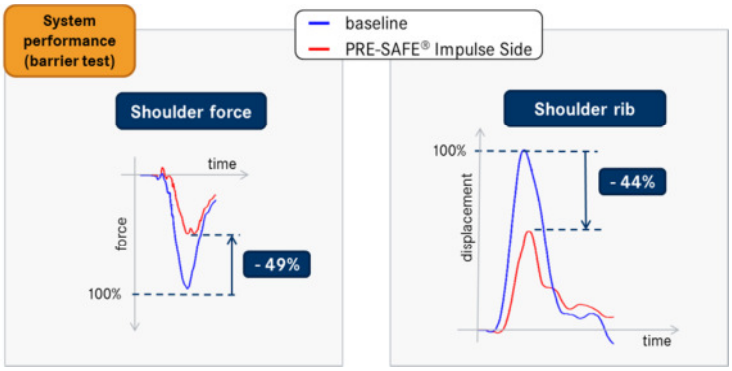


*Figure 4: Benefit of PRE-SAFE® Impulse Side system for barrier test configuration*

This improvement can further be observed on the thorax and the abdominal ribs. The PRE-SAFE® Impulse Side effect in the lower thorax region is also less pronounced than in the upper one in this load scenario, same tendency as for the pole load case (Figure 5).

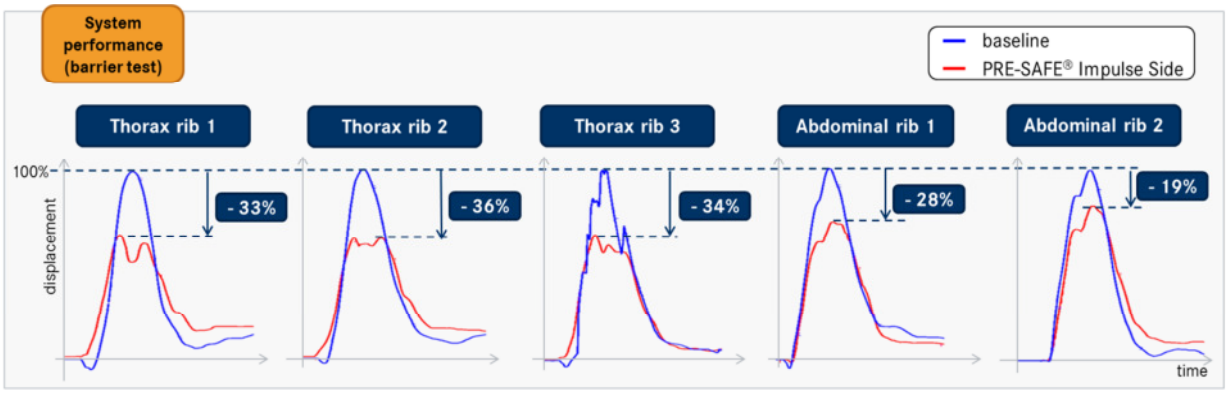


*Figure 5: Benefit of PRE-SAFE® Impulse Side in barrier test configuration*

## System robustness

As PRE-SAFE® Impulse Side is the very first pre-triggered restraint system it was crucial to realize a robust system. The robustness of the system regarding to variation of the triggering time was analyzed. Investigations were undertaken in a PRE-SAFE® Impulse Side actuator time window starting from half a second prior to crash up to t0. An optimal operating point has been found and the response of the system around this point has been analyzed.

With a 25% error in the triggering time of the actor, the benefit compared to the baseline remains significant, showing the robustness of the PRE-SAFE® Impulse Side system (figure 6).

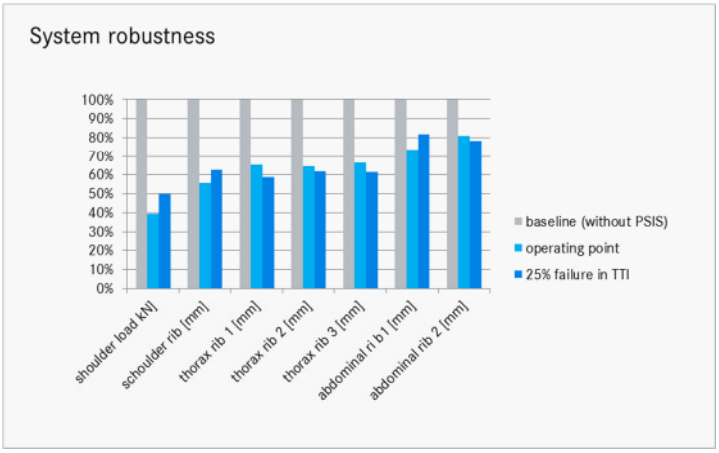


*Figure 6: System robustness: Displacement of SID2s Dummy with 25% failure in TTI (time to impact)*

## SENSOR SYSTEM AND AREAS OF COVERAGE

Capturing and recording the environment, which primarily encompasses radar sensors, but also cameras and ultrasonic sensors, has established itself as an enabler for assistance systems in modern vehicles.

These sensors as used for driver assistance systems could also be used to develop spin-off applications that offer protection in an accident.

For this purpose, special algorithms were created that analyze the sensor data to detect directly "collision objects". Such detection can be realized independently of the assistance functions and operating status of the vehicle. The overarching objective is to detect "objects on a collision course", whereby this detection refers to the vantage point of the respective sensor. From this perspective, a passing vehicle in oncoming traffic is just as much an "object on a collision course" as a bridge pillar that the appropriate vehicle is approaching. Potential collision objects can also be detected when the vehicle is stationary.

The relevant space of time for detecting collision objects begins nearly half a second before the impact. From this time onwards it is possible to predict whether the collision is unavoidable or not. As a consequence the short distance area to the vehicle (typically under 15 meters) must be covered by the sensor system for such functions.

In the event of an impending frontal or rear-end collision, graduated preventive safety measures are activated. These measures are up to now always reversible in line with the underlying idea of the PRE-SAFE® concept.

Current Mercedes-Benz carlines equipped with a driving assistance package utilize targeted algorithms to detect collision using forward-facing sensors and the sensor in the rear bumper.

To realize the PRE-SAFE® Impulse Side function sensors that monitor the side area near to the car are needed. Accident analysis data were used to establish a basis for the observation area. Figure 7 (left) shows the distribution of impact angles in side crashes based on analysis of GIDAS (German In-Depth Accident Study) compared with today crash test scenarios required by regulations and ratings.

These areas on both side of the car have to be covered by the sensors. Figure 7 right illustrates the installation location and visibility of these sensors, whereby angles α and β depend on the exact application constraints and sensor concept.

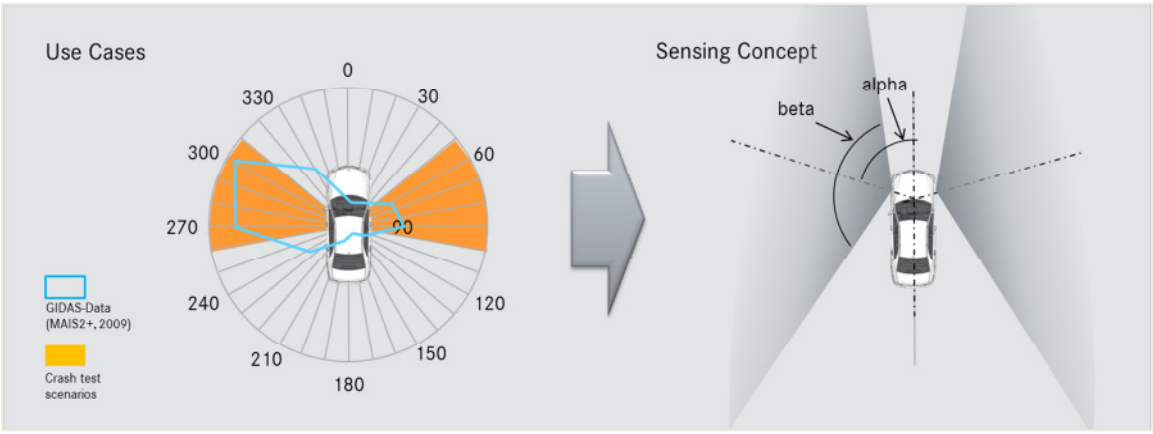


***Figure 7: Schematic illustration of the sensor visibility areas required for PRE-SAFE® Impulse Side***

The sensors needed for the PRE-SAFE® Impulse Side function filled the existing gap in the sensor coverage (Figure 7) achieving a 360-degree monitoring of the car surroundings.

## SYSTEM RELIABILITY

### Driving assistance

While the functional development for so-called "fire cases" (collisions that are detected in the pre-crash phase and for which a system enable is required on demand) is typically conducted on test tracks and using corresponding "soft targets", validation against false deployment must be handled parallel in two ways.

First, specially equipped test vehicles – as is the case with the development of driving assistance systems – are operated in normal, international road traffic in order to encounter as many different traffic and road-based situations as possible. As actual, "accident-critical" situations only arise very rarely, however, this type of testing must be supplemented with deliberately induced accident scenarios conducted on test tracks. In the process, very close drive-by or swerving situations must also be taken into account as well as conceivable special or misuse situations.

Testing and validating these "no-fire cases" is very expansive in scope when it comes to development.

As "PRE-SAFE® Impulse Side" and all other PRE-SAFE® measures always refer to additional, proactive measures that supplement the conventional basic occupant protection system, a deployment strategy must be chosen that prevents firing, or enabling, in the event of uncertain situations. PRE-SAFE® Impulse Side will help to further reduce occupant loads, however.

### Customer Acceptance Study

Due to the triggering character of the PRE-SAFE® Impulse Side system, the function could be activated in the absence of a subsequent crash in isolated cases. Should this happen, the design of the system has to ensure that the driver is not influenced in his or her driving task.

To investigate this issue, the moving based driving simulator was used to analyze the effect of PRE-SAFE® Impulse Side activation completely free of risk and with a high rate of reproducibility.

During the driving simulator study, the driver's response to PRE-SAFE® Impulse Side activation in normal driving situations and the resulting reactions were assessed. Acceptance of false deployment was likewise examined. Three driving situations were constructed to activate the function and verify two driving situations with comparative natural disruptions (crosswind and flying stones). The driving route consists of urban scenarios, country road, and highway sections. The situation was incorporated into the route with 4 variants.

Data of objective measurement for assessing the driver response (driver behavior, driving dynamics, lane tracking, and environment) were recorded. In the study 175 PRE-SAFE® Impulse Side deployments and 54 comparative disturbances were evaluated.

PRE-SAFE® Impulse Side activation during the driving study has not shown any influence on lane tracking in the urban scenarios. On highway, the influence of PRE-SAFE® Impulse Side is less disturbing than experiencing a crosswind while passing another vehicle. Activation of the PRE-SAFE® Impulse Side induces driver responses that do not lead to critical driving situations and can be compared with natural disturbances such as crosswinds.

## CONCLUSIONS

To date, occupant protection measures have only been actively deployed after the accident has started to transpire. In response to this, Mercedes-Benz launched PRE-SAFE® in 2002, the first reversible protection system that acts before the accident starts to take place.
As future possibilities encompass the opportunity to reliably detect accidents in advance, the time window in which restraint systems can offer protection increases dramatically. This, in turn, leads to great potential for further improving occupant protection in a passenger car.
To this end, the PRE-SAFE® Impulse Side pre-impacting restraint system utilizes initial information about the unavoidable side impact to optimally prepare the vehicle's occupants. This is achieved by coordinating actions with the 360-degree environment sensor system, which senses the relevant areas of the vehicle and provides the required signals and information for triggering the protective system.
With PRE-SAFE® Impulse Side a defined force and energy is exerted to actively integrate the occupant in the side impact at an early stage when the vehicle has not yet started to decelerate or has just begun to slow down. Analysis in numerical simulation, sled and vehicle testing, show that occupant loads could be significantly reduced by the benefit of the system.
As PRE-SAFE® Impulse Side is a preventive protection system and false deployment of it cannot be ruled out entirely, a driving simulator study was conducted to investigate the effects on a driving situation and the driver's acceptance of undesired activation.
To ensure adequate validation, the highest priority and challenge is to avoid undesired deployment, even if this means missing an opportunity to deploy when needed.
As PRE-SAFE® Impulse Side is an "on top" protection system, when it does not deploy, all protection capability of the side airbag will be still there.
Automated driving functions directly or indirectly will change the basic conditions associated with passive safety. Synergies with sensor technologies and situation assessment enable further innovative occupant protection strategies, like PRE-SAFE® Impulse Side, to be implemented in the future.

**REFERENCES**

[1] F. Kramer, U. Franz, B. Lorenz, J. Remfrey, R. Schöneburg. 2013. "Integrale Sicherheit von Kraftfahrzeugen: Biomechanik - Simulation - Sicherheit im Entwicklungsprozess“. Vieweg Verlag, 4. Ausgabe, Mai 2013
[2] U. Mellinghoff, T. Breitling, R. Schöneburg, H.G. Metzler, Daimler AG. 2009. “The Mercedes-Benz Experimental Safety Vehicle 2009“. The 21st International Technical Conference on the Enhanced Safety of Vehicles Conference (ESV) – (Stuttgart, Germany, June 15–18).
[3] K.-H. Baumann, R. Schöneburg, Daimler AG. 2010. “PRE-SAFE Pulse: Die Erweiterung des Insassenschutzes durch Nutzung der Vorunfallphase”. 12. VDA Technischer Kongress (Ludwigsburg, Germany, March 24-25).
[4] T. Heinrich, R. Schöneburg, R. Bachmann, U. Merz, M. Fehring, Daimler AG. 2010. “PRE-SAFE® Impulse – Early Interacting Occupant Restraint System”. 10th International Symposium and Exhibition on Sophisticated Car Occupant Safety Systems (Karlsruhe, Germany, December 6 – 8).
[5] J. Richert, M. Fehring, R. Schöneburg, Daimler AG. 2014. “On the way from a preventive to a pre-impacting restraint system”. SAE 2014 GOVERNMENT/INDUSTRY MEETING. (Washington, D.C., January 21-24)
[6] T. Unselt, M. Fehring, R. Schöneburg, Daimler AG. 2013. “Insassen- und Partnerschutz unter den Rahmenbedingungen der Einführung autonomer Fahrzeugsysteme“. 9. VDI Tagung „Fahrzeug-sicherheit“. (Berlin, Germany, November 20 - 21).
[7] M. Paurevic, R. Schöneburg, J. Richert, R. Bogenrieder, Daimler AG. 2014. “PRE-SAFE® IMPULSE SIDE: A PREVENTIVE PRE-IMPACTING RESTRAINT SYSTEM”. 12th International Symposium and Exhibition on Sophisticated Car Occupant Safety Systems (Karlsruhe, Germany, December 1 – 3).
[8] GIDAS (German In-Depth Accident Study). 2009. “MAIS2+ injured passenger in near side collisions”

# COUNTERMEASURES TO ADDRESS MISUSE IN CHILD RESTRAINT INSTALLATIONS: FROM TECHNICAL SOLUTIONS TO REAL WORLD EVALUATION

**Farid Bendjellal**
Britax Childcare Group
Germany

Paper Number 15-0375.

## ABSTRACT

Misuse has been reported in various studies as an important issue in countries where local legislation requires a mandatory use of child restraint systems. It has been shown that the rate of incorrect fitting of the CRS to the car may vary between 60 to 80% (1 Bendjellal, 2006).
However research has not confirmed that all misuse scenarios result in critical occupant loading but a combination of several misuse situations may lead to an improper occupant restraint (2 Bilston, Brown, 2011). It is therefore important to develop technical solutions aiming at reducing the risk of misuse in real-world. Slack in vehicle seat belts when securing the CRS to the vehicle and improper occupant restraint within the CRS are among the top 5 misuse situations according to Bennett study (3 Bennett, 2011) and in NHTSA 2005 survey (4 NHTSA, 2006).
Two technical solutions are presented in this paper, these are:

- A system (called A) that enables improving the attachment of the CRS to the vehicle by assisting the user to tighten properly the vehicle seatbelt
- A system (called B) that was developed: to improve the attachment of the CRS to the vehicle by tightening the vehicle seat-belt (mechanical solution); and (for harness seats) to reduce slack in the harness in riding conditions (electronic solution).

Operating modes of both systems are described. User trials were conducted to assess further the functionality of the systems as well as getting consumer feedback when utilizing them in real world. Key findings from these are also provided in the paper. Both systems show promising results in terms of assisting the users in installing CRSs.

## INTRODUCTION

In previous papers, mechanical and / or visual systems were presented and these enabled the tension of the harness of the CRS to be adjusted by the caregiver. The Safe Strap system was developed in 2006 with the aim to provide such indication. The system is mounted on one of the straps of the CRS harness and comprises 2 members which are pivotally coupled. The upper member as shown in Figure 1 is equipped with visual pictograms illustrating the status of the harness tension. When the desired tension is not achieved the member is in a raised position thereby indicating that the tension is not correct. Pulling the adjuster strap of the CRS will reduce the slack and increase the tension in the harness; the upper member is then deflected to a flat position that is parallel with the harness strap. Pictograms are provided as indicators of the correct or incorrect tension.

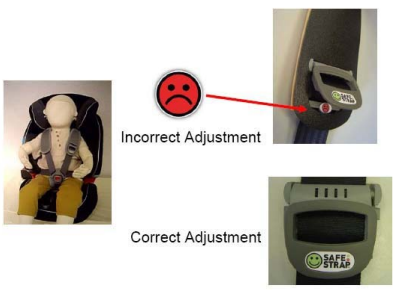


*Figure 1: Safe Strap System*

*Figure 2: Audible system to help user adjusting correctly the harness*

Another technical solution consists in providing the user an audible signal that indicates a correct level of harness adjustment was reached. Such a solution, called Click & Safe™ was introduced in 2008 on Group 1 seats. When pulling the adjuster strap forward and upwards audible clicks indicate that there is no slack or a minimum slack and, that an optimum tension in the harness was achieved. An illustration is provided in Figure 2. Based on lessons learned with these systems, new features were developed which are presented in the following. This paper focuses on CRS systems which use: the vehicle's 3-point seat belt to secure the CRS to the vehicle; and an integrated harness system to secure the child occupant within the CRS.

**Installing car seats in vehicles requires 3 steps –** First reading the user guide of both the vehicle and the CRS by the caregiver; second- installing the seat into the car and securing the CRS with the seat-belt with a properly routed belt, third-installing the child in the seat and placing the harness and tightening it. It is important that all these 3 steps are carried out properly. But in reality parents tend to speed up the first step, hence the risk to oversee important information. User manuals in general contain a lot of information, required by regulation but can be intimidating for parents. The second step is essential to ensure that the CRS is adequately secured to the car. That means a correct belt routing and getting the belt tight enough to retain the CRS. This part of the installation can be challenging as parents, once the belt is properly routed, often exert less or much effort to tighten the belt, only to find as they check their work that the child restraint still feels loose. Isofix system was introduced to address this potential problem and provide an effective solution for parents. However there are still many countries around the world where this attachment is not available in vehicles. For seats which use harness systems, the 3rd step involves tightening the harness with sufficient force to properly restrain the child.

## ENHANCING THE CHILD ATTACHMENT WITH THE SEAT-BELT- SYSTEM A

Introduced in 2000 on a forward facing CRS, the system features a tensioning arrangement for the lap strap of a vehicle seat belt, consisting of side limbs and levers. When the seat shell is moved from the raised position illustrated in Figure 3 by the letter (a), to its position of normal use (c) , the levers are pushed downwards so that the side limbs (position b) deflect the lap strap from the direct path of the belt guides.

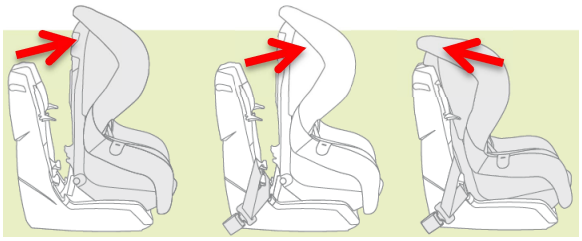

a b c

*Figure 3: A tensioning system of the seat-belt introduced in 2000 on a Forward Facing CRS*

Recently a system called Click-Tight (System A) was developed and introduced on a US convertible platform. It features a large tensioning arm that opens completely to allow for easy and clear routing of the belt from the front of the seat with easy access forward or rearward facing. With the system, there is only one installation method necessary regardless of the size of the child, or which orientation (FWF or RWF).

Once the belt is routed properly through the simple and accessible belt path, the tensioning arm can be easily closed over the vehicle belt. Once the tensioner clicks closed, the mechanism is locked and the belt is properly tensioned. Figure 4 illustrates the operating mode of the Click Tight.

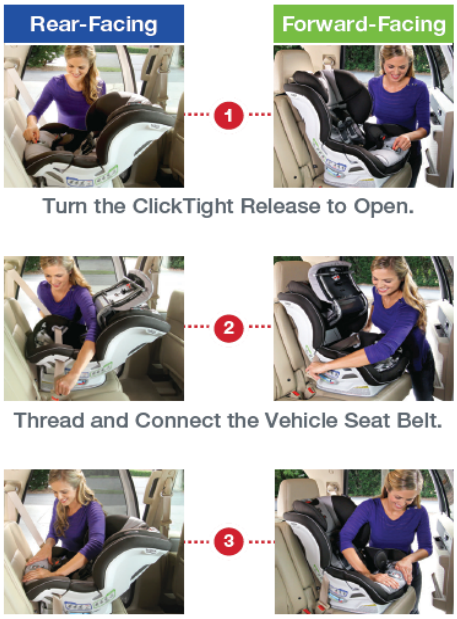


*Figure 4: Click Tight Feature*

**ENHANCING THE CHILD TO CRS ATTACHMENT - SYSTEM B**

The system was developed for child restraint systems with integrated harness and was introduced in EU in 2014 on a Group I platform (9-18 kg mass range). The CRS was equipped with seat-belt tightening system. The feature described here is included in the 'safety loop' of the integral harness and comprises harness straps, an adjuster, a buckle, energy absorbing chest pads and 4 key elements that are part of the innovation, called Automatic Tensioning System:

- A bezel as the communication interface to consumers showing the status of the child restraint system,
- An integrated retractor system that bridges the harness and the adjuster,
- Sensor that detects the occupant presence and controls automatically power supply,
- Software and electronic components.

The Automatic Tensioning System supports the installation of the child by a real time measured tension control on the integrated harness with respective feedback to the caregiver. The resulting tension on the safety loop of the child restraint system is kept over time by the Automatic Tensioning System in real time as well, independent from movements of the child or any other unintentional effect, which could cause loss of tension.
For extreme situations, e.g. unintended buckle release, the system is equipped with electromechanical alert devices, communicating with the caregiver. The key steps in utilizing the ATS are shown in Figure 5.
Once the user has placed the child into the seat, the system is automatically detecting that a child has been placed into the seat. The seat can detect this by the means of a sensor that is located underneath the seating surface. After a pre-defined time the bezel lights up red, as shown in Figure 6, which indicates to the user that the system is activated.

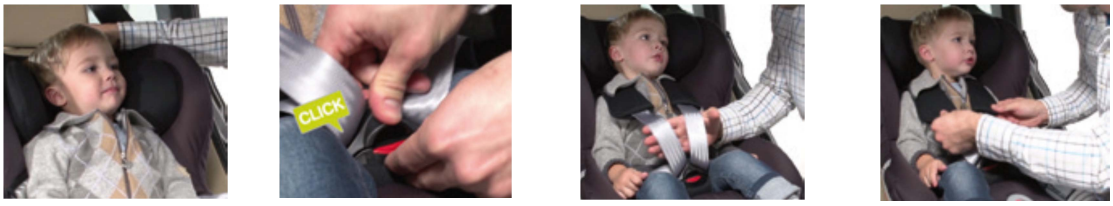


*Figure 5: Key steps in utilizing the Automatic Tensioning System*

*Figure 6: The bezel lights up red and no audible signal indicates that the system is activated.*

*Figure 7: The bezel lights up green and audible signal can be heard.*

Would the user leave the child un-buckled in the child seat or would not harness the child to the correct harness tension an audible alert will be activated after a pre-defined time. This is comparable to the seat belt reminder installed in vehicles that will deliver an audible alert if the driver forgets to buckle up.

In normal operating, a user would harness the child in a similar process as for comparable 5 point safety harnesses. The shoulder straps would be placed over the shoulders and the buckle tongs would be brought together and placed into the buckle. The tightening of the harness can be done by pulling the adjustor strap. The user needs to pull the adjustor strap till the bezel, as shown in figure 7, is lighting-up green and giving an audible signal.

Besides that the system is guiding the user to a proper harness fit the system has two additional functions. The mechanical part of the system has the capability to take slack out of the harness system. The system is able to remove this slack or looseness of the harness within a defined range. The system is designed to ensure that the harness fit remains at the same level of tension as at the moment of harnessing or increases in tension to the required level over time. In case the defined range of compensation has been reached the system will alert the user that the system will not compensate further. Where further tension is required (in normal usage, this should not be necessary as the fit should be equal or better than the original harness tension) or desired by the user, the system can be reloaded again by pulling again the adjustor strap, till the bezel lights-up green, as shown in Figure 7.

Another function that the system provides is that, once the system is fully loaded, it can alert the user in case the child is escaping or unbuckling itself. The bezel will light up red and an audible signal will alert the user. Allowing users to pull over and harness the child correctly.

## CLICK TIGHT SYSTEM VALIDATION

The system A was evaluated in consumer trials that took place in different geographic locations. Consumers were asked to read the user guide, install the CRS in the vehicle and then use the Click Tight system. Both rear facing and forward facing installation were used. The key result: participants found the system easy to understand and operate, and felt satisfied with the resulting tension of the seat-belt once the tensioning arm was locked.

## AUTOMATIC TENSIONING SYSTEM VALIDATION

The ATS system has been tested during the development multiple times in various conditions, ranging from mechanical tests to electronic tests. Besides all relevant component / seat testing related to the homologation of the seat has been tested as well with consumer at different development stages. Some of the main research questions were: would users be able to use the ATS system, would the comfort of the child be influenced by the continuous retracting of the ATS system, would the perceived fit of the harness be rated as sufficient?

The system has been tested with consumers in two different ways. Pre-homologation of the seat the test took place in a car clinic environment. Multiple groups with more than 30 users tested different models during the development in this controlled environment, as shown in Figure 8. The consumers were asked to perform pre-

defined tasks like placing the child into the seat while the car seat was installed into a car. During this test children wore different types of clothes. Children age ranged from 9 months to 4 years.

*Figure 8: Car clinic of fitting test.*

After the seat has been homologated it has been tested in a large scale combined qualitative and quantitative test. More than 100 consumers participated for a prolonged period of time. The main objective of the research was to gain a deep understanding of the user experience. The field investigation consisted of 3 different stages.

In the first stage the consumers have been trained similar to the training they would get in a retail environment. After this the same predefined tasks has been performed as in the car clinic tests. In the second stage the test persons tested the seat in their own car for more than 3 weeks. During this period a group of 40 users had an application installed on their smart-phones to give real-time feedback about the ATS. They have been asked to perform some predefined tasks of harnessing their child before and after their journey, to rate this and make pictures of these situations. As last stage of the field test all test persons have been interviewed to gain quantitative and qualitative feedback on the seat.

**FINDINGS /RESULTS**

The system A (Click Tight) shows very good results in terms of:

- Facilitation the task of seat-belt routing and seat-belt tensioning when installing a convertible CRS,
- Reducing the slack in the vehicle seat belt
- This holds true for both rear facing and forward facing installation as the same tensioning arm is utilized for both configurations.

For the system B (ATS) results of the research highlighted that all users understood the functions of the system and could perform the task to harness their child correctly. In summary:

- 96% of the users rated the harness fit as correct.
- 27% of the users responded even that they would harness their child now tighter than before after discovering and using the ATS system.
- 90% of the users rated that the ATS system fulfilled the comfort expectations for their children.

**CONCLUSIONS/PERSPECTIVE**

The objective of this study was to present 2 features that were developed respectively to enhance the CRS to vehicle attachment, and to improve both CRS to vehicle attachment and securing the child to the CRS. The first system, called Click-Tight, was developed to help the user to get the appropriate tension of the vehicle seat-belt. A key component of the feature, i.e. a large tensioning arm helps to reach the correct tension of the seat-belt. In addition, the system works for both rear facing and forward facing installation. Feedback from consumer trials allowed assessing the system at various stages of the program. The system was launched in 2014 on a convertible CRS.

The 2nd system called “Automatic Tensioning System” was developed to help the care giver to install the child into the seat by providing a real time feedback on the harness tension. The ATS includes electronic as well as mechanical components, and has been developed and introduced on a R44 Group I platform. That platform was already equipped with a seat-belt tensioning system. The ATS among others features a sensor that detects the occupant presence. Once the child is installed and attached with harness, the ATS assists the user, when the

later pulls the adjuster strap, with visual and sound indicators to reach the appropriate harness tension. The system has also the capability to remove the slack in the harness in real time. In addition an alert signal is initiated when a large slack is detected or when the seat buckle is released.

The ATS has been validated during various evaluation trials with consumers which were divided into 2 phases: a pre-homologation phase where the consumer trials took place in a car clinic environment. The second phase (post-homologation) involved more than 100 consumers. The key results from the whole consumer trial research shows that 96% of the participants rated the harness fit as correct and about one third responded that they would harness their child now tighter, and 90% of the users rated the ATS fulfilling the comfort expectations for their children.

Based on the consumer trials and experience gained in developing both systems; the next step will be to extend their application to other platforms.

**ACKNOWLEDGEMENTS**

The author wishes to thank all members of Britax Römer and Britax US who participated to the ATS project.
The views expressed here are those of the author and not necessarily those of BRITAX GROUP and its entities.

**REFERENCES**

[1] Farid Bendjellal, Mark Bennett, Shaun Carine 2006. “Reducing Misuse of Child Restraint Systems – An attempt to treat loose Harness Problems.”
Presented at: 4th Conference Protection of Children in Cars, Munich, December 2006.
[2] Lynne E. Bilston, Julie Brown 2011. „The cumulative effect of multiple forms of minor incorrect use in Forward Facing Child Restraints on head injury risk”.
Presented at: ESV Conference, Washington D.C., 2011.
[3] Mark Bennett, Farid Bendjellal 2011. “Misuse: Recent Evaluations in Ireland”.
Presented at: 9th International Conference Protection of Children in Cars, Munich, December 2011.
[4] Lawrence E. Decina, Kathy H. Lococo, Charlene T. Doyle: Child Restraint Use Sur-vey: LATCH Use and Misuse, NHTSA, 2006.

**The Australian Child Restraint Evaluation Program: An Update on Dynamic Assessment Protocols and Observed Dynamic Performance of Child Restraint Systems**

**Julie Brown**
NeuRA Injury Prevention Research Centre and University of NSW
Australia

**Basuki Suratno**
**Dan Leavy**
Transport for NSW
Australia

**Paul Kelly**
**Michael Griffiths**
Road Safety Solutions
Australia

**Peter Aquilina**
Roads and Maritime Services, Crashlab
Australia

**Michael Paine**
Vehicle Design & Research
Australia

**Jack Haley**
NRMA Motoring and Services
Australia

**Blake Harris**
RACV
Australia

Paper Number 15-0376

## ABSTRACT

The purpose of the Australian Child Restraint Evaluation Program (CREP) is to provide consumers with independent safety information; and to apply commercial and public consumer pressure on manufacturers to deliver child restraint systems (CRS) that perform well beyond the requirements of the Australian Standard. This paper describes the evolution of the dynamic assessment protocols and presents a summary of areas where improvement in dynamic performance has occurred. Areas of dynamic performance where there is still room for improvement, are also reviewed.

The dynamic assessment protocol has evolved from a system that separately scored the performance of CRS in frontal, 90 degrees and 66 degrees simulated impacts to a system that provides a single overall score for front and side impact tests to determine CRS ratings. The current protocols also nominate a number of 'Critical' 'Performance Aspect' (PAs) and a CRS is limited to one star if a score of '0' is achieved for any critical PA. There have also been significant changes to the dynamic test and assessment methods over the years to ensure assessment methods are as objective as possible, and some variation in the types of performance features assessed. For rearward facing infant restraints, CREP currently assesses the ability of the CRS to retain the head and torso in front and side impacts, control upward and rotational displacement of the CRS in rebound and distribute the load over the back of the dummy, in frontal testing, , manage dummy head and torso energy in frontal testing and manage dummy head energy in side impact. Similar assessments of dummy and head retention and energy management are used in the rating of forward facing child restraints. These assessments also include head and knee excursion. For booster seats, the ability of the booster to provide and maintain good sash belt geometry, and to prevent submarining in frontal

impacts. Assessments of head retention and energy management in side impact and dummy retention both in near and off-side impacts are also included for booster seats. There have been substantial improvements in the side impact protection features of rearward facing and forward facing child restraints observed in the program, and increasingly better performance of booster seats in maintaining good seat belt geometry in frontal impact. However, there is a need for more attention to head energy management in side impact, particularly among rearward facing restraints. Among rearward facing restraints, there are also concerns about poor performance of most restraints to adequately distribute crash forces through the back of the torso in frontal impact. Among forward facing restraints, there are concerns over head containment during rebound in frontal impact.

While there have been significant improvements to the test and assessment methods used in CREP there is a possibility that some aspects of good performance are being overstated and aspects of poor performance understated due to limitations in the assessment and rating procedures. Areas for possible future refinements of the protocols are also discussed.

## INTRODUCTION

A child restraint evaluation program (CREP) has been operating in Australia since 1994. The concept of the program has been described previously (Kelly et al, 1996). According to Kelly et al (1996) the program was introduced following laboratory crash test observations of substantial variations in the performance of child restraint systems coming onto the Australian market in 1993. All child restraint systems sold in Australia since 1978 have had to comply with Australia/New Zealand Standard 1754 (AS/NZS 1754 had). The Australian Standard sets a minimum level of required performance and the relatively small number of restraints on the Australian market prior to 1993 generally exceeded this level of performance in the laboratory and in the field. The observation that some new restraints from new manufacturers that were coming on the market appeared to be just meeting the minimum requirements of the Standard raised concerns that these restraints may not provide the same level of protection to children in the real world (Kelly et al, 1996). The very first iteration of the program (CREP-Stage 1) included additional tests and performance criteria to those prescribed by the Standard to establish any differences in performance beyond the minimum requirements of the Standard of restraints being sold in Australia at that time , and to bring these differences to the attention of consumers.

The results of Stage 1 were published in a national subscription consumer magazine and wider consumer access was facilitated through a publically available brochure. According to Kelly et al (1996) there was clear consumer interest in the program. It also became clear that the published information was being used by consumers as a tool in making purchasing decisions with manufacturers reporting increases in sales of restraints that ranked well, and decreases in sales of those that were rated poorly. This established the value of the program as a mechanism to apply commercial and public consumer pressure on manufacturers to deliver child restraint systems (CRS) that performed well beyond the requirements of the Australian Standard.

Two further releases of CREP results occurred in 1996 (Stage 2) and 2000 (Stage 3). These used the same general test methods, approach to assessing performance and publication strategies used in Stage 1.

In 2004 the program underwent a major review that resulted in a revised dynamic test protocol and a new approach to the overall assessment of the restraints using an objective point based method (Brown et al, 2007). Results of assessments using these new protocols were released as CREP Stage 4a & CREP Stage 4b. The assessment method was further enhanced in 2009, and the results from Stages 4A to 4D were rescored to the enhanced method and released in 2010, together with the results for CREP 4E.

Following the introduction of substantive changes to the Australian Standard in 2010 the test protocols were again reviewed in 2012 to ensure CREP stayed true to its original aim of assessing the performance of restraints sold in Australia beyond the minimum requirements of the Australian Standard. This resulted in more significant changes to the test method and inclusion of some additional performance assessments. The resulting test procedures and assessment protocols were adopted and have been used in the CREP 5 ratings. The CREP 5 rating procedures remain current with some slight modifications to allow for the assessment of ISOFIX compatible restraints.

This paper describes the evolution of the dynamic assessment protocols and presents a summary of the areas where improvement in dynamic performance has occurred. Areas of dynamic performance where there is still room for improvement are also reviewed.

## EVOLUTION OF THE DYNAMIC ASSESMENT PROTOCOL

Throughout the first three releases of CREP results (CREP1-3) the assesment procedure remained relatively stable, however significnat changes were introduced in CREP 4 and CREP 5. These are summarised below.

### Test Methods

While the intention of CREP since its inception has been to assess the performance of restraint systems beyond the minimum requirements of the Australian Standard, the test methods have been heavily based on the test methods included in the Standard. The test orientations and test pulses used in each iteration of the program are summarised in Table 1.

**Table1.**
**Evolution of crash tests included in CREP assessment procedures**

| Sled Test | CREP Stage 1-2 (1994-1996) | CREP Stage 2 (1996-1999) | CREP Stage 3 (2000-2004) | CREP Stage 4 (2005-2012) | CREP Stage 5 (2012-present) |
|---|---|---|---|---|---|
| Frontal 48km/h 24g | RF, FF, Boosters | RF, FF, Boosters | RF, FF, HBB | - | - |
| Frontal 56km/h 34g | RF, FF, Boosters | RF, FF, Boosters | RF, FF | RF, FF, Boosters | RF, FF, Boosters |
| NS Side 90° [+] | RF, FF, Boosters | RF, FF, Boosters | RF, FF, HBB | RF, FF, Boosters | RF, FF, Boosters |
| NS Side 45° [+] | RF, FF, Boosters | RF, FF, Boosters | RF, FF, HBB | - | - |
| NS Side 66 ° [+] | - | - | - | RF, FF, Boosters | RF, FF |
| FS Side 90 ° [+] | - | - | - | - | Boosters |
| Rear Impact[+] | RF, FF | RF, FF | RF, FF | - | - |
| Inverted[++] | RF | RF | RF | - | - |

*RF – Rearward facing infant restraint; FF – Forward facing child seat; LBB – Low back/backless booster; HBB – High back booster; Booster – any booster seat; NS – Near side; FS – Far side.
[+] Impact pulse is 32km/h 14g and static side door structure incorporated in test set up; [++] Impact pulse 16km/h 8g

Initially (Stages 1-3) CREP included two frontal impact tests; one that equaled the minimum deceleration and velocity change requirements of the Australian Standard (48km/h, 24g), and one that attempted to more closely match the assessment of adult restraint systems in the Australian New Car Assessment Program (Kelly et al, 1996). The more severe pulse used a velocity change of 56km/h and a deceleration that was as near as possible to the maximum acceleration allowed by the Australian Standard test method (34g). However in the review of the protocols prior to CREP 4, the lower severity test was removed from the protocol as this test was not producing any worthwhile information for making comparisons of performance beyond that required by the Standard.

The side impact tests included in all iterations of CREP have used the same pulse requirements as that included in the Australian Standard. The Australian Standard has required a 90 degree side impact test since 1975. However, the assessment of performance in side impact in the Standard was originally related to the restraint's ability to retain the dummy and maintain structural integrity in this orientation. To allow restraint performance to be assessed beyond this, a side door structure was added to the test set up in CREP Stage 1 and as described below, this continues to CREP 5 with some modification to the structure. The additional 45 degree side impact test was included in CREP Stage 1 in acknowledgement of field data that indicated that most side impacts included some forward component of force. In the review conducted prior to CREP 4 it was felt that there was also no worthwhile comparable information being collected from the 45° tests, and it was unclear what proportion of real world impacts this orientation was actually simulating. To maintain the intention of being

able to assess performance under oblique loading but with some justification for the orientation being used, a decision was made to move to a 66° impact as that more closely resembled the US NCAP side impact conditions at that time.

Up until CREP Stage 5, all side impact testing simulated near side impacts. In the early stages of CREP 1-4, many high back boosters demonstrated inadequacies in the retention of test dummies during rebound in these near side impacts. To address this and allow the performance of different booster seats on the market to be compared, a far side impact was included for booster seats in CREP 5.

Rear and inverted tests included in CREP Stages 1-3 were basically mimicking the tests carried out as part of compliance testing for the Standard and were not providing any information on performance beyond that required by the Standard. These tests were discontinued after CREP Stage 3.

As shown in Table 1, there has been some variation in the restraint types subjected to different tests throughout the evolution of the program. As described by Brown et al (2007), all restraints were subjected to all frontal and side impact tests in the first Stage of CREP (Stage 1). The performance of most boosters on the market in Australia at that time (early 90's) was quite poor in that first series of tests. Based on this poor performance, subsequent early CREP series treated boosters differently. High back boosters were exempted from the higher severity frontal tests due to this poor performance and test house concerns regarding the robustness of the test TNO P10 dummy in CREP Stages 2 & 3. However trials conducted prior to CREP Stage 4 alleviated these concerns and these restraints were again subjected to the higher severity frontal impact in later stages. Booster cushions (i.e. backless boosters) were excluded from CREP Stages 2 and 3 due to their inherent inability to provide any measurable protection in side impact. This was reversed in the lead-up to CREP Stage 4, as changes made to the Australian Standard prior to the commencement of CREP 4 basically removed booster cushions or backless boosters from the Australian market. As described below, the change to the Australian Standard that impacted booster cushions/backless boosters was the adoption by Standards Australia of the CREP side impact test method and assessment procedure. Therefore no backless boosters have been included in any CREP series since Stage 1.

Booster seats were never included in the rear impact or inverted tests, and forward facing restraints were always excluded from the inverted tests.

**Test rig**

The test equipment used throughout all stages of CREP is the same as that used in Standards testing of child restraints in Australia. This involves a test bench in compliance with the Australian standard mounted on a rebound sled. For side impact tests, a side door structure is also mounted to the sled. There has been some evolution of the side door structure over the course of the program and this is described below.

As described by Kelly et al (1996) in the original CREP (Stage 1) the side door structure attempted to replicate a simplified rear door of a large sedan in size and shape, and included an inner door skin and 'window'. The structure was fabricated from square wall tubing, the inner skin from thin sheet metal and the 'window' from 6mm Polycarbonate sheeting. The inner skin was replaced after each test. A side door structure, comprising a metal frame and polycarbonate panels, was added to the Australian Standard test procedure in 2004. The addition of this structure, together with a requirement that all restraints prevent contact between the test dummy's head and the side door meant that by CREP Stage 4 many restraints on the Australian market were able to contain the head to some extent. To this point, head accelerations and Head Injury Criteria (HIC) were being recorded in the CREP tests but not being used in scoring. Even allowing for the unknown biofidelic nature of the dummy's head, the generally very high HICs being recorded indicated a distinct lack of energy attenuating materials in CRS side structures. This led to discussion about the possibility of including some assessment of the head energy management in side impact. However, the non-uniform nature of the side door structure prevented this from being achieved. Research programs that had attempted to alter the energy absorption properties of restraint side wings were not able to measure significant differences in dummy head acceleration and HIC (Bilston et al, 2005), because altering the side wings resulted in differences in head or restraint impact location on the door. As the stiffness of the original door varied with location, any variations due to modification of the side wings were masked by changes in where the door was struck. To counter this, a new door structure with uniform stiffness was introduced in CREP Stage 5.

**Dummies**

The dummies used in CREP also conform to the requirements of the Australian Standard and largely belong to the TNO P series family of dummies. However, there have been changes to the types of dummies used to test different restraint types, and to how some dummies are have been used over the evolution of the program. Table 2 summarises the test dummies used by restraint type and impact condition across the history of CREP.

**Table2.**
**Test dummies used in CREP assessment procedures**

| Restraint type | Impact | CREP Stage 1 (1994-1996) | CREP Stage 2 (1996-1999) | CREP Stage 3 (2000-2004) | CREP Stage 4 (2005-2012) | CREP Stage 5 (2012-present) |
|---|---|---|---|---|---|---|
| Rearward Facing Infant | Front | P3/4 (9kg) | P3/4 (9kg) | P3/4 (9kg) | P3/4 (9kg) or P1 ½ (11kg)* | P3/4 (9kg) or P1 ½ (11kg)* |
| | Side | P3/4 (9kg) | P3/4 (9kg) | P3/4 (9kg) | P3/4 (9kg) | P3/4 (9kg) |
| | Rear/Inverted | Taru T# (4kg) | Taru T# (4kg) | Taru T# (4kg) | - | - |
| Forward Facing Child | Front | P6 (22kg) | P6 (22kg) | P6 (22kg) | P6 (22kg) | P6 (22kg) |
| | Side | P3 (15kg) | P3 (15kg) | P3 (15kg) | P3 (15kg)+ | P3 (15kg)+ |
| | Rear | P6 (22kg) | P6 (22kg) | P6 (22kg) | - | - |
| Booster (Type E)^ | Front | P6 (22kg) or P10 (32kg)* | P6 (22kg) or P10 (32kg)* | P6 (22kg) or P10 (32kg)* | P10 (32kg) | P6 (26kg)++ |
| | Side | P3 (15kg) | P3 (15kg) | P3 (15kg) | P6 (22kg)+ | P6 (22kg)+ |
| Booster (Type F)^ | Front | - | - | - | - | P10 (32kg) |
| | Side | - | - | - | - | P10 (32kg)+ |

*Choice of test dummy depended on maximum occupant mass specified by manufacturer. +Seated height modified to better represent seated height of children at upper end of restraint size range (P3 boosted to 605mm, P6 increased by 40mm).++ P6 dummy weight is boosted to match upper mass range of Type E Booster. ^ A new type of booster was specified in the Australian Standard in 2010. # Taru Theresa.

The most important changes to the dummies occurred with the introduction of CREP 4 and were related to a realization that restraints on the market at that time (pre-2005) were often too small to accommodate the full size range of children to which they were marketed. This manifested, in many cases, as poor side impact protection, as the tops of the side wings of many restraints were below the seated height of the children using them. As shown in Table 2, the P3 dummy continued to be used to assess forward facing restraints, and the P6 to assess booster seats in CREP 4. However, the seated heights of these dummies were boosted to match the seated height of the upper age ranges of children using these types of restraints.

For booster seats, the size of the dummy used to assess performance in frontal impacts was reduced from the P10 in CREP 4 to the P6 in CREP 5. This occurred in response to manufacturers concerns that the P10 dummy is significantly bigger and heavier than the largest size of child for which these restraints were designed. There was evidence of this in CREP 4, with a few boosters observed to be unable to properly accommodate the larger dummy. Furthermore, since the primary objective of the booster is to improve seat belt geometry for small occupants who would not be adequately restrained by the belt without the booster, it was felt that the smaller P6 dummy would provide a more suitable assessment. However, the P6 dummy's weight is below that of the upper limit of the weight range of these restraints. Therefore, the P6 is weighted to match the upper limit of the mass range of Type E boosters, by adding material to the chest and pelvic areas. This is done to ensure there is good assessment of the structural integrity of these restraints in the frontal impact.

**Performance assessment**

The areas of performance assessed throughout the CREP history have remained relatively unchanged. Since its inception, the program has assessed a number of areas of performance common to all restraint types. These include structural integrity of the restraint and dummy retention. For rearward facing restraints there has also always been an assessment of the restraint's ability to distribute crash loads across the back of the dummy. 'The need to distribute the crash forces in this way arises from concerns about the potential for neck injury resulting

from axial loading of the spine, particularly in young infants with their combination of a relatively large head and weak neck. Head displacement and head energy management (HIC 36) in frontal impact has always been assessed in rearward facing and forward facing restraints and head protection in side impact has been common across all restraint types throughout the entire history of the program. However, there have been changes in what restraints are subjected to these assessments and the way head protection in side impact is monitored. There have also been other areas of performance assessment added for some restraints, over time.

Head displacement and head energy management were originally assessed in all restraint types but these assessments were eventually dropped for booster seats as these measures were found to be heavily influenced by lap belt and sash strap position. Low head excursion occurs when there is submarining. Although low head excursion is desirable, submarining in booster seats is not.

In the original Stage 1 of CREP, head protection in side impact was monitored in two ways. Firstly there was an assessment of whether or not the dummy's head was allowed to strike the side door structure, and secondly HIC 36 was used to gauge the severity of the impact between the dummy's head and the door structure. The head strike assessment has been continued through the subsequent stages of CREP to the present time, and retention requirement that restraints must prevent a head strike with the side door structure was included in the Australian Standard in 2004. In 2010, the Standard was revised to require that no observable part of the dummy head could be within 10mm of the door. No attempt was made to assess head injury management in side impact during the early stages of the CREP due to the non-uniform stiffness of the original door structure. However, HIC 36 values continued to be routinely collected to monitor the severity of head impacts and to gain an indication as to whether any meaningful energy attenuation measures were being implemented by manufacturers.

Following the introduction into the Australian Standard of the side door structure and the requirement for all restraints to prevent head to door contact, all devices coming onto the Australian market began to provide some degree of head containment. To capture the variability in the degree of head containment that was being observed, CREP Stage 4 introduced a graded score of this performance. As described by Brown et al (2007), the highest score is given if the head remains completely within the confines of the side wings and a low score is given if the head becomes exposed over the rim of the side wings. A '0' score is assigned to head contact with the door.

Assessment of side impact head energy management was introduced for CREP 5, using HIC 36 as the assessment criteria. This required the introduction of a new side door structure with uniform stiffness.

Significant additions to the assessment of booster seat performance were also made in CREP 4. As described by Brown et al, (2007) the assessment procedures introduced in CREP 4 placed a high priority on the ability of a booster seat to provide the test dummy with good seat belt geometry and for the dummy's upper torso to remain satisfactorily restrained throughout the impact. Assessments were therefore included for the pre-impact seat belt sash strap geometry on the dummy and for the maintenance or otherwise of good sash strap and lap belt geometries during impact. Similar assessments were subsequently incorporated into AS/NZS 1754:2010.

**Scoring Systems**

In CREP 1 and 2, "Preferred Buy" ratings were given to a number of devices in each category that were rated as performing well in a number of pre-defined areas. However, the method used to make these judgments was subjective and there was little documentation of the protocols used. This led to a significant difference in how preferred buys were awarded in CREP 3. In CREP 3 evaluations were based mainly on technical compliance with requirements, and little weight was given to the more desirable features of performance used in making assessments in CREP 1 & 2.

To address this, an objective point scoring system for CREP was first introduced in CREP 4. The scoring system used in Stage 4 involved the use of a ratings matrix, using an approach derived from methods used in the ease of use assessment by the North American National Highway Safety Traffic Administration (NHTSA), and is discussed below.

Basically, the features assessed in the dynamic component were divided into a set of performance categories. Within each category, there were a set of items or individual performance aspects (PA). Each PA was given a weight between 1 and 4 based on the importance in terms of offering crash protection in the real world. A numerical scale of 4 (good) to 0 (unacceptable) was used to rate the outcome for each PA. Scores for each PA

were obtained by multiplying the outcome score by the weight for that PA. Category scores were calculated by adding the scores obtained for that category and calculating what percentage this was of the maximum possible score for that category. Initially, each category was then awarded an A, B, C or D ranking based on the breakpoints set out in Table 3 below.

These breakpoints were set on the basis that any device scoring less than or equal to 50% of the maximum score was judged as 'unacceptable' and given a 'D' ranking. The range between 50% and 100% was then divided into 3 equal ranks.

The overall score was calculated by averaging the sum of the normalised scores for each component. That is [(% score Frontal) + (% score Side 66) + (% score Side 90)/3]. The overall score was then also awarded a ranking using the same breakpoints illustrated in Table 3. One limiting rule was also applied to category and overall rankings. This rule was that if any device receives two or more '0' scores (i.e. an 'unacceptable') score, that device could not be awarded an A or B ranking for that category or for an overall ranking.

**Table 3 Ranking Score Calculations – CREP Dynamic Testing**

| 'Performance Aspect' Set Score | Overall Score |
|---|---|
| The 'PA' set score ≥ 83% of maximum 'PA' scores that could be obtained for the set | The sum of the 'PA' scores ≥ 83% of the sum of the maximum scores that could be obtained for all the 'Performance Aspects' |
| The 'PA' set score < 83% but ≥ 67% maximum 'PA' scores that could be obtained for the set | The sum of the 'PA' scores ≥ 66% but < 83% of the sum of the maximum scores that could be obtained for all the 'Performance Aspects' |
| The 'PA' set score < 66% but ≥ 50% of maximum 'PA' scores that could be obtained for the set | The sum of the 'PA' scores ≥ 50% but < 66% of the sum of the maximum scores that could be obtained for all the 'Performance Aspects' |
| The 'PA' set score < 50% of maximum 'PA' scores that could be obtained for the set | The sum of the 'PA' scores < 50% of the sum of the maximum scores that could be obtained for all the 'Performance Aspects' |

While the scoring system introduced in CREP 4 was relatively successful in providing comparative ratings of restraints on the market, some child restraint systems were observed to perform unexpectedly poorly in some important areas. Some of the observed failures were not anticipated when the CREP 4 protocols were introduced and the resulting ratings did not adequately reflect their poor performance. The lack of a 'balancing' feature in calculating the overall score from the component dynamic tests also added to the problem. Poor performance in one of the dynamic tests e.g. side impact could be masked by very good performance in the other tests e.g. frontal impact.

The scoring system was then modified and the revamped system introduced part way through CREP 4. It has not changed since. This new method has three important characteristics; 1. The assessment of performance in three different test orientations are combined into a single group of assessments; 2. A number of critical performance areas were identified where poor performance in one of those areas limits the overall score, and 3. A 5 star rating system replaces the 4 category A-D ranking system.

The method of calculating an overall score by averaging the sum of the normalized scores from each of the three dynamic tests was therefore abandoned and this addressed the need for any 'balancing' feature. As shown in Table 4, the three dynamic tests continued to be included and scored individually. However performance aspects that are common to two or more tests are grouped into a single score, with the lowest score in any test used in the ratings. Performance aspects that are not common across two or more tests are kept as separate items, with two exceptions. These are 'Head Retention' for forward facing seats and boosters; and dummy

retention in booster seats. While the assessment of 'Head Retention' for forward facing seats and boosters is common to both side impact tests, restraints often demonstrate very different performance in the two tests.

**Table4.**
**Assessment features in the combined scoring system introduced during CREP4**

| Rearward facing infant restraints | Forward facing child restraints | Booster Seats |
|---|---|---|
| Head Retention - Front & Side Impact Testing* | Forward Head Excursion – Frontal Impact Testing* | Seat Belt Sash Strap Location - Frontal Testing |
| Dummy Retention - Front & Side Impact Testing* | Forward Knee Excursion – Frontal Impact Testing | Head Retention – 90 Side Impact Testing |
| Upward and/or Rotational Displacement of the CRS in Rebound – Frontal Impact Testing | Head Retention – Frontal and Side Impact Testing | Dummy Retention – Frontal Testing* |
| CRS Security and Integrity - Front & Side Impact Testing* | Dummy Retention - Front & Side Impact Testing* | Dummy Retention 90 Side Impact Testing |
| Load Distribution - Frontal Impact Testing | CRS Security & Integrity - Front & Side Impact Testing* | Head Energy Management -Side Impact Testing with the seat belt sash strap over the shoulder adjacent to the *Side Impact Door* |
| Head Energy Management - Frontal Impact Testing | Operation of Quick Release Device – Frontal Impact Testing* | Submarining - Frontal Impact Testing |
| Head Energy Management -Side Impact Testing* | Head Energy Management - Frontal Impact Testing | CRS Security & Integrity - Front & Side Impact Testing* |
| Torso Energy Management - Frontal Impact Testing | Head Energy Management - Side Impact Testing | |
| Adjuster Slip - Front & Side Impact Testing* | Torso Energy Management - Frontal Impact Testing | |
| | Upward Displacement of CRS in Rebound - Frontal Impact Testing | |
| | Adjuster Slip - Front & Side Impact Testing* | |

Good performance in a 90 degrees test would almost certainly be negated by universally poor performance in the 66 degrees tests. Therefore, a decision was made to continue to treat these separately. Similarly, dummy retention in booster seats is quite often starkly different between frontal and side impact testing. Therefore, dummy retention in frontal impact continues to be treated differently from dummy retention in side impact.

In this new method of scoring the overall performance, the overall score is calculated by taking the sum of points achieved divided by the maximum number of possible points and expressing this as a percentage.

A number of performance aspects have been nominated as critical features to ensure extremely poor performance in any of the tests is adequately captured. If a restraint scores a 0 in any one of the critical features (highlighted with * in Table 4) the restraint is limited to a 1 star rating.

The five star rating system was achieved by dividing the range of scores between 50 and 100. This resulted in the following breakpoints:-

- 5 stars – ≥ 87.5%
- 4 stars – ≥ 75% < 87.5
- 3 stars - ≥ 62.5% < 75%
- 2 stars - ≥50% <62.5%
- 1 star - <50%

**OBSERVED IMPROVEMENTS IN CHILD RESTRAINT SYSTEM PERFORMANCE**

There have been a number of important and quite clear improvements in child restraint performance observed over the course of the CREP. The most important of these have been the improvements in side impact protection provided by forward facings seats and booster seats, and the performance of booster seats in frontal impact. As detailed below these have largely occurred following significant enhancements in restraint design.

**Side impact protection**

In the first series of the CREP (Stage 1), 40% (4/10) of forward facing restraints and 100% (5/5) of the high back booster seats, allowed a head strike. This was despite the fact that in this test series there was no increase in the seated height of the dummies to match the upper limit of the seated height range of children who would be using the restraints. An improvement in side impact protection is evident from review of the results coinciding with the beginning of CREP Stage 4 and the boosting of the dummy seated heights.

In the first series of CREP 4 (4a), most forward facing restraints and high back booster seats allowed head contact with the door. While this poor performance continued for most of CREP Stage 4 there was some improvement observed, see Figure 1. However, by CREP 5 no head contact with the side door occurred in any restraint in the 90° tests.

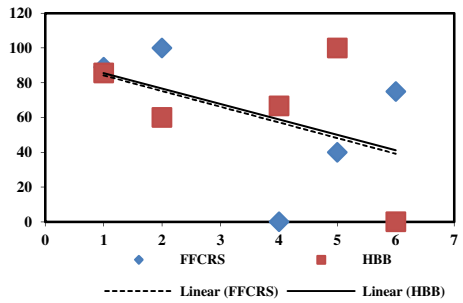


***Figure1. Performance of restraints in each series of CREP 4 from CREP4a (1) to CREP 4B (2) shown as percentage of restraints that allowed head contact with side door in each series. FFCRS - Forward facing child restraint; HBB – High Back Booster***

Typical side wing height change on FFCRS over CREP4-CREP5

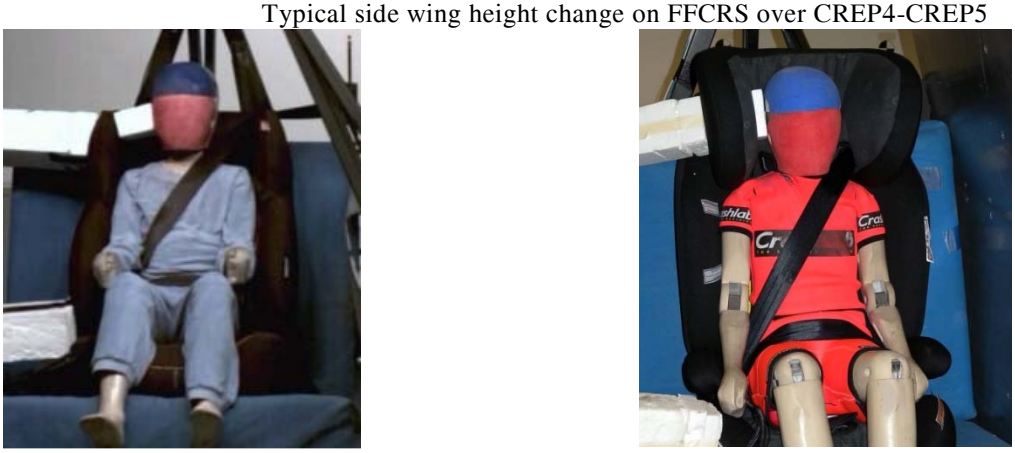

Typical side wing height change on HBB over CREP4-CREP5

***Figure2. Typical changes in side wing height in forward facing child restraints (FFCRS) and high back boosters (HBB) from CREP 4 (2005-2012) to CREP 5 (2012-)***

As shown in Figure 2, the driver in these improvements is an increase in side wing height in both forward-facing child restraints, and high back booster seats. The movement towards higher side wings is likely to be a result of the combination of the adoption of the CREP side impact test procedure and a similar assessment method into the Australian Standard in 2004 together with additional requirements included in the Standard for minimum seat back heights for all restraint types in 2010. The restraint dimension requirements were written to support laws requiring appropriate restraint use by Australian children. Restraint back and (for rearward & forward facing restraints) shoulder harness slot heights were defined to ensure that forward facing restraints could accommodate children up to the 95$^{th}$ percentile 4 years old, and booster seats could accommodate children up to the 95$^{th}$ percentile 8 year old.

**Frontal crash protection in booster seats**

The ability of high back booster seats to provide good seat belt geometry and to maintain good torso restraint during frontal impact began to be assessed in CREP from Stage 4. Results from the first 17 high back booster seats from these assessments have been published previously (Brown et al, 2009). As described by Brown et al (2009), 10 of the 17 ( 59%) demonstrated static lap belt positions low down on the dummy abdomen, adjacent to the dummy thighs, and only 5 of the 17 (29%) boosters were able to maintain good lap belt positioning throughout the frontal impact. Furthermore, Brown et al (2009) noted a wide variation in the static position of the sash part of the belt in these boosters, with only two restraints positioning the sash over the mid-shoulder region of the dummy, and contact between the sash belt and the dummy shoulder was maintained during the impact in only 9 of the 17 boosters (53%).

The results presented by Brown et al (2009) represent the first half of the CREP 4 test series, and as shown in Figure 3, some improvement was beginning to be observed by the end of CREP 4. Fifteen boosters were tested in the second half of CREP 4, good lap belt positioning was maintained in 8 of the 15 boosters (53%) and contact between the sash belt and dummy shoulder maintained in 13/15 boosters (87%).

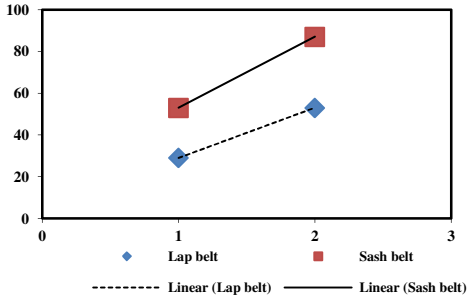


***Figure3. Percentage of boosters maintaining good lap belt and sash belt position during dynamic frontal testing in the first half (1) and second half (2) of CREP 4 (2005-2012)***

Requirements related to the static pre-impact position of the lap belt were included in the Australian Standard in 2010 – and more recently knee excursion limits have been added as a defacto measure of submarining. (2013). This means that all booster seats now sold on the Australian market must demonstrate the ability to provide good lap belt positioning and minimize submarining in frontal impact testing.

As described above, the dummy being used to assess most booster seats was changed to the P6 in CREP Stage 5. In CREP 5 there has only been one booster that has failed to maintain good lap belt position using the P6 dummy, and all have demonstrated an ability to maintain contact between the sash belt and the shoulder throughout testing.

## AREAS IDENTIFIED FOR FURTHER IMPROVEMENT IN RESTRAINT PERFORMANCE

While there have been some notable improvements in performance as described above, some issues of concern remain. These include the level of side impact protection for the head and load distribution management in frontal testing in rearward facing restraints and head protection in forward facing restraints during rebound in frontal testing.

### Head protection in side impact in rearward facing restraints

Head energy management assessment in side impact commenced in CREP 5. This involves the use of HIC36 to comparatively assess how well restraints attenuate energy once the dummy's head is contained within the side structure of the restraint in the 90° impact. As shown in Figure 4, there are some substantial variations being observed in how well different restraints appear to be able to do this. It is unknown whether the variations in performance being observed reflect any variation in performance in the real world, but the magnitude of the differences suggest this may be an area worthy of further investigation

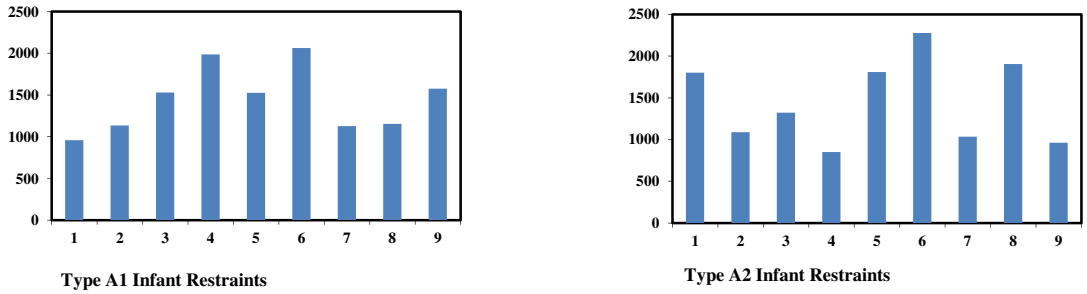


*Figure4. HIC36 measured in 90° side impact with TNO P3/4 (Type A1) & TNO P1 ½ (Type A2)*

**Distribution of crash load in rearward facing restraints**

Another area of concern in the performance of rearward facing restraints is their ability to distribute the crash load over the back of the dummy. A primary design goal of a rearward facing restraint should be to distribute most of the load in a frontal crash through the back of the head and torso. The Australian Standard carries a note to this effect, and as such it is not a mandatory requirement of the Standard. This feature has been assessed in CREP since its inception by calculating the force distributed through the back of the torso as a percentage of the force along the longitudinal axis of the torso. The larger the value, the better the restraint is in achieving the design goal. Figure 5 illustrates the results achieved by rearward facing restraints tested during CREP 5. There is clearly one restraint that is substantially superior in being able to distribute the greater proportion of the load through the back of the dummy. Significantly, 17 of the 27 (63%) of the restraints tested to dated in CREP 5 have not been able do so. Again the effect this is having in the real world is currently unknown, but the results indicate further investigation is warranted.

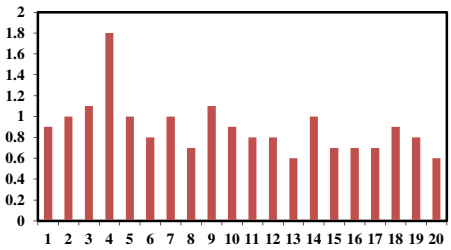


*Figure5. Performance of rearward facing restraints in distributing crash loads over back of dummy head and torso in frontal impact (from CREP 5)*

**Head protection in forward facing restraints during rebound**

While we have seen significant increases in the height of the side wings in forward facing restraints, and the full height of the side wings being comprised of structurally robust material, there appears to have been a tendency for manufacturers to not extend this height/structural integrity to the back of their restraints. In CREP 5, the behavior of the dummy's head during rebound in frontal testing has been assessed in forward facing restraints. This has captured a previously unreported potentially poor aspect of performance of many modern forward facing restraints. This involves the dummy's head being allowed to rotate over the top of the seat back (see Figure 6). This occurs in restraints where the height of the restraint back reduces between the side wings, as well as in restraints where the material at the top of the seat back fails to adequately support the dummy's head. The latter has commonly been seen in restraints incorporating internal adjustable head restraints (see Figure 6).

Head rotates overs 'dip' in seat back  No structural support at top of back  Head rest fails to support head

***Figure6. Poor support of dummy head in rebound during frontal impact***

## AREAS IDENTIFIED FOR FURTHER ENHANCEMENT OF THE SCORING PROTOCOLS

On the introduction of an objective point system based assessment method in CREP 4, the focus for booster seats was primarily on the ability of boosters to achieve their primary design goal of improving seat belt geometry for the children using them. As described above, there have been substantial improvements in this regard in boosters introduced onto the Australian market over the last decade or so. There have also been significant enhancements to the Australian Standard related to the required levels of performance in maintaining good seat belt geometry in frontal impact. Changes made to the booster seat protocols prior to CREP 5 in response to the modifications made to the Australian Standard, may have left the protocols needing more refinement to better communicate variations in performance beyond that related to front impact protection.

Some boosters are performing in a far superior manner to others in containing the dummy's head in side impact and managing the energy, as measured by HIC36 (see Figure 7). Currently, the scoring system being used in CREP 5 is not capturing this variation in performance as well as it might. Five star boosters should be expected among the higher performing restraints in all aspects, and as shown in Figure 7, one restraint in particular has measured HIC >1000 in side impact but has still managed to score a 5 star rating. Similarly there are two restraints that have measured HICs among the highest values seen in this series and these restraints have still managed to score 4 stars. Further refinements of the assessment and scoring protocol are planned to try to adequately capture this type of performance in ratings. Moreover, consideration is being given to making the head energy management in side impact a critical feature. In that way this type of poor performance would limit the overall score the restraint could achieve. It is important that manufacturers be encouraged to seriously consider the energy attenuation provided by their restraint systems in side impact.

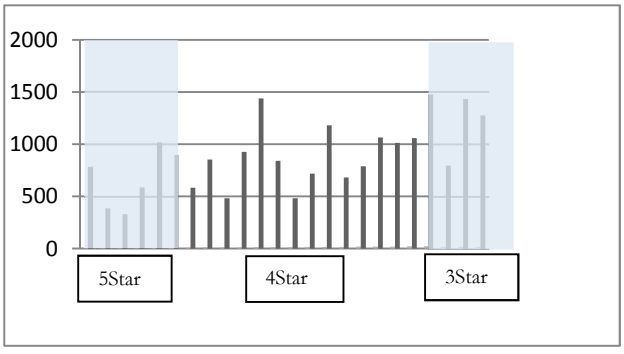


***Figure7. Head energy management as measured by HIC3g in boosters in side impact in CREP 5***

## CONCLUSIONS

The Australian CREP program has evolved dramatically over the last 20 years. It is now a comprehensive and objective rating system providing important advice to consumers about the performance of restraints beyond the minimum performance level required by the Australian Standard for child restraints.

There have been innovative test methods and assessment procedures incorporated into the CREP since its inception and these have continued to evolve with the program. In addition to providing consumers with important information and encouraging manufacturers to continually improve their products, the CREP has also driven improvement in the minimum performance required by the Australian mandatory product Standard. Together, this has worked to influence some dramatic improvements in the performance of child restraints now available on the Australian market. This is most notably seen in the head protection provided in side impact in forward facing restraints and high back boosters; and the performance of high back boosters in frontal impact.

The program also continues to highlight emerging areas of concern. Currently this includes the head protection provided by rearward facing restraints in side impact, the inability of rearward facing restraints generally to adequately distribute crash forces in frontal impact, and the tendency for poor head containment in forward facing restraints during rebound in frontal testing. While it is clear that there are substantial variations in performance of restraints currently on the market in these areas, the impact of this on the real world crash protection of children remains unclear. Further investigation is warranted.

Finally, there may be some aspects of poor performance still not adequately being captured by the current protocols and work continues to further enhance the protocols.

## REFERENCES

Bilston, Lynne E, Brown, Julie, & Kelly, Paul. (2005). Improved protection for children in forward-facing restraints during side impacts. *Traffic injury prevention, 6*(2), 135-146.

Brown, Julie, Kelly, Paul, Suratno, Basuki, Paine, Michael, & Griffiths, Michael. (2009). The need for enhanced protocols for assessing the dynamic performance of booster seats in frontal impacts. *Traffic injury prevention, 10*(1), 58-69.

Brown, Julie, Paine, Michael, Paine, David, Kelly, Paul, Griffiths, Michael, Magadera, Nimmi, Soames, J. (2007). *Revised assessment protocols and scoring methods for the Australian Child Restraint Evaluation Program.* Paper presented at the 20th Enhanced Safety of Vehicles Conference, Lyon.

Kelly, P, Griffiths, M, Booth, M, Lemon, J, Crothers, N, & Franks, C. (1996). *Child restraint evaluation program.* Paper presented at the Proceedings: International Technical Conference on the Enhanced Safety of Vehicles.

# THE POTENTIAL FOR ADAPTIVE SAFETY THROUGH IN-VEHICLE BIOMEDICAL AND BIOMETRIC MONITORING

**Stephen A. Ridella**
**Julie J. Kang**
National Highway Traffic Safety Administration
USA

**Satoshi Kitazaki**
University of Iowa
USA

Paper Number15-0377

## ABSTRACT

A 2009 study by the National Highway Traffic Safety Administration identified certain medical conditions as contributing factors in crash causation (Hanna 2009). It was found that about 1.3% of all crashes included in the National Motor Vehicle Crash Causation Survey (NMVCCS) were precipitated by driver reported medical emergencies and 84% of the drivers in crashes precipitated by medical emergencies experienced seizures ( epileptic and others), blackouts (non-diabetic), and diabetic reaction prior to the crashes. Drivers who had crashes precipitated by medical emergencies were more likely to sustain severe injury (28% for incapacitating injury and death for crashes with medical emergency; 11% for crashes without medical emergency). Thus, the premise exists that there may be benefit to identify the driver (and other occupants) of the vehicle as well as monitor their current health status through passive or active methods. This monitoring could take into account chronic conditions (such as bone mineral density) through driver input or through initial vehicle startup measurements which could be used to provide optimal comfort or safety system performance. Additional information about the driver's health or behavioral conditions could be interpreted from blood pressure, heart and respiration rate, blood glucose levels and other physiological parameters and could lead to vehicle intervention in driving and/or alert EMS or police of the impending health condition that may affect driving or cause a crash. This monitoring could be done in many ways such as the recent rapid growth in wearable technology with the ability to pair to apps.

This paper will discuss issues related to driver behavioral and health monitoring and review potential technologies for monitoring and as well as methods for biometric identification. Recent publications on driver crash risk due to chronic and acute health conditions will be summarized. Finally, applications that may be associated with the monitoring will be discussed.

## INTRODUCTION

Driver state is an important factor affecting safe driving behavior. Detection and intervention of drowsiness, distraction and drunkenness have been studied by many up to now. The decline of an individual driver's health is another potential cause for a significant proportion of crashes. Researchers as early as 1967 recognized medical impairment as a possible contributor to traffic "accidents" (Waller, 1967). In his report, Waller outlined seven criteria that should be adhered to in a study of this subject, including "there must be a reasonable mechanism for identifying most of the high risk persons, and for doing so early enough to avoid a substantial portion of their accident experience". In a recently released report, the National Highway Traffic Safety Administration reviewed crashes from the National Motor Vehicle Crash Causation Survey (NMVCCS) to determine the "critical reason, which is the last event in the crash causal chain, and concluded that driver was that reason for 94% of crashes in that nationally represented survey (NHTSA, 2015). Of those 94% of crashes (representing over 2 million crashes), seven percent, or 145,000 crashes were attributed to a driver "non-performance error", which could be drowsiness or an acute medical condition. Using the same data set, Hanna (2009) found that 1.3% of all crashes involving light passenger vehicles in NMVCCS were precipitated by a driver's medical emergency and 84% of the drivers in crashes precipitated by medical emergencies had experienced seizures (related to epilepsy and other conditions), blackouts (non-diabetic), and diabetic reaction prior to the crashes (Figure 1). Hanna found that the drivers who had crashes precipitated by medical emergencies were more likely to be more severely injured (i.e. 28% suffered incapacitating injury and death in crashes with a medical emergency compared to 11% in crashes without medical

emergency). Although the ratio of the crashes related to acute medical emergencies was small in the study, there were many other disease-related cognitive and psychomotor impairments (chronic) that may have increased the risk of crash. The Federal Motor Carrier Safety Administration (FMCSA) commissioned a series of studies to determine risk of motor vehicle crash for a variety of medical disorders based on reports and medical expert panel opinions provided by) (Table 1, FMCSA, 2007-2011). The table shows a statistically significant increased risk for a crash based on a driver having one of several disorders. Obstructive sleep apnea (OSA) is shown to have the highest relative risk (1.30-5.72). Another general consideration is that some diseases such as type II diabetes, cardiovascular disease, mild cognitive impairment (MCI) and Alzheimer's disease are associated with aging. Now that the aging population is growing rapidly in the US, crash rates of occupants with those diseases may see increases despite the recent report by the Insurance Institute for Highway Safety (IIHS) indicating that fatal crash involvement rates of older drivers were decreasing faster than those of younger drivers (IIHS Status Report, 2014). NHTSA's 5-year plan for traffic safety for older people (NHTSA, 2013) also highlights older drivers' risk in association with increased medical problems.

Advances in vehicle electronics have made it possible for drivers and passengers to customize their driving experience in many ways. Personalized settings for seat position, as well as heating/cooling/ventilation and entertainment (separated for drivers and passengers) have been available for many years. Recent technological progress in diversity, sensitivity, data capacity and miniaturization of biometric and biomedical instrumentation sensors and devices are enabling the general public to have more real-time access to personal health status as well as enjoy more security for their personal electronic devices. Recent development has resulted in devices that can be embedded anywhere such as clothes, wristbands, watches, vehicle interiors, etc. to detect and report medical information such as body temperature, heart, respiration and perspiration rates, blood glucose and oxygenation levels, and other physiological functions. This data combined with user identification through recognition of fingerprints, iris, facial and/or voice inputs can provide a rapid analysis of a person's state of health. The availability and use of this information has implications in many markets and significant potential to increase driving comfort and safety when embedded into appropriate algorithms related to vehicle design and performance. For example, a vehicle that senses that the driver has an elevated body temperature and has increased his/her respiration rate significantly may automatically open windows or increase interior ventilation to improve comfort. Also, providing input to the vehicle that the driver is 75 years old and thus has reduced bone mineral density, the vehicle may adjust restraint system parameters to optimize occupant protection in the event of a crash. The same vehicle system could also forward the driver's vital information to first responders and other health professionals even before they reached the scene of the crash.

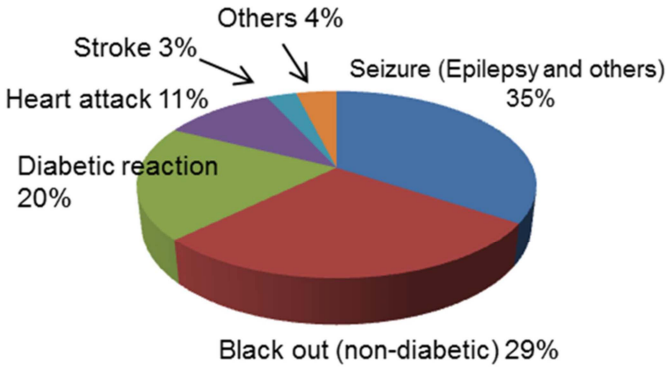


***Figure 1 . Type of medical conditions which precipitated crashes (Hanna, 2009).***

This paper will present the current state of passive personal identification and monitoring of a person's health status, as well as the expected developments of such systems in the future. A discussion of how these devices could influence vehicle comfort and safety will be provided through a summary of the technology available or in development, the challenges of integrating the devices to the vehicle, the potential use, accuracy, standardization and privacy of data as well as other policy implications of this technology. Practical examples will be given to exemplify

the market readiness of technology and the potential for diversification of products and applications and their breadth and depth.

## HEALTH CONDITIONS THAT MAY AFFECT DRIVING

Medical conditions are generally divided into two categories, chronic and acute problems. Some diseases have either chronic or acute problems and some have both. Effective in-vehicle interventions for these two aspects are different. The driver is at extremely high risk of crash in the case of acute health decline which shows distinctive physiological and behavioral changes. An in-vehicle system that detects a decline and controls the vehicle for an unresponsive driver may help to to avoid a crash. On the other hand, chronic health problems develop slowly and degrade cognitive and behavioral performance of the driver over time, resulting in higher general risk of crash. In-vehicle systems that increase the safety margin of the vehicle based on individual's driving ability may minimize the increased risk. The following discussion describes medical conditions that may affect driving.

**Table 1.**
**Summary of motor vehicle crash risk for various medical disorders (FMCSA, various reports 2007-2011, Rizzo, 2011)**

| Medical Condition | Relative Risk (95% Confidence Interval) |
|---|---|
| Cardiovascular Disease | 1.43 ( 1.11-1.84) |
| Diabetes Mellitus | 1.28 ( 1.12-1.47) |
| Obstructive Sleep Apnea | 1.30-5.72 (pooled studies) |
| Seizure Disorders | 1.13-2.16 (pooled studies) |
| Traumatic Brain Injury | 1.32 (0.77-2.25) |

### Diabetes

The likelihood that a person has diabetes (type II) increases with age. Wild *et al*., (2004) estimated that the number of people over 65 years old with diabetes in developed countries will increase by 80% between 2000-2030 and the total number of people over the age of 46 with diabetes will be nearly 80 million people by 2030. An acute risk factor for driving is hypoglycemia (it can lead to coma) which can be caused mainly by insulin-dependent Type 1 diabetes, whereas the chronic risk factors for driving are neuropathy (decreased sensation at feet and hands), retinopathy (vision loss), and encephalopathy (cognitive decline), all of which can be caused by both Type 1 and Type II diabetes (Rizzo,2011). However, scientific evidence for drivers with diabetes being at greater risk for crashes is not conclusive. Tregear et al. (2007) reviewed and conducted meta-analysis of thirteen studies, comparing crash risk among drivers with diabetes to drivers without diabetes, and found that the risk for crash among drivers with diabetes was 19% greater than the risk among drivers without diabetes (within the range published by FMCSA in Table 1). On the other hand, Tregear *et al*. found no statistically significant evidence to suggest that insulin-treated individuals are at higher risk for crash than individuals with diabetes not being treated with insulin. It seems that diabetes increases the crash risk but contributions from the acute symptoms and the chronic symptoms to the increased risk are not yet known. The American Diabetes Association (ADA) states that diabetes management and education of both patients and health care professionals is the important intervention to the driving risk due to hypoglycemia (American Diabetes Association, 2012).

### Obstructive sleep apnea (OSA)

There is strong evidence that the highest relative risk of motor vehicle crash is for OSA, ranging between 1.30 and 5.72 (FMCSA, 2007, Table 1). There is evidence that OSA affects a significant portion of the population regardless whether it is diagnosed or undiagnosed. Hiestand et al. (2006) conducted a telephone interview of 1506 US adults using the Berlin questionnaire and found that 26% of respondents met the criteria indicating a high risk of OSA. NHTSA estimated that 1.4% of total crashes and 1.75% of fatal crashes were related to sleepiness (NHTSA, 1985). However, Leger (1994) suggested that NHTSA's estimation was underestimated and provided a new estimation of sleep-related crash rates as 41.6% of total crashes and 36.1% of fatal crashes. Because of potential under-reporting and inability to determine post-mortem that drowsiness or micro-sleep episodes contributed to the crash, there is no clear-cut estimation of crash rate related to OSA. However, considering the high risk factors which were estimated

in strictly controlled driving simulator studies, OSA should be one of the conditions that can contribute to a risk of a vehicle crash.

Another important aspect of OSA is the fact that the disease remains undiagnosed in many individuals. Hiestand et al. (2006) concluded that the prevalence of OSA in the US was estimated to be between 5% and 10%, but only 1 in 10 of those with OSA were adequately diagnosed and screened for Continuous Positive Airway Pressure (CPAP) treatment. Untreated OSA can cause daytime somnolence, cognitive impairment, loss in work productivity with a typical symptom of microsleep and increase risk of motor vehicle crashes. It should be also noted that some sleepy drivers are not aware of their impaired status, possibly because of related cognitive impairment of an altered frame of reference for fatigue (Rizzo, 2011).

Effects of OSA on driving performance have been investigated in driving simulator experiments by some researchers. It was found by Paul at al. (2005) and Boyle et al. (2008) that untreated OSA patients showed greater variation in steering, lane position and TLC (Time-to-Lane-Crossing) during micro-sleep episodes, and degree of driving performance decrement was correlated with microsleep duration, particularly on curved roads. Risser and Ware (1999) found that untreated OSA patients demonstrated increased lane position variability and road departure incident which were positively correlated with frequency and duration of attention lapses (sleeps). Drowsy driver detection and alert systems are commercially available now. However, it remains unknown to what extent the current technology detects the critical state of drivers with OSA featured by frequent occurrence of micro-sleep episodes and to what extent the technology can mitigate the risk of crash.

Other Disease Conditions

In addition to insulin dependent diabetes (typically Type I) and OSA, other diseases such as cardiovascular disease, seizure disorders and traumatic brain injury can also expose the driver to an increased crash risk due to acute symptoms (e.g.: heart attack and stroke, epileptic seizure). With cardiovascular disease, there are increasingly more middle-age and older drivers being treated for symptoms associated with atrial fibrillation and congestive heart failure. Also, conditions associated with respiratory health such as Chronic Obstructive Pulmonary Disease and asthma are becoming increasingly common in the adult population. These conditions can turn from chronic to acute without warning. Each acute health decline is associated with distinctive physiological and behavioral changes from the normal condition and it is important to have the ability to detect such declines of the occupant while in the vehicle to activate an in-vehicle intervention.

More long-term degenerative conditions include osteoporosis and mild-to-severe cognitive degeneration such as Alzheimer's disease. Ridella et al. (2012) found that osteoporosis or poor bone quality was the most significant contributing factor to injury, specifically, incidence of rib fractures, in older occupants involved in an injury-producing car crash. These crashes typically involved lower crash speeds than did crashes involving younger injured drivers and occupants. While treatable with many medications, bone quality continues to diminish with age with evidence that the pace of bone loss is more significant in women than men. Cognitive impairments are more difficult to determine in real-time without an adequate baseline or history for comparison.

## REVIEW OF CURRENT TECHNOLOGIES USING DRIVER MONITORING

### Occupant Identification

A first step in the process of monitoring is passive, non-invasive identification of the driver and perhaps passengers. The driver's identification would be useful in a host of different applications. Establishing identity may allow for the vehicle to create a baseline of the occupant's health status that can be used in current as well as future driving tasks. Algorithms may be developed for the vehicle to learn how it is driven in certain situations and the associated physiological measurements specific to that person. Also, there may be situations where several drivers share a single vehicle such as the use of a family car, where there may be a range of driving abilities. A teenager who is enrolled in a graduated licensing program may have certain vehicle restrictions put upon them whereas other members of the family may enjoy the full privileges of driving. Therefore, based on the driver's identity, a monitoring system would adjust the vehicle's abilities or monitor highly complex driving tasks more closely.

In addition, a history of the driver's performance would also lend insight into the longitudinal data for comparative purposes. This information could be used to determine long-standing trends in performance such as declining mental capacities (e.g. Alzheimer's or dementia), health issues, changes in driving performance, etc.

Technology to determine identity has grown exponentially in the past few years due to consumer demand for greater security of data. Much of this technology has the ability to be adapted to the vehicle environment or brought in through portable devices. Camera-based technology can be used for identification through facial recognition or iris analysis software. Fingerprint, vascular pattern and voice-recognition scanning are other methods of uniquely identifying an individual. An alternative to passive identification is the driver's userprovided information through a key card, implantable radiofrequency ID or RFID or other device that uniquely identifies an individual.

**Behavioral Monitoring (DrIIVE)**

Driver Monitoring of Impairments and Inattention using Vehicle Equipment (DrIIVE) is a current NHTSA project that uses driver monitoring data. DrIIVE is focused on the development of an algorithm that can accurately identify and distinguish among different forms of inattention or impaired driving including alcohol-impaired, drowsy, and distracted driving. DrIIVE determines driver behavior data from vehicle measures such as steering and pedal inputs, lane variability, and compares signatures of normal driving with impaired driving. The goal is to use the DrIIVE algorithm to identify and evaluate the effectiveness of driver monitoring countermeasures on impaired driving behavior.

**Alcohol Impairment (DADDS)**

In 2008, NHTSA launched a cooperation program to develop in-vehicle technology that could accurately, precisely, and reliably measure a driver's blood alcohol concentration. in a non-invasive way in a very short time. (Monk, 2012). Now in it's second phase, two subsystems have been developed and are being integrated into a research vehicle for further testing. One system is breath based and continually samples the area around the driver for alcohol and carbon dioxide through an infra-red sensor whose measurements can be converted into a blood alcohol concentration. A second subsystem is touch-based and can measure the absorbed near infra-red light in a person's finger and derive an alcohol concentration. These systems have the dramatic potential to reduce crashes and fatalities involving drunk drivers by denying the driver the ability to start and drive the vehicle.

**Physiology/Health Monitoring**

Monitoring driver health should be non-invasive and passive. Both in-vehicle and wearable technology have been developed, however, only wearable technology has been commercialized to date. As sensor technology has become smaller and less expensive, a vast array of sensor applications have been developed or published. Ford Motor Company, working with a restraint and sensor supplier, developed a prototype vehicle to measure a variety of physiological signals (Watson et al, 2011). Figure 2 below indicates that they were looking at both comfort (temperature difference) and real-time physiology (heart and respiration rate). They indicated that the signals could be integrated for use in assessing driver performance as a function of wellness, workload, and stress. Ford also has demonstrated an in-vehicle glucose monitoring system that could detect a driver's possibility for a diabetic episode (Ford, 2011).

Demonstrations of blood oxygenation measurements using a variant of typical finger-tip pulse oximeters, Meditech 2011), blood pressure and bone mineral density bring more information about driver/occupant health into the vehicle. The BOSCOS (BOneSCanning for Occupant Safety, Hardy et al, 2005) project created an in-dashboard ultrasound sensor that could deduce bone strength based on measurements taken from the distal third of a finger when inserted into the device.

Wearable devices or mobile human health monitoring is a maturing area of health awareness particularly in the sports medicine market. Miniaturized electronics or MEMS technology has allowed for creation of wearable wrist bands, head bands, even undergarments that are capable of accurately measuring heart rate, respiration, sweat production, etc. These devices are usually coupled to a portable electronic device application to record daily exercise results and associated physiological responses. The applications have algorithms to detect medical issues and

performance progress with the person wearing the technology as well as determine stress or anxiety levels. The cost of these devices has dropped dramatically in the past several years with many devices selling in the $50-$150 range. The sophistication, accuracy and reliability of these devices is steadily improving such that some diagnosis of heart and respiratory health may be deduced from the signals rather than just the instantaneous rates that are reported by the devices.

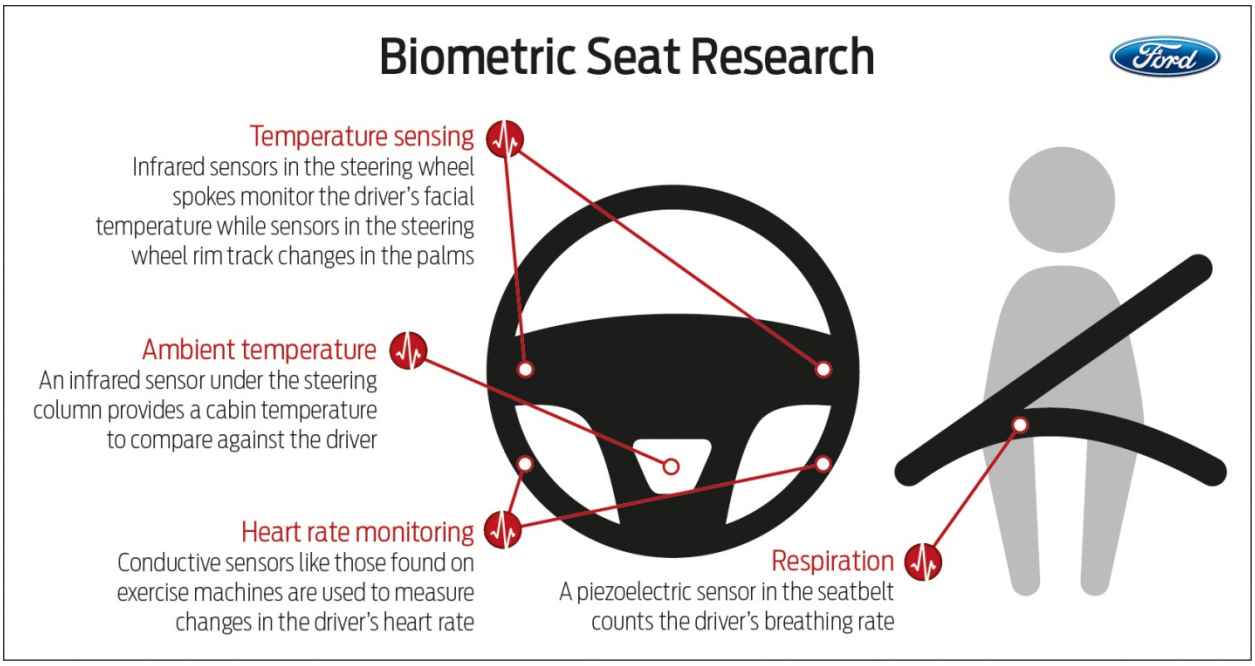


***Figure 2. Examples of prototype health monitoring sensors embedded in vehicle components (Wired , 2011)***

**Establishing a Baseline**

Another new challenge within the scope is connection and integration of monitoring the state of the driver in the home (off board) and in the vehicle (on board). Monitoring a person's life in the home through so called "Smart Home" or "Wearable sensors" is becoming important for "Aging in Place" or "Tailor-made Health Care" and it is actively being tested by research projects for its effectiveness and clarification of system and social requirements. However, there are no systems / research projects focusing on integration of on and off board driver monitoring. Early signs of an acute health problem may be detected in the home before driving and such data can be brought into the vehicle to provide the in-vehicle monitoring system with an initial parameter set to raise the sensitivity of detection. For example, lower glucose level data or poor sleep quality data measured in the home may be used in the vehicle for earlier detection of hypoglycemia and frequent micro-sleep occurrence (Table 2). Driver state monitored in the home and in the vehicle can also make use of cause-effect relationships. For example, failure to take medicines in the home may increase the possibility of occurrence of hypoglycemic episodes or epileptic seizure behind the wheel. Such behavioral data measured in the home can also be brought into the vehicle to enhance or change the in-vehicle intervention strategy (e.g. failure to take anti-seizure medicine locks the ignition). Integration of on- and off-board driver monitoring will increase accuracy of detection of drivers' health problems and strengthen the intervention strategy to avoid crash.

Another example of driving performance data being brought into the off-board network involves continuous monitoring of the driving environment. Driving includes many complex and parallel cognitive and physical tasks under certain levels of stress that may magnify certain aspects of a driver's chronic health problems (e.g. cardiovascular diseases). Therefore, a driver's state measured in the vehicle can be brought into a hospital or a smart home to be integrated with other behavioral and physiological data measured in the home to diagnose the chronic health state with better accuracy or in an earlier phase.

**IMPLEMENTATION/APPLICATION**

Evolution of the current driver state monitoring technology and integration with vehicle-embedded biometric sensors or wearable sensors with wireless connection to the vehicle (on-board monitoring) should be able to detect some or all of the acute health declines in real time. Candidates for on-board biometric sensors for each of the driver's acute health decline are summarized in Table 2. Most of the biometric sensors for on-board monitoring shown in Table 2 are still under research or development. Applicability of these sensors to the detection of acute symptoms needs to be investigated with consideration for the cost and the user acceptance.

If the driver-state monitoring can detect early signs of a decline while the driver is still conscious, a multilayered intervention strategy using information and assistive vehicle control could be taken. When the driver fails to take actions to avoid a crash or if the system fails to detect early signs of the decline due to too rapid decline, future autonomous vehicle technology will be the key to avoiding crashes by bringing the vehicle safely to a stop on the hard shoulder of the road for the driver who is likely to be unconscious (i.e. Autonomous Emergency Stop System or AESS, Shunk, 2009, Nissan, 2013). Stopping a vehicle in busy traffic or high speed traffic could induce additional crashes involving other vehicles. Vehicle-to-vehicle communication to broadcast the emergency signal to surrounding and following vehicles could be included in the AESS. Accuracy of detection also needs to be high. Integration of environmental sensors with driver-state monitoring could be considered so that the system activates the Autonomous Emergency Stop System when the driver is in a health decline and the risk of crash is imminent (Figure 3).

The contributing factors and co-morbidities associated with the most common injuries also point to interventions that could benefit the older occupant. While knowing age of a driver or occupant may help in some driving task assistance, it is less of an indicator of overall health. Sensing occupant bone quality can lead to real-time adaptive restraint systems that lower the loads on the poorer quality bones of older or less healthy occupants and could help reduce incidence of rib injuries. Newer technologies such as 4-point belt systems and inflatable seat belts also help to reduce or distribute chest loading (Ridella, 2012).

Driver-state data measured in the vehicle can be also brought out of the vehicle to the off-board network. Advanced Automatic Collision Notification System (AACN) is an example that automatically sends notification of a collision event together with vehicle and driver-state data from the pre-crash phase to a hospital so that the ER will have sufficient preparation time prior to arrival of the casualties.

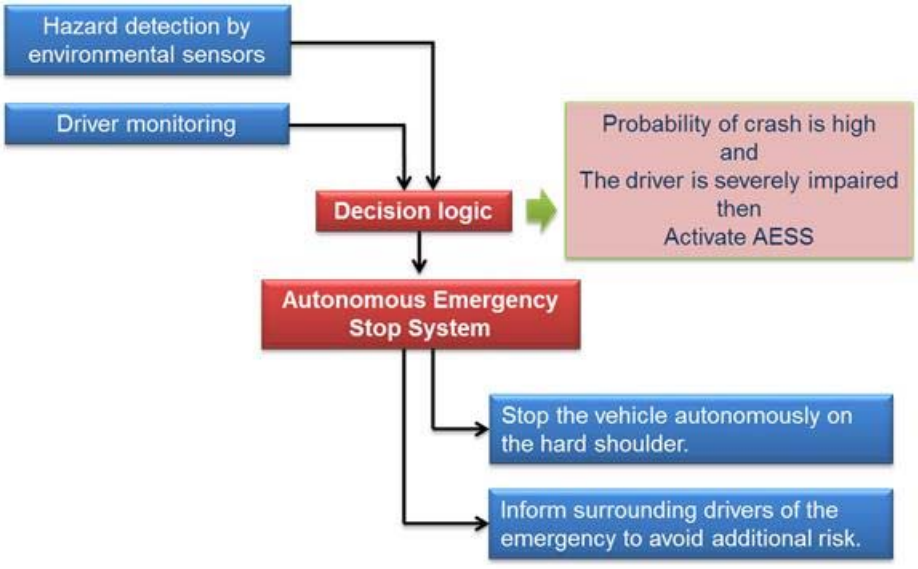


***Figure 3 . Functional flow of Autonomous Emergency Stop System.***

## ISSUES

### Privacy, protection and malicious intent

Since the devices and other instrumentation in the vehicle or on the occupant are measuring, monitoring, transmitting, and/or recording health status information, concerns arise regarding the protection and privacy of this data. The Health Insurance Portability and Accountability Act of 1996 (HIPAA) sets rights for an individual's health information and prescribes rules and limits over who can review and receive that information. This rule applies to any form of the information whether it is oral, written or electronic. The information that is envisioned to be collected may not necessarily be covered by HIPAA depending on how it is collected and used. For example, it may be that the data is only used in a non-identifiable, real-time manner to inform the vehicle that the occupant is drowsy or has an abnormal condition. In other cases, when linked to driver/occupant identification technology, the data is personal and possibly subject to HIPAA. It could also be recorded and/or transmitted depending on application if there is a need to interpret the data in real-time by a health professional or to review the data by law enforcement at a later date should an event occur. HIPAA rules are very specific about cases such as this, however, it is likely an interpretation of HIPAA in the vehicle environment may need further review as this technology develops.

Another consideration is the malicious use of the health information data. Security of the data, whether stored in the vehicle, in a portable device or other form needs to be protected from other sources that could use or manipulate the data in harmful ways. For example, a baseline health information data set could be altered either through direct intervention or electronic methods such that an abnormal event would not be detected by the vehicle or software. An intervention or denial of service could occur during driving, thus making the system inoperative. There are endless scenarios that could occur depending on sophistication of the system. Current cybersecurity research regarding other vehicle communications should include the possibility of how the health and driver monitoring activities can be protected from mischievous intent.

### Performance

Performance of such a system would require extensive testing for reliability, repeatability and reproducibility. In his short article nearly fifty years ago, one of Waller's criteria for monitoring for physical impairment was that "few persons of low accident risk should be falsely categorized in the high accident risk group". That is, the number of false-positive identifications should be minimized and conversely, the number of true-positives should be maximized. It is imperative that these devices are calibrated properly or can be re-calibrated based on manual feedback from the driver/occupant or perhaps periodically from a software "push" through an application or other connected technology whether portable or vehicle-based.

### Cancelable

Finally, the driver and/or other occupants may reserve the right to cancel or not participate in real-time identification and monitoring. This may apply when a vehicle is not driven by an owner or designated driver for whom baseline data exists. Also, rental cars may either not be equipped with such devices or a driver may opt out from participation.

## SUMMARY

The paper discussed the premise that identification of a vehicle driver (and/or occupants) as well as monitoring their health, mood or behavioral status while driving, may have significant value for safety. It is documented that health conditions may contribute to increased crash risk and that those with conditions have poorer outcomes should a crash occur. By monitoring a driver's health status in real time, possibly comparing to a baseline value, acute conditions may be detected and a warning , intervention, or other countermeasure may be applied. There is abundant technology in development as evidenced by manufacturs' documented research. Also, both traditional and non-traditional automotive suppliers have been involved in the early vehicle-based technology research, however, the sports market has dominated the wearable monitoring device development and production. Research projects in driver behavior, alcohol detection and a host of other technologies in development may lead to new advances in safety as the population of driver's age and people are more aware of their own health status.

**REFERENCES**


1. American Diabetes Association. (2012). Diabetes and Driving. *Diabetes Care*, Vol.35, *Supplement* 1, ppS81-S86.

2. Badugu,R., Lakowicz,J.R., and Geddes,C.D. (2004). Noninvasive continuous monitoring of physiological glucose using a monosaccharide-sensing contact lens. *Analytical Chemistry*, Vol.76, No.3, pp610-618.

3. Baig,M.M., Gholamhosseini,H., and Connolly,M.J. (2013). A comprehensive survey of wearable and wireless ECG monitoring systems for older adults. *Medical & Biological Engineering & Computing* Vol. 51, No. 5, pp485-495.

4. Balanou,E., Gils,M.V., and Vanhala,T. (2013). State-of-the-art of wearable EEG for personalized health applications. Presentation material at 10th InternationalConference on Wearable Micro and Nano Technologies for Personalized Health. Retrieved February 20, 2014 from http://phealth2013.eu/uploads/keepitsimple/E.Balanou.pdf

5. Boyle,L.N., Tippin,J., Paul,A., and Rizzo,M. (2008). Driver performance in the moments surrounding a microsleep. *Transportation Research* Part F 11, pp126–136.

6. Casson,A.J., Yates,D.C., Smith,S.J.M., Duncan,J.S., and Rodriguez-Villegas,E. (2010). Wearable Electroencephalography. *IEEE engineering in medicine and biology magazine* (2010, May/June), pp44-56.

7. FMCSA. (2007) Expert Panel Recommendations: Cardiovascular Disease and Commercial Motor Vehicle Driver Safety. Evidence Report. Presented to FMCSA, April 2007.

8. FMCSA. (2007). Expert Panel Recommendations: Seizure Disorders and Commercial Motor Vehicle Driver Safety. Evidence Report. Presented to FMCSA, November, 2007.

9. FMCSA. (2007) Expert Panel Recommendations: Obstructive Sleep Apnea and Commercial Motor Vehicle Driver Safety. Evidence Report. Presented to FMCSA, November, 2007.

10. FMCSA. (2009) Expert Panel Recommendations: Traumatic Brain Injury and Commercial Motor Vehicle Driver Safety. Evidence Report. Presented to FMCSA, March, 2009.

11. FMCSA. (2011) Expert Panel Recommendations: 2010 Update Diabetes and and Commercial Motor Vehicle Driver Safety.Evidence Report. Presented to FMCSA, May ,2007.

12. Ford (2011, May). *Ford In-Car Health and Wellness Solutions*. Retrieved February 20, 2014 from http://medicaldesign.com/site-files/medicaldesign.com/files/archive/medicaldesign.com/Medtronic-fact-sheet-HR.pdf

13. Hanna, R. (2009). The contribution of medical conditions to passenger vehicle crashes. *DOT Report*, DOT HS 811 219.

14. Hardy, R.N., Watson, J.W., Cook, R., Zioupos, P., Forrester, B., Frampton, R., Page, M., Kennedy, A., Peach, S., Sproston, P. Development and Assessment of a Bone Scaning Device to Enhance Restraint Performance. In: Proceedings of the 19th International Conference on the Enhanced Safety of Vehicles. Washington, D.C.

15. Hiestand,D.M., Britz,P., Goldman,M. and Phillips,B. (2006). Prevalence of symptoms and risk of sleep apnea in the US population. *CHEST Journal*, Vol.130., No.3, pp780-786.

16. Insurance Institute for Highway Safety. (2014). Status Report, Vol. 49, No. 1.

17. Iowa State University (2005). *Smart Home Lab*. Retrieved February 20, 2014 from http://smarthome.cs.iastate.edu/Demos.html

18. Leger,D. (1994). The cost of sleep-related accidents: a report for national commission on sleep disorders research. *Sleep*, Vol.17, No.1, pp84-93.

19. Meditech (2011). *Finger Pulse Oximeter*. Retrieved February 20, 2014 from http://www.meditech.com.cn/Finger-Pulse-Oximeter

20. Misugi,K., Kanamori,H., and Atsumi,B. (2003). Toyota's program for universal design in vehicle development. Universal design for the Toyota "RAUM", *Toyota Motor Corporation, "Raum" press information*

21. Monk,C (2012, August). *Driver Alcohol Detection System for Safety (DADSS).* Retrieved February 20, 2014 from https://secure.hosting.vt.edu/www.apps.vtti.vt.edu/PDFs/NDRS-2012-presentations/DADSS%20VTTI%20Naturalistic%20Conference%20Presentation%202012%20v3.pdf

22. NHTSA (1985). Transportation-related sleep research. CAR files study. *Report to the Senate Committee on Appropriations and House Committee on Appropriations*. Washngton,DC., US Department of Transportation.

23. NHTSA (2013). Traffic safety for older people - 5-year plan. DOT HS 811 837.

24. NHTSA (2015). Critical Reasons for Crashes Investigated in the National Motor Vehicle Crash Causation Survey. DOT HS 812115.

25. Nijsen,T.M.E., Arends,J.B.A.M., Griep,P.A.M., and Cluitmans,P.J.M. (2005). The potential value of three-dimensional accelerometry for detection of motor seizures in severe epilepsy. *Epilepsy & Behavior,* Vol. 7, pp74-84.

26. Nissan (2013, August). *Nissan Autonomous Drive: Emergency Stop*. Retrieved February 20, 2014 from http://nissannews.com/en-US/nissan/usa/releases/nissan-announces-unprecedented-autonomous-drive-benchmarks/videos/nissan-autonomous-drive-emergency-stop

27. Paul,A., Boyle,L.N., Tippin,J., and Rizzo,M. (2005). Variability of driving performance during microsleeps. *Proceeding of the third International driving Symposium on Human Factors in Driver Assessment, Training and Vehicle Design*. pp18-24.

28. Pautan.org (2011, May). *Ford Develops Heart Rate Monitoring Car Seat*. Retrieved February 20, 2014 from http://paultan.org/2011/05/26/ford-develops-heart-rate-monitoring-car-seat/

29. Positive ID (2013). *Non-Invasive Breath Glucose Detection Device*. Retrieved February 20, 2014 from http://www.positiveidcorp.com/products_breathglucosedetection.html

30. Quick,D. (2009, January). *Implantable Sensor Simplifies Blood Pressure Readings*. Retrieved February 20, 2014 from http://www.gizmag.com/tiny-sensor-simplifies-blood-pressure-readings/10846/

31. Ridella, S.A., Rupp, J.R., and Poland, K. Age-Related Differences in AIS 3+ Crash Injury Risk, Types, Causation and Mechanisms. In: Proceedings of the 2012 International IRCOBI Conference on the Biomechanics of Injury, pp. 43-59, Dublin, Ireland, September 2012.

32. Ridelust (2011, January). *Ferrari Working On Driver Monitoring Technology*. Retrieved February 20, 2014 from http://www.ridelust.com/ferrari-working-on-driver-monitoring-technology/

33. Risser,M.R. and Ware,J.C. (1999). Driving simulation with EEG monitoring in nomals and obstructive sleep apnea patients. *Sleep,* Vol. 23, No.3, pp393-398.

34. Rizzo,M. (2011). Impaired driving from medical conditions: A 70-year-old man trying to decide if he should continue driving. *JAMA*, March 9, 2011, Vol.305, No.10, pp1018-1026.

35. Shunk,C. (2009, June). *BMW Working On System That Stops Vehicles During A Medical Emergency*. Retrieved February 20, 2014 from http://www.autoblog.com/2009/06/05/bmw-working-on-system-that-stops-vehicles-during-a-medical-emerg/

36. Skubic,M., Alexander,G., Poppescu,M., Rantz,M., and Keller,J. (2009). A smart home application to eldercare: Current status and lessons learned. *Technology and Health Care* 17, pp183-201.

37. Tregear,S.J., Rizzo,M., Tiller,M., Schoelles,K., Hegmann,K.T., Greenberg,M.I., Phillips,B. and Anderson,G. (2007). Diabetes and motor vehicle crashes: a systematic evidence-based review and meta-analysis. *Proceedings of the Fourth International Driving Symposium on Human Factors in Driver Assessment, Training and Vehicle Design*. pp343-350.

38. University of Florida. *The Gator Tech Smart House (GTSH). Retrieved February 20, 2014 from http://www.icta.ufl.edu/gt.htm#1*

39. University of Rochester Medical Center (2014). *University Creates Medical "Smart Home" To Study Future Health Technology*. Retrieved February 20, 2014 from http://www.urmc.rochester.edu/news/story/index.cfm?id=-103

40. Waller, J.A. (1967). The Contribution of Medical Impairment to Traffic Accidents. In: The Prevention of Highway Injury, Selzer, M.L., Gikas, P.W. and Huelke, D.F. (eds). , Highway Safety Research Institute, Ann Arbor, MI.

41. Watson, T. , Krause J., Le, J. and Rao, M.K. (2011). Vehicle Integrated Non-Intrusive Monitoring of Driver Biological Signals. SAE Paper No. 2011-01-1095., SAE International, Warrendale, PA.

42. Wild,S., Roglic,G., Green,A., Sicree,R. and King,H. (2004). Global prevalence of diabetes; Estimates for the year 2000 and projections for 2030., *Diabetes Care*, Vol.27, No.5.

43. Wired. (2012). http://www.wired.com/2012/06/ford-workload/

**Table 2.**
**Monitoring technologies and application to driver's state**

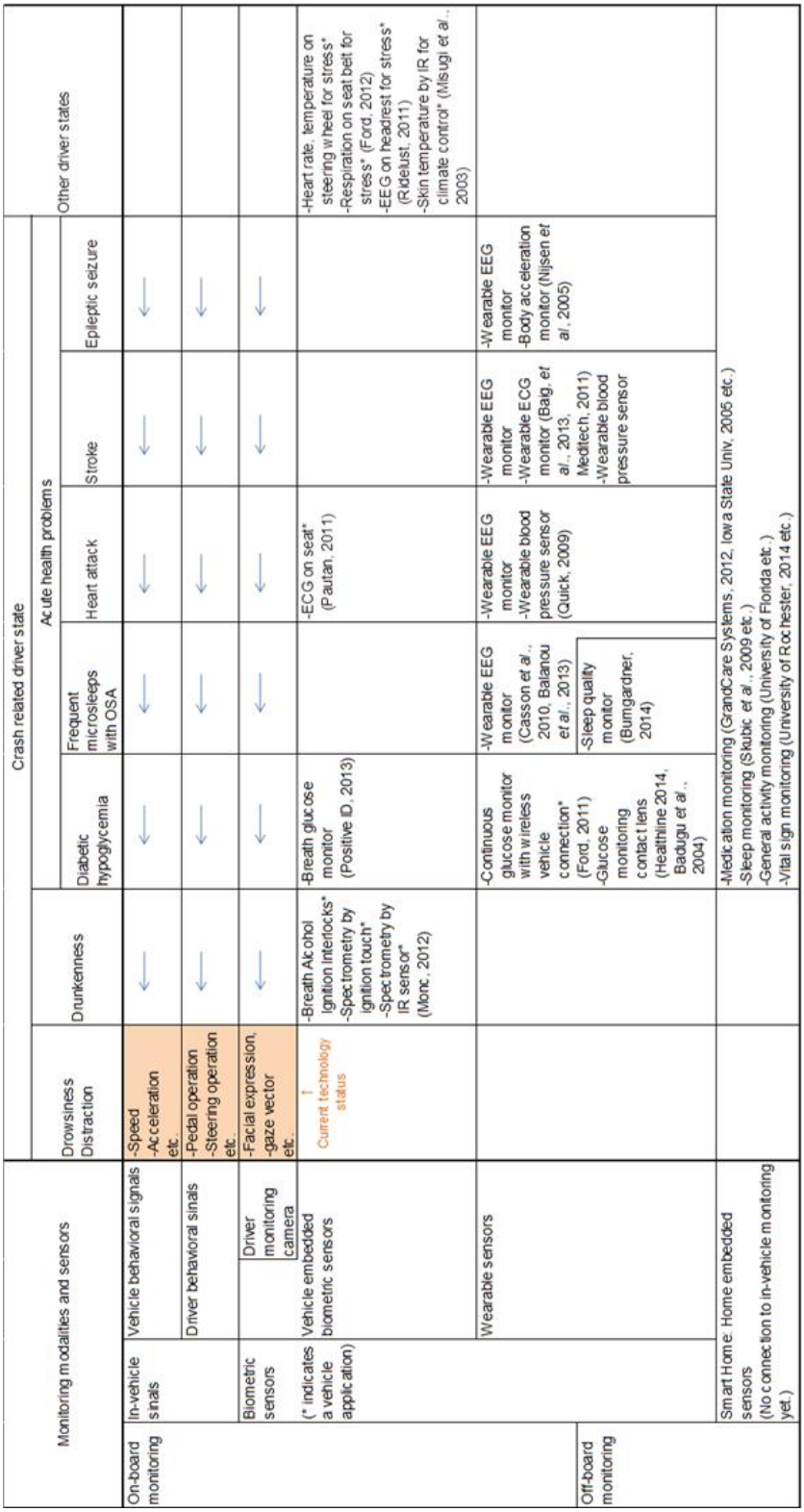

# DEVELOPMENT OF A BASIC SAFETY MESSAGE FOR TRACTOR-TRAILERS FOR VEHICLE-TO-VEHICLE COMMUNICATIONS

**Alrik L. Svenson**
National Highway Traffic Safety Administration
United States

**Gordon Peredo**
**Luca Delgrossi**
Mercedes-Benz Research & Development North America, Inc.
United States

Paper Number 15-0379

## ABSTRACT

Currently the Basic Safety Message (BSM) used by heavy truck tractor-trailers was developed for Vehicle-to-Vehicle (V2V) communications in the U.S. DOT Safety Pilot and uses a simplified bounding box algorithm for conveying the position and heading of the tractor-trailer. However, because of the articulated behavior inherent in a tractor-trailer, this approach does not accurately identify the trailer position or vehicle space for V2V safety applications in all situations. Consequently, in certain situations this can lead to an unacceptable number of false and missed warnings to drivers in surrounding connected vehicles. The U.S. DOT, in partnership with the Crash Avoidance Metrics Partnership (CAMP) and Mercedes-Benz Research & Development North America, Inc. (MBRDNA) conducted a project, Tractor-Trailer Basic Safety Message Development (TT-BSM), to develop technical solutions to this location identification problem for heavy truck tractors with one or more articulated trailers. TT-BSM developed several BSM enhancement approaches to more accurately represent tractor-trailer articulation. Furthermore, the team also completed the system and performance requirements and an assessment of the enhanced BSM impact on internal vehicle platform (On-Board Equipment, OBE, necessary vehicle sensors on the tractor and the trailer) and external systems (e.g. communications channel loading, other OBE-equipped vehicles, and backend systems). The enhanced BSM can more accurately transmit position and heading for articulated tractor-trailers and thus allows for better safety warnings and fewer false and missed warnings to drivers.

## INTRODUCTION

Over the last several years, the United States Department of Transportation (U.S. DOT) and the Crash Avoidance Metrics Partnership (CAMP) Vehicle Safety Communications 3 (VSC3) Consortium (Ford Motor Company, General Motors Corporation, Honda R&D Americas, Inc., Hyundai-Kia America Technical Center, Inc., Mercedes-Benz Research & Development North America, Inc., Nissan Technical Center North America, Inc., Toyota Motor Engineering & Manufacturing North America, Inc., and Volkswagen Group of America) have collaborated in the area of Vehicle-to-Vehicle (V2V) communications for the Safety Pilot program. [1] V2V safety systems generally rely on Dedicated Short Range Communications (DSRC) transmissions to share position, kinematic, and vehicle information with neighboring vehicles that are similarly equipped and warn their drivers of potential imminent dangers. The Safety Pilot Model Deployment (MD) launched August 21, 2012 running through 2013 provided insight into public perception, acceptance, and effectiveness of active safety systems that could be supported by the use of low-cost technologies, specifically 5.9 GHz DSRC and the Global Positioning System (GPS). This was demonstrated in MD on different prototype vehicles, including tractor-trailers, that hosted multiple DSRC-based safety applications aimed at addressing several crash categories, such as rear-end, lane change, intersecting, or oncoming. [2-3]

Three Class 8 tractor-trailers were equipped with fully integrated on-board equipment (OBE) and used in Driver Clinics held in Ohio and California under the V2V Safety Pilot project. [4] The results of the clinics showed the promise of the technology for heavy vehicles while under controlled conditions on a test track. These trucks were then included in the Model Deployment field test in Ann Arbor, Michigan. [5] For Model Deployment, the position and heading of the tractor-trailer in the Basic Safety Message (BSM) was derived by a simplified bounding box

algorithm which treated the tractor-trailer as a single rigid body. However, because of the articulated behavior inherent in a tractor-trailer, this approach can lead to an unacceptable number of false and missed warnings to drivers in surrounding connected vehicles, especially when the vehicle is in a turn. The U.S. DOT in partnership with CAMP and Mercedes-Benz Research & Development North America, Inc. has developed technical solutions (enhanced BSM) to this issue and established system and performance requirements. Furthermore, the partnership also completed an assessment of the enhanced BSM's impact on the internal vehicle platform (On-Board Equipment, OBE, necessary vehicle sensors on the tractor and the trailer) and external systems (e.g. communications channel loading, other OBE-equipped vehicles, and backend systems). The objective of this paper is to describe these team efforts and results.

**Background**

V2V communications based on 5.9 GHz DSRC allow vehicles to be aware of other nearby similarly equipped vehicles and assess collision risks by exchanging safety messages describing vehicles' current status. These communications can deliver information beyond on-board sensors' range or field of view and high-quality information such as vehicle weight, size, and brake status. As of now, research has mostly focused on DSRC-based systems aimed at alerting the driver of imminent dangers. A recent NHTSA report shows that just two of many possible V2V safety applications, Intersection Movement Assist (IMA) and Left Turn Assist (LTA), would on an annual basis potentially prevent 25,000 to 592,000 crashes, save 49 to 1,083 lives, avoid 11,000 to 270,000 Maximum Abbreviated Injury Scale 1-5 injuries, and reduce 31,000 to 728,000 property-damage-only crashes by the time V2V technology had spread through the entire fleet. [6]

The first prototype applications developed as part of several CAMP projects sponsored by the U.S. DOT included:

- Emergency Electronic Brake Lights (EEBL)
- Forward Collision Warning (FCW)
- Lane Change Warning (LCW) / Blind Spot Warning (BSW)
- Do Not Pass Warning (DNPW)
- Intersection Movement Assist (IMA)
- Control Loss Warning (CLW)

These V2V applications share a common concept of operations: using BSMs that are periodically broadcast by other similarly-equipped vehicles to track nearby vehicles and assess the risks of collision. BSMs include information on vehicle position, speed, heading, brake status, and size. This small set of information is sufficient to support most V2V safety applications for collision prediction.

Collision prediction algorithms need accurate information on the space occupied by each vehicle over time as well as its movements. This requires a model to represent vehicles and the space they occupy as they travel and execute driving maneuvers on the road. In current V2V systems developed by CAMP, vehicles are modeled as rigid body rectangles with a length and width. The BSM position transmitted over the air corresponds to the vehicle center expressed in terms of latitude, longitude, and elevation. Each vehicle calculates its center as an offset from the physical position of the GPS antenna (typically installed on the roof of the vehicle). V2V applications can tolerate errors in absolute position estimates to a certain degree as long as the relative position estimates meet application accuracy requirements. The V2V positioning system typically supports lane-level (< 1.5m) accuracy.

The recent CAMP projects focused solely on rigid body vehicle representations, as noted above. Unfortunately, the model does not sufficiently describe the space occupied by articulated vehicles during turn maneuvers. This problem can affect any articulated V2V-equipped commercial, transit, or passenger vehicle and will be discussed further in this paper.

**V2V with Articulated Vehicles**

Understanding how V2V applications generate warnings to the driver provides a foundation for the discussion on articulated vehicles. For example, FCW tracks one or more Remote Vehicles (RVs) ahead of the Host Vehicle (HV) traveling in the same general path and issues a warning to the HV driver if there is an imminent danger of collision

with an RV. FCW compares the HV predicted path (based on its location, speed, heading, and other parameters) with the RV path history. This path history comes from a trail of recent RV positions and is included in its BSM. This vehicle center point is calculated as an offset from the vehicle's GPS antenna (i.e. a constant offset in a rigid body).

When vehicle articulation is considered, additional factors must be included to process V2V applications correctly. In vehicle dynamics terminology, as in Figure 1 below, a vehicle's heading refers to the direction of the forward longitudinal axis of the vehicle's body with respect to a global reference. Its course heading is its instantaneous direction of travel with respect to a global reference. During steering maneuvers, the course heading will always differ from the vehicle heading. This difference is called the side slip angle, or β. When traveling on a straight road, the side slip angle is essentially zero. In addition, the vehicle's articulation angle is defined as the difference between the tractor and trailer headings.

For a light vehicle, reporting the course heading as the vehicle heading is an acceptable approximation. The instantaneous direction of travel (course heading) is far more meaningful to other DSRC-equipped vehicles than the vehicle heading since those vehicles use the direction of travel to predict its future path. This future path helps other vehicles calculate intercepts. This simplification becomes a problem when the broadcasting vehicle has articulation angles between multiple bodies.

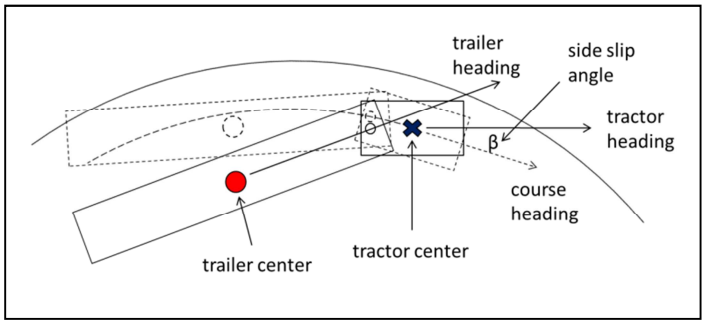


***Figure 1. Articulated Vehicle Terminology.***

For an articulated vehicle, it became apparent that correcting for articulation angle was not sufficient to accurately represent the location of the trailer. The vehicle is represented as a box, oriented in the direction of its course heading irrespective of the vehicle heading and rotated about its geometric center. Since both the true tractor and trailer poses are rotated about the center of the tractor (since the GPS antenna was mounted on the tractor) by the side slip angle, the DSRC system needed to correct for both the side slip angle and the articulation angle in order to accurately represent the location of the trailer. Without this correction, the error in the trailer orientation would be significant, especially as trailer length or number of trailers increase. Modeling could be further improved with filtering of other error sources (e.g. GPS, yaw rate, etc.), but was not the goal of this project and was omitted.

In the articulated vehicle used for this project, the GPS antenna was mounted on the roof of the tractor so when the vehicle changed direction, this offset remained constant even though the trailer swung in an arc relative to the tractor. As a result, the articulated vehicle path history can be significantly offset from the actual trailer position and orientation. As this erroneous 'ghost' trail was laid behind the vehicle, another approaching vehicle could wrongly trigger or suppress a warning. False warnings might occur when the HV is driving in the neighboring lane and the RV is going into a curve or turn. If the RV trail is in the path ahead of the HV when it is actually to the right of the HV while the road curves to the right, the HV may get a false FCW warning.

V2V safety applications on long, non-articulated vehicles such as city buses may also need to correct for vehicle versus course heading differences. In large steering angle maneuvers, such as pulling out of a bus stop, the vehicle may develop very large side slip angles. These side slip angles could be as much as 60°. It is unclear what impact this problem would have on warning application performance for long vehicles. That question merits further investigation, yet lies outside the scope of this paper.

The TT-BSM project was initiated to address these shortcomings due to misrepresentations of the space occupied by articulated vehicles. The main focus of the project was to derive the position and heading of each part of the articulated vehicle, define over-the-air messages to convey this information to nearby vehicles, and implement and test the solution in an actual vehicle; all with a minimum impact on the existing V2V system and communications standards.

### TT-BSM Solution Sets

The TT-BSM project considered three alternative approaches to describe position and heading for each part of an articulated vehicle. The results of these alternatives were compared to the baseline rigid body approach, i.e., the initial rigid body model developed in previous CAMP projects (Figure 2a). This approach was included for comparison and had the advantage of not requiring changes to the V2V safety applications or Standards, but offered a simplistic and inaccurate representation of the trailer position. The second approach (multi-DGPS approach, Figure 2b) used distinct rigid body representations for the tractor and trailer where separate, independent rectangles represented the actual locations of each body of the articulated vehicle. A multi-DGPS receiver system was used to derive these locations. In the third approach (best fit rigid body, Figure 2c), the length and width of the rigid body model was kept the same, but translated its position laterally and longitudinally so that the rectangle is centered in a weighted average of the articulated tractor-trailer's planar area. Even though this solution broadcasts a rigid body model, it still required knowledge of the articulation angle. Finally, the fourth approach (algorithm approach, Figure 2d) used separate rectangles, as in the second approach, but no sensors are used to determine the actual position of the trailer. Rather, this is calculated through a kinematics algorithm. The yaw rate of the tractor is derived from DGPS. This is translated into a lateral velocity at the tractor hitch point (fifth wheel) and, since the trailer hitch point is fixed to the tractor hitch point, this translates into a trailer yaw rate. The trailer yaw angle is then numerically integrated from the trailer yaw rate. The trailer heading and center location are then calculated from the known geometry.

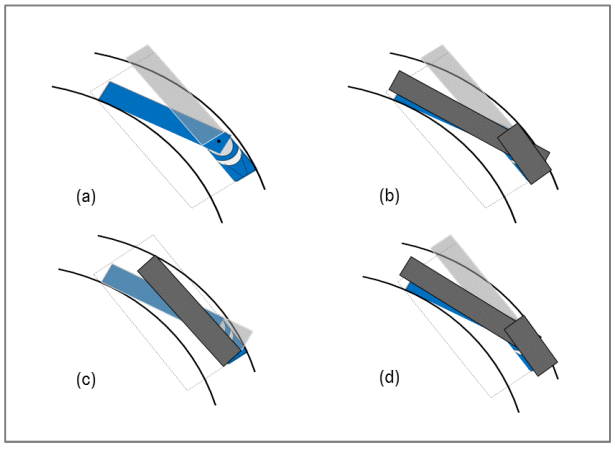


***Figure 2. TT-BSM Project Solution Set.***

In terms of packaging the trailer description into over-the-air messages, approaches 1 and 3 do not require any changes to the BSM or the safety applications: the baseline is the default light vehicle approach, while the third solution would simply offset the location of the rigid body tractor-trailer representation. Approaches 2 and 4 would require a BSM that could include a separate package of information for trailers in addition to the tractor. In order to select a workable approach for implementation, numerous simulations were developed and run to assess the pros and cons of each.

### Simulations

In order to compare the solution approaches, scenarios were first developed to highlight their differences. Since the intention was to address potential problems caused by vehicle articulation, the scenarios incorporated conditions where the tractor-trailer bodies were at different headings, creating a non-zero articulation angle between them.

Furthermore, the vehicle was limited to turning from a thru lane and not a left or right turn pocket. This accentuated the rigid body model misrepresentation of the trailer position and heading by minimizing vehicle offset from the thru lane of travel as close to the intersection as possible.

Once scenarios were defined, tractor and trailer models as well as vehicle motion models simulating vehicle dynamics in the selected scenarios were constructed in the TruckSim simulation tool. At the same time, Matlab and Simulink were used to create models of each approach and V2V safety application functions within the on-board DSRC platform. The result of each simulation was a target classification and threat level for each component of the articulated tractor-trailer relative to the specific approach used. The results for each approach, as applied to a specific scenario, were overlaid and visualized in animations, providing clear comparisons of the various approaches in a simulated environment.

In all, four scenarios were used in the simulations. These included a constant radius of curvature road, two types of right hand turns, and a fast lane change at highway speeds. In all scenarios, the HV is following the tractor-trailer on the same road. The following describes these scenarios and relevant parameters in more detail.

For curved roads, such as a highway cloverleaf exit, the tighter or smaller the curve radius, the more likely the false alert due to misrepresentation of trailer articulation. Conversely, a large radius curve more closely approximates a straight road, reducing articulation angles and the chances for a false alert. In this scenario, a tractor-trailer was driven in a constant radius of curvature turn at steady-state conditions. This modeled pure articulation while removing transient vehicle steering dynamics from consideration. This case was used to determine if using a rigid body model could cause the vehicle to protrude into an adjacent lane virtually and, conversely, if any of the approaches represented the tractor-trailer pose correctly, so as to prevent false warnings.

In the second scenario, multi-lane right hand turns, the tractor-trailer is driven in a typical (for the U.S.) wide intersection turn of 90 degrees. A left hand turn scenario is not used since this is typically done from a left turn pocket or suicide lane and does not fulfill the more stressing condition where the vehicle turns from a thru lane.

For single lane right hand turns, the third scenario, the tractor-trailer makes a 90 degree turn onto a narrow intersecting road. In order to successfully negotiate the tight turn, the tractor-trailer swerves onto the adjacent left lane before turning right. This is more typical in urban settings where narrow roads may be lined with parked cars.

The last scenario involves a fast lane change at highway speeds where the tractor-trailer undergoes high speed negative offtracking. This is a well understood phenomenon for articulated vehicles engaged in evasive lateral maneuvers at highway speeds. This is the only situation in which negative offtracking is anticipated for standard tractor-trailers in typical driving conditions in the U.S.

These scenarios represent the range of kinematics and dynamics of articulation angle in combination tractor-trailers in typical driving conditions. Since tractors and trailers come in many sizes, considerations for their lengths must be made since this directly impacts the BSM information and potential for false alerts. Tractor and trailer sizes considered were limited to those available in the CCV-IT and V2V-MD projects, but represent a large proportion of existing vehicles in U.S. commercial fleets.

For the constant radius of curvature scenario, the likelihood of getting a false warning was maximized when the articulation angle between the two bodies was maximized. In turn, the articulation angle was maximized when the tractor wheelbase was minimized and the trailer wheelbase was maximized. This represented a worst case articulation angle for typical tractor-trailer combinations.

In the right hand turn scenarios, the articulation angle is a dynamic function of position in the turn path. The likelihood of getting a false warning depended on where the tractor was in the turn as well as what the articulation angle was at that point in the turn. The relationship between these two factors and the determination of which of the two factors was dominant depended heavily on the radius of curvature of the turn. In each case, the likelihood of getting a false warning was maximized when the articulation angle was maximized and the total straight-line trailer length was maximized.

For the fast lane change scenario, the likelihood of getting a false warning was maximized when the lane change time and distance were minimized and the articulation angle of the rear-most trailer was maximized. The tractor-trailer essentially acted as a pendulum, with the lateral motion of the tractor acting as an impulse input to the pendulum. A tractor with a shorter wheelbase was able to turn faster and should therefore result in a greater lateral impulse input to the trailer. A trailer with a shorter wheelbase would also result in a greater articulation angle for a given impulse input, but multiple trailers will amplify this effect down the longitudinal axis of the combined tractor trailer system.

TruckSim was used in a co-simulation environment with Matlab/Simulink, as noted previously. A constant velocity target was sent from Simulink to TruckSim for each vehicle in each scenario. TruckSim then simulated the dynamics of the vehicle in the specific run case of the scenario. In all cases, the tractor-trailer was the remote vehicle, leading the host vehicle on the same road. The analysis required certain conditions, including the presence of vehicle articulation and the potential for collisions. As such, FCW proved most relevant to false alerts since articulation could be produced in turns and curved roads and collisions could be possible from a trailing vehicle. As such, the simulations evaluated the approaches against this specific safety application.

The output that TruckSim sent back to Simulink was a series of reference points that were attached to specific points on the vehicle bodies; most important were the volumetric centers of the vehicle bodies. Simulink/Matlab were then used to compute lateral offsets between HV and RV, RV path history, and lane boundaries so the HV could classify the RV target information. The Simulink/Matlab model was reconfigurable to run the baseline rigid body model or any of the other three approach models. Finally, the data were run through a model of FCW to determine if a warning occurred.

Tractor and trailer models were designed in TruckSim to match up with each of the scenarios and their various run cases. They were also designed to coincide with vehicles that may be available for live testing, where possible, so that TruckSim results could be compared to test results. This resulted in some cases where the tractor-trailer configuration that was optimal for trapping false warnings was not used.

In developing the models, another consideration further constrained the list of scenarios. The purpose of the fast lane change scenario was to trap the effects of high speed negative offtracking since this is the only scenario in which negative offtracking would be expected to occur. A model of a fast lane change was created in TruckSim to analyze this scenario. It was determined from simulations that a lane change would have to occur at an unreasonably fast and dangerous lateral speed in order to induce articulation angle dynamics that could have the potential for false warnings. As a result, the fast lane change at highway speeds was removed from the scenario list and was not considered further in this project.

The simulations showed that some approaches consistently performed better than others. Figure 3 shows examples of simulation results. In all cases, the tractor-trailer was the RV and a light vehicle was the HV. The tractor-trailer color varied by approach: yellow for the baseline rigid body, light blue for multi-DGPS, light brown for the best fit rigid body, and semitransparent black for the algorithm approach. Similarly colored lines were drawn to show the breadcrumb trails of the HV and RV. In all cases, the breadcrumb trails also precede the vehicles due to the limitations of pictures versus animations. Several of the approaches were overlaid in the same graphic in order to show comparisons. A legend was also included to indicate how the HV classified (e.g. ahead, ahead left, ahead right) each target (i.e. tractor, trailer1, and in cases with doubles, trailer2). In the cases where the classification is surrounded by a red border, the HV received an FCW warning for that target. Since both rigid body models (original and best fit) treat the tractor and trailer(s) as a single rigid body, the target classification in the legend is only reflected under the tractor column. It is important to note that the light blue, multi-DGPS approach was considered to be the most accurate method to determine the true pose of the tractor and trailer(s) since this relied on direct DGPS measurements for each. As such, the closer another approach lined up with the multi-DGPS representation and target classification, the more accurate and less likely to generate false alerts that approach was considered.

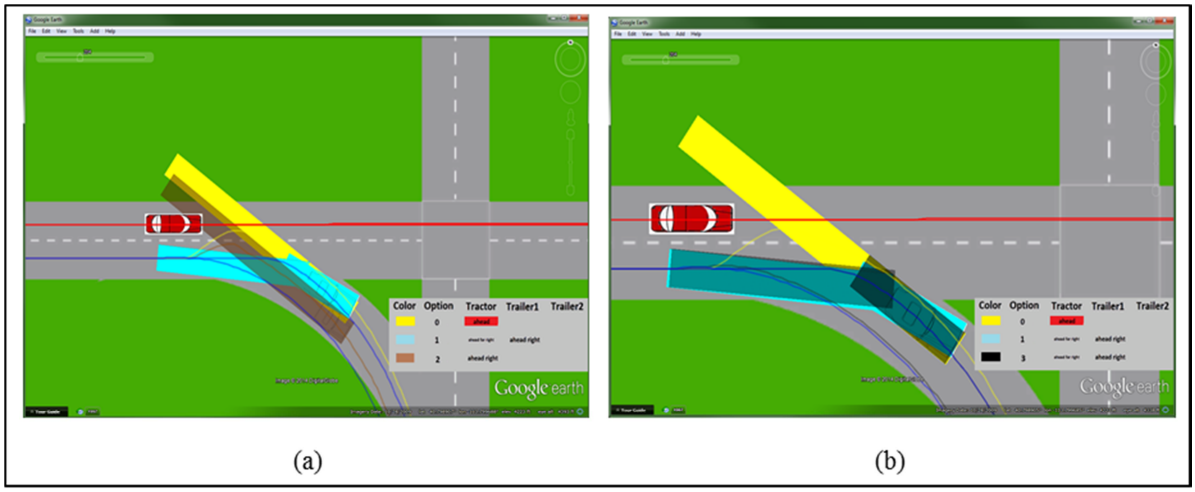


Source: Google Earth. Used with permission

***Figure 3. Sample TT-BSM Simulation Results.***

In Figures 3a and 3b, a tractor-trailer is making a right turn and a light vehicle is approaching it from behind in the adjacent lane. This represents the same simulation, but is split into two parts to provide better clarity. The baseline and multi-DGPS solutions remain the same in both, but Figure 3a includes the best fit rigid body approach, whereas Figure 3b shows the algorithm approach. In this case all non-baseline approaches perform better than the baseline since they did not warn inappropriately. From this example and many more similar results, it became clear that the multi-DGPS and algorithm approaches are superior to the baseline and best fit rigid body approaches. They track and classify the tractor and trailer(s) more accurately and do not cause FCW to falsely warn or fail to warn. The best fit rigid body does perform better than the baseline rigid body approach, but not nearly as well as the other two.

**Testing**

Road tests were designed to verify the accuracy of the proposed solutions to the articulated vehicle BSM problem. The tests enabled comparisons between actual recorded tractor and trailer data and the proposed enhancement to the BSM rigid body model. As part of this project, one of the above approaches was selected for further investigation and implementation. This was the algorithm approach. For comparison purposes, the study team also implemented the baseline rigid body and multi-DGPS approaches. The test system was designed such that multiple approaches could be tested on the road simultaneously. This was the surest way to develop comparable results without having to focus undue energies on precise repetition of test parameters.

Three scenarios were used for testing: constant radius curve, multilane right turn, and single lane right turn. These were based on the simulation scenarios and optimized for a test track environment. The Constant Radius Curve scenario simulated a freeway cloverleaf or other long/wide curve road geometries. This was a steady state scenario in which the truck followed a curved path of constant radius. The centerline of the path driven by the tractor-trailer had a curve radius of 30m. The Multi-lane Right Turn scenario simulated typical wide intersection road geometries in which a truck driver could have multiple lanes available to execute a turn without entering the opposing lanes of travel. A turn radius of 20m was used. This scenario required the use of two, two-lane roads forming a perpendicular intersection. The Single Lane Right Turn scenario simulated the wide-turn strategy truck drivers utilize when turning in very constricted road geometries. In this circumstance it was necessary for the truck to encroach on neighboring lanes, sometimes oncoming, in order to execute a turn such that the trailer does not off-track onto a sidewalk.

Table 1 shows results for tests conducted in this project where a warning was expected. A ‘pass’ meant that a warning was generated when it should have and a ‘fail’ meant that a warning did not occur as it should have. Each cell represents a separate test run. It is clear that the algorithm approach performed best while the rigid body baseline approach fared the worst. This is in line with the simulation results, though the multi-DGPS approach was expected to have better performance. During some of the testing, DGPS readings were inconsistent and may account for the multi-DGPS test failures.

*Table 1. Test Results.*

| | Multi-lane Right Turn | | | | | Single Lane Right Turn | | | | | Constant Radius Curve | | | | |
|---|---|---|---|---|---|---|---|---|---|---|---|---|---|---|---|
| **Rigid** | Fail | Fail | Pass | Fail | Pass | Fail | Fail | Pass | Pass | Fail | Pass | Fail | Fail | Fail | Fail |
| **Multi-DGPS** | Fail | Pass | Pass | Pass | Pass | Pass | Pass | Fail | Fail | Pass | Pass | Fail | Pass | Pass | Pass |
| **Algorithm** | Pass | Pass | Fail | Fail | Pass | Pass | Pass | Pass | Pass | Pass | Pass | Pass | Pass | Pass | Pass |

In addition to road testing, a general assessment of the approaches was conducted in order to determine whether other factors may influence the results and either strengthen or undermine the algorithm approach effectiveness. Table 2 contains the summary of this general assessment. Each approach was compared based on various implementation factors. These included potential changes to the BSM structure, the accuracy of tractor and trailer positional representation, additional sensor measurements, changes to computational load, and changes to V2V safety applications. While no approach was perfect in all categories, the algorithm approach performed well and did not impose an insurmountable burden for implementation. Data frames and elements must be defined and added to the BSM Part II structure and some changes are required in supporting V2X software modules, but none of the V2V safety applications required modification for this project. The algorithm approach BSM is backward compatible with existing V2V safety applications, though these will only decipher the tractor information. Vehicles receiving the enhanced BSMs will need to understand the new data frames and elements in order to correctly act on the information they contain.

*Table 2. General Assessment of Approaches Relative to Implementation Factors.*

| | | Communication Changes | | Representational Accuracy | | Required Knowledge | | Tractor Calculations | Trailer Calculations | Application Changes |
|---|---|---|---|---|---|---|---|---|---|---|
| **Approach** | **Description** | Change to BSM Part I | BSM Part IIs | Tractor Pose | Trailer Pose | Real-Time Hitch Angle | Real-Time Beta Angle | Tractor Pose | Trailer Pose | HV's Target Classifier |
| Baseline Rigid | Default - single rigid-body, fixed on the tractor | None | 0 | Good | Poor - no off-tracking | No | No | None | None | None |
| Multi-DGPS | Two separate bodies, exactly matching tractor and trailer poses | Limited to tractor only | 1 | Good | Good | Yes | Yes | Heading (beta angle) | Heading (articulation angle) | Must track two bodies |
| Best Fit Rigid | Single rigid-body, best fit in curve with weighted average of bodies | None | 0 | Fair - incorrect lateral location | Fair - partial off-tracking | Yes | No | Lateral Location | Lateral location | None |
| Algorithm | Two separate bodies, estimate tractrix of the curve of trailer | Limited to tractor only | 1 | Good | Good | No | No | None | Heading (articulation angle) | Must track two bodies |

**Basic Safety Message Enhancements**

The BSM format is specified as part of the SAE J2735 DSRC Message Set standard. [7] A BSM consists of data elements (DEs) and data frames (DFs). A data element is a basic building block and a data frame comprises one or more data elements or other data frames. Data elements and data frames can be used to form BSMs similar to words in a sentence. For this reason, the SAE J2735 standard is often referred to as the data dictionary for V2V communications. Although BSMs are intended for use over the 5.9 GHz DSRC spectrum, their specification is independent of any frequency bands and they can be effectively used in other communication contexts. It is generally accepted that broadcasting BSMs at 10 Hz is sufficient to meet the requirements of the most demanding V2V safety applications.

The BSM format was carefully designed to minimize the message size. Smaller messages can help reduce DSRC channel congestion. To keep BSM sizes small, their content is structured into two parts. Part I – known as Basic Vehicle State – is mandatory and contains those data elements and data frames that must always be included in a BSM. BSM Part I has a fixed size of 39 bytes.

***Table 3. BSM Part I Data Elements and Data Frames.***

| BSM Data Item | Sequence | BSM Part | Type | Bytes |
|---|---|---|---|---|
| Message ID | | I | Data Element | 1 |
| Message Count | | I | Data Element | 1 |
| Temporary ID | | I | Data Element | 4 |
| Time | | I | Data Element | 2 |
| Latitude | PositionLocal3D | I | Data Element | 4 |
| Longitude | | I | Data Element | 4 |
| Elevation | | I | Data Element | 2 |
| Positioning Accuracy | | I | Data Frame | 4 |
| Transmission & Speed | Motion | I | Data Frame | 2 |
| Heading | | I | Data Element | 2 |
| Steering Wheel Angle | | I | Data Element | 1 |
| Accelerations | | I | Data Frame | 7 |
| Brake System Status | Control | I | Data Frame | 2 |
| Vehicle Size | VehicleBasics | I | Data Frame | 3 |

Part II, which includes the Vehicle Safety Extensions and Vehicle Status data frames, is optional. Typically, vehicles periodically broadcast BSM Part I only: specific events, such as emergency braking and control loss, can be described by setting the corresponding event flag in BSM Part II.

The Tractor-Trailer Basic Safety Message (TT-BSM) project developed BSM extensions to accurately represent articulated vehicles in V2X communications to reduce the potential for false warnings in the DSRC-based safety applications developed as part of the previous Connected Commercial Vehicle – Integrated Truck (CCV-IT) and

Connected Commercial Vehicle – Retrofit Safety Device (CCV-RSD) projects. When creating extensions to the current BSM format, several design goals were considered. In particular, special efforts were made to:

- accurately represent the position of articulated vehicle bodies in V2X BSMs
- minimize false warnings in nearby V2X-equipped vehicles
- minimize changes to the current SAE J2735 BSM structure
- minimize changes to existing V2X safety applications and equipment

The algorithmic approach from the proposed solutions produced by the TT-BSM project was selected since it met the goals better than the other solutions. In the algorithmic approach, the trailer dynamics during a turn maneuver are calculated in real-time. The trailer hitch point is fixed to the tractor hitch point. The yaw rate of the tractor is derived from GPS; this is translated into a lateral velocity at the hitch point; and this is translated into a yaw rate of the trailer. The trailer yaw angle is then numerically integrated from the trailer yaw rate. The trailer heading and center location are then calculated from the available geometry. A significant advantage of this approach is that no extra sensors are required. In initial testing and simulations, it performed nearly as well as the multi-DGPS solution without the associated long-term costs and complexity of the multi-DGPS solution. It can effectively represent vehicle articulation in multiple tractor-trailer configurations and in several representative scenarios, far better than the existing rigid body approach. Also, it is implementable with reasonable changes to supporting software modules without affecting the function of the safety applications.

With the algorithmic approach, no changes are necessary to BSM Part I, which remains a fixed size of 39 bytes. This ensures a high degree of backward compatibility with existing V2X systems. A new data frame, *DF_TrailerInfo*, is introduced to describe the trailer position and heading. The *DF_TrailerInfo* data frame is optional and is to be included in BSM Part II only when necessary, e.g. when one or more trailers are attached to a tractor. *DF_TrailerInfo* is comprised of a *DE_TrailerCount* data element and one or more *DF_TrailerDetail* data frames, depending on the number of trailers. *DE_TrailerCount* is a new data element that indicates how many *DF_TrailerDetail* data frames follow. *DE_TrailerCount* represents the number of trailers attached to the tractor. Each *DF_TrailerDetail* data frame is formed by elements and frames that are part of the existing BSM specifications.

***Table 4. DF_TrailerDetail Items.***

| DF_TrailerDetail Item | Sequence | Type | Bytes |
|---|---|---|---|
| Latitude | PositionLocal3D | Data Element | 4 |
| Longitude | | Data Element | 4 |
| Elevation | | Data Element | 2 |
| Positioning Accuracy | | Data Frame | 4 |
| Transmission & Speed | Motion | Data Frame | 2 |
| Heading | | Data Element | 2 |
| Steering Wheel Angle | | Data Element | 1 |
| Accelerations | | Data Frame | 7 |
| Brake System Status | Control | Data Frame | 2 |
| Vehicle Size | VehicleBasics | Data Frame | 3 |
| Path History | | Data Frame | Varies |
| Path Prediction | | Data Frame | Varies |
| Vehicle Height | VehicleData | Data Element | 1 |
| Bumpers Heights | | Data Frame | 2 |
| Vehicle Mass | | Date Element | 1 |
| Trailer Weight | | Data Element | 2 |
| Vehicle Type | | Data Element | 2 |

If any trailers exist, then the correspondent *DF_TrailerInfo* data frames shall be included in BSM Part II as necessary. *DF_TrailerInfo* will include as a minimum *DE_TrailerCount* and *DF_TrailerDetailOne*. The size of the *DF_TrailerInfo* data frame varies due to the inclusion of variable size frames such as Path History and Path Prediction and based on the number of articulations. Since the fixed portion of the *DF_TrailerInfo* data frame is 40 bytes, the resulting size roughly compares with the size of BSM Part I for a tractor with a single trailer. In case of multiple trailers, the size of this data frame could reach the double or triple of BSM Part I.

Introducing a new data frame for BSMs may raise concerns about increased over-the-air data traffic and consequent effects on channel load. Even if larger than BSM Part I, this is still a fairly small amount of data and it can be included in a single DSRC packet. It should also be noted that tractor-trailer vehicles represent a very small fraction of overall vehicles on the road.

Additionally, the position of the trailer needs to be described through BSM Part II only during turn maneuvers, which represent a small fraction of the driving time. When an articulated vehicle follows a straight path with small variations of the heading direction, it can describe its dynamics through the long rigid body model, thus broadcasting BSM Part I for a longer body. The onboard V2V system could continuously monitor the trailer articulation angle and adopt the strategy to broadcast BSM Part II only when this angle is larger than a certain threshold.

It should also be observed that the tractor-trailer combination broadcasting BSM Part I (to describe the tractor dynamics) and BSM Part II (to describe the trailer dynamics) contributes to channel load roughly equally to a pair of vehicles closely following each other and occupying the same space on the road. In other words, an articulated vehicle occupies a portion of the road that, in a congested traffic scenario, would be occupied by a pair of light vehicles broadcasting two BSM Part I messages to describe its dynamics. Based on all the above considerations, it can be concluded that introducing the proposed scheme to accurately describe the trailer position and heading does not result in additional over-the-air traffic able to significantly impact DSRC channel load.

## CONCLUSIONS

This study investigated solutions to improve the tractor-trailer position algorithm used in the current BSM and proposed an enhanced BSM for articulated vehicles by integrating trailer information into Part II of the BSM. This approach was successful in transmitting this information to surrounding vehicles using V2V communications once trailer parameters were known While only tested with one safety application, the enhancement to the tractor-trailer body model is likely applicable to others as well. Further work on an automated method of obtaining trailer parameters may be necessary to fully implement this solution for articulated commercial vehicles in service.

## REFERENCES

[1] Ahmed-Zaid, F., et al. 2011. "Vehicle Safety Communications –Applications (VSC-A) Final Report," National Highway Traffic Safety Administration, Report No. DOT HS 811 492A, Washington, D.C.
[2] Peredo, G. 2014. "Connected Commercial Vehicles—Integrated Truck Project Applications Requirements Final Technical Report," U.S. Department of Transportation, Report No. FHWA-JPO-13-106, Washington, D.C.
[3] Pape, D., J. Holdridge, and D. Stephens. 2014. "Connected Commercial Vehicles—Retrofit Safety Device Kit Project: Final Report," U.S. Department of Transportation, Report No. FHWA-JPO-14-111, Washington, D.C.
[4] Pape, D., J. Holdridge, and D. Stephens. 2014. "Connected Commercial Vehicles—Integrated Truck Project Driver Clinics, Performance Tests, and Lessons Learned Final Reports," U.S. Department of Transportation, Report No. FHWA-JPO-13-110, Washington, D.C.
[5] LeBlanc, D., S. E. Bogard, and R. Goodsell. 2014. "Connected Commercial Vehicles—Integrated Truck Project Model Deployment Operational Analysis Report," U.S. Department of Transportation, Report No. FHWA-JPO-13-111, Washington, D.C.

[6] Harding, J., G. R. Powell, R. Yoon, J. Fikentscher, C. Doyle, D. Sade, M. Lukuc, J. Simons, and J. Wang. 2014. "Vehicle-to-Vehicle Communications: Readiness of V2V Technology for Application," National Highway Traffic Safety Administration, Report No. DOT HS 812 014 Washington, D.C.
[7] DRAFT SAE J2735 DEDICATED SHORT RANGE COMMUNICATIONS (DSRC) MESSAGE SET DICTIONARY, (http://standards.sae.org/j2735_200911/), SAE International, November 19, 2009.

# INTRODUCTION OF A SOLID STATE, NON-INVASIVE HUMAN TOUCH BASED ALCOHOL SENSOR

**Leonard Cech**
**Mallik Nagolu**
**Dennis Rumps**
TK Holdings, Inc.
U.S.

**Ben Ver Steeg**
**Derek Treese**
**Bentley Laaksonen**
**Stephanie Tehseldar**
**Trent Ridder**
TruTouch Technologies, Inc.
U.S.

Paper Number 15-0380

## ABSTRACT

This paper presents an overview of the theory and implementation of a touch-based optical sensor (TruTouch sensor) for monitoring the alcohol concentration in the driver of a vehicle. This novel sensor is intended to improve driver safety by providing a non-intrusive means of notifying a driver when their blood alcohol concentration may be too high to operate a vehicle safely. The optical alcohol detection system has successfully completed several stages of development and validation. A commercially available, industrial version of the system (TruTouch 2500, or Mark 1) has undergone extensive clinical testing and field validation. Under the DADSS (Driver Alcohol Detection System for Safety) Program, a compact semiconductor version (Mark 2) of the optical system has been developed targeting use in consumer vehicles. Based on proven semiconductor laser technologies, the Mark 2 sensor system has demonstrated excellent spectral accuracy and precision and is currently undergoing laboratory validation testing. A demonstration vehicle version of the system has been designed and will be implemented following completion of the laboratory validation testing.

## INTRODUCTION

The negative societal impact of alcohol (ethanol) impaired vehicle driving has been established through numerous clinical studies [1] and confirmed by accident statistics over many years [2]. Currently, the primary means of mitigating alcohol impaired driving is through education and legal enforcement. The percentage of alcohol in the blood circulatory system at any given time can be directly correlated with the neurological sensory, cognitive and reactive performance of the driver. Legal limits for alcohol concentration have been established for drivers of both private and commercial vehicles [3]. Today, the use of alcohol detection technology for driver safety is limited to law enforcement testing (post-accident, during traffic stops / checkpoints) or in the case of previously convicted DUI offenders through the installation of a breath based vehicle interlocks. These systems work well for the purpose of law enforcement but are unsuitable for routine use by consumers. The goal of the current sensor development is to produce a system that is seamlessly integrated into the vehicle's infrastructure, providing consumers with the knowledge of their alcohol concentration without imposing inconvenience to their daily driving experience. In order to accomplish this, a human machine interface (HMI) design has been proposed that incorporates the optical sensor into the vehicle start button. Advances in automotive buttons and touchscreens make it feasible to integrate skin based sensors and achieve appropriate visual, audio, and haptic feedback without compromising function [4]. During routine vehicle operation, the driver's alcohol concentration could be measured and communicated to the driver so that appropriate choices can be made (e.g. delay drive, alternate driver or alternate transportation method). The use of existing vehicle occupancy sensors combined with advanced signal processing supports a simple and practical anti-spoofing method, improving the safety and efficacy of the system.

## SENSOR THEORY OF OPERATION

The TruTouch alcohol measurement technology has been validated using multiple approaches including *in vitro* (test tube) studies of multi-component samples, clinical studies involving alcohol dosing of humans, and real-world measurements by customers in a variety of challenging environments. The validation efforts are exemplified by multiple peer-reviewed journal articles and a strong intellectual property base.

### Scientific Basis of the TruTouch Measurement

The TruTouch technology employs near-infrared (NIR) absorption spectroscopy to measure skin tissue. The NIR spectral region typically spans the portion of the electromagnetic spectrum between the visible, which is generally considered to end at 0.7 µm, and the infrared, which begins at 2.5 µm. However, for measuring alcohol *in vivo* (in human), some portions of the NIR are more advantageous than others. The features most commonly observed in the NIR are overtones and combinations of fundamental vibrations of hydrogen bonded to carbon, nitrogen, and oxygen [5,6,7,8,9].

The absorbance spectrum of alcohol shows features over the NIR region (see figure 1). The 1.25- µm 2.5 µm region contains the 1st overtone and combination bands of the carbon-hydrogen and oxygen-hydrogen bonds. The 0.7-1.25 µm region contains higher order overtones of these bonds. Examination of Figure 1 and its inset shows that the 0.7-1.25 µm region is 400 times weaker than the signal in the longer wavelength, 1.25- 2.5 µm region.

Furthermore, the utility of the visible region (0.3 to 0.7 µm) and the 0.7-1.25 µm part of the NIR are limited by the presence of skin pigmentation (melanin) that creates large differences between people, particularly of different ethnicities. In contrast, the longer wavelength region is virtually unaffected by pigmentation [10]. As a result of the larger signal and absence of pigmentation, the TruTouch technology is designed to measure the longer wavelength (1.25-2.5 µm) region.

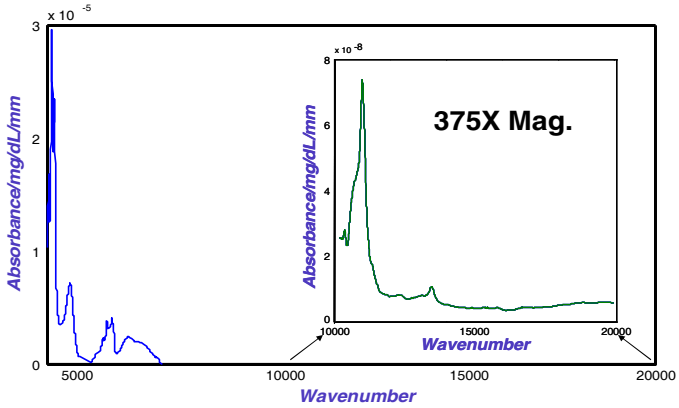


**Figure 1. Absorptivity of alcohol in the NIR and visible.**

In addition to the aforementioned advantages, the NIR spectral region (4000-8000 cm-1 or 1.25-2.5 µm) is of prime interest for non-invasive alcohol measurements because it offers specificity for a number of analytes, including alcohol and other organic molecules present in tissue, while supporting optical path lengths of several millimeters with acceptable absorbance characteristics [11,12,13,14,15]. Comparing NIR spectra (normalized to unit concentration) of alcohol and water collected using a TruTouch system, demonstrates the effect of molecular structure on NIR absorption spectra and indicates spectral regions of separation (see Figure 2a).

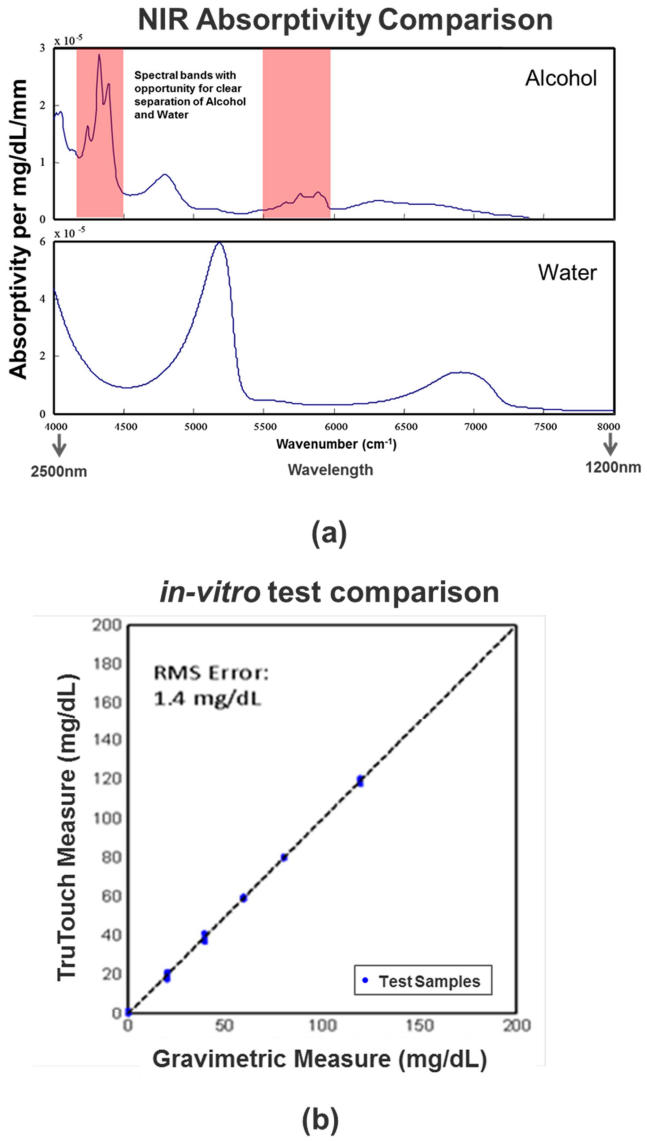


***Figure 2. Comparison of Alcohol, Water in NIR (a);* Ethanol Test Results: 98 *in-vitro* samples *(b).***

TruTouch systems (including Mark 1) are based on a Michelson interferometer Fourier Transform IR (FTIR) instrument that delivers NIR radiation to the skin and underlying tissue and collects the diffusely reflected signal using a fiber-based optical probe. The collected light contains spectral information which allows the determination of the subject's alcohol concentration directly from the measurement. Specific details of the industrial version of the optical alcohol detection system can be found in several issued United States Patents and applications [16,17,18,19,20].

**Laboratory and Clinical Validation**

The objectives of any analytical measurement procedure are high sensitivity and high selectivity for the target analyte (e.g. alcohol concentration). Sensitivity refers to a method's ability to respond to quantity changes in the target analyte, while selectivity is the extent to which a method erroneously responds to changes in interfering analytes (e.g. water, collagen, proteins, and other chemicals present in the body). Ensuring the

selectivity of an analyte measurement can be notoriously challenging in complex systems such as human tissue [21, 22]. Accordingly, careful design and controlled experiments are required to verify the validity of any measurement approach.

Historically, researchers have used *in-vitro* experiments to assess the sensitivity and selectivity of methods for quantifying analytes at physiological concentrations [23,24,25,26,27,28,29]. These experiments are useful diagnostics for the validity of a measurement approach because sample composition and the experimental conditions are controlled by the practitioner; allowing direct assessment of measurement sensitivity and selectivity. For laboratory validation of the alcohol sensor, an optically scattering tissue phantom was developed using 0.3 micron diameter polystyrene microspheres to mimic the optical properties of human skin.

To validate the Mark 1 sensor, a validation study comparing sensor measurements with tissue phantom samples containing gravimetric prepared ethanol, urea, creatinine, albumin, and saline was carried out. The study demonstrates the high degree of accuracy achievable with the touch based sensor (see figure 2b).

### *In Vivo* Clinical Results

In order to demonstrate the accuracy of the sensor with human subjects, controlled clinical trials were conducted on the commercially available version of the system (TruTouch 2500, Mark 1). In these trials, venous blood samples were collected and sent to a certified forensic grade lab for gas chromatography analysis. Comparison data were collected on the TruTouch sensor, evidentiary grade breath sensor, and both compared against the venous blood samples. Alcohol excursions were induced in 108 subjects at Lovelace Scientific Resources (Albuquerque, NM) following overnight fasts. Written consent was obtained from each participant following explanation of the IRB-approved protocols (Quorum Review). Baseline blood and touch NIR alcohol measurements were taken upon arrival in order to verify zero initial alcohol concentration. The alcohol dose for all subjects was ingested orally with a target peak blood alcohol concentration of 120 mg/dL (0.12%). The mass of the alcohol dose was calculated for each subject using an estimate of total body water based upon gender and body mass [29]. The test results (see figure 3), indicate a strong correlation between the touch based sensor and venous blood measurements [30].

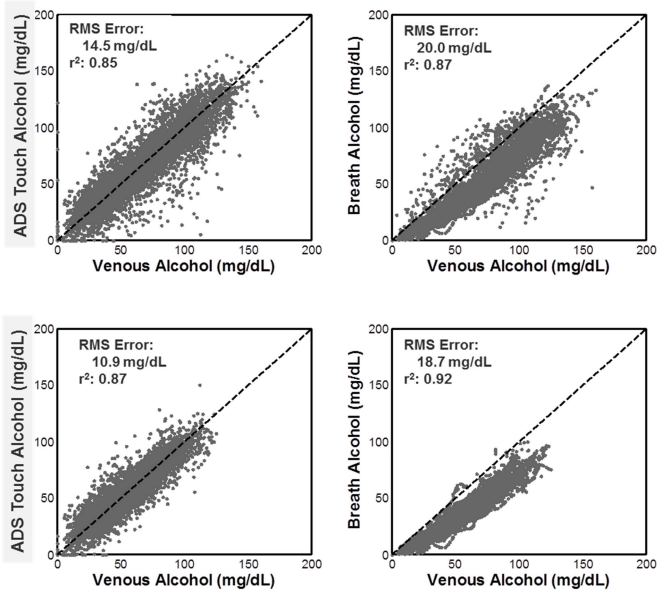


***Figure 3. Human Subject (in-vivo) study results.***

The top two plots compare the TruTouch sensor to venous blood measurements, and an evidential grade breath test to venous blood measurements, respectively. The bottom plots compare data, limited to the "elimination phase" of the alcohol excursion (e.g. after the initial rapid physiological alcohol uptake which is governed by gastric emptying and absorption of the alcohol in the small intestine during and after consumption).

## SOLID STATE TOUCH SENSOR (MARK 2)

The Mark 2 sensor under development for potential application to vehicle operation uses standard automotive electronic design (see figure 4a) and discrete semiconductor lasers to encode the specific spectral information necessary for alcohol measurements.

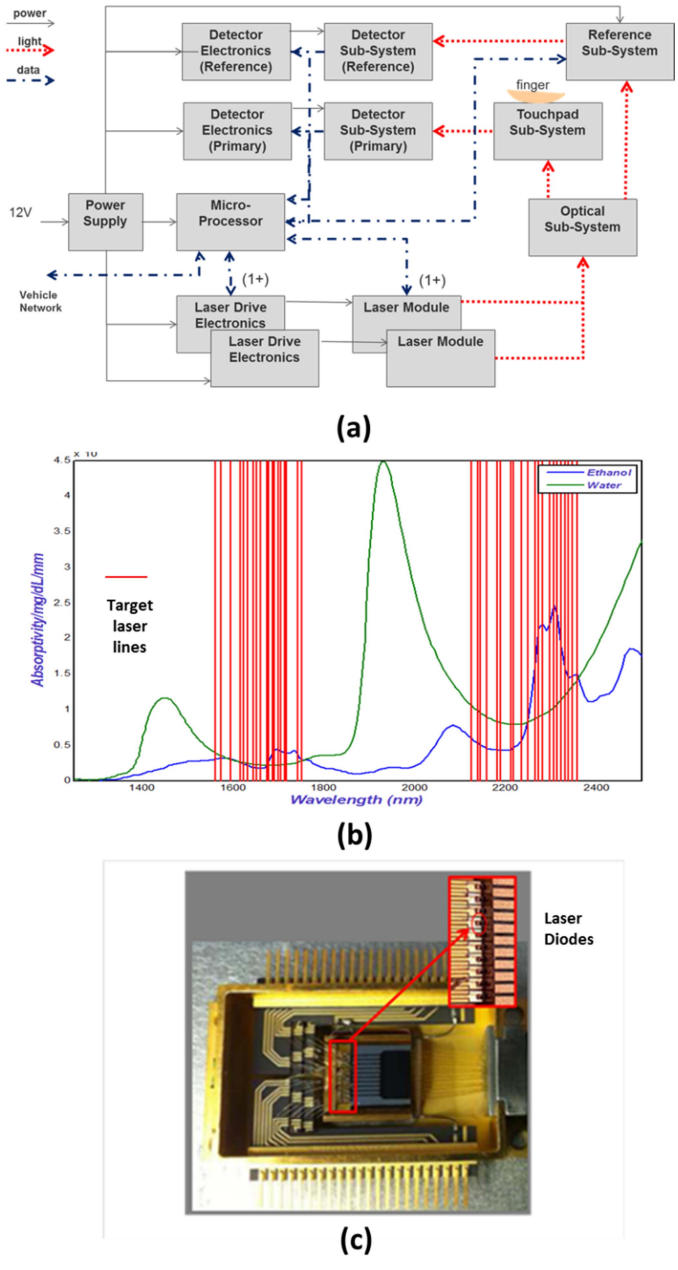


**Figure 4. Solid State Design (a), Laser line targets (b), Prototype Multi laser Module (c).**

In contrast to the Mark 1 sensor, which measures a semi-continuous spectrum, the new design uses discrete, narrow-band spectral lines specifically chosen through analysis of several hundred thousand *in-vivo* alcohol tests. The laser wavelengths are targeted to spectral regions where ethanol and water absorbance levels are separable (see figure 4b), optimizing ethanol detection while avoiding the strong water absorbance features.

The use of multiple discrete lasers to interrogate spectral information allows for a highly integrated, compact optical module. For the Mark 2 design, a custom 12 laser prototype module was developed with individual controllable laser die mounted on ceramic substrates (see figure 4c). The inset detailed view shows the individual laser die mounted on the ceramic substrate. The design is compact, even at the prototype phase, and can be further integrated using packaging techniques developed for laser applications in other industries.

To show the spectral measurement accuracy of the Mark 2 system, several standard benchmark measurements have been performed and compared to both the Mark 1 system and to laboratory grade FTIR spectrometers (see figure 5). Measurements to date indicate good agreement with laboratory grade and Mark 1 system measurements. Additional testing is ongoing and planned including *in-vitro* and *in-vivo* studies similar to those previously described to verify performance that exceeds all previous FTIR systems and approaches performance targets for a vehicle based system.

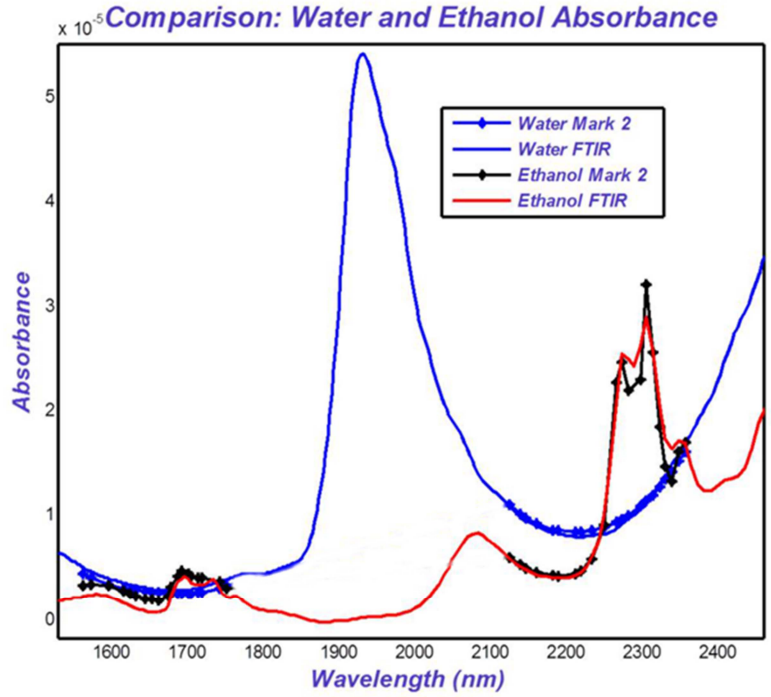


***Figure 5. Mark 2 Measurement performance comparison compared to FTIR.***

## AUTOMOTIVE ADS SYSTEM CONSIDERATIONS

Although significant progress has been made towards establishing the feasibility of a non-invasive touch based alcohol measurement system, continued research and development is necessary to achieve a production automotive system that can meet aggressive targets for performance, measurement time, reliability and robustness. Several key considerations in the touch based design are explored further below.

**Human Machine Interface** A touch based sensor provides a natural opportunity to integrate the sensor touchpad into a standard starter ignition switch. Inclusion of proximity and/or touch sensors in the design supports the ability to enable alcohol measurements only when appropriate. Inclusion of a haptic actuator(s) and/or light(s) provides for natural HMI feedback (see figure 6). For example, light and haptic actuators can be used to provide driver feedback on proper finger placement, measurement initiation, measurement result and other desired HMI feedback.

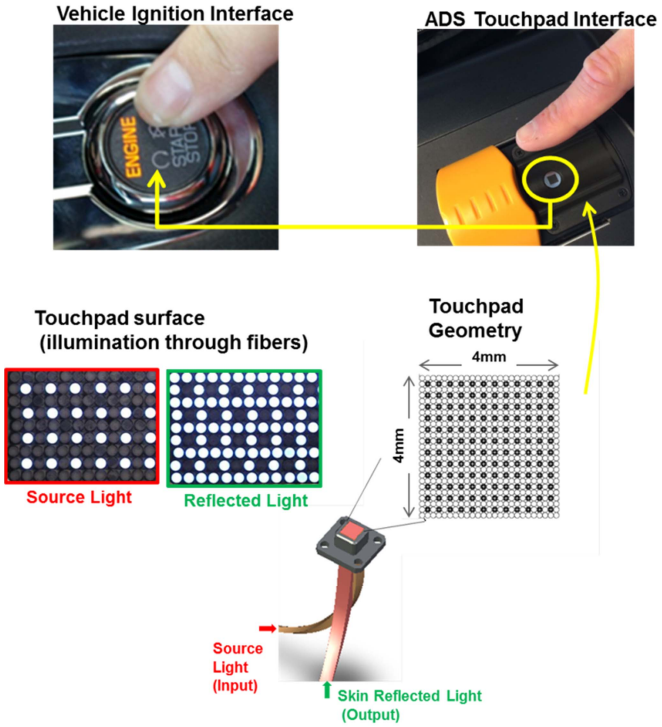


***Figure 6. Prototype alcohol measurement ignition switch integration concept.***

A vehicle ignition system provides one natural touch based measurement location; other viable locations throughout a vehicle exist where a driver/operator skin touch interface might be used for initial or periodic alcohol measurements.

**Anti-Spoofing Concept**

Based on the proposed ignition switch HMI integration, there is the potential for non-impaired occupants to try and test (start the vehicle) on behalf of another person, who intends to drive, but is impaired. To mitigate this situation, a simple anti-spoofing method can be achieved through the integration of an electric field Occupant Classification System (OCS) within the driver seat. Such systems are often used in production vehicles for the front passenger seat to satisfy a regulatory requirement to distinguish child seats from empty or full size human occupants. The information is often used to suppress airbag deployment in the case of child seats or empty seats. Electric field based OCS systems emit a controlled signal in proximity to the seat occupant. This harmless signal is influenced by the seated occupant and is transmitted through anything that the occupant touches. Because the ignition switch is touched by the driver, detection of this OCS signal can be used to distinguish the seated driver from others touching the ignition switch. The alcohol measurement control logic can be configured to require a new ignition touch (measurement) for all driver seat occupancy state changes (e.g. ingress/egress). This anti-spoofing concept could be further enhanced through signal integrity methods currently used in secure, safety automotive systems.

## Environmental, Life and Ruggedness

The Mark 2 design is based on electro-optical components widely used in aerospace, defense, communications and commercial industries requiring high accuracy and precision in a rugged environment and over long operational life. Lasers and detectors of the type utilized have been verified for long term operation through military specification environmental and ruggedness testing [31, 32]. However, the Mark 2 application, introduces new technical and commercial challenges. For example, the measurement touch probe surface must be designed to operate with a wide range of finger surface chemicals and mechanical abuse such as scratching or impact. In addition, the system must be capable of reliable and accurate operation over full vehicle life, despite natural sub-system aging and drift. To mitigate these effects, the Mark 2 design incorporates an absolute chemical reference to allow for variance, bias and drift removal from measurements, over the course of the system life, in addition to providing a method to verify measurement quality and viability. Such techniques are widely used in other safety critical automotive sensors.

## Commercial Challenges

The primary technical limiting factor in the development of the Mark 2 system is the fabrication and manufacturing base immaturity of the laser module and supporting optical interfaces. While advancements in the field of lasers is widespread [33,34], particularly due to new applications and markets evolving quickly, there are currently limited fully developed applications for semi-conductor lasers with the target wavelengths and optical powers targeted for the Mark 2 system.

To date, many of the target high laser wavelengths are only required in small volume specialized applications or in clinical research. On the contrary, many of the lower wavelength lasers required for the Mark 2 design are used in high volume, high reliability, and moderate to low cost packages for high bandwidth telecommunications. Lessons learned in the evolutionary technology and manufacturing growth of laser diodes can help accelerate the maturity and availability of higher wavelength diodes for use in this application. Research and development in non-invasive medical sensing is accelerating, driving new applications and markets; organically increasing manufacturing base and test investment necessary to lead to competition for low cost, high reliability automotive quality laser modules for non-invasive alcohol sensing.

## CONCLUSIONS

Establishing the technical feasibility for a touch based sensor that could be used to accurately and precisely measure blood alcohol concentrations is a key initial step towards providing technical solutions to reduce alcohol impaired driving. The solid state Mark 2 system prototype provides a technically feasible architecture based on initial testing, with concepts to achieve naturalistic HMI and an anti-spoofing method. However, additional testing and design iteration are required towards a system that is capable of meeting automotive requirements.

## ACKNOWLEDGMENTS

The authors would sincerely like to thank the DADSS program (and their sponsors) as well as Lovelace Clinical Research center for their continuing support on this project.

## REFERENCES

[1] Compton and Benning, DOT HS 812 117 Behavioral Safety Research February 2015 “Drug and Alcohol Crash Risk”
[2] DOT HS 812 017 May 2014, “State Alcohol-Impaired-Driving Estimates”
[3] Blood Alcohol Limits Worldwide, http://www.icap.org/Table/BACLimitsWorldwide
[4] SAE# 2014-01-026, April 2014, Lisseman et al. “Touchscreen Concepts Revisited: Approaches and Possibilities”

[5] Wheeler OH (1959). "Near Infrared Spectra of Organic Compounds". Chem. Rev. 59: pp.629-666.
[6] Fletcher AN, Heller CA (1968) ."The Alcohol Self-Association Dimer and the Absorption Band near [7]1.53 µm". Journal of Physical Chemistry 72: pp. 1839-1841.
[8] Iwamoto R, Shigetoshi A, Saito Y, Samura H (2001). "FT-NIR Spectroscopic Study of OH Groups in Ethylene-Vinyl Alcohol Copolymer". Applied Spectroscopy 55(7): pp.864-870.
[9]Alam MK, Callis JB (1994). "Elucidation of Species in Alcohol-Water Mixes Using Near-IR Spectroscopy and Multivariate Statistics". Analytical Chemistry 66(14): pp.2293-2301.
[10] RR Anderson, JA Parrish, "The Optics of Human Skin" The Journal of Investigative Dermatology, Vol. 77, No. 1., pp. 13-19, 1981
[11]Wheeler OH (1959)." Near Infrared Spectra of Organic Compounds". Chem. Rev. 59: pp.629-666.
[12]Fletcher AN, Heller CA (1968) ."The Alcohol Self-Association Dimer and the Absorption Band near 1.53 µm". Journal of Physical Chemistry 72: pp. 1839-1841.
[13]Iwamoto R, Shigetoshi A, Saito Y, Samura H (2001). "FT-NIR Spectroscopic Study of OH Groups" in Ethylene-Vinyl Alcohol Copolymer. Applied Spectroscopy 55(7): pp.864-870.
[14] Alam MK, Callis JB (1994). "Elucidation of Species in Alcohol-Water Mixes Using Near-IR Spectroscopy and Multivariate Statistics". Analytical Chemistry 66(14): pp.2293-2301.
[15] Smith AW, Boord CE (1926). "Infrared Absorption in Ethers, Esters, and Related Substances". J. Am. Chem. Soc. 48: pp.1512-1520.
[16] Abbink, RE et al. (2003). "System for noninvasive measurement of glucose in humans". U.S. Patent#6,574,490.
[17]Messerchmidt RG, Abbink RE (2003)." Interferometer Spectrometer with Reduced Alignment Sensitivity." United States Patent #6,504,614.
[18]T.Ridder, J. Maynard (2003). "Method and apparatus for optical spectroscopy incorporating a vertical cavity surface emitting laser as an interferometer reference," United States Patent #6,654,125.
[19] C. Gardner, T. Ridder, W. Gruner (2004). "Non-invasive determination of direction and rate of change of an analyte," US Patent #7,016,713.
[20] T. Ridder, J. Maynard, et al (2004). "Noninvasive determination of alcohol in tissue," US Patent App. #10/852415.
[21] Brown C, and Ridder T, "A Definition of Multivariate Selectivity: Part 1: Theoretical and Practical Merits", Applied Spectroscopy, 59(6), pp. 787-803, 2005.
[22] Ridder T, and Brown C, "A Definition of Multivariate Selectivity: Part 2: Experimental Applications", Applied Spectroscopy, 59(6), pp. 804-815, 2005.
[22]McShane MJ, Cote G (1998). "Near-Infrared Spectroscopy for Determination of Glucose, Lactate, and Ammonia in Cell Culture Media." Applied Spectroscopy 52(8): pp.1073-1078.
[23]Wabomba MJ, Small GW, Arnold MA (2003). "Evaluation of selectivity and robustness of near-infrared glucose measurements based on short-scan Fourier transform infrared interferograms." Analytica Chimica Acta 490: pp.325-340.
[24]Arnold MA, Small GW, Xiang D, Qui J, Murhammer DW (2004). "Pure Component Selectivity Analysis of Multivariate Calibration Models from Near-Infrared Spectra." Analytical Chemistry 76(9): pp.2583-2590.
[25]Rhiel M, Cohen MB, Murhammer DW, Arnold MA (2002). "Nondestructive Near-Infrared Spectroscopic Measurement of Multiple Analytes in Undiluted Samples of Serum-Based Cell Culture Media." Biotechnology and Bioengineering 77(1): pp.73-82.
[26]Riley MR, Arnold MA, Murhammer DW (2000). "Effect of Sample Complexity on Quantification of Analytes in Aqueous Samples by Near-Infrared Spectroscopy." Applied Spectroscopy 52(2): pp.255-261.
[27]Wehlburg CM, Haaland DM, Melgaard DK, Martin LE (2002). "New Hybrid Algorithm for Maintaining Multivariate Quantitative Calibrations of a Near-Infrared Spectrometer." Applied Spectroscopy 56(5): pp.605-614.
[28]Melgaard DK, Haaland DM, Wehlburg CM (2002). "Concentration Residual Augmented Classical Least Squares (CRACLS): A Multivariate Calibration Method with Advantages over Partial Least Squares." Applied Spectroscopy 56(2): pp.615-624.
[29] B.T. Davies and C.K. Bowen, "Peak Blood Alcohol Prediction: An Empirical Test of Computer Models," Journal of Studies on Alcohol, 61, 187-191 (2000).

[30] Ridder T, Ver Steeg B, Laaksonen B, Radigan W, "Robust Calibration Transfer in Noninvasive Ethanol Measurements, Part II: Modification of Instrument Measurements by Incorporation of Expert Knowledge (MIMIK)," Applied Spectroscopy, 68(8), (2014)
[31] ICSO 2010 Rhodes, Greece, International Conference on Space Optics 4 - 8 October 2010; S. Tornow et Al; "QUALIFICATION OF AN EVALUATED BUTTERFLY-PACKAGED DFB LASER DESIGNED FOR SPACE APPLICATIONS"
[32] Proc. of SPIE Vol. 5465, Reliability of Optical Fiber Components, Devices, Systems, and Networks II, Y. Deshayes et Al; "Estimation of lifetime distributions on 1550 nm DFB laser diodes using Monte-Carlo statistic computations"
[33] V. K. Kononenko; Stepanov Institute of Physics NASB 2010, "History and Developments of Semiconductor Lasers"
[34] http://www.laserfocusworld.com/articles/print/volume-51/issue-01/features/laser-marketplace-2015-lasers-surround-us-in-the-year-of-light.html; "Laser Marketplace 2015: Lasers surround us in the Year of Light"

# INNOVATIVE RESTRAINTS TO PREVENT CHEST INJURIES IN FRONTAL IMPACTS

**Francisco J. Lopez-Valdes**
**Oscar Juste-Lorente**
Institute of Engineering Research (I3A), University of Zaragoza
Spain

Paper Number 15-0381

## ABSTRACT

By 2050, 21% of world population is expected to be older than 60 years. This age shift poses a serious challenge to the protection of car occupants, as fragility and frailty are associated to increasing age. Advanced restraint systems that aim to reduce chest loading by implementing load limiters or inflatable parts have been introduced in the market over the last years. This paper investigates the kinematics and dynamics of two surrogates (THOR dummy, Post Mortem Human Surrogates or PMHS) in 35 km/h impacts under the action of two different restraints: a pretensioning, force-limiting seat belt (PT+FL) and a concept design consisting of two separate shoulder and lap belt bands (split buckle system or SB). Three repeats per condition where done with the THOR dummy, while only one PMHS was tested per restraint system. With respect to the PT+FL, the results from the THOR tests showed that the SB seat belt decreased chest deflection significantly without a substantial increase of the forward displacement of the head. The PT+FL belt allowed the pelvis of the PMHS to move forward preventing the rotation of the torso and therefore reducing the forward excursion of the head. The PMHS test with the SB resulted in improved kinematics compared with the PT+FL. A complete understanding of the kinematics and dynamics induced by these restraints would require additional PMHS tests.

## INTRODUCTION

Life expectancy in Europe rose by eight years between 1960 and 2006 [1]. Additionally, the number of births has declined continuously over the last decades, resulting in an increase of the proportion of elderly people in the European population. While in 2012 about 17% of all Europeans were aged 65 and older, the share of those over age 65 will rise to 28% in 2020 [2]. According to United Nations, the same trend is observed in the whole world although it is particularly important in Eastern Asia (Japan, China, Mongolia), Europe and North America. Interestingly, fast population ageing will take place mainly in the less developed regions. Globally, it is forecasted that world's population age 60 years or over will increase over the following years to reach 21% in 2050 [3].

In 2010, 6,563 elderly people were killed in road traffic accidents in the 24 European Member States for which CARE data is available [4]. This constitutes 21.7% of fatalities of all ages in 2010. What is even more significant is that the the proportion of elderly fatalities has been increasing steadily for the last 10 years. While this increase is undoubtely related to a higher exposure of this age group, it is also true that increased frailty and fragility are associated to aging. Contemporary research has shown that should the injury risk of the elderly was similar to that of a 20-year-old car occupant, some 10,000 lives could be saved in the United States [5]. Therefore, given the existing trend of a growing proportion of elderly road users, it is mandatory to recognize their physiological differences and to incorporate their peculiarities into the design of more effective restraints. A review of AIS3+ injuries within NASS CDS shows that as age increases from 15 to 75+ years old, the incidence of thoracic injuries increases and becomes the most frequent serious injury among car occupants older than 46 years old, and accounting for more than 35% of all AIS3+ injuries in people aged 75 years and above [6]

Force-limiting seatbelts in combination with airbags have been shown to reduce significantly chest loading and consequently chest injuries, without increasing the risk of a head impact [7,8]. The combination of pretensioners and force limiters in rear seat restraints has been also shown to allow greater torso rotation of the occupant without increasing significantly the peak forward excursion of the head and therefore without increasing the risk of head contact [9,10]. In recent years, inflatable seatbelts have been discussed as a countermeasure that can reduce the risk of chest injuries even further by increasing the area of the torso on which the seatbelt force is applied and incorporating a damping effect in addition to the elastic component of conventional belt webbing [11-14]. These innovative restraints have been shown to modify substantially the kinematics of the occupants, challenging existing knowledge about the

optimal seatbelt geometry and position of belt anchorages [14]. With the continuous improvement of finite element human body models (HBM), parametric analyses constitute an effective methodology to optimize the design of innovative restraint systems. Real testing with Anthropomorphic Test Devices (ATD) also allows to confirm that existing testing tools are sensitive to newly designed restraint systems. However, it is also necessary that both surrogates (HBM and ATD) are able to capture the effects of these restraints on real human subjects. Thus, Post Mortem Human Surrogate (PMHS) testing is advisable to acquire a more accurate picture of the potential benefit that these system can bring to elderly car occupants.

The present study discusses the performance of the THOR ATD and the mechanical response of two PMHS exposed to a frontal impact and restrained by two different seatbelt solutions. The kinematics and dynamics of both surrogates will be compared with the goal of assessing if a new seatbelt concept is capable of reducing chest deflection without increasing other important performance indices.

## METHODS

Eight sled tests in matching conditions were performed at the crash test facility of the Institute of Enginering Research (I3A) of the University of Zaragoza. Two Post Mortem Human Surrogates (PMHS) were exposed to a 35 km/h (nominally) frontal impact, using two different restraints. Then, the THOR dummy was exposed to nominally the same test conditions and using the same two types of restraints than in the PMHS tests. Three repeats were done per restraint type with the THOR dummy. The test matrix is shown in Table 1. The time history of sled deceleration is included in Figure A1 and Figure A2 in the Appendix.

**Table1.**
**Test matrix.**

| Occupant type | # runs | Restraint | Impact speed (km/h) |
|---|---|---|---|
| PMHS | 1 | SB | 37.7 |
| PMHS | 1 | PT+FL | 34.6 |
| THOR | 3 | SB | 34.8±0.2 |
| THOR | 3 | PT+FL | 34.7±0.0 |

### Test setup

The test fixture consisted of a rigid metallic frame allowing complete visual access to the occupant while preserving the basic geometry of a standard seating position of a passenger car. This test fixture has been used elsewhere as a reasonable approximation to the passenger posture in the study of ATD biofidelity and in the development of thoracic injury criteria [15,16]. The seat consisted of a flat steel plate with two pelvic supports at the rear. Forward motion of the occupant was restrained by two different seat belts: a retractor pretensioned (2 kN), force-limiting (4 kN) belt (PT+FL) and an innovative belt consisting on two independent shoulder and lap bands (SB). The SB shoulder belt band was retractor pretensioned (3 kN) and the lap belt band was pretensioned at 3.5 kN bilaterally. The position of the buckle of the lower shoulder belt band was forward of that of the inner buckle of the lap belt with the goal of unloading the lower part of the rib cage. As for the position of the D-ring, it was modified accordingly to the specific dimensions and anthropometry of the different surrogates to ensure that the upper shoulder belt angle measured between the shoulder of the occupant and the D-ring was the same. Belt tension was measured at several locations both on the shoulder and on the lap seat belts for each system. Sensor data in the ATD and PMHS tests were captured at 10,000 Hz with an external data acquisition system (PCI-6254, National Instruments; Austin, TX). The kinematics of the surrogates were recorded by a lateral and a frontal high-speed imager at 1,000 Hz.

### THOR tests

The THOR ATD used in this study is the THOR-NT upgraded within the THORAX project (European 7th Framework Program) to improve biofidelity and injury assessment capabilities [17,18]. This THORAX THOR (further denoted as simply THOR) is similar to the U.S version THOR Mod Kit with SD3 shoulder.

ATD head was instrumented with a 6-degree-of-freedom (DOF) cube including three linear accelerometers and three angular rate sensors (ARS) oriented in perpendicular directions acoording to SAE J211 recommendations. Two 6-axis load cells were present at the upper and lower neck locations. Chest instrumentation included four 3D IR-TRACCs (Infra-Red Telescoping Rod for the Assessment of Chest Compression) and 72 strain gauges distributed from rib 2 to rib 7 bilaterally (equally spaced along the rib). The dummy was equipped with a 96-channel digital on-board data acquisition system to supplement the external one.

A high-speed motion capture system consisting of 10 cameras was used to track the position of retroreflective spherical markers within a calibrated 3D volumen at 1,000 Hz (Vicon, TS series, Oxford, UK). A calibration procedure, performed prior to testing, established the position and orientation of each camera in a reference coordinate system at a laboratory fix location. A local coordinate system moving with the test buck was defined so that the relative motion between the occupant and the buck could be resolved. The local X axis pointed forward in the direction of the sled motion and the local Z axis pointed upwards. Displacements were calculated with respect to the local coordinate system. Reflective markers were attached to several relevant anatomical locations in the dummy, although only the head ones (attached bilaterally and over the line passing through the center of gravity of the head) were used in this study.

**PMHS tests**

The two PMHS tests used in this study as comparison with the THOR dummy were carried out within the 7th Framework Program Marie Curie Action BIO-ADVANCE [19]. The procurement and handling of PMHS were done according to the internal procedures of the laboratory of the I3A (University of Zaragoza). These procedures were reviewed and approved by the laboratory Oversight Committee and by the Ethical Commission for Clinical Trials of Aragon (CEICA), which is the officially appointed regional committee that supervises the ethics of all clinical trials performed within the region. CEICA is totally independent from the University of Zaragoza and reports directly to the Health Commissioner of the Regional Government.

Triaxial accelerometers were rigidly attached to the head, T1, T8, L2 and the pelvis. ARS were added to the head and T1. Linear acceleration was measured at the location of the sternum body. Photo targets were used to identify relevant landmarks, including the location of the external auditory meatus bilaterally. These photo targets were used to track the displacement of the center of gravity of the head in the sagittal plane.

**RESULTS**

**Upper shoulder belt force**

Figure 1 shows the time history plot of the belt tension measured at the upper shoulder belt location in the THOR sled tests. Red solid lines correspond to the SB seatbelt while blue solid lines are the forces measured in the PT+FL belt tests. Apart from the greater pretensioner force of the SB seatbelt, two out of the three tests with the SB seatbelt resulted in a higher peak force than in the case of the PT+FL seatbelt (PT+FL: 5465.7 ± 212.7 N; SB: 6124.7 ± 706.6 N). Figure 1 also shows that the SB seatbelt induced a bimodal force curve on the ATD with the first and higher peak ocurring at around 100 ms followed by a smaller peak at approximately 135 ms. The second maximum observed when the SB seatbelt was used contributed to the longer interaction between the occupant and the restraint: while the magnitudes of the force-time traces of the PT+FL seat belt are almost negligible at t=120 ms, the curves corresponding to the SB seatbelt indicate that the occupant was still being restrained by the seatbelt up to t=150 ms.

The time traces in Figure 2 show the time history of the upper shoulder belt forces in the PMHS tests. The peak force sustained by the occupant when the SB seat belt was used was higher than in the case of the PT+FL seat belt (6109.7 N vs. 4133.51 N). the longer interaction of the occupant with the restraint that was observed with THOR is also present in the PMHS tests, although there is no secondary peak in this case.

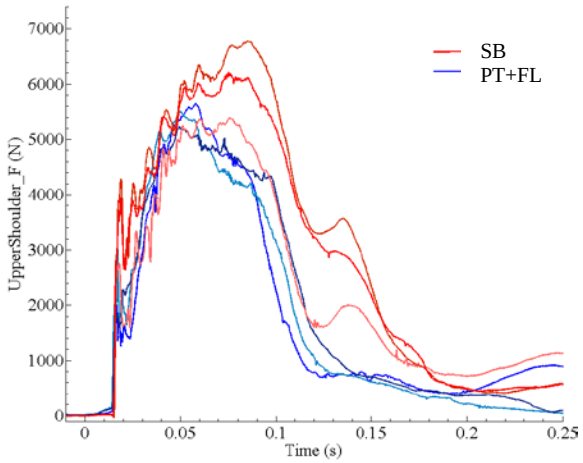


***Figure 1 Time history of the upper shoulder belt force measured in the dummy tests***

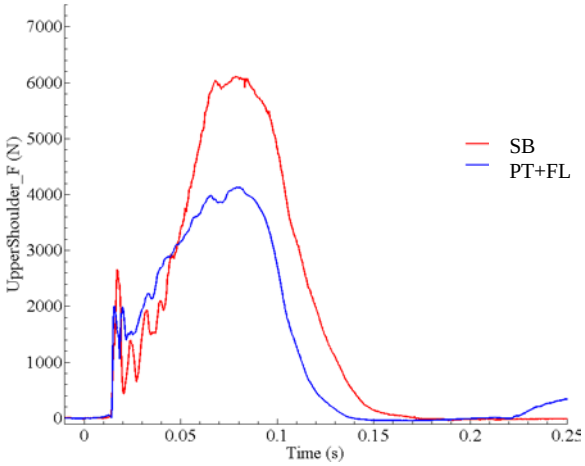


***Figure 2. Time history of the upper shoulder belt force estimated in the PMHS tests.***

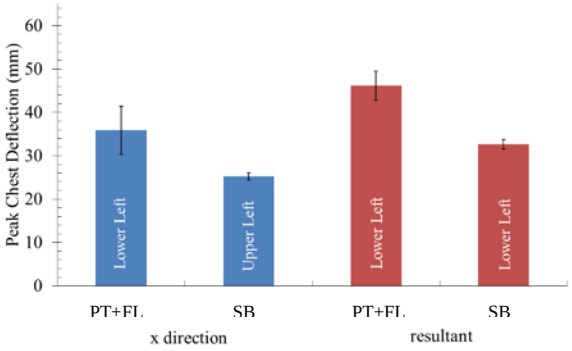


***Figure 3 THOR peak chest deflection in mm in the local x-direction (blue bars) and resultant (red bars) as measured by the IRTRACCs, with error bars corresponding to the standard deviation. Labels within the bars indicate the IRTRACC sensor recording the peak deflection.***

**THOR chest deflection**

The peak chest deflection in the local x-direction (initially aligned with the motion of the sled, but moving with the ATD torso) was measured at the lower left IRTRACC when the PT+FL seatbelt was used while it ocurred at the location of the upper left IRTRACC with the SB due to the higher forces applied to the shoulder of the occupant. In addition, the peak deflection was greater with the PT+FL seatbelt (35.9 ± 5.6 mm vs. 25.2 ± 0.8 mm). When the three components of the deflection were combined into the calculation of the peak resultant deflection, still the PT+FL seatbelt resulted in a greater magnitude (46.2 ± 3.4 mm vs. 32.7 ± 1.1 mm). However, the resultant peak deflection was measured at the lower left chest location regardless of the restraint used.

**Head displacement in the sagittal plane**

The displacement in the sagittal plane of the center of gravity of the head of THOR and the PMHS is shown in Figure 4 and Figure 5. Blue solid lines correspond to the PT+FL seatbelt and red solid lines to the SB seatbelt.

Peak forward displacements of the head center of gravity of THOR were not significantly different for the two restraints under analysis (PT+FL: 390.7 ± 11.1 mm; SB: 406.4 ± 6.7 mm). Figure 4 illustrates that the nature of the trajectory of the head center of gravity was similar under the action of the two different restraints. Other than slight differences in magnitude, it is not possible to identify different trends or behaviors. Regardless of the restraint, the head center of gravity moved straight forward and slightly downwards up to t=50 ms and then it started to describe a curvilinear trajectory.

As the statures of the two PMHS were different, trajectories were length-scaled to those of a 50$^{th}$ male percentile (nominally, 175 cm). Figure 5 shows the comparison of the scaled trajectories followed by the center of gravity of the PMHS head depending on the seatbelt used. The use of the SB resulted in a greater forward excursion (306.1 mm vs. 188.8 mm). The maximum vertical excursion of the two seatbelts were not substantially different. The shape of the trajectories differed importantly. While the use of the SB seatbelt resulted into an initial forward displacement of the center of gravity of the head that occurred parallel to the local X axis for about 70 ms, the use of the PT+FL seatbelt caused the PMHS head to describe a curvilinear trajectory from the first instants of the deceleration. The analysis of the high-speed video images indicated that while the SB seatbelt allowed the spine of the dummy to pitch forward and rotate, the PT+FL seatbelt impeded the flexion of the PMHS spine resulting into the curvilinear motion of the head center of gravity in which the lower neck acted as fulcrum of the rotation. There are two reasons that contribute to the differences observed in the kinematics of the spine of the PMHS. The first one is that the higher lap belt forces of the SB seatbelt facilitated that the pelvis of the PMHS almost did not move forward during the impact, while the pelvis of the PMHS that was restrained with the PT+FL slid during the deceleration over the flat surface of the seat. The forward pelvic motion caused the occupant to adopt a slouched position and prevented the torso from pitching forward as it would have been desirable. The second reason is that the analyses of the lower shoulder belt forces show that even if the peak force is much higher when the SB seatbelt was used (4729.0 N vs. 3461. 6 N, see Table 2), the PT+FL lower shoulder belt force was higher up to t=70 ms and therefore the torso of the occupant was subjected to a higher force that could have impeded the rotation during the first stages of the deceleration. In fact it is around t=70 ms that the torso of the PMHS restrained with the SB belt stopped its rotation and the head started to describe a curvilinear trajectory.

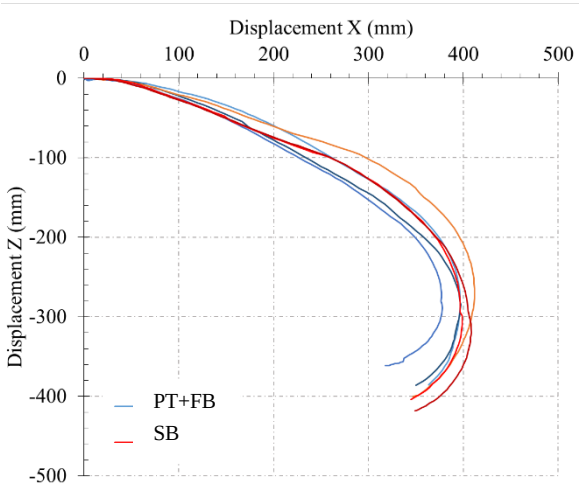


***Figure 4 Displacement of the center of gravity of THOR head in the sagittal plane.***

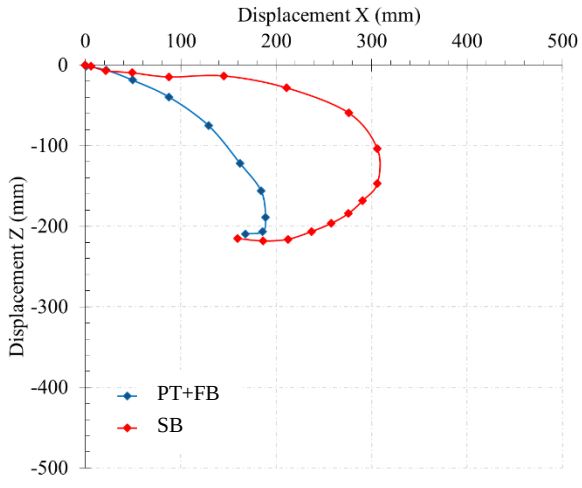


***Figure 5 Displacement of the center of gravity of the PMHS head in the sagittal plane. Trajectories are scaled to represent a 50$^{th}$ male percentile.***

## DISCUSSION

The concept design of the split buckle restraint system (SB) intended to increase the loading on anatomical parts that are potentially more likely to bear higher loads (i.e. clavicle, pelvis) so that the amount of restraint loading on the chest could be lowered without modifying significantly the forward displacement of the head. The assessment of the system was done using two different occupant surrogates: the THOR dummy and PMHS in sled frontal impacts with a delta-v = 35 km/h (nominally). A pretensioned, force limiting seatbelt (PT+FL) was

used as reference for the assessment. The data generated in these tests can be used to benchmark numerical models, so that parametric studies can be done to find the optimal geometry of the split buckle seat belt [20].

The tests with the THOR dummy showed that the use of the SB belt system resulted into slightly higher upper shoulder belt forces, considerably higher lower shoulder forces and higher bilateral lap belt forces as well. However, resultant chest deflection and local x-axis chest deflection as measured by the IRTRACCs of the dummy were reduced for all measurement locations with the exception of the upper left IRTRACC, in which the magnitudes were not significantly different. Comparable results regarding belt forces were observed also in the PMHS tests, confirming the predictions given by THOR. Despite the associated higher SB shoulder belt, the duration of the engagement between belt and occupant was longer than in the PT+FL case, which resulted in smaller sternal deceleration of the occupant (see Table 2).

As for the displacement of the head in the sagittal plane, Figure 4 illustrates that THOR did not capture significant differences in nature between the two belt systems. In addition, the peak forward displacement of the center of gravity was similar regardless of the belt used (PT+FL: 390.7±11.1 mm vs. SB: 406.4±6.7 mm). The tests with the PMHS showed very different results in this case. While the SB system resulted in a trajectory in which the head moved forward first parallel to the local X axis and then underwent a curvilinear translation, when the PT+FL system was used, there was almost no forward motion of the torso of the PMHS resulting into a curvilinear translation of the head from the beginning of the deceleration. Consequently, the magnitude of the peak forward displacement of the head was smaller in this case (PT+FL: 188.8 mm vs. SB: 306.1 mm). However, the analysis of the high-speed video images showed that while the SB lap belt prevented the forward displacement of the PMHS pelvis, the PT+FL belt allowed the pelvis of the occupant to move forward. The forward motion of the pelvis associated to the lack of torso pitch are indicative of poor occupant kinematics that could result in submarining. Of course, the flat design of the seat is playing an important role in the deficient control of the motion of the pelvis as indicated in previous work using the same test fixture [21]. These differences in the kinematics of the pelvis and the torso were not observed in the sled tests with the THOR dummy. Even if the pelvis of the dummy moves forward during the initial instants of the deceleration until it is arrested by the lap belt, the torso of the dummy rotates up to the moment of maximum shoulder belt tension in which the head starts to undergo flexion. Regardless of the seatbelt used, the analysis of the kinematics of THOR does not indicate that submarining occurred in the tests.

The test fixture, except for the restraint type used, is a replica of that used in previous studies aiming to assess the biofidelity of THOR and to develop a new chest injury criterion for this ATD [22]. In the present study, the knee bolster used in [22] was removed. The only other set of PMHS and dummy tests that were run with this fixture without knee bolster compared the kinematics of the Hybrid with the kinematics of PMHS in frontal impacts conducted at 9 km/h [23]. In this case, non-pretensioned, non force-limiting seat belts were used. Recorded peak upper shoulder belt forces were in the range between 1000 kN and 1250 kN, and peak forward head displacement of the three tested PMHS ranged between 280 and 310 mm. Two remarks are relevant from this study. First, the nature of the motion of the head was similar to that observed in the present study for the SB seat belt: an initial trajectory parallel to the sled X-axis followed by a curvilinear trajectory once the upper shoulder force peaked. Secondly, while THOR predicted greater forward head excursion compared to the PMHS, the Hybrid III (178±2 mm) fell short to predict the displacement of the PMHS heads.

The magnitude of the upper and lower neck reactions (forces and moments) in THOR were similar regardless of the seat belt system used in the test. Measured values were considerably smaller than those proposed in existing IARV (Mx=143 Nm; My=190 Nm; Mz=96 Nm; Fz=4 kN; Fx=Fy=3.1 kN) [24]. Neck reaction forces were not calculated for the PMHS, but the comparison of the values measured for the acceleration and angular rate of the head indicated that the SB belt induced higher linear acceleration than the PT+FL seat belt, and consequently the upper neck loads would have been slightly greater.

**Table 2.**
**Peak value comparison of selected parameters between the PT+FL and the SB belt.**

| | PT+FL | | SB | |
|---|---|---|---|---|
| | **THOR test*** | **PMHS test** | **THOR test*** | **PMHS test** |
| Head acceleration** (g) | | | | |
| x | -19.8±2.8 | 10.4 | -22.7±1.4 | 28.5 |
| y | 3.9±1.0 | 29.8 | 2.3±0.5 | -58.1 |
| z | 32.9±2.0 | 33.5 | 38.4±7.0 | 50.7 |
| Head angular rate (deg/s) | | | | |
| x | -767.1±22.8 | -2170.0 | -635.4±99.5 | 2078.1 |
| y | -1798.9±92.0 | 579.8 | -2079.6±149.8 | 419.8 |
| z | -681.5±18.1 | 300.4 | -639.5±110.7 | 1001.0 |
| Upper neck | | | | |
| Fx (kN) | 1.2±0.4 | - | 1.1±0.0 | - |
| Fy (kN) | 0.2±0.0 | - | 0.2±0.1 | - |
| Fz (kN) | 1.4±0.1 | - | 1.8±0.1 | - |
| Mx (Nm) | -21.7±3.1 | - | -19.0±96.8 | - |
| My (Nm) | 22.0±0.2 | - | 21.6±2.1 | - |
| Mz (Nm) | -5.4±0.6 | - | 2.9±1.3 | - |
| Lower neck | | | | |
| Fx (kN) | 0.6±0.2 | - | 0.5±0.1 | - |
| Fy (kN) | 0.5±0.3 | - | 0.2±0.1 | - |
| Fz (kN) | -1.2±0.2 | - | -1.6±0.1 | - |
| Mx (Nm) | 55.0±8.0 | - | 58.8±5.2 | - |
| My (Nm) | 23.8±8.3 | - | 25.5±0.8 | - |
| Mz (Nm) | -18.4±4.1 | - | -19.1±4.3 | - |
| Chest acceleration (g) | - | -143.0 | - | -106.1 |
| Pelvis acceleration (g) | | | | |
| x | -11.3±0.6 | -38.7 | -15.5±0.9 | -59.4 |
| y | -9.3±4.5 | -36.4 | -8.6±4.1 | 27.7 |
| z | -18.3±1.7 | -25.7 | -19.0±2.1 | -22.6 |
| Head maximum forward displacement (mm) | 390.7 ± 11.1 | 188.8 | 406.4 ± 6.7 | 306.1 |
| IRTRACC (Resultant, mm) | | | | |
| Upper Left | 31.8±1.5 | - | 32.1±0.8 | - |
| Lower Left | 46.2±3.4 | - | 32.4±1.0 | - |
| Upper Right | 31.7±2.9 | - | 31.8±1.4 | - |
| Lower Right | 26.6±2.9 | - | 21.4±1.0 | - |
| IRTRACC (x direction, mm) | | | | |
| Upper Left | 24.2±0.5 | - | 25.1±0.9 | - |
| Lower Left | 35.9±5.6 | - | 24.5±1.8 | - |
| Upper Right | 17.0±14.3 | - | 8.0±0.9 | - |
| Lower Right | 18.1±8.0 | - | 12.3±0.2 | - |
| Upper shoulder belt force (N) | 5465.7 ± 212.7 | 4133.5 | 6124.7 ± 706.6 | 6109.7 |
| Lower shoulder belt force (N) | 3998.5±156.0 | 3461.6 | 5055.5±575.7 | 4729.0 |
| Right lap belt force (N) | 2001.8±20.6 | 1634.5 | 3133.3±48.0 | 2053.5 |
| Left lap belt force (N) | 2059.3±542.6 | 3324.7 | 2971.9±22.6 | 7367.7 |

* Values for THOR shown as average ± standard deviation.

** Magnitude measured with respect to a local coordinate system with origin in the head attachment plate, not transferred to the head center of gravity.

**Limitations**

Even if the test fixture has been utilized before in the assessment of the biofidelity of ATD and in the development of thoracic ATD injury criteria, it is questionable its utility in the assessment of restraint systems. The simple geometry and the completely rigid structure of the seat facilitated the forward motion of the pelvis of the PMHS restrained with the PT+FL and the subsequent differences in torso pitch with respect to the other seatbelt solution. A regular production seat would have reduced the forward motion of the pelvis and contributed to increase the forward rotation of the torso.

Some channels of the external data acquisition system malfunctioned during the THOR tests. In particular, the upper shoulder belt load cell did not measure correctly the tension of the belt. To overcome this issue, a methodology was developed so that the magnitude of the belt tension at the upper shoulder location could be estimated using the measurement from the lower shoulder belt. The methodology is explained within the Appendix, and it was built using previously sled tests ran with both restraint systems. The correlation factor of the relationship found between the upper and lower belt tension magnitudes were $R^2$= 0.98 (PT+FL) and $R^2$= 0.99 (SB).

One additional limitation is the magnitude variability observed in the deceleration pulse between the two PMHS experiments that reached almost 4g at its peak difference. Although this difference would have hindered a detailed quantitative comparison between the performance of the two systems, the differences in the nature of the kinematics suggest that these differences were not related to just a change in the magnitude of the mechanical insult but to the way in which the restraints interacted with the PMHS. Interestingly, these differences were not observed when the surrogate chosen was THOR.

## CONCLUSIONS

The present study compares the kinematics and dynamics of the THOR dummy and two PMHS in frontal impacts at 35 km/h using two different seat belts. One belt was a pretensioned force-limiting seatbelt that was used to benchmark a new concept consisting of two separate shoulder and lap bands, equipped with pretensioners at the shoulder belt retractor and at both lap belt anchorages. The aim of the SB model was to increase the load on the clavicle and pelvis to unload the chest region, without increasing significantly the forward displacement of the head comparing to the benchmark. The sled tests performed with THOR confirmed the intended performance of the concept belt and the chest deflection measured by the IRTRACC was substantially lower in comparison with the PT+FL seatbelt. The two PMHS exhibited very different kinematics depending on the seatbelt used. While the PT+FL seatbelt allowed the pelvis to move forward, reducing torso pitch and therefore inducing a curvilinear motion of the head, the SB allowed substantial torso pitch resulting on increased forward excursion of the head that moved initially in a rectilinear fashion undergoing a curvilinear trajectory only once the torso motion was completely arrested. Given the limited number of PMHS tests, it is not possible to conclude if the particularities of the individual PMHS were the cause of the differences or if THOR failed to capture the kinematics of an actual subject under the action of these seat belts.

## ACKNOWLEDGEMENTS

Autoliv Research collaborated in this study providing access to the THOR dummy and the restraint systems. It was partially funded by the Instituto Aragones de Fomento of Gobierno de Aragon via the "Collaborative agreement to foster research on impact biomechanics", signed on Feb 11th, 2015. The PMHS tests were performed within the BIO-ADVANCE project (Marie Curie Actions, FP7/2007-2013, REA grant agreement no. 299298). More information about this project and its goals can be found in [19]. The analyses presented here were not generated during the project and do not represent necessarily the position of the researchers involved in BIO-ADVANCE. This study shows solely the interpretation of the authors and is not necessarily the view of Autoliv Research or the Instituto Aragones de Fomento.

## REFERENCES

[1] European Commission. Commission Communication - The demographic future of Europe – From challenge to opportunity (2006)

[2] EuroStat. Fertility rates - Statistics explained (2013): http://epp.eurostat.ec.europa.eu/statistics_explained/index.php/Fertility_statistics#Publications. Last accessed: 01/02/2014.
[3] United Nations, Department of Economic and Social Affairs, Population Division (2013). World Population Ageing 2013. ST/ESA/SER.A/348
[4] European Road Safety Observatory (ERSO) Website, Factsheet the Elderly (> 64 years) Traffic Safety Basic Facts 2012, DACOTA Project.
[5] Kent R, Trowbridge M, Lopez-Valdes FJ et al. How many people are injured and killed as a result of aging? Frailty, fragility, and the elderly risk-exposure tradeoff assessed via a risk saturation model. Annals of Advances in Automotive Medicine, 2009. Vol. 53, 40-50.
[6] Scarboro M. Real World Older Occupant Injury. SAE Government / Industry meeting. January 2014. Washington DC, USA. Available at : http://www.nhtsa.gov/Research/Public+Meetings/SAE+2014+Government+Industry+Meeting.
[7] Kent R, Crandall JR, Bolton J, Prasad P, Nusholtz G, Mertz H. The influence of superficial soft tissues and restraint conditions on thoracic skeletal injury prediction. Stapp Car Crash J. 2001;45:183–204.
[8] Walz M. NCAP test improvements with pretensioners and load limiters. Traffic Inj Prev. 2004;5:18–25.
[9] Forman JL, Michaelson J, Kent R, Kuppa A, Bostrom O. Occupant restraint in the rear seat: ATD responses to standard and pre-tensioning, force-limiting belt restraints. AnnAdvAutomotMed. 2008;52:141–154.
[10] Forman JL, Lopez-Valdes F, Lessley D, et al. Rear seat occupant safety: an investigation of a progressive force-limiting, pretensioning 3-point belt system using adult PMHS in frontal sled tests. Stapp Car Crash J. 2009;53:49–74.
[11] Forman JL, Lopez-Valdes F, Dennis N, Kent R, Tanji H, Higuchi K. An inflatable belt system in the rear seat occupant environment: investigating feasibility and benefit in frontal impact sled tests with a 50th percentile male ATD. Ann Adv Automot Med. 2010;54:111–126.
[12] Kent R, Lopez-Valdes FJ, Dennis NJ, et al. Assessment of a three-point restraint system with a pre-tensioned lap belt and an inflatable, force limited shoulder belt. Stapp Car Crash J. 2011;55:141–159.
[13] Sundararajan S,Rouhana SW, Board D, et al. Biomechanical assessment of a rear-seat inflatable seatbelt in frontal impacts. Stapp Car Crash J. 2011;55:161–197.
[14] F. J. Lopez-Valdes, O. Juste, B. Pipkorn, I. Garcia-Muñoz, C. Sunnevång, M. Dahlgren & J. J. Alba (2014) A Comparison of the Performance of Two Advanced Restraint Systems in Frontal Impacts, Traffic Injury Prevention, 15:sup1, S119-S125, DOI: 10.1080/15389588.2014.936410
[15] Lopez-Valdes FJ, Lau A, Lamp J, et al. Analysis of spinal motion and loads during frontal impacts. Comparison between PMHS and ATD. Ann Adv Automot Med. 2010;54:61–78.
[16] Shaw G, Parent D, Purtsezov S, et al. Impact response of restrained PMHS in frontal sled tests: skeletal deformation patterns under seat belt loading. Stapp Car Crash J. 2009;53:1–48.
[17] Hynd D, Carroll J, Davidsson J, Vezin P. Biofidelity Requirements for the THORAX Project. THORAX D2.1 European Commission DG RTD 7th Framework Program.
[18] Lemmen P, Been B, Carroll J, et al. An advanced thorax–shoulder design for the THOR dummy. In: Proceedings of the 23rd ESV Conference, Seoul, Korea, 2013.
[19] BIO-ADVANCE (Advancing traffic safety through the investigation of human tolerance to impact). Marie Curie Actions. Final Report. Project No. 299298. 2014. European Commission.
[20] Pipkorn B, Lopez-Valdes FJ, Lundgren C, Brase D, Sunnevang C. Advanced seat belt system for reduced chest deflection. Paper No. 15-0371. 24th International Technical Conference on the Enhanced Safety of Vehicles (ESV). Gothenburg, Sweden, June 8-11, 2015
[21] Lopez-Valdes FJ, Juste Lorente, O, Pipkorn B, Garcia I, Sunnevang C, Dahlgren M, Alba J. (2014) A comparison of the performance of two advanced restraint systems in frontal impacts. Traffic Injury Prevention. Volume 15, Supplement 1, 2014: S119-S125.
[22] Shaw G, Parent D, Purtsezov S, Lessley D, Crandall J, Kent R, Guillemot H, Ridella S, Takhounts E, Martin P. Impact Response of Restrained PMHS in Frontal Sled Tests: Skeletal Deformation Patterns Under Seat Belt Loading. Stapp Car Crash Journal.Vol. 53, pp 1-48, 2009.
[23] Lopez-Valdes FJ, Lau A, Lamp J, Riley P, Lessley DJ, Damon A, Kindig M, Kent R, Balasubramanian S, Seacrist T, Maltese M, Arbogast K, Higuchi K, Tanji S (2010). Analysis of spinal motion during frontal impacts. Comparison between PMHS and ATD. Ann Adv Automot Med. 2010;54:61-78.
[24] Mertz HJ, Irwin AL, Prasad P. Biomechanical and scaling bases for frontal and side impact injury assessment reference values. Stapp Car Crash Journal, Vol. 47 (October 2003), pp. 155-188.

## APPENDIX

### Sled deceleration

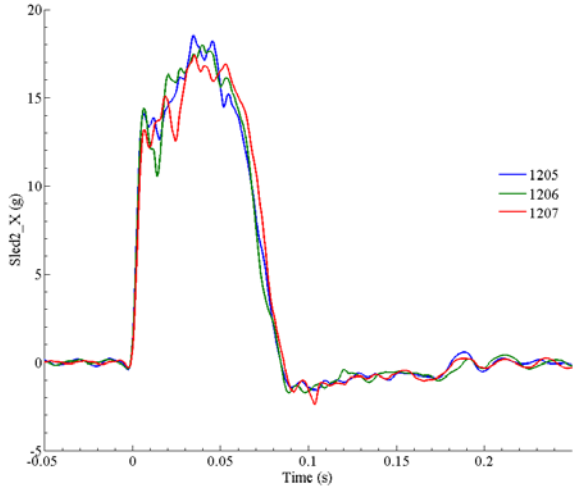


*Figure A1. Time history of the deceleration of the sled. THOR tests.*

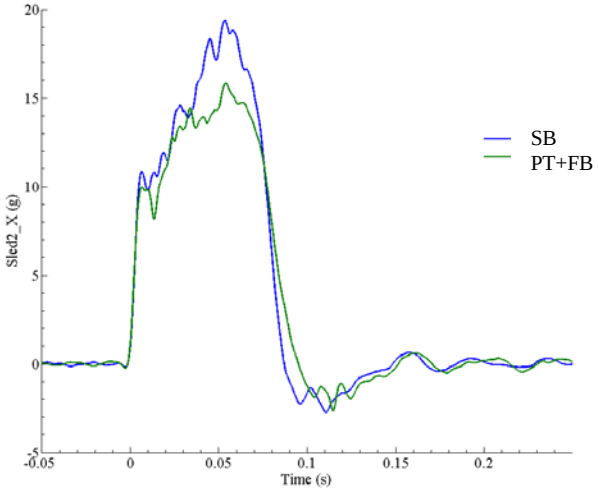


*Figure A2. Time history of the deceleration of the sled. PMHS test.*

### Estimation of upper shoulder belt forces (THOR tests)

The channel associated to the measurement of the tension at the upper shoulder belt location failed during the THOR tests. The input voltage fluctuated during the tests and, consequently, the measure of belt force was erroneous. To provide a reasoned estimation of the tension of the belt at this location, previous sled tests performed using the same deceleration pulse and the THOR dummy were used to find a correlation between the tension of the shoulder belt at the upper (close to the clavicle) and lower locations (close to the abdomen). It was found that a linear relationship could be established between these two measurements and therefore, the upper shoulder force could be estimated based on the measurement obtained at the lower location. The correlation factors obtained in the estimation of the upper shoulder belt force were $R^2$= 0.98 (FL+PT belt) and $R^2$=0.99 (SB belt) (see Figures A3 and A4).

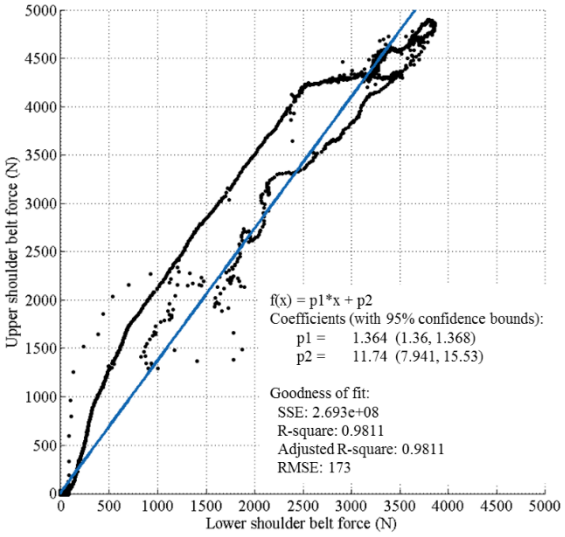


*Figure A3. Linear relationship (blue solid line) existing between the shoulder belt forces measured at the upper and lower locations. FL+PT belt.*

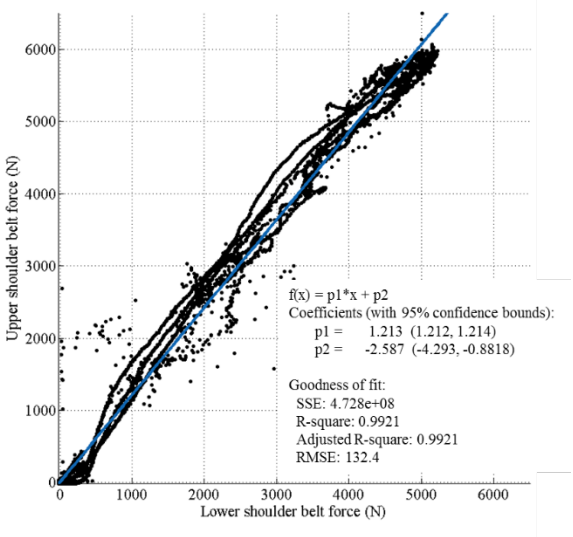


*Figure A4. Linear relationship (blue solid line) existing between the shoulder belt forces measured at the upper and lower locations. SB belt.*

# GENDER DIFFERENCES IN OCCUPANT POSTURE AND MUSCLE ACTIVITY WITH MOTORIZED SEAT BELTS

**Hattie Cutcliffe**
Duke University, Department of Biomedical Engineering
USA

**Karin Brolin**
**Jonas Östh**
**Jóna Marín Ólafsdóttir**
**Johan Davidsson**
Chalmers University of Technology, Department of Applied Mechanics
Sweden

Paper Number 15-0384

## ABSTRACT

The aim of this study was to assess gender differences in the posture and muscular activity of occupants in response to pretension from motorized seatbelts. Male and female vehicle occupants were tested in both front seat positions during normal driving and autonomous braking. This data is useful for the development of human body models (HBM), and increases the understanding of the effects of motorized belts.

Kinematics and electromyography (EMG) were analyzed for 18 volunteers (9 male, 9 female) subjected to autonomous braking (11 $m/s^2$ deceleration) during real driving on rural roads. Two restraint configurations were tested: a standard belt and a motorized belt, activated 240 ms before the initiation of braking. Statistical comparison of volunteers' posture and normalized EMG amplitudes was performed to understand differences incurred by the motorized belts, as well as to compare response across gender and role (occupant position within the vehicle). Data was analyzed both prior to and at vehicle deceleration, which occurred 240 ms after motorized belt onset.

Motorized belts significantly affected all postural metrics, and significantly elevated the activity of all muscles compared to typical riding. Though increases in muscle activity were small at deceleration onset compared with typical riding for male occupants and female passengers, female drivers demonstrated significantly larger increases in muscular activity: between 5 and 13% of the maximum voluntary contraction (MVC). At deceleration onset, standard belts showed little change in posture or muscle activation, with the median changes being well within the ranges exhibited during typical riding for all groups (i.e. not distinguishable from typical riding). Typical riding postures of males and females were similar, as were muscular activation levels—generally less than 5% of the MVC. However, drivers exhibited significantly higher muscular activity in the arm and shoulder muscles than passengers.

Limitations include the repeated nature of the testing, as prior work has shown that habituation across trials alters occupant response compared to that of unaware occupants. However, randomization of the trial order helped mitigate potential habituation effects. Another limitation is the sample size of 18 volunteers.

An important finding of this study is that the increase in occupant muscular activation seen with motorized belts was gender-specific: at deceleration, the change in activation of most muscles was significantly different across gender and belt type, with female drivers exhibiting larger increases in muscular activation than male drivers or passengers of either gender, particularly in the arm muscles. These activations appeared to be startle responses, and may have implications for interactions with the steering wheel and motion during a braking or crash event. This warrants further studies and stresses the importance of quantifying male and female subjects separately in future studies of pre-crash systems.

Keywords: Gender; driver, passenger; reversible, motorized seat belt; braking; EMG

## INTRODUCTION

Vehicle safety has improved significantly since the 1950s. Early interventions were in-crash systems; for example, improved vehicle structures and occupant restraints. The three-point seat belt was first introduced in 1957, and reported injury reduction was 40–90% (Bohlin 1967) and more than 35% (Norin et al. 1984). Later, Cummings et al. (2003) estimated a 61% lower risk of death for belted front seat occupants compared to unbelted occupants, based on accident data from 1986–1998. More recently, accident avoidance and pre-crash systems that avoid or mitigate the severity of accidents have been implemented on a large scale. Autonomous braking systems have been introduced (Coelingh et al. 2007; Distner et al. 2009; Schittenhelm 2009). Autonomous braking is beneficial by reducing the vehicle's kinetic energy. However, for impacts with equivalent speed, pre-crash braking increases chest deflection and belt forces (Antona et al. 2010), indicating that injury prevention can be improved with integrated safety systems that reposition the occupant before the impact. One example is autonomous braking in combination with reversible seat belt pretension, which removes belt slack and secures the occupant prior to an impact (Schöeneburg et al. 2011). Motorized seat belts provide reversible pretension before the crash and have the potential to reposition the occupant to an optimal pre-crash position.

Reversible seat belt pretension has been studied in combination with driver emergency braking (Tobata et al. 2003), lateral maneuvers (Mages et al. 2011), pre-impact braking (Woitsch and Sinz 2014), and stationary conditions (Good et al. 2008a; Good et al. 2008b; Develet et al. 2013). In these studies, volunteers or anthropomorphic test devices (ATDs) were used. ATDs have severe limitations as they are too stiff to represent relaxed occupants in low loading conditions (Beeman et al. 2012). Increasingly, computational human body models (HBMs) are used in vehicle safety assessment. Currently available HBMs have mainly been developed and validated in the crash loading regime. Active HBMs, which include occupant muscle response and are validated for braking and similar scenarios (Östh et al. 2015), have the potential to become strong tools for the development and assessment of integrated safety systems. However, the active HBM of Östh et al. (2015) represents the $50^{th}$ percentile male and there are no active HBMs representing female occupants. Therefore, to study gender differences in occupant response with integrated safety systems, volunteers are the best option to date. With increased knowledge from volunteer experiments, future HBMs can be developed to represent gender differences and study integrated safety systems for the full sequence from pre-crash to crash.

The aim of this study was to analyze how pretension with motorized seatbelts changed occupant posture and muscle activity, and to assess differences in response based on gender and occupant position in the vehicle. This was done with statistical analyses of volunteer data from drivers and front seat passengers with and without motorized seat belt pretension prior to autonomous braking interventions. The results have the potential to enhance traffic safety for all occupants, males and females, by providing an increased understanding of how motorized belts affect occupants and by providing data for enhancement of simulation tools, such as HBMs representing both genders.

## METHODS

This study analyzed data from volunteer experiments, approved by the Ethical Review Board at the University of Gothenburg, Sweden, where 20 volunteers were exposed to 29 braking interventions (11 $m/s^2$) as drivers (Östh et al. 2013) and passengers (Ólafsdóttir et al. 2013). Volunteers with incomplete data sets were excluded, and therefore 9 females and 9 males were incuded in this study. For each volunteer, 18 braking interventions were analyzed (12 driver, 6 passenger). The tests were conducted in a passenger car equipped with a motorized belt. Interventions were performed in a randomized order with two seat belt retractor configurations: a standard configuration that locked at 4 $m/s^2$ vehicle deceleration or when the belt pay out acceleration was 15 $m/s^2$ (subsequently denoted "standard"), and a reversible configuration where the electrical motor provided 170 N of belt pretension force at an approximate maximum retraction speed of 300 mm/s (subsequently denoted "motorized"). Each braking intervention was triggered without prior notification to the volunteer. Data were analyzed for two different time periods, before triggering the intervention (termed "typical riding") and at the onset of vehcile deceleration (termed "initial braking"). Vehicle deceleration occurred on average 350 ms after triggering; for trials with the motorized belt, pretension occurred on average after 110 ms.

Prior to testing, volunteers' anthropometry was measured (Table 1). Sitting height was the distance between the superior aspect of the head and the seated surface in the mid-sagittal plane, with volunteers sitting on a stool (Schneider et al. 1983). Surface electromyography (EMG) electrodes were applied bilaterally to the volunteers (Figure 1). Volunteers were positioned in a Maximum Voluntary Contraction (MVC) rig, designed to provide a posture that resembled the driving position, and three repetitions of MVC were performed for each tested muscle (Östh et al. 2013). Within the test vehicle, volunteers could partially adjust the driver seat and steering wheel to find a comfortable driving position and were told to keep their hands symmetrically on the steering wheel. Allowed adjustments were translation of the seat, change of the inclination angle of the seat back, and steering wheel position and angle. The passenger seat was fixed (in the mid fore/aft position with a seat back angle of 22°), and volunteers were instructed to keep their feet symmetrical to the midline of the footwell and rest their hands on their lap.

Surface EMG was recorded with a sampling rate of 2048 Hz using a Compumedics Grael (Compumedics, Abbotsford, Australia) for eight muscle groups: sternocleidomastoid, cervical paravertebrals, rectus abdominis, lumbar paravertebrals, biceps brachii, triceps brachii, anterior deltoid, and posterior deltoid (Figure 1). EMG data were normalized using MVC. In typical riding, EMG data were averaged over a one-second interval, from 1.5 to 0.5 s before trigger. In initial braking, EMG data were averaged over a 20 ms interval starting at deceleration onset. The change in activation in initial braking compared to typical riding was investigated per trial as the the absolute increase or decrease in activation. Then, the median change across trials of a given condition was used to represent each volunteer's response.

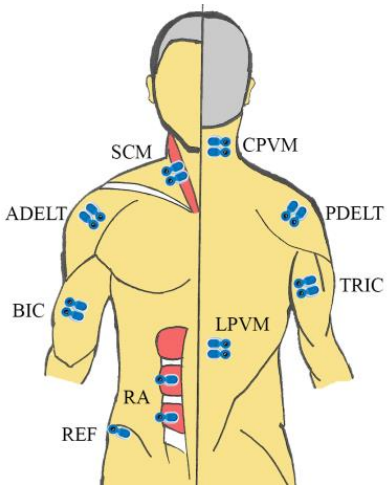


***Figure 1. EMG electrode placement (anterior locations on left, posterior locations on right). SCM: sternocleidomastoid; CPVM: cervical paravertebrals; ADELT: anterior deltoid; PDELT: posterior deltoid; BIC: biceps brachii; TRIC: triceps brachii; LPVM: lumbar paravertebrals; RA: rectus abdominis; REF: reference electrode. Adapted from Östh et al. (2013) by permission of The Stapp Association.***

Kinematic data was acquired at 50 Hz through film analysis (TEMA Automotive, Image Systems, Linköping, Sweden). Posture was measured with video tracking of markers on the volunteer's head and chest. In the present study, the head center of gravity (CG) position was calculated from film markers close to the ear and eye (Östh et al. 2013). Kinematic posture data were collected in a vehicle-fixed coordinate system, with positive X forward and positive Z upward (Figure 2). Head rotation was the angle between the horizontal plane and the Frankfort plane, in the sagittal plane, with positive rotation representing extension. Relative head-to-sternum distance was the difference between the calculated head CG and the chest marker, effectively measuring the posture of the neck: an individual with a larger head-to-sternum X in one position compared to another would have a more retracted posture in the former. Head-to-head restraint distance was the difference between the head CG and the mid-point on the anterior surface of the head restraint, in the mid-sagittal plane. For typical riding, kinematic data was analyzed and defined as the average value over the first 100 ms after trigger. The median across all trials of a given condition was used to represent each volunteer's response. For initial braking, the postural metrics were collected at deceleration onset. For each trial, the volunteer's change in metric was taken as the difference between the response at deceleration onset and at typical riding, with the median change across all trials of a given condition representing each volunteer's response.

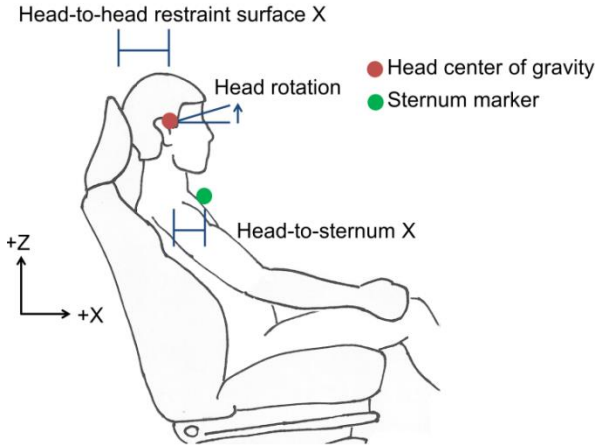


***Figure 2. Schematic of postural metrics used in this study.***

Statistical analysis included a normality and homoscedasticity assessment and a general test for group differences: either a parametric repeated-measures ANCOVA, with sitting height as a covariate, or a nonparametric Friedman test (when data did not meet normality or homoscedasticity assumptions). A 5% significance level was used. For typical riding, two-way repeated measures designs were used, with factors being role (driver or passenger) and gender. For initial braking, three-way repeated measures designs were used, with belt type (motorized or standard) as an additional repeated measure. To compensate for the seat belt loading asymmetry, outboard muscles of the drivers and passengers were compared, and likewise for inboard muscles. Data processing was performed in MATLAB (Version 8.0.0, MathWorks, Natick, MA), while statistical analyses were implemented in SAS (Version 9.3, SAS Institute Inc., Cary, NC).

## RESULTS

The volunteer sitting height was normally distributed (919 ± 39 mm). A post-hoc t-test indicated a significant difference ($p < 0.05$) in male and female sitting height, with females (894 ± 33 mm) being shorter than males (945 ± 27 mm). Table 1 lists the average anthropometric measurements for females and males.

**Table 1.**
**Volunteer anthropometric data. SD: Standard deviation.**

| Volunteers | Age (years) | Height (cm) | Weight (kg) | Sitting Height (mm) |
|---|---|---|---|---|
| Male Mean (SD) | 34.1 (12.7) | 178.1 (4.8) | 77.2 (5.8) | 945 (27) |
| Female Mean (SD) | 28.8 (5.9) | 166.6 (5.0) | 59.4 (5.2) | 894 (33) |

Motorized belts significantly affected all postural metrics (Figure 3). The occupant position at initial braking with motorized belts is illustrated in Figure 4 for one male and one female volunteer. Notably, the median sternal X location was shifted posteriorly by more than 10 mm (depending on gender and role) with motorized belts, and the median head-to-sternum X distance was reduced by 12 to 13 mm for females (depending on role) and by 6 to 7 mm for males. The lower values for males may be due to the higher inertia (mass) of male volunteers compared to female volunteers. The range (difference between the 75$^{th}$ and 25$^{th}$ percentiles) of change in postural metrics seen with standard belts during initial braking was well within the range exhibited during typical riding, for all comparable metrics, indicating that there were no other factors except the belt influencing the occupant response. The typical riding position did not seem to depend on gender, as the only significant effect of gender was found for the head-to-sternum X, which also showed significant covariance with sitting height. Role had a significant effect on the head-to-sternum X, indicating differences in neck curvature. Passengers had more than 20 mm larger median head-to-sternum X distances than drivers.

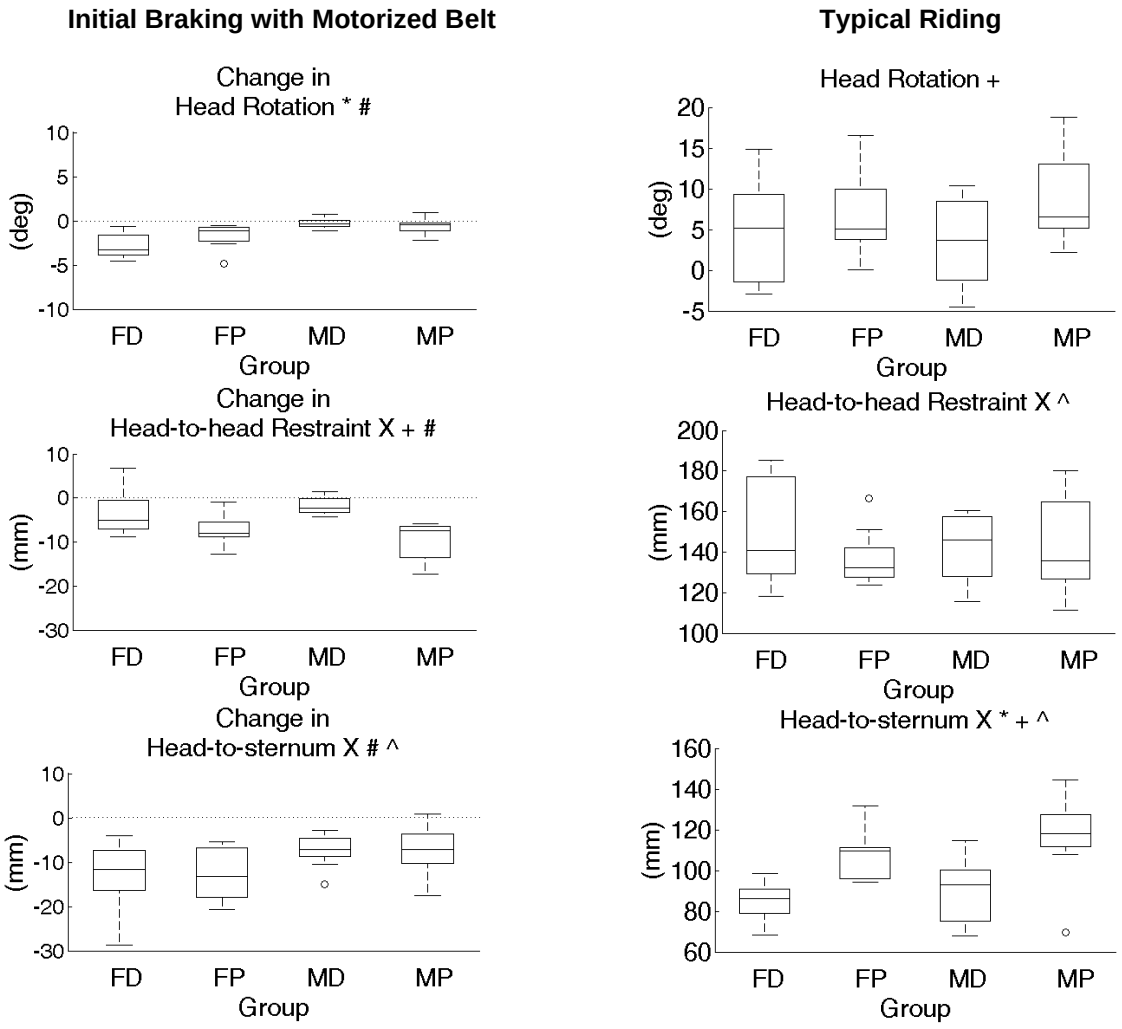


***Figure 3. Median change in postural metrics with motorized belts for initial braking compared to typical riding (left) and median postural metrics during typical riding (right). The interquartile ranges are indicated with boxes and outliers by circles. All head metrics are defined at the head center of gravity. FD: female drivers; FP: female passengers; MD: male drivers; MP: male passengers. *=significant main effect of gender, +=significant main effect of role, #=significant main effect of belt type, ^=significant covariance with sitting height.***

***Figure 4. Pictures of one female (left) and one male (right) volunteer in the driver (top) and passenger (bottom) position during initial braking with a motorized seatbelt (~250 ms after belt pretension).***

Gender differences were not found for the muscle activity during typical riding (Table 2). Muscle activity was not normally distributed, and was analyzed nonparametrically. Drivers exhibited significantly higher acivity in the arm and shoulder muscles than passengers. Though nonsignificant, this trend was evident for most neck and trunk muscles. Notably, while muscles generally displayed interquartile ranges of less than 5% MVC, the lumbar paravertebral muscles had muscle activity up to 20% MVC. With standard belts, the median changes in muscle activity during initial braking were well within the ranges during typical riding for all groups (typically <1% MVC, LPVM <5% MVC), in line with the postural metrics.

Motorized belts significantly increased muscle activity for all muscles (Figures 5 and 6, Table 3). Gender generally displayed significant effects on the arm, shoulder, and trunk muscles, with females showing larger changes than males. The increase in muscle activity was generally small (less than 5% MVC), except for female drivers. In the group of female drivers, for the measured muscles activity increased by 5-13% MVC, and inboard muscles typically displayed slightly larger increases in activity than outboard muscles. With motorized belts, a trend of drivers displaying larger median changes in muscle activity than passengers was seen for most muscles. The lumbar paravertebral muscle had higher increases in activity with motorized belts compared to the other muscles: 9-11% MVC for female drivers, 7-11% for female passengers, 6% for male drivers, and 2-5% for male passengers (Figure 6). Role significantly affected the outboard and inboard cervical paravertebral muscles, with drivers showing larger changes than passengers (Figure 6). Role also significantly affected the outboard rectus abdominis and inboard anterior deltoid.

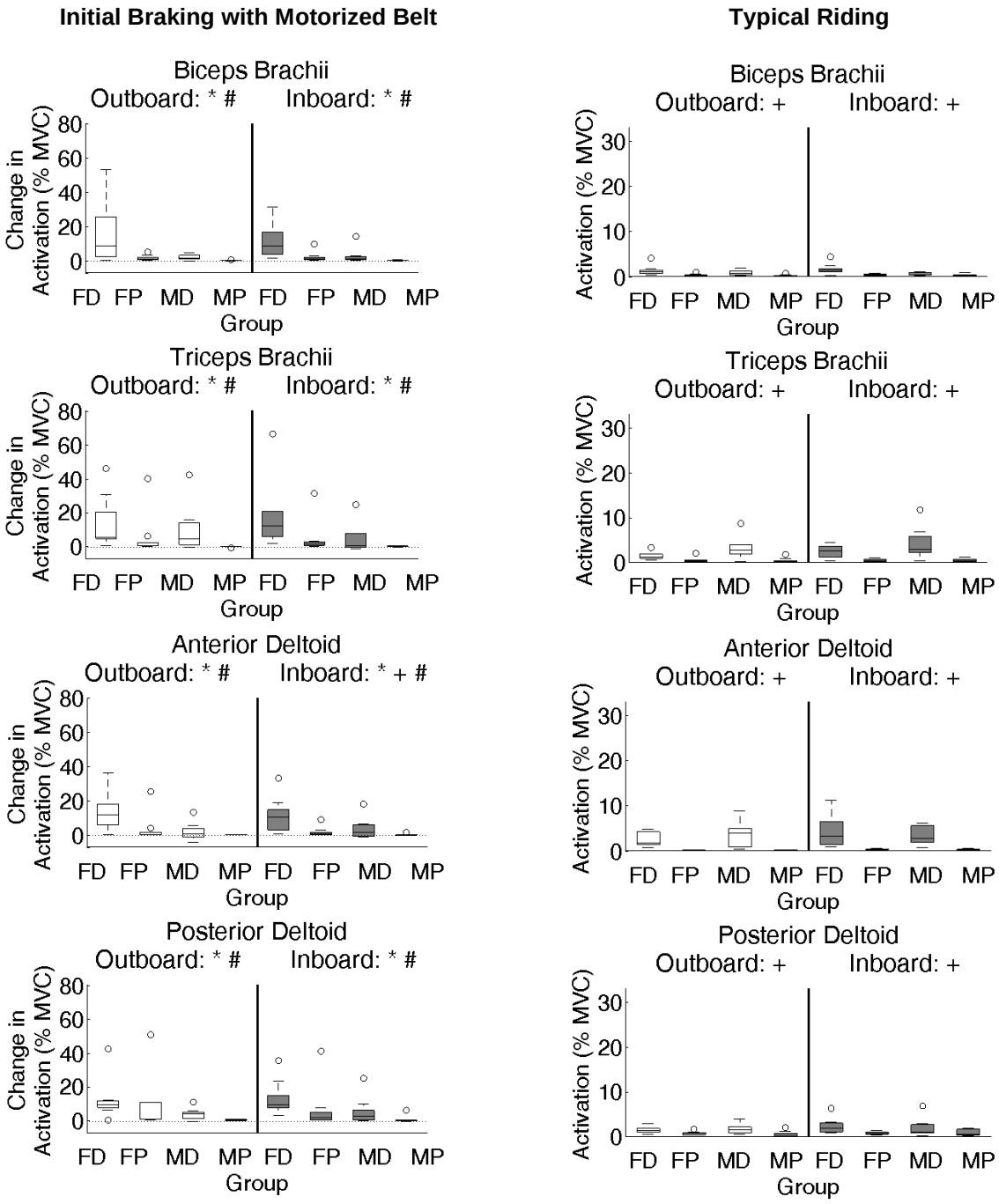


***Figure 5. Median change in arm and shoulder muscle activity with motorized belts for initial braking compared to typical riding (left) and median muscle activity during typical riding (right). The interquartile ranges are indicated with boxes (white for outboard muscles, grey for inboard muscles) and outliers by circles.***

***FD: female drivers; FP: female passengers; MD: male drivers; MP: male passengers.***

****=significant main effect of gender, +=significant main effect of role, #=significant main effect of belt type.***

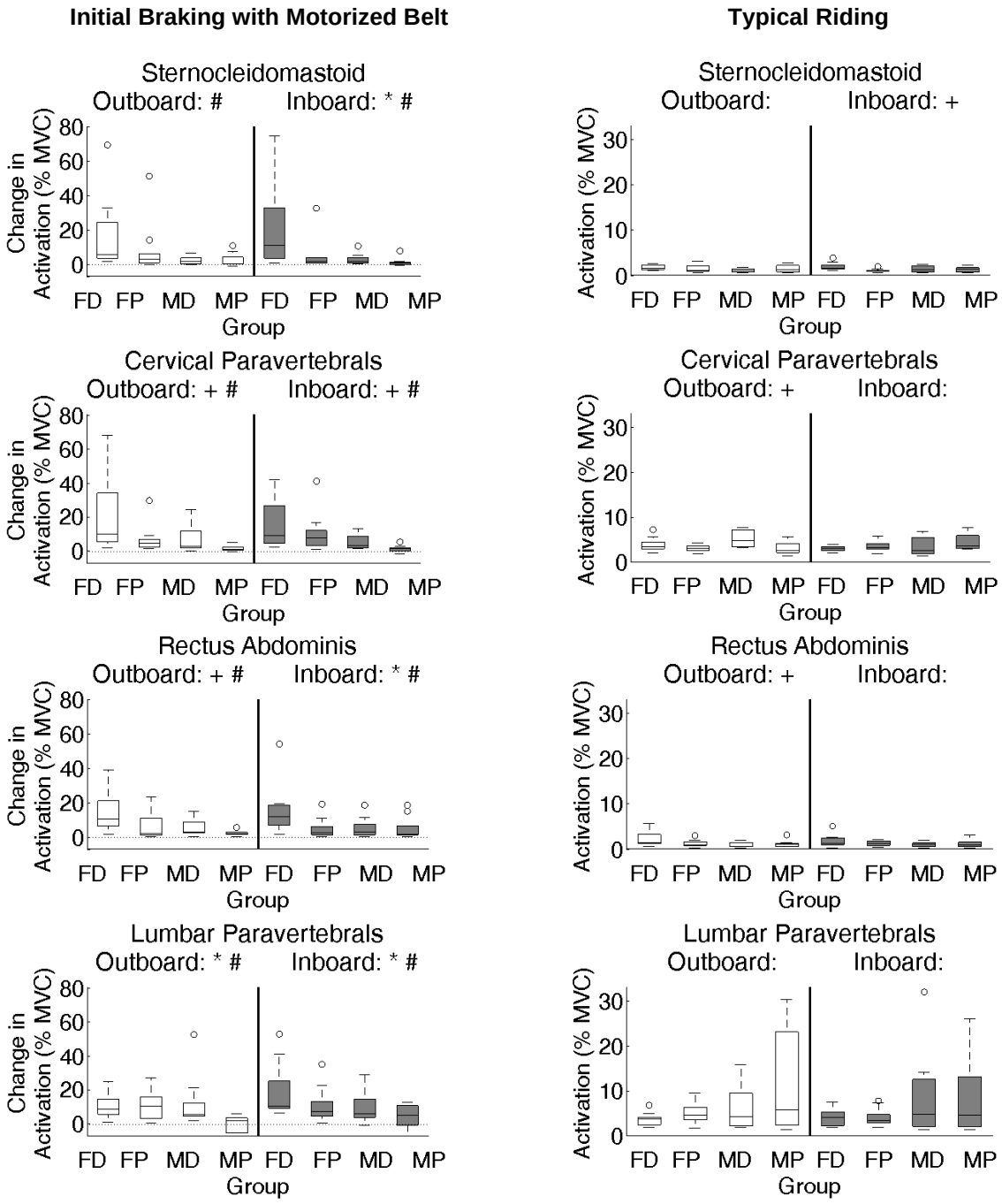


***Figure 6. Median change in neck and trunk muscle activity with motorized belts for initial braking compared to typical riding (left) and median muscle activity during typical riding (right). The interquartile ranges are indicated with boxes (white for outboard muscles, grey for inboard muscles) and outliers by circles.***

***FD: female drivers; FP: female passengers; MD: male drivers; MP: male passengers.***

****=significant main effect of gender, +=significant main effect of role, #=significant main effect of belt type.***

**Table 2.**
**Median (25th, 75th percentile) Muscle Activity (%MVC) in Typical Riding.**
* significant main effect of gender, + significant main effect of role.

| Group | SCM | CPVM | RA | LPVM | BIC | TRIC | ADELT | PDELT |
|---|---|---|---|---|---|---|---|---|
| Outboard muscles | | | | | | | | |
| | | + | + | | + | + | + | + |
| Female Drivers | 1.6 (1.3, 2.3) | 3.4 (3.0, 4.5) | 1.4 (1.2, 3.3) | 3.8 (2.5, 4.2) | 1.0 (0.7, 1.4) | 1.2 (1.0, 1.9) | 1.7 (1.4, 4.3) | 1.5 (1.0, 1.9) |
| Female Passengers | 1.1 (0.9, 2.1) | 3.1 (2.7, 3.6) | 1.0 (0.8, 1.7) | 4.7 (3.6, 6.4) | 0.3 (0.2, 0.5) | 0.4 (0.3, 0.5) | 0.2 (0.1, 0.2) | 0.7 (0.5, 1.0) |
| Male Drivers | 1.1 (0.7, 1.5) | 4.8 (3.4, 7.1) | 1.4 (0.6, 1.5) | 4.4 (2.3, 9.5) | 0.7 (0.4, 1.3) | 2.7 (2.0, 3.9) | 4.0 (0.9, 5.1) | 1.7 (0.9, 2.2) |
| Male Passengers | 1.2 (0.8, 2.2) | 2.6 (2.2, 4.2) | 1.0 (0.5, 1.3) | 5.8 (2.4, 23.1) | 0.1 (0.1, 0.3) | 0.3 (0.2, 0.5) | 0.2 (0.1, 0.3) | 0.5 (0.2, 0.8) |
| Inboard muscles | | | | | | | | |
| | + | | | | + | + | + | + |
| Female Drivers | 1.6 (1.4, 2.3) | 3.1 (2.6, 3.5) | 1.3 (1.0, 2.5) | 4.2 (2.3, 5.4) | 1.4 (1.1, 1.9) | 2.6 (1.2, 3.6) | 3.3 (1.4, 6.5) | 2.0 (1.1, 3.1) |
| Female Passengers | 1.0 (0.9, 1.2) | 3.2 (3.0, 4.2) | 1.2 (0.8, 1.8) | 3.4 (2.9, 4.7) | 0.4 (0.3, 0.5) | 0.5 (0.3, 0.7) | 0.4 (0.3, 0.5) | 0.8 (0.6, 1.1) |
| Male Drivers | 1.3 (0.8, 2.2) | 2.6 (2.0, 5.5) | 1.1 (0.6, 1.4) | 4.8 (2.1, 12.5) | 0.5 (0.4, 0.9) | 3.0 (2.2, 5.8) | 2.7 (1.9, 5.6) | 1.0 (0.9, 2.7) |
| Male Passengers | 1.4 (0.7, 1.7) | 3.6 (3.1, 5.9) | 1.0 (0.5, 1.6) | 4.6 (2.0, 13.1) | 0.3 (0.2, 0.5) | 0.5 (0.2, 0.8) | 0.3 (0.2, 0.4) | 0.5 (0.4, 1.7) |

**Table 3.**
**Median (25th, 75th percentile) Change of Muscle Activity (%MVC) with Motorized Belts.**
* significant main effect of gender, + significant main effect of role, # significant main effect of belt type.

| Group | SCM | CPVM | RA | LPVM | BIC | TRIC | ADELT | PDELT |
|---|---|---|---|---|---|---|---|---|
| Outboard muscles | | | | | | | | |
| | # | + # | + # | * # | * # | * # | * # | * # |
| Female Drivers | 5.5 (3.6, 24.3) | 10.4 (5.5, 34.1) | 10.7 (6.4, 21.2) | 8.9 (5.9, 14.7) | 8.7 (5.6, 5.0) | 5.6 (5.0, 20.5) | 12.0 (5.9, 18.2) | 9.6 (8.1, 12.0) |
| Female Passengers | 2.9 (1.0, 6.2) | 4.9 (2.7, 7.0) | 2.2 (1.2, 11.0) | 10.6 (3.4, 16.0) | 1.3 (0.6, 2.2) | 1.0 (0.6, 2.5) | 0.4 (0.3, 1.8) | 1.4 (1.1, 10.9) |
| Male Drivers | 1.6 (0.2, 3.7) | 3.0 (2.1, 11.9) | 3.1 (2.7, 8.7) | 5.6 (4.6, 12.3) | 1.6 (1.0, 3.2) | 5.0 (1.5, 14.3) | 1.0 (-1.1, 3.7) | 4.6 (1.5, 5.2) |
| Male Passengers | 0.4 (0.2, 4.1) | 1.5 (0.9, 2.8) | 2.2 (1.5, 2.8) | 2.1 (-5.1, 3.8) | 0.2 (0.1, 0.3) | 0.2 (0.2, 0.4) | 0.2 (0.2, 0.4) | 0.7 (0.4, 1.1) |
| Inboard muscles | | | | | | | | |
| | * # | + # | * # | * # | * # | * # | * + # | * # |
| Female Drivers | 11.1 (3.6, 32.6) | 9.3 (4.7, 26.8) | 11.7 (6.9, 18.6) | 10.5 (9.4, 25.2) | 8.9 (3.7, 16.7) | 12.5 (5.9, 20.8) | 10.6 (3.2, 14.8) | 9.7 (7.9, 15.2) |
| Female Passengers | 1.6 (0.8, 3.9) | 7.9 (3.5, 12.2) | 2.7 (1.4, 6.1) | 7.4 (4.9, 13.4) | 1.2 (0.6, 2.0) | 1.8 (1.0, 3.2) | 0.8 (0.3, 1.5) | 2.3 (0.9, 5.5) |
| Male Drivers | 1.6 (0.8, 4.0) | 3.6 (2.3, 8.9) | 2.8 (1.4, 7.6) | 6.4 (4.1, 14.7) | 1.3 (0.7, 2.7) | 0.7 (0.1, 7.9) | 1.6 (-0.4, 6.3) | 3.0 (0.9, 6.4) |
| Male Passengers | 0.6 (0.0, 1.2) | 1.7 (0.4, 2.2) | 1.8 (1.4, 6.5) | 5.2 (-0.5,10.9) | 0.2 (0.1, 0.4) | 0.2 (0.2, 0.6) | 0.1 (0.1, 0.3) | 0.5 (0.3, 0.7) |

## LIMITATIONS

There are limitations inherent in the experimental procedure, such as the use of a specific test vehicle or the level of autonomous deceleration applied. With respect to the current investigation, all braking events analyzed were autonomous events with volunteers who were unaware of the impending deceleration. As prior work has shown that habituation across trials alters occupant response compared to that of unaware occupants (Blouin et al. 2003a, Siegmund et al. 2003b), the repeated nature of the testing introduces some limitations. However, randomization of the trial order helped mitigate potential habituation effects. As the passenger seat was fixed, the typical passenger riding posture does not take into account potential gender differences in seat adjustment. However, it is plausible that passengers adjust the seats to a lesser extent than drivers during real driving. On the other hand, the driver data capture differences in seat adjustment and are more representative of real life driving postures. Another limitation is the sample size of 18 volunteers.

The change in occupant metrics due to the motorized seat belt was evaluated approximately 250 ms after the start of pretension. At this time, the deceleration had started to build up and was a few percent of the maximum value. It was assumed that the deceleration during initial braking would not influence the occupant response. To ensure that the influence of factors other than the belt pretension was negligible, braking interventions with a standard belt were analyzed at initial braking and compared to the typical riding metrics. The small changes (often less than 1%MVC) in muscular activation from typical riding values seen with standard belts are consistent with the studies by Ejima et al. (2007, 2008, and 2009), which did not find major muscle activity between 0 and 100 ms after deceleration initiation for the muscles tested. They are also in line with trends seen in frontal perturbations, in which normalized integrated EMG values from the sternocleidomastoid and cervical paravertebral muscles were less than 5% and 15%MVC, respectively, for the first 25 ms after deceleration initiation (Blouin et al. 2003b). The reported median changes were within the $25^{th}$ -$75^{th}$ percentiles of values for the typical riding (i.e. not distinguishable from typical riding) for comparable metrics. Hence, the change in muscle activity compared to typical riding can be considered an effect of motorized belt pretension, and not of deceleration onset.

## DISCUSSION

During typical riding, posture and muscular activity was similar across gender. Differences were seen between drivers and passengers. Drivers displayed significantly smaller (by over 20 mm) head-to-sternum X values than passengers, meaning that drivers adopted a more protracted head posture than passengers. The typical riding postures found here are in line with other studies. For instance, Carlsson and Davidsson (2011) reported an average head-to-sternum X distance of approximately 82 mm in a similar study, which is slightly below our median values of 86 - 118 mm depending on group. Likewise, a significant effect of role was seen for muscles in the arm, which is expected due to driver interactions with the steering wheel. However, though significant differences in activation across role were present, median activation levels during typical riding were low: all median values were below 6% MVC and many were below 2% MVC. These values are in line with the maximum pre-impact activation levels of 1-5% MVC reported in the rear impact tests of Szabo and Welcher (1996) for the muscles investigated (sternocleidomastoid, suboccipital cervical extensors, superior trapezius, and paralumbar muscles). They are also in line with reported median muscle activation levels prior to sled perturbation of between 0.6 and 3.7% MVC (Ólafsdóttir et al. 2014), for several cervical muscles (sternocleidomastoid, trapezius, levator scapulae, splenius capitis, semispinalis capitis, semispinalis cervicis, and multifidus).

Motorized belts significantly altered all postural metrics. Though the median changes seen with motorized belts were small for metrics associated with the head, they were slightly larger for metrics associated with the sternum. Indeed, the sternum marker moved typically more than 10 mm posteriorly with the motorized belts, likely because of the direct interaction between the belt and the sternum. These differences were present throughout the braking event: occupants with motorized belts displayed significantly less forward displacement than occupants with standard belts (Ólafsdóttir et al. 2013, Östh et al. 2013). Similarly, Schöeneburg et al. (2011) reported that reversible belt tension reduced the median peak forward chest and neck displacements of volunteers with 42% and 34%, respectively, in braking tests with reversible belt tension compared to tests without.

Likewise, motorized belts significantly increased muscle activity. The changes were interesting as they occurred early in time relative to the total braking event, as steady-state deceleration levels were not reached until 0.8 seconds post-trigger (Ólafsdóttir et al. 2013, Östh et al. 2013). Since motorized belt pretension fires before deceleration starts, it is hypothesized that these muscular reactions occur as part of a startle or reflex response to the belt (Ólafsdóttir et al. 2013, Östh et al. 2013). Such startle contractions would result in higher muscle activity at deceleration onset with motorized belts compared to standard belts, which is an important consideration for human body modeling. To the best of the authors' knowledge, there are no comparable studies investigating muscular effects of motorized belts.

Furthermore, the effect of motorized belts appeared to be gender-specific. The gender difference in the current study was largely driven by female drivers, whose changes in muscle activity ranged between 5 and 13% MVC. As passengers, their changes were less than 5% MVC for all muscles except the lumbar paravertebrals. Also, male changes in muscle activity were typically less than 5% MVC, both as drivers and passengers. However, gender differences in reflex time and activation onset may be contributing to the differences observed in this study. Females have faster stretch reflex times than males for neck flexor (sternocleidomastoid) and extensor (semispinalis capitis, splenius capitis) muscles (Foust et al. 1973). Furthermore, Siegmund et al. (2003a) found significantly different muscle onset times between males and females in a series of frontal sled tests, with female activation occurring 5 and 3 ms before male activation for the sternocleidomastoid and cervical paraspinal muscles, respectively. Taken together, these effects could contribute to the gender differences in activation observed in the current study.

Though the presence of startle was not rigorously investigated in this study, the results presented here indicate that the initial muscular activity provoked by motorized belt pretension is different between males and females. These differences are consistent with differences found later in the braking event, where average activation levels during steady-state braking were higher for females than males for drivers (Östh et al. 2013) and passengers (Ólafsdóttir et al. 2013). Hence, we recommend further investigation of female drivers, exploring the potential startle effect that motorized belt pretension seems to induce for this group of occupants.

## CONCLUSIONS

Motorized belts significantly changed the occupant posture, especially with respect to the chest, and significantly increased muscle activity. Gender did not seem to influence the typical riding postural metrics or muscle activation levels. In contrast, drivers and passengers had significantly different metrics for posture and muscle activity in typical riding. The effect of motorized belt pretension was gender-specific. When belt pretension was applied, though changes in postural metrics were similar for males and females, significant differences in activation were observed across gender. This gender difference at initial braking was driven by high changes in activation for female drivers. Therefore, further studies with a focus on female drivers are needed to explore the startle effect that motorized belt pretension seems to induce for this group of occupants.

## ACKNOWLEDGEMENTS

The authors would like to thank the Whitaker Foundation for supporting this work with a stipend for Hattie Cutcliffe to visit Chalmers. Additionally, the authors would like to thank the other project partners and co-funders: Autoliv Research AB, Umeå University, Volvo Group, and Volvo Car Corporation and the funding by VINNOVA – Swedish Governmental Agency for Innovation Systems through the FFI – Vehicle and Traffic Safety research programme. The work was carried out at SAFER – Vehicle and Traffic Safety Centre at Chalmers, Gothenburg, Sweden.

## REFERENCES

[1] Antona J, Ejima S, Zama Y. (2010) Influence of the Driver Conditions on the Injury Outcome in Front Impact Collisions. Proceedings of the JSAE Conference; Tokyo, Japan.

[2] Beeman SM, Kemper AR, Madigan ML, Franck CT, Loftus SC. (2012) Occupant Kinematics in Low-speed Frontal Sled Tests: Human Volunteers, Hybrid III ATD, and PMHS. Accident Analysis and Prevention 47:128–139.

[3] Blouin J, Descarreaux M, Bélanger-Gravel A, Simoneau M, Teasdale N. (2003a) Attenuation of human neck muscle activity following repeated imposed trunk-forward linear acceleration. Exp Brain Res. 150:458-464.
[4] Blouin J, Descarreaux M, Bélanger-Gravel A, Simoneau M, Teasdale N. (2003b) Self-initiating a seated perturbation modifies the neck postural responses in humans. Neuroscience Letters 347:1-4.
[5] Bohlin N. (1967) A Statistical Analysis of 28,000 Accident Cases with Emphasis on Occupant Restraint Value. Proceedings of the 11th Stapp Car Crash Conference; Anaheim, CA, USA.
[6] Carlsson S, Davidsson J. (2011) Volunteer occupant kinematics during driver initiated and autonomous braking when driving in real traffic environments. Proceedings of the IRCOBI Conference; Krakow, Poland.
[7] Coelingh E, Jakobsson L, Lind H, Lindman M. (2007) Collision Warning with Auto Brake – A Real-life Safety Perspective. Proceedings of the 20th ESV Conference; Lyon, France.
[8] Cummings P, Wells JD, Rivara FP. (2003) Estimating Seat Belt Effectiveness using Matched-pair Cohort Methods. Accident Analysis and Prevention 35:143–149.
[9] Develet J-A, Carlsson A, Svensson M, Fredriksson R, Bråse D, Holcombe S. (2013) Evaluation of the Biofidelity of the BioRID-II and THOR-NT Anthropometric Test Devices under Seatbelt Pre-Pretensioner Loading in Stationary Conditions. Proceedings of the Ohio State University Injury Biomechanics Seminar; Columbus, OH, USA.
[10] Distner M, Bengtsson M, Broberg T, Jakobsson L. (2009) City Safety – A System Addressing Rear-End Collisions at Low Speeds. Proceedings of the 21st ESV Conference; Stuttgart, Germany.
[11] Ejima S, Ono K, Holcombe S, Kaneoka K, Fukushima M. (2007) A study on occupant kinematics behavior and muscle activities during pre-impact braking based on volunteer tests. Proceedings of the IRCOBI Conference; Maastricht, the Netherlands.
[12] Ejima S, Zama Y, Satou F, Holcombe S, Ono K, Kaneoka K, Shiina I. (2008) Prediction of physical motion of the human body based on muscle activity during pre-impact braking. Proceedings of the IRCOBI Conference; Bern, Switzerland.
[13] Ejima S, Zama Y, Ono K, Kaneoka K, Shiina I, Asada H. (2009) Prediction of pre-impact occupant kinematic behavior based on the muscle activity during frontal collision. Proceedings of the 21st ESV Conference; Stuttgart, Germany.
[14] Foust DR, Chaffin DB, Snyder RG, Baum JK. (1973) Cervical range of motion and dynamic response and strength of cervical muscles. Proceedings of the 17th Stapp Car Crash Conference; Coronado, CA.
[15] Good CA, Viano DC, Ronsky JL. (2008a) Biomechanics of Volunteers Subject to Loading by a Motorized Shoulder Belt Tensioner. Spine 33:E225–E235.
[16] Good CA, Viano DC, Ronsky JL. (2008b) The Hybrid III Dummy Family Subject to Loading by a Motorized Shoulder BeltTensioner. SAE International Journal of Passenger Cars-Mechanical Systems 1(1):383–395.
[17] Mages M, Seyffert M, Class U. (2011) Analysis of the Pre-Crash Benefit of Reversible Belt Pre-pretensioning in Different Accident Scenarios. Proceedings of the 22nd ESV Conference; Washington, D.C., USA.
[18] Norin H, Carlsson G, Korner J. (1984) Seat Belt Usage in Sweden and Its Injury Reducing Effect. SAE Technical Paper No. 840194. Society of Automotive Engineers, Warrendale, PA.
[19] Ólafsdóttir JM, Östh JKH, Davidsson J, Brolin KB. (2013) Passenger kinematics and muscle responses in autonomous braking events with standard and reversible pre-tensioned restraints. Proceedings of the IRCOBI Conference; Gothenburg, Sweden.
[20] Ólafsdóttir JM, Brolin K, Blouin J, Siegmund GP. (2014) Dynamic spatial tuning of cervical muscle reflexes to multidirectional seated perturbations. Spine 40(4):E211-E219.
[21] Östh J, Brolin K, Bråse D. (2015) A Human Body Model with Active Muscles for Simulation of Pre-Tensioned Restraints in Autonomous Braking Interventions. Traffic Injury Prevention 16(3):304-313.
[22] Östh J, Ólafsdóttir JM, Davidsson J, Brolin K. (2013) Driver kinematic and muscle responses in braking events with reversibly pre-tensioned and standard restraints: Validation data for human models. Stapp Car Crash Journal 57:1-41.
[23] Schittenhelm H. (2009) The Vision of Accident Free Driving – How Efficient are We Actually in Avoiding or Mitigating Longitudinal Real World Accidents. Proceedings of the 21st ESV Conference; Stuttgart, Germany.
[24] Schneider LW, Robbins DH, Pflug MA, Snyder RG. (1983) Development of anthropometrically based design specifications for an advanced adult anthropomorphic dummy family, Vol. 1. National Highway Traffic Safety Administration Report No. UMTR 1-83-53-1, Washington, DC.

[25] Schöeneburg R, Baumann K, Fehring M, Daimler AG. (2011) The efficiency of PRE-SAFE systems in pre-braked frontal collision situations. Proceedings of the 22nd ESV Conference; Washington, D.C.
[26] Siegmund GP, Sanderson DJ, Myers BS, Inglis JT. (2003a) Awareness affects the response of human subjects exposed to a single whiplash-like perturbation. Spine 28(7):671-679.
[27] Siegmund GP, Sanderson DJ, Myers BS, Inglis JT. (2003b) Rapid neck muscle adaptation alters the head kinematics of aware and unaware subjects undergoing multiple whiplash-like perturbations. Journal of Biomechanics 36:473-482.
[28] Szabo TJ, Welcher JB. (1996) Human subject kinematics and electromyographic activity during low speed rear impacts. Proceedings of the 40th Stapp Car Crash Conference; Albuquerque, NM.
[29] Tobata H, Takagi H, Pal C, Fukuda S. (2003) Development of Pre-Crash Active Seatbelt System for Real World Safety. Proceedings of the 18th ESV Conference; Nagoya, Japan.
[30] Woitsch G, Sinz W. (2014) Influences of Pre-Crash Braking Induced Dummy – Forward Displacements on Dummy Behaviour during EuroNCAP Frontal Crashtest. Accident Analysis and Prevention 62:268-275.

# UNVEILING THE STRUCTURAL RESPONSE OF THE RIBCAGE: CONTRIBUTION OF THE INTERCOSTAL MUSCLES TO THE THORACIC MECHANICAL RESPONSE

**David Poulard**
Center for Applied Biomechanics, University of Virginia
USA

**Damien Subit**
Institut de Biomécanique Humaine Georges Charpak, Arts et Métiers ParisTech
France

Paper Number 15-0387

## ABSTRACT

Current finite element (FE) models of the human body do not properly include the contribution of the intercostal muscles (ICM), which is believed to limit their rib fracture prediction capabilities. In the present study, an existing full body model for a seated 50th-percentile male was evaluated under five cases of loading: point loading of the denuded ribcage, frontal pendulum impact tests, lateral and oblique pendulum impact tests and table top tests. The sensitivity of the model to changes in material model of the ICM was evaluated by using two material models: an isotropic linear elastic material model and a foam model defined by a single uniaxial load curve extracted from a recent literature. The performance of these models compared to the experiments was assessed quantitatively through a correlation analysis on the force and chest deflection time histories. The simulations found that that the material properties of the ICM have little effect on the externally measured impact force and chest deformation except in point loading.

## INTRODUCTION

Thoracic injuries are the most common blunt trauma sustained by restrained occupants in motor vehicle crashes [1]. Amongst thoracic injuries, rib fractures are commonly used as an indicator of a crash severity as these fractures are relatively straight forward to detect and the increase of their number was shown to be associated to an increase of the risk of sustaining more severe injuries to the internal organs (aorta, lungs, heart). The structure of the thoracic segment structure is complex because of its geometry and the material heterogeneity: it consists of the ribcage, the viscera, the musculature and the skin, and its mechanical response results from the contribution of these tissues, soft and hard. Understanding how the thorax deforms under dynamic solicitations is an active area of research.

Finite element (FE) models of the human thorax or the entire body have been developed to investigate the structural response of the thorax and establish its injury tolerance [2-9]. These models rely on two types of data: the material and geometrical information to build them, and the experimental data required to evaluate their biofidelity, i.e. their ability to predict a mechanical response under dynamic loading similar to what would experience a real person. In both cases, post-mortem human (PMHS) data are used, and the capabilities of the models depend on the availability of the experimental data.

Material constitutive models and the required data to validate the models created for the isolated thoracic components are available for nearly all the tissues: clavicle [10, 11], ribs [12-14] and costal cartilage [15, 16]. However, there is little information in the literature for the intercostal muscles (ICM), and therefore the FE models currently available use material properties reported on in by [17]. This study lists properties of some thoracic muscles, such as the pectoralis major and the trapezius but not specifically identify intercostal material properties. Therefore, as thoracic muscle structure differs along the thorax, modeling the ICM using properties of other thoracic muscles may be not appropriate. It was found from animal experiments that the intercostal muscles could generate substantially less tensile force than other muscles like the diaphragm [18, 19]. Recently, Kindig et al. [20] found that decreasing the elastic modulus of the intercostal muscles of a FE ribcage model alter significantly the ribcage

deformation under quasi-static point loading and dynamic sternal loading. Moreover, while an isotropic linear elastic material model is commonly used for modeling the ICM, it was found from cadaver tests that ICM exhibit a hyperelastic behavior in tension [21]. Thus, it appears that the FE models currently available do not properly include the contribution of the intercostal muscles, which is believed to limit the rib fracture prediction capabilities of the thorax model.

Therefore, the goal if this present study is to examine the sensitivity of a thorax FE to the changes in intercostal muscle material constitutive model based on recent literature. To do, a parametric analysis was performed to evaluate the sensitivity of the thorax to the constitutive models used for the ICM using a human body model (HBM). The different versions of the HBM were exercised under several loading conditions with various constitutive models for the ICM and their performance was assessed quantitatively to experiments through a correlation analysis.

## METHODOLOGY

### Finite Element Body Model Overview

The HBM used in this study was the version 4.1 of the seated 50th-percentile male, developed in LS-DYNA for the Global Human Body Models Consortium (GHBMC). This full model has been described in a previous study [9, 14, 22] and evaluated under various loading environments (antero-posterior rib bending, point loading of the denuded ribcage, omnidirectional pendulum impact and table top) through a correlation metric tool (CORA) based on linearly independent signals [9].

The intercostal muscles were defined as a single layer of triangular planar shell elements of 1.5 mm thickness which were attached between adjacent ribs. The membrane element formulation was used since it was assumed that the intercostal could not support a through-thickness bending load. By default, an isotropic linear elastic material model with E=0.5 MPa, was used for these elements. This material model was changed in the present study.

### Defining new material properties for the intercostal muscles

Material Type 181 (*MAT_SIMPLIFIED_RUBBER/FOAM) was used for a new model of the behavior of the ICM. This material model provides a rubber and foam model defined by a single uniaxial load curve defining the force versus actual change in a gauge length. The single uniaxial load curve was defined to cover the complete range of expected loading.

In tension, the load curve was defined from the hyperelastic behavior of the ICM found in [21]. In this study, tensile tests were performed on three ICM samples harvested from one cadaver at different locations: one sample (#A) located between ribs 8 and 9 from the anterior aspect of the rib cage, and two samples (#B and #C) located between ribs 9 and 10 in the lateral and posterior aspects of the rib cage. For the three samples, a toe region was observed, followed by quasi-linear response after about 30 % of stretch and failure at 60%. An average stress-strain response from the three samples was extracted and converted to a load-displacement curve by assuming a specimen gauge length, width and thickness of 1 mm.

Figure 1 shows the stress-strain curve used in the rubber/foam model, the experimental curves used for its definition and the stress-strain curve based on the default material for comparison. In compression, the load curve was defined to eliminate the compressive action since the ICM exhibit similar behavior [21]. Nevertheless, stiffen up the material stress-strain curve at large compression ($\varepsilon<0.8$) was found essential for avoiding negative volume.

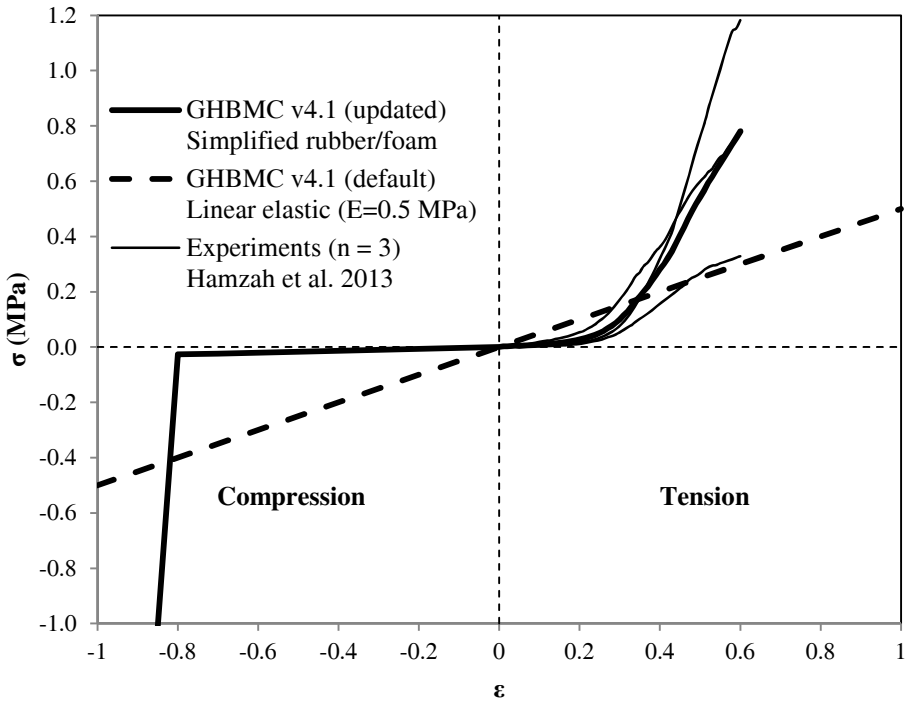


***Figure1. Stress-strain curves used in the ICM for the updated version the GHBMC model, the experimental curves used for its definition and the stress-strain curve based on the default material for comparison.***

**Evaluation cases**

The influence of the ICM material on thoracic mechanical response was evaluated from the denuded ribcage to the full body model using four sets of experiments. These experimental cases were selected based on their previous use for the validation of the HBM [9]. The experimental tests and model validation process are described below.

**Point loading of the eviscerated ribcage** Quasi-static point loading of the ribcage was simulated, using the method outlined in Kindig et al. [23]. The FE model of the ribcage was positioned oriented in an upright position similar to the experiment and the six degrees of freedom of the thoracic vertebrae were constrained. The spherical segment was positioned and oriented such that the contact surfaces on the sphere did not initially penetrate the ribcage mesh (Figure 2a). The loading plate was positioned initially in contact with the contact surface of the sphere and aligned such that the vector normal to the plate was directed along the average vector direction used in the experiments at this particular loading location. The plate was constrained to translate along this vector only, with no rotation allowed, consistent with the experimental boundary conditions. The plate was displaced at a constant 200 mm/sec up to the prescribed displacement used in the experiment (varied with the loading location). The loading rate to 200 mm/sec provided a reasonable simulation time while maintaining stable contact forces. To avoid strain-rate effects, the Cowper-Symonds yield-stress scaling in the bone material models was disabled. The reaction force onto the plate nodes was outputted for comparison with experiment.

Simulations were performed at the lower and upper sternum levels and the costochondral junction (CCJ) of rib levels 1, 3, 4, 6, and 9 (Figure 2b). The average value of the maximum normalized displacement obtained in experiments for each location was used to define the maximum displacement reached in simulation and

consequently the termination time. No modifications were made on the force and displacement obtained from simulations.

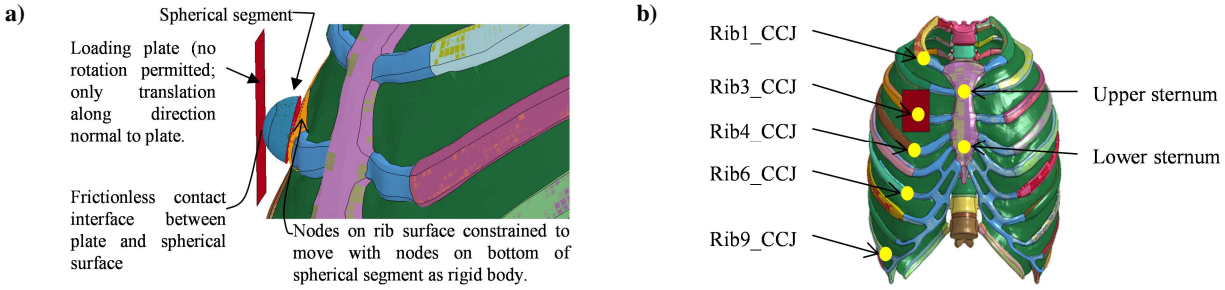


***Figure2. Setup for point loading simulation [9]. (a) Close-up at loading site (b) anterior view.***

**Frontal pendulum impact** The FBM was exercised under frontal pendulum impact [24]. In the simulation, the FBM was seated on a rigid plate and the impactor positioned at the midsternum level (Figure 3a). An initial velocity of 4.3 m/s was imposed on the impactor. The impact force was measured as the contact force between the impact and model. Chest deflection was defined as the variation of length between the middle of two nodes taken on the pectoral muscles and a node taken on the skin at T8 level [9]. The impact force chest deflection curve from the FE model simulations was compared to the experimental corridors normalized to the 50th percentile male developed by Lebarbé and Petit [25] to evaluate the response of the thorax model.

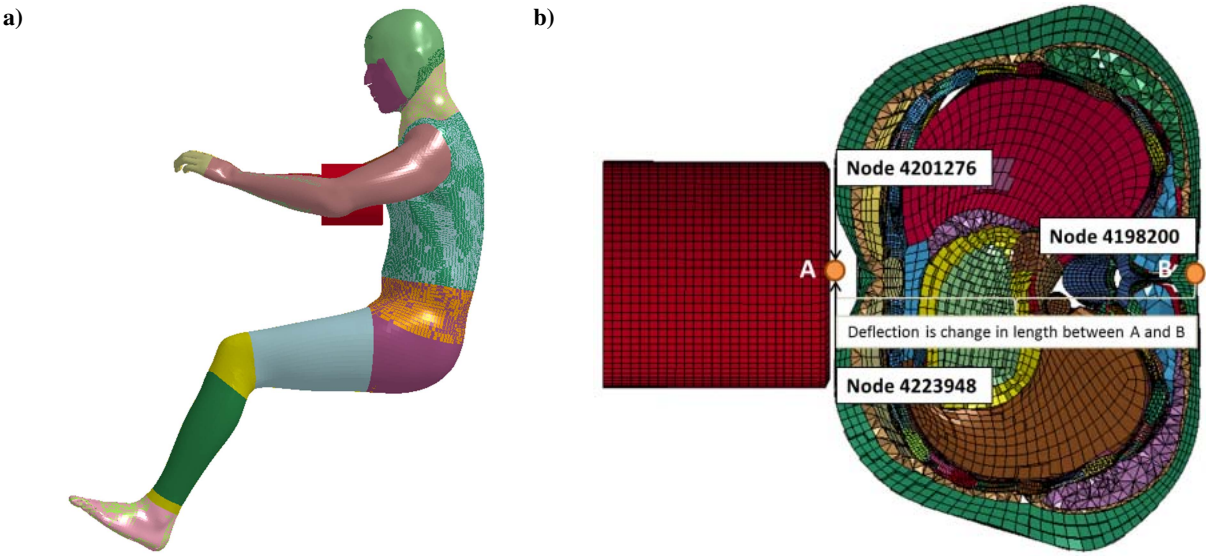


***Figure3. Setup for frontal pendulum impact [9]. (a) Lateral view, (b) Superior view of the cross-section of the thorax at the mid-sternum showing the points used to measure the chest deflection.***

**Pure lateral impact** The FBM was further run according to a pure lateral impact configuration available in the literature [26]. In the simulation, the FBM was seated on a rigid plate and the impactor positioned under the axiliary level, similar to the experiments (Figure 4a). The cylindrical impactor with a diameter of 152 mm, a mass of 23.4 kg and an initial impact velocity of 2.5 m/s was centered with the transverse plane through the fourth interspace of the ribcage. The impact force was measured as the contact force between the impactor and model. The chest deflection was defined as the change in length between two bilateral nodes aligned with the center of the impactor (Figure 4b).

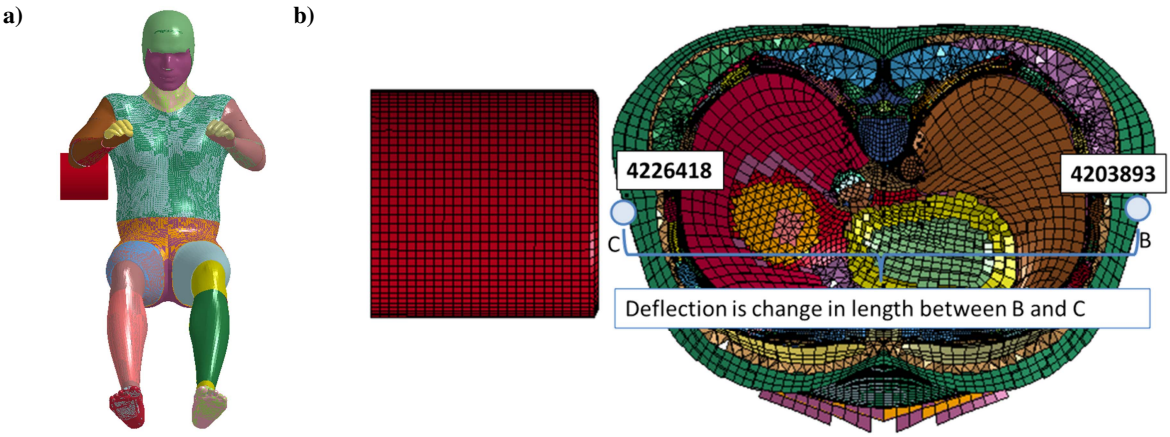


***Figure4. Setup for lateral pendulum impact [9]. (a) Frontal view, (b) Superior view of the cross-section of the thorax at the level of sternum the fourth interspace showing the points used to measure the chest deflection.***

In a qualitative evaluation, the force-deflection curve from the FE model was compared to the experimental corridors normalized to the 50th percentile male developed by Shaw et al. [26]. For the quantitative evaluation, the force/time and deflection/time histories were used.

**Table top tests** The FBM was set-up to simulate four tabletop restrained configurations [27]:

- hub loading, where the hub was simulated as a cylindrical rigid body with a diameter of 152 mm,
- belt loading, where single and double diagonal belts were modeled by a layer of 2-mm thick shell elements,
- distributed loading, where an extra-wide belt was modeled by a layer of 2-mm-thick shell elements and was 203-mm wide.

The pulley system used in the experiments was simulated by slip ring elements and several 1-D belt elements so that the loading angles of the 1D-belt elements were maintained and consistent with experimental configurations (Figure 6a). These tabletop models were loaded using the displacement-time history reported on in Kent et al. [27] up to 20% of chest compression (non-injurious level) for all the four loading conditions (Figure 6b). The displacement was applied symmetrically to the extremities of the single, double and distributed loading, and to the hub. Prior to applying the loading, the models were allowed to settle on the table for 100 ms under its own weight. The settling process was applied in a pre-simulation and the initial stress was imported in the FBM for the table top simulations. The limbs were cut to reduce the computation time.

The reaction force was defined as the contact force between the support table and the model. The compression was defined as the ratio of the Z-displacement of a node taken on midsternum (A, Figure 6a) divided by the initial distance between A and the support table.

The reaction force versus compression curves were then compared to the thoracic response corridors developed from the fifteen PMHS tested by Kent et al. [27].

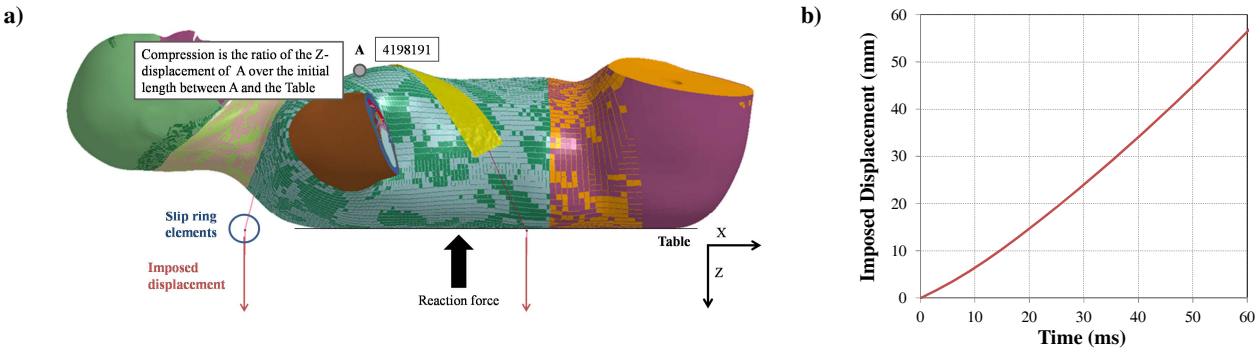


***Figure5. Setup for single belt table top test [9]. (a) Lateral view, (b) Displacement imposed to the loading structure.***

**Quantitative assessment of the response of the model**

A quantitative assessment of the response of the models compared to the five sets of experiments was performed through metrics obtained with the CORA software (CORelation and Analysis, Parternship for Dummy Technology and Biomechanics). Each of these metrics is given a score and the weighed sum of these score is the CORA score ranging between 0 and 1. A CORA score above 0.8 is considered as a good fit between the model and the experimental response [28]. As CORA calculates the correlation of each signal separately, those single ratings were combined to a global model rating by calculating the mean value of all the ratings. Table 1 shows which data were used to establish the rating for each load cased. Ratings with a score of 0.8 or higher were assumed as good.

The experimental response was defined from the average response and inner/outer corridors derived from the experimental results [9].

**Table1.**
**`Signals used in the correlation analysis [9].**

| Load case | Sub load case(s) | Signals |
|---|---|---|
| Point loading of the ribcage | Lower sternum, Rib1_CCJ, Rib3_CCJ, Rib4_CCJ, Rib6_CCJ, Rib9_CCJ, Upper sternum | 1. Force vs. Displacement* |
| Frontal pendulum impact | Impact velocity 4.3 m/s | 1. Force vs. Time<br>2. Deflection vs. Time |
| Lateral pendulum impact | Impact velocity 2.5 m/s | 1. Force vs. Time<br>2. Deflection vs. Time |
| Table top | Hub, Single Belt, Double Belt, Distributed Loading | 1. Force vs. Compression* |

*: Equivalent to Force vs. Time in CORA, as displacement and chest compression were the independent variables.

**RESULTS**

**Point loading of the eviscerated ribcage**

The scaled force versus scaled deflection curves predicted by the HBM after ICM modification different from the baseline model (Figure 6). In all tested locations, the model after modification was found to be more compliant, up to be out of the corridors. Quantitatively, the average CORA model score was 0.73 ± 0.12 after modification was lower than the baseline model (0.80 ± 0.12)(Table 2).

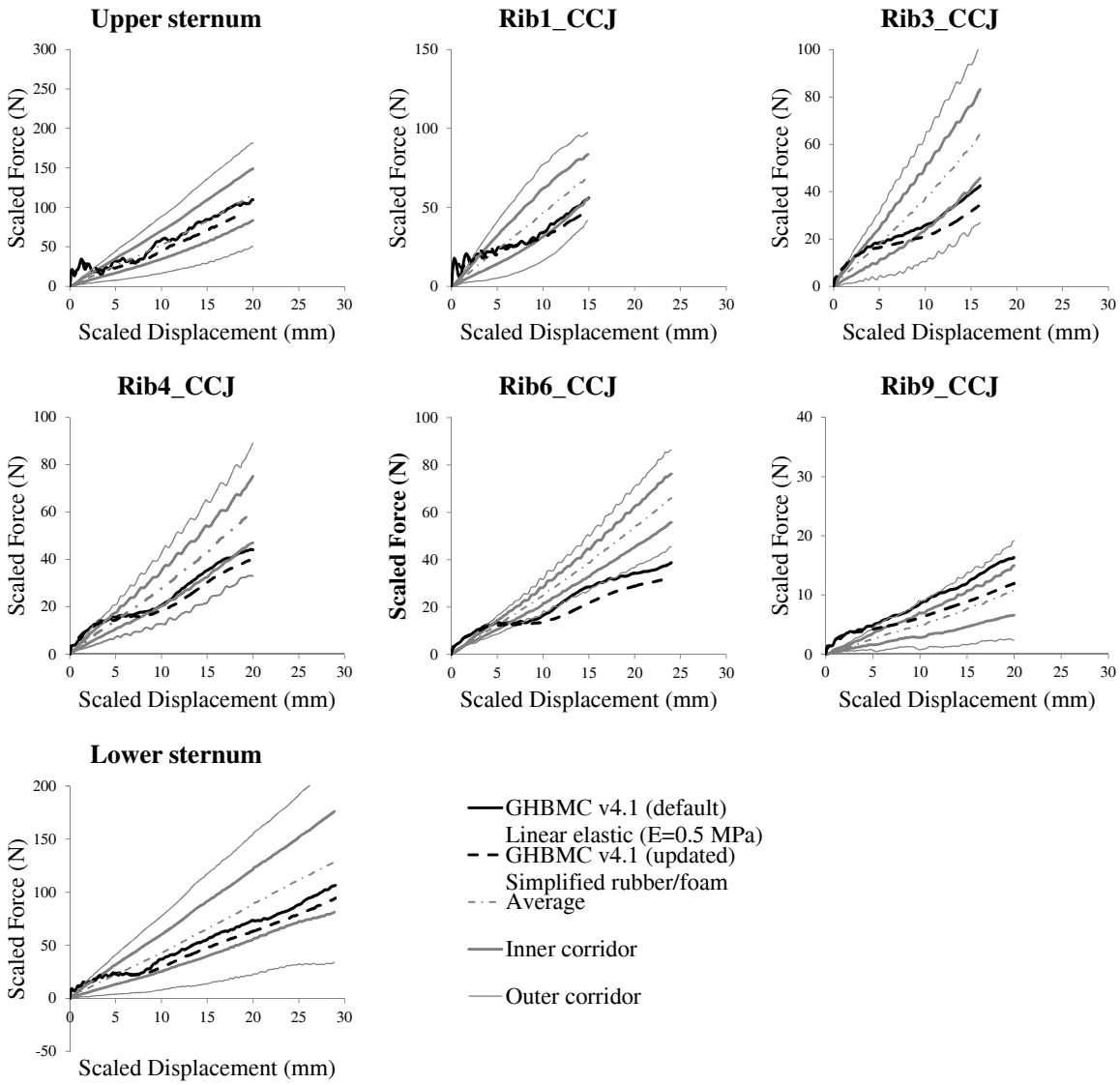


***Figure6. Model performance for point loading of the denuded ribcage. Scaled Force-Scaled Displacement. Experimental corridors are adapted from [23].***

**Frontal and lateral pendulum tests**

The reaction force versus chest deflection curves predicted by the HBM after ICM modifications was really close to the baseline model (Figure 7 and 8). CORA model scores after modifications were 0.86 in frontal and 0.89 in lateral close to the scores obtained with the baseline model (0.84 and 0.89 respectively) (Table 2).

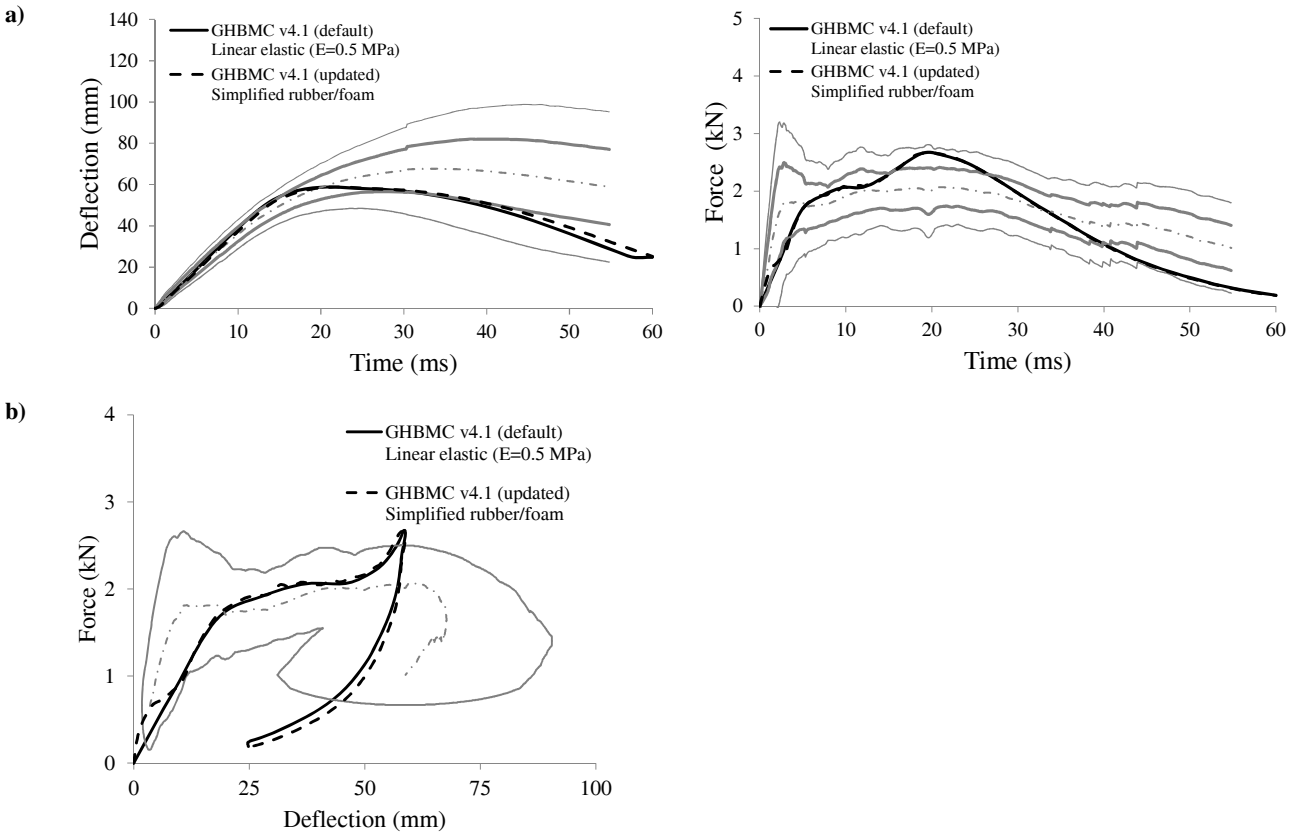


***Figure7. Model performance for frontal pendulum tests. (a) Deflection-Time and Force-Time histories, (b) Force-Deflection, (c) CORA ratings. Experimental corridors are adapted from [24] and [25].***

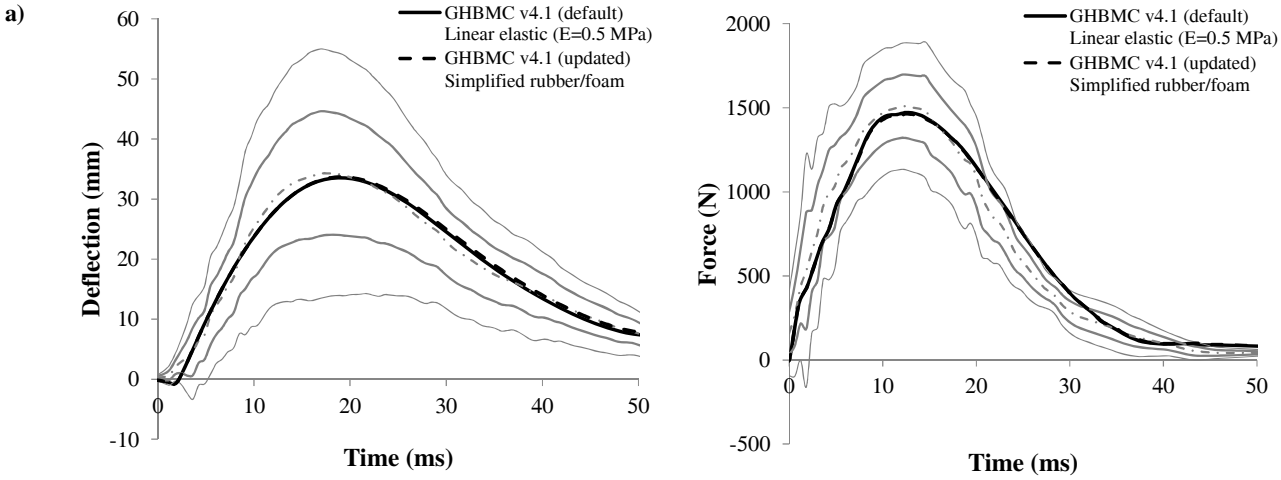

b)

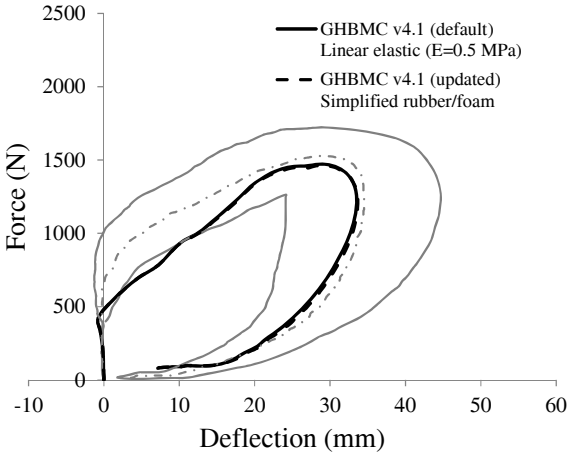


***Figure8. Model performance for lateral pendulum tests: (a) Deflection-Time and Force-Time histories, (b) Force-Deflection. Experimental corridors are adapted from [26].***

**Table top tests**

The reaction force versus chest compression curves predicted by the HBM after modifications closely agreed with the response obtained by the baseline model for all configurations (Figure9). The average CORA model score obtained by the model after modifications was 0.83 ± 0.10, slightly lower than the baseline model (0.86 ± 0.10) (Table 2).

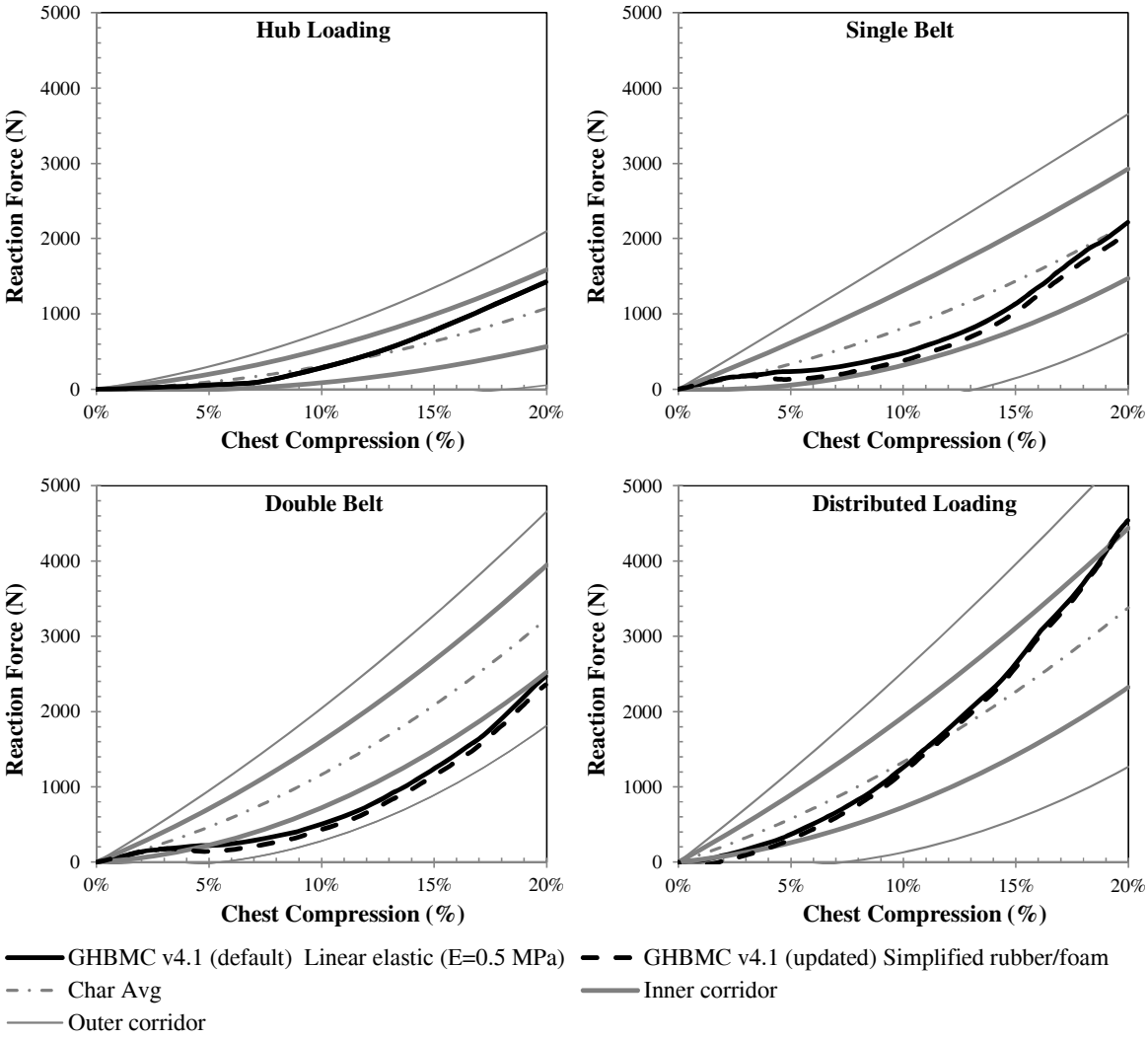


***Figure9. Model performance for table top tests. (a) Reaction Force-Chest Compression, (b) CORA ratings. Experimental corridors are adapted from [27].***

**Table2.**
**CORA scores.**

| | Model | Subload Case | Signal | Corridor Score | Cross-correlation | | | | Signal Score | Model Score |
|---|---|---|---|---|---|---|---|---|---|---|
| | | | | | Phase Score | Size Score | Progression Score | Score | | |
| Point loading of the ribcage | 1* | Lower sternum | Force | 1.00 | *Ignored* | 0.54 | 1.00 | 0.77 | 0.89 | 0.80 |
| | | Rib1_CCJ | Force | 0.89 | *Ignored* | 0.51 | 0.98 | 0.75 | 0.82 | |
| | | Rib3_CCJ | Force | 1.00 | *Ignored* | 0.31 | 0.99 | 0.65 | 0.83 | |
| | | Rib4_CCJ | Force | 0.93 | *Ignored* | 0.46 | 0.99 | 0.73 | 0.83 | |
| | | Rib6_CCJ | Force | 0.44 | *Ignored* | 0.41 | 1.00 | 0.70 | 0.57 | |
| | | Rib9_CCJ | Force | 0.44 | *Ignored* | 0.93 | 1.00 | 0.96 | 0.70 | |
| | | Upper sternum | Force | 1.00 | *Ignored* | 0.79 | 1.00 | 0.90 | 0.95 | |
| | 2** | Lower sternum | Force | 1.00 | *Ignored* | 0.44 | 1.00 | 0.72 | 0.86 | 0.73 |
| | | Rib1_CCJ | Force | 0.86 | *Ignored* | 0.50 | 0.97 | 0.74 | 0.80 | |
| | | Rib3_CCJ | Force | 0.85 | *Ignored* | 0.22 | 0.98 | 0.60 | 0.72 | |
| | | Rib4_CCJ | Force | 0.72 | *Ignored* | 0.35 | 0.99 | 0.67 | 0.69 | |
| | | Rib6_CCJ | Force | 0.15 | *Ignored* | 0.27 | 0.99 | 0.63 | 0.39 | |
| | | Rib9_CCJ | Force | 0.69 | *Ignored* | 0.77 | 0.98 | 0.87 | 0.78 | |
| | | Upper sternum | Force | 0.99 | *Ignored* | 0.56 | 1.00 | 0.78 | 0.88 | |
| Frontal | 1 | N/A | Deflection | 0.89 | *Ignored* | 0.68 | 0.99 | 0.84 | 0.86 | 0.84 |
| | | | Force | 0.67 | *Ignored* | 0.94 | 0.98 | 0.96 | 0.82 | |
| | 2 | N/A | Deflection | 0.93 | *Ignored* | 0.70 | 0.99 | 0.85 | 0.89 | 0.86 |
| | | | Force | 0.67 | *Ignored* | 0.95 | 0.98 | 0.96 | 0.82 | |
| Lateral | 1 | N/A | Deflection | 0.97 | *Ignored* | 0.99 | 1.00 | 1.00 | 0.98 | 0.89 |
| | | | Force | 0.61 | *Ignored* | 1.00 | 1.00 | 1.00 | 0.80 | |
| | 2 | N/A | Deflection | 0.96 | *Ignored* | 0.98 | 1.00 | 0.99 | 0.98 | 0.89 |
| | | | Force | 0.61 | *Ignored* | 1.00 | 1.00 | 1.00 | 0.80 | |
| Table top | 1 | Hub loading | Force | 1.00 | *Ignored* | 0.64 | 1.00 | 0.82 | 0.91 | 0.86 |
| | | Single belt | Force | 1.00 | *Ignored* | 0.74 | 0.91 | 0.83 | 0.91 | |
| | | Double belt | Force | 0.73 | *Ignored* | 0.40 | 0.99 | 0.70 | 0.71 | |
| | | Distributed loading | Force | 0.98 | *Ignored* | 0.71 | 1.00 | 0.85 | 0.92 | |
| | 2 | Hub loading | Force | 1.00 | *Ignored* | 0.65 | 0.99 | 0.82 | 0.91 | 0.83 |
| | | Single belt | Force | 1.00 | *Ignored* | 0.62 | 0.99 | 0.80 | 0.90 | |
| | | Double belt | Force | 0.58 | *Ignored* | 0.36 | 0.99 | 0.67 | 0.63 | |
| | | Distributed loading | Force | 0.89 | *Ignored* | 0.73 | 0.99 | 0.86 | 0.88 | |

* 1: GHBMC v4.1 (default) | Linear elastic (E=0.5 MPa). ** 2: GHBMC v4.1 (updated) | Simplified rubber/foam.

## DISCUSSION

The version 4.1 of the GHBMC model was modified to include more realistic material definition of the intercostal muscles (ICM) based on recent published experiments. Its performance was evaluated qualitatively and quantitatively by comparison of the simulation results to the experiments based on signal correlation analysis. Overall, the material properties of the ICM have little effect on the externally measured impact force and chest deformation except in point loading. Sensitivy of the ICM in point loading was already observed in a previous study [20], but it is the first time such influence is studied on a thorax model at multiple length scales.

The use of a correlation method such as CORA allows to perform a multi-configuration evaluation of a FE model, and it is the first time such a method is applied to evaluate the influence of modification on a thorax model at multiple length scales. Nevertheless, not all the CORA ratings obtained for each test configuration was high, therefore a degree of caution is needed when we evaluated the influence of a specific parameter. Consequently, the relative assessment of different versions of the same model using CORA may be more pertinent that an absolute evaluation of a specific version. Thus, this method was used during this study for the different versions of the model.

As the current assessment of the model response focused on global response, its ability to predict rib fracture, a common feature in whole body FE models, was not evaluated. Fractures were reported in some tests but not in the point loading of the eviscerated ribcage which is the only load case displaying a sensitivity to a change in ICM material. An interesting contribution of this study will be to report the strain distribution within the ribcage to evaluate the influence of the ICM. Nevertheless, as no experimental data is currently available to evaluate strain distribution biofidelity, it will not possible to assess the capability of the model to appropriately predict the strain distribution in the ribs for these loading cases.

## CONCLUSIONS

In the present study, an existing full body model for a seated 50th-percentile male was evaluated under five cases of loading: point loading of the denuded ribcage, frontal pendulum impact tests, lateral and oblique pendulum impact tests and table top tests. The sensitivity of the model to changes in material model of the intercostal muscles (ICM) was evaluated by using two material models: an isotropic linear elastic material model and a foam model defined by a single uniaxial load curve extracted from a recent literature. The performance of these models compared to the experiments was assessed quantitatively through a correlation analysis on the force and chest deflection time histories. The simulations found that that the material properties of the ICM have little effect on the externally measured impact force and chest deformation except in point loading suggesting that the ICM has localized effect. This localized effect may be captured by analyzing the strain distribution in the ribcage.

## ACKNOWLEDGEMENTS

The funding for this study was provided by the Global Human Body Models Consortium.

## REFERENCES

[1] Carroll, J., et al. 2009. “A comparison between crash test results and real-world accident outcomes in terms of injury mechanisms and occupant characteristics.”
THORAX project GA (218516).
[2] Robin, S.2001. “HUMOS: human model for safety–a joint effort towards the development of refined human-like car occupant models.”
In Proceedings of the. 17th Enhanced Safety of Vehicles Conference.
[3] Iwamoto, M., et al. 2002. “Development of a finite element model of the total human model for safety (THUMS) and application to injury reconstruction.”
In Proceedings of the International Research Council on the Biomechanics of Injury conference.
[4] Kimpara, H., et al., 2005. “Development of a Three-Dimensional Finite Element Chest Model for the 5 (th) Percentile Female”

Stapp Car Crash J. 49: p. 251-269.
[5] Zhao, J. and G. Narwani. 2005. “Development of a human body finite element model for restraint system R&D applications.”
In the 19th International Technical Conference on the Enhanced Safety of Vehicles (ESV).
[6] Song, E., Trosseille, X. and Baudrit P. 2009. “Evaluation of thoracic deflection as an injury criterion for side impact using a finite elements thorax model.”
Stapp Car Crash J, 53: p. 155-191.
[7] Ito, O., Dokko Y., and Ohashi K. 2009. “Development of adult and elderly FE thorax skeletal models.”
SAE Technical Paper.
[8] Vezin, P. and Berthet F. 2009. “Structural characterization of human rib cage behavior under dynamic loading.”
Stapp car crash journal, 53: p. 93-125.
[9] Poulard, D., et al., 2015. “Thoracic response targets for a computational model: A hierarchical approach to assess the biofidelity of a 50th-percentile occupant male finite element model.”
J Mech Behav Biomed Mater, 45C: p. 45-64.
[10] Kemper, A., et al., 2005. “Biomechanical response of the human clavicle subjected to dynamic bending. “
Biomedical sciences instrumentation, 42: p. 231-236.
[11] Duprey, S., K. Bruyere, and J.-P. Verriest, 2008. “Influence of geometrical personalization on the simulation of clavicle fractures.”
Journal of biomechanics, 41(1): p. 200-207.
[12] Charpail, E., et al., 2005. “Characterization of PMHS Ribs: A New Test Methodology.”
Stapp car crash journal, 49: p. 183-198.
[13] Li, Z., et al., 2010. “Rib fractures under anterior–posterior dynamic loads: experimental and finite-element study.”
Journal of biomechanics, 43(2): p. 228-234.
[14] Li, Z., et al. 2010. “Development of finite element model of 50th percentile male using multiblock hex meshing approach.”
In Proceedings of the 6th Annual World Congress on Biomechanics, Singapore.
[15] Guo, B.-y., et al.,2007. “Age and gender related changes in biomechanical properties of healthy human costal cartilage.”
Clinical Biomechanics, 22(3): p. 292-297.
[16] Forman, J.L., et al. 2010. “The contribution of the perichondrium to the structural mechanical behavior of the costal-cartilage. “
Journal of biomechanical engineering, 132(9): p. 094501.
[17] Yamada, H. and F.G. Evans, 1970. “Strength of biological materials.”
[18] Farkas, G.A., 1991. “Mechanical properties of respiratory muscles in primates. “
Respiration physiology, 86(1): p. 41-50.
[19] Kelly, N.G., R. McCarter, and G. Barnwell, 1993. “Respiratory muscle stiffness is age-and muscle-specific.”
Aging Clinical and Experimental Research, 5(3): p. 229-238.
[20] Kindig, M., et al., 2015. “Effect of intercostal muscle and costovertebral joint material properties on human ribcage stiffness and kinematics.”
Comput Methods Biomech Biomed Engin, 18(5): p. 556-70.
[21] Hamzah, M., et al. 2013. “An Inverse Finite Element Approach for Estimating the Fiber Orientations in Intercostal Muscles.”
In Proceedings of the Impact Research Council on the Biomechanics of Impact (IRCOBI). Gothenburg, Sweden.
[22] Gayzik, F.S., et al., 2009. “A multi-modality image data collection protocol for full body finite element model development.”
SAE Technical Paper.
[23] Kindig, M.W., et al., 2010. “Structural response of cadaveric ribcages under a localized loading: stiffness and kinematic trends.”
Stapp Car Crash J, 54: p. 337-80.

[24] Kroell, C., D. Schneider, and A. Nahum, 1971. “Impact tolerance and response of the human thorax, in biomechanics of impact injury and injury tolerances of the thorax-shoulder complex.” SAE paper 710851.
[25] Lebarbé, M. and Petit, P. 2012. “New biofidelity targets for the thorax of a 50th percentile adult male in frontal impact.”
In Proceedings of the Impact Research Council on the Biomechanics of Impact (IRCOBI).
[26] Shaw, J.M., et al., 2006. “Oblique and lateral impact response of the PMHS thorax. ”
Stapp Car Crash J, 50: p. 147-167.
[27] Kent, R., Lessley, D. and Sherwood, C. 2004. “Thoracic response to dynamic, non-impact loading from a hub, distributed belt, diagonal belt, and double diagonal belts. “
Stapp Car Crash J, 48: p. 495-519.
[28] Gehre, C., Gades, H. and Wernicke, P. 2009. “Objective rating of signals using test and simulation responses.”
In Proceeding of the 21st International Technical Conference on the Enhanced Safety of Vehicles, Stuttgart, Germany.

# RESULTS OF FIRST FIELD TEST OF TELEMETRY BASED INJURY SEVERITY PREDICTION

**Stewart C. Wang, MD PhD**
**Carla J. Kohoyda-Inglis, MPA**
**Joel B. MacWilliams**
University of Michigan International Center for Automotive Medicine
USA
**Kathryn F. Anderson**
**Julie A. Kleinert**
**Anthony G. Melocchi**
**Lisa A. Stacey**
General Motors
USA
**Jeffery W. Joyner**
OnStar
USA

15-0388

## ABSTRACT

Identification of severely injured occupants is of utmost urgency following a crash event. Advanced automatic collision notification (AACN) has great potential to improve post-crash care if the risk of severe injury to a vehicle's occupants can be accurately predicted. The National Expert Panel for Field Triage set a 20% risk of Injury Severity Score (ISS) 15+ injury [1] as the threshold for urgent transport to a trauma center. The objective of this study was to field test real world performance of the published injury severity prediction (ISP) algorithm in collisions involving recent model GM vehicles equipped with OnStar.

This study was approved by the IRB of the Michigan Department of Community Health. There were 924 occupants in 836 crash events, involving vehicles equipped with AACN capabilities, in the state of Michigan which were identified from the OnStar records. The police crash report corresponding to the event was identified in the State of Michigan database and used to confirm data sent by telemetry from the vehicle. The injury status of all occupants in the case vehicles was determined. Occupants not transported for medical evaluation were assumed to have ISS<15. For occupants transported from the scene for evaluation and treatment, medical records and imaging data were obtained from the treating facility. Case reviews were conducted to jointly analyze crash, vehicle telemetry, and injury outcome data. The algorithm was used to calculate the predicted risk of injury based on transmitted telemetry data and this prediction was compared to the observed injury outcome for each vehicle as well as each occupant.

In this field study, the ISP algorithm's ability to predict whether a vehicle had a seriously injured (ISS>15) occupant was, in terms of sensitivity, at 63.64% compared to the model sensitivity of 39.6% and it also came very close to expectations of specificity at 96.12% compared to the model specificity of 98.3% with use of age and gender data. Without use of age and gender, for ISP calculation, the sensitivity performance was 45.45% while the specificity improved slightly to 97.58%. Detailed analysis of cases suggests that further performance gains could be obtained with more detailed definition of crash direction, seating position, and occupant age.

There were 184 candidate crash occupants in 167 vehicles not included in the study analysis due to: A) missing Police accident reports, n=77 in 75 crashes; B) inability to retrieve medical records, n = 71 in 61 crashes; or C) rollover event, n=36 in 31 crashes. Analysis of these excluded cases did not reveal any bias in crash severity or injury that would confound the current study findings.

This study confirms for the first time under real-world field conditions that occupant injury severity can be predicted using vehicle telemetry data. The ISP algorithm's ability to predict a 20% or greater risk of severe (ISS15+) injury was better than anticipated and confirms ISP's utility for the field triage of crash subjects. This analysis suggests that AACN technology can greatly facilitate the collection of field data with ISP also serving as a baseline for potential monitoring of the benefits resulting from vehicle safety design changes.

## INTRODUCTION

Over 1.2 million people died worldwide as a result of road traffic accidents in 2009. While many countries do not have data for injuries sustained in motor vehicle crashes (MVC), estimates from the WHO indicate the total number of non-fatal injuries sustained in a MVC is between 20 and 50 million. [2]

In 2013, the most recent year for which US data is currently available, there were 32,719 road traffic fatalities in the United States alone. Additionally, 2,313,000 people were injured (732 per 100,000). [3]

While some vehicle occupants sustain immediately fatal injuries, a substantial portion expire subsequently during transport or in the emergency department as a result of traumatic shock from injuries that compromise oxygenation and ventilation or cause bleeding. Minimizing the time between injury and treatment is absolutely critical to reducing mortality and morbidity. [4] It is therefore crucial to get first responders to the scene quickly – with the appropriate equipment to initially treat the injuries sustained and then to triage and transport the occupants to the appropriate medical center for further care. Level 1 trauma centers are resourced and staffed to provide definitive trauma care. Severely injured patients have a 25% reduction in mortality if transferred to a Level I trauma center versus if they are transported to a non-Trauma center [5]

At the injury scene, EMS providers determine the severity of injury, initiate medical management and identify the most appropriate medical facility destination through a process called "field triage." [6] In 2009, the Centers for Disease Control and Prevention (CDC) convened the National Expert Panel on Field Triage to review and make recommendations for improving the American College of Surgeons Field Triage Decision Scheme which served as the basis for triage protocols used by state and local EMS systems across the United States. [4] The goal of the field triage process is to get the right person to the right place in the right time. Not every MVC victim needs to be transported to a level I trauma center, but for those who do, it is vital that the first responders on the scene recognize this and move quickly. The first two steps of the Field Triage Decision scheme use anatomic (Step 1) and physiologic criteria (Step 2) to identify the most severely injured patients. Step 3 uses mechanism of injury, for which the National Expert Panel targeted a 20% risk of ISS>15 injury. MVCs were the most significant mechanism of injury addressed in Step 3 and the Panel recommended the inclusion of "vehicle telemetry consistent with high risk of injury". This criterion was included in the 2006 revision as a placeholder in anticipation of more widespread adoption of AACN equipped vehicles. [4].

The CDC subsequently convened a subcommittee of the National Expert Panel over 2007-2008 to coordinate the use of vehicle telemetry. [4] This Expert Panel on the Advanced Automatic Collision Notification and Triage of the Injured Patient concluded that AACN showed promise in improving outcomes to severely injured crash patients by a) predicting the likelihood of serious injury in vehicle occupants, b) decreasing response times by pre-hospital care providers, c) assisting with field triage destination and transportation decisions, d) decreasing time to definite trauma care and e) decreasing death and disability from MVCs. This panel recommended that pilot studies be conducted using vehicle telemetry data including

- Delta V (crash severity)
- Principal direction of force (PDOF)
- Seatbelt usage
- Crash with multiple impacts
- Vehicle type.

Additionally, it recommended that voice communication be established with the vehicle occupants to determine the presence of injuries and also to collect additional information such as age and gender that might affect injury risk. The panel also recommended that injury risk should be calculated with all available data and that if the occupant is at 20% or greater risk of ISS>15 injury, the relevant Public Safety Answering Point (PSAP) should be notified that the occupant meets the Field Triage Decision Scheme's Step 3 criterion for "vehicle telemetry consistent with high risk of injury" and appropriate resources dispatched. [4]

Based on these recommendations an ISP algorithm was developed using a logistic regression model of nationally representative crash data (NASS-CDS from calendar years 1999-2008). [7] Vehicle safety systems are constantly evolving, including changes to the vehicle structure and the restraint systems; as such the risk of injury may also evolve as the vehicle fleet changes. Since AACN equipped vehicles are newer and NASS-CDS contains crash data from many model years, NASS-CDS was filtered to include model year 2000 and newer cars, light trucks, and vans. Only planar non-rollover crash events were used as the ISP algorithm is not designed for rollover crashes. Delta-V is calculated within the current generation of Event Data Recorders (EDRs) and is utilized in the ISP algorithm because delta-V has been shown to be predictive of injury within planar crashes; this same relationship has not been demonstrated in rollover crashes. [6]. For the logistic regression model, crash PDOF was binned into four crash directions (front, left, right and rear). Frontal crashes were defined as those with PDOF of 11, 12 or 1 o'clock, right side as those from 2 to 4 o'clock, rear from 5 to 7 o'clock, and left from 8 to 10 o'clock. The ISP algorithm was

designed to predict the probability that a crash-involved vehicle will contain one or more occupants with severe injury (ISS>15). Analysis of the logistic regression model and resultant ISP algorithm targeting 20% or greater risk of ISS>15 injury showed that crash direction, seat belt use and Delta-V were the most important predictors of serious injury. The NASS-CDS dataset estimates delta-V on an energy-based calculation using post-crash vehicle deformation.

The ISP model sensitivity, based on the NASS-CDS dataset, was 40% and specificity was 98% using an injury probability cutoff of 20% risk of ISS >15.

The current study was undertaken as a pilot to analyze the field performance of the ISP algorithm for newer AACN-equipped GM vehicles involved in crashes. Study objectives also included assessment of the effects of 1) limiting data collection to a single vehicle manufacturer (GM); 2) substitution of transmitted Delta-V from crash sensors in place of vehicle deformation based crash severity; and 3) substitution of transmitted PDOF from crash sensors in place of vehicle deformation based crash direction.

**Methods**

Any vehicle involved in a MVC, which had a current subscription to the OnStar telematics program, was eligible for inclusion. The ICAM team received permission from the Michigan Department of Community Health (MDCH) to access medical records for any patient involved in one of these crashes. Both vehicle and occupant identification remained anonymous to GM and OnStar.

For this pilot study, ICAM received a convenience sample of 1,003 OnStar crash cases that took place in the state of Michigan from January 2008 through August 2011. These data included information provided by the SDM to the PSAP. Also included is the latitude and longitude of the scene, delta direction, delta velocity, whether and which airbags deployed, whether multiple impacts occurred, whether a rollover event occurred, vehicle category and type.

As a research institution, ICAM requested and was granted access to the Michigan Department of Transportation User website. With the time and location data from the OnStar, staff members were able to pinpoint each crash and retrieve the Police Accident Report (PAR). The PAR provides extensive detail about the vehicle, crash, and occupants. In order to request medical records, it was necessary to gather the occupants' names and birthdates as well as where they were transported if they needed further care. Matching the vehicle identification number (VIN) from the OnStar data to the PAR, the ICAM team ensured they were looking at the report for the correct vehicle and crash. 1,108 candidate crash occupants were identified using this process.

With names and birthdates, the treating hospitals were contacted to request medical records (EMS transport sheets, Emergency Department notes, operative notes, radiology reports, and discharge notes) as well as radiological data – specifically any computed tomography scans performed on the occupants. ICAM nursing staff then abstracted injury information from the medical records and created a list of injuries sustained for each transported occupant. If occupants were not transported, it was assumed that their injury severity score (ISS) was <15.

Of the 1,003 candidate crash cases, there were 184 occupants in 167 vehicles that were not included in the study analysis due to: A) missing police accident reports, n=77 in 75 crashes; B) inability to retrieve medical records, n = 71 in 61 crashes; or C) rollover event, n=36 occupants in 31 crashes. Analysis of these excluded cases did not reveal any bias in crash severity or injury that would confound the current study findings. In the end 836 crash vehicles with 924 occupants were available for analysis.

The implementation of the ISP Algorithm for seatbelt usage uses a base case of 0 if the seat belt is not used or its use is unknown, for any occupied seat. In this study approximately 40% of the crash incidents did not have complete seat belt information so the base case was applied in these cases in the same way that the OnStar application would process these cases. See Appendix B for relative weights of NASS sample to the convenience sample for key variables.

Concurrently, ICAM's crash investigator with more than 30 years of experience in the crash industry crosschecked the OnStar telemetry data against the PARs for each case. He confirmed that the SDM data matched the PAR data. Any incongruous data was marked for further review.

Study subject confidentiality was protected by having all records and medical data tagged with an anonymous study ID by ICAM medical staff before crash review of GM/OnStar engineers. No subject identifiable data collected by ICAM was made available to GM/OnStar.

A multidisciplinary review panel including ICAM medical and research personnel as well as automotive engineers with previous medical training from GM and OnStar was convened to review all cases where an occupant was transported to a medical center. Furthermore, cases with incongruities between predicted ISP and observed outcomes were reviewed in depth with consideration of all the following factors:

Crash Factors

1. Configuration
    a. PDOF
    b. Angled
    c. Offset (Vehicle Overlap)
    d. Narrow object
2. Compatibility
    a. Mass
    b. Geometry
    c. Stiffness
3. Multiple impacts
4. Rollover
5. Occupant seating position
6. Ejection
7. Entrapment

Vehicle factors

1. Deployment of Airbags
    a. Curtain
    b. Thorax
    c. Pelvic/thorax
    d. Knee
    e. Second stage co-deploy
2. Safety belt restraint
    a. Use
    b. Loading locations on occupant
3. Deployment of Pre-tensioners
    a. Dual
    b. Single
    c. Location (on retractor, buckle, or outboard lap anchor)
4. Head rest configurations
5. SDM
    a. Supplier
    b. Generation

Occupant factors

1. Age
2. Gender
3. Morphomics
    a. Anthropometry
    b. BMD
    c. Muscle Quality/Mass
    d. Fat Distribution/Mass
4. Co-morbidities
5. Stature

**RESULTS**

As some telematics providers do not collect age and gender information, we examined ISP performance with and without inclusion of age and gender data.

**ISP calculated with Known Age/Gender**

SENSITIVITY – 63.64%

SPECIFICITY – 96%

| | **Low ISS** | **High ISS** | |
|---|---|---|---|
| **Low ISP** | **792** | **4** | 796 |
| **High ISP** | **33** | **7** | 40 |
| | 825 | 11 | 836 |

**Table 1 ISP with Known Age & Gender**

ISP TRUE NEGATIVES (ISP<.2, no occupant in vehicle with ISS>15): The majority of the vehicle cases were, as expected, those in the low ISP/low ISS category. In fact, there were 792 cases in this category using age and gender when calculating the ISP. The occupants in these vehicles were not transported to a hospital and were considered uninjured. The ICAM panel did not review these cases, as they were considered true negatives.

ISP TRUE POSITIVES (ISP >.2, at least one occupant in vehicle with ISS>15): The initial expectation that there would be few cases with a high ISP and high ISS (true positives) was confirmed. There were seven such cases when age and gender were included in the ISP calculation. (Table 2)

| ID | (Age/ Gender) | Veh Occ | PDOF | ISP | ISS |
|---|---|---|---|---|---|
| 721 | (75 M) | Drive | Right | 0.31 | 29 |
| 2541 | (18 F) | 2nd row right | Right | 0.4 | 75 |
| 749 | (48 F) | Driver | Front | 0.58 | 43 |
| 772 | (20 M) | Driver | Left | 0.66 | 16 |
| 2030 | (81 F) | RFP | Right | 0.27 | 22 |
| 965 | (46 F) | Driver | Front | 0.29 | 29 |
| 1522 | (55 F) | Driver | Right | 0.61 | 17 |

**Table 2 ISP True Positive Cases**

ISP FALSE NEGATIVES: There were four cases in the low ISP/high ISS category. The average age of these case occupants was 46.75. The calculated ISP in this false negative group ranged from 0.03 to 0.19 (3% to 19% risk of ISS>15 injury). The average ISP was 0.12. The average ISS in this group was 24.5. All the cases in this group involved females.

We looked at each of these cases in depth to determine if we could discern potential reasons for the discrepancy between prediction and outcome. As stated previously severely injured patients with ISS>15 require the highest level of care and rapid identification of this group is essential. (Table 3)

| ID | (Age/ Gender) | Veh Occ | PDOF | ISP | ISS |
|---|---|---|---|---|---|
| 1430 | (45 F) | RFP | Rear | 0.15 | 26 |
| 964 | (40 F) | Driver | Rear | 0.19 | 34 |
| 1806 | (52 F) | 2d row right | Right | 0.03 | 17 |
| 1403 | (50 F) | Driver | Left | 0.12 | 21 |

**Table 3 ISP False Negative Cases**

**Case 1430**

This case occupant was the 45-year-old, female, 3-point-belt restrained, right front passenger of a mid-size sport utility vehicle. The vehicle was involved in a severe rear impact from a semi-truck, followed by a minor frontal impact. The driver of the vehicle, a 50-year-old male, sustained lung injuries, an ISS of 10. The case occupant sustained severe head and chest injuries and had an ISS of 26. The telemetry did not report multiple impacts (it did not meet the 15 mph ΔV notification cutoff for a frontal impact). However, clearly there were multiple collisions (rear followed by front). A potential contributing factor is the incompatibility in terms of stiffness, mass, and geometry between the two vehicles.

**Case 964**

This case occupant was the 40-year-old, female, with unknown belt status, driver of mid-size sport utility vehicle. The case vehicle was struck in a rear-end fashion by a large semi-truck, which caused the case vehicle to travel diagonally through the intersection and over a curb. She sustained severe head, abdominal, and pelvic injuries and received an ISS of 34, with a calculated ISP of 0.19. The information from OnStar had 2 high ΔVs (>40 mph); the crash was not identified as a multiple impact, but was classified as a rollover. There was no indication on the PAR that a rollover had taken place; the vehicle was on its wheels at the time of the report, hence this case was included for consideration. A potential contributing factor is the large difference in terms of stiffness, mass, and geometry between the two vehicles.

**Case 1806**

The case occupant was the 52-year-old, female, 3-point-belt restrained, right rear passenger of a mid-size passenger car. The impact was a right sided, T-type impact, essentially occurring at her seating position. Her ISS was 17, due to chest injuries and pelvic fractures and the calculated ISP was 0.03. Both front-seat passengers were belted so the ISP was calculated utilizing their belted status. ISP correctly predicted the outcome for the front seat occupants, however, not correctly for this rear-seated occupant. The current algorithm was designed to predict the probability that a crash-involved vehicle will contain one or more occupants with severe injury (ISS>15) and therefore

underweights the injury risk of right sided impacts when there is an occupant located on the right side of the vehicle. Since most of the vehicles in the NASS-CDS dataset used in the previous study to develop the ISP algorithm did not have right front or rear seat passengers, the ISP may underweight the injury risk of passengers at those locations and could be evolved to include a right front passenger variable.

**Case 1403**

The case occupant was the 50-year-old, female, 3-point-belt restrained, driver of a mid-size passenger car. The case vehicle was struck on the left side, forward of the A-pillar by a school bus and was categorized as a left-side impact in the OnStar data. This very thin occupant sustained severe head injuries, an ISS of 21 and a calculated ISP of 0.12. A potential contributory factor is the case occupant's stature. In our past research, we have found that thin occupants often sustain more serious head injuries than heavier occupants. [8] Another potential contributing factor is the incompatibility in terms of stiffness, mass, and geometry between the two vehicles.

ISP FALSE POSITIVES: There were 33 cases in the high ISP/low ISS category. We analyzed these on a case-by-case basis to assess any potential trends. Twenty-two of these cases were determined to be single impacts and eleven of the cases sustained multiple impacts. Nineteen of the cases (57.6%) were transported to a medical center. The average age in this group was 39.56, which was younger than the 46.75 average age of the ISP false negative group. The average ISP for this group was 0.36, and the average ISS was 3.09. (Appendix A)

## DISCUSSION

The results of this field study confirm the utility of vehicle telemetry data transmitted by AACN systems for identification of crash vehicles that contain seriously injured occupants. Multiple models have been developed in the past, but they have all relied on vehicle-deformation based measurement of crash severity and data obtained from the NASS-CDS dataset. This study is the first to utilize actual telemetry data transmitted from vehicles involved in wide variety of crashes to assess real world injury prediction.

The field performance of the Injury Severity Prediction algorithm utilizing the OnStar dataset using age and gender data showed 63.64% sensitivity and 96% specificity. Without age and gender data, sensitivity is 45.45%, while specificity improved slightly to 97.58%. Sensitivity is defined as the probability that a test result will be positive (ISP≥0.2) when the condition (ISS>15) is present. The observed sensitivity performance was better than the 40% performance that the ISP algorithm achieved when applied to the NASS-CDS dataset. There may be several reasons for this including more consistent and accurate measurement of crash severity, more accurate determination of restraint use and more consistent vehicle safety performance as all the crash vehicles were from a single manufacturer and were newer models.

The specificity performance of the ISP in this study was 96%. Specificity is defined as the probability that a test result will be negative (ISP<0.2) when the condition (ISS>15) is not present. The observed specificity performance was slightly less than the 98.3% performance that the algorithm achieved when applied to the NASS-CDS dataset. While the overall number of cases studied is relatively small, there were fewer ISS>15 injured cases observed than would have been expected based on the number of cases, configuration and crash-severity mix of the crashes included in this study. This trend might be the result of continuously improving vehicle safety performance in the study fleet versus the NASS-CDS fleet used to calibrate the algorithm. The average age of the study fleet was younger than the average age of the vehicles in NASS-CDS.

The results of this field study confirm the importance of age and gender data and also suggest that it may be important to utilize more granular age data than a single threshold at age 55. The sensitivity of the ISP algorithm improved from 45.45% to 63.64% with the inclusion of age and gender data and the false negative group was slightly older on average than the false positive group (46.75 vs. 39.56). It is well known that the increased crash injury risk accelerates with advancing age rather than plateauing at age 55. [5, 9-11] The current ISP algorithm includes age (>55) and gender (presence of a female in the vehicle) as variables. However, SDMs do not have the capability to capture these data. It has been suggested that when the telematics provider contacts the occupants in the crashed vehicle, they can ask questions about who is in the vehicle. In this way, they can obtain age and gender data to send to the PSAPs. The results of the current study confirm the importance of age and gender in injury risk calculation and highlight the importance of collecting this data. Several of the false negative (low ISP/high ISS) cases involving very elderly patients as well as the overall aging population trend suggest that sensitivity might be further improved by including more granular age parameters in the ISP than a single threshold of age 55. Similarly, the younger age in the false positive (high ISP/low ISS) cases suggest that decreasing the risk coefficients for young

occupants might also improve ISP performance. These potential benefits must be weighed against the increased time and potential confusion that may result in attempts to obtain this information.

The original algorithm was developed from data culled from the National Automotive Sampling System (NASS) and defined crash direction into only four categories (front, left, right, and rear). This study followed that convention. However, real world crashes do not always fit precisely into these categories, and frequently fall into offset or narrow configurations that may have a different impact on the occupant injury risk. The large number of offset frontal and sideswipe cases among our false positives suggests that improving telemetry data to better differentiate these crash configurations may help improve ISP performance.

Right oblique and right side impact crashes are underweighted in the original ISP algorithm. Our data with 1 of the false negative cases involving right side occupant suggest that it may be beneficial to adjust the right side impact coefficients to reflect a higher risk of severe injury if it is determined by telemetry or communication that right sided seats are occupied in a right oblique or side impact crash.

Telemetry data regarding possible occupant ejection would also be very useful if automotive grade sensors for this application are created.

While the study covered all types of vehicles, from compact car to large pickup, we limited the specific vehicle models in order to see injury patterns more clearly. The type of vehicle can affect the pattern and risk of injury, especially in two-vehicle crashes where there is vehicle incompatibility in terms of mass and geometry. The sensitivity of this study is better than originally predicted (40%) possibly in part due to the consistency of the vehicles from a single manufacturer with a consistent occupant protection strategy.

While the specificity of this study is a little less than expected, it is quite good for a preliminary study. This specificity performance may allow very large potential savings as technology becomes more comprehensive and reliable. The observed specificity performance in the field by the ISP suggests that it may become possible to decrease the dispatch of limited EMS resources to the scenes of low risk crashes. With new safety systems coming on line within the next few years as well as enhancements in the SDM systems, we anticipate continued improvements in ISP specificity performance.

**Study Limitations**

When selecting for convenience samples, it is important to recognize that there are limitations to the collection and reporting of the data.

One significant challenge for collection of telemetry crash data is that the SDMs can vary from vehicle to vehicle, depending on the vehicle model year and the evolution of module hardware/software upgrades. In order to build the sample, OnStar collected data on vehicles where the SDMs were known to have the capability needed to support the algorithm calculation. As such, the mix of vehicles in the study differs slightly from the NASS-CDS ISP development sample and has a higher percentage of sport utilities and a lower percentage of pickups and vans compared to the development sample. See Appendix B for the full weighting comparison.

Another limitation of the study relates to seat belt status. For any front occupied seat, the ISP algorithm assumes a base case if the seat belt is *unbelted* or its use is *unknown.* The probability of injury severity is lowered if the belt status is determined to have been buckled. Therefore, in the case of unknown belt status, the ISP will have a higher probability of injury severity than if the algorithm assumed the belt was used. In this study, approximately 40% of the crashes did not have complete seat belt information and for these cases the *unknown* base case was applied – as ISP algorithm would code them in a real-world situation. It should be understood that had seatbelt status been known and if the occupants in these cases were belted, the outcome of the study could have been slightly different. For the seven cases classified as High ISP/High ISS (true positive), it is possible that some of these cases would have had a lower ISP and been classified as a false negative, thereby reducing sensitivity. Similarly, for the 33 cases in the High ISP/Low ISS category (false positive), some of those cases would have possibly been classified as true negative, thereby increasing specificity. The cases with Low ISP/Low ISS (true negative) and Low ISP/High ISS (false negatives) would be unaffected as reducing the ISP would not change the categorization of these cases.

Another limitation is that the "multiple impacts indicator" is an element that varies fairly significantly from NASS-CDS to GM's telemetry protocols. In NASS-CDS, multiple impacts are flagged anytime a vehicle has two impacts regardless of their severity. For example, in NASS-CDS, if a vehicle hits a mailbox and subsequently hits a tree, both events are recorded and the multiple impacts indicator is turned on. At GM/OnStar multiple impacts is turned on if two or more qualifying events occur in the same ignition cycle. A qualifying event is an event that has a Delta V over a predefined level. In our example the impact with the mailbox would not have a Delta V significant enough to be a qualified event and the multiple event indicator would not be turned on. See Appendix B for the full weighting comparison.

Finally, due to IRB limitations, the study was conducted using only state of Michigan crashes. However the sample does include crashes from varying years, seasons, weather conditions, times of day, and days of the week.

## CONCLUSION

The level of sensitivity for severe injury achieved by ISP in this field study was a remarkable 63.64%. This performance is impressive from a medical perspective, especially considering that it is achieved with only data or communication transmitted from the vehicle and before dispatch of EMS to the scene.

Since the consequence of missing a severe injury is immediately life-threatening, sensitivity has generally received the highest priority in trauma care. The longstanding Field Decision Scheme has been used as the basis for triage protocols in state and local EMS systems across the United States for many decades. The combined sensitivity of the first two steps (Physiologic and Anatomic) of the Decision Scheme has consistently remained around between 40-50% with field data collected first hand by EMS during the pre-hospital phase of care. [12-15] Newer crash sensors may also support improvements in the performance of the ISP algorithm. As the SDM systems in vehicles change and more detailed telemetry data collection is possible, ICAM anticipates improvements in risk prediction. The fleet is in constant flux with new safety systems as well as enhanced SDMs. [16, 17]

Michigan, parts of the United States, and the world all have many rural areas where reports of crash events to public safety may be delayed, leading to slow response by EMS. [18, 19] These same areas are also characterized by long transport distances that will delay the transfer of the severely injured to medical facilities. Automatic collisions notification alone, without additional vehicle telemetry for injury prediction, can save significant lives [20]. Time is of the essence in these cases and getting these occupants to the proper medical destination capable of definitive trauma care is essential. Transmitted telemetry data from AACN can not only provide notification that a crash has occurred, it can also alert the local first responders as to what type and how severe of crash they are responding to – they will know what equipment to bring in order to best triage and treat the occupants. There is potential also to immediately initiate air transport and get them to the scene quickly as well.

The resources utilized in the emergency care of crash injuries place a significant burden on local communities, especially rural ones. Over triaging patients without severe injuries to trauma centers or other medical centers for unnecessary evaluation is expensive and wasteful. The recent changes to Step 3 (mechanism of injury) of the Field Triage Decision Scheme is estimated to provide yearly US savings of over $500 million in medical costs alone. [21] With widespread use of AACN, those savings can be multiplied.

**REFERENCES**


1. AAAM, *Abbreviated Injury Scale 2005*. 2005, 2007 updates ed, ed. T.A. Gennarelli and E. Wodzin. 2005, Barrington, Illinois: AAAM. 167.
2. World Health Organization, *Global Status Report on Road Safety: Time for Action*. 2009, World Health Organization: Geneva. p. 301.
3. NHTSA, *Traffic Safety Facts 2013*. 2013, Washington, DC: US Department of Transportation, National Highway Traffic Safety Administration.
4. Sasser, S.M., et al., *Guidelines for field triage of injured patients. Recommendations of the National Expert Panel on Field Triage.* MMWR Recomm Rep, 2009. **58**(RR-1): p. 1-35.
5. MacKenzie, E.J., et al., *A national evaluation of the effect of trauma-center care on mortality.* N Engl J Med, 2006. **354**(4): p. 366-78.
6. Bailey, B. and S. Sasser, *Automatic Crash Notification's Role in Triage.* Jounal of Emergency Medical Services, 2011.
7. Kononen, D.W., C.A.C. Flannagan, and S.C. Wang, *Identification and validation of a logistic regression model for predicting serious injuries associated with motor vehicle crashes.* Accident Analysis & Prevention, 2010. **43**(1): p. 112-22.
8. Wang, S.C., et al. *Increased Depth of Subcutaneous Fat is Protective Against Abdominal Injuries in Motor Vehicle Collisions*. in *Annual Proceedings for the Association for the Advancement of Automotive Medicine*. 2003: AAAM.
9. Champion, H.R., et al., *The Major Trauma Outcome Study: establishing national norms for trauma care.* J Trauma, 1990. **30**(11): p. 1356-65.
10. Grossman, M.D., et al., *When is an elder old? Effect of preexisting conditions on mortality in geriatric trauma.* J Trauma, 2002. **52**(2): p. 242-6.
11. Morris, J.A., Jr., E.J. MacKenzie, and S.L. Edelstein, *The effect of preexisting conditions on mortality in trauma patients.* JAMA, 1990. **263**(14): p. 1942-6.
12. Wang, S.C., *CIREN Data Review for CDC Field Triage Committee*. 2006, University of Michigan: Ann Arbor.
13. Santaniello, J.M., et al., *Mechanism of injury does not predict acuity or level of service need: field triage criteria revisited.* Surgery, 2003. **134**(4): p. 698-703; discussion 703-4.
14. Henry, M.C., et al., *Incremental benefit of individual American College of Surgeons trauma triage criteria.* Acad Emerg Med, 1996. **3**(11): p. 992-1000.
15. Bond, R.J., J.B. Kortbeek, and R.M. Preshaw, *Field trauma triage: combining mechanism of injury with the prehospital index for an improved trauma triage tool.* J Trauma, 1997. **43**(2): p. 283-7.
16. Clark, D.E. and B.M. Cushing, *Predicted effect of automatic crash notification on traffic mortality.* Accid Anal Prev, 2002. **34**(4): p. 507-13.
17. Hunt, R.C., *Emerging communication technologies in emergency medical services.* Prehosp Emerg Care, 2002. **6**(1): p. 131-6.
18. Champion, H.R. and B. Cushing, *Emerging technology for vehicular safety and emergency response to roadway crashes.* Surg Clin North Am, 1999. **79**(6): p. 1229-40, vii.
19. NHTSA, *National Highway Safety Administration. Automatic collision notice field test summary.* Ann Emerg Med, 2001. **38**(4): p. 453-4.
20. Lahausse, J.A., et al., *The potential for automatic crash notification systems to reduce road fatalities.* Ann Adv Automot Med, 2008. **52**: p. 85-92.
21. Faul, M., et al., *Large cost savings realized from the 2006 Field Triage Guideline: reduction in overtriage in U.S. trauma centers.* Prehosp Emerg Care, 2012. **16**(2): p. 222-9.

Appendix A

| UMID | Age | Gender | Veh Occ | PDOF | Veh Type | ISP | ISP A/G | ISS | Mult | Trans | Review Notes |
|---|---|---|---|---|---|---|---|---|---|---|---|
| 633 | 37 | F | Driver | Front | CAR | 0.16 | 0.23 | 4 | N | Y | near-side offset frontal |
| 2105 | 21 | F | Driver | Left | CAR | 0.18 | 0.25 | 0 | N | N | near-side sideswipe |
| 2106 | 32 | F | Driver | Left | CAR | 0.14 | 0.20 | 0 | N | N | full frontal |
| 644 | 16 | M | Driver | Left | CAR | 0.71 | 0.71 | 1 | Y | Y | near-side offset front corner hit, into a near-side sideswipe |
| 716 | 49 | F | Driver | Front | UTILITY | 0.17 | 0.24 | 0 | Y | Y | near-side offset frontal (tree) |
| 1233 | 17 | F | Driver | Left | UTILITY | 0.27 | 0.36 | 1 | N | Y | near-side L-type front |
| 743 | 56 | F | Driver | Left | CAR | 0.21 | 0.52 | 2 | N | Y | near-side T-type (21 mph delta V) |
| 751 | 18 | F | Driver | Front | CAR | 0.18 | 0.26 | 10 | N | Y | full frontal |
| 837 | 80 | F | Driver | Front | UTILITY | 0.26 | 0.59 | 11 | N | Y | full frontal |
| 1248 | 99 | M | Driver | Front | CAR | 0.16 | 0.35 | 0 | N | N | severe frontal into a guardrail/barrier |
| 863 | 50 | F | Driver | Right | CAR | 0.29 | 0.39 | 0 | N | N | full frontal |
| 892 | 20 | F | Driver | Right | CAR | 0.14 | 0.21 | 0 | N | N | minor near-side sideswipe followed by far-side offset frontal into tree |
| 551 | 53 | F | Driver | Front | CAR | 0.41 | 0.52 | 11 | Y | Y | near-side frontal into mailbox (minor) followed by center frontal into tree |
| 919 | 40 | M | Driver | Front | CAR | 0.26 | 0.26 | 0 | Y | Y | near-side offset frontal followed by a near-side offset frontal tree impact |
| 938 | 17 | M | Driver | Front | UTILITY | 0.37 | 0.37 | 1 | Y | Y | full frontal |
| 946 | 48 | F | Driver | Front | UTILITY | 0.24 | 0.33 | 14 | N | Y | near-side sideswipe, followed by offset near-side frontal |
| 1253 | 18 | M | Driver | Left | CAR | 0.57 | 0.57 | 1 | Y | Y | near-side sideswipe (minor), followed by offset near-side frontal |
| 955 | 62 | F | Driver | Front | CAR | 0.12 | 0.36 | 5 | Y | Y | 3 impacts (front, left, and rear) with a ditch |
| 957 | 43 | F | Driver | Front | UTILITY | 0.13 | 0.29 | 2 | N | Y | frontal |
| 997 | 26 | F | Driver | Front | UTILITY | 0.22 | 0.31 | 0 | Y | N | near-side L-type rear followed by minor frontal into tree |
| 1001 | 39 | F | Driver | Right | UTILITY | 0.28 | 0.38 | 9 | N | Y | far-side T-type |
| 1024 | 36 | F | Driver | Front | UTILITY | 0.33 | 0.43 | 1 | N | Y | full frontal |
| 1027 | 57 | M | Driver | Left | CAR | 0.12 | 0.27 | 14 | N | Y | near side T-type |
| 1040 | 58 | F | Driver | Front | UTILITY | 0.08 | 0.28 | 0 | N | N | offset frontal |
| 2533 | 59 | F | Driver | Left | CAR | 0.17 | 0.47 | 0 | N | N | near-side T-type |
| 1078 | 23 | F | Driver | Front | CAR | 0.27 | 0.36 | 0 | N | N | full frontal |

| UMID | Age | Gender | Veh Occ | PDOF | Veh Type | ISP | ISP A/G | ISS | Mult | Trans | Review Notes |
|---|---|---|---|---|---|---|---|---|---|---|---|
| 1172 | 22 | F | Driver | Left | CAR | 0.22 | 0.30 | 0 | Y | N | near-side from pickup, followed by narrow frontal into pole/tree |
| 1186 | 24 | M | Driver | Front | CAR | 0.53 | 0.53 | 10 | N | Y | near-side offset frontal |
| 1221 | 62 | F | Driver | Right | CAR | 0.08 | 0.26 | 5 | Y | Y | far-side T-type, followed by near-side T-type |
| 1291 | 22 | F | Driver | Front | CAR | 0.22 | 0.31 | 0 | N | N | far-side offset frontal |
| 1521 | 35 | F | Driver | Left | UTILITY | 0.22 | 0.31 | 0 | N | N | near-side offset frontal |
| 2107 | 43 | F | Driver | Left | CAR | 0.30 | 0.40 | 0 | N | N | near-side L-type front |
| 1768 | 24 | M | Driver | Left | PICKUP | 0.28 | 0.28 | 0 | Y | N | near-side sideswipe followed by offset frontal |

Appendix B

**Seat Belt Usage**
The implementation of the ISP Algorithm for seatbelt usage uses a base case of 0 if the seat belt is not used or its use is unknown, for any occupied seat. For seat belt usage by all occupants the belt usage coefficient is used in the ISP calculation. In this study approximately 40% of the crash incidents did not have complete seat belt information so the base case was applied in these cases in the same way that the OnStar application would process these cases. In those cases where seat belt information was unavailable and the Police report indicated belt use, or the injury patterns indicated belt use, then the belt usage coefficient was used in the ISP calculation.

**Vehicle Models**
The vehicle makeup in this study is influenced by the fact that all of the accidents were confined to the state of Michigan. The original study, by Kononen, Flannagan, and Wang, relied on a much larger source of information (NASS/CDS). It is important to understand the differences in vehicle types.

**Multiple Impacts**
Multiple impacts were determined by the availability of secondary delta V data. If the secondary delta v was null then the accident was a determined to be a single impact.

**See following table for full comparison to NASS-CDS development data set.**

| | | Average Values | | |
|---|---|---|---|---|
| | | All Cases | Complete Cases | Complete Cases |
| **Variable** | | **NASS-CDS** | **NASS-CDS** | **ICAM Sample** |
| | **ISS15+** | 0.124 | 0.108 | 0.012 |
| | **Median ln(Delta-V mph)** | 2.820 | 2.820 | 2.606 |
| **Direction** | **Front** | 0.800 | 0.780 | 0.695 |
| | **Left** | 0.082 | 0.088 | 0.100 |
| | **Right** | 0.074 | 0.080 | 0.122 |
| | **Rear** | 0.044 | 0.052 | 0.083 |
| **Vehicle_Type** | **Car** | 0.675 | 0.676 | 0.700 |
| | **Utility** | 0.168 | 0.174 | 0.2810 |
| | **Pickup** | 0.101 | 0.093 | .0780 |
| | **Van** | 0.057 | 0.056 | 0.000 |
| | **Multiple Events** | 0.395 | 0.364 | 0.021 |
| | **RFP Present** | 0.274 | 0.278 | 0.318 |
| | **all_belted** | 0.774 | 0.793 | 0.345 |
| | **any_female** | 0.573 | 0.597 | 0.573 |
| | **maxvehage2** | 0.192 | 0.196 | 0.269 |

# MPDB-Mobile offset progressive deformable barrier

A new approach to cover compatibility and offset testing

**Volker, Sandner**
**Andreas, Ratzek**
ADAC e.V
Germany

Paper Number 15-0389

**ABSTRACT**

For more than 25 years the German Automobile Club ADAC is conducting tests to show the consumers and Industry the compatibility of passenger cars. With the upcoming off road vehicles in the 90´s, the structural and mass difference between the compact and the small executive cars according the Off roaders was huge. The geometries in the vehicle front structures were totally different and did not align in case of a frontal impact. In combination with less performing structures for offset crashes the outcome in a car to car offset frontal impact tests was dramatically worse. Not only the smaller and lighter car showed poor performance also the crash structure of the large off roader failed. A decade later the passenger cars have become much safer due to consumer test programs and regulatory demands. But still these cars are showing a different behaviour in a car to car impact than in a car to barrier impact.
The different results of ODB tests, car to car impacts and the accident analyse showed that there is a need to find a test solution which will show this performance in a full size crash and allow analysing and rating the result.
Several tests with vehicles, barriers and different test conditions have been carried out to find a solution to reproduce real life behaviour and a possibility to rate the vehicle according its aggressiveness and compatibility, which lead to a mobile barrier solution with a progressive deformable element.

## INTRODUCTION

Passenger cars have become much safer over the last years, not least thanks to comprehensive consumer testing programmes. The vehicles comply with most of the requirements of the Euro NCAP standard crash configurations.

The Euro NCAP frontal impact assesses the vehicle's self protection potential under the precondition that the car's supporting structure is ideally hit in the crash. Since single-vehicle accidents account for over 50%[1] of road deaths and over 40% of severely injured occupants, self protection is a decisive aspect of passive safety. ADAC accident research data shows, however, that severe injuries may be due to the fact that the supporting vehicle structures fail to meet. To ensure optimal accident protection, it is essential that the supporting vehicle structure is hit and that the crumple zone absorbs energy while the cabin remains stable. However, ADAC accident research data shows that this is not always the case. In many collisions, e.g. the longitudinal member is not hit (*Figure 1*) or the cross member detaches from the frame. In such case, the crumple zone cannot be fully utilised and the cabin deforms. This reduces survival space which means that the restraint systems fail to prevent the occupants from hitting the steering wheel or dashboard and sustaining severe injuries.

***Figure 1:*** ***If the supporting vehicle structure is not hit in a crash, the impact energy causes cabin deformation***

In 2010, ADAC introduced a new test set-up to assess the compatibility of vehicles. The test procedure should address the majority of the collisions not covered by the standard. In the test, the test vehicle impacts a special, honeycomb-shaped element, leaving a characteristic indentation whose surface is scanned for evaluation after the test. The indentation scan allows an assessment of a vehicle's sensitivity to nonstandard crash constellations. Moreover, the test assesses the partner protection of the vehicle's crumple zone and the load the vehicle causes to smaller vehicles in a collision. This vehicle to mobile barrier test with a progressive deformable Element was named ADAC compatibility test or MPDB test.

To achieve additional reductions in the injury risk of car occupants, extended research into passive safety will be required. Assessing a vehicle's self protection potential under ideal load conditions will no longer be sufficient. The effective interaction of different vehicles ("compatibility") and a large front-end shield are becoming increasingly important.

## ACCIDENT STATISTICS

In 2009, 183,785 car occupants [1] were in a road accident involving a maximum of two parties: approx. 64% of them were in a car-to-car accident, 23% in single-vehicle accidents, 9% in accidents involving HGV and buses and approx. 4% in accidents involving other road users.

Considering exclusively accidents causing severe or fatal injuries, the percentage of single-vehicle accidents increases considerably (see Table 1 and Figure 2).

***Table 1:***

***Car occupants involved in accidents in Germany by crash opponent and injury severity***

| **Crash opponent** | **Car occupants** (single-vehicle and two-vehicle accidents) | | | |
|---|---|---|---|---|
| | **No. of occupants involved in accidents** | of which | | |
| | | **killed** | **severely injured** | **slightly injured** |
| Single-vehicle | 42,773 | 932 | 10,962 | 30,879 |
| Passenger car | 118,173 | 516 | 11,630 | 106,027 |
| HGV, bus | 16,425 | 307 | 2,435 | 13,683 |
| Other | 6,414 | 51 | 757 | 5,606 |

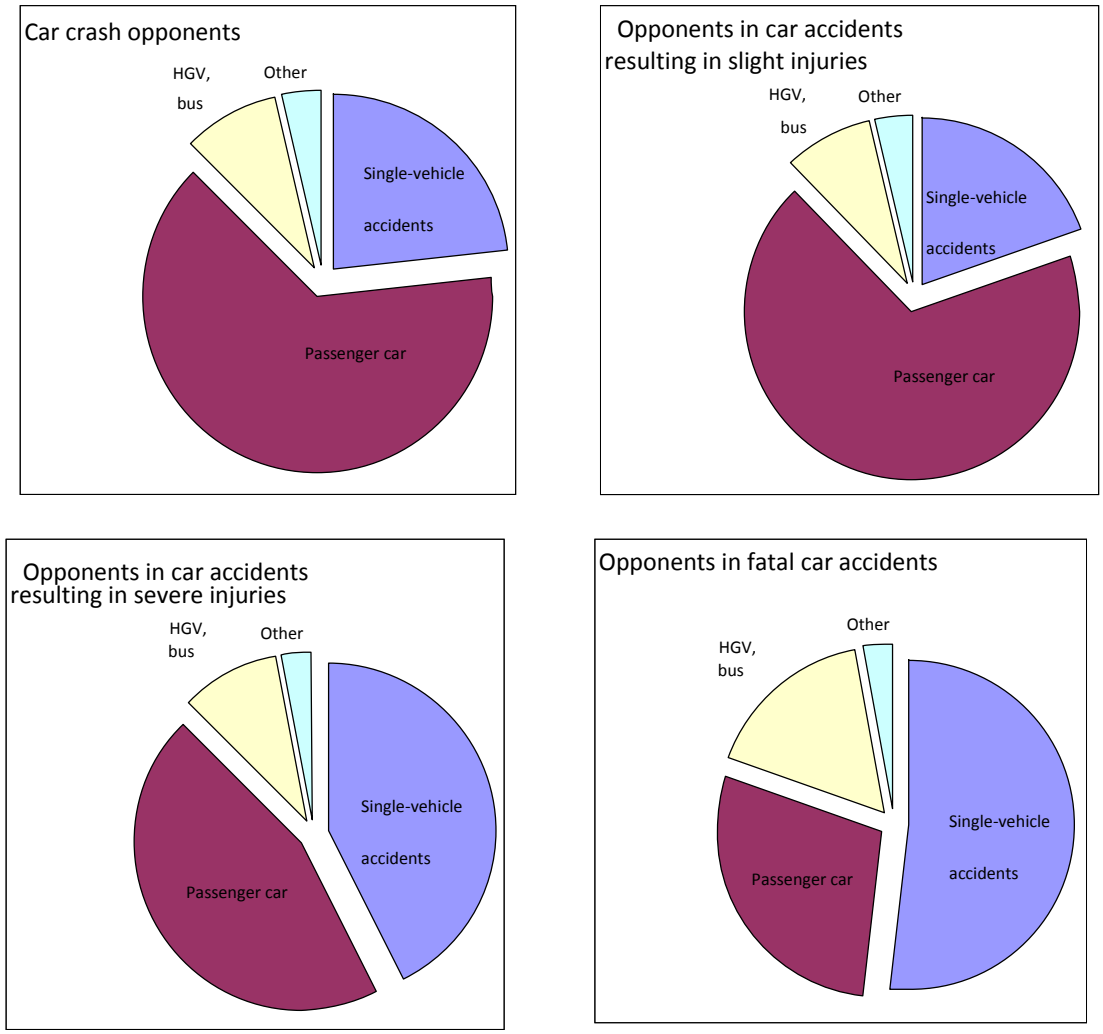


***Figure 2: Car crash opponents (top left) and crash opponents by injury severity of car occupants*** *Fehler! Textmarke nicht definiert.*

According to ADAC accident research data, the vehicle class only has a minor influence on the severity of the injuries car occupants sustain (Table 2). There are two reasons:

- ADAC accident research concentrates on severe accidents; approx. 39% of them are single-vehicle collisions and 14% involve utility vehicles. In these two types of accidents, the vehicle's self protection potential is essential while the high vehicle weight and a more rigid front end have little advantage. The only asset is the larger crumple zone of large cars.
- The analysis considers all types of collisions. Large vehicles have the greatest advantage in front-end collisions.

**Table 2:**

**Percentage of slightly, severely and fatally injured car occupants (ADAC accident research; vehicles built in 2000 or later)**

| | Supermini | Family | Luxury |
|---|---|---|---|
| Slightly injured | 37% | 38% | 45% |
| Severely injured | 60% | 60% | 53% |
| Fatally injured | 3% | 2% | 2% |

Considering exclusively two-car front-end collisions, it becomes obvious that injury severity is relatively strongly affected by vehicle mass. Figure 3 shows that the risk of getting seriously or fatally injured in a crash is approximately twice as high in very light vehicles (<950kg) (over 27%) as in very heavy vehicles (>1750kg).

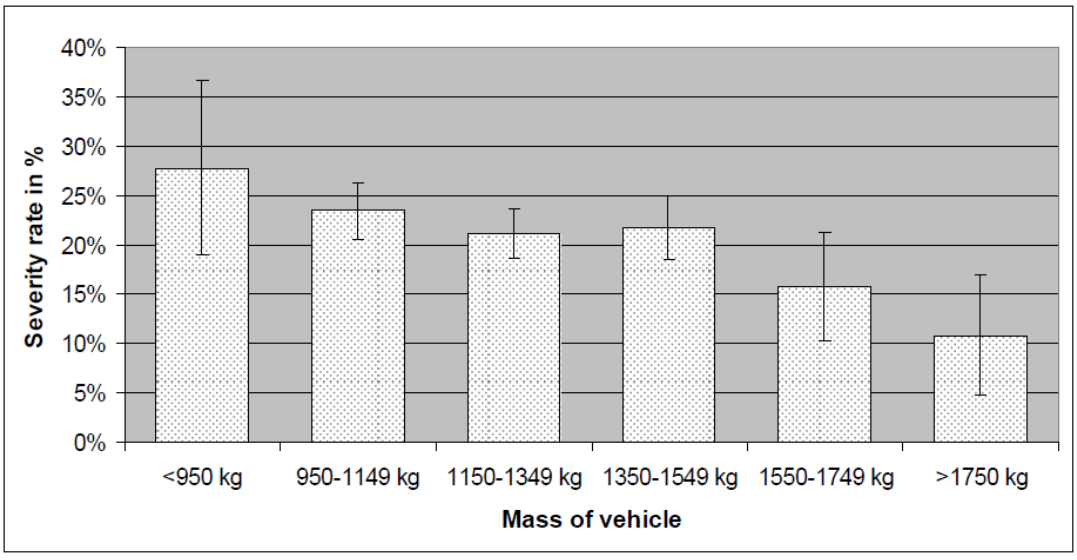


: severity rate in frontal impact according to the mass of the vehicle.
Vehicle designed since 2000 or registered since 2004.

**Figure 3: Percentage of severely and fatally injured in car-to-car front-end collisions by vehicle mass[2]**

**WHAT DOES COMPATIBILITY INCLUDE**

Compatibility refers to the interaction of colliding vehicles. The following issues are especially important:

- **Weight difference:**

  When two vehicles of different weight crash into each other at identical speed, both vehicles will move in the heavier car's direction of travel. While the impact causes the lighter car to brake to a standstill and then accelerate rearward, the heavier car is braked from its speed of travel to a residual speed.

  Vehicle deceleration depends on the change in speed during the crash (delta v = pre-crash speed of travel – post-crash residual speed) and is a decisive factor for determining accident severity and the occupants' injury risk. Since speed change is smaller in the heavier passenger car, loads on the occupants are lower in the heavier than in the lighter vehicle.

***Figure 4: Upon impact, the heavy SUV causes the light supermini to skid rearward***

- **Different front-end rigidity:**

  The test set-up used for vehicle approval based on ECE R94 and the Euro NCAP frontal impact includes an offset collision between two cars of identical weight which travel at the same speed. For this test, it is essential that impact energy is absorbed by the crumple zone before the cabin starts to deform. To ensure that the vehicle's own "pushing" mass causes only the crumple zone to deform, heavy vehicles have higher front-end stability than light vehicles. Although heavy vehicles usually have a longer deformation distance, the structural force required to cause front-end deformation is significantly higher in heavy vehicles than in light vehicles.

  If two different vehicles crash into each other, the crumple zone of the lighter car will be the first to deform because of the vehicles' different rigidities. As a result, the load on the small vehicle may become too high relatively quickly while the crumple zone of the larger vehicle remains mostly intact.

***Figure 5:*** ***Post-crash deformation is considerably stronger in the small vehicle (left) than in the more rigid large vehicle (right)***

- **Different front-end geometries:**

  The deformable element used in the Euro NCAP frontal impact and the ECE R94 vehicle approval is comparatively soft and absorbs only little energy while maximum load is exerted. Modern vehicles penetrate the element (blue in Figure 6), and the longitudinal member transfers the impact energy directly to the metal plate behind.

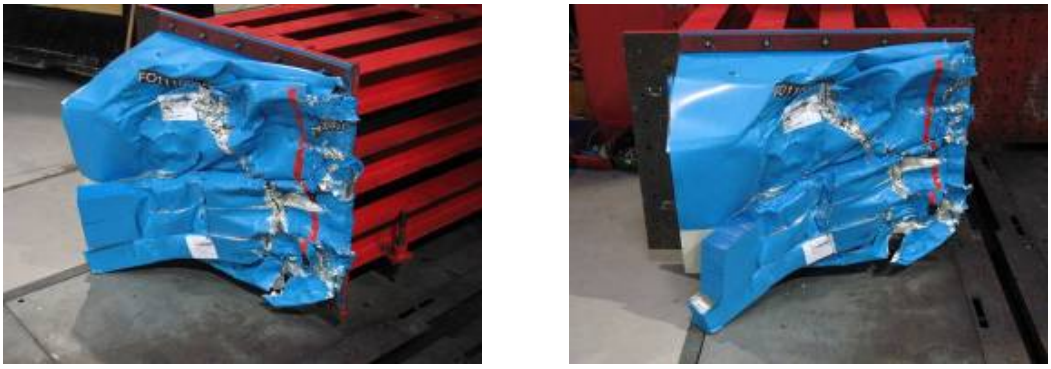

***Figure 6:*** ***Since the current front-end element absorbs only little impact energy, energy is transferred to the large and stable metal plate behind the element***

Longitudinal member position and dimensions as well as transverse member stability (cross members connecting the left and right longitudinal members; red in Figure7) are of minor significance. In this standard crash, even a single longitudinal member jutting out of the vehicle like a spear can transfer the impact energy to the large metal plate behind the deformable element.

***Figure 7:*** ***The dimensions and position of supporting structures in modern cars vary considerably***

More often than not, cars colliding head-on cannot support each other because their supporting structures do not meet, causing the crumple zone to remain mostly intact while the cabin deforms. In most cases, this results in very severe injuries to the occupants (Figure 8). The smaller the front-end overlap and the higher the collision speeds, the more serious are the consequences of geometric discrepancies. An approach by IIHS is covering exactly this kind of small overlap situation, by using just 25% of the vehicle width.

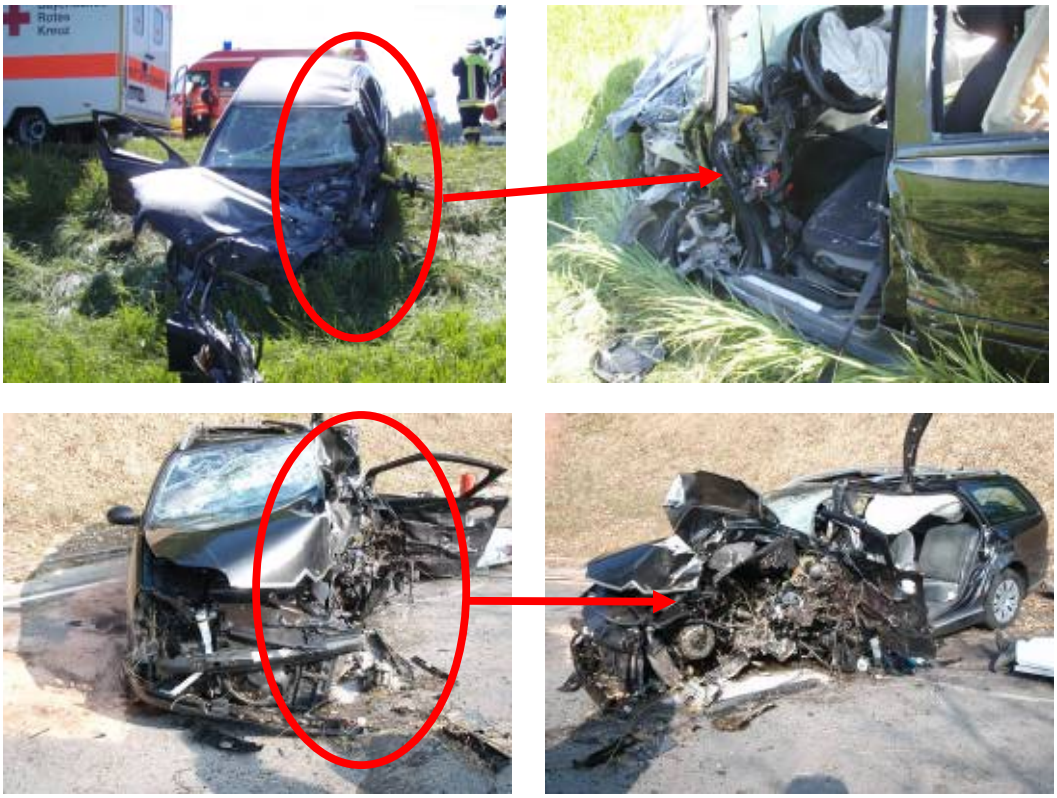

***Figure 8:*** ***If the supporting vehicle structure is not hit in a crash, the impact energy causes cabin deformation***

## DEVELOPMENT OF CAR TO MOBILE DEFORMABLE BARRIER TEST

As the car to car impact was the starting point the initial setup of the car to barrier test should be close as possible. The impact speed of 56kph and the overlap of 50% of the small car were taken over. In several European projects, such as APROSYS, the actual average mass of passenger cars in Europe were discussed for the side impact barrier. While taken into account the number and type of cars actual on the market as well as actual selling numbers, the compact car class, shows the highest number actual on European roads. In driving condition these class will be approximately 1400kg heavy. The mass of the mobile barrier was set to this weight, which is already covered by the FMVSS 208 side impact barrier, which is the base for the impacting trolley.

### First impact tests

The initial starting point for the test specification was the car to car impact test between two cars of the same mass range and size. This test was carried out according the actual car to car impact specifications with 50% overlap of the small car and 56kph impact speed. In this test, also the vehicles were out of the same vehicle class, both longitudinal did not match (see Figure 9)

***Figure 9: car to car impact at 56kph***

In a second test the yellow car was replaced by the mobile barrier equipped with the PDB Element. All other parameters were not changed (see Figure10)

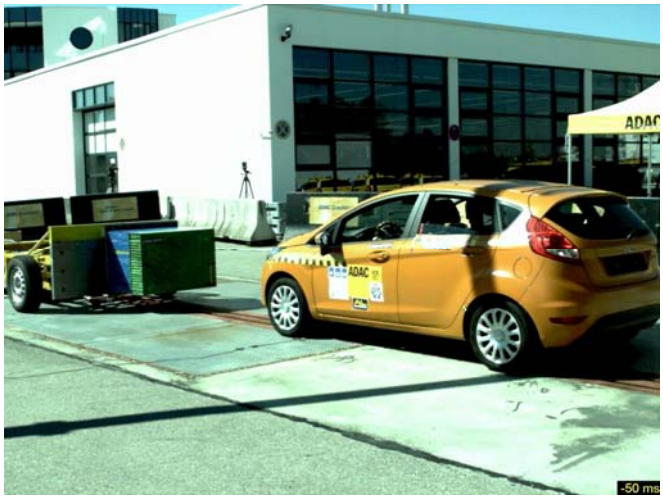


***Figure 10: car to mobile barrier impact at 56kph***

**Comparison of deformations:**

A direct comparison between the vehicle pulses, the vehicle deformations and the 3D measurement showed that the MPDB test loaded the tested vehicle in a different way than in the car to car impact.

***Figure 11 : car to car test (left picture), car to MPDB test (right picture):***

Differences detected after the impacts were are more or less undeformed footwell area, the trans facia beam and A-pillar section showed rupture, the instrument panel intruded the passenger compartmented. Compared to cases of the ADAC accident research and also compared to the car to car test those deformations are quite uncommon and lead to the decision to implement changes in the test setup and improve the performance of the test results.

The top of the PDB element is compareably high (appr. 900 mm) and in the upper part more or less undeformed. So it is quite likely that the upper part of the PDB is stiffer than an average car. During the test, the PDB put a lot of energy into the car, especially in the area of the waist line. Following changes were applied to the barrier due to that fact.

1. **reduce the ground clearance of the PDB by 75 mm**
2. **reduce the overall height of the PDB by 135 mm**

3. **reduce the test speed to 50 kph**

A second impact test with the changes mentioned was performed and the vehicle pulse as well as the 3D measurement and the deformation of the car were quite close and comparable see deformation pictures in Figure 12.

***Figure 12: Comparison of deformations car to car test (left picture), new car to MPDB test (right picture):***

The overall result of the new test setup could be recognized after the detailed analyses of the vehicle tested according the new boundaries. Not only the overall picture shows a comparable deformation, also the detailed view below the dashboard, the deformation of the A-pillar and the intact trans facia beam offer no big differences between the 2 tests. But there are still less deformations in the footwell area of the MPDB tested car. The conclusion is, that deformations of the PDB are more homogeneous – the upper part is also loading the tested vehicle.

**Test setup car to MPDB**

The new test setup of compatibility crash test simulates a head-on collision with a 50% overlap between the vehicle to be assessed and an approx. 1400kg moving trolley with a PDB, made of alloy, representing a typical, widely used small family car (see Figure 13). The vehicle and the trolley are travelling at identical speed.

The ground clearance of the PDB barrier is 150mm while the height of the barrier is 750mm above the ground and one alloy box with a stiffness of 0,34MPa and a second block with progressive stiffness, both covered with an alloy sheet.

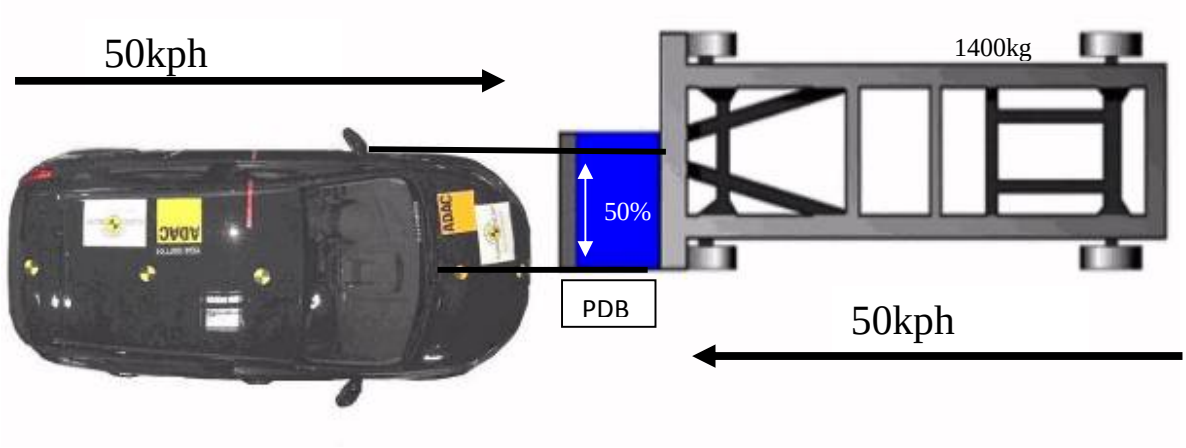


***Figure 13: Test set-up of the compatibility crash test***

To assess the occupants' injury risk, two 50% H3 dummy on each of the two front seats and restrained a Q6 child dummy in an appropriate CRS on the right rear seat were installed. Dummy installation and instrumentation as well as vehicle load and measurement were in compliance with the Euro NCAP test protocol. Also the Dummy assessment was carried out according Euro NCAP assessment protocols.

**METHODE OF THE COMPATIBILITY ASSESSMENT**

The compatibility assessment includes the analysis of the indentation the colliding vehicle leaves on the deformation element upon the impact as well as the change in trolley speed. The assessment comprises the steps below:

1. **Determining the assessment area:**

   The first step includes determining the area of the PDB that is relevant for assessment in dependence of the vehicle dimensions and other framework conditions:

   **Width** Ideally, the front-end shield spans the entire width of the passenger car to be able to absorb impact energy in the crumple zone also in accidents where overlap is minor. To take this into account, the assessment area represents 45% of the vehicle width.
   Because of the crash kinematics (rotation of the vehicle and trolley), force is exerted on the side edges of the deformation element which, as transverse load, causes unrealistic deformation to the honeycomb structure. As a result, the edges cannot be assessed and the assessment area ends 200mm from the PDB's side edges.

   **Height** To ensure that the structures of the colliding vehicles meet upon the impact and to lower the risk of overriding or underriding the barrier, the supporting structure must be mounted between 250 and 650mm above the ground. This takes the different vehicle classes into account and complies with additional requirements (e.g. RCAR bumper test, HGV underrun protection).

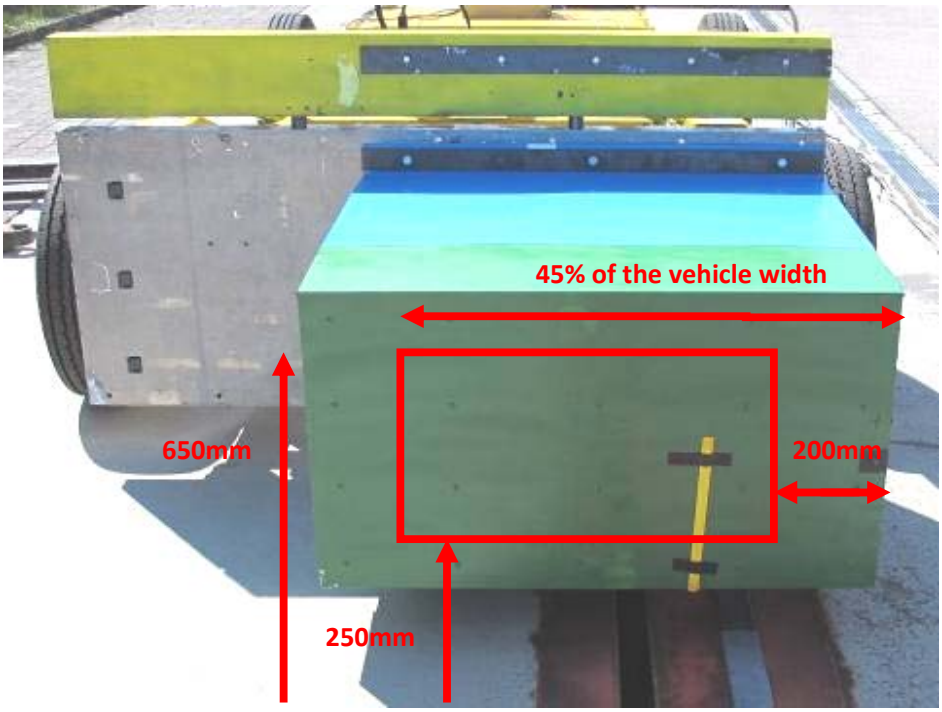


*Figure 14: Determining the assessment area*

**2. Assessing indentation homogeneity/geometry:**

Ideally, the vehicle front end should have homogeneous rigidity in the entire assessment area (see Figure 14). Both very rigid longitudinal members that penetrate the colliding vehicle like a spear and very soft areas that do not provide support for the colliding vehicle and barely dissipate or absorb energy are a disadvantage. A vehicle meets the above criteria if it leaves a homogeneous and large indentation in the PDB.

The homogeneity assessment comprises a statistical evaluation of the intrusion depth in the area under assessment. For this purpose, the average intrusion depth and the standard deviation (a measure for the mean variation of the measured values around the average) are determined. A greater standard deviation means a more inhomogeneous deformation of the barrier and results in a poorer homogeneity rating.

**3. Assessment of the energy impacting on the colliding vehicle:**

Two criteria are used to assess front-end rigidity and the energy impacting on the colliding vehicle:

- **Energy impacting in the PDB assessment area:** Great differences in the rigidity of colliding vehicles may cause impact energy to be absorbed only by the less rigid vehicle while the crumple zone of the more stable vehicle remains intact. Very high front-end rigidity therefore has a detrimental effect on partner protection. PDB deformation depth enables the assessment of front-end rigidity and impact energy. To lower the risk of excessive loads on the colliding vehicle, it is essential that the vehicle tested absorbs kinematic energy in its own crumple zone.
- **Change in trolley speed:** Since for technical reasons impact energy assessment focuses only on the assessment area as defined above, we do not consider the entire amount of energy impacting on the colliding vehicle in our test. Therefore, we also assess the change in trolley speed. While a change by less than 50kph is a plus, a change by more than 50kph is a drawback.

**Examples of different front structures**

The following tables will show the results of 3 family cars tested in the last test series and according the latest version of the assessment. All cars have been tested also by IIHS according the small overlap test. The results in the compatibility test are showing very different behaviour of front structures. In the 1st example the vehicle shows a single load path of extreme stiffness and a very weak cross member. While example 2 has several load pathes in height and is also covering the outside areas of the longitudinal. This vehicle scores well in the small overlap and the compatibility test. The 3rd vehicle shows also 2 load pathes in the front, but also a weak cross member. The longitudinal is too stiff, but less aggressive than in example 1. The 3rd car has a good rating in small overlap tests too.

**Table 3:**

**Example 1 family car**

| | |
|---|---|
| Post-crash vehicle | The vehicle is a family car with a very inhomogeneous crumple zone consisting of two longitudinal members which are interconnected by an unstable aluminium cross member. The cross member spans the width of the longitudinal members, leaving the area in front of the front wheels unprotected. In front of the suspension strut domes, the vehicle has two short, but rather flat, longitudinal members (shotguns). However, they are placed too far to the rear and top to absorb deformation energy in the test.<br>Maximum deceleration of the vehicle upon the impact was 38g. The change in speed was |

| | | |
|---|---|---|
| | 57kph.<br> | |
| Post-crash PDB | PDB deformation upon the impact is extremely inhomogeneous with the longitudinal member punching a deep hole into the barrier and the engine block causing strong deformation to the PDB edges (on the right in the photo). Where the vehicles front wheel impacts the PDB, intrusion of the PDB which absorbs approx. 93kJ is, however, minimal. The PDB trolley's maximum deceleration upon impact was 35g. The change in speed was 63kph. | 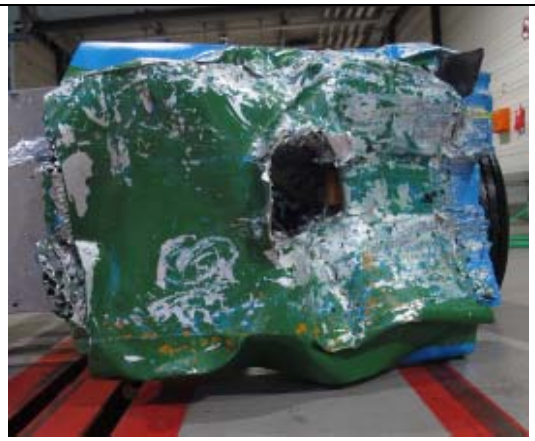 |
| Digitised post-crash PDB front | This illustration shows the entire front of the PDB and the different intrusion depths. Intrusion depth colour scheme:<br>Orange 0 to 160mm<br>Yellow 160 to 320mm<br>Green 320 to 480mm<br>Red >480mm | 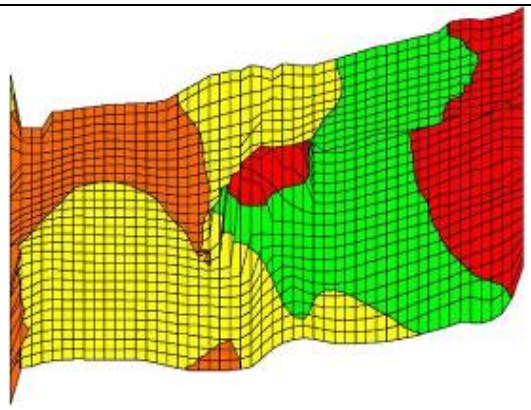 |
| Post-crash PDB assessment area | This illustration shows the PDB area that is relevant for compatibility assessment.<br>The green area of the indentation left by the Audi's front end is well-suited to absorb energy in a crash, while the red area is much too rigid. On the other hand, the yellow and orange areas are too soft. | 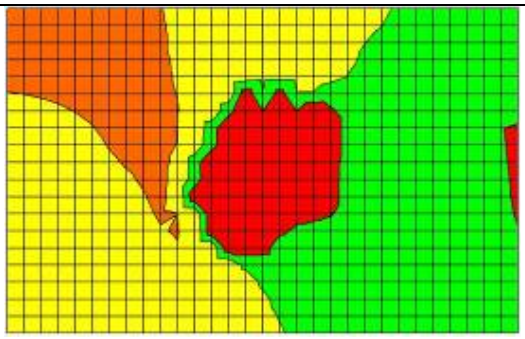 |

**Table 4:**

**Example 2 family car**

<table>
<tr><td>Post-crash vehicle</td><td>The vehicle is a family car with a relatively homogeneous crumple zone. It consists of three horizontal planes connected on the right and left with vertical profiles:<ul><li>The main load path consists of two longitudinal members interconnected by a steel cross member. There is an additional connection from the longitudinal members to the suspension strut domes in front of the wheels.</li><li>A steel lock support of somewhat weaker dimensions is located above the main load path and is connected to the suspension strut domes on either side.</li><li>Below the main load path is another steel cross member which spans the width of the longitudinal members.</li></ul>What makes the vehicle design unique are its structures located outside the longitudinal members and in front of the front wheels. These structures are intended to dissipate the impact energy over a large area and absorb energy in crashes with little overlap.<br>Maximum deceleration of the vehicle upon the impact was 71g. The change in speed was 58kph.<br> </td></tr>
<tr><td>Post-crash PDB</td><td>Rather large areas of the element are deformed by the impact. There are no major holes in the surface, but the individual members on the vehicle front have left visible indentations. The PDB trolley’s maximum deceleration upon impact was 29g. The change in speed was 58kph. The barrier absorbs 76kJ of energy in the crash test.<br> </td></tr>
</table>

| | | |
|---|---|---|
| Digitised post-crash PDB front | This illustration shows the entire front of the PDB and the different intrusion depths. Intrusion depth colour scheme:<br>Orange 0 to 160mm<br>Yellow 160 to 320mm<br>Green 320 to 480mm<br>Red >480mm | 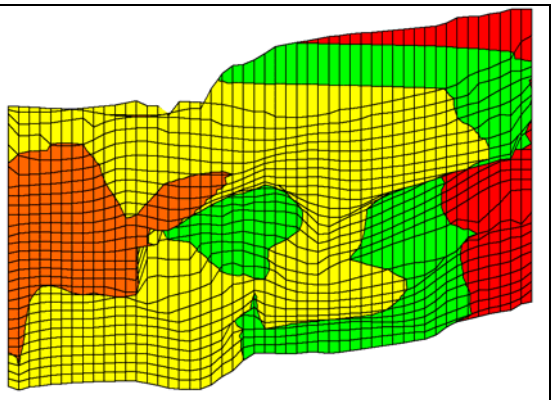 |

**Table 5:**

**Example 3 family car**

| | | |
|---|---|---|
| Post-crash vehicle | The front end of the vehicle comprises several load paths:<br>• The main load path consists of two longitudinal members connected by a steel cross member.<br>• Underneath the longitudinal members, there is an additional steel cross member whose outer edges rest on the chassis sub-frame.<br>• In front of the suspension strut domes, the vehicle has two additional short, longitudinal members (shotguns) stably connected to the main load path. These members are intended to protect the cabin in crashes with little overlap.<br>Maximum deceleration of the Vehicle upon the impact was 33g. The change in speed was 51kph.<br> | |
| Post-crash PDB | The main load path of the vehicle leaves a vertical bend and a much deeper indentation than the other supporting structures. In this test, the PDB element absorbed 92kJ of energy. The PDB trolley's maximum deceleration upon impact was 38g. The change in speed was 58kph. | |

| | | |
|---|---|---|
| Digitised post-crash PDB front | This illustration shows the entire front of the PDB and the different intrusion depths. Intrusion depth colour scheme:<br>Orange 0 to 160mm<br>Yellow 160 to 320mm<br>Green 320 to 480mm<br>Red >480mm | 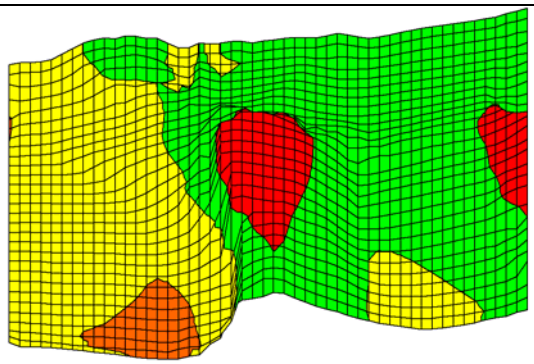 |

## CONCLUSIONS

Compliance with Euro NCAP frontal impact requirements is essential for good occupant protection. However, even vehicles with a very inhomogeneous front-end design may pass this test. In the event of a two-vehicle accident (or single-vehicle accident such as vehicle-tree collision), poor front end structural design may result in excessive local loads on the vehicle or its opponent and serious injuries for the occupants. Vehicle designers must therefore take additional requirements into account:

- **Adapted front-end geometries**

  In today's vehicles, there is no standard for the mounting height of front-end supporting structures, i.e. mounting height may vary greatly from manufacturer to manufacturer and from car model to car model. Cross members are usually very flat and do not span the entire width of the vehicle. In addition, they are unstable, failing to dissipate the impact energy. As a result, there is poor energy absorption potential for the colliding vehicles.

  Equipping a vehicle with a front shield consisting of wide multiple cross members (see Figure 15) may dramatically improve partner protection and self protection (e.g. when crashing into a tree). It helps dissipate the impact energy throughout a large area so that most of it is absorbed in the crumple zone. The shield should protect the area between 250mm and 650mm above the ground and ideally span the entire width of the vehicle. This construction will not only help for partner protection, also small overlap scenarios will be addressed with this construction.

***Figure 15:*** ***Frontal impact protection: disadvantageous (left) vs. advantageous (right) front-end construction***

- **Adapted front-end stability**

  Vehicle mass has no influence on the deformation distance required to keep vehicle deceleration at an acceptable level. The long nose of a large and heavy vehicle can therefore be divided into a soft partner protection area and a rigid self protection area. This ensures that in a head-on collision with a light vehicle, the crumple zone of the large vehicle is able to absorb most of the energy rather than the small vehicle.

If the vehicle designers bear the above issues in mind, they will contribute to considerably lowering the injury risk in single-vehicle and car-to-car accidents. The risk of getting seriously or fatally injured is likely to decrease by approx. 7%[1] This would prevent over 150 road deaths and some 2100 serious injuries to car occupants on German roads each year.

The Euro NCAP roadmap for 2017-ff will also include an updated frontal impact scenario and will have to deal with the question self and partner protection. Possible frontal scenarios were examined in the last 5 years which will be taken into account for a new consumer frontal impact test scenario in 2020.

.

## REFERENCES

[1] Federal Statistical Office Germany; road accidents 2012
[2] IRCOBI Conference 2010; C. Chauvel, S. Cuny, G. Favergon, N. Bertholon, P. Delannoy: Self-Protection and Partner-Protection for new vehicles

# A MULTIPLE TARGET TRACKING STRATEGY USING MOVING HORIZON ESTIMATION APPROACH

**Runxiao Ding**
**Miao Yu**
**Wen-Hua Chen**
Department of Aeronautical and Automotive Engineering
Loughborough University
United Kingdom

Paper Number 15-0390

## ABSTRACT

Tracking multiple road users is playing a significant role in autonomous vehicles and advanced driver assistance systems. Different from Multiple Target Tracking (MTT) in aerospace, the motion of the ground vehicles is likely constrained by their operational environment such as road and terrain. This information could be taken as additional domain knowledge and exploited in the development of tracking algorithms so as to enhance tracking quality and continuity.This paper proposes a new MTT strategy, Multiple Hypothesis Tracking using Moving Horizon Estimation approach (MHE-MHT), for tracking ground vehicles aided by road width constraints. In this strategy, tracking association ambiguity is handled by MHT algorithms which are proved as a preferred data association method for solving the data association problem arising in MTT. Unlike most of the MTT strategies, which solve target state estimation using Kalman filter (and its derivations), we propose a new solution using the moving horizon estimation (MHE) concept. By applying optimization based MHE, not only nonlinear dynamic systems but additional state constraints in target tracking problems such as road width can be naturally handled. The proposed MHE-MHT algorithm is demonstrated by a ground vehicle tracking scenario with an unknown and time varying number of targets observed in clutter environments. Using the optimal subpattern assignment metric, numerical results are presented to show the advantages of the constrained MHE-MHT structure by comparing it with the Kalman filter based MHT.

*Keywords*: Multiple target tracking, Multiple hypothesis tracking, Moving horizon estimation, Inequality constraints, Autonomous vehicles

## INTRODUCTION

Multiple target tracking (MTT) is an important research topic in automated vehicle field. Although a number of MTT algorithms have been developed, e.g. [1], it is still a quite challenging task to implement MTT in realistic situations, especially when suffering from low visibility of sensors, high clutter and high target density. One promising approach that has drawn a great deal of attention recently is to improve the performance of tracking algorithms by utilizing trajectory and other constraints/knowledge imposed from environments including available road maps. It has become a consensus that prior nonstandard information such as target speed constraints, road network and terrain information can be exploited in the tracker to reduce estimaiton error and provide better tracking accuracy [2]. For instance, a vehicle travelling on a road is expected to move within the road boundaries and follow its speed limitation. In other words, the performance of tracking systems is often limited if ignoring or not taking use of this additional source of informaiton. Even for the cases of low signal quality with high clutter density, the incorporation fo such constaint information is sufficient enough to get a relatively good tracking performance [11].

### A. Constrained state estimation

One effective approach of solving the road constrained MTT is to incorporate the constraint-related information into a standard filter algorithm (state estimation process) as state constraints. For most MTT structures, Kalman filtering and its variations are commonly used to estimate the state of a target based on its state process and measurement models. However, when the road state constraints cannot fit easily into the structure of a Kalman filter, they are often ignored or dealt with heuristically [3Although constrained Kalman filter methods are relatively easy in implementation, these methods have several disadvantages even for basic linear and equality constraints [3]. Recently, some other methods, for example, see [7], [8], [9], [10], are also developed based on optimization and truncation approaches. The majority of filters proposed to solve the constrained estimation problems focus on linear (in)equality or nonlinear equality constraints. A little research has been conducted on nonlinear inequality

constraints so far. However, (non)linear inequality constraints have played an important role for most tracking scenarios in ground vehicle tracking problems,, e.g. roundabout boundary.
More specifically, Rao et al. [10] have proposed a constrained state estimation for nonlinear discrete-time systems. It is based on a moving horizon concept based state estimation known as moving horizon estimation (MHE). The basic strategy of MHE in determining the optimal state estimation is to reformulate the estimation problem as an optimisation problem using a fixed-size estimation window. This method has been widely used in chemical engineering. Other applications include hybrid system, distributed, network system, large-scale system and so on. However, the implementation of moving horizon approach based estimation method in target tracking is still relatively an uncharted area. Advantages for using MHE to solve target tracking state estimation could be significant. Since the method is optimization based, road constraints or similar in target tracking problems can be naturally handled by MHE as additional (non)linear and/or (in)equality constraints on linear or nonlinear systems under consideration. In addition to state constraints, MHE is also able to incorporate constraints on the state process and/or observation noises. In vehicle tracking, such constraints are typically used to model bounded disturbance or truncated distribution/density representing the influence of the operation environment on vehicle movement such as vehicle acceleration and deceleration.
Another advantage of using MHE as a state estimation method in target tracking is that it always considers a window of $N$ latest measurements. Such feature is very meaningful in target tracking problems especially when targets are occluded by each other/static obstacles which leads to no reliable measurement at specific time step/steps. MHE utilizes the measurements in a receding horizon window could reduce the effect of unreliable measurements such as in the above situation in state estimation. Simulation results in [4] show that MHE achieves the smallest estimation error for nonlinear systems and nonlinear constraints. Theoretically, for a linear system without constraints and with a quadratic cost, MHE reduces to Kalman filtering algorithms when an infinite horizon window is considered.

**B. Multiple target tracking problem**

The problem of estimating the position of moving targets, also known as MTT, has become an important part in autonomous vehicles and advanced driver assistance systems. Knowledge about the state of moving objects can be taken as powerful information to improve the level of autonomy for vehicles. MTT techniques are required in a number of automotive applications including Advanced Driver Assistance Systems (ADAS), Collision Avoidance Systems, and Vehicle-automation Systems. Such systems can incorporate functions such as adaptive cruise control, lane keeping, precise manoeuvring, pedestrian detection and so on [12] aiming for achieving an improved collision avoidance behaviour and safe road driving even in populated environments. By using state-of-the-art on-board sensors such like radar, lidar, GPS and camera vision systems together with accurate global and local maps, different levels of automation could be achieved in automotive applications, from individual autonomous functionalities to fully automated vehicles.
Several approaches for MTT have been developed over the last decades, overviews can be found in Pulford [13] and Christophe [14]. Basically, these methods can be divided into two categories – the data association based 'classic' methods and the more recent finite set statistics (FISST) based approaches. The data association based methods are largely based on probability, stochastic processes and estimation theory. Existing methods include Nearest Neighbour Standard Filter (NNSF) [15], Global Nearest Neighbour (GNN) approach [16], Joint Probabilistic Data Association (JPDA) [17] and Multiple Hypothesis tracking (MHT) algorithm [18]. Among them, MHE is a more complex approach that considers data association across multiple scans and multiple hypotheses. In other words, MHT algorithm attempts to keep all possible association hypotheses over multiple frames of data. This results in an exponentially growing number of hypotheses and thus a NP-hard problem. Cox [19] in 1997 developed an efficient implementation by using polynomial time optimization algorithm to find the k-best solutions to an assignment problem along with pruning and merging techniques to reduce the number of low probability hypotheses. MHT essentially keeps a set of multiple hypotheses and thus the assignment ambiguity will be resolved in future when subsequent new observations are arrived. In this case, hard decisions are not made until they need to be with the fact of using more information, rather than just the current data frame, thus possible error association could be corrected when more evidences are updated. Such features along with the dramatic increases in computational capabilities have made MHT a preferred data association method for modern systems [20].
Until very recent, a new concept has been introduced in MTT area - the random finite set statistics (FISST) [27]. While the conventional MTT methods try to solve the problem explicitly by expending single target tracking with data association capabilities, the number of targets is also considered as a random variable (random set) and explicit data association are avoided in FISST. The innovation of FISST is to model both the system and measurement as

random finite sets (RFSs) and directly apply the Bayes recursion to these set-valued random variables and thus solving the data association problem implicitly. In contrast to explicit data association methods, conventional probability-mass functions are replaced by belief-mass functions. Probability hypothesis density filter (PHD) [28] and multi-target multi-Bernoulli (MeMBer) [29] filter proposed by Mahler have successfully implemented the FISST concept into MTT.

The objective of this paper is to derive an efficient strategy for road-constrained MTT. The main contribution of this work is twofold: 1) a constrained MHE algorithm is proposed to solve the state estimation problem arising in road maps assisted target tracking. Since MHE is an optimization based method, it provides a natural way to handle nonlinear systems and incorporate various inequality constraints that may be difficult to be dealt with in other state estimation algorithms. 2) The work is further extended from single target tracking into MTT. A new MTT strategy for tracking multiple ground vehicles, namely MHE-MHT, is proposed, where moving horizon concept is combined with MHT to incorporate various road and other environment information. In this combined strategy, tracking association ambiguity is handled by MHT algorithms that have been proved as a preferred data association method while constrained state estimation is solved by MHE.

The paper is organized as follows. After presenting the introduction in road map constrained MTT, MHE based single target tracking is proposed for incorporating the road and other possible constraints. This work is further extended to MTT by combing with MHT in the following section In order to verify the efficiency of the proposed algorithms, simulation results of multiple target tracking with inequality road width constraints are presented . Finally, this paper ends with conclusions.

## MHE BASED TARGET TRACKING WITH ROAD CONSTRAINT

In the operation of automated vehicles, it is necessary to track all the nearby road users to make sure the safety of the vehicles and other road users. Tracking road users is in fact a constrained estimation problem as the objects of interest must be on the road. In this section, both the road constrained state estimation problem and MHE based target tracking are described.

### A. System specification

Consider the movement of objects of interest described by the discrete system:

$$x_{k+1} = f(x_k) + \omega_k \qquad (1)$$

and the observation equation:

$$y_k = h(x_k) + v_k \qquad (2)$$

where the time point $k$ takes integer values, $f: \mathbb{R}^n \to \mathbb{R}^n$ is the nonlinear system function and $h: \mathbb{R}^n \to \mathbb{R}^m$ is the nonlinear measurement model. $x_k \in \mathbb{R}^n$ is the state vector, $y_k \in \mathbb{R}^m$ is the vector of available measurements. The vectors $\omega_k \in \mathbb{R}^n$ and $v_k \in \mathbb{R}^m$ are Gaussian noises of the process and the measurement described by independent pdfs $p(\omega_k) = N(0, Q)$ and $p(v_k) = N(0, R)$, respectively, where $Q$ and $R$ are covariance matrices. It is commonly assumed that the initial pdf of the state vector is known as a Gaussian pdf $p(x_0) = N(\tilde{x}_0, \tilde{P}_0)$. Let $F_k$, $G_k$ and $H_k$ be the Jacobian matrices with respect to $x_k$, $\omega_k$ and measurement states, respectively.. Then the system described in (1) and (2) is now equivalent to a linear system.

### B. Target tracking road width constraints

As discussed in Introduction, ground targets are constrained when moving along a road network. Thus the knowledge of terrain database and road maps can be used as constraints and incorporated into the tracking algorithm. In most existing techniques, the road map constraints target motion in a one-dimensional physical space [30] (by ignoring the road width) and incorporate them as equality constraints. This is fairly good approach when an observer is far away from the moving objects such as in the scenario of unmanned aircraft tracking a ground vehicle. However in automated vehicles, only objects in proximity are of interests. The road width is comparable to the measurement accuracy (high accuracy sensors such as lidar). In this paper, road network information is considered as road width inequality constraints and the target motion is restricted by these physical constraints in both straight and curved segments.

**Linear state inequality constraints** Suppose that at each time step $k$, $x_k$ is subject to the following linear inequality constraint:

$$a_k \leq C_k(x_k) \leq b_k \qquad (3)$$

where $C_k$: $\mathbb{R}^n \to \mathbb{R}^c$, $a_k$, $b_k \in \mathbb{R}^c$, and the inequality $\leq$ holds for all elements of the vectors and $a_k \neq b_k$, $\forall k$. $C_k$ is a known $c \times n$ matrix, $a_k$ and $b_k$ are the known vectors each with a dimension of $c \times 1$ representing the lower and upper road boundary individually, $c$ is the number of constraints, $n$ is the number of states, and $c \leq n$. $C_k$ is supposed to be of full rank. For target tracking with straight (linear) road width constraint shown in Figure 1, Eq (3) is expressed as:

$$\begin{bmatrix} -I \\ I \end{bmatrix} * T_{g,l}(x_k) \leq \begin{bmatrix} -ub \\ lb \end{bmatrix} \qquad (4)$$

where $T_{g,l}$ is known as the transformation matrix representing the rotation from the global coordinate to the road network local coordinate (with orientation along and orthogonal to the road) by rotation angle $\theta$.

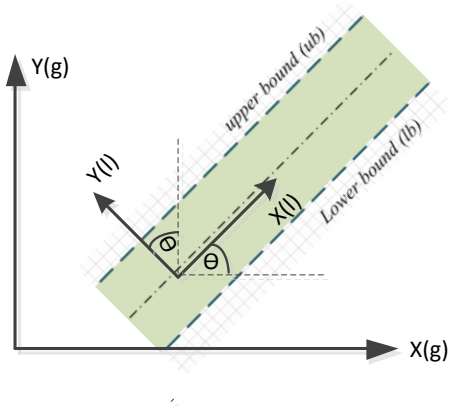


***Figure 1. Straight road width linear constraint***

**Nonlinear state inequality constraints** In the same fashion as the linear road width constraint shown in (3), a circular or curved road segment shown in Figure 2 can be represented as a nonlinear inequality constraint as

$$r_1 \leq \sqrt{{x_{1,k}}^2 + {x_{2,k}}^2} \leq r_2 \qquad (5)$$

The road is defined by two arcs with radii $r_1$ and $r_2$ representing the lower/upper road boundary, with the center at the origin of the Cartesian coordinate system. At each time step $k$, target position state $x_{1,k}$ and $x_{2,k}$ are subject to the following nonlinear inequality constraint

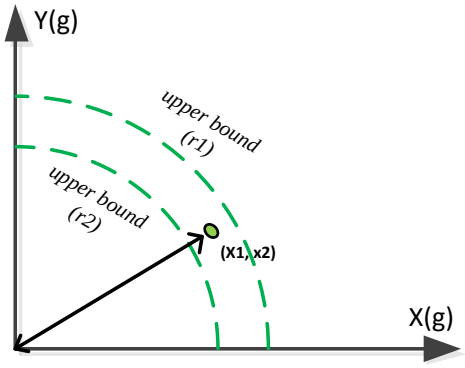


***Figure 2. Curved road width nonlinear constraint***

### C. Moving horizon estimation with constraints

MHE is an optimization approach based state estimation method that can take into account the constraint during estimation process and provide a constrained estimate directly. Essentially, MHE follows Bayes rule which maximizes the probability density function of the past states given the measurements in a fixed length of horizon . Considering a horizon length of *N* past time steps, the joint conditional density is then given by:

$$p(X_N|Y_N) \propto p(Y_N|X_N)\, p(X_N|Y_{0:k-N-1}) , \qquad (6)$$

where $p(X_N|Y_{0:k-N-1}) = p(x_{k-N}, \dots, x_{k-1}|y_0, \dots, y_{k-N-1})$, is the *a priori* state density given the measurements before the horizon; $p(Y_N|X_N) = p(y_{k-N}, \dots, y_{k-1}|x_{k-N}, \dots, x_{k-1})$ is the joint measurement likelihood function. Assuming that $X_N$ is a first order Markovian chain, the *a posteriori* joint conditional density of (6) is:

$$p(X_N|Y_N) = c \prod_{j=k-N}^{k-1} p\left(y_j|x_j\right) \prod_{j=k-N}^{k-1} p\left(x_{j+1}|x_j\right) p(x_{k-N}|Y_{0:k-N-1}) , \qquad (7)$$

where *c* is the constant and $p\left(y_j|x_j\right)$ is the likelihood function for each measurement within the horizon. $p\left(x_{j+1}|x_j\right)$ is the state transition probability density function and $p(x_{k-N}|Y_{0:k-N-1})$ is the *a priori* density of the initial state of the horizon. For system (1) and (2), the state transition pdf is defined as $p(x_{k+1} - f(x_k))$:

$$p(x_{k+1}|x_k) = p(\omega_k) = p(\mathrm{x}_{\mathrm{k+1}} - \hat{x}_{k+1}) = p(x_{k+1} - f(x_k)) , \qquad (8)$$

where $\omega_k$ is the system process noise defined by $N(0, Q)$, and the likelihood function is defined by $p(y_k - h(x_k))$

$$p(y_k|x_k) = p(v_k) = p(y_k - \hat{y}_k) = p(y_k - h(x_k)) , \qquad (9)$$

where $v_k$ is the measurement noise of $N(0, R)$. Now by applying negative logarithm to joint density (7), we obtain the MHE cost function for system (1)-(2) which is a quadratic programming (optimization) problem:

$$\phi_T^* = \min_{x_0, \{\omega_k\}_{k=0}^{T-1}} \phi_T(x_0, \{\omega_k\}) = \arg \min_{z, \{\omega_k\}_{k=T-N}^{T-1}} \sum_{k=T-N}^{T-1} \|\omega_k\|_{Q^{-1}}^2 + \|v_k\|_{R^{-1}}^2 + \Gamma_{T-N}(z) , \qquad (10)$$

where $\|\alpha\|_A^2 = \alpha^T A \alpha$ for quadratic form. $x_k := x(k; z, \{\omega_j\}_{j=T-N}^{k-1})$ denotes the solution of (10) for system (1),(2) at time *k* with initial state *z* and process noise $\{\omega_j\}_{j=T-N}^{k-1}$ in horizon length. $\Gamma_{T-N}(z)$ is referred to as arrival cost which plays an important role in summarizing the effect of the past measurements $\{y_k\}_{k=0}^{T-N-1}$ as *a priori* information on the state $x_{T-N}$ ( $\Gamma_{\mathrm{T-N}}(\mathrm{z}) = -\log\left(\mathrm{p}(x_{k-N}|Y_{0:k-N-1})\right)$ ). However, the initialization of MHE with the best choice of the arrival cost term is an open issue. In this paper, the arrival cost is approximated using the EKF with the following form:

$$\Gamma_{\mathrm{T-N}}(\mathrm{z}) \approx (z - \bar{x}_{T-N}^{mh})' P_{T-N}{}^{-1} (z - \bar{x}_{T-N}^{mh}), \qquad (11)$$

where $\bar{x}_{T-N}^{mh}$ is the optimal estimate at time *T-N* generated in (10) given measurements from time 0 to *T-N-1*, the covariance matrix $P_{T-N}$ is an estimate of the covariance of $\bar{x}_{T-N}^{mh}$ calculated by EKF. Typically any nonlinear filter capable of propagating the conditional mean and covariance could be used to compute the arrival cost in MHE such as unscented Kalmen filters, particle filters and cell filters.
Since MHE is an optimization framework based state estimation algorithm, the physical road width constraints discussed above could be easily imposed on the MHE state variables.

## MHE BASED MULTIPLE HYPOTHESIS TRACKING (MHE-MHT)

In this section, we first review the original MHT algorithm described by Reid [18] and Cox [19]. Then the formation of MHE-MHT structure is set forth explicitly.

### A. Multiple hypothesis tracking structure

The original MHT algorithm is a deferred decision logic which forms alternative association hypotheses in order to deal with observation to track assignment uncertainties. According to Reid's paper, the hypothesis based MHT keeps the past hypotheses in the memory between consecutive time steps. MHT has the advantage of being able to deal with track creation, confirmation, occlusion and deletion in a probabilistically consistent way. The original MHT framework contains three main processes: hypothesis generation, probability calculation and hypothesis reduction. When a new measurement is received, observations that fall within the gate region set a possible measurement to track assignment thus an existing hypothesis is extended to a set of new hypotheses by considering all possible tracks to measurements assignments. Several assumptions are made when generating hypothesis:

**Assumption 1**

(i) Each hypothesis contains a set of compatible observation to track assignments,
(ii) Assignments are defined as 'compatible' if they have no measurements in common which means in each Hypothesis, each measurement can only update with one of the existing tracks.

**B. MHE-MHT framework**

In Figure 3, we present the flow diagram of MHE-MHT algorithm. Let $Y_k = \{y_i^k\}_{i=1}^{m_k}$ denote the set of $m_k$ measurements received at time k. Each of the measurement has three possible hypotheses:

- The measurement starts a new target
- The measurement is a false alarm
- The measurement belongs to an existing target

1) Gate Check: First the distance between the predicted priori target and the current measurements is calculated known as measurement prediction error/innovation. The prediction of target position is done by KF prediction update and the distance is defined as the Mahalanobis distance:

$$\left(y_m^k - \hat{y}_{k/k-1}\right)^T S_{k/k-1}\left(y_m^k - \hat{y}_{k/k-1}\right) \leq Gating, \qquad (12)$$

where $y_m^k$ is the measurement *m* at time *k*, $\hat{y}_{k/k-1}$ is the predicted target position and $S_{k/k-1}$ is the covariance of innovation vector , ${S^{-1}}_{k/k-1} = H\, P_{(k)} H + R$ both are calculated by KF. $Gating$ is a matrix of binary values which indicates maximum possible distance between measurement and targets. Only the measurements inside the gate are considered for assignment. Later, these statistical differences are used in data association.

2) Data association: MHE-MHT implements the same data association process as the Reids algorithm[18] which has been explained above. The assignment matrix is generated to represent all possible target-to-measurement associations. Then each new hypothesis contains a set of potential target-to-measurement assignments, leading to an exhaustive approach of enumerating all the possible assignment combinations. To solve this problem, the Murty's algorithm [19] is used to find the *k*-best assignment/new hypotheses generated from each parent hypothesis. To further reduce the computational cost, a merging algorithm is also implemented in to prevent hypotheses from being considered if the ratio of their probability to the best hypothesis becomes too small.

3) Target Maintenance: For ground target tracking scenarios, vehicles may enter or leave the surveillance field of view during the tracking process. Moreover, occlusion or miss detection is also possible when a vehicle is hidden behind another one. In order to achieve a fully functional tracking algorithm, we implement target maintenance logic in MHE-MHT structure. Basically, there are three possible status for a set of targets in this logic: target initiation, confirmation/deletion and maintenance. The implementation is based on track-oriented approach. The targets present at a time step are a combination of existing targets from the parent tracks and any new targets resulting from the set of measurement associations. For any targets in existence at time *k*-1, the possible associations at time *k*:

- Target initiation: If the measurement is associated with a new target and the new target hypothesis appears in the current *k*-best hypotheses. Add a target *lifetime* index to the target with value 1.
- Target confirmation/deletion: The new target is confirmed only if the detected target appears along the same track over a consecutive iterations of *Ct* times. The *lifetime* index is accumulated by 1whenever the tentative target is detected and will become *Ct* (confirmation threshold) when confirmed. On the contrary, the *lifetime* index for any existing target is reduced by 1 whenever the target is not associated with the current measurement and will be permanently deleted from target list when the *lifetime* is 0.
- Target maintenance: The confirmed target may be temporally occluded or undetected by the sensor.

For this situation, the track measurement for unassociated targets is updated according to the predicted position of the target last associated states.

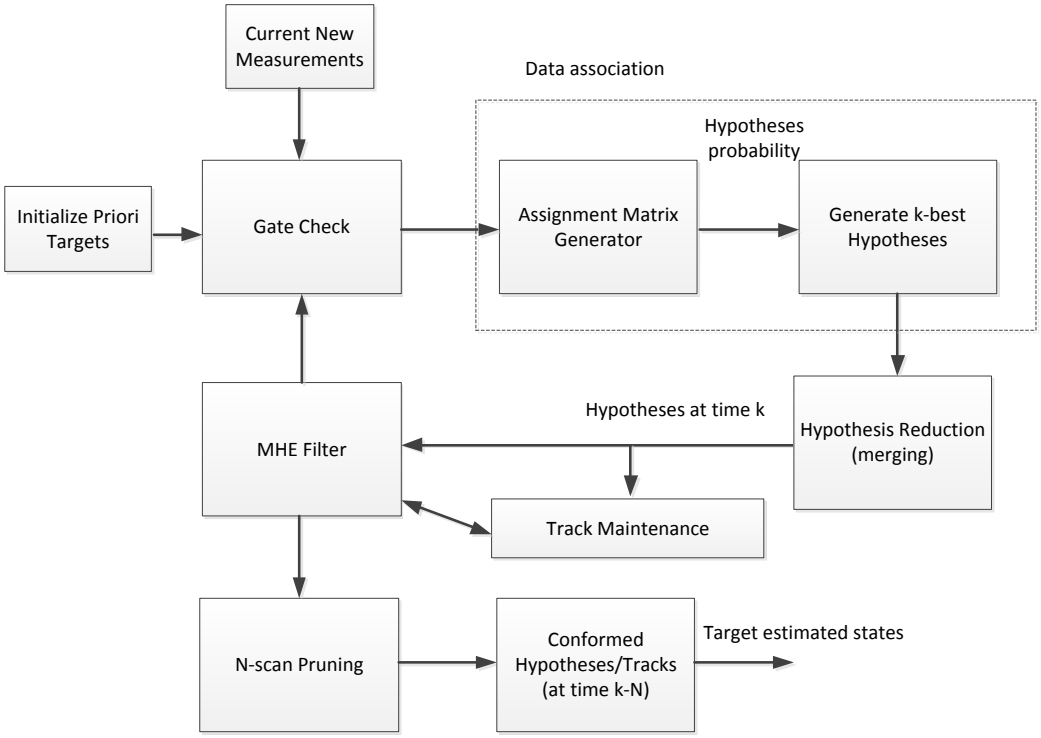


***Figure 3. Flow diagram of MHE-MHT algorithm***

4) MHE filter: The details about implementing MHE for constrained target tracking have been discussed in previous section in this paper. In this part, the main work will focus on comparing the difference between MHE and KF under the MHT structure. In the original MHT, the 'Filter' process is based on Kalman state estimation including two individual steps: prediction update and measurement update. However, the two steps are combined in MHE and solved directly by optimization solver. In MHE, the state estimation is determined online by solving a finite horizon state estimation problem. To determine new estimate of the target state, the finite horizon of latest measurements are resolved while the problem is solved recursively with only the current step measurement being considered in KF. Assuming that at time $k$, $x_k \coloneqq x(k; z, \{\omega_j\}_{j=T-N}^{k-1})$ denotes the solution of MHE optimization function (10) for a linear, time-invariant discrete-time system with initial state $z$ and process noise $\{\omega_j\}_{j=T-N}^{k-1}$ in horizon length $N$. Then the estimation result is:

$$x(k; z, \{\omega_j\}_{j=T-N}^{k-1}) = F^k z + \sum_{j=0}^{k-1} F^{k-j-1} G \omega_j \quad , \qquad (13)$$

and if considering the road linear inequality constraint in (3), an additional MHE state constraint is consideredas

$$a_k \leq H_{C_k} F^k z + H_{C_k} \sum_{j=0}^{k-1} F^{k-j-1} G w_j + \sum_{j=0}^{k-1} v_j \leq b_k, \qquad (14)$$

where $F$ is the linear state transition matrix, and $H_{C_k}$ is the linear constraint matrix. $\{v_j\}_{j=T-N}^{k-1}$ is the estimated measurement noise for $N$ horizon length.

The filtering process would be similar to KF if measurements are always detected and updated with the target, However, a problem arises when miss detection happens among a horizon of measurements, since there is no individual predict update process in MHE and the estimation problem is solved by an optimization solver. In the MHE-MHT algorithm, the missing target measurement is presumed as one step predicted state calculated by KF: $x_k = F x_{k-1}$ and thus the estimated process noise $\omega_j$ and measurement noise $v_j$ for time $k$ is taken as null. This

assumption is equivalent the one used in KF-MHT for missed detection which treats the non-available posterior measurement updated estimate as the prior predicted state. The proof is shown below:

- For Kalman filter at time *k*
  Prediction Update: $\hat{x}_{k|k-1} = F\hat{x}_{k-1|k-1}$
  Measurement Update: $\hat{x}_{k|k} = \hat{x}_{k|k-1} + K_k(y_k - \hat{y}_{k|k-1})$
- If at time *k*, measurement $y_k$is missing, then the predicted state $\hat{x}_{k|k-1}$ is taken as estimated state $\hat{x}_{k|k}$, In other words, the measurement update step is rejected
- So $K_k(y_k - \hat{y}_{k|k-1}) = 0$, and thus $y_k = \hat{y}_{k|k-1}$, where $\hat{y}_{k|k-1}$ is predicted target $\hat{y}_{k|k-1} = HF\hat{x}_{k-1|k-1}$
- In this case, for system :
  $x_{k+1} = Fx_k + \omega_k$
  $y_k = Hx_k + v_k$
- So $y_k = \hat{y}_{k|k-1} = HFx_k$ and thus $\omega_k$ *and* $v_k$are null

Correspondingly, the high level logic for MHE-MHT target maintenance is shown below in Table 1:

**Table 1.**

**High level logic for MHE-MHT target maintenance**

```
 -- At time k, for nExistedTarg number of existing target in a hypothesis
For k=1: nExistedTarg
    (Case one: permanent deleted targets)
    If LifePoint == 0
       Continue; (the target is permanently deleted/already disappeared)
    End
    (Case two: target maintenance—target updating with measurement or temporally miss detection)
    If Targ≠asso (Target not associated with current measurement)
       LifePoint=LifePoint-1;
         If LifePoint>0
            Implement KF prediction for MHE estimation
         End
    Else (Target associated with current measurement)
       Implement MHE update;
         If LifePoint<MaxLifePoint
            LifePoint= LifePoint+1;
        End
    End
    (Case three: target initialization)
For k=1: nNewTarg (measurement is associated to a new target)
     Use current measurement as initial position;
     LifePoint=0;
End
```

5) N-scan pruning: The key principle of the MHT method is that difficult data association decisions are deferred until more data are received, which could be achieved by using N-scan pruning. The structure provides a convenient mechanism for implementing deferred decision logic and for presenting a coherent output from the MHT. The continued growth of the tracks is also controlled by N-scan pruning technique by keeping only the N previous scans in the trees. The hypotheses with low probability are deleted after N-scan pruning. The survive target after pruning process are predicted using the new measurements obtained and reformed into new hypotheses. In MHE-MHT the number of N scans is chosen as the same value for horizon length in MHE. As a result, the association uncertainty at time k-N is resolved by the hypotheses given at time k and meanwhile the estimation process considers all measurements within the last N scans.

## SIMULATION and RESULTS

In this section, the proposed algorithm is evaluated by means of two examples. The first example is aimed at illustration of handling nonlinear inequality road constraint using a MHE based approach, using a single target circular road tracking scenario. The second one which is inspired by [28] is a complex multiple target tracking scenario incorporating road inequality constraints for an intersection scenario.

### A. Target tracking with nonlinear road inequality constraints

In the first example, we follow the previous study of [8] in 2012 to set up the test scenario. A moving vehicle on a circular road section is considered as shown in Figure 4. The road is defined by two boundaries with two arcs of *r1*=96m and *r2*=100m, respectively, centered at the origin of a Cartesian coordinate system. The vehicle dynamics is described by a white noise acceleration motion model.

$$x_{k+1} = \begin{bmatrix} 1 & T & 0 & 0 \\ 0 & 1 & 0 & 0 \\ 0 & 0 & 1 & T \\ 0 & 0 & 0 & 1 \end{bmatrix} x_k + \begin{bmatrix} T^2/2 & 0 \\ 0 & T^2/2 \\ T & 0 \\ 0 & T \end{bmatrix} \omega_k \qquad (15)$$

where the state vector $x_k = [x_{1,k}, x_{2,k}, \dot{x}_{1,k}, \dot{x}_{1,k}]^T$ consists of the vehicle position and velocity in x and y directions, $T = 1$ is the sampling interval, and $\omega_k$ is a two-dimensional Gaussian process noise with zero mean and covariance matrix $Q = eye(2)$. The initial state of the vehicle is $x_0 = [98,0,0,10]^T$. The vehicle is supposed to move for $k = 1, \dots, K$ with $K = 20$.
The vehicle is tracked by range and bearing sensors modelled as:

$$z_k = \begin{bmatrix} \sqrt{x_{1,k}^2 + x_{2,k}^2} \\ arctan\left(\frac{x_{2,k}}{x_{1,k}}\right) \end{bmatrix} + v_k \qquad (16)$$

where $v_k$ is a two-dimensional Gaussian zero-mean measurement noise with a diagonal covariance matrix $R = diag\{8, 10^{-3}\}$. Given the road boundaries, the state inequality constraint is shown in (5): $r_1 \leq \sqrt{{x_{1,k}}^2 + {x_{2,k}}^2} \leq r_2$.

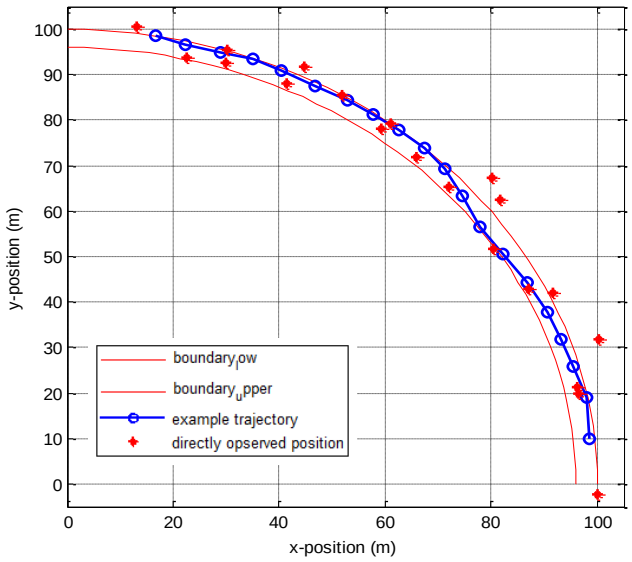


***Figure 4. Tracking scenario for example 1***

The performance of constrained MHE filter was measured using the mean-square error (MSE):

$$MSE = \left(2(K+1)\right)^{-1} \sum_{k=0}^{K} \sum_{i=1}^{2} (x_{1,k} - \hat{x}_{i,k})^2 \qquad (17)$$

We compare the performance of constrained MHE (cMHE) with different horizon length (N=2 and 8) with some other conventional filters. In [8], Straka compared several conventional filters including the unscented Kalman filter (UKF), divided difference filter (DFF), the Gaussian mixture filter (GMF), constrained particle filter (cPF) and the truncated versions tUKF, tDDF, and tGMF. The results are shown in table.2:

**Table 2.**

**Estimation performance of filters for example 1**

| | UKF | DDF | GMF | tUKF | tDDF | tGMF | cPF($10^3$samples) | cMHE (N=2) | cMHE(N=8) |
|---|---|---|---|---|---|---|---|---|---|
| MSE | 7.79 | 20.27 | 6.31 | 4.23 | 4.90 | 3.63 | 4.29 | 4.46 | 3.98 |
| Time (s) | 0.019 | 0.027 | 0.042 | 3.280 | 3.458 | 6.612 | 9.28 | 1.09 | 2.97 |

It can be seen from Table 2 that the tUKF, tDDF, tGMF outperform their unconstrained conventional filters UKF, DDF and GMF. The cPF provides high quality estimates however at an expense of high computational cost. The proposed constrained MHE in this paper provides reasonable good performance especially when increasing the horizon length. When N=8 the cMHE provides the second best MSE=3.98 among all filters in Table.2 which is slightly worse than tGMF with MSE=3.63 however cMHE provides a much better the computational cost with only half time taken for tGMF by using *fmincon* server in MATLAB.

### B. Multiple target tracking for intersecting road scenario

In the second example, we set up a multiple target tracking simulation for interacting scenario. As illustrated in Figure5, the region of interest is [-1000m,1000m] x [-1000m,1000m] with an unknown and time varying number of targets observed in a clutter environment. The vehicle dynamics is described the same as (15) and the state vector $x_k = [x_{1,k}, x_{2,k}, \dot{x}_{1,k}, \dot{x}_{1,k}]^T$ consists of the vehicle position and velocity while the measurement model is defined as a noisy position in x and y directions. $T = 1$ is the sampling interval and the two-dimensional Gaussian process noise has covariance matrix $Q$ of 5 m/$s^2$ standard deviation. Initially, two targets start moving in the environment with initial state $x_{1,0} = [250,250,0,0]^T$ and $x_{2,0} = [-250,-250,0,0]^T$. The target initial covariance is defined as $P_0 = diag[100,100,25,25]^T$ for both two targets. Each target is detected with a probability of $P_d = 0.98$, and the Gaussian noise based position measurement has a standard deviation of 10m in both directions. The detected measurements are immersed in clutter that can be modeled as a Poisson distribution with clutter density of $\beta_{FA} = 12.5 * 10^{-6}$ over the $4 * 10^6 m^2$ region (i.e., 50 clutter returns over the region of interest). As shown in Figure 5, Target 1 and 2 appear at the same time in different locations, traveling along straight lines and cross each other at K=53s. A new target spawns from Target 1's trajectory at time K=66s. The total simulation time is K=100s.
The target trajectories are supposed to be constrained by road boundaries, each with a width of 6 meters using the road inequality constraint in (4). The position estimates are shown in Figure 6, it can be seen that the constrained MHE-MHT algorithm provides accurate tracking performance. Moreover, the algorithm not only tracks Target 1 and 2 but also able to detect and track the spawned Target 3. The lifetime threshold is defined as 4, which means any new target can only be confirmed if successfully detected in 4 sequential time steps. The horizon length used in MHE in chosen as 4 and so as for N-scan pruning. At each time 3-best hypothesis are generated from each parent hypothesis.

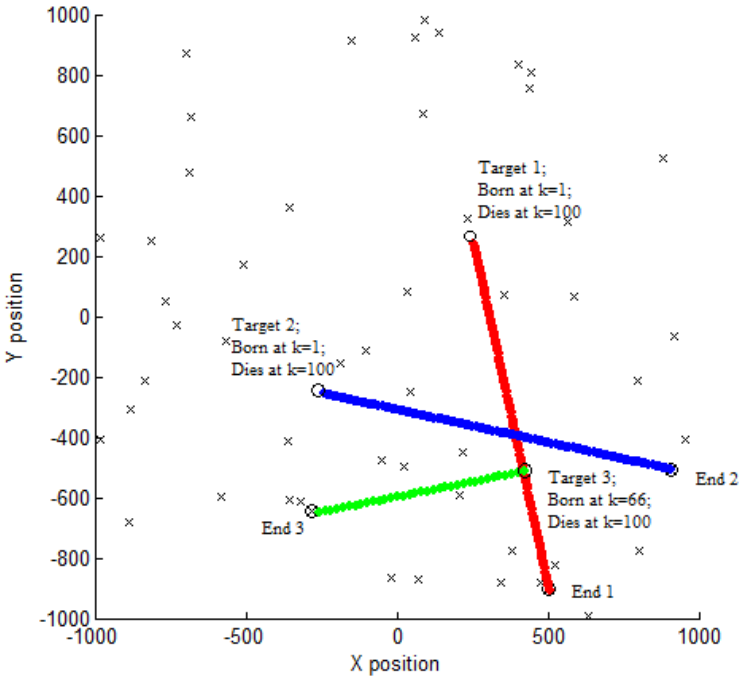


***Figure 5. Target trajectories for scenario 2***

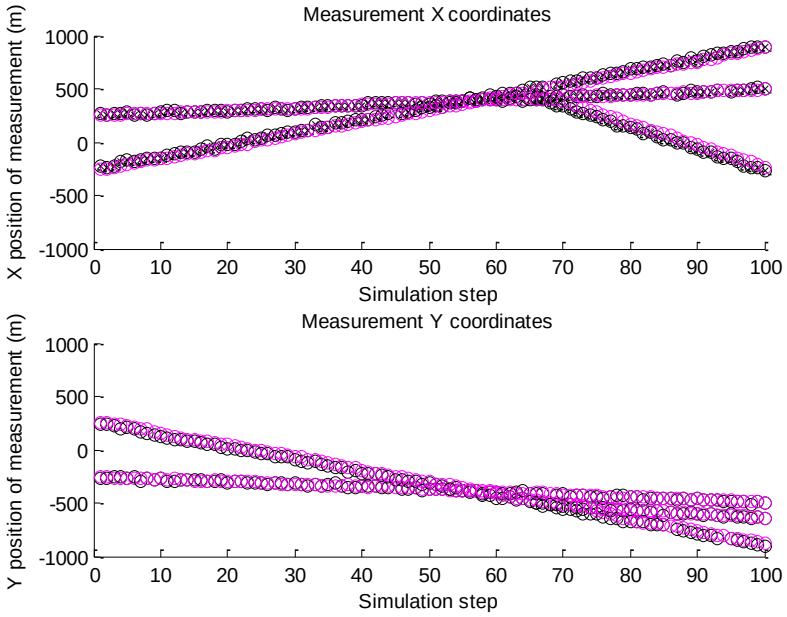


***Figure 6. Position estimation for MHE-MHT***

To further analysis our algorithm, Figure7 shows a comparison between original Kalman filter based MHT and constrained MHE-MHT using the optimal subpattern assignment metric (OSPA) [31] which considers not only the estimation performance but also association accuracy.

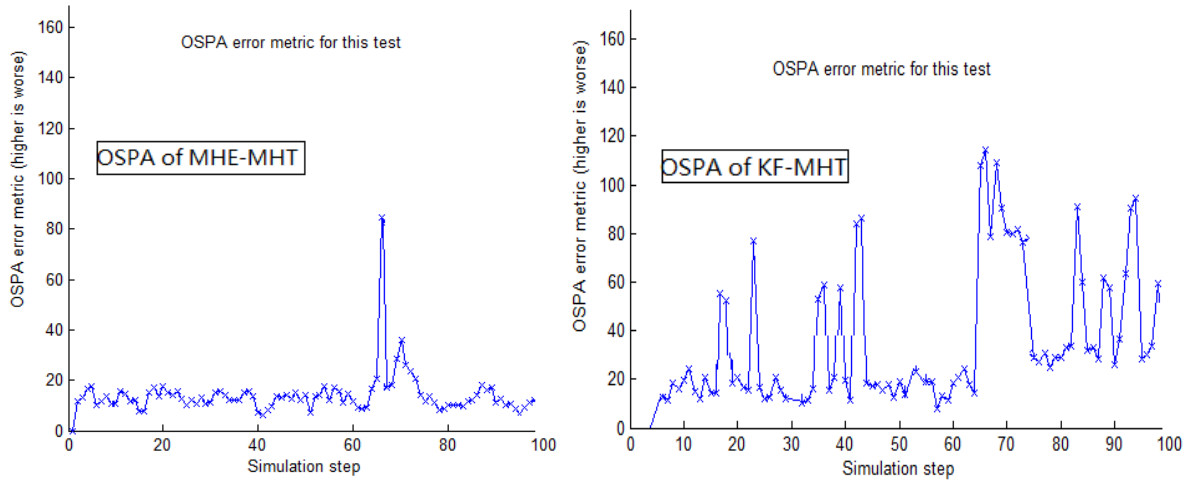


***Figure 7. OSPA performance for MHE-MHT and KF-MHT algorithm***

From the results, it can be seen that the MHE-MHT algorithm performance is more stable than KF-MHT which is concluded by the variation of the OSPA distance over time. This is because of the more accurate state estimation performance for constrained MHE which also affects the accuracy of new target detection and data association. In the original KF-MHT, road width constraint is not considered which makes the predicted target more likely to associate with clutter and thus generate false new targets. At time k=66, the new target appears which makes OSPA increase significantly. However, the faulty association hypotheses are soon discarded in MHE-MHT by the correct one which has higher hypothesis probability.

## CONCLUSION

In this paper, we propose a novel MHE-MHT algorithm for constrained multiple target tracking problems. External road information is employed by MHE filters in state estimation process. A target maintenance logic is designed for MHE-MHT algorithm to track multiple targets efficiently and accurately. Initial simulation studies have shown the effectiveness of the proposed algorithm against conventional algorithms.
The future work will focus on incorporating extra domain knowledge in the MHE-MHT structure especially for target interaction problems since the target are considered moving independently in most target tracking algorithms without having interacting behaviors with other targets or physical environment. Experimental research combing real sensor data and digital map information will also be carried out.

## REFERENCES

[1] Blackman, SS. "Multiple hypothesis tracking for multiple target tracking." Aerospace and Electronic Systems Magazine, IEEE 19.1 (2004): 5-18.
[2] Ristic, B., S Arulampalam, and N Gordon. Beyond the Kalman filter: Particle filters for tracking applications. Vol. 685. Boston: Artech house, 2004.
[3] Simon, D, and Tli Chia. "Kalman filtering with state equality constraints."Aerospace and Electronic Systems, IEEE Transactions on 38.1 (2002): 128-136.
[4] Simon, D. "Kalman filtering with state constraints: a survey of linear and nonlinear algorithms." IET Control Theory & Applications 4.8 (2010): 1303-1318.
[5] Yang, C, M Bakich, and EBlasch. "Nonlinear constrained tracking of targets on roads." Information Fusion, 2005 8th International Conference on. Vol. 1. IEEE, 2005.
[6] Yang, C, and E Blasch. "Kalman filtering with nonlinear state constraints." Aerospace and Electronic Systems, IEEE Transactions on 45.1 (2009): 70-84.

[7] Luenberger, David G., and Yinyu Ye. Linear and nonlinear programming. Vol. 116. Springer Science & Business Media, 2008.
[8] Straka, O, J Duník, and M Šimandl. "Truncation nonlinear filters for state estimation with nonlinear inequality constraints." Automatica48.2 (2012): 273-286.
[9] Shao, X, B Huang, and J Lee. "Constrained Bayesian state estimation–A comparative study and a new particle filter based approach." Journal of Process Control 20.2 (2010): 143-157.
[10] Rao, Christopher V., James B. Rawlings, and David Q. Mayne. "Constrained state estimation for nonlinear discrete-time systems: Stability and moving horizon approximations." Automatic Control, IEEE Transactions on 48.2 (2003): 246-258.
[11] Ulmke, M, and W Koch. "Road-map assisted ground moving target tracking." Aerospace and Electronic Systems, IEEE Transactions on 42.4 (2006): 1264-1274.
[12] Bishop, R. "A survey of intelligent vehicle applications worldwide."Intelligent Vehicles Symposium, 2000. IV 2000. Proceedings of the IEEE. IEEE, 2000.
[13] Pulford, G. W. "Taxonomy of multiple target tracking methods." Radar, Sonar and Navigation, IEE Proceedings-. Vol. 152. No. 5. IET, 2005.
[14] Stiller, C, FLeòn, and Marco Kruse. "Information fusion for automotive applications–An overview." Information fusion 12.4 (2011): 244-252.
[15] Rong Li, X., & Y Bar-Shalom. "Tracking in clutter with nearest neighbor filters: analysis and performance." Aerospace and Electronic Systems, IEEE Transactions on 32.3 (1996): 995-1010.
[16] Blackrnan, S, & House. "Design and analysis of modern tracking systems." Boston, MA: Artech House (1999).
[17] Fortmann, Thomas E., Y Bar-Shalom, and M Scheffe. "Sonar tracking of multiple targets using joint probabilistic data association." Oceanic Engineering, IEEE Journal of 8.3 (1983): 173-184.
[18] Reid, D. "An algorithm for tracking multiple targets." Automatic Control, IEEE Transactions on 24.6 (1979): 843-854.
[19] Cox, J., and S. Hingorani. "An efficient implementation of Reid's multiple hypothesis tracking algorithm and its evaluation for the purpose of visual tracking." Pattern Analysis and Machine Intelligence, IEEE Transactions on 18.2 (1996): 138-150.
[20] Blackman, S S. "Multiple hypothesis tracking for multiple target tracking." Aerospace and Electronic Systems Magazine, IEEE 19.1 (2004): 5-18.
[21] S, Roy L., and Tod E. Luginbuhl. Probabilistic multi-hypothesis tracking. No. NUWC-NPT-TR-10428. NAVAL UNDERWATER SYSTEMS CENTER NEWPORT RI, 1995.
[22] Moon, Tod K. "The expectation-maximization algorithm." Signal processing magazine, IEEE 13.6 (1996): 47-60.
[23] Rago, C, P Willett, and R Streit. "A comparison of the JPDAF and PMHT tracking algorithms." Acoustics, Speech, and Signal Processing, 1995. ICASSP-95., 1995 International Conference on. Vol. 5. IEEE, 1995.
[24] Hue, C, J-P. Le Cadre, and P Pérez. "Tracking multiple objects with particle filtering." Aerospace and Electronic Systems, IEEE Transactions on38.3 (2002): 791-812.
[25] Vermaak, J, Simon J. G, and P Perez. "Monte carlo filtering for multi target tracking and data association." Aerospace and Electronic Systems, IEEE Transactions on 41.1 (2005): 309-332.
[26] Tonissen, S M., and R J. Evans. "Peformance of dynamic programming techniques for Track-Before-Detect." Aerospace and Electronic Systems, IEEE Transactions on 32.4 (1996): 1440-1451.
[27] Vo, B, S Singh, and A Doucet. "Sequential Monte Carlo methods for multitarget filtering with random finite sets." Aerospace and Electronic Systems, IEEE Transactions on 41.4 (2005): 1224-1245.
[28] Vo, B, and W Ma. "The Gaussian mixture probability hypothesis density filter." Signal Processing, IEEE Transactions on 54.11 (2006): 4091-4104.
[29] Vo, Ba-T, Ba-N Vo, and A Cantoni. "The cardinality balanced multi-target multi-Bernoulli filter and its implementations." Signal Processing, IEEE Transactions on 57.2 (2009): 409-423.
[30] Yang, C, M Bakich, and E Blasch. "Nonlinear constrained tracking of targets on roads." Information Fusion, 2005 8th International Conference on. Vol. 1. IEEE, 2005.
[31] Schuhmacher, D, B Vo, and B Vo. "A consistent metric for performance evaluation of multi-object filters." Signal Processing, IEEE Transactions on 56.8 (2008): 3447-3457.

# PEDESTRIAN RESPONSE WITH DIFFERENT INITIAL POSITIONS DURING IMPACT WITH A MID-SIZED SEDAN

**Huipeng Chen**
**David Poulard**
**Jeff R. Crandall**
**Matthew B. Panzer**
Center for Applied Biomechanics, University of Virginia
United States of America

Paper Number 15-0391

## ABSTRACT

Real-world pedestrian impacts occur with highly-variable or unknown initial conditions of the pedestrian. However, experimental pedestrian tests and computational pedestrian impact simulations mainly focus on the response of the subject using specific initial conditions. The objective of this study is to investigate computationally the influence of posture and impact direction angle on pedestrian response during an impact. The 50$^{th}$ male THUMS pedestrian model was integrated with a mid-sized sedan finite element model initially travelling at 40 km/h. The influence of the pedestrian position during impact was investigated by varying 9 orientations (relative to the vehicle) and 3 standing/gait postures, for a total of 27 impact configurations simulated. Pedestrian kinematics and injury were assessed and compared across all simulations. Substantial variations were observed on the pedestrian torso rotation (-68.9°~57.6°), and head impact conditions (head impact time 111~139 ms, and head impact velocity 10.7~15.3 m/s). The head impact velocity was found to correlate with the impact direction angle, where facing towards or away from the vehicle would result in greater head impact velocity than when struck in a purely-lateral impact.

## INTRODUCTION

Although significant improvements have been achieved in mitigating pedestrian fatalities, there are still over 400,000 pedestrians killed each year worldwide [1]. Epidemiological reviews have highlighted that 66-82% of pedestrians were hit by passenger cars and 60-77% of pedestrians were struck by the vehicle front [2], and serious injuries occur frequently at speeds between 25 and 55 km/h [3]. More than 60 % of the pedestrian accidents occurred at a vehicle speed of 40 km/h or less, and impacts with the bumper, hood, and windshield were believed to be the leading sources of pedestrian injury [4]. This suggests that an indepth understanding of the complex interaction between the pedestrian and vehicle is essential to ensure effective countermeasures.

The response of the human body to vehicle impact has been extensively studied using post-mortem human specimens (PMHS) on component tests [5] and vehicle-impact tests [6- 9]. These tests are the primary source of data for the development of physical and computational surrogates (anthropomorphic test devices and human body models, respectively). Understandably, studies involving vehicle-pedestrian impact using PMHS have focused on well-defined situations such as pure-lateral vehicle impact direction and specific pedestrian posture.

The most common pedestrian-vehicle impacts occur when pedestrians are crossing the road, and the amount of pedestrians struck laterally varies between 65-89% of all impact cases [2,3,10]. However, an accurate pedestrian impact angle may not always be reported and it is reasonable to assume that the pedestrian impact direction is not purely lateral. In addition, prior to an accident, pedestrians often move in different ways: 71-79 % of pedestrians involved in accidents are standing upright and moving across the road [11], while 65% of pedestrians are walking and 20% are running [2]. Reaction to an oncoming vehicle will also influence the initial orientation and posture of a pedestrian [12]. Changes to pedestrian orientation and posture from the purely-lateral stance may greatly affect the ensuing kinematics, injury risk, and pattern during a vehicle-pedestrian impact.

Compared to experimental tests performed with PMHS which differ in age and anthropometry, simulations with human computational models have the potential to evaluate the impact response of a single individual while introducing extrinsic variability. Peng et al. [13] used the stances for different gait parameters developed in a previous pedestrian sensitivity study by Untaroiu et al. [14] to investigate the effects of gait on pedestrian head

kinematics. However, this study did not investigate the whole-body kinematics and injury mechanism because a simplified multibody ellipsoid model was used. Finite element (FE) models of a human body offer some promising advantages for studying injury biomechanics, including the prediction of injury mechanisms and injury criteria and a large potential for customization. One the existing human body models (HBMs) that have been developed is the Total Human Model for Safety (THUMS) pedestrian model, which has been used to investigate the biomechanics of vehicle-pedestrian impact [15- 21]. While these studies focused on the risk of injury to a specific body part (brain: [19], shoulder: [21]) or the influence of specific parameters such as car type, vehicle speed, and pedestrian size [17-20], there were no studies on the influence of posture and impact orientation.

The hypothesis of this study is that changes to the pedestrian posture and orientation at the time of impact will significantly affect the resulting responses and distribution of injury predicted for the pedestrian. Thus, the objective of this study is to computationally investigate the influence of posture and impact orientation on pedestrian kinematics and injury during an impact with a mid-sized sedan.

## METHODS

### Model Setup

The THUMS pedestrian model (50$^{th}$ male, version 4.01) was integrated with a FE model of the front-end structure of a mid-sized sedan (Figure 1). The vehicle model is the same vehicle used in a previous experimental PMHS pedestrian test series at UVA reported by Subit et al. [9] . All boundary conditions and mass distributions assigned to the FE vehicle model were consistent with those of the test series. An initial velocity of 40 km/h was applied on the vehicle and was allowed to impact the pedestrian. The friction coefficient between the HBM and the vehicle was 0.5, and was 0.6 between the feet and ground [13]. The simulation time was 200 ms, using the code LS-DYNA v971 7.1.1.

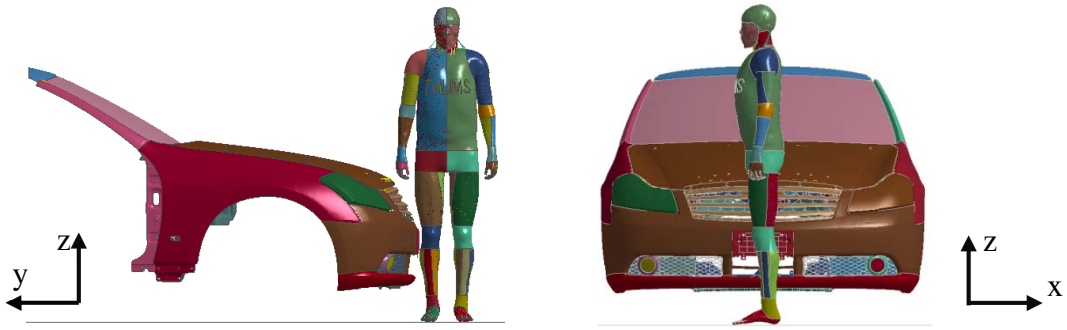


***Figure1. Simulation set up (Baseline model S0).***

### Alteration of posture

Three human postures were created from the original HBM (Figure 2). A baseline model “S”, which is the default position of the THUMS pedestrian model, was defined as a standing posture with arms down and legs aligned. Two additional models were defined with walking postures, referred to as “RF” and “LF”, and were derived from a normal gait-cycle of 0% (right leg forward) and 50% (left leg forward) respectively [14]. Positioning of the THUMS pedestrian model for the RF and LF postures was done using pre-simulation to match the angles of the hips, knees, shoulders and elbows.

*Standing (S)* *Right leg forward (RF)* *Left leg forward (LF)*

***Figure 2. Pedestrian postures.***

**Impact direction**

Nine pedestrian impact orientations were defined in the study, with the pedestrian center of gravity (CG) located along the centerline of the vehicle. The baseline impact orientation was the pure-lateral case (Figure 1) with an associated impact direction angle of 0 degrees. Eight additional impact directions were created from the baseline orientation by rotating the pedestrian relative to the vehicle by ±15° ("near lateral"), ±30° and ±60° ("non-lateral"), and ±90° ("facing toward" or "facing away") (Figure 3). Due to the nearly symmetric geometry of the vehicle and HBM, these cases represent a full 360° array of pedestrian impact orientation relative to the vehicle.

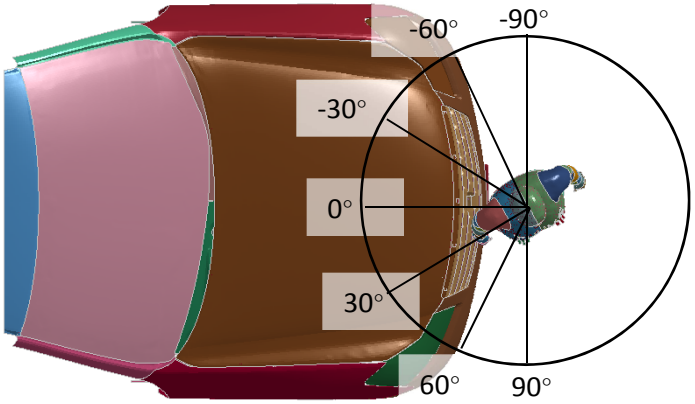


***Figure3. Impact direction angles. The model shown is S30.***

**Simulation matrix**

By varying the three pedestrian postures and nine impact directions, a matrix of 27 cases in total was created and simulated (Table 1).

**Table 1. Simulation Matrix**

| | Simulation ID | | | | | | | | |
|---|---|---|---|---|---|---|---|---|---|
| Impact direction angle | **0** | **15** | **30** | **60** | **90** | **-15** | **-30** | **-60** | **-90** |
| Standing posture | S0 | S15 | S30 | S60 | S90 | SN15 | SN30 | SN60 | SN90 |
| Right leg forward posture | RF0 | RF 15 | RF 30 | RF 60 | RF90 | RFN15 | RFN30 | RFN60 | RFN90 |
| Left leg forward posture | LF0 | LF15 | LF30 | LF60 | LF90 | LFN15 | LFN30 | LFN60 | LFN90 |

**Pedestrian Kinematics**

Head impact velocity $V_h$ was defined as the relative velocity between the head center gravity and the vehicle CG after initiation of contact (Equation 1). The head impact location was categorized by 4 areas on the vehicle according to the wrap around distance (WAD) [23], which was measured as the sum of the distance from the ground to bumper, bumper to hood leading edge, and hood leading edge to head impact location. For the vehicle used in this study, the head impact location could be classified by the 4 areas illustrated on Figure 4.

$$V_{relative} = |\vec{V}_{head} - \vec{V}_{car}| \qquad \text{[Equation 1]}$$

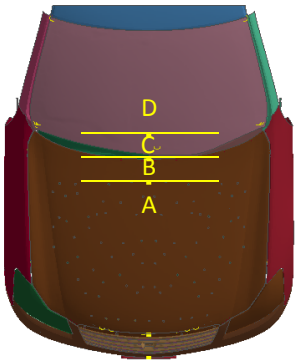


***Figure4. Wrap around distance (WAD) categories.*** A: WAD < 1800 mm (hood), B: 1800 ⩽ WAD<1950 (cowl), C: 1950 ⩽ WAD< 2100 (windshield frame), D: WAD ⩾ 2100 mm (windshield).

Torso rotation was calculated by change in the line formed by the left and right acromion, from the initial and final (when torso impacts vehicle) pedestrian facing angle to the vehicle (Equation 2) and Figure 5.

$$\theta_{initial} = accsin(\frac{L_x}{L}) \qquad \theta_{final} = accos(\frac{L_z}{L}) \qquad \text{[Equation 2]}$$

***Figure5. Initial torso angle and final torso angle (Configuration SN30).***

### Bony Fracture and Ligament rupture

The injuries predicted to occur in the simulations were bone fractures and ligament ruptures, and strain-based injury criteria were used for predicting these types of injuries. A 3% principal strain fracture criterion was used to predict all the cortical bone fracture (except for hands and feet), and 16% principal strain injury criterion was used for knee ligament rupture [20, 22]. These values are representative of a 40 year-old subject [20]. Tissue-level injury prediction was done in the post-processing stage of the simulation, since element deletion was not activated during the simulations to ensure stability of the models.

### Statistical Analyses

The response variables in this study were the pedestrian kinematics obtained from the models: head impact time, head impact site, head velocity Vh, torso impact angle, torso rotation. Descriptive statistics were given for all variables as mean ± one standard deviation (SD). Posture and impact direction effects were explored using a general linear regression model with the pedestrian kinematics as the dependent variables. Student's t-tests were performed on the regressed coefficients and $p < 0.05$ was considered statistically significant.

## RESULTS

### Pedestrian Kinematics

Pedestrian kinematics for each simulation are listed in Table 2. Considerable variability was found with the observed head impact time of 111~139 ms, head impact velocity of 10.7~15.3 m/s, and torso rotation of -68.9°~57.6°. All head impact locations were between the cowl and windshield frame, with the WAD ranging from 1900 to 2100 mm. In all 27 configurations, 8 experienced shoulder impact, and 14 experienced elbow impact (4 experienced both), while only 9 did not experience either impact. In Figure 6, $V_h$ is displayed crossed impact direction angle and absolute impact direction angle according to the respective posture. The head impact velocity $V_h$ was higher in cases where the pedestrian was turned away from the purely-lateral orientation (Figure 6). No trend was observed for the amount of torso rotation experienced by the pedestrian as a factor of impact direction angle (Figure 7).

Linear regression coefficients of the pedestrian kinematics are shown in Table 3. Posture was a significant predictor for head impact site ($p=0.029$), torso impact angle ($p=0.049$) and torso rotation ($p=0.049$). Impact direction angle was a significant predictor for head impact site ($p<0.0001$) and torso impact angle ($p<0.0001$). There was a trend that impact direction may be predictor for head impact velocity $V_h$ ($p=0.066$). The absolute impact direction angle was found to be a significant predictor ($p<0.0001$) for the head impact velocity Vh.

**Table 2. Pedestrian kinematics**

| Cases | Head impact time (ms) | Head impact site | Head impact location | $V_h$ (m/s) | Torso impact angle (°) | Torso rotation (°) | Upper extremity impact |
|---|---|---|---|---|---|---|---|
| S0 | 139 | lateral | C | 11.6 | 15 | 15 | both |
| S15 | 139 | occipital | C,D | 10.8 | 72.6 | 57.6 | elbow |
| SN15 | 135 | frontal | C | 10.8 | -83.9 | -68.9 | elbow |
| S30 | 134 | occipital | C | 11.8 | 84.0 | 54.0 | elbow |
| SN30 | 125 | frontal | C | 12 | -89.0 | -59.0 | elbow |
| S60 | 123 | occipital | C | 14.6 | 77.6 | 17.6 | - |
| SN60 | 117 | frontal | B,C | 13.4 | -88.3 | -28.3 | - |
| S90 | 117 | occipital | C | 15.3 | 87.9 | -2.1 | - |
| SN90 | 111 | frontal | B | 14.0 | -88.6 | 1.4 | - |
| RF0 | 128 | occipital | C | 12.2 | 29.5 | 29.5 | shoulder |
| RF15 | 124 | occipital | C | 12.7 | 47.6 | 32.6 | shoulder |
| RFN15 | 129 | lateral | B,C | 13.6 | 8.5 | 23.5 | shoulder |
| RF30 | 125 | occipital | B,C | 12.7 | 75.5 | 45.5 | elbow |
| RFN30 | 129 | lateral | B | 14.9 | -27.0 | 3.0 | shoulder |
| RF60 | 123 | occipital | B,C | 13.5 | 77.5 | 17.5 | elbow |
| RFN60 | 130 | frontal | B,C | 12.5 | -86.5 | -26.5 | - |
| RF90 | 130 | occipital | B | 15 | 87.0 | -3.0 | - |
| RFN90 | 129 | frontal | B,C | 13.3 | -75.0 | 15.0 | - |
| LF0 | 132 | frontal | C | 11.7 | -40.0 | -40.0 | both |
| LF15 | 132 | lateral | C | 12.5 | 11.8 | -3.2 | both |
| LFN15 | 131 | frontal | C | 11.2 | -76.0 | -61.0 | elbow |
| LF30 | 130 | lateral | B,C | 13.9 | 23.9 | -6.1 | both |
| LFN30 | 118 | frontal | B,C | 10.7 | -77.6 | -47.6 | elbow |
| LF60 | 134 | occipital | B,C | 13.3 | 90.0 | 30.0 | - |
| LFN60 | 124 | frontal | B | 12.1 | -52.2 | 7.8 | elbow |
| LF90 | 132 | occipital | B, C | 15.4 | 88.2 | -0.8 | - |
| LFN90 | 129 | frontal | B | 13.2 | -106.0 | -16.0 | elbow |

*A: WAD < 1800 mm (hood), B: 1800 ⩽ WAD<1950 (cowl), C: 1950 ⩽ WAD< 2100 (windshield frame), D: WAD ⩾ 2100 mm (windshield).

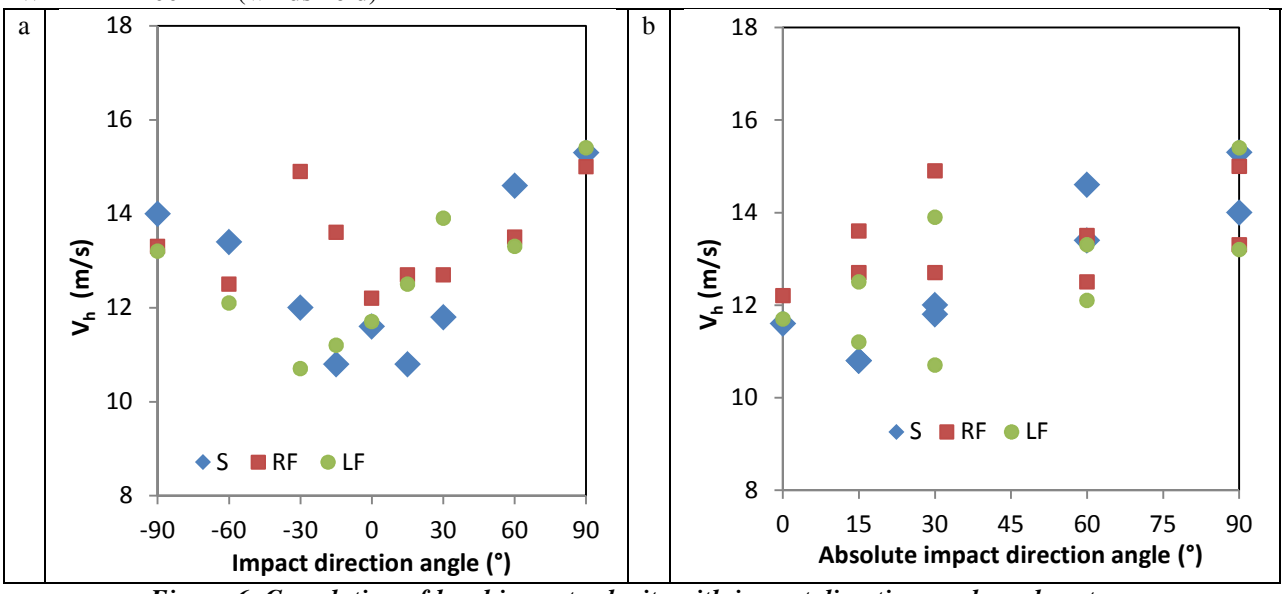


*Figure 6. Correlation of head impact velocity with impact direction angle and posture*

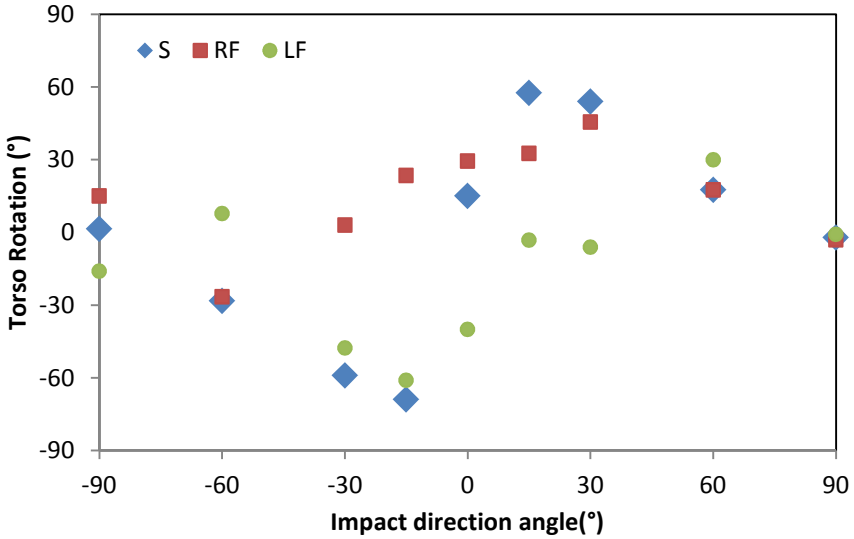


*Figure7. Correlation of torso rotation with impact direction angle and posture*

**Table 3. Linear regression analysis of pedestrian kinematics**

| Variables | Coefficients | S.D. | t-Stat | P-value | Lower 95% | Upper 95.0% |
|---|---|---|---|---|---|---|
| Head impact time | | | | | | |
| Posture | -0.83 | 1.60 | -0.52 | 0.607 | -4.13 | 2.46 |
| Impact direction angle | 0.03 | 0.02 | 1.04 | 0.310 | -0.03 | 0.08 |
| Head impact site | | | | | | |
| Posture* | -0.33 | 0.14 | -2.32 | 0.029 | -0.63 | -0.04 |
| Impact direction angle* | -0.01 | 0.00 | -6.39 | 0.0000 | -0.02 | -0.01 |
| Head impact velocity $V_h$ | | | | | | |
| Posture | 0.36 | 0.31 | 1.15 | 0.263 | -0.28 | 1.00 |
| Impact direction angle | 0.01 | 0.00 | 1.92 | 0.066 | 0.00 | 0.02 |
| Absolute impact direction angle* | 0.03 | 0.01 | 4.94 | 0.000 | 0.02 | 0.04 |
| Torso impact angle | | | | | | |
| Posture* | 15.28 | 7.36 | 2.08 | 0.049 | 0.09 | 30.46 |
| Impact direction angle* | 1.19 | 0.11 | 10.61 | 0.0001 | 0.96 | 1.43 |
| Torso rotation angle | | | | | | |
| Posture* | 15.22 | 7.36 | 2.07 | 0.049 | 0.04 | 30.40 |
| Impact direction angle | 0.19 | 0.11 | 1.73 | 0.097 | -0.04 | 0.43 |

*p< 0.05

**Bony Fracture and Ligament Rupture**

The observed cortical bone fractures and knee ligament ruptures are listed in Table 4. The skeletal fractures and ligament ruptures were mainly found in the skull and knee ligaments. Skull fractures were observed in every case except three cases (cases S15, R30, and RN30). Only two upper neck (C2) fractures were observed, and one of them (case RFN30) experienced a shoulder impact causing the neck to sustain a substantial bending moment. In three cases, there was a single rib (upper thorax) fracture and in one case a sternum fracture was observed. Only one upper extremity fracture (right ulna during an elbow impact in S30) and two thoracic spine fractures occurred. Shoulder injuries were found and included four cases of scapular fracture and one clavicle fracture. All cases with shoulder injury experienced oblique torso impact with the hood (facing down, with torso impact angle -40°~ -76°), but in the case RFN90 and LFN60, the scapula fractures did not happen on the impacted side.

Pelvis fractures occurred in four cases, all on the right acetabulum occur. Those cases were pure-lateral or near-lateral impacts. There were no thigh and leg fracture observed in these cases, and in all cases except S90 a knee ligament rupture occurred. There was a correlation between the number of knee ligament ruptures and the impact direction (Figure 8). Most knee ligament ruptures occurred when the pedestrian was facing towards the vehicle (creating a hyperextension of the knees) and least ruptures occurred when the pedestrian was facing away from the vehicle (creating a flexion of the knees).

**Table 4. Bony fractures and ligament ruptures**

| Cases | Head/ Neck | Upper Extremity | Chest/spine /shoulder | Pelvis | Thigh /Leg | Knee ligaments rupture (R/L/Number) |
|---|---|---|---|---|---|---|
| S0 | Skull/- | - | - | R Hipbone Acetabulum | - | (ACL, MCL)/ (ACL, PCL, LCL)/5 |
| S15 | - | - | Sternum, L 1st rib /-/- | - | - | (ACL, MCL)/(ACL, LCL)/4 |
| SN15 | Skull/- | - | - | - | - | (All)/(ACL, LCL, PCL)/7 |
| S30 | Skull/- | R ULNA | - | - | - | (MCL)/(LCL, ACL)/3 |
| SN30 | Skull/- | - | - | - | - | (MCL,ACL,PCL)/(ACL,LCL,PCL),6 |
| S60 | Skull/- | - | - | - | - | /(ACL, LCL)/2 |
| SN60 | Skull/- | - | - | - | - | ( All)/(ACL, LCL, PCL)/7 |
| S90 | Skull/- | - | - | - | - | -/-/0 |
| SN90 | Skull/- | - | - | - | - | All/All/8 |
| RF0 | Skull/- | - | - | R Hipbone Acetabulum | - | (ACL, MCL)/ (ACL, LCL)/4 |
| RF15 | Skull/- | - | - | - | - | (MCL)/(ACL, LCL)/3 |
| RFN15 | Skull/- | - | - | - | - | (MCL,ACL,PCL)/(ACL,LCL)/5 |
| RF30 | - | - | R 2nd rib/-/- | - | - | (MCL)/(LCL, ACL)/3 |
| RFN30 | -/C2 | - | - | - | - | (MCL, ACL, PCL)/ (ACL, PCL, LCL)/6 |
| RF60 | Skull/- | - | - | - | - | -/(ACL, LCL)/2 |
| RFN60 | Skull/- | - | - | - | - | (MCL, ACL, PCL)/(All)/7 |
| RF90 | Skull/- | - | - | - | - | (LCL)/-/1 |
| RFN90 | Skull/- | - | -/-/L scapula | - | - | All/All/8 |
| LF0 | Skull/- | - | -/-/R scapula | R Hipbone Acetabulum | - | (ACL, MCL)/ (ACL, LCL, PCL)/5 |
| LF15 | Skull/- | - | R 3rd rib/T3/- | - | - | (MCL)/(ACL, LCL, PCL)/4 |
| LFN15 | Skull/- | - | -/-/R clavicle, R scapula | R Hipbone Acetabulum | - | (ACL, MCL)/ (ACL, LCL, PCL)/5 |
| LF30 | Skull/- | - | -/T3/- | - | - | (ACL,MCL)/(ACL,LCL,PCL)/5 |
| LFN30 | Skull/- | - | - | - | - | (ACL,MCL,PCL)/(ACL,LCL,PCL)/6 |
| LF60 | Skull/- | - | - | - | - | (ACL, LCL)/(ACL, LCL)/4 |
| LFN60 | Skull/- | - | -/-/R scapula | - | - | (ACL,MCL,PCL)/(ACL,LCL,PCL)/6 |
| LF90 | Skull/C2 | - | - | - | - | -/(LCL)/1 |
| LFN90 | Skull/- | - | - | - | - | (ACL, LCL, PCL)/(All)/7 |

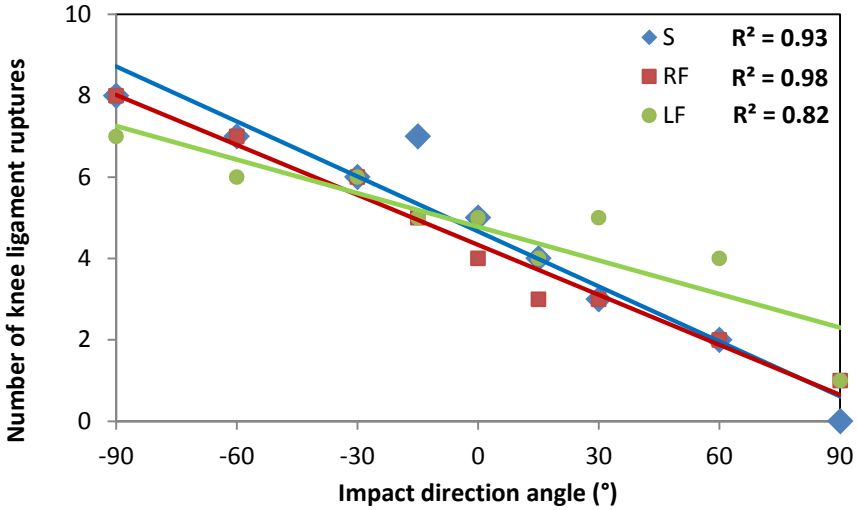


*Figure 8. Correlation of the number of knee ligament ruptures with impact direction angle and posture.*

## DISCUSSION

### Pedestrian Kinematics

**Torso rotation** Pedestrian torso rotation was caused by the impact of the vehicle initially striking the pedestrian leg at a location away from the body CG, which depended on the initial impact direction and human posture. Generally, a positive initial impact orientation caused positive torso rotation and vice versa. For the standing posture cases, the torso rotation entirely depended on the initial impact direction. However, for the right leg forward (RF) and left leg forward (LF) cases, the torso rotations were jointly determined by the initial impact direction and human posture. In RF cases, the initial contact point was anterior to the body CG even in pure-lateral impact, and as a result, case RF0 obtained 29.5° torso rotation; while in LF cases, the initial contact point was posterior to the body CG in pure-lateral impact, and case LF0 obtained -40° torso rotation. Consequently, only one negative torso rotation was observed in all 9 RF cases, and only two positive torso rotations were observed in all LF cases (Figure 7).

**Shoulder impact and elbow impact** In most of the pedestrian experimental tests [6-9], the PMHS hands were attached to each other prior to the pure-lateral impact. As a result, substantial elbow impact and shoulder impact were seen in the tests conducted [6-8]. In this study, the occurance of shoulder impact depended on the initial impact direction. All the cadaver tests were pure-lateral impact and all experienced shoulder impact. In the simulations, fewer shoulder impacts were observed and they were mainly from cases with a purely-lateral or near-lateral orientation. The occurance of elbow impact depended on both the initial impact direction and arm posture. Eleven of 14 cases with elbow impacts occurred with an initial impact direction from 0° ~ 30°. The cases with right leg forward (RF) posture (Figure 1-2) had less occurrence of elbow impact. All those cases without shoulder or elbow impact were with initial impact angles of ±60° and ±90°.

The experiments revealed that elbow and shoulder impacts had considerable influence on head kinematics [6-9]. Elbow impact influences torso rotation and changes the proceeding head kinematics. In the simulations, those configurations with elbow or shoulder impact had much lower head impact velocity (12.3±1.2 m/s, while 14.1±1.0 m/s for cases without elbow or shoulder impact) and later head impact time (average 129.2±5.5 ms, while average 124.8±8.1 ms for cases without elbow or shoulder impact).

**Head impact condition** In 11 cases, the head impact sites are at the occipital portion of the head, and in the other 11 cases the head impacts are frontal portion of the head. Only 5 of 27 cases resulted in a lateral impact to the head. Different phenomenon can explain this finding. Firstly, facing toward or away from the vehicle resulted in the head impact direction in the frontal and occipital regions respectively. Secondly, the torso rotation, due to the initial impact direction and human posture, resulted in the oblique torso impact with the hood. The torso would continue to rotate around the shoulder during the impact which resulted in the head impact striking the vehicle either in the frontal portion of the head or the occipital portion, not an oblique

impact (posterior-lateral or anterio-lateral). In a typical example (case RF15), the pre-impact, shoulder-impact, and head impact shown in Figure 9, and illustrates the torso rotation and the following head impact. Consequently, the lateral head impacts only happen when the torso impact was lateral (S0, RFN15, RFN30, LF15 and LF30), which account for a very low proportion of the simulated cases (5/27). Interestingly, the head impact velocity of cases resulting in occipital head impacts was 13.4±1.5 m/s, while cases with frontal head impact was slightly lower at 12.3±1.1 m/s.

*0 ms (torso yaw 15°)* *110 ms (torso yaw 47.6°)* *135 ms (torso yaw 63.1°)*

***Figure 9. Torso rotation and head impact direction (case RF15).***

The head impact velocity was sensitive to the initial impact direction, and increased as the initial impact angle increased (in magnitude). The head impact velocity was 11.8±0.3 m/s in pure-lateral impact, 11.9±1.2 m/s in near-lateral impact, 13.0±1.2 m/s in non-lateral impact, and 14.4±1.0 m/s in facing toward and facing away impacts. The head impact velocity was not sensitive to human posture, and was 12.7±1.67 m/s in standing postures, 13.4±1.0 m/s in RF postures, and 12.7±1.5 m/s in LF postures.

**Directional dependence** In standing and LF posture cases, the near-lateral cases had different torso rotation than pure-lateral cases. The head velocity was found to correlate with the impact direction angle ($p=0.029$). Since the head impact velocity was found to greatly influence the head injury risk [22], the head injury risk might be substantially influenced by the impact direction angle.

**Posture dependence** The directions of torso rotation were fundamentally different for various postures; torso rotation was found correlated to the posture ($p=0.049$). Therefore evaluating a pedestrian model in only one posture as in previous studies [18, 20] may not sufficiently encompass all likely head injury responses.

**Bony Fracture and Ligament Rupture**

Frequent skull fractures in these simulation could be attributed to the high stiffness of the impact locations (cowl and windshield frame) and the severity of the vehicle impact. In one of the three cases without skull fracture (S15), the head contacted the windshield, which is the softest area in all the head impact locations in this study. In the studies by Watanabe et al. [19, 20], skull fracture was not observed in centerline impact (at 40 km/h), but observed in corner impacts in which the head impact location was the A pillar. In the simulation study by Han et al., more than 70% AIS 4+ head injury risk (based on HIC value) was observed for a 50$^{th}$ percentile male impacted by a medium-sized sedan (centerline) at 40 km/h.

Very few rib fractures were observed in this study, but this is consistent with the pedestrian impact literature. In a simulation study by Han et al., the risk of chest injury was low [17, 18]. Likewise, no rib fractures were observed in the studies by Watanabe et al. [19, 20]. In the PMHS experiments, Subit et al. reported that subjects impacted by the small city car sustained more rib fractures than the subjects impacted by the mid-sized sedan [9].

In this study, the height of pedestrian knee was approximately at the center of the vehicle bumper causing a substantial bending effect at the knee joint and exposing the knee to severe impact. Knee ligament injury was very sensitive to impact direction. The most severe knee injuries were in the facing toward impacts where the knee was hyperextended, while the facing away impact rarely resulted in knee ligament ruptures because the knee flexed. In most of pure-lateral and near-lateral impacts, the valgus knee sustained MCL an ACL rupture,

and the varus knee sustained ACL and LCL rupture. As a result, ACL was the most frequently injured knee ligament in the pedestrian impacts because it happens on both knees, while MCL ruptures were mainly on valgus knee and LCL were mainly on varus knee.

**Limitations**

In this study, the influence of pre-crash posture was investigated using a standing posture and two walking postures representing the most distinct upper and lower extremity postures during the entire gait cycle [14]. An extension of this study, where intermediate gaits are added to the study will help to confirm the results presented in this paper.

The vehicle model was designed to reproduce the pedestrian impact buck used in Subit et al. [9] and did not contain an engine which might affect the pedestrian kinetics while in contact with the hood. However in another pedestrian impact study, Han et al. reported that the clearance between the hood and the engine in a mid-sized sedan was large enough to prevent the hood from impacting against the engine during a pedestrian impact [17, 18].

Finally, injury modeling using element deletion was not used to ensure numerical stability of the model. Thus, the results of this study would rely on the assumption that the influence of bone fracture on the ensuing pedestrian kinematics and kinetics would be negligible.

## CONCLUSIONS

In the present study, a $50^{th}$ pedestrian human body model was subjected to impact with the centerline of a mid-sized sedan at 40 km/h. Three postured models were created from the original HBM: one matching the standard posture and two matching extreme walking gait postures. Nine impact directions were also investigated. A substantial variety of responses was observed when the impact direction and human posture were varied, including the pedestrian torso rotation, head impact condition, and knee ligament rupture. The patterns observed in the responses of the postured HBM indicate that the shoulder and elbow impact occurred frequently and substantially influenced the head kinematics. The head impact velocity was found to correlate with the impact direction angle, where facing towards or away from the vehicle would result in greater head impact velocity than when struck in a purely-lateral impact.

## ACKNOWLEDGEMENTS

The authors would like to acknowledge support from Toyota Collaborative Safety Research Center (Toyota CSRC). The authors would like to acknowledge Aaron Steinhilb and Robert Panek (Toyota Motor Engineering & Manufacturing, North America) for their contribution to the design of the study. Note: the views expressed in this paper are those of the authors and do not necessarily represent or reflect the views of the sponsors.

## REFERENCES

[1] Naci, H., Chisholm, D., and Baker, T. D. 2009. “Distribution of road traffic deaths by road user group: a global comparison”. Injury Prevention, 15(1), 55-59.
[2] Hardy, R. 2009. "APROSYS - Final Report for the Work on "Pedestrian and Pedal Cyclist Accidents" (SP3), AP-90-0003", Cranfield Impact Centre.
[3] Yang, J. 2005. “Review of injury biomechanics in car-pedestrian collisions”. International Journal of Vehicle Safety, 1(1), 100-117.
[4] Chen, H.P., Fu, L.X., and Zheng, H.Y. 2009. “A comparative study between China and IHRA for the vehicle-pedestrian impact”, SAE International Journal of Passenger Cars-Mechanical Systems 2, 1108–1115.
[5] Kerrigan, J. R., Drinkwater, D. C., Kam, C. Y., Murphy, D. B., Ivarsson, B. J., Crandall, J. R., and Patrie, J. 2004. “Tolerance of the human leg and thigh in dynamic latero-medial bending”. International Journal of Crashworthiness, 9(6), 607-623.
[6] Schroeder, G., Konosu, A., Ishikawa, H., and Kajzer, J. 2000. “Injury Mechanism of Pedestrians During a Front-End Collision with a Late Model Car”. JSAE Spring 2000.

[7] Kerrigan, J. R., Crandall, J. R. and B. Deng. 2007. "Pedestrian kinematic response to mid-sized vehicle impact." International Journal of Vehicle Safety 2(3): 221-240.
[8] Kerrigan, J., Murphy, D. B., Drinkwater, D. C., Kam, C. Y., Bose D., and Crandall, J. R. 2005. "Kinematic Corridors for PMHS Tested in Full-Scale Pedestrian Impact Tests". Enhanced Vehicle Safety (ESV), Washington D.C., US.
[9] Subit, D., Kerrigan, J., Crandall, J. R., Fukuyama, K., Yamazaki, K., Kamiji, K., and Yasuki, T. 2008. "Pedestrian-vehicle interaction: kinematics and injury analysis of four full scale tests". In Proceedings of the International Research Council on the Biomechanics of Injury conference (Vol. 36, pp. 275-294). International Research Council on Biomechanics of Injury.
[10] Simms, C., and Wood, D. 2009. "Pedestrian and cyclist impact: a biomechanical perspective" (Vol. 166). Springer Science & Business Media.
[11] Maki, T., Kajzer, J., Mizuno, K., and Sekine, Y. 2003. "Comparative analysis of vehicle-bicyclist and vehicle-pedestrian accidents in Japan". Accident Analysis and Prevention 35(6): 927-940.
[12] Soni, A., Robert, T., Rongieras, F., and Beillas, P. 2013. "Observations on pedestrian pre-crash reactions during simulated accidents". Stapp car crash journal, 57, 157-183.
[13] Peng, Y., Deck, C., Yang, J., and Willinger, R. 2012. "Effects of pedestrian gait, vehicle-front geometry and impact velocity on kinematics of adult and child pedestrian head." Int. J. Crashworthiness 1 (2012), pp. 1-9
[14] Untaroiu, C. D., Meissner, M. U., Crandall, J. R., Takahashi, Y., Okamoto, M., and Ito, O. 2009. "Crash reconstruction of pedestrian accidents using optimization techniques". International Journal of Impact Engineering, 36(2), 210-219.
[15] Tamura, A., Nakahira, Y., Iwamoto, M., Watanabe, I., Miki, K., Hayashi, S., and Yasuki, T. 2006. "The Influence of the Traction Force Due to Inertia of the Brain Mass on Traumatic Brain Injury during SUV-to-Pedestrian Impact." International Research Council on the Biomechanics of Impacts. IRCOBI.
[16] Yasuki, T., and Yamamae, Y. 2010. "Validation of Kinematics and Lower Extremity Injuries Estimated by Total Human Model for Safety in SUV to Pedestrian Impact Test". Journal of Biomechanical Science and Engineering 5(4): 340-356.
[17] Han, Y., Yang, J., Nishimoto, K., Mizuno, K., Matsui, Y., Nakane, D., and Hitosugi, M. 2012. "Finite element analysis of kinematic behaviour and injuries to pedestrians in vehicle collisions." International Journal of Crashworthiness, 17(2), 141-152.
[18] Han, Y., Yang, J., Mizuno, K., and Matsui, Y. 2012. "Effects of vehicle impact velocity, vehicle front-end shapes on pedestrian injury risk." Traffic injury prevention, 13(5), 507-518.
[19] Watanabe, R., Miyazaki, H., Kitagawa, Y., and Yasuki, T. 2011. "Research of Collision Speed Dependency of Pedestrian Head and Chest Injuries using Human FE Model (THUMS Version 4)." 22nd ESV, 11-0043.
[20] Watanabe R., Katsuhara, T., Miyazaki, H., Kitagawa, Y., and Yasuki, T. 2012 "Research of the Relationship of Pedestrian Injury to Collision Speed, Car-type, Impact Location and Pedestrian Sizes using Human FE model (THUMS Version 4)". Stapp Car Crash journal, Vol 56, pp. 269- 321.
[21] Paas, R., Davidsson, J., and Brolin, K. 2015. "Head Kinematics and Shoulder Biomechanics in Shoulder Impacts similar to Pedestrian Crashes–a THUMS study." Traffic injury prevention, 16(5):498-506. doi: 10.1080/15389588.2014.968778.
[22] Peng, Y., Deck, C., Yang, J., Otte, D., Willinger, R. 2013. "A study of adult pedestrian head impact conditions and injury risks in passenger car collisions based on real-world accident data". Traffic injury prevention, 14(6), 639-646.

# ANALYSIS AND SIMULATION OF OCCUPANT INJURY RISK AT NASS/CDS

**Jaeho Shin**
Kyungil University
Korea

**Hyung Yun Choi**
Hongik University
Korea

**Chang Jin Oh, Jin Ho Bae**
Hyundai and Kia Motor Company
Korea

Paper Number 15-0394

## ABSTRACT

The body regional injury information from the head, thorax, abdomen, upper and lower extremities of vehicle occupant due to the restraints and interior parts were extracted from 2009-2012 NASS/CDS data base. For those cases with high occurrence frequency, detailed and comprehensive data analysis was performed to find significances between the accident, occupant, vehicle, and injury data. A numerical frontal impact sled model with Hybrid III dummy and GHBMC human body model is constructed to simulate and identify those injury risks at NASS/CDS.
Among the 5,734 body regional injuries from frontal crash accidents, lower extremity (27.8%), upper extremity (21.3%), thorax (15.1%), face (10.9%), spine (8,7%), head (7.3%), and abdomen (6.9%) were found in order of frequent occurrence. The main injury sources of the head were windshield, side structure, and steering wheel. For thorax and abdomen, they were seat belt and steering wheel. Instrument panel was for the lower extremity. Body regional injury patterns for head were concussion and contusion. For thorax, they were vessel laceration and lung contusion. For abdomen, laceration and contusion of organs were major injury patterns. Bone fracture and ligament rupture were found at the lower extremity. Steering wheel and seat positions were main factors affect head and thorax injury risks. From the sled impact simulation, high injury risks of the head and thorax were assessed respectively at conditions of steering column tilt down and rear most seat positions, which correlated well with the findings at NASS/CDS data analysis.

## INTRODUCTION

Occupant injury rate at crash accidents has not been decreased in proportion to the advancing vehicle safety technology and design. Crash injury occurs occasionally by restraint system, i.e., seat belt and airbag. When seat belt excessively restraints the occupant, it may bring rib fractures and abdominal organ ruptures. In the opposite case, the insufficient restraining would allow second impact and consequent injuries, i.e., from the impact of occupant against interior parts. Airbag can be a life threatening device when it becomes an injury source at a relatively lower speed crash. This study focuses on identifying injury sources of anatomical body regions of vehicle occupant and associated vehicle parameters. The representative scenarios of occupant's crash injury are also developed for the reconstruction of the injury risk with a numerical simulation that can further elucidates the outcomes of the study.
Pintar et al. [1] reported that the head injury risk became the least when both airbag and seat belt were used together. The multiple injuries at brain and skull are the most frequent head injury for those unbelted occupant with deployed airbag. Wallies and Greaves [2] presented that the airbag induced injury tended to increase with more airbag in use (i.e., deployed). The risk of skull fracture reduced by 42% due to the airbag [3], whereas the brain injury risk rather increased [4]. The increasing facial fracture risk by airbag at front seat passengers was reported by Murphy et al. [5]

The study of eye injury by airbag was done by Duma et al. [6] The growth of minor head injury (AIS 1) risk by the depowered airbag was analyzed by Huber et al. [7] Cerebrovascular injuries due to the airbag deployment were reported by Davis et al. [8]

Untatoiu et al. [9] has investigated the biomechanical response and injury outcome to the abdominal regions in static deployment tests using two pre-tensioner systems. The high belt (pre-tensioning) forces may increase the risk of abdominal injuries to the vehicle occupant since abdominal injuries (spleen lacerations) were observed in two PMHS with higher BMI. Using the whole lower limb FE model, sensitivity study was performed by Yue et al. [10] to evaluate the effect of the hip joint angle (occupant posture variation) to acetabulum injury tolerance in frontal impact. They reported the tolerance of the hip acetabulum (cortical bone) showed greater sensitivity to the hip extension angle than to the abduction angle.

Bostrom and Kruse [11] proposed a cost effective method of sled test to assess a head injury risk at small overlap crash. They found the dominating head injury mechanisms were head impact at interior part, i.e., A-pillar or at the external objects. It was also reported that the THOR dummy was an appropriate surrogate for the small overlap test while the Hybrid III was not.

The body regional AIS3+ (or 2+) injury information along head, thorax, abdomen, upper and lower extremities due to the restraints (airbag and seat belt) and interior parts (instrument panel, steering wheel, windshield, and etc.) were extracted from 2009-2012 NASS (National Automotive Sampling System)/CDS (Crashworthiness Data System) data base. The data were limited to the frontal crash (10-2 O'clock direction), driver and front seat passenger, and adult. And thus this filtering reduced the total number of injuries in the analysis from 17,915 to 5,734. For those cases with high occurrence frequency, detailed and comprehensive analysis was performed for accident (vehicle and accident types, vehicle speed), occupant (gender, height, weight, and position), vehicle (vehicle size and restraints), and injury (body region, type, and AIS) data.

Numerical frontal impact sled models with Hybrid III dummy and GHBMC(Global Human Body Models Consortium [12]) human body model were constructed to simulate and identify those injury risks at NASS/CDS data. The numerical injury simulations were proceeded in two steps. In the first step, the frontal crash sled simulation was performed with Hybrid III dummy to predict overall kinematics of the driver. In the following step, the same frontal crash sled model used at the first step applied but the driver model was substituted with anatomically detailed human body model, i.e., GHBMC model for more biomechanical injury prediction. The relatively simple composition of Hybrid III finite element dummy model (about 5k elements) in the first step facilitated more comprehensive parametric analysis while the second step with GHBMC human body model (about 2 million elements) was focused for few selected cases due to the heavy computational load.

Among the 5,734 body regional injuries from frontal crash accidents, lower extremity (27.8%), upper extremity (21.3%), thorax (15.1%), face (10.9%), spine (8,7%), head (7.3%), and abdomen (6.9%) were found in order of frequent occurrence. The main injury sources of the head were windshield, side structure, and steering wheel. For thorax and abdomen, they were seat belt and steering wheel. Instrument panel was for the lower extremity. Body regional injury (AIS 2+) patterns of head were concussion and contusion. For thorax, they were vessel laceration and lung contusion. For abdomen, laceration and contusion of organs were major injury patterns. Bone fracture and ligament rupture were found at the lower extremity. From the sled impact simulation, high injury risks of the head and thorax were assessed at conditions of steering wheel down and rear most seat position, respectively.

## METHOD

### Analysis of Parameters Effecting on Injury Risk

Using NASS/CDS database of 2009-2012, the frequency analysis of injury risk was performed along the anatomical body regions, i.e., head, face, neck, thorax, abdomen, spine, upper extremity, lower extremity, and unspecified. The injury types, organs in each body region were subsequently analyzed. The injury source such as instrument panel, steering wheel, windshield, airbag, seat belt, and etc. was also identified for those injuries with high levels (AIS 2 or 3+). Lastly, the detailed investigation to find a correlation of injury risk with other

parameters, i.e., accident type, vehicle closing speed, Delta V, occupant gender, age, and anthropometry, restraining condition, vehicle size, seat position, and steering column tilt angle were further carried out. Figure 1 shows the procedure of injury risk analysis in this study.

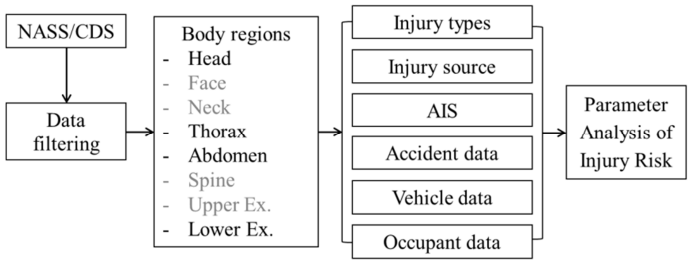


***Figure 1. Procedure of injury risk analysis at NASS/CDS.***

**Numerical Simulation Model to Reconstruct Injury Risk**

In order to verify the analyzed result of injury risk at NASS/CDS, numerical simulation using frontal impact sled model consists of driver side vehicle compartment including an aribag and seat belt were performed. Modeling parameters for airbag and seat belt such as mass flow rate, pretensioner and load limiter were calibrated against a medium sedan. Dummy kinematics such as head and chest accelerations and the belt force were validated against US NCAP test result of the target vehicle. Sled pulses at 56, 68, and 79 kph closing speed at a frontal crash were emulated to represent 25G, 30G, and 35G of vehicle peak decelerations, respectively. However, this sled model was only validated for upper body kinematics of driver due to the limited for the evaluation of head and thorax injury risks but none at lower extremity.

There were four main parameters in the sled simulation: 1. three restraining conditions, i.e., with/without airbag deployment and belted/unbelted (no case of unbelted without airbag deployment), 2. two seat positions, i.e., center and rear most, 3. three steering column tilt angles, i.e., -3/0/3 degrees, and 4. three impact speeds, i.e., 56, 68, and 79 kph. The modeling of the occupant restraining by airbag and seat belt, e.g., firing time, vent hole size, pretensioner, limit load, and etc. were identically applied to all simulation cases.

There were two kinds of occupant models (Figure 2) adopted in the sled simulation to respectively predict overall kinematics and biomechanical injury of driver at frontal crash. As a first analysis in two-step procedure of sled simulations, Hybrid III medium size male dummy model was used for predicting overall occupant kinematics and interactions with vehicle interior and restraints. The preliminary injury risk was assessed by quantifying the contact forces on various vehicle interior such as windshield, steering wheel against head and chest and HIC and amount of chest deflection at the Hybrid III dummy model. The effects of simulation parameters on injury risk were correlated with the result from data analysis of NASS/CDS. The GHBMC human body model with medium male size was also adopted to predict more biomechanical injury such as number of rib fractures for the thorax injury risk. No assessment of skull fracture, brain injury, abdomen organ rupture were included in the current study and it remains as on-going and future study.

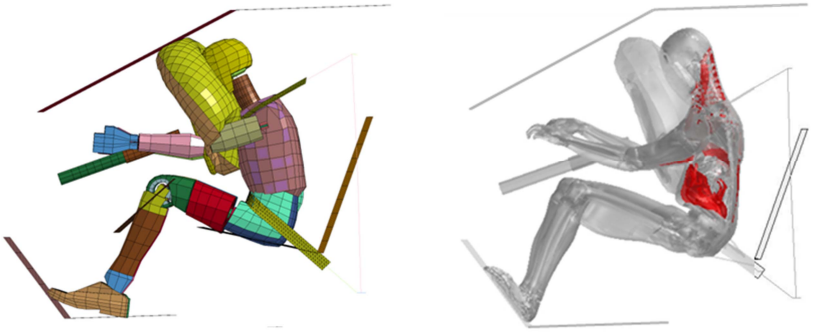

***Figure 2. Frontal impact sled model with Hybrid III model (left) and GHBMC human body model (right).***

## RESULTS

### Frequency Analysis of Body Regional Injury Risk

The body regional injury risk at frontal crash from 2009-12 NASS/CDS data is listed in Table 1. Among 5,734 injuries which is limited to adult driver and front seat passenger, lower extremity was the most frequent body region (27.8%) followed by upper extremity (21.3%), thorax (15.1%), face (10.9%), spine (8.7%), head (7.3%), abdomen (6.9%), and neck (1.3%).

**Table 1. Body regional injury risk from 2009-2012 NASS/CDS.**

| Body regions | Injury frequency | Ratio (%) |
|---|---|---|
| Head | 419 | 7.3 |
| Face | 627 | 10.9 |
| Neck | 74 | 1.3 |
| Thorax | 865 | 15.1 |
| Abdomen | 396 | 6.9 |
| Spine | 501 | 8.7 |
| Upper Extremity | 1,222 | 21.3 |
| Lower Extremity | 1,595 | 27.8 |
| Unspecified | 35 | 0.6 |
| Total | 5,734 | 100.0 |

Other than four main body regions (head, thorax, abdomen, and lower extremity), face, neck, spine, and upper extremity were not included at the further detailed analysis due to the relatively lower injury severity (AIS 2-) even with high occurrence rates.

The major injury sources and associated injury patterns of head are investigated (Table 2). Top three head injury sources, i.e., windshield, side structure, and steering wheel showed a similar occurrence rate. The most significant factor with the windshield became airbag and unbelted condition, especially for AIS 3+ head injury (90%, 9 out of 10 cases). The full down position of steering column was also an effective variable (80%, 4 out of 5 cases). In case of side structure to head injury risk, airbag and belted (66%, 19 out of 29 cases of AIS 3+ head injury) and rear most seat position (57%, 13 out of 23 cases) were dominant variables. Unbelted (58%, 18 out of 31 cases of AIS 3+ head injury) and full up steering column position (69%, 11 out of 16 cases) were prominent factors with steering wheel. For instrument panel, the controlling variables are airbag and belted (52%, 13 out of 25 cases of AIS 3+ head injury) and rear most seat position (65%, 15 out of 23 cases). The airbag as head injury source was affected by age and gender but quantitative analysis was not feasible. Figure 3 shows an example NASS/CDS case (2009-73-074) of head injury due to the steering wheel.

**Table 2. Head injury source and pattern.**

| Injury source | Injury freque | Ratio (%) | Major lesion | Restraint | Injury variable |
|---|---|---|---|---|---|
| Windshield | 74 | 17.7 | Contusion* | Airbag & Unbelted | Steering column position (full down) |
| Side structure | 67 | 16.0 | Contusion* | Airbag & Belted | Occupant position (rear most) |
| Steering wheel | 66 | 15.8 | Contusion* | Unbelted | Steering column position (full up) |
| Instrument panel | 40 | 9.5 | Concussion** | Airbag | Occupant position (rear most) |
| Airbag | 26 | 6.2 | Concussion** | Airbag & Belted | Occupant age and sex (old and female) |
| Etc. | 146 | 34.8 | - | - | - |
| Total | 419 | 100 | - | - | - |

* Contusion: 27.2% of head injuries

** Concussion: 25.1% of head injuries

***Figure 3. NASS/CDS case (2009-79-074) of head injury due to the steering wheel: unbelted driver, Delta V 46 kph, Head AIS 5, ISS 30.***

The results of thorax injury with major sources and associated patterns are summarized in Table 3. The belt web was the most frequent injury source (62%) to the thorax of which airbag was deployed for all AIS 3+ injuries (100%, 28 out of 28 cases). And the rear most seat position was another dominant variable (82%, 14 out of 17 cases). In case of steering wheel, airbag and unbelted was the most common restraining condition for AIS 4+ injury level (71%, 24 out 30 cases) and the upright seat back angle was also marked a variable (52%, 12 out of 23 cases). For instrument panel, the controlling variables are airbag and belted (92%, 11 out of 12 cases of AIS 4+ thorax injury) and rear most seat position (82%, 9 out of 11 cases). The quantitative analysis for inner trim, seat back, and airbag as injury source was not feasible. Figure 4 shows an example NASS/CDS case (2010-79-070) of thorax injury due to the belt web.

**Table 3. Injury pattern and source of thorax.**

| Injury source | Injury frequency | Ratio (%) | Major lesion | Restraint | Injury variable |
|---|---|---|---|---|---|
| Belt web | 538 | 62.2 | Laceration*, Fracture** | Airbag & Belted | Occupant position (rear most) |
| Steering wheel | 176 | 20.3 | Laceration* | Airbag & Unbelted | Occupant posture (seat back angle) |
| Instrument panel | 55 | 6.4 | Laceration*, Contusion# | Airbag & Unbelted | Occupant position (rear most) |
| Inner trim | 47 | 5.4 | Laceration*, Contusion# | Airbag & Belted | Impact direction |
| Seat back | 20 | 2.3 | Laceration* | Airbag & Unbelted | Other passengers |
| Airbag | 19 | 2.2 | Fracture** | Airbag & Belted | Occupant position (fore most) |
| Etc. | 10 | 1.1 | - | - | - |
| Total | 865 | 100 | - | - | - |

* Laceration: 5.8% of thorax injuries

** Fracture: 14.7% of thorax injuries

# Contusion: 62.0% of thorax injuries

***Figure 4. NASS/CDS case (2010-79-070) of thorax injury due to the belt web: belted passenger (rear most seat position) with airbag, Delta V 51 kph, Thorax AIS 6, ISS 75.***

The major injury sources and associated injury patterns of abdomen are investigated (Table 4). Similar to thorax injury, the belt web was most frequent injury source (64%) followed by steering wheel (22%). For belt web, airbag was deployed for all AIS 3+ injuries (100%, 12 out of 12 cases) and the rear most seat position was also a dominant variable (64%, 7 out of 11 cases). In case of steering wheel, airbag and belted was the most common restraining condition for AIS 3+ injury level (52%, 12 out 23 cases) and the foremost seat position was a distinct variable (46%, 10 out of 22 cases). Other injury sources such as instrument panel, inner trim, airbag, and armrest showed relatively low occurrence frequencies. Figure 5 shows an example NASS/CDS case (2012-49-063) of abdomen injury due to the steering wheel.

**Table 4. Injury pattern and source of abdomen.**

| Injury source | Injury frequency | Ratio (%) | Major lesion | Restraint | Injury variable |
|---|---|---|---|---|---|
| Belt web | 252 | 63.6 | Laceration* | Airbag & Belted | Occupant position (rear most) |
| Steering wheel | 87 | 22.0 | Laceration*, Contusion** | Airbag & Belted | Occupant position (fore most) |
| Instrument panel | 15 | 3.8 | - | - | - |
| Inner trim | 10 | 2.5 | - | - | - |
| Airbag | 9 | 2.3 | - | - | - |
| Armrest | 9 | 2.3 | - | - | - |
| Etc. | 14 | 3.5 | - | - | - |
| Total | 396 | 100 | - | - | - |

* Laceration: 22.7% of abdomen injuries

** Contusion: 58.1% of abdomen injuries

***Figure 5. NASS/CDS case (2012-49-063) of abdomen injury due to the steering wheel: belted driver (fore most) with airbag, Delta V 64 kph, Abdomen AIS 5, ISS 57.***

The results of lower extremity are listed in Table 5. Instrument panel was most frequent injury source (50%) followed by floor (15%). In case of instrument panel, airbag and belted was the most common restraining condition for AIS 3 injury level (61%, 41 out 67 cases) and the reclined seat back was the main variable (75%, 50 out 67 cases). Lower extremity injury due to floor had airbag and belted condition (AIS 3 84%, 16 out of 19 cases) and fore most seat position (39%, 5 out 13 cases). The overweight of obese occupant was also a common variable at both instrument panel and floor. In case of foot controls, airbag and belted condition (AIS 3, 88%, 7 out of 8 cases) and rear most seat position (63%, 5 out 8 cases) are the most common restraint condition and the main variables. For belt web, airbag and belted condition (AIS 2, 100%, 4 out of 4 cases) and rear most seat position (67%, 2 out 3 cases) were obtained. Figure 6 shows an example NASS/CDS case (2012-09-012) of lower extremity injury due to instrument panel.

**Table 5. Injury pattern and source of lower extremity.**

| Injury source | Injury frequency | Ratio (%) | Major lesion | Restraint | Injury variable |
|---|---|---|---|---|---|
| Instrument panel | 789 | 49.5 | Laceration*, Fracture** | Airbag & Belted | Occupant posture (reclined) |
| Floor | 242 | 15.2 | Fracture** | Airbag & Belted | Occupant position (fore most) |
| Foot controls | 151 | 9.5 | Fracture** | Airbag & Belted | Occupant position (rear most) |
| Belt web | 148 | 9.3 | Fracture** | Airbag & Belted | Occupant position (rear most) |
| Glove box door | 95 | 6.0 | - | - | - |
| Steering wheel | 62 | 3.9 | - | - | - |
| Etc. | 108 | 6.8 | - | - | - |
| Total | 1595 | 100 | - | - | - |

* Laceration: 7.0% of lower extremity injuries

** Fracture: 26.3% of lower extremity injuries

***Figure 6. NASS/CDS case (2012-09-012) of lower extremity injury due to the instrument panel: unbelted driver with airbag, Delta V 54 kph, Lower extremity AIS 3, ISS 34.***

## Numerical Simulation Model for Reconstruction of Injury Risk

Figure 7 shows the result of frontal sled impact simulation with various parameters in which the instantaneous motion at 80 milliseconds was selected for the comparison of dummy motion among simulation parameters, i.e., three restraining conditions, two seat positions, and three steering column tilt angles. The dummy kinematics and interactions with vehicle interior parts were interpreted by contact forces between body regions and airbag, steering wheel, and windshield and were summarized in Table 6. Since shoulder belt forces at all 18 cases were saturated to its limit force (about 5.0 kN) and thus it was not included at in the analysis.

- Head contact to steering wheel: Some cases (cases 2, 5, and 6) with belt+airbag condition at 68 and 79 kph impacts. With unbelted condition (cases 7-12) at all three impact speeds except case 11 (center position of seat and -3 degree of steering wheel tilt angle). With no airbag condition (cases 13-18), rear most seat position (Cases 14, 16, and 18) showed significant higher (89% at 56 kph, 20% at 68 kph, and 43% at 79 kph) contact forces between head and steering wheel than with center seat position (cases 13, 15, and 17) at all three impact speeds mainly due to the large excursion of the head.
- Head contact to windshield: No contact was observed with belted condition (cases 1-6, and 13-18). In all unbelted condition (cases 7-12) except case 9 (center position of seat and +3 degree of steering column tilt angle), contact forces between head and windshield were calculated.
- Chest contact to steering wheel: No contact was observed with belt+airbag condition (cases 1-6) at all three impact speeds. In unbelted with airbag condition (cases 7-12) at two higher impact speeds (i.e., 68 and 79 kph) except case 11 (center position of seat and -3 degree of steering wheel tilt angle), contact forces between chest and steering wheel were calculated. Belted with no airbag condition (cases 13-18) showed a mild contact between chest and steering wheel. Rear most seat position (cases 8, 10, 12, 14, 16, and 18) showed higher (48% at 56 kph, 27% at 68 kph, and 44% at 79 kph) contact forces between chest and steering wheel than center seat position (cases 7, 9, 11, 13, 15, and 17) at all three impact speeds.

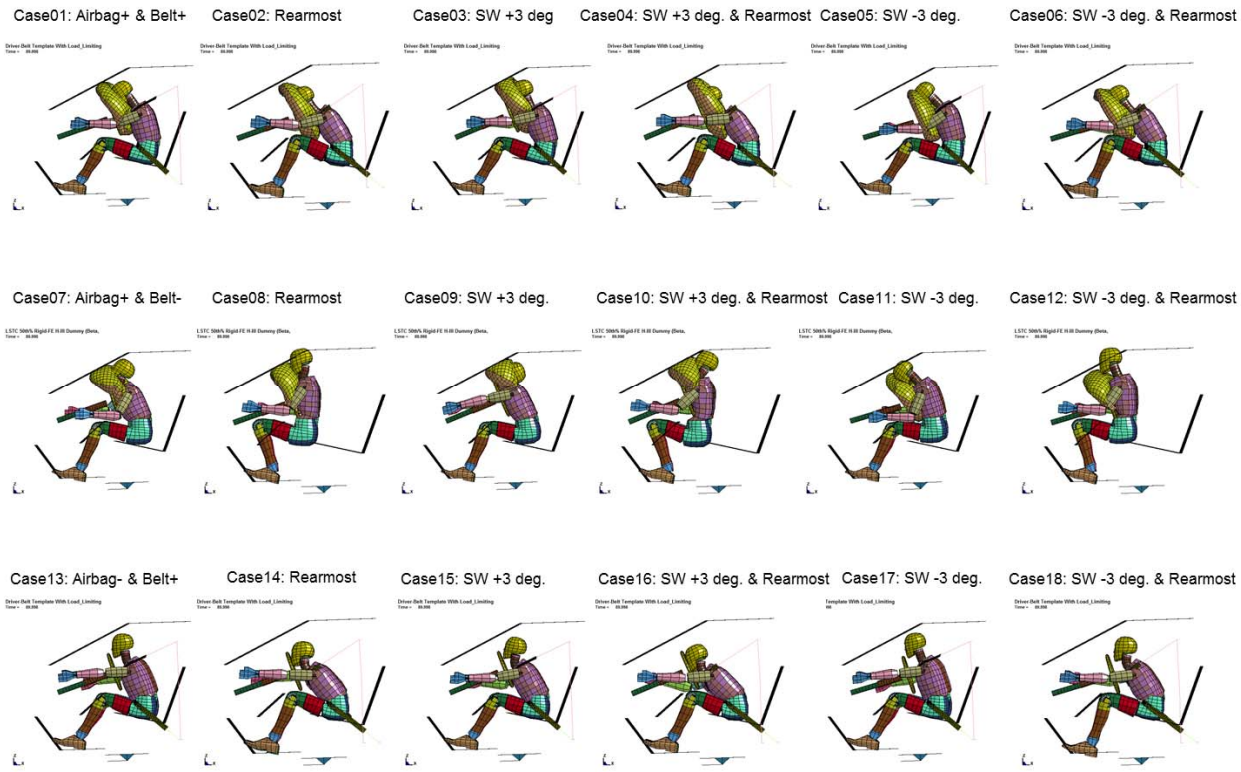


***Figure 7. Simulation result with Hybrid III dummy model: 18 cases at 80msec with 56 kph impact speed.***

**Table 6. Result of frontal sled impact simulation with Hybrid III dummy.**

| Case No. | Air bag | Seat belt | Steering column Tilt angle (degree) | Seat position | Max. head contact force (kN) | | | Max. chest contact force (kN) | | HIC | Max. chest deflection (mm) |
|---|---|---|---|---|---|---|---|---|---|---|---|
| | | | | | Airbag | Steering wheel | Wind shield | Airbag | Steering wheel | | |
| 56 kph impact | | | | | | | | | | | |
| 1 | + | + | 0 | Center | 1.24 | 0 | 0 | 1.53 | 0 | 367 | 32.85 |
| 2 | + | + | 0 | Rearmost | 1.91 | 0 | 0 | 1.15 | 0 | 619 | 47.68 |
| 3 | + | + | +3 | Center | 1.75 | 0 | 0 | 1.33 | 0 | 402 | 30.23 |
| 4 | + | + | +3 | Rearmost | 2.08 | 0 | 0 | 1.08 | 0 | 639 | 46.36 |
| 5 | + | + | -3 | Center | 1.10 | 0 | 0 | 1.48 | 0 | 367 | 35.55 |
| 6 | + | + | -3 | Rearmost | 1.62 | 0.2 | 0 | 1.17 | 0 | 634 | 50.17 |
| 7 | + | - | 0 | Center | 1.26 | 0 | 7.02 | 2.14 | 0 | 776 | 10.90 |
| 8 | + | - | 0 | Rearmost | 1.21 | 0 | 8.13 | 3.16 | 0 | 1,365 | 14.81 |
| 9 | + | - | +3 | Center | 8.3 | 0 | 0 | 6.06 | 1.69 | 2,044 | 13.41 |
| 10 | + | - | +3 | Rearmost | 6.88 | 0 | 7.19 | 3.33 | 1.9 | 2,227 | 12.33 |
| 11 | + | - | -3 | Center | 4.87 | 11.05 | 7.28 | 2.71 | 0 | 1,729 | 17.89 |
| 12 | + | - | -3 | Rearmost | 0.78 | 0 | 8.94 | 2.49 | 0 | 1,227 | 15.35 |
| 13 | - | + | 0 | Center | 0 | 6.85 | 0 | 0 | 0 | 2,678 | 16.81 |
| 14 | - | + | 0 | Rearmost | 0 | 13.7 | 0 | 0 | 0 | 7,319 | 44.62 |
| 15 | - | + | +3 | Center | 0 | 9.83 | 0 | 0 | 0 | 4,403 | 18.71 |
| 16 | - | + | +3 | Rearmost | 0 | 20.39 | 0 | 0 | 0 | 10,790 | 45.27 |
| 17 | - | + | -3 | Center | 0 | 8.25 | 0 | 0 | 0 | 2,982 | 18.70 |
| 18 | - | + | -3 | Rearmost | 0 | 12.94 | 0 | 0 | 0 | 14,570 | 41.09 |
| 68 kph impact | | | | | | | | | | | |
| 1 | + | + | 0 | Center | 1.51 | 0 | 0 | 1.58 | 0 | 648 | 36.35 |
| 2 | + | + | 0 | Rearmost | 4.14 | 1.70 | 0 | 1.29 | 0 | 1,625 | 56.74 |
| 3 | + | + | +3 | Center | 1.78 | 0 | 0 | 1.72 | 0 | 522 | 33.29 |
| 4 | + | + | +3 | Rearmost | 2.95 | 0 | 0 | 1.42 | 0 | 1,304 | 55.94 |
| 5 | + | + | -3 | Center | 2.34 | 5.92 | 0 | 2.41 | 0 | 985 | 38.34 |
| 6 | + | + | -3 | Rearmost | 7.97 | 6.79 | 0 | 1.27 | 0 | 2,856 | 54.49 |
| 7 | + | - | 0 | Center | 6.21 | 0 | 6.88 | 6.94 | 1.66 | 2,817 | 39.47 |
| 8 | + | - | 0 | Rearmost | 5.25 | 0 | 8.76 | 9.93 | 9.56 | 3,062 | 48.89 |
| 9 | + | - | +3 | Center | 11.71 | 0 | 0 | 13.50 | 5.52 | 3,804 | 51.59 |
| 10 | + | - | +3 | Rearmost | 7.00 | 0 | 7.59 | 7.81 | 6.14 | 3,761 | 77.47 |
| 11 | + | - | -3 | Center | 5.46 | 10.67 | 7.92 | 3.58 | 0 | 2,732 | 14.97 |
| 12 | + | - | -3 | Rearmost | 0.93 | 0 | 10.16 | 7.53 | 4.59 | 2,073 | 51.28 |
| 13 | - | + | 0 | Center | 0 | 13.45 | 0 | 0 | 0.59 | 10,160 | 20.81 |
| 14 | - | + | 0 | Rearmost | 0 | 19.43 | 0 | 0 | 0 | 20,260 | 46.91 |
| 15 | - | + | +3 | Center | 0 | 16.74 | 0 | 0 | 3.74 | 9,164 | 22.34 |
| 16 | - | + | +3 | Rearmost | 0 | 16.16 | 0 | 0 | 0 | 9,599 | 47.39 |
| 17 | - | + | -3 | Center | 0 | 11.99 | 0 | 0 | 0 | 9,865 | 22.33 |
| 18 | - | + | -3 | Rearmost | 0 | 14.78 | 0 | 0 | 0 | 24,740 | 42.60 |
| 79 kph impact | | | | | | | | | | | |
| 1 | + | + | 0 | Center | 1.8 | 0 | 0 | 1.75 | 0 | 1,367 | 40.32 |
| 2 | + | + | 0 | Rearmost | 10.95 | 9.37 | 0 | 1.38 | 0 | 5,615 | 60.37 |
| 3 | + | + | +3 | Center | 2.04 | 0 | 0 | 1.56 | 0 | 1,232 | 38.57 |
| 4 | + | + | +3 | Rearmost | 12.94 | 0 | 0 | 2.18 | 0 | 4,109 | 59.43 |
| 5 | + | + | -3 | Center | 2.09 | 8.07 | 0 | 1.94 | 0 | 1,573 | 44.05 |
| 6 | + | + | -3 | Rearmost | 6.66 | 19.75 | 0 | 1.07 | 0 | 10,100 | 62.98 |
| 7 | + | - | 0 | Center | 6.4 | 0 | 7.58 | 6.2 | 3.19 | 2,812 | 50.18 |
| 8 | + | - | 0 | Rearmost | 5.33 | 0 | 9.27 | 8.06 | 24.2 | 4,275 | 77.08 |
| 9 | + | - | +3 | Center | 8.13 | 0 | 2.46 | 12.48 | 10.01 | 3,489 | 75.03 |
| 10 | + | - | +3 | Rearmost | 8.81 | 0 | 8.12 | 9.23 | 11.5 | 5,898 | 91.52 |
| 11 | + | - | -3 | Center | 1.56 | 11.09 | 9.39 | 5.73 | 0 | 1,762 | 47.31 |
| 12 | + | - | -3 | Rearmost | 1.07 | 0 | 10.18 | 11.66 | 21.09 | 2,935 | 81.76 |
| 13 | - | + | 0 | Center | 0 | 15.11 | 0 | 0 | 4.72 | 20,070 | 30.20 |
| 14 | - | + | 0 | Rearmost | 0 | 25.76 | 0 | 0 | 0 | 43,930 | 52.72 |
| 15 | - | + | +3 | Center | 0 | 16.3 | 0 | 0 | 7.37 | 1,4170 | 43.83 |
| 16 | - | + | +3 | Rearmost | 0 | 14.04 | 0 | 0 | 0.85 | 9,926 | 49.93 |
| 17 | - | + | -3 | Center | 0 | 12.83 | 0 | 0 | 1.36 | 15,180 | 25.94 |
| 18 | - | + | -3 | Rearmost | 0 | 23.22 | 0 | 0 | 0 | 37,370 | 43.55 |

The body regional injury risk was also assessed by two injury indices, i.e., HIC and chest deflection as follows:

**Effect of restraining** With belt+airbag condition (cases 1-6) at 56 kph impact, HIC values for all seat positions and steering column tilt angles were calculated under 1,000, the injury threshold in a compliance test and also showed a gradual increase with the impact speed. However, the belt only condition showed much higher HIC values at all three impact speeds than the other two restraining conditions mainly due to the head contact to steering wheel and windshield. This result shows the protection effect of airbag that becomes more significant at a higher impact speed. It is also noticeable that the increasing rate of chest deflection with airbag only condition is relatively much higher than the other two restraining conditions. In Figure 8and 9, mean values of HIC and chest deflection are respectively displayed with three restraining conditions and at three impact speeds. Each one represents average value with six variations (2 seat positions X 3 steering column tilt angles, Figure 9). Therefore the heights of error bar at mean value represent a degree of scattering (e.g., standard deviation) in six data points simulated with other two parameters, i.e., seat positions and steering column tilt angles.

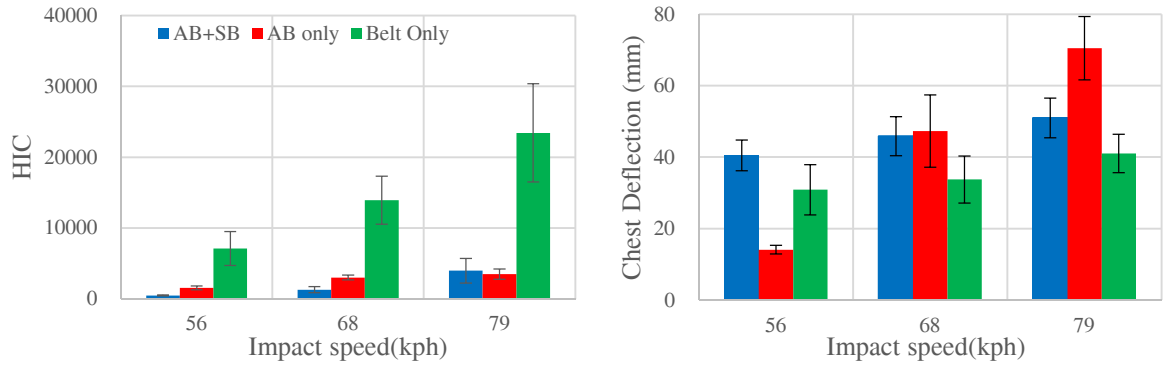


***Figure 8. Head and thorax injury risks with restraining condition.***

**Effect of seat position** Both HIC and chest deflection increased respectively by 100% and 60% at the rear most seat position compared to center position at all three impact speeds.

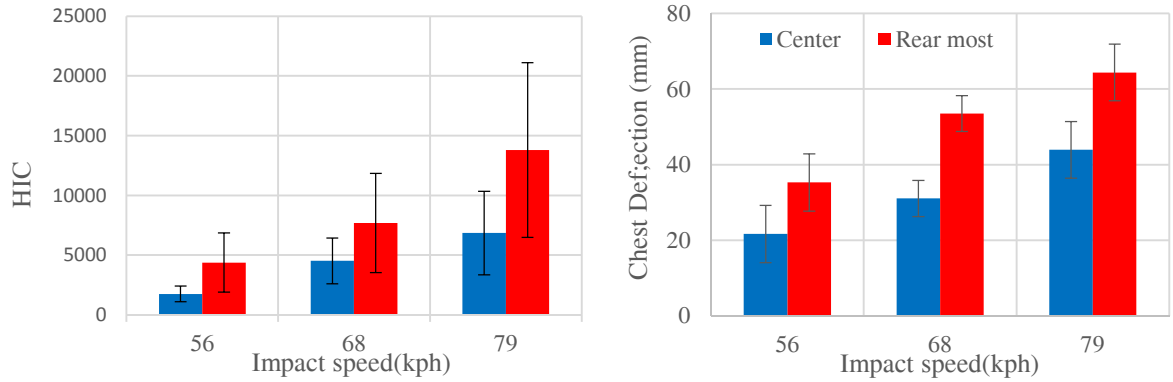


***Figure 9. Head and thorax injury risks with seat position.***

**Effect of steering column tilt angle** **The** HIC values showed quite different patterns at different impact speeds, i.e., respectively V shape, step up, and inverse V shape as a steering column is tilted in upper (+3 degree), middle(0 degree), or lower (3 degree, Figure 10). The chest deflections at 56 kph impact speed are in similar levels for all three tilt angles, while they became substantially higher with +3 degree case than two other tilt angles at 68 and 79 kph impact speeds.

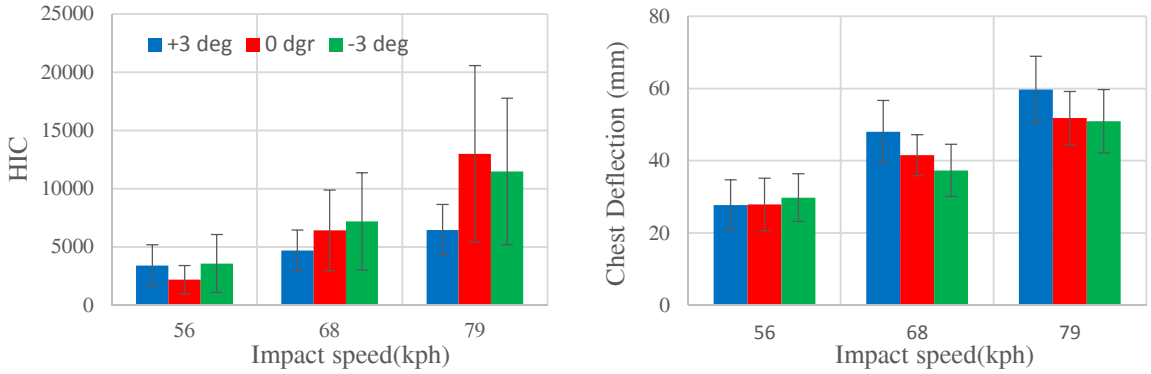


***Figure 10. Head and thorax injury risks with steering column tilt angle.***

**Correlation of injury risk between NASS/CDS data analysis and sled impact simulation** The windshield was the leading head injury source for unbelted driver with the full down steering column tilt position (Table 2). The predicted HIC values from sled impact simulation at 56 kph speed between center and full down steering column positions, i.e., cases 1 and 7 versus cases 5 and 11 showed much higher head injury risk at full down steering column position, especially with unbelted condition (Figure 11(a)). However this correlation becomes not so consistent at two other sled impact speeds.

The belt web was the most frequent injury source for thorax with airbag and rear most seat position (Table 3). The predicted chest deflection at all three sled speeds between center and rear most seat positions, i.e., cases 1, 3, and 5 versus cases 2, 4, and 6 shows much higher head injury risk at rear most seat position (Figure 11(b)).

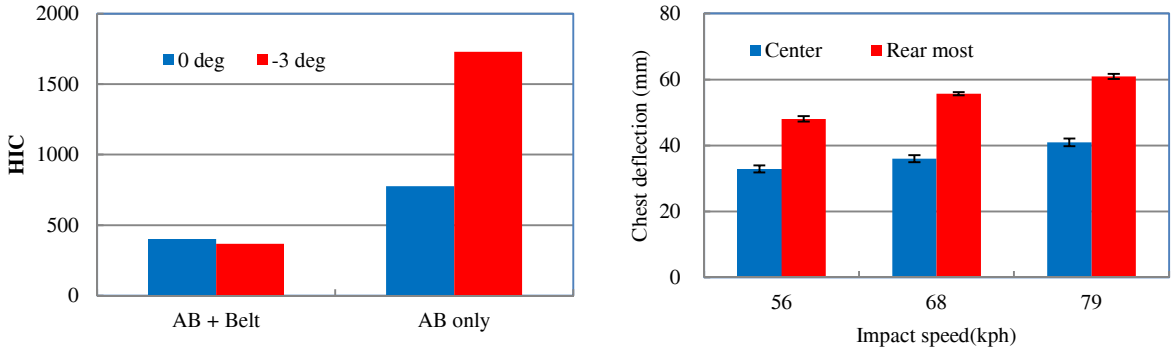


(a) Head injury risk (b) Thorax injrury risk

***Figure 11. Head and thorax injury risks for correlation with NASS/CDS analysis result.***

**Numerical Simulations using Human Body Model**

Three configurations of the sled modeling in Figure 7, cases 1, 5, and 6 were selected for substituting the dummy model with the anatomically detailed human body model, i.e., GHBMC model (Figure 12). The comparison of thorax injury risk at a frontal impact between two drivers model were made at 68 kph impact speed. The thorax injury risks were assessed by number of rib fractures and chest deflection respectively from the GHBMC human body model and the Hybrid III dummy model. As listed in Table 7, the GHBMC model predicted 80% increase of thorax injury risk with the change of steering column tilt angle and seat position by 5 to 9 rib fractures while 40% increase of chest deflection by the Hybrid III dummy model.

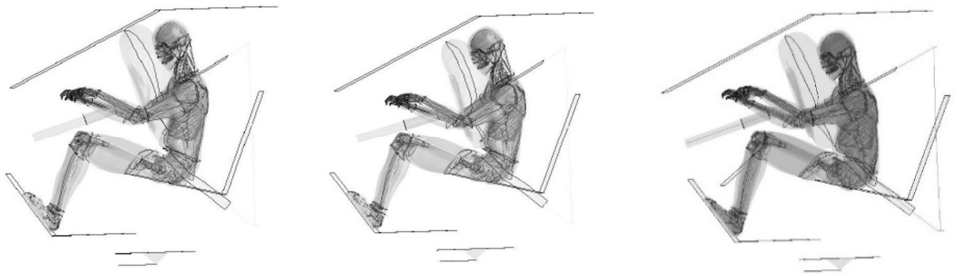

**Case 1** **Case 5** **Case 6**

***Figure 12. Front sled impact simulation with GHBMC human body model at 68 kph speed (Case 1: baseline model, Case 5: -3 steering column tilt, Case 6: -3 steering col1mn tilt + rear most seat position).***

**Table 7. Comparison of thorax injury risk between Hybrid III dummy and GHBMC human body model.**

| Steering column tilt | Seat position | GHBMC | Hybrid-III |
|---|---|---|---|
| | | No. of rib fracture | Chest deflection (mm) |
| Mid | Center | 5 (base) | 36.35 (base) |
| Down | Center | 6 (+20%) | 38.34 (+6%) |
| Down | Rear most | 9 (+80%) | 54.49 (+40%) |

## CONCLUSIONS

The body regional injury risks of driver and front seat passenger at a frontal impact were investigated using 2009-2012 NASS/CDS data. Numerical sled impact simulations using two driver models, the Hybrid III dummy and the GHBMC human body model, were used to confirm the change of injury risk with restraining condition, steering column tilt angle, and seat position. Some of distinctive findings in this study are as follows:

- Windshield, side structure, and steering column equally contribute head injury risk as injury sources.
- Belt web is a dominant injury sources at thorax and abdomen injury risks.
- Instrument panel is main injury source at lower extremity injury risk.
- 80% of AIS 3+ head injuries by windshield as a injury source was found at the full down position of steering column tilt.
- 69% of AIS 3+ head injuries by steering wheel as a injury source was found at the full up position of steering column tilt.
- 65% of AIS 3+ head injuries by instrument panel as a injury source was found at the rear most seat position.
- 82% of AIS 3+ thorax injuries by belt web as a injury source was found at the rear most seat position.
- 64% of AIS 3+ abdomen injuries by belt web as a injury source was found at the rear most seat position.

- 75% of AIS 3 lower extremity injuries by instrument panel as a injury source was found at the reclined seat back.
- Both Hybrid III dummy and GHBMC human body model predict the increasing thorax injury risk at steering column down tilt angle and rear most seat positions. However, the GHBMC human body model was more sensitive, i.e., prediction of higher injury value than the Hybrid III dummy model.

In the future, the real world accident data analysis will be extended to side impact and the numerical sled simulation with GHBMC human body model for more biomechanical injury risk prediction, e.g., CSDM(Cumulative Strain Damage Measure) to predict DAI(Diffuse Axonal Injury) of head.

## REFERENCES


[1] Pintar, F. A., Yoganandan, N., Gennarelli, T. A. 2000. "Airbag Effectiveness on Brain Trauma in Frontal Crashes", 44th AAAM Annual Conference.

[2] Wallis, L. A. and Greaves, I. 2002. "Injuries Associated with Airbag Deployment", Emerg Med J, Vol. 19, 490-493.

[3] Cuerden, R., Hill, J., Kirk, A., Mackay, M. 2001. "The Potential Effectiveness of Adaptive Restraints", Proceedings of the IRCOBI Conference, Isle of Man.

[4] Frampton, R. J., Welsh, R., Kirk, A., Fay, P. 2000. "Effectiveness of Airbag Restraints in Frontal Crashes – What European Field Studies Tell Us", Proceedings of the IRCOBI Conference, Montpellier, France.

[5] Murphy, R. X. Jr., Birmingham, K. L., Okunski, W. J., Wasser, T. 2000. "The Influence of Airbag and Restraining Devices on the Patterns of Facial Trauma in Motor Vehicle Collisions", Plast Reconstr Surg, Vol. 105(2), 516-520.

[6] Duma, S. M. and Jernigan, M. V. 2003. "The Effects of Airbags on Orbital Fracture Patterns in Frontal Automobile Crashes", Ophthal Plast Reconstr Surg Vol. 19(2), 107-111.

[7] Huber, C. D., Lee, J. B., Yang, K. H., King, A. I. 2005. "Head Injuries in Airbag-Equipped Motor Vehicles with Special Emphasis on AIS 1 and 2 Facial and Loss of Consciousness Injuries", Traffic Inj Prev, Vol. 6(2), 170-174.

[8] Davis, R. P., McGwin, G. Jr., Melton, S. M., Reiff, D. A., Whitley, D., Rue, L. W. 3rd. 2004. "Specific Occupant and Collision Characteristics are Associated with Motor Vehicle Collision-Related Blunt Cerebrovascular Artery Injury", J Trauma, Vol. 56(1), 64-67.

[9] Untaroiu, C., Bose, D., Lu, Y-C., Riley, P., Lessley, D., Sochor, M. 2011. "Abdominal and Thoracic Response to Loading of Pretensioner Restraint Systems", Proceedings of the IRCOBI Conference, Krakow, Poland.

[10] Yue, N. and Untaroiu, C. 2014. "A Numerical Investigation on the Variation in Hip Injury Tolerance with Occupant Posture during Frontal Collisions", Traffic Injury Prevention, Vol. 15, 513-522.

[11] Bostrom, O. and Kruse, D. 2011. "A Sled Test Method for Small Overlap Crashes and Fatal Head Injuries", Paper Number 11-0369, 22nd Enhanced Safety of Vehicle Conference, Washington DC.

[12] Global Human Body Models Consortium, www.ghbmc.com.

# SAFETY ASSESSMENT PROCEDURE FOR ADVANCED EMERGENCY BRAKING SYSTEM

**Taewoo Kim**
**Taeyoung Lee**
**Kyongsu Yi**
School of Mechanical and Aerospace Engineering, Seoul National University
Korea

**Jaewan Lee**
Korea Automobile Testing & Research Institute, Korea Transportation Safety Authority
Korea

Paper Number 15-0395

## ABSTRACT

This paper suggests a safety assessment procedure for evaluation of enhanced longitudinal safety by Advanced Emergency Braking (AEB) system in Korea. The objective of project is to suggest safety evaluation procedure of the AEB system with the consideration of Korean road condition and physically meaningful situation.
To develop the impact assessment procedure of the AEB system, the AEB test vehicle as well as the test scenario should be designed. Before the development of the test procedure, this paper reviews the international regulation of AEB system and traffic accident statistics, and develops domestic safety standards and evaluation requirements. Test scenario has been developed to assess the safety performance of AEB systems for the reductions in collision frequency and severity by using the Korea's traffic accident statistics. Also, the test scenario is designed to represent the real driving condition and to evaluate the safety performance of AEB system in various situations. The AEB test vehicle comprises of a millimeter wave radar sensor, CCD camera and pre-developed AEB algorithm of which are processed to judge the collision risk. To evaluate the collision avoidance performance of the AEB test vehicle, pre-performance test was conducted by using the NCAP-AEBS draft test procedure and proposed test scenario.
From the traffic accident statistics and the field test result, it is shown that proposed AEBS test scenario represents not only the frequently occurred collision case but also physically meaningful situation in terms of expected control performance of the AEB system. Also, it has been shown that AEB system of prior study can reduce the collision velocity and provide the greatest real world benefits. Because of the limitation of test equipment and safety, test scenario about Cut-in vehicle could not be included in the test results of the proposed test procedure. However, by using the analysis methods and simulation test, the safety effect for enhanced longitudinal safety of the AEBS with respect to Cut-in case has been assessed scientifically.
In this paper, the safety assessment procedure for AEB system has been described to evaluate the safety performance of the AEB system. The test procedure according to AEB system provides objective safety performance level of each AEB system. Also, these tests are expected to be a strong driver of improved safety in the real world.

## INTRODUCTION

Since the passive safety systems, such as seat belts, airbags or active head-rest, etc., became part of almost every vehicle, the demands of vehicle active safety system had been also getting larger. Therefore, many automakers are trying to help drivers to avoid or mitigate collision using active safety system. Several systems are already commercialized including Adaptive Cruise Control (ACC), Traffic Jam Assist (TJA), Lane Keeping Support (LKS), Lane Change Assist (LCA), Blind Spot Detection (BSD), Automated Parking Assist (APA) and Forward Collision Warning System (FCWS). [1]~[6] Especially, Advanced Emergency Braking (AEB) system is one of the active safety system which is supposed to be able to significantly contribute to reduce the number of road fatalities.
After AEB system was developed and commercialized, the number of vehicles with AEB system have been increased and is predicted to be increased more. Also, as AEB system became one of the most interesting topic for researchers and automakers, there have been many studies to improve the performance of AEB system. Therefore, each of AEB systems developed in different ways which means it is difficult to compare the performance between

each AEB systems. Hence, the studies to evaluate the performance of these AEB systems are required. Governments and research centers of many countries such as Euro NCAP and International Organization for Standardization (ISO) have been studied about the regulation of AEB system and some of them already announce a standard regulation. The regulation of ISO is already using as a standard of safety performance for the commercialization of AEB system. Euro NCAP provides objective standards about the safety performance of AEB system. [7] However, these regulations are still not perfect to guarantee the safety by AEB system in various situation.
In the case of Korea, there is no specific regulation about the performance of AEB system. According to the National Policy statistics in Korea, the total number of deaths in 2010 caused by traffic accidents in Korea was 5,505 which means about 2.6 per 10,000 cars experianced the fatal accident. It was the twice the OECD average of 1.3. [8] In 2009, Traffic Accident Analysis Center of Korea reports that almost 60 percent of traffic accident was longitudinal accident. Hence, the regulation which is based on the Korean road condition is required to reduce the collision frequency and severity.
In this paper, the international regulation of AEB system and the traffic accident statistics are reviewed. The typical factors which should be considered for the development of AEB test scenario are summarized.Then, we present the AEB test scenario which contains the characteristics of traffic accident of Korea and represents not only the frequently occurred collision case but also physically meaningful situation. Last of all, the proposed test scenario is verified via computer simulation and vehicle test.

## TRAFFIC ACCIDENT STATISTICS AND THE STATUS OF REGULATION OF AEB

In this chapter, traffic accident statistics and the international regulations of AEB are reviewed.

### Traffic Accident Statistics

To develop the test scenario for the evaluation of the performance of AEB systems which is appropriate to the case of Korea, traffic accident statistics of Korea should be studied. In this section, the type of traffic accident of Korea is reviewed based on the reports of Traffic Accident Analysis Center of Korea. Also, to determine the specific ratio of each type of collision which was not exists in the case of Korea, international traffic accident statistics is also reviewed.

**Korea** Lee analyzed the traffic accident of Korea from 2005 to 2009 based on the reports of Traffic Accident Analysis Center of Korea. [9], [10] He analyzes and classifies the traffic accident statistics based on the two topics: violation of law and human factor. Based on the case of violation of law, almost 50 percent of all traffic accident was caused by the violation of the duty to drive safely. Signal violation and safe distance violation was followed. Safe distance violation which is closely related with the longitudinal safety was 13.7 percent of traffic accident. According to the classification based on the human factors, almost 60 percent of traffic accident was caused by the negligence in forward-looking which is also closely related with the longitudinal safety.

**International** NHTSA reports about the situation and driving condition of traffic accident. [11] According to the report of NHTSA, traffic accident which occurred in America can be classified into 7 categories, and 39 percent of total traffic accidents were longitudinal collision. Also, in order to analyze the situation of traffic accident, NHTSA classify the traffic accident into 45 kinds of typical scenarios. Five of them were closely related with the longitudinal safety, which are about 28.9 percent of total traffic accidents.

### Regulation of AEB system

Research centers of many countries have been studied about AEB system for the announcement of regulation of AEB system. In this section, the regulation of Euro NCAP and ISO are introduced.

**Euro NCAP** Euro NCAP classifies the AEB test procedure into 2 cases: City and Inter-Urban test procedure. [12] For AEB City test scenario, they evaluate the performance of AEB in low speed region while

the preceding vehicle is at standstill. For AEB Inter-Urban test scenario, they evaluate the performance of AEB in low and high speed region for the cases of which the preceding vehicle is stationary, slowly moving and braking with constant deceleration. The scoring of each test procedure was developed based on the statistical data about the frequency and severity of traffic accident at each speed region. However, they only regulate the performance of AEB in the case of straight road and simple target condition. Hence, the performance of AEB in curve or other driving situation cannot be guaranteed. Also, they focused only on the avoidance and mitigation of the collision which means the excessive control of AEB system cannot be verified through their regulation.

**ISO** ISO also announce the regulation of AEB system. They evaluate the performance AEB with the vehicle speed from 15 km/h to the maximum available speed. They suggest that the AEB system should be able to reduce the impact speed more than 20 km/h for the stationary target, and to avoid the collision for the moving target with the speed of 12 km/h. Also, they regulate about the warning timing of AEB system. However, they also regulate the performance of AEB only in simple cases: straight road and single target condition.

## REPRESENTATIVE FACTORS OF AEB TEST SCENARIO

For the evaluation of the performance of AEB system, test scenario should represent not only the frequently occurred collision case but also physically meaningful situation. Hence, many factors such as driving mode, road type, environment, and AEB system element should be considered to evaluate the performance of AEB system. The typical factors are summarized in fig. 1. The AEB test scenario should contains these factors to varify the performance of AEB in various situation.

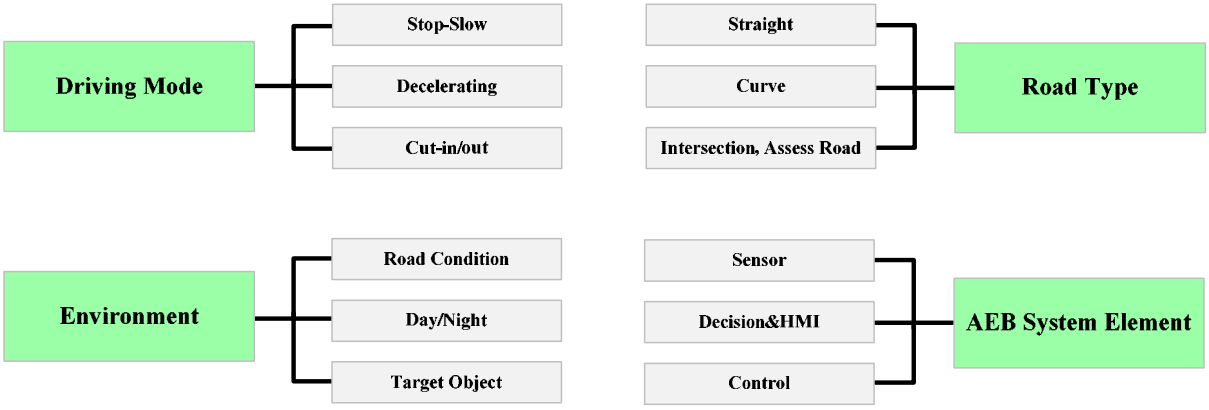


*Figure1. Representative factors of AEB scenario.*

### Driving Mode

The performance of AEB should be guaranteed in various kinds of driving condition especially about the behavior of preceding vehicle. To evaluate the performance of AEB, the vehicle with AEB should be tested in both normal and severe conditions. The typical examples of these driving modes are introduced in this section.

**Preceding Stop-Slow Vehicle** In city-driving condition, lots of crashes occur between the stationary or stop preceding vehicle and following vehicle. Hence, the response of AEB about the slow or stop preceding vehicle should be evaluated.

**Preceding Decelerating Vehicle** Many drivers do not use large deceleration in normal driving condition. However, dangerous situation makes driver to use large deceleration which can make a secondary accident with the following vehicle. If the preceding vehicle is decelerating with large deceleration in some reasons, it is difficult to react quickly for the driver of following vehicle. Hence, AEB should indicate the danger to the driver and should determine to decelerate the vehicle automatically in proper moment unless the driver reacts about the dangerous situation. Although the AEB cannot prevent the crash perfectly, it should decrease the severity of the accident. Hence, the performance of AEB about the preceding decelerating vehicle should be verified.

**Preceding Cut-in/out Vehicle** Sudden Cut-in or Cut-out situation can be a risk to the following vehicle. In this situation, the flexible reactions about each case are very important. If the Cut-in or Cut-out situation makes the situation dangerously, the proper reaction of the driver is required. In this situation, AEB should indicate the danger to the driver and determine to decelerate the vehicle in proper moment to avoid the crash or decrease the severity of the crash unless the driver reacts about the danger. Hence, the performance of AEB in Cut-in or Cut-out situation should be also evaluated. Also, if the Cut-in/out situation is not dangerous to the following vehicle, AEB should not be activated. The undesired and unnecessary reaction of AEB could disturb the driver. Hence, the deactivation of AEB in safe Cut-in/out situation should be verified.

**Road Type**

In City road condition, various types of road are exists which could effect on the performance of the AEB. Including the straight road condition, AEB should guarantees the performance on curve or other road types.

**Straight Road** According to the NHTSA's report, for about 40 percent of the collision was longitudinal collision. [11] Hence, the performance of AEB in longitudinal collision situation should be evaluated importantly

**Curve** In slow speed condition, dangerous situation is occurred when the distance between the vehicles is relatively small. In this situation, the effect of curvature of the road is small because the lateral offset of the preceding vehicle at dangerous situation is relatively small. However, in high speed region, the effect of curvature of the road is not negligible. AEB system should classify the vehicles which are on the same lane and which are not. If AEB system is failed to recognize the preceding vehicle on the same lane in curve, AEB could not response about the danger at proper moment which can lead to an accident. If AEB response about the vehicle on other lane and decelerate the vehicle, it can disturb the driver. Hence, deactivation of the AEB by the vehicle on other lanes should be also verified as well as the activation by the vehicle on same lane.

**Other Road (Intersection, Access Road)** Various types of road condition including the mentioned situation are exists in normal city driving condition. Although the straight and curve road condition are more frequent, complex road conditions such as intersection and assess road is more dangerous. However, the performance of AEB cannot be guaranteed perfectly in these complex situations due to the limitation of the perception range of AEB system. Hence, the evaluation of the performance of AEB in complex driving mode such as intersection and assess road is not considered in this paper. However, these topics are suggested to be considered on the evaluation of the performance of advanced active safety system or advanced driver assistance systems (ADAS).

**Environment**

AEB should also guarantee the performance in unusual environment. Although the performance of AEB on unusual environment cannot be perfect, AEB should guarantee a certain level of safety performance. Hence, AEB performance on unusual environment condition should be evaluated.

**Road Condition** Braking distance of the vehicle became longer in wet road condition. In this situation, AEB should response about the danger quickly than usual situation. Even if AEB cannot estimate the road condition, it should guarantee a certain level of safety performance on the wet road condition.

**Day/Night Condition** In night-time driving condition, driver's sight became narrow which makes the required time to recognition and decision became larger. Hence, AEB system should indicate the danger to the driver and response about the danger properly in night-time driving condition. However, some kind of sensors such as vision sensors are vulnerable to a night condition. Also, although vehicles are visible at night due to the headlight and taillight of the vehicle, pedestrian or other kind of obstacles are not visible. Hence, the performance of AEB in night-time driving condition is suggested to be evaluated.

**Target Object** In city-driving condition, pedestrian or other obstacles on the road can lead to an accident. Hence, AEB should perceive the pedestrian or other obstacles as well as the preceding vehicles. Especially, AEB should be able to perceive the pedestrian and response about the danger because car to pedestrian accident can lead to a fatal accident. Hence, the performance of AEB about the pedestrian target should be verified.

**AEB System Element**

AEB system should contain four parts: sensor part, decision and Human Machine Interface (HMI), control, and actuator. The characteristics and general requirements of each part are explained in this section.

**Sensor** Sensor part perceives the target in the range. It should classify the target type such as preceding vehicle, pedestrian and other kind of obstacles and it also should be able to classify the two-wheeled vehicle or other specific targets. It should provide the target information including the type of target, target position, and preceding vehicle relative velocity. Multi-target perception and tracking should be available. The longitudinal and lateral perception range of sensors should satisfy the range requirement for the operation of AEB. Certain level of accuracy in unusual driving condition should be also guaranteed as well as in normal driving condition.

**Decision & Human Machine Interface (HMI)** Decision part selects the proper target between the perceived multi targets and recognizes the risk. Decision part should be able to track the multi-target simultaneously and select the proper target to response in dangerous situation. Hence, this target selecting ability should be also guaranteed in multi-vehicle condition and curve or other complex driving conditions. Also, tracking ability including the tracking delay about new target should be evaluated. In order to evaluate the safety performance of AEB, warning and decelerating timing can be a standard of evaluation.
HMI is the part which indicates the danger to the driver and responses about the drivers input. HMI should indicate to the driver visually, acoustically, or in other ways to make driver react about the danger. In this situation, HMI should perceive the change of driver's behavior. If driver react about the danger, HMI should hand over the control authority to the driver. This change of control authority should be evaluated as well as the safety performance of AEB with and without driver's braking input: for example, if the amount of brake of the driver is not enough, AEB should make the vehicle to decelerate more.

**Control** Control part decelerate the vehicle in proper amount of deceleration for each situation. Although a small amount of deceleration can be lead to an accident, large amount of deceleration can disturb the driver and make driver inconvenient. The appropriate range of deceleration which doesn't make driver inconvenient

is difficult to be determined theoretically. Hence, driving data based determination is usually suggested to guarantee the comfort of driver as well as the safety performance of AEB.

**Actuator** In order to guarantee the performance in real driving condition, the actuator part should be durable. Hence, the durability about vibration, repetitive decelerating condition, and environmental change should be guaranteed.

## AEB TEST SCENARIO

Based on the international AEB regulation and the typical factors of AEB test scenario which are mentioned in previous chapters, the required AEB test scenario for the evaluation of the performance of AEB system can be determined. However, although the exact performance of AEB system in various situation can be evaluated through a great number of test scenarios, limited test is available due to the limitations. Hence, significant and necessary test scenario should be selected. The summarized test scenario for the evaluation of the performance of AEB system is described in table 1. In this chapter, only three cases of test scenario is explained.

**Table1.**
**AEB test scenario.**

<table>
<tr><th>Item</th><th>Preceding Vehicle</th><th colspan="2">Specifics</th><th>Test No.</th></tr>
<tr><td rowspan="6">Test No. 1<br>Straight</td><td rowspan="3">Stop Vehicle</td><td rowspan="2">Vehicle Target</td><td>Dry Asphalt</td><td>1-1D</td></tr>
<tr><td>Wet Asphalt</td><td>1-1W</td></tr>
<tr><td colspan="2">Pedestrian Target</td><td>1-1P</td></tr>
<tr><td colspan="3">Slow Vehicle</td><td>1-2</td></tr>
<tr><td colspan="3">Decelerating Vehicle</td><td>1-3</td></tr>
<tr><td colspan="3">Cut-in Vehicle</td><td>1-4</td></tr>
<tr><td>Test No. 2<br>Curve</td><td colspan="3">Stop Vehicle</td><td>2-1</td></tr>
</table>

### Straight Road Preceding Decelerating Vehicle

The main purpose of AEB system is avoidance or mitigation of the collision in longitudinal direction. Preceding deceleration vehicle is one of the typical scenario of longitudinal traffic accident.

**Scenario** In straight road, the large deceleration of preceding vehicle can cause an accident. Especially, if the driver of subject vehicle fails to recognize the deceleration of the preceding vehicle, it can lead to a fatal accident. Hence, warning and braking of the AEB system in this situation should be evaluated.

**Performance evaluation** In straight road preceding vehicle decelerating situation, AEB should indicate the danger to the driver. Also, unless the driver reacts about the danger, AEB should determine to decelerate the vehicle automatically to avoid or mitigate the danger. For this, AEB should be able to perceive the target in proper range and recognize the danger. Hence, the warning and decelerating timing of the AEB system should be evaluated. Also, the relative speed of the impact and the reduction of the subject vehicle speed should be in safe region.

**Straight Road Preceding Cut-in Vehicle**

AEB system should be able to response about sudden change of traffic condition such as cut-in case.

**Scenario** The test scenarios of the Euro-NCAP and ISO already include the preceding stop, slow, and decelerating vehicle. However, these three scenarios cannot evaluate the response about an unexpected obstacle or vehicle. Preceding cut-in vehicle situation is one of the representative situations of the danger caused by unexpected obstacles or vehicles. However, in normal driving condition, cut-in vehicle with similar speed does not always lead to an accident. In this situation, the response of AEB system could disturb the driver and make the driver inconvenient. Hence, the response of AEB system about both safe and dangerous Cut-in cases should be verified.

**Performance evaluation** When the preceding vehicle cuts in with deceleration, AEB should be able to recognize the danger and indicate the danger to the driver. Unless the driver reacts about the danger, AEB system should determine to decelerate the vehicle automatically to avoid or mitigate the collision. However, if the cut-in of preceding vehicle doesn't cause a danger, AEB system should not be activated. Hence, the deactivation of AEB system in safe Cut-in situation should be evaluated as well as the activation of AEB system in dangerous Cut-in situation. In the case of cut-in with decelerating situation, the warning and decelerating timing should be checked as well as the collision avoidance or reduction of the impact speed. Also, in the case of safe cut-in situation, the deactivation of AEB should be verified.

**Curve Road Preceding Stop Vehicle**

Regulation of Euro-NCAP and ISO evaluate the performance of AEB only in straight road condition. However, in city and inter-urban case, the driver should meet lots of curves. Hence, AEB performance in curve road also should be evaluated.

**Scenario** City and Inter-Urban condition contains lots of curve road situation. Hence, AEB system should guarantee the safety performance in curve road condition to guarantee the safety in city or inter-urban driving condition. For this, AEB system performance in curve road condition should be evaluated. In curve road situation, target perception and decision part is the most important part while other performance of AEB can be also evaluated in the case of straight road condition. Curve road stop vehicle situation is the most typical and simple scenario between the curve road situation.

**Performance evaluation factor** In the case of curve road stop vehicle scenario, the most important part is perception and recognition of the target on same lane. For this, activation by the preceding vehicle on same lane and deactivation by the obstacle on other lanes should be assessed. The effect of curvature became larger at high speed region. Hence, the performance of AEB system should be evaluated in high speed region. For the same lane stationary obstacle, perception and recognition of the AEB system should be evaluated as well as warning and decelerating timing. Since the test should be proceeded in high speed region, impact speed and relative impact speed also should be verified. For the stationary obstacle on other lanes, failure of the perception or recognition should be verified.

## SIMULATION AND VEHICLE TEST RESULT

In this chapter, the simulation and field test result of the proposed AEB test scenario is proposed. For this, AEB algorithm which is presented in previous research is introduced in the first section. Using this AEB algorithm, computer simulation was conducted using simulation toll Carsim and MATLAB/Simulink. Also, vehicle test was also conducted. However, cut-in and curve test scenario couldn't be included due to the limitation of test equipment and safety.

**AEB Algorithm**

In the study of Lee, AEB algorithm based on a new safety index was proposed. [Lee 2015] The new safety index was developed by using time to collision (TTC) and warning index (x). TTC and warning index is defined as:

$$TTC = \frac{C}{v_{rel}} \qquad \textbf{(1)}$$

$$x = \frac{C - d_{br}}{d_w - d_{br}} \qquad \textbf{(2)}$$

where $C$ is clearance, $v_{rel}$ is relative velocity, and $d_{br}$, $d_w$ are braking-critical and warning-critical distances which are defined as follows. [13]

$$d_{br} = v_{rel} \cdot t_{brake} - \frac{{v_{rel}}^2}{2a_{\max}}$$
$$d_w = v_{rel} \cdot t_{thinking} + v_{rel} \cdot t_{brake} - \frac{{v_{rel}}^2}{2a_{partial}} \qquad \textbf{(3)}$$

where $t_{brake}$ is system delay, which is given by the brake-system hardware, $a_{\max}$ is the maximum deceleration of the vehicle under driving conditions, $t_{thinking}$ is the delay in human response between recognition and manipulation. [14] Using these indices, new longitudinal safety index can be defined as follows. [7]

$$S_{Longi} = \sqrt{\left(\frac{TTC - TTC_{Partial}}{TTC_{Emergency} - TTC_{Partial}}\right)^2 + \left(\frac{x - x_{Partial}}{x_{Emergency} - x_{Partial}}\right)^2} \qquad \textbf{(4)}$$

where $TTC_{Partial}$, $TTC_{Emergency}$, $x_{Partial}$, $and$ $x_{Emergency}$ are the thresholds for the control mode selection of AEB system which can be determined physically:Warning mode, Partial braking mode and Emergency braking mode.
Based on this new longitudinal safety index, AEB algorithm select the control mode: warning mode determines to indicate the danger to the driver, partial braking mode determines to decelerates the vehicle with small deceleration, and emergency braking mode determines to decelerate the vehicle with the maximum deceleration.

**Simulation Result**

Computer simulation was conducted using simulation tool Carsim and MATLAB/Simulink. In this paper, the simulation result of Cut-in with decelerating vehicle scenario is presented.

**Simulation Case: Cut in with Decelerating Vehicle** The simulation result of Cut-in with decelerating vehicle scenario is shown in fig.2. Initially, radar sensor of subject vehicle failed to detect the preceding vehicle due to the lateral offset of preceding vehicle. After the preceding vehicle started to cut in, lateral offset decreased and radar based target perception became possible. However, since the preceding vehicle was decelerating during the cut-in, clearance between the preceding vehicle and subject vehicle is smaller than 10 m when the preceding vehicle started to be detected. Hence, as described in fig.2 (d), AEB started to indicate the danger, and started to decelerate the vehicle due to the assumption that driver didn't look forward at that moment. As described in fig.2 (a), collision was avoided and the velocity of subject vehicle was successfully decelerated. This result shows that the proposed AEB system performs well in the Cut-in with decelerating vehicle scenario.

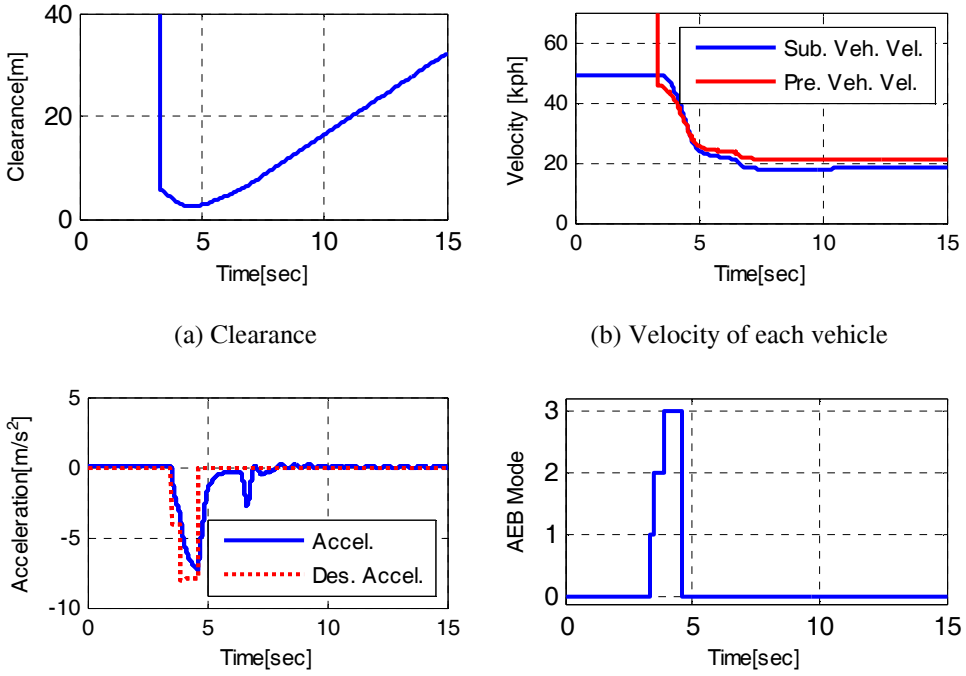


(a) Clearance

(b) Velocity of each vehicle

(c) Acceleration

(d) AEB Control Mode

***Figure2. Simulation result of AEB system in preceding cut-in with decelerating vehicle scenario.***

**Vehicle Test**

To confirm that the proposed AEB test scenario is realistic and physically meaningful, vehicle test have been conducted. The proposed AEB algorithm is implemented on vehicle. A millimeter wave radar sensor and carge-coupled device (CCD) camera are equipped to detect the preceding tret, pedestrian, and obstacles. The Euro-NCAP vehicle target which is physically linked with another vehicle was used as a preceding vehicle target for the preceding moving target cases. In this section, test result of the straight road decelerating vehicle scenario which is also included in the regulation of Euro NCAP is presented.

**Test Case: Straight Road Decelerating Vehicle** The test result of the straight road decelerating vehicle scenario is shown in fig.3. The initial speed of subject and preceding vehicle was 50 km/h and initial clearance was about 50m. As shown in fig.3, after the preceding vehicle started to be decelerated with constant deceleration of 0.2g, clearance between the preceding vehicle and subject vehicle was also decreased. However, the subject vehicle maintained the initial speed according to the assumption that there was no reaction of driver about the danger. Therefore, AEB system indicates the danger to the driver which is expressed as AEB Mode 1, and AEB system started to decelerate the vehicle automatically which is expressed as AEB Mode 2. Fig.3 shows that proposed AEB algorithm performed well in the straight road preceding decelerating vehicle situation.

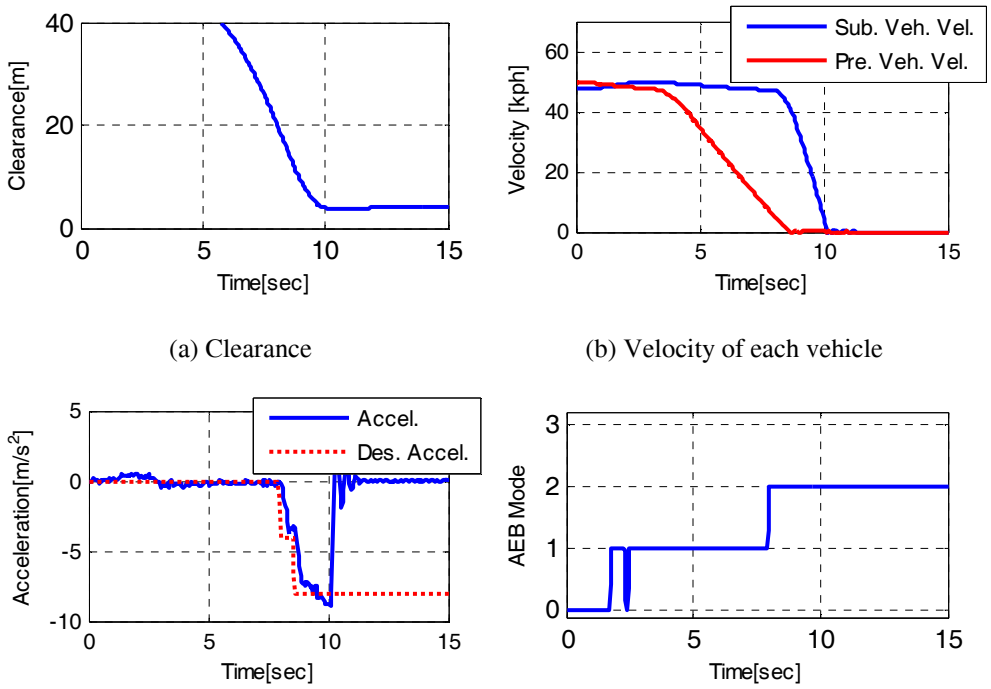


(a) Clearance

(b) Velocity of each vehicle

(c) Acceleration

(d) AEB Control Mode

***Figure3. Test result of AEB system in preceding decelerating vehicle scenario.***

## CONCLUSIONS

In this paper, a safety assessment procedure for evaluation of enhanced longitudinal safety by Advanced Emergency Braking (AEB) system has been developed. The proposed AEB test scenario consists of 7 cases which include straight road cut-in vehicle scenario and curve road stop vehicle scenario. In order to determine the AEB test scenario which represents the real driving condition, the typical factors such as driving mode, road type, environment, and AEB system element should be considered to guarantee that the proposed AEB test scenario represent not only the frequently occurred situation but also physically meaningful situation. The proposed AEB test scenario has been validated based on the investigation on international regulation of AEB system and traffic accident statistics. In order to verify the proposed AEB test scenario, AEB algorithm of prior study was conducted via computer simulation and vehicle test. The simulation and vehicle test results show that the proposed AEB test scenario was realistic and physically meaningful.
In order to develop the specific regulation such as rating criteria and detail procedure of each test scenario, additional experimental test should be conducted with various AEB systems.

* This work was supported by the BK21 program, the Korea Ministry of Land, Infrastructure and Transport; the Korea Agency for Infrastructure Technology Advancement (Project No. 14PTSI-C054118-06), SNU-IAMD, and the National Research Foundation of Korea(NRF) grant funded by the Ministry of Science, ICT & Future Planning (MSIP) (No. 2009-0083495)

## REFERENCES

[1] N. Minoiu,. M. Netto, S. Mammar, B. Lusetti,. "Driver Steering Assistance for Lane Deperture Avoidance" Control Engineering Practice, Vol. 17,pp.642-651, 2009

[2] X. An, M. Wu, H. He, "A Novel Approach to Provide Lane Departure Warning Using Only One Forward-Looking Camera", Proc. Int. Symp. Collaborative Technologies and Systems, pp. 356-362, 2006.
[3] S. Moon, I. Moon, and K. Yi, "Design, tuning, and evaluation fo a full-range adaptive cruise control system with collision avoidance", Control Engineering Practice, Vol. 17, No. 4, pp. 442-445, 2009.
[4] P. Seiler, B. Song, and J. K. Hedrick, "Development of a Collision Avoidance System", Proc. SAE Conference, pp. 97-103, 1998.
[5] A. Vahidi, and A. Eskandarian, "Research Advences in Intelligent Collision Avoidance and Adaptive Cruise Control", IEEE Transactions on Intelligent Transportation Systems, Vol. 4, No. 3, pp.143-153, 2003.
[6] M. Rimini-Doering, T. Altmueller, "Effect of Lane Departure Warning on Drowsy Drivers' Performance and State in a Simulator", PROCEEDINGS of the Third International Driving ymposium on Human Factors in Driver Assessment, Training & Vehicle Design, pp. 88-95, 2005.
[7] Robust Autonomous Emergency Braking Algorithm using the Tire-road Friction Estimation and the Sensor Uncertainties
[8] Inseong, Choi, Seongwoo, Cho and Byungdo, Kang, "An Overview on Establishing Safety Assessment Standard of Longitudinal Active Safety System in Korea", ESV 2013-0490
[9] T. Lee, K. Yi, and J. Lee, "Safety Index for the Analysis of the Longitudinal Safety Effect", pp 1283-1288, KSAE
[10] "Road Traffic Accidents in Korea 2009", Traffic Accident Analysis Center, Road Traffic Authority, Korea
[11] NHTSA, “NHTSA: Pre-Crash Scenario Typology for Crash Avoidance Research”. 2007
[12] Euro NCAP, "Euro_NCAP_2014_AEB_Test_Protocol", 2013
[13] K. Yi, K. Hedrick, and S. C. Lee, "Estimation of tire-road friction using observer based identifiers", Vehicle Syst. Dyn., vol. 31, pp. 233-261, 1999.
[14] Wanki Cho, Seungwuk Moon, Sihyoung Lee, and Kyongsu Yi, 2010, "Intelligent Vehicle Safety Control Based on Index plane", AVEC 2010

**Occupant Behavior and Brain Injury in NHTSA Oblique Test**

**Jeong Keun, Lee**
Hyundai Mobis
Republic of Korea

**Hyo bae, Lee**
**Hun hee, Jeong**
Hyundai Mobis
Republic of Korea

Paper Number 15-0397

## ABSTRACT

The National Highway Traffic Safety Administration (NHTSA) found that a large number of fatalities occurred in crashes involving poor structural interaction between the striking and the struck vehicles, such as corner impacts, oblique crashes, or impacts with narrow objects.
NHTSA proposed the oblique test that can reproduce vehicle crush, occupant kinematics, and risk of injury in vehicle-to-vehicle crashes, an offset impact between a research moving deformable barrier (RMDB) and a stationary vehicle at a 15 degree angle.
Recent research for NHTSA oblique test with THOR ATD showed the lateral movement of both occupants, so that the driver's head contact with door or between door and steering wheel. For the far-side occupant, the head contact with center IP and the brain injury risk predicted using BrIC is higher than SOI.
The objective of this paper is to investigate and understand the effect of airbag performance on the occupant kinematics and related injury during NHTSA oblique tests. This paper focuses on effect of various airbag parameters corresponding to the dynamic stiffness.
The research integrated the injury analysis with a crash testing and computer simulation. MADYMO was used to create a NHTSA oblique test environment. Both 50th percentile THOR ATD and Hybrid III in MADYMO were respectively used to simulate occupant kinematics and injuries for the driver and passenger occupant. Airbag models for curtain airbag and passenger airbag are used in the simulations in order to understand the effect of various restraint system concepts on occupant kinematics and injuries.
In this paper, driver side airbag and passenger side airbag are investigated for both near-side occupant and far-side occupant. CAE models are used to show their advantages and limitations. Further enhancements are proposed to improve the correlation of these occupant models. Passenger side airbag and driver side airbag are investigated to reduce the brain injury and head contact with compartment. NHTSA oblique test case is used to demonstrate the effectiveness of the airbag variations.
Limitations of the current airbag model used for NHTSA oblique test were highlighted. Vent hole was modified to improve the head injury.
For reducing the brain injury risk of occupant in an NHTSA oblique test, it was found counter measures which didn't cause head rotation was effective.

## INTRODUCTION

The past several years, most vehicles have achieved the good ratings in the IIHS frontal tests, and NHTSA's frontal NCAP. This aroused the IIHS and NHTSA to investigate further test configurations for frontal impacts in order to improve the occupant safety. The Small Overlap Impact (SOI) test shown in Figure 1 has been introduced by IIHS, that is a 64 km/h frontal crash test in which 25% of the front-end of a vehicle is overlaped by a rigid barrier. The vehicle structural performance, restraints and dummy kinematics, and dummy injury measures are used to rate the vehicle's overall safety performance as Good, Acceptable, Marginal or Poor. Four groups of dummy injury ratings utilize the instrumentation in the dummy's head and neck, chest, hip and thigh, and legs and feet. The vehicle structural rating is based upon the pre-test and post-test measurements of seven various locations. Prior to the designing a NHTSA oblique test, shown in Figure 1, the NHTSA investigated fatal frontal crashes in the NASS database in which the occupants were belted non-ejected and the vehicles were equipped with frontal airbags. A large number of fatalities occurred in crashes involving poor structural interaction between the striking and the

struck vehicles in the report published in 2009[1]. On the other hand, full-frontal or offset-frontal impacts with good structural interaction ended in less fatalities, unless the crashes were of extreme severity or the occupants were exceptionally vulnerable. As a result of the NHTSA study, the agency stated its intent to further analyze small overlap and oblique frontal crashes [2]. NHTSA had conducted a large number of frontal crash tests, and developed a moving deformable barrier crash test, shown in Figure 1. The ″research" moving deformable barrier (RMDB) impacts the target vehicle at 90 kph (56 mph) and the stationary vehicle is positioned such that the angle between the RMDB and the vehicle is 15 degrees and the overlap is 35 percent on the driver side of the vehicle[3]. The RMDB's mass is 2490.7 kg (5491 lb.).

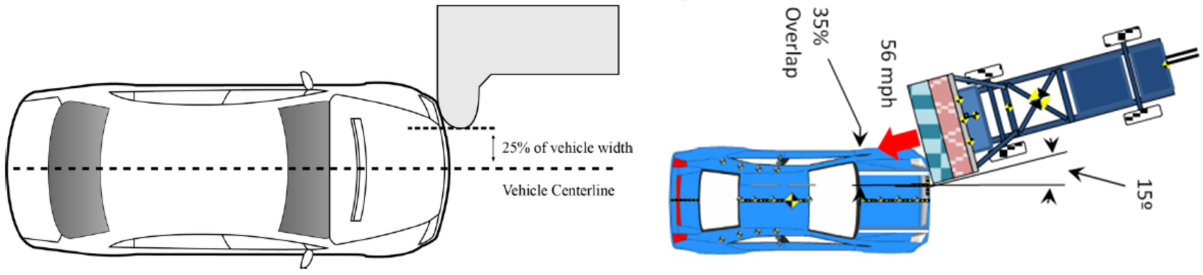


*(a) IIHS Small Overlap* *(b) NHTSA RMDB*

***Figure1. Scheme of IIHS Small Overlap and NHTSA RMDB.***

The hybrid III frontal crash test dummy is developed at 1970's and the development of an advanced frontal crash test dummy with improved biofidelity under frontal impact conditions and with expanded injury assessment capabilities is needed. Under these circumstances, in 2001 an advanced frontal crash test dummy THOR (Test Device for Human Occupant Restraint) - Alpha version was developed in the United States[4]. After the THOR Alpha, later upgraded to the THOR-NT in 2005. A modification package ("Mod Kit") intended to enhance the biofidelity, repeatability, durability, and usability of the THOR was introduced in 2011 and installed as an upgrade kit on the NHTSAowned fleet of THOR-NT ATDs[5]. Recent research showed that THOR dummy injury measures are closer to those of the post mortem human surrogates (PMHS) than the Hybrid III By continuous improvement of THOR dummy[6]. Comparing responses of the THOR and the Hybrid III with the same conditions, the upper body of the THOR moved forward more, compared to the Hybrid III, and the torsion about the z-axis was also larger than the Hybrid III. As a result, the head acceleration of the THOR and the Hybrid III showed different responses. NHTSA Oblique RMDB crash tests included an anthropomorphic test device (ATD) seated in the driver (near-side) and passenger(far-side) position. These ATDs are a 50$^{th}$ percentile male THOR. Due to the test configuration of NHTSA Oblique RMDB, both side occupants responses in NHTSA's tests showed rotational head velocities and resulted in high risk of brain injury. Rotational motion of the head can cause the brain injury and rotational kinematics experienced by the head may cause axonal deformations large enough to induce their functional deficit[7].

## OBJECTIVES

The objectives of this study are:

1. Estimate the CAE simulation method of the oblique RMDB test for correlation refer to the dummy kinematics and the brain injury comparision between CAE result and test data.
2. Compare the dummy injury responses between THOR and Hybrid III in Oblique RMDB tests.
3. Estimate the sensitivity of the brain injury to different parameters of airbag .

## METHODOLOGY

A correlated NHTSA NCAP model was used to build a NHTSA oblique RMDB baseline model. Modeling method for RMDB occupant analysis was constructed using both deceleration method and rigid body motion method as shown in Figure 2. The deceleration method is commonly used modeling method for FMVSS208 and NHTSA NCAP. The rigid body motion method is constructed by using the test motion of the tested vehicle. Structural intrusion data was extracted from a full vehicle test. The vehicle intrusion at struck side during test was used to replicate the vehicle test and to correlate the low extremity injuries and dummy kinematics. Hybrid III 50th percentile dummy was used first as a driver and a passenger occupants in order to compare the injury responses of THOR and Hybrid III dummy. This model used driver side airbag, passenger side airbag, curtain airbag, retractor and pre-tensioner as a restraint system.

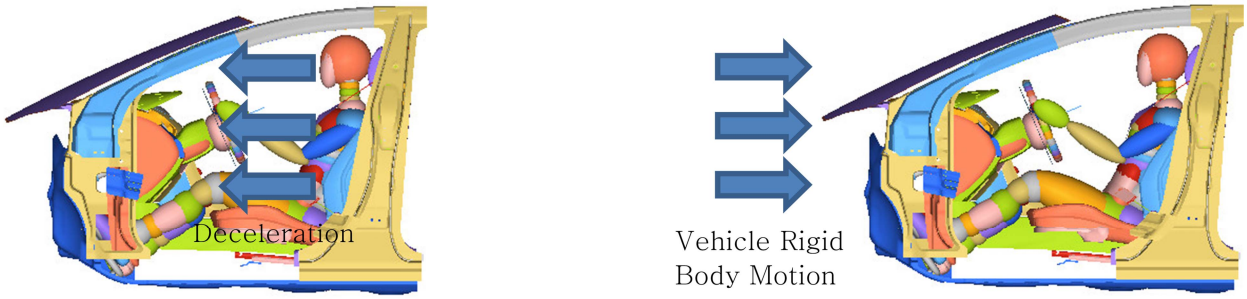


***Figure2. Occupant Simulation Modeling Methods for RMDB.***

Both baseline models used for this study demonstrated good correlation with NHTSA Oblique RMDB test. Validation index is unique index for evaluating the injury correlation rating of CAE model. Validation indices for the deceleration method and the rigid body motion method are 89 and 90 points respectively. This means both modeling methods give the similar injury response in peak and phase. For NHTSA Oblique RMDB test condition, occupant kinematics of the rigid body motion method showed better correlation with the test. This occupant kinematic correlation is shown in Figure 3.

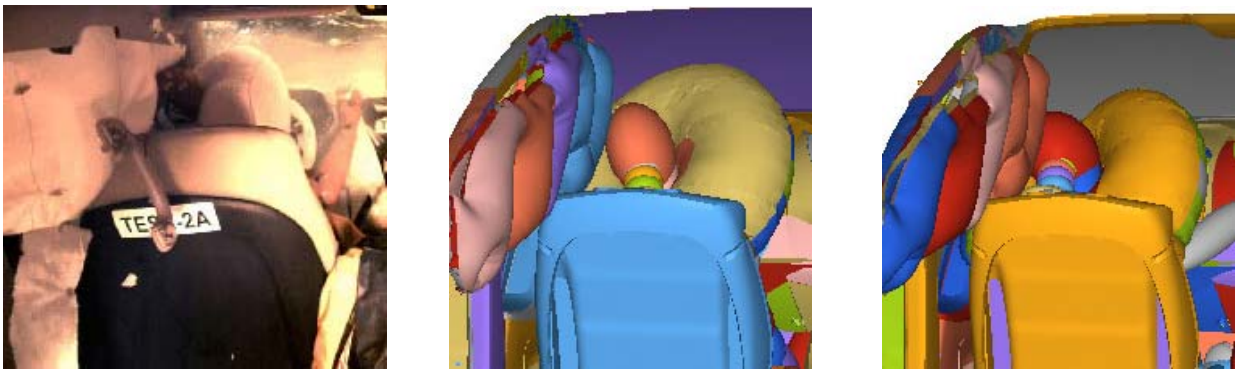

***(a) Test*** ***(b) Simulation w/Deceleration*** ***(c) Simulation w/Rigid Body Motion***

***Figure3. Dummy Kinematics.***

With this correlated model using the rigid body motion method, further study was conducted in order to understand the injury trends and occupant kinematics with variation of parameters. The passenger side occupant kinematics of the rigid body motion method showed good correlation with the test in Figure 4.

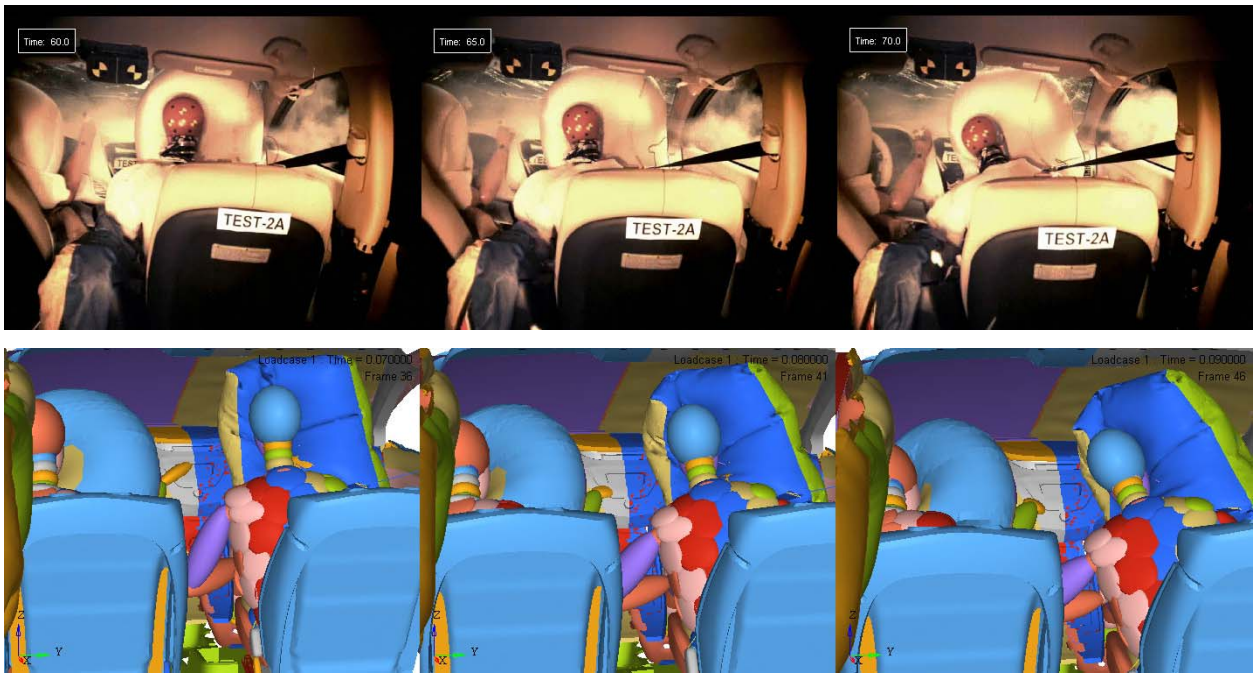


*Figure4. Comparison of Passenger Dummy Kinematics between Test and Simulation.*

**RESULTS**

This study evaluated the kinematic and the brain injury responses of a THOR and the 50th percentile Hybrid III in the NHTSA Oblique RMDB frontal impact condition. The 50th percentile Hybrid III dummy is replaced by the THOR in the baseline model and then compared with the test results and the injury tendency. It was observed from the CAE simulation result data that the brain injury of the THOR dummy tended to increase about 30~51% with respect to the Hybrid III dummy. Figure 5 compares injuries for THOR dummy and Hybrid II dummy. BrIC values were higher for THOR dummy in both driver and passenger. This increasing tendency of the brain injury is also observed in the tests. The differences of neck joints between THOR dummy and Hybrid III dummy caused the increasing of the BrIC.

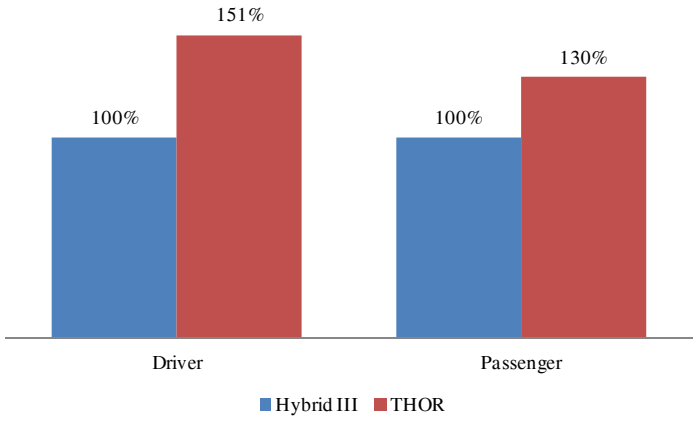


*Figure5. BrIC Response of THOR and Hybrid III*

The purpose of this parameter study was to understand the effectiveness of the restraint system based on airbag's internal pressure. To achieve this, airbag's outer vent was varied at every 5 mm step.

Figure 6 compares internal pressure and BrIC for various vent hole size. Outer vent hole size variation analysis showed that as internal pressure decreased, BrIC is increased. Head X travel and Y rotational velocity were increased with decrease in internal pressure level of DAB. Since DAB's reaction force was reduced, it allowed dummy head and chest to travel farther increasing the dummy's forward movement.

From the internal pressure analysis of PAB, it was observed that with decrease in internal pressure level of PAB, BrIC was decreased slightly. It was seen at the lowest level of BrIC for 60mm outer vent. The lower internal pressure result in decreasing Z rotational velocity of the passenger's head.

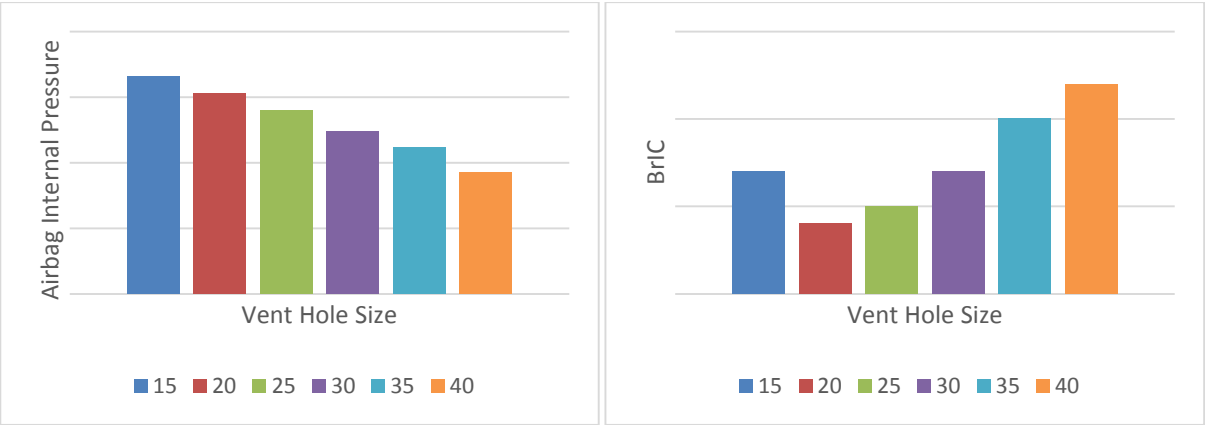


***Figure6. Driver BrIC w.r.t Outer Vent Size.***

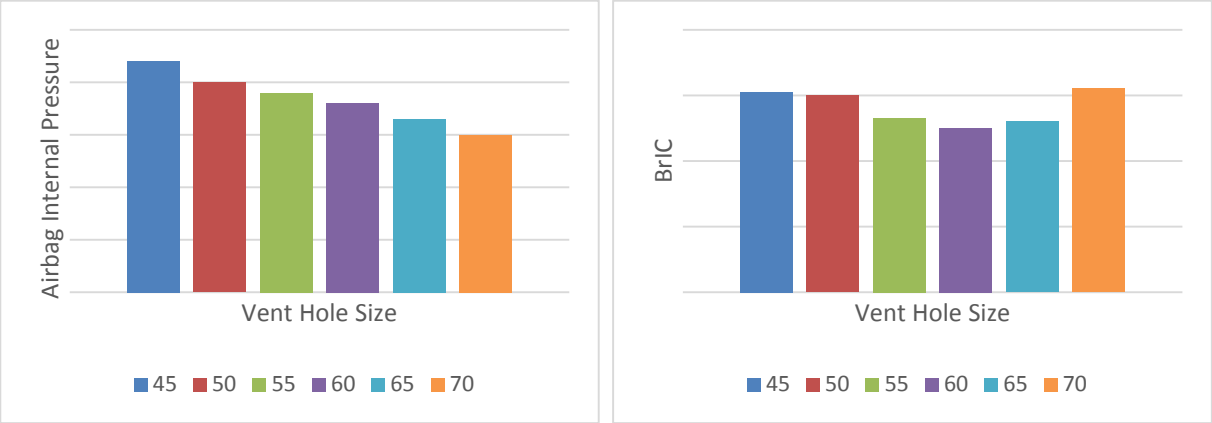


***Figure7. Passenger BrIC w.r.t Outer Vent Size.***

## CONCLUSIONS

1. For dummy injury response, there is slight difference between the deceleration method and the rigid body motion method. The rigid body motion method for CAE modeling gives better correlation in dummy kinematics with the test both driver side and passenger side occupants.

2. It was observed from CAE simulation result data that the brain injury of the THOR dummy tended to increase about 30~51% with respect to the Hybrid III dummy. This increasing tendency of the brain injury is also observed in the tests.
3. Head rotational velocity depends on the internal pressure of the airbag, the pressure stratage should be used for major component of BrIC. The strategy for achieving highest injury rating in NHTSA NCAP should be modified to meet the NHTSA Oblique RMDB BrIC requirements.

**REFERENCES**

[1] Bean, J., Kahane, C. K., Mynatt, M., Rudd, R. W., Rush, C. J. and Wiacek, C. 2009. "Fatalities in Frontal Crashes Despite Seat Belts and Air Bags- Review of All CDS Cases- Model and Calendar Years 2000-2007 – 122 Fatalities." Report No. DOT HS 811 102. US DOT, Sept. 2009.

[2] Saunders, J., Craig, M. and Parent, D. 2012. "Moving Deformable Barrier Test Procedure for Evaluating Small Overlap/Oblique Crashes." SAE World Congress, Paper No. 2012-01-0577.

[3] Saunders, J. and Parent, D. 2013. "Assessment of an Oblique Moving Deformable Barrier Test Procedure." Paper No.: 13-0402, 23rd ESV Conference, Seoul, Korea.

[4] Haffner M., Eppinger R., Rangarajan N., Shams T., Artis M., Beach D. 2001. "Foundations and Elements of the NHTSA THOR Alpha ATD Design," Proceedings of the 17th International Technical Conference on the Enhanced Safety of Vehicles.

[5] Daniel P. Parent, Matthew Craig, Stephen A. Ridella, Joseph D. McFadden. 2013. ), "Thoracic Biofidelity Assessment of the THOR mod kit ATD", Paper No.: 13-0327, 23rd ESV Conference, Seoul, Korea.

[6] Greg Shaw, David Lessley, Joe Ash, Jeff Crandall and Dan Parent. 2013. "Response Comparison for the Hybrid III, THOR Mod Kit with SD-3 Shoulder, and PMHS in aSimulated Frontal Crash" Paper No.: 13-0130, 23rd ESV Conference, Seoul, Korea.

[7] Erik G. Takhounts, Matthew J. Craig, Kevin Moorhouse, Joe McFadden and Vikas Hasija. 2013. "Development of Brain Injury Criteria (BrIC)" Stapp Car Crash Journal, Vol. 57, 243-266

# RELIABILITY IMPROVEMENT NEEDED IN THE EYE GLANCE MEASUREMENT USING DRIVING SIMULATOR TEST

**Mikael Ljung Aust**
**Annie Rydström**
**Robert Broström**
**Trent Victor**
Volvo Car Corporation
Sweden

Paper Number 15-0398

## ABSTRACT

To improve the interface design of in-vehicle infotainment systems, robust evaluation methods are required. The Eye Glance measurement using Driving Simulator test (EGDS) defined in the Visual-manual NHTSA Driver Distraction Guidelines for in-Vehicle Electronic Devices is a promising candidate. However, the present study indicates that EGDS needs further refinement to become sufficiently robust. When two randomly selected groups of 24 drivers tested the same ten in-vehicle tasks following the EGDS protocol, test outcomes were not the same for the two groups. The analysis showed this to be a consequence of how the EGDS pass/fail criteria are calculated. As currently formulated, they make test outcomes highly dependent on between-driver variability. To assess the problem magnitude with repeated EGDS testing, another eight virtual test groups were created by for each group randomly selecting 24 of the 48 participants' test scores. The analysis showed that EGDS outcomes were 60 % consistent between these ten groups. While six tasks consistently passed or failed, the outcome for the other four depended on which group had tested them. This EGDS reliability problem could possibly be overcome by matching the criteria calculation principles to the underlying population variability.

## INTRODUCTION

Naturalistic driving studies indicate that looking away from the forward roadway for more than a certain period of time is a key crash contributing factor (Dingus et al, 2006; Klauer et al, 2006; Victor and Dozza, 2011; Liang et al, 2012). This fact, combined with the societal transition towards ubiquitous use of information technology, has put driver distraction on top of the traffic safety agenda.

From a vehicle design point of view, many potential sources of distraction such as eating, drinking and interacting with passengers lie outside the vehicle manufacturers' influence. However, they do control the design of all in-vehicle systems that involve visual-manual interaction while driving. To guide the design of these system, several design guidelines have been published. These include the European Statement of Principles (European Commission, 2008), the JAMA guidelines (JAMA, 2004) and the Alliance of Automobile Manufacturers guidelines (AAM, 2006).

These guidelines are sometimes difficult to apply, because while they may propose thresholds that in-vehicle tasks need to meet to be allowed while driving, they rarely propose methods for testing task compliance with those thresholds. For example, the AAM guidelines (AAM, 2006) suggest that each visual-manual task should require less than 2 seconds in mean glance duration and maximum 20 seconds total eyes off-road time, but there is no associated test method.

The latest addition, i.e. the Visual-manual NHTSA Driver Distraction Guidelines for in-Vehicle Electronic Devices (NHTSA, 2013), departs from the above tradition. It specifies both specific performance criteria against which in-vehicle tasks should be evaluated as well as specific test methods for testing criteria compliance. This paper is focused on the Eye Glance Measurement Using Driving Simulator Test Procedure, or EGDS (NHTSA, 2013). In EGDS, 24 randomly recruited test participants drive a lead vehicle following scenario on the highway while performing the in-vehicle tasks under evaluation. Their off-road glance durations during task performance are measured and assessed against the following Acceptance Criteria (AC), (NHTSA, 2013):

- *AC1: For at least 21 of the 24 test participants, no more than 15 percent (rounded up to the next whole number) of each participant's total number of eye glances away from the forward road scene have durations of greater than 2.0 seconds while performing the testable task one time.*

- *AC2: For at least 21 of the 24 test participants, the mean duration of all eye glances away from the forward road scene is less than or equal to 2.0 seconds while performing the testable task one time.*

- *AC3: For at least 21 of the 24 test participants, the sum of the durations of each individual participant's eye glances away from the forward road scene is less than or equal to 12.0 seconds while performing the testable task one time.*

If the tested task does not fulfil AC1-AC3, it should not be accessible while driving.

The publication of the NHTSA guidelines is very timely and will drive certainly drive vehicle safety forward. However, when looking closer into EGDS in its current formulation, there are indications that EGDS test outcomes may not be robust, i.e. that repeatability is low.

Two of the clearest indications come from two previous studies of off-road glance durations during interaction with in-vehicle tasks. Both Ljung Aust et al (2013) and Broström et al (2013) found that a significant portion of the test participants in their studies exhibited traits in their off-road glance behaviour that, if prevalent in the driver population at large, would lead to non-robust outcomes when testing in-vehicle tasks with the EGDS method. Both predicted that test outcomes would depend more on who the randomly selected test participants happened to be, rather than on the design of the task being tested.

These study results can be explained in two ways. One is methodological differences. Since both studies differed in setup and sampling procedure from the protocol in EGDS, it is possible that methodological differences are driving the conclusions rather than problems with the EGDS criteria.

Another possible explanation is that it is the way in which the acceptance criteria are calculated that leads to low robustness. Support for this latter explanation comes from a peculiar property of how the criteria are set up. In a general human factors study context, EGDS can be characterized as a between-group methodology, i.e. a new group of test participants are recruited for each test condition (e.g. each new set of task to be tested).

In terms of statistics, between-group designs are typically analysed on a group level. The data points for each test group are averaged or treated in some other way before comparisons between groups are made. Moreover, the important step, where sophisticated statistical methods such as ANOVA are used, is to assess if a difference in mean group values is significant. This step normally includes assessing whether the variability in each groups' test data is small enough to conclude that the observed mean value difference makes the groups significantly different. However, the EGDS acceptance criteria neither make the assessment on the group level, nor judge the outcome dependent on sample variability. Criteria fulfillment is instead determined by counting the frequency of individual outcomes.

In itself, a frequency counting approach does not lead to low test repeatability, as long as the variability in the tested group(s) does not overlap with acceptance criteria thresholds. If the thresholds however do overlap with population variability, it becomes a very different story.

To illustrate the problem, assume you want to performance test the height of manufactured door frames, and that the acceptance criteria state that anybody up to 10 ft. tall should be able to pass through. With this threshold, any randomly selected group of test participants is suitable for the assessment of frame heights, because even though people's normal height variability is several ft., nobody comes near the threshold limit.

However, if the threshold is lowered to 6'2", the situation changes. Now, the tested door frame will fail if any person in the test group is taller than 6'2", and pass if nobody is. Under this threshold, who comes to the lab becomes crucially important for test outcome. Given random participant selection and peoples' normal height

variability, the same 6'2" frame would pass the acceptance criteria on some days and fail on others, despite being 6'2" all the time.

For off-road glance duration measurements, there seems to exist a conceptual equivalent to tall people in the door frame example above. These drivers, aptly named "long glancers" (Broström et al, 2013), are ones who in general take their time in each step of an in-vehicle task interaction, quite independently of which task they are performing. Since long glancers were found to often look away for more than 2.0 seconds when doing in-vehicle tasks, and the current EGDS thresholds are set at 2.0 seconds, Broström et al (2013) predicted that the relative prevalence of such "long glancers" in an EGDS test group would have a large influence on the outcome. Essentially, if there are 4-5 long glancers in a test group of 24, any tested task tested would likely fail, regardless of how well designed it was.

Other studies also indicate that long glancers exist, and that their typical off-road glance durations overlap with EGDS criteria. One on-road study found that older drivers often glanced at the task display for more than 2 seconds at a time when doing in-vehicle tasks (Wikman and Summala, 2005). Donmez et al (2010) found in a simulator study that drivers could be divided into three visual strategy clusters where the "high risk cluster" looked away from the road for the longest periods, with mean off-road glance duration values over 1.6 seconds. Recently, Rydström et al (Rydström, 2015) found that when comparing two different groups of 24 randomly selected test participants performing the same ten tasks following the EGDS protocol in detail, the between group outcome was similar for less than half the tested tasks.

In light of the above, the first aim of the current study was to assess whether there exists an overlap between EGDS criteria thresholds and normal off-road glance duration variability when EGDS tests are performed fully according to the specified protocol (NHTSA, 2013). In addition, if an overlap was found, a second aim was to examine what level of robustness could be expected if the EGDS method would be used to assess 10 identical vehicles.

## METHODOLOGY

Two full EGDS tests were performed at the test facilities of Ergoneers GmbH in Manching, Germany. A total of 48 participants, i.e. two test groups of 24 persons each, were recruited in the area around Manching in Germany. Each sample conformed to the EGDS recommendations (NHSTA, 2013) regarding general criteria, participant impartiality, age mix and gender balance.

### Equipment

The test was conducted in an Ergoneers Sim-Lab left-hand drive, fixed base and open cab driving simulator (Figure 1). The simulator is designed as a replica of an actual production vehicle and was adapted to the EGDS driving simulator recommendations.

***Figure 1: The Ergoneers Sim-Lab driving simulator***

Participants drove a lead vehicle following scenario on an undivided, four lane, highway with a speed limit of 50 mph. The Ergoneers Dikablis head mounted eye tracking system was used to record participants' eye

movements. A touch-screen tablet containing a prototype infotainment system was mounted at the center panel of the simulator. Tasks 1-9 (see below) were performed on the tablet. An additional, conventional Panasonic car stereo was also installed to test the AAM radio manual tuning reference task (AAM, 2006).

**Tasks performed**

The prototype infotainment system was designed to replicate a typical in-vehicle center stack interface. Nine basic tasks were selected for assessment, and a manual radio tuning reference task was added to test a conventional car stereo (see Table 1).

***Table1: Descriptions of the ten tasks used in the two EGDS tests***

| Task no. | Task | Task description |
|---|---|---|
| 1 | Activate vehicle function | Access menu and activate a specific vehicle function (on/off option) |
| 2 | Activate USB | Access menu and activate USB |
| 3 | Set new destination | Access navigation menu and activate a search field and tap in a destination of 10 characters and start guidance |
| 4 | Set favorite destination | Access navigation menu and a favorite menu, choose a specific destination and start guidance |
| 5 | Select and play music from USB | Access menu and activate USB and find a specified song in a list |
| 6 | Call contact from recent calls list | Access phone menu and recent calls list and choose a specified contact in the list to call |
| 7 | Dial known phone number manually | Access phone menu and keypad and tap in a well known 10 digit phone number and call |
| 8 | Change temperature | Access climate and increase temperature with 2 degrees |
| 9 | Set seat heat | Access seat heat and set it to a mid-level |
| 10 | AAM reference task - Manual radio tuning | Access FM1 and adjust to 106.7 (starting position FM3, preset 97.4) |

**Procedure**

The test procedure, including test participant training, followed the EGDS protocol (NHTSA, 2013). Upon arriving to the test facilities, participants were given a brief description on the test procedure and asked to fill in a consent form, as well as a demographic questionnaire. Then they were asked to sit down in the simulator and adjust the seat. Next they put on the eye tracking glasses, and the eye tracking system was calibrated. The user interface and tasks were demonstrated to the participants and they were then instructed to practice each task as many times as they wanted to. Next, participants were given instructions on how to drive in the driving scenario, and got to practice driving it. When they felt comfortable driving, they got to practice performing the ten tasks while driving, as many times as they felt they needed. After training, data collection began. All tasks started from a home screen view, and ended when the task had been correctly executed.

**Glance data analysis**

After data collection was completed, the durations of all off-road glances for each test person during each task were calculated. This data set was then analysed to assess its basic properties and variability.

**Acceptance test robustness analysis**

To contextually frame the robustness analysis, it was assumed that NHTSA may test 10 vehicles in 2017, when the guidelines come into effect. Thus, a procedure was employed where 24 out of the 48 test participants from the current study were randomly selected using Matlab's random function to form a "virtual test group". The virtual test group essentially represents what the test outcome would have been if another combination of the 48 participants than the actual two is study had happened to been selected. The random selection of 24 participants was repeated 8 times, thus generating 8 virtual test groups in addition to the two real test groups.

Outcomes on the acceptance criteria were then evaluated for all 10 groups (the two real plus the eight virtual). Since the tested tasks were identical for all groups, this corresponds to a situation where 10 different test groups are brought in to evaluate the same vehicle 10 times over. Following the above example, this would correspond to NHTSA testing 10 vehicles with identical infotainment systems installed. For a method with high repeatability, one would expect very similar outcomes between all groups under these conditions.

**RESULTS**

The off-road glance duration distributions for the two tested groups are quite similar, as can be seen in Figure 2 below.

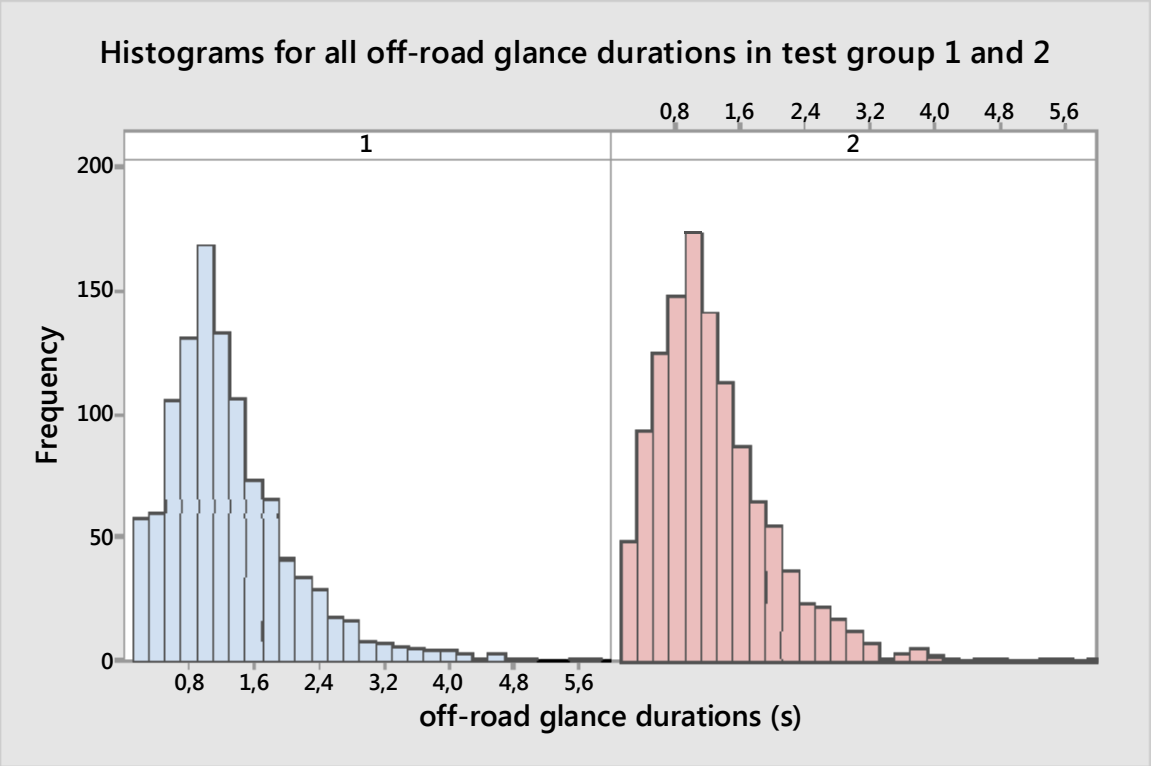


*Figure 2: The histograms for the two groups show that they have similar off-road glance duration distributions*

The glance duration data is also similar for the two groups in terms of means and standard deviations (Table 2).

*Table 2: Means and standard deviations for off-road glance durations in the two groups*

| Group | Nr of glances | Mean | StDev |
|---|---|---|---|
| 1 | 1085 | 1,3211 | 0,9023 |
| 2 | 1187 | 1,2605 | 0,7833 |

From Table 2, it is clear that the variability in the dataset overlap with the EGDS 2.0 second limits, since that lies within one standard deviation for both test groups.

The standard deviation indicates that the variability has a quite wide span. This is captured in Figure 2, which shows the average off-road glance duration value across all tasks for each test participant. As can be seen, the drivers with the shortest mean glance durations have values well below 1.0 second, while those with the longest are above 2.0 seconds.

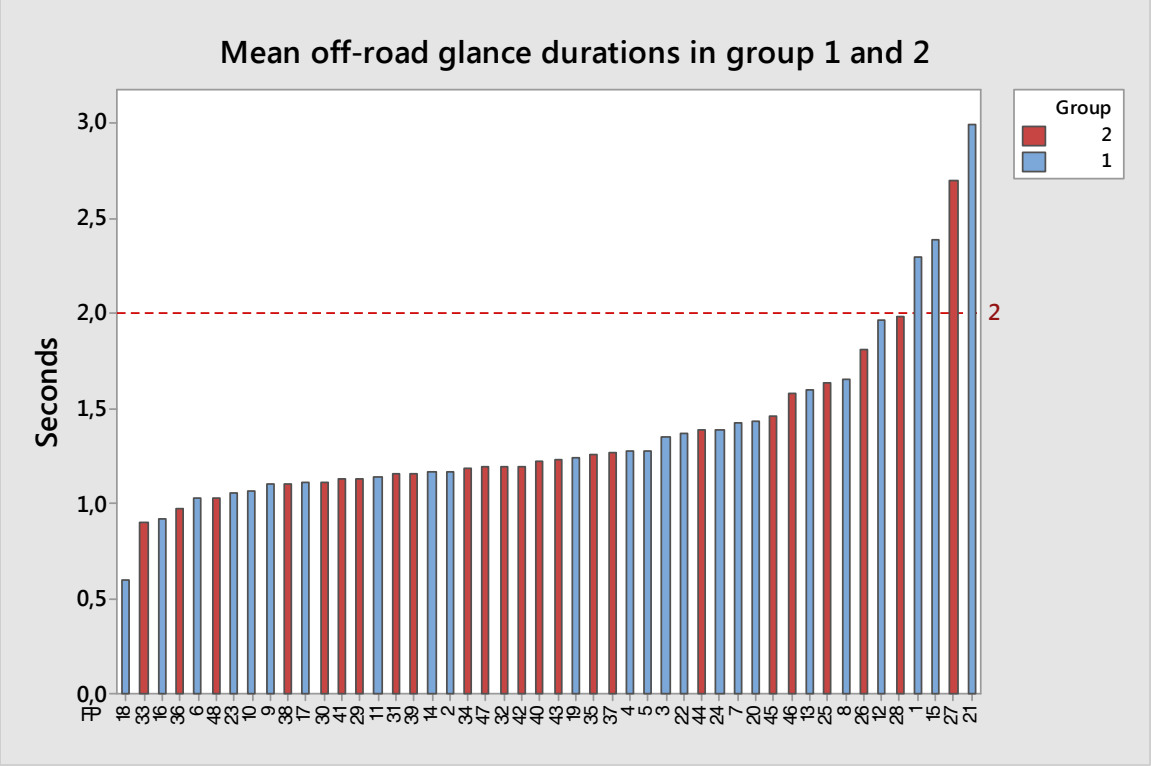


*Figure 3: Mean off-road glance durations across all tasks for each test person, ranked according to duration. The reference line indicates the 2.0 s threshold in EGDS.*

The performance outcome on the acceptance criteria for the two real test groups (RG1 and RG2) and the eight re-sampled groups (VG1-8) are shown in Table 3.

The results in Table 3 illustrate that the 10 tasks used in the study spans the whole range from difficult to simple. Setting a new destination fails on every criteria in almost every test group, while setting the seat heat and activating USB pass on all criteria in all test groups. The task set selected for this study thus seem to cover a relevant span for a reliability analysis.

Table 3 also indicates that testing with the EGDS method as currently formulated is not robust. For AC1, the outcome is inconsistent for 5 of 10 tasks. For AC2, the outcome is inconsistent for 7 of 10 tasks. For AC3, the outcome is inconsistent for 2 of 10 tasks.

When all three acceptance criteria are jointly considered on a per task basis, the inconsistencies remain. If the results of Table 3 were applied to the hypothetical test of 10 vehicles with identical infotainment systems in 2017 conjectured above, six tasks would consistently be allowed or prohibited while driving, while for the other four, it would depend on the group of test participants that tested them. Thus, the EGDS criteria yield 60 % consistency between groups in testing.

| | | Activate vehicle function | Activate USB | Set a new destination | Set a favorite destination | Select and play music from USB | Call contact from recents list | Dial known phone number manually | Change temp. | Set seat heat | AAM ref task: Manual radio tuning |
|---|---|---|---|---|---|---|---|---|---|---|---|
| **AC1 For each driver, max 15% glances > 2.0 s** | RG1 | 2 | 3 | 8 | 2 | 8 | 3 | 11 | 6 | 1 | 5 |
| | RG2 | 3 | 1 | 10 | 4 | 6 | 4 | 10 | 2 | 0 | 3 |
| | VG1 | 2 | 0 | 8 | 3 | 7 | 2 | 6 | 3 | 0 | 3 |
| | VG2 | 2 | 2 | 7 | 3 | 7 | 5 | 10 | 4 | 1 | 4 |
| | VG3 | 2 | 3 | 7 | 0 | 5 | 4 | 9 | 4 | 0 | 3 |
| | VG4 | 2 | 1 | 7 | 4 | 4 | 2 | 7 | 3 | 1 | 4 |
| | VG5 | 4 | 2 | 7 | 4 | 10 | 5 | 10 | 5 | 1 | 5 |
| | VG6 | 2 | 2 | 8 | 2 | 5 | 2 | 9 | 3 | 1 | 2 |
| | VG7 | 1 | 3 | 7 | 3 | 9 | 3 | 9 | 4 | 1 | 4 |
| | VG8 | 4 | 2 | 7 | 4 | 8 | 3 | 9 | 5 | 1 | 7 |
| | | | | | | | | | | | |
| **AC2 For each driver, mean glance duration < 2.0 s** | RG1 | 2 | 3 | 6 | 6 | 6 | 4 | 9 | 6 | 1 | 2 |
| | RG2 | 3 | 1 | 4 | 2 | 3 | 3 | 3 | 2 | 0 | 1 |
| | VG1 | 2 | 0 | 4 | 1 | 4 | 1 | 2 | 1 | 0 | 0 |
| | VG2 | 2 | 2 | 4 | 3 | 5 | 6 | 7 | 4 | 0 | 0 |
| | VG3 | 2 | 2 | 4 | 3 | 2 | 3 | 5 | 4 | 0 | 2 |
| | VG4 | 2 | 1 | 2 | 1 | 2 | 3 | 4 | 3 | 1 | 2 |
| | VG5 | 3 | 3 | 6 | 5 | 6 | 4 | 7 | 5 | 1 | 2 |
| | VG6 | 2 | 2 | 2 | 2 | 4 | 2 | 5 | 3 | 1 | 0 |
| | VG7 | 1 | 3 | 5 | 5 | 5 | 4 | 6 | 4 | 1 | 1 |
| | VG8 | 4 | 3 | 5 | 3 | 6 | 4 | 7 | 5 | 1 | 2 |
| | | | | | | | | | | | |
| **AC3 For each driver, total glance time < 12.0 s** | RG1 | 0 | 0 | 9 | 0 | 3 | 0 | 3 | 0 | 0 | 12 |
| | RG2 | 0 | 0 | 13 | 0 | 1 | 0 | 3 | 0 | 0 | 16 |
| | VG1 | 0 | 0 | 11 | 0 | 1 | 0 | 5 | 0 | 0 | 10 |
| | VG2 | 0 | 0 | 7 | 0 | 2 | 0 | 3 | 0 | 0 | 11 |
| | VG3 | 0 | 0 | 13 | 0 | 1 | 0 | 1 | 0 | 0 | 17 |
| | VG4 | 0 | 0 | 13 | 0 | 3 | 0 | 4 | 0 | 0 | 15 |
| | VG5 | 0 | 0 | 8 | 0 | 3 | 0 | 3 | 0 | 0 | 13 |
| | VG6 | 0 | 0 | 11 | 0 | 4 | 0 | 3 | 0 | 0 | 13 |
| | VG7 | 0 | 0 | 12 | 0 | 3 | 0 | 4 | 0 | 0 | 14 |
| | VG8 | 0 | 0 | 9 | 0 | 3 | 0 | 1 | 0 | 0 | 14 |

*Table 1: Outcome on the EGDS acceptance criteria for the two real and eight virtual test groups*

## DISCUSSION

The first aim of the current study was to assess whether an overlap between EGDS thresholds and normal off-road glance duration variability is present when EGDS tests are performed fully according to protocol (NHTSA, 2013). The results show that an overlap does exist.

Both Broström et al (2013) and Ljung Aust et al (2013) found that off-road glance lengths when performing in-vehicle tasks while driving were quite individual and task independent, i.e. the between driver variability on the

glance metrics was much larger than the within driver variability. The results in Figure 3 show this to be the case also in the current study. While the drivers with the shortest mean values are well below 1.0 seconds, those with the longest are well above 2.0 seconds.

Since the present study followed the proscribed EGDS procedure in detail, this indicates that this is not an artefact of the test set up, which one possible explanation for the Broström et al (2013) and Ljung Aust et al (2013) results. Rather it seems to be attributable to properties of the tested population. In other words, drivers seem to have their own, personal, pace by which they performed in-vehicle tasks while driving, and this is reflected in how long their off-road glances are.

As Figure 3 illustrates, for some drivers this individual pace result in off-road glance durations that make them prone to fail on acceptance criteria 1 and 2 regardless of which task is being tested. The likelihood of a task passing the EGDS test thus becomes highly dependent on how many long glancers happen to be included in the participant sample.

The second aim of this study was to examine what the effect of the overlap would be on a series of EGDS tests. Here, it was found that the effect was substantial. On a per task level, EGDS was only 60 % consistent between test groups, which seems low for a test meant to determine which in-vehicle tasks should be allowed while driving.

However, reliability levels could probably be improved with only minor alterations to EGDS. The current study illustrates that there is a mismatch between how the EGDS criteria are currently calculated and the underlying population variability. This mismatch could potentially be resolved by using other approaches than a frequency count to calculate criteria fulfilment. For example, one could study what reliability level is reached if thresholds are calculated on a group mean level, perhaps with additional thresholds determined by standard deviations. This is an urgent topic for future research.

A limitation of the current study is that it only involves two test groups, so more studies are naturally needed. Another limitation is that the re-sampling used to construct the 8 virtual test groups may lead to underestimation of observed variability. However, since this would lead to an over- rather than underestimation of robustness, the above method reliability analysis is likely a conservative one.

**REFERENCES**

Alliance of Automobile Manufacturers. 2006. “Statement of Principles, Criteria and Verification Procedures on Driver-Interactions with Advanced In-Vehicle Information and Communication Systems”, Driver Focus-Telematics Working Group, Washington, DC., June 26, 2006 update.

Broström, R., Bengtsson, P., & Axelsson, J. (2011). Correlation between safety assessments in the driver–car interaction design process. *Applied Ergonomics, 42(4)*, 575-582.

Broström, R., Ljung Aust, M., Wahlberg, L., & Källgren, L. (2013). What drives off-road glance durations during multitasking – capacity, practice or strategy? In *3rd International Conference on Driver Distraction and Inattention*. Gothenburg, Sweden.

Dingus, T.A., Klauer, S.G., Neale, V. L., Petersen, A. et al. 2006. “The 100-Car Naturalistic Driving Study, Phase II – Results of the 100-Car Field Experiment.” Cambridge: U.S. Department of Transportation, John A. Volpe National Transportation Systems Center.

Donmez, B., Boyle, L. N., & Lee, J. D. (2010). Differences in Off-Road Glances: Effects on Young Drivers’ Performance. *Journal of Transportation Engineering*, *136*(5), 403–409. doi:10.1061/(ASCE)TE.1943-5436.0000068

European Commission. 2008. “Commission Recommendation of 26 May 2008 on Safe and Efficient In-Vehicle Information and Communication Systems; Update of the European Statement of Principles on Human-Machine Interfaces.”

JAMA. 2004. “Guideline for In-Vehicle Display Systems, Version 3.0”. Japan Automobile Manufacturers Association, Tokyo, Japan, August 2004.

Klauer, S. G., Dingus, T. A., Neale, V. L., Sudweeks, J., & Ramsey, D. J. 2006. “The impact of driver inattention on near-crash/crash risk: An analysis using the 100-Car Naturalistic Driving Study data.” Blacksburg, VA: Virginia Tech Transportation Institute, 2006.

Liang, Y., Lee, J.D., Yekhshatyan, L. 2012. “How dangerous is looking away from the road? Algorithms predict crash risk from glance patterns in naturalistic driving”. Published online before print, *Human Factors: The Journal of the Human Factors and Ergonomics Society*, June 15, 2012.

Ljung Aust, M., Dombrovskis, S., Kovaceva, J., Svanberg, B. & Ivarsson, J. (2013) “An Empirically Based Suggestion for Reformulating the Glance Duration Criteria in NHTSA's Visual-Manual Interaction Guidelines”, in the proceedings of SAE 2013 World Congress, 15-18 April, Detroit, USA. Paper no 2013-01-0444.

Rydström, A., Ljung Aust, M., Broström, .R., & Victor, T. (2015) Repeatability of the NHTSA Visual-Manual Guidelines Assessment Procedure, paper nr 15-0240, ESV 2015.

Victor, T. and Dozza, M. “Timing matters: Visual behavior and crash risk in the 100-Car online data”. Presentation given at the 2nd International Conference on Driver Distraction and Inattention, Gothenburg, Sweden, Sept 5-7, 2011. Accessed 120125 at http://www.chalmers.se/safer/ddi2011-en/

Wikman, A., & Summala, S. (2005) Aging and Time-Sharing in Highway Driving. Optometry and Vision Science, 82, 716-723.

Visual-manual NHTSA Driver Distraction Guidelines for in-Vehicle Electronic Devices (2013). Docket no. NHTSA-2010-0053, National Highway Traffic Safety Administration, April 2013.

# Probabilistic Prediction based Automated Driving Control in Urban Traffic Situation

**Junyung Lee[1], Jongsang Suh[1], Dongwook Kim[1], Kyuwon Kim[1], Boemjun Kim[1], Inseong Choi[2], Kyongchan Min[2], and Kyongsu Yi[1]**
[1]School of Mechanical and Aerospace Engineering, Seoul National University
599 Gwanangno, Gwanak-Gu, Seoul, 151-742, Korea
[2]Korea Automobile Testing & Research Institute, Korea Transportation Safety Authority
Korea

Paper Number 15-0402 (same as abstract ID provided by MIRA)

## ABSTRACT
This paper represents an automated driving control algorithm in urban traffic situation. In order to achieve a development of a highly automated driving control algorithm in urban environments, the research issues can be classified into two things. One of the issues is to determine a safe driving envelope with the consideration of probable risks and the other is to achieve robustness of control performance under disturbances and model uncertainties. While human drivers maneuver a vehicle, they determine appropriate steering angle and acceleration based on the predictable trajectories of the surrounding vehicles. Therefore, not only current states of surrounding vehicles but also predictable behaviors of surrounding vehicles and potential obstacles should be considered in designing an automated driving control algorithm. In order to analyze the probabilistic behaviors of surrounding vehicles, we collected driving data on a real road. Then, in order to guarantee safety to the possible change of traffic situation surrounding the subject vehicle during a finite time-horizon, the safe driving envelope which describes the safe driving condition over a finite time horizon is defined in consideration of probabilistic prediction of future positions of surrounding vehicles and potential obstacles. Since an automated driving control algorithm is required to operate in a wide operating region and limit the set of permissible states and inputs, a model predictive control (MPC) approach has been used widely in designing an automated driving control algorithm. MPC approach uses a dynamic model of the vehicle to predict the future states of the system and determines optimal control sequences at each time step to minimize a performance index while satisfying constraints based on the predicted future states. Since the solving nonlinear optimization problem has computational burden, we design an architecture which decides a desired steering angle and longitudinal acceleration parallel to reduce the computational load. For the guarantee of the robustness of control performance, a robust invariant set is used to ensure robust satisfaction of vehicle states and constraints against disturbances and model uncertainties. The effectiveness of the proposed control algorithm is evaluated by comparing between human driver data and proposed algorithm.

## I. Introduction
Recently, the interest of automotive industry changes from the passive safety system to the active safety system and, by extension, automated driving system due to advances in sensing technologies. For example, active safety applications, such as vehicle stability control (VSC), adaptive cruise control (ACC), lane keeping assistance (LKA) and lane change assistance (LCA) system, have been extensively researched [1]. In order to enhance safety and achieve zero fatalities, many researches have been undertaken to integrate individual active safety systems for the development of an automated driving system [2].
In developing an automated driving system which is required to operate in a wide operating region and limit the set of permissible states and inputs, MPC approach has been used widely because of its capability to handle system constraints in a systematic way [3], [4]. MPC approach uses a dynamic model of the plant to predict the future states of the system and determines optimal control sequences at each time step to minimize a performance index while satisfying constraints based on the predicted future states [5]. The first term of this optimal control sequences is applied to the system. At next time step, new optimal control sequences is calculated over a shifted prediction horizon. In [6], Falcone et al. present a MPC based active steering controller for tracking the desired trajectory as close as possible while satisfying various constraints. In this research, it is assumed that the desired trajectory over a finite horizon is known. Erlien et al. use a safe driving envelope which means a safe region of states in which the system should be constrained [7]. In this research, the safe driving envelope consists of a stable handling envelope to ensure vehicle stability and an environmental envelope to constrain the position states for the collision avoidance. The environmental envelope is defined based on the current states of surrounding environment of the subject vehicle. In order to compensate the effect on the control performance by model uncertainties and exogenous

disturbances, robust MPC approach which adds a linear feedback control input to the nominal control inputs based on the analysis of robust invariant sets have been introduced and used to design an autonomous control algorithm [8].

In order to develop a highly automated driving system, the research issues can be classified into two things. One of the issues is to enhance safety under the possible change of the behaviors of neighboring vehicles in the future. Human drivers maneuver the vehicle predicting possible surrounding vehicle's trajectories. Therefore, not only current states of surrounding environment of the subject vehicle but also predicted behaviors of surrounding environment should be considered to control the vehicle autonomously [9]. Furthermore, since probable behaviors of surrounding vehicles should be considered to prevent a potential collision accident in the future, a probabilistic prediction is required [10]. The other issue in designing an automated driving system is to achieve robustness of control performance under disturbances and model uncertainties due to inaccurate or time varying parameters [6].

In this research, we focus on designing an automated control algorithm which handles probable risky situations due to the possible change of traffic situation surrounding the subject vehicle while satisfying a robust control performance with respect to model parameter uncertainties and exogenous disturbances. In order to enhance safety with respect to the potential behaviors of surrounding vehicles, a safe driving envelope which describes the safe driving condition over a finite time horizon is defined in consideration of probabilistic prediction of future states of surrounding environment. Then MPC problem is formulated to determine the desired steering angle and desired longitudinal acceleration while maintaining the subject vehicle into the safe driving envelope. A tube-based robust MPC approach is used to guarantee robust performance under model uncertainties and exogenous disturbances.

This paper is structured as follows: The overall architecture of the proposed automated driving control algorithm is described in Section II. In Section III, the lateral dynamics model for the determination of the desired steering angle and longitudinal dynamics model for the determination of the desired longitudinal acceleration are derived briefly. In Section IV, probabilistic prediction of surrounding vehicle behaviors and the description of the safe driving envelope is described briefly. Then the controller is designed based on robust MPC approach in Section V. Section VI shows the vehicle test results for the evaluation of the performance of the proposed algorithm. Then the contribution of this research and introduction of future works are summarized in Section VII.

## II. Overall Architecture

The overall architecture of the proposed automated driving control algorithm is shown in Fig. 1. In the integrated perception layer, the information which is required to determine the desired driving mode and safe driving envelope is refined using measurements from various sensors. In order to assess the driving situation precisely, states of the subject vehicle and surrounding vehicles should be estimated from various measurements via exterior sensors, such as vision and radar sensors. Then, the probable behaviors of the surrounding vehicles over a finite prediction horizon are predicted using the information of current states of surrounding vehicles. Using the estimated states of the subject vehicle and the ranges of probable behaviors of the surrounding vehicles over a finite prediction horizon, a desired motion or desired driving mode of the subject vehicle is determined in the risk management layer. Since the goal of the automated driving control algorithm proposed in this paper is to control the vehicle autonomously on the road, the required driving mode is classified into lane keeping and lane change mode. The desired driving mode is determined with the consideration of not only current states of traffic situation surrounding the subject vehicle but also predictable situations among the potential changes of traffic situation surrounding the subject vehicle. Then the safe driving envelope is determined based on the desired driving mode. Then the controller is designed to determine the desired steering angle and the desired longitudinal acceleration separately while satisfying reliability. Using robust MPC approach, the desired control inputs are determined to improve safety and ride comfort while satisfying constraints of states and inputs.

## III. Vehicle dynamics model

In order to obtain the desired control inputs separately based on MPC approach, the lateral dynamics model and longitudinal dynamics model should be derived. In this research, the lateral dynamics model is designed by combining the bicycle model and error dynamics with respect to a road. Furthermore, the longitudinal dynamics model is designed by integrating the inter-vehicle dynamics and longitudinal actuator's dynamics.

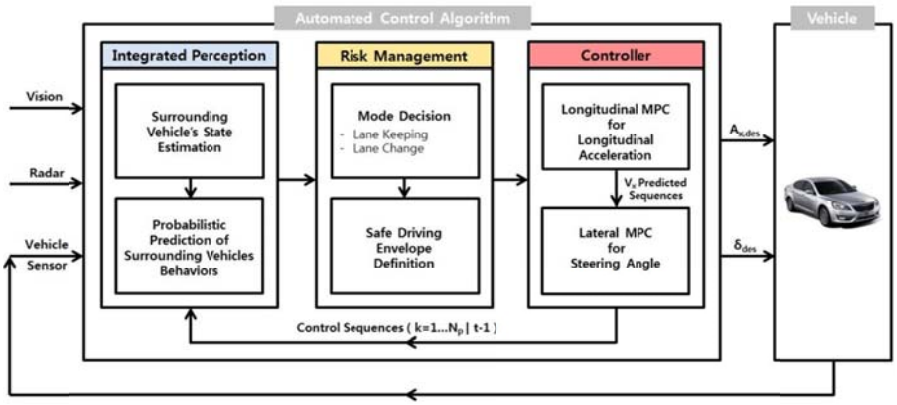


***Fig. 1 Overall architecture of the proposed automated driving control algorithm***

### *A.* Lateral dynamics model

A classic bicycle model is usually used to design a lateral control law [3]. However, since an automated driving system should operate in a wide operating region, a classic bicycle model which assumes small slip angles of tires could not be suitable as a predictive model. On the other hand, if we use a nonlinear tire model to build a dynamic model, a nonlinear optimization problem should be solved at each time step. However, a computational burden to solve a nonlinear MPC problem is a critical barrier for its implementation [6]. In order to cope with this drawback, we apply a saturated linear tire model to reflect a tire saturation characteristic [11]. Then the bicycle model could be modified as follows:

$$\begin{bmatrix}\dot{\beta}\\ \dot{\gamma}\end{bmatrix}=\begin{bmatrix}a_{11} & a_{12}\\ a_{21} & a_{22}\end{bmatrix}\begin{bmatrix}\beta\\ \gamma\end{bmatrix}+\begin{bmatrix}b_1\\ b_2\end{bmatrix}\delta_f \tag{1}$$

$$a_{11}=-\frac{2k_{\alpha f}C_f+2k_{\alpha r}C_r}{mv_x},\ a_{12}=-1+\frac{-2k_{\alpha f}C_f l_f+2k_{\alpha r}C_r l_r}{mv_x^2},$$
$$a_{21}=\frac{-2k_{\alpha f}C_f l_f+2k_{\alpha r}C_r l_r}{I_z},\ a_{22}=-\frac{2k_{\alpha f}C_f l_f^2+2k_{\alpha r}C_r l_r^2}{I_z v_x}, \tag{2}$$
$$b_1=\frac{2k_{\alpha f}C_f}{mv_x},\ b_2=\frac{2k_{\alpha f}C_f l_f}{I_z}$$

where, $k_{\alpha f}$ and $k_{\alpha r}$ are the cornering stiffness adjustment coefficients to reflect a tire saturation characteristic. These adjustment coefficients are assumed to be known exactly in this paper.

In order to control the vehicle in the lateral direction, the modified bicycle model is combined with the error dynamics which describes error with respect to a road. Therefore, the complete model used to design a MPC controller is defined as shown in (3) and a diagram of the vehicle model is depicted in Fig. 2.

$$\dot{x}_{lat}=A_{lat}x_{lat}+B_{lat}u_{lat}+F_{\rho,lat}\rho_{ref} \tag{3}$$

$$A_{lat}=\begin{bmatrix}a_{11} & a_{12} & 0 & 0\\ a_{21} & a_{22} & 0 & 0\\ 0 & 1 & 0 & 0\\ v_x & 0 & v_x & 0\end{bmatrix},\ B_{lat}=\begin{bmatrix}b_1\\ b_2\\ 0\\ 0\end{bmatrix},\ F_{\rho,lat}=\begin{bmatrix}0\\ 0\\ -v_x\\ 0\end{bmatrix} \tag{4}$$

where, the state vector is $x_{lat}=\begin{bmatrix}\beta & \gamma & e_\psi & e_y\end{bmatrix}^T$, the control input is $u_{lat}=\delta_{f,des}$, $e_\psi$ is the orientation error of the vehicle with respect to the road, $e_y$ denotes the lateral offset with respect to the center line of the lane, and $\rho_{ref}$ is the road curvature.

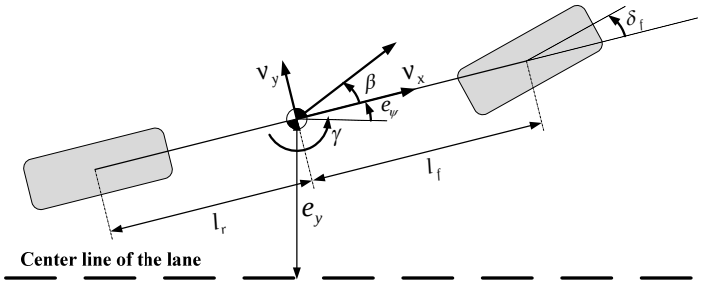


***Fig. 2 Diagram of lateral dynamics model***

In order to solve a receding horizon optimization problem, the continuous differential equation (3) should be discretized. (1) can be converted as follows:

$$x_{lat}(k+1|t) = A_{lat,d}(k|t)x_{lat}(k|t) + B_{lat,d}(k|t)u(k|t) + F_{\rho,lat,d}(k|t)\rho_{ref}(t) \tag{5}$$

$$A_{lat,d} = e^{A_{lat}T_s},\ B_{lat,d} = \left(\int_0^{T_s} e^{A_{lat}\tau}d\tau\right)B_{lat},\ F_{\rho,lat,d} = \left(\int_0^{T_s} e^{A_{lat}\tau}d\tau\right)F_{\rho,lat} \tag{6}$$

where, $T_s$ is the sampling time. The system matrices of the lateral dynamics model, such as $A_{lat,d}(k|t)$, $B_{lat,d}(k|t)$, and $F_{\rho,lat,d}(k|t)$, are obtained using the predicted sequences of the longitudinal velocity during a finite time-horizon.

### *B.* Longitudinal dynamics model

In designing a longitudinal dynamics model of the subject vehicle, an actuator delay between the desired longitudinal acceleration and the response of the actual longitudinal acceleration is considered as follows [11]:

$$a_x = \frac{1}{\tau_{ax}s+1}a_{x,des} \tag{7}$$

where, $\tau_{ax}$ is a time-constant chosen as 0.4 sec based on the analysis of the vehicle test platform.

In this research, two variables, such as distance error $\Delta d$ and relative speed $\Delta v_x$, are used to define the inter-vehicle dynamics.

$$\begin{aligned} &\Delta d = C_x - C_{x,des},\ \ C_{x,des} = \tau_h \cdot v_x + C_{x,safe} \\ &\Delta v_x = v_{x,\text{target}} - v_x \end{aligned} \tag{8}$$

where, $C_x$ and $C_{x,des}$ are the actual clearance and desired clearance between the subject vehicle and the target vehicle respectively, $\tau_h$ indicates the time gap, $C_{x,safe}$ is the minimum safety longitudinal clearance and $v_{x,\text{target}}$ is the longitudinal velocity of the target vehicle. In this research, in order to embrace driving characteristics of all of the drivers, the time gap, $\tau_h$, is chosen as 1.36 sec which is the mean value of time gap for collected driving data in steady-state following situation [1]. Furthermore the minimum safety longitudinal clearance, $C_{x,safe}$, is chosen as 2 meters which is identical with the mean value of the clearance at the zero speed for all of the drivers [1]. The method how to select the target vehicle among the surrounding vehicle would be described in Section IV.

The derivative of the equation (8) could be derived as shown in (9)

$$\begin{aligned} &\Delta\dot{d} = \Delta v_x - \tau_h \cdot a_x \\ &\Delta\dot{v}_x = a_{x,\text{target}} - a_x \end{aligned} \tag{9}$$

Combining equation (7) and equation (9), the longitudinal dynamics model could be described as follows:

$$\dot{x}_{long} = A_{long}x_{long} + B_{long}u_{long} + F_{long}a_{x,\text{target}} \tag{10}$$

$$A_{long} = \begin{bmatrix} 0 & 1 & -\tau_h \\ 0 & 0 & -1 \\ 0 & 0 & -1/\tau_{ax} \end{bmatrix}, B_{long} = \begin{bmatrix} 0 \\ 0 \\ 1/\tau_{ax} \end{bmatrix}, F_{long} = \begin{bmatrix} 0 \\ 1 \\ 0 \end{bmatrix} \tag{11}$$

where, the state vector is $x_{long} = \begin{bmatrix} \Delta d & \Delta v_x & a_x \end{bmatrix}^T$ and the control input is $u_{long} = a_{x,des}$.

As similar as the lateral dynamics model, the discretization of the continuous state equation (10) is conducted through the ZOH method as follows:

$$x_{long}(k+1) = A_{long,d}\, x_{long}(k) + B_{long,d}\, u_{long}(k) + F_{long,d}\, a_{x,\text{target}}(k) \tag{12}$$

$$A_{long,d} = e^{A_{long} T_s},\ B_{long,d} = \left( \int_0^{T_s} e^{A_{long}\tau} d\tau \right) B_{long},\ F_{\rho,long,d} = \left( \int_0^{T_s} e^{A_{long}\tau} d\tau \right) F_{\rho,long} \tag{13}$$

## IV. Safe driving Envelope

Generally, human drivers monitor surrounding environment and predict the future states of surrounding environment based on the current states of that. Then drivers estimate the threat level of possible actions and decide the maneuver of the subject vehicle in consideration of the predicted states of surrounding vehicles during a finite time-horizon. Therefore, in order to develop a highly automated driving system, a safe driving envelope which indicates the drivable boundaries for safe driving over a finite prediction horizon should be determined with the consideration of not only current states of traffic situation surrounding the subject vehicle but also probable future states of that simultaneously [9]. Considering probable future states of surrounding vehicles, it could be expected that the automated driving control algorithm could handle probable risky situation during a finite time-horizon and enhance safety. Furthermore, if we define the safe driving envelope based on the probabilistic prediction, it is expected that an automated driving control algorithm which reflects human driver's driving characteristics with an acceptable ride comfort could be developed. Firstly, the method of the probabilistic prediction method is presented in Section III-A. Then the determination of the desired driving mode and the safe driving envelope is represented in Section III-B.

### A. Probabilistic prediction of surrounding vehicle's behavior

One of common approach to predict the future states of traffic situation surrounding the subject vehicles is a deterministic prediction which assumes that the surrounding vehicles maintain its current movement during a finite time horizon. Since this approach ignores the probability of all possible movements of surrounding vehicles, this could cause incorrect interpretation of the current driving situation.

In order to compensate the shortcomings of the deterministic prediction of the behaviors of surrounding vehicles, the possible behaviors of surrounding vehicles are predicted and the risky behaviors among the possible behaviors of other vehicles surrounding the subject vehicle are considered in determining the safe driving envelope.

For the prediction of the reasonable and realistic behaviors of surrounding vehicles, the interaction between vehicles and the restriction on surrounding vehicle's maneuver due to the road geometry should be considered [12]. Moreover, it is assumed that drivers of the surrounding vehicles obey general traffic rules [13]. It means that the surrounding vehicle's behavior is assumed to keep the lane or change one lane at a time, not two or more lanes at a time. If one of surrounding vehicles changes the lane, then that vehicle is assumed to keep the relevant lane in the far-off future. Furthermore the violation of the centerline of surrounding vehicles is prohibited.

In predicting reasonable ranges of the future states of surrounding vehicles, driving data are collected on test track and real road to analyze the probabilistic movement characteristics of the vehicle [14]. For the implementation of these assumptions, a path-following model is designed while interacting with a vehicle state predictor during one cycle of the prediction process. In the vehicle state predictor, the vehicle's probable position and its error covariance over a finite time horizon are predicted by *Extended Kalman Filter* using the desired yaw rate obtained by the path-following model as the virtual measurement.

Fig. 3 depicts the overall architecture of probabilistic prediction of surrounding vehicles. Using measurements from the various sensors, such as vehicle sensor, radar and vision sensor, the range of the predicted states with corresponding uncertainty is determined as shown in Fig. 3. $p_x$ is the longitudinal position of the vehicle, $p_y$ is the lateral position of the vehicle, $N_p$ denotes the prediction horizon, and subscript '*j*' means the *j*-th objects. In predicting the position of the surrounding vehicle, it is assumed that the size of the object is equivalent to the subject vehicle. The ellipse in Fig. 3 indicates the predicted probable range of the center gravity of the vehicle at the prediction time. A detailed description on the computational procedures to predict the probabilistic range of future states during a finite time horizon is described concretely in [10], [15].

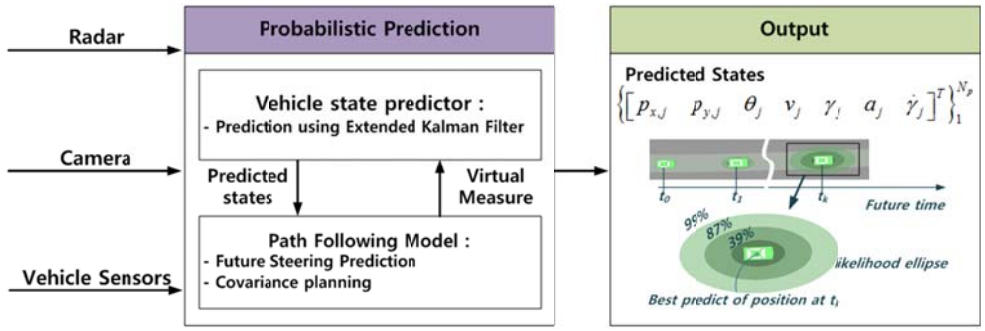


***Fig. 3 Overall architecture of probabilistic prediction of surrounding vehicle's behavior***

### B. Driving mode and Environmental envelope decision

For the determination of the environmental envelope to improve safety, first of all, a potential risky situation should be considered. The risky situation among the probable behaviors of the surrounding vehicles could be classified roughly into three types. Firstly, if the preceding vehicle in the originating lane of the subject vehicle decelerates abruptly, then the potential risk of collision between the preceding vehicle and the subject vehicle would increase. Secondly, if the approaching vehicle in the adjacent lane accelerates during a lane change maneuver of the subject vehicle, then the collision between the approaching vehicle in the adjacent lane and the subject vehicle could be expected. Thirdly, there could be a potential risk of collision due to a sudden cut-in vehicle. Therefore, for the enhancement of safety, not only current states of surrounding environment of the subject vehicle but also these risky behaviors of the surrounding vehicles over a finite prediction horizon should be considered in determining the environmental envelope to improve safety.

Since the environmental envelope should be defined based on the desired motion, we should determine the desired motion or desired driving mode of the subject vehicle before the decision of the environmental envelope. The required driving mode could be approximately classified into lane keeping and lane change mode on an auto road. If there is no preceding vehicle in the originating lane which has a potential risk of collision during a finite prediction horizon, the desired driving mode could be determined as a lane keeping mode. In this case, the environmental envelope is determined to keep the originating lane while maintaining safety with respect to the surrounding vehicle. If the longitudinal or lateral clearances expected at the prediction time step $k$ between the subject vehicle and surrounding vehicle are larger than predefined threshold value, then the collision risk is low and the environmental envelope for $e_y$ is determined to prevent a lane departure. On the other hand, if the longitudinal or lateral clearances at the prediction time step $k$ are expected to be smaller than thresholds, then the collision risk is high. Therefore the environmental envelope for $e_y$ is determined to keep the originating lane while evading the approaching vehicle in the adjacent lane. The decision process of the environmental envelope for a lane keeping mode and the environmental envelope to keep the originating lane while maintaining safety with respect to the surrounding vehicles are described in Fig. 4-(a). In Fig. 4-(a), the pink rectangle indicates the region of the possible behavior of surrounding vehicles and the violet rectangle indicates the region of the possible behavior of surrounding vehicles with the consideration of sensor uncertainty.

On the other hand, there could be a preceding vehicle in the originating lane which has a collision risk during a finite prediction horizon or one of the surrounding vehicles in the adjacent lane is expected to change the lane into the originating lane of the subject vehicle during the prediction time horizon. In this case, the lane change of the subject vehicle from the originating lane to the adjacent lane might be required. Then the feasibility of the lane change and safety after the lane change should be considered. If there is no vehicle is in the adjacent lane when the lane change of the subject vehicle is required, then the lane change could be permitted. Otherwise, we should investigate the minimum longitudinal clearance between the subject vehicle and the vehicle in the adjacent lane to which the subject vehicle change the lane from the originating lane over a finite prediction horizon. If the minimum longitudinal clearance between the subject vehicle and the vehicle in the adjacent lane is larger than the minimum safety longitudinal clearance over a finite prediction horizon, then the collision between the subject vehicle and the vehicle in the adjacent lane would be avoided over a finite prediction horizon. Therefore, the lane change of the subject vehicle could be permitted and the desired driving mode could be determined as a lane change mode. On the

contrary, if the minimum longitudinal clearance between the subject vehicle and the vehicle in the adjacent lane is smaller than the minimum safety longitudinal clearance over a finite prediction horizon, there could be a collision between the subject vehicle and the vehicle in the adjacent lane during a finite time-horizon and the lane change of the subject vehicle should not be permitted. The decision process of the environmental envelope for a lane change mode is described in Fig. 4-(b).

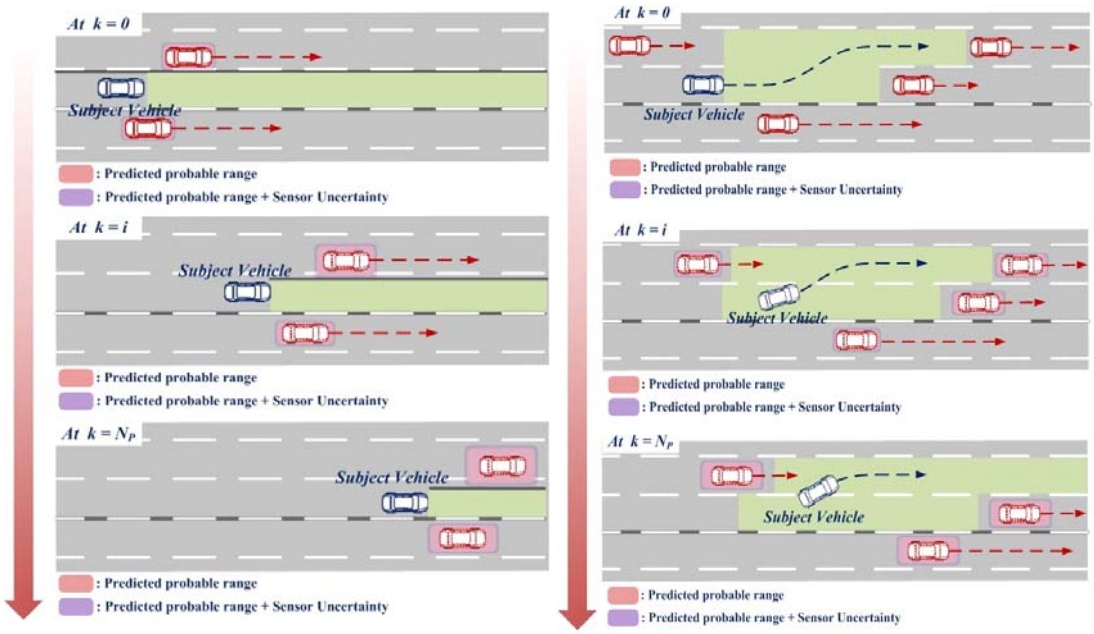


***(a) Lane keeping mode*** ***(b) Lane Chang mode***

***Fig. 4 Decision process of the environmental envelope***

Consequently, the condition of limitation of the lateral deviation, $e_y$, to satisfying the environmental envelope can be written as follows:

$$H_{env} \cdot x(k) \le G_{env,upper,bound}(k), \quad k = 1,\ldots,N_p$$
$$G_{env,lower,bound}(k) \le H_{env} \cdot x(k), \quad k = 1,\ldots,N_p \qquad (14)$$

*where,*

$$H_{env} = \begin{bmatrix} 0 & 0 & 0 & 1 \end{bmatrix}$$

Before the determination of the environmental envelope to guarantee the longitudinal safety, we need to define the state of the target vehicle for the control of the longitudinal acceleration. In the case of a lane keeping mode, if the width of the environmental envelope for $e_y$ over a finite prediction horizon is large enough, it means that possible behaviors of surrounding vehicles in the adjacent lane are predicted to keep their lane. Then the preceding vehicle in the originating lane is chosen as the target vehicle for the control of the longitudinal acceleration. If there is no preceding vehicle in the originating lane or the clearance between the subject vehicle and the preceding vehicle is too far, then the virtual vehicle to follow the desired velocity is chosen as the target vehicle for the control of the longitudinal acceleration.

On the other hand, one of adjacent vehicles could be expected to approach to the originating lane of the subject vehicle or change the lane into the originating lane of the subject vehicle. In this case, the width of the environmental envelope for $e_y$ could be smaller than minimum safety width. It means that the subject vehicle could not keep the lane only with the steering maneuver. Generally, when drivers recognize that the neighboring vehicle in the adjacent lane is entering into the lane of the subject vehicle, drivers generally tend to release the throttle pedal or apply the brakes to decelerate [16]. According to the previous research [16], the target vehicle is generated by combining the preceding vehicle in the originating lane and the meaningful vehicle in the adjacent lane. Based on this research, the clearance and relative speed between the subject vehicle and the meaningful vehicle in the adjacent lane are integrated with those between the subject vehicle and the preceding vehicle in the originating lane for the generation of the target vehicle's information. For instance, if the width of the environmental envelope for

$e_y$ at the prediction time step $j$ is expected to be smaller than minimum safety width as shown in Fig. 8, then the weighting factor, $\omega_{LK}$, to determine the target vehicle's state for the longitudinal acceleration control is determined as shown in (15).

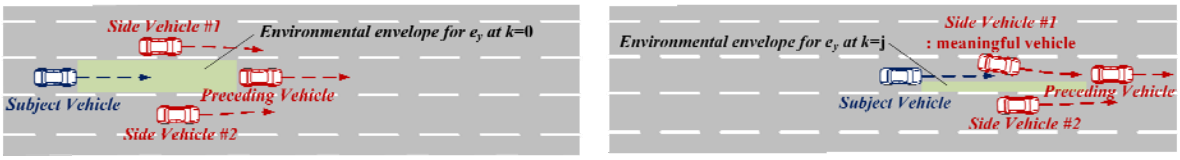


***(a) Environmental envelope at the prediction time step k = 0***

***(b) Environmental envelope at the prediction time step k = j***

***Fig. 5 Determination of the target vehicle for the longitudinal acceleration control in a lane keeping mode***

$$\begin{aligned}\omega_{LK} &= f(n, \mathbf{Risk}), \quad (0 < \omega_{LK} \le 1) \\ &= \max\left(\max\left(\frac{\min\left(TTC^{-1}, TTC^{-1}{}_{th}\right)}{TTC^{-1}{}_{th}}\right|_n, 1 - \frac{\min\left(\mathbf{x}, \mathbf{x}_{th}\right)}{\mathbf{x}_{th}}\Big|_n\Big)\right)\end{aligned} \tag{15}$$

where, $TTC$ means the time to collision and $\mathbf{x}$ indicates the non-dimensional warning index [1]. $n$ in (15) indicates the prediction time step at which the width of the environmental envelope for $e_y$ is smaller than minimum safety width.

Consequently, the integration between the preceding vehicle in the originating lane and meaningful vehicle in the adjacent lane is defined as shown in (16).

$$\begin{bmatrix} C_x(t) \\ v_{x,\mathbf{target}}(t) \\ a_{x,\mathbf{target}}(t) \end{bmatrix} = \omega_{LK} \cdot \begin{bmatrix} C_{x,\text{meaningful}}(j|t) \\ v_{x,\text{meaningful}}(j|t) \\ a_{x,\text{meaningful}}(j|t) \end{bmatrix} + (1-\omega_{LK}) \cdot \begin{bmatrix} C_{x,inlane}(t) \\ v_{x,inlane}(t) \\ a_{x,inlane}(t) \end{bmatrix} \tag{16}$$

In the case of a lane change mode, the target vehicle's states are determined by the integration between the preceding vehicle and the surrounding vehicle in the adjacent lane of the lane change direction. For instance, if the lane change direction is left, then the target vehicle's states are determined by the integration between the preceding vehicle in the originating lane and the surrounding vehicle in the left lane. The weighting factor for the integration in a lane change mode, $\omega_{LC}$, is defined as shown in (17). Then the integration for the determination of the target vehicle's states to control a longitudinal acceleration during a lane change mode is defined as shown in (18).

$$\omega_{LC} = \frac{|e_y|}{2/3 \cdot W_{road}}, \quad (0 < \omega_{LC} \le 1) \tag{17}$$

$$\begin{bmatrix} C_x(t) \\ v_{x,\mathbf{target}}(t) \\ a_{x,\mathbf{target}}(t) \end{bmatrix} = \omega_{LC} \cdot \begin{bmatrix} C_{x,sidelane,LC} \\ v_{x,sidelane,LC} \\ a_{x,sidelane,LC} \end{bmatrix} + (1-\omega_{LC}) \cdot \begin{bmatrix} C_{x,inlane}(t) \\ v_{x,inlane}(t) \\ a_{x,inlane}(t) \end{bmatrix} \tag{18}$$

where, the subscript 'side-lane' means the vehicle in the adjacent lane to which the subject vehicle changes the lane from the originating lane and $W_{road}$ is the road width which could be known from the vision sensor.

After the determination of the state of the target vehicle for the control of the longitudinal acceleration, then we could define the environmental envelope to guarantee the longitudinal safety. In order to avoid the collision over a finite prediction horizon, the clearance between the subject vehicle and the target vehicle should be larger than minimum safety longitudinal clearance, $C_{x,safe}$, as shown in (19).

$$C_x(k|t) \ge C_{x,safe}, \quad k = 1, \ldots, N_p \tag{19}$$

To satisfy the condition described in (19), the constraint of the distance error between the actual clearance and desired clearance could be defined as follows:

$$\Delta d(k|t) \ge C_{x,safe} - C_{x,des}(k|t) = -\tau_h \cdot v_x, \quad k = 1, \ldots, N_p \tag{20}$$

Moreover, for the improvement of the longitudinal safety, the relative speed between the subject vehicle and the

target vehicle should be larger than the threshold of the relative speed, $\Delta v_{x,\min}$, as shown in (21).

$$\Delta v_x(k|t) \geq \Delta v_{x,\min}, \quad k = 1,\ldots,N_p \tag{21}$$

Consequently, the environmental envelope to guarantee the longitudinal safety could be represented as the linear inequality as shown in (22).

$$H_{long} \cdot x_{long,d}(k|t) \geq G_{long,\min}, \quad k = 1,\ldots,N_p \quad where, \; H_{long} = \begin{bmatrix} 1 & 0 & 0 \\ 0 & 1 & 0 \end{bmatrix}, \; G_{long,\min} = \begin{bmatrix} -\tau_h \cdot v_x \\ \Delta v_{x,\min} \end{bmatrix} \tag{22}$$

## V. Robust MPC based Controller design

As mentioned in Section I, distributed control architecture which is composed of the lateral control law based on robust MPC approach and the longitudinal control law based on robust MPC approach is adopted. In this research, the sampling time, $T_s$, is chosen as 0.1 second and the length of the prediction horizon, $N_p$, is chosen as 20. These receding horizon optimization problems are solved at each time step and the first terms of the optimal control sequences are applied to the system. Then receding horizon optimization problems for a shifted prediction horizon are solved to obtain new optimal control inputs at next time step. To solve MPC problem in MATLAB, CVXGEN which is designed to be utilizable in MATLAB is used as solver [17]. The MPC problem is defined using CVXGEN syntax, and the CVXGEN returns convex optimization solver for the defined optimization solver for the defined optimization problem.

### A. Background on Robust Model Predictive Control

In this section, we present the background on robust MPC which is used to decide the desired control inputs for the robust control performance. The control problem based on robust MPC is classified into a feedforward control input for the nominal system and a linear feedback control input to reduce the error between the actual state and the nominal state predicted by model of the plant.

Then the control law can be written as follows:

$$u(k) = \bar{u}(k) + K(x(k) - \bar{x}(k)) = \bar{u}(k) + Ke \tag{23}$$

where, $K \in \mathbf{R}^{m \times n}$ is the linear state feedback gain and $e := (x(k) - \bar{x}(k))$ is the error between the actual state and the predicted nominal state. In this paper, the control law of the state feedback gain is LQR.

### B. Desired Steering Angle Decision

As mentioned above, in order to obtain the desired steering angle to keep the vehicle in the safe driving envelope while satisfying the robustness of the control performance under model uncertainties and exogenous disturbances, a feedforward steering input for the nominal lateral dynamics model and a feedback steering input for the compensation of the error between the actual states and the predicted nominal states should be integrated. For the determination of a feedforward steering input, we design the cost function as follows:

$$J = \sum_{k=1}^{N_p-1} \bar{x}_{lat}(k|t)^T W_{\text{cost},lat}\, \bar{x}_{lat}(k|t) + R_{lat,\Delta u} \sum_{k=0}^{N_p-2} \left\| \bar{u}_{lat}(k+1|t) - \bar{u}_{lat}(k|t) \right\|_2 + \left( H\, \bar{x}_{lat}(N_p|t) - y_{des} \right)^T W_{N_p} \left( H\, \bar{x}_{lat}(N_p|t) - y_{des} \right) + R_{lat} \sum_{k=0}^{N_p-1} \left\| \bar{u}_{lat}(k|t) \right\|_2$$

*where,*

$$H = \begin{bmatrix} 0 & 0 & 1 & 0 \\ 0 & 0 & 0 & 1 \end{bmatrix} \tag{24}$$

where, $W_{\text{cost},lat}$ is predefined weighting matrix, which penalize the differences between states and zero, $W_{N_p}$ is predefined weighting matrix to reduce the differences between the final position of the vehicle over a finite prediction horizon and the desired position, $R_{lat}$ and $R_{lat,\Delta u}$ are predefined weighting matrices for the reduction of magnitudes of steering angle control sequences and the rate of change in steering angle control sequences respectively. These matrices are positive-definite symmetric. $W_{N_p}$ is defined as shown in (25).

$$\begin{aligned} y_{des} &= \begin{bmatrix} 0 & W_{road} \end{bmatrix}^T : \; Left \;\; Lane \;\; Change \\ y_{des} &= \begin{bmatrix} 0 & -W_{road} \end{bmatrix}^T : \; Right \;\; Lane \;\; Change \end{aligned} \tag{25}$$

Since the actuator has a limitation to operate, the control input and there derivatives need to be constrained. These constraints are given as follows:

$$\begin{aligned} &\left|u_{lat}(k|t)\right| \le u_{lat,\max}, && k=0\ldots N_p-1 \\ &\left\|u_{lat}(k+1|t)-u_{lat}(k|t)\right\|_\infty \le S_{lat}, && k=0\ldots N_p-2 \end{aligned} \tag{26}$$

where, $u_{lat,\max}$ is the maximum magnitude of the steering control input and $S_{lat}$ is the maximum magnitude of the rate of change of the steering control input.

In order to ensure the stability of the vehicle, the side slip angle and lateral acceleration should be restricted for the stability of the vehicle. Therefore the condition for the stability of the vehicle can be written as follows:

$$\left|\beta(k|t)\right| \le \beta_{\max} = \tan^{-1}\left(0.02\mu g\right), \quad k=1,\ldots,N_p \tag{27}$$

$$\left|\gamma(k|t)\right| \le \gamma_{\max} = \frac{A_{y,\max}}{v_x}, \quad k=1,\ldots,N_p \tag{28}$$

where, $\mu$ denotes tire-road friction coefficient and $A_{y,\max}$ is the threshold of the lateral acceleration, which is chosen as 8m/s$^2$.

The constraints for the stability of the vehicle which are defined in (27) and (28) can be represented as the linear inequality as shown in (29).

$$\left|H_{veh}\cdot x_{lat}(k|t)\right| \le G_{veh,\max}, \quad k=1,\ldots,N_p \quad \textit{where, } H_{veh}=\begin{bmatrix}1&0&0&0\\0&1&0&0\end{bmatrix},\ G_{veh,\max}=\begin{bmatrix}\beta_{\max}\\ \gamma_{\max}\end{bmatrix} \tag{29}$$

Then MPC problem for the determination of the feedforward steering input could be defined by combining (5), (14), (24), (26) and (29) as follows:

$$\begin{aligned} &\min\ (24) \\ &s.t.\ (5),(14),(26),(29) \end{aligned} \tag{30}$$

In order to design the robust MPC while reducing complexity, the effect of model parameter uncertainties and exogenous disturbances on the linear dynamics model in (5) is represented as an additive equivalent disturbance. Then the lateral dynamics model including the additional disturbance term is written as follows:

$$x_{lat}(k+1) = A_{lat,d}\,x(k) + B_{lat,d}\,u(k) + F_{\rho,lat,d}\,\rho_{ref}(k) + w_{lat,eq} \tag{31}$$

where, $w_{lat,eq} \in \mathbf{R}^{4\times 1}$ is the additive equivalent disturbance on the lateral dynamics model. The equivalent disturbance $w_{lat,eq}$ is unknown but assumed to be bounded as shown in (32).

$$w_{lat,eq} \in W_{lat},\ \left|w_{lat,eq}\right| \le \left[0.05, 0.05, 0.5\cdot\frac{\pi}{180}, 0.1\right]^T \tag{32}$$

### C. Desired Longitudinal Acceleration Decision

Similar to the lateral control law, the longitudinal control law should be designed to obtain the desired longitudinal acceleration to keep the vehicle in the safe driving envelope while ensuring the robust control performance. Therefore the desired longitudinal acceleration is determined by combining a feedforward input for the nominal longitudinal dynamics model and a feedback input to attenuate the effect on the system by model parameter uncertainties or external disturbances.

In order to determine the feedforward control input for the longitudinal control of the vehicle, we design the cost function as shown in (33).

$$J_{long} = \sum_{k=1}^{N_p} \bar{x}_{long}(k|t)^T W_{\text{cost},long}\,\bar{x}_{long}(k|t) + R_{long}\sum_{k=0}^{N_p-1}\left\|\bar{u}_{long}(k|t)\right\|_2 + \left|\bar{u}_{long}(0|t)-a_x\right| + R_{long,\Delta u}\sum_{k=0}^{N_p-2}\left\|\bar{u}_{long}(k+1|t)-\bar{u}_{long}(k|t)\right\|_2 \tag{33}$$

where, $W_{\text{cost},long}$ is predefined weighting matrix for the minimization of the differences between states and zero, $R_{long}$ is predefined weighting matrix to reduce the magnitudes of longitudinal acceleration sequences and $R_{long,\Delta u}$ is predefined weighting matrix to prevent abrupt change of longitudinal acceleration in sequences. These weighting matrices are positive-definite symmetric.

The constraints on the range of the longitudinal acceleration control input and change rate during a finite prediction horizon are written as follows:

$$\begin{aligned} &\bar{u}_{long,\min} \le \bar{u}_{long}(k|t) \le \bar{u}_{long,\max}, && k=0\ldots N_p-1 \\ &\left\|\bar{u}_{long}(k+1)-\bar{u}_{long}(k)\right\|_\infty \le \bar{S}_{long}, && k=0\ldots N_p-2 \end{aligned} \tag{34}$$

where, $\bar{u}_{long,\min}$ and $\bar{u}_{long,\max}$ are the minimum and maximum magnitude of the longitudinal acceleration control

input respectively. $\overline{S}_{long}$ is the maximum magnitude of the rate of change of the longitudinal acceleration control input.

Then MPC problem for the determination of the feedforward longitudinal acceleration input could be formulated by combining (10), (22), (33) and (34) as follows:

$$\begin{aligned} &\min\ (33) \\ &s.t.\ (10),(22),(34) \end{aligned} \tag{35}$$

In order to determine a feedback control input for the longitudinal control of the vehicle, an additive equivalent disturbance is included in (10) to represent the effect on the system by model parameter uncertainties or external disturbances.

$$x_{long}(k+1) = A_{long,d}\,x_{long}(k) + B_{long,d}\,u_{long}(k) + F_{long,d}\,a_{x,\text{target}}(k) + w_{long,eq} \tag{36}$$

where, $w_{long,eq} \in \mathbf{R}^{3\times 1}$ is the additive equivalent disturbance on the longitudinal dynamics model. Similar to the equivalent disturbance on the lateral dynamics model, it is assumed that the equivalent disturbance on the longitudinal dynamics model, $w_{long,eq}$, is unknown but bounded as shown in (37).

$$w_{long,eq} \in W_{long},\ \left|w_{long,eq}\right| \le \left[0.05, 0.1, 0.05\right]^T \tag{37}$$

## VI. Vehicle test results

The proposed automated driving control algorithm is evaluated through computer vehicle tests. In order to evaluate the proposed algorithm on a real test vehicle, Hyundai-Kia Motors K7 is used as a test vehicle platform. Figure 6 shows the test vehicle configuration. In order to measure DLC, heading angle and road curvature, a Mobileye camera system is equipped on the test vehicle. The proposed algorithm has been implemented on "dSPACE Autobox", which is used for the real-time application and equipped with a DS1005 processor board. Delphi radars are equipped on the test vehicle to perceive surrounding environments. The hardware components mentioned above communicate through a CAN bus.

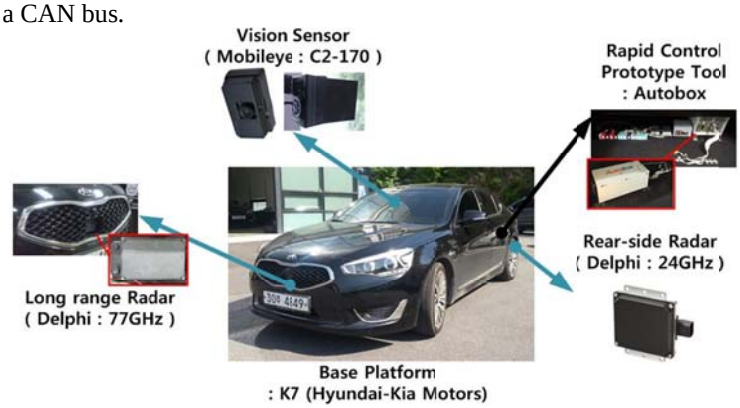


***Fig. 6 Test vehicle configuration***

The test track is a straight road. The road-tire friction coefficient is assumed to be 0.85, since the road of the test track is a dry asphalt road. Two cases of experiments have been conducted. In order to evaluate the performance of the proposed algorithm under lane change situation, the scenario of experiment is designed to evaluate the performance of the proposed algorithm under overtaking situation as shown in Figure 7.

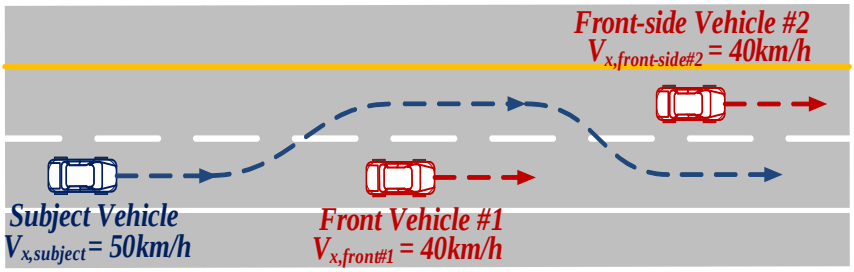


***Fig. 7 Experiment scenario for overtaking***

The simulation results are presented in Figure 8. As shown in Figure 8, it can be known that the controller shows quite similar performances to the human driver while changing lane. Based on these results, it has been shown that the proposed algorithm could reflect human driver's driving characteristics. It means that the proposed algorithm could provide acceptable ride comfort in general driving situations. Since lateral offset is measured by camera sensors, lateral offset is plotted as discontinuous as shown in Figure 8-(a). Figure 8-(b) and (c) depict steering angle and longitudinal acceleration comparing results between the human driver and the controller. Lateral acceleration has reasonable magnitude as shown in Figure 8-(d).

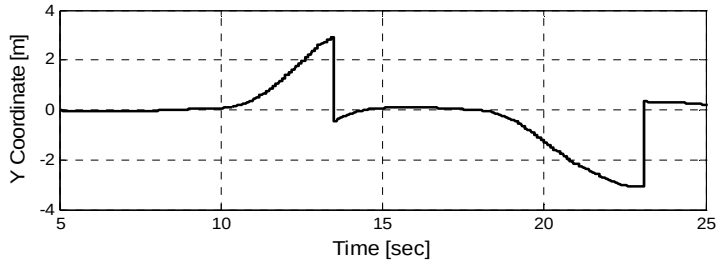


***(a) Lateral offset***

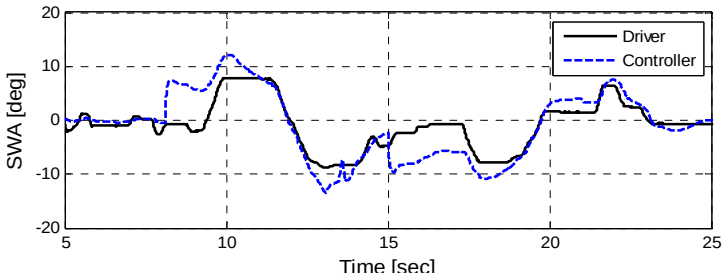


***(b) Comparison of the steering angle between the driver and the controller***

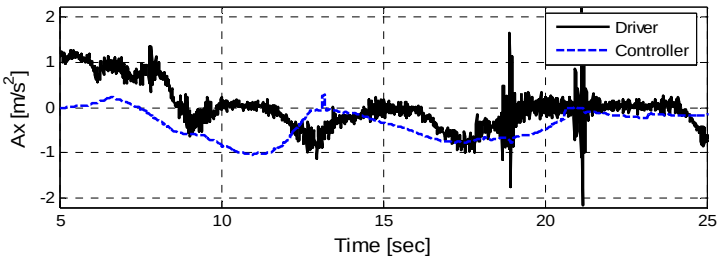


***(c) Comparison of the longitudinal acceleration between the driver and the controller***

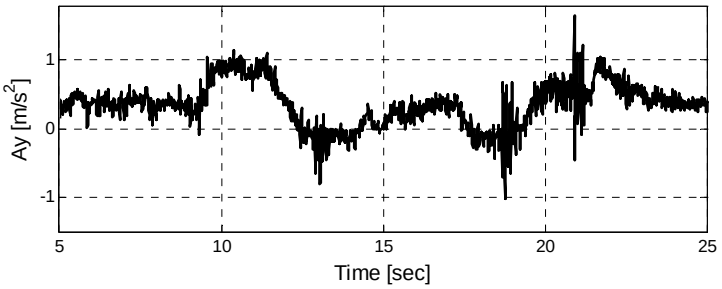


***(d) Lateral acceleration***

***Fig. 8 Comparison between the driver and the proposed algorithm under overtaking situation***

## VII. Conclusion

A robust MPC based vehicle speed and steering control algorithm has been developed to enhance safety and ensure constraint satisfaction under model uncertainties and external disturbances. In order to cope with potential risky situation, not only current states of surrounding environment but also potential risky behaviors of that during a finite time horizon are considered simultaneously in determining the desired driving mode and the safe driving envelope. Then distributed control architecture based on robust MPC approach is used to determine the desired steering angle and desired longitudinal acceleration separately while satisfying reliability and reducing a computational burden.

In order to verify the effectiveness of the proposed control algorithm, computer simulations have been conducted. The simulation results show that the proposed control algorithm enhances safety with respect to the potential risk and provides permissible ride comfort. Furthermore it has been shown that robust vehicle control performance can be obtained in the presence of additional disturbances by using the proposed algorithm.

In the future, we should verify the performance of the proposed algorithm via vehicle tests.


### ACKNOWLEDGMENT

This work was jointly supported by the Hyundai Motors Company, SNU-IAMD, the BK21 program, and the National Research Foundation of Korea(NRF) grant funded by the Ministry of Science, ICT & Future Planning (MSIP) (No. 2009-0083495).


## REFERENCES


[1] S. Moon, and K. Yi, “Human driving data-based design of a vehicle adaptive cruise control algorithm,” Vehicle System Dynamics, vol. 46, no. 8, pp. 661-690, 2008.

[2] A. Eskandarian, 2012, Handbook of Intelligent Vehicles, London: Springer London

[3] A. Gray, Y. Gao, J. Hedrick, and F. Borrelli, “Robust predictive control for semi-autonomous vehicles with an uncertain driver model,” IEEE Intelligent Vehicles Symposium, Gold Coast, Australia, pp. 208-213, 2013.

[4] P. Falcone, M. Tufo, F. Borrelli, J. Asgari, and H. E. Tseng, “A linear time varying model predictive control approach to the integrated vehicle dynamics control problem in autonomous system,” Proceedings of the 46th IEEE Conference on Decision and Control, New Orleans, USA, pp. 2980-2985, 2007.

[5] D. Mayne, J. Rawlings, C. Rao, and P. Scokaert, “Constrained model predictive control: Stability and optimality,” Automatica, vol. 36, no. 6, pp. 789-814, June 2000.

[6] P. Falcone, F. Borrelli, J. Asgari, H. E. Tseng, and D. Hrovat, “Predictive active steering control for autonomous vehicle systems,” IEEE Transactions on Control System Technology, vol. 15, no. 3, pp. 566-580, May 2007.

[7] S. Erlien, S. Fujita, and J. Gerdes, “Safe driving envelopes for shared control of ground vehicles,” in 7th IFAC Symposium Advances in Automotive Control, Tokyo, Japan, 2013.

[8] M. Kothare, V. Balakrishnan, and M. Morari, “Robust Constrained Model Predictive Control using Linear Matrix Inequalities,” Automatica, vol. 32, no. 10, pp. 1361-1379, 1996.
[9] D. Ferguson, and D. Dolgove, “Modifying behavior of autonomous vehicle based on predicted behavior of other vehicles,” Pat. no. 20130261872A1, United States, 2013.
[10] B. Kim and K. Yi, “Probabilistic states prediction algorithm using multi-sensor fusion and application to Smart Cruise Control systems,” IEEE Intelligent Vehicles Symposium, Gold Coast, Australia, pp. 888-895, June 2013.
[11] D. Zhang, K. Li, and J. Wang, “A curving ACC system with coordination control of longitudinal car-following and lateral stability,” Vehicle System Dynamics, vol. 50, no. 7, Mar. 2012.
[12] M. Althoff, O. Stursberg, and M. Buss, “Model-based probabilistic collision detection in autonomous driving,” IEEE Transactions on Intelligent Transportation System, vol. 10, no. 2, pp. 299-310, June 2009.
[13] B. Vanholme, D. Gruyer, B. Lusetti, S. Glaser, and S. Mammar, “Highly automated driving on highways based on legal safety,” IEEE Transactions on Intelligent Transportation System, vol. 14, no. 1, pp. 333-347, Mar. 2013.
[14] T. Lee, K. Yi, and C. Jeong, “Integrated stochastic driver model for evaluation of the vehicle active safety systems,” Fast-zero 2011, Tokyo, Japan, 2011.
[15] B. Kim, and K. Yi, “Probabilistic and Holistic Prediction of Vehicle States Using Sensor Fusion for Application to Integrated Vehicle Safety Systems,” IEEE Transactions on Intelligent Transportation Systems, vol. 15, no. 5, pp. 2178-2190, 2014.
[16] S. Moon, H. Kang, and K. Yi, “Multi-vehicle target selection for adaptive cruise control,” Vehicle System Dynamics, vol. 48, no. 11, pp. 1325-1343, 2010.

**Comparison between Occlusion Methods for Measuring Distraction Caused by Smartphone Interaction**

**Christian Jernberg**
**Pontus Larsson**
Driver Environment & Human Factors, Advanced Technology & Research, Volvo Group Trucks Technology, SE-40508 Göteborg, Sweden (christian.jernberg@volvo.com)
Paper Number 15-0404

## ABSTRACT

**Research Question/Objective**
The occlusion method is an established method for measuring the visual demand from in-vehicle interfaces. The method is usually employed by means of occlusion glasses which can be automatically made opaque or transparent. However, occlusion can also be achieved by turning on and off the screen of the interface being studied. It can be hypothesized though, that glasses-occlusion requires more visual re-orientation efforts after each occluded interval which may give longer Total Shutter Open Times (TSOTs) than the method where only the interface screen is occluded.

**Methods and Data Sources**
Two experiments were conducted, with 10 participants (5 female) in Experiment 1 and 14 participants (7 female) in Experiment 2. In both experiments, participants were seated in a truck mockup and performed tasks on a smartphone. Two occlusion conditions were employed: 1) Occlusion with glasses, and 2) Embedded occlusion (turning the screen of the smartphone on/off). Participants also performed a baseline condition with no occlusion. In Experiment 1, five different tasks were performed in each condition: destination selection, dialing a phone number, dialing a contact, changing radio frequency and setting the alarm clock. For each task, a note showing the data to be entered was posted next to the smartphone, e.g. the number to be dialed.
The four tasks used in Experiment 2 were: visual-manual text entry, make changes in a truck driving log, dial a phone number and select item from a map (using pinch/swipe operations). The participants did not have support from any note but had to remember the data to enter for each task.
For both experiments, TSOTs and Resumability (R) were submitted to separate ANOVAs to reveal differences between occlusion and tasks.

**Results**
The results of Experiment 1 showed a main effect of occlusion type on TSOT ($p < .05$), where Glasses resulted in longer TSOTs ($M = 8.1$s) than Embedded ($M = 7.4$s). However, the interaction between occlusion and task was also significant ($p < .01$), and suggested that mainly the phone dialing task caused the difference in TSOTs. An explanation to this could be that tasks requiring more visual-spatial reorientation are more difficult to perform with glasses occlusion. A simpler explanation could be that participants needed to look at the note while dialing – which can be done during the occluded intervals with the embedded method. The results from experiment 2 did not show any statistically significant effect of occlusion on TSOTs which suggests that the effects found in Experiment 1 were caused by the fact that participants had to look at the paper note while dialing.

**Discussion and Limitations**
The current experiments indicate that the embedded method gives TSOTs comparable to the glasses-occlusion method. However, one must be aware of the fact that there are practical differences between the methods which can lead to diverging TSOTs. The current experiments show that such divergence can occur when instructions are given visually.

**Conclusions and Relevance to Session Submitted**
The embedded occlusion method for evaluating distraction is nonetheless promising since it is easy to use and can be integrated in app developers' toolkit.

## INTRODUCTION

The occlusion method is well adopted and established for measuring the visual demand of in-vehicle information systems (IVIS). The method dates back to the late 60s and was developed by Senders et al.[1] in order to find a suitable surrogate for the more expensive and time consuming eye-tracking method.

The International Organization for Standardization (ISO) state in their guideline for occlusion that when using the occlusion method, the system that are being tested should work as intended and be fitted in a vehicle, simulator buck, or mock up in a design which duplicates the placement of the system in its intended environment. The viewing angle and the placement of the controls in relation to the driver should be the same as in the finished product[2]. Before testing the system the participant should be allowed to practice until he or she can adequately handle the system. A rule of thumb is mentioned as between two and five test trials per function, including two with occlusion. After the practice, a total of five test trials should be performed with similar end state of the system. Each function should be practiced and evaluated separately before moving on to the next.

The ISO standard specifies three possible ways to use occlusion, and these are as follows:

1 – Occlusion glasses
2 – Display blanking
3 – Mechanically or electronically operated shutters.

All these methods have in common that they are not allowed to interfere with the manual controls of the IVIS and the change from occluded to un-occluded state (opaque to transparent) or vice versa cannot take longer than 20 ms. The length of the interval during which the shutter is open or closed is 1.5s.

The two most relevant measurements used in this type of evaluation are the Total Shutter Open Time, TSOT, and the Resumability Ratio, R. The TSOT value represents an estimation of how long the driver would have to avert the gaze from the road to perform a task and R is a measurement of how easy it is for the driver to continue a dialogue after it is interrupted. R is calculated as the ratio between the TSOT and the total task time unoccluded ($TTT_{unoccl}$).

The occlusion method is accepted by ISO, the Society of Automotive Engineers (SAE)[3], the National Highway Traffic Safety Administration (NHTSA)[4], the Alliance of Automobile Manufacturers (AAM)[5] and the Japan Automobile Manufacturers Association (JAMA)[6] to determine if a system is safe enough to be used while driving. However, the criteria for how the method should be used might vary slightly. In the ISO standard the criteria is up to the person who is performing the evaluation or developing the interface. JAMA on the other hand say that the limit for total task time is 8 seconds, which make the maximum acceptable TSOT 7.5 seconds. For the NHTSA and AAM guidelines the maximum TSOT are twice as long, 15 seconds.

Occlusion should be optimal for evaluations in the early phases of the design process[7]; the main reason being that it is comparably cheap and simple to perform. Therefore, it is possible to have a larger number of participants for several design loops and iterations compared to when the eye-tracking method is used for example. So even though the occlusion method is not as precise in measuring where the most problematic areas of an IVIS are as the eye-tracking method, it can still give an indication of which concept that is the least distracting when comparing different ones[8]. Furthermore, if the display blanking variant of occlusion can be integrated in software development packages, it should even further simplify the process of iteratively developing and testing new in-vehicle interfaces.

In this study, the focus lies mainly with comparing the occlusion glasses to display blanking (hereafter referred to as “embedded occlusion”), and it is hypothesized that there are some differences between these which may lead to that the different methods result in different TSOT- and R values. For example, with the glasses there should be a short period of time where the eyes need to adjust to a new focal distance; something not needed when it is only the screen of the IVIS that is turned blank. Also, while the glasses do not interfere with the manual controls, it covers these as well as the hand of the operator. This is not the case with embedded occlusion and thus it should be easier to resume a task or even continue a task during the occluded interval (so

called 'blind operating') since there is still the ability to see where the fingers are positioned relative to the edge of the IVIS. This hypothesis is tested in two experiments presented in the following paragraphs in which a set of apps in a regular smartphone is evaluated using both the glasses-occlusion method and a smartphone-embedded method.

## METHODS AND DATA SOURCES

Two experiments were conducted, between which the main differences were that Experiment 2 included tasks of higher difficulty and that participants did not receive any visual instructions during the tasks.

### Experiment design

For both experiments, a within-group factorial design was used with Occlusion type (None/ Glasses / Embedded), Task (1-5 for Experiment 1 or 1-4 for Experiment 2) and Task repetition (5) as independent variables. The order of conditions was balanced between participants in order to avoid order effects.

### Participants

In Experiment 1, 10 participants (5 female) took part. Their mean age was 39.5 years (*SD* = 9.25). Two participants were over 50 years old. In Experiment 2, 14 participants (7 female) took part. Their mean age was 36.7 years (*SD* = 6.98). All participants were recruited from within the company.

### Apparatus and equipment

Apparatus and equipment was identical for the two experiments. A Samsung I9001 Galaxy S Plus smartphone was used as the main interface with which the participants would perform the task. The smartphone was positioned in a cradle mounted to the dashboard of a truck cab mockup. The truck cab mockup consisted of a truck seat, in which the participants were seated during the whole experiment, a steering wheel, and a complete dashboard (see Figure 1).

Occlusion was accomplished with PLATO visual occlusion spectacles for the glasses-occlusion conditions (see Figure 2) and with a custom app for the embedded occlusion conditions. Timing of the tasks was accomplished with a regular stop watch app in a smartphone.

***Figure 1. Truck cab mockup used in both experiments***

***Figure 2. Person wearing occlusion glasses.***

**Tasks**

In both experiments, five variations of each task were to be completed (which is according to the ISO standard), for example: call five different phone numbers or select five different destination addresses.

In Experiment 1, five different tasks were to be conducted in each occlusion condition. For each task in Experiment 1, a note showing the data to be entered was posted next to the smartphone, e.g. the number to be dialed. The tasks were:

1. Change radio frequency: In the smartphone's built-in radio app, the participants had to repeatedly tap either a left or right arrow until a frequency given by the paper note had been reached. In total, the arrow had to be tapped 31 times to complete each variation of the task.

2. Select destination: In the navigation app "Waze", the participants had to tap to open the menu, tap "navigate", scroll through a list and select one of five pre-defined destinations and then finally tap to start navigation.

3. Set the alarm clock: In the smartphone's built-in clock app, the participants had to first tap "create alarm", then tap the hour digits and through the appearing on-screen keyboard enter one out of five given times (20:00, 00.00, 17:00, 10:00, 18:00), tap "next", tap "repetition of alarm", tap "every day" and finally tap "Save" twice.

4. Dial a phone number: In the smartphone's regular phone interface, the participants had to manually enter one out of five phone numbers – all containing a long push "+" and 13 digits (e.g.: +49 157 3943 3782) and then tap the green phone symbol to call the number.

5. Dial a contact: In the smartphone's regular contact list, the participants had to scroll to one out of five names, tap the name, and finally tap the contact's phone number. All names started with the letter "M" and the participants had to scroll down approximately 30 contacts before the target contact became visible.

In Experiment 2, four different tasks were to be conducted in each occlusion condition. In this experiment, no note displaying the target data (i.e. phone number, destination address etc.) to be entered was used; the participants had to remember the data to be used in each task, and this was given verbally by the test leader before each task. The tasks were:

1. Enter destination: In the navigation app "Waze", the participants had to tap to open the menu, tap "navigate", tap in the search field and manually enter one out of five addresses given by the test leader with the on-screen keyboard, then tap the search icon, select the appropriate destination address from the list appearing and tap "drive" twice to start navigation. The addresses were Importgatan, Planetgatan, Teknikgatan,

Kvillegatan, and Londongatan (all selected from the vicinity of the test site so that no time lag would occur after the search/navigate icon had been tapped.)

2. Change time in log: In the app "TimeBook" (a tool for truck drivers to record their working and resting times), the participants had to tap "list" to open a list with logs, then tap one out of five specific logs (identified by the number of tasks they contained – between 21-25) , scroll to the last task in that log, tap the task, tap "end time" for the task and tap the "+" icon twice to extend the task by 2 hours and finally press "enter".

3. Dial a phone number: In the smartphone's regular phone interface, the participants had to manually enter one out of five phone numbers – all containing a long push "+", the numbers "495" and then 10 digits. Since the participants had to remember the number sequences by heart, logical number sequences were used (e.g.: +495 24 68 10 12 14). When the number had been dialed, the participants had to tap the green phone symbol to call the number.

4. Call dealer: In the app "DealerLocator" (a tool for truck drivers to find nearby truck dealers), the participants had to use multiple swipe / pinch-zoom operation to navigate a digital map, starting from Göteborg, Sweden and find one out of five dealers in the Barcelona, Spain region. Once the dealer had been located, the participant had to tap the dealer marker, and finally tap the dealer's phone number to make a call.

## Procedure

The procedure was identical for both experiments. Participants arrived individually to the test lab. They were firstly introduced to the study, the smartphone, the occlusion glasses and the embedded occlusion app. Then, the tasks to be performed during the test were demonstrated.

The actual test then started. Before each task, participants practiced the task (using other data entries than the ones used in the experiment trials) until they could perform them without error. They then got to practice the task also with occlusion (either embedded or glasses depending on the condition) before an actual trial was conducted during which the task completion time was recorded by the test leader. The test leader instructed the participants verbally to start each task by saying "start… now" and the participant notified when he/she was finished with a task by saying "done". If the task was not completed without errors, they were asked to perform the task once more. After all tasks had been completed, participants were debriefed and thanked for their participation.

## RESULTS

Using the acquired Total Task Times (TTT), the measures Total Shutter Open Time (TSOT) and Resumability ratio (R) were first calculated according to:

$$TSOT = 0.75 \cdot \left(INT\left(\frac{TTT}{1.5}\right)\right) + 0.5 \cdot MOD\left(INT\left(\frac{TTT}{1.5}\right), 2\right) + MOD\left(\frac{TTT}{1.5}, 1\right) \cdot \left(1 - MOD\left(INT\left(\frac{TTT}{1.5}\right), 2\right)\right) \quad (1)$$

$$R = \frac{TSOT}{TTT_{unoccluded}} \quad (2)$$

TSOT and R values were then submitted to separate 2x5x5 - occlusion (embedded/glasses) x (task number) x (task repetition) and 2x4x5 - occlusion (embedded/glasses) x (task number) x (task repetition) - repeated measures Analyses of Variance (ANOVAs) for Experiment 1 and Experiment 2 respectively.

## Experiment 1 results

Considering TSOT, a statistically significant main effect of occlusion was found: $F(1,8) = 8.323$, $p = .02$. Post hoc test using Bonferroni's adjustment for multiple comparisons showed that the Glasses occlusion condition resulted in longer TSOTs than the Embedded occlusion ($M = 8.122$, $SE = 0.423$ compared to $M = 7.397$, $SE = 0.436$).

A main effect of task was also found: $F(4,32) = 61.843$, $p < .001$ (Sphericity assumed). Post hoc test showed that task 4 (dial phone number) resulted in statistically significantly longer TSOTs than all the other tasks (Bonferroni's method used to adjust for multiple comparisons). The effect of task on TSOT is shown in Figure 3 below.

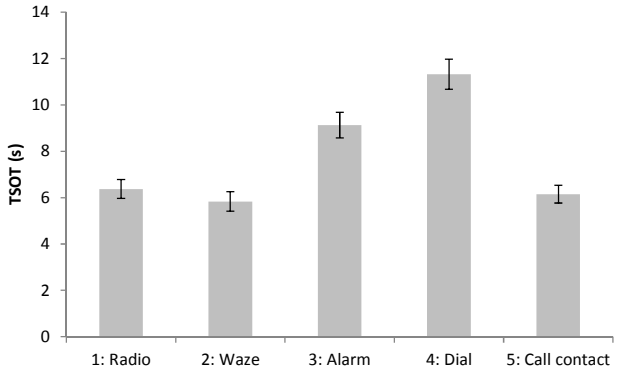


***Figure 3. TSOT as function of Task for Experiment 1. Whiskers show standard error.***

However, a statistically significant interaction effect between occlusion and task was also found: $F(4,32) = 6.143$, $p = .001$, Sphericity assumed. The effect is visualized in Figure 4 below, where it can be seen that it seems it is mainly Task 4 (Dial a phone number) for which the occlusion types differ.

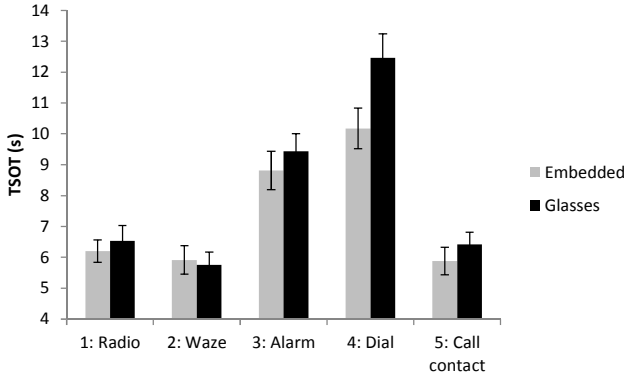


***Figure 4. Interaction between occlusion and task for TSOT, experiment 1. Whiskers show standard error.***

For Repetition, a main effect was found ($F(4,32) = 6.495$, $p = .001$), and from the result of a Bonferroni-adjusted post hoc test, one could see that this effect was due to repetition 4 resulting in a statistically significantly lower TSOT compared to repetition 1 ($M = 7.485$, $SE = 0.423$ vs $M = 8.313$, $SE = 0.516$, respectively, $p = .01$).

For R, no main effect of occlusion was found, although a trend could be noted indicating that Glasses occlusion could give higher R than embedded occlusion ($M = 0.849$ vs $M = 0.791$, $p = .067$). A similar trend was found for the interaction between task and occlusion. A statistically significant main effect was however found for task: $F(4,28) = 7.579$, $p < .001$. Figure 5 below shows that it was mainly the

difference between Task 1/ 2 (Radio / Waze) compared to Task 3 (Alarm) and the difference between Task 1 and 4 (Dial) which caused this effect (Bonferroni's method used to adjust for multiple comparisons). No other effects were found.

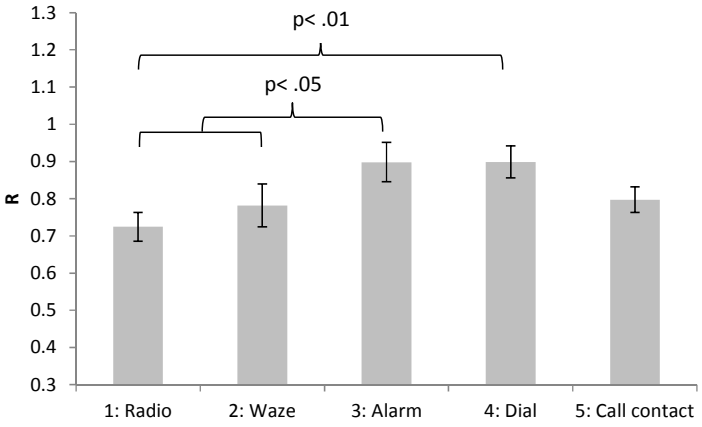


***Figure 5. R as function of task for R, Experiment 1. Whiskers show standard error.***

Taken together, the Dial and Alarm tasks seemed to require more glance time and were also more difficult to resume compared to the other tasks. The Dial task seemed to be the reason why a main effect of occlusion on TSOT was found. The reason for this effect may be that more difficult tasks, which require more visual reorientation than simpler tasks, are more difficult to perform with the glasses occlusion. A much simpler explanation could be that the Dial task required the participants to look at the paper note to be able to complete the task (the data to be entered for the other tasks were much simpler to remember). This could obviously not be done while the glasses were shut, compared to the Embedded occlusion where participants could read the number to be dialed also during blanked-sceen intervals.
These explanations were the reason for conducting Experiment 2, in which more difficult tasks were included and the participants did not have the paper note to read off.

**Experiment 2 results**

There was no effect of Occlusion on TSOT in experiment 2 ($F(1,13) = .160$, $p = .695$, $M = 15.163$ for embedded occlusion and $M = 15.708$ for glasses occlusion, $p = .695$). A main effect of Task on TSOT was however found: $F(1.637, 21.284) = 56.4$, $p < .001$ (Greenhouse-Geisser corrected). Post hoc test using Bonferroni's method of adjustment showed that all tasks differed from each other ($p < .01$); means and standard errors are visualized in Figure 6 below. Here it can also be seen that the Dial task, when performed with numbers in a logical sequence, resulted in lower mean TSOTs compared to Experiment 1, when the participants had to read on the paper note (of course not statistically tested here however). Interestingly, a similar effect of repetition as found in Experiment 1 was also found in Experiment 2: $F(4,52) = 4.401$, $p = .004$. Again, it seemed that Repetition 4 resulted in the lowest TSOTs, but also that the last repetition gave longer TSOTs than the others. The general trends for repetition for both Experiment 1 and 2 are shown in Figure 7.

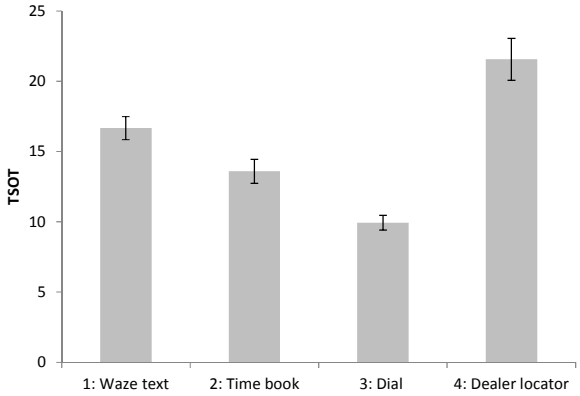


**Figure 6. TSOT as function of task, experiment 2. Whiskers show standard error.**

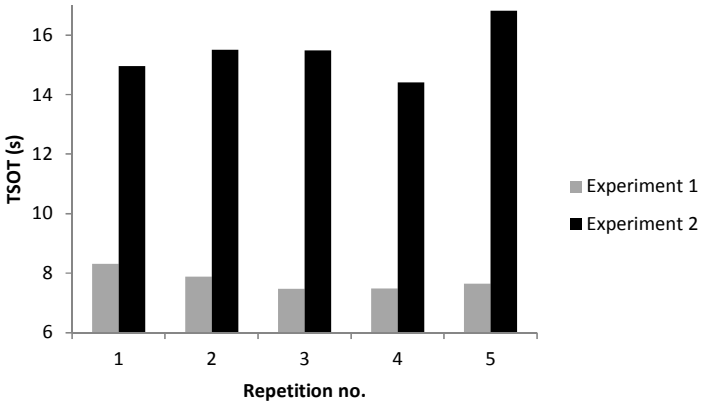


**Figure 7. TSOT as function of repetition comparing both experiments.**

No statistically significant effect of Occlusion on R was found: $F(1,12) = .013$, $p = .912$. Moreover, there were neither any statistically significant effects of Task ($F(3,36) = 2.348$, $p = .089$) or Repetition ($F(4,48) = 1.599$, $p = .190$) on R.

## DISCUSSION AND LIMITATIONS

In Experiment 1, a statistically significant effect of occlusion on TSOT was found. However it was suspected that this effect was only due to one of the tasks, namely "Dial phone number". One possible explanation was that the use of visual instructions (a paper note with the number to be dialed) caused this effect. In case of the embedded occlusion, the phone number could obviously be read also during screen blanking, but when wearing the glasses the number can only be read during shutter-open intervals. Another explanation was that the occlusion types generate different results only for more difficult tasks which require visual reorientation, in turn which could be more difficult when the whole scene is blanked out as in the glasses-occlusion situation.

Experiment 2, in which there was no paper note to be read from, did not result in any differences in TSOT depending on occlusion type. Experiment 2 also included more difficult tasks, especially one involving interacting with a map which one would expect to be more difficult for the glasses occlusion - but even the measures obtained from this task did not seem to be affected by occlusion type. Thus, we can be fairly certain that the two occlusion methods will not generate different results, if visual instructions are avoided. It is important to note however, that the current set of experiments has not considered visual instructions and task difficult as factors in a factorial design (since this was not the purpose/hypotheses of the experiments from the beginning). To be able to draw firm conclusions,

another experiment should be conducted where visual instructions and task difficulty are independent variables.

## CONCLUSIONS AND RECOMMENDATIONS

Our conclusion is that the occlusion method is a good way to early on determine if a system is too distracting for a driver or not. Even though it is not as accurate as eye-tracking, the simplicity with which it can be performed makes it ideal for app-developers to use while developing automotive applications. With the embedded occlusion method, they could test their systems before presenting them to a vehicle manufacturer and thus save time and resources for both parties.

However, a recommendation would be to add in the ISO guideline that the occlusion method should not allow visual instructions (apart from such that are presented in the actual interface under study) during the trials as this could interfere with the results of the evaluations.

## ACKNOWLEDGEMENTS

The work presented in this paper was conducted as a part of the ongoing project SICS (Safe Interaction, Connectivity and State), co-financed by the Swedish Governmental Agency for Innovation Systems (VINNOVA).

## REFERENCES

[1] Senders, J.W., Kristofferson, A.B., Levison, W.H., Dietrich, C.W. and Ward, J.L. 1967. "The attentional demand of automobile driving."
Highway Research Record, No 195: 15-33

[2] ISO 16673:2007. "Road vehicles – Ergonomic aspects of transport information and control systems – Occlusion method to assess visual demand due to the use of in vehicle systems."
Available for purchase at: http://www.iso.org/iso/catalogue_detail.htm?csnumber=38035. Accessed March 3, 2015.

[3] SAE J2364, 2004. "Navigation and Route Guidance Function Accessibility While Driving".
Available for purchase at: http://standards.sae.org/wip/j2364/. Accessed March 3, 2015.

[4] NHTSA: National Highway Traffic Safety Administration, 2013. "Guidelines for Reducing Visual-Manual Driver Distraction during Interactions with Integrated, In-Vehicle, Electronic Devices, Version 1.01 Docket No. NHTSA-2010-0053".
Available at: https://www.distraction.gov/download/11302b-Visual_Manual_Distraction_Guidelines_V1-0_010815_v1_tag.pdf. Accessed March 13, 2015.

[5] Driver Focus-Telematics Working Group, 2006. "Statement of principles, criteria and verification procedures on driver interactions with advanced in-vehicle information and communication systems."
Alliance of Automobile Manufacturers, Washington, DC.

[6] JAMA: Japan Automobile Manufacturers Association Inc., 2004 "Guidelines for In-Vehicle Display Systems - Version 3.0."
Available at: http://www.jama-english.jp/release/release/2005/jama_guidelines_v30_en.pdf. Accessed March 13, 2015

[7] Young, K, Lee, J.D. and Regan, M.A. 2008. "Driver Distraction: Theory, Effects and Mitigation"
CRC Press, Boca Raton, FL: 123-134

[8] Kroon, M. 2006. “Comparison Between Visual Occlusion and Eye-movement based visual demand assessment of in-vehicle information systems”
Departure of Computing Science, Umeå University, Sweden

# GENERAL VIRTUAL TESTING METHODOLOGY FOR TYPE IV CNG TANKS

**Ralf Matheis**
**Helmi Murnisya**
Forschungsgesellschaft Kraftfahrwesen mbH Aachen
Germany

**Roberto Puppini**
Centro Ricerche Fiat S.C.p.A.
Italy

Paper Number 15-0405

## ABSTRACT

The project MATISSE funded by European Commission's 7th Framework Programme (FP7) aims to make a significant step forward in the capability of the automotive industry to model, predict and optimise the crash behaviour of mass produced fibre reinforced polymers (FRP) with the focus set on components for alternatively powered vehicles (APV). One of the project's main research goals is the development of a general virtual testing methodology (VTM) for the development of APV driven by compressed natural gas (CNG) equipped with composite FRP tanks of Type IV.
Due to the increasing legislative demands on the emission of future vehicles, the development of APVs that are in this regard superior to conventional internal-combustion engines (ICE) driven by petrol or diesel fuel is currently in the centre of attention of the automotive industry. Here, the usage of ICE with CNG supply offers advantages in comparison to other concepts, since it requires only moderate modifications of the conventional drive train. Because of the high mechanical demands on the required high-pressure storage tanks and the need for lightweight structures, which also contributes to the emission reduction, the usage of material of high specific material properties is required. Especially the full composite tanks of the Type IV show a high potential in this regard. Since these high-pressure storage components form a significant safety hazard, the accurate analysis of the mechanical demands during relevant crash load cases is of great importance. For the proper and optimal integration of the tanks into the vehicle during the APV design and development process at industrial level, moreover the predictability of the material and component behaviour using the finite element method (FEM) is indispensable.
Within the MATISSE project a new overall approach for the crash analysis of CNG tanks is proposed. This paper describes the main aspects of this VTM:
First, a FRP material modelling approach for wet wound CNG tanks, that makes use of the so-called "reverse FEM" as well as of novel physically based material models that are fed with calculative as well as literature based material values and are validated on three point bending tests of wound tubes was defined.
Then, the derived material models for glass and carbon fibre were subsequently used for the modelling of FEM tank models, whereby different steps of optimisation of on the one hand the accuracy and on the other hand the simulation time were conducted.
In a next step, different relevant load cases on a full vehicle model of a compact car equipped with a CNG tank where simulated and analysed. The detected highest mechanical demands were thereupon transferred to a component test programme on a tank-subsystem that depicts the loads obtained by the tanks. Here again, the FEM model of the tank is used to find the appropriate boundary conditions.
The developed test programme was subsequently conducted on a series of physical tanks and the simulation approach and thus the VTM was validated on the results.

## INTRODUCTION

Increasing energy costs, limitation of crude oil resources as well as constantly intensifying emission targets (especially w.r.t. $CO_2$) are a pivotal driver for current automotive research and development [1]. In this regard alternatively powered vehicles (APV) with drive-trains that differ from conventional internal-combustion engines (ICE) supplied with petrol or diesel fuel show high potential for energy economical and environmentally friendly propulsion [2]. On the other hand lightweight structures are a fundamental requirement in order to achieve a low demand of energy and to compensate possible higher structural masses of alternatively powered drive-trains [3].
An alternatively powered drive-train that is on the one hand cost efficient since it requires comparatively minor design changes to conventional vehicles (primarily ignition and valve-train system) and on the other hand has a perspective to evoke low $CO_2$ emissions, is an ICE operated with compressed natural gas (CNG) [4], [5]. This energy source requires high-pressure storage tanks that have to withstand the high mechanical

demands of internal pressures of 200 bars to 250 bars. In order to achieve energy storage that is simultaneously light and safe, pressure vessels of the Type IV that are entirely made of fibre reinforced polymers (FRP) are currently state of the art [6].
For the proper and optimal integration of the tanks into the vehicle during the APV design and development process at industrial level, moreover the predictability of the material and component behaviour using the finite element method (FEM) is indispensable [7]. Besides analyses of the passenger and partner safety of the vehicle, the simulation of the component loading behaviour and subsequent analysis of the material stresses and damage allows an optimisation of components concerning weight. Especially FRP laminates offer a potential for optimisation as well as numerous influence parameters [8].
One of the major advantages of FEM simulations is that, once a model validated on test results is established, analyses for different scenarios or design changes can be carried out virtually. This can reduce the development expenses as well as development cycles drastically. However, approval tests are obligatory for the final vehicle or respectively component [9].

## MOTIVATION

Although virtual methods like FEM analyses have become an integral part of the automotive industry, they still lack in broad acceptance concerning their reliability. Especially, when it comes to unconventional materials like FRP, the development is characterised by conventional component tests. With regard to CNG tanks, the InGAS project identified the following open issues:

- No crash simulation models are available for such complex composite structures
- No standardised test procedures are available
- No validated methods are available to transfer the test results to the crash situation in a vehicle [10]

In order to overcome these issues and to make a step forward in the capability of the automotive industry to model, predict and optimise the crash behaviour of vehicles equipped with Type IV tanks, a virtual testing methodology (VTM) was developed within the project MATISSE funded by European Commission's 7$^{th}$ Framework Programme. As a demonstrator a belly mounted CNG tank consisting of a combined carbon fibre reinforced polymer (CFRP) and glass fibre reinforced polymer (GFRP) wet wound structure with a polyamide (PA) liner and aluminium bosses was used. However, the feasibility of the approach was also verified for a neck mounted design.

The physical tanks used as reference within the VTM are produced and provided by the MATISSE partner Xperion Energy & Environment GmbH and are approved for vehicle application.

All simulations within the VTM are carried out using the explicit FEM solver LS-DYNA which is provided by the MATISSE partner DYNAmore Nordic AB.

## VTM APPROACH

The here presented VTM approach aims to achieve an adequate level of prediction of the failure behaviour of composite high-pressure storage tanks (HST) under crash loading conditions, both at component and vehicle level. This general VTM involves four main steps:

- Identification of relevant (full vehicle) crash scenarios.
- Their numerical simulation through FEM codes.
- Analysis of results obtained from these simulations and extraction of the envelope of crash loading conditions of interest insisting on HST.
- Definition of simplified/reduced test set-ups capable of generating, on the isolated HST, loading conditions that are equivalent and/or representative of the ones that are seen by the composite tank within the vehicle during full car crashes of interest (the above mentioned envelope), so that corresponding physical test-rigs

can be designed in detail and subsequently built for experimental testing campaigns on the composite tanks.

The general VTM is illustrated in Figure 1.

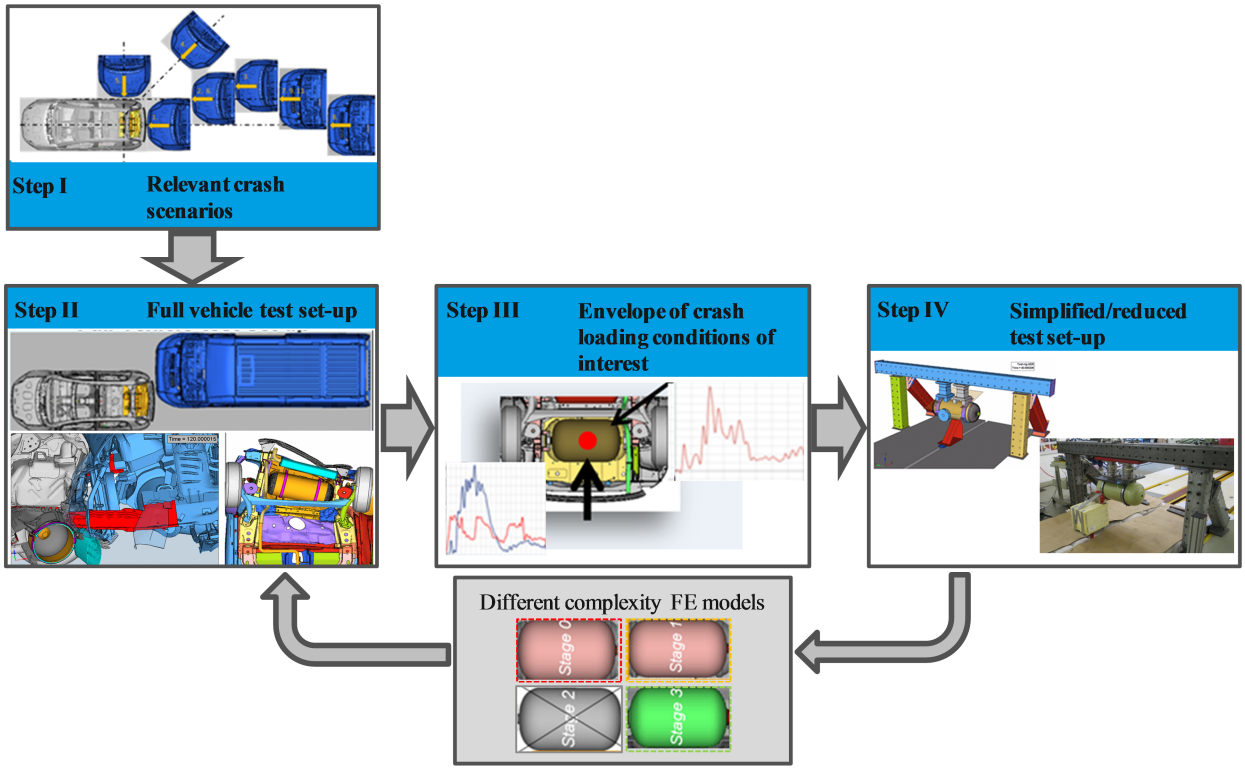


*Figure1. Schematic diagram of the VTM*

## SIMULATION TOOLS

In order to successfully pass through these steps, a special focus has to be set on the CNG tank model, which is considered to be the key element of the methodology. The model is based on geometry and material information for the components liner and bosses as well as the winding and material information for the CFRP and GFRP winding layers. In order to achieve the highest precision of results but on the other hand to allow an efficient course of the project, here four different stages of modelling complexity are applied in the steps of the VTM. For the validation of the material model a so-called reverse FEM approach is applied.

### Reverse FEM Approach

Based on the applied wet winding production process used to manufacture Type IV CNG tanks, a rather unconventional simulation approach has to be carried out, since the process does not allow the production of flat or ring shaped specimens for standardised quasi-static tests (for general data acquisition as it is usually done for FRP materials). In order to use a material structure that is windable and comparable to the investigated tanks, several tubes with different layer set-ups are tested in a quasi-static three point bending (3PB) test, with two circular lateral constraints and a cylindrical central indenter with a constant velocity of 1 mm/s. The material model for the simulation is defined using calculated literature or assumed values and then calibrated on the test results of the 3PB and checked for plausibility on virtual quasi-static coupon tests (that consider tensile, compression and shear loading). Furthermore, the delamination failure criteria are virtually validated by the simulation of an end notch flexure (ENF) test and a double cantilever beam (DCB) test. In order to achieve robust modelling different laminate set-ups are tested in the 3PB. The MATISSE modelling approach is presented in Figure 2.

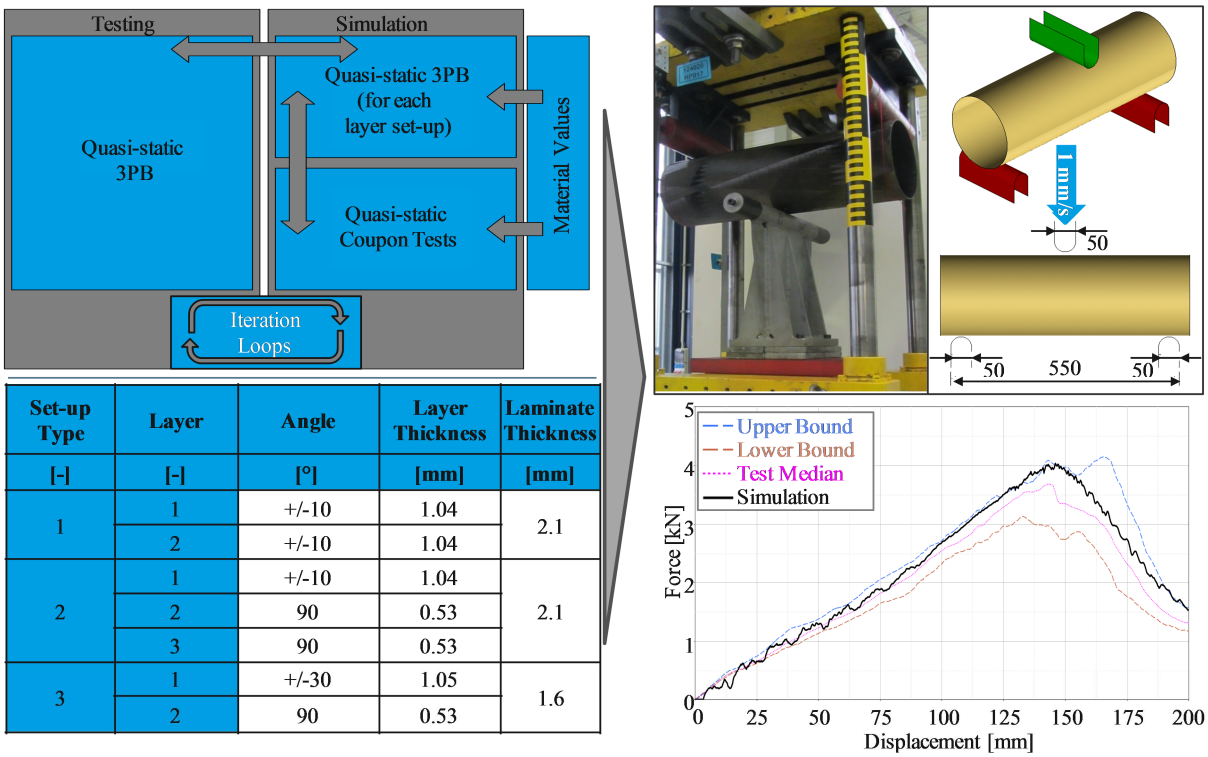


| Set-up Type | Layer | Angle | Layer Thickness | Laminate Thickness |
|---|---|---|---|---|
| [-] | [-] | [°] | [mm] | [mm] |
| 1 | 1 | +/-10 | 1.04 | 2.1 |
| | 2 | +/-10 | 1.04 | |
| 2 | 1 | +/-10 | 1.04 | 2.1 |
| | 2 | 90 | 0.53 | |
| | 3 | 90 | 0.53 | |
| 3 | 1 | +/-30 | 1.05 | 1.6 |
| | 2 | 90 | 0.53 | |

***Figure2. Reverse FEM approach***

**Stage 0 tank model**

Stage 0 defines a rough CNG tank model that has the geometry of the tank to be analysed but is meshed rather coarse with shell elements (average size of 10 mm) and assumes only elastic and isotropic material behaviour, without any failure criteria for the composite layers. The bosses are modelled as solid elements with elastic and isotropic material properties, too. However, the mechanical properties of the composite part of the vessel are correspondent to the in-fibre properties of the materials applied (average Young's modulus and density). The stage 0 derives from the past FP7 project InGAS and is applied in order to evaluate the crash conditions in a very early stage of the project since it does not require in-depth information of the materials and the winding set-up (see Figure 3).

**Stage 1 tank model**

For a more sophisticated evaluation of the crash behaviour the stage 1 model is applied. The model is provided with the geometry and winding information of the tank to be analysed and uses a much finer shell mesh of 3 mm with layer definition applied to different integration points. The shell mesh is used in order to allow time efficient modelling and calculation. However, the section of the wound areas of the tank show thicknesses up to 22.5 mm and thus exceeding the limitations of the shell theory. Furthermore, it is modelled with a special composite material model (*MAT_58) that considers material moduli and strength values for the fibre and transversal direction as well as for shear. The liner is considered to be elastic and the bosses are modelled as rigid. All material values are based on either literature research or calculations (see Figure 3).

**Stage 2 tank model**

The stage 2 represents the most complex tank model of the VTM and is used for the second loop of step IV. It uses the same component geometry and winding information as stage 1 but is meshed with several layers of thick shell elements with layer definition applied to different integration points. It uses a novel continuum damage model (*MAT_262). The model considers material moduli and strength values for the fibre and transversal direction as well as for shear and material damage mechanisms that are physically based and consider fracture toughness values.

Furthermore, the structural failure due to delamination is adressed using cohesive elements between the thick shell elements that consider different failure modes (see Figure 3).

**Stage 3 tank model**

Stage 3 is a predictive composite model suitable for the use within full car crash FE simulations and applied in a third loop of step 1 and respectively step IV of the VTM . It is based on the Stage 2 but comprises a set of simplifications such as coarsening, layer clustering and numerically more efficient elements. It derives from a number of simplification and subsequent simulation loops within step IV that are evaluated in comparison to the Stage 2 simulation results. After each measure of simplification the simulation results are compared and the accuracy and efficiency of the measure is evaluated. If the related gain in efficiency is considered to be worth the loss in accuracy a simplification measure is kept. If not, the measure is withdrawn and another measure is applied (see Figure 3).

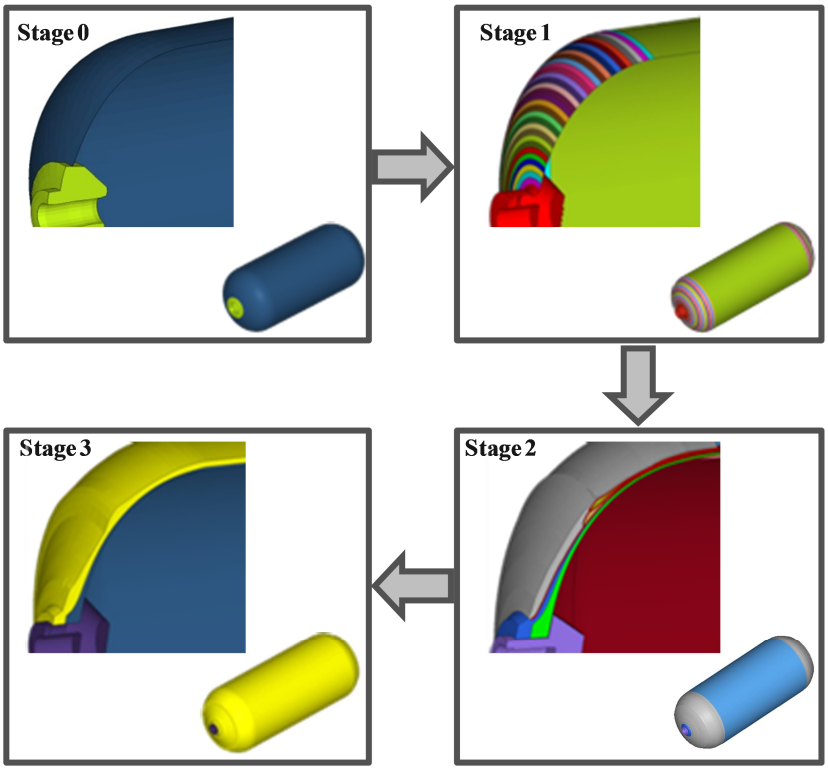


*Figure3. Stages of CNG tank model*

**STEPS OF THE VTM**

In the following the different steps of the VTM are described in detail and their application within the MATISSE project is presented.

**Step 1: Identification of Relevant Crash Scenarios**

The identification of the crash scenarios is not primarily based on statistical relevance since the focus of the VTM is not set on the most likely load cases but on crash scenarios that are relevant w.r.t. the potential to induce damages on the composite CNG tanks. For this concern numerous crash situations are proposed and evaluated by crash experts concerning their severity but also w.r.t. to probability.
More precisely, for the here described reference case eleven full car-to-car collisions involving a B-class vehicle equipped with an unpressurised CNG tank system and two different types of opponents (bullet vehicles) were chosen. As relevant bullet vehicles a B-class car and a van were considered. The target car is always assumed to be

stationary with released brakes. For the target car three different types of muffler locations/lay-outs were considered. The eleven load cases are as follows:

Target car without muffler between the tank and the rear crossbeam; bullet: B-class car impacting at 55 km/h
1. Rear impact, “full overlap”
2. Rear impact, “50% overlap”
3. Rear impact, “25% overlap”
4. Side impact, from the right side, “oblique”
5. Side impact, from the right side, “perpendicular”

Target car with muffler between the tank and the rear crossbeam; bullet: B-class car and van impacting at 55 km/h
6. Rear impact by car , “50% overlap”
7. Rear impact by van, “50% overlap”
8. Rear impact by van, “full overlap”

Target car with muffler between the tank and the rear crossbeam but with reduced distance w.r.t. tank; bullet: van impacting at 55 km/h
9. Rear impact by van, “50% overlap”
10. Rear impact by van, “full overlap”

Target car with muffler with reduced distance to tank; bullet: van impacting at 80 km/h
11. Rear impact by van, “50% overlap”

In this step of the VTM neither simulations nor physical tests are applied. However, the choice of relevant load cases forms the basis for the fully virtual step 2.

**Step 2: Numerical Simulation of Relevant Crash Scenarios**

Subsequently in the second step of the VTM all the considered collision scenarios are simulated and the results are evaluated concerning their severity. This includes the stresses and strains of the tank structure but also general endangerments of these components due to impacts on sharp or rigid components as well as the loading in the valve area.

In the reference case the simulation was carried out in LS-DYNA using existing models for the B-class car and the van. The model of the impacted vehicle is equipped with a tank model as well as the corresponding environment structure. In a first loop of the step 2, the stage 0 model was used due to the fact that the complex modelling and reverse FEM activities made a very early availability of stage 1 model within the project not possible. As the stage 1 model was released, the general conclusions of the simulations could be verified and refined in a second loop using this more significant model.

The results obtained from the numerical simulation campaign confirmed that the most severe loading conditions for the CNG composite tank are achieved when the reference vehicle is impacted by the van. In particular, impact configuration no. 9 resulted to be the worst one. Due to the offset and to the “aggressivity” of the van (stiffer and higher main rails, almost double vehicle mass) w.r.t. the reference car, the latter is subjected to very high rear intrusions with the van front structure arriving to interact directly with the tank. Configuration no. 11 (in practice the no. 9 repeated with the speed increased at 80 km/h), despite being more severe in terms of overall target vehicle deformations, was almost similar to configuration no. 9 in terms of loading conditions on the composite tank. This is the case mainly due to the fact that the extra energy introduced by the speed increase was absorbed essentially through more deformation of the vehicle structure in front of the tank area. The deformations for the target vehicle in this crash configuration are presented in Figure 4.

Again no physical tests are foreseen in this step of the VTM.

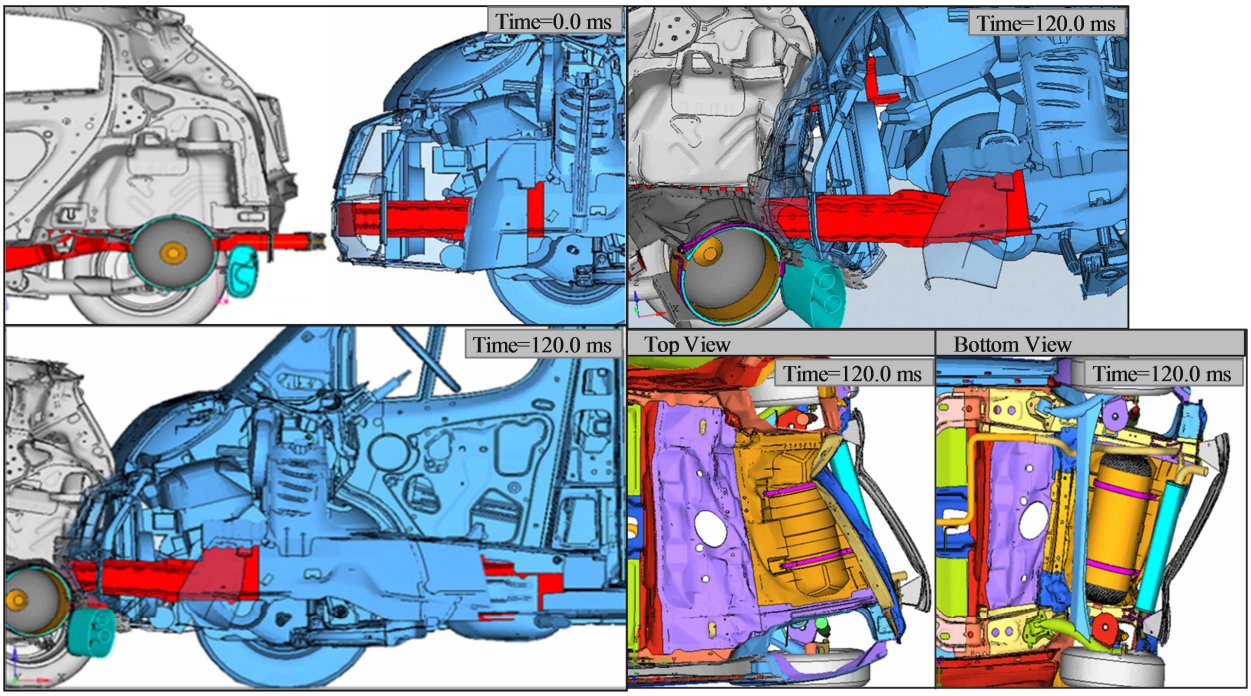


***Figure4. Configuration 9: Deformations on target vehicle equipped with Stage 1 tank model***

**Step 3: Envelop of Crash Loading Conditions**

In the third step of the VTM there is a more in depth analysis of the loading to the tank, especially on areas that have potential of hazard to the environment due to damage or even leakage and burst. This includes for example:

- accelerations in different points
- global contact force and maximum interface resultant force
- interface normal pressure
- section forces on the tank
- section forces on tank fixations

Furthermore, this analysis gives information about which boundary conditions and subsystems of the full vehicle impact have to be transferred to the subsequent definition of an adequate simplified test that is significant for the loading of the tank.

Then, the third step of the VTM led to the identification of some important indications towards the definition of an equivalent simplified/reduced subsystem test set-up.

Such indications are recalled in the following:

- An equivalent simplified test-rig should have the possibility to impact the tank on different locations and from different directions.
- This possibility should be realised by an impactor capable to reproduce similar normal pressures on the tank and global contact forces (i.e. having the proper shape and energy level).
- The simplified test-rig should have the possibility to allow some deformation of the tank anchorage points, by acting on their stiffness/strength within a proper range, in order to reproduce the boundary condition seen by the tank when mounted on the specific reference vehicle.

**Step 4: Simplified Test Set-up**

The step 4 of the VTM is a pivotal step for the application of this methodology since it is not only carried out in the virtual environment but is also performed on physical tanks, thus providing the input for a comparison between the simulation and the tests and allowing a subsequent validation of the approach. In step 4 the task is to accurately reflect the boundary conditions of loading conditions considered to be relevant and significant (i.e. like the already mentioned full vehicle configuration 9) with a test rig that can be set up on the one hand simple and easy and on the other hand reproducible, in order to avoid expensive and complex full vehicle tests. The validation by the experimental test results obtained with such a test-rig shall provide a tank model that can be applied in a validated full vehicle model in order to obtain information about the crash saftey of the CNG tank system. For these in-vehicle applications, the validation process should comprise a final simplification of the tank model in order not to affect the simulation costs too significantly (i.e. the already described stage 3 model).

Starting from the reference case (i.e. the full vehicle configuration 9) a suitable test rig for a crash test facility, considering the above mentioned indications, was developped in several loops of iteration leading to a flexible set-up that allows the application of different tank sizes and mounting systems (e.g. belly and neck mounting) as well as different impact orientations, positions, masses, surfaces and velocities. As a result of such test-rig flexibility, other impact configurations than the one corresponding to the reference case (named test-rig configuration 6) were explored at numerical simulation level, so that a possible test-matrix for the experimental campaign with the reduced set-up was proposed. Among these test-rig configurations, four (including the reference case) were identified as the most relevant ones and subsequently for complexity reasons only this subset of configurations was tested (see test-rig configurations 2, 5, 6 and 7 in Figure 5). The specimen is mounted as it is applied in the vehicle but upside down, since this allows the highest flexibility and accuracy of the test rig set-up on a crash test facility. Here, the tests are documented using load-cells at the mounting plate and high-speed video cameras from different positions.

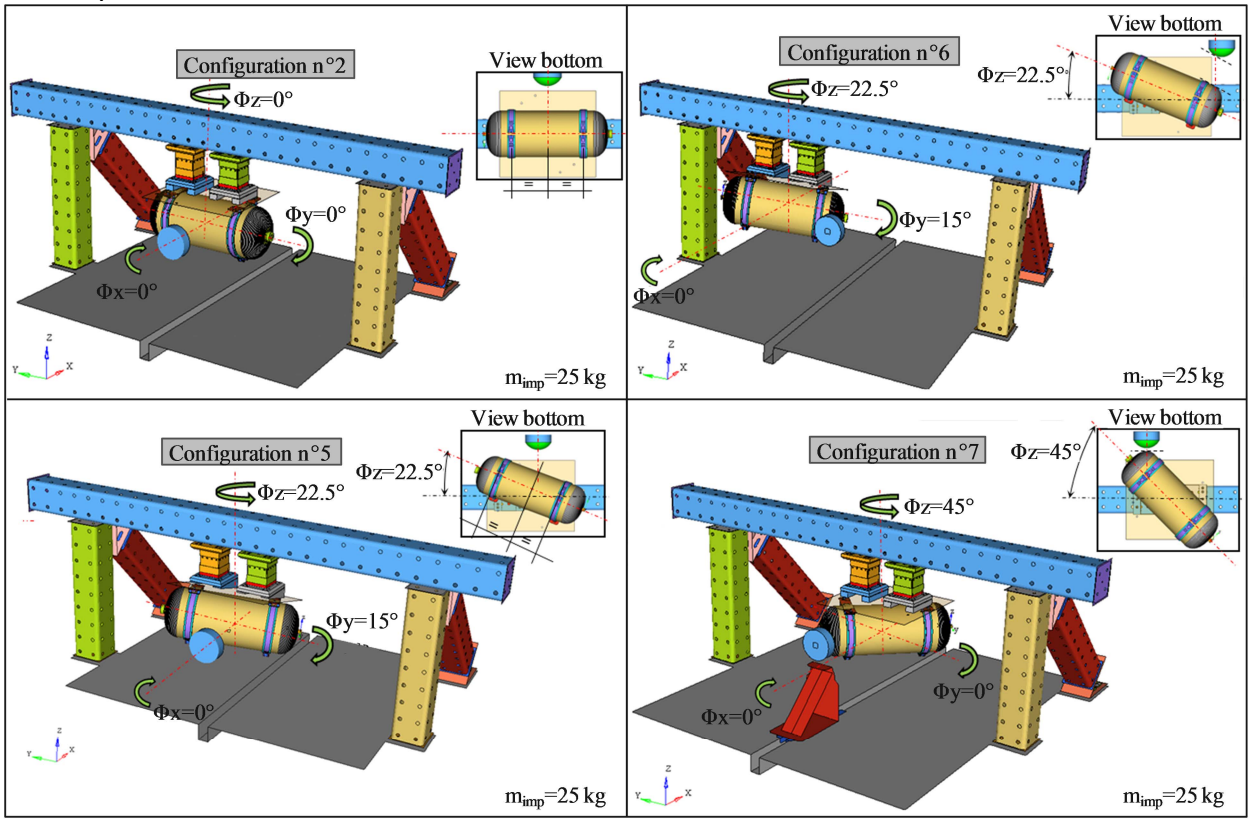


***Figure5. Simplified test set-up and analysed impact configurations***

After the conduction of the tests several evaluations were carried out. These were analysis of force and acceleration curves measured on the test rig, optical check of tank surface as well as of the mounting straps and interior, microscopy and CT of cut-out specimens as well as burst pressure and cycling pressure tests in order to understand the failure criteria and to see potential areas of hazard (see Figure 6). Furthermore, the experimental results were applied in order to validate the stage 2 model and to subsequently derive the simplified stage 3 model, i.e. the final one that is suitable for the application in all the VTM steps, then closing the methodology loop for potential future structural optimisation or evaluation of different vehicle and tank structures.

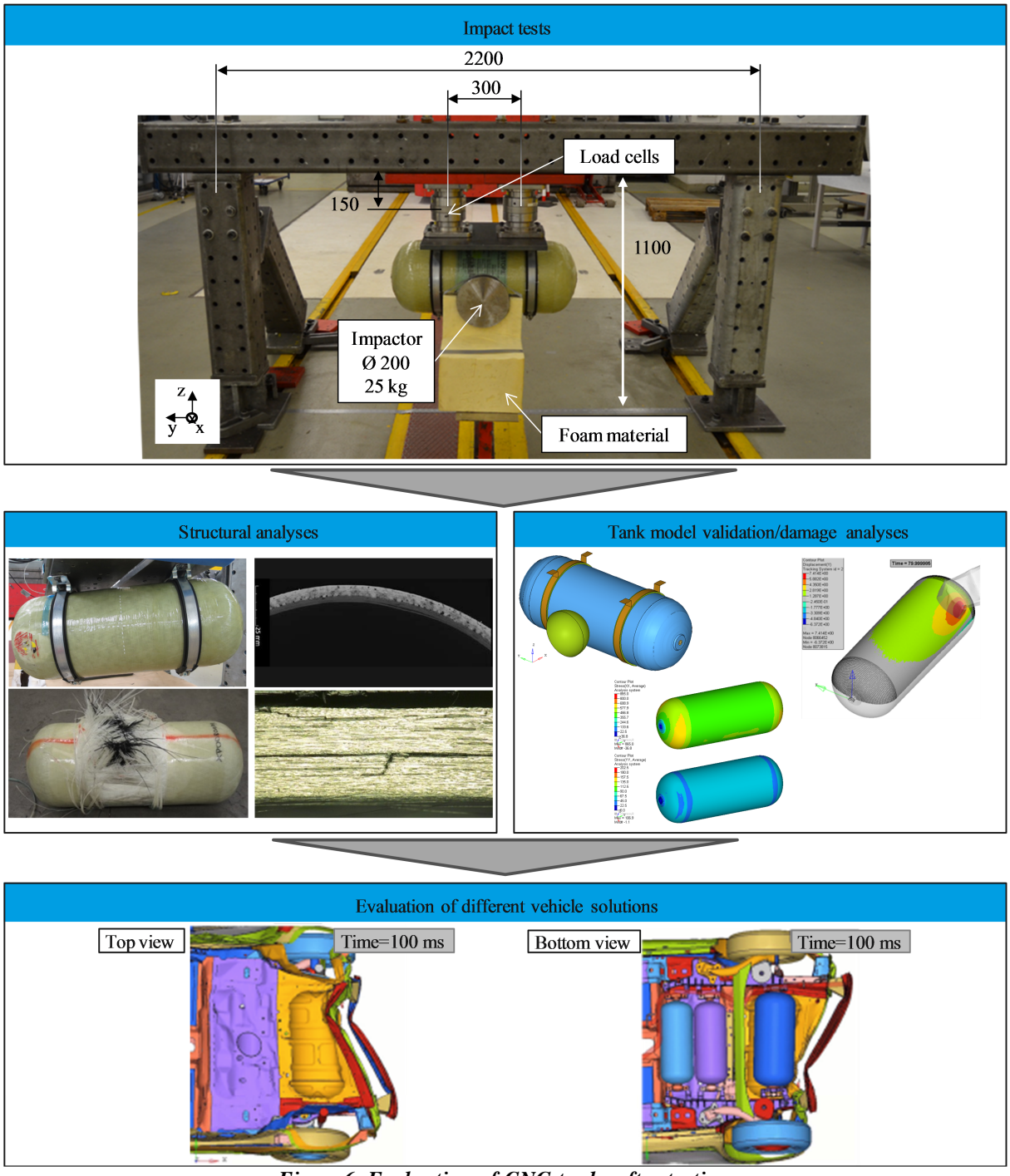


***Figure6. Evaluation of CNG tanks after testing***

## CONCLUSIONS

A stepwise virtual testing methodology for the evaluation and optimisation of vehicles equipped with CNG tanks was developed in the MATISSE project. This methodology allows a reduction of the development effort related to the crash safety design of such a type of APV, on the basis of a validated vehicle simulation model and a simplified experimental test rig set-up that is suitable for the evaluation of the tank crash behaviour as well as for the validation of an appropriate tank model for the crash simulation.

In the course of the methodology a set of relevant crash load cases (at full vehicle level) was defined and subsequently modelled in the FEM environment by using the vehicle model of interest that includes the adopted tank model(s) according to the specific lay-out solution to be examined. Based on the simulation results from this scenario, the most relevant loading conditions acting on the tank(s) can be isolated and further analysed. The results of such an analysis can be used for the definition of a suitable simplified and equivalent test-rig configuration as well as for an adequate experimental test programme. With the conduction of physical tests according to that test programme and together with their corresponding FEM simulations, a tank model can be improved/refined to cover adequately the composite behaviour under impact conditions. Furthermore, it can be validated against the obtained experimental results and subsequently reduced/simplified in order to be more efficiently applied in full vehicle simulations, by maintaining at the same time an appropriate level of failure prediction/detection during the industrial development process of CNG tanks and vehicles equipped with such systems.

## ACKNOWLEDGEMENT

All the presented work was carried out within the project MATISSE funded by European Commission's 7$^{th}$ Framework Programme.

The authors would like to acknowledge the MATISSE partners Xperion Energy & Environment GmbH and DYNAmore Nordic AB for the collaboration since the very beginning of the project.

**REFERENCES**

[1] Eichhorn, U. 2012. “Mobility for the Future”
Proceedings, 21st Aachen Colloquium Automobile and Engine Technology 2012
[2] Wu, J.; Dunn, S. C. 1995. “Environmentally responsible logistics systems“
International Journal of Physical Distribution & Logistics Management, Vol. 25 Iss: 2, pp.20 – 38
[3] N.N.. 2012. “Fortschrittsbericht der Nationalen Plattform Elektromobilität (Dritter Bericht)“
Bundesministerium für Umwelt, Naturschutz, Bau und Reaktorsicherheit, Germany
[4] da Silveria, B. H.; Benvenuti, L. H.; Werninghaus, E.; Coelho, E. P. D.; Silva, C. D.; de Olivera, F. R.; Silva,m J. C. S. 2004. “Development of a Concept Vehicle for Compressed Natural Gas”
SAE Technical Paper Series, Paper No. 2004-01-3452
[5] Gaudio, R.; Volpi, E. 2009. “Position Paper: Natural Gas and $CO_2$ - Natural gas is a champion in road transport and also saving $CO_2$ emissions”
Position Paper of NGVA Europe
[6] Hansen, G. P.; Sato, M.; Yan, Y. 2010. “Pressure Vessels for Hydrogen Vehicles: An OEM Perspective”
International Hydrogen Fuel and Pressure Vessel Forum, Beijing
[7] Liu, G. R.; Quek, S. S. 2003. “Finite Element Method – A Practical Course”
Elsevier B.V.
[8] Venkataraman, S.; Haftka, R. T.1999. „Optimization of Composite Panels – A Review”
Proceedings, American Society for Composites
[9] Bueno, P.; Mallen, J.; Rodrigo, J.; Cordero, R.; Garcia, J. 2012. “D3.2 – Overview on accreditation procedures in Europe”
Project Deliverable, imviter Project, FP7–2007–SST–218688
[10] N.N. http://www.ingas-eu.org INGAS Project Final Report and INGAS second annual report - Publishable Executive Summary

# ENHANCEMENT OF OCCUPANT SAFETY IN OFFSET FRONTAL VEHICLE COLLISION: USING NOVEL MATHEMATICAL MODELLING ALONGSIDE VEHICLE DYNAMICS CONTROL SYSTEMS

**Mustafa, Elkady**
Lebanese International University,
Lebanon
Ain Shams University,
Egypt

**Ahmed, Elmarakbi**
**John, MacIntyre**
University of Sunderland,
UK

15-0409

## ABSTRACT

Occupant safety is one of the most important issues for vehicle manufacturing. Active safety plays an important role to protect the occupant during the crash events. In this paper, vehicle dynamics control systems (VDCS) are used to enhance the occupant safety in offset frontal vehicle collision. VDCS are activated to optimize the vehicle in impending collision. A new mathematical modelling of the vehicle alongside VDCS is developed to study the effect of vehicle dynamics control systems on vehicle collision mitigation. A multi -body occupant mathematical model is developed to capture the occupant kinematics during frontal offset collision. Different cases of vehicle dynamics control systems have been used to show their effect on the occupant dynamic response. The occupant deceleration and the occupant's chest and head rotational acceleration are used as injury criteria. It is shown from the numerical simulations that the occupant behaviour can be captured and analysed quickly and accurately. Furthermore, it is shown that the VDCS can affect the crash characteristics positively and the occupant safety is improved.

## INTRODUCTION

The most well-known pre-collision method is the advance driver assistant systems (ADAS). The aim of ADAS is to mitigate and avoid vehicle frontal collisions. The main idea of ADAS is to collect data from the road (i.e. traffic lights, other cars distances and velocities, obstacles, etc.) and transfer this information to the driver, warn the driver in danger situations and aide the driver actively in imminent collision. There are different actions may be taken when these systems detect that the collision is unavoidable. For example, the brake assistant system (BAS) [1] and the collision mitigation brake system (CMBS) [2] were used to activate the braking instantly based on the behaviour characteristics of the driver, and relative position from the most dangerous other object for the moment.

During frontal vehicle collision, it is found that the vehicle body pitch and drop play an important role in driver's neck and head injury [3, 4]. Vehicle body pitch and drop have normally been experienced in frontal crash tests. Chang et al. [3] investigated frame deformation upon full-frontal impact using a finite element (FE) method and discussed the cause and counter-measures design regarding vehicle body pitch and drop. It was found that downward bending generated from the geometric offsets of the frame rails in the vertical direction during a crash is the key feature of the pitching of the vehicle body.

Using mathematical models in crash simulation is useful at the first design concept because rapid analysis is required at this stage. In addition, the well-known advantage of mathematical modelling provides a quick simulation analysis compared with FE models. Vehicle crash mathematical modelling is used to represent the vehicle front structure [5]. Also, other analyses and simulations of vehicle-to-barrier impact using a simple mass spring model were established by [6]. A simple lumped-parameter model is used, discussed the applicability of providing variable energy-absorbing properties as a function of the impact speed [7]. The occupant can also be modelled mathematically as a one-mass model [8], a two-mass model [9], a three-mass mode [10] or a multi-mass model [11]. In the most of these studies, the researchers claimed that simple occupant mathematical models can obtain usefully similar results to sophisticated analytical and experimental work.

Vehicle dynamics control systems (VDCS) play an important role in improving vehicle stability, ride characteristics, and passenger safety. On the other hand, the effect of VDCS on vehicle crashworthiness and collision mitigation is considered in several studies. The influence of the braking force on vehicle impact dynamics in low-speed rear-end collisions was studied [12] and this confirmed that the braking force was not negligible in high-quality simulations of vehicle impact dynamics at low speed. The effect of vehicle braking and anti-pitch control systems on the crash routine have been investigated by Hogan [13], who also investigated the possibility of using VDCS to improve vehicle collision performance in full and offset frontal vehicle to barrier collision.

However, there are no studies have been found that investigate the effect of VDCS on the occupant safety. From the existing literature, it is clear that research work done on the effect of VDCS on the occupant safety is rare. Hereafter the current study is fulfilled to determine the occupant response in offset crash scenario with different cases of VDCS. To accomplish this study, a mathematical multi-body occupant model has been developed.

## THE NEW VEHICLE DYNAMICS/CRASH MATHEMATICAL MODELLING FOR PRIMARY IMPACT

The primary impact indicates the collision between the front-end structure of the vehicle and an obstacle (another vehicle in this paper). This section describes a 6-DOF vehicle dynamics/crash-mathematical model, shown in Figure 1, which has been former developed by the author [14], for one vehicle and in case of a crash scenario between the two vehicles, where subscript *a* denotes vehicle (a) which is equipped with the VDCS and a subscript *b* denotes vehicle (b) which is used in a free rolling case for all crash scenarios. This model has been used to study the effect of vehicle dynamics control systems on vehicle collision mitigation.

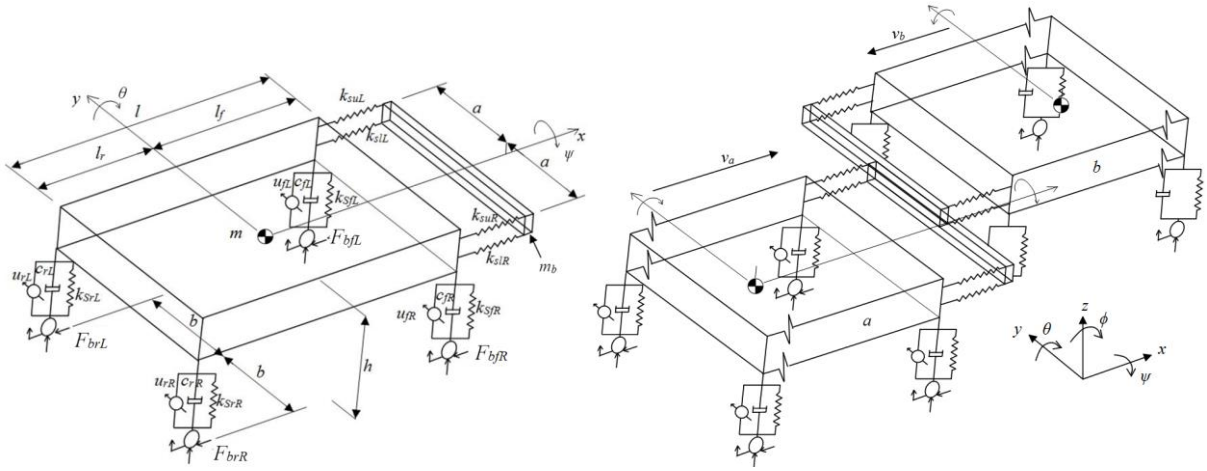


***6-DOF one vehicle model*** ***vehicle-to-vehicle offset crash scenario***

***Figure 1. Vehicle dynamics/crash-mathematical model***

As shown in Figure 1, four spring/damper units are used to represent the conventional vehicle suspension system. Each unit has a spring stiffness $k_S$ and damping coefficient c. The subscripts *f, r, R* and *L* denote the front wheels, real wheels, right wheels and left wheels, respectively. The ASC system is co-simulated with the conventional suspension system to add or subtract an active force element u, and the ABS is co-simulated with the mathematical model using a simple wheel model to generate the braking force $F_b$. To represent the front-end structure of the vehicle, four nonlinear springs with stiffness $k_s$ are proposed. Two springs represent the upper members (rails) and two springs represent the lower members of the vehicle frontal structure. The subscripts u denotes the upper rails while the subscript *l* denotes the lower rails. The bumper of the vehicle is represented by a lumped mass $m_b$ and it has only a rotational motion about the point of collision. The equations of motion and control systems have been described in details in a previous study by the author [14] to predict the vehicle deceleration, pitching angle and acceleration, and yawing angle and acceleration. These outputs from the vehicle model are used as input data for the occupant model.

**MULTI-BODY OCCUPANT MODEL (SECONDARY IMPACT)**

The occupant biodynamic model, with its different views before and after the crash shown in Figure 2, is developed to evaluate the occupant kinematic behaviour during the secondary impact. The secondary impact is the interaction between the occupant and the restraint system and/or the vehicle interior due to vehicle collisions. The human body model consists of three bodies, with masses $m_1$, $m_2$ and $m_3$. The first body (pelvis), with mass $m_1$, represents the legs and the pelvic area of the occupant and it is considered to have a translation motion in the longitudinal direction and rotation motions (pitching, rolling and yawing) with the vehicle body. The second body (chest), with mass $m_2$, represents the occupant's abdominal area, the thorax area and the arms and it is considered to have a translation motion in the longitudinal direction and rotation motion around the pivot between the pelvis and the chest bodies (pivot 1). The third body (head), with mass $m_3$, represents the head and neck of the occupant and it is considered to have a translation motion in the longitudinal direction and rotation motion around the pivot between the chest and the head (pivot 2). A rotational coil spring is proposed at each pivot to represent the joint stiffness between the pelvis and the chest areas and between the chest and the head areas, respectively. The seatbelt is represented by two linear spring-damper units between the compartment and the occupant; the frontal and side airbags are represented by tow linear spring-damper units for each one.

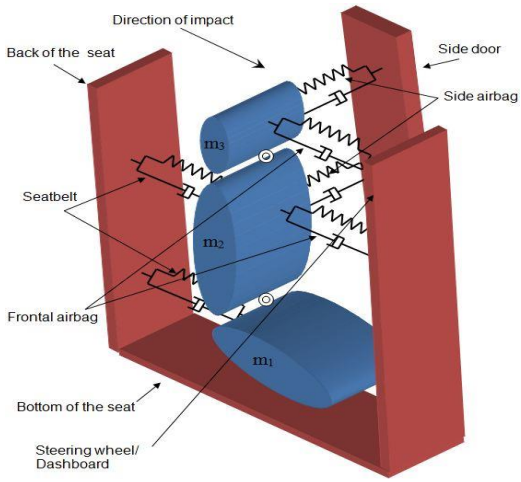


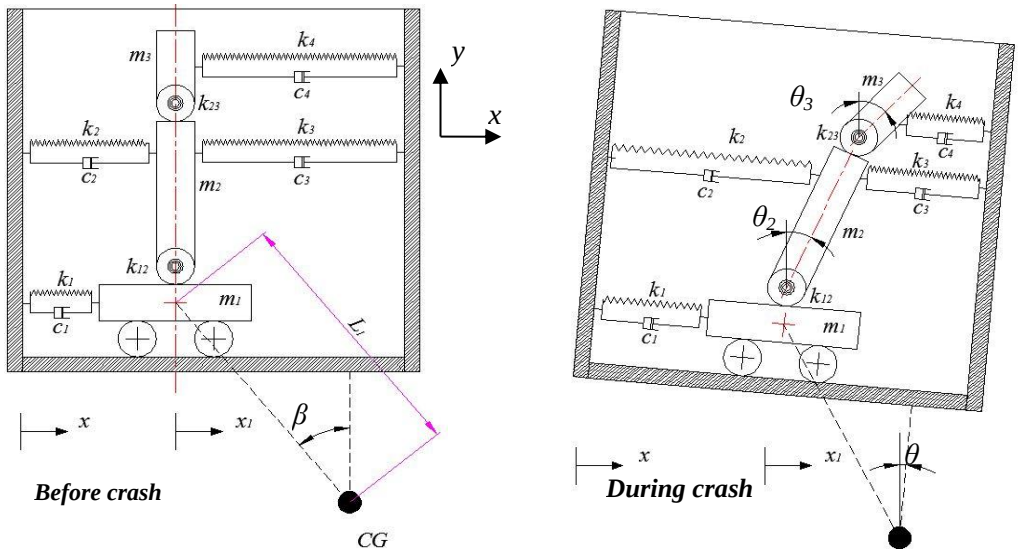


***Side view of the occupant model***

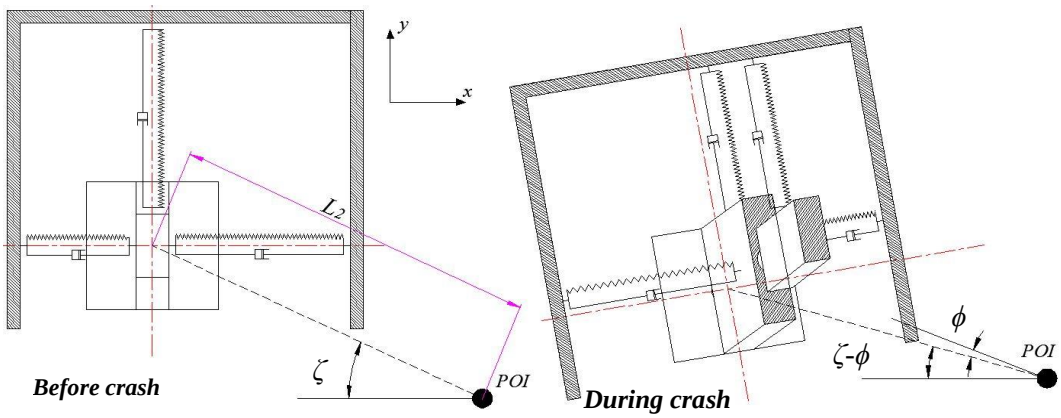


***Top view of the occupant model (POI: Point of Impact)***

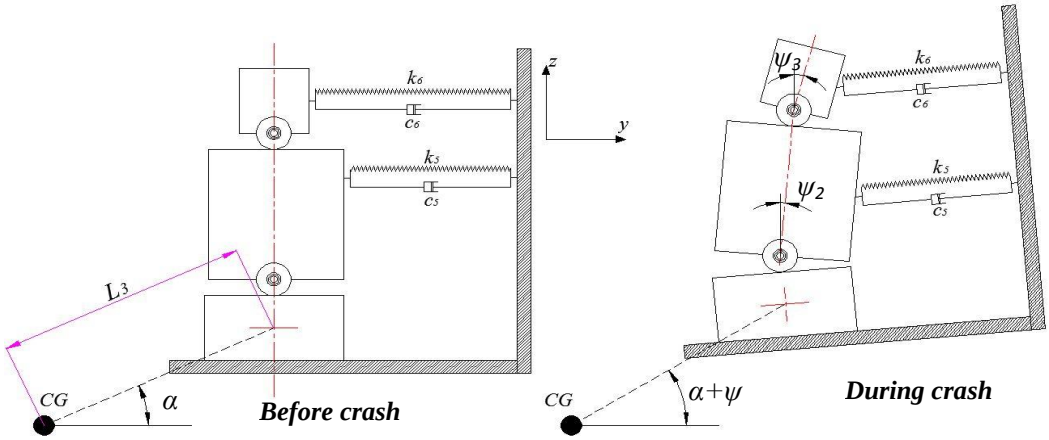


***Frontal view of the occupant model***

***Figure 2. Multi-body occupant model (secondary impact) and its different views before and during the crash***

**Equation of Motion (EOM) of the Human Body Model**

Due to the complexity of obtaining the equation of motions directly from the system, Lagrange's equations have been used to describe the general motions of the multi-body human model as follows:

$$\frac{d}{dt}\left(\frac{\partial E}{\partial \dot{x}_1}\right)-\frac{\partial E}{\partial x_1}+\frac{\partial V}{\partial x_1}+\frac{\partial D}{\partial \dot{x}_1}=0 \tag{1}$$

$$\frac{d}{dt}\left(\frac{\partial E}{\partial \dot{\theta}_2}\right)-\frac{\partial E}{\partial \theta_2}+\frac{\partial V}{\partial \theta_2}+\frac{\partial D}{\partial \dot{\theta}_2}=0 \tag{2}$$

$$\frac{d}{dt}\left(\frac{\partial E}{\partial \dot{\theta}_3}\right)-\frac{\partial E}{\partial \theta_3}+\frac{\partial V}{\partial \theta_3}+\frac{\partial D}{\partial \dot{\theta}_3}=0 \tag{3}$$

$$\frac{d}{dt}\left(\frac{\partial E}{\partial \dot{\psi}_2}\right)-\frac{\partial E}{\partial \psi_2}+\frac{\partial V}{\partial \psi_2}+\frac{\partial D}{\partial \dot{\psi}_2}=0 \tag{4}$$

$$\frac{d}{dt}\left(\frac{\partial E}{\partial \dot{\psi}_3}\right)-\frac{\partial E}{\partial \psi_3}+\frac{\partial V}{\partial \psi_3}+\frac{\partial D}{\partial \dot{\psi}_3}=0 \quad (5)$$

where *E, V* and *D* are the kinetic energy, potential energy and the Rayleigh dissipation function of the system, respectively. $x_1$, $\theta_2$, $\theta_3$, $\psi_2$ and $\psi_3$ are the longitudinal movement of the occupant's pelvis, the rotational angle of the occupant's chest about (*y*) axis, the rotational angle of the occupant's head about (*y*) axis, the rotational angle of the occupant's pelvis about (*x*) axis and the rotational angle of the occupant's head about (*x*) axis, respectively. $\dot{x}_1$, $\dot{\theta}_2$, $\dot{\theta}_3$, $\dot{\psi}_2$ and $\dot{\psi}_3$ are their velocities, respectively. To get the components of the equations 1, 2, 3, 4 and 5, the differentiations of the kinetic energy, potential energy, and Rayleigh dissipation function are determined. To solve these equations, they have been put in an integratable form and then rewritten in a matrix form. After that, different occupant's bodies responses ($x_1$, $\theta_2$, $\theta_3$, $\psi_2$ and $\psi_3$) can be determined based on the input data from the vehicle model by solving the equations numerically.

**NUMERICAL SIMULATIONS OF VEHICLE-TO-VEHICLE OFFSET-COLLISION SCENARIO**

Two different cases of VDCS are investigated in this section and their associated results are compared with the free rolling case scenario. These different VDCS cases are described as follows:

Case 1: Free rolling: - in this case the vehicle collides with a barrier/vehicle without applying any types of control.
Case 2: Anti-lock braking system (ABS): - in this case the anti-lock braking system is applied before and during the collision.
Case 6: Anti-lock braking system alongside under-pitch control system (ABS + UPC): - in this case, the vehicle is taken a reverse pitching angle before crash using an ASC system.

The injury criteria in this paper have been taken as occupant's pelvis deceleration, occupant's chest rotational acceleration, and head rotational acceleration. The vehicle output data (deceleration and pitching and yawing acceleration) due to the collision [14] are transferred to the occupant as a sudden deceleration to all the body. The following data is used in the numerical simulation: $m_1$ = 26.68 kg, $m_2$ = 46.06 kg, $m_3$ = 5.52 kg, $k_{R12}$ = 280 Nm/rad, $k_{R23}$ = 200 Nm/rad, $l_2$ = 0.427 m, $l_3$ = 0.24 m [10]. The total stiffness of the two seatbelt springs is 98.1 kN/m with a damping coefficient of 20% [8], and then it distributed between the upper and lower seatbelt springs by ratio of 2:3, respectively [15]. Airbag's spring stiffness is 5 kN/m and the damping coefficient is 20%. The slacks of the seatbelt springs are assumed zero, and the slack of the airbag is 0.05 m.

For the occupant's pelvis relative displacement for vehicle (a), it is shown that it increases forward to reach its maximum position and then returns due to the lower seatbelt springs. It is observed that there are insignificant differences between the values of the maximum relative displacement of the occupant's pelvis in the different cases of VDCS. Regarding to the lower-body deceleration of the vehicle (a), it is shown that it increases during the collision to reach its maximum values at the end of impact and then reduces after the effect of collision is ended. There is a sudden decrease of the deceleration at the end of collision, this is due to the reverse effect of the braking force when the vehicle changes its direction and starts to move backward. It is observed that the maximum deceleration is almost the same for all cases with very small differences. These small differences mean that the VDCS do have an insignificant effect on the pelvis relative displacement and deceleration.

The rotation angle of the occupant's chest about y axis for all cases of vehicle (a) is shown in Figure 3. The occupant's chest starts the collision with different rotational angles according to each case of the VDCS. The occupant takes this angle in the period of 1.5 sec prior collisions when the VDCS is applied. After that, the rotational angle of the occupant's chest remains constant for about 0.03 sec, then it increased to reach its maximum value after the end of the collision. The maximum rotation angle is observed in case 2, while the minimum one is observed in case 3 (ABS + UPC). The rotational acceleration about y axis of the occupant's chest is captured. The chest rotational acceleration increases gradually to reach its maximum positive value and then reduces to reach its maximum negative value. The maximum positive rotational acceleration is monitored in case 1 and the minimum one occurred in case 2, while the maximum negative rotational acceleration is shown in case 3 and the minimum is in case 2.

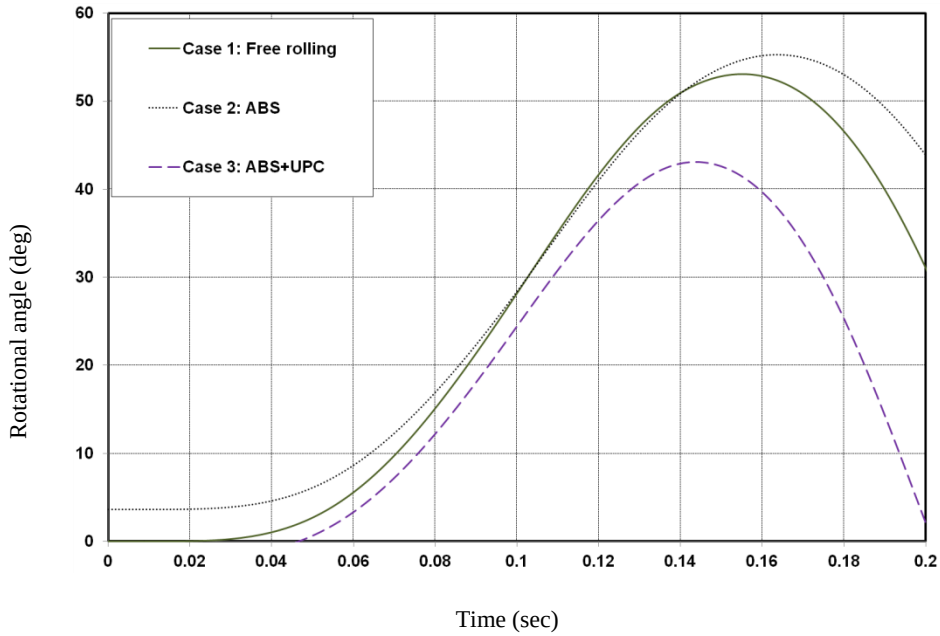


***Figure 3.*** **Rotational angle of the occupant's chest about y axis (Offset frontal vehicle-to-vehicle impact), vehicle (a)**

The rotation angle of the occupant's head about y axis is depicted in Figure 4. The head rotation angle increases rapidly for a period of time, which occurred during the increase of the chest rotation. Then, it increases fast due to the return of the occupant's chest to reach its peak value (maximum value). The peak value of the head rotational angle is observed in case 2, while the minimum one is detected in case 3. The rotational acceleration of the occupant's head is also shown, the acceleration increases with a different manner according to each case to reach its maximum value. These maximum values occurred in different time related to each case. In other words, the maximum acceleration in cases 1 and 3 occurs approximately at 0.07 sec, while in case 2 it occurs approximately at 0.08 sec. The minimum negative acceleration is observed in cases 2, while the maximum negative values are seen in cases 1 and 3.

The rotation angle about x axis of the occupant's chest for all cases of vehicle (a) is depicted in Figure 5. When the occupant's chest reaches its maximum rotational angle, it stays in this position for a period of time while the vehicle rotates around the point of impact. The maximum rotation angle is observed in case 1 (free rolling) while the minimum angle is observed in cases 3 (ABS + UPC). The rotational acceleration of the occupant's chest about x axis for all cases of vehicle (a) is obtained. There are three sudden changes in the acceleration during collision. The first one is due to the activation of the side airbag, while the second one is due to the reverse braking force. The third sudden change of the chest acceleration is due to the deactivation of the vehicle's front-end springs, which causes a sudden decrease of the vehicle pitching, yawing and rolling. The maximum positive rotational acceleration of the occupant's chest about x axis is observed in cases 1, while the minimum value occurs in case 3. The maximum negative rotational acceleration happens in case 1 and the minimum is observed in case 3. These negative acceleration values occur due to the force generated by the lower spring-damper system of the side airbag.

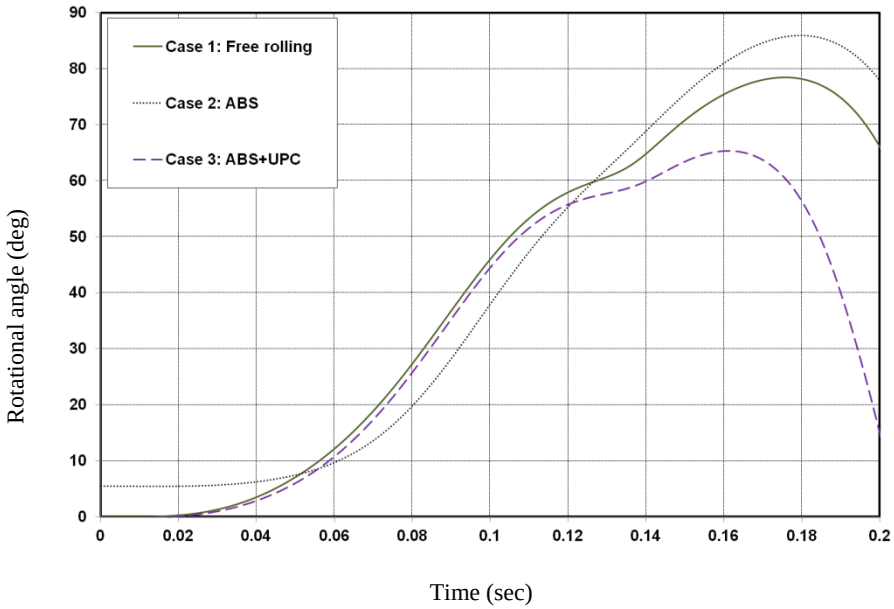


***Figure 4. Rotational angle of the occupant's head about y axis (Offset frontal vehicle-to-vehicle impact), vehicle (a)***

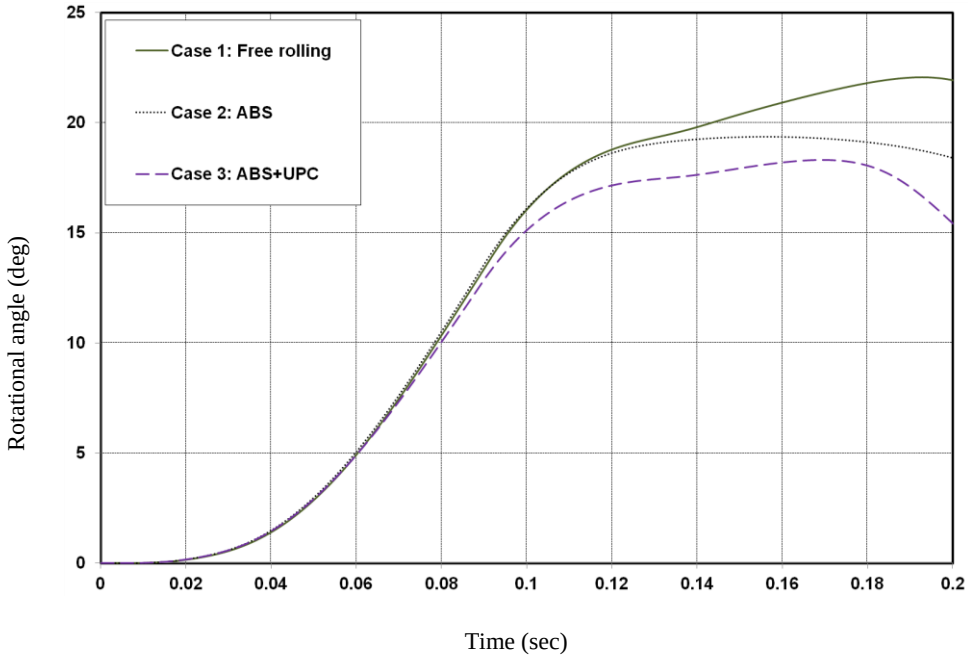


***Figure 5. Rotational angle of the occupant's chest about x axis (Offset frontal vehicle-to-vehicle impact), vehicle (a)***

The rotation angle about x axis of the occupant's head for the vehicle (a) is shown in Figure 6. At the beginning of the collision, while the chest takes a positive acceleration and starts rotating towards the vehicle's side door, the head takes a different negative small rotation value related to each case, all these values are close to 5 deg. The positive maximum value of the head rotational angle is observed in case 3, while the minimum peak angle is seen in case 2. The rotational acceleration about x axis of the occupant's head in all cases has been gained. The effect of the reverse braking force is observed at the end of the collision. The maximum positive acceleration (in the period from 0.06 to 0.1 sec) is almost the same for all cases, while the maximum negative acceleration (in the period from 0.1 to 0.16 sec), caused by the side airbag force, is observed in case 1 with relatively a higher value. The minimum negative acceleration is detected in case 2.

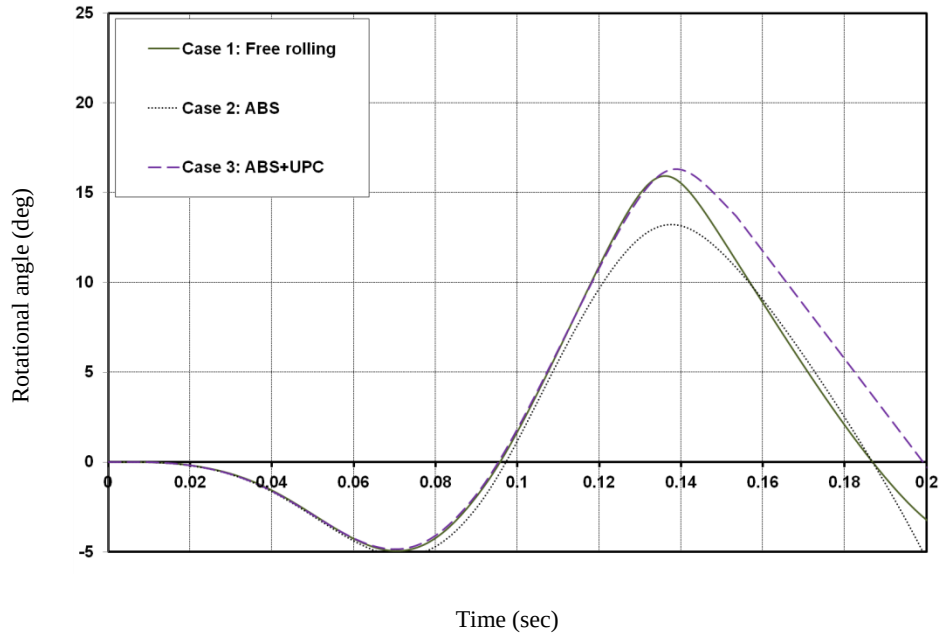


***Figure 6. Rotational angle of the occupant's head about x axis (Offset frontal vehicle-to-vehicle impact), vehicle (a)***

The occupant behaviour of the occupant of the vehicle (b) is also captured for all cases of the VDCS. It is shown that applying the VDCS for vehicle (a) has insignificant effect on the other vehicle.
Related to the occupant injury criteria, the occupant's head rotational accelerations appeared to be the major cause of strain-induced brain injury which it contributed to more than 80% of the brain strain and the peak amplitude of rotational acceleration must not exceed 9.4 krad/s$^2$ (538.5 kdeg/s$^2$) [16]. The results show some improvement in the occupant injury criteria, which makes the crash event more survivable. Use of under pitch technique (case 3) can help reduce the chest and head rotation angle, and head rotational acceleration. The VDCS affects the occupant's behaviour with different ways related to the applied case, and it can be seen that the applied of frontal UPC alongside ABS (case 3) can be taken as the best case due to its effect on the occupant's head (the most important part of the occupant's body). The future study, as extensions to this work, will be focused on the optimization of using different integrated VDCS.

## CONCLUSIONS

A multi-body occupant mathematical model has been developed to study the effect of VDCS on the occupant dynamic response during vehicle collision. Different cases of the VDCS have been investigated in case of vehicle-to-vehicle frontal offset collision. The results obtained from a previous vehicle model have been used as the input data for the occupant model. The results show that the effect of the VDCS is quite minimal in terms of occupant relative displacement and deceleration. However, there are a significant effect on the rotations angle and acceleration of the occupant chest and head, which are greatly enhanced.

## ACKNOWLEDGMENT

The authors would like to thank the Egyptian Government and the Faculty of Engineering, Ain Shams University for supporting this research.

## REFERENCES

[1] Tamura, M., Inoue, H., Watanabe, T., Maruko, N. Research on a Brake Assist System with a Preview Function. SAE International, Warrendale, PA, 2001, SAE Technical Paper 2001-01-0357
[2] Sugimoto, Y., Sauer, C. Effectiveness Estimation Method for Advanced Driver Assistance System and Its Application to Collision Mitigation Brake System. Proceeding 19th International Technology Conference, Enhanced Safety Vehicles, 2005, pp. 1–8.

[3] Chang J. M, Rahman M, Ali M, Tyan T, El-Bkaily M. and Cheng, J. Modeling and design for vehicle pitch and drop of body-on frame vehicles. SAE World Congress & Exhibition, Detroit, MI, USA, 2005, Paper No. 2005-01-0356.
[4] Chang J. M, Ali M, Craig R, Tyan T, El-bkaily M. and Cheng J. Important modeling practices in CAE simulation for vehicle pitch and drop. SAE World Congress & Exhibition, Detroit, MI, USA, 2006, Paper No. 2006-01-0124.
[5] Emori R. I. Analytical approach to automobile collisions. SAE World Congress & Exhibition, Warrendale, USA, 1968, Paper No. 680016.
[6] Kamal M. M. Analysis and simulation of vehicle to barrier impact. SAE World Congress & Exhibition, Detroit, USA, 1970, Paper No. 700414.
[7] Khattab, A. Steering system and method for independent steering of wheels (Ph.D. Thesis), The department of Mechanical and Industrial Engineering, Concordia University Montreal, Quebec, Canada, 2010.
[8] Elmarakbi, A. and Zu, J. Dynamic analysis of smart structures for vehicle-to vehicle frontal collision alleviation. Transaction of Society of Automotive Engineers of Japan, 2004, 35: 151-156.
[9] Renneker DN. A basic study of 'energy-absorbing' vehicle structure and occupant restraints by mathematical model. SAE International, Warrendale, PA, 1967, SAE paper 670897.
[10] Ilie, S. and Tabacu, S. Study of the occupant's kinematics during the frontal impact. Annals of the Oradea University, Fascicle of Management and Technological Engineering, 2007, VI (XVI).
[11] Roberts VL and Robins DH. Multidimensional mathe- matical modeling of occupant dynamics under crash con- ditions. SAE International, Warrendale, PA, 1969, SAE paper 690248,.
[12] Mastandrea M. and Vangi D. Influence of braking force in low-speed vehicle collisions. Proceedings IMechE, 2005, 219 (2): 151-164.
[13] Hogan I. and Manning W. The use of vehicle dynamic control systems for automotive collision mitigation [J]. 3rd Institution of Engineering and Technology Conference, Warwick, UK, 2007: 1-10.
[14] Elkady M, Elmarakbi, A and Crolla, D. A numerical study for optimizing vehicle dynamics control systems in offset impacts [J]. SAE World Congress & Exhibition, Detroit, USA, 2011, Paper No. 2011-01-0954.
[15] Paulitz, T. J., Blackketter, D. M. and Rink, K. K. Constant force restraints for frontal collisions [J]. Proceedings of the Institution of Mechanical Engineering, Part D: Journal of Automobile Engineering, 2006, 220(9): 1177-1189.
[16] Zhang, J. and Pintar, F. Brain Strains in Vehicle Impact Tests [J]. Annual Proceedings Associated Advanced Automotive Medicine, 2006, 50: 1-12.

# The RELATIONSHIP between BAC and BrAC of HEALTHY KOREAN MALE

**Seung-Hwan, Yi**
**Sang-Ho, Lee**
Department of Mechanical Eng., KNUT (Korea National University of Transportation)
Republic of Korea

**Beom-Woo, Nam**
**Jeong-Seok, Seo**
**Bo-ram, Lee**
**Min-Choul, Ahn**
Department of Psychiatry, Konkuk University Hospital
Republic of Korea

**Byong-Do, Kang**
**Jeong-Min, In**
KATRI (Korea Automotive Testing & Research Institute)
Republic of Korea

Paper Number 15-0410

**ABSTRACT**

BrACs (Breath alcohol concentrations) are often converted to the corresponding BACs (blood alcohol concentrations) by multiplying a partition ratio, Q. However, according to the previous researches, it has been revealed that it depended upon the nations. So, the partition ratio (or Q-factor) of healthy Korean adult males and its correlation to some variables including TBW (total body water), BMI (body mass index), BFM (body fat mass), and PBF (percentage of body fat) were revealed. The average of partition ratio did show particular difference around 100 when the subjects were divided with two sets: below and above the average of TBW. The partition ratio of Korean healthy males showed 1,913 (95 % confidence interval (CI) from 1,889 to 1,937) for whole time intervals. However, when Q was averaged after peak BACs, it gave 2,011 (95 % CI range from 1,982 to 2,040). Bland-Altman plots revealed the compatibility of measurement method of multi-gas analyzer, and the biases according to the partition ratios (Q=2,100 and Q=1,913) gave -0.0052 (95 % CI from -0.0059 to -0.0045) and -0.0004 (95 % CI from –0.0011 to +0.0003), respectively. From this study, the partition ratio of Korean healthy males has been reported for the first time with massive medical experiments.

**INTRODUCTION**

The vehicles are getting more and more important in modern life for traveling, commuting, and logistics etc.. As the numbers of automobiles increase, however, road traffic safety become a national-wide matter in order to diminish road traffic accidents and also fatalities. In Sweden, they declared Vision Zero slogan in order to eliminate any victom from the road traffic accidents [1]. Among the road traffic accidents, alcohol-related crashes and fatalities are the major issues around the world in terms of improving more safe road traffic situation. In order to alleviate alcohol-related accidents, most of nations use alcohol sensing appartus for screening drunken drivers and it measures BrAC by using optical components or fuel-cell type devices [2, 3].
Currently, the breathalyzers for monitoring BrAC are widely used in the world in order to screen impaired drivers at the roadside. The regal limit for impairments are 0.08 % in U.S. and 0.05 % in most European countries. Although, Sweden adopted a 0.05 % BAC limit in 1950s, the regal limit of BAC has been recently lowered to 0.02 % in order to improve traffic safety further. By lowering regal limit, James and Robert reported that fatal crashes and severe personal injuries have been decreased and settled down more safe road traffic situation than ever [4]. In 1962, Korean government legitimated the road traffic law in order to enforce alcohol-impaired driving. After four decades, BrAC analysis for road traffic offences is regulated in 2006, setting a regal BAC limit of 0.05 % for driving. Also, there were several trials to decrease the regal limit of BAC to 0.03 % for road traffic safety and for decreasing alcohol-related fatalities.

Since the consumed alcohol is eliminated from the body also through the exhaled air that is coming from deep lungs [5, 6], the measurement of BrAC has been evaluated to analyze BAC for decades. The relationship between BAC and BrAC has been studied for long time, so BAC is currently converted from BrAC by multiplying by a BAC/BrAC ratio known as partition ratio or conversion factor, Q. The US NHTSA (National Highway Traffic Safety Administration) uses a conversion factor, Q, as 2,100 [7], this value was also adopted for converting BrAC to BAC in Korea. However, Jones and Andersson reported that most countries adopt a conversion factor of 2,000 to 2,300 [8]. Furthermore, the recent study showed that the conversion factor could be ranged from 2,225 to 2,650; Jones and Andersson reported the average conversion factor was 2,448 in their article [9], Pavlic et al. presented the time dependency of Q ranged from 2,225 to 2,650 [10], and Lindberg et al. showed that the BAC/BrAC ratio was 2,251 in case of Swedish subjects [1].
Since the conversion factor, Q, is relavant to BAC determined from breathalyzer and also it is relatively different from country to country, the aim of this study is to identify the BAC/BrAC ratio of Korean healthy males and its correlation to some variables: TBW, BMI, BFM, and PBF in this research.

## MATERIALS AND METHODS

### Subjects

One hundred and one individuals, whole healthy males, were enrolled in this study as paid volunteers. Ages ranged from 20 to 50 years and body weights ranged from 55 to 78 kg. Whole subjects were not heavy consumers of alcoholic beverages (less than two bottles of Soju (20 % (v/v) in their regular lifestyle). The study was approved by the Ethics committee of Konkuk University Hospital, Korea.

### Experiment procedures

The volunteers were recruited by posting announcement through internet or public board. The volunteers were screened by psychiatric doctor with basic medical and psychiatric checkup containing physical examination, vital sign, CBC (complete blood count), LFT (liver function test), vital sign check, Alcohol Use Disorder Identification Test-Korea (AUDIT-K), CAGE (cut-down, annoyed, guilty, eye-opener) survey. Finally, 101 individuals were selected and participated in this research. Whole participants checked up their current physical status by measuring weight, height, TBW, BFM, PBF, and BMI, which were analyzed by InBody 720 (InBody Co., LTD.). Since it roughly took 2 minutes to analyze one breath sample, the volunteers were divided into ten groups. The volunteers belonged to each sub-group were randomly selected and each subject was asked to consume 0.35 mg/ml/kg or 0.7 mg/ml/kg Soju (30 % (v/v)) for 15 minutes. After consuming alcohol, they are allowed to rinse the mouth with drinking water in order to ensure the absence of mouth alcohol before the first testing, however, not allowed to drink water until 2 hours after consuming whole alcohol. The samples (one blood and two breath) were obtained at timed intervals of 15, 30, 45, 60, 90, 120, 180, 240 minutes after drinking alcohol in order to reveal the relationship between BAC and BrAC for healthy Korean males. The BAC/BrAC ratio was analyzed according to the four body index (TBW, BFM, PBF, and BMI). In order to avoid complexity in subsequent data interpretation, no food and mixing of different alcohol were allowed, furthermore, violent physical activity was not allowed during the experiment also.

### Collection of blood and BAC analysis

After drinking of alcohol within 15 minutes, a blood sample of 2 mL was drawn from the proximal stopcock which is connected to the indwelling catheter at each timed interval as mentioned earlier and injected into a 3 mL Vacutainer tube (BD Franklin, Lake NJ, USA), containing EDTA (Ethylene-diamine tetra-acetic acid). The tubes were stored in a refrigerator at 4 to 6 °C and brought to Neodin medical Institute located in Seoul the day after the experiments were finished for each sub-group. Each delivered blood sample was analyzed by enzymatic methods (COBAS Integra 800, Roche USA) twice times in order to reveal BAC.

### BrAC Measurements

One breath sample for each volunteer was collected with 3 liter non-odor bag (TK005-N-003, BMS Corp., Japan) at the same time the blood sample drawn from the indwelling catheter and analyzed with INNOVA-1312 multi-gas analyzer (LumaSense Technologies, Denmark). The analyzer used in this study consists of two main components:

optical and acoustical measurement units. By adopting photo-acoustic measuring principles, it could analyze gases from ppb to ppm level. So, this analyzer has been selected as a reference BrAC measurement apparatus in this study. However, in order to enhance the measurement reliability, the multi-gas analyzer was sent back to the manufacturer for adding a new filter (for ethanol measurement) and was calibrated in order to secure the accuracy of measurement. After measuring each breath sample three times with multi-gas analyzer, the average BAC has been converted ppm level to percentage level by multiplying conversion factors. The other breath samples for each person were measured by using four portable breathalyzers (AL9000, Sentech Corp., Korea) at timed intervals of 15, 30, 45, 60, 90, 120, 180, 240 minutes after drinking alcohol. Then four-measured values were averaged after finishing tests for comparison. Each portable breathalyzer was also calibrated before the experiments to alleviate the reliability issues raised in fuel-cell type breathalyzer.

**Calculation of Q**

The partition ratio, Q, was individually calculated for each subject from the ratio of the mean BAC value to the average BrAC value determined from the multi-gas analyzer in this study. However, the ratio of BAC to BrAC value, Q, assumed to be 2,100 in portable breathalyzer because Korean jurisdiction admitted this value currently. All statistical parameters such as average, standard deviations of average and 95 % confidence intervals for the calculated parameters were acquired with MS Excel 2013 and also Sigma Plot 12.5.

**RESULTS and DISCUSSION**

After arranging BAC results according to the elapsed times, Korean adult males show three characteristic alcohol metabolisim patterns as shwon in Figure 1: left-shifted, standard, and right-shifted patterns (five mixed patterns are excluded in this analysis). The numbers of subjects belonged to each category denote as n in Figure 1. Compared to Figure 1 b), left-shifted pattern reveals no peak of alcohol concentration in their blood, however, right-shfited (also standard) type presents a peak alcohol concentration after 90 mins later in this subject. As can be inferred from Figure 1, the alcohol metabolism of Korean adult males could be divided into three characteristic patterns.

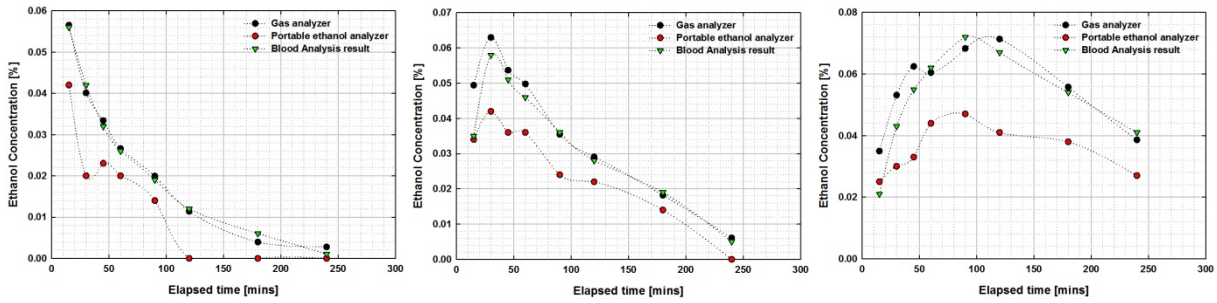


***Figure 1. Three characterisitic patterns of BAC: a) left-shited (n=29), b) standard (n=52), c) right-shfited(n=15).***

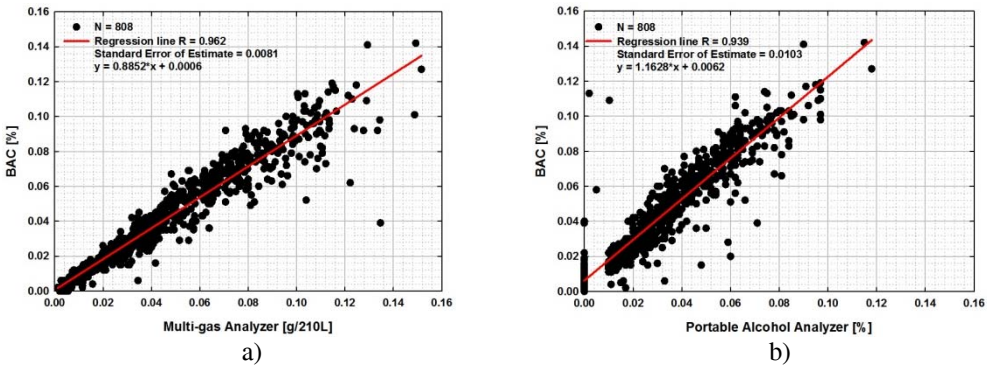


***Figure 2. Relationship between BAC and BrAC with two different BrAC measurements.***

Figure 2 shows the relationship between BACs and BrACs measured by two different apparatus: multi-gas analyzer and portable breathalyzer with an assumed partition ratio, Q=2,100 (N=808, numbers of whole measured values). In case of multi-gas analzyer, BACs are overestimated as depicted in Figure 1 a); regression line *y=0.8852x+0.0006 with R=0.962*. However, when breath alcohol concentrations are measured with portable breathalyzer, BACs were underestimated as can be seen in Figure 1 b); regression line *y=1.1628x+0.0062, wih R=0.939*. Even though there was small bias that is roughly 10 % of the error (± 0.005 %) with the measurement of multi-gas analzyer, the data measured by breathalyzer showed little higher offset value in BAC measurement. Furthermore, even BACs had some meaningful values, the breathalyzer didn't monitor the actual BACs in some subjects.

Since there were some differnces between BAC and BrAC measurements in both cases when the partition ratio, Q, was used as 2100, the partition ratio was calculated according to the elapsed time. Low BACs which are less than 0.01 % are excluded in this analysis in order to increase the accuracy of partition ratio. Also, the average value of $T_{max}$, which means the average time that BAC reaches the highest value after consuming alcohol in this study, was 55 mins [11], so the partition ratios were calculated with this time reference and showed as in Figure 3. During the absorption period (which was less than 60 mins after consuming alcohol), average of Q was 1,779. However, after 60 mins (this time intervals belonged to the digestion of alcohol), the average partition ratio was 2,011. Furthermore, when whole data were calculated without the time limitation, the average partition ratio of healthy Korean males was calculated as 1,913.

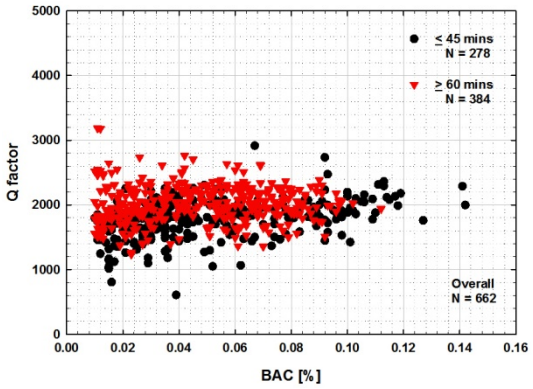


***Figure 3. Partition ratio as a function of BAC***

When total body waters were above and below the average value (42.4 Liters), the average of Q-factor was 1,903 (95% C.I. 1,870 to 1,938) and 1,999 (95% C.I. 1,966 to 2,033), respectively. In terms of BMI, the average of BMI was 25 for healthy Korean male. When BMI was above the average value, the partition ratio showed 1,935 (95% C.I. 1,887 to 1,983). When the partition ratios were categorized into body fat mass (BFM) and percentage body fat (PBF), the averages of partition ratio presented 1,950 (95 % C.I. 1,916 to 1,983) and 1,957 (95 % C.I. 1,924 to 1,990) when BFM and PBF are above the average values, respectively. The data related to partition ratio according to body index were listed in *Table 1*.

***Table 1. Partition ratio according to body index (excluded BACs less than 30 mins)***

| Categories | | BMI | | TBW | | BFM | | PBF | |
|---|---|---|---|---|---|---|---|---|---|
| | | Above Ave. | Below Ave. | Above Ave. | Below Ave. | Above Ave. | Below Ave. | Above Ave. | Below Ave. |
| Average values | | 1,935 | 1,951 | 1,903 | 1,999 | 1,950 | 1,941 | 1,957 | 1,934 |
| 95 % C.I. | Lower Limit | 1,887 | 1,924 | 1,870 | 1,966 | 1,916 | 1,905 | 1,924 | 1,898 |
| | Upper Limit | 1,983 | 1,979 | 1,938 | 2,033 | 1,983 | 1,976 | 1,990 | 1,979 |
| Standard Deviation | | 315 | 284 | 308 | 267 | 285 | 304 | 284 | 305 |

The partition ratio (Q=2,011 after 60 mins later) would be a important factor in order to calculate the estimated BAC when the extrapolated BAC is needed to evaluate initial BAC value [12] by police. Also the average partition ratio, after drinking alcohol without time limit, would be essential to the manufacturer of BAIIDs (breath alcohol ignition interlock devices) since the user of BAIIDs would be requested to pass the rolling retest during driving [13, 14]. So, it would be valualbe to know the relationship between BACs and BrACs as a parameter of partition ratio and showed their relationship in Figure 5. As can be seen in Figure 5, when

Q=2,100 was adopted to calculate the BACs, the actual BACs would be overestimated by the exhaled breath samples. The regression line showed *y= 0.8615x+0.0023* with R=0.944 in this case (Q=2,100). It would be certain that the measurement results can be not favorable to Korean healthy males. However, when the partition ratio is less than 2,100, as denoted in Q=1,913 (depicted in red dots), BrACs product by Q showed more favorable matches that the previous results with regression line, *y= 0.9457x+0.0023*, with R=0.944.

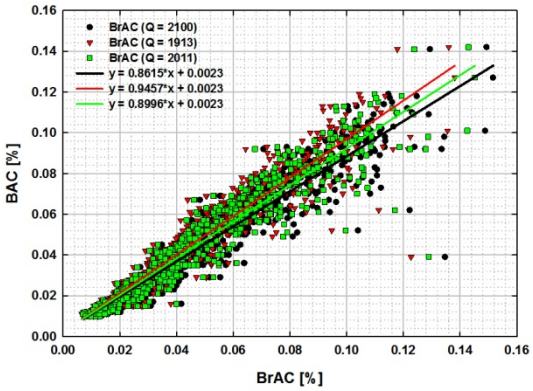


***Figure 5. BAC vs. BrAC according to the partition ratio, Q.***

In order to assure the capability of replacement of invasive BAC measurement, Bland-Altman plots according to the partition ratios (Q=2,100 and Q=1,913) have been presented in Figure 6. If there is no or small bias in Bland-Altman plot, it is well known that a new experimental apparatus or device could be replaceable in medical checkup etc. As described in Figure 6 a), when the partition ratio, Q, was used as 2,100, there was a bias with -0.0052 and showed its 95 % CI from -0.0059 to -0.0045. Also the limits of agreement ranged from -0.0242 to 0.0138. Even though it is not shown in this article, when Q=2,011 is adopted, the bias showed -0.0029 and its 95 % CI marked from -0.0036 to -0.0022. However, when Q=1,913 was multiplied to BrACs in order to calculate BACs, the bias showed -0.0004 and revealed its 95 % CI from –0.0011 to +0.0003. Furthermore, the limits of agreement of evaluation ranged from -0.0179 to +0.0171. Since the limit of agreement had offset toward negative value in case of Q=2,100, the measured values from multi-gas analyzer would clearly exaggerate BACs as mentioned in Figure 5. From the results mentioned above in Figure 5 and Figure 6, it is clear that the average value of partition ratio calculated with the whole time interval BAC/BrAC ratio will be more reasonable than the value of Q (=2,100) used in current breathalyzer for Korean adult males.

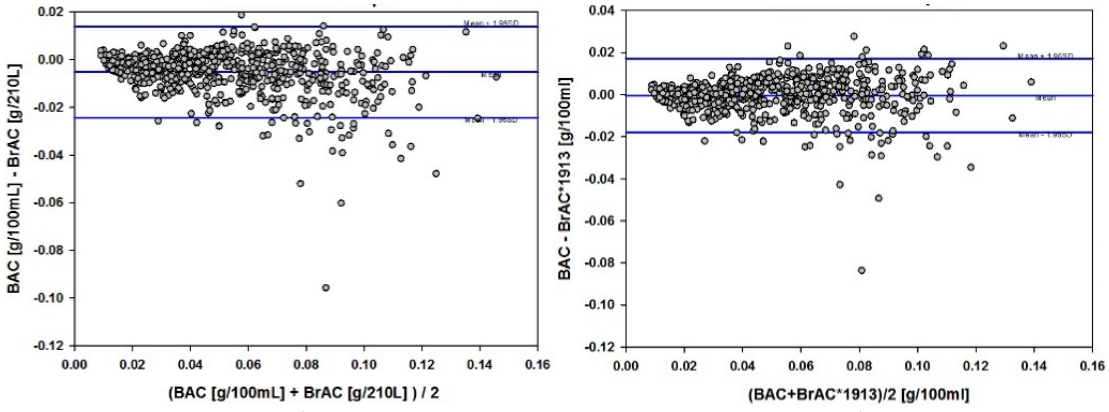


**a)** **b)**

***Figure 6. Bland-Altman plots according to the partition ratio, Q: a) Q=2,100, b) Q=1,913.***

## CONCLUSIONS

In order to reveal the relationship between BAC and BrAC of healthy Korean males, the huge medical experiments has been executed for the first time in Korean medical study. Korean healthy males showed three characteristic BAC patterns, however, more than 50 % subjects (52 out of 101 individuals) participated in this

study showed a standard pattern with BAC peak around 50 mins. Even though there was no big differences in partition ratio in terms of BMI, BFM, and PBF, however, there was a meaningful gap in partition ratio when TBW is divided into two categories: above and below the average value. Since the partition ratio differed from the conventional value (Q=2,100) in case of Korean healthy males, it would be better to consider a new value (Q=1,913) or execute more profound research activities in order to calculate BACs from BrACs for Korean healthy males. The more reasonable partition ratio included Korean females will be reported shortly in the near future.

## ACKOWLEDGEMENTS

This research is supported by a grant from Ministry of Land, Infrastructure and Transportation (Grant number: 13TLRP-C067560-05-000000).

## REFERENCES

[1] Swedish Transport Administration, 2012. "Analysis of road safety trends 2012: management by objective for road safety work, towards the 2020 interim targets", December 2013.
[2] Lindberg, L., Brauer, S., Wollmer, P., Goldberg, L., Jones, A.W., Olsson, S.G., 2007. "Breath alcohol concentration determined with a new analyzer using free exhalation predicts almost precisely the arterial blood alcohol concentration.", Forensic Science International, 168, 200-207.
[3] Edna, S., David, S., 2011. "An analysis of alcohol breath tests results with portable and desktop breath testers as surrogates of blood alcohol levels.", Accident Analysis and Prevention, 43, 2188-2194.
[4] James, C.F., Robert, B.V., 2006. "The effectiveness of reducing illegal blood alcohol concentration (BAC) limits for driving: Evidence for lowering the limit to 0.05 BAC", J. Safety Research., 37, 233-243.
[5] Marion, P., Petra, G., Kathrin, L., and Walter, R., 2007. "Elimination rates of breath alcohol." Forensic Science International, 171, 16-21.
[6] Hlastala, M.P., 1998. "The alcohol breath test-a review.", American Physiological Society, 401-408.
[7] Federal Register, 1993. "Highway safety programs; Model specifications for devices to measure breath alcohol.", Federal Register/Vol.58, No. 179, pp.48705-48710/Friday, September 17, 1993
[8] Jones, A.W., Andersson, L., 1996. "Variability of the blood/breath alcohol ratio in drinking drivers." J. Forensic Science, 41, 916-921.
[9] Jones, A.W., Andersson, L., 2003. "Comparison of ethanol concentrations in venous blood and end-expired breath during a controlled drinking study.", Forensic Science International, 132, 18-25.
[10] Pavlic, M., Grubwieser, P., Brandstatter, A., Libiseller, K., Rabl, W., 2006. "A study concerning the blood/breath alcohol conversion factor Q: concentration dependency and its applicability in daily routine." Forensic Science International, 158, 149-156.
[11] Nam, B.W., Yi, S.H., Seo, J.S., Lee, B.R. 2014. "Alcohol pharmacokinetics in Korean healthy male", J. European College of Neuropsychopharmacology, 24, supplement 2, S661.
[12] Altman, D.G., Bland, J.M. 1983. "Measurement in medicine: the analysis of method comparison studies", Statistician, 32, 307-317.
[13] Federal Register, "Model specifications for breath alcohol ignition interlock devices (BAIIDs)", vol.57, no.67, Tuesday, April 7, 1992.
[14] National Research Council Canada, "Technical standard for vehicular breath alcohol interlock devices in Canada", Project 54-A3948, August 9, 2011.

# PILOT STUDY ON ADVANCED AUTOMATIC COLLISION NOTIFICATION AND HELICOPTER EMERGENCY MEDICAL SERVICE SYSTEM IN JAPAN

**Toru Kiuchi**
Toyota Motor Corporation
Japan

**Yuichi Motomura, Hitoshi Matsumoto**
Nihon Medical University, Chiba Hokusoh Hospital
Japan

**Kunihiro Mashiko**
Minamitama Hospital
Japan

Paper Number 15-0415

## ABSTRACT

This paper focuses on the pilot study on Advanced Automatic Collision Notification (AACN) and Helicopter Emergency Medical Service (HEMS) systems in Japan. The pilot study was carried out in Chiba prefecture by the AACN Committee in affiliation with Emergency Medical Network of Helicopter and Hospital (HEM-Net).

There were many opinions that Japanese accident data was preferable to develop a Japanese AACN algorithm. Then, the Occupant Injury Predict Algorithm newly developed by Nihon University was utilized for the study. About 2.8 million Japanese accident data (so called ITARDA Macro Data) were used to define logistic regression risk curves of fatal and severe injuries to car occupants. To validate this algorithm, the in-depth accident case study by Nihon University and Nihon Medical University at the Chiba Hokusoh Hospital was used. Moreover, to decide the threshold value, this in-depth accident study was also used.

Regarding the AACN prototype system, HELPNET infrastructures already developed for existing Japanese ACN service were used for sending vehicle data to the HELPNET center. In the simulated accident, Event Data Recorder (EDR) data was added on usual HELPNET data and transmitted from a car to a HELPNET server at the HELPNET center. The AACN server got vehicle data such as Delta V and seatbelt status as input to the algorithm.

The result was transmitted to a Tablet PC at the Fire Department Head Quarters and Chiba Hokusoh hospital simultaneously. An operator of HELPNET made an Emergency Call to both the Fire Department and Hokusoh hospital individually.

In case of severe injury, a Tablet PC indicated the situation and a doctor dispatched to the accident spot by a helicopter. After a helicopter with a doctor took off, verbal communications between the helicopter and Fire Department started to decide a rendezvous point nearby the crash spot. After landing, the doctor contacted the injured occupant who was carried by an ambulance there. The AACN prototype system for a limited area, only in Chiba prefecture, was developed.

AACN transmitting tests were carried out at some spots in Chiba prefecture within the jurisdiction of two headquarters individually. The prototype AACN system operated as intended. Within a minute from the airbag deployment signal, the algorithm result screen arrived simultaneously on AACN Tablet PCs at Chiba Hokusoh hospital, Chiba prefecture Fire Department H.Q. and also at the transmitting spot. The next step of AACN transmitting test should be that AACN activates HEMS of Chiba Hokusoh hospital. To expand cover area in Japan, collaborations of other HEMS base hospitals in other prefectures should be planed soon.

## INTRODUCTION

In Japan, casualties of traffic accidents are recently decreasing. According to the National Police Agency, 573,824 traffic accidents occurred in Japan in 2014. Compairing with 2012, this was a decrease of 55,179. These crashes killed 4,113 peoples (decrease of 260) and injured 711,374 people (decrease of 70,120). Since 2004, the decreasing trend seems to continue, however, the situation is still serious [1].

Under continued conditions, it would be very difficult to achieve Japanese Gorverment Target, which was that the traffic accident fatalities in Japan should be 2,500 or less by 2018 and realize the safest road traffic society in the world by 2020, decided in the Cabinet in 2013.

**Automatic collision notification (ACN)**

To decrease casualties of motor vehicle crashes, many technologies such as pre-crash and post-crash seem to be effective. Beside such technologies, collision notification technologies are also helpful to decrease dispatch of emergency medical service (EMS). In Japan, an automatic collision notification (ACN) service called HELPNET started in 2005. The scheme of HELPNET is provided in Figure 1.

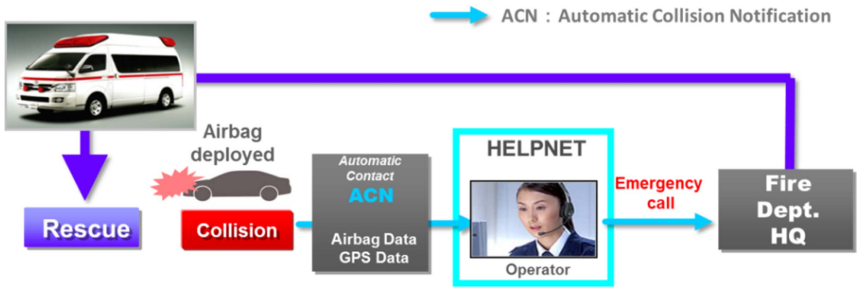


*Figure 1. Existing ACN service in Japan*

In case of a collision with airbag deployment, the ACN system automatically contacts the HELPNET center and collision information such as airbag deployment data and Global Positioning System (GPS) data are sent to HELPNET server. An operator of HELPNET calles drivers of vehicles with a deployed airbag using aDigital Comunication Module (DCM). If there is no answer from the driver, the operator calls the nearest Fire Depertment Head Quarter.

**Advanced automatic collision notification (AACN)**

Life saving potential of an advanced automatic collision notification (AACN) system is expexted in Japan[2,3].

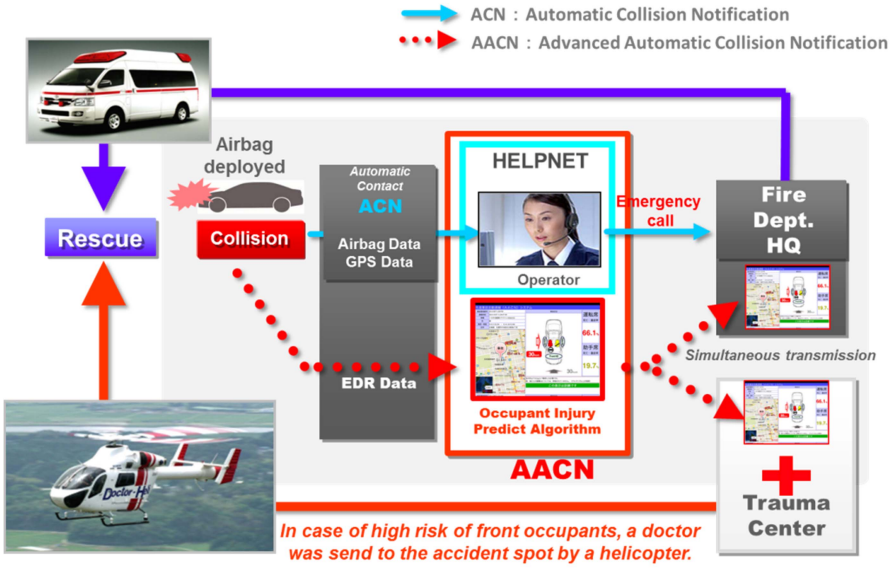


*Figure 2. Developing AACN and HEMS system in Japan.*

The scheme of AACN and HEMS system is provided in Figure 2. In December, 2011, the authors carried out a demonstration test of AACN and HEMS system at a test site of the Japan Automobile Research Institule (JARI). A crash test using a prototype vehicle with an AACN system was carried out. The vehicle with dummies struck a crash barrier at 50 kph. EDR's data was transmitted to the server. Occupant Transportation Decision Algorithm (OTDA) of Wake Forest University [4] used these data to determine the kind of hospital to which the injured driver is to be transffered. From Chiba Hokusoh hospital, a helicoper with a doctor took off and landed at a rendezvous spot next to the barrier. The doctor contacted the dummy representing an injured driver after 21 minutes from the collision.

Three years have passed from this demonstration test. An AACN committee in affiliation with Emergency Medical Network of Helicopter and Hospital (HEM-Net) continued activities to realize AACN and HEMS systems in Japan. Dr. Mashiko was the chairman of the committee and all authors of this paper were involved in activities targeting a real service of AACN and HEMS systems in Chiba prefecture.

## OBJECTIVES

The objectives of this study was to develop AACN and HEMS systems, using infrastructure already prepared for the existing ACN (HELPNET) service. At the beginning, after the development of the system, some real accident cases were considered to be used to examin real effectiveness of AACN and HEMS system. However, there were many restrictions of a real accident case usage without proper ammendments of the terms of HELPNET service. Then, the study using real accidents was abondoned and the study of data transmitting simulation in Chiba prefecture for HELPNET, Chiba Fire Department. H.Q. and Hokusoh hospital was planed.

## METHODS

To develop AACN and HEMS systems in Japan, the principal elements are described individually in the following.

### Algorithm to estimate occupant injury

In this study, the TOYOTA-Nihon University algorithm was developed and utilized [5]. For the demonstration at JARI in Dec. 2011, OTDA developed by Wake Forest University was used. It was developed based on NASS-CDS data. Recently, at JSAE GIA Forum and JSAE comitte on the AACN, many attendees eager to develop Japanese algorithm made by Japanese accident data[2,3]. About 2.8 million of accidents from ITARDA Macro Data in Japan were used to define logistic regression risk curves of fatal and severe injured car occupants. Risk factors of the algorithm are summarized on Table 1. In order to validate this algorithm, combined data from the hospital based in-depth accident study by Nihon University and Nihon Medical University at the Chiba Hokusoh Hospital was used.

**Table 1.**
**TOYOTA-Nihon University Algorithm used for the pilot study in Chiba prefecture.**

| TOYOTA Nihon University model | | | | |
|---|---|---|---|---|
| Risk factors | | Model 2_Type 1 | Model 2_Type 1_P | Model 2_Type 1_K |
| Intercept | | -4.888 | -4.931 | -5.195 |
| Delta $V_{pseudo}$ | [km/h] | 0.094 | 0.097 | 0.091 |
| Crash Direction | Front | -0.047 | -0.335 | 0.328 |
| | Near side | 1.167 | 1.069 | 1.342 |
| | Far side | 1.024 | 0.755 | 1.361 |
| | Rear | - | - | - |
| Age | Under 54 years | - | - | - |
| | 55-64 years | 0.585 | 0.437 | 0.759 |
| | Over 65 years | 1.027 | 0.879 | 1.171 |
| Belt use | Yes = 1, No = 0 | -1.818 | -1.901 | -1.738 |
| Multiple crash | Yes = 1, No = 0 | 0.120 | 0.082 | 0.169 |
| Vehicle type | Passenger car | -0.288 | | |
| | Kei car | - | | |

Examples of major risk curves are provided in Figure 3. These curves depict injury probabilities for Frontal impact without seatbelt, Frontal impact with seatbelt and Near Side impact with seatbelt. For a delta V of 40 kph, the risk of fatal and severe injury was 53%, 16% and 25%,respectively.

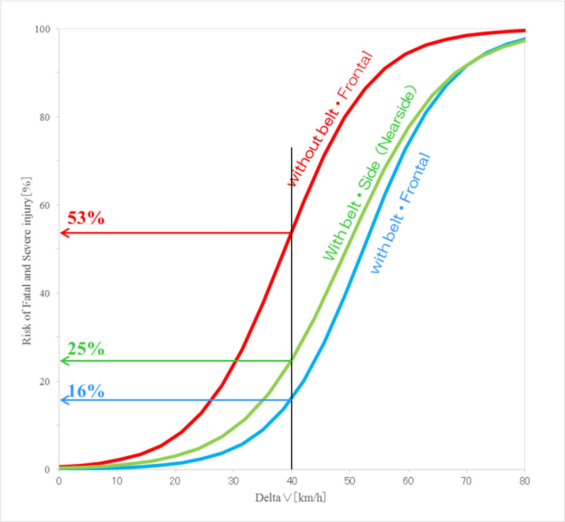


*Figure 3. Risk curves of the algorithm used for the pilot study*

**Threshold for dispatch decision**

The threshold for dispatch decision was analyzed and decided using the in-depth accident study by Nihon University and Nihon Medical University at the Chiba Hokusoh Hospital again. Doctors at Hokusoh hospital decided a decision threshold value after analyzing over triage rate and under triage rate for in-depth accident study cases. The decision threshold value seemed to be depended on a HEMS base hospital at which AACN and HEMS systems are used.

**Algorithm result screen design**

A sample algorithm result ( in Japanese language) is provided in Figure 4. The screen consisted of four areas. At the upper left part, there was text information on Accident ID and time, name and color of the involved vehicle, GPS data and address of the accident spot. At the lower left part, there was a map showing the accident spot. At the upper right, there were crash conditions, such as Delta V and airbag deployment and risk of fatal and severe injury of front occupants. Finally, at the lower right, some comments were added.

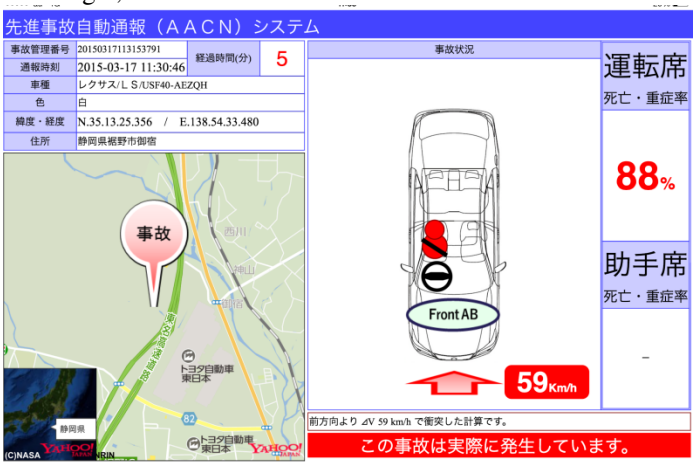


*Figure 4. An algorithm result transferred to Tablet PC*

**AACN scheme in Chiba prefecture**

A prototype AACN scheme for the pilot study in Chiba prefecture is provided in Figure 5. The circled numbers in the figure represent the step by step process of the AACN scheme. There were two DCMs in the test vehicle. One was an original DCM initially equiped and the other was an additional DCM for the pilot study. Each step follows below.

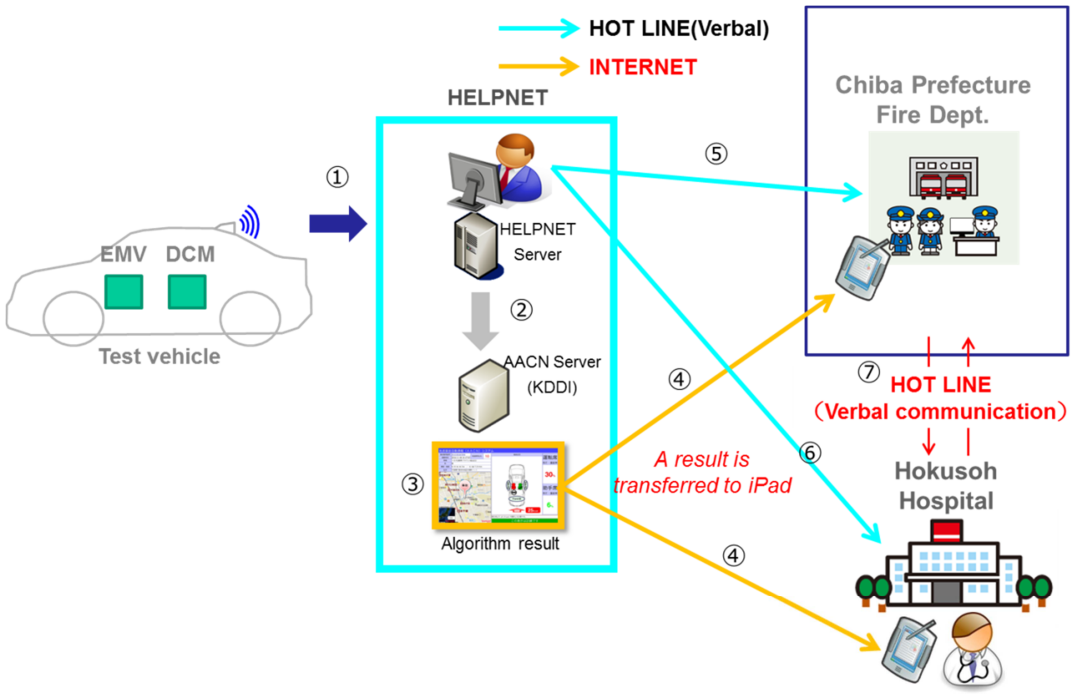


***Figure 5. AACN scheme for the pilot study in Chiba prefecture***

**Step 1** The AACN scheme was triggered by an airbag deployment signal. EDR data of a test vehicle was transmitted to HELPNET server. GPS data and vehicle ID were also transmitted.

**Step 2** AACN server received vehicle data to input the algorithm from HELPNET server every 30 seconds. Other information, such as accident time, vehicle ID and GPS information were also received.

**Step 3** AACN server calculated a risk of front occupants using the algorithm and arranged an algorithm result screen.

**Step 4** AN algorithm result screen was transmitted to Tablet PCs at Chiba prefecture Fire Department H.Q. and Chiba Hokusoh hospital simultaneously (also at the accident spot).

**Step 5** HELPNET operator called Chiba prefecture Fire Department H.Q. by HOT LINE. This step was usual HELPNET ACN operation. In addition, in case of AACN, HELPNET operator confirmed the arrival of an algorithm result screen on Tablet PC at the H.Q..

**Step 6** After a call to Chiba prefecture Fire Department H.Q., HELPNET operator called Chiba Hokusoh hospital by HOTLINE. In case of high risk of the front occupant, a doctor was send to the accident spot by a helicopter.

**Step 7** Verbal communication was made between Chiba Hokusoh hospital and Chiba prefecture Fire Department H.Q. to decide a rendezvous spot for a helicopter and an ambulance.

## RESULTS

A total of 6 cases of transmission from 2 accident spots were carried out during the first pilot test period in March, 2015. No error transmission occurred and of the AACN system seemed to function as intended. Within a minute from the airbag deployment signal, the algorithm result screen arrived simultaneously on Tablet PCs at both Chiba Hokusoh hospital and Chiba prefecture Fire Department H.Q.

The effectiveness of AACN and HEMS systems are not established yet because a transmission test with HEMS activated by AACN was not finished at the time of writing this paper.

## DISCUSSIONS

This study was orgnized by the AACN committee under Emergency Medical Network of Helicopter and Hospital (HEM-Net). It was natural that Chiba Hokusoh hospital, as a pioneer of HEMS base hospital in Japan, contributed a fundermentl part of this study. In Japan, there are 47 helicopters for HEMS and 49 HEMS base hospitals, as of March, 2015. In order to cover all of Japan, the number of cooperative HEMS base hospitals should be increased step by step. The authors had selected 6 HEMS base hospitals from Hokkaido to Kyusyu in Japan. A similar pilot study should be planed for each hospital.

Regarding the AACN algolithm, the authors adopted a newly developed algorithm by Nihon University in this study. Based on ITARDA macro accident data, logistic regression risk curves were produced. Many other algorithm were based on in-depth accident data such as NASS-CDS [6-14]. Comparing with in-depth accident data, ITARDA macro accident data had limited information. For example, there is no information on CDC-code, Delta V, MAIS, ISS etc.. However, ITARDA macro data seemed to be suitable for algorithm risk factors used in this study according to evaluation result using in-depth accident study carried out between Nihon University and Nihon Medical University Chiba Hokusoh hospital.

Regarding the threshold for dispatch decision, the authors adopted a decision value calculated using in-depth accident study at the same hospital. The over triage rate and the under triage rate were analyzed. It became obvious that a decision threshold value depended on each HEMS base hospital. However, there was no other HEMS base hospital which conducted an individual accident study. This issue needs to be solved in future.

## CONCLUSIONS

The AACN and HEMS pilot system in Chiba prefecture was developed in cooperation with Nihon Medical University Chiba Hokusoh hospital, which was a pioneer of HEMS base hospitals, and Chiba prefecture Fire Department Head Quarters.

At some spots in Chiba prefecture, transmitting tests were carried out and prototype system operated as intended. Within a minute from airbag deployment signal, the algorithm result screen arrived on Tablet PCs at both Chiba Hokusoh hospital and Chiba prefecture Fire Department Head Quarters simultaneously.

To expand this pilot study on AACN and HEMS system widely, the next step was scheduled among other HEMS base hospitals in Japan.

## ACKNOWLEDGEMENTS

The authors thank Prof. Nishimoto of Nihon University for a contribution to development and evaluation of the algorithm used in this study and continuous in-depth accident study collaboration with Nihon Medical University Chiba Hokusoh hospital.

**REFERENCES**

[1] National Police Agency: Statistics of Traffic Accident 2014.
[2] Society of Automotive Engineers of Japan: Proceeding of GIA Forum. JSAE Spring Session; 2013
[3] Society of Automotive Engineers of Japan: Proceeding of GIA Forum. JSAE Spring Session; 2014
[4] Stitzel JD, Martin RS, et al. Research on Estimation of Occupant Injuries by Utilizing ACN Technology – Final Report. November 30, 2010
[5] Tominaga S, Nishimoto T, Motomura U, Matsumoto H, Lubbe N, Kiuchi T. Injury Prediction Algorithm for AACN based Japanese Road Accident Data 20145822, JSAE Autumn Session;2014.
[6] Kononen DW, Flannagan CA, Wang SC. Identification and validation of a logistic regression model for predicting serious injuries associated with motor vehicle crashes. Accid Anal Prev. 2011;43:112-22.
[7] Augenstein J, Digges K, Ogata S, Perdeck E, Stratton J. Development and validation of the URGENCY algorithm to predict compelling injuries. Enhanced Safety of Vehicles2001.
[8] Bahouth G, Digges K, Schulman C. Influence of injury risk thresholds on the performance of an algorithm to predict crashes with serious injuries. Ann Adv Automot Med. 2012;56:223-30.
[9] Bahouth GT, Digges KH, Bedewi NE, Kuznetsov A, Augenstein JS, Perdeck E. Devleopment of URGENCY 2.1 for the prediction of crash injury severity. Top Emerg Med. 2004;26:157-65.
[10] Rauscher S, Messner G, Baur P, Augenstein J, Digges K, Perdeck E, et al. Enhanced automatic collision notification system - improved rescue care due to injury prediction - first field experience. Enhanced Safety of Vehicle Conference. Stuttgart, Germany2009.
[11] Augenstein J, Perdeck E, Bahouth GT, Digges KH, Borchers N, Baur P. Injury identification: priorities for data transmitted. Enhanced Safety of Vehicles2005.
[12] Weaver AA, Barnard RT, Kilgo PD, Martin RS, Stitzel JD. Mortality-based quantification of injury severity for frequently occuring motor vehicle crash injuries. Ann Adv Automot Med. 2013;57:235-45.
[13] Schoell SL, Doud AN, Weaver AA, Talton JW, Barnard RT, Martin RS, et al. Development of a time sensitivity score for frequently occurring motor vehicle crash injuries. Journal of the American College of Surgeons. 2014.
[14] Schoell SL, Doud AN, Weaver AA, Barnard RT, Meredith JW, Stitzel JD, et al. Predicting patients that require care at a trauma center: analysis of injuries and other factors. Injury. 2014.

# FINITE ELEMENT STUDY OF EFFECTIVENESS OF MODIFIED FRONT-END STRUCTURE WITH ALUMINIUM FOAM IN REDUCING PEDESTRIAN INJURY

**Wachirut,Kongsakul**
Faculty of Engineering, King Mongkut's University of Technology North Bangkok
Thailand

**Julaluk, Carmai**
The Sirindhorn International Thai-German Graduate School of Engineering
King Mongkut's University of Technology North Bangkok
Thailand

**Sujeepapha, Charoenthong**
Faculty of Engineering, King Mongkut's University of Technology North Bangkok
Thailand

Paper Number 15-0416

## ABSTRACT

Pedestrians are vulnerable road users. Unlike Occupant in cars, they do not have protection equipment and are often involved in serious accidents leading to fatalities. The reduction of pedestrian injuries has recently become one of the most important road traffic accident priorities. For the bonnet type of vehicle, leg and head injuries are the most prevalent type of injury associated with car-to-pedestrian collision. The possible reduction of leg and head injuries can be done through the design of vehicle bumper structure. Strong and stiff front structure of vehicle usually leads to severe injury to pedestrians in the accident. The use of new class of material like aluminium foam as part of bumper structure can provide better energy absorption capability and hence reduction of impact force to pedestrians. However, in order to design or modify the front structure to be safer for pedestrians, it is necessary to understand kinematics and injury mechanisms of car-pedestrian collisions, which are usually analyzed through costly full scale crash tests of a dummy or a cadaver. Finite element simulations with a human body model are an alternative mean, which offers information of post-crash kinematics and injury mechanisms. This paper has therefore employed the finite element model of pedestrian-city car collisions to study the effectiveness of the modified front-end bumper with aluminium foam in reducing the level of pedestrian injuries. The front bumper structure has preliminary been modified to include the aluminium foam as part of energy absorber. Two relative densities of aluminium foam were selected. The lower density one gave a better injury reduction performance. It was used to simulate a crash with THUMS to study detail injuries of pedestrian. The modified bumper model showed improved performance of injury reduction. The results exhibited the potential use of low density Al-foam in minimizing pedestrian injury and the benefit of using the human body finite element model which provides detailed injury information to help in the design and development of vehicle for pedestrian safety with cheaper cost compared to the actual full-scale crash tests.

## INTRODUCTION

Road traffic injuries are a significant global public health problem around the world. Accidents which involve pedestrians mostly result in severe injury or death. Most of car manufacturers have given less priority to pedestrian safety. This is due to the fact that many countries in particularly developing countries have no such regulations. However, many regional New Car Assessment Programs (NCAP) have included pedestrian safety assessment into their car-rating system. This has encouraged many car manufacturers to develop cars with better pedestrian protection. NCAP has assessed pedestrian safety through the impact tests of the front structure with legform and headform since the front structure of vehicle is the part that mostly hits pedestrians. Strong and stiff front structure of vehicle usually leads to severe injury to pedestrians in the accident. Impactor crash test is poor in giving information about the injury mechanisms and kinematics of the pedestrian during crash. Car manufacturers have lately begun to use design principles that have proved successful in protecting car occupants to develop vehicle design concepts that reduce the likelihood of injuries to pedestrians in the event of a car-pedestrian crash. There is a possibility to protect a pedestrian

lower limbs during impact by introducing an appropriate cushion and support of the lower extremities for example the bumper energy absorber. Aluminium foam is a material which has excellent energy absorption capacity. It has been recently introduced to automotive industry to make a crashbox for crashworthiness design [1]. This paper aims at introducing aluminium foam to the front-end structure of a passenger car to study its potential in reducing pedestrian injury level. For purpose of vehicle development, full-scale crash tests are required. However, the actual crash tests are costly compared to alternative computer simulations. Finite element (FE) analysis has been employed widely in vehicle components design and optimization. It is therefore, introduced in this work to simulate pedestrian-car collisions. By firstly, simplified the vehicle model to include only necessary components to reduce computation time. The simplified vehicle model was validated against the actual crash test. The front-end structure of this simplified model was modified by introducing aluminium foam with two relative densities aiming to minimise the pedestrian injury level. The modified bumper structure with two relative densities were numerically assessed with legform impactor. The best safety performance one was selected for car-to-pedestrian simulation. The dynamic responses and injury level were compared with those obtained from the original front-end structure.

## SIMPLIFIED FE MODEL OF A PASSENGER CAR

A passenger car finite element model was taken from the National Crash Analysis Center (NCAC) [2]. In the present study, only frontal collision with a pedestrian was considered. Therefore, some unnecessary components were deleted to simplify the car model. The main body in white structure were kept upto the B-pillar. The doors were removed. All components below the hood were kept in place. Since some components and structures were removed, extra mass needed to be added and distributed correctly to obtain the same mass and Centre of Gravity (C.G.) location as in the actual car. Figure 1 shows the simplified FE vehicle model and comparisons of mass and C.G. location with the complete vehicle model. All extra nodes that carried extra mass were constrained to the C.G. of the car. All nodes at area A and B in figure 1 were not allowed to translate in *y* and *z* directions also not to rotate around *x* and *z* axes. The mass and the C.G. of the simplified model were almost identical to the complete model. In order to validate the simplified car model, a full frontal wall crash was simulated and compared the results with the actual crash test data of NHTSA [3]. The car model was set to impact a rigid wall at 56 km/h. The overall global deformation of the actual car was very similar to the actual crash test as shown in figure 2. The acceleration response taken from the engine top and bottom were compared as shown in figure 3. Reasonably good agreement can be seen.

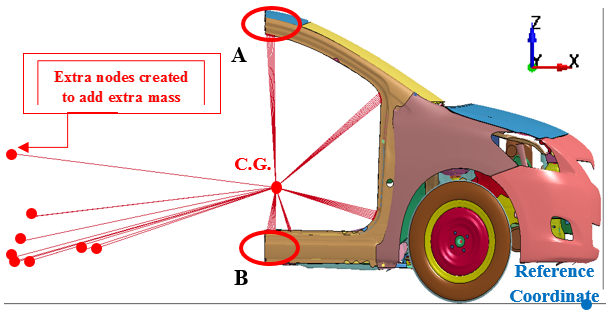


***Figure 1. Simplified finite element model of Toyota Yaris sedan***

## FRONT-BUMPER MODIFICATION TO IMPROVE PEDESTRIAN

For the bonnet-type vehicle, leg and head are body regions that have high risk of severe injuries. The proposed design modification aims at illustrating the potential application of aluminium foam (Al-foam) together with add-on stiffeners to primarily reduce lower extremity injury. Three components made of Al-foam were attached to the front-end of the car as shown in figure 3. They were upper and lower stiffeners as well as a cushion part attached in front of the bumper beam. Two relative densities of Al-foam were used. Material behaviour of Al-foam was required for finite element implementation. The Crushable Foam material model in LSDYNA [4] was employed for this purpose. It requires mass

density, Young's modulus, Poisson's ratio and stress-strain curve. Compression tests of Al-foam were conducted for relative densities of 0.051 and 0.185.

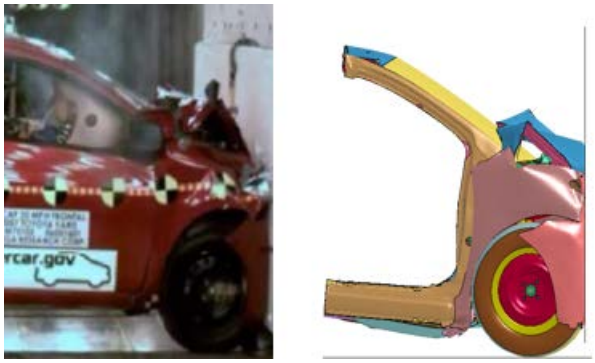

a)

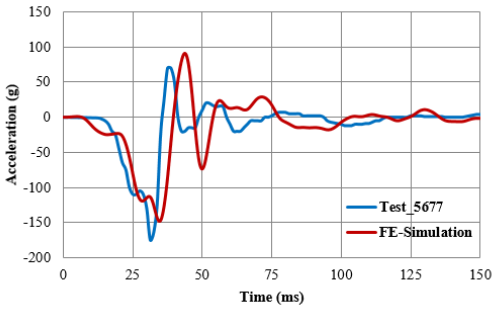


b)

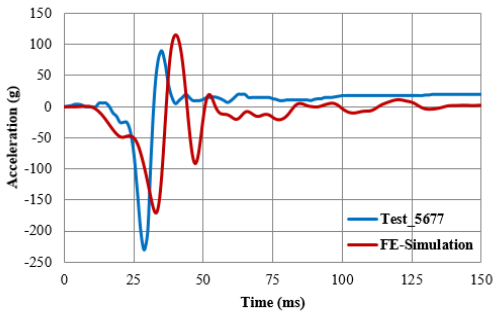


c)

***Figure 2. Comparisons of a) global deformation b) engine top acceleration c) engine bottom acceleration.***

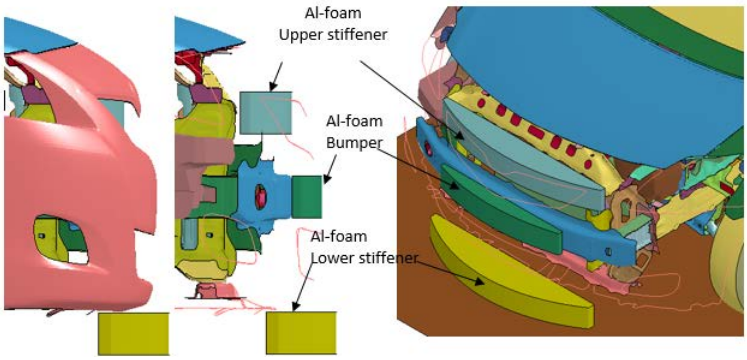


***Figure 3. Front bumper modification with aluminium foam parts.***

## PEDESTRIAN CRASH FINITE ELEMENT MODEL SET UP

Two configurations of crash tests were simulated in this paper. One was legform-car impact test, the other was car-to-pedestrian crash test. A 50 percentile Total Human Body Model for Safety (THUMS) was employed for pedestrian model in this paper. THUMS model is capable of predicting detail injury of brain ligament, bones and internal organs. The set-up of both configurations are shown in figure 5. The legform-to-car model was set up according to the Euro NCAP protocol [5]. The legform was set to move towards the centre of the car bumper at a speed of 40km/hr. For the car-to-pedestrian model, the human body model was initially positioned in front of the car centerline. The car was set

to impact the pedestrian from the right side at a speed of 40 km/hr. The contact friction coefficient between THUMS and the car was 0.3 and the ground friction coefficient was 0.9. Both the car and THUMS were placed in the acceleration field of gravity.

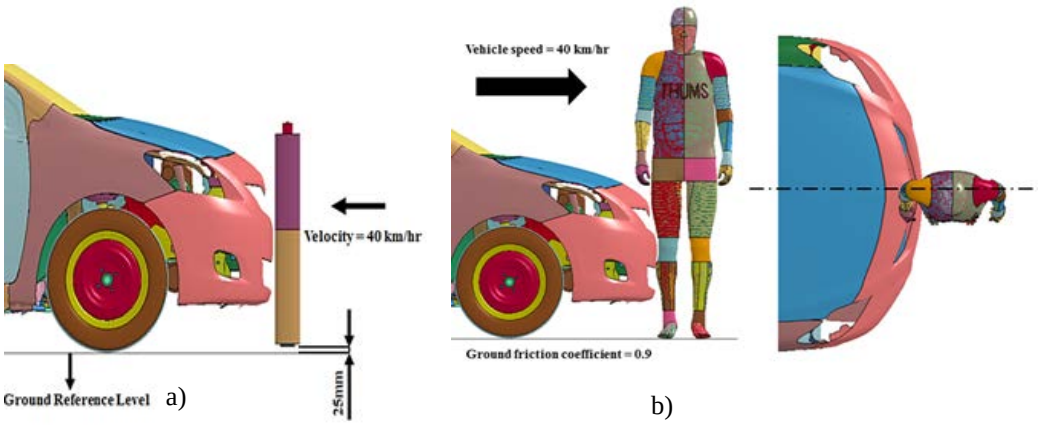


***Figure 4. FE model of a) Car-to-Legform impact set-up b) Car-to-Pedestrian collision set-up.***

## SIMULATION RESULTS

Two set of simulation results are presented. The first set was from the car-to-legform impact test which was employed to assess performance of the original bumper structure and the modified bumper structure with two relative densities of Al-foam. The best performance among the two relative densities was selected to crash with THUMS for detail injury analysis which provided the second set of simulation results.

### Legform-car impact simulations

Three cases were conducted. According to the Euro-NCAP protocol [5], three injury parameters including the upper tibia acceleration, the knee shearing displacement, the knee bending angle were used to assess the pedestrian protection performance of the front-end bumper. The maximum value of each injury parameter for each cases are given in table 1. It is obvious that the modified structure with 0.051 relative density Al-foam has all values of injury parameters below the limit specified by Euro NCAP.

**Table 1.**
**The maximum value of each injury parameters for each simulation cases.**

| Injury parameters | Euro NCAP limit [5] | Original structure | Modified structure with 0.051 relative density al-foam | Modified structure with 0.185 relative density al-foam |
|---|---|---|---|---|
| Tibia acceleration (g) | 150 | 228 | 117.7 | 208.08 |
| Knee shear displacement (mm) | 6 | -4.8 | -1.54 | -2.47 |
| Knee bending angle (degree) | 15 | 30 | 12.06 | 20.36 |

### Car-to-pedestrian simulations

Two cases were simulated. The first one used the original structure of the car to hit with THUMS in order to obtain the baseline results. The second one used the modified structure with 0.051 relative density al-foam to hit with THUMS. The detail injury were compared and analysed.

**Post-crash kinematics behaviour and dynamic responses** Figure 5 shows a comparison of kinematics behaviour of pedestrian crashed by the car with original front-end structure and with modified front-end structure. For both cases, the knee was firstly struck by the bumper followed by the thigh and the tibia almost at the same time. The front bumper deformed and the lower extremities bent along the car frontal contour. The upper body rotated around the vehicle front area leading to the pelvis collision with the bonnet leading edge. The elbow were collided with the lower windshield portion. The chest and shoulder collided with the windshield portion at the back end of the hood. Since the neck behaved like a joint which allowed rotation degree of freedom, the head was angularly accelerated and made contact with the windshield. Finally the whole body bounced off the car. The differences can be seen clearly at 40ms, the simulation with the modified bumper model shows less knee bending angle than the original design. In addition, at 60 ms the left leg started to project away from the right leg. This was because the lower part of tibia was in contact with the lower stiffener which tried to resist the tibia movement. The left leg moved away from the car faster than the right leg because some of the right leg energy was absorbed by the lower stiffener aluminum foam. The time and location of head impact were also different. At 130 ms, the one with original bumper structure hit the windshield at 442 mm from the lower end of windshield where are the one with the modified bumper structure hit to the windshield at 410 mm.

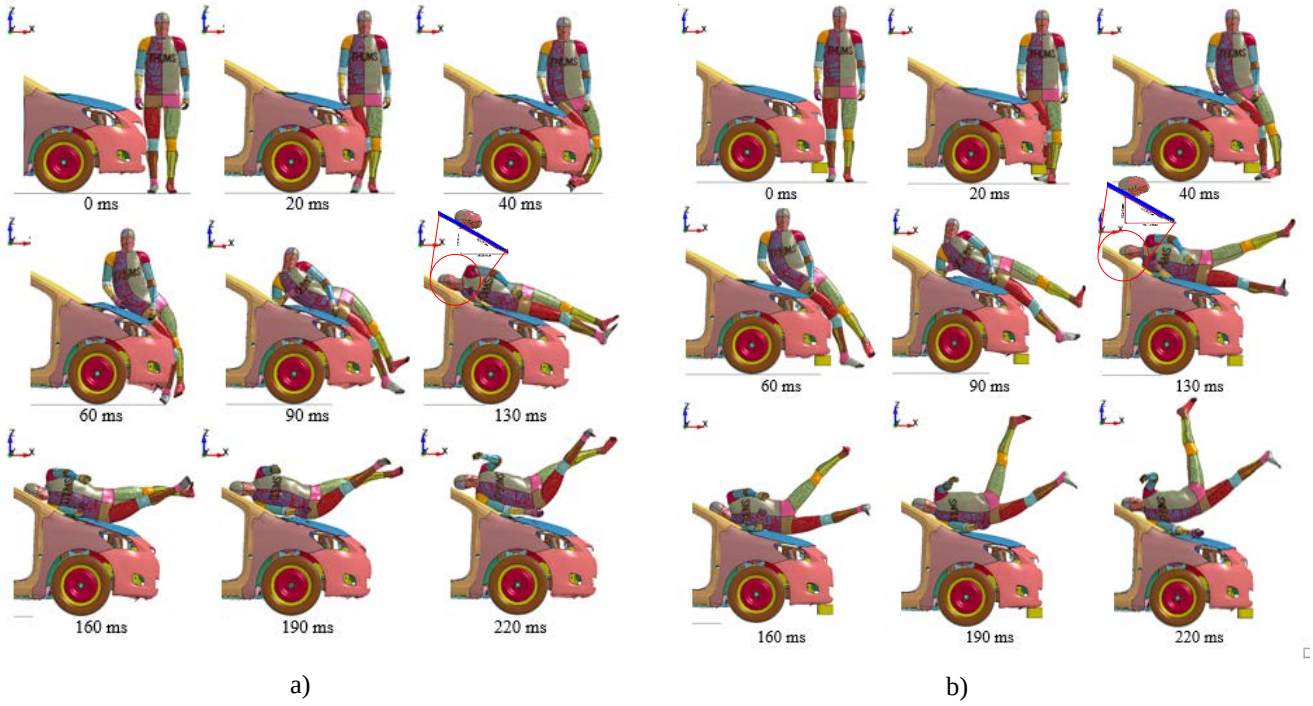


***Figure 5. Pedestrian kinematics obtained a) original bumper model b) modified bumper model.***

Figure 6 shows comparisons of dynamic responses. The patterns of contact force during collision were similar. The graphs consisted of 5 peak forces corresponding to the impact of plastic cover-leg, bumper beam-leg, elbow-lower part of windshield, chest-hood and head-windshield respectively. The highest peak force was when bumper beam in contact with the knee. The contact force obtained from simulation with the modified bumper was in overall less than those of the original bumper model except the highest peak. This was due to the introduction of the lower stiffener which tried to resist the movement of the lower part of the tibia causing the high contact force at the knee area. The introduction of bumper foam components slowed down the pedestrian body as observing from head and chest relative velocity graphs. The head impact acceleration was decreased from 175.7g to 150g. The $HIC_{15}$ obtained from the simulation with original bumper model was 1059 which implied high risk of severe head injury with AIS3 50% injury

risk [6]. The $HIC_{15}$ was reduced to 913.8 for simulation with the modified bumper model, hence lower risk of head injury.

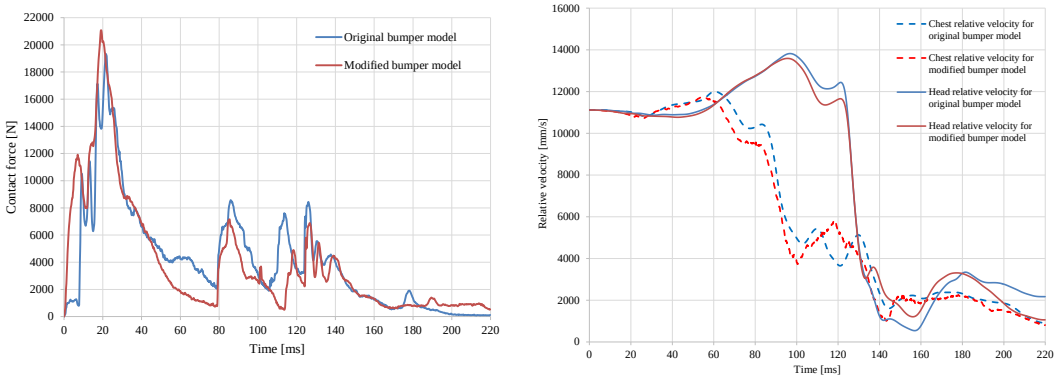


***Figure 6. Dynamic response a) the contact reaction force during collision b)relative velocity.***

**<u>Pedestrian injuries</u>** Figure 7 shows comparisons of bending moment and resultant force time histories at various height along the lower extremity. The threshold for 50% injury risk of AM50th was 447 Nm for femur [7-8] ,134 Nm for knee [7-8] and 340 Nm for tibia [9]. The patterns of bending moment were different. For the original bumper model, the maximum bending moment of the right lower extremity was the largest at the tibia height 400 mm above ground. It was 256.52 Nm but still within the tolerance limit of tibia for 50% injury risk of AIS2. While at the knee area with height of 500 mm above ground the maximum bending moment was 231.45 Nm. This value exceeded the tolerance limit of knee for 50% injury risk. The maximum bending moment of the femur was lower than that of tibia and knee. The values were still within the tolerance limit for 50% injury of AIS3. However, for the modified bumper model, the highest maximum bending moment of 400 Nm was shifted to the femur. This value was still within the limit of femur fracture. The knee and tibia bending moment taken from the modified bumper simulations had lower value than the original bumper model. They were all within the limit of bone fracture and knee joint damage.

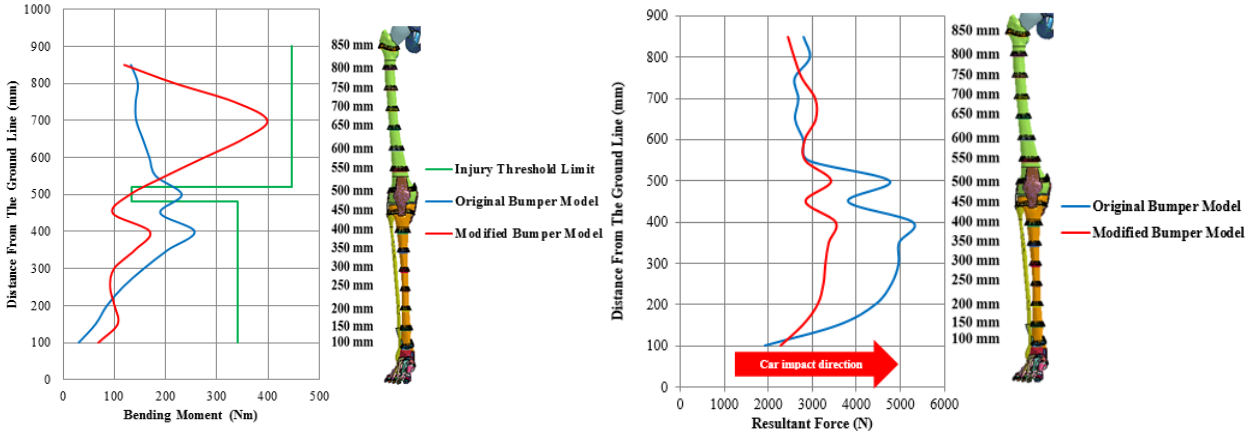


a) b)

***Figure 7 a) bending moment and b) resultant force along the right lower extremity.***

Resultant force expressed the same trend as shown in figure 7 b). The resultant force obtained from the simulation with the modified bumper was less than those of the original bumper for every distance.

Apart from dynamic responses, the biofidelity of the human body model can also give detailed injuries of all parts of the pedestrian body. Figure 8 shows comparisons of stress and strain distributions on the extremities. For the original bumper design, high stress of 141 MPa occurred at the front fibula and tibia. However, the magnitude of the stress was still within the bone fracture stress threshold of 150 MPa [10-12]. It was found that stress distribution changed for the simulation with the modified bumper. High stress occurred on femur rather than on the tibia. The highest magnitude was 122.67 MPa which was still below the femur fracture limit of 150 MPa. However, the overall magnitude of stress within the lower extremities was reduced for the simulation with the modified bumper. The maximum strain on knee ligaments for the case of the original bumper was at 0.25 which was beyond the rupture strain limit of 0.16 [13]. The simulation with the modified bumper structure showed improvement of the strain value. The maximum strain value reduced to 0.18. Very high stress also found at the humerus (upper part of an arm) due to the impact of elbow to the lower part of the windshield. For the original bumper simulation case, the stress was 232.5 MPa which exceeded the bone fracture limit of 150 MPa. For the modified bumper case, the stress value was much lower. The modified bumper model helped reducing the injury risk of humerus fracture.

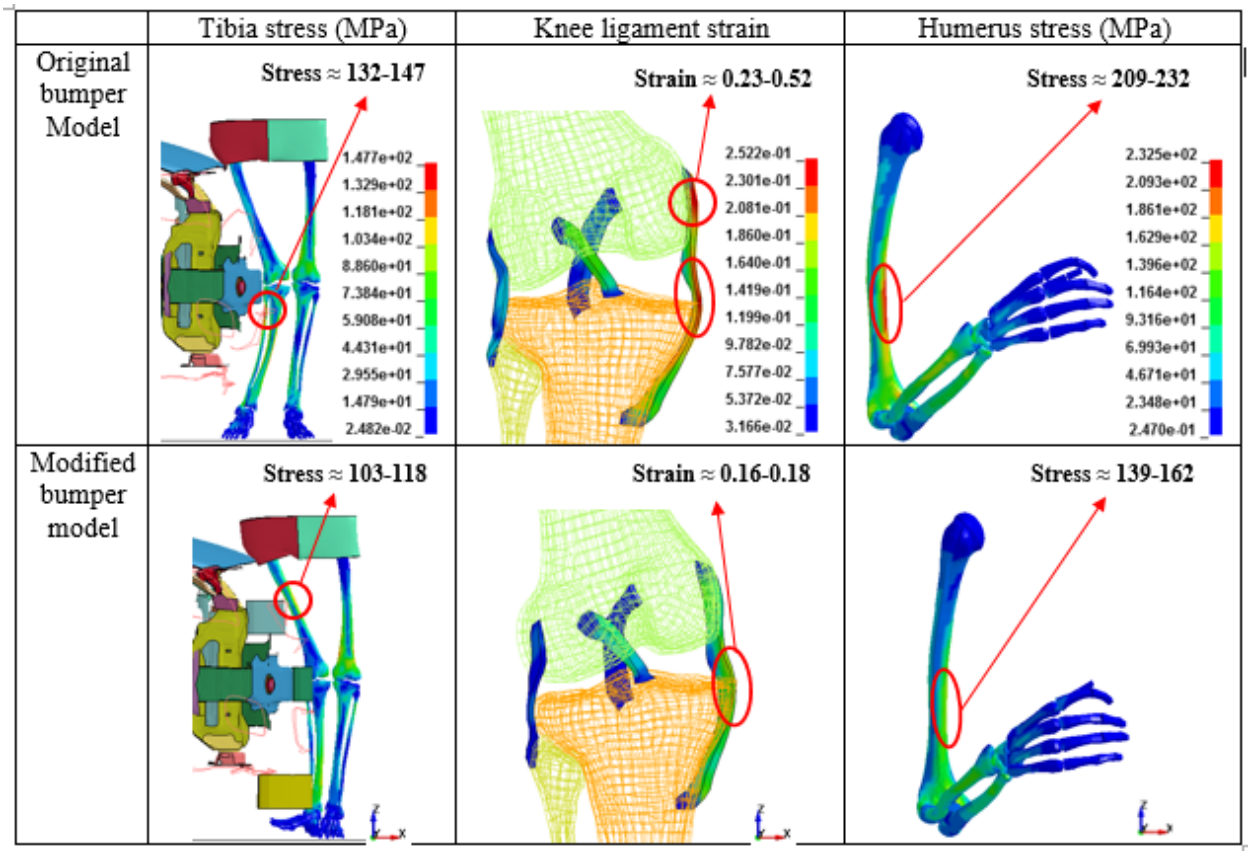


***Figure 8. comparisons of stress and strain distributions on the extremities.***

Figure 9 shows comparisons of detailed injury for the upper body. The thorax experienced high stress due to the impact of thorax to the back of the hood. For the original bumper model, two ribs, number 3 and 5 had quite high effective stress of around 149.2 MPa which was at the borderline for rib fractures. This impact also induced high pressure within the lung as shown in figure 9. The limit of human lung usually uses pressure to define threshold [12]. The limit is at ±10 kPa. From the simulation results, the red area represents the area that pressure exceeds 10kPa and the dark blue area represents area that pressure is less that -10kPa. The right lung showed damage as the pressure was greater than 10 kPa for almost all area of the right lung. With the modified bumper model, a drastically improvement was seen for

the ribcage stress and the lung pressure. The maximum stress on rib number 5 reduced to 94 MPa which was much below the fracture limit. In addition, the pressure within the lung was also considerably reduced. However, when comparing strain on brain, it was found that the strain within the brain expressed advert effect. For the case with modified bumper, the strain increased to 0.52 which exceeded the limit value of 0.3 for soft tissue damage. This implied that the modified bumper structure induced brain contusion. Although, the head acceleration and HIC value were reduced, the brain strain did not follow the same trend. The argument is that the HIC is calculated from the translation acceleration. There have been some studies illustrating that the relational velocity and acceleration have effects on the brain injury [13-14]. Since post-crash kinematics of head were different, it could affect the strain pattern and magnitude

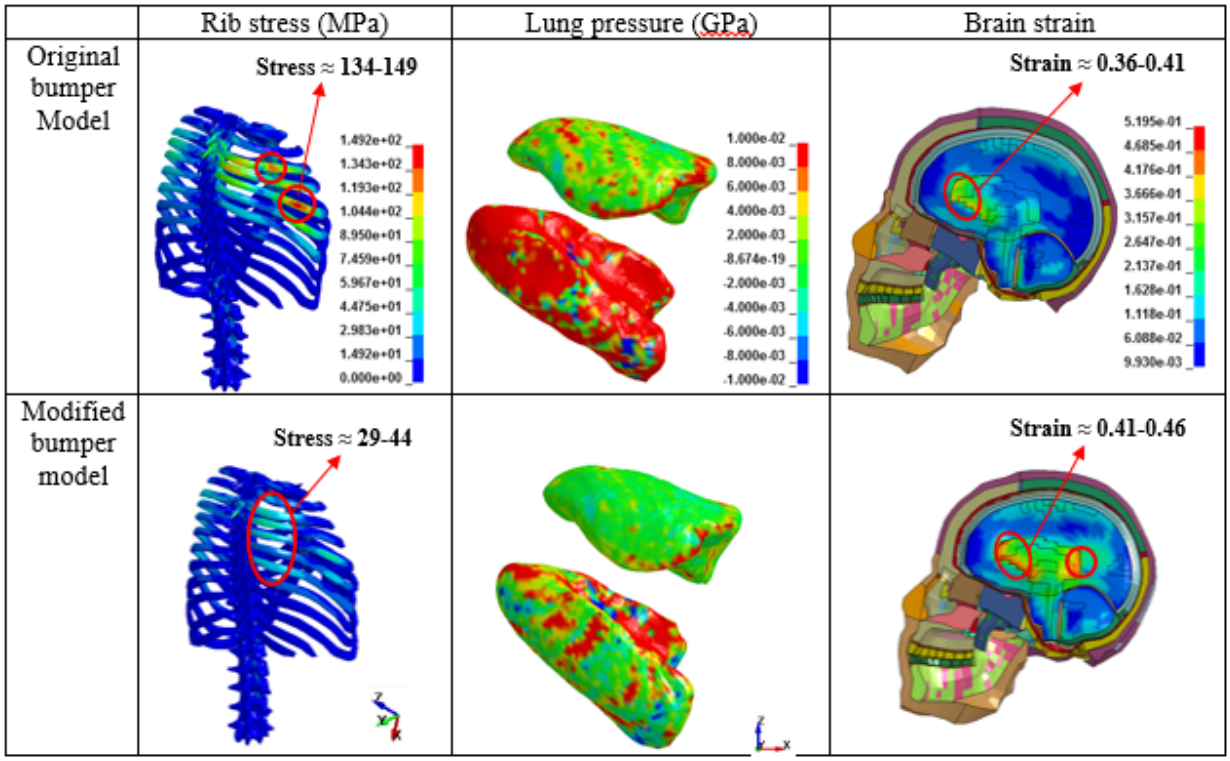


***Figure 9. Comparisons of stress and strain distributions for upper body part.***

## CONCLUSIONS

This paper aimed at studying the potential use of aluminium foam as part of front-end structure to reduce pedestrian injury. The detail injury analysis was performed though the use of finite element human body model. A modification to the bumper structure was done but with limitation of the shape of the bumper cover of the existing car. Three components made of aluminium form were added to the front bumper structure as part of energy absorber. Two relative densities of aluminium foam, 0.051 and 0.185, were considered. The modified design with lower relative density of 0.051was selected based on the legform injury parameters performance. It was used to simulate a crash with THUMS in order to study detailed injuries of pedestrian. The post-crash kinematics showed some differences at the lower extremities and head. The dynamic responses and level of injury were improved with the modified front bumper using low density aluminium foam. However, when simulating car-to-THUMS collision, some detailed injury information showed that the modified bumper caused slight problem in brain area. The results illustrated that the low density aluminium foam could be employed in the design for pedestrian friendly vehicle. The design and development process needed to take into account the injury of other body regions also especially the brain

which could not be simulated using a headform or a dummy. The current study also supported the benefit of using THUMS in the design development of pedestrian friendly bumper.

## REFERENCES


[1] Cymat Technologies. “Aluminum Foam Technology Applied to Automotive Design”

[2] NCAC. 2011. “Development and Validation of a Finite Element Model for a 2010 Toyota Yaris Sedan” NCAC 2011-T-001, prepared for FHWA.

[3] MGA Research Corporation. 2006. “Final Report of New Car Assessment Program Testing of a 2007 Toyota Yaris.” NHTSA Test No. 5677.

[4] LS-DYNA. 2012. “Keyword User’s Manual Volume II Material Models” Version 971 R6.1.0, Livermore Software Technology Corporation (LSTC).

[5] Euro NCAP. 2013. “Pedestrian Testing Protocol V.6.2.1.” (Belgium, Feb).

[6] Prasad P and Mertz H. 1985. “The Position of the United States Delegation to the ISO Working Group 6 on the Use fo HIC in the Automotive Environment.” SAE Government/Industry Meeting and Exposition, SAE paper no. 851246.

[7] Kerrigan, J.R., et al. 2003. “Experiments for Establishing Pedestrian-Impact Lower Limb Injury Criteria.” SAE World Congress & Exhibition.

[8] Ivarsson, J., et al. 2004. “Dynamic response corridors and injury thresholds of the Pedestrian lower extremities.” International IRCOBI Conference on the Biomechanics of Impact.

[9] United Nations Economic and Social Council. 2012 “Proposal for amendmentsto global technical regulation No. 9 ECE/TRANS/WP.29/GRSP/2010/2.” (Usa).

[10] Han,Y., Yang, J. and Mizuno, K. 2011. “Virtual Reconstruction of Long Bone Fracture in Car to Pedestrian Collisions Using Multi body System and Finite Element Method.” Chinese journal of mechanical engineering, 1-12.

[11] Han, Y., et al. 2012. “A study on chest injury mechanism and the effectiveness of a headform impact test for pedestrian chest protection from vehicle collisions.” Safety Science, 1304-1312.

[12] Shigeta, K., Kitagawa, Y. and Yasuki, T. 2009. “Development of Next Generation Human FE Model Capable of Organ Injury Prediction.” Enhanced Safety of Vehicles, 1-20.

[13] Watanabe, R., et al. 2011. “Research of collision speed dependency of pedestrian head and chest injuries using human FE model (THUMS Version 4).” Enhanced Safety of Vehicles, 1-13.

[14] Kimpara, H. and Iwamoto, M. 2012. “Mild traumatic brain injury predictors based on angular accelerations during impacts.” Annals of Biomedical Engineering, 114-126.

# IMPLICATION OF CHILDREN IN ROAD ACCIDENTS IN FRANCE IN 2011

**Philippe Lesire**
**Franck Léopold**
**Cyril Chauvel**
Laboratory of Accidentology Biomechanics and Human behaviour PSA Peugeot-Citroën / RENAULT
France

**Véronique Hervé**
**Sophie Cuny**
European Centre for Safety Studies and Risk Analysis
France

Paper Number 15-0418

## ABSTRACT

This study intends to present the analysis of all road accidents that occurred in France during the year 2011 in which children (0-13y incl.) have been involved. Based on the data collected and coded in the French safety project (VOIESUR) accidents with children have been analysed by experts. Then, these data have been weighted to be representative of the French situation.

The paper proposes an analysis of the accident data for 5 categories of road users that are light vehicle occupants, pedestrians, cyclists, motorbike passengers and buses and coaches' occupants. A distribution of the different parameters of the accident and its outcomes such as the children's injury severity is available per different road user categories.

The repartition of children across the previously described user categories shows that the most common accident for children is being light vehicle occupants (64%), then cyclists (17%) and finally pedestrians (15%). Buses and PTW occupants are representing a very small proportion (approximately 2% each).

On the 101 fatally injured children, the repartition is different and as follow: 61% are light vehicle occupants, 11% are cyclists and 26% are pedestrians. No power two wheels (PTW) passengers or coach and bus occupants have been fatally injured in 2011 in France. The remaining 2% are not belonging to any of these categories of road users.
For each category, a comparison of accident data between fatal cases and the others is proposed ending in a list of some remarkable differences. Countermeasures for fatal accidents are also proposed in each respective category.
For light vehicle occupants, the analysis of usual data such as infrastructure and journeys have been completed by a sociological profile of children's drivers and specific psychological items such as alcohol and drug consumption, atmosphere in the vehicle. Concerning children involved in cars, the sample size for children in cars is 654 that once weighted to make it representative of reality correspond to 17748 children including 62 that were killed. Evidence of a restraint system used by children has been coded for 69% of children, but in only 44% of the cases, the restraint system was appropriate and correctly used.

For children in the other road user categories, the analysis is a little bit more limited but it includes the age distribution, infrastructure and journeys data, the responsibility of involved parts (including children). The presence of protection device such as helmets: it is about 8% for cyclists and about 82% for PTW passengers. For pedestrian children they sustained their accident while they were using a crosswalk in only 5% of the cases, and in 50% of the cases they were running across the road.

Conclusion: This paper opens the field of considering all children involved in a road traffic accident in a national safety study, not focusing only on fatal cases and not limited to the situation of children in cars. Even if some limitations due to the use of weighting factors exist, it gives a comprehensive picture of the situation in France.

## INTRODUCTION

This paper is presenting two visions of the implication of children in road accidents in France. First, the global picture for all children and secondly it is focusing on the characteristics of accidents per types of road users. It is based on the one year collection data done in the VOIESUR project that have been weighted to be representative of the French situation. The official indication of the implication of children in road accidents that have occurred in France in 2011 is given in the publication of the National data results for the year 2011. The figures shows there are lower than the ones presented in this study. This is due to the fact that this kind of data when collected on police report is underestimating the proportion of slightly injured and uninjured occupants, especially children (generally not interviewed by the police). That's why the weighting factors have been adjusted to be representative of the observed situation based on observations in hospitals. More information about the context has already been detailed precisely in the publication [1] presented at the 11th International Conference of child safety in cars.

### VOIESUR project

Despite a sharp reduction of the number of fatalities on French roads since 2000, road accidents are still one of the priorities of the French government. VOIESUR (Vehicle, Occupants, Infrastructure, Environment, and Safety of Users of the Road) is a National project of 40 months started in January 2012. This project, partly funded by the Agence Nationale de la Recherche (National Agency for Research) and the MAIF foundation fits with the EU declaration of the "Decade of Road Safety". Its consortium is composed of 4 partners: LAB - Laboratory of Accidentology, Biomechanics and Human behaviour, CEESAR - European Centre for Safety Studies and Risk Analysis, CEREMA - National Centre For Studies and Expertise on Risks, Environment, Mobility, and Urban and Country planning , IFSTTAR - French institute of science and technology for transport, development and networks. Among its multiple objectives, the VOIESUR project has a key-point: to keep moving forward in the field of road safety and thus place France among the safest countries in the world. To do so it is necessary to have complete and accurate information in line with current issues such as vulnerable road users. In the VOIESUR project, a new database of road accidents that occurred during the year 2011 in France has been built with the aim to be representative of the national situation. Based on in-depth police report studies, VOIESUR expands the fields of observation not only to fatal accidents but also to traffic accidents with injuries. The project is updating the comprehensive information system on road safety that dates from 2000. It is based on reports established by the police in France during the year 2011 related to road accidents in which at least one person was injured.
People concerned by the coding will be all French fatalities, all Rhône area accident injuries and 1/20 random of national accident injuries. The database includes the details of the accidents and when available the full medical records of the people involved. A match between the VOIESUR database and the Rhône register injury database provides the basis for a data recovery methodology to propose a correction of the underreporting in the French national data.
The analysis of this database, allows to improve the general knowledge in accidentology and to focus on specific road users such as pedestrians, two-wheelers, children, seniors or to look at the evolution of the road safety in France over the last thirty years by comparison with data previously coded and analysed. In addition, this database is used to evaluate the method of data recovery and to suggest a correction on national data. The realization of thematic studies supplies a better safety diagnosis on specific road users and in the end these studies is providing row material to elaborate new safety systems and to base statements to establish new road safety regulations.
The version of the database used for this study is v19, on which the version 2 of weighting factors has been applied.
One of the thematic studies of the VOIESUR project is dealing with the situation of children involved in road accidents. The motivations and the work organisation of that part of the project have been reported in the Child safety culture workshop held in 2012 prior to the Munich conference "children in cars", and are explained in the proceeding of the conference [2].

## METHOD

Every accident is described in details using general variables in three areas (vehicle, occupant, and infrastructure) and specific safety variables are coded by experts in the domain to understand all aspects of the accident. Up to 450 variables usable for future studies are coded for each accident. The analysis of injured children in a road accident that occurred in 2011 has been conducted using the VOIESUR database. Victims have been classified according to 5

categories, light vehicle occupants, cyclists, powered two wheels passengers, buses and coaches' occupants and pedestrians. Over-accidents have been excluded from the sample has the same person can change of user category between two events and make the analysis too complex.

In the VOIESUR database, medical data of injured road users has been coded using AIS code revision 98 [3] when available. But in fact, there are not so many cases that contain such data as autopsy or complete medical report of people involved in road accident in France, because this is not mandatory but only performed if required by the justice. External post mortem inspections are sometimes performed but cannot be considered as a detailed medical report. They do not present a complete list of injuries, but can be useful for the determination of locations of impact across the children's bodies, and in a certain way the determination of restraint conditions for vehicle occupants. The present study focusses on all child injury levels including those fatality and such medical inspection reports are included in the sample. Children involved in a road accidents are split in four injury level categories: Uninjured, slightly injured, seriously injured, and killed, with clear definitions for each of them.

**Weighting factors**

The purpose of this study is to be as far as possible representative of French situation. As it has been already highlighted in previous National projects, a recording gap between the number of accidents recorded by the police and the number of accidents that actually occurred in 2011. Thus, weightings have been determined in the VOIESUR project to correct the record found error. The document [4] refers to the VOIESUR deliverable explaining the calculation of these weightings.

Sampling at 1/20th the personal road accidents led us to the creation of the first correction factor. It is therefore assigned to each injury accident a weight of 20 to return to a condition called exhaustive (All fatal accidents have been coded, no correction is applied to them). After that, a recording gap in the sharing between the different entities of the security forces was found, which led us again to the creation of another correction factor to restore the right proportions. Finally, an under recording of some accidents has been also found while comparing the exhaustive list of hospital recordings of admissions following a road accident and the list of people recorded by the police. This last factor is depending on the category of road users, the injury severity level and the unit of police in charge of reporting the event. Therefore, on all the following results, the three weightings were applied to correct the raw data. There are of course limitations to use such factors to make the data representative of the real road situation, and questions on the validity of these factors for the situation of children on the road are sometimes possible. For example, children cyclists in the original sample are not very numerous, but they are also rarely recorded by the police if none of the people implied in the accident is severely injured. Therefore, the weighting factors to scale these cases to the road reality are often high. Unlike fatalities, the information obtained for personal accidents are not exhaustive, this can have an influence on the quality of the analysis that is performed.

## GENERAL RESULTS

The sample size for this chapter is 31636 children (0-13 years of age) involved in roads accidents in France in 2011. The material is coded data for 915 children on whom corrector factors were applied to obtain this sample representative of road situation reality. It is composed of all type of users and all injury severity levels.

**Proportion of children involved in road accident in France -2011 per road user categories**

The distribution between the categories of road users is shown on Figure1and can be read as follow: 64% are light vehicle occupants, 17% are cyclists and 15% are pedestrians. PTW passengers and bus and coach occupants represent a little less than 2% each. The remaining children (0,5%) are not belonging to any of these categories of road users.

**Implication of children in accidents occurring in France in 2011**

The situation of children needs to be compared with the one of adults involved in road accidents to underline differences. Children represent 6% of the total number of people involved in road accidents in France in 2011. Having a look on the proportions of children in the different user categories, it clearly appears that for the categories of PTW and "other vehicles", children are representing very low figures (less than 1%), but they represent 18% of the total number of the pedestrians having accidents, and 8% of cyclists. This underlines the fact that when they have to take decisions, such as crossing a street, being able to stop at crossroads, or riding

a bike in the traffic, they more often fail than adults. Children represent 7% of all people involved in road accident as occupant of a light vehicle.

The part of children considered in categories of vulnerable road users is 34% of the total number of children. The same figure for adults is 40%, but excluding PTW makes this proportion going down to 17% for adults while it remains to 32% for children. Therefore, accidents with children need to be treated with special cares.

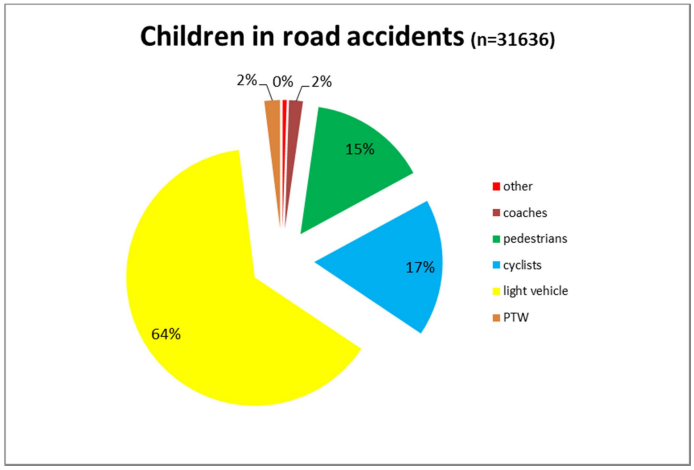


***Figure1. Proportion of children involved in personal road accident in France -2011 per road user categories***

**Distribution of injury severity per different road user categories.**

Once the implication of children across the different road users categories, it becomes important to analyse the severity of the injuries of children consecutively to their accidents. It is what is shown on Figure2. For that a relative simple way is to consider the duration of hospitalization of children, which is the official way to do it in France. Some children do not go to the hospital at all, they are considered as not injured, some others are conducted by rescue teams or parents to hospital but their stay there is shorter than 24 hours, these ones are considered as lightly injured. Children staying more than 24 hours are considered as severely injured, except for those who do not survive within the period of 30 days following the accident. In some cases, only the information that the child was transported to the hospital is available in the police report without any other indication of the injuries they sustained (from hospitals nor parents).These have been put in a separate category named injured NFS, but very often, not reported injuries are of a low level of severity.

The proportion of children fatally injured is 0,3% of the total number of children involved in road accidents. This proportion can be considered as relatively low as compared to the one of adults that is 0,8%, but it is important to remind the psychological impact of children's fatality in the society and the relative costs. For the category of severely injured road users, children are showing lower figures (4,3%) than the ones of adults (7,7%). If just looking at the proportion of road users involved in a road accident but not injured, the proportion for adults and children is similar with 30% in each category and the proportion of light injured population is also very close (50%). The proportion of children for who no information at all on injury severity are available is higher than for adults.

The previously described repartition is not uniform across all the road user categories. Details are on Figure2. The proportion of uninjured children is very high for bus and coach occupants with 77%, followed by light vehicle occupants for which the proportion is 44%. This proportion dramatically goes down when children are part of the most vulnerable road user categories such as pedestrians, PTW passengers, and cyclists. For these two last ones, the proportion of light injuries is very high, with respectively 80% and 90%. Pedestrians are showing the largest proportion of severely injured children with nearly 15%, and also have the higher rate of fatally injured children with 0,6%. They are followed by the light vehicle occupants with a fatality rate of 0,3% and finally by cyclists with 0,2%.

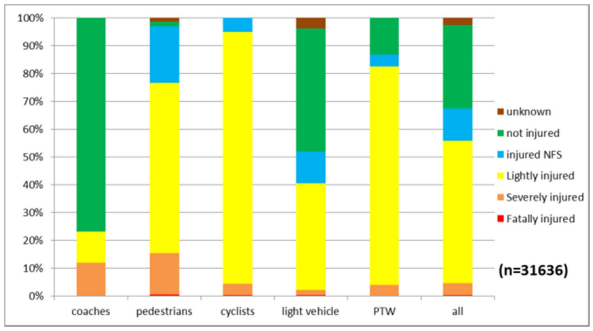


***Figure2. Injury severity per different road user categories for children involved in a personal accident***

As children passengers of light vehicles are representing nearly 2/3 of the total number of children involved in road accidents, even if showing a rate of fatality lower than pedestrians, their number is higher. On the 101 fatally injured children, 61% are light vehicle occupants, 26% are pedestrians and 11% are cyclists. No PTW passengers or coach and bus occupant has been fatally injured in 2011 in France. The remaining 2% of children fatally injured are not belonging to any of these categories of road users.

An important point in terms of protection of children as road users is to know the location and if possible the injury mechanisms that occurred during their accidents. To evaluate the injury severity, the AIS scale is used. In order to eliminate the lightest injuries, the present analysis is focussing on AIS3+ injuries that are defined on this scale as serious injuries. The number of AIS3+ injuries in the sample once weighted is 996. But having a look of their distribution makes no sense if they are not spread per user categories. Figure3 gives an overview for the categories of road users for which the number of severe injuries was sufficient to be dispatch across the different body segments. It is more detailed in the analysis for the different road user's categories, but what clearly appears is that limbs and more particularly lower limbs are the most often injured body segments at AIS3+ level, for all categories of road users and that this represents more than half of the total number of severe injuries for children pedestrians and cyclists. This has to be balanced with the fact that fatal cases of children are not often containing autopsy report, so fatal injuries or combination of injuries are missing in the database, but some external examinations can report injuries such as opened fractures. The head remains the first vital body segment in terms of frequency of severe injuries for cyclists and light vehicle occupants while this is the chest for pedestrians.

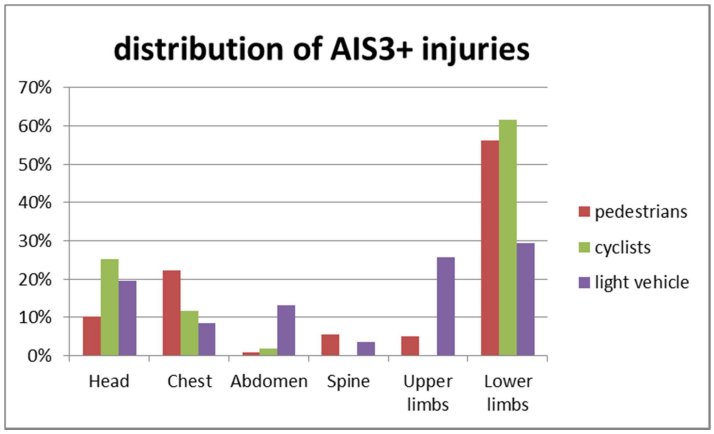


***Figure3. Distribution of AIS3+ injuries per body segments for the different road user categories (n=996)***

**RESULTS PER USER CATEGORIES:**

From this point, the analysis is only considering the children for who the age is known. Their number is 28851 for the 5 categories of road users considered in the following analysis. When distributed according to the age of children it clearly appears that globally implication of children in road accidents is slowly growing as children get older from birth to 10 years of age, and that the increase is much faster from 11 to 13 years. This

is mainly coming from a combination of the fact that if the number of light vehicle occupant and pedestrians is more or less stable up to 10 years old and then going up, the number of cyclists, PTW passengers and occupant of buses and coaches is concentrated around 10 year old children and more, which is re-enforcing this phenomena. This statement can be attributed to the appearance of the child's autonomy and need of mobility.

**Light vehicle occupants**

The number of children occupant of a light vehicle that has been involved in a road accident in 2011 in France is 17748. Children from birth to 10 years of age are more or less equally involved in road accidents as light vehicle occupants with an average value of 1200 for each year of age. As the sample is based on only one year of data collection, gaps and peaks are existing but could certainly be limited using a multi-annual sample. The extrapolation cannot be effective for the data that is missing in the sample. For children after 10 years of age, the number is rising up regularly to reach 2300 for children that are 13 year old.

**Infrastructure and accident conditions** About 50% of the accidents involving a child as light vehicle occupant occurred in built up areas. 75% happened during the day, 22% during the night and 3% at dawn or twilight. The most common obstacle is another light vehicle in 53% of the cases. Fixed obstacles represent 27% of the sample, 2 wheels 10% and 6% is heavy utility vehicles that are mainly trucks. Pedestrians have been coded as opposite obstacle for 2% of the cases. The 2% remaining of opposite obstacles belongs to the categories of "other vehicles".

52% of the accidents occurred on primary roads, one third on secondary roads, highways are "only" totalizing 16% of the total of accidents with children as car occupants. The typology of accidents is different according to the different road categories for children accidents. For highways, the most common accident type is roll-overs with 40% of the cases to which 10% of tip-overs could be added. Frontal impacts represent 32% and rear impacts 10%. Side impact is only scoring 4%, on this type of road. On primary roads, frontal impacts are the first accident type with 58%, rear impacts are following 19%, then side impacts with 11%. Roll-overs on such roads are only 5% of the sample and side swipe counts for 3%. On secondary roads, Frontal and side impacts are equivalent with 39% each, rear impacts are coming then with 14%. Very few roll-overs and tip-overs has been mentioned for this category of roads, but it has to be said that side swipe are showing their higher score with 6%. This can be explained partially by the fact that roads from this category are certainly narrower than the other ones, facilitating this kind of impacts.

30% of accidents occurred in or close to an intersection. From this particular configuration, 61% of the drivers intended to cross the intersection and 25% had the wish to turn left or right. It has to be noticed that 7% were stopped prior or in the intersection at the moment of the accident. For the 70% of accidents that did not happened at intersections it has to be noticed that in 71% of the cases, the vehicle was going strait, without any intension of changing direction, 8% are overtaking another vehicle, other 8% are slowing down, 5% are changing of lane and finally, 7% are stopped.

From that point, it is important to notice that for the analysis accident of light vehicles against pedestrians and two wheels (with and without engine) have been excluded as the loads are very often very low for the light vehicle occupants in this kind of road accidents. The number of children in the following analysis is 15236.

**Type of impacts** The distribution of the type of impacts for children light vehicle passengers is as follow: 51% of the children are involved in frontal impact, side impacts and rear impacts are very close one to the other with respectively 16 and 17%. Roll-overs count for 10% and tip-overs for 2%. Side swipe, falls and other accident configuration are representing approximately 1% all together.

**Sociological profile of children's drivers:** This point is not always considered in analysis of topics related to road safety and more particularly child safety in cars. The part of technical data is of course crucial to understand the situation and define axes of progress, but the knowledge of sociological and psychological data are also essential to be efficient in the communication campaigns and educational programs. [5] The number of variable that can be used for that and being present in the police reports are not so numerous. For example, the school level is not available, and information such as profession of the driver is not always reported, which makes more difficult the definition of a sociological profile. Nevertheless professional activity, the level of responsibility in the accident, the fact of having

an insurance for the vehicle, the relationship between child and the driver, the type journey, and the main reason of the accident have been coded in the VOIESUR database for accidents in which children were involved.
In 94% of the cases, vehicles in which children were transported were covered by an insurance policy. This is not totally surprising as this is mandatory in France to have one to use a vehicle.
Journeys for children are unknown for 31%, which is limiting a little bit the use of this data, but it's interesting to notice that leisure activities comes to the first range of known journeys with 21%, closely followed by the visit to family that scores 20%. Departures to holidays are not a negligible part of the accident with children in light vehicles with 10%. What can appear to be surprising in this list is that the activities conducted every day such as the travel to school, or nursery is only representing 4% of the total and that shopping activities is scoring 6%.

Drivers in a very large majority of cases are the parents or parents in law of the transported children mothers representing 49% of the cases and fathers 31%. The other members of the family such as grand-parents, sisters and brothers, uncles and aunts represent additional 8%. This means that information on child safety as to be focussed on the familial environment. Friends and neighbours are driving in 9% of the cases. They can also be good vectors for forwarding safety messages to parents of children but also need to receive information on the right way to transport children in cars.

Looking at the driving experience, the variable used to determine this parameter is the number of years of driving licence which is available for 78% of cases. The figures are showing that drivers with a shorter experience have tendency of being more involved in accidents with children and that the percentage of implication is going down as the number of years of driving license is increasing.: 33% for less than 10 year, 26% between 11 and 20 years, and 19% for more than drivers with more than 20 years of driving licence. This can be a bias due to the fact that people having children to transport are relatively young and therefore are relatively young in their driving experience.
59% of drivers have a professional activity, 20% are non-actives, and the professional situation is unknown for 21%.
The responsibility in the accident has been coded using different method in the VOIESUR project. For this analysis, it is proposed to use the judgement of the expert on this point as when coding, he knows the facts and the involvement of the different parts in the accident. As results, the driver of the vehicle in which the child is transported is responsible in 47% of the cases. In 50% the driver has not responsibility in the accident. For 2% the responsibility is shared between parts and in 1% it was not possible to determine this parameter.

**Psychological items:** The consumption of alcohol or drugs prior to driving have been considered in the psychological profile of drivers. Other parameters sometimes more difficult to evaluate, or subject to interpretation have been when possible coded by experts such as the atmosphere in the vehicle, the influence of the presence of the child on the driving performance, and the time pressure on the driver to make the journey. Personal data for drivers such as the stability of the professional situation and the recent change of family status have also been taken into account.

First of all, the data is showing that the driver behaviour in terms of restraint use has a huge influence on the fact that the child is restrained or not: when the driver is using the seatbelt only 5% of the children are not restrained that has to be compared with a rate of unrestrained children of 26% when the driver is not belted.

Going one step further, the proportion of children that seems to be correctly restrained with the limitations indicated in the section dedicated to this item, is only 1% when the driver is not restrained versus 46% for the cases in which the driver is wearing the vehicle seatbelt.
The measure of the level of alcohol for drivers compulsory in France after an accident occurred, so this data is available for 91% of the cases of our sample. The maximum authorized alcohol level is 0,5 g/l of blood, which correspond to a limit of 0,25g/l of expulsed air. For 20% of the accidents, alcohol has been found for one of the drivers, and at least 8% of the drivers with children on board were over the legal limit.
The consumption of drugs in France is not legalized and if no medical treatment is declared, no drug should be found for drivers. The control of presence is not mandatory in all accidents, but more on request of the legal department in severe cases. Up to now the cost of such control was high. This could change in the coming years with

the apparition of saliva tests that seems to give satisfying results. The data is missing for 27% of the drivers in our sample. For 72%, drivers have shown no evidence of drug consumption but the test was positive for 1% of them. About 5% of the drivers with children on board had a recent change in their family status, to be compared with 69% for which no evidence of change has been recorded. This data is missing for the remaining 26%. Figures are relatively similar for the stability of the professional situation, with 67% without any change, about 5% recorded with a recent change and with 28% unknown.
The atmosphere in the vehicle at the moment of the accident is determined by expert according to the statement of the drivers when available, and by other occupant's and witnesses reports if any. In 27% of the cases, the data was not possible to determinate. It was considered as neutral if no evidence of one of the category was reported, or if the statements report that nothing special was on-going in the vehicle. This comes in the first row with 59%. On-going conversations are the second configuration with 5%, and playing or laughing is reported in 3% of the cases. Another category is that all passengers in the car are sleeping, this happened in 1% of the case. Some cases of fights or violent discussions between adults have also been reported but they are isolated cases. The 5% remaining were coded as other situations and a more in-depth investigation of these cases could be interesting but is not available at this day.
Another point partially link with the previous one was the estimation of the influence of the presence of the child in the following of events ending by accident. Experts have stated that for 90% of cases, children had no influence in the accident story, but they also stated that in 4% of the cases the child is clearly involved in the chain of events ending into the accident and that in other 4% they had potentially influence the driving performance. In 2% of the cases, it was not possible to status due to a lack of information.
The last point that has been studied is the fact that the driver was under time pressure to make the journey, which was the case for only 6% of them.

**Restraint conditions:** The use of restraint systems and the quality of use of these systems while travelling in light vehicles is one of the key point in the definition of ways of progress in child safety studies [6]. Data collections since years are reporting that the number of correctly installed children is very low. Even recent studies stated that this figure is between one quarter and one third, depending on the studies and their relative methods of collection [7].
On the sample of 15536 children, the restraint conditions are unknown for 25% of them, because no indication in the police report can help experts to status on this point. About 6% of the children were not restrained at all; this is not far from the figures obtained in real life observations previously stated as references. For the 69% remaining, experts have coded that restraint systems were used by children, and for 44%, it seems that the restraint system was correctly used. Misuse of restraint systems have been identified for only 2% of children of the sample, which is not close to the real situation. This clearly shows the limitation of the analysis that can be conducted on such detailed points by only using police reports, even if coded by accidentologists. For the remaining 23%, no indication was available to make a decision on the quality of use of the restraint systems.

**Injuries:** Injuries or absence of injury have been coded using the AIS scale for more than 10000 children involved in accidents as light vehicle occupants. This can give a more precise picture than the length of hospitalization used in the official national statistics, as it is based most of the time on medical information reported by hospital or in the statement of parents. The level of protection seems to be already high and 49% of the children have not been injured. 43% other percent receive injuries of a minor level. 6% of the remaining children received moderate injuries. The 2 % remaining received severe, serious, critical or fatal injuries
It is important to focus and these particular children and have a look on the repartition of these injuries of having a high level of severity. Looking at Figure3, it is clear that limbs represent a high percentage of them, but the head that is scoring 20%, the abdomen with 13% and also the chest are vital body segments that need to be better protected.

**Remarkable points between all accidents / fatal accidents:** This paragraph is presenting the main differences between all accidents and the fatal ones in which children are involved as light vehicles occupants. All the following statements on these differences are statistically significant.

First of all, fatal accidents occur for 94% in non-built up area which as to be compared the fact that this proportion is 50% for all accidents. Fatal accidents occur more often than other during the night time (35% versus 22%). Their proportion representing highways is a little bit higher with 20% against 16%, but the main difference in terms of road categories comes from the secondary roads that are two times higher than for non-fatal cases.

Focusing now on the driver, in terms of responsibility in the accident, the ones in fatal accidents have a part of responsibility in 70% of the cases to be compared with the 47% in other accidents. The proportion of drivers with alcohol is twice higher in fatal accidents than for others, and the same observation is done concerning the consumption of drugs. Human factors and more particularly psychological points are different when comparing fatal and non-fatal accidents: the change in family status is 13% in the first case and 5% in the second one. A similar observation is done concerning the professional stability. Drivers involved in accidents being not fatal for children have had a recent change in their professional activity for 5% and for the ones driving a light vehicle in which a child is killed this rate is 16%, which is more than 3 times higher.

Finally when looking at children themselves, two remarkable points: the number of unrestrained children is also different with 6% in accidents versus 22% in fatal cases and the proportion of children that are sleeping is 2% in non-fatal accidents and reach 26% in fatal cases.

**Main countermeasures for fatal accidents:** This part is an extract from the deliverable of the VOIESUR project dedicated to the situation of children fatally injured in road accident as light vehicle occupants [8]. More details are available on the referenced document. Countermeasures can belong to different categories, such as infrastructure, primary or passive safety devices. For the first two, the counter-measures are not specific to child safety but may also apply to all road users. It is important also to mention that multiple proposals could have been made for each accident. For the infrastructure, being not expert in the domain, this value has only been chosen when the infrastructure could have clearly been safer. For example, the separation in the traffic between train, trucks and light vehicles is the best possible solution to avoid collisions between them as there are few chances for car occupants to survive in an accident against a train. More simply to apply, in some cases the mere presence of guardrail could have avoided the vehicle to fall in water or in ravines. For the primary safety, systems based on the communication between cars and infrastructures with the decision of action such as automatic stops in case of a stopped vehicle in front, or arriving at a stop line could be helpful, automatic speed adaptation systems to location or weather conditions could also be beneficial in a large number of cases, and so would be systems keeping a safe distance between vehicles. The other types of systems that could participate to the reduction of the number of children killed in light vehicles are the ones giving information to the driver that something wrong is happening. For example line departure warnings, trajectory control aids and “falling asleep” control systems could be applied in some cases of this study.

In terms of passive safety, looking at the number of unrestrained children in vehicles, it is clear that the use of a restraint system is in this area the first and necessary thing to be done. Then the choice of the appropriate CRS and its correct use are the following step. It seems that these two first points could improve the situation in more than 40% of the fatalities. Once correctly used, restraint systems both on the car and CRS could be improved. Of course some countermeasures for the drivers are also necessary such as reinforcing the law application with regard to alcohol consumption or speeding.

Globally there is a big need of safety information for drivers, to respect the rules in terms of speed, distance between vehicles, and to adapt their driving to conditions. Messages dealing with the use of restraint systems for all car occupants are needed in combination with the message of adapted correctly used restraint systems.

### Pedestrians

4696 children have been involved as pedestrians in road accidents in 2011 in France. This represents 15% of the total number of children and 18% of the total number of pedestrians of all ages recorded. The number of children killed as pedestrians represent 26% of the total number of children killed on the road.

The distribution of ages of children pedestrians for all injury severities shows that as soon as they are able to walk, children are involved as pedestrians in road accidents. Their number is stable across the different ages but for the data of 2011 a peak is visible only for the 12 years old children without any evident reason for that.

**Infrastructure**

Nearly all accidents of children pedestrians have occurred in built up areas (98%), and mainly during the day time (86%). Night accidents are representing 9% to which 3% that have happened at the dawn or twilight as for the light vehicle occupants.

Concerning the moment to which the accident occurs, there is no big differences between the months of the year, the two first ones being June and April with 13% each and the month with the lower number of accident being July with only 2%. Children pedestrians' accidents mainly took place on the week working days. Week-ends are only counting for 11% of the total. A large part of children pedestrians accidents happened between 4 and 6 pm, a peak is also visible at 8 am. Nearly no accident between 8pm and 8 am.

2/3 of the accidents, took place on primary roads, 30% in smaller streets and 3% on highways. About 1% occurred on other road categories such as private or public parking places.

About 71% of children are impacted by the front of the vehicle and about 22% are in contact with the side of the vehicle. In about 5% children are overpassed by one of the wheel not necessarily with another impact with the vehicle. In 58% of the cases, the child pedestrian is impacted by a light vehicle. The second category of opposite vehicles is motorbikes that are surprisingly involved in 27% of the accidents of pedestrian children. Heavy vehicles come third with 10%, and bicycles are representing 2%. The 3% remaining belongs to the category "other vehicles".

Figure 4 shows the distribution of the children's actions when the accident happened. About ¾ of them were simply crossing the street perpendicularly. To this it is necessary to add another 11% that were crossing not necessary perpendicularly which make this action at the top place with 85%. For children crossing the road, in 44% of the cases, it was noted that the child was crossing on a crosswalk, but in 47% it was coded that the child was crossing outside of cross walk. The data is unknown for the remaining 9%. This underlines that there is still a need of education for children to cross in fit areas. 13% of the children were walking along the street or road and have been impacted by an incoming vehicle and 1% of the children were just standing.

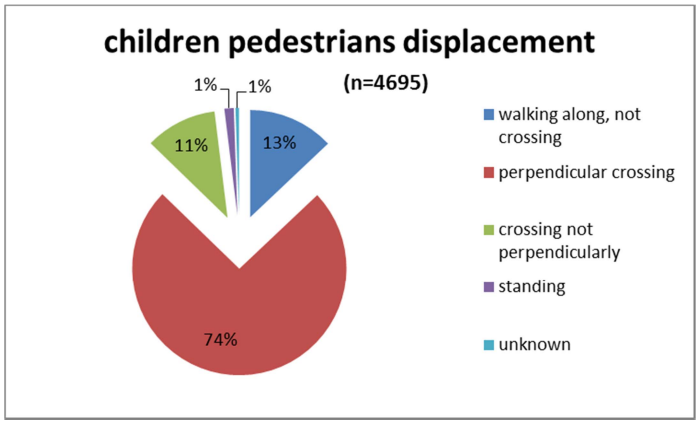


***Figure4: distribution of the displacement of the children pedestrians at the moment of the accident***

**Human factors** As for all accidents of the VOIESUR database, the responsibility of all parts involved in road accidents have been established by expert, based on the infrastructure configuration, the behaviour and actions of each part. As results it appears that children have been considered as the most responsible part in 49% of the cases, to which 6% have to be added for shared responsibility. It is important to look then at the children's activity when the accident occurred and on the journey they were doing. For that, one variable available in the database gives indication of the speed of the pedestrian at the moment of the impact. This data is unknown for 12% of the children but in 50% of the accidents, children were running while 31% were walking. In the 7% missing, the data has been coded as other, which can indicate that the child was not moving, or was trying to catch something under a car, or hidden in a game...

For 16% of them children have been coded as escaping from the vigilance of an adult. This shows the important not only to deliver safety messages to children but also to the accompanying people. It has to be underline that 90% of them are under 6 year old.
In terms of "journey", child pedestrian accidents happened for 38% in a leisure activity and for 32% on their way from home to school or back. In 11% the variable is coded as other, 6% were going shopping, 3% were on their way to visit their family and this data is unknown for 10% of the cases.

**Injuries** 9% of the children have been over passed by the vehicle that is involved in the accident, 5% without any other impact, the others having being first impacted and then overpassed. The recording of injury severity using the AIS98 code has allow to have an overview of the severity of all children pedestrians involved in road accidents. Very few children are reported as not injured (only 2%) but the level of injury severity is unknown for 40% of the children. In this category all fatal accidents without autopsy are counted but also all the cases for which no medical data was available in the police report, very often because the injury severity if any if very low. This is confirmed when looking at the Figure2 for which the rate of lightly injured is 61% to which a large number of cases from the category of "injured NFS" that is scoring 20% could be added. For moderate and severe injuries, that are globally more reported in the police documentation, injuries of AIS2 level represent 13%, the ones of AIS3, 7% and the ones of AIS4, 2%
A distribution of AIS 3+ injuries across the body segments has been done to determine priorities in terms of protection for children as pedestrians based on the road reality. The sample is composed of 597 AIS3+ injuries, among which the most commonly body segment is lower limbs with 56%. It is followed by the chest with 22% and then by the head with 10%. The spine is representing 6%, upper limbs 5% and the abdomen about 1%.

**Remarkable points between all accidents / fatal accidents** As for the light vehicle occupants, this paragraph intends to show the biggest difference between accidents of all severities with children and the fatal ones. For pedestrians, there are more similitudes than differences for the infrastructure, the light, the fact that half of the children are running.

The repartition between the accident locations is a little bit different between all children pedestrian accidents that happen for 98% in built-up areas to be compared with 88% "only" for fatal accidents.

The order in the distribution of the pedestrian displacements is totally different. For fatal accidents, crossing not perpendicularly reaches 68% instead of 11% while perpendicularly is representing 4%, instead of 75% for all accidents. A bigger proportion of static pedestrians is also visible in the fatality sample with 16% versus 1%.
The proportion of children that have been over passed is far higher in the fatality cases for which this injury mechanism represents 44% of the sample while it is only 9% when considering the totality of accidents.

**Main countermeasures for fatal accidents:** this part is an extract from the deliverable of the VOIESUR project dedicated to the situation of children fatally injured road accident in the section pedestrians [8]. Educational programs are needed: to change their general behaviour while being on the road is not a game place, and that you need to cross without running and after having check that no vehicle is coming. Some infrastructure could also be arranged: to slow down the speed of vehicles at crossing points would be effective; manage a clearer area so the vision of drivers could be better at pedestrian crossing points. This will be effective only if children are using these points to cross the street. To better arrange sidewalks in a way that it is only possible to cross the streets at given points. Solutions proposed on the infrastructure side can be combined for a better efficiency and would not only be profitable for children, but for all pedestrians. In addition, the detection of vulnerable road users is now becoming more common on vehicles but collision avoidance systems will only be effective if children (cyclists or pedestrians) are not hidden. The proportion of children being over passed by the vehicle in the sample of fatally injured children is 44%, and for them, no passive safety action is possible.

**Cyclists**

5472 children have been involved in a road accident as cyclists in France in 2011. This makes the cyclists being at the second user category with 17% of the total number of children the road accident. By cyclist it is understood than the children were riding the bicycle. The number of children fatally injured in the sample is 11 that are representing 11% of the total number of children killed.
The youngest child in the sample is 4 year old but the number of children cyclists becomes more consistent after 8 years of age and regularly increase with the age from that point.

**Infrastructure**
Nearly all (99%) of the children cyclist accidents happened in built up areas, and during the daylight period. Looking at road categories, most of the accidents occurred on primary roads (68%) and 31% on secondary roads, the last 1% occurred on roads of other types. It has to be noticed that the presence of intersection has been coded for 84% of the cases. In 91% of cases children were going straight even at intersections, in 7% of the cases they intend to turn, but not necessary at intersections! 77% of cyclists have been involved in a frontal impact, 22% impacted on their side.
The light vehicles represent the first kind of obstacle, followed by heavy vehicles and fixed obstacles.

**Human factors**
Children cyclist accidents are concentrated around April, May and June. They also happened more on Saturdays and Wednesdays which are days without school for children younger than 14 years of age. The proportion of accidents also recorded on Sundays is not negligible. All accidents happened between 11am and 9pm.
The journeys that children were doing are distributed as follow: visit to family comes at the first row with 93%, far behind come leisure activities with 3%, going or coming back from school only represent 1%, and shopping is at the same level with also 1%. The data is unknown for 2%.
Experts have coded the responsibility in the happening of the accident of the children as vulnerable road users and of the driver of the opposite vehicle for every accident case. 3 levels of responsibility have been defined: full, share, and none. Of course this is subject to interpretation bias but in the case of accidents of children on bicycles, the information is considered as reliable as accident scenarios were not too complex. Children on their bicycles have been found to be fully responsible in 96% of the cases, the responsibility was shared with another part in 1% of the cases and in only 3% the children were considered as not responsible at all.

**Protection** In France, the use of a helmet is only mandatory for riders of motorized two wheels. Cyclists are not included in this category and can therefore ride without any helmet. The only obligation for them is to wear reflecting jacket if they ride by night outside of urban areas. Bicycle helmet legislation appears to be effective in increasing helmet use and decreasing head injury rates in the populations for which it is implemented. However, there are very few high quality evaluative studies that measure these outcomes [9, 10]. Nevertheless, it is highly recommended by authorities to use a homologated helmet when cycling [11], especially for children as in half of their falls injuries to head occurred. Even if this seems to be an appropriate protection device, helmets approved for cycling are recognized to be efficient for falls up to 20 kph. Children are normally not riding very fast compared to adults but this could limit the number of cases for which helmets are useful. The proportion of children using a helmet in the sample is 8%, and the proportion not wearing any is 84%. The data is unknown for the remaining 9%. It is not possible to measure any efficiency of the system due to the low sample of children wearing protecting device.

**Injuries:** As for other road user categories, injuries have been coded using AIS98 code. None of the cyclists in the sample are uninjured, 85% only sustained light injuries, 10% received moderate injuries. Children cyclists seriously injured counts for 1%, the level of injury is unknown for 4% of the children.
As visible on Figure3, the repartition of the serious injuries (AIS3+ level) indicates that the lower limbs is the most often seriously injured body segment with 61%. Then comes the head with 25%, the chest with 12% and finally the abdomen with 2%.

**Remarkable points between all accidents / fatal accidents:** This paragraph is presenting the main differences between all accidents and the fatal ones in which children are involved as cyclists. All the following statements on these differences are statistically significant.
The main difference is the location of the accident that is occurring only for 44% at intersection for fatal accident while it happens 84% for all cases.
None of the children involved in the fatal cases was wearing a helmet. This has led to a case by case analysis of the cases concluding that a very limited benefit of helmet would be expected on the sample of fatal cases.

**Main countermeasures for fatal accidents:** this part is an extract from the deliverable of the VOIESUR project dedicated to the situation of children fatally injured road accident in the section cyclists [8].
Educational programs are needed: for children to better behave when riding bicycles and a need of awareness of for parents on the fact that their children are not necessary ready to be left alone in the road traffic.
To improve the visibility of the children on their bikes would allow a better prevention of their behaviours for other road users. It is known that separating road users ones from the others is one of the safest solution: it is necessary to encourage the development of dedicated infrastructures for riding bicycles with crossroads infrastructures specific for bicycle. In addition, as for pedestrians, the detection by vehicles of cyclists using Intelligent Technical Systems would also limit the number of fatalities of cyclists and by the way of children cyclists. Considering children killed on their bicycles it has to be remind that they are nearly all perpendicular to the opposite vehicle trajectory.

**Powered Two Wheels passengers**

The number of children present as PTW passengers in the database is equivalent to 624 children that have been involved in 2011 in France. No fatality of children has been recorded as PTW passenger in the year 2011. The youngest children are 6 years old and it seems that the tendency of implication is growing with the age of children. Looking at the type of the vehicles on which children are passengers, the sample is composed about a little bit more than 1/3 by mopeds, the others being motorcycles. 30% of the PTW are fitted with engine lower than 50cc, 46% have an engine that is between 50 and 125cc, 15% are on motorbikes with an engine bigger than 125cc. The size of the engine is unknown for 9% of the cases.

**Infrastructure:** 95% of the accidents in this category happened in build-up areas. 78% mostly during the daytime, dawn and twilight represent 15% of the cases and 6% happened during the night time.
Looking at the road categories, there is a good balance between primary and secondary roads. The majority of collisions with PTW took place at intersections. Finally, concerning the opposite obstacle, it is very often another vehicle, light vehicles coming at the first row. Impacts against fixed obstacles count for 10%.

**Human factors:** Experts have coded the responsibility in the happening of the accident of the drivers of the PTW riding with children. The same levels as for the other children road users categories are used in this section. Globally the balance between responsible or not clearly goes for not responsible in the case of accident with children passengers of PTW. The distribution of the type of journey, when known, shows that leisure and rides come first, and that visit to family or friends is at the second row. Shopping is very far behind and no accident riding to or from school was registered.

**Protection use:** 91% of the children of the sample are wearing a helmet when being transported on a PTW. It has to be noticed that for 9% of them the helmet is not attached to the head and the data is unknown for the last 9%. Due to the low number of children on PTW with injuries, it is not possible to compare the situation of children travelling with and without helmets.

**Injuries:** Injuries, when known have been coded using the AIS scale. Very few AIS3+ injuries have been noted, and only 13% of the children involved in such accidents are uninjured, but the number of children that have being staying in hospital less than 24 hours is 79%. The seriously and severely injured children represent 4% of the

sample and the injury severity is not known and cannot be estimated for the last 4%. Results have to be taken with a lot of caution as the original number of children is not very high.

**Bus and coach occupants**

**General data on buses and coaches:** The definition used in the analysis is the same as the one used in the French National data: buses are city buses in which you can either be seated or be standing. Coaches are vehicles in which only seated passengers can be transported and since 2009 have to use a restraint system if the vehicle is equipped. Transportation of children to school in France is done by bus inside the big city and their close suburbs but in rural areas, it is normally done using coaches. In the VOIESUR database, for buses and coaches, 6606 occupants of all ages are present. Frontal impact is first impact type with more than 40%, followed by side impact about 30%. Rear collision scores 15% of the total and surprisingly roll-overs only represent 2%. For frontal impact, most of the time, the accident severity, coded in EES (Equivalent Energy Speed) in the database is not known.

The projection at national level for children is 311. This represents 2% of the total number of children involved in road accident in a year. Of course, the number of accident with such vehicle can show fluctuation from one year to another one, so conclusions are only valid for the year 2011. What is remarkable in this year is that no fatality of children in buses and coaches has been observed in France. In addition, it can be noted that there is no child under the age of 4 in the sample. Children in the following analysis are all between 4 and 14 years of age.

**Infrastructure:**

A very large proportion (93%) of buses and coaches accidents with children on board happened in built-up areas, and for 97% during the day. They took place on primary roads for 85%.
The typology of accidents for the buses and coaches are globally at low severity. Some of them were against pedestrians that represent no real physical impact for the bus occupants. In other cases, some children standing in the vehicle felt down on the door and were ejected without any impact of the bus, but just during a steering manoeuvre. Some frontal cases are reported but most of them have a very low EES (Equivalent Energy Speed) which means that their occupants are submitted to relatively low loads. Very few cases with a EES over 15 kph, are part of the sample. That's the main reason why it has not been possible to study the efficiency for children of restraint systems in such vehicles. For that a sample big enough containing restrained and non-restrained children in different crash scenarios is needed. May be the VOIESUR database is one of the brick to build the scientific knowledge on this point, but the project itself cannot bring any conclusion on that point.

**Injuries:** Children from 4 to 11 are all uninjured or are slightly injured only, no severe injury was observed for this age group. For children from 12 to 14 years, the sample contains different levels of injuries and a part of non-injured children. The injury severity for all children involved in accidents as bus or coach occupants has been coded using the AIS code version 1998. This parameter is known for 91% of the children of the sample. 59% of them are uninjured, and 20% only sustained AIS1 level injuries (cuts, skin abrasions, contusions,…). Severe AIS3 injuries have been observed on lower limbs, but no cerebral injury, chest fracture, spine injury or abdominal injury has been reported.

## CONCLUSIONS

It is difficult to consider a global road child safety message as children involved in road accidents belongs to different kind of roads users in which they do not have the same level of responsibility. Children are globally not able to take decision by themselves to properly behave in the road traffic. That's an additional reason for them to be treated as vulnerable road users. But when adults are deciding for children as for example in cars, it is clearly shown that the way children are protected is not satisfying mostly because the restraint systems are not adapted or not correctly used.
Globally, children involved in road accidents are for a large proportion not injured or slightly injured but the proportion of severely injured is sometimes over 10% as for pedestrians. The type of severe injuries that can be sustained by children is linked to the category of road user as reminded on Figure3. In the VOIESUR sample, a

large proportion of severe injuries has been attributed to the lower and upper limbs. This is somehow surprising as this is not necessary the conclusions issued from the CASPER accident database [12] that was orientated to biomechanical works research and for which the data collection was not representative of the road reality. Nevertheless, it appears that to improve the protection of children the head is always an important body segment whatever the type of road user, that for pedestrians it seems important to consider the chest while for car occupants, the abdomen seems also to be one of the priorities.
Works on the infrastructures are possible but it has to be reminded that children's road accidents do not occur in the same locations, especially the ones leading to severe injuries or fatalities. This would be helpful to focus on pedestrians and cyclists in cities and on the communication that is forwarded to both parents and children in order that they improve their behaviour while walking or riding in the streets. For children car occupants, the most urgent points to improve the situation are the improvement of the quality of use of the restraint systems and the protection of vital body segments such as the head and the abdomen.
This study has some limitations because of the use of weighting factors calculated for each child. This is helpful when considering the complete data set but it can become a bias when working on selection of data in which one of the children is representing a large proportion of the total. In addition, this study is limited in terms of the size of the sample because it contains only one year of data collection, which is representing a large amount of data but relatively few for each category of road users. In addition, a multi-annual data collection would allow to eliminate the bias of exceptional events that are may be in the sample, and some other rare configurations that are not there. One speaking example could be a coach accident with multi fatality of children. This would completely change the picture compared to the one of the VOIESUR data set.
This study has shown a picture that it representative of the situation of accidents with children in France compared them as different types of road users, and have brought data to construct ways of progress.

## ACKNOWLEDGEMENTS

The authors would like to acknowledge the VOIESUR partners (LAB, CEESAR, CEREMA , IFSTTAR) for their support during the duration of the project, and the Association Nationale de la Recherche, and the FONDATION MAIF for their financial support.

## REFERENCES

[1] Léopold & al. 2013. "VOIESUR: Analysis of all children's fatal road accidents in France in 2011"
11th Conference of child safety in cars (Munich 2013)
[2] Léopold & al . 2012. "VOIESUR: Focus on child safety specificities"
10th Conference of child safety in cars (Munich 2012)
[3] The Abbreviated Injury Scale – AIS, version 98
[4] Amoros &al. 2014. "VOIESUR: L3 "Methodology Data recovery and extrapolation"
ANR project reference: ANR-11-VPTT-0007
[5] Langlois & al. 2012. "D3.1.1 Report on Social approach of Child Safety"
CASPER project – FP7 – GA218564
[6] Lesire & al. 2010. "D1.2-2 –Misuse effect analysis – Results of dynamic testing program"
CHILD project – FP5 - G3RD-CT-2002-00791
[7] Muller& al. 2012. "D3.1.2 –Report on misuse and relative tests"
CASPER project – FP7 - GA218564
[8] Lesire &al. 2014. "VOIESUR: L4.6.1 Report on the children fatally injured on the road"
ANR project reference: ANR-11-VPTT-0007
[9] Macpherson & al. 2008 « *Bicycle helmet legislation for the uptake of helmet use and prevention of head injuries* »
Cochrane Database of Systematic Reviews, no 3
[10] Swedish official data 2009 – "Målstyrning av trafiksäkerhetsarbetet – Analys av trafiksäkerhetsutvecklingen"
[11] http://www.economie.gouv.fr/dgccrf/Publications/Vie-pratique/Fiches-pratiques/Casque/
[12]Kirk & al. 2012.DEL CASPER accident database analysis
CASPER project – FP7 – GA218564

# AN INVERSE MONTE-CARLO BASED METHOD TO ESTIMATE PRE-CRASH DISTRIBUTION FOR VRU SAFETY

**Hariharan, Sankara Subramanian**
**Sudipto, Mukherjee**
**Anoop, Chawla**
Indian Institute of Technology Delhi
India

**Dietmar, Goehlich**
Technical Universitaet Berlin
Germany

Paper Number 15-0421

## ABSTRACT

Current safety standards are based on maximum stiffness measures over a grid on the frontal surface of a vehicle. The safety of VRU is also influenced by the overall shape of the impacting vehicle. "Initial conditions" [IC] from the dominant crash scenarios are used for CAE simulations in Industrial practice to tweak designs. The IC's to design for are decided based on cluster analysis from reconstructions of crash data. Currently, CAE methods to predict the outcomes (final resting state of interacting elements) of a crash deterministically, given the initial conditions are available. But there are no established methods to do the inverse process, that is ascertain the conditions at the initiation of the crash given the final static state of the interacting elements. Recorded data being the final resting state of the interacting elements, the inverse problem is of significance, and is usually tackled by heuristics and iterations augmenting physical laws. While reconstructions of specific cases require detailed observation and experienced personnel, it is hypothesized that estimating a distribution of the pre-impact measures in crashes is more robust with respect to a distribution of the post impact observation than that of individual crashes.
Individual cases from crash reconstruction, approximated to a Gaussian "normal" probability density function, were assumed for the probability of occurrence of individual cases. Crash physics was captured using a multibody simulation in MADYMO solver. An inverse Monte Carlo [MC] simulation with MADYMO solver as the system under study was modelled in "FME" module in statistical software "R".
A set of post-crash data on head hit location [O1] was generated using forward MC simulation. The variable parameters were four different vehicle profiles, relative position of 50M along vehicle lateral axis [I2] and the relative orientation of with respect to vehicle. The pedestrian represented using one 50th percentile male [50M] pedestrian model was not varied.
Starting with the distribution of "O1" and an "I2" distribution perturbed by up to 20% in mean value as input, an I2 was computed using inverse MC. The "I2" distribution from inverse MC showed less than 10% deviation from the original v3 data set mean with randomized values of untracked variables.
During the inverse MC process, the quality of "fit" to a desired O1 distribution was tracked using the sum of root mean square of differences between normalized density coefficients and a "relaxation parameter" computed as squared logarithmic probability to a normal distribution. The stabilization of the tracking parameter indicated a robust solution.

## INTRODUCTION

Vulnerable Road Users (VRU) is a term used to collectively refer to pedestrians, bicyclists and motorcyclists. Report by WHO (World Health Organisation 2013) shows bicyclists and pedestrians to constitute over a quarter (27%) of the total traffic related fatalities in the world. VRU safety in crash scenarios involving cars has remained an active area of research with safety tests put in place for pedestrian safety using body-form impact on the vehicle front to estimate the potential injury risk. One of the components of VRU – pedestrians - represent a majority of VRU exposed to traffic threats. Data from (World Health Organisation 2013) also indicate pedestrian fatalities to be 22% of total road fatalities. Pedestrian safety has been addressed by regulatory and rating tests like Euro-NCAP

(Hobbs and Mcdonough 1998) and by indirect indicators for threats to pedestrians from car fronts. These rating and regulatory tests have been modelled for estimating threats to target human populations and crash scenarios selected based on data in crash databases. Current safety standards are based on maximum stiffness measures over a grid on the frontal surface of a vehicle. It is however well understood that safety of VRU is also influenced by the overall shape of the impacting vehicle (Crandall et al. 2002).
Advancement in CAE has led to crash simulations being used as a method for virtually replicating crashes. In industrial practice, CAE simulations are used to model using "initial conditions" [IC] from the dominant crash scenario to tweak designs. The IC's to design for are decided based on cluster analysis from reconstructions of crash data. Lack of clear data from post-crash scenes limit the efficiency of replications of crashes through computer simulations. Crash reconstructions of specific cases require detailed observations of the crash scene and experienced personnel to apply heuristics and iterate on simulations. It is hypothesized that estimating a distribution of the pre-impact measures in crashes is more robust with respect to a distribution of the post impact observation than inferring the IC's of individual crashes through reconstructions. We also note that for design or standard setting purposes, it is the statistics as opposed to specific cases which is of relevance.
The authors (S subramanian et al. 2014) have proposed a method based on inverse Monte Carlo to estimate pre-crash variables using limited post-crash data. This work evaluates the robustness of the inverse Monte Carlo method using a synthetic randomized post-crash data to estimate pre-crash data.

## METHODOLOGY

Crash simulation using computational techniques work on uni-directional physics of crash. The post-crash effects can be estimated using known pre-crash conditions. This work will discuss verification of previously proposed methodology to estimate pre-crash variables to model crash simulations. The first step of this study was to generate synthetically randomized crash data equivalent. Vehicle velocity (I1), vehicle category denoted by vehicle profile (I2), location of pedestrian in lateral plane of vehicle (I3) and orientation of pedestrian with respect to vehicle with pedestrian hit on left or right (I4) were selected for variation. The output of the crash simulation (O1) was captured. The present objective was to estimate most likely lateral position of pedestrian in front of vehicle (I3). An inverse Monte Carlo based on 'Mu' measure was executed with O1 distribution to estimate variable I3.

### Crash simulation

Vehicle to pedestrian crash was simulated using multibody MADYMO solver with pedestrian represented by 50th percentile male pedestrian model. Vehicle was represented using multibody model for vehicle front and the crash scenario was similar to previous work by authors (S subramanian et al. 2014).

### Generation of synthetic crash data

A synthetic randomized crash data was generated using forward Monte Carlo (FMC) simulation using sensitivity study module of OptiSlang (Dynardo Gmbh 2011) with 500 samples. The input variables I1 to I4 were classified as discrete and continuous variables with ranges of values shown in Table 1. I1 and I4 were discrete variables with three and four levels of values respectively. I2 and I3 were varied continuously in the range indicated. The input variable I2 was initialized with two values for every set of I1, I3 and I4. Two values of I2 was generated to simulate a "left" and "right" side impact of pedestrian with all other variables in same level for one iteration.

**Table1.**
**Input variables to Monte Carlo simulations**

| | Unit | Variable Type | Range |
|---|---|---|---|
| Velocity (I1) | m/s | Discrete | 30,40,50 |
| Angle (I2) | Degrees | Continuous | -30 to +30 |
| Location (I3) | m | Continuous | 0.2 to 1.8 |
| Category (I4) | No unit | Discrete | A, B, D or generic |

The FMC study had an objective of data distribution generation of the head hit location of pedestrian (O1). An overview of the process is shown in Figure 1. The variables I1 to I4 form the input to vehicle-pedestrian crash

simulation in MADYMO. MADYMO solver output files were read back by OptiSlang for the estimated primary head hit point on the vehicle by tracking the head and vehicle front positions through the simulation.

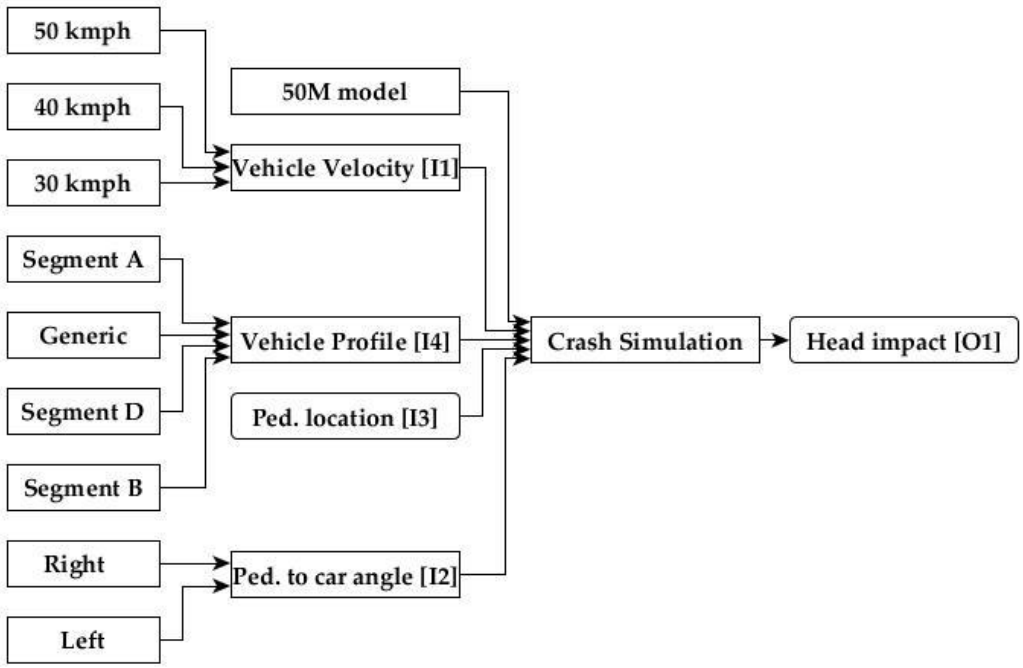


***Figure1. Methodology for a synthetic data generation using Monte Carlo forward method***

The data generated during FMC study of the I3 and O1 were exported from OptiSlang and a normal distribution was "fitted" to the data using modules in open source software R. The estimates of O1 distribution mean and variance obtained by the end of FMC would be used to provide an "expected" distribution of O1 for Inverse Monte Carlo method to estimate for I3 distribution. A normal distribution fitted to O1 had a mean of

**Estimation of a pre-crash variable**

Inverse Monte Carlo (IMC) based simulation was setup using FME module(Soetaert and Petzoldt 2010) in R language. The system under study was MADYMO solver with output being processed to provide O1 values. Most of the fine-tuning variables of FME were in default values. The number of iterations of this sample study was restricted to 500 iterations.
A 'μ' [Mu] measure was formulated based on the suggestions in FME documentations. μ was sum of RMS difference in density coefficients of present IMC iteration O1 values and similar values output from FMC along with a logarithmic normal probability of the I2 on expected normal probability function. The application μ in this work is shown in equation (1). A detailed discussion of μ can be found in (S subramanian et al. 2014).

**Sample calculation of μ**

$\mu = CF*RMS*100 + RP$ **(1)**

Where,

RMS - Root mean square difference in density coefficients between FMC and IMC
CF – Correction Factor
RP – Relaxation Parameter = -2 * log (Normal Probability)

For a specific I2 value of 145cm, the Normal distribution for RP has mean of 100cm and standard deviation of 45cm.
The normal probability of I2 = 4.9e-5
2*log (Normal probability) = RP = -8.6137
RMS calculated between FMC and IMC values of I2 were 0.015. The RMS values are multiplied by a factor of 100 in this case to make them significant in comparison to the RP.
**μ = 0.015*100-8.6137 = 10.19**

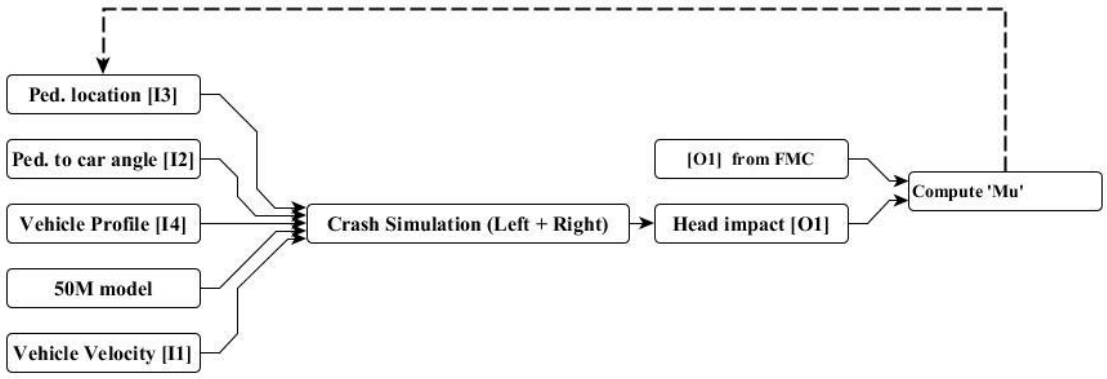


***Figure2. Methodology to estimate pre-crash variable using inverse Monte Carlo method***

## RESULTS AND DISCUSSION

### Variation of μ

The parameter 'μ' is expressed as a sum of CF*RMS and RP. During IMC simulations, the best possible solution can be obtained when the value of 'μ' reduces to minimum. The variation of RMS is indicative of global variation of O1 from IMC with corresponding value from FMC. The variation in RMS is shown in Figure 3, which indicate the value to stabilize over 300 iterations.
The value of RP was controlled by the new data point generated by randomized number generator of Monte Carlo process. The variation of RP and μ (Mu) is shown in Figure 4. The variation of RP between 15 and 20 is the direct result of normal probability calculation. The influencing part, μ, was the global parameter CF*RMS which stabilized by 300 iterations and was relatively stable beyond that point. It was concluded that iterations beyond 600 may not be necessary.

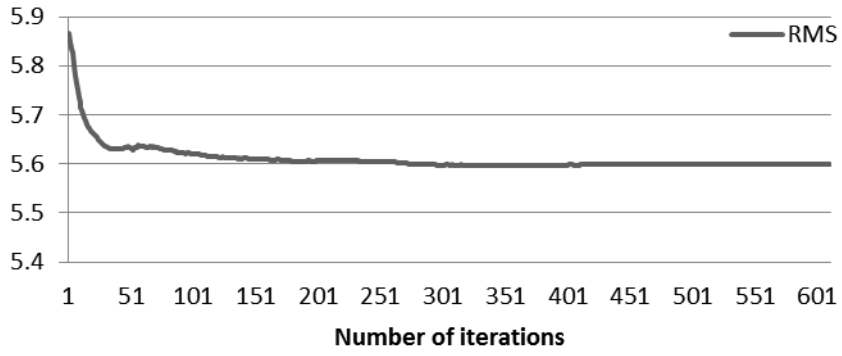


***Figure3. Variation of RMS in IMC***

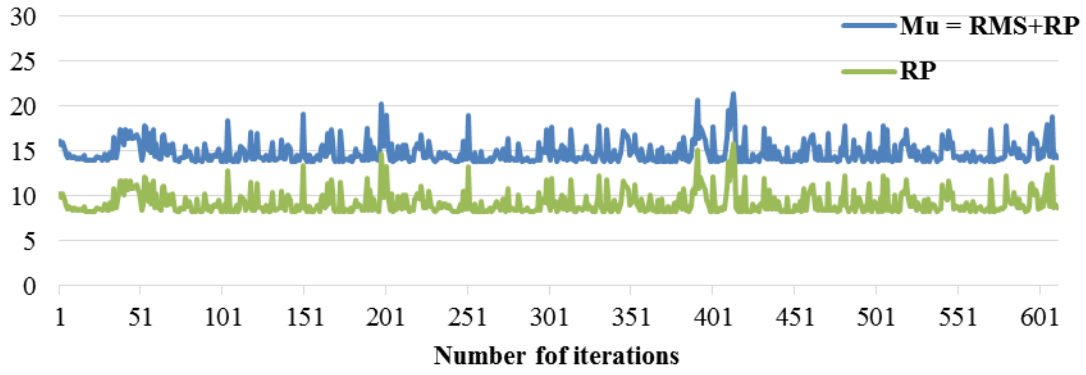


***Figure4. Variation of 'μ' in IMC***

**Variation of O1**

The objective of IMC simulation was to estimate the I2 distribution based on output distribution O1 processed from FMC simulations. In this study, a Gaussian normal probability function was assumed for all variables .Every head hit location (O1) was recorded and their density coefficient was obtained. The O1 density distribution obtained from FMC indicated a non-normal behavior as shown as dark shaded bars in Figure 5. The O1 distribution obtained from IMC process is indicated using lighter shades of bars in Figure 5, which show a mixed match with O1 from FMC. The O1 obtained from IMC process was generated with influence of normal probability which is evident with a peak near the middle of the O1 graph of density coefficients. The variation of the density coefficients of O1 distribution of FMC and IMC showed a Pearson coefficient of 0.83.

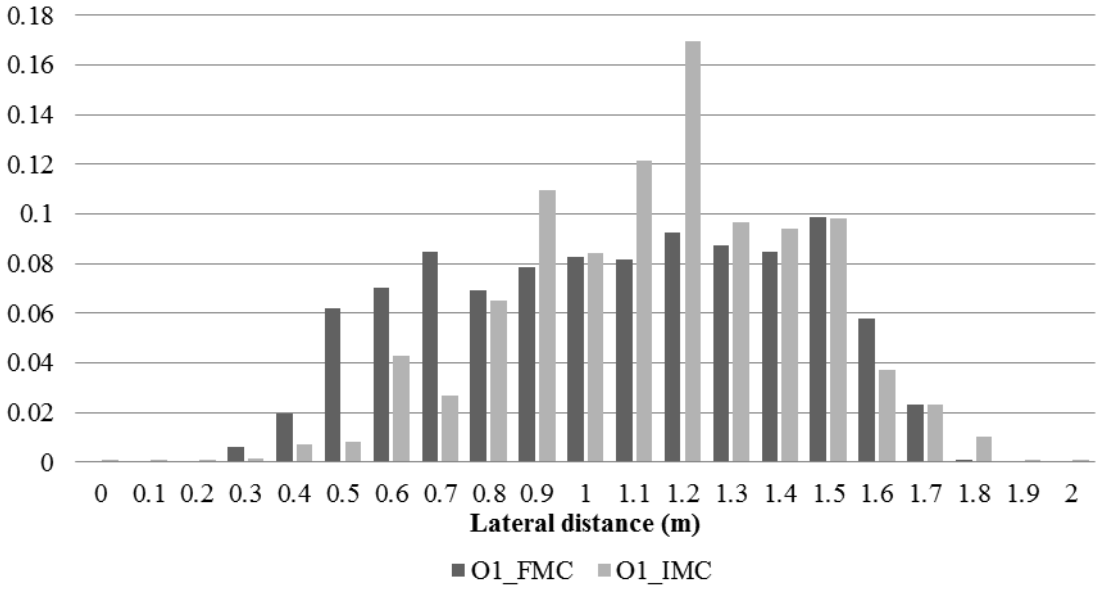


***Figure5. Comparison density coefficients of O1 from FMC and IMC***

The I2 variable was fitted to normal distributions by similar methods as O1 and their mean and variances were compared. Table 2 shows variable I2's normally distributed mean and standard deviation from FMC and IMC processes. Mean of I2 from IMC varies under 10% from the mean of I2 from FMC. The assumed normal distribution for comparison of I2 had mean at 1.10m and standard distribution of 0.25m. The initial value of I2 in IMC was assumed to be 1.45m. There was a significant shift in overall distribution towards FMC values.

**Table2.**
**Comparison of I2 from FMC and IMC**

| | FMC | IMC |
|---|---|---|
| Mean I2 (m) | 1.01 | 1.08 |
| Variance I2 (m) | 0.34 | 0.24 |

**Limitations**

A Gaussian normal distribution was assumed for all variables to estimate the probability. With clearer data available on specific variables, a better prediction probability function can be incorporated. The μ measure remains sensitive to the units of length used and appropriate correction factors need to be updated for better convergence. Sample runs of higher than 500 were not studied as the simulations trend was visible with shift in mean towards expected values.
The comparison was based on kinematic distributions, both at the input and output. The point of real concern is predicting trauma levels. An increased performance, when extended to HBM's applications (with significantly enhanced degrees of freedom) in conjunction with injury models has to be attempted.

## CONCLUSIONS

During the inverse MC process, the quality of "fit" to a desired O1 distribution was tracked using the sum of root mean square of differences between normalized density coefficients and a "relaxation parameter" computed as squared logarithmic probability to a normal distribution. The stabilization of the tracking parameter indicated an optimal solution.
This methodology combined with advanced tools like FE human body model will improve injury prediction efficiency of CAE tools.

## REFERENCES


[1] Crandall, J.R. et al. 2002. Designing road vehicles for pedestrian protection. *BMJ* (324), pp. 1145–1148.
[2] Dynardo Gmbh 2011. *Dynardo Gmbh OPTISLANG - The optimizing structural language v3.2.1*. Weimar, Luthergasse 1 D, Germany: Dynardo Gmbh.
[3] Hobbs, C.A. and Mcdonough, P.J. 1998. Development of the European New Car Assesment Programme (Euro NCAP). In: *ESV 98-S11-O-06*.
[4] S subramanian, H. et al. 2014. Methodology for estimation of probable location of VRU before impact using data from post-crash analysis. In: *IRCOBI conference 2014*.
[5] Soetaert, K. and Petzoldt, T. 2010. Inverse Modelling , Sensitivity and Monte Carlo Analysis in R Using Package FME. *Journal of statistical software* 33(3), pp. 1–28.
[6] World Health Organisation 2013. *Global status report on road safety 2013: supporting a decade of action*.

# DRIVER BEHAVIOR DURING LANE CHANGE FROM THE 100-CAR NATURALISTIC DRIVING STUDY

**Rong Chen**
Virginia Tech
United States

**Kristofer D. Kusano**
Virginia Tech
United States

**Hampton C. Gabler**
Virginia Tech
United States

Paper Number 15-0423

## ABSTRACT

Lane changes with the intention to overtake the vehicle in front are especially challenging scenarios for forward collision warning (FCW) designs. These overtaking maneuvers can occur at high relative vehicle speeds and often involve no brake and/or turn signal application. Therefore, overtaking presents the potential of erroneously triggering the FCW. A better understanding of lane change events can improve designs of human-machine interface and increase driver acceptance of FCW. The objective of this study was to characterize driver behavior during lane change events using naturalistic driving data.

The analysis was based on data from the 100-Car naturalistic driving study, collected by the Virginia Tech Transportation Institute. The 100-Car study contains approximately 1.2 million vehicle miles of driving and 43,000 hours of data collected from 108 primary drivers. In order to identify overtaking maneuvers from a large sample of driving data, our study developed and validated an algorithm to automatically identify overtaking events. The lead vehicle and minimum time to collision (TTC) at the start of lane change events was identified using radar processing techniques developed in a previous study. The lane change identification algorithm was validated against video analysis which manually identified 1,425 lane change events from approximately 126 full trips.

Forty-five (45) drivers with valid time series data was selected from the 100-Car study. From the sample of drivers, our algorithm identified 326,238 lane change events. Lane change events were evenly distributed between left side and right side lane change. The characterization of lane change frequency and minimum TTC was divided into 10 mph speed bins for vehicle travel speeds between 10 mph to 90 mph. A total of 90,639 lane change events were found to involve a closing lead vehicle. For all lane change events with a closing lead vehicle, the results showed that drivers change lanes most frequently in the 50-60 mph speed range. Minimum TTC was found to increase with travel speed, and the variability in minimum TTC between drivers also increased with travel speed.

## INTRODUCTION

One of the most frequent crash modes on the roadway is rear end collisions. The National Highway Traffic Safety Administration (NHTSA) reported 1.8 million rear end crashes occurred in the United States in 2012 [1]. Forward collision warning (FCW) systems have great potential to reduce rear end collisions on the roadway. Studies have estimated that FCW can reduce the number of fatally injured drivers by as much as 29% [2]. However, driver acceptance of the systems is paramount to the effectiveness of a FCW system. If a system delivers the warning too early the driver may be annoyed and turn off the system.

Lane changes with the intention to pass the vehicle in front are especially challenging scenarios for FCW designs because these overtaking maneuvers can occur at high relative vehicle speeds and often involve no brake and/or turn

signal application. Therefore, overtaking presents the potential of prematurely triggering the FCW. A better understanding of lane change events can increase driver acceptance of FCW and improve the effectiveness of FCW systems. The objective of this study is to characterize driver behavior during lane change events using the 100-Car Naturalistic Driving Study.

## METHOD

### The 100-Car Naturalistic Driving Study

The 100-Car study was a landmark large-scale Naturalistic Driving Study (NDS) conducted by the Virginia Tech Transportation Institute (VTTI) from 2001 to 2004. The study contains approximately 1.2 million vehicle miles of driving and 43,000 hours of data collected from 108 primary drivers and 299 secondary drivers [3]. Drivers were recruited from the Washington D.C. metropolitan area. No restrictions were used to select subjects, e.g. excluding those with traffic violations. Younger drivers, i.e. under 25 years, and self-reported high mileage drivers were, however, sought and oversampled [4].

Vehicles were instrumented with cameras and inertial measurement devices and equipped with a PC-based computer to collect and store the data. The data collection box housed a yaw rate sensor, dual axis accelerometers, and a GPS navigation unit. In addition, radar sensors were mounted on the front and rear of the vehicle that were able to track other vehicles. The data collection box was usually installed on the roof of the trunk of the vehicle in order to be unobtrusive. All data were sampled at a rate of 10 samples per second. Some of the sensors had lower sample rates. These data were still sampled at 10 samples per second but would have multiple samples with equal magnitude.

There were five (5) cameras that offered continuous views in and around the vehicle. An exemplar view is shown in Figure 1. The upper left frame shows a view of the driver's face and upper body, blurred to protect the identity of the driver in Figure 1. The lower left pane is an over-the-shoulder view of the driver, the upper right pane is a forward view out the front of the vehicle, and the lower right pane is split between a view out the passenger side of the vehicles and out the rear of the vehicle. The video was useful in the study in interpreting vehicle instrumentation data.

***Figure 1. Combined Video Views from the 100-Car Naturalistic Study*** [4]**.**

### Overall Study Approach

Our approach for the current study was broken down into three subtasks, as shown in Figure 2. The first subtask of the study was to find the lane change maneuvers and determine the start and finish of the lane change events. Since not all lane change events involve braking and/or turn signal use, we have developed an algorithm which used the lane tracking instrumentation data to identify lane change events. The second subtask of the study was to identify whether a lead vehicle was present during lane change events. Lastly, minimum Time to Collision (TTC) was computed for each lane change maneuver.

***Figure 2. Overall Project Approach***

**Automated Search Algorithm Development**

The identification of lane change events was based on the lane change signal recorded by the on-board lane tracking system. The lane change signal was triggered when the vehicle center line met the lane edge as the vehicle moved across the lane. In addition to the distance of vehicle centerline relative to the lane boundary, the lane tracking system also records the confidence level, from 0 to 100%, that the lane tracking system was providing correct distance evaluation. The following conditions must have been met in order to be accepted as a valid lane change: the duration of the lane change maneuver was greater than 0.3 seconds, no aborted lane change signals, vehicle speed above 10 mph, and average lane tracking confidence greater than 30% during the duration of lane change.

Figure 3 shows the definition of lane change duration used in this study. The start of lane change was defined as the time when the vehicle leading edge met the lane edge, and the end of lane change event was defined as the time when the vehicle was completely within the boundaries of the adjacent lane.

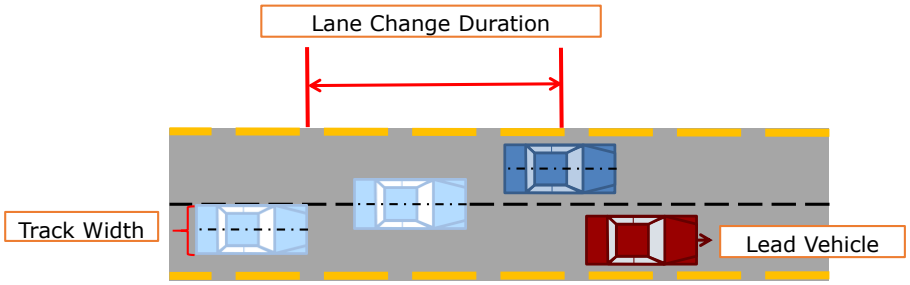


***Figure 3 Definition of Lane Change Duration.***

The lead vehicle identification algorithm developed in this study was based on a previously methodology [5]. The lead vehicle detection algorithm utilizes the on-board instrumentation, such as radar, vehicle speed, vehicle azimuth, and vehicle acceleration, to identify the correct lead vehicle at the start of a lane change event.

For each lane change with a lead vehicle present, the TTC was calculated as the range divided by range rate at the start of the lane change event, as shown in Equation (1).

$$TTC = \frac{x}{\dot{x}} \quad (1)$$

**Algorithm Validation**

Both the lane change identification and lead vehicle detection algorithm were validated against a sample of 1,425 manually identified lane change events. The sample of validation lane change events was examined from inspection of 126 trips, containing nearly 50 hours of video footage.

Table 1 shows the distribution of lane change maneuvers and the presence of lead vehicles in the validation sample. Merging lane change maneuvers include entering and exiting the highway. Lane changes involving drivers changing lanes to pass a lead vehicle were considered overtaking events. All other events were labeled "Lane

Change – Other". Examples of "Lane Change – Other" include events when drivers change lanes but do not overtake any vehicle. As shown by Table 1, 94% of the passing lane change events included the presences of a lead vehicle, as identified by reviewer. However, only 42% of merging events and 37% of lane change events had lead vehicle presence. By our definition, overtaking events should always have a lead vehicle. However, during the validation process, if the reviewer could identify a lead vehicle in the video but the on-board radar did not identify a lead vehicle, the particular lane change event was marked as not having a lead vehicle. Based on the large percentage of merging events and the low incidence of lead vehicle presence during merging events, this sample of validation data suggest that in most lane change event there will not be a lead vehicle present.

**Table 1.**
**Lane Change Maneuver and Presence of Lead Vehicle**

| Maneuver | Total Number of Lane Changes | Lead Vehicle Present (Count) | Lead Vehicle Present (% of Lane Changes) |
|---|---|---|---|
| Merging | 439 | 184 | 42% |
| Overtaking | 420 | 395 | 94% |
| Lane Change - Other | 566 | 209 | 37% |
| Total | 1425 | 788 | 55% |

## RESULTS

### Algorithm Validation

The performance of the lane change detection algorithm was evaluated based on contingency matrix shown in Figure 4. The sensitivity (% of correctly detected true positives) and specificity (% of correctly detected true negatives) of the algorithm was calculated as the ratio of true positive and true negative to the corresponding lane change maneuver.

Table 2 summarizes the comparison of the video and lane tracking indicated lane change events. For all valid lane changes with sufficient lane tracking information (i.e. lane tracking confidence > 30%, vehicle speed > 10 mph, and headway < 3 s). The lane change detection algorithm performed very well. The sensitivity of the algorithm was 0.87 and the specificity of the algorithm was 0.98.

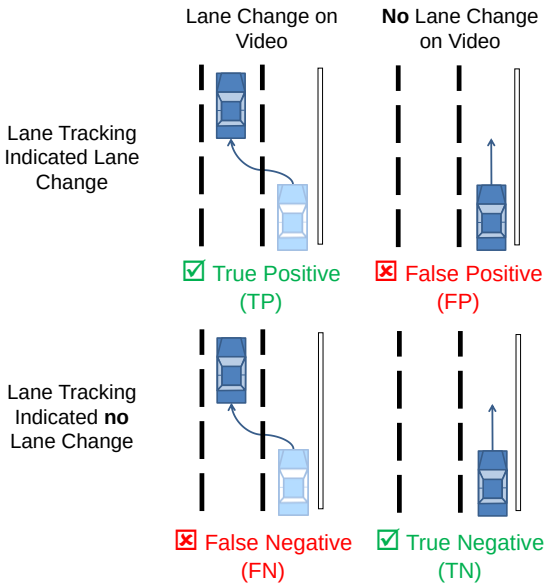


***Figure 4: True Positive and False Negative Matrix***

**Table 2.**
**Comparison Results of Video and Lane Tracking Indicated Lane Changes**

| | |
|---|---|
| Lane changes with sufficient lane tracking information | 645 |
| $Sensitivity = \frac{TP}{TP + FN}$ | 0.87 |
| $Specificity = \frac{TN}{TN + FP}$ | 0.98 |

The lead vehicle detection algorithm correctly identified the car following situation in 84% of the lane changes in the validation sample. Figure 5 shows the lead vehicle identification algorithm performance in five different car following scenarios. Scenario a) is the correct identification of a lead vehicle when there is lead vehicle present, b) is the correct determination of no lead vehicle, c) is the identification of a lead vehicle when no lead vehicle is present, d) is no lead vehicle is identified when a lead vehicle is present, and e) is identifying the wrong vehicle as the lead vehicle.

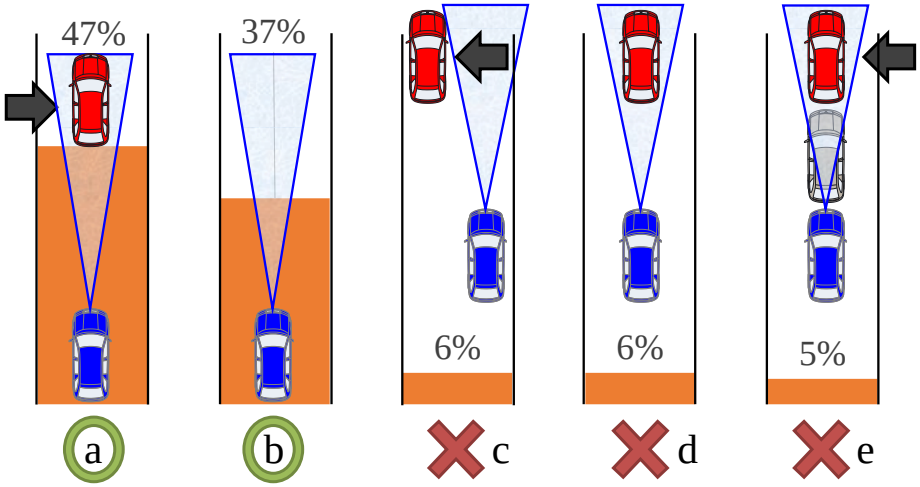


***Figure 5: Lead Vehicle Detection Scenarios***

**Driver Selection**

A total of 108 primary drivers and 299 secondary drivers were included in the 100-Car study period in which all driving in an instrumented vehicle was recorded [3]. Primary drivers were the primary owners or leasers of the instrumented vehicles. Secondary drivers occasionally drove the vehicles. Primary drivers accounted for 89% of all miles driven during the study period. The entire 100-Car database contains approximately 1.2 million miles of driving, 1,119,202 miles of which were driven by primary drivers in 139,367 trips [3]. Some primary drivers drove in multiple vehicles. For the current study only trips where a primary driver was driving in the vehicle that he or she most frequently drove during the study, i.e. their primary vehicle, were selected.

Prior to the analysis, the status of all time-series data was inspected. Instrumentation data, including front facing radar, vehicle speed, brake switch status, yaw rate signals, and lane tracking, were checked for missing or invalid data. The current study only included vehicle which had valid data in at least 60% of all trips and 60% of all distance traveled. Table 3 summarizes the sample of trips with valid sensor data. A total of 46,250 trips from 45 drivers were used in this study.

**Table 3.**
**Driver Selection with Valid Sensor Data**

| | |
|---|---|
| Number of Drivers | 45 |
| Number of Trips | 46,250 |
| Total Miles Driven | 406,606.7 |
| Median Trip Distance (miles) | 4.6 |
| Median Trip Duration (minutes) | 11.4 |

**Population Distribution of TTC at Lane Change**

Table 4 shows the result of the lane change detection algorithm for all drivers with valid sensor data, organized by lane change scenarios. A total of 326,238 lane changes were found in the 46,250 trips. The distribution of left side and right side lane changes was essentially even. A total of 90,639 lane changes involved a closing lead vehicle. Closing lead vehicles was defined to be lane change events where the driver was moving closer to the lead vehicle. As shown in the table, lane changes with closing lead vehicle accounted for approximately 28% of all lane change events. Similar to the distribution of all lane change events, left side lane change accounted for approximately 52% of all lane changes with closing lead vehicle, and right side lane changes was approximately 48% of all lane changes with closing lead vehicle.

**Table 4.**
**Lane Change Scenario Distribution**

| | **All Lane Changes (% of All Lane Changes)** | **Lane Change with Closing Lead Vehicle (% of Lane Change with Closing Lead Vehicle)** |
|---|---|---|
| Left Side Lane Change | 171,519 (52.6%) | 47,420 (52.3%) |
| Right Side Lane Change | 154,719 (47.4%) | 43,219 (47.7%) |
| Total Lane Change | 326,238 (100%) | 90,639 (100%) |

Table 5 summarizes the distribution of lane change frequency. The zero $10^{th}$ percentile values in each of the measurements in the table resulted from the fact that no lane changes were detected in approximately 35% of the trips.

**Table 5.**
**Lane Change Frequency Distributions**

| **Measurement** | **$10^{th}$ Percentile** | **Median** | **$90^{th}$ Percentile** |
|---|---|---|---|
| Lane change per trip | 0 | 3 | 19 |
| Lane change per mile | 0 | 0.8 | 2.3 |
| Lane change per hour | 0 | 19.7 | 58.4 |

Figure 6 shows the distribution of total number of lane changes with a closing lead vehicle within each speed bin. The label above the figure shows the number of driver who made lane changes within the speed bin, e.g. n = 45 drivers in the 10-20 mph speed bin. Not all drivers made lane changes within each speed bins, therefore not all speed bins had 45 drivers. The figure shows a skewed left distribution, suggesting that lane change events with closing lead vehicles are more likely to occur at higher travel speeds, such as suburban roads with speed limits

ranging from 35-45 mph, and highways with speed limits ranging from 55-65 mph. As shown in the figure, the speed bin with the most number of lane changes is the 60-70 mph range. This speed range corresponds to the highest highway speed limit surrounding the Washington D.C. metropolitan area, and could be the result of frequent driver movement through traffic gaps in congested area. However, this total is skewed by one outlier driver, who had more than 4,000 lane changes in the 60-70 mph speed range.

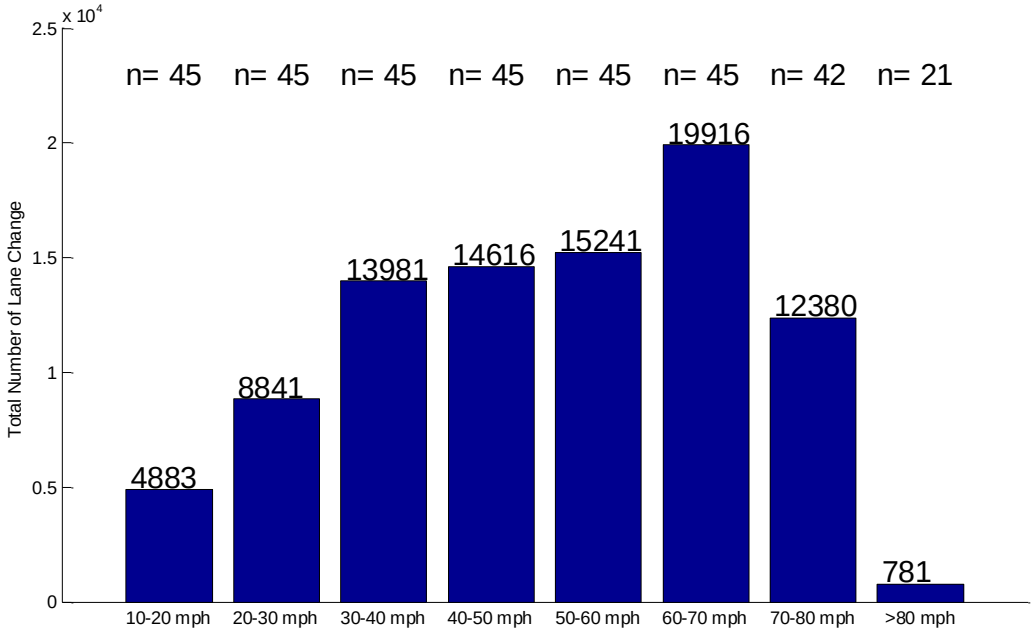


***Figure 6: Distribution of Lane Change with Closing Lead Vehicle and TTC (90,639 total lane changes)***

Figure 7 shows the distribution of minimum TTC by driver in each speed bin. Each driver has one point in each 10 mph speed bin. The cumulative distribution of minimum TTC for each driver are plotted below for each speed bin. In Figure 7, TTC was computed as the TTC at the start of lane change, and minimum TTC for each driver refers to the lowest (closest to zero) TTC for trips within each speed bin.

In general, the minimum TTC increases with travel speed. The variability in minimum TTC between drivers also increases with travel speed. The plot shows the number of drivers who made lane changes with a closing lead vehicle in each speed bin (ex. N = 45 in the 60-70 mph bin). Due to the relatively low percent of lane change at high speeds, not all drivers had lane changes with a closing lead vehicle in the >80 mph speed range.

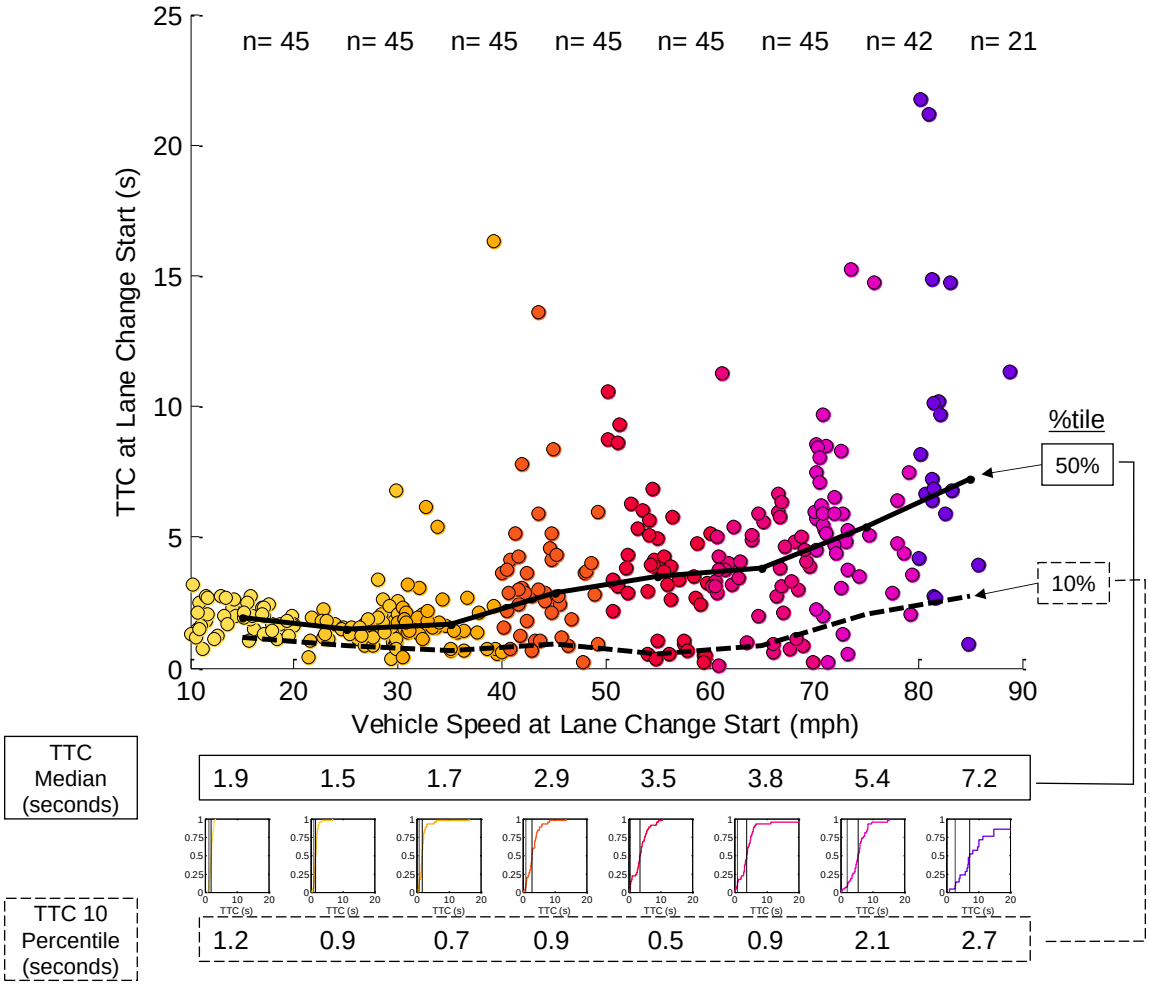


***Figure 7: Minimum TTC for Each Driver by Travel Speed Bin (n =90,639 lane changes)***

## CONCLUSIONS

The objective of this study was to characterize driver behavior during lane change events. This study presented a methodology to detect lane change events and a methodology to identify lead vehicle in lane change events in the 100-Car NDS. The performance of these two algorithms was validated against 126 trips, in which the researchers manually examined the video footage to determine the time frame of lane change and lead vehicle presence. Finally these algorithms were applied to the 100-Car NDS dataset to obtain the distribution of TTC at lane change with a lead vehicle in front of the subject car.

In 126 randomly selected validation trips, the researcher manually reviewed the trip video and identified 1,425 lane change events. 420 events were found to be overtaking event, in which the video shows a driver passing a lead vehicle. A total of 439 merging lane change was found in the sample, in which a closing lead vehicle was present in about 42% of the merging events. For lane change events other than overtaking and merging (566 events), a closing lead vehicle was present in 37% of these events. Overall, the lane change detection algorithm performed very well. For lane changes with sufficient lane tracking information, the validation process showed that the automated lane change algorithm had a sensitivity of 0.87 and a specificity of 0.983. The lead vehicle identification algorithm also

performed reasonably well, and correctly identified the car following situation in 84% of the validation sample of lane change events. Our lane change detection algorithm is highly dependent on the presence of lane markings, therefore our analysis was restricted to marked roadways. It is currently uncertain how our results will be generalized to roads with poor lane markings.

A total of 326,238 lane change events were identified by the algorithm in 46,250 trips, totaling over 400,000 miles of driving. In addition, the breakdown of lane change frequency by speed bin also shows that drivers are more likely to change lanes in travel speeds ranging from 30-60 mph. The lower lane change frequency in the lower speed range bins can potentially be due to several reasons. First, it is likely that lane changes events in lower speed ranges (i.e. lower than 30 mph) were on roads with lower speed limit and were 2-lane roads with no adjacent lanes to change into. We also hypothesize that when drivers initiate lane change maneuvers in lower speed ranges, they were more likely to speed up and thus are grouped into higher speed bin ranges. An example scenario would be during congested traffic conditions in the Washington D.C. area, the instrumented vehicle are in a lane with slow moving traffic but speeds up to change into the adjacent lane in order to move ahead of traffic.

The distribution of TTC showed that minimum TTC, as well as variability of TTC between drivers, generally increased with travel speed. The increase in TTC can be attributed to drivers generally becoming more cautious and increase following distance as travel speed increases. As driver begins to increase following distance, lead vehicles are more likely to be outside of the range of the front radar. Although our study was highly dependent on the radar to detect lead vehicle, therefore biased towards what the radar can "see", the results are still relevant in improving the effectiveness of a FCW system in a crash imminent situation.

The characterization of lane change events presented in the current study will provide active safety system designers further understanding of driver action in overtaking maneuvers and can improve designs of FCW systems. Specifically, the results of this study show that the frequency and TTC in lane change events vary by vehicle speed. The large variability in minimum TTC between drivers shows the need for FCW systems to implement several different warning thresholds depending on different driving style.

## ACKNOWLEDGEMENTS

The authors would like to acknowledge the Toyota Collaborative Safety Research Center (CSRC) and Toyota Motor Corporation for funding this study. Our special thanks to Rini Sherony, Hiroyuki Takahashi, and Satoshi Taniguchi of Toyota for sharing their technical insights and expertise throughout the project. We also gratefully acknowledge Stephen Hunter and Stephani Martinelli, our Virginia Tech undergraduate research assistants, for their greatly appreciated contributions to the search algorithm validation.

## REFERENCES

[1] National Highway Traffic Safety Administration, "Traffic Safety Facts 2012: A Compilation of Motor Vehicle Crash Data From the Fatalit Analysis Reporting System and the General Estimation System." U.S. Department of Transportation, Washington, DC, Report no. DOT HS 812 032, 2014.

[2] K. D. Kusano and H. C. Gabler, "Safety Benefits of Forward Collision Warning, Brake Assist, and Autonomous Braking Systems in Rear-End Collisions," *IEEE Trans. Intell. Transp. Syst.*, vol. 13, no. 4, pp. 1546–1555, Dec. 2012.

[3] J. McClafferty and J. Hankey, "100-Car Reanalysis : Summary of Primary and Secondary Driver Characteristics." The National Surface Transportation Safety Center for Excellence, Blacksburg, VA, p. Report Number 10–UT–007, 2010.

[4] T. Dingus, S. Klauer, V. Neale, A. Petersen, S. E. Lee, J. Sudweeks, M. Perez, J. Hankey, D. Ramsey, S. Gupta, C. Bucher, Z. . Doerzaph, J. Jermeland, and R. . Knipling, "The 100-Car Naturalistic Driving Study, Phase II – Results of the 100-Car Field Experiment," Report no. DOT HS 810 593, 2006.

[5] K. D. Kusano, J. Montgomery, and H. C. Gabler, "Methodology for identifying car following events from naturalistic data," *IEEE Intell. Veh. Symp.*, pp. 281–285, 2014.

# RUN OFF ROAD SAFETY

**Lotta Jakobsson**
**Anders Axelson**
**Magnus Björklund**
**Pär Nilsson**
**Trent Victor**
Volvo Car Corporation
Sweden

Paper Number 15-0424

## ABSTRACT

Run off road events are frequent and can result in severe consequences. The reasons for leaving the road are numerous and the sequence the car is subjected to differs in most events. The aim of this study is to holistically address safety improvement in run off road events, presenting methods for evaluation as well as examples of countermeasures for the whole sequence from normal driving to post-crash.
Real world data, comprising statistical and in-depth crash data as well as driving data from Volvo Cars' database in Sweden, forms the basis for understanding of influencing factors and mechanisms related to occurrence of the event as well as occupant injury. Countermeasures are presented along with the test methods which were developed based on the mechanisms identified. The test methods include road off road avoidance test methods, complete vehicle crash tests, and rig tests; such as occupant positioning using a robot rig and vertical loading tests using a drop tower rig.
Countermeasures addressing run off road safety are developed and verified using the identified test methods and integrated into vehicle design. Examples of systems addressing road departure avoidance aspects are Driver Alert Control and Lane Keeping Aid. Countermeasures specifically addressing occupant protection are occupant positioning by detecting run off road events and activating an electrical reversible safety belt pretensioner, as well as unique energy-absorbing functionality in the seat. Post-crash measures are enhanced by added activation of eCall in some run off road scenarios.
Optimally, avoiding the run off road is most beneficial and this study provides some initial steps illustrated by production systems. However, if run off road occurs, one priority is to reduce vertical occupant loadings when landing on the wheels after a free-flight, a rollover or when going into a ditch and impacting an embankment. This type of loading could result in thoracic-lumbar spine fractures. The design of the unique energy absorbing functionality in the seat, put into production 2015, will help provide important enhanced occupant protection.
Additionally, injury outcome is influenced by the occupant position during the event: head and arms flinging around impacting the interior, bent postures reducing the tolerances of spinal injuries, and sub-optimal occupant positioning relative to protection systems. The unique run off road detection and safety belt pretensioning early in the events, together with the seat backrest's side supports, will assist the occupant to stay positioned during the event and help improve protection.
This study is based on a holistic approach to safety, covering the whole event from normal driving to crash care, introducing world first production technology enhancing occupant protection in these diverse and complex events. It goes beyond standardized safety evaluation of today and it provides an illustrative example on how safety systems can take action across the entire crash sequence and the interaction of different types of systems adding to the effect of addressing real world protection needs.

## INTRODUCTION

Run off road events are frequent and can result in severe consequences. In the United States, single vehicle roadway departure crashes accounted for about 20% of all police-reported crashes (Wang and Knipling, 1994). In Germany, 33% of all fatal crashes were run off road crashes (Statistisches Bundesamt, 2011). In Sweden since 2003, single car crashes is the most common type when it comes to fatal accidents (Hillerdal, 2011). Injuries can be sustained to any body part (Jakobsson et al. 2014). Among injury types highlighted as related to run off road events are thoracic and lumbar spine injuries. Although found in all crash situations, Jakobsson et al. (2006) showed that AIS2+ thoracic and lumbar injuries were mostly found in multiple events; a high proportion of the cases being run off road crashes.

Occupant posture, such as forward bending was highlighted as an influencing factor, with the injury mechanism of spinal axial loading with different degree of flexion leading to compression and anterior wedge fractures, especially seen in run off road events with complex occupant kinematics.
In the context of crash avoidance, numerous test methods and evaluation procedures address situations triggering potential run off road crashes, such as sleepiness (Anund et al., 2009 and 2011, Fors et al, 2013) and distraction (NHTSA, 2010, Hanowski, 2011, Fitch et al. 2013). Additionally, test methods evaluating specific technology such as Electronic Stability Control (ESC) and Lane Departure Warning (LDW) are found within legal and public domain testing. However broad test methods addressing run off road safety effectiveness on multiple factors influencing causation (driver behaviors, friction, weather, etc) in the avoidance phase are scarcer, although first steps are taken e.g. within the Advanced Crash Avoidance Technologies Program at NHTSA (Gordon et al., 2010).
Leaving the road can result in a variety of more or less complex events. While some vehicles quickly come to a rest position without any severe event, other vehicles leave the road into a free flying event, landing on the wheels or continue into a roll or turn-over event or interact multiple times with the environment. In-depth studies in Austria highlight the effect of guardrails leading the vehicle to "take off" as well as vehicles jumping into road side objects such as traffic sign poles or overpasses (Tomasch et al., 2010). Jakobsson et al. (2014) reported that important mechanisms addressing run off situations include drifting and avoidance of animals on the road. Being a complex event, not one single test method addresses this whole area of concern. Some parts of some events, such as skidding sideways and impacting a tree, are addressed in standardized lateral pole impact tests. Additionally, standardized frontal barrier tests address parts of events ending up into a large rock or a brick wall. However, neither influence of potential change in occupant posture before impact, nor reasons for leaving the road are covered in these standardized crash tests.
Addressing run off road safety poses a variety of challenges, ranging from understanding the reasons for leaving the road to means of evaluating the potential injury outcome, all put into the overall context of run off road safety. The objective of this study is to address run off road events, presenting methods for evaluation as well as examples of countermeasures addressing the whole sequence from normal driving to post-crash. This is done by summarizing influencing factors and mechanisms to target when developing test methods; and briefly presenting some newly developed test methods along with production systems/technology addressing run off road safety.

## INFLUENCING FACTORS AND MECHANISMS

Based on real world data, crash causation mechanisms and injury causing mechanisms were identified and presented by Jakobsson et al. (2014). The purpose of these mechanisms was to, in a structured way, address the complex and diverse area of run off road safety and to guide development of test methods with a holistic approach.
There are several reasons for leaving the road exemplified by driver distraction, sleepiness and fatigue, inadequate speed and vehicle interaction in relation to the traffic situation and maneuver for avoidance of animal crashes and other objects on the road (Najm et al., 2002, Liu and Subramanian, 2009, Jakobsson et al., 2014). Factors potentially influencing crash causation of run off road events are essential to take into account in test method developments targeting evaluation of road departure avoidance.
For the run off road situations, especially occupant kinematics as well as occupant retention were highlighted and differ from on-road occupant protection situations. The occupant kinematics, longer duration and less acceleration as compared to on-road crashes, exposes especially the upper extremities and the head for non-optimal positions from a protection point of view. Occupant retention addresses the upper body positioning during the run off road event. Several potential injury causing mechanisms are seen during the wide and diverse types of events. Analyzing real world data, Jakobsson et al. (2014), highlighted the different types of environments, such as rough terrain, ditch types and whether multiple events occur, as important mechanisms contributing to the occupant injury. Numerous different impact objects are probable as well as differences in impact configuration, including complex rollover events. Complex vehicle kinematics due to the run off road environment, occupant kinematics and occupant retention affect the occupant posture which depending on the impact, influences the occupant injury consequences in run off road crashes. Important occupant protection mechanisms concern impacts to interior structures, vertical loading on the occupant through the seat, as well as keeping the occupant in a favorable position during the event (Jakobsson et al. 2014 and 2015).

## TEST METHODS

Based on the identified factors and mechanisms, a variety of test methods were developed to address occupant protection aspects as well for evaluating technology assisting the driver to stay on the road. The whole context is

described in Jakobsson et al. (2014) and the test methods specifically addressing the countermeasures presented in the present study will be covered in this chapter.

**Road Departure Avoidance Test Methods**

Systems addressing road departure avoidance aspects, such as Driver Alert Control (DAC) and Lane Keeping Aid (LKA), are tested with virtual methods, simulator tests as well as test track and on-road tests. Driver representation is important in all types of test methods. Depending on the level of critical event and repeatability issues, the choice of method is made.
The virtual test methods consist of virtual representations of the driver as well as the vehicle and environment (Gordon et al., 2010; Markkula, 2015; Benderius, 2014). The driver model is designed based on knowledge from testing with drivers in specific real world situations, and can be more or less advanced, depending on the application. Virtual test methods allow that a large number of tests can be performed using the same model just varying the vehicle systems or the environment. Other benefits are the possibilities to use it in early phase technology developments.
In tests evaluating warnings (e.g. Driver Alert Control) and vehicle interventions to prevent road departures by drifting (e.g. LKA), driver reactions on these warnings and interventions are evaluated. The driver reactions can be tested both on test tracks and in driving simulators (Petersson and Svanberg, 2013) while the whole run off road scenario only can be tested in a driving simulator for test repeatability as well as safety reasons. Data from the test track tests can be used to build a driver model to incorporate into a virtual test method, which provides an additional tool beneficial when evaluating a large number of specific scenarios of e.g. run off road speeds and angles. The evaluation target in this testing is to avoid road departures as such, with a special focus on the drifting behavior.
The Driver Alert Control and Lane Keeping Aid systems target pre-crash driver states such as sleepiness, fatigue and distraction as these are identified as important pre-crash parameters in run off road crashes. Test methods evaluating these aspects comprise test track and on-road testing and using driving simulators. For sleepiness testing the set-up is usually a several hour long drive on a highway (speed limit 110km/h) where the driver just drives the car, with no critical situations or distraction tasks induced. The tests can be designed using different levels of sleep deprivation (over several days) and the characteristics of the participants are carefully selected. The evaluation target during the test is typically to decrease the time driving in a sleepy state. For distraction testing, the driver is asked to repeatedly perform a number of secondary tasks sequentially, exemplified by using in-vehicle HMI, such as phone or radio. The evaluation target is to increase drivers' eyes-on-road and reduce glances over a certain duration time on the secondary tasks. A description of a related test method is described in Ljung Aust et al (2013).

**Occupant Protection Complete Vehicle Test Methods**

Three complete vehicle crash test track methods, called Ditch, Airborne and Rough Terrain were developed to simulate some main run off road vehicle kinematics potentially causing occupant injury. These methods can be used for evaluating the consequences of combination of low acceleration and high acceleration parts of the event on vehicle and restraint system performance as well as provide insight into potential occupant kinematics. The tests were run at Volvo Cars Safety Centre in Sweden, using Test Track 2 which is a moveable covered test track with semi-directional electrical propulsion system. The tests were run towards the outdoor crash test environment, where different run off road scenarios are built. The car is launched from the test track, just before entering the run off road scenario, by a position triggered system. Crash test dummies are used as human representation in the tests. Important feature of a crash test dummy for this purpose is good flexibility in shoulders and upper body, hence the Thor dummy with modified shoulder (Törnvall et al., 2008) was used.
During the Ditch method the vehicle is launched at 80 km/h and drifts with an angle of 12-15 degrees into a ditch (Figure 1). The ditch is 80 cm deep with a slope of 30-40% from the road surface. Approximately 20 m after leaving the road, entering the ditch and traveling along the bottom of the ditch, an embankment is reached forcing the vehicle into an upward motion. The embankment has the same slope as the ditch, and represents a crossing road. This test method captures the characteristics seen in real world cases when the vehicle is drifting into the ditch in a rather narrow angle, travels in the ditch, thereafter impacting an embankment leading to underbody interaction to ground, causing high vertical loading into the occupant through the seat.
During the Airborne method the vehicle is launched at 50-80 km/h leaving the road in a range of angles (30 degrees in Figure 1) into a steep slope introducing a phase of free flight of the vehicle, before landing on smooth surface and continue onwards. The height difference is 80 cm, resulting in a hard impact on the wheels, causing vertical forces.

During the test method called Rough Terrain the vehicle is launched at 70-80 km/h perpendicular from the road into a rough terrain environment (Figure 1). The rough terrain causes a bumpy ride producing substantial lateral vehicle motions (rolling motions) in combination with vertical and longitudinal vehicle motions.
In all the three crash test track methods, the occupant will be subjected to acceleration changes in different directions and intensities through the event, due to the vehicle kinematics in several directions simultaneously. This could expose the different parts of a restrained occupant (especially the upper extremities and head) to potential impacts to the interior, partial ejection as well as changes in upper body positions posing the spine into flexed postures.

***Figure 1. The complete vehicle Run off road crash test methods; Ditch (top), Airborne (middle) and Rough Terrain (bottom).***

**Occupant Protection Rig Test Methods**

Rig test methods were developed to replicate sequences from the whole vehicle test methods in a repeatable and reproducible way. The two main areas of interest were the occupant kinematics when subjected to varieties of loading directions and intensity, and the vertical occupant loading. Two rig test methods were designed to address these two areas.
A robot controlled test setup, called 'Robocoaster', was used to simulate occupant kinematics. It provides a flexible and multi-purpose test set-up evaluating occupant positioning and occupant retention. A vehicle seat and restraint system is mounted on a multi-axial robot (ABB IRB 6600 industrial robot) and can be used together with a crash test dummy (Figure 2). The robot can be programmed to, in repeatable manner, simulate the occupant kinematics in one of the three test track methods, or any variations of a run off road crash, within the limitations of the robot used.

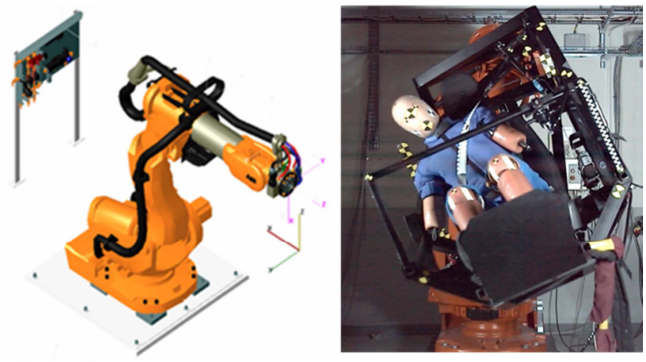

*Figure 2. Rig test method 'Robocoaster'.*

A rig test method simulating the vertical loading through the seat was developed (Figure 3). It provides a simplified and repeatable test set-up for vertical occupant loading, which can occur at hard landing on the wheels after a free flight or during the undercarriage interaction, e.g. with the embankment in the Ditch method. A seat is attached to a frame which moves on vertical rails on a drop tower. The desired vertical acceleration in the physical test set-up is achieved by releasing the frame from a specific height and stopped using the deceleration-sled principle of bending steel. The rig test method also has a virtual counterpart. A crash test dummy is positioned in the seat during test. For the physical test, a HIII 50%-ile male dummy is used while in the virtual test-set up the BioRID (50%-ile male) is used. The z-component of the pelvis accelerometer is monitored and used as the injury criteria measure 'vertical occupant acceleration'. The test method is described in detail in Jakobsson et al. (2015).

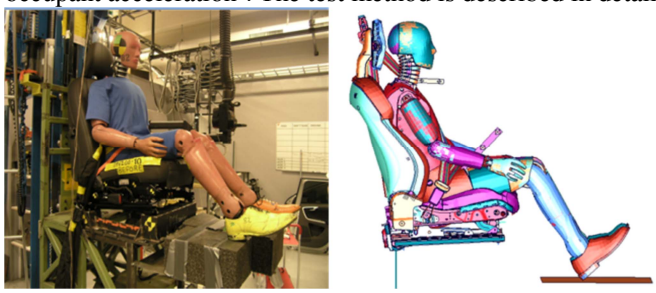

***Figure 3. Rig test methods for vertical occupant loading; physical test setup (left) and virtual test setup (right).***

## COUNTERMEASURES

Countermeasures addressing run off road safety, which are integrated into vehicle design, were developed and verified using the test methods. As illustrated in Figure 4, the countermeasures address run off road safety in a holistic way. Examples of production systems addressing run off road avoidance aspects during normal driving are Driver Alert Control and Lane Keeping Aid. Countermeasures specifically addressing occupant protection are occupant positioning by detecting run off road events and activating an electrical reversible safety belt pretensioner, as well as unique energy-absorbing functionality in the seat. Post-crash measures are enhanced by added activation of eCall in some run off road scenarios.

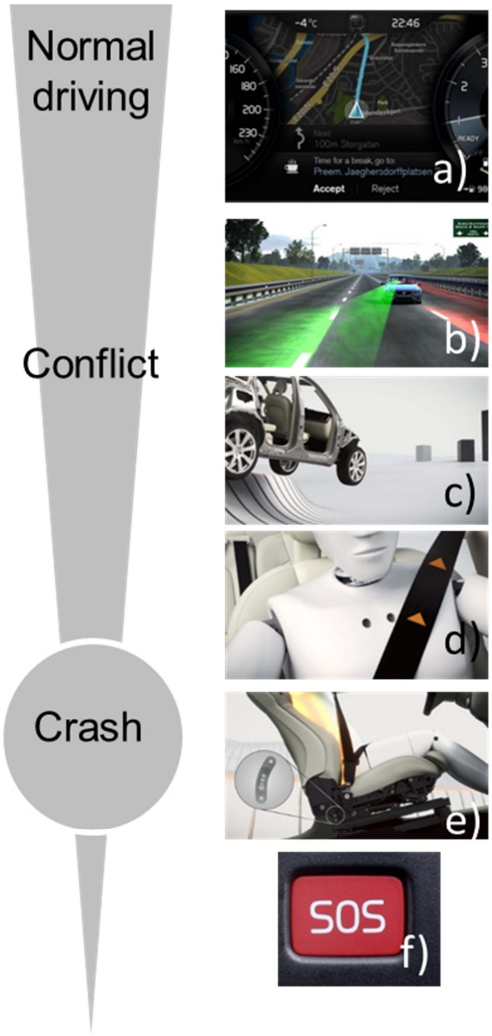


***Figure 4. Holistic approach including countermeasures; Driver support system exemplified by a) Driver Alert Control with Rest Stop Guidance and b) Lane Keeping Aid, occupant protection systems exemplified by c) run off road detection, d) electrical reversible safety belt pre-tensioning and e) energy absorbing functionality in seat, and f) post-crash measure such as eCall activation***.

Driver Alert Control detects and warns tired or inattentive drivers. In the 2015 Volvo XC90, it is enhanced with a new Rest Stop Guidance (Figure 4a), which directs the driver to the nearest rest area. Lane Keeping Aid (Figure 4b) helps the driver stay on track by applying extra steering torque if the car is about to leave the lane unintentionally. As a post-crash measure, eCall offers safety benefits in providing information to the Call Center who can contact the occupants in the car as well as call for assistance when needed (Figure 4f). Real world activation of eCall is dependent of detection capabilities including interpretation of the detection. Conventional triggering of eCall is based on activation levels for pyrotechnical devices, e.g. pretensioners and airbags. Triggering in situations beyond those requires knowledge of the event. Run off road events are challenging being diverse and complex. The test methods developed and presented in this study provide such knowledge and have been used to further refine the eCall activation capabilities included in the 2015 Volvo XC90.
For occupant protection, controlling the occupant position together with the energy absorbing functionality provides benefits in a large range of situations. By keeping the occupant in an upright posture while cushioning a potential vertical enables a combined benefit since the spine in more tolerable when straight. The details on detection algorithm and activation logic, as well as the electrical reversible safety belt pretensioner and seat design are presented below.

**Detection Algorithms and Activation Logic**

The new detection algorithms in the restraint control module are able to detect new run off road scenarios, such as Ditch, Airborne, and Rough Terrain. This is enabled by using sensor data from the vehicle's restraint control module along with information from the vehicle bus. As compared to prior vehicles, no hardware is added, while extensive work on algorithms has been carried out. A major challenge is to address all relevant real world crash scenarios and take action to help protect the vehicle occupants accordingly. The sensor functionality is an important step towards addressing crashes beyond the standardized crash test methods. In order to make this happen and to control the triggering, data from complete vehicle real world like events are necessary. Hence, the development of the complete vehicle test methods was essential for this important functionality. Sensor data gathered from the complete vehicle crash tests was taken as input to the calibration process, wherein algorithm parameters were tuned in multiple simulation loops. The input data set included both scenarios where activation of one or more protection components is required (Fire tests), and scenarios where there shall be no activation of protection components (No Fire tests), in order to assess the robustness of the algorithm methods and the calibration. The development of detection algorithms and activation logic is further described in Nilsson et al. (2014).

**Electrical Reversible Safety Belt Pretensioner**

If a run off road scenario is detected, an electrical reversible safety belt pretensioner is activated, provided the occupant is belted. The safety belts are electrically tightened to retract and keep the occupants in position (Figure 4d). The electrical reversible pretensioner has two force levels, which are used depending on the estimated severity of the scenario (i.e. medium force in low severity events, high force in high severity events). Full retraction is achieved within 250 ms, belt force is up to 300 N, and the belts are kept firmly tightened as long as the car is in motion. Once the run off road scenario has ended, as determined by global acceleration level, the belt tension is released. The electrical reversible pretensioner forces are strong enough also to retract forward leaning occupants (Lorenz et al. 2001, Develet et al. 2013).
In case of a sufficiently severe secondary impact in the course of a run off road scenario, e.g. to a tree, an embankment, another obstacle or a rollover event; the pyrotechnical safety belt pretensioners will be activated on all seven seating positions, provided the occupants are belted. Additionally, other restraints, such as airbags and inflatable curtains will be activated when needed.

**Seat Design**

An important part of the run off road safety package is the all new seat design as introduced in the 2015 Volvo XC90. The protruding side bolsters of the seat backrest helps to provide occupant support together with the safety belt retraction. The seat has been designed addressing spinal protection in case of a vertical load through the seat. A deformation element is built into the inner rear part of the seat connection to the seat frame. In case of vertical loads, the seat will slide in the slot while deforming the deformation element (Figures 4e and 5). The deformation element allows for a controlled vertical deformation of up to 25 mm. The space under the seat is cleared to allow for total occupant movement up to 150 mm. This movement is achieved mainly by compressing the seat foam and extending the springs in the seat cushion, which together with the deformation element provide energy absorption. The deformation element is triggered by force during the event. The force is dependent on occupant weight in combination with acceleration amplitude and direction. Vertical forces of a certain limit will trigger the deformation of the element as well as allow the occupant to move into the seat cushion. These vertical forces can occur in rollover events when landing on the wheels, as a result of a free flight event or any other crash sequence where there is a vertical force component, such as in the Ditch test situation. The deformation element also plays a part in the Whiplash protection system (WHIPS), activated by the torque occurring when the occupant sinks into the seat backrest during the rear end impact event.

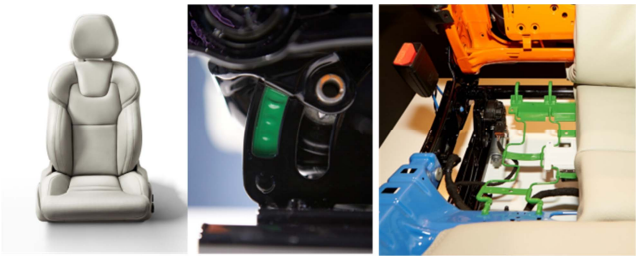

***Figure 5. Overview of seat design including side bolsters (left). Close-up views of energy absorption functionality; side view of deformation element (middle), top view of seat cushion including springs (right).***

Figure 6 shows a comparison of vertical occupant acceleration, comparing the new seat design to a prior Volvo seat, available in e.g. Volvo S40, XC70, S80, S60 model years 2011-2013. The rig test method for vertical occupant loading, simulating a sequence from the embankment interaction during the Ditch whole vehicle test, is used for this comparison. The seat is exposed to a maximum acceleration of approximately 90m/s2, pulse duration about 100ms and 'change of velocity' of 6,5m/s. In this loading situation, the vertical occupant acceleration is reduced by 32% in the new seat design as compared to the reference seat. The chosen situation is representative of a situation where spinal injuries can occur in real world crashes.

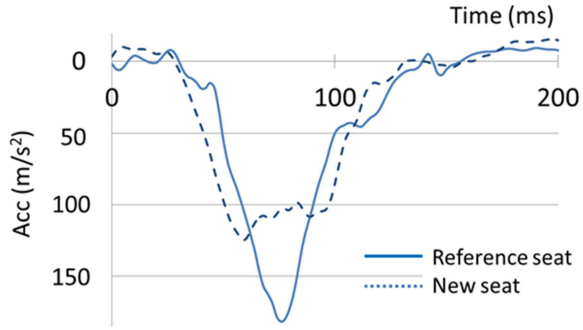


***Figure 6. Pelvis vertical acceleration comparing new seat and reference seat using the virtual loading rig test method (Jakobsson et al. 2015).***

## DISCUSSION

This study addresses the area of run off road events which has, up until now, been in limited focus within automotive development. Test methods as well as countermeasures addressing the whole sequence in run off road events present a first step within this area and will help to reduce real world consequences. The study presents a holistic approach, including production systems addressing run off road avoidance aspects during normal driving, countermeasures specifically addressing occupant protection post-crash measures.

A holistic approach is necessary when addressing run off road safety. The reasons for running off the road are several and the characteristics of the events are numerous. The way behind this study was to base the knowledge of real world situations, identifying influencing factors and possible mechanisms, developing test methods and by this creating both a deeper understanding as well as countermeasures. This process is described further in Jakobsson et al. (2014).

Optimally, avoiding a run off road event is most beneficial and this study provides some initial steps illustrated by the Lane Keeping Aid and Driver Alert Control production systems. Further steps are needed to address all the reasons for running of the road and offer support in those situations. In addition, prototype road departure avoidance technologies have been presented, however so far not ready for production. The challenges mainly concern detection issues; identifying the large variety of different types of road edges and to separate them from e.g. cracks and other damages on the road.

Figure 6 shows that by adding energy absorbing functionality in the seat together with improved clearance under the seat, vertical occupant acceleration can be substantially reduced in situations where thoracic and lumbar spine injuries could occur in real world situations (Jakobsson et al. 2015). Combining this with keeping the occupant in an upright posture will help reduce spinal injuries even further. Injury outcome is influenced by the occupant position

during the event: head and arms flinging around impacting the interior, bent postures reducing the tolerances of spinal injuries, and sub-optimal occupant positioning relative to protection systems. The unique run off road detection and safety belt pretensioning early in the events, will assist the occupant to stay positioned during the event and help improve protection. This is a robust way of addressing occupant protection in run off road situations, keeping the occupant in a controlled position, enabling the protective safety systems to help the occupant in different upcoming events.
The present study goes beyond standardized safety evaluations of today. Firstly, it is an area that still is to be addressed in regulatory and consumer testing. Secondly, it combines in an effective way safety of the total sequence of an event; including active, integrated and passive safety technology. Both of these are necessary in order to improve the relatively large amount of injuries occurring in these types of events. Obviously, run off road being complex and diverse events, a limitation of this study is that not all events and potential consequences are addressed. However, the approach of this study and methods developed based on influencing factors, provide a path to build further studies and countermeasures on. Going beyond standardized safety evaluation of today, it provides an illustrative example on how safety systems can take action across the entire crash spectrum and the interaction of different types of systems adding to the effect of addressing real world protection needs.

## CONCLUSIONS

This study is based on a holistic approach of safety, covering the whole event from normal driving to crash care, introducing world-first production technology enhancing occupant protection in these diverse and complex events. It goes beyond standardized safety evaluation of today and it provides an illustrative example on how safety systems can take action across the entire crash spectrum and the interactive play of different types of systems adding on the effect of addressing real world protection needs.
Unique test methods including complete vehicle run off road crash tests, and rig tests addressing occupant positioning and vertical loading using a robot rig and a drop tower rig, respectively, are developed to evaluate the countermeasures as introduced in the 2015 Volvo XC90. The world-first run off road protection package includes detection of run off road events and activation of an electrical reversible safety belt pretensioner, together with unique energy-absorbing functionality in the seat. The cascade of countermeasures covering the whole event from normal driving to crash care systems, also including systems acting to avoid crashes such as Driver Alert Control and Lane Keeping Aid as well as added activation of eCall will provide improved safety in an important number of run off road events.

## REFERENCES


Anund, A., Kircher, A. & Tapani, A. (2009). The effect of milled rumble strips versus virtual rumble strips on sleepy drivers – a driving simulator study. *VTI report No 645A*, Swedish Road and Traffic Research Institute (VIT), Linköping, Sweden, (www.vti.se)

Anund, A., Kecklund, G. & Åkerstedt, T. (2011). Sleepiness, crashes and the effectiveness of countermeasures, Consolidated report within ERANET node 1. *VTI report No 12A-201*, Swedish Road and Traffic Research Institute (VTI), Linköping, Sweden, (www.vti.se)

Benderius, O. (2014). Modelling criver steering and neuromuscular behaviour. PhD Thesis. Chalmers University of Technology. ISBN 978-91-7597-090-5

Develet, J.-A., Carlsson, A., Svensson, M., Fredriksson, R., Bråse, D. & Holcombe, S. (2013). Evaluation of the biofidelity of the BioRID-II and THOR-NT anthropomorphic test devices under seatbelt pre-pretensioner loading in stationary conditions. *2013 Ohio State University Injury Biomechanics Symposium*, p. 1-15

Fitch, G.M., Soccolich, S.A., Guo, F., McClafferty, J., Fang, Y., Olson, R.L., Perez, M.A., Hanowski, R.J., Hankey, J.M. & Dingus, T.A. (2013). The impact of hand-held and hands-free cell phone use on driving performance and safety-critical event risk, NHTSA Technical Report, DOT HS 811757

Fors, C., Hallvig, D., Hasselberg, E., Kovaceva, J., Sörner, P., Krantz, M., Grönvall, J-F. & Anund, A. (2013) Investigation of driver sleepiness in FOT sata, Final Report of the project SleepEYE II, part 2, VIP Publication 2013-2, Swedish Road and Traffic Research Institute (VTI), Linköping, Sweden (www.vti.se)

Gordon, T., Sardar, H., Blower, D., Ljung Aust, M., Bareket, Z., Barnes, M., Blankespoor, A., Isaksson-Hellman, I., Ivarsson, J., Juhas, B., Nobukawa, K., & Theander, H. (2010). Advanced Crash Avoidance Technologies (ACAT) Program – Final Report of the Volvo-Ford-UMTRI Project: Safety impact methodology for lane departure warning – Method development and estimation of benefits, NHTSA Technical Report, DOT HS 811405

Hanowski, R.J. (2011). The naturalistic study of distracted driving: Moving from research to practice, *SAE Int. J. Commer. Veh*. 4(1), SAE Paper No 2011-01-2305

Hillerdal I. (2011). Passenger cars in fatal single vehicle accidents on Swedish roads. UPTEC STS11011, Uppsala University, Uppsala, Sweden

Jakobsson, L., Bergman, T. & Johansson, L. (2006). Identifying thoracic and lumbar spinal injuries in car accidents. *Proc of IRCOBI Conference on Biomechanics of Impacts*, Madrid, Spain, 2006: 61-71

Jakobsson, L., Lindman, M., Axelson, A., Lökensgård, B., Petersson, M., Svanberg, B. & Kovaceva, J. (2014). Addressing run off road safety. *SAE Int. J. Passeng. Cars - Mech. Syst*. 7(1). doi:10.4271/2014-01-0554

Jakobsson, L., Björklund, M. & Axelson, A. (2015). Vertical occupant loading in car crashes; Test methods and countermeasures, *SAE Technical Paper*, 2015-01-1459

Liu, C., & Subramanian, R. (2009). Factors related to fatal single-vehicle run-off-road crashes. *NHTSA Technical Report*, DOT HS811 232

Ljung Aust, M., Dombrovskis, S., Kovaceva, J., Svanberg, B. et al. (2013). An empirically based suggestion for reformulating the glance duration criteria in NHTSA's visual-manual interaction guidelines, *SAE Int. J. Passeng. Cars - Electron. Electr. Syst*. 6(2):444-453. doi:10.4271/2013-01-0444

Lorenz, B.K., Strohbeck-Kuehner, P., Mattern, R., Class, U. & Lueders, M. (2001). Volunteer tests on human tolerance levels of pretension for reversible seatbelt tensioners in the pre-crash-phase. Phase I results: test using a stationary vehicle. *Proceedings of the International Research Council on the Biomechanics of Injury Conference (IRCOBI),* Isle of Man, UK, p 311-322

Markkula, G. (2015). Driver behavior models for evaluating automotive active safety - from neural dynamics to vehicle dynamics. PhD Thesis. Chalmers University of Technology, Göteborg, Sweden. ISBN 978-91-7597-153-7

Najm, W., Koopmann, J., Boyle, L. & Smith D. (2002). Development of test scenarios for off road way crash countermeasures based on crash statistics. *NHTSA Technical Report*, DOT HS 809 505

NHTSA. (2010). Driver Distraction Program, *NHTSA Technical Report*, DOT HS 811299

Nilsson, P., Jakobsson, L., Axelson, A., Hardå, P. & Wogel, A. (2014). Complex world safety: Detection of run off road scenarios using inertial sensors. *Airbag 2014*: 12th International Symposium and Exhibition on Sophisticated Car Occupant Safety Systems, Karlsruhe, Germany

Petersson, M. & Svanberg, B. (2013). Driver reaction for evaluating autonomous interventions - A test-track method. *International Conference on Biomechanics of Impacts (Ircobi),*Göteborg, Sweden

Statistisches Bundesamt. (2011) Fachserie 8 Reihe 7, Verkehrsunfälle

Tomasch, E., Hoschopf, H., Gobald, M., Steffan, H., Nadler, B., Nadler, F., Strnad. B. & Schneideret, F. (2010). Single vehicle run-off-road accidents colliding rurned down terminals of guardrails. *Transport Research Board* (TRB)

Törnvall, F.V., Holmqvist, K., Davidsson, J., Svensson, M.Y., Gugler, J., Steffan, H. & Haland, Y. (2008). Evaluation of dummy shoulder kinematics in oblique frontal collisions. *International Conference on Biomechanics of Impacts* (Ircobi)

Wang, J.S. & Knipling, R.R. (1994). Single vehicle roadway departure crashes: Problem size assessment and statistical description. *NHTSA Technical Report*, DOT HS 808 113

# ASSESSING MECHANISMS OF INJURY AS PREDICTORS OF SEVERE INJURY FOR ADULT CAR AND TRUCK OCCUPANTS

**Ruben Buendia**[1,2,3]
**Stefan Candefjord**[1,2,3]
**Bengt-Arne Sjöqvist**[1,2,3]
[1]SAFER Vehicle and Traffic Safety Centre at Chalmers
[2]Department of Signals and Systems, Chalmers University of Technology, 412 96, Gothenburg, Sweden
[3]MedTech West, Sahlgrenska University Hospital, Röda Stråket 10 B, 413 45 Gothenburg, Sweden

Paper Number 15-0427

## ABSTRACT

This study evaluates Mechanisms of Injury (MOI) that can be rapidly assessed at the scene of accident and may be used as predictors of severe injury for traffic accidents involving occupants in cars or trucks. The objective is to increase the knowledge of how MOI can be used to differentiate whether a patient is severely injured or not. This knowledge can be used to improve trauma triage systems. Furthermore, an objective is to analyze safety differences between cars and light/heavy trucks. The scope is adult occupants of cars, light and heavy trucks injured in accidents registered in the Swedish Traffic Accident Data Acquisition (STRADA) database from 2003 to 2013. Partition between severe and non-severe injury was done according to the Injury Severity Score (ISS) with ISS > 15 as definition of severe injury. The MOIs considered were: belt use, airbag deployment, posted speed limit, elderly occupant (age ≥ 55 years), sex, type of accident (single, intersection, turning, head-on, overtaking, rear end, tram/train, wild animal or other) and location of the accident (urban or rural). The different MOI were evaluated individually using univariate chi-square tests and together using multivariate logistic regression models. Results show that belt use is the most crucial factor determining risk of severe injury for all vehicle types. Age is the second most important factor, with elderly occupants exhibiting a higher risk. Head-on accidents are the most dangerous for cars and light trucks while single accidents are the most dangerous for heavy trucks. Belt use compliance is much lower for truck occupants. This appears to be the main reason for the frequency of severe injury being higher for truck occupants than for car occupants.

## INTRODUCTION

Rapid transport of severely injured trauma patients to a trauma center substantially decreases mortality [1, 2]. Medical examination of the patient with support from a triage protocol and observations of characteristics of the accident are the main tools emergency personnel have for recognizing patients with severe injury. Schoell et al. [3] stated that improvement of triage systems is nowadays the most important area to address to continue reducing fatal and severe injuries for motor vehicle accidents. Therefore, maintaining, updating and improving trauma triage systems is of utmost importance.

Triage systems are in general primarily based on physiological and anatomical criteria and secondly on Mechanisms of Injury (MOI). The value of MOI is to detect occult injuries and reduce undertriage. A study with around one million trauma patients concluded that using physiologic and anatomic criteria alone lead to undertriage [4]. This strongly supports the use of MOI in triage systems.

In Sweden RETTS [5] is the most widespread triage system. The MOI that apply for motor vehicle crashes are: occupant ejected from vehicle, vehicle rollover, person entrapped, and deployment of airbag. For car accidents there is an additional criteria: estimated speed > 60 km/h. We believe that risk for severe injury can be predicted with higher precision, i.e. with reduced overtriage and/or undertriage, by adding complementary MOI to the triaging process.

In order to improve triage systems for traffic accidents this study evaluates the predictive power of severe injury for MOI that can rapidly be assessed at the scene of accident. In addition a comparison between cars, light and heavy trucks of how these MOI relate to injury severity was performed.

The scope of the study is adult occupants in cars, light and heavy trucks for accidents registered in the Swedish Traffic Accident Data Acquisition (STRADA) database for eleven years, from 2003 to 2013. The evaluation of the predictors is performed by comparing the proportion of patients with severe injury for each level of the

variable, univariate analyses of association with probability of severe injury using chi-squared tests and multivariate analyses using logistic regression models. The logistic regression models were developed in the studies by Buendia, Candefjord et al. [6, 7].

## METHODS

STRADA is the Swedish Transport Administrations national information system for traffic accidents occurring on the public roads of Sweden. It included two sources of data, independent reports from the police and the hospital treating the patient. The database is contained in a Microsoft Access® database file. An introduction to STRADA is available in [8].

Between calendar years 2003 to 2013 near 650 000 injured persons can be found in STRADA. Each accident has a unique ID which is shared between the police report and the hospital report and is the link between accident and patients. We included only accidents involving injured occupants traveling in a car or a truck where both a police and a hospital report were available. In the case of cars, subjects with missing information in any predictor considered were not included.

The observations were divided into cars, light trucks, i.e. trucks with total weight up to 3500 kg, and heavy trucks, i.e. trucks with a total weight over 16 500 kg, according to the Swedish official classification of trucks. Trucks of medium weight were not considered because they were not sufficient in numbers to feed a model with enough statistical power.

The total number of accident victims was 29 128 for cars, 2 775 for light trucks and 922 for heavy trucks. They were injured in 22 607, 2 608 and 903 accidents for cars, light trucks and heavy trucks, respectively.

Casualties were classified as severely injured or not according to the Injury Severity Score (ISS) with ISS > 15 used as definition of severe injury, i.e. a victim with ISS > 15 is classified as severely injured and a victim with ISS < 15 is classified as non-severely injured. This was the dependent variable for all analyses. The proportion of severely injured was 2.0 % for cars, 2.9 % for light trucks and 4.0 % for heavy trucks. The MOI used as predictors are detailed in Table I.

The software used for the statistical analysis was IBM SPSS Version 22. Chi-squared tests were used to assess the univariate association with probability of severe injury for each predictor, where the null hypothesis was no association. $p < 0.05$ was considered statistically significant, casting doubts over the null hypothesis. The multivariate analyses were performed using logistic regression modelling. *p*-values and odds ratio (OR) for each predictor were derived. Logistic regression is a maximum-likelihood method commonly used in studies of traffic accidents, see e.g. [9, 10].

**Table 1: MOI description. For each MOI level the percentage of casualties having that characteristic is given.**

| Predictor | Levels | Frequency | | | Description |
|---|---|---|---|---|---|
| | | Cars (%) | Light Trucks (%) | Heavy Trucks (%) | |
| **Belt Use** | Unknown<br>Unbelted<br>Belted | <br>94<br>5.9 | 12<br>8.7<br>79 | 17<br>28<br>55 | Whether the casualty was using the seat belt at the moment of the accident |
| **Airbag Deployment** | Unknown<br>Undeployed<br>Deployed<br>No Airbag | <br>60<br>38<br>2.1 | 33<br>38<br>26<br>2 | 50<br>45<br>1.6<br>2.9 | Whether the airbag was deployed at the moment of the accident in case there was an airbag in the seat of the casualty |
| **Accident Type** | Turning<br>Intersection<br>Head-on<br>Overtaking<br>Single<br>Tram/Train<br>Rear End<br>WLA<br>Other | 23*<br>23*<br>13*<br>13*<br>31<br>0.2<br>27<br>3.2<br>3.1 | 4.4<br>13<br>11<br>2.2<br>34<br>0.5<br>28<br>2.8<br>4.2 | 1.7<br>2.8<br>13<br>1.3<br>61<br>1.2<br>14<br>0.8<br>3.8 | Classification according to the following types of accident: Intersection, collision of vehicle in an intersection; Turning, collision with a vehicle on a turning maneuver; Head-on, frontal collision of vehicles; Overtaking, collision with a vehicle on a overtaking maneuver; Single, vehicle collides with stationary object or departs from the road; Rear End, one vehicle collide with another from behind, Tram/Train, a vehicle collide with a tram or a train, WLA, a vehicle collide with a WLA, Other, other kind of accident. |
| **PSL** | Unknown<br>30<br>40<br>50<br>60<br>70<br>80<br>90<br>100<br>110<br>120 | <br>1.2<br>0.8<br>29<br>1<br>31<br>4.3<br>20<br>2.9<br>8.8<br>0.7 | 11<br>1.1<br>0.7<br>18<br>1.2<br>30<br>4.4<br>18<br>3.9<br>9.7<br>0.9 | 12<br>0.5<br>0.3<br>12<br>0.3<br>26<br>5.5<br>29<br>2.7<br>12<br>1.2 | Posted Speed Limit in the segment of road where the accident took place |
| **Accident Place** | Unknown<br>Urban<br>Rural | <br>38<br>62 | 8.8<br>27<br>64 | 8<br>15<br>76 | Whether the accident took place in an urban or rural environment, i.e. in or out a population center. Circumvallation roads are considered urban. |
| **Elderly** | Under 55<br>Over 55 | 78.4<br>21.6 | 84<br>16 | 83<br>17 | The age 55 years old was used because the National Expert Panel's decision to retain age 55 as a criterion for consideration in the Field Triage Decision Scheme (Sasser et al., 2012). |
| **Sex** | Male<br>Female | 54<br>46 | 82<br>18 | 92<br>7.6 | Whether the victim was male or female |

***For car accidents Overtaking was merged with Head-on and Turning was merged with Intersection.**

## RESULTS

Belt use and its relation to frequency of severe injury are shown in Figures 1 and 2 respectively. Results of the univariate analyses are shown in Table 2 which includes degrees of freedom, *p*-value for each predictor and the percentage of severely injured patients associated with each predictor level. Table 3 shows the results for the multivariate logistic regression models. For each predictor the statistical significance (*p*-values), β-coefficients for the regression equation and OR are shown.

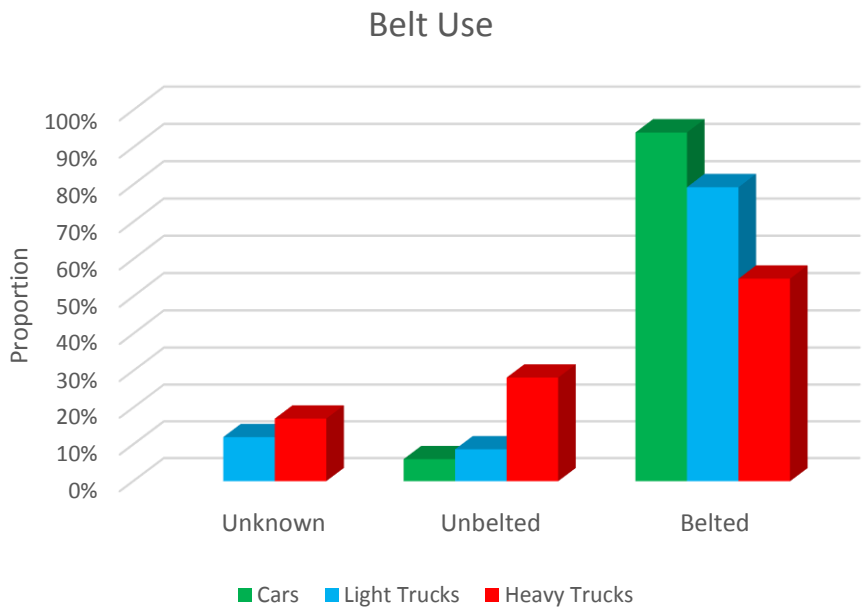


***Figure 1: Belt use compliance for the different occupant groups. Note that subjects classified as unknown were removed in cars.***

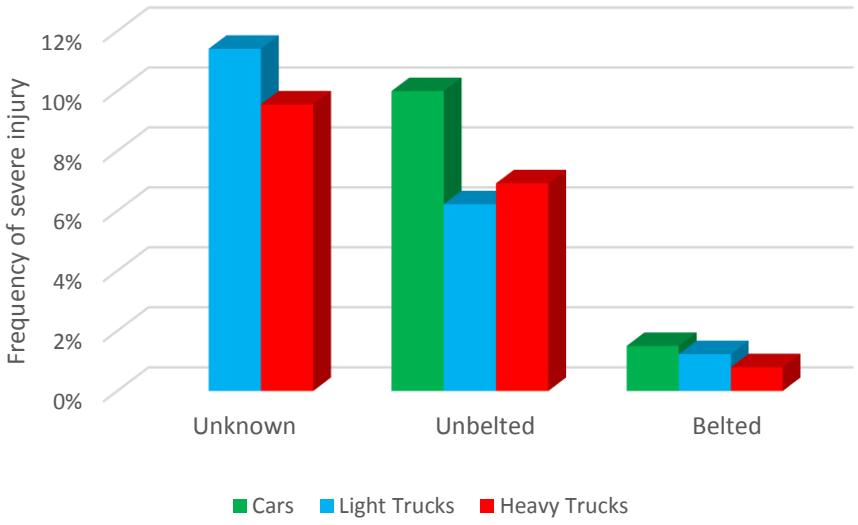


***Figure 2: Frequency of severe injury versus belt use. Note that subjects classified as unknown were removed in cars.***

**Table 2: Univariate analysis of MOI using chi-square tests of association. *p*-values and percentage of severely injured patients associated with each of its levels are shown.**

| Variable | *p* | | | Variable Levels | Percent of subjects suffering severe injury for each variable level | | |
|---|---|---|---|---|---|---|---|
| | Cars | Light Trucks | Heavy Trucks | | Cars (%) | Light Trucks (%) | Heavy Trucks (%) |
| **Belt Use** | < 10e-4 | < 10e-4 | < 10e-4 | Unknown<br>Unbelted<br>Belted | <br>10<br>1.5 | 11<br>6.2<br>1.2 | 9.6<br>6.9<br>0.8 |
| **Airbag Deployment** | 0.0030 | < 10e-4 | 0.18 | Unknown<br>Non-deployed<br>Deployed<br>No Airbag | <br>1.8<br>2.3<br>2.6 | 5.4<br>1.1<br>2.2<br>3.6 | 5.4<br>2.6<br>0.0<br>3.7 |
| **Accident Type** | < 10e-4 | < 10e-4 | 0.17 | Turning<br>Intersection<br>Head-on<br>Overtaking<br>Single<br>Tram/Train<br>Rear End<br>WLA<br>Other | 1.2*<br>1.2*<br>6.1*<br>6.1*<br>2.4<br>2<br>0.3<br>2<br>1.9 | 0.8<br>1.7<br>9.2<br>0<br>3<br>27<br>0.9<br>1.3<br>4.3 | 0<br>0<br>0.8<br>0<br>5.5<br>9.1<br>3<br>0<br>0 |
| **PSL** | < 10e-4 | 0.24 | 0.62 | Unknown<br>30 Km/h<br>40 Km/h<br>50 Km/h<br>60 Km/h<br>70 Km/h<br>80 Km/h<br>90 Km/h<br>100 Km/h<br>110 Km/h<br>120 Km/h | <br>0.6<br>0.8<br>0.9<br>1.0<br>2.1<br>2.5<br>4.1<br>1.1<br>0.9<br>1.1 | 3.5<br>0<br>0<br>1.6<br>0<br>3.1<br>1.7<br>4.4<br>0.9<br>3.3<br>4 | 3.7<br>0<br>0<br>7.4<br>0<br>5.1<br>2.0<br>2.6<br>0.0<br>3.7<br>9.1 |
| **Accident Place** | < 10e-4 | 0.23 | 0.17 | Unknown<br>Urban<br>Rural | <br>1<br>2.6 | 3.3<br>2<br>3.2 | 0<br>4.9<br>4.3 |
| **Elderly** | < 10e-4 | 0.0001 | 0.45 | Under 55<br>Over 55 | 1.6<br>3.6 | 2.4<br>5.7 | 3.8<br>5.1 |
| **Sex** | < 10e-4 | 0.18 | 0.60 | Male<br>Female | 1.4<br>2.5 | 3.1<br>2 | 4.1<br>2.9 |

***For car accidents Overtaking was merged with Head-on and Turning was merged with Intersection.**

**Table 3: Multivariate analysis of MOI using logistic regression models. *p*-values, β coefficients and odds ratio are shown.**

| **Predictors** | **β** | | | ***p*** | | | **$e^{\beta}$** | | |
|---|---|---|---|---|---|---|---|---|---|
| | **Cars** | **Light Trucks** | **Heavy Trucks** | **Cars** | **Light Trucks** | **Heavy Trucks** | **Cars** | **Light Trucks** | **Heavy Trucks** |
| **Belt** (Unbelted) | | | | < 10e-4 | < 10e-4 | < 10e-4 | | | |
| Belted | -2.1 | -2 | -2.4 | | | | 0.18 | 0.14 | 0.090 |
| Unknown | | 0.22 | 0.33 | | | | | 1.2 | 1.4 |
| **Airbag** (Non-deployed) | | | | 0.33 | 0.20 | 0.28 | | | |
| Deployed | 0.10 | 0.31 | -16 | | | | 1.4 | 1.4 | < 10e-4 |
| No Airbag | 0.34 | 1.4 | 2.1 | | | | 1.6 | 4.0 | 8.2 |
| Unknown | | 0.64 | 0.60 | | | | | 1.9 | 1.8 |
| **Over55/Under55** | 0.92 | 0.78 | 0.48 | < 10e-4 | 0.0050 | 0.29 | 2.7 | 2.2 | 1.6 |
| **Female/Male** | 0.33 | -0.32 | -0.18 | < 10e-4 | 0.39 | 0.82 | 1.4 | 0.73 | 0.84 |
| **Place** (Urban) | | | | < 10e-4 | 0.28 | 0.60 | | | |
| Rural | 0.48 | 0.48 | 0.51 | | | | 1.6 | 1.6 | 1.7 |
| Unknown | | 0.53 | -18 | | | | | 1.7 | < 10e-4 |
| **ATC** (Head-on) | | | | < 10e-4 | < 10e-4 | .85 | | | |
| Intersection | -1.5* | -1.5 | -16 | | | | 0.23* | 0.22 | < 10e-4 |
| Other | -1.2 | -1.1 | -17 | | | | 0.29 | 0.33 | < 10e-4 |
| Overtaking | **Ref*** | -19 | -16 | | | | **Ref *** | < 10e-4 | < 10e-4 |
| Rear end | -2.7 | -2.4 | 1.5 | | | | 0.07 | 0.09 | 4.7 |
| Single | -1.1 | -1.4 | 2.0 | | | | 0.34 | 0.24 | 7.3 |
| TramTrain | -0.43 | 0.90 | 2.0 | | | | 0.65 | 2.5 | 6.5 |
| Turning | -1.5* | -2.5 | -16 | | | | 0.23* | 0.080 | < 10e-4 |
| Wild | -1.4 | -2.6 | -17 | | | | 0.25 | 0.072 | < 10e-4 |
| **PSL** ( Unknown ) | | | | < 10e-4 | 0.25 | 0.85 | | | |
| 30 Km/h | **Ref†** | -17 | -19 | | | | **Ref†** | < 10e-4 | < 10e-4 |
| 40 Km/h | 1.1 | -16 | -18 | | | | 2.9 | < 10e-4 | < 10e-4 |
| 50 Km/h | 0.6 | -0.85 | 1.1 | | | | 1.8 | 0.43 | 2.9 |
| 60 Km/h | 0.87 | -18 | -17 | | | | 2.4 | < 10e-4 | < 10e-4 |
| 70 Km/h | 1.0 | -0.14 | .50 | | | | 2.7 | 0.87 | 1.7 |
| 80 Km/h | 1.2 | -0.72 | .040 | | | | 3.5 | 0.49 | 1.0 |
| 90 Km/h | 1.5 | 0.51 | -0.27 | | | | 4.4 | 1.7 | 0.76 |
| 100 Km/h | 0.85 | -0.18 | -18 | | | | 2.3 | 0.83 | < 10e-4 |
| 110 Km/h | 0.40 | 0.55 | -0.14 | | | | 1.5 | 1.7 | 0.87 |
| 120 Km/h | 0.86 | 0.84 | 0.26 | | | | 2.4 | 2.3 | 1.3 |

***For car accidents Overtaking was merged with Head-on and Turning was merged with Intersection.**

**†30 Km/h was the reference for cars unlike for trucks where the reference was "Unknown".**

## DISCUSSION

### Proportion of severely injured subjects versus belt use

The proportion of severely injured subjects was higher for trucks than for cars, and higher for heavy trucks than for light trucks. The frequencies were 4.0 % for heavy trucks, 2.9 % for light trucks and 2.0 % for cars. These results were surprising because larger vehicles, especially heavy trucks, were expected to be safer due to heavier weight and the occupant compartment being placed higher above the wheelbase. Large differences in compliance of belt use were found to be the cause of these surprising results. These differences can be observed in Figures 1 and 2. Figure 1 shows that the percentage of belted subjects is much higher in cars than in trucks, and the compliance is particularly low at 55 % for heavy truck occupants. Figure 2 indicates that for belted and unbelted occupants, cars are less safe than both types of trucks.

In both types of trucks a significant percentage of cases had belt use registered as unknown, which is probably a consequence of that it was reported by the patient himself/herself. Figure 3 shows that cases where belt use was unknown have even higher frequency of severe injury than unbelted cases, a surprising finding for which we currently have no explanation. However, it is likely that most of these cases were unbelted. For cars, cases where belt use was reported as unknown were not included in the analyzed data since a high discrimination power was achieved when eliminating cases with missing information.

Belt use was by far the most significant predictor for all vehicle types. Moreover it was the only variable that was statistically significant for heavy trucks ($p < 0.05$). It should be noted that the statistical significance of the predictors is highly influenced by the size of the datasets, e.g. more predictors were statistically significant for cars. Nevertheless a comparison of the predictors between different vehicle types can be made according to their ranking within a vehicle type.

### Association of the different predictors with probability of severe injury

It is difficult to draw conclusions regarding airbag as being a valuable predictor of severe injury. One reason is that the level was unknown for many truck accidents, another is that airbag deployment is likely to be biased towards more severe crashes. Moreover for heavy trucks only 15 cases had deployed airbag, with no severely injured occupants. However, it can be concluded that the association of airbag deployment with probability of severe injury is much smaller than for belt use. We recommend that use of airbag deployment and not belt use as criteria in RETTS should be reconsidered and further evaluated in field studies.

Regarding type of accident note that for cars overtaking accidents were merged with head-on and turning accidents were merged with intersection [6]. The effect of merging these types of accidents is weak because the number of accidents classified as overtaking and turning were relatively small. For cars and light trucks head-on accidents are the most dangerous ones, whereas rear-end accidents are the most common but the least dangerous. The results are very different for heavy trucks where single accidents are by far the most common as well as the most dangerous. It is surprising that for heavy trucks rear-end accidents showed a higher probability of severe injury than head-on accidents. These results show that different types of accidents have similar consequences for cars and light trucks but are very different for heavy trucks.

In all types of vehicles the majority of accidents included in this study occurred in roads with PSL 50, 70, 90 and 110 km/h, with over half of the accidents taking place on roads with PSL 70 and 90 km/h. Roads with PSL 90 km/h are most dangerous for cars and light trucks, whereas roads with PSL 50 km/h have the highest risk of severe injury for heavy trucks, which was unexpected. This result should be interpreted with caution since it is based only on 100 subjects.

Rural environments produced a substantially higher proportion of severely injured than urban environments for all types of vehicles. Despite that heavy trucks showed a higher proportion of severely injured in urban environments, after adjusting for all other predictors, i.e. in the multivariate logistic regression model (Table 3), the OR showed that rural environments are a risk factor with positive association. This may partially be due to that PSL 50 km/h, which was the PSL with highest associated risk of severe injury for heavy trucks, was correlated with urban environment.

Occupants over 55 years old has a substantially higher probability of being severely injured than younger occupants in all three types of vehicle. However this factor is more prominent for cars than for light and heavy trucks. Regarding sex, women have a higher risk of sustaining severe injury for cars but a lower risk for trucks. In principle women are more vulnerable to trauma than men [10], however for trucks this result points in the opposite direction.

## CONCLUSIONS

Belt use is the most important factor influencing the risk of sustaining severe injury for occupants in cars and trucks involved in traffic accidents. We recommend including belt use as criteria for triage protocols. There is a need for information campaigns and other means for increasing belt use compliance for cars and trucks, in particular for heavy trucks.

The finding that single accidents account for over 60 % of all heavy truck accidents that produce injuries, and that this is the most dangerous type, point to a need for innovations to reduce them.

## REFERENCES


[1] Haas, B., Gomez, D., Zagorski, B., Stukel, T.A., Rubenfeld, G.D. and Nathens, A.B., 2010. "Survival of the Fittest: The Hidden Cost of Undertriage of Major Trauma." Journal of the American College of Surgeons 211, 804-811.

[2] MacKenzie, E., Rivara, F., Jurkovich, G., Nathens, A., Frey, K., Egleston, B., Salkever, D., Scharfstein, D., 2006. "A national evaluation of the effect of trauma-center care on mortality." New England Journal of Medicine 354, 366-378.

[3] Schoell, S. L., Doud, A. N., Weaver, A.A., Talton, J.W., Barnard, R.T., Martin, R.S., Meredith, J.W. and Stitzel, J. D., 2014. "Development of a Time Sensitivity Score for Frequently Occurring Motor Vehicle Crash Injuries." Journal of the American College of Surgeons.

[4] Brown, J.B., Stassen, N.A., Bankey, P.E., Sangosanya, A.T., Cheng, J.D., Gestring, M.L., 2011. "Mechanism of Injury and Special Consideration Criteria Still Matter: An Evaluation of the National Trauma Triage Protocol." Journal of Trauma-Injury Infection and Critical Care 70, 268, 38-45.

[5] Widgren, B.R., Jourak, M., 2011. "Medical Emergency Triage and Treatment System (METTS): A New Protocol in Primary Triage and Secondary Priority Decision in Emergency Medicine." Journal of Emergency Medicine 40, 623-628.

[6] Buendia, R., Candefjord, S., Fagerlind, H., Bálint, A., Sjöqvist, B.A. 2015. "On Scene Injury Severity Prediction (OSISP) Algorithm for Car Occupants." Submitted to Accident Analysis and Prevention.

[7] Buendia, R., Candefjord, S., Fagerlind, H., Bálint, A., Wege, C., Sjöqvist, B.A. 2015. "On Scene Injury Severity Prediction (OSISP) Algorithm for Truck Occupants." Submitted to Traffic Injury Prevention.

[8] Howard, C. and Linder, A., 2014. "Review of Swedish experiences concerning analysis of people injured in traffic accidents." Swedish National Road and Transport Research Institute (VTI) VTI Report, 7A-2014, 1-34.

[9] Harrell, F.E., 2001. "Regression modeling strategies, with applications to linear models, survival analysis and logistic regression." Springer Science and Business Media, Inc., New York.

[10] Kononen, D.W., Flannagan, C.A.C., Wang, S.C., 2011. "Identification and validation of a logistic regression model for predicting serious injuries associated with motor vehicle crashes." Accident Analysis & Prevention 43, 112-122.

# HUMAN FACTORS EVALUATION OF LEVEL 2 AND LEVEL 3 AUTOMATED DRIVING CONCEPTS

**Paul, Rau**
National Highway Traffic Safety Administration
United States

**Myra, Blanco**
**Jon, Atwood**
**Holland, Vasquez**
**Tammy, Trimble**
**Vikki, Fitchett**
**Josh, Radlbeck**
**Gregory, Fitch**
**Sheldon, Russell**
Virginia Tech Transportation Institute
United States

Paper Number 15-0428

## ABSTRACT

This project evaluates how drivers interact with different automated vehicle functions under various concepts of Level 2 and Level 3 automation. The objective is to determine whether principles for human-machine interface (HMI) design for automated vehicles could be based on things such as timing, sequence, and presentation of automated functions produced by this study. Methods involve test track evaluations of participants using three distinct automation concepts, two involving automation Level 2 and one involving automation Level 3 (as defined by the National Highway Traffic Safety Administration [NHTSA] policy paper on vehicle automation; NHTSA, 2013). Data sources included both objective and subjective data from participants' responses to the different portions of the experimental protocols. Results will be produced from parametric linear regression analyses and qualitative evaluations of participants' subjective responses to questionnaires. Where appropriate, statistical techniques will be applied for conditioning the sample data to ensure that the assumptions underlying these analyses are met. The detailed timing, sequence, and presentation measurements from the various research efforts involved herein will be used to specify human factors design principles for automated vehicle HMIs. The resulting principles would benefit from subsequent naturalistic evaluations for fine-tuning the performance metrics, and for addressing any gaps or new questions arising from this research. Crash avoidance technologies are evolving rapidly toward increasing automation, involving a higher complexity of interoperability between user and vehicle functions than what has previously been known. Understanding the detailed human factors capabilities and limitations of these users and the impacts of the timing, sequence, and presentation of information presented to the users will be important for shaping the safety policies.

## INTRODUCTION

Technological advancements over the past decade have led to the emergence of advanced driver assistance systems. Current features such as Adaptive Cruise Control (ACC), collision warning, and automatic braking systems are becoming commonplace in modern automobiles. Furthermore, automated systems that combine limited lateral and longitudinal control over a vehicle are becoming commercially available. Some of these systems incorporate various methods to ensure driver participation.

While automated systems offer the potential for increased safety and reduced human error, their use may create issues which could benefit from further investigation. These issues may include negative adaptations based on misunderstanding, misuse, over-reliance on the automated systems, and distractions from the driving task due to interaction with the automated system. These issues should be examined in order to address any potential for unforeseen consequences of increased automation.

Of specific interest is how an automated system will impact operators' willingness to engage in non-driving-related tasks. As noted in previous work, (e.g., Llaneras, Salinger, & Green, 2013), the current generation of automated systems is designed to support, rather than replace, the driver. The presence of automated systems may create the perception to free an operator's attention, which may then be directed at non-driving tasks. The redirection of the operator's attention to non-driving tasks may also impact an operator's situational awareness, including the ability to perceive critical factors in the environment or to detect issues with the automated systems (e.g., system state changes or failures).

As automated driving technology advances, the "driver's" role is shifting from active vehicle control to passive supervision of the automated system and/or the environment. The current study focused on the human factors issues that arise when vehicles equipped with automation technologies shift the human from the role of driver to that of operator. Automated vehicle systems must be designed to instruct and prompt the operator to act, if and when needed, in a timely and appropriate way in order to ensure safety. This study investigated how operators interact with partial automation under National Highway Traffic Safety Administration (NHTSA) Levels 2 and 3 (NHTSA, 2013). Level 2 (Combined Function Automation) and Level 3 (Limited Self-Driving Automation) were of particular interest because this is the point at which the driver's role transitions from one of driving to one of operation.

**Objective**

The purpose of this study was to examine the interaction between human users and automated vehicle systems. Specifically: how do human users interact with vehicles that have L2 and L3 automated systems, can these users take over control of the driving task when required, and can they determine the acceptable balance between controlling the vehicle when necessary and letting the automated system function as designed to perform the driving task when appropriate? The ultimate goal of this research was to ascertain how operators interact with automated vehicles and determine how automated vehicle technology can best support safe driving.

**Project Research Questions**

This study centered on six key research questions developed by NHTSA. The focus of this research was to address each question based on sound empirical research findings. The research questions were:

1. How do drivers interact with and operate vehicles that offer Level 2 and Level 3 automation; e.g., what is the driver performance profile over length of time in continuous or sustained automation?
2. What are the system performance risks from driver involvement with, and interruption from, secondary tasks (such as portable electronic device use) that could arise when operating Level 2 or Level 3 automated vehicle systems?
3. What are the most effective hand-off strategies between the system and the driver, including response to faults/failures?
4. How do drivers engage, disengage, and reengage with the driving task in response to the various states of Level 2 and Level 3 automation?
5. How do drivers perform under various operational concepts within Level 2 and Level 3 automation, such as systems intended for everyday driving on open roadways in mixed traffic or systems intended for dedicated roadway-vehicle applications (e.g., automated lanes, remote highways)?
6. What are the most effective human-machine interface concepts, guided by human factors best practices, which optimize the safe operation of Level 2 and Level 3 systems?

The six aforementioned research questions were addressed in three experiments. Experiment 1 examined how best to alert operators to regain control of the vehicle, Experiment 2 examined the system prompt effectiveness (i.e., how effectively the HMI communicated to the operator) over time, and Experiment 3 examined operator behavior over time. Experiments 1 and 2 were conducted using a vehicle equipped with an L2 system, while Experiment 3 was conducted with a vehicle equipped with an L2 system that can simulate L3 driving on a test track. The details of the experiments and their expected findings are presented in the following sections.

## EXPERIMENT 1: ALERTING OPERATORS TO REGAIN CONTROL OF AN L2 AUTOMATED VEHICLE

### Purpose

There are numerous ways to notify operators that they need to regain control of a partially automated vehicle. The purpose of this experiment was to investigate which human-machine interface (HMI) characteristics are most effective at issuing a Take-Over Request (TOR) and to identify the transition times between the operator and the automated functions in regard to the driving tasks.

### Participants

Data were collected from 35 participants recruited from the greater Detroit, Michigan area; however, 10 participants were considered invalid (i.e., session cancellation due to adverse weather, track closures, or technical issues associated with the prototype vehicle). As such, the analysis will represent data from 25 participants (16 males, 9 females). The mean age of participants was 44.3 years old (S.D. = 19.24), with ages ranging from 18 to 72 years old.

### Method

A single, long-exposure, experiment was conducted. Participants were provided with a thorough familiarization of the vehicle and its operation, followed by a single, approximately 90-minute, exposure to the vehicle in L2 automated driving. During the driving session, participants were instructed to perform non-driving-related tasks (e.g., e-mail, web browsing) and were, at times, presented with alerts stating that they must take control of the vehicle. Three forms of alerts were presented: Cautionary, Imminent, and Staged. The Cautionary alerts provided information to the participants that a potential problem was detected. The Imminent alerts provided the participants with a message that an active fault was detected. The Staged alerts transitioned from a cautionary alert phase to an imminent alert phase. Participants' reactions to these messages, both in duration and method of response, were among the variables examined in this experiment.

### Experimental Design

The study was performed as a within-subject design. All participants completed one 90-minute driving session during which they received a total of 19 system alerts. For each of the alert types, participants experienced three unimodal alerts (visual only) and three multimodal alerts (visual + haptic). The study was designed to mimic worst-case scenarios when the operator was not monitoring the roadway due to the non-driving tasks.

The alerts were presented to participants in six different orders. Each order consisted of the six different combinations of alert type and alert modality, and this was repeated three times within the experimental session. Using all six possible alert type and alert modality combinations, a Latin square was developed to create six different orders of alert presentation. The order was repeated three times within the 90-minute driving session, resulting in 18 alerts. After receiving these 18 alerts, each participant received an Imminent multimodal alert coupled with an experimenter-triggered lane drift, resulting in a total of 19 alerts. The alerts were presented at random times between 2 and 8 minutes; thus, participants were less likely to be able to anticipate when they would occur.

### Venue

This experiment was conducted at the Milford Proving Ground circle track in Milford, Michigan. This facility is owned and maintained by General Motors (GM) and includes a 4.5-mile banked circle track with five travel lanes. The travel speed for each lane falls within a designated speed range, with the innermost lane allowing for stop and go traffic and the outermost lane being restricted to speeds of 100 mph and above. Experiment 1 was conducted in Lane 3, which allowed speeds of between 50 - 70 mph.

**Vehicle**

A 2009 Chevrolet Malibu equipped with a prototype L2 automated driving system was used (See Figure 1). As part of the automated driving system, several HMI components were installed and the vehicle was modified to include ACC and lane centering along with a flexible driver interface. Additionally, the vehicle was equipped with a researcher's control console, which was designed to allow the in-vehicle experimenter to trigger various displays and to change the operation of the automation systems, including simulating erroneous behavior and equipment failures.

***Figure1. 2009 Chevrolet Malibu with a prototype L2 system used in Experiment 1.***

The vehicle was also equipped with a data collection and recording device. These key variables were collected: status of the automation (e.g., off, on and actively controlling, failure mode), vehicle speed, lane position, and flags indicating the presentation of messages and system failures. In addition, video views which included the operator's face, forward roadway, and HMI were collected.

**Study Session**

Prior to beginning the study session, participants were provided with a static orientation to the experimental vehicle, which included information about the basic controls and the L2 automation features. Following this, participants received an on-track orientation consisting of four laps on the test track. During the 90-minute driving session, participants were instructed to perform a variety of non-driving tasks using a tablet computer when the L2 automation was activated. Participants were presented with three types of non-driving tasks to complete using the tablet computer: navigation, email, and web-browsing. At approximately 5-minute intervals (in random values ranging from 2 to 8 minutes), participants were provided with unimodal (visual only) or multimodal (visual + haptic seat vibration) alerts (Cautionary, Imminent, or Staged) instructing them to take control of the vehicle. Details pertaining to the Cautionary, Imminent, and Staged alert timings are depicted in Figure 2.

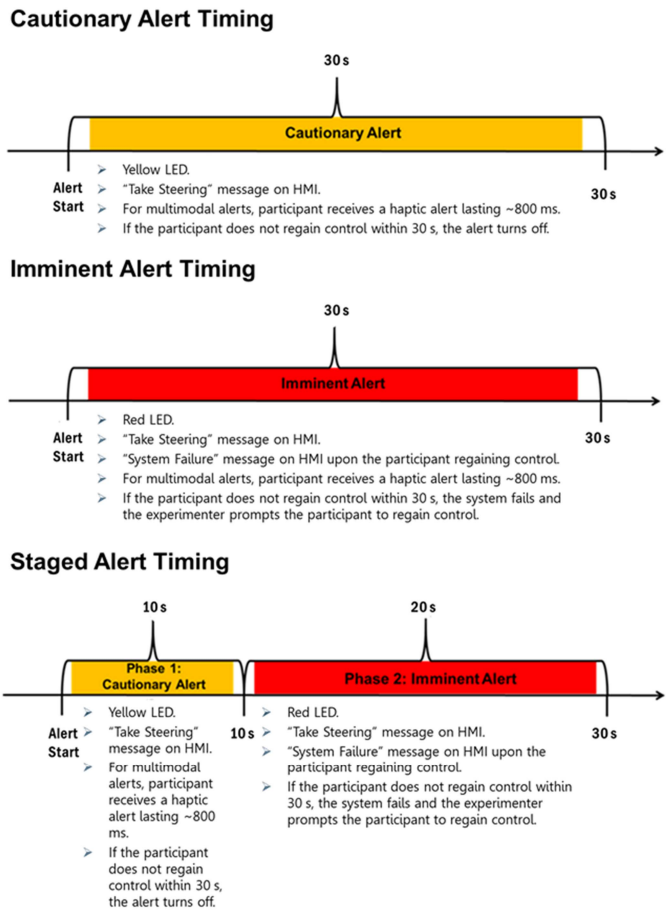


***Figure2. Cautionary, Imminent, and Staged take control alert timelines for Experiment 1.***

A trust scale was administered 10 times throughout the experimental session at approximately 9-minute intervals. Participants were asked to rate their trust in the ability of the automation to function properly while they engaged in non-driving tasks using a 7-point Likert-type scale. In addition to the 10 trust ratings collected throughout the experimental session, participants were asked to complete the after-experience trust scales and participate in an open-ended interview upon completing the driving session. Compensation was provided for participation in the study.

## EXPERIMENT 2: SYSTEM PROMPT EFFECTIVENESS OVER TIME

### Purpose

The second experiment investigated how to prompt operators to monitor the driving environment when engaged in a non-driving-related task during the operation of an L2 automated vehicle. A secondary purpose was to investigate the effectiveness of the prompts over time.

### Participants

Data were collected from 56 participants recruited from the greater Detroit area (28 males, 28 females) with a mean age of 41 years old (S.D. = 16.3), with ages ranging from 18 to 72 years old.

## Method

A single, long-exposure experiment was conducted. Participants were provided with a brief familiarization with the vehicle and its operation, followed by three 60-minute experimental sessions. During the sessions, participants were given tasks to be completed using a tablet computer. During these tasks, participants received prompts based on their predetermined prompt condition (either 2-second, 7-second, or No Prompts). For the 2- or 7-second prompt conditions, participants received prompts after periods of inattention to the driving environment for the corresponding amount of time. Participants given the No Prompts condition did not receive any prompts and they were free to behave as they thought was appropriate.

In addition to these prompts, at a random time during one predetermined session, the participant received an alert for a surprise left lane drift, consisting of a haptic seat alert and a flashing red LED. In a different predetermined session, the participant experienced a surprise lane drift with no alert, which consisted only of a left lane drift without any alert and with the prompting system disabled. The experimenter-injected lane drift was used to simulate a lane-keeping performance issue combined with a failure of the prompting system. Note that, to the participants with the 2-second and 7-second prompt conditions, the alert that they received along with the lane drift was indistinguishable from the prompts that they had been receiving based on their attention state. Participants' reactions to these prompts, alerts, and lane drifts, both in duration and method of response, were examined in this experiment.

## Experimental Design

The study was performed as a 3 x 3 x 3 mixed factorial design. Each participant completed three successive driving sessions, and each session included one of the following: a lane drift with an alert, a lane drift without an alert, or no lane drift. Participants experienced each of these conditions once during the experiment. In addition, there were also three different prompt conditions that were used with the driver monitoring system, and each participant experienced only one prompt condition, either: 2-second, 7-second, or No Prompts. The prompt timing was based on previous distraction research (2-second prompts) (e.g., Klauer et al., 2006) and expert opinion (7-second prompts). Additionally, the study was designed to mimic worst-case scenarios when the operator was not monitoring the roadway due to the non-driving tasks.

## Venue

As was the case for Experiment 1, Experiment 2 was also conducted at GM's Milford Proving Ground circle track in Milford, Michigan. However, this experiment utilized Lane 2, which allowed speeds of between 30-50 mph.

## Vehicle

A 2010 model year Cadillac SRX equipped with a prototype L2 automated driving system was used as the experimental vehicle (See Figure 3). As part of the automated driving system, several HMI components were installed. These included an instrument panel binnacle-mounted screen providing information on the automated driving system, and two steering wheel buttons to control the automation: one ACC button, and one button for the lane-centering system, a prototype automated vehicle system.

***Figure3. 2010 Cadillac SRX with a prototype L2 system used in Experiment 2.***

The vehicle was equipped with Virginia Tech Transportation Institute's (VTTI) data acquisition system (DAS). The variables collected by the DAS included status of the automation, vehicle speed, and lane position. In addition, video views including the operator's face, forward roadway, and HMI were collected.

**Study Session**

Prior to beginning the study session, participants were provided with a static orientation to the experimental vehicle, which included the basic controls and the L2 automation features. Following this, participants received an on-track orientation consisting of four laps on the test track. Participants then completed three driving sessions, with each lasting approximately 60 minutes. Participants were instructed to begin interacting with a variety of non-driving tasks during the driving session upon activating the L2 automation. Participants were presented with three types of non-driving tasks: navigation, email, and web-browsing. These tasks were similar in terms of the visual/manual demand required and they were presented in a random order.

Each participant was assigned a prompt condition: either 2-second, 7-second, or No Prompts. The driver monitoring system provided three stages of prompts based on the assigned prompt condition and the participant's attention state. If the participant's attention state was not on the driving environment, the system provided alerts based on the assigned prompt condition. For the 2-second prompt condition, the prompts began after the participant's attention state was not on the driving environment for 2 s. For the 7-second prompt condition, the prompts began after the participant's attention state was not on the driving environment for 7 s. Participants who were assigned to the No Prompts condition did not receive any prompts. The driver monitoring system provided three progressive stages of alerts. Details pertaining to the prompt stages are detailed in Figure 4 below.

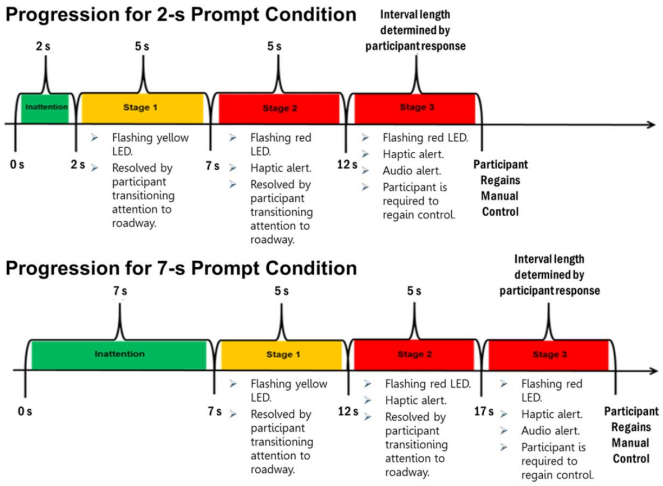


***Figure4. Alert timelines for 2-second & 7-second prompt conditions for Experiment 2.***

During the experiment, each participant experienced both types of lane drift (with and without an alert) and no lane drift—one time each—in different driving sessions, and at random times. All of the surprise lane drifts were prescribed and injected into the condition of interest using the experimenter console. The lane drifts with the alerts represent the condition of a lane-keeping performance issue in which the system warns the vehicle operator in order for him/her to regain control. The situations with no alerts represent conditions where there is a lane-keeping performance issue and a simultaneous failure of the prompt system, but the system does not warn the vehicle operator. Participant responses to the attention state prompts and experimenter-injected lane drifts were measured using visual evidence from the DAS. After completing three driving sessions, participants were instructed to exit the circle track and return to the preparation area. Participants were then interviewed, asked to complete the after-experience trust scales and interview, and provided with a debriefing as to the purpose of the study. Compensation was provided for participation in the study.

## EXPERIMENT 3: HUMAN-AUTOMATION SYSTEM PERFORMANCE OVER TIME

The purpose of the third experiment was to investigate what HMI characteristics are effective at alerting operators to regain control of an L3 automated vehicle and to identify the transition times between the operator and the automated functions in regard to the driving tasks.

### Participants

Data were collected from 37 participants recruited from the greater Roanoke, Virginia area; however, 12 participants were considered invalid (i.e., session cancellation due to adverse weather or technical issues associated with the DAS or the prototype vehicle). The analysis will consist of data from 25 participants. The mean age of the participants was 38.8 years old (S.D. = 13.77), with ages ranging from 18 to 69 years old.

### Method

A single-exposure experiment was performed. Participants were provided with a thorough familiarization with the vehicle and its operation, including use of the automated features. Training was followed by three 30-minute experimental sessions. During the sessions, participants had free exposure to a non-driving-related task (i.e., use of their own cell phone or the provided tablet, as they felt was appropriate) and were presented with a message stating that they must take control of the vehicle. Participants' reactions to these messages, both in duration and method of response, were examined in this experiment.

**Experimental Design**

The study was performed as a within-subject design. Each participant completed three successive driving sessions, each session with one of three alert types; all participants received all alert types exactly once. The three alert types were: Staged, Imminent–No External Threat, and Imminent–External Threat. They received a Staged alert in the absence of an external threat, an Imminent alert in the absence of an external threat, and an Imminent alert in response to an external threat (i.e., a revealed box on the road). The Staged alert was composed of four phases: 1) a short tone followed by an informational message asking operators to prepare for manual control (including a countdown timer), 2) a Cautionary verbal alert played in addition to an animated HMI display with the instruction to "please turn off autodrive" presented for 10 s, 3) a repeated cautionary tone played in addition to an orange visual alert stating to "turn off autodrive now" presented for 10 s, and 4) a repeated imminent tone played in addition to a red visual alert stating to "turn off autodrive now" presented for 10 s combined with the automation beginning to apply the brakes. The Imminent alert was composed of a red visual alert stating to "turn off autodrive now" presented for 10 s along with the automation applying the brakes.

**Venue**

This experiment was conducted on the Virginia Smart Road test track, which is located at VTTI in Blacksburg, Virginia. The test track is constructed to state and federal roadway standards and has a length of 2.2 mi, with looped turns at either end. The straight section of the track is approximately 0.5 mi in length. Two lanes run the duration of the track, with the exception of the looped turns. Wireless Internet coverage is available on the track. The facility is closed to outside traffic and only study-related vehicles were present during the experiment.

**Vehicle**

A 2012 Lexus RX450h was used as the experimental vehicle for Experiment 3 (See Figure 5). This L2 vehicle was equipped with a prototype automated driving system that can simulate L3 driving on a test track. As part of the prototype system, several HMI components were installed. These included an instrument panel binnacle-mounted screen providing information on the automated driving system, and two steering wheel buttons to control the automation: one ON button on the left side of the wheel and one OFF button on the right side of the wheel.

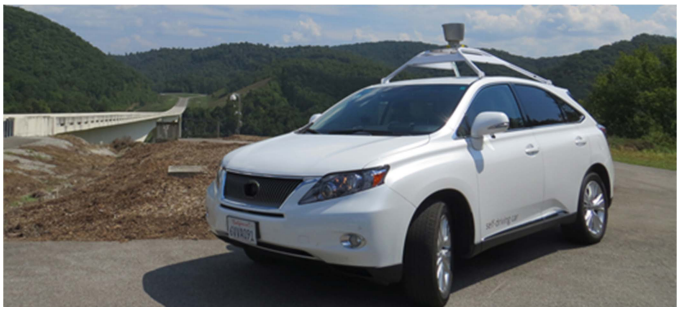

***Figure5. 2012 Lexus RX450h with a prototype L3 system used in Experiment 3.***

The vehicle was instrumented with VTTI's DAS. The variables collected by the DAS included throttle/brake input and automation state. In addition, video views including the operator's face, the forward roadway, and the HMI were collected.

**Study Session**

Prior to receiving any hands-on training, the participants viewed a 10-minute video summarizing the vehicle's features with a specific focus on the automated components and operation of the vehicle. This video was a training requirement of the automated vehicle provider and was consistent with the recommendation in NHTSA's *Preliminary Statement of Policy Concerning Automated Vehicles* in the section entitled "Recommendations Concerning State Activities Related to Self-Driving Vehicles" (NHTSA, 2013; pp. 10-11). This video was intended to detail the prototype system's operating capabilities and limitations. The participants were also shown the different

types of the alerts (i.e., Staged, Imminent–External Threat, and Imminent–No External Threat) during the video. Following this, participants received an on-track orientation consisting of four laps on the test track.

The experiment consisted of three 30-minute driving sessions. Participants were able to freely engage in non-driving tasks (i.e. tablet computer and cell phone use) when the automated system was activated. At a randomly selected point within each session, one of the three alert types was presented: Staged, Imminent–External Threat, or Imminent–No External Threat. The alerts happened at a predetermined location and participants experienced all three alert types during the experimental session. While each participant experienced all of the alert types, they were not always experienced in the same order. Details pertaining to Staged and Imminent alert timing and presentation are shown in Figure 6.

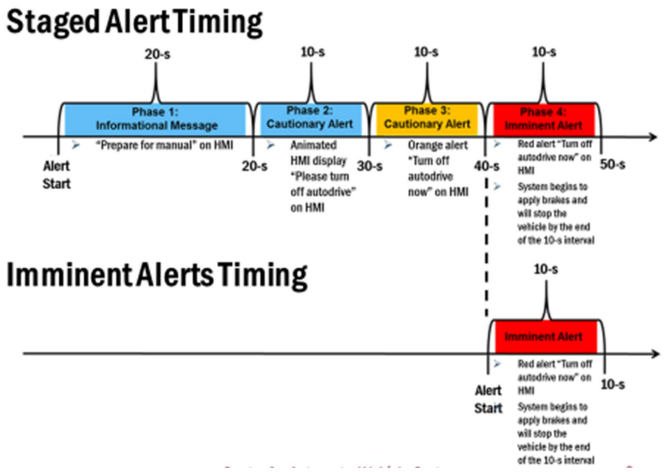


***Figure6. Staged and Imminent take control alert timelines for Experiment 3.***

A 15-minute break was offered after each session to allow for participant comfort; however, some participants chose to forgo the breaks. The maximum speed for all sessions was 45 mph, with lower speeds used for the turns at both ends of the track.

The trust scale was presented at 10-minute intervals during each session (at the beginning of the session, followed by administrations after 10, 20, and 30 minutes). Upon completion of the third session, the participant was instructed to deactivate the vehicle's automation, assume manual control over the vehicle, exit the track, and return to the preparation area. An interview was performed at that point. Compensation was provided for participation in the study.

## PLANNED STATISTICAL ANALYSES

Because the data are measured repeatedly on participants over time, longitudinal statistical methods—used widely in experiments with repeated measures—can be used to analyze the data. For the variables that involve a time until the participant performs some action (such as regaining control of the vehicle), continuous data methods can be used, although the presence of extreme values may require the use of a data transformation (such as the logarithmic transformation) to effectively normalize the data to help fulfill the assumptions of these techniques. For other types of variables, such as the number of non-driving-related glances (which are counts) and the monitoring rate (a proportion), more general longitudinal methods can be used that account for the wide variety of distributions that these variables follow.

## EXPECTED RESULTS

The detailed timing, sequence, and presentation measurements from the various research efforts involved herein could be used to develop human factors design principles. Crash avoidance technologies are evolving rapidly toward

increasing automation, involving a higher complexity of interoperability between user and vehicle functions than has previously been known. Understanding the detailed human factors capabilities and limitations of these users and the impacts of the timing, sequence, and presentation of information presented to the users will be important for shaping the safety policies.

## REFERENCES


Klauer, S.G., Dingus, T.A., Neale, V.L., Sudweeks, J.D., & Ramsey, D.J. (2006). *The impact of driver inattention on near-crash/crash risk: An analysis using the 100-car naturalistic driving study data* (No. HS-810 594). Washington, DC: National Highway Traffic Safety Administration, USDOT.

Llaneras, R.E., Salinger, J., & Green, C.A. (2013). Human factors issues associated with limited ability autonomous driving systems: Drivers' allocation of visual attention to the forward roadway. *Proceedings of the International Driving Symposium on Human Factors in Driver Assessment, Training, and Vehicle Design, 7*, 92-98.

NHTSA. (2013). *Preliminary statement of policy concerning automated vehicles*. Retrieved from http://www.nhtsa.gov/staticfiles/rulemaking/pdf/Automated_Vehicles_Policy.pdf

# CORRELATION BETWEEN THOR BrIC AND TBI RISK FROM FULL BODY HUMAN MODEL

**Maika Katagiri**
**Ning Zhang**
**Jay Zhao**
**Jialou Hu**
**Mike Scavnicky**
**Bernd Cyliax**
**Ingo Mueller**
**Torsten Steiner**
TAKATA Corporation
United States, Germany, Japan

Paper Number 15-0249

## ABSTRACT

The Brain Injury Criteria (BrIC) was recently developed by using two human head models (SIMon and GHBMC) and ATD impact and crash test data. This study used a system simulation approach to further investigate correlations between BrIC from the THOR sled tests in the NHTSA Advanced Adaptive Restraint Program (AARP) and the human occupant traumatic brain injury (TBI) AIS 4+ risks estimated with a full body human model.

Eleven sled tests for the 50$^{th}$percentile male THOR Mod Kit dummy performed in AARP were selected as the basis for this analysis. The measured THOR BrIC values from these tests ranged from 0.49 to 1.89. For each of the THOR sled tests, a FE system model was built and the correlation was confirmed with the physical test data. The full body human model, a combination of the GHBMC head model and the in-house Takata human body model (TKHM), has been validated at component and full body levels. The THOR dummy model was then replaced with the full body human model in the system and the sled test simulations for the human under the same test conditions were conducted. The maximum principal strain (MPS) and the cumulative strain damage measure (CSDM) from the human head model were calculated from deformation of the brain tissue elements. The risks of AIS 4+ TBI injuries per the CSDM and MPS measures were compared with those estimated with BrIC from the THOR sled tests using paired student t-tests.

Overall, good agreement of the head, chest and pelvis translational accelerations and the head rotational velocities between the THOR dummy and the human body model were found for the full frontal sled cases. Differences between the two were observed for the head rotational velocities under the oblique sled test conditions. The results of additional simulations where an impactor struck laterally the face-jaw of the THOR, TKHM and GHBMC indicated that the THOR head-neck twisted more and faster than the human models, which could be a major cause of the inconsistency in the oblique cases.

Linear correlations between the THOR BrIC and the AIS 4+ TBI risk estimations from CSDM and MPS outputs of the human model were observed (with $R^2$ score of 0.81 for CSDM and $R^2$=0.85 for MPS). The TBI risks estimated from the THOR sled tests and the human model were similar in the full frontal, while the BrIC from the THOR sled tests overestimated the TBI risks.

## INTRODUCTION

Great efforts have been made in the past decade to reduce death and injury in motor vehicle crashes (MVC). New FMVSS and NCAP test protocols have been implemented by the National Highway Traffic Safety Administration (NHTSA), and more advanced restraint system devices such as dual stage frontal airbags, curtain airbags, knee airbags, seatbelt pretensioners, seatbelt load limiters, etc. have been introduced into the vehicle fleet. Nevertheless, according to the Center for Disease Control and Prevention, prevalence for TBI has increased in the past decade, and more than 50% of TBI related deaths were due to MVC. Therefore, more work has been needed to reduce TBI related injuries and deaths associated with motor vehicle traffic accidents.

Takhounts et al. 2013 explained the possible root causes for TBI being among the most frequent injury and death related to MVC: the current regulated testing protocols may not represent real world crash scenarios associated with TBI injuries; the Anthropomorphic Test Device (ATDs) used in the lab tests may not represent the human responses to crash loadings; and the current injury assessment methods may not represent the injury mechanism with TBI at

the organ and tissue level. The industry has been working diligently to address this issue. To improve the regulated testing protocol, small overlap and oblique vehicle crash test configurations were extensively investigated by NHTSA and IIHS. The newly developed THOR dummy significantly improves bio-fidelity compared to the Hybrid-III dummy, which is the current test standard. The Brain Injury Criteria (BrIC), a head rotational velocity-based injury measure for TBI, was recently proposed [Takhounts et al. 2013] as a compliment to the existing translational acceleration-based HIC, which mainly acounts for contact-induced brain injury.

In development of BrIC, Takhaunts et al. used a series of linear impactor tests for the head-neck complex from the Hybrid III 50th male and 5th female dummies, THOR 50th male dummy, ES-2re, SID-IIs, WorldSID 50th Male and 5$^{th}$ Female, and 223 NCAP and frontal offset tests with 7 ATDs, in combination with simulation analysis using the two human head FE models (Simon and GHBMC), which were validated against various human brain response datasets, to develop correlation between BrIC for all ATDs and the human TBI risks estimation with the human head models. The head kinematics, including linear and angular accelerations measured from the dummy, were directly applied as the loading conditions to the human head FE models to calculate the brain tissue deformation. Such an approach for developing the TBI risks vs. BrIC relationship potentially over-looked or inaccurately estimated possible differences between the dummy-human kinematics responding to different crash conditions, and the dummy-human interactive forces with the restraint system (seatbelt and airbags), especially for the head-neck complex. These differences might significantly affect the TBI risk estimation with the human head models. To better understand and quantify the dummy-human kinematics difference, we were motivated to conduct further investigation at the system level using physical THOR sled test data and a reliable full body human model.

Two main tools were employed to conduct this study. First, FE models developed as part of the NHTSA-funded Advanced Adaptive Restraints Program (AARP) were utilized. In this research, the influence of multiple system variables on the baseline restraint system performance were investigated, such as the crash pulse severity in full frontal and oblique loading directions, different occupant sizes, positions and postures, and restraint configurations [Cyliax et al. 2015]. Dozens of AARP sled tests using the THOR Mod Kit dummy under different impact conditions were performed. For each of the baseline THOR sled tests, a sled system FE model was constructed and correlated. The THOR sled tests with the advanced adaptive restraint system (AARS) were simulated, and the AARS system models were verified by conducting sled tests. The second tool employed was an in-house mid-sized male human body FE model (TKHM) [Zhao et. al. 2007, Zhang et al. 2013].

The objectives of this study were:

1) To obtain a better understanding of the THOR 50$^{th}$percentile male dummy and human 50$^{th}$percentile male occupant kinematics and responses under the AARP sled test conditions, and how the kinematics differences between the human occupant and the ATD affect the brain injury prediction.
2) To investigate the correlation between the BrIC values resulting from the AARP sled test cases with the THOR dummy and the and the TBI risks estimated with the full body human model in the same AARP sled test cases.

## METHODS

The current study took several steps to accomplish. First, a set of AARP sled tests for the driver male 50$^{th}$percentile THOR dummy using various sled test pulses and ATD positions/postures and the restraint configurations were performed and analyzed. Second, for each of the THOR test cases, a correlated driver sled system FE model was developed. Third, the THOR sled test model was replaced with a validated human full body model, and the sled test with the human model was simulated for the same test conditions. Finally, the human model results were analyzed to estimate the tissue level human brain injuries. Correlations between the measured BrIC from the AARP THOR sled tests and the CSDM or MPS based TBI risks from the whole human body models were investigated.

### AARP THOR Sled Tests

For this study, eleven driver-side sled tests using the THOR Mod Kit dummy from the AARP were selected. In selecting the tests, the following considerations were made: 1) the measured THOR BrIC values, which were calculated using Eq. (1) [Takhounts et al. 2013], covered a wide range; 2) the corresponding sled system FE model correlated well to the corresponding sled test. Table 1 lists the selected driver THOR sled tests and the measured HIC and BrIC values, with the "soft" pulse representing a 35mph crash of an average mid-sized passenger car in the current fleet, the "hard pulse" representing a 35mph crash of a sub-compact car, 0 degree sled representing the full frontal crashes, and the left 15 degree angled sled simulating for the oblique crashes. In all the sled tests in Table 1, the THOR dummy was seated in the mid-track seat position, with a "normal" posture (as per the FMVSS-208 seating protocol), or a "forward leaning" posture. From the tests, the BrIC values ranged from 0.46 to 1.89, and the HIC ranged from 116 to 547.

$$BrIC = \sqrt{\left(\frac{\omega_x}{\omega_{xC}}\right)^2 + \left(\frac{\omega_y}{\omega_{yC}}\right)^2 + \left(\frac{\omega_z}{\omega_{zC}}\right)^2} \qquad \begin{matrix}\omega_{xC} = 66.25 \\ \omega_{yC} = 56.45 \\ \omega_{zC} = 42.87\end{matrix} \qquad \textbf{(1)}$$

$\omega_x, \omega_y, \omega_z$: *maxmum of absolute angular velocities*

***Table 1. AARP sled tests selected for this study (Seatbelt: SB, Driver Airbag: DAB, Curtain Airbag: CAB, Knee Airbag: KAB)***

| Test Number | Sled Pulse | Sled Angle [deg] | Driver posture | Restraint System | BrIC | HIC15 |
|---|---|---|---|---|---|---|
| BDSJ0141 | Soft | 0 (Full-Frontal) | Normal | SB, DAB, KAB | 0.59 | 232 |
| BDSK0372 | Soft | | Normal | SB, DAB, KAB | 0.46 | 185 |
| BDSJ0179 | Hard | | Normal | SB, DAB, KAB | 0.80 | 301 |
| BDSK0066 | Hard | | Normal | SB, DAB, KAB | 0.63 | 311 |
| BDSK0108 | Hard | | Normal | SB, DAB, KAB | 0.68 | 283 |
| BDSK0297 | Hard | | Normal | SB, DAB, KAB | 0.62 | 226 |
| BDSJ0173 | Soft | | Forward leaning | SB, DAB, KAB | 0.49 | 116 |
| BDSJ0180 | Hard | Left-15 (Oblique) | Normal | SB, DAB, KAB | 1.74 | 400 |
| BDSK0109 | Hard | | Normal | SB, DAB, KAB, CAB | 1.54 | 547 |
| BDSK0124 | Hard | | Normal | SB, DAB, KAB, CAB | 1.89 | 326 |
| BDSK0341 | Hard | | Normal | SB, DAB, KAB, CAB | 1.13 | 237 |

**AARP THOR Sled System Model**

For each of the sled tests in Table 1, a FE system model was built with Ls-dyna 971 v6.1.2 (LSTC, Livermore, CA), and was validated at both the component level and the system level.

At the component level, all the restraint components used in the AARP driver system, including the baseline and adaptive driver airbags, knee airbag, curtain airbag, the baseline and adaptive seat belt, steering wheel and column were tested, and the FE models representing these components were validated with various impact tests. The THOR dummy model (V2.0beta, NHTSA) was updated and validated with the certification tests and the AARP sled tests [Zhao et al. 2015].

The validated component models were integrated into the AARP driver sled system models. For each of the driver THOR sled tests in Table 1, a system model was set up per the test configuration and the sled test simulation was conducted. The system model was then validated with the sled test data. Correlations were made for the dummy kinematics, the time-histories of the dummy measurements, and the injury measures between the test and the model. Quality of the correlations were accessed with the same methods and criteria developed for evaluation of the THOR Mod Kit dummy model system performance [Zhao et al. 2015]. Appendix-A (Figures A-1 through A-11) show the correlations of the accelerations of the head CG, chest CG, pelvis CG, and the head rotational velocities for all the cases in Table 1.

**Full Body Human Model**

The Takata Human Model (TKHM) version v5.3 was developed and used for this study. The model is a combination of the main body (excluding the head) of the TKHM version v4.3 and the same GHBMC (Global Human Body Model Consortium) head model v3.5 used in the BrIC study [Takhounts, 2013]. Prior to this study, the TKHM v4.3 model was extensively validated at component and full body levels [Zhao, 2007, Zhang, 2013], and the GHBMC head model [Mao, 2013] was correlated to PMHS intracranial pressure data [Nahum et al, 1977 and Trosseille et al 1992], brain motion tests [Hardy et al. 2001, 2007], and facial bone impact data [Nyquist et al. 1986, Allsop et al. 1988].

In this study, additional validations were made for the integrated neck-head assembly responses at both segment and full head-neck assembly levels to assure the biofidelity of the head-neck complex model.

At the cervical spine segment level, simulations were made for the motion segments of C1-C2 and C2-C3 in extension, flexion, lateral-bending, and torsion loadings at a maximum rotational speed of 0.00873 rad/sec

achieved at 36 msec. Figure B-1 (Appendix-B) shows the model predicted motion segment stiffness of C1-C2 and C2-C3 in extension, flexion, lateral-bending, and torsion compared to the test data [Ashton-Miller et al. 1997]. It is seen that the model predicted stiffness for the simulated loading cases were within the test data corridors.
At the neck-head assembly level, five PMHS test configurations [Wismans et al. 1986, Thunnissen et al. 1995, Davidsson et al. 1998, Hynd et al. 2007, Deng 1999] used for the GHBMC neck model validations were simulated with the updated head-neck assembly model. Figure B-2 (Appendix-B) shows the model predicted full head-neck complex responses to extension, flexion, lateral-bending, and torsion compared to the test data. It is seen that the model responses of these validation cases are within or close to the test data corridors or targets.
The integrated full body model v5.3 was further validated for the whole body responses in the PMHS sled tests performed at UVA [Kent et al. 2006]. The PMHS driver sled test for the test subjects #533, #544, #546 was simulated. Figure B-3 shows the correlation of the traces of histories of the head CG, T1, chest CG, and pelvis CG between the human body model and the test data. The human model kinematics responding to the sled test conditions was close to the PMHS in the test.

**AARP Sled Tests Simulations with Full Body Human Model**

Case by case the AARP sled models were updated by replacing the Thor dummy model with the full body human model. The same H-point and pelvis angle of THOR dummy positioning were used to position the human model. The head CG, knee centers, and ankle positions were further verified to have matched the two positions. The seat foam was fit using a positioning simulation, and the seat belts were re-routed across the human model torso. The contacts were defined between restraints, seat, environment and the human body. All the other system parameters for the THOR sled models were kept the same for the human sled model.
Sled simulations with the human body model were conducted for all corresponding THOR sled tests in Table 1. Occupant kinematics among the physical THOR sled test, the numerical THOR sled test, and the numerical sled test with the human body sled model were compared. The time-histories of head CG, T1, chest CG, and pelvis CG outputs were correlated.

**Development of Correlation between THOR BrIC and Brain Tissue Criteria (MPS and CSDM)**

From the human model sled test simulation results for each test case, the CSDM and MPS were calculated from the deformation of the brain tissue elements. The MPS and CSDM based risks of AIS 4+ TBI injuries ($P_{human,MPS}$, $P_{human,CSDM}$) were calculated according to Takhounts et al, 2013 by Eq. (2) and (3) respectively.
From the THOR sled test results, the BrIC based risks of AIS 4+ TBI injuries corresponding to the MPS and CSDM measures ($P_{THOR,MPS}$, $P_{THOR,CSDM}$) were calculated by Eq. (4) and (5) [Takhounts et al., 2013] respectively. Each pair of the risks ($P_{human,MPS}$ vs. $P_{THOR,MPS}$, and $P_{human,CSDM}$ vs. $P_{THOR,CSDM}$) were compared with linear curve regression and paired student t-tests using Excel Data Analysis ToolPak (Microsoft Office 2010, Redmond, WA).

$$P_{human,MPS}(AIS\ 4) = 1 - exp\left(-\frac{MPS}{1.010}\right)^{2.84} \quad \textbf{(2)}$$

$$P_{human,CSDM}(AIS\ 4) = 1 - exp\left(-\frac{CSDM}{0.600}\right)^{1.8} \quad \textbf{(3)}$$

$$P_{THOR,MPS}(AIS\ 4) = 1 - exp\left(-\frac{BrIC}{1.204}\right)^{2.84} \quad \textbf{(4)}$$

$$P_{THOR,CSDM}(AIS\ 4) = 1 - exp\left(-\frac{BrIC-0.523}{0.647}\right)^{1.8} \quad \textbf{(5)}$$

## RESULTS

### Kinematics Analysis

For all the cases in Table 1, the video camera views in the THOR tests and the screenshots of the animation in the full body human model simulations were compared. Furthermore, the correlations of the time histories of accelerations of the head CG, the chest CG, and the pelvis CG and the head rotational velocities (Appendix-A) were also processed for quantitative comparison of the kinematics. It was seen that in all the full frontal test cases, the kinematics of the THOR model were similar to the human model, while in all the oblique cases, the kinematics of the THOR and the human model were different. As two examples, Figure 1.a and Figure 1.b show the kinematics comparisons for the full frontal test case BDSJ0179 and the oblique case BDSK0124 respectively. Figure 2.a and Figure 2.b compare the head angular displacements between the THOR sled test and the human model sled simulation for the two cases BDSJ0179 and BDSK0124 respectively. Taking the oblique test case BDSK0124 as an example, until the head-airbag contact at about 60 ms, both the drivers moved forward and outboard to the left at about the same speed. After the contact, the THOR head and neck twisted more to the right (inboard) at a higher rotational velocity compared to the human model head.

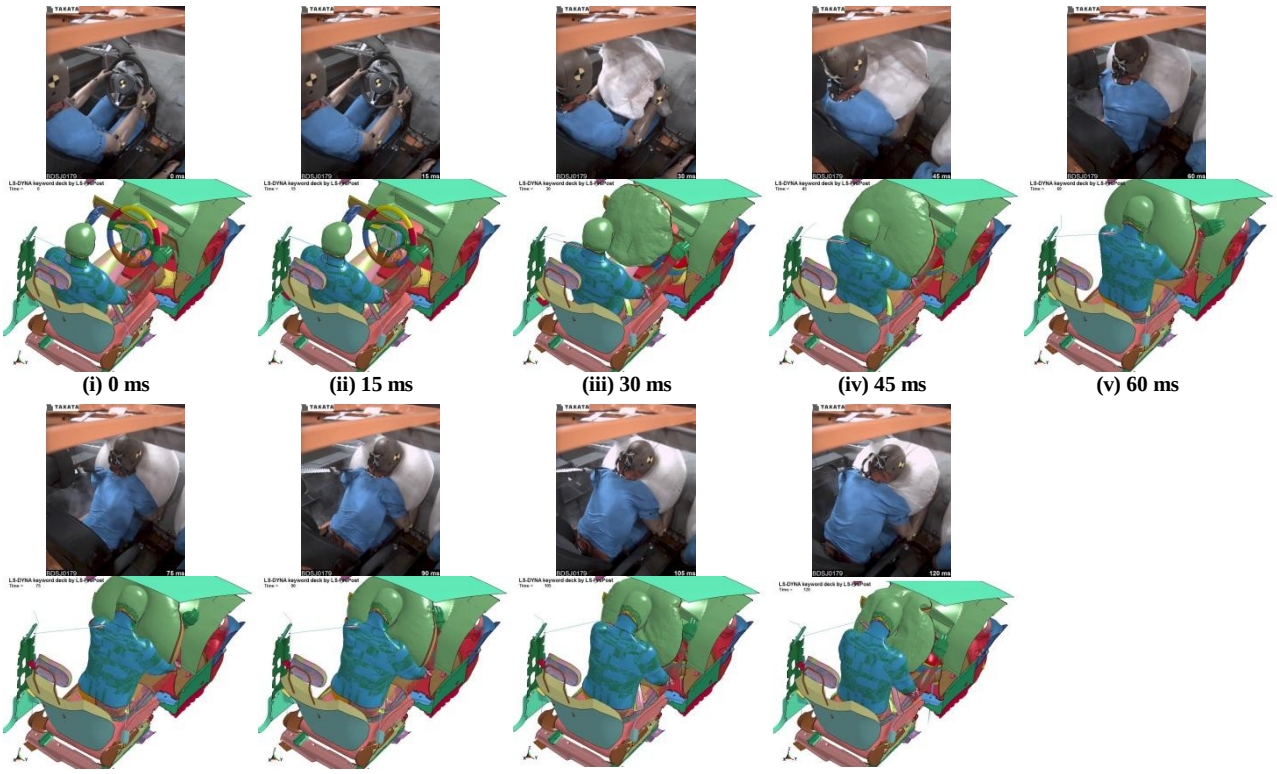

**(i) 0 ms** **(ii) 15 ms** **(iii) 30 ms** **(iv) 45 ms** **(v) 60 ms**

**(vi) 75 ms** **(vii) 90 ms** **(viii) 105 ms** **(ix) 120 ms**

**(a) Full Frontal Hard Pulse (BDSJ0179)**

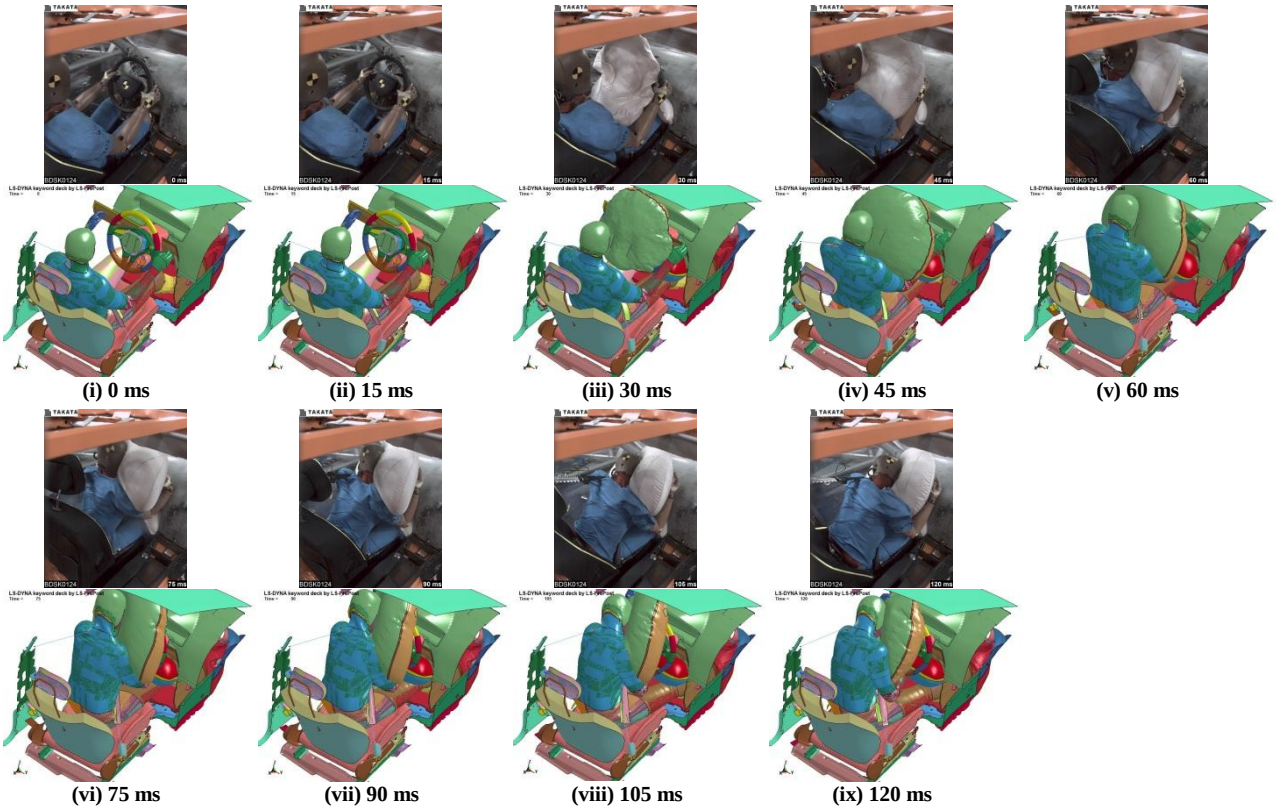

(i) 0 ms (ii) 15 ms (iii) 30 ms (iv) 45 ms (v) 60 ms

(vi) 75 ms (vii) 90 ms (viii) 105 ms (ix) 120 ms

**(b) Oblique Hard Pulse (BDSK0124)**

***Figure 1. Comparison of the kinematics between the video camera views in the THOR sled test and the screenshots of animation in the same sled test with the full body human model***

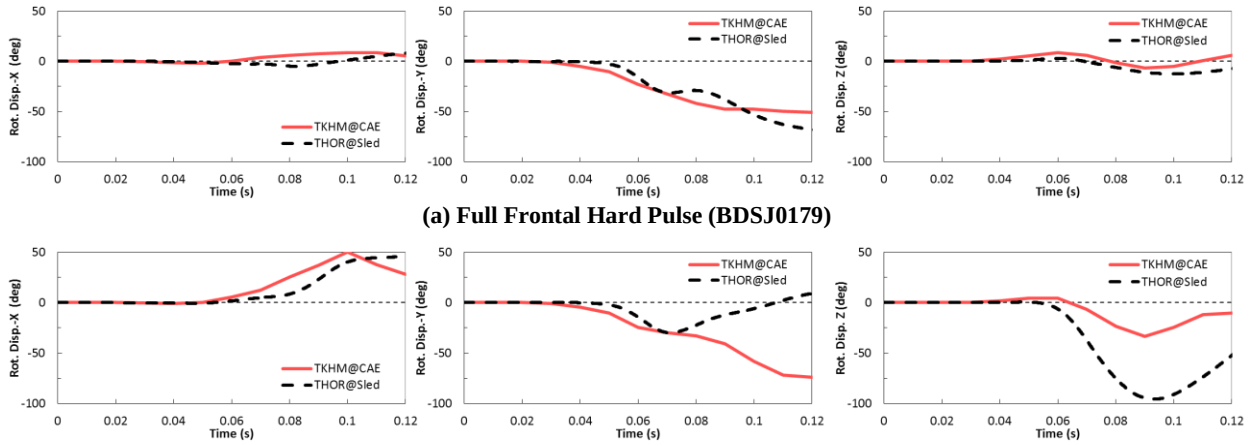


**(a) Full Frontal Hard Pulse (BDSJ0179)**

**b) Oblique Hard Pulse (BDSK0124)**

***Figure 2. Comparison of the head angular displacements between the THOR sled test and the human model sled simulation. The dashed black curves were from the THOR, and the solid red lines were from the human model.***

Figure 3.a and 3.b compare the head-airbag interaction forces of x-, y-, z- components between the THOR sled test simulation and the human model sled simulation for the two cases BDSJ0179 and BDSK0124 respectively. It was seen that in the full frontal case, the human head experienced the higher x- (longitudinal) force from the driver airbag than the THOR, while in the oblique case, the human head experienced the less y- (lateral) force than the THOR before 100 msec and got the higher force after that.

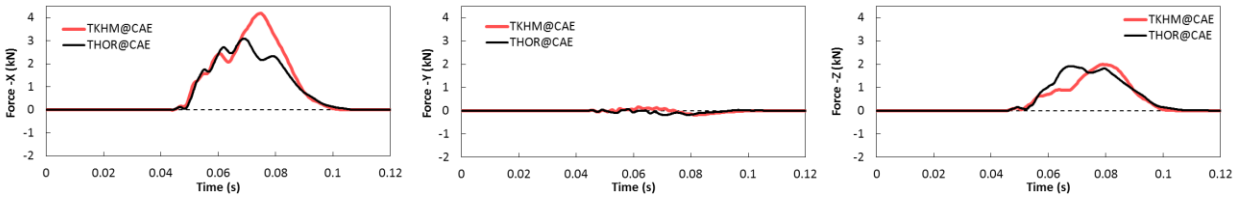


**(a) Full Frontal Hard Pulse (BDSJ0179)**

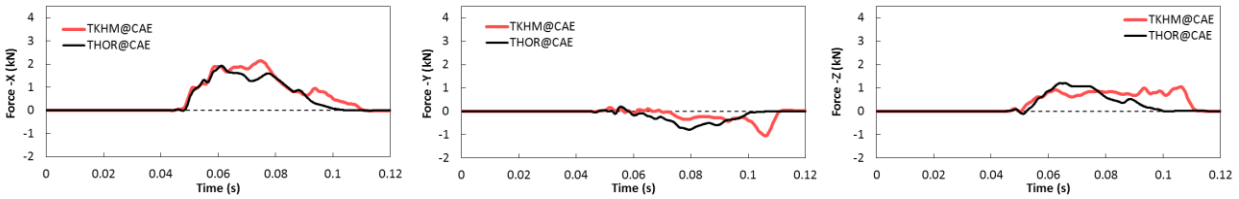


**b) Oblique Hard Pulse (BDSK0124)**

***Figure 3. Comparison of the head-airbag contact forces between the THOR sled simulation and the human model sled simulation.***

### BrIC Values of THOR and Human Model

The BrIC obtained from the human model sled test simulations were compared to the THOR BrIC measured from the tests. Figure 4 depicts the correlation between these two groups of BrIC values. In Figure 4, all the THOR BrIC values of less than 0.8 were from the full frontal cases, and all the others above 0.8 were the oblique cases. It is seen that the BrIC from the human model were similar to the THOR in the full frontal group, but were much lower than the THOR in the oblique group.

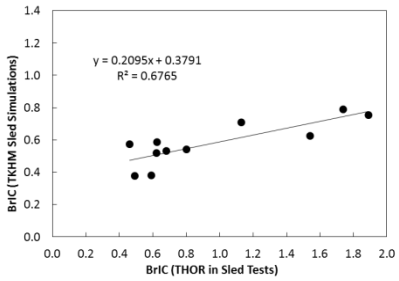


***Figure 4. Comparison of BrIC between from the physical THOR sled tests and from the numerical sled tests with the full body human model***

The bigger difference of the THOR BrIC values compared to the human head in the oblique cases was mainly due to the head Z-rotational velocity difference. Figure 5 compares the differences of the maximum of absolute head x-, y-, and z- angular velocities of the human model outputs subtracted by those of the THOR tests. It is seen that in the full frontal group such differences were small, while in the oblique cases, the z- angular velocities of the THOR were much higher than the human model, which were consistent with the kinematics difference analyzed above.

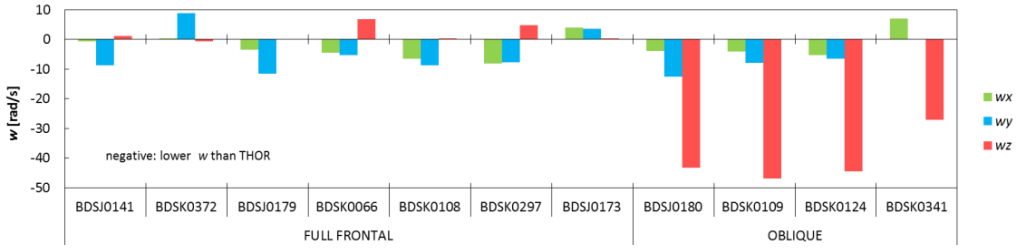


***Figure 5. Differences of the maximum of absolute head angular velocities of the human model outputs subtracted by those of the THOR sled tests***

**AIS 4+ TBI Risks**

Figure 6.a and 6.b respectively show the correlation between the pair of the TBI AIS 4+ risks ($P_{human,MPS}$ vs. $P_{THOR,MPS}$, and $P_{human,CSDM}$ vs. $P_{THOR,CSDM}$), where $P_{human,MPS}$ and $P_{THOR,MPS}$ are the MPS based risk from the human body model and the THOR BrIC measured from the sled tests respectively, and $P_{human,CSDM}$ and $P_{THOR,CSDM}$ are the CSDM based risk from the two respectively. Overall good correlations of each pair of these two were observed, with the correlation coefficient $R^2$ score of 0.85 for the MPS based risks and 0.81 for the CSDM based risks.

**(a) MPS** **(b) CSDM**

***Figure 6. Comparison of AIS 4+ TBI risks between from the physical THOR sled tests and from the sled simulations with full body human model***

**DISCUSSIONS**

**Kinematics Difference between THOR and Human Model**

The results of this study indicated that in all the oblique sled cases occupant kinematics differences in the head rotation between the human body model and the THOR were mainly due to the Z-rotation difference, One cause for such a difference was due to the less y- (lateral) airbag force applied to the human head than that to the THOR, as shown in Figure 3.b. Another cause could be the occupant head-neck models' torsional response to the impacts. To quantify the occupant head-neck models' torsional characteristics, additional numerical simulations for the quasi-static and dynamic loadings were performed for both the THOR and the human models.

The quasi-static loading cases per the Duke University study [Parent, 2015] were set up for the THOR Mod Kit head-neck assembly model, the human head-neck model (TKHMv5.3), and the GHBMC head-neck model (GHBMCv4.0), respectively, where the GHBMC head-neck model was taken as a reference for the comparison. Figure 7.a shows the simulation results of the torsional response of the THOR model and the two human models (TKHMv5.3 & GHBMCv4.0), compared to the Duke University PMHS tests data set [Parent, 2015]. It is seen that the torsional moments of T1 at the rotation angle of 63 degree of the THOR model, TKHMv5.3 and GHBMCv4.0 were in the corridors of the tests. The two human models' responses were very close and they all were lower than that of the THOR. The nonlinearities of the torsional stiffness were different between the dummy and human models. While the rotational moment at T1 of THOR increases almost linearly with the head rotation, the T1 moments of the human models were lower at the early stage of the rotation and increased nonlinearly.

Virtual linear impactor tests were set up for the THOR head-neck assembly model, the human head-neck model (TKHMv5.3), and the GHBMC head-neck model (GHBMCv4.0) respectively, in which a rigid cylinder with 43 mm diameter and a 5 kg mass laterally impacted the jaw of the head at an impact speed of 5 m/s. The T1 and below of each of the three head-neck assembly models in the test setup were constrained as fixed. Figure 6.b shows the simulation results of the torsional responses of the THOR model and the two human models to such an impact condition. Notably, the THOR rotational response (velocity and displacement) was approximately twice that of the human models under the same dynamic loading. These studies suggested that although the torsional stiffness of the human head-neck models was lower than the THOR under quasi-static loading, under dynamic loading, the THOR head-neck rotated more easily compared to the human model. Such

torsional characteristic differences between the THOR and the human head-neck could be a major cause of the occupant kinematics differences observed in the oblique sled cases.
Currently there is no published PMHS test data in this simulated dynamic loading. The simulated human model behaviors could be validated if such test data were available.

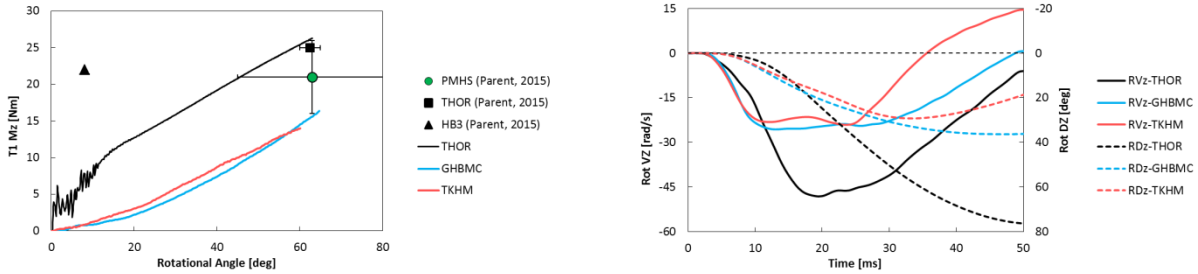


**(a) Quasi-Static loading** **(b) Dynamic impact**

***Figure 7. Torsional responses of the THOR model, and the human models (TKHM & GHBMC) to the quasi-static and dynamic loadings***

**AIS 4+ TBI Risk Estimation Difference between THOR and Human Model**

This study indicated that in all the full frontal sled test cases, the TBI 4+ risks estimated from Takhounts' risk function with the THOR BrIC from the sled tests were close to the MPS or CSDM based TBI 4+ risks from the human model. However, in all the oblique sled test cases, the THOR BrIC derived TBI 4+ risks were higher than those from the human model, which could be mainly due to the head-neck torsional characteristic difference discussed in the prior section.

**Limitations of this Study**

This study used a system simulation approach which requires high quality validated sled test models for the THOR as well as for the human body. In this study, the THOR sled models for all the test cases were well or fairly correlated with the test data. However, the corresponding human sled test models were not validated directly with PMHS sled tests since such data do not exist. The calculated CSDM and MPS values from the human model, which affect significantly the TBI injury risks outcomes, could be further verified.
This study observed significant head-neck torsional kinematic differences between the THOR and the human model in all the oblique sled test cases. The simulated face-jaw linear impactor tests for the THOR and the PMHS indicated that the THOR-human head-neck torsional characteristic differences under the dynamic impact condition could be a major cause. Compared to the THOR, the human head-neck has a lower torsional stiffness under quasi-static loading, exhibits a stiffer torsional response compared to the THOR under dynamic loading. These findings need verification to corresponding PMHS tests using the same face-jaw linear impactor test protocol.
Finally, this study used a relatively small sample size. More data points could provide further insight into the BrIC response with the THOR ATD.

**CONCLUSIONS**

A systematic method to use THOR sled tests and a full body human model to assess TBI risks was developed. This study confirmed that the BrIC from the THOR sled tests is a statistically significant indicator or measure for AIS 4+ TBI risk.
In the full frontal sled test cases, the occupant kinematics and the TBI 4+ injury risks between the THOR and the human model were similar.
In the oblique sled test cases, the BrIC and the AIS 4+ TBI injury risk from the THOR were higher than those estimated from the human model, which indicates the TBI risk in oblique crash scenarios using THOR could be over-estimated. This difference is possibly due to the observed difference of the head-neck rotational responses under dynamic torsional impact between the THOR and the human model. The dynamic impactor simulations indicate the human model head-neck exhibits a stiffer torsional response compared to the THOR.

**ACKNOWLEDGEMENTS**

The AARP project was funded by NHTSA Contract #DTNH22-12-C-00266. The authors greatly appreciate the support from NHTSA, especially James Saunders, Stephen Summers, and Dan Parent.

**REFERENCES**

Allsop, DL., Warner, CY., Wille, MG., Schneider, DC., Nahum, AM., 1988, "Facial Impact Response – A Comparison of the Hybrid III Dummy and Human Cadaver", In Proc. 32nd Stapp Car Crash Conference, SAE Paper No. 881719.

Ashton-Miller JA., and Schultz, AB. 1997. "Biomechanics of the Human Spine", Basic Orthopaedic Biomechanics, 2nd ed.

Cyliax, B., Scavnicky, M., Mueller, I., Zhao, J., and Aoki, H. 2015. "Advanced Adaptive Restraints Program Individualization of Occupant Safety Systems", SAE 2015 Government/Industry Meeting, Washington, DC.

Davidsson, J., Deutscher, C., Hell, W., Linder, A., Lovsund, P., Svensson, M., et al., 1998, "Human Volunteer Kinematics in Rear-end Sled Collisions", In Proc. IRCOBI conference, 289-301

Deng, B., 1999 "Kinematics of human cadaver cervical spine during low speed rear end impacts", PhD Thesis, Wayne State University.

Hardy, WN., Foster, C., Mason, M., Yang, K., King, A., Tashman, S., 2001, "Investigation of Head Injury Mechanisms Using Neutral Density Technology and High-speed Biplanar X-ray", Stapp Car Crash Journal 45: 337-368.

Hardy, WN., Mason, MJ., Foster CD., Shah, CS., Kopacz, JM, Yang, K, King, A, Bishop, J., Bey, M., Anderst, W., Tashman, S., 2007, "A Study of the Response of the Human Cadaver Head to Impact", Stapp Car Crash Journal 51: 17-80.

Hynd, D, Svensson, M, Trosseille, X, van Ratingen, M., and Davidsson, J., 2007, "Dummy Requirements and Injury Criteria for a Low-speed Rear Impact Whiplash Dummy", European Enhanced Vehicle-Safety Committee, EEVC WG12 #505A.

Kent, R., Forman, J., et al., 2006, "Whole-body Kinematic and Dynamic Response of Restrained PMHS in Frontal Sled Tests", Stapp Car Crash Journal 50: 299-336.

Mao, H., Zhang, L., Jiang, B., et al., 2013, "Development of a Finite Element Human Head model Validated with Forty Nine Loading Cases from Experimental and Real World Impacts", J Biomech Eng. 135(11), Paper No: BIO-12-1302.

Nahum, AM., Smith, R., and Ward, CC., 1977, "Intracranial Pressure Dynamics During Head Impact", In Proc. 21st Stapp Car Crash Conference, SAE Paper No. 770922.

Nyquist, GW., Cavanaugh, JM., Goldberg, SJ, King, A., 1986, "Facial Impact Tolerance and Response", In Proc. 30th Stapp Car Crash Conference", SAE Paper No. 861896.

Parent, D., 2015, "NHTSA THOR Update", THOR Public Meeting, Washington, DC.

Takhounts, E., Craig, JC., Moorhouse, K., and McFadden, J., 2013, "Development of Brain injury Criteria (BrIC)", Stapp Car Crash Journal 57: 343-266.

Thunnissen, J., Wismans, J., Ewing, C., and Thomas, D., 1995, "Human Volunteer Head-Neck Response in Frontal Flexion: A New Analysis", SAE Paper No. 952721.

Trosseille, X., et al., 1992, "Development of a F.E.M. of the Human Head According to a Specific Test Protocol, In Proc. 36th Stapp Car Crash Conference, SAE Paper No. 922527.

Wismans, V., Oorschot, H., and Woltring, H., 1986, "Omni-Directional Human Head-Neck Response" SAE Paper No. 861893.

Zhang, N., Katagiri, M., and Zhao, J. 2014. "TBI Risk Assessment with AARP THOR Sled Tests and a Full Body Human Model." The 42th International Workshop on Human Subjects for Biomechanical Research.

Zhao, J., Zhang, N., and Hu J. 2015. "Implementation of THOR FE Model in AARP Project", NHTSA Public Meeting Concerning Test Device for Human Occupant Restraint, Washington, DC.

Zhao, J., Narwani, G. 2007. "Biomechanical Analysis of Hard Tissue Responses and Injuries with Finite Element Full Human Body Model." ESV 07-0354.

## APPENDIX A: AARP Sled Models Correlations

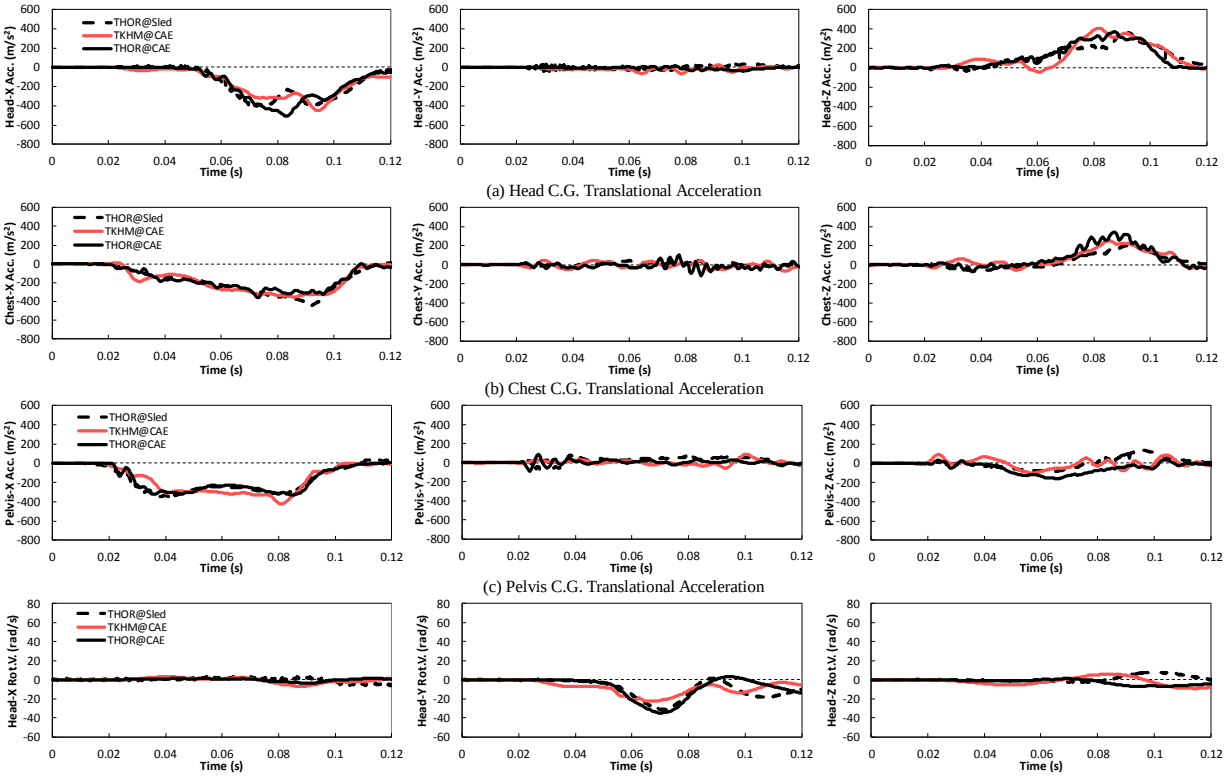


(a) Head C.G. Translational Acceleration

(b) Chest C.G. Translational Acceleration

(c) Pelvis C.G. Translational Acceleration

(d) Head C.G. Rotational Velocity

***Figure A-1. Full Frontal Soft Pulse (BDSJ0141)***

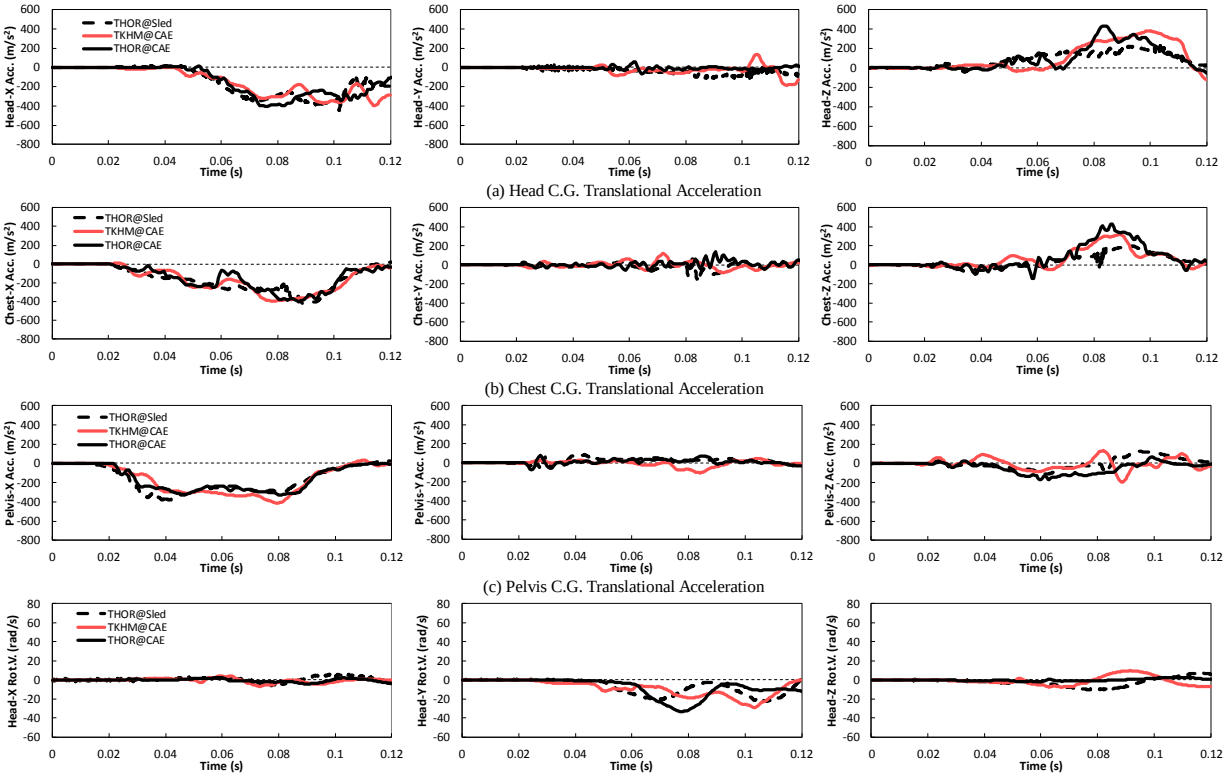


(a) Head C.G. Translational Acceleration

(b) Chest C.G. Translational Acceleration

(c) Pelvis C.G. Translational Acceleration

(d) Head C.G. Rotational Velocity

***Figure A-2. Full Frontal Soft Pulse with AARS (BDSK0372)***

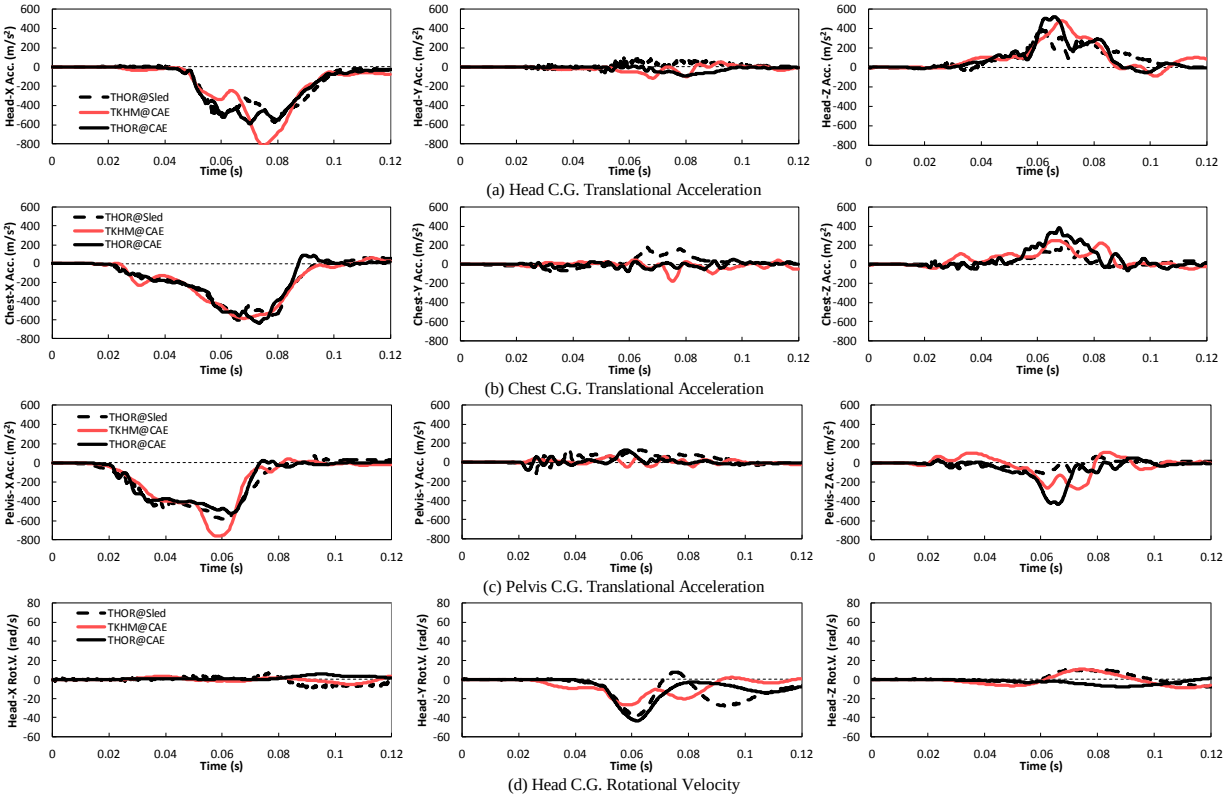


(a) Head C.G. Translational Acceleration

(b) Chest C.G. Translational Acceleration

(c) Pelvis C.G. Translational Acceleration

(d) Head C.G. Rotational Velocity

***Figure A-3. Full Frontal Hard Pulse (BDSJ0179)***

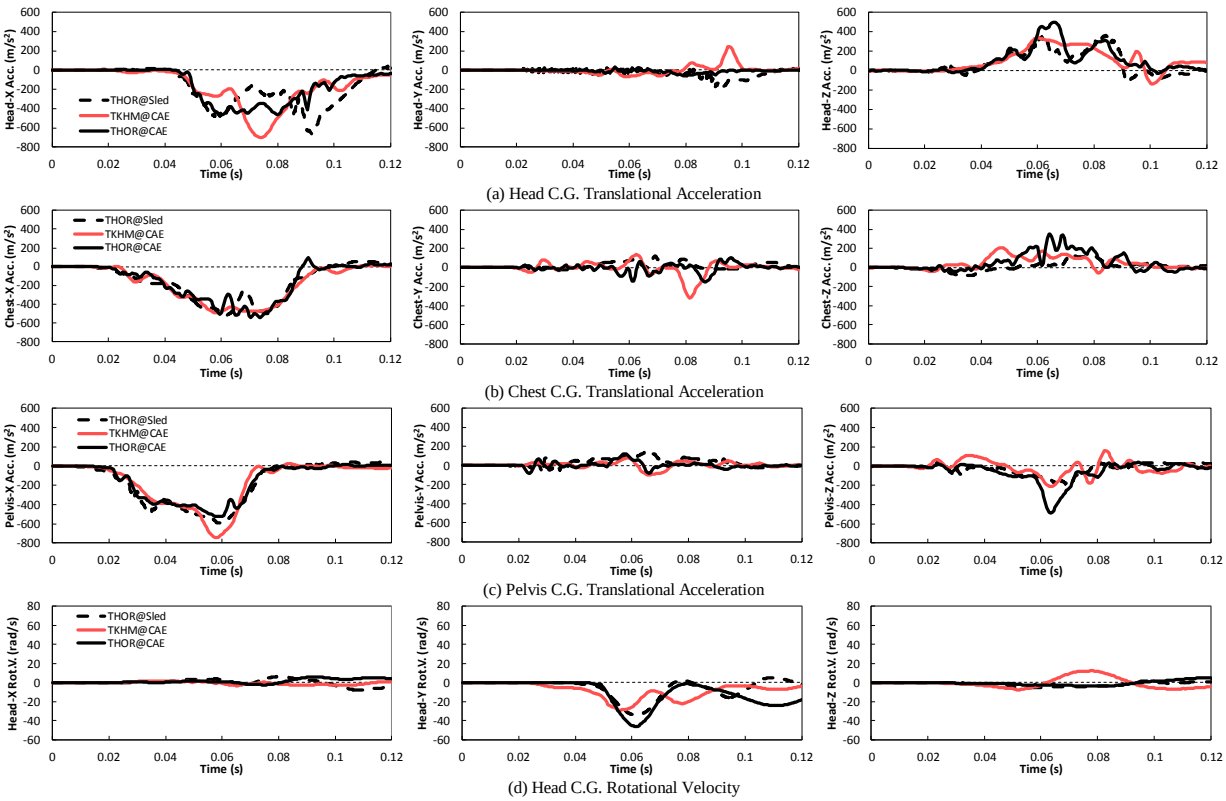


(a) Head C.G. Translational Acceleration

(b) Chest C.G. Translational Acceleration

(c) Pelvis C.G. Translational Acceleration

(d) Head C.G. Rotational Velocity

***Figure A-4. Full Frontal Hard Pulse with AARS (BDSK0066)***

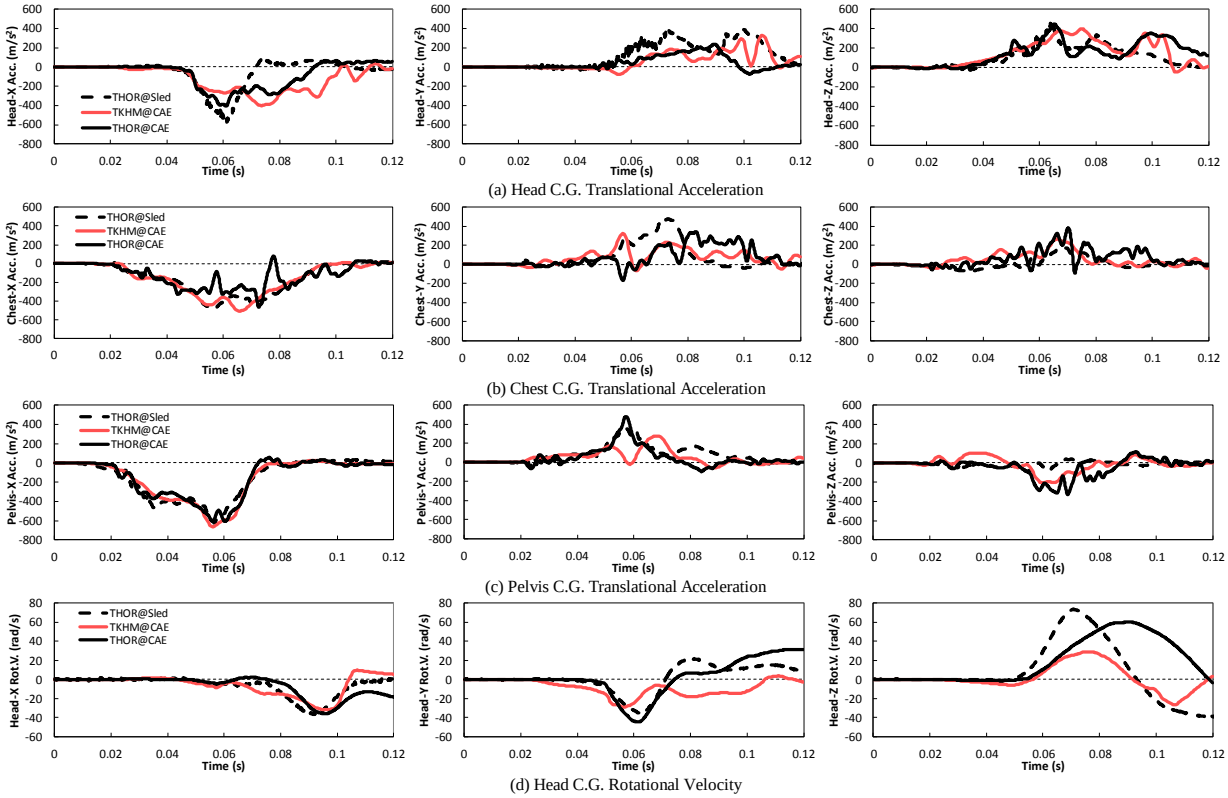


(a) Head C.G. Translational Acceleration

(b) Chest C.G. Translational Acceleration

(c) Pelvis C.G. Translational Acceleration

(d) Head C.G. Rotational Velocity

***Figure A-5. Full Frontal Hard Pulse with AARS (BDSK0108)***

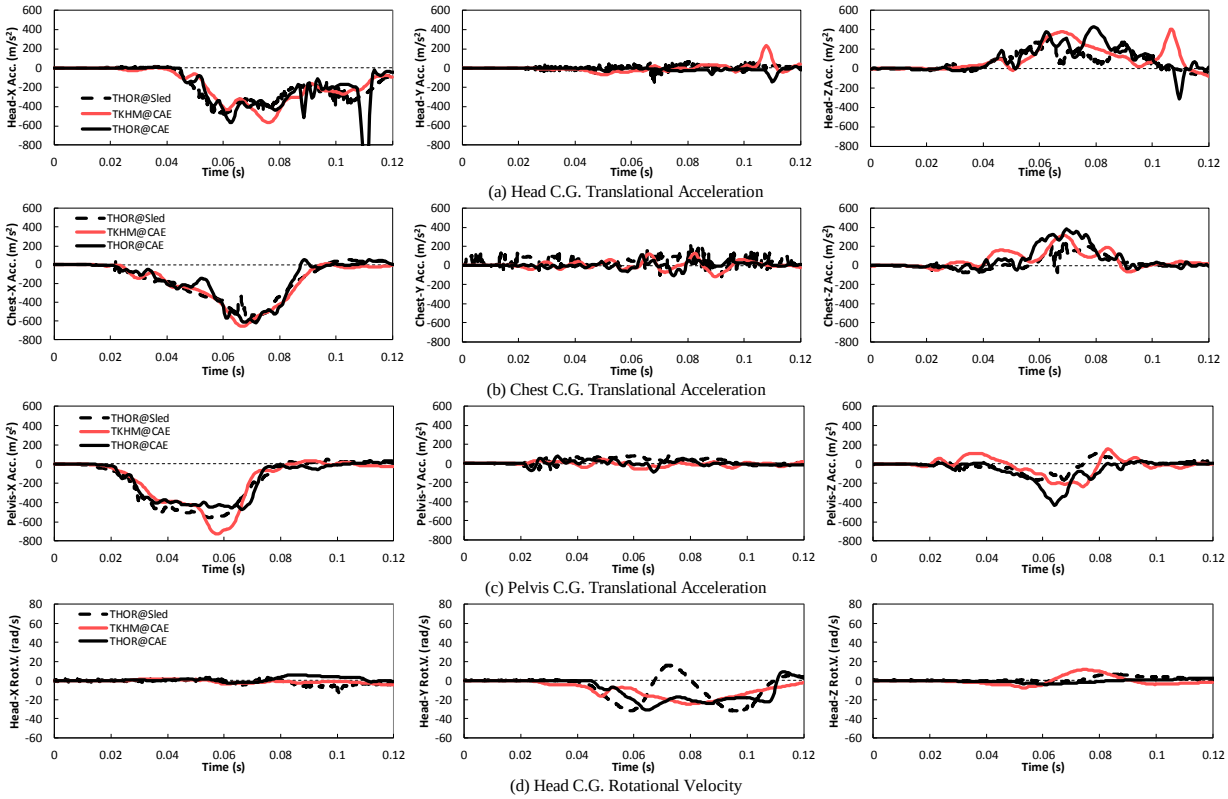


(a) Head C.G. Translational Acceleration

(b) Chest C.G. Translational Acceleration

(c) Pelvis C.G. Translational Acceleration

(d) Head C.G. Rotational Velocity

***Figure A-6. Full Frontal Hard Pulse with AARS (BDSK0297)***

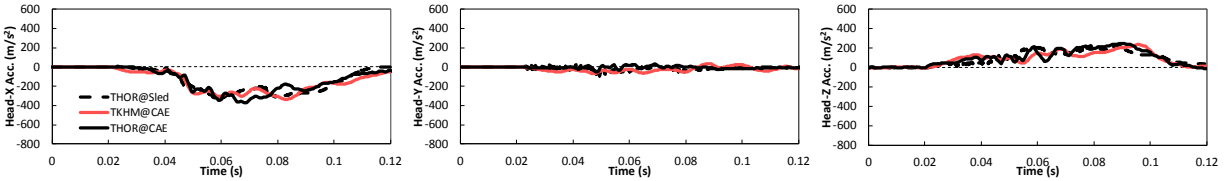


(a) Head C.G. Translational Acceleration

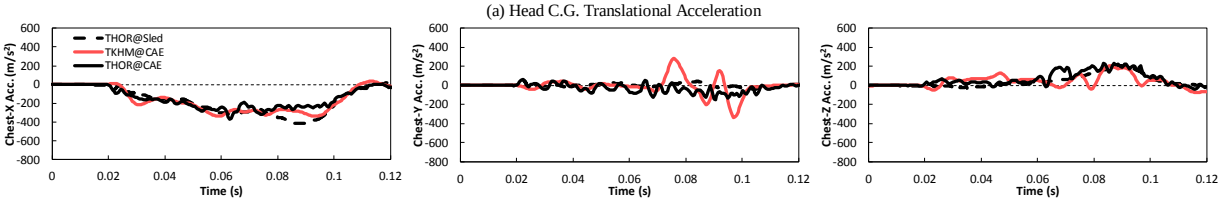


(b) Chest C.G. Translational Acceleration

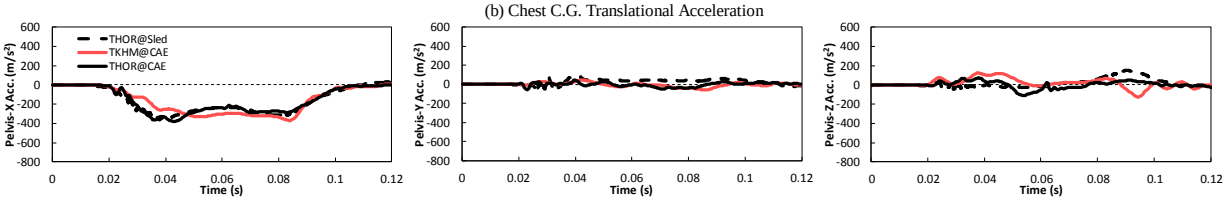


(c) Pelvis C.G. Translational Acceleration

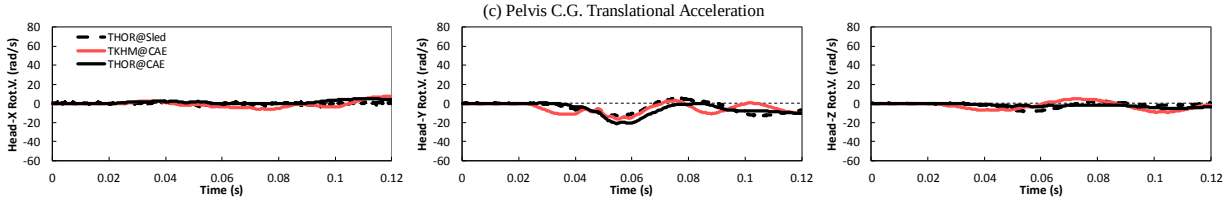


(d) Head C.G. Rotational Velocity

***Figure A-7 Full Frontal Soft Pulse in Forward Position (BDSJ0173)***

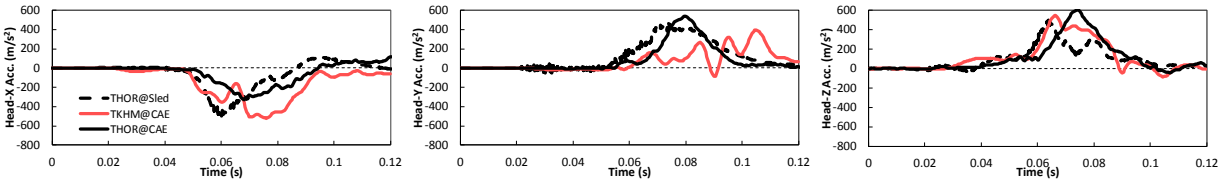


(a) Head C.G. Translational Acceleration

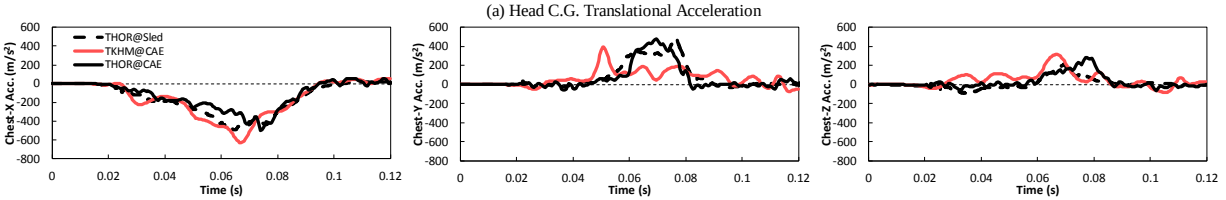


(b) Chest C.G. Translational Acceleration

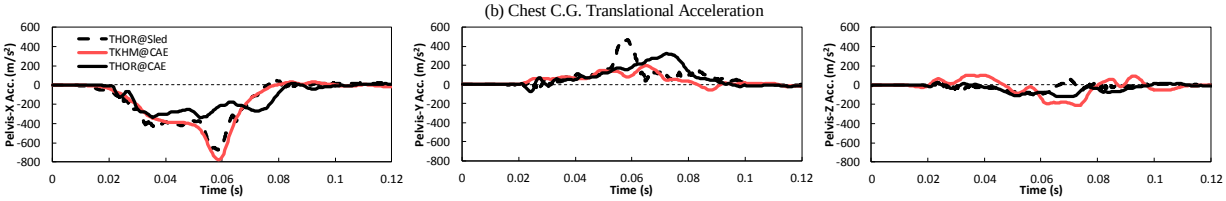


(c) Pelvis C.G. Translational Acceleration

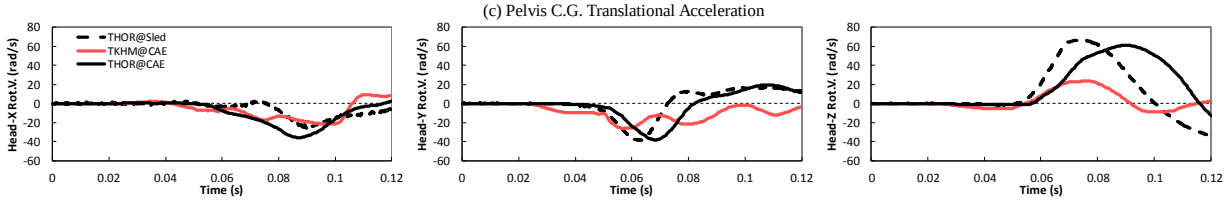


(d) Head C.G. Rotational Velocity

***Figure A-8. Oblique Hard Pulse (BDSJ0180)***

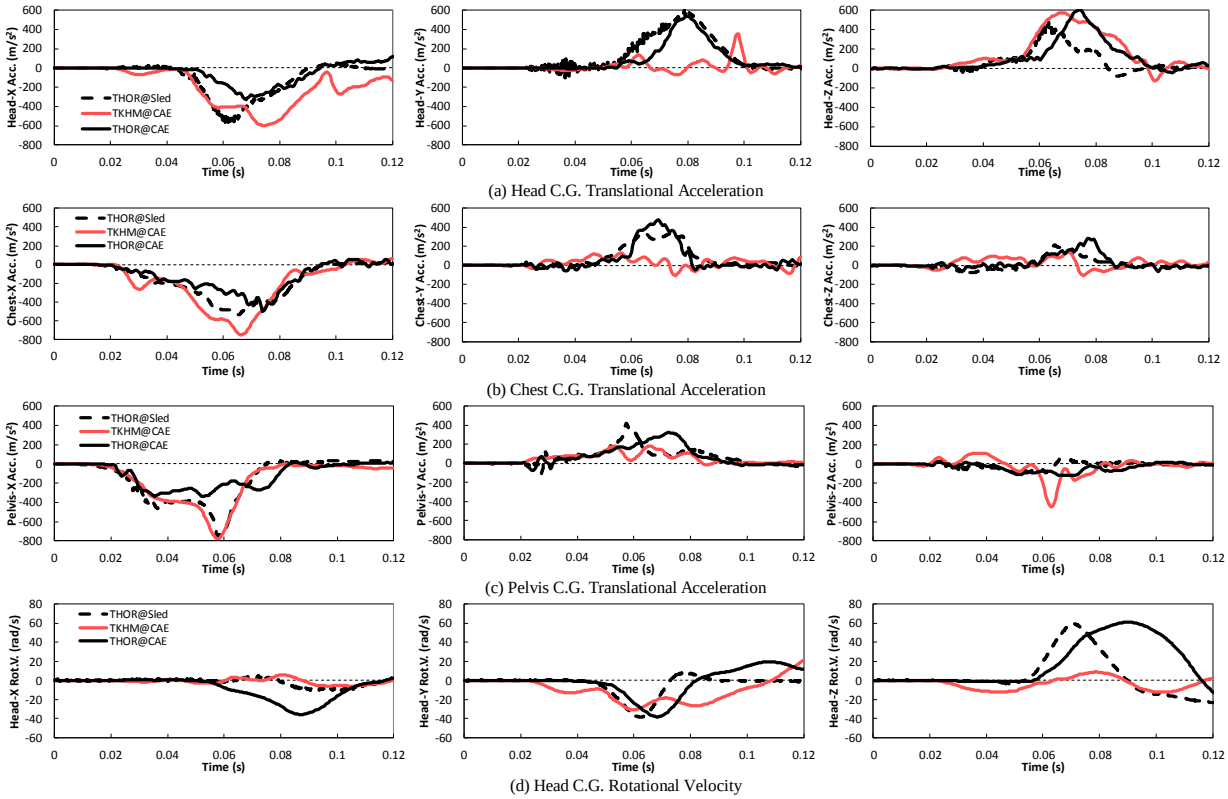


(a) Head C.G. Translational Acceleration

(b) Chest C.G. Translational Acceleration

(c) Pelvis C.G. Translational Acceleration

(d) Head C.G. Rotational Velocity

***Figure A-9. Oblique Hard Pulse with AARS (BDSK0109)***

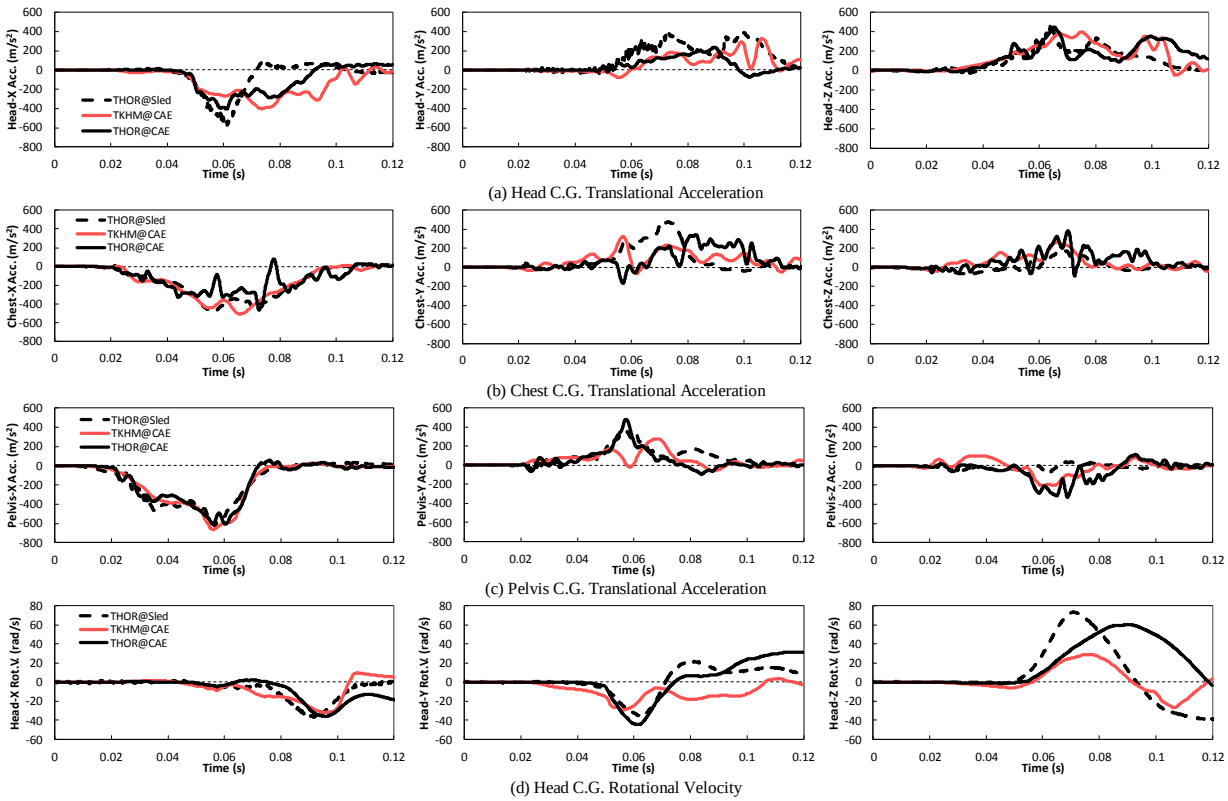


(a) Head C.G. Translational Acceleration

(b) Chest C.G. Translational Acceleration

(c) Pelvis C.G. Translational Acceleration

(d) Head C.G. Rotational Velocity

***Figure A-10. Oblique Hard Pulse with AARS (BDSK0124)***

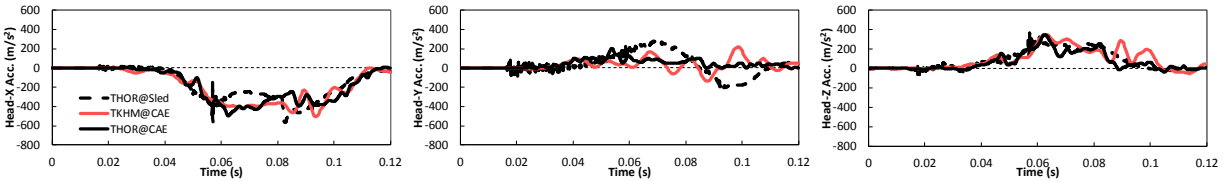


(a) Head C.G. Translational Acceleration

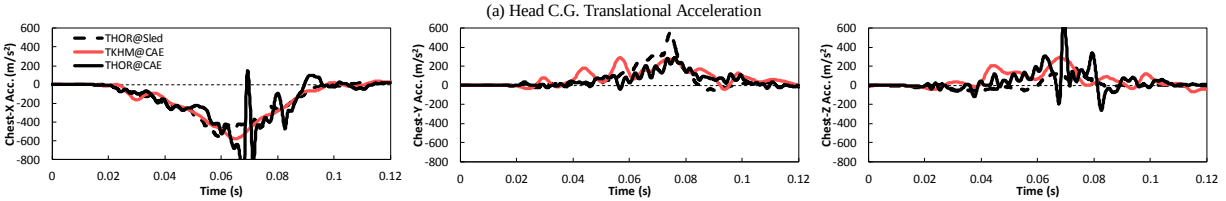


(b) Chest C.G. Translational Acceleration

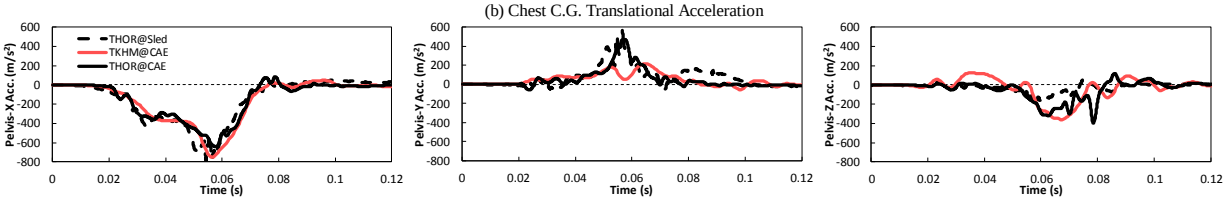


(c) Pelvis C.G. Translational Acceleration

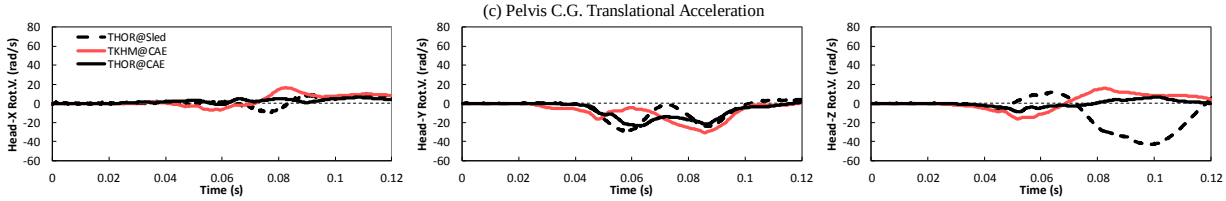


(d) Head C.G. Rotational Velocity

***Figure A-11. Oblique Hard Pulse with AARS (BDSK0341)***

## APPENDIX B: TKHM v.5.3 Validations

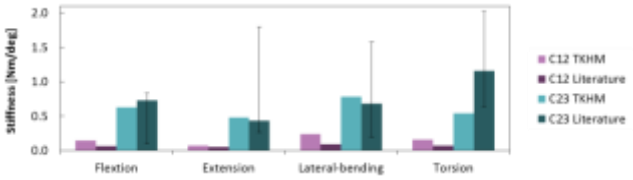


***Figure B-1. Validation Results against Cervical Vertebra Tests***

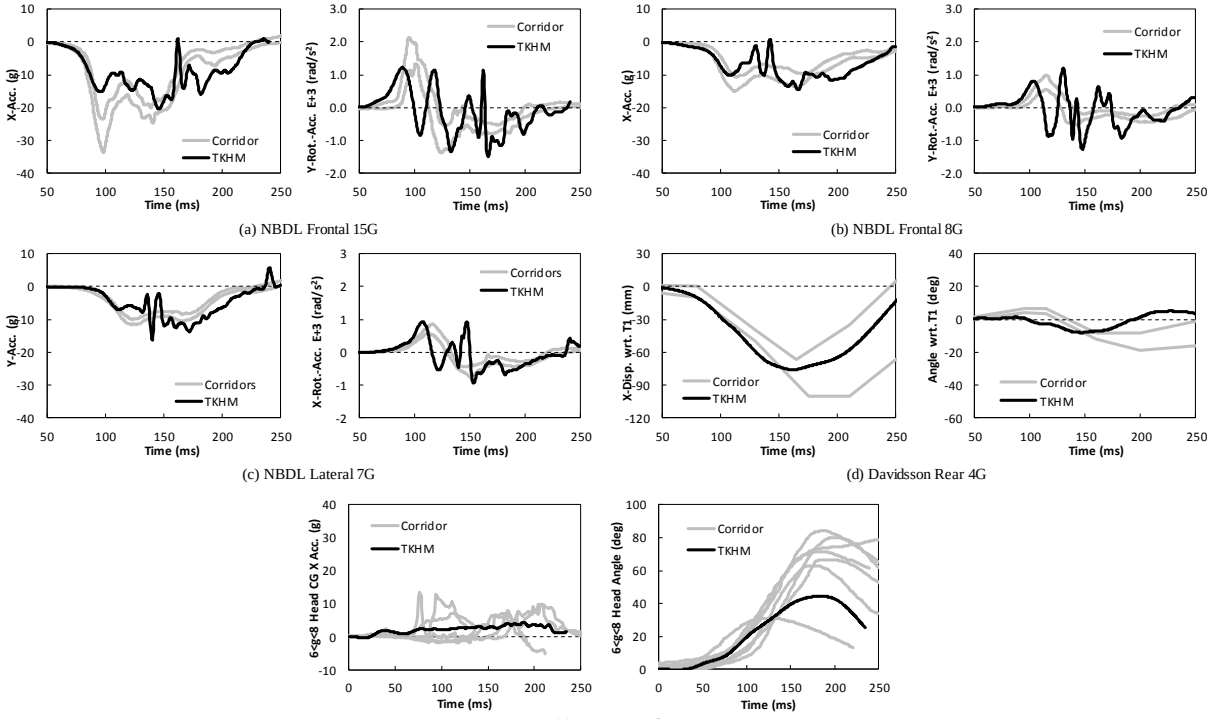


(a) NBDL Frontal 15G

(b) NBDL Frontal 8G

(c) NBDL Lateral 7G

(d) Davidsson Rear 4G

(e) Deng Rear 7G

***Figure B-2. Validation Results against Head-Neck Component Tests***

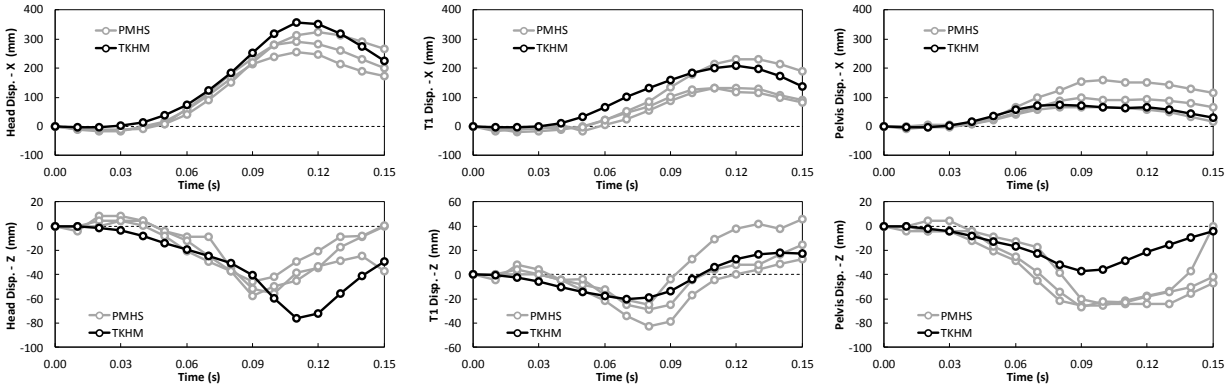


(a) Head C.G

(b) T1 C.G

(c) Pelvis C.G

***Figure B-3. Validation Results against UVA PMHS Sled Tests***

**Target Crash Population of Automated Vehicles**

**Paul Rau**
National Highway Traffic Safety Administration
USA

**Mikio Yanagisawa**
**Wassim G. Najm**
Volpe National Transportation Systems Center
USA

Paper Number 15-0430

## ABSTRACT

This paper describes a method to determine the target crash population that could be addressed by automated vehicles. The method maps specific automated vehicle functions to five layers of crash information including crash location, pre-crash scenario, driving conditions, travel speed, and driver condition. The focus of this paper is on automated vehicle functions at automation levels 2 through 4 as defined by the National Highway Traffic Safety Administration. This paper identifies the automated vehicle functions and their automation levels, operational characteristics and conditions, and applicable pre-crash scenarios through literature review and relevant research programs. This paper also identifies the approach to query the crash data and account for level 0 and level 1 automated vehicle functions when estimating target crash populations for automated vehicle functions at levels 2 through 4. The application of this method, using the General Estimates System and Fatality Analysis Reporting system crash databases, would express the target crash populations in terms of the annual frequency of all crashes, fatal-only crashes, and involved persons at different injury levels.

## INTRODUCTION

Automated vehicles have the potential to reduce motor vehicle crashes and mitigate the severity of injuries by performing driving controls effectively without the constraint of driver inputs. The target crash population (TCP) depends on the automated vehicle function and the level of automation. The National Highway Traffic Safety Administration (NHTSA) has defined the following five levels of automation that are distinguished by the degree of shared control and monitoring authority between the driver and the vehicle [1]:

- *Level 0 – No Automation (L0)*: This level accounts for crash warning systems and secondary automated controls such as wipers, headlights, etc.
- *Level 1 – Function-Specific Automation (L1)*: This level involves one or multiple specific control functions operating independently from each other. The driver has overall control, and is solely responsible for safe operation, but can choose to cede limited authority over a primary control (e.g., adaptive cruise control), the vehicle can automatically assume limited authority over a primary control (e.g., electronic stability control), or the vehicle can provide added control to aid the driver in certain normal driving or crash-imminent situations (e.g., automated emergency braking).
- *Level 2 - Combined Function Automation (L2)*: The driver cedes primary control of at least two primary control functions designed to work in unison in certain limited driving situations, but is still responsible for monitoring and safe operation of the vehicle. The driver is expected to be available at all times to control the vehicle.
- *Level 3 - Limited Self-Driving Automation (L3)*: The driver can cede full control and monitoring authority of all safety-critical functions under certain traffic and environmental conditions. The driver is expected to be available for occasional control of the vehicle.

- *Level 4 - Full Self-Driving Automation (L4)*: The driver provides navigation input but is not expected to be available for control of the vehicle. The vehicle is designed to safely perform all safety-critical driving functions and monitor roadway conditions for an entire trip.

This paper is focused on the target crash population for L2-L4 automation levels in light vehicles (e.g., passenger cars, vans and minivans, sport utility vehicles, and pickup trucks with gross vehicle weight rating less than 10,000 pounds). It describes a method to determine the target crash population that could be addressed by L2-L4 automated vehicles in general and the incremental target crashes that could not be addressed by crash avoidance applications or L0-L1 automation levels. Using NHTSA's General Estimates System (GES) and Fatality Analysis Reporting System (FARS) crash databases, the application of this method would express the TCP in terms of the annual frequency of all target crashes, fatal-only crashes, and involved persons at different injury levels. The potential safety benefits of automated vehicles would then be projected by multiplying the TCP values with estimates of the crash avoidance effectiveness of various automated vehicle functions. These crash avoidance effectiveness estimates need to be derived from research studies that collect and analyze driver-vehicle-roadway performance data for various automated vehicle systems.

**Previous Research**

NHTSA has conducted a crash causal study that analyzed 5,471 passenger vehicle crashes within the United States between 2005 and 2007. This analysis determined the pre-crash events and critical factors related to the actions that led to a crash [2]. Results from this study suggest that human error is the critical reason for 93% of crashes. Human errors were categorized into recognition (e.g., inattentive, distracted), decision (e.g., too fast, gap misjudgment), performance (e.g., overcompensation, poor control), and non-performance (e.g., sleepy, ill) errors. Thus, it has been alluded that automated vehicles at all levels of automation can potentially address a part of these crashes by supporting driver attention and response, and providing automatic vehicle control in both normal driving tasks and crash-imminent situations [3].

By compensating for driver error, many presentations and articles viewed the 93% of crashes as a preliminary estimate for the potential target crash population of automated vehicles. This general estimate is made independent of the prospective automated vehicle functions and their automation levels (i.e., L2-L4), and does not account for the crashes that would be avoided with crash avoidance systems and other motor vehicle safety applications (i.e., L0-L1). For example, forward crash warning (FCW) systems (i.e., L0) alert drivers to a potential crash with a slower or stopped lead vehicle. Rear-end crashes are the target crash population for FCW within the operational conditions of the system. On the other hand, an L2 automated car-following function, which controls the headway to lead vehicles and keeps the vehicle within the travel lane, would also target rear-end crashes mostly on highways. Hence, the analysis in this paper seeks to refine this general estimate of target crashes (93% of crashes) by describing a method that identifies target crash populations for individual automated vehicle functions and levels of automation, finds target crash overlaps among automated vehicle functions, and accounts for incremental target crashes between L0-L4 automation levels.

**Approach**

This paper first identifies and describes the operational conditions of prospective L2-L4 automated vehicle functions as reported in the literature. In addition, this paper lists L0 and L1 systems of interest that may share target crashes with higher levels of automated vehicle functions. Then, these automated vehicle functions and their operations are mapped to the crash information where they may apply. The applicability to crash information is dependent on the operational capabilities of each automated vehicle function and the availability of pertinent information. Key crash information includes the pre-crash scenarios and their characteristics, crash contributing factors of the driving environment and vehicle, and detailed crash causes of the driver. The query of the GES and FARS crash databases

would then yield the numbers of all police-reported and fatal-only crashes, as well as the numbers of injured persons and their injury levels, which could be addressed by L0-L4 functions individually and incrementally. The authors believe that the results will provide reasonable and defendable target crash populations and thus subsequent safety benefit estimates for automated vehicles. This will be accomplished by accounting for safety benefits as estimated from previous benefits studies addressing foundational crash avoidance technologies.

## AUTOMATED VEHICLE FUNCTIONS

The automation of primary control systems in motor vehicles can generally support safe driving by improving driver performance overall. As examples of driver support, L2-L4 automated vehicle functions [4]:

- Can aid in driver vigilance; e.g., watch for forward collision or ensure vehicle heading.
- Can decrease total driver workload and mitigate driver fatigue.
- Monitor the driving environment at a constant level of alertness, which may eliminate small driver errors such as steering reversal.
- May offer some protection from distraction.
- May correct or prevent poor decisions of novice drivers.

In above examples, automated vehicle functions may address motor vehicle crashes in any pre-crash scenario caused by driver physiological impairment or driving task errors including driver recognition, decision, and action errors.

Specific L2-L4 automated vehicle functions may have the potential to address target driving situations and pre-crash scenarios caused by different factors. Examples of automated vehicle functions include [5]:

- *Adaptive Cruise Control (ACC) with Lane Keeping, Lane Centering, Lane Change, and/or Merge*: L2 automated functions that keep the vehicle in its intended lane of travel and at desired headway, and perform lane change and/or allow other vehicles to merge onto the roadway.
- *Automatic Parking*: L2-L4 automated functions that assist the driver or fully controls the parking of a motor vehicle.
- *Automated Roadwork Assistance*: L2 automated function that navigates the vehicle through a work zone at limited speeds.
- *Automated Shuttles/Taxis*: L4 automated functions that operate at relatively slow speeds in designated zones including city streets and campuses.
- *Close-Headway Platooning*: L3 automated function that controls the longitudinal and lateral dynamic aspects of the vehicle on highways at all speeds including entering and leaving the platoon.
- *Emergency Stopping Assistant*: L3-L4 automated function that detects incapacitated drivers and safely maneuvers the vehicle to park on the side of the roadway.
- *Highway Driving*: L2-L4 automated functions that perform all driving tasks on highways at varying degrees of complexity relative to the automation level.
- *Traffic Jam Assist*: L2 automated function that performs car-following (i.e., longitudinal control) and lane keeping (i.e., lateral control) on highways at slow speeds.

Table 1 lists key automated vehicle functions for different levels of automation including L0 systems that are considered for the estimation of target crash population. Applicable operational conditions and roadways are also indicated to help map these functions to target crashes. This analysis considers the following L0 functions:

- *Alcohol Detection Technology*: limits the operation of a vehicle if above-limit alcohol levels are detected for the driver.
- *Back-Up Systems*: warns driver of objects and persons when backing up.

- *Blind Spot Warning/Lane Change Warning (BSW/LCW)*: alerts drivers to the presence of vehicles approaching or in their blind spot in the adjacent lane.
- *FCW*: warns drivers of stopped, slowing, or slower vehicles ahead.
- *Intersection Movement Assist (IMA)*: warns drivers of vehicles approaching from a lateral direction at an intersection.
- *Left Turn Assist (LTA)*: warns drivers to the presence of oncoming, opposite-direction traffic when attempting a left turn.
- *Road Departure Crash Warning (RDCW)*: warns drivers of unintentional lane departure. This function also warns drivers when approaching a curve at unsafe speeds.

L1 automated vehicle functions under consideration include automatic parking, automated roadwork assistance, ACC, cooperative ACC (CACC), electronic stability control (ESC), automated emergency braking (AEB), and pedestrian crash avoidance and mitigation (PCAM).

Information about the operational conditions of the automated vehicle functions listed in

MAPPING OF AUTOMATED FUNCTIONS TO CRASH DATA

For specific automated vehicle functions, it is important to determine their applicable crash characteristics. Figure 1 illustrates the process used to map the specific automated vehicle functions to the crash data. This process correlates automated vehicle functions and their capabilities to the crash information available. It should be noted that deficiencies exist in the data collection and reporting process for GES and FARS databases. When applying this mapping process, circumventing these deficiencies would limit the quantity of available data. The following key crash characteristics help to decide on the applicability of automated vehicle functions: crash location, pre-crash scenario, driving environmental conditions, vehicle travel speed, and driver condition.

**Location**

The location of a crash easily identifies the applicability of an automated vehicle function to a crash. For example, an L0 IMA warning would only be issued at an intersection, L1 automated roadwork assistance function would only activate in a dedicated work zone, or L2 Highway Driving would be limited to highways. Furthermore, the general location of the crash within the crash data can be obtained from variables in the GES and FARS crash databases (e.g., dedicated work zone, non-junction, intersection, entrance/exit ramp, etc.).

**Table 1** reflects details available from the literature at the time of this analysis (e.g., maximum speeds). This paper assumes that each automated vehicle function will mature in a timely manner and uses the intended operational capabilities when estimating target crash population (e.g., Close-Headway Platooning was only tested at a speed of 53 mph (85 km/h) and gaps of 5-15 meters, but platooning would plausibly occur at higher highway speeds).

Some automated vehicle functions (e.g., Highway Driving and Automatic Parking) transcend multiple levels of automation. These functions may be designed for minimal or full automation at the discretion of the manufacturer. An automatic parking feature may only control lateral motion when parallel parking or can allow the driver to leave the vehicle and have the vehicle park itself. The information obtained from this analysis was compared to variables in the GES and FARS crash databases to develop a mapping system that enables the correlation of automated vehicle functions to historical crash information.

## MAPPING OF AUTOMATED FUNCTIONS TO CRASH DATA

For specific automated vehicle functions, it is important to determine their applicable crash characteristics. Figure 1 illustrates the process used to map the specific automated vehicle functions to the crash data. This process correlates automated vehicle functions and their capabilities to the crash information available. It should be noted that deficiencies exist in the data collection and reporting process for GES and FARS databases. When applying this mapping process, circumventing these deficiencies would limit the quantity of available data. The following key crash characteristics help to decide on the applicability of automated vehicle functions: crash location, pre-crash scenario, driving environmental conditions, vehicle travel speed, and driver condition.

### Location

The location of a crash easily identifies the applicability of an automated vehicle function to a crash. For example, an L0 IMA warning would only be issued at an intersection, L1 automated roadwork assistance function would only activate in a dedicated work zone, or L2 Highway Driving would be limited to highways. Furthermore, the general location of the crash within the crash data can be obtained from variables in the GES and FARS crash databases (e.g., dedicated work zone, non-junction, intersection, entrance/exit ramp, etc.).

**Table 1.**

**Summary of L0-L4 Automated Vehicle Functions.**

| Automation Level | AV Functions | Operational Conditions | Roadways |
|---|---|---|---|
| L0 | Warning Systems (FCW, IMA, LTA, BSW/LCW, RDCW) | Speeds > 25 mph | All Roads |
| | Back-Up Systems | Reverse Only<br>Low Speeds | All Roads |
| | Alcohol Detection Technology | Drunk Driver | All Roads |
| L1 | Automated Roadwork Assistance 1 | Low Speeds | Work Zone |
| | Automatic Parking 1 | Low Speeds | Urban |
| | Pedestrian Crash Avoidance and Mitigation | Speeds < 45 mph | All Roads |
| | Adaptive Cruise Control (ACC) | High Speeds | Highway |
| | Cooperative Adaptive Cruise Control | High Speeds | Highway |
| | Electronic Stability Control | Loss of Control | All Roads |
| | Automated Emergency Braking | Imminent Crash | All Roads |
| L2 | Automated Roadwork Assistance 2 | Low Speeds | Work Zone |
| | Automatic Parking 2 | Low Speeds | Urban |
| | Traffic Jam Assist | Speeds ≤ 37 mph | Urban |
| | ACC w/Lane Keeping and Lane Change | Speeds < 75 mph | Highway |
| | ACC w/Lane Keeping, Lane Change and Merge | Speeds ≤ 81 mph | Highway |
| | ACC w/Lane Centering | Speeds ≤ 100 mph | Highway |
| | Highway Driving 2 | High Speeds | Highway |
| L3 | Automatic Parking 3 | Low Speeds | Urban |
| | Close-Headway Platooning | Speeds ≤ 56 mph | Highway |
| | Highway Driving 3 | High Speeds | Highway |
| | Emergency Stopping Assistance 3 | Incapacitated Driver | Highway |
| L4 | Automatic Parking 4 | Low Speeds | Urban |
| | Automated Shuttles/Taxis | Low Speeds | Urban |
| | Emergency Stopping Assistance 4 | Incapacitated Driver | All Roads |

**Pre-Crash Scenario**

The pre-crash scenarios depict specific vehicle movements and dynamics as well as the critical event occurring immediately prior to the crash [6]. Crash scenarios and their corresponding crash types. Some L0-L1 automated vehicle functions are primarily designed to prevent specific pre-crash scenarios (although secondary pre-crash scenarios may benefit from the same function). For example, an L0 FCW function is designed to prevent rear-end crashes and an L1 PCAM function is designed to prevent pedestrian crashes. Some L2-L4 automated vehicle functions indirectly address specific pre-crash scenarios based on the vehicle maneuvers that are automatically performed. For example, L2 ACC with Lane Centering would prevent rear-end, drifting, and road departure crashes.

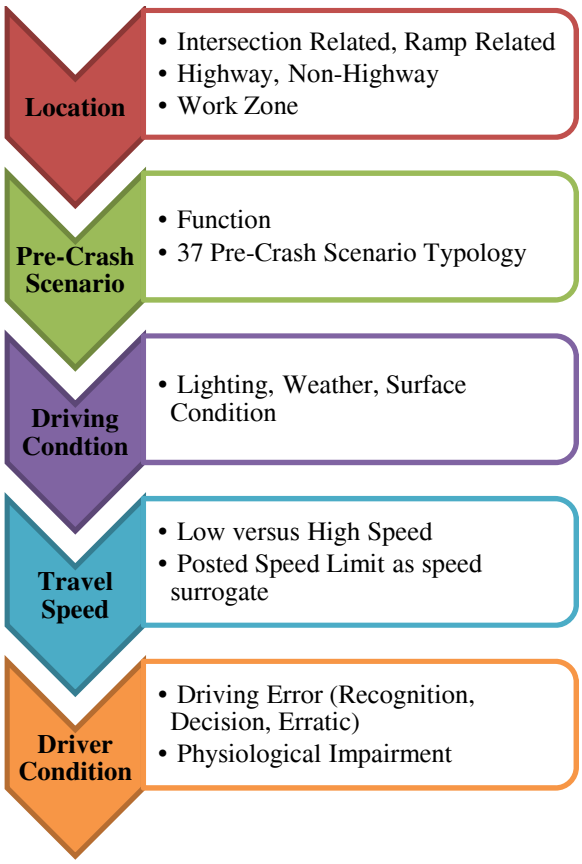


***Figure 1. Breakdown Process to Correlate Automated Vehicle Functions to Crash Data.***

**Table 2.**

**List of Pre-Crash Scenarios and Corresponding Crash Types.**

| No | Pre-Crash Scenario | Crash Type |
|---|---|---|
| 1 | Vehicle Failure | Run-Off-Road |
| 2 | Control Loss with Prior Vehicle Action | |
| 3 | Control Loss without Prior Vehicle Action | |
| 4 | Running Red Light | Crossing Paths |
| 5 | Running Stop Sign | |
| 6 | Road Edge Departure with Prior Vehicle Maneuver | Run-Off-Road |
| 7 | Road Edge Departure without Prior Vehicle Maneuver | |
| 8 | Road Edge Departure While Backing Up | |
| 9 | Animal Crash with Prior Vehicle Maneuver | Animal |
| 10 | Animal Crash without Prior Vehicle Maneuver | |
| 11 | Pedestrian Crash with Prior Vehicle Maneuver | Pedestrian |
| 12 | Pedestrian Crash without Prior Vehicle Maneuver | |
| 13 | Pedalcyclist Crash with Prior Vehicle Maneuver | Pedalcyclist |
| 14 | Pedalcyclist Crash without Prior Vehicle Maneuver | |
| 15 | Backing Up into Another Vehicle | Backing |
| 16 | Vehicle(s) Turning – Same Direction | Lane Change |
| 17 | Vehicle(s) Parking – Same Direction | |
| 18 | Vehicle(s) Changing Lanes – Same Direction | |
| 19 | Vehicle(s) Drifting – Same Direction | |
| 20 | Vehicle(s) Making a Maneuver – Opposite Direction | Opposite Direction |
| 21 | Vehicle(s) Not Making a Maneuver – Opposite Direction | |
| 22 | Following Vehicle Making a Maneuver | Rear-End |
| 23 | Lead Vehicle Accelerating | |
| 24 | Lead Vehicle Moving at Lower Constant Speed | |
| 25 | Lead Vehicle Decelerating | |
| 26 | Lead Vehicle Stopped | |
| 27 | LTAP/OD at Signalized Intersections | Crossing Paths |
| 28 | Vehicle Turning Right at Signalized Intersections | |
| 29 | LTAP/OD at Non-Signalized Intersections | |
| 30 | Straight Crossing Paths at Non-Signalized Intersections | |
| 31 | Vehicle(s) Turning at Non-Signalized Intersections | |
| 32 | Evasive Action with Prior Vehicle Maneuver | Run-Off-Road |
| 33 | Evasive Action without Prior Vehicle Maneuver | |
| 34 | Non-Collision Incident | Other |
| 35 | Object Crash with Prior Vehicle Maneuver | Object |
| 36 | Object Crash without Prior Vehicle Maneuver | |
| 37 | Other | Other |

By mapping the operational roadway of an automated function to the location of a crash, the pre-crash scenarios are naturally filtered out (e.g., crossing-path crashes don't occur on a highway for Highway Driving functions). The pre-crash scenarios are derived from various pre-crash event variables within the GES and FARS databases.

**Driving Condition**

The driving condition seeks to identify the environment in which the crash occurred. The environment is simplified to lighting, atmospheric conditions, and roadway surface conditions. All these conditions are readily available within GES and FARS databases. The described breakdown maps automated vehicle functions to crash data regardless of the technology used. However, it is possible that some technologies may be limited or suppressed in severe driving conditions. For example, a camera-based L2 ACC with lane keeping may not be available for operation on snow-covered roadways or an L3 Close-Headway Platooning may not operate at high speeds on wet or slippery roadway surfaces. When projecting the potential safety benefits in the future, driving conditions are crucial to estimating the crash avoidance effectiveness of these automated vehicle functions.

**Travel Speed**

Some automated vehicle functions are active at certain speeds. For example, an L1 PCAM function may not operate at speeds above 45 mph (72 km/h) or an L2 ACC with lane keeping may not work at speeds less than a typical highway speed (~50 mph or 80 km/h). Although travel speed is not as readily available or accurate in the crash data, this information can be deduced from other variables in the GES and FARS databases. For instance, it can be assumed that the driver is traveling at the speed limit if the travel speed is not a contributing factor to the crash (GES and FARS variable) on a roadway with certain posted speed limit (GES and FARS variable). On the other hand, if speed were referenced as a crash contributing factor, then it is assumed that the driver would be traveling at least +10 mph (16 km/h) over the speed limit. This analysis considers the 45 mph (72 km/h) travel speed as the threshold between “low” and “high” speed categories.

**Driver Condition**

Ideally, if full automation (L4) were to replace the driver in all motor vehicles then all crashes caused by the driver would be avoided given that the automation performs safely under all these crash conditions. Figure 2 illustrates a detailed breakdown of primary causal factors for light-vehicle crashes. It can be surmised that full automation (L4) could target up to 90% of motor vehicle crashes caused by driver error in driving tasks (i.e., recognition, decision, and action errors) and driver physiological condition (i.e., drunk, asleep, and ill) [7]. This is congruent to the results from the previously mentioned NHTSA study; however, the information provided in Figure 2 is a more detailed breakdown of primary causal factors based on 1992-1993 data from NHTSA crash databases.

Driving task errors in Figure 2 encompass:

- Recognition errors such as inattention, looked but did not see, and obstructed vision.
- Decision errors such as tailgating, unsafe passing, gap/velocity misjudgment, excessive speed, and trying to beat yellow light or other vehicle.
- Erratic actions such as failure to control vehicle, prior evasive maneuver, deliberate violation of traffic control device, and willful unsafe driving act.

Since the reported driver condition can be subjective depending on the combination of information provided in the crash data (e.g., drunk, inattentive, excessive speed) and that extensive human factors testing may be necessary to fully understand the capabilities of these automated vehicle functions as they relate to the driver, this analysis relegates the driver condition to the last layer of the breakdown.

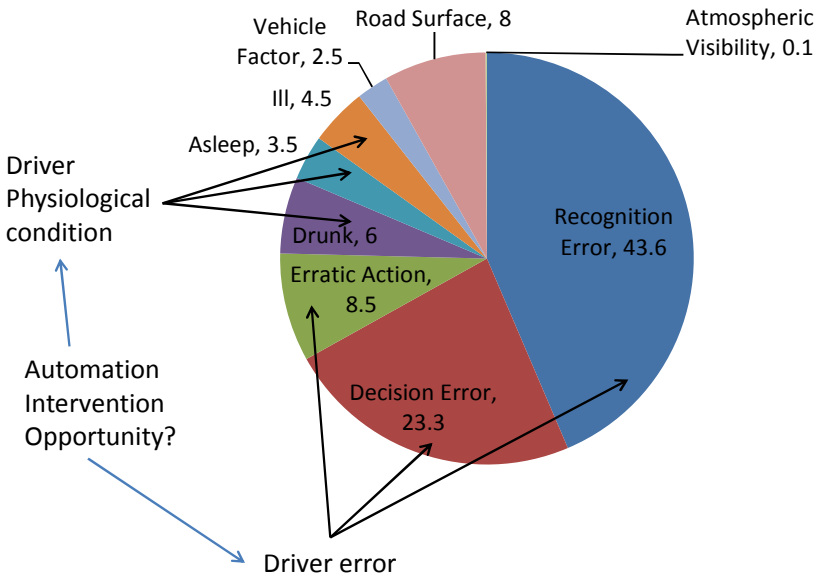


***Figure 2. Critical Causal Factors for Light Vehicle Crashes (in % crashes).***

## Mapping Results

Table 3 shows the results of mapping the L2-L4 automated vehicle functions under consideration to the five layers of crash characteristics. The automated vehicle functions are categorized by level of automation. This mapping aggregates the results for individual automated vehicle functions to their levels of automation. Many of the listed automated vehicle functions overlap on many variables. By applying this method, the analysis should first map each automated vehicle function individually and later aggregate the results so as to directly trace and account for the overlaps.

**Table 3.**

**Mapping of L2-L4 Automated Vehicle Functions to Crash Characteristics.**

| Automation Level | AV Functions | Location | Pre-Crash Scenarios | Driving Conditions | Travel Speed | Driver Conditions |
|---|---|---|---|---|---|---|
| L2 | Automated Roadwork Assistance 2 | Work Zone | Rear-End, Pedestrian | All | Low Speed | Recognition, Decision, Erratic |
| | Automatic Parking 2 | Non-Highway | Parking | All | Low Speed | Recognition, Decision, Erratic |
| | Traffic Jam Assist | Highway | Rear-End, Drifting | All | Low Speed | Recognition, Decision, Erratic |
| | ACC w/Lane Keeping and Lane Change | Highway | Road Departure, Rear-End, Changing Lanes, Drifting | All | High Speed | Recognition, Decision, Erratic |
| | ACC w/Lane Keeping, Lane Change and Merge | Ramp, Highway | Road Departure, Rear-End, Changing Lanes, Drifting | All | High Speed | Recognition, Decision, Erratic |
| | ACC w/Lane Centering | Highway | Road Departure, Rear-End, Drifting | All | High Speed | Recognition, Decision, Erratic |
| | Highway Driving 2 | Highway | Road Departure, Rear-End, Changing Lanes, Drifting | All | High Speed | Recognition, Decision, Erratic |
| L3 | Automatic Parking 3 | Non-Highway | Parking | All | Low Speed | Recognition, Decision, Erratic |
| | Close-Headway Platooning | Highway | Road Departure, Rear-End, Changing Lanes, Drifting | All | High Speed | Recognition, Decision, Erratic |
| | Highway Driving 3 | Highway | Road Departure, Rear-End, Changing Lanes, Drifting | All | High Speed | Recognition, Decision, Erratic |
| | Emergency Stopping Assistance 3 | Highway | | All | All | Physiological Impairment |
| L4 | Automatic Parking 4 | Non-Highway | Parking | All | Low Speed | Recognition, Decision, Erratic |
| | Automated Shuttles/Taxis | Intersection, Non-Highway | Crossing Paths, Road Departure, Rear-End, Opposite Direction, Turning, Chagning Lanes, Drifting, Pedestrian, Pedalcyclist | All | Low Speed | All |
| | Emergency Stopping Assistance 4 | All Roads | | All | All | Physiological Impairment |

## TARGET CRASH POPULATIONS

The main focus of the method in this paper is to determine the target crash populations of L2-L4 automated vehicle functions. However, it is logical to consider L0 and L1 functions that are or will be simultaneously implemented in the light-vehicle fleet and will potentially provide considerable safety benefits. Table 4 lists the L0 and L1 functions and their corresponding mapping to crash data. Further research would provide detailed system effectiveness estimates for the listed applications.

**Table 4.**

**Mapping of L0-L1 Automated Vehicle Functions**

| Automation Level | AV Functions | Location | Pre-Crash Scenarios | Driving Conditions | Travel Speed | Driver Conditions |
|---|---|---|---|---|---|---|
| L0 | FCW | Work Zone, Ramp, Intersection, Non-Highway, Highway | Rear-End | All | High Speed | Recognition, Decision |
| | IMA | Intersection | Straight and Turning Crossing Paths | All | High Speed | Recognition, Decision |
| | LTA | Intersection | Left Turn Across Path / Opposite Direction | All | High Speed | Recognition, Decision |
| | BSW/LCW | Work Zone, Ramp, Highway, Non-Highway | Turning and Changing Lanes/ Same Direction | All | Low Speed High Speed | Recognition, Decision |
| | RDCW (CSW and LDW) | Work Zone, Ramp, Highway, Non-Highway | Road Departure, Drifting (Same Direction and Opposite Direction) | All | High Speed | Recognition, Decision |
| | Back Up Systems | Non-Highway, Non-Trafficway | Road Departure Backing, Backing into Vehicle | All | Low Speed | Recognition, Decision |
| | Alcohol Detection Technology | | | | | Physiological (Alcohol) |
| L1 | Automated Roadwork Assistance 1 | Work Zone | Rear-End, Pedestrian | All | Low Speed | Recognition, Decision, Erratic |
| | Automatic Parking 1 | Non-Highway | Parking | All | Low Speed | Recognition, Decision, Erratic |
| | PCAM | Work Zone, Intersection, Non-Highway | Pedestrian | All | Low Speed | Recognition, Decision, Erratic |
| | ACC | Highway | Rear-End | All | High Speed | Recognition, Decision, Erratic |
| | CACC | Highway | Rear-End | All | High Speed | Recognition, Decision, Erratic |
| | ESC | All Roads | Control Loss, Rollover | All | All | Recognition, Decision, Erratic |
| | AEB | All Roads | Rear-End, Pedestrian, Opposite Direction | All | All | Recognition, Decision, Erratic |

Accounting for the potential safety benefits of L0 and L1 functions as mapped to crash data in Table 4, L2-L4 automated vehicle functions would target the residual or remaining crashes not addressed or avoided by L0 and L1 functions. The TCP estimates can then be characterized by the level of automation incrementally (i.e., accounting for residual crashes) and independently (i.e., not accounting for target crashes or safety benefits by other levels).

## CONCLUSION

This paper described a method to estimate the target crash populations for automated vehicle functions at levels 2 through 4 while accounting for the potential safety benefits that could be accrued from the full deployment of some selected L0 and L1 functions. This method correlated specific automated vehicle functions to five layers of crash data. This paper identified specific automated vehicle functions with detailed operational conditions and mapped each automated vehicle function through five filters within the crash data. Follow-on application of this method by querying the GES and FARS crash databases will generate the TCP estimates.

Automated vehicle functions at all levels of automation were identified and detailed, which included operational speeds, ranges, and locations. The five layers of crash data consisted of crash location, pre-crash scenario, driving condition, travel speed, and driver condition. This paper developed a method to estimate the TCP values that could be addressed by automated vehicle technology. The multiplication of these TCP values with estimates of the crash avoidance effectiveness would project the potential safety benefits of the various automated vehicle functions.

Further research is needed to estimate the crash avoidance effectiveness by analyzing driver-vehicle-roadway performance data collected from past and future research studies for various automated vehicle systems.

## REFERENCES


[1] National Highway Traffic Safety Administration. 2013. "Preliminary Statement of Policy Concerning Automated Vehicles."

[2] "National Motor Vehicle Crash Causation Survey. Report to Congress." 2008. National Highway Traffic Safety Administration, DOT HS 811 059.

[3] Expert testimony by John Maddox. 2014. U.S House of Representatives Committee on Science, Space and Technology - Subcommittee on Research and Technology. Future of Transportation Technology.

[4] Marinik, A., Bishop, R., Fitchett, V., Morgan, J.F., Trimble, T.E., and M. Blanco. 2014. "Human Factors Evaluation of Level 2 and Level 3 Automated Driving Concepts: Concepts of Operation." National Highway Traffic Safety Administration, DOT HS 812 044.

[5] Trimble, T.E., Bishop, R., Morgan, J.F., and M. Blanco. 2014. "Human Factors Evaluation of Level 2 and Level 3 Automated Driving Concepts: Past Research, State of Automation Technology, and Emerging System Concepts." National Highway Traffic Safety Administration, DOT HS 812 043.

[6] Najm, W.G., Smith, J.D., and M. Yanagisawa. 2007. "Pre-Crash Scenario Typology for Crash Avoidance Research." National Highway Traffic Safety Administration, DOT HS 810 767.

[7] Najm, W.G., Mironer, M., Koziol, J. Jr., Wang, J.-S., and RR. Knipling. 1995. "Synthesis Report: Examination of Target Vehicular Crashes and Potential ITS Countermeasures." National Highway Traffic Safety Administration, DOT HS 808 263.


## ACRONYMS

| | |
|---|---|
| **ACC** | Adaptive Cruise Control |
| **AEB** | Automated Emergency Braking |
| **BSW/LCW** | Blind Spot Warning/Lane Change Warning |
| **CACC** | Cooperative Adaptive Cruise Control |
| **ESC** | Electronic Stability Control |
| **FARS** | Fatality Analysis Reporting System |
| **FCW** | Forward Crash Warning |
| **GES** | General Estimates System |
| **IMA** | Intersection Movement Assist |
| **LTA** | Left Turn Assist |
| **Lx** | Automation Level x |
| **NHTSA** | National Highway Traffic Safety Administration |
| **PCAM** | Pedestrian Crash Avoidance and Mitigation |
| **RDCW** | Road Departure Crash Warning |
| **TCP** | Target Crash Population |

# Improve Road Safety Using Combined V2V and Pre-Collision Systems

**Mingxin Liu, Stanley Chien, and Yaobin Chen**
Transportation Active Safety Institute, Indiana University–Purdue University Indianapolis, USA

Paper Number 15-0431

## ABSTRACT

In current vehicle to vehicle (V2V) communication systems, each vehicle broadcasts its motion status and receives information from other vehicles in order to make safety decisions and actions. State-of-the-art pre-collision systems (PCS) utilize onboard sensors to collect potential crash object information for making safety action decisions. This V2V-PCS combination enables a vehicle to not only send its own motion information, but also its PCS detected information to other vehicles. Conceptually, the additional information should help a V2V enabled vehicle make its safety related decisions more accurately and efficiently. The objective of this study is to find if a combined V2V and PCS system (V2V-PCS) can further improve the safety of not only V2V-PCS enabled vehicles but also other non V2V-PCS enabled vehicles on the road. This paper describes a process that can be used to analyze pedestrian and vehicle scenarios, and determine whether or not the safety of pedestrians could be improved by a V2V-PCS system. It also gives an analytical method for determining the benefit of using V2V-PCS. The environments set up for V2V-PCS simulation and real vehicle testing are also described.

**Keyword**: Pre-collision systems, V2V

## 1. Introduction

Based on statistics from the 2005-2008 National Automotive Sampling System (NASS) General Estimates System (GES) crash databases, V2V-based safety applications would potentially address about 4,336,000 police-reported light-vehicle crashes annually, with the 95 percent confidence interval between 3,691,000 and 4,981,000 [1]. The advancement in computation power and communication capability enables the practical implementation of vehicle to vehicle communication (V2V) systems. The advantage of V2V systems has been well discussed in many literatures. Pilot V2V implementation programs are conducted in several countries [2, 3]. The fundamental advantage of V2V is its capability of exchanging vehicle information that enables the intelligent decisions regarding road safety and efficiency. V2V-based safety applications predominantly apply to crashes that involve multi-vehicle pre-crash scenarios. This analysis is conducted with support from the Intelligent Transportation System's program for safety and mobility applications based on V2V and vehicle-to-infrastructure (V2I) communications [4]. To improve the intelligence of V2V systems, there are studies for incorporating information from traffic lights and road sensors through vehicle to infrastructure (V2I) systems, vehicle to pedestrian (V2P) systems into V2X systems. However, the current development of V2X systems is based on the concept that each participant provides its own operating information to the V2X system. There will be a long time period that V2V capable and non-V2V vehicles coexist on roads. The current design of the V2X systems does not benefit non-V2X equipped objects (vehicle and pedestrians) since the information of these objects cannot be entered into the V2X systems. To solve this problem, there should be a way to gather the information of non-V2V enabled objects on the road, transmit this information the V2X system, and use the information to improve the safety of all objects on the road.

PCS system is an active safety component in many commercially available vehicles. A PCS has sensors (video camera, radar, lidar, etc.) to detect vehicles, pedestrians and bicyclist. The sensor information is presently used for collision imminent warning, automatic braking and maneuvering. If the PCS sensor information of a vehicle can be broadcast to a V2V network, other V2V enabled vehicles may use the information to improve the safety of the sensed objects. This paper discusses the future technology development in combining V2V and PCS together to enable a V2V vehicle to broadcast its PCS detected information and use recieved information to make better crash avoidance decisions. The combined V2V-PCS can effectively extend the information gathering range of V2V vehicles and enables all V2V vehicles to get information of non-V2V enabled objects.

This paper describes a systematic process to investigate all V2V-PCS scenarios that potentially benefit the pedestrians with the adoption of the combined V2V-PCS systems. First the variables and their values relevant to V2V-PCS scenarios are identified. Then all scenarios generated from the combination of the variable values are examined to determine if they can improve pedestrian safety. The computation method for determining if the V2V-PCS improves the pedestrian safety for each scenario is described. The calculation of the first appearance location of the pedestrian to the vehicle and time to collision due to the location of the obscure object is described. The result of this study serves three purposes, (1) it provides a baseline to describe the usefulness of a V2V-PCS system, (2) it provides all pedestrian V2V-PCS simulation scenarios and crash calculation for future study and demonstration, and (3) it supports the establishment of testing scenarios for the performance evaluation of the V2V-PCS enabled vehicles.

## 2. Environment description and scenario categorization

It is assumed that there are three types of vehicles on the road: vehicles without V2V capability, vehicles with V2V capability but no PCS capability, vehicles with both and V2V and PCS capabilities. Each vehicle can be either moving or stationary. It is also assumed that pedestrians and stationary objects on the road do not have V2V capability. To describe V2V-PCS scenarios for pedestrian safety, the objects in the scenarios include pedestrians, vehicle potentially crashes the pedestrians (crashing vehicle), and V2V-PCS enabled vehicle that broadcast the pedestrian information and objects that obscure the view of the crashing vehicle. To describe the scenarios that a V2V-PCS system could show pedestrian safety advantage, following variables are identified:

1. *Crash Location* – The crash location variable has four relevant values: not-at-intersection, before-intersection in-intersection, after intersection.
2. *Crashing Vehicle Motion Direction*: possible values are *straight forward, turn left, turn right, merge left, and merge right*. In not-at-intersection scenarios, crashing vehicles cannot turn left or right so there are only three possible values: *straight forward, merge left, and merge right*; in intersection related scenarios, merging while turning is equivalent to turning with a different radius, so there are only three possible values: *straight forward, turn left, and turn right*.
3. *Pedestrian motion direction relative to the crashing vehicle*: Four possible values are *Left to Right, Right to Left, Along Traffic, and Against Traffic*.
4. *Obscure object*: There are seven interested values for this variable: no obscure object, stationary/moving obscure objects on left/front/right. The presence of obscure objects blocks the view of the crashing vehicle and shortens the reaction time to a potential collision.

For the convenience of describing the V2V-PCS scenarios, the notations for these variables and their values are defined in Table 1.

*Table 1. Variables and values relevant for describing V2V-PCS scenarios*

| **Crash location** | **Crashing vehicle direction** | **Pedestrian direction respect to crashing vehicle** | **Obscure object- location with respect to crashing vehicle (M=motion, S=Stationary)** |
|---|---|---|---|
| IB – before intersection | VLT – left tern | PLR – left to right | OS/M – obscure obj. |
| IA - after intersection | VRT – right turn | PRL – right to left | OS/M – obscure obj. |
| II – in intersection | VST - straight | PAL – along traffic | OS/M – obscure obj. |
| IN – not in intersection | VLM – left merge | PAG –against traffic | ON – no object |
| | VRM –right merge | | |
| | VLC – left curve | | |
| | VRC –right curve | | |

168 different scenarios can be identified based on the combination of all possible values of environment variables as described in Table 1. In which 108 are intersection related and 60 are non-intersection related. 108 intersection related cases are calculated as 1(intersection)*3(Before, In, or After intersection)*3(Turn left, Turn right, Straight Forward)*4(Left to Right, Right to Left, Along Traffic, Against Traffic)*3(moving obscure objects, stationary obscure objects, no obscure object) . 60 non-intersection scenarios are calculated as 1(non-intersection)*5(Curve

left, Curve right, Straight Forward, Merge left, Merge right) *4(Left to Right, Right to Left, Along Traffic, Against Traffic)*3(moving obscure objects, stationary obscure objects, no obscure object).

Each of these 168 scenarios was studied to determine if it could benefit from the use of V2V-PCS systems. The basic idea is to check if the crashing vehicle can get potential crash information earlier when a V2V-PCS system is adopted. The crashing vehicle may not be able to see the pedestrian for various reasons. If there is another vehicle (the informing vehicle) that has the PCS capability to detect the pedestrian and send the information to the crashing vehicle, the crashing vehicle may able to take measures in advance to avoid the collision. Here it is assumed that pedestrians do not detect the potential danger and cannot send their location information to vehicles. According to the selection criteria described above, 96 scenarios (listed in Table 2) are able to benefit from V2V-PCS systems and 72 Scenarios will not benefit from V2V-PCS systems.

*Table 2. 96 scenarios that the V2V-PCS system can improve the pedestrian safety*

| Location | Vehicle | Pedestrian and the Obscure object |
|---|---|---|
| IB | VLT | PLR_OS; PLR_OM; PLR_ON; PRL_OS; PRL_OM; PRL_ON; PAL_ON; PAG_ON |
| | VRT | PLR_OS; PLR_OM; PLR_ON; PRL_OS; PRL_OM; PRL_ON; PAL_ON; PAG_ON |
| | VST | PLR_OS; PLR_OM; PLR_ON; PRL_OS; PRL_OM; PRL_ON; PAL_ON; PAG_ON |
| IA | VLT | PLR_OS; PLR_OM; PLR_ON; PRL_OS; PRL_OM; PRL_ON; PAL_ON; PAG_ON |
| | VRT | PLR_OS; PLR_OM; PLR_ON; PRL_OS; PRL_OM; PRL_ON; PAL_ON; PAG_ON |
| | VST | PLR_OS; PLR_OM; PLR_ON; PRL_OS; PRL_OM; PRL_ON; PAL_ON; PAG_ON |
| II | | None |
| IN | VST | PLR_OS; PLR_OM; PLR_ON; PRL_OS; PRL_OM; PRL_ON; PAL_ON; PAG_ON |
| | VLC | PLR_OS; PLR_OM; PLR_ON; PRL_OS; PRL_OM; PRL_ON; PAL_ON; PAG_ON |
| | VRC | PLR_OS; PLR_OM; PLR_ON; PRL_OS; PRL_OM; PRL_ON; PAL_ON; PAG_ON |
| | VLM | PLR_OS; PLR_OM; PLR_ON; PRL_OS; PRL_OM; PRL_ON;<br>PAL_OS; PAL_OM; PAL_ON; PAG_OS; PAG_OM; PAG_ON |
| | VRM | PLR_OS; PLR_OM; PLR_ON; PRL_OS; PRL_OM; PRL_ON;<br>PAL_OS; PAL_OM; PAL_ON; PAG_OS; PAG_OM; PAG_ON |

*Table 3. 72 Scenarios that the V2V-PCS cannot improve the pedestrian safety*

| Location | Vehicle | Pedestrian and the Obscure object |
|---|---|---|
| IB | VLT | PAL_OS; PAL_OM; PAG_OS; PAG_OM |
| | VRT | PAL_OS; PAL_OM; PAG_OS; PAG_OM |
| | VST | PAL_OS; PAL_OM; PAG_OS; PAG_OM |
| IA | VLT | PAL_OS; PAL_OM; PAG_OS; PAG_OM |
| | VRT | PAL_OS; PAL_OM; PAG_OS; PAG_OM |
| | VST | PAL_OS; PAL_OM; PAG_OS; PAG_OM |
| II | VLT | PLR_OS; PLR_OM; PLR_ON; PRL_OS; PRL_OM; PRL_ON;<br>PAL_OS; PAL_OM; PAL_ON; PAG_OS; PAG_OM; PAG_ON |
| | VRT | PLR_OS; PLR_OM; PLR_ON; PRL_OS; PRL_OM; PRL_ON;<br>PAL_OS; PAL_OM; PAL_ON; PAG_OS; PAG_OM; PAG_ON |
| | VST | PLR_OS; PLR_OM; PLR_ON; PRL_OS; PRL_OM; PRL_ON;<br>PAL_OS; PAL_OM; PAL_ON; PAG_OS; PAG_OM; PAG_ON |
| IN | VST | PAL_OS; PAG_OS; PAL_OM; PAG_OM |
| | VLC | PAL_OS; PAG_OS; PAL_OM; PAG_OM |
| | VRC | PAL_OS; PAG_OS; PAL_OM; PAG_OM |
| | VLM | None |
| | VRM | None |

To make the graphical description easier, following icons are used in figures:

The pedestrian sign represents the pedestrian without the capability to communicate with vehicles.

The red vehicle represents the crashing vehicle equipped with V2V (may have PCS capability).

The yellow vehicle represents the informing vehicle equipped with both PCS and V2V.

The blue vehicle represents the stationary vehicle equipped with both PCS and V2V

The hexagon represents the obscure object.

Figure 1A demonstrates a situation that the use of a V2V-PCS system could improve the safety of a pedestrian. The red car (crashing vehicle) is going straight forward. The stationary blue car is waiting for a left turn signal and obscures the view of the red car. The pedestrian is walking across the road from left to right. The red car may not be able to stop due to the short reaction time. If the yellow car (the informing vehicle) coming from the other side or the blue car has pedestrian PCS and V2V capability, they can detect the pedestrian and send the pedestrian motion information to the red car so that the red car can take measures in advance to avoid potential crash to the pedestrian. If the red car is equipped with V2V but no PCS, it can generate warning to the driver, and or generate pre-braking command to the brake system to be ready for real brake. If the red car has both PCS and V2V capabilities, it can pay special attention to the location where the pedestrian is expected to appear and make quicker and better decisions. The V2V-PCS is useful even if the obscure blue car is not present (Figure 1B). If the pedestrian is far from the fast moving red car, the sensors in the red car may not be able to detect the pedestrian so the PCS on the red car may not be able to make effective braking decision. Since the pedestrian is much closer to yellow car, the V2V-PCS of the yellow car can provide pedestrian information before the red car can recognize the pedestrian.

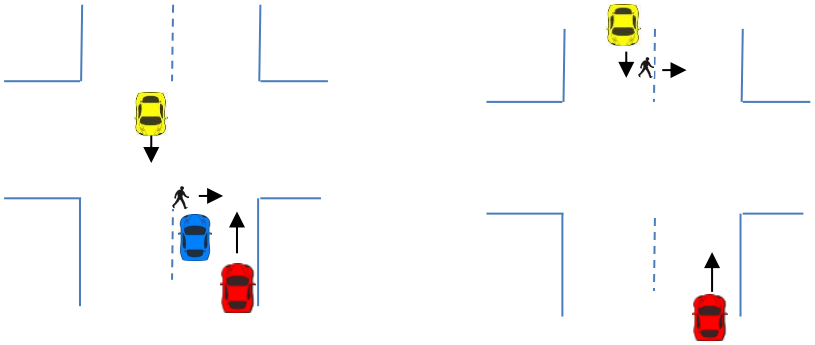

*(A) IB-VST-PLR-OS* *(B) IA-VST-PLR-ON*

*Figure 1. Example scenarios showing that the V2V-PCS system may prevent a crash to the pedestrian.*

Figure 2 demonstrates a scenario that the V2V-PCS system cannot improve the safety of a pedestrian. The red car (crashing vehicle) is going straight forward. The obscure blue car is in front of the red car. The pedestrian is walking along the road. Even the pedestrian information sent by the blue car and received by the red car, there is not a situation that the red car can crash to the pedestrian.

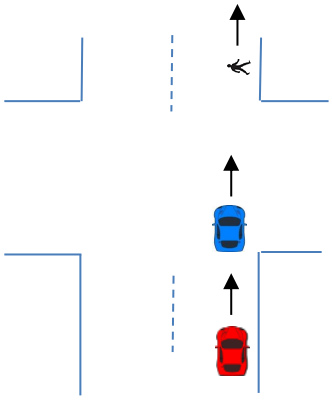

*Figure 2. A scenario IA-VST-PAL-OM showing the scenarios at the V2V-PCS system does not help pedestrian safety.*

## 3. Analysis of scenarios

All scenarios that V2V-PCS systems improve the safety of the pedestrians are identified in last section. The next step is to answer two practical questions quantitatively,

A. Given any scenario as described in Table 2 with detailed motion information of all objects, how do we know if there is a crash or not? The answer to this question is useful for developing a V2V-PCS warning/braking strategy.

B. Given any scenario as described in Table 2 with the positions and speeds of all objects except the initial position of the crashing vehicle, what is the initial position of the crashing vehicle so that there is a crash to the pedestrian at a specific location of the vehicle? The answer to this question is useful for setting up the test scenario for evaluating the effectiveness of the V2V-PCS systems.

To answer these questions, scenarios in Table 2 are reorganized into three categories based on the vehicle motion direction: vehicle move straight, vehicle change/merge lanes, and vehicle move in a curved lane.

### 3.1. The straight moving vehicle crashes a pedestrian crossing a street

This subsection provides a method to check if there will be a crash when a pedestrian is crossing the road and vehicle is moving straight. This method is essential for evaluating whether or not a V2V-PCS system is capable of improving a pedestrian's safety. Figure 3 depicts a situation where a straight moving vehicle crashes into a pedestrian crossing the street. The red car is moving straight forward with center at the y-axis, while a pedestrian crosses the road from left to right with an angle of Θ to x-axis. Assuming the crash location is at the origin of the coordinate system, the following equations can answer the aforementioned two questions.

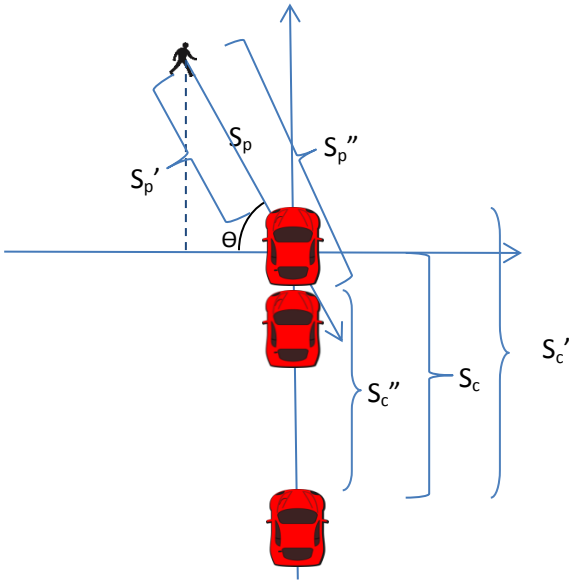


*Figure 3. The straight moving vehicle crashes a pedestrian crossing a street.*

Definition of notations in Figure 3:

Θ: The angle of the pedestrian's motion with respect to x axis

$L_c$: The length of the vehicle

$W_c$: The width of the vehicle

$S_c$: The distance between the vehicle's initial position (front center) and the potential collision point

$S_c'$: The distance between vehicle's initial position (front left corner) and the potential collision point

$$S_c' = S_c + 0.5W_c \tan \Theta$$

$S_c''$: The distance between vehicle's initial position (front right corner) and the potential collision

$$S_c'' = S_c - 0.5W_c \tan \Theta$$

$S_p$: The distance between pedestrian's initial position (front center) and the collision point

$S_p'$: The distance between the pedestrian's initial position and the collision point with vehicle's front left corner

$$S_p' = S_p - 0.5W_c/\cos \Theta$$

$S_p''$: The distance between pedestrian's initial position and the collision point with vehicle's front right corner

$$S_p'' = S_p + 0.5W_c/\cos \Theta$$

$v_p$: The velocity of the pedestrian (Assume the pedestrian is moving at a constant speed)
$v_c$: The initial velocity of the vehicle
$a_c$: The acceleration of the vehicle

**A. Determine if there is a collision between the vehicle and the pedestrian**

According to Figure 3, potential crash time $t_c$ is bounded by two conditions, one where the pedestrian is struck at the left front corner of the vehicle and one where the pedestrian is struck at the right front corner of the vehicle. The time interval for the pedestrian to move between these two points can be expressed as [ $t_p$', $t_p$"], and the time interval for the vehicle to move between these two points can be shown as [ $t_c$', $t_c$"]. Vc crashes to the pedestrian when [$t_c$', $t_c$"] overlaps [$t_p$', $t_p$"].

$t_p$' and $t_p$" can be calculated as $S_p$'/$v_p$ and $S_p$"/$v_p$, respectively.
$t_c$' and $t_c$" can be calculated using Newton's laws of motion: $t = (-v_c \pm sqrt(v_c^2 + 2a_cS_c)) / a_c$,
If $a_c > 0$, If $sqrt(v_c^2 + 2\ a_cS_c) \geq v_c > 0$, Then $t = (-v_c + sqrt(v_c^2 + 2a_cS_c)) / a_c$
If $v_c > sqrt(v_c^2 + 2a_cS_c') > 0$, Then no positive t, invalid for this application.
If $a_c < 0$, If $v_c \geq sqrt(v_c^2 + 2a_cS_c') > 0$, Then $t = (-v_c + sqrt(v_c^2 + 2a_cS_c')) / a_c$
If $0 < v_c < sqrt(v_c^2 + 2a_cS_c')$, Then $t = (-v_c + sqrt(v_c^2 + 2a_cS_c')) / a_c$
If $a_c = 0$, $t = S_c/v_c$

**Example 3.1.A:**

Given the situation in Figure 2 and the variable values in the following table

| $a_c$ | $v_c$ | $v_p$ | Θ | $L_c$ | $W_c$ | $S_p$ | $S_p$' | $S_p$" | $S_c$ | $S_c$' | $S_c$" |
|---|---|---|---|---|---|---|---|---|---|---|---|
| 5m/s$^2$ | 13.5m/s | 1.5 m/s | 60$^o$ | 4.8m | 1.8m | 7.5m | 5.7m | 9.3m | 55m | 56.56m | 53.44m |

The calculation of ($t_p$', $t_p$") is (3.8 sec, 6.2sec), and ($t_c$', $t_c$") is (3.96 sec, 4.18 sec). Since there is an overlap time range which is [3.96 sec, 4.18 sec], it there is collision between the pedestrian and the crashing vehicle during this time interval.

**B. Determine the initial positions of Vc and the pedestrian that guarantee a crash**

According to Figure 3, the crashing vehicle is on y-axis and the crash point is at the origin, so the initial position of the vehicle is (0, -$S_c$) and the initial position of pedestrian is (-$S_p$cosΘ, $S_p$sinΘ). To guarantee a crash for vehicle testing, the initial position of the vehicle can be decided according to the initial position of the pedestrian and vice versa. In other word, the travel time for the pedestrian to reach origin should be the same as that for the vehicle. If the desired crash point is not at the middle front of the vehicle, the path of vehicle in the y-direction can be shifted along the-x axis accordingly.

**3.2 The vehicle crashes a pedestrian crossing a street while change lanes**

This section provides the method to check if there is a crash when a pedestrian is crossing the road and vehicle is changing lanes. Figure 4 depicts the situation that a vehicle crashes into a pedestrian crossing the street while changing lanes. The red car Vc is changing to the left lane centered at y-axis while a pedestrian crosses the road from left to right with an angle of Θ to x-axis. The definitions of the notations in Figure 4 are the same as that in Section 3.1. The additional notation α is the angle between y-axis and the line from the vehicles initial position to origin.

**A. Determine if there is a crash between Vc and the pedestrian**

Practically, in the vehicle changing lanes cases, the distance that the vehicle moves forward is much longer than the distance that the vehicle moves laterally (equals the width of a lane). Thus the width of the lane that the vehicle merges can be ignored so that these cases can be regarded as the vehicle moving straight forward as described in Section 3.1. So the method described in Section 3.1 can be used for these change lanes cases.

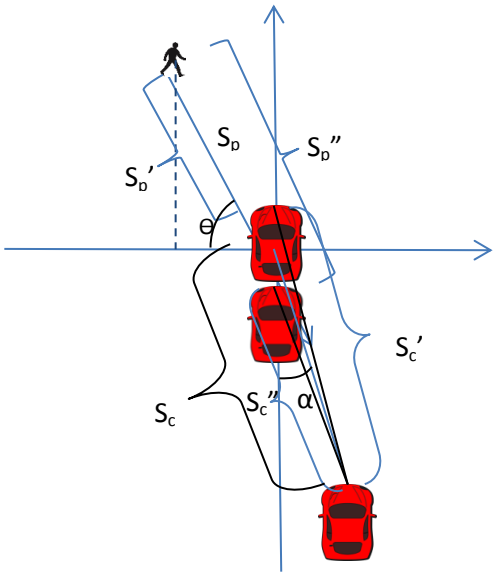


*Figure 4. The vehicle changes lanes and crashes a pedestrian crossing a street.*

### B. Determine the initial positions of Vc and the pedestrian for vehicle V2V-PCS performance evaluation

According to Figure 3, the initial position of Vc is ($S_c\sin\alpha$, $-S_c\cos\alpha$) and the initial position of the pedestrian is ($-S_p\cos\Theta$, $S_p\sin\Theta$). To guarantee a crash in V2V-PCS evaluation, the initial position of the vehicle needs to be decided according to the initial position of the pedestrian and vice versa. In other words, the travel time for the pedestrian to reach origin should be the same as that for the vehicle. If the desired crash point is not at the middle front of the vehicle, the path of vehicle in the y-direction can be shifted along the-x axis accordingly.

## 3.3 The vehicle crashes the pedestrian while following a curved road

This subsection provides the method to check if there will be a crash when a pedestrian is crossing the road and vehicle is moving along a curved road (depicted in Figure 5). The red car is curving with center at y-axis while a pedestrian crosses the road from left to right with an angle of Θ to x-axis. It is assumed that the crash location will be at the origin of the coordinate. The curved lane in a non-intersection location can be considered as a straight lane in terms of traveling distance and time. Therefore, the method described in section 3.1 for determining if there is a collision between the vehicle and the pedestrian can be directly applied is this case. The method described in Section 3.2 for determining the initial positions of Vc and the pedestrian that guarantee a crash also can be directly applied is this case.

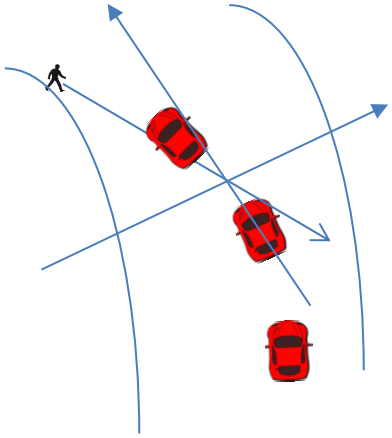

*Figure 5. The vehicle crashes a pedestrian crossing a street while curving.*

## 4 Add obscuring objects to the scenarios

The presence of obscuring objects does not change the collision time. However, they would delay a vehicles ability to recognize the pedestrian, which leads to less time for the vehicle to react to imminent crash to the pedestrian. To analyze the effect of the obscuring objects, the following question needs to be answered:

*Given the path of the pedestrian and the location of the obscuring objects, how could the locations of the obscuring objects be determined so that the object obscures the vehicles view of the pedestrian?*

By answering this question, the time between the first appearance point of the pedestrian and a collision, or time to collision (TTC), can be calculated. If PCS systems are obscured then vehicles must rely more on V2V systems. Figure 6 will be used to describe the effect of the location of obscuring objects on potential crashes. For the simplicity of explanation, it is assumed that the camera is located at the front center of each vehicle. Notations in Figure 6 are defined as follows

Lvs & Wvs: The length and width of the blocking vehicle Vs.
Pp: The coordinates of the pedestrian.
Pvc: The front center position of Vc.
Pvc'& Pvc": The initial position and the final position that Vc is blocked by Vs.
Pvs-fr: The coordinates of the front right corner of Vs
Pvs-rl: The coordinates of the rear left corner of Vs

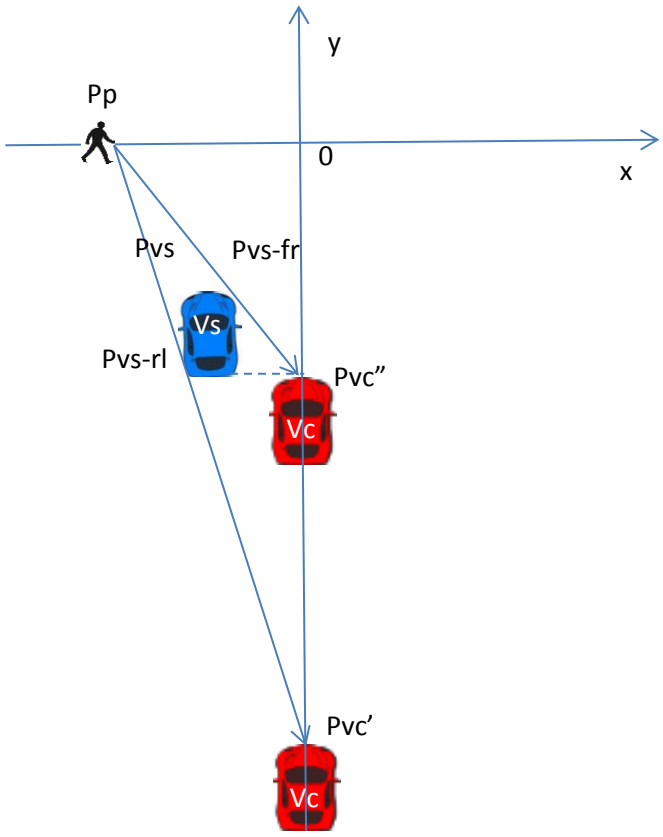


*Figure 6. Add obscure vehicle Vs to scenarios*

According to Figure 6, the range of positions that the blocking vehicle Vs blocks the crashing vehicle Vc's view of the pedestrian is from Pvc' to Pvc". For a given Pvs, Lvs and Wvs, Pvs-fr and vs-rl can be calculated. If Pp is given, Pvc' can be calculated as the point on y-axis and on the line of PpPvs-rl, and Pvc" can be calculated as the point on y-axis and on the line of PpPvs-fr. If Pvc is between Pvc'and Pvc", Vc cannot see the pedestrian.

## 5 Conclusion

This paper used an exhaustive analysis method to identify the scenarios that a combined PCS and V2V system can improve the pedestrian safety theoretically. 96 out of 168 pedestrian related scenarios can benefit from V2V-PCS system. The method for determining if there is a potential crash for all 96 cases for given vehicle and pedestrian motion parameters is described. The method for creating a crash condition for V2V-PCS system evaluation is also described. The calculation of the first appearance location of the pedestrian to the vehicle and time to collision due to the location of the obscure object is described. These results lay a good foundation for further V2V-PCS system studies.

**Acknowledgement**

This project is funded by the US Department of Transportation, Crash Imminent Safety (CrIS) University Transportation Center (UTC).

## REFERENCES

[1] Najm, W.G., Koopmann, J., Smith, J.D. and J. Brewer. 2010. "Frequency of Target Crashes for IntelliDrive Safety Systems." DOT HS 811 381, U.S. Department of Transportation, National Highway Traffic Safety Administration, Washington, DC.

[2] Harding, J., Powell, G., R., Yoon, R., Fikentscher, J., Doyle, C., Sade, D., Lukuc, M., Simons, J., & Wang, J. (2014, August). Vehicle-to-vehicle communications: Readiness of V2V technology for application. (Report No. DOT HS 812 014). Washington, DC: National Highway Traffic Safety Administration.

[3] Frost & Sullivan, http://www.frost.com/prod/servlet/press-release.pag?docid=289374477, Daimler and Volvo Take Lead in Implementation of V2V Communication Systems in Europe.

[4] Najm, W.G., Ranganathan, R., Srinivasan, G., Smith, J.D., Toma, S., Swanson, E. and A. Burgett. 2010. "Description of Light Vehicle Pre-Crash Scenarios for Safety Applications Najm 10 Based on Vehicle-to-Vehicle Communications." To be published, U.S. Department of Transportation, National Highway Traffic Safety Administration, Washington, DC.

# INJURIES AND KINEMATICS: RESPONSE OF THE CERVICAL SPINE IN INVERTED IMPACTS

**Carolyn Roberts**
**Jason R. Kerrigan**
University of Virginia, Center for Applied Biomechanics
United States of America

Paper Number 15-0432

## ABSTRACT

Given the frequency and severity of cervical spine injuries resulting from rollover crashes, it is critical to analyze the mechanism of cervical spine injury in this loading condition. In rollover crashes, roof-to-ground impacts can generate axial compression of the cervical spine, which can result in paralysis and death. This study was performed to compare injury type and severity between component and full body inverted vertex impact tests with post-mortem human surrogates (PMHS); a secondary aim was to determine how changes in vertebral kinematics resulted in changes in hear reaction loads. Five PMHS were suspended in an inverted seated position and then dropped from two heights to achieve 2 m/s (one subjects once and another twice) and 4.4 m/s (all subjects) at impact. The subjects were dropped on a padded five-axis load cell to record the reaction force from impact. Each PMHS was instrumented with three blocks (each containing three accelerometers and three angular rate sensors) rigidly mounted along the upper thoracic spine and on the head. Injuries were determined using both CT scans and dissection following testing. Vertical force traces from the load cell reflect a similar two peak shape seen in previous full-body and component tests. High-speed (1000 Hz) X-ray video analysis shows the neck retains in its initial orientation but becomes increasingly compressed during the loading portion of the first peak. At the first peak, the cervical spine begins to curve, putting the cervical spine into extension, with the center of curvature around C3 or C4, and continues into bending during the unloading of the first peak. The head then translates forward and the neck moves into flexion during the second peak. Each PMHS achieved a flexion injury in the upper thoracic spine or the lower cervical spine during the testing, which occurred during the second peak of the force trace, contradicting previous theories that injury occurs at the first peak, where maximum force occurs. These tests suggest that the direction of torso loading, impact velocity, and boundary conditions at the ends of the cervical spine all affect the kinematics during impact as well as the resulting injuries, and should all be taken into account when determining appropriate injury criteria and developing biofidelic ATDs to predict injuries in crash tests.

## INTRODUCTION

Occupant-to-roof impact can cause some of the most severe injuries in rollover crashes; these injuries have been shown to be related to the amount of roof intrusion into the occupant compartment and the post-crash headroom in the vehicle (Ridella et al. 2008). Occupant-roof interaction generates axial compression in the cervical spine, which is responsible for many rollover crash-induced injuries. Although there are multiple head-neck PMHS compoment studies focused on cervical spine injuries caused by axial compression, few full-body PMHS tests have been performed (Sances et al., 1981; Nusholtz, 1983; Yoganandan et al., 1991; Kerrigan et al. 2014). Viano combines the data from studies by Sances, Nusholtz, and Yoganandan and reports full-body PMHS testing consistently produced injury above 4.0 m/s and consistently resulted in no injury below 2.0 m/s, and more data is needed between the 2.0 and 4.0 m/s range (Sances et al., 1981; Nusholtz, 1983; Yoganandan et al., 1991; Viano & Parenteau , 2008).

Previous head-neck component vertex-impact testing that employed a fixed torso mass (16 kg) and a constraint on the motion of the T1 vertebra has produced severe injury at or above 3.1 m/s (Nightingale et al. 1996, 1997). A more recent study escrived vertex impacr experiments with four full-body PMHS in an impact conditions between 3.0 amd 3.6 m/s, with a goal of generating the same impact positioning and condition achieved by Nightingale in component testing (Nightingale et al. 1996, 1997; Kerrigan et al. 2014). These velocity conditions were also chosen in order to help fill the void of data identified by Viano and Parenteau (Viano & Parenteau 2008). However, the

study found that injuries were significantly less severe than in the Nightingale studies, with only one fracture in the full-body drop tests related to the first 100 ms after impact, and hypothesized these differences in injury severity were due to contraints on T1 (Nightingale et al., 1996, 1997).

This study aimed to expand on the study by Kerrigan et al. (2014) by subjecting five more PMHS to inverted vertex impact. Conditions were the same as the previous study, but tests were performed at 2.0 and 4.4 m/s to compare the results of these recent whole body tests to those of the literature ((Sances et al., 1981; Nusholtz, 1983; Yoganandan et al., 1991) that utilized similar velocities. Specific aims of the cyrrent study included determination whether injuries, in general, can be produced when impact velocity is 4.4 m/s, comparison of injury severity and type to those recorded in previous component and whole body tests, and to identify how abrupt changes in vertebral kinematics are represented in impact force data.

## TESTING METHODS

Five male PMHS were selected for this study; while all subjects were tested with a 4.4 m/s impact velocity; two subjects were tested at 2 m/s to examine the effect of impact velocity on spinal dynamics and repeatability of response (Table 1).

**Table 1.**
**Physical information and test matrix for each post-mortem human surrogate (PMHS) tested.**

| Subject Number | Age (years) | Height (mm) | Weight (kg) | Bone Density (DXA) | First Test (Impact Velocity) | Second Test (Impact Velocity) | Third Test (Impact Velocity) |
|---|---|---|---|---|---|---|---|
| *#582* | 71 | 1780 | 68.04 | 0.8 | 4.4 m/s (Test 6) | - | - |
| *#534* | 71 | 1715 | 93.16 | 0.8 | 2.0 m/s (Test 7) | 4.4 m/s (Test 8) | |
| *#606* | 62 | 1803 | 51.71 | -0.3 | 2.0 m/s (Test 9) | 2.0 m/s (Test 10) | 4.4 m/s (Test 11) |
| *#610* | 48 | 1721 | 61.69 | -2.6 | 4.4 m/s (Test 12) | - | - |
| *#693* | 47 | 1780 | 64.49 | -1.3 | 4.4 m/s (Test 13) | - | - |

### PMHS Preparation and Instrumentation

The PMHS were obtained and treated in accordance with the ethical guidelines established by the Human Usage Review Panel of the National Highway Traffic Safety Administration, and all testing and handling procedures were reviewed and approved by the Center for Applied Biomechanics Biological Protocol Committee and an independent Oversight Committee at the University of Virginia.

**PMHS Preparation** The upper extremities of each subject were removed at the sternoclavicular joint. Mounting plates for instrumentation cubes were screwed into the right and left sides of the parietal bones using wood screws. Three sets of mounting hardware were screwed into T1, T4, and T8, and static x-rays and geometric calculations were used to confirm that each mount was rigidly attached to the correct vertebra. After surgical preparation, each subject was wrapped in a thin layer of mechanically adhesive wrap (Coban, 3M, St. Paul, MN, USA) and outfitted with a tactical body harness (355 Extraction Harness, Yates Gear Inc, Redding, CA, USA). A post-preparation CT scan was taken to ensure no damage was done to the cervical spine and to confirm mount locations.

**Instrumentation** The instrumentation on the spine consisted of three blocks, rigidly attached to T1, T4, and T8 with the mounting hardware. Each block allowed for the attachment of three accelerometers (7264B-2000, Endevco, San Juan Capistrano, CA, USA) and three angular rate sensors (ARS-8K, DTS, Seal Beach, CA, USA). Two more of instrumentation blocks were also affixed to either side of the head onto the mounting plates. Other instrumentation used in the test included two load cells; one padded six-axis load cell (Denton B-3868-D, Humanetics Innovative Solutions, Plymouth, MI, USA) onto which the subjects landed, and another cable load cell that allowed for determination of drop release time. On the top plate of the six-axis load cell, a piece of 25.4 mm thick light-density closed-cell, polyvinyl chloride general purpose foam (V700 Series 1.00", Gaska Tape Inc., Elkhart, IN, USA), was adhered to the steel plate. This foam was used previously (Frechede et al. 2009) to mimic the foam used by Nightingale et al. (1996).

### Testing Area Setup and Procedures

Each subject was suspended in an upside-down seated position (Manary et al., 1998) using a system of strings and taut ties (small plastic pieces to adjust the length of each string). All of the strings were looped around a single carabineer, from which the cadaver was suspended. Multiple strings allowed for control over the position, and the subject's torso was rotated until the superior endplate of T1 was oriented at a 25 degree angle from parallel to ground, and the cervical spine was flexed until the Frankfurt plane was oriented parallel to the ground (Nightingale et al., 1996). The subject was positioned such that vertex of the head was centered over the padded load cell. Following final positioning, a ROMER arm scanner (ROMER Absolute Arm with Integrated Scanner, Hexagon Metrology, North Kingstown, RI, USA) was used to collect the orientation and position of all of the accelerometers, angular rate sensors, and the padded load cell onto which each subject landed. After recording this final position with the scans, the subject was released with a solenoid release mechanics to sustain impact with the load plate affixed to the floor.

X-Ray imagery was captured at 1000 Hz in all of the impact tests via positioning the subjects between an image intensifier connected to a high speed digital imager (GX-1, NAC Inc., Japan). Video images were also captured at 1000 Hz from lateral and superior views of the subjects.

A post-test CT was taken, followed by a dissection to confirmed the bony fracture seen in the CT scan and to display ligamentous and facet joint damage.

## DATA ANALYSIS

### Coordinate Transformations of Data

Head and T1 acceleration data were transformed to local coordinate systems (defined by anatomical landmarks) using the rigid body assumption. The vertebral and head coordinate systems were generated using CT imagery to find the location and orientation of the mount relative to vertebral anatomy. In the vertebral coordinate system, the y-axis was generated by creating a vector from the most lateral point of the left to the most lateral point of the right transverse process. The x-axis was defined to point from the most posterior point of the spinous process to a point on the y-axis such that the x- and y-axes were perpendicular. The z-axis was found by taking the cross product of the x and y vectors. The local head coordinate system was determined using 3 screws (right, left and posterior) that generated the plane in which the cg of the head laid. The y-axis was found by finding the vector of the location of the left screw, L and to the location of the right screw, R. Next the x-axis of the head was determined by finding the perpendicular line to the y-axis on which point P, the posterior of the head, lies. The positive x-axis was found my taking the cross product of the positive x-axis and the positive y-axis. After all of the local data had been found, time histories of the head and T1 local-to-global coordinate system transformations were determined from the angular rate data (Beard & Schlick, 2003).

### High Speed X-ray video analysis

Changes to the shape of cervical spine over the first 80 ms (2.0 m/s impact velocity tests) or 175 ms (4.4 m/s impact velocity tests) after impact were determined by tracking the motion of the connection between the vertebral body and the spinous process for each of the cervical vertebrae in each test using X-ray images. The times when abrupt changes in cervical curvature were seen were compared to the head/load plate loads to facilitate dynamic response analysis.

## RESULTS AND DISCUSSION

### Head Forces

The vertical force traces measured by the padded load cell during impact follow the general double peak shape seen in other studies, both full-body and component, that axially load the cervical spine (Figure 1). Comparing the force results from this test to the previous full-body tests in the literature, the duration, magnitude and peak forces attained during the test closely match (Sances et al., 1981; Nusholtz, 1983; Yoganandan et al., 1991). However, comparing to component tests, increasing the impact velocity by 38% (from 3.2 m/s to 4.4 m/s), resulted in an increased force of 200-250% (Nightingale et al., 1996, 1997). The previous whole body study showed similar peak forces as the component tests, yet no or only subtle injuries (Kerrigan 2014). If this were solely due to rate sensitivity, then it would be at a level that exceeds documented rate sensitivity for all other human tissues. The higher impact force is likely due more of the upper body mass being recruited in the initial impact because there is less time for it to move or articulate away from the load path.

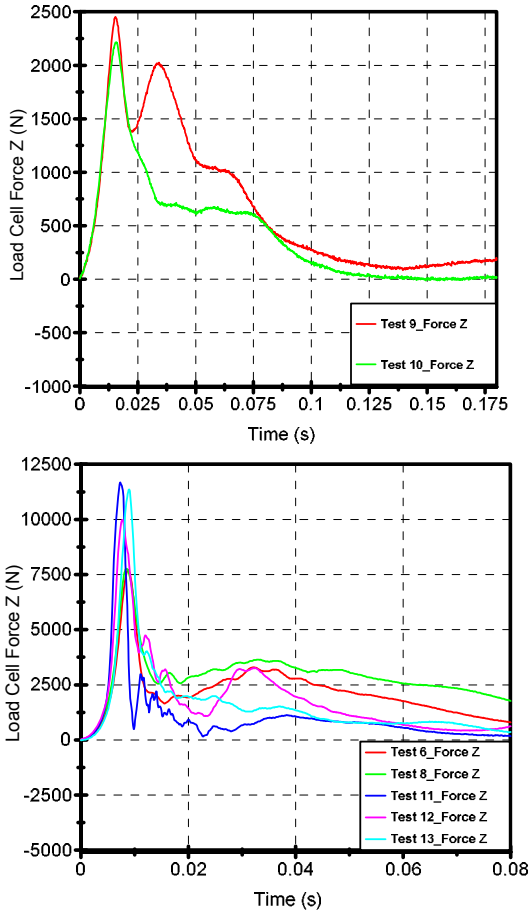


***Figure 1. Vertical force traces for each tests. The 2.0 m/s impact velocity tests are depicted in the top graph, and the 4.4 m/s impact velocity tests are depicted in the bottom graph***

**Kinematics of the torso, neck, and head**

Using high-speed X-ray video, it is possible to see the position of the cervical spine as a whole throughout the entire loading period resulting from the impact (both peaks in the vertical force trace). The relative positions of the cervical spine, torso, and head at different times during the vertical force trace are depicted in Figure 2.

In part 1, the PMHS has just initiated contact with the load cell; T1 looks as if it is 25 degrees from horizontal, as it was initially positioned, and the cervical spine is fairly straight with the exception of C1 and C2 (this is probably due to the initial position of the Frankfurt plane at 0 degrees). In part 2, the force trace shows a dramatic increase towards its maximum peak; the cervical spine remains in the same position, but begins to compress slightly. This is the only time during the test where the neck is in pure axial compression. At this time, the torso continues to translate downwards and the head remains fixed in its initial position. In part 3, the maximum Z-force is reached, and the curvature of the neck begins to increase, specifically around C3-C4. In part 4, the vertical force decreases as the neck continues to increase more and more in curvature. In other words, the load decreases at the geometry of the neck changes. In part 5, the vertical force increases once again, and the cervical spine begins to straighten as the head translates forward, and again, the torso continues to translate downward. In part 6, the force reaches a second peak as the neck straightens, and the head continues to translate even further forward, and the torso continues to move down. This puts the neck in shear loading, especially at the C7/T1 interface. In part 7, the Z-force is decreasing, and the bottom of the neck is in flexion with shear loading, the head continues to move forward, and begins to rotate up towards the torso. In 8, the head has almost left the load cell, and the head continues to rotate upwards, while the torso continues to translate downwards and also posteriorly. This rotation and translation of the head continue until the head leaves the load cell and the magnitude of the Z-force is zero.

As was noted before, these general kinematics occurred for every subject with the exception of Subject 582 in Test 6. In Test 6, the Subject's torso loaded the head and neck more vertically. This meant that the head was unable to translate forward and then rotate out of the way of the torso that was loading it.

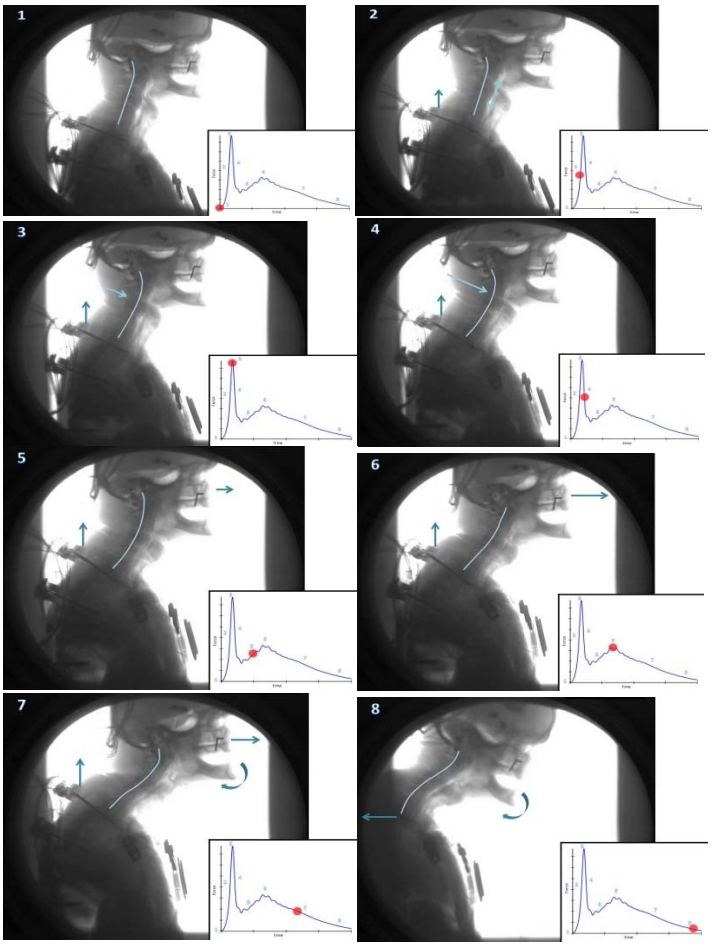


***Figure 2. Time step of X-ray video to show the kinematics of the cervical spine with respect to the force trace shape. A light blue curve is drawn along the cervical spine, connecting the location where the spinous process meets the body of each vertebra. Arrows are also shown to depict the general motion of the head and torso of the subject. This figure shows the representative general kinematics that all subjects underwent (with the exception of Subject 582). The red dot on the force trace of each image denotes the relative time at which each motion in the picture is occurring. Each image is also labeled in chronological order (1-8).***

**Injuries**

Table 2 is a collection of the injuries found in all of the subjects. It is very clear that most of the injuries occur in the lower cervical spine and thoracic spine and, it is important to note that only one compression injury in the upper cervical spine was attained during this test. All of the subjects did not attain bony fracture, but all were all injured during testing, most at the 4.4 m/s impact velocity.

**Table 2.**
**Location and type of injuries attained for each subject during testing.**

| Injury Location ↓ | Subject # 582 | Subject # 534 | Subject # 606 | Subject # 610 | Subject # 693 |
|---|---|---|---|---|---|
| **C1 Vertebra** | Anterior arch fracture | | | | |
| **C2 Vertebra** | | | | | |
| **C3 Vertebra** | | Two fractures in the vertebral body | | | |
| **C3/C4 Joint** | | | | Anterior longitudinal ligament tear | |
| **C4 Vertebra** | | | | | |
| **C5 Vertebra** | | | | | |
| **C6 Vertebra** | | | Acute fracture of inferior endplate | | |
| **C6/C7 Joint** | | | | Small tear in anterior longitudinal ligament | |
| **C7 Vertebra** | | | Acute fracture of superior endplate | | |
| **C7/T1 Joint** | | Supraspinous ligament tear<br>Interspinous ligament tear<br>Ligamentum flavum tear | Supraspinous ligament tear<br>Interspinous ligament tear<br>Facet disruption | Supraspinous ligament tear<br>Interspinous ligament tear<br>Ligamentum flavum tear<br>Partial tear of anterior longitudinal ligament<br>Facet disruption | Supraspinous ligament tear<br>Interspinous ligament tear<br>Partial tear of posterior longitudinal ligament |
| **T1 Vertebra** | Acute fracture of inferior endplate | Lamina fracture | | | |
| **T1/T2 Joint** | | | | | Facet disruption |
| **T2 Vertebra** | Acute fracture of inferior endplate<br>Acute fracture of superior endplate | Lamina Fracture | | | |
| **T3 Vertebra** | Acute fracture of superior endplate | | | | |
| **T4 Vertebra** | | Lamina Fracture | | | |
| **T5 Vertebra** | | Lamina Fracture | | | |

Most of the injuries at the C6, C7, T1 and T2 level were located anterior, suggesting they were flexion injuries. Given the mode of injury is flexion, and from the X-ray videos it is clear that the cervical spine does not go into flexion until the second peak of loading, it makes sense that these injuries occur during the second peak of the vertical force trace, not at the point of maximum vertical force. This suggests that simply measuring and then using a maximum force as an injury criterion would not be effective, as these injuries occur nowhere near the maximum force. These injuries are likely due to difference in stiffness between the neck and torso; more motion is allotted for the vertebrae in the cervical spine, and the resistance to motion of the more rigid thoracic spine could cause stress concentrations that resulted in fracture or excessive stretching of ligaments causing tearing.

The ligamentous injuries and fractures in C3 and C4 were located posterior, suggesting their mode of injury was extension. Extension of the cervical spine occurs during the unloading portion of the first peak of the vertical force trace, so it is likely that these extension injuries occurred just following the maximum measured force.

One injury is an outlier to this injury data set: the anterior arch fracture of C1 from subject 582. In the test of this subject, the head was unable to move away from the torso as it descended, and therefore the loading on the cervical spine due to the torso was directed more vertical than in the other tests. As seen in the time step videos in Appendix A, as well as Figure 3 the cervical spine remains straight for a longer portion of the test than in all of the other tests. It is likely that a higher axial force was experienced in the upper cervical spine in test 9, which explains this anterior arch fracture of C1. This injury is likely the only injury resulting from reaching a maximum vertical force where pure axial compression is the only load on the cervical spine.

Subject #606 attained an injury at the C7/T1 joint during test 9, the first 2.0 m/s impact velocity test for this subject. The injury could be seen on the high-speed X-ray video, and occurred after the 175 ms test time. The injury was not initially seen, so Test 10 (at 2.0 m/s impact velocity) and Test 11 (at 4.4 m/s impact velocity) were still performed. The magnitude of Z force between Test 9 and 10 are extremely close, suggesting that the first peak of loading is not affected by the C7/T1 extension injury. There is a distinct difference between the two tests as Test 10 lacks a distinct second peak; there is also a lack of a second peak in Test 11. The lack of the second peak in vertical force coupled with an extension injury further reinforces the idea that flexion injuries occur during the second peak, and that the prior damage to the C7/T1 joint allowed for greater motion between the cervical and thoracic spines, allowing the neck to more easily rotate away from the torso, and decreasing the vertical loading recorded by the load cell.

**Differences in kinematics between subjects**

Subject 582 had the largest divergence from the generalized kinematics and injuries explained above. Although this subject achieved an axial compression injury, the maximum force in Test 6 has the lowest magnitude of the 4.4 m/s impact velocity tests, yet Subject 582 has the second highest mass. Given all other subjects attained higher maximum forces, but no axial compression injuries, there was likely a difference in position of the cervical spine throughout impact, which could be seen through high speed X-ray imagery (Figure 3). One of the most significant discrepancies is the difference in the head position. In the top image, the head of Subject 582 is trapped almost directly under the torso, whereas in the bottom image, Test 12, the subject's head has translated to the right in the X-ray video, and the neck and torso still have room to translate downwards, because the head has moved out of the way. Another significant difference is the difference between the curvature of the cervical and thoracic spines between the two tests. There is a sharp bend between the cervical and thoracic spines in the bottom figure (the location where Subject 610 attained a flexion injury), whereas the curvature at this location in the top photo is much less severe.

Although the two subjects were initially positioned in the same manner, differences in kinematics and injuries are likely due to geometric differences in the thorax of each subject, which could change the anterior-posterior position of the center of mass of the torso, and thus change the direction of the force that loads the neck.

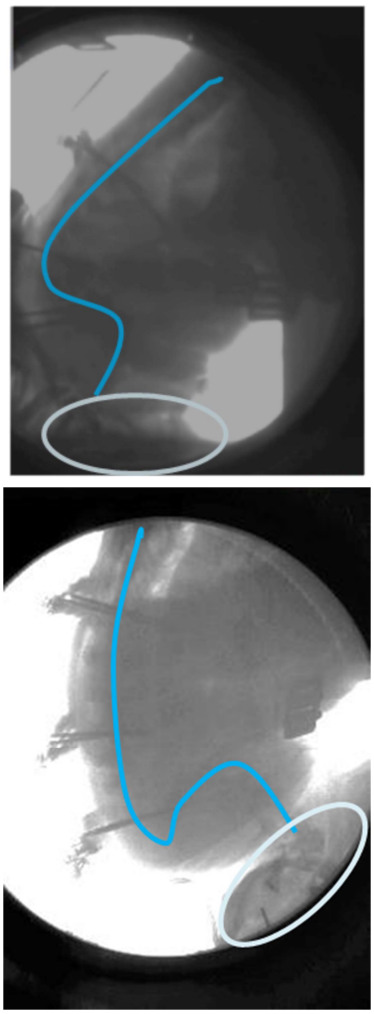

***Figure 3. Kinematic differences between the spine and head between Subject 582, Test 6 (top) versus Subject 610, Test 12 (bottom) both at 40ms after impact under the same velocity conditions. The blue line shows a trace of the cervical and thoracic spine shapes and the white circle shows the approximate location and orientation of the head.***

**Boundary Conditions of the Cervical Spine**

It is well established that cervical spine boundary conditions have a substantial effect on the injury tolerance and type in compressive loading (Nightingale et al., 1991). By performing full body-drop tests, one of these boundary effects can be measured in vitro, by measuring the motion of T1 using an instrumentation mount with three accelerometers and three angular rate sensors (Figure 4). There was substantial rotation of the T1 vertebra, especially in the roll (over a 15 degree change).

Given the magnitude of these rotations it is possible that the assumptions made for the boundary conditions by Nightingale in head-neck complex tests. Allowing T1 to only translate in the global Z direction drastically limits the motion that is seen in the full body. By restricting the motion of T1, more severe injuries could have been generated in the cervical spine at a lower impact velocity, and could have been created at different times or different locations than if T1 were allowed to be free to rotate.

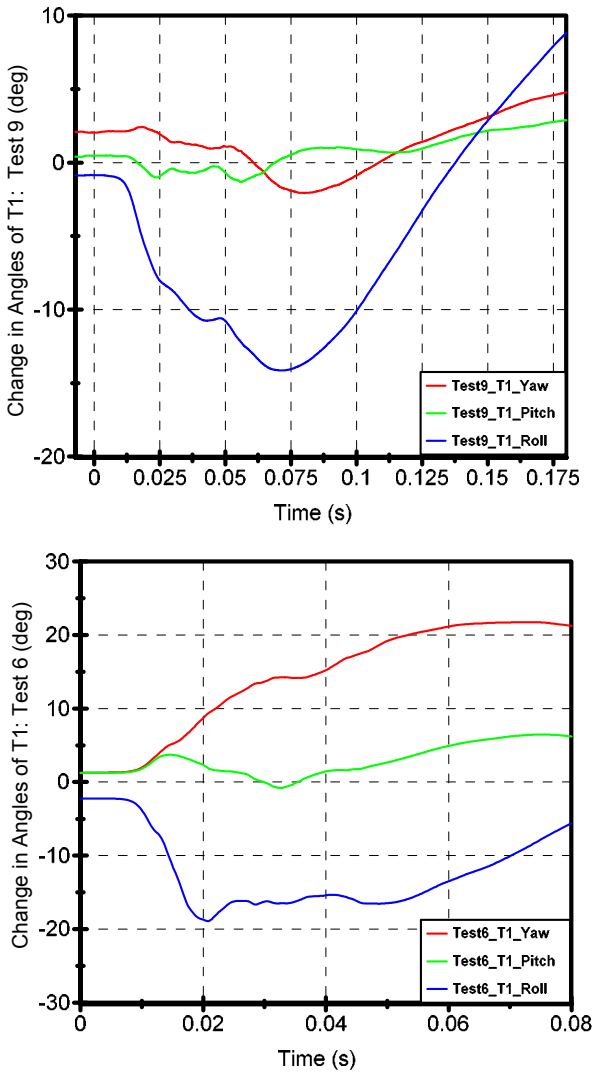


***Figure 4. Local vertebral coordinate system angular velocities depicting the motion of T1 during tests are shown. The plot on the top shows the x, y and z angular rates for a 2.0 m/s impact velocity test, and the plot on the bottom shows the same angular rates for a 4.4 m/s impact velocity test.***

## CONCLUSIONS

Five whole body PMHS were subjected to inverted vertex impacts at 2.0 m/s and 4.4 m/s to examine their response relative to other subjects tested at different velocity tests and component tests that constrained subject motion. The goals of this study included evaluation of whether a 4.4 m/s impact velocity was sufficient to cause injuries, comparison of injury severities and types to those seen in previous tests, and determination of how changes in vertebral kinematics are represented in impact force. The results of this study allowed the following conclusions to be drawn:

Results showed that:

- In general, the PMHS were injured at the 4.4 m/s impact velocity level
- The PMHS injuries generated in these tests were less severe than injuries produced in component test studies conducted at lower impact velocities around 3.2 m/s
- Substantially higher head forces (first peak) were generated in this study than in the previous whole body and component test studies at 3.2 m/s (7500-11500 N vs. 4500 N).

- Injuries, in general, do not occur as a result of the peak impact force; the peak head force does not indicate injury tolerance of the subject
- T1 rotates out of the way during the time period between initial impact, the peak force, and the time when the injury occurs, which suggests that constraining its motion will affect the load response and additionally the injury tolerance of the spine

A next steps in this research could be to evaluate how well existing ATDs represent human respinse by sunjecting ATDs to matched experiments. Aditionally, these data could be used to inform computational analyses aimed at evaluating human body computational models and/or using them to examine the effects of muscle tension on head/neck/torso response.

**REFERENCES**


[1] Beard, D. A., and Schlick, T. (2003). Unbiased Rotational Moves for Rigid-Body Dynamics. Biophysical Journal, 85, 2973-2976.

[2] Frechede B; McIntosh A; Grzebieta R; Bambach M. (2009) Hybrid III ATD in inverted impacts: influence of impact angle on neck injury risk assessment. Annals of Biomedical Engineering, 37(7): 1403-1414.

[3] Kerrigan, J., Foster, J., Forman, J., Toczyski, J., Roberts, C., Crandall, J. (2014). Axial Compression Injury Tolerance of the Cervical Spine: Initial Results. Traffic Injury Prevention.

[4] Manary M., Reed M., Flannagan C., Schneider L. (1998). ATD Positioning Based on Driver Posture and Position. 42nd Stapp Car Crash Conference. 1-13.

[5] Matsushita T, Sato TB, Hirabayashi K, Fujimura S, Asazuma T, Takatori T. X-ray study of the human neck motion due to head inertia loading. Proceedings of the 38th Stapp Car Crash Conference, 55-64, 1994.

[6] Nightingale RW, Meyers BS, McElhaney J, Richardson WJ, Doherty BJ. (1991) The Influence of End Condition of Human Cervical Spine Injury Mechanisms. SAE 912915, Society of Automotive Engineers.

[7] Nightingale R., McElhaney J., Richardson W., Myers B. (1996). Dynamic responses of the head and cervical spine to axial impact loading. J Biomechanics, 29: 307–18.

[8] Nightingale R., McElhaney J., Camacho D., Kleinberger M., Winkelstein B., Myers B. (1997) The dynamic responses of the cervical spine: buckling, end conditions, and tolerance in compressive impacts. Proceedings of the 41st Stapp Car Crash Conference. Paper number 973344. 451-71.

[9] Nusholtz, G.., et al. (1983). Cervical spine injury mechanisms. No. 831616. SAE Technical Paper.

[10] Ridella, S., and A. Eigen. "Biomechanical investigation of injury mechanisms in rollover crashes from the CIREN database." proceedings of the 2008 International IRCOBI Conference, Bern, Switzerland. 2008.

[11] Sances Jr A, Myklebust J, Cusick JF, Weber R, Houterman C, Larson, SJ, Walsh P, Chilbert M, Prieto T, Zyvoloski M, Ewing C, Thomas D. (1981) Experimental Studies of Brain and Neck Injury. Proceedings of the 25th Stapp Car Crash Conference, Society of Automotive Engineers.

[12] Viano D., Parenteau C. (2008). Analysis of head impacts causing neck compression injury. Traffic Injury Prevention, 9(2):144-52.

[13] Yoganandan N, Pintar FA, Sances A Jr and Maiman DJ. (1991) Strength and kinematic response of dynamic cervical spine injuries, Spine, Vol. 16, No. 10S, pp. 511–517.

## APPENDIX A: STILL FRAME IMAGES OF TEST VIDEO

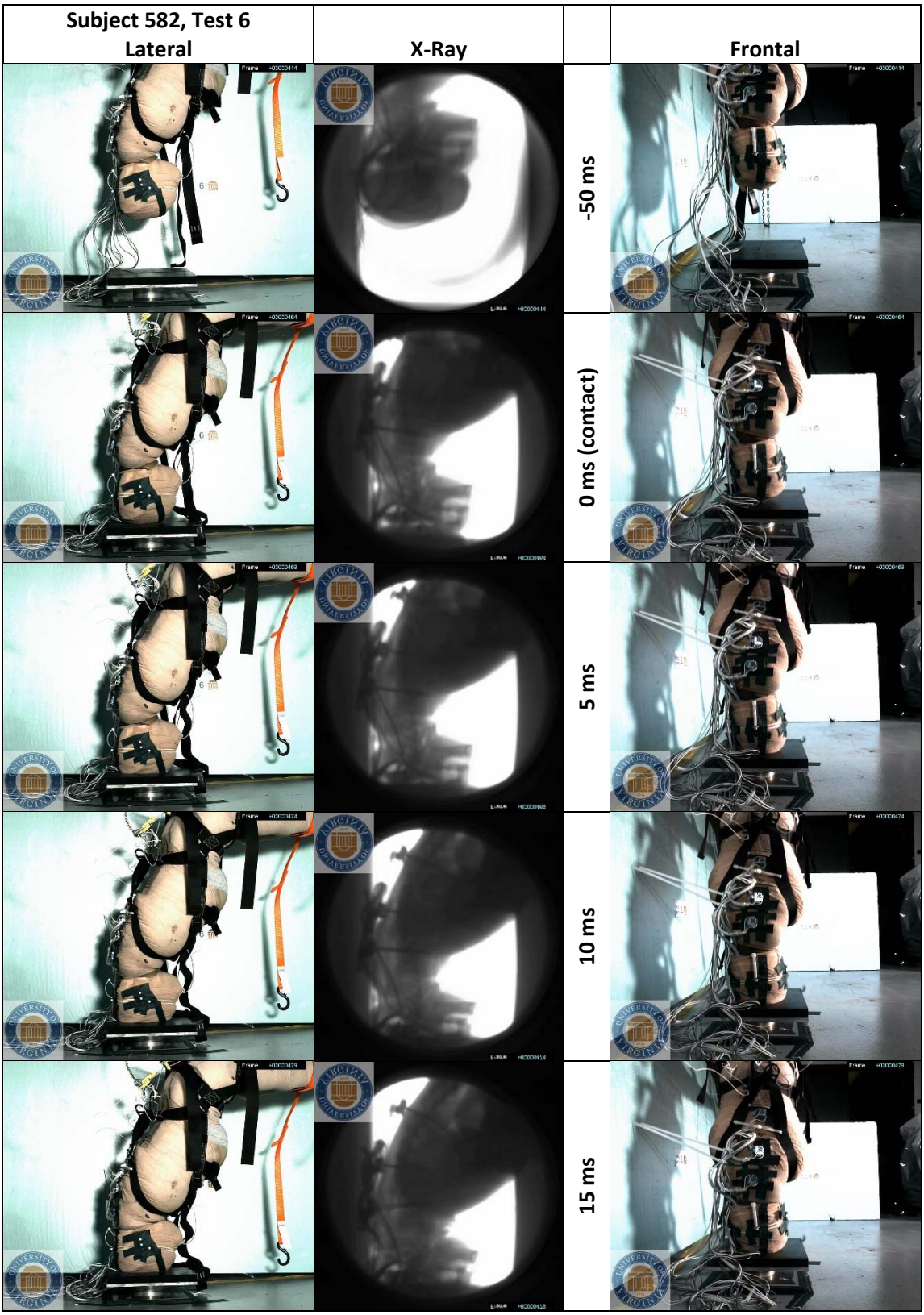

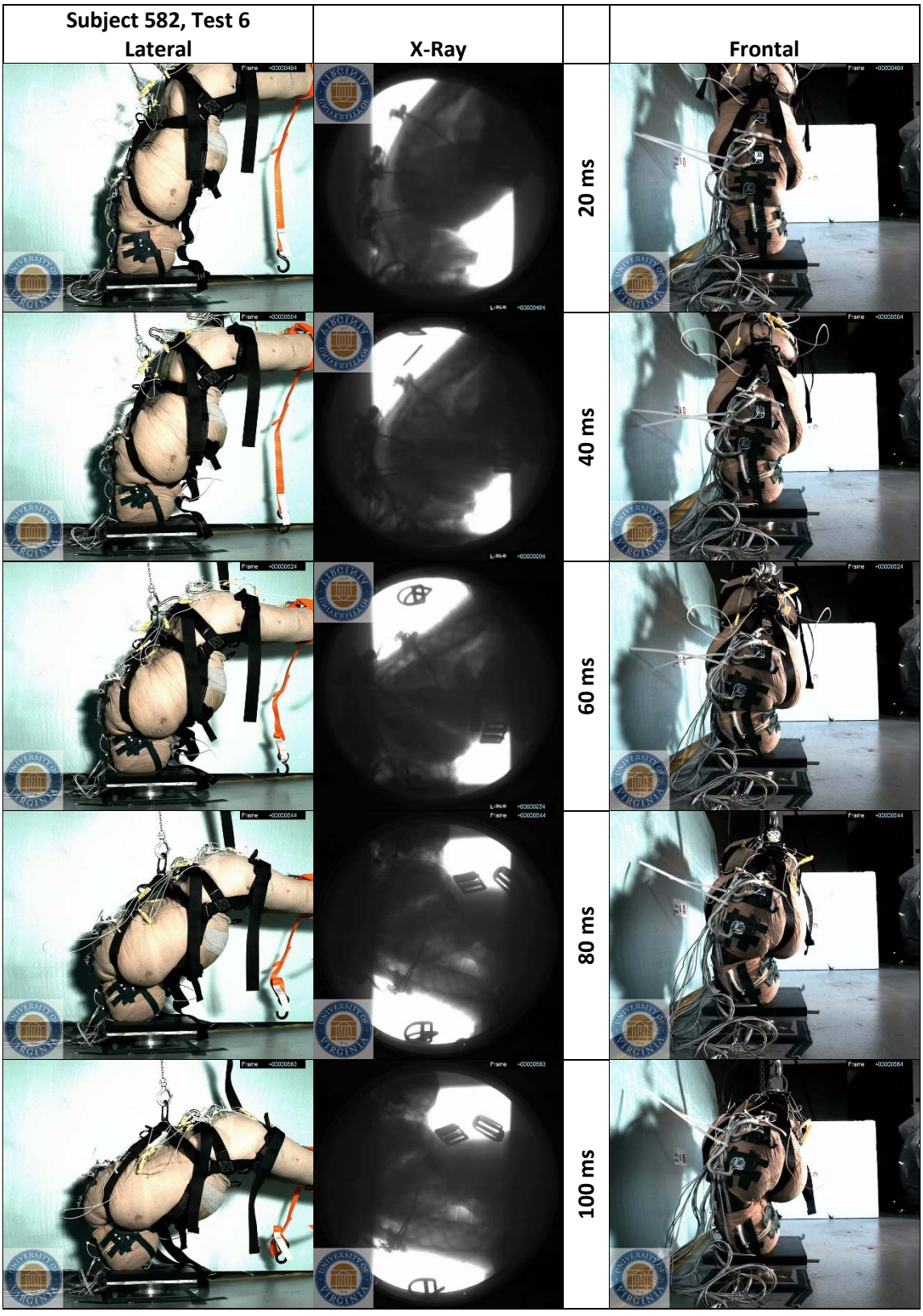
Subject 582, Test 6
Lateral
X-Ray
Frontal
20 ms
40 ms
60 ms
80 ms
100 ms

| Subject 534, Test 8<br>Lateral | | Frontal |
|---|---|---|
| 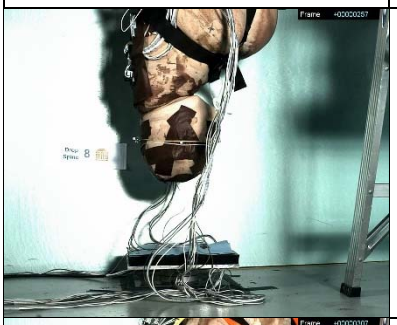 | -50 ms | 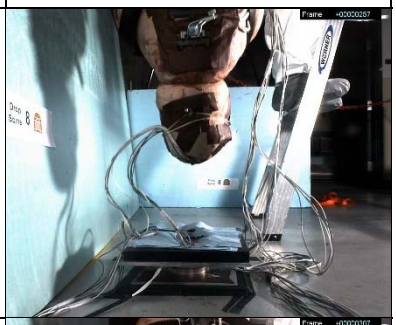 |
| | 0 ms (contact) | |
| | 5 ms | 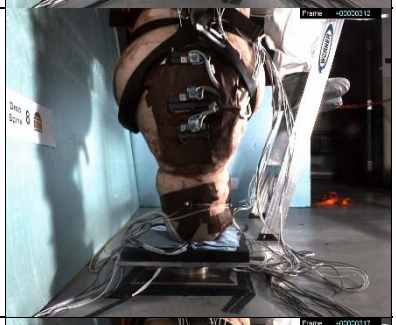 |
| | 10 ms | |
| | 15 ms | |

| Subject 534, Test 8<br>Lateral | | Frontal |
|---|---|---|
| 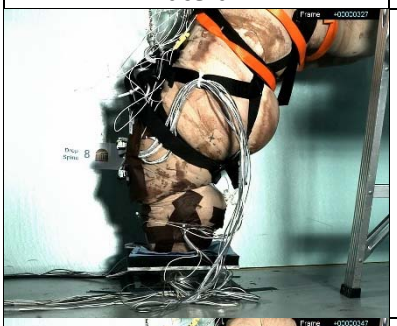 | 20 ms | 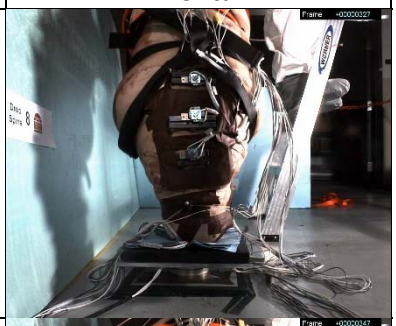 |
| | 40 ms | 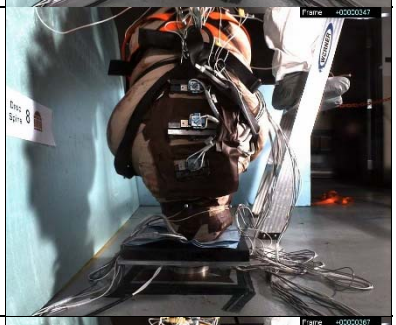 |
| | 60 ms | 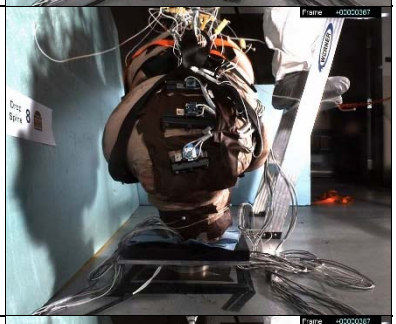 |
| | 80 ms | |
| | 100 ms | |

| Subject 606, Test 9<br>Lateral | X-Ray | | Frontal |
|---|---|---|---|
| 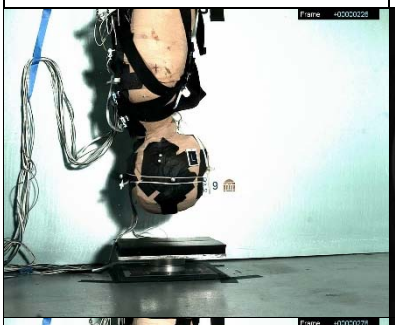 | | -50 ms | 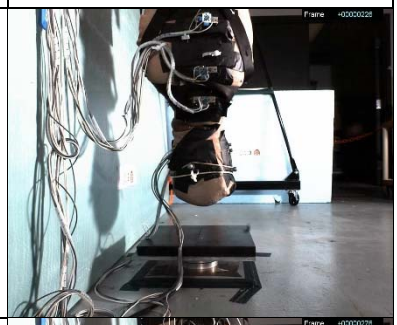 |
| | | 0 ms (contact) | |
| | | 5 ms | |
| 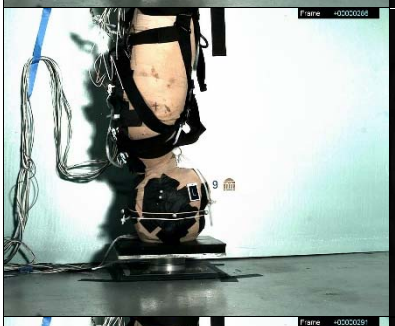 | | 10 ms | |
| 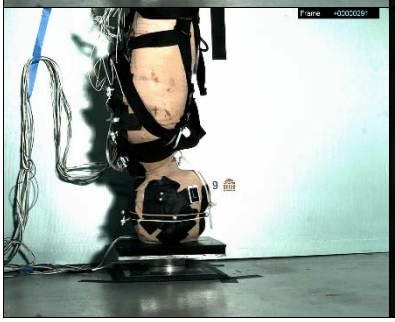 | | 15 ms | 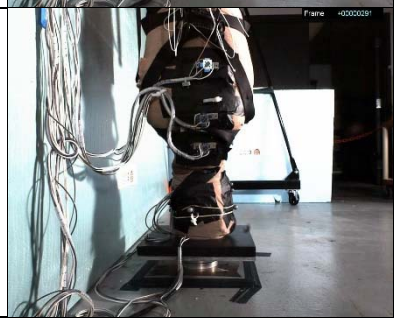 |

| Subject 606, Test 9<br>Lateral | X-Ray | | Frontal |
|---|---|---|---|
| 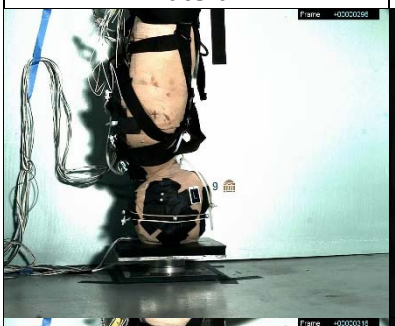 | | 20 ms | 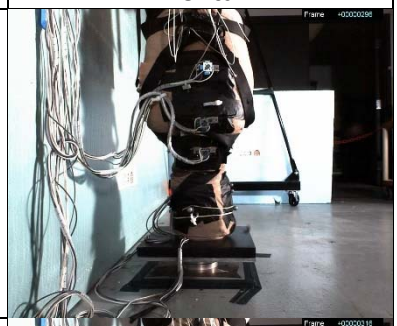 |
| 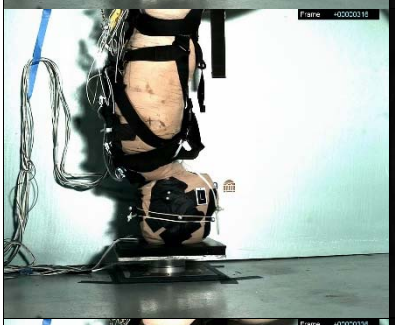 | 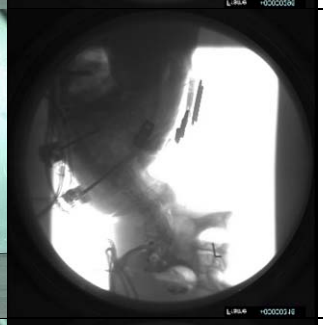 | 40 ms | |
| 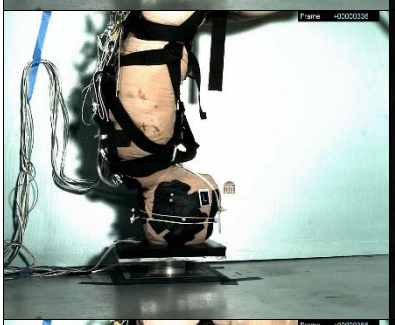 | | 60 ms | |
| 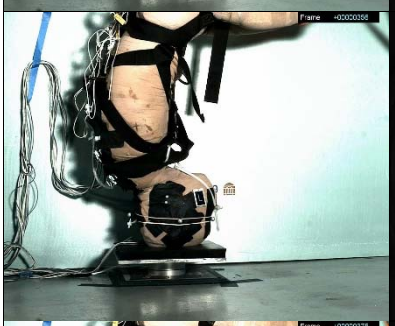 | | 80 ms | |
| | | 100 ms | 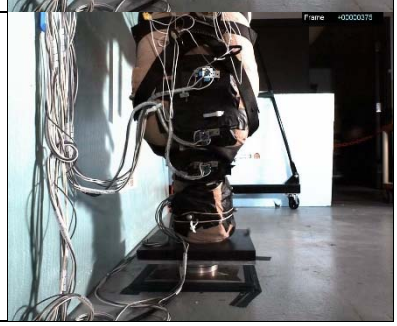 |

| Subject 606, Test 10<br>Lateral | X-Ray | | Frontal |
|---|---|---|---|
| 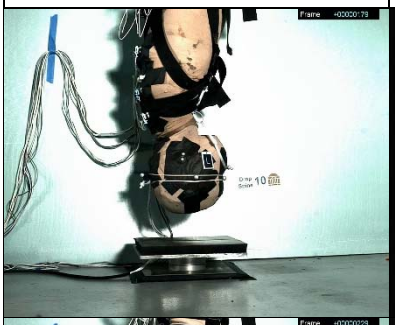 | 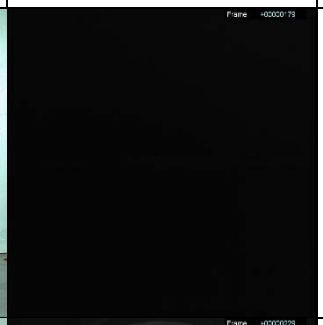 | -50 ms | 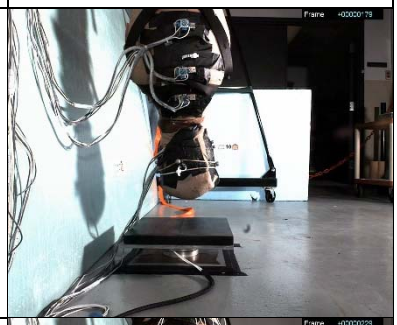 |
| | | 0 ms (contact) | |
| | | 5 ms | |
| | | 10 ms | 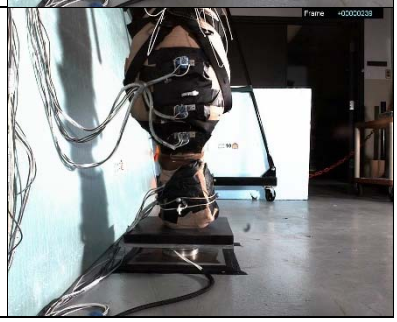 |

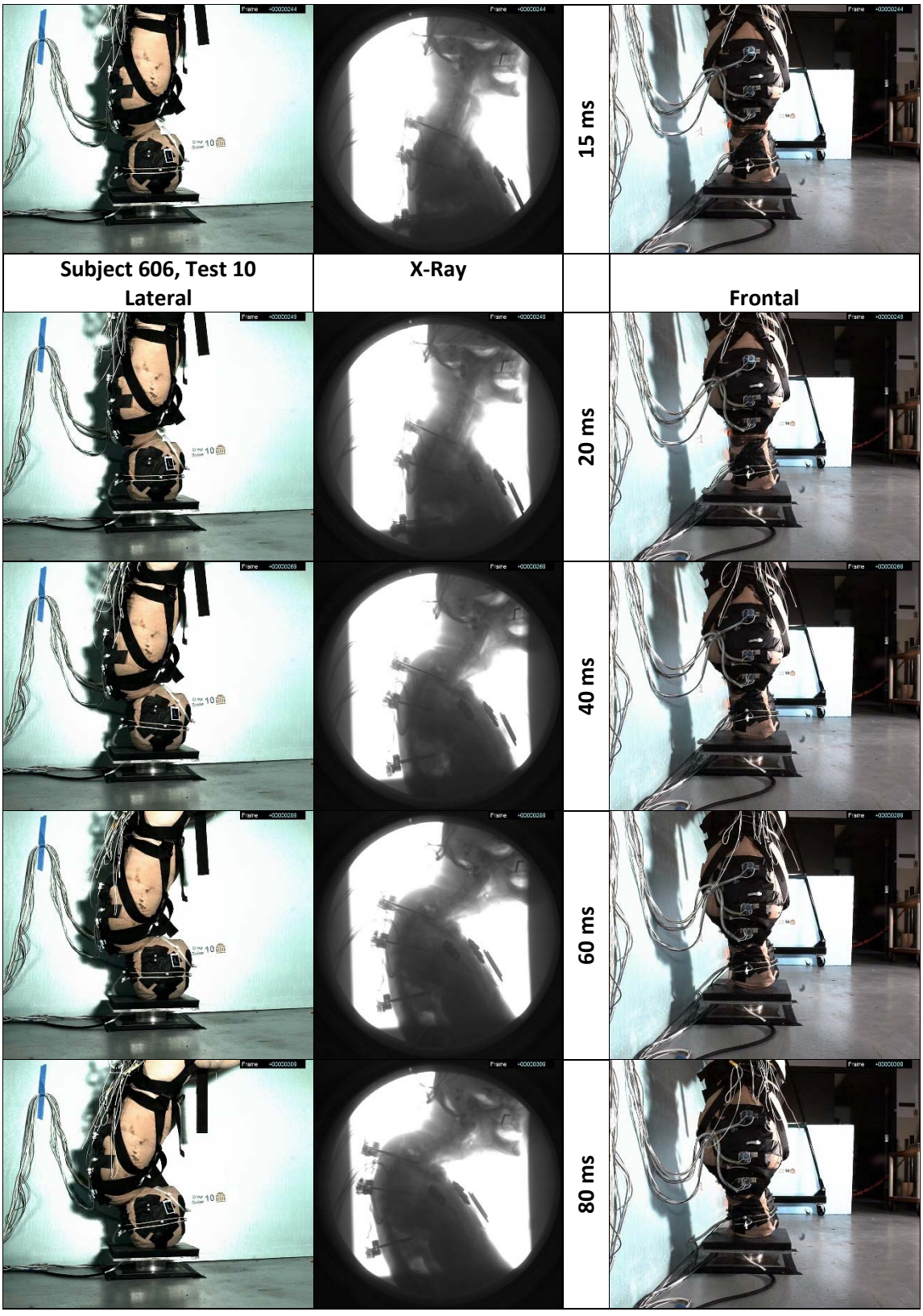
Subject 606, Test 10
Lateral
X-Ray
Frontal
15 ms
20 ms
40 ms
60 ms
80 ms

| Subject 606, Test 11<br>Lateral | X-Ray | | Frontal |
|---|---|---|---|
| 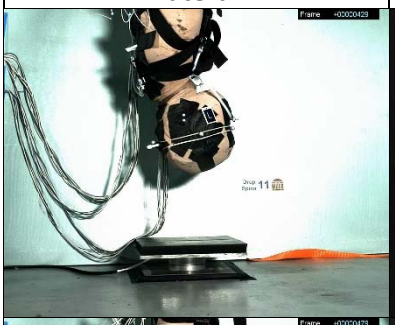 | 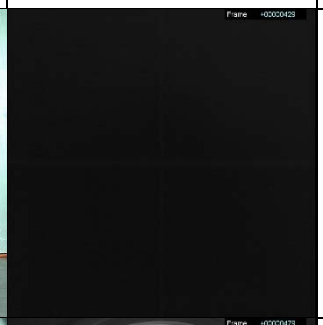 | -50 ms | 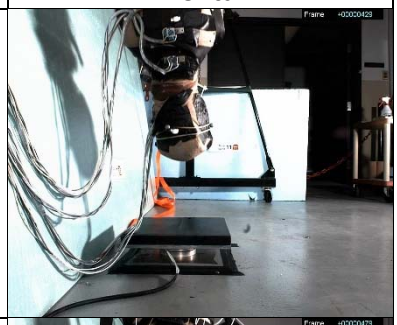 |
| | | 0 ms (contact) | |
| | | 5 ms | |

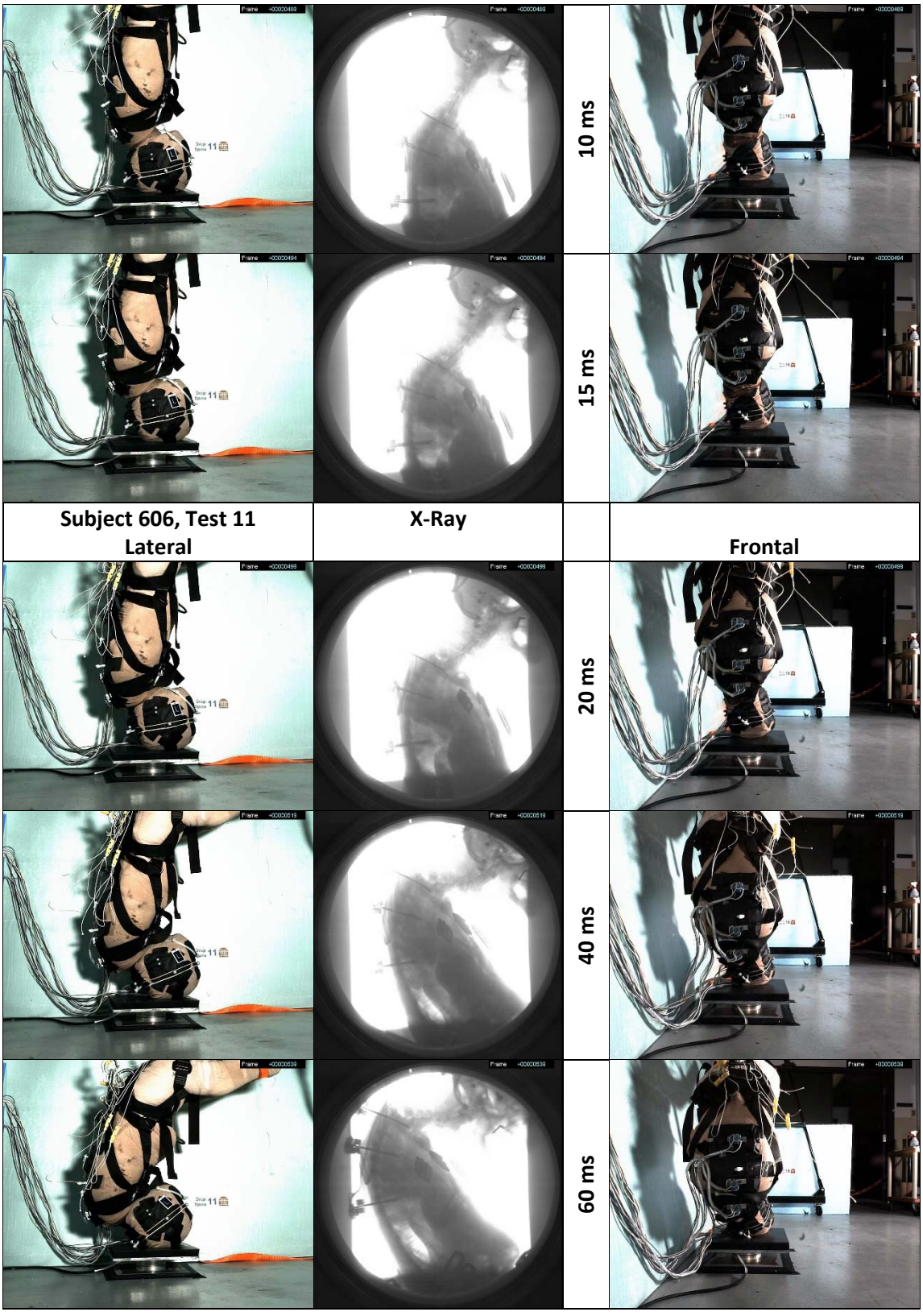
10 ms
15 ms
Subject 606, Test 11
Lateral
X-Ray
Frontal
20 ms
40 ms
60 ms

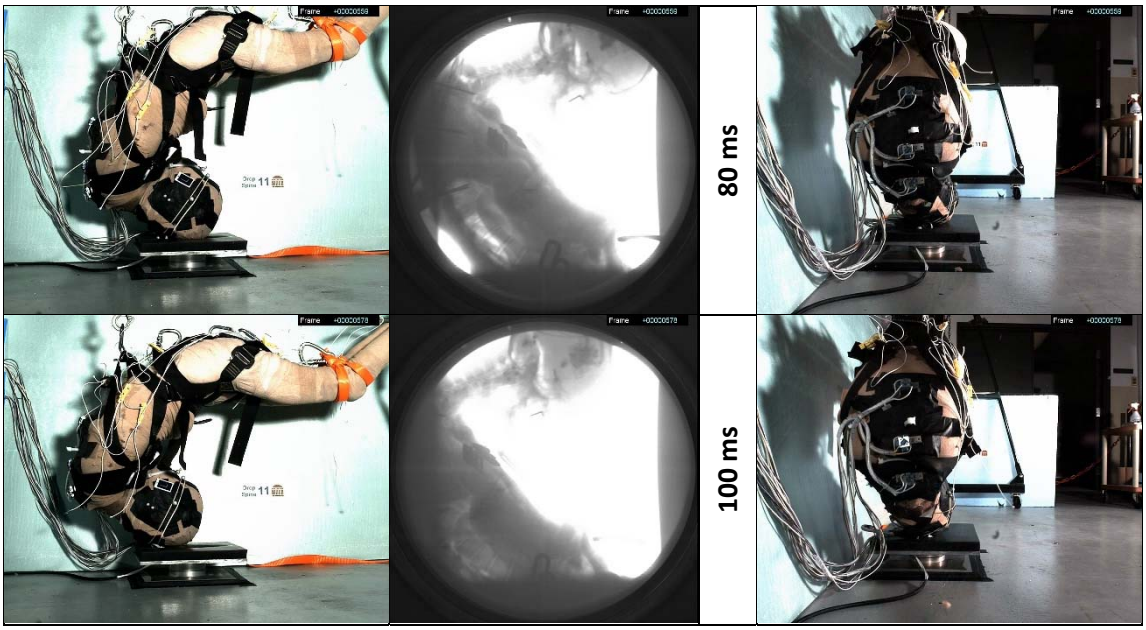


| Subject 610, Test 12<br>Lateral | X-Ray | | Frontal |
|---|---|---|---|
| | 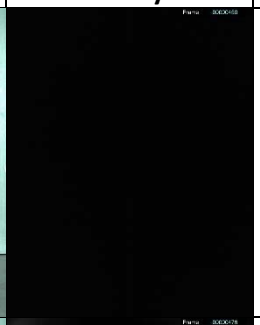 | -50 ms | 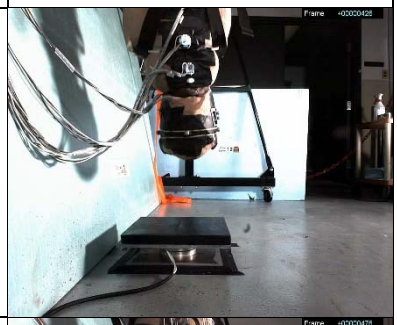 |
| | | 0 ms (contact) | 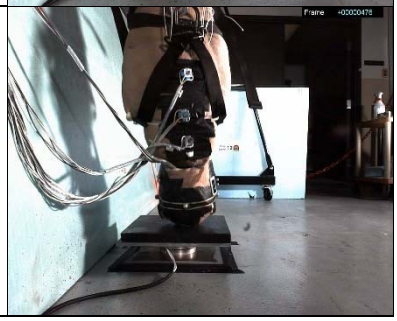 |

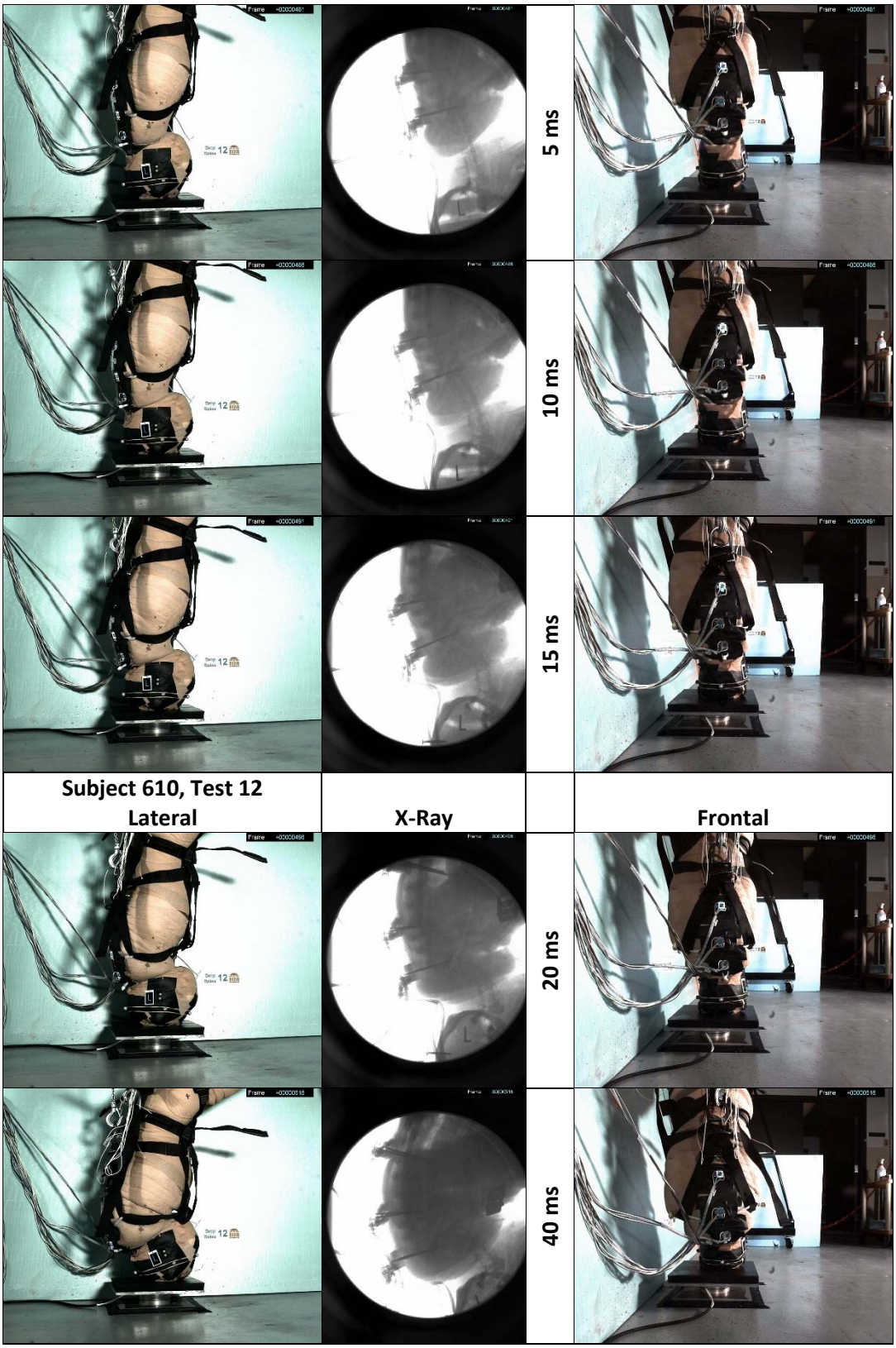
5 ms
10 ms
15 ms
Subject 610, Test 12
Lateral
X-Ray
Frontal
20 ms
40 ms

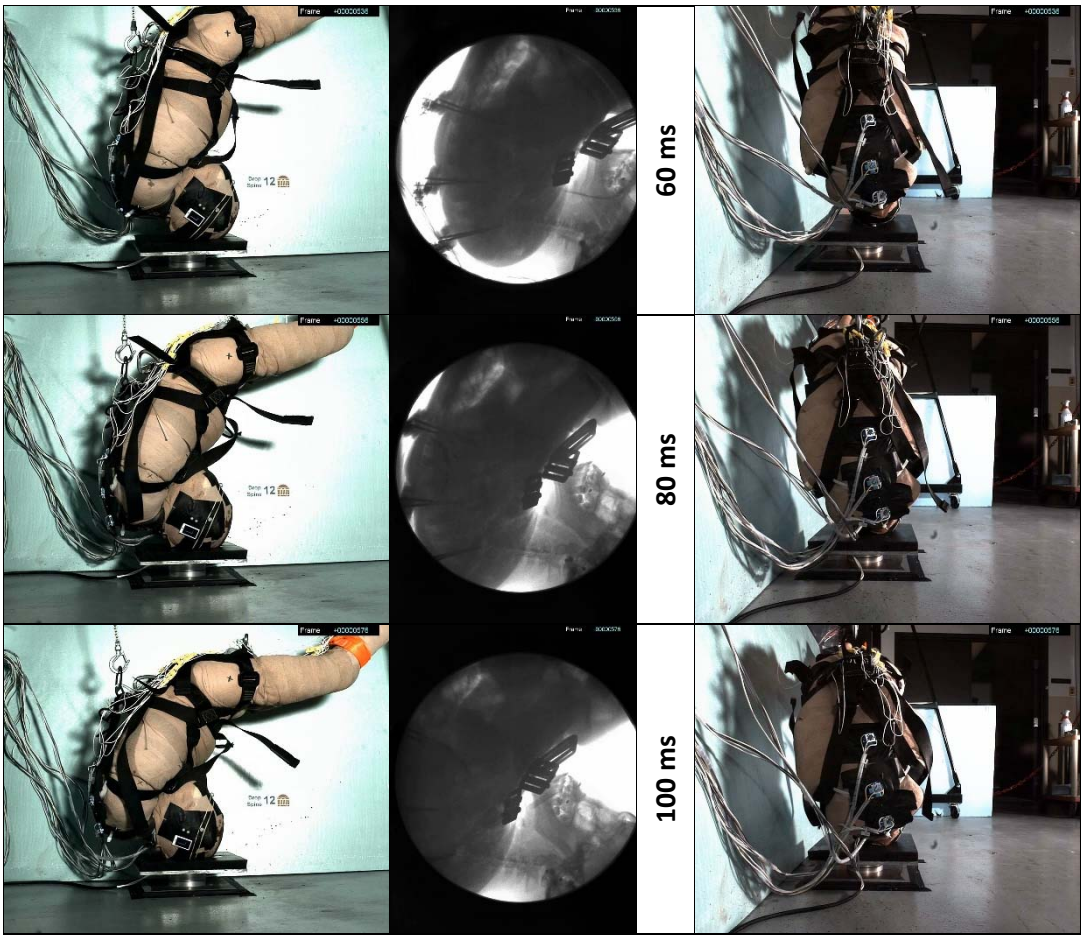


| Subject 693, Test 13<br>Lateral | X-Ray | | Frontal |
|---|---|---|---|
| 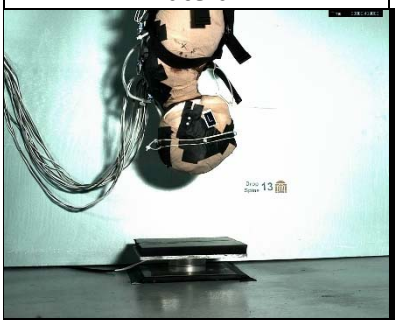 | 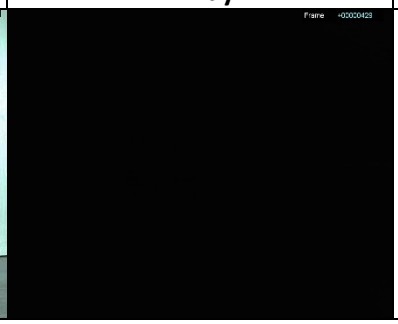 | -50 ms | 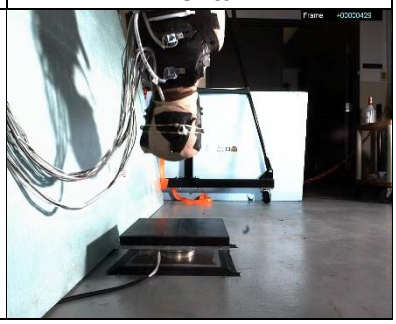 |

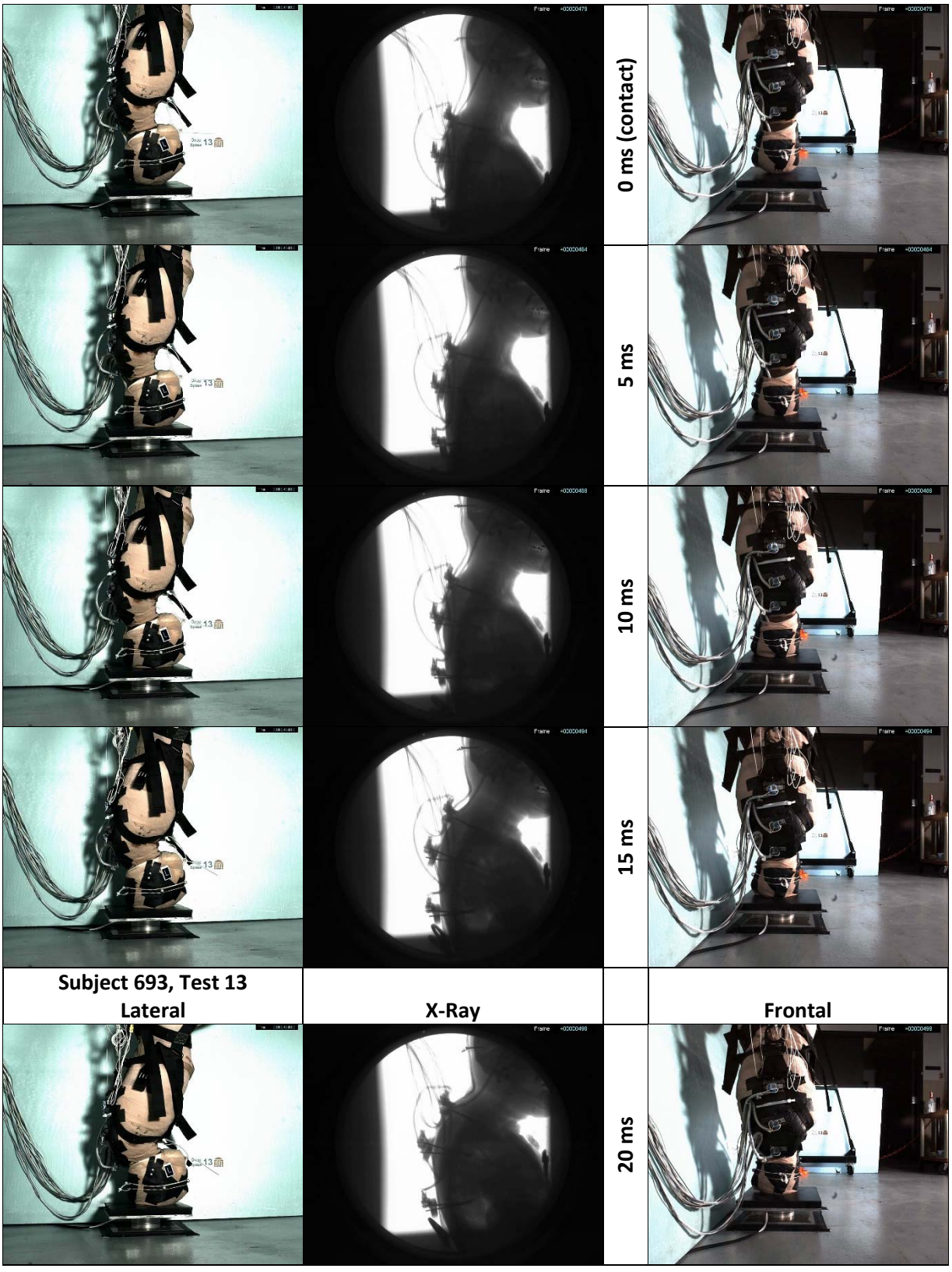
0 ms (contact)
5 ms
10 ms
15 ms
20 ms
Subject 693, Test 13
Lateral
X-Ray
Frontal

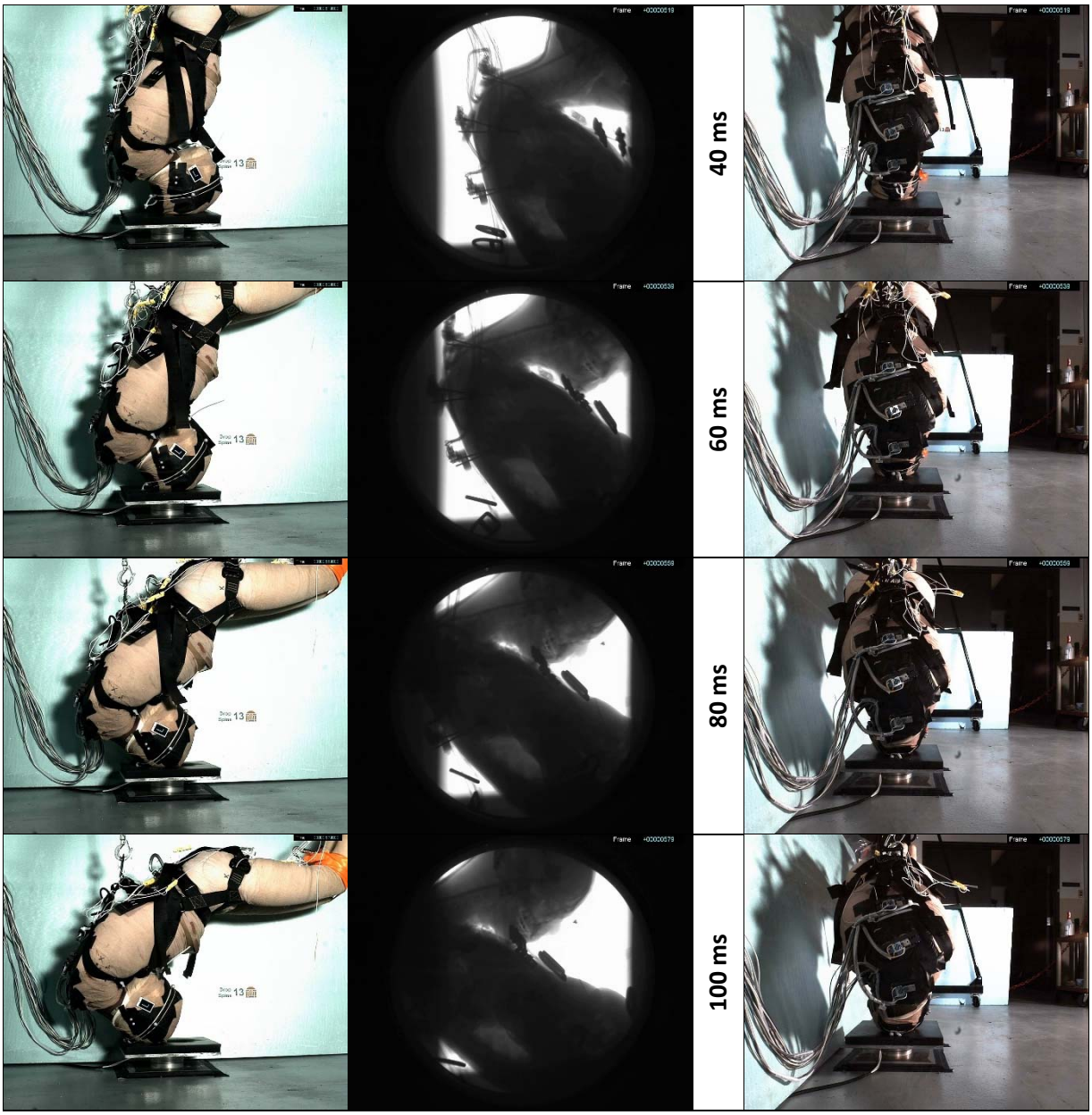
40 ms
60 ms
80 ms
100 ms

# IMPROVEMENTS TO THE FLEXIBLE PEDESTRIAN LEGFORM IMPACTOR: THE DEVELOPMENT OF NEW BONE CORES

**Thomas KINSKY**, Adam Opel AG / General Motors Europe Engineering, Germany*)
**Martin FRITZ**, 4a Engineering GmbH, Austria
**Peter LESSMANN**, BGS Boehme and Gehring GmbH, Germany
**Franz ROTH**, AUDI AG, Germany*)

*) representing the Task Force Pedestrians of the European Automobile Manufacturers' Association (ACEA)

Paper No. 15-0433

## ABSTRACT

During the first decade of the 21st century, pedestrian safety in general was one of the main subjects of vehicle safety development. For the legform testing, the impactor developed by the European Enhanced Vehicle-Safety Committee was the standard impactor but experts from Japan introduced a new impactor, the so-called Flexible Pedestrian Legform Impactor (FlexPLI). The FlexPLI is capable to quantify the load of a human long bone, which is a significant advantage when developing vehicles with reduced bone fracture risk.

With the impactor being developed by a single company spare part availability was limited. In addition, potential improvement in terms of robustness in maximum load were identified. Therefore, a joint project was initiated, in which automobile manufacturers and their partners developed universal spare parts for the FlexPLI bone cores. These parts can withstand higher bending loads, are available from stock and do not need to be adapted to a specific legform. Furthermore, a reduction in variation of properties due to a different production process was achieved. This reduces performance variation within the legs and is comparable to the initial bone core mean performance. The document introduces the details of the project.

## INTRODUCTION

During the first decade of the 21st century, pedestrian safety in general was one of the main subjects of vehicle safety development. For the legform testing, the legform impactor developed by the working groups of the European Enhanced Vehicle Safety Committee (EEVC) was state of the art at that time. However, to enhance the representation of a true human leg, experts from Japan introduced a new legform impactor when others still tried to understand how to work with EEVC Legform Impactor (EEVC LFI).

The new Japanese impactor, nowadays called Flexible Pedestrian Legform Impactor (FlexPLI), provides one significant advantage compared to the EEVC LFI: In addition to the assessment of knee injuries, it is able to also assess injury risks to the long bones of a human leg.

To promote the introduction of the new legform and to allow experts of other regions also contributing to the development, the Japan Automobile Research Institute (JARI) and the Japan Automobile Manufacturers Association (JAMA) lend different build levels of the impactor to labs outside Japan.

The European Automobile Manufacturers' Association (ACEA) was equipped with several FlexPLI's by Japan for several years. This allowed ACEA members to conduct tests at different labs such as Concept Technologie GmbH in Austria (Concept), the Bundesanstalt fuer Strassenwesen / Federal Highway Safety Research Institute (BASt) and BGS Boehme and Gehring GmbH[1] as well as Bertrandt Ingenieurbuero GmbH (Bertrandt) in Germany. During those tests, learnings and expertise were generated. These were brought into the activities of the UNECE Informal Group on Pedestrian Safety (INF GR PS) (working from 2002 to 2006), the UNECE Technical Evaluation Group (TEG) (working from 2005 to 2010) as well as the UNECE Informal Group on gtr No. 9 – Phase 2 (IG GTR9-PH2) (working from 2011 to 2013).

[1] BGS Boehme und Gehring GmbH is the company operating the test laboratory of the German Bundesanstalt fuer Strassenwesen / Federal Highway Safety Research Institute (BASt).

Finally, the efforts of the working groups mentioned before led to the introduction of the FlexPLI into UN Regulation 127 as of January 2015 as well as to a corresponding draft amendment for the gtr No. 9, which is in the process of adoption. The design of the FlexPLI has achieved a build level that will allow its future use for regulatory purposes. However, room for further improvements to this build level is seen and one of the respective solutions is presented in this document.

## CONCERNS WITH THE DESIGN OF THE FLEXIBLE PEDESTRIAN LEGFORM IMPACTOR

During one of the first test series conducted on behalf of ACEA by the company Concept in 2004, Knotz reported about concerns with the – at that time too low – stiffness of the FlexPLI. Knotz tested an early version, the version 2003, of the new impactor. He noted that the legform had a tendency to bend extremely and to follow the contour of the tested vehicles (Knotz 2004, page 25). Experts of ACEA members raised the concern whether this could result in damages to the bone cores of the FlexPLI and whether this indeed represents the behavior of a human leg.

From their testing with the next generation of the FlexPLI, the version 2004, Mallory, Stammen and Legault reported about damages to the bone cores of the impactor in three out of five tests (Mallory, Stammen, Legault 2005, page 8).

Feedback generated in such tests lead to one major design change that was introduced in 2005 with the FlexPLI version G: Starting with this version, all FlexPLIs have a squared design of tibia and femur sections, compared to the round tibias and femurs of the earlier versions. In the corners of the respective sections, steel cables are placed to limit the maximum bending of tibia and femur and therefore prevent the impactor from being excessively bent.

Figure 1 shows a principal drawing of the latest build level of the new impactor. “The FlexPLI consists of a femur and a tibia, which are composed of bone cores made of fiber glass, and several nylon segments attached to them. The overall design of femur and tibia represents the human bones and their ability to be bent. Strain gauges, glued to the fiber glass core, are used to measure the bending moments at the different segments and thereby assess the risk of bone fractures. The knee element consists of two complex blocks, where string potentiometers represent the human knee ligaments. Their elongations assess the risk of ligament injuries… Human skin and flesh are formed by several layers of rubber and neoprene sheets. To closer follow the geometry of a human leg, the number of layers is different for femur, knee and tibia…” (Kinsky, Friesen, Buenger 2011, page 2ff.)

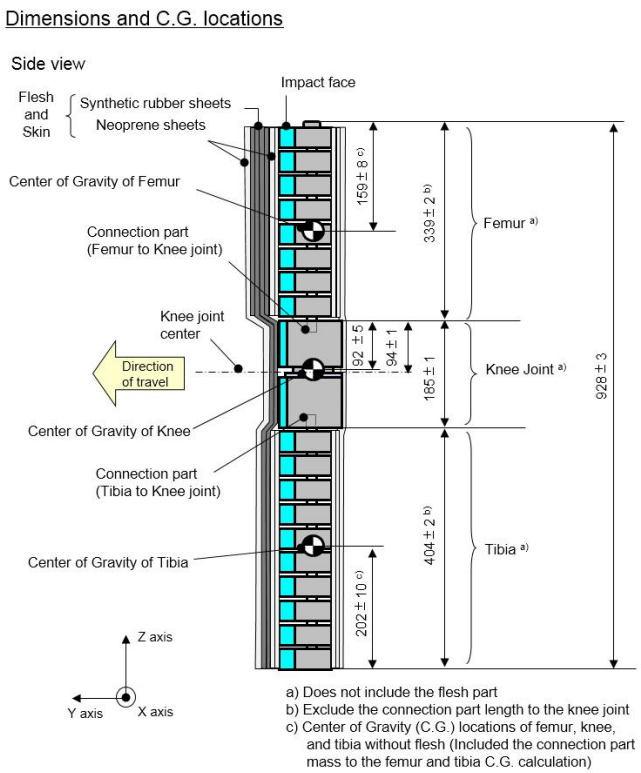


Figure 1: Latest design of the FlexPLI as introduced in the 01 series of amendments to UN R127 (UNECE 2015, page 26)

In 2008, Been and colleagues summarized the development status of the FlexPLI in its intended final version GTR[2] (Been et al. 2008). Been and colleagues introduced the 3-point quasi-static bending test applied to the bone cores individually as well as to the total assemblies to prove the material robustness. This test was carried into calibration and certification procedure of the assemblies for official impact tests. However, in all these tests the bone cores were, by that time, never loaded with bending moments of more than 400 Nm – moments, which could be expected frequently when considering that the maximum bending moments in discussion at that time were in this range. Been et al. also explained that the plastic material surrounding the glass fibers was changed at that time from polyester to vinylester to improve the durability (Been et al. 2008, page 34) and that the old and the new bone core material had been overload-tested with bending moments of 500 Nm to prove the optimization (Been et al. 2008, pages 35ff.). However, experts from ACEA members felt that this still will not be sufficient for development tests were the initial performance of new cars may still to be quantified.

In 2011, Kinsky reported on a first long-time durability assessment with one of the prototypes of the FlexPLI version GTR (Kinsky 2011). Kinsky noted significant wear and visible white cracks on the surface of the bone cores by matrix failure in the bone core material (Kinsky 2011, pages 13 ff.). The report raised also concerns about the availability of spare parts for the impactor.

Additionally, experts of Humanetics, producing the FlexPLI version GTR, stated in 2011 that the fiberglass bone cores are tailor-made for each single legform (Humanetcis 2011). This was explained with the production process of the fiberglass material that cannot guarantee stable material properties. The material is produced in a pultrusion process as a straight profile (see figure 2). Since, according to Humanetics, the glass fibers are not necessarily orientated in line and the thickness of the profile is reduced by machining by about one third, the final batch of material has varying quality (high variation of strength and stiffness). Therefore, the bone cores are produced as blanks and then are slightly reworked to fine-tune the performance in the tibia and femur assemblies. According to the drawings, the bone cores finally vary in thicknesses between 10.3 and 10.9 mm (Humanetics 2015), which in principle makes each bone being unique. Also, the experts of Humanetics stated that the ultimate strength of the straight profile is foreseen for a maximum of 250 MPa (which approximately corresponds to a bending moment of 185 Nm) but that Humanetics tested them up to 400 Nm bending moment (which would require a minimum strength of 540 MPa)

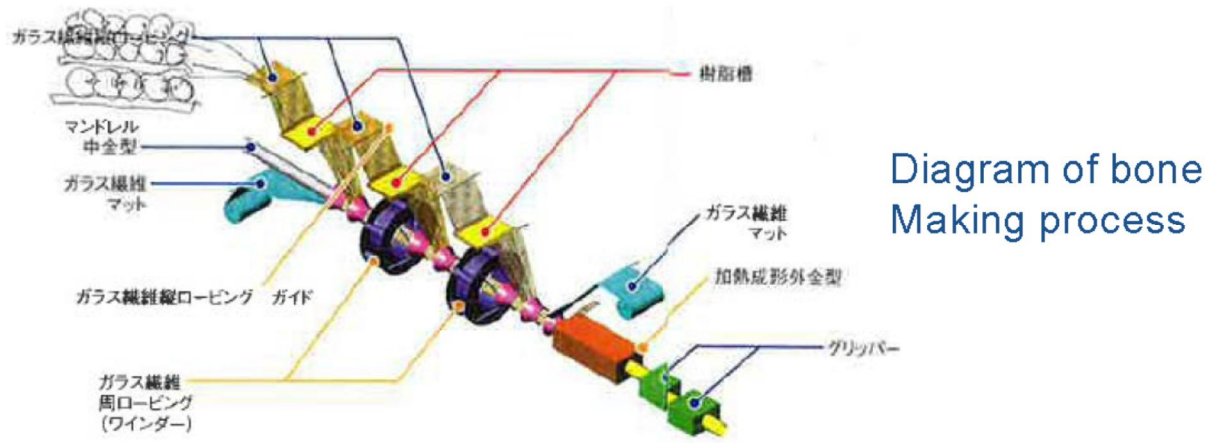


Figure 2: Diagram of the production process for the bone core material, which is then processed in several further steps to the tailor-made bone core for each FlexPLI (Humanetics 2011, page 21)

Based on the statements of Humanetics, concerns were raised by automobile industry experts: Will the FlexPLI withstand higher loads then the legislation limits, also if these loads occur more than once? Will spare parts be available on short notice? How can the required impactor's finite elements (FE) model address variation of the actual parts? Etc.

[2] Early versions of the FlexPLI had been named according to their year of introduction. Since 2005, the new versions were named G, then GT and finally GTR, indicating that the development steps should lead to the use in the global technical regulation (gtr) on pedestrian safety.

**DEVELOPMENT OF NEW BONE CORES FOR THE FLEXPLI**

Experts of ACEA finally decided to support enabling alternative suppliers of the bone cores. The product specifications included:

- The new bone cores should have the ability to withstand bending moments of at least 20 percent above the limits foreseen for legislation (with legislation limits still being in final discussion at that time);
- The material behavior should be reproducible with just small variations in the product performance;
- The dimensions of the new bone cores should fit the dimensions of the other parts of the FlexPLI to avoid a need of further modifications to the impactor;
- The new bone cores should preferably be available as spare parts on stock, without a need to fine-tune them for their use in a specific legform impactor;
- The new bone cores should allow for the use of the different data acquisition systems already in use by different ACEA members;
- A material model should be made available for the simulation;
- Further improvements to the bone cores as well as to the whole FlexPLI could be discussed, if possible.

A preceding project on this topic had been conducted by Partnership for Dummy Technology and Biomechanics (pdb) in Ingolstadt/Germany and Adam Opel AG in Ruesselsheim/Germany with the company 4a Engineering GmbH (4a) in Traboch/Austria. Therefore, ACEA decided for a joint project also with 4a. 4a is a technically oriented research and development company with the focus on plastics engineering and composite material science. They choose to cooperate with the well-experienced test labs BGS in Bergisch Gladbach/Germany and partially also with Bertrandt in Gaimersheim (near Ingolstadt)/Germany. Both labs were experienced in testing the FlexPLI. BGS conducted tests with all earlier versions of the FlexPLI since 2004 and contributed to joint projects with ACEA aiming to improve the impactor. Bertrandt was one of the very first owners of the latest FlexPLI version in Europe and conducted many tests with this version that also helped to improve the design.

After an initial assessment, following objectives were defined for 4a to achieve: The bone cores should be made of a new composite material with narrow variation of the material properties. The fiber matrix combination in this material should be optimized for maximum fatigue strength. Also, the cross section and the bending behavior should be optimized compared to the original bone cores. Finally, 4a also suggested using an improved fixation concept for the bones, taking into account the anisotropy of the material.

In a first step, 4a sourced a new fiberglass material for the bones. The new material is specifically produced for the purposes of the legform impactor with a thickness very close to the final dimensions of the bone cores. Then, the surfaces are grinded down just a few tenth of a millimeter to have flat surfaces that allow the attachment of the strain gauges. The new material has a bending strength of at least 750 MPa (corresponding to 550 Nm bending moment), compared to 250 MPa of the original part as mentioned before. Also, 4a guarantees that the new bone cores are produced with very narrow production tolerances while having the specified material properties.

The strain gauges are bonded to the front and rear surfaces of the bone cores. Initially, the concept of using wires for each single strain gauge was maintained. However, during the frequent assembling and disassembling of the bone cores during the project it was noted, that the wiring always causes a risk of failure due to pinching, braking etc. 4a therefore finally developed folia-printed flexible circuit boards (PCB's) that are attached to the bone core surfaces and that allow minimized wiring. Just one wire per PCB is needed that is placed on the non-struck side close to the knee element.

Using the PCB's also solved issues with the electrical resistance, specifically the bridge resistors. It was observed that in some cases Wheatstone bridges for the strain gauges were also fitted to the data logger board, in addition to resistors in the plugs. The respective wiring depended on the data acquisition system and was impactor specific. Therefore, in these cases the sensors could not be calibrated without the data acquisition system. This would have created issues when producing the bone cores as universal spare parts. The PCB now allows placing all bridge resistors on the PCB, independent of the data logger or the plugs used. Of course, affected FlexPLIs need to be modified accordingly in the beginning but this finally guarantees easy supply of spare parts.

Finally, the bones are covered by heat-shrink tubes. This guarantees the proper dimensions of the bone cores while, at the same time, protecting the strain gauges and the PCB's as well as the bone cores' surfaces from external damaging.

To attach the bone cores to the FlexPLI knee, 4a developed new clamps. Those clamps make contact over the full width of the bone core – in contradiction to the original ones that just contact the bones locally. Due to this, seating stress can be significantly reduced and much higher clamping forces can be achieved.

Figure 3 shows the two major parts as well as the final assemblies of the 4a bone core spare parts (see figure 3). The parts have the same attachment dimensions as the original parts and the same mass, they have a similar test performance, but they provide a better robustness and durability. However, especially the latter details needed to be proven by tests.

Figure 3: Final assembly of 4a femur bone core and 4a tibia bone core spare part, the PCB for a tibia as well as a tibia blank (from left to right) (photograph: 4a Engineering GmbH)

## COMPARISON TESTS WITH THE NEW BONE CORES

During the development of the new bone cores, numerous tests had been conducted at BASt by BGS as well as by Bertrandt. The final tests confirming the usability were conducted by BGS. Besides the FlexPLI certification tests on component as well as on assembly level, the project partners decided to conduct tests against a test rig that was configured to represent a sedan-type vehicle. The test rig is a standard test rig that had been developed for validation purposes and was also used for other ACEA projects.

For the certification, quasi-static bending tests of the bone cores for sensor calibrate, certification tests of tibia, femur and knee assemblies as well as final certification tests of the complete legform impactor, have to be conducted. All tests were passed without issues using three different impactors. These three impactors were equipped with three different data acquisition systems. For the certification of the impactor, both tests configurations as foreseen in the UN R127 were conducted: the so-called pendulum testing as well as the so-called inverse testing.

Also, BGS conducted tests against the test rig that was designed to represent the typical load paths of a sedan-type passenger car (see figure 4). During these tests, no unexpected results were achieved and testing proceeded without any noticeable problems.

The test results from the certification tests and against the test rig are shown in annexes 1 to 3. Observed differences in elongation values of the knee are not influenced by long bones and are impactor specific since the knee section of the different impactors had not been modified.

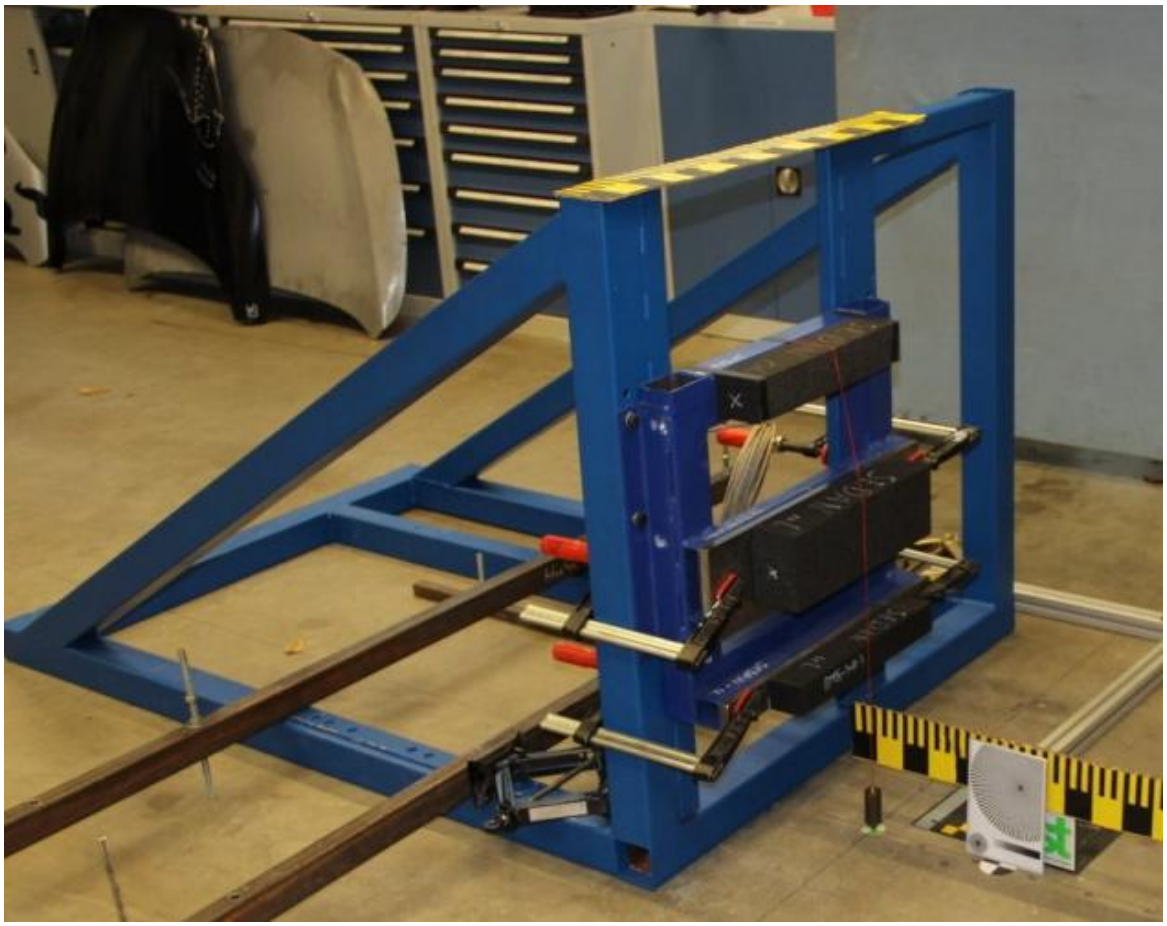

Figure 4: Test rig representing the typical load paths of a sedan-type passenger car (photograph: BASt/BGS Boehme and Gehring GmbH)

After finalizing the tests described above, two further impactors have been equipped with the new 4a bone cores. In addition, these impactors work properly without any abnormalities. After evaluating the data generated in the tests, the project partners finally concluded that the new spare parts can be made available for industrial use.

## REMAINING ISSUES

One major issue coming up during the activities described above were the connector plugs used for the data acquisition systems (including the wiring) of the different legforms. These plugs were observed to be not suitable for the usage in such an impactor and are subject to frequent failure (breakages of the plugs, breakage of the strain relief, disconnections during the acceleration of the impactor, etc.). In addition, these plugs are uncommon (at least in Europe) and acquiring spare parts turned out to be a serious challenge due to limited availability. Therefore, future users of the new 4a bone cores are recommended to also replace the connector plugs to ensure availability of the test tool for vehicle development. Substitution of the Wheatstone bridges may need additional efforts in the beginning but it ensures an uncomplicated and easy supply of spare parts afterwards.

In addition, the project partners noted that several further improvements to the FlexPLI may be possible, aiming at the improvement of the handling, the durability and the robustness of the whole impactor. It was therefore decided to further investigate possible improvements to the impactor in new projects.

Finally, further steps will be needed to develop the FE model of the FlexPLI. Currently, no validated model exists. As soon as this issue is solved, the new 4a bone cores will need to also be provided as supplements to this model. However, from the project team no further issues are expected with this.

## CONCLUSIONS

In this joint project, ACEA together with 4a, BGS, Bertrandt as well as pdb developed universal spare parts for the FlexPLI bone cores. These parts can withstand higher bending loads than the original bone cores and have no influence on the certification output. They are available from stock and there is no need for legform-specific adaptations. In addition, the new parts are produced with higher accuracy so that no variation of their performance needs to be expected. Some further improvements to the electric equipment of the impactor as described above will allow the universal usage of the new bone cores.

## ACKNOWLEDGEMENTS

Several experts have – actively or passively – supported this project. The authors would like to thank specifically BASt, Bertrandt with Mr. Jan-Christopher Kolb and his team, pdb with Mr. Klaus Bortenschlager and his team as well as the experts of the ACEA Task Force Pedestrians for their support, especially Mr. Benjamin Buenger.

## FREQUENTLY USED ABBREVIATIONS

| | |
|---|---|
| ACEA | European Automobile Manufacturers' Association |
| EEVC | European Enhanced Vehicle-Safety Committee [originally founded as European Experimental Vehicle Committee] |
| FE | finite element |
| ff. | and the following |
| FlexPLI | Flexible Pedestrian Legform Impactor |
| JAMA | Japan Automobile Manufacturers Association |
| JARI | Japan Automobile Research Institute |
| LFI | Legform Impactor |
| PCB | printed circuit boardUNECE United Nations Economic Commission for Europe |

## REFERENCES

Been u.a. 2008:
Been, Bernard; N.N. (JAMA); N.N. (JARI): First Technology Safety Systems / FLEX-PLI-GTR Development Prototypes. Add. 1 JAMA-JARI / Improvement of Durability of Bone Core; Add. 2 JAMA /JARI Development of A Dynamic Assembly Calibration Test Procedure for Flex-GTR using an FE Flex-GT-prototype model. Working document TEG-071 with annexes 1 and 2 for the 7th meeting of the FlexPLI Technical Evaluation Group, Bergisch Gladbach, 8 December 2008. – Available in internet: http://www.unece.org/trans/main/wp29/wp29wgs/wp29grsp/ pedestrian_flexpli.html (2015-02-27).

Humanetics 2011:
N.N. (Humanetics): FLEX PLI Upgrade Status / TEG Webex Meeting / May 11, 2011. Working document for the (planned) 13th meeting of the FlexPLI Technical Evaluation Group". – Not publically available since the meeting finally never took place. However, the document had been shared in advance with all experts involved in the TEG activities.

Humanetics 2015:
N.N. (Humanetics): Reviewed FlexPLI version GTR drawing package, Rev. 4 (final version status Feb. 2015). – Available in internet: https://www2.unece.org/wiki/display/trans/GTR9-2+9th+session (2015-02-27)

Kinsky 2011:
Kinsky, Thomas: FlexPLI Version GTR Prototype SN-02 – Durability Assessment. Working document GTR9-1-04c for the 1st meeting of the Informal Group on gtr No 9 –Phase 2 (IG GTR9-PH2), Geneva/Switzerland, 1 – 2 December 2011. – Available in internet: https://www2.unece.org/wiki/display/trans/GTR9-2+1st+session (2015-02-27).

Kinsky/Friesen/Buenger 2011:
Kinsky, Thomas; Friesen, Flavio; Buenger, Benjamin: The Flexible Pedestrian Legform Impactor and its Impact on Vehicle Design. Document 11-0328 for the 22nd ESV Conference, Washington D.C., 13 – 16 June 2011. – Available in internet: http://www.nhtsa.gov/ESV (2015-02-27).

Knotz 2004:
Knotz, Christoph: Comparison Tests Using a TRL Legform Impactor and a JARI Flexible Pedestrian Legform Impactor. Test Report Nr. 10160/FGS/01 Rev.2 of Concept Technologie GmbH under contract of the European Automobile Manufacturers' Association ACEA. – Gratkorn, 07.06.2004.

Mallory/Stammen/Legault 2005:
Mallory, Ann; Stammen, Jason; Legault, France: Component leg testing of vehicle front structures. Document 05-0194 for the 19th ESV-Konferenz, Washington D.C., 6 – 9 June 2005. – Available in internet: http://www.nhtsa.gov/ESV (2015-02-27).

UNECE 2015:
United Nations Economic Commission for Europe: Regulation No. 127 / 01 series of amendments to the Regulation – Date of entry into force: 22 January 2015 / Uniform provisions concerning the approval of motor vehicles with regard to their pedestrian safety performance. Document R127r1e of the addenda to UN Vehicle Regulations 1958 Agreement. – Available in Internet: http://www.unece.org/trans/main/wp29/wp29regs121-140.html (2015-02-27).

## ANNEX 1 – TEST RESULTS PENDULUM CERTIFICATION

Test results for 3 different legforms with 3 repetitions each, the most right bar in each block represents the mean value.

Pendulum: Femur A3

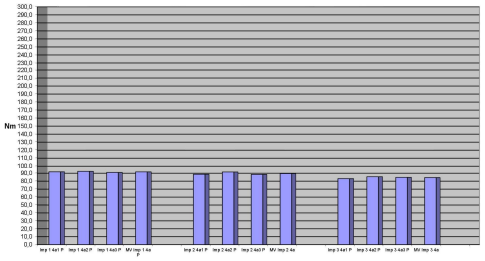


Pendulum: MCL

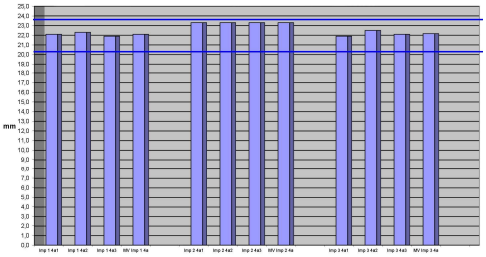


Pendulum: Femur A2

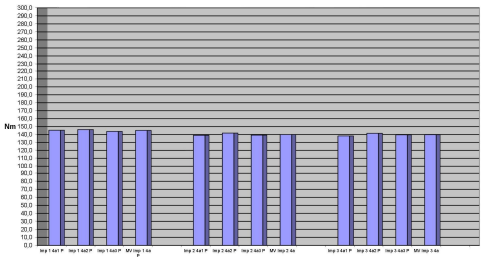


Pendulum: Tibia A1

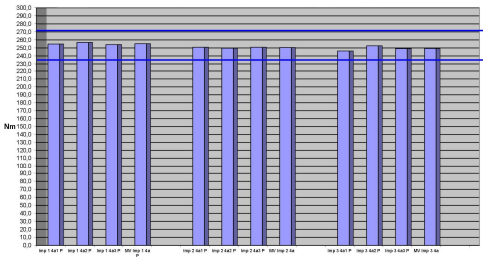


Pendulum: Femur A1

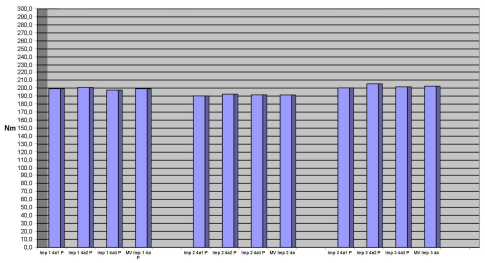


Pendulum: Tibia A2

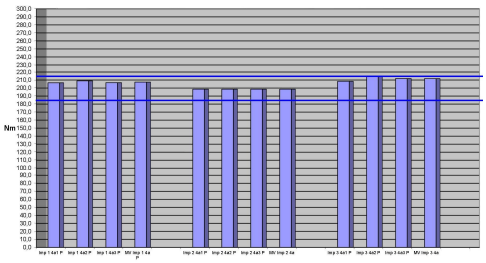


Pendulum: ACL

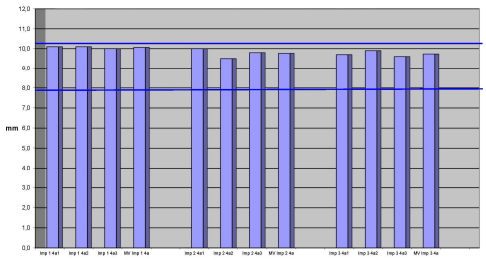


Pendulum: Tibia A3

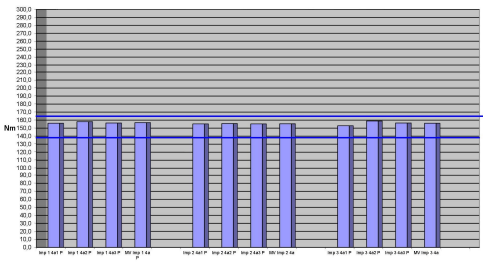


Pendulum: PCL

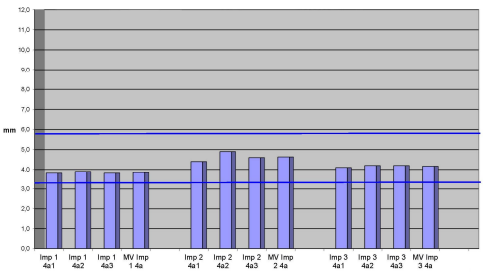


Pendulum: Tibia A4

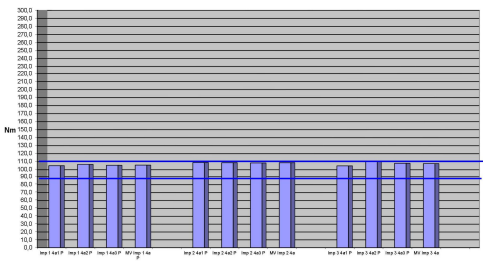

## ANNEX 2 – TEST RESULTS INVERSE CERTIFICATION

Test results for 3 different legforms with 3 repetitions each, the most right bar in each block represents the mean value.

Invers: Femur A3

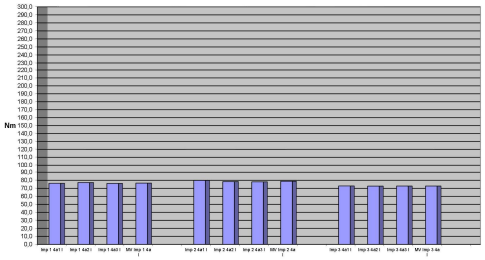


Invers: MCL

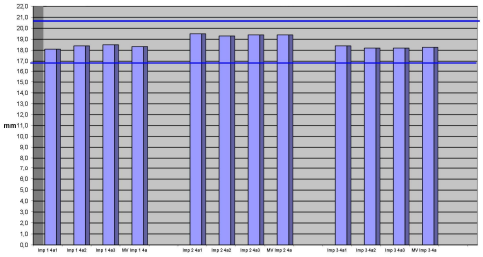


Invers: Femur A2

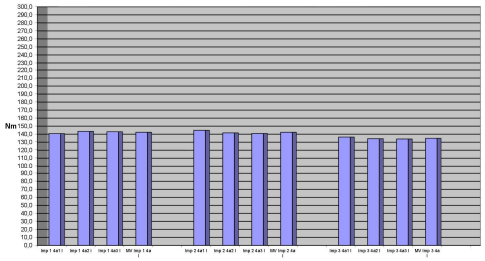


Invers: Tibia A1

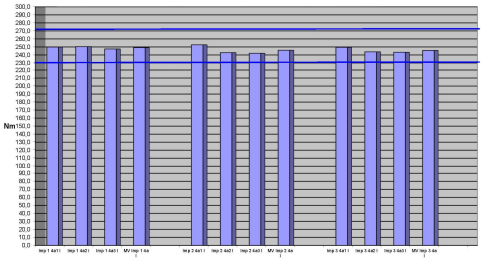


Invers: Femur A1

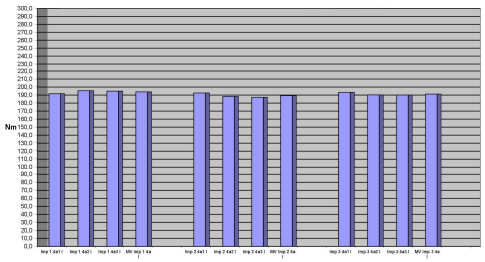


Invers: Tibia A2

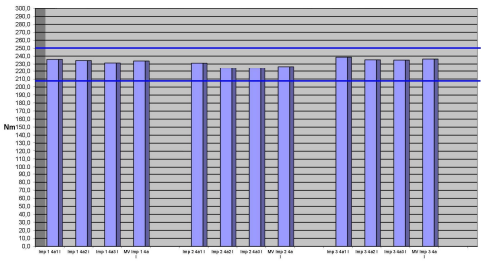


Invers: ACL

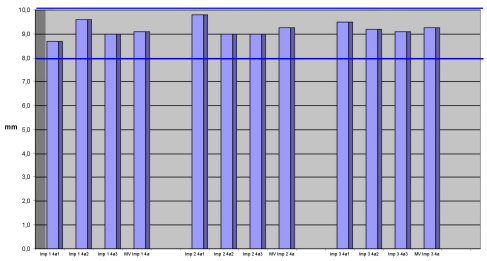


Invers: Tibia A3

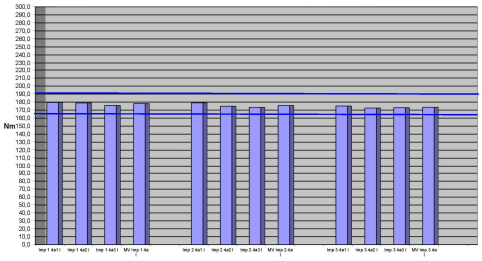


Invers: PCL

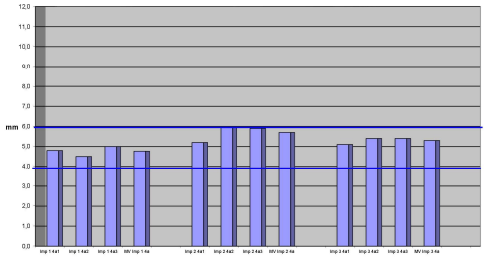


Invers: Tibia A4

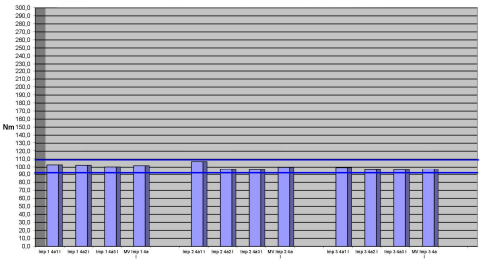

## ANNEX 3 – TEST RESULTS SEDAN TEST FRAME

Test results for 3 different legforms equipped with 4 a bone cores with 3 repetitions each (left blocks in each diagram), in comparison with 3 legforms equipped with the original bone cores (right blocks). The most right bar in each block represents the mean value.

Sedan Test Frame: Femur A3

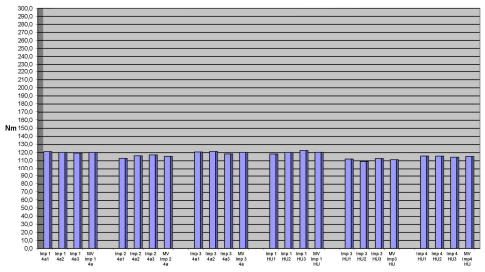


Sedan Test Frame: MCL

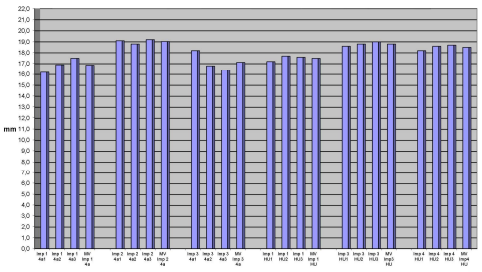


Sedan Test Frame: Femur A2

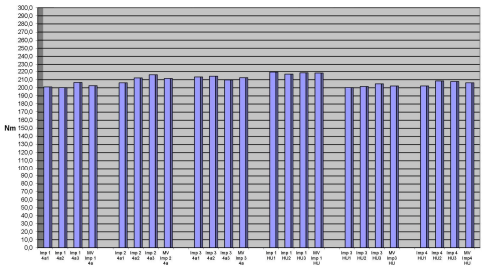


Sedan Test Frame: Tibia A1

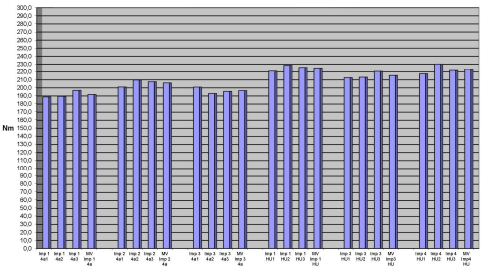


Sedan Test Frame: Femur A1

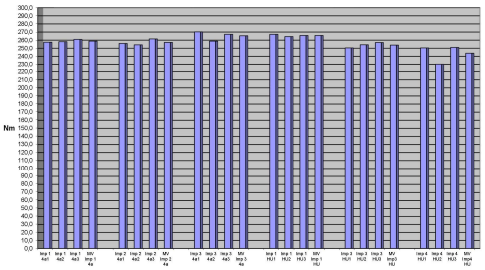


Sedan Test Frame: Tibia A2

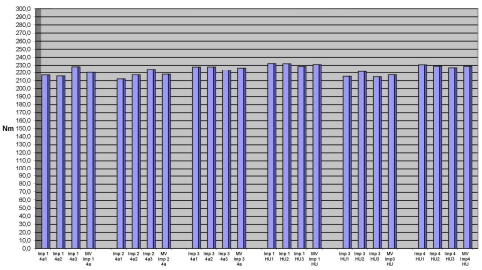


Sedan Test Frame: ACL

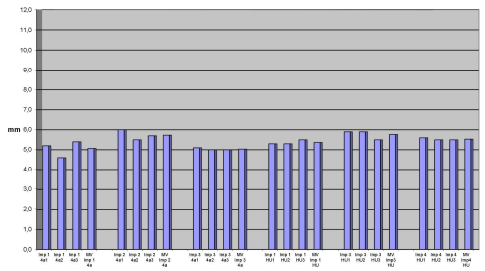


Sedan Test Frame: Tibia A3

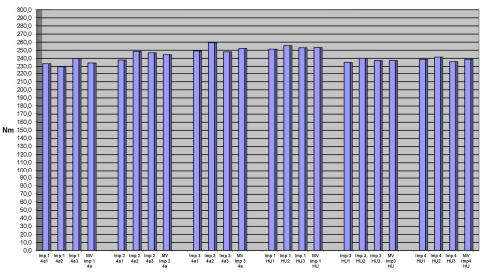


Sedan Test Frame: PCL

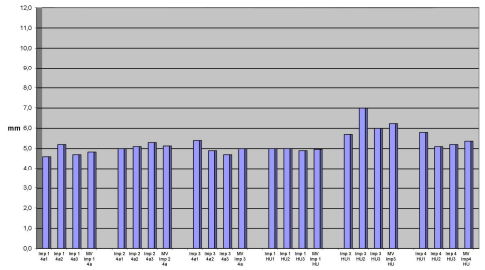


Sedan Test Frame: Tibia A4

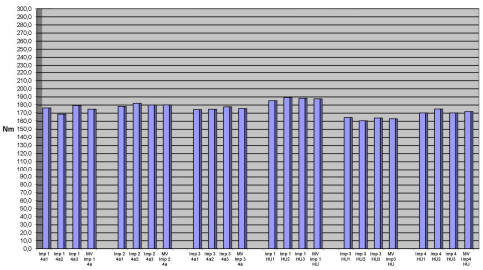

# A CONCEPT FOR NATURALISTIC DATA COLLECTION FOR VULNERABLE ROAD USERS USING A SMARTPHONE-BASED PLATFORM

**Leif Sandsjö**
MedTech West/University of Borås, Borås
SAFER Vehicle and Traffic Safety Centre, Chalmers University of Technology, Gothenburg
Sweden

**Bengt Arne Sjöqvist**
**Stefan Candefjord**
SAFER Vehicle and Traffic Safety Centre, Chalmers University of Technology, Gothenburg
MedTech West/Dept. of Signals and Systems, Chalmers University of Technology, Gothenburg
Sweden

Paper Number 15-0435

## ABSTRACT

This paper presents a smartphone-based platform for large-scale, low-cost, long-term naturalistic data collection aimed at vulnerable road users (VRUs). The approach taken is to collect naturalistic movement data from VRUs based on information from the embedded sensors in high-end smartphones. The Smartphone application, *LogYard*, developed in the current study, allows the recording of high quality data (tri-axial acceleration and rotation at 100 Hz plus GPS position and velocity each second). This way, large data quantities from ATV drivers' movements during daily use in different use cases, can be transferred from a large number of users and accumulated in a cloud-based server for off-line analysis.

Apart from the description on how data is recorded and managed in the smartphone-based platform, also a procedure on how to include participants to studies and how private integrity issues and informed consent can be handled from a distance is presented. By means of the presented smartphone based platform, large number of participants taking part in several parallel on-going studies can be easily administered. This makes the platform a powerful tool to use in large-scale, low-cost, long-term studies providing data from large groups of study participants.

The information made available this way can be used to develop automatic crash notification (ACN) systems directed to VRUs based on identifying movements outside what is "normal" for bicyclists, mopedists, motorcyclists and ATV users.

## INTRODUCTION

Almost half of the over 1.2 million deaths in road traffic accidents worldwide each year strike vulnerable road users (VRUs) (WHO, 2009), i.e. pedestrians, bicyclists, moped drivers, and motorcyclists. The typical accident scenario that comes in mind is that the VRU collide with a car. Contrary to such preconceptions, statistics show e.g. that 8 out of 10 bicycle accidents are single vehicle accidents, and that these are often due to bad maintenance or slippery road conditions (Niska and Eriksson, 2013). Single bicycle accidents produce about ¾ of the severe injuries (Niska and Eriksson, 2013) and single accidents account for almost half of the fatalities for motorcyclists (Strandroth and Persson, 2005). An accident with a two-wheel vehicle may, even at fairly low velocities, lead to the driver getting unconscious or in other ways incapable of calling for help, and the accident may stay unnoticed for a long time if happening on small roads or during low traffic.

There is obviously a lot to gain if road users could be equipped with a system or function that not only can detect an accident or emergency situation but also can inform about this by sending an automatic alarm in case the driver is incapable of calling for help. Such an Automatic Crash Notification (ACN) system was first developed for cars by General Motors and installed in their luxury models under the brand name OnStar. Today, OnStar, or similar systems, is installed in millions of vehicles from different manufacturers. These systems automatically send an alarm to a call center in case of a crash triggering the airbag to be deployed. Further development of ACN systems was initiated by US researchers in the late 90s (Champion, et al., 2003), showing that it is possible to use the information available from vehicle sensors such as accelerometers to not only detect crashes but also estimate the severity of the crash and predict how the impact may have affected the passenger(s). In the European Union an ACN initiative is

expected to be introduced in 2018; this service shall work in all member countries and is referred to as *eCall*. Although the *eCall* initiative is first and foremost aimed at automobiles, an adaptation of the system targeting also motorcycles is in progress.

In line with the *eCall* concept for cars, also riders of bicycles, mopeds, motorcycles or all-terrain vehicles (ATVs) can be equipped with sensors that are connected to e.g. a smartphone application (the embedded sensors in the smartphone may be good enough) that triggers an alarm when sudden changes in position or velocity outside what is considered normal for the specific type of vehicle is detected. Although this approach is similar to the *eCall* initiative, it differs significantly as the sensors preferably should be worn by the driver, as it is more relevant to trace what happens to the driver than the vehicle. This approach is further pronounced when considering the opportunity to use GPS information to find not only the site of the accident, but also the exact position of the driver who may be far separated from the vehicle after an accident.

The *Postcrash* group at SAFER foster a general interest in ACN systems and how these can be used to improve the rescueing activities after an accident. Since VRUs is an important group to target in order to reduce road traffic injuries it is highly relevant to extend the current ACN initiatives now starting to be commonly available in automobiles also to other categories of road users.

In order to test the feasibility of an ACN system for VRUs, we performed a pilot study to test the hypothesis that the built-in/embedded sensors of a high-end smartphone can be used to detect a bicycle accident. We found that the smartphone sensors (accelerometers, gyroscopes, and GPS system) can provide information about the movements during bicycling and that a smartphone app can use this information to evaluate falls or crash events in real time (Candefjord, et al., 2014). The study, demonstrated a smartphone app ("jalp!", available from GooglePlay) for detecting bicycle accidents on the Android platform using a Google Nexus 4 smartphone. Although a number of simulated crash situations were used during the development, the main approach was to collect motion data from bicycle use in different situations (on different surfaces, with different bicycles and persons, different placements of the smartphone, on rural roads and in city environments, seated and standing position, etc.). This information was then used to develop an algorithm capable of distinguishing crashes from normal cycling (Candefjord, et al., 2014).

We are now taking this smartphone based ACN concept further by adapating the algorithm for other VRUs. The next in line is ATVs. ATVs have become popular and are commonly used as a light-weight tractor and transportation means in agriculture, forestry, and leisure activities on- and off-road. Unfortunately, the use is associated with a high prevalence of accidents and serious injuries (even fatal). This can be explained by the driver being unprotected, ATVs being heavy (which becomes dangerous if overturning), and, despite the four wheels, having poor driving properties in regular traffic.

As ATV use is more diverse than bicycling we need to learn more about what signifies normal ATV use. In line with the approach taken in the development of the bicycle app described above, extensive data collection can provide a base for what can be considered safe. Movements beyond normal use will then indicate potentially riskful situations that can be used to warn the ATV driver but also send an alarm if an integrated automatic evaluation of all available sensor signals indicate an accident. However, such large-scale collection of naturalistic data to provide a pool of, in this case, "normal ATV use" is generally considered both time consuming and expensive due to the extra mobile equipment needed to follow the driver/vehicle over time. As we use smartphones to detect accidents by means of the developed app for bicycle use, there is just some additional software needed to also record the high-quality accelerometer and gyroscope signals as well as the GPS-information. We have developed the smartphone app "LogYard" (available from Google Play and App Store) that takes the sensor signals from the embedded sensors at 100 Hz, and GPS information every second, and store them for later upload to a cloud-based server.

The aim of this paper is to present a smartphone based platform for low-cost collection of large-scale naturalistic movement data and ways to do this while adhering to established integrity levels for the participating VRUs.

## METHODS

Methodological issues relating to large-scale collection of naturalistic movement data from VRUs concerns individual recordings of VRUs activities, ways of contributing additional metadata, and anonymity/privacy.

### Recordings of activities

Individual recordings of movement data is performed by means of the developed smartphone app "LogYard" available from Google Play (Android) and App Store (iOS). The study participant simply starts the recording of data from the embedded sensors (accelerometers, gyroscopes, GPS) of the smartphone by pressing "start" on the app. The recording goes on until it is stopped by activating the "stop" button shown on the smartphone screen during recording.

### Ways to contribute metadata

Additional information about the recording can be provided by keying in short text messages during the ride, or afterwards to each file containing the recorded information when presented to the user in upload mode. By means of this function, metadata about the recording (road conditions, special events, etc) can be added and made available to the analyst in the analysis. The upload functionality also provide the user with options about which files (i.e. recordings) that should be uploaded and which should be deleted and not made available to the analysis.

### Participants' anonymity

The recording of driver movements or behaviour during regular use of any vehicle in order to improve safety might at first be considered unproblematic. However, the experiences from introducing systems that enable postcrash analysis in cars tells us that many car customers are reluctant to such initiatives as it can provide data that may be incriminating to the driver. The use of GPS-information can also be considered sensitive and highly intrusive. Thus, high volume recording of VRUs' movements must comply to *good research practice* and be able to adhere to different levels of anonymity/privacy according to the purpose of the study and the participants' interest.

Three anonymity/privacy levels can easily be discerned:

i) No need for anonymity/privacy: This is trivial in the sense that no measures needs to be taken to govern the privacy or anonymity of the participants taking part in the study. However, the validity of data collected under these circumstances may be questioned as participants may choose to leave out information or avoid activities when not acting under the cover of anonymity.

ii) Complete anonymity/privacy: Although there are many applications where anonymously provided data can be of interest, the design of systems that can ensure complete anonymity based on data provided by smartphones is beyond the scope of this presentation. Even though measures are taken to secure anonymity, we have learned that virtually no system can stand hostile attacks from a resourceful intruder.

iii) High demands on anonymity/privacy: In the research community, good research practice has established a high level of anonymity that, for all intents and purposes, come close to complete anonymity. This level of anonymity allows research personnel to handle sensitive information from individuals by using individual codes and the link between the code and the actual person (the key) is kept hidden and only available to the person being responsible for the study and act under vow of silence/confidentiality. This means that it is only in exceptional cases where it is in all concerned parties' interest to connect specific data to the actual person, that the key information is used. In a clinical study, for instance, it might be that the analysis has identified a serious condition that needs to be treated.

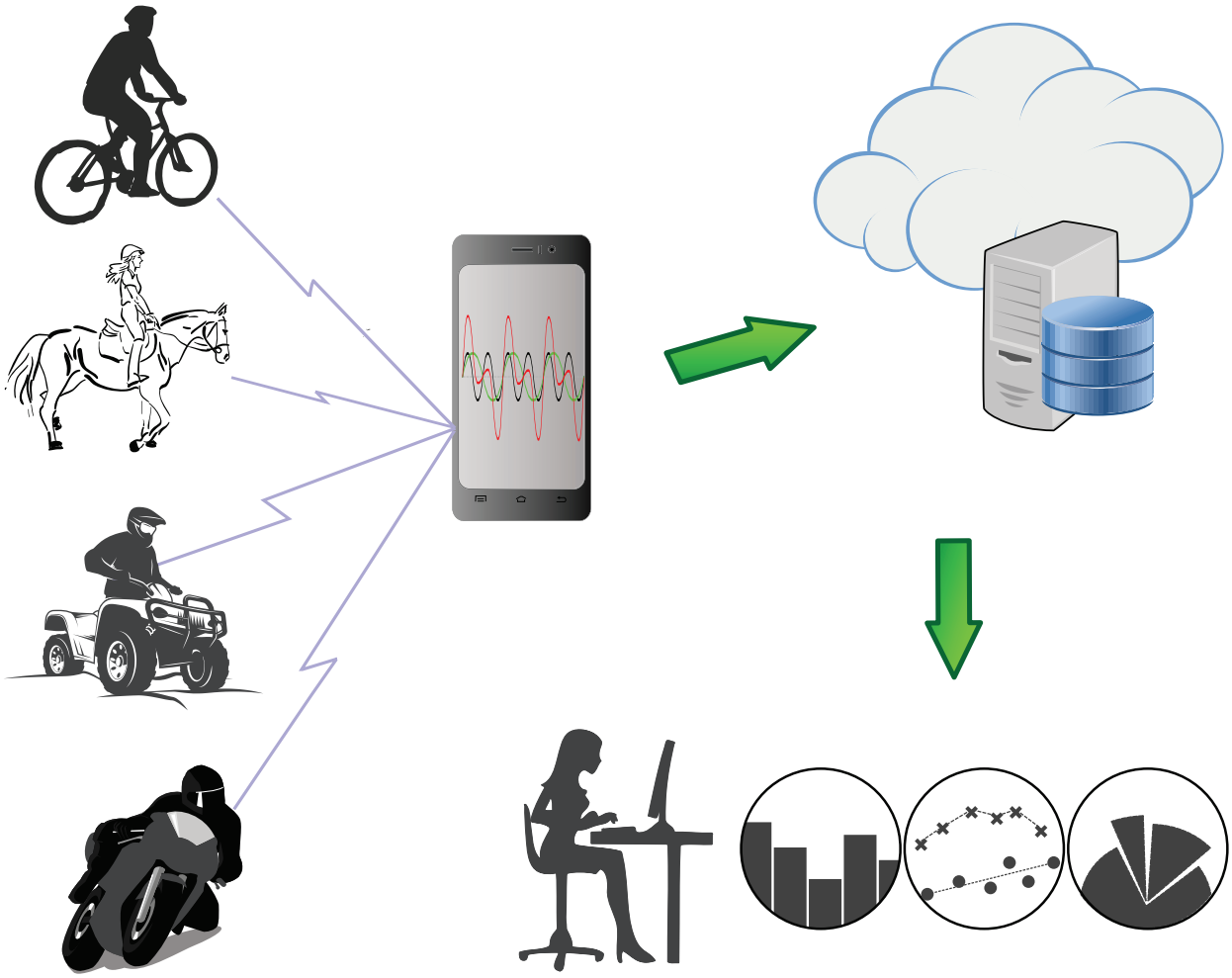

*Figure 1: Participants taking part in a study can record movement data (from the smartphone embedded tri-axial accelerometer, gyroscopes and GPS –system) during their everyday transportation/spare time activities (left). The participants upload their activity files of choice to the "cloud". Researchers and other stakeholders associated to a specific study can easily access all the study data and download it for analysis but cannot connect a participants' data to the actual person. Data upload/download is secured via an encrypted file transfer protocol (FTP).*

## RESULTS

The suggested smartphone based-platform for large-scale recording of VRUs movement data is presented in Figure 1. All information collected from the users can be uploaded to a cloud-based server. The data integrity is provided by means of an individual key that is sent out to each study participant which establish the link to the cloud-based server where the information is organized according to study and participant.

### Procedure to establish an "Informed consent" in high-volume data collection

The procedure to establish an individual "informed consent" from a distance to many participants is shown in Figure 2. The start is always to find and send out information to potential participants. This can be done by sending out flyers or posting invitations on the web. Interested and eligible persons are included in the study after signing the "informed consent" document where the study is described and the study candidate is informed about that the

participation in the study is voluntary and the particiapant's right to at any time leave the study without being asked to explain why.

If the informed consent form is not signed in paper, an email response from the study candidate on the outgoing message providing the necessary information from the study coordinator/principal investigator stating that a response saying "I have read the information and confirm participation in the study" is considered as a signed informed consent. The study candidate thereby becomes a study participant. The principal investigator can then send out the study code that the participant should enter in the LogYard app which then is linked to the specific study in future uploads of LogYard data to the cloud-based server while keeping the participant anonymous to the research staff.

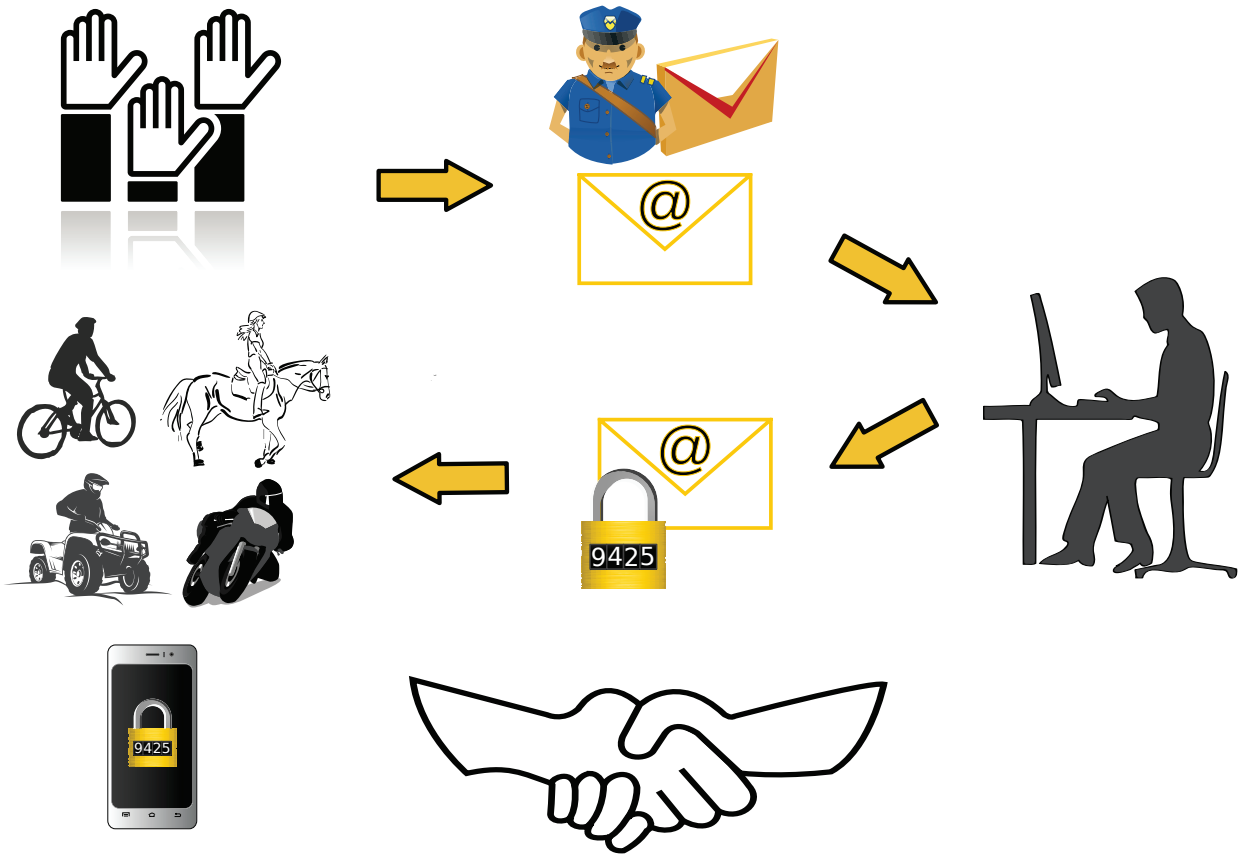


*Figure 2: Each participant's privacy is assured according to the procedure shown in the figure. Those that have gotten information about the study and are interested to take part (raised hands) send the signed informed consent form by regular mail (or a corresponding confirmation by email) confirming the will to participate in the study. The principal investigator/person responsible for the study returns the unique study code to the participant. When this code is entered in the smartphone app the link to the cloud-based server is established and the participant can then record and upload data to the study server (as shown in Figure 1). Only the principal investigator knows and has access to the "key" connecting the subject study code to the participating person.*

## CONCLUSIONS

The infra-structure for large scale, long-term, low-cost smartphone based naturalistic data collection developed in this study can provide large quantities of high quality data from different VRUs use cases and studies. We believe that this information can be used not only to learn about everyday use but also potentially dangerous situations. This information can be used to increase awareness of safer driving behavior based on movement data and the accompanying comments, but also allow automatic crash notification systems for vulnerable road users, similar to the eCall initiative for cars, to be developed.

## ACKNOWLEDGEMENT

This study was funded by Länsförsäkringsbolagens forskningsfond, Stockholm, Sweden.

## REFERENCES

Candefjord, S. Sandsjö, L. Andersson, R. Carlborg, N. Szakal, A. Westlund, J. Sjöqvist, B.A. (2014) Using Smartphones to Monitor Cycling and Automatically Detect Accidents – Towards *eCall* Functionality for Cyclists. Proceedings, International Cycling Conference, 18-19 November, Göteborg, Sweden.

Champion HR, Augenstein JS, Blatt AJ, Digges KH, Hunt RC, Lombardo LV & Siegel JH. (2003) "Reducing Highway Deaths and Disabilities with Automatic Wireless Transmission of Serious Injury Probability Ratings from Vehicles in Crashes to EMS" Proceedings of the 18th International Technical Conference on the Enhanced Safety of Vehicles (ESV).

Niska, A. & Eriksson, J. (2013) "VTI rapport 801: Statistik över cyklisters olyckor - Faktaunderlag till gemensam strategi för säker cykling".

Strandroth, J. & Persson, J. (2005) "Motorcykelolyckor med dödlig utgång - Analys av Vägverkets djupstudiematerial 2000-2003 (Utgåva 2)".

World Health Organization (2009) "Global status report on road safety: time for action" ISBN 978 92 4 156384 0.

# DEVELOPMENT OF A STANDARDIZED METHOD FOR MAKING CHARACTERISTIC RADAR MEASUREMENTS OF EXAMPLE VEHICLES AND SURROGATE TARGETS

**Jordan Y. Silberling**
**John W. Zellner**
**Joseph Kelly**
**John F. Lenkeit**
Dynamic Research, Inc.
United States of America

Paper Number 15-0437

## ABSTRACT

Testing of Advanced Driver Assistance Systems (ADAS) often requires the use of a surrogate vehicle to represent a real vehicle in conflict scenarios. Use of a surrogate vehicle is required if there is a potential for a collision during testing. In order to ensure that the test results are representative of what will occur on the road, the surrogate vehicle should appear to the test vehicle as a real car.

This paper describes a method and equipment developed for measuring and analyzing the radar signature of typical vehicles and surrogate targets. The method was then applied to eight small passenger cars to better understand what the radar signature of representative passenger vehicles are.

A special-purpose trolley was designed to serve as a portable, self-contained measurement, data acquisition and power platform. It consists of a wheeled trolley base and a vertical structure to which the various equipment are attached. The sensor trolley has 3 retractable feet that are used to make it a stationary device during measurements. The front two feet can be used for fine roll adjustment and the rear foot can be used for fine pitch adjustment. Mounted to the trolley are a commercial production 6-77 GHz RADAR sensor, a sensor bracket with roll angle level and scope sight, a data acquisition system, a laptop computer, a 12 volt battery and a power distribution box.

Eight small passenger cars were measured, three sedans, three hatchbacks, and two microcars. Small passenger cars may represent a worst case in terms of vehicle visibility. The representative vehicle radar measurements were made taken from five viewing angles and at three distances for each angle. The data from these measurements are presented.

## INTRODUCTION

Testing of Advanced Driver Assistance Systems (ADAS) often requires the use of a surrogate vehicle to represent a real vehicle in conflict scenarios. In order to ensure that the test results are representative of what will occur on the road, the surrogate vehicle should appear to the test vehicle sensors as a real car.

Many ADAS technologies use data from several types of sensors, including camera, radar and laser. The task of making a surrogate vehicle appear to be a real vehicle to ADAS sensors requires that the surrogate vehicle be representative of a real production vehicle to each of the sensors being used. To support surrogate target and test procedure development, a need exists for standardized methods for measuring and reporting the sensed properties of examplar real world vehicles and candidate surrogate targets. This method should be conducive to obtaining repeatable, reproducible and representative results.

This document describes a method for measuring and analyzing the radar signature of representative production vehicles in order to quantify the radar signatures of typical small light passenger vehicles. The method may also be applied to candidate surrogate vehicles.

Previous studies have have described some of the fundamental difficulties involved in characterizing vehicle radar reflection characteristics. Based on measurements of twenty five vehicles using high-resolution instrumentation operating in the 91-97 GHz frequency range, Buller et al (Ref 1) indicated that rear aspect principal reflection sources typically originate from components such as bumpers, license plate shelters, rear-axle components, mufflers, tail-lights, etc., and that secondary reflection sources which contribute to some of the signatures include chassis supports, rear-window joins with roof, rear-spoilers, side-view mirrors and roof racks. The equipment used in making measurements is often very costly research-grame radar measurement systems. It is common in the defense industry to use specially designed anechoic chamber for making measurements (Ref. 2). In support of the development of NHTSA's Strikable Surrogate Vehicle (SSV) measurements were made of twenty six vehicles using W-band (90-98 GHz) instruments, and a subset of these were also analyzed at Ka-band (26.5-36.5 GHz) (Ref 3). Measurements were also made of various surrogate design candidates. The measurement results were used to guide the modification of the radar reflection characteristics of the surrogate to be representative of typical vehicles involved in rear end crashes.

Vehicle systems that depend on radar are implemented using production, automotive-grade sensors that are relatively small and low cost in comparison to research grade systems. The vehicle systems interpret the incoming signals to determine whether or not they represent a vehicle. Ultimately, it is these types of system that must respond properly to a surrogate. A goal of the study reported here was to develop a system for making radar measuremens that is based on typical automotive-grade equipment and processing. The system developed uses an automotive-grade radar sensor mounted to a mobile sensor trolley to allow for fast in-field radar measurements.

## MEASUREMENT METHODS

### Measurement Equipment

**Radar Sensor** A Bosch LRR3 Long-Range Radar sensor was used for making measurements. The Bosch sensor is an in-production automotive-grade sensor that is currently in use in production vehicles. Using an automotive-grade sensor, as opposed to a research-grade sensor, allows for the data to be representative of what will be used in typical ADAS's in terms of sensor quality, resolution and field of view. Figure 1 shows the LRR3 sensor and Table 1 lists the key features.

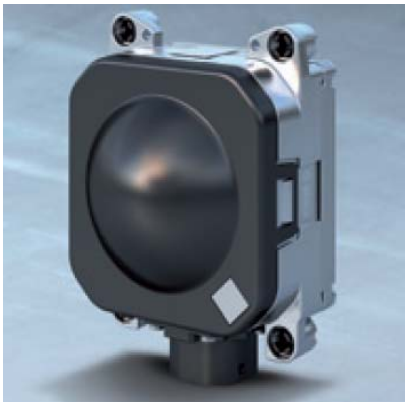

***Figure1. Bosch LRR3 Radar Sensor.***

**Table1.**
**Bosch LRR3 Features**

| Technical Feature | Value |
|---|---|
| Frequency range | 76-77 GHz |
| Distance | 0.5-250 m |
| Accuracy | ±0.1 m |
| Horizontal visual range | 30° (-3 dB angle) |
| Vertical visual range | 5° (-3 dB angle) |
| Typical cycle time | 80-100 ms |

The sensor was provided by Bosch with a custom firmware upgrade that included a CAN message output of the calculated Radar Cross Section (RCS) area of each of the detected objects. The RCS output of the sensor includes corrections for antenna gain, antenna azimuth characteristics, and object distance.

**Sensor Trolley** A purpose built trolley was designed to provide a compact and portable mount for the main system components. The trolley consisted of a wheeled trolley base and a vertical structure which holds the sensor bracket and a laptop. The sensor trolley has 3 leveling feet that are used to make it a stationary device during measurements. The front two feet can be used for fine roll adjustment and the rear foot can be used for fine pitch adjustment. The sensor trolley also contains a 24 GHz radar sensor from Smart Micro and a laser scanner from IBEO, however, this document only discusses the Bosch LRR3 sensor that is more typical of contemporary radar sensors used in production vehicles. The components that are part of the sensor trolley are:

- 12 volt battery (item 1 in Figure 2),
- Power distribution box (item 2),
- dSpace MicroAutoBox II, used for data acquisition of CAN messages (item 3, mounted behind the sensor bracket),
- Bosch LRR3 sensor, set at 18 inches off the ground to represent a typical radar installation height (item 4),
- Sensor bracket with roll angle level and scope sight (item 5),
- Scope sight (item 6), and
- Laptop for data capture and review (item 7).

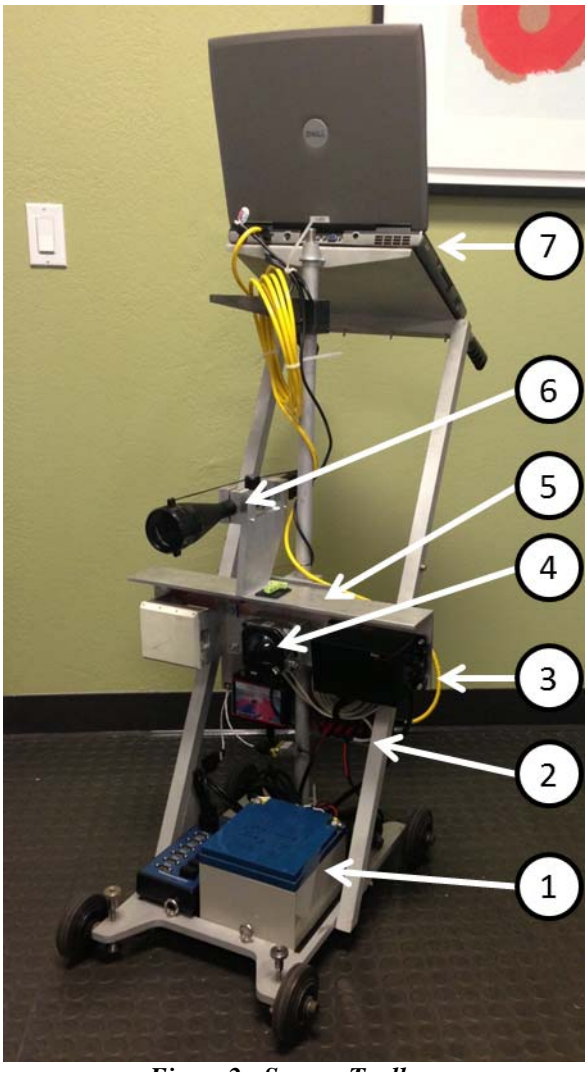


***Figure2. Sensor Trolley.***

The radar sensor is aligned with the sensor bracket, which is calibrated to be parallel to the radar sensor. This is accomplished by using an alignment device (Figure 3) that contains a laser and a visual target that has the same lateral and vertical offset as the scope does relative to the mirror on the Bosch sensor. Note that the alignment device uses the same tripod base as the scope sight device (Figure 4) except the lateral and vertical offset of the target is relative to the sensor center instead of the sensor mirror. The steps to accomplish the alignment are:

1. Point the laser at the mirror on the Bosch sensor.
2. Adjust the pitch and yaw of the sensor trolley and/or bracket in order to cause the laser to reflect back onto itself.
3. Adjust the horizontal and elevation adjustments of the scope sight so that it is pointed at the visual target.

***Figure3. Sensor Alignment Device.***

**Sensor Alignment to Representative Vehicle**

In order to obtain repeatable results it is necessary to carefully aim the sensor at the vehicle. The procedure described in this section is used for aligning the sensor with the vehicle and minimizes any misalignment due to variation in the roadway surface or other sources of error.

1. The vehicle is placed with its geometric center at a known location (referred to as the origin). The vehicle heading angle can be in any direction relative to the sensor.
2. The sensor trolley is then positioned at a known distance from the origin and facing the vehicle.
3. Place the scope sight device centered over the line connecting the vehicle geometric center to the sensor (marking this with a chalk line is recommended). The scope sight device is similar to the alignment device in Figure 4, except that the offsets are based on the center of the sensor box itself as opposed to the sensor mirror.

***Figure4. Scope Sight Device.***

4. Extend the three leveling feet on the sensor trolley so that the wheels of the sensor trolley are not touching the ground.

5. Adjust the two front leveling feet to level the sensor bracket in roll using the bubble level.
6. Adjust pitch angle using the rear leveling foot such that the scope sight is vertically aligned with the visual target.
7. Adjust the sensor yaw using a fine yaw adjustment plate, which changes the relative yaw angle between the sensor bracket and the trolley.
8. Confirm that the scope sight is aligned with the target.

***Figure5. Scope Sight After Target Alignment.***

9. Move the scope sight device and any other equipment away from the vehicle to prevent confounding the radar measurement data.
10. Record the sensor data.

**Measurement Matrix**

In order to capture the radar signature of the entire vehicle, the radar measurements were taken from five viewing angles as shown in Figure 6. In addition, the measurements were taken from distances of 20, 40, and 60 m. This will result in 15 measurements of each vehicle.

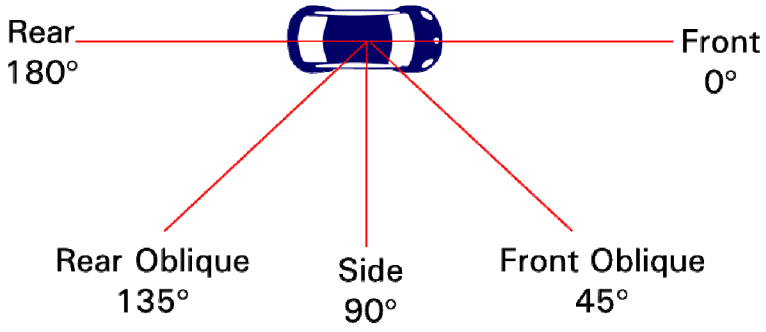


***Figure6. Radar Measurement Viewing Angles.***

**Table2.**
**Test Matrix**

| Viewing Angle | | Ranges (m) |
|---|---|---|
| Front | 0° | 20, 40, 60 |
| Front Oblique | 45° | 20, 40, 60 |
| Side | 90° | 20, 40, 60 |
| Rear Oblique | 135° | 20, 40, 60 |
| Rear | 180° | 20, 40, 60 |
| Front | 0° | 20, 40, 60 |

**Data Collection**

The Bosch LRR3 reports the data using CAN bus communication. For these measurements, a MicroAutoBox from dSpace was used to capture and record the data from the Bosch sensor. The sensor can track as many as 32 objects at a time and transmits the data approximately every 80 ms. For each object the following data were recorded:

- Longitudinal position (m)
- Lateral position (m)
- Probability of existence (0-1)
- Object validity (binary)
- RCS (dB-$m^2$)

**REPRESENTATIVE VEHICLES**

Eight small light passenger vehicles were measured for this analysis, including three sedans, three hatchbacks, and two microcars. Small light passenger vehicles represent a worst case in terms of vehicle visibility to radar and other sensors as compared to midsize and large light passenger vehicles and medium and heavy trucks.

Table 3 lists the vehicles that were used. Figure 7 provides a photograph of each of the measured vehicles. These vehicles include several vehicles from the same generation as vehicles that were previously measured by the Michigan Tech Research Institute (MTRI) using a high resolution research grade radar device as reported in Ref 1. These vehicles were selected to provide maximum overlap between this document and the MTRI report (Ref 1). Other vehicles, such as the Smart Fortwo and Scion iQ were measured because they were under consideration for being used as models for a surrogate vehicle.

**Table3.**
**Test Matrix**

| Make and Model | Model Year |
|---|---|
| Toyota Corolla | 2010 |
| Honda Civic | 2010 |
| Ford Fiesta Sedan | 2012 |
| Ford Fiesta Hatchback | 2014 |
| Toyota Matrix | 2014 |
| Honda Fit | 2013 |
| Smart Fortwo | 2014 |
| Scion iQ | 2014 |

***Figure7. Representative Vehicles.***
***a) Toyota Corolla; b) Honda Civic; c) Ford Fiesta Sedan; d) Ford Fiesta Hatchback;***
***e) Toyota Matrix; f) Honda Fit; g) Smart Fortwo; h) Scion iQ.***

## DATA ANALYSIS METHODS

The recorded data for each measurement was processed using a two-step procedure. First, the raw data is filtered to remove any invalid measurements such as measurements of the surrounding environment. Second, the detected objects that appear to be inconsistent are removed.

This section describes the data filtering in detail as well as the data analysis methods used to objectively quantify the RCS of a group of representative vehicles.

**Data Filtering**

The raw data for each 5-second time epoch was first filtered to remove any invalid measurements or measurements not related to the representative vehicle. The invalid measurements were removed using the "Object Validity" output from the Bosch sensor. Additionally, the raw data points were spatially filtered by removing all data points that did not fall within an area around the vehicle. The size of the area was chosen to be a 9 meters long by 4 meters wide rectangle, which helped to ensure that there were no objects within the valid area except for the vehicle being measured, as shown in Figure 8.

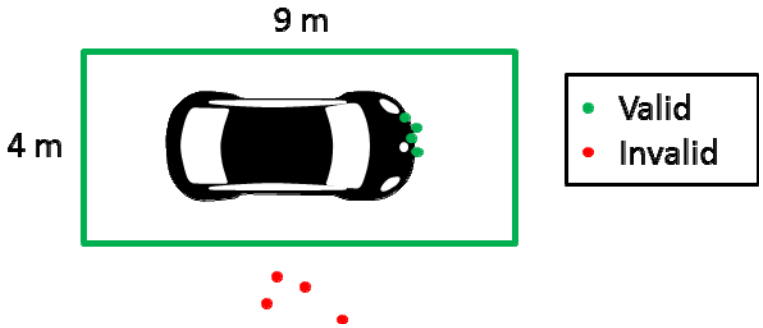


***Figure8. Spatial Data Filtering.***

The data were then filtered to ensure that the detected objects were real and consistently visible. This was accomplished by examining the duration of visibility for each of the detected objects. All data points for an object were removed from the measurement if the object was not detected for at least 25% of the measurement epoch. This had the benefit of removing measurement outliers that appeared for only a few frames, as shown in Figure 9.

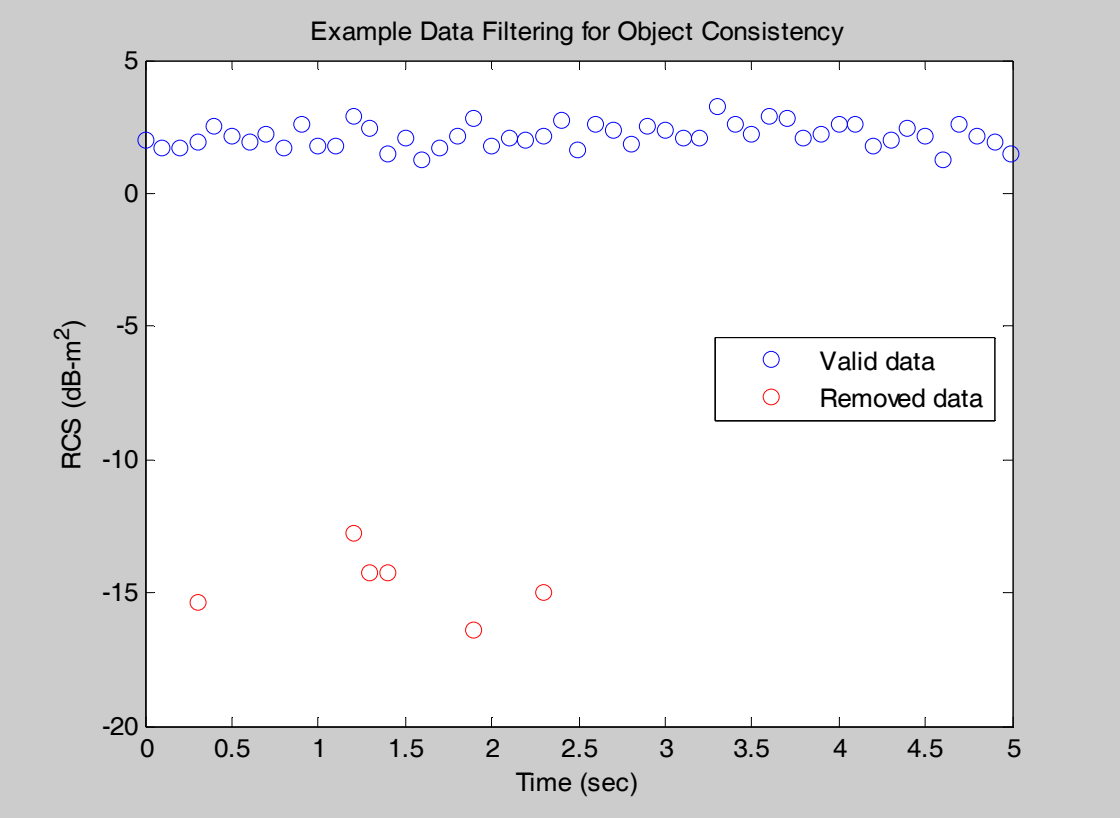


***Figure9. Example Data Filtering for Object Consistency.***

**Data Analysis**

After filtering, the data contained only measurements for consistently visible "objects" associated with the representative vehicle. Use of the term "objects" in this section refers to the detected objects remaining in a data set after the filtering has been applied. In most cases, it appeared that each detected "object" corresponded to a sub-structure or surface of the vehicle that had, for a variety of reasons, relatively strong radar reflectance.

**Number of Detected Objects** Each of the 120 measurements (15 measurements per vehicle times 8 vehicles) resulted in 1 to 4 objects being detected. Based on the reported spatial data it is clear that the dominant object was typically the nearest portion of the vehicle. However, for numerous measurements, other objects were visible further within or on the far side of the vehicle. Figure 10 shows the breakdown of the number of detected objects for all measurements (all viewing angles and ranges). Less than 5% of the measurements resulted in 3 or 4 objects while 60% had 1 object.

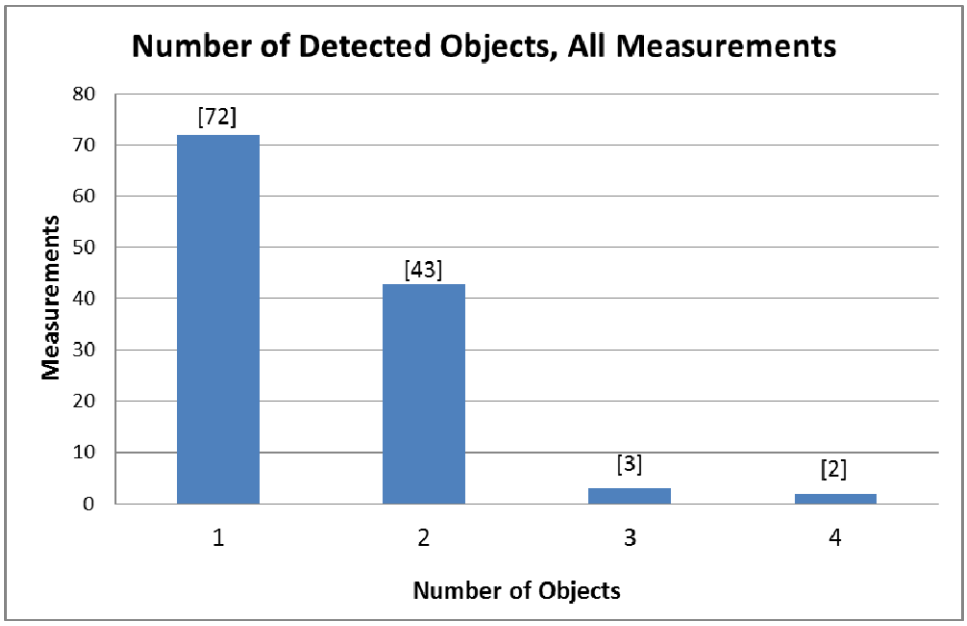


*Figure10. Example Data Filtering for Object Consistency.*

Looking at the data by viewing angle, Figure 11 shows that the oblique views are much more likely to result in more than one object being detected. The two oblique views (front and rear) resulted in 34 out of 48 measurements with 2 or more objects (over 70%). The direct viewing angles (front, side, and rear) resulted in 14 out of 72 measurements with 2 or more objects (less than 20%).

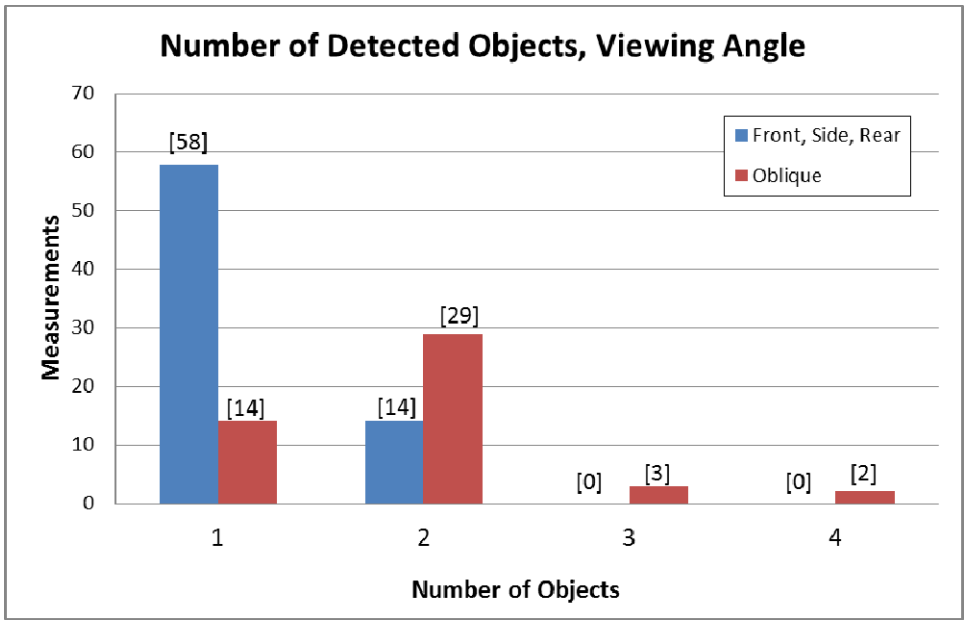


*Figure11. Number of Detected Objects by Viewing Angle.*

The number of detected objects can also be dependent on range. Figure 12 shows that measurements taken from a range of 20 meters are more likely to have multiple objects (over 50%) than measurements taken from 40 or 60 meters (less than 40%). This might be due to the fact that, at closer range, the reflections from the vehicle cover a larger angular field of view for the sensor, which might cause the sensor to classify the reflections as separate objects. It might also be the result of the higher power reflections that are detected by the sensor at closer range (i.e., radar power drops off with the 4th power of distance (Ref 1)).

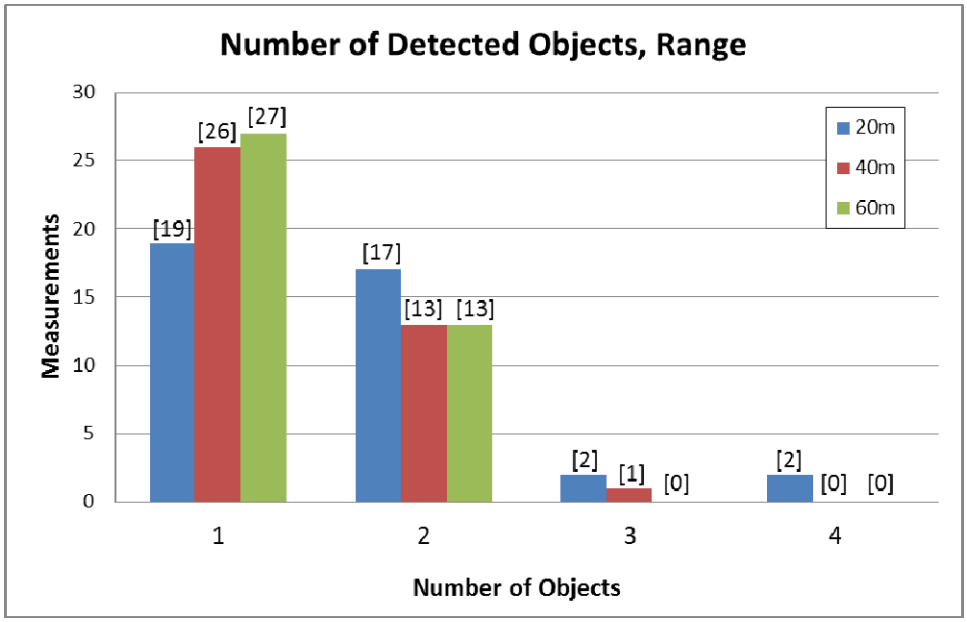


***Figure12. Number of Detected Objects by Range.***

The presence of multiple sensed objects must be accounted for when developing an index for the RCS of representative vehicles. The sensor itself reports an RCS value for each object, so the presence of multiple detected objects associated with a single vehicle requires some additional steps be taken to be able to assign an RCS value to a given vehicle.

**Classification of the Primary Object** In order to reduce the RCS variation caused by relatively lower power reflections from the far side of the vehicle, it was decided that only one object for each measurement should be used for the analysis. The "primary object", as it is referred to, was selected as the object with the largest average RCS on the "near side" of the vehicle. As shown in Figure 13, for front, rear, and side measurements the near side of the vehicle was defined as the area between the sensor and the geometric center of the vehicle; for oblique measurements the near side of the vehicle was defined as the area between the sensor and the longitudinal centerline of the vehicle.

Figure 14 shows an example of a measurement that had multiple objects. For this rear view measurement, Object 1 was detected as the rear of the vehicle. Object 2 was detected as being on the far side of the vehicle with a relatively lower RCS. In this example, Object 1 was classified as the primary object and the data associated with Object 1 were used for further analysis.

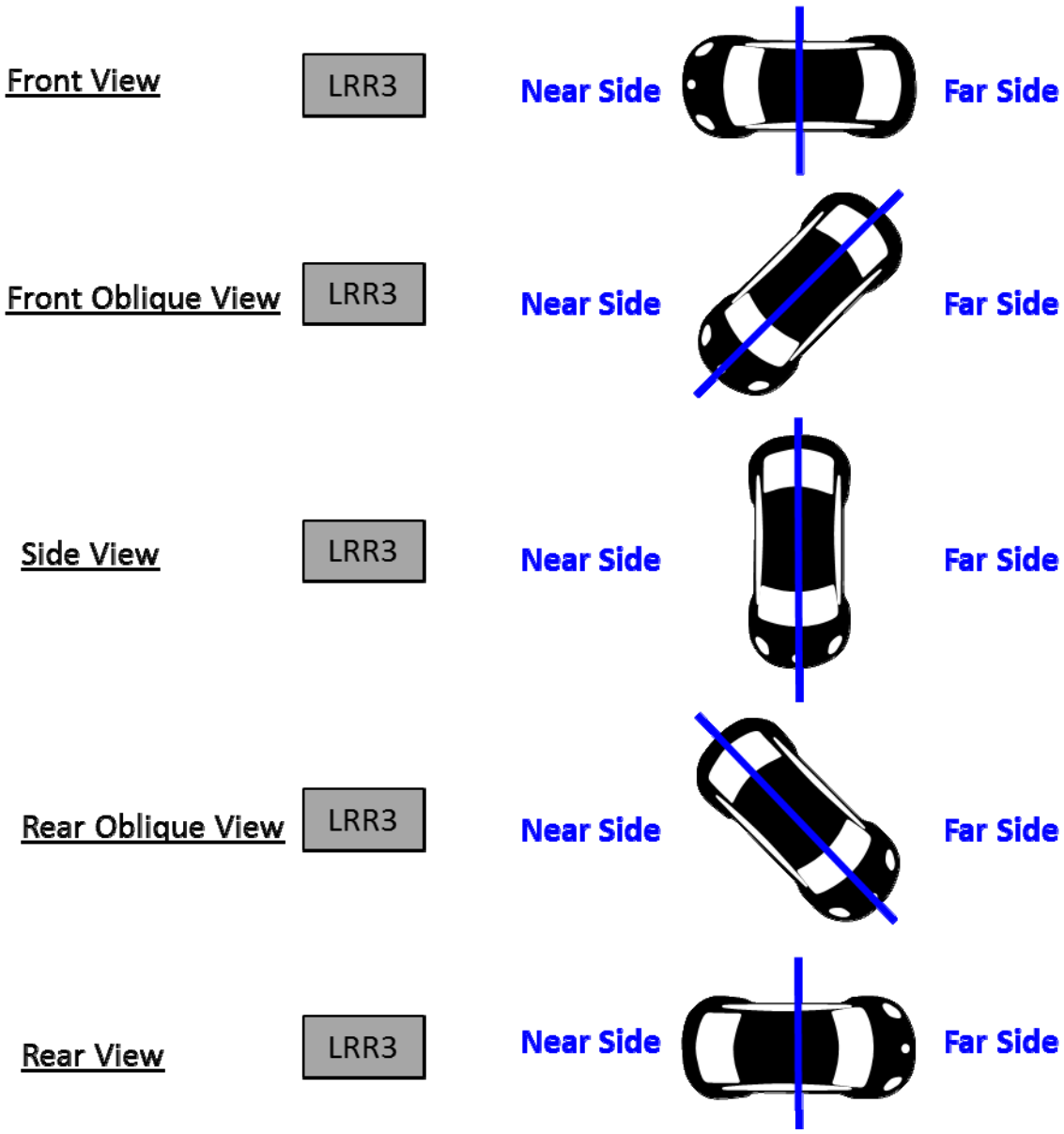


*Figure13. Definition of Near-Side and Far-Side Objects.*

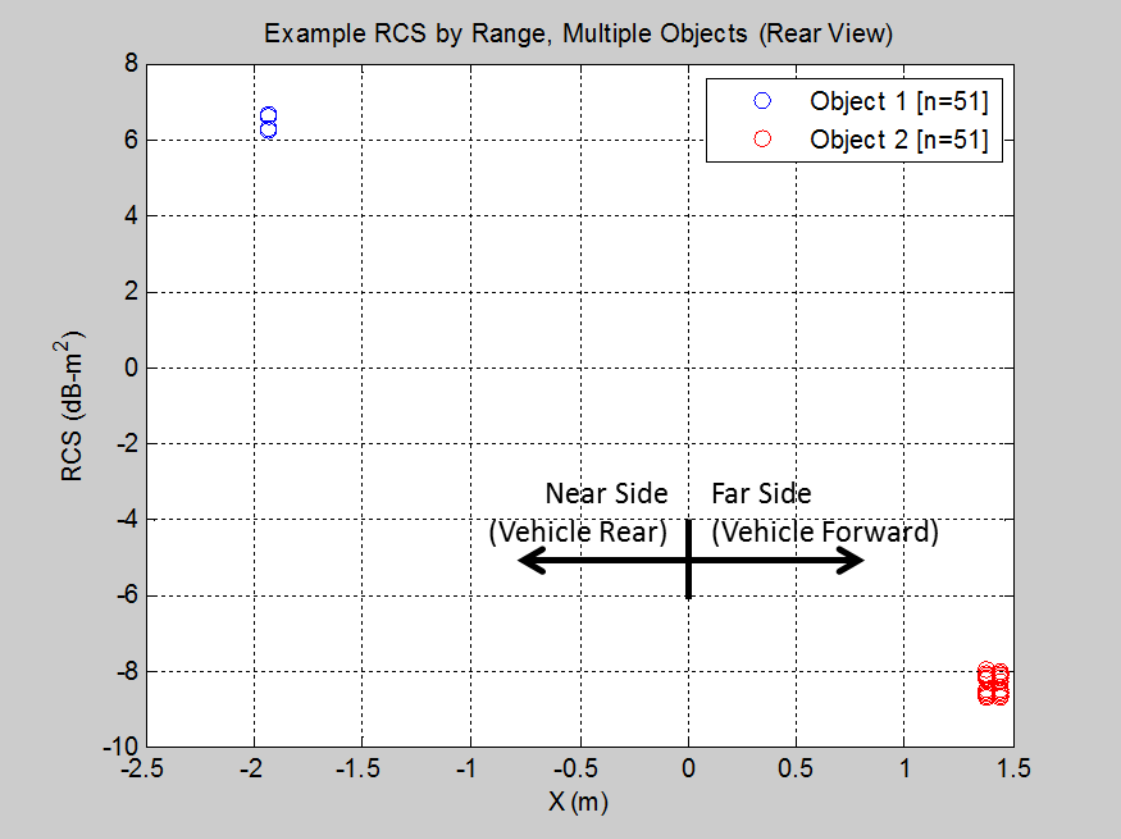


***Figure 14. Example of Primary Object Classification (for One Vehicle, One Distance and One Viewing Angle).***

Of the 120 measurements, 25 measurements contained at least one near-side object and one far-side object. On average, the near side object had a higher RCS than the far side object by an average of 11.26 dB-m$^2$. However, 5 of the measurements had a far side object with a larger RCS than the near side object. These measurements were all for the oblique views (4 rear, 1 front) and had an average difference in RCS of 1.57 dB-m$^2$ with a maximum difference of 2.44 dB-m$^2$.

Additionally, 5 of the 120 measurements resulted in only a far side object being detected. These were all rear oblique view measurements and were not included in the current analysis (i.e., there was assumed to be no primary object). However, in the future, it may be reasonable to consider the far side objects in these cases when classifying which object is the primary object for analysis.

**Statistical Analysis** The data have been processed to include only data points for the primary object from each measurement. These data can then be used to calculate the statistical properties of the RCS for the representative vehicles. For each set of measurements at a given viewing angle and range, the RCS mean and standard deviation were calculated. These values are used to create an RCS band at each viewing angle to represent the range of RCS values for the representative vehicles.

## MEASUREMENT RESULTS

The average RCS across all of the representative vehicles at each range and viewing angle is provided in Figure 15. In addition, the ±1-sigma (standard deviation) and ±2-sigma ranges are shown.

The mean RCS (μ) values for all of the measurements at each of the tested ranges varied from -11.5 to 15.0 dB-m$^2$, with standard deviations ranging from 2.4 to 7.6 dB-m$^2$. The side view had the largest mean RCS values, ranging

from 6.4 to 15.0 dB-$m^2$, with a standard deviations ranging from 3.5 to 6.1 dB-$m^2$. The oblique views (front and rear) had the smallest mean RCS values, ranging from -11.5 to -6.7 dB-$m^2$, with relatively small standard deviations, ranging from 2.4 to 4.8 dB-$m^2$.

Table 4 provides a numeric summary of the data that are depicted in Figure 15.

In addition to the summary figure provided in this section, raw histogram and cumulative distributions plots are provided in Appendix A.

**Table4.**
**Summary of RCS by Range and Angle**

| Angle | Range (m) | RCS Mean ($\mu$) [dB-$m^2$] | RCS Std. Dev. ($\sigma$)[dB-$m^2$] |
|---|---|---|---|
| Front | 20 | 0.13 | 4.74 |
| | 40 | 6.07 | 7.62 |
| | 60 | 8.15 | 2.55 |
| Front | 20 | -10.26 | 2.40 |
| Oblique | 40 | -8.68 | 4.82 |
| | 60 | -6.66 | 3.91 |
| Side | 20 | 6.41 | 3.45 |
| | 40 | 10.37 | 4.99 |
| | 60 | 14.99 | 6.06 |
| Rear | 20 | -11.51 | 2.45 |
| Oblique | 40 | -7.19 | 3.32 |
| | 60 | -8.16 | 3.15 |
| Rear | 20 | 2.15 | 3.39 |
| | 40 | 6.85 | 3.50 |
| | 60 | 2.22 | 6.36 |

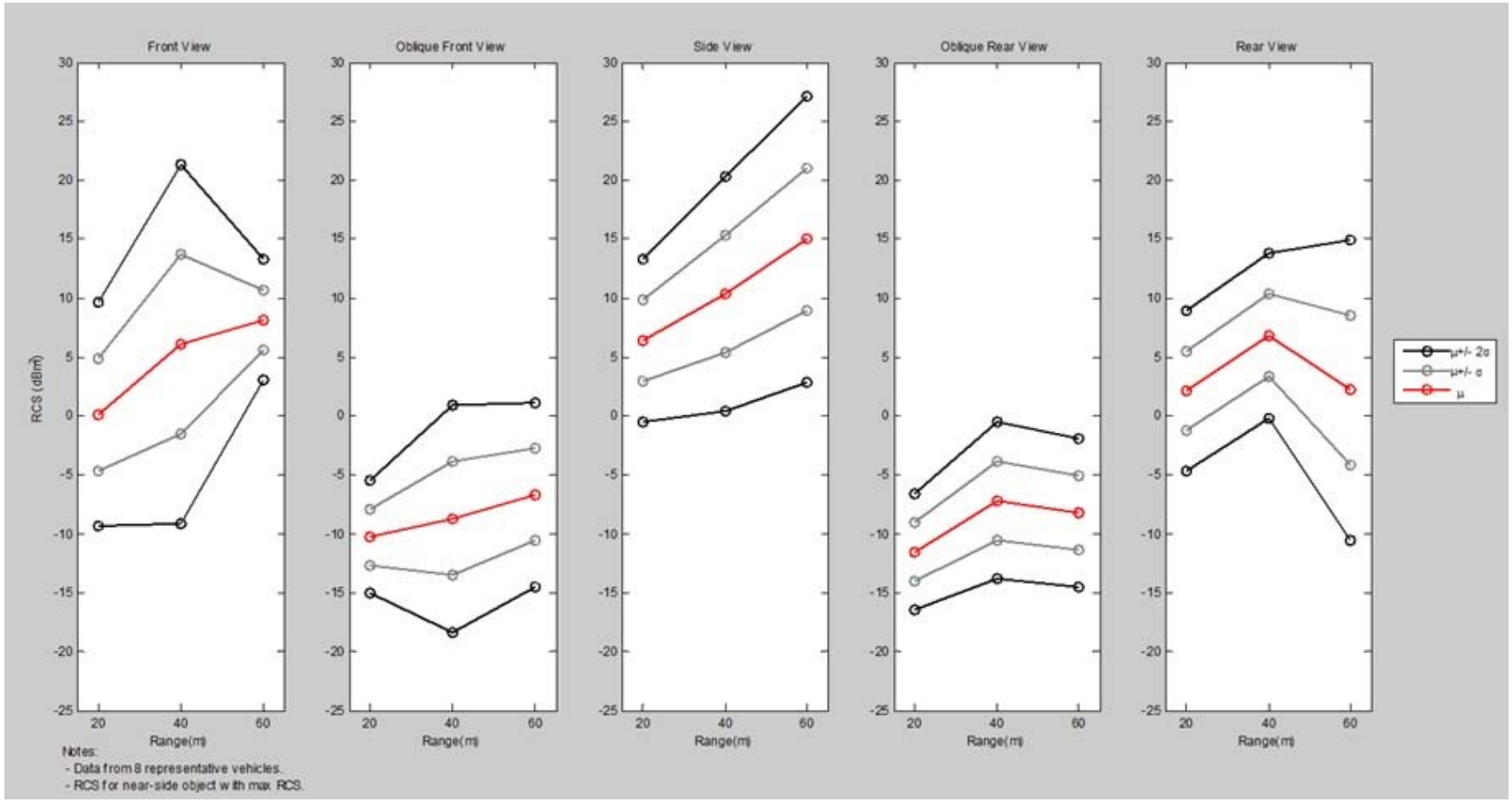


***Figure15. Summary of RCS by Range and Angle.***

## CONCLUSION

A system was developed for making radar measuremens that is based on typical automotive-grade equipment and processing. The system developed uses an automotive-grade radar sensor mounted to a mobile sensor trolley to allow for fast in-field radar measurements. The system was then used to measure the radar characteristics of eight small passenger cars from five viewing angles and at three distances for each angle.

The data in this document indicate that the side view of a vehicle will generally have the largest RCS, the front and rear views of a vehicle will have a moderately high RCS, and the oblique views will have a very small RCS. These results seem intuitive because the side view provides the largest reflection surface and that surface is oriented mostly perpendicular to the sensor. The orientation of the oblique views is such that the radar will tend to be reflected away from the sensor. Because of the strong dependence of RCS on viewing angle, surrogate vehicles that are representative of passenger vehicles from all angles are more realistic for testing ADAS technologies that may function at one or more ranges of angles.

It is also evident from the data that there is a large variation in RCS between vehicles. The rear view RCS of one vehicle may be much smaller or larger than the rear view RCS of another vehicle, even if the vehicles are a similar size and similarly shaped. Therefore, it is important for ADAS's to be able to accommodate large variations in radar signatures in order to be effective under real-world conditions.

The RCS measurement results for the representative vehicles that are presented here can be compared to similar measurements for surrogate vehicles. This method will confirm whether the RCS signature (i.e., from all angles and ranges) of a given surrogate vehicle is similar to and representative of real-world vehicles.

## REFERENCES

[1] W. Buller, et al, Radar Scattering Design Elements for a Pre-Collision System Surrogate TargetVehicular Technology Conference (VTC Spring), 2013 IEEE 77th

[2] V.G., Borkar, A. Ghosh, and N. Chourasia, "Radar Cross-section Measurement Techniques," Defense Science Journal, Vol. 60, pp 204-212, March 2010.

[3] W. Buller, B. Wilson, J. Ebling, L. van Nieuwstadt, and B. Hart., Radar Measurements of NHTSA's Surrogate Vehicle SS_V, US DOT Docket NHTSA-2012-0057-0034, DTNH11-12-P-01638, December 2012.

# INVESTIGATION OF REAR SEAT OCCUPANT POTENTIAL INJURY RISK BASE ON SEAT BELT CONFIGURATIONS

**Younghan Youn**
**Haesun Kim**
**Jiyang Park**
Korea University of Technology and Education

**Jaewan Lee**
**Siwoo Kim**
Korea Automotive Testing and Research Institute
Korea, Republic of

Paper Number 15-0443

## ABSTRACT

The occupants of all ages and sizes can be seated in the rear seats. But legal requirements regarding the qualification of the second seat row restraint system with anthropomorphic test devices (ATDs) currently do not exist. The protection of frontal seat passengers in both driver and front seated occupant has been more focused from the auto industries as well as regulatory bodies more than 40 years. Fortunately, their interests have been extended to rear seat occupants especially children and female occupants in recent years. However, the current available safety devices for the rear seat occupants are standard seat belt system only. Also, the majority of the rear seat occupant studies were focused to evaluate and protect child either CRS or using seat belt restrained in rear seat. The rear seat seemed to offer the greatest protection to children 0–12 years. Children seated in the rear seat had a lower risk of death compared with front seat passengers whether or not they were restrained. However, among adolescent and adult passengers, the rear seat offered less protection with increasing age and when restraints were used.
As a pilot project in Korea, total 452 accident cases have been collected and numbers of injured occupants (in patient) were 698. Drivers were 383 (54.9%), front passengers were 164, 2nd row left side seat were 47 (6.7%), 2nd row right side seat were 82 (11.6%), 2nd row middle seat were 15 (2.1%), and the remains are 3rd and 4th row seat occupants. Results from ISS injury severity analysis, the occupant of driver seating position has the highest ISS scores, 7.8±10.3, while front passenger (7.7±12.9), $2^{nd}$ middle seat (6.3±7.7), $2^{nd}$ left seat (6.1±9.3), $2^{nd}$ right seat 6±11.7), $3^{rd}$ left seat (6±0.0), $3^{rd}$ middle seat (5±0.0), and $3^{rd}$ left seat (2.8±1.7). Although the analysis was based on the limited numbers of data set, the safety of the rear seat adult occupants can't be ignored. Especially, the majority of rear seat potential occupants may be vulnerable occupants such as child, female with children, pregnant woman, and elderly.
In this study, the rear seat belts anchorage locations of the current domestic passenger vehicles were investigated to evaluate the influence of rear seat belt anchorage geometrical configurations in terms of the rear seat passenger safety. The sled type simulation models are developed with three point belts are fitted on the HybridⅢ 5th percentile dummy and HybridⅢ 50th percentile dummy. The injury value, particularly HIC15 and Chest deflection were examined to evaluate the contribution of rear seat belt anchorage locations.

## INTRODUCTION

Accident statistics over the last decades have shown a continuous reduction of killed and severely injured in the road traffic accidents. Historically the driver and front seat occupant have been the highest priority because these positions are occupied most often and therefore account for the greatest numbers of casualties. The introduction of airbags, seat belts and other advanced safety systems in front seating positions, along with vehicle structural improvements, has led to a significant reduction in the number of casualties and fatalities among vehicle occupants. This development was driven forward by new legislative requirements and the introduction and continuous progress on worldwide consumer test programs like the Euro-NCAP. The user's consciousness on safety is continually increasing due to publications and public discussion of road safety issues. Car manufacturers, in cooperation with suppliers, have taken massive action in order to achieve a top rating in consumer tests. The equipment rate of active and passive elements is steadily increasing and allows predicting further positive effect on road safety for the future. In newer model vehicles, occupant protection is achieved through the utilisation of a 'system'; a combination of vehicle crush characteristics, enhanced seat and seat belt technologies, such as seat belt pretensioners and load limiters, and airbags. This has largely been a result of consumer and regulatory assessments evaluating the performance of the system, rather than regulating the presence of any single component. Since these assessment

programs evaluate the protection provided in the front seat only, there has been less motivation for vehicle manufacturers to develop and implement these technologies in the rear seat, and the extent to which such technologies are available in the rear seat is not documented. Less attention has been paid to the rear seat. It was due to the rear seat has been considered safer than the front seat. Recently, however, a number of recent studies have been conducted showing instances of lower levels of protection for rear seat occupants compared to front seat occupants in the frontal crash test.

On the rear seat, the occupants of all ages and sizes can be seated. But the legal requirements regarding the vehicle safety issues of the second seat row restraint system with anthropomorphic test devices (ATDs) currently do not exist. Only consumer tests such as EuroNCAP, JNCAP and C-NCAP with respect to rear occupant protection systems have been adopted as a part of safety performance evaluations. Several recent publications discuss the passenger safety of the second row. Kuppa et al. indicates higher mechanical loads on rear seat passengers during a crash and deduce a higher injury risk compared to drivers and passengers in the first row. Restraint components like inflatable cushions (airbags) in order to protect the head and thorax or the lower extremities as well as pyrotechnical pre-tensioners partly with multi-stage load limiters for belt retractors are standard equipment in the front seat row. The next generation of advanced restraints system for first row occupants is already under development. Individualized restraint systems, like those providing adaptive pressure control of the airbag pressure and multi-stage belt force limitation concepts, are pending market introduction. These systems enable tailored restraint performance depending on crash severity and occupant size. In contrast to this, a 3-point belt retractor without pretension and force limitation is still the standard for the back seat passengers.

Consumer protection organizations incorporated adult passengers on the rear seat in their frontal test programs. The Hybrid III ATD with the 5th percentile is already an element of a test configuration for China-NCAP and Japan-NCAP. Euro-NCAP has been announced a follow up in 2015.

From 2014 national survey of seat belt usages, the wearing rate of dirver and front passenger was 78%, but only 22% of rear occupant was belted. It is significant improved from 2011's 5% rate of the belted rear seat occupant. To further promote usage of rear seat belts, the traffic regulation for wearing all seated passenger is effected in 2015. According to the survey, the one of main reason for unbelted was inconvenience of fitting and geometrical diffculty of buckle-up in the rear seat.To protect the rear seated occupants, MLIT granted a research project as a part of ASV program. This research program is part of a project intended to understand the optimal rear seat environment for rear seated adults and old child passengers who use the vehicle belt for primary restraint. Therefore, the objectives of this study were development of test protocols for rear seat occupant protection in future KNCAP plan. The total domestic 39 passenger vehicles including SUVs of the second rows seat's belt-anchorage geometrical configuration are investigated and compared with the KMVSS 102 (similar to FMVSS 210) criteria. To estimate injury risk of rear seat occupant, the sled type frontal crash simulations has been conducted with 5th female H3 and 50th male H3 dummies based on KNCAP crash pulse.

## ACCIDNT DATA ANALYSIS

A numerous researchers have been studied to focus on the relationships between the safety of the front and rear seat passengers. The most of these studies were limited to evaluate and protect child either CRS or adult seat belt restrained in rear seat. On the basis of the analysis of injuries of the road accident victims (injured and killed), it has been estimated that the risk of death of a rear seat passenger was smaller by 26–41% compared to a front seat one, even without the seat belts. On the average, the risk of death was 21% lower among passengers in the rear seat compared with front seat passengers. This apparent protection varied with age, restraint use, and airbag presence. The rear seat seemed to offer the greatest protection to children 0–12 years. Children seated in the rear seat had a lower risk of death compared with front seat passengers whether or not they were restrained. Among adolescent and adult passengers, the rear seat offered less protection with increasing age and when restraints were used. Restraints offered more protection to both front and rear seat passengers in vehicles with a front passenger airbag. In addition, restraints offered greater protection to front seat passengers compared with rear seat passengers.

Improving road safety, the first step in the process is identifying significant safety enhancement areas and the mechanisms of accidents and/or injuries that govern the problem. As a pilot project, total 452 accident cases have been collected from 3 different regional hospitals during last 11months period of traffic accident investigations. The sizes of 3 cities are from 210,000 to 450,000 populations which are typical medium size city. The total collected numbers of injured occupants (in patient) were 698. Drivers were 383 (54.9%), front passengers were 164, 2nd row left side seat were 47 (6.7%), 2nd row right side seat were 82 (11.6%), 2nd row middle seat were 15 (2.1%), and the remains are 3rd and 4th row seat occupants. Results from ISS injury severity analysis, the occupant of driver seating position has the highest ISS scores, 7.8±10.3, while front passenger (7.7±12.9), 2$^{nd}$ middle seat (6.3±7.7), 2$^{nd}$ left

seat (6.1±9.3), 2nd right seat 6±11.7), 3rd left seat (6±0.0), 3rd middle seat (5±0.0), and 3rd left seat (2.8±1.7) as shown in Table 1. In this analysis, un-belted occupants were not discriminated. Although the analysis was based on the limited data set, safety of the rear seat occupants can't be ignored. Therefore, the safety of rear seat occupant is equally important and must be seriously considered in terms of overall vehicle safety concepts from all related stock holders such as government body, auto makers, insurance agencies, and NGO. Especially, the majority of rear seat potential occupant may be vulnerable occupants such as child, female with children, pregnant woman, and elderly.

Table 1 ISS injury severity by the different occupant seating positions

| (n, %)/Seating position | Driver | F. Pass | 2nd row Left | 2nd row Right | 2nd row Middle | 3rd row Left | 3rd row Right | 3rd row Middle | 4th row Left |
|---|---|---|---|---|---|---|---|---|---|
| Total (698, 100) | 383 (54.9) | 164 (23.5) | 47 (6.7) | 81 (11.6) | 15 (2.1) | 1 (0.1) | 4 (0.6) | 1 (0.1) | 2 (0.3) |
| ISS (mean±std) | 7.8 ±10.3 | 7.7 ±12.9 | 6 ±11.7 | 6.1 ±9.3 | 6.3 ±7.7 | 6 ±0.0 | 2.8 ±1.7 | 5 ±0.0 | 1.5 ±0.7 |
| ISS (median) | 4 | 3 | 3 | 2 | 5 | 11 | - | - | - |
| ISS (interquartile range ) | 2-9.8 | 2-12.3 | 2-10.3 | 1-3 | 2-11 | 3-22.8 | - | - | - |

## LEGAL REQUIREMENTS FOR REAR SEAT BELT ANCHORAGES

Recent work at the University of Michigan Transportation Research Institute (UMTRI) has demonstrated that belt anchorage locations have a strong effect on occupant kinematics. More-rearward or higher lower anchorages (flatter lap belt angles) tend to reduce lower-body excursion, except when submarining occurs due to the belt slipping off the pelvis and into the abdomen. More-forward and higher upper anchorage locations tend to increase head excursion, except when submarining occurs.

In Korea, the locations of the anchorages of seat belt systems are regulated by Korea Motor Vehicle Safety Standard (KMVSS) 102 which is similar to FMVSS 210. Anchorage locations are referenced to the seating reference point (SgRP), which is measured using the SAE J826 H-point manikin. Lap belt anchorages must be positioned such that a vector from the anchorage to the SgRP in side view forms an angle of between 30 and 75 degrees with the horizontal. Upper anchorages must be located within a side-view zone defined with respect to the SAE J826 two-dimensional template with the template H-point aligned with the SgRP.

SHOULDER BELT ANCHORAGES:

| SEAT | SEATING POSITION | SPECIFIED ANGLE RANGE ABOVE OR BELOW HORIZONTAL | MEASURED ANGLE |
|---|---|---|---|
| FRONT | Left | 0 - 80 degrees above | |
| | | 0 - 40 degrees below | |
| | Right | 0 - 80 degrees above | |
| | | 0 - 40 degrees below | |
| REAR | Left | 0 - 80 degrees above | |
| | | 0 - 40 degrees below | |
| | Right | 0 - 80 degrees above | |
| | | 0 - 40 degrees below | |

LAP BELT ANCHORAGES:

| SEAT | SEATING POSITION | SPECIFIED ANGLE RANGE ABOVE HORIZONTAL | MEASURED ANGLE | | DOES BELT SECURELY FIT ON PELVIS? |
|---|---|---|---|---|---|
| | | | I/B | O/B | |
| FRONT | Left | 30 to 75 degrees | | | |
| | Center | 30 to 75 degrees | | | |
| | Right | 30 to 75 degrees | | | |
| REAR | Left | 30 to 75 degrees | | | |
| | Center | 30 to 75 degrees | | | |
| | Right | 30 to 75 degrees | | | |
| THIRD | Left | 30 to 75 degrees | | | |
| | Center | 30 to 75 degrees | | | |
| | Right | 30 to 75 degrees | | | |
| SIDE FACING | Left Side | 30 to 75 degrees | | | |
| | Right Side | 30 to 75 degrees | | | |

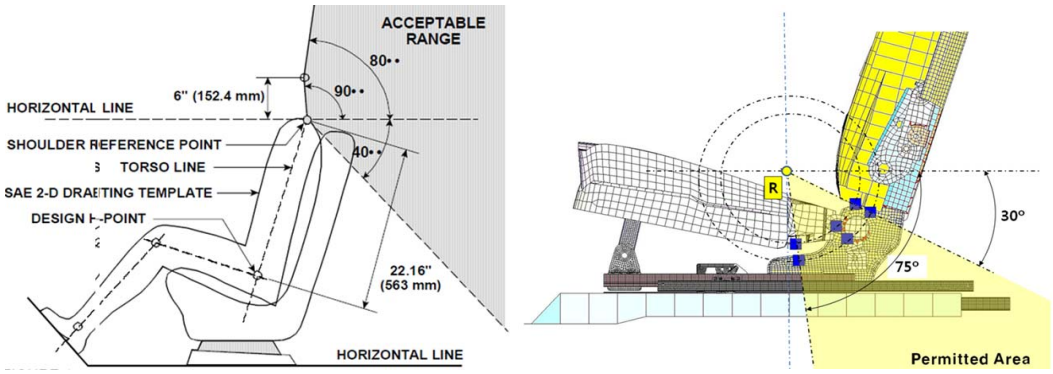


Fig. 1 KMVSS 102 requirements for rear seat belt anchorage points

## SIMULATION MODEL FOR REAR SEAT OCCUPANT

To assess safety of rear seat occupants, sled type simulation was conducted with calculated average value of 2010 - 2012 KNCAP 33 tested vehicles crash pulses to normalize crash severity as shown in Fig 4. The physical rear seat of each vehicle was manufactured differently due to different vehicle configuration as well as characteristic of vehicle model.

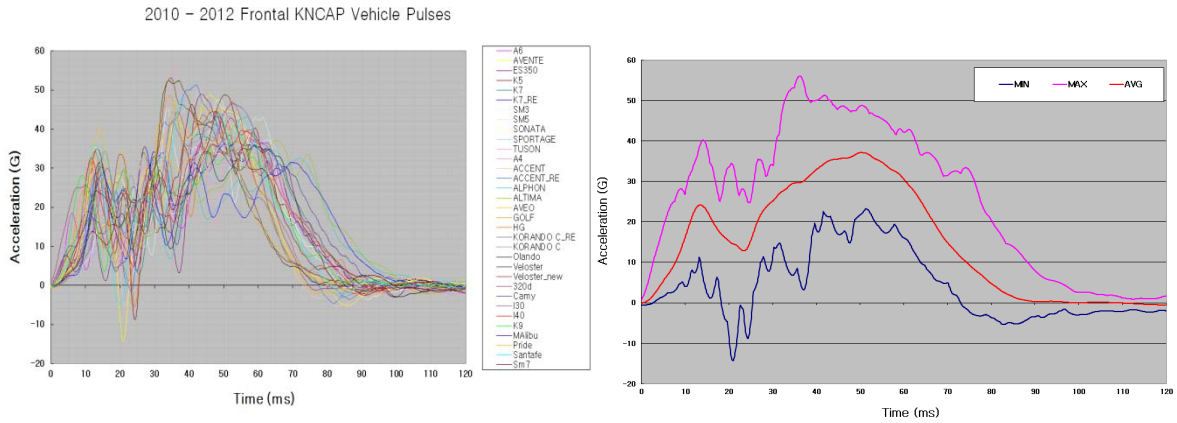


Fig. 4 Vehicle pulses of 2010-2012 KNCAP test and average pulse

In this simulation, the rear seat was modeled according to UN R44 as a standard seat model in order to eliminate seat variation, only focus to observe influence of seat belt anchorage configurations. The standard rear seat and polyurethane foam were modeled as shown in Fig 5. The webbing of seat belt was modeled as having 7% elongation material property. The pre-tensioner and load limiter of rear seat belt were not available for most of current production vehicle. These devices were not modeled.

Also, in the simulation model, to examine kinematics of occupants and injury levels of the different types of dummies during the crash event, the front seat was modeled as shown in Fig 6. Injuries of 5th H3 and 50th H3 dummies were compared with different seat belt anchorage locations.

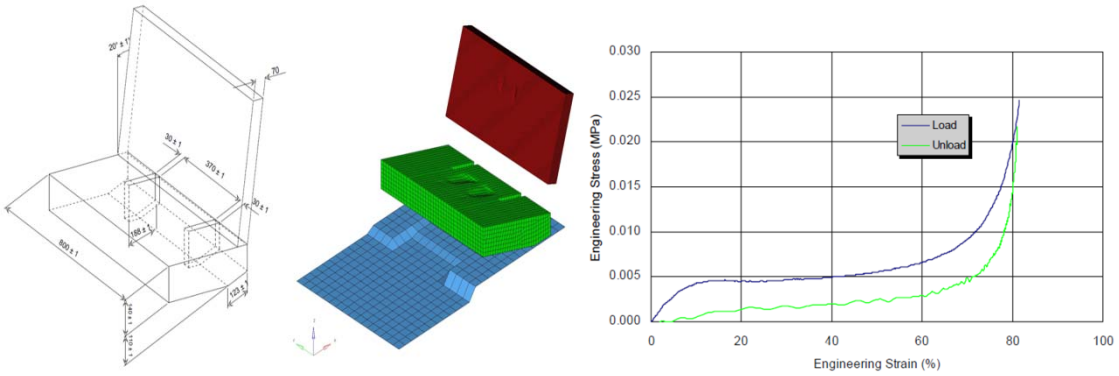


Fig. 5 Standard rear seat model and seat cushion characteristics

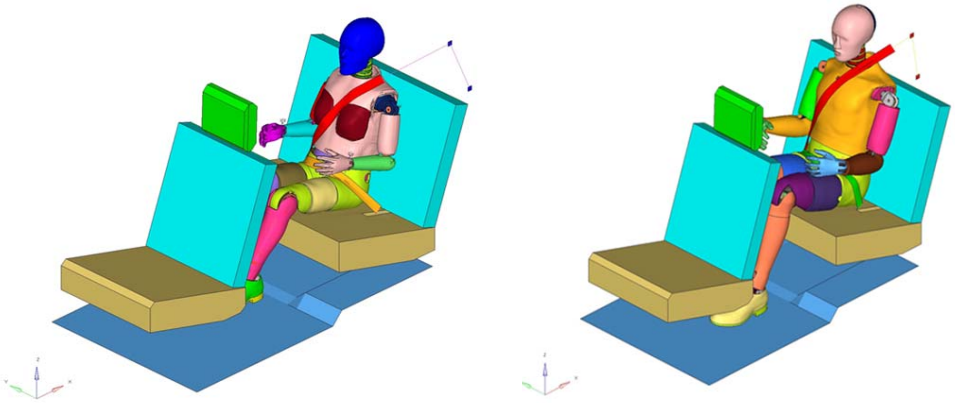

Fig. 6 Rear seat frontal impact simulation model for 5%tile and 50%tile dummies

## RESULTS

In this study, the total 39 passenger vehicles (sedan and SUV) from the 5 domestic car manufactures were examined. These vehicles were consisted in 3 sub-compacts, 3 compacts, 11 mediums, 9 large vehicles, and 12 SUV vehicles. In geometric data collection process, the coordinate of upper and lower anchorages were calculated from CAD data without any physical measurements due to availability of all vehicles. Fig. 1 shows the current KMVSS 102 requirements for the rear seat belt anchorages.

Table 2 and Fig 2 and 3 show the calculated seat belt anchorage locations relative to SgRP according to KMVSS 102 allowable zones. The red dots were average locations of examined vehicles. The lower anchorage locations scattered the entire allowable range of side-view angles. Upper anchorage locations also spanned a wide range, reflecting the wide variety of upper belt anchorage configurations, including those mounted in the C-pillar, package shelf, and integrated into the seat. But, the distributions of Z directional range were relatedly narrowed due to accommodate from 5th H3 to 95th H3 dummies. Inboard, buckle-side lower anchorages had slightly steeper (higher) lap belt angles, and the inboard anchorage was generally closer to the occupant centerline than the outboard anchorage. Since the distributions of all 39 vehicle's anchorages location were calculated only based on the CAD geometric data, it is not intended to verify fulfillment of requirements of regulation for out-ranged vehicle's anchorage locations.

Table 2 Relative coordinates of rear seat belt anchorage points (reference point: SgRP in mm)

| | vehicle Type | D-ring Coordinate | | | Lower Outboard | | | Lower Inboard | | | Seat Angle |
|---|---|---|---|---|---|---|---|---|---|---|---|
| | | X | Y | Z | X | Y | Z | X | Y | Z | |
| **01** | Small | -679.4 | -216.5 | 471.1 | -48.3 | -354.4 | -156.2 | -122.4 | 177.3 | -142.6 | 27 |

| | | | | | | | | | | | |
|---|---|---|---|---|---|---|---|---|---|---|---|
| **02** | Medium | -675.9 | -206.4 | 509.3 | -64.1 | -263.1 | -174.8 | -157.5 | 170.0 | -135.5 | 25 |
| **03** | Large | -675.9 | -206.4 | 509.3 | -64.1 | -263.1 | -174.8 | -171.3 | 195.5 | -125.1 | 28 |
| **04** | SUV | -251.3 | -276.0 | 654.8 | -132.1 | -338.0 | -173.9 | -210.5 | 159.5 | -222.5 | 25 |
| **05** | Mini | -442.1 | -275.3 | 549.3 | -52.5 | -300.5 | -92.8 | -117.6 | 141.5 | -147.8 | 26 |
| **06** | Compact | -504.7 | -293.2 | 599.0 | -101.7 | -221.3 | -146.9 | -75.3 | 162.0 | -157.1 | 25 |
| **07** | Small | -539.0 | -230.0 | 519.0 | -62.0 | -336.5 | -141.9 | -137.0 | 200.4 | -129.3 | 27 |
| **08** | Medium | -450.7 | -255.5 | 471.8 | -50.0 | -340.3 | -125.0 | -129.5 | 125.3 | -143.8 | 27 |
| **09** | Large | -460.6 | -225.4 | 452.8 | -60.0 | -310.3 | -144.0 | -139.5 | 155.3 | -162.8 | 25 |
| **10** | SUV | -412.4 | -312.3 | 580.5 | -249.9 | -318.0 | -230.2 | -196.3 | 181.4 | -160.9 | 25 |
| **11** | SUV | -306.6 | -304.2 | 638.2 | -109.3 | -270.4 | -217.2 | -196.3 | 181.4 | -162.8 | 25 |
| **12** | SUV | -482.3 | -296.6 | 567.4 | -85.7 | -254.5 | -184.2 | -84.4 | 183.3 | -204.6 | 25 |
| **13** | Large | -520.4 | -309.6 | 592.3 | -127.6 | -308.7 | -135.7 | -105.5 | 233.6 | -112.4 | 27 |
| **14** | Large | -382.4 | -261.5 | 561.1 | -2.5 | -275.0 | -147.3 | -53.3 | 208.4 | -202.3 | 27 |
| **15** | SUV | -444.1 | -192.8 | 542.6 | -375.0 | -236.6 | -287.4 | -67.0 | 191.4 | -118.2 | 15 |
| **16** | SUV | -393.4 | -265.1 | 618.4 | -130.3 | -315.0 | -62.3 | -82.2 | 240.9 | -97.1 | 15 |
| **17** | SUV | -405.9 | -271.4 | 615.6 | -47.4 | -331.0 | -133.1 | -138.9 | 120.0 | -202.9 | 15 |
| **18** | Compact | -392.5 | -201.0 | 577.5 | -103.5 | -250.2 | -106.4 | -127.1 | 156.0 | -114.1 | 26 |
| **19** | Small | -522.7 | -243.0 | 496.9 | -72.7 | -286.5 | -72.7 | -128.5 | 187.4 | -87.4 | 26 |
| **20** | Small | -471.5 | -271.1 | 501.6 | -86.7 | -275.1 | -112.2 | -152.1 | 152.9 | -125.6 | 26 |
| **21** | Small | -419.5 | -212.8 | 541.1 | -112.4 | -275.1 | -87.1 | -150.9 | 184.0 | -116.0 | 27 |
| **22** | Medium | -410.0 | -226.0 | 545.0 | -54.5 | -368.2 | -112.8 | -51.7 | 130.1 | -154.3 | 27 |
| **23** | Medium | -457.2 | -279.5 | 524.3 | -98.8 | -355.8 | -107.7 | -124.9 | 201.2 | -135.3 | 26 |
| **24** | Large | -413.4 | -220.4 | 538.6 | -66.6 | -359.2 | -107.9 | -63.6 | 139.5 | -152.0 | 27 |
| **25** | Large | -438.7 | -210.7 | 534.4 | -49.2 | -256.7 | -78.5 | -70.1 | 215.2 | -109.7 | 26 |
| **26** | Large | -494.1 | -195.0 | 540.3 | -88.5 | -256.1 | -89.9 | -108.2 | 219.5 | -126.2 | 27 |
| **27** | SUV | -261.7 | -263.7 | 631.1 | -88.7 | -254.4 | -146.6 | -53.5 | 171.9 | -145.0 | 25 |
| **28** | SUV | -221.7 | -263.7 | 631.1 | -48.7 | -254.4 | -146.6 | -13.5 | 171.9 | -145.0 | 25 |
| **29** | SUV | -246.8 | -256.9 | 633.6 | -130.9 | -197.9 | -170.0 | -142.5 | 171.4 | -157.3 | 23 |
| **30** | Mini | -332.7 | -249.8 | 584.5 | -78.0 | -215.0 | -118.7 | -139.8 | 108.7 | -110.9 | 24.5 |
| **31** | Mini | -350.8 | -267.8 | 598.5 | -198.0 | -207.0 | -119.0 | -70.4 | 186.8 | -119.7 | 21 |
| **32** | Compact | -409.2 | -234.2 | 625.0 | -105.5 | -249.3 | -97.4 | -94.2 | 164.1 | -135.7 | 26 |
| **33** | Small | -443.3 | -208.2 | 561.6 | -108.3 | -272.6 | -87.1 | -157.1 | 185.1 | -124.3 | 27 |
| **34** | Medium | -415.7 | -226.6 | 537.7 | -56.8 | -363.0 | -111.4 | -51.7 | 130.2 | -153.4 | 27 |
| **35** | Large | -436.2 | -220.2 | 543.8 | -61.6 | -359.2 | -107.9 | -58.7 | 139.7 | -151.4 | 27 |
| **36** | Large | -436.7 | -195.0 | 533.0 | -59.6 | -242.5 | -88.3 | -80.0 | 225.5 | -116.6 | 27 |
| **37** | SUV | -315.4 | -270.2 | 618.0 | -94.9 | -255.7 | -168.6 | -84.7 | 187.6 | -162.8 | 25 |
| **38** | SUV | -353.0 | -244.4 | 607.4 | -157.4 | -298.8 | -187.5 | -93.0 | 183.0 | -88.8 | 23 |
| **39** | SUV | -410.7 | -252.4 | 612.8 | -130.9 | -197.9 | -170.0 | -142.5 | 171.4 | -157.3 | 23 |

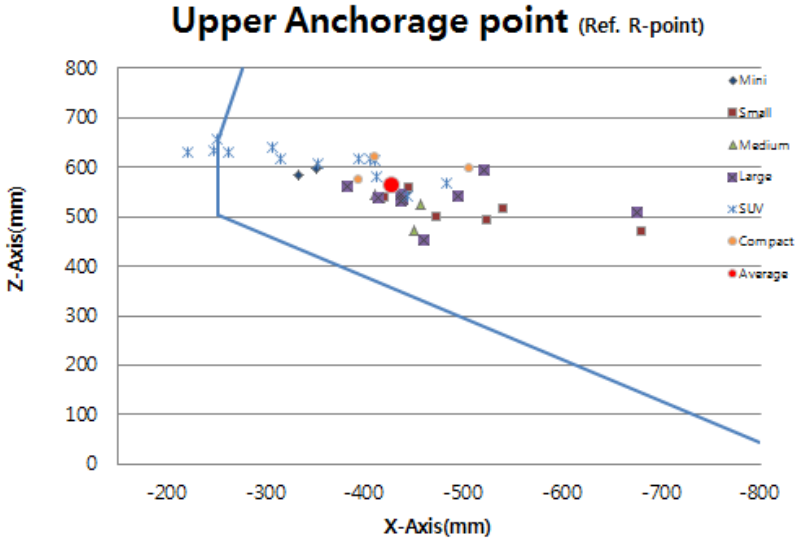


Fig. 2 Side views (y direction) of rear seat belt upper anchorage locations

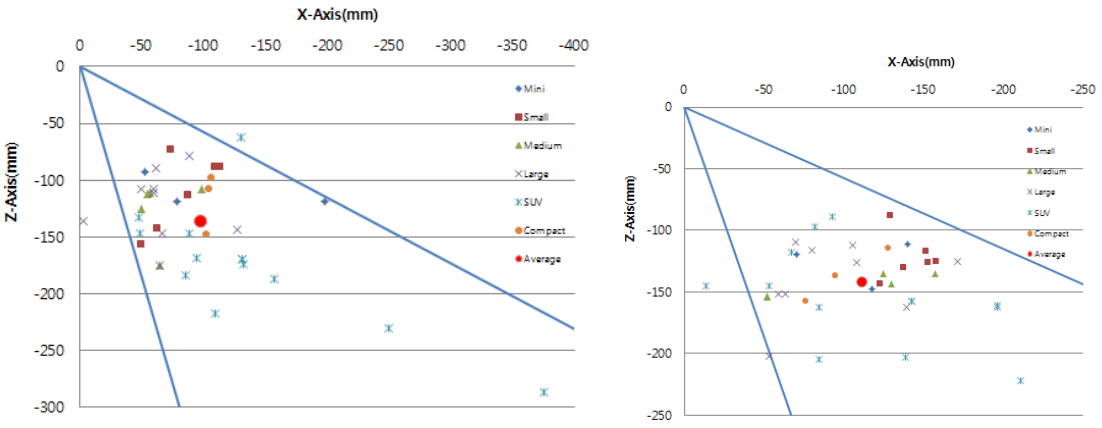


Fig. 3 Side views (y direction) of rear seat belt lower outboard and inboard anchorage locations

## DISCUSSIONS

### Geometrical distribution of seat belt anchorages

Normally, the belt geometry in rear seats is less favorable than in front seats. This is due on the one hand to vehicle geometry, which does not permit optimal belt-anchoring points, for example, the rear wheel house restricts the possibilities of fastening the anchor fitting. On the other hand, the rear seat running all the way through results in restrictions in fastening buckles. The seat position of the occupant in the rear seat is also different from in the front seat. Due to the restricted foot space extending to the front seat, the knees bend further causing the pelvis to tilt further backwards. The geometry of belts and the seat position result in the angle between the lap belt and the pelvis normally becoming comparatively small. As a consequence, the risk in a head-on collision of the lap belt slipping over the wings of ilium is evident, i.e., submarining can occur. The upper fastening point of the shoulder belt, which has frequently been positioned far to the rear, also promotes submarining.

In this study, the second-row belt anchorage locations for 39 domestic passenger vehicles using CAD geometric data were examined. The results indicate that seat belt anchorage locations in second rows vary widely. The range of upper anchorage locations were relatively widely spread in X direction compared with Y and Z directions as shown in Fig 7. In Z direction, the most of SUV type vehicles were in higher location of upper anchorage points. Due to absence of separated trunk wall in SUVs, the upper anchorage points were attached to the C-pillar. In general, upper anchorage locations may affect the risk of torso rollout in frontal crashes and also can contribute to discomfort due to contact between the belt and the occupant's neck if the anchorage is too high or too far from inboard. The fore-aft location of the anchorage can also affect head excursion and chest loading in frontal crashes.

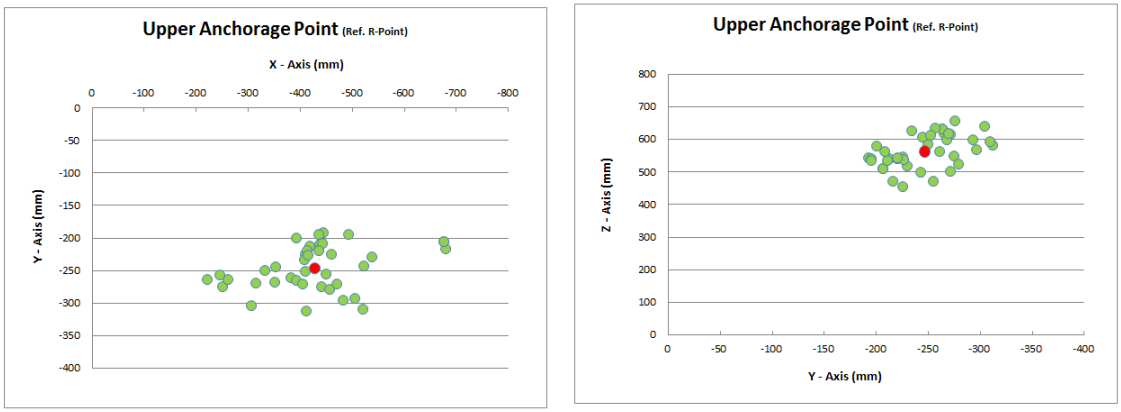


Fig. 7 Distribution of upper anchorage points in y-x and z-y planes

Fig 8 shows the range of lower anchorages, which spans the allowable range, is of particular concern for belt performance in frontal impact. In general, flatter belt angles are associated with better pelvis restraint but a higher likelihood of submarining, although submarining is influenced by many other factors. Steeper lap belt angles are needed to prevent submarining for smaller occupants, particularly children seated on vehicle seats with long seat cushions that produce slouched postures.

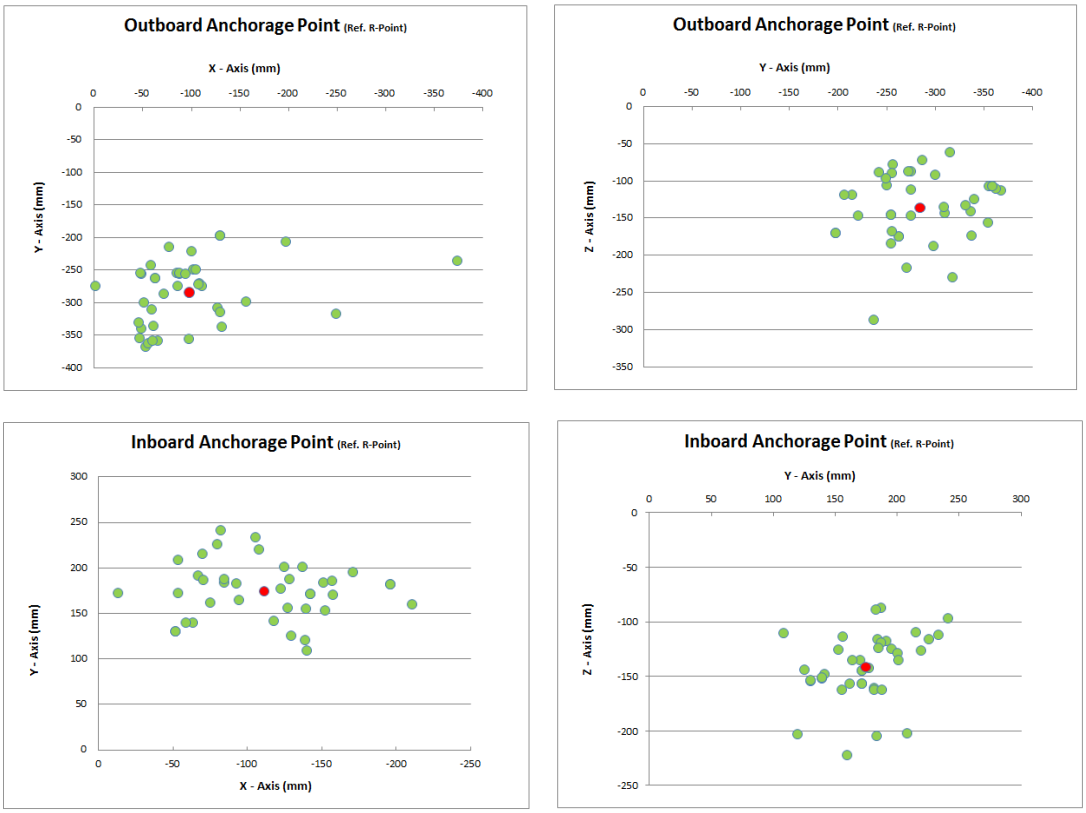


Fig. 8 Distribution of lower anchorages points in x-y and z-y planes

**Dummy seating position with different seat belt fitting**

As shown in Fig. 9 and 10, the seated position of 5%tile and 50%tile dummies were based on case 28 configuration which is foremost X direction of upper anchorage. The shoulder belt can't hold firmly upper torso of female dummy compared with same upper anchorage for 50%tile male dummy.

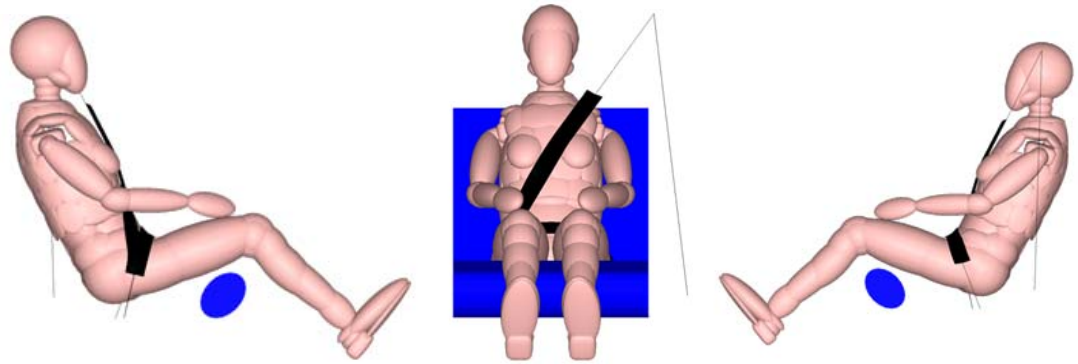

Fig. 9 5%tile female dummy Seated configuration of case 28

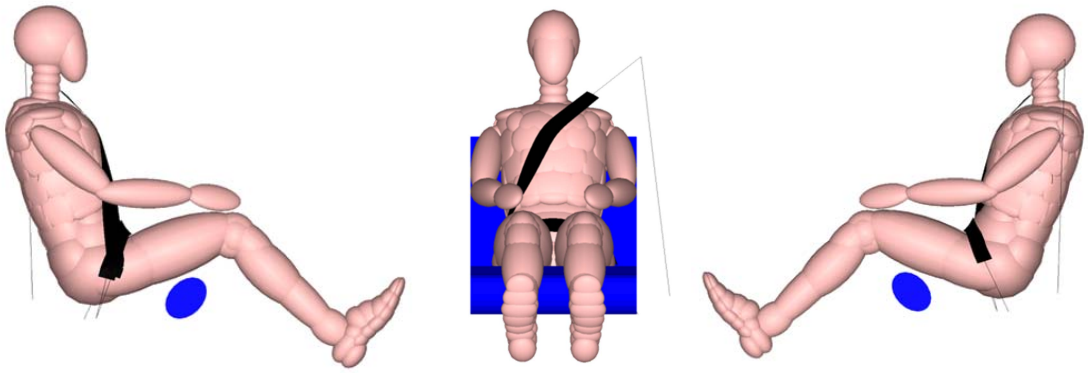

Fig. 10 50%tile male dummy Seated configuration of case 28

**Injury assessment for rear seat belt anchorage location**

Results from the sled simulation, injury values reveal that the most dominate factor is x directional location of upper anchorage point both in 5$^{th}$ H3 and 50$^{th}$ as shown in Table 3, Fig. 9 and 10. The more rearward locates upper anchorage point shows the less HIC values. Since regulation required at least suitable for 5$^{th}$ female dummy, less affecting coordinate in HIC is z directional point. For the chest deflection, also x coordinate of upper anchorage is influencing factor.

Table 3 Injury assessment for different rear seat belt anchorage points

| | Type | Hybrid Ⅲ 5%tile Female Dummy | | | | | Hybrid Ⅲ 50%tile Male Dummy | | | | |
|---|---|---|---|---|---|---|---|---|---|---|---|
| | | Head | Chest | Neck | | | Head | Chest | Neck | | |
| | | $HIC_{15}$ | Deflection (mm) | Tension (kN) | Compression (kN) | $N_{ij}$ | $HIC_{15}$ | Deflection (mm) | Tension (kN) | Compression (kN) | $N_{ij}$ |
| **01** | Small | 600.8 | 35.5 | 2.8 | 1.6 | 1.2 | 694.6 | 22.4 | 3.1 | 2.6 | 0.7 |
| **02** | Medium | 607.9 | 35.8 | 2.6 | 1.6 | 1.2 | 748.3 | 30.2 | 3.6 | 2.6 | 0.8 |
| **03** | Large | 556.4 | 39.8 | 2.4 | 1.6 | 1.1 | 725.2 | 51.5 | 2.9 | 2.6 | 0.7 |
| **04** | SUV | 1132.0 | 44.4 | 3.1 | 1.4 | 1.3 | 1358.6 | 44.4 | 4.4 | 2.2 | 1.0 |
| **05** | Mini | 987.4 | 40.4 | 2.7 | 1.7 | 1.5 | 1060.7 | 58.5 | 3.6 | 2.8 | 0.8 |
| **06** | Compact | 988.8 | 46.1 | 3.1 | 1.6 | 1.0 | 1061.8 | 53.0 | 3.5 | 2.4 | 0.9 |
| **07** | Small | 511.3 | 39.1 | 2.5 | 1.5 | 1.1 | 861.4 | 59.1 | 3.4 | 2.6 | 0.8 |
| **08** | Medium | 709.3 | 54.2 | 2.6 | 1.7 | 1.0 | 1029.9 | 64.7 | 3.4 | 2.4 | 0.9 |
| **09** | Large | 724.0 | 42.9 | 2.5 | 1.5 | 1.2 | 924.2 | 55.1 | 3.5 | 2.8 | 0.8 |
| **10** | SUV | 931.3 | 54.7 | 2.8 | 1.6 | 1.2 | 981.1 | 52.3 | 3.4 | 2.7 | 0.8 |
| **11** | SUV | 991.4 | 56.1 | 2.9 | 1.4 | 1.1 | 1167.4 | 64.6 | 3.7 | 2.5 | 0.8 |
| **12** | SUV | 823.8 | 53.0 | 2.4 | 1.4 | 1.1 | 836.0 | 50.7 | 3.0 | 2.4 | 0.9 |
| **13** | Large | 932.1 | 47.0 | 2.7 | 1.7 | 1.3 | 929.9 | 44.7 | 3.3 | 2.7 | 0.8 |
| **14** | Large | 933.4 | 53.5 | 2.9 | 1.5 | 1.2 | 924.5 | 53.7 | 3.1 | 2.5 | 0.8 |
| **15** | SUV | 737.7 | 40.6 | 2.4 | 1.6 | 1.2 | 907.0 | 45.3 | 3.2 | 2.6 | 0.9 |
| **16** | SUV | 916.9 | 46.4 | 2.7 | 1.5 | 1.5 | 975.6 | 45.5 | 3.4 | 2.6 | 0.7 |
| **17** | SUV | 1082.5 | 52.9 | 3.0 | 1.6 | 1.4 | 1090.2 | 63.6 | 3.7 | 2.7 | 0.8 |
| **18** | Compact | 687.7 | 37.7 | 2.5 | 1.4 | 1.3 | 898.6 | 56.6 | 3.3 | 2.6 | 0.8 |
| **19** | Small | 527.8 | 47.3 | 2.5 | 1.7 | 1.2 | 756.5 | 47.1 | 3.6 | 2.6 | 0.8 |
| **20** | Small | 765.6 | 43.8 | 2.6 | 1.6 | 1.4 | 921.0 | 57.2 | 3.5 | 2.6 | 0.9 |
| **21** | Small | 783.6 | 44.9 | 2.5 | 1.7 | 1.2 | 811.5 | 52.2 | 3.2 | 2.5 | 0.8 |
| **22** | Medium | 1023.0 | 51.5 | 2.7 | 1.7 | 1.3 | 1097.4 | 64.1 | 3.6 | 2.4 | 0.8 |
| **23** | Medium | 667.0 | 52.3 | 2.4 | 1.6 | 1.0 | 927.7 | 51.8 | 3.3 | 2.6 | 0.9 |
| **24** | Large | 966.6 | 51.0 | 2.8 | 1.6 | 1.3 | 966.5 | 62.0 | 3.6 | 2.5 | 0.9 |
| **25** | Large | 644.1 | 43.2 | 2.5 | 1.5 | 1.3 | 809.0 | 45.5 | 3.1 | 2.6 | 0.7 |
| **26** | Large | 524.2 | 38.8 | 2.3 | 1.4 | 1.0 | 728.2 | 43.8 | 2.9 | 2.6 | 0.7 |
| **27** | SUV | 1162.4 | 53.8 | 3.3 | 1.5 | 1.2 | 1171.8 | 52.7 | 3.6 | 2.3 | 0.9 |
| **28** | SUV | 1204.5 | 56.6 | 3.2 | 1.4 | 1.0 | 1156.4 | 65.1 | 3.6 | 2.3 | 0.9 |
| **29** | SUV | 1176.8 | 52.1 | 3.1 | 1.5 | 1.2 | 1218.5 | 48.6 | 3.8 | 2.5 | 0.9 |
| **30** | Mini | 1087.8 | 49.2 | 3.1 | 1.6 | 1.5 | 1065.7 | 61.9 | 3.7 | 2.4 | 0.9 |

| | | | | | | | | | | | |
|---|---|---|---|---|---|---|---|---|---|---|---|
| **31** | Mini | 947.3 | 53.6 | 2.7 | 1.4 | 1.1 | 1144.5 | 48.9 | 3.7 | 2.6 | 0.8 |
| **32** | Compact | 1015.2 | 46.6 | 2.9 | 1.6 | 1.4 | 1027.8 | 50.6 | 3.5 | 2.6 | 0.8 |
| **33** | Small | 706.0 | 41.4 | 2.5 | 1.7 | 1.2 | 706.0 | 41.4 | 3.2 | 2.7 | 0.8 |
| **34** | Medium | 929.6 | 55.2 | 2.6 | 1.8 | 1.0 | 1081.9 | 60.8 | 3.5 | 2.5 | 0.8 |
| **35** | Large | 991.5 | 49.7 | 2.7 | 1.7 | 1.3 | 1072.1 | 60.1 | 3.6 | 2.6 | 0.8 |
| **36** | Large | 628.5 | 42.1 | 2.3 | 1.5 | 1.1 | 772.3 | 43.5 | 3.0 | 2.6 | 0.8 |
| **37** | SUV | 1005.6 | 52.0 | 3.2 | 1.4 | 1.2 | 1144.1 | 50.1 | 3.6 | 2.5 | 0.9 |
| **38** | SUV | 880.7 | 47.8 | 2.8 | 1.5 | 1.3 | 957.1 | 52.0 | 3.3 | 2.6 | 0.8 |
| **39** | SUV | 952.5 | 44.7 | 2.9 | 1.6 | 1.3 | 969.2 | 57.7 | 3.4 | 2.5 | 0.8 |

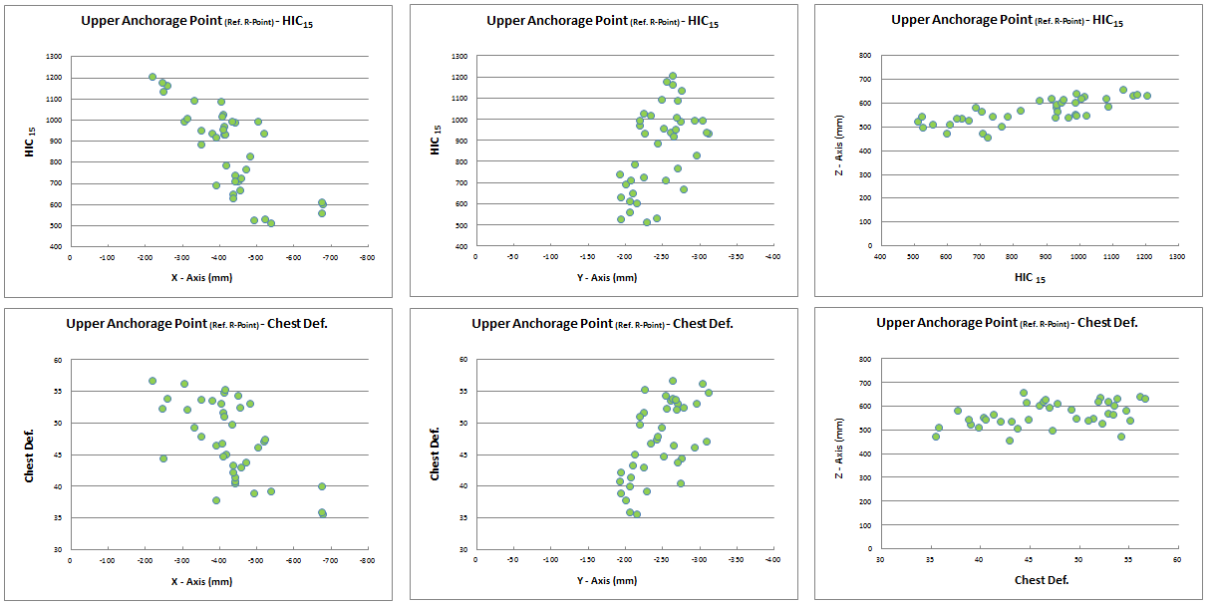


Fig.9 Injury severity of 5%tile female dummy based on distribution of upper anchorage locations

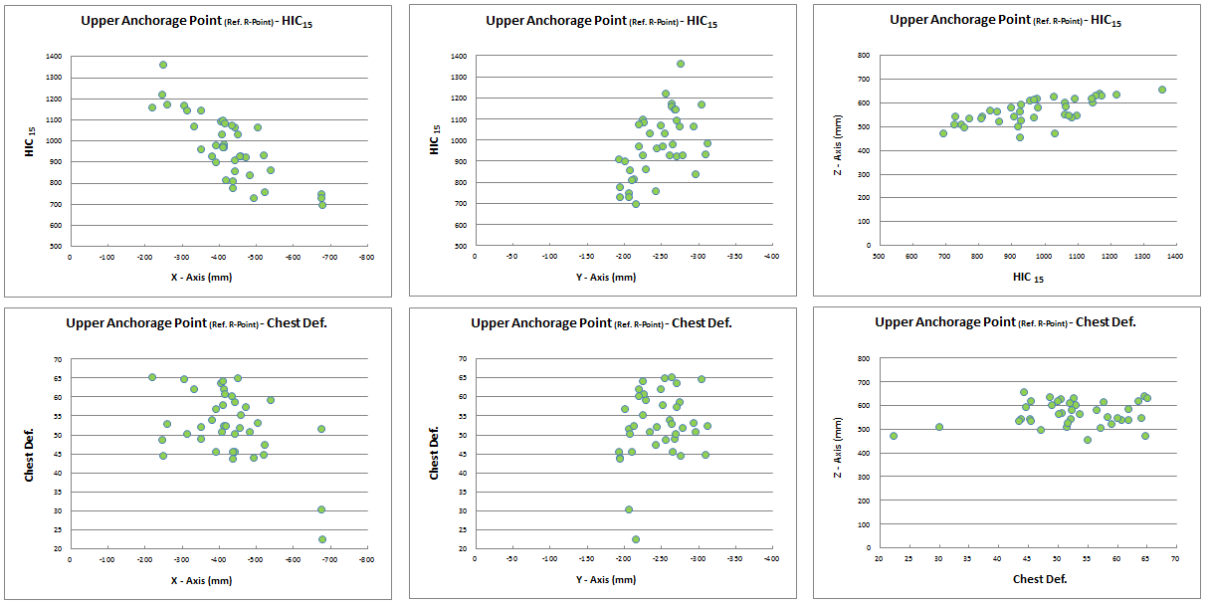


Fig. 10 Injury severity of 50%tile male dummy based on distribution of upper anchorage locations

## CONCLUSIONS

A significant increase has been observed in the number of installed restraint technologies available to front seat occupants as compared to rear seat technologies over the last couple of decades. With current research suggesting that the front seat is becoming relatively more effective at mitigating injuries [6-9], there is scope to improve the rear seat occupant protection system. The implementation of already available supplemental restraints available in the front seat and/or novel technologies, are potentially effective methods of improving safety in the rear seat.

In this study, the second-row belt anchorage geometric data were examined. Based on the geometric locations of rear seat belt anchorage, a standard frontal impact simulation was conducted to assess the influence of these belt anchorage points in rear seat occupant between 5%tile female H3 dummy and 50%tile H3 male dummy. From results from geometric calculation, the rear seat belt anchorages were widely scattered especially in X directional upper anchorage point. Some of vehicles were even out ranges of regulation requirements. The results indicate that seat belt anchorage locations in second rows vary widely. The range of upper anchorage locations were relatively wider spread in x direction compared with y and z directions. In injury assessments, the upper anchorage point strongly influences the motion of upper body. Results from the sled simulations, injury values reveal that the most dominate factor for HIC is x directional location of upper anchorage point both in $5^{th}$ H3 and $50^{th}$. The more rearward location of upper anchorage point shows the lower HIC values. Since regulation required at least suitable for $5^{th}$ female dummy, less affecting coordinate in HIC is z directional point. For the chest deflection, also x coordinate of upper anchorage is influencing factor.

## ACKNOWLEDGEMENTS

This research has been supported by a grant from MLIT and KAIA(11PTSI-C54118-03) of Korean government

## REFERENCES

[1] Schönebeck S., Schepers A., Pöppel-Decker M., Leipnitz C., Fitschen A. Voraussichtliche Entwicklung von Unfallanzahlen und Jahresfahrleistungen in Deutschland, Ergebnisse 2011 Bundesanstalt für Straßenwesen

[2] Kuppa S., Saunders J., Fessahaie O. Rear Seat Occupant Protection in Frontal Crashes International Technical Conference of the Enhanced Safety of Vehicles, 2005

[3] Forman J., Michelson J., Kent R.; Kuppa S., Bostrom O. Occupant Restraint in the Rear Seat: ATD Responses to Standard and Pre-Tensioning, Force –Limiting Belt Restraints 52nd AAAM Conference, 2008

[4] Stegmeier M., Bausch H. Rear Seat Protection for Occupants Sizes from Q6 to HIII 95%ile in Frontal Crashes 9th International Conference Protection of Children in Cars, 2011

[5] Klinich, K.D., Reed, M.P., Orton, N.R., Manary, M.A., and Rupp, J.D. (2011). Optimizing Protection for Rear Seat Occupants: Assessing Booster Performance with Realistic Belt Geometry using the Hybrid-III 6YO ATD. Technical Report 2011-40. University of Michigan Transportation Research Institute, Ann Arbor, MI.

[6] Website China-NCAP http://www.c-ncap.org.cn/C-NCAP/index.htm

[7] Website Japan-NCAP http://www.nasva.go.jp/mamoru/en/index.html

[8] Website EuroNCAP http://www.euroncap.com/home.aspx

[9] Smith, K. M., Cummings, P., Passenger seating position and the risk of passenger death in traffic crashes: a matched cohort study, Injury Prevention No. 12, pp. 83–86, USA 2006

[10] R. Kent*, et al.*, "The feasibility and effectiveness of belt pretensioning and load limiting for adults in the rear seat," *International Journal of Vehicle Safety,* vol. 2, pp. 378-403, 2007.

[11] Klinich, K.D., Reed, M.P., Orton, N.R., Manary, M.A., and Rupp, J.D. (2011). Optimizing Protection for Rear Seat Occupants: Assessing Booster Performance with Realistic Belt Geometry using the Hybrid-III 6YO ATD. Technical Report 2011-40. University of Michigan Transportation Research Institute, Ann Arbor, MI.

# OPPORTUNITIES FOR REDUCING FAR-SIDE CASUALTIES

**George T. Bahouth**
**Dennis Murakhovskiy**
Impact Research, LLC
United States

**Kennerly H. Digges**
The George Washington University
United States

**Holger Rist**
**Richard Wiik**
TAKATA Corporation

Paper Number 15-0444

## ABSTRACT

This paper uses NASS 2004-2013 to estimate the population of belted front seat occupants exposed to far-side crashes and those with serious injuries. The use of the most recent ten years of NASS data permitted an update of the characteristics of far-side crashes that are associated with serious injuries among belted front seat occupants. When compared with earlier studies, it was found that the vehicle category that includes SUV's, pickups and vans, has increased as the collision partner in far-side crashes. There has likewise been an increase in the median crash severity for MAIS 3+ injured. For the 2004-2013 NASS CDS data, the median crash severity for MAIS 3+ injured was a lateral delta V of 36 kph. Chest/abdominal injuries accounted for 43% and head injuries accounted for 23% of the AIS 3+ injuries. Drivers accounted for 79% of the MAIS 3+ injured belted front outboard occupants that were involved in far-side crashes. About 53% of front outboard occupant's chest injuries were caused by contacts with the vehicle center stack or seat back and 21% were associated with contacts with the far-side structure. In regards to head injuries, the far side structure accounts for more than 60% of the AIS 3+ injuries. Of the far side crash involved occupants analyzed, they sustained AIS3+ head or chest injuries from the far side of the vehicle more than 4.4 times more often than were attributed to occupant to occupant contact. Another striking trend is the disproportionate number of AIS3+ injured occupants in light passenger cars where belted front outboard occupants sustained severe injuries at a rate 2.7 times higher than exposed. Finally, this study identified that only 3.1% of belted AIS3+ injured occupants involved in far-side collisions sustained their injuries due to head to head contact with another front seat occupant.

## INTRODUCTION

A purpose of this paper is to investigate the characteristics of belted occupants with MAIS 3+ injuries who were exposed to far-side crashes. Although there is a history of research in far-side analysis and test criteria, this crash mode has not been addressed by safety regulations or consumer information ratings. An extensive international collaborative research project on far-side safety was completed in 2009 [Gabler 2005, Pintar 2007, Fildes 2009, Digges 2009]. Since the 2009 study was published, there have been changes in the composition of the US passenger vehicle fleet and in the safety of the vehicles. Regulatory changes include an increased penetration of vehicles that comply with a near-side impact standard requiring dynamic crash tests and related consumer information tests (FMVSS 214). It is appropriate to update the earlier analyses with the latest decade of NASS CDS data to include the possible affect of these changes, with the goal of understanding the evolution of the far side crash scenario in recent years.

There have been a number of international and US studies of far-side crash data that can provide a basis for comparing how the safety environment in far-side crashes has changed.

Mackay [1991] examined 193 crashes with belt restrained far-side occupants in Birmingham England during the period 1983-1989. The 193 cases contained 150 AIS 2 injuries and 15 AIS 3+ injuries. Among those with AIS 2+ head injuries, 35% came out of the shoulder belt. For those with AIS 2+ abdominal injuries, 72% were from contact with the safety belt. Contact with the belt system was the most frequent source of chest injuries to all involved occupants (59%).

A study using the Australian field data gathered between 1989 and 1992 examined 198 side impact crashes involving 234 occupants [Fildes et al. 1994]. These authors reported that 38% of the injured occupants were on the far side.

Frampton [1998] studied 295 crashes with belt restrained far-side occupants in England between June 1992 and April 1996. These cases included 46 MAIS 2 and 33 MAIS 3+ injuries. The MAIS 2 median delta V was 25 kph. The median MAIS 3+ delta V was 35 kph. Frampton found that the head and chest were the most frequently injured body regions.

Three US studies of far-side crashes [Digges 2001, 2006; Gabler 2005 and Yoganandan 2014] used different years of NASS CDS data. Each of the studies used similar controls that included the following: Passenger Cars or LTVs Only, GAD = Left or Right Side, No Rollovers, Occupant on Opposite Side of Impact, 3-Point Belt Restrained Occupants, Front Seat Outboard Occupants.

An early US analysis of far-side belted occupants in NASS CDS 1988-1998 was reported in a 2001 ESV paper [Digges, 2001]. The paper reported that a median lateral delta-V for AIS 3+ injuries was 30 kph. The most frequently AIS 3+ injured body regions were: chest/abdomen, 58%; head, 24% and spine 16%. The body region/contact combinations associated with the most frequent AIS 3+ injuries were: chest/abdomen to seatbelt, 20.6% and chest/abdomen to seatback and side interior, 17.2%. Occupant to occupant contacts accounted for less than 4%.

Gabler [2005], analyzing NASS CDS 1993-2002 data, showed that the median lateral delta-V for belted front seat occupants exposed to a far side impact was 12 km/hr. The median lateral delta-V for serious (AIS 3+) injuries was 28 km/hr. A principal direction of force of 60 degrees was most likely to be associated with serious injury. A PDOF of 60 degrees +/- 15 degrees was experienced by 60% of the seriously injured persons. The body regions with the highest number of AIS 3+ injuries were: chest/abdomen, 41% and head/face, 32%. The contacts for AIS 2+ head injuries were widely distributed with no source exceeding 10%. AIS 2+ head injuries from contacts with other occupants constituted 4.8% of the injuring sources. Unlike head injuries, the contacts for AIS 2+ chest and abdominal injuries were concentrated. For AIS 2+ chest injuries, 48% were attributed to the seat back and 24% to the safety belt. For AIS 2+ abdominal injuries, 87% were caused by the safety belt.

Yoganandan [2013] analyzed the NASS CDS database for the years 2009 to 2012 limited to vehicles of model year less than or equal to 10 years old at the time of the collision. Ejections were excluded. Injuries were coded using AIS 2005 and 2008. For the 519,195 weighted far-side occupants in the database, the authors found that the median lateral delta-V for belted front seat occupants exposed to a far-side impact was 19 km/hr. The median lateral delta-V for serious injuries was 42 km/hr. The most frequently injured body regions at the AIS 3+ level were: thorax, 69%; head, 50%; spine, 14% and abdomen, 13%.

## APPROACH

The present study examines far-side occupants in NASS CDS 2004 to 2013. Far-side crashes were selected based on the damage region (left or right side) for the most severe impact event (GAD1) where the occupant was seated in

the front row in the outboard position opposite the damaged side of the vehicle. Additionally far-side crashes that were preceded or followed by a rollover were excluded from this analysis. This was the same criteria used by the three studies listed previously. The resulting population of weighted far-side occupants in this new data set was 1,595,533. This larger data set allowed improved resolution for the far-side analysis, including the examination of injuring contacts, which was not available in the Yoganandan paper.

NASS CDS researchers code occupant injury contacts into one of more than 120 possible categories based on evidence within inspected vehicles and the nature of injuries sustained. A listing of the possible contact categories for drivers and right front passengers is included in the Appendix, Table A1. For the purpose of this study, contact sources and populations have been aggregated into 22 categories to allow for a simplified analysis of this data.

In order to maintain a consistent injury coding during the entire NASS period studied, AIS 1998 was applied in each year. The use of the 1998 coding permitted an analysis that was not influenced by changes in the injury coding and it allowed a better comparison with the results of earlier papers by Gabler and Digges. The 2005 and 2008 editions of the AIS code generally result in reducing the severity of selected injuries in the 1998 AIS code. A principal effect of the recent AIS coding changes on longitudinal studies has been to improve the apparent safety performance of vehicles in NASS CDS. This improvement is purely due to the injury coding and not to vehicle safety or human factors. When applied to 2010-2013 far-side data, the AIS 2008 code increased frequency of MAIS 3+ injuries by about 2 kph over the crash severity range from 25 to 50 kph. A comparison of the same NASS CDS data coded with the two different AIS coding systems is shown in Figure 1. The data is for belted MAIS 3+ injured front outboard occupants in far-side crashes. The comparison indicates how the use of two different AIS coding systems in a study can introduce confounding influences.

Beginning in 2010, NASS researchers began coding CDS applicable occupant injuries using AIS 2008 and retained AIS 1998 codes as well. The AIS 2008 coding definitions introduced new injury codes and adjusted AIS injury severity for a subset of existing injuries. The impact of this change was evaluated to determine its effect on the injured population distribution involved in far-side crashes. Figure 1 below shows the cumulative distribution curve for MAIS3+ injured versus lateral deltaV comparing the same population of cases coded in AIS 1998 versus AIS 2008.

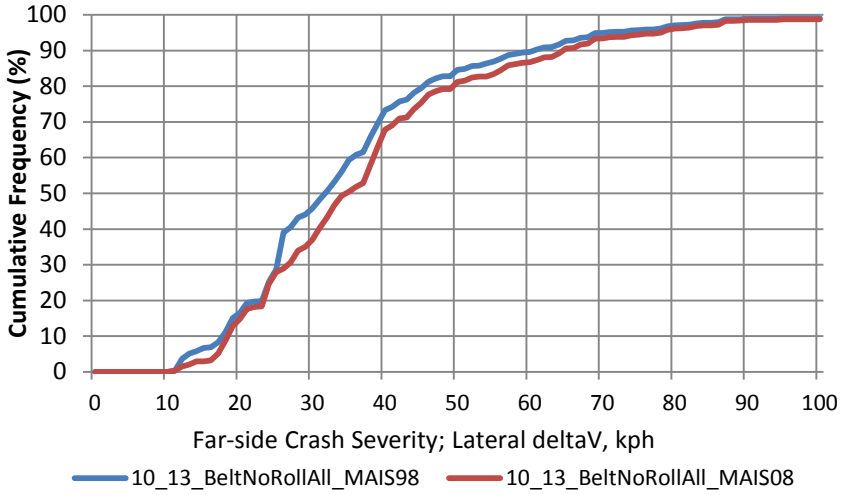


***Figure 1. Comparison of NASS CDS 2010-2013 far-side data coded with AIS 1998 and AIS 2008 – Cumulative frequency of MAIS 3+ injured***

**RESULTS**

An overview of the NASS CDS 2004 to 2013 data relative to far-side crash and injury frequency is presented in Table 1. Far side crashes that comply with the data restriction of the study constitute 9.5% of the crashes and 8.3% of the MAIS 3+ injured.

**Table 1. Exposed Occupants and MAIS 3+ Injured (AIS 1998) for All Crashes and Far-side by Crash Year (weighted data)**

| Crash Year | All Crashes | Far-side Crashes | Far-side % | All MAIS 3+ | Far-side MAIS 3+ | Far-side MAIS 3+ % |
|---|---|---|---|---|---|---|
| 2004 | 3,885,615 | 430,156 | 11% | 97,190 | 6,781 | 7% |
| 2005 | 3,760,785 | 379,505 | 10% | 93,079 | 8,300 | 9% |
| 2006 | 3,867356 | 393,353 | 10% | 101,351 | 9,261 | 9% |
| 2007 | 3,941238 | 405,134 | 10% | 113,438 | 9,310 | 8% |
| 2008 | 3,316723 | 369,800 | 11% | 92,317 | 8,767 | 9% |
| 2009 | 1,994830 | 196,864 | 10% | 51,883 | 3,847 | 7% |
| 2010 | 1,731751 | 162,610) | 9% | 30,466 | 1,984 | 7% |
| 2011 | 1,687834 | 181,933 | 11% | 27,346 | 2,722 | 10% |
| 2012 | 3,157945 | 203,417 | 6% | 24,438 | 1,308 | 5% |
| 2013 | 3,164383 | 334,753 | 11% | 34,295 | 2,674 | 8% |
| 2004-2013 | 30,508,460 | 2,894,915 | 9.5% | 665,803 | 54,954 | 8.3% |

Figure 2 shows the NASS CDS 2004 to 2013 populations of far-side crashes by vehicle model year. As shown, the majority of findings here involve model year 2000-2008 vehicles with a reduced contribution from earlier and later model years. The increased crash count for older vehicles is a function of increased time exposure and does not indicate a reduction in far-side crash involvement for new vehicles as it appears in Figure 2.

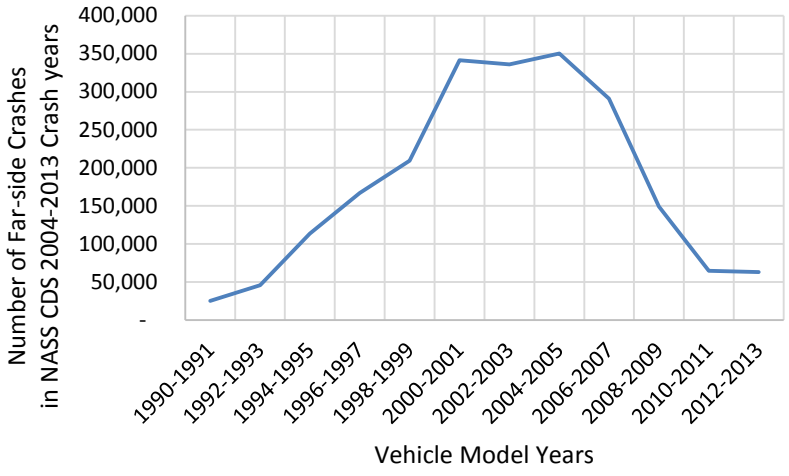


.

***Figure 2. Population of NASS CDS 2004-2013 light vehicles involved in far-side crashes by vehicle model year***

Figure 3a and Figure 3b show the distribution of outboard front seat occupants and the resulting MAIS 3+ injured populations in far-side crashes respectively. Crashes involving rollovers were excluded. The figure shows that 75% of far-side involved occupants are drivers, and drivers make up 79% of MAIS3+ injured occupants.

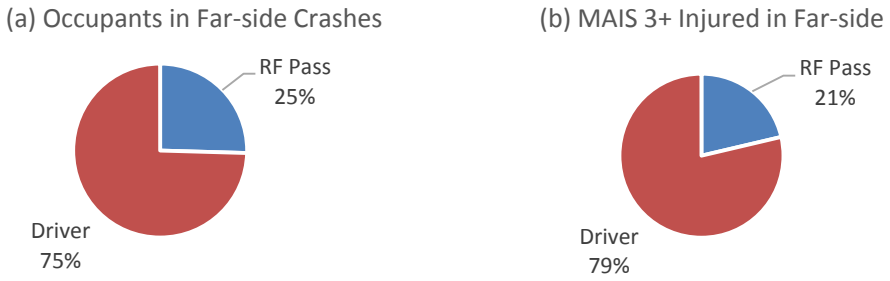


***Figure 3. (a) Distribution of belted outboard front seat occupants and (b) MAIS 3+ injured (AIS 1998) belted front seat occupants in far-side crashes NASS CDS 2004 to 2013.***

Figure 4 through Figure 10 use NASS CDS years 2004-2013 restricted to belted far-side occupants in front outboard seats with rollovers and ejections excluded. The MAIS3+ injured population includes AIS 3-6 and fatally injured coded using AIS 1998 unless otherwise noted.

Figure 4 shows the resulting cumulative frequency of exposed and MAIS 3+ injured occupants. The median delta V for exposed occupants was 15 kph. There has been an increase in the median delta V for MAIS3+ injured occupants since the earlier analyses. The current data shows a delta V increase to 36 kph compared with 28 kph reported in the Gabler study. This implies that 50% of the MAIS3+ population sustained their injuries during crashes with a total deltaV at or below 36 kph.

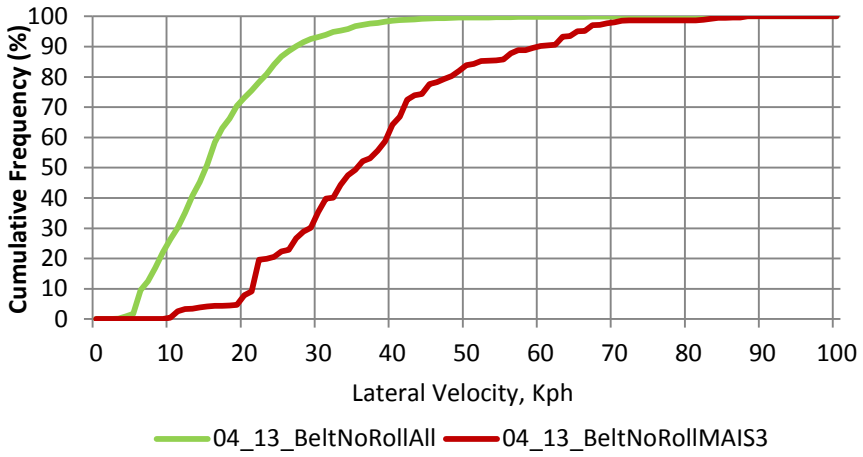


***Figure 4. Cumulative frequency of belted outboard front seat occupants and those with MAIS 3+ injuries (AIS 1998) in far-side crashes NASS CDS 2004 to 2013***

The distribution of occupants and MAIS 3+ injured by crash impact angle is displayed in Figure 5. For this figure, the left and right impacts angles are both measured as positive angles relative to the frontal direction at zero degrees. For example, pure lateral left side impacts are coded as 270 degrees in NASS but as 90 degrees for this plot. This approach permits left side and right side impacts be overlaid. The most frequent crash and injury direction of 60

degrees is consistent with the earlier findings of Gabler. In the Gabler analysis 60% of the MAIS 3+ injuries occurred at 60 degrees compared with 54% in the NASS CDS 2004 to 2013 data.

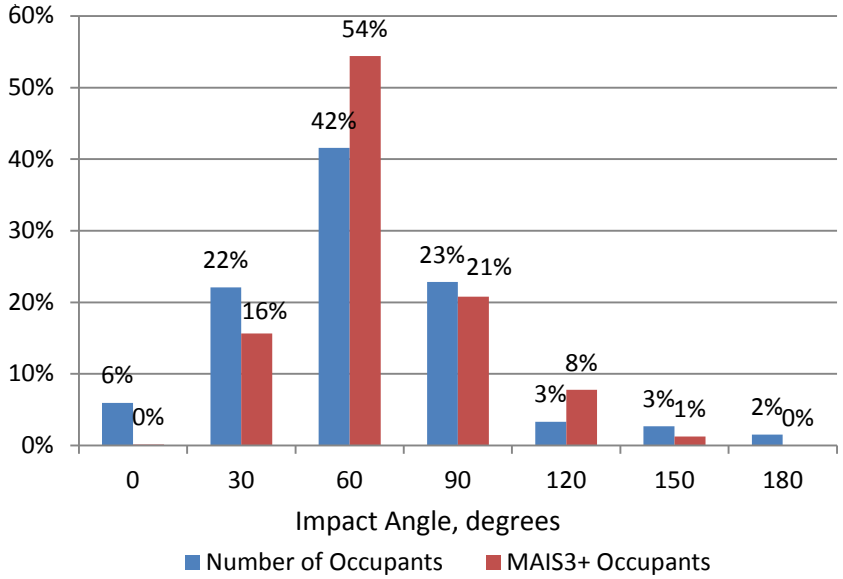


***Figure 5. Distribution of belted outboard front seat occupants and those with MAIS 3+ injuries (AIS 1998) in far-side crashes by crash direction, NASS CDS 2004 to 2013***

Figure 6 presents the horizontal damage area distribution for far-side belted occupants. The horizontal damage area is based on an SAE standard that defines the various horizontal areas of the vehicle as shown in the Figure 6 illustration. The most frequent crash and injury damage area at the Y location is consistent with the earlier findings of Gabler. In the Gabler analysis 42% of the MAIS 3+ injuries occurred in Y damage crashes compared with 34% in the NASS CDS 2004 to 2013 data. The largest change in the recent data was an increase in the MAIS 3+ injuries that occurred with distributed (D) damage. The distributed population of MAIS 3+ increased from 10% in Gabler to 20% in this later analysis.

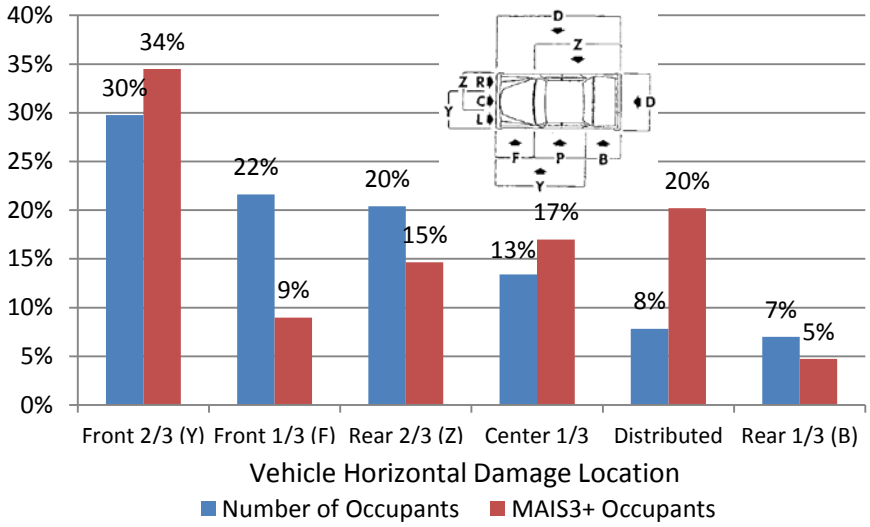


***Figure 6. Distribution of belted outboard front seat occupants and those with MAIS 3+ injuries (AIS 1998) in far-side crashes by horizontal damage area, NASS CDS 2004 to 2013***

Figure 7 compares the distribution of far-side occupants(a) , MAIS 3+ injured (b) and fatally injured (c) by collision partner and compares the results using older and newer data sets. NASS CDS 1993-2002 crash years were included for comparison with the 2004-2013 crash data. The newer data shows an increase in the population percentage of crashes with LTV's as the collision partner and an increase in the proportion of theMAIS 3+ injured and fatally injured for these collisions. In addition, the population percentage of fatalities during far-side crashes is significantly higher for fixed object crashes in the recent data compared with the earlier crash years.

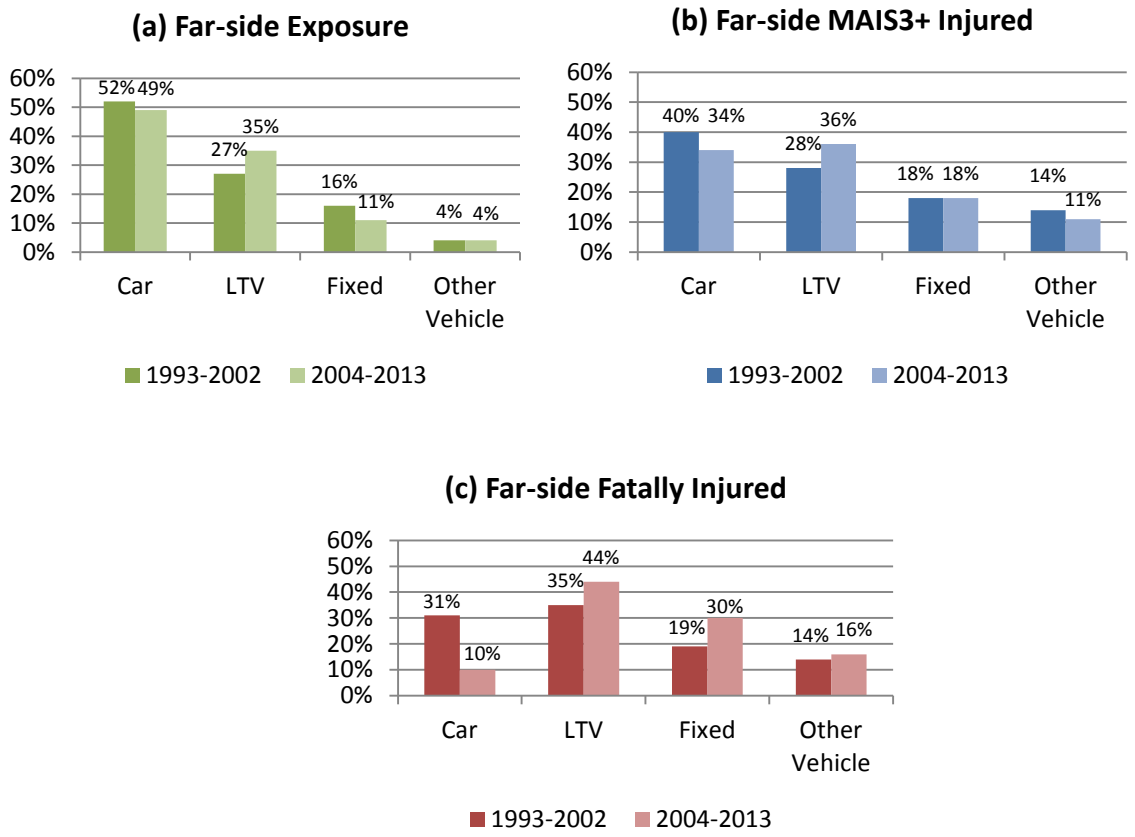


***Figure 7. (a) Distribution of belted outboard front seat occupants by collision partner, (b) those with MAIS 3+ injuries (AIS 1998) and (c) those fatally injured in far-side crashes by collision partner, NASS CDS (1993-2002 vs. 2004 to 2013).***

Figure 8 shows the annualized distribution of AIS3+ injuries in the population of exposed far-side occupants by injured body region. The injury distribution is generally consistent with earlier studies. Chest+Abdomen accounts for 43 % and head for 23%. In the earlier paper by Gabler, MAIS 3+ chest injuries were reported at 34 % and head injuries at 27%, showing a shift towards chest injuries in the more recent data.

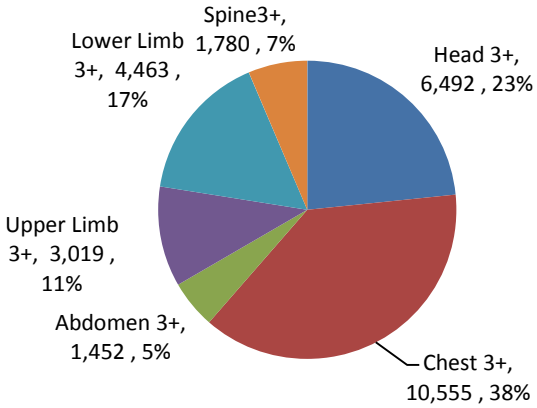


***Figure 8. Distribution of AIS 3+ injuries (AIS 1998) by body region, belted front seat outboard occupants in far-side crashes NASS CDS 2004-2013 (Annualized data, weighted).***

Figure 9 and Figure 10 display the aggregated injuring contacts for head and chest injuries. For belted front outboard occupants, occupant to occupant contact is responsible for 13.6% of the AIS 3+ head injuries and 4.9% of the AIS 3+ chest injuries suffered in far-side crashes. The far side structure was by far the most frequent head injury contact, causing close to 62% of the AIS3+ injuries. The front seat back was the most frequent source of chest injuries and in combination with the center stack, accounted for over 53% of the AIS3+ injuries, followed by the far side structure and belt/restraints.

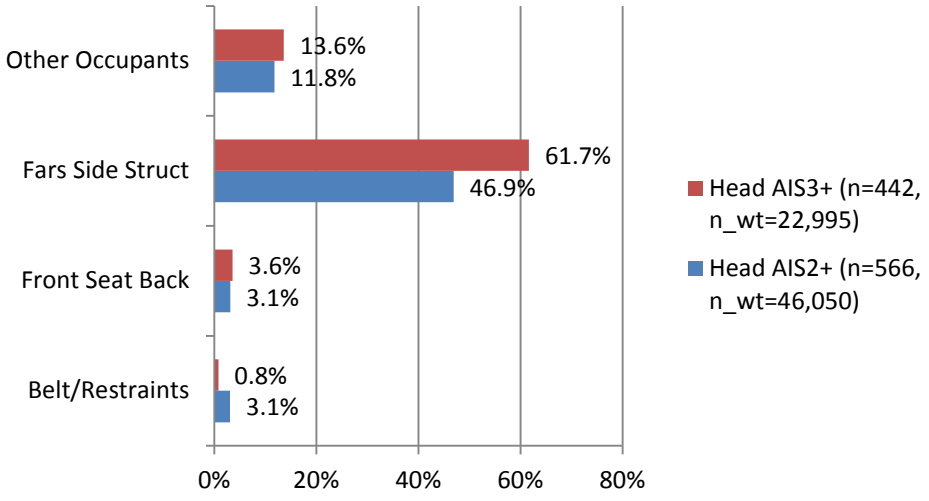


.

***Figure 9.Top 4 Contributors Amenable to Far-side Countermeasures: AIS 2+ and AIS 3+ head injuries (AIS 1998) by injuring contact for belted front outboard seat occupants in far-side crashes NASS CDS 2004-2013***

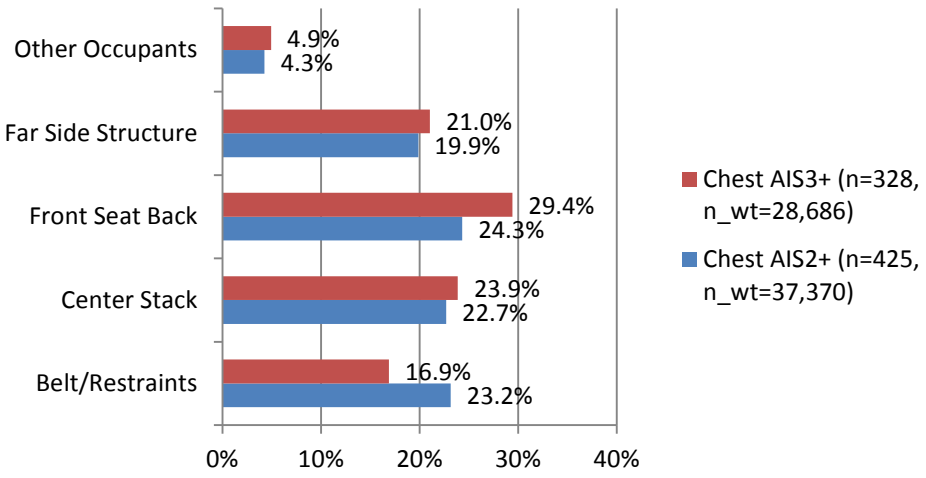


***Figure 10. Top 5 Contributors Amenable to Far-side Countermeasures: AIS 2+ and AIS 3+ chest injuries (AIS 1998) by injuring contact for belted front outboard seat occupants in far-side crashes NASS CDS 2004-2013***

An in-depth review was conducted including all NASS CDS 2004-2013 cases where more than one front seat occupant was present and one or more AIS3+ head injury was sustained by either occupant. Overall, 310 raw cases representing 17,047 MAIS3+ injured occupants were analyzed. Overall, 528 total weighted occupants (3.1% of all MAIS3+ injured) were flagged as having AIS3+ head injuries with evidence of head to head contact within this sample.

Figure 11and Figure 12 compare crash severity for occupants and MAIS 3+ injured when exposed to near-side and far-side crashes. The median crash severity for the exposed populations was 15 kph vs 17 kph for near-side vs. far-side belted front outboard occupants. For the MAIS 3+ injured, the median near-side crash severity was 31.5 kph compared with 36 kph for far-side occupants.

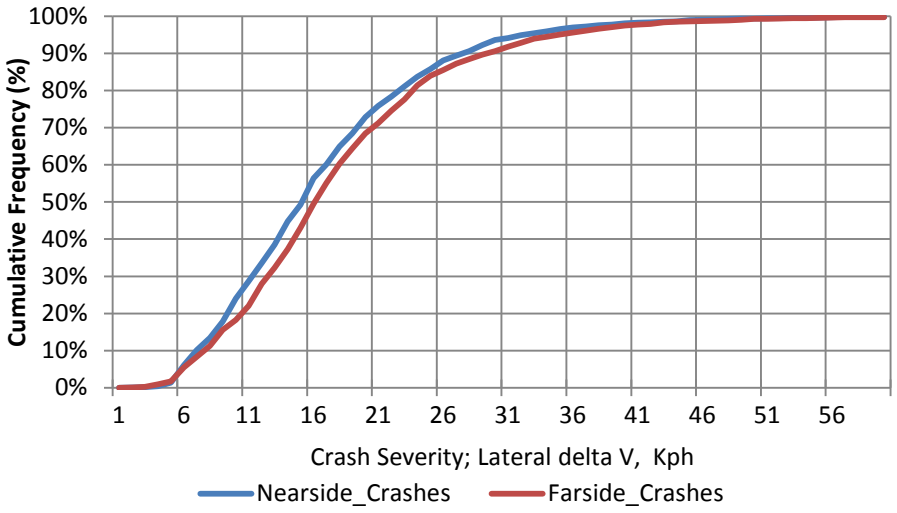


***Figure 11. Cumulative frequency of belted outboard front seat occupants in near-side and far-side crashes NASS CDS 2004 to 2013***

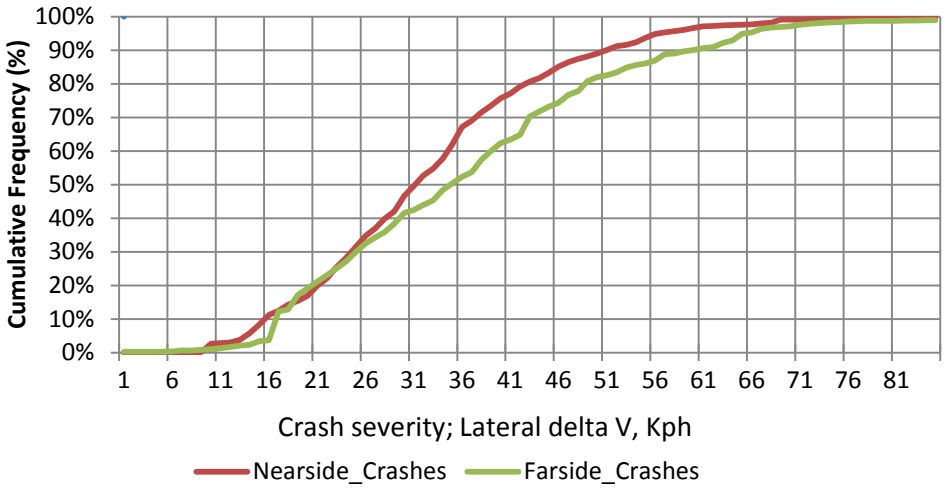


***Figure 12. Cumulative frequency of belted outboard front seat occupants with MAIS 3+ injuries in near-side and far-side crashes NASS CDS 2004 to 2013***

Figure 13 provides a summary of the odds of MAIS3+ injury by model year grouping. This result is based on a multivariate logistic regression model controlling for deltaV, specific horizontal location of damage to the vehicle, extent of damage, occupant age and model year group. The comparison group is the model year 2000-2004 category controlling for other factors. As shown, there is a statistically measurable decrease in the odds of MAIS3+ injury during nearside crashes for the model year 2005-2014 group, which cannot be seen in the far side crash data set.

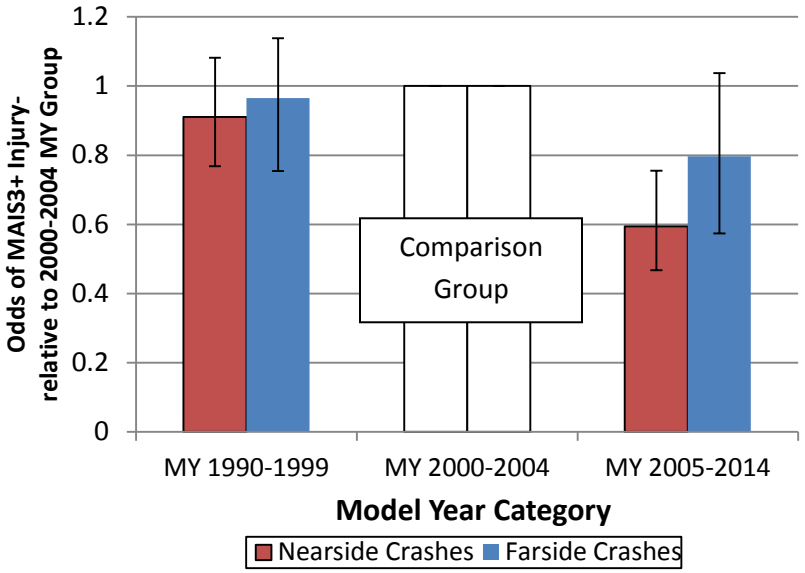


***Figure 13. Far-side involved versus MAIS 3+ injuries by vehicle model year group NASS CDS 2004 to 2013***

Figure 14 compares front outboard crash involved populations with MAIS3+ injured population by US NCAP vehicle size category for the impacted vehicle. Category sizes are as follows:

- Passenger cars mini (PC/Mi) (1,500–1,999 lbs.)
- Passenger carslight(PC/L) (2,000–2,499 lbs.)
- Passenger cars compact(PC/C) (2,500–2,999 lbs.)

- Passenger cars medium (PC/Me) (3,000–3,499 lbs.)
- Passenger cars heavy (PC/H) (3,500 lbs. and over)
- Sport utility vehicles(SUV)
- Pickup trucks(PU)
- Vans(VAN)

As seen in Figure 14, the light vehicle population is overrepresented in the MAIS3+ injured category relative to the occupants exposed (7.4% of the involved and 20.0% of the MAIS3+ injured). Due to the reduced occupant comparment size for Passenger cars in the Light vehicle category, improved far-side crash protection may have an even greater impact on occupants riding in vehicles within this category.

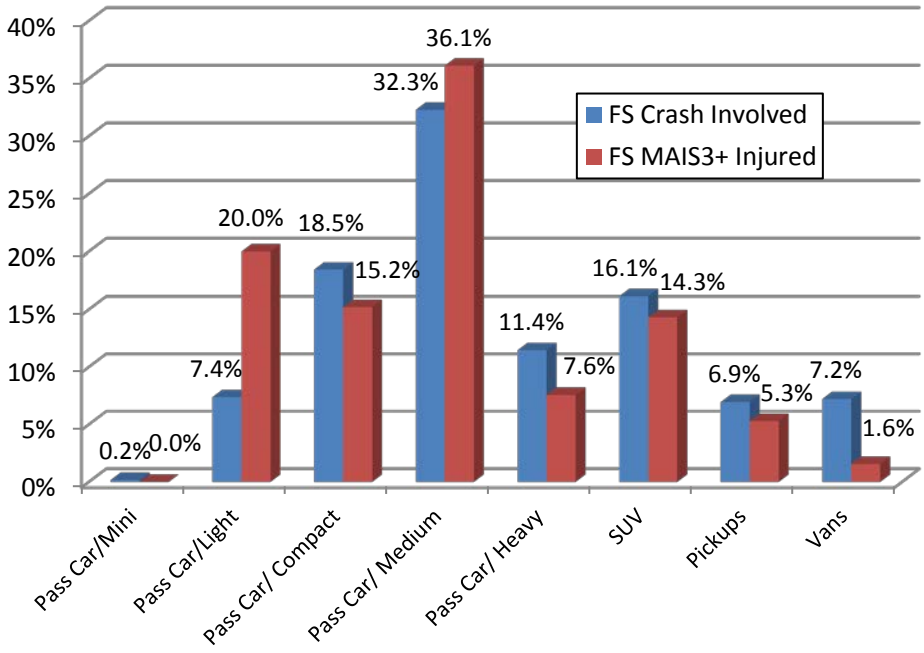


***Figure 14. Far-side involved versus MAIS 3+ injuries by NCAP Vehicle Class NASS CDS 2004 to 2013***

**DISCUSSION**

The use of the AIS 1998 coding for the MAIS 3+ injuries in NASS years 2004 to 2013 permitted a comparison of the analyses conducted under this study with the earlier comprehensive analysis that used 1993 to 2002 data [Gabler 2005]. As shown in Figure 1, the use of different AIS coding introduces confounding factors that obfuscate the influence of vehicle safety changes. The use of AIS 2008 coding tended to reduce the exposed delta V for MAIS 3+ injured in far side crashes by about 2 kph over the crash severity range of 25 to 50 kph lateral delta V.

The NASS 2004 to 2013 data shows that 75% of far-side involved occupants are drivers, and drivers make up 79% of MAIS3+ injured occupants. This data indicates that drivers are over represented among the MAIS 3+ injured occupants.

The recent decade of data (Figure 5) shows that the most frequent impact angle is 60 degrees and the most frequently damaged area of the vehicle side is the forward 2/3, known as the Y damage pattern. These results are consistent with the earlier findings of Gabler. However, the frequency of MAIS 3+ injured in vehicles with distributed damage increased from 10% in the 1993-2002 data to 20% in the 2004-2013 data.

Figure 7 shows a difference in far-side crash characteristics that has occurred in recent data years. In earlier data years passenger cars were the most frequent crash partner for both exposure and MAIS 3+ injuries. In the recent years, passenger cars have been replaced by light trucks and vans (LTV) as the most frequent crash partner for MAIS 3+ injuries. Since LTV's are generally heavier than passenger cars, the crash severity of the struck vehicle would be expected to increase, all other factors being equal. This was found to be the case. In the Gabler study, the median delta V lateral velocity for MAIS 3+ injured was 28 kph. In contrast, the present study found the median velocity to be 36 kph. The higher distributed damage frequency in recent vehicles with MAIS 3+ injured occupants may also be influenced by the increased frequency of LTV's as the striking vehicle.

Both the present and the earlier studies found that the chest was the body region most frequently injured at the MAIS 3+ level. The chest/abdomen AIS 3+ constituted 41% of the injuries in the Gabler study and 43% in this study. The head/face accounted for 32% of AIS 3+ in Gabler and 23% in this study.

Gabler found that occupant to occupant contact was attributed to 4.8 % of the AIS 2+ head injuries compared with 11.8% in this study as shown in Figure 9. Of note is the fact that the current study aggregates driver and right front passenger injury contact data while previous studies report driver experience alone. For AIS 2+ chest injuries, occupant to occupant contact was associated with 3.7% of the chest injuries compared with 4.3% in this paper as shown in Figure 10. In both data sets the AIS 2+ injuries from occupant to occupant contact is small.

As shown in Figure 9 and Figure 10, the percentage of AIS 3+ head and chest injuries from occupant to occupant contact was 13.6% and 4.9% respectively. Protection opportunities limited to head to head contact would address about 3.1% of the far-side AIS 3+ injured for belted front outboard seated far side occupants.

The occupant to occupant protection opportunities are extremely modest when compared to the 65.3% of AIS 3+ head injuries caused by contact with the seat back and far side interior. For the driver AIS 3+ chest injury contacts, 53.3% could be addressed by mitigating occupant contacts with the seat back and center stack and another 21.0% are associated with far side interior contacts. Finally, 16.9% are attributed to safety belt contacts.

Countermeasures that reduce the excursion of the upper body and mitigate the severity of contacts with the seat back, center stack, and far-side interior offer the possibility of addressing at least 65.3% of the head injuries and 74.3% of the chest injuries at the AIS 3+ level.

Belt loading was associated with 16.9% of the MAIS 3+ chest injuries. Earlier studies of occupant kinematics in far-side crashes indicate that the occupant frequently comes out of the shoulder restraint and the upper body translates across the vehicle [Digges 2001, Alonzo 1999, Pintar 2006, 2007]. In a study of post mortem human specimens in far-side sled tests at 16 and 34 kph, Kent found that increased engagement of the shoulder belt decreased the lateral head excursion but increased the risk of chest injury (Kent 2013). The authors observed that in the tests a substantial portion of the belt loading passed through the lower portion of the contralateral rib cage; a region with lower injury resistance to the oblique loading when compared to loading of the superior ribs and shoulder in frontal crashes by the belt. A related type of belt loading in low severity real world crashes has been shown to produce severe liver injuries to drivers restrained by 2 point belts (Augenstein 2000). The tests conducted by Kent also demonstrated that effective restraint engagement of the chest can generate lateral bending of the cervical spine sufficient to generate injury from head inertia. These research results suggest the need for carefully monitoring the risk of chest and abdominal injuries from belt loading when evaluating far-side countermeasures.

Figure 11 and Figure 12 show crash severity comparisons of populations exposed to near-side and far-side crashes. For the far-side crashes, the median crash severity is 17 kph; about 2 kph higher than for the near-side population. For the MAIS 3+ injured population the median far-side crash severity is 36 kph; 4.5 kph higher than for the near-side MAIS 3+ population.

Figure 13 suggests that there is a statistically measurable decrease in the odds of MAIS3+ injury during nearside crashes for the model year 2005-2013 group. A non-significant and reduced improvement is observed for 2005-2013 model year far-side involved vehicles. This suggests that countermeasures and design changes have been introduced and have impacted nearside occupant protection while greater opportunities remain to improve far-side protection.

As shown in Figure 14, light passenger vehicles are overrepresented in the MAIS3+ injury category per crash involvement. This observation follows logically from the fact that occupant compartment sizes are smaller as vehicle mass decreases increasing the risk for far-side compartment contact by the head during far-side crashes and through interaction with intruding structures in some cases.

## CONCLUSIONS

One major change in the far-side crashes in newer vs. older NASS CDS data years has been an increase in the frequency of pickups, SUV's and vans as the collision partner. In the recent NASS CDS years reported in this paper, the median crash severity for MAIS 3+ belted front seat outboard occupants has increased by 4.5 kph. For the MAIS 3+ population, the frequency of distributed damage (damage to the entire side of the struck vehicle) has increased from 10% to 20%.

The following characteristics are the most representative NASS CDS 2004-2013 the crash conditions associated with MAIS 3+ injured belted front seat outboard occupants exposed to far-side crashes:

MAIS 3+ injury exposure: 79% driver; 21% right front passenger

Median crash severity – lateral delta V; 36 kph.

Most frequent crash directions -

- 54% of MAIS 3+ at 60 degrees
- 21% of MAIS 3+ at 90 degrees

Most frequent vehicle horizontal damage areas for AIS3+ injured occupants-

- Front 2/3 (Y) - 34%
- Distributed (D) - 20%
- Center passenger compartment - 17%

Body region injured (belted outboard front seat occupants):

- 43% of AIS 3+ is to the Chest/Abdomen
- 23% of AIS 3+ is to the Head

Most frequent head injuring contacts for 23% of MAIS 3+ (belted outboard front seat occupants,)

- Far-side structure - 61.7%
- Other occupant – 13.6%

Most frequent chest/abdomen injuring contacts for 43% of MAIS 3+ (belted outboard front seat occupants,)

- Front seat and center stack - 53.3%
- Far-side structure – 21.0%
- Safety belt - 16.9%
- Other occupant – 4.9%

As belt systems improve in upper body retention for far-side protection, excessive lateral loading of the lower ribs is undesirable due to the increased vulnerability of this body region to injury. Additional studies are recommended to assess suitable belt loading criteria for far-side crashes.

Only 3.1% of belted AIS3+ injured occupants involved in far-side collisions sustained their injuries due to head to head contact with another front seat occupant. Overall, these findings suggests that greater opportunities to reduce injuries exist in limiting occupant lateral movement when compared to the benefits of preventing head to head contact alone when more than one front outboard occupant is present.

## REFERENCES


[1] The Abbreviated Injury Scale. Des Plaines, IL: Association for the Advancement of Automotive Medicine; 1998

[2] The Abbreviated Injury Scale. Des Plaines, IL: Association for the Advancement of Automotive Medicine; 2005.

[3] The Abbreviated Injury Scale. Des Plaines, IL: Association for the Advancement of Automotive Medicine; 2008.

[4] Alonso, B, Digges, K, and Morgan, R, Far-side vehicle simulations with MADYMO", SAE 2007-01-0378, April 2007.

[5] Augenstein J, Perdeck E, Bowen J, et al. Injuries to restrained occupants in far-side crashes. Annu Proc Assoc Adv Automot Med 1999;43:139–158.

[6] Augenstein, J, Digges, K., and others, "Dummy Measurements of Chest Injuries Induced by Two-Point Belt Systems", 44th Annual Proceedings of the Association for the Advancement of Automotive Medicine, October, 2000.

[7] Digges KH, Dalmotas D. Injuries to restrained occupants in far-side crashes. In: Proceedings of the International Conference on Enhanced Safety of Vehicles, Amsterdam, The Netherlands; 2001.

[8] Digges, KH, Echemendia, C, Fildes, B, and Pintar, F, A safety rateing for far-side crashes, Paper Number 09-0217, Proceedings of the 21st ESV Conference, Washington DC, June 2009.

[9] Digges KH, Gabler HC. Opportunities for reducing casualties in far-side crashes. In: Proceedings of the SAE Conference, Warrendale, PA: SAE; 2006.

[10] Digges KH, Gabler HC, Mohan P, Alonso B. Characteristics of the injury environment in far-side crashes. Annu Proc Assoc Adv Automot Med. 2005;49:185–197.

[11] Fildes BH, Fitzharris M, Gabler CH, Digges K, Smith S. Chest and abdominal injuries in far-side crashes. In: Proceedings of the ESV Conference, 2007:43–56.

[12] Fildes, B, and Digges, K, (editors), Occupant protection in Far-side Crashes, Final Report on International Collaborative Research on Far-side Protection, GW University and Monash University Report, June 2009. http://autosafetyresearch.org/pdfs/Far-side%20final%20report%20Finalx.pdf

[13] FMVSS-214. Side Impact Protection. Washington, DC: US Government Printing Office; 1990. 49 CFR; Parts 571. FMVSS-214. Washington, DC: US Government Printing Office; 2008 49 CFR: 571.214.

[14] Frampton R, Brown R, Thomas P, Fay P. The Importance of non-struckside occupants in collisions. 42nd Annu Proc Assoc Adv Automot Med. 1998;303–320.

[15] Gabler HC, Digges K, Fildes BH, Sparke L. Side impact injury risk for belted far-side passenger vehicle occupants. Journal of Passenger Car - Mechanical Systems. 2005;114:1–9.

[16] Kent, R, Forman, J, Lessey, D, Arbogast, K, Higuchi, K, A parametric study of far-side mechanisms, Proceedings of the 23rd ESV Conference, Seoul, Korea, May 2013.

[17] Mackay M, Parkin S, Hill JR, Munns J. Restrained occupants on the nonstruck side in lateral collisions. 35th Annu Proc Assoc Adv Automot Med. 1991;35:119–131.

[18] Newland, C., Belcher, T., Bostrom, O., Gabler, H., Cha., J., Wong, H., Tylko, S., and Dal Nevo, R., “Occupant-to-Occupant Interaction and Impact Injury Risk in Side Impact Crashes”, Stapp Car Crash Journal, Vol 52, pp..327-347, 2008.

[19] Pintar FA, Yoganandan N, Stemper BD, et al. Comparison of PMHS, WorldSID, and THOR-NT responses in simulated far side impact. Stapp Car Crash J. 2007;51:313–360.

[20] Pintar FA, Yoganandan N, Stemper BD, et al. WorldSID assessment of far side impact countermeasures. Annu Proc Assoc Adv Automot Med. 2006;50:199–219.

[21] Thomas P, Frampton R. Injury patterns in side collisions—a new look with reference to current test methods and injury criteria. In: Proceedings of the 43rd Stapp Car Cash Conference, 1999:13–24.

[22] Yoganandan, N, Arun, M, Halloway, D, Pintar, F, Maiman, D, Szabo, A, Rudd, A, Crash characteristics and injury patterns of restrained front seat occupants in far-side impacts, . Annu Proc Assoc Adv Automot Med. 2014;58:27-34

## APPENDIX

### Table A.1

| Injury_Source_Cat | Injury Source | Injury_Source_Category | Injury Source |
|---|---|---|---|
| Belt/Restraints | Belt Restraint Webb/Buckle | Left Side Struct (Far Side Structure) | Left Forward Upper Quadrant |
| | Belt B Pill Atch | | Left Forward Lower Quadrant |
| | Oth Restr Sys Compon | | Left Rear Upper Quadrant |
| Center Stack | Floor Or Console Transmiss Lever | | Left Rear Lower Quadrant |
| Dr Side Bags_Any | Air Bag-Dr Side | | Left Armrest/Hardware In Forward Upper Quadrant |
| | Bag-Dr Side+Eyew | | Left Armrest/Hardware In Forward Lower Quadrant |
| | Bag-Dr Side+Jlry | | Left Armrest/Hardware In Rear Upper Quadrant |
| | Bag-Dr Side+Obj | | Left Armrest/Hardware In Rear Lower Quadrant |
| | Bag-Dr Side+Mout | | Roof Left Rail |
| | Bagcover-Dr Side | Oth Vehicle_Ext Struc | Other Exterior Surface Or Tires |
| Front Seat Back | Seat, Back Support | | Unk Exterior Obj |
| | Head Restraint Sys | | Omv Front Bumper |
| Glass_Noncontact | Flying Glass | | Omv Hood Edge |
| | Other Noncontact Inj Source | | Omv Other Front Of Veh |
| Ground | Ground | | Omv Hood |
| Instr Panel Ctr | Center Panel | | Omv Windshield, Roof Rail, A-Pillar |
| | Center Ins Panel | | Omv Side Surface |
| | Ce Low Instru Panel | | Omv Side Mirrors |
| Instr Panel Left | Left Pane; | | Omv Side Protrus |
| | Knee Bolster | | Omv Rear Surface |
| | Left Instr Panel | | Omv Und/Carriage |
| | Low Lt Instru Panel | | Omv Tires/Wheels |
| Instr Panel Rt | Right Panel | | Omv Oth Exterior |
| | Glove Compartment Door | | Omv Unk Exterior |
| | Right Ins Panel | | Oth Obj |
| | Rl Instru Panel | Other Occupants | Other Occupants |
| Left Side Struct (Far Side Structure) | Left Interior | Pass Side Bags_Any | Air Bag-Ps Side |
| | Left Hardware | | Bag-Ps Side+Eyew |
| | Left A (A1/A2)Pillar | | Bag-Ps Side+Jry |
| | Left B Pillar | | Bag=Ps Side+Obj |
| | Oth Left Pillar | | Bag=Ps Side+Mout |
| | Left Window Glas | | Bagcover-Ps Side |
| | Left Window Fram | | Bagcvr-Psside+Ey |
| | Left Window Sill | | Bagcvr-Psside+Ob |
| | Left Window+Oth | Right Side Struct (Far Side Structure) | Right Interior |
| | Left Side Glass Reinforced By Ext Obj | | Right Hardware |
| | Left Side Panel Forward Of A1/A2 Pillar | | Right A (A1/A2) Pillar |
| | Left Side Panel Rear Of The B-Pillar | | Right B Pillar |

**Table A.1, continued**

| Injury_Source_Cat | Injury Source | Injury_Source_Category | Injury Source |
|---|---|---|---|
| Right Side Struct (Far Side Structure) | Oth Right Pillar | Steer Assembly | Steering Wheel Combo Of Rim And Hub/Spoke |
| | Right Side Wind Glass | | Steering Column, Transmission Selector Lever |
| | Right Side Wind Frame | | Hand Ctrls For Braking/Accel |
| | Right Side Window Sill | | Steering Ctrl Devices |
| | Right Side Window+Oth | | Steering Knob Att To Steering Wheel |
| | Right Side Panel Forward Of A1/A2 Pillar | | Repl Steer Whl |
| | Right Side Panel Rear Of The B-Pillar | | Joy Stick Steering Ctrl |
| | Right Forward Upper Quadrant | Toe/Floorpan Pan | Floor (Includ Toe Pan) |
| | Right Forward Lower Quadrant | | Foot Controls Includ Parking Brake |
| | Right Rear Upper Quadrant | Unknown | Inj, Unknown Source |
| | Right Rear Lower Quadrant | Windshield/Fr Header | Windshield |
| | Right Armrest/Hardware In Fwd Upper Quadrant | | Mirror |
| | Right Armrest/Hardware In Fwd Lower Quadrant | | Sunvisor |
| | Right Armrest/Hardware In Rear Upper Quadrant | | Windshld Dr Side Only |
| | Right Armrest/Hardware In Rear Lower Quadrant | | Windshld Ps Side Only |
| | Roof Right Rail | | Reinforced Wndsh By Ext Obj |
| Roof | Roof/Convertible Top | | Sunvisor Reinforced By Ext Obj |
| Steer Assembly | Steering Wheel Rim | | Front Header |
| | Steering Wheel Hub/Spoke | | |

# SAFETY 2.0 – POTENTIALS OF COOPERATIVE SAFETY BY VEHICLE-TO-X COMMUNICATION

**Dr. Gunnar Juergens**
**Dr. Bernhard Klumpp**
**Dr. Ralf Schnupp**
**Dr. Ulrich Staehlin**
Continental, Chassis & Safety Division, Passive Safety & Sensorics Business Unit
Germany

Paper Number 15-0447

## ABSTRACT

Safety Technology has evolved significantly over the last decades. The technological progress, based on the continuous advances in vehicle crash worthiness, restraint systems and active safety functions have made traffic safer than ever before. Latest development has led to a sharp increase in the equipment rates for advanced surrounding sensors, so that on-board surrounding sensors such as camera, radar and lidar sensors have become standard equipment in modern vehicles. Surrounding sensors can provide safety critical information to a vehicle and are thus a pre-requisite for new integrated safety functions such as Forward Collision Warning (FCW) or Emergency Brake Assist (EBA). What if vehicles could communicate with each other and create a network for safety critical information in traffic? What if my vehicle gets real-time information on sudden braking maneuvers 500 meters ahead? What if a vehicle camera detects a cyclist approaching at an urban intersection and shares the cyclist position information with other vehicles? What if vehicles share their mass, velocity and position before a crash to optimize the strategy of airbag deployment? Wouldn`t all this open a new dimension of safety in future traffic – Safety 2.0?
This paper promotes cooperative safety as a new approach based on the exchange of safety critical information in traffic. The underlying thesis is that cooperative safety would dramatically increase the safety for a large number of traffic participants, including vehicles without on-board surrounding sensors and vulnerable road users (VRUs) like children, pedestrians and cyclists.

## INTRODUCTION

Traditionally, vehicle users rely on the seat belt and airbag to protect them from harm during an accident, just like a safety net would protect the fall of an acrobat in a circus. Today's approach goes far beyond this safety net. Advanced Driver Assistance Systems (ADAS), tailored to specific driving situations, help to avoid accidents, should the driver fail to take proper action. ADAS are doing an excellent job of this because they have traits that make them perfect co-pilots: They do not get distracted, they don't suffer from mood swings, they don't drink, and they never become tired. The EU commission has in its Vision Zero set the ambitious goal for halving road casualties down to 15,750 by 2020 and moving close to zero fatalities in road transport by 2050 [1]. An increasing number of ADAS is a significant move towards more driving safety, fewer accidents, and fewer fatalities – towards the EU target of Vision Zero.

So, are we nearly there yet? No, we are not. After all, on-board surrounding sensors are subject to similar limitations as they apply to the human senses. Due to many reasons the practical range of an automotive sensor can be limited just as much as human eyesight, for instance. Ultimately, the human eyesight needs a "line of sight" to detect objects, traffic signs or road markings. At low visibility e.g. due to bad weather or fog, with the support of different surrounding sensor technology, ADAS can help to recognize vehicles and obstacles more accurately than the human eye could do. However, hidden objects, like approaching vehicles hidden by trucks, or vehicles behind buildings in an inner-city crossing situation, cannot be recognized. Even the most advanced surrounding sensors have a line of sight. If there is no such line of sight, ADAS cannot help.

This is a non-satisfying situation, considering the enormous benefit that could be reaped, if the "line-of-sight" problem was finally overcome. According to a study of the U.S. Department of Transportation (DOT), Federal Highway Administration [2], in 2007, approximately 2.4 million intersection-related crashes occurred in the U.S.A., representing 40% of all crashes and 21.5 % of traffic fatalities. Therefore, the ultimate integrated approach to driving safety needs to address just that – integrating new technologies to close the gaps of visibility and enable powerful and effective safety functions.

The answer lies in an exchange of safety critical data between vehicles (V2V) and between vehicles and infrastructure (V2I). Such V2X communication is based on IEEE 1609 Standard (in EU: ITS-G5) [3], also known as automotive WLAN technology. In V2X communication vehicles become cooperative by exchanging relevant information with each other and with the infrastructure (like traffic lights, construction sites, etc.). Based on cooperative safety, imminent collisions can be recognized and prevented, even when collision objects are hidden and even at higher speeds over a broader range than vision and radar based systems can do.

## SHORT RANGE AND LONG RANGE COMMUNICATION

With the use of V2X communication a wider scope of cooperative safety functions can be evaluated and initiated, ideally before a situation even gets critical. This data flow can take driving safety to a whole new dimension that can be called “Safety 2.0”.

As the timeline for this type of V2X communication can be very short, and initiating a safety function may have to be done in split seconds, it is unlikely that drivers will want to rely on the instantaneously available bandwidth for internet access and a communication flow via a backend. True, this long-range networking of vehicles will be of immense importance during normal driving. Actually, vehicle drivers and passengers will probably consider being “always on” to be the most useful part of wireless communication. However, when there is immediate danger to life and health, short range V2X is essential. Long and short range communication complement each other because they have different strengths to offer during different driving scenarios (see figure 1).

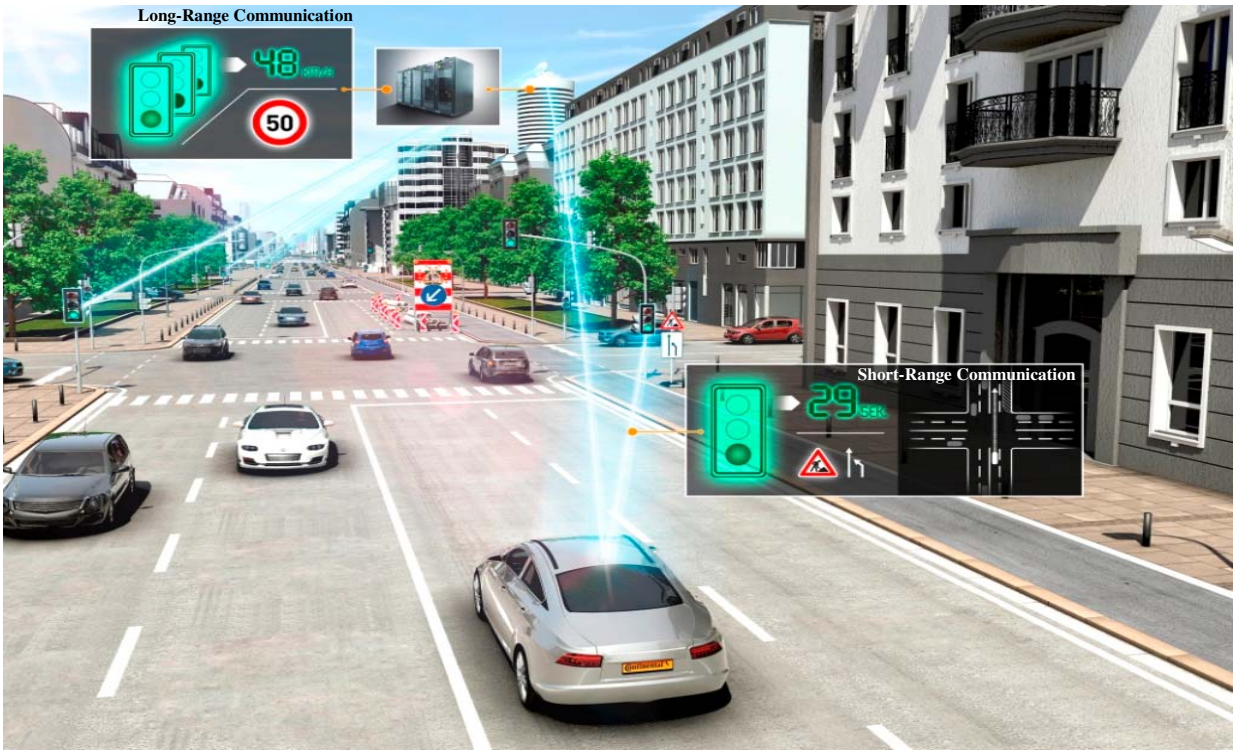


***Figure1. Short range V2X communication and long range communication via backend complement each other***

## VEHICLE-TO-X HAS PASSED THE TEST

Short range V2X is no longer a vision. Since the successful conclusion of the Safety Pilot field trial in the US and the large sim$^{TD}$ (Safe Intelligent Mobility – Field Test Germany) pilot project on V2V communication in Germany [4], it is clear that the underlying technology works. A V2X unit has been developed during the sim$^{TD}$ project and is close to serial production at Continental. With this unit safety critical data such as vehicle speed, location, precise time (time stamp), or brake status, can be communicated within a spontaneous "ad-hoc" network of vehicles (compare ETSI specification [5]). As a further enhancement, objects or traffic situations (e.g. broken vehicles, accidents or slippery road conditions) detected by the sensors of another vehicle, can also be communicated to the ego vehicle before the situation becomes visible to that vehicle. By receiving and processing data from other vehicles, V2X communication turns into a new cooperative "sensor" that complements the existing on-board surrounding sensors.

Imagine a scenario, where a truck and a sports utility vehicle are at risk of colliding because the drivers are unable to see one another approaching the intersection (the stop sign is disabled). With V2X, both drivers would receive warnings of a potential collision, allowing them to take actions to avoid it. The Intersection Movement Assist (IMA) warns the driver of a vehicle when it is not safe to enter an intersection due to a high probability of colliding with one or more vehicles at intersections both where a signal is present (a "controlled" intersection) (see figure 2) and at those where only a stop or yield-sign is present (an "uncontrolled" intersection).

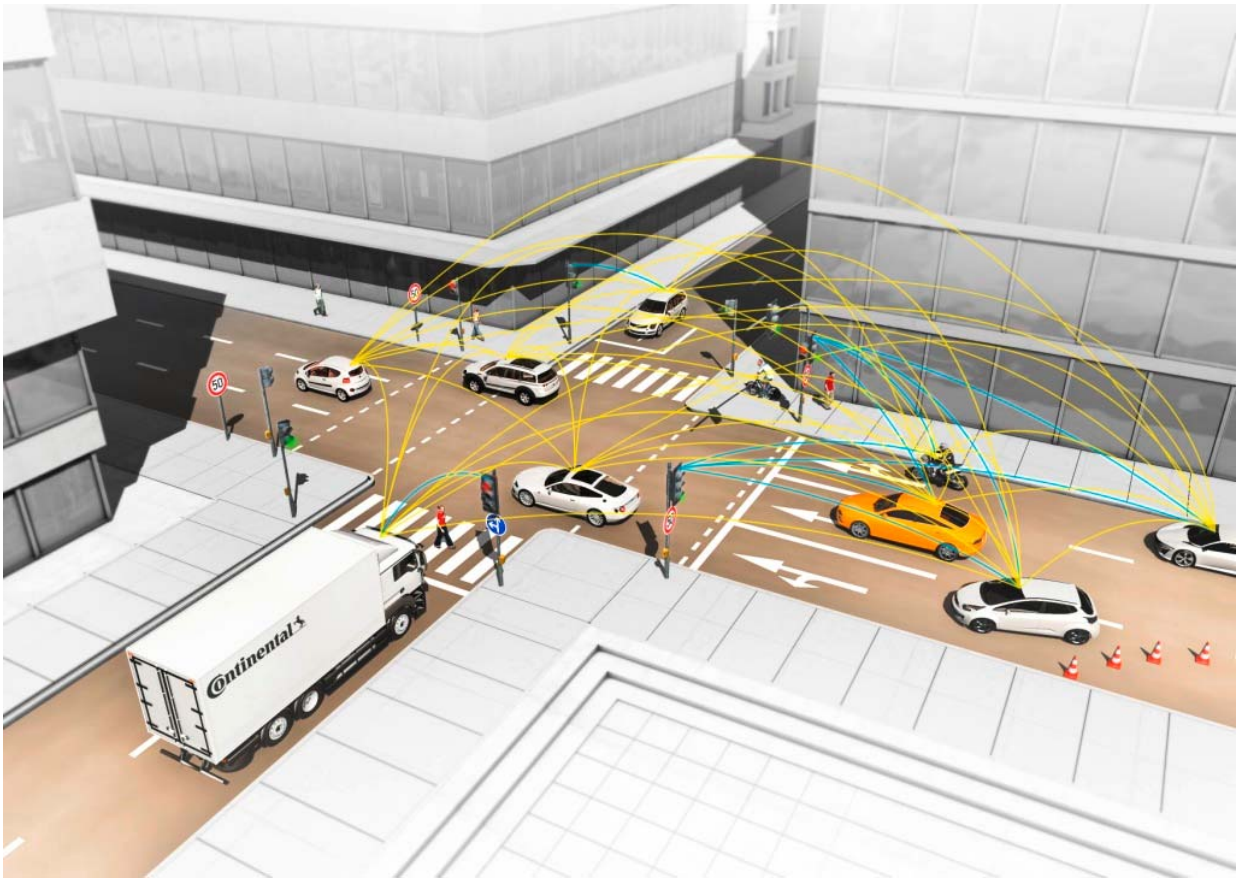


***Figure2. Example of V2V Intersection Movement Assist warning scenario***

Also scenarios with oncoming traffic in the opposite direction can be addressed: A Left Turn Assist (LTA) can warn the driver of a vehicle, when they are entering an intersection, not to turn left in front of another vehicles traveling in the opposite direction. Even in overtaking scenarios hidden "blind spot" vehicles driving in the opposite direction can be detected and signalized with a warning. A cooperative V2X communication can even detect a vehicle traveling towards you when it is hidden behind a curve (see figure 3).

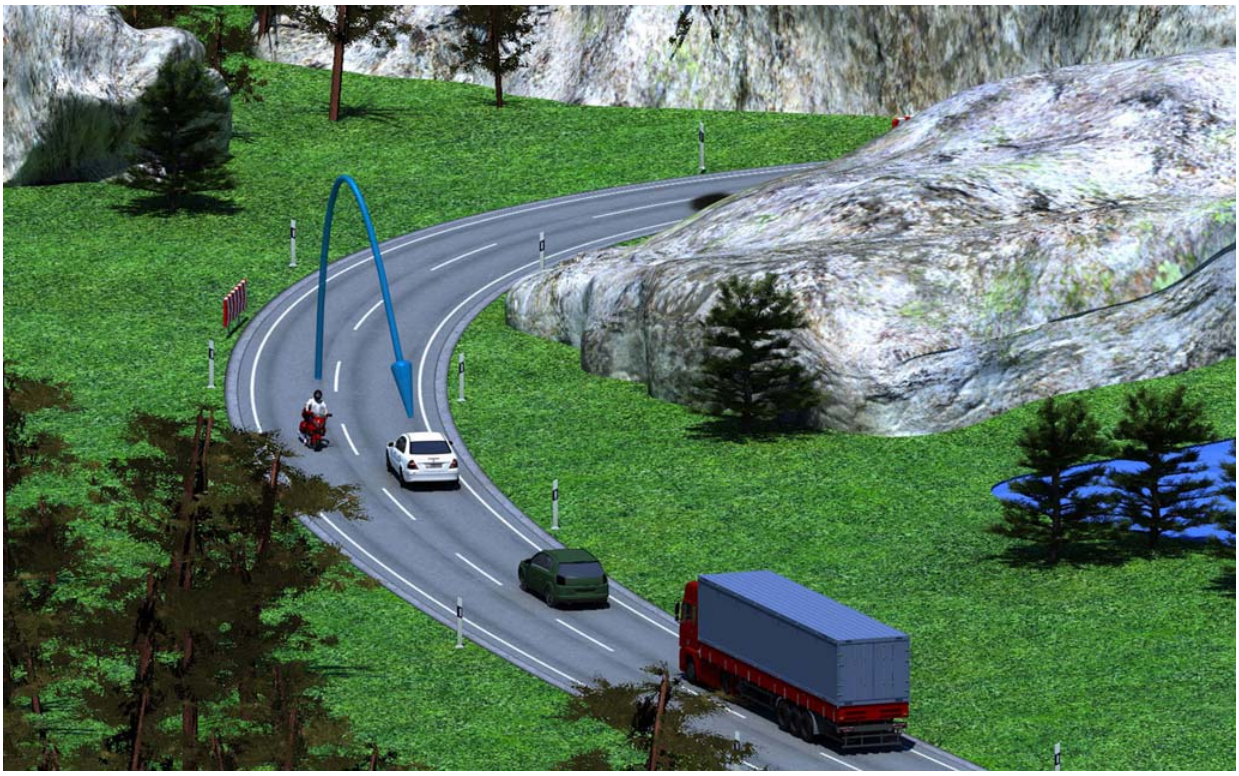

***Figure3. Avoiding an accident at a hazardous location through short range V2X (image courtesy of Car2Car Communication Consortium)***

Imagine a motorway where traffic going in the opposite direction will have passed an accident on the ego vehicle's side of the motorway long before the ego vehicle gets to the accident (see figure 4). As soon as this information is available, the driver can be warned and the lateral and longitudinal dynamics of the ego vehicle can be adjusted to the situation. Other use cases include crossroads where another vehicle may have a good field of vision while the ego vehicle next to it has not. The other vehicle will therefore be able to detect the approaching truck and will share this bit of information with the vehicles around. During this mutual information sending and retrieval process one vehicle tells the other what it "sees".

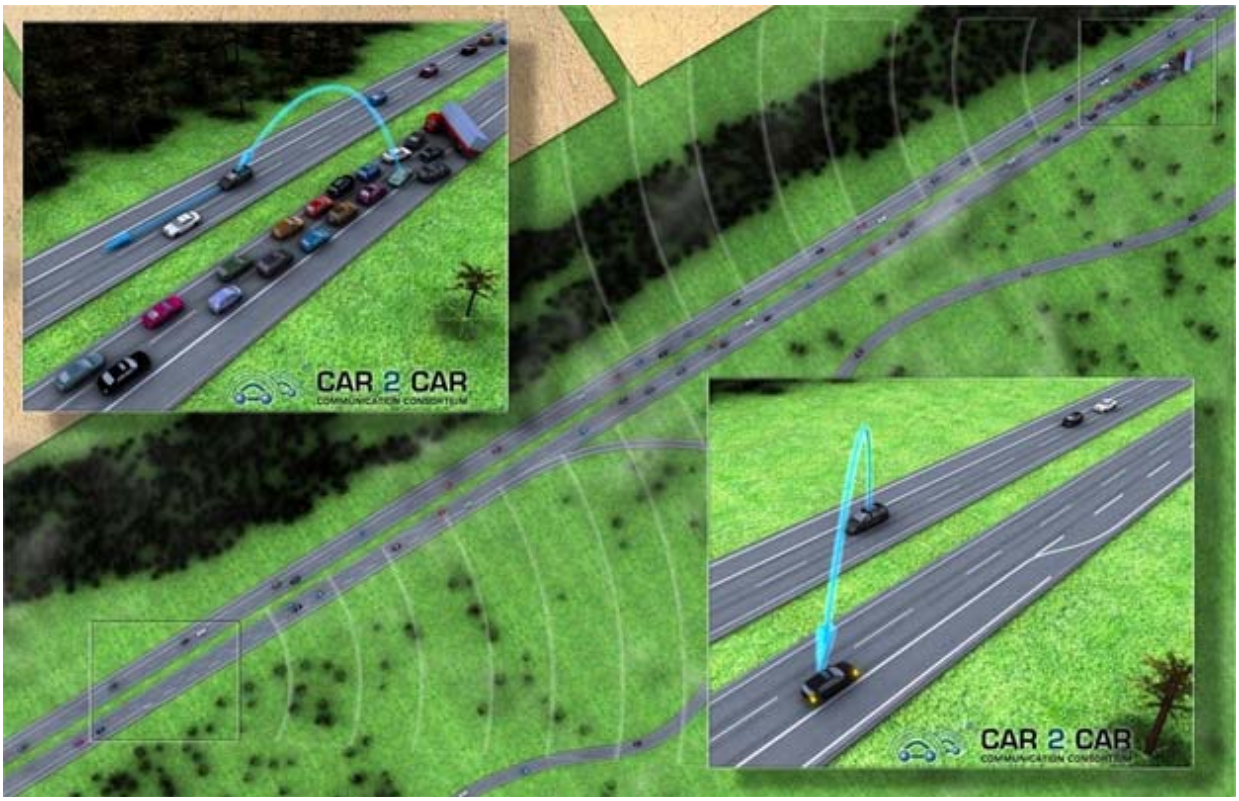


***Figure4. Avoiding a traffic jam through short range V2X (image courtesy of Car2Car Communication Consortium)***

**NHTSA STUDY ON EFFECTIVENESS OF V2V COMMUNICATION**

According to a new report on the readiness of V2V technology, initiated by DOT's National Highway Traffic Safety Administration (NHTSA) [2], V2V safety technology can help drivers avoid or reduce the severity of four out of five unimpaired vehicle crashes.

In order to measure the potential impact of V2V technology, the NHTSA report looks at rear end collision scenarios, lane change scenarios and intersection scenarios (see figure 5). In the scenarios new safety functions based on V2V communication help to avoid accidents. These functions include Forward Collision Warning (FCW), Intersection Movement Assist (IMA) and Left Turn Assist (LTA). In terms of safety impacts, the report estimates that Intersection Movement Assist and Left Turn Assist would per year prevent up to 592,000 crashes and save up to 1,083 lives. And in addition the severity of accidents would be reduced significantly [2].

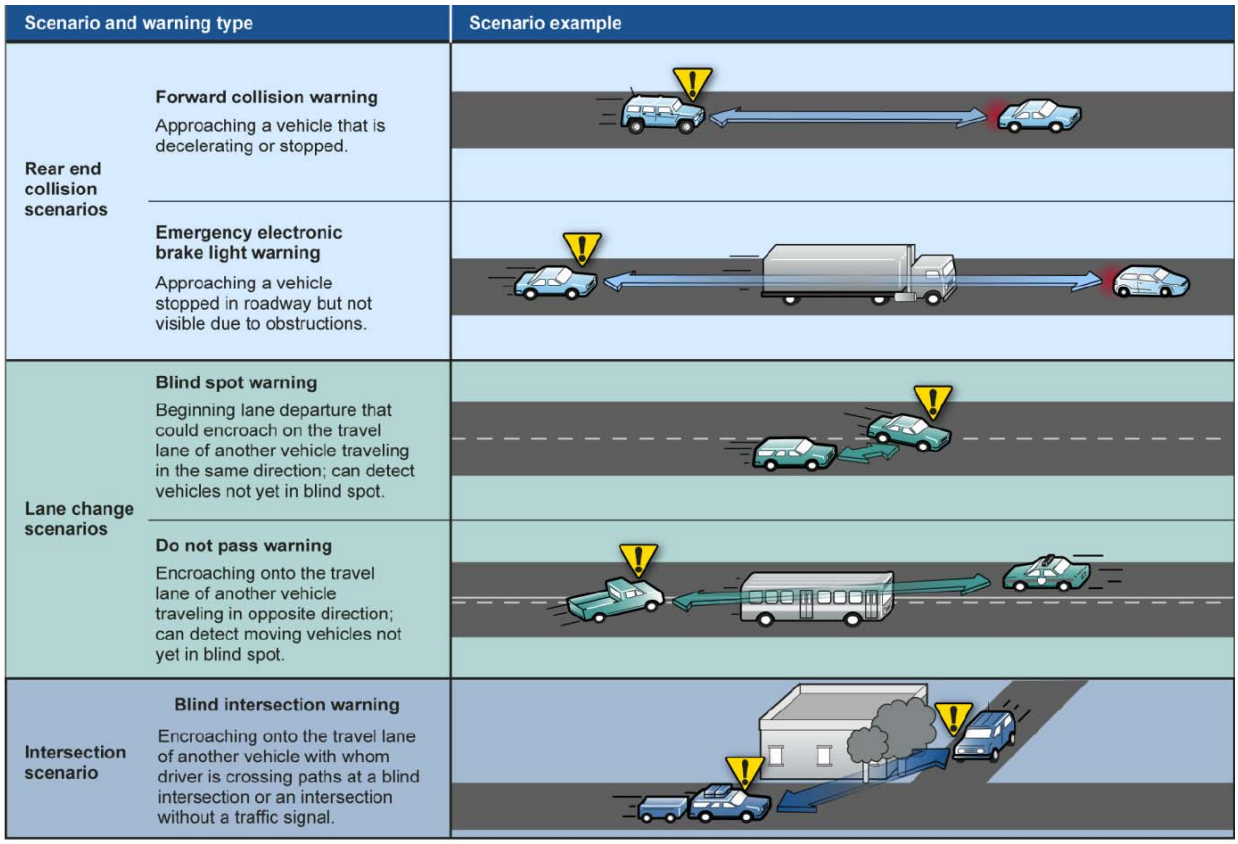


***Figure5. Examples of crash scenarios and Vehicle-to-Vehicle applications (image courtesy of [2])***

## PROTECTION FOR VULNERABLE ROAD USERS (VRU)

Let's turn to another important group of road users besides vehicles and their drivers and passengers: vulnerable road users (VRUs) such as children, pedestrians and cyclists, suddenly appearing from behind an object, are one of the major concerns to developers. In comparison to vehicles, they have no or almost no protection systems, but they operate in more complex traffic scenarios: between two parking vehicles, behind an obstacle, in a crowd, at crossings, etc.

Vision or radar based sensors can detect VRUs as long as the "line of sight" (compare above) is given. Is the VRU hidden by other objects, V2X communication can help to identify VRUs and to trigger the right warning or vehicle function. At Continental several technological approaches are under research. Within the German Ko-FAS research project Continental has developed and tested new hardware and software which facilitates an innovative approach to cooperative driving safety. In addition to conventional radar the research vehicles were equipped with a secondary radar system. In principle this is aircraft technology that has been modified for automotive requirements. A transponder (receiver and transmitter), called Ko-TAG 2.0, installed in each vehicle sends out an interrogating signal and receives active replies from other road users [6]. During the project pedestrians were equipped with an early version of a Safe-TAG 1.0 transponder so that they too could be identified and located. During extensive testing, which included equipping a complex crossroads in the town of Aschaffenburg (Germany) with stationary transponders, this type of tagging and short range V2X communication demonstrated enormous accident avoidance potential. Alternative technologies to the transponder developed in Ko-TAG could be promising for an ad-hoc communication between the vehicle and the VRU [7].

## BUILDING SAFETY 2.0

The vehicle architecture required for Safety 2.0 adds new sensors and controllers to the vehicle. As described by the above mentioned NHTSA report [2], a typical setup of a V2X system would consist of DSRC (Dedicated Short Range Communication) radios and a GNSS receiver (see figure 6). Furthermore a V2X Control Unit is needed to process and interpret all sensor data and to trigger required safety functions.

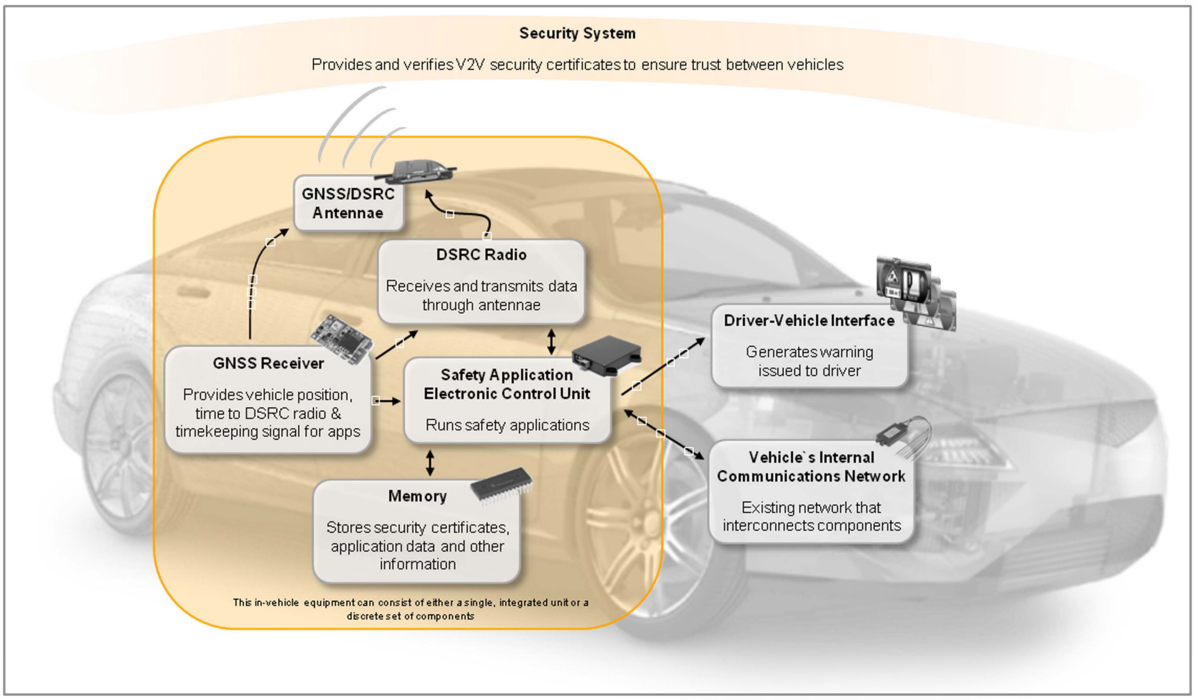


***Figure6. In-Vehicle components of a generic V2V System (based on [2])***

## ACCURATE POSITION IDENTIFICATION IS BECOMING AVAILABLE

In Safety 2.0 knowing the exact position of vehicles will become essential to any cooperative safety function. Up to now, the guidance of the vehicle was realized by the identification of landmarks and traffic – by the driver. Two main challenges can be distinguished: to reach the desired target by choosing the best routes (macro navigation) and to guide the vehicle in order to follow the route, which means longitudinal and lateral guidance while keeping the traffic regulations, avoid collisions etc. (micro navigation).

Safety 2.0 is addressing cooperative safety at the level of micro navigation. To achieve this, the position of all vehicles involved in the V2X communication network needs to be known at all times. Continental has developed the sensor "M2XPro®" (Motion Information to X Provider), which is designed to fulfill positioning requirements of V2X functions and of future systems for automated driving.

In order to achieve an effective and affordable solution, the concept of the M2XPro® positioning algorithm builds on existing standard sensors in the vehicle. By fusion of the vehicle-typical sensors Inertial Measurement Unit (IMU), Wheel Speed Sensors, Steering Angle Sensors (Odometry) and GNSS sensor, the existing redundancy of these sensors can be utilized to determine the accurate position of a vehicle.

Sensors can be disturbed due to their measuring principles, depending on the surrounding conditions. Using a fusion approach, those disturbances can be compensated by the strengths of the other sensors. For example wheel-slip or a

reduced number of visible satellites of the GNSS sensor can be weighted lower based on their increased noise or the given sensor information can be canceled out of the motion calculation by means of plausibilization.

This M2XPro® sensor can either be used as a stand-alone unit, or it can be integrated into a specific V2X unit – whichever suits the architecture best (compare [8]). The data provided by M2XPro® is completed by an integrity measure, which indicates what sensor data is actually available and how consistent the sensors are to each other and to the values the algorithm has calculated. The integrity measure is of high value for any safety function. At a high integrity measure a safety function can produce a precise warning or can trigger the correct reaction of the vehicle. However, at a low integrity measure a safety function might decide to stop any further execution due to uncertainty.

Overall the concept of M2XPro® leads to a significant improvement for information on the position and motion of a vehicle. Compared to a GNSS-only position information M2XPro® is improving availability, accuracy and reliability. Thereby M2XPro® is a requirement to any safety function in Safety 2.0.

## OUTLOOK

As safety technology has evolved and modern ADAS contribute to a safe driving in most traffic scenarios, V2X communication can close a missing gap: by the cooperative exchange of safety critical data, other vehicles or Vulnerable Road Users (VRU) become visible, even when they are out of the "line of sight" for the on-board surrounding sensors. Closing this gap carries the potential of developing a new level of cooperative safety functions - Safety 2.0. Eventually this new level of functions will bring us a big step further towards the vision of zero accidents.
V2X technology is ready to be applied and with the underlying potential of this technology it will be exciting to develop new safety functions. To speak with the words of David Strickland, NHTSA Administrator: "[…] Vehicle-to-vehicle communication has the potential to be the ultimate game-changer in roadway safety" [9].

## REFERENCES

[1] European Commission, Roadmap to a Single European Transport Area – Towards a competitive and resource efficient transport system, White Paper, 2011.
[2] Harding, J., Powell, G., R., Yoon, R., Fikentscher, J., Doyle, C., Sade, D., Lukuc, M., Simons, J., & Wang, J. (2014, August). Vehicle-to-vehicle communications: Readiness of V2V technology for application. (Report No. DOT HS 812 014). Washington, DC: National Highway Traffic Safety Administration.
[3] ETSI EN 302 663 V1.2.0 (2012-11): Intelligent Transport Systems (ITS); Access layer specification for Intelligent Transport Systems operating in the 5GHz frequency band.
[4] http://www.simtd.de/index.dhtml/enEN/news/events/news/201303_simTD-Abschluss2.html
[5] ETSI EN 302 637-2 V1.3.0 (2013-08): Intelligent Transport Systems (ITS); Vehicular Communications; Basic Set of Applications; Part 2: Specification of Cooperative Awareness Basic Service.
[6] D. Westhofen, C. Gruendler, K. Doll, U. Brunsmann, S. Zecha: Transponder- and Camera-based advanced driver assistance system, IEEE Intelligent Vehicles Symposium (IV), Alcalá de Henares, 2012
[7] http://media.gm.com/media/us/en/gm/news.detail.html/content/Pages/news/us/en/2012/Jul/0726_pedestrian.html
[8] S. Guenthner, B. Schmid, U.Staehlin, G. Juergens (2014): Sensorsysteme für Car2X, Herausforderungen für die Fahrzeugarchitektur, 30. VDI/VW Gemeinschaftstagung Fahrerassistenz und Integrierte Sicherheit, Wolfsburg 2014
[9] NHTSA 34-12, Press release, August 21, 2012: DOT Launches Largest-Ever Road Test of Connected Vehicle Crash Avoidance Technology

# Key Considerations in the Development of Driving Automation Systems

Crash Avoidance Metrics Partnership (CAMP) Automated Vehicle Research (AVR) Consortium
Andy Christensen, Nissan - North America
Andrew Cunningham, Volkswagen (VW) Group of America
Jerry Engelman, Ford Motor Company
Charles Green, General Motors
Charles Kawashima, Mercedes-Benz
Steve Kiger, CAMP
Danil Prokhorov, Toyota Motor Engineering & Manufacturing North America, Inc.
Levasseur Tellis, Ford Motor Company
Barbara Wendling, Volkswagen (VW) Group of America
Frank Barickman, National Highway Traffic Safety Administration

## Abstract

The historical roles of drivers, vehicle manufacturers, federal and state regulators, and law enforcement agencies in automotive safety is well understood. However, the increasing deployment of driving automation technologies to support various comfort, convenience, efficiency, productivity, mobility, and possibly safety features has the potential to alter this understanding. In order to facilitate clarity in discussing the topic of driving automation with other stakeholders and to clarify the level(s) of automation on which the agency is currently focusing its efforts, the National Highway Traffic Safety Administration (NHTSA) released a Preliminary Statement of Policy (SOP) concerning Automated Vehicles that included its automation levels.

In this paper, we present key factors for consideration in each automation level which are based upon SAE J3016. These factors focus on adding more specificity with regard to the distribution of the driving tasks between the driver and the automation system. The result of this effort has led to a refinement of our understanding of the automation levels based on the nature of the vehicle control aspect provided by the feature, the nature of the environmental sensing and response, the fallback strategy employed, and the feature's scope of operation.

## Introduction

The Automated Vehicle Research (AVR) for Enhanced Safety Project (i.e., the AVR Project) was initiated in September 2013. The project is being conducted by the Crash Avoidance Metrics Partnership (CAMP) AVR Consortium (Ford, General Motors, Nissan, Mercedes-Benz, Toyota, and Volkswagen/Audi). It is sponsored by the National Highway Traffic Safety Administration (NHTSA) through NHTSA Cooperative Agreement No. DTNH22-05-H-01277, Project Order 0009 and is scheduled to run 19 months through April 30, 2015.

The AVR Project, initiated within the electronic control systems segment of NHTSA's research program, has the following goals:

- Develop a list of potential driving automation applications that may be emerging on vehicles in the future
- Develop detailed functional descriptions for emerging operational concepts within each automation level
- Develop potential test and evaluation methods that map to the functional description of the automation levels
- Coordinate activities with other driving automation research projects

Task 3 focused on describing functional characteristics of driving automation systems. It also maps the sets of automation functions to the defined automation levels. This report presents the results of the work conducted in Task 3.

The AVR project is focusing on the functional building blocks and interactions between functions at the vehicle level as well as the dependencies on, and interaction with, the environment which define different levels of automation.

**Rationale on Why Driving Automation Levels Are Needed**

The increasing deployment of driving automation systems may begin to alter the historical roles of drivers, vehicle manufacturers, federal and state regulators, and law enforcement agencies in maintaining automotive safety. Maintaining safety throughout this transition is an important concern. In order to support the development and deployment of driving automation technologies it is important to consider and communicate the way in which these roles may change. The task of driving can be divided into three types of activities necessary to operate a vehicle (Michon, 1985):

- Operational behaviors such as longitudinal and lateral control as well as object and event detection and classification
- Tactical behaviors such as speed selection, lane selection, object and event response selection, and maneuver planning
- Strategic behaviors including destination planning and route planning

The operational behaviors of longitudinal and lateral control refer to the actions that drivers traditionally perform using closed-loop control of vehicle speed (using the accelerator and/or brake pedals) and position within the driving lane (using the steering wheel). Object and event detection, classification, and response (OEDR) refers to the perception of any circumstance relevant to the immediate driving task, and the appropriate reaction to such circumstance. In the remainder of this report, object and event detection, classification, and response is referred to as OEDR.

Within the overall task of driving, the operational and tactical behaviors relate directly to the dynamic aspects of driving and are thus grouped into what is referred to as the dynamic driving task, or DDT (SAE, 2014). An examination of changes in the driver's role can become the basis for categorizing driving automation systems.

It is important to clarify the difference between the systems for which these categories are intended and those for which these categories are not intended. For purposes of this paper, driving automation systems are designed to provide sustained operation of those subtasks of the DDT allocated to the system for extended periods of time, thus changing the driver's role. (The driver's continued involvement includes such things as engaging the system and resuming control.) Non-driving automation systems do not complete a subtask of the DDT, but do provide temporary or partial support to the driver by augmenting driver operation or intervening in critical situations, and hence the driver's role does not change. For example, a system such as electronic stability control (ESC) only provides temporary support to the driver for short periods of time by intervening in specified situations, enhancing the driver's performance rather than altering their role. Thus driving automation systems differ fundamentally from non-driving automation systems in their intent, extent and/or duration, and the role of the driver.

Traditionally, the design of the machine or automobile has focused around responding to the driver inputs in a predictable and prescribed way with high reliability. The use of the machine and the commands issued to the machine are a role entirely performed by the driver based upon their perception, experience, and desired outcomes. Figure 1 depicts the combined man-machine interface that constitutes the traditional DDT for human operation of a vehicle without a driving automation system.

Automation of elements of the DDT is not new to the automotive industry. However, successful automation to date has focused on rather specific functions designed to provide assistance to the driver while he or she otherwise maintains overall authority of the vehicle. These functions improve the interface between the driver and the vehicle in such a way as to provide better control or more convenient operation but do not fundamentally alter the roles of the driver and vehicle in executing the DDT. Consider conventional cruise control as an example. The driver must turn the feature on and select a desired speed. Once turned on, the automation system (conventional cruise control) will maintain that speed until cancelled by the driver. The automation system is not assessing the driving environment to decide appropriate speed limits, nor making an attempt to assess the safe speed for the current conditions. The automation system is also not considering potential collisions with other vehicles or infrastructure objects.

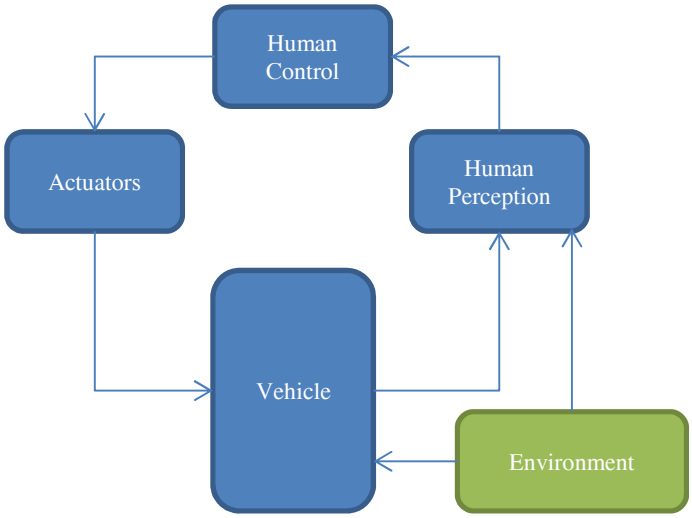


**Figure 1: Human Operation of a Traditional Vehicle – the Dynamic Driving Task**

Thus for conventional cruise control, avoiding safety-related hazards is a role entirely performed by the driver even though the machine executes its task, i.e., maintains the driver set speed. In this sense, safety is an outcome of the man-machine combination executing all facets of the DDT in unison. The advent of new driving automation technologies which enable additional portions of the driving task to be reallocated from the driver to the vehicle could potentially alter the traditional driver-vehicle relationship. Consider Figure 2 where both the human driver and the machine may have the ability to control the vehicle.

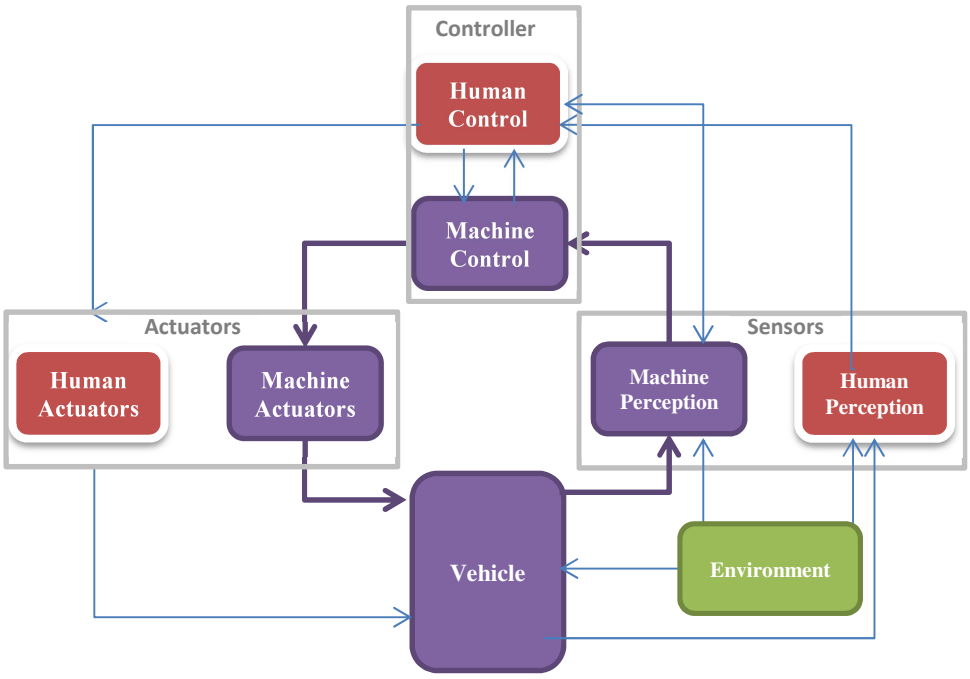


**Figure 2: The Introduction of Machine Automation to the Dynamic Driving Task**

As previously noted, the DDT includes lateral control, longitudinal control, and object and event detection and response (OEDR). These have not necessarily been altered in number or scope but they may now be expected to be

performed by the human driver, the automated machine, or both. It is this design allocation of the various subtasks which make up the DDT (and the subsequent role of the machine and the human driver in performance of the DDT) that motivates the discussion of categories or "levels" of automation. Engineers, designers, and policy makers benefit by having a way to categorize degrees of automation of the DDT in order to assist in communications between these stakeholder groups. However, it may also help drivers understand their role in the DDT in relation to the designers' intended usage of a driving automation system. The coordination of the driver and the driving automation system in the execution of the DDT (i.e., which elements of it are distributed between man and/or machine) is key to the safe operation of the vehicle.

Consider, for example, an automated parallel parking application. Some current production implementations require the driver to engage the system to look for a parking space on a particular side of the vehicle. Upon scanning an available parking space, the system provides either a confirmation of the ability to park or a denial if no suitable physical space is found. If the system finds a space and the driver confirms the desire to park, the system will automate the lateral control portion of the DDT to enter the space while the driver performs the longitudinal control as well as OEDR portions of the DDT. In making the decision to allow the vehicle to park, the driver is also judging the performance of the automation and ultimately maintaining control of the vehicle. If the steering might lead to a collision or makes the driver uncomfortable, the driver has the ability and is expected to stop the parking maneuver. The system is assisting the driver in executing a steering maneuver just as cruise control assists the driver in maintaining a desired speed, but the driver has the role and ability to make decisions and take actions to avoid collisions. The elements of Figure 2 are preserved, but the functions expected of the driver and system are different than parallel parking executed according to Figure 1.

As driving automation technologies begin to alter the allocation of subtasks that make up the DDT between driver and vehicle, the coordination of the driver and the driving automation system in the execution of the DDT is key to the safe operation of the vehicle. The automation system manufacturer should be conscious of all aspects of the DDT when considering the safety of these systems and consider how the system and the driver individually or together perform all of the dynamic driving task.

This paper discusses the categorical divisions (or "Levels") for driving automation based on the different roles for the driver and driving automation system.

**Rationale for Specific Levels of Driving Automation**

As discussed in the prior section, the driving automation system and the driver must individually or together perform all facets of the DDT. In addition, it should be noted that this may occur in some or all driving conditions, modes, and/or geographical locations. Under all these circumstances, either the driver or the automation system needs to provide fallback capability in the event that the automation system reaches the limits of its operational authority, or an automation system or vehicle failure occurs.

The most basic level of driving automation only has the functional capability to perform either longitudinal or lateral control with limited sensing capability. With these systems, the driver continues to perform the other motion control task (lateral or longitudinal) as well as the remainder of the object and event detection and response subtask of the DDT. Such systems have been widely researched and deployed (e.g., adaptive cruise control and advanced parking assistance (steering only) systems). Thus, with less capable driving automation where only part of the DDT can be automated, the functional capability to perform either or both longitudinal and lateral control is the relevant distinction to determining the level of the automation. With somewhat more capable driving automation, the system performs both longitudinal and lateral control simultaneously, but cannot perform the complete OEDR subtask. With these systems, the driver continues to perform the remainder of the OEDR subtask.

With highly capable driving automation, the systems can perform the complete DDT, providing appropriate responses to relevant objects and events. However, some systems may only be operational under specific driving conditions, such as during specific driving modes, under prescribed conditions, and/or in limited geographical locations. These systems have "conditionality." Additionally, such a system expects the driver to be able to take over in the event certain types of failures occur (i.e., under conditions that exceed its operational capabilities).

More capable automation systems are able to bring the vehicle to a "minimal risk condition" ( SAE, 2014) without driver action in the event that the system is no longer operating in the conditions for which it is designed or the system and/or vehicle experiences a failure, and no driver intervenes. This is also sometimes referred to as "fallback" capability. Thus, conditionality and "fallback" capability are the characteristics that separate higher

levels of automation. Therefore, the automation levels are differentiated according to the following functional characteristics (which are further defined within SAE J3016 as well as German BASt documents):

- These subtasks of the Dynamic Driving Task:
  - Lateral control subtask
  - Longitudinal control subtask
  - OEDR subtask
- These Functional Capabilities:
  - Driving mode, circumstance and location capabilities
  - Fallback capability

Using these functional characteristics, and considering that higher degrees of automation exceed and include lesser automation capabilities, the following defines step-wise levels of increasing driving automation that provide a framework for creation of an automation classification method.

Table **1** provides a visual overview of the SAE/BASt levels and illustrates the distribution of functions by automation level to either the driver or the automation system. Following the table is a detailed description of each level in the taxonomy that are used for the purposes of our research project.

**Table 1: Distribution of Functions by SAE/BASt Driving Automation Level**

| Automation Level Name | Dynamic Driving Sub-Tasks | | Functional Capability | |
|---|---|---|---|---|
| | Sustained Execution of Lateral and/or Longitudinal Control | Object & Event Detection and Response (OEDR) | Fallback Performance of Dynamic Driving Task | Driving Mode Circumstance, Location Capabilities |
| **0 No Automation** | Driver | Driver | Driver | None of the DDT is automated |
| **1 Driver Assistance** | Driver and system | Driver | Driver | Some driving modes |
| **2 Partial Automation** | System | Driver | Driver | Some driving modes |
| **3 Conditional Automation** | System | System | Driver | Some driving modes |
| **4 High Automation** | System | System | System | Some driving modes |
| **5 Full Automation** | System | System | System | All driving modes |

**Level 0: No Automation –** Vehicle features in this level do not automate any of the dynamic driving subtasks on a sustained basis. Thus, it has no driving automation. The driver of a vehicle without any automation performs the complete dynamic driving task. The driver provides the appropriate responses to all driving conditions. Additionally, alert systems that support the driver's OEDR performance, and systems that intervene momentarily in affecting lateral and/or longitudinal control of the vehicle to prevent or mitigate collision (e.g., crash imminent braking systems, electronic stability control, anti-lock brake systems, dynamic brake support, etc.) are included in this level of automation, as they do not automate any part of the DDT on a sustained basis.

**Level 1: Driver Assistance –** Driving automation systems in this level automate, on a sustained basis, either the lateral control subtask of the DDT, or the longitudinal control subtask of the same. It does not automate both simultaneously. In conjunction with performance of either the lateral or longitudinal control subtask, a Level 1 automation system does perform part, but not all, of the OEDR subtask associated with that aspect of vehicle control. That is, the driver of a vehicle equipped with an active Level 1 automation system performs the remainder of the DDT in all on-road conditions.

**Level 2: Partial Automation –** Driving automation systems in this level automate, on a sustained basis, both the lateral and longitudinal control subtasks of the DDT simultaneously. In conjunction with performance of the lateral and longitudinal control subtasks, a Level 2 automation system may also perform part, but not all, of the OEDR subtask. That is, the driver of a vehicle equipped with an active Level 2 automation system performs the remainder of the dynamic driving task (i.e., the remainder of the OEDR subtask) in all on-road conditions.

**Note on Terminology**

It should be noted that at this point in the hierarchy of levels, we are distinguishing preceding and following levels. Namely, Levels 0-2 encompass features that automate either none or some of the DDT, but not all of it, whereas Levels 3-5 encompass features that automate the entire dynamic driving task, whether on a part-time basis (limited range of on-road operational capability) or full-time basis (unlimited range of on-road operational capability). Because automation systems in Levels 3-5 are capable of performing the complete DDT, providing appropriate responses to relevant objects and events, they are referred to in this report as higher automated vehicle systems.

**Level 3: Conditional Automation –** Higher driving automation systems in this level automate the complete DDT, providing appropriate responses to relevant objects and events. However, the automation is situationally-limited in functional capabilities both in terms of driving modes, circumstances, and/or locations and in terms of fallback performance capability. That is, Level 3 higher driving automation system applications are capable of performing the complete DDT under limited conditions, outside of which the driver performs the complete DDT. In the event that the driving automation system is nearing the end of its operating capabilities (i.e., is about to transition out of the driving mode, conditions, and/or location(s) for which it is designed or experiences a relevant failure in the automation system), the system will warn the driver of the need to resume performance of the DDT far enough in advance to permit an orderly and controllable transfer. If the driver fails to respond in time to such a takeover warning, the automation system may not be able to achieve a minimal risk condition in all cases. In addition, the driver's fallback role includes detecting vehicle failures. The driver's role here includes passive monitoring, both for automation system-initiated takeover requests. Active supervision of the automation operation or the driving environment is not part of the driver's role in Level 3 automated operation. This differentiation may be operationalized with respect to driver visual attention. The driver's visual attention is not required to monitor the roadway for purposes of performing the OEDR subtask of the DDT in Level 3 operation. However the driver still has the role to sense (through visual, auditory, haptic and/or kinesthetic senses) if there is a takeover request issued by the automated driving system. The details of this driver fallback capability are a human factors topic and is outside the scope of the project. Other NHTSA research efforts (e.g., the current Human Factors Evaluation of Level 2 and Level 3 Automated Driving Concepts Project) will address some of the issues in this topic.

**Level 4: High Automation –** Driving automation systems in this level automate the complete dynamic driving task, providing appropriate responses to relevant objects and events. However, the automation is situationally-limited in operational capabilities in terms of driving modes, circumstances, and/or locations. In the event that the system is nearing the end of its operating capabilities (i.e., is about to transition out of the driving mode, conditions, and/or location(s) for which it is designed *or* a relevant failure in the system and/or vehicle occurs), the automation system

will warn the driver of the need to resume performance of the DDT far enough in advance to permit an orderly transfer. If the driver fails to respond in time to a such a takeover warning, the system will automatically achieve a minimal risk condition. (Note that the difference between a Level 3 and a Level 4 driving automation system is that the latter will reliably achieve a minimal risk condition without driver support, whereas the former will not reliably do so.)

**Level 5: Full Automation** – A driving automation system in this level automates the complete dynamic driving task, providing appropriate responses to relevant objects and events without situational limits in functional capabilities. That is, Level 5 systems are capable of completely performing the dynamic driving task under all on-road conditions in which a human driver can legally drive a motor vehicle today.

**Methodology for Classifying Features to Driving Automation Levels and Example Classifications**

As shown previously in

Table **1**, there are four important characteristics, which differentiate the levels of automation:

1. The performance of the DDT (lateral and longitudinal subtasks)
2. The nature of immediate, situationally-relevant environmental sensing and response
3. The fallback capability
4. The scope and range of operational capability

By their very nature, these factors address the system design and driver role in mitigating the hazards associated with on-road performance of the complete dynamic driving task (DDT). The basic hazards to be considered are as follows:

1. Staying on the road surface
2. Avoiding collisions with other objects on the roadway
3. Maintaining the stability and controllability of the vehicle during normal operation
4. Maintaining the stability and controllability of the vehicle in failed conditions

**Discussion of Levels**

A Level 0 feature is characterized by no sustained automation of the DDT, it is the driver's role to execute the basic functions of, and to mitigate the basic hazards associated with, the DDT at all times. Vehicle design can support the driver with these roles through intervention and monitoring aids such as stability control, forward and/or lateral collision warning or crash imminent braking, but the driver performs the DDT.

As automation begins to relieve the driver of certain functions such as longitudinal spacing or lateral positioning, the role of the machine and the driver in avoiding hazards may become less easily distinguishable. It is, therefore, through these definitions of higher automation levels that we seek to clearly define the distribution of driving tasks between the driving automation system and the driver at each level of automation.

A Level 1 driving automation system is characterized by sustained longitudinal or lateral control subtask performance of the DDT. It may be capable of avoiding some collisions within its control and sensing capabilities but it cannot completely avoid all possible crashes with objects. Thus, the driver supervises the automated vehicle system performance and intervenes as necessary to perform all remaining aspects of the DDT. For instance, adaptive cruise control traditionally performs longitudinal control within limits of maximum acceleration to mitigate stability issues on wet or slippery roads. However, it cannot make lateral avoidance maneuvers nor unlimited braking applications. It may also only respond to metallic objects moving within certain operational constraints. The feature automates a limited scenario and the driver is tasked with maintaining lateral control to stay on the road, maintain lanes, and avoid objects laterally and longitudinally if required. By the nature of the driver's role in the complete system operation, drivers are attentive to the external driving environment (ACAS FOT, 2005). Objects not within the defined operational set, such as accelerations required above the system limitations and vehicle dynamics limitations due to road surface conditions, are monitored, and responded to, by the driver. The vehicle

may warn if adverse conditions are detected but the driver intervenes when the system limitations are, or imminently may be, exceeded.

A Level 2 driving automation system is characterized by sustained lateral and longitudinal control subtask performance of the DDT but again within a defined boundary of operation. For example, pending conditions, the system may see some road lines but perhaps not road edges. It may see vehicles with large metallic content but it may not see pedestrians or small animals particularly those entering the scene laterally from behind an occluding structure. A Level 2 system has lateral and longitudinal control capability that may appear expansive but has limits both in actuator and sensing capability that may make it suitable only for some specific automation tasks and only under prescribed operating conditions. Drivers still monitor the external environment and make judgments about the suitability for use of the automation with Level 2 systems. Drivers intervene as needed if the limits of the automation system's design range of authority are reached, or if a system or vehicle failure occurs, to ensure all possible hazards are mitigated.

A Level 3 driving automation system has full sensing and actuation capability to mitigate all of the DDT -associated hazards but within a prescribed operating envelope. An example might be low-speed parking operations with all vehicle functions operating normally, or an application designed to operate the vehicle in dense traffic conditions on limited access freeways. The driver does not monitor the driving environment but responds to prompts from the automation system directing him/her to resume control in a reasonable time frame. These prompts would occur in the event that the system operational range has been exceeded (e.g., no longer in a parking area), or a relevant system or vehicle malfunction has occurred. It is worth noting that at the machine level, the appearance of a Level 2 and a Level 3 feature may be indistinguishable to drivers not aware of the design intent. Subtle limits of sensing capability or handling of particular vehicle failures might distinguish a Level 2 from a Level 3 system and without detailed design documentation and access to specific internal data, a driver may not be able to properly classify a new feature.

Level 4 and Level 5 driving automation systems are distinguished from lower levels because the driver does not intervene or play any role in the avoidance of the hazards associated with the DDT. A Level 4 system may have a limited scope of operation such as highways only, but it will have authority to achieve its mission and avoid all hazards associated with that mission within its scope of operation and also have the capability to reach a minimal risk condition. A Level 5 system will have these same capabilities except without a limit of scope other than the confines of the legal road system and infrastructure. Thus it will provide full-function, point-to-point driving automation with the ability to use all surface streets as it deems appropriate to the mission.

Given these characteristics of driving automation features and automation levels, the following methodology can be used to assign a new automation feature to one of the automation levels described above Figure 3 shows a flow-chart which distills the methodology for classifying automation features to levels of automation. The encircled numbers shown in the figure are the automation levels, resulting from following the Y(es) or N(o) paths when answering the specified questions sequentially from top to bottom.

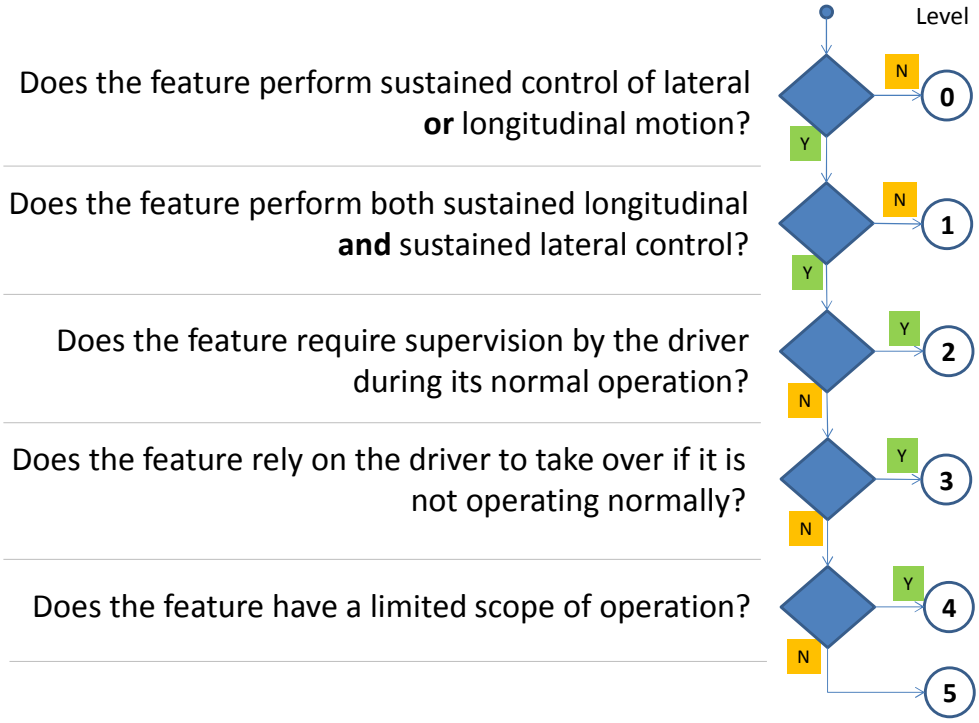


**Figure 3: Flow Chart Illustrating the Methodology for Classifying Automation Features to Levels of Automation**

**Example Classification of Driving Automation Features Using the Methodology**

The following list of driving automation features is provided to illustrate the use of the classification methodology. The descriptions are reproduced from the corresponding references, whenever available:

- Cruise Control (CC): Once this feature is engaged, the vehicle will perform longitudinal control (i.e., maintain the driver specified speed) within a limited driving domain (e.g., speed range, acceleration and deceleration/coast capability) until disengaged by the driver or due to a detected fault
- Adaptive Cruise Control (ACC): While engaged, it performs longitudinal control within a limited driving domain (e.g., speed range, acceleration and deceleration/coast capability, environmental conditions). ACC may perform distance (headway) control to some detected objects (again within its limited domain) in addition to its speed control capabilities. As with conventional cruise control, the driver supervises.
- Cooperative Adaptive Cruise Control (C-ACC): Same as ACC except the ACC-equipped vehicle and other vehicles in front of it are equipped with vehicle-to-vehicle (V2V) communication capabilities so as to inform each other of their current speed and other operationally relevant parameters (Nowakowski et al., 2010).
- Super Cruise: "Super Cruise is capable of semi-automated driving including hands-off lane following, braking and speed control under certain driving conditions. The system is designed to ease the driver's workload on freeways only, in bumper-to-bumper traffic and on long road trips; however, the driver's attention is still required" (General Motors, 2013).
- Automatic Parking:
    - "Toyota's Intelligent Parking Assist (IPA): This system assists with the steering wheel operation while parallel parking or parking in garages. When the driver sets the designed parking position on the monitor, the system assists the steering wheel operation" (Toyota Motor Corporation, 2014).

    - "The Audi technology works through a mobile app. A driver exits the car at the entrance to a parking garage, then simply touches the app on a mobile device so the driverless car can scour the garage for an open space. It then parks itself. When the driver returns, he or she simply selects the app again and like valet parking, the car returns to the entrance" (Mearian, 2013).

- Traffic Jam Assistant: "The traffic jam assistant helps you in monotonous situations on the motorway. In dense traffic at speeds of up to 40 km/h, the system allows you to move easily along with the traffic and stay relaxed. It automatically maintains the desired distance from the vehicle ahead and regulates the car's speed right down to standstill – as well as providing active steering support, too. This helps you stay on track, providing you keep at least one hand on the steering wheel" (BMW AG, 2013).
- Highway Driving Assist: "Toyota's Automated Highway Driving Assistant: The first part of the system is the Cooperative-adaptive cruise control, essentially a next-gen automated cruise control. The system uses 700 MHz band vehicle-to-vehicle ITS communications to gather acceleration/ deceleration data from the vehicles ahead and maintain a safe, uniform following distance. The second part of AHDA is Lane Trace Control, which Toyota described to us as a more advanced form of its Lane Keeping Assist system. Current-generation lane systems simply provide a warning or minimal amount of steering feedback when the vehicle begins to stray from the lane, but Toyota's Lane Trace adjusts the steering angle, torque and braking in order to maintain a driving line within the lane" (Weiss, 2013).
- Closed Circuit Automatic Shuttle/Delivery Vehicle: A vehicle that drives along a fixed route (i.e., a particular form of limited driving domain, limited to a specific route; the system may have other domain limitations such as weather conditions). The passenger (or goods) can enter and exit the vehicle at a set of stops (i.e., point-to-point). The system does not need an on-board driver control interface to operate within specified operational conditions.

Table 2 illustrates example features derived from the automation features listed above, as well as additional information available to the project team. A generic description based on the information above is provided for each feature in the table. Automation feature descriptions are also provided to illustrate the nature of the variation and facilitate classification of the feature to an automation level. The feature descriptions needed to categorize the levels are shown in the columns on the right side of the table.

**Table 2: Exemplar Driving Automation Features**

| | | Descriptions required to categorize levels | | | |
|---|---|---|---|---|---|
| | | | | Only required if driver does not have supervisory role | |
| Feature | Description | Sustained Control | Sensing and Response Capability (Driver's supervisory role) | Fallback | Operational conditions |
| Cruise control | Once this feature is engaged, the vehicle will perform longitudinal control (i.e., maintain the driver specified speed) within a limited driving domain (e.g., speed range, acceleration and deceleration/coast capability) until disengaged by the driver or due to a detected fault (see also in Section 2 of this report). | Sustained Longitudinal control | Driver must supervise | | |
| Adaptive Cruise Control (ACC) | While engaged, it performs longitudinal control within a limited driving domain (e.g., speed range, acceleration and deceleration/coast capability, environmental conditions). ACC may perform distance (headway) control to some detected objects (again within its limited domain) in addition to its speed control capabilities. As with conventional cruise control, driver supervision is required (see also in Section 6.1 of this report). | Sustained Longitudinal control | Driver must supervise | | |
| Cooperative Adaptive Cruise Control (C-ACC) | Same as ACC except the ACC-equipped vehicle and other vehicles in front of it are equipped with vehicle-to-vehicle (V2V) communication capabilities so as to inform each other of theirs current speed and other parameters (Nowakowski et al., 2010). | Sustained Longitudinal control | Driver must supervise | | |
| GM Super Cruise | "Super Cruise is capable of semi-automated driving including hands-off lane following, braking and speed control under certain driving conditions. The system is designed to ease the driver's workload on freeways only, in bumper-to-bumper traffic and on long road trips; however, the driver's attention is still required" (General Motors, 2013). | Sustained Lateral and Longitudinal control | Driver must supervise | | |
| Toyota Intelligent Parking Assist | "This system assists with the steering wheel operation while parallel parking or parking in garages. When the driver sets the designed parking position on the monitor, the system assists the steering wheel operation" (Toyota Motor Corporation, 2014). | Sustained Lateral control | Driver must supervise | | |
| Audi Parking System | "The Audi technology works through a mobile app. A driver exits the car at the entrance to a parking garage, then simply touches the app on a mobile device so the driverless car can scour the garage for an open space. It then parks itself. When the driver returns, he or she simply selects the app again and like valet parking, the car returns to the entrance" (Mearian, 2013). | Sustained Lateral and Longitudinal control | No driver required, therefore no supervisory requirements | Driver is not required | Low speed, parking lot only |
| Traffic Jam Assistant | "The traffic jam assistant helps you in monotonous situations on the motorway. In dense traffic at speeds of up to 40 km/h, the system allows you to move easily along with the traffic and stay relaxed. It automatically maintains the desired distance from the vehicle ahead and regulates the car's speed right down to standstill – as well as providing active steering support, too. This helps you stay on track, providing you keep at least one hand on the steering wheel" (BMW AG, 2013). | Sustained Longitudinal control | Driver must supervise | | |
| Toyota Highway Driving Assistant | "Toyota's Automated Highway Driving Assistant: The first part of the system is the Cooperative-adaptive cruise control, essentially a next-gen automated cruise control. The system uses 700 MHz band vehicle-to-vehicle ITS communications to gather acceleration/ deceleration data from the vehicles ahead and maintain a safe, uniform following distance. The second part of AHDA is Lane Trace Control, which Toyota described to us as a more advanced form of its Lane Keeping Assist system. Current-generation lane systems simply provide a warning or minimal amount of steering feedback when the vehicle begins to stray from the lane, but Toyota's Lane Trace adjusts the steering angle, torque and braking in order to maintain a driving line within the lane" (Weiss, 2013). | Sustained Lateral and longitudinal control | Driver must supervise | | |
| Robotic Taxi | A vehicle that can pick up passengers (or goods), then drive them to the place of their choosing (i.e., point-to-multi-point). The system is not required to have an on-board driver control interface to operate within specified operational conditions. The system does not have limited domains of operation, it can operate within any legal road system and under any environmental conditions deemed acceptable by road system authorities (i.e., when roads are open). This hypothetical vehicle is claimed to be one of the future products of Google's self-driving car program (see, e.g., Fitzsimmons, 2013). | Sustained Lateral and Longitudinal control | No driver required, therefore no supervisory requirements | No driver required | any publicly available roads |
| Closed Circuit Automatic Shuttle/Delivery Vehicle | A vehicle that drives along a fixed route (i.e., a particular form of limited driving domain, limited to a specific route; the system may have other domain limitations such as weather conditions). The passenger (or goods) can enter and exit the vehicle at a set of stops (i.e., point-to-point). The system is not required to have an on-board driver control interface to operate within specified operational conditions. | Sustained Lateral and Longitudinal control | No driver required, therefore no supervisory requirements | No driver required | fixed route |

Table 3 illustrates the application of the developed methodology to map the features into the automation levels. The methodology question from Figure 3 is shown in the first row. The feature's automation level results from answering "Yes" or "No" to the appropriate question. The arrows indicate whether to move to the next question (right-arrow) or to stop at the resulting level (up-arrow). Comments are also provided regarding assumptions made based on the feature description, whenever necessary.

It should be noted for the given feature, it is very important to have sufficient information in the description to be able to answer the methodology questions unambiguously. Consider Toyota's Automated Highway Driving Assistant as an example of classifying a feature to an automation level. According to the flow chart in Figure 3, the first question asked is whether the feature is capable of sustained control of either lateral or longitudinal motion in lieu of the driver. Clearly, the answer is yes, therefore, the logical flow proceeds to the next question. The answer to the second question is again yes, because the feature can control the vehicle both laterally and longitudinally on a sustained basis in lieu of the driver, according to the feature's description. The next question is whether the feature requires a driver's supervision during its normal operation. The feature description as provided above is not complete, however Toyota's current view is that the human supervision is necessary, meaning that the answer is yes and that the feature is thus classified as Level 2.

**Table 3: Mapping Automation Features into Driving Automation Levels**

| **Automation Methodology Question** | Sustained Lateral **OR** Longitudional control? | Sustained Lateral **AND** Longitudional Control? | Driver supervision required? | Driver required outside normal operation? | Limited scope of operation? | |
|---|---|---|---|---|---|---|
| Automation characteristic | **Control** | | **Sensing and response** | **Fallback** | **Operational conditions** | |
| Answer confirms level or proceeds to next question | Yes → | Yes → | No → | No → | No → | |
| | No ↑ | No ↑ | Yes ↑ | Yes ↑ | Yes ↑ | |
| **Automated level** | **0** | **1** | **2** | **3** | **4** | **5** |
| Cruise control | Yes → | No ↑ | | | | |
| Adaptive cruise control (ACC) | Yes → | No ↑ | | | | |
| Cooperative Adaptive cruise control (C-ACC) | Yes → | No ↑ | | | | |
| GM Super Cruise | Yes → | Yes → | Yes ↑ | | | |
| Toyota Intelligent Park Assist | Yes → | No ↑ | | | | |
| Audi Parking System | Yes → | Yes → | No → | No → | Yes ↑ | |
| Traffic Jam Assist | Yes → | No ↑ | | | | |
| Toyota Highway Driving Assistant | Yes → | Yes → | Yes ↑ | | | |
| Robotic Taxi | Yes → | Yes → | No → | No → | No → | ↑ |

## Conclusions

The introduction of higher levels of driving automation technologies has the potential to alter the traditional driver-vehicle relationship. However, in order to facilitate discussion about automated vehicle technologies, it is beneficial to define categorical divisions for driving automation based on the functional capabilities of the automation and the role of the driver in the DDT.

While there are several different automation level definitions under consideration at the time of this writing, this paper and the methodologies discussed have been based on the SAE J3016 (2014) and BASt levels. In addition, the automation levels developed in this research, including supporting terms and definitions, focus on:

a) The functional capability of the automation system (and the subsequent role of the driver vs. the automation system) to perform the complete DDT

b) The ability of the driver and the automation combined to provide the appropriate responses to relevant objects and events

c) The driving mode

d) The fallback capability of the automation system

Once a clear definition of the automation is provided, the minimum set of automation functions for each level of automation can be defined. It is important to note that the higher levels of driving automation include those functional capabilities found at the lower levels of automation, and that each increasing level of automation includes functions aimed at reducing the driver's role in completing the DDT.

Lastly, the methodology in this report that allows classification of new automation applications into the automation levels is based on the automation functions provided by the feature. These functions include the nature of the vehicle control aspect provided by the feature, the nature of the environmental sensing and response, the fallback strategy employed, and the feature's scope of operation. Given this information about an automation application, it is possible to classify potential automation features to an automation level by following the approach outlined in this paper. However, a detailed understanding of the driving automation system design is needed to make this classification correctly.

## References


Billings, C. E., Lauber, J. K., Funkhouser, H., Lyman, G., and Huff, E. M. (1976). NASA Aviation Safety Reporting System (Tech. Rep. TM-X-3445). Moffett Field, CA: NASA Ames Research Center.

BMW AG. (2013). Traffic Jam Assistant. Retrieved March 24, 2014 from http://www.bmw.com/com/en/newvehicles/x/x5/2013/showroom/driver_assistance/traffic_jam_assistant.html#t=l

Fitzsimmons, M. (2013). Google may be crafting its own self-driving cars, tinkering with robo-taxis. In techradar. Retrieved on March 24, 2014 from http://www.techradar.com /news/car-tech/google-may-be-designing-its-own-self-driving-cars-tinkering-with-robo-taxis-1175511

General Motors Corporation. (2005). *Automotive Collision Avoidance System Field Operational Test (ACAS FOT) Final Program Report* (Report No. DOT HS 809 886). Washington, DC: National Highway Traffic Safety Administration.

General Motors. (2013). 'Super Cruise' Takes on Real-World Traffic Scenarios, Cadillac's semi-automated vehicle technology undergoes further testing. Retrieved March 24, 2014 from http://media.gm.com/media/us/en/gm/news.detail.html/content/Pages/news/us/en/2013/Apr/0429-cadillac-super-cruise.html

Llaneras, R. E., Salinger, J. and Green, C. A., (2013). Human Factors Issues Associated with Limited Ability Autonomous Driving Systems: Drivers' Allocation of Visual Attention to the Forward Roadway. In *Proceedings of the 7th International Driving Symposium on Human Factors in Driver Assessment, Training, and Vehicle Design.* Paper presented at Driving Assessment 2013, Bolton Landing, New York (pp. 92-98). Iowa City, IA: University of Iowa Public Policy Center.

Mearian, L. (2013). Audi tech automatically finds vacant parking spot, sans driver. In *Computerworld.* Retrieved March 24, 2014 from http://www.computerworld.com /s/article/9242138/Audi_tech_automatically_finds_a_vacant_parking_spot_sans_driver_

Michon, J. A., (1985). A Critical Review of Driver Behavior Models: What Do We Know, What Should We Do? In L. Evans and R. C. Schwing (Eds.), *Human Behavior and Traffic Safety* (pp. 485-520). New York, NY: Plenum Press.

National Highway Traffic Safety Administration, (2013). "*Preliminary Statement of Policy Concerning Automated Vehicles*." Washington, DC: Author. Retrieved March 18, 2014 from http://www.nhtsa.gov/staticfiles/rulemaking/pdf/Automated_Vehicles_Policy.pdf.

Nowakowski, C., Shladover, S., Cody, D., Fanping, B., O'Connell, J., Spring, J., Dickey, S., and Nelson, D. (2010). *Cooperative Adaptive Cruise Control: Testing Drivers' Choices of Following Distances* (California PATH Research Report No. UCB-ITS-PRR-2010-39. Berkeley, CA: University of California, California PATH Program. Retrieved March 24, 2014 from http://www.path.berkeley.edu/PATH/Publications/PDF/PRR/2010/PRR-2010-39.pdf

Parasuraman, R.; Riley, V. (1997). "Humans and Automation: Use, Misuse, Disuse, Abuse." Human Factors 39: 230–253.

SAE International On-Road Automated Vehicle Standards Committee, (2014). SAE Information Report: (J3016) *"Taxonomy and Definitions for Terms Related to On-Road Motor Vehicle Automated Driving System."* Warrendale, PA: SAE International.

Salinger, J., Green, C., Reid, B., Widmann, G. R., Prieto, R., Llaneras, E., Chen, Y., Koskie, S., Rajput, V. S., Tian, R., Bolourchi, F., and Prabhuswamy, S. (In Publication). *"Human Factors for Limited Ability Autonomous Driving Systems (HF4LAADS), FHWA Cooperative Agreement # DTFH61-08-R-00006, Deliverable 8 – Final Report* ." Washington, DC: Federal Highway Administration.

Toyota Motor Corporation. (2014). Technology that Supports Parking. Retrieved March 24, 2014 from http://www.toyota-global.com/innovation/safety_technology/safety_technology/parking/

Weiss, C. C. (2013). Toyota details its Automated Highway Driving Assist system. Gizmag. Retrieved on March 24, 2014 from http://www.gizmag.com/toyota-automated-highway-driving/29378/

# Driver Vehicle Interface Design Assistance for Vehicle-to-Vehicle Technology Applications

**Christian Jerome, Ph.D.**
**Chris Monk, Ph.D.**
National Highway Traffic Safety Administration
U.S. Department of Transportation
United States

**John Campbell, Ph.D.**
Battelle
United States

**Paper Number 15-0452**

**ABSTRACT**

This paper provides an overview of the program of research involved in the development of a set of driver-vehicle interface (DVI) design assistance intended for vehicle-to-vehicle (V2V) technology applications. The research reviewed and performed under the NHTSA sponsored program of research (Human Factors for Connected Vehicles (HFCV), Safety Pilot DVI Evaluations, Driver Issues, and Integration Strategy) will culminate in a DVI Design Assistance Document for V2V technology applications. The results of the research will inform this document, which will be a set of Design Assistance topics and will describe appropriate human-centric design attributes for the DVI.

## INTRODUCTION

Automotive DVI research in general has typically focused on the design of safety system DVIs. Therefore, the available research used to inform this DVI Design Assistance Document is primarily drawn from safety research. However, the basic design assistance that this document provides may help inform the design of non-safety related DVIs (i.e., infotainment and driver convenience systems) for V2V. Additionally, this document provides information from recent and ongoing research in the emerging field of V2V technology.

### Objectives

The overall objective of the HFCV research program is for V2V technologies and applications to have DVIs that effectively communicate safety information while managing driver workload and minimizing distraction. This objective will be realized with the product of this research program, the DVI Design Assistance Document, and will aid in the design of relevant system interfaces to be more effective without increasing distraction or creating high workload.

### Goals

The goal of the DVI Design Assistance Document is to aid the design of interfaces that are effective without increasing distraction**.** Warning system interfaces are effective if they (1) attract the driver's attention, (2) communicate the intended information, (3) communicate the information in a way that is immediately understandable so the driver can process the information, and (4) directs attention to a threat in time for the driver to take corrective action. The DVI Design Assistance Document were informed by previous research and current ongoing research performed in the course of the HFCV research program. The research program and design assistance provide information for a better understanding of driver behavior, improved driver assistance

technologies, interface design assistance for vehicle-to-vehicle communications technologies aimed at passenger vehicles, heavy trucks, and transit vehicles. The NHTSA's primary concern is safety applications, but the research and design assistance also cover some mobility and sustainability applications for V2V.

In order to realize these goals and objectives, the research program approach included a number of phases and simultaneous tracks that informed the DVI Design Assistance Document. The program began with a definition of the problem, which split into two main tracks of research: one focusing on V2V information and how it should be integrated and managed to better suit the driver's needs, and the other focused on characterisitcs of the DVI and how different safety messages should be delivered to the driver. The HFCV program also engaged stakeholder throughout the DVI Design Assistance development in order to improve the format and content of the DVI Design Assistance Document.

## DVI DESIGN ASSISTANCE DOCUMENT

The topics within the V2V DVI Design Assistance Document are informed by the best available scientific research, and the DVI Design Assistance Document is a collection of focus areas uncovered by research that are intended to inform and assist DVI designers in making decisions regarding potential issues with various aspects of the DVI. Each focus area includes an introduction that first defines the topic and how it might be problematic, then the focus area summarizes the functional design goal with supporting design assistance. The focus area then includes a discussion of the practical design issues and the supporting available scientific research.Each focus area of the V2V DVI Design Assistance Document is organized into an easy-to-read, two-page format.

Overall, this document provides goals and assistance for the design and development of V2V DVIs, for both light- and heavy-vehicles, based on knowledge of driver capabilities and limitations. It consists of a series of chapters containing DVI design assistance. Each chapter provides a set of subtopics relevant to a specific design characteristic or element. Chapter 2 provides an overview of the format and content of these design-specific chapter topics (Chapters 3 through 11). Following the design chapters are a set of reference chapters with supplemental information (Chapters 12 through 18), including tutorials, a glossary, an index, lists of abbreviations and equations used in the document, a list of additional standards and other documents related to DVI design, and a complete reference list of articles and reports used to develop the design assistance and tutorials. Figure 1 below provides a high-level overview of the chapters and topics included in the DVI Design Assistance Document.

*Figure 1. Overview of the Contents of the DVI Design Assistance Document.*

In the V2V DVI Design Assistance Document, a consistent two-page format is used to present the individual human factors topics provided in Chapters 3 through 10. On each page, the chapter title is indicated by centered, bold type within the header. As described in more detail below, the left-hand page presents the title of the topic; an introduction and overview of the topic; a high-level design goal; supporting design assistance; and a graphic, table, or figure that augments the text information. The right-hand page provides the more detailed supporting rationale for the topic, as well as special design considerations, cross-references to related topics, and a list of references. A sample topic, with key features highlighted, is shown below in Figure 2:

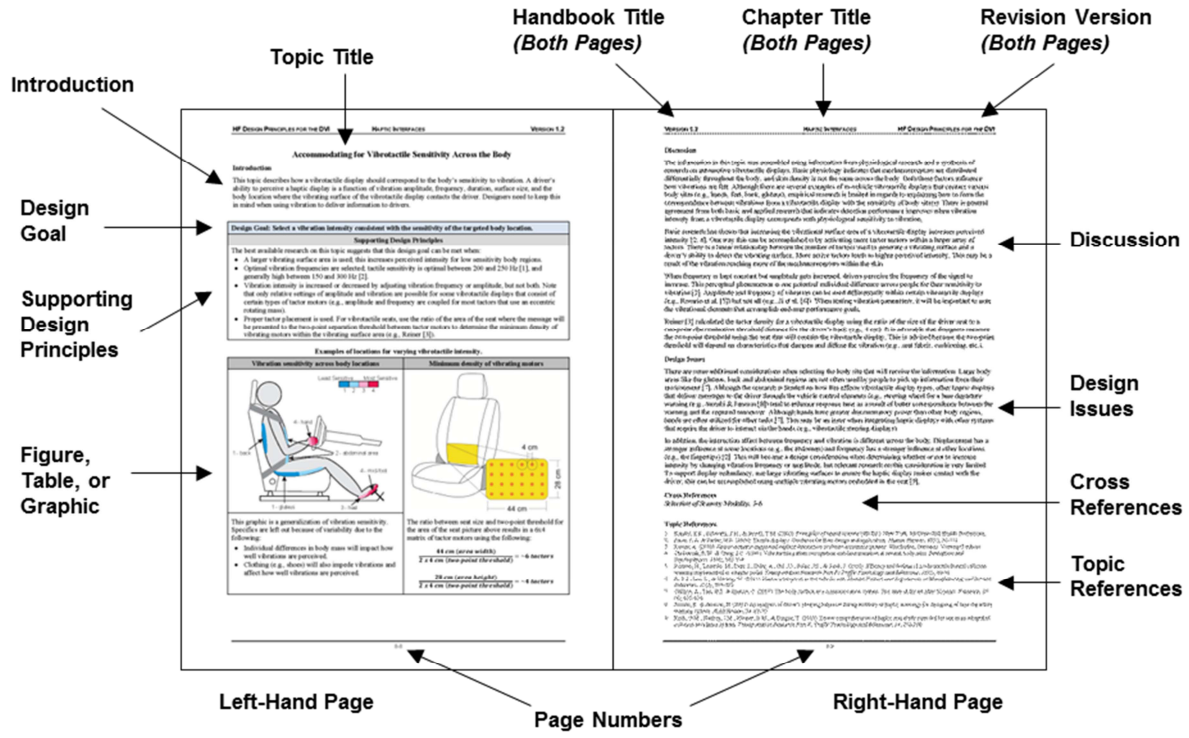


*Figure 2. Topic format used in the design assistance document.*

**Overview of Example Topics**

Below, we have summarized the contents from a small sample of the design topics addressed in the DVI Design Assistance Document:

- Locating a Visual Display,
- Perceived Urgency of Auditory Warnings,
- Accommodating for Vibrotactile Sensitivity Across the Body, and
- Selection of Sensory Modality for Heavy Vehicle Warnings

Only 4 of the 52 design topics were included in the interest of the limits of this publication, and these particular 4 topics were chosen due to the expected high interest in them (i.e., they are key topics of interest in current trends for DVI design).

**Locating a Visual Display**

This topic discusses the issues related to the location of a display where it will be easily seen and comprehended by drivers. As new warning and information systems on the market can increase dashboard complexity, selecting an appropriate location for a visual display is important to minimize information-seeking behavior that distracts from the driving task. Recommended design assistance to facilitate rapid extraction of information while minimizing eyes-off-road glances and negative impacts on driving performance are:

- Critical displays for continuous vehicle control or critical warnings related to vehicle forward path are located within ± 15 degrees of the central line of sight but as close to the central line of sight as practicable. ISO (1984) recommends that messages that require immediate detection be located within 5 degrees of the forward view when possible. (A).
- Displays are placed in locations that are generally compatible with established expectations or with location cues from other warnings, such as auditory or haptic (B).
- The display location is compatible with the desired response, such as a display in the mirror for alerts for looking to the blind spot; a Head-Up Display (HUD) that is used to direct attention to the forward view for critical warnings (C).
- The design and location minimizes glare from external sources or other displays in the vehicle (e.g., in the instrument panel or under a protective cover; D).

Figure 3 below illustrates potential visual display locations.

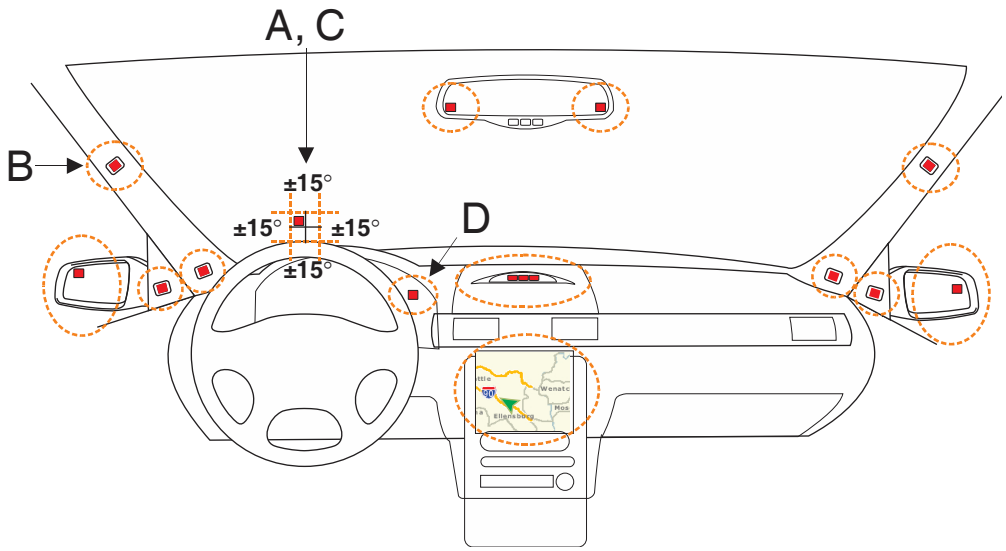


*Figure 3. Potential Locations for Visual Displays*

Additional discussion in this design topic includes research results and recommendations for keeping warnings near to the driver's line of sight, use of color, and correspondence between the driver's gaze and directional hazard location. Benefits of highly compatible display-response relationships include development of strong mental models by the operator as to how the system works, reduced driver response times, and fewer response errors. Also noted, is the lack of current data or standards regarding messages in heavy vehicle (HV) applications.

**Perceived Urgency of Auditory Warnings**

This topic discusses and recommends a number of design assistance topics to create auditory warnings that clearly communicate a level of urgency consistent with the urgency of the hazard. Auditory attributes that can be engineered to higher or lower levels of urgency include:

**To increase the perceived urgency:**

- Use faster auditory signals (e.g., 6 pulse/sec).
- Use regular rhythms (all pulses equally spaced).
- Use a greater number of pulse burst units (e.g., 4 units).
- Use auditory signals that speed up.
- Use high fundamental frequencies (e.g., ≥1000 Hz).
- Use random or irregular overtones.
- Use a large pitch range (e.g., 9 semitones).
- Use a random pitch contour.
- Use an atonal musical structure (random sequence of pulses).
- Use more urgent words (e.g., "Danger").

**To decrease the perceived urgency:**

- Use slower auditory signals (e.g., 1.5 pulse/sec).
- Use irregular rhythms (pulses not equally spaced).
- Use a fewer number of pulse burst units (e.g., 1 unit).
- Use auditory signals that slow down.
- Use low fundamental frequencies (e.g., 200 Hz).
- Use a regular harmonic series.
- Use a small pitch range (3 semitones).
- Use a down or up pitch contour.
- Use a resolved musical structure (from natural scales).
- Use less urgent words (e.g., "Caution").

Figure 4 below provides a visual comparison of higher urgency auditory signal characteristics (tops) with lower urgency signal characteristics (bottom).

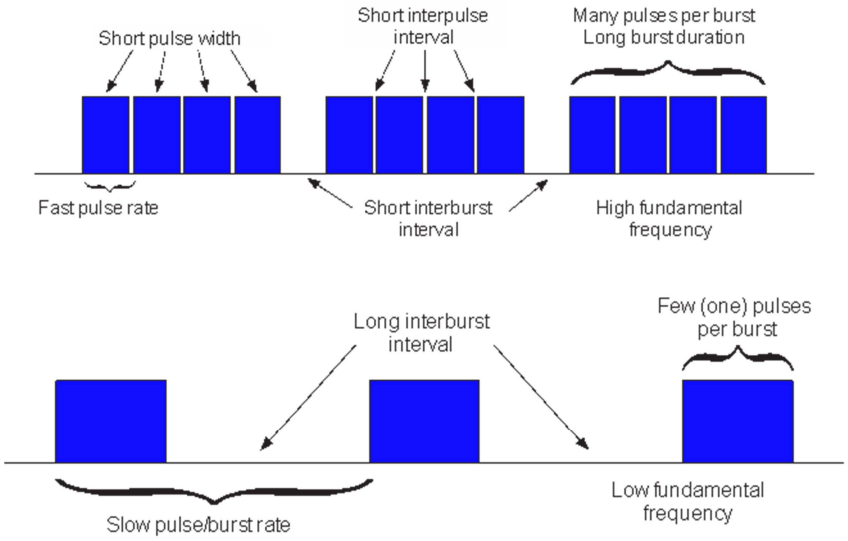


*Figure 4. Comparison of Auditory Signal Characteristics Associated with Higher vs. Lower Levels of Perceived Urgency Characteristics*

The discussion for this topic includes research results and recommendations indicating that accurate urgency mapping leads to more effective driver response. While more urgent signals are associated with faster reaction

times, confusion, startle responses, or distraction can result if the perceived urgency is higher than the situation demands.

Some of the design trade-offs to be considered include compatibility with other signals, driver annoyance, and distinctiveness of the signal. Message semantics for both signals and speech can affect driver response. Study findings suggest that perceived urgency can be increased using high-urgency semantics (whether with speech or with familiar non-speech signals) into auditory messages that have lower-urgency acoustic characteristics (Guilluame et al. 2002; Baldwin & May, 2011).

**Accommodating for Vibrotactile Sensitivity Across the Body**

This topic provides design assistance for how to design vibrotactile displays so that they correspond to the body's sensitivity to vibration. Vibrotactile display attributes include vibration amplitude, frequency, duration, surface size, and the body location of the vibrating surface. Displays are most effective when they are readily perceived by the driver thus matching vibrotactile intensity with the differing sensitivity of various body locations will increase detection.

Figure 5 below provides examples of body locations for varying vibrotactile intensity.

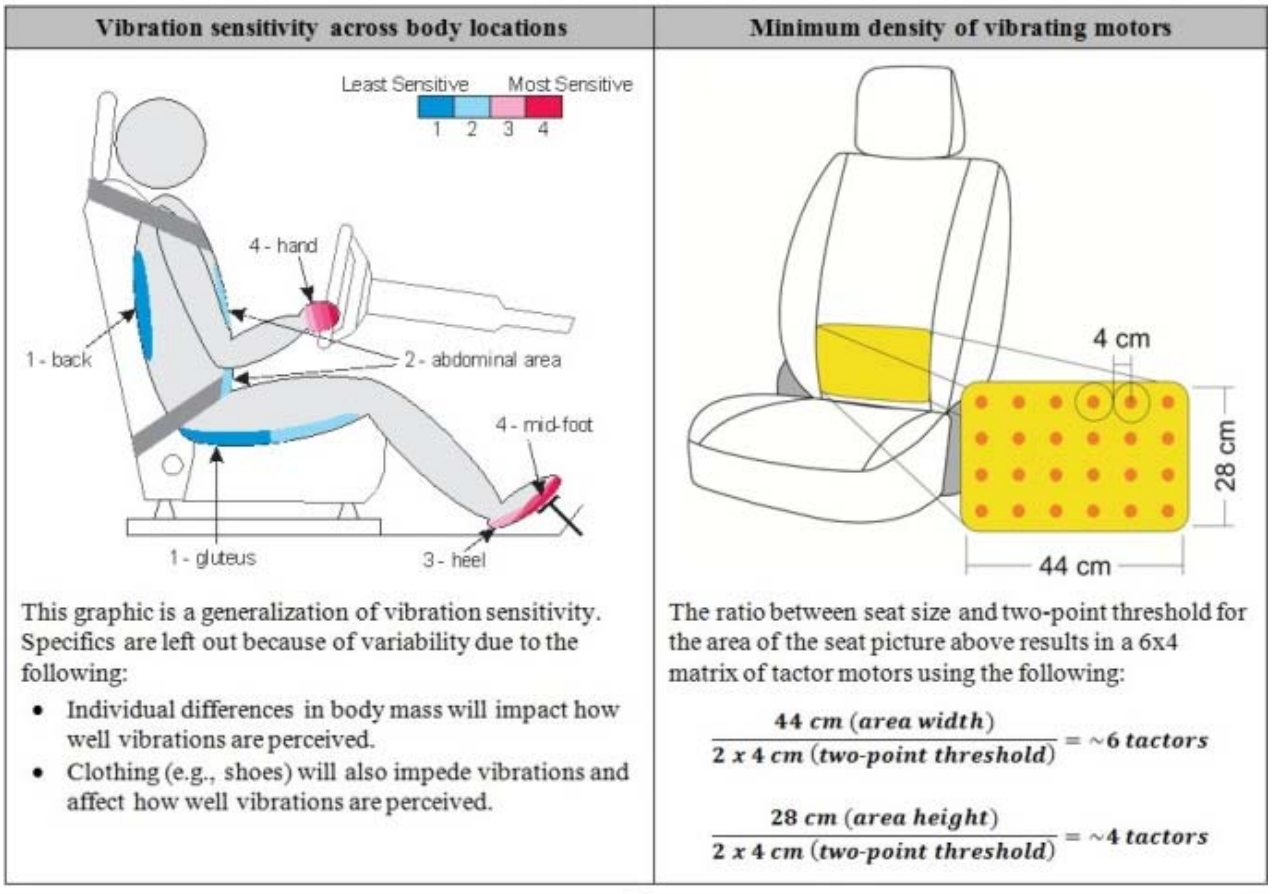


*Figure 5. General Design Assistance for Vibrotactile Displays*

Information on this topic is derived from research on both physiological responses to vibration and vibrotactile message delivery to drivers. As mechanoreceptors are distributed differentially throughout the body, and skin density is not the same across the body, vibrations are felt differently at different body sites. Both basic research and applied research indicate detection of the vibrotactile signal is improved when the vibration intensity corresponds with the physiological sensitivity to vibration.

Generally, drivers perceive increased intensity by either: 1) increasing surface area or number of tactors activated within the surface area, or 2) increasing the amplitude of a constant frequency. A two-point discrimination threshold can be used. Prototype testing using the exact seat to be used with the device is recommended as the threshold will be affected by the fabric, cushioning and other characteristics of the seat.

Additional design issues for consideration include driver familiarity, i.e., most drivers are not used to receiving information via vibrotactile sensation to large body areas such as the gluteus. Using the steering wheel to deliver a haptic cue for lane change warning, for example, would obtain a quicker response due to the correspondence between the warning and the corrective action. Consider also that signals to the hands, while effective sensation-wise, may be less effective when other driver activities using the hands interfere with reception of the signal. Display redundancy can be supported by using larger vibrating surfaces such as the seat.

**Selection of Sensory Modality for Heavy Vehicle Warnings**

This topic discusses how to select an appropriate presentation, such as visual, auditory, or haptic, for use in a heavy vehicle (HV) environment. The nature of heavy vehicle driving creates additional issues to be considered in light of higher visual scanning demands, the long-term exposure to alerts, and passenger needs. The selected DVI modality should be consistent with HV driver tasks, needs, and expectations. Table 1 below provides a summary of the recommendations for CWS functions and control types. In addition:

- Avoid using exclusively visual warnings for imminent collision warnings.
- Use auditory or haptic signals as the primary mode of conveying collision warning information. Use an auditory or haptic signal in conjunction with a visual display to increase warning conspicuity. Auditory signals have been shown to provide effective cautionary and imminent warnings, particularly as part of multimodal warnings.
- The use of haptic signals may be preferred over auditory signals in transit bus applications because they are less obtrusive and less likely to be noticed by passengers. However, haptic signals have additional considerations to ensure they are perceived. Design Assistance for Haptic Displays in Heavy Vehicles in the DVI Design Assistance Document provides issues, caveats, and recommendations associated with using haptic signals in heavy vehicles.

**Table 1.**
**Recommendations and Design Assistance for Collision Warning Systems (CWS) in the Heavy Vehicle Cab**

| CWS Function | Recommendation | Use Discrete Control | Use Continuous Control |
|---|---|---|---|
| **On/Off**<br>Enables and disables the CWS.<br>*Note:* Drivers should be notified of system status for automatic system startup (i.e., ignition activated systems). | Not Recommended | Yes | Not Applicable |
| **Sensitivity (Warning Timing, Warning Threshold, Range, TTC)**<br>Controls the physical or temporal proximity threshold for which warnings are activated. | Neutral Recommendation<br>(i.e., can use if desired).<br>Limited Range of Settings[1] | Yes<br>Between 2 and 6 Sensitivity Settings | Yes<br>Precise Adjustment |
| **Master Intensity**<br>Master control for intensity of all displays within a modality (i.e., visual, auditory, or haptic). May include non-warning displays (e.g., IP brightness). | Recommended<br>Limited Range of Settings[2] | Yes<br>Multi-position | Yes<br>Limited Range |
| **Auditory Intensity**<br>Controls the intensity of the auditory warning signals. | Recommended<br>Limited Range of Settings[2] | Yes<br>Multi-position | Yes<br>Limited Range |
| **Visual Luminance**<br>Controls the intensity of the visual warning signals. | Recommended<br>Limited Range of Settings[2] | Yes<br>Multi-position | Yes<br>Limited Range |

Most current passenger vehicle CWSs allow disablement of the system by drivers; some current HV CWSs do as well. Disablement of the system, however, defeats the purpose of the fleet owner/operator. Additionally, some research notes that most drivers would not disable the system and prefer an integrated CWS system.

Allowing adjustments to CWS systems can accommodate both owner and driver needs. For example, reducing system sensitivity in a cluttered driving environment would correspondingly reduce the frequency of nuisance alarms, although this may mean a delayed alert which would not provide enough time for response. Another example is the decibel level of alarms, which can cause driver annoyance if set too loud. While research indicates that, for a forward imminent-only crash warning, 87dBA was rated appropriately high by 81% of drivers, 15% did not consider it loud enough (Tidwell et al., in press).

These design assistance topics recommend that HV system sensitivity could be reduced temporarily by drivers to mitigate nuisance/false alarms, through duration and frequency of reduction limits, and based on a standard sensitivity setting using empirical analysis of driver response times and vehicle stopping distances. Minimum audible and luminous settings could employ adaptive capability to accommodate varying levels of ambient noise and nighttime or low luminance conditions.

**Involvement of the DVI Design Community**

**Stakeholder Groups** The process for developing the DVI Design Assistance Document included participation of the DVI design community through two stakeholder groups: one for light vehicles and one for heavy vehicles. The stakeholder groups included individuals from OEMs, suppliers, and other industry companies and organizations.

**Information Gathering and Sharing** When each new organization joins a stakeholder group, the first activity they participate in is a User Requirements Analysis. This activity provides: 1) an opportunity to get a better understanding of the organization's needs as end-users, 2) information on how the DVI Design Assistance Document might fit into the design process at the organization, and 3) a first opportunity for an organization to provide feedback on the general content, format, and organization of the document. Other means of communicating and working with stakeholders was through webinars, workshops, and group or individual interviews.

Feedback and input from the community was used to:

- Support development of the content, format, and organization of the DVI Design Assistance,
- Provide insight into the DVI design process at their organization,
- Evaluate preliminary concepts and plans for the materials,
- Suggest additional research studies and source materials, and
- Review and provide comments on draft materials.

Key questions presented to the stakeholders covered all aspects of the final DVI Design Assistance, were organized around four main topics. Below each of the following topics include some of the main issues discussed:

- What content would you find useful?
  - Key needs for human factors information across a range of in-vehicle issues and applications.
  - Requests for design assistance on specific topics.
  - Data sources that we should use to develop the design assistance.
  - When, where, how, and how often the design assistance would be used.
  - Degree to which initial ideas for content meet the information needs of end-users.
- What format would work best?
  - Overall presentation of the V2V DVI Design Assistance Document – how to best achieve clarity, relevance & ease-of-use.
  - Layout of individual sections or topics.
  - Amount of text vs. non-text elements.
  - Flow and structure of text portions.
  - Use of graphics, figures, and tables.
  - Length and consistency of individual sections or elements.
  - Presentation of constraints and trade-offs.
  - Presentation of supporting materials.
- How would you like to see the information organized?
  - End-user ideas and preferences for overall organization of the materials.
  - Degree to which final organization of the V2V DVI Design Assistance Document:
    - Matches the design process.
    - Matches information needs.
    - Facilitates understanding of the design assistance.
    - Facilitates overall ease-of-use.
- When and how would this information be used within your organization?
  - During initial specification of the driver-vehicle interface
  - During testing and evaluation
  - During a final quality check

**CONCLUSIONS**

The V2V DVI Design Assistance Document provides a set of 52 human factors design assistance for driver-vehicle interfaces (DVIs) of systems for V2V communication. The design assistance are based on the findings of current high-quality research (including both the best-available scientific literature, and current research being conducted by agencies of the United States Department of Transportation), as well as basic human factors concepts. These design assistance are provided as a tool and a complementary resource to other documents and resources, as well as an expansion to industry research and existing guidance from the National Highway Traffic Safety Administration. The information within this document may be useful to researchers, designers, and original equipment manufacturers and Tier-1 suppliers seeking to ensure that V2V DVIs are designed to better reflect driver limitations and capabilities.

**Discussion and Limitations**

While DVI design assistance topics such as these can be a valuable tool and resource for designers, they are not without limitations. Many factors must be considered, and tradeoffs examined, prior to finalizing a DVI design. Some of these factors include regulation and industry or international standards. These design assistance topics are intended to support developers as they design DVIs for V2V communication systems. Note that this document is not meant to serve as a standard or design guideline. Resources such as Federal Motor Vehicle Safety Standards (FMVSS), SAE and ISO standards, and the Visual-Manual NHTSA Driver Distraction Guidelines for In-Vehicle Electronic Devices (NHTSA, 2013) exist that provide design guidance for DVIs. Instead, this document it is meant to serve as a complementary resource for original equipment manufacturers (OEMs), Tier-1 suppliers, and the automotive research community in designing V2V DVIs that enable rapid, consistent, and reliable communication between the vehicle and driver.

**REFERENCES**


Baldwin, C. L. & May, J. F. (2011). Loudness interacts with semantics in auditory warnings to impact rear-end collisions. *Transportation Research Part F: Traffic Psychology and Behaviour, 14*(1), 36-42.

Guilluame, A., Drake, C., Rivenez, M., Pellieux, L., & Chastres, V. (2002). Perception of urgency and alarm design. *Proceedings of the 8th International Conference on Auditory Display*.

International Organization for Standardization (ISO) (1984). *Development and principles for application of public information symbols.* (ISO/TR 7239). Geneva: Author.

Tidwell, S.A., Blanco, M., Trimble, T., Atwood, J., & Morgan, J.F. (in press). *Evaluation of heavy vehicle crash warning interfaces* (Report No. DOT HS XXX XXX). Washington, DC: National Highway Traffic Safety Administration.

# MITIGATING DROWSINESS: LINKING DETECTION TO MITIGATION

**Chris Schwarz**

**Timothy L. Brown**

**John Gaspar**

**Dawn Marshall**

The University of Iowa

USA

**John Lee**

The University of Wisconsin

USA

**Satoshi Kitazaki**

The University of Iowa

USA

**Julie Kang**

National Highway Traffic Safety Administration

USA

Paper Number 15-0453

ABSTRACT

Drowsy driving contributes towards up to 24% of crashes and near crashes observed; 886 fatal crashes per year can be attributed to drowsy, fatigued or sleeping drivers. Drowsiness mitigation technology is composed of a detection algorithm and a mitigation component. This paper is primarily concerned with the latter, specifically for a driving simulation study about mitigating drowsy driving. The study is part of NHTSA's Driver Monitoring of Inattention and Impairment using Vehicle Equipment (DrIIVE) program. The detection algorithm incorporates time series probabilistic estimation using a Hidden Markov Model, so a drowsiness prediction at any time is dependent on a previous history of observations. Two mitigation methods are designed for testing in the simulation study. One is a three stage audio/visual alert that requires a driver response through a button press. The second is a binary haptic alert that uses a vibrating seat. Additionally, each mitigation will include three varying levels of sensitivity: a nominal model, an over-sensitive model, and an under-sensitive model. These variations will expose drivers to different numbers of false alarms while also potentially missing episodes of drowsiness. Various parameters in the detection algorithm were tested and the vote thresholds of two Random Forest models were selected for variation. It was observed how these parameters affected the output of the detection and mitigation system using previously collected drowsy driving data. Three specific levels were chosen as candidates for the experiment. It is hoped that the study will answer questions about how effective a mitigation system is at changing driving performance, whether drivers willfully ignore the mitigation, and how many alerts are too many.

## INTRODUCTION

The National Highway Traffic Safety Administration (NHTSA) estimates that 83,000 crashes per year and 886 fatal crashes per year can be attributed to drowsy, fatigued, or sleeping drivers (NHTSA, 2011). The 100-car naturalistic driving study found that drowsy driving contributed to 22% to 24% of crashes and near-crashes observed (Klauer, Dingus, Neale, Sudweeks, & Ramsey, 2006). Other studies suggest that despite known dangers many drivers continue to drive drowsy and fall asleep behind the wheel (MacLean, Davies, & Thiele, 2003; McCartt, Rohrbaugh, Hammer, & Fuller, 2000). Technology may be able to address some of these risks.

Drowsiness mitigation technology consists of two subsystems, a drowsiness detection system and a driver feedback system. The drowsiness detection system or algorithm collects data from the driver or vehicle, processes this data with a detection algorithm, and makes predictions about the alertness of the driver. The feedback system activates when the detection system predicts that the driver is drowsy and alerts the driver in order to prevent a drowsiness related crash. With some exceptions, research on drowsiness mitigation technology has largely focused on the detection algorithm. This piece of the system is critical because it strongly influences drivers' trust and reliance on the mitigation technology and constrains the design space of the feedback system (Balkin, Horrey, Graeber, Czeisler, & Dinges, 2011).

Research on drowsiness detection algorithms can be differentiated by the input data, prediction algorithm, and ground truth definition of drowsiness. Input data typically consists of camera-based eye measures (Dinges & Grace, 1998; Grace et al., 1996; Ji, Zhu, & Lan, 2004), electric potential measures from the brain (Lal, Craig, Boord, Kirkup, & Nguyen, 2003; Lin et al., 2005; Wali, Murugappan, & Ahmmad, 2013), or driver input to the vehicle such as steering wheel angle (Krajewski & Sommer, 2009; McDonald, Lee, Schwarz, & Brown, 2013a; Sayed & Eskandarian, 2001). Prediction algorithms vary from simple thresholds (Dinges & Grace, 1998), to more complex graphical models (Ji et al., 2004). The ground truth definitions also vary between studies and range from general levels of drowsiness associated with lack of sleep (Sayed & Eskandarian, 2001; J. H. Yang, Tijerina, Pilutti, Coughlin, & Feron, 2009), to more episodic measures of drowsiness such as drowsiness-related lane departures (McDonald et al., 2013a). Recent research primarily focuses on innovations in the prediction algorithm dimension. One prominent development in this dimension is a transition from static prediction algorithms to time-based prediction algorithms (Ji, Lan, & Looney, 2006; G. Yang, Lin, & Bhattacharya, 2010; J. H. Yang et al., 2009). These time-based prediction algorithms allow predictions to account for well-understood temporal effects of drowsiness: for example, a drowsy driver is likely to stay drowsy and an alert driver is likely to stay alert. Additionally, they can be built around previously non-temporal (or static) algorithms to improve predictions (Ji et al., 2006, 2004). The success of these algorithms and their strong basis in the theory of drowsy driving suggests that it could be helpful to enhance other non-temporal models by incorporating them into temporal frameworks.

Mitigation systems are the critical link between the detection system and influencing driver behavior. While the detection system aims to accurately assess driver state, the aim of the mitigation system is to present driver state information to the driver in a way that is likely to persuade the driver to make choices that improve safety. This process involves the translation of the raw detection system outputs for use by the mitigation system. These systems can theoretically take many forms, from a simple audible chime or visual icon to more complex displays that relay different levels of performance or instruction to the driver. Although the same algorithm might be used across systems, the type of the interface will dictate the required adaptation of the raw data.

The topic of this paper is the design of a mitigation system to provide feedback to the driver about the system's perception of their state of drowsiness. The mitigation system should help the driver become more aware of their drowsiness. In the short term, it may help them to improve their driving performance; however, the ultimate desired effect would be to cause them to pause their trip and take a rest.

There are several drowsiness alert systems on the market currently (see Figure 1). Many are binary alerts that display a coffee cup icon and play a chime when the alert is triggered. Some systems attempt to provide a more continuous, or at least multi-level discrete, scale of drowsiness to the driver. Some systems require the driver to press a button to acknowledge the alert.

***Figure 1. Example Mitigation interfaces from Volvo, Mercedes-Benz and Ford***

## PRIOR WORK

The NHTSA DrIIVE program focuses on the detection and mitigation of driver impairment from drowsiness and distraction. Several models were generated in phase 1 of the DrIIVE program, including a Bayesian Network, a time-to-lane-crossing (TLC) model, and a Random Forest model based on steering wheel angle (McDonald, Lee, Schwarz, & Brown, 2013b). A Random Forest model that incorporates temporal steering information into a static algorithm was trained on drowsy lane departure data (2013a), (Brown, Lee, Schwarz, Fiorentino, & McDonald, 2014).

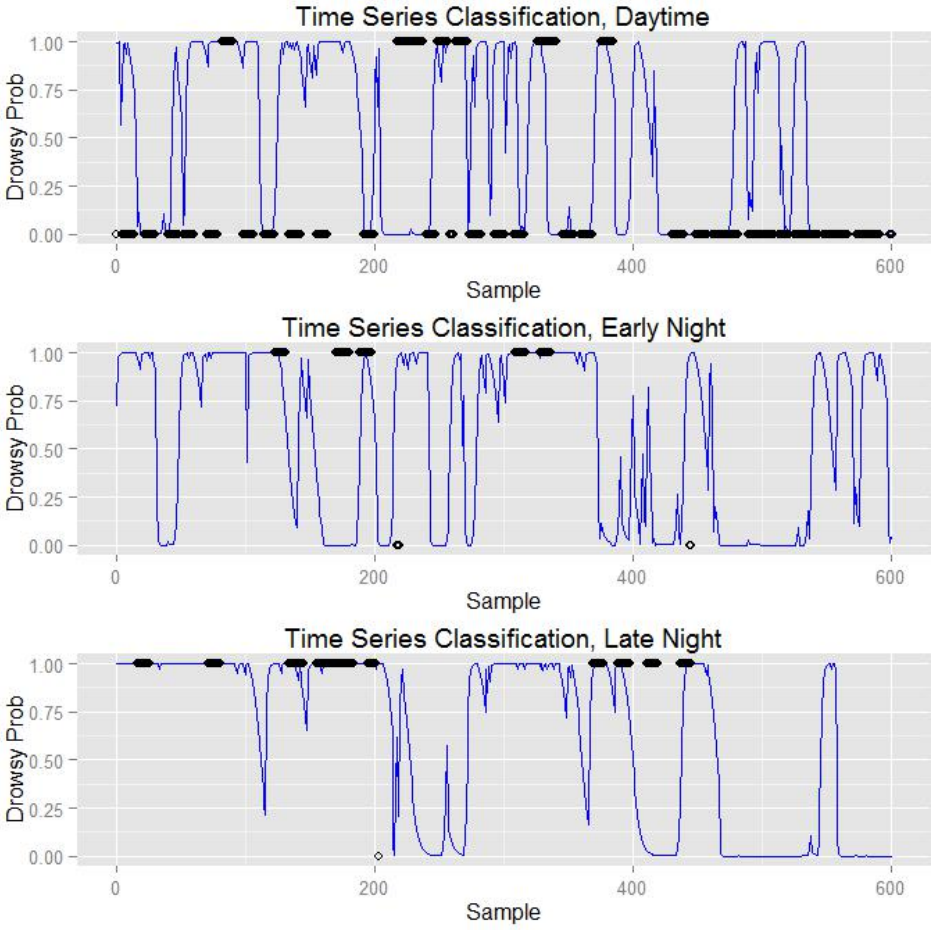


***Figure 2. Example Time Series: ground truth markers and drowsiness HMM output***

This initial algorithm was then extended by placing the static steering algorithm into a temporal prediction framework and exploring the effect of this approach on the timeliness of the detection algorithm (Schwarz,

McDonald, Lee, & Brown, *submitted*). The enhancements produced a set of Random Forest (RF) models that were fed into a Hidden Markov Model (HMM) capable of capturing the heuristic that an awake driver is more likely to remain awake in the near future, while a drowsy driver is likely to remain drowsy.

The Random Forest models were trained in the open source statistical software R (R Development Core Team, 2009) using the caret package (Kuhn, 2008). Normally, a classification is inferred using an RF model by running all the decision trees and using the majority vote as the output. However, if one keeps track of the vote count for each instance the model is run, then the vote count can be used as the continuous predictor in a Receiver Operator Characteristics (ROC) analysis. Then, an optimal threshold on the vote count may be computed from the ROC curve using Youden's Index (Powers, 2007). An optimal set of RF models was produced using vote thresholds of 162 votes for the steering RF model and 151 votes for the pedals RF model, where all RF models had 500 decision trees.

A Hidden Markov Model (HMM) was designed to include the effect of historical observations and accept inputs from the RF models, and was trained using the HMM library in R (Himmelmann, 2010). A regular time interval of six seconds is selected as the model frequency. Two pieces of evidence are provided, one from the steering RF classification, and the other from the pedal RF classification. The output of the HMM, shown in Figure 2 is compared to a threshold to classify each time sample as a drowsy or awake. The threshold value was selected from an ROC curve to be 0.74. The RF models along with the HMM complete the drowsiness detection algorithm.

METHOD

Two mitigation systems were designed for use as between subject conditions in a new drowsiness mitigation study. The first is a three stage audio/visual alert with driver interaction through a button. The second is a binary haptic alert that vibrates the driver's seat. Three levels of the drowsiness detection system are included in the experimental design as a between-subjects dependent variable. The three levels will include a nominal design, a design that is more sensitive, and one that is less sensitive. These levels will expose drivers to different numbers of false alerts, while perhaps also failing to detect the drowsiness in some cases.

**MITIGATION DESCRIPTIONS**

The audio-visual alert is a three stage warning. The threshold value used to trigger each stage is the same for each stage. If drowsiness is detected while in the nominal state of no mitigation, then a stage 1 warning is issued. This warning is a white coffee cup icon with an OK button for driver acknowledgement (Figure 3a) and an audio chime that plays when the icon appears. Once the driver presses the button, the icon is removed. The mitigation will remain in stage 1 for a minimum period of time; and during that time the detection algorithm may remain in a classification of drowsy state or return to an awake state. If the detection algorithm classification returns to awake, then the mitigation will abate after a fixed delay. However, if another drowsy episode is detected before the mitigation abates, or the drowsy state persists for 60 seconds, then the mitigation escalates to stage 2. On entry into stage 2, a stage 2 warning is issued using the visual icon in Figure 3b along with an audio beep. This icon is removed once the driver acknowledges the warning with a button press. Exactly the same logic is applied during stage 2 until the mitigation either abates back to stage 1 or escalates to stage 3. A stage 3 alert consists of the icon in Figure 3c, and a repeated audio beep. There cannot be any more escalations from stage 3, but the warning may be reissued if the drowsy state persists or soon repeats. Only incremental escalations and abatements are allowed. This mitigation has the chance to capture the driver's attention by varying the stimulus on repeated warnings; but it also has the potential to be a nuisance to a driver who is already self-aware or not drowsy.

The haptic alert is a binary alert system that provides a counterpoint to the three stage alert. It also differs in modality by providing a haptic alert through seat vibration, thus making it a more subtle, and potentially less annoying, cue. The same logic for stage escalation is applied in the binary alert to either trigger the initial alert or repeat it after 60 seconds. Once the drowsy detection expires, the mitigation naturally abates back to the nominal driving state.

## MITIGATION SENSITIVITY MANIPULATIONS

A significant question addressed in this paper is: how can we vary the sensitivity of the algorithm / mitigation system? Random Forest models are especially opaque and little intuition about why a given parameter set works is available to the designer. Hidden Markov models are slightly easier to intuit, but are nonetheless complicated. There are several choices that were considered, most of which were either discarded or found to not have a significant effect upon the final outcome of the classification and mitigation performance. The Random Forest models are considered first.

(a) (b) (c)

***Figure 3. Visual Mitigation Icons: (a) stage 1 interactive, (b) stage 2 interactive, (c) stage 3 interactive***

Two Random Forest models are used in the drowsiness detection algorithm, one for steering and one for pedals. Each Random Forest is composed of 500 decision trees; and each decision tree may have on the order of 100 nodes. Therefore, it is not feasible to try to tune those parameters individually. One could think about a strategy of retraining new RF models with the intent of changing the sensitivity; but then there may be other performance differences between them that are confounded with sensitivity. The other parameter one can think about tuning is the voting threshold for output classification. Normally, RF models are majority rule, meaning that more than 250 trees in a 500 tree RF would have to agree to set a class output. This vote threshold number may be allowed to vary and we used it as a threshold variable in an ROC analysis in our prior modeling work. The lower the value of the vote threshold, the more trees potentially need to be run to gather up the required number of votes, thus potentially increasing the computational demand of the model by some small amount. For example, with a threshold of 100, one may have to evaluate as many of 400 of the trees to guarantee that there are not 100 votes for drowsiness.

Hidden Markov Models have fewer parameters than RF models and they are more intuitive than trying to tune a decision tree. The state transition probabilities set the probability of an HMM changing state from awake to drowsy or vice-versa at any time step. The probabilities in each direction can be set independently. The emission probabilities set the chances that any of the observed variables of the HMM, or combinations thereof, indicate the value of the state. The state transition model is the base of the HMM with the prior probabilities, while the emission model conditions the state transitions with the presence of evidence. We estimated values for the emissions probabilities by counting the presence of RF model classification and their likelihood of correlating with a drowsy driving ground truth state. The final parameter that could be varied is the threshold we apply to the posterior probability, the output of the HMM, to set a final classification for the detection algorithm.

We chose not to attempt to tune the emission probabilities, for essentially the same reason we did not tune each decision tree. It would change the characteristics of the model and defeat the purpose of the machine learning training routines that optimize model parameters. We experimented with varying the state transition probabilities, the effect of which is similar to that of changing a low pass filter cutoff frequency that is filtering the HMM output (Figure 2). A lower transition probability will produce a more filtered signal that has a longer rise (or fall) time. Ultimately, the effect of varying these probabilities, while measurable, did not effect a significant change in the algorithm output.

Similarly, we explored the final HMM threshold value. This value was obtained previously as the optimal operating point on an ROC curve obtained after a model optimization process conducted on the RF and HMM models. This parameter is the easiest to understand, effectively dividing Figure 2 into an upper and a lower region that corresponds to drowsy and awake predictions, respectively. Unfortunately, the variation of this last threshold has the least effect out of all the parameter tuning that was tried. This is likely because most state transitions changed the posterior probability all the way from zero to one and vice versa. The number of cases where a transition changed direction partway was fewer than one might have expected. In that situation, we can only shift the edges of the state transition by a few seconds by varying the output threshold.

The parameters that had the greatest effect on the drowsiness detection algorithm were the vote thresholds of the two RF models. An RF model with a higher vote threshold simply requires more of its constituent decision trees to agree on the output classification. Setting this threshold above the majority value may be problematic because it may then be that neither class gathers enough votes to meet the threshold. Ten levels of parameters for the RF vote thresholds were set. Values for the Steer RF model are: {162, 170, 180, 190, 200, 210, 220, 230, 240, 250}. Values for the Brake RF are: {151, 160, 170, 180, 190, 200, 210, 220, 230, 240}. The parameters are always varied together, not independently. Level one values correspond to the optimal threshold obtained in prior work to optimize the ROC curve indicators of model performance. The subsequent levels step up the values of each threshold until the steering RF value reaches majority rule. Notice that the relationship between the two values is essentially maintained through the levels such that the steer RF threshold is always greater than the brake RF.

This particular range of parameters fits nicely with the goals of our model variation exercise. The optimal values gave the best performance when compared to the awake and drowsy ground truth data points; however, the majority of time history samples are not associated with any ground truth because there was no lane departure. Therefore, the algorithm performance at these points is difficult to judge. We did observe however, that many of these in-between points are classified as drowsy and thus contribute to the overall number of mitigation warnings. We would therefore consider this parameter set as being on the sensitive side. To make the models less sensitive, we wish to make it harder for the RF models to issue drowsy classifications, which means requiring more models to agree on drowsiness. Therefore we increase the values of the vote thresholds up to the majority rule value, but no further.

The different levels of RF models were run on the DrIIVE Phase I drowsiness data with all other parts of the detection algorithm held constant. Some simple metrics were calculated on the detection / mitigation system in order to compare across levels. A mitigation was considered to be in a ‘correct’ stage at each ground truth data point if it was in stage 0 (no mitigation) at an awake point or in any stage of mitigation at a drowsy point.

The system was designed to operate at speeds greater than 40 mph, so the percentage of time that the vehicle was traveling faster than this limit was calculated as a reference for other measures. A variable, *timeAtSpeed*, was calculated as the amount of time in the drive that the car was traveling above this limit. A variable, *timeInMitigation*, was calculated as the amount of time that the mitigation system was in any mitigation stage. Then a normalized measure was calculated as

$$Time\ in\ Mitigation\ (\%) = \frac{timeInMitigation}{timeAtSpeed} \times 100$$

Confining ourselves to only those samples with ground truth data, we counted which of those points were in the ‘correct’ stage of mitigation, as described above. This may be expressed in an indicator variable, $I_C$, of zeros and ones of length $N$, where $N$ is the number of ground truth points in a drive. The percentage of correctly mitigated ground truth points was then computed in each drive as

$$Accuracy\ (\%) = \frac{100}{N} \sum_{1}^{N} I_C$$

This coarse metric does not indicate whether a ground truth data point falls in the first or last part of a mitigation, nor which stage of mitigation is active, nor whether an incorrectly mitigated ground truth point falls just before or after a period of mitigation. The accuracy metric, together with the time-in-mitigation metric, provide an idea of how parametric variations affect the output of the detection / mitigation system, and create a tradeoff between sensitivity and accuracy.

RESULTS

Ten levels of vote thresholds for the Steer RF and Pedals RF model were tested on the DrIIVE Phase I drowsiness data, which was all collected in unmitigated conditions. Both the three stage audio-visual mitigation as well as the binary haptic mitigation were run on each drive in the three conditions of that study: Day, Early Night, and Late Night. Since it was not possible to provide human interaction with the button response, an automatic button response was programmed after one second; therefore, the simulations do not account for unresponsive drivers.

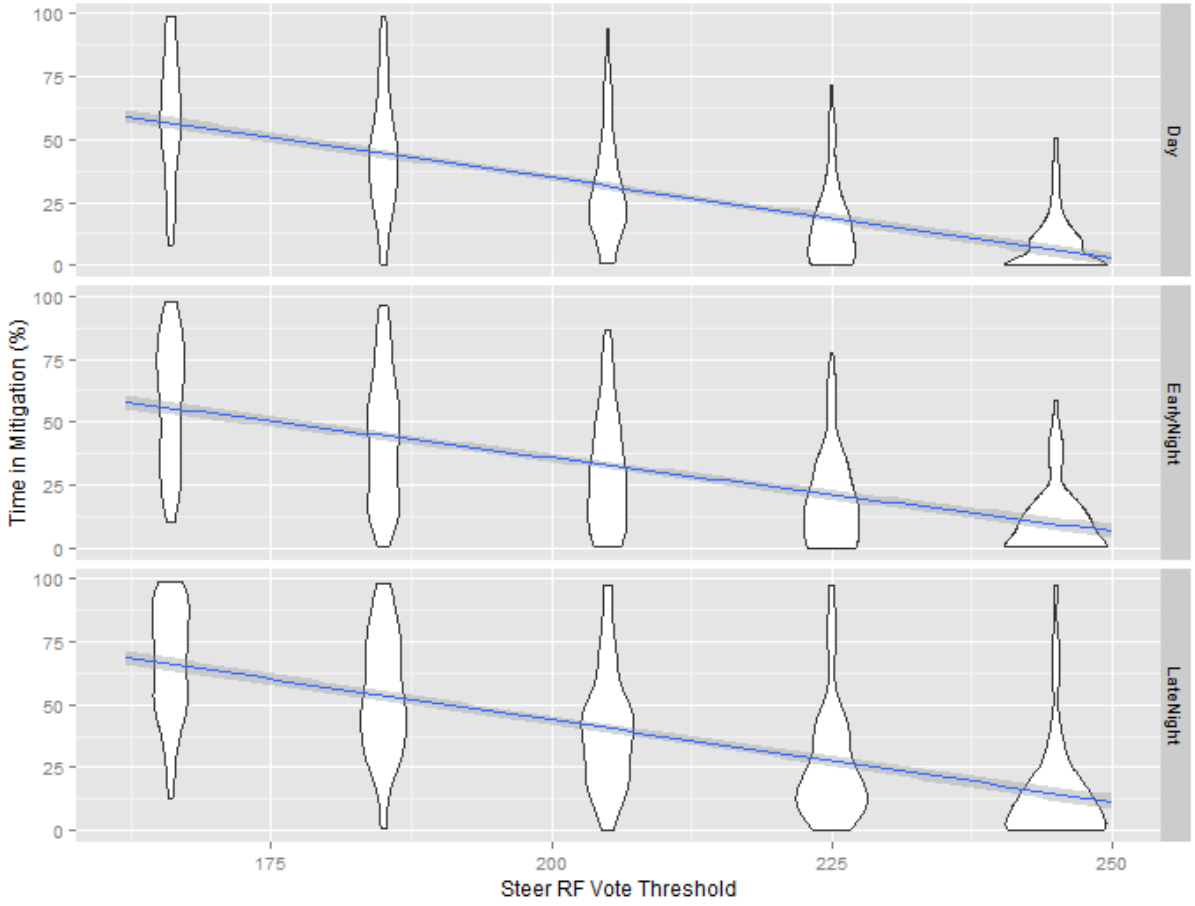


***Figure 4. Violin plot and linear fit of the percentage of time in a drive that the mitigation is active for the audio/visual alert mode***

The Time in Mitigation and Accuracy metrics are displayed for the three stage mitigation in Figure 4 and Figure 5, respectively. These figures show an overlay of a violin plot with a line fit, the latter with confidence intervals represented by a gray band. A violin plot shows information similar to a box plot, but shapes the sides of each 'box' according to the probability density of the sample points (Hintze & Nelson, 1998). The wider the shape is, the denser the points are at that location in the plot. The ggplot2 library (Wickhan, 2009) in R was used to generate the plots; and the plotting function was allowed to bin the horizontal axis from ten levels into just five bins, making the figure somewhat less dense and easier to comprehend.

The violin plot in Figure 4 shows the density of samples of the Time in Mitigation measure decreases as the vote threshold increases. This result holds across all three conditions and is completely intuitive. As more votes are required for the RF models to issue drowsy classifications, it becomes more difficult for the algorithm to transition into the drowsy state; and less time is spent in all stages of mitigation. The time in

mitigation at level ten for the Day, Early Night, and Late Night conditions is approximately 5%, 10%, and 12% respectively.

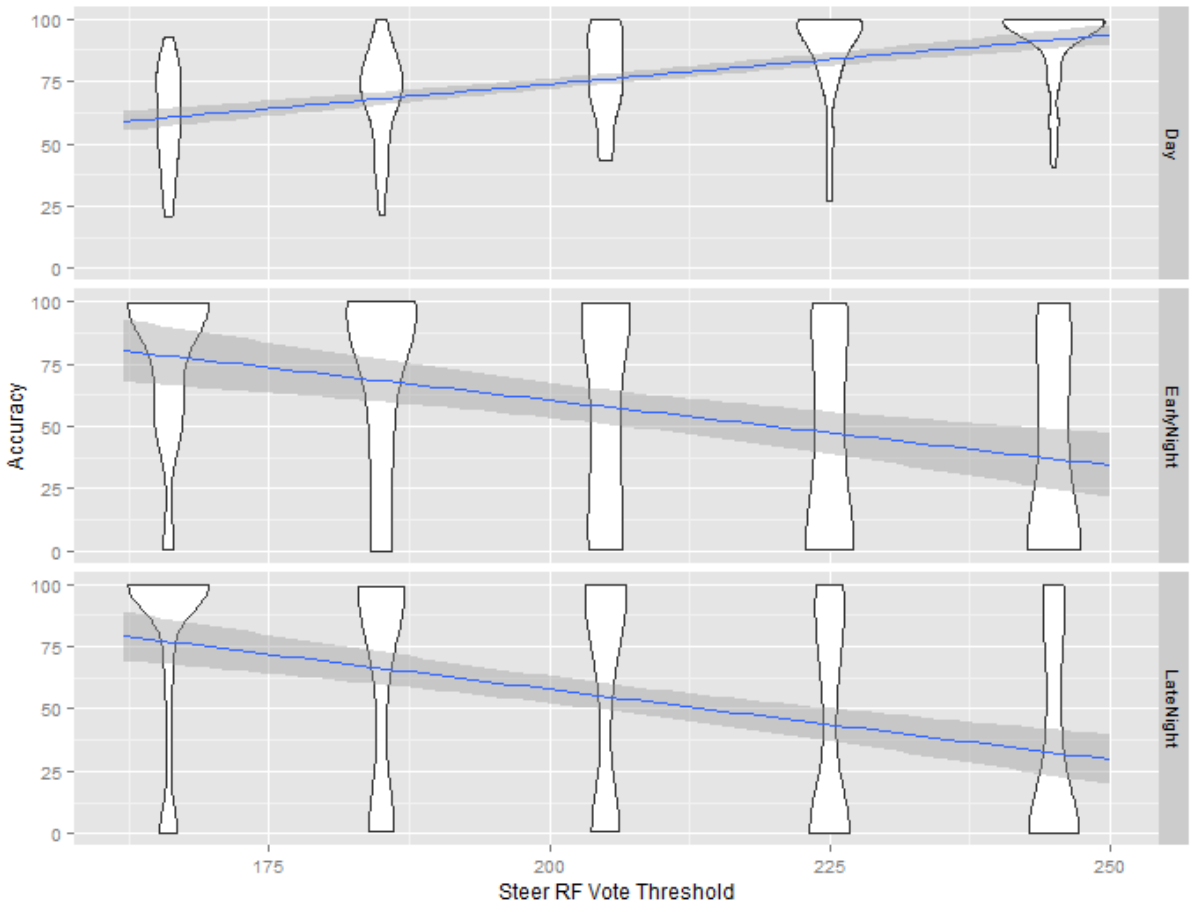


***Figure 5. Violin plot and linear fit of the percentage of ground truth points that are correctly mitigated for the audio/visual alert mode***

The violin plot in Figure 5 shows the density of samples of varying Accuracy as a function of the Steer RF vote threshold. The line fit serves to make clear the shift in the density of samples as the vote thresholds are increased. The accuracy in the Day condition actually rises as the RF models become more conservative. The explanation for this result is that almost all of the ground truth points in the Day conditions are awake points. Then it becomes clear that a simplistic approach of turning off the mitigation altogether would increase the accuracy in this condition to almost 100%. On the other hand, the accuracy is seen to drop for both night conditions as the vote threshold is increased, as expected. At the far end of the test, where vote thresholds for steering and pedals are 250 and 240 respectively, the estimated accuracy in the Day, Early Night, and Late Night conditions is 90%, 38%, and 30% respectively.

A similar pattern of results was obtained for the binary haptic mitigation, though the haptic system had smaller overall values for the Time in Mitigation metric. The different logic of the binary mitigation as compared to the more complex three-stage system result in less time spent in mitigation.

**THREE SENSITIVITY LEVELS**

The drowsiness mitigation study will have Early Night and Late Night conditions, but will not include Day drives. However three levels of sensitivity will be designed for each of the two mitigation types. Previous work resulted in trained models and an ROC curve evaluation of the models to optimize a drowsiness detection

algorithm. This 'optimal' model corresponds to the level one parameter set described in this paper. As discussed earlier, that optimization only considered ground truth points and classifications on in-between points were not part of the evaluation. In reality, the in-between samples make up a majority of the data in most drives and therefore contribute significantly to the number of mitigation alerts. All three conditions were in some stage of mitigation over half the time, which is especially surprising for the Day condition.

A commercial system would most likely condition the algorithm output on other factors such as time of day, driving style, traffic density, and perhaps other variables. Since we are not collecting additional Day drives, conditioning by day/night is not necessary at this time. Three mitigation models were selected for the two modalities with the purpose of obtaining a wide spread in the *timeInMitigation* and *accuracy* metrics. The starting point was to choose three target accuracy values. Those values then mapped to corresponding time in mitigation and RF model vote thresholds. The values selected for the three models are summarized in Table 1. These models are spaced far enough apart that they offer a clear distinction to the drivers who experience them.

***Table 1. Three levels of mitigation selected using Late Night data for audio/visual and haptic modes***

| Level | Steer RF Votes | | Pedal RF Votes | | Time in Mitigation (%) | | Accuracy (%) | |
|---|---|---|---|---|---|---|---|---|
| | Visual | Haptic | Visual | Haptic | Visual | Haptic | Visual | Haptic |
| Over sensitive | 170 | 162 | 160 | 151 | 63 | 40 | 75 | 70 |
| Nominal | 190 | 175 | 180 | 165 | 50 | 38 | 63 | 63 |
| Under-sensitive | 215 | 195 | 205 | 185 | 38 | 30 | 50 | 50 |

## CONCLUSIONS

Two mitigation systems, a three stage audio/visual and a binary haptic, were designed to use the output of a previously designed drowsiness detection algorithm. Additionally, three levels of each system were obtained to provide a good range of system sensitivity to drowsiness. In this way, a range of false alarm rates will be generated from the study and questions about the effectiveness of the mitigation might be differentiated from questions about the nuisance factor of the mitigation alerts.

The ultimate desired outcome for a drowsiness mitigation system is that the driver would realize their own impairment and pause the trip to rest. Such an outcome is not allowed for however in the protocol of the simulator experiment. On the other hand, a primary interest of the DrIIVE program is to study vehicle-based measures of impairment. Having determined that such measures are useful for classifying drowsiness, the data from the upcoming study may be used to test whether a mitigation system also causes detectable differences in driving performance as measured by vehicle-based sensors.

REFERENCES


Balkin, T. J., Horrey, W. J., Graeber, R. C., Czeisler, C. A., Dinges, D. F. (2011). The challenges and opportunities of technological approaches to fatigue management. *Accident Analysis & Prevention*, *43*(2), 565–72.

Brown, T., Lee, J., Schwarz, C., Fiorentino, D., McDonald, A. (2014). *Assessing the Feasibility of Vehicle-based Sensors to Detect Drowsy Driving* (Final Report No. DOT HS 811 886). Washington, DC: NHTSA.

Dinges, D. F., & Grace, R. (1998). *PERCLOS: A valid psychophysiological measure of alertness as assessed by psychomotor vigilance. Federal Highway Administration*. Washington D.C.

Grace, R., Byrne, V. E., Bierman, D. M., Legrand, J.-M., Gricourt, D., Davis, B. K., Carnahan, B. (1996). A drowsy driver detection system for heavy vehicles. In *17th DASC. AIAA/IEEE/SAE. Digital Avionics Systems Conference. Proceedings,* Vol. 2, pp. I36/1–I36/8.

Himmelmann, L. (2010). HMM: HMM - Hidden Markov Models (Version 1.0). Retrieved from http://cran.r-project.org/web/packages/HMM/index.html

Hintze, J. L., & Nelson, R. D. (1998). Violin Plots: A Box Plot-Density Trace Synergism. *The American Statistician*, *52*(2), 181–184.

Ji, Q., Lan, P., & Looney, C. (2006). A probabilistic framework for modeling and real-time monitoring human fatigue. *IEEE Transactions on Systems, Man, and Cybernetics - Part A: Systems and Humans*, *36*(5), 862–875.

Ji, Q., Zhu, Z., & Lan, P. (2004). Real-Time Nonintrusive Monitoring and Prediction of Driver Fatigue. *IEEE Transactions on Vehicular Technology*, *53*(4), 1052–1068.

Klauer, S., Dingus, T., Neale, V., Sudweeks, J., Ramsey, D. (2006). *The impact of driver inattention on near-crash/crash risk: An analysis using the 100-car naturalistic driving study data. Analysis*. (Report No. DOT HS 810 594). Washington D.C.: National Highway Traffic Safety Administration.

Krajewski, J., & Sommer, D. (2009). Steering wheel behavior based estimation of fatigue. In *Proceedings of the 5th International Driving Symposium on Human Factors in Driver Assessment and Design* (pp. 118–124).

Kuhn, M. (2008). Building Predictive Models in R Using the caret Package. *Journal of Statistical Software*, *28*(5).

Lal, S. K. L., Craig, A., Boord, P., Kirkup, L., Nguyen, H. (2003). Development of an algorithm for an EEG-based driver fatigue countermeasure. *Journal of Safety Research*, *34*(3), 321–328.

Lin, C., Wu, R., Liang, S., Chao, W., Chen, Y., Jung, T. (2005). EEG-based drowsiness estimation for safety driving using independent component analysis. *IEEE Transactions on Circuits and Systems I: Regular Papers*, *52*(12), 2726–2738.

MacLean, A. W., Davies, D. R. ., Thiele, K. (2003). The hazards and prevention of driving while sleepy. *Sleep Medicine Reviews*, *7*(6), 507–521.

McCartt, A. T., Rohrbaugh, J. W., Hammer, M. C., Fuller, S. Z. (2000). Factors associated with falling asleep at the wheel among long-distance truck drivers. *Accident Analysis & Prevention*, *32*(4), 493–504.

McDonald, A. D., Lee, J. D., Schwarz, C., Brown, T. L. (2013a). Steering in a Random Forest: Ensemble Learning for Detecting Drowsiness-Related Lane Departures. *Human Factors: The Journal of the Human Factors and Ergonomics Society*.

McDonald, A. D., Lee, J. D., Schwarz, C., Brown, T. L. (2013b). Steering in a Random Forest Ensemble Learning for Detecting Drowsiness-Related Lane Departures. *Human Factors: The Journal of the Human Factors and Ergonomics Society*.

NHTSA. (2011). *Drowsy Driving* (Traffic Safety Facts No. DOT HS 811 449). Washington, DC: NHTSA.

Powers, D. M. W. (2007). *Evaluation: From Precision, Recall and F-Factor to ROC, Informedness, Markedness & Correlation* (Technical Report No. SIE-07-001). Adelaide, Australia: Flinders University.

R Development Core Team. (2009). *{R: A language and environment for statistical computing}*. Vienna, Austria: R Foundation for Statistical Computing.

Sayed, R., & Eskandarian, A. (2001). Unobtrusive drowsiness detection by neural network learning of driver steering. *Proceedings of the Institution of Mechanical Engineers, Part D: Journal of Automobile Engineering*, *215*(9), 969–975.

Schwarz, C., McDonald, A., Lee, J. D., & Brown, T. L. (submitted). Time Series Classification of Drowsiness from Driving Input Signals. *IEEE Journal on Intelligent Transportation Systems*.

Wali, M., Murugappan, M., & Ahmmad, B. (2013). Wavelet Packet Transform Based Driver Distraction Level Classification Using EEG. *Mathematical Problems in Engineering*.

Wickhan, H. (2009). *ggplot2: elegant graphics for data analysis*. New York: Springer.

Yang, G., Lin, Y., & Bhattacharya, P. (2010). A driver fatigue recognition model based on information fusion and dynamic Bayesian network. *Information Sciences*, *180*(10), 1942–1954.

Yang, J. H., Tijerina, L., Pilutti, T., Coughlin, J. F., Feron, E. (2009). Detection of Driver Fatigue Caused by Sleep Deprivation. *IEEE Transactions on Systems, Man, and Cybernetics - Part A: Systems and Humans*, *39*(4), 694–705.

**An Overview of NHTSA's Electronics Reliability and Cybersecurity Research Programs**

Authors(s): Arthur Carter, David Freeman, and Cem Hatipoglu

National Highway Traffic Safety Administration (NHTSA)

**Paper ID 15-0454**

**Abstract**

This paper provides an overview of the National Highway Traffic Safety Administration's (NHTSA) research programs in electronic control systems reliability and automotive cybersecurity. The agency's electronics reliability research covers methods and voluntary standards both inside and outside the automotive industry. The research looks for such standards and methods that assess, identify, and mitigate potential new hazards that may arise from the increasing use of electronics and electronic control systems in the design of modern automobiles. Cybersecurity, within the context of road vehicles, is the protection of vehicular electronic systems, communication networks, control algorithms, software, users, and underlying data from malicious attacks, damage, unauthorized access, or manipulation.

## BACKGROUND

### NHTSA's safety role

NHTSA is responsible for developing, setting, and enforcing regulations for motor vehicles and motor vehicle equipment. Many of the agency's regulations are Federal Motor Vehicle Safety Standards (FMVSSs) with which manufacturers must self-certify compliance when offering motor vehicles and motor vehicle equipment for sale in the United States. NHTSA also studies behaviors and attitudes in highway safety, focusing on drivers, passengers, pedestrians, and motorcyclists. Additionally, NHTSA identifies and measures behaviors involved in crashes or associated with injuries, and working with States and other partners develop and refine countermeasures to deter unsafe behaviors and promote safe alternatives. Further, the agency provides consumer information relevant to motor vehicle safety. For example, NHTSA's New Car Assessment Program (NCAP) provides comparative safety information for various vehicle models to aid consumers in their purchasing decisions (e.g., the 5-star crash test ratings). The purpose of the agency's programs is to reduce motor vehicle crashes and their attendant deaths, injuries, and property damage.

### Progression of electronics use in vehicles

The first common use of automotive electronics dates back to 1970s and by 2009 a typical automobile featured over 100 microprocessors, 50 electronic control units, five miles of wiring and probably contains close to 100 million lines of code [1]. Use of electronics has enabled safer and more fuel-efficient vehicles for decades and also facilitated convenience functions demanded by the consumers. Electric and hybrid vehicles could not have been developed and produced without the extensive use of electronics. Other proven safety technologies such as electronic stability control could also not be implemented without electronics.

Over time, growth of electronics use has accelerated and this trend is expected to continue as the automotive industry develops and deploys even more advanced automated vehicle features. This trend

results in increased complexities in the design, testing, and validation of automotive systems. Those complexities also raise general challenges in the areas of reliability, security, and safety assurance of increasingly networked vehicles that leverage electronics within a distributed, embedded and real-time control system architecture.

Growing system complexity and abundance of design variants even within one manufacturer over model years and across classes of vehicles raise general questions over whether manufactures can ensure the functional safety of existing processes. Further, anomalies associated with electronic systems—including those related to software programming, intermittent electronics hardware malfunctions, and effects of electromagnetic disturbances—may not leave physical evidence. Thus, they are difficult to investigate without a record of data from the electronic systems. As a result, NHTSA, industry members, and other interested parties are actively researching this issue to better understand these potential new functional safety challenges and identity methods to help address them.

**National Research Council Study**

In 2010, the National Highway Traffic Safety Administration (NHTSA) funded a National Research Council (NRC) study on how the agency's regulatory, research, and defect investigation programs can be strengthened to help address the safety assurance and oversight challenges arising from the expanding functionality and use of automotive electronics. Proceedings of this research through the NRC appointed 16-member committee was published in the Transportation Research Board (TRB) Special Report 308 [7] by the National Academies of Sciences (NAS) in 2012. It identified five main challenges for the safety of future electronic control systems:

1) An increased amount of complex software that cannot be exhaustively tested;
2) The highly interactive nature of the electronic control system—more interactions exist among system components, and the outcome may be difficult to anticipate;
3) The growing importance of human factors consideration in automotive electronic control system design;
4) The potentially harmful interaction with the external environment including electromagnetic interference; and
5) The novel and rapidly changing technology.

Further, the study offered recommendations to NHTSA on the actions that the agency could take to meet the six challenges they identified. These include:

1. Becoming more familiar with and engaged in standard-setting and other efforts (involving industry) that are aimed at strengthening the means by which manufacturers ensure the safe performance of their automotive electronics systems
2. Convening a standing technical advisory panel; undertaking a comprehensive review of the capabilities that the agency will need in monitoring and investigating safety deficiencies in electronics-intensive vehicles
3. Ensuring that Event Data Recorders (EDRs) become commonplace in new vehicles
4. Conducting research on human factors issues informing manufacturers' system design decisions

5. Initiating a strategic planning effort that gives explicit consideration to the safety challenges resulting from vehicle electronics that give rise to an agenda for meeting them
6. Making the formulation of a strategic plan a top goal in NHTSA's overall priority plan

The program plans we outline in this paper primarily respond to the first NAS recommendation.

**Electronics Systems Safety Research**

Informed by the NRC study and other internal deliberations on this topic, NHTSA established the Electronic Systems Safety Research Division within the Office of Crash Avoidance and Electronic Controls Research. While our existing investigative and rulemaking processes do cover electronic system (they emphasize performance metrics that apply regardless of whether the vehicle uses a mechanical or electronic way of achieving the performance), we also recognize the increasing industry focus, and processes that govern the safety assurance associated with vehicle systems that are mostly electronic in nature. This type of research can help enhance our understanding of various functional safety issues, fail-safe operations, diagnostics, software reliability, hardware validation, on-board tamper-resistance enhancements, hacking, and malicious external control. Along these themes, NHTSA has developed and is conducting new research in the areas of electronics reliability and automotive cybersecurity (including how these topics affect vehicle automation research). Given the close relationship between electronics reliability, cybersecurity, vehicle automation, our Electronic Systems Safety Research Program are closely considers the relationship between all three topics.

In support of our efforts, NHTSA started building in-house applied electronics research capabilities at its testing facility at the Vehicle Research and Test Center (VRTC) in East Liberty, OH. The purpose of these capabilities is to support testing of electronic systems and potential countermeasures towards developing objective test procedures for electronics related standards, requirements, guidelines, principles, or best practices.

Further, the agency established a Council on "Vehicle Electronics, Vehicle Software, and Emerging Technologies" to coordinate and share information on a broad array of topics related to advanced vehicle electronics and emerging technologies. The Council is managed by senior NHTSA officials. Its mission is to (1) broaden, leverage, and expand the agency's expertise in motor vehicle electronics; (2) to continue ensuring that technologies enhance vehicle safety; (3) review and advise the research program on electronics topics.

The primary goals of the electronics reliability and automotive cybersecurity research programs are similar. The five primary goals are to

1. build a knowledge base to establish comprehensive research plans for automotive electronics reliability/cybersecurity and develop enabling tools for applied research in these areas
2. strengthen and facilitate the implementation of safety-effective voluntary industry-based standards for automotive electronics reliability / cybersecurity

3. foster the development of new system solutions for improving automotive electronics reliability / cybersecurity
4. identify potential minimum performance-based vehicle safety requirements and/or principles for electronics reliability / cybersecurity
5. create foundational materials for future potential NHTSA policy and regulatory decision activities

## ELECTRONICS RELIABILITY PROGRAM

NHTSA's electronics reliability research program covers various safety-critical applications deployed on vehicles today, as well as those envisioned on future vehicles that may feature more advanced forms of automation and connectivity.
NHTSA's electronics reliability research activities in support of our five aforementioned primary goals include the following projects.

### Functional Safety Process and Requirements Research

This project focuses on examining ISO 26262 process standard and how it can improve the electronics reliability and security through encouraging design best practices at manufacturers. The scope of automotive functional safety, as defined within the ISO 26262 standard, only covers a portion of safety assurance activities associated with the design and manufacturing of a safe vehicle. More specifically, the ISO 26262 process addresses the safety related requirements necessary to meet the identified safety integrity levels of vehicle functions under electrical and electronic failures. While this process is only a piece of the overall vehicle safety assurance process, it is of great interest, because it adds a streamlined functional safety component to the standard systems engineering process that deals with the growingly complex portion of the vehicle architecture, namely the electronics, control system and software design. NHTSA continues to evaluate the ISO 26262 standard [8] and its process steps as well as other approaches used in the industry and those emerging in academic settings such as System Theoretic Process Analysis (STPA).

The agency has research underway that is applying the ISO 26262 standard in conjunction with STPA to safety critical automotive systems that directly govern the motion controls of a vehicle. More specifically, we are researching safety requirements associated with electronic throttle control (various propulsion system variations such as internal combustion engine, diesel, hybrid, electric), electronic brake control, electronic steering control (through electric power steering, pure steer-by-wire and differential braking), and rechargeable energy storage system controls.

### Reliability Enhancing Systems Solutions

NHTSA is currently researching areas of advanced diagnostics and prognostics as they pertain to predicting impending system failures (prognostics) and logging critical fault code data (diagnostics) in safety-critical automotive electronic control systems. The agency is seeking to identify the safety improvement opportunities that may be gained from the development and use of enhanced diagnostics and prognostics in automotive applications.

NHTSA is also conducting an assessment of failure-response mechanisms that could help ensure that automotive, safety-critical, electronic control systems are (1) fail safe(i.e. allow driving in a safe-state to

mitigate loss or partial loss of functionality); (2) fail operational(i.e. allow normal driving with loss-of-function warning); and (3) fail secure i.e. disallow the vehicle to be used in the advent of a catastrophic failure. The agency is seeking to gain and provide insight into how automotive technologies address safety beyond system reliability practices (i.e. in addition to preventing the failure, how do systems react to failures?).

Another area of research is the human-factors challenges associated with driver interactions during system failures in safety-critical automotive electronic control systems. Driver notifications/warnings pertaining to an electronic control system failure would ideally be timely, appropriate, and effective.

## AUTOMOTIVE CYBERSECURITY PROGRAM

As stated before, NHTSA established five primary goals, based on a systems engineering process, to address cybersecurity challenges associated with the secure operation of motor vehicles equipped with advanced electronic control systems.

Our automotive cybersecurity research activities in support of these goals include the following activities:

### Establishing an Automotive Cybersecurity Knowledge-base

NHTSA has been actively researching cybersecurity standards, principles and best practices in automotive and other industries. A mature knowledge base in cybersecurity exists primarily in the information technology (IT) domain, which provides valuable insights for the protection of automotive electronic assets, however, principles adopted from IT security may not fully address the security and safety requirements of cyber-physical systems[1] (CPS) [4]. Because security risks can result in imminent safety concerns in case of CPS such as an automobile, risk tolerance associated with security vulnerabilities differ significantly -particularly for systems that govern the motion controls of a vehicle. As a result, we investigated various threat modeling approaches used in other industries and researched potential threat modeling and characterization methods that may apply to vehicle controls [3].

We also investigated design and quality control processes that focus on cybersecurity challenges throughout the lifecycle of a product. For instance we reviewed various National Institute of Standards and Technology (NIST) publications, and particularly studied NIST's Cybersecurity Risk Management Framework and how it may be applied to modern automobiles [2].

### Industry Standards, Best Practices and Cybersecurity Initiatives

To facilitate security-by-design through quality assurance processes, the automotive manufacturers, suppliers, and other stakeholders are collaborating through SAE International to examine the emerging vehicle cybersecurity concerns and considering actions that could include the development of voluntary standards, guidelines, or best practices documents. NHTSA encourages these activities and provides feedback to SAE International Standards committees, such as the Vehicle Electrical System Security committee, and the Electrical Hardware Security committee.

[1] Cyber-physical systems (CPS) are engineered systems that are built from, and depend upon, the seamless integration of computational algorithms and physical components. [National Science Foundation's definition of CPS]

Another industry activity that NHTSA strongly encourages is the recent joint effort undertaken by Alliance of Automotive Manufacturers and the Association of Global Automakers with the goal of establishing a voluntary information sharing and analysis center (ISAC) or other comparable program for the automobile industry sector.

NHTSA studied the ISAC model [5] for safeguarding against cybersecurity risks and threats in other industries such as financial services, information technology, and communications. Our analyses indicate that an automotive sector specific information sharing forum, such as an ISAC, is beneficial to pursue. It could advance the cybersecurity awareness and countermeasure development effectiveness among public and private stakeholders. ISACs have a unique capability to provide comprehensive inter- and intra-sector coverage to share critical information pertaining to sector analysis, alert and intelligence sharing, and incident management and response.

Our research across other industries indicates that the *complete prevention* of cyber-threats is unlikely. This fact and the successful use of ISACs in other industry sectors, suggest that it might also be effective for the auto industry to have mechanisms in place to expeditiously exchange information related to cyber-threats, vulnerabilities, and countermeasures among industry stakeholders when threats occur. Such a mechanism would enhance the ability of the automotive sector to prepare for, respond to, and recover from cybersecurity

**System Solutions for Automotive Cybersecurity**

In terms of system solutions, here are four major pieces to the agency's research approach.

6. *Preventive solutions*: This group of techniques helps to harden the design of automotive electronic systems and networks such that it would be difficult for malicious attacks to take place. Using structured security process standards could help identify vulnerabilities such that necessary design improvements can be identified and implemented during the design phase of the product. These vulnerabilities include possible entry points through accessible physical interfaces (such as the OBD-II port, USB ports, CD/DVD players), short range wireless interfaces, (such as Bluetooth, Wi-Fi, or Dedicated Short Range Communications (DSRC)), and long-range wireless interfaces such as cellular or satellite-based connectivity to the vehicle). Examples of design improvements could include the use of:

    a. encryption and/or authentication of messages on communication networks;
    b. different communication approaches, architectures or protocols;
    c. segmentation/isolation of safety-critical system control networks;
    d. redundant communications , direct measurements and/or message authentication or source validation for safety critical system inputs that can influence the motion controls of a vehicle;
    e. strong authentication controls for remote access vectors to vehicles;
    f. gateway controls and firewalls between interfaced vehicle networks;

g. formal methods for the specification, development and validation of embedded systems; etc.

The primary intents of this category of activities are (1) to significantly reduce the probability of cyber risks; and (2) to limit the impacts of a potential cybersecurity breach (e.g. one part of one vehicle or just one vehicle as opposed to an entire fleet).

7. *Real-time intrusion detection methods*: As a complement to the preventative measures, detecting intrusions into the system would help provide more comprehensive protection. A cybersecurity breach would likely take place on or through a communication network. From an intrusion detection perspective, vehicular network communications are considered fairly predictable and may be well-suited for real-time monitoring to detect anomalous activity with respect to nominal expected message flows. We are initiating research in 2015into real-time monitoring technologies targeted for use in the automotive sector.

8. *Real-time response methods*: Once a potential intrusion is detected, having practical strategies in place would help mitigate potential harmful impacts. Depending on the potential risks and level of intrusion detection confidence, the vehicle architecture could be designed to take a variety of actions such as: (1) temporarily or permanently shutting down the communication network(s) (at the potential cost of disabling various safety functions); (2) informing the driver; (3) recording and transmitting before-and-after trigger point data for further analysis; (4) and counter-measure development, etc. The purpose of this category of cybersecurity defense is to mitigate the potential harmful consequences of detected anomalous activity on the vehicle experiencing the potential breach.

9. *Treatment methods*: While the previous paragraph discussed response methods (dealing with fail-safe operation of the vehicle where an intrusion is detected), treatment methods deal with distributing information related to the subject risk to other potential vulnerable entities even before cybersecurity threat reaches them. Treatment methods involve timely information extraction from impacted parties, their analysis, development of countermeasures, and timely dissemination of that countermeasure to all relevant stakeholders (such as through an ISAC).

**Applied Cybersecurity Research**

NHTSA's primary objective through the cybersecurity program is to develop cybersecurity performance requirements, principles, best practices, and objective tests to assess conformance with such standards.

In support of this goal, NHTSA has been building applied cybersecurity testing capabilities and a cybersecurity laboratory at its Vehicle Research and Testing Center (VRTC) in East Liberty, OH. Current capabilities support communication bus and RF monitoring, CAN and GPS spoofing, firmware analysis and limited ECU penetration-testing. Planned future capabilities include RF disruption research, which will explore robustness associated with LTE, DSRC, GPS and Radar signals.

## SUMMARY

The growth in electronics and software use in the design of automobiles is likely to continue because they support advanced

safety, efficiency, and convenience features. Along with this trend, come the challenges associated with managing safety and security of growingly complex automotive electrical architectures and networks.

NHTSA is continuing to conduct research on safety-critical automotive electronic control systems and collaborating with public and private sector stakeholders to advance its safety mission. The security for safety critical control systems remain a major area of interest for the Agency. Our main goal is to develop facts-based safety and security requirements or guidance for safety assurance of critical automotive systems.

In response to the Moving Ahead for Progress in the 21st Century Act (MAP-21) [6], NHTSA published a Federal Register notice outlining its examination of the need for safety standards with regard to electronic systems in passenger motor vehicles [9] in October 2014 and received public comments. We are in the process of writing a report to Congress, as required by MAP-21, which will also incorporate the received comments.

We have plans to extend ongoing electronics reliability research and cybersecurity research into emerging technologies that offer varying levels of vehicle automation as outlined in NHTSA's Preliminary Statement of Policy Concerning Automated Vehicles [10]. We are conscious of the increased role that electronic systems will play in the driving task in these future vehicles. Thus, NHTSA continues to design its research plans accordingly.

## REFERENCES


1) Charette, R.N. (2009). This car runs on code. IEEE Spectrum.
2) McCarthy, C., & Harnett, K. (2014, October). National Institute of Standards and Technology Cybersecurity Risk Management Framework Applied to Modern Vehicle. (Report No. DOT HS 812 073). Washington, DC: National Highway Traffic Safety Administration.
3) McCarthy, C., Harnett, K., & Carter, A. (2014, October). Characterization of potential security threats in modern automobiles: A composite modeling approach. (Report No. DOT HS 812 074). Washington, DC: National Highway Traffic Safety Administration.
4) McCarthy, C., Harnett, K., & Carter, A. (2014, October). A summary of cybersecurity best practices. (Report No. DOT HS 812 075). Washington, DC: National Highway Traffic Safety Administration.
5) McCarthy, C., Harnett, K., Carter, A., & Hatipoglu C. (2014, October). Assessment of the Information Sharing and Analysis Center Model, (Report No. DOT HS 812 076). Washington, DC: National Highway Traffic Safety Administration.
6) Moving Ahead for Progress in the 21st Century Act, Public Law 112-141 (Jul. 6, 2012), § 31402.
7) National Research Council of the National Academies. (2012). The Safety Promise and Challenge of Automotive Electronics, insights from unintended acceleration, (ISBN 978-0-309-22304-1).
8) Van Eikema Hommes, Q.. (2012). Review and Assessment of the ISO 26262 Draft Road Vehicle—Functional

Safety. (SAE Technical Paper: 2012-01-0025)
9) NHTSA. (2014). Federal Register Notice: Automotive Electronic Control Systems Safety and Security. (NHTSA-2014-0108)
10) NHTSA. (2012). Preliminary Statement of Policy Concerning Automated Vehicles.

# AUDITORY ALERTS IN VEHICLES: EFFECTS OF ALERT CHARACTERISTICS AND AMBIENT NOISE CONDITIONS ON PERCEIVED MEANING AND DETECTABILITY

**Jeremiah Singer**
**Neil Lerner**
Westat
USA

**Carryl Baldwin**
George Mason University
USA

**Eric Traube**
National Highway Traffic Safety Administration
USA

Paper Number 15-0455

## ABSTRACT

Two complementary studies were conducted. In Study 1 (categorical perception of alerts), a series of experiments examined the key parameters that result in listeners perceiving a given sound as an urgent warning versus other less urgent message categories. Initial perceptual sorting experiments identified the most significant parameters and subsequent driving simulator experiments confirmed and refined the findings. Study 1 found that four auditory characteristics accounted for most of the variance in classification of auditory alerts as urgent warnings. Sounds were classified as alarms over 90 percent of the time when they had a peak-to-total-time-ratio (ratio of the time that the sound is at full intensity to the entire pulse duration including onset and offset) of greater than or equal to .7, an interburst interval of less than or equal to 125 ms, at least 3 harmonics, and a base frequency of greater than or equal to 1000 Hz. These results were observed initially in laboratory studies, and replicated during simulated driving. In Study 2 (warning perception in ambient noise environments), an experiment was conducted to investigate the effects of different in-vehicle ambient noise conditions on auditory signal detection and perception. Participants driving on a freeway experienced three ambient noise conditions (windows closed and no music, music playing, front windows open). Fifteen auditory alerts, presented at 65 or 75 decibels (A-weighted), occasionally occurred. Participants pressed a button as soon as they detected the sound, then provided ratings of the noticeability, urgency, and intended meaning of the sound. Study 2 found significant main effects for ambient noise condition and for alert sound for perceived noticeability, urgency, and response time to alert. Detection was impaired by the presence of music, and even more so with the front windows open. Even when auditory signals were heard, noise conditions modified their perceived urgency and meaning. There were also interactions between ambient noise condition and sound, indicating differences in how well sounds of similar loudness tolerated interference from noise. Results also demonstrate that the perceived urgency and meaning of auditory messages can change under noisier ambient conditions, and some features of more noise-resistant signals were suggested by the data. The findings of this research may help interface designers to create auditory signals that indicate the appropriate type and urgency of message.

## INTRODUCTION

Advanced technologies in vehicles and on mobile devices when used to complete the driving task such as smartphones are expanding the amount of informtion available to drivers. Information is increasingly available about safety-critical events, vehicle status, traffic and navigation, and so forth. In this increasingly information-dense environment, it is important that drivers can quickly and easily recognize and distingish time-critical safety information from other, less urgent information.

This paper describes two complementary studies conducted within the National Highway Traffic Safety Administration's (NHTSA) Crash Warning Interface Metrics (CWIM) research program. The CWIM program included a series of research studies intended to address research needs related to the driver-vehicle interface for advanced crash warning systems. Study 1 (Categorical Perception of Alerts) included a series of research tasks designed to establish criteria regarding the key characteristics of a warning sound that would enable the sound to be quickly and reliably perceived as representing a highly urgent collision warning. Study 2 (Warning Perception in Ambient Noise Environments) investigated the effects of different in-vehicle ambient noise conditions on auditory signal detection and perception. Together, these two studies provide insights into the criteria required for an acoustic

signal to be unambiguously interpreted as an urgent warning with the consideration of the effects of varied in-vehicle ambient noise conditions on the detection and interpretation of signals.

## STUDY 1: CATEGORICAL PERCEPTION OF ALERTS

This study, which was led by George Mason University (GMU), included a series of research tasks designed to establish criteria regarding the key characteristics of a warning sound that enable the sound to be quickly and reliably categorized as an urgent warning rather than a vehicle status message or a social notification. Three methodologies were implemented across six research tasks to specifically examine the range of key parameters that result in 85 percent of listeners perceiving a given sound as an urgent collision warning. The 85-percent criterion was selected because it is a common de facto criterion to establish a boundary of typical behavior or perception.

Before beginning the experiments, the research team conducted a survey of forward collision warning (FCW) sounds currently in use in automobiles. The objective of this task was to collect an inventory of warning sounds that could be used to develop an initial list of characteristics common among acoustic warnings. A focus was placed on obtaining representative OEM FCW sounds (i.e., those with the greatest vehicle fleet penetration). Once obtained, the sounds were analyzed in terms of their acoustic properties (e.g., spectral frequency components, pulse duration, onset and offset, harmonics, tempo, etc.). From this inventory, as well as existing published guidelines (e.g., Campbell, Richard, Brown, & McCallum, 2007), a list of key parameters was developed and examined in subsequent experiments. Select non-warning sounds (e.g., vehicle status notifications, ringtones) were also surveyed and recreated for use in this research.

The first four research tasks in this study were a sort task and a series of three method-of-adjustment laboratory tasks. These studies were designed to define and refine the key acoustic characteristics that cause individuals to categorize a message as an urgent crash warning as opposed to other less urgent categories, using the characteristics identified in the inventory of existing in-vehicle warning sounds as a starting point. Specifically, the research team sought to define the key parameters that would be associated with at least 85 percent of listeners perceiving the sounds as a highly urgent, time-critical collision warning. The final two tasks validated the findings of the first four tasks using a sort task and a driving simulation task, respectively. Methods and results for each of the six research tasks are briefly discussed below.

### Perceptual Space Sort Task

**Introduction** The goal of this series was to define the perceptual space associated with a highly urgent FCW sound. Specifically, the research team sought to define the key parameters that would be associated with at least 85 percent of listeners perceiving the sounds as a highly urgent, time-critical collision warning.

**Method** Twenty-one GMU students participated in this research task. Stimuli initially included in the Perceptual Space Sort Task were 29 varying driver-vehicle interface (DVI)-related sounds. Sounds were created in Adobe Audition CS5.5 and Audacity and were based closely on sounds used in real, in-vehicle systems. Stimuli included sounds from many categories of in-vehicle system including those similar to FCW, LDW, backup warning, fatigue alerts, door open, low fuel, seatbelt, and park assist sounds. Stimuli were equated for loudness using Adobe Audition and were presented at 84 decibels, A-weighted (dBA).

Sounds were embedded in a large Microsoft PowerPoint slide such that they could be played by clicking on the sound and a pressing a small play triangle. After a participant played a sound, he or she could move it using the cursor into one of four categories. The available categories were “Warnings,” “Alerts,” “Status Notifications,” and “Social Notifications.” Each category also held a small section labeled “Prototype.” Under each category were two text boxes. The first text box held the text “Click here to tell us why…” and was intended to allow participants to give justification for how or why they grouped sounds together. The second box held the text “Best Urgency Level:” and was intended to allow participants to give a numerical rating of the desired urgency level for each category between 1 and 100.

Participants were instructed to play each sound and then categorize it into one of the four available categories. “Warning” sounds were suggested to “include sounds that you believe to be time-critical, collision warning sounds.” “Alert” sounds were suggested to “include non-critical alerting sounds, for example, a sound that might indicate a

lane departure or a parking assist sound." "Status Notifications" were suggested to "include sounds that indicate something about the status of your car, for example, low windshield wiper fluid or low tire pressure." "Social Notifications" were suggested to "include sounds used by a car's social media system to indicate a social media (like Facebook or email) notification." Participants were instructed that they could have as many sounds as they desired in each category but must have at least one sound in every category. Participants were further instructed that after categorizing each sound, they should play every sound again and choose one sound that was the most prototypical of each category and move it into the "Prototype" section. Participants were finally instructed that they should then attempt to explain their grouping choices and choose an urgency level for each category between 1 and 100. After the practice task, participants were given the experimental task which was identical to the practice but with more sounds.

**Results** Results were first analyzed only in terms of the percentage of times each sound was placed in a given category. While participants distinguished between warnings and alerts as opposed to status or social notifications, there was little agreement on what constituted a warning or an alert. This was further made obvious based on explanations for categorization where it was possible for two participants to categorize based on the same criteria but to choose opposite categories for which those criteria apply. Therefore, all "warning" and "alert" categorizations were reclassified into a new category called "alarms" after data collection.

The four most important (i.e., explaining the most variance) properties that related most to alarm-like warnings were determined using a backward stepwise logistic regression to predict membership in the category "alarm." These properties were interburst interval (IBI), base spectral frequency, number of harmonics (which contributed to the harshness of the tone) and peak to total time ratio. These properties explained 58 percent of the variance in alarm classification ($R = .800$, adj. $R^2 = .581$). Peak to total time ratio defines a property to encompass the perceptions created by longer or shorter onset or offset values. IBI is the gap between multiple bursts of sound, which contributes to the perceived tempo of a sound.

Using the results of the backward stepwise regression, criteria were defined in order of decreasing importance for each property of interest and cutoffs were determined. Cutoffs allowed the researchers to organize the data in terms of whether or not it met each criterion sequentially, and eliminate any sound that did not pass at each level. Cutoffs in this case were based partially on results from the subsequent Method of Adjustment experiments and partially based on the research team's experiences from previous studies and examples from the literature. Sounds that met all four of the criteria below were classified as alarms by at least 90 percent of the listeners. The criteria identified were:

- Peak to total time ratio $\geq .7$
- Interburst interval (IBI) $\leq 125$ ms
- Number of harmonics $\geq 3$
- Base frequency $\geq 1000$ Hertz (Hz)

**Method of Adjustment – Single Parameter**

**Introduction** The primary purpose of this experiment was to see at what point participants perceived an auditory tone to either be a highly urgent time-critical collision warning sound or to no longer be a highly urgent time-critical collision warning sound. A psychophysical method of adjustment procedure was implemented using ascending and descending thresholds for the key parameters. Participants began with a high or low parameter value and then adjusted it up or down, respectively, until the parameter fell within what they perceived to be a level consistent with a critical warning. For this experiment, frequency, IBI, pulse duration, and pulses per burst were examined one at a time. Averages of the crossover points using an ascending and descending series of parameter adjustments could then be used to further define the perceptual space. Furthermore, these results could be compared to the parameters obtained from the previously described Sort Task and any similar parameter values for the cutoffs would validate the Sort Task results.

**Method** Twenty GMU students participated in this experiment. The base sound used for this experiment was a single 300 Hz tone lasting 200 ms with a 20 ms onset and offset. The tone was repeated eight times with 118 ms between each burst, lasting for a total time of 2426 ms. The sound was played through Sennheiser headphones via a Matlab program. The Matlab program allowed participants to adjust the sound by frequency, pulse duration, tempo

(IBI), or pulses per burst. Sounds were presented at 84 dBA. All parameters included a minimum and maximum possible value with a set increment by which the parameter could be adjusted. For this experiment participants only adjusted one parameter at a time. Each screen indicated which parameter would be adjusted and whether the parameter should be adjusted to sound like a highly urgent, time-critical collision warning or no longer like a highly urgent, time-critical collision warning. Participants adjusted each parameter six times. In a randomized order participants adjusted each parameter three times in ascending order to make it sound like a highly urgent, time-critical collision warning sound and three times in descending order to make it no longer sound like a highly urgent, time-critical collision warning sound. Participants received real-time feedback, such that each time an adjustment was made, a new sound was played based upon the adjustment. Participants could continue to make adjustments until they were satisfied that the sound sounded like or no longer sounded like a highly urgent, time-critical collision warning.

**Results** Table 1 shows the mean and 85th percentile values at which at least 85 percent of participants found the sound to be a highly urgent, time-critical warning.

**Table 1.**
**Mean values for parameters and value in which at least 85 percent of all participants found the sound to be a highly urgent, time-critical warning**

| Parameter | Mean Value | 85% Value |
|---|---|---|
| Frequency | 931.71 Hz | 1200 Hz |
| Tempo (IBI) | 330 ms | 240 ms |
| Pulse Duration | 460 ms | 360 ms |
| Pulse Per Burst | 2.73 | 4 |

**Method of Adjustment – Multiple Parameters**

**Introduction** This experiment was conducted to explore the possibility that some acoustic parameters may play a stronger role than others in shaping the perceptual space. This experiment allowed individuals to adjust all four parameters simultaneously, allowing them to change the parameter they felt was more important and thus dictating their perception. Furthermore, this experiment makes it possible for the participant to always make a sound seem like or unlike a highly urgent, time-critical collision warning sound, where in the single parameter adjustment it was possible that someone may not have been able to effectively create a highly urgent sound by changing levels of only one parameter. For example, it is possible that participants could not adjust the sound enough to perceive it as being either a highly urgent, time-critical collision warning sound or no longer being a highly urgent, time-critical collision warning sound..

**Method** Twenty GMU students participated in this experiment. For this experiment the same base sound from the Single Adjustment Task was used in addition to two DVI-related FCW sounds. Sounds were played through Sennheiser headphones via a Matlab program. The Matlab program allowed participants to adjust the sound on frequency, pulse duration, tempo (IBI), and pulses per burst simultaneously (by the same values as presented for the Single Adjustment Experiment). Sounds were presented at approximately 78 dBA. This sound pressure level was 6 dBA lower than used in the previous Method of Adjustment study. This change was made to reduce signal loudness to a level closer to what might be found in vehicles.

The procedure was exactly the same as the Single Adjustment Task with the exception that participants in this experiment were asked to adjust each of the four parameters for a single sound. Participants were allowed to adjust all four parameters at the same time, allowing them to freely choose which parameter to adjust first and allowed them to continually switch between parameters until they were satisfied with the resulting sound. As in the previous adjustment study, participants were instructed that their task was to make the sound presented seem either like a highly urgent, time-critical collision warning (in the ascending trials) or to no longer sound like a highly urgent, time-critical collision warning (in the descending trials).

**Results** Table 2 shows the average value for each parameter as well the value at which at least 85 percent of participants found the sound to be a highly urgent, time-critical collision warning. The table shows that the values were similar to those found in the previous method of adjustment experiment.

**Table 2.**
**Average values for parameters and value in which at least 85 percent of all participants found the sound to be a highly urgent, time-critical collision warning**

| Parameter | Average Value | 85% Value |
|---|---|---|
| Frequency | 1094.17 Hz | 1300 Hz |
| Tempo (IBI) | 500 ms | 360 ms |
| Pulse Duration | 510 ms | 440 ms |
| Pulse Per Burst | 3.03 | 4 |

**Method of Adjustment – Prototype Development**

**Introduction** The primary purpose of this experiment was to gain information regarding what values of each of the key parameters would result in individual perceptions of that sound being the "ideal or prototypical" collision warning sound.

**Method** Twenty-five GMU students participated in this experiment. For this experiment the same base sound from the "Method of Adjustment – Single Parameter" task was used. The sound was played through Sennheiser headphones via a Matlab program. The Matlab program allowed participants to adjust the sound on frequency, pulse duration, tempo (IBI), and pulses per burst simultaneously. Sounds were presented at approximately 78 dBA.

The procedure was the same as the Multiple Adjustment Task with the exception that participants were now asked to adjust the sound until it matched their prototype of the ideal highly urgent, time-critical collision warning sound.

**Results** Table 3 shows the average value for each parameter as well as the value at which at least 85 percent of participants found the sound to be a highly urgent, time-critical collision warning. Compared to the results of the previous method of adjustment task, these results show that an "ideal" collision warning sound has a higher frequency, faster tempo, and faster pace than a "threshold" collision warning.

**Table 3.**
**Average values for parameters and value in which at least 85 percent of all participants found the sound to be a highly urgent, time-critical collision warning**

| Parameter | Average Value | 85% Value |
|---|---|---|
| Frequency | 1576 Hz | 1900 Hz |
| Tempo (IBI) | 254 ms | 40 ms |
| Pulse Duration | 398 ms | 200 ms |
| Pulse Per Burst | 4.16 | 5 |

**Validation Sort Task**

**Introduction** The primary purpose of the Validation Sort Task was to validate the results of the initial sort task and the method of adjustment tasks. To do so, researchers chose to investigate parameters that were found to be important in the previous tasks. Since only one of the previously-evaluated sounds met all four of the criteria established in the first Sort Task, the researchers directly manipulated key acoustic aspects of several sounds to create new sounds designed to examine the robustness of criteria cutoff values. Specifically, the number of harmonics present in several sounds was manipulated by adding harmonic components to sounds that previously had only one harmonic. The presence of multiple harmonics was found in the previous tasks to influence the "harshness"

of the sound, and indirectly, perceived urgency or importance. Further, it was found in the first sort task that some sounds were inadvertently disproportionately long. Therefore in this validation task, sounds were recreated to be of more similar lengths; approximately 1500 ms.

**Method** Fifteen GMU students participated in this experiment. Stimuli for the Validation Sort Task were similar to the Perceptual Space Sort Task but included additional stimuli using added harmonics such that 52 total stimuli were presented to participants. All apparatus and presentation methods were identical to the Perceptual Space Sort Task discussed above.

**Results** Results were analyzed identically to the Perceptual Space Sort Task, using the same criteria and cutoffs. A backwards stepwise regression was able to account for 61 percent of the variance in Alarm classification ($R=.802$, adjusted $R^2=.612$). Sounds that met all criteria (or even criteria after the first cutoff) were much more likely to be considered "alarm" sounds than status or social sounds.

**Rapid Categorization under Divided Attention**

**Introduction** The Rapid Categorization under Divided Attention task was designed to extend and provide additional validation of the results from the earlier tasks in this series. It has previously been shown that cognitive load can degrade participants' responses to warnings while driving (Lewis, Penaranda, Roberts, & Baldwin, 2013; Santangelo & Spence, 2007). Therefore, this task was designed to examine whether or not people's rapid categorization of sounds into critical and noncritical categories differed when they were experiencing the multiple demands of simulated driving while being engaged in a distracting secondary task. In this experiment, participants first completed a sort task similar to the two reported earlier in this study. Then they were asked to categorize sounds by providing a behavioral response (either a brake or button press) while they were concurrently engaged in both a simulated driving task and an n-back number recall task. The n-back task is described in the Method section.

**Method** Twenty-two GMU students participated in this experiment. For the sort task, 26 sounds were used, with specific emphasis placed on those sounds that were shown to be consistently categorized across the sort tasks. The sort task was similar to the two previous sort task experiments with some small changes. In this case the separate categories of "warning" and "alert" were merged into one single "alarm" category, as previous experiments indicated that there is little consistent differentiation between "warnings" and "alerts" by sound parameters. The prototype section of the experiment was removed; otherwise, all aspects of the sort task were identical to the previous sort tasks.

Upon completion of the sort task, participants were seated in the driving simulator. A Realtime Technologies desktop driving simulator was used, with a Logitech Driving Force GT steering wheel. Ambient sound was presented via two monaural computer speakers at 60 dBA. Sounds were presented via a pair of Bose computer speakers at 75 dBA. The same sounds were used as in the sort task. All sounds were repeated twice except for some of the social sounds, which were repeated four times to increase the temporal gap between more urgent sounds. This set of sounds included several sounds based on criteria that were earlier established and were expected to consistently be classified as alarms. Additionally, several sounds were used that shared several but not all attributes of an alarm. The research team theorized that these sounds would be more difficult to classify and potentially result in not being classified as an alarm and/or requiring more time to make a classification response.

Participants practiced driving while maintaining a speed of 45 mph and holding a steady lane position. Once participants were comfortable with the simulator they were instructed that they would be doing a visual 1-back task. For this task, numbers between 1 and 10 were presented on a small screen to the right of the steering wheel. Participants responded via the steering wheel positively or negatively depending on whether or not each number matched the number presented directly before it. After a variable amount of time on the 1-back task, a sound played and participants indicated via the brake, left button, or plus button whether they considered the sound to be an alarm, a status notification, or a social notification, respectively. For the initial practice task, instead of actual signals, the experimenter spoke the words "alarm", "status" or "social." Participants then repeated the category name that they heard. This allwed participants to become familiar with the response actions without exposing them to actual signals or requiring them to make a decision about the categorization of a signal. Midway through the practice, participants began driving and practiced all three tasks simultaneously. After completing the practice task, participants completed the experimental task. The experimental task was similar to the practice task with the main difference

being that sounds were now abstract tones (drawn from sounds used in the sort task experiments). Participants were instructed to make their classifications as quickly as possible while maintaining control of the vehicle.

**Results** Results from the sort task, using the same cutoffs and criteria as in the Perceptual Space Sort Task and Validation Sort Task, indicate that the sounds from Rapid Categorization Under Divided Attention are categorized similarly to previous experiments and that the criteria and cutoff results are highly predictive of alarm categorization (R=.865, adj. $R^2$=.701). If the abstract sound met the first two of the previously-established criteria (peak to total time ratio > .7; IBI < 125 ms) it was classified as an alarm at least 70 percent of the time. Sounds that met all four of the previously-established criteria (ratio and IBI, plus number of harmonics > 3; base frequency > 1000 Hz) were classified as alarms nearly 90 percent of the time. Note that these results are highly similar to the results of the previous two sort tasks. This provides additional support for the reliability and validity of the previous results. The next aim of the current study was to determine if the previously-established alarm criteria were also predictive of alarm perception under divided attention rapid categorization conditions.

Figure 1 shows the results of the rapid categorization task while participants were engaged in the driving and 1-back distraction task. Results are remarkably similar to those obtained from the sort task without concurrent load. Alarm categorization in the sort task obtained while driving was highly correlated with alarm categorization during the rapid categorization task (Pearson correlation=0.962, p<0.001). Additionally, status and social categorization during the sort task were highly correlated with status and social categorization during the rapid categorization task (Pearson correlation for status categorization =0.934, p<0.001 and for social categorization =0.982, p<0.001).

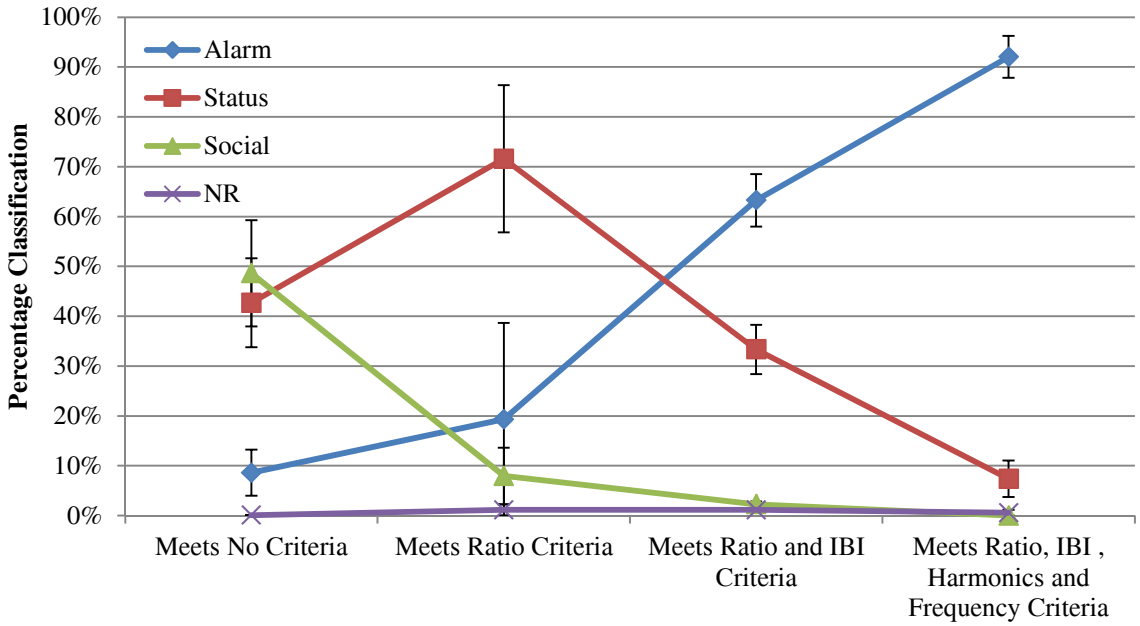


***Figure 1. Percent categorization while driving by criteria met during driving and distraction task performance.***

Results indicate that the number of criteria met was indicative of response times, where the fastest response times were for sounds that met all four of the previously-established alarm criteria, and slowest response times were for sounds that met only the ratio criterion. These results show that when a sound matches with the criteria, people are able to decide more quickly whether or not the sound is a critical alarm relative to a "status" or "social" sound.

Additionally, the more likely a sound was to be classified as an alarm, the faster the response time for that alert, with alarm classification being significantly predictive of lower response times, B = -0.398, p=0.004. Further, alarm classification even in the sort task was significantly predictive of faster response times during the driving task, B = -0.296, p=0.031. These results indicate that the more homogenous the classification (the more participants classify a sound as an alarm), the faster participants are able to respond to that sound. There was a potential confound, however, because participants categorized sounds by pressing a different button on a steering wheel for

each category. Therefore, differences in button response times could have potentially influenced results, though there is no direct evidence that this was the case.

**Study 1 Discussion**

The primary aim of this series of perceptual space investigations was to determine the key acoustic characteristics and the parameter values associated with sounds being unambiguously perceived as being or not being highly urgent collision warnings. Toward this aim, the research team employed three methodologies across a series of research tasks. The first task (Perceptual Space Sort) employed regression techniques to identify key characteristics that accounted for a substantial amount of the variance in category classifications (see Perceptual Space Sort Task Results section). Cutoff scores for each of these key parameters were then established by examining the values of each characteristic that resulted in an 85 percent probability of classification as an alarm. The cutoffs established were a peak to total time ratio of greater than or equal to .7, an IBI of less than or equal to 125 ms, at least three harmonics, and a base frequency of greater than or equal to 1000 Hz. When all four of these criteria were met, the sound was classified as an alarm over 90 percent of the time. Meeting only the first of these criteria (peak to total time ratio greater than or equal to .7) resulted in an alarm classification rate of 70 percent. However, because only one sound in the initial set actually met all four criteria and since the criteria were established by the same data set that was being used to examine classification performance, further validation was warranted.

Using alternative methodologies (method of adjustment with single and multiple parameters) yielded results that confirmed several of the parameters (base frequency, presence of at least three harmonics). Though not specifically manipulated, the peak to total time ratio parameter was also met by the resulting sound created in each of the method of adjustment procedures. Though the method of adjustment yielded a longer IBI than the criteria had established, it could reasonably be determined to be an artifact of the fact that when adjusting IBI, participants were actually listening to bursts that contained three pulses that each had onset and offset times of 20 ms. Using criteria established in IEC 60601-1-8 (a medical alarm standard) a sound with onset and offsets create the perception of tempo when they alternate in and out of 90 percent of their peak amplitude. Therefore, the sounds being adjusted would have inadvertently yielded a tempo within the criteria established in the first sort task.

A final validation in the series examined the predictive capabilities of these criteria while participants were engaged in a simulated driving task and were concurrently performing a distraction task consisting of a visual version of an n-back task. The criteria had strong predictive capabilities under these conditions. Sounds that met all four of the criteria were classified as alarms over 90 percent of the time. Furthermore, when exposed to sounds meeting all four criteria participants were able to make their classifications much faster than when they met only one to three of the criteria. This suggests that sounds meeting these criteria not only have a high probability of being understood to be a warning but also that participants come to this understanding much faster than sounds that meet only a few of the criteria.

Together, the results of this research suggest that it is possible to define key characteristics and associated parameter values that could yield effective alarms for use in collision warning systems. A limitation of this research is that the laboratory methods had participants categorize sounds rather than respond to them in a more ecologically valid context (e.g., orientation and response to a perceived threat while driving). Follow-up research funded by NHTSA, and conducted by Westat and GMU, is ongoing to investigate signal categorization and response to unexpected signals during simulated and on-road driving. This follow-up research also includes haptic signals, a wider range of acoustic signals, and a broader age range of participants.

## STUDY 2: WARNING PERCEPTION IN AMBIENT NOISE ENVIRONMENTS

### Introduction

This study, which was conducted by Westat, was an experiment to measure aspects of driver perception of warnings and alerts under a range of ambient noise driving conditions on actual roads. Considerable research has addressed perceptions of in-vehicle warnings and messages, but the vast majority of this work has been conducted under relatively benign in-vehicle ambient noise conditions. Warnings, however, must remain effective under the likely range of noise conditions that may be anticipated in vehicles. Very little information exists on perception of meaning and urgency in noise.The characteristics and sound level of in-cab ambient noise may vary due to the vehicle's physical characteristics, the road surface, surrounding traffic, travel speed, and interior noise sources.

### Method

**Design** The experiment was a three-factor design, with one between-groups factor (vehicle type) and two within-groups factors (interior noise condition, acoustic signal). Three different vehicles were used in the experiment in order to provide a representative range of vehicle types: (1) a small car, (2) a larger sedan, and (3) an SUV. Each participant drove only one of these vehicles. During the drive, data were collected under three different interior noise conditions: (1) windows up, music off; (2) windows open, music off; and (3) windows up, music on. The order in which each noise condition block was presented to participants was counterbalanced within each vehicle condition.

A set of 15 different acoustic signals was presented under each ambient noise condition. These included three unique voice messages and eight unique non-voice sounds. All eleven of the unique sounds and voices were presented at a sound pressure level (SPL) of approximately 65 dBA as measured near the driver's right ear. One of the voice messages and three of the non-voice sounds were also presented at 75 dBA, with the resultant total of 15 signals. The lower 65 dBA level is representative of a number of acoustic alerts as measured in production vehicles (Lin & Green, 2013). The higher 75 dBA level is more consistent with human factors guidance (e.g., Campbell, Richman, Carney, & Lee, 2004), assuming a moderate level of ambient vehicle cab noise.

Four different dependent measures were recorded to evaluate driver response. These included: (1) a measure of reaction time for the participant to detect the occurrence of a signal; (2) a rating of signal noticeability; (3) a rating of signal urgency; and (4) perceived meaning of the signal (chosen from a set of four alternatives).

**Participants** Participants included 34 drivers aged 22 to 49, with 13 males and 21 females. No participants reported having hearing decrements or using hearing assistive devices. All drove regularly, held valid U.S. driver's licenses, and passed a screener of their motor vehicle records.

**Vehicles** Three different classes of passenger vehicles were used in order to provide a range of vehicle types. These types were small car (2013 Hyundai Accent GLS), sedan (2013 Toyota Camry LE), and SUV (2013 GMC Terrain SLT). The specific vehicles used were selected from among the best-selling models in their class and with good rental availability. Twelve participants drove the small car, 11 drove the sedan, and 11 drove the SUV.

**Roadway** Data collection took place on a limited access toll highway (Maryland Route 200) with a 60 mph speed limit. This is a relatively new highway with smooth and uniform asphalt over most of its length. It is also generally free-flowing, without congestion. These attributes permitted good control over ambient road noise and speed conditions. The roadway has three travel lanes in each direction. Participants were instructed to travel in the right lane except when needing to pass slower vehicles.

**Noise conditions** All drives were conducted during clear weather on dry roads, with a target speed of 60 mph. The fan on the climate control system was set to a low, inaudible setting. During the baseline condition, all windows were closed and music was off. During the "windows open" condition, the front windows on both sides of the vehicle were fully opened. During the "music on" condition, the smooth jazz song "Café Amore" by Spyro Gyra played in a continuous loop. The volume of the music was adjusted by the participant to the volume they would typically use for their own music while driving alone in their own car. However, the experimenter required participants to set the volume at a level equating to at least 60 dBA, as measured in an otherwise silent vehicle

interior. The minimum SPL was established to ensure that the music could potentially affect participants' detection and ratings of messages.

**Auditory signals and stimulus presentation** Fifteen auditory signals were compared. There were 11 unique alerts presented at approximately 65 dBA. Four of these sounds were also presented at approximately 75 dBA. All sounds were initially volume-adjusted to these levels, but were then adjusted for perceptual equivalence of loudness, as determined by a jury of six individually tested raters. Thus, the 65 dBA sounds were of subjectively equivalent loudness to a 65 dBA continuous pink noise signal (i.e., a signal of random noise containing equal amounts of energy per octave). The 75 dBA sounds were digitally amplified by 10 dB from the 65 dBA level.

The alerts used in this experiment were adapted from examples of current in-vehicle warnings and alerts of various types, other sounds found in various sources, and synthetic speech messages created using an online text-to-speech generator.[1] It is important to note that the signals that were sourced from current in-vehicle systems were presented using a different speaker in a different vehicle interior, and are not necessarily presented at the same SPL as the original alerts. Therefore, the results of this experiment do not necessarily reflect upon the messages as used in their native vehicle environments. The alerts used in this experiment are briefly described below. Alerts 1 through 8 are sounds presented at the 65 dBA level; alerts 9-11 are voice messages at the 65 dBA level; and alerts 12-15 are the subset of alerts presented at the 75 dBA level.

1. FCW 1: One burst of 20 fast beeps with a relatively high frequency profile.
2. FCW 2: Four bursts of four fast beeps with a relatively low frequency profile.
3. Blind spot warning: Three bursts of four fast beeps, each with a smoothed onset and offset and a sustained low intensity sound between beeps.
4. Pedestrian warning: A single sustained beep with a duration of 2 s.
5. Seat belt alert 1: A single chime that decays to silence in the span of about 2 s, with intensity varying in a wavelike pattern.
6. Seat belt alert 2: Two chimes, each of which decays to silence in the span of about 1 s.
7. Park assist 1: One burst of eight beeps.
8. Park assist 2: Two bursts of three beeps.
9. Female voice – not urgent: Female voice says "Attention."
10. Female voice – urgent: Female voice says "Warning, warning."
11. Male voice – urgent: Male voice says "Warning, warning."
12. FCW 1 (high): Same as FCW 1, but presented at 75 dBA.
13. Blind spot (high): Same as (3), but presented at 75 dBA.
14. Park assist 1(high): Same as (7), but presented at 75 dBA.
15. Female voice – urgent (high): Same as (10), but presented at 75 dBA.

During the experimental drives, the auditory signals were presented by an X-Mini II XAM4 capsule speaker mounted on top of the dashboard immediately behind the steering wheel.

Within each noise condition block, the experimental control software generated a random presentation order for the 15 auditory signals. The software provided a random time gap that ranged from 10 to 50 s and averaged 30 s from the completion of the previous sound's ratings to the presentation of the next sound. Once the random time had passed, the software indicated to the experimenter that the next signal could be activated. The actual triggering of the trial was done by the experimenter, who first determined that there were no unusual acoustic circumstances (e.g., a large truck passing or a patch of noisier roadway surface). When the participant detected the signal they pressed a microswitch button, worn on their finger or thumb, to provide a response time. The data collection system recorded the response time and then cued the experimenter, who was seated in the right rear seat, to verbally present a series of rating and choice questions. The participants rated:

- Noticeability (defined as "The sound is easily noticeable among other sounds and noises in the vehicle"); 1=not very; 7=extremely

[1] http://www.oddcast.com/home/demos/tts/tts_example.php

- Urgency (defined as "The sound conveys a sense of importance, motivating you to make an immediate response"); 1=not very; 7=extremely
- Perceived meaning. The sound was placed in whichever of four categories the participant felt best matched the meaning conveyed by the signal
    1. Urgent crash warning
    2. Safety information (other than urgent crash warnings)
    3. Information not related to safety
    4. Incoming personal communication (e.g., call, text message, email)

If the participant did not respond to the alert by pressing the microswitch within eight seconds of signal initiation, the participant was deemed to have failed to detect the signal and no rating questions were asked. The participant received no feedback that there was a missed signal.

**Results**

Driver perception of the auditory signals was influenced by both the nature of the signal and the ambient noise background. Figure 2 shows the percentage of signals detected by the driver for each signal under each ambient noise condition. Few participants missed any signals in the baseline condition (windows up, music off). In the music condition, a few signals were detected in the 70 percent or fewer range, but most were detected at least 80 percent of the time. The open windows condition interfered with detection more dramatically. All four of the signals presented at the 75 dBA level continued to be detected well even with the windows open, but for the 65 dBA signals there was a wide disparity in performance, with a few detected by more than 90 percent of participants and three others detected by only around 10 percent of participants.

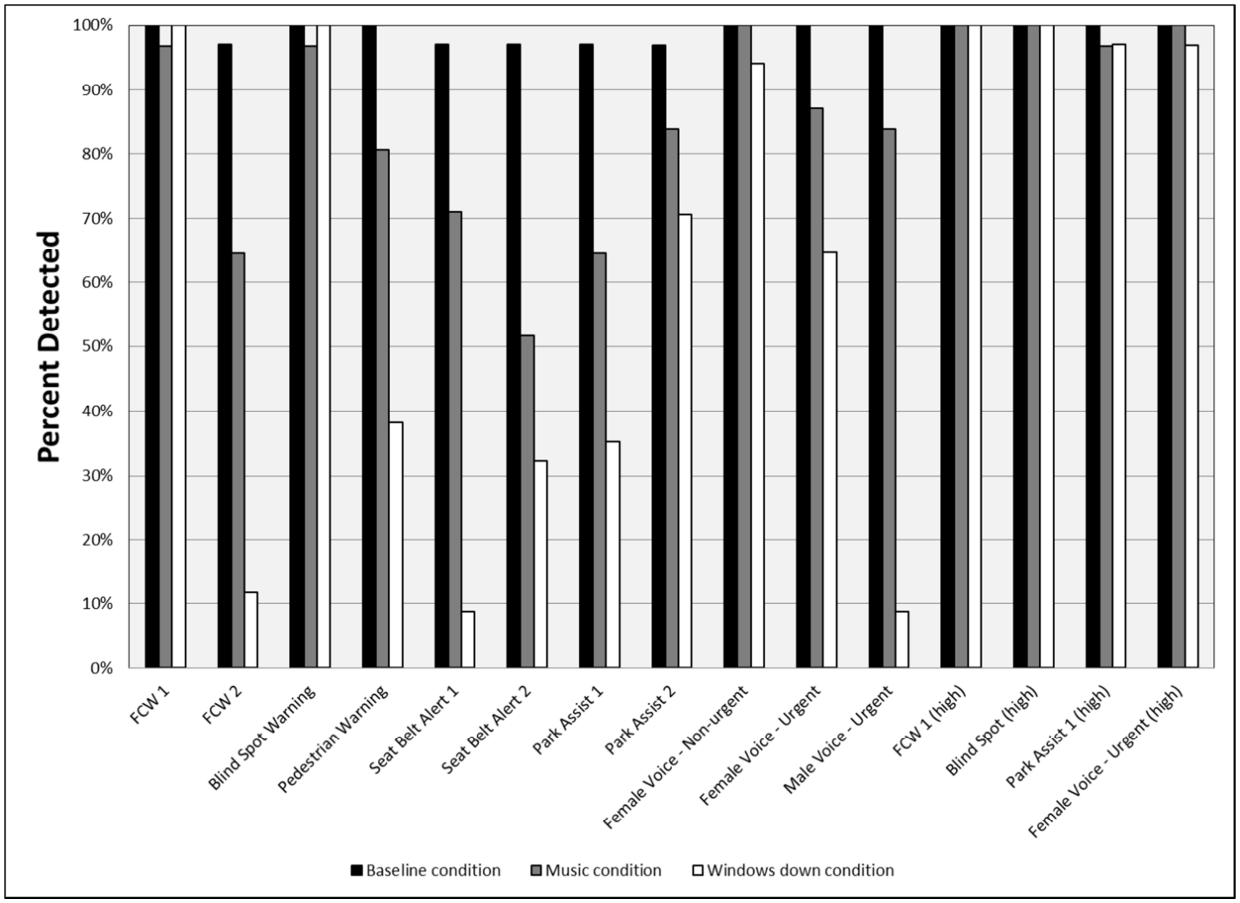


***Figure 2. Percentage of participants who detected alerts under each ambient noise condition.***

Three-factor (signal, ambient noise background, vehicle type) ANOVAs were conducted for the measures of rated noticeability, rated urgency, and response time. The three parallel analyses yielded identical conclusions. Signal, noise condition, and their interaction were all statistically significant ($p<0.0001$). There was no main effect of vehicle type and no interaction of vehicle type with ambient noise background. There was a significant interaction of signal with vehicle type, though there was no clear pattern of effects. It may be expected that due to the complex and varied geometry of the vehicle cabin space and the nature of the reflective and absorbing materials, the differences in the acoustic space might differentially affect some signals. There was no three-way interaction. Figure 3 shows the group mean rating of urgency for each signal under each ambient noise condition. The figure shows that there were dramatic differences in perceived urgency, even among sounds that were equated for similar perceived loudness under relatively quiet conditions.

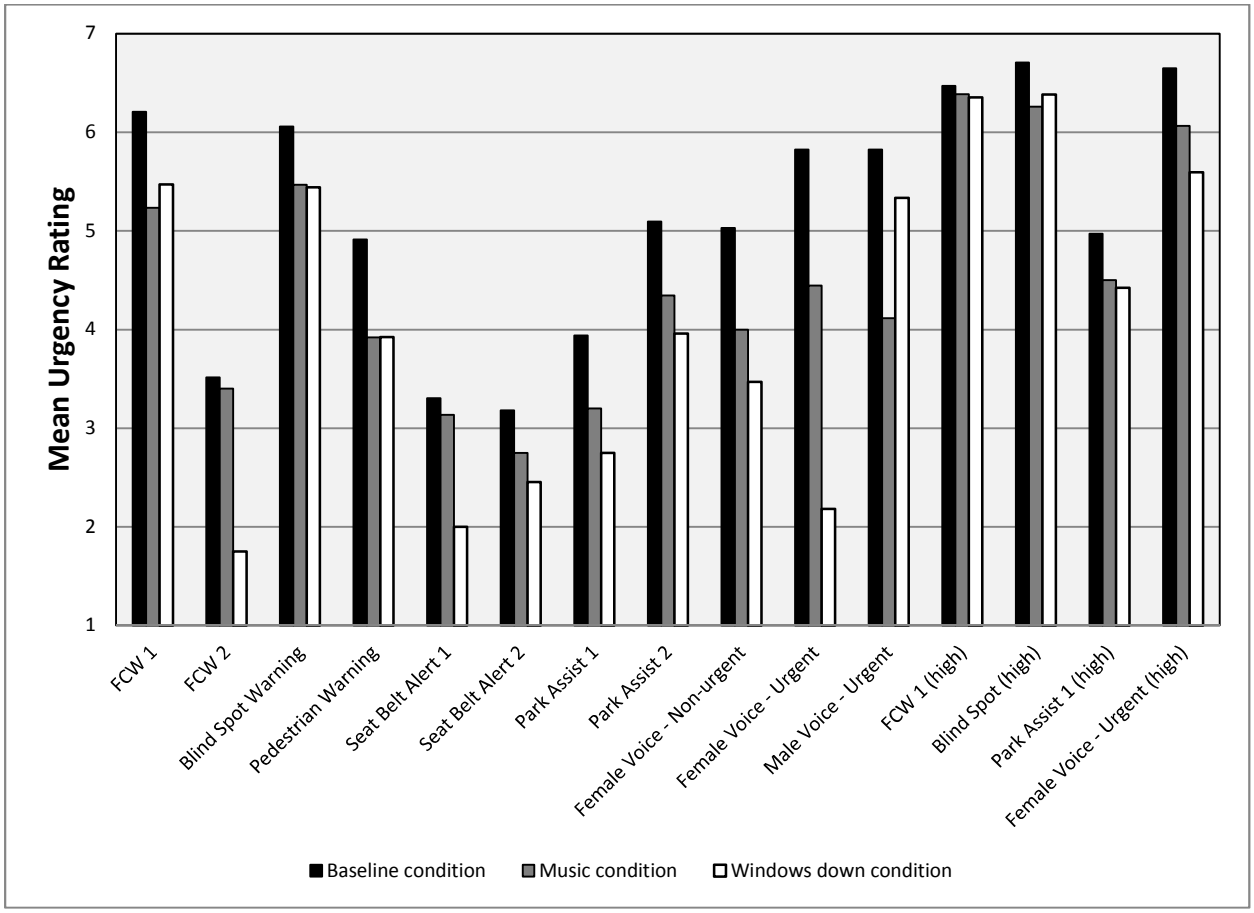


***Figure 3. Mean urgency rating for each combination of signal and ambient noise condition.***

The ambient noise condition influenced the category of meaning that a listener assigned to a particular alert. Participants had the option of classifying a given alert as "urgent crash warning," "safety information," "information not related to safety," and "incoming personal communication." As expected, the various alerts differed in terms of how they were interpreted, with some predominantly viewed as urgent crash warnings and others predominantly view as unrelated to safety at all. Multinomial logistic regression was used to analyze the perceived meaning classifications. Multinomial logistic regression is used to predict the probability of category membership on a dependent variable based on multiple independent variables. This approach is an extension of binary logistic regression that allows for $k>2$ categories of a dependent variable. Maximum likelihood estimation is used to evaluate the probability of category membership. The current model analysis was performed in SAS and used a cumulative logit model with Fisher's scoring as an optimization technique. Differences of least square means are reported with Sidak adjusted p-values. The analysis found signficant effects of ambient noise ($p=0.0036$), acoustic signal ($p<0.0001$), and an interaction between these two factors ($p<0.0001$). The key outcome to note here is that

ambient noise condition had a significant effect on participants' categorization of signals, and the significant interaction term reveals that different signals were affected in different ways by the various ambient noise conditions, revealing a complex relationship between ambient noise and acoustic signals with regard to perceived category of meaning.

**Study 2 Discussion**

As an initial study on this topic, the experiment demonstrated very sizable effects of ambient noise conditions that might reasonably be expected to occur on occasion. Background noise from music, and especially from open windows, interfered with the perception of auditory signals presented at 65 dBA. Interference was not very pronounced for the set of 75 dBA signals, although only four signals were included at this level. The set of sounds and voice messages equated for approximately equal loudness under relatively quiet listening conditions differed substantially in noticeability and urgency even under the baseline condition and even more under the music and open windows conditions. Under noise conditions, 65 dBA signals were less likely to be detected, and when they were detected they typically lost much of their perceived urgency, which may compromise their effectiveness as urgent crash warnings. Some sounds suffered low detection rates under noise, particularly the windows open ambient condition.

This experiment was designed to provide an initial examination of the extent to which possible ambient noise conditions might interfere with signal detection and meaning. It was not intended to provide any systematic evaluation of signal features or parameters regarding their resistance to noise effects. However, based on the limited sample of sounds and conditions, it appeared that the predominant frequencies that characterize a signal may relate to perceived urgency under noise. Sounds with base frequencies below 1000 Hz generally performed worst and those with base or significant components above 1500 Hz performed best. However, this observation is based on a limited sample of sounds that also differed in a number of other respects, and so it should be considered tentative. A series of follow-up laboratory investigations conducted within NHTSA's CWIM research program replicated and extended the findings of this on-road study by investigating additional sounds, ambient noise conditions, and sound pressure levels.

## CONCLUSIONS

The National Highway Traffic Safety Administration's Crash Warning Interface Metrics program included a series of research studies intended to address research needs related to the driver-vehicle interface for advanced crash warning systems. The two complementary studies described in this paper investigated the signal characteristics that lead to people clearly distinguish urgent alert sounds from other message categories (Study 1), and how the effects of various in-vehicle ambient noise conditions affect the detection and perceived meaning of signals (Study 2).

In Study 1 (Categorical Perception of Alerts), a wide range of parameters was systematically tested, and four parameters were found to be most important in influencing categorization as a warning or safety alert: base frequency, number of harmonics, IBI, and peak to total time ratio. The cutoff values at which a sound becomes unambiguously perceived as an alarm were refined and validated in a series of tasks including a driving simulator task under cognitive load. The findings can potentially help designers create in-vehicle systems in which intended crash warnings are reliably perceived as urgent and critical and in which intended lower urgency message types do not lead to confusion with urgent warnings.

In Study 2 (Warning Perception in Ambient Noise Environments), a set of 15 sounds was presented to drivers under three ambient sound conditions. Results show that many sounds that were easily detected and perceived as urgent in a relatively quiet vehicle interior were much less likely to be detected or perceived as urgent in a louder vehicle interior (e.g., with windows open). Main effects of detection rate for sound stimulus suggest that sounds adjusted for equal loudness in a quiet environment are not necessarily equally loud in a vehicle environment. The presence of interactive effects between different sounds and ambient noise conditions suggests that some sounds are more resistant to the interfering effects of elevated ambient noise than others.

Taken together, the results of these two studies show that the acoustic characteristics that cause a sound to be unambiguously interpreted as an urgent alarm or other category are quantifiable, but that the ambient noise condition in which sounds are heard can have a significant effect on signal detection and interpretation. In-vehicle acoustic

signals, then, should be quickly and unambiguously interpreted with the meaning intended by the designer, and should maintain their detectability and meaning in a variety of ambient noise conditions. Study 2 found that sounds played at 75 dBA were substantially less impaired by elevated ambient noise than sounds played at 65 dBA, suggesting that alerts presented at approximately 65 dBA, as is common in production vehicles, might not always maintain their detectability and meaning under elevated ambient noise. The limited number of stimuli investigated in this study does not provide enough data to suggest an ideal loudness, nor suggest features that might make a given sound more detectable or more reliably categorized at a given loudness.

These studies have some notable limitations. As noted above, signal loudness has a substantial effect on signal detection and interpretation, especially in elevated ambient noise. Study 1 did not systematically manipulate signal loudness, and Study 2 only manipulated loudness at two levels for five signals. Study 2 also only investigated three ambient noise conditions. These studies also involved participants focused on an experimental task without the context of a real on-road information environment. As such, there were no conditions or hazards associated with signals, nor were participants expected to react or respond to signals (other than by providing a categorical response). Follow-up research conducted within NHTSA's CWIM program has continued the ambient noise line of research by replicating the on-road findings in a laboratory setting and extending the research to investigate additional sounds, ambient noise conditions, and sound pressure levels. A separate study conducted within NHTSA's Connected Vehicle program will extend the categorical perception research by investigating additional sounds, as well as haptic signals, in driving simulator and on-road experiments.

## REFERENCES

Campbell, J.L., Richard, C.M., Brown, J.L., & McCallum, M. (2007). Crash warning system interfaces: Human factors insights and lessons learned. Report no. DOT HS 810 697. Washington, DC: National Highway Traffic Safety Administration.

Campbell, J.L., Richman, J.B., Carney, C., & Lee, J.D. (2004). In-vehicle display icons and other information elements, Volume I: Guidelines. Report no. FHWA-RD-03-065. McLean, VA: Federal Highway Administration.

Lewis, B.A., Penaranda, B.N., Roberts, D.M., & Baldwin, C.L. (2013). Effectiveness of bimodal versus unimodal alerts for distracted drivers. Paper presented at the International Conference on Driving Assessment, Bolton Landing, NY.

Lin, B., & Green, P. (2013). Measurements of driver-assistance warning-signal characteristics in 2013 cars. Report no. UMTRI-2013-03. Ann Arbor, MI: University of Michigan Transportation Research Institute.

Santangelo, V., & Spence, C. (2007). Multisensory cues capture spatial attention regardless of perceptual load. Journal of Experimental Psychology: Human Perception and Performance, 33(6), 1311-1321.

# Analysis of Vehicle-Based Security Operations

**Jason M. Carter, Ph.D.**
**Nathanael Paul, Ph.D.**
Oak Ridge National Laboratory
United States

**Jenny Zhang**
National Highway Traffic Safety Administration
United States

**Paper 15-0457**

## Abstract

Vehicle-to-vehicle (V2V) communications promises to increase roadway safety by providing each vehicle with 360 degree situational awareness of other vehicles in proximity, and by complementing onboard sensors such as radar or camera in detecting imminent crash scenarios. In the United States, approximately three hundred million automobiles could participate in a fully deployed V2V system if Dedicated Short-Range Communication (DSRC) device use becomes mandatory. The system's reliance on continuous communication, however, provides a potential means for unscrupulous persons to transmit false data in an attempt to cause crashes, create traffic congestion, or simply render the system useless. V2V communications must be highly scalable while retaining robust security and privacy preserving features to meet the intra-vehicle and vehicle-to-infrastructure communication requirements for a growing vehicle population.

Oakridge National Research Laboratory is investigating a Vehicle-Based Security System (VBSS) to provide security and privacy for a fully deployed V2V and V2I system. In the VBSS an On-board Unit (OBU) generates short-term certificates and signs Basic Safety Messages (BSM) to preserve privacy and enhance security. This work outlines a potential VBSS structure and its operational concepts; it examines how a vehicle-based system might feasibly provide security and privacy, highlights remaining challenges, and explores potential mitigations to address those challenges.

Certificate management alternatives that attempt to meet V2V security and privacy requirements have been examined previously by the research community including privacy-preserving group certificates, shared certificates, and functional encryption. Due to real-world operational constraints, adopting one of these approaches for VBSS V2V communication is difficult. Timely misbehavior detection and revocation are still open problems for any V2V system. We explore the alternative approaches that may be applicable to a VBSS, and suggest some additional research directions in order to find a practical solution that appropriately addresses security and privacy.

## Section 1: Introduction

Dedicated Short-Range Communication (DSRC) can support V2V and V2I communications; however, bandwidth and range limitations challenge integration of safety and privacy features. In order to ensure interoperability between different OEMs, vehicle safety messages (i.e., Basic Safety Messages or BSMs) must be trusted while protecting the identity of the driver or vehicle.

In a traditional public key infrastructure (PKI), participants create, receive, manage, and revoke certificates. A certificate encapsulates a participant's public key and identifies that participant within the system. Each participant signs data using their private key. When a message recipient receives a signed message, the recipient verifies the message signature using the sender's public key to ensure the message has not been altered. Assuming that the sender's private signing key has not been compromised or exposed, the recipient will trust that the sender signed and sent the received message.

The proposed Public Key Infrastructure (PKI) for the Intelligent Transportation System (ITS) Vehicle-to-Vehicle (V2V) safety initiative will be the largest PKI ever deployed. The PKI needs to address the basic security properties (authentication, integrity, and non-repudiation) of a traditional PKI while protecting individual privacy. In the rest of this document, assume that unless otherwise stated, a PKI refers to a PKI for use in a transportation infrastructure and will be used for V2V and V2I. As in most PKIs, revocation is

needed. Revocation typically requires participant identification. For this PKI, the revocation authority would be identifying certificates associated with a particular vehicle or device.

Participant population estimates in a PKI provide a foundation for network traffic, storage, and infrastructure analyses. Using a linear model of U.S. vehicle registration numbers from 2000 to 2012 [FHWA11], the number of registered vehicles in 2016 will be approximately 257 million; this includes public and private automobiles, buses, and trucks. The population of private and public vehicles will be dynamic; vehicles will be added and removed from the system for several reasons. U.S. vehicle population increases on average 1.97 million vehicles per year. This implies that more than 15 million new vehicles are purchased on average each year in the U.S. [NADA14]. When the V2V system is fully deployed, the VPKI system is expected to accommodate more vehicles as the overall U.S. vehicle population is projected to grow. Furthermore, the VPKI needs to manage certificates from the end-of-life, misbehaving, and/or malfunctioning vehicles in order to ensure the integrity of the V2V system and protect the remaining participants from mishaps. The 2011 Automotive Recycling Association Report estimated 12.61 million vehicles are recycled per year; this value is very close to our end-of-life vehicle projections (i.e., 12.96 million per year). The certificates in end-of-life vehicles may potentially be compromised and used maliciously. Vehicles that intentionally use compromised certificates maliciously, or unintentionally malfunction, are classified as misbehaving vehicles; this class of vehicles may cause mishaps intentionally or unintentionally based on their broadcast safety messages.

The deployment of a PKI system relies on a supporting infrastructure. The components and authorities within this infrastructure manage and distribute certificates so participants can communicate in a trustworthy way. However, addressing privacy concerns requires a different certificate management and distribution approach from a traditional PKI that uses inherently identifying credentials. A recently proposed Security Credential Management System (SCMS) for North America adds infrastructure components to provide privacy protection. [Whyte13] attempts to address privacy by building an infrastructure whose architectural design mitigates the possibility of an internal privacy breach, and this work is the basis for the current VPKI, the Security Credential Management System (SCMS) being explored for North America. Several promising alternative strategies have been developed that may allow

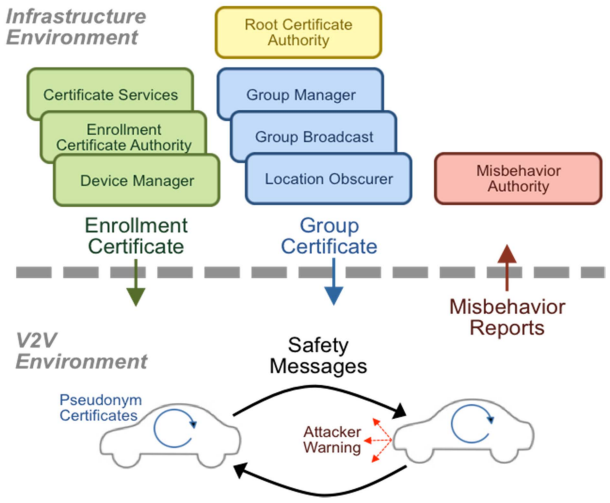


**Figure 1: Vehicle-Based Security System**

for a reduced level of infrastructure and associated communications with the vehicle. These include privacy-protecting group credentials, shared certificates, and functional encryption [Delgrossi12].

To reduce the supporting infrastructure size and to increase a vehicle's independence from the infrastructure, ORNL has been investigating the potential for a Vehicle-Based Security System (VBSS) to provide security and privacy at the scale of a fully deployed V2V system. Figure 1 is an overview of the operations and components in our VBSS concept.

Communication between the infrastructure components does happen but is not illustrated. Instead of a trusted authority issuing ephemeral certificates, the proposed VBSS uses group credentials, and they facilitate short-lived pseudonym certificate generation on the vehicle. Vehicles form groups, and a vehicle will sign a message using its group signing key while maintaining anonymity. Unlike a traditional PKI message, in order to verify a message, a recipient does not need to know who exactly signed a message.

Group credentials also integrate mechanisms to add and remove participants in an efficient way; this feature can be used for vehicle revocation.

This paper outlines the VBSS structure and its operational concepts; it examines how a vehicle-based system might feasibly provide security and privacy, highlights remaining challenges, and explores potential mitigations to address those challenges. We suggest some additional research directions that will further validate a vehicle-based approach to V2V credential management.

## Section 2: Towards a Feasible VBSS

A PKI that addresses privacy must also scale to meet the needs of the U.S. vehicle population. In a PKI, identifying a signer is counter to the goal of maintaining a driver's (signer's) privacy. We assume that a driver wants to ensure the safety messages they transmits cannot be used to expose private details about that individual's movements. If a vehicle used a single private key to sign every safety message, then the associated, publicly available, certificate could be used to identify that driver's safety messages. Such a PKI must manage over 250 million identifying credentials. Scaling to manage this many credentials is a significant challenge. Short-lived pseudonym certificates have been adopted as a way to obfuscate an individual's identity; numerous pseudonyms are used by each driver, multiplying the credential management challenge.

There are many potential cryptographic approaches to achieving a PKI that addresses privacy and scalability. These include functional encryption, shared certificates, and group signatures [Delgrossi12]. Although functional encryption in Vehicle Ad-hoc NETworks (VANETs) has recently received attention [Huang09], the maturity of the technology lags behind the other two approaches.

With shared certificates, a collection of vehicles (sharing group) share a single unique private key to sign safety messages. The verifying certificate of all vehicles within the sharing group provides equal anonymity; however, revoking a single bad participant will have the collateral effect of revoking all the members in the sharing group. To mitigate this collateral damage, each vehicle is given multiple keys. A new shared private signing key can be selected from the "backup" keys when the signing key being used is revoked. With this scheme, all of a vehicle's signing keys could be revoked without any evidence of the vehicle's misbehavior (i.e., a vehicle that unintentionally has behavior that does not conform to an expected adjudicated behavior). While no one has data on the expected or actual misbehaving vehicle rate, we anticipate that the number of misbehaving vehicles will be large requiring extensive mitigation of the collateral damage effect.

Group signatures have been prototyped in VANETs, although they can be computationally demanding. However, other work shows that the computational burden of group signatures does not preclude its use in vehicular networks: Instead of using group credentials to sign each and every message, they could be used to anchor ECDSA certificate trust [Calandriello11]. The group signatures are combined with Elliptical Curve Digital Signature Algorithm (ECDSA) signatures to decrease computational and network consumption. With this strategy, the vehicle acts as a subordinate certificate authority and generates its own ephemeral ECDSA certificates: each vehicle signs a generated ECDSA public key with its group signing key.

The combined use of ECDSA and group signatures is shown in Figure 2. In Figure 2, Alice creates a BSM and signs that BSM with a private pseudonym ECDSA signing key, $k_A$. This yields the signature Sig $k_A$ (BSM). In this example, Alice also signs the pseudonym certificate with her group signing key and attaches the corresponding signature, $<A>_G$. Then, Alice sends the message and signatures to Bob. If Bob has received a message from Alice in the past, then Bob will trust the message once he verifies the BSM's signature. If Bob has not previously received a message from Alice, Bob will first verify the group

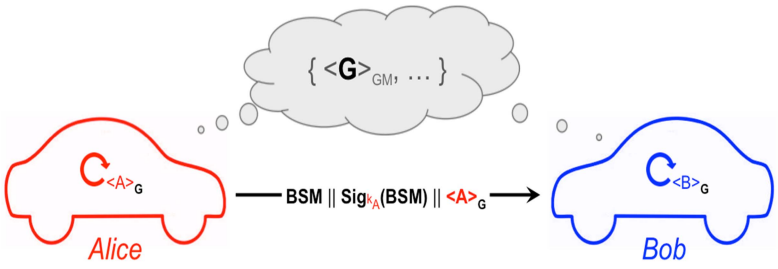


**Figure 2: Two Vehicles Communicating Using Group Signed Pseudonyms**

signature of the pseudonym, $<A>_G$, by using the group public key. Then, Bob can check the BSM signature using <A>. The circular arrow in Figure 2 signifies the vehicle's ability to generate pseudonyms. Pseudonyms can be created on-demand or in small, custom-sized batches. When a sender transitions to a new pseudonym certificate, the BSM recipient must obtain and verify that certificate prior to authenticating messages.

## Section 3: A Group-Based VBSS

In a group signature scheme, a group manager has a role similar to a root certificate authority [Chaum91, Ateniese00, Bellare05]. Any party in the PKI may receive a message signed by a particular group member. If the message recipient is in the same group as the message sender, then their common group public key can be used to authenticate the message. If the message recipient is in a different group from the message signer, he or she must first obtain the sender's group public key and then verify the message (We anticipate that it will be feasible to store all group public keys on a vehicle, and every vehicle starts with all group public keys). Group signatures are anonymous: the group public key, or certificate, only identifies the group and not an individual. When verifying a message, the recipient verifies that the message signer was a valid group member when they signed the message, but no additional identifying information about the message signer is learned.

To form a group, a group manager must be designated and several public parameters chosen. When a potential participant requests assignment to a group, the participant's private pseudonym signing key must either be self-generated or generated by the group manager. In earlier work [Ateniese00], a group member takes part in an interactive group join protocol and receives a membership certificate tuple: a signature in the form of a pair, $(A_i, e_i)$; $A_i$ is computed as part of a zero-knowledge proof (ZKP) that shows that the prospective member knows a secret value, and random prime integer, $e_i$, usable for member revocation. The group manager creates groups, manages revocations, and identifies group members when needed by revealing a particular signatory. Using the group membership certificate, a participant sends and signs messages. Message verification proves the message signer is part of the group; no other details are provided by the sender.

The number and size of groups is a design choice. Some of the factors that might be used in determining how the U.S. vehicle population is partitioned include: geographic boundaries, vehicle manufacturer, and vehicle make. In other PKI systems, designers have created revocation mechanisms that can address vehicle recalls. Similarly, large subsets of a vehicle population can be revoked directly by removing an entire group when the group partitioning strategy is designed properly.

Table 1 details an example nation-wide group design in the U.S. In this design, there are fifteen thousand groups (and 15,000 corresponding group public keys). This design facilitates recalling a specific make and model of a vehicle in certain geographic regions. In the Table, Local Group Size accounts for all the groups within one of the fifty geographic regions, a state.

| Description | Quantity |
|---|---|
| U.S. States | 50 |
| U.S. Automobile Manufacturers | 30 |
| Manufacturer Models | 10 |
| Groups | 15,000 |
| System Participants | 250,000,000 |
| Participants Per Group | 16667 |
| Local Group Size | 300 |

**Table 1: Notional VPKI Group Design (U.S.)**

One issue with the group credential approach is internal privacy. The group manager can determine who signed a message using the signature and the information it retains about the entire group, a breach of internal privacy. However, internal privacy could be enhanced by splitting the group manager into two logical (or physical) entities; the collusion of both entities would be needed to identify a particular message signatory. In the most recent SCMS specification document [SCMS14], a Trusted Platform Module (TPM) was suggested to isolate and protect linkage authority operations, and this could be done in the same machine. A similar approach could be used to provide internal privacy for the group credential approach.

**Group Revocation.** Three alternative approaches to revoke a group member using Certificate Revocation List (CRL) are considered. A CRL is a list that grows and shrinks to ideally contain all those participants that could possibly be acting in the system and should be ignored. In one approach, the group manager

issues a CRL to identify revoked participants. The CRL also contains updated group public keys [Ateniese02]. Each unrevoked user uses the same CRL to identify revoked participants and verifies new messages. These CRLs have high overhead and transmission bandwidth costs. More specifically, verification is linear to the number of revoked participants, and the CRL is .proportional to the number of revoked participants [Ateniese02]

In a more recent approach, a revocation list is issued that includes each revoked participant's private key [Boneh04]. This approach may allow an adversary to link messages to a single vehicle. This linking weakness is eliminated in another scheme at the cost of increased computation [Nakanishi05].

In a different approach [Camenisch02], each group public key characterizes its members by accumulating individual, identifying member values; however, the final accumulated value cannot be used to identify any single member. When a group member signs a message, their signature contains a proof, verifiable using the group public key, that some member of the group generated the signature. A group member can be removed, or revoked, from a group. The group manager revokes the member by removing their identifying number from the accumulated value included in the group public key. Although the revoked group member can still sign messages, message recipients will not be able to authenticate the message using the new group public key, since the individual has been removed from the group. New group public keys must be distributed efficiently to all participants that may receive a message from the revoked participant to facilitate this revocation alternative .

## Section 4: Trusted Hardware

The cryptographic operations for VBSS will require high performance on-board vehicle computation to sign messages at 10Hz and verify messages at 1000Hz. In research trials, 400 MHz [DOT811492D], 1 GHz, and 3 GHz (i.e., a desktop CPU [DOT811492D]) processors have been used to experimentally evaluate system performance requirements. Exact hardware computational requirements are yet to be established. However, due to added computational burden from group signatures, the VBSS concept may require a custom Application Specific Integrated Circuit (ASIC) to perform trust-critical computation along with another processor (or a core) for additional general computation. We anticipate a 10-15x speedup with new ASICs.

We discuss three possible options for protecting on-board security elements and increasing computation: a TPM, the ARM TrustZone [ARM09], and a Hardware Security Module (HSM). Of these three options, TPMs will not meet the needs of VBSS, since they are resource-limited in computation and I/O. For instance, the ST19NP18-TPM can store only nine keys [ST13]. TPMs often interface over the Low Pin Count (LPC) bus (33 MHz). This limited interface can potentially create a bottleneck for computation. While TPMs are resource constrained, they are an attractive option with an estimated cost of about $1 [Kursawe04].

If ARM chips are used for computation (over 50 billion ARM chips have been produced [ARM14]), the ARM TrustZone architecture could potentially meet VBSS requirements. ARM TrustZone is a proprietary trusted computing architecture that is integrated in many modern ARM chips. In the ARM TrustZone architecture, applications execute in two zones: a Secure World and a Normal World. Sensitive computations are executed in the Secure World. However, when multiple applications execute in the Secure World, establishing trust among secure world applications will add complexity to the system. Some manufacturers are already making automotive compute platforms based on ARM chips [NVIDIA15].

An HSM is a separate and distinct trustworthy computing device. Depending on the HSM, it may have more mitigations against physical tampering, and it may have more powerful computational capabilities. Depending on the features, it may meet VBSS message signing, message verification, key management, and policy enforcement operational constraints. HSM cost varies from the IBM 4765 [IBM4765] that costs several thousand dollars to HSMs for more specific applications cost less. For this application, a custom design produced at scale should be cheaper than more general HSMs; the cost should be feasible for connected vehicle technology. Additional HSM experimentation is needed to verify HSM suitability.

## Section 5: VPKI Revocation Goals

The trust among vehicles will be depend on the effectiveness of misbehavior detection and revocation subsystems within the PKI. With imperfect revocation, vehicles may trust an untrustworthy BSM. Traditional CRLs attempt to address all abnormal actors. There are three basic problems with this approach: first, list growth; second, determining when an actor on the list can be removed; and third, checking the list efficiently. These basic problems are particularly hard to contend with in a large, dynamic

environment. There are several properties of this environment that may call for examination of different methods to revoke misbehaving vehicles:

**Area of Concern**: Vehicles are only concerned about those vehicles that are immediately within their range (e.g., 300m to 1000m range for DSRC is realistic); this area is small, and it is always changing.

**Population of Concern**: For most drivers, the subset of vehicles that they will encounter over the life of their vehicle will be significantly smaller than the set of all participating vehicles. In other words, most traditional CRL-identified actors are irrelevant for particular drivers. The core challenge is the variation in participating vehicle travel patterns in the U.S. Some drivers will encounter significantly more actors on the CRL than others; therefore, placing restrictions on which misbehaving vehicles are added to the CRL based on geography may cause drivers to trust vehicles they should not.

**Immediacy of Concern**: Of those vehicles within our area of concern, V2V systems should only focus on vehicles whose trajectory will bring them close to our immediate position; a vehicle may be in our area of concern but its trajectory may never pose a safety problem to our vehicle.

**Duration of Concern or Duration of Misbehavior**. Malfunctions may occur in the devices that provide data to include in safety messages and in devices used to corroborate vehicle misbehavior. Malfunctions may be short-lived. In the case of a short-lived malfunction, it would be a huge inconvenience for the driver to have to re-enroll in the VPKI for something that was caused by environmental factors.

The misbehavior and revocation goals for a PKI follow. Many of these goals may not be completely achievable in a system of this scale:

*Correct detection and classification of participants.* In an ideal system, the false positive (incorrectly labeling a vehicle as misbehaving when it is not misbehaving) rate is zero. The false negative rate (not labeling a vehicle as misbehaving when it is misbehaving) is also zero. If there are too many false positives, drivers may ignore safety warnings. With too many false negatives, the opportunity for accidents grows but well-behaved participants may never notice the existence of the unrevoked bad actors. In both cases, trust erodes. In addition to perfect actor classification, an ideal system should correctly identify unintentionally misbehavior and intention misbehavior.

*Immediate removal of misbehaving participants.* This goal relates to the immediacy of revocation – ideally, detection and revocation happen simultaneously along with notifying the remaining participants in the system of the revocation. In short, identified misbehaving vehicles are immediately unable to interact with others in the PKI; there is no delay. With a system of this scale, this goal cannot be met.

*Removed unintentional abnormal actors can immediately rejoin after their vehicle is fixed.* If an unintentional misbehaving vehicle is revoked and then fixed, the driver would expect that the vehicle's communication would be restored. Authenticating the unintentional misbehavior is important; this relies on correct detection and classification of participants, and it may be difficult to do.

*Upon one or more revocations, remaining non-revoked vehicles continue to function without interruption or extra work*. When a vehicle is revoked, the good vehicles that remain should be able to participate in the PKI without interruption and without extra work (except CRL use). In some potential VBSS schemes [Tengler07, White09, Haas09], a normal non-misbehaving vehicle may have to do some amount of extra work to remain in the system. When comparing revocation systems, the amount of extra work that a non-misbehaving vehicle must perform to remain part of the PKI is a potential metric of comparison.

## Section 6: Misbehavior Detection: From Local to Global

The number of vehicles that will be revoked over some defined time period is a valuable estimate when determining the feasibly of a vehicular credential management system. In a traditional PKI, revocation strategies are used to handle inappropriate or malicious use of credentials. In a VPKI, revocation strategies are needed to address malfunctioning vehicles, as well as malicious vehicles that could cause vehicle mishaps. Since this system has not been realized or simulated at scale to our knowledge, estimates are hard to derive and justify. Four classes were identified to stratify the broader estimation problem. These numbers are used to estimate the degree to which revocation will be required in the VPKI being considered for the U.S.

*Malicious vehicle*. Total elimination of malicious actors is improbable. A malicious participant may avoid detection by learning how global misbehavior detection is performed, for instance the period of time over which misbehavior reports are retained. We hypothesize vehicle credential compromise will be very difficult initially based on the diversity of vehicles, hardware, access points, and communication protocols.

The security posture in this domain makes it hard to estimate the likelihood of certificate compromise. We anticipate that this number will be low compared to the population of malfunctioning vehicles.

*Malfunctioning vehicles*. Electronic components typically fail early in their lifecycle due to manufacturing defects that escaped quality control and much later when the device reaches its time-to-failure. In between those times, component failure rates remain fairly constant. Component failure rate is also hard to estimate, since many of the components used in these systems are still being developed. Depending on a component's function, it may be possible for the vehicle to self-validate information and avoid broadcasting inaccurate BSMs. Assuming that this capability is possible, we anticipate that the number of resulting revocations will be low.

*Environmental-Impacted Malfunctioning Vehicles – vehicles whose component accuracies are affected by environmental conditions*. Environmental conditions could lead to a wide range of issues. We do not estimate the impact here.

*End-of-life Vehicles*: This class of vehicles presents a dilemma: on one hand, we can assume that these vehicles have been completely removed from the system; on the other hand, parts are routinely harvested from end-of-life vehicles and security credentials are potentially valuable resources for bad actors. When the credentials do have value, attackers may harvest certificates from end-of-life vehicles, and then find a way to use them to broadcast targeted messages. We estimated that there are approximately 1 million end=-of-life vehicles per month. Identifying these vehicles and revoking them is a challenge.

Previous estimates put the total population estimates from these three vehicle populations at a relatively low value [Whyte13].

Figure 3 identifies the infrastructure entities involved with misbehavior detection and revocation. The operations involved in misbehavior detection and revocation start with local misbehavior detection and misbehavior reporting. Misbehavior reports are generated by a vehicle that detects an anomalous safety message; the message has a prescribed format; it is encrypted and sent through the infrastructure to the

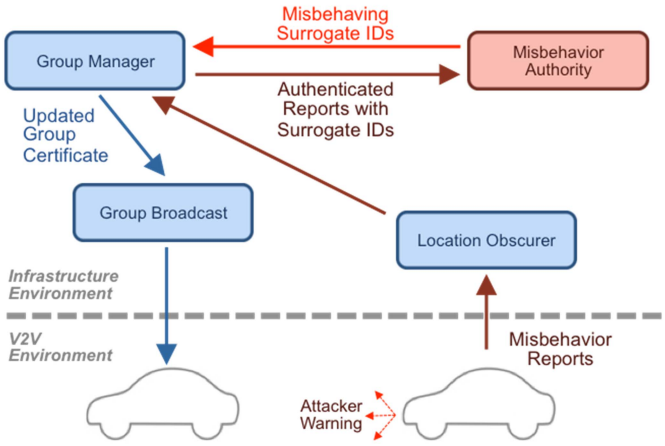


**Figure 3: Misbehavior Reporting and Group Certificate Updates**

group manager. Global misbehavior detection operates on a collection of misbehavior reports. Finally, group credentials must be modified and redistributed to the participant population.

Local misbehavior detection is a vehicle's intrinsic ability to use on-board hardware (e.g., vehicle-resident sensors) and software to detect safety messages that do not conform to physical reality. This locality is opposite a global system where a central networked system performs misbehavior detection. Local misbehavior detection can be done using software that detects simple safety message anomalies, or in a more complex system corroborate information collected from a vehicle's organic sensors (e.g., radar, lidar, sonar) with received safety messages to determine irregularities more accurately. In global misbehavior detection, other infrastructure components (e.g., a RSU or misbehavior authority) determine if a vehicle is misbehaving.

In recent work, using vehicle-resident sensors, researchers have explored attacker-warning systems that can be used independently or in conjunction with misbehavior reporting and revocation [Calandriello11]. The attacker-warning concept that we outline can extend the range of a vehicle's inherent warning sensors; on-

board sensors may have line-of-sight range or be blocked by surrounding vehicles. Attacker warnings need be within the range of DSRC communications. One of the challenges in realizing an attacker-warning system is trust. Much of the information is provided by sensors whose readings may be suspect (e.g., GPS). Additionally, this is a consensus-based concept without a central trusted authority; this is a significant obstacle. A conceptual attacker warning might employ three operations:

1. Local, or inherent, misbehavior detection
2. Warning transmission: Vehicles and roadside equipment should broadcast warning messages over DSRC to other vehicles in their area of concern. The following information may be important for vehicles able to receive these warnings:
    - The actor's pseudonym certificate. Although these certificates are short-lived, one or two certificates may be sufficient to span the time over which the warned vehicle may encounter the actor.
    - Report time. Due to immediacy of concern and duration of misbehavior, it may be appropriate to limit a warning message's valid time.
    - Reporter position. A vehicle's location changes and may not impact a given situation. This proximity information may help validate the warning or the need to consider the warning. While this could impact privacy, there may be ways to not report the position globally but use this information locally.
    - Consensus information. As a measure to improve warning system trust, warning recipients could rebroadcast validated warning messages with an updated confidence value. Warnings with higher confidence should be more trustworthy.
3. Warning processing: Vehicles should be able to receive and evaluate warnings, and then use these warnings in conjunction with safety messages to improve their safety posture.

There are motivations to combine several approaches. A vehicle can enforce a local policy based on local misbehavior detection. Local misbehavior adjudication helps use valuable DSRC resources more efficiently, decreases the computation required during global adjudication, and it has the potential to reduce global misbehavior detection errors.

Since the effectiveness of using any revocation scheme is unknown in this large-scale VPKI deployment, an incremental approach to handling misbehavior may be worth consideration. In this incremental approach, local misbehavior detection is the most critical; an attacker-warning system might be introduced next; finally, misbehavior reporting to a global authority might be required to improve the overall trustworthiness of the system at the expense of significant communication and processing overhead.

Each misbehavior report contains details from one or more safety messages that the vehicle used to determine local misbehavior. The reporting vehicle must sign all reports to avoid malicious reports from being processed; encryption may also be necessary to maintain the confidentiality of the reporter. In our conceptual VBSS, misbehavior reports flow through a network traffic obfuscator, similar to one that was previously introduced [Whyte13]. Reports are then handed off to the group manager. The group manager verifies the report using the appropriate version of the group certificate making sure the reporting vehicle has not been removed from the group. Then, the group manager will "open" a signed BSM to identify the misbehaving vehicle that signed that BSM and assign it an ephemeral proxy identifier. The purpose of the proxy identifier is to provide a way for the misbehavior authority to aggregate reports on a specific vehicle and not have secret information on a particular driver. A collection of reports on a vehicle does not automatically imply misbehavior; therefore, the misbehavior authority should know as little as possible about the identity of the vehicles it is analyzing in the aggregate. Proxy identifiers will be short-lived, so they do not become unique persistent identifiers and allow the misbehavior authority to break the privacy of vehicles that are found to be behaving correctly. Authenticated reports with a proxy identifier are then passed to the misbehavior authority.

The Misbehavior Authority is responsible for gathering misbehavior reports globally from all the participants in the connected vehicle system. Ideally, the misbehavior authority should be a central entity within the infrastructure; however, misbehavior authorities that are collocated with distributed group managers should be investigated. Global misbehavior detection algorithms are an open area of research [Delgrossi12]; however, one critical property of these algorithms will be their true positive and true negative rate.

Once the misbehavior authority has identified misbehavior, the group manager will remove that vehicle from the group by distributing updated public data including an updated group certificate that will disallow revoked vehicles from continued participation. A removal operation is performed for each validated misbehavior report. In other words, the number of operations necessary to update the trust elements in the

system is linear in the number of revoked vehicles. After a number of removals have been made, group certificate updates will be distributed to system participants. However, the size and number of trust elements is fixed with groups.

## Section 7: VBSS Revocation

If a BSM sender or receiver has an outdated group certificate, messages sent between the parties may not be verifiable. This issue holds with many of the group signature schemes. One way to address this issue is to assign vehicles to multiple groups. Assume that a given vehicle is a member of two groups. If one of its two group public keys is old, then the user can use the other corresponding private signing key to create message signatures that can be authenticated. Alternatively, assume both group public keys are old (i.e., the group manager has revoked at least one member in each group). The user may not be able to communicate with other users that are using the most recent public group keys.

As a possible alternative to addressing unsynchronized public key updates, we propose that revocation be staggered. For example, rather than each group member storing a single group public key for a given group, the group member stores the current group public key and the previous group public key. If a group member updates her group public key, she can then verify messages from senders that have updated to the latest group public key, and she can also verify messages from senders who use the previous group signing key. By staggering group public key updates, the immediacy of user updates can be relaxed.

In a traditional PKI, participants may submit certificates to a central authority to check whether they are on the CRL. CRLs may be broadcast to users, so users can check the certificates they receive locally. CRL updates are usually promulgated using delta lists to decrease the amount of communication overhead. When short-lived certificates are used, a central authority can utilize a blacklist to identify those participants whose certificate expirations should not be extended or renewed. The primary issues with these traditional approaches are list management (additions and removals), list size, and list distribution. CRLs have global context: all participants must have knowledge of the complete list since they may interact with a revoked participant.

In a group-based VBSS, the group manager can identify a message sender, since they can "open" a de-identified group signature on a pseudonym certificate. Their role can be split to further distribute the trust elements and make it harder to break privacy, but ultimately when a misbehaving vehicle has been identified its privacy is assumed to be forfeit.

Misbehavior reporting, adjudication, and revocation synchronization challenges exist in the real-time and distributed V2V environment. Because the identification and revocation of a bad participant is not immediate, we now examine how delayed revocation impacts a group revocation system. Figure 4, depicts the evolution of the V2X environment over a period of time where two vehicles have been reported as misbehaving and subsequently revoked from the group. While this figure illustrates some of the synchronization challenges in a VBSS based on groups, other designs [Whyte13] may be susceptible to synchronization issues. In the Figure, time progresses from left to right; the dotted arrow delineates the state of the infrastructure (top) and the state of the vehicular environment (bottom). For simplicity, all vehicles are part of one group. Both environments start in a good state (green) at the left: all parties are using group certificate one (GC1).

In VBSS, vehicle revocation can only occur when misbehavior has been reported, and the misbehavior authority classifies the identified vehicle as misbehaving. These actions will not occur instantaneously. In the Figure, there is a time gap between the Vehicle A misbehavior report and misbehavior adjudication and creation of GC2. Since we have perfect hindsight and Vehicle A is truly misbehaving, the trust state of the V2V environment is degraded at the point in time when Vehicle A started misbehaving – Vehicle A will be

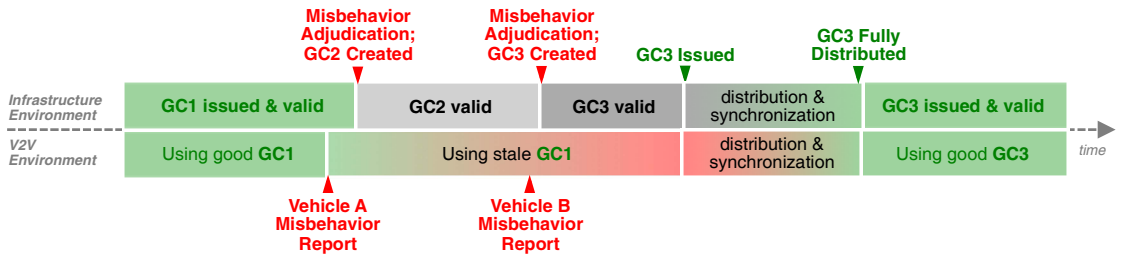


**Figure 4: Misbehavior Reporting and Revocation Synchronization**

trusted by other vehicles, but it will be transmitting potentially untrustworthy messages that will be verified by recipients. The gradual transition from green to red in the lower portion of the Figure illustrates the effect of this state; more and more vehicles encounter the misbehaving vehicle and will trust its broadcast safety messages. In an ideal system, this transition would not exist; however, misbehavior reporting, misbehavior adjudication, and distribution of updated credential will require time. Decreasing the transition from green to red and back to green is a goal.

When a vehicle is revoked, the group public key must be updated. The infrastructure may not issue new group certificates every time a vehicle is revoked. The propagation of new group certificates consumes communication resources and time.

The gray color in the Figure indicates the time period when the infrastructure's group certificate state differs from the group certificate's state in the V2V environment, because GC2 was not issued by the infrastructure. After the second misbehavior adjudication has been integrated into the group certificate, GC3 is ready to be issued. The group manager then re-issues updated group certificates on a schedule to minimize synchronization problems. Once new credentials are released, vehicles and roadside equipment can transmit these updates to vehicles that have not received the update yet.

In the Figure, the trust of the system is degraded from the time the first vehicle misbehaves until GC3 has been fully distributed. At this point, both environments are synchronized. Any group-signed messages the misbehaving vehicles broadcast will not be verifiable using the updated credentials.

To protect against misbehaving vehicles that have not been revoked, local misbehavior detection is a potential first line of defense. During the distribution and synchronization period, the system gradually returns to a fully trusted state. Certificate caching can be introduced to alleviate the problem of unsynchronized group certificates. Let $GC_x$ be group certificate $x$, and let each vehicle cache two GC versions: $GC_{x-1}$ and $GC_x$. We assume the sender is using pseudonyms generated using their most recent GC. Each signature includes a signed identifier (e.g., the value one for a message signed by $GC_1$, the value two for a message signed by $GC_2$, etc.). A vehicle can quickly check if it has the most recent GC by checking the identifier.

We consider six abnormal cases where four GC versions have been issued ($GC_1$, $GC_2$, $GC_3$, and $GC_4$), where $GC_4$ is the most recent GC. In each case, vehicle A is sending a basic safety message to a receiver, vehicle B. Both vehicles can store up to two certificates. To enable communication between two vehicles, they must have at least one $GC_x$ in common.

**Case 1: Functioning with Old Certificates.** Both vehicles have cached $GC_1$ and $GC_2$. Vehicle B can validate vehicle A's message. If vehicle A has not been revoked, their interaction is equivalent to the case where the most recent update is $GC_2$ despite both vehicles being out of synchronization with the infrastructure. If vehicle A has been revoked, $GC_3$ or $GC_4$ should reflect their removal from the group. However, in their current state vehicle B's trust will be misplaced. To remedy this situation, B should update to $GC_4$ as quickly as possible.

**Case 2: Delay in Revocation.** Both vehicles have $GC_3$ and $GC_4$. B can validate A's message. It is possible that A could have been reported as misbehaving, but a new update has not been issued – this case must be handled by local misbehavior detection.

**Case 3: Partially Unsynchronized Old Sender.** A has $GC_1$ and $GC_2$ in its cache; B has $GC_2$ and $GC_3$ in its cache. B can validate A's message using $GC_2$. If A has not been revoked, the exchange is equivalent to the case where the most recent update is $GC_2$. If A has been revoked in $GC_3$ or $GC_4$, then B's trust will be misplaced. In all situations, B can notify A that its certificates are out of date since it had to use an outdated certificate to validate the pseudonym. This should cue A to pull the $GC_4$ update (from a road-side unit or nearby vehicle) and generate new pseudonyms. This case is the main reason more than one GC is cached. B could not verify A's messages if B could only store the latest GC, $GC_3$. With the caching of GCs, A and B can still communicate.

**Case 4: Partially Unsynchronized Old Receiver.** Vehicle A has $GC_2$ and $GC_3$; vehicle B has $GC_1$ and $GC_2$. B can only verify A's signatures if A is using old pseudonyms; this would be abnormal for A. If A were using updated pseudonyms, B will not be able to authenticate A's pseudonyms. In the first case (A uses $GC_2$), B would still be unaware that it needs to update its certificate but could continue communicating with A; in the later case, B will know to update its certificate when it finds $GC_3$ was used.

**Case 5: Unsynchronized Old Receiver:** A has $GC_3$ and $GC_4$; B has $GC_1$ and $GC_2$. B cannot verify any signed messages from vehicle A. This does not mean that vehicle A's messages are untrustworthy. The signature identifier is a cue for B to check for an updated GC.

**Case 6: Unsynchronized Old Sender.** A has $GC_1$ and $GC_2$; B has $GC_3$ and $GC_4$. B cannot validate messages from A. This may mean that A's messages cannot be trusted, or if A is trustworthy it is due to B not having $GC_2$ in its cache. The signature identifier cues B to obtain an updated group certificate.

Significant communication savings may be possible by using group certificate revocation strategies instead of more traditional certificate revocation lists. When a new vehicle joins a VBSS, it will receive an initial load of group certificates that enable it to authenticate the vehicles within its geographic area. However, only being able to communicate to vehicles in its own geographic area may be insufficient for vehicles that travel outside of their local area. How groups are determined and established is an important area of research. The design must incorporate several factors including the type of large-scale revocation (e.g., recalls) that might be required, laws, and the capabilities of stakeholders to perform certain group manager functions. One possible configuration involves dividing the vehicle population by states, manufacturer, and model.

Because the size of the group certificate is fixed, the storage needed for all of the group certificates is the constraining factor. A group certificate is approximately 900 bytes [Calandriello11] (could potentially use smaller key sizes for reduced certificate sizes). We can use this information to reason about how many groups a VBSS should support. Based on our notional group partitioning strategy, vehicles must store 15,000 group certificates to cover the entire U.S. This will be unnecessary for almost all vehicles in the system. However, if these certificates were stored on the vehicle, the total storage capacity needed would be approximately 13 MB. If we cache the previously used group certificate, then the total amount of storage would be almost 27 MB. These certificates are public and not identifying, so they do not need to be stored in memory whose access is restricted to trusted software and hardware. Our concept includes a mechanism for distribution of trust updates; therefore, storage of this number of group certificates may not be necessary.

**End-of-life vehicles.** Scaling to address end-of-life vehicle revocation is difficult. As previously noted, there are approximately 1 million vehicles that reach their end-of-life each month in the U.S. Adding these vehicles to a traditional revocation list is prohibitive. To address these vehicles in a group PKI, group certificate size remains fixed independent of the number of updates. The group update distribution process benefits from the fixed group public key size. Traditional CRLs grow linearly in the number of vehicles. In a traditional PKI approach, accommodating end-of-life revocations will make revocation infeasible.

## Section 6: Conclusion

Traditional PKIs have been designed and used for specific types of problems where privacy is not a concern (e.g., email). This lack of privacy is an issue for a vehicle PKI. Parties in a traditional PKI will exchange keys and later send and receive messages. When a recipient verifies a message, they assumes that the sender is trustworthy. In a vehicle PKI, a receiver must trust the sender without identifying the sender – the sender should remain anonymous. This is a challenging problem at a large scale, and a different way of approaching the problem is needed. To provide privacy at a large scale, we suggest the use of a group-based approach for VBSS. Our initial analysis shows that using groups in a vehicle PKI helps mitigate some of the issues that we see in other systems.

A great deal of work has been done to address vehicle security and privacy; however, more work and field trials are necessary. Trustworthy hardware may be required on all connected vehicles to protect credentials; it will certainly be necessary to protect a group signing key and the pseudonym generation process in a VBSS. The BSM transmit and receive rates envisioned in high density V2V environments may require high performance trustworthy hardware in vehicles. This system's trust is predicated on the acceptable operation of a misbehavior detection and revocation system. The right balance of local and global misbehavior detection is critical, and more misbehavior simulation and experimental results will help us establish what will be an acceptable operational state. By integrating group certificates, VBSS may address some of the revocation overhead issues in a system of this size; staggered (or cached) group certificate updates offer additional benefits.

An operational VPKI that provides an acceptable level of security and privacy would be a groundbreaking achievement. We are optimistic about the possible solutions VBSS offers: Putting pseudonym generation in the vehicle has benefits; the inherent privacy preserving properties of group signature cryptography mitigates certain types of infrastructure growth. We encourage research that enables a vehicle to produce its own ephemeral certificates while protecting privacy. Using groups, vehicle privacy is maintained through the anonymity afforded by a group. As vehicle PKI research and technology becomes more focused, the unique challenges this environment presents will be addressed and the promise of safer vehicles will be realized.

## Acknowledgements

This research was funded by the National Highway Traffic Safety Administration (NHTSA). To date, NHTSA has posed questions and provided insight that has helped guide this work. We would also like to thank Lawrence MacIntyre and Jarilyn Hernandez, our colleagues at the Oak Ridge National Laboratory, for their valuable feedback on this research.

## Section 7: References

**[Al-Fuqaha07] A. Al-Fuqaha and O. Al-Ibrahim. Geo-encryption Protocol for Mobile Networks. *Computer Communications*. 30(11-12):2510-2517. Sept. 2007.**

**[ARM09] ARM. ARM Security Technology: Building a Secure System using TrustZone Technology. Available at http://infocenter.arm.com/help/topic/com.arm.doc.prd29-genc-009492c/PRD29-GENC-009492C_trustzone_security_whitepaper.pdf. 2009.**

**[ARM14] ARM. http://next100billionchips.com. *Internet Archive Wayback Machine*. July 15, 2014. Available at https://web.archive.org/web/20140715212213/http://www.next100billionchips.com/.**

**[Ateniese00] G. Ateniese, J. Camenisch, M. Joye, and G. Tsudik. A Practical and Provably Secure Coalition-resistant Group Signature Scheme. In *Proceedings of the 20th Annual Crypto Conference (CRYPTO)*. August 2000.**

**[Ateniese02] Giuseppe Ateniese, Dawn Song, Gene Tsudik. Quasi-Efficient revocation of Group Signatures. *Financial Cryptography*. March 2002.**

**[Bellare03] Mihir Bellare, Daniele Micciancio, Bogdan Warinschi. Foundations of Group Signatures: Formal Definitions, Simplified Requirements, and a Construction Based on General Assumptions. In *Advances in Cryptology – EUROCRYPT 2003*, *Lecture Notes in Computer Science (LNCS) Vol. 2656, E. Biham ed, Springer-Verlag, p. 614-629.* May 2003.**

**[Bellare05] Mihir Bellare, Haixia Shi, Chong Zhang. Foundations of Group Signatures: The Case of Dynamic Groups. In *Topics in Cryptology – CT-RSA 2005, Lecture Notes in Computer Science (LNCS) Vol. 3376, A. Menezes ed, Springer-Verlag,* 2005.**

**[Boneh04] Dan Boneh and Hovav Shacham. Group Signatures with Verifier-Local Revocation. In *Proceedings of the 11th ACM Conference on Computer and Communications Security* (CCS). p. 168-177. October 2004.**

**[Calandriello11] Calandriello, G.; Papadimitratos, P.; Hubaux, J.-P.; Lioy, Antonio, "On the Performance of Secure Vehicular Communication Systems," *Dependable and Secure Computing, IEEE Transactions on* , vol.8, no.6, pp.898-912, Nov.-Dec. 2011. [Camenisch02] Jan Camenisch and Anna Lysyanskaya. Dynamic Accumulators and Application to Efficient Revocation of Anonymous Credentials. In *Advances in Cryptology – CRYPTO 2002*. *Lecture Notes in Computer Science (LNCS 2442).* p. 61-76. September 2002.**

**[Chaum91] David Chaum and Eugene van Heyst. Group Signatures. In *Advances in Cryptology – EUROCRYPT 1991 (LNCS 547). p. 257-265.* April 1991.**

**[Delgrossi12] Luca Delgrossi and Tao Zhang. Vehicle Safety Communications. *Wiley.* 1st ed. October 2012.**

**[DOT811492D] DOT. Vehicle Safety Communications – Applications (VSC-A). Final Report: Appendix Volume 3 Security. *CAMP*. DOT HS 811492D. Sept. 2011.**

**[FHWA11] Federal Highway Administration's Office of Highway Policy Information, Highway Statistics Series, http://www.fhwa.dot.gov/policyinformation/statistics/2011/. September 2011, Accessed 2014.**

**[Haas09] Jason J. Haas, Yih-Chun Hu, Kenneth P. Laberteaux. *Security and Communication Networks*. John Wiley & Sons, Ltd. September 2009.**

**[Help14] HelpScout. 75 Customer Service Facts, Quotes & Statistics. Available at http://www.helpscout .net/75-customer-service-facts-quotes-statistics/.**

**[Huang09] Dijiang Huang, Mayank Verma. ASPE: attribute-based secure policy enforcement in vehicular ad hoc networks. In *Ad Hoc Networks*. 7(8):1526-1535. November 2009.**

**[IBM4765] IBM. IBM 4765 PCIe Cryptographic Coprocessor. Available at https://www-03.ibm.com/security/cryptocards/pciecc/pdf/PCIe_Spec_Sheet.pdf.**

**[Kursawe04] Klaus Kursawe. Trusted Computing and its Applications: An Overview. In *ISSE 2004 – Securing Electronic Business Processes*. Springer. September 2004.**

**[Nakanishi05] Toru Nakanishi and Nobuo Funabiki. A Short Verifier-Local Revocation Group Signature Scheme with Backward Unlinkability from Bilinear Maps. In *ASIACRYPT 2005. Springer-Verlag, LNCS 3788.* p. 533-548. December 2005.**

**[NADA14] NADA. NADA DATA Annual Financial Profile of America's Franchised New-Car Dealerships. www.nada.org. 2014.**

**[NHTSA14] National Highway Traffic Safety Administration (NHTSA), USDOT. U.S. Department of Transportation Announces Decision to Move Forward with Vehicle-to-Vehicle Communication for Light Vehicles. *Press Release*. Available at http://www.nhtsa.gov/About+NHTSA/Press+Releases /2014/USDOT+to+Move+Forward+with+Vehicle-to-Vehicle+Communication+Technology+for+Light+ Vehicles. February 3, 2014.**

**[NVIDIA15] NVIDIA. Buy Jetson TK1 DevKit. Available at https://developer.nvidia.com/jetson-tk1.**

**[Raya06] Maxim Raya, Daniel Jungels, Panos Papadimitratos, Imad Aad, Jean-Pierre Hubaux. Certificate Revocation in Vehicular Networks. *LCA Technical Report*. 2006.**

**[ST13] STMicroelectronics. ST19NP18-TPM Data Brief. Available at http://www.st.com/st-web-ui/static/active/en/resource/technical/document/data_brief/DM00039003.pdf. November 2013.**

**[Tengler07] Steve Tengler, Scott Andrews, Ronald Heft. Digital Certificate Pool. *U.S. Patent US20070223702 A1*. Sept. 2007.**

**[White09] Robert G. White, et al. Privacy and Scalability Analysis of Vehicular Combinatorial Certificate Schemes. In *Proceedings of Consumer Communications and Networking Conference*. January 2009.**

**[Whyte13] William Whyte, Andre Weimerskirch, Virendra Kumar, Thorsten Hehn. A Security Credential Management System for V2V Communications. In Proceedings of the Vehicular Networking Conference (VNC). December 2013.**

# UNOBTRUSIVE BREATH ALCOHOL SENSING SYSTEM

**Bertil Hök**
Hök Instrument AB
Sweden

**Håkan Pettersson**
Autoliv Development AB
Sweden

**Jonas Ljungblad**
Hök Instrument AB
Sweden

Paper Number 15-0458

## ABSTRACT

Although the vast majority of vehicle drivers are sober, drunk driving remains to be a major contributor to fatal accidents. Massive deployment of unobtrusive breath alcohol sensing systems could potentially save tens of thousands of lives worldwide every year by preventing drunk driving [1]. The work reported here is ultimately aiming at such a system. The technical performance of the present sensing system with respect to automotive requirements is summarized, and new results towards unobtrusive breath alcohol determination within vehicle compartments are presented.

Breath alcohol concentration (BrAC) can be determined unobtrusively if (i) the sensing system provides real-time signals with adequate accuracy corresponding to the local concentrations of both alcohol and a tracer gas, e g $CO_2$, (ii) the dilution of the breath is not excessive in relation to background concentrations, (iii) the sensor location can be seamlessly integrated into the interior of a vehicle cabin. All three of these aspects are addressed in the present paper.

More than a hundred prototypes based on infrared spectroscopy were fabricated and subjected to automotive qualification tests in the full temperature range -40 … +85$^0$C. In the majority of tests, adequate performance was noted. Measures are now being taken to fill remaining performance gaps. Test results with human subjects were positive and in accordance with expectations with respect to physiological variations. In-vehicle tests showed that for the best sensor position, passive breath samples allowed BrAC to be determined at a resolution of 2-4% of the US legal limit, providing proof-of-principle for unobtrusive testing. Nevertheless, vehicle integration remains to be the major technological challenge to the objective of deployment on a large scale of unobtrusive driver breath alcohol determination.

The feasibility of unobtrusive breath alcohol determination in vehicles, and adequate performance of a sensor system based on infrared spectroscopy have been experimentally demonstrated. The alcohol sensing system may advantageously be integrated into vehicles, and may also be combined with other technologies to monitor driver impairment.

## INTRODUCTION

Although the vast majority of vehicle drivers are sober, drunk driving remains to be a major contributor to fatal accidents. Many informative and persuasive initiatives have been undertaken. Devices for the determination of breath alcohol concentration (BrAC) are commercially available for screening and evidential purposes, and alcohol interlocks are being increasingly used [2]. However, according to the driver alcohol detection system for safety (DADSS) initiative [3, 4], there is a need for radical improvement in order to make such devices acceptable on a

larger scale. The technology needs to be unobtrusive to the sober driver, and it should determine whether the driver's blood alcohol concentration (BAC) is above or below the legal limit with high accuracy. Deployment of such a technology on a large scale could potentially save tens of thousands of lives every year by preventing drunk driving.

Our research towards less obtrusive sensor systems for BrAC determination started in 2005. The envisioned system will unobtrusively and accurately detect alcohol in the driver's breath before the vehicle may be started, or while driving. In earlier publications, we have demonstrated methods and system solutions for contactless determination of BrAC [5, 6] in screening applications where sobriety is expected to be the norm. The physiological rationale of using a tracer gas, e.g. carbon dioxide ($CO_2$), for contactless determination was examined [7], and the usefulness of this technique in patients with reduced consciousness was demonstrated [8]. Recently, further progress towards unobtrusive and highly accurate BrAC determination in automotive applications has been demonstrated [9, 10, 11].

In this paper, an updated review of the methods and technology for unobtrusive and highly accurate breath alcohol determination is provided. New experimental results are presented on the technical performance of the sensing system with respect to automotive requirements. Results from human tests and in-vehicle unobtrusive testing are summarized and discussed in view of the overall objectives.

## METHODS AND TECHNOLOGY

### *Basic system function*

Breath alcohol concentration (BrAC) can be determined unobtrusively if (i) the sensing system provides real-time signals with adequate accuracy corresponding to the local concentrations of both alcohol and a tracer gas, e g $CO_2$, (ii) the dilution of the breath is not excessive in relation to background concentrations of both alcohol and the tracer gas, (iii) the sensor location can be seamlessly integrated into the interior of a vehicle cabin without undue influence from passengers or other sources of interference. These three aspects will be addressed throughout the paper.

The requirements of unobtrusiveness and high accuracy are seemingly contradictory. A key to resolving this contradiction is to introduce a two-step procedure, in which the first unobtrusive step is providing a preliminary result whether the driver's BrAC is above, say half the legal limit, or not. If below, the vehicle immediately becomes drivable ('green'). If BrAC is much higher than the legal limit, the drivability will be locked ('red'). A sober driver, and one with BrAC clearly above the legal limit, will thus perceive the system to be unobtrusive. If the unobtrusive BrAC reading is in the 'yellow zone' in between, the driver will be offered the possibility of providing an active breath test in order to determine BrAC with high accuracy.

Figure 1 schematically shows a typical time sequence starting by automatically switching on the sensor system when the car is unlocked. The sensor is staying in a standby mode until the door to the driver's seat is first opened and then closed. This is the point when the sensor is activated. The occurrence of a $CO_2$ peak is used as an indicator of a breath above the background level. If a corresponding peak of ethyl alcohol (EtOH) is detected at basically the same point in time, it is possible to estimate BrAC using the following equation

$$BrAC = EtOH_{meas} * DF = EtOH_{meas} * (CO2_{et}\text{-}CO2_{background}) / (CO2_{meas}\text{-}CO2_{background}) \quad (1).$$

The subscript 'meas' denotes the measured peak values, and '$CO2_{et}$' the end tidal $CO_2$ concentration, which is believed to approach the alveolar concentration, typically 4.8±0.5 vol% [7, 12]. DF is the dilution factor, ranging from one in highly concentrated air close to the mouth of the subject, to large numbers at a large distance. The background $CO_2$ concentration is typically less than 0.1 vol%. The standard measurement unit for BrAC is mg/L, which relates to blood alcohol concentration (BAC, %) by the approximate relation 1 mg/L BrAC = 0.2%BAC [13]. The US legal limit of 0.08%BAC thus corresponds to a BrAC value of 0.4 mg/L.

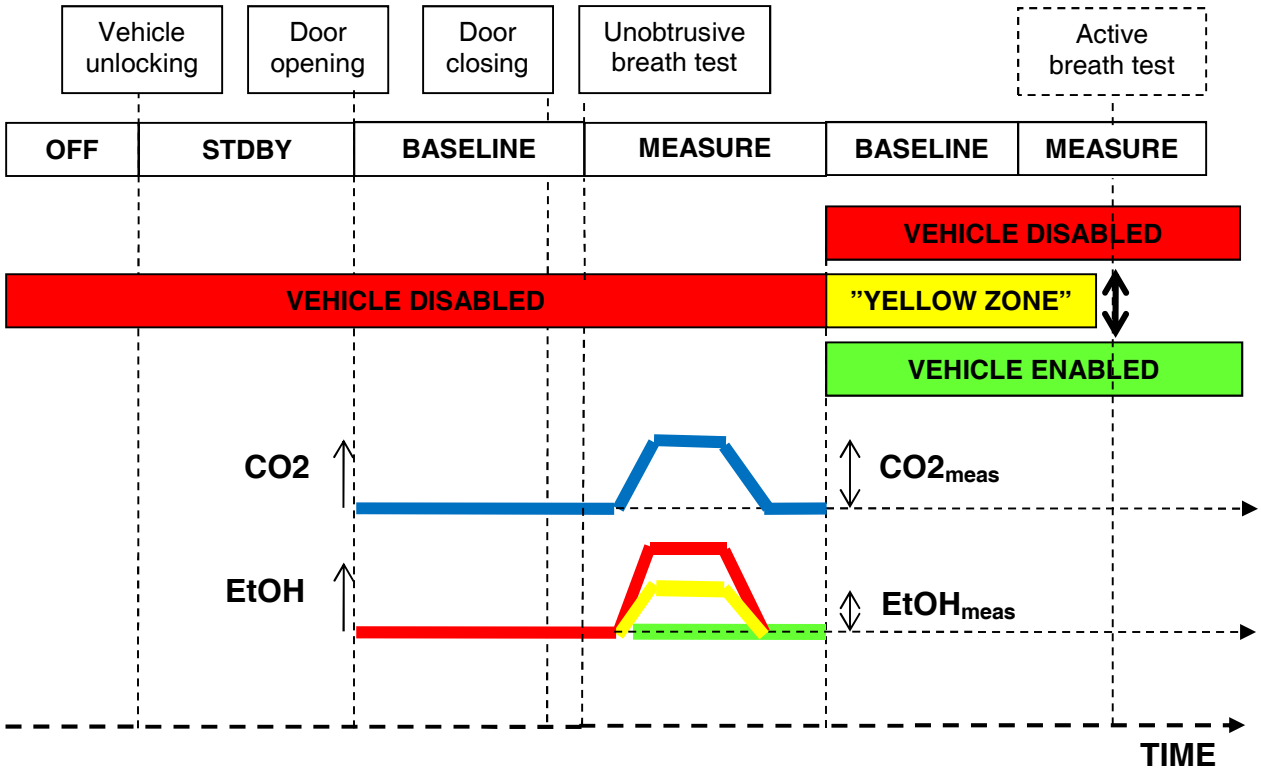


*Figure 1. Schematic time sequence of unobtrusive breath test.*

The active test to be performed when the unobtrusive test results in a "yellow zone" BrAC value, is expected to distinguish with a high accuracy whether or not the legal limit is exceeded. Then it is necessary to provide an undiluted breath sample (DF=1 in equation (1), independent of $CO2_{meas}$). It should be noted that continuous or intermittent monitoring using basically the same scheme is also possible during driving. Accumulating data over time adds to the accuracy of the system.

***System implementation***

The sensor system includes the following critical parts:

- Air inlet defining the sampling point at which air is continously being withdrawn, and fed to:
- A measuring cell including optical and sensing elements for real-time infrared transmission measurement for the selective detection of $CO_2$ and EtOH, respectively
- Signal processor for digitizing the sensor signals into a standard, calibrated format corresponding to local gas concentrations
- Auxiliary sensor elements to distinguish between a true breath and possible interference
- Main processor performing algorithms for breath recognition and BrAC determination, including eq. (1).

Three prototype generations of the system have been implemented so far. The 3rd generation devices were miniaturized compared to generation 2, with approximate dimensions 120 x 40 x 20 mm, packaged for handheld use

vehicle integration. Figure 2 shows photographs of the unpackaged device, a handheld implementation, and a possible future integration of the device into the A-pillar of a vehicle.

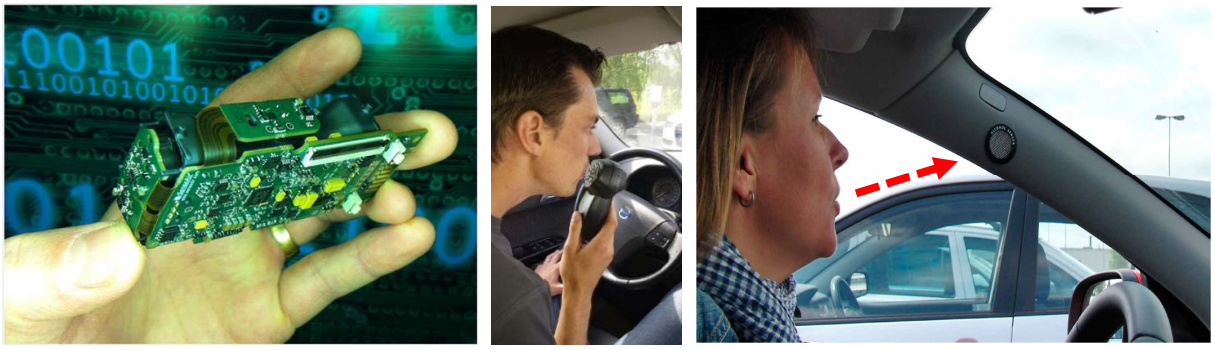

***Figure 2 Photographs of an unpackaged sensor (left), a handheld device (middle), and a device integrated into the A-pillar of a vehicle (right).***

With a handheld device operated at 3-5 cm distance, the dilution factor DF will be in the range 1.5-2.5. For a less obtrusive breath at 15-20 cm distance DF is typically 5-10.

***Experimental tests***

Extensive tests have been performed on the device and system levels, with experimental settings involving both artificial and human objects. The device level included automotive qualification tests, and tests on human subjects. More details of these tests are provided in the Results section.

In-vehicle system tests were performed in order to provide an understanding of the critical boundary conditions relating to unobtrusive breath alcohol determination. The breath flow is expected to be influenced by other flow sources, including ventilation, air conditioning, passengers, and obstacles within a vehicle compartment. The in-vehicle tests included theoretical simulations using finite element methods, and experimental visualization of breathing pattern using a phantom and water mist as an optical contrast medium. A third method was to position sensor prototypes at various locations within a vehicle compartment, and to record and analyze the sensor signals upon entrance of a human subject into the driver's seat.

## RESULTS

This section will provide a summary of results from automotive qualification tests, tests on human subjects, and in-vehicle tests.

### Automotive qualification test results

When possible, the tests were performed according to industrial standards. However, in several cases more stringent specifications were adopted [14, 15] compared to requirements according to current industrial standards. This was especially the case when the requirements related to measurement accuracy and startup time were examined in view of unobtrusive and highly accurate BrAC determination. More than a hundred complete devices of generation 2 and 3 have been fabricated and tested.

The test results are summarized in table 1, including columns of the test types, relevant limit values, standards, and test result. In total 18 test types were included, all of which primarily relate to the device performance. The majority of tests were performed on generation 2 devices. Results from generation 3 are underway and will be added in due course.

**Table1.**
**Results of automotive qualification tests.**

| Test | Limit | Standard | Test result |
|---|---|---|---|
| Unit-unit calibration error EtOH | ±5% | [14, 15] | Pass |
| Unit-unit calibration error $CO_2$ | ±5% | [14, 15] | Pass |
| Resolution | 2µg/L | [14, 15] | Pass |
| Linearity | ±2% | [14, 15] | Pass |
| Startup time at room temp | 5 sec | [14, 15] | - |
| Startup time at -40°C | 20 sec | [14, 15] | - |
| Power consumption | 70W peak, 8W cont. | [14, 15] | Pass |
| Function test 0°C … +85°C | ±0.03 mg/L | [14, 15] | Pass |
| Function test -40°C | ±0.03 mg/L | [14, 15] | - |
| Cross sensitivity | Acetone, … | EN50436-1,2 | Pass |
| Barometric pressure | 0.8 ... 1.1 bar | EN50436-1,2 | Pass |
| Manipulation, circumvention | - | EN50436-1,2 | Pass |
| Vibration test | - | ISO16750 | Pass |
| Mechanical shock | - | ISO16750 | Pass |
| Accelerated aging | Corr. to 15 yrs of use | [14, 15] | Pass |
| Corrosive atmosphere | $NO_x$, $SO_x$ … | [14, 15] | Pass |
| EMC | 200V/m immunity | [14, 15] | Pass |
| Application-like long term test | - | [14, 15] | Pass |

Table 1 summarizes the fact that the results met or exceeded the requirements in the majority of tests. There is still a gap between actual and required performance at extremely low temperature, and some improvement is required for the startup time.

**Human subjects study**

The human subject tests were motivated by the fact that the proposed technique represents a new method in need of experimental evidence. The results summarized here have recently been published in more detail elsewhere [10].

Thirty adult volunteers with an age distribution from 19 to 70 years were enrolled for the test and provided their informed consent to participation. The study was approved by the Swedish Ethical Review Board in Uppsala (dnr 2013-089). Each subject was instructed to consume alcohol with a target intoxication level of 0.06 to 0.10 %BAC (BrAC 0.3 to 0.5 mg/L) within 15 minutes. The dosage was decided using body weight as the main parameter. During the elimination phase, the subjects performed breath tests every 20 minutes, using generation 2 devices both in a contacting mode or operation with a mouthpiece, and without a mouthpiece at a distance varying from 3 to approximately 15 cm. On each of these occasions a reference BrAC value was obtained with an evidential breath analyzer, Evidenzer (Nanopuls AB, Uppsala, Sweden). A total number of 1,465 breath tests were performed.

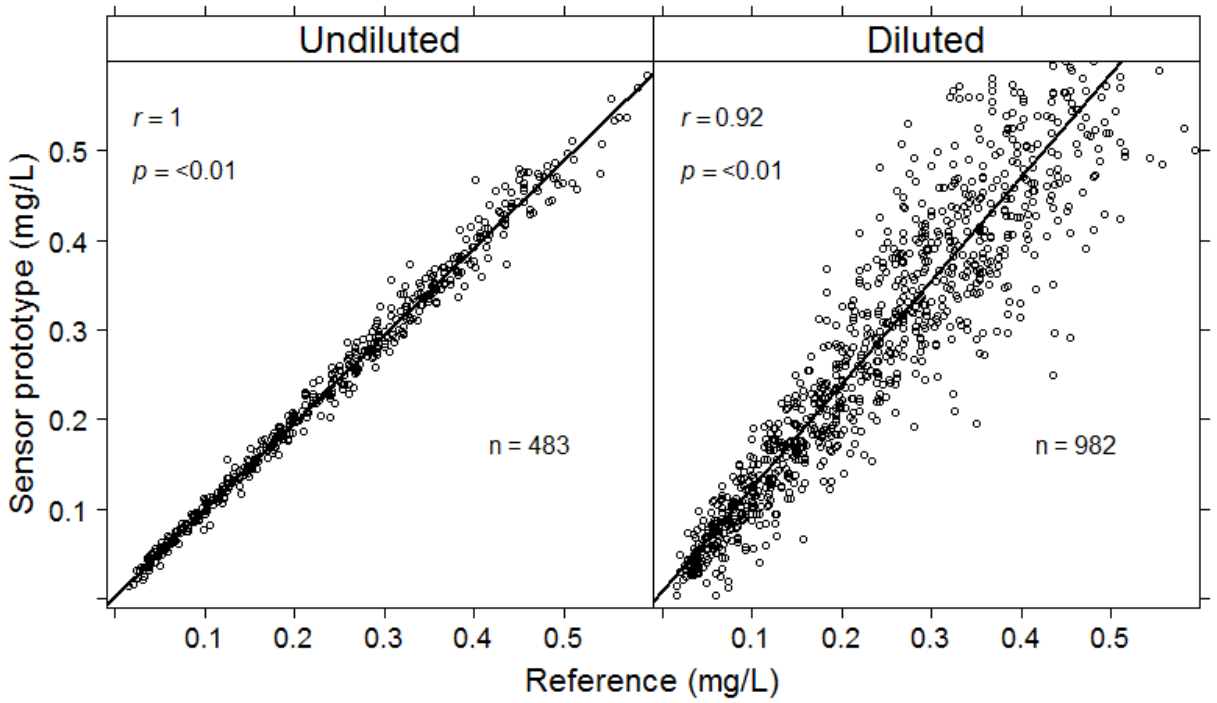


*a)* *b)*

***Figure 3 Results of human subjects test of thirty volunteers. The graph a) represents active tests with a mouthpiece and b) tests performed at 3-15 cm distance. Both graphs show measurement results with generation 2 devices (y-axis) compared to an evidential breath analyzer (x-axis).***

The results of the human subject study are summarized in Figure 3. The correlation between active tests (undiluted, DF=1, graph 4 a)) is excellent with a correlation coefficient of 1.00, providing experimental support of the technical performance summarized in the previous subsection.

As shown in Figure 3 b), the human tests performed at 3-15 cm distance exhibited much larger variations than the undiluted breath tests. In this graph, eq. (1) was used for calculation of BrAC. A striking feature is that the distribution is shifted upwards from the identity line. This can be understood from a systematic deviation between the end tidal value and the alveolar $CO_2$ concentration [7, 11, 12]. The distribution has a funnel shape, increasing with concentration. This is a direct result of eq. (1) and the dominating variability of $CO2_{et}$. Not shown in the presented graphs is that the sensor distance did not influence the distribution, despite the large variation from 3 to 15 cm [11].

**In-vehicle test results**

A theoretical model was designed for simulation of relevant phenomena relating to in-vehicle air flow dynamics using finite element methodology (ANSYS). The model represented an idealization of a real-world occupant compartment geometry in order to enable the study of basic mechanisms and phenomena at moderate requirements of processing capacity and computing time. Figure 4 a) shows a simulated breath flow being deflected by a stronger guide flow passing to the left of the driver's head. The guide flow is attracting the breath flow, thus creating a possibility to control the flow direction.

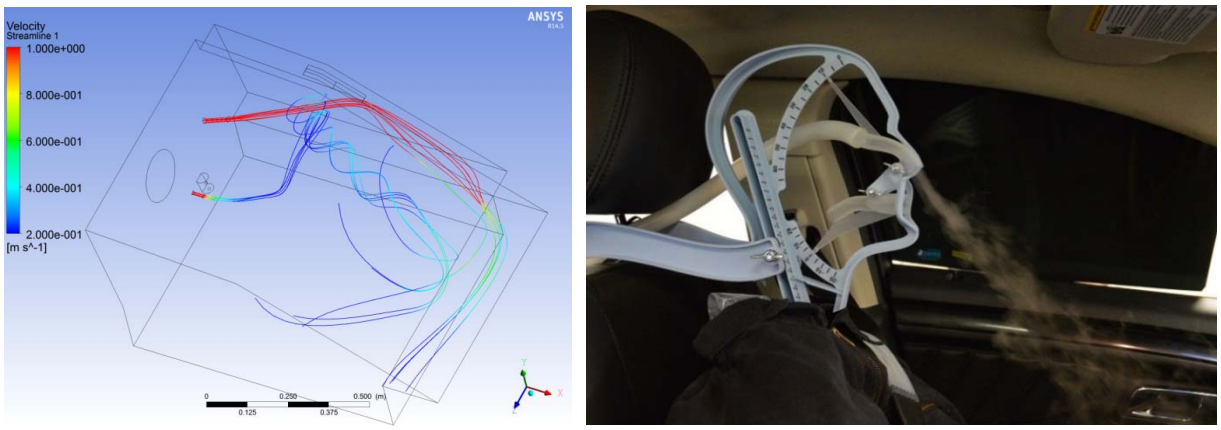


***Figure 4. a) Visualization of in-vehicle breath flow using FEM simulation (left). b) Breath flow from driver phantom visualized by a mist of water droplets (right).***

The experimental setup shown in Figure 4 b) was designed to enable air flow patterns to be visualized using a driver phantom, providing a realistic breathing pattern. A mist of water droplets injected into the flow was used as an optical contrast medium. Both mouth and nose breathing could be simulated using this setup.

The results of in-vehicle measurements using human subjects are summarized in Figure 5, showing graphs of measured EtOH concentration as a function of the dilution factor DF. A parabolic relationship between measured EtOH concentration and dilution is observed at given levels of BrAC, and is evident from eq. (1). Figure 5 a) also includes data of the range of dilution factors observed in a completely passive mode of operation. The in-vehicle tests were performed with volunteers instructed to control their exhalation either by nose or mouth. Data from the most favorable positions are included: Seat belt, sun shield, and steering column.

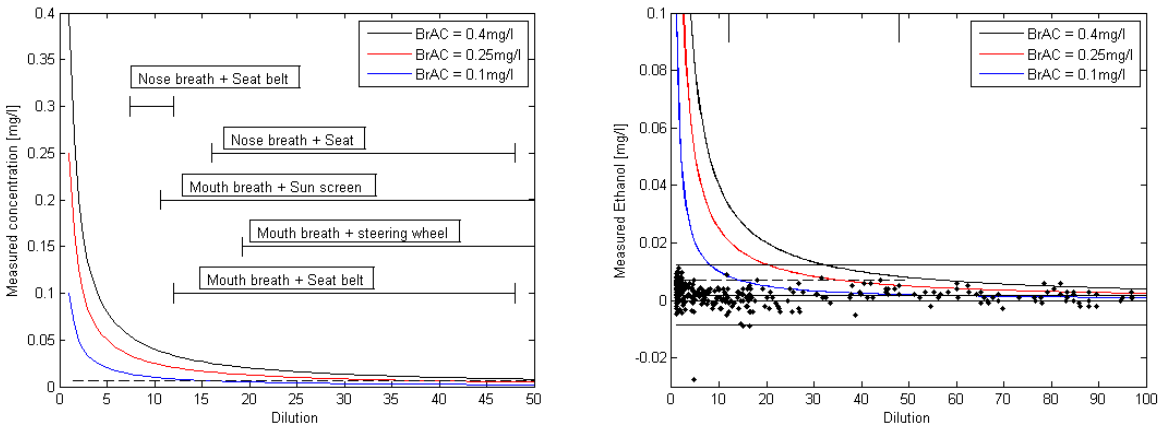


***(a)*** ***(b)***

***Figure 5. Measured EtOH concentration as a function of dilution for various settings.***
***a) Theoretical curves at different BrAC levels are superimposed with measured dilution data from various in-vehicle positions. The dashed line corresponds to the $3\sigma$ resolution.***
***b) Basically the same graph as a) but with different scaling, and measured data (dots, see text).***

Figure 5 b) includes experimental data from the sensor positions seat belt, steering column, and side door. The 420 data points from 38 volunteers indicate that DF needs to be below 20-30 in order to obtain adequate resolution.

## DISCUSSION

The automotive test results were positive for the majority of test cases conducted. Measures are now being taken to shut the remaining performance gaps concerning startup time and accuracy at extreme temperatures. This work is underway and is expected to provide overall fulfillment of the present specification [14, 15].

The system performance in human subjects is adequate in view of the suggested two-step procedure, in which the first unobtrusive step is a provisional BrAC determination (Figure 1). The observed variability of contactless measurements can be understood from the corresponding variability between individuals of alveolar $CO_2$ concentration [7].

The test results on unobtrusive in-vehicle determination indicated (Figure 4 a) that for the best sensor position in a vehicle setting, the seat belt position, typical dilution factors of 8-15 were observed by passive detection in several individuals, resulting in a BrAC resolution of 2-4% of the US legal limit. This observation is believed to constitute proof-of-principle for passive BrAC determination according to the scheme of Figure 1. However, the seat belt position is not considered suitable from an integration perspective. In other positions, the dilution is much larger.

Besides truly passive detection the option of a directed breath from a distance to a sensor integrated in the vehicle, as depicted in Figure 2 c), should also be considered. It may be argued that this option is also unobtrusive to the sober driver, since it only takes 1-2 seconds of the driver's attention, similar to pressing a button. This reflection notwithstanding, aspect (iii) related to vehicle integration remains as the most compelling technical challenge compared to (i) and (ii) (see subsection on basic system function) to the objective of unobtrusive breath alcohol determination.

Several initiatives are underway to integrate breath alcohol sensor systems with other technologies, including the already mentioned DADSS program [3, 4], and the Drive Me project directed towards evaluation of new technologies for autonomous vehicles [16].

## CONCLUSIONS

The feasibility of unobtrusive breath alcohol determination in vehicles, and adequate performance of a sensor system based on infrared spectroscopy have been experimentally demonstrated. The alcohol sensing system may advantageously be integrated into vehicles, and may also be combined with other technologies including autonomous driving.


## ACKNOWLEDGEMENTS

Financial contributions from the Automotive Coalition for Traffic Safety (ACTS), the National Highway Traffic Safety Administration, NHTSA, the Swedish Knowledge Foundation, and Vinnova, The Swedish Innovation Agency, are gratefully acknowledged. The authors also wish to express their thanks to all members of the project team at Autoliv, SenseAir, and Hök Instrument, for their excellent contributions.


## REFERENCES


[1] National Highway Traffic Safety Administration (NHTSA), *The Economic and Societal Impact of Motor Vehicle Crashes 2010*, Report DOT HS 812 013, May 2014.

[2] Harding P, Zettl R (2008) Methods for breath analysis (Chapter 7). Garriott JC (Ed.) Garriott's Medicolegal Aspects of Alcohol (5th Ed.). Lawyers & Judges Publishing Company, Tucson, AZ. p. 229-253.

[3] A Zaouk, Driver Alcohol Detection System for Safety, Transportation Research Board 90th Annual Meeting, Washington D. C., Jan. 25, 2011.

[4] S Ferguson, A Zaouk, N Dalal, C Strohl, E Traube, R Strassburger, Driver Alcohol Detection System for Safety (DADSS) – Phase I Prototype Testing and Findings, Proc. 22nd Int. Conf. Enhanced Safety of Vehicles, February 2012, Paper No 11-0230.

[5] B Hök, H Pettersson, G Andersson Contactless measurement of breath alcohol, Proc. Micro Structure Workshop, MSW 2006, May 2006, Västerås, Sweden.

[6] B Hök, H Pettersson, Annika Kaisdotter Andersson, S Haasl, P Åkerlund, Breath Analyzer for Alcolocks and Screening Devices, IEEE Sensors Journal, vol. 10 (2010), p. 10-15.

[7] A Kaisdotter Andersson, Improved Breath Alcohol Analysis with Use of Carbon Dioxide as the Tracer Gas, Ph. D. Thesis No. 83, Mälardalen University, Västerås-Eskilstuna, Sweden, September 2010.

[8] A Kaisdotter Andersson, B Hök, D Rentsch, G Rücker, M Ekström, Improved Breath Alcohol Analysis in Patients with Depressed Consciousness, Med. Biol. Eng. Comput. 2011.

[9] A Kaisdotter Andersson, B Hök, A Karlsson, H Pettersson, Unobtrusive Breath Alcohol Testing, International Conference on Alcohol, Drugs and Traffic Safety, ICADTS 2013, August 25-28, 2013, Brisbane, Australia, Paper No. 2Bi.

[10] J Ljungblad, B Hök, M Ekström, Critical Performance of a New Breath Analyzer for Screening Applications, Intelligent Sensors, Sensor Networks and Information Processing (ISSNIP), 2014 IEEE Ninth International Conference on, Singapore, 21-24 April 2014, doi: 10.1109/ISSNIP.2014.6827626.

[11] B Hök, J Ljungblad, A Kaisdotter Andersson, M Ekström, M Enlund, Unobtrusive and Highly Accurate Breath Alcohol Determination Enabled by Improved Methodology and Technology, J. Forensic Investigation, 2014;2(4) 8.

[12] A B Lumb, Nunn's Applied Respiratory Physiology, 6th Ed., Elsevier, 2005, p. 157-158.

[13] AW Jones (2010) The relationship between blood alcohol concentration (BAC) and breath alcohol concentration (BrAC): A review of the evidence. (Road Safety Web Publication No. 15). Department of Transport, London.

[14] T Eklöv et al, Autoliv Design Goal Document for Alcohol Sensor (unpublished document, 2011).

[15] T Eklöv et al, Autoliv Test Specification for Alcohol Sensor (unpublished document, 2012).

[16] http://www.slashgear.com/volvo-drive-me-project-brings-100-autonomous-cars-to-the-road-02307359/.

# GOVERNMENT STATUS REPORT OF JAPAN

**Hidenobu KUBOTA**
Director,
Technical planning Office,
Engineering Planning Division,
Engineering and Safety Department,
Road Transport Bureau,
Ministry of Land, Infrastructure, Transport and Tourism of Japan (MLIT)

## TRENDS OF THE ROAD TRAFFIC ACCIDENTS IN JAPAN

The number of fatalities (those who died within 24 hours) resulting from traffic accidents in 2014 was 4,113. This represents the fourteenth consecutive year that the number of fatalities has been decreasing. This number was about one-fourth the 16,765 fatalities in 1970, which was the year in which the number of fatalities reached a peak. In addition, the number of accidents resulting in injury or death and the number of injured persons decreased for the tenth consecutive year in a row since 2004, when the numbers were at their worst.

However, the number of fatalities and injured persons and the number of accidents resulting in injury remained high in 2014, as there were approximately 710,000 fatalities and injured persons, and approximately 570,000 accidents resulting in injury or death.

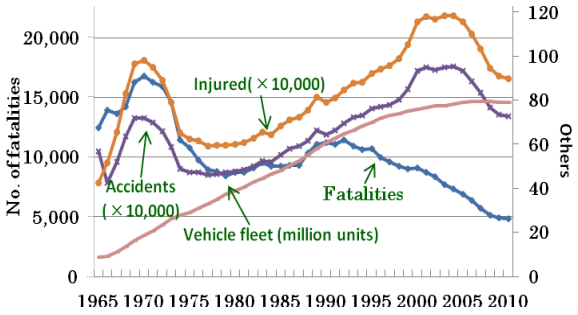


**Figure 1. Trends of the road traffic accidents in Japan**

New targets were established: to reduce the number of fatalities to below 3,000 (those who died within 24 hours) and to below around 3,500 (those who died within 30 days) by 2015 in the Ninth Fundamental Traffic Safety Program for 2011–2015.

The road transport environment is beginning to change greatly due to the change in types of traffic accident victims reflecting the aging society and the introduction of new technologies including electric vehicles for a low carbon society.

Therefore, on 1 June 2011 the Working Group on Technology and Vehicle Safety of the Council for Transport Policy of the Ministry of Land, Infrastructure, Transport and Tourism (MLIT) reported a new target for 2020 to reduce the number of fatalities by implementing vehicle safety measures and evaluating their effect, and setting the policy for reaching the new target.

Future direction of safety measures includes the following:

1) Correspondence to declining birthrate and a growing proportion of elderly people
2) Reduction of traffic accident victims for pedestrian and bicycle crew's
3) Correspondence to new mobility such as EV, micro mobility
4) Measures against grievous accident in which heavy duty vehicles are involved

## FUTURE RESEARCH IN FINDING SOLUTIONS TO THE SAFETY PROBLEMS IDENTIFIED

To reduce the number of traffic accidents, approaches will be made towards the following measures upon speculating future changes in social structures, such as future developments in IT and the progression of declining birthrates and an aging society.

- Promotion of safety measures for pedestrians;

- Promotion of neck injury prevention measures;
- Introduction of standards on crash compatibility;
- Research on advanced technologies, etc.

Concrete approaches regarding each of the measures are introduced below.

## 1. Promotion of safety measures for pedestrians

With regard to accidents involving pedestrians, which account for a high percentage of the number of fatalities caused by traffic accidents in Japan, it is necessary to implement popularization and promotion of pedestrian protection performance standards. As a result, with regard to measures for pedestrians, pedestrian head protection standards were introduced in 2004, and were also adopted pedestrian leg protection standards in January 2015. At the same time, a global technical regulation for pedestrian leg protection has been discussed at GRSP under WP.29 and Japan continues actively contributing to those activities.

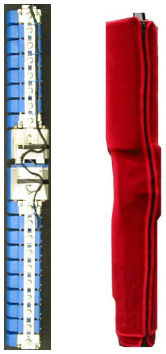

**Figure 2. FLEX-PLI**

According to rapidly spreading of hybrid cars, Japan judged that measures are needed to address the quietness of hybrid cars. And then the MLIT set up a study committee to investigate the problem of quietness.

In 2010, this committee reported to the MLIT on a future direction and specifically recommended that these vehicles should emit a sound. Based on these results, the MLIT published a guideline on Acoustic Vehicle Alarting Systems (AVAS) for short, which are designed to solve the quietness of HVs and similar vehicles.

WP.29 established a guideline in March 2011 based on Japan's guideline and now expects to develop it as a global technical regulation (gtr).

**Figure 2. Demonstration of sound devices that could equip "silent cars"**

## 2. Promotion of neck injury prevention measures (standardization of dummies)

Accidents involving neck injury account for more than half of the total number of accidents, and as there is an increasing trend in the number of such accidents in recent years, the enhancement of standards for headrests, etc. is being promoted as measures for neck injuries.

At the same time, with regard to assessments of whiplash injuries, which 80% of occupants in rear-end collisions suffer, the mechanism behind the occurrence of whiplash is complex, and as a result, there is not enough scientific clarification and it is also unclear as to which dummies should be used and what items to assess.

In particular, with regard to dummies, there are concerns regarding the consistency of assessments due to differences in structures, etc. of the dummies, and it is necessary for dummies to be standardized by having the research institutions, etc. of each country make approaches by contributing to efforts to elucidate the mechanism behind the occurrence of whiplash injuries and decide on assessment standards and indicators.

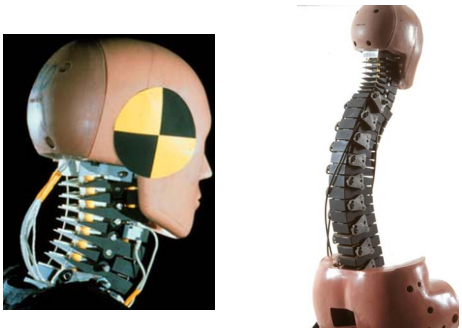

**Figure 3. Standardization of dummies**

## 3. Introduction of standards on crash compatibility, etc.

In addition to the above, crash compatibility measures for accidents involving frontal collision are also one of the passive damage mitigation measures for which approaches should be made. Japan considers measures for mini vehicles as being necessary. For the short-term, reviews are currently being conducted on the installation height of structural members so that the structural members interlock when there is a frontal collision.

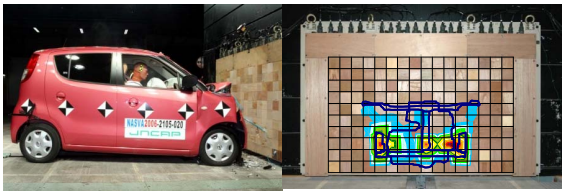

**Figure 4. Crash Compatibility**

Standards relating to performance for protecting occupants from electric shock after the collision of an electric vehicle or hybrid vehicle were introduced in 2007, and based on these regulations, UNECE regulations were established at WP.29 in 2010. Currently, a global technical regulation for electric vehicles is now being discussed at GRSP under WP.29 and Japan continues actively contributing to those activities.

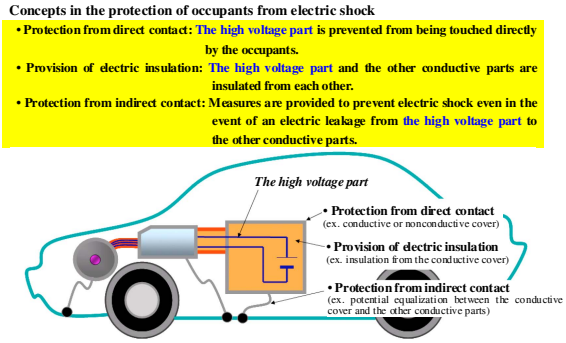


**Figure 5. Concepts in the protection of occupants from electric shock**

## 4. Research on advanced technologies

In order to effectively reduce traffic accidents, the MLIT began in FY 1991 a project on vehicles equipped with advanced safety technologies (Advanced Safety Vehicle, or ASV), and has been promoting the deployment of ASVs for more than 20 years. ASV technologies such as the Advanced Emergency Braking System (AEBS), Adaptive Cruise Control (ACC) and Lane Keep Assistance System (LKAS) were put into practice as a result. Phase 5 of the project, which began in FY 2011, aims to reduce traffic accidents even further. The project promotes the development of ASV technologies and next-generation communication-based systems such as vehicle-to-vehicle (V2V) and vehicle-to-pedestrian (V2P), as well as driver assistance systems in case of emergency.

In addition to the ASV project, the MLIT has been working on the development and promotion of automated driving technologies through various activities. One example is the Cross-ministerial Strategic Innovation Promotion Programme (SIP), which was established based on the Japan Revitalization Strategy (JRS, cabinet approval on June 14, 2013) and Comprehensive Strategy on Science, Technology and Innovation (cabinet approval on June 7, 2013). The SIP aims to encourage innovation by promoting research and development at all stages by enhancing cross-ministerial cooperation. The Council for Science, Technology and Innovation designates research themes based on their expected impact

on solving societal issues and enhancing economic growth. Among the ten SIP programmes is the Innovation of Automated Driving for Universal Services. Automated driving is thus being discussed in line with the road map drawn up by the JRS.

Under WP.29, the ITS Informal Working Group had been the group to discuss various technical issues regarding the vehicle part of Intelligent Transport System (ITS). The group has so far developed common understandings relating to automated driving technologies such as the definition of automated driving technology, Guidelines on establishing requirements for high-priority warning signals, and Design Principles for Control Systems of Advanced Driver Assistance Systems (ADAS). Meanwhile, the Working Party on Brakes and Running Gear (GRRF) under WP.29 has developed UN Regulations for advanced technologies, such as R130 on lane departure warning systems (LDWS) and R131 on AEBS.

## IDEAS FOR POTENTIAL COLLABORATIVE RESERCH INTER NATIONALLY

In addition to above mentioned, Japan would like to collaborate internationally to establish regulation against head restraint because accidents involving neck injury account for a high percentage of the number of fatalities in Japan as mentioned above. And also global technical regulations on new technologies like QRTV, RESS, AEBS and ITS in general could be established and in order to do so it would be needed to collaborate internationally by doing so, we could surely promote smooth diffusion of safe and convenient vehicles with equipments utilizing above mentioned advanced automotive technologies.

## CONCLUSION

Measures that are being taken in Japan have been described above, but in order to promote international harmonization in the aspects of further advancing safe and environmentally friendly vehicles in the future, it is perceived that approaches made in coordination with the ESV Conference, WP.29, ITS World Congress, etc. will become increasingly important.

# 24th ESV Government Status Report

Nat Beuse
Associate Administrator for Vehicle Safety
USA

The 24th International Technical Conference
on the Enhanced Safety of Vehicles
**June 8-11, 2015 Gothenburg, Sweden**

# U.S. Fatalities and Fatality Rate, by Year

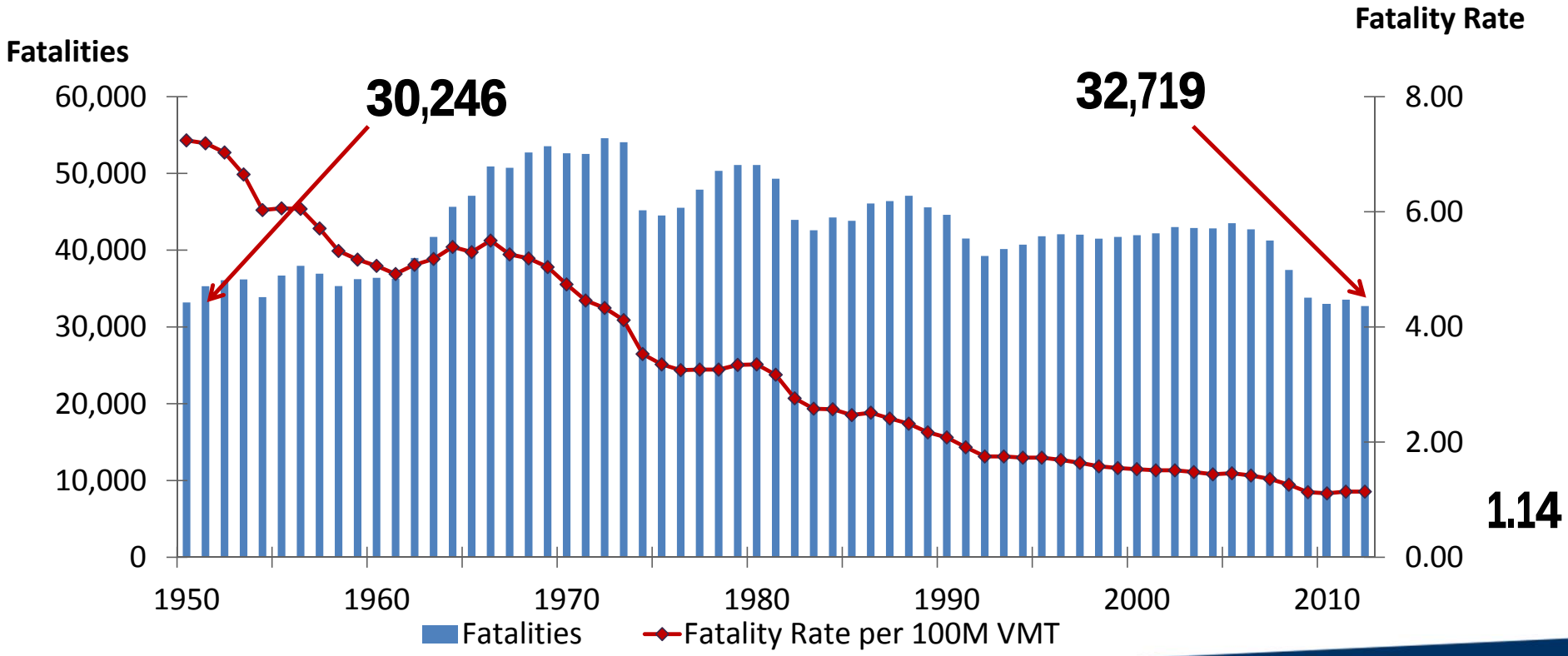


Motor vehicle crashes cost nearly $871 billion

# Many Recent Advances in Safety ~ US Market

- Standards recently just taking full effect or soon to take effect
  - Upgraded Side Impact Standard
  - Electronic Stability Control
  - Improved Roof Crush Resistance
  - Ejection Mitigation
  - Improved Rear Visibility
  - Motorcoach Seat Belts
- Enhancements to Consumer Information
  - Driving improved performance without regulation
  - New tests, rating protocol, and new advanced technologies

# Evolving Strategy

- Crashworthiness still Important
  - Advanced dummies, new restraints, and new fuels to name a few
- Opportunities for new technologies to help
  - Driver behavior very much part of the issue
- Convergence of Crash Avoidance Systems
  - Crash Warning and Mitigation Systems
  - Vehicle-to-vehicle communications
  - Self-driving vehicles (eg limited and full)

# Key Crashworthiness Research Programs

- Crash Safety
  - New Test Dummies and Crash Modes: Agency Decision 2015
  - Seat Belt Reminders and Interlocks: Results in 2016
  - Adaptive and Rear Seat Restraints: Results in 2016
  - Research to complete rulemakings related to children 2016
- New Fuels
  - Batteries: Research supporting the GTR
  - Hydrogen: Research to implement the GTR
- Improving Understanding
  - CIREN
  - Human Body Modeling

# Key Crash Avoidance Research Programs

- Vehicle-to-Vehicle Communications
  - Complete Research in 2015: Proposal in 2016
- Vehicle Automation
  - Automatic Emergency Braking: Test Procedures ~ 2015
  - Human Factors and Operational Concepts; Results ~ 2015
- Impairment
  - Distraction Guidelines for Portable Devices: Proposal ~ 2015
  - Alcohol Detection Technology: Research Vehicle ~ 2015

**GOVERNMENT STATUS REPORT, SWEDEN 2015**

**Anders Lie**
**Johan Strandroth**
**Claes Tingvall**
Swedish Transport Administration
Sweden

## SWEDISH ROAD SAFETY ORGANISATION

The Ministry of Enterprise and Innovation is responsible for road traffic safety in Sweden. But due to the decentralised structure in Sweden, the Ministry works with budget, goals, and policy related issues while the operations are managed by the **Swedish Transport Administration** based on the directions from the ministry. The administration is responsible for the planning of the entire transport system with all modes of transport. It is also responsible for the building and maintenance of roads and railroads. The Swedish Transport Administration, also has an overarching role in the development of long term strategies and plans for all modes of transport in the transport system, contributing to the goals set up by the government for the transport sector. The Transport Administration holds responsibility for research within the fields of mobility, environment and traffic safety. It is also performing in-depth studies of fatal crashes within the road traffic system. If co-operation with other actors in society is necessary to effectively achieve its goals the Administration may work together with these actors.

The other authority in the sector is the **Swedish Transport Agency** which has overall responsibility for regulations within air, sea, rail road and road traffic. Within the Swedish Transport Agency the Road and Railway Department formulates regulations, examines and grants permits, as well as exercise supervision within the field of road transport over e.g. road traffic, vehicles, driving licences and commercial transport. The agency also conducts analyses of road traffic and supply information about injuries and accidents within the road transport system. Swedish Transport Agency is also maintains vehicle and driver licence registers.

The Swedish Transport Administration and the Swedish Transport Agency are both responsible to work towards the transport policy goals.

In Sweden the main other bodies active in road traffic safety efforts are the police and the local authorities. Other important parties are the NGOs for example the National Society for Road Safety (NTF), with its member organisations, and transport industry organisations. The Group for National Road Safety Co-operation (GNS) is a central body that co-ordinates the co-operation between the Swedish Transport Administration and Agency, the local authorities the authority for occupational health and safety and the police. The NTF is an additional member of this group, as well as some other key partners from the traffic safety sector.

## ROAD TRAFFIC FATALITIES

The Swedish overarching long-term safety objective within the road transport system was settled in 1997, when the Swedish parliament voted for the "Vision Zero". This vision states that ultimately no one should be killed or seriously injured in the road transport system (Johansson, 2009). The design and function of the system should be adapted to the conditions required to meet this goal.

Since Sweden introduced a visionary goal in the middle of the 1990s several jurisdictions have taken the same approach. In some jurisdictions the name has been changed to Safe Systems Approach to avoid the strong focus on the number zero (OECD, 2008).

The Commission of the European Communities has in its White Paper on transports set out the goal "By 2050, move close to zero fatalities in road transport. In line with this goal, the EU aims at halving road casualties by between 2010 and 2020. Make sure that the EU is a world leader in safety and security of transport in all modes of transport" (EC, 2011. Page 10).

Sweden as member of the European Union was part of the union's target of a 50% reduction of fatalities between 2001 and 2010. For Sweden that target meant a maximum 271 fatalities year 2010.

In the year 2010 the number of fatalities in Sweden was 266. The road toll in Sweden thus did reach the 50% EU target for 2010. Great progress was also made in other countries in the EU. Latvia, Estonia, Lithuania, Spain, Luxembourg, Sweden, France and Slovenia all reached the EU 2010 target. Portugal very nearly made it with a reduction of 49.4%.

With significantly less than 300 fatalities per year Sweden is one of the safest countries when it comes to road traffic, with a level of 2.7 fatalities per 100.000 inhabitants in 2013. This is about half of the European Union risk average (5.2 fatalities per 100 000 inhabitants year 2013). In Sweden fatalities related to distance travelled is 3.6 fatalities per billon vehicles-kilometres (2013) which can be compared with the 7.1 fatalities per billion –vehicle kilometres (2013) in USA (IRTAD 2014).

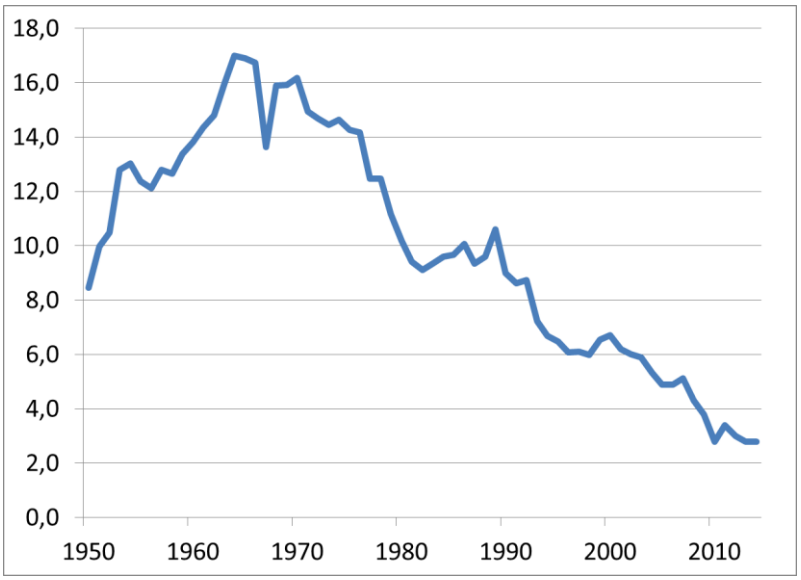


**Figure 1. Road fatalities per 100 000 inhabitants in Sweden 1950-2014**

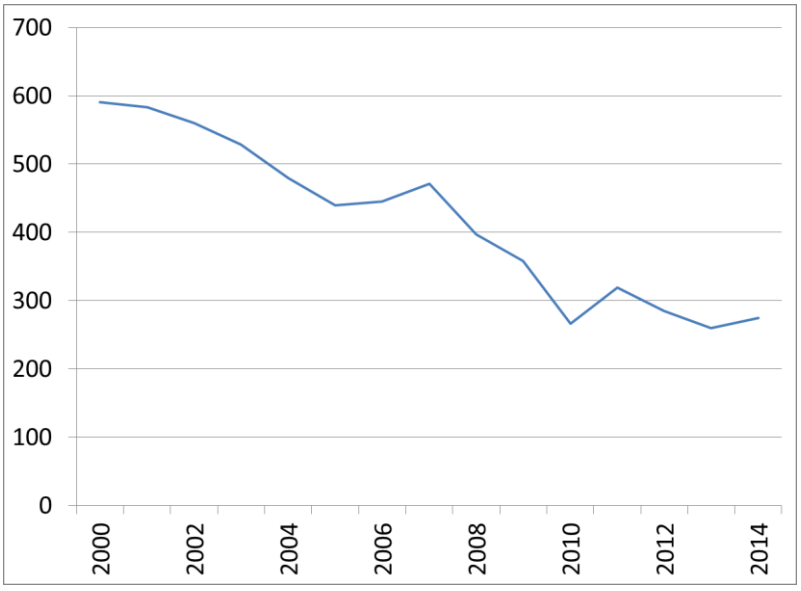


**Figure 2. Road fatalities in Sweden 2000 to 2014**

## INTERIM TRAFFIC SAFETY TARGET FOR 2020

Sweden has a long tradition in setting quantitative road traffic safety targets. In 2009 the Swedish government stated a target of 50% reduction of fatalities and 25 % reduction of severe injuries from 2007 to 2020. This target would demand Sweden to be at a maximum of 220 fatalities in the year 2020. This interim target towards the Vision Zero is a part of an updated continuing road safety operation in collaboration with other stakeholders (The Group for National Road Safety Co-operation, GNS).

After Sweden decided on a target for 2020 the European Union has decided on a 50% fatality reduction between 2010 and 2020. For Sweden this would mean a maximum of 133 fatalities in the year 2020 (because of the good safety performance in 2010). This new European ambition is significantly higher than the Swedish target. Thus, Sweden so far has not committed to the EU target.

The partners of GNS have made an analysis on whether the 133 goal could be achieved and what status a set of Safety Performance Indicators (SPI) would have to be at to support the goal. From this analysis it seems that the goal is achievable.

In 2012 the new interim road safety target for 2020 was proposed to the Swedish Government by the Swedish Transport Administration (STA, 2012). One important element in the revision was to predict the benefits of future interventions for road safety in order to facilitate the prioritisation of road safety measures. One way of doing that is to evaluate safety technology with retrospective analysis of crashes. However, by using retro-spective data there is the risk of adapting safety innovations to scenarios irrelevant in the future. Also, challenges arise as safety interventions do not act alone but are rather interacting components in a complex road transport system. Therefore a new method to consider possible impact of safety interventions was developed (Strandroth, 2014).

The key point was to project the chain of events leading to a crash today into the crashes for a given time in the future. Assumptions on implementation on safety technologies were made and these assumptions were applied on the crashes of today. It was estimated which crashes would be prevented and the residual was analysed to identify the characteristics of future crashes. The Swedish Transport Administration's in-depth studies of fatal crashes and hospital admission data translated into risk of permanent medical impairment were used in the calculations.

It was estimated that the number of road fatalities would be reduced with approximately 40 percent from 2010 to 2020 with the current planned interventions for this period. The main part of the reduction originated from the gradual replacement of the vehicle fleet. The analysis also suggested that it would be possible to strengthen the targets to a reduction of the number of fatalities by 50 percent to 133 fatalities between 2010 and 2020. But that would require measures above and beyond those that are included in the prediction. Through this new method not only quantitative estimations were made but also valuable information regarding the characteristics of future crashes was found. The current Swedish road safety operation is based on a system of management by objectives. This system is based on cooperation between stakeholders, targets on SPI:s, and annual result conferences where road safety developments and targets are followed up. The aim is to create long-term and systematic road safety operation together with the other stakeholders.

The road SPI:s that are monitored is speed compliance, sober driving, seat belt use, helmet use, safe vehicles, ABS on motorcycles, safe national roads, safe municipal streets and maintenance standard on municipal streets. These indicators each have a target for 2020 which makes possible to prioritize between measures easier for stakeholders.

## DEVELOPMENT TOWARDS THE GOAL 2020

The role of the vehicles to contribute to the target is further discussed later in this paper. However, it is worth noticing that the replacement of the car fleet gave the biggest contribution to the results 2010 and in the near future.

The development towards the target is annually evaluated at a result conference in April. So far there have been six conferences making it possible for all stakeholders to meet and discuss further work towards the interim target and Vision Zero.

## ISO-MANAGEMENT SYSTEM FOR ROAD TRAFFIC SAFETY

In the spirit of the Tylösand Declaration, Sweden has been an initiator to get a new work within International Organization for Standardization (ISO). The work is aiming at developing a Road-Traffic Safety Management System standard. (ISO/TC 241 - Project Committee: Road-Traffic Safety Management System). Sweden is through the Swedish Standards Institute (SIS) holding the secretariat.
The vision of the International Management Systems Standard is:
• Elimination of death and serious injury in the road transport system is the overarching goal.
• A voluntary and complimentary tool to legislation, addressing all organizations interacting with road traffic and driven by the needs of interested parties, including market forces.
• An approach to utilize and disseminate ”best practice”.
• Knowledge transfer from Traffic safety experts to the intended user community of the standard.

All requirements of the International Standard are generic and are intended to be applicable to all organizations regardless of type, size, products and services provided.
The standard was delivered in 2012 as ISO 39001 Road traffic safety (RTS) management systems - Requirements with guidance for use.

## PENETRATION OF SOME SAFETY SYSTEMS IN SWEDEN

Electronic Stability Control (ESC) has been proven to be very effective in reducing crashes related to loss of control (Erke, 2008, Ferguson, 2007, Lie et al. 2006).
The first studies of the effectiveness of ESC were published in the ESV conference 2003. Several studies followed in 2004 and 2005 establishing a scientific ground for declaring that ESC was effective. A study of fatal crashes in Sweden has shown that ESC is reducing fatal loss-of-control crashes with 74% (Lie. 2012). As these crashes constitute about 36% of all fatal crashes for cars without ESC, the overall effect is around 27% risk reduction. This is higher than previous estimates based on crashes with a lower severity level.

The first mass market car with ESC was introduced late 1998. ESC was from then on gradually implemented on executive mid-size and large cars and reached a 15 % new car sales penetration in mid 2003. Sweden has been world leading in getting a high degree of ESC penetration in new car sales. In December 2014, all new passenger cars were equipped with ESC. Even with this rapid introduction of ESC predictions show that it will be year 2017 before 90% of the traffic will be performed in cars with ESC.
Sweden has actively been part of Euro NCAP since the start of the organisation. Over the years since Euro NCAP started, the average scores have improved both for occupant protection as well as for pedestrian protection. Swedish Transport Administration has done an evaluation of the relation between Euro NCAP results and the risk of injury and fatality in real life crashes. The study shows a 70% fatality risk reduction between a Euro NCAP 2 star car and a 5 star car (Kullgren et al. 2010). A Swedish study shows the relation between Euro NCAP pedestrian score and real life impairment risks for pedestrians and bicyclists (Strandroth et al. 2014). Results show that the injury severity for pedestrians and bicyclists hit by cars with three and four star pedestrian protection compared to cars with just one star was significantly reduced (24-56%) for all body regions. Regarding injuries of higher severity the reduction was most evident for head injuries. The injury reduction grows with higher levels of medical impairment and in lower impact speeds.
In December 2014 99% of the new car sales had a seat belt reminder according to Euro NCAP specification for the driver. 98% had a reminder for the passenger and 78% a system to monitor seat belt use in the rear seat. Seat belt reminders are reducing the number of unbelted driver in city traffic with 80% in Europe (Lie et al. 2008). A Swedish study has shown that seat belt reminders living up to Euro NCAP’s specification is increasing seat belt use in fatal crashes with 80%. (Lie, 2012). This is very promising.

## THE CONTRIBUTION OF NEW VEHICLES

With a rapid development of vehicles safety there has been of interest to calculate the yearly benefit of the exchange of the vehicle fleet. With about 140 fatalities in cars every year, the exchange of slightly fewer than 7% of the vehicle fleet results in around 7 “saved” lives in 2014. Out of these about two

thirds comes from the better crash protection and one third from the ESC systems.

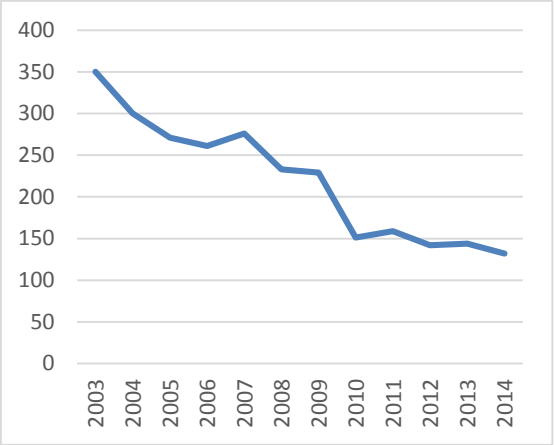


**Figure 3. Road fatalities in passenger vehicles Sweden 2003 to 2014**

## ABS ON MOTORCYCLES

Anti-lock Brakes (ABS) has been proved by several studies to significantly reduce motorcycle crashes by some 20-50% depending on injury severity (Teoh, 2011; HLDI, 2009; Rizzi et al., 2009). A study on US insurance data (HLDI, 2014) also shows that the benefit with ABS was even higher in combination with Combined Brake System (CBS). As technology evolves more advanced ABS-system is expected and in 2013 Bosch introduced Motorcycle Stability Control (MSC) with enables full braking in a cornering manoeuvre. In 2014 two motorcycle models with MSC was available in the Swedish market.

Earlier studies have focused primarily on heavier motorcycle models. In 2014 a new study was therefore performed in order to confirm if the results applies to lighter motorcycles, i.e. scooters, as well (Rizzi et al., 2014). The study involved crashes from Sweden but also from Italy and Spain, i.e. countries in southern Europe were motorcycles are often used for transportation. An induced exposure approach was used and the material includes more than 10,000 casualty crashes with motorcycles. Results show that the effectiveness of motorcycle ABS in reducing injury crashes ranged from 24% in Italy to 29% in Spain, and 34% in Sweden. The reductions in severe and fatal crashes were even greater, at 34% in Spain and 42% in Sweden. The overall reductions of crashes involving ABS-equipped scooters (at least 250 cc) were 27% in Italy and 22% in Spain.

It was concluded that at this stage, there is more than sufficient scientific-based evidence to support the implementation of ABS on all motorcycles, even light ones.

Many stakeholders have been encouraging the fitment of ABS on new motorcycles (STA, 2012). In Sweden the fitment rate has increased from approximately 15% in 2008 to 85 % in 2014. According to Bosch Corporation (2012) the installation rate in Europe for ABS in production on motorcycles with engine size larger than 250 cc has increased from 27% in 2007 to 36% in 2010. Since the European Parliament also has voted for a legislation which makes ABS mandatory for all new motorcycles over 125cc from 2016, the fitment rate is likely to increase even more in the years to come.

## FFI – STRATEGIC VEHICLE RESEARCH AND INNOVATION

Transport, mobility and accessibility are of major importance for quality of life and growth. If society is to continue its positive development, transport solutions must be safe and environmentally sustainable. Safe electric cars, smarter logistics and resource-efficient production technology are examples of the innovation and renewal which can help the Swedish automotive industry meet this challenge. To drive the development forwards, Sweden's government together with the industry have initiated a long-term partnership within FFI – Strategic Vehicle Research and Innovation (R&D). Sweden has a long and positive experience of such co-operation between authorities, the industry and academia. FFI funds R&D that focuses on climate, environment and safety. The effort is ongoing and includes some €100 million per year, half of which comes from public funds through VINNOVA, the Swedish Transport Administration and the Swedish Energy Agency. An equivalent amount is invested by the four industrial partners: Volvo, FKG (Scandinavian Automotive Suppliers), Scania and Volvo Cars. This collaboration between public bodies, industry, educational establishments and research institutes is intended to provide high-quality results and contribute to positive social development. In order to keep the focus and to strive for the goals, the members in collaboration have developed a road map defining safety concepts and mile posts for the years 2020, 2025 and 2030.

The road maps will be updated as progress is achieved.

FFI funds for projects are divided so that two thirds of the money is allocated to climate and environment while one third to safety. An FFI board is responsible for setting a balance between targeted projects and more long-term efforts which can deliver ground breaking results. The board's duties also include promoting constructive cooperation between the various actors in the road traffic system.

The investments in FFI take place through various collaborative programmes. One is "traffic safety and automated vehicles". Sweden is a world leader in traffic safety. The programme will contribute to the continued development of vehicles with active systems to prevent accidents as well as passive ones to mitigate the consequences of those accidents where a vehicle is involved. Initiatives have a systemic approach so as to get roads, vehicles and road- users to interact well.

## IMPORTANT FIELDS FOR FURTHER RESEARCH

Many fatalities in Sweden as well as globally are related to impaired driving. In Sweden 2011, 18% of killed vehicle drivers had illegal levels of alcohol on their bodies (Swedish Transport Administration 2012). As many other countries Sweden has an alcolock programme for offenders. There is also some 85000 alcolocks used in Sweden in trucks, buses and taxis on a voluntary basis. There are even some installations made in trams, ferries and locomotives. These alcolocks are used on an emerging market for safe transports. Both buyers of transports and suppliers have found these alcolocks attractive to ensure sober drivers. There is an ongoing technology development both in terms of new basic technologies for alcolocks and forms for a reliable and non-intrusive sobriety support systems.

Alcohol consumption is not the only reason for impaired driving. Often fatigue, distraction, legal and illegal drugs are also lumped into the term impaired driving. Vehicle systems that detect distraction and fatigue are out on the market. These systems are using signals from the vehicle to analyse the state and driving pattern for the driver. Already today the cars have an idea about when driving isn't up to standards. The systems as of today have weak feed back to the driver and uses signal lamps of haptic feedback. Not far away in time the vehicle will have a good estimate of the potential impairment of the driver. The question is how a vehicle, on its own, can restrict and guide the driver into a safe driving envelope. The most evident way is to limit the speed of the vehicle and putting safety systems into a more nervous mode. This makes a potential crash avoided and less harmful. There is an evident need in society to research this field and to develop guide lines for a safe shut down sequence.

The layout of infrastructure and the properties of it are becoming important for modern safety technologies. Already today lane departure warning systems are using lane markings as a critical component. In the near future crash avoidance by steering will need even better environmental awareness from lines and other road furniture. More and more cars are reading traffic signs and speed restriction signs are used to help drivers from speeding. As identified by the European Council, there is an urgent need for better co-operation between vehicle manufacturers and suppliers, and road authorities. Rules, standards and strategies for line painting and road signs could be aligned with the properties of modern vehicle systems to better achieve good functionality and safety.

As traffic is developing into a more automated mode of transport the need for close co-operation between all actors in the field is becoming urgent. Automation in traffic demands co-operation.

Speed management is a key element to achieve good safety. More and more countries are using speed cameras and section control to diminish illegal speeding. In Sweden more than 1000 speed cameras or as it is called in Sweden, "road safety cameras" have been put up the last years. The aim of the camera system in Sweden is to support drivers in making a safe speed choice and, through a change in speed behaviour among a large proportion of the traffic create a new social norm with respect to what is an appropriate speed (Belin et al 2010). This has generated an emerging market demand for support systems helping users not to speed. Already many years ago nomadic Satnavs indicated the speed limit. The same approach is now entering integrated navigations systems. Some vehicle manufacturers are also using cameras to read speed signs. As an effect of the marker development the consumer crash test program Euro NCAP has developed a protocol to assess Speed Assistance Systems (SAS) and is using the protocol since January 2013. A better compliance with speed

limits will give significant environmental benefits through lower fuels consumption.
Just like vehicle safety and road safety have been two to a large degree separate cultures, vehicle safety and ITS (intelligent Transport System) have been driven by different groups in industry and society. There are high expectations from the ITS side to solve traffic safety problems. Further research is needed in which vehicle safety experts and ITS experts more clearly define the areas of potential for improved safety. This should be done for the different stages of a driving process leading up to a potential crash. The connected vehicle is probably more important to strategic decisions in the driving than for support in emergency situations. A reasonable balance must be achieved between safety from connectivity, active and passive safety. This balance should be further investigated and communicated.

Although the road traffic injuries is a very complex problem a comprehensive knowledge have been developed over the years about the magnitude of the road safety problem, knowledge about important risk factors and both theoretical knowledge and practice experience about effective road safety strategies and measures . However, we are still lacking systematic knowledge about the way different public authorities, private organizations in different time periods try to tackle this major public health problem. We do not seem to have an adequate understanding and interpretation of the dynamics of the process aimed at formulating and implementing road safety polices and how sound road safety interventions are diffused in the society. Improving road safety requires knowledge about implementation processes, measures known to be effective and how and where in other sectors of society road safety aspects can be mainstreamed and partnerships built. It also requires the ability to choose the strategies and approaches that best fit the specific conditions of different countries Racioppi 2004, Belin 2012).

The safety development for car users is impressive over the last decade. We have in Sweden seen a drop of in car fatalities with more than 50 %. But there is still a need to further improve.
For other road users the same positive development isn't seen. The fatalities in the group of vulnerable road users is proportionally growing. When looking at impairing injuries, pedestrians together with bicyclists have as many injuries as car users. This will impact traffic safety work in the future, both from the road design and the vehicle perspective.

## CONCLUSIONS

When it comes to traffic Sweden is one of the safest countries in the world. The Vision Zero approach has further boosted a good safety culture.

The exchange of vehicles in combination with improved vehicle technology is a major contributor to achieve ambitious traffic safety targets. As more than 50% of new sales cars are sold to companies and other non-private buyers, active strategies to convince large fleet buyers to choose best safety standard is of outmost importance.

Road users have a responsibility to operate within the safety limits of the road transport system where vehicle industry in its role as system designer partner can support the road user. Intelligent seat belt reminders, systems alerting drivers when speeding and alcohol starter interlocks are important systems to further develop and put on the market in large scale.

The ISO 39001 management system standard for traffic safety will give organisations a possibility to work focused with traffic safety.

Vehicle manufacturers and organisations responsible for infrastructure must develop better co-operations to ensure that the modern road offers a useful interface to modern vehicle technology such as lane departure warning and traffic sign recognition.

A safe system is achieved when user capabilities, vehicle safety, road design and speed limits all are in harmony. A holistic perspective on road safety is under development and is important when prioritizing research efforts.

More general information is available at the following pages
http://www.trafikverket.se/eng
http://www.transportstyrelsen.se/en
http://www.vinnova.se/en/ffi/

## REFERENCES


Belin, M-Å., Tillgren, P., Vedung, E., Cameron, M., Tingvall, C. (2010) Speed cameras in Sweden and Victoria, Australia – a case study. Accident, Analysis and Prevention. Vol. 42:6 pp. 2165-2170.

Belin, M.-Å., Tillgren, P. & Vedung, E. 2011. Vision Zero – a road safety policy innovation. International Journal of Injury Control and Safety Promotion, 1-9.

Belin, M-Å. (2012) Public Road Safety Policy Change and its Implementation – Vision Zero a road safety policy innovation. PhD thesis. Karolinska Institutet, Stockholm 2012.

EC (Commission of the European Communities) (2011). Roadmap to a Single European Transport Area – Towards a competitive and resource efficient transport system SEC(2011) 391 final. Brussels.

European Council's conclusion on "Communication from the Commission to the European Parliament, the Council, the European Economic and Social Committee and the Committee of the Regions: "Towards a European road safety area: policy orientations on road safety 2011-2020".

Highway Loss Data Institute. (2009) Motorcycle Antilock Braking System (ABS). Insurance Special Report, December 2009 A-81.

Highway Loss Data Institute. (2014) Evaluation of motorcycle antilock braking systems. Bulletin, Vol. 31, No. 11: Sept 2014.

IRTAD Annual Report 2014
OECD/ITF, Paris 2014

Johansson, R (2009). Vision Zero – Implementing a policy for traffic safety. Journal of Safety Science, 47(6): 826–831.

Kullgren A, Lie A, Tingvall C Comparison between Euro NCAP Test Results and Real-World Crash Data. 2010 Traffic Injury Prevention, 11: 6, 587 — 593

Lie A. Nonconformities in real world fatal crashes - electronic stability control and seat belt reminders. Traffic Injury Prevention, 13:3, 308-314. 2012

Lie A, Tingvall C, Krafft M, Kullgren A. The Effectiveness of Electronic Stability Control (ESC) in Reducing Real Life Crashes and Injuries. Traffic Injury Prevention, Vol. 7:1 pp38-43 2006.

Lie A, Kullgren A, Krafft M, Tingvall C. Intelligent Seatbelt Reminders. Do They Change Driver Seat Belt Use In Europe. Paper No. 07-0388. Proc 20th ESV Conf. Lyon 2007 Also revised in Traffic Injury Prevention, 9:446–449, 2008

OECD (2008). Towards Zero: Ambitious road safety target and the safe system. OECD/ITF. ISBN 978-92-821-0195-7. Paris.

Racioppi, F. 2004. Preventing road traffic injury: a public health perspective for Europe, World Health Organization Regional Office for Europe.

Rizzi, M., Strandroth, J. and Tingvall, C. 2009. "The Effectiveness of Antilock Brake Systems on Motorcycles in Reducing Real-Life Crashes and Injuries". Traffic Injury Prevention,10:5, 479-487.

Rizzi M., Strandroth J., Kullgren A., Tingvall C., Fildes B. (2015) Effectiveness of Motorcycle Antilock Braking Systems (ABS) in Reducing Crashes, the First Cross-National Study. Traffic Injury Prevention (2015) 16, 177–183.

Strandroth J, Sternlund S, Lie A, Tingvall C, Rizzi M, Kullgren A, Ohlin M, Fredriksson R. The Correlation between Euro NCAP Pedestrian Test Results and Injury Severity in Real-Life Crashes with Pedestrians and Bicyclists. Stapp Car Crash Journal, vol. 58, 2014.

Strandroth J, Rizzi M, Sternlund S, Johansson R, Kullgren A, Tingvall C. A new method to evaluate future impact of vehicle safety technology in Sweden. Stapp Car Crash Journal, vol. 56, 2012.

Strandroth J. Identifying the potential of combined road safety intervention – A method to evaluate future effects of integrated road and vehicle safety technologies. Thesis. Chalmers Technical University 2015.

Swedish Transport Administration (2010). Bilbältesanvändning i dödsolyckor (Seat belt use in fatal crashes), En analys av vägtrafikolyckor i Sverige 2005-01-01 till 2009-06-30.

Swedish Transport Administration. (2012) Översyn av etappmål och indikatorer för säkerhet på väg mellan år 2010–2020 [Review of interim road safety targets and safety performance indicators for the period 2010-2020].

Swedish Transport Administration. (2012) Analys av trafiksäkerhetsutvecklingen 2011 [Analysis of the traffic safety development 2011Teoh ER. (2011) Effectiveness of Antilock Braking Systems in Reducing Motorcycle Fatal Crash Rates. Traffic Injury Prevention, 12:2, 169-173.

Tingvall C, Ifver J, Krafft M, Kullgren A, Lie A, Rizzi M, Sternlund S, Stigson H and Strandroth J. The Consequences of Adopting a MAIS 3 Injury Target for Road Safety in the EU: a Comparison with Targets Based on Fatalities and Long-term Consequences. 09/2013; In proceeding of: Int. IRCOBI Conf. on the Biomechanics of Injury, ISSN: 2235-3151.

Trafikanalys. Vägtrafikskador 2013. Stockholm 2013. Accessed 2014-03-02 at http://trafa.se/PageDocuments/Vaegtrafikskador_2013.pdf

# STATUS REPORT, FEDERAL REPUBLIC OF GERMANY

**President and Professor**
**Stefan Strick**
Federal Highway Research Institute
Germany

**24th ESV-Conference**

Gothenburg, Sweden, June 8-11, 2015

## 1 STATUS AND TRENDS

### 1.1 Road accidents in Germany

The total number of police registered road accidents has stagnated for the last 10 years – between 2.2 and 2.4 million road accidents. There were slight increases in single years such as 2004, 2007 or 2010, but as well slight decreases in 2002 or 2011. On the long run, there is an increase since 2000 by 2.7 percent in 2013. The forecast for 2014 thus indicates a decrease in accident figures by roundabout 2 percent (2013: 2.41 million road accidents).
The number of road accidents with personal injury has decreased by 24 % since 2000, resulting in 291,105 road accidents with personal injury in 2013. For 2014 a slight increase of almost 2.5 percent to approximately 298,000 injury accidents is expected.
Casualty figures have also decreased, with lower reductions for slight injuries and higher reductions for severe injuries and fatalities. The total number of casualties has decreased by more than 26 percent from 511,577 in 2000 to 377,481 in 2013. For 2014 the increased number of injury accidents will lead also to an increased number of casualties of approximately 2.5 percent compared to 2013 – to about 387,000 casualties in 2014.
Since 2000, the number of severe injuries has been reduced by nearly 37 percent to 64,057 seriously injured road users in 2013 and the number of slight injuries has been reduced by nearly 23 percent to 310,085 slightly injured road users. Fatalities have decreased by 55 percent from 7,503 fatalities in 2000 to 3,339 fatalities in 2013. A slight increase to approximately 3,360 fatalities has been predicted for 2014.
According to the positive development on the long term, the year 2013 showed the lowest number of fatalities since introduction of accident statistics. And also for the number of injury crashes and casualties the year 2013 was the second best after 2010, when accident figures were even lower than 2013.
But the forecast for 2014 with stagnating or even increasing numbers shows, that the positive development cannot be taken for granted. While many factors concerning e.g. safety behavior or vehicle and infrastructure safety play an important role for the long term development of fatality and crash figures, short-term increases result mainly from changes in mobility and traffic behavior due to different and extreme weather conditions. The year 2014 was characterized by an early and mild spring, resulting in high accident and fatality figures concerning mainly motorized and non-motorized two-wheelers.

### 1.2 Socio-economic costs due to road traffic accidents in Germany

The Federal Highway Research Institute (BASt) calculates the costs of road accidents on an annual basis. The costs of road traffic accidents to Germany's national economy include personal injuries and damage to goods.
The calculated costs include direct costs (e.g. for medical treatment, vehicle repair/replacement), indirect costs (for police services, the legal system, insurance administration, replacement of employees), lost potential growth (including the shadow economy), lost added value of housework and voluntary work, humanitarian costs, costs of monetised travel time losses due to accidents on motorways. Using the developed calculation model an analysis of very severe injuries and the effect of underreporting on total accident costs could be accomplished.
The calculated total accident costs for 2012 amounted to approximately 32.11 billion Euro.
Furthermore, personal injuries amounted to 13.54 billion Euro. Costs of about 18.57 billion Euro were caused by damage to goods.

The costs per person add up to 1.62 million Euro for a fatality, 116,151 Euro for a severely injured person and 4,829 Euro for a slightly injured person.

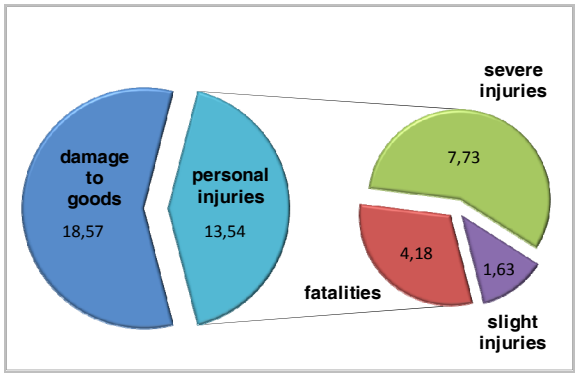


***Figure 1: Costs due to road traffic accidents in 2012 (billion Euro)***

### 1.3 German Road Safety Programme

The German Road Safety Program was launched in autumn 2011 and will be running for ten years until 2020. The principal aim of the program is to enable safe, ecologically sensitive and sustainable mobility for all road users in Germany. It comprises a wide range of road safety measures addressing road users, vehicles and the road infrastructure.
The program addresses new challenges (e.g. demographic change and mobility of elderly) and aims at safeguarding the efficiency of the road network. At the same time, it reflects recent technological developments in vehicles such as driver assistance systems, cooperative vehicle systems or new engine concepts. In these latter areas, the main focus lies on ensuring that the development of vehicle technology induces safety gains rather than safety risks. Activities also focus on rural roads and on reducing not only the number of fatalities, but also the number of serious injuries.
For the first time, a quantitative target of -40% for fatalities by the year 2020 was set. The target was defined on the basis of scientific research regarding the expected development of road safety until the year 2020 (R. Maier et al., 2012 a). The monitoring and assessment of road safety measures and the development towards the target is done by the Road Accident Prevention Report, which is prepared every two years and submitted to the German Bundestag. In 2015, a Midterm Report will be launched, taking stock of the first half of the road safety program. Until 2013 the number of fatalities has been reduced by 16,7 % since 2011. On condition of a prolongation of this trend into the coming years Germany is well on its way to achieve the reduction of 40 % by 2020.

## 2 RESEARCH

### 2.1 Finished projects

#### 2.1.1 AsPeCSS

The ASPECSS project (Assessment methodologies for forward looking integrated pedestrian and further extension to cyclists safety systems) focused on passenger cars' forward looking safety systems that are designed to address pedestrian and cyclist accidents. The project's aim was to deliver harmonised test procedures as input for further regulatory and consumer rating activities as well as to develop a methodology to assess the integrated safety systems (benefit of the linkage from both vehicle's active and passive safety systems). Other initiatives that contributed to the definition of test and rating procedures were the AEB (Autonomous Emergency Braking) group and the vFSS (vorausschauende Frontschutzsysteme / advanced forward looking safety systems) group. Final test procedures had been discussed and defined within Euro NCAP, based on input of all of these initiatives. The four final test cases for pedestrian AEB systems had then undergone extensive validation and verification testing by various test labs, and as a result, the test procedure has proven to be able to compare the performance of different types of pedestrian AEB systems.
In parallel to the work done by ASPECSS, AEB group and vFSS, specifications for a propulsion system as well

as for the pedestrian dummy had been defined. A proper combination of propulsion system and dummy is now available for testing. It is expected that testing within Euro NCAP will start as announced by beginning of 2016.

***Figure 2: Testing of pedestrian AEB system.***

### 2.1.2 InteractIVe

After almost four years of work, the integrated project interactIVe has reached its completion, marking major progress towards the realisation of advanced safety systems for Intelligent Vehicles.
The main achievement is the creation and evaluation of integrated ADAS (Advanced Driver Assistance Systems), characterised by outstanding capabilities for supporting the driver in varied traffic scenarios, and specifically for avoiding hazardous situations. Several new safety functions have been implemented in six passenger cars and one truck, based on the following pillar concepts: continuous driver support, collision avoidance, and collision mitigation. These vehicles have granted a comprehensive validation in a large set of field trials, in some cases combined with driving simulator experiments. Special attention has been given to low cost solutions for all the vehicle segments.
Multiple integrated functions were developed for continuous driver support, but also for executing active interventions for collision avoidance and collision mitigation purposes are served by an integrated perception layer. The primary objective was to extend the ADAS scenarios range and usability by introducing a unique access point, the so-called perception layer, where not only different fusion approaches will fit into the same concept, but also all applications have an access to sensor-, digital maps- and communication data through a common interface: the Perception Horizon.
Different types of sensors were used ranging from radars, cameras and lidars to GPS receivers for the extraction of the electronic horizon.
In parallel to this, work was also initiated by the development of detailed use-cases. The use-cases describe how the functions in the different demonstrator vehicles should resolve so called target (accident) scenarios. This work led to Information, Warning and Intervention (IWI) strategies. The IWI strategies should be applicable both to the specific demonstrator vehicles in the interactIVe project as well as to ADAS beyond the project.
The general IWI strategies can be seen as Human Factors guidelines or general functional requirements for ADAS. The development of IWI strategies was carried out iteratively. The use-cases and initial requirements from the vertical sub-projects served as a starting point in order to define the functions. Strategies were evaluated in different simulator and test track experiments and updated based on the outcome of the experiments.
The analysis of legal aspects for broad exploitation of the interactIVe applications was carried out. This work clearly identified the current steering system regulation UN-R 79 as being the most relevant hurdle for the introduction of new, more automated ADAS technologies.

### 2.1.3 Global technical regulation on pedestrian safety

An Informal Working Group on GTR9 Phase 2 chaired by Germany and with intensive contributions of BASt has prepared both, a second phase for a global technical regulation on pedestrian safety as well as the 01 series of amendments of UN regulation 127, both introducing a new flexible pedestrian impactor (FlexPLI), better reflecting the human response and kinematic behaviour of a pedestrian in case of an impact. In the meantime, UN-R 127.01 has been adopted by WP.29 and is being applied by the contracting parties since January 2015.

In parallel, a Task Force of the IWG redefined the bumper area being subjected to tests with the FlexPLI. A proposal of the Task Force, in principle stating the hard structure under the bumper fascia to define the width of the test area, has been already endorsed by GRSP at its December 2014 session.

### 2.1.4 Pedestrian safety

Within the Euro NCAP consortium, a technical working group updated the pedestrian test and assessment protocols. Amongst other things, the FlexPLI has been introduced and is being assessed against injury criteria and performance limits proposed by BASt. The new upper legform test is now focusing on the injured body region pelvis and femur rather than on the injury causing part. A new test with the child headform impactor against the bonnet leading edge was proposed by BASt and was introduced in 2015 as monitoring test for defined vehicle heights.

### 2.1.5 Cyclist safety

Cyclists as the second group of vulnerable road users are currently not addressed by provisions of passive safety. Therefore, BASt initiated the development of a test and assessment procedure for passive cyclist safety, revising, where necessary, the pedestrian test procedures by addressing the particularities of vehicle to cyclist accidents in terms of boundary conditions, following real world accident data and impact kinematics.

### 2.1.6 Motorcycle helmets

The numbers of accidents involving motorcycles with severe or fatal injuries are still on a very high level compared to other traffic participants. Motorcycle helmets are a substantial part of the protection devices in accidents. Requirements for motorcycle helmets are specified in the UN-R 22 with regard to visibility, shock absorption and others.
In order to reduce this high number of seriously injured or killed motorcycle riders a research project was conducted to establish recommendations for an improvement of the UN-R 22 concerning the type of test, test equipment, test criteria and limits.
Therefore, national and in-depth accident data (GIDAS) were analyzed and supplementary computer based FEM simulations were performed to better understand the injury mechanism and injury pattern of helm protected head injuries. In addition, different new head injury criteria and head finite element models were discussed.
The statistics from national accident data have shown that in 2013, 641 riders were killed and 12,034 were seriously injured in a total number of 42,427 PTW (powered-two-weheeler) accidents. The analysis of motorcycle accidents in GIDAS was based on a subgroup of motorcycle drivers with MAIS 3+ injuries (n=199). In most cases, a protective helmet had been used. In 18%, the main injuries were located in the region of the head; in 48%, the victims had no head injuries but serious to critical or fatal injuries to the body. About 10% of the motorcycle riders had no helmet at all or used an absolutely unsuitable helmet.
Recommendations with regard to the type of testing, test velocities, test temperature and test criteria have been made.

### 2.1.7 Rear Underrun Protection

UN-R 58 governs the design and installation of rear underrun protection devices on vehicles of categories N2, N3, O3 and O4. Nevertheless, rear end collisions – especially those involving vehicles of category M1 – with the aforementioned categories of commercial vehicles are characterized by a high level of accident severity. Germany thus submitted a proposal to the UNECE suggesting that the regulation be amended. This would include, inter alia, increasing test forces and reducing ground clearance. Using an injury risk model based on German national accident statistics, it is estimated that these measures could reduce the number of fatalities by 53 to 78 % and the number of seriously injured casualties by 27 to 49 % in such accident constellations, which is equivalent to 20 fatalities and 95 seriously injured casualties per year. In monetary terms, the benefit would be 35.7 million euros. The costs for the goods vehicles and trailers affected each year would be between 5 and 20 million euros, depending on how the costs are estimated. Thus, the benefit-cost ratio for the proposed measures is between 1.78 and 7.
Related to relevant accidents at EU 27 level based on a CARE database analysis, the benefit is estimated to be higher than in Germany by at least a factor of 9, whereas fleet-dependent costs would only exhibit a factor of 4. Thus, for the European commercial vehicle fleet and the accidents in which they are involved, it can be estimated that the effectiveness at EU 27 level would be at least as high as in Germany.
Against the background of the problems associated with HGV rear underrunning, the question arises as to whether passenger car emergency braking systems can, in the near future, represent an effective and efficient alternative for improving the situation of rear underrun accidents. For Germany the benefit from introducing an

ideal emergency braking system for all passenger cars would be around 842 million euros per year, while the costs for 3 million newly registered vehicles per year in Germany would be between 489 and 917 million euros. This produces a benefit-cost ratio of 0.9 to 1.7. By comparison, improving the Rear Underrun Protection Regulation would prevent 38 % (20 of 53) of the fatalities theoretically addressed by an emergency braking system but would only cause 2 % of the costs of passenger car emergency braking systems.

### 2.1.8 Impact of age related changes on injury biomechanics and test tools/procedures

The demographic change results in a higher participation of older people in traffic which leads to increased risk of accidents and injury of this particularly vulnerable group. The passive vehicle safety still shows potential for improvement to address this increasing challenge. BASt is supporting this in particular by contribution to research towards the optimization of test tools and procedures for passive vehicle safety in regulation and consumer testing. To enable this, BASt has been involved in a variety of research projects and regulatory activities in particular addressing to age-related conditions of road users.
E.g. as part of the revision of the UN-R 94 for frontal impact of cars the injury criteria of the Hybrid III dummies were adjusted to take into account the injury tolerance of older car occupants. Further a research project addressing injury biomechanics of elderly was funded by BASt, which was completed in 2014. The aim of this project was to identify age-related anthropometric differences of the bony thorax based on medical imaging methods (Figure 4). The results allow the adaptation of a numerical human model to represents an older vehicle occupant. This model can be used for further simulation-based investigations to improve the passive vehicle safety for elderly occupants.

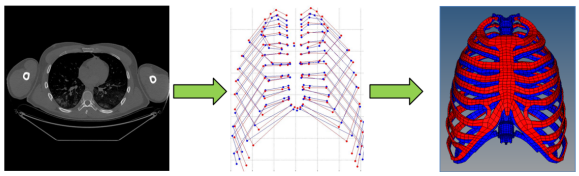

***Figure 3: Age-related anthropometric differences of the human bony thorax***

On February 12, 2014 the symposium "Trauma biomechanics of older road user - Challenges of Demographic Change" was held at BASt with around 70 participants. The event focused on biomechanical age-related changes of older road users, which may have an effect on accident risk and road safety in general of elderly road users. During the symposium, studies were presented based on current accident data indicating the priorities of the injuries of older road users. In addition, recent biomechanical research results were presented. Furthermore possible technical solutions of vehicle safety systems to take into account biomechanical differences of elderly car occupants were discussed.
BASt will continue to investigate the impact of demographic change on a necessary adaptation of testing and evaluation methods of passive vehicle safety. Specifically, this means a further contribution towards an optimization of wheelchair restraint systems as well as in the development of frontal impact test methods and the frontal impact dummy THOR with corresponding age-related injury criteria. This will be supported by increased use of numerical simulation models of human body.
Some of these research activities including further work on the THOR dummy will take place in the EU funded research project SENIORS (Safety-Enhancing Innovations for Older Road Users). The project will start in June 2015 with a duration of about 3 years under the coordination of BASt. It is based on an integrated approach to improve the safe mobility of older road users in the context of demographic change. All relevant modes of transport are taken into account in the road with a focus on vehicle occupants as well as pedestrians and cyclists.

### 2.1.9 Child restraint systems

The work of the UNECE/GRSP Informal Group “Child Safety” deals with the new regulation UNECE R129 for child restraint systems (CRS). A step by step approach is implemented. The Phase 1 dealing with with ISOFix Integral “Universal” CRS (“i-Size”) is finalized. The new regulation includes side impact testing, an updated test bench and the use of the Q-dummies. The weight group system has changed to a standing height based system which is easier to understand by users. Up to an age of 15 month an “i-size” CRS has to be rearward facing. The new regulation gives the possibility to have universal rearward facing CRS with ISOFix anchorages. The use of CRS homologated according to the UNECE R129 is implemented in the German regulation. To support the use of the CRS and explain the new regulation a brochure “Kindersicherheit im Auto” will be published by BASt. The brochure will be also available for download in English (“Child Safety in Cars”).

### 2.1.10 Smoke and toxicity in bus fires

Bus fires occur frequently but are usually not accompanied with severely injured persons. In most of the cases the fire starts in the engine compartment and does not affect any passengers because they can leave the bus in time. However single accidents, in which the fire enters the passenger compartment, resulted in a high number of fatalities. More dangerous than the fire itself is the toxicity of smoke gases due to burning interior parts made of plastic materials.
BASt therefore initiated a research project with regard to the fire safety performance of buses including smoke development and its toxicity. The study was elaborated by BAM (Bundesanstalt für Materialforschung und -prüfung, Federal Institute for Materials Research and Testing, Germany) and was published recently. Burning behaviour tests were carried out with small specimen of bus interior material, with complete seats and using whole buses in order to examine possibilities to further increase bus fire safety and to determine how far it is possible to transfer and adapt existing rail requirements to buses.
Some of the outcome of the experiments is already incorporated into international legislation. Especially UN-R 107 and 118 cover bus fire safety performance. E. g. fire detection systems in the engine compartment and smoke detection systems in separate interior compartments which turned out to be very useful are already required. Also testing of certain properties of insulation materials to repel fuel or lubricant as well as testing vertical burning rates for vertically mounted parts is specified in the UN regulations.
The most important results of the work concern smoke development and toxicity of smoke gas components which are still not covered by legislation. As demonstrated in the experiments, in case of a fire the air in a passenger compartment of a bus is quickly filled with large amounts of opaque smoke that impair visibility. Requirements limiting smoke density and toxic smoke gas concentrations would help to increase the time of escape for passengers in case of a bus fire so that they are not exposed to the toxic components that are produced when bus parts are burning. It is not sufficient to limit all components together by a weighted sum as in the current rail standard since single gases might be lethal although the sum limit is not exceeded. It is rather recommended to limit concentrations for each single component. The study further recommends that the concept to use fire suppression systems in the engine compartment should be persued further.
The transposition of the recommendations of this study into UN regulations is currently discussed on national level. The report is available for download: http://www.bast.de/DE/FB-F/Publikationen/Download-Publikationen/Downloads/F1-busFireProject.pdf.

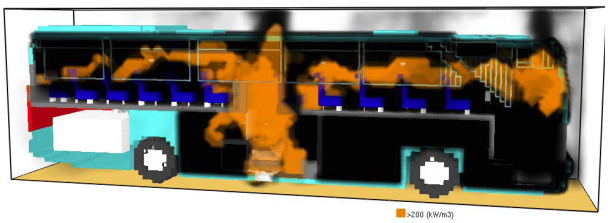

***Figure 4: Bus fire simulation (source: BAM)***

### 2.1.11 Periodic Roadworthiness Tests

The current Directive 2009/40/EC includes minimum standards for the periodic roadworthiness tests of motor vehicles (regular vehicle checks required by law) and will be replaced by the Directive 2014/45/EC. The current Directive 2009/40/EC is repealed with effect from 20 May 2018.
The current Directive applies to passenger cars, buses, coaches, light and heavy goods vehicles and their trailers (with more than 3,5 tons maximum authorized mass), but not to scooters, motorbikes, tractors and other smaller trailers.
In the Directive 2014/45/EC (Official journal of the European Union / L127 / 29$^{th}$ of April 2014, Volume 57) the scope of vehicles to be tested is extended to two- or three-wheel vehicles from 1. January 2022 (vehicle categories L3e, L4e, L5e and L7e, with an engine displacement of more than 125 cm) and wheeled tractors of category T5. These two categories of vehicles are currently not compulsory under EU law. Also vehicles of historic interest have now been more precisely defined. Other aspects such as the minimum training of inspectors and the common data exchange are also part of the Directive. The still outstanding implementing acts will cover the verification of the electronic vehicle safety systems, such as Adaptive Cruise Control and the exchange of data between the Member States.
The European Commission contracted a consortium led by CITA including BASt to undertake a project to develop and evaluate roadworthiness inspection methods for the inspection of the functionality and performance of Electronically Controlled Safety Systems (ECSS) and perform a cost benefit analysis for their potential introduction into European legislation.

For this purpose 2,654 tests on electronic systems were performed during field tests. The stored error messages of the tested vehicles cannot be associated with existing defects or are only relating to a low voltage of the vehicle. Therefore those error messages of the electronic systems are not suitable for the purpose of Periodic Technical Inspection at this time. In addition, it has been found, that the reference value method is a suitable additionally method to assess the deceleration and the brake force distribution. The final report was transmitted in July 2014 to the Directorate General MOVE of the European Commission: http://www.cita-vehicleinspection.org/Home/Studies/ECSS/tabid/560/Default.aspx.

***Figure 5: scan tool used in ECSS***

### 2.1.12 EVERSAFE

The objective for EVERSAFE was to provide safety requirements for electrically propelled vehicles, thus answering the current need for standardization within the area. This was achieved through the investigation of potential safety issues of electric vehicles and further complemented with a study of user safety concerns. This allowed for the identification of real and perceived safety risks which were needed to be addressed by the developed safety requirements. Under the scope of the EVERSAFE project, safety issues were categorized in two groups:

• Active/Primary Safety: Under this topic vehicle stability was addressed under fault conditions which would not arise in a conventional vehicle, i.e. failures in wheel hub motors, faulty regenerative braking systems.

• Passive/Secondary Safety: Within this area, the focus was set on the fields of crash compatibility (conventional fleet meets electric fleet) and Energy Storage Systems behaviour under and after crash loads (focusing on Li-ion batteries). Major results were recommendations for the safe testing of electric vehicles and/or their main components in regulations and standards as well as an updated safe handling procedure for rescue services to be considered in case of a severely damaged electric vehicle in crash.

To mitigate the safety issues identified by EVERSAFE, the delivered safety recommendations also revealed needs for further research efforts and comprised suggestions for standardization to be implemented by both industry and legislation.

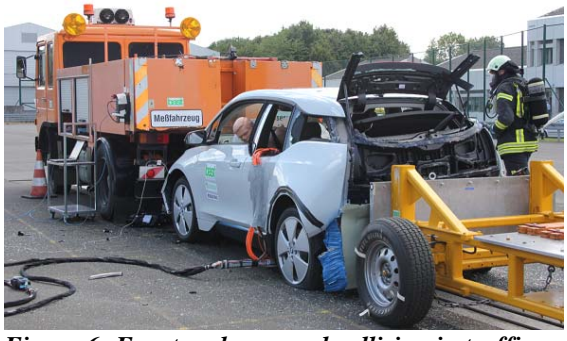


***Figure 6: Front and rear-end collision in traffic congestion scenario***

## 2.2 Ongoing research

### 2.2.1 Turning Assist Systems for trucks

Accidents between right turning trucks and straight riding cyclists often show massive consequences. Accident severity is much higher than in other accidents. The situation is critical especially due to the fact that, in spite of the mirrors that are mandatory for ensuring the field of view for the truck drivers, cyclists in some situations

cannot be seen or are not seen by the driver. Either the cyclist is overlooked or is in a blind spot area that results from the turning manoeuvre of the truck and its articulation if it is a truck trailer or truck semitrailer combination.
At present driver assistance systems are discussed that can support the driver in the turning situation by giving a warning when cyclists are riding parallel to the truck just before or in the turning manoeuvre. Such systems would generally bear a high potential to avoid accidents of right turning trucks and cyclists no matter if they ride on the road or on a parallel bicycle path. However, performance requirements for such turning assist systems or even test procedures do not exist yet.
BASt therefore carries out a research project in order to develop a testing method and elaborate requirements for turning assist systems for trucks. In-depth accident data was evaluated case by case in order to find out which are representative critical situations. These findings served to determine characteristic parameters (e.g. boundary conditions, trajectories of truck and cyclist, speeds during the critical situation, impact points). Based on these parameters and technical feasibility by current sensor and actuator technology, representative test scenarios and pass/fail-criteria are defined.
After having fixed the set of test cases and parameters a validation phase has to follow. For that purpose trucks equipped with turning assist system will be used. It will be examined if the system is able to inform the driver when necessary and how far it is still annoying due to possibly given false warnings.
It can be expected that a turning assist system that fulfils the requirements and tests elaborated in this study will have a very positive influence on accident figures concerning right turning trucks and cyclists. The test procedure is meant to be the basis for an international discussion on introducing turning assist systems in vehicle regulations at UNECE level.

### 2.2.2. Study on Camera-Monitor-Systems

Within the automotive context camera monitor systems (CMS) can be used to present views of the traffic situation behind the vehicle to the driver via a monitor mounted inside the cabin. This offers the opportunity to replace classical outside and inside rear-view mirrors and therefore to implement new design concepts, aerodynamically optimized vehicle shapes and to reduce the width of the vehicle. Further, the use of a CMS offers the potential to implement functionalities like warnings or situation-adaptive fields of view that are not feasible with conventional rear-view mirrors. Despite these potential advantages, it is important to consider the possible technical constraints of this technology and its effect on driver perception and behavior. On the technical side besides the field of view and the robustness of the system, aspects as its functionality at day and night as well as under varying weather conditions were object to a scientific investigation conducted by BASt. Concerning human machine interaction the perception of velocities and distances of approaching vehicles were considered as they might be different for CMS as compared to conventional rear-view mirrors. Potential influencing factors as the position of the display or drivers' age were taken into account. Within the BASt study CMS was tested under controlled conditions as well as in real traffic for passenger cars and heavy goods vehicles.
In general, it was shown that it is possible to display the indirect rear view sufficiently for the driver, both for cars and trucks, using CMS which meet specific quality criteria. Depending on the design, it is even possible to receive more information about the rear space from a CMS than is possible with mirror systems. It was also shown that the change from mirrors to CMS requires a certain period of familiarisation. However, this period is relatively short and does not necessarily result in safety-critical situations.
Currently the UN-R 46 (Devices for indirect vision) is under revision by an informal group on Camera-Monitor Systems, in which above mentioned results are considered.

### 2.2.3 Study on winter tyres

Winter tyre use for passenger cars is mandatory in Germany if there is snow or ice on the road. Commercial vehicles are required to have tyres with winter characteristics only fitted to their driven axles, and no specific limits for tyre wear and age are set for any vehicles' winter tyres.
Since wear and age of tyres might have a considerable effect on their friction coefficients, BASt was asked to perform an extensive study on winterly road surfaces to identify reasonable limits. In general, passenger car tyre properties decrease substantially with profile depths below 4 mm, but not with age. This effect had not been found with commercial vehicle tyres.
Theoretical considerations suggest that specific winter tyres on trailer and steering axles might contribute to better braking behavior of commercial vehicles. The steering axle has a large influence on empty truck-and-trailer combinations, while the trailer axles have a high effect on fully loaden vehicles. The current regulation on tyres UN-R 117 does not define any tests or winter requirements for steering axle or trailer tyres, so no robust estimation on the improvement of traffic safety can be done.

It seems that a situational requirement to fit belt chains to driven axles could improve the climbing ability of commercial vehicles in specific situations. Since a large amount of traffic jams on German highways in winterly conditions is due to trucks being stuck, this could in fact improve winterly traffic flow.

### 2.2.4 Accessibility in long distance buses

In order to deregulate passenger transport, German long-distance bus operators are now allowed to compete against one another and against rail transport. To meet the requirements of all passenger groups in the light of inclusion, their buses will have to provide two wheelchair spaces by 2020 (by 2016 for vehicles first registrations). These requirements build not only towards the German wide aspiration to reduce accessibility barriers, but also towards the goal to avoid barriers systematically in the future. So far, it is not clear if other specifications for equipment going beyond those accessibility requirements in long-distance buses are needed to ensure an appropriate degree of accessibility. For that purpose BASt initiated a research project carried out by Human Factors Consult, Berlin. After having defined accessibility in this context, the main goal of the research project is to derive recommendations for measures to be taken when designing and building accessible long distance buses as a basis for international discussion on harmonised regulations. The project therefore includes two subordinate tasks: first to gather stakeholder requirements and define accessibility which is both done using questionnaires and workshops and second to compose recommendations for respective measures. Different kinds and degrees of disabilities have to be regarded. The measures shall focus on the vehicle itself, the operation of the long-distance buses and on operation personnel. Road infrastructure issues shall be demonstrated using examples for best practice. Deriving measures shall also take into account the state of the art technology for barrier free access and examples coming from the rail sector. In the end also costs, feasibility (technical limits) and practicability have to be considered when assessing the measures proposed.
First intermediate and preliminary results show that for the technical requirements for the bus UN-R 107 Annex 8 can serve as a good basis which might be amended. It turned out and should be paid attention to that accessibility in the view of disabled people often can be reached by the use of support addressing at least two sensory channels. It seems equally important to consider needs and requirements of different user groups (individuals differently challenged and unchallenged in kind and degree (of impairment), senior citizens, children, parents, etc.) in a design for everyone and to focus not only on the accessibility of the vehicles but equally on a barrier-free travel chain as a whole.
The project is planned to be finished in the course of the year 2015.

### 2.2.5 GTR on head restraints

For several years, work is in progress with regard to develop an improved regulatory dynamic test procedure for head restraints with the aim of mitigation of neck injuries. The dynamic test option in the current GTR No. 7 on head restraints foresees the use of a Hybrid III dummy using the test pulse as described in FMVSS 202a. According to several studies like those from EEVC, the Hybrid III is lacking biofidelity under rear impact conditions and is not humanlike enough for seat or head restraint testing. In consumer test programs like Euro NCAP or IIHS, the BioRID is used for many years for the dynamic assessment of seat performance under rear impact conditions. However, several concerns have been raised about the repeatability and reproducibility of the BioRID. As the anthropometric test device (ATD) is the crucial factor in a dynamic test a suitable dummy needs to be defined for use in regulation. Several studies have shown that out of the available dummies (Hybrid III, THOR, RID3D, BioRID) the BioRID seems to be the best dummy for low speed rear impact seat testing.
Within the framework of the Informal Working Group on a GTR No. 7 on head restraints phase 2 a BioRID Technical Evaluation Group (TEG) has been given the task to improve the BioRID and to develop the necessary specifications and documentation for regulatory purposes. The BioRID TEG started its work in January 2010 and most of the meetings are hold as WebEx meetings with some joint face to face meetings with the GTR No. 7 group. The BioRID TEG is chaired by BASt. The TEG has made significant progress and quite a lot of issues have been discussed, investigated further and addressed in the meantime e.g. by technical bulletins released by the dummy manufacturer (Humanetics). A drawing package is now available on the UNECE website as well as an improved certification procedure; a built level check list has been published as well as a PADI (Procedures for Assembly, Disassembly and Inspection). Work is ongoing with the aim of reducing the response corridors during certification and refining the certification procedure. A new certification test (GEN-X test) has been developed and some further refinements are ongoing. The improvements developed and proposed by the TEG and the new certification procedures are indented to be used by Euro NCAP and IIHS, too. The aim is a worldwide harmonized BioRID for testing under rear impact conditions for regulatory purposes as well as consumer testing. A really challenging task of the GTR No. 7 group and the BioRID TEG is the development of validated injury or seat performance criteria addressing the risk of cervical spine distorsions. In September 2014 a special GTR No. 7 / BioRID TEG Group of Experts Whiplash Injury Criteria Meeting was chaired by BASt.

The group recommended a set of potential injury criteria for regulatory purposes. However, those injury criteria are still under discussion and further research.

### 2.2.6 Child restraint systems

BASt is further supporting the work of the UNECE/GRSP Informal Group "Child Safety" in the development of Phase 2 of the new regulation UN-R 129. This phase deals with the implementation of universal booster seats (with and without backrest), were the child is secured by the vehicle 3-point belt, in the regulation. This will also include the stature based system and will be connected to the standing height of the child. After finalization of Phase 2, the group will work on other CRS types in a third phase.
In addition BASt is participating in the "Chest and Abdomen Injury Criteria Task Force", dealing with the Q-dummies. This work includes the reconstruction of accidents with children involved as car occupants The Task Force will give input for the UNECE/GRSP Informal Group "Child Safety" and the Euro NCAP Child Safety Working Group.
After the implementation of the CRS-car interface compatibility assessment protocol, Euro NCAP now works on the replacement of the dummies representing smaller children by dummies representing older children in the dynamic test. BASt is involved in the development of the new protocol which will include the Q6 and the Q10 dummies as rear seat occupants in dynamic ODB and side impact tests. The aim is to improve the protection of larger children respectively small adults on rear seats.

### 2.2.7 Urban Space: User oriented assistance systems and network management

Together with 30 partners including automobile and electronics manufacturers, suppliers, communication technology and software companies as well as research institutes and cities BASt has joined the national project UR:BAN[1] which started in 2012 running for a four-years-term until April 2016. The project is funded by the Federal Ministry of Economics and Technology. UR:BAN focuses on the development of advanced driver assistance and traffic management systems for cities and pays special attention to the human being in all aspects of mobility and traffic.
UR:BAN also covers the evaluation and prediction of vulnerable road users´ (pedestrians and cyclists) behaviour and movements. With regard to the complexity of urban traffic UR:BAN aims at supporting the driver in performing maneuvers such as driving in narrow or obstructed streets, resolving conflicts with opposing traffic and performing lane changes. By means of novel panoramic sensing and prediction capabilities collisions can be avoided by automatic braking and/or swerving. BASt is involved here with legal expertise since the legal implications of the functions developed in UR:BAN – such as functions performing automated swerving manoeuvres in critical traffic situations – have to be identified and examined.
Furthermore, UR:BAN takes the human being into account by incorporating adaptive support into the design of vehicle controls and displays. BASt is involved in the examination of the aspect of controllability of new driver assistance systems with psychological and legal expertise.

### 2.2.8 AdaptIVe

Automated driving systems as defined in the EU-project AdaptIVe accomplish surplus operations compared to Advanced Driver Assistance Systems currently in use. They automatically take over operational manoeuvres and "drive" the vehicle longitudinally and cross-ways. Depending on level of automation they differ in terms of tasks still allocated to the driver.
AdaptIVe has the vision of a widespread application of automated driving to improve road safety and address inefficiency in traffic flow. The project approved by the European commission involves 29 research institutes, suppliers and industrial partners. The project develops new and integrated automated functions to improve traffic safety by minimizing the effects of human errors. The general objective of AdaptIVe is to develop new functionalities provided by partially-automated and highly-automated vehicles. Major AdaptIVe-functions are foreseen for different settings, namely highways, urban traffic, and specific close-range manoeuvres. Continuously automated systems like Adaptive Cruise Control and/or Lane-keeping Systems are well established in the market for Driver Assistance Systems today. In combination of these systems, for example the motorway chauffeur, the driver would additionally not required to constantly monitor the "drive" by the function any longer. In legal terms the question is being raised whether legislation is keeping pace with these technological advancements.
Therefore, in addition to the technological aspects, AdaptIVe will address important legal issues that might have impact on the market introduction of automated systems. It will identify the legal implications for manufacturers and drivers and identify boundaries lying in current regulation. Today's legal framework was developed based

[1] www.urban-online.org

on the concept that safe driving is a task of the driver only. Consequently it is likewise a basic legal assumption as well as requirement that the driver must be able to control his vehicle at all times. With a move to automated driving, the driver might temporarily, under certain conditions no longer be needed permanently in this role. Contradictions of such a development with the current legal situation need to be identified.
The main goal of this project is to collect and summarise the important aspects from legislation for different EU-member states on this technology. The secondary objective, from a legal perspective, is to foster mutual understanding and identify the possibly necessary harmonization within the EU member states. This objective shall be achieved by a comprehensive review of the current legal framework regarding automated systems. The review shall cover regulatory law (e.g. national road traffic law), the Vienna Convention on Road Traffic and road traffic liability (of the driver/ vehicle owner). If possible, corresponding aspects of criminal law (specific for the field of road traffic) and administrative offences can be investigated.
Another contribution of BASt is to provide input on impact analysis methology with focus on accident data from the CARE and GIDAS database.

### 2.2.9 KO-HAF

In 2015 a new research project concerning cooperative, highly automated driving (Ko-HAF) starts. BASt joins a national consortium with automobile and electronics manufacturers, suppliers, communication technology and software companies, research institutes and road administrations. The project aims on development of cooperative, highly automated driving on motorways, i.e. for high speed ranges on well constructed road infrastructure. This includes a significant improvement of forecasts for environmental detection in addition to the automation of the longitudinal and lateral control of vehicles.
The driver can not be taken entirely out of the loop during highly automated driving. Therefore, the readmission of the driving task by the human within a certain lead time will be researched in Ko-HAF as well. Several test vehicles will be constructed for testing and demonstration of highly automated driving under normal conditions and in case of system failure. The new vehicle operation will take place on test tracks and on public roads.
Key activities of BASt – in an academic part – are the evaluation of usability of external data for the highly automated driving, the design of data exchange with third parties and the evaluation of data protection issues.
In a practical part, BASt will conduct driving tests to determine the effect of different levels of automation on the driver's fatigue by EEG (electroencephalography) brain wave measurement and test the effectiveness of possible countermeasures in a second step.

### 2.2.10 aFAS

The project "aFAS" is funded by the Federal Ministry of Economics and Technology. Following the successful introduction of assisted driving funktions (up to level 2 of the BASt definitions) the next major step will be the integration of innovative driving functions in high and full automated levels. Against this background, the project „aFAS" was built by a consortium of eight partners. The name stands for a driverless mobile warning truck in case of temporary road works. Temporary road works present a danger for employees of road maintenance services. Accidents often occur because motor vehicles crash into the contruction site. The focus is therefore to build a driverless fully automated truck to improve safety for the employees of road maintenance services. The prototype of "aFAS" will be tested on the hard shoulder of the freeway in real traffic. A particular challenge in this project is to meet the requirements of functional sefety and quality of the steering system and the brake system. Also the sensor system has strict quality standards. BASt is involved with legal expertise in respect to driverless automation. Furthermore, BASt is involved in the application for a special license needed for the driverless vehicle. The limited speeds required for road maintenance provide ideal conditions for the first technical realization of driverless driving.

### 2.2.11 Frontal Impact

With regard to impact direction the frontal impact is still the most relevant one in terms of injury causation for passenger vehicles. Accident data has shown that the stability of passenger compartments has been improved substantially in recent years, even for lighter vehicles. However, the performance of the restraint system becomes now even more important because vehicles are getting stiffer which is leading to a higher deceleration pulse. Additionally, in real-world car-to-car impacts the lighter of the two vehicles has to withstand higher loadings than the heavier vehicle due to the principle of linear momentum.
Therefore, a research project is ongoing to investigate different types of frontal impact test procedures. The objectives are focused on restraint system tests and include tests with a mobile deformable barrier as well. Different anthropomorphic test devices are used to evaluate the protection capability of occupant restraint systems in particular with regard to the prevention of thoracic injuries.

Furthermore, the benefit of different frontal test procedures will be estimated based on real world accident data.

***Figure 7: Comparison of two full width frontal impact tests.***

### 2.3 Perspective

As the finished studies show, vehicle safety research is an international issue. Therefore BASt participated in applying for calls of the European framework research programme “Horizon 2020”. In addition national projects complement the work addressing specific research topics. BASt was successful with regard to the projects mentioned below.

#### 2.3.1 SENIORS

Given the demographical change today’s society is facing, a european funded research project named SENIORS (Safety-ENhancing Innovations for Older Road userS) under the HORIZON 2020 framework programme will investigate the safety need for combining different transport modes being used by the elderly as the most vulnerable road users. The consortium consists of a governmental entity, Euro NCAP laboratories, research institutes, dummy manufacturers, OEMs and vehicle suppliers. The project with kick-off on 1 June 2015 has a running time of 36 months. BASt acts as project coordinator.

#### 2.3.2 PROSPECT

Several vehicles that are currently on the market feature automatic emergency braking (AEB) systems either as standard or optional fitment. Assessment procedures for these systems are under development or already available. Their expected positive effect on accident figures is taken into account in consumer testing.
However, current systems suffer from a few limitations. Their intervention in critical driving situations occurs shortly before this event - at a time when the vehicle driver has almost no chance to avoid the accident by itself. As a consequence, this late reaction time makes it difficult for the AEB system to avoid (e.g. vehicle comes to a full stop just in front of the threat), in particular in high speed scenarios and scenarios with obscured pedestrians. If the braking intervention would start too early, there would be plenty of false activations in regular traffic, even in perfectly normal situations - which is not acceptable for traffic flow, from a safety perspective, and last but not least for the driver. Also, current systems only have access to vehicle braking systems. There's no automatic steering system in production (some prototypes are available).
Proactive safety systems especially for pedestrians and cyclists can be more effective, if they tune their intervention timing better to the traffic situation and driver fatigue, and if they use steering intervention additionally to braking intervention.
This is where the PROSPECT (Proactive Safety for Pedestrians and Cyclists) project comes in: PROSPECT will develop advanced Human-Machine Interfaces (HMI) as well as advanced vehicle control strategies for combined steering and braking. The advanced HMI will monitor the driver's directional attention and for instance intervene earlier in cases where the threat is out of the driver's focus. The control systems will make use

of a tremendously increased radial sensor range to find the optimal combination of steering and braking, and advanced sensor interpretation systems will allow to better judge the intention of pedestrians along the vehicle route with respect to their direction of movement.
To estimate the benefit for these new functions, advanced testing and validation methods need to be developed. Current validation of automatic brake systems is carried out on a test track, without irritating objects, road clutter, road signs or lines; thus, in rather artificial surroundings. PROSPECT will not only introduce novel realistic surrogate targets, but also perform testing in realistic surroundings including other moved objects, infrastructural facilities, clutter and the like.
Final output of PROSPECT will be three vehicle demonstrators, to be tested in detail using state-of-the art surrogate targets for pedestrians and newly developed surrogate targets for bicycles and their riders.

### 2.3.3 CODECS

The deployment preparation of Cooperative Intelligent Transport Systems (C-ITS) involves many stakeholders, including the automotive industry, National Road Authorities and road operators (including their suppliers), automobile clubs and organisations promoting ITS as a tool to safer, smarter and more environmental friendly mobility. COoperative ITS DEployment Coordination Support is a 36 month support action (kick off 1 June 2015) where core stakeholders support the deployment coordination activities on European scale (Amsterdam Group, EC C-ITS Deployment Platform). Beyond elements of aligning deployment roadmaps and of strategy coordination one important planned output will consist in the profiling of standards which are relevant for C-ITS services with infrastructure involvement. This technically important output for ensuring interoperability represents the focus of the BASt involvement in the CODECS support action.

**GOVERNMENT STATUS REPORT**

**Vehicle Safety Standards Branch**

**Department of Infrastructure and Regional Development**

**AUSTRALIA**

## INTRODUCTION

Australia is in the fourth year of a co-ordinated national strategy on road safety, and continues a downward trend in road crash fatalities. However, the trend is not consistent across all road user categories, leaving a number of areas for continued improvement.

***Figure 1*** **- National Fatality Rates and Road User Type**

## THE NATIONAL ROAD SAFETY STRATEGY 2011-2020

The National Road Safety Strategy 2011–2020 was released on 20 May 2011 and presents a 10-year plan to reduce the annual numbers of both deaths and serious injuries on Australian roads by at least 30 per cent. Figure 2 shows the target in conjunction with current fatality rates.

***Figure 2*** **- National Road Safety Strategy**

The strategy outlines broad directions for the future of Australian road safety, planned initiatives for the first three years and a range of options for further consideration as the strategy progresses. The initiatives and options are set out in four key areas—Safe Roads, Safe Speeds, Safe Vehicles and Safe People.

The strategy included a requirement for a thorough review to be carried out after three years. The review was conducted by Austroads in 2014 under Terms of Reference approved by Australian Commonwealth, State and Territory Transport Ministers. These called for:

An assessment of progress made during the first three years of the NRSS (2011–2013)

A review of the ongoing suitability of the 'high level' content of the NRSS

Identification of implementation priorities and key actions for the next three years.

The review was largely informed by an independent study commissioned from the Centre for Automotive Safety Research(CASR) at the University of Adelaide.

The main findings of the review were:

Good statistical progress was made in the first three years of the NRSS, as measured by overall changes in annual road fatality counts. The number of deaths in 2013 represented a 16.5% reduction relative to the strategy baseline period (2008–2010).

Fatality trends were less positive for certain sub-groups of road users, particularly cyclists, motorcyclists and older drivers.

Progress in reducing serious injury numbers was difficult to determine because of the lack of reliable, nationally consistent, non-fatal crash data. Available hospital data provided some evidence that serious injury levels had not declined in concert with the general downward trend in deaths.

The review found that progress in implementing the 59 'first steps' actions in the NRSS was varied, though there was evidence that most had been actively progressed to some extent and that there had been a number of clear achievements. Progress had been particularly strong in the vehicle safety area.

The review concluded that the 'high-level' content of the NRSS – its guiding vision, targets, key directions and Safe System principles – remain valid and appropriate for the 10-year strategy.

The review identified a range of 'priority areas' where road safety progress appears to have been lagging or where there is opportunity to make significant future gains. These areas included a mix of high-risk road user groups, countermeasure priorities and capacity building activities, and are discussed in some detail in the report prepared by CASR.

The review also concluded that the next phase of NRSS delivery should be guided by a more concise action plan than the initial 'first steps' agenda: it should focus on issues that clearly warrant national attention and that can be addressed through specific national actions.

**Action Plan 2015–2017**

The main outcome of the review is the three-year Action Plan described in this document.

In developing the content of the Action Plan, an over-arching principle was to focus on actions that will deliver or support significant long-term improvements in the safety of the road transport system – especially through strategic investment in infrastructure safety, vehicle safety and capacity building work.

This gives rise to some important qualifications about the content of the plan:

The Action Plan is not intended to directly target every higher-risk road user or community group identified in the NRSS review. By focusing on actions with system-wide impacts, it is expected that all groups will benefit from the plan.

The Action Plan is not intended to replace the content of the NRSS, but to ensure that national (or nationally-agreed)efforts are focused on strategically important initiatives. Many of the original 'first steps' actions in the NRSS remain important and will continue to be progressed at a jurisdictional level.

The Action Plan covers a number of broad categories:

Prioritizing our investments in infrastructure;

Improving the safety of Australia's vehicle fleet;

Encouraging safer road use; and

Advancing the safe system.

Improvements in the safety of vehicles on Australian roads are therefore fundamental to the Plan and particularly seek to implement priority vehicle safety standards (through the Australian Design Rules) and to accelerate the market uptake of vehicle technologies with significant safety potential.

The specific regulatory actions listed are to consider the mandating of:

Pole side impact occupant protection standards for new vehicles;

Antilock brake systems for new motorcycles; and

Electronic stability control for new heavy vehicles.

Targeted new technologies include Autonomous Emergency Braking, Lane Departure Warning and Intelligent Speed Advisory systems. These are to be promoted through collaboration between ANCAP (the Australasian New Car Assessment Program), individual jurisdictions (including the Commonwealth and States and Territories) and other stakeholders.

More detail on Australia's National Road Safety Strategy 2011-2020 and Action Plan 2015-2017 are available at https://www.infrastructure.gov.au/roads/safety/national_road_safety_strategy/index.aspx.

**ANCAP**

The Australian Government continues to be a member and major supporter of the Australasian New Car Assessment Program, with financial support being confirmed at least until 2015-16. ANCAP is currently in a period of transition, with testing and rating protocols to be aligned with those of Euro NCAP from 2018. ANCAP ratings remain significant in Australian consumer choice, with 81 percent of light vehicles sold carrying a 5-star rating (December 2014). In this period, an ANCAP rating was available for 92 percent of light vehicles sold.

**REVIEW OF THE MOTOR VEHICLE STANDARDS ACT 1989**

On 16 January 2014 the Assistant Minister for Infrastructure and Regional Development, the Hon Jamie Briggs MP, announced a comprehensive review of the Motor Vehicle Standards Act 1989, with a view to reducing regulatory costs to business and individuals and improving the safety and environmental performance of road motor vehicles.

The last major review of the *Act* was conducted in 1999. Since this time there has been significant change in the domestic and global environment of vehicle manufacturing, in vehicle technologies and in purchasing preferences of consumers. A public consultation process was conducted in late 2013 to seek feedback from interested parties on the need for a review and on the currency and operation of the legislation.

The review is currently in progress and has involved a public submission process along with consultations on possible future options for the Act. An Options Discussion paper was prepared and a number of public workshops were conducted in order to facilitate the process. The public submissions are being used to develop recommendations to Government and to prepare a Regulation Impact Statement for any proposed changes to vehicle regulation.

More detail on the review is available at
https://www.infrastructure.gov.au/roads/safety/national_road_safety_strategy/index.aspx.

## HARMONISATION OF ADRS WITH INTERNATIONAL STANDARDS

Pending the outcome of the review, the Australian Government has accelerated harmonization of the Australian Design Rules (ADRs) with international standards, in particular by application of a further round of UN Regulations in anticipation of the advent of International Whole Vehicle Type Approval.

Application of UN Regulations means that in effect relevant ADRs are automatically updated when UN Regulations are updated, providing immediate access to the Australian market to vehicles featuring the latest safety technology.

Australia is committed to an international system for developing vehicle standards and is active participant of the UN World Forum for Harmonization of Vehicle Regulations.

## REGULATORY DEVELOPMENTS

The ADR program works towards an agreed set of priorities in line with international regulations through UN WP29 activities and also Australia's National Road Safety Strategy 2011-20.

*Brake Assist Systems (BAS)*

In November 2013, Australia mandated BAS for light passenger vehicles and light commercial vehicles. Requirements will apply to new model vehicles from November 2015, to all new light passenger vehicles from November 2016 and all new light commercial vehicles from November 2017.

BAS has been shown to reduce the number and severity of crashes involving vulnerable road users, but can have broader application to other types of crashes where braking is a factor.

*Electronic Stability Control (ESC)*

In 2009Australia mandated ESC for light passenger vehicles. Requirements applied from November 2011 to new model vehicles and from November 2013 to all new vehicles.

In November 2013, Australia extended requirements for ESC to light commercial vehicles. As for BAS, these requirements will apply from November 2015 to new model vehicles and from November 2017 to all new vehicles.

*Antilock Brake Systems (ABS) and the National Heavy Vehicle Braking Strategy (NHVBS)*

Australia has diverse range of heavy vehicles and some heavy vehicle combinations that are not common in other countries. It is therefore important to ensure that braking technologies are compatible and suited to the combinations used in Australia, and the Australian road environment.

The NHVBS was released in 2008 and has been incorporated into the NRSS. Under Phase I of the NHVBS, Australia has mandated ABS for heavy trucks and buses and ABS or load proportioning brake systems for heavy trailers. Requirements have applied to new model vehicles from July 2014 and to new vehicles from January 2015. As part of these requirements:

- Trucks and buses equipped for towing must have facilities to power Electronic Braking Systems (EBS) (such as ABS/ESC) for the trailer, as well as provide the correct signaling for EBS operation where fitted.

Trailers with rear couplings must provide wiring suitable to transmit ABS/ESC/EBS functions to follow-on trailers.

There are expected to be significant safety benefits resulting from these changes.

*Pole Side Impact*

Vehicle occupant side impact fatalities account for around 20% of the road toll in a number of studied countries for example: Australia, Germany, the United Kingdom, the Republic of Korea and the United States).Australia proposed development of a Global Technical Regulation (GTR)on Pole Side Impact in 2010 and chaired the informal working group that developed the GTR.

GTR 14on Pole Side Impact was adopted by Working Party 29 on 13 November 2013. The GTR was subsequently transposed into a UN Regulation, which was adopted in November 2014.

EuroNCAPalso introduced test requirements based on the GTR on 1 January 2015, showing how regulatory and non-regulatory approaches can work effectively together.

Australia has commenced the domestic rulemaking process, in line with the NRSS and Action Plan 2015-2017. A Regulatory Impact Statement expected to be released shortly.

The performance requirements of the GTR (and UN Regulation) will reduce vehicle occupant injury risk (particularly head injury risk) in pole side impact crashes as well as vehicle-to-vehicle and other side impact crashes.

*ABS for motorcycles*

The case for mandating ABS for motorcycles is being considered, in line with the NRSS and Action Plan 2015-2017. Research on the real-world effectiveness of ABS in reducing road trauma is underway in conjunction with the Victorian Government in Australia. This research is expected to be finalized by mid- 2015.

*ESC and the NHVBS*

The case for mandating ESC for heavy vehicles is being considered, in line with Phase II of the NHVBS and the NRSS and Action Plan 2015-2017. Consultation is underway and the work is expected to be finalized by early 2016.

# STATUS REPORT, EUROPEAN ENHANCED VEHICLE-SAFETY COMMITTEE (EEVC)

**Bernd Lorenz**
EEVC Secretary General
Federal Highway Research Institute (BASt)
Germany

## INTRODUCTION

The European Enhanced Vehicle-Safety Committee (EEVC) was formed in February 1971 in Rome and has been active in participating in the ESV-programme since that time. EEVC comprised 8 members representing the administrations in charge of vehicle safety regulation from France, Germany, Italy, the Netherlands, Poland, Spain, Sweden and the United Kingdom.
During those four decades the environment of pre-regulatory research in the field of vehicle safety in Europe (and world-wide) has considerably evolved and it was necessary to realign EEVC to keep up with the future challenges. Therefore the EEVC Steering Committee agreed on new Transient Terms of Reference [1] which allow more flexibility and open EEVC to non-EEVC countries.

## NEW TRANSIENT TERMS OF REFERENCE

EEVC, which has contributed to the former IHRA activities from the beginning, is convinced that pre-regulatory safety vehicle research has to be approached at a world-wide level; within that objective the Steering Committee of EEVC has confirmed that non-EEVC countries can participate at WG level to share their research.

The EEVC Steering Committee had an internal reflection on its future and how to determine future research directions and priorities.
As a result of the discussion new Transient Terms of References (TToR) were agreed.
According to the new TToR the objectives of EEVC are:

- to provide impartial scientific advice to support the development of European vehicle safety standards and legislation,
- to co-ordinate European research activities with regard to harmonised vehicle safety regulations,
- to support specific research, evaluate technical proposals and define scientific tools (such as biomechanical criteria, test dummies, test procedures) needed for further development of technical standards and legislation,
- to advise European governments, the United Nations Economic Commission for Europe (UNECE) World Forum for Harmonisation of Vehicle Regulations (WP29), and the European Commission including their groups of experts on vehicle safety, in the area of vehicle safety improvement,
- to organise, upon request, European representation to international research groups in the area of vehicle safety,
- to advise other groups if called upon, on issues related to vehicle safety,
- to promote enhanced vehicle safety by publishing research results

The government of any EU member state, which has sufficient scientific capacity to carry out practical research relevant to vehicle safety and is willing and able to contribute effectively to coordinated EEVC research programmes, may become a full member of EEVC.
Application for membership by the government administration in charge of vehicle safety regulation of an EU member state shall demonstrate that it has sufficient scientific capacity or is in a position effectively to contribute to EEVC research. Application shall be made to full members who shall agree to its membership unless one-third of the existing full members object.
At the end of each year, the secretary general shall ask all the full members to indicate to each other their volunteer to continue and to participate actively to the EEVC work for the year to come.
In case of negative answer of a full member, this full member shall be designated as “sleeping full member” and shall not be part of the steering committee for the year to come with no possibility to vote.
The full members of the year 2015 are France, Germany, Italy, the Netherlands, Poland, Spain and the United Kingdom. It is worthwhile to note that some of these members are members of Euro NCAP, too.

The EEVC Steering Committee has decided that the setting of the research agenda is the critical parameter in the further work of the EEVC, for both the scope of its activities and its priorities. It was agreed that short term and longer term research needed to be considered together.

## NEW EEVC WEBSITE

The old EEVC website has been subject to major hacker attacks and was shut down for this reason. In 2014, the new EEVC website (www.eevc.org ) has been launched. The web site serves as an information platform for all interested parties, both EEVC members and external, with a broad pool of documents/publications. Moreover, it is a useful tool for coordination and publication of the EEVC work, as well as for the internal data and information exchange. Each working group/task force has it is own member area with the opportunity to promote their work, share documents and make it available for the members before it will be published in the public area of the website.

## ADVANCED ANTHROPOMETRIC CRASH DUMMIES (WG 12)

This working group is the longest active Working Group within EEVC. The scope of the Working Group includes adult as well as child crash dummies and corresponding injury criteria.

### Child Dummies

The main work of EEVC WG12 during the last years was related to child safety. From a study completed in 2008 [2] it was concluded that the Q dummies offer a major step forward compared to the current P dummies used in UNECE Regulation 44. The Q family consists of a new born, a 9 month, a 1.5 year, a 3 year and a 6 year old dummy. The 10 year old version of the Q dummies was developed within the framework of the European project EPOCH [3].

The objective of the work of WG12 was to advise on the Q family for child safety in the new UNECE regulation 129 on “Enhanced child restraint systems”.

The main focus of the work was on the Q10 dummy. One report regarding the Q10 dummy was finalized so far "Q10 dummy Report - Advanced Child Dummies and Injury Criteria for Frontal Impact" [4]. The purpose of this report was to advise on an upper limit child dummy for frontal impact including advise on abdominal load sensing and injury criteria and corresponding tolerance.

Currently EEVC WG12 is working on a second report regarding the Q10 dummy, "Advice on the Q10 dummies for side impact testing". It will focus on the side impact biofidelity improvement of the Q10 dummy updated by a side impact kit. The dummy with this kit was evaluated in pendulum and Heidelberg type side impact sled tests and showed an improved biofidelity compared to the standard Q10.

WG12 will continue to work on a third deliverable "Advice on the use of the thoracic compression criteria balanced with possible abdominal pressure", which will be mainly based on review of the work conducted by a EEVC task group especially dedicated to this topic (see below).

### Whiplash Dummies/Seat Performance Criteria

After completion in 2008 of an extensive evaluation of various crash dummies for low-speed rear impact, from which it was concluded that the BIORID is the most suitable dummy for this type of accident [5]; WG 12 has focused its activities on seat performance criteria (whiplash criteria). In Dec. 2010 an interim report on the analyses of real world (insurance) data was finalized. The main finding of this preliminary study was that the neck injury criterion NIC and upper neck shear force seem to be the best predictors for short and long term neck complaints following a rear-end impact.

The work on this topic continued using a larger insurance database and new seat tests with the BIORID dummy in order to verify and further elaborate on these initial findings. This EEVC WG12 report “Evaluation of Seat Performance Criteria for Future Rear-end Impact Testing” was provided to the UNECE GTR no. 7 informal group on head restraints and the BioRID Technical Evaluation Group (BioRID TEG) to serve as a basis for discussion [6] at a Group of Experts Whiplash Injury Criteria Meeting in September 2014 in Berlin in advance of the IRCOBI conference. However, the discussion on suitable injury criteria for whiplash associated disorders for regulatory purposes is still ongoing.

**Further Work of WG12**

In 2009 a status report concerning the 50th percentile adult male WorldSID dummy was completed [7] and in 2010 a status report concerning the 5th percentile female WorldSID dummy [8]. The development of the 5th percentile female WorldSID dummy has been carried out within the European R&D project APROSYS. An extensive international evaluation of this female dummy is still taking place and members of EEVC are participating in the Informal Working Group for Side Impact dummies that is considering the appropriateness of the 5th percentile female WorldSID for future regulations.

However, the 50th percentile adult male WorldSID dummy has been adopted as a regulatory tool for the GTR No. 14 on Pole Side Impact which was established in the Global Registry on 13th November 2013 [9].

Since the beginning of 2015 Euro NCAP is also using the 50th percentile adult male WorldSID dummy in its updated side [10] and pole test procedure [11].

Further work of EEVC WG12 during the last years includes advice on injury criteria for frontal impact dummies. Proposed injury criteria for the Hybrid-III 5% female to be used in an updated ECE R94 test procedure including a full width frontal test were revived. Furthermore the use of a proposed chest deflection criterion DEQ based on chest deflection measured in Hybrid III dummies and seat belt force was discussed within WG12.

## SIDE IMPACT PROTECTION

The car side impact problem in Europe remains substantial and a frequent cause of fatal and serious injury. For this reason, the EEVC's Working Group 13 has been active over years in providing advice concerning measures to reduce the risk of injury to road vehicle occupants in the event of a side impact and issued a report in March 2010. In this latest period, the working group focussed on determining the accident and casualty profile of European side impact accidents, and considered the development of a modified barrier based, pole and interior headform test procedures. The societal benefits and associated costs of a series of potential options for the modification of UNECE Regulation 95 were also considered.

French, Swedish and UK national data were analysed and showed that around one quarter of car occupant casualties are injured as a result of a side impact. However, this rises to between 29% and 38% for those fatally injured, illustrating the more injurious nature of this type of collision. In side impacts 60% of casualties are 'struck side' (SS) occupants and 40% are 'non-struck side' (NSS). The proportion of fatal casualties in simple car to car or car to pole impacts is substantial, 50% and 67% for the United Kingdom and France, emphasising both the relevance and importance of the mobile deformable and pole impact tests.

An analysis to estimate the likely societal benefits for modifications to UNECE Regulation 95 was completed for Great Britain; this highlighted that there is still much benefit to be gained from the side impact safety measures in place today for Europe (i.e. UN-ECE Regulation 95 and Euro NCAP). However, the introduction of a regulatory pole test (to the current Euro NCAP specification with full dummy assessment) into the existing UN-ECE Regulation 95 would deliver significant benefits to society in terms of fatal and serious injuries.

Whilst the configuration of the current Regulation 95 barrier based test remains relevant, it is accepted that a more representative barrier is desirable and supportable from a safety perspective. Key characteristics of a revised test have been defined, though further work is needed to finalise the specification of the AE-MDB barrier Version 3 before it can be considered for use.

An analysis of National and in-depth data has been identified as the requisite first step towards better understanding of the injuries to non-struck side occupants, their associated mechanisms and determining the effectiveness of potential countermeasures.

Euro NCAP has taken the outcome of the AE-MDB research on board. An expert group of former WG13 and APROSYS members preceded the work after WG13 was formally put on hold.

Based on the recommendation of the expert group Euro NCAP focussed on the final stiffness corridor design followed by an accreditation process for the barrier manufacturers.

From 2015 onwards the AE-MDB replaces the ECE R95 barrier in Euro NCAP testing [10].

## IMPROVEMENT OF CAR CRASH COMPATIBILITY AND FRONTAL IMPACT

The working group on compatibility was initiated in 1996 and worked with methods to test and evaluate compatibility in frontal impacts as well as improve frontal impact protection. Compatibility within the working group is understood as both partner and self protection as compatibility should not compromise existing safety levels.

Research activities included national research programs as well as European projects like the 5th Framework project VC-Compat and the FP7 Project FIMCAR. WG 15 conducted experimental tests, computer simulations,

and analyses of different databases to understand and describe the key issues in crash compatibility including structural interaction, global force levels, and compartment strength.
The results of the FIMCAR project identified the need for both full width and offset frontal impact tests in regulations. Test protocols, evaluation criteria, and benefit analyses were developed in the project and provided to the UNECE Informal Working Group on Frontal Impact. Although not all results for the FIMCAR project were accepted the incorporation of a full width rigid barrier test is under final review by the UNECE working party on passive safety (GRSP).

## EEVC CURRENT ACTIVITIES

### Restart of WG21

On its December 2014 meeting the EEVC Steering Committee decided to reactivate EEVC WG 21. It was the feeling of the Steering Committee that an independent look on the current accident data is needed with regard to detect research priorities on vehicle (and road) safety for the future. There might be still white spots but also a critical review of what has been reached in the last decade shall be undertaken.
The outcome of this research shall help to determine future research directions and priorities.

### THOR Task Force

The main role on this work item of WG 12 was to advise on an advanced frontal dummy for regulatory use with appropriate injury risk functions. For this purpose WG 12 followed closely the international activities concerning the THOR dummy taking into account the recommendations formulated by EEVC in 2006 [12]. Specific to lower leg injuries, EEVC WG 12 published a study in March 2009 addressing the THOR-Lx Design and Performance [13].
Meanwhile the production version of the 50% percentile male THOR-M is available and the first THOR-M dummies have been delivered to Europe. There are also some older THOR upgraded with a special THOR ModKit. NHTSA is in the process of the federalization of the THOR.
Euro NCAP has recently published an updated roadmap [14] in which the use of the THOR in an advanced frontal impact test procedure is announced.
However, there are still a lot of open issues related to the use of the THOR for regulatory purposes and consumer testing. Therefore a new EEVC task force which is open to all interested parties willing to contribute shall work on those open questions.

### Q Dummy Chest and Abdominal Injury Task Force

The CASPER project failed to develop injury risk functions for the Q-dummies' chest because there were only few valid accident cases available with AIS 3+ injuries for frontal impact and only 2 valid cases with AIS 3+ injuries for lateral impact. In addition in a number of accident reconstruction cases chest deflection measurement data was not available.
Abdominal injury risk functions were developed within the CASPER project for Q3 and Q6 only due to a lack of instrumented dummies of other sizes.
Accident reconstruction was outside the scope of the EPOCh project in developing the Q10.
This is why some interested parties (BASt, Britax, Dorel, Humanetics, IFSTTAR, LAB, TRL, TUB/VFSB, UTAC, VTI) started a Q Dummy Chest and Abdominal Injury Criteria Task Force in April 2013. No funding was available for the program at this status. All partners are contributing on a voluntary basis or are securing support by their own means. After the start of the Task Force other organizations joined (e.g. ADAC, BMW, PDB).
It was the feeling of some of the involved parties that a more formal structure or umbrella was needed to improve the support and speed up the work of the group. This is why EEVC has taken this task force under its wings. The task force is chaired by Dr. Heiko Johannsen.
Results shall be reported to UNECE GRSP for further consideration on regulation, EEVC WG12 and Euro NCAP.
The objective of the task force is to deliver a scientific basis for the definition of chest and abdomen performance criteria. The participants agreed to concentrate on the objectives and to collaborate openly in order to reach the objectives.
New partners that contribute resources to the work described above are welcome.

**Further Work**

Virtual testing / human body models

The possible use of virtual testing was discussed within WG12. This could be a future work item of a working group. Based on the results of the EC funded project IMVITER project the use of the virtual testing for the regulatory process was discussed. Based on the EU 371/2010 a flow chart was obtained within IMVITER. The developed methodology has been applied with 3 regulatory pilot tests. Both the Virtual Tests and the reference Tests are merged to obtain a response corridor where the model needs to be "included". As possible application of virtual testing in a regulatory context three options were identified, which could be further evaluated by the working group

- Use the Digital Human Body Models in current type approval process to provide supplementary information where dummies or experimental tools show limitations.
- Use of virtual testing as aid for the definition of test tool based procedures, improving experimental test tool, e.g. impactors or dummies
- Only virtual testing based approval including Digital Human Body Models.

Injury criteria for elderly

EEVC has signed a letter of support for the EC Horizon 2020 SENIORS project (Safety Enhanced Innovations for Older Road Users). The SENIORS project is expected to start in June 2015.

The efforts put the last years in road safety derived to a reduction of almost 48% of total fatalities in Europe, and the number of elderly fatalities due to road accidents has also decreased. However, among all the road fatalities, the proportion of elderly is steadily increasing. SENIORS aims at providing the needed knowledge and enable the suitable tools to reduce the number of elderly fatalities and serious injuries suffered in road traffic accidents in the near future. The increase of the level of protection for the elderly road users will be achieved by the in-depth understanding of the injury causation and mechanisms of this particular sub-group of VRU by enhancing the introduction of advanced safety systems through the implementation of assessment tools for elderly protection based on PMHS studies, volunteer testing and accident data (thus real-based).

The main goal of SENIORS project is to improve the safe mobility of the elderly, including obese, using an integrated approach and real-based knowledge that includes the main modes of transport as well as the particularities of this vulnerable road user group.

Thus, this project will investigate and assess the injury reduction that can be achieved through innovative tools and safety systems targeting the protection of the elderly as passenger car occupants, external road users (pedestrians, cyclists, e-bike riders) and while using other means of transport (such as public buses).

As such EEVC is looking forward to a good cooperation with SENIORS initiative. This is preferably to be established via joined meetings, active contribution in the course of the dissemination activities, next to the participation in Advisory Board meetings.

**European part of the Student Safety Technology Design Competition**

Three finalist teams from each region (Asia, Europe, North America) compete for top honors at this 24th ESV Conference in Gothenburg where their prototype devices/demonstrators will be on display in the exhibition hall.

EEVC has taken over the responsibility for organizing the European part of the student competition ten teams from Europe submitted abstracts. A panel of five judges from Spain, Poland, Germany, France and Sweden reviewed and evaluated the abstracts.

Based on the evaluation some teams have been selected for the competition. In March/April 2015 a panel of judges – members of the EEVC Steering Committee - shall visit the selected teams' universities to evaluate the developed safety concept and functional design model. Based on the evaluation three teams have been selected for the competition.

The European Commission is sponsoring the European part of the student competition.

**CONCLUSION**

Since the start of EEVC in 1971 the environment of pre-regulatory research in the field of vehicle safety in Europe (and world-wide) has considerably evolved. EEVC has now realigned and agreed on new Transient Terms of Reference to keep up with the future challenges. The new TToR allow more flexibility and open EEVC to non-EEVC countries. Therefore EEVC is inviting non-EEVC countries to contribute to its activities like the new THOR and the Q dummy chest and abdominal injury task forces.

**REFERENCES**


1) European Enhanced Vehicle-Safety Committee: Transient Terms of Reference. www.eevc.org
2) Advanced Child Dummies and Injury Criteria for Frontal Impact, EEVC WG12 Report, Doc. 514, April 2008, see www.eevc.org
3) http://www.epochfp7.org
4) Q10 dummy Report - Advanced Child Dummies and Injury Criteria for Frontal Impact, EEVC WG12 Report Doc642, January 2015, www.eevc.org
5) Summary Report: Requirements and Assessment of Low-Speed Rear Impact Whiplash Dummies, EEVC WG12 Report , Doc. 505C, Oct. 2008, see www.eevc.org
6) Evaluation of Seat Performance Criteria for Future Rear-end Impact Testing, EEVC WG12, March 2013, Doc WCWID-1-09e.pdf, https://www2.unece.org/wiki/display/trans/BioRID+TEG
7) Status of WorldSID 50th Percentile Male Side Impact Dummy, EEVC WG12 Report Doc547 March 2009, www.eevc.org.
8) Status of WorldSID 5th Percentile Female Side Impact Dummy, EEVC WG12 Report Doc557 April 2010, www.eevc.org.
9) Global technical regulation no. 14 on pole side impact, ECE/TRANS/180/Add.14, http://www.unece.org/fileadmin/DAM/trans/doc/2014/wp29grsp/ECE-TRANS-180a14e.pdf , Established in the Global Registry on 13 November 2013
10) Euro NCAP Side Impact Mobile Deformable Barrier Testing Protocol Version 7, June 2014, http://www.euroncap.com/en/for-engineers/protocols/adult-occupant-protection
11) Euro NCAP Oblique Pole Side Impact Testing Protocol Version 7, June 2014, http://www.euroncap.com/en/for-engineers/protocols/adult-occupant-protection
12) EEVC Recommendations on the Future of the Harmonised THOR Dummy, Report on the outcome of the Special Workshop on “Harmonization of THOR – The Advanced Frontal Dummy”, held 4-5 May 2006 at TRL, UK, www.eevc.org.
13) Report on THOR-Lx Design and Performance, EEVC WG12 Report Doc. 546, March 2009, www.eevc.org
14) Euro NCAP 2020 Roadmap Rev. 1, March 2015, http://www.euroncap.com/en/for-engineers/whats-new/

# KOREA GOVERNMENT STATUS REPORT

**Hyun-Sung, Shin**
Deputy Director, Ministry of Land, Infrastructure and Transport
Republic of Korea

Paper Number 15-0470

## ABSTRACT

Korea has maintained its status as the world's fifth largest player in auto production. Development of both the domestic economy and the auto industry has led to quantitative growth of the auto market with the number of registered car exceeding 20 million. However, Korea still lags behind advanced countries in terms of reducing the number of road traffic accidents and fatalities. Under the circumstance, the Korean government set comprehensive measures to reduce traffic deaths and has put cross-ministry efforts to meet the challenge. In this context, the government is devoted to harmonizing domestic vehicle safety regulations with international regulations while improving the domestic regulations to better fit with the traffic environments of the country. In addition, the government is inducing vehicle manufacturers to produce safer vehicles by strengthening the New Car Assessment Program.

## GENERAL STATUS OF KOREAN VEHICLES

Korea has managed to maintain its place as the fifth largest global player in vehicle manufacturing for a decade from 2005 to 2014 (see Figure1.). Such achievement has been possible thanks to the significant progress achieved by the domestic vehicle industry coupled with steady economic growth during the period.
After reaching 1 million in 1985, the number of registered vehicles in Korea had continuously increased and hit 20 million mark in 2014 while the ratio of citizens per vehicle has dropped to 2.5 (see Figure2.).

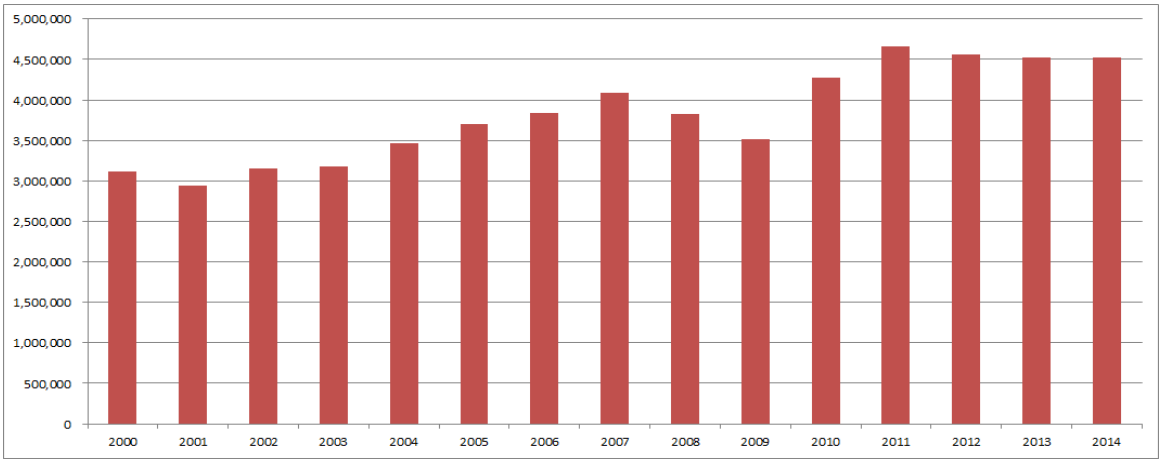


***Figure1. Number of vehicles manufactured***

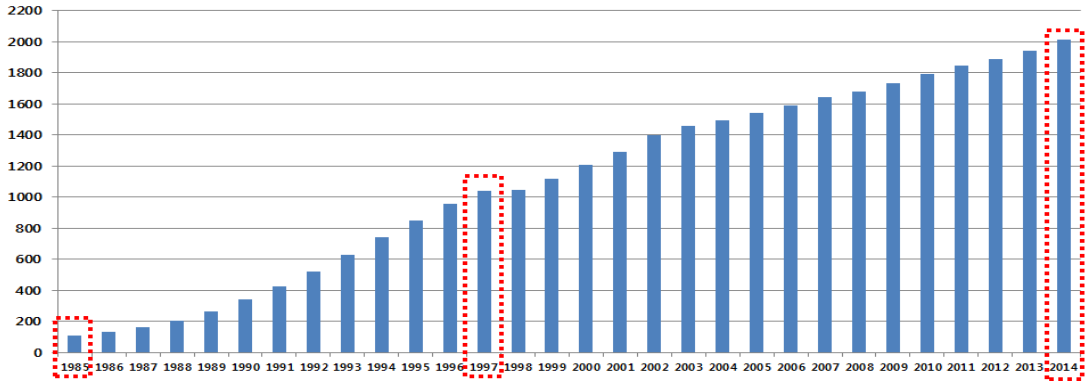


*Figure2. Total number of registered vehicles*

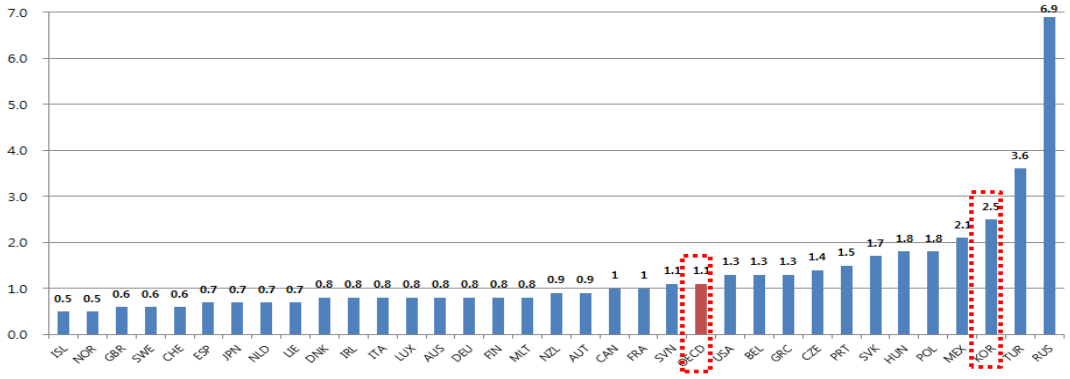


*Figure3. Number of deaths from traffic accidents per 10,000 vehicles*

Despite the growth of domestic auto market, the traffic fatality per every 10,000 vehicles is 2.5 persons as of the end of 2011, which is one of the lowest ranks among the OECD member countries (see Figure3.).
However, the number of deaths caused by road traffic accidents has decreased steadily since 2004 and recorded less than 5,000 for the first time in 2014 (see Figure 4.).

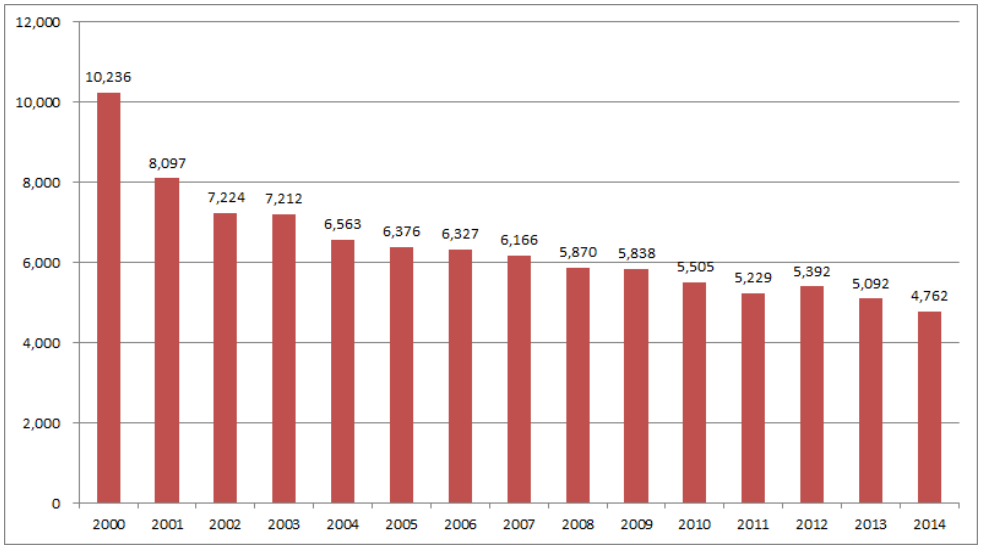


*Figure4. Number of deaths from traffic accidents*

The recent two years recorded the fastest decline in the traffic-related death rate in a decade. The average annual decline rate of road traffic deaths was 2.4% from 2004 to 2012 and 6.0% during the recent two years. The average annual road traffic death rate dropped by 2.4% from 2004 to 2012 and 6.0% during the recent two years. The road traffic fatality rate also went down from 2.41% in 2012 to 2.36% in 2013 and further declined to 2.1% in 2014. The government's efforts to reduce traffic accidents and fatalities played an important role in cutting the road traffic death rate. In particular, the Comprehensive Plan to Reduce Traffic Fatalities 2013-2017 was released in July 2013 and has been implemented to enhance vehicle safety, promote public awareness on traffic safety and improve road infrastructure.

With the goal of cutting road traffic fatality rate by 30% by 2017, five strategies were set under the Comprehensive Plan to Reduce Traffic Fatalities. Main action plans to achieve the strategies include obligating the use of safety belt for all vehicle passengers on expressways, conducting campaigns with active involvement of citizens and establishing institutional basis for Emergency Call System(e-call system) to further advance the accident response system.

**Table1. Comprehensive plan to reduce traffic fatalities**

| **Strategies & Action Plans** |
|---|
| 1. Creating the culture of valuing people the most to promote traffic safety<br>- Advancing traffic regulations and applying stricter punishment for traffic violations<br>- Advancing insurance systems and rooting out illegally registered cars under someone else's name<br>- Strengthening education on traffic safety<br>- Conducting traffic safety campaigns with the participation of citizens |
| 2. Expanding infrastructure to promote safety<br>- Eliminating causes of traffic accidents by securing safety infrastructure in the road environments<br>- Realization of smarter and safer roads<br>- Securing safety on the road for safer daily lives of pedestrians<br>- Strengthening vehicle safety regulations and expanding the application of advanced safety devices |
| 3. Establishing customized measures for relatively vulnerable groups in the transportation sector<br>- Strengthening safety management to prevent accidents caused by senior citizens<br>- Spreading customized safety education programs and creating culture of considering others<br>- Strengthening traffic safety for children<br>- Strengthening traffic safety for families with multi-cultural backgrounds and foreigners residing in Korea |
| 4. Enhancing traffic safety for vehicles used for business purposes and advancing the accident response system<br>- Strengthening safety management for vehicles used for business purposes<br>- Tightening enforcement on traffic violations related to vehicles for business use and providing guidance to traffic offenders<br>- Providing information on road safety and building up the capacity of professionals in the related fields<br>- Introduction of the Emergency Call System and prevention of secondary accidents |
| 5. Improving the system of traffic safety policies<br>- Strengthening managing and adjusting functions of traffic safety policies<br>- Enhancing local governments' capacity for traffic safety<br>- Securing stable financial resources for traffic safety programs<br>- Providing more support for traffic safety programs of local governments |

The following is the recent legal development in vehicle regulations, in terms of their improvement and harmonization to international regulations and the New Car Assessment Program aimed at improving vehicle safety.

## IMPROVEMENT IN VEHICLE REGULATIONS

### Safety-belt reminder for unbuckled passengers

In the case of vehicle crash, whether a passenger fastens a seatbelt or not is a crucial determinant of how seriously the passenger is injured. It was found that the fatality and serious injury rates surged by more than nine times when seat belts were not worn by passengers on the rear seat in collision tests conducted by KATRI in 2010. Even though the use of seat belts by all vehicle passengers is mandatory on expressways, the rate of buckled rear seat passengers remains at 19%[1]. So, with the aim of promoting the use of seat-belts, the government plans to make audible warning devices that send alarms to unrestrained rear seat passengers as one of evaluation items of the new car assessment starting from 2015.
In addition, Korea proposed the mandatory installation of Safety-belt Reminders for rear seats at the WP.29 Working Party on Passive Safety in December 2014[2]. The rationale is the low safety-belt wearing rate for rear seats in nations such as Korea, which becomes all the more important for such nations where occupancy rate for rear seats is relatively higher.

### Mandatory installment of a Daytime Running Lamp (DRL) for all vehicles

After the introduction of DRL in 2010, installment of DRL was initially optional and became mandatory in June 2014.
The mandatory use of DRL is based on results of studies that suggest the positive impact of DRL on ensuring the field of visions of drivers and road users under foggy, rainy, dusty and other adverse weather conditions during daytime as well as in the evening and at dawn. A study shows that mandatory installation of DRL would reduce the regional traffic accidents by 19% in average, suggesting an expectative traffic-accident prevention effect [3].

### Strengthening safety regulations for vehicles used for commuting school children

The MOLIT enhanced vehicle safety regulations to prevent accidents involving backing school bus, traversing children after getting off the school bus or children accidentally stuck in the school bus. Major strategies to prevent accidents caused by those vehicles include installing automatic stop signal devices near the driving seat to catch the attention of other drivers who try to overtake the vehicle and installing Rear view camera and backup audible warning devices. In addition, wide-angle mirrors which are currently installed on the right side of the driver's seat will also be extended on the left to minimize blind spot areas for drivers [4].

| Stop signal devices | Wide-angle mirror | Rear view camera |
|---|---|---|
| 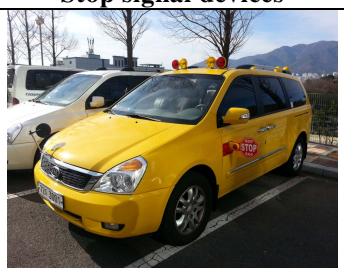 | | |

*Figure5. Commuting school children applied Strengthening safety regulations*

### Strengthening performance requirements for Endurance (Auxiliary) Braking System for the safety of vehicles used for commercial purposes

A series of road accidents has claimed many lives in Korea as large-sized passenger vehicles carrying groups of students deviated from steep and winding downhill roads in local areas or plunged off mountain roads. In this regard, given the geographical features of Korea, the government strengthened the endurance (auxiliary) braking regulation in June 2014. While Endurance (Auxiliary) Braking System is usually used to support service brakes, researchers suggest that Auxiliary Braking System can also be used to prevent brake fade on steep downhill roads.

In this regard, the use of high-performing Endurance (Auxiliary) Braking System is expected to contribute to enhanced braking performance on steep downhill roads.

## HARMONIZATION OF VEHICLE REGULATIONS

As a member country of the 1958 Agreement and the 1998 Agreement, Korea has updated the domestic regulations in accordance with international regulations since 1996. As a result, 47 UN Regulations and 9 UN GTRs were reflected on domestic regulations. The table below shows the updates made in the domestic regulations.

**Table2. Status of harmonization in Korea**

| Year | UN Regulations | UN GTRs |
|---|---|---|
| 2006 | - UN R13H : Passenger vehicle brake<br>- UN R19 : Front fog lamp | - GTR No.1 : Door locks & Retention |
| 2008 | - UN R14 : Safety Belt Anchorages<br>- UN R53 : Motorcycle Installation<br>- UN R57 : Motorcycle Headlamps<br>- UN R107 : Safety Inclination Angle<br>- UN R39 : Speedometer<br>- UN R95 : Side Collision<br>- UN R123 : Semi-AFS | - GTR No.3 : Motorcycle Brake<br>- GTR No.9 : Pedestrian Safety |
| 2009 | - UN R48 : Hazard Warning Signal<br>- UN R73 : Lateral Protection | - |
| 2010 | - UN R6 : Side Direction Indicator<br>- UN R10 : EMC<br>- UN R13 : Spring Brake<br>- UN R46 : Rear View Mirror<br>- UN R79 : Steering Effort<br>- UN R87 : DRL(Optional)<br>- UN R112 : Asymmetric Headlamps<br>- UN R123 : Full AFLS<br>- UN R125 : Field of Vision | - GTR No.6 : Safety Glazing<br>- GTR No.7 : Head Restraint<br>- GTR No.8 : ESC |
| 2011 | - UN R64 : TPMS<br>- UN R85 : Engine and Net Power<br>- UN R42 : Bumper<br>- UN R91 : Side Marker Lamp | - |
| 2012 | - UN R1,2,8,20,72,112,113 : Headlamps for Motorcycle<br>- R53 : Light & Lighting devices for Motorcycle<br>- UN R13 : Brake Assist System(BAS)<br>- UN R107 : Minimum Turning Radius | - GTR No.4 : WHDC<br>- GTR No.11 : Engine emissions for Non-Road Machinery |
| 2014 | - UN R30, 54 : Pneumatic Tyres<br>- UN R100 : Electric Powertrain<br>- UN R73 : Lateral Protection<br>- UN R58 : Rear Underrun Protection<br>- UN R55 : Coupling Components<br>- UN R21 : Power-operation of windows<br>- UN R119 : Cornering Lamps<br>- UN R7 : Front & Rear position Lamps, Stop lamps and End-outline Marker Lamps<br>- UN R3 : Retro-reflecting devices<br>- UN R4 : Rear Registration plate lamps<br>- UN R23 : Reversing lamps<br>- UN R70 : Rear Marking plates | - GTR No.5 : ODB |
| **Total** | **47** | **9** |

Researches on 14 items including brake lining, wheels and camera monitoring systems for replacing mirrors will be conducted in 2015 to harmonize domestic regulations with international ones. In addition, medium and long term plans (2016-2019) for researches on autonomous vehicles and related new technologies along with vehicle regulations are being developed.

## STRENGTHEN NEW CAR ASSESSMENT PROGRAM (NCAP)

The Korean government is encouraging the production and sale of safer vehicles and is providing information about safety of vehicles by implementing New Car Assessment Program and disclosing its result. A total of 127 types of vehicles have been evaluated by 2014 since the New Car Assessment Program was introduced in 1999. The government has upgraded the assessment program by widening the pool of evaluated vehicle types ranging from compact cars to vans and trucks and by adding evaluation items. The Comprehensive Grading System was expanded as they are now in 2013 to help consumers to make more informed decisions. The applied percentage of evaluations items was also changed based on data about domestic traffic accidents. As a result, the percentage of pedestrian safety was set at 25% given the high fatalities of pedestrians (see Table3.).

**Table3. Sample of the Comprehensive Grading System of KNCAP**

| Evaluated Fields | | Crash worthiness [65%] | | | | | Pedestrian safety [25%] | Driving safety [10%] | | Accident prevention safety [additional point 1.0] | | |
|---|---|---|---|---|---|---|---|---|---|---|---|---|
| Evaluation items / Vehicle Type | | Full frontal impact [16.0] | Offset impact [16.0] | Side impact [16.0] | Seat [10.0] | Pole side [+2.0] | Pedestrian safety [30] | Rollover resistance [5.0] | Braking [5.0] | Forward collision [0.4] | Lane departure [0.3] | Seat belt [0.3] |
| Small | **xxx** | 15.9 (99.4%) | 13.5 (84.4%) | 16.0 (100.0%) | 8.7 (87.0%) | 2.0 (100.0%) | 17.0 (56.7%) | 4.4 (87.7%) | 3.9 (78.0%) | | | |

The mid-to-long term road map was established in 2014. The main strategies under the road map include the introduction of advanced airbags and an evaluation system for the relatively vulnerable groups in the transportation sector such as women and children. Enhancing assessment procedures in such areas as broadside collisions and adding six evaluation items including proactive safety devices are also expected to be included in the scheme (see Table4.).

**Table4. The Roadmap of Korean New Car Assessment Program (KNCAP)**

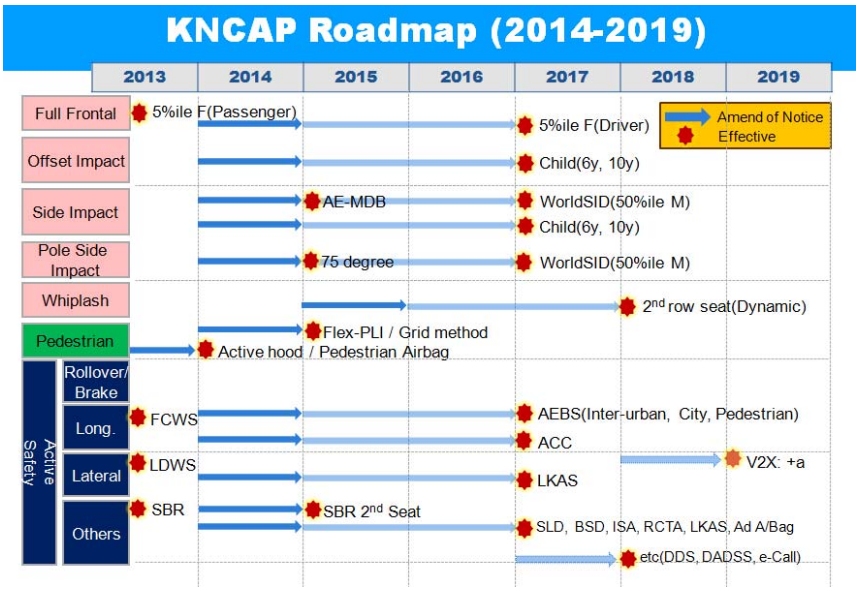

## CONCLUSIONS

The Korean government is putting efforts to improve traffic safety by establishing “The Comprehensive Plan to Reduce Traffic Fatalities 2013-2017” following the “Reduce Traffic Fatality by Half". Improvement of vehicle regulations and the New Car Assessment Program to facilitate the production of safer vehicles provide a basis for such efforts. To that end, exchanging information and setting the right direction through international discussion are also as important as maintaining the potential of continuous improvement of vehicle safety by promoting the development and application of advanced technologies.

## REFERENCES

[1] Statistical Analysis Result: "The usage rate of Seatbelt on the road in Korea", 2015, KATRI
[2] http://www.unece.org/trans/main/wp29/wp29wgs/wp29grsp/grspinf56.html ; GRSP-56-02
[3] "2007 Vehicle Regulations Harmonization Research Report", 2007, KATRI
[4] The Amendment of KMVSS (Korean Motor Vehicle Safety Standard), 2014.2.21

**GOVERNMENT STATUS REPORT - POLAND**

Wojciech Przybylski
Motor Transport Institute (ITS), Poland

## INTRODUCTION

The following report contains information on the progress achieved in Poland with regard to aspects of road traffic safety since the time of 22nd ESV Conference (Washington DC, 2011). This period was generally characterised as the intentional effort towards the traffic safety items within all its main system fields taking into account priorities drawn from analysis of domestic and international accident statistics. The current accident statistics for the last ten years are given on Figure 1, and Figure 2 and in Table 1.

In 2014 on Polish roads 34 970 road accidents occurred resulted in 3 202 fatalities and 42 545 injured persons which gives for the years between 2010 and 2014 as follows:

- 3 862 less road accidents (- 9.9%),
- 705 less fatalities (- 18%),
- 6 407 less injured (- 13,1%),

Even if the last four years on our roads were not that bed still Poland demonstrate the higher level of danger on the roads in comparison to other EU countries.

## I. The diagnosis of Road Safety in Poland.

Over the past 10 years (2005÷2014) more than 45 thousand people died and approximately 532 thousand were injured (of which about 25% seriously injured) on Polish roads. During this decade, the number of accidents decreased by 27%, the number of fatalities by 41%, and the number of injured by 30%.

**Figure 1. Accident Data in Comparison with the Vehicle Stock in Poland in the Period 2005-2014**

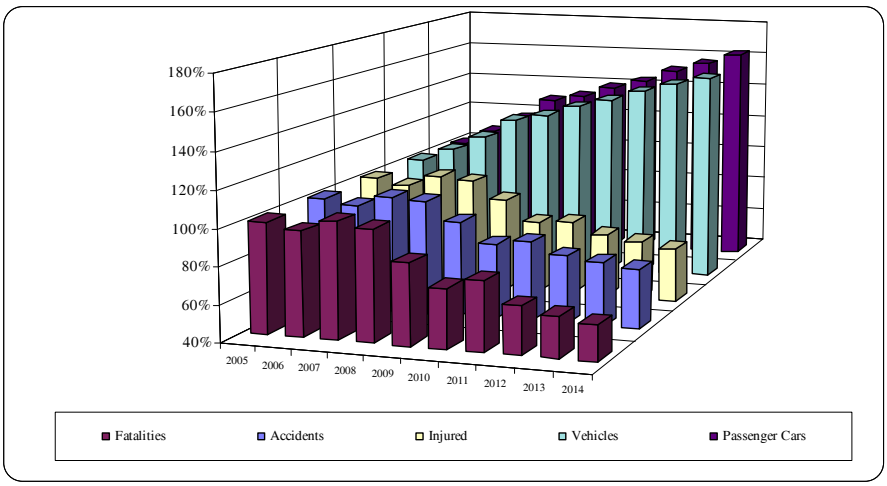


By: Anna Zielińska, Motor Transport Institute

**Figure 2. Current trend in accident data and the car stock in Poland**

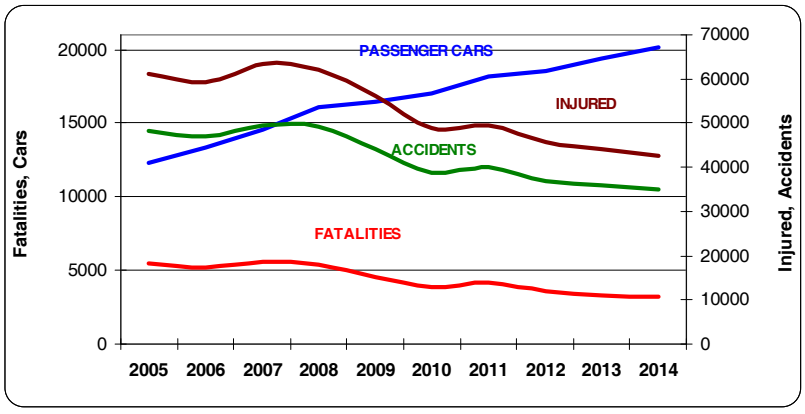


By: Anna Zielińska, Motor Transport Institute

**Table 1. Accident Data in Comparison with the Vehicle Stock and Population in Poland in the Period of 2005÷2014**

| Year | No. of accidents | No. of fatalities | No. of injured | No. of vehicles (thousands) | No. of cars (thousands) | Polish population (thousands) | Fatality factor (No. of fatalities / 1 mln of inhabitants) | Accident severity (No. of deaths / 100 of accidents) | No. of cars / 1000 inhabitants |
|---|---|---|---|---|---|---|---|---|---|
| 2005 | 48 100 | 5 444 | 61 191 | 16 816 | 12 339 | 38 157 | 143 | 11 | 323 |
| 2006 | 46 876 | 5 243 | 59 123 | 18 035 | 13 384 | 38 126 | 138 | 11 | 351 |
| 2007 | 49 536 | 5 583 | 63 224 | 19 472 | 14 589 | 38 116 | 146 | 11 | 383 |
| 2008 | 49 054 | 5 437 | 62 097 | 21 337 | 16 079 | 38 136 | 143 | 11 | 422 |
| 2009 | 44 196 | 4 572 | 56 046 | 22 025 | 16 495 | 38 167 | 120 | 10 | 432 |
| 2010 | 38 832 | 3 907 | 48 952 | 23 037 | 17 240 | 38 530 | 101 | 10 | 447 |
| 2011 | 40 069 | 4 189 | 49 506 | 23 853 | 17 872 | 38 538 | 109 | 10 | 464 |
| 2012 | 37 046 | 3 571 | 45 792 | 24 876 | 18 744 | 38 533 | 93 | 10 | 486 |
| 2013 | 35 847 | 3 357 | 44 059 | 25 684 | 19 389 | 38 496 | 87 | 9 | 504 |
| *2014* | *34 970* | *3 202* | *42 545* | *26 455* | *20 164** | *38 484** | *83* | *9* | *524* |

*Preliminary data estimated as of March 2015 by Motor Transport Institute*
* Central Statistical Office data as of June 30, 2014

By: Anna Zielińska Motor Transport Institute

## II. The existing programme for road traffic safety and a bit of history

In **2005** the National Road Safety Programme GAMBIT 2005 was adopted by the government. In the programme it was established that:

1. The Polish far-reaching and ethically empowered vision of road safety will be the ZERO VISION.
2. The main objective to be attained by the year 2013 is a decrease in the number of fatalities by 50% over 10 years, i.e. the number of fatalities is to drop to 2800 in the year 2013.
3. In Poland, the high-risk groups most likely to be killed in a road accident include: vulnerable road users (pedestrians, cyclists, motorbike drivers, motorcyclists), children, and young drivers.
4. The main problems regarding road safety include:
   a) dangerous behavior of road users,
   b) poor quality of road infrastructure,
   c) lack of an effective system of road safety management.

In order to reach the main objective, 15 groups of priority actions and 144 tasks grouped into five detailed objectives were established:

1. Creation of a basis for conducting effective and far-reaching operations enhancing road traffic safety.
2. Shaping safe behaviors of road users.
3. Protection of pedestrians, children and cyclists.
4. Construction and maintenance of safe road infrastructure.
5. Reduction of the severity of accidents.

The assessment of the *GAMBIT 2005* Programme implementation, as per its status in the year 2014 indicates that:

1. In what concerns national roads, the set objective has not been attained - the objective was to reduce the number of fatalities down to 770 (the target value was exceeded by 82%).
2. As for the remaining road categories, the stage objectives were attained - the number of fatalities for these road categories is 4÷15% below predictions.
3. In relation to the base year (2003) a decrease of 19%÷40% in the number of fatalities occurred in all districts.
4. In three districts the objective for the year 2010 has been attained.

In the years 2008÷2010 a very encouraging decrease in the number of fatalities could be noticed. It was due to the actions undertaken in that period, as well as to the long-term effects of the changes and measures undertaken in preceding years.

During the period in which the *GAMBIT 2005* Programme was in force, many educational, preventive and infrastructural actions, in line with the programme directions, were undertaken at the national level. Unfortunately, only 84 out of 144 (58%) planned tasks were undertaken. At the same time, in many cases, political and administrative decisions were incompatible with the *GAMBIT 2005* Programme. In Poland, road accidents are still not perceived as a sufficiently important problem, and the poor effectiveness of actions at the institutional level is the result of the principle of shared collective responsibility for the problems with road safety management. Despite the problems mentioned above, a systematic decrease in the number of fatalities due to road accidents is taking place in Poland. An increased activity of Polish experts on the international arena may be observed, as well as a fairly extensive number of the undertaken actions for road traffic safety, within which the *GAMBIT 2005* Programme continues to play an essential role.

**Conclusions related to GAMBIT**

1. The strategy and action plans for road safety were properly developed under the GAMBIT programmes.
2. Trainings for road safety professionals increase the number of experts in this area at different levels. Poland participated in certain trainings conducted abroad (the Netherlands, France, Sweden) and is a well-informed member of the international community handling road safety issues.
3. One essential problem was the failure to implement actions *en masse* under the *GAMBIT 2005* Programme and the lack of assessment of their effectiveness. Unfortunately, sources of funding for these actions were also very limited. As a result, the scope of the undertaken actions was not extensive.
4. The existing regional GAMBIT programmes were properly developed, but the effective implementation of actions under such programmes requires the support from the central level, improvement of databases and performance assessment.
5. The identification of agencies leading in the governmental structures (leaders), performing the tasks regarding road safety indicated an insufficient political will behind the actions for road safety (lack of a political and operational leader, and the institutional problems in the area of cooperation).

## III. Current situation

**Scope and characteristics of the problem.** Based on the available statistical data, it can be stated that per 100 accidents on Polish roads, there are approximately: 9 fatalities, 31 seriously injured persons, and 92 moderately and lightly injured persons.

**Poland against the background of the European Union.** Since 2007 Poland has been an inglorious leader among the European Union countries as regards the number of fatalities in road accidents. The share of Poland in the total number of fatalities amounts to 11%, although Polish population accounts for only around 7% of the total number of residents in the European Union. The risk of loss of life on Polish roads was twice as high as the European average in this respect, and over three times higher than in the countries leading in the area of road traffic safety, such as Great Britain, the Netherlands, or Sweden. The most frequently used rate for international comparisons is the mortality rate, which is the number of annual fatalities per 1 million inhabitants, and this rate for Poland amounted to 83 fatalities. Therefore, in 2014 Poland was one of leaders among all the countries of the European Union in this classification.

**Types of accidents.** For many years now, most people killed in road accidents (over 33% of the total number of fatalities) die in accidents connected with running over a pedestrian, which sets us apart negatively not only from Europe, but also from the world. These are the accidents connected with pedestrians moving on a street. Another group of accidents with a high mortality rate (15÷20%) are accidents caused by a head-on collision, the reason for which is often the lack of divided roads. There are frequent side collisions on intersections and entries/exits, which can also have fatal consequences. Equally dangerous are the accidents connected with driving into an obstacle (a tree or a post) located too close to the edge of the road.

**Victims of road accidents - groups of high risk.** From all the victims of road accidents, pedestrians represent the largest group (33.6% of fatalities and 27.8% of seriously injured) (Figure 3). Among drivers, the largest group of victims are the drivers of passenger cars (27.6% of fatalities and 22.5% of seriously injured). Cyclists should be taken into consideration, as they amount to approximately 7.5% of fatalities and 9.2% of seriously injured, while their share in the road traffic accounts for around 1%. The share of motorcyclists (2.3 % of fatalities and 4,2% of seriously injured) and moped drivers (2.0% of fatalities and 7.1% of seriously injured) in the number of road accidents victims is also increasing. The accidents in which pedestrians are the victims take place mainly in urban areas, while accidents in which drivers and passengers of vehicles are the victims take place mainly on country roads. However, a huge severity of the accidents with the participation of pedestrians (25% fatalities and 30% seriously injured in comparison to the total number of victims) takes place on the national roads.

**Figure 3. Victims of road accidents - groups of high risk.**

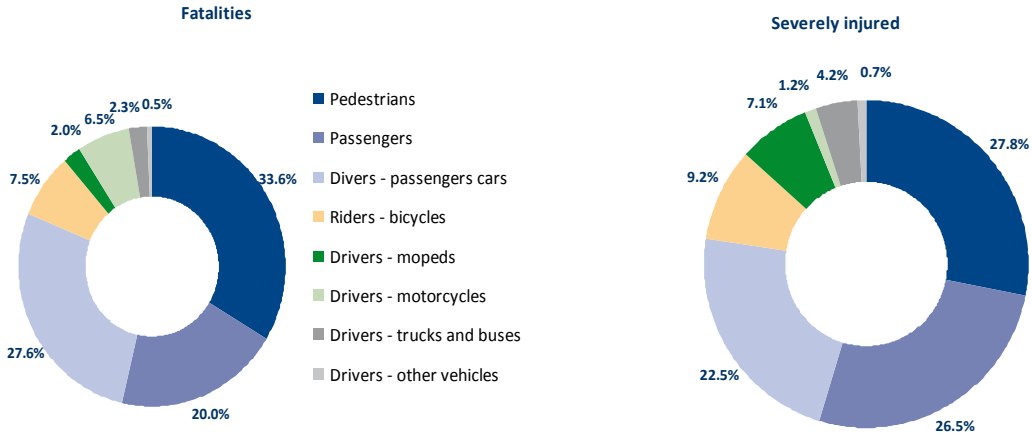


**The age of the victims of accidents.** The highest mortality rates (number of fatalities per 1 million of inhabitants) refer to young people (aged 15 to 24) and people over 65 years old.

**The circumstances and causes of road accidents.** The circumstances which lead to road accidents with fatalities most often include:

- the behavior of road users (maladjustment of speed, failure to give the right of way, incorrect overtaking, incorrect behavior towards a pedestrian, drunk driving and the lack of protection among road traffic users);
- external conditions (mainly: limited visibility and adverse weather conditions).

**The geography of accidents and their victims.** The largest number of fatalities is recorded in the Mazowieckie District, and then in the following districts: the Wielkopolskie, Śląskie, Łódzkie and Małopolskie Districts. The combined number of fatalities in these five districts accounts for over 50% of the all road accident fatalities in Poland. However, in relation to the number of inhabitants, the highest mortality rate in road accidents and, consequently, the highest risk (Figure 1.9) exists in the Świętokrzyskie and Mazowieckie Districts. It is also quite high in the Podlaskie, Łódzkie, Warmińsko-Mazurskie, Wielkopolskie, Lubelskie, Lubuskie and Kujawsko-Mazurskie Districts. It results, among others, from the low standard of the road network, high transit traffic in these districts, and inappropriate behaviors of road traffic users.

**Socio-economic cost of road accidents.** Since 2012 the cost of road accidents in Poland is estimated by a commission of the National Road Safety Council. The method of the valuation of the costs of road accidents is based on the generally accepted practice in transport economics and comprises of the following components: medical costs, cost of the lost productivity power (lost production), cost of damage to property and administrative costs. This method does not factor in the cost of human suffering resulting from road accidents. Additionally, the research conducted by the Road and Bridge Research Institute does not take account of the cost of collisions, i.e. accidents without any victims (estimated cost of 8 billion Polish zloty). In the future, this element should be included in the methodology of accident costs valuation. Latest estimation of total yearly road accidents costs for 2013 year amount to 49.1 billion Polish zloty (research of Road and Bridge Research Institute). According to the data from 2011, the greatest share of the annual accident cost in Poland is represented by the costs related to the injuries (57.3%). The costs related to fatalities account for 1/3 of the annual total (32.6%). The smallest share is represented by the cost of material losses (10.1%).

**Unfavorable forecast.** Forecasts regarding demography and motorization in Poland indicate that, in the years **2011÷2020**: the number of inhabitants may decrease by 1÷4%, the number of vehicles may increase by 15÷25%, i.e. reach the number of 30 million vehicles, and mobility of citizens (measured by transport performance) may increase by 30–35%. The stagnation or the limitation of preventive activities in the following years may halt the decreasing tendency in terms of the number of road accidents and the fatalities resulting from them. It is estimated that, in such a situation, over 40 thousand people may be killed and over half a million may be injured in road accidents by 2020. The value of both property and social loss of these road occurrences may reach 225 billion of Polish zloty. Therefore, it is necessary to take effective steps in order to protect the lives and health of road users.

**Diagnostic conclusions.** The research allowed for the identification of main problem areas in road safety in Poland:

1. Protection of pedestrians in road traffic.
2. Shaping the habits of driving with an allowed speed.
3. Shaping safe behaviors of road users.

4. Adaptation of road infrastructure to basic standards of road safety.
5. Promotion and use of safe vehicles.
6. Development of road rescue system.
7. Development of road safety management system as a basis for the effective solution of the aforementioned problems.

On the base of the diagnosis national programme was developed within the context of other existing, accepted and planned programmes and strategies - both international (UN and EU) and national documents.

## IV NATIONAL PROGRAMME

Despite international documents the following national documents were taken into account to build Polish National Road Safety Programme 2013÷2020.

**National Development Strategy 2020.** In this document, it is stated that, due to high risk of road fatalities in Poland, programmes for the improvement of Road Safety are to be developed and implemented. Such programmes are to be in line with works on the improvement of infrastructure and information and education campaigns concerning traffic rules and the promotion of safe behavior of road users. Most important tasks include:

- construction and development of automatic traffic monitoring systems,
- development of an integrated system of accidents management,
- development of an integrated system of passenger service and goods transport,
- improvement of forms and channels of communication with society in terms of road traffic safety, Intelligent Transportation Systems,
- development of systems for financing investments within the scope of road traffic safety.

**Transport Development Strategy until 2020.** Apart from the general goals which take account of the new concepts of EU common transport policy and of the main guidelines of Polish transport policy developed recently, the document indicates strategic trends in the area of road traffic safety:

- safe behavior of road users,
- safe road infrastructure, safe vehicles,
- effective system of road rescue and medical assistance.

**Efficient State Strategy 2020.** The document underlines seven detailed objectives. Objective number seven: *Provision of a high standard of safety and public order*, determines the following directions for intervention associated with road traffic safety:

- counteracting road risks,
- road rescue and protection of the population (fire protection; preventive, rescue and firefighting actions),
- implementation and improvement of the rescue alert system,
- improvement of the functioning of the Medical Rescue Alert system.

The aforementioned intervention directions include several issues, such as the development of a national Road Safety programme, unification of the law, raising existing infrastructure standards, improvement of the functioning of structures and of the enforcement of procedures.

**National Health Programme for the years 2007÷2015.** Road accidents are considered a health related problem of the society. The third strategic goal of the National Health Programme is the reduction of the frequency of injuries resulting from road accidents and the limitation of their consequences. Reaching this goal calls for the reduction of the number of deaths resulting from road accident injuries. The need for preventive measures has also been identified.

**National Programme for Prevention and Solving of Alcohol-Related Problems for the years 2011÷2015**. The document determines plans for the following actions directed at limiting the number of vehicle drivers under the influence of alcohol:

- increase the number of sobriety tests carried out during standard road checks,
- development of a strategy concerning the problem of drunk driving, development and implementation of a unified programme for drivers detained for driving under the influence of alcohol,
- public education actions concerning the influence of alcohol on human body and the risk of damages arising as a result of driving vehicles under the influence of alcohol.

**Programme structure.** The Polish National Road Safety Programme 2013÷2020 and its structure of intervention is based on the following five pillars:

- safe behaviors of road traffic users,
- safe road infrastructure,
- safe speed,
- safe vehicles,
- rescue and medical assistance system.

Effective implementation of activities within the above mentioned pillars is conditioned by the improvement of the management system for road safety. Therefore, the Programme indicates also the activities which are essential for planning, implementation, coordination and monitoring activities within its particular pillars. In every pillar, based on the diagnosis of the existing status of road safety, three priority directions (priorities) reflecting fundamental problems of road safety in Poland were distinguished, as well as conditions for their implementation. However, every priority accumulates activities covering:

- Engineering - understood as technical solutions for:
  — road network, which upgrade road safety and make roads "forgive" human errors,
  — vehicles, which protect drivers, passengers and other road users, as well as diminish possible damages of an accident.
- Supervision - understood as visible supervision and control aiming at the verification of existing regulations and prevention of non-compliance.
- Education - understood as enhancing awareness of road safety by identification and understanding the risk. The objective of education is to change attitudes and behaviors at the individual level, as well as at the level of certain communities or at the organizational level.

## V. SAFE VEHICLES

Bearing in mind the very technological profile of ESV Conference I would like to give more information on road safety related to vehicle. According to the statistical data, vehicles are in Poland quite rarely the main cause of a road accident (less than 1% of total), but their technical condition more often assist to other causes and significantly influences the severity of accidents.

**Figure 4. The main reasons of accidents attributable to technical failures in vehicles.**

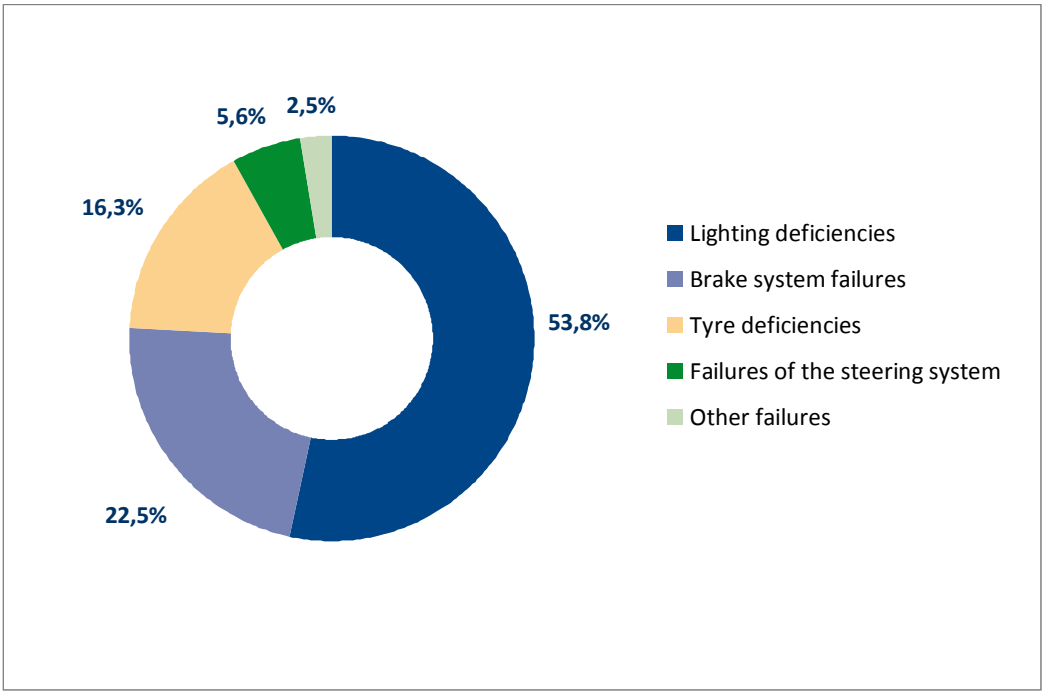


In addition estimations of the Motor Transport Institute indicate that in 2009, the average age of the vehicles in use in Poland was around 13 years. For comparison: the average age of vehicles at this time in Sweden was just under 10 years, in Finland - over 11 and in the USA - 11 years. Research shows that the average number of failures significant in terms of the safety of road traffic increases with the age of the vehicle. At the same time, it is noticeable that the older the car is the more failures posing a risk to road safety.

**Risk factors**

Vehicle safety directly influences the number of fatalities and the scale of consequences of accidents. For this reason, solutions in this area should be constantly sought and implemented, especially through equipping cars with elements supporting the driver (active safety) and elements protecting the persons participating in road occurrences (passive safety).

**Technical condition of the vehicle.** Pursuant to the law in force, the technical condition of vehicles is periodically revised by motor vehicle inspection stations (MVIS). However, an inspection carried out by the

Supreme Chamber of Control revealed that supervision over these inspection stations is insufficient. Nearly two thirds of obligatory devices of the MVIS is not certified. In Poland, the low technical culture is also a problem. It translates into neglect of the technical condition of vehicles, especially in what regards elements influencing the safety, such as brakes, lighting, shock-absorbers, steering system, tire pressure.

**Lighting.** Lighting deficiencies are among the most frequently listed failures (54%). This allows us to define the lighting issues as one of priorities in those actions for improvement of road safety which are linked with the technical condition of vehicles. Regulations regarding lighting-related technical requirements for vehicles are not in step with the technological progress and the low awareness of drivers is an additional factor, as they usually do not know that even formally proper lighting may not illuminate the way sufficiently.

**Spare parts.** Another problem is related to the spare parts used in vehicles. Technical requirements which should be met by parts and subassemblies used as replacement of original parts are not regulated by European laws. It has been estimated, based on examination of spare parts, that the quality of over 50% of parts currently on the market, as well as of various operating fluids (including brake fluid) poses a potential direct hazard to the safety of vehicle use.

**Equipment - modern safety devices.** Currently, all the newly manufactured vehicles in the European Union are equipped with basic safety systems, such as seat belts, ABS system or air bags for the driver. Additionally, thanks to advanced technologies, it is possible to equip cars with more systems supporting the driver in a risky situation on the road. This allows drivers to avoid collisions or to mitigate their consequences, both for the driver and for the passengers, as well as for other road users. Examples of such systems are: electronic traction control (which assists the driver in recovering from skids), camera systems limiting the so-called blind spot or e-Call (a system installed in the car, which automatically notifies rescue services about an accident). These solutions form part of the "e-Safety System". Vehicle producers subject their technical solutions to safety tests and strive to rank as high as possible in consumer rankings, such as Euro NCAP, which helps to popularize these solution and make them more readily available in new cars. Also cars driven in Poland, both imported as used vehicles (mostly from other EU states), are largely equipped with systems enhancing road traffic safety thanks to which a vehicle may limit the consequences of human-made errors and it technical shortcomings are rarely the cause of accidents.

**Priorities and directions of actions** (Table 2.).The diagnosis of the current state, as well as the experiences of model states of the European Union (in terms of road safety considerations), lead us to adopt two priorities under the Safe Vehicle pillar:

- Priority 1 - Enhancement of actions regarding vehicle technical condition inspections,
- Priority 2 - Improvement of safety systems in vehicles.

**Enhancement of actions regarding vehicle technical condition inspections** aims to, above all, reduce the risk of accidents caused by poor technical condition of vehicles and to limit their severity.

**Improvement of safety systems in vehicles** aims to implement such construction solutions so as to render the vehicle capable of protecting its driver and passenger, as well as other road users, to prevent human errors and to minimize the dangers when these errors are made.

**Conditions for the performance of these actions.** Basic conditions for the successful performance of the actions related to vehicle safety are legislative measures and support resulting from research and exchange of experiences.

**Legislative measures** aims for development of:

- a concept for a modernized national system for the inspection of the technical condition of all vehicles.
- provisions regarding the professional supervision over the equipment of motor vehicle inspection stations and monitoring their work.
- technical requirements unequivocally and objectively guaranteed by technical tests of vehicles.
- legal base for the implementation of a system (certification, homologation) to supervise the introduction into trade and use in cars of parts and operating fluids.

**Research and exchange of experiences**

- Introduction of the common practice of using the technologies of objective exploitation tests with the use of devices allowing for precise and quick exploitation measurements. Conducting in-depth research on road traffic accidents, including the analyses of the influence of the technical condition of vehicles for the occurrence of accidents. Conducting development works related to defined groups of advanced technology products. Research, development and pilot implementation of intelligent transport systems related to the cooperation of devices with which roads and vehicles are equipped.
- International cooperation regarding the improvement of legal regulations related to the systems of testing and assessment of spare parts, operating fluids and participation in international research regarding pilot implementation of modern solutions within the scope of active and passive safety.

**Table 2. Priorities and directions of actions within the *Safe Vehicle* pillar**

| Priority | Direction of actions | | |
|---|---|---|---|
| | **Engineering** | **Supervision** | **Education** |
| **Enhancement of actions regarding vehicle technical condition inspections** | Implementation of modern technologies and techniques at motor vehicle inspection stations;<br><br>Improvement of technical homologation and use requirements regarding vehicle equipment; | Modernization of the system of supervision of motor vehicle inspection stations and monitoring their work;<br><br>Modernization of the system for verification of equipment and parts in cars which affect their safety in road traffic;<br><br>Certification of the obligatory equipment of motor vehicle inspection stations; | Education within a complex education system[I] regarding maintenance of the proper technical condition of vehicle and how it affects the safety of all road users;<br><br>Running, within the system of promoting road traffic safety[II], information campaigns and campaigns to promote maintenance of the proper technical state of vehicles[III];<br><br>Periodic trainings for diagnosticians and supervisors of motor vehicle inspection stations[IV]; |
| **Improvement of safety systems in vehicles** | Equipping the vehicles with modern safety devices[V];<br><br>The implementation of obligation of using devices blocking the vehicle start-up for professional drivers in cases when alcohol content in exhaled air exceeds | The implementation of supervision on proper use of obligatory safety devices installed in vehicle (e.g. child safety seats); | Popularization among the car owners of modern vehicle safety systems; |

I. *System of education* included in whole within the *System of road safety management* (tab. 9.1)
II. *System of promotion* included in whole within the *System of road safety management* (tab. 9.1)
III. Including the popularization of the significance of lighting on the road safety and promotion of better quality lighting.
IV. *System of education* for road safety staff, included in whole within the *System of road safety management* (tab. 9.1)
V. Including systems to raise the safety of vulnerable road users, such as automated braking systems, external air bad.

**Rescue service and post-crash response.** Rescue service are the activities taken up under conditions of sudden or extraordinary danger to life and health, and also to property and environment, performed immediately. The main characteristics of rescue service are the suddenness of the incident preceding the action, for example, of the forces of nature or human, and the urgent course of reaction. Among numerous rescue fields, medical rescue service and post-crash care process are essential for the road safety, because they concern the health and lives of the injured, and, what is more, they require the involvement of many parties.

More detailed information on The Polish National Road Safety Programme 2013÷2020 are presented on website of the National Road Safety Council (http://www.krbrd.gov.pl/en/).
I am also glad to inform you that accordingly to the request from National Road Safety Council the Motor Transport Institute established Polish Road Safety Observatory and is its operator.

**I would like to wish all of you a good co-operation and fruitful exchange of knowledge during this very important scientific international ESV conference being one of the important bases for improvement of everyday life - improvement of vehicle safety and thus road traffic safety.**

# Road Safety Vademecum

## Road safety trends, statistics and challenges in the EU 2010-2013

**March, 2014**

**European Commission**
**DG for Mobility and Transport**
**Unit C.4 – Road Safety**

# Contents

Summary of findings ..... 2

1. Introduction ..... 3

2. The road safety situation in the EU today ..... 4

3. The road users ..... 7

4. The vehicles ..... 9

5. The infrastructure ..... 10

6. New Member State: Croatia ..... 13

7. Concluding remarks ..... 14

Disclaimer
This report is an internal working material produced by unit C.4, DG MOVE, summarising preliminary EU road safety information for 2013 and final detailed data up to 2012.

# Summary of findings

- In 2013, slightly more than **26,000** road fatalities were reported in the EU.
- This is a decrease of around **8%** compared to 2012.
- In total, there were **52 road deaths** per million inhabitants in 2013 in the EU.
- The top road safety performers (lowest number of road deaths per year and million inhabitants) in 2013 were **the UK, Sweden and Denmark**.
- The highest number of road fatalities in 2013 was found in **Romania, Latvia, Poland and Lithuania.**
- Over the period 2010-2012, the two main improvements are seen for **young road users** and for **car occupants**:
    - The number of young victims (aged 18-24) decreased by 19% to compare to the percentage reduction of elderly road users (above 65 years) of only 2% for the same period.
    - The number of car occupants killed decreased by 13% from 2010 to 2012, a stronger development than that for vulnerable road users.

# 1. Introduction

The Transport White Paper announced a strategic target for EU road safety for the period 2011-2020: to reduce the number of road deaths by half.

In 2010, some 31,500 people lost their lives on the roads in the 28 EU Member States. This figure is the baseline for the strategy objective and the target is to have less than 15,750 road deaths in 2020. If the target is achieved, more than 90,000 lives would have been saved in total during the decade.

Following a slow year in 2011, the number of road fatalities is now again substantially decreasing. The preliminary data for 2013 bring the EU development in line with the target curve.

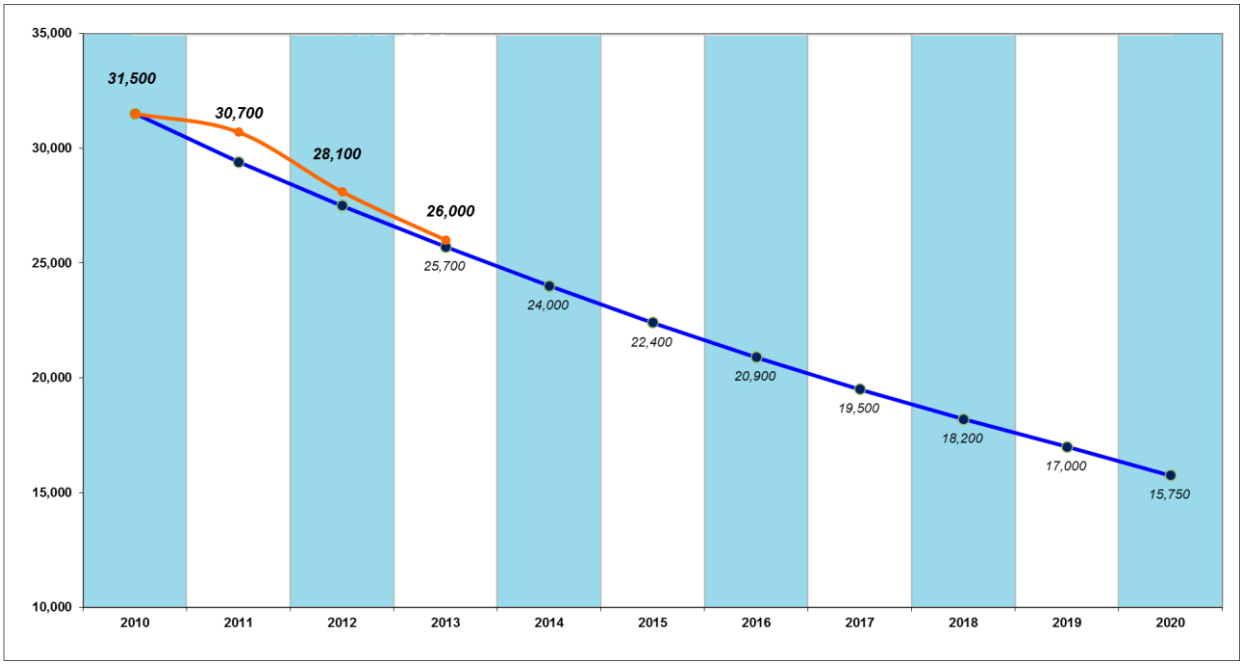


*Development over time: reduction of number of fatalities in the EU 2010-2020*
*(blue line = target, orange line = actual number of fatalities reported)*

This text provides an overview of the latest road safety data and the main road safety developments in the EU. It presents the first provisional figures reported for 2013, where available, complemented with the final detailed data for 2012.

## 2. The road safety situation in the EU today

In 2013, a provisional total of 26,200 road fatalities were reported in the EU. This is a decrease of around 8% compared to 2012.

The EU average road fatality rate in 2013 is 52 people killed per million inhabitants, to compare to the baseline year 2010 with 62 dead per million inhabitants.

| | **Fatalities/million inhabitants** | |
|---|---|---|
| **Member State** | **2010** | **2013** |
| Austria | 66 | 54 |
| Belgium | 77 | 65 |
| Bulgaria | 105 | 82 |
| Croatia | 99 | 86 |
| Cyprus | 73 | 53 |
| Czech Republic | 77 | 63 |
| Denmark | 46 | 32 |
| Estonia | 59 | 61 |
| Finland | 51 | 48 |
| France | 62 | 50 |
| Germany | 45 | 41 |
| Greece | 112 | 81 |
| Hungary | 74 | 59 |
| Ireland | 47 | 42 |
| Italy | 70 | 58 |
| Latvia | 103 | 86 |
| Lithuania | 95 | 85 |
| Luxembourg | 64 | 87 |
| Malta | 36 | 54 |
| Netherlands | 32 | - |
| Poland | 102 | 87 |
| Portugal | 80 | 62 |
| Romania | 117 | 92 |
| Slovakia | 69 | 42 |
| Slovenia | 67 | 61 |
| Spain | 53 | 37 |
| Sweden | 28 | 28 |
| United Kingdom | 30 | 29 |
| **EU** | **62** | **52** |

The best road fatality rate is reported from the Sweden and UK, with 28 and 29 dead per million inhabitants respectively. Both countries have defended this top position since the start of the strategy period. They are followed by Denmark with 34 reported dead per million inhabitants.

Slovakia has made the most impressive improvement from 2012 to 2013 with 24% fewer road deaths, giving a new fatality rate of 42 dead per million inhabitants. This brings Slovakia from 10th to shared 7th position among Member States, overtaking Finland and Malta.

| | **Evolution of total number of fatalities** | |
|---|---|---|
| **Member State** | **average percentage change/year 2000-2010** | **Percentage change 2012-2013** |
| Austria | -6% | -15% |
| Belgium | -6% | -7% |
| Bulgaria | -3% | 0% |
| Croatia | - | -6% |
| Cyprus | -5% | -14% |
| Czech Republic | -5% | -12% |
| Denmark | -6% | 8% |
| Estonia | -10% | -7% |
| Finland | -5% | 3% |
| France | -8% | -11% |
| Germany | -7% | -7% |
| Greece | -4% | -12% |
| Hungary | -6% | -2% |
| Ireland | -7% | 19% |
| Italy | -6% | -6% |
| Latvia | -10% | 1% |
| Lithuania | -9% | -15% |
| Luxembourg | -8% | 32% |
| Malta | -1% | 100% |
| Netherlands | -7% | - |
| Poland | -4% | -6% |
| Portugal | -6% | -9% |
| Romania | 0% | -9% |
| Slovakia | -5% | -24% |
| Slovenia | -7% | -4% |
| Spain | -9% | -10% |
| Sweden | -8% | -7% |
| United Kingdom | -7% | -1% |
| **EU** | **-6%** | **-8%** |

The highest number of road fatalities per inhabitants is found in Romania, followed by Latvia and Lithuania. However, Lithuania has made a substantial improvement of -15% road fatalities since 2012, reporting the second best percentage change over the year after Slovakia, same as Austria.

Malta and Luxembourg reported large percentage increases from 2012 to 2013 but have few road deaths in total numbers so the percentage change over a single year is not statistically significant. Also Ireland (+19) and Denmark (+8%) report large negative developments since last year.

In sum, the year 2013 was a year of great diversity, with some Member States reporting large improvements and other reporting a worrying deterioration of the road safety situation.

# 3. The road users

| Road user group | Change 2010-2012 |
|---|---|
| Pedestrians | -8% |
| Cyclists | +6% |
| Moped riders | -15% |
| Motorcycle riders | -13% |
| Car occupants | -13% |
| Heavy goods vehicle drivers | -10% |
| **All road deaths** | **-11%** |

*Evolution over time: per road user group 2010-2012*

During the years 2010-2012 pedestrian road deaths only decreased by 8%, three percentage points less than the total percentage improvement for all road deaths. The best improvement among pedestrians is seen for the age groups 50-64 years and 65 years and above.

For cyclists, the trend is even worse: the number of cyclists killed actually increased by 6% from 2010 to 2012. This is explained at least partly by an increased total number of cyclists on the roads. Among cyclists, the age factor is quite striking. While the number of young and children who die while biking decrease, the number of killed grown-up bicyclist is on the increase. Among those older than 50 years, the number of fatalities increased by alarming 10% from 2010-2012.

For car occupants and motorcyclists, the fatalities decreased more than average. This is commented further upon in the following chapter on vehicles.

**Risks per age groups**
While the decade 2001-2010 could be called the decade of improved child safety with great improvements in safety for those younger than 15 years, the biggest improvement since 2010 is seen in the safety for people aged 18-24.

| Age group | Change 2010-2012 |
|---|---|
| < 15 | -14% |
| 15-17 | -18% |
| 18-24 | -19% |
| 25-49 | -18% |
| 50-64 | -9% |
| >65 | -2% |
| **All road deaths** | **-11%** |

*Evolution over time: per age group 2010-2012*

On the other hand, the development for those older than 65 is less encouraging. This is partly linked to the demographic trend of an ageing society and the increase of the number of elderly in the EU over time.

**The gender aspect**
Male fatalities are still clearly over-represented in road traffic crashes. In 2012, 76% of all road fatalities were male and 24% were female. Among car driver fatalities, 82% were male.

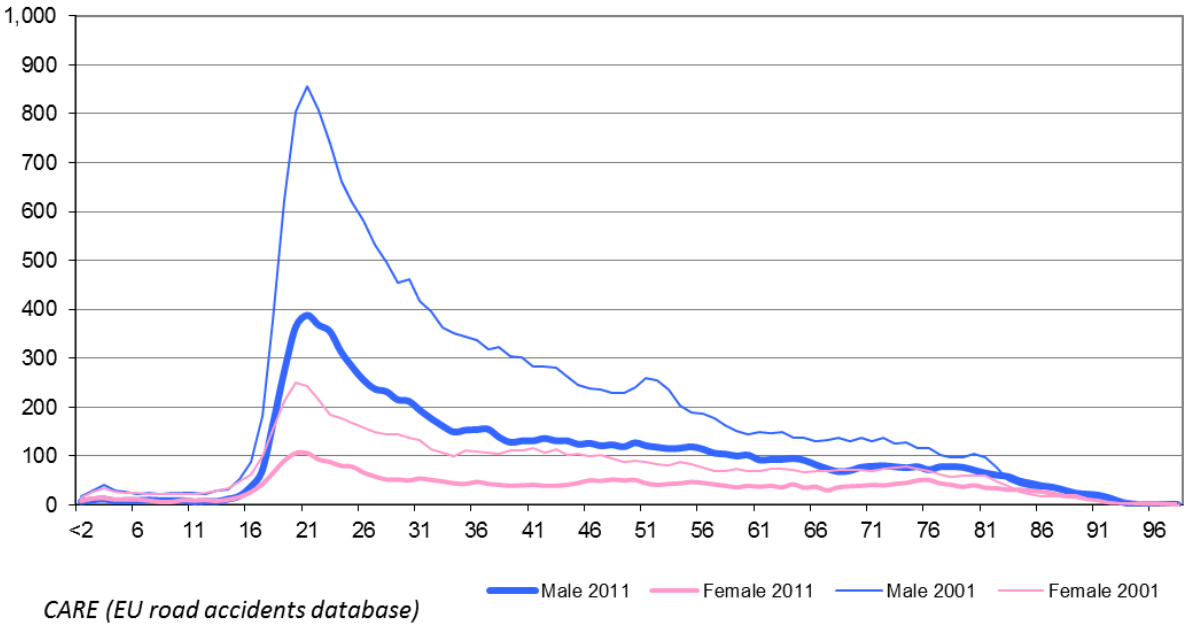


*Number of car occupant fatalities by gender and age.*

Women are more often than men involved in fatal road accidents as pedestrians, whereas men are more often than women involved in fatal road traffic crashes as car drivers.

# 4. The vehicles

**Powered two-wheelers**
Motorcycle fatalities have been an issue of great concern the last years, considering the large over-representation of motorcyclists among road fatalities. Most fatalities of motorcyclists and moped drivers occur on rural or urban roads.

To some degree, the trend has now turned and also the number of motorcyclist road deaths decreased more than average from 2010-2012, thanks to an increased focus on the safety of this road user group.

Countermeasures during the last years have included a legislative change in the EU driving licence directive to ensure a gradual access to the heaviest motorbikes for young people. Development and increased use of protective clothing and protective devices is another important action area, studied by an on-going EU-funded project. From 2016, the EU type approval requirements for motorcycles will include the more advanced braking systems such as ABS.

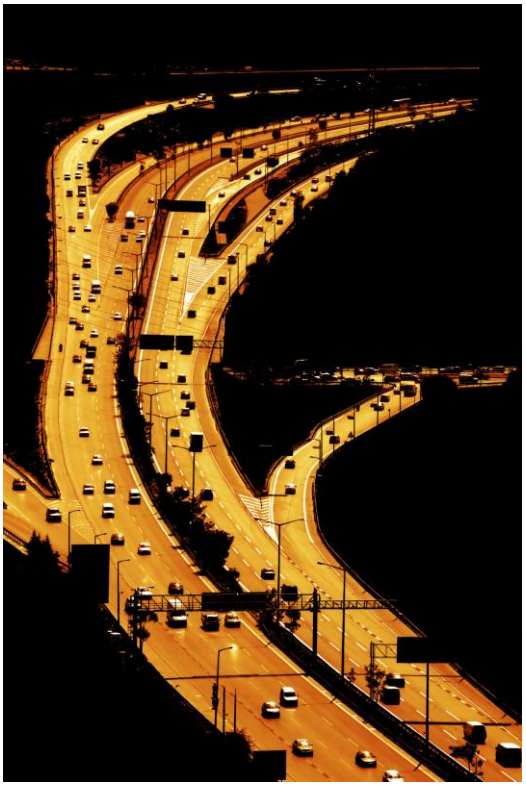

**Cars**
The road safety evolution for car drivers is stronger than for most other road user groups.

Cars are becoming safer, better equipped and more thoroughly tested for technical defects. Seat belt use is going up; the DaCoTA project reported that EU average seat belt use rates are around 85% in the front seat and 60% in the rear seat.

EuroNCAP, initiated as a study commissioned by the Commission Road Safety Unit, has led to a general fitting of airbags in cars. Technical developments for efficient enforcement of traffic rules in combination with better quality of driver training and road user education also have contributed to the positive development.

**Heavy goods vehicles**
The motorised vehicle category which defies the general trend is the heavy goods vehicles. The number of heavy goods vehicle driver fatalities decreased by only -7% 2010-2012, which is an even slower improvement than that of pedestrians. However, the total number of heavy goods vehicle drivers killed is also already quite low. Fatalities as consequences of crashes involving trucks or buses are more common on rural roads and motorways and less common inside the urban areas.

To further improve the situation, the Commission has initiated a review of the directive regulating minimum training and qualification requirements for professional drivers. The aim is to simplify and clarify the requirements and, where needed, to optimise the conditions for road safety training of professional drivers.

# 5. The infrastructure

Different types of accidents happen on different kinds of roads and the road fatalities are unevenly distributed on the different road types.

The situation also varies across the EU due to differences existing among Member States on traffic flows, population density and quality of road infrastructure. For example, in Romania, Cyprus, Croatia the highest share of fatalities occurred on urban roads while in Finland, Ireland, Luxembourg and Spain the majority of fatalities were on rural roads. Spain and Belgium reported the highest percentage of fatalities on the motorways.

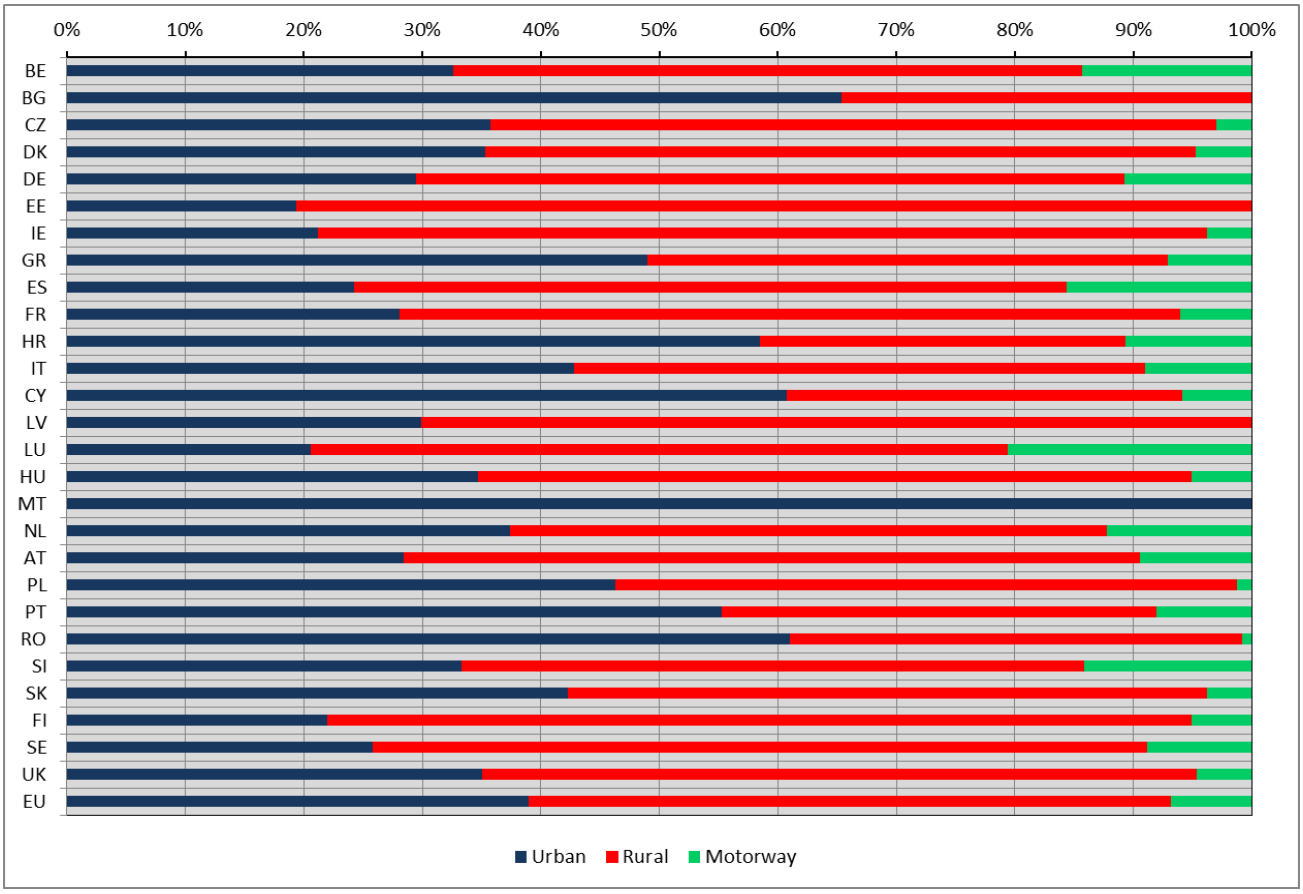


*Fatalities per road type (2012)*

**Urban areas**

The urban areas are characterised by frequent interaction between motorised vehicles and unprotected road users such as pedestrians and cyclists. However, the speed is also normally lower in the urban areas and the severity of road traffic crashes therefore somewhat lower. It is inside the urban areas that most of the less serious accidents occur. Of all fatal road traffic crashes however, only around 40% happen on urban roads. From 2010 to 2012, it was on the urban roads that the number of road fatalities decreased the most.

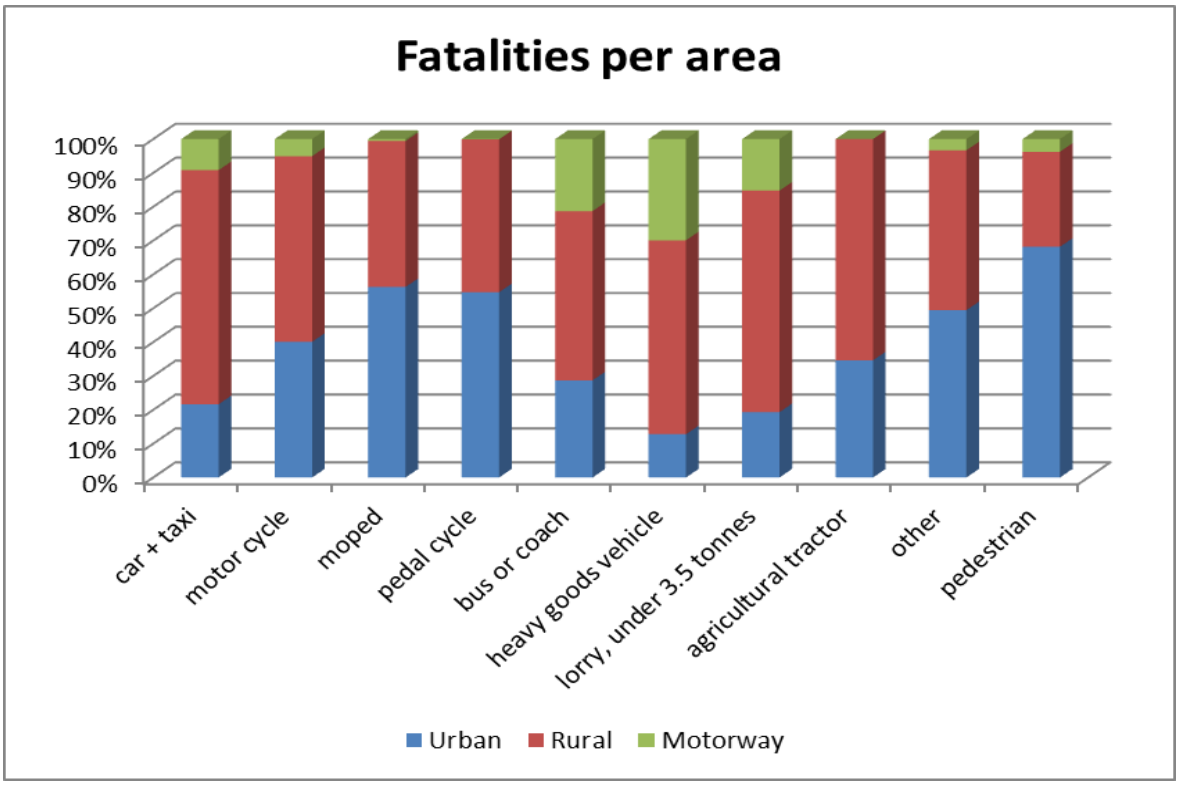


*Type of fatality per road category*

**Rural roads**

Rural roads normally have higher speeds than urban roads but lower speeds than motorways. The infrastructure standards are not as well regulated for rural roads as for motorways. It is on the rural roads that most of all fatal road traffic crashes take place: more than 50% of all the fatal crashes.

**Motorways**

Motorways and expressways are typically designed to accommodate long distance traffic travelling on a higher speed. In spite of the speed, only 5% of the total number of accidents took place on the motorways, but on the other hand, the consequences of each single crash are more serious and around 7% of all road fatalities occur on the motorways.

| | **Urban** | **Rural** | **Motorway** |
|---|---|---|---|
| Accidents | 68% | 27% | 5% |
| Fatal accidents | 40% | 53% | 7% |
| Fatalities | 39% | 54% | 7% |
| Injured | 65% | 29% | 6% |
| Seriously injured | 55% | 39% | 6% |
| Ratio victims(*)/accidents | 1.2 | 1.4 | 1.5 |

*(*) Victims includes both injured and fatalities*

**Infrastructure safety management: the legislative framework**

Directive 2008/96/EC[1] provides the EU legislative framework for the safety management of road infrastructure. The directive establishes management procedures aimed to ensure that the road network is safe. It applies to the trans-European road network[2] but Member States are highly encouraged to apply the principles also on the secondary road network, notably where EU funding is provided to road infrastructure investments.

| TEN-T Comprehensive Network (2013) | | TEN-T Core Network (2013) | |
|---|---|---|---|
| | **Length (km)** | | **Length (km)** |
| Completed | 123.459 | Completed | 56.016 |
| To Be Upgraded | 43.723 | To Be Upgraded | 17.334 |
| New Construction | 13.247 | New Construction | 3.614 |

*Trans-European road network: length of roads*

For new roads, the directive provides that safety impact assessments and audits have to be carried out at different stages of planning and construction. For already existing roads, a periodic safety ranking to find the most dangerous sections (*blackspots*) and periodic safety inspections are mandatory. The results of these inspections should then be the starting point for targeting maintenance and improvements of the network.

The infrastructure safety management directive does not prescribe in detail what methods Member States should use to assess the safety of their roads. However, it lists a number of aspects that the assessments need to cover. Member States are also obliged to establish guidelines for the practical steps to be followed by national authorities or infrastructure managers in assessing the safety of roads.

A specific legislation is also currently in place for ensuring a minimum safety standard of tunnels[3]. Following the deadly accidents and fires of Mont Blanc, Tauern and St. Gotthard at the end of the 1990s and the early 2000s, systematic procedures and technical solutions have been established in EU legislation for tunnels longer than 500 meters.

[1] Directive 2008/96/EC of the European Parliament and of the Council of 19 November 2008 on road infrastructure safety management OJ L 319, 29.11.2008, p. 59–67

[2] Regulation (EU) No 1315/2013 of the European Parliament and of the Council of 11 December 2013 on Union guidelines for the development of the trans-European transport network and repealing Decision No 661/2010/EU

[3] Directive 2004/54/EC of the European Parliament and of the Council of 29 April 2004 on minimum safety requirements for tunnels in the Trans-European Road Network, OJ L 167, 30.4.2004, p. 39-9

# 6. New Member State: Croatia

The newest EU Member State, Croatia, has taken on the challenge of reducing the number of road deaths by half until 2020. This strategic target is adopted in the *National road safety programme 2011 – 2020* which is closely aligned with the policy objectives of the European Commission.

Since around 2008, Croatia has succeeded in achieving a steep reduction of the number of road fatalities. In 2001, the number of dead per million inhabitants was 146; by 2013 this was down to 86 dead per million inhabitants compared to the EU average of 52.

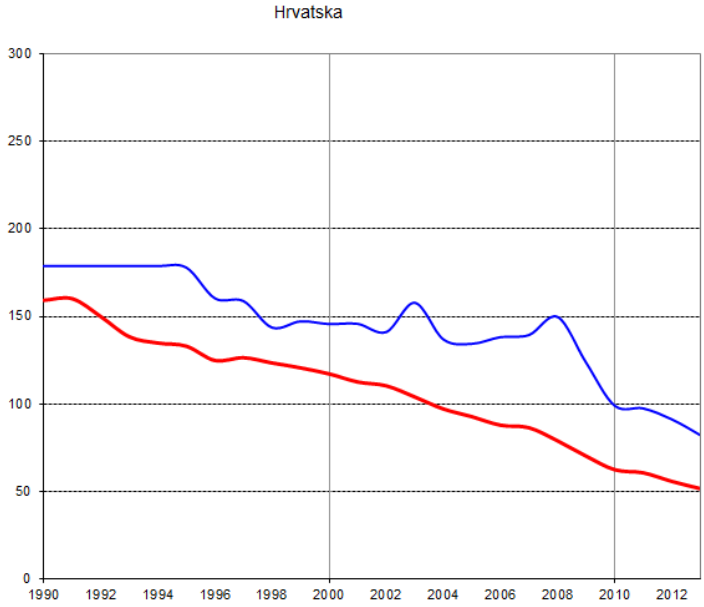


*Number of road deaths per million inhabitants 1990-2012 in Croatia.*
*Red line shows EU average.*

The majority of road traffic crashes and fatalities in Croatia take place in urban areas: 80% of the accidents happen inside urban areas (EU average 68%) and 59% of fatalities (EU average 39%).

Croatia has only a partial zero tolerance policy on alcohol: a 0.0‰ limit for young drivers (16 to 24 years old) and professional drivers but for other drivers the 0.5‰ limit applies.

# 7. Concluding remarks

The main trends between 2010 and 2012 are *the safety of young road users* and *the safety of cars.*

The young car drivers are especially important since they have been largely over-represented among road fatalities and because their big share of the road safety problem means that a large percentage decrease gives substantial effect to the total numbers.

The reduction of car occupant fatalities can be linked both to driver education efforts, to enforcement campaigns and to the increased safety and improved equipment of vehicles today – not least with advanced driver assistance technology for road safety.

**Future developments**

For the coming years some additional focus on the unprotected road users seems to be called for. The low percentage improvements for pedestrians and cyclists indicate that more needs to be done. Among pedestrians, the increased use of smart phones and mobile phones as road user distractions is one risk factor to be further investigated. The Commission therefore launches a study on this during 2014.

The ageing Europe is mirrored also in the road safety statistics with the elderly making up an increasing share of the total number of road safety fatalities. Elderly pedestrians but also elderly car drivers face too high risks in road traffic today. To find solutions to the problem, the Commission initiates studies on road safety for elderly during the coming year.

The number of fatal motorway crashes no longer decreases at the same speed as other accidents. To investigate what more can be done to bring the improvement rate back on track, the Commission considers a review of the infrastructure safety management directive. A similar review is prepared for the professional driver training and qualifications directive, seeing that the number of heavy goods vehicle drivers killed is also decreasing less than average.

More information about these and many other planned and implemented road safety measures can be found on http://ec.europa.eu/roadsafety.

# ESV CONFERENCE 2015 - ITALIAN GOVERNMENT STATUS REPORT

Dr. Antonio Erario
Head of Division, International Regulatory Affairs
Ministry of Infrastructure and Transport
Department for Transport
Italy

## ABSTRACT

This paper provides an overview of the main results achieved by Italy in the field of road safety during recent years. It focuses on the "National Plan on Road Safety" adopted in 1999, on its follow-up, in particular on its last edition titled "Horizon 2020".

After a general introduction of main road safety results, this paper describes the principal measures adopted during the last period, focusing on regulatory policies and enforcement.

A brief description of the research activities in the field of vehicle safety is given as well as a summary of the main recommended actions to improve road safety.

## GENERAL

### Road Safety in Italy

In the period 2001-2010 Italy has reduced its fatality rate from 125 fatalities/$10^6$ inhabitants to 68 fatalities/$10^6$ inhabitants which is about 46% reduction. Figure 1 shows the reduction of mortality rate recorded in the same period in the Europe Union [EU 27] Member States.

Between 2001 and 2013, Italy recorded a 52% reduction of fatalities (from 7,096 to 3,385) as well as 31% reduction of injured. It should be highlighted that the reduction of fatalities is more significant in the recent years since in the period 2001 – 2010 it was about 42%.

Looking at the percentage variation of number of deaths and injured between 2001 and 2013 by mode of transport, an inhomogeneous trend results for different categories of road users. In the case of mopeds there is a significant reduction in both the number of deaths and injured. Other categories, such as passenger cars and goods vehicles, show a modest reduction of the number of injured while reaching a significant reduction of the number of deaths (more than 50%). Cyclists and pedestrians, show a reduction of the number of deaths and an increase of the number of injured Finally, motorcycles show a slight decrease in the number of deaths (3%) and an increase in the number of injured (+ 19%).

In spite of the progress made, Italy remains a European country with high number of fatalities (3,385 in the year 2013); therefore further and continuous improvements are necessary.

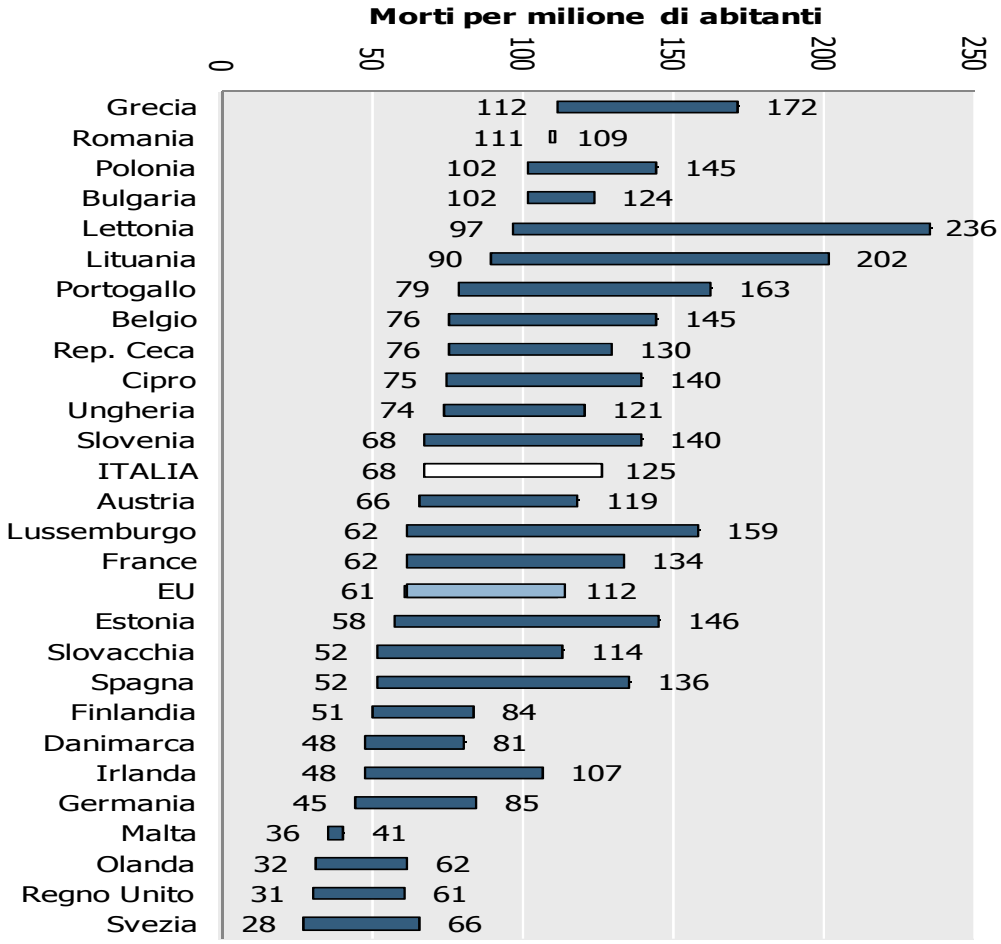


**Figure 1 – Fatalities rate in EU 27 in period 2001-2010**

## THE MAIN ADOPTED MEASURES

The first National Plan on Road Safety covered the period 2001-2010 with the following strategic actions:

### 1. Regulatory policies

The main regulatory policies were represented by changes to the national highway code. In particular, the three major changes concerned:

- The introduction in 2003 of a penalty point system based driving license (Law No. 151/03). During the first two semesters of applications a reduction of 1,846 deaths was recorded as shown in figure 2.
- More empowerment to police agents and higher penalties, especially for "drink and drugs" drivers (Law No. 160/07).
- Zero tolerance for alcohol in case of young drivers (18-21 aged) and professional drivers.

2. Better enforcement

The main adopted enforcement actions were the following

- Increased number of checks on drink and driving. Between 2007 and 2012 the number of these checks increased by 220%
- The installation of automatic control systems (made by cameras and radars). The Italian automatic system to check average speed - so called "Tutor"- started to be implemented in 2004. In 2012 the system was in operation on about 3000 km of the highway network (the Italian highway road network is about 6700 km). In the period 2004-2011 a 48 % reduction of fatalities on highways was recorded.

3. Better road safety risk awareness

The adoption at national and local level of information campaigns has increased driver's awareness with regard to drink driving, speeding, use of helmets and safety belts. The main national campaigns are:

- "The guardian angel" campaign" which was conducted in the period 2003-2004.
- "On the good road" campaign which was conducted in the period 2009-2011.

The above campaigns resulted in an increase of the road risk awareness and in a behavioural change; this emerged by interviewing two samples of people (respectively 3000 and 5000 people).

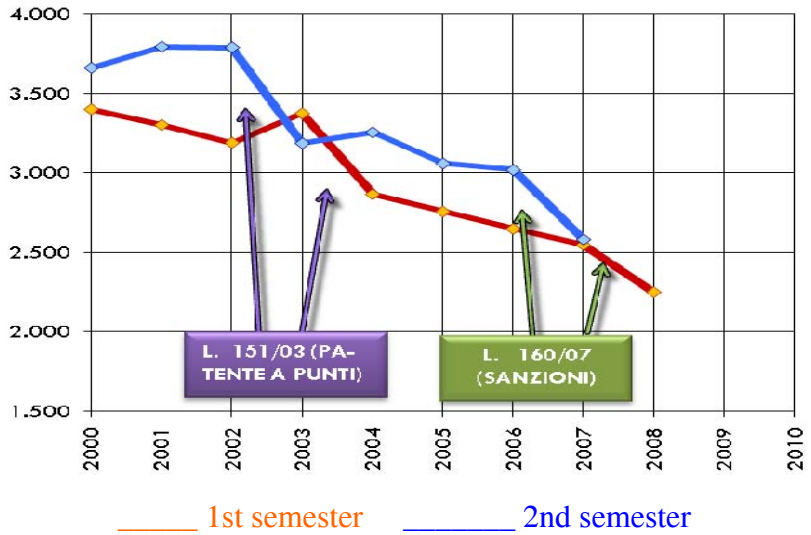


**Figure 2 - The effect of introduction of a penalty point system based driving license**

HORIZON 2020

The National Plan on Road Safety for 2001-2010 (hereinafter called NPRS 2001-2010) was developed in order to meet the goal fixed by the EU level of halving the number of fatalities in the EU.

Instead of a fixing a general target, the National Plan on Road Safety Horizon 2020 (briefly Horizon 2020) has set two levels of goals:

I. **General goals** concerning the level of safety of the whole road network where the final goal is the reduction of number of fatalities. The first target is to halve the number of fatalities by 2020 according to the European target. In terms of figure that means to reach a fatalities rate of 33 fatalities/$10^6$ inhabitants.

II. **Specific goals** defined according to the road user categories with higher level of risks. The categories which were identified are: pedestrians, cyclists, two-wheeler motor vehicle users and accidents of commuters. The result of a study shows the following:

- Pedestrians have an accident rate 6.7 time higher than car users;
- Cyclists have an accident rate 9,4 time higher than car users;
- Two-wheeler motor vehicle users have an accident rate 12,0 time higher than car users;
- The fatalities of commuters are about 6% of total road fatalities but they have risen by 52,1% between 2001 and 2010

Moreover, "Horizon 2020" adopted the principle of "no child dead on the road" aiming to involve all citizens to adopt a new culture of life.

WHAT TO BE CHECKED

The analysis of risk factors shows that the main factors triggering a road accident are the following.

- The high vehicle speed – both the absolute speed and relative speed between users – is the main factor causing about 30% of fatal accidents and is responsible for 17% of the accidents occurred in suburban area as recorded by police in 2012.
- The visibility is a main factor especially for vulnerable road users (pedestrian, cyclist and children).
- The "drink and drug" driving is a main factor especially for young drivers. According to a study conducted during 2008 and 2011 about 10% of drivers do not observe drink limit value.
- Use of safety protection systems. In the period 2009-2011, only 64% of front seats occupants used seat belt against a European average of about 78%. In the rear seat, the seat belt use rate is very low, around 10%. With regard the use of helmets it is estimated at about 90 %.
- The environmental factors are mainly related to the design and road maintenance. In 2012, 16% of deaths in road accidents occurred on wet or slippery road.
- Mass and shape of the vehicles is an important factor especially for vulnerable road users (cyclists, pedestrians and motorcyclists).
- Lack of experience leading to underestimation of risk and overestimation of their abilities are factors typically associated with young drivers and novice drivers. In Italy, 36% of young drivers aged up to 24 declare they over speed when driving, compared to a European average of 31%.
- Fatigue, stress and distractions while driving. It is estimated that drowsiness/fatigue is one of the causing factor in 10-20% of all road accidents, with an almost twice mortality rate compared to accidents due to other causes. The distraction is often linked to the use of mobile phones while driving. It is estimated that in Italy about 9% of people use a mobile phone when driving without a headset.

VEHICLE SAFETY RESEARCH

Research in the field of vehicle safety is mainly carried out in the framework of the activities of the European Enhanced Vehicle-safety Committee – EEVC of which Italy is member.

Researches conducted by EEVC are taken into account by the European Commission when preparing new legislation on road vehicle safety and by the UNECE which adopts technical regulations under the framework of the 1958 and 1998 Agreements.

The EEVC technical work is made by nine working groups, six of them dealing with passive safety, two with active safety and one with accidentology.

In the future, further progress in vehicle safety is mainly expected in the area of active safety rather than passive safety, but also in the field of integrated safety (combining passive and active safety for a more realistic performance evaluation). A key role is expected to be played by accidentology that will allow the definition of testing scenarios as well as real world assessment of active and passive systems.

Several are the ongoing actions.

With reference to accidentology and data collection Italy, through Florence University and FCA, is involved in the **IGLAD** (Initiative for the Global Harmonisation of Accident Data) **Consortium**. IGLAD was initiated in 2010 by European car manufacturers and is a consortium for harmonisation of global in-depth traffic accident data to improve road and vehicle safety. Main objectives of the consortium are the data collection and the recoding of data according to a standardized data scheme to enable comparison between datasets. At present, information on 75 variables regarding accidents, roads, participants (vehicles or VRU's), occupants and safety systems have been harmonized.

In the field of active safety, with more emphasis on the driver monitoring, a relevant Italian research project is **DRIVE IN$^2$** Project (DRIVEr Monitoring: Technologies, Methodologies and IN-vehicle INnovative systems for a safe and eco-compatible driving), which is coordinated by FCA Italy and involves several Universities.
The project received the Smart Communities award at SMAU (Salone Macchine, Attrezzature Ufficio, -exhibition of machinery and equipment for office) the most important Italian event dedicated to Information & Communication Technology- Naples, 2014. The objective is to develop advanced methodologies, technologies and systems for driver-vehicle interaction that help prevent accidents and reduce polluting emissions, with particular emphasis on the role of the driver. A key strength of the project is its multi-disciplinary approach, which includes:

- cognitive and behavioural analysis to identify factors having the greatest impact on the level and quality of driver awareness;
- monitoring of physical and psychological condition of drivers, including alcohol and/or drug use;
- application of data fusion and data mining techniques for an integrated analysis of vehicle variables;
- monitoring of driving style to determine maximum efficiency thresholds for key vehicle performance parameters.

One of the most interesting results from the project was the development of the SIM-Panda, the first prototype for safe road testing of driver monitoring systems. The vehicle enables realistic testing of systems that monitor the effects of fatigue, intoxication etc., without the dangers associated with real non-controlled driving conditions.

The Italian Ministry for Transport and Infrastructure recognized the DRIVE IN2 project as one of best practice, according to the National Action Plan for Intelligent Transport Systems (ITS), which was adopted by Ministerial Decree of 12 February 2014.

In the field of integrated safety, a relevant Italian project is **APPS4Safety** (Active Preventive Passive Solutions for Safety). The project is co-founded by Research Ministry and is included in the programs of DATTILO (the transport and logistic district), in the Campania Region. The project is coordinated by FCA (Italy), and is developed in collaboration with universities, several engineering firms and SAPA, an automotive parts supplier. APPS4Safety is focused on increasing the use of virtual engineering tools and methodologies in the automotive design and validation process to achieve a more integrated approach to safety challenges.

This multidisciplinary approach includes use of accidentology data, advanced components for non-conventional crashes (i.e., small overlap and pedestrian crash), new active and preventive safety technologies and systems, driving simulators, and new procedures for testing in the laboratory, on the vehicle or in a virtual environment.

With reference to ADAS evaluation Italy, is involved in the "Harmonization Group on Prospective Effectiveness Assessment for Road Safety (PEARS)". The objective of the group is to provide an open platform to discuss methodologies to evaluate the real-world effectiveness of advanced driver assistance systems in potentially hazardous traffic scenarios through virtual simulation. This cooperative research and development initiative involves major automakers, universities and automotive research institutes in Europe.

With reference to new test procedures Italy, is involved into the **CATS consortium** (Cyclist Autonomous emergency braking Testing System). The Consortium is working into the definition of a new testing procedure to assess Cyclist AEB (Autonomous Emergency Braking) systems and consumer tests of those systems.

Finally, Italy is involved in the field of tertiary safety on the work about new ISO 17840-1 for emergency rescue sheets.

## ACTIONS TO BE TAKEN

Italy has been experiencing the greatest and most relevant amelioration process in the field of road safety during the last 30 years, which made it possible to re-align with the other EU countries.

A series of actions have been recommended by the transport administration and are being considered at political level.

First of all, in order to improve the effectiveness on road safety it is necessary to reinforce the action and ensuring a better coordination at central, regional and local level

In this respect, the Directorate General for Road Safety of the Ministry of Infrastructure and transport

plays a pivotal role. This organisation is linked to the corresponding regional offices which makes it possible to deal with road safety in a more systematic way.

Secondly, it is clear that the enforcement action is producing positive effects; therefore, we expect to continue to increase the number of controls on the roads with a better and dissuasive enforcement of traffic rules.

Another priority is the creation of a road safety culture, starting from school level with the aim of making the young population more aware of the need of careful and responsible driving. This priority should also concern administrations dealing with road safety in order to better train the existing human resources and prepare the new professionals to better deal with the subject.

The Road Safety National Plan has strongly recommended the adoption of a monitoring network based on local administrations and coordinated at national level. The aim of the monitoring is to have a better knowledge of the state and the evolution of road safety, the road safety measure adopted during the years and the results which have been achieved, to assess the effectiveness of the adopted measures.

---